ANGEWANDTE CHEMIE
International Edition in English
Volume 28 · Number 1
January 1989
Pages 1–134

Chemical Aspects of Fusion Technology

By Hans J. Ache

Managing thermally controlled nuclear fusion will certainly be regarded one day as one of the most successful accomplishments in nuclear physics. At the same time, however, it will represent a technical achievement unparalleled in the history of science and engineering. This in turn would mean, in retrospect, that decisive contributions had to come from a number of disciplines as diverse as materials and engineering sciences and classical chemistry, and that the same collaboration will have to continue in the future in order to reach the ultimate goal, to construct a reactor capable of producing energy from almost inexhaustible source materials (fuels), such as deuterium and lithium. What is the chemist's role in this development? Similarly as in the development of fission reactors, i.e., the nuclear power plants currently in operation, chemists will have to ensure the existence of a reliable fuel cycle—starting from the availability, storage and reprocessing of the fuel through to the provision for safe storage of the waste. In this review article an attempt will be made to outline the problems associated with these tasks and the approaches to be made by the chemist in solving them.

1. How Does a Fusion Reactor Work?

The underlying principle of nuclear fusion is that atomic nuclei are brought together close enough to fuse despite the repelling electric forces of their two identical charges. In D-T fusion, i.e., the fusion reaction at present standing the best chance of technical realization, this process requires deuterons and tritons with a mean thermal energy of about 10 keV. Consequently, a temperature of ca. 100 million K must be produced in the fuel mixture (plasma) of such a fusion reactor.

[*] Prof. Dr. H. J. Ache
Kernforschungszentrum, Institut für Radiochemie
Postfach 3640, D-7500 Karlsruhe (FRG)
and
Lehrstuhl für Instrumentelle Analytik und Radiochemie der Universität
Kaiserstrasse 12, D-7500 Karlsruhe (FRG)

Fusion of a deuterium nucleus and a tritium nucleus leads to the production of a He-4 nucleus (α-particle) and a high-energy neutron (14.1 MeV).

$$D + T \longrightarrow {}^4He(3.5\ MeV) + n(14.1\ MeV) \quad (1)$$

The neutron, which carries some 80% of the energy released in the reaction, leaves the plasma without undergoing any major interactions, penetrates the first wall of the reactor, transfers its energy by collisions in the blanket, and produces the tritium necessary to maintain the fuel cycle (Fig. 1) in nuclear reactions with the Li-bearing breeding material in the blanket. This means that 80% of the energy produced in the fusion process is no longer available to maintain the temperature required in the plasma. Consequently, it is imperative that the remaining 20% available

 © VCH Verlagsgesellschaft mbH, D-6940 Weinheim, 1989 0570-0833/89/0101-0001 $ 02.50/0

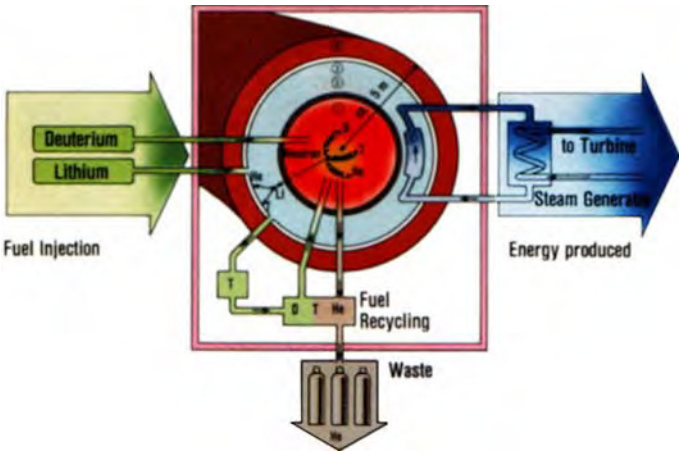


Fig. 1. Schematic diagram of a Tokamak-type fusion reactor (from [1a]): ① = Plasma; ② = First wall; ③ = Blanket; ④ = Magnet coils; ⑤ = Heat exchangers.

as kinetic energy of the α-particles be used most efficiently for plasma heating so as to make up for the heat flow delivered to the outside in the steady-state mode of operation by radiation, thermal conduction, and convection. This is done in the so-called Tokamak reactor,[1] (Tokamak being a russian abbreviation for toroidal magnet chamber), where strong magnetic fields—produced by superconducting magnets—permeate the burning plasma. These magnetic fields are aligned so that the electrically charged plasma particles are compelled to move helically along the magnetic flux lines, thus largely preventing any contact between these particles and the chamber wall and, hence, any heat transport to the wall. The plasma is first heated by induction currents (ohmic heating), a technique which can now attain plasma temperatures of ca. 10^7 K. As this temperature is still one order of magnitude lower than the 10^8 K required for fusion, additional heating techniques are under development, such as the injection of accelerated particles and exposure to electromagnetic waves. In order to keep within tolerable limits the heat release by the plasma through radiation, continuous removal of the helium produced and of any other impurities contained in the plasma chamber must be ensured.

The tritium generated in the blanket by fast neutrons reacting with lithium is extracted in a suitable way, purified, and supplied to the combustion chamber as a fuel together with deuterium. The energy deposited in the blanket by the fast neutrons is extracted by heat exchangers. The heat is used for conventional electricity generation.

2. Preparation of Source Materials

In principle, a number of nuclear reactions can be considered for nuclear fusion. Table 1 lists some of these reactions together with data of importance in practical applications, such as the energy released in the reaction E_2, the required ignition energy E_1 (each expressed in keV as unit of ion temperature), and the ratio of the energy produced in such a reaction relative to the energy required for the reaction to proceed.[2]

Table 1. Fusion reactions.

Reaction	Energy yield E_2 [keV]	Ignition energy E_1 [keV]	E_2/E_1
$D + T \rightarrow {}^4He + n$	17600	10	1760
$D + D \rightarrow {}^3He + n$	3300	50	66
$D + D \rightarrow T + p$	4000	50	80
$D + {}^3He \rightarrow {}^4He + p$	18300	100	183
$p + {}^{11}B \rightarrow 3\,{}^4He$	8700	300	29

There are two parameters in favor of the D–T reaction: on the one hand, the relatively high energy yield associated with it and, on the other hand, the comparatively low ignition energy of 10 keV, which is certainly a very decisive factor for technical implementation.

What about the supplies of source materials required for this reaction? Deuterium is available in sufficient quantities as D_2O/HDO in water; the reserves are good for millions of years, and deuterium can be separated from light water H_2O at relatively little expense. The other fuel, tritium, is the radioactive isotope of hydrogen with a half-life of ca. 12 years. It must be synthesized by means of nuclear reactions, preferably from lithium because of the high cross sections for the appropriate reactions.[3,4] Lithium is also available in sufficient quantities in the crust of the earth and in sea water. The problem is thus reduced to the question of whether sufficient tritium can be produced from lithium, and to whether this can be achieved economically. The nuclear reactions in question are (2) and (3).

$$^6Li + n_{slow} \longrightarrow T + {}^4He \quad (2)$$

$$^7Li + n_{fast} \longrightarrow T + {}^4He + n_{slow} \quad (3)$$

Now, existing fission reactors could be used to irradiate lithium with slow neutrons and produce tritium in this way. This process is actually carried out on a small scale, albeit mainly for military purposes. Normally the source materials used are Li–Al alloys containing a few percent by weight of the highly enriched Li-6 isotope in aluminum. The tritium in this case is driven off at temperatures of ca. 600 K together with the helium produced in the same reaction.[5]

However, in terms of energy, this way of generating tritium would be extremely wasteful, considering that the fission of a ^{235}U or ^{239}Pu nucleus by slow neutrons already releases some 196 MeV of energy [Eq. (4)]. Even if one neutron were available for the Li(n,α)T reaction (2) after each fission, subsequent fusion with deuterium of the tritium atom produced in this way would generate only 17.6 MeV of energy, which is not even 10% of the energy produced in a fission reactor per fission event [Eq. (4)]. Under these circumstances, it would be more reasonable to continue making direct use of the energy produced by fission.

$$^{235}U + n \longrightarrow \text{fission products} + \text{neutrons} + 196\ \text{MeV} \quad (4)$$

It follows, therefore, that a fusion reactor is purposeful only if the tritium is generated directly in it by the fast neutrons produced in the fusion reaction [Eq. (1)]. However, as

only one neutron occurs per fusion, and not all of these neutrons can be expected to be involved in tritium production, nuclear reactions or a sequence of nuclear reactions must be used which are able to generate more than one tritium atom per fast neutron produced in the fusion process. Fortunately, lithium not only contains the Li-6 isotope, which produces tritium with slow neutrons [Eq. (2)], but also the Li-7 isotope, which has an isotopic abundance in lithium of ca. 92.5%. Li-7 reacts with fast neutrons in accordance with Equation (3), giving rise not only to a tritium atom, but also to a slow neutron, which can undergo another reaction, this time with Li-6, producing more tritium as shown in Equation (2). Consequently, the tritium yield may be increased considerably and a tritium breeding factor, i.e., a ratio of tritium produced to tritium consumed, in excess of 1 may be achieved.

Attaining a tritium breeding factor clearly in excess of unity is decisive for a fusion reactor. Hence, one of the first and foremost tasks for chemists, and especially radiochemists, was to provide the cross-sections of all nuclear reactions possible with these potential breeding materials as a function of neutron energy, which are required to calculate the tritium breeding factor. Many thousands of measurements had to be carried out for reliable predictions to be made of the suitability of a compound as a blanket material, the greatest difficulties being encountered especially in measurements of the energy and angular distribution of nuclear reactions producing secondary neutrons. Earlier reports frequently showed discrepancies in the findings published by various laboratories. However, it has meanwhile been possible to clear up most of them.

The database now available can be regarded as quite reliable, allowing neutron physicists to calculate a variety of blanket concepts, i.e., various arrangements of the blanket material.[6] These have shown that breeding factors considerably in excess of unity can be achieved in pure lithium as the blanket material. A detailed assessment of the influence of existing uncertainties in the relevant cross-sections on the determination of the tritium breeding factor led to a final uncertainty of only 2–6% in the tritium breeding factor.[7]

Should the use of "breeding" materials other than elemental Li, such as Li-silicates, Li-titanates, etc., result in the number of neutrons not being sufficient because of competing reactions of the neutrons with other elements, so that a breeding ratio in excess of unity could not be guaranteed, so-called neutron multipliers will have to be considered; these are elements which undergo nuclear reactions with fast neutrons and thereby produce several neutrons. The elements beryllium and lead, in particular, would be eligible for this purpose.

Although it may thus seem possible to maintain a fuel cycle, it must be emphasized here that not too many neutrons are available for tritium production and that the tritium produced must be handled very economically.

3. Fuel Cycle in a Tokamak Reactor

Whereas the fundamental considerations for the production of tritium could be treated quite independently of the type of reactor involved, the fuel cycle can be discussed only with reference to a specific type of reactor. The first energy-producing fusion reactors, as provided for in the European Fusion Program,[8] will be based on the Tokamak principle[1] (Fig. 1), i.e. the fusion of deuterium and tritium in a plasma. Two parameters are decisive for the ignition and maintenance of the plasma: the product of plasma confinement time and plasma density, and the temperature (Fig. 2). According to *Lawson*,[9] certain minimum levels of these parameters must be ensured for ignition to take place reliably and for the thermonuclear fire to be maintained. Since helium is produced in the fusion, the plasma becomes "diluted," which decreases the product of confinement time and density; consequently, helium must be removed in order to maintain the thermonuclear fire.

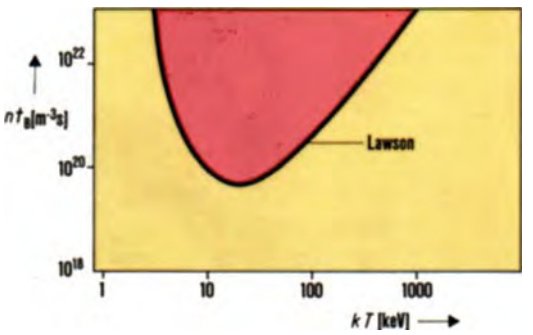


Fig. 2. Lawson diagram: The product of plasma density, (n), and plasma confinement time, (t_B), is plotted as a function of the ion temperature, kT, of the particles in the plasma. The orange area indicates the range in which a thermonuclear fire can be maintained. "Dilution" of the plasma [formed according to Eq. (1)] leads to "extinction" of the plasma. The burnup is thereby limited.

The burnup, i.e., the amount of helium produced, must not exceed a certain level, which may vary between 2% and 20%, depending on the design of the plasma chamber. This implies a continuous throughput through the plasma chamber, coupled with a continuous separation of helium from the unspent fuel mixture. A schematic diagram of such a fusion reactor is shown in Figure 1.

According to the law of conservation of momentum, the energy released as kinetic energy in reaction (1) is distributed in the ratio of 1 :4 between the α-particle (^{4}He) and the neutron. It is imperative that the majority of the α-particles with two positive charges be prevented from leaving the plasma, as their kinetic energy is required to maintain the high plasma temperature needed for the fusion process. This objective can be achieved to a large extent, but not completely, by the method of magnetic confinement used in the Tokamak principle.

The neutrons produced in the fusion process can leave the plasma, pass through the first wall and release their energy in the breeding blanket, where tritium is produced. This energy, and the energy released in the ^{6}Li(n,α)T and ^{7}Li(n,nα)T nuclear reactions, the latter of which contributes some 12% to the total energy, is "extracted" by means of a coolant, probably water. Of course, it cannot be ruled out in this process that the tritium produced in the

blanket will diffuse into the water. Such an exchange must also be taken into account in the cooling of the first wall.

The complete fuel cycle in a fusion reactor is shown in Figure 3. A distinction can be made between an inner and an outer fuel cycle: combustion in the plasma, exhaust pumping, exhaust purification, and tritium recovery from the impurities, plus downstream hydrogen isotope separation and storage in the inner fuel cycle; tritium generation in the blanket, tritium extraction and purification in the outer fuel cycle; finally, the recovery of tritium from the coolant must also be considered.

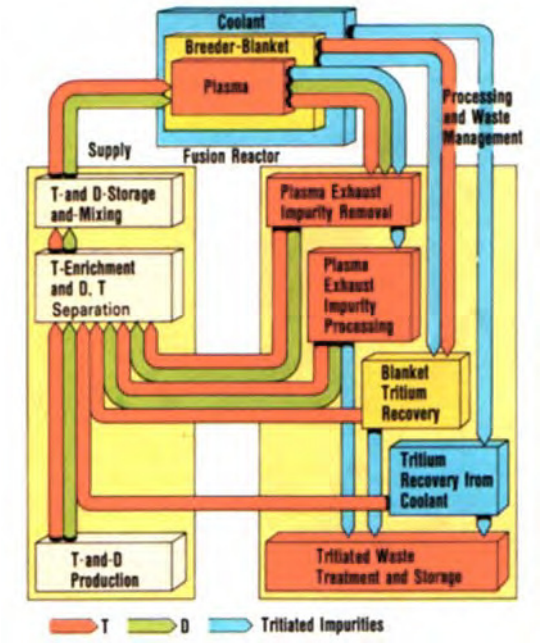


Fig. 3. Fuel cycle in a fusion reactor.

Model calculations have been carried out in order to assess the tolerable rate of total tritium losses in the system on the basis of a tritium breeding factor given by the blanket concept, and to detect those points at which losses are particularly important.[10,11] First of all, the minimum tritium breeding factor (B_{min}) required to maintain the fuel cycle had to be determined [Eq. (5)]; it is a function of the tritium loss in the system (V) and the radioactive decay of the tritium inventory ($\lambda\tau$), where λ is the decay constant of tritium and τ is the average retention time of the tritium in the system.[10]

$$B_{min} = 1 + V + \lambda\tau \tag{5}$$

The retention time, τ, (in days) is given by the tritium inventory divided by the daily tritium consumption. The total loss not due to decay can be subdivided into the losses arising in the different subsystems [Eq. (6)].

$$V = (1-f)\,V_B + V_K + (1/A - 1)\,V_R \tag{6}$$

V_B = loss in T production from the blanket; V_K = loss in T recovery from the cooling water; V_R = losses in plasma exhaust purification; f = fraction of T transferred to the cooling water in the blanket; A = T burnup in the plasma; $(1/A-1)$ = factor taking into account the fact that, for a given quantity of fuel, more runs through the system or purification steps are necessary at low burnup than at high burnup.

If $V_B \approx V_K \approx V_R$, the total loss is largely determined by $(1/A-1)\,V_R$, i.e. the losses arising in plasma exhaust purification seem to play a major role. This is explained by the fact that a given quantity of fuel required to produce energy in a power reactor will need more cycles or purification steps at low burnup than at high burnup. V_R is thus weighted by the factor of $(1/A-1)$, which is already 49 at $A = 2\%$ (Table 2). Let us explain the situation once more: If 90 g of tritium is burnt in the NET (*N*ext *E*uropean *T*orus) reactor per day, 1.8 kg of tritium must be purified each day at a burnup of 5%, whereas it would be only 0.45 kg per day at a burnup of 20%. Obviously, considerably higher tritium losses would arise in the former case. At a given breeding factor of $B \leq 1.1$ and a burnup of 5%, including radioactive decay, the losses in plasma purification can be estimated to be in the region of less than 0.1%.

Table 2. Relation between T-burnup and T-loss in the cycle [Eq. (6)].

A	$(1/A-1)$
0.1	9
0.05	19
0.02	49

For the chemist, this poses the following questions: What possibilities are there for increasing the burnup? How can losses in plasma exhaust purification be kept low enough? Or, even better, how can both objectives be met? As mentioned in Figure 2, the burnup factor is limited first by the dilution effect of the helium produced. But that is not all.

In addition to the uncharged fast neutrons produced in fusion, a considerable number of charged and uncharged helium and hydrogen particles which have escaped magnetic confinement impinge upon the "first wall" surrounding the plasma. The estimated flux in an energy producing reactor is 10^{14}–10^{15} neutrons $cm^{-2}\ s^{-1}$ and ca. 10^{16} charged or neutral hydrogen and helium particles.[12] This

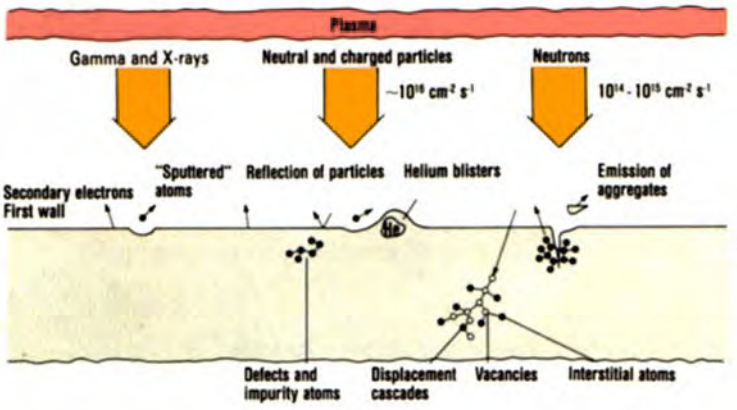


Fig. 4. Summary of the events occurring in the plasma-wall interaction.

irradiation of the first wall is certainly one of the most difficult problems in fusion and has not yet been solved satisfactorily. The interaction of these particles with the first wall may give rise to a number of chemical and physical processes, sputtering, etc., all of which will cause wastage and embrittlement of the material of the wall (Fig. 4).[13]

In addition to these materials problems, sputtering will introduce impurities into the plasma. A particularly critical situation in maintaining the fusion process arises if the plasma gas is contaminated by elements of higher atomic numbers, since their presence results in increased energy diffusion from the plasma. As a consequence, additional energy will have to be supplied to the plasma from the outside or, in other words, the ignition temperature in the plasma must be raised, as can be seen from Figure 5, where the ignition temperature is plotted as a function of the concentrations of various elements.

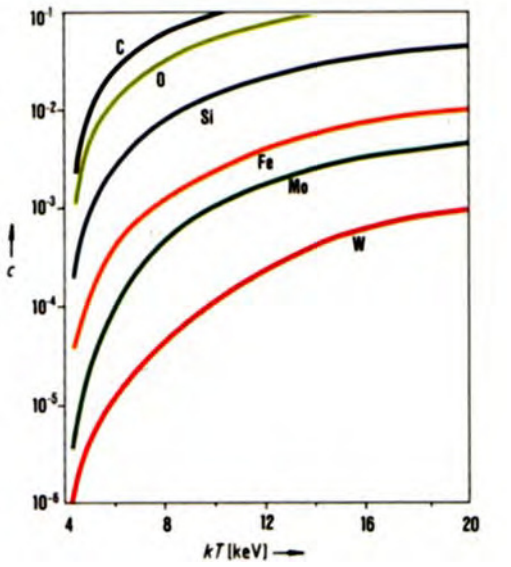


Fig. 5. Relationship between the ignition temperature kT and the impurity concentration c [atomic fraction] in the plasma for various heavy elements.

The additional burdening of the plasma with these impurities, which, like helium, must be removed continuously, means that the burnup will be decreased beyond the limit set by the dilution with the helium produced in the fusion process. If this contamination of the plasma could be prevented, it would be possible to increase the burnup and in this way also reduce the tritium losses in the plasma exhaust purification by reducing the number of cleaning steps.

In the present concept implemented already, e.g., in such experimental reactors as TFTR, TEXTOR, and JET,[14] the plasma chamber, which, at least according to current designs, would be made of stainless steel or alloys of elements of high atomic numbers, because of the extremely large mechanical and thermal stresses, is covered with a protective coating of materials of low atomic numbers, for which preferably graphite or C–H films with an H/C ratio of 0.4 can be used.[15]

4. Chemistry of the First Wall

Two aspects of the wall protection are of particular interest to chemists: what about the uptake of hydrogen in carbon? Is it possible that a tritium inventory is built up in the graphite or in the C–H films, which would create difficulties in plasma ignition, especially in the early phase, because of the adsorption of fuel in larger quantities? What kinds and what volumes of impurities get into the plasma?

These aspects have been the subject of numerous studies,[16] which have shown that hydrogen, unless it is reflected by the graphite surface, is retained in the graphite until a saturation concentration of 0.4 H/C has been reached. If more hydrogen is made available at temperatures of 900–1200 K, hydrogen is released again as H_2. When the graphite was implanted with hydrogen up to saturation, bombardment with deuterium released first pure H_2, then HD and, finally, after saturation, D_2.[17] This aspect is significant especially if the plasma chamber had been carburized, i.e., the carbon had been applied to the first wall by means of a glow discharge in a mixture of CH_4 and H_2 (Fig. 6).[18] In this case, there is again a carbon

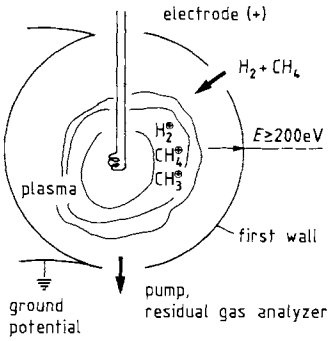


Fig. 6. Method of carburization to produce a protective carbon coating on the first wall. The plasma discharge in a mixture of CH_4 and H_2 produces a deposition of carbon films on the first wall.

layer saturated with hydrogen in a ratio of H/C ≈ 0.4. If a D–T mixture is used to ignite a fusion reactor prepared in this way, it may well be that the fuel is unduly diluted in the initial stage by H_2 released from the bombardment of the wall with D or T. It has therefore been proposed to choose the composition of the C–H film in such a way that its hydrogen isotope composition corresponds to the fuel mixture, which might be achieved, e.g., by a glow discharge in mixtures of CD_4 and T_2.[19] In addition, the diffusion of tritium into the inner layers of graphite was also of interest, as this could have led to an undesirable increase in the tritium inventory in the first wall. These studies, all of which were conducted to improve our knowledge of the chemical and physical bonding of hydrogen in graphite or, even better, in carbon, and which also included Raman and photoelectron spectroscopic as well as secondary ion mass spectrometric studies, resulted in a number of empirical models, which also took into account migration through the pores into the inner regions of the graphite. Such models for graphite are summarized schematically in

Figure 7.[16] They allow the T inventory bound in the graphite to be estimated, and show that this quantity can be considered as unimportant compared to the overall T-inventory.

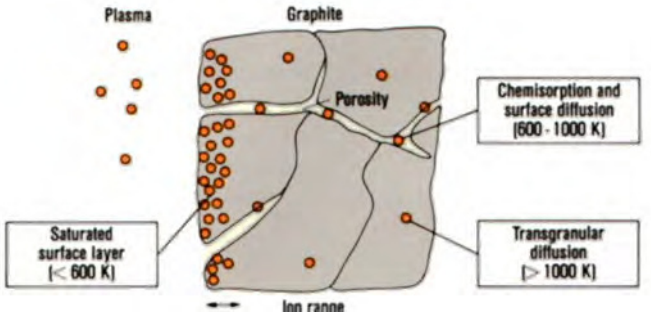


Fig. 7. Schematic diagram of the uptake of hydrogen in graphite (from [16]): Graphite produces a surface coating saturated with hydrogen (H/C = 0.4). If more hydrogen is supplied, this will be incorporated, while simultaneously releasing a corresponding amount of hydrogen already present.—Diffusion of hydrogen into the pores and transgranular diffusion on a larger scale occur only at higher temperatures.

From the results of the above experiments it was to be expected that there is no serious tritium storage during the plasma burning time, when the temperature of the graphite layer is ca. 1500 K. As a realistic upper limit, the tritium inventory bound in the graphite of the plasma chamber walls in the NET reactor is assumed to be ca. 10^{18} tritium atoms/cm^2, which adds up to a negligible quantity of 10^{25} tritium atoms for a total surface area of 10^7 cm^2.[20]

Strictly speaking, however, these conclusions relate only to the processes arising in the interaction between hydrogen and the solid graphite matrix. More recent studies have shown that the erosion to be expected to occur in graphite plates is due in approximately equal parts to physical sputtering, chemical sputtering by hydrogen, chemical reactions with oxygen, and a combination of various other effects.[21] Oxygen contamination can never be absolutely excluded in a plant as complicated as a fusion reactor. Physical sputtering leads to the formation of graphite deposits on large surface areas in the reactor, and the entrainment of large quantities of tritium in these deposition layers e.g., bound by co-deposition cannot be ruled out. In this connection it should also be pointed out that physicochemical quantities, such as the solubility of hydrogen in graphite at temperatures of ca. 1500 K, are still unknown and need to be studied before any final statements can be made about the hydrogen storage capacities of graphite or similar materials.

The release of tritium as T_2 is not the only possibility resulting from an interaction between hydrogen and a graphite surface saturated with hydrogen. In addition to the absorption and desorption of hydrogen, also the products formed as a consequence of the reactions between energetic hydrogen particles and carbon are of interest, as they result in contamination of the plasma. Studies on the reactions of thermal and energetic hydrogen atoms or ions with graphite and with carbon films (H/C = 0.4) have shown that the chemical erosion of carbon includes the production of hydrocarbons,[22,23] especially of methane or

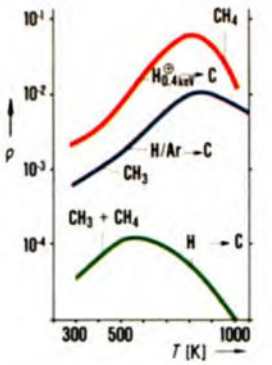


Fig. 8. Reactions of thermal and energy-rich hydrogen with graphite (from [24]): Thermal hydrogen produces mainly CH_3; energy-rich hydrogen produces CH_4; ρ = reaction yield per H atom, T = target temperature.

methyl radicals. Figure 8 shows a plot of the hydrocarbon yield as a function of the target temperature T for several kinetic energies of the impinging particles, atomic hydrogen or hydrogen ions. It can be seen that, in an equilibrium state, i.e. in the presence of a surface saturated with hydrogen (H/C = 0.4) the yield of CH_4 upon irradiation with hydrogen ions of 0.4 keV energy is 4×10^{-2} CH_4 per $H^{\oplus}$ at 800 K.[24] The desorption of H_2 is always roughly two orders of magnitude higher, under otherwise unchanged conditions. It would be extremely important to find materials in which the formation of hydrocarbons and, hence, the contamination of the plasma and also erosion is diminished. However, for the time being it must be assumed, as has been borne out by experiments in JET, that the plasma exhaust will contain 10% of the tritium bound to methane at a burnup of 5%, which leaves it to the chemists' creative imagination to find ways of purifying the exhaust and recovering the tritium, and do all this at a loss of less than 0.1%.

5. Chemistry of the Internal Fuel Cycle—Tritium Recovery

Regarding the plasma exhaust purification process, the chemist is presented with the following tasks: firstly, the process should be so designed that it proceeds effectively and as quickly as possible at the lowest possible temperature so that diffusion losses are avoided and, secondly, the process should not involve any appreciable formation of tritiated waste, and thus not cause any loss of tritium.

Irrespective of the first wall being covered with a protective coating or not, as described in Section 4, methane must in any case be considered as a possible impurity in the plasma gas. However, it certainly will not be the only impurity. First and foremost, outgassing of various materials at the high operating temperatures encountered will also cause compounds other than methane, e.g., CO, CO_2 and H_2O, to enter the plasma. Moreover, in a machine as large and complicated as this, minor leakages can never be excluded entirely, which means that minute quantities of nitrogen and oxygen will penetrate into the plasma chamber, thus probably causing further contamination of the plasma with nitrogen compounds such as nitrogen oxides and ammonia.

A suitable purification procedure must therefore provide for all these components of the plasma exhaust. Moreover, the hydrogen flux resulting from this process must not contain more than 100 ppm of He and 1 ppm of other impurities, since otherwise there will be difficulties in downstream low-temperature rectification of the hydrogen isotopes.

Since such quantities as the daily throughputs of tritium and deuterium, the volume of blanket material and the like are also of importance in choosing the process techniques, the operating conditions assumed in the NET concept will serve as a basis for the following discussions.

NET is the successor to JET (Joint European Torus) and will serve as a basis for the construction of a demonstration machine (DEMO).[7] While the JET program is primarily geared to resolving problems in the physics sector, the NET program is designed to generate a burning plasma and, concomitantly, to serve as a test-bed for the more important reactor components, such as the first wall, blanket, and the tritium generation and purification systems. DEMO is planned to be a reactor capable of generating energy and breeding its own tritium, albeit as yet not optimized economically.

A peak power of 747 MW has been estimated for NET with a duty cycle of 0.8, which corresponds to plasma burning times of ca. 1000 s interrupted by down-times of ca. 250 s. At an availability of 100%, this results in a tritium consumption of 91 g and a deuterium consumption of 60.8 g per day. At a burnup of 5%, i.e., if the respective burning of tritium and of deuterium in the plasma is to be limited to 5%, this means a daily througput of 1824 g of tritium and 1217 g of deuterium.[25] These quantities must be purified daily.

5.1. Primary Purification of the Plasma Exhaust

There are essentially four techniques[26] which can be applied to separate hydrogen from the impurities in the inner fuel cycle, each of them raising interesting questions for the chemist.

5.1.1. Palladium-Silver Membranes

The first of these techniques is based on the application of palladium-silver membranes, which are permeable to hydrogen at elevated temperature (>600 K), while retaining impurities.[27] The major advantage of this technique, which is shown schematically in Figure 9, lies in its continuity; however, two critical problem in particular arise from the application of this technique to fusion technology:

1. Embrittlement of the palladium–silver alloy by helium (produced as tritium decays within the membrane) and by frequent temperature changes, as are required when the purification system is started up and turned off.
2. Reversible or irreversible coating of the membrane surface with substances which impede the passage of hydrogen (membrane poisoning).

While the mobility of helium and, hence, outgassing from the membrane, is considered to be sufficient at the operating temperature of the membrane, it is not yet known what maximum contamination of potential poisons to the phase transit reaction is tolerated by the membrane. For carbon monoxide, for example, it was observed that, up to concentrations of 8.2×10^{-3} mol L^{-1}[28] and even higher contents of other gases, such as ammonia, carbon dioxide, and nitrogen, there was no reduction in the flow of hydrogen; methane does not impair the membrane surface even at concentrations up to 40%.[29] More extensive (surface) studies must be carried out in this area in order to gain a better understanding of these poisoning phenomena and, thus, embark on specific further developments in the production of these membranes.

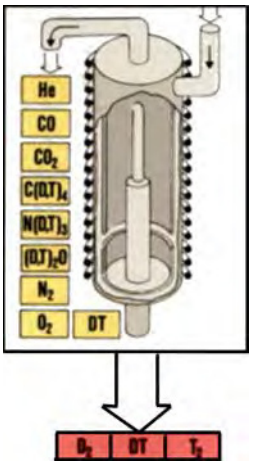


Fig. 9. Schematic diagram of the removal of impurities from the plasma exhaust by means of the Pd/Ag membrane. Advantage: continuous process; disadvantages: the waste stream contains T, embrittlement with changes in temperature, poisoning by certain compounds.

A fundamental problem associated with membrane techniques is the possibility of obtaining a hydrogen flow free from impurities, but not a flow of impurities free from hydrogen. That is, the recovery of tritium from the flow of impurities in a second process step is indispensable.

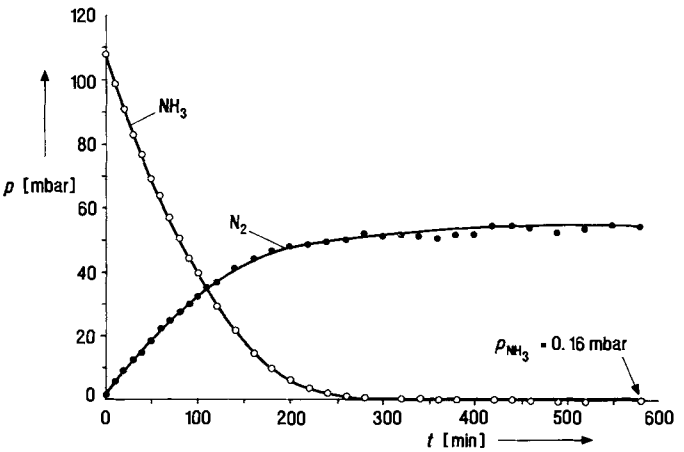


Fig. 10. Catalytic decomposition of ammonia on the surface of a Pd/Ag permeator [29].

A special advantage associated with the use of palladium–silver membranes is the catalytic decomposition of ammonia, one of the expected impurities in the reactor exhaust, on the surface of the permeator. This reaction has been observed and quantified in connection with experiments performed on the decomposition of ammonia by transition metal catalysts.[29] Figure 10 shows typical curves for the concentrations of ammonia and nitrogen while a helium/ammonia mixture is being circulated, and Figure 11 shows the dependence of the decomposition rate on pressure as determined from the experiments. Hydrogen is separated simultaneously, thus shifting the chemical equilibrium of reaction (7)

$$2\,NH_3 \rightleftharpoons N_2 + 3\,H_2 \qquad (7)$$

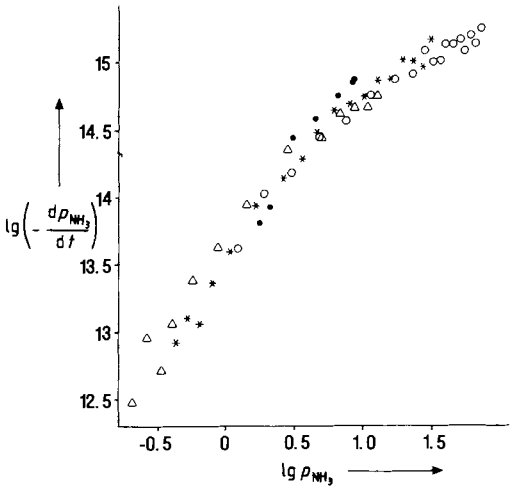


Fig. 11. Kinetics of ammonia decomposition in a Pd/Ag permeator [29]. Initial pressure p [mbar] of NH_3: ○ = 108.1, * = 60.4, ● = 49.7, △ = 32.9. dp_{NH_3}/dt in molecules $cm^{-2}\,s^{-1}$.

in the direction of the elements. As shown in Section 5.2, tritium bound to nitrogen and deuterium can be recovered in the same way.

An arrangement for the separation of deuterium and tritium from the reactor exhaust, which would be suitable for NET, would be a bundle of 250 or 300 palladium–silver tubes of ca. 1.6 mm diameter and roughly 40 cm long, which would be operated at ca. 600 K and an inlet pressure not exceeding 1 bar. The hydrogen partial pressure on the outlet side could be kept below 1 mbar, thus allowing the hydrogen isotopes to be separated as quantitatively as possible in the very first process step.[25]

5.1.2. Hot Metal Getters

The second method of hydrogen separation uses hot metal getters. Purifying various gases is possible, in principle, by selective getter reactions in specific solids. Thus, various metals such as uranium, titanium, and zirconium or some of their alloys react, partly at high temperatures, with hydrocarbons, carbon oxides, ammonia, nitrogen, hydrogen, water, and oxygen in irreversible reactions producing carbides, nitrides and oxides, and in reversible reactions producing hydrides,[30–35] as is shown schematically in Figure 12. The reactivity depends very much on temperature,

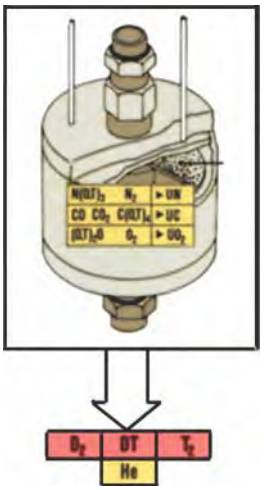


Fig. 12. Schematic diagram of the removal of impurities from the plasma exhaust by means of hot metal getters. Advantages: continuous method, irreversible retention of nitrogen, carbon, and oxygen, negligible retention of hydrogen at higher temperatures; disadvantages: requires high temperatures, produces large amounts of waste.

the state and size of the surface area, and the composition of the getter material. Figure 13 shows the coexistence lines for thermodynamic equilibrium of uranium and titanium with their respective hydrides, and, for a zirconium–aluminum alloy commercially available as ST 101 getter material,[36] a pressure limit for hydrogen above which the material will embrittle at the respective temperature due to reaction with hydrogen. It should be noted that the logarithmic pressure scale in Figure 13 covers more than 10 orders of magnitude.

Whereas uranium no longer produces hydride above 650 K at the hydrogen partial pressures under discussion

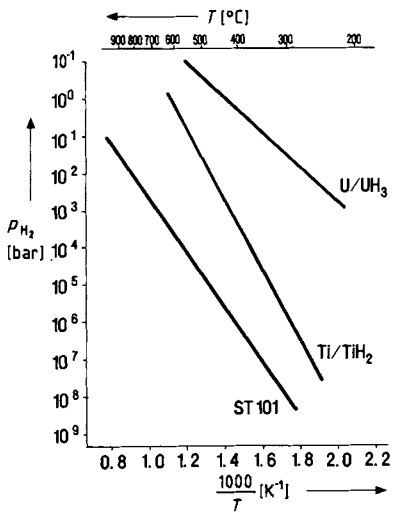


Fig. 13. Hydrogen equilibrium pressures as a function of temperature in various metal/metal-hydrogen systems [29].

($p_{H_2} \leq 0.1$ bar) and thus no longer binds any hydrogen (aside from its sparing solubility), in the case of titanium this is true only for temperatures above 850 K; the zirconium-aluminum alloy would even have to be used at temperatures above 1200 K in order to minimize the hydrogen inventory of the getter and avoid embrittlement.

The lower temperature limit for the formation of uranium carbide from hydrocarbons or carbon oxides is estimated to be around 1100 K[32,37] for kinetic reasons and, especially, because of the rate of diffusion of the reaction product into the interior of the solid. Similar temperatures apply for titanium and zirconium-aluminum alloys.[38,39] Also ammonia and nitrogen are converted into metal nitrides only above ca. 900 K.[38,39] The metal oxides are, by comparison, produced relatively easily by reaction with water or oxygen: in the case of uranium, e.g., the oxide formed on the metal surface at only 450 K does not act as a protective coating for the base metal. The reaction with water may also lead to formation of uranium hydride, independently of the partial pressure and the temperature.[32]

When using these hot-metal getters in fusion technology it must be borne in mind that prolonged use, e.g., of uranium, leads to saturation by the nitride, carbide, etc., which reduces the efficiency of the getter; normally, this point is reached when about 10% of the uranium metal has been used. This means that the getter must be replaced periodically, thus giving rise to considerable amounts of radioactive waste. Since uranium is relatively expensive and is pyrophoric when finely distributed, it should as far as possible be replaced by other getter materials, e.g. zirconium-aluminum alloys (SAES getters) or zirconium-cobalt alloys. Therefore, in the search for suitable substitutes, of primary interest regarding the potential systems are the determination of physicochemical data, such as hydrogen solubility, diffusion constants, phase diagrams, and the kinetics and thermodynamics of their reactions with hydrogen, carbon, oxygen, and nitrogen. In particular, a knowledge of the kinetics of formation and decomposition of these compounds is of decisive importance in deciding whether a material can be used as a getter or not. Moreover, getter-poisoning by certain compounds or elements also plays a role, which, in turn, necessitates surface chemistry studies being carried out in order to elucidate the reactions occurring under these conditions. The advantage of plasma gas purification by getters without a further tritium recovery step, as would be required in the use of Pd/Ag membranes, is offset by the disadvantage that most of these getters require high temperatures, thus raising problems of tritium diffusion to the outside. Current efforts are claimed at finding getter materials which are already effective at low temperatures. Furthermore, this technique requires separation of the helium before the hydrogen isotope mixture can be separated by low-temperature rectification.

5.1.3. Molecular Sieves

The third method is based on the adsorption of impurities on molecular sieves at temperatures around 300 K and 75 K, respectively,[40,41] as shown schematically in Figure 14. Although this method is rather simple in principle, it is a batch process also requiring subsequent separation of the helium, which can be achieved by conversion of the tritium into uranium tritide and pumping off the unbound helium. The impurities adsorbed in the molecular sieve are pumped off periodically at elevated temperatures and need to be processed further (see Section 5.2).

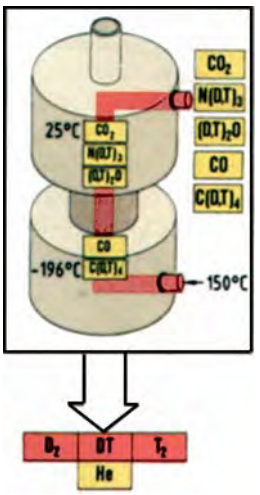


Fig. 14. Schematic diagram of the removal of impurities from the plasma exhaust by means of molecular sieves. Advantage: proven technique; disadvantages: the waste stream contains T, batch process.

A problem associated with the use of adsorbers, such as zeolites, is the possibility of an isotope exchange between the tritium adsorbed, e.g., as water, and the residual water content in the zeolites, which cannot be removed even at higher temperatures.[42] To what extent this process may result in an undesirable increase in the tritium inventory in the adsorber is presently the subject of numerous investigations.

5.1.4. Selective Freezing

The fourth method makes use of selective freezing of the plasma exhaust in cryopumps,[26,43] which are also used to pump off the plasma. In order to achieve CH_4 separation down to the 0.1 ppm level required for subsequent removal of the hydrogen isotopes, temperatures of <45 K are necessary; the corresponding temperature for the separation of N_2 and CO is 28 K. Calculations have shown that also significant quantities of DT and T_2 are frozen out together with these impurities,[26] which means that the impurities separated need to be reprocessed, as in the molecular sieve and Pd/Ag membrane methods. Estimates have shown that approximately ten times more DT/T_2 enters the waste stream to be reprocessed than is the case with the Pd/Ag membrane.

5.2. Recovery of Tritium from the Plasma Exhaust Impurities

As explained in Section 5.1.1, separation of the plasma exhausts by means of the Pd/Ag membrane technique pro-

duces a gas stream containing not only the impurities that have been removed from the plasma, but also slight quantities of tritium as DT or T_2. According to a quantitative estimate, this stream will amount to 1–6% of the plasma exhaust stream. Further purification by the membrane technique does not seem to be feasible because of the increased hazard of membrane poisoning as a result of the high concentration of impurities. Consequently, other methods will have to be envisaged for the reprocessing of such a stream and the recovery of tritium from its tritium-bearing components.

A similar stream of impurities arises upon regeneration of molecular sieves if the plasma exhausts are purified by cryoadsorption (see Section 5.1.3) or cryopump techniques are used. The decisive aspect to be borne in mind when selecting the methods for recovery of tritium from the impurities is, as also in exhaust purification itself, the minimization of tritium losses into the open, i.e., in cooling systems, laboratory or reactor spaces, and also in the form of radioactive waste. Consequently, first and foremost, diffusion must be minimized and, since this is determined by the temperature, also the temperature must be kept as low as possible in all reactions; secondly, the catalysts and getters etc. must be chosen especially from the point of view of their regenerability, so as to limit the accrual of radioactive waste. That is, the complex composition of the reactor exhaust so far as a simple and quantitative recovery of deuterium and tritium is concerned, requires a sophisticated combination of a variety of physicochemical processes. Even the sequence of possible steps is in no way trivial. In principle, only a minimum number of process steps should be sought for, at temperatures as low as possible and involving a minimum of radioactive inventory; not only are high decontamination levels in the process exhaust called for, but also minimization of secondary wastes.

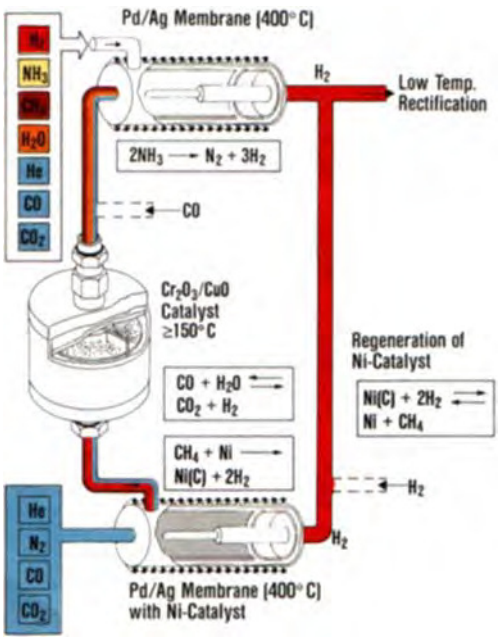


Fig. 15. Flowsheet for the removal of impurities from the plasma exhaust by means of a combined Pd/Ag membrane-catalyst-Pd/Ag membrane (cracking) process [42].

Recently,[29] a combination of several process steps was reported which seems to optimally fulfill the requirements regarding lowest possible process temperatures and minimum accrual of waste. The flowsheet is shown in Figure 15.

Since the reactor exhaust consists mainly of unburnt deuterium and tritium, the most reasonable first process step must surely be the removal of the bulk of these two species. Because of the advantages of low operating temperature (ca. 650 K), the very low stationary tritium inventory, the high efficiency of tritium removal, and, especially, the high purity of the product, this is done in the concept discussed here by means of a palladium/silver permeator, which is so dimensioned that the hydrogen content can be reduced to 1%.[25] At the same time, the small amounts of ammonia to be expected in the reactor exhaust are catalytically converted into the elements on the palladium/silver tubes, and the hydrogen reaction product is removed together with the main process gas.

In general, the concentration of impurities is low at the inlet of the permeator, which makes poisoning rather unlikely. It is known that water does not reduce the permeation rate.[29,44] The permeability in the presence of higher concentrations of CO is decreased only at temperatures below 575 K. The concentrations of both compounds are coupled via the reactions (8), (9) and (10).

$$2\,CO + 2\,H_2 \rightleftharpoons CH_4 + CO_2 \quad (8)$$

$$CH_4 + H_2 \rightleftharpoons CO + 3\,H_2 \quad (9)$$

$$CO + H_2O \rightleftharpoons H_2 + CO_2 \quad (10)$$

Molecular oxygen is not expected to arise, because of the large excess of hydrogen and because of the catalytic activity of palladium in the generation of water. Consequently, the removal of hydrogen in the Pd/Ag permeator will shift the thermodynamic equilibrium in the direction of carbon dioxide production.

Water present in the exhaust can be catalytically reduced by means of CO, which would have to be added, on

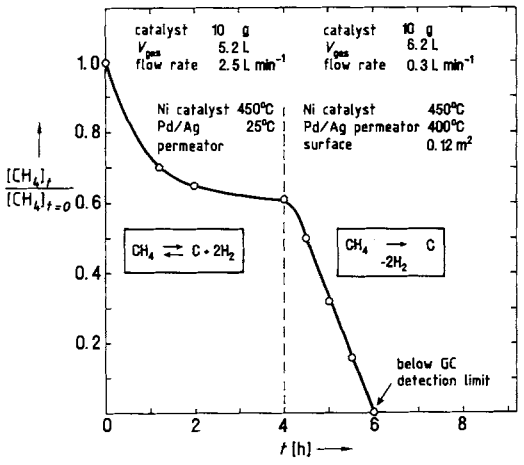


Fig. 16. The methane cracking reaction in a closed circuit at 450°C on a nickel catalyst, first without (left) and then with hydrogen removal by a Pd/Ag membrane (right) [29].

a Cr_2O_3/CuO bed at about 420 K. The final process step is the conversion on a bed consisting of palladium/silver permeator and nickel/aluminum oxide catalyst.

Figure 16 shows the results of equilibration experiments[29] which were run in a closed loop with a mixture of 40 vol.% methane (0.093 mol) in helium on a 10 g nickel/aluminum oxide catalyst at 720 K. It follows from Figure 16 that the mixture can be thermodynamically equilibrated within four hours.

Calculation of the methane equilibrium concentration as a function of pressure and temperature using thermodynamic standard data (Fig. 17) gives an excellent agreement

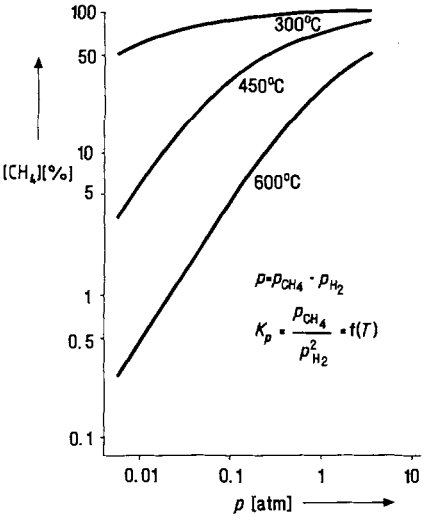


Fig. 17. Methane equilibrium concentrations at various temperatures as a function of the total pressure [29].

of the value calculated at 720 K for $p = 580$ mbar with that measured in the experiment described above. As the temperature of the catalyst is raised or lowered, the methane concentration follows the calculated curve, that is the reaction is reversible. A palladium/silver permeator integrated into the circuit and operated at ca. 675 K allows selective removal of the hydrogen produced, thus shifting the equilibrium to methane concentrations below the limit of gas chromatographic detection (Fig. 16). Because of the reversibility of the reaction, the carbon deposited on the catalyst during methane decomposition can be reconverted into methane by reaction with hydrogen at temperatures of 720–770 K.

This direct combination of cracking reactions and hydrogen permeation is likely to produce very high decontamination levels. Furthermore, no sizable amounts of waste, at least of waste which cannot be regenerated should be formed in this process, and thus loss of tritium ought to be minimized.

The hydrogen recovered and purified in one of the methods described above (decomposition of NH_3 and CH_4, reduction of H_2O with CO) can be decomposed into its isotopes either by cryogenic distillation,[45] thermodiffusion, or by means of gas chromatographic techniques.[46,47]

A fourth method of tritium enrichment by photochemical dissociation of tritiated trifluoromethane or similar compounds using laser radiation is still in the early stages of development and will therefore not be covered in greater detail here.[48] The basic principle of this technique is the excitation of the molecule, by means of a pulsed CO_2 laser, to such a level that it dissociates into CF_2 and TF. The reactive TF can be removed from the hydrocarbon stream by well-known techniques.

Also the question of tritium storage has largely been solved. In all modern techniques the tritium gas is converted at relatively low temperatures into a solid metal hydride (metal tritide) [Eq. (11)],[49] the metals used being preferably uranium, zirconium, and titanium. At higher temperatures, these metal hydrides again decompose into tritium and metal.

$$M + \frac{x}{2} T_2 \rightleftharpoons MT_x \qquad (11)$$

For instance, under equilibrium conditions, the tritium pressure across the UT_3/U system is 3.5×10^{-4} torr at 350 K and ca. 5×10^2 torr at 670 K.

The kinetics of hydride formation and decomposition, and the influence of gaseous impurities, such as air, or that of the decay of tritium (according to $T \xrightarrow{\beta^-} {}^3He$) producing ^3He, have been studied in great detail. One of the important considerations is that these metal tritides are stable under the usual storage conditions; thus, e.g., for zirconium hydride in air an ignition temperature between 720 and 830 K was observed, whereas uranium hydride is more pyrophoric.

The tritium stored in this way can now be released again as a gas and, after having been mixed with deuterium in a 1:1 ratio, can be fed back into the plasma chamber of a Tokamak reactor, where it can be ignited at high temperature (ca. 10^8 K). The rates of feeding the fuel and extracting the plasma gases are determined by the rated power of the reactor and the burnup of tritium and deuterium.

6. Blanket Chemistry

The blanket serves three purposes; firstly, it must not only accommodate the energy of the fusion neutrons, whose kinetic energy amounts to some 80% of the fusion energy, but also the energy released in the exothermal neutron capture reactions (such as $^6Li(n,\alpha)T$), which contributes another 12% to the total fusion energy, and convert this energy into heat to be removed from the blanket in a way suitable for further use. Secondly, it, i.e. its lithium part, represents the target material, with which the neutrons produced in the fusion reaction undergo nuclear reactions, to furnish the fuel required for fusion, namely tritium. Finally, the blanket also serves, at least in part, as a shield for the immediate environment of the fusion reactor, including the relatively sensitive superconducting magnets, against neutron radiation.

These criteria result in the following boundary conditions for the proper choice of blanket material:

1. It must enable a tritium breeding factor in excess of 1 to be achieved.

2. Extraction from the blanket of the tritium bred should be easy. It should be possible to minimize the tritium inventory in the blanket.
3. It may neither react with the material of the vessel nor with the coolant transferring the thermal energy from the blanket, e.g., to a steam generator.

As already mentioned in Section 3, the second part of the fuel cycle concerns the extraction of tritium from the breeding blanket, the purification of the tritium bred and its introduction into the plasma. An assessment, for this external fuel cycle, of the tritium breeding ratio vs. the losses and the retention time in the same way as made for the internal fuel cycle [Eq. (5)], and under the assumption that the losses can be restricted to 0.1%, as in the inner cycle, should give rise to the expectation that this time, the radioactive decay should play a more important role because of the expected longer retention time of the tritium in the blanket and especially if larger quantities are transferred to the cooling water ($f \geq 0.5$). For the chemist, this raises the problem of investigating those parameters for the potential breeder materials which determine the retention time and thus also the tritium inventory in the breeder blanket. In principle, two types of blankets are under consideration:[50]

1. The "liquid" blanket consisting of lithium metal or the eutectic lithium–lead mixture.
2. The solid blanket, for which mainly lithium compounds can be used, such as lithium silicates, titanates, aluminates, etc.

6.1. Liquid Metal Blankets

Let us first consider the case of a "liquid" blanket. In this category, only the so-called liquid metal blankets consisting of pure lithium metal or the eutectic lithium–lead mixture, $Li_{17}Pb_{83}$ (m.p. 508 K), must be seriously taken into account.[50,51] For both these materials a breeding factor in excess of unity has been predicted. Various methods of tritium extraction have been proposed for this type of blanket. The successful development of an extraction technique, however, requires that the fundamental physicochemical data be known, such as the solubility or distribution equilibria of the compounds to be extracted between the phases involved in extraction. Hydrogen is known to be dissolved in metals generally on an atomic basis. Its distribution between the metal and the gas phases is determined by the Sievert equation [Eq. (12)], K_S being defined by Eq. (13).

$$S = K_S p^{1/2} \tag{12}$$

$$\lg K_S = A + \frac{B}{T} \tag{13}$$

where S = solubility of hydrogen in the metal in atom-ppm (appm). K_S = Sievert's constant (appm torr$^{-1/2}$), p = hydrogen partial pressure (torr), A and B are constants (B is related to the dissolution energy).

The first task for the chemist, therefore, was to clarify whether this relation also applies under the conditions of fusion technology, i.e., at extremely low tritium concentrations and high temperatures. Investigations showed[52,53] that the equation (12) does indeed apply under all conditions related to fusion. At the same time, it was observed that the solubility of hydrogen in $Li_{17}Pb_{83}$ is several orders of magnitude lower than it is in pure Li metal.[53] This is due to the fact that the Li activity responsible for the solubility of hydrogen is largely reduced in the mixture as compared to pure Li. To illustrate these differences, let us assume that 1 appm of hydrogen is dissolved in each of these materials at 773 K; this results in an equilibrium partial pressure of hydrogen over Li metal of 2×10^{-11} torr, while, in the case of the Li–Pb mixture, it is already 4×10^{-2} torr.[54] From this standpoint it would seem much simpler to extract tritium from the $Li_{17}Pb_{83}$ mixture than from lithium metal.

Despite the relatively high solubility of tritium in lithium metal, recent mass spectrometric investigations[55] have drawn attention to a possibility of separating tritium from lithium by high-temperature distillation. Experiments have shown that the tritium compounds formed at temperatures above 1300 K are mainly those of the LiT and Li_2T types, whose equilibrium partial pressures are a factor of 40 and more above that of T_2 over the metal. It should therefore be possible to remove the tritium from the Li metal by high-temperature distillation outside the blanket (in a secondary circuit).

Another method of T extraction could make use of the freezing out of tritium in a cold trap at 78 K.[51] However, as the solubility of tritium in lithium is still very high at that temperature (estimates range between 200 weight-ppm (wppm) and 2700 wppm), the tritium inventory in a lithium blanket of 1630 m^3 typical for an energy producing power reactor would still be unrealistically large (160–2200 kg), and it is for this reason that the application of this technique is no longer under serious consideration.

More opportunities are thought to lie in the application of getters for the extraction of tritium from Li metal.[51] The passage of liquid lithium over a bed of porous getter materials is under discussion. Various metals such as yttrium and cerium and their alloys are at present under investigation regarding their gettering capabilities.[56] For removal of tritium from and regeneration of the getters, they are removed from the lithium stream and heated in a vacuum. The problems associated with this technique, and relevant exploratory studies still to be carried out will be dealt with in greater detail in the discussion of Li–Pb blankets.

Another technique is tritium extraction into a salt melt.[57] In this case, the liquid lithium metal is brought into close contact with a melt of LiF–LiCl–LiBr, with which Li metal is not miscible, outside the blanket at 445 °C. Since tritium has a much higher solubility in the salt melt than in the metal, this method of extraction can reduce the tritium concentration in Li metal to less than 0.5 wppm, i.e., at an assumed blanket volume of 1630 m^3, the tritium inventory in the blanket would represent an acceptable level of ca. 400 g. However, one grave disadvantage of this method is the presence of halogen ions in the blanket material and the associated hazard of enhanced corrosion of the structural materials.

The extraction of tritium from the Li–Pb alloy, $Li_{17}Pb_{83}$, can be achieved by techniques similar to those employed in the extraction of tritium from Li metal.[26] One major advantage is the considerably higher tritium equilibrium partial pressure over the metal mixture. Therefore, the tritium can conceivably be removed by simply pumping off the gas phase over the metal phase or by permeation through suitable membranes.[58] However, there is still the drawback of the equilibrium pressure not being established fast enough for practical application, because of the relatively slow kinetics of the diffusion process. Efforts are under way to accelerate this process by scrubbing the tritium in the Li–Pb alloy with helium gas in a countercurrent flow process.[59] At present, this is believed to be the most promising process.

As in the extraction of tritium from Li metal, in this case also the removal of tritium by means of suitable getters is under discussion; given the low solubility of T in $Li_{17}Pb_{83}$, this technique should be easier than with lithium metal.[57] Yttrium for example has a solubility for tritium at 500°C which exceeds that of $Li_{17}Pb_{83}$ by a factor of 2×10^5; i.e., if 1800 t of blanket material (tritium equilibrium partial pressure, 10^{-4} torr) is brought into contact with only 20 kg of yttrium getter, only 1.3 g of tritium would remain in the blanket, while 6.7 g of tritium would be taken up by the getter, provided that there is always enough time for the equilibrium to adjust. The use of getters has so far always failed because very little is known about the compatibility of the getter materials envisaged, such as U, Zr, Ti, and their alloys, with the Li–Pb mixture. Also the kinetics of the tritium uptake by the getters is largely unknown, although this is a factor of decisive importance for their practical application. Furthermore, very little information is available about the extent to which the effectiveness of getters is influenced by the presence of impurities such as O, N, C, etc. in the Li–Pb mixture.

6.2. Solid Blankets

In the case of solid blankets, mainly ceramic materials, such as lithium compounds of the type Li_2O, γ-$LiAlO_2$, Li_5AlO_4, Li_2SiO_3, Li_2TiO_3, Li_2ZrO_3, and Li_4SiO_4 are to be used. In all these cases, perhaps with the exception of LiO_2, neutron multipliers, such as beryllium, will be required to achieve a breeding factor >1. Once again the chemists contribution to this field primarily concerns the determination of the physicochemical data of these materials, as these are most important both in the successful planning of tritium extraction and in the selection of the structural material that comes into contact with the blanket. Criteria influencing the choice of material in this case are, inter alia, the rate of tritium release and the expected tritium inventory in the blanket, which is determined by the tritium adsorbed, dissolved and bound to defects, and by the thermal stability. All these parameters are summarized schematically in Figure 18. Especially the fraction of tritium bound to defects is likely to depend very strongly on structural changes of the material in the radiation field.

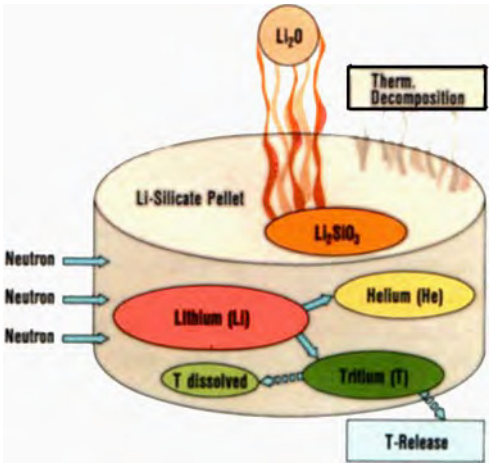


Fig. 18. Schematic diagram of the thermal decomposition of the blanket material (Li_2SiO_3) and of the processes associated with the generation and release of tritium.

Of particular interest in this connection[60] are the studies in which the production and the release of the tritium generated in the $^6Li(n,\alpha)T$ reaction in Li_2O has been monitored. In the author's opinion, the tritium may initially be present in Li_2O both as a neutral atom as well as a positively or a negatively charged ion (Fig. 19). The neutral

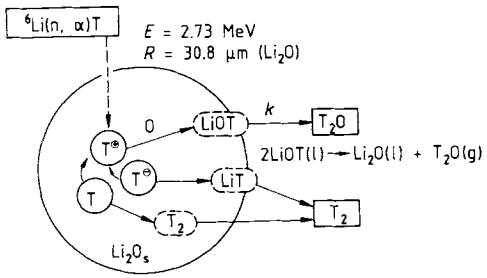


Fig. 19. Schematic representation of the reactions associated with the generation of tritium and its subsequent release in Li_2O [60].

particles produce molecular T_2, which diffuses out of the crystal, while the positively charged tritium on the surface produces first LiOT and then T_2O. Consequently, the negatively charged tritium should produce LiT as an intermediate stage on the surface, and then finally T_2. The rate-determining step in the release of T_2O at low temperatures ($T<570$ K) is the dissociation of LiOT on the surface, whereas, at higher temperatures, it is the diffusion of $T^{\oplus}$ which determines the course of the reaction. In agreement with numerous other findings it can be summarized that the transport of tritium inside the compounds under investigation is determined by diffusion at fusion-related temperatures. Some of these findings are reproduced in Figure 20,[61] where the diffusion constant is plotted as a function of temperature for a variety of possible breeder materials. It follows, e.g., that the diffusion constant of tritium is several orders of magnitude higher in the liquid blanket materials than in the ceramics, as was to be expected.

These studies also revealed that the activation energy for the diffusion is relatively high,[62] that, e.g., in β-Li_5AlO_4 particles with a diameter of 200 μm an average retention time of 4 s was measured at 1273 K, whereas at 873 K it was a factor of 100 greater. However, as there will always be temperature gradients, because of the geometry of the blanket, clear differences in tritium retention in various regions of the blanket must be expected, which must be taken into account in calculating the tritium inventory.

A factor of decisive importance with regard to the suitability of a ceramic material as a blanket material is its low solubility for hydrogen. Although data on the diffusion of hydrogen isotopes in ceramic blanket materials have been published by several groups of authors (see Fig. 20),[61,63]

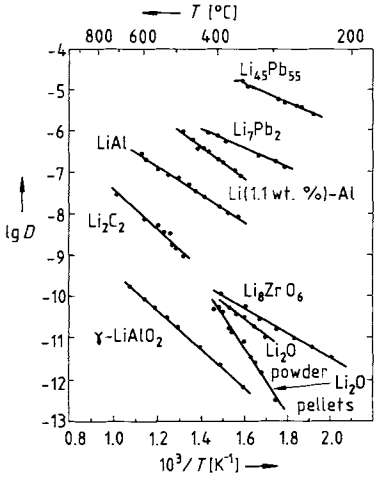


Fig. 20. Diffusion constant D [$cm^2\ s^{-1}$] of tritium as a function of temperature in a number of potential blanket materials [61].

very little has thus far been reported about the physical solubility of tritium in such materials.[64] One main reason for this lack of information obviously lies in the basic difficulties of measuring these quantities.

More recent volumetric measurements, and measurements with radioactive tracers,[65] indicate very low solubilities of ca. 10^{-5} mol hydrogen/mol Li_2SiO_3 at temperatures between 720–820 K. The results are reproduced in Figure 21 together with the hydrogen solubilities in some other solids.[65] The measurements also showed, however, that impurities in these ceramics may lead to clearly different results. Very little is known at present about the effects of radiation induced defects on the solubility.

The diffusion measurements available to date seem to favor a lower blanket operating temperature of 570–600 K, i.e., a temperature at which a sufficiently rapid hydrogen transport may be expected. The upper temperature limit is given by another property of these materials, namely their property of losing their porosity, or of sintering, at higher temperatures.[50] This normally occurs at temperatures above 0.8 T_m, T_m being the temperature of the absolute melting point. Above this temperature the thermal sintering process begins, generally between 1070–1570 K. Since it is known that radiation effects can lead to the so-called closure of porosity even at low temperatures, detailed investigations must be carried out in the future into the influence of radiation on the thermal stability of these compounds. At present, very little is known about these effects, nor about the question as to what extent radiation-induced defects may influence the diffusion of tritium, or what kind of barriers they represent to T diffusion.

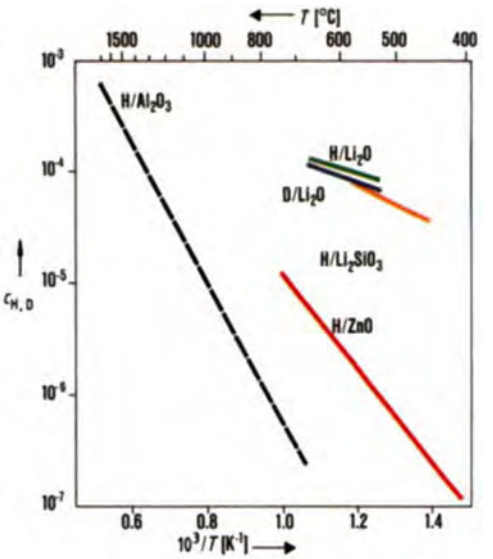


Fig. 21. Hydrogen solubility c [mole fraction] as a function of temperature in various ceramics [65].

As far as the process of thermal release is concerned, the rate-determining step is the diffusion of tritium through the interior of the solid, as has been explained above (Fig. 19). In this connection it should be pointed out that in studies in which T was produced in the reaction $^6Li(n,\alpha)T$, this tritium occurred as HTO if the reaction took place in oxygen-bearing compounds,[60] whereas it was found as HT in oxygen-free compounds.[66] Since the range of the recoil tritium particle generated in the nuclear reaction is very short, and since tritium cannot be expected to diffuse through the interior of the solid as HTO, it may be concluded that the reaction between the "hot" recoil T particles and their environment has only very little influence on the form in which tritium leaves the solid. Especially at the high temperatures prevailing in the blanket, there will be surface reactions between the tritium compound and the blanket materials which will determine the final chemical form of the tritium extracted or released.

A conclusive answer to the question of whether and with what efficiency tritium can be extracted from various blanket materials, can best be found by appropriate exploratory experiments. Such experiments are at present under way in various places. The results so far have been quite encouraging. For instance, a research team from the Argonne National Laboratory has been able to show in a neutron irradiation experiment conducted in the Oak Ridge research reactor that more than 99.9% of the theoretical amount of tritium to be expected can be extracted as tritium gas from a solid Li ceramic at temperatures between 860 and 920 K.[93]

In a ceramic blanket, extraction of tritium by means of the propellent gas flow (helium) seems to be the simplest method.[25,67] Separation of the tritium, which, as has been

borne out in the Argonne experiments, is present as T_2, perhaps together with small amounts of HTO, can be achieved by a variety of processes, whereby similar considerations apply as for the methods used in plasma exhaust purification (Section 5).[26] One such process is based on the catalytic combustion of tritium to produce HTO or T_2O and its subsequent condensation in a cold trap or on a molecular sieve.[68] The water arising must be decomposed either by reduction on a hot metal bed (uranium)[69] or—as has recently been proposed—electrolytically, before the hydrogen mixture can be subjected to isotope separation.

The reduction step with uranium is expensive and gives rise to waste problems, as has been mentioned in Section 5.1.2. The electrolysis of tritiated water with a high specific activity of T, however, raised a number of problems, for which a solution was found only recently in the development of new types of electrolysis systems. In conventional electrolysis systems using aqueous KOH as the electrolyte, the tritium–hydrogen exchange, e.g., would result in considerable tritium enrichment in the electrolyte, thus increasing the tritium inventory to unduly high levels. In addition, there would be the problems of waste disposal and tritium recovery from the electrolyte. More recent developments in this field therefore depart from a particularly compact design with extremely low electrolyte volumes.[70] In a different type of electrolyzer using solid electrolytes, such as synthetic polymers, there is the problem of radiation-induced damage to these membranes, and no satisfactory solutions have as yet been found for long-term operation.

Another modern development, high-temperature electrolysis,[71] uses an inorganic solid electrolyte of stabilized ZrO_2-ceramics (Fig. 22), which remains in place and undergoes no change during operation of the electrolytic plant. The plant can be run at 370–1270 K. The water vapor supplied is decomposed on the cathode side of the electrolysis membrane under the influence of the applied voltage.

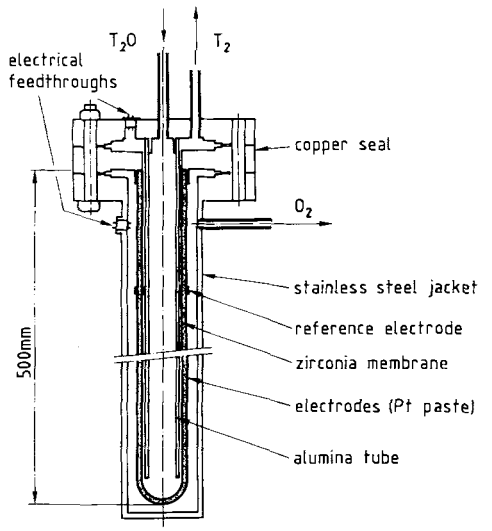


Fig. 22. Schematic representation of a high-temperature cell for the electrolysis of tritiated water [71].

With regard to the thermal stability of blanket materials, there is not only the question already dealt with of changes in porosity as a function of temperature, but also the problem of thermal decomposition of the compounds and the associated formation of aggressive products which could contribute to corrosion in the structural materials. Such studies[72–75] have been and are being carried out with Knudsen effusion cell mass spectrometers, which allow the species generated at higher temperatures to be identified and quantified (vapor pressure). The compounds to be studied are heated to a precisely set high temperature in the Knudsen cell and the gaseous species are fed into the ionizing chamber of the mass spectrometer, ionized, and measured. A vapor-pressure curve measured in this way for Li over Li_2SiO_3 as a function of temperature is shown, for example, in Figure 23.[76]

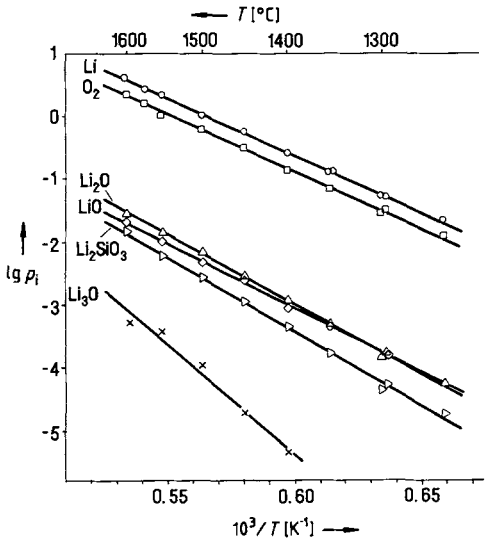


Fig. 23. Partial saturation vapor pressures p_i [Pa] over Li_2SiO_3 as a function of temperature [76].

The other purpose of the blanket is to transform the kinetic energy of the neutrons produced during fusion into heat, and to transport this heat to a steam generator. This requires a coolant, which probably will be water, because of its widely known advantages. Another possibility would be helium gas.

6.3. Tritium Removal from the Coolant

The problem associated with the use of water is that, because of the low solubility of tritium in most blanket materials, which is one of the very reasons for this choice of material, the equilibrium partial pressure of the tritium over the liquid or solid blanket will be relatively high. This means that there will be substantial diffusion of tritium through the walls of the pipes into the cooling water at the blanket temperatures of more than 600–800 K. The extent of this diffusion will be illustrated by way of an example: for a hydrogen concentration of 1 appm in the lithium metal, the equilibrium partial pressure of hydrogen over the metal is 2×10^{-11} torr at 770 K. *Sievert*'s constant for stainless steel (SS 316) is 9.1, which leads to a diffusion of

4×10^{-5} cm^3 of hydrogen per hour (at STP) through a wall area of 1 m^2 at a wall thickness of 1 mm. This corresponds to ca. 10^{-4} Ci of tritium per hour.[54] In the case of $Li_{17}Pb_{83}$, where the partial pressure of the oxygen is considerably higher under the same conditions (4×10^{-2} torr), the same line of reasoning will lead to a diffusion of 1.8 cm^3 or 4.8 Ci per hour (at STP). Naturally, this equilibrium partial pressure will not be attained if the tritium gas over the blanket is continuously extracted or removed by means of helium gas. However, it must be assumed that considerable quantities of tritium will probably enter the cooling water, and will have to be removed periodically; in addition to this, there is the cooling water used for cooling the first wall, into which also major amounts of tritium are going to diffuse (Fig. 24). Other tritium-bearing aqueous solutions arise during decontamination of the exhaust air from rooms and boxes by oxidation of the tritium.

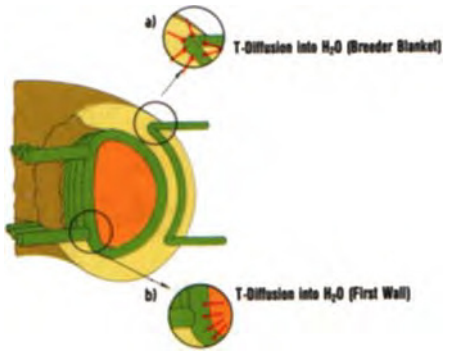


Fig. 24. Schematic diagram of tritium diffusion into the cooling water. a) Tritium diffusion into the cooling water of the breeding blanket (heat decrease); b) tritium diffusion into the cooling water of the first wall.

At present, only very crude approximations of the permeation of tritium into the cooling water can be made. In a power-producing reactor, an equilibrium permeation rate into the cooling water of 10^2–10^4 Ci of tritium per day is generally assumed. It has been suggested that the tritium concentration in the cooling water should be limited to 2–10 Ci per liter, which could be achieved by the detritiation of ca. 1000 liters per day for the cooling water volumes assumed above. Various methods are available for this purpose. Fractional distillation of water, a step used in water treatment or as the final process step in the production of heavy water, where the dilution factor (the ratio D/H or T/H in the water) is between 10^{-1} and 10^{-2}, cannot be used for the depletion of tritium in cooling water because the dilution factor in this case will be below 10^{-7}. Consequently, more effective enrichment processes must be used before the tritium-enriched hydrogen stream is subjected to cryogenic fractionation. Three of the procedures studied most intensively in this connection will be briefly discussed here.

The first process is *v*apor *p*hase *c*atalytic *ex*change (VPCE),[77] in which the catalytic exchange is brought about in the countercurrent flow [see Eq. (14)] at operating

$$HTO_{gas} + H_2 \overset{cat.}{\rightleftharpoons} H_2O_{gas} + HT \qquad (14)$$

temperatures of ca. 500 K, i.e., with superheated steam. The advantage of the method lies in the fact that the catalyst is not inactivated by liquid water. On the other hand, there is the disadvantage that the process needs to be run in several cascades, thus requiring a relatively extensive system including repeated evaporation, superheating, and condensation of the water, and involving a considerable consumption of energy.

The second process is *l*iquid *p*hase *c*atalytic *ex*change (LPCE)[78] on a hydrophobic catalyst [Eqs. (15) and (16)].

$$HTO_{liquid} + H_2O_{gas} \overset{cat.}{\rightleftharpoons} H_2O_{liquid} + HTO_{gas} \qquad (15)$$

$$HTO_{gas} + H_2 \overset{cat.}{\rightleftharpoons} H_2O_{gas} + HT \qquad (16)$$

In the process, tritium is exchanged between tritiated water and gaseous hydrogen in a countercurrent flow process.

The third process is *c*ombined *e*lectrolysis–*c*atalytic *ex*change (CECE). In this case, as shown in Figure 25, the cooling water is supplied to the column containing the hydrophobic catalyst. It exchanges with the tritium-bearing hydrogen stream generated in the electrolyzer, whereby tritium is further enriched in the water [Eq. (17)].

$$HT + H_2O_{liquid} \overset{cat.}{\rightleftharpoons} HTO_{liquid} + H_2 \qquad (17)$$

The tritium-enriched liquid water enters the electrolyzer, where it is dissociated again. Part of the tritium-bearing hydrogen stream enters the low-temperature rectification column, while the remainder, as described above, is passed to the catalytic column for exchange with the tritiated water. The hydrogen stream is burnt with oxygen at the head of the exchange column.

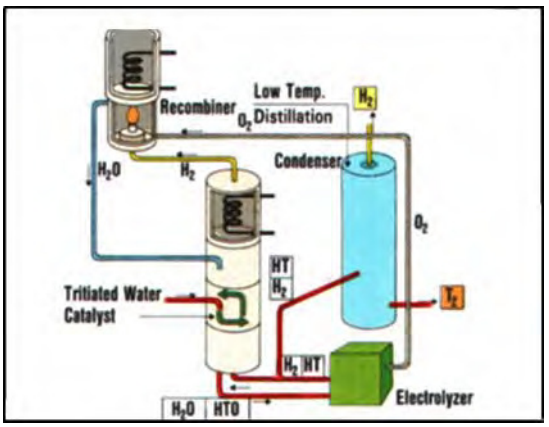


Fig. 25. Schematic diagram of tritium enrichment by the CECE method [79].

Prerequisite for the successful application of the latter two processes was the development of a hydrophobic catalyst,[29,80] which also had to meet stringent criteria of stability, abrasion resistance, radiation stability, and relative insensitivity to impurities because of the problems associated with the waste management of material contaminated with tritium. Catalysts of this kind, which work on a Pt–carbon–teflon basis, have been known for some time. Specific further development of these materials has enabled catalysts

to be developed which fully satisfy the aforementioned criteria.

Other procedures which have been proposed for the separation of tritium from aqueous solutions are based on the application of lasers, e.g., the process of selective dissociation of the C-T bond in trifluoromethane, in which case a transfer of the tritium bound in the water to the trifluoromethane gas must first be achieved,[48] or the photochemical dissociation of tritiated water in the presence of solid-state catalysts such as Pt on TiO_2, which are distributed as colloids in the aqueous phase.[81] The catalytic reduction of tritiated water by carbon monoxide (water-gas reaction) is also envisaged.

However, if the diffusion of larger quantities of tritium into the coolant must be reckoned with, the choice of procedure will depend on the respective characteristic retention time of tritium or on the tritium inventory in the individual systems. In this respect, the CECE process is likely to surpass all other procedures, except perhaps the laser separation.

7. Analysis

The analytical problems arising in the fuel cycle of a fusion reactor have been hinted at very briefly under the headings of the different systems. Thus, in the case of plasma exhaust purification, aside from plasma diagnostics, concentration assays of the tritiated impurities must carried out quickly and, whenever possible, under flow conditions. Conventional methods may be employed for this purpose, such as mass spectrometry, FT-IR spectrometry and laser Raman spectrometry, but they will all have to be adapted to special conditions, especially for on-line operation.[82]

Determination of the properties of materials, diffusion, etc. requires the use of thermochemical methods such as thermogravimetry, X-ray diffraction, electrochemical Knudsen effusion cell mass spectrometry and, in particular, techniques of surface analysis, such as ESCA and Auger spectroscopy, and secondary ion mass spectrometry, to study the reactions largely proceeding on the surfaces of getters.[83] Quality control, e.g., in the production of blanket materials, is achieved in the usual way by optical spectrometry (AAS, AES, AFS, etc.) and also by X-ray fluorescence and neutron activation analysis.

Difficulties arise, however, in the continuous checks for impurities in a liquid metal blanket, for which no methods are as yet available that have been tested under realistic conditions. As already mentioned in Section 6, one important aspect in the choice of the blanket is its compatibility with the structural materials surrounding it. In a liquid metal blanket there is also the influence of impurities on the aggressiveness of the blanket material towards the structural material, which may lead, e.g., to locally enhanced corrosion. There is. therefore, the urgent need to monitor continuously for such impurities as nitrogen, hydrogen, oxygen, and carbon in the liquid metal blanket.

For hydrogen and carbon, monitors have been proposed[84] which are based on the principle of the diffusion of these impurities through suitable membranes at elevated temperatures. As is seen in Figure 26, such an in-line hydrogen monitor consists of an α-Fe membrane, which, at an operating temperature of 350°C, permits the diffusion of hydrogen, which is then pumped off in a controlled way. The resultant hydrogen partial pressure is measured.

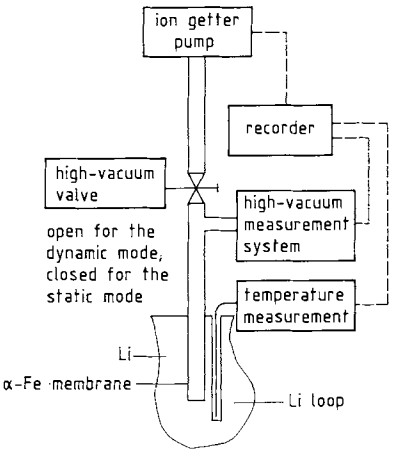


Fig. 26. Schematic diagram of the in-line hydrogen monitor [84].

In the carbon monitor, the carbon likewise diffuses through an α-Fe membrane, but at a temperature of 500°C. The iron oxide coating on the inside oxidizes the diffusing carbon to CO, which is determined by flame photometry either in this form or after catalytic conversion into CH_4.

The in-line oxygen and nitrogen monitors,[84] which are still at the experimental stage, are based on the electrochemical principle. A measuring setup of this kind is outlined in Scheme 1 for the case of oxygen, and in Scheme 2 for the case of nitrogen.

$$\mathrm{Li(O)\ //\ \overset{\text{solid electrolyte}}{ZrO_2\cdot MgO}\ //\ \overset{\text{reference electrode}}{In-In_2O_3}}$$

or

$$\mathrm{Li_{17}Pb_{83}(O)\ //\ (ZrO_2-MgO\ or\ ThO_2-Y_2O_3)\ //\ In-In_2O_3}$$

Scheme 1. Measuring set-up of an in-line oxygen monitor.

$$\left.\begin{matrix}\mathrm{Li(N)}\\ \text{or}\\ \mathrm{Li_{17}Pb_{83}(N)}\end{matrix}\right\}\ \mathrm{//}\ \overset{\text{solid electrolyte}}{(AlN)}\ \mathrm{//}\ \overset{\text{reference electrode}}{(Cr-Cr_2N)}$$

Scheme 2. Measuring set-up of an in-line nitrogen monitor.

In both cases the problem is the lack of compatibility of the solid electrolytes with the liquid metals, Li or $Li_{17}Pb_{83}$, which leads to rapid decomposition. The development of more resistant systems will pose major problems to electrochemists.

8. Safety Aspects in Fusion Reactor Operation

As unavoidable as the diffusion of tritium into the cooling water will be the release of non-negligible quantities into the glove-box atmosphere, in which many of the processes described here will have to be carried out, and, of course, into the environment of the fusion reactor.

Removing tritium from a glove-box atmosphere no longer poses any problems. The procedure is based on the catalytic combustion of hydrogen and subsequent adsorption of the water onto suitable materials.[26] Another method, which has already been used for test purposes, employs the catalytic addition of hydrogen to a carbon–carbon double bond in suitable organic compounds, such as linoleic acid.[85] In this case, the glove-box atmosphere is pumped in a countercurrent flow through a linoleic acid solution containing a platinum catalyst. From the waste disposal point of view, however, the addition to a solid compound would be preferable. Consequently, certain types of organometallic compounds have been proposed which might act as getters for T_2 or HT. In this case, the tritium is expected to attach to a carbon–carbon double bond or triple bond in the compound, with this step being catalyzed by a heavy metal atom present in the molecule.[86] However, investigations with these compounds showed that, in the presence of oxygen, the same catalyst also promotes the oxidation of tritium to water, thus destroying the advantage of the method, which is the immobilization of tritium in a solid form without producing the radiologically more dangerous intermediate product, water. As a consequence, these materials surely cannot be used for the detritiation of the exhaust air from rooms, for which so far the conventional method of catalytic combustion of tritium and subsequent absorption in molecular sieves is foreseen.

It would be worthwhile, however, to find a catalyst able to induce an effective combustion of small quantities of tritium in air at room temperature, because it is uneconomical, although still required at the present time, to maintain a large catalytic bed at elevated temperatures. Some recent studies[87] have already improved our understanding of the kinetics controlling the oxidation of tritium to tritiated water with atmospheric oxygen; progress has been made in the development of catalysts meeting the required specifications on the basis of platinum/Al_2O_3, palladium/kaolin and palladium/zeolite. However, they have not yet reached the stage of development for use as reliable emergency purification systems. In all these processes, the water produced is subsequently adsorbed on molecular sieves.

Monitoring the tritium activity in the reactor building as well as the amount of tritium released into the environment with the exhaust air requires detectors which can measure maximum concentrations of tritium as HTO of 5×10^{-10} g T per m^3 of air, which is the maximum permissable exposure level for working in controlled areas, up to 10^{-12} g/m^3 in controlled areas outside reactors which is the maximum permissible exposure level for personnel not under occupational surveillance.

The most sensitive technique in use at the present time operates in the batch mode and is based on the catalytic combustion of the gaseous, tritium-bearing substances encountered, such as T_2, HT, etc., the adsorption of the HTO produced, and the measurement of its amount by liquid scintillation spectrometry.

Continuous monitoring for gaseous T-compounds, especially of HT or T_2 in the presence of γ-radiation and in the presence of radioctive noble gases, such as Kr-85, Xe-133, etc., is possible with most monitors now commercially available. The simplest versions consist of three ionization chambers in a sandwich structure and work according to the principle of anticoincidence counting.[88] The smaller inner chamber is dimensioned so as to be just large enough to absorb quantitatively the soft β-radiation from tritium (< 0.018 MeV). It is permeated by the gas stream to be monitored. The more energetic radiation or external γ-radiation emitted by the other radioactive noble gases (fission product gases, etc.) penetrates the wall of this counting chamber and is registered in one of the two closed outer counting chambers. Only signals resulting from the inner counting chamber, which are not coincident with signals from one of the outer counting chambers, are due to the decay of tritium and are registered.

Depending on their design, the dynamic range of such detectors is between 10^{-2} and 10^{7} μCi m^{-3} in the presence of γ-radiation and radioactive noble gases, and thus includes the permissible concentration of 5×10^{-3} Ci of HT or T_2 in controlled areas. Another type of detector[89] is based on the following principle: The pulse rise time in a proportional counter is a function of the speed at which the electrons (β-particles) arrive at the counting wire. The shorter the range of the β-particles the smaller will be the fluctuations in their arrival time. If one plots the observed relative count rate as a function of the pulse rise time (Fig. 27), two clearly different regions are found, in which only the signals registered under A are due to the decay of tritium and will be registered. When using counters of this type with a volume of 3 L, 2×10^{-8} g m^{-3} or 2×10^{-1} μCi m^{-3} of tritium can be detected in the presence of comparable Kr-85 activities.

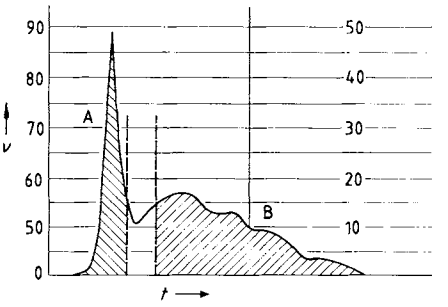


Fig. 27. Relative count rate ν vs. pulse rise time t in a Berthold-type tritium monitor [89]. Background: 1000 cpm (counts per minute); T: 300 cpm; measuring time 20 min; relative flowrate air/methane = 1/4.

In this connection, reference should also be made to the need to detect tritium separately in all its forms, because its radiological toxicity depends strongly on its presence, e.g., as HT or T_2 or as the much more dangerous HTO or T_2O.[90]

The radiological toxicity of tritiated water is roughly a factor of 25000 greater than that of HT or T_2, because most of the inhaled tritium is exhaled again, and the permeability of human tissue is lower for HT than for HTO.

In the tritium flow monitors used so far, a selection of the tritium compounds was achieved by a two-chamber system in which one chamber measured the bulk tritium, while the other measured only tritium present as HT or T_2,

after water had been removed in an upstream molecular sieve.[88] A more recent discovery[88] makes use of the property of Nafion, a polymeric fluorohydrocarbon, whose permeability for water is up to a factor of 10^4 higher than it is for hydrogen. The principle of such a monitor can be seen from Figure 28. It consists of two concentric cylinders with a partition wall made of Nafion. The gas stream under investigation, which contains HTO, HT, and possibly radioactive noble gases, flows into the inner cylinder, HTO enters the outer cylinder through the membrane and is scavenged into a separate detector, while HT and the noble gases are measured in a conventional T-detector, as explained above.

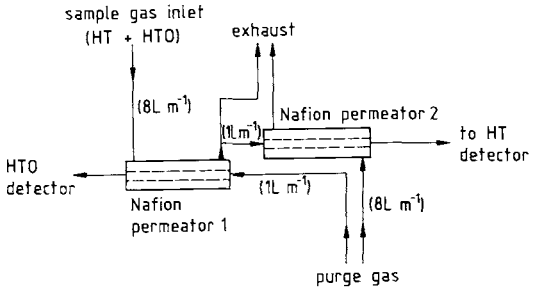


Fig. 28. Schematic diagram of a tritium monitor for simultaneous measurement of tritium gas and tritiated water [88].

A very decisive factor in the operation of a fusion reactor will be the minimization of tritium losses to the environment. As has been discussed above in more detail, this is necessary, on the one hand, for economic reasons. On the other hand, however, the acceptance of this new way of generating energy will also depend on our ability to ensure that radioactive contamination of the environment is minimized by the retention of tritium in a fusion reactor, e.g., by a system of in-depth containments. According to current technical experience in this sector[91] it would seem possible to limit the escape of tritium into the atmosphere to 2 g of tritium annually during the normal operation of a fusion reactor. On this basis, a maximum radiation dosage under the most adverse conditions and for the most highly exposed person permanently staying at a distance of 1 km from the reactor would be 1.5 mrem/a. The average exposure level for those living within a radius of 50 km from the reactor would then be 0.001 mrem/a. These levels correspond to some 0.75 and 0.005%, respectively, of the average natural radioactive dose of 200 mrem/a in the Federal Republic of Germany and are clearly well below the local variations in dose levels due to natural radioactivity.[90]

Chemists must, however, devote special attention also to those measures which can contribute to a minimization of tritium-bearing and tritium-contaminated wastes. In designing flowsheets and selecting the methods available for each process step, the handling of radioactive wastes and their disposal must also be taken into account. In addition, the decontamination of surfaces contaminated with tritium is of special importance, particularly if one considers the huge dimensions of the components of a future fusion reactor. Consequently, chemists will also have to develop new and more effective methods of surface decontamination, which in turn demands a better knowledge of the chemical processes leading to contamination.

The fusion reactor will not only produce tritium but also a number of other radioactive products arising as a consequence of the irradiation of structural and blanket materials with neutrons.[90,92] The amount of radioactivity generated in this way will depend largely on the elemental (and isotopic) compositions of the materials used. It is to be expected that it will be possible, in the course of future developments, to manufacture materials containing mainly those isotopes of the elements used which, like the Mo isotopes of masses 95, 96 and 97, will produce only limited amounts of radioactive nuclides or, at least, no long-lived radionuclides upon neutron irradiation. Another important factor will be the use of blanket material of extremely high purity; this will lead to a substantial reduction in the radioactivity produced by neutron bombardment of the impurities. It should also be pointed out that, in contrast to the radioactive wastes arising in fission reactors, in the case of fusion reactors no long-lived α-emitters are produced.

The influence of the material of the first wall on its specific activity is shown in Figure 29. If current commercial steel grades, such as AISI 316 are used, the activity inventory will be roughly 10^{10} Ci after five full-load years, with a loading of the first wall of 10 MW per year and m^2.[90] This corresponds to the activity inventory of a fission reactor of the same electric power. If low-activation materials are used, such as a vanadium-chromium-titanium alloy (V15Cr5Ti), this inventory is already one order of magnitude lower. Further development in this direction seems to be possible.

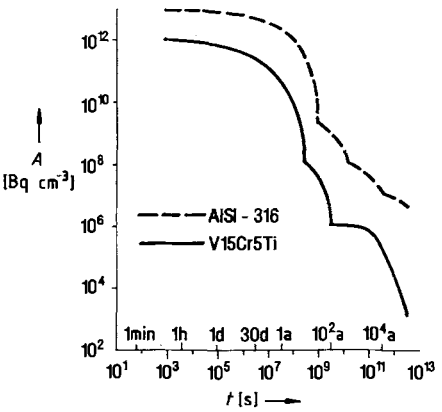


Fig. 29. Specific activity A of the first wall of a fusion reactor for two different wall materials as a function of time [90].

9. Concluding Remarks

An attempt has been made in this article to outline the problems that chemists have been faced with, and will be facing, in the development of fusion technology. These problems will continue to make very great demands on the capabilities of chemists. The challenge is great but not insurmounable given the possibilities and facilities of modern chemical research and process engineering.

The author would like to express his deep gratitude to his staff at the Institute for Radiochemistry, and especially to Drs. Penzhorn, Ihle, Glugla, Albrecht and Willin, for their enthusiasm and valuable assistance in drafting the manuscript and to Ms. Pfennig for her help in reviewing the manuscript and compiling the references.

Received: November 14, 1987 [A 704 IE]
German version: *Angew. Chem. 101* (1989) 1

[1] For an introduction to the engineering and construction of fusion reactors see for example: a) J. Eidens, G. H. Wolf, *ATW Atomwirtsch. Atomtech. 27* (1982) 138; b) R. W. Conn, *Spektrum Wiss. 12* (1983) 50; c) T. Kammash: *Fusion Reactor Physics,* Ann Arbor Science Publishers, Ann Arbor, MI, USA 1976.
[2] D. A. Dingee, *Chem. Eng. News (NY) 86* (1979) No. 7, p. 30.
[3] D. I. Garber, R. R. Kinsey, *Brookhaven Natl. Lab. Rep. BNL 325* (1976), 3rd edit., Vol. 2. p. 11.
[4] V. S. Crocker, S. Blow, C. J. H. Watson, *U.K. At. Energy Auth. Res. Group Culham Lab. Rep. CLM-P 240* (1970).
[5] P. Hugony, H. Sauvage, E. Roth, *Bull. Inf. Sci. Tech. Commis. Energ. At. (Fr.) 178* (1973) 3.
[6] U. Fischer, *Kernforschungszent. Karlsruhe Ber. KfK-4255* (1987).
[7] M. Z. Youssef, M. A. Abdou, *Fusion Technol. 9* (1986) 286.
[8] See *JET Annu. Rep. 1986, EUR 111 14 EN; JET Prog. Rep. 1986, EUR 111 13 EN; NET Status Rep. 1985, Rep. 51.*
[9] J. D. Lawson, *Proc. Phys. Soc. London Sect. B70* (1957) 1.
[10] F. Carré, E. Proust, A. Rocaboy, *Nucl. Technol. Fusion 4* (1983) 93.
[11] M. A. Abdou, E. L. Vold, C. Y. Gung, M. Z. Youssef, K. Shin, *Fusion Technol. 9* (1986) 250.
[12] G. L. Kulcinski, J. R. Young, *Radiat. Eff. Tritium Technol. Fusion React. Proc. Int. Conf. 1975, Vol. 2,* p. 38.
[13] K. Ehrlich, D. Kaletta, *KfK-Nachr. 11* (1979) No. 2, p. 25.
[14] TFTR = Tokamak Fusion Test Reactor in Princeton, NJ, USA; TEXTOR = Tokamak Experiment for Technology Oriented Research, Jülich (FRG); JET = Joint European Torus, Culham, UK; NET = Next European Torus.
[15] K. Sonnenberg, K. J. Dietz, P. Kupschus, *JET Prog. Rep. 1986, EUR 111 13 EN,* 292.
[16] K. L. Wilson, W. L. Hsu, *J. Nucl. Mater. 145–147* (1987) 121.
[17] B. L. Doyle, W. R. Wampler, D. K. Brice, S. T. Picraux, *J. Nucl. Mater. 93–94* (1980) 551.
[18] J. Winter, *J. Nucl. Mater. 145–147* (1987) 131.
[19] B. L. Doyle, *J. Nucl. Mater. 144* (1986) 280.
[20] G. M. McCracken, Lecture at the Symposium "Plasma-Wall Interaction (H-Isotopes with Graphite)", Garching 1984.
[21] E. Vietzke, V. Philipps, *Nucl. Instrum. Methods Phys. Res. Sect. B23* (1987) 449.
[22] a) V. Philipps, E. Vietzke, M. Erdweg, K. Flaskamp, *J. Nucl. Mater. 145–147* (1987) 292; b) E. Vietzke, K. Flaskamp, V. Philipps, G. Esser, P. Wiengold, J. Winter, *ibid. 145–147* (1987) 443.
[23] P. T. Dawson, *CFFTP* (Canadian Fusion Fuels Technology Project) *Rep. G-85038* (1984).
[24] a) E. Vietzke, K. Flaskamp, V. Philipps, *J. Nucl. Mater. 128–129* (1984) 545; b) E. Vietzke, V. Philipps, *Int. Hot Atom Chem. Symp. 13th* (Mount Fujy, Japan 1987), Abstract No. 32.
[25] P. J. Dinner, M. Chazalon, S. K. Sood, O. K. Kveton, *Fusion Technol. 8* (1985) 2228.
[26] S. K. Sood, O. K. Kveton, *CFFTP Rep. G-86020* (1986).
[27] H. Yoshida, S. Konishi, Y. Naruse, *Nucl. Technol. Fusion 3* (1983) 471.
[28] R.-D. Penzhorn, R. Rodriguez, M. Glugla, K. Günther, H. Yoshida, S. Konishi, *Fusion Technol. 14* (1988) 450.
[29] R.-D. Penzhorn, M. Glugla, *KfK-Nachr. 19* (1987) No. 1, p. 23.
[30] W. M. Müller, J. P. Blackledge, G. G. Libowitz, *Met. Hydrides 1968.*
[31] T. Tanabe, T. Yamamoto, S. Imoto, *J. Less-Common Met. 89* (1983) 393.
[32] J. J. Katz, E. Rabinowitch: *The Chemistry of Uranium* (*Natl. Nucl. Energy Ser. Manhattan Proj. Tech. Sect. Div. 8* (1951) Vol. 5.1).
[33] E. A. Gulbransen, K. F. Andrew, *Met. Trans. 185* (1949) 741.
[34] H. Heimbach, H. R. Ihle, C. H. Wu, *Comm. Eur. Communities Rep. EUR 9183 EN* (1984), Vol. 1, p. 421.
[35] R. E. Wilson, C. Barnes, R. Koonz, L. Baker, *Nucl. Sci. Eng. 25* (1966) 109.
[36] SAES Getters, Milan, Italy.
[37] F. H. Spedding, H. A. Wilhelm, *Mon. Tech. Rep. Ames Project CC 1524* (1944).
[38] E. Willin, M. Sirch, R.-D. Penzhorn, M. Devillers, *Fusion Technol. 14* (1988) 756.
[39] L. Rosai, M. Borghi, *J. Vac. Sci. Technol. 11* (1974) 347.
[40] J. L. Anderson, *Proc. IEEE 69* (1981) 1069.
[41] J. L. Anderson, *Nucl. Technol. Fusion 4* (1983) No. 2, Part 2, p. 75.
[42] M. Glugla, K. Günther, R.-D. Penzhorn, *Trans. Int. Conf. ENS/ANS 4th 1986,* Vol. 3, p. 197.
[43] J. L. Anderson, R. H. Sherman, *Los Alamos Natl. Lab. Rep. LA-6855* (1977) 193.
[44] R.-D. Penzhorn, M. Glugla, R. Rodrigúez, D. Herbrechter, *Jahrestagung Kerntechnik 1988 (Travemünde).*
[45] J. R. Bartlit, W. H. Denton, R. H. Sherman, *Proc. Top. Meet. Technol. Controlled Nucl. Fusion 3* (1978) 778.
[46] A. Neubert, H. Heimbach, H. R. Ihle, *Comm. Eur. Communities Rep. EUR 9183 EN* (1984), Vol. 1, p. 417.
[47] H. Frischmuth, J. Perchermeyer, A. Stimmelmayr, H. Weichselgartner, *Comm. Eur. Communities Rep. EUR 7983 EN* (1982), Vol. 1, p. 549.
[48] J. A. O'Neill, K. B. Woodall, J. R. Robins, F. E. Bartoszek, H. D. Morrison, *Fusion Technol. 8* (1985) 2273.
[49] W. J. Holtslander, J. M. Yaraskavitch, *At. Energy Can. Ltd. Rep. AECL-7151* (1981).
[50] M. Abdou, *Argonne Natl. Lab. Rep. FPP-82-1,* Vol. 1.
[51] J. A. Blink, O. H. Krikorian, N. J. Hoffman in J. L. Gole, W. C. Stwally (Eds.): *Metal Bonding and Interactions* (*ACS Symp. Ser. 179* (1982)), p. 497.
[52] A. Neubert, K. F. Zmbov, *High-Temp. Sci. 6* (1974) 303.
[53] H. R. Ihle, A. Neubert, C. H. Wu, *Comm. Eur. Communities Rep. 6215* (1978), Vol. 2, p. 639.
[54] H. Feuerstein (Kernforschungszentrum Karlsruhe), private communication.
[55] H. R. Ihle, C. H. Wu, *J. Phys. Chem. 79* (1975) 2386.
[56] J. B. Talbot, P. W. Fisher, S. D. Clinton, *J. Nucl. Mater. 103–104* (1981) 681.
[57] W. F. Calaway, *Nucl. Technol. 39* (1978) 63.
[58] R. E. Buxbaum, *Sep. Sci. Technol. 18* (1983) 1251.
[59] G. Pierini, F. Masetti, C. Rizello, *Comm. Eur. Communities Rep. EUR 9183 EN* (1984), Vol. 1, p. 463.
[60] H. Kudo, K. Okuno, *J. Nucl. Mater. 133–134* (1985) 192.
[61] a) H. Kudo, *J. Radioanal. Chem. 67* (1981) 82; b) H. Kudo, K. Okuno, S. O'Hira, *J. Nucl. Mater. 155–157* (1988) 524; c) H. Kudo, K. Okuno, *Radiochim. Acta 33* (1983) 223.
[62] D. Guggi, H. R. Ihle, U. Kurz, D. Brüning, *Comm. Eur. Communities Rep. EUR 7035 EN* (1980), Vol. 1, p. 553.
[63] D. Brüning, D. Guggi, H. R. Ihle, A. Neubert, *Comm. Eur. Communities Rep. EUR 9183 EN* (1984), Vol. 1, p. 427.
[64] H. Katsuta, S. Konishi, H. Yoshida, *J. Nucl. Mater. 116* (1983) 244.
[65] M. Glugla, K. H. Simon, R.-D. Penzhorn, *J. Nucl. Mater. 155–157* (1988) 513.
[66] H. Kudo, K. Kushita, K. Okuno, *J. Nucl. Mater. 116* (1983) 78.
[67] M. Dalle-Donne, S. Dorner, *Comm. Eur. Communities Rep. EUR 9183 EN* (1984), Vol. 1, p. 173.
[68] J. Reimann, S. Malang, *Kernforschungszent. Karlsruhe Ber. KfK-4105* (1986).
[69] H. Yoshida, H. Takeshita, S. Konishi, H. Ohno, T. Kurasawa, H. Watanabe, Y. Naruse, *Nucl. Technol. Fusion 5* (1984) 178.
[70] A. Rahier, R. Cornelissen, A. Bruggeman, W. Goossens, L. Baetsle, *Fusion Technol. 8* (1985) 2035.
[71] S. Konishi, H. Yoshida, H. Ohno, Y. Naruse, D. O. Coffin, C. R. Walthers, K. E. Binning, *Fusion Technol. 8* (1985) 2042.
[72] A. Neubert, D. Guggi, *J. Chem. Thermodyn. 10* (1978) 297.
[73] H. R. Ihle, H. Kudo, C. H. Wu, *Thermodyn. Nucl. Mater. Proc. Symp. 1979* (1980), Vol. 2, p. 31.
[74] C. H. Wu, H. R. Ihle, K. Zmbov, *J. Chem. Soc. Faraday Trans. 2 76* (1970) 447.
[75] D. Guggi, H. R. Ihle, A. Neubert, *Comm. Eur. Communities Rep. EUR 5602* (1976), Vol. 1, p. 635.
[76] R.-D. Penzhorn, H. R. Ihle, P. Schuster, K. Zmbov, *J. Nucl. Mater. 155–157* (1988) 471.
[77] M. Damiani, *Sulzer Tech. Rev. 4* (1972).
[78] J. P. Butler, J. H. Rolston, W. H. Stevens in H. K. Rae (Ed.): *Separation of Hydrogen Isotopes* (*ACS Symp. Ser. 68* (1978)), p. 93.
[79] H. J. Fiek, J. Romaker, U. Schindewolf, *Chem. Ing. Tech. 52* (1980) 892.
[80] F. Rückert, unpublished.
[81] K. J. Monserrat, L. M. D'Souza, *CFFTP Rep. G-85016* (1985); *AECL-8751* (1985).
[82] E. Roth, J. Veau, *Fresenius Z. Anal. Chem. 322* (1985) 130.
[83] H. Moers, G. Pfennig, H. Klewe-Nebenius, R.-D. Penzhorn, M. Sirch, E. Willin, *Kernforschungszent. Karlsruhe Ber. KfK-4449* (1988).
[84] J. Dekeyser, F. Casteels, H. Tas, H. Soenen, M. Alberty, *Comm. Eur. Communities Rep. EUR 9183 EN* (1984), Vol. 1, p. 1037.
[85] H. Weichselgartner, *Comm. Eur. Communities Rep. EUR 7983 EN* (1982), Vol. 1, p. 573.
[86] H. H. Miller, E. R. Bissell, R. T. Tsugawa, P. C. Sauers, *Proc. Tritium Technol. Fission Fusion Isot. Appl. Am. Nucl. Soc. Natl. Top. Meet. 1980,* 208; *J. Nucl. Mater. 101* (1981) 238.
[87] A. E. Sherwood, B. G. Monahan, R. A. McWilliams, F. S. Uribe, C. M. Griffith, *Univ. Calif. Radiat. Lab. Rep. 52811* (1979).
[88] A review of the instruments available can be found, e.g., in W. G. Dickie, D. F. Wormald, R. C. Macphee (Eds.): *Canadian Tritium Experience* (Canadian Fusion Fuels Technology Project), Ontario Hydro, Mississauga, Ontario, Canada 1984, p. 69.
[89] F. Berthold: Tritium in air, measurements by pulse shape discrimination, in Lab. Prof. Berthold, Publication, Wildbad/Schwarzwald.
[90] A. Fiege, W. Gulden, W. Kramer, *KfK-Nachr. 19* (1987) No. 1, p. 3.
[91] *Environmental Impact and Economic Aspects of Nuclear Fusion,* EUR-FU BRU/XII 828/86 (1986). Issued by the Commission of the European Community.
[92] J. Gruber, *Environ. Sci. Technol. 17* (1983) 425.
[93] R. G. Clemmer, R. F. Malecha, I. T. Dudley, *Nucl. Technol. Fusion 4* (1983) 83.

Main-Chain Chirality and Optical Activity in Polymers Consisting of C–C Chains**

By Günter Wulff*

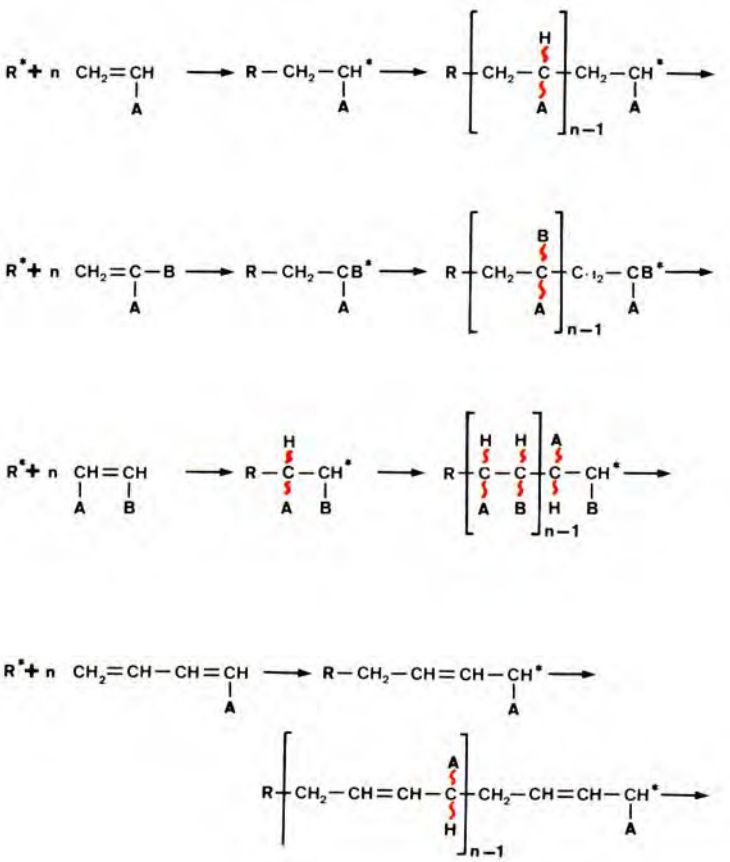
Main-chain chirality is the optical activity resulting from the configurational or conformational arrangement in the main chain of a polymer. The chirality of the most important types of structures has been investigated on the basis of systematic considerations of symmetry. This has led to the surprising result that even in polymers derived from 1-substituted or nonsymmetric 1,1-disubstituted olefins (the technologically most important polymers) several types of chiral structures exist, which are expected to result in optical activity if a particular enantiomer is favorably formed. By carrying out an asymmetric cyclopolymerization, it has been possible to obtain certain structural types in the form of optically active copolymers or homopolymers (e.g., copolymers of styrene with methyl methacrylate, or even the homopolymer of styrene). Another new group of optically active polymers consists of the atropisomeric helical polyisocyanides, poly(trityl methacrylates), and polychlorals. Optically active polymers are already used as adsorbents for the chromatographic separation of racemic mixtures. Further applications are likely to emerge.

1. Introduction

Polymers consisting of C–C chains are mainly obtained by polymerization of unsaturated monomers (e.g., ethylene, 1-substituted or 1,2-disubstituted olefins, butadiene, or substituted 1,3-dienes). Polymers formed from 1-substituted olefins are usually termed, according to the nature of the substituents, polyolefins, vinyl polymers, or polyacrylates; those formed from 1,1-disubstituted olefins are called polyolefins, vinylidene polymers, or polymethacrylates. For the substituted monomers, as can be seen from Scheme 1, each propagating step during the polymerization results in the formation of a new stereogenic center[***] with four different substituents. This holds good for free radical, anionic, cationic, or coordination polymerization. With increasing degree of polymerization the number of possible diastereomers rises rapidly.

Following the discovery of stereoregular polymerization using Ziegler–Natta catalysts,[5] the stereochemistry of such chains was studied in great detail (for reviews see, e.g., Refs. [6–9]; an excellent review article on this topic by *Farina*[10] has been published recently). The tacticity of polymer chains (i.e., the uniformity of successive configurational arrangements in the main chain[11]) is now well known, thanks mainly to NMR spectroscopic studies.[6–10]

On the other hand, it was still not certain whether polymers could show optical activity as a result of chirality due to the configurational arrangements in the main chain (known as main-chain chirality). While evidence for such phenomena was subsequently found for 1,2-disubstituted olefins and certain substituted dienes,[12–14] until recently it was thought that, for polymers based on 1-substituted and nonsymmetric 1,1-disubstituted olefins, main-chain chirality would not give rise to optical activity.[15–19] These latter types of polymers are by far the most important classes of polymeric materials, both technologically and scientifically. Optical activity in such polymers was only observed for



Scheme 1. Initiation and growth in the free radical polymerization of different types of monomers, resulting in the formation of diastereomers. The radical is indicated by an asterisk.

[*] Prof. Dr. G. Wulff
Institut für Organische Chemie und
Makromolekulare Chemie der Universität
Universitätsstrasse 1, D-4000 Düsseldorf (FRG)

[**] On the Chirality of Polyvinyl Compounds, Part 8. Part 7: [1].

[***] An atom bearing several substituents is described as *stereogenic* if interchanging two of its substituents results in a stereoisomer (such an atom is said to form a stereocenter). Notations such as chiral C atom or chiral center, which have been used customarily up to now, should be avoided [2–4].

polymers obtained from 1-substituted olefins bearing an optically active side chain (for reviews on optically active polymers in general see, e.g., Refs. [10, 15–24]).

Only recently has optical activity arising from the main-chain configuration been shown to occur for polymers of 1-substituted and nonsymmetric 1,1-disubstituted olefins.[25–30] Furthermore, it has been possible to synthesize a completely new type of optically active polymer, whose chirality results from a sort of atropisomerism in the main chain. In this manner one can obtain polymers with a predetermined single-handed helical structure.[31–36]

The considerable delay in investigating the chirality of vinyl polymers was due to the special stereochemical features associated with very long chains. Firstly, it is not always possible to determine the symmetry properties of such systems in a simple way, and secondly, stereoregular polymers with complicated tacticity can be synthesized only with difficulty. Moreover, the relationship between chirality and optical activity is more complex for polymers than for low-molecular-weight substances. For many chiral polymers, even pure enantiomers, optical activity is not expected for fundamental reasons.

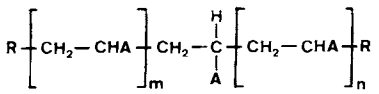
In the present survey, the symmetry properties of polymers consisting of C–C chains will be systematically reviewed in Section 2, in which the relationship between chirality and optical activity in polymers will also be discussed. Section 3 will deal with the different types of optically active polymers known so far. The problem of atropisomerism in polymer chains will be discussed in detail in Section 4. The treatment will be limited throughout to polymers whose optical activity results from chirality due to the configuration or conformation in the main chain. Polymers with optical activity arising from the configuration of side chains (for reviews see Refs. [10, 17, 20, 21, 37, 38]) and optically active polymers with heteroatoms in the main chain[10, 17–21, 39, 40] are not included.

The main emphasis in this article will be on polymers of 1-substituted and 1,1-disubstituted olefins, since a significant amount of new information has recently been gathered on these polymers.

2. Symmetry Considerations for Polymers Consisting of C–C Chains

2.1. Statement of the Problem

Symmetry properties are more difficult to recognize in polymer chains made up of uniformly repeating units than in low-molecular-weight compounds. The macromolecule usually contains stereocenters, either at each carbon atom of the chain or at alternate carbon atoms, each of which bears four different substituents. In the vinyl polymer **1**, for example, two of the substituents are the group A and the hydrogen atom. The other two substituents consist of the chain ends of different length.



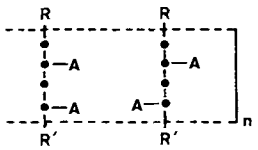
1

Optical activity is not expected to result from this structure alone, since, on the one hand, stereocenters with two different, but very long, substituents (e.g., in natural fats) show practically no optical rotation and, on the other, for each stereocenter in the chain there is one on the other side of the chain with the opposite configuration. This implies that the chain residues of differing length in **1** are exchanged; $n > m$ instead of $n < m$. Any optical activity found must therefore be caused by other structural features.

In addition to this fundamental problem there exists another one of a more practical nature. Whereas compounds of low molecular weight are in general uniquely defined with regard to their constitution and configuration, leaving the conformation as the sole variable about which one must make assumptions, this is not the case for macromolecules. The existence of structural defects in the chains, of differences in the chain ends, and of a distribution of molecular weights, as well as the fact that the configuration is almost never completely uniform, even in stereoregular polymers, forces one to use simplified models. (For a discussion of the need to use models in dealing with real molecules, see *Mislow* and *Bickart*[41].)

2.2. Selection of Suitable Models

At first, the macromolecules are assumed to possess an ideal stereoregular structure: i.e., they are made up of repeating units with identical constitution and configuration. Such ideal stereoregular polymers are usually described by specifying the smallest regularly repeating configurational unit (called an *n*-ad).[6–11] For the well-known stereoregular vinyl polymer types, namely, isotactic and syndiotactic, these units are termed the *meso* diad and the racemic diad, respectively.[*]



2 **3**

For ideal stereoregular polymers the following two models, which have also been used in previous work,[10, 15, 16, 28, 30] will be employed here:

a) A very long finite chain with identical chain ends;
b) An infinite (i.e., unlimited) chain. This is a useful model for true high polymers and has been shown to be particularly valuable for stereochemical considerations. In this case all the units of a stereoregular polymer are

[*] Throughout this article macromolecular formulas are shown in the normal Fischer projection, since chains of known absolute configuration are dealt with. This differs from the IUPAC Macromolecular Division's recommendations [11], which suggest that for polymers the 90°-rotated Fischer projection should be used. Furthermore, for greater clarity the carbon atoms of the chain are represented by dots, and the hydrogen atoms are omitted. Different substituents on the main chain are denoted by A, B, D, and E. The substituents themselves are regarded as having rotational symmetry with respect to the substituent-to-chain axis.

exactly identical, and there are no longer any end groups.

Considerations of symmetry in both these models are based on the conformation with the highest symmetry, which is usually the zigzag chain conformation. For the sake of simplicity, the normal Fischer projection will usually be employed here.

For the finite chain model a, with identical chain ends, the chirality can be determined in the usual manner by point group symmetry considerations, although for long chains this is often not easy. For the infinite chain model b, the symmetry properties of stereoregular polymers can be described using the one-dimensional space group (line group), since this model involves a three-dimensional body having periodicity in one direction. This method of describing the polymer chain has been used mainly in calculations related to spectroscopic studies.[16,42-48] When using space groups it is necessary to take into account, in addition to the symmetry operations of the point groups, translational and other symmetry operations combined with translation (glide planes, transverse mirror planes, and screw symmetry axes).[46-50] A one-dimensional space group is chiral if it contains neither a mirror symmetry plane nor a glide plane of symmetry.[16]

For symmetry considerations an infinite chain can be replaced by a ring, which may be regarded as an endless chain with a finite number of units.[51,52] *Farina, Peraldo,* and *Natta*[16] have applied this principle very successfully to determine the symmetry properties of complex stereoregular polymers, especially polymers of 1,2-disubstituted olefins and 1,3-dienes. In these studies they placed the *n*-ads in a ring containing the corresponding number of units. The ring, assumed to be planar, together with its substituents, has symmetry properties comparable to those of the infinite chain model b, but can be described in terms of point group symmetry. An example is the triad in a stereoregular homopolymer of a vinyl monomer; this triad is represented as the three-membered ring structure **4** (in this case the CH_2 groups do not contribute to the symmetry properties and are omitted from the ring representation). The triads **5a-f**, shown as Fischer projections (Fig. 1), are equivalent and describe the same stereoregular polymer chain in the infinite chain model (in this case, only the repeating configurational unit without end groups is shown).

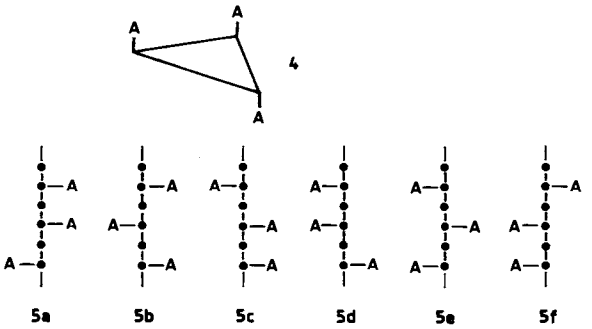


Fig. 1. Different triad representations for the same stereoregular polymer (the triads 5 form an infinite chain).

2.3. Types of Chiral Polymers

2.3.1. Stereoregular Homopolymers

Here we shall discuss polymers of 1-substituted olefins (CH_2=CHA) and of nonsymmetric 1,1-disubstituted olefins (CH_2=CAB), which have the same symmetry properties. Since polymers of symmetric 1,2-disubstituted olefins (ACH=CHA) have comparable symmetry properties, they can also be treated here.

It has long been recognized that the usual types of stereoregular homopolymers of these monomers, namely, the isotactic and syndiotactic polymers, are achiral.[6-10,15-21] For the finite chain model it can be seen that the isotactic chain **6** (Fig. 2) possesses a mirror plane and is therefore a *meso* form. (The difference between R and CH_2-R at the chain ends is neglected here.) The tertiary carbon atoms of the chain can be assigned an absolute configuration in which, in addition to A and H, the substituents are the two chain ends of different lengths. If, for example, one assigns to carbon atom a) the (*R*) configuration and then considers a tertiary carbon atom on the other side of the chain, the chain end that was previously the shorter one now becomes the longer and, accordingly, one obtains the (*S*) configuration for b). In an isotactic chain, therefore, one-half is (formally) in the (*R*) configuration and the other half in the (*S*) configuration.

The mirror symmetry in isotactic polymers can be eliminated[25,26] if, starting near the middle of the chain, substituents are switched to the opposite side of the chain with respect to the Fischer projection (**7**). The stereogenic centers in the chain now have continuous sequences of either (*R*) or (*S*) configuration. Since each section of the chain is strictly isotactic, we have proposed to describe such structures as "inverse biblock isotactic".[25,26] Structure **7** has only a twofold axis of symmetry and can therefore be regarded as chiral. A structure of this type cannot be represented by the infinite chain model. In high polymers with such structures optical activity is not expected solely on the basis of configurational effects. One needs to determine experimentally, by synthesizing model compounds, the upper limit of molecular weight for which optical rotation can occur, in certain cases as a result of the formation of a chiral long-range ordering (e.g., a single-handed helix).[53]

Syndiotactic polymers **8**, as represented by the infinite chain model, possess a glide mirror plane and translational mirror planes perpendicular to the chain axis. Thus the syndiotactic chain is achiral.

The above conclusions pertaining to symmetry also apply to isotactic polymers **9** and syndiotactic polymers **10** obtained from 1,2-disubstituted olefins (ACH=CHA), which are accordingly achiral.[16]

As was mentioned previously, isotactic and syndiotactic polymers have structures which can be characterized in terms of *meso* and racemic diads **2** and **3**, respectively. For longer structural units such as triads, a triad characteristic of an isotactic polymer also exists, in addition to the triads **5**. Placed in a ring (see **4**), such a triad gives rise to mirror symmetry. Similarly, investigation of the possible tetrads and pentads reveals only achiral configurations. Only for a

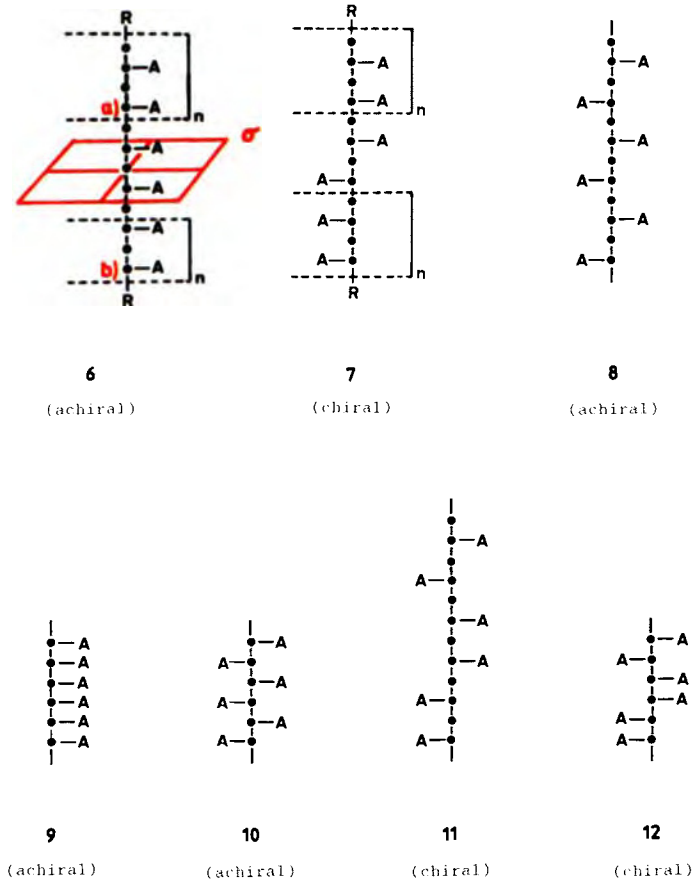


Fig. 2. Chiral and achiral homopolymers: **6** and **9** isotactic; **8** and **10** syndiotactic; **7** inverse biblock isotactic; **11** and **12** have chiral hexads.

regularly repeating structural unit made up of six monomer units is one of the eight possible hexads (see **11**) chiral, with C_2 symmetry. When arranged in a six-membered ring, the hexad has symmetry properties similar to those of the hexitols, of which only chiroinositol is chiral. This conclusion is also true for vinyl and vinylidene compounds and for the triads in polymers of symmetrically 1,2-disubstituted olefins **12**.[10,16] When longer structural units (heptads, octads) are considered, the number of possible chiral structures increases.

2.3.2. *Stereoregular Copolymers*

In stereoregular copolymers a much greater proportion of the structures are chiral. However, for the simplest cases of the alternating copolymers of 1-substituted olefins, the possible diads **13** and **14**, as well as all the conceivable tetrads, are achiral (Fig. 3). This also holds good for the corresponding homopolymers of nonsymmetric 1,2-disubstituted olefins.[54]

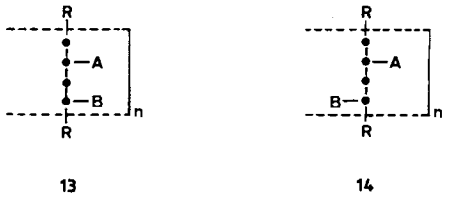


Fig. 3. Achiral diads in copolymers.

Of the three possible triads **15**–**17** with the sequence AAB, one structure is chiral and asymmetric,[25] namely, **17**. Figure 4 shows the three possible configurations in the ring form. In the asymmetric triad **17** the chirality is determined by the diad which carries the A substituents. Although the carbon atom with the B substituent is in a chiral environment (i.e., it is "chirotopic"[3]), it does not constitute a stereogenic center in this triad (compare **17a** and **17b**).

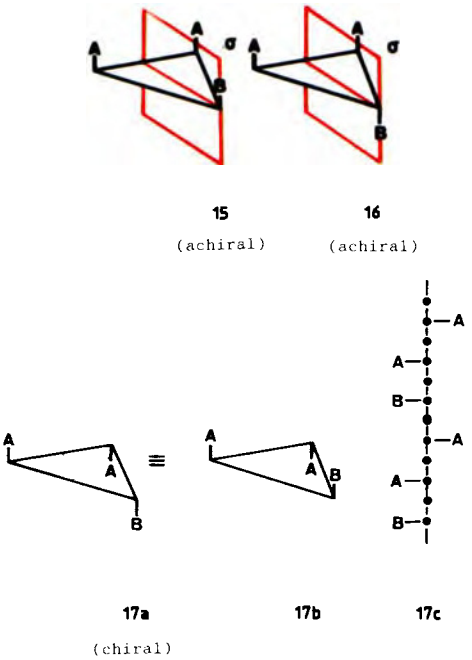


Fig. 4. Possible triads with the sequence AAB.

All four possible triads **18**–**21** (Fig. 5) in a stereoregular terpolymer are chiral and asymmetric. Of the five possible tetrads with the sequence AABB, three (**22**–**24**) are chiral (Fig. 6). Chiral polymers having this type of symmetry

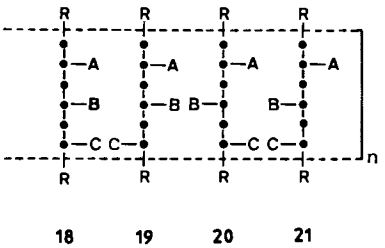


Fig. 5. Chiral terpolymers.

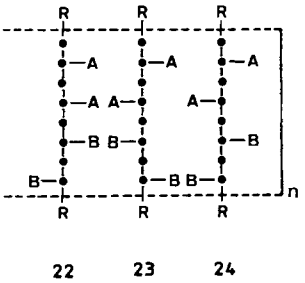


Fig. 6. Chiral tetrads.

(without the CH_2 groups of **22**–**24**) can in principle also be obtained by alternating copolymerization of ACH=CHA with BCH=CHB.

When the investigation of the symmetry properties of stereoregular copolymers further includes tetrads with other arrangements of the substituent (e.g., A_3B) or different substituents (A, B, D, E) or includes longer structural units (pentads, hexads, etc.), the proportion of chiral configurations is greatly increased. For example, for tetrads made up of three or four different monomers with different substituents, all the possible configurations in a stereoregular polymer are chiral.

2.3.3. Chiral Polymer Structures Resulting from Breakdown of Translational Symmetry

In the foregoing section chiral structures in stereoregular polymers were identified mainly by putting the repeating units into a ring structure. In other cases they can be derived in a more straightforward manner by introducing intermediate units along the chain to remove the mirror symmetry in the direction perpendicular to the translational axis (see Fig. 7).

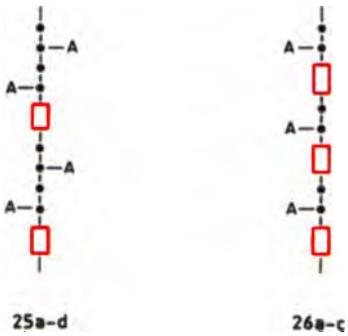


Fig. 7. Removal of translational symmetry by inserting intermediate groups. Intermediate units in **25a**, one or more comonomer units; in **25b**, atactic homopolymer; in **25c**, heteroatoms; in **25d**, double bonds. Intermediate units in **26a**, double bonds; in **26b**, 1,2-disubstituted comonomers; in **26c**, heteroatoms.

An achiral, syndiotactic polymer **8** can be converted into a chiral chain by separating the A–A structural units from each other (**25**). In the chain **17c** such a separation has been achieved by introducing a comonomer unit with the substituent B. It is especially easy to obtain polymers of this type by introducing heteroatoms into the chain to afford chiral polyesters, polyamides, polyethers, polyimines, etc. (which will not be discussed further here). Since in the case of the copolymers **17c**, the carbon atom bearing the substituent B is not decisive for the chirality, the AA diads can also be separated from each other by chains of any comonomer which can be either stereoregular or atactic.[29] This gives rise to a very important question with regard to the optical activity of homopolymers: Do chiral chains result when AA diads of a given absolute configuration (e.g., (*S*,*S*)) are separated from each other by atactic sequences of the same monomer, and could, for example, polystyrene be optically active under these circumstances?

A detailed statistical analysis of all possible arrangements in polymers of this type shows that, in fact, 25–50% of the stereogenic carbon atoms in the diads are present in chain segments which could contribute to the optical activity of the polymer.[57] The occurrence of chiral arrangements with uniform absolute configurations in these partially atactic polymers is due to the fact that each stereogenic center of the diads has one adjacent center with a uniquely predetermined absolute configuration, whereas the configuration of the stereogenic center on the other side changes in a random manner. Thus, in addition to polymers with chiral hexads **11**, it is also possible to obtain chiral homopolymers when diads with a uniform absolute configuration are distributed within a polymer chain which is otherwise atactic (**25b**). (The arrangement in the hexad **11** can also be described by means of chiral diads separated from each other by a monomer unit with alternating absolute configuration.) However, the optical rotation exhibited by such polymers is noticeably smaller than for other types of chiral polymers.[57]

As shown in **25** and **26**, many different ways of separating the diads have already been known for some time; important contributions to this problem have been made by *Arcus*,[15] *Schmitt* and *Schuerch*,[58] and *Natta* and *Farina*.[16,59] Polymers that have been particularly well studied are those of 1,2-disubstituted olefins (and also of cyclic olefins). Thus, when a comonomer CH_2=CHB or even ethylene is used to achieve the separation in such syndiotactic polymers, the chiral structures **27** and **28** can be obtained (Fig. 8). It should also be possible for structural elements of the type shown in **28** to be formed in the polymerization of 1-substituted olefins, if some head-to-head linkages occur. This provides another possible route for obtaining optically active, albeit nonregular, homopolymers from 1-substituted olefins.[25]

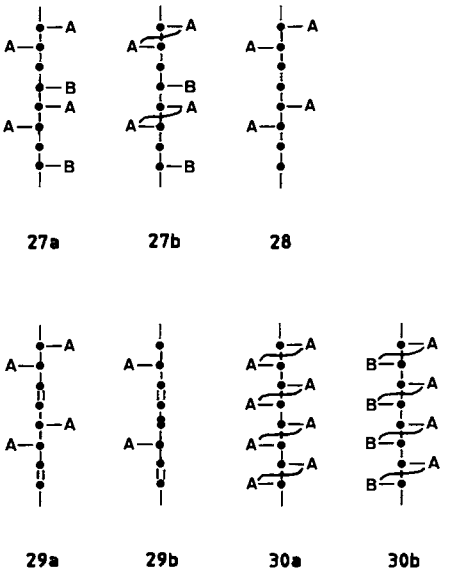


Fig. 8. Types of chiral structures resulting from elimination of the translational symmetry.

A double bond is also suitable as an intermediate unit in **25** (see **25d**). From 1,4-A_2-butadienes one can construct chiral polymers with structures of the type **29a**, while from 1-A-butadienes chiral polymers like **29b** are obtained.

The mirror planes perpendicular to the translational axis in syndiotactic polymers from 1,2-disubstituted olefins can also be eliminated by forming a ring structure, as shown in **30a**. In this case no intermediate unit is introduced; instead, the two chain substituents on a stereogenic carbon atom are nonequivalent because one of the neighbors is in the same ring structure while the other is outside. The existence of this type of structure has been verified particularly for the case of two different substituents (**30b**).[13,16] For clear representation of the stereochemical situation, one can also put the structural units of **27**–**30** (Fig. 8) into a ring structure.[16]

2.3.4. Atactic Polymers

Atactic polymers contain chiral centers with equal numbers of (*R*) and (*S*) configurations distributed in a random sequence along the chain.[11] In this case only the finite chain model can be used, and a detailed analysis is best carried out using statistical methods. Clearly, the model for such a chain will be chiral, but molecules of this kind do not in fact show optical activity. In 1984 *Green* and *Garetz*[60] calculated the probability of finding both enantiomers of a diastereomer in a sample of an atactic polymer. They found that, with a degree of polymerization (X_n) of 70 or greater, the molecules of an atactic polymer in principle must be present as pure enantiomers, since the number of possible diastereomers is far greater than the total number of molecules present. This leads to the paradoxical conclusion that, in a polymerization carried out under achiral conditions, pure enantiomers are formed. According to *Green* and *Garetz*, optical activity in such cases is not observed owing to intermolecular compensation of the rotational contributions from the different diastereomeric species.[60] However, it should be pointed out that the arrangement in atactic polymers is cryptochiral (i.e., the model of the molecule is chiral, but the substance is in actuality achiral)[41] and therefore even a single chain of this polymer is not expected to show optical activity.

3. Polymers with Optical Activity Caused by Chirality of the Main-Chain Configuration

3.1. Polymers of 1-Substituted and Nonsymmetric 1,1-Disubstituted Olefins

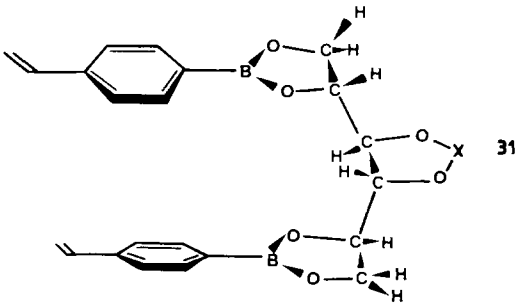
3.1.1. General Considerations

The initial attempts to synthesize optically active polymeric vinyl compounds were made at a time when the types of chain configurations necessary for chirality were not yet clear. Based on the negative results obtained in these experiments[61,62,65–67] it was assumed that polymers of 1-substituted olefins could not be obtained in forms exhibiting optical activity due to main-chain chirality.[15,17–19,61]

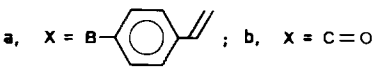
The discussion in Section 2 has shown that a great many structures in this class of polymers are indeed chiral. One only needs to consider how structures such as **11**, **17**–**24**, **25a**, or **25b** can be prepared as single enantiomers. In all these cases, if there is a predominance of one absolute configuration, optical activity is expected to occur. Admittedly, though, these structures are not very easy to synthesize.

3.1.2. Asymmetric Copolymerization

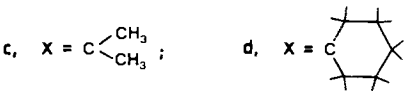
Of the chiral structures deduced in Section 2, the copolymer of the type **17c**, with an asymmetric triad, should be most easy to obtain in practice. In this case, the deciding factor for optical activity is the configuration of the diad carrying the substituent A. An attempt was therefore made to link two monomer units to a chiral template molecule to give, for example, **31**, followed by copolymerization with another monomer. A suitable chiral template is D-mannitol, to which 4-vinylphenylboronic acid was bonded at the 1,2 and 5,6 positions. The 3,4 position contains a five-membered ring, which stabilizes the spatial conformation of the molecule.[25,27,29]



31



a, X = B ; b, X = C=O



c, X = C(CH$_3$)$_2$; d, X = C

The template monomer (e.g., **31d**[29]) was subjected to free radical polymerization with various comonomers and, after splitting off the template, a soluble linear copolymer with a molecular weight of about 100000 was obtained.

The polymers obtained using a comonomer ratio of 1:1 show a very pronounced optical rotation in some cases, with $[\alpha]_{365}^{30}$ values from −56.0 to +145 [degree dm^{-1} g^{-1} cm^3] (see Table 1). Notwithstanding their different directions of rotation, both the positively and negatively rotating polymers possess the same absolute configuration. For example, polymer No. 10 with 4-vinylbenzaldehyde as the comonomer gave, after reduction with $LiAlH_4$, a polymer which had a structure corresponding to that of copolymer No. 6 obtained using 4-vinylbenzyl alcohol as comonomer. Both these polymers showed almost the same negative optical rotation value.[68] Similar relationships were also observed in other cases. Circular dichroism studies have shown that the positive rotations are caused by large Cot-

Table 1. Optical rotation values for copolymers of **31d** with various comonomers, measured after splitting off the template molecules [29, 68, 69]. The free-radical-initiated copolymerization, with the comonomers in a molar ratio of approximately 1:1, was continued until 10–20% of the monomers had reacted.

No.	Comonomer	$[\alpha]_{365}$ [degree $dm^{-1} g^{-1} cm^3$]
1	Methacrylonitrile	− 56.0
2	Methyl methacrylate	− 33.8
3	Styrene	− 23.0
4	3-Methylstyrene	− 18.8
5	4-Methylstyrene	− 7.7
6	4-Vinylbenzyl alcohol (4-hydroxymethylstyrene)	− 7.0
7	4-Chlorostyrene	+ 1.5
8	4-Nitrostyrene	+ 20.7
9	4-Vinylbenzonitrile (4-cyanostyrene)	+ 27.0
10	4-Vinylbenzaldehyde (4-formylstyrene)	+ 39.0
11	2-Vinylnaphthalene	+ 56.0
12	4-Vinylstilbene	+ 145

ton effects arising from the conjugated chromophore of the comonomer. Presumably the comonomers are forced by the chiral diads into an asymmetric conformation, a phenomenon already documented in the case of polymers bearing chiral side chains.[38]

The detailed copolymerization behavior of **31d** with methyl methacrylate is illustrated by the copolymerization diagram in Figure 9, in which the composition of the polymer is plotted as a function of that of the comonomer mixture. It can be clearly seen that the template monomer is preferentially incorporated into the polymer. The diagram also shows the optical rotation values of the resulting polymers. The specific rotation value reaches its maximum of about −80° when the copolymer contains about 25 mol% of **31d**.[27,29]

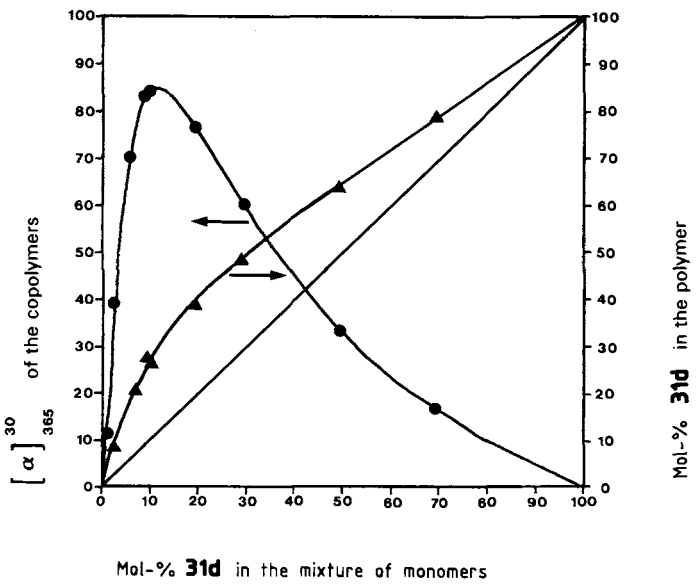


Fig. 9. Constitution of copolymers of **31d** with methyl methacrylate (Table 1, No. 2) and their optical rotation after splitting off the template molecules. The composition of the monomer mixture is plotted as the abscissa.

More detailed studies on the mechanism of this asymmetric copolymerization have shown[29] that **31d** undergoes a cyclopolymerization; i.e., the two double bonds in **31d** are incorporated into the polymer chain one after the other through the formation of a 19-membered ring. Figures 9 and 10 show the crucial step after the addition of the growing "macroradical" to **31d**. The benzyl radical thus generated can only react with the second double bond in the conformation shown in Figures 10 and 11. A further monomer can then only react from below, resulting in the formation of an (*S,S*) distyryl diad. For a different conformation of the first double bond one obtains an (*R,S*) diad, which is a *meso* form and does not contribute to the optical activity.

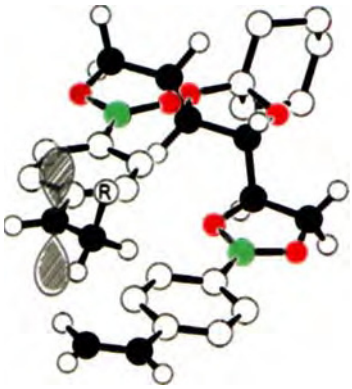


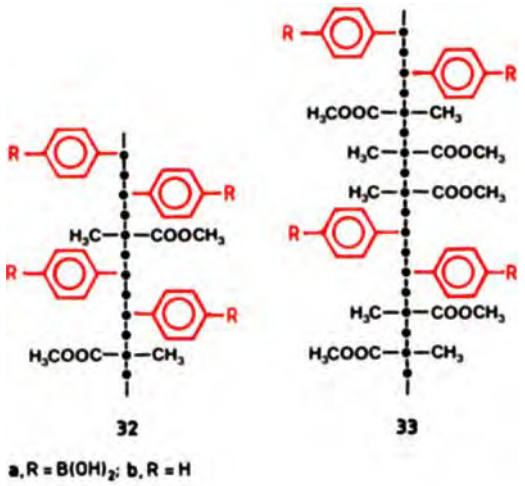
Fig. 10. Possible arrangement of the styryl radical from **31d** after reacting with a free radical R* according to a ball-and-stick model. For clarity the carbon atoms of mannitol and the vinyl group are shown in black and the hydrogen atoms of the phenyl ring and the cyclohexyl group are omitted (boron, green; oxygen, red).



Fig. 11. The CPK space-filling model of the same intermediate as in Fig. 10 shows that after the reaction of this free radical with the second double bond a further monomer unit can only add from below (boron, green; oxygen, red).

After the template molecules are split off, copolymers of methyl methacrylate with **31d** contain the idealized structure **32a**, or, in the case of an excess of the comonomer, the structure **33a**.

Boric acid can be quantitatively removed from these polymers using $AgNO_3/NH_3$, resulting in styrene–methyl methacrylate copolymers **32b** or **33b**, which are especially suitable for ^1H and ^{13}C NMR studies.[29,70] The structure



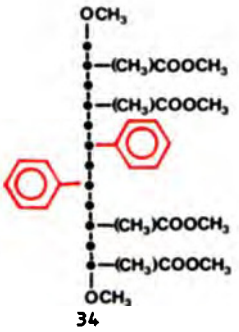


Fig. 12. Optically active copolymers **32**, **33** and an optically active model compound **34**. For **33**, a portion of the chain in which the configurations of the methacrylate units are randomly arranged is shown. The same is true of the methacrylate units in **34**.

and absolute configuration of the polymers **32b** and **33b** have been unambiguously determined by comparison of their NMR and circular dichroism spectra with those of newly synthesized model compounds (e.g., **34**).[29,71] The polymer chains, as predicted from conformational analysis, do in fact contain (*S,S*) distyryl diads, along with a certain amount of (*R,S*) *meso*-diads.

Polymers of the types **32b** and **33b** can be subjected to various functionalization reactions,[1] namely, nitration, bromination, chloromethylation, or acetylation at the *para* position of the distyryl diads, as well as reduction of the ester groups. In an analogous manner modified materials can be obtained from methacrylonitrile-based copolymers. These reactions afford a wide variety of optically active, soluble polymers bearing different functional groups with optical activities arising from main-chain chirality.

3.1.3. Optically Active Homopolymers

In a number of cases optically active homopolymers could also be obtained; however, their specific optical rotation values (reported for the polymers based on methacrylate,[22,72–75] vinylcarbazole,[76,77] *m*-tolylvinylsulfone,[78] and benzyl[79]) were quite small. The structure and mechanism of formation of such polymers are still unclear. In some cases the optical activity was attributed to chiral conformations, since configurational chirality in the main chain did not appear to be possible.

A systematic synthesis of homopolymers made up of chiral hexads **11** would probably be difficult. On the other hand, polymers of the type **25b** have now been prepared.[57] For this purpose **31d** was copolymerized with styrene: after splitting off the 3,4-*O*-cyclohexylidene-D-mannitol used as a template, an optically active 4-vinylphenylboronic acid–styrene copolymer **35** was obtained, with a specific optical rotation $[\alpha]_{365}^{30} = -35$ [degree dm^{-1} g^{-1} cm^3]. Quantitative deboronation of **35** gave the styrene homopolymer **36**, with a specific optical rotation $[\alpha]_{365}^{30} = -3$ [degree cm^{-1} g^{-1} cm^3] (Fig. 13). The homopolymer synthesized by this method contains asymmetric distyryl diads of uniform configuration within an otherwise atactic styrene polymer. It is thus the first example of an optically active homopolymer of this class with defined structure and configurational main-chain chirality.

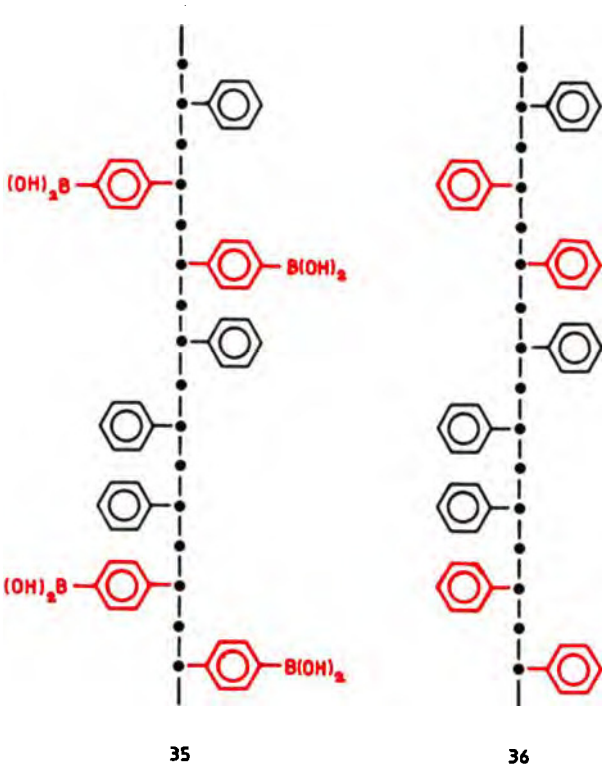
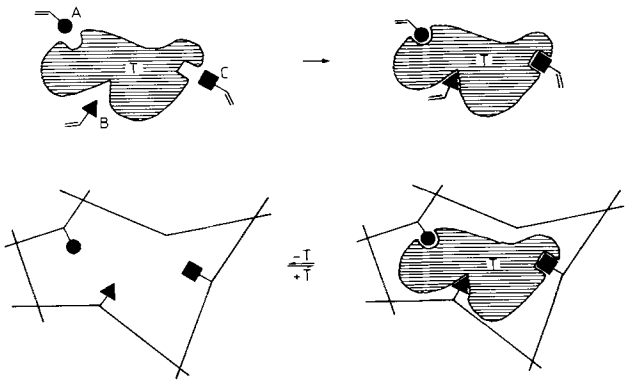


Fig. 13. The optically active co- and homopolymers **35** and **36** (portion of the chain).

3.1.4. Branched and Cross-linked Polymers

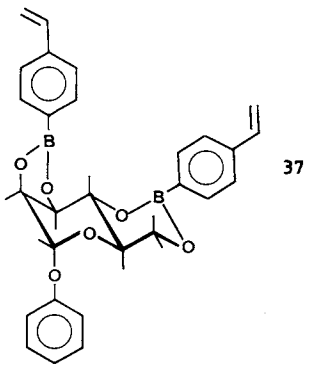
Quite apart from chirality due to the configurational arrangement of substituents along the main chain of linear polymers, it should be possible for branched polymers to generate asymmetric configurations at branching positions arising from the different lengths of the chains. However, up to now no examples are known.

On the other hand, we have been successful in obtaining chiral arrangements in cross-linked polymers.[80–83] For this purpose polymerizable vinyl monomers containing functional groups were attached to suitable optically active template molecules, which were subsequently copolymer-



Scheme 2. Schematic representation of polymerization in the presence of a template (T).

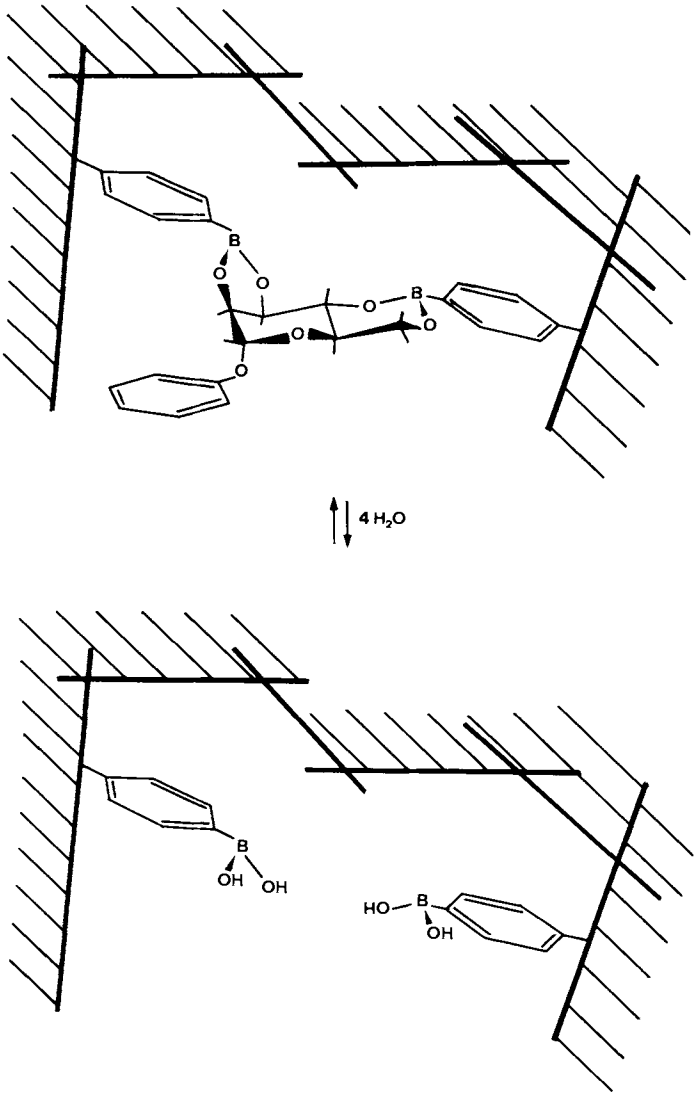
ized, in the presence of solvents and relatively large concentrations of cross-linking agents, to give macroporous polymers. Removal of the template molecules (see Scheme 2) left behind chiral cavities in the polymer, the cavity shape and the arrangement of the functional groups being determined by the template molecules. An example is the polymerization of the monomer **37**, where phenyl-α-D-



37

mannopyranoside acts as a template to which two molecules of 4-vinylphenylboronic acid are linked as diesters of boronic acid. After polymerization and removal of the template (Scheme 3), chiral cavities are left behind, each with two boronic acid groups. Polymers of this type are optically active. The optical activity is measured for a suspension of the polymer in a solvent having the same refractive index as the polymer, a technique which was developed for other types of insoluble polymers. Figure 14 depicts the incorporation of the template into the polymer. The asymmetry of the cavities can be recognized from the excellent racemate resolution ability for the template compound. For the present system α values (the ratio K_D/K_L of the solvent/polymer partition coefficients for the L and D forms) greater than 4.5 were obtained.[83]

The chirality of the cavities is stabilized by means of the cross-linking points in the polymer chain. This chirality can arise from the configuration of the cross-linking points as well as from asymmetric conformations of the polymer chain which are stabilized by cross-linking. In the case of **37**, the chiral configurations of the linear portions of the chain do not contribute to the asymmetry of the cavity.



Scheme 3. Schematic representation of the removal of the template molecule phenyl-α-D-mannopyranoside from a highly cross-linked copolymer of **37**.

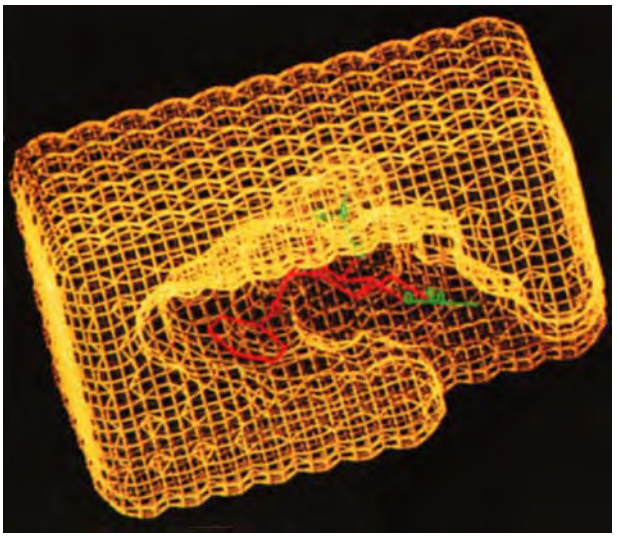


Fig. 14. Computer-generated representation of the imprinting caused by phenyl-α-D-mannopyranoside as a template (see Schemes 2 and 3).

This method of molecular inprinting has now been extensively applied with many different templates, and numerous other research groups have reported important applications based on this principle. (Further details are described in several recent review articles.[85-88])

3.2. Polymers of 1,2-Disubstituted Olefins

In contrast to vinyl polymers, optically active polymers with main-chain chirality obtained from 1,2-disubstituted olefins have been quite systematically studied.[10, 15-21] Three principal methods have been used for asymmetric induction during polymerization:

a) During copolymerization, monomers with optically active substituents that can be subsequently removed have been used. In this case the substituent controls the stereochemistry of each step during chain growth.
b) Polymerization can be carried out in the presence of an optically active catalyst. This method cannot, however, be applied to free radical polymerization with optically active initiators.[61, 62]
c) Another possibility involves polymerization in a chiral medium such as an optically active solvent or clathrate-forming compound.

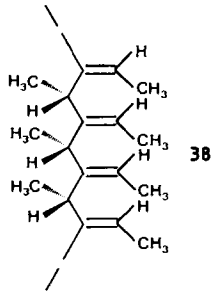
Using (*S*)-(−)-α-methylbenzyl methacrylate and maleic anhydride (method a, structural type **27b**), *Beredjick* and *Schuerch*[12] were the first to obtain optically active polymers consisting of C–C chains with main-chain chirality. Several more examples have been reported in recent years.[89-93] *Natta, Farina* et al.[13] succeeded in obtaining polymers of the type **30b** (thought to be predominantly in the *threo*-diisotactic configuration[10]) with strong optical activity by cationic polymerization of benzofuran in the presence of an optically active catalyst.

3.3. Polymers of Substituted 1,3-Dienes

Natta and co-workers[14, 46] carried out the anionic polymerization of methyl sorbate using an optically active initiator and thereby obtained the first optically active homopolymer consisting of C–C chains with main-chain chirality (the structures of the 12 possible regular stereoisomers are given in Ref. [10]). A polymer with a chiral structure of the type **29b** was obtained[95] by asymmetric polymerization of 1,3-pentadiene (here A = CH_3). The γ-radiation-induced polymerization of dienes immobilized in a chiral host lattice (e.g., perhydrotriphenylene[96, 97] or deoxycholic acid[98, 99]) has proved to be a better method. It appears that in these cases the asymmetric induction by the chiral host lattice could be a through-space effect.[97] Optically active polymers have also been obtained by the free radical polymerization of 2,4-pentadienoic acid in the presence of (*S*)-(−)-α-phenylethylamine.[100]

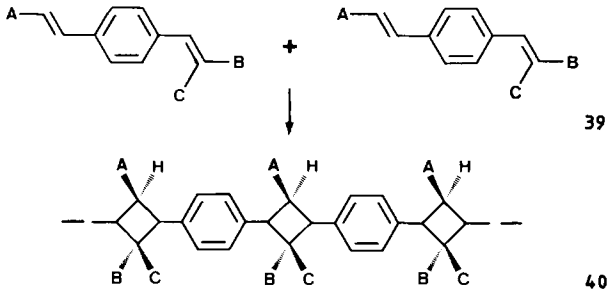
3.4. Other Structural Types

Two optically active polymers with special structures should be mentioned here. The first was obtained by polymerization of optically active (*R*)-2,3-pentadiene using π-allylnickel iodide. Of the four possible structures, the predominant one is thought to be **38**.[101]



38

In the second instance *Addadi, Lahav* and co-workers[102, 103] photopolymerized unsaturated dicarboxylic acid derivatives of the type **39** in the crystalline phase (Fig. 15). They used achiral monomers which, however, could be obained as a chiral crystal modification. The photopolymerization gave optically active cyclobutane derivatives with the structure **40**, with a relatively low degree of polymerization.



39

40

Fig. 15. Photochemical polymerization of cinnamic acid derivatives in the crystalline phase. For example, A = $COOsBu$, B = COOEt, C = CN.

4. Chiral Conformations and Atropisomers

4.1. General Considerations

In contrast to the assumptions made regarding molecular models in Section 2, real polymer molecules in solution constantly undergo rapid conformational changes; they exist, for example, as random coils or in partially regular helical conformations.[10, 104-106] (For reviews on helical molecules and helicity see Refs. [107, 108].) The probability of finding achiral conformations is vanishingly small, and therefore in practice all real chain molecules (even polyethylene) are present in chiral conformations. However, these chiral conformations do not in general produce measurable optical activity, since conformations with positive and negative optical rotations are present in equal amounts (i.e., the polymers are "stochastically achiral").[41]

In the crystalline phase many isotactic polymers are present in helical form.[10, 47, 109] The helices can have either right-handed or left-handed structures, the two forms (en-

antiomorphic conformations) having equal energy. When helices of this kind (e.g., in polypropylene) are formed, they do not possess C_2 symmetry, since all the substituents are oriented along one direction of the helix (unidirectional helix).[10, 109] In principle, under chiral conditions it may be possible to produce helices with predominantly one screw sense in the crystalline phase or other solid phase and thus to obtain a solid with optical activity (see, e.g., Refs. [110, 111]). However, for high-molecular-weight polymers of this kind the optical activity should be lost immediately and completely upon dissolving or melting, since the conformational equilibrium results in the formation of helices with both the screw senses in equal amounts (in addition to random components). In solution, however, a one-screw-sense helicity in chains with achiral substituents can be induced by a pendant optically active catalyst[112] or through the presence of a small number of optically active substituents.[38, 113a] Helices with a single screw sense can be formed even when the stereogenicity of the optically active substituents is due to an isotope effect, e.g., H and D.[113b]

A different case arises when an isotactic polymer chain possesses bulky substituents which impose severe steric hindrance. Now it becomes possible to stabilize the helix by these groups. As a result, there is no longer any conformational equilibrium at room temperature, or perhaps even at higher temperatures. For every individual chain only one type of helix occurs. Following the success of *Nolte, Drenth* and co-workers with polyisocyanides,[31, 32] of *Vogl* et al.[35] with polychlorals, and of *Okamoto, Yuki, Hatada* and co-workers[33, 34] with poly(trityl methacrylate), there have been considerable developments in obtaining optically active polymers with stable, one-screw-sense helices derived from achiral monomers. This type of isomerism can be described as atropisomerism, since it is a form of conformational isomerism in which particular isomers are stabilized by rotational hindrance about single bonds.

The particular case of poly(trityl methacrylate) illustrates the complexity of the stereochemical problems associated with the formation of such helices. The helix is actually formed during the polymerization reaction (Fig. 16). Under achiral conditions left-handed (*M*) and right-handed (*P*) helices are formed in equal amounts, but with optically active catalysts mostly or exclusively one of these two is formed in certain circumstances. If one considers a single step during the chain growth, the monomer molecule with a prostereogenic center can add to the growing *M*-type helix in either the (*R*) or the (*S*) configuration. The two intermediate states **41a** and **41b** are diastereomers.

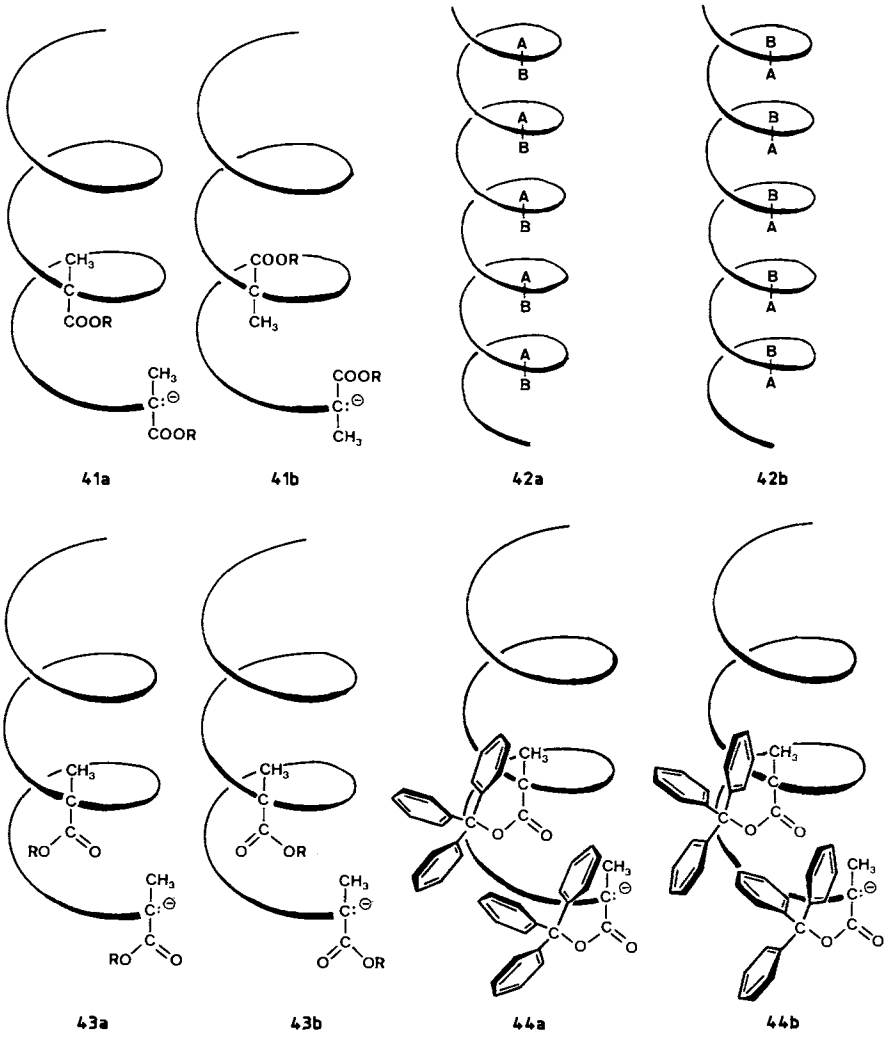


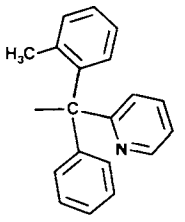
Fig. 16. Schematic representation of the stereochemical situation during the growth of an (*M*) trityl methacrylate helix. For clarity the carbanion, instead of the ester enolate is shown in each case. Structures **41a** and **41b** show the incorporation of a monomer unit in the (*R*) and (*S*) configuration, respectively, while **42a** and **42b** show the identities of the completed helices so formed, **43a** and **43b** show the two preferred conformations of the ester group, and **44a** and **44b** show the two helical forms of the trityl propeller.

Studies on oligomers suggest that the monomer always adds to the helix in the same configuration.[63,64,114] However, in the completed helix of a high polymer, where the influence of the end groups can be neglected, the two configurations *M*(*R*) and *M*(*S*) are indistinguishable, and they no longer constitute diastereomers (cf. **42a** and **42b**). An analogous situation exists for the *P*-type helix.

These conclusions are only valid if the substituents on the polymer chain can be assumed to have rotational symmetry with respect to the substituent-to-chain axis. However, this is not the case for poly(trityl methacrylate). Conformational analysis shows that the ester groups can have two different conformations in the helix, namely, **43a** and **43b**. Examination of CPK space-filling molecular models suggests that the rotation about the bond linking the carboxyl carbon to the polymer-chain carbon is partially or completely restricted and that for steric reasons all the groups must have the same conformation.

One must also take into consideration that the trityl group, which is in the propeller form, should have the same sense of helicity (i.e., (+) or (−)) in all the trityl groups, and that this sense is already established during the polymer growth reaction (**44a** and **44b**). (For the stereochemistry of molecular propeller forms see Ref. [115a], and for the preferred conformation of the trityl group see Ref. [115b].) Consequently, for the actual growth reaction in the presence of an optically active catalyst, each growth step has a total of 16 possible diastereomeric intermediate states. Steric considerations suggest that one of these is preferred. It is not yet known to what extent the side groups (ester and trityl group) retain conformational mobility, which would enable them to rearrange into the most thermodynamically stable configuration after the helix has been formed. In the completed polymer itself there are a total of four possible diastereomeric *d,l* pairs which could occur (as atropisomers or conformers).

The situation becomes further complicated when the propeller consists of three different "blades", as *Okamoto* et al.[116] recently reported for polymerization of a methacrylate containing the optically active propeller structure **45**. Owing to the occurrence of both planar and point chirality,[115a] in addition to the propeller chirality, the propeller structure **45** alone has eight possible diastereomeric *d,l* pairs.[115a] As a result, a single enantiomer of **45** gives rise to a total of 32 possible diastereomeric configurations for the helices in the polymer. Thus, in this case, a complete determination of the configuration and conformation of the helix will not be easy.



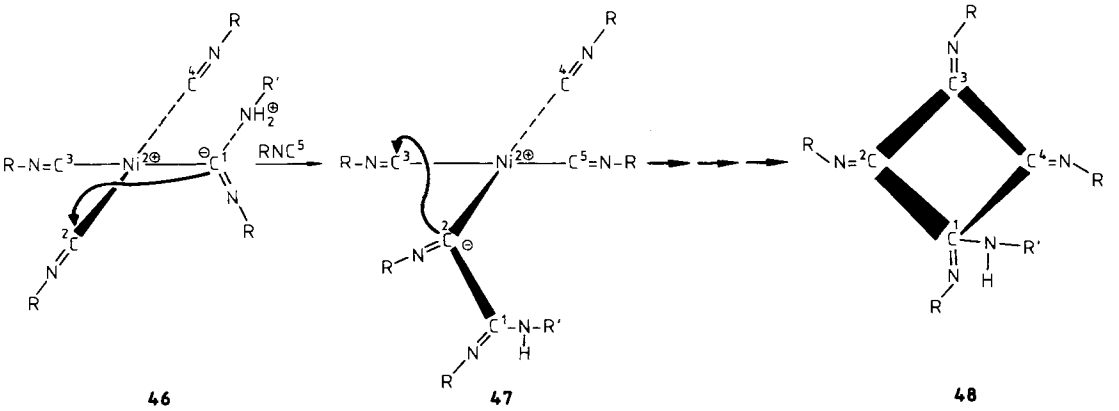
45

4.2. Chiral Atropisomeric Polymers

4.2.1. Helical Polyisocyanides

Polyisocyanides **48**, also termed poly(carbonimidoyls) or polyiminomethylenes (see Refs. [32, 36, 117–119] for reviews), have a structural type which is highly unusual in polymers, with each carbon atom of the chain having a double bond to a nitrogen atom. This brings about a restricted rotation about the C–C single bonds of the chain and hence results in the formation of stable, rigid helices.[120a] *Nolte, Drenth* et al.[31] have succeeded in separating the right- and left-handed helices of poly(*tert*-butyl isocyanide) chromatographically, using a polymer prepared from optically active (*S*)-*sec*-butyl isocyanide as the stationary phase. Circular dichroism studies and calculations using *Tinoco*'s exciton theory suggest that the negatively rotating polymers have a *P*-type helix and the positively rotating polymers an *M*-type helix.[36a]

The polymerization of isocyanides takes place, for example, in the presence of Ni^{II} salts (Fig. 17). In this case, a planar $[Ni(CNR)_4]^{2\oplus}$ complex (**46**) is initially formed. The reaction itself is initiated by attack from a nucleophile such as an amine, which increases the nucleophilicity of the carbon in **46** sufficiently to allow the attack of an adjacent coordinated isocyanide ligand (**47**). The reaction then continues as a succession of insertion steps in the same direction around the Ni center (the so-called merry-go-round mechanism).[32]



46 **47** **48**

Fig. 17. Mechanism of polymerization and helix formation in polyisocyanide **48** (cf. Fig. 18) [36].

This leads readily to the formation of a very tight helical structure (**48a**, Fig. 18), since the isocyanide units on the nickel ion are in the desired geometrical arrangement. The insertion reaction can proceed in either a clockwise or a counterclockwise direction, giving rise to right- or left-handed 4_1 helices, respectively. In principle the substituent can be in either the *syn* or the *anti* position during the growth process. It is assumed that all the substituents during the chain growth are in fact oriented in the same direction; hence, in this case, the helical polymers resulting from either the *syn* or the *anti* configuration would be identical.[120b]

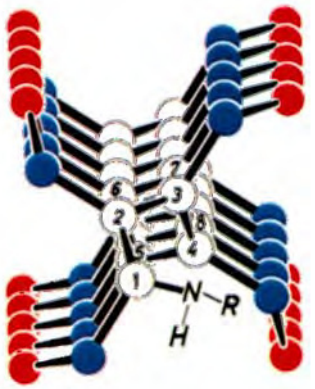


Fig. 18. Stereo view of the helix of **48** (cf. Fig. 17). The computer drawing of the helix was prepared according to data obtained from *R. J. M. Nolte*, Nijmegen, and *W. Drenth*, Utrecht.

It has recently been found[36a, 121] that use of an optically active amine as the initiating nucleophile results in the formation of a one-screw-sense helix with an optical yield of up to 85%. It is also possible, in the presence of small amounts of slowly polymerizing optically active isocyanides, to convert the achiral isocyanide into a nearly uniform homopolymer with a high degree of optical enrichment.[36a, 122]

4.2.2. *Helical Poly(trityl methacrylates)*

By anionic polymerization of trityl methacrylate in toluene at −78 °C using a butyllithium/(−)-sparteine complex (initiator/ligand complex), *Okamoto* et al.[33] obtained helical poly(trityl methacrylates) showing large positive optical rotation values (Fig. 19 and Table 2). When the very bulky trityl group was replaced by a methyl group, the optical rotation completely disappeared and highly isotactic poly(methyl methacrylate) (*meso* form) was obtained. The

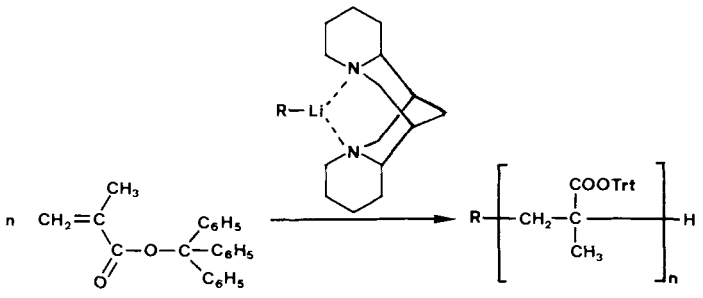
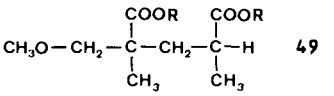


Fig. 19. Polymerization of trityl methacrylate to give helical polymers using alkyllithium/(−)-spartein.



49

Table 2. Helical polymers of methacrylate monomers; polymerizations of $CH_2=C(CH_3)COOR$ were carried out in toluene at −78 °C. Abbreviations: DPEDA = *N,N'*-diphenylethylenediamine; DDB = 2,3-dimethoxy-1,4-bis(dimethylamino)butane; Li-(*R*)-PAN = lithium-(*R*)-*N*-(1-phenylethyl)anilide; TMEDA = *N,N,N',N'*-tetramethylethylenediamine.

R	Initiator	Ligand	$[\alpha]_D$ [a] [degree $dm^{-1} g^{-1} cm^3$]	Ref.
Trityl	BuLi	(−)-spartein	+363	[124b]
Trityl	DPEDA-Li	(*R,R*)-(−)-DDB	−335	[124a]
Trityl	Li-(*R*)-PAN	—	− 70	[125]
Trityl	Li-(+)-**49**	TMEDA	−120	[114]
Trityl	Li-(−)-**49**	TMEDA	+120	[114]
(+)-**45**	BuLi	in THF	+395 → −321	[116]
(+)-**45**	DPEDA-Li	(*S,S*)-(+)-DDB	+509 → −357	[116]

[a] Optical rotations measured in THF for the THF-soluble component. Results given for *R* = **45** are for initial rotation at −78 °C, and final rotation after quenching the reaction with methanol and allowing the reaction mixture to stand at −20 °C.

chirality must therefore be attributed to a type of atropisomerism which is stabilized by the trityl group.[123] By using other optically active ligands in the initiator complex—e.g., (*R,R*)-(−)-2,3-dimethoxy-1,4-bis(dimethylamino)butane ((−)-DDB)[124a]—it has also become possible to obtain a poly(trityl methacrylate) showing negative optical rotation (see Table 2).

Optically active polymers can also be prepared using an optically active initiator, lithium (*R*)-*N*-(1-phenylethyl)anilide, although in this case the specific rotation is smaller.[124b] The diphenyl(2-pyridyl)methyl group[125, 126] and the optically active propeller group (+)-phenyl(2-pyridyl)(*o*-tolyl)methyl **45**[116] have also been used as bulky ester groups. The methacrylic ester of **45** has some unusual properties. Polymerization of the optically active monomer at −78 °C, even without the introduction of a chiral ligand into the achiral initiator, gives a polymer with strong positive optical rotation. After quenching the reaction with methanol and allowing the product to stand at −20 °C, it is slowly converted into a polymer showing negative optical rotation (see Table 2). This behavior is unaltered when (+)-DDB is introduced as the ligand during the polymerization. Apparently, the initial product, formed under kinetic control, is subsequently converted into the thermodynamically more stable form by an alteration of the conformation of the side chains[116] (see Section 4.1 with regard to the several possible isomeric forms in this case).

Relatively little is known regarding the mechanism of formation of helical poly(trityl methacrylates). It is well known that during polymerization under achiral conditions both types of helices are formed simultaneously and can be separated chromatographically on optically active poly(trityl methacrylate) as stationary phase.[127] Further details have been obtained from studies on the oligomers formed during the early stages of the polymerization.[63, 64, 114] In contrast to high polymers, isotactic oligomers at this stage do not form *meso* compounds. One can therefore study the absolute configuration following the

first addition steps. Thus it was possible for the first time to obtain optically active oligomers ($X_n = 1$–4) of trityl methacrylate and of methyl methacrylate (after transesterification of the oligomers).[63] The extent of asymmetric induction during the first addition step in the presence of (−)-spartein was only 20 to 40% depending on the reaction conditions.[114] The two enantiomers thus formed undergo further reaction at different rates, yielding oligomers with an isotacticity of over 90%.

The stereochemistry of the addition of the monomer at the chain end is controlled firstly by the last chiral center in the chain (backbone control) and secondly by the chiral ligands of the initiator complex (chelate control). In order to study the influence of the former factor, pure samples of the four possible "dimers" ((+) and (−) *threo* and (+) and (−) *erythro*), e.g., (+) form of **49**, were synthesized and, after deprotonation with lithium diisopropylamide (LDA), were used as initiators.[114] In the presence of an achiral chelating agent, the (+) and (−) forms of **49** gave polymers exhibiting opposite optical rotations (see Table 2). However, addition of (−)-sparteine was found to control completely the direction of optical rotation of the resulting polymer.

There is some evidence that the helix contains four monomeric units per turn.[63] The rate of reaction increases markedly after the formation of oligomers with $X_n = 4$ and $X_n = 8$.[63,64] Beyond $X_n = 9$, the stereochemistry of further chain growth is controlled by the preformed helix (in a manner similar to the helix control mechanism[128a]). Accordingly, the growing end of a preformed single-handed helix incorporates only one antipode of a racemic monomer.[127b] Figure 20 shows a computer-generated representation of the structure with four monomeric units per turn of the helix, in one of its possible conformations. The severe crowding of the substituents is clearly evident.

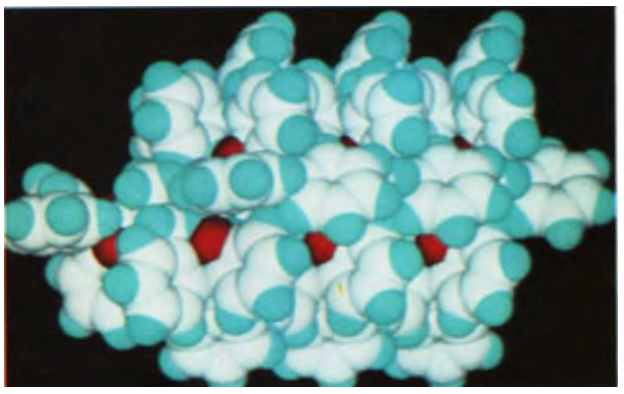
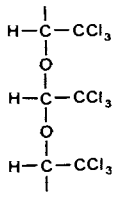


Fig. 20. Computer-generated representation of helical poly(trityl methacrylate) with four monomer units per turn and all trityl ester groups in the same configuration (this is one of eight possible structures).

4.2.3. Helical Polychlorals

Although polychlorals **50** are not C–C polymers, they will be mentioned briefly here, since their symmetry properties are similar to those of the polyvinyl compounds. Using optically active anionic initiators, *Vogl* and co-workers[35,36b,128,129] were able to obtain insoluble polymers of chloral. Films of these polymers show an extremely large optical rotation, with $[\alpha]_D$ values up to +3000°. Here again it is assumed that the helices are present in only one screw sense. The insolubility of the polymers presents considerable obstacles for further detailed studies.

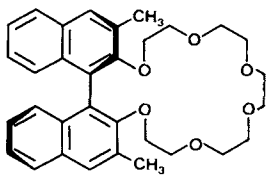


50

4.3. Optical Activity Caused by Flexible Chiral Conformations in the Main Chain

Contrary to atropisomers which are stabilized by large sterically crowded groups, one-screw-sense helical conformations of the chain in common polymers may be only stable in the solid phase or are stabilized by chiral catalysts, head groups, or side groups. Although unambiguous examples of the first case are not yet known, the polymerization of propylene in the presence of (*S*)-ethylenebis(tetrahydroindenyl)zirconium dichloride and methylalumoxane $(MeAlO)_n$ in toluene produces a highly isotactic polypropylene.[110,111] It has been shown, by studies during the early stages of the polymerization, that the oligomers in this polymerization are optically active and are essentially isotactic.[130a,b]

Cram and *Sogah*[112a] polymerized various esters of methacrylic acid (methyl, *tert*-butyl, benzyl) anionically in the presence of optically active binaphthyl crown ethers (e.g., **51**) to give oligomers ($X_n = 4.8$–12) which at first, in



51

the presence of the initiator,[112b] showed considerable optical activity. After removal of the catalyst, however, the optical rotation became considerably smaller, a fact which was attributed to an unwinding of the helices in the chain.[112] It appears that the helicity in this case is caused solely by the anchored catalyst and that the remaining optical rotation in these oligomers could be due to configurational effects, as in the case of optically active oligomers of methyl methacrylate[63] and propylene.[130]

5. Outlook

In this survey it has been shown that, contrary to previous assumptions, even the technologically most important polymers (i.e., those based on 1-substituted and nonsymmetric 1,1-disubstituted olefins) can exist in optically active forms. One of the factors that can give rise to optical activity in these polymers is the configurational arrange-

ment of the stereogenic centers along the main chain. Chirality due to the main-chain configuration is by no means unusual. In fact, when all conceivable structures are taken into consideration, it occurs very frequently. However, because of cryptochirality, atactic polymers, in particular, cannot occur in optically active forms, even when enantiomers of a single type are present. In stereoregular polymers, on the other hand, many optically active structures are conceivable; some of these have been realized experimentally and show very strong optical activity in some cases. In addition to optically active vinyl and vinylidene polymers with configurational main-chain chirality, further new groups of optically active polymers have been synthesized with optical activity arising from helical, atropisomeric structures.

The immediate objectives of the present investigations are essentially of scientific interest directed towards a general and deeper understanding of the stereochemistry of polymers. In addition, a very interesting question arises: Does optical activity in enantiomerically pure or enriched polymers introduce new interesting properties, leading to novel practical applications? Despite the very short time since the synthesis of these materials, some interesting applications have already begun to emerge.

Optically active poly(trityl methacrylate),[131-135] polychloral,[136] and cross-linked polymethacrylates prepared through the template approach[137-139] have been successfully used as adsorbing media for chromatographic separation of racemates. Chromatographic columns consisting of poly(trityl methacrylate) supported on silica gel[132] are now commercially available. Further emerging applications of these materials include their use as chiral reagents in asymmetric synthesis, as chiral catalysts or model enzymes, and as components of membranes and vesicles. For such applications selectivity can sometimes be considerably enhanced by the combination of side-chain chirality with main-chain chirality.[140]

The physical properties of pure optically active forms of polymers can differ considerably from those of racemates, as has been observed in the case of poly(α-methylbenzyl methacrylates).[141] There is particular interest in these materials for possible applications based on their piezoelectric, ferroelectric, or nonlinear optical properties. In particular, at the present time the nonlinear optical properties of optically active polymers are being thoroughly investigated in several laboratories. Generally speaking, interactions of electromagnetic fields with substances showing nonlinear optical properties generate new fields with altered phase, frequency, and amplitude as well as other characteristics of propagation. Materials of this kind are used to an increasing extent for the construction of optical switches and elements for signal processing, for positioning and guiding of laser beams, and for second harmonic generation in lasers.[142]

The use of polymers instead of inorganic or organic crystals offers several advantages. They are mechanically stable, can be easily produced and processed, and can be readily modified to introduce functional groups giving rise to high nonlinear optical coefficients.[142-144] More challenging is to obtain a noncentrosymmetric phase structure of the polymers, which is necessary for achieving nonlinear effects. For this purpose oriented rodlike molecules can be used in thin layers.[145] Helical, optically active polymers could also be used. Noncentrosymmetric arrangements can also be obtained in bulk using liquid crystals exhibiting the chiral smectic C-phase.[146] Since, in this case, the polymers have to be chiral and optically active, this offers an important application of the polymers described in this article.

Special thanks are due to my co-workers who have been involved with me in research on this topic and who, through their commitment and their ideas, have contributed to an important share of these results. We received financial support from the Deutsche Forschungsgemeinschaft, the Minister of Science and Research in the State of Nordrhein-Westfalen, and the Fonds der Chemischen Industrie. In preparing this review I have benefited from detailed discussions with K. Mislow (Princeton), M. M. Green (New York), M. Farina (Milan), Y. Okamoto (Osaka), and R. Bareiss (Mainz). The computer graphics in Figures 14 and 19 were obtained with the help of Dr. Hövel (Bayer AG, Leverkusen) and those in Figures 10, 11, and 18 were produced with the help of Dipl.-Chem. T. Stach, Düsseldorf, to both of whom I express my sincere thanks. Thanks are also due to Dr. P. K. Dhal, Düsseldorf, for his help in the preparation of this manuscript.

Received: December 16, 1987 [A 705 IE]
German version: *Angew. Chem. 101* (1989) 22
Translated by *Jack Becconsall*, Gwynedd, UK

[1] G. Wulff, P. K. Dhal, *Makromol. Chem. 188* (1987) 2847.
[2] K. Mislow, J. Siegel, *J. Am. Chem. Soc. 106* (1984) 3319.
[3] G. E. McCasland: *A General System for the Naming of Stereoisomers*, Chemical Abstract Service, Columbus, OH 1953, p. 2.
[4] D. J. Brand, J. Fisher, *J. Chem. Educ. 64* (1987) 1035.
[5] K. Ziegler, *Angew. Chem. 76* (1964) 545; G. Natta, *ibid. 76* (1964) 553.
[6] A. D. Ketley (Ed.): *The Stereochemistry of Macromolecules, Vol. 1-3*, Dekker, New York 1967-1968.
[7] F. A. Bovey: *Polymer and Configuration*, Academic Press, New York 1969.
[8] R. W. Lenz, F. Ciardelli (Eds.): *Preparation and Properties of Stereoregular Polymers*, Reidel, Dordrecht 1980.
[9] F. A. Bovey: *Chain Structure and Conformation of Macromolecules*, Academic Press, New York 1982.
[10] M. Farina, *Top. Stereochem. 17* (1987) 1.
[11] IUPAC Macromolecular Division, Commission on Macromolecular Nomenclature: *Stereochemical Definitions and Notations Relating to Polymers*, *Pure Appl. Chem. 53* (1981) 733.
[12] N. Beredjick, C. Schuerch, *J. Am. Chem. Soc. 80* (1958) 1933.
[13] G. Natta, M. Farina, M. Peraldo, G. Bressan, *Makromol. Chem. 43* (1961) 68.
[14] G. Natta, M. Farina, M. Donati, M. Peraldo, *Chim. Ind. (Milan) 42* (1960) 1363.
[15] C. L. Arcus, *Prog. Stereochem. 3* (1962) 264.
[16] M. Farina, M. Peraldo, G. Natta, *Angew. Chem. 77* (1965) 149; *Angew. Chem. Int. Ed. Engl. 4* (1965) 107.
[17] R. C. Schulz, E. Kaiser, *Adv. Polym. Sci. 4* (1965) 236.
[18] P. Pino, *Adv. Polym. Sci. 4* (1965) 393.
[19] M. Goodman, A. Abe, Y.-L. Fan, *Makromol. Rev. 1* (1967) 1.
[20] P. Pino, G. P. Lorenzi in [8], Chapter 1.
[21] E. Selegny (Ed.): *Optically Active Polymers*, Reidel, Dordrecht 1979.
[22] Y. Minoura in [21], p. 159.
[23] H. Sumida, *Kobunshi Kako 34* (1985) 486; *Chem. Abstr. 104* (1986) 110207.
[24] H. Suda, *Kobunshi 35* (1986) 688; *Chem. Abstr. 105* (1986) 134354.
[25] G. Wulff, K. Zabrocki, J. Hohn, *Angew. Chem. 90* (1978) 567; *Angew. Chem. Int. Ed. Engl. 17* (1978) 535.
[26] G. Wulff, J. Hohn, *Macromolecules 15* (1982) 1255.
[27] G. Wulff, R. Kemmerer, J. Vietmeier, H. G. Poll, *Nouv. J. Chim. 6* (1982) 681.
[28] G. Wulff, *Nachr. Chem. Tech. Lab. 33* (1985) 956.
[29] G. Wulff, R. Kemmerer, B. Vogt, *J. Am. Chem. Soc. 109* (1987) 7449.

[30] a) M. Fontanille, A. Guyot (Eds.): *Recent Advances in Mechanistic and Synthetic Aspects of Polymerization*, Reidel, Dordrecht 1987; b) G. Wulff in [30a], p. 399.

[31] R. J. M. Nolte, A. J. M. van Beijnen, W. Drenth, *J. Am. Chem. Soc. 96* (1974) 5932.

[32] W. Drenth, R. J. M. Nolte, *Acc. Chem. Res. 12* (1979) 30.

[33] Y. Okamoto, K. Suzuki, K. Ohta, K. Hatada, H. Yuki, *J. Am. Chem. Soc. 101* (1979) 4763.

[34] Y. Okamoto, K. Ohta, K. Hatada, H. Yuki in J. E. McGrath (Ed.): *Anionic Polymerization: Kinetics, Mechanism and Synthesis, ACS-Symp. Ser. 166* (1981) 353.

[35] L. S. Corley, O. Vogl, *Polym. Bull. (Berlin) 3* (1980) 211.

[36] a) R. J. M. Nolte, W. Drenth in [30a], p. 451; b) O. Vogl, G. D. Jaycox, *Polymer 28* (1987) 2179.

[37] F. Ciardelli, C. Carlini, R. Solaro, A. Altomare, O. Pieroni, J. L. Houben, A. Fissi, *Pure Appl. Chem. 56* (1984) 329.

[38] F. Ciardelli, P. Salvadori, *Pure Appl. Chem. 57* (1985) 931.

[39] A. Leborgne, N. Spassky, J. Kops in E. J. Goethals (Ed.): *Cationic Polymerization and Related Processes*, Academic Press, London 1984, p. 227.

[40] C. G. Overberger, C. X. Lu, C. C. Chen, *J. Polym. Sci. Polym. Chem. Ed. 24* (1986) 75.

[41] K. Mislow, P. Bickart, *Isr. J. Chem. 15* (1977) 1.

[42] M. C. Tobin, *J. Chem. Phys. 23* (1955) 891.

[43] S. Krimm, C. Y. Liang, G. B. B. M. Sutherland, *J. Chem. Phys. 25* (1956) 549.

[44] B. K. Vainshtein, *Kristallografiya 4* (1959) 842.

[45] S. Krimm, *Fortschr. Hochpolym.-Forsch. 2* (1960) 51.

[46] G. Natta, M. Farina: *Struktur und Verhalten von Molekülen im Raum*, Verlag Chemie, Weinheim 1976, p. 221.

[47] H. Tadokoro: *Structure of Crystalline Polymers*, Wiley, New York 1979, p. 23.

[48] J. B. Bozovic, M. Vujivic, F. Herbut, M. Damnjanovic in J.-M. Andre, J. L. Brédas, J. Delhalle, J. Ladek, C. Moser (Eds.): *Recent Advances in the Quantum Theory of Polymers*, Springer, Berlin 1980, p. 80.

[49] A. V. Shubnikov, V. A. Koptsik: *Symmetry in Science and Art*, Plenum Press, New York 1974, p. 79.

[50] I. Hargittai, M. Hargittai: *Symmetry Through the Eyes of a Chemist*, VCH Verlagsgesellschaft, Weinheim 1986, p. 327.

[51] M. Born, T. von Kármán, *Phys. Z. 13* (1912) 297.

[52] High polymers can also be obtained in the form of macrocycles, which are good models for the study of certain properties. See, e.g., G. B. McKenna, G. Hadziioannou, P. Lutz, G. Hild, C. Strazielle, C. Straupe, P. Rempp, A. J. Kovacs, *Macromolecules 20* (1987) 498; R. Roovers in R. M. Ottenbreiter, L. A. Utracki, S. Inoue (Eds.): *Current Topics in Polymer Science, Vol. 1*, Hanser, München 1987, p. 45; S. J. Clarson, K. Dodgson, J. A. Semlyen, *Polymer 26* (1986) 930; D. Geiser, H. Höcker, *Macromolecules 13* (1980) 653; H. Horbach, H. Vernaleken, K. Weirauch, *Makromol. Chem. 181* (1980) 111; J. A. Semlyen (Ed.): *Cyclic Polymers*, Elsevier, New York 1986.

[53] G. Wulff, J. Petzold, unpublished results.

[54] C. L. Arcus, *J. Chem. Soc. 1957*, 1189.

[55] In this case the new term "chirogen" for the designation of chiral partial structures could be used, a chirogen is a stereocenter that is not identical with its mirror image [56].

[56] J. H. Brewster, *J. Org. Chem. 51* (1986) 4751; P. G. Mezey, *J. Am. Chem. Soc. 108* (1986) 3976.

[57] G. Wulff, P. K. Dhal, *Angew. Chem.*, in press.

[58] G. J. Schmitt, C. Schuerch, *J. Polym. Sci. 45* (1960) 313.

[59] G. Natta, M. Farina, *Tetrahedron Lett. 1963*, 703.

[60] M. M. Green, B. A. Garetz, *Tetrahedron Lett. 25* (1984) 2831.

[61] H. L. Frisch, C. Schuerch, M. Szwarc, *J. Polym. Sci. 11* (1953) 559.

[62] F. Ciardelli, E. Chiellini, C. Carlini in [21], p. 83.

[63] G. Wulff, R. Sczepan, A. Steigel, *Tetrahedron Lett. 27* (1986) 1991.

[64] Y. Okamoto, E. Yashima, T. Nakano, K. Hatada, *Chem. Lett. 1987*, 759.

[65] C. S. Marvel, C. G. Overberger, *J. Am. Chem. Soc. 66* (1944) 475.

[66] N. Beredjick, C. Schuerch, *J. Am. Chem. Soc. 78* (1956) 2646.

[67] C. L. Arcus, D. W. West, *J. Chem. Soc. 1959*, 2699.

[68] G. Wulff, P. K. Dhal, *Macromolecules 21* (1988) 571.

[69] G. Wulff, P. K. Dhal, unpublished results.

[70] G. Wulff, R. Kemmerer, B. Vogt, P. K. Dhal, A. Steigel, unpublished results.

[71] G. Wulff, R. Kemmerer, B. Vogt, *Freiburger Makromolekulares Kolloquium*, March 1986, Abstracts p. 31.

[72] S. Kataoka, T. Ando, *Kobunshi Ronbunshu 37* (1980) 185; *Chem. Abstr. 92* (1980) 198833.

[73] S. Kataoka, T. Ando, *Polym. Commun. 25* (1984) 24.

[74] K. Nozaki, Y. Matsubara, M. Yoshihara, T. Maeshima, *Makromol. Chem. Rapid Commun. 5* (1984) 723.

[75] N. Kunieda, S. Yamane, H. Taguchi, M. Kinoshita, *Mem. Fac. Eng. Osaka City Univ. 24* (1983) 195; *Chem. Abstr. 102* (1985) 46289.

[76] J. Asakura, M. Yoshihara, T. Maeshima, *Makromol. Chem. Rapid. Commun. 4* (1983) 103.

[77] K. Nozaki, J. Asakura, M. Yoshihara, T. Maeshima, *J. Macromol. Sci. Chem. A 21* (1984) 1405.

[78] F. Toda, K. Mori, *J. Chem. Soc. Chem. Commun. 1986*, 1059.

[79] Y. Sugaya, K. Nomiya, M. Miwai, *Seikei Daigaku Kogakubu Kogaku Hokoku 32* (1981) 2187; *Chem. Abstr. 96* (1982) 52735.

[80] G. Wulff, A. Sarhan, *Angew. Chem. 84* (1972) 364; *Angew. Chem. Int. Ed. Engl. 11* (1972) 341.

[81] G. Wulff, A. Sarhan, K. Zabrocki, *Tetrahedron Lett. 1973*, 4329.

[82] G. Wulff, W. Vesper, R. Grobe-Einsler, A. Sarhan, *Makromol. Chem. 178* (1977) 2799.

[83] G. Wulff, J. Vietmeier, H.-G. Poll, *Makromol. Chem. 188* (1987) 731.

[84] a) G. Wulff, G. Kirstein, C. Beyer, unpublished; b) P. Pino, J. Bartus, O. Vogl, *Polym. Prepr. (Am. Chem. Soc. Div. Polym. Chem.) 29* (1988) 254.

[85] G. Wulff, A. Sarhan in B. S. Green, Y. Ashani, D. Chipman (Eds.): *Chemical Approaches to Understanding Enzyme Catalysis*, Elsevier, Amsterdam 1982, p. 106.

[86] G. Wulff, *Pure Appl. Chem. 54* (1982) 2093.

[87] G. Wulff in A. J. Laskin, G. T. Tsao, L. B. Wingard (Eds.): *Enzyme Engineering 7, Ann. NY Acad. Sci. 434* (1984) 327.

[88] G. Wulff in W. T. Ford (Ed.): *Polymeric Reagents and Catalysts, ACS Symp. Ser. 308* (1986) 186.

[89] T. Doiuchi, Y. Minoura, *Makromol. Chem. 181* (1980) 1081.

[90] N. Kunieda, S. Yamane, H. Taguchi, M. Kinoshita, *Makromol. Chem. Rapid Commun. 4* (1983) 57.

[91] M. Yoshihara, J. Asakura, H. Takahashi, T. Maeshima, *J. Macromol. Sci. Chem. A 20* (1983) 123.

[92] T. Oishi, N. Okamoto, M. Fujimoto, *J. Polym. Sci. Polym. Chem. Ed. 24* (1986) 1185.

[93] E. Kobayashi, S. Matsumura, J. Furukawa, *Polym. Bull. 3* (1980) 285.

[94] H. Yamaguchi, T. Doiuchi, K. Kawamoto, *Macromolecules 18* (1985) 2120.

[95] M. Mijata, Y. Kitahara, K. Takemoto, *Makromol. Chem. 184* (1983) 1771.

[96] G. Natta, L. Porri, S. Valenti, *Makromol. Chem. 67* (1963) 225.

[97] M. Farina, G. Audisio, G. Natta, *J. Am. Chem. Soc. 89* (1967) 5071.

[98] M. Farina, G. Di Silvestro, P. Sozzani, *Makromol. Chem. Rapid Commun. 2* (1981) 51.

[99] M. Miyata, Y. Kitahara, K. Takemoto, *Polym. J. (Tokyo) 13* (1981) 111.

[100] Yu. B. Monakov, N. G. Marina, O. I. Kozlova, F. Ya. Kanzafarov, G. A. Tolstikov, *Dokl. Akad. Nauk SSSR 292* (1987) 405.

[101] L. Porri, R. Rossi, G. Ingrosso, *Tetrahedron Lett. 1971*, 1083.

[102] L. Addadi, M. Cohen, M. Lahav, *J. Chem. Soc. Chem. Commun. 1975*, 471.

[103] L. Addadi, M. Lahav, *J. Am. Chem. Soc. 101* (1979) 2152.

[104] P. J. Flory: *Statistical Mechanics of Chain Molecules*, Wiley, New York 1969.

[105] H. Morawetz: *Macromolecules in Solution*, Wiley, New York, 2nd ed. 1975.

[106] H. V. Volkenstein: *Configurational Statistics of Polymeric Chains*, Wiley, New York 1963.

[107] K. P. Meurer, F. Vögtle, *Top. Curr. Chem. 127* (1985) 10.

[108] J. H. Brewster, *Top. Curr. Chem. 47* (1974) 29.

[109] P. Corradini, G. Guera, B. Pirozzi in [8], pp. 317, 387.

[110] W. Kaminski, *Angew. Makromol. Chem. 145/146* (1986) 149.

[111] W. Kaminski, K. Külper, S. Niedoba, *Makromol. Chem. Macromol. Symp. 3* (1986) 377.

[112] a) D. J. Cram, D. Y. Sogah, *J. Am. Chem. Soc. 107* (1985) 8301; b) D. Y. Sogah (Wilmington, DE), personal communication.

[113] a) F. Ciardelli, M. Aglietto, G. Roggeri in [30a], p. 409; b) M. M. Green, C. Andreola, B. Muñoz, H. P. Reidy, *J. Am. Chem. Soc. 110* (1988) 4063.

[114] G. Wulff, B. Vogt, J. Petzoldt, *Polym. Mater. Sci. Eng. 58*, (1988) 859.

[115] a) K. Mislow, D. Gust, P. Finocchiaro, R. J. Boettcher, *Top. Curr. Chem. 47* (1974) 1; b) W. Clegg, J. C. Lockhart, *J. Chem. Soc. Perkin Trans. 2 1987*, 1621.

[116] Y. Okamoto, E. Yashima, K. Hatada, *J. Polym. Sci. Polym. Lett. Ed. 25* (1987) 297.

[117] F. Millich, *Macromol. Rev. 15* (1980) 207.

[118] F. Millich in [8], p. 195.

[119] R. B. King, *Polym. News 12* (1987) 166.

[120] a) F. Millich, R. G. Sinclair, *J. Polym. Sci. Part C 22* (1968) 33; b) for possible *syn-anti* isomerisation see M. M. Green, R. A. Gross, F. C. Schilling, K. Zero, C. Crosby, *Macromolecules 21* (1988) 1839.

[121] P. C. J. Kramer, R. J. M. Nolte, W. Drenth, *J. Chem. Soc. Chem. Commun. 1986*, 1789.

[122] T. Harada, M. C. Cleij, R. J. M. Nolte, A. M. F. Hezemans, W. Drenth, *J. Chem. Soc. Chem. Commun. 1984,* 726.
[123] Similar behavior is shown by *N,N*-disubstituted acrylamides: Y. Okamoto, M. Adachi, H. Shohi, H. Yuki, *Polym. J. (Tokyo) 13* (1981) 175.
[124] a) Y. Okamoto, H. Shohi, H. Yuki, *J. Polym. Sci. Polym. Lett. Ed. 21* (1983) 601; b) Y. Okamoto, K. Suzuki, H. Yuki, *J. Polym. Sci. Polym. Chem. Ed. 18* (1980) 3043.
[125] Y. Okamoto, M. Ishikura, K. Hatada, H. Yuki, *Polym. J. (Tokyo) 15* (1983) 851.
[126] For hydrolytically more stable derivatives of poly(trityl methacrylates) see: Y. Okamoto, E. Yashima, M. Ishikura, K. Hatada, *Polym. J. (Tokyo) 19* (1987) 1183.
[127] Y. Okamoto, I. Okamoto, H. Yuki, *J. Polym. Sci. Polym. Lett. Ed. 19* (1981) 451.
[128] a) P. Doty, R. D. Lundberg, *J. Am. Chem. Soc. 79* (1957) 2338; b) E. Yashima, Y. Okamoto, K. Hatada, *Macromolecules 21* (1988) 854.
[129] a) O. Vogl, L. S. Corley, W. J. Harris, G. D. Jaycox, J. Zhang, *Makromol. Chem. Suppl. 13* (1985) 1; b) O. Vogl, G. D. Jaycox, *CHEMTECH 16* (1986) 698; c) J. Zhang, G. D. Jaycox, O. Vogl, *Polymer J. 19* (1987) 603.
[130] a) P. Pino, P. Cioni, J. Wei, *J. Am. Chem. Soc. 109* (1987) 6189; b) W. Kaminski, Hamburg, personal communication; c) D. Sogah, Wilmington, DE, personal communication.
[131] H. Yuki, Y. Okamoto, I. Okamoto, *J. Am. Chem. Soc. 102* (1980) 6356.
[132] Y. Okamoto, S. Honda, I. Okamoto, H. Yuki, S. Murata, R. Noyori, H. Tanaka, *J. Am. Chem. Soc. 103* (1981) 6971.
[133] Y. Okamoto, E. Yashima, K. Hatada, K. Mislow, *J. Org. Chem. 49* (1984) 557.
[134] Y. Okamoto, S. Honda, K. Hatada, H. Yuki, *J. Chromatogr. 350* (1985) 127.
[135] a) L. Crane, M. Zief (Eds.): *Chromatographic Chiral Separations,* Dekker, New York 1988; b) Y. Okamoto, K. Hatada in [135a], p. xxx.
[136] K. Hatada, S. Shimizu, H. Yuki, W. Harris, O. Vogl, *Polym. Bull. 4* (1981) 179.
[137] G. Wulff, H.-G. Poll, M. Minárik, *J. Liquid Chrmatogr. 9* (1986) 385.
[138] a) G. Wulff, M. Minárik, *HRC CC, J. High Resolut. Chromatogr. Chromatogr. Commun. 9* (1986) 607; b) G. Wulff, M. Minárik in [135a], p. 15.
[139] a) M. Glad, O. Norrlöw, B. Sellergren, N. Siegbahn, K. Mosbach, *J. Chromatogr. 347* (1985) 11; b) B. Sellergren, M. Lepisto, K. Mosbach, *J. Am. Chem. Soc. 110* (1988) 5853.
[140] a) H. G. J. Visser, R. J. M. Nolte, W. Drenth, *Marcomolecules 18* (1985) 1818; b) Y. Fujii, K. Matsutani, K. Kikuchi, *J. Chem. Soc. Chem. Comm. 1985,* 415.
[141] H. Hatada, S. Shimizu, Y. Terawaki, K. Ohta, H. Yuki, *Polymer J. 13* (1981) 811.
[142] D. J. Williams, *Angew. Chem. 96* (1984) 637; *Angew. Chem. Int. Ed. Engl. 23* (1984) 690.
[143] D. S. Chemla, J. Zyss (Eds.): *Nonlinear Optical Properties of Organic Molecules and Crystals, Vol. 1 and 2,* Academic Press, New York 1987.
[144] G. Khanarian, A. Artigliere, R. Keoszian, E. W. Choe, R. De Martino, D. Stuetz, C. C. Teng, *Proc. SPIE Int. Soc. Opt. Eng. (Mol. Polym. Optoelectron. Mater. Fundam. Appl.) 682* (1987) 153.
[145] See, e.g., T. Arndt, C. Bubeck, G. Duda, T. Sauer, G. Wegner, *Freiburger Makromolekulares Kolloquium,* March 1988, Abstracts p. 40.
[146] N. A. Plate, R. V. Talrose, Ya. S. Freidzon, V. P. Shibaev, *Polymer J. 19* (1987) 135.

Intramolecular, Stoichiometric (Li, Mg, Zn) and Catalytic (Ni, Pd, Pt) Metallo-Ene Reactions in Organic Synthesis

New Synthetic Methods (75)

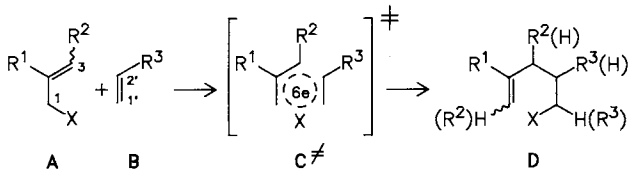
By Wolfgang Oppolzer*

Dedicated to Professor Elias J. Corey on the occasion of his 60th birthday

Metallo-ene reactions, hardly recognized until very recently, have experienced a breathtaking development when applied in an intramolecular sense. Efficient regio- and stereoselective magnesium-ene cyclizations have served as a cornerstone for numerous syntheses of structurally diverse natural products (e.g., sesquiterpenes of marine or plant origin, alkaloids, fragrances, insect defense compounds, and a fungitoxin). A brilliant example is the synthesis of the elusive odorant (+)-khusimone which outshines 20 years of work in the field of tricyclovetivane synthesis. Palladium-, platinum-, and nickel-catalyzed versions of the metallo-ene reaction are in a comparatively early stage of exploration, but, nevertheless, reveal intriguing potential. Hence an almost 100% stereospecific C–O→C–Pd→C–C chirality transfer permits simple and selective, *cis*- or *trans*-annelation processes. The mild cyclization conditions are compatible with various functional groups, such as nitrogen moieties, which offer interesting perspectives for the preparation of heterocycles (e.g., alkaloids) difficult to obtain by other methods. Carbon monoxide insertion reactions of the cyclized σ-metal intermediates were shown to afford annelated cyclopentanones and cyclopentenones with concomitant stereocontrolled formation of four carbon–carbon bonds. These and other observations, highlighted in this article, provide a platform for further extensions and applications of this powerful method in organic synthesis.

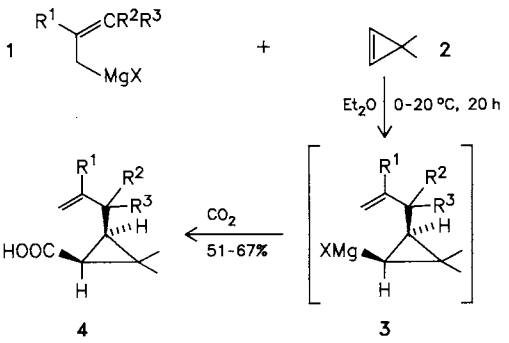
1. Introduction

The ene reaction, discovered 45 years ago by *Alder* et al.,[1] usually involves the thermal reaction of an olefin containing an allylic hydrogen (ene) with an electron-deficient unsaturated compound (enophile) to form 1:1 adducts via a cyclic 6e transition state (e.g., **A** + **B** → **C**$^{\neq}$ → **D**, X = H, Scheme 1).



Scheme 1. X = H: ene reaction. X = M: metallo-ene reaction.

Starting in 1970, *Lehmkuhl* et al.[2] systematically studied the analogous addition of allylic Grignard reagents **A**, X = MgCl, to alkenes or alkynes. Kinetic measurements showed negative activation entropies of $\Delta S^{\neq} = -18$ to -24 cal K^{-1} mol^{-1}.[2b] Further evidence for a concerted suprafacial reaction via transition state **C**$^{\neq}$, X = MgL_n, was provided by the addition of 2-alkenylmagnesium halides **1** to 3,3-dimethylcyclopropene **2**; subsequent carboxylation with CO_2 yielded *cis*-2-allylcyclopropanecarboxylic acids **4**[2c] (Scheme 2). Given that the configuration of a cyclopropyl-magnesium bond is stable and is carboxylated (CO_2) with retention,[3] it follows that the allyl unit and the metal are transferred to the same face of the cyclopropene **2** to furnish intermediate **3**.



R^1, R^2, R^3 = Me, H; X = Cl, Br

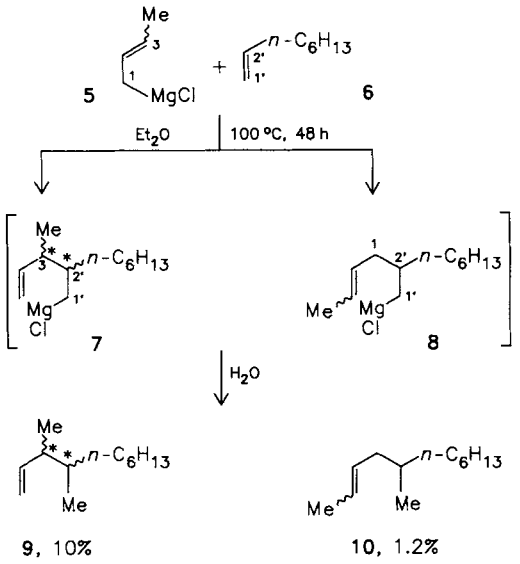
Scheme 2.

This more than formal analogy with the classical ene process has prompted us to classify transformations like **A** + **B** → **D**, X = metal, as metallo-ene reactions. Indeed, closely related additions of allylzinc,[4] -aluminum,[5] and -boron reagents[6] to (strained) alkenes, acetylenes, allenes, and enol ethers have appeared in the literature since 1971.

Despite the extensive work of *Lehmkuhl*, the magnesium-ene reaction has received virtually no attention as a strategic tool in organic synthesis. Problems of low regio- and stereoselectivity and low overall efficiency may limit the applicability of the bimolecular reactions, as exemplified by the addition of crotylmagnesium chloride to 1-octene[2a,d] (Scheme 3).

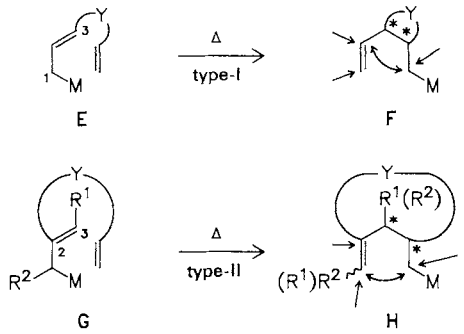
[*] Prof. Dr. W. Oppolzer
Département de Chimie Organique, Université de Genève
30, quai E. Ansermet, CH-1211 Genève 4 (Switzerland)

 © VCH Verlagsgesellschaft mbH, D-6940 Weinheim, 1989 0570-0833/89/0101-0038 $ 02.50/0



Scheme 3.

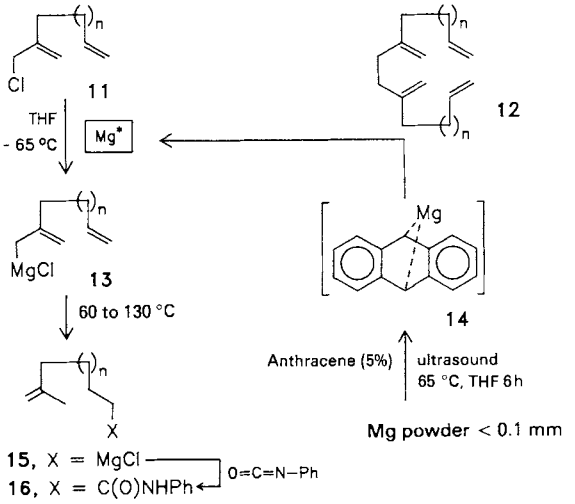
In contrast, similar to intramolecular [4+2] cycloadditions[7] and ene reactions,[8] intramolecular versions of the metallo-ene process may be regio- and stereoselective, entropically favored, and thus more efficient. This holds for two different modes of cyclization (Scheme 4) in which the enophile is linked by a suitable bridge, either to the terminal carbon atom (C-3, type I) or to the central carbon atom (C-2, type II) of the metallo-ene unit.



Scheme 4. Type I: The bridge Y links the enophile to C-3 of the metallo-ene. Type II: The bridge Y links the enophile to C-2 of the metallo-ene.

Essential for the practicality of such processes was, furthermore, a convenient preparation of the 2-alkenylmetal precursors **E** and **G**. In particular, the conventional treatment of allylic halides with Mg turnings in Et_2O frequently led to coupling products: e.g., **11** → **12** (Scheme 5).

Magnesium, activated by evaporation[9] or, much more conveniently, by sonication with anthracene (5%),[10] usually accomplished the metalation of 2-alkenyl chlorides (e.g., **11**) at −65°C in THF without significant coupling.[11] The resulting, clean, alkali-metal- and alkali-halide-free solutions of Grignard reagents **13** are compatible with the thermal cyclization/trapping sequence **13** → **15** → **16**.[11] This easy preparation of the starting 2-alkenylmagnesium chlorides, as well as the propensity of the cyclized alkylmagnesium intermediates **F** and **H** for further functionalizations and cyclizations involving the metalated and the two olefinic sites, offers a considerable potential in organic synthesis.



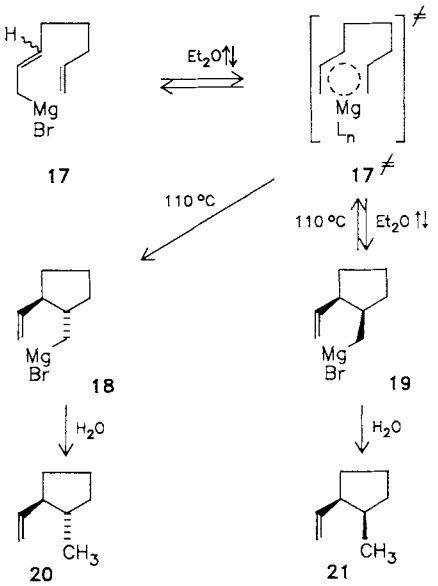
Scheme 5. The yield of **16**, n = 2, was 69% based on **11**.

2. Intramolecular Magnesium- and Lithium-Ene Reactions

2.1. Type-I Reactions

2.1.1. Initial Studies

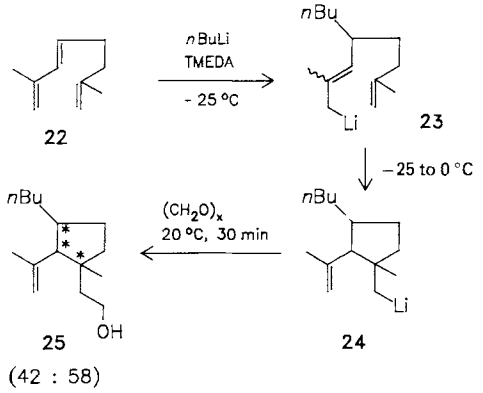
The first encouraging example of an intramolecular type-I magnesium-ene reaction dates back to 1972. As described by *Felkin* et al.,[12a] 2,7-octadienylmagnesium bromide **17** cyclized in boiling Et_2O to give, after aqueous workup, selectively *cis*-1-methyl-2-vinylcyclopentane **21** in 67% yield. Heating the solution of the transient Grignard product **19** to 110°C (sealed tube, 24 h) furnished, after hydrolysis, mainly the thermodynamically more stable *trans*-cyclopentane **20** (**20** : **21** = 11 : 1), indicating the re-



Scheme 6.

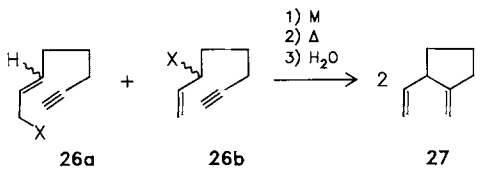
versibility of the cyclization **17** ⇌ **19** at a higher temperature.[12b] It is worth noting that **17** could be obtained in situ from 1,3-butadiene, *n*PrMgBr and $[(PPh_3)_2NiCl_2]$ (2 mol%) and that **18** and **19** were also trapped by D_2O or acetone. The conversion **17** → **19** → **21** was also reported in a patent.[12c]

Two years later, the transformation of the isoprene dimer **22** to **25** (mixture of stereoisomers) was observed and interpreted as a conjugate addition of *n*BuLi to diene **22** followed by a (surprisingly smooth) intramolecular lithium-ene addition **23** → **24**.[13]



Scheme 7. The yield of **25** was 58% based on **22** (two stereoisomers).

A comparative study demonstrated the relative efficiency of a metalation/cyclization/hydrolysis reaction sequence to give **27** from enynyl bromides and phenyl ethers **26a** and **26b**.[14] These reactions obviously involve intramolecular zinc-, magnesium-, and lithium-ene additions to a terminal acetylene unit (Scheme 8, Table 1).



Scheme 8.

Table 1. Cyclizations of alkynes **26a** and **26b** to give **27** via intramolecular metallo-ene reactions.

X	Metal M	Solvent	*T* [°C]	*t* [h]	Yield **27** [%]
Br	Zn	THF	20	2	43
Br	Mg	Et_2O	[a]	2	15
OPh	Li	THF	50	2–24	50

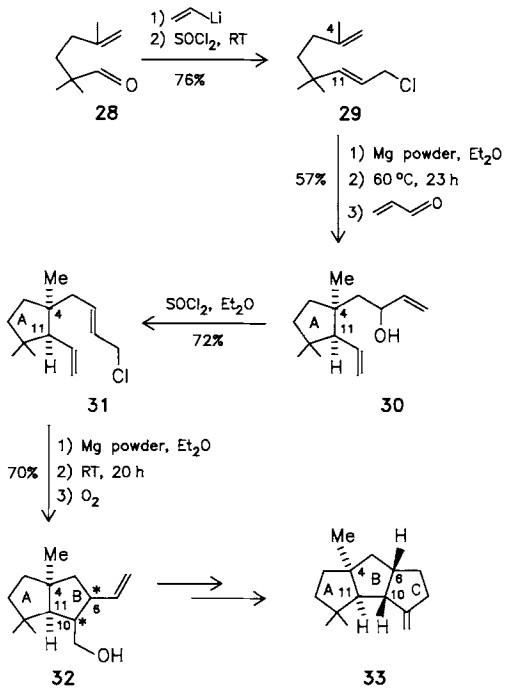
[a] Heated under reflux.

Also the cyclization of 1 : 2 adducts of allyl Grignard derivatives to 1,3-butadiene or isoprene giving divinylcyclohexylmethylmagnesium halides (mixtures of stereoisomers) has been ascribed to an intramolecular magnesium-ene process.[2e]

2.1.2. *Applications to Syntheses of Natural Products*

After these more or less isolated reports it was the challenge of natural product synthesis which spurred the most relevant exploration and extensions of the intramolecular magnesium-ene reaction. Its strategic role in synthesis is also illustrated by the following examples.

The synthesis of $\Delta^{9(12)}$-capnellene **33**, published in 1982,[15] addressed the issue of rendering this process iterative to assemble polycyclopentanoid systems (Scheme 9).

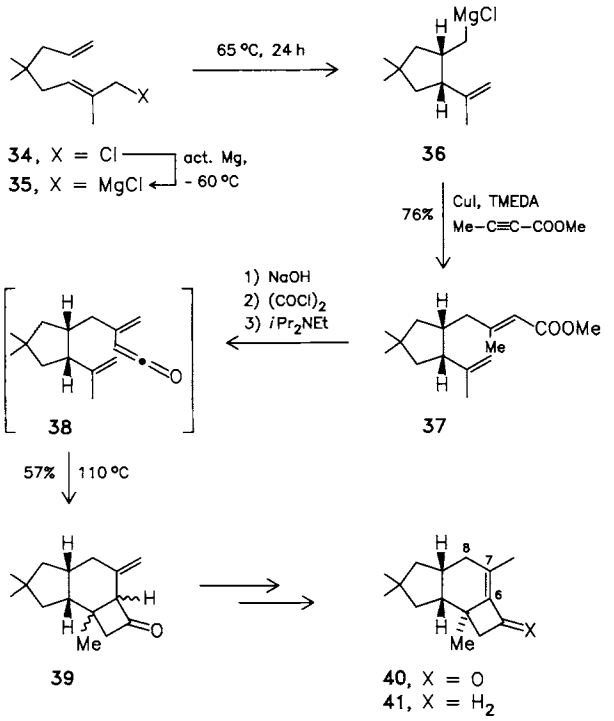


Scheme 9.

Thus, in the first key step **29** → **30**, the sterically congested bond between C-4 and C-11 was formed with high stereochemical control. Trapping of the cyclized Grignard intermediate with acrolein set the stage for the second magnesium-ene cyclization which occurs at room temperature. Scavenging the bicyclic magnesium-ene product with oxygen furnished alcohol **32** as a 3 : 2 mixture of stereoisomers. This kinetically derived lack of diastereoselection was of minor importance since the remaining closure of ring C was accomplished by an intramolecular aldolization with thermodynamic control over the configuration at C-6 and/or at C-10. Hence, the mixture **32** was channeled efficiently into the pure *cis-anti-cis*-triquinane **33**.

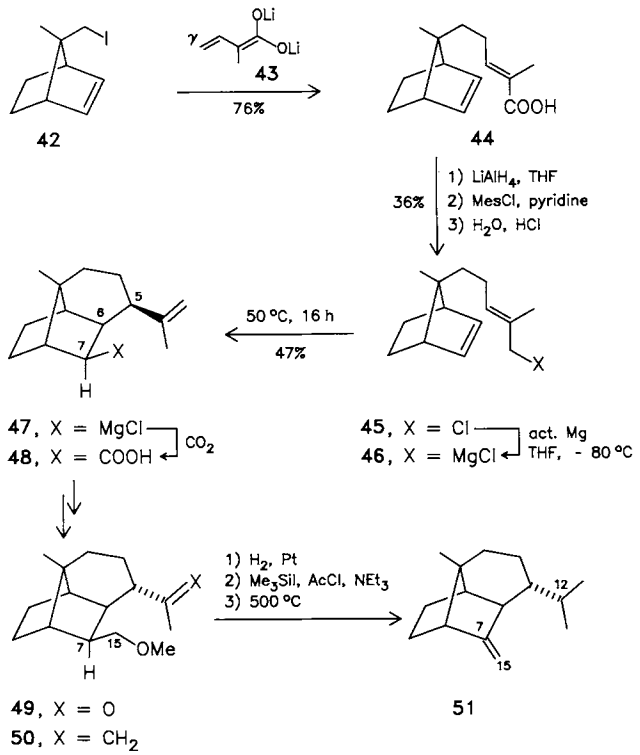
Highly diastereocontrolled formation of a *cis*-1,2-disubstituted five-membered ring was again observed in the key step **35** → **36** of the synthesis of (±)-6-protoilludene **41**[16] (Scheme 10).

Copper-promoted trapping of the cyclized organomagnesium species **36** by 1,4 addition to methyl 2-butynoate furnished the conjugated ester **37** in *one* synthetic operation from **34** (76%). The thus generated 1,2-*cis*-disposed functionalities in **37** were ideally suited to form the remaining six- and four-membered rings simultaneously by an intramolecular vinylketene/alkene cycloaddition (**38** → **39**). The carbonyl group in **39** (chromatographically



Scheme 10.

purified), furthermore, directed the olefin bond into the 6(7) position (instead of the otherwise favored 7(8) position). Although the [2+2] addition (**38**→**39**) did not show the desired high stereoselectivity, this approach to the protoilludene skeleton **39** in only two or three synthetic operations from the readily available acyclic dienyl chloride **34** exemplifies the *general* potential of magnesium-ene cyclizations when coupled with cycloaddition processes.

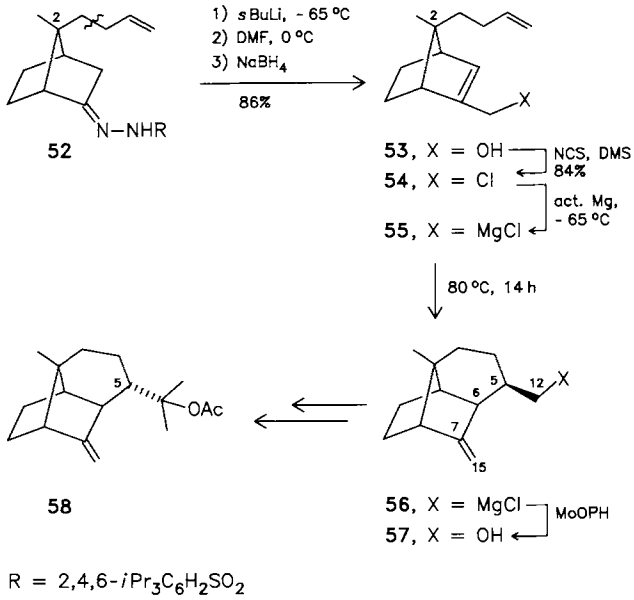


Scheme 11.

Another approach to an unusual sesquiterpene, sinularene **51**,[17] involves the diastereocontrolled formation of a six-membered ring by a magnesium-ene process (Scheme 11).

Thus, selective γ-alkylation of the dianion **43** by the iodide **42** gave the (*E*)-carboxylic acid **44**, which was converted into allylic chloride **45**. Successive treatment of **45** with activated magnesium, heating to 50 °C, and CO_2 trapping led to the formation of the bond between C-5 and C-6 and that between C-7 and C-15, giving the crystalline carboxylic acid **48** (47% overall yield) in a single operation. In this case, however, the kinetically controlled *cis* relation of magnesium-donor and -acceptor sites in **47** required an epimerization at C-5 (KOH treatment of **49**) to give, via a final ester pyrolysis, the target molecule **51**.

A related synthesis of 12-acetoxysinularene **58**[18] differs in that the magnesium-ene unit is part of the norbornene skeleton which carries the enophilic chain at C-2 (Scheme 12).

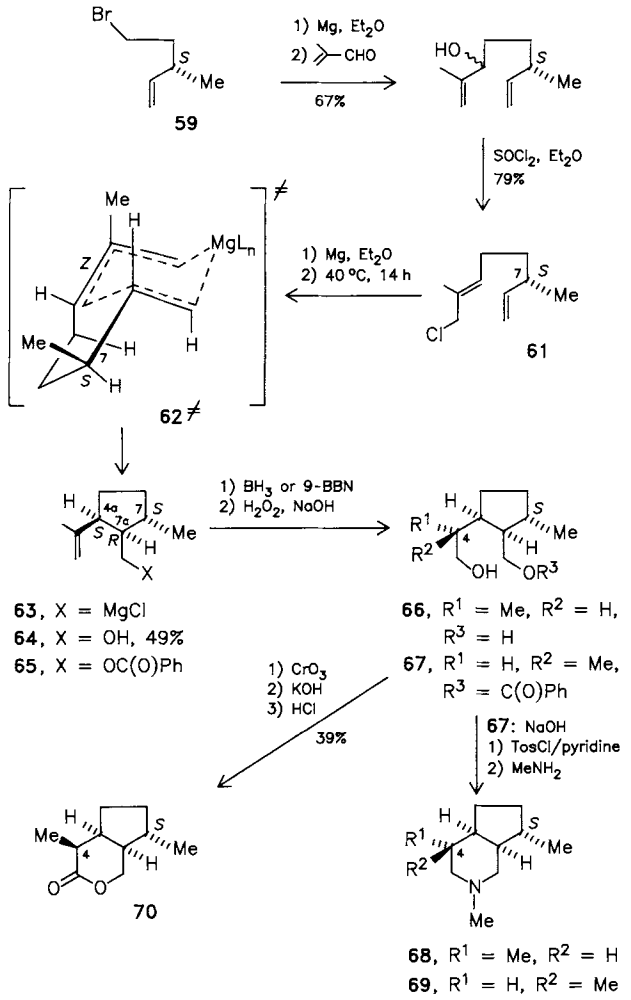


Scheme 12. NCS = *N*-chlorosuccinimide, DMS = dimethyl sulfide, MoOPH = MoO_5-pyridine-hexamethylphosphoramide complex.

Hence, by reversing the relative positions of the reaction partners, the bond between C-5 and C-6 was closed in the key step **55**→**56** with simultaneous formation of both the methylene group and the C-12 Mg functionality. Accordingly, one synthetic operation provided alcohol **57** in 62% yield from chloride **54**. (Again, the initial *cis* relation of C-12 and C-7 was altered thereafter by an epimerization at C-5.)

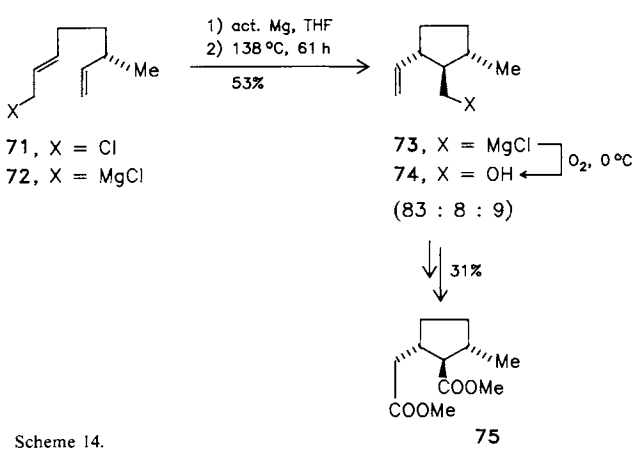
The stereodirecting bias of a preexisting stereogenic center on the intramolecular magnesium-ene reaction is illustrated by the enantioselective syntheses of (+)-α-skytanthine **68** and (+)-δ-skytanthine **69**, as well as of (+)-iridomyrmecine **70**[19] (Scheme 13).

Bromide **59**, easily accessible in 94% enantiomeric purity via an asymmetric 1,4 addition of vinylcopper to a chiral *O*-crotylenoate, was converted into the allylic chloride **61**. Metalation of **61** with commercial Mg powder and



Scheme 13. 9-BBN = 9-borabicyclo[3.3.1]nonane.

heating of the resulting solution under reflux followed by oxidative trapping of **63** with MoOPH at −78 °C yielded an 88.4/5.9/3.0/1.4 stereoisomer mixture of cyclized alcohols (58%). The major isomer **64**, isolated by flash chromatography (49% from **61**), has the desired (4a*S*,7a*R*) configuration. This result is consistent with a favored transition state **62**≠ (with the C-7 methyl group oriented toward the convex face) assuming that 2,3-substituted 2-alkenylmagnesium halides react in their (*Z*) form (cf. Section 2.2.1). Stereoconvergent control over the remaining center C-4 was achieved by hydroboration(BH_3)/oxidation of the free alcohol **64** to give diol **66** which was cyclized to give (+)-skytanthine **68**; alternatively, hydroboration(BBN)/oxidation of the benzoate **65** furnished predominantly the C-4-epimer **67** which was transformed into either (+)-δ-skytanthine **69** or (+)-iridomyrmecine **70**.



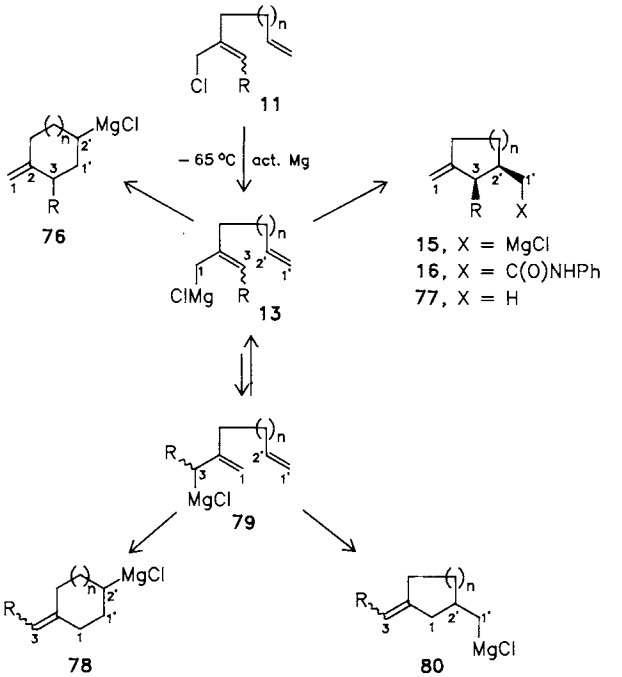
Scheme 14.

Whereas all foregoing applications rely on a kinetically determined stereoselectivity of magnesium-ene cyclizations, it is apparently a thermodynamic control which governs the cyclization **72**→**73** at 138 °C over 61 h to give, after oxidative quenching with O_2, an 83 : 8 : 9 mixture of stereoisomers. The major all-*trans* alcohol **74** was converted into the dimethyl ester of *trans,trans*-boschnialic acid **75**[20] (Scheme 14).

2.2. Type-II Magnesium-Ene Cyclizations

2.2.1. Systematic Investigations

This version, in which the enophilic chain is attached to the central atom C-2 of the magnesium-ene moiety was not described until 1982 (see Scheme 15). A systematic investigation dealing with the efficiency as well as the regio- and stereoselectivity of this reaction[21] (Scheme 15, Table 2) involved heating 2-alkenylallylmagnesium chlorides **13** followed by quenching of the cyclized Grignard reagents with phenyl isocyanate (Table 2, entries 1–5) or water (entry 6).



Scheme 15.

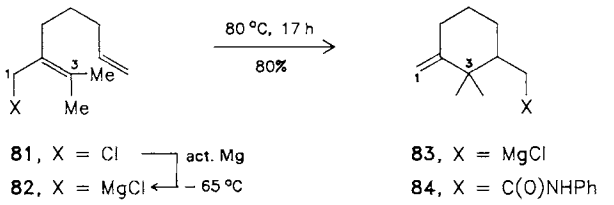
Table 2. Intramolecular type-II magnesium-ene reactions **11**→[**13**→**15**]→**16** or **77**.

Entry		n	R	*T* [°C]	*t* [h]	Product	Yield [%]
1	**a**	1	H	130	23	**16a**	71
2	**b**	2	H	80	17	**16b**	72
3	**c**	3	H	130	17	**16c**	71
4	**d**	3	CH_3	130	23	**16d**	40 [a]
5	**e**	2	CH_3	80	17	**16e**	86
6	**f**	2	n-C_6H_{13}	80	17	**77f**	81

[a] 20% of noncyclized dienylanilide isolated.

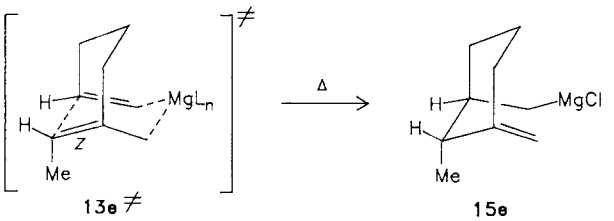
It is worth noting that a six-membered ring (entries 2, 5, 6) was formed more readily than a five-membered (entry 1) or a seven-membered ring (entries 3, 4), reflecting the counterplay of entropic and angle-strain factors.

This study also revealed an astonishing *regioselectivity* insofar as only products **16** or **77** (but no isomers derived from **76** or **78**) were observed, regardless of the distance between the reactive units. Accordingly, the magnesium was transferred to the distal site C-1′ of the *enophile* and the new C–C bond was formed at the proximal C-2′ site. As to type-II cyclizations of nonsymmetrically substituted *magnesium-ene* species (entries 4–6), a rapid 1,3-metal migration, **13**⇆**79**,[22] leaves two possibilities: C–C bond formation with either the more or less substituted ene terminal C-3 (**13**→**15**) or C-1 (**79**→**80**) of which only the former regiochemistry was observed. Also the 3,3-dimethyl-substituted magnesium-ene component of **81** underwent C–C bond formation only to C-3 (generating a quaternary center) to give **84** (80%, Scheme 16).



Scheme 16.

Focusing on the *stereochemistry* it is interesting to note that only *cis* isomers **16** and **77** were observed; this indicates highly selective olefin "insertion" into a (*Z*)-ene unit **13** (Scheme 17) which is in a rapid equilibrium with (*E*)-**13** (via the 1,3-Mg shift **13**⇆**79**; see Scheme 15).

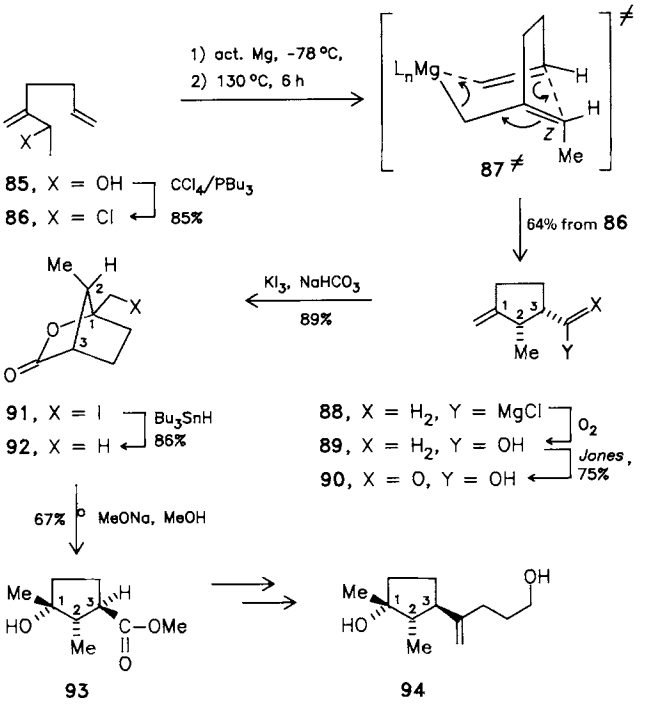


Scheme 17.

2.2.2. *Applications to the Syntheses of Natural Products*

The above-mentioned type of stereocontrol is exploited in a synthesis of the fungitoxin (±)-chokol-A **94**[23] (Scheme 18).

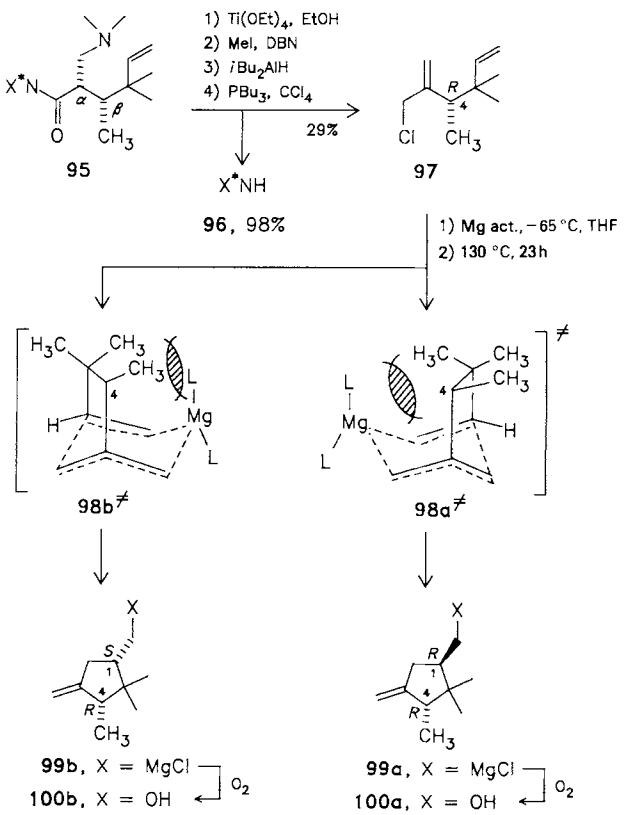
Alcohol **85** (easily prepared from 1-hexen-5-one in two steps) efficiently gave allyl chloride **86** (CCl_4/PBu_3; 85% yield). The metalation/cyclization/oxidation step **86**→**87**≠→**88**→**89** (described in detail) furnished *cis*-cyclopentylmethanol **89** (64% from **86** together with 2% of its *trans* epimer and 6% of a positional isomer derived from **80**); **89** was then oxidized to *cis*-carboxylic acid **90**. Iodolactonization/reduction, **90**→**91**→**92**, assured the desired *cis* disposition of the C-1-hydroxyl and C-2-methyl groups



Scheme 18.

in **93**. Basic methanolysis of lactone **92**, accompanied by C-3 epimerization, furnished the *trans*-related 3-methoxycarbonyl substituent, which was transformed into the pentenol side chain of **94**.

By contrast, no diastereoselectivity was found in the type-II magnesium-ene cyclization/oxidation **97**→**98**≠→

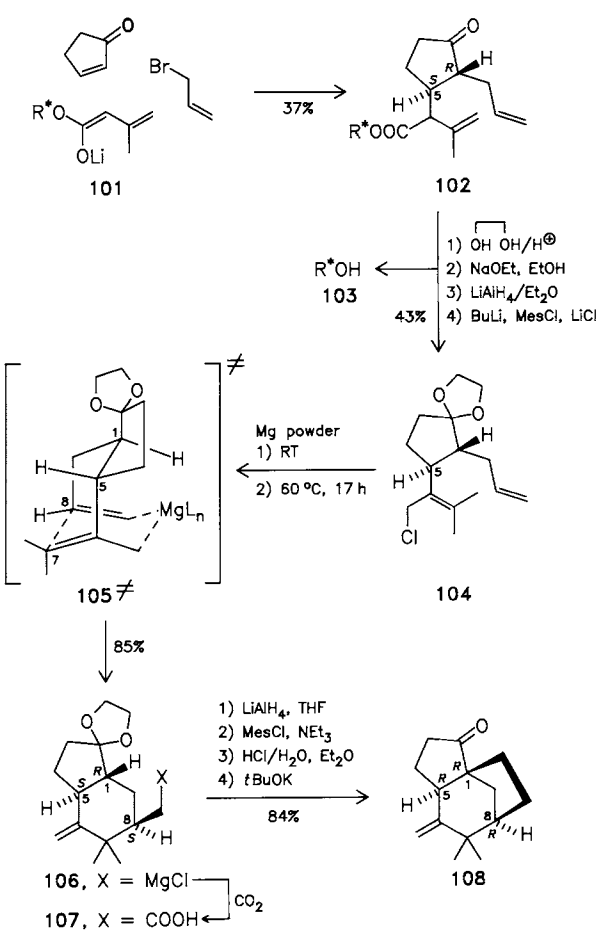


Scheme 19. DBN = 1,5-diazabicyclo[4.3.0]non-5-ene.

99 → **100**, which afforded the carrion beetle defense compound β-necrodol **100a** together with its C-1 epimer **100b** (61%, 1:1 mixture).[24] This is not surprising since transition states **98a**$^{\neq}$ (→ **100a**) and **98b**$^{\neq}$ (→ **100b**) suffer similar steric crowding due to the *gem*-dimethyl substitution (Scheme 19).

Nevertheless, **95**, obtained in enantiomerically pure form via a methylcopper addition/Mannich reaction of a chiral *N*-crotonoylsultam, provided (4*R*)-**97**, which yielded, after separation from **100b**, optically pure β-necrodol **100a**, thus enabling an assignment of the absolute configuration of the natural product.

A culmination of the type-II magnesium-ene cyclization methodology is its ideal application to the regio-, diastereo-, and enantioselective synthesis of the otherwise elusive, odoriferous norsesquiterpene (+)-khusimone **108**[25] (Scheme 20).

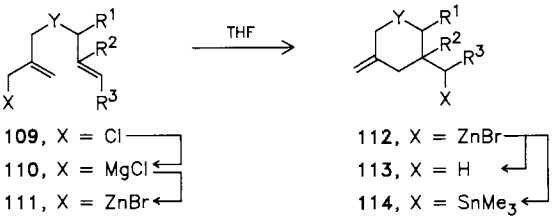


Scheme 20.

Conjugate addition of a chiral dienolate **101** to cyclopentenone, coupled with an enolate trapping by allyl bromide, chromatography, and crystallization, directly gave enantiomerically pure **102** (37% from cyclopentenone), which was readily converted into allylic chloride **104**. Slow addition of **104** to Mg powder (Merck) in THF, heating the solution at 60 °C for 17 h, and quenching with CO_2 gave, after crystallization, bicyclic carboxylic acid **107** (85% from **104**). No regio- or stereoisomer of **107** was found in the mother liquor. This particularly strong influence of the preexisting centers C-5 and C-1 in **104** on the generation of the stereogenic center C-8 conforms with the sterically least congested transition state **105**$^{\neq}$. Hence, the magnesium-ene step provided the thermodynamically unstable, sterically encumbered 7,7-dimethyl-6-methylene moiety with perfect control over the chirality at C-8.

2.3. Type-II Zinc-Ene Cyclizations

The thermal type-II cyclizations of olefinic allylzinc bromides **111** show interesting possibilities; the latter were prepared in situ from chlorides **109** via transmetalation of the Grignard intermediates **110** with $ZnBr_2$ (1.5 equiv.). Quenching of the cyclized alkylzinc species with H_2O (→ **113**) or $ClSnMe_3$ (→ **114**) provided oxygen and nitrogen heterocycles[26] (Scheme 21, Table 3).



Scheme 21.

Table 3. Intramolecular type-II zinc-ene reactions **111** → **112** → **113** or **114** in THF.

Entry		Y	R^1	R^2	R^3	*T* [°C]	*t* [h]	Product	Yield [%] [a]
1	**a**	O	H	H	H	80	23	**114a**	57
2	**b**	O	H	H	CH_3	80	45	**113b**	80
3	**c**	O	H	CH_3	H	130	22	**113c**	50
4	**d**	O	C_6H_5	H	H	80	48	**113d**	76 [b]
5	**e**	OCH_2	H	H	H	80	24	**114e**	62
6	**f**	O	$-(CH_2)_3-$		H	130	22	**113f**	0
7	**g**	NCH_3	H	H	H	80	24	**114g**	64

[a] Based on **109**. [b] 2:1 *trans/cis* mixture.

Analogous attempts to cyclize the allylmagnesium chlorides **110** failed, except for the transformation **110g** → **114g** (76%). On the other hand, the less nucleophilic zinc derivatives **111** cyclized readily at 80 °C, even with a terminally methyl-substituted alkenyl unit (although at 130 °C, entry 3); however, the reaction failed with a cyclohexenyl enophile unit (entry 6).

2.4. Conclusions

The following trends can be seen from the available evidence.

Ring size: The ease of cyclization decreases in the following order relative to the size of the developing ring:

type I: $5 > 6 \gg 7$
type II: $6 > 5 \approx 7 \gg 8$

Regioselectivity: Carbon–carbon bonds are preferentially formed between the proximal sites of ene and eno-

phile in the type-I process and between the more substituted ene terminal and the proximal enophile site in the type-II version.

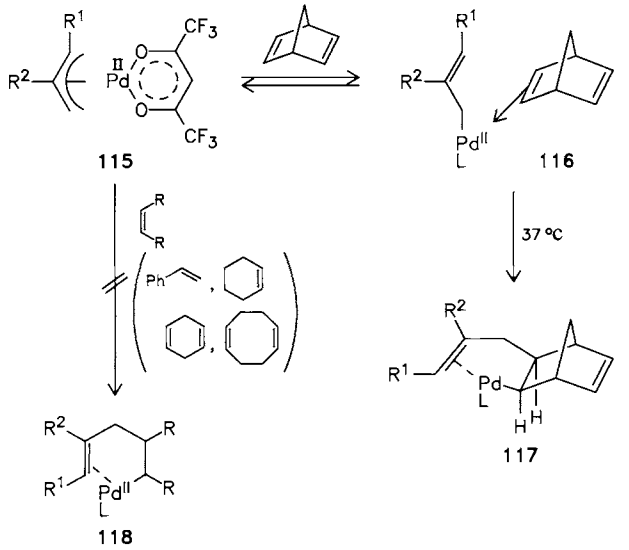
Stereoselectivity: Type-I cyclizations usually furnish, under kinetic control, predominantly five- and six-membered rings carrying *cis*-disposed magnesium-donor and -acceptor units even when a quaternary center is generated. 2,3-Dialkyl-substituted allylmagnesium moieties react preferentially in their (*Z*) form, inducing a *cis* relation of the C-3 substituent and the magnesium acceptor site in type-II cyclization products. However, the stereoselectivity of type-I and type-II magnesium-ene cyclizations can be greatly diminished by severe steric hindrance, for example, by critically placed *gem*-dimethyl groups (cf. **31**, **98**).

Limitations: The above examples involve only terminal (or strained, cf. **46**) olefinic enophile units since intramolecular insertions of 1,2-dialkyl, trialkyl, and cyclic alkenes into allylmagnesium compounds could not be achieved. Furthermore, attempts to apply these cyclizations to the preparation of pyrrolidines have so far failed. Nevertheless, type-II cyclizations of allylzinc derivatives show potential in overcoming some of these limitations.

3. Palladium-, Nickel-, and Platinum-Catalyzed Intramolecular Metallo-Ene Reactions

3.1. Palladium-Catalyzed Metallo-Ene Reactions

As a more interesting concept to circumvent these and other constraints of magnesium-ene cyclizations, we envisaged the exploration of *catalytic* intramolecular palladium-ene reactions. Indeed, stoichiometric amounts of allylpalladium complexes **115** and norbornadiene have been reported to undergo rapid, reversible formation of the σ-allyl complexes **116**, which at 37 °C yielded the *cis*-insertion products **117**[27] (Scheme 22).

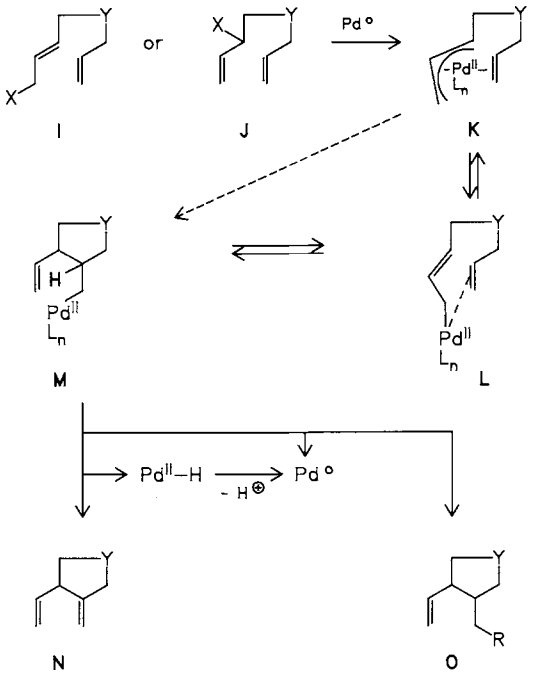


Scheme 22. L = hexafluoroacetylacetonate.

Similar stoichiometric additions of allylpalladium species to norbornene[28] and 1,3-dienes[29] are also known, whereas simple olefins (e.g., styrene, cyclohexene, 1,4-cyclohexadiene, and 1,5-cyclooctadiene) did not undergo this reaction.[27]

3.1.1. Type-I Cyclizations

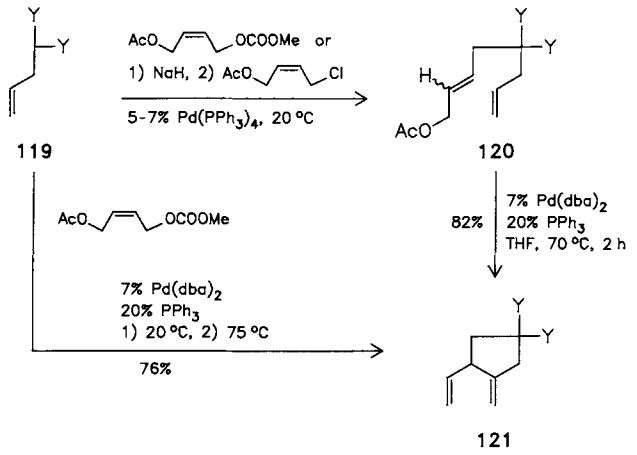
However, we assumed that the intramolecular ene process **L** → **M** would be entropically favored and that a subsequent irreversible β-elimination **M** → **N** would withdraw the ene product **M** from the equilibrium **L** ⇆ **M**.[30a] A further option is insertion/reductive elimination **M** → **O**.[30b] The thereby regenerated Pd^0 should continue the catalytic cycle by oxidative addition to allyl derivatives **I** or **J** (e.g., X = OR), thus providing in situ the olefinic allylpalladium intermediates **K** (Scheme 23).



Scheme 23.

Acetoxydienes **120** were readily obtained, predominantly as their (*E*) isomers, via $Pd(PPh_3)_4$-catalyzed alkylation[31] of disulfones **119a** (Y = SO_2Aryl) or malonates **119b** (Y = COOMe) with 4-acetoxy-2-butenyl methyl carbonate. Heating diene **120a** (Y = Tos) with $Pd(dba)_2$ (0.07 equiv.)/PPh_3 (0.2 equiv.) in THF at 70 °C gave the expected cyclized 1,4-diene **121a** in 83% yield. Even more conveniently, product **121a** was obtained (76% yield) in *one* operation from **119a** via Pd^0-catalyzed alkylation/cyclization[30] (Scheme 24, Table 4, entry 2).

Solvent effects significantly influence this novel ene process, as illustrated by the cyclization of the malonate **120b** (→ **121b**). Whereas no reaction took place in toluene, dichloromethane, or *N,N*-dimethylformamide, the rate and yield increased on proceeding from THF (20%) to methanol (65%) to acetic acid (77%, entries 3–5).[30] Interestingly, the presence of the phosphane turned out to be indispensable for the transformation **120b** → **121b**.



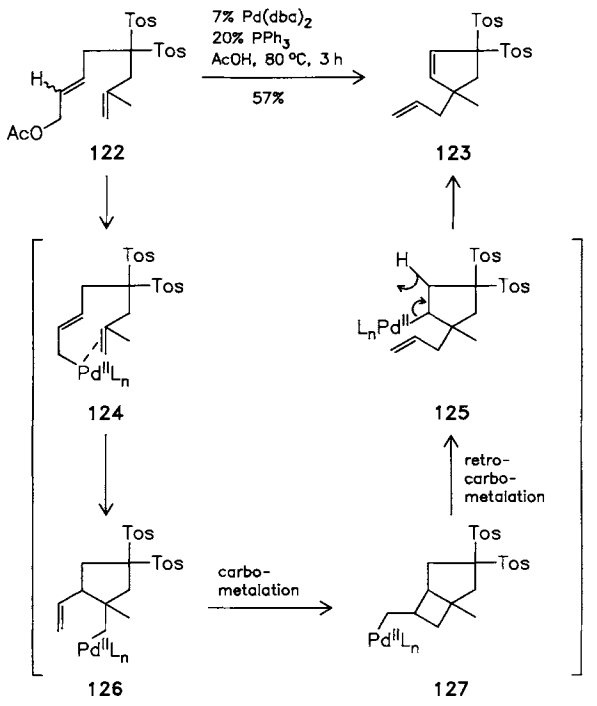
Scheme 24. dba = dibenzylideneacetone.

Table 4. $Pd(dba)_2/PPh_3$-catalyzed cyclizations **120** → **121**.

Entry		Y	Solvent	T [°C]	t [h]	Yield **121** [%]
1	**a**	Tos	THF	70	2	82
2 [a]	**a**	Tos	THF	one-pot [a]		76
3	**b**	COOMe	THF	80	40	20
4	**b**	COOMe	MeOH	80	8	65
5	**b**	COOMe	AcOH	80	1.5	77

[a] One-pot reaction from **119a**.

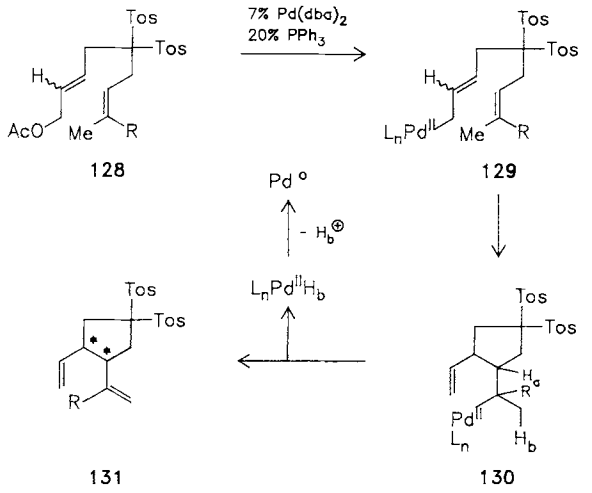
Intramolecular insertion of a 1,1-dialkylalkene into an allylpalladium unit (**124** → **126**) proceeded under the usual conditions as illustrated by the cyclization **122** → **123**[32] (Scheme 25).



Scheme 25.

It appears that the cyclized alkylpalladium intermediate **126**, unable to undergo β-elimination, carbometalates the adjacent vinyl group to give the transient **127**, which undergoes retro-carbometalation/β-elimination **127** → **125** → **123**.

In striking contrast to 8-alkyl-substituted 2,7-dienylmagnesium halides, which did not cyclize (cf. Section 2.1), the allylpalladium unit of **129** inserted readily into a terminally mono- and even dimethyl-substituted olefinic bond to give the transients **130** (Scheme 26, Table 5).

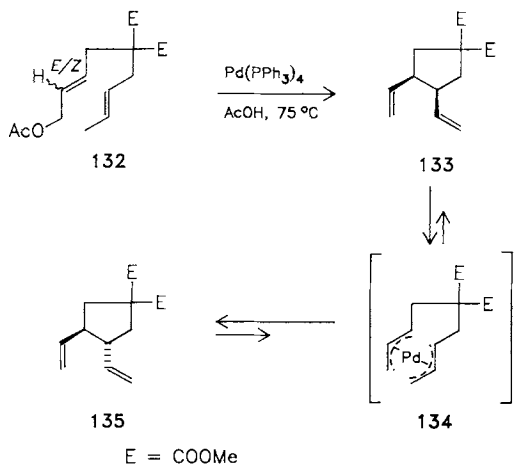


Scheme 26.

Table 5. $Pd(dba)_2/PPh_3$-catalyzed cyclizations **128** → **131**.

Entry		R	Solvent	T [°C]	t [h]	Yield **131** [%]
1	**a**	H	THF	75	15	80
2	**a**	H	AcOH	75	1.5	91
3	**b**	Me	THF	85	40	40
4	**b**	Me	AcOH	75	1.5	71

The efficient Pd^0-catalyzed cyclizations (AcOH, 75 °C, 1.5 h) of acetoxydienes **128a** and **128b** furnished, in each case, a single 1,5-diene product, **131a** (91%) and **131b** (71%), respectively. It follows that the cyclic alkylpalladium intermediates **130** eliminate the exocyclic H_b prefer-



Scheme 27.

Table 6. Stereochemistry of $Pd(PPh_3)_4$-catalyzed cyclizations **132** → **133** + **135**.

Entry	**132** $E:Z$	Equiv. $Pd(PPh_3)_4$	t [h]	Yield [%] **133** + **135**	**133** : **135**
1	0 : 100	0.05	5	70	36 : 64
2	60 : 40	0.05	5	67	36 : 64
3	60 : 40	0.07	2	26 (80) [a]	32 : 68
4	60 : 40	0.10	24	52	10 : 90

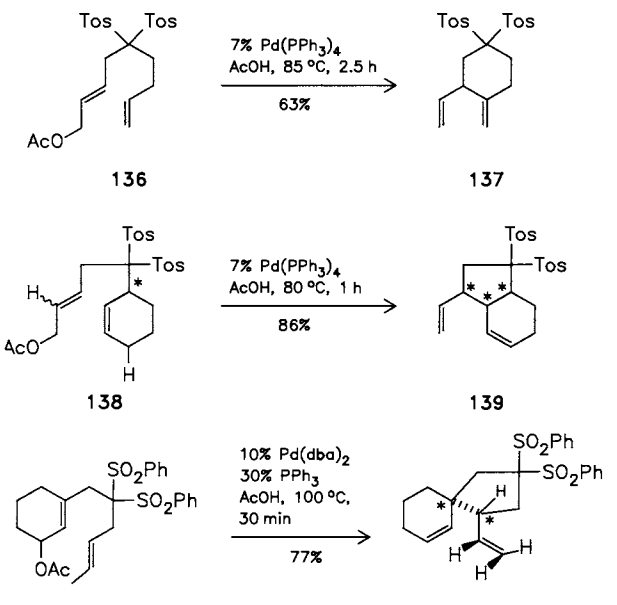
[a] Yield in parentheses based on recovered **132**.

entially over H_a in agreement with the conformational constraints of a *syn* β-elimination process. Again, acetic acid proved to be a better solvent than THF (cf. entries 1, 2 and 3, 4).[30]

The cyclization **132** → **133** + **135** showed a kinetically controlled 2 : 1 preference for the formation of the *trans*-divinylcyclopentane (independent of the ene *E*/*Z* configuration (cf. Scheme 34); the ratio increased to 9 : 1 when more catalyst and a longer reaction time were employed[32] (Scheme 27, Table 6).

This useful predominance of the thermodynamically more stable *trans* product **135** (entry 4) presumably involves a palladium-catalyzed "Cope-type" equilibration (**133** ⇆ **134** ⇆ **135**).

As expected, $Pd(PPh_3)_4$ also proved to be a suitable catalyst for intramolecular palladium-ene reactions (Scheme 28).

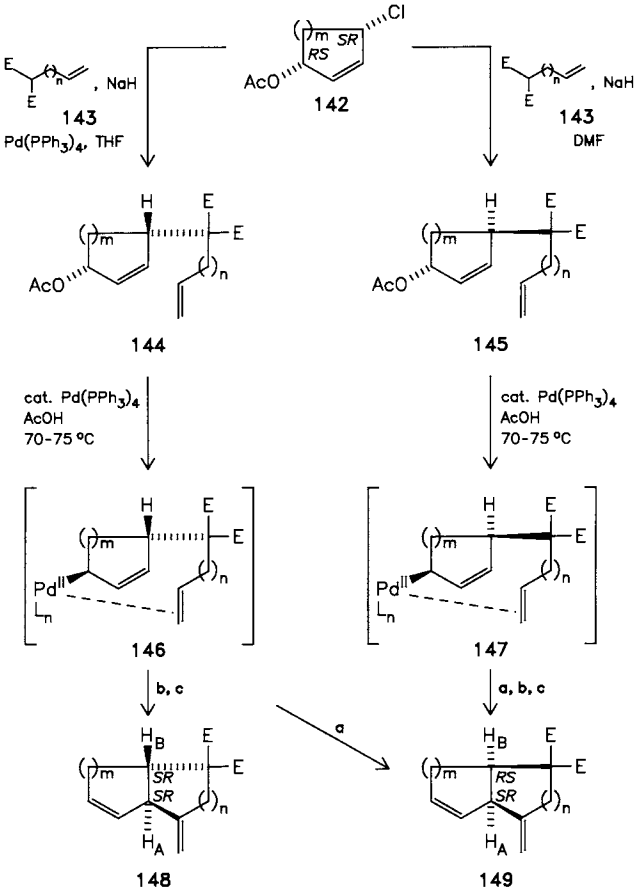


Scheme 28.

Conversion **136** → **137** illustrates the feasibility of this method for six-membered ring formation. Acetoxydiene **138**, containing a cyclic enophile unit, furnished stereoselectively the bicyclic product **139** in 86% yield.[30]

The palladium-ene unit may also be part of a ring, as shown by the stereoselective formation of a spiro system (**140** → **141**).[32a,33]

Stereochemically even more striking are the cyclizations depicted in Scheme 29 and Table 7.



Scheme 29.

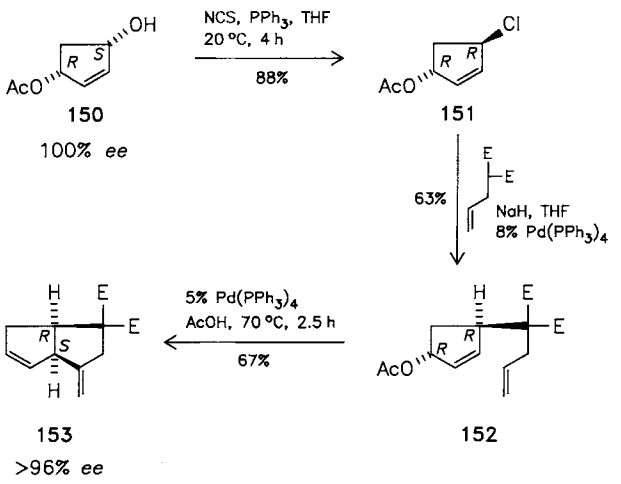
Table 7. Stereocontrolled syntheses of bicyclo[4.3.0]-, [4.4.0]-, and [5.3.0] ring systems by Pd-catalyzed cyclizations of acetoxydienes **144** and **145** (in AcOH).

Entry [a]	Starting material	m	n	t [h]	Yield **149** + **148** [%]	**149** : **148**
1	**145a**	2	1	1.1	84	≥98 : ≤2
2	**144a**	2	1	4	55	≥98 : ≤2
3	**145b**	2	2	3	60	>99 : <1
4	**144b**	2	2	3	69	5 : 95
5	**145c**	3	1	4	73	99 : 1
6	**144c**	3	1	1.8	80–92	2 : 98

[a] Entries 1–4: 7 mol% $Pd(PPh_3)_4$, 75 °C. Entry 5: 10 mol% $Pd(PPh_3)_4$, 70 °C. Entry 6: 5 mol% $Pd(PPh_3)_4$, 70 °C.

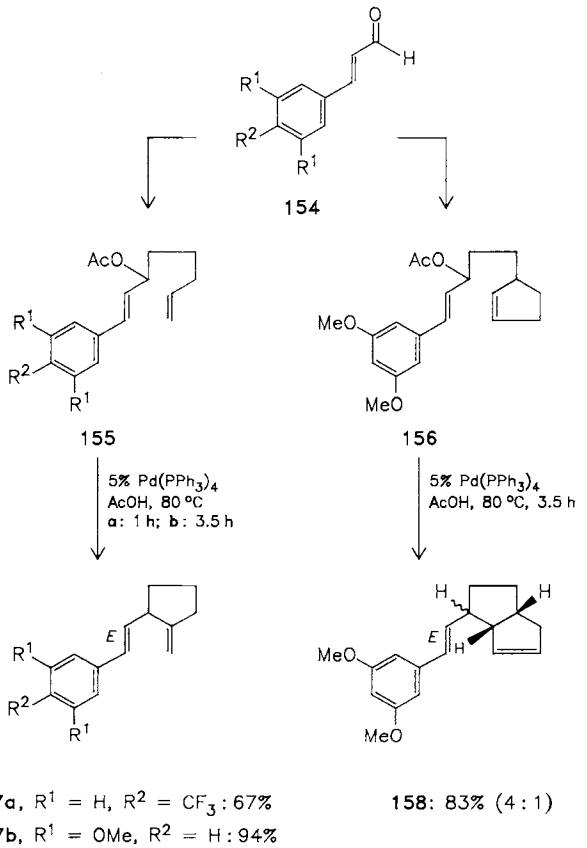
Comparison of entries 1 and 2 shows that the *trans*- or *cis*-olefinic cyclohexenyl acetates **145a** or **144a**, respectively, gave the same *cis*-annelated hexahydroindene **149a**.[30] However, the conversion **144a** → **149a** is significantly slower, presumably due to the relatively slow *trans*/*cis* isomerization **146** → **147**. It appears that, in initially formed **146a**, coordination of the Pd atom with the *trans*-disposed enophile is highly unfavorable, which prevents its conversion to **148a**. However, a longer bridge or a larger preexisting ring should permit allylpalladium/olefin coordination even in the *trans* intermediates **146**. Indeed, the *trans*-acetoxydiene **145b** furnished exclusively the *cis*-fused octahydronaphthalene **149b**, whereas the *cis*-acetoxydiene **144b**

gave, with 95% stereospecificity, the *trans*-annelated product **148b** (entries 3, 4).[33,34] This interesting C-O→C-Pd→C-C chirality transfer also provides selective routes to *cis*- or *trans*-fused octahydroazulenes **149c** or **148c**, respectively (entries 5, 6).[32,34] These findings confirm that the olefin inserts predominantly into the σ-(or π-)allylpalladium unit *cis* relative to the Pd atom (i.e., in a suprafacial manner).



Scheme 30.

Scheme 30 exemplifies the analogous enantiospecific preparation of a hexahydropentalene **153** from a readily available, optically pure hydroxy acetate **150**.[32,34]

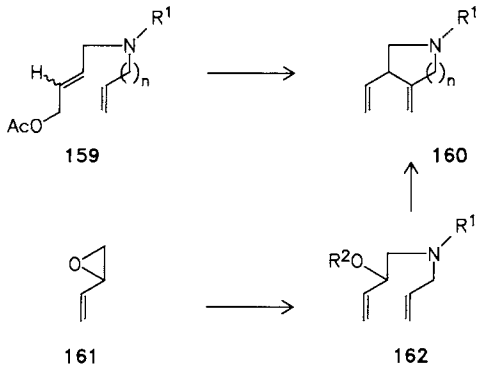


Scheme 31.

The *gem*-disulfone and malonate functionalities described above facilitate the preparation of the "palladium-ene" precursors **I** (Scheme 23) and can be readily removed or modified but they *are not essential* for the cyclization process. Thus, 3-acetoxy-substituted 1,7-octadienes **J** (e.g., **155**, **156**) containing simple carbon bridges are very readily accessible and undergo smooth Pd-catalyzed cyclizations[32] (Scheme 31).

Only products **157** and **158** containing an (*E*)-olefinic bond were found, indicating the ene-type reaction of (*E*)-allylpalladium intermediates.

Catalytic Pd-ene cyclizations may also open new perspectives in alkaloid synthesis, as shown by the smooth formation of pyrrolidines and piperidines.[33,35]



Scheme 32.

Table 8. Synthesis of pyrrolidines and piperidines by Pd^0-catalyzed cyclizations **159**→**160** and **162**→**160** (AcOH, 80 °C, 5 mol% $Pd(PPh_3)_4$).

Entry	Starting material	R^1	R^2	n	*t* [h]	Yield **160** [%]
1	**159a**	CH_2Ph	—	1	3	72
2	**159b**	$COOCH_2Ph$	—	1	1	69
3	**159c**	Tos	—	1	0.5	72
4 [a]	**159d**	Tos	—	2	4	77
5	**162e**	C(O)Ph	C(O)Ph	1	0.5	81
6	**162f**	Tos	H	1	3.5	78

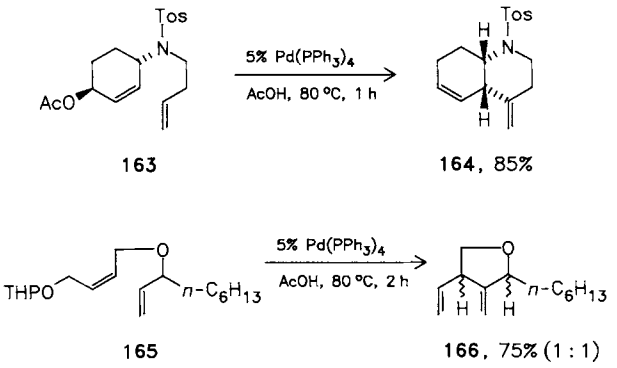
[a] 7 mol% of $Pd(PPh_3)_4$ used.

Scheme 32 and Table 8 illustrate the cyclizations of "palladium-ene" precursors **I** (**159**, entries 1-4) and **J** (**162**, entries 5, 6) containing a nitrogen atom as part of the bridge. The leaving group in **162** can even be a simple hydroxyl group (entry 6).[35]

Stereospecific formation of the *cis*-fused octahydroquinoline **164** (85%) is depicted in Scheme 33, which also shows the conversion of diallyl ether **165** to a 1:1 *cis*/*trans* mixture of tetrahydrofurans **166** (75%).[35]

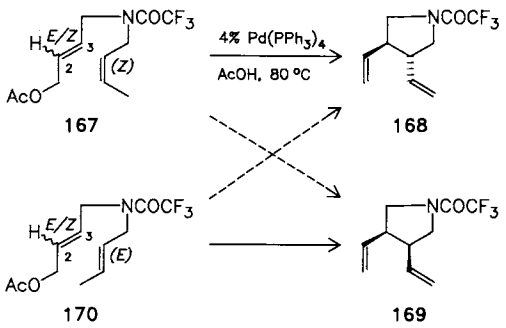
It is worth noting that the initial oxidative addition of Pd^0 to **165** proceeded with selective substitution of the allylic acetal group whereas the allylic ether moieties remained intact.

Pd^0-catalyzed cyclizations of (*E*,*Z*)-, (*Z*,*Z*)-, (*E*,*E*)-, and (*Z*,*E*)-*N*-trifluoroacetamides **167** and **170** (Scheme 34, Table 9) again represent the insertion of terminally methyl-



Scheme 33. THP = tetrahydropyranyl.

substituted olefinic bonds into (*E*)-allylpalladium components followed by β-elimination of a methyl hydrogen atom[35] (Scheme 34, Table 9).



Scheme 34.

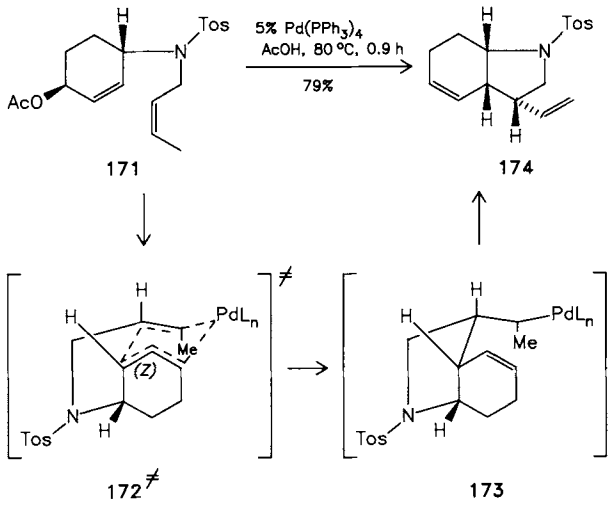
Table 9. Pd^0-catalyzed cyclizations **167** → **168** + **169** and **170** → **168** + **169**.

Entry	Starting material	*E/Z* C-2–C-3	*t* [h]	Yield **168** + **169** [%]	**168** : **169**
1	**167**	*E*	0.6	76	88 : 12
2 [a]	**167**	*E*	20	75	88 : 12
3	**167**	*Z*	1.9	59	91 : 9
4	**170**	*E*	2	67	28 : 72
5 [a]	**170**	*E*	52	62	30 : 70
6	**170**	*Z*	2.5	51	30 : 70

[a] 10 mol% of [polymer-C_6H_4-$P(C_6H_5)_2]_4Pd$ (Fluka).

Entries 2 and 5 exemplify the use of a polymer-supported palladium(0)-phosphane catalyst which may offer, in general, practical advantages for carrying out palladium-catalyzed ene-type cyclizations.[36] As to the *stereochemistry*, dienes **167**, containing a (*Z*)-enophile, gave, under kinetic control, predominantly the *trans*-divinylpyrrolidine **168** (≈8 : 1, entries 1–3), whereas dienes **170**, containing an (*E*)-enophile, afforded, less selectively (2.5 : 1), the *cis* product **169** (entries 4–6). This stereochemical outcome was independent of the *E/Z* configuration of the allyl acetates **167** and **170** in agreement with an (*Z*)-→(*E*)-allylpalladium isomerization prior to the insertion (indeed, isomerizations (*Z*)-**167** → (*E*)-**167** and (*Z*)-**170** → (*E*)-**170** were observed under the cyclization conditions).

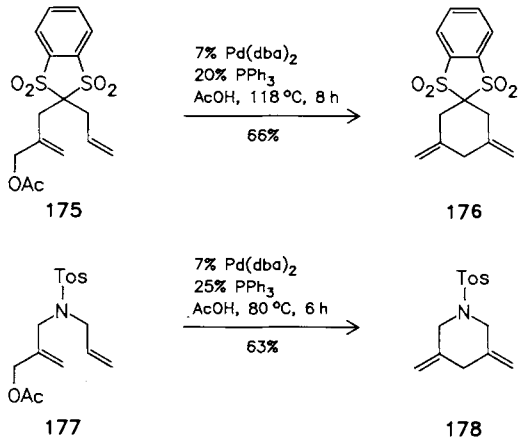
By contrast, if the (*Z*) configuration of the allylpalladium unit (e.g., in **172**$^{\neq}$) is enforced by incorporation into a ring, only *cis*-substituted insertion products are expected, as confirmed by the annelation **171** → **174**[35] (Scheme 35).



Scheme 35.

3.1.2. *Type-II Cyclizations*

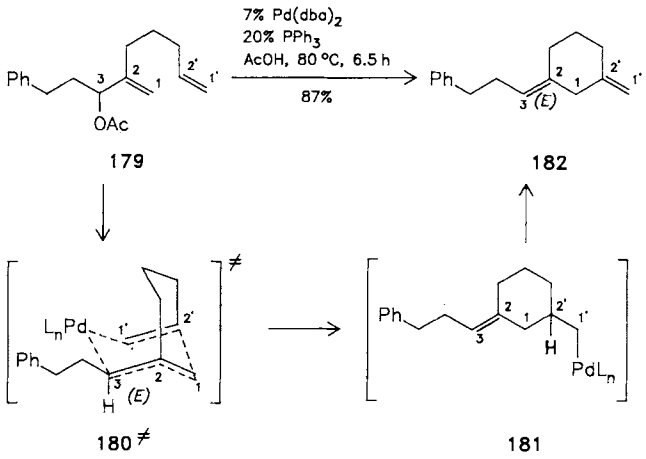
Scheme 36 illustrates the feasibility of carrying out catalytic type-II palladium-ene cyclizations, for example, the transformation **175** → **176** (118 °C, 8 h, 66% yield).[33,37] Cyclization of **177** proceeded under milder conditions (80 °C, 6 h) to give piperidine **178** (63%).[37]



Scheme 36.

Also, dienyl acetate **179** (readily prepared from 6-hepten-2-one and lacking the disulfone moiety) was easily transformed into (*E*)-1,4-diene **182** (87%)[33,37] (Scheme 37).

This regiochemistry parallels that of stoichiometric additions of allylpalladium complexes to norbornadiene,[27] but was subject to uncertainty in view of the relatively fast 1,3-Pd migration[31] (formally analogous to the equilibrium **13** ⇆ **79**; Scheme 15, Section 2.2.1). Accordingly, the conversion **179** → **182** demonstrates a new stereocontrolled access to exocyclic trisubstituted alkenes involving C–C bond formation at the less substituted allylpalladium ter-

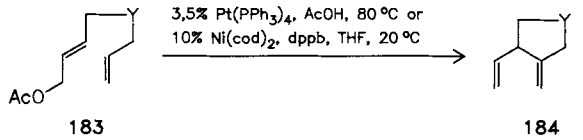


Scheme 37.

minal and thus showing a regio- and stereochemistry *opposite* to the type-II magnesium-ene process (Scheme 15, **13** → **15**).

3.2. Platinum- and Nickel-Catalyzed Reactions

The above concept of catalytic metallo-ene cyclizations (Scheme 23) may also be extended to platinum and nickel. Norbornene has already been reported to undergo stoichiometric, bimolecular addition of a preformed allylnickel complex followed by carbomethoxylation of the adduct,[28a] as well as a nickel-catalyzed allylation/rearrangement/elimination.[38] Allylnickel/olefin insertions are apparently involved in Ni-catalyzed polymerizations and oligomerizations of 1,3-butadiene[39] such as the dimerization to 1-methylene-2-vinylcyclopentane.[40]



Scheme 38. cod = 1,5-cyclooctadiene; dppb = *P,P'*-tetramethylenebis(diphenylphosphane).

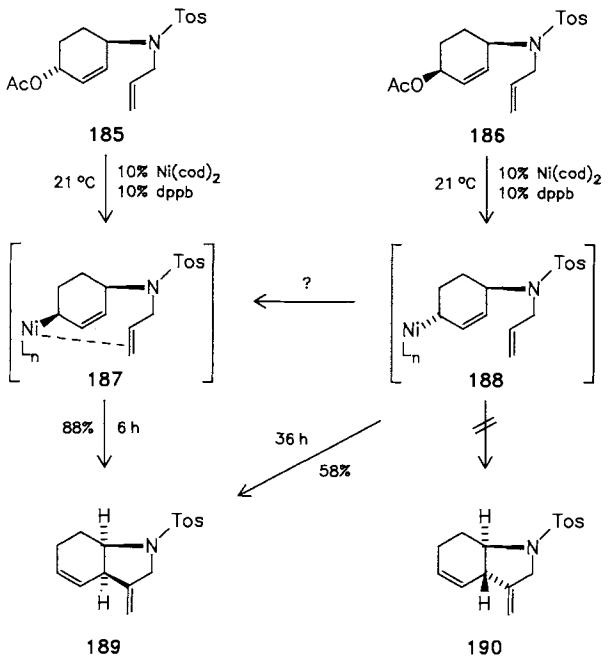
Table 10. Pt^0- and Ni^0-catalyzed cyclizations **183** → **184**. Pt^0 catalysis: 3.5 mol% $Pt(PPh_3)_4$, AcOH, 80 °C. Ni^0 catalysis: 10 mol% $Ni(cod)_2$, dppb, THF, 20 °C.

Entry		Y	Cat.	Solvent	T [°C]	t [h]	Yield [%]
1	**a**	$C(SO_2Ph)_2$	Pt^0	AcOH	80	5	85
2	**a**	$C(SO_2Ph)_2$	Ni^0	THF	20	3	83
3	**b**	N–Tos	Ni^0	THF	20	12	76
4	**c**	$N–CPh_3$	Ni^0	THF	20	0.7	92

Heating dienyl acetate **183a** with 3.5 mol% of $Pt(PPh_3)_4$ in acetic acid at 80 °C furnished the expected cyclopentane **184a** in 85% yield[33,41] (Scheme 38, Table 10, entry 1).

The feasibility of Ni^0 complexes as catalysts for intramolecular metallo-ene reactions was, despite the encouraging precedents, not straightforward and depended strongly on their ligands. Systematic studies showed a 1:1 mixture of $Ni(cod)_2$/dppb to catalyze (10 mol%) the allylation/elimination **183** → **184** at 20 °C in THF with a synthetically useful efficiency (76–92%, entries 2–4).[33,41]

The catalyst [Ni(cod)dppb], formed in situ, induced smooth conversion of monocyclic *trans*-acetoxydiene **185** to the *cis*-fused 3-methylene-hexahydroindole **189** (88%), which is also formed much more slowly (58%) from the *cis*-precursor **186**[41] (Scheme 39).



Scheme 39.

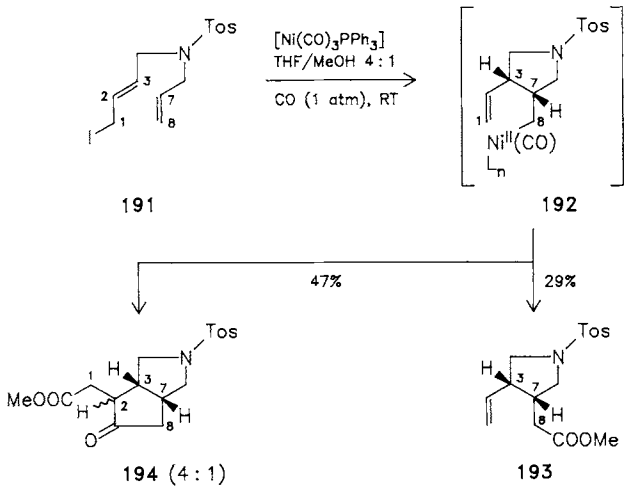
This indicates a preferred *cis*-allylnickel/olefin insertion **187** → **189** analogous to the closely related palladium-catalyzed annelations **146a** or **147a** → **149a**.

Coupling of an intramolecular nickel-ene process with a methoxycarbonylation should regenerate a Ni^0 species to continue the catalytic cycle analogous to the originally envisaged sequence **I** or **J** → **K** → **L** → **M** → **O** (Scheme 23).

Tricarbonyl(triphenylphosphane)nickel[42] (25 mol%), a stable, easy to handle solid (versus the highly volatile and toxic $Ni(CO)_4$) readily catalyzed the conversion of dienyl iodide **191** (THF/MeOH 4:1, 1 atm CO, room temperature) to the monocyclic *cis*-substituted pyrrolidine **193** (29%) and the bicyclic compound **194** (47%, 4:1 mixture of isomers, Scheme 40).[41]

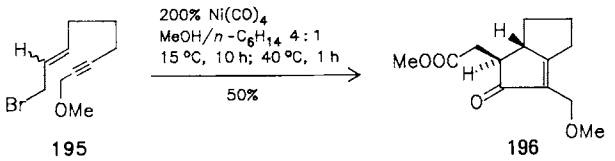
It thus appears that the nickel-ene process **191** → **192** is stereoselective and that **192** forms a *C*-acylnickel intermediate which inserts either methanol (→ **193**) or the internal olefinic bond giving, after final methoxycarbonylation, ketoester **194**. It is interesting to note that both insertion pathways are preferred over a β-elimination of **192**.

Direct β-elimination cannot interfere with allylnickel/alkyne insertion–carbonylation sequences. Very recently, the



Scheme 40.

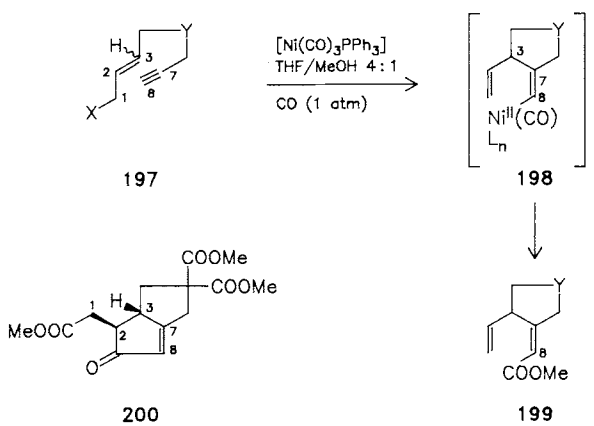
bicyclization of (*E*)- and (*Z*)-**195** to **196** (50%), promoted by 200 mol% of $Ni(CO)_4$ at 40°C, has been reported[43] (Scheme 41).



Scheme 41.

Use of 25 mol% of the more practical $[Ni(CO)_3PPh_3]$ catalyst under CO (1 atm, THF/MeOH 4:1, room temperature) resulted in exclusive monocyclization of enynyl iodide **197a** to **199a**[41] (Scheme 42, Table 11, entry 1).

This unusual stereocontrolled approach to an exocyclic trisubstituted olefinic bond is consistent with a suprafacial allylnickel/acetylene insertion **197** → **198**. Malonate **197b** yielded, under similar reaction conditions, the monocyclic ester **199b** (41%) and the bicyclic diester **200** (36%) in a stereospecific manner (entry 2). Bicyclization (→ **200**, 62%) was more prominent when starting with bromide **197c**, which required a higher reaction temperature (entry 3).[41]



Scheme 42.

Table 11. $[Ni(CO)_3PPh_3]$-catalyzed intramolecular allylation/carbonylation of alkynes **197** → **199** (+ **200**). 20–25 mol% catalyst, 1 atm CO.

Entry		*E/Z* of **197**	Y	X	*T* [°C]	*t* [h]	Yield **199** [%]	Yield **200** [%]
1	**a**	*E*	N–Tos	I	RT	20	69	–
2	**b**	*E*	$C(COOMe)_2$	I	RT	20	41	36
3	**c**	*Z*	$C(COOMe)_2$	Br	[a]	[a]	14	62

[a] 48 h at RT then 12 h at 50°C.

3.3. Conclusions

Intramolecular metallo-ene reactions may be catalyzed not only by complexes of Pd^0 but also by those of the other d^{10} transition metals, Pt^0 and Ni^0. Nickel(0) requires an inert atmosphere and a more subtle choice of ligands but provides *cis*-diastereoselectivity in the cyclization step (proceeding at room temperature in THF) and offers numerous possibilities in synthesis when combined with CO-insertion reactions. The stereochemical evidence cited above is not consistent with radical (cf. Scheme 29) or metallocyclic intermediates (cf. Scheme 34), but is in agreement with a suprafacial σ-allylmetallo-ene type process or a direct π-allylmetal/alkene(alkyne) insertion pathway. The compatibility of this reaction with nitrogen atoms as part of the bridge offers interesting perspectives for alkaloid syntheses.

4. Summary and Outlook

Stoichiometric, intramolecular metal-ene reactions (M = Li, Mg, Zn) involving terminal or strained alkene enophile units have served extensively as a cornerstone in efficient syntheses of natural products. Most of this work centers on allylmagnesium/alkene cyclizations because of their diastereoselectivity, the accessibility of the starting materials, and the propensity of the cyclized Grignard intermediates to be trapped by a vast array of electrophiles. On the other hand, the use of Mg is incompatible with several functionalities (e.g., certain heteroatoms) in the acyclic precursor. Zinc-ene cyclizations seem to surmount some of these limitations.

However, d^{10}-transition-metal-catalyzed versions promise, at the moment, an even wider range of possibilities. The need to maintain the catalytic cycle by continuous regeneration of the zerovalent metal limits, however, the functionalizability of the metalated center in the cyclized intermediate. For the same reasons, the readily accessible starting materials may contain various functional groups which are compatible with the reaction conditions and which may be of value for the syntheses of complex heterocycles such as alkaloids. The suprafacial nature of the process permits a useful C–O→C–Pd→C–C chirality transfer.

The exploration of this field is still in its infancy and has focused mainly on the palladium-catalyzed process which is easier to carry out and apparently more versatile (e.g., regarding the substitution pattern of the enophile unit) than the less expensive nickel-catalyzed version. Already,

complementary regio- and stereoselectivities of intramolecular magnesium-, palladium-, and nickel-ene type processes have been recognized which may be put to advantage in organic synthesis.

The future will supply more insight into the mechanisms; nevertheless, the depicted rationalizations have proved to be of predictive value. The range of synthetically useful insertion reactions which are to regenerate the catalytic species will certainly be expanded, as will the nature of the metal, ligands, and starting materials. In particular, the application and development of chiral ligands for achieving asymmetric metallo-ene cyclizations is a considerable challenge. Finally, strategic use for the synthesis of naturally occurring or new structures, difficult to obtain by other methods, is expected to reveal the realistic and full potential of the transition-metal-catalyzed versions.

It is a privilege to acknowledge the crucial contributions of my co-workers whose names are cited in the appropriate references. We thank the Swiss National Science Foundation, Sandoz AG, Basel, and Givaudan SA, Vernier, for generous support of this work.

Received: September 28, 1988 [A 706 IE]
German version: *Angew. Chem. 101* (1989) 39

[1] K. Alder, F. Pascher, A. Schmitz, *Ber. Dtsch. Chem. Ges. 76* (1943) 27.
[2] a) H. Lehmkuhl, D. Reinehr, *J. Organomet. Chem. 25* (1970) C47; review: H. Lehmkuhl, *Bull. Soc. Chim. Fr. Part II 1981*, 87; b) H. Lehmkuhl, E. Janssen, *Justus Liebigs Ann. Chem. 1978*, 1854; c) H. Lehmkuhl, K. Mehler, *ibid. 1978*, 1841; d) H. Lehmkuhl, D. Reinehr, D. Henneberg, G. Schomburg, G. Schroth, *ibid. 1975*, 119; H. Lehmkuhl, W. Bergstein, D. Henneberg, E. Janssen, O. Olbrysch, D. Reinehr, G. Schomburg, *ibid. 1975*, 1176; e) H. Lehmkuhl, D. Reinehr, K. Mehler, G. Schomburg, H. Kötter, D. Henneberg, G. Schroth, *ibid. 1978*, 1449.
[3] H. M. Walborsky, A. E. Young, *J. Am. Chem. Soc. 86* (1964) 3288; *88* (1966) 3437; H. G. Richey, Jr., R. M. Bension, *J. Org. Chem. 45* (1980) 5036.
[4] H. Lehmkuhl, N. Nehl, *J. Organomet. Chem. 60* (1973) 1; Y. Frangin, M. Gaudemar, *Bull. Soc. Chim. Fr. 1976*, 1173; F. Bernadou, L. Miginiac, *Tetrahedron Lett. 1976*, 3083; E. Negishi, J. A. Miller, *J. Am. Chem. Soc. 105* (1983) 6761; G. A. Molander, *J. Org. Chem. 48* (1983) 5409; P. Knochel, J. F. Normant, *Tetrahedron Lett. 27* (1986) 1043.
[5] A. Stefani, *Helv. Chim. Acta 56* (1973) 1192.
[6] B. M. Mikhailov, Yu.. N. Bubnov, *Tetrahedron Lett. 1971*, 2127; Yu. N. Bubnov, O. A. Nesmeyanova, T. Yu. Rudashevskaya, B. M. Mikhailov, B. A. Kazansky, *ibid. 1971*, 2153.
[7] W. Oppolzer, *Angew. Chem. 89* (1977) 10; *Angew. Chem. Int. Ed. Engl. 16* (1977) 10; E. Ciganek, *Org. React. 32* (1984) 1; A. G. Fallis, *Can. J. Chem. 62* (1984) 183; D. Craig, *Chem. Soc. Rev. 16* (1987) 187.
[8] W. Oppolzer, V. Snieckus, *Angew. Chem. 90* (1978) 506; *Angew. Chem. Int. Ed. Engl. 17* (1978) 476.
[9] W. Oppolzer, E. P. Kündig, P. M. Bishop, C. Perret, *Tetrahedron Lett. 23* (1982) 3901.
[10] H. Bönnemann, B. Bogdanović, R. Brinkmann, D.-W. He, B. Spliethoff, *Angew. Chem. 95* (1983) 749; *Angew. Chem. Int. Ed. Engl. 22* (1983) 728.
[11] W. Oppolzer, P. Schneider, *Tetrahedron Lett. 25* (1984) 3305.
[12] a) H. Felkin, J. D. Umpleby, E. Hagaman, E. Wenkert, *Tetrahedron Lett. 1972*, 2285; b) H. Felkin, L. D. Kwart, G. Swierczewski, J. D. Umpleby, *J. Chem. Soc. Chem. Commun. 1975*, 242; c) H. Fukutani, M. Takizawa, H. Okada, *Jpn. Pat.* 7239, 034 (1972); *Chem. Abstr. 78* (1973) 111498.
[13] A. D. Josey, *J. Org. Chem. 39* (1974) 139.
[14] G. Courtois, A. Masson, L. Migniac, *C. R. Séances Acad. Sci. Ser. C 286* (1978) 265.
[15] W. Oppolzer, K. Bättig, *Tetrahedron Lett. 23* (1982) 4669.
[16] W. Oppolzer, A. Nakao, *Tetrahedron Lett. 27* (1986) 5471.
[17] W. Oppolzer, H. F. Strauss, D. P. Simmons, *Tetrahedron Lett. 23* (1982) 4673.
[18] W. Oppolzer, T. Begley, A. Ashcroft, *Tetrahedron Lett. 25* (1984) 825.
[19] W. Oppolzer, E. J. Jacobsen, *Tetrahedron Lett. 27* (1986) 1141.
[20] W. Oppolzer, T. Inokuchi, unpublished results.
[21] W. Oppolzer, R. Pitteloud, H. F. Strauss, *J. Am. Chem. Soc. 104* (1982) 6476.
[22] J. E. Nordlander, W. G. Young, J. D. Roberts, *J. Am. Chem. Soc. 83* (1961) 494.
[23] W. Oppolzer, A. F. Cunningham, Jr., *Tetrahedron Lett. 27* (1986) 5467.
[24] W. Oppolzer, P. Schneider, *Helv. Chim. Acta 69* (1986) 1817.
[25] W. Oppolzer, R. Pitteloud, *J. Am Chem. Soc. 104* (1982) 6578; W. Oppolzer, R. Pitteloud, G. Bernardinelli, K. Bättig, *Tetrahedron Lett. 24* (1983) 4975.
[26] J. van der Louw, J. L. van der Baan, H. Stieltjes, F. Bickelhaupt, G. W. Klumpp, *Tetrahedron Lett. 28* (1987) 5929.
[27] R. P. Hughes, J. Powell, *J. Organomet. Chem. 30* (1971) C45.
[28] a) M. C. Gallazzi, T. L. Hanlon, G. Vitulli, L. Porri, *J. Organomet. Chem. 33* (1971) C45; b) R. C. Larock, J. P. Burkhart, K. Oertle, *Tetrahedron Lett. 23* (1982) 1071.
[29] Y. Takahashi, S. Sakai, Y. Ishii, *J. Organomet. Chem. 16* (1969) 177; *Inorg. Chem. 11* (1972) 1516; R. P. Hughes, T. Jack, J. Powell, *J. Organomet. Chem. 63* (1973) 451; J. Kiji, Y. Miura, J. Furukawa, *ibid. 140* (1977) 317.
[30] a) W. Oppolzer, J.-M. Gaudin, *Helv. Chim. Acta 70* (1987) 1477; b) W. Oppolzer, *Pure Appl. Chem. 60* (1988) 39.
[31] Preparations and other reactions of allylpalladium derivatives, reviews: J. Tsuji, *Pure Appl. Chem. 53* (1981) 371; B. M. Trost, T. R. Verhoeven in G. Wilkinson, F. G. A. Stone, E. W. Abel (Eds.): *Comprehensive Organometallic Chemistry, Vol. 8*, Pergamon Press, Oxford 1982, p. 799; J. Tsuji, *Tetrahedron 42* (1986) 4361; J. P. Collman, L. S. Hegedus, J. R. Norton, R. G. Finke, *Principles and Applications of Organometallic Chemistry*, University Science Books, Mill Valley, CA 1987, p. 881.
[32] a) W. Oppolzer, J. M. Gaudin, R. E. Swenson, J.-P. Barras, presented (W. O.) at the 3e Congrès national de la Société Française de Chimie, Nice, September 5, 1988; b) W. Oppolzer, R. E. Swenson, W. Pachinger, Helv. Chim. Acta, in press.
[33] W. Oppolzer, *Chimia 42* (1988) 6.
[34] W. Oppolzer, J.-M. Gaudin, T. N. Birkinshaw, *Tetrahedron Lett. 29* (1988) 4705.
[35] W. Oppolzer, J.-M. Gaudin, M. Bedoya-Zurita, J. Hueso-Rodriguez, T. M. Raynham, C. Robyr, *Tetrahedron Lett. 29* (1988) 4709.
[36] W. Oppolzer, D. Kuo, unpublished results.
[37] W. Oppolzer, R. E. Swenson, J.-M. Gaudin, *Tetrahedron Lett. 29* (1988) 5529.
[38] M. Catellani, G. P. Chiusoli, E. Dradi, G. Salerno, *J. Organomet. Chem. 177* (1979) C29.
[39] Review: G. Wilke, *Angew. Chem. 100* (1988) 189; *Angew. Chem. Int. Ed. Engl. 27* (1988) 185.
[40] J. Kiji, K. Masui, J. Furukawa, *Bull. Chem. Soc. Jpn. 44* (1971) 1956.
[41] W. Oppolzer, M. Bedoya-Zurita, C. Y. Switzer, *Tetrahedron Lett.*, in press.
[42] R. A. Schunn, *Inorg. Synth. 15* (1974) 5.
[43] F. Camps, J. Coll, J. M. Moreto, J. Toras, *Tetrahedron Lett. 28* (1987) 4745.

When submitting manuscripts, authors of articles intended for publication as "Communications" are requested to read the "Notice to Authors" reproduced in the January issue of the journal following the list of contents; upon request, a copy can be obtained from the editorial office.

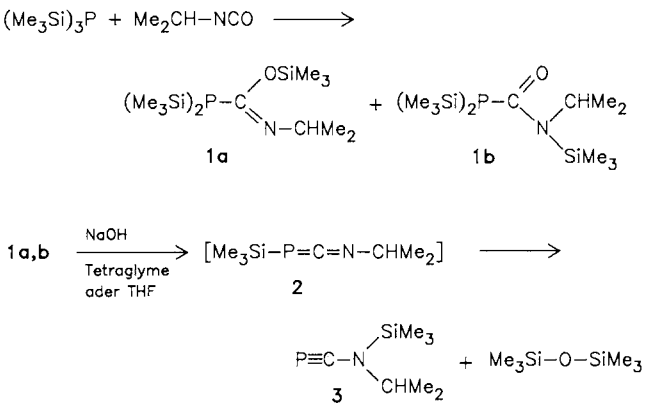
A Stable Amino-Substituted Phosphaalkyne**

By *Rolf Appel** and *Michael Poppe*

Dedicated to Professor Hans Bock on the occasion of his 60th birthday

The stabilization of phosphaalkynes[1a] at room temperature requires the use of bulky organic groups such as isopropyl, methylcyclohexyl, methylcyclopentyl, neopentyl,[1b] *tert*-butyl,[2] tri-*tert*-butylphenyl,[3] adamantyl,[4] or triptycyl.[5] Phosphaalkynes containing small groups[6] or heteroatoms, such as F–C≡P[7] or $(CH_3)_3Si$–C≡P,[8] are unstable and can only be characterized spectroscopically. The existence of stable bromo-, hydroxy-, or amino-substituted phosphaalkynes, described in the literature,[9] has been questioned.[10]

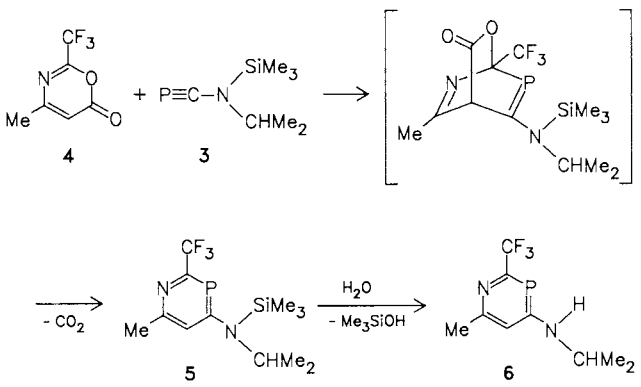
We have now found that the stable amino-substituted phosphaalkyne **3** is formed by NaOH-induced elimination of hexamethyldisiloxane from the adduct of tris(trimethylsilyl)phosphane with isopropyl isocyanate. According to the elemental analysis and spectroscopic data, **1** is a tautomeric mixture **1a**, **b**.[11] The ^{31}P NMR spectrum shows two resonances at $\delta = -123$ (broad) and -151 (broad) in a ratio of 1:9. In the ^{13}C NMR spectrum, the quaternary C atom is characterized by the resonance at $\delta = 160.1$ (d, $^1J_{CP} = 43.2$ Hz); a phosphaalkene isomer could not be detected.



Mechanistically, the formation of **3** from **1** can be explained in terms of the intermediary formation of the non-isolable 1-aza-3-phosphaallene **2**, which rearranges very rapidly to the phosphaalkyne. Analogies are known from carbodiimide chemistry.[12]

The empirical formula $C_7H_{16}NPSi$ for **3** was established by the elemental analysis and the high-resolution mass spectrum. The ^{31}P NMR spectrum displays a singlet at $\delta = -140$; the alkyne C atom gives rise to a doublet at $\delta = 154$ ($^1J_{CP} = 18.3$ Hz) in the ^{13}C NMR spectrum. These data are in agreement with the observation that P and C atoms of phosphaalkynes absorb at higher field than P and C atoms of phosphaalkenes.[2]

Constitutional isomers of **3** with phosphacarbodiimide or cyanophosphane structure can be ruled out by the ^1H NMR and IR spectra. In the IR spectrum of **3** (neat), neither a cumulene nor a C≡N stretching vibration is present. Instead, one observes a strong absorption at $\tilde{\nu} = 1588$ cm^{-1}, which may be assigned to the P≡C stretching vibration. For *t*Bu–C≡P and F–C≡P, characteristic IR absorptions at 1533 cm^{-1} and 1660 cm^{-1}, respectively, have been reported.[2,7] In the ^1H NMR spectrum, the protons of the trimethylsilyl group give rise to a singlet at $\delta = 0.04$ and the proton of the isopropyl group gives rise to a septet of doublets at $\delta = 2.7$ ($^3J_{HH} = 6.6$ Hz; $^4J_{HP} = 2.8$ Hz) due to coupling between the protons of the methyl groups and the P atom.



Further structural proof is provided by the [4+2] cycloaddition with an electron-poor heterodiene.[13] As expected, **3** reacts with the oxazinone **4**[14] to give the 1,3-aza-λ^3-phosphinine **5**, which, owing to its ready hydrolysis, can only be isolated in pure form as the NH compound **6**.

The phosphaalkyne **3** is stable both in pure form and in solution; a solution of **3** in toluene can be heated under reflux for 10 min without apparent change (^{31}P NMR). Upon contact with air, the initially colorless liquid turns first yellow then orange.

Experimental Procedure

1: Tris(trimethylsilyl)phosphane (14.5 g, 58 mmol) and isopropyl isocyanate (6.4 g, 75 mmol) were stirred in 20 mL of ether for 3 d. After removal of all volatiles under oil-pump vacuum, the residue was distilled. B.p. 38–40°C/10^{-4} torr. Yield: 16.9 g (87%, based on tris(trimethylsilyl)phosphane) of a colorless, spontaneously flammable liquid. ^1H NMR (400 MHz, C_6D_6): $\delta = 0.30$–0.33 (27 H, $Si(CH_3)_3$), 1.15 (d, 6 H, $J_{HH} = 6$ Hz, $N(CH_3)_2$), 3.98 (sept, 1 H, $^3J_{HH} = 6$ Hz, NCH); ^{13}C NMR (23 MHz, C_6D_6): $\delta = 0.9$, 1.1, 1.5 ($Si(CH_3)_3$), 24.2 (s, $(CH_3)_2$), 53.8 (d, $^3J_{CP} = 27.7$ Hz, NC), 160.1 (d, $^1J_{CP} = 43.2$ Hz, CP). ^{31}P NMR (32.4 MHz, C_6D_6, H_3PO_4 ext.): $\delta = -151.2$, -123.1. MS (70 eV, 70°C): *m/z* 335.1687 ($M^{\oplus}$).

[*] Prof. Dr. R. Appel, M. Poppe
Anorganisch-chemisches Institut der Universität
Gerhard-Domagk-Strasse 1, D-5300 Bonn 1 (FRG)

[**] Low-Coordinate Phosphorus Compounds, Part 71. Part 70: R. Appel, N. Siabalis, *Phosphorus Sulfur*, in press.

3: Finely ground NaOH (ca. 1 g) was added to a solution of **1** (7.1 g, 21 mmol) in 15 mL of tetraglyme. At the end of the reaction, the solution was deep red. All components that were volatile at room temperature were condensed under high vacuum in a trap cooled to −78°C. Repeated condensation from the trap afforded pure **3**. Yield: 2 g (56%) of a colorless liquid, b.p. 39–40°C/1.5 torr. ^{1}H NMR (90 MHz, C_6D_6): $\delta = 0.04$ (s, 9 H, $Si(CH_3)_3$), 1.13 (d, 6 H, $^3J_{HH} = 6.6$ Hz, $(CH_3)_2$), 2.7 (sept., d, 1 H, $^3J_{HH} = 6.6$ Hz, $^4J_{HH} = 2.8$ Hz, NCH). ^{13}C NMR (23 MHz, C_6D_6): $\delta = -1.47$ (s, $Si(CH_3)_3$), 21.06 (s, $(CH_3)_2$), 48.62 (d, $^3J_{CP} = 6.6$ Hz, NC), 153.9 (d, $^1J_{CP} = 18.31$ Hz, PC). ^{31}P NMR (32.4 MHz, C_6D_6, H_3PO_4 ext.): $\delta = -140$; IR (KBr, neat, selected absorption): $\tilde{\nu} = 2930$ (s), 1588 (vs), 1251 cm^{-1} (vs). MS (70 eV, 150°C): 173.0789 ($M^{\oplus}$), molecular weight (cryoscopic in benzene): 169.

5/6: **3** (560 mg, 3.2 mmol) and **4** (580 mg, 3.2 mmol) were heated together without solvent at 70°C for 45 min, resulting in the evolution of gas and the formation of **5**. ^{1}H NMR (90 MHz, C_6D_6): $\delta = 0.15$ (s, 9 H, $Si(CH_3)_3$), 1.18 (d, 6 H, $^4J_{HP} = 6.6$ Hz, $(CH_3)_2$), 2.42 (d, 3 H, $^5J_{HP} = 2$ Hz, CH_3), 3.95 (m, 1 H, NCH), 6.72 (d, 1 H, $^3J_{HP} = 2.8$ Hz, Aryl-H). ^{19}F NMR (84.6 MHz, C_6D_6, $CFCl_3$ ext.): $\delta = -66.8$ (d, $^3J_{FP} = 38.6$ Hz). ^{31}P NMR (32.4 MHz, C_6D_6, H_3PO_4 ext.): $\delta = 133.8$ (q, $^3J_{PF} = 38.6$ Hz). Compound **5** is hydrolyzed by even traces of water with cleavage of the Si-N bond to give **6**, b.p. 55°C/10^{-4} torr. Yield: 325 mg (43% based on **3**) of a yellow oil. Appropriate spectroscopic data were obtained for **6**.

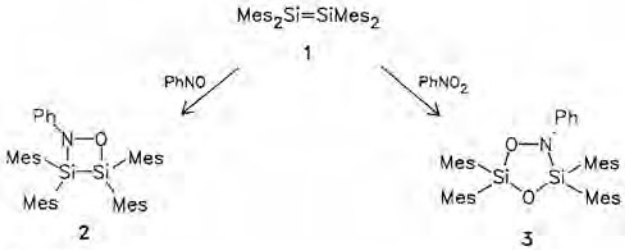
Received: July 27, 1988 [Z 2887 IE]
German version: *Angew. Chem. 101* (1989) 70

[1] a) Review: M. Regitz, P. Binger, *Angew. Chem. 100* (1988) 1541; *Angew. Chem. Int. Ed. Engl. 27* (1988) 1484; b) W. Rösch, U. J. Vogelbacher, T. Allspach, M. Regitz, *J. Organomet. Chem. 306* (1986) 39.
[2] G. Becker, G. Gresser, G. Uhl, *Z. Naturforsch. B36* (1981) 16.
[3] G. Märkl, H. Sejpka, *Tetrahedron Lett. 27* (1986) 171.
[4] T. Allspach, M. Regitz, G. Becker, W. Becker, *Synthesis 1986*, 31.
[5] G. Märkl, H. Sejpka, *Tetrahedron Lett. 26* (1985) 5507.
[6] a) T. E. Gier, *J. Am. Chem. Soc. 83* (1961) 1769; b) M. J. Hopkinson, H. W. Kroto, J. F. Nixon, N. P. C. Simmons, *Chem. Phys. 42* (1976) 460; c) NMR data for a) and b): B. Pellerini, J. M. Denis, J. Perrocheau, R. Carrié, *Tetrahedron Lett. 27* (1986) 5723; d) T. A. Cooper, H. W. Kroto, J. F. Nixon, O. Ohashi, *J. Chem. Soc. Chem. Commun. 1980*, 333; e) J. C. T. R. Burckett St. Laurent, T. A. Cooper, H. W. Kroto, J. F. Nixon, O. Ohashi, K. J. Ohno, *J. Mol. Struct. 79* (1982) 215.
[7] H. W. Kroto, J. F. Nixon, N. P. Westwood, N. P. C. Simmons, *J. Am. Chem. Soc. 100* (1978) 446; H. E. Hosseini, H. W. Kroto, J. F. Nixon, S. Brownstein, J. R. Morton, K. F. Preston, *J. Chem. Soc. Chem. Commun. 1979*, 653.
[8] R. Appel, A. Westerhaus, *Tetrahedron Lett. 22* (1981) 2159; B. Solouki, H. Bock, R. Appel, A. Westerhaus, G. Becker, G. Uhl, *Chem. Ber. 115* (1982) 3747.
[9] I. S. Matveev, *Khim. Tekhnol. 6* (1974) 49; *Khim. Prom-st. Ser.: Reakt. Osobo Chist. Veshchestva 6* (1979) 33; *Chem. Abstr. 93* (1980) 95347a.
[10] M. Regitz in *Houben-Weyl: Methoden der Organischen Chemie, Bd. E 1*, Thieme, Stuttgart 1982, pp. 23 and 25.
[11] Cf. G. Becker, J. Härer, G. Uhl, H. J. Wessely, *Z. Anorg. Allg. Chem. 520* (1985) 120.
[12] I. Ruppert, *Tetrahedron Lett. 1977*, 1987.
[13] R. Appel, M. Grosse-Bley, H. Souady, W. Steglich, *Phosphorus Sulfur 30* (1987) 757.
[14] E. Buschmann, *Dissertation*, Technische Universität Berlin 1975.

Synthesis of the Novel Ring Systems 1,2,3,4-Oxazadisiletidine and 1,3,4,2,5-Dioxazadisilolidine**

By *Gregory R. Gillette, Jim Maxka*, and *Robert West**

The reactions of disilenes[1] have led to the isolation of many novel cyclic organosilanes.[2] Here we report the reactions of tetramesityldisilene **1** (Mes = 2,4,6-$Me_3C_6H_2$) with nitrosobenzene and nitrobenzene to yield the title compounds **2** and **3**, which, to the best of our knowledge, represent the first examples of these structures for organosilicon compounds (Scheme 1).



Scheme 1.

The addition of a blue solution of nitrosobenzene in C_6D_6 to a yellow solution of **1** in the same solvent resulted in slow decolorization of the solution. A single new product was observed in the ^{29}Si-NMR spectrum having resonances at $\delta = 27.2$ and 9.75.[3] The colorless solid obtained after work-up gave spectral data consistent with the structure of the [2+2] cycloadduct **2**.[4] To further characterize **2** an INEPT-INADEQUATE ^{29}Si-NMR experiment was conducted to determine the coupling constant between the two nonequivalent silicon atoms.[5] The spectrum obtained for **2** is shown in Figure 1 (top). The value of 108 Hz for the coupling constant in **2** is larger than the usual 80–90 Hz for $^1J_{Si-Si}$ in organodisilanes and implies a larger amount of s character in the Si–Si bond of **2** than is found in typical disilanes. The $^1J_{Si-Si}$ of **2** is similar to that for the isoelectronic 1,2-dioxadisiletane[6] and may be indicative of unusual bonding in these ring systems.

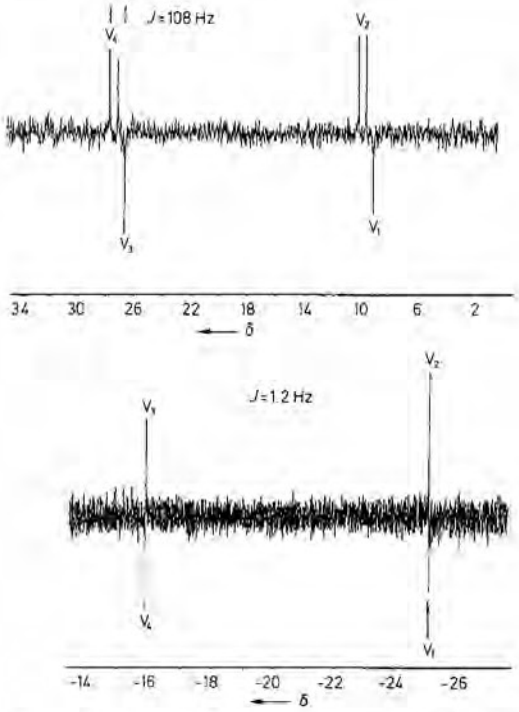


Fig. 1. Top: INEPT-INADEQUATE ^{29}Si-NMR spectrum for **2**, $J = 108$ Hz. Bottom: INEPT-INADEQUATE ^{29}Si-NMR spectrum of **3**, $J = 1.2$ Hz.

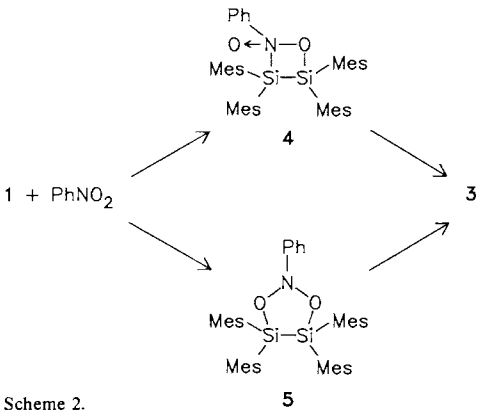
Addition of nitrobenzene to a solution of **1** in C_6D_6 resulted in immediate decolorization of the yellow solution. Analysis of the solution by ^{29}Si-NMR spectroscopy showed that only one product was formed with ^{29}Si resonances at $\delta = -15.8$ and -24.9. The colorless solid obtained after work-up gave analytical data consistent with structure **3**,[7] although the *N*-oxide **4** could not be excluded.[8] The INEPT-INADEQUATE ^{29}Si-NMR spectrum of the product is shown in Figure 1 (bottom). The ob-

[*] Prof. Dr. R. West, Dr. G. R. Gillette, Dr. J. Maxka
Department of Chemistry, University of Wisconsin
Madison, WI 53706 (USA)

[**] Dedicated to Professor *Hans Bock* on the occasion of his 60th birthday. This work was supported by the Air Force Office of Scientific Research Air Force Systems Command, USAF (contract No. F49620-86-0010) and by the 3M Company.

served value of 1.2 Hz for the coupling constant is in the range of known $^2J_{(Si-O-Si)}$ values (1–4 Hz)[9] and is consistent with structure **3**. As further proof of the structure **3**, we found that **2**, when oxidized with 1 equiv. of *m*-chloroperbenzoic acid at −78 °C also yields **3**.

With the structure of **3** established as the 1,3,4 isomer, the question remains as to how it is formed. Two possible pathways can be envisioned (Scheme 2): a [2+2] cycloaddition of $PhNO_2$ with **1** would lead to the *N*-oxide **4**, while



Scheme 2.

[3+2] addition would lead to the 1,3,2-dioxazolidine isomer **5**. Preliminary studies of the reaction at low temperature indicate that **5** may be a precursor to **3**.[10] Further studies are necessary in order to determine the mechanism of this rearrangement.[11]

Received: August 24, 1988 [Z 2940 IE]
German version: *Angew. Chem. 101* (1989) 90

[1] R. West, M. J. Fink, J. Michl, *Science (Washington, DC) 214* (1981) 1343.

[2] For reviews of disilenes see: R. West, *Angew. Chem. 99* (1987) 1231; *Angew. Chem. Int. Ed. Engl. 26* (1987) 1201; G. Raabe, J. Michl, *Chem. Rev. 85* (1985) 419; R. West, *Pure Appl. Chem. 56* (1984) 163.

[3] All spectra were recorded on a Bruker AM 360 (71.55 MHz for ^{29}Si) spectrometer using either the INEPT or INEPT-INADEQUATE pulse sequences and complete proton decoupling. Chemical shifts (δ-values) are reported in ppm from a tetramethylsilane external reference.

[4] Experimental procedure for **2**: A solution of nitrosobenzene (50 mg, 0.46 mmol) in 1 mL C_6D_6 was added to a solution of **1** (250 mg, 0.46 mmol) in 1 mL C_6D_6. The yellow solution slowly decolorized after addition. The benzene was removed in vacuo and the residue was recrystallized from hexane (5 mL) to yield the colorless solid **2**. Yield: 176 mg (59%), m.p. 280–284 °C; correct elemental analyses. MS: calcd. ($M^{\oplus}$) 639.3340, found 639.3347 (2.45%); ^1H-NMR (270 MHz, C_6D_6): δ = 7.85 (d, 2H), 7.38 (d, 1H), 7.30 (t, 2H), 6.84 (s, 4H), 6.82 (s, 4H), 2.73 (s, 12H), 2.61 (s, 12H), 2.28 (s, 6H), 2.24 (s, 6H).

[5] For a discussion of the INEPT-INADEQUATE experiment as applied to ^{29}Si NMR, see: H. B. Yokelson, A. J. Millevolte, B. R. Adams, R. West, *J. Am. Chem. Soc. 109* (1987) 4116.

[6] M. J. Michalczyk, R. West, J. Michl, *J. Chem. Soc. Chem. Commun. 1984*, 2525–26. The magnitude of $^1J_{Si-Si}$ for 1,2-dioxadisiletanes ranges from 96–98 Hz.

[7] Experimental procedure for **3**: To a solution of **1** (400 mg, 0.75 mmol) in C_6D_6 at room temperature was added 76 µL (0.75 mmol) of nitrobenzene. The yellow solution immediately decolorized upon addition. The benzene was removed in vacuo and the residue was recrystallized from hexane to yield the colorless solid **3**. Yield: 310 mg (63%), m.p. 257–260 °C; correct elemental analyses; MS: calcd. ($M^{\oplus}$) 655.3289, found 655.3322 (100%); ^1H NMR ($CDCl_3$): δ = 7.08 (t, 2H), 6.86 (d, 2H), 6.72 (t, 1H), 6.69 (s, 4H), 6.68 (s, 4H), 2.28 (s, 12H), 2.23 (s, 6H), 2.20 (s, 6H), 2.06 (s, 12H).

[8] The IR spectrum did not distinguish unambiguously between **3** and **4**.

[9] G. Pfisterer, H. Dreeskamp, *Ber. Bunsenges. Phys. Chem. 73* (1969) 654; R. K. Harris, B. J. Kimber, *J. Magn. Reson. 17* (1975) 174.

[10] Reaction of **1** with 1 equiv. of $PhNO_2$ at −50 °C yields one new product according to ^{29}Si NMR having a resonance of δ = 0.64 (C_7D_8). After the solution is warmed to room temperature the peak at +0.64 ppm vanishes and is replaced by two new peaks at δ = −15.8 and −24.9, the same chemical shifts as were found for **3**.

[11] Recently we have learned, by private communication from Prof. *M. Weidenbruch*, that the addition of an isocyanate to tetra-*tert*-butyldisilene proceeds with a similar rearrangement to give an analogous five-membered ring product. Editorial note: see M. Weidenbruch, B. Flintjer, S. Pohl, W. Saak, *Angew. Chem. 101* (1989) 89; *Angew. Chem. Int. Ed. Engl. 28* (1989) 95.

$[(Me_3Si)_2CHGe]_6$, the First Hexagermaprismane**

By *Akira Sekiguchi, Chizuko Kabuto,* and *Hideki Sakurai**

Dedicated to Professor Hans Bock on the occasion of his 60th birthday

Highly symmetrical polyhedral alkanes, such as tetrahedrane, cubane and prismane, have been the subject of considerable interest because of their unusual physical and chemical properties.[1] The synthesis of polyhedranes consisting of framework of atoms other than carbon is also intriguing as a challenging synthetic target as well as from being of theoretical interest. Theoretical calculations, limited to polyhedral silicon compounds at present, suggest that hexasilaprismane is the most stable valence isomer of H_6Si_6.[2] The replacement of the silicon atoms by germanium, should not alter this situation.[2] In this respect, it was of particular interest to prepare silicon or germanium analogues of prismane. We describe herein the synthesis of the first hexagermaprismane, **2**, as well as its X-ray crystal structure analysis.

For the synthesis of strained molecules, such as hexagermaprismane, it is of prime importance to choose an appropriate protecting group. After several unsuccessful attempts, we have found the bis(trimethylsilyl)methyl group to be best suited for hexagermaprismane [Eq. (a)]. A solu-

$$\underset{\mathbf{1}}{(Me_3Si)_2CHGeCl_3} \xrightarrow[Li]{THF} \underset{\mathbf{2}}{[(Me_3Si)_2CHGe]_6} \qquad (a)$$

tion of bis(trimethylsilyl)methyltrichlorogermane **1** (2035 mg, 6.02 mmol) in THF (20 mL) was added dropwise to a stirred suspension of lithium powder (153 mg, 21.9 mmol) in THF (10 mL) at −78 °C under argon.[3] The color of the solution turned deep dark-brown. The reaction mixture was stirred for an additional 6 h at −78 °C and then overnight at room temperature. The reaction mixture was concentrated and then carefully chromatographed on silica gel with hexane (R_f = 0.75), to afford yellow-orange crystals of the hexagermaprismane **2** (166 mg, 12%). After isolation and purification, the prismane **2** was unexpectedly stable to atmospheric oxygen and moisture, although it partially decomposed upon heating to 200 °C.

The prismane structure of **2** was deduced on the basis of the following spectroscopic properties: the FD mass spectrum contained the $M^{\oplus}$ cluster in the range *m/z* 1388–1402 in agreement with that calculated for $C_{42}H_{114}Si_{12}Ge_6$. The molecular weight was determined as 1375 (calcd. 1390.8) by vapor pressure osmometry. Correct elemental analyses were also obtained. The ^1H, ^{13}C and ^{29}Si NMR spectra are fully consistent with the highly symmetrical structure: ^1H NMR (200 MHz, C_6D_6): δ = 0.62 (s, 18H, $SiMe_3$), 1.37 (s,

[*] Prof. Dr. H. Sakurai, Dr. A. Sekiguchi, Dr. C. Kabuto
Department of Chemistry, Faculty of Science
Tohoku University
Sendai 980 (Japan)

[**] Chemistry of Organosilicon Compounds, Part 252.—Part 251: H. Sakurai, K. Ebata, K. Sakamoto, Y. Nakadaira, C. Kabuto, *Chem. Lett. 1988*, 965.

1H, Si_2CHGe); ^{13}C NMR (50 MHz, C_6D_6): $\delta = 4.08, 29.8$; ^{29}Si NMR (40 MHz, C_6D_6): $\delta = -1.95$.

An absorption maximum at 280 nm ($\varepsilon = 3.22 \times 10^4$, hexane), tailing into the visible region (~ 500 nm), was observed in the electronic spectrum. The prismane **2** exhibits thermochromism. Crystals of **2** reversibly change color from pale yellow at -196 °C to intense orange at 200 °C.

The X-ray structure determination unequivocally established the prismane structure of **2** (Fig. 1). Because of a limited data set, there is some uncertainty in the positions of the methyl substituents.[4] However, the prismane structure consisting of six germanium atoms was determined with sufficient accuracy to discuss its geometrical features.

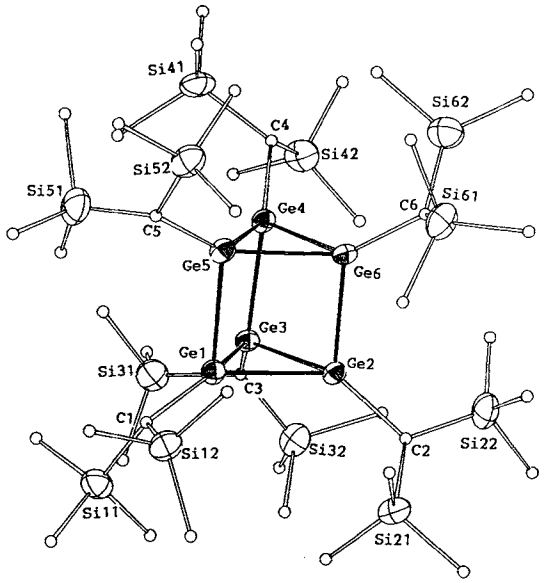


Fig. 1. Crystal structure of **2** (ORTEP). Selected bond lengths [Å] and angles [°]: Ge1-Ge2 2.584(6), Ge1-Ge3 2.580(6), Ge2-Ge3 2.580(5), Ge4-Ge5 2.579(6), Ge4-Ge6 2.579(5), Ge5-Ge6 2.578(6), Ge1-Ge5 2.526(6), Ge2-Ge6 2.516(6), Ge3-Ge4 2.523(4); Ge2-Ge1-Ge3 60.0(1), Ge1-Ge2-Ge3 60.0(1), Ge1-Ge3-Ge2 60.1(1), Ge5-Ge4-Ge6 60.0(2), Ge4-Ge5-Ge6 60.0(2), Ge4-Ge6-Ge5 60.0(2), Ge2-Ge1-Ge5 89.9(2), Ge3-Ge1-Ge5 88.5(2), Ge1-Ge2-Ge6 89.8(2), Ge3-Ge2-Ge6 91.4(1), Ge1-Ge3-Ge4 91.4(2), Ge2-Ge3-Ge4 88.5(2), Ge3-Ge4-Ge5 88.6(2), Ge3-Ge4-Ge6 91.2(2), Ge1-Ge5-Ge4 91.3(2), Ge1-Ge5-Ge6 89.7(2), Ge2-Ge6-Ge4 88.7(2), Ge2-Ge6-Ge5 90.3(2).

The molecule has D_{3h} symmetry. The prismane skeleton is constructed from two regular triangles (Ge-Ge 2.578(6)–2.584(6) Å, av. 2.58 Å and Ge-Ge-Ge 60.0(2)–60.1(1)°, av. 60°) and three regular squares (Ge-Ge 2.516(6)–2.526(6) Å, av. 2.52 Å and Ge-Ge-Ge 88.5(2)–91.4(2)°, av. 90°). All the Ge-Ge bonds are considerably longer than the Ge-Ge bond lengths in other polygermanes (2.374–2.465 Å). It is surprising that the bond lengths in the triangles are longer than those in the squares, since calculations for C and Si prismanes have predicted the opposite trend[2] as was found in the structures of the carbon analogues.[5]

Received: August 24, 1988 [Z 2939 IE]
German version: *Angew. Chem. 101* (1989) 97

[1] A. Greenberg, J. F. Liebman: *Strained Organic Molecules*, Academic Press, New York 1978.

[2] a) S. Nagase, T. Kudo, M. Aoki, *J. Chem. Soc. Chem. Commun. 1985*, 1121; b) A. F. Sax, R. Janoschek, *Phosphorus Sulfur 28* (1986) 151; c) A. F. Sax, R. Janoschek, *Angew. Chem. 98* (1986) 634; *Angew. Chem. Int. Ed. Engl. 25* (1986) 651; d) S. Nagase, M. Nakano, T. Kudo, *J. Chem. Soc. Chem. Commun. 1987*, 60; S. Nagase, H. Teramae, T. Kudo, *J. Phys. Chem. 86* (1987) 4513; A. F. Sax, J. Kalcher, R. Janoschek, *J. Comput. Chem. 9* (1988) 564.

[3] Compound **1** was prepared by the reaction of bis(trimethylsilyl)methylmagnesium chloride with tetrachlorogermane in ether in 80% yield. B.p. = 112–115 °C/10 torr; ^1H NMR ($CDCl_3$): $\delta = 0.40$ (s, 18H, $SiMe_3$), 1.07 (s, 1H, Si_2CHGe); MS: m/z 323 ($M^{\oplus} - Me$); Correct CH-analyses.

[4] Fairly good crystals were obtained from a hexane/ethanol solution. The crystals belong to the orthorhombic space group *Imm*2 ($Z = 4$). However, the crystals contained hexane and became opaque immediately upon loss of solvent. Even when the crystal was sealed in a glass capillary under an atmosphere saturated with solvent, data collection was not possible. Crystals for X-ray analysis were obtained from benzene/ethanol solution. Although most of the crystals were twinned, we were able to find one single crystal of size $0.1 \times 0.1 \times 0.3$ mm. Since the crystal gradually decomposed in the X-ray beam, the data were measured at a high speed ($2\theta - \omega$ scan mode, ω-scan speed 8°/min) on a Rigaku AFC5-R diffractometer with a rotating anode (50 kV, 200 mA) using graphite monochromatized $Mo_{K\alpha}$ radiation. A total of 3016 reflections within $2\theta = 30°$ with significant intensity were collected. The direct structure determination was rather complicated because of the pseudosymmetry about the Ge atom positions on the crystal axes as well as insufficient data. The correct solution was finally obtained by combining use of the Negative Quartet Invariant method. The final R factor was 0.084 for 1966 reflections with $F_0 \geq 3\sigma(F_0)$ ($R = 0.098$ for all reflections). Crystal data of **2**: $C_{42}H_{114}Si_{12}Ge_6$, $M_r = 1390.8$, $a = 22.456(5)$, $b = 25.858(8)$, $c = 13.042(7)$ Å, $\beta = 102.30(3)°$, $V = 7399.2(52)$ Å^3, space group $P2_1/n$, $Z = 4$, $\rho_{calcd} = 1.25$ g/cm^3, $Mo_{K\alpha} = 25.9$ cm^{-1}. Further details of the crystal structure investigation can be obtained from the Fachinformationszentrum Energie, Physik, Mathematik, D-7514 Eggenstein-Leopoldshafen 2, on quoting the depository number CSD-53423, the names of the authors, and the journal citation.

[5] a) R. R. Karl, Y. C. Wang, S. H. Bauer, *J. Mol. Structure 25* (1975) 17. b) G. Maier, I. Bauer, U. Huber-Patz, R. Jahn, D. Kallfass, H. Rodewald, H. Irngartinger, *Chem. Ber. 119* (1986) 1111. c) H. Wingert, G. Maas, M. Regitz, *Tetrahedron 42* (1986) 5341. d) H. Irngartinger, D. Kallfass, E. Litterst, R. Gleiter, *Acta Crystallogr. C43* (1987) 266. e) R. Srinivasan, Y. Hu, M. F. Farona, E. A. Zarate, W. J. Youngs, *J. Org. Chem. 52* (1987) 1167.

K_4P_3, a Compound Containing the Radical Anion $P_3^{4\ominus}$ **

By *Hans Georg von Schnering,* Martin Hartweg, Ute Hartweg,* and *Wolfgang Hönle*

Dedicated to Professor Hans Bock on the occasion of his 60th birthday

The alkali metals M form many compounds with phosphorus, which exhibit differing structures and properties[1] and have been particularly well characterized for $M : P \leq 1$. As early as 1956, however, there was evidence, from the work of *Korte* and *Klemm*,[2,3] for the existence of other well-defined compounds between K_3P and KP although they could not be unambiguously identified. This is due, to a considerable extent, to the exceptional stability of yellow K_3P_7,[4] which is the only detectable intermediate in the thermal decomposition of K_3P. We have now synthesized and characterized one of the intermediate phases, the compound K_4P_3.

Sufficient quantities of pure K_4P_3 are obtained only if an excess of potassium is used in the synthesis from the elements (K, P_{red}, $K : P = 1.5$–2.0; 400 °C, Nb- or Solidex ampoule; glove box with integrated gas purification; < 0.1 ppm H_2O; < 1 ppm O_2). Although the crystals of K_4P_3 are partly embedded in potassium or in green-reflecting K_3P

[*] Prof. Dr. H. G. von Schnering, Dr. M. Hartweg, Dipl.-Chem. U. Hartweg, Dr. W. Hönle
Max-Planck-Institut für Festkörperforschung
Heisenbergstrasse 1, D-7000 Stuttgart 80 (FRG)

[**] Chemistry and Structural Chemistry of Phosphides and Polyphosphides, Part 50. This work was supported by the Fonds der Chemischen Industrie. We thank Prof. Dr. *H. C. Wolf* (ESR), Dr. *R. Kremer* (SQUID-magnetometer), Dr. *K. Peters* (X-ray data) and Dr. *M. Somer* (IR), all Stuttgart, for the measurements.—Part 49: G. Fritz, H.-W. Schneider, W. Hönle, H. G. von Schnering, *Z. Naturforsch. B43* (1988) 561.

after the reaction, they can be easily isolated by mechanical separation. For K : P ratios of ca. 1.5, another phase, in addition to K_4P_3, is produced as a black, micro-crystalline powder, from which K_4P_3 can also be readily separated. Up to now, stoichiometric reactions have led to mixtures of other phases. This explains why marked quantities of K_4P_3 are observed, in almost all cases, in the synthesis of K_3P. The excess alkali metal is apparently necessary to compensate for the high decomposition pressure and losses through reaction with the wall of the reaction vessel.

K_4P_3 forms blue-black, metallically gleaming platelets, which are very air- and moisture-sensitive. **Caution**: reaction products having K : P > 1 have a tendency to undergo **explosive decomposition** upon grinding even under an inert atmosphere with the formation of a potassium mirror on the wall of the mortar. This tribochemical reactivity increases with aging of the product under the influence of light. Samples, which have been carefully sealed in Schlenk-tubes, often explode after several weeks of storage. Whether these properties are attributable to K_4P_3 or to traces of other compounds is, as yet, unclear. However, the electronic structure of K_4P_3 suggests that it is responsible for this behavior.

The crystal structure of K_4P_3 was determined from single crystal data.[5] K_4P_3 crystallizes in the W_3CoB_3 type of structure[6] (Fig. 1). Characteristic is the bent P_3-chain with relatively short bond lengths (d_{P-P} = 218.3 pm) and a large

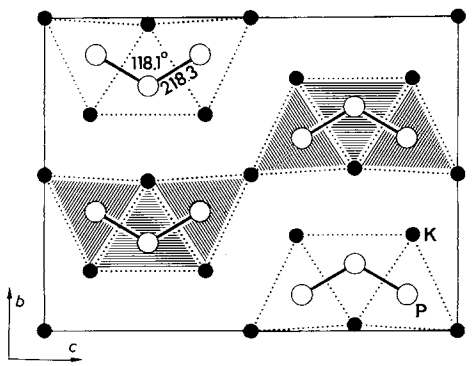


Fig. 1. Projection of the K_4P_3 structure on (100). The hatched structural units are displaced by $a/2$ with respect to each other. d_{P-P} in pm.

bond angle (P-P-P = 118.1°) (compare, e.g., $P_3^{5\ominus}$ in LaP_2: 222.0 pm/107.5°[7]). Each P atom lies in the center of a trigonal prism built up of 6 K atoms with tricapped rectangular faces, such that the terminal P atoms are coordinated by 8K + 1P and the central P atom by 7K + 2P (d_{K-P} = 332.1–336.3 pm). Figure 1 shows the characteristic condensation of three prisms and their further connection to form a two-dimensional, infinite, corrugated, layered structure. Noteworthy is the relationship with the structure of K_4P_6,[8] in which trigonal prismatic coordinated P atoms are assembled as isolated $P_6^{4\ominus}$ rings. According to the simple electron-transfer model of *Zintl* and *Klemm*,[9] K_4P_3 contains the 19-valence electron $P_3^{4\ominus}$ radical anion. It is the first triatomic 19-electron system, without the involvement of a second-row element, to be isolated and is isoelectronic and topologically directly comparable to $S_3^{\ominus}$, ClO_2 and the $O_3^{\ominus}$ radical of the alkali metal ozonides.[10] The tribochemical lability mentioned above is consistent with this picture.

The expected paramagnetism of K_4P_3 could be detected. The temperature dependence is, however, complex and does not follow the simple Curie-Weiss law (Fig. 2), un-

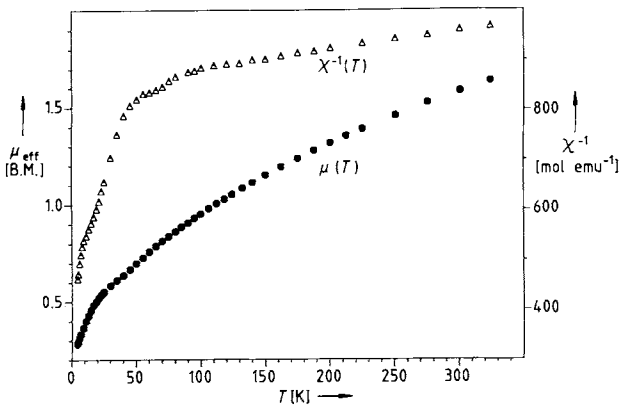


Fig. 2. Variation of the reciprocal magnetic susceptibility χ^{-1} (△) and the effective magnetic moment μ_{eff} (●) with temperature T.

like, for example, the above-mentioned ozonides.[10] At 300 K, an effective magnetic moment of $\mu = 1.6$ B.M. is attained but the temperature dependence of the curve does not lead one to expect a convergence at the expected value for $S = 1/2$ ($\mu = 1.74$ B.M.). On the contrary, the dependence of the reciprocal magnetic susceptibility χ^{-1} upon the temperature T shows a gradient typical for a doublet state ($S = 1/2$) only in the range $50 < T < 100$ K. Above 100 K, χ^{-1} exhibits, with good precision, the behavior of a quartet state ($S = 3/2$). Initial quantum mechanical calculations[11] (Hartree-Fock, SCF) show that the lowest-lying doublet and quartet states have almost the same energy so that a $^2\Gamma \rightarrow {}^4\Gamma$ excitation seems to be possible even at low temperatures. The first doublet-doublet transition is expected at ca. 10000 cm^{-1}. ESR measurements (300 K, powder sample, 0.2 mg) showed a signal at $g = 2.02$ with linewidth ca. 80 G but with only 15–20% of the expected intensity (cf. $S_3^{\ominus}$: $g = 2.028$; 160 G[12]). The loss of intensity could be explained either by the occurrence of a quartet state or by high electrical conductivity. Because of the extreme sensitivity of the compound one can not exclude the possibility of a partial decomposition of the substance, particularly upon weighing out small quantities. For this reason, quantitative statements will have to await the results of further investigations.

Two of the three possible normal vibrations of the P_3 moiety are observed in the FIR spectrum at 300 K, the asymmetric stretch at 438 cm^{-1} and the deformation at 163 cm^{-1}. This represents a shift of ca. 30–40 cm^{-1} to higher wave numbers compared with other P-P stretching frequencies which is in accord with the increased P-P bond-order.

Received: September 7, 1988 [Z 2958 IE]
German version: *Angew. Chem. 101* (1989) 98

[1] H. G. von Schnering, W. Hönle, *Chem. Rev. 88* (1988) 243.
[2] D. Korte, *Diplomarbeit*, Universität Münster 1956; *Dissertation*, Universität Münster 1960.
[3] W. Klemm, *Proc. Chem. Soc. (London) 1958*, 329; *Trab. Reun. Int. React. Sólidos, 3rd, 1956*, Vol. 1, p. 447.
[4] R. P. Santandrea, Ch. Mensing, H. G. von Schnering, *Thermochim. Acta 98* (1986) 301.
[5] Crystal structure data: K_4P_3; $M_r = 249.33$; $a = 504.9(1)$; $b = 1119.7(2)$; $c = 1478.8(3)$ pm; space group *Cmcm* (No. 63); $Z = 4$; $V = 125.84$ cm^3

mol^{-1}; $\rho_{calcd} = 1.981$ g cm^{-3}; measurement: Syntex P3 four-circle diffractometer, graphite monochromator, scintillation counter, $3.5° < 2\theta < 55.0'$, ω-scan, variable scan speed dependent on I, 296 K; $Mo_{K\alpha}$ radiation; ψ-scan; seven reflections hkl, program SHELX76, direct methods, least squares refinement, full matrix, 27 variables; $N(hkl) = 577$, 418 with $I > 3\sigma(I)$; $R_{iso} = 0.042$, $R_{aniso} = 0.032$. Further details of the crystal structure determination can be obtained from the Fachinformationszentrum Energie, Physik, Mathematik GmbH, D-7514 Eggenstein-Leopoldshafen 2, on quoting the depository number CSD-53310, the names of the authors and the journal citation.

[6] H. Jedlicka, F. Benesovsky, H. Nowotny, *Mh. Chemie 100* (1969) 844.

[7] H. G. von Schnering, W. Wichelhaus, M. Schulze Nahrup, *Z. Anorg. Allg. Chem. 412* (1975) 193.

[8] H.-P. Abicht, W. Hönle, H. G. von Schnering, *Z. Anorg. Allg. Chem. 519* (1984) 7.

[9] Compare: H. Schäfer, B. Eisenmann, W. Müller, *Angew. Chem. 85* (1973) 742; *Angew. Chem. Int. Ed. Engl. 12* (1973) 694; H. G. von Schnering, *ibid. 93* (1981) 44 and *20* (1981) 33; H. Schäfer, *Annu. Rev. Mater. Sci. 15* (1985) 1.

[10] W. Schnick, M. Jansen, *Angew. Chem. 97* (1985) 48; *Angew. Chem. Int. Ed. Engl. 24* (1985) 54; M. Lueken, M. Deussen, M. Jansen, U. Hesse, W. Schnick, *Z. Anorg. Allg. Chem. 553* (1987) 179.

[11] U. Wedig, Stuttgart, unpublished results.

[12] F. Seel, H. J. Guettler, *Z. Naturforsch. B 30* (1975) 88.

$Na_xMg_{5-x}Ga_9$, a New Intermetallic Phase as a Link Between Zintl Phases and Metals

By *Reinhard Nesper**

Dedicated to Professor Hans Bock on the occasion of his 60th birthday

Binary compounds of the alkali metals with the elements of group 13 such as NaTl belong to the classical Zintl phases,[1] i.e., they are compounds with defined compositions.

In contrast, the ternary compounds of the alkali or alkaline earth metals with group 13 elements often exhibit a phase width, with which the dependence of bonding relationships upon the valence-electron number can be studied. The binary phases NaGe,[2] Na_7Ga_{13},[2,3] $Na_{22}Ga_{39}$,[4] Mg_5Ga_2,[5] Mg_2Ga,[6] MgGa,[7] $MgGa_2$[8] and $MgGa_5$[9] are known border members of the ternary system Na/Mg/Ga. In the course of systematic studies of this system, we have discovered the new ternary compound $Na_xMg_{5-x}Ga_9$, which is not a derivative of the binary phases. The compound exhibits, typical for intermetallic compounds, a phase width $2 \leq x \leq 3$.

The synthesis was carried out by heating a mixture of the pure elements in welded niobium ampoules to 1100 K and then cooling over a period of 24 h. The product has a metallic luster and is both air- and moisture-sensitive. The compound is not ductile but hard and brittle, resembling in this respect the classical valence compounds and Zintl phases. The compound exhibits, however, a specific resistance of $\rho(300\ K) \simeq 10\ \Omega$ cm, which lies within the range of resistances found for metals and increases with rising temperature. $Na_xMg_{5-x}Ga_9$ gives an X-ray powder pattern which is distinctly different from those of the binary phases $NaGa_4$, Na_7Ga_{13}, $Na_{22}Ga_{39}$, MgGa and $MgGa_2$. Single-crystal photographs show predominantly the Laue symmetry $6/mmm$ (Table 1), which is modulated by composition-dependent superstructures.

$Na_xMg_{5-x}Ga_9$ crystallizes in a new structure type, in which the Ga-atoms form a three-dimensional framework of linked icosahedra and Friauf polyhedra (truncated tetrahedra, cf. Fig. 1). These two types of polyhedron are typical for intermetallic phases. The Ga framework is not significantly influenced by the superstructure and the cation positions within the framework are all localized unambiguously. The mean distances between the Ga atoms of the icosahedra are similar (2.69–2.73 Å), while that of Ga5 in the Friauf polyhedra is ca. 0.1 Å longer (2.81 Å). Although these distances are somewhat longer than the sum of the covalent radii ($2r_{cov} = 2.52$ Å), quantum mechanical calculations have shown that this effect does not necessarily lead to the loss of countable local bonds. In related aluminides, whose electronic structures follow, to a large extent, the valence rules according to quantum mechanical calculations,[10] bonds which are about 0.2 Å longer than $2r_{cov}$ are also found.

The superstructure results essentially from changes in the region of the six-fold tube. A further Ga atom is located here, which is terminally bound to the icosahedron and shows a significant elongation of its electron density (Fig. 2). This nonuniformity can be well described by three different Ga positions (Ga1, Ga1′ and Ga1″), each of which is bound in a different manner to the neighboring Ga atoms. Thus, by combination of the positions Ga1, Ga1′ and Ga1″, limiting cases for the local chemical bonding can be

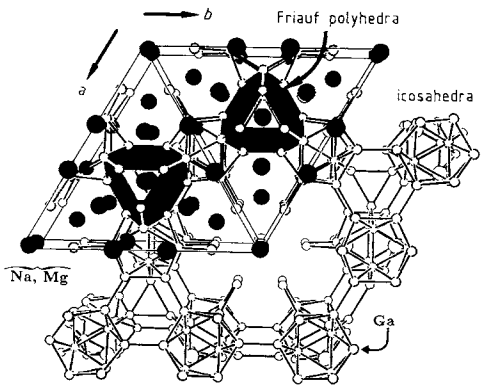


Fig. 1. Projection of the hexagonal structure of $Na_xMg_{5-x}Ga_9$ along the c-axis [14]: Ga, open circles; Na, Mg, full circles; Friauf polyhedra, black; metal atoms outside of the unit cell are not shown.

Table 1. $Na_xMg_{5-x}Ga_9$; structural parameters: space group $P6/mmm$-D_{6h}^1 (No. 191), $Z = 6$, $a = 15.43(1)$, $c = 8.998(6)$ Å; single-crystal structure solution: four-circle diffractometer, 461 reflections hkl, $R_w(aniso) = 0.056$ [13]. The relatively large standard deviations of the occupation factors of the split positions are attributed to strong correlation of the closely-neighboring positions in the structure refinement. This does not, however, alter the fact that split positions are present.

Atom	Position	x	y	z	$U_{iso/equi}$	Occupancy
Ga1	12(n)	0.2062	0	0.2000	315(26)	0.72(14)
Ga1′	12(n)	0.2000	0	0.1600	315(26)	0.18(14)
Ga1″	12(n)	0.168(5)	0	0.2300	315(26)	0.10(14)
Ga2	12(n)	0.353(1)	0	0.3600	219(18)	0.58(2)
Ga2′	12(n)	0.351(2)	0	0.3300	219(18)	0.42(2)
Ga3	12(q)	0.4911(4)	0.1596(4)	1/2	101(26)	1
Ga4	12(o)	0.4501(2)	0.9002(4)	0.2578(8)	196(21)	1
Ga5	6(l)	0.3958(3)	0.7915(6)	0	98(32)	1
M1	2(e)	0	0	0.260(3)	722(230)	0.12(10)
M1′	2(e)	0	0	0.340(3)	722(230)	0.88(10)
M2	6(m)	0.130(1)	0.261(2)	1/2	218(119)	1
M3	12(o)	0.2088(7)	0.418(1)	0.191(2)	299(89)	1
M4	6(j)	0.387(2)	0	0	343(134)	1
M5	4(h)	1/3	2/3	0.306(4)	212(117)	1

[*] Dr. R. Nesper
Max-Planck-Institut für Festkörperforschung
Heisenbergstrasse 1, D-7000 Stuttgart 80 (FRG)

formulated, in which one, two or three bonds per Ga atom are attained (Ga1, one bond: Ga1-Ga2; Ga1′, two bonds: Ga1′-Ga1′, -Ga1′; Ga1″, three bonds: Ga1″-Ga1″, -Ga1″, -Ga2′; cf. Fig. 2). Mean distances of 2.60–2.83 Å are also obtained for these limiting cases.

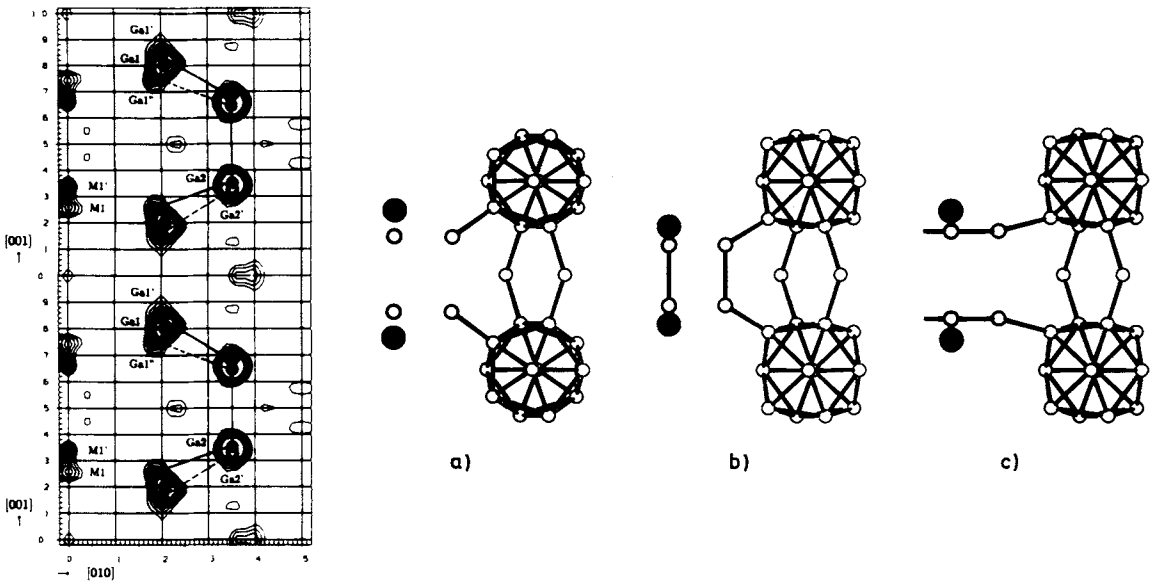


Fig. 2. Electron density of the plane (0*yz*). The distribution of the electron density of Ga1 can be described by three positions, which have bond orders of one, two and three to the neighboring Ga atoms (cf. a, b, c; Ga: open circles; Na, Mg: full circles).

The differentiation between Na and Ga exclusively on the basis of the crystallographic data is, in this case, not possible. The distances M–Ga lie in the range 3.2 to 3.5 Å and give coordination numbers of 10 to 12 for all M atoms except for M1 and M1′, which have only six neighbors. A decision between Na–Ga and Mg–Ga contacts is not possible on this basis. If one, however, sets the requirement that the balance of charge between the Ga polyanions and the cations has to be satisfied locally as is found, for example, in Zintl phases, then all the positions cannot be occupied by Mg atoms. In order to analyze the electron balance using the Zintl-Klemm concept,[11] the icosahedra were treated as *closo*-polyhedra as described by *Wade*.[12] The icosahedron is coordinated in the first coordination sphere by four metal atoms, only half of which are at its disposal ($M_{4/2}Ga_{12}^{2\ominus}$). The X_{12} framework of the Friauf polyhedron can be understood in terms of classical, two-electron two-center bonds.[10] Since the polyhedron is linked to three icosahedra, only three Ga-atoms, each of them four-bonded, remain per formula unit. They are not part of the icosahedra. Accordingly, the following electron balance can be written for the basic framework:

$$6\,Na^{\oplus} + 1.5\,Ga_{12}^{2\ominus\ \text{icosahedron}} + 3\,Ga^{\ominus\ \text{Friauf}}$$

The charge required for the basic framework is already satisfied by six of the metal positions even if these are occupied only by Na atoms. A variable charge for the remaining atoms (Na or Mg) can only be compensated on the local level by the bond order of Ga1 (Ga1′, Ga1″).

A further metal position (M1) lies in the center of the large tube and is a direct neighbor of Ga1. Depending on the occupancy of this position (Na or Mg), Ga1, Ga1′ and Ga1″ receive differing amounts of transferred charge, to which the different bonding situations are correlated. Consequently, Ga1 can be formulated as a 7e-, 6e- or 5e-species according to (1b)$Ga^{4\ominus}$, (2b)$Ga^{3\ominus}$ and (3b)$Ga^{2\ominus}$. The observed displacements of the electron density with formation of the superstructure(s) indicate those positions which represent different bonding situations.

The phase width of $Na_xMg_{5-x}Ga_9$ includes the formulas with $2 \le x \le 3$, as revealed in this structural chemical study. $Na_xMg_{5-x}Ga_9$ possesses the typical properties (silver metallic luster, electrical conductivity) and the typical structural building blocks of intermetallic phases. Nevertheless, its bonding can be understood in terms of classical valence rules and the Zintl-Klemm concept.[11] These findings are supported by experimental and quantum mechanical studies of related ternary aluminides.[10]

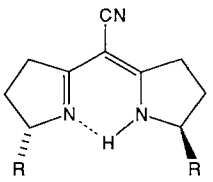
Submitted: September 13, 1988 [Z 2964 IE]
German version: *Angew. Chem. 101* (1989) 99

[1] E. Zintl, J. Goubeau, W. Dullenkopf, *Z. Phys. Chem. A 154* (1931) 1; E. Zintl, A. Harder, *ibid. A 154* (1931) 47; E. Zintl, W. Dullenkopf, *ibid. B 16* (1932) 183; E. Zintl, H. Kaiser, *Z. Anorg. Allg. Chem. 211* (1933) 113.
[2] U. Frank-Cordier, G. Cordier, H. Schäfer, *Z. Naturforsch. B 37* (1982) 119; G. Bruzzone, *Acta Crystallogr. B 25* (1969) 1206.
[3] Sh. R. Zhakupov, *Russ. J. Phys. Chem. 54* (1980) 584.
[4] U. Frank-Cordier, G. Cordier, H. Schäfer, *Z. Naturforsch. B 37* (1982) 127; R. G. Ling, C. Belin, *Acta Crystallogr. B 38* (1982) 1101.
[5] K. Schubert, K. Frank, R. Gohle, A. Maldonado, H. G. Meissner, A. Raman, W. Rossteutscher, *Naturwissenschaften 50* (1963) 41.
[6] K. Frank, K. Schubert, *J. Less-Common Metals 20* (1970) 215.
[7] K. Schubert, F. Gauzzi, K. Frank, *Z. Metallkd. 54* (1963) 422.
[8] G. S. Smith, K. F. Mucker, Q. Johnson, D. H. Wood, *Acta Crystallogr. B 25* (1969) 549.
[9] B. Predel, D. W. Stein, *J. Less-Common Metals 18* (1969) 203; G. S. Smith,. Q. Johnson, D. H. Wood, *Acta Crystallogr. B 25* (1969) 554.
[10] R. Nesper, *Habilitationsschrift*, Universität Stuttgart 1988.
[11] W. Klemm, *Proc. Chem. Soc. (London) 1959*, 329; W. Klemm: *Festkörperprobleme*, Vieweg, Braunschweig 1963; E. Mooser, W. B. Pearson, *Phys. Rev. 101* (1956) 1608.
[12] K. Wade, *Adv. Inorg. Chem. Radiochem. 18* (1976) 1, 67.
[13] G. M. Sheldrick, E. Egert: *SHELXS Programs for Crystal Structure Solution*, Universität Göttingen 1984; G. M. Sheldrick, *SHELX-76 Programs for Crystal Structure Determination*, University of Cambridge 1976.
[14] C. K. Johnson, *ORTEP II, Thermal Ellipsoid Plot Program*, Oak Ridge, TN, USA 1976.

Enantioselective Reduction of α,β-Unsaturated Carboxylates with $NaBH_4$ and Catalytic Amounts of Chiral Cobalt Semicorrin Complexes**

By *Urs Leutenegger, Andrew Madin,* and *Andreas Pfaltz**

Chiral C_2-symmetric chelate ligands having the structure type of semicorrins **1**–**3** are readily accessible in enantiomerically pure form starting from pyroglutamic acid.[1] The substituents at the two chirality centers can be varied quite easily and are held firmly in position by the rigid ligand skeleton in immediate proximity to the coordination center of the ligand. Semicorrins of this type therefore appeared to offer ideal prerequisites for use in enantioselective catalysis with chiral metal complexes. As a first example of a metal-catalyzed process that proceeds enantioselectively under the influence of chiral semicorrin ligands, we have investigated the cyclopropanation of olefins with diazo compounds. With copper complexes of the ligand **3** as catalysts we obtained enantioselectivities of up to 97% *ee*.[1] We now report on the enantioselective reduction of α,β-unsaturated carboxylates with sodium borohydride in the presence of cobalt-semicorrin complexes as catalysts.



1 R = CH_2OSiMe_2tBu
2 R = CH_2OEt
3 R = CMe_2OH

Our studies in this direction were stimulated by the work of *Fischli* et al.,[2] who had shown that α,β-unsaturated carbonyl compounds can be reduced selectively at the CC double bond with optical yields between 0 and 33% with zinc/acetic acid and cobalamine as catalyst.[3] In our case, sodium borohydride in ethanol/dimethylformamide (DMF) proved to be the better choice as reducing agent.[4] The ester **4a** employed as test substrate[2] is virtually inert to this reagent at room temperature in the absence of a catalyst (<5% conversion after 48 h). In the presence of catalytic amounts (1 mol-%) of the semicorrin complex formed in situ from $CoCl_2$ and the ligand **1**, on the other hand, a smooth, remarkably uniform reduction to the optically active ester (+)-**5a** is observed, which proceeds to completion at room temperature within 1–2 d (crude product: >99.8% **5a** according to GC).[5] The enantiomeric purity of the product was reproducible at 94% *ee* in a series of experiments.[6] The other substrates investigated so far, with the exception of the phenyl-substituted derivatives **4d** and **6d**, react with similarly high enantioselectivity (cf. Table 1). The (*E*)- and (*Z*)-isomers each afford products of opposite configuration. Ethyl geranate **4b** and the (*Z*)-isomer **6b** are selectively reduced at the conjugated CC double bond, whereas the isolated double bond remains untouched. Upon work-up, the ligand **1** forms a (catalytically inactive) cobalt-bis(semicorrinate) complex, and can be recovered in good yield by decomplexation with acetic acid.

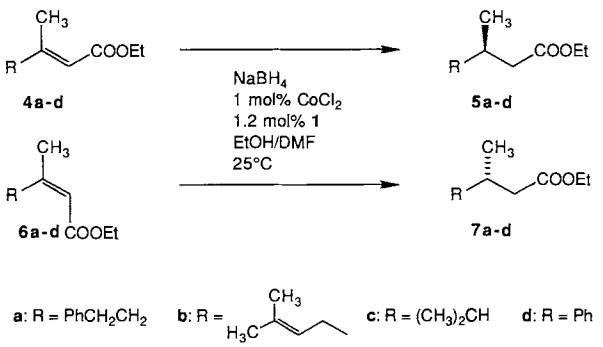


Table 1. Enantioselective reduction of the α,β-unsaturated carboxylates **4a**–**d** and **6a**–**d** [5].

Starting compound	Product	Yield [%] [a]	Enantioselectivity [% *ee*] [b]	Configuration [c]
4a	(+)-**5a**	97	94	*R*
6a	(−)-**7a**	95	94	*S*
4b	(+)-**5b**	95	94	*R*
6b	(−)-**7b**	94	94	*S*
4c	(−)-**5c**	84 [d]	96	*S*
6c	(+)-**7c**	86 [d]	90	*R*
4d	(+)-**5d**	95	81	*S*
6d	(−)-**7d**	97	73	*R*

[a] Product isolated after column chromatography. [b] Estimated accuracy ± 1%. Determined by ^{1}H-NMR spectroscopy with Eu(hfc)$_3$ after reduction to the corresponding alcohol with $LiAlH_4$ and acetylation [2]. The *ee* values of **5a**,**b** and **7a**, **b** were checked by HPLC analysis (Techsil 5 μ; pentane/AcOEt 5:1) of the corresponding (*R*)-1-(1-naphthyl)ethylamides [7]. [c] Assignment based on optical rotation; for **5a**, **7a**: according to Ref. [2]; **5b**, **7b**: [8]; **5c**, **7c**: [10]; **5d**, **7d**: [11]. [d] Loss of substance because of volatility of the product.

The method described here for the enantioselective reduction of α,β-unsaturated carboxylic acid esters can be carried out very easily on a laboratory scale. It has numerous possible applications in organic synthesis; e.g. isoprenoid chains, as occur inter alia, in the vitamins E and K_1, can be synthesized stereoselectively in this way[7,8] (cf. the reactions **4b**→**5b** and **6b**→**7b**). The enantioselectivities lie in the same range as in the catalytic hydrogenation of structurally related α,β-unsaturated carboxylic acids and allylic alcohols with the Ru^{II}-BINAP catalysts developed by *Nojori* et al.[7] In contrast to the enantioselective catalytic hydrogenation with chiral rhodium- and ruthenium-phosphane complexes,[7,9] which afford high optical yields only in the presence of a free carboxy, amide or hydroxy function in the proximity of the CC double bond, in the reduction with cobalt-semicorrin complexes, carboxylic esters can be used. The mechanism of the cobalt-catalyzed reaction and its applicability to other classes of substrates are presently the subject of further investigations.

Received: August 2, 1988 [Z 2900 IE]
German version: *Angew. Chem. 101* (1989) 61

[*] Priv.-Doz. Dr. A. Pfaltz, U. Leutenegger, A. Madin [+]
Laboratorium für Organische Chemie der ETH
ETH-Zentrum, CH-8092 Zürich (Switzerland)
[+] Exchange student from the Imperial College, London.

[**] This work was supported by the ETH Zürich and Hoffmann-La Roche & Co., Basel.

[1] H. Fritschi, U. Leutenegger, A. Pfaltz, *Angew. Chem. 98* (1986) 1028; *Angew. Chem. Int. Ed. Engl. 25* (1986) 1005; H. Fritschi, U. Leutenegger, K. Siegmann, A. Pfaltz, W. Keller, C. Kratky, *Helv. Chim. Acta 71* (1988) 1541; H. Fritschi, U. Leutenegger, A. Pfaltz, *ibid. 71* (1988) 1553.
[2] A. Fischli, D. Süss, *Helv. Chim. Acta 62* (1979) 48; *ibid. 62* (1979) 2361; A. Fischli, J. Daly, *ibid. 63* (1980) 1628.

[3] Examples of enantioselective cobalt-catalyzed hydrogenations of α,β-unsaturated carbonyl compounds with H_2 (7–50% *ee*) are also known: S. Takeuchi, Y. Ohgo, J. Yoshimura, *Chem. Lett. 1973*, 265; Y. Ohgo, S. Takeuchi, Y. Natori, J. Yoshimura, *Bull. Chem. Soc. Jpn. 54* (1981) 2124.
[4] No reaction was observed with molecular hydrogen (2–100 atm, 25–100°C). In the presence of Zn/AcOH or Zn/NH_4Cl the cobalt-semicorrin complex was decomplexed.
[5] *Procedure:* A solution of the α,β-unsaturated ester (9.2 mmol) in EtOH (3.7 mL) under N_2 was treated successively with $CoCl_2 \cdot 6H_2O$ (0.092 mmol dissolved in 1 mL of EtOH), **1** (0.11 mmol in 1.9 mL of EtOH; color change from bluish-violet to dark blue), and $NaBH_4$ (18 mmol in 5.5 mL of DMF; color change to brown). The slightly turbid reaction mixture was degassed under high vacuum by repeated freezing and thawing, and finally stirred for 48 h at ca. 25°C in a vacuum-tight, sealed ampule fitted with Teflon stopper. After addition of H_2O, the mixture was extracted with methylene chloride and the organic phase washed three times with water to remove DMF. The yellow, crude product was purified by flash chromatography [12] (silica gel, 2 × 15 cm; hexane/Et_2O 15:1).
[6] On using the ligand **2** the *ee* value of **5a** was 90%. The ligand **3** does not form a cobalt complex under the reaction conditions (presumably for steric reasons).
[7] H. Takaya, T. Ohta, N. Sayo, H. Kumobayashi, S. Akutagawa, S. Inoue, I. Kasahara, R. Noyori, *J. Am. Chem. Soc. 109* (1987) 1596; T. Ohta, H. Takaya, M. Kitamura, K. Nagai, R. Noyori, *J. Org. Chem. 52* (1987) 3174.
[8] D. Valentine, Jr., K. K. Johnson, W. Priester, R. C. Sun, K. Toth, G. Saucy, *J. Org. Chem. 45* (1980) 3698.
[9] K. E. Koenig: *The Applicability of Asymmetric Homogeneous Catalytic Hydrogenation* in J. D. Morrison (Ed.): *Asymmetric Synthesis, Vol. 5* ("Chiral Catalysis"), Academic Press, Orlando, FL, USA 1985, p. 71.
[10] L. Lardicci, R. Menicagli, A. M. Caporusso, G. Giacomelli, *Chem. Ind. (London) 1973*, 184.
[11] V. Prelog, H. Scherrer, *Helv. Chim. Acta 42* (1959) 2227.
[12] W. C. Still, M. Kahn, A. Mitra, *J. Org. Chem. 43* (1978) 2923.

Nickel Complexes Containing Sterically Demanding Thiolate Ligands: $[Ni_8S(SC_4H_9)_9]^{\ominus}$, a Mixed-Valence Nickel Sulfide Thiolate Cluster, and $[Ni_4(SC_3H_7)_8]$, a Homoleptic Nickel Thiolate**

By *Thomas Krüger, Bernt Krebs,* and *Gerald Henkel**

In terms of their complex chemistry, numerous metalloproteins belong to the class of metal thiolates or metal sulfide thiolates. Prominent examples are the metallothioneins, the iron-sulfur proteins, and the nitrogenases (cf., e.g., Ref. [1]). The investigation of the structure and function of these biomolecules has been accompanied over the past two decades by an unprecedented development of the chemistry of iron, copper, zinc, molybdenum, cadmium, and mercury complexes containing sulfur ligands (cf., e.g., Ref. [2]).

Nickel was recently added to the list of biologically important elements; partial sulfur coordination has been reported for the nickel centers in certain enzymes.[3] The catalytic activity of nickel-containing hydrogenases and CO dehydrogenases appears to be related to the redox properties of the nickel center; metal oxidation states of +1 to +4 have been discussed.[3–5]

The known mixed nickel sulfide thiolate complexes, like the homoleptic nickel thiolates, contain the metal in its divalent form (cf. Ref. [6] and references cited therein). The synthesis of the mixed-valence compound **1** has now demonstrated for the first time that sterically demanding ligands such as 2-methyl-2-propanethiolate are capable of stabilizing unusual oxidation states of nickel in complexes with complete sulfur coordination.

Complex **1** is prepared by reaction of $NiCl_2$ with NaS*t*Bu in methanol and is obtained, after addition of Ph_4PBr, as black needles of the complex salt **2**.[7]

$[Ni_8S(StBu)_9]^{\ominus}$ **1**
$[Ph_4P][Ni_8S(StBu)_9] \cdot MeOH$ **2**
$[Ni_4(SiPr)_8]$ **3**

According to an X-ray structure analysis,[8] crystals of **2** contain, in addition to undistorted $Ph_4P^{\oplus}$ ions and solvate molecules, two symmetry-independent octanuclear anions **1** having the novel $Ni_8(\mu_6\text{-}S)(\mu_2\text{-}SR)_9$ framework. The

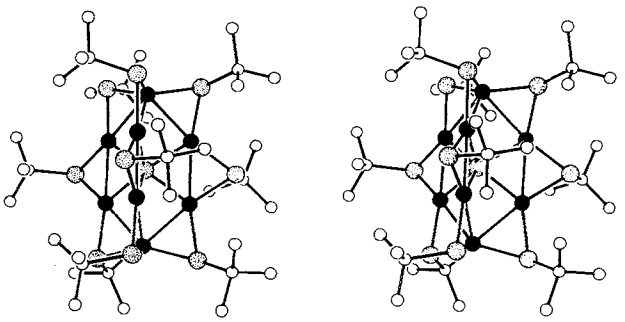


Fig. 1. Stereoscopic view of the structure of **1** in crystals of **2** (hydrogen atoms omitted). Nickel, black; sulfur, dotted; carbon, white.

structure of **1** (H atoms omitted) is shown in Figure 1. The central Ni_8S_{10} unit of **1** is given in Figure 2. Six nickel atoms (Ni^P, black) form a trigonal prism, whose triangular faces are capped by two further nickel atoms (Ni^K,

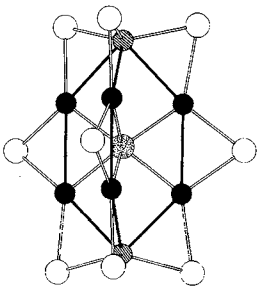


Fig. 2. Schematic drawing of the Ni_8S_{10} framework of the complex anion **1**. Nickel, black and hatched; sulfur, dotted and white. For details see text.

hatched). The average oxidation state of the metal centers is +1.25 and can be formally ascribed to six $Ni^{\oplus}$ and two $Ni^{2\oplus}$. The diamagnetic behavior of **1** (symmetry C_3, slightly distorted) indicates a delocalized electron system, so that an assignment of integral oxidation states to individual metal centers is problematical. Indeed, in addition to unusually short distances between the capping nickel atoms (hatched) and their neighbors (black; average 2.471 Å), we observe three further short distances between the nickel atoms of opposite triangular faces of the metal prism (average: 2.444 Å), which we ascribe to nickel–nickel bonds. Moreover, all nickel pairs with short distances also have thiolate bridges, resulting in a total of nine (μ_2-SR) functions (white). The edges of the triangular faces of the prism have an average length of 3.122 Å and are not

[*] Prof. Dr. G. Henkel, Dipl.-Chem. T. Krüger, Prof. Dr. B. Krebs
Anorganisch-chemisches Institut der Universität
Wilhelm-Klemm-Strasse 8, D-4400 Münster (FRG)

[**] This work was supported by the Bundesminister für Forschung und Technologie (grant 05339GAB/3), by the Minister für Wissenschaft und Forschung des Landes Nordrhein-Westfalen, and by the Fonds der Chemischen Industrie.

bridged by ligands. With a total of 114 skeletal electrons in the Ni_8S_{10} framework, a "magic" electron count[9] is achieved.

The center of the nickel prism is occupied by a unique sulfur atom (dotted) bonded simultaneously to six nickel atoms. This represents the first example of the stabilization of a sulfide ion in a complex, in which it is encapsulated by six equivalent metal atoms. The $(\mu_6\text{-S})Ni_6$ fragment represents a slightly distorted portion of the structure of hexagonal NiS. The average $(\mu_6\text{-S})$–Ni bond length is 2.179 Å. Thus, despite the high coordination number of the sulfur atom, this length is even slightly shorter than the average (SR)–Ni^k bond length of 2.196 Å. In contrast, the average (SR)–Ni^p bond length is only 2.157 Å.

Just as unusual as the oxidation state of the nickel centers is their coordination. The ligands are arranged in such a way that each nickel atom is surrounded by three sulfur atoms in a nearly trigonal-planar fashion. The deviation of the capping nickel atoms from the plane of the sulfur atoms is very large (0.439 Å), presumably due to the bonds to the three metal neighbors. A similar effect is not observed for the nickel atoms of the central metal prism, because their direct metal neighbors lie in the same plane as the sulfur ligands. In this case, the deviation is only 0.095 Å.

The reaction of $(Et_4N)_2[NiBr_4]$ with NaS*i*Pr in acetone or acetonitrile does not result in the formation of a mononuclear nickel thiolate ion, even when a large excess of thiolate is used; only the cyclic, neutral complex **3**, isolated as black crystalline material is formed instead.[7] According to the X-ray structure analysis,[8] **3** is a tetranuclear molecule (idealized D_{4h} symmetry) with a cubane-like Ni_4S_8 framework (Fig. 3). An analogous condensation

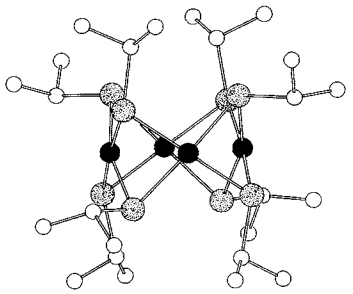


Fig. 3. Crystal structure of **3** (hydrogen atoms omitted). Nickel, black; sulfur, dotted; carbon, white.

is observed for the nickel thiolates $[Ni_4(SC_5H_9NMe)_8]$[10] and $[Ni_4(SC_6H_{11})_8]$.[11] All three compounds share a common feature: they all contain ligands of the secondary thiolate type (2-propanethiolate, *N*-methylpiperidine-4-thiolate, cyclohexanethiolate). The preferential formation of tetranuclear, neutral nickel thiolate complexes might therefore be due to specific chemical properties of secondary thiolate ligands.

Received: July 19, 1988 [Z 2871 IE]
German version: *Angew. Chem. 101* (1989) 54

[1] P. Harrison (Ed.): *Metalloproteins, Part 1* and *Part 2*, VCH Verlagsgesellschaft, Weinheim 1985, and references cited therein.
[2] I. G. Dance, *Polyhedron 5* (1986) 1037, and references cited therein.
[3] C. T. Walsh, W. H. Orme-Johnson, *Biochemistry 26* (1987) 4901, and references cited therein.
[4] P. A. Lindahl, N. Kojima, R. P. Hausinger, J. A. Fox, B. K. Teo, C. T. Walsh, W. H. Orme-Johnson, *J. Am. Chem. Soc. 106* (1984) 3062.
[5] M. Teixeira, I. Moura, A. V. Xavier, B. H. Huynh, D. V. DerVartanian, H. D. Peck, Jr., J. LeGall, J. J. G. Moura, *J. Biol. Chem. 260* (1985) 8942.
[6] a) W. Tremel, M. Kriege, B. Krebs, G. Henkel, *Inorg. Chem. 27* (1988) 3886; b) W. Tremel, G. Henkel, *ibid. 27* (1988) 3896.
[7] *Experimental procedure:* All operations were carried out in degassed solvents under a pure nitrogen atmosphere. **2**: 2-Methyl-2-propanethiol *t*BuSH (4.50 g, 50 mmol) was added under a stream of nitrogen to a solution of sodium (1.15 g, 50 mmol) in 70 mL of methanol. The solution was stirred at room temperature until the reaction was complete (10 min) and then treated with $NiCl_2$ (1.30 g, 10 mmol). After stirring for 3 d, the solution was filtered. Addition of ca. 1 g of Ph_4PBr resulted in the formation of needle-shaped crystals of **2** within 12 h. Yield: 0.62 g (29.6%). Correct C,H analysis. **3**: A slurry of $(Et_4N)_2[NiBr_4]$ (3.19 g, 5 mmol) in 70 mL of acetone was added slowly to a suspension of sodium 2-propanethiolate NaS*i*Pr (2.45 g, 25 mmol) in 40 mL of acetone. After stirring for 16 h, the dark brown solution was filtered and allowed to stand at room temperature. Black platelets of **3** formed within 24 h. Yield: 0.27 g (25.8%). Correct C,H analysis.
[8] Crystal structure analysis: Syntex $P2_1$ four-circle diffractometer, $Mo_{K\alpha}$ radiation, graphite monochromator, scintillation counter, $T = 150$ K, empirical absorption correction, EXTL and SHELXTL programs, direct methods, least-squares fit. **2**: Triclinic, space group $P\bar{1}$, $a = 14.893(6)$, $b = 15.389(6)$, $c = 32.790(10)$ Å, $\alpha = 87.92(3)$, $\beta = 89.77(3)$, $\gamma = 89.65(3)°$, $V = 7510.1$ Å^3, $Z = 4$, $\rho_{calcd} = 1.48$ g cm^{-3}, $\mu(Mo_{K\alpha}) = 22.7$ cm^{-1}, crystal dimensions $0.12 \times 0.14 \times 0.32$ mm^3, ω-scan, $2\theta_{max} = 44°$, 18417 unique reflections, R (R_w) = 0.056 (0.051) for 13731 reflections with $F_0 > 3.92\sigma(F_0)$ [1459 variables, all non-hydrogen atoms refined with anisotropic temperature factors, phenyl H atoms calculated at idealized positions ($U(H) = 1.2\,U_{eq}(C)$). Methyl H and hydroxyl H atoms not included, one scaling factor]. **3**: Monoclinic, space group $P2/n$, $a = 12.746(2)$, $b = 10.067(2)$, $c = 14.494(2)$ Å, $\beta = 93.78(2)°$, $V = 1855.8$ Å^3, $Z = 2$, $\rho_{calcd} = 1.50$ g cm^{-3}, $\mu(Mo_{K\alpha}) = 24.3$ cm^{-1}, crystal dimensions $0.05 \times 0.25 \times 0.35$ mm^3, $\theta - 2\theta$ scan, $2\theta_{max} = 54°$, 4096 unique reflections, R (R_w) = 0.024 (0.023) for 3416 reflections with $F_0 > 3.92\sigma(F_0)$ [164 variables, H atoms calculated at idealized positions ($U(H) = 1.2\,U_{eq}(C)$), all other atoms refined with anisotropic temperature factors, one scaling factor]. Further details of the crystal structure investigation may be obtained from the Fachinformationszentrum Energie, Physik, Mathematik GmbH, D-7514 Eggenstein-Leopoldshafen 2 (FRG), on quoting the depository number CSD-53370, the names of the authors, and the journal citation.
[9] D. M. P. Mingos, *Acc. Chem. Res. 17* (1984) 311.
[10] W. Gaete, J. Ros, X. Solans, M. Font-Altaba, J. L. Brianso, *Inorg. Chem. 23* (1984) 39.
[11] M. Kriege, G. Henkel, *Z. Naturforsch. B42* (1987) 1121.

Heterogeneous, Metathesis-active Schrock-type Carbene Complexes by Reaction of Carbyne Tungsten(VI) Complexes with Silica Gel**

By *Karin Weiss** and *Georg Lössel*

We have recently reported the preparation of heterogeneous, bimetallic metathesis catalysts by reaction of Fischer-type carbene or carbyne tungsten(0) complexes with the reduced Phillips catalyst, a silica gel-Cr^{II} compound.[1-3] The carbene and carbyne complexes presumably undergo a [2+1]-cycloaddition of the W=C or W≡C bond to the surface Cr^{II} atoms; the complexes exhibit no reactivity towards silica gel. As an extension of this study, we have now investigated the activation of Schrock-type carbyne tungsten(VI) complexes by reduced Phillips catalyst.

In homogeneous solution, the carbyne tungsten(VI) complexes exhibit varying degrees of metathesis activity, depending on the other ligands at the W center. Thus, for example, $[Cl_3(dme)W{\equiv}C\,t\text{Bu}]$[4] (dme = dimethoxyethane) catalyzes the metathesis of linear and cyclic olefins at

[*] Dr. K. Weiss, G. Lössel
Laboratorium für Anorganische Chemie der Universität
Postfach 101251, D-8580 Bayreuth (FRG)

[**] Investigations of Polymerization and Metathesis Reactions, Part 15. This work was supported by the Deutsche Forschungsgemeinschaft. Part 14: [3].

room temperature,[5,6] while $[(t\mathrm{BuO})_3\mathrm{W}{\equiv}\mathrm{C}t\mathrm{Bu}]$[4] (Np = neopentyl) shows no metathesis activity. We tested whether the metathesis activity of the carbyne complex $[(t\mathrm{BuO})_3\mathrm{W}{\equiv}\mathrm{C}t\mathrm{Bu}]$ could be enhanced by reaction with reduced Phillips catalyst as described below. The carbyne complex was stirred with an equimolar (Cr : W) quantity of the reduced Phillips catalyst [Merck silica gel 7733, activated with O_2 at 800 °C, reduced with CO at 350 °C, ca. 1% Cr^{II}, preparation as described in Ref. [7]] suspended in hexane at 0 °C. After 2 h, the bimetallic catalyst was collected by filtration, washed with hexane and dried in vacuo. For comparison, the reaction of silica gel, which had been subjected to the same preparative steps as the reduced Phillips catalyst, with the exception of Cr-doping, with the carbyne complex was also investigated. In each case, $[(t\mathrm{BuO})_3\mathrm{W}{\equiv}\mathrm{C}t\mathrm{Bu}]$ was quantitatively adsorbed.

The metathesis activity of the two products was tested by reaction with 1-octene in hexane at 69 °C. The metathesis of 1-octene affords tetradecene C_{14} and ethylene C_2 [Eqn. (a)]

$$\underset{C_8}{2\,C_6H_{13}CH{=}CH_2} \overset{cat}{\rightleftharpoons} \underset{C_{14}}{C_6H_{13}CH{=}CHC_6H_{13}} + \underset{C_2}{H_2C{=}CH_2} \qquad (a)$$

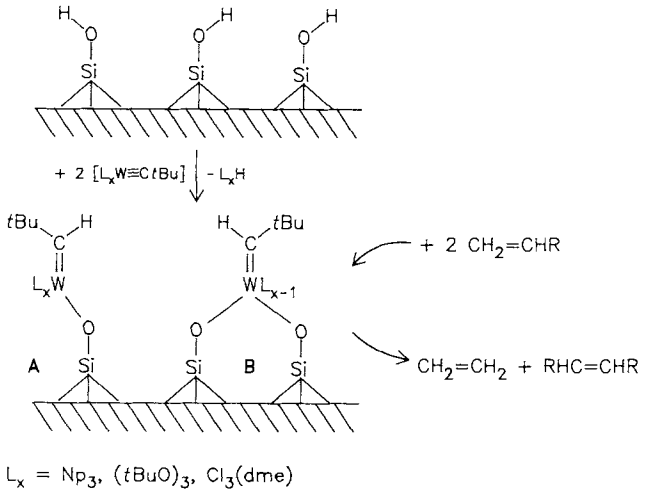
The results showed, surprisingly, that the product derived from the carbyne complex and silica gel has greater catalytic activity (Fig. 1b) than the bimetallic catalyst (Fig. 1c). We therefore conclude that $[(t\mathrm{BuO})_3\mathrm{W}{\equiv}\mathrm{C}t\mathrm{Bu}]$ is activated by reaction with the silica gel and not by reaction with the surface Cr atoms of the reduced Phillips catalyst. After reaction with the carbyne complex, the Phillips catalyst no longer exhibited polymerization activity indicating that $[(t\mathrm{BuO})_3\mathrm{W}{\equiv}\mathrm{C}t\mathrm{Bu}]$ had reacted with the surface Cr atoms. Thus, in the case of the reduced Phillips catalyst, the SiOH groups and the chromium atoms compete for reaction with the carbyne complex.

The activation by silica gel can be explained by reaction of the carbyne complex with the Si–OH protons. *Schrock* et al.[8] have shown that carbyne tungsten(VI) complexes react with Brønsted acids HX to give carbene tungsten(VI) complexes; this reaction is generally used for the synthesis of Schrock carbene complexes. In the reaction with excess HX, the anion $X^{\ominus}$ may displace one of the ligands (e.g., $t\mathrm{BuO}^{\ominus}$) from the W center [Eqn. (b)].

$$[(t\mathrm{BuO})_3\mathrm{W}{\equiv}\mathrm{C}t\mathrm{Bu}] + 2\,\mathrm{HX} \longrightarrow [\mathrm{X}_2(t\mathrm{BuO})_2\mathrm{W}{=}\mathrm{CH}t\mathrm{Bu}] + t\mathrm{BuOH} \qquad (b)$$

X = PhO, Cl, RCOO etc.

The surface SiOH protons of silica gel could react with the carbyne tungsten(VI) complexes to give either a "one-legged" surface anchored carbene complex (Scheme 1, structure **A**) or, via ligand displacement, to afford a "two-legged" surface anchored complex (Scheme 1, structure **B**). The surface carbene W^{VI} complexes are both coordinatively unsaturated and in each case the electrophilic character of the W center is further increased by the coordination of SiO groups.



L_x = Np_3, $(t\mathrm{BuO})_3$, $Cl_3(dme)$

Scheme 1. Reaction of carbyne tungsten(VI) complexes with silica gel to form heterogeneous carbene tungsten(VI) complexes.

The synthesis of heterogeneous carbene tungsten(VI) complexes can be extended to $[Np_3\mathrm{W}{\equiv}\mathrm{C}t\mathrm{Bu}]$ and $[Cl_3(dme)\mathrm{W}{\equiv}\mathrm{C}t\mathrm{Bu}]$. The quantity of HCl produced in the reaction between $[Cl_3(dme)\mathrm{W}{\equiv}\mathrm{C}t\mathrm{Bu}]$ and silica gel was determined acidimetrically. One mol of HCl is eliminated per mol of carbyne complex suggesting that the adsorbed carbene complexes have the structure **B**.

The solid-state ^{13}C NMR spectrum of the product from $[(t\mathrm{BuO})_3\mathrm{W}{\equiv}\mathrm{C}t\mathrm{Bu}]$ and kieselgel exhibited resonances at $\delta = 28.8$ and 73.9 (tBuO) and 31.9 ($=\mathrm{C}(\mathrm{C}CH_3)_3$). Carbene tungsten(VI) complexes exhibit similar chemical shifts in solution. We have, until now, been unable to detect the signal for the carbene carbon atom, perhaps because of splitting into several rotational side bands.

The metathesis activity of the heterogeneous carbene complexes was tested by reaction with 1-octene at 69 and 122 °C. Their activity was compared with that of the analogous carbene and carbyne complexes in homogeneous solution (Table 1, Fig. 2). Of the complexes tested, only the heterogeneous carbene complexes proved to have high catalytic activity. Thus, for example, the system SiO_2/$[Np_2\mathrm{W}{=}\mathrm{CH}t\mathrm{Bu}]$ had a turnover rate of 830 mol 1-octene per mol W at 122 °C. In contrast, the carbene and carbyne complexes in solution had smaller turnovers or showed no activity at all. Raising the reaction temperature generally led to an increase in the rate of reaction.

Schrock[9] and *Osborn* et al.[10] have shown that metathesis-inactive carbene tungsten(VI) complexes can be activated by the addition of Lewis acids or by substitution of

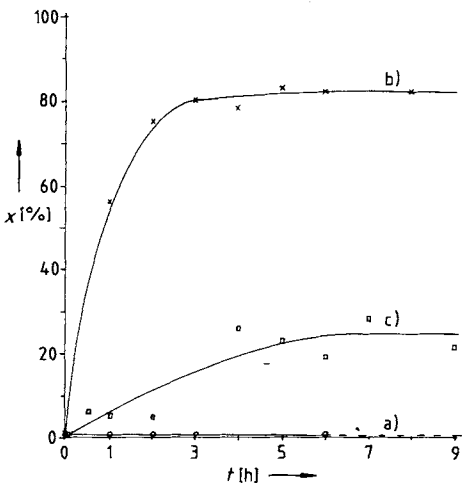


Fig. 1. Metathesis of 1-octene with $(t\mathrm{BuO})_3\mathrm{W}{\equiv}\mathrm{C}t\mathrm{Bu}$ at 69 °C; x = turnover of 1-octene; molar ratio 1-octene : W = 10^4 : 1. a) in hexane solution; b) carbyne complex, fixed on silica gel; c) carbyne complex, fixed on reduced Phillips catalyst.

Table 1. Metathesis of 1-octene with hetero- and homogeneous carbene and carbyne tungsten(VI) complexes. x = turnovers per minute (mol 1-octene/mol W). Starting concentration 1-octene : W = 10^4 : 1.

	Turnover [%] at 69 °C	at 122 °C
a) Heterogeneous catalysts		
$SiO_2/[Cl_2W{=}CHtBu]$	30	200
$SiO_2/[(tBuO)_2W{=}CHtBu]$	60	140
$SiO_2/[Np_2W{=}CHtBu]$	260	830
b) Homogeneous catalysts		
$[Cl_3(dme)W{\equiv}CtBu]$	5	50
$[(tBuO)_3W{\equiv}CtBu]$	1	5
$[Np_3W{\equiv}CtBu]$	0	0
$[(tBuO)_2(PhO)_2W{=}CHtBu]$	0	0

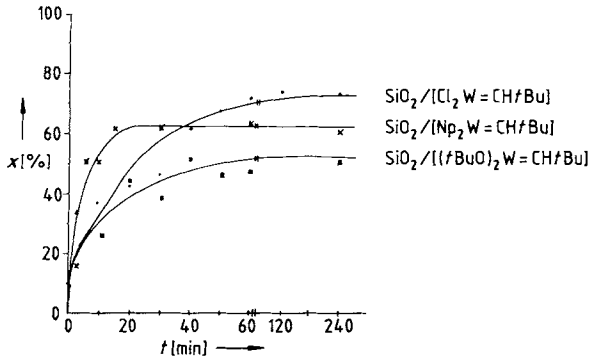


Fig. 2. Metathesis of 1-octene with heterogeneous carbene tungsten(VI) complexes at 122 °C; x = turnover of 1-octene; molar ratio 1-octene : W = 10^4 : 1.

the alkoxy ligands by strongly electron-withdrawing perfluoroalkoxy or imido ligands. In this way, the electronegative character of the W center is increased, favoring addition of olefins to the W=C bond so that metathesis can more readily occur. A similar effect is clearly also achieved by coordination on the SiO_2 surface.

The heterogeneous carbene complexes can be stored at −30 °C for several weeks without loss of catalytic activity. After one week at 20 °C, $SiO_2/[Np_2W{=}CHtBu]$ still had its original activity.

Alkene isomerization becomes significant only when the molar ratio W : 1-octene becomes greater, i.e. with decreasing 1-octene concentration. A similar behavior has been observed for the heterogeneous bimetallic catalysts prepared from carbene or carbyne tungsten(0) complexes and the reduced Phillips catalyst.[1-3]

Carbene tungsten complexes in high oxidation states have long been postulated to be the catalytically active species in the metathesis of olefins by heterogeneous tungsten catalysts.[11] The results reported here support this theory and make it possible to study these catalysts systematically.

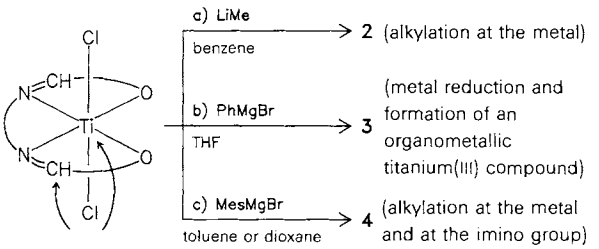
Submitted: August 8, 1988 [Z 2917 IE]
German version: *Angew. Chem. 101* (1989) 75

[1] K. Weiss, W. Guthmann, S. Maisuls, *Angew. Chem. 100* (1988) 268; *Angew. Chem. Int. Ed. Engl. 27* (1988) 275.
[2] K. Weiss, W. Guthmann, M. Denzner, *J. Mol. Catal. 46* (1988) 341.
[3] K. Weiss, M. Denzner, *J. Organomet. Chem. 355* (1988) 273.
[4] R. R. Schrock, D. N. Clark, J. Sancho, J. H. Wengrovius, S. M. Rocklage, S. I. Pedersen, *Organometallics 1* (1982) 1645.
[5] K. Weiss, *Angew. Chem. 98* (1986) 350; *Angew. Chem. Int. Ed. Engl. 25* (1986) 359.
[6] K. Weiss, G. Lössel, R. Goller, *J. Mol. Catal. 46* (1988) 267.
[7] H. L. Krauss, B. Rebensdorff, U. Westphal, *Z. Anorg. Allg. Chem. 414* (1975) 97.
[8] J. H. Freudenberger, R. R. Schrock, *Organometallics 4* (1985) 1937.
[9] R. R. Schrock, *J. Organomet. Chem. 300* (1986) 249.
[10] M. T. Youinou, J. Kress, J. Fischer, A. Aguero, J. A. Osborn, *J. Am. Chem. Soc. 110* (1988) 1488.
[11] V. Dragutan, A. T. Balaban, M. Dimonie: *Olefin Metathesis and Ring Opening Polymerisation of Cycloolefins*, Wiley, New York 1985.

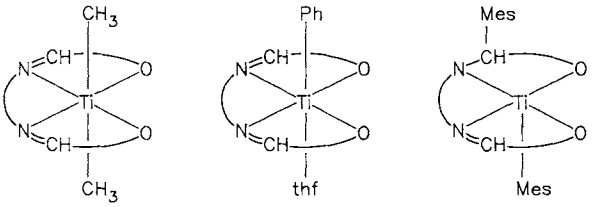
A *trans*-Dimethyl Derivative of Octahedral Ti^{IV}: Alkylation and Arylation of Ti^{IV}-Schiff Base Complexes**

By *Carlo Floriani,* Euro Solari, Fabio Corazza, Angiola Chiesi-Villa,* and *Carlo Guastini*

The chemistry of the titanium–carbon bond is still having a major impact in organometallic chemistry for both metal-induced stoichiometric[1,2] and catalytic transformations.[3b] Many of its characteristics are, however, associated with the presence of cyclopentadienyl ligands at a tetrahedrally coordinated metal center.[3c] Since the chemical behavior of the Ti–C bond towards substrates is largely affected by the steric and electronic constraints imposed by the ancillary ligands, we turned our attention to a rigid ligand, such as salen [salen = *N*,*N*′-ethylenebis(salicylideneiminato) dianion], whose use has many precedents, almost exclusively in the organometallic chemistry of cobalt(III).[4] Several organic derivatives of early transition metals with tetradentate ligands have been reported recently.[5,6] $[Ti(salen)Cl_2]$ **1**[7] seemed to be an excellent starting material for the preparation of organometallic derivatives.



1, $[Ti(salen)Cl_2]$



2, $[Ti(salen)(Me)_2]$ 3, $[(Ph)Ti(salen)(thf)]$ 4, $[Ti(salenMes)(Mes)]$

Scheme 1. Mes = 2,4,6-$Me_3C_6H_2$. The arrows indicate the possible alkylation sites in **1**.

[*] Prof. Dr. C. Floriani, Dr. E. Solari, Dr. F. Corazza
I.C.M.A., Université de Lausanne
Place du Château 3, CH-1005 Lausanne (Switzerland)
Prof. Dr. A. Chiesi-Villa, Prof. Dr. C. Guastini
Istituto di Strutturistica Chimica
Centro di Studio per la Strutturistica Diffrattometrica del CNR
Università di Parma, I-43 100 Parma (Italy)

[**] This work was supported by the Fonds National Suisse de la Recherche Scientifique (S. N. F. 2.131-0.86).

The alkylation and arylation reactions were much more complex than expected because of the presence of electrophilic sites in the salen ligand. Depending upon the nucleophile and the solvent, the reaction can follow three different pathways a)–c) to form complexes **2**–**4** (Scheme 1). The reaction is influenced by a considerable number of variables, of which the polarity of the solvent is probably the major factor determining the reaction pathway. Alkylation of **1** using LiMe in benzene led to the dimethyl derivative **2**,[8] whose structure is shown in Figure 1.[9] The structure shows a nearly *trans* arrangement of the two methyl groups ($C1_{Me}$–Ti–$C2_{Me}$ 154.9(6)°). The Ti–C bond distances,[3] as well as the structural parameters for the [Ti(salen)] moiety, are in the usual ranges.[7b] **2** is a red crystalline solid, which is stable in the solid state but undergoes decomposition in solution at room temperature. This instability might be due to the self-labilization of two alkyl groups *trans* to each other.

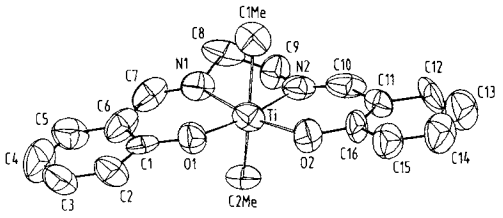


Fig. 1. Molecular structure of **2**. Bond lengths [Å]: Ti–O1 1.83(1), Ti–O2 1.86(1), Ti–N1 2.14(1), Ti–N2 2.15(1), Ti–C1Me 2.15(2), Ti–C2Me 2.15(1); bond angles [°]: O1–Ti–O2 110.9(4), N1–Ti–N2 76.5(6), N1–Ti–O1 86.5(5), N2–Ti–O2 86.1(5), N1–Ti–O2 162.6(5), N2–Ti–O1 162.8(5), C1Me–Ti–C2Me 154.9(6).

When the reaction was carried out using either CH_3MgI or LiMe in THF, reduction to titanium(III) was observed. When **1** was reacted with PhMgBr in THF, complex **3** was isolated and structurally characterized.[10] **3** is much more thermally stable than **2**, both in the solid state and in solution. Reduction of **1** was also observed using MesMgBr (Mes = 2,4,6-$Me_3C_6H_2$) in THF. When the same reaction was carried out in toluene or dioxane,[11] **4** was isolated. The structure of complex **4** is shown in Figure 2.[12] One of the mesityl groups is bonded to the metal atom (Ti–C 2.142(3) Å), while the other is bound to one of the imino carbon atoms. The titanium atom has a pseudo-square pyramidal coordination, with the metal atom lying 0.487(1) Å out of the N_2O_2 plane of the salen ligand, which is distorted due to alkylation at the imino carbon atom. The alkylation leads to the trianionic [salenMes] ligand, and would account for the significant differences observed between the two Ti–N and Ti–O bond lengths. Additionally, the ^{1}H NMR spectrum shows the inequivalence of the mesityl groups, and of the two *o*-methyl substituents of the mesityl group attached to the metal atom.[11]

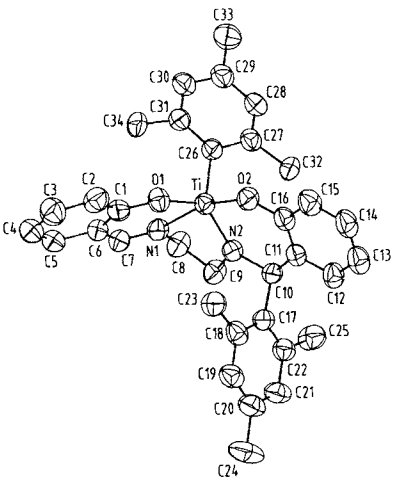


Fig. 2. Molecular structure of **4**. Bond lengths [Å]: Ti–O1 1.874(3), Ti–O2 1.822(3), Ti–N1 2.151(3), Ti–N2 1.927(3), Ti–C26 2.142(3); bond angles [°]: O1–Ti–O2 100.5(1), N1–Ti–N2 76.4(1), N1–Ti–O1 81.7(1), N2–Ti–O2 89.6(1), N1–Ti–O2 162.2(1), N2–Ti–O1 132.7(1).

The results raise the question of whether complexes **3** and **4** have a diaryl metal complex as a common precursor. The formation of **3** can then be readily explained by homolytic cleavage of a Ti–C bond. Migration of an alkyl group to the imino functionality may account for the formation of **4**. The thermal decomposition of **2**, as followed by ^{1}H NMR spectroscopy, clearly shows migration of one of the methyl groups to the imino carbon atom. We cannot, however, exclude a direct alkylation at the imino group. Although this has not been observed in the alkylation of cobalt(III) complexes,[4] the electrophilicity of the imino groups is significantly higher in **1**.

Received: July 1988 [Z 2882 IE]
German version: *Angew. Chem. 101* (1989) 91

[1] M. T. Reetz, *Organotitanium Reagents in Organic Synthesis*, Springer, Berlin 1986.

[2] B. Weidmann, D. Seebach, *Angew. Chem. 95* (1983) 12; *Angew. Chem. Int. Ed. Engl. 22* (1983) 31; D. Seebach, B. Weidmann, L. Widler in R. Scheffold (Ed.): *Modern Synthetic Methods, Vol. 3*, Wiley, New York 1983.

[3] a) M. Bottrill, P. D. Gavens, J. M. Kelland, J. McMeeking in G. Wilkinson, F. G. A. Stone, E. W. Abel (Eds.): *Comprehensive Organometallic Chemistry, Vol. 3*, Pergamon, Oxford 1982; b) [3a], Chap. 22.5; c) [3a], Chaps. 22.3 and 22.4.

[4] J. M. Pratt, P. J. Craig, *Adv. Organomet. Chem. 11* (1973) 404.

[5] C. Floriani, S. Ciurli, A. Chiesi-Villa, C. Guastini, *J. Chem. Soc. Chem. Commun. 1986*, 1401; *Angew. Chem. 99* (1987) 56; *Angew. Chem. Int. Ed. Engl. 26* (1987) 70.

[6] S. Gambarotta, M. Mazzanti, C. Floriani, A. Chiesi-Villa, C. Guastini, *J. Chem. Soc. Chem. Commun. 1985*, 829.

[7] a) Very easy synthesis of **1**: G. Dell'Amico, F. Marchetti, C. Floriani, *J. Chem. Soc. Dalton Trans. 1982*, 2197; b) structure of **1**: G. Gilli, D. W. J. Cruickshank, R. C. Beddoes, O. S. Mills, *Acta Crystallogr. Sect. B 28* (1972) 1889.

[8] *Experimental procedure* for **2**: To a suspension of **1** (3.25 g, 8.44 mmol) in benzene (200 mL) was added a solution of LiMe (16.88 mmol) in Et_2O dropwise at room temperature. The very insoluble complex **1** dissolved completely giving a red-brown solution. After 2 h, LiCl was filtered off, and the solution allowed to stand for 24 h to give **2** (1.80 g, 50.5%). Crystals suitable for X-ray analysis were obtained by recrystallizing **2** from toluene to give **2**·C_7H_8. ^{1}H NMR (CD_2Cl_2): $\delta = -0.25$ (s, 6H), 4.31 (s, 4H), 7.02 (m, 4H), 7.35 (s, 4H), 8.37 (s, 2H).

[9] **2**: orthorhombic, space group $P2_12_12_1$, $a = 22.795(2)$, $b = 14.734(1)$, $c = 6.849(1)$ Å, $V = 2300.3(4)$ Å^3, $Z = 4$, $\rho_{calcd} = 1.26$ g cm^{-3}, $F(000) = 920$, $\lambda(Mo_{K\alpha}) = 0.71069$ Å, $\mu(Mo_{K\alpha}) = 3.88$ cm^{-1}; crystal dimensions $0.19 \times 0.31 \times 0.72$ mm^3. The structure was solved by the heavy atom method and refined anisotropically for all non-hydrogen atoms except for the toluene carbon atoms. The methyl carbon atom of toluene was found to be statistically distributed over two positions and was isotropically refined with site occupancy factors of 0.5. All hydrogen atoms, apart from those in the disordered methyl groups, were placed in geometrically calculated positions and introduced into the final refinement as fixed contributors ($U_{iso} = 0.08$ Å^2). 882 unique observed reflections [$I > 2\sigma(I)$] collected at room temperature ($6° < 2\theta < 46°$) were used, $R = 0.038$ [13].

[10] *Experimental procedure* for **3**: A solution of PhMgBr (14.07 mmol) in THF (11.7 mL) was added to a suspension of **1** (2.71 g, 7.04 mmol) in THF (70 mL). **1** dissolved giving a green-blue solution. After adding dioxane (2.5 mL, 30.0 mmol) and allowing the solution to stand at room temperature for 5 h, magnesium salts crystallized and were removed by filtration. After 2 d green-blue crystals of **3**·1.5 thf had formed (2.28 g, 70%). $\mu_{eff} = 1.77$ BM at 294 K. The solid state structure shows a pseudooctahedral coordination for titanium with the Ph group *trans* to the THF molecule; the salen ligand forms the equatorial plane.

[11] *Experimental procedure* for **4**: A solution of MesMgBr (21.0 mmol) in THF (18.6 mL) was added to a suspension of **1** (4.05 g, 10.5 mmol) in dioxane (100 mL) at room temperature. A green solution formed with an insoluble white solid. The solid was removed by filtration, and the solution allowed to stand for 24 h at room temperature to give yellow-orange crystalline **4**·$C_4H_8O_2$ (4.14 g, 65%). The reaction in toluene gave solvent-free **4** (70%) without any reduction to titanium(III) (green solution). ^{1}H NMR of **4** (from toluene) (C_6D_6): $\delta = 1.60$ (s, 3H), 2.03 (s, 3H), 2.12 (s, 3H), 2.43 (s, 3H), 2.49 (s, 6H), 2.70 (m, 1H), 3.17 (m, 1H), 3.39 (m, 1H), 4.29 (m, 1H), 6.30–7.25 (a series of multiplets, 12H), 7.28 (s, 1H).

[12] **4**: monoclinic, space group $P2_1/n$, $a = 12.804(1)$, $b = 26.566(3)$, $c = 10.014(1)$ Å, $\beta = 95.27(1)°$, $V = 3391.9(6)$ Å^3, $Z = 4$, $\rho_{calcd} = 1.255$ g cm^{-3}, $F(000) = 1360$, $\lambda(Cu_{K\alpha}) = 1.54178$ Å, $\mu(Cu_{K\alpha}) = 24.56$ cm^{-1}; crystal dimensions $0.21 \times 0.21 \times 0.65$ mm^3. Solution of the structure as for **1** (see [9]). The hydrogen atoms, partly located by difference methods, partly placed in calculated positions, were introduced as fixed contributors into the final refinement ($U_{iso} = 0.12$ Å^2). 3625 unique observed reflections [$I > 2\sigma(I)$] collected at room temperature ($6° < 2\theta < 130°$) were used, $R = 0.057$. The intensities were corrected for absorption [13].

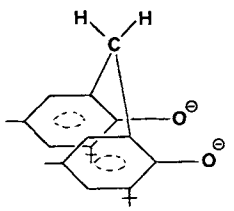
[13] Further details of the crystal structure investigation are available from the Director of the Cambridge Crystallographic Data Centre, University Chemical Laboratory, Lensfield Road, Cambridge CB2 1EW (England) on quoting the full literature citation.

A Sensitive Spectroscopic Probe for Monitoring Changes in the Coordination Sphere of Titanium: Eight-Membered Dioxatitanacycles and Their Organometallic Derivatives**

By *Carlo Floriani,* Fabio Corazza, William Lesueur, Angiola Chiesi-Villa* and *Carlo Guastini*

Is there a method for efficiently monitoring changes in the coordination sphere of a metal ion via spectroscopy? One possibility is to enclose the ion in a heterocycle and to study changes in the structure and their dependence upon changes in the metal coordination sphere. The 2,2′-methylenebis(6-*tert*-butyl-4-methylphenolato) dianion (MBP) proved to be a suitable probe for these effects in organotitanium chemistry.

MBP can also act as an oxo matrix for anchoring organometallic functionalities and as a O⌒O′ bidentate ligand which can adapt its interaction with the metal atom to changes in the coordination sphere and can form very stable metallacycles. Additionally, MBP contains methylene hydrogen atoms which may be influenced by the proximity of a metal atom.



MBP

[(MBP)TiCl$_2$]	[CpTiCl(MBP)]	[(MBP)TiCl$_2$L]	[(MBP)TiR$_2$]
1	**2**	**3**, L = *t*BuNC	**5**, R = Me
		4, L = THF	**6**, R = Ph

[*] Prof. Dr. C. Floriani, Dr. F. Corazza, Dipl.-Chem. W. Lesueur
I.C.M.A., Université de Lausanne
Place du Château 3, CH-1005 Lausanne (Switzerland)
Prof. Dr. A. Chiesi-Villa, Prof. Dr. C. Guastini
Istituto di Strutturistica Chimica
Centro di Studio per la Strutturistica Diffrattometrica del CNR
Università di Parma, I-43100 Parma (Italy)

[**] This work was supported by the Fonds National Suisse de la Recherche Scientifique (S.N.F. 2.131-0.86). We thank Prof. *V. Bertolasi* for the collection of X-ray data for complex **5** and Dr. *S. Pastor* (Ciba-Geigy) for helpful discussions.

We report the synthesis of functionalizable eight-membered dioxatitanacycles and some of their organometallic derivatives emphasizing the relevance of the use of the ancillary ligand MBP. The importance of organotitanium compounds with oxo ligands in organic synthesis,[1,2] organometallic chemistry[1-3,4a] and catalysis[4b] is well known.

The reaction of $TiCl_4$ with $MBPH_2$ in *n*-hexane proceeded with spontaneous evolution of HCl to give red crystals of [(MBP)TiCl$_2$] **1**.[5] **1** is fairly soluble in a large number of organic solvents. The boat conformation of the metallacycle **1** in the solid state is shown in Figure 1.[6] The structure exhibits some interesting structural peculiarities: the Ti–O bond distances are exceedingly short in agreement with a very high Ti–O bond order (probably > 2).[3b] Accordingly, the oxo ligands must be considered to be donors of more than two electrons, and the Ti–O bond order and the electron donation from the oxo ligand to titanium should vary with the coordination number of the metal.[3] The coordination number of the metal was increased either by replacing one chlorine by a Cp ligand [Cp = η^5-C_5H_5], or by adding a monodentate ligand to **1**. Reaction of $MBPNa_2$ with $CpTiCl_3$ gave [CpTiCl(MBP)] **2**[7] while the addition of a monodentate ligand L to **1** [L = *t*BuNC, THF] led to the adducts [(MBP)TiCl$_2$L] **3**, L = RNC and **4**, L = THF. Preliminary crystallographic results show that complex **2** has a similar boat structure to **1** with the Cp ligand in a pseudo-axial position; the Ti–O bond distance in **2** (Ti–O 1.82(2) Å) is significantly longer than that in

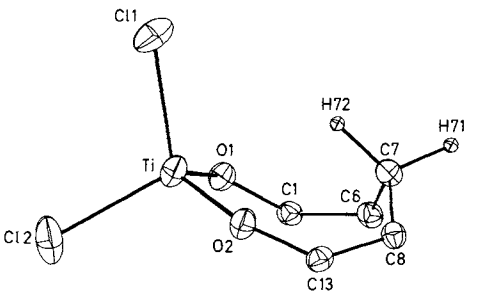


Fig. 1. Molecular structure of [(MBP)TiCl$_2$] **1** (ORTEP, 50% probability ellipsoids). Bond lengths [Å] and angles [°]: Ti–Cl1 2.215(2), Ti–Cl2 2.206(2), Ti–O1 1.760(4), Ti–O2 1.742(4); O1–Ti–O2 106.5(2), Cl2–Ti–O2 108.1(2), Cl2–Ti–O1 110.6(2), Cl1–Ti–O2 111.0(2), Cl1–Ti–O1 111.1(2), Cl1–Ti–Cl2 109.5(1), Ti–O1–C1 143.6(4), Ti–O2–C13 155.8(4).

1.[9] The ^{1}H NMR resonances of the CH_2 group proved to be an excellent probe for the detection of metallacycle formation and are very sensitive to changes in the metal coordination sphere within the metallacycle.[10] The two protons appear as a singlet in the free phenol, but give rise to a pair of well-separated doublets in the metallacycle. The separation of the two doublets, which ranges from 0.34 in **1**, to 0.72 in **2**, 1.03 in **3**, and 1.13 ppm in **4**, increases with increasing coordination number of the metal. It is as yet unknown whether this variation is due to a change in the conformation of the metallacycle in solution, since **2** has a boat conformation in the solid state, while [Cp_2Zr(MBP)], which exhibits two doublets separated by 1.07 ppm, has a solid-state chair conformation.[9] It is however clear that changes in the coordination sphere of the titanium atom are revealed by a change in the separation of the two doublets in the ^{1}H NMR spectrum. Thus, the interaction of a substrate with the metal center can be observed during

metal-assisted reactions. Reaction of **1** with LiMe or LiPh led to the thermally stable organometallic compounds [(MBP)$TiMe_2$] **5**[11] and [(MBP)$TiPh_2$] **6**.[12] An X-ray structural analysis[13] of **5** showed that it also has a boat conformation (Fig. 2). The molecule has a plane of symmetry containing the $TiMe_2$ and CH_2 groups. The structural parameters are very similar to those of **1**. The ^1H NMR at room temperature shows the non-equivalence of the two methyl groups and of the two methylene protons. The separation of the two doublets ($\Delta\delta = 0.17$) and the short Ti–O bond distance (1.799(3) Å) are as expected for tetracoordinate titanium.

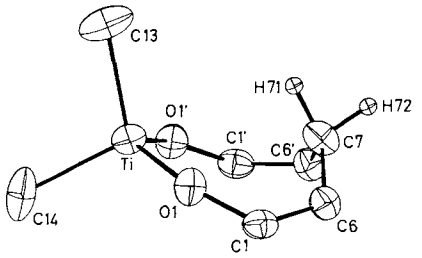


Fig. 2. Molecular structure of [(MBP)$TiMe_2$] **5** (ORTEP, 50% probability ellipsoids). Bond lengths [Å] and angles [°]: Ti–O1 1.799(3), Ti–C13 2.090(9), Ti–C14 2.030(10); O1–Ti–O1′ 112.7(2), C13–Ti–C14 105.8(5), C14–Ti–O1 109.0(1), C13–Ti–O1 110.0(1), Ti–O1–C1 145.7(3). Atoms marked (′) are generated by the transformation $x, 1/2-y, z$.

Received: August 8, 1988 [Z 2911 IE]
German version: *Angew. Chem. 101* (1989) 93

[1] a) M. T. Reetz: *Organotitanium Reagents in Organic Synthesis*, Springer, Berlin 1986; b) B. Weidmann, D. Seebach, *Angew. Chem. 95* (1983) 12; *Angew. Chem. Int. Ed. Engl. 22* (1983) 31; D. Seebach, B. Weidmann, L. Widler in R. Scheffold (Ed.): *Modern Synthetic Methods, Vol. 3*, Wiley, New York 1983.

[2] S. F. Pedersen, J. C. Dewan, R. R. Eckman, K. B. Sharpless, *J. Am. Chem. Soc. 109* (1987) 1279, and references cited therein.

[3] a) L. R. Chamberlain, L. D. Durfee, P. E. Fau, P. E. Fanwick, L. Kobriger, S. L. Latesky, A. K. McMullen, I. P. Rothwell, K. Folting, J. C. Huffman, W. E. Streib, R. Wang, *J. Am. Chem. Soc. 109* (1987) 390, 6068 and references cited therein; L. D. Durfee, P. E. Fanwick, I. P. Rothwell, K. Folting, J. C. Huffman, *ibid. 109* (1987) 4720; b) T. V. Lubben, P. T. Wolczanski, *ibid. 109* (1987) 424 and references cited therein.

[4] a) M. Bottrill, P. D. Gavens, J. M. Kelland, J. McMeeking in G. Wilkinson, F. G. A. Stone, E. W. Abel (Eds.): *Comprehensive Organometallic Chemistry, Vol. 3*, Pergamon, Oxford 1982; b) [4a], Chap. 22.5; c) Chap. 22.3 and 22.4.

[5] *Procedure* for **1**: $TiCl_4$ (6.5 mL, 61.8 mmol) was added dropwise to a solution of $MBPH_2$ (21.0 g, 61.8 mmol) in *n*-hexane (300 mL). The resulting red solution, on standing at room temperature for 12 h, gave red crystals of **1** (yield 24.9 g, 88.0%). ^1H NMR (200 MHz, CD_2Cl_2): $\delta = 7.22$ (d, 2H, Ph), 7.03 (d, 2H, Ph), 4.08 (d, 1H, $J_{HH} = 14.4$ Hz, CH_2), 3.74 (d, 1H, $J_{HH} = 14.4$ Hz, CH_2), 2.34 (s, 6H, Me), 1.47 (s, 18H, *t*Bu). Some titanacycles containing other heteroatoms are described in [4b].

[6] Structure of **1**: triclinic, space group $P\bar{1}$, $a = 9.704(1)$, $b = 12.938(2)$, $c = 9.514(1)$ Å, $\alpha = 92.45(1)$, $\beta = 94.0(1)$, $\gamma = 85.97(1)°$, $V = 1187.8(3)$ Å^3, $Z = 2$, $\rho_{calcd} = 1.279$ g cm^{-3}, $\lambda(Mo_{K\alpha}) = 0.71069$ Å, $\mu(Mo_{K\alpha}) = 5.97$ cm^{-1}: crystal dimensions $0.08 \times 0.45 \times 0.78$ mm^3. The structure was solved by the heavy atom method (Patterson and Fourier synthesis) and refined by full-matrix least-squares. For 1427 unique observed structure amplitudes [$I > 2\sigma(I)$, no correction for absorption] collected at room temperature on a Philips PW 1100 diffractometer in the range $6 < 2\theta < 46°$ the *R* value was 0.038 (unit weights). All the hydrogen atoms were located in a difference Fourier map and introduced as fixed contributors in the final stage of refinement [14].

[7] *Procedure* for **2**: Solid $CpTiCl_3$ (10.71 g, 48.83 mmol) was added to a suspension of $MBPNa_2$ (48.83 mmol) in benzene (300 mL) and the mixture gently heated. The resulting suspension was kept at room temperature for 12 h, then heated and filtered while hot to remove NaCl. **2** crystallized upon concentration of the solution (yield 15.0 g, 63.0%). ^1H NMR (200 MHz, CD_2Cl_2): $\delta = 7.04$ (d, 2H, Ph), 6.91 (d, 2H, Ph), 6.83 (s, 5H, Cp), 4.16 (d, 1H, $J_{HH} = 13.6$ Hz, CH_2), 3.44 (d, 1H, $J_{HH} = 13.6$ Hz, CH_2), 2.24 (s, 6H, Me), 1.31 (s, 18H, *t*Bu).

[8] *Procedure* for **3**: *t*BuNC (0.33 mL, 2.95 mmol) was added to a solution of **1** (1.35 g, 2.95 mmol) in *n*-hexane (80 mL). The color changed from red to deep-red. The solution was cooled to 4 °C for 48 h to afford deep-red microcrystalline **3** (yield 1.50 g, 94%). IR: $\tilde{\nu}$(CN) (nujol) = 2223 cm^{-1}, $\tilde{\nu}$(CN) (C_6D_6) = 2211 cm^{-1}; ^1H NMR (200 MHz, CD_2Cl_2): $\delta = 7.09$ (d, 2H, Ph), 6.95 (d, 2H, Ph), 4.52 (d, 1H, $J_{HH} = 13.9$ Hz, CH_2), 3.49 (d, 1H, $J_{HH} = 13.9$ Hz, CH_2), 2.26 (s, 6H, Me), 1.55 (s, 9H, *t*BuNC), 1.41 (s, 18H, *t*Bu).

[9] C. Floriani et al., unpublished.

[10] Detailed conformational studies have been carried for a number of heterocycles with phosphorus, silicon and boron in the same diphenoxo skeleton; see: S. D. Pastor, J. D. Spivack, R. K. Rodebaugh, D. Bini, *J. Org. Chem. 49* (1984) 1297; S. D. Pastor, J. D. Spivack, *J. Heterocycl. Chem. 20* (1983) 1311; P. A. Odorisio, S. D. Pastor, J. D. Spivack, L. Steinhuebel, R. K. Rodebaugh, *Phosphorus and Sulfur 15* (1983) 9; *ibid. 19* (1984) 285; H. S. Rzepa, R. N. Sheppard, *J. Chem. Res. 5* (1988) 102 and references cited therein.

[11] *Procedure* for **5**: A suspension of **1** (1.55 g, 3.36 mmol) in pentane (50 mL) at −30 °C was reacted with a solution of LiMe (6.72 mmol) in Et_2O. The yellow solution was warmed to room temperature and LiCl removed by filtration. The resulting solution gave, on cooling at −30 °C for 12 h, yellow crystalline **5** (yield 0.61 g, 43.6%). ^1H NMR (200 MHz, C_6D_6): $\delta = 6.99$ (d, 4H, Ph), 3.38 (d, 1H, $J_{HH} = 14.2$ Hz, CH_2), 3.21 (d, 1H, $J_{HH} = 14.2$ Hz, CH_2), 2.11 (s, 6H, *p*-Me), 1.60 (s, 18H, *o*-*t*Bu), 1.38 (s, 3H, Me), 1.36 (s, 3H, Me).

[12] *Procedure* for **6**: **1** (3.70 g, 8.70 mmol) was added to a solution of LiPh (17.5 mmol) in Et_2O (100 mL) at room temperature. The resulting solution was allowed to stand for 12 h, then evaporated to dryness. The resulting solid was dissolved in pentane (50 mL) and LiCl removed by filtration. The pentane solution, upon cooling to −30 °C, gave crystalline green **6** (yield 1.79 g, 38.0%). ^1H NMR (200 MHz, CD_2Cl_2): $\delta = 8.02$ (m, 4H, Ti-Ph), 7.25 (m, 6H, Ti-Ph), 7.19 (d, 2H, Ph), 7.04 (d, 2H, Ph), 3.68 (d, 1H, $J_{HH} = 14.5$ Hz, CH_2), 3.56 (d, 1H, $J_{HH} = 14.5$ Hz, CH_2), 2.31 (s, 6H, *p*-Me), 1.59 (d, 18H, *t*Bu).

[13] Structure of **5**: orthorhombic, space group *Pnma*, $a = 11.982(2)$, $b = 23.753(5)$, $c = 8.375(1)$ Å, $V = 2383.6(7)$ Å^3, $Z = 4$, $\rho_{calcd} = 1.161$ g cm^{-3}, $\lambda(Mo_{K\alpha}) = 0.71069$ Å, $\mu(Mo_{K\alpha}) = 3.69$ cm^{-1}; crystal dimensions $0.21 \times 0.27 \times 0.40$ mm^3. The structure was solved by the heavy atom method (Patterson and Fourier synthesis) and refined by full-matrix least-squares. For 1631 unique observed structure amplitudes [$I > 3\sigma(I)$] collected at room temperature on a CAD4 diffractometer in the range $4 < 2\theta < 54°$ the *R* value was 0.080 (unit weights). Most of the hydrogen atoms were located in a difference Fourier map and introduced as fixed contributors in the final stage of refinement. All calculations were carried out using SHELX 76 [14].

[14] Further details of the crystal structure investigation are available from the Director of the Cambridge Crystallographic Data Centre, University Chemical Laboratory, Lensfield Road, Cambridge CB2 1EW (England) on quoting the full journal citation.

3-Arylsulfonyloxazolidines as Chiral Templates; Asymmetric Synthesis of 2-Substituted 2-Hydroxycyclohexanecarbaldehydes from 2-Hydroxymethylenecyclohexanone**

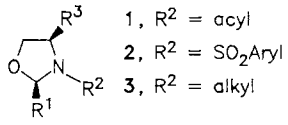
By *Inga Hoppe, Dieter Hoppe,* Christian Wolff, Ernst Egert,** and *Regine Herbst*

Enantiomerically pure mono- and bicyclic 3-acyloxazolidines are suitable as chiral templates for asymmetric synthesis.[1–4] Our attempts to use **1** more generally for intra- and intermolecular reactions at R^1 and R^2, however, revealed serious disadvantages to this approach:[5] (1) changing stereoselectivities in the condensation step;[4–6] (2) lack of stability toward several organometallic reagents; (3) low tendency for crystallization and difficult NMR-spectro-

[*] a) Prof. Dr. D. Hoppe, Dr. I. Hoppe, Dr. C. Wolff
Institut für Organische Chemie der Universität
Olshausenstrasse 40-60, D-2300 Kiel 1 (FRG)
b) Prof. Dr. E. Egert, R. Herbst
Institut für Organische Chemie der Universität
Tammannstrasse 4, D-3400 Göttingen (FRG)

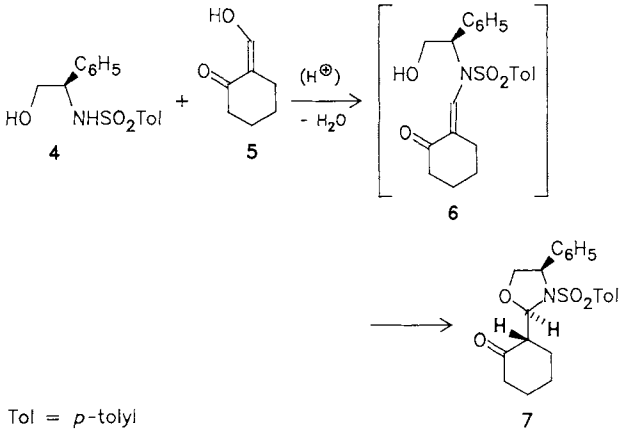
[**] This work was supported by the Fonds der Chemischen Industrie and Bayer AG, Leverkusen (donation of chemicals).

scopic structural elucidation owing to slowly interconverting amide rotamers.



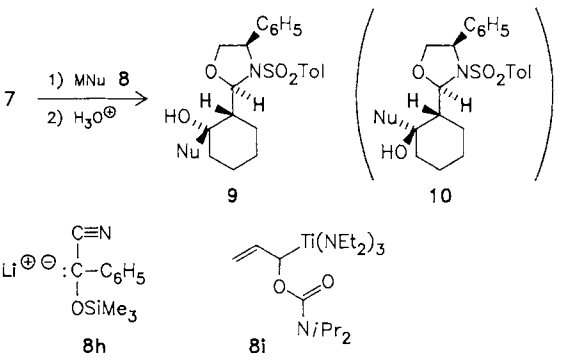
R^1 = alkyl, alkenyl, aryl; R^3 = alkyl, phenyl

We have now found that the 3-arylsulfonyloxazolidines **2** are not only free of these limitations but also have further advantages. We present here the first example of their application in enantioselective synthesis. (*R*)-*N*-(4-Toluenesulfonyl)phenylglycinol **4** undergoes acid-catalyzed condensation with 2-hydroxymethylenecyclohexanone **5** to give a single crystalline *cis*-oxazolidine **7** (yield 71%); less than 5% of the other three possible diastereoisomers are present in the crude product.[7] The *cis* selectivity of formation observed for 3-alkyloxazolidines **3**[8] thus remains valid. In addition, the formation of a third stereogenic center is induced in the cyclohexane ring. We assume that this is the result of an intramolecular *anti* addition of the OH group in the intermediary (*E*)-enamide **6**.



Tol = *p*-tolyl

The addition of widely differing nucleophiles MNu **8** to the keto group of the six-membered ring usually leads to diastereoisomerically pure adducts **9** (Table 1); only the reduction of **7** with diisobutylaluminum hydride (DIBAH) or sodium borohydride affords, in addition to **9a**, a second diastereoisomer, presumably **10a** (99%, 43:57, and 72%, 48:52, respectively).



The configuration of the methyl adduct **9b**—(1′*R*,2*R*,2′*S*,4*R*)—was determined by an X-ray structure analysis.[12] Noteworthy is the pyramidal configuration of N-3 (sum of angles 344.5°; Fig. 1) and the fact that the aryl moiety of the sulfonyl group covers the "bottom face" of the five-membered ring.

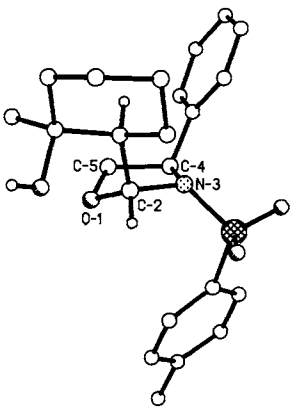


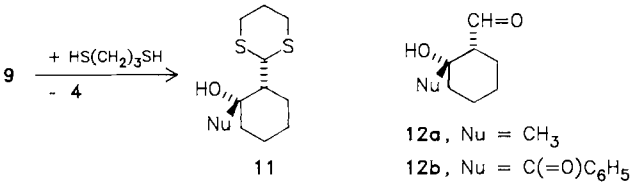
Fig. 1. Molecular structure of **9b**. The five-membered ring adopts an envelope conformation, with O-1 lying 50 pm outside the plane formed by the four other ring atoms.

Table 1. Yields, melting points, and optical rotations for the synthesized oxazolidines **9** and *ent*-**9**.

Starting material	MNu	Product **9** [a, b]	Nu	Yield [%] [c]	M.p. [°C] [d]	$[\alpha]_D^{20}$ [e]
7	$Zn(BH_4)_2$ **8a**	**9a**	H	99	60 (decomp.)	−563
7	$ClMgCH_3$ **8b**	**9b**	CH_3	89	171	−112.8
ent-7	$ClMgCH_3$ **8b**	*ent*-**9b**	CH_3	91	171	+113.0
7	$BrMgC_6H_5$ **8c**	**9c**	C_6H_5	80	161	− 79.4
7	$BrMgCH{=}CH_2$ **8d**	**9d**	$CH{=}CH_2$	95	55	− 96.7
ent-7	$Li^{\oplus}CH_2{=}C(O^{\ominus}){-}OtBu$ **8e**	*ent*-**9e**	CH_2CO_2tBu	70	169	+ 80.4
ent-7	$Li^{\oplus}(CH_3)_2C{=}C(O^{\ominus}){-}OMe$ **8f**	*ent*-**9f**	$C(CH_3)_2CO_2Me$	50	147	+ 95.6
ent-7	Li–C(OMe)=CH_2 [9] **8g**	*ent*-**9g**	C(OMe)=CH_2	52	56 (decomp.)	+ 86.3
ent-7	**8h** [10]	*ent*-**9h** [f]	(C=O)Ph	67	181	+ 56.4
ent-7	**8i** [11]	*ent*-**9i**	(*Z*)-$CH_2CH{=}CHOCb$ [g]	68	71	+ 45

[a] All products **9** were obtained in analytically pure form (C ±0.3, H ±0.3). [b] A second diastereomer could not be detected in any case by ^1H NMR spectroscopy, ≥95% *ds*. [c] After chromatographic purification. [d] From ether/petroleum ether. [e] CH_2Cl_2, $c = 1$. [f] Isolated and characterized as $OSiMe_3$ derivative. [g] OCb = (C=O)N*i*Pr_2.

The amino acetals **9** correspond to (2-substituted) 2-hydroxycyclohexanecarbaldehydes **12**. As we showed by converting *ent*-**9b** and *ent*-**9h** into the enantiomerically pure dithianes *ent*-**11b** (85%) and *ent*-**11h** (80%), respectively, the removal of the chiral auxiliary occurs smoothly with 1,3-propanedithiol, even for dehydration-sensitive derivatives.[3]



The method described here allows the general and simple synthesis of enantiomerically pure aldehydes of type **12**; usually, diastereoisomer separations of the intermediates are not required. The good crystallizability of **9** simplifies purification, when necessary in specific cases. Functionalized nucleophiles, such as enolates (**8e**, **8f**), synthetic equivalents of acylanions, **8g**[9] and **8h**,[10] and of homoenolates (e.g., **8i**[11]), also react facilely, thereby allowing the synthesis of bicyclic compounds in subsequent reactions. The enantiomers *ent*-**11** are also accessible with the L-valinol congener (*ent*-**7**, $(CH_3)_2CH$ instead of C_6H_5).

Experimental Procedure

7: 4-Å molecular sieves (10 g) and methanesulfonic acid (0.15 g) were added sequentially to a solution of **4** (2.91 g, 10 mmol) and **5** (1.26 g, 10 mmol) in 50 mL of dichloromethane. The reaction mixture was stirred slowly for 24 h at 20–25 °C; solid potassium carbonate (0.4 g) was then added and the solids were filtered off, followed by removal of the solvent under vacuum. Crystallization from ether and chromatography of the mother liquor on silica gel with ether/pentane (1:1) afforded 2.84 g (71%) **7**, $R_F = 0.13$, m.p. 144 °C, $[\alpha]_D^{20}$ −136.1 (CH_2Cl_2, $c = 1$). *ent*-**7**, $[\alpha]_D^{20}$ +136.0, was obtained in the same way from *ent*-**4**. Selected spectroscopic data. ^{1}H NMR ($CDCl_3$): $\delta = 3.82$ and 3.90 (ABX, $J_{gem} = 9.1$ Hz, $J_{cis} = 7.3$ Hz, $J_{trans} = 5.8$ Hz, 5-H_2), 4.75 (dd, 4-H), 5.73 (d, $J = 8.5$ Hz, 2-H). ^{13}C NMR ($CDCl_3$): $\delta = 54.6$ (C-1′), 62.1 (C-5), 71.1 (C-4), 91.5 (C-2), 209.9 (2′-C=O); IR (KBr): $\tilde{\nu} = 1660$ (C=O), 1355 and 1165 cm^{-1} (NSO_2).

ent-**9b**: A 2 M solution of methylmagnesium chloride in THF (3 mL, 6 mmol) was added to a solution of *ent*-**7** (2.00 g, 5.00 mmol) in THF below −70 °C and the resulting mixture was stirred for 24 h in an acetone/dry ice bath. The solution was then warmed to room temperature and the solvent removed under vacuum. The residue was worked up with dichloromethane/saturated ammonium chloride solution. Crystallization from toluene/ether and chromatography of the mother liquor on silica gel with ether/pentane (1:1) afforded 1.89 g (91%) *ent*-**9b**, $R_F = 0.15$. A second diastereomer could not be detected. ^{1}H NMR ($CDCl_3$): $\delta = 1.25$ (s, 2′-CH_3), 2.25 (s, OH), 3.87 and 4.00 (ABX part, $J_{gem} = 9.0$ Hz, $J_{cis} = 7.8$ Hz, $J_{trans} = 7.1$ Hz, 5-H_2), 5.63 (d, $J = 8.5$ Hz, 2-H). ^{13}C NMR ($CDCl_3$): $\delta = 29.5$ (2′-CH_3), 21.4 (C-4′), 24.7 (C-5′), 25.2 (C-6′), 40.8 (C-3′), 47.4 (C-1′), 62.0 (C-4), 70.77 (C-2′), 70.84 (C-5), 90.4 (C-2).

ent-**11b**: A solution of *ent*-**9b** (208 mg, 0.50 mmol), 1,3-propanedithiol (0.080 mL, 0.80 mmol), and methanesulfonic acid (15 mg) in dichloromethane (2.5 mL) was refluxed under argon for 3 h and, after cooling, neutralized with potassium carbonate (40 mg). Chromatography on silica gel with ether/pentane (1:5) afforded 98 mg (85%) *ent*-**11b**, m.p. 68 °C (pentane), $[\alpha]_D^{20}$ +63.4 (CH_2Cl_2, $c = 1.5$). *ent*-**11h**: Yield 80%, m.p. 99 °C, $[\alpha]_D^{20}$ +1.96, $[\alpha]_{436}^{20}$ −91.5 (CH_2Cl_2, $c = 1$).

Received: August 8, 1988 [Z 2912 IE]
German version: *Angew. Chem. 101* (1989) 65

[1] A. I. Meyers, B. A. Lefker, *Tetrahedron 43* (1987) 5663, and references cited therein.
[2] D. Seebach, J. D. Aebi, *Tetrahedron Lett. 25* (1984) 2545.
[3] A. Bernardi, S. Cardani, G. Poli, C. Scolastico, *J. Org. Chem. 51* (1986) 5041.
[4] Cf. also: M. E. Jung, L. J. Street, *Heterocycles 27* (1988) 45.
[5] a) U. Ries, *Diplomarbeit*, Universität Göttingen 1985; b) H. Hoffmann, *Diplomarbeit*, Universität Kiel 1987.
[6] W. Ando, Y. Igarashi, L. Huang, *Chem. Lett. 1987*, 1361.
[7] If the reaction of **4** and **5** is carried out in refluxing benzene, up to 50% of a second diastereomer of **7** with (1′*R*) configuration in the six-membered ring is formed. M.p. = 53–55 °C (ether), $R_F = 0.20$ (ether/petroleum ether 1:1), $[\alpha]_D^{20}$ −92.7 (CH_2Cl_2, $c = 0.4$). ^{1}H NMR ($CDCl_3$): $\delta = 3.64$ and 4.09 (ABX part, $J_{gem} = 9.1$ Hz, $J_{cis} = 6.7$ Hz, $J_{trans} = 3.3$ Hz, 5-H_2), 4.63 (dd, 4-H), 5.54 (d, $J = 2.1$ Hz, 2-H).
[8] a) L. Neelakantan, *J. Org. Chem. 36* (1971) 2256; b) A. H. Beckett, G. R. Jones, *Tetrahedron 33* (1977) 3313; c) G. Just, P. Potvin, P. Uggowitzer, *J. Org. Chem. 48* (1983) 2923; d) M. Huche, J. Aubouet, G. Pourcelot, J. Berlan, *Tetrahedron Lett. 24* (1983) 585; e) H. Abdallah, R. Grée, R. Carrié, *ibid. 23* (1982) 503; f) P. Mangeney, A. Alexakis, J. F. Normant, *ibid. 24* (1983) 373; g) C. Agami, F. Couty, *ibid. 28* (1987) 5659, and references cited therein; h) H. Takahashi, Y. Chida, K. Higashiyama, H. Onishi, *Chem. Pharm. Bull. 33* (1985) 4662, and references cited therein.
[9] U. Schöllkopf, P. Hänssle, *Justus Liebigs Ann. Chem. 763* (1972) 208; J. E. Baldwin, G. A. Höfle, O. W. Lever, Jr., *J. Am. Chem. Soc. 96* (1974) 7125.
[10] S. Hünig, M. Öller, *Chem. Ber. 114* (1981) 959.
[11] Li-reagent: D. Hoppe, R. Hanko, A. Brönneke, F. Lichtenberg, E. van Hülsen, *Chem. Ber. 118* (1985) 2822; Ti-reagent analogous to: R. Hanko, D. Hoppe, *Angew. Chem. 94* (1982) 378; *Angew. Chem. Int. Ed. Engl. 21* (1982) 372.
[12] Crystal structure analysis of **9b** ($C_{23}H_{29}NO_4S$): space group $P2_12_12_1$, $a = 1027.9(1)$, $b = 1307.2(1)$, $c = 1612.6(2)$ pm, $V = 2.167$ nm^3, $Z = 4$; crystal dimensions, $0.7 \times 0.8 \times 1.0$ mm^3, 4360 measured reflections, $2\theta_{max} = 50°$ ($Mo_{K\alpha}$), empirical absorption correction; structure solution by direct methods (SHELXS-86), 3684 symmetry-independent reflections with $|F| > 3\sigma(F)$ used for the anisotropic refinement (272 parameters), H atoms localized by difference electron density determination and refined using a riding model or "restraints", $R = 0.033$ [$R_w = 0.043$, $w^{-1} = \sigma(F)^2 + 2 \times 10^{-4} F^2$]; absolute configuration confirmed by η-refinement [$\eta = 1.0(1)$]; crystal packing stabilized by intermolecular O-H···O(S) hydrogen bonds. Further details of the crystal structure investigation may be obtained from the Fachinformationszentrum Energie, Physik, Mathematik GmbH, D-7514 Eggenstein-Leopoldshafen 2 (FRG), on quoting the depository number CSD-53267, the names of the authors, and the journal citation.

Asymmetric Homoaldol Reaction by Enantioselective Lithiation of a Prochiral 2-Butenyl Carbamate**

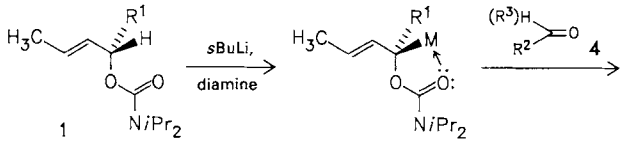
By *Dieter Hoppe** and *Oliver Zschage*

Enantiomerically pure *secondary* 2-alkenyl carbamates such as **1a** are deprotonated by alkyllithium-TMEDA with retention of configuration to give the corresponding chiral lithium derivatives **2a**·TMEDA.[1] The latter are configurationally stable below −70 °C and thus of preparative value. After metal exchange with tetra(isopropoxy)titanium, which also occurs with retention, the titanium complex **3a** adds to aldehydes **4** with 1,3-chirality transfer in the allyl moiety—coupled with enantiofacial differentiation at the carbonyl group (transition state **A**)—to afford, after aqueous work-up, the optically active homoaldol adducts **5**.[1–3]

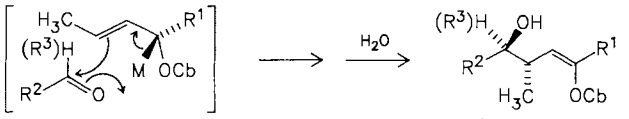
Nonracemic 1-unsubstituted enol carbamates such as **6**, valuable building blocks for the synthesis of diastereoisomerically pure γ-lactones,[4,5] are not accessible in this way, since their synthesis requires (prochiral) *primary* alkenyl carbamates like **1b** as starting materials. We have now found a surprisingly simple approach to generate (*R*)-**2** by deprotonation of **1b** in the presence of an enantiomerically pure diamine as complex-forming agent. Second-order asymmetric induction[6] results in the crystallization of only one enantiomer of **2b**, as a diamine complex, from a solution of the configurationally labile, racemic lithium

[*] Prof. Dr. D. Hoppe, Dipl.-Chem. O. Zschage
Institut für Organische Chemie der Universität
Olshausenstrasse 40–60, D-2300 Kiel (FRG)

[**] This work was supported by the Deutsche Forschungsgemeinschaft and the Fonds der Chemischen Industrie.



1–3: a, $R^1 = CH_3$; b, $R^1 = H$ — 2, M = Li · diamine; 3, M = $Ti(OiPr)_4^{\ominus}\ Li^{\oplus}$



A — 5, $R^1 = CH_3$; 6, $R^1 = H$

Cb = $C(=O)N(iPr)_2$

4,6: a, $R^2 = CH(CH_3)_2$, $R^3 = H$; b, $R^2 = CH_3$, $R^3 = H$; c, $R^2 = (CH_2)_3CH_3$; $R^3 = H$; d, $R^2 = R^3 = CH_3$

compound *rac*-**2b**. The solid product is then transmetalated to give the configurationally stable titanium derivative **3b**, which adds enantioselectively to aldehydes and ketones.

Reaction of (*E*)-2-butenyl carbamate **1b** with a solution of equivalent molar amounts of *sec*-butyllithium and (−)-sparteine[7] **7** below −70°C in pentane/cyclohexane results, within only a few minutes, in the crystallization of a lithium complex. Upon addition of four equivalents of tetra(isopropoxy)titanium,[8] the complex goes into solution; subsequent reaction with achiral aldehydes **4a–c** or with acetone (**4b**) gives the diastereomerically pure adducts **6a–d** in 90–95% yield and with 80–84% enantiomeric excess[9] (see Table 1).

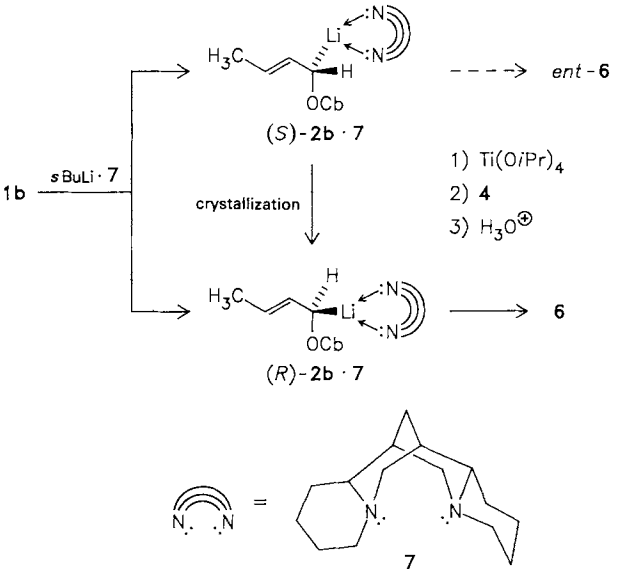
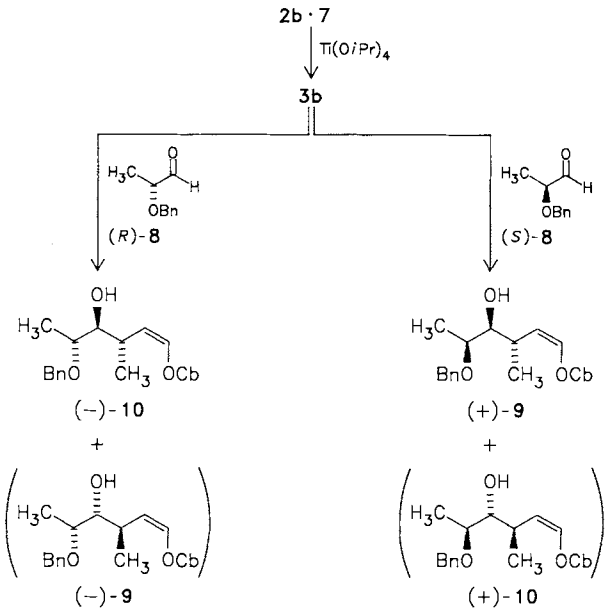


Table 1. Yields, enantiomeric excesses, and optical rotations for the homoaldol adducts **6**, **9**, and **10**.

Product	R^2	R^3	Yield [%]	*ee* [%]	$[\alpha]_D^{20}$ [a]
6a [5a]	$(CH_3)_2CH$	H	95	83	+15.2
6b [5a]	CH_3	H	95	80	+22.0
6c [4a]	*n*-C_4H_9	H	92	82	+ 5.1
6d [4b]	CH_3	CH_3	93	84	+48.0
(+)-**9** [5b]	(*S*)-$CH_3CH(OBn)$	H	90 [b]	>95	+33.0
(−)-**10** [5b]	(*R*)-$CH_3CH(OBn)$	H	79 [c]	>95	− 9.8

[a] Methanol, $c = 2.0$–2.5. [b] Besides 4% (+)-**10**. [c] Besides 14% (−)-**9**.

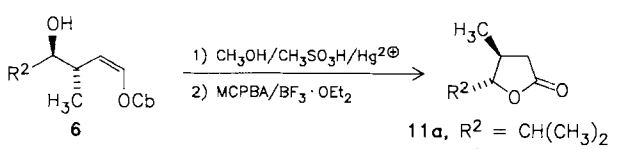
The same reaction with (*S*)-2-benzyloxypropanal (*S*)-**8** leads to formation of the diastereoisomers[5b] (+)-**9** and (+)-**10** (95:5, yield 94%), whereas with (*R*)-**8** the enantiomers (−)-**9** and (−)-**10** are obtained in almost the opposite ratio (15:85, yield 93%).[1b,10] The configuration at C-3 and C-4 of the diastereoisomers formed in excess, (+)-**9** and (−)-**10**, which is related to that of **3** through the transition state **A**,[1] leads to assignment of an (*R*) configuration to the reacting titanium species **3b**.[11] The average enantiomeric ratio attained for **6**/*ent*-**6** (91:9) reflects the minimal diastereoisomeric ratio of the sparteine complexes (*R*)-**2b**·**7**:(*S*)-**2b**·**7** in the reaction mixture.



The same result is obtained when the racemate *rac*-**2b**·DME (DME = dimethoxyethane) is first generated and (−)-sparteine **7** is then added (92% **6a** with 82% *ee*). On the other hand, in experiments in which crystallization did not occur, **6a** was obtained in the same yield but with maximally 20% *ee*.

Thus, the following interpretation is compelling: the enrichment of (*R*)-**2b**·**7** is the consequence of a second-order asymmetric induction;[6] i.e., the diastereoisomeric complexes (*R*)- and (*S*)-**2b**·**7** are configurationally labile in solution and equilibrate through an epimerization; (*R*)-**2b**·**7** is removed from the equilibrium by crystallization and, as a solid, is configurationally stable. The transmetalation with $Ti(OiPr)_4$ apparently occurs directly with the solid. Thus, it is not possible to determine whether **1b** is deprotonated by *s*BuLi·**7** with enantiotopic differentiation—although this was our original conception.

Methanolysis and Grieco oxidation[4a] of **6** afford the optically active lactones **11**. We obtained (+)-**11a**[12] in 87% and (+)-**11c**[12] (Quercus lactone A)[13] in 90% yield.



6 — 11a, $R^2 = CH(CH_3)_2$; 11c, $R^2 = (CH_2)_3CH_3$

This method offers a fundamentally new and very simple route to nonracemic allyllithium derivatives. Thus, (*R*)-**2b** should be of interest not only as a chiral homoenolate reagent but also (after ozonolysis[14] of **6**) as an *anti*-selective propanal enolate equivalent that adds with good reagent-controlled stereoselectivity.[15]

Experimental Procedure

A ca. 1.4 M solution of *sec*-butyllithium (2.2 mmol) in cyclohexane/isopentane was added to a solution of (−)-sparteine (**7**) (2.2 mmol) in pentane (7 mL) and cyclohexane (1 mL) [16] cooled in a dry ice/acetone bath. **1b** (2.0 mmol) [4b] in 2 mL of pentane was then added to the stirred solution. After 10 min, the precipitate formed on the wall of the flask was brought into suspension by removing the flask briefly from the cooling bath (internal temperature max. −60 °C!) and the flask was cooled once again at −70 °C. After 30 min, 8.8 mmol of tetra(isopropoxy)titanium was added and, after another 30 min, 2.5 mmol of the carbonyl compounds **4** or **8**. After stirring for 4 h, the reaction mixture was allowed to warm to 0 °C and 2 N hydrochloric acid and ether (40 mL each) were added, followed by the usual workup. Purification was accomplished by flash chromatography on silica gel with ether/pentane (1:8 to 4).

Received: August 8, 1988 [Z 2913 IE]
German version: *Angew. Chem. 101* (1989) 67

[1] a) D. Hoppe, T. Krämer, *Angew. Chem. 98* (1986) 171; *Angew. Chem. Int. Ed. Engl. 25* (1986) 160; b) T. Krämer, D. Hoppe, *Tetrahedron Lett. 28* (1987) 5149.

[2] Reviews: a) D. Hoppe, *Angew. Chem. 96* (1984) 930; *Angew. Chem. Int. Ed. Engl. 23* (1984) 932; b) D. Hoppe in M. P. Schneider (Ed.): *Enzymes as Catalysts in Organic Synthesis*, Reidel, Dordrecht 1986, p. 176.

[3] Other methods for asymmetric homoaldol reactions: a) H. Roder, G. Helmchen, E.-M. Peters, H.-G. von Schnering, *Angew. Chem. 96* (1984) 895; *Angew. Chem. Int. Ed. Engl. 23* (1984) 898; b) V. J. Jephcote, A. J. Pratt, E. J. Thomas, *J. Chem. Soc. Chem. Commun. 1984*, 800; c) R. W. Hoffmann, S. Dresely, *Tetrahedron Lett. 28* (1987) 5303.

[4] a) D. Hoppe, A. Brönneke, *Tetrahedron Lett. 24* (1983) 1687; b) D. Hoppe, R. Hanko, A. Brönneke, F. Lichtenberg, E. van Hülsen, *Chem. Ber. 118* (1985) 2822.

[5] a) J. Lüssmann, D. Hoppe, P. G. Jones, C. Fittschen, G. M. Sheldrick, *Tetrahedron Lett. 27* (1986) 3595; b) D. Hoppe, G. Tarara, M. Wilckens, P. G. Jones, D. Schmidt, J. J. Stezowski, *Angew. Chem. 99* (1987) 1079; *Angew. Chem. Int. Ed. Engl. 26* (1987) 1034.

[6] J. D. Morrison in J. D. Morrison (Ed.): *Asymmetric Synthesis, Vol. 1*, Academic Press, New York 1983, p. 1.

[7] (−)-Sparteine has already been used for chiral modification of "cations" of organometallic compounds containing *achiral* "carbanion" moieties: see, for example, M. Guetté, J. Capillon, J.-P. Guetté, *Tetrahedron 29* (1973) 3659. It is important to note that the asymmetric induction in that case is caused by the orientation of the starting materials with respect to the cation. Thus, the direction and extent of the asymmetric induction cannot be predicted. Application to a chiral Grignard compound gave only a slight enantiomeric exess (7% *ee*), cf. S. Harvey, P. C. Junk, C. L. Raston, G. Salem, *J. Org. Chem. 53* (1988) 3134.

[8] Reviews: M. T. Reetz, *Organotitanium Reagents in Organic Synthesis*, Springer, Berlin 1986; D. Seebach, B. Weidmann in R. Scheffold (Ed.): *Modern Synthetic Methods 1983*, Salle, Frankfurt 1983, p. 217.

[9] Determined by ^{1}H NMR spectroscopy in ca. 0.2 M $CDCl_3$ solution with 10–40 mol% of tris[(3-heptafluoropropylhydroxymethylene)-d-camphorato]europium(III) [Eu(hfpc)$_3$]. The 1-H signal of **6** is shifted 0.2–0.5 ppm downfield compared with that of *ent*-**6**.

[10] For the problem of double stereodifferentiation in the addition of chiral organometallic compounds, see R. W. Hoffmann, J. Lanz, R. Metternich, G. Tarara, D. Hoppe, *Angew. Chem. 99* (1987) 1196; *Angew. Chem. Int. Ed. Engl. 26* (1987) 1145, and references cited therein.

[11] In control experiments, the lithium complex **2b**·**7** also gave **6a** (62% *ee*) in excess in addition to α adducts and the γ-*syn* diastereomer. This demonstrates that the metal exchange with Ti(O*i*Pr)$_4$ occurs with retention.

[12] **11c**: $[\alpha]_D^{20}$ +52.1 (methanol, $c = 1$). The optical purity of 62%, determined by comparison of the optical rotation with that of the natural product [13a], is presumably incorrect, since the transformation of **6c** (83% *ee*) cannot be accompanied by racemization. **11a** (83% *ee*): $[\alpha]_D^{20}$ +31.8 (methanol, $c = 2.5$).

[13] a) M. Masuda, K. Nisimimura, *Chem. Lett. 1981*, 1333; b) enantioselective synthesis: R. M. Ortuño, R. Merce, J. Font, *Tetrahedron 43* (1987) 4497.

[14] D. Hoppe, F. Lichtenberg, *Angew. Chem. 94* (1982) 378; *Angew. Chem. Int. Ed. Engl. 21* (1982) 372; *Angew. Chem. Suppl. 1982*, 961.

[15] Reviews on the use of crotylmetal compounds as propanal enolate equivalents; a) R. W. Hoffmann, *Angew. Chem. 99* (1987) 503; *Angew. Chem. Int. Ed. Engl. 26* (1987) 489; b) R. W. Hoffmann, *Pure Appl. Chem. 60* (1988) 123; c) Y. Yamamoto, *Acc. Chem. Res. 20* (1987) 243.

[16] The crystallization of (*R*)-**2b**·**7** is induced by cyclohexane. It is still not clear whether the cyclohexane is incorporated into the crystal lattice or only serves as a crystallization seed. As we have shown for **6a**, after addition of cyclohexane, *n*-butyllithium in hexane can also be used for the deprotonation, giving the same results.

Retention of Configuration in the Non-Darwinian Evolution of Cytochrome c

By *Shosuke Kojo**, *Koushi Fukunishi*, and *Ikuyo Tsukamoto*

Cytochrome c from eukaryotes characteristically has two sulfide bonds between the cysteine residues of the apoprotein and the hemin group. Acid hydrolysis of cytochrome c affords the prosthetic group hemin c **1**, whose structure is shown in Figure 1. Since cytochrome c is distributed in a wide range of organisms, it has been especially useful as a probe for the study of molecular evolution, particularly with regard to changes in the amino acid sequence.[1,2] These studies are related to the idea of non-Darwinian,[3] i.e., neutral evolution,[4] in which variations in homologous proteins are attributed to a genetic drift without selective advantage. Thus, for example, the cytochrome c of a horse differs from that of baker's yeast in 45 of the ca. 110 amino acid residues.[5] This number is very large, considering that, in many cases, even a single amino acid alteration is sufficient to cause a dramatic change in the function of the protein.

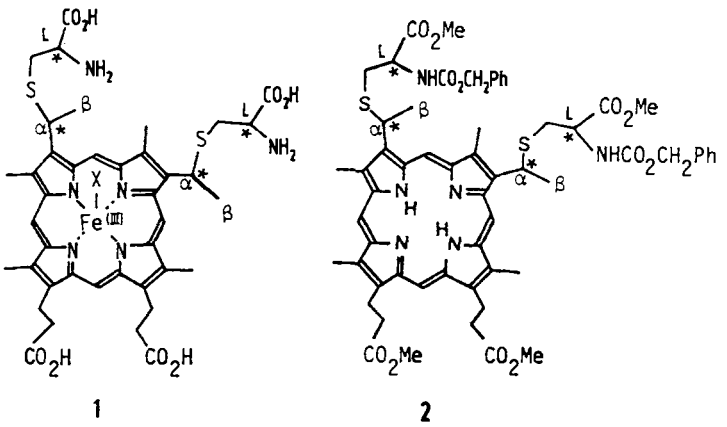


Fig. 1. Hemin c **1** and bis(*N*-benzyloxycarbonyl)porphyrin-c tetramethylester **2**. The chiral carbon atoms are indicated by asterisks. The letter L indicates that the cysteinyl group is the L-isomer. X represents a ligand; in compound **1**, X = Cl.

Cytochrome c is located in a respiratory system, whose origin is very old. Furthermore, its fundamental reaction mechanism has not changed during biological evolution.

[*] Prof. Dr. S. Kojo
Laboratory of Food Chemistry and Nutrition
Department of Life and Health Sciences
Hyogo University of Teacher Education
Shimokume, Yashiro, Hyogo 674-14 (Japan)
Prof. Dr. K. Fukunishi
Department of Chemistry, Kyoto Institute of Technology
Kyoto 606 (Japan)
Prof. Dr. I. Tsukamoto
Department of Food Science and Nutrition, Nara Women's University
Nara 630 (Japan)

Accordingly, some structural similarities are expected to be exhibited by the various cytochrome c forms even after considerable neutral evolution. Such similarities must be closely related to the function of the protein, which transports electrons from cytochrome c_1 to cytochrome oxidase in the mitochondrial membrane. The functional similarity of eukaryotic cytochromes c is demonstrated by the fact that many of them react equally rapidly with beef heart cytochrome oxidase in spite of them having considerable differences in the amino acid sequence.[6] In order to exhibit this functional similarity in interaction with neighboring proteins, cytochrome c must retain its redox potential and molecular properties, such as size and charge distribution as well as the environment and orientation of the active site. The retention of the redox potential is, as is already well-known, ensured by the presence of sulfide bonds and of similar ligands bound to the iron atom of the hemin group. The retention of the molecular properties is expected to be dependent on the configuration of the two chiral α-C atoms bearing the sulfide bonds. As shown by X-ray studies,[2] the small protein of cytochrome c just covers the porphyrin ring, one edge of which even projects into the solvent. For this reason its molecular shape (especially in the vicinity of the active site) is assumed to be strongly influenced by the configuration of the two chiral C atoms at the junction of the hemin group and the apoprotein. Since the hemin group contains two chiral carbon atoms, four diastereomers are possible.

We have developed a chemical method[7] to investigate this stereochemical problem and have established unambiguously that hemin c **1** of horse cytochrome c consists of a single isomer.[1] A mixture of the four diastereomers of **1**[8] was prepared and converted into the tetramethylesters **2**[9] (Fig. 1). The four components of **2** were separated by HPLC. We also prepared isomers of **1** starting from D- or D,L-cysteine, and used these compounds to check for racemization of the cysteine part of **1** using HPLC; no racemization was found. Moreover, cytochrome c was converted to **2** via stereospecific reactions and its HPLC chromatogram compared with that of the chemically prepared diastereomers. This showed that horse cytochrome c contained only one of the four possible diastereomers.[7] The same method was applied to cytochrome c from chicken, tuna and *Saccharomyces cerevisiae*. All of these cytochromes c were shown to have the same stereochemistry at the chiral carbon atoms as the horse cytochrome c. Although only a limited number of examples is available, these results strongly suggest that the configuration in the positions α- to the sulfide bonds is retained during the evolution of eukaryotic cytochrome c and that this—as mentioned above—may be essential for the retention of protein function. In other words, neutral evolution was apparently only possible if the stereochemical requirements were fulfilled.

Received: July 19, 1988 [Z 2872 IE]
German version: *Angew. Chem. 101* (1989) 64

[1] W. M. Fitch, E. Margoliash, *Science (Washington) 155* (1967) 279.
[2] R. E. Dickerson, R. Timkovich in P. D. Boyer (Ed.): *The Enzymes, Vol. 11*, Academic Press, New York 1975, p. 397–547.
[3] J. L. King, T. H. Jukes, *Science Washington 164* (1969) 788.
[4] E. Kimura, *Nature (London) 217* (1968) 624.
[5] M. O. Dayhoff, *Atlas of Protein Sequence and Structure, Vol. 5*, National Biomedical Research Foundation, Washington, DC, USA 1972.
[6] L. Smith, M. E. Nava, E. Margoliash, *Oxidases Relat. Redox Syst. Proc. Int. Symp. 2nd 1971 (1973)* 629–647.
[7] S. Kojo, S. Sano, K. Fukunishi, *J. Chem. Soc. Chem. Commun. 1981*, 1223.
[8] S. Kojo, S. Sano, *J. Chem. Soc. Chem. Commun. 1977*, 249.
[9] S. Kojo, S. Sano, *J. Chem. Soc. Perkin Trans. 1 1981*, 2864.

Model of a Solvent-Shared Ion Pair with N-H···C Hydrogen Bonds between Amine and Carbanion—Crystal Structure of [Fluorenyllithium·2 Ethylenediamine]$_\infty$**

By *Stefan Buchholz, Klaus Harms, Michael Marsch, Werner Massa,* and *Gernot Boche**

In the majority of organolithium compounds $Li^\oplus$ is bound directly to C or heteroatoms (N, O, S) of the carbanion ("contact ion pairs").[1] In a few exceptional cases $Li^\oplus$ is chelated by two 12-crown-4[2] or tetramethylethylenediamine (TMEDA) molecules.[3] Herein we report on the solid state structure of [fluorenyllithium·2 ethylenediamine]$_\infty$ **1**.[4] The ethylenediamine (EDA) ligands in this complex form a network structure with the fourfold coordinated $Li^\oplus$ ions in which the "naked" fluorenyl anions are embedded; the structure is stabilized by N-H···C hydrogen bonds (Fig. 1).[5]

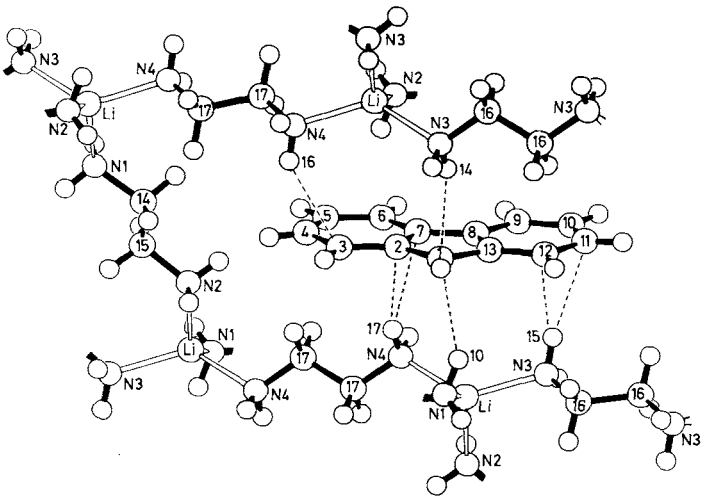


Fig. 1. Section of the crystal structure of [fluorenyllithium·2 ethylenediamine]$_\infty$ **1** [8] with N-H···C hydrogen bonds <280 pm. Two of the three crystallographically different EDA molecules lie on inversion centers. Important bond lengths [pm]: C1-C2 139.9(4), C2-C3 142.6(5), C3-C4 136.3(6), C4-C5 139.6(6), C5-C6 139.9(6), C6-C7 138.7(4), C7-C8 143.6(4), C8-C9 141.7(4), C9-C10 137.7(5), C10-C11 139.8(5), C11-C12 138.0(4), C12-C13 141.4(4), C13-C1 142.7(4), C14-C15 152.0(4), C16-C16′ 152.9(4), C17-C17′ 151.9(4), C14-N1 148.4(4), C15-N2 148.0(4), C16-N3 146.9(4), C17-N4 146.7(4), Li-N1 207.1(5), Li-N2 209.8(5), Li-N3 208.0(5), Li-N4 207.7(5), Li···C13 403.6(6), Li′-C2 406.0(6), Li′···C3 407.5(7); N-H···C hydrogen bonds with H···C distances <280 pm: C1-N3′ 331.1(4), C1-H14′ 250(4), H14′-N3′ 87(4), C7-N4 332.9(4), C7-H17 259(3), H17-N4 90(3), C1-N1 342.9(5), C1-H10 257(3), H10-N1 97(3), C3-N4′ 349.5(4), C3-H16′ 274(3), H16′-N4′ 90(3), C12-N3 350.8(4), C12-H15 271(3), H15-N3 95(3), C2-N4 357.0(4), C2-H17 269(3), H17-N4 90(3), C11-N3 359.4(9), C11-H15 267(3), H15-N3 95(3); bond angles [°]: N1-Li-N2 126.2(3), N1-Li-N3 101.2(2), N1-Li-N4 102.5(2), N2-Li-N3 103.5(2), N2-Li-N4 99(2), N3-Li-N4 127.5(3); N-H···C hydrogen bonds: C1-H14-N3 156(3), C7-H17-N4 140(3), C1-H10-N1 148(2), C3-H16′-N4′ 141(3), C12-H15-N3 142(2), C2-H17-N4 166(3), C11-H15-N3 164(2); torsion angles [°]: N1-C14-C15-N2 175.5(2), N3-C16-C16′-N3′ 180, N4-C17-C17′-N4′ 180.

Each $Li^\oplus$ ion is surrounded by four EDA molecules, which are present in antiperiplanar conformation (torsion angles 180, 180 and 175.5°). The N-Li-N bond angles (99.0 to 127.5°) are closer to the tetrahedral angle than in a

[*] Prof. Dr. G. Boche, Dipl.-Chem. S. Buchholz, Dr. K. Harms, M. Marsch, Priv.-Doz. Dr. W. Massa
Fachbereich Chemie der Universität
Hans-Meerwein-Strasse, D-3550 Marburg (FRG)

[**] This work was supported by the Deutsche Forschungsgemeinschaft and the Fonds der Chemischen Industrie. *S. B.* thanks the Studienstiftung des Deutschen Volkes for a scholarship.

chelate.[9] $Li^{\oplus}$ is not bound to a C atom of the fluorenyl anion, the shortest distance Li–C13 is 403.6 pm (in the solid state structure of the contact ion pair fluorenyllithium·2quinuclidine[10] the following Li–C distances were found: 233.3, 247.1 and 279.4 pm). In contrast, the fluorenyl anion **1** exhibits hydrogen bonding with the amine hydrogen atoms of the EDAs, of which only those with H···C distances <280 pm are shown in Figure 1. The bonds H14–C1 (250 pm), H10–C1 (257 pm) and H17–C7 (259 pm), in particular, are significantly shorter than the sum of the van-der-Waals radii of H and C (290 pm).[11] According to semiempirical calculations[10, 12] C1 exhibits the highest charge density, that of C7 also being high. Up to now the presence of H bonds to carbanions was mainly concluded from kinetic investigations;[13] spectroscopic detection was possible in only a few cases.[14] Investigations by *Seebach* et al.[15] and *Tamm* et al.[17] show the significance of N–H bridged amide, ester, and ketone enolates, which were prepared by deprotonation with lithium amides, in alkylation or deuteration (degree of deuteration up to <1%). *Dunitz* and *Seebach* et al. first found an N–H···C bond X-ray crystallographically in the lithium enolate $[t\mathrm{BuC(OLi)CH_2}\cdot\mathrm{TriMEDA}]_2$.[15b]

Our findings are in agreement with the UV/VIS spectrum of fluorenyllithium in ethylenediamine, from which the presence of N–H···C hydrogen bonds had already been concluded;[18] the absorption maximum $\lambda_{max}=368$ nm[19] is shifted hypsochromically compared to that of the solvent-separated ion pair ($Fl^{\ominus}$, THF, $Li^{\oplus}$, −30°C, $\lambda_{max}=373$),[20] and the contact-ion pair ($Fl^{\ominus}$, $Li^{\oplus}$, THF, 25°C) absorbs at 349 nm.[19]

Marcus[21] recently made a distinction between "solvent separated", "contact" and "*solvent shared*" ion pairs. In a solvent-separated ion pair each ion has its own solvent shell, whereas in a solvent-shared (solvent-bridged) ion pair both ions share the solvent molecules. The solid state structure of **1** is thus a model for a solvent-bridged ion pair. In this case in particular it is also to be expected that the N–H bonds participating in H-bonds are additionally polarized by the $Li^{\oplus}$–N interaction and thus better hydrogen bond donors. Solvent-shared ion pairs of the type described here should therefore be of general importance in polar organometallic compounds in solvents which contain N–H or O–H groups.

Received: August 3, 1988 [Z 2902 IE]
German version: *Angew. Chem. 101* (1989) 57

[1] a) W. N. Setzer, P. von R. Schleyer, *Adv. Organomet. Chem. 24* (1985) 353; b) G. Boche, *Angew. Chem. 101* (1989) in press; *Angew. Chem. Int. Ed. Engl. 28* (1989) in press.

[2] $Ph_3C^{\ominus}Li^{\oplus}(12\text{-crown-4})_2$ and $Ph_2CH^{\ominus}Li^{\oplus}(12\text{-crown-4})_2$: M. M. Olmstead, P. P. Power, *J. Am. Chem. Soc. 107* (1985) 2174; $^{\ominus}CH_2C_6H_2(3,5\text{-}Me_2)(4\text{-}BMes_2)Li^{\oplus}(12\text{-crown-4})_2$: R. A. Bartlett, P. P. Power, *Organometallics 5* (1986) 1916; $^{\ominus}CH_2BMes_2Li^{\oplus}(12\text{-crown-4})_2$: M. M. Olmstead, P. P. Power, K. J. Weese, R. J. Doedens, *J. Am. Chem. Soc. 109* (1987) 2541; review: P. P. Power, *Acc. Chem. Res. 21* (1988) 147.

[3] $BH_3(Me_2)P{-}C^{\ominus}H{-}P(Me_2)BH_3Li^{\oplus}(TMEDA)_2$: H. Schmidbaur, F. Weiss, B. Zimmer-Gasser, *Angew. Chem. 91* (1979) 848; *Angew. Chem. Int. Ed. Engl. 18* (1979) 782; $^{\ominus}CH_2Ni(C_2H_4)_2Li^{\oplus}(TMEDA)_2$: K. Jonas, K. R. Pörschke, C. Krüger, Y.-H. Tsay, *Angew. Chem. 88* (1976) 682; *Angew. Chem. Int. Ed. Engl. 15* (1976) 621.

[4] Procedure for **1**: A solution of fluorene (55 mg, 0.33 mmol) in dimethoxyethane (5.0 mL) was treated at 20°C with 2.2 mL (1 equiv.) of *n*BuLi in hexane and 0.8 mL (36 equiv.) of ethylenediamine. Crystals of **1** suitable for an X-ray structure analysis separated out in ca. 15 h.

[5] X-ray structure analysis: $C_{13}H_9Li\cdot2(C_2H_8N_2)$: $M=292.35$, monoclinic, space group $P2_1/c$, $a=1472.4(3)$, $b=856.1(2)$, $c=1326.7(3)$ pm, $\beta=104.11(2)°$, $Z=4$, $\rho_{calcd}=1.197$ g cm^{-3}. Measurements on an Enraf-Nonius CAD4 diffractometer with $Cu_{K\alpha}$ radiation (graphite monochromator) at −65°C; 2119 independent reflections with $F>4\sigma(F)$ and $\theta=3$–60°. Solution by direct methods [6], refinement [7] to $R=0.0614$, $R_w=0.0557$, all non-hydrogen atoms with anisotropic, H atoms with common isotropic temperature factors (all H atoms localized). Further details of the crystal structure investigation are available on request from the Fachinformationszentrum Energie, Physik, Mathematik GmbH, D-7514 Eggenstein-Leopoldshafen 2 (FRG) on quoting the depository number CSD-53270, the names of the authors, and the journal citation.

[6] G. M. Sheldrick, *SHELXS-86, Program for Crystal Structure Solution*, Göttingen 1986.

[7] G. M. Sheldrick, *SHELX-76, Program for Crystal Structure Determination*, Cambridge 1976.

[8] E. Keller, *SCHAKAL-86B, A FORTRAN Program for the Graphic Representation of Molecular and Crystallographic Models*, Freiburg 1986.

[9] In LiBr·2EDA the N-Li-N chelate angle is 86.0 (±1.2)°, in LiCl·2EDA 88.3 (±0.6)°; non-chelated as well as chelated EDA molecules are present in the crystal structures of both compounds; P. F. Durmond, P. Piret, M. Van Meerssche, *Acta Crystallogr. 23* (1967) 780; see also R. Zerger, W. Rhine, G. D. Stucky, *J. Am. Chem. Soc. 96* (1974) 5441.

[10] J. J. Brooks, W. Rhine, G. D. Stucky, *J. Am. Chem. Soc. 94* (1972) 7339.

[11] A. Weiss, H. Witte: *Kristallstruktur und chemische Bindung*, Verlag Chemie, Weinheim 1983, p. 329.

[12] S. Buchholz, *Diplomarbeit*, Universität Marburg 1988.

[13] D. J. Cram: *Fundamentals of Carbanion Chemistry*, Academic Press, New York 1965, p. 86–103; A. Streitwieser, J. A. Hudson, F. Mares, *J. Am. Chem. Soc. 90* (1968) 648; M. Schlosser, J. Hartmann, *ibid. 98* (1976) 4674; H. F. Koch, D. B. Dahlberg, G. Lodder, K. S. Root, N. A. Touchette, R. L. Solsky, R. M. Zuck, L. J. Wagner, N. H. Koch, M. A. Kuzemko, *ibid. 105* (1983) 2394; S. Hoz, M. Livneh, *ibid. 109* (1987) 7483; H. F. Koch: *Reactions of Hydrogen-bonded Carbanion Intermediates* in E. Buncel, T. Durst (Eds.): *Comprehensive Carbanion Chemistry, Part C*, Elsevier, Amsterdam 1987.

[14] L. Greifenstein, G. A. Pagani, *J. Org. Chem. 46* (1981) 3360; U. T. Mueller-Westerhoff, A. Nazzal, W. Prössdorf, *J. Am. Chem. Soc. 103* (1981) 7678; G. Caldwell, M. D. Rozeboom, J. P. Kiplinger, J. E. Bartmess, *ibid. 106* (1984) 4660; d) P. Ahlberg, B. Johnsson, I. McEwen, M. Rönneqvist, *J. Chem. Soc. Chem. Commun. 1986*, 1500.

[15] a) D. Seebach, J. D. Aebio, *Helv. Chim. Acta 68* (1985) 1507, and references cited therein; b) T. Laube, J. D. Dunitz, D. Seebach, *ibid. 68* (1985) 1373. The position of the bridging hydrogen atom was calculated; an assumed N–H distance of 101 pm gives H···C contacts of 262 and 273 pm. The H···C distances measured by us, however, are not to be compared with these. Namely, if the H atom in an N–H···C hydrogen bond is localized X-ray crystallographically too short a N–H and thus too long a H···C distance is expected to result [16]. The measured N–H distance, e.g. in the N3–H14···Cl hydrogen bond in **1**, is only 87 pm. Review: D. Seebach, *Angew. Chem. 100* (1988) 1685; *Angew. Chem. Int. Ed. Engl. 27* (1988) 1624.

[16] R. Taylor, O. Kennard, *Acta Crystallogr. B 39* (1983) 133.

[17] P. Strazewski, C. Tamm, *Helv. Chim. Acta 69* (1986) 1041.

[18] J.-P. Pascault, J. Golé, *J. Chim. Phys. 68* (1971) 442, 453.

[19] R. Smyk, *M. S. Thesis*, College of Forestry, Syracuse University, Syracuse, NY, USA 1968, cited in J. Smid: *Spectrophotometric Studies of Ion-Pair Equilibria* in M. Szwarc (Ed.): *Ions and Ion Pairs in Organic Reactions, Vol. 1*, Wiley-Interscience, New York 1972, p. 106.

[20] For the solvent-separated ion-pair, *Smid* [19] assumed a distance of the cation from the fluorenyl anion of ca. 450 pm. This means that a shorter Li–C distance (Li–C13 403.6 pm!) could (jointly) determine the hypsochromic shift in the UV/VIS spectrum of fluorenyllithium in ethylenediamine [19].

[21] Y. Marcus: *Ion Solvation*, Wiley, New York 1985, p. 218ff. We thank Herrn Prof. *C. Reichardt*, Universität Marburg, for this reference.

Hydrogen Bonds between an $NH_4^{\oplus}$ Ion and a Carbanion—Crystal Structure of Ammonium 1,2,4-Tricyanocyclopentadienide**

By *Stefan Buchholz, Klaus Harms, Werner Massa,* and *Gernot Boche**

Although the structures of numerous alkali metal organo compounds have been elucidated in the past few

[*] Prof. Dr. G. Boche, Dipl.-Chem. S. Buchholz,
Dr. K. Harms, Priv.-Doz. Dr. W. Massa
Fachbereich Chemie der Universität
Hans-Meerwein-Strasse, D-3550 Marburg (FRG)

[**] This work was supported by the Deutsche Forschungsgemeinschaft and the Fonds der Chemischen Industrie. *S. B.* thanks the Studienstiftung des deutschen Volkes for a scholarship.

years,[1] very little information is available about their ammonium equivalents (carbanions with ammonium counterions).[2] Herein we report on the crystal structure of ammonium 1,2,4-tricyanocyclopentadienide **1**.[3]

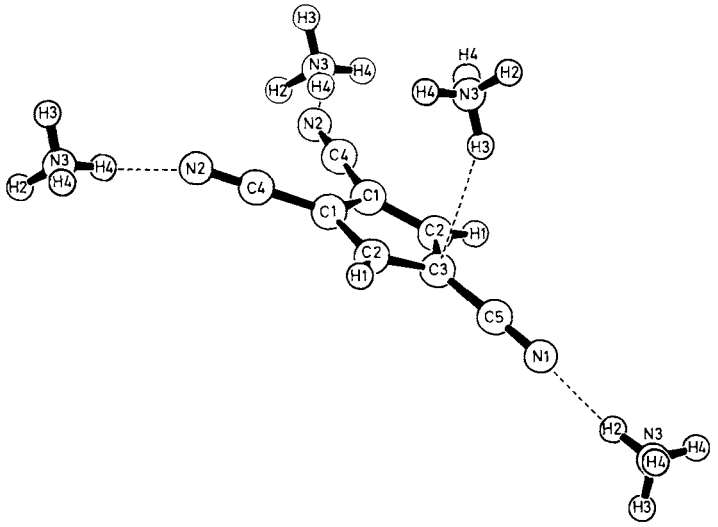


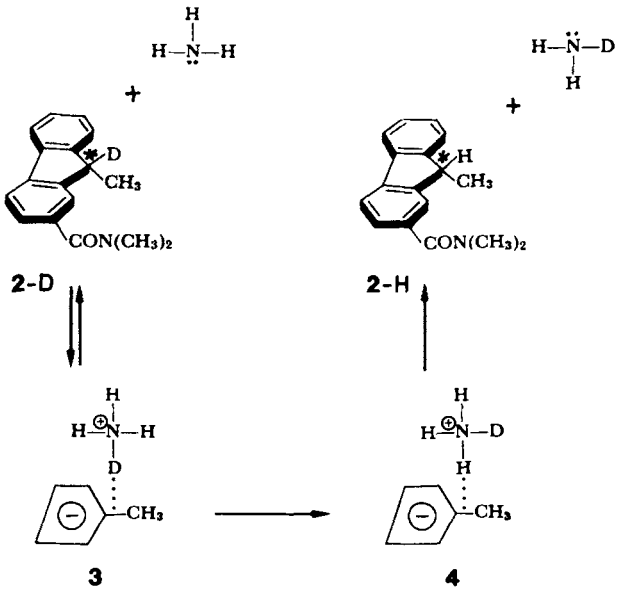
Fig. 1. Section of the crystal structure **5** of ammonium 1,2,4-tricyanocyclopentadienide **1** [8], showing the interactions of a 1,2,4-tricyanocyclopentadienide ion with the four nearest ammonium ions (atoms with the same numbers are symmetry equivalent); cation and anion lie on crystallographic mirror planes, that of the anion being perpendicular to the ring plane. Important bond lengths [pm]: C1-C1′ 142.9(2), C1-C2 139.0(3), C2-C3 141.6(2), C1-C4 142.0(3), C4-N2 115.3(2), C3-C5 142.2(4), C5-N1 114.8(3); hydrogen bonds [pm]: N3···N1 291.2(3), H2···N1 195(4), N3-H2 97(3), N3···N2 295.4(2), H4···N2 206(2), N3-H4 90(2), N3···C3 341.8(3), H3···C3 258(4), N3-H3 98(4); important (bond) angles [°]: ring plane-C1-C4 2.8(2), ring plane-C3-C5 3.6(2), ring plane-C4-N2 4.7(1), ring plane-C5-N1 4.7(2), ring plane-N2-N3 5.45(2), ring plane-N1-N3 5.06(2); hydrogen bond angles [°]: N3-H2···N1 171(3), N3-H4···N2 174(2), N3-H3···C3 144(3).

As shown in Figure 1, each nitrile N-atom is bound via a hydrogen bond to an $NH_4^{\oplus}$ ion, and each $NH_4^{\oplus}$ ion forms three hydrogen bonds to nitrile N-atoms and one hydrogen-bond to a cyclopentadienide C-atom (C3).

The N-H···N hydrogen bonds are almost linear (N3-H2···N1 171(3)°; N3-H4···N2 174(2)°), and the H···N distances are markedly shorter (H2···N1 195(4), H4···N2 206(2) pm) than the sum of the van-der-Waals radii of H and N (275 pm).[9] The N atoms of the $NH_4^{\oplus}$ ions participating in the N-H···N bridges lie "below" the five-membered ring plane[10] (N3 47.4(5), N3′ 52.2(8) pm), so that the nitrile groups are also bent "downwards" (distances to the ring plane: C4 7.0(4), N2 16.4(0.4), C5 9.0(6), N1 18.4(7) pm). The CN bond lengths in the nitrile groups (115.3(2) pm) are almost exactly as long as in acetonitrile (115.7 pm[11]), and are thus consistent with the crystal structure of [(α-cyanobenzyllithium·TMEDA)$_2$·benzene][12] and underscore the chiefly inductive stabilization of a negative charge.

Also remarkable about the structure of **1** is the hydrogen bonding of an $NH_4^{\oplus}$ ion to a C atom of the 1,2,4-tricyanocyclopentadienide (N3-H3···C3).[13] The bond angle is 144(3)°, and the distances N3-H3 and H3···C3 are 98(4) and 258(4) pm, respectively. The H3···C3 distance corresponds to the H···C distances measured for [fluorenyllithium·2ethylenediamine]$_\infty$.[14] The H-bond to C3 is consistent with the results of an MNDO calculation, according to which C3 (−0.196) has a much higher negative charge than C1 (−0.130) and C2 (−0.032).

Cram explained the high degree of D/H exchange with retention compared to the racemization found in the reaction of the optically active fluorene derivative **2**-D with NH_3 (0.3 mol L^{-1} NH_3 in THF at 145°C: $k_{ex}/k_{rac}=148$!) in terms of deuterium (hydrogen) bonding of $NDH_3^{\oplus}$ to the fluorenyl anion (see Scheme 1; similar observations were made with propyl and dipropylamine as bases).[15a]



Scheme 1. D/H exchange with retention (predominant) in the reaction of the optically active **2**-D with NH_3 [15a].

Whereas the N-D···C bridge in **3** leads back to the optically active **2**-D, on rotation of the $NDH_3^{\oplus}$ ion about an N-H axis an N-H···C bridged ion pair **4** is obtained from which **2**-H is formed by proton transfer with retention. Hydrogen bonds also play a decisive role in the isoracemization example: PhEtCDCN in THF/1.5 M *t*BuOH with tripropylamine as base: $k_{ex}/k_{rac}=0.05$!); the tertiary amine takes the $D^{\oplus}$ ion on a "conducted tour" from one side of the molecule via a nitrile N···$DN^{\oplus}Pr_3$ bridge (!) to the other, without $D^{\oplus}$ wandering into the solvent.[15b] The crystal structure of **1** may tentatively be regarded as a suitable solid-state model for both D/H exchange reactions in solution. In the sense of the correlation principle[16] the solid state structure of **1** represents the initial phase of proton transfer from N3 to C3 (or the final phase of the deprotonation of the corresponding CH acid by NH_3), and the observed structure can be assigned to a point on the reaction coordinate.

Received: August 3, 1988 [Z 2903 IE]
German version: *Angew. Chem. 101* (1989) 58

[1] W. N. Setzer, P. von R. Schleyer, *Adv. Organomet. Chem. 24* (1985) 353; P. Jutzi, *ibid. 26* (1986) 217; C. Schade, P. von R. Schleyer, *ibid. 27* (1987) 169; G. Boche, *Angew. Chem. 101* (1989) in press; *Angew. Chem. Int. Ed. Engl. 28* (1989) in press.

[2] X-ray crystallographically characterized $NH_4^{\oplus}$ compounds: $NH_4C(CN)_3$: R. Desiderato, R. L. San, *Acta Crystallogr. 18* (1965) 1; $NH_4(NC)_2C(NC)C-(CH)_3C(CN)C(CN)_2$: J. Edmonds, J. K. Herdklotz, R. L. Sass, *ibid. B26* (1970) 1355; $NH_4C(CN)_2NO_2$: O. Simonsen, *ibid. B37* (1981) 344; ammonium 5-chlorodinitromethyltetrazole: E. A. Goiko, N. V. Grigor'eva, G. V. Makarenko, N. V. Margolis, A. A. Mel'nikov, T. K. Strochkina, I. V. Tselinski, *Zh. Strukt. Khim. 25* (1984) 180.

[3] Procedure for **1**: 1.0 g (5.5 mmol) of potassium 1,2,4-tricyanocyclopentadienide **4** was dissolved in 50 mL of methanol and converted by chromatography on a cation exchanger loaded with $NH_4^{\oplus}$ (Lewatit S100; column volume ca. 150 mL) into the ammonium salt **1** (yield 88%). Crystals

suitable for an X-ray structure analysis were obtained by recrystallization from water (under N_2). Decomp. at 230°C: 300-MHz ^{1}H-NMR ([D$_6$]dimethyl sulfoxide): $\delta = 7.08$ (s, 4H), 6.66 (s, 2H); 75-MHz ^{13}C-NMR: $\delta = 122.1$ (2C; C2), 119.5 (1C; C3), 118.4 (2C; C1), 92.2 (2C; C4), 90.1 (1C; C5).

[4] O. W. Webster, *J. Am. Chem. Soc. 88* (1966) 3045.

[5] X-ray structure analysis: $C_8H_6N_4$, $M = 158.16$, orthorhombic, space group *Pnma*, $a = 1294.1(2)$, $b = 945.0(1)$, $c = 645.9(1)$ pm, $Z = 4$, $\rho_{calcd} = 1.330$ g cm^{-3}. Measurements on an Enraf-Nonius CAD4 diffractometer with $Cu_{K\alpha}$ radiation (graphite monochromator) at -120°C. 603 independent reflections with $F > 4\sigma(F)$ and $\theta = 3$–60°. Solution by direct methods [6], refinement [7] to $R = 0.0434$, $R_w = 0.0364$, non-hydrogen atoms with anisotropic, H atoms with isotropic temperature factors (H atoms located). Further details of the crystal structure investigation are available on request from the Fachinformationszentrum Energie, Physik, Mathematik GmbH, D-7514 Eggenstein-Leopoldshafen 2 (FRG), on quoting the depository number CSD-53217, the names of the authors, and the journal citation.

[6] G. M. Sheldrick, *SHELXS-86, Program for Crystal Structure Solution*, Göttingen 1986.

[7] G. M. Sheldrick, *SHELX-76, Program for Crystal Structure Determination*, Cambridge 1976.

[8] E. Keller, *SCHAKAL-86B, A FORTRAN Program for the Graphic Representation of Molecular and Crystallographic Models*, Freiburg 1986.

[9] A. Bondi, *J. Phys. Chem. 68* (1964) 441.

[10] Least squares plane; the maximum deviation of a ring atom (C3) is 0.2(5) pm; A. L. Spek, *Platon 88, Program for Geometrical Analysis of Crystal Structures*, Utrecht 1988.

[11] C. C. Costain, *J. Chem. Phys. 29* (1958) 864.

[12] G. Boche, M. Marsch, K. Harms, *Angew. Chem. 98* (1986) 373; *Angew. Chem. Int. Ed. Engl. 25* (1986) 373.

[13] It must be pointed out that the hydrogen bond of the $NH_4^{\oplus}$ ion to C3 could be (jointly) caused by the hydrogen bonds to the three nitrile N atoms also present and the resulting arrangement thereby, especially since cation and anion lie on crystallographic mirror planes.

[14] S. Buchholz, K. Harms, M. Marsch, W. Massa, G. Boche, *Angew. Chem. 101* (1989) 57; *Angew. Chem. Int. Ed. Engl. 28* (1989) 72.

[15] a) D. J. Cram: *Fundamentals of Carbanion Chemistry*, Academic Press, New York 1965, p. 88ff.; b) *ibid.* p. 98ff.

[16] H. B. Bürgi, J. D. Dunitz, *Acc. Chem. Res. 16* (1983) 153.

A New Oxygen Sensor Based on the Thermoelectric Power of Solid Solutions of Nb_2O_5 and Bi_2O_3**

By *A. V. Chadwick, W. Zhou,* and *J. M. Thomas**

There is a growing general demand for sensitive sensors, especially those like some of the biosensors in commercial use that can function at relatively low temperatures. Moreover, in view of its potentially pervasive practical importance, a new, robust material suitable for monitoring the partial pressure of oxygen is of particular interest.

Currently favored oxygen sensors of inorganic type are often based on solid electrolytes, such as alkaline-earth stabilized zirconia (ZrO_2(Ca)) in which anion vacancies abound. An electrochemical concentration cell is used,[1] and this requires a reference pressure of oxygen for its operation. Many other non-stoichiometric mixed oxides are potentially viable oxygen sensors, one example being the stabilized δ-phase of Bi_2O_3, which is said[2] to be a 'thermogalvanic' oxygen gauge. There are, however, other inorganic oxygen sensors, e.g., semiconductors, which do not require a reference system.

During the course of an extensive study[3–6] of the solid-state structural and catalytic chemistry of solid solutions derived from Bi_2O_3, we have discovered what appears to be a powerful new oxygen sensor; and which, because it entails measurement of thermoelectric power, dispenses with the need for a reference pressure of oxygen. It consists of a dilute solid solution (1:60) of Nb_2O_5 in Bi_2O_3, which has the previously recognized structure of the β-phase of Bi_2O_3[7] (Fig. 1).

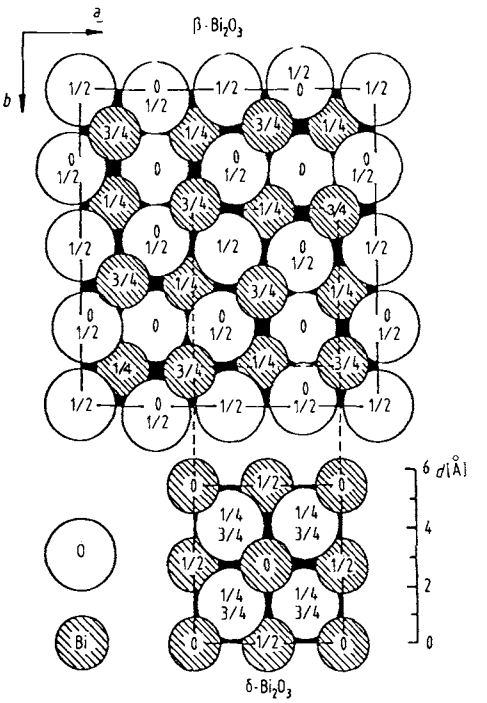


Fig. 1. Schematic representations of the crystal structures of β- (above) and δ-Bi_2O_3 (below). The β-phase may be regarded as a distorted form of the δ-phase which, in turn, may be regarded as the fluorite structure with a quarter of the normal $O^{2\ominus}$ sites left vacant.

For an essentially ionic solid, the thermoelectric power θ, defined as the ratio of the voltage difference ΔV to the temperature difference ΔT between two faces of a sample in a temperature gradient, has two components.[8,9] One is the so-called homogeneous thermoelectric power arising from the thermo-migration of ions, thereby generating a separation of charge; the other, heterogeneous component arises from the temperature dependence of the crystal-electrode contact potential. The usual arrangement[10] employed for recording θ entails the following cell (Scheme 1).

inert metal, O_2 (M = Pt, Au, etc.)	metal oxide (the sensor)	O_2, inert metal (M = Pt, Au, etc.)

Scheme 1.

The comprehensive relationship between θ and the various transport parameters and concentration of point defects is rather complicated.[6] But for a purely anionic conductor there is a simple dependence between θ and the oxygen pressure p_{O_2} [Eq. (a)]

$$\theta \sim \frac{1}{4}\frac{R}{F}\ln p_{O_2} \qquad \text{(a)}$$

[*] Prof. Dr. J. M. Thomas
Davy Faraday Research Laboratory, The Royal Institution
21, Albemarle Street, London W1X 4BS (UK)
A. V. Chadwick
University Chemical Laboratory, University of Kent
Canterbury, Kent CT2 7NH (UK)
W. Zhou
Department of Physical Chemistry, University of Cambridge
Lensfield Road, Cambridge CB2 1EP (UK)

[**] We thank Dr. *D. A. Jefferson* for helpful discussions, Dr. *E.-S. Hammmam* for assistance with the thermoelectric measurements and Fudan University for support to *W. Z.*

where R is the gas constant and F the Faraday constant. The origin of the factor of 1/4 is the equation (b),

$$\frac{1}{2}O_{2,g} + 2e^{\ominus}_{M} \rightleftharpoons O^{2\ominus}_{\text{surface of metal oxide}} \quad (b)$$

from which it can be seen that one electron equates with one quarter of an O_2 molecule.

Previous studies[8,9] of the thermoelectric power of the stabilized δ-phase of Bi_2O_3 in the system $Y_2O_3 \cdot Bi_2O_3$ show that the solid solutions are purely ionic, and plots of θ versus $\ln p_{O_2}$ do indeed have the expected slope $1/4(R/F)$ with θ itself being essentially temperature dependent. We find that the thermoelectric power of the δ-phase of pure Bi_2O_3 exhibits ionic behaviour for $p_{O_2} > 2 \times 10^{-3}$ atm, but not so at lower pressures.

In the present study, samples of $Nb_2O_5 : Bi_2O_3$ (1:60) were prepared as pressed pellets (ca. 1 mm thick, 13 mm diameter) by mixing the pure component oxides and sintering in air at 1023 K for prolonged periods. Gold foil sheets (0.01 mm thick) were pressed onto the faces of a sample and the sandwich so formed was placed between the platinum electrodes of a conductivity cell. The temperature at each face was determined by Pt-Pt/13% Rh thermocouples spot welded to each electrode. The thermocouple EMF at each electrode was monitored with a digital voltmeter and the voltage across the sample was measured with a high impedence electrometer.[10] The pressure of air in the cell could be varied from 10^{-8} to 1 atm. The sign convention used is that θ is positive if the polarity of the hotter electrode is positive. Initial experiments showed that ΔV versus ΔT plots passed through the origin so that rapid measurements of θ could be determined from a single value of ΔT. Additional measurements of conductivity were taken using AC techniques. The sample was annealed in the cell at 1000 K for ca. 12 h to ensure a good electrical contact between it and the electrodes.

The conductivity measurements showed a transition at 900 K, decreasing by two orders of magnitude with decreasing temperature, which indicates the change from high temperature δ-phase to low temperature β-phase. The transition was very slow when the sample was held a few degrees above or below 900 K and it took several hours for the conductivity to reach a constant value.

The plot of θ versus $\ln p_{air}$ for a sample in the δ-phase at 1033 K (Fig. 2) is very similar to that observed for pure Bi_2O_3 showing a slope of $1/4(R/F)$ at high p_{air}, suggesting predominantly ionic conduction. The plot reverses slope at low p_{air}. With the β-phase, however, the results were very unusual. A typical plot for θ versus in $\ln p_{air}$ is shown in Figure 2 for a sample at 768 K. The slope is $4.7(R/F)$ and the results were reversible and characterized by a rapid response (the voltage settles after a few seconds on cycling p_{air}). Similar results were observed down to 573 K.

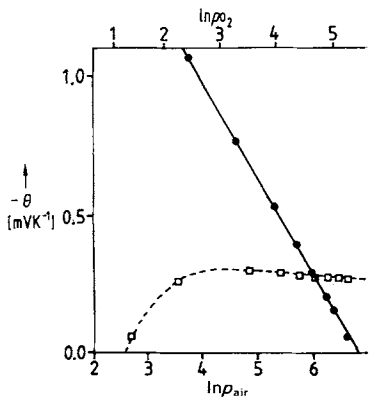


Fig. 2. The dependence of the thermoelectric power θ on air pressure p [torr] for $Nb_2O_5 : Bi_2O_3$ (1:60). Empty squares: δ-phase at 1033 K; filled circles: β-phase at 768 K.

We do not know the origin of the observed dependence of θ on $\ln p_{air}$ in the β-phase. The exponent of 4.7 is too large to be explained on the basis of any simple reaction involving gaseous O_2 and defects. The phenomenon is presumably associated with the generation of electronic carriers either within the sample or at the sample-electrode interfaces.

Although the origin of the observations for the β-phase is at present unclear, the magnitude, speed and reproducibility of the changes in thermoelectric power with varying p_{air} points to potential application in oxygen monitoring. The enhanced response of $Nb_2O_5 : Bi_2O_3$ solid solutions make them attractive materials as oxygen sensors, and worthy of future investigation.

Received: July 4, 1988 [Z 2845 IE]
German version: *Angew. Chem. 101* (1989) 69

[1] W. C. Maskell, B. C. H. Steele, *J. Appl. Electrochem. 16* (1986) 475.
[2] J. H. W. De Wit, T. Honders, G. H. J. Broers in P. Vashishta, J. N. M. Mundy, G. K. Shenoy (Eds.): *Fast Ion Transport in Solids*, Elsevier, New York 1979, p. 675.
[3] W. Zhou, D. A. Jefferson, J. M. Thomas, *Proc. Soc. London Ser. A 406* (1986) 173.
[4] W. Zhou, D. A. Jefferson, M. Alario Franco, J. M. Thomas, *J. Phys. Chem. 91* (1987) 512.
[5] W. Zhou, D. A. Jefferson, J. M. Thomas, *J. Solid State Chem. 70* (1987) 129.
[6] A. Harriman, J. M. Thomas, W. Zhou, D. A. Jefferson, *J. Solid State Chem. 72* (1988) 126.
[7] A. F. Wells: *Structural Inorganic Chemistry*, University Press, Oxford 1984, p. 889.
[8] A. R. Allnatt, P. W. M. Jacobs, *Proc. R. Soc. London Ser. A 260* (1961) 350.
[9] A. R. Allnatt, P. W. M. Jacobs, *Chem. Rev. 67* (1967) 681.
[10] A. V. Chadwick, E.-S. Hammam, B. Zeqiri, F. Beech, *Mater. Sci. Forum 7* (1986) 317.

Investigation of the Tautomerism of ^{15}N-Labeled Hydroporphyrins by Dynamic NMR Spectroscopy**

By *Martin Schlabach, Helmut Rumpel,* and *Hans-Heinrich Limbach**

The problem of the mechanism of the thermal- and light-induced tautomerism of porphyrin, P (Fig. 1, top left) and its derivatives is of current interest.[1-10] Information about the different reaction pathways shown in Figure 1 (top left) has mainly been obtained from dynamic NMR studies of kinetic HH/HD/DD isotope effects[4,5] and of solid state effects,[8] as well as from theoretical studies.[10] Unfortunately, it has not yet been possible so far to significantly increase or decrease the reaction barrier by variation of the chemical structure,[2,5,7] a technique which

[*] Prof. Dr. H.-H. Limbach, Dipl.-Chem. M. Schlabach
Institut für Physikalische Chemie der Universität
Albertstrasse 21, D-7800 Freiburg (FRG)
Dr. H. Rumpel
Ciba-Geigy AG
CH-4002 Basel (Switzerland)

[**] This work was supported by the Deutsche Forschungsgemeinschaft, the Stiftung Volkswagenwerk and the Fonds der Chemischen Industrie. We thank Prof. Dr. *H. Fritz* for time on the Bruker AM400 NMR spectrometer of Ciba-Geigy AG, Basel, Switzerland.

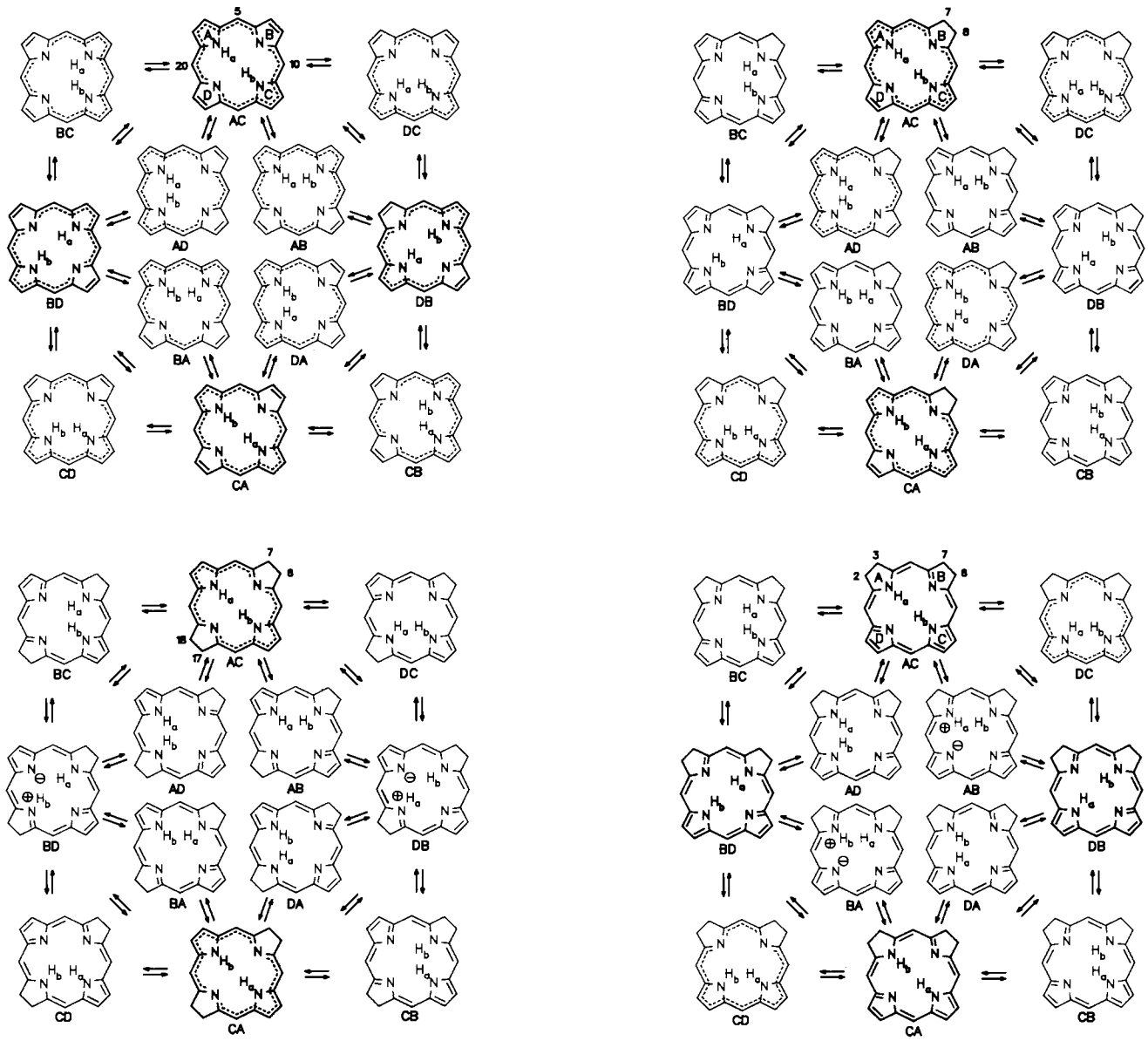


Fig. 1. Proton transfer pathways in the parent compounds porphyrin (formerly porphine [27]) (top left), chlorin (top right), bacteriochlorin (bottom left), and isobacteriochlorin (bottom right). The different pyrrole rings are labeled clockwise with the capital letters A to D. The nitrogen atoms in these rings are labeled as N-21, N-22, N-23 and N-24. The various tautomers are represented here, in a way similar to that proposed in [18], by the pairs XY, with X, Y = A–D. X refers to the pyrrole ring on which the inner proton H_a is located and Y characterizes the location of H_b. All tautomers XY and YX are degenerate with exception of the case where one proton is substituted by deuterium. Tautomeric structures which have been spectroscopically assigned are boldfaced. The dashed lines indicate, as usual, "aromatic" 18 π electron delocalization pathways [3, 7]. Only one zwitterionic structure is shown for the tautomers BD and DB and for AB and BA in Figures 1c and 1d.

usually provides interesting insights into reaction mechanisms. We show here that this goal can be achieved by specific hydrogenation of the pyrrole rings of porphyrins, which leads to the biologically important hydroporphyrins chlorin, C (Fig. 1, top right), bacteriochlorin, Bc (Fig. 1, bottom left) and isobacteriochlorin, iBc (Fig. 1, bottom right).[11–22] Although some evidence for tautomerism[1a] and phototautomerism[21] of chlorins, and for phototautomerism of isobacteriochlorins[22] has been reported, the proton transfer processes occurring in these compounds have not yet been characterized. The different reaction dynamics of hydroporphyrins observed here can be explained by the gain or loss of aromatic resonance energy during the different reaction steps shown in Figures 1. In particular, we have performed ^{1}H NMR line shape analyses of the ^{15}N-labeled hydroporphyrins TPC,[23] TPBc,[24] and TPiBc[25] dissolved in organic solvents.

The ^{1}H NMR spectra of TPC in $C_2D_2Cl_4$ contain only one signal at $\delta \approx -1.5$ ppm for the two inner protons H_a and H_b. This δ-value signifies that TPC experiences an aromatic, porphyrin-type ring current.[28] As shown in Figure 2, the signal is split at room temperature into a ^{1}H-^{15}N doublet. These results are consistent only with the presence of the two degenerate tautomers AC and CA which exchange slowly at room temperature within the NMR timescale. For the case of fast exchange, the signal should exhibit a triplet structure as found for other ^{15}NH$\cdots{}^{15}$N $\rightleftharpoons$ ^{15}N$\cdots$H^{15}N proton transfer systems.[4, 29] In fact, a doublet→triplet interconversion is observed at elevated temperatures (Fig. 2, top).[30] The rate constants were obtained by line shape analysis [Eq. (a)].[31]

$$k_{AC\rightarrow CA} \cong 10^{11.8} \exp(-61.3\ \mathrm{kJ\ mol^{-1}}/RT) \qquad \text{(a)}$$

Thus, the energy of activation of the tautomerism increases to about 20 kJ mol^{-1} upon hydrogenation of one

 © VCH Verlagsgesellschaft mbH, D-6940 Weinheim, 1989 0570-0833/89/0101-0077 $ 02.50/0

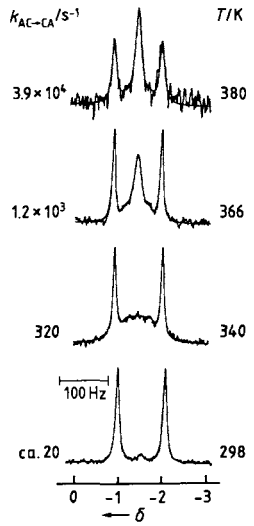


Fig. 2. Superposed experimental and simulated 90.02 MHz ^{1}H NMR spectra of 95% ^{15}N-enriched TPC [23], dissolved in $C_2D_2Cl_4$, as a function of temperature T. 4 μs $\pi/2$ pulses, 2 kHz spectral width, 2.1 s repetition time, 2000 scans on average.

pyrrole ring of porphyrin, an effect which can be explained by the loss of the aromatic resonance energy during the course of the reaction AC→CA.

The ^{1}H-^{15}N doublet of the inner protons of TPBc dissolved in [D_8]toluene appears at $\delta \approx -1.25$ ppm. Thus, this compound also experiences a porphyrin-type ring current. This finding confirms the model of the aromatic electron delocalization pathways[3,7] indicated in Figure 1 by dashed lines. In contrast to TPC, however, the TPBc ^{1}H-^{15}N doublet does not show any sign of conversion into a triplet even at 140°C. Thus, the process AC→CA must be much slower in TPBc than in TPC. This is understandable because not only is aromatic resonance energy lost during the interconversion AC→CA (Fig. 1, bottom left), there is also the additional energy required for charge separation, when the formally zwitterionic intermediates BD and DB are formed.

The greatest surprise is, however, provided by the temperature dependent signals of the inner protons of TPiBc, shown in Figure 3. At −100°C, two exchange broadened

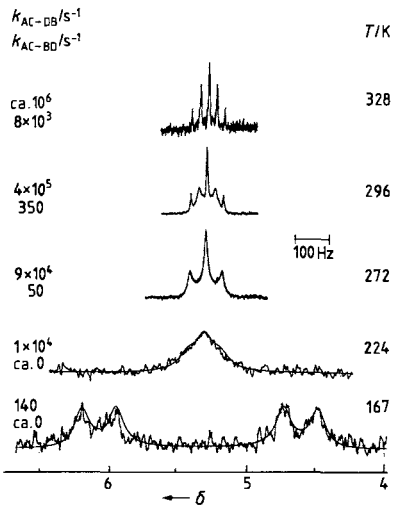


Fig. 3. Superposed experimental and simulated 400.12MHz ^{1}H NMR spectra of 95% ^{15}N-enriched TPiBc [25], dissolved in [D_8]toluene, as a function of temperature T. 3 μs $\pi/2$ pulses, 7 kHz spectral width, 2.1 s repetition time, 8000 scans on average.

^{1}H-^{15}N doublets[32] of equal intensity are observed at $\delta = 4.6$ and 6.1. This low-field shift of the inner proton signals indicates that the porphyrin-type ring current is largely suppressed in TPiBc.[28] The observation that H_a and H_b are inequivalent[33] can only be explained by the presence of the degenerate non-aromatic *trans*-forms AC, DB, CA and BD (Fig. 1, bottom left). As the temperature is raised, however, coalescence of the H_a and H_b doublets into a single exchange-broadened triplet is observed (Fig. 3, middle). These signal changes are expected for the processes AC→DB (and CA→BD). The processes AC→BD (and CA→DB) would not render H_a and H_b equivalent but would lead to two ^{1}H-^{15}N triplets at $\delta = 4.6$ and 6.1. It is, however, surprising that the latter processes are not completely suppressed but lead at higher temperatures to a triplet→quintet interconversion of the ^{1}H-^{15}N signal (Fig. 3, top). The rate constants were obtained by line shape analysis [Eqs. (b) and (c)].[34]

$$k_{AC\rightarrow DB} \cong 10^{10.3} \exp(-27\,\mathrm{kJ\,mol^{-1}}/RT) \quad (b)$$

$$k_{AC\rightarrow BD} \cong 10^{11.1} \exp(-49.2\,\mathrm{kJ\,mol^{-1}}/RT) \quad (c)$$

^{1}H NMR spectra of deuterated and partly deuterated TPiBc showed that both processes are affected by major kinetic HH/HD/DD isotope effects. In addition, preliminary experiments using the ^{15}N CP/MAS NMR technique[8a-f] indicate that the process AC→DB also takes place in the solid state. These results establish TPiBc as the first intramolecular proton transfer system characterized by two symmetric double minimum potentials of unequal height.

The finding that in TPiBc the process AC→DB is much faster than the process AC→BD could perhaps be explained in terms of weak hydrogen bonds between the rings A and D and between C and B although there is no evidence at present for such phenomena in this class of compounds.[12,15,16] The assumption of a step-wise rather than a concerted reaction mechanism provides, however, a more plausible explanation of the experimental results. According to Figure 1 (bottom right), one expects the process AC→DC in TPiBc to be assisted by a considerable gain of resonance energy in the two transition states separating the aromatic *cis*-intermediate DC from the non-aromatic *trans*-tautomers AC and DB. Such a stabilization is neither expected for pathway AC→BD nor for the concerted proton transfer steps. Further experimental and theoretical studies are, however, necessary in order to confirm the first experimental indications for a stepwise reaction mechanism for the tautomerism of porphyrins obtained in this work.

Received: August 2, 1988 [Z 2898 IE]
German version: *Angew. Chem. 101* (1989) 84

CAS Registry Numbers:
TPC, 118070-81-8; TPBc, 118102-31-1; TPiBc, 118102-32-2; TPP, 71771-09-0.

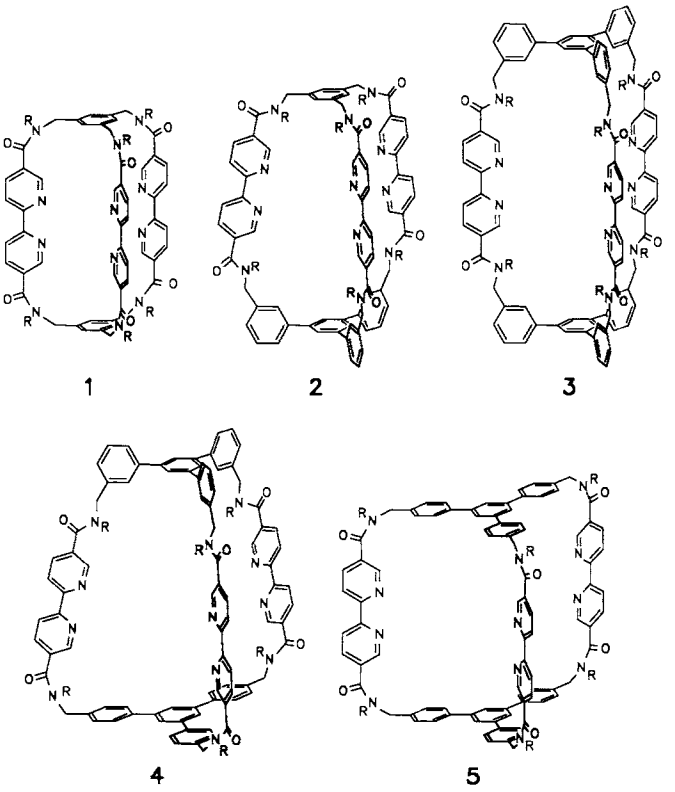
[1] a) C. B. Storm, Y. Teklu, *J. Am. Chem. Soc. 94* (1972) 1745; b) *Ann. N. Y. Acad. Sci. 206* (1973) 631; c) R. J. Abraham, G. E. Hawkes, K. M. Smith, *Tetrahedron Lett. 1974*, 1483; d) *J. Chem. Soc. Perkin Trans. 2 1974*, 1483; e) H. J. C. Yeh, M. Sato, I. Morishima, *J. Magn. Reson. 26* (1977) 365; f) D. Gust, J. D. Roberts, *J. Am. Chem. Soc. 99* (1977) 3637; g) C. S. Irving, A. Lapidot, *J. Chem. Soc. Chem. Commun. 1977*, 184; h) H.-H. Limbach, J. Hennig, *J. Chem. Soc. Faraday Trans. 2 75* (1979) 752; i) J. Hennig, H.-H. Limbach, *J. Magn. Reson. 49* (1982) 322.
[2] S. S. Eaton, G. R. Eaton, *J. Am. Chem. Soc. 99* (1977) 1601.
[3] P. S. Clezy, C. J. R. Fookes, S. Sternhell, *Aust. J. Chem. 31* (1978) 639.
[4] H.-H. Limbach, J. Hennig, D. Gerritzen, H. Rumpel, *Faraday Discuss. Chem. Soc. 74* (1982) 822.
[5] M. Schlabach, B. Wehrle, H.-H. Limbach, E. Bunnenberg, A. Knierzinger, A. Y. L. Shu, B. R. Tolf, C. Djerassi, *J. Am. Chem. Soc. 108* (1986) 3856.

[6] a) P. Stilbs, M. E. Moseley, *J. Chem. Soc. Faraday Trans. 2 76* (1980) 729; b) P. Stilbs, *J. Magn. Reson. 58* (1984) 152; c) J. Hennig, H.-H. Limbach, *J. Am. Chem. Soc. 106* (1984) 869.
[7] a) M. J. Crosswell, M. M. Harding, S. Sternhell, *J. Am. Chem. Soc. 108* (1986) 3608; b) M. J. Crosswell, L. D. Field, M. M. Harding, S. Sternhell, *ibid. 109* (1987) 2335.
[8] a) H.-H. Limbach, J. Hennig, R. D. Kendrick, C. S. Yannoni, *J. Am. Chem. Soc. 106* (1984) 4059; b) H.-H. Limbach, B. Wehrle, H. Zimmermann, R. D. Kendrick, C. S. Yannoni, *ibid. 109* (1987) 929; c) *Angew. Chem. 99* (1987) 241; *Angew. Chem. Int. Ed. Engl. 26* (1987) 247; d) B. Wehrle, H.-H. Limbach, M. Köcher, O. Ermer, E. Vogel, *ibid. 99* (1987) 914 and *26* (1987) 934; e) B. Wehrle, H. Zimmermann, H.-H. Limbach, *Ber. Bunsenges. Phys. Chem. 91* (1987) 941; f) H.-H. Limbach, B. Wehrle, M. Schlabach, R. D. Kendrick, C. S. Yannoni, *J. Magn. Reson. 77* (1988) 84; g) L. Frydman, A. C. Olivieri, L. E. Diaz, B. Frydman, F. G. Morin, C. L. Mayne, D. M. Grant, A. D. Adler, *J. Am. Chem. Soc. 110* (1988) 336; h) L. Frydman, A. C. Olivieri, L. E. Diaz, A. Valasinas, B. Frydman, *ibid. 110* (1988) 5651.
[9] a) S. Völker, J. H. van der Waals, *Mol. Phys. 32* (1976) 1703; b) S. Voelker, R. Macfarlane, *IBM Res. Dev. 23* (1979) 547.
[10] a) J. Almlöf, *Int. J. Quantum Chem. 8* (1974) 915; b) H.-H. Limbach, J. Hennig, *J. Chem. Phys. 71* (1979) 3120; c) H.-H. Limbach, J. Hennig, J. Stulz, *ibid. 78* (1983) 5432; d) H.-H. Limbach, *ibid. 80* (1984) 5343; e) V. A. Kusmitsky, K. N. Solovyov, *J. Mol. Struct. 65* (1980) 219; f) A. Sarai, *J. Chem. Phys. 76* (1982) 5554; g) *ibid. 80* (1984) 5431; h) G. I. Bersuker, V. Z. Polinger, *Chem. Phys. 86* (1984) 57; i) K. M. Merz, C. H. Reynolds, *J. Chem. Soc. Chem. Commun. 1988*, 90; j) Z. Smedarchina, W. Siebrand, T. A. Wildman, *Chem. Phys. Lett. 143* (1988) 395; k) D. C. Rawlings, E. R. Davidson, M. Gouterman, *Theor. Chim. Acta 61* (1982) 227.
[11] H. W. Whitlock, R. Hanover, M. Y. Oester, B. K. Bower, *J. Am. Chem. Soc. 91* (1969) 7485.
[12] C. K. Chang, *Biochemistry 19* (1980) 1971.
[13] H. Scheer, J. J. Katz in K. M. Smith (Ed.): *Porphyrins and Metalloporphyrins*, Elsevier, Amsterdam 1975, p. 440ff.
[14] a) Y. Harel, J. Manassen, *J. Am. Chem. Soc. 100* (1978) 6228; b) A. M. Stolzenberg, M. T. Stershic, *Magn. Reson. Chem. 25* (1987) 256; c) Y. Harel, J. Manassen, *Org. Magn. Reson. 16* (1981) 290; d) A. M. Stolzenberg, L. O. Spreer, R. H. Holm, *J. Am. Chem. Soc. 102* (1980) 364; e) R. Thomas, *Dissertation*, Braunschweig 1967; f) W. Hoppe, G. Will, J. Gassmann, H. Weichselgartner, *Z. Kristallogr. 128* (1969) 18.
[15] W. B. T. Cruse, P. J. Harrison, O. Kennard, *J. Am. Chem. Soc. 104* (1982) 2376.
[16] K. M. Barkigia, J. Fajer, C. K. Chang, G. J. B. Williams, *J. Am. Chem. Soc. 104* (1982) 315.
[17] K. M. Barkigia, J. Fajer, L. D. Spaulding, G. J. B. Williams, *J. Am. Chem. Soc. 103* (1981) 176.
[18] F. A. Burkhalter, E. C. Meister, U. Wild, *J. Phys. Chem. 91* (1987) 3228.
[19] a) K. M. Smith, D. A. Goff, R. J. Abraham, J. E. Plant, *Org. Magn. Reson. 21* (1983) 505; b) R. J. Abraham, K. M. Smith, *J. Am. Chem. Soc. 105* (1983) 5737.
[20] J. D. Keegan, A. M. Stolzenberg, Y. C. Lu, R. E. Linder, G. Barth, A. Moscowitz, E. Bunnenberg, C. Djerassi, *J. Am. Chem. Soc. 104* (1982) 4305.
[21] S. Voelker, R. M. Macfarlane, *J. Chem. Phys. 73* (1980) 4478.
[22] L. W. Johnson, M. D. Murphy, C. Pope, M. Foresti, J. R. Lombardi, *J. Chem. Phys. 86* (1987) 4335.
[23] TPC (= 5,10,15,20-tetraphenyl[$^{15}N_4$]chlorin = 5,10,15,20-tetraphenyl-[$^{15}N_4$]-7,8-dihydroporphyrin) was prepared, in a similar way as described in [11] for the unlabeled material, from TPP (= 5,10,15,20-tetraphenyl[$^{15}N_4$]porphyrin); TPP was prepared according to [26], [^{15}N]pyrrole synthesized as described in [8d]. Note that the name 5,10,15,20-tetraphenyl[$^{15}N_4$]-2,3-dihydroporphyrin proposed in the IUPAC recommentations [27] is not consistent with the findings of this study. The ^{15}N labeling of all compounds in this study was performed in order to obtain reliable results which are not affected by intermolecular proton exchange and ^{14}N quadrupole relaxation.
[24] TPBc (= 5,10,15,20-tetraphenyl[$^{15}N_4$]bacteriochlorin) was prepared, in a way similar to that described in [11] for the unlabeled material, from TPP.
[25] TPiBc (= 5,10,15,20-tetraphenyl[$^{15}N_4$]isobacteriochlorin) was prepared, in a way similar to that described in [11] for the unlabeled material, from TPP.
[26] F. R. Longo, E. J. Thorne, A. D. Adler, S. Dym, *J. Heterocycl. Chem. 12* (1975) 1305.
[27] G. P. Moss, *Pure Appl. Chem. 59* (1987) 779.
[28] R. J. Abraham, C. J. Medforth, K. M. Smith, D. A. Goff, D. J. Simpson, *J. Am. Chem. Soc. 109* (1987) 4786.
[29] G. Otting, H. Rumpel, L. Meschede, G. Scherer, H.-H. Limbach, *Ber. Bunsenges. Phys. Chem. 90* (1986) 1122.
[30] Intermolecular proton transfer would lead to breakdown of the ^{1}H-^{15}N splitting pattern [29].
[31] The activation parameters were obtained from a total of 16 spectra of TPC in $C_2D_2Cl_4$ and [D_8]toluene in the temperature range 298 to 406 K; no solvent effects were observed.
[32] In monodeuterated TPiBc, these signals are sharp at -100°C due to a kinetic HH/HD isotope effect which indicates that the broadening in the bottom spectrum of Figure 3 stems from proton transfer and not from slow rotational diffusion [6].
[33] We tentatively assign the signal at $\delta = 4.6$ to H-21 and the signal at $\delta = 6.1$ to H-23. For the atomic numbering scheme see legend to Figure 1.
[34] $k_{AC \rightarrow DB}$ was obtained from 7 spectra between 170 and 280 K, $k_{AC \rightarrow BD}$ from 4 spectra between 270 and 320 K. Note that the line shape of the outer proton signals, which are not shown here, is sensitive only to the process AC→DB and not to the process AC→BD.

Selective Molecular Recognition of Trihydroxybenzenes**

By *Frank Ebmeyer* and *Fritz Vögtle**

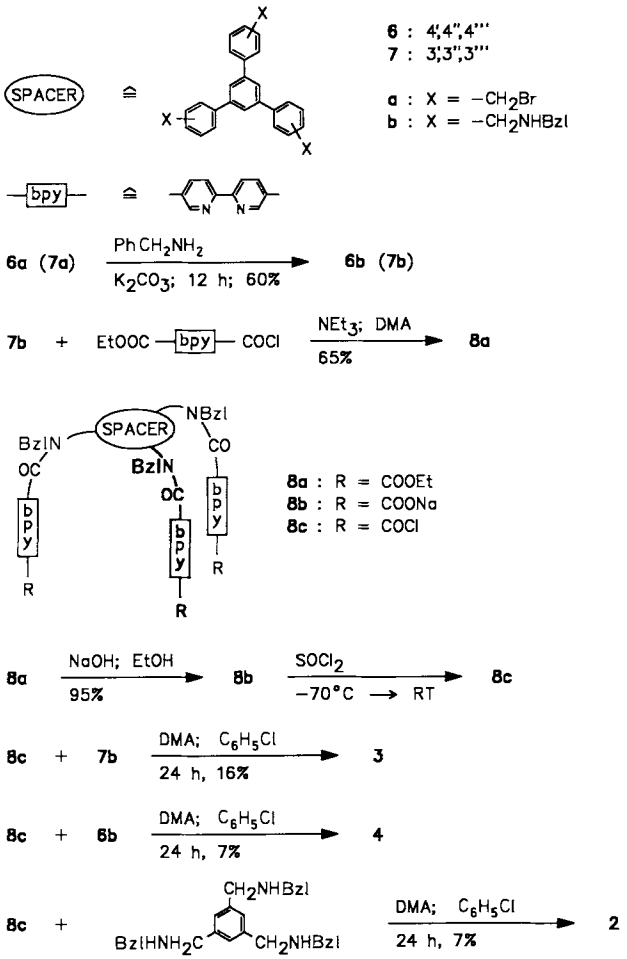
The complexation of organic molecules in nonaqueous media is currently being intensively investigated.[1] We report here on the synthesis and complexation properties of the macrobicyclic compounds **2**–**4**,[2] which exhibit a remarkable selectivity for phenolic substrates, in particular trihydroxybenzenes. Although the bipyridine ligand **1**, synthesized in 1986, strongly complexes small metal cations,[3] it does not bind organic molecules. The successive expansion of the host cavity with the C_3-symmetric spacers introduced by us[4] leads to the new complex-forming molecules **2**–**4** having larger cavities.



[*] Prof. Dr. F. Vögtle, Dipl.-Chem. F. Ebmeyer
Institut für Organische Chemie und Biochemie der Universität
Gerhard-Domagk-Strasse 1, D-5300 Bonn 1 (FRG)

[**] This work was supported by the Deutsche Forschungsgemeinschaft and the Fonds der Chemischen Industrie and by Bayer AG, Leverkusen, BASF AG, Ludwigshafen, Hoechst AG, Frankfurt, and Degussa AG, Hanau (donation of chemicals). *F. E.* thanks the Stiftung Volkswagenwerk for a Kekulé Stipendium. We thank Dr. *J. Peter-Katalinić* (Physiologisch-chemisches Institut der Universität Bonn) and Finnigan/MAT (Bremen) for FAB mass spectra, Dr. *G. Eckhart* and *C. Schmidt* for EI mass spectra and NMR spectra, respectively, Dipl.-Chem. *Ch. Seel* for the drawings, and Mrs. *A. Bail* for assistance.

Attempted transfer of the reaction conditions used in the cyclization to **1**[3] to the expanded tris(bipyridine) compound **5** (containing the 4′,4″,4‴-triphenylbenzene spacer) was unsuccessful. Only upon employing the *meta*-substituted spacer—under modified conditions[5]—was the large-cavity compound **3** obtained in 16% yield.[6] The macrobicyclic compounds **2** and **4** with conical cavities[8] were obtained similarly, in yields of 7% each (Scheme 1).

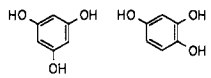
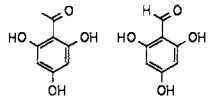
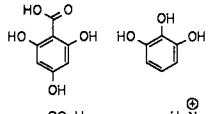
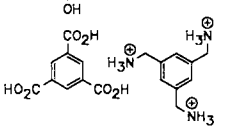


Scheme 1. Bzl = benzyl, DMA = dimethylacetamide.

The new ligands, hexadentate in the cavity,[9] are tailor-made for incorporating complementary trifunctional guest molecules. However, attempts to form inclusion complexes with tricarboxylic acids such as 1,3,5-benzenetricarboxylic acid or the tris(ammonium) salt of 1,3,5-tris(aminomethyl)benzene as guests (dichloromethane as solvent) were unsuccessful. On the other hand, several trihydroxybenzenes were complexed. The guest substances, which are insoluble in dichloromethane, dissolved after addition of the host compounds **2**–**4**; the ^{1}H NMR spectra of the filtered solutions display signals of host *and* guest molecules. The simple pattern of the guest signals—not split in the 400 MHz spectrum—indicates a symmetrical complexation.[10]

Integration of the NMR absorptions reveals a 1 : 1 stoichiometry of the host–guest complexes, even when starting with nonstoichiometric ratios of host and guest molecules. A 1 : 3 stoichiometry was found for the guests picric acid (2,4,6-trinitrophenol) and nitrophloroglucinol (1,3,5-trihydroxynitrobenzene), which do not fit into the cavities of **2**–**4**. The complexation of the phenolic guests is selective. As shown in Table 1, only certain trihydroxybenzenes are complexed, but not structurally related compounds or the isomer pyrogallol (1,2,3-trihydroxybenzene). These findings reflect a marked guest selectivity found earlier in other studies.[11]

Table 1. Host/guest selectivities (+, complexation; −, no complexation). Host concentrations ca. 2×10^{-3} mol L^{-1}; solvent CD_2Cl_2, 25 °C.

Guest	2	3	4
	+	+	−
	+	+	+
	−	−	−
	−	−	−

Selectivity is also observed upon varying the host compounds: whereas neither the host **1** nor its open-chain precursor **8a** complexes phloroglucinol and 1,2,4-trihydroxybenzene, these compounds are indeed complexed by **2** and **3** (but not by the isomer **4**). This finding supports the notion of hydrogen bonding between host and guest in a suitably sized cavity. In agreement with this, the hosts **2**, **3**, and **4** also discriminate between phloroglucinol derivatives: even a small structural change such as the introduction of a methyl or a carboxyl group results in loss of complexation.

A gravimetric method[12] revealed an appreciable association constant of 11 000 ± 2000 (in dichloromethane) for

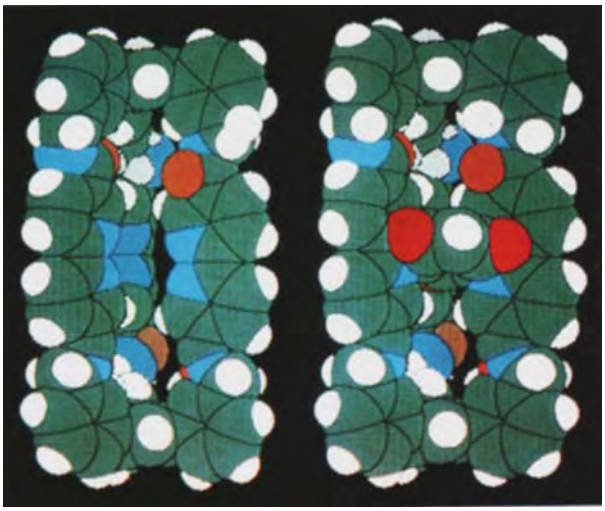


Fig. 1. Left: Host molecule **3** with empty cavity. Right: Space-filling model of the phloroglucinol complex of **3**; the phloroglucinol guest molecule lies perpendicular to the plane of the page between the three bipyridine units of the host **3** [16].

 © VCH Verlagsgesellschaft mbH, D-6940 Weinheim, 1989 0570-0833/89/0101-0080 $ 02.50/0

the complex of **3** with phloroglucinol; this high value can be explained by the formation of multiple hydrogen bonds between host and guest in the cavity. The exact fitting of the guest into the interior of the "receptor molecules" **2–4** is supported not only by the marked host/guest selectivities and the high association constants, but also by the fact that irradiation of the resonance of the bipyridine protons results in a small but significant NOE effect (−0.5%) for the guest protons.

Compounds **1–4** illustrate that the cavity of host compounds can be changed selectively with respect to size and shape by variation of the spacer, allowing the direct synthesis of selective complex-forming molecules.[13] The conical shape of the cavity, the high selectivity in the molecular recognition of trihydroxybenzenes, and the stabilization of phenolic guests toward oxidants[14] have hardly been achieved so far in a synthetic "receptor molecule".[15]

Received: August 9, 1988 [Z 2918 IE]
German version: *Angew. Chem. 101* (1989) 95

[1] a) Reviews: F. Diederich, *Angew. Chem. 100* (1988) 372; *Angew. Chem. Int. Ed. Engl. 27* (1988) 362; cf. also J.-M. Lehn, *ibid. 100* (1988) 91 and *27* (1988) 89; b) R. E. Sheridan, H. W. Whitlock, Jr., *J. Am. Chem. Soc. 110* (1988) 4071.

[2] Host compounds of this type belong neither to the crowns and cryptands nor to the spherands, hemispherands, cryptophanes, or cavitands.

[3] a) S. Grammenudi, F. Vögtle, *Angew. Chem. 98* (1986) 1119; *Angew. Chem. Int. Ed. Engl. 25* (1986) 1122; b) S. Grammenudi, M. Franke, F. Vögtle, E. Steckhan, *J. Inclusion Phenom. 5* (1987) 695. c) Photophysics of the **1**-$Ru^{2\oplus}$ complex: L. De Cola, F. Barigelletti, V. Balzani, P. Belser, A. v. Zelewsky, F. Vögtle, F. Ebmeyer, *J. Am. Chem. Soc. 110* (1988) 7210.

[4] P. Stutte, W. Kiggen, F. Vögtle, *Tetrahedron 43* (1987) 2065; cf. T. Merz, H. Wirtz, F. Vögtle, *Angew. Chem. 98* (1986) 549; *Angew. Chem. Int. Ed. Engl. 25* (1986) 567.

[5] The higher the dilution, the greater the amount of dimethylacetamide (DMA) in the solvent mixture; different eluent for chromatography, cf. [6].

[6] a) *Experimental procedure* for **3**: Solutions of the acid chloride **8c** (4.34 g, 3.10 mmol) in 250 mL of DMA (Fluka, puriss.) and the triamine **7b** (4.11 g, 6.20 mmol) in 250 mL of dry chlorobenzene were simultaneously added dropwise under argon over 12 h to a mixture of chlorobenzene (750 mL) and DMA (250 mL) at room temperature [7]. The reaction mixture was then stirred for an additional 12 h and the resulting precipitate was filtered off. The red solution was concentrated and the residue was carefully dried under vacuum. Dichloromethane was then added to form a slurry, which was transferred to a silica gel column and chromatographed (eluent, dichloromethane/methanol 20:1), affording 1.00 g of **3** (16% yield, $R_F = 0.28$). b) All new macrocyclic compounds gave suitable elemental analyses, FAB mass spectra, and ^1H and ^{13}C NMR spectra and exhibited the following R_F values (eluent: dichloromethane/methanol 20:1): 0.20 (**2**), 0.28 (**3**), 0.28 (4).

[7] Synthesis of the precursors: a) F. Vögtle, N. Sendhoff, *Chem. Ber. 121* (1988), in press; b) N. Sendhoff, *Dissertation*, Universität Bonn 1988; c) cf. [3b].

[8] Compare with the conical cavities of cyclodextrins and some macrotetracyclic hexalactams: F. Vögtle, B. Dung, *J. Inclusion Phenom. 6* (1988) 429.

[9] The pyridine rings in **2–5** freely rotate around their long axis according to the NMR findings; in the free ligands, some of the pyridine nitrogen atoms are presumably directed outwards—in analogy to the situation for crown ethers and cryptands.

[10] We consider a rapid exchange to be unlikely in view of the size of the host molecule and the multiple bonding sites. Compare the three-dimensional bonding and the similarly high complexation constants of cryptands toward ions.

[11] a) F. Vögtle, W. M. Müller, U. Werner, H.-W. Losensky, *Angew. Chem. 99* (1987) 930; *Angew. Chem. Int. Ed. Engl. 26* (1987) 901; b) cf. [1b].

[12] a) F. Diederich, K. Dick, *J. Am. Chem. Soc. 106* (1984) 8024; b) T. W. Bell, J. Liu, *ibid. 110* (1988) 3673.

[13] The ligands **2–4** can also be used to complex transition metals. We thank Prof. *A. von Zelewsky*, Fribourg, and Prof. *V. Balzani*, Bologna, for fruitful discussions.

[14] Solutions of phloroglucinol and **3** in dichloromethane do not turn dark upon daylong exposure to light and air, as is the case for aqueous solutions without host (the trihydroxybenzenes are only sparingly soluble in CD_2Cl_2 without addition of host).

[15] Cf. also: D. Heyer, J.-M. Lehn, *Tetrahedron Lett. 27* (1986) 5869; T. Fujita, J.-M. Lehn, *ibid. 29* (1988) 1709.

[16] The two pictures in Figure 1 were drawn with the "Atom 87" program, Oxford University Press, Beta-test version, October 1987.

A Silicogermanate with a Si : Ge Ratio ≥ 2 —an MFI Zeolite of Novel Composition**

By *Zelimir Gabelica** and *Jean-Louis Guth*

The pore volume, acidity and sorptive properties of zeolites can be modified and controlled by substitution of the framework atoms. We report herein results dealing with the substitution of Si by Ge in pure Si-bearing zeolites. A series of crystalline, microporous solids containing Si and Ge in an MFI type tetrahedral framework have been synthesized under hydrothermal conditions in the presence of $Pr_4N^{\oplus}$ ions as structure directing agents, over the whole pH range in the absence of alkali metal or ammonium cations. The unit cell composition of these solids, after removal of included organics, is $Si_{96-x}Ge_xO_{192}$, where $x \leq 34 \pm 4$. It is concluded that such a framework is built up from the 5-1 secondary building units (SBU) in which at least two tetrahedral centers are occupied by Ge. Such a high degree of substitution of Si by another tetravalent element has, until now, not been observed for an MFI type structure. Our method opens new pathways for preparing other highly substituted zeolites.

Both amorphous (glasses) and crystalline solid solutions are known in the binary system SiO_2–GeO_2.[1-2] In contrast to the open zeolitic structures, these phases, which were obtained at high temperature (>700 °C), are not microporous. The frameworks of the natural zeolites[3] and of most of the synthetic molecular sieves[4] contain Si and Al atoms in the tetrahedral positions. Framework substitution by other tetravalent and trivalent elements is also well-known.[4] Recently, a series of zeolite structures containing only Si were reported.[5,6] In the case of Si-MFI, the incorporation of $Ti^{4\oplus}$ in the framework has been reported but the degree of substitution was very low (ca. 2.5 wt.%).[7] Substitution of Si by Ge was, until now, not reported; clearly, this could only be achieved when a trivalent element (e.g., $Al^{3\oplus}$) was present in the framework.

The novel (Si,Ge)-MFI zeolites are obtained by heating an aqueous solution of the Si and Ge reactants at 60–220 °C in the presence of a structure directing agent such as $Pr_4N^{\oplus}$. The crystallization time depends markedly on temperature, pH and the presence of fluoride ions. Typically, a mixture having the molar composition $GeCl_4$–SiO_2–HF–$0.5\,Pr_4NBr$–$8\,CH_3NH_2$–$35\,H_2O$ is heated in the presence of MFI seeds for 15 h at 180 °C in PTFE coated autoclaves. The resulting solid, as identified by X-ray diffraction, has an MFI type structure. The unit cell composition, after calcination in air at 550 °C for 10 h, is $Si_{63}Ge_{33}O_{192}$, as determined by atomic absorption and spot EDX analysis of individual crystallites.[8] In neutral or acidic media, other oxides, which contain most of the Ge, coprecipitate with the

[*] Dr. Z. Gabelica
Facultés Universitaires Notre-Dame de la Paix
Department of Chemistry
61, Rue de Bruxelles, B-5000 Namur (Belgium)
Dr. J. L. Guth
Laboratoire Matériaux Minéraux, E.N.S.C.Mu
F-68093 Mulhouse (France)

[**] This work was carried out in Mulhouse and supported by the Noelting Foundation E.N.S.C.Mulhouse (*Z. G.*).

MFI zeolite. In very basic media, the formation of soluble germanates also limits the extent of Ge incorporation in the zeolite. Moreover, if the basic pH value is adjusted by alkali metal or ammonium hydroxides, the corresponding germanates precipitate together with MFI crystallites, whose frameworks consist mostly of Si. These problems can be avoided by adjusting the pH to about 10 using short chain alkyl amines such as CH_3NH_2. Under these conditions, pure (Si,Ge)-MFI crystals can be synthesized in good yield with a wide range of compositions. A further addition of fluoride ions, which are known to advantageously reduce the mobilizing effect of $OH^{\ominus}$ ions,[9] reduces the crystallization time considerably. The crystal size of the silicogermanate zeolite increases with decreasing pH, provided that $F^{\ominus}$ ions are present. At pH 10–11, Si-MFI precipitates in Ge-free media, as tiny elongated platelets ($10 \times 3 \times 0.5$ μm), whereas the habitus of the Ge-rich phases is nearly isometric ($6 \times 4 \times 4$ μm for $x = 33$).

The freshly prepared silicogermanate crystals are orthorhombic but become monoclinic at room temperature (±20°C), provided that the included organic molecules are first removed by heating to 500°C in air. The monoclinic-orthorhombic transition temperature increases linearly with increasing Ge content (Fig. 1). For conventional

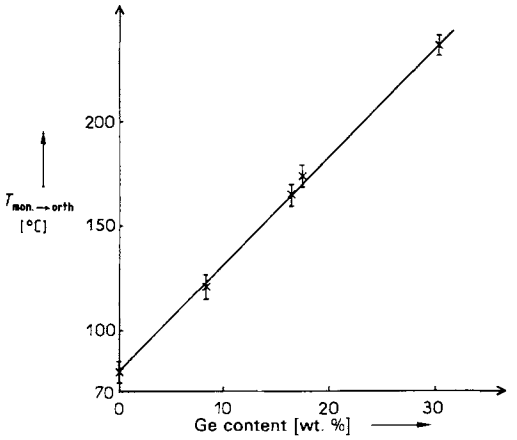


Fig. 1. Dependence of the orthorhombic-monoclinic phase transition temperature upon Ge content for calcined MFI samples. The samples were prepared at pH 10–11. Data were collected by temperature-dependent X-ray structure analysis.

MFI zeolites in which Si is substituted by a trivalent element (Al, B, ...), the opposite is observed, i.e., the transition temperature decreases with increasing substitution.[10] The lattice constants and the unit cell volume also increase with increasing substitution (Table 1).

Table 1. Dependence of the lattice constants and the unit cell volume upon the Ge content x for the monoclinic phase.

x [wt. %]	a [Å]	b [Å]	c [Å]	β [°]	V [Å^3]
0	13.379	20.098	19.878	90.58	5345
17.1	13.428	20.137	19.939	90.58	5391
32.8	13.455	20.180	19.968	90.51	5428

Differential thermal analysis (DTA) has been used to detect organic templates in MFI frameworks.[11,12] Using DTA, we were able to detect $Pr_4N^{\oplus}$ ions, whose decomposition temperature in the MFI framework is different from that of $Pr_4N^{\oplus}F^{\ominus}$ ion pairs.[12] Since they are not expected to occur in regular TO_2 frameworks containing only tetravalent elements, their presence indicates the formation of framework defects of the type $T\text{-}O^{\ominus}$. The stronger acidic character of Ge, compared to Si, reduces its tendency to (poly)condense into regular Ge-O-T framework bridges, especially in basic media. Upon thermal decomposition of the $Pr_4N^{\oplus}$ ions, the formation of an increasing number of T-O-T bridges results in a marked decrease in the number of $T\text{-}O^{\ominus}$ defects. This phenomenon was studied by comparing the high resolution solid-state MAS ^{29}Si NMR spectra of the freshly prepared and calcined Si-MFI and (Si,Ge)-MFI phases (Fig. 2). As expected, the calcined

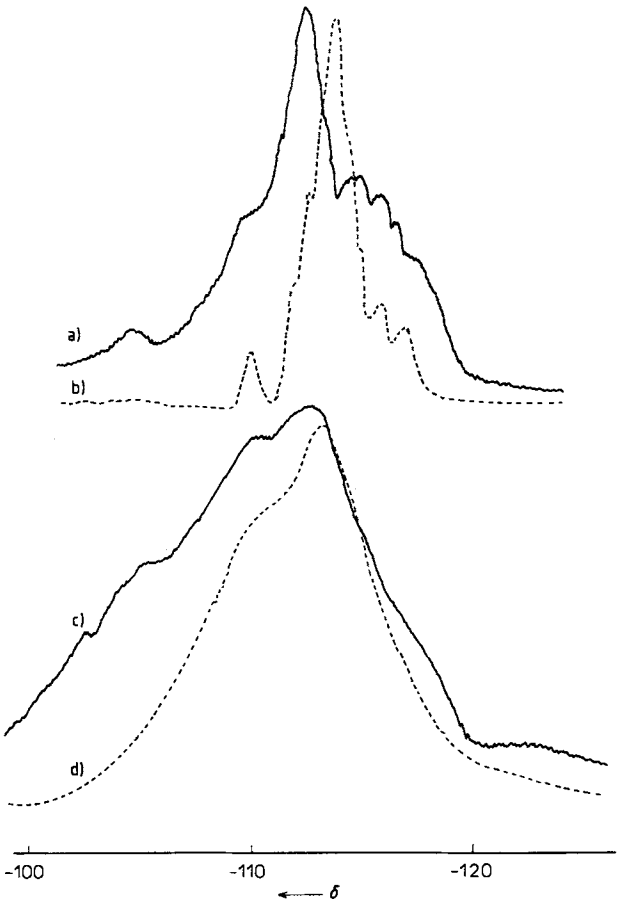


Fig. 2. High resolution solid-state MAS ^{29}Si NMR spectra (Bruker MSL 300 MHz spectrometer) a) untreated Si-MFI; b) its calcined form; c) untreated (Si,Ge)-MFI (Si : Ge ≈ 2); d) its calcined form.

phases show better resolved spectra. The signals are also narrower for the pure Si-MFI than for the silicogermanate zeolite, especially in the high field region. When Ge is present in T sites, the increasing number of Si(nGe) configurations results in a spectral broadening in the low field region (Ge is less electronegative than Si). The presence of defect groups, which are characterized by an NMR resonance at $\delta \approx -105$[13] was not clearly detected. Nevertheless, the shoulder observed between $\delta = -108$ and -110 for both freshly prepared and calcined (Si,Ge) phases suggests the presence of Si(nGe) framework configurations in these zeolites.

Our investigations allow germanium to be added to the already wide range of elements which can occupy T sites in MFI frameworks. The unexpectedly high Ge contents exceed the degrees of Si substitution achieved up to now. The upper limit of the Si:Ge ratio of about 2 can be understood on the basis of the assumption that the formation of Ge-O-Ge linkages is avoided; they have also not been detected in solution.[14] Consequently, a pure Ge-MFI zeolite is expected to be difficult to synthesize.

Received: July 4, 1988;
Revised: September 23, 1988 [Z 2841 IE]
German version: *Angew. Chem. 101* (1989) 60

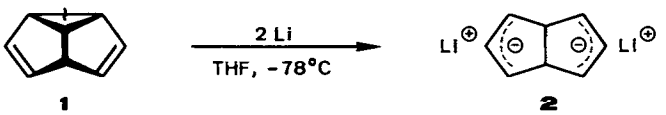
[1] W. S. Miller, F. Dachille, E. C. Shafer, R. Roy, *Am. Miner. 48* (1963) 1024.
[2] B. Z. Shalumov, L. A. Zhukova, E. A. Ryabenko, N. G. Chernaya, Y. V. Oboznenko, *Izv. Akad. Nauk. SSSR Neorg. Mater. 22* (1986) 966.
[3] G. Gottardi, E. Galli, *Natural Zeolites*, Springer, Berlin 1985, p. 409.
[4] R. M. Barrer: *Hydrothermal Chemistry of Zeolites*, Academic Press, London 1982, p. 543.
[5] E. M. Flanigen, J. M. Bennett, R. W. Grose, J. P. Cohen, R. L. Patton, R. M. Kirchner, J. V. Smith, *Nature (London) 271* (1978) 512.
[6] H. Gies, R. R. Gunawardane, *Zeolites 7* (1987) 442.
[7] G. Perego, G. Bellussi, C. Corno, M. Taramasso, F. Bounomo, A. Esposito in Y. Murakami, A. Iijima, J. W. Ward (Eds.): *New Developments in Zeolite Science and Technology*, Kodansha, Tokyo 1986, p. 129.
[8] Z. Gabelica, N. Blom, E. G. Derouane, *Appl. Catal. 5* (1983) 227.
[9] J. L. Guth, H. Kessler, R. Wey in Y. Murakami, A. Iijima, J. W. Ward (Eds.): *New Developments in Zeolite Science and Technology*, Kodansha, Tokyo 1986, p. 121.
[10] D. G. Hay, H. Jaeger, *J. Chem. Soc. Chem. Commun. 1984*, 1433.
[11] Z. Gabelica, J. B. Nagy, P. Bodart, A. Nastro, *Thermochim. Acta 93* (1985) 749.
[12] M. Soulard, S. Bilger, H. Kessler, J. L. Guth, *Zeolites 7* (1987) 463.
[13] J. B. Nagy, Z. Gabelica, E. G. Derouane, *Chem. Lett. 1982*, 1105.
[14] C. T. G. Knight, R. J. Kirkpatrick, E. Oldfield, *J. Am. Chem. Soc. 109* (1987) 1632.

Stable Open-Chain 1,3-Dilithium Compounds by Reaction of Methylenecyclopropanes with Lithium Powder: 2,4-Dilithio-1-butenes**

By *Adalbert Maercker** and *Klaus-Dieter Klein*

Dedicated to Professor Gerhard Hesse on the occasion of his 80th birthday

Polylithium organic compounds[1] can be prepared by reductive cleavage of a cyclopropane σ bond with lithium, provided that a resonance-stabilized system is formed; for example, the dilithium "semibullvalenediide" **2** is obtained by treatment of semibullvalene **1** with lithium in



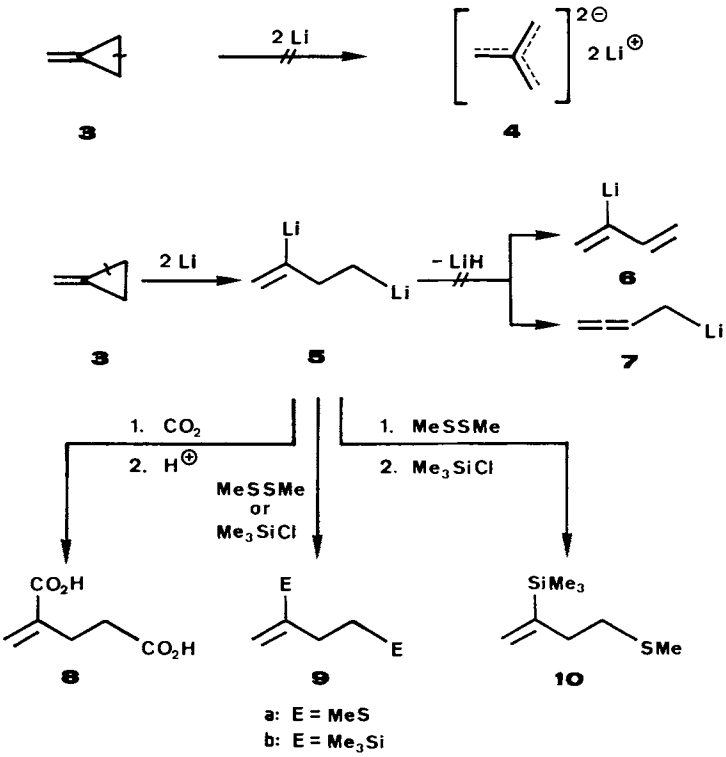
1 **2**

THF or dimethyl ether at −78°C.[2] The homologous barbaralane reacts analogously, that is, again with formation of a bis(allyllithium) compound.[3]

[*] Prof. Dr. A. Maercker, Dipl.-Chem. K.-D. Klein
Institut für Organische Chemie der Universität
Adolf-Reichwein-Strasse, D-5900 Siegen (FRG)

[**] Polylithium Organic Compounds, Part 9. This work was supported by the Minister für Wissenschaft und Forschung des Landes Nordrhein-Westfalen and by the Fonds der Chemischen Industrie.—Part 8: A. Maercker, F. Brauers, W. Brieden, M. Jung, H. D. Lutz, *Angew. Chem. 100* (1988) 413; *Angew. Chem. Int. Ed. Engl. 27* (1988) 404.

We have now found that methylenecyclopropane **3** also reacts smoothly with lithium powder, both neat at its boiling point (10°C, 1 h) and in diethyl ether at room temperature (1/2 h). However, cleavage of the weakest cyclopropane bond to form the extremely stable, Y-delocalized trimethylenemethane dianion **4**[4] does not occur. Instead, the 2,4-dilithio-1-butene **5**, combining both vinyl and homoallyl character, is the sole product (Scheme 1).



Scheme 1.

Table 1. Important physical data for the compounds **5**, **8**, **9a,b**, and **10** [a].

5: ^{1}H NMR (80 MHz, [D$_{10}$]Et$_2$O): δ = 6.03, 5.21 (2 d, br, ^2J = 5.5 Hz; H$_2$C=), 2.89 (t, br, ^3J = 7.2 Hz; CH$_2$C), −0.75 (t, ^3J = 7.2 Hz; CH$_2$Li). ^{13}C NMR (20.1 MHz, [D$_{10}$]Et$_2$O): δ = 204.4 (=CLi), 119.8 (H$_2$C=), 49.5 (CH$_2$C), 11.4 (CH$_2$Li). ^{6}Li NMR (58.9 MHz, [D$_{10}$]Et$_2$O, standard 1 M LiCl in THF, external): δ = 1.6 (s, br)

8: ^{1}H NMR (80 MHz, [D$_6$]DMSO): δ = 12.27 (s, br; 2 CO$_2$H), 6.07, 5.62 (2 d, br, ^2J = 1.5 Hz; H$_2$C=), 2.43 (s, br; 2 CH$_2$). ^{13}C NMR (20.1 MHz, [D$_6$]DMSO): δ = 173.5, 167.7 (2 CO$_2$H), 139.7 (=C), 124.6 (H$_2$C=), 32.6, 26.7 (2 CH$_2$). MS (70 eV): *m/z* 144 (*M*$^\oplus$, 2%), 126 (82), 98 (100), 69 (46), 55 (48), 53 (62), 45 (39). M.p. 128–133°C. Cf. [5]

9a: ^{1}H NMR (80 MHz, CDCl$_3$): δ = 5.07, 4.65 (2 s, br; H$_2$C=), 2.76–2.38 (m; 2 CH$_2$), 2.24, 2.12 (2 s; 2 SCH$_3$). ^{13}C NMR (20.1 MHz, CDCl$_3$): δ = 145.0 (=C), 104.8 (H$_2$C=), 37.0, 33.2 (2 CH$_2$), 15.1, 14.1 (2 SCH$_3$). MS (70 eV): *m/z* 148 (*M*$^\oplus$, 18%), 133 (28), 101 (23), 85 (15), 61 (100), 53 (14), 45 (15). B.p. 86–88°C/10 torr. Correct elemental analysis

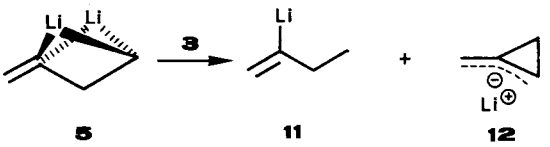
9b: ^{1}H NMR (80 MHz, CDCl$_3$): δ = 5.59, 5.30 (2 dt, ^2J = 3.0, ^4J = 1.5, 1.1 Hz; H$_2$C=), 2.16 (m; CH$_2$C), 0.62 (m; CH$_2$Si), 0.11, 0.01 (2 s; 2 SiMe$_3$). ^{13}C NMR (100.6 MHz, CDCl$_3$): δ = 154.9 (=C), 122.3 (H$_2$C=), 29.9, 16.1 (2 CH$_2$), −1.3, −1.7 (2 SiMe$_3$). MS (70 eV): *m/z* 200 (*M*$^\oplus$, 8%), 113 (5), 112 (44), 97 (33), 74 (18), 73 (100), 45 (14). B.p. 65–66°C/12 torr. Cf. [6]

10: ^{1}H NMR (80 MHz, CDCl$_3$): δ = 5.59, 5.39 (2 m; H$_2$C=), 2.62–2.39 (m; 2 CH$_2$), 2.13 (s; SCH$_3$), 0.09 (s; SiMe$_3$). ^{13}C NMR (100.6 MHz, CDCl$_3$): δ = 150.7 (=C), 125.1 (H$_2$C=), 35.6, 33.8 (2 CH$_2$), 15.6 (SCH$_3$), −1.5 (SiMe$_3$). MS (70 eV): *m/z* 174 (*M*$^\oplus$, 32%), 159 (100), 105 (74), 73 (68), 61 (37), 59 (16), 45 (11). B.p. 75–76°C/10 torr. Correct elemental analysis

[a] DMSO = dimethyl sulfoxide.

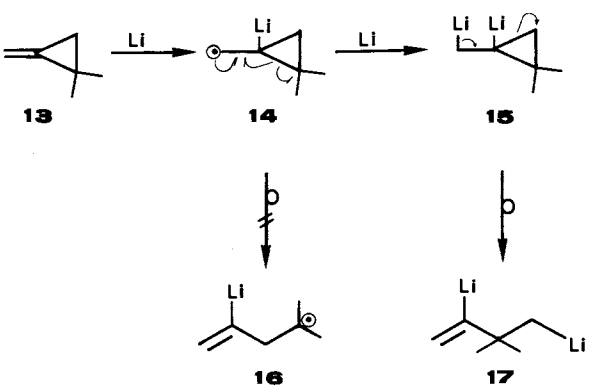
 © VCH Verlagsgesellschaft mbH, D-6940 Weinheim, 1989 0570-0833/89/0101-0083 $ 02.50/0

Derivatization of **5** with carbon dioxide, dimethyl disulfide, and chlorotrimethylsilane leads to formation of the expected products **8** (50%), **9a** (53%), and **9b** (67%), respectively, which were characterized by NMR spectroscopy and mass spectrometry (Table 1); dimethyl sulfate affords 2-methyl-1-pentene in 68% yield. Since the two anionic centers of **5** differ in their reactivity, the reaction can also be carried out stepwise with two different electrophiles, for example, first with one equivalent of dimethyl disulfide and then with chlorotrimethylsilane. The formation of **10** (Scheme 1, Table 1) in 25% yield proves that—as expected—the homoallyl position is more reactive than the vinyl position. This is further supported by the tandem reaction with methanol and chlorotrimethylsilane, which gives mainly 2-trimethylsilyl-1-butene[7] (33%). However, the presence of traces of 2-lithio-1-butene **11** always has to be taken into consideration, since still unreacted **3** is in part metalated by **5**.



Compound **5** is remarkably stable toward diethyl ether as solvent, a property already observed for 1,3-dilithiopropane[8] and, as in that case, presumably due to a doubly bridged structure.[9] However, in contrast to 1,3-dilithiopropane,[8] which rapidly eliminates lithium hydride (half-life period of 1 h at room temperature), **5** does not display such reaction behavior at all—neither 2-lithio-1,3-butadiene **6** nor its tautomer **7** (Scheme 1) could be detected. It was therefore possible to carry out detailed NMR studies on the orange-red solution of **5** (Table 1). However, no conclusions could be drawn regarding association and bridging, since the $^{6}Li,^{13}C$ coupling constants could not be derived from the spectra. The appearance of several signals in the ^{6}Li NMR spectrum recorded between -20 and $-80\,^{\circ}C$ is not compelling evidence against a doubly bridged structure, but might also indicate the simultaneous presence of different aggregates. Unfortunately, the crystals obtained so far have not been suitable for an X-ray structure analysis.

The reaction of 2,2-dimethylmethylenecyclopropane **13** with lithium powder under the same conditions, yielding **17**, provided clues as to the mechanism of cleavage of **3** with lithium (Scheme 2). The formation of **17** indicates that, before ring-opening occurs to give **16**, the initially formed radical anion **14** reacts with a second lithium atom to give the 1-lithiomethylcyclopropyllithium **15**. As a cyclopropylcarbinyllithium derivative, **15** then undergoes the known[10] anionic rearrangement with ring-opening to form the primary homoallyllithium derivative **17**.[11]



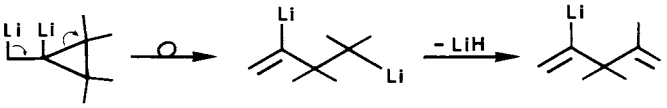
Scheme 2.

Experimental Procedure

Approximately 10% of a solution of **3** (8.0 g, 0.15 mol) [12] in 50 mL of diethyl ether was added dropwise, initially at room temperature, to a suspension of lithium powder (2.5 g, 0.36 mol, 2% sodium) in 50 mL of diethyl ether, the reaction being carried out under argon. After the reaction had begun—the reaction solution turned yellow and began to reflux—the remaining solution of **3** was added at ice-bath temperature so as to avoid partial evaporation of **3** (b.p. 10°C). The reaction mixture was then stirred for 1/2 h at room temperature and the excess lithium was filtered off under inert gas. Yield: 70–75% **5**; very stable (half-life period of decomposition, 27 d at room temperature).

Received: July 22, 1988 [Z 2881 IE]
German version: *Angew. Chem. 101* (1989) 63

[1] Review: A. Maercker, M. Theis, *Top. Curr. Chem. 138* (1987) 1.
[2] M. J. Goldstein, T. T. Wenzel, G. Whittaker, S. F. Yates, *J. Am. Chem. Soc. 104* (1982) 2669; M. J. Goldstein, T. T. Wenzel, *J. Chem. Soc. Chem. Commun. 1984*, 1654, 1655.
[3] R. Trinks, K. Müllen, *Chem. Ber. 120* (1987) 1481.
[4] Reviews: J. Klein, *Tetrahedron 39* (1983) 2733; *ibid. 44* (1988) 503.
[5] J. Kagan, L. Tolentino, M. G. Ettlinger, *J. Org. Chem. 40* (1975) 3085.
[6] P. Cros, C. Triantaphylides, G. Buono, *J. Org. Chem. 53* (1988) 185.
[7] B.p. 30–32°C/10 torr; appropriate ^{1}H and ^{13}C NMR and mass spectra. Cf. Yu. K. Grishin, N. M. Sergeyev, Yu. A. Ustynyuk, *Org. Magn. Reson. 4* (1972) 377.
[8] J. W. F. L. Seetz, G. Schat, O. S. Akkerman, F. Bickelhaupt, *J. Am. Chem. Soc. 104* (1982) 6848.
[9] P. von R. Schleyer, A. J. Kos, E. Kaufmann, *J. Am. Chem. Soc. 105* (1983) 7617.
[10] Cf. P. T. Lansbury, V. A. Pattison, W. A. Clement, J. D. Sidler, *J. Am. Chem. Soc. 86* (1964) 2247.
[11] The corresponding tetramethyl derivative of **3**, on the other hand, leads only to a monolithium compound, since, after ring-opening, the initially formed product eliminated lithium hydride. The reason for this secondary reaction might be the formation of a tertiary homoallyllithium center occurring for the first time:



[12] R. Köster, S. Arora, P. Binger, *Justus Liebigs Ann. Chem. 1973*, 1219.

Structures of Quino[7,8-*h*]quinoline and Quino[8,7-*h*]quinoline**

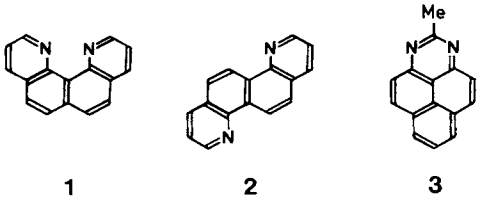
By *Claus Krieger, Ian Newsom, Michael A. Zirnstein,* and *Heinz A. Staab**

Recently, we described a new type of "proton sponge", quino[7,8-*h*]quinoline **1**.[2] The two nitrogen atoms of **1** are mutually oriented as in 1,8-bis(dimethylamino)naphthalene ("proton sponge"); in contrast to the earlier "proton sponges", however, **1** lacks the hydrophobic shielding of the basic centers and thus of the hydrogen bond in the *mono*protonated cation, which was responsible for the low

[*] Prof. Dr. H. A. Staab, C. Krieger, Dr. I. Newsom,
Dipl.-Chem. M. A. Zirnstein
Abteilung Organische Chemie
Max-Planck-Institut für medizinische Forschung
Jahnstrasse 29, D-6900 Heidelberg (FRG)

[**] New "Proton Sponges", Part 8.—Part 7: H. A. Staab, M. Höne, C. Krieger, *Tetrahedron Lett. 29* (1988) 1905.

rate of proton transfer observed for the "proton sponges" known so far. Accordingly, **1**, whose basicity constant is eight powers of ten larger than that of quinoline, is also a kinetically active base.[3]



1 **2** **3**

The first synthesis of **1**, reported in 1950, began with the nitration of benzo[*h*]quinoline, whereby the authors thought they had obtained 10-nitrobenzo[*h*]quinoline; the corresponding amine was then converted by Skraup reaction into a compound which they held to be **1**.[4] In fact, the nitration afforded a mixture of products, from which the desired 10-nitro compound was not obtained but probably instead the 7-nitro compound. Therefore, the compound formed in the Skraup reaction was presumably a structural isomer of **1**, the quino[8,7-*h*]quinoline **2**.[5] In 1967, *Buu-Hoï* et al.[6] reported the synthesis of **1** from 1,8-bis(acetamido)naphthalene by double Skraup reaction. Upon repetition of this procedure, we found that neither MS nor NMR data were in agreement with the structure **1**, but instead were in complete agreement with the suggestion of *Sauvage* et al.,[7] made at the time of our studies (1985), that this reaction does not yield **1** but, rather unexpectedly, 2-methyl-1,3-diazapyrene **3**. In addition, however, we obtained a further compound (m.p. 219–221 °C) in this reaction in small yield; its elemental analysis, mass spectrum [*m/z* 230 (100%, $M^{\oplus}$), 202, 115 (5, $M^{2\oplus}$)] and ^{1}H NMR spectrum [$\delta = 7.60$ (dd, 2H; 3-H), 8.05 (d, 2H; 5-H), 8.35 (dd, 2H; 4-H), 9.10 (dd, 2H; 2-H), 9.45 (d, 2H; 6-H); $CDCl_3$, 80 MHz] established the structure of a quinoquinoline. Based on the synthetic route, we first suspected **1**. However, the number of lines in the fully decoupled ^{13}C NMR spectrum, containing only three signals for quaternary C atoms, indicated the presence of **2**. Its formation is apparently, as in the earlier attempts to synthesize **1**, due to the preferred introduction of the nitrogen functions into the synthetic precursors in the 1,5 instead of the desired 1,8 positions of the central "naphthalene system".

The decade-old uncertainties concerning the synthesis and structural assignment of **1** and **2** could now be resolved by X-ray structural analysis of the two compounds. Furthermore, the structure of **1** was of particular interest because of its "proton sponge" properties.[2]

Evaporation of a solution of **1** in acetone afforded crystals containing 1/2 molecule of water per molecule of **1**. Figure 1 shows the molecular structure of **1** viewed from above the quinoquinoline system. The bond lengths around the periphery of the molecule and, in particular, the alternations of these bond lengths, largely correspond to the bonding in other quinoline systems (e.g., **2**; see below). Noteworthy in the inner region, characterized by the close proximity of N(1) and N(12), is the increase in the central external angle of the "naphthalene unit" (125.4°), which results in an increase in the N···N distance to 272.8 pm. Despite the interaction between these nitrogen atoms, there is only a very slight deviation of the molecule from

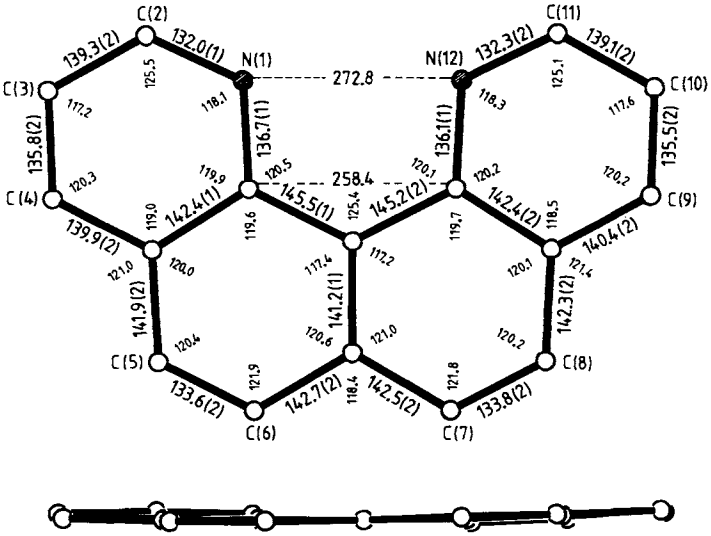


Fig. 1. Molecular structure of **1** viewed from above the plane of the quinoquinoline (above) and from the side (bottom). The upper part of the figure shows bond lengths [pm] and angles [°] (standard deviation of the last decimal place in parentheses). Tetragonal space group $I4_1/a$, $a = 1446.0(2)$, $c = 2213.9(4)$ pm; $Z = 16$, $\rho_{calcd} = 1.373$ g cm^{-3}; 2860 measured reflections, 1854 with $I \geq 2.00\sigma(I)$ observed; structural solution by direct methods (MULTAN), $R = 0.046$ [8].

planarity, as shown in the side view (Fig. 1, bottom): the largest deviations from the "least-squares plane" through the ten "naphthalene" C atoms are 13 and 12 pm for C(2) and C(3), respectively; the two nitrogen atoms lie only 7 pm above and 6 pm below this plane. Since, owing to interactions between the basic groups, all other strong "proton sponges" (e.g., 1,8-bis(dimethylamino)naphthalene, corresponding to **1**) exhibit a strong steric deformation of the free base, which is reduced by the N···H···N hydrogen bond upon protonation,[1] the largely planar structure of **1** is very surprising. This planarity is undoubtedly due to the incorporation of the nitrogen atoms into the tetracyclic aromatic system. Figure 2 shows the crystal packing of **1** · 1/2 H_2O in the projection along the *c* axis.

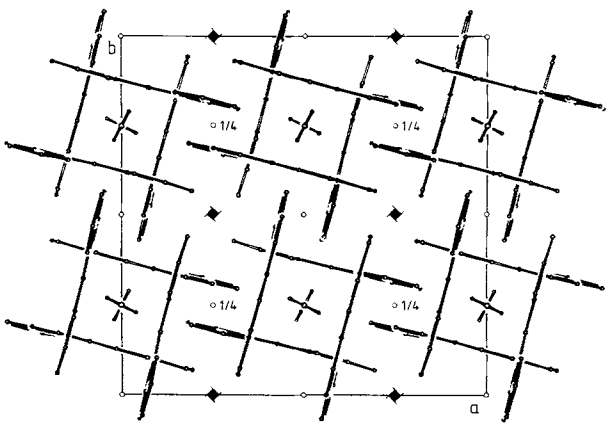


Fig. 2. Crystal packing of **1** · 1/2 H_2O in the projection along the *c* axis.

ing of **1** and also reveals the positions of the molecules of crystal water on the $\bar{4}$ axis. Because of the large separation from the nitrogen atoms of **1** and the unfavorable arrangement referred to the "lone pairs" of these atoms, the water molecules do not engage in specific hydrogen-bond interactions with **1**.

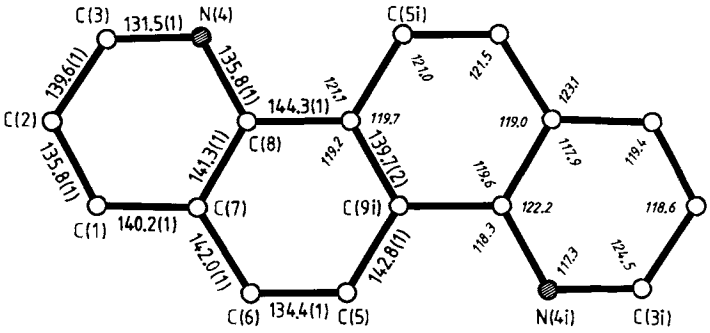


Fig. 3. Molecular structure of **2** as viewed from above the quinoquinoline plane with bond lengths [pm] and bond angles [°] (standard deviations of the last decimal place in parentheses). Monoclinic prisms from ethanol/water, space group $P2_1/c$, $a=450.5(1)$, $b=971.7(2)$, $c=1233.5(2)$ pm, $\beta=93.29(2)°$, $Z=2$, $\rho_{calcd}=1.418$ g cm^{-3}; 1354 reflections, 976 observed with $I \geq 2.00\sigma(I)$; structure solution by direct methods (MULTAN), $R=0.037$ [8].

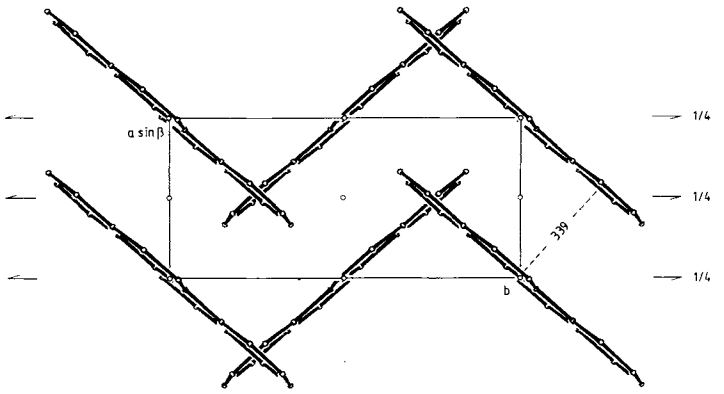


Fig. 4. Crystal packing of **2** in the projection along the *c* axis.

Figure 3 shows the molecular structure of **2** viewed from above the tetracyclic ring system. The bond lengths and bond angles of the centrosymmetric molecule do not deviate significantly from those of other quinoline compounds. The molecule is nearly perfectly planar with maximal deviations of 2 pm [for C(6) and N(4)] for the least-squares plane formed by the 18 ring atoms. The crystal packing (Fig. 4) shows the "herring-bone pattern" often observed for polycyclic aromatic compounds. The molecules are stacked along the *a* axis, the stacking axis forming an angle of 41.4° with the plane of the molecules; the interplanar distance between neighboring molecules within the stack is 339 pm.

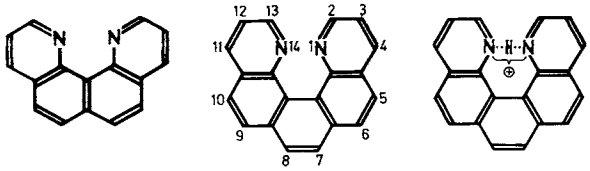
Received: August 18, 1988 [Z 2928 IE]
German version: *Angew. Chem. 101* (1989) 72

[1] Review: H. A. Staab, T. Saupe, *Angew. Chem. 100* (1988) 895; *Angew. Chem. Int. Ed. Engl. 27* (1988) 865.
[2] M. A. Zirnstein, H. A. Staab, *Angew. Chem. 99* (1987) 460; *Angew. Chem. Int. Ed. Engl. 26* (1987) 460.
[3] R. W. Alder, P. S. Bowman, W. R. S. Steele, D. R. Winterman, *Chem. Commun. 1968*, 723; further references in [1].
[4] I. Iwai, S. Hara, *J. Pharm. Soc. Jpn. 70* (1950) 32.
[5] I. Iwai, S. Hara, S. Sayegi, *J. Pharm. Soc. Jpn. 71* (1951) 1152.
[6] M. Dufour, N. P. Buu-Hoï, P. Jacquignon, *J. Chem. Soc. C 1967*, 1415.
[7] A. Edel, P. A. Marnot, J. P. Sauvage, *Tetrahedron Lett. 26* (1985) 727.
[8] Further details of the crystal structure investigations may be obtained from the Fachinformationszentrum Energie, Physik, Mathematik GmbH, D-7514 Eggenstein-Leopoldshafen 2 (FRG), on quoting the depository number CSD-53273, the names of the authors, and the journal citation.

Benzo[1,2-*h* : 4,3-*h'*]diquinoline ("1,14-Diaza[5]helicene"): Synthesis, Structure, and Properties**

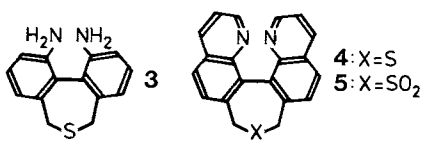
By *Heinz A. Staab,* Michael A. Zirnstein,* and *Claus Krieger*

Our synthesis of quino[7,8-*h*]quinoline **1** provides a "proton sponge"[1] whose basic centers, as well as the N···H···N hydrogen bond (in the cation formed by protonation of **1**), are not hydrophobically shielded by *N*-alkyl groups.[2] In the preceding communication, we described the molecular structure of **1**.[3] In the same way that **1** is related to 1,8-bis(dimethylamino)naphthalene, the actual "proton sponge"[4] benzo[1,2-*h* : 4,3-*h'*]diquinoline **2** is related to 4,5-bis(dimethylamino)phenanthrene, whose synthesis, structure, and "proton-sponge" properties we have also described.[5] Whereas a largely planar structure was found for **1**,[3] compound **2**, whose basic structure is that of a [5]helicene, should display strong helical deformation. This should be reflected in the N···N distance, the preferential orientation of the nitrogen "lone pairs", and thus the N···H···N hydrogen bond in the monocation **2a** derived from **2**.



1 **2** **2a**

To synthesize **2**, 1,11-diamino-5,7-dihydrodibenzo[*c*,*e*]-thiepin **3**, synthesized earlier by us,[5] was converted into 7,9-dihydrothiepino[3,4-*h* : 6,5-*h'*]diquinoline **4** (24% yield) in a double Skraup reaction (glycerol, arsenic acid, conc. sulfuric acid; 30 min, 145–150°C). Oxidation with trifluoroperoxyacetic acid in trifluoroacetic acid (2 h, 0–20°C) led to the *S*,*S*-dioxide **5** in 72% yield. A variant of the Ramberg–Bäcklund rearrangement[5,6] with KOH and CCl_4 in *t*BuOH (3–5°C, then 2.5 h, 40°C) resulted in conversion of **5** into the desired **2** (m.p. 271–273°C; 13% yield, 16% re-



isolation of **5**). The structure of **2** was established by correct elemental analysis, mass spectrum [*m/z* 280 (100%, $M^{\oplus}$), 279 (24), 252 (24), 140 (11, $M^{2\oplus}$); high-resolution MS: $M^{\oplus}$ 280.0997 corresponding to $C_{20}H_{12}N_2$] and ^{1}H NMR data [$\delta=7.59$ (dd, $J=8.1$ and 4.2 Hz, 2H; 3,12-H), 8.10 and 8.12 (AB, $J=8.5$ Hz, 2H each; 5,10- and 6,9-H), 8.19 (s, 2H, 7,8-H), 8.43 (dd, $J=8.1$ and 1.7 Hz, 2H; 4,11-H), 8.56 (dd, $J=4.2$ and 1.7 Hz, 2H; 2,13-H; 500 MHz, [D_6]dimethyl sulfoxide (DMSO)].

[*] Prof. Dr. H. A. Staab, Dipl.-Chem. M. A. Zirnstein, C. Krieger
Abteilung Organische Chemie
Max-Planck-Institut für medizinische Forschung
Jahnstrasse 29, D-6900 Heidelberg (FRG)

[**] New "Proton Sponges", Part 9.—Part 8: [3].

The molecular structure of **2**, which has C_2 symmetry in the crystal, is shown in Figure 1. Bond lengths and angles (Fig. 1, top) do not reveal any unusual features in comparison to planar **1** or its isomer.[3] The middle of Figure 1 shows the considerable helical deviation of the planar arrangement; this is seen even more clearly in the side view along the central bond C(17)–C(17i) (Fig. 1, bottom). The consequence of this helical deformation is an increase in the N···N distance to 270.5 pm, which is only slightly shorter than the N···N distance in planar **1** (272.8 pm). Figure 2 shows the lattice packing of **2**, which is present as a racemate.

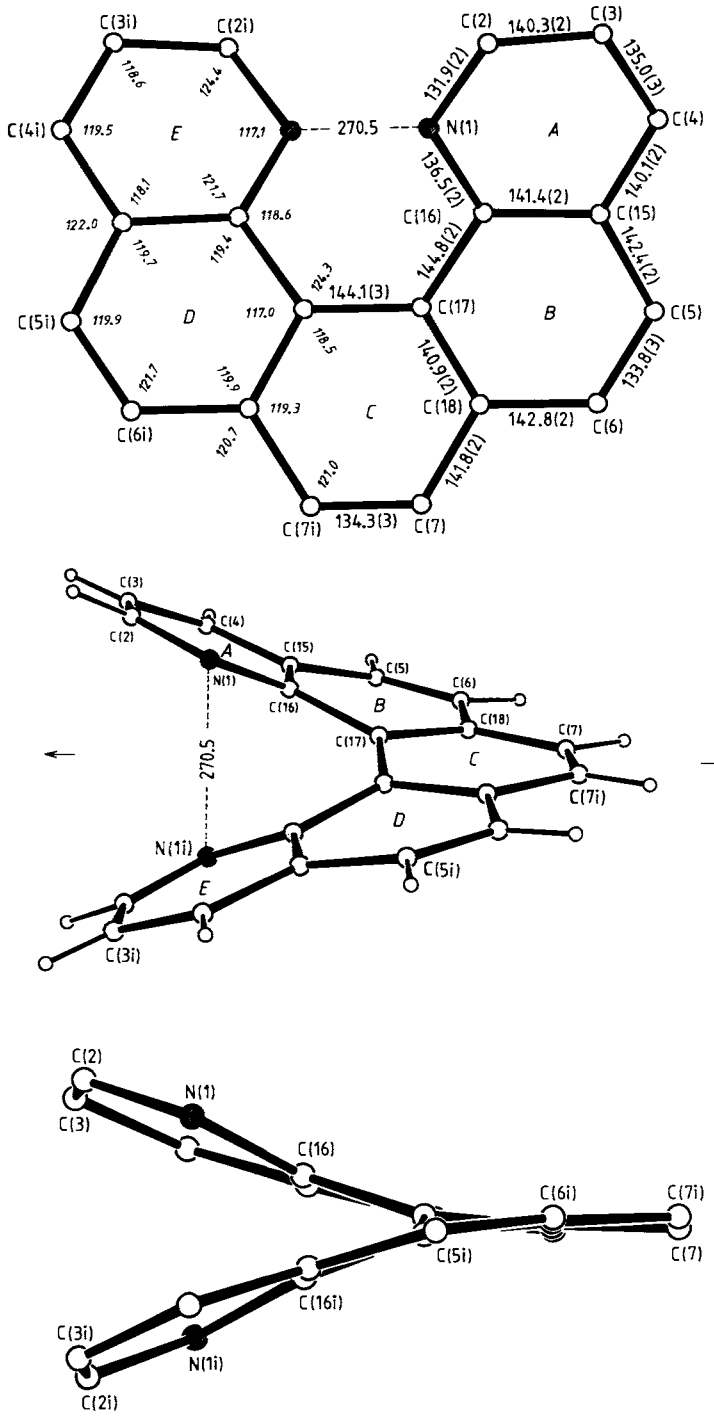


Fig. 1. Molecular structure of **2** viewed from above the average plane of the central six-membered ring C (top), from the side of and somewhat above the pentacyclic system (middle), and from the side along the central C(17)–C(17i) bond (bottom); bond lengths [pm] and valence angles [°] (standard deviations of the last decimal place in parentheses) are given above. Crystal of **2** from ethyl acetate, space group $C2/c$; $a = 1213.0(3)$, $b = 905.8(2)$, $c = 1279.2(3)$ pm, $b = 106.28(2)°$; $Z = 4$, $\rho_{calcd} = 1.380$ g cm^{-3}; 1613 symmetry-independent reflections to $\sin\theta/\lambda = 6.8$ nm^{-1}, 910 observed with $I \geq 2\sigma(I)$ [7]. The structure was solved starting from that of [5]helicene [8] by placing the molecule on the twofold axis and optimizing its position by variation of the y coordinate and rotation around the twofold axis; $R = 0.039$.

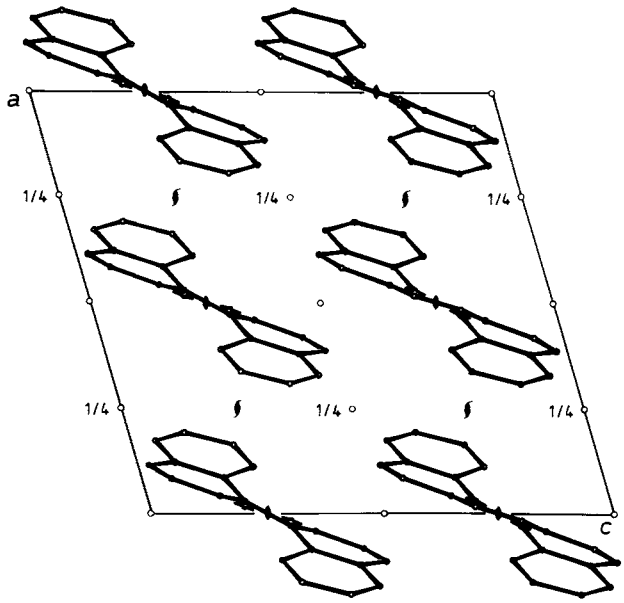


Fig. 2. Crystal lattice packing of **2** (racemate) in the projection along the b axis.

Upon addition of 70% perchloric acid in excess to **2** in dichloromethane, a perchlorate is formed which can be recrystallized from methanol/water (3:1) (64% yield; m.p. ≥ 320 °C, dec.). The elemental analysis and the ^{1}H NMR spectrum [$\delta = 8.28$ (dd, $J = 7.8$ and 4.7 Hz, 2H; 3,12-H), 8.44 and 8.49 (AB, $J = 8.4$ Hz, 2H each; 5,10-H and 6,9-H), 8.59 (s, 2H; 7,8-H), 9.15 (dd, $J = 8.0$ and 1.6 Hz, 2H; 4,11-H), 9.59 (dd, $J = 4.6$ and 1.6 Hz; 2,13-H), 23.89 (br. s, 1H, N···H···N); 500 MHz, [D$_6$]DMSO] confirm the expected presence of the *mono*cation **2a**. Compared to **2**, all signals in **2a** are shifted downfield by the protonation. Most noteworthy is the chemical shift of the hydrogen-bond proton (to almost $\delta = 24$!). Although we find a strong downfield shift for all N···H···N hydrogen bonds in the "proton sponges", the value found for **2a** shows that here the anisotropy effect of the helical aromatic bonding system is additionally important.

^{1}H NMR spectroscopic determination of the signal intensities in transprotonation experiments with 1,8-bis(dimethylamino)naphthalene[1] gave a pK_a value of 10.3 ± 0.2 for **2**. In these experiments, only averaged signals were found for **2** and **2a**, so that, in this case, the rate of proton transfer is rapid relative to the time scale of the NMR method. This is not true for typical "proton sponges", whose basic centers and N···H···N hydrogen bonds are hydrophobically shielded by *N*-alkyl groups.[1] The behavior of **2**/**2a** is in complete agreement, however, with that of **1**/**1a**. Thus, **2** is also an example of a kinetically active "proton sponge". That the basicity constant of **2** is nearly two powers of ten smaller than that of **1**,[2] although the N···N distance in **2** (270.5 pm) is somewhat shorter than

in **1** (272.8 pm)[3], is presumably due to the helical structure of **2** (see Fig. 1, middle). This structure nearly removes the destabilizing "lone-pair" interaction of the nitrogen atoms in the free base and, for **2a**, hinders the formation of an N···H···N hydrogen bond along the favored direction of the nitrogen "lone pairs".

Received: August 18, 1988 [Z 2929 IE]
German version: *Angew. Chem. 101* (1989) 73

[1] Review on "Proton Sponges": H. A. Staab, T. Saupe, *Angew. Chem. 100* (1988) 895; *Angew. Chem. Int. Ed. Engl. 27* (1988) 865.
[2] M. A. Zirnstein, H. A. Staab, *Angew. Chem. 99* (1987) 460; *Angew. Chem. Int. Ed. Engl. 26* (1987) 460.
[3] C. Krieger, M. A. Zirnstein, I. Newsom, H. A. Staab, *Angew. Chem. 101* (1989) 72; *Angew. Chem. Int. Ed. Engl. 28* (1989) 84.
[4] R. W. Alder, M. R. Bryce, N. C. Goode, N. Miller, J. Owen, *J. Chem. Soc. Perkin Trans. 1 1981*, 2840; the name "Proton Sponge" was introduced by Aldrich Chemicals Co., Milwaukee, as the commercial name of this compound.
[5] T. Saupe, C. Krieger, H. A. Staab, *Angew. Chem. 98* (1986) 460; *Angew. Chem. Int. Ed. Engl. 25* (1986) 451; for the X-ray structure analysis see [1].
[6] C. Y. Meyers, A. M. Malte, W. S. Matthews, *J. Am. Chem. Soc. 91* (1969) 7510; C. Y. Meyers, W. S. Matthews, G. J. McCollum, J. C. Branca, *Tetrahedron Lett. 1974*, 1105.
[7] Further details of the crystal structure investigation may be obtained from the Fachinformationszentrum Energie, Physik, Mathematik GmbH, D-7514 Eggenstein-Leopoldshafen 2 (FRG), on quoting the depository number CSD-53274, the names of the authors, and the journal citation.
[8] R. Kuroda, *J. Chem. Soc. Perkin Trans. 2 1982*, 789; cf. also A. O. McIntosh, J. M. Robertson, V. Vand, *J. Chem. Soc. 1954*, 1661.

Methylboron Oxide, $H_3C-B{\equiv}O$**

By *Hans Bock,* Lorenz Cederbaum,* W. von Niessen, Peter Paetzold,* Pavel Rosmus,* and *Bahman Solouki*

Dedicated to Professor Heinz Georg Wagner on the occasion of his 60th birthday

Organoboron oxides (organo(oxo)boranes) RBO are kinetically unstable with respect to their cyclic trimers[2-4] and, therefore, in contrast to the isoelectronic iminoboranes RBNR[5] and methyleneboranes $RBCR_2$,[6] they were previously unknown. The title compound is of particular interest with regard to its electron distribution; containing 16 valence electrons, it should thus have a linear CBO framework[7] and can be compared with numerous well-known compounds, such as $H_3C-C{\equiv}CH$ and $H_3Si-C{\equiv}CH$[8] as well as $H_3C-C{\equiv}N$.[9]

Methylboron oxide was generated by pyrolysis of 2-methyl-1,3,2-dioxaborolane-4,5-dione at 1100 K, optimized by PE-spectroscopic real-time gas analysis[1] (Fig. 1), and the PE spectrum of the "pure" compound (Fig. 1, bottom) was obtained by digital subtraction ("spectra stripping") of the ionization patterns of the thermodynamically favored fragmentation molecules CO and CO_2.[10] The radical cation states were assigned on the basis of the total energy differences determined from a highly-correlated calculation according to the algebraic diagrammatic construction(3) procedure (ADC(3) procedure).[11]

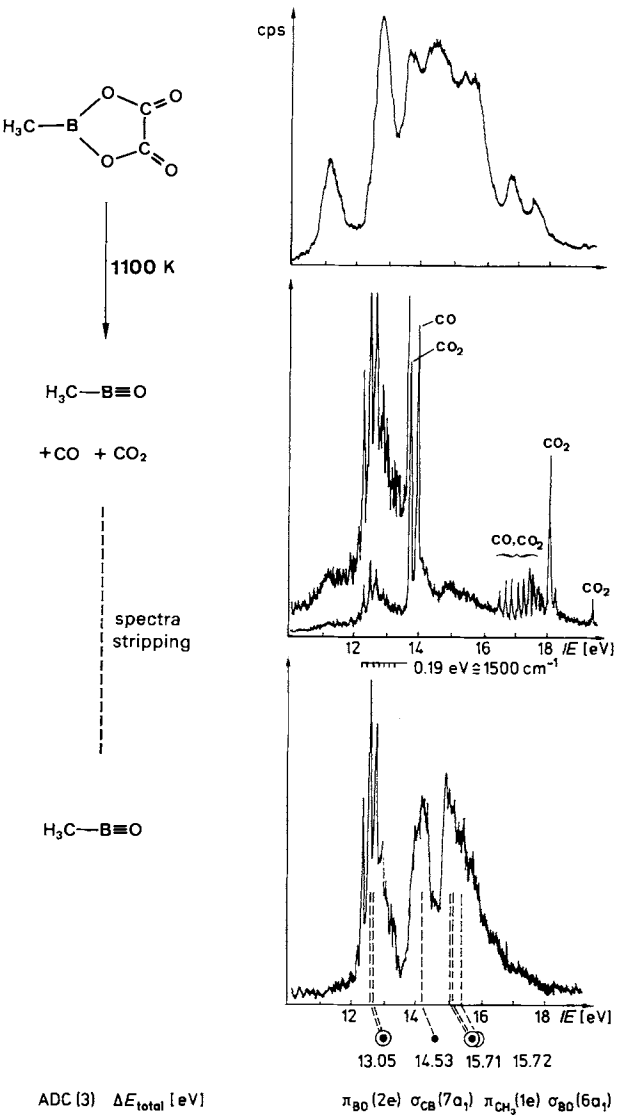


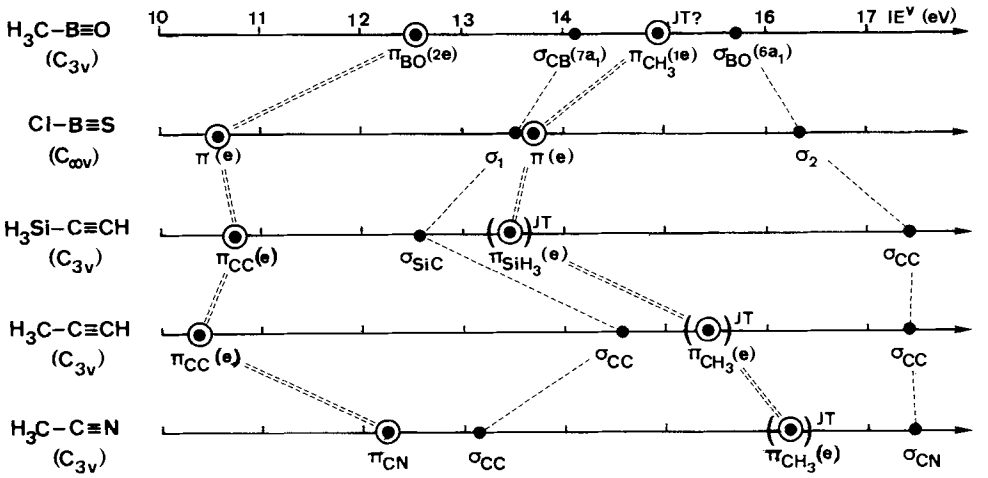
Fig. 1. He(I) PE spectra of 2-methyl-1,3,2-dioxaborolane-4,5-dione at 330 K (top), of its pyrolysis products at 1100 K (middle), and—after digital subtraction of the ionization patterns of CO and CO_2—of methylboron oxide (bottom) [10]. Assignment of the six radical cation states in the measuring range on the basis of ADC(3) total energy differences [11].

A comparison of the radical cation states of $H_3C-B{\equiv}O$ with equivalent states[12] of the iso(valence)electronic molecules $Cl-B{\equiv}S$,[4] $H_3Si-C{\equiv}CH$,[8] $H_3C-C{\equiv}CH$,[8] and $H_3C-C{\equiv}N$[9] (Scheme 1) corroborates the ADC(3) assignment (Fig. 1) and furthermore provides, on the basis of first- and second-order perturbation arguments, insights into its electron distribution (JT: center of gravity of Jahn-Teller-split bands).

The sequences of the radical cation states of the iso(valence)electronic molecules $H_3C-B{\equiv}O$ and $Cl-B{\equiv}S$ are, as expected, in agreement and therefore support the independently made assignments.[4, 11] The lower π(e) ionization energies can be explained by the differences in the effective nuclear charges $Z_{eff}(S) < Z_{eff}(O)$, and the larger π and σ splittings by the differences $Z_{eff}(Cl-S) < Z_{eff}(O-C)$ as

[*] Prof. Dr. H. Bock, Dr. P. Rosmus, Dr. B. Solouki
Institut für Anorganische Chemie der Universität
Niederurseler Hang, D-6000 Frankfurt am Main 50 (FRG)
Prof. Dr. L. S. Cederbaum, Prof. Dr. W. von Niessen
Physikalisch-chemisches Institut der Universität
Im Neuenheimer Feld, D-6900 Heidelberg (FRG)
Prof. Dr. P. Paetzold
Institut für Anorganische Chemie der Technischen Hochschule
Templergraben 55, D-5100 Aachen (FRG)

[**] Gas-Phase Reactions, Part 70. This work was supported by the Deutsche Forschungsgemeinschaft, the Fonds der chemischen Industrie, and the State of Hessen. Part 69: [1].



Scheme 1.

well as the thereby increased second-order perturbations ($\Delta E \approx 1/\Delta Z_{eff}$).[12] An analogous argument, $Z_{eff}(Si) \ll Z_{eff}(C)$, allows a comparison with and among the H_3Si- and H_3C-acetylene derivatives, for which the "hyperconjugative" π_{CC}/π_{EH_3} interactions can be estimated from the ionization energies by means of the following equation:[8, 12]

$$\beta^{\pi}_{CC/EH_3} = \sqrt{(IE_1(HC{\equiv}CH) - IE_1)(IE(e, H_3EEH_3) - IE_1)}$$

$$\beta^{\pi}_{CC/CH_3} = -2.1\ \text{eV} \gg \beta^{\pi}_{CC/SiH_3} = -1.4\ \text{eV}$$

Omitting first-order perturbation corrections[8, 12] for $H_3C-B{\equiv}O$, the following value is obtained:

$$\beta^{\pi}_{BO/CH_3} = \sqrt{(\approx 13.4 - 12.5)(14.3 - 12.5)} \approx -1.3\ \text{eV}$$

This hyperconjugative interaction parameter is in agreement with the observed small π splitting $\Delta\pi(e) = 2.5$ eV (cf. Scheme 1: $H_3C-C{\equiv}CH$ 5 eV; $H_3Si-C{\equiv}CH$ 2.7 eV). Extremely close comparability exists with H_3CCN due to the isoelectronic relationship between $B{\equiv}O$ and $C{\equiv}N$: the first two vertical ionization energies differ from each other only by $\Delta IE_1 \approx 0.3$ eV and $\Delta IE_2 \approx 0.9$ eV; the π interaction, $\beta^{\pi}_{CN/CH_3} \approx -1.8$ eV[9] is larger by 0.5 eV.

The comparison of the radical cation states (Scheme 1) thus provides the following clues: The C_{3v} molecule $H_3C-B{\equiv}O$ contains, according to chemical parlance, a "true BO triple bond"[5] and its ionization pattern, cum grano salis, is identical with that of the isoelectronic $H_3C-C{\equiv}N$.[13] The two compounds are also similar with respect to the vibrational fine structure ($\tilde{\nu}^{\oplus} \approx 1500\ \text{cm}^{-1}$; H_3C-CN, $\tilde{\nu}^{\oplus} \approx 1430\ \text{cm}^{-1}$[9]) visible in the first ionization band (Fig. 1) and due presumably to an H_3C deformation. MNDO calculations[14] predict a largely balanced charge distribution

$$H_3C^{+0.19}-B^{-0.06}{\equiv}O^{-0.13}$$

and a negative enthalpy of formation $\Delta H_f \approx -90$ kcal mol^{-1}. In view of the experimentally determined (Fig. 1: generation temperature $T \approx 1100$ K) thermodynamic stability of $H_3C-B{\equiv}O$, the kinetic instability of organoboron oxides[2] is presumably caused by the energetically favored oligomerization, for example, to give six-membered ring compounds $(RBO)_3$, and it should be possible to isolate derivatives with bulky alkyl or aryl groups.

Received: August 1, 1988 [Z 2894 IE]
German version: *Angew. Chem. 101* (1989) 77

CAS Registry numbers:
H_3CBO, 79723-21-0; 2-methyl-1,3,2-dioxaborolane-4,5-dione, 34221-87-9.

[1] Cf. the review on PE-spectroscopic detection of reactive intermediates in the gas phase: H. Bock, B. Solouki, S. Aygen, M. Bankmann, O. Breuer, R. Dammel, J. Dörr, M. Haun, T. Hirabayashi, D. Jaculi, J. Mintzer, S. Mohmand, H. Müller, P. Rosmus, B. Roth, J. Wittmann, H.-P. Wolf, *J. Mol. Struct. 173* (1988) 31–49.

[2] M. Groeteklas, P. Paetzold, *Chem. Ber. 121* (1988) 809, and references cited therein. Cf. also P. Paetzold, P. Bohm, A. Richter, E. Scholl, Z. *Naturforsch. B31* (1976) 754; P. Paetzold, W. Scheibitz, E. Scholl, *ibid. 26* (1971) 646.

[3] HBO as well as FBO, ClBO, and BrBO have been isolated in a matrix and/or detected in flow experiments by mass spectrometry; cf. Y. Kawashina, K. Kawaguchi, Y. Endo, E. Hivota, *J. Chem. Phys. 87* (1987) 2006 or D. C. Frost, C. Kirby, W. M. Lau, A. McDowell, N. P. C. Westwood, *J. Mol. Struct. 100* (1983) 87, and references cited therein.

[4] Of the iso(valence)electronic derivatives of XBS, HBS has been prepared by reaction of H_2S with B_∞ at $T > 1300$ K (R. W. Kirk, P. L. Timms, *Chem. Commun. 1967*, 8) and characterized by PE spectroscopy (T. P. Fehlner, D. W. Turner, *J. Am. Chem. Soc. 95* (1973) 7175; H. W. Kroto, R. J. Suffolk, N. P. C. Westwood, *Chem. Phys. Lett. 22* (1973) 495). The ionization energies correlate with those of FBS, ClBS, and BrBS (cf. H. W. Kroto, *Chem. Soc. Rev. 11* (1982) 457, and references cited therein; small amounts of H_3CBS can be detected by microwave spectroscopy in reaction mixtures of $H_3CSSCH_3 + B_\infty$ at $T > 1300$ K.

[5] Review: P. Paetzold, *Adv. Inorg. Chem. 31* (1987) 123–170, and references cited therein; derivatives RBNH are also unknown.

[6] Cf. H. Lukasch, G. Schmidt-Lukasch, U. Lippold, A. Berndt, *Angew. Chem. 100* (1988) 959; *Angew. Chem. Int. Ed. Engl. 27* (1988) 960, and references cited therein, especially for derivatives $RBCH_2$ with $R = OCH_3$, $N(CH_3)_2$.

[7] A. D. Walsh, *J. Chem. Soc. 1953*, 2260–2331; cf. also R. J. Buenker, S. D. Peyerimhoff, *Theor. Chim. Acta 24* (1972) 132.

[8] W. Ensslin, H. Bock, G. Becker, *J. Am. Chem. Soc. 96* (1974) 2757. Cf. also: H. Bock, B. Solouki: *Photoelectron Spectra of Silicon Compounds* in S. Patai, Z. Rappoport (Eds.): *The Chemistry of Organic Silicon Compounds*, Wiley, London 1988, in press.

[9] Cf. H. Stafast, H. Bock: *Photoelectron Spectra of Cyano Compounds* in S. Patai (Ed.): *The Chemistry of the Cyano Group*, Wiley, London 1983, pp. 137–185, and references cited therein.

[10] Leybold Heraeus UPG 200 PE spectrometer with electron-bombardment short-path oven [1], on-line recording with PDP 11/40; measuring pressure, 10^{-4} mbar; resolution, 20 meV; intensity, 10^5 cps (Ar); calibration: $^2P_{3/2}(Ar) = 15.76$ eV and $^2\Sigma^+(CO) = 14.01$ eV and $^2\Pi_g(CO_2) = 13.78$ eV. The vertical He(I) ionization energies of H_3CBO are (in eV): 12.54, 14.12, 14.95 (Jahn/Teller 15.7?) and > 15.7 (Fig. 1; overlapping bands). The vibrational fine structure of the first band displays splittings of 0.19 eV = 1530 cm^{-1}.

[11] J. Schirmer, L. S. Cederbaum, O. Walter, *Phys. Rev. A 28* (1983) 1237; W. von Niessen, J. Schirmer, L. S. Cederbaum, *Comp. Phys. Rep. 1* (1984) 59. Molecular geometry of H_3CBO optimized by the Hartree-Fock method with the assumption of C_{3v} symmetry: $d_{BO}=121.6$ pm, $d_{C-B}=153.2$ pm, $d_{C-H}=108.6$ pm, $\sphericalangle HCB=110.8°$; basis set (cf. T. H. Dunning, *J. Chem. Phys. 53* (1970) 2823; *55* (1971) 3958): each C, B, O 9s/5p contracted to 3s/2p and each H 4s contracted to 3s. HF energies [eV]: −13.88 (2e), −15.86 ($7a_1$), −16.72 (1e), −17.08 ($6a_1$), −27.53 ($5a_1$), −36.38 ($4a_1$). ADC(3) single-particle energies [eV] (configurations and pole strengths in parentheses): 13.051 ($2e^{-1}$, 0.899), 14.529 ($7a_1^{-1}$, 0.902), 15.172 ($1e^{-1}$, 0.922), 15.724 ($6a_1^{-1}$, 0.892), 25.079 ($5a_1^{-1}$ and $3(2h^{-1}p)$), 34.921 and 34.955 ($4a_1^{-1}$ and $4(2h^{-1}p)$, 0.179 and 0.178); Ionization energies with pole strengths <0.1 were not included. *F. Tarantelli* and *H.-G. Weikert* helped with the calculations.

[12] H. Bock, *Angew. Chem. 89* (1977) 631; *Angew. Chem. Int. Ed. Engl. 16* (1977) 613, and references cited therein.

[13] Starting from the structure in the gas phase (determined by electron diffraction), the following MNDO eigenvalues were calculated for H_3CCN: −12.8 eV (2e), −14.1 eV ($4a_1$), −15.5 eV (1e), and −18.5 eV ($3a_1$) (cf. Scheme 1). The resulting charge distribution

$$H_3C^{+0.20}-C^{-0.11}\equiv N^{-0.08}$$

leads to a dipole moment $\mu=2.6$ D ($\mu_{exp}=3.9$ D [9]).

[14] MNDO geometry optimization for $H_3C-B\equiv O$ gave $d_{CB}=153$ pm, $d_{BO}=118$ pm, $d_{CH}=111$ pm and $\sphericalangle HCB=110°$, and $\mu=2.4$ D as dipole moment. The eigenvalues −13.6 eV (2e), −14.4 eV ($4a_1$), −15.6 eV (1e), and −17.7 eV ($3a_1$) reflect the ionization pattern despite differing Koopmans' defects [11] (cf. also 4-31-G ab initio results G. Raabe, W. Schlieker, W. Strassburger, E. Heyne, J. Fleischhauer, *Z. Naturforsch. B42* (1987) 1027).

The Structure of Hexaaminobenzene**

By *David A. Dixon,* Joseph C. Calabrese,* and *Joel S. Miller**

The quest for molecular organic ferromagnets has culminated in the characterization of the complex $[Fe^{III}(C_5Me_5)_2]^{\oplus}[TCNE]^{\ominus}$ as a bulk ferromagnet.[1,2] Totally p-orbital based ferromagnets require stable radical cations or anions with D_{2d} symmetry or with a rotation axis of three or greater,[2] such as hexaaminobenzene **1**.[3] Donor-acceptor systems based on substituted $\mathbf{1}^{\oplus}$ have yet to be characterized as exhibiting ferromagnetic behavior;[4] however, this high symmetry, low ionization potential donor is of fundamental interest. Herein we report the X-ray structural analysis and redox properties of **1**.

Hexaaminobenzene was prepared by a literature route from 1,3,5-triamino-2,4,6-trinitrobenzene.[3b] Crystals suitable for single crystal X-ray diffraction[5] were obtained from nitromethane under an inert atmosphere. The molecule has six identical CNH_2 groups (Fig. 1). The geometrical parameters are given in Table 1. A packing diagram is depicted in Figure 2. The crystal packing is dominated by weak intermolecular NH···N interactions such that the nitrogen lone pair is positioned between adjacent hydrogens of nearby molecules. This results in an arrangement in which each molecule is surrounded by twelve other molecules in three different orientations. The vibrational spectrum of **1** is quite simple, consistent with its high molecular symmetry. Characteristic infrared absorptions (Nujol; for IR data in KBr see [3a]) are given in Table 2.

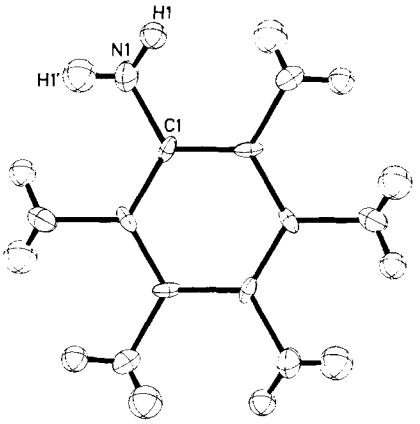


Fig. 1. ORTEP drawing of **1** (50% ellipsoids).

Unlike hexaazaoctadecahydrocoronene, which exhibits four reversible one-electron oxidations,[6,7] **1** exhibits only one reversible one-electron oxidation at −0.11 V (vs. SCE in $MeNO_2$) corresponding to $\mathbf{1}^{\oplus}e^{\ominus} \rightleftharpoons \mathbf{1}$. Although an irreversible oxidation to $\mathbf{1}^{2\oplus}$ occurs at ca. +0.56 V, chemical oxidation has not yet led to crystalline solids suitable for single crystal X-ray analysis.

Table 1. Bond lengths and angles for **1** (see Fig. 1 for the numbering scheme).

between	Bond lengths [Å] experimental	calculated D_{3d} [a]	calculated S_6 [a]	calculated S_6 [b]	definition	Bond angles [°] experimental	calculated D_{3d} [a]	calculated S_6 [a]	calculated S_6 [b]
N1-C1	1.432(8)	1.457	1.459	1.426	C1-N1-H1	112(4)	108.6	108.1	110.1
N1-H1	0.879(56)	1.03	1.031	1.001	C1-N1-H1′	116(5)	108.6	107.9	110.1
N1-H1′	0.841(67)	1.03	1.032	1.004	H1-N1-H1′	110(5)	104.8	104.7	106.0
C1-C1 [c]	1.383(6)	1.396	1.395	1.392	N1-C1-C1 [d]	120(1)	120.0	119.5	119.2
					N1-C1-C1 [c]	120(1)	120.0	120.5	120.8
					C1[c]-C1-C1 [d]	120.00(2)	120.0	119.9	119.9
					CC-NH [e]		35.3	22.1, 48.2	10.9, 52.5

[a] STO-3G. [b] 6-31G*(N). [c] $1/2-z, -1/2+x, y$. [d] $1/2+y, z, 1/2-x$. [e] Torsion angle.

Ab initio molecular orbital calculations were carried out with the program GRADSCF[8] on a CRAY-XMP/24 computer using both the minimal STO-3G basis set[9] and the 6-31G* (N) basis set (168 orbitals).[10] The geometry of **1** was gradient optimized[11] and force fields were calculated analytically.[12]

[*] Dr. J. S. Miller, Dr. D. A. Dixon, Dr. J. C. Calabrese
Central Research and Development,
E. I. du Pont de Nemours and Co., Inc.
Experimental Station E328, Wilmington, DE 19880-0328 (USA)

[**] We are indebted to *D. Bruce Chase, Ray Richardson, William Marshall, Carlos Vazquez,* and *Daniel Wipf* for assistance in obtaining physical measurements as well as preparing samples.

Table 2. Experimental and calculated vibrational spectra [a].

IR spectrum					Raman spectrum				
$\tilde{\nu}_{exp}$	$\tilde{\nu}_{calcd}$ scaled [b]	$\tilde{\nu}_{calcd}$ unscaled	I_{calcd}	symmetry [c]	$\tilde{\nu}_{exp}$	$\tilde{\nu}_{calcd}$ scaled [b]	$\tilde{\nu}_{calcd}$ unscaled	I_{calcd}	symmetry [c]
3341 s	3363	4101	4	e_u	1625 s	1650	2014	—	e_g
						1596	1946	—	e_g
3263 br	3218	3924	8	e_u	1391 s	1374	1676	—	a_g
1625 br	1629	1986	64	a_u	1192 w	1168	1424	—	e_g
1490 s	1482	1807	213	e_u	1081 w	1052	1283	—	e_g
1199 w	1196	1458	39	e_u	890 m	901	1099	—	e_g
						899	1096	—	a_g
925 m	940	1144	632	e_u	835 m				
840 s	827	1008	236	e_u	820 m				
					720 w	704	859	—	a_g
					579 s	577 [d]	641	—	a_g

[a] $\tilde{\nu}$ in cm^{-1}; I in km mol^{-1}. [b] Scaling factor = 0.82. [c] Qualitative assignment of the motion of the normal coordinate. [d] Scaling factor = 0.90.

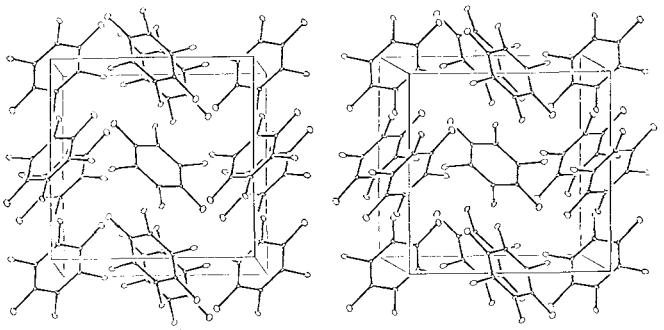


Fig. 2. Stereoview of a unit cell of **1** (hydrogens omitted for clarity).

The calculated metric parameters for **1** are given in Table 1. The structure was initially calculated with exact D_{3d} symmetry using the STO-3G basis set. This structure is not an energy minimum, but has a negative direction of curvature characterized by an imaginary frequency of 93i cm^{-1}; i.e., it is a transition state. When the structure was reoptimized following the direction of negative curvature, a minimum energy structure with S_6 symmetry was obtained. This S_6 structure is 0.2 kcal/mol lower in energy at the Hartree-Fock level and 0.4 kcal/mol lower at the MP-2 level with the STO-3G basis set[13] than the D_{3d} structure. The S_6 structure has the NH_2 groups rotated by 13° away relative to the D_{3d} structure about the C–N bond axis. Consistent with the small energy difference, the geometry parameters for the two structures are essentially the same. We reoptimized the S_6 structure with the much larger 6-31G* (N) basis set. The calculated C–C bond distance is only 0.009 Å longer. The calculated C–N distance is in even better agreement and is 0.006 Å shorter than the experimental value. The experimental N–H bonds are too short compared to the theoretical values, a well-known phenomenon.[14] The calculated values for θ(CCC) and θ(CCN) are 120 ± 1.0°, consistent with the experimental results. The NH_2 groups are calculated to be more pyramidal than the experimental values. This is not surprising considering the difficulty in assigning the hydrogen positions in the crystal structure. With the 6-31G* (N) basis set, the NH_2 groups are even further twisted away from the D_{3d} structure with CCNH torsion angles of 11° and 52° giving an average twist of 21° for the NH_2 groups. The calculated rotation away from the D_{3d} structure about the C–N bond is consistent with the observed values considering the errors in the positions of the hydrogens (Fig. 1). The STO-3G structure is in good agreement with the 6-31G* (N) structure except that the C–N and N–H bond distances are too long with the smaller basis set.

The vibrational frequencies calculated with the STO-3G basis set need to be scaled in order to account for basis set deficiencies, correlation effects and anharmonicity.[15] Scale factors of 0.8 to 0.9 are typical and a value of 0.82, based on comparing our calculated spectra with the experimental one, was used. Scaled and unscaled values with the calculated infrared intensities are presented in Table 2 together with their symmetry assignments. At this level of calculation, the intensities are only given for qualitative comparison. Twelve bands between 3370 (scaled) cm^{-1} and 3210 (scaled) cm^{-1} corresponding to the N–H stretches were calculated. The scaled positions of the most intense N–H stretches agree with the experimental values. The agreement is best for the lower frequency bands.

The scaled bands at 1629, 1482 and 1196 cm^{-1} are predicted to be intense in the IR and correspond to motions of the NH_2 groups, e.g., scissoring, and to C–C ring stretches and deformations. The most intense IR band in this region is the one at 1482 cm^{-1} according to both theory and experiment. There are three Raman bands in this same spectral region. The broad band observed at 1625 cm^{-1} is probably due to two overlapping e_g bands calculated at 1650 and 1596 (scaled) cm^{-1} with possibly some contribution from the intense a_u (IR-active) band at 1629 cm^{-1}. The most intense IR band (predominantly NH_2 motion) is calculated to be at 940 cm^{-1} and a less intense band is predicted at 827 cm^{-1}. This latter band has a significant component of C–N bond motion. The experimental intensities for this pair are reversed. We also calculate an intense a_u band at 894cm^{-1} (scaled) with I = 145 km/mol involving significant motion of the NH_2 group. The Raman band at 890 cm^{-1} is a combination of an a_g band (ring deformation) and an e_g band (NH_2 group motion). The Raman bands near 830 cm^{-1} could be due to the very strong IR-active e_u band at 840 cm^{-1}. The weak Raman band at 720 cm^{-1} is of a_g symmetry, as is the most intense Raman band at 579 cm^{-1}. The a_g band at 579 cm^{-1} is the symmetric C–N stretch.

Received: August 2, 1988 [Z 2899 IE]
German version: *Angew. Chem. 101* (1989) 79

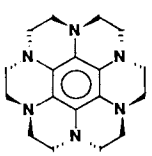
[1] J. S. Miller, J. C. Calabrese, H. Rommelmann, S. Chittapeddi, J. H. Zhang, W. M. Reiff, A. J. Epstein, *J. Am. Chem. Soc. 109* (1987) 769; S. Chittapeddi, K. R. Cromack, J. S. Miller, A. J. Epstein, *Phys. Rev. Lett. 58* (1987) 2695.

[2] J. S. Miller, A. J. Epstein, W. M. Reiff, *Chem. Rev. 88* (1988) 201; *Acc. Chem. Res. 21* (1988) 114; *Science (Washington) 240* (1988) 40.
[3] a) B. Kohne, K. Praefcke, *Liebigs Ann. Chem. 1987*, 265; b) D. Z. Rogers, *J. Org. Chem. 51* (1986) 3905.
[4] a) R. Breslow, *Pure Appl. Chem. 54* (1982) 927; b) R. Breslow, B. Jaun, R. Q. Klutz, C.-Z. Xia, *Tetrahedron 38* (1982) 863; c) R. Breslow, *Mol. Cryst. Liq. Cryst. 125* (1985) 261; d) T. J. LePage, R. Breslow, *J. Am. Chem. Soc. 109* (1987) 6412.
[5] **1**: cubic, $a=9.192(4)$ Å, $V=776.2$ Å^3, *Pca*3 (No. 205), $Z=4$, $\mu(Mo_{K\alpha})=0.94$ cm^{-1}, $T=-70$°C, $\rho_{calcd}=1.433$ g cm^{-3}, $R=0.03$, $R_w=0.025$% for 66 unique reflections [$I>3\sigma(I)$] to $2\theta_{max}=55$° on Enraf-Nonius CAD4 diffractometer. Further details of the X-ray structure analysis can be obtained from the director of the Cambridge Crystallographic Data Centre, University Chemical Laboratory, Lensfield Road, Cambridge CB2 1EW (England), on quoting the names of the authors and the journal citation.
[6] R. Breslow, P. Maslak, J. S. Thomaides, *J. Am. Chem. Soc. 106* (1984) 6453; B. Kohne, K. Praefcke, A. Reichmann, *Chem. Ztg. 109* (1985) 17; J. S. Thomaides, P. Maslak, R. Breslow, *J. Am. Chem. Soc. 110* (1988) 3970.
[7] J. S. Miller, D. A. Dixon, J. C. Calabrese, *Science (Washington) 240* (1988) 1185.
[8] GRADSCF is an ab initio gradient program system designed and written by *A. Komornicki* at Polyatomics Research, Mountain View, CA (USA).
[9] W. J. Hehre, R. F. Stewart, J. A. Pople, *J. Chem. Phys. 51* (1969) 2657.
[10] R. Ditchfield, W. J. Hehre, J. A. Pople, *J. Chem. Phys. 54* (1971) 724. An exponent of 0.8 was used for the 3d exponent of N.
[11] a) P. Pulay in H. F. Schaefer, III (Ed.): *Applications of Electronic Structure Theory*, Plenum, New York 1977, Chap. 4; b) A. Komornicki, K. Ishida, K. Morokuma, R. Ditchfield, M. Conrad, *Chem. Phys. Lett. 45* (1977) 595.
[12] H. F. King, A. Komornicki, *J. Chem. Phys. 84* (1986) 5645.
[13] a) C. Møller, M. S. Plesset, *Phys. Rev. 46* (1934) 618; b) J. A. Pople, J. S. Binkley, R. Seeger, *Int. J. Quantum Chem. Symps. 10* (1976) 1.
[14] T. A. Halgren, R. J. Anderson, D. S. Jones, W. N. Lipscomb, *Chem. Phys. Lett. 8* (1971) 547.
[15] J. S. Miller, J. H. Zhang, W. M. Reiff, D. A. Dixon, L. D. Preston, A. H. Reis, Jr., E. Gebert, M. Extine, J. Troup, A. J. Epstein, M. D. Ward, *J. Phys. Chem. 91* (1987) 4344.

The Structure of the Tetracation of Hexaazaoctadecahydrocoronene, A Simple Substituted Benzene

By *David A. Dixon,* Joseph C. Calabrese, Richard L. Harlow,* and *Joel S. Miller**

The molecular and electronic structure of benzene and its derivatives have fascinated chemists for many years. Due to the high symmetry of benzene, the dication of benzene or of highly symmetrical benzene derivatives was postulated[1] to play the role of the degenerate triplet cationic species in *McConnell*'s model[2] for organic ferromagnets. *Breslow* et al.[3a-c] and *Praefeke* et al. [3d] have synthesized the highly symmetric derivative (D_{3d} point group) hexaazaoctadecahydrocoronene **1** and have generated its dication.[3a-c]



1

[*] Dr. D. A. Dixon, Dr. J. S. Miller, Dr. J. C. Calabrese, Dr. R. L. Harlow
Central Research and Development,
E. I. du Pont de Nemours and Co., Inc.
Experimental Station E328, Wilmington, DE 19880-0328 (USA)

[**] We are indebted to *W. Marshall, R. S. McLean, D. Wipf,* and *C. Vazquez* for assistance in obtaining physical measurements and preparing samples and to *P. J. Krusic, M. D. Ward,* and *E. Wasserman* for stimulating discussions.

In the solid state, the dication exhibits a singlet ground state as observed by magnetic susceptibility and EPR measurements consistent with the X-ray structures of several $\mathbf{1}^{2\oplus}$ salts which show a distorted structure with C_{2v} symmetry.[4] Other EPR studies suggest that the spin of the ground state of materials containing $\mathbf{1}^{2\oplus}$ can be strongly dependent on the environment.[3c] **1** can be further oxidized to yield $\mathbf{1}^{4\oplus}$ as shown by cyclic voltammetry.[3b,4] We have succeeded in crystallizing $\mathbf{1}^{4\oplus}$ as the salt $[\mathbf{1}][SbF_6]_4\cdot MeCN$[5] and herein report the first structural determination of a benzene derivative in the +4 oxidation state.

The salt crystallizes in the monoclinic space group $C2/m$[6] and the tetracation lies on a $2/m$ site in the asymmetric unit. In Table 1, the heavy atom bond distances for $\mathbf{1}^{4\oplus}$ are compared with those of **1**.[4] The structure of $\mathbf{1}^{4\oplus}$ (Fig. 1) is only slightly distorted from the idealized D_{3d}

Table 1. Observed and calculated average bond distances [Å] for $\mathbf{1}^n$ (n = 0, 4⊕).

[a]	n = 0		n = 4⊕	
	Exp.	Calcd.	Exp.	Calcd.
C_B-C_B	1.397	1.401	1.436	1.475
C_B-N	1.416	1.453	1.318	1.330
N-C_H	1.442	1.474	1.472	1.506
C_H-C_H	1.492	1.537	1.518	1.542

[a] C_B: C atoms of benzene ring; C_H: aliphatic C-atoms.

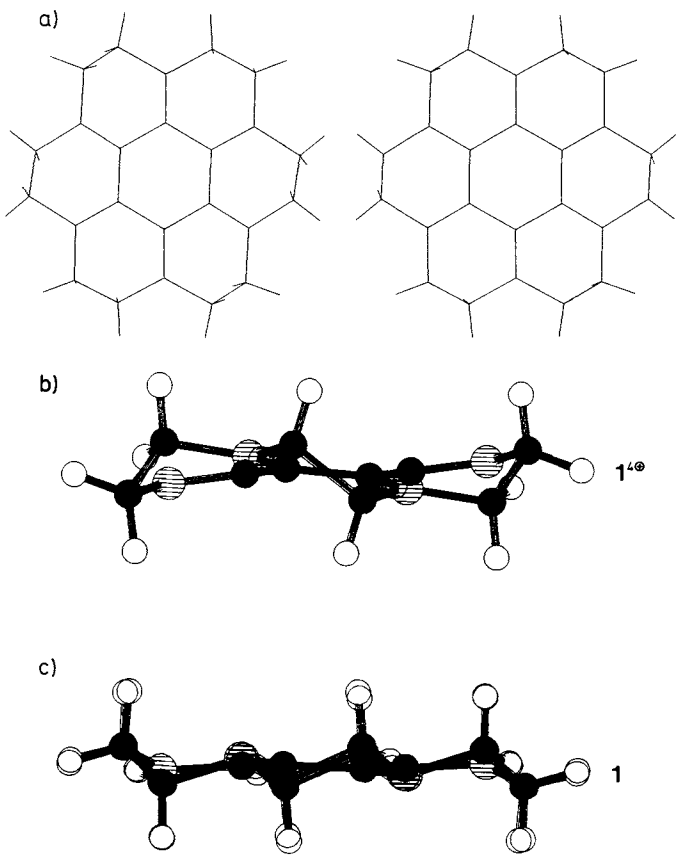


Fig. 1. Structure of $\mathbf{1}^{4\oplus}$ in crystals of **1** $[SbF_6]_4\cdot MeCN$. a) Stereoview down the approximate 3-fold axis of $\mathbf{1}^{4\oplus}$. b) Side view of $\mathbf{1}^{4\oplus}$. c) Side view of **1**. Note the higher planarity of **1** compared to $\mathbf{1}^{4\oplus}$.

symmetry. All the C_B–C_B bond distances are equal within experimental error as are the C_B–N bond distances. The C_B–C_B bond distances are 0.04 Å longer in the tetracation as compared to the neutral molecule, whereas the C_B–N bond distances are 0.10 Å shorter in the tetracation. Both the N–C_H and C_H–C_H bond distances are 0.03 Å longer in the tetracation. The $(C_B)_6N_6$ central region of the tetracation is significantly nonplanar as compared to the planarity of the moiety in **1** (Fig. 1b, c). The average C_B and N displacements from the C_6 least squares plane are 0.053 and 0.245 Å in $[HAOC]^{4\oplus}$ as compared to 0.013 and 0.116 Å for HOAC.

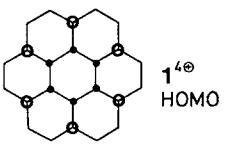
The "π orbitals" of **1** can be formally generated by adding the benzene π orbitals (Scheme 1, left) to the orbitals of the N lone pairs (Scheme 1, right). The exact mixing



Scheme 1. Left: π-orbitals of benzene. Right: orbital scheme for the nitrogen lone-pairs, obtained by linear combination of the N-atom orbitals. The energy scales, left and right are different.

depends on a variety of factors such as overlap, electron repulsion, etc. Although the HOMO of **1** is degenerate, it has significant electron density on both C and N. Thus, when four electrons are removed from **1**, remixing of the orbitals could occur, leading to an e^2 occupancy and a triplet state for $\mathbf{1}^{4\oplus}$. Magnetic susceptibility measurements showed, however, that $\mathbf{1}^{4\oplus}$ is diamagnetic between 2 and 320 K with no evidence for a triplet state contribution.

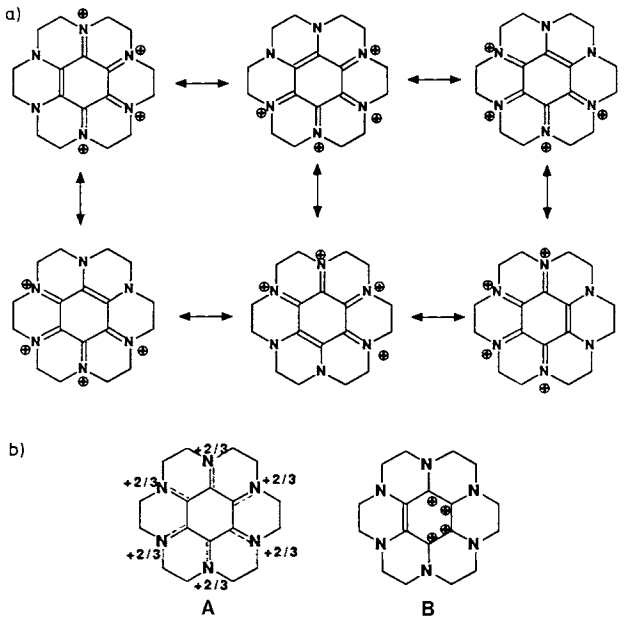
The geometry of $\mathbf{1}^{4\oplus}$ was gradient optimized[7] as a singlet with the STO-3G basis set[8] and represents an energy minimum as shown by analytical second derivative[9] calculations.[10] Even though the charge is redistributed, the HOMO for $\mathbf{1}^{4\oplus}$ is nondegenerate, and is predominantly an out-of-plane p orbital on C_B and N (Scheme 2). The



Scheme 2. Out-of-plane p orbitals on C_B and N, which dominate in the HOMO of $\mathbf{1}^{4\oplus}$.

LUMO is a degenerate pair of orbitals. The calculated bond distances for HAOC and $[HAOC]^{4\oplus}$ are listed in Table 1. The calculated C_B–C_B bond distance in $\mathbf{1}^{4\oplus}$ is 0.04 Å longer than the average experimental value. The other calculated bond distances in $\mathbf{1}^{4\oplus}$ are 0.012–0.034 Å longer than the experimental values and show the identical trends found when comparing the experimental **1** and $\mathbf{1}^{2\oplus}$ geometry parameters.[4] (The expanded calculated external C_H–C_H and C_H–N bond distances allow the calculated internal C_B–C_B and C_B–N bond distances also to be longer.) The calculations also show the increase in nonplanarity of the $(C_B)_6N_6$ moiety in going from **1** to $\mathbf{1}^{4\oplus}$ that was observed experimentally (see Fig. 1b, c).

The calculated charge distribution for $\mathbf{1}^{4\oplus}$ shows C_B with a charge of 0.19 $e^{\ominus}$ and N with a charge of -0.17 $e^{\ominus}$. The group charges for the C_H groups are 0.37 $e^{\ominus}$. These can be compared to the charges in **1** of 0.06 $e^{\ominus}$ on C_H, -0.28 $e^{\ominus}$ on N and 0.11 $e^{\ominus}$ on the C_H groups. Clearly the largest change in the charge distribution is on the external portion of the molecule. The charge removed from C_B and N is approximately equal. Considering the excess charge on the C_H groups, most of the charge was removed from the nitrogen region rather than from the benzene ring. This is consistent with the modest lengthening of the C_B–C_B bond distances as compared to the dramatic decrease in the C_B–N bond distances which is approaching the C–N bond distance found in protonated imines (1.29 Å).[11] This is also consistent with the coefficients in the LUMO of $\mathbf{1}^{4\oplus}$ being larger on N than on C_B. From the above results, the most important resonance structures for $\mathbf{1}^{4\oplus}$ are shown in Scheme 3.[12] Note that the charges are on the nitrogen atoms (as in **A**) rather than on the carbon atoms (as in **B**).



Scheme 3. a) The most important resonance structures of $\mathbf{1}^{4\oplus}$. b) **A** = charge distribution in $\mathbf{1}^{4\oplus}$ derived from the resonance structures; **B** = charge distribution in $\mathbf{1}^{4\oplus}$ based on the $(4n+2)\pi$-electron rule.

Received: August 30, 1988 [Z 2947 IE]
German version: *Angew. Chem. 101* (1989) 81

[1] a) R. Breslow, *Pure Appl. Chem. 54* (1982) 927; b) R. Breslow, B. Jaun, R. Q. Klutz, C.-Z. Xia, *Tetrahedron 38* (1982) 863.

[2] H. M. McConnell, *Proc. R. A. Welch Found. Chem. Res. 11* (1967) 144; J. S. Miller, A. J. Epstein, *J. Am. Chem. Soc. 109* (1987) 3850; *NATO Adv. Studies Ser. B168* (1988) 159; J. S. Miller, A. J. Epstein, W. M. Reiff, *Chem. Rev. 88* (1988) 201; *Acc. Chem. Res. 21* (1988) 114; *Science (Washington) 240* (1988) 40.

[3] a) R. Breslow, *Mol. Cryst. Liq. Cryst. 125* (1985) 261; b) R. Breslow, P. Maslak, J. S. Thomaides, *J. Am. Chem. Soc. 106* (1984) 6453; c) J. S. Thomaides, P. Maslak, R. Breslow, *ibid. 110* (1988) 3970; d) B. Kohne, K. Praefcke, A. Reichmann, *Chem. Ztg. 109* (1985) 17.

[4] J. S. Miller, D. A. Dixon, J. C. Calabrese, *Science (Washington) 240* (1988) 1185.

[5] **1** was prepared from hexaaminobenzene via a modified literature route [3b]. A solution of HAOC in CH_2Cl_2 was added to a solution of $[NO][SbF_6]$ in CH_3CN (1:4 molar ratio). Crystals were grown by diffusion of diethyl ether into the acetonitrile solution.

[6] **1** $[SbF_6]_4 \cdot MeCN$: monoclinic, $a = 14.357(1)$, $b = 11.652(1)$, $c = 12.070(1)$ Å, $\beta = 114.74(1)°$, $V = 1833.8$ Å^3, $C2/m$ (No. 12), $Z = 2$, $\mu(Mo_{K\alpha}) = 30.82$ cm^{-1}, $T = -70$°C, $\rho_{calcd} = 2.396$ g cm^{-3}, $R = 0.026$, $R_w = 0.028$ for 2226 unique reflections [$I > 3\sigma(I)$, $2\theta_{max} = 60°$] for $Mo_{K\alpha}$ radiation ($\lambda = 0.71069$ Å) on a Enraf-Nonius CAD4 diffractometer. Further details

of the crystal structure determination can be obtained from the director of the Cambridge Crystallographic Data Centre, Lensfield Road, Cambridge CB2 1EW (England) by quoting the names of the authors and the journal citation.

[7] a) P. Pulay in H. F. Schaefer, III (Ed.): *Applications of Electronic Structure Theory*, Plenum, New York 1977, Ch. 4; b) A. Komornicki, K. Ishida, K. Morokuma, R. Ditchfield, M. Conrad, *Chem. Phys. Lett. 45* (1977) 595.

[8] W. J. Hehre, R. F. Stewart, J. A. People, *J. Chem. Phys. 51* (1969) 2657.

[9] H. F. King, A. Komornicki, *J. Chem. Phys. 84* (1986) 5645.

[10] The calculations were performed with the program GRADSCF on a CRAY-XMP/24 computer. GRADSCF is an ab initio gradient program system designed and written by *A. Komornicki* at Polyatomics Research Mountain View, CA (USA).

[11] R. A. Eades, D. A. Weil, M. R. Ellenberger, W. E. Farneth, D. A. Dixon, C. H. Douglass, Jr., *J. Am. Chem. Soc. 103* (1981) 5372; P. A. Kollman, *Adv. Org. Chem. 9* (1976) 1.

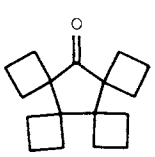
[12] Although the $(4n+2)$ π-electron counting rule can be applied to substituted benzenes, it is inappropriate to apply it to the structure of $1^{4\oplus}$ for determining the charge distribution. The $4n+2$ rule would place four positive charges in the benzene ring, whereas the excess positive charges are clearly found in the regions of the nitrogens.

From Tetraspiranes to Bispropellanes**

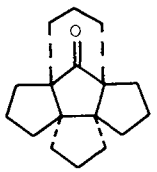
By *Lutz Fitjer** and *Ulrike Quabeck*

In memoriam David Ginsburg

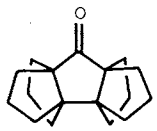
Upon reaction with acid the tetraspiroketone **1** rearranges via a fivefold 1,2-shift to the pentacyclic ketone **2** ($\Delta H_f = -53.1$ kcal mol^{-1}).[1] Formation of the isomeric bispropellanone **3** ($\Delta H_f = -53.1$ kcal mol^{-1})[1] is not observed even if equilibrium conditions are maintained. We have now found that the relative stabilities of **2** and **3** can be altered to such an extent by replacement of the carbonyl oxygen by alkylidene groups that rearrangements of the corresponding tetraspiranes (**4a,b**) to bispropellanes (**8a,b**) are possible.



1



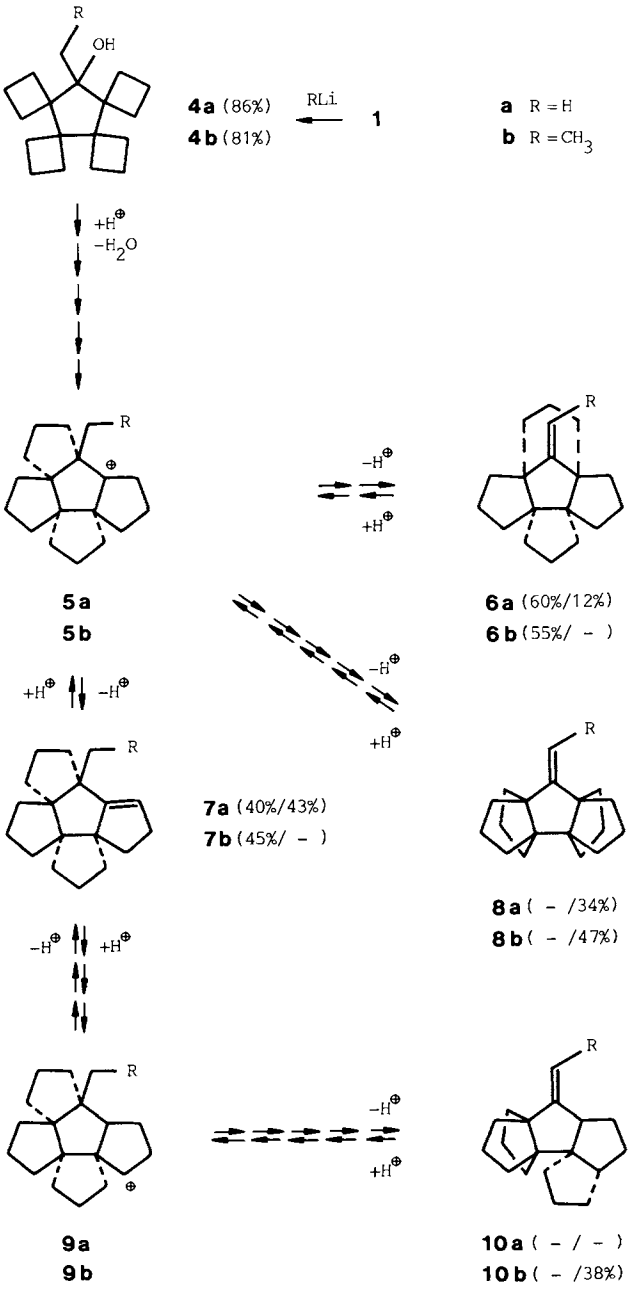
2



3

Evidence of this was afforded by force field calculations[2] on **6a,b**, **7a,b** and **8a,b** as potential products of a rearrangement of **4a,b** via **5a,b** (see Scheme 1). **8a** ($\Delta H_f = -5.80$ kcal mol^{-1}) and **8b** ($\Delta H_f = -13.07$ kcal mol^{-1}) are so distinctly favored over their isomers **6a** and **7a** ($\Delta H_f = -2.32$ kcal mol^{-1} and -3.82 kcal mol^{-1}) and **6b** and **7b** ($\Delta H_f = -5.80$ and -5.86 kcal mol^{-1}) respectively, that we have prepared **4a** and **4b** and used them in rearrangement experiments.

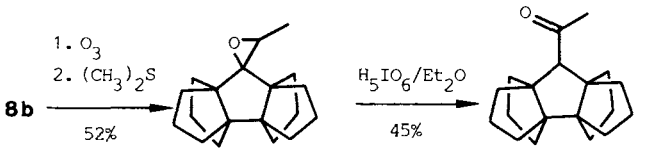
We obtained **4a** (m.p. 110–111 °C, yield 86%[3] and **4b** (m.p. 25–27 °C, yield 81%)[3] by reaction of the tetraspiroketone **1**[1] with methyl- and ethyllithium, respectively. For the rearrangement we chose conditions favoring the kinetically and thermochemically controlled reactions A and B, respectively. In the case of reaction A, 0.38 molar benzolic solutions of **4a** and **4b** were heated together with 2 gram equivalents of Nafion NR 50[4] at 70 °C for 30 min, and, in the case of reaction B, 0.10 molar benzolic solutions with 40 gram equivalents of Nafion NR 50 at 70 °C for 6 h. Reaction A afforded, in the case of **4a** and **4b**, mixtures of **6a** (m.p. 202–206 °C, 60%)[3] and **7a** (m.p. 118–121 °C, 40%)[3] and **6b** (m.p. 182–184 °C, 55%)[3] and **7b** (liq., 45%),[3] respectively. Reaction B in the case of **4a** furnished a mixture of **6a** (12%), **7a** (43%) and **8a** (m.p. 176–178 °C, 34%)[3] and in the case of **4b** a mixture of **8b** (m.p. 121–123 °C, 47%)[3] and **10b** (m.p. 156–160 °C, 38%).[3] The formation of **10b** was unexpected, as this requires involvement of the secondary carbenium ion **9b** as intermediate and could be associated with a considerably higher activation energy than all the other products.[5] All rearrangement products were separated by thin-layer chromatography on silica gel doped with silver nitrate[6] in dichloromethane.



[*] Prof. Dr. L. Fitjer, Dipl.-Chem. U. Quabeck
Institut für Organische Chemie der Universität
Tammannstrasse 2, D-3400 Göttingen (FRG)

[**] Polyspiranes, Part 18. Rearrangement Cascades, Part 13. This work was supported by the Deutsche Forschungsgemeinschaft and the Fonds der Chemischen Industrie.—Parts 17 and 12: L. Fitjer, A. Kanschik, M. Majewski, *Tetrahedron Lett. 29* (1988) 5525.

The structures of **6a** (C_s), **7a** (C_1), **8a** (C_{2v}) and **10b** (C_1) were deduced from the number and multiplicity of their ^{13}C-NMR signals. The structures of **6b** (C_1) and **7b** (C_1) could be assigned on the basis of the coupling patterns of their vinyl proton signals (**6b**: $\delta = 5.32$, dd, $J = 1.6$ and 3.3 Hz, 1H; **7b**: $\delta = 4.94$, q, $J = 8.0$ Hz, 1H). **8b** (C_s) was identified by comparison of its ^{13}C-NMR spectrum with that of **8a**. Attempts to oxidatively cleave the double bond of **8b** have thus far failed. Ozonolysis afforded the epoxide **11** (m.p. 145°C, 52%),[3,7] while an attempted subsequent cleavage with periodic acid in anhydrous ether[8] furnished the ketone **12** (m.p. 155°C, 45%).[3]



11 12

These findings show that suitably substituted tetraspiranes can be used for the synthesis of bispropellanes. The realizability of such transformations had already been predicted by *Ginsburg*.[9] A verification of the equilibria via equilibration experiments with **6a,b**, **7a,b**, **8a,b** and **10b** has not yet been carried out. The route to trispropellanes, however, would appear open.

Received: July 18, 1988;
supplemented: September 18, 1988 [Z 2870 IE]
German version: *Angew. Chem. 101* (1989) 55

[1] L. Fitjer, U. Quabeck, *Angew. Chem. 99* (1987) 1054; *Angew. Chem. Int. Ed. Engl. 26* (1987) 1023.

[2] Program MM2: N. L. Allinger, *J. Am. Chem. Soc. 98* (1977) 8127. In the case of **6a** (**6b**) 6(8), in the case of **7a** (**7b**) 8(24), and in the case of **8a** (**8b**) 7(10) conformations had to be optimized symmetrywise in their geometry and investigated with regard to their enthalpy of formation before the respective global minima were established. In the case of **6a** and **6b** only chair conformations were considered.

[3] All the new compounds (**4a,b**, **6a,b**, **7a,b**, **8a,b**, **10b**, **11**, **12**) gave correct analyses and/or high-resolution mass spectra. The IR, ^{1}H-, ^{13}C-NMR and mass spectra are consistent with the given structures. The stereochemistry quoted for **10b** is based on force-field calculations and is tentative. ^{13}C-NMR data 20 and 50 MHz (**4a**, **7a,b**): **4a** (C_6D_6): $\delta = 16.59$, 17.03, 25.61, 25.64, 25.81 (C_{sec}), 25.88 (C_{prim}), 27.18 (C_{sec}), 54.55, 57.56, 80.68 (C_{quart}); **4b** (C_6D_6): $\delta = 8.65$ (C_{prim}), 16.39, 16.70, 25.62, 25.67, 26.01, 26.65, 31.29 (C_{sec}), 55.02, 57.75, 81.82 (C_{quart}); **6a** ($CDCl_3$): $\delta = 19.07$, 27.83, 33.31, 34.32, 38.02, 38.35 (C_{sec}), 59.46, 62.00 (C_{quart}), 96.82 (C_{sec}), 169.32 (C_{quart}); **6b** ($CDCl_3$): $\delta = 12.97$ (C_{prim}), 19.14, 24.80, 26.03, 27.72, 33.18, 34.32, 35.41, 35.75, 36.94, 38.56, 39.09, 39.53 (C_{sec}), 60.07, 60.89, 62.19, 62.78 (C_{quart}), 108.18 (C_{tert}), 159.18 (C_{quart}); **7a** ($CDCl_3$): $\delta = 24.51$ (C_{prim}), 25.14, 25.90, 26.39, 33.74, 38.09, 38.22, 38.52, 38.78, 39.27, 39.81, 41.41 (C_{sec}), 50.30, 61.72, 68.37, 71.19 (C_{quart}), 116.55 (C_{tert}), 165.08 (C_{quart}); **7b** ($CDCl_3$): $\delta = 10.12$ (C_{prim}), 24.80, 26.14, 26.71, 28.99, 33.77, 34.87, 37.39, 38.05, 38.58, 39.37, 39.85, 40.27 (C_{sec}), 54.40, 61.63, 68.38, 71.27 (C_{quart}), 117.16 (C_{tert}), 164.36 (C_{quart}); **8a** ($CDCl_3$): $\delta = 26.93$, 39.12, 43.66 (C_{sec}), 65.08, 71.13 (C_{quart}), 104.15 (C_{sec}), 173.91 (C_{quart}); **8b** (C_6D_6): $\delta = 15.22$ (C_{prim}), 27.21, 27.73, 39.32, 39.66, 43.10, 44.45 (C_{sec}), 64.78, 67.03, 69.47, 72.15 (C_{quart}), 114.91 (C_{tert}), 164.32 (C_{quart}); **10b** ($CDCl_3$): $\delta = 14.24$ (C_{prim}), 19.56, 24.02, 25.64, 28.34, 28.75, 31.12, 34.54, 36.71, 38.40, 39.18, 40.27, 46.26 (C_{sec}), 50.22, 55.43 (C_{quart}), 58.13 (C_{tert}), 59.35 (C_{quart}), 109.91 (C_{tert}), 149.31 (C_{quart}); **11** ($CDCl_3$): $\delta = 15.27$ (C_{prim}), 25.82, 26.34, 26.95, 27.26, 34.90, 37.12, 37.91, 38.56, 38.64 (coincidence of two lines), 40.46, 41.00 (C_{sec}), 54.24 (C_{tert}), 65.47, 66.78, 67.75, 68.85, 73.67 (C_{quart}); **12** ($CDCl_3$): $\delta = 25.21$, 26.41, 31.56, 37.78, 37.93 (coincidence of two lines), 41.82, 67.07, 67.12, 69.29, 209.62.

[4] Nafion NR50 (Aldrich-Chemie, D-7924 Steinheim (FRG)) was activated for 12 h at 105°C/20 torr immediately before use.

[5] M. Saunders, J. Chandrasekhar, P. von R. Schleyer in P. de Mayo (Ed.): *Rearrangements in Ground and Excited States, Vol. 1*, Academic Press, New York 1980, p. 4.

[6] W. K. Wilson, G. J. Schroepfer, Jr., *J. Org. Chem. 53* (1988) 1713.

[7] Cf. also P. S. Bailey: *Ozonation in Organic Chemistry, Vol. 1*, Academic Press, New York 1978, p. 197ff.

[8] L. F. Fieser, M. Fieser: *Reagents for Organic Synthesis, Vol. 1*, Wiley, New York 1967, p. 817.

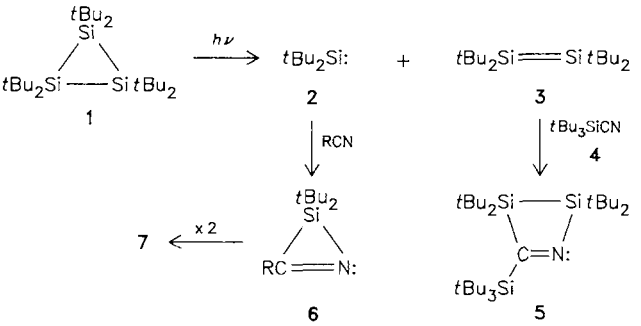
[9] D. Ginsburg, *Top. Curr. Chem. 137* (1987) 1.

Disilene *versus* Silanediyl ("Silylene") Additions to CN and NCO Bonds**

By *Manfred Weidenbruch,* Bolko Flintjer, Siegfried Pohl,* and *Wolfgang Saak*

Despite bulky ligands, which are necessary for the stabilization of the SiSi double bond ("embedded double bonds"), disilenes are more reactive than alkenes bearing sterically less demanding substituents, and, in some cases, undergo reactions atypical for CC double bonds.[1] For example, alkenes do not undergo [2+2]-cycloadditions with nitriles.[2] We have now found, however, that tetra-*tert*-butyldisilene **3**, formed on photolysis of hexa-*tert*-butylcyclotrisilane **1**,[3] reacts smoothly with tri-*tert*-butylsilyl cyanide **4**[4] to give the 2,3-disila-1-azetine **5**.

In contrast, nitriles RCN with smaller substituents R react with **2** to give preferentially azasilirenes **6**, which spontaneously undergo σ-dimerization to give 1,4- or 1,3-diaza-2,5-disila-1(6),3-cyclohexadienes **7**.[5] Formation of the intermediates **6** could be confirmed indirectly by the analogous reaction with phosphalkynes, from which stable phosphasilirenes are isolable.[6] Apparently the bulky



tBu_3Si group prevents addition of **2** to **4** to give the ring-strained **6** (and its dimerization to **7**) and thus favors the [2+2]-cycloaddition to give **5**. The formation of **5** by addition of **2** to **4** (→ **6**) with subsequent silanediyl insertion in the Si–C or Si–N bond cannot be completely ruled out. However, such insertion reactions only take place at higher temperatures[7] and should, in this case, be further impaired by the bulky substituents.

The spectroscopic data contribute very little to an elucidation of the constitution of **5**,[8] for the C=N stretching vibration, which normally appears between 1560 and 1605 cm^{-1} in the case of SiC=NSi compounds,[5] is not ob-

[*] Prof. Dr. M. Weidenbruch, B. Flintjer, Prof. Dr. S. Pohl, Dipl.-Chem. W. Saak
Fachbereich Chemie der Universität
Carl-von-Ossietzky-Strasse 9–11, D-2900 Oldenburg (FRG)

[**] Silicon Compounds with Strong Intramolecular Steric Interactions, Part 34. This work was supported by the Deutsche Forschungsgemeinschaft and the Fonds der Chemischen Industrie.—Part 33: M. Weidenbruch, A. Schäfer, H. Marsmann, *J. Organomet. Chem. 354* (1988) C 12.

served. An X-ray structure analysis of **5**[9] (Fig. 1), on the other hand, revealed some especially informative features: The four ring atoms and the exocyclic Si atom lie exactly in a plane. The steric crowding of the molecule not only forces a stretching of all ring bonds but also leads to a substantial widening of the Si2–C1–Si3 angle to 144°. As expected, the smallest bond angles inside the ring occur at the Si atoms.

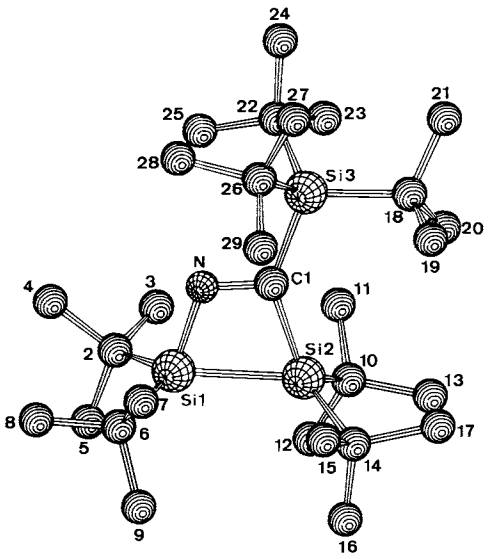
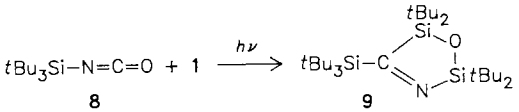


Fig. 1. Crystal structure of **5** (without H atoms). Selected bond lengths [pm] and angles [°] (standard deviations): Si1-Si2 179.8(2), C1-N 130.4(3), C1-Si2 199.6(3), C1-Si3 195.4(3); Si1-N-C1 109.7(2), N-C1-Si2 104.8(2), C1-Si2-Si1 69.5(1), N-Si1-Si2 75.8(1), Si2-C1-Si3 143.9(1).

Less unambiguous from the mechanistic standpoint is the photolysis of **1** in the presence of tri-*tert*-butylsilyl isocyanate **8**,[4] which we have investigated as first example for the reaction behavior of **3** (or also of **2**) towards cumulated double-bond systems. Here again a compound is isolated which is formally composed of **3** and **8** in a ratio of 1:1. The obvious assumption that the product[10] is formed by [2+2]-cycloaddition of **3**, either at the CO or at the CN double bond,[11] is disproved by the X-ray structure analysis[9] (Fig. 2), which rather indicates that multiple cleavage and recoupling of bonds leads to formation of the 3-aza-1-oxa-2,5-disilacyclopent-3-ene derivative **9**. The



8 **9**

formation of **9** not only requires rupture of the CO bond and insertion of the oxygen between two Si atoms, but also migration of the bulky tBu$_3$Si group from the N atom to the C atom. All the more astonishing is that the rearrangement takes place under the mild reaction conditions chosen here. Attempts to trap intermediates with other isocyanates have so far failed.

West et al.[12] recently found that the reaction of the stable tetramesityldisilene with nitrobenzene is initiated by a [2+3]-cycloaddition of the Si=Si bond to the oxygen atoms of the nitro group at which, as in the case of **9**, a rearrangement with formation of the disiloxane finally takes place. This can be regarded as indicative of a similar reaction of **8** with **3**.

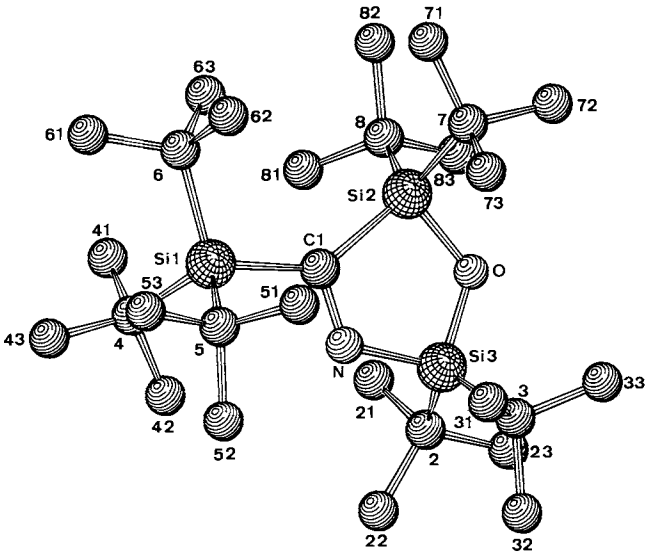


Fig. 2. Crystal structure of **9** (without H atoms). Selected bond lengths [pm] and angles [°] (standard deviations): C1-Si2 202.2(3), Si2-O 166.2(2), O-Si3 165.6(2), Si3-N 177.4(2), N-C1 129.0(3), C1-Si1 196.7(3); C1-Si2-O 93.8(1), Si2-O-Si3 118.4(1), O-Si3-N 99.2(1), Si3-N-C1 118.5(2), N-C1-Si2 110.1(2).

Experimental

5: A solution of **1** (0.65 g, 1.53 mol) and **4** (1.00 g, 450 mL) in 70 mL of *n*-hexane was irradiated with a mercury high-pressure lamp (Heraeus TQ150) until the initially yellow solution was almost colorless. The residue remaining after removal of *n*-hexane by distillation furnished, after repeated recrystallization from *n*-pentane, 0.35 g of crystalline **5** (30% yield, based on **3**). Additional **5** remained unpurified in the mother liquor (NMR signals).

9: Analogously to the synthesis of **5**, a solution of **1** (0.85 g, 2.0 mmol) and **8** (1.40 g, 5.9 mmol) in 60 mL of *n*-hexane afforded 0.32 g (20%) of crystalline **9**. Similarly as in the case of **5**, according to an NMR analysis additional **9** remained unpurified in the mother liquor.

Received: August 1, 1988 [Z 2897 IE]
German version: *Angew. Chem. 101* (1989) 89

[1] Review: R. West, *Angew. Chem. 99* (1987) 1231; *Angew. Chem. Int. Ed. Engl. 26* (1987) 1201.
[2] See, for example: G. Tennant in D. Barton, W. D. Ollis, I. O. Sutherland (Eds.): *Comprehensive Organic Chemistry, Vol. 2*, Pergamon Press, Oxford 1979, p. 385; D. E. Davies, R. C. Storr in A. R. Katritzky, C. W. Rees, W. Lwowski (Eds.): *Comprehensive Heterocyclic Chemistry, Vol. 7, Part 5*, Pergamon Press, Oxford 1984, p. 237.
[3] A. Schäfer, M. Weidenbruch, K. Peters, H. G. von Schnering, *Angew. Chem. 96* (1984) 311; *Angew. Chem. Int. Ed. Engl. 23* (1984) 302.
[4] M. Weidenbruch, H. Pesel, *Z. Naturforsch. B33* (1978) 1465.
[5] M. Weidenbruch, A. Schäfer, K. Peters, H. G. von Schnering, *J. Organomet. Chem. 314* (1986) 25.
[6] A. Schäfer, M. Weidenbruch, W. Saak, S. Pohl, *Angew. Chem. 99* (1987) 806; *Angew. Chem. Int. Ed. Engl. 26* (1987) 776.
[7] T. J. Barton, J. A. Kilgour, *J. Am. Chem. Soc. 98* (1976) 7746; D. Seyferth, D. C. Annarelli, D. P. Duncon, *Organometallics 1* (1982) 1288.
[8] **5**: orange-yellow platelets, m.p. 117–119°C; ^{1}H-NMR (300 MHz, C_6D_6): δ = 1.29 (s, 18H), 1.345 (s, 45H); (C_6D_{12}): δ = 1.297 (s, 27H), 1.322 (s, 18H), 1.335 (s, 18H); MS (CI, isobutane): m/z 510 (MH$^\oplus$, 100%), correct C,H,N analysis.
[9] **5**: monoclinic, space group $P2_1/c$ (No. 14). a = 1712.9(1), b = 1119.1(1), c = 1793.8(1) pm; β = 104.06(1)°. V = 3335.5 · 10^6 pm^3; Z = 4, ρ_{calcd} = 1.016 g cm^{-3}, 4852 independent reflections observed ($I > 2\sigma(I)$) 4237, number of variables 298, empirical absorption correction, R = 0.055, R_w = 0.054.—**9**: triclinic, space group $P\bar{1}$ (No. 2). a = 894.3(1), b = 1176.1(1), c = 1605.2(1) pm, α = 98.06(1), β = 90.90(1), γ = 92.89(1)°. V = 1669.1 · 10^6 pm^3; Z = 2, ρ_{calcd} = 1.023 g cm^{-3}, 5167 independent reflections observed ($I > 2\sigma(I)$) 3566, number of variables 433, R = 0.047; R_w = 0.043.—Further details of the crystal structure investigations are available on request from the Fachinformationszentrum Energie, Physik, Mathematik GmbH, D-7514 Eggenstein-Leopoldshafen 2 (FRG), on quoting the depository number CSD-53309, the names of the authors, and the journal citation.

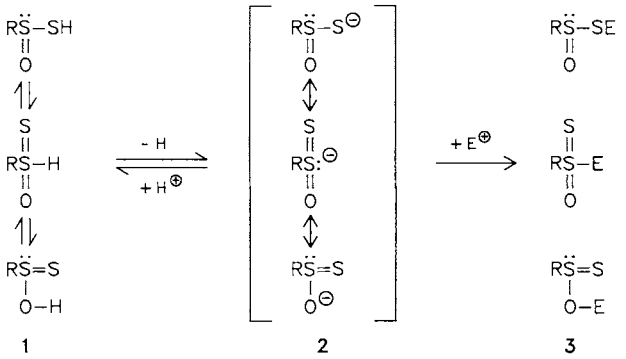
[10] **9**: pale green platelets, m.p. 191–194°C; ^{1}H-NMR (300 MHz, C_6D_6): $\delta = 1.24$ (s, 18H), 1.26 (s, 18H), 1.345 (s, 27H); MS (CI, isobutane): m/z 526 ($MH^{\oplus}$, 100%); correct C,H,N analysis.
[11] M. Weidenbruch, B. Flintjer, S. Pohl, W. Saak, J. Martens, *J. Organomet. Chem. 338* (1988) C 1.
[12] R. West, private communicastion (August 9, 1988). Editorial note: see G. R. Gillette, J. Maxka, R. West, *Angew. Chem. 101* (1989) 90; *Angew. Chem. Int. Ed. Engl. 28* (1989) 54.

Thiosulfinic Acids: a New Class of Chiral Organosulfur Compounds**

By *Marian Mikołajczyk,* Piotr Łyżwa, Józef Drabowicz, Michał Wieczorek,* and *Grzegorz Bujacz*

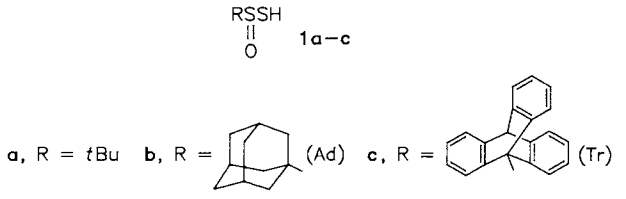
Dedicated to Professor Friedrich Cramer on the occasion of his 65th birthday

The well-known sulfinic acids RSO_2H[1,2] are effectively achiral because their anions are symmetrical and therefore achiral. Replacement of one of the two oxygen atoms in this anion by sulfur formally leads to the thiosulfinic acids RSOSH **1**, for which both the acid and its anion are chiral. However, to the best of our knowledge this class of organosulfur compounds has not yet been described. The only known compounds, which may be regarded to be formally derived from thiosulfinic acids, are the thiosulfinates RS(O)SR,[3] which were also obtained in optically active form.[4]



Scheme 1.

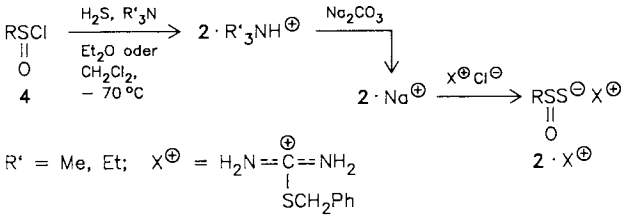
The chiral thiosulfinate anion can be described by three mesomeric forms (Scheme 1). Therefore, protonation could lead to three tautomeric forms of the acid **1** and the reaction with an electrophile $E^{\oplus}$ could result in the formation of three isomeric products.



[*] Prof. Dr. M. Mikołajczyk, P. Łyżwa, Dr. J. Drabowicz
Centre of Molecular and Macromolecular Studies,
Polish Academy of Sciences
Boczna 5, 90-362 Łódź (Poland)
Dr. M. Wieczorek, G. Bujacz
Institute of General Chemistry, Technical University
Żwirki 36, 90-524 Łódź (Poland)

[**] This work was supported by the Polish Academy of Sciences and the Ministry of National Education (CPBP 01.13 and RP.II.10).

We now report the first synthesis and characterization of the relatively stable salts of thiosulfinic acids **1a–c**, whose stability may be due to the sterically demanding substituents at the central sulfur atom.



Reaction of the sulfinyl chlorides **4a–c** with hydrogen sulfide and trialkylamines at −70°C in ether or dichloromethane gave, in high yields (75–87%), the ammonium salts of the acids **2**. For ease of characterization these salts were converted first into sodium and then into *S*-benzylthiuronium salts. ^{1}H and ^{13}C NMR spectra of the salts thus obtained are consistent with the thiosulfinic acid structure (Table 1).

Table 1. Selected ^{1}H and ^{13}C NMR data for salts of the thiosulfinic acid **1**.

2a · $Me_3NH^{\oplus}$ [a]: ^{1}H NMR (60 MHz, TMS_{int}, $CDCl_3$): $\delta = 1.15$ (s, 9H; Me_3C), 2.80 (s, 9H; Me_3N); $^{13}C\{^1H\}$ NMR (22.63 MHz, $CDCl_3$): $\delta = 22.74$ (Me_3C), 43.53 (Me_3N), 52.7 (Me_3C–)

2b · $X^{\oplus}$ [b]: ^{1}H NMR (60 MHz, TMS_{int}, CD_3OD): $\delta = 1.7$–2.5 (m, 15H; Ad), 4.40 (s, 2H; CH_2Ph), 4.85 (s, 4H; NH_2), 7.40 (s, 5H; Ph); $^{13}C\{^1H\}$ NMR (38.93 MHz, $CDCl_3$): $\delta = 30.65$, 36.61, 43.89 (Ad), 36.75 (CH_2Ph), 66.33 (C-1 of Ad), 128.08, 129.48, 129.72, 130.07 (Ph), 138.04 ($C(NH_2)_2$)

2c · $Na^{\oplus}$ [c]: ^{1}H NMR (300 MHz, TMS_{int}, CD_3OD): $\delta = 5.34$ (s, 1H; H10), 7.21–7.35 (m. 6H), 7.59–7.66 (m, 3H), 8.54–8.57 (m, 1H), 8.98–9.01 (m, 2H); $^{13}C\{^1H\}$ NMR (38.93 MHz, CD_3OD): $\delta = 56.16$ (C10), 75.56 (C9), 123.90, 124.22, 125.29, 143.64, 143.87, 148.29, 149.67

[a] We have not been able to isolate an analytically pure salt because of slow decomposition. [b] m.p. 135–140°C (from ethanol); correct C,H,S,N analyses were obtained. [c] **2c** · $Et_3NH^{\oplus}$; m.p. 223–225°C (from chloroform/*n*-pentane); we have not been able to isolate the analytically pure salt because of facile oxidation to the corresponding thiosulfonate.

A final proof of the structure was provided by an X-ray structure analysis (Fig. 1) of the *S*-benzylthiuronium salt of adamantanethiosulfinic acid **2b**.[6] It showed a slightly distorted tetrahedral arrangement of the substituents (carbon, oxygen, sulfur and lone electron pair) around the central sulfur atom in the anion under discussion. The S1–O and S1–S2 distances of 1.536 and 2.025 Å suggest delocalization of the negative charge in the anion.

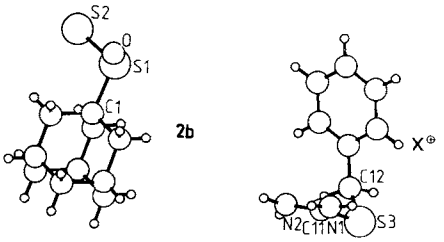
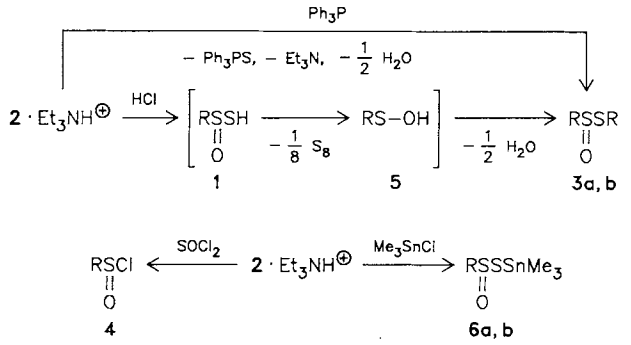


Fig. 1. Molecular structure of **2b** · $X^{\oplus}$. Important bond lengths [Å] and bond angles [°]: C1–S1 1.845(3), S1–O 1.536(2), S1–S2 2.025(9), C11–S3 1.759(3), C11–N1 1.302(4), C11–N2 1.318(4), C12–S3 1.826(3); S2–S1–O 109.70(8), S2–S1–C1 104.74(8), O–S1–C1 103.12(9), N2–C11–S3 120.9(2), N1–C11–S3 116.9(2), N2–C11–N1 122.2(2).

Some chemical reactions of the triethylammonium salts of **2** are summarized in Scheme 2.

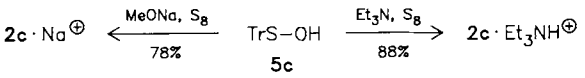


Scheme 2.

The free acids **1a** and **1b** obtained upon acidification undergo a fast and almost quantitative conversion into the thiosulfinates **3a** and **3b** via the sulfenic acids **5a** and **5b**. The only exception is triptycenethiosulfinic acid **2c**, which gives, after elimination of sulfur, the stable triptycenesulfenic acid **5c**.[7] The conversion of the triethylammonium salts of **2a** and **2b** into **3a** and **3b** may also be achieved by using triphenylphosphine as a desulfurization agent. Triethylammonium salts of **2** react with thionyl chloride to give the sulfinyl chlorides **4** in high yields (60–77%). Trimethyltin chloride reacts with the ammonium salts of **2a** and **2b** to give the stannyl derivatives **6a** and **6b**[8]. Their thiolo-structure was supported by a strong IR absorption band at 1050 cm^{-1} characteristic for the S=O grouping.

Taking advantage of the fact that the sulphenic acid **5c**[7] is stable, we also found that it reacts easily with elemental sulfur in the presence of triethylamine or sodium methoxide to give the corresponding salts of **2c**.

This reaction resembles the well-known addition of elemental sulfur to dialkyl phosphites to afford monothiophosphates[9].



Experimental Procedure

2b · $Na^{\oplus}$: Triethylamine (0.46 g, 4.55 mmol) in ether (5 mL) was added to a solution of **4b** (0.5 g, 2.28 mmol) in dry ether (30 mL) at −70°C, after which hydrogen sulfide (0.08 g, 2.28 mmol) was passed through the reaction mixture. After stirring for 5 min at −70°C, triethylammonium chloride was filtered off and the ethereal solution shaken with a solution of sodium hydrogen carbonate (0.12 g, 1.13 mmol) in water (5 mL). The aqueous phase was washed with ether (2 × 10 mL) and evaporated under vacuum to give **2b** · $Na^{\oplus}$ as a white powder. Yield 0.35 g (74%).

2b · $X^{\oplus}$: *S*-Benzylthiuronium chloride $X^{\oplus}Cl^{\ominus}$ (0.49 g, 2.42 mmol) in water (10 mL) was added to a solution of **2b** · $Na^{\oplus}$ (0.5 g, 2.42 mmol) in water (10 mL) at 5°C. After 12 h at 5°C, the precipitate of **2b** · $X^{\oplus}$ was collected by filtration and recrystallized from ethanol. Yield: 0.55 g (69%); m.p. 135–140°C.

Received: July 4, 1988 [Z 2843 IE]
German version: *Angew. Chem. 101* (1989) 87

CAS Registry Numbers:
1a, 34637-29-1; **1b**, 118112-80-4; **2a**, 118112-83-7; **2a** · $Me_3NH^{\oplus}$, 118112-19-7; **2b**, 118112-84-8; **2b** · $X^{\oplus}$, 118112-81-5; **2b** · $Na^{\oplus}$, 118112-90-6; **2c**, 118112-87-1; **2c** · $Na^{\oplus}$, 118112-82-6; **3a**, 31562-40-0; **3b**, 42809-69-8; **4a**, 31562-43-3; **4b**, 21280-43-3; **4c**, 118112-78-0; **5a**, 4719-19-1; **5b**, 118112-85-9; **5c**, 87656-34-6; **6a**, 118112-88-2; **6b**, 118112-89-3; hydrogen sulfide, 7783-06-4.

[1] a) *Huben-Weyl-Müller: Methoden der Organischen Chemie, Vol. XI E*, Thieme, Stuttgart 1985; b) E. Krauthausen in [1a], p. 614.
[2] K. K. Andersen in D. N. Jones (Ed.): *Comprehensive Organic Chemistry, Vol. 3*, Pergamon, Oxford 1979, p. 317.
[3] E. Krauthausen in [1], p. 651.
[4] M. Mikołajczyk, J. Drabowicz, *Top. Stereochem. 13* (1982) 333.
[5] For the sake of simplicity only one tautomeric form of **1** and one mesomeric form of **2** are used.
[6] **2b** · $X^{\oplus}$: $C_{18}H_{26}N_2S_3O$, m.p. = 135–140°C (from EtOH); triclinic, space group $P\bar{1}$, $Z=2$, $a=6.385(2)$, $b=9.459(1)$, $c=16.445(2)$ Å, $\alpha=82.45(1)$, $\beta=82.78(2)$, $\gamma=78.88(1)°$; $V=960.96$ Å^3, $\mu=3.8$ cm^{-1}; $\rho_{calcd}=1.32$ g cm^{-3}. The intensities of 3519 reflections were measured on an Enraf-Nonius CAD-4 diffractometer using $Mo_{K\alpha}$ radiation ($\lambda=0.71073$ Å), graphite monochromator; range of measurement: $1 \leq \theta \leq 25°$; $\omega/2\theta$ scan; no absorption correction; structure solution by direct methods; H-atoms refined with isotropic thermal parameters, all other atoms refined with anisotropic thermal parameters; refined by full-matrix least-squares method to $R=0.033$ for 3157 observed reflections with $I \geq 3\sigma(I)$ ($R_w=0.037$, $w^{-1}=\sigma(F^2)$). Further details of the crystal structure investigation may be obtained from the Fachinformationszentrum Energie, Physik, Mathematik GmbH, D-7514 Eggenstein-Leopoldshafen 2 (FRG), on quoting the depository number CSD-53495, the names of the authors, and the full journal citation.
[7] N. Nakamura, *J. Am. Chem. Soc. 105* (1983) 7172.
[8] **6a**: Sublimation at ca. 110°C; m.p. = 184–185°C (from chloroform/*n*-hexane); ^{1}H NMR (60 MHz, TMS_{int}, $CDCl_3$): $\delta=0.55$ (s, 9H; Me_3Sn), 1.25 (s, 9H; Me_3C); $^{13}C\{^1H\}$ NMR (38.93 MHz, TMS_{int}, $CDCl_3$): $\delta=-2.44$ (Me_3Sn), 23.77 (Me_3C), 60.40 (s, Me_3C–); correct C,H,S analyses. **6b**: Sublimation of ca. 135°C; m.p. = 200°C (from chloroform/*n*-hexane); ^{1}H NMR (60 MHz, TMS_{int}, $CDCl_3$): $\delta=0.45$ (s, 9H; Me_3Sn), 1.22–1.40 (m, 6H; Ad), 1.43–1.55 (m, 6H; Ad), 1.60–1.71 (m, 3H; Ad); $^{13}C\{^1H\}$ NMR (38.93 MHz, TMS_{int}, $CDCl_3$): $\delta=-9.37$ (Me_3Sn), 29.83, 35.96, 37.00 (Ad), 62.03 (C1 of Ad); correct C,H,S analyses.
[9] B. Gallenkamp, W. Hofer, B.-W. Krüger, F. Maurer, T. Pfister in *Houben-Weyl-Müller: Methoden der Organischen Chemie, Vol. XII/E 2*, Thieme, Stuttgart 1982, p. 663.

Self-Reduction of $[Ph_4P][Nb(SCH_2CH_2CH_2S)_3]$ with Formation of a Nb_2^{IV} Complex**

By *Kazuyuki Tatsumi,* Yoitsu Sekiguchi, Michiyo Sebata, Akira Nakamura,* Roger E. Cramer,* and *Thomas Chung*

The usefulness of dithiolate ligands lies partly in their ability to form transition metal complexes of diversified structural types with varying nuclearity. In spite of this advantage, the relevant chemistry of group 5 metals has not been well developed. We have recently reported the syntheses and characterization of anionic tris(dithiolato) complexes $[M(SCH_2CH_2S)_3]^{\ominus}$, $[M(SCH_2CH_2CH_2S)_3]^{\ominus}$, and $[M(SCH{=}CHS)_3]^{\ominus}$, M = Nb^V and Ta^V.[1] The 1,2-ethanedithiolato complexes undergo an unusual intramolecular rearrangement in DMF, in the presence of a trace amount of water, methanol or phenol, yielding $[MS(SCH_2CH_2S)(SCH_2CH_2SCH_2CH_2S)]^{\ominus}$.[2] In this reaction, the pentavalent metal oxidation state is retained. In contrast, in the case of the homoleptic 1,3-propanedithiolato complex of Nb^V, an interesting self-reduction was found to take place in acetonitrile to give an Nb^{IV}–Nb^{IV} binuclear complex, which in turn afforded another binuclear species when treated with methanol.

When a concentrated acetonitrile solution of $[Ph_4P][Nb(SCH_2CH_2CH_2S)_3]$ **1** was allowed to stand at room

[*] Prof. Dr. A. Nakamura, Dr. K. Tatsumi, Y. Sekiguchi, M. Sebata
Department of Macromolecular Science
Faculty of Science, Osaka University
Toyonaka, Osaka 560 (Japan)
Prof. Dr. R. E. Cramer, T. Chung
Department of Chemistry, University of Hawaii
Honolulu, Hawaii 96822 (USA)

[**] *R. E. C.* and *T. C.* at the University of Hawaii are thankful for partial support by the National Science Foundation (Grant CHE 85-19289) and by the donors of the Petroleum Research Fund administered by the American Chemical Society.

temperature under Ar for approximately one month, the color of the solution changed from reddish-orange to red. During this time, the characteristic UV-VIS absorption bands of **1** [$\lambda_{max}(\varepsilon)$: 344 (15000), 403 (11000), 482 sh (6500)] were replaced by three new bands. From this solution, we isolated a red crystalline powder (70% yield), which was formulated as $[Ph_4P]_2[Nb_2(SCH_2CH_2CH_2S)_5]$ **2** on the basis of elemental analysis and the IR and NMR spectra.[3a,b] Treatment of **2** with methanol led to the formation of another binuclear complex **3** containing methoxy groups as dark-red crystals.[3a,c] The UV-VIS spectra of **2** and **3** are rather similar but are distinguishable, and the conversion **2** → **3** was observed to occur spontaneously. Both **2** and **3** are diamagnetic and moderately air- and moisture sensitive. Treatment of **1** with methanol did not, however, lead to formation of **3** and only an uncharacterizable powder precipitated.

$$[Ph_4P][Nb(SCH_2CH_2CH_2S)_3] \xrightarrow[CH_3CN]{1\ month} [Ph_4P]_2[Nb_2(SCH_2CH_2CH_2S)_5]$$

1 **2**

$$\xrightarrow[MeOH]{} [Ph_4P][Nb_2(OMe)_3(SCH_2CH_2CH_2S)_3]$$

3

A single crystal X-Ray structural analysis[4] showed that **3** consists of discrete phosphonium cations and binuclear niobium anions. The ORTEP plot for the anion is shown in Figure 1. The two niobium atoms are bridged by one

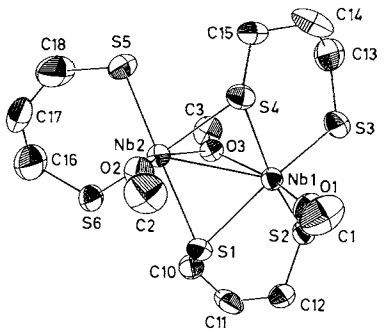


Fig. 1. The structure of the complex anion of **3** shown with 50% probability ellipsoids. Selected bond distances [Å] and angles [°]: Nb1–Nb2 2.901(1), Nb1–S1 2.537(2), Nb1–S2 2.494(2), Nb1–S3 2.457(2), Nb1–S4 2.516(2), Nb2–S1 2.568(2), Nb2–S4 2.564(2), Nb2–S5 2.464(2), Nb2–S6 2.459(2), Nb1–O1 1.860(4), Nb1–O3 2.091(3), Nb2–O2 1.846(4), Nb2–O3 2.088(4); S1–Nb1–S2 85.7(1), S4–Nb1–S3 91.3(1), S5–Nb2–S6 91.1(1), Nb1–O3–Nb2 87.9(1), Nb1–S1–Nb2 69.2(0), Nb1–S4–Nb2 69.6(0), Nb1–O1–C1 156.6(5), Nb2–O2–C2 158.7(5).

oxygen and two sulfur atoms, to provide a rare example of a triply bridged Nb^{IV} dimer. The metal–metal distance of 2.901(1) Å indicates the presence of a single bond, which accounts for the diamagnetism of **3**. The Nb^{IV}–Nb^{IV} bond length is comparable with those found in the related binuclear species $[Nb_2X_4(\mu\text{-}S)(\mu\text{-}S_2)(C_4H_8S)_4]$ (X = Cl, 2.844(2) Å; X = Br, 2.830(5) Å),[5] the semiconductor $Nb(S)(S_2)$ (3.037(3) Å),[6] and the quadruply-bridged Nb^{IV} dimer $[Nb_2Cl_4(\mu\text{-}Cl)_4(PMe_3)_4]$ (2.833(1) Å);[7] in contrast, the complex $[Cp_2Nb_2(CO)_4(\mu\text{-}S)_3]$ has a very long metal–metal distance (3.555(1) Å).[8] The more-common doubly-bridged Nb^{IV} dimers also exhibit differing Nb–Nb distances, e.g., $[Nb_2Cl_4(\mu\text{-}OMe)_2(OMe)_2(MeOH)_2]$ (2.781(1) Å),[9] $[Nb_2Cl_2(\mu\text{-}S)_3(NCMe)_4]$ (2.864(3), 2.872(3) Å),[10] and $[Cp_4Nb_2(\mu\text{-}S)_2]$ (3.2340(8) Å).[11]

The three dithiolates cause an asymmetry in the structure of **3** with two of them acting as half-bridging ligands and one as a terminal ligand.[12] Although the two pseudo-octahedrally coordinated niobium atoms are nonequivalent, their local coordination environments are similar. The oxygen and niobium atoms are nearly coplanar, with a maximum deviation (dev.) of 0.01 Å from the least-squares plane to which the S1–S2–S3–S4 (dev. 0.04 Å) and S1–S4–S5–S6 (dev. 0.07 Å) planes are perpendicular (89.5° and 89.4°, respectively). The dihedral angle between the two S_4 planes is 118.0°. Nb(1) is displaced by 0.23 Å out of the first S_4 plane towards the terminal methoxy group, while Nb(2) lies 0.24 Å out of the second S_4 plane. The Nb–O1 and Nb–O2 bonds are shorter than expected for a single bond, possibly due to $O\text{-}p_\pi\text{-}Nb\text{-}d_\pi$ donation. The Nb–S(terminal) distances resemble those in **1** (2.442(4)–2.466(4) Å), but the S–Nb–S bite angles are notably larger than those in **1** (83.9° av.) and $[Nb(SCH_2CH_2S)_3]^{\ominus}$ (81.9° av.).

The room temperature ^1H NMR spectrum of **3**[3c] shows three singlet peaks (1:1:1) for the methoxy protons and two complicated multiplets (1:2) for the dithiolate protons. This implies that the asymmetric structure is retained in solution and that the coordination geometry is rigid. For **2**, according to the ^1H NMR spectrum,[3b] the coordination mode of one dithiolate differs from that of the other four. It is possible that one dithiolate occupies a bridging position and the others terminal positions.

In the formation of **2**, the reduction of Nb is probably induced by reductive elimination of a dithiolate ligand from **1**. It should be noted here that neither $[Nb(SCH_2CH_2S)_3]^{\ominus}$ nor $[Ta(SCH_2CH_2CH_2S)_3]^{\ominus}$ gave a reduced dimer under similar conditions. In the case of the Ta^V complex, the reduction potential of −1.59 V ($E_{1/2}$ vs. SCE, quasi-reversible, in DMSO) lies well below that of **1** (−1.25 V, quasi-reversible),[1b] so that its propensity for resisting self-reduction is understandable. The reduction potentials of $[Nb(SCH_2CH_2S)_3]^{\ominus}$ (−1.20 V) and **1** are, however, very similar. Therefore, the different behavior of the two Nb^V chelates must be due to other factors, e.g., the chelate ring size. 1,2-Ethanedithiolate, which forms smaller rings than 1,3-propanedithiolate, is perhaps less well-suited for occupying a bridging or a half-bridging position in Nb^{IV} dimers, and/or is less likely to be eliminated as a cyclodithiaalkane.

Submitted: August 2, 1988 [Z 2901 IE]
German version: *Angew. Chem. 101* (1989) 83

[1] a) K. Tsutsumi, Y. Sekiguchi, A. Nakamura, R. E. Cramer, J. J. Rupp, *Angew. Chem. 98* (1986) 95; *Angew. Chem. Int. Ed. Engl. 25* (1986) 86; b) K. Tatsumi, I. Matsubara, Y. Sekiguchi, A. Nakamura, C. Mealli, *Inorg. Chem. 28* (1989), in press.

[2] K. Tatsumi, Y. Sekiguchi, A. Nakamura, R. E. Cramer, J. J. Rupp, *J. Am. Chem. Soc. 108* (1986) 1358.

[3] a) All manipulations were carried out under argon using water-free solvents. **2** and **3** gave satisfactory elemental analyses. b) **2**: red crystalline powder; ^1H NMR (400 MHz, $CDCl_3$, room temperature): δ = 1.91 (quintet, 8H, $SCH_2CH_2CH_2S$), 2.30 (quintet, 2H, $SCH_2CH_2CH_2S$), 2.67 (t, 16H, $SCH_2CH_2CH_2S$), 3.13 (t, 4H, $SCH_2CH_2CH_2S$); UV/VIS (DMF): $\lambda_{max}(\varepsilon)$ = 316 sh, 391 (16000), 470 (4100) nm; far-IR (Nujol mull): 363 (w), 345 (w), 331 (m), 311 (m), 292 (m), 283 (m), 263 (w) cm^{-1}. We have not yet been able to develop a rational synthesis for **2**. For instance, when an acetonitrile solution of **1** was refluxed for one day, formation of **2** was observed, but a large amount of uncharacterizable powder also precipitated. c) **3**: dark-red crystals; ^1H-NMR (400 MHz, $CDCl_3$, room temperature): δ = 2.29 ppm (m, 4H, $\mu\text{-}SCH_2CH_2CH_2S$), 2.36 (m, 2H, $SCH_2CH_2CH_2S$), 2.8 (m, 4H, $\mu\text{-}SCH_2CH_2CH_2S$), 3.15 (m, 4H, $SCH_2CH_2CH_2S$), 3.4 (m, 2H, $\mu\text{-}SCH_2CH_2CH_2S$), 3.57 (s, 3H, $\mu\text{-}OCH_3$), 3.74 (m, 2H, $\mu\text{-}SCH_2CH_2CH_2S$), 3.85 (s, 3H, OCH_3). The signals of the dithiolate protons were tentatively assigned on the basis of sequential decoupling experiments. UV/VIS (DMF): $\lambda_{max}(\varepsilon)$ = 316 (6600), 379 (11000), 460 (1400) nm; far-IR (Nujol mull): 423 (m), 354 (m), 336 (w), 317 (m), 297 (w), 287 sh, 263 (w) cm^{-1}.

[4] A single crystal of **3** was mounted in a glass capillary and sealed under argon. Monoclinic, space group $P2_1/n$, $a=18.593(4)$, $b=14.558(5)$, $c=15.894(3)$ Å, $\beta=105.99(2)°$, $\rho_{calcd}=1.505$ g cm^{-3}, $Z=4$, $\mu(Mo_{K\alpha})=5.45$ cm^{-1}. X-ray data were collected on a Syntax $P\bar{1}$ diffractometer in the $\theta/2\theta$ mode using graphite-monochromated $Mo_{K\alpha}$ radiation. The data were corrected for Lorentz and polarization effects, and an empirical absorption correction was applied. Of the 8831 measured reflections ($3<2\theta<50°$), 5343 observed reflections with $F_0^2>3.0\sigma(F_0^2)$ were used for the structure analysis. The structure was solved by MULTAN 80 and the standard Patterson heavy atom technique and refined to $R=0.0448$ and $R_G=0.0475$ using the SHELX 76 program. The phenyl rings of $Ph_4P^{\oplus}$ were treated as semi-rigid bodies, while the other non-hydrogen atoms were described anisotropically. A difference Fourier map after the final cycle of refinements showed a maximum residual peak of 0.8 e/Å^3 in a phenyl ring. Further details of the crystal structure investigation can be obtained from the Fachinformationszentrum Energie, Physik, Mathematik GmbH, D-7514 Eggenstein-Leopoldshafen 2, by quoting the depository number CSD-53344, the name of the authors, and the journal citation.

[5] a) M. G. B. Drew, I. B. Baba, D. A. Rice, D. M. Williams, *Inorg. Chim. Acta 44* (1980) L217; b) M. G. B. Drew, D. A. Rice, D. M. Williams, *J. Chem. Soc. Dalton Trans. 1983*, 2251.

[6] J. Rijnsborp, F. Jellinek, *J. Solid State Chem. 25* (1978) 325.

[7] F. A. Cotton, S. A. Duraj, W. J. Roth, *Inorg. Chem. 23* (1984) 3592.

[8] W. A. Herrmann, H. Biersack, M. L. Ziegler, B. Balbach, *J. Organomet. Chem. 206* (1981) C33.

[9] F. A. Cotton, M. P. Diebold, W. J. Roth, *Inorg. Chem. 24* (1985) 3509.

[10] A. J. Benton, M. G. B. Drew, R. J. Hobson, D. A. Rice, *J. Chem. Soc. Dalton Trans. 1981*, 1304.

[11] Yu. V. Skripkin, I. L. Eremenko, A. A. Pasynskii, Yu. T. Struchkov, V. E. Shklover, *J. Organomet. Chem. 267* (1984) 285.

[12] This type of half-bridging 1,3-propanedithiolate has been observed previously for the complexes $[Ph_4P][Mo_2O_2N_3(SCH_2CH_2CH_2S)_3]$ and $[Ph_4P]_2[Mn_3(SCH_2CH_2CH_2S)_5]$: P. T. Bishop, J. R. Dilworth, J. Hutchinson, J. A. Zubieta, *J. Chem. Soc. Chem. Commun. 1982*, 1052 and J. L. Seela, K. Folting, R.-J. Wang, J. C. Huffman, G. Christou, H.-R. Chang, D. N. Hendrickson, *Inorg. Chem. 24* (1985) 4454, respectively.

BOOK REVIEWS

Book reviews are written by invitation from the editor. Suggestions for books to be reviewed and for qualified book reviewers are welcome. Publishers should send prospects or (better) books to the following address: Redaktion Angewandte Chemie, Postfach 101161, D-6940 Weinheim, Bundesrepublik Deutschland. The editor reserves the right of selecting which books will be reviewed. Uninvited books not chosen for review will not be returned.

Organometallic Chemistry. An Overview. By *J. S. Thayer*. VCH Verlagsgesellschaft, Weinheim/VCH Publishers, New York 1988. xii, 170 pp., hard cover, DM 68.00.—ISBN 3-527-26196-6/0-89573-121-5

This book is written for people with a reasonably good background in chemistry who may be interested in learning something about organometallic chemistry. Since the very definition of an "organometallic" compound is neither uniform nor completely consistent, the author has chosen to include in the "metal" portion of "organometallic" any element whose electronegativity is less than that of carbon. This definition will include elements (boron, silicon, germanium, phosphorus, arsenic and tellurium) that are often termed "metalloids".

After a brief introduction to the concept of organometallic chemistry and its nomenclature and historical development, the classification of organometallic compounds used in this book is explained. This is based on the type of bonding as follows: ionic metal–carbon bond (with a metal cation and a carbanion), electron-deficient (when an electron pair on a single carbon is shared with two metal atoms), covalent, and synergistic (involving interaction of π-electrons of an olefin—or nonbonding electrons on a divalent carbon atom—with empty orbitals on metal atoms). Chapter 2 (11 pages) describes the general methods of synthesis of the metal–carbon bond, including those using elemental metals as well as metal compounds. Chapters 3 (8 pages) and 4 (8 pages) deal with ionic and electron-deficient metal–carbon bonds, respectively. Metal–carbon σ-bonds are discussed in Chapters 5 to 7 (41 pages), divided into the reactive metals (e.g. Zn, Cd, Ga, most transition metals, many derivatives of Be, Mg and Al), the heavy metals (those of the last two rows of the Periodic Table, with relatively high electronegativities, including Hg, Ir, Tl, Sn, Pb, Sb, Bi, Pt and Au), and the metalloids (B, Si, Ge, P, As, Se, Te and higher-valent Br and I). The organization of these chapters is clear, and provides the reader with a rapid and concise view of the essential features. They cite specific literature references (up to 1985), as well as general books and reviews. Synergistic metal–carbon bonds are discussed in Chapters 8 to 10 (29 pages), including mononuclear compounds of divalent carbon, mononuclear complexes of unsaturated hydrocarbons, and polynuclear compounds. These chapters are again well presented, although additional references should have been cited in Chapter 10. To show the role of polynuclear complexes in catalysis and surface sciences, the classical reviews by *Muetterties* and *Krause* (*Angew. Chem. Int. Ed. Engl.* 1983) or by *Muetterties, Rhodin* et al. (*Chem. Rev.* 1979) would have been most appropriate (rather than a series of *nine* articles by *Maught* in *Science* 1983). The importance of organometallic compounds in biology is very well illustrated in Chapters 12 to 14 (32 pages), including pharmaceutical and biochemical uses, toxicological and biocidal aspects, and environmental occurrence and transformation. These chapters are most welcome, and will convince the reader of the broad scope of organometallic chemistry. Thus, for example, Vitamin B_{12} coenzyme was shown in 1961 to con-

tain a Co–C bond, making it the first organometallic compound known to be formed as a product of biological metabolism; or again, the first report that methylmercuric compounds can be generated by the action of microorganisms on inorganic mercury compounds appeared in 1968. Chapter 14 (5 pages) serves as a postscript, in which selected topics and papers which appeared during the preparation of the preceding chapters are mentioned. This includes synthetic aspects, compounds involving metal–metal multiple bonding, and organometallic compounds in the environment, with references up to 1986. A subject index (6 pages), an author index (6 pages) and a compound index (10 pages), all very useful, conclude the book.

Despite obvious omissions (the late *R. S. Nyholm* and *J. Lewis* should have been cited for their pioneering work on carbonyl and metal–metal bonded complexes), and some awkwardly drawn figures (e.g. erroneous perspective in Figs. 6.1 and 9.2, ring unsaturation not shown in Fig. 10.1, inconsistent representation of the carbonyl ligands in Fig. 10.3), this book is very well written and presented.

The author has emphasized topics such as organometalloid chemistry, and industrial and biological applications, which should attract the interest of a broader audience. It therefore represents a useful addition to the many monographs already available in this area, and will certainly be very helpful to beginners in organometallic chemistry, who will be further encouraged by the conciseness of the book (170 pages). More advanced students or researchers will find more detailed information in, for example, "Organotransition Metal Chemistry" by *A. Yamamoto* (Wiley, New York 1986) or in "Organometallchemie" by *Ch. Elschenbroich* and *A. Salzer* (B. G. Teubner, Stuttgart 1986).

Finally, the publisher should be complimented for the high quality at the reasonable price of 0.40 DM/page for a hard-cover book.

Pierre Braunstein [NB 927 IE]
Laboratoire de Chimie de Coordination
Université Louis Pasteur
Strasbourg (France)

Inorganic Mass Spectrometry. Edited by *F. Adams, R. Gijbels,* and *R. Van Grieken.* Wiley, Chichester 1988. xi, 404 pp., bound, £ 57.50.—ISBN 0-471-82364-3

The editors of this book, who together head the Center for Microanalysis and Trace Analysis at the University of Antwerp, deserve credit for having satisfied a long-felt need for an up-to-date review on inorganic mass spectrometry; it is published as Volume 95 in the series "Chemical Analysis". As the editors themselves state in the introduction, the book appears at a time when there is considerable renewed interest in inorganic mass spectrometry (MS) in research, development and applications, and the indications of a rapid growth in its importance to the analytical chemist are unmistakable.

The first chapter (*I. Cornides*, 16 pp., 87 references) gives a chatty and amusing account of the historical background to the inorganic mass spectrometry of solids. Chapter 2 (*G. Ramendik, J. Verlinden* and *R. Gijbels*, 68 pp., 267 references) is a detailed and accurate report on spark source MS (SSMS). The principle of the method and the instrumentation are described, with an appropriately detailed treatment of the physical background. In addition to the main area of application of this method in multielement analysis of bulk samples, its capabilities for microanalysis, local analysis and depth profile analysis are discussed.

Chapter 3 (*W. W. Harrison*, 40 pp., 93 references) is concerned with glow discharge MS (GDMS), a method whose application to analysis is still quite new. It offers a very informative means for directly analyzing conducting and semiconducting solids, and commercial instruments using this method are now available. The article only covers the literature up to 1985, and is therefore not completely up-to-date, especially with regard to applications. Also the advantages of the method are a little over-generalized in places, and the disadvantages are rather played down. It turns out that a more complete and up-to-date review article on GDMS, with *W. W. Harrison* as one of its authors, has already been published elsewhere this year, which suggests that publication of the book has been delayed.

Secondary ion MS (SIMS), a method with a particularly high sensitivity, has been used for many years in surface analysis. Chapter 4 (*A. Lodding*, 48 pp., 103 references) describes the latest instrumental developments in the method, and the resulting application possibilities, including imaging SIMS. An impressive and concise account of the current state of techniques and knowledge in SIMS is presented; altogether the chapter is an excellent introduction and overview for the non-specialist.

The following chapter on laser microprobe MS (*A. H. Verbueken, F. J. Bruynseels, R. Van Grieken* and *F. Adams*, 124 pp., 303 references) is much concerned with minute details. The extent of this is apparent from such trivial statements as that the effects of electrostatic lenses are governed by the laws of ion optics, or that with the help of a computer one can easily undertake even tasks that are lengthy and laborious when carried out manually. However, when the applications are reached the information content improves, although even here the overview of the topic tends to become lost in the wealth of detail, leaving the impression that less quantity would have resulted in better quality.

Chapter 6 (*A. L. Gray*, 44 pp., 38 references) deals with MS using an inductively coupled radiofrequency plasma as the ion source (ICP/MS), giving in a relatively modest amount of space an excellent introduction and review. The basic principles and the design and functioning of the instrument are described fully in an easily understandable and very clearly presented way. With regard to the applications and the special sample introduction techniques needed, the capabilities of the method are convincingly shown using well chosen examples with detailed explanations.

Chapter 7 (*K. G. Heumann*, 76 pp., 232 references) gives a clear, precise and comprehensive account of the principles and applications of the isotope dilution method. The description of the applications is very detailed and even includes procedural rules, and consequently this contribution offers much more than just an introductory survey. This approach seems to be well justified, since the isotope dilution method can in principle give sufficient accuracy in any isotope-specific measurement problem, and it is therefore of prime interest in this context.

The eighth and last chapter (*R. Gijbels* and *F. Adams*, 18 pp., 55 references) gives an assessment of trends for the future development of inorganic MS.

The currently topical theme of MS on sputtered neutral particles (SNMS), which offers better quantitative measurements together with better depth resolution than is possible with other methods for surface and depth profile analysis, has unfortunately not been covered in this mono-

graph. Furthermore, it can be seen just by scanning the list of contents that the individual methods have received very unequal treatment as regards length, without there being, in the introduction for example, any indication of the reasons for this or of the editors' aims. The suspicion that is thereby raised, that this is a rather heterogeneous collection of review articles of different sorts, is reinforced when reading the book. The individual contributions vary greatly in breadth of coverage and in depth and quality of treatment, and also in the extent to which they are up-to-date.

As is only to be expected from a collection of individual articles, there can be no uniformity of style and presentation in this book, and it cannot offer the majority of readers a balanced treatment of the different methods included. It would certainly have helped if the editors had exercised a tighter coordination of the individual contributions, although the resulting delay in publication would have made the book less up-to-date. Its appearance should nevertheless be welcomed, as it has at present no competitor in the analyst's bookshelves, and the numerous references give rapid access to the original papers.

Dietmar Stüwer [NB 935 IE]
Institut für Spektrochemie und
angewandte Spektroskopie
Dortmund (FRG)

Arzneimittel—Fortschritte 1972 bis 1985. Edited by *A. Kleemann, E. Lindner* and *J. Engel.* VCH Verlagsgesellschaft, Weinheim 1987. xiv, 1517 pp., bound, DM 540.00.—ISBN 3-527-26329-2

This book is a supplementary volume which updates and extends the five-volume work "Arzneimittel—Entwicklung, Wirkung und Darstellung", by *Ehrhart* and *Ruschig,* which was published in its second edition in 1972. In twenty chapters by numerous experts the book deals with the progress made in pharmaceutical chemistry in the thirteen years from 1972 to 1985.

The volume begins with a short survey of drug design by *J. K. Seydel,* which in 51 pages summarizes the theory of structure-activity relationships, continuing up to molecular modelling and computer graphics.

In the second chapter (59 pp.) on enzyme inhibitors *H. Tschesche* reports on reversible proteinase inhibitors, including the renin- and angiotensin-converting enzyme inhibitors and the microbial α-glucosidase inhibitors, but makes no reference whatever to irreversible enzyme inhibitors such as α-difluoromethylornithine (see, for example, C. Walsh, *Tetrahedron 38* (1982) 871-909). However, some of these enzyme inhibitors are discussed later, along with mechanisms, when antihormones are treated in Chapter 18.

In the third, quite short, chapter (36 pp.) *T. Y. Shen* and *P. Davies* summarize the latest developments in the area of anti-inflammatory agents and the most important methods for synthesizing them.

In Chapter 4, which is also short (28 pp.), *J. A. Vida* reports on progress in psychotropic drugs, from the neuroleptics to the anxiolytic drugs.

Next, in Chapter 5 (281 pp.), several groups of authors in turn deal with new cardiovascular drugs. A short section on sympathomimetics and positive inotropic substances is followed by a very detailed discussion of the cardiac glycosides. Next antihypertensives are discussed; in addition to the pure α_1-adrenoreceptor antagonists such as Prazosin, Ketanserin is also included. After covering the centrally acting α_2-adrenoreceptor agonists of the clonidine type, the new dopamine agonists such as Fenoldopam are briefly discussed, followed by drugs with direct myogenic vasodilatory activity such as Hydralazine and Minoxidil. Also included under this class of substances is the new, very interesting potassium dilator BRL-34915, although the mechanism of its activity was not clarified until after the chapter was written.

The tables that follow listing substances with activity on the renin-angiotensin system illustrate the large number of similar and highly active ACE inhibitors that are currently being developed, and they also give evidence of the beginning of the very active phase of development in the area of renin inhibitors and angiotensin-II antagonists. Next comes a brief description of the chemical syntheses of most of the cardiovascular drugs that are listed here. The section which follows gives a survey of the development of beta-receptor blockers, with tables giving in each case the important intrinsic sympathomimetic activity (ISA). In the discussion of anti-anginal and anti-hypertensive drugs (23 pp.), the very important calcium antagonists and their syntheses are unfortunately only treated very briefly. The sections that follow summarize developments in vasoactive drugs and nootropics.

In Chapter 6 (21 pp.) *D. Bormann* and *R. Muschaweck* report briefly on developments in diuretics, but they fail to mention, in addition to the usual sulfonamide diuretics, the aldosterone antagonists of the spironolactone-spirorenone type; these are, however, discussed in Chapter 9 on steroid hormones.

In Chapter 7 (28 pp.) *A. Novakova-Banet, H. Feier, J. Müller* and *H. Zilg* discuss blood factors and clotting, and also fibrinolytics (although the plasminogen activators were not yet known at the time), and finally blood substitutes.

Chapter 8 (42 pp.) by *E. Granzer* deals with lipid regulators, briefly describing Compactin and Mevinolin, and also their use with advantage in combination with bile acid binding resins such as Cholestipol.

The first part of Chapter 9, by *W. König*, consists of more than 200 pages on regulatory peptides, and is a small monograph in itself. The treatment of the topic ranges from Somatostatin via ANF (atrial natriuretic factor), the encephalins and insulin, through to the interleukins and tumor necrosis factors (TNF); even structure-activity relationships are discussed for the important peptides. In the careful and accurate review of progress in steroid hormones by *U. Stache* in Chapter 9, Part 2 (41 pp.), the only important development missing is that of the aromatase inhibitors for future treatment of breast and prostate carcinomas, which had already emerged at the time of the review; however, this is briefly covered in Chapter 18.

The discussion of oral hypoglycemic drugs in Chapter 10 (18 pp.) by *W. Hitzel* and *R. Weyer* includes, in addition to stimulators of endogenic insulin synthesis, a brief account of some new substances such as Acarbose and Sorbinil which reduce the blood glucose level.

In Chapter 11 (87 pp.) *G. Beck* gives an overview of developments in prostaglandins, thromboxanes and leukotrienes, and assesses their likely future applications in fertility control, and in the treatment of gastric ulcers, and more especially of cardiovascular disease. Data on the new thromboxane-synthetase inhibitors and thromboxane antagonists, together with the 5-lipoxygenase inhibitors and leukotriene antagonists are summarized in short tables.

In Chapter 12 (33 pp.) *U. Achterrath-Tuckermann, G. Dressen, M. Mollière* and *J. Engel* report on progress in

respiratory drugs. In addition to the antitussives and β_2-stimulators there is a brief account of the anti-asthmatic/anti-allergic drugs, but surprisingly the very important cromoglycic acid disodium salt (Intal), although mentioned briefly in the text, does not appear in the corresponding table. In the discussion of the latest developments the potentially very important PAF antagonists are mentioned only in a single sentence, and the thromboxane antagonists are not mentioned at all, despite the fact that they might have a very important role in asthma therapy, as well as the leukotriene antagonists which are discussed in some detail.

In Chapter 13 (30 pp.) *J. Szelenyi* and *H. Schickaneder* describe the most important anti-ulcer drugs, from antiacids via histamine-H_2 antagonists to the new K^+-H^+-ATP-ase inhibitors.

Chapter 14 (118 pp.) by *W. Schröck* on antibiotics is confined to a detailed discussion of antibiotics of the β-lactam, aminoglycoside, macrolide and peptide types; all other antibiotics, e.g. tetracyclins, are either omitted or dealt with in Chapter 15 by *H. Plümpe* (65 pp.), which covers compounds with antiparasitic activity; here the latest developments in treatments against protozoa and in anthelmintics are described, including the remarkable results obtained using Praziquantel.

In Chapter 16 (33 pp.) *M. Plempel* and *J. Stetter* summarize progress on new antimycotics, and in Chapter 17 (27 pp.) *J. Hilfenaus* describes developments in antiviral agents, continuing up to Aciclovir as an inhibitor of the viral thymidine kinase; this chapter was written before work related to the AIDS virus came into prominence.

In the report on anti-tumor agents (Chapter 18, 72 pp.) *W. P. Brade* and *U. Niemeyer* discuss the cytostatic drugs, including the new platinum complexes. They then describe progress in hormones and antihormones, and discuss, amongst other topics, the biosynthesis of oestrogen and the aromatase inhibitors—including the irreversible "suicide inhibition", mention of which was omitted from Chapter 2 on enzyme inhibitors. The LHRH analogs such as Buserelin, which are also interesting in this context, receive only a brief mention here, but they were discussed earlier in Chapter 9 on regulatory peptides.

In Chapter 19 (66 pp.) a group of authors examine progress in immune stimulation and immune suppression. After discussing the immune system and how it can be stimulated by muramyl dipeptides and substances such as Levamisol or Azimexon, special attention amongst immunosuppressives is given, as expected, to cyclosporin, which represents a notable therapeutic breakthrough in this field.

In the 20th and last chapter (11 pp.), *H. G. Schwick* gives an overview of antibody serums and vaccines, without, however, mentioning monoclonal antibodies.

Leaving aside the many gaps and omissions in the material covered—e.g. chemotherapeutic compounds such as the highly effective gyrase inhibitors are missing—one finds that in many of the chapters the literature cited extends only up to 1981 or 1983, and only a few of the articles list references to work published in 1985 and 1986.

Looking at the volume as a whole, many of the chapters give very good summaries of the topics covered, and there are only a very few printing errors. Moreover, most of the authors have tried to give fair evaluations of other pharmaceutical products in addition to those made by their own firms, and to give them their rightful place.

It remains a mystery why this work, which is aimed at all scientists working in the pharmaceutical field, has been written and published in German, with the exception of the two chapters by English-speaking authors (Chapter 3 by *Chen* and *Davies* and Chapter 4 by *Vida*); this limits its readership to those who can read German texts, and these are relatively few in international terms. It inevitably limits the distribution of the work, and this in turn makes the price so high as to be prohibitive for many. For these reasons such works should in future, as a general principle, be published only in English, and it should further be borne in mind that all publications on progress in the pharmaceutical field must compete with, for example, the series "Annual Reports in Medicinal Chemistry", which is good value for money and is nearly always very up-to-date.

Helmut Vorbrüggen [NB 926 IE]
Schering AG, Berlin

Ions in Solution: Basic Principles of Chemical Interactions. By *J. Burgess*. Ellis Horwood, Chichester/Halsted Press, New York 1988. 191 pp., bound, £ 15.95.—ISBN 0-7458-0172-2/0-470-21059-1

Following the comprehensive monograph "Metal Ions in Solution" (Ellis Horwood, Chichester 1978, 480 pp.), the same author has now written a shorter version on the same topic, which nevertheless includes additional material and has been updated. It is aimed mainly at chemistry students, and is accompanied by two audio-cassettes (obtainable from the Royal Society of Chemistry, Distribution Centre, Letchworth SG6 1HN, Great Britain).

The contents of the book are conveniently arranged in 13 chapters. The first half deals with all the important aspects of the solvation of ions, the main emphasis being on a detailed description of the behavior of metal cations in aqueous solution. After an introductory chapter which is devoted to the dissolution of salts and the hydration of metal cations and of simple and complex anions, the second chapter introduces solvation numbers, and describes how these can be determined by NMR spectroscopy or by measuring ionic mobilities. Chapter 3 describes the types of information that can be obtained from X-ray and neutron diffraction measurements on electrolyte solutions (radial distribution functions, ion-solvent distances), and Chapter 4 gives an account of the use of spectroscopic and thermochemical methods to determine the strength of intermolecular ion-solvent interactions.

This is followed in Chapter 5 by a description of the Brønsted acid/base behavior of aqua-metal ions, their hydrolysis, and their polymerization to form polynuclear bridged aqua-complexes, and their stability constants are discussed in Chapter 6. An appropriate amount of attention is given here to selective cation solvators such as coronands, cryptands and naturally occurring crown ethers (valinomycin, monactin, monensin). Concluding this half of the book, Chapter 7 deals with the redox potentials of the aqua-metal ions and of the complexes derived from them by ligand exchange.

The second half of the book is concerned with kinetic and thermodynamic aspects of ion solvation. The first topics treated are solvent exchange reactions between solution and solvento-metal ions (Chapter 9), complex formation between solvento-metal ions and polydentate open-chain or macro(poly)cyclic ligands (Chapter 10), associative and dissociative substitution in complex ions (Chapter 11), and redox reactions involving an "inner sphere" and "outer sphere" electron transfer mechanism (Chapter 12).

The 13th and last chapter, "Past, Present and Future", summarizes the current state of research and the developments to be expected in a few selected areas of the chemistry of ions in solution (e.g. direct NMR spectroscopy of metal ions, the synthesis and applications of new highly selective macrocyclic ligands, and the importance of activation volumes for determining reaction mechanisms). At the end of the book is a useful glossary with definitions of frequently used terms, a bibliography which should encourage further reading, and a brief subject index. The book is well written from a teaching standpoint, and contains 77 tables and 93 figures. It was apparently based on a series of lectures and a workbook accompanied by audiocassettes. The sections of the book dealing with complex formation by metal ions in solution, and with the kinetics of solvent exchange between solvated metal ions and the bulk of the solvent—topics on which the author has himself made significant research contributions—are especially good.

Unfortunately a few printing errors that could confuse beginners in the field have crept in: incorrect formulas are given for ethylenediamine tetraacetate and hexamethylphosphoric acid triamide (p. 13) and for the metabisulfite ion (p. 71).

This book provides valuable, though quite demanding, reading for both the beginner and the advanced student wishing to become acquainted with the chemistry of ions in solution.

Christian Reichardt [NB 923 IE]
Fachbereich Chemie
der Universität Marburg (FRG)

Architecture of Eukaryotic Genes. Edited by *G. Kahl.* VCH Verlagsgesellschaft, Weinheim/VCH Publishers, New York 1988. xiv, 518 pp., bound, DM 195.00.—ISBN 3-527-26835-9/0-89573-809-0

This book contains a summary of the symposium on "Chromatin Structure of Plant Genes", which took place in Frankfurt/Main in 1986. Accordingly it consists of 27 individual articles based on the main lectures of the symposium, arranged under seven topic areas. Eight articles are concerned with structure and function of genes within plants or obtained from plants, while 17 articles describe, for genes from higher eukaryotic organisms other than plants, principles of structure and function that have been intensively studied, and may be generally applicable; a final article deals with the nucleosome fine structure of the lower eukaryotic organism *Saccharomyces cerevisiae*. At the beginning is an article on the structural and topological polymorphism of DNA, which is relevant to all types of organisms. The book concludes with an attempt at a general perspective on current trends in research on chromatin structure and chromatin activation in plant cells.

With the arrangement of topics adopted here the reader is first familiarized with the general DNA structure, and particularly with the organization, sequences and activity of expression signals in plant genes, then with higher level regulation mechanisms. Next comes a chapter on the properties of the DNA binding proteins in the chromatin and the structure of their genes, followed by an overview of protein-DNA interaction effects in the chromatin. Next is a chapter of central importance which describes the relationships between chromatin structure and expressional activity for a few particular genes, followed by another dealing with the transcriptional activity of the DNA and its dependence on the degree of methylation of its regulator sequences, with several examples. The last two topics covered are the long-range geometrical structure of the chromatin in the nuclear matrix, and the genetic and physical mapping of high molecular weight chromosomes.

Obviously a book dealing with such a wide range of topics in areas where intensive research is continuing can only present a snapshot of the situation, which is all that is intended, and it therefore cannot be expected to be up-to-date and complete in every detail. Instead the value of the book lies more in the insights which the individual articles give for specialists in neighboring areas, and in the very useful drawing together of these different topics under the general theme of chromatin structure and gene expressional activity, in a form which, to the best of my knowledge, is new and unique. Some of the individual articles are structured along the lines of reviews, and so have the inherent disadvantage that for the specialist their topicality lasts only until the next review article appears; others consist of summaries of the authors' own researches, and these can serve as examples for the application of similar ideas to other genes and organisms.

Because of the variety of material contained in the book, and its relatively advanced level, which in some cases is even highly specialized, the potential readership extends from the advanced student with some previous knowledge of molecular genetics, who wishes to study the organization of DNA in chromatin and the structural and mechanistic dynamics involved when genes are activated, to the specialist in a particular area who wants to have a collection of reviews of related areas at hand for consulting when needed. Both these groups of readers will be able to obtain an overview from this book, and the plentiful references provided will enable them to follow this by reading up on individual topics in greater depth. The book is also of undoubted value to the university teacher preparing specialist lectures on eukaryotic molecular genetics, and he will also find here reviews to help in course planning, and specific examples to use in his lectures. Whilst I anticipate that those buying their own copy of the book will be limited to specialists in the field, it is beyond question that it should be available in the library of every molecular genetics laboratory, both for the general education of those working in the area, and to provide reviews of the specialist topics covered.

Wolfgang Hillen [NB 924 IE]
Institut für Mikrobiologie und Biochemie
der Universität Erlangen-Nürnberg (FRG)

Solvents and Solvent Effects in Organic Chemistry. 2nd edition, revised and enlarged. By *C. Reichardt.* VCH Verlagsgesellschaft, Weinheim 1988. 534 pp., bound, DM 108.00.—ISBN 3-527-26805-7

It was not until the last few decades that values of the acidities, basicities and reactivities of organic compounds determined by mass spectrometry showed that many properties that had formerly been attributed to the reactants are to a large extent determined by the solvents. The study of solvent effects has therefore come to occupy a central role in the whole of (organic) chemistry. For this reason alone the first edition of this book, published in 1979, was assured of success, which was further increased by the excellent preparation and presentation of the material.

The many new results and the greatly extended knowledge that have been gained in this field during the last eight years (including publications up to the beginning of 1987) have been incorporated into this considerably enlarged new edition, maintaining the same high standard. Since new facts and views concerning the solvents themselves have also come to light, the title has been extended to take account of this.

The original division into seven chapters has been retained, but the relative emphases have shifted considerably. The book begins with a chapter on "Solute-Solvent Interactions" (45 pp., 303 references), in which those currently held concepts that are of general validity are summarized. In addition important effects such as solvophobic interactions and micelle formation are discussed. "Classification of Solvents" (26 pp., 171 references) deals with their classification according to their various physical and chemical properties (e.g. acids and bases). Also included here are specific solvation effects, and recent attempts using multivariant statistical methods (chemometrics) to arrive at a rational classification of solvents.

The chapter on "Solvent Effects on the Positions of Homogeneous Chemical Equilibria" (41 pp., 229 references) covers not only the classical effects on acid-base and keto-enol equilibria (including the most recent data, with also gas phase data for comparison), but also solvent effects on conformational, valence isomerization and electron transfer equilibria. The next chapter on "Solvent Effects on the Rate of Homogeneous Chemical Reactions" (171 pp., 769 references) has undergone the greatest enlargement, as is evident from the remarkably large bibliography alone. Qualitative observations, quantitative measurements and theories are discussed, with examples from a very wide range of reaction types, and effects produced by external pressure, molecular sieve action and liquid crystalline reaction media are described.

The important topic "Solvent Effects on Absorption Spectra of Organic Compounds" (53 pp., 434 references) has also been updated to the latest situation. In addition to the classical effects on UV-VIS and IR spectra, solvent effects on ESR and NMR spectra are also described. The final chapter "Empirical Parameters of Solvent Polarity" (66 pp., 287 references) has been rewritten because of the large number of new papers that have been published. The description of the now well-known Y, Z and E_T scales has been enlarged to include also some newer characteristic quantities, and properties specific to the solvents, e.g. acceptor and donor properties. The comparison of different empirical scales and the detailed discussion of the controversial multiparameter relationships is especially helpful.

There is a welcome addition in the form of an appendix which contains numerous tables listing the properties of solvents, methods for purification, and areas of use in spectroscopy and synthesis; information on toxicities is also included.

It can already be seen from this brief description of the contents of the book that one could scarcely imagine any other monograph which would treat the whole field of solvent effects so comprehensively without becoming unacceptably long. One gets the impression that the literature has been very carefully reviewed and evaluated. The well chosen examples enable the reader to quickly understand each type of problem, and the detailed bibliography allows him to extend his reading both in breadth and depth. Anyone wishing to learn about solvent effects or to investigate them, or who wishes to find typical examples of effects on equilibria and reactions, will find this book to be good value. For these reasons it belongs not only in every library but also at the chemist's bench, and an economical paperback edition of the book would be a very welcome addition.

Siegfried Hünig [NB 937 IE]
Institut für Organische Chemie
der Universität Würzburg (FRG)

Zur Konformation des Cyclohexans. (Ostwalds Klassiker der exakten Wissenschaft, Band 274.) By *H. Sachse* and *E. Mohr*. Akademische Verlagsgesellschaft Geest & Portig, Leipzig 1987. 152 pp., paperback, DM 21.00.—ISBN 3-321-00025-3

In 1885 *Adolf von Baeyer* assumed in his strain theory that all cycloalkanes had a planar ring of carbon atoms. This view was challenged five years later by *Hermann Sachse*, who proposed non-planar chair and boat structures for the important case of cyclohexane. He also correctly recognized the possibility of chair inversion in cyclohexane, yet overestimated the strain requirements, and concluded that inversion could not occur at room temperature. This led him to describe the *cis*- and *trans*-cyclohexane-1,4-dicarboxylic acids as conformational rather than configurational isomers. As a corollary of this, he further concluded that for monosubstituted cyclohexanes one should expect two stable and separable isomers with axial and equatorial orientation of the substituent respectively. Since this could not be backed by experiment, and probably also as a consequence of the eminent authority of *von Baeyer*, the work of *Sachse* gained no recognition and fell into oblivion for many years to come. It was not until 25 years later (1915), long after *Sachse*'s premature death in 1893, that *Ernst Mohr* again took up the cyclohexane problem, and made it clear that "no objection whatsoever" could be raised against *Sachse*'s ideas regarding the non-planar structure of cyclohexane, provided the inversion barrier is low enough. A breakthrough in favor of the non-planar structure of cyclohexane eventually came from the firm conclusion reached by *Mohr* in 1922 that *both* stereoisomers of decalin should exist, followed almost immediately (1923) by *Walter Hückel*'s experimental verification of this prediction. On this matter, *Mohr* had engaged in a controversy with *Richard Willstätter*, one of *von Baeyer*'s former students and late supporter of a planar structure of cyclohexane, who shortly earlier (1921) had declared *trans*-decalin could not be made due to excessive strain.

The present booklet is preceded by an introduction by editor *Horst Remane*, describing some elements of conformational analysis (9 pages): present-day significance, some basic facts, historical developments. Biographical details and an account of the scientific achievements of *Hermann Sachse* and *Ernst Mohr* follow (13 pages). Mention is made here of both pioneers' grave personal lives overshadowed by serious illness. *Sachse* died at an age of only 31, *Mohr* at 53. The central part of the book is, of course, taken up by the reprints of *Sachse*'s two key publications and three relevant papers by *Mohr*:

1) H. Sachse: Über die geometrischen Isomerien der Hexamethylenderivate, *Berichte der Deutschen Chemischen Gesellschaft 23* (1890) 1363–1370.
2) H. Sachse: Über die Konfigurationen der Polymethylenringe, *Zeitschrift für Physikalische Chemie 10* (1892) 203–241.

3) E. Mohr: Die Baeyersche Spannungstheorie und die Struktur des Diamanten, *Journal für Praktische Chemie 98* (1918) 315–353.
4) E.Mohr: Zur Theorie der *cis—trans*-Isomerie des Decahydronaphthalins, *Berichte der Deutschen Chemischen Gesellschaft 55* (1922) 230–231.
5) E. Mohr: Zwei spannungsfreie Cycloheptanmodelle, *Journal für Praktische Chemie 103* (1922) 316–328.

The original papers are annotated with comments by the editor, which make up the last 13 pages, including an author index.

Some critical comments follow concerning the editing of the little book. The introductory section on fundamentals of conformational analysis appears somewhat drab and outdated. The origin of the rotation barrier in ethane (p. 8) is actually pretty clear (R. M. Pitzer, *Acc. Chem. Res. 16* (1983) 207). It is rather disconcerting to detect just in *this* text that the characterization of the stationary points of the inversion process of cyclohexane has not been gotten right (p. 10, Fig. 5).

The editor has taken much care in supplementing the old nomenclature by more recent conventions, but in my view has gone a little too far, as the present historical context demands a tender approach indeed. For example, on page 14 it is noted *expressis verbis* "... Jod [Iod, H. R.]"; *un peu de trop*, it seems to me! Again, wherever the name "Hexamethylen" occurs in the original papers, and this happens frequently, of course, the reader is invariably and relentlessly instructed that the glorious modern term is "Cyclohexan". In favor of the editor, let us assume that the editing program of a computer has performed its stubborn task here! I found the alteration of "Benzol" in the original papers to "Benzen" very irritating, since even modern German usage on the whole still prefers the old "classical" variant. The editor had indeed better avoided this inept interference, especially since he ultimately refrained from introducing the new word in the titles of the cited publications (see, for example, the bizarre situation on p. 82, ref. 12).

As the original papers have not been directly reproduced, but have instead been newly type-set and annotated, some errors have naturally crept in here and there. For example, in connection with note [5] on p. 30 the proper spelling is "Kohlenstoffatom*e*." It is to be hoped that the numerous analytical relationships in *Sachse*'s second paper have not suffered; one error at least is perceptible in the first expression on p. 54. In Fig. 1 and, more particularly, Fig. 2 of the first paper by *Mohr*, the perspective is wrong, while Figs. 4, 6 and 20 are turned upside-down.

On p. 144 it is stated in note [42] that the twist forms of cyclobutane interconvert by pseudorotation. In actual fact, this process is to be referred to as a ring inversion, since the planar four-membered ring allows only a single type of non-planar deformation (normal coordinate), which necessarily cannot be degenerate. A pseudorotatory degree of freedom corresponds to a double degeneracy, which is only possible in rings with five or more members.

Despite all this criticism, it is to be welcomed that the publishers of the series "Ostwalds Klassiker" have devoted a volume to the history of elucidation of the cyclohexane structure, and thereby also to the core of conformational analysis. The booklet is recommended to everyone interested in the history of the development of basic concepts of modern chemistry, especially as the price is within reach of even small purses.

Otto Ermer [NB 921 IE]
Institut für Organische Chemie
der Universität Köln (FRG)

Registered names, trademarks, etc. used in this journal, even when not marked as such, are not to be considered unprotected by law.
© VCH Verlagsgesellschaft mbH, D-6940 Weinheim, 1989.
Printed in the Federal Republic of Germany by Zechnersche Buchdruckerei, Speyer/Rhein.

All rights reserved (including those of translation into foreign languages). No part of this issue may be be reproduced in any form – by photoprint, microfilm, or any other means – nor transmitted or translated into a machine language without written permission from the publishers. Only single copies of contributions, or parts thereof, may be made for personal use. This journal was carefully produced in all its parts. Nevertheless, authors, editors and publisher do not warrant the information contained therein to be free of errors. Readers are advised to keep in mind that statements, data, illustrations, procedural details or other items may inadvertently be inaccurate.

Valid for users in the USA: The appearance of the code at the bottom of the first page of an article in this journal (serial) indicates the copyright owner's consent that copies of the article may be made for personal or internal use, or for the personal or internal use of specific clients. This consent is given on the condition, however, that the copier pay the stated per-copy fee through the Copyright Clearance Center, Inc., for copying beyond that permitted by Sections 107 or 108 of the U.S. Copyright Law. This consent does not extend to other kinds of copying, such as copying for general distribution, for advertising or promotional purposes, for creating new collective works, or for resale. For copying from back volumes of this journal see 'Permissions to Photo-Copy: Publisher's Fee List' of the CCC.

Paving the Way ...

ADVANCED MATERIALS has made a successful start. In 1989 it will continue to be part of ANGEWANDTE CHEMIE but may be subscribed to separately and will be available in its own specially designed cover,[*] which shows an idealized picture of a microfabricated structure of a kind commonly used in microelectronics. The decision to pave the way for ADVANCED MATERIALS to become a journal in its own right has been made in response to many requests by scientists and engineers from various disciplines other than chemistry, bearing witness to the accuracy of the message conveyed in the first editorial in May last year:

Modern science and technology rely on specialists. Nevertheless, the complexity of many problems is all too often an obstacle to gaining a deeper understanding of physical and chemical phenomena. In particular, the development of advanced materials and new technologies requires the joint efforts of many specialists from a variety of disciplines. The nature of ceramics, polymers, composites and other new materials is such that successful processing must integrate the individual steps of molecular and microstructural design, engineering, testing and manufacturing. The once common distinction between the product, its function in a system, and the material from which it is made has lost its meaning in a context wherein new materials are created on demand to serve special requirements. This implies that a multidisciplinary team of experts is more likely to be successful in the development and application of advanced materials than are individual researchers working within the limits of their special field.

It is always surprising to see that despite the diversity of all the materials in use and under development, the concepts, phenomena and transformations involved in making and using ceramics, metals, polymers and composites are strikingly similar. Important features are phase equilibria, phase transformation mechanisms, defect structures, flow and fracture mechanisms, structures of crystals and glasses and their relationships, internal boundaries and their contribution to macroscopic behavior, the motion or confinement of charge carriers, the statistical mechanics of assemblies of subsystems; these features not only serve to characterize the individual materials in which they were first studied, but also determine the behavior and performance of other materials which at first sight are totally unrelated.

It is this intellectual relationship between the phenomena that are seen in different materials and between the seemingly distinct features that are found in the same material, which has given birth to *Materials Science* as a discipline in its own right. One of the most challenging tasks is to provide the link between the thinking of the chemist who considers materials mainly in terms of structure and dynamics on the atomic and molecular scale and the concepts of the physicist whose models are often based on the continuous nature of matter. Moreover, materials science integrates important aspects of engineering in so far as certain properties of materials arise solely from the process of manufacturing owing to the physical and chemical methods of handling. The latter is most obvious in modern polymer materials where the supermolecular structure of the constituent chain molecules is entirely determined by the processing methods.

Recent years have witnessed an unprecedented explosion of new structural materials. Today the place of technological change due to the availability of more and more specialized high performance materials is rapid. We are only beginning to realize the opportunities provided by the new materials. In addition to changing the engineering landscape, advanced structural materials have also altered traditional policies regarding materials. Historically, national interests in materials have centered around the problem of shortages of supply of certain "critical" ores and minerals. The potential of the new materials such as high performance composites goes far beyond substitution. They provide performance and manufacturing advances which cannot be achieved with traditional metals and they are often the key for new technologies. Therefore, an active governmental role in accelerating the development and commercialization of such materials is seen in all major industrialized countries.

Contents

Paving the Way ... 107
Notice to Authors 109
G. Heimke
Advanced Ceramics for Biomedical Applications 111
J. P. Rabe
Surface Chemistry with the Scanning Tunneling Microscope 117
Research News
R. W. Cahn
Aluminum-rich Metallic Glasses 123
Conference Reports
H. Jäger
High-Temperature Superconductors in Strasbourg ... 124
... and Colorado Springs 125
Conference Calendar 129

[*] Illustration & Design, Mannheim, FRG.

ADVANCED MATERIALS

Advanced materials are now ranked together with microelectronics and biotechnology as the most promising "high-tech" industries of the future. With the rise of materials science as a recognizable discipline, many new journals covering different aspects of the field have been founded, all of them publishing either original papers or long, in-depth reviews. In addition, there exist series of books, a plethora of monographs and even an encyclopedia for this new discipline. What the materials community is still lacking is a truly international journal that concomitantly provides stimulating short reviews comprehensible to the many subgroups of the discipline and highly topical short communications that are of interest to more than one discipline; such a journal should also present highlights from the recent original literature, conference reports, book reviews, information about funding programs and materials science institutes, as well as other important news, i.e., all those ingredients that make a journal enjoyable and timely. ADVANCED MATERIALS is intended to serve this purpose.

The program is illustrated best by presenting the authors and titles of the reviews published in the first six issues:

H. Möhwald
Controlling the Microstructure of Monomolecular Layers

J. G. Bednorz, K. A. Müller
Perovskite-Type Oxides—the New Approach to High-T_c Superconductivity (Nobel Lecture)

W. A. Kaysser, G. Petzow
Advanced Materials by Powder Metallurgy

M. T. Reetz
Anionic Polymerization of α-Activated Olefins

J. W. Rabalais et al.
From Carbon Beams to Diamond Films

D. Haarer, A. Blumen
Polymeric Photoconductors—New Concepts

H. Yanagida
Intelligent Materials—A New Frontier

R. Schöllhorn
From Electronic/Ionic Conductors to Superconductors: Control of Material Properties

Z. Yoshida, T. Sugimoto
New Donors of Molecular Organic (Super)Conductors

M. Antonietti
Microgels—Polymers with a Special Molecular Architecture

H. Inokuchi
New Organic Superconductors

Thus ADVANCED MATERIALS covers all aspects of materials science, but especially genuine new materials and methods for their preparation, modification and investigation; important theoretical concepts are also discussed. Attention is always focused on an interdisciplinary approach. The key question is, what does the physicist want to know from the chemist and vice versa, and what do both have to communicate to the materials scientists? ADVANCED MATERIALS is planned to stimulate fruitful discussions and to promote cooperation between scientists from different disciplines.

Finally, it is important to note that ADVANCED MATERIALS now accepts short communications for publication (see Notice to Authors on the following pages). With this addition to the publishing program ADVANCED MATERIALS features

- editorial essays
- short reviews
- short communications
- highlights from the literature ("research news")
- news from the materials science scene
- book reviews
- conference reports
- conference calendar

and serves the needs of a rapidly growing materials science and engineering community. It should help to pave the way for fruitful cooperation.

Peter Gölitz
Weinheim (FRG)



ADVANCED MATERIALS

Notice to Authors

1. General Information

ADVANCED MATERIALS appears monthly as part of Angewandte Chemie and publishes short review articles, communications, research news, conference reports, book reviews, a conference calendar and correspondence. Contributions for all sections must be submitted in English. Manuscripts (original and one copy) should be submitted to the following address:

ADVANCED MATERIALS
Postfach 101161
D-6940 Weinheim
Federal Republic of Germany

Authors of review articles and communications will receive immediate acknowledgement of receipt of their manuscript.

2. Type of Contributions

2.1. Review Articles

Review articles should deal with topics of current interest in any area of materials science and engineering, and should be written in such a way that they are comprehensible to the large and heterogeneous readership of ADVANCED MATERIALS. Rather than an assemblage of detailed information with a complete literature survey, a critically selected treatment of the material is desired; unsolved problems and possible developments can also be discussed, applicational aspects should be highlighted. Although review articles are generally written upon invitation, unsolicited manuscripts are also welcome provided their contents are in keeping with the character of the journal; in any case, authors wishing to write a review article should contact the editor as early as possible.

A review article should be clearly structured. A *lead-in* (maximum length half a page of manuscript), which should not be a mere summary of the article, but rather an "appetizer," must precede the text itself; this should arouse the readers' interest—particularly those not familiar with the area. The first section of the review article itself, the *introduction*, should primarily introduce the nonspecialist to the subject in as clearly and lively a way as possible. A review article should conclude with a section entitled *summary and outlook*.

Length: A review article should consist of a manuscript having up to 15 pages of pure text (A4 format, *double* spacing, ca. 60 typewriter strokes per line); footnotes and literature citations, tables, formulas, schemes, and figures, in a number appropriate to the text and topic should be submitted on separate sheets. If a longer article is planned, the agreement of the editor should be sought as early as possible. Short review articles (8–10 manuscript pages of pure text) are *highly welcome* and are generally published more rapidly.

2.2. Communications

Communications are short notes describing preliminary or complete results of experimental or theoretical studies covering all branches of materials science and engineering including materials related chemistry and physics. A communication must be of general interest with respect to its significance, novelty, or wide applicability; it must at least contribute to the development of an important area of research and should be written in such way that the nonspecialist is able to recognize the significance the author attaches to his results. Contributions which do not satisfy these criteria will not be accepted for publication even if they are factually and formally beyond reproach. In reaching a decision the interest of the reader, and not that of the author, is paramount. *Therefore, the first paragraph of a communication should give a short explanation of what is being reported, why the investigation was undertaken, and what findings have been made.*

Usually, the quality of each communication is assessed by two independent referees. In general, a decision to accept or reject a communication will be made within four to six weeks; the result is then communicated to the author immediately. Authors who are requested to alter their manuscripts should send the revised version within three months to the editorial office; otherwise, a communication could be considered to have been withdrawn.

Justification: A short text justifying why a preliminary communication should appear in ADVANCED MATERIALS must accompany the manuscript. The justification should facilitate making a decision to either accept or reject the article.

Length: Inclusive of all literature citations, footnotes, and tables, a communication should consist of a manuscript of not more than six pages (A4 format, *double* spacing, ca. 60 typewriter strokes per line); a limited number of figures and formulas may be added. Longer communications will be accepted only if their quality warrants special consideration; otherwise, they will be returned immediately.

Only publications that have already been published or are in the press should be cited; copies of publications in press should be submitted along with the manuscript. Unpublished results and lectures should only be cited for exceptional reasons. Details that could be of importance to the referees, but that are unlikely to be of interest to the reader, can be submitted as an enclosure.

2.3. Research News, Conference Reports and Book Reviews

Research news, conference reports and book reviews are usually written on invitation. Suggestions for research results to be highlighted, conferences to be covered and books to be reviewed and for authors are welcome.

3. Manuscript Preparation

To prepare their manuscript formally beyond reproach, authors are requested to carefully study comparable articles in a recent issue of the journal; this is conducive to a speedy handling of a manuscript. American spellings should be used throughout: consult *Webster's Third New International Dictionary of the English Language*, G. and C. Merriam, Springfield MA, 1965. Useful, general hints for preparing manuscripts are to be found in such books as

The ACS Style Guide. American Chemical Society, Washington 1986; *The Chicago Manual of Style*, 13th edition, University of Chicago Press, Chicago 1982. H. F. Ebel, C. Bliefert, W. E. Russey, *The Art of Scientific Writing*, VCH Verlagsgesellschaft, Weinheim 1987.

Review articles should be divided into sections and subsections (1. ..., 1.1. ..., 1.1.1. ...) which are to be provided with headings. The section numbers should be referred to in cross references.

Communications should not be divided into sections. However, experimental details should be summarized separately under the heading *Experimental Procedure*. The literature references and footnotes should have as little text as possible.

Manuscripts should be typed on one side of A4 format paper using *double spacing* and ca. 60 typewriter strokes per line; a ca. 3-cm margin should be left free at the top, bottom, and left-hand side of each page, and a ca. 2-cm margin on the right-hand side. Italics are designated by single underlining, bold type by double underlining.

3.1. First Page

Both the title, *which should be as succinct as possible*, and the *full* fore- and surnames of the authors should be typed using lower and upper case letters. An asterisk after the name of the author to whom correspondence should be sent refers to a footnote at the bottom of the same page where the respective address can be found. This footnote contains the names of the authors with their academic titles. If necessary, a second footnote on this page should contain the series title and series number as well as the reference of the last article in the series. In addition, this footnote should also contain, if necessary, the names of institutions, companies, and individuals who have supported the work.

3.2. Nomenclature, Symbols, and Units

The rules and recommendations of the International Union of Pure and Applied Chemistry (IUPAC) and the International Union of Pure and Applied Physics (IUPAP) should be adhered to.

3.3. Abbreviations and Acronyms

Abbreviations and acronyms should be used sparingly and consistently. Where they first appear in the text they should—apart from the best known exceptions—immediately follow the complete term in parentheses. In review articles where a number of abbreviations and acronyms occur these can be explained in a footnote on the first page.

3.4. Chemical Formulas

Chemical formulas should be sketched with stencils or prepared with a printer using a computer graphics program. Formulas should be numbered consecutively with Arabic numerals and Roman lower case letters; these are to be doubly underlined in text, e.g., 1, 2a. Abbreviations such as Me, Et, *n*Br, *i*Pr, *s*Bu, *t*Bu, and Ph (not ϕ) may be used in formulas; however, their use should be consistent.

3.5. Equations

Mathematical, physical and chemical equations should if possible be numbered consecutively with Roman lower case letters in parentheses. Greek letters and special characters must be clearly recognizable (if necessary, an annotation should be supplied in the margin, e.g., Greek small case psi); in addition, it must also be evident whether a symbol should lie on the line or appear as a sub- or superscript, whether it should be in italics or boldface.

3.6. Figures

Originals are required if line drawings or photographs (sharply defined, high-contrast, without masking screen, black-and-white) are used. All figures are to be numbered with Arabic numerals in the sequence in which they are referred to in the text and are to be supplied with a comprehensive legend. Color photographs can be reproduced.

Formulas and figures should be capable of being reduced either to widths of 5–8 cm or 14–17 cm. *Symbols and captions must be 1.5–2.0 mm large after the reduction process.* Insofar as possible, all lettering should roughly have the same size.

3.7. Tables

Tables should be provided with a brief title and should only be subdivided by three horizontal rules (head rule, neck rule, foot rule). Tables having only one or two columns and columns having only one or two entries are to be avoided. For footnotes in tables, Roman lower case letters set in square brackets are to be used. All tables are to be numbered using Arabic numerals in the sequence in which they are referred to in the text.

3.8. Literature References, Footnotes

References to literature or to footnotes in the text are to be set in square brackets (e.g., [1], [2a, b], or [1–3]). References and footnotes are to be numbered *consecutively* and arranged at the end of the manuscript. Mode of citation: forenames (initials) and surnames of all authors, abbreviated form of the title of the journal (singly underlined; abbreviated according to *Chemical Abstracts Service Source Index*, volume number (singly underlined), year of publication in parentheses, page number (on which the publication begins). Example: a) B. Müller, A. Smith, Angew. Chem. 95 (1983) 24; Angew. Chem. Int. Ed. Engl. 22 (1983) 19; b) C. von Zeta, J. Chem. Soc. Chem. Commun. 1983, 5312. When citing a book, its title should be underlined. Example: B. Müller in A. Smith (Ed.): Chemistry, An Introduction, publisher, publisher's location and year of publication, page number.

4. Galley Proofs and Reprints

The author to whom correspondence should be addressed will receive two galley proofs of both the German and the English versions of an article; one copy of *each* version should be corrected and returned immediately together with the duly completed forms for ordering complimentary (30 for review articles, 25 for communications) and extra reprints.

Advanced Ceramics for Biomedical Applications

Bioinert Ceramics
Bioactive Ceramics
Glass and Oxide Ceramics
Implant Devices

By Günther Heimke*

1. Introduction

The broad exploration of the possible improvement of hard tissue replacements by the application of ceramic materials was initiated by *Hulbert*[1] and *Hench*[2] in the late 1960's. It was soon realized that, from the large number of ceramic materials, only a few have a combination of properties which made them reasonable candidates for uses in reconstructive surgery. These few have been grouped into two main categories according to the reactions they provoke in the surrounding bony tissue: The one does not or nearly not influence the adjacent tissue biochemically. Therefore, it was termed "bioinert". The materials in the other group were found to have a really fascinating ability; they can bond to living bony tissue in the sense of a gluing effect, but without the addition of an adhesive. They are called "bioactive" materials.

From the point of view of the introduction of these ceramics into medicine it might be called a happy coincidence that, at about the time these materials became available to implantology, some inadequacies of the previously used materials and material combinations were realized: In the mid 1960's, total hip replacements had become a standard treatment after the introduction of polymethylmethacrylate (PMMA) as the so-called bone cement.[3] By 1970, increased reoperations stimulated efforts to find the causes for the failures. In the early 1970's, it was widely agreed that the soft tissue layer, which separates the surface of the PMMA along most parts of the interface from the normally proliferating bony tissue, is the weakest link in this chain.[4] It was also recognized that polyethylene wear particles contributed, among other things, to a thickening of the soft tissue layer and, therefore, to implant loosening. In dentistry, a direct correlation exists between the thickness of the soft tissue interlayer, the mobility of the implant, the pocket depth of the gingiva surrounding the implant, and the probability of implant failure.[5] At that time, it was generally assumed that a basic cause for the formation of the soft tissue interlayer was the chemical instability of the materials used, mainly the stainless steels, cobalt-based alloys, and the PMMA. This instability resulted in solution products (metal ions or monomers) disturbing the highly sensitive differentiation processes necessary for undisturbed bone formation.

The particular type of ceramic biocompatibility raised hopes of avoiding such soft tissue interlayers and thereby achieving direct anchorage of implant devices. Soft tissue free implant fixation was termed osseo-integration. For joint replacements, the low friction and high wear resistance of alumina ceramics offered an additional advantage.

2. Bioinert Ceramics

The main representative of the bioinert materials is the high purity, high density alumina ceramic. Other oxide and mixed oxide ceramics have also been tested for their biological responses but were found only to approach the compatibility and the other favorable combination of properties of the alumina ceramic.[6, 7]

Soon after the early publications several groups extended and detailed the studies of these new materials in different directions: *Boutin*[8] immediately commenced clinical trials and, thus, was the first to insert a hip prosthesis containing an alumina ceramic component into humans, and *Griss* and *Heimke*, as summarized in a review,[9] began detailed studies of the tissue reactions and the possibilities for cement-free anchorage of hip joint components.

Their initial experiments, in which the test pieces were placed in the bony tissue under nearly load-free conditions, confirmed the high degree of tissue compatibility of high-purity alumina and the adequacy of the definition of the term "bioinert" given in Table 1. It was recognized that the reorganization of the bony tissue adjacent to an alumina implant follows exactly the same sequence of reactions characteristic of fracture healing. Further experi-

Table 1. The concept of a bioinert material.

Requirement	Result
"Nothing goes into solution": leakage of ions or other matter from the implant into the surrounding tissue below detectability by the cells and without any systemic effects	No biochemical influence on cell differentiation and proliferation No biochemical information to the cells about the presence of the implant
Strong and fast absorption of molecules contained in body fluent so that the surface of the implant is completely covered (coated) by the body's own matter	No enzyme reactions The implant is "camouflaged" against the host's immune system No foreign body reactions

[*] Prof. Dr. G. Heimke
Department of Bioengineering
Clemson University
301 Rhodes Eng. Res. Center
Clemson, SC 29634-0905 (USA)

ments with fully functional total hip replacements in sheep and dogs revealed the influence of an incompletely stable initial implant fixation and enabled the design criteria to be defined, allowing for a stable and reliable anchorage of the joint components in the adjacent bony tissue. Simultaneously, alumina wear particles were tested biologically as well as the carcinogenicity of this material.[9]

The essential biomechanical requirement for fracture healing is to avoid any shear motion along the interface. In addition to fracture healing, however, it was found that, for maintaining the close bone contact with such a bioinert prosthesis, it is essential to preserve this condition of motionlessness along the interface concerned for the entire lifetime of the prosthesis.

Basically, there are only two mechanical situations allowing for a motionless contact: the load-free situation and an orientation of the interface perpendicular to the forces acting along this interface. Thus, all load-bearing implants must present to the adjacent bony tissue sufficiently large interfaces that are transmitters of mostly pure pressure. Surfaces along which the forces are mainly transmitted parallel (resulting in shear along the interface) are separated by a soft tissue interlayer from the surrounding bone and therefore cannot contribute to osseo-integration and load transmission. Figure 1 summarizes this concept schematically. Clinical experience has shown that the requirement of perpendicularity of the forces meeting the interface allows for a deviation of up to $\approx 15°$.

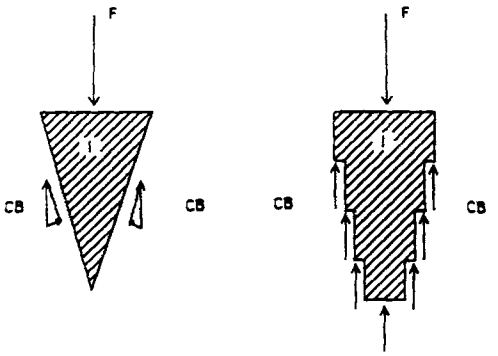


Fig. 1. Schematic representation of the shape dependence of the forces (F) acting along the interfaces of implants (I). Left: large tangential component resulting in shear along the interface; right: pure pressure at the surfaces of the steps, avoiding tangential movements along these surfaces (CB = cancellous bone).

The validity of the concept of the purely stress-and-strain-field controlled tissue reactions along the interface to implants of a bioinert material like Al_2O_3 ceramic was confirmed by the discovery of the "load-line-shadow effect" by *Büsing* et al.,[10] in 1979. The essentials of this effect are schematically described in Figure 2.

According to the previously described requirements for close bone contact, such contact could not be expected along mainly tangentially loaded interfaces such as the cylindrical surfaces of the Tübingen dental implants shown in Figure 3. However, evaluation of the tissue surrounding two implants, which had been in situ and functioning well for many years and which became available for inspection because of an accident the patient suffered, revealed a close bone apposition not only along the pressure transmitting interfaces (the surfaces of the steps connecting the cylinders of different diameters) but also along the cylindrical, mainly tangentially loaded areas. Because of the interlocking effect, due to the presence of the lacunae, and because of the much higher stiffness of the implant as compared with the surrounding, mostly cancellous bone,

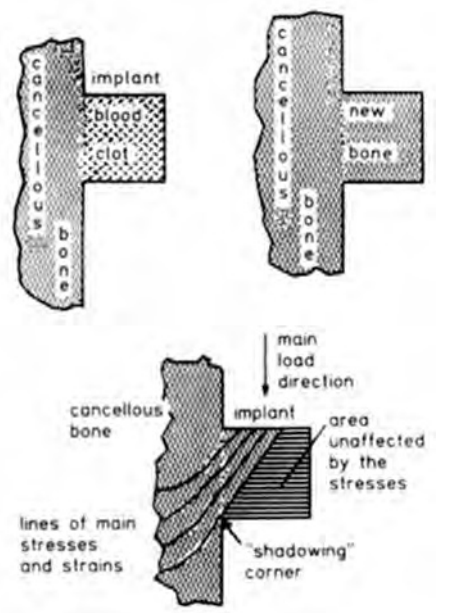


Fig. 2. The Load-Line-Shadow Effect. Top left: after press-fitting the implant, the lacunae are filled with a blood clot. Top right: during the healing-in phase the blood clot serves as a scaffold for new bone formation, filling the lacunae homogeneously. Bottom: After loading, the bony tissue reorganizes according to the stress and strain field present, resulting in an area of decalcification where no stresses are acting, the area which is "shadowed" from the load lines.

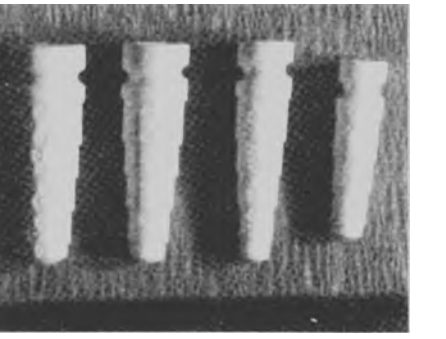


Fig. 3. Frialit Dental Implant, Tübingen type, made of medical grade alumina ceramic. Note the stepped shape of the intraosseous portion with lacunae along the cylindrical surfaces. The grooves parallel to the axis are for additional rotational stabilization. The circular groove around the coronal part is to accommodate the margin of the gingiva.

ADVANCED MATERIALS

the relative movements created by all load changes are accommodated by the elastic deformation of these bony structures some distance from the surface of the implant rather than by shear movements along the interface. Thus, an interdependence exists between the shape of the implant and the reactions of the bony tissue surrounding it. To achieve a stable and reliable osseo-integration, the shape of the implant must be chosen so that the stress and strain field created by its insertion allows for remodeling reactions resulting in a close bone contact along as many interfaces as possible.

3. Bioactive Ceramics

A fascinating bond formation was observed between bony tissue and some Ca-phosphate containing glasses and glass ceramics. It was studied in detail by *Hench* et al.[2] and *Blenke* et al.[11] Some time after the insertion into bony tissue, the formation of a silica rich zone along the interface was observed from which some sodium, calcium and phosphate ions had obviously leached out. It was hoped that this zone would act as a diffusion barrier, preventing the leaching out of these ions from continuing. The mechanical strength of the interface in tension or shear was tested after the animals were sacrificed; high forces were needed and the samples mostly ruptured inside the glass or the bone. This mechanically strong bond was found after a healing-in period during which the condition of motionlessness along the interfaces, as in fracture healing, was observed. It was maintained under loading conditions as long as the forces transmitted through the interfaces concerned were mainly perpendicularly oriented, as was the case in the early experiments of *Hench* et al.[2] Along mainly tangentially loaded interfaces, however, the bond could not be maintained reliably. It appears that the silica-rich layer is disturbed again and again by shear forces, resulting in a continuation of the leaching process.

A similarly strong attachment of bony tissue had been observed with some Ca-phosphate ceramics by the mid-1970's. The details of bonding, however, were found to be very different from the bond to the glasses. A summary of information gained after the first decade was given by *Jarchow*[12] and *de Groot*.[13] The main representatives of these bioactive ceramics are hydroxylapatite $Ca_{10}(PO_4)_6(OH)_2$, which, with some variations, is identical with the mineral phase of bony tissue and tricalciumphosphate $Ca_3(PO_4)_2$; this can, with some approximation, be regarded as the dehydrated version of hydroxylapatite. Both materials have been tested biologically in dense and porous versions.

If inserted into bony tissue, a layer of body deposited hydroxylapatite covers most of the implant surface relatively early during the healing-in period. The crystals immediately underneath appear to have lost much of their integrity; organic matter can be detected down to a depth of several crystal layers along grain boundaries.[14] In areas not in contact with bony tissue, the initial resorption processes which also precede the deposition of the bony layers do not cease. The influences of the chemical and phase compositions, crystal structure, and ceramic processing parameters on the tissue responses have been evaluated by several groups. Dense hydroxylapatite and tricalciumphosphate ceramics were found to be relatively stable in the bony environment; for the porous versions, different resorption rates have been found.

The present state of knowledge about the reactions of these bioactive materials in the body environment can be presented in the following three statements:

a) The initial flexural strength cannot be increased to much more than 100 MPa for the Ca-phosphate ceramics and to 200 MPa for the glasses.[15]
b) In the body environment the strength is reduced considerably by corrosion and fatigue.
c) The bond of bony tissue to dense hydroxylapatite can withstand several years of functional loading by shear forces.

4. Clinical Applications of Ceramics in Medicine

The low mechanical strength of the bioactive ceramics and its further reduction by fatigue excludes their uses in most of the load bearing applications. A clinical trial in which the low mechanical strength is believed to be compensated by pre-compressing the hydroxylapatite ceramic of cylindrical dental implants is, with some various after early failures from other reasons, still in progress.[13]

Many attempts have been made to compensate for the poor mechanical properties of these bioactive materials by coating them onto high strength substrates in order to use the bone bonding ability of the bioactive ceramics for the

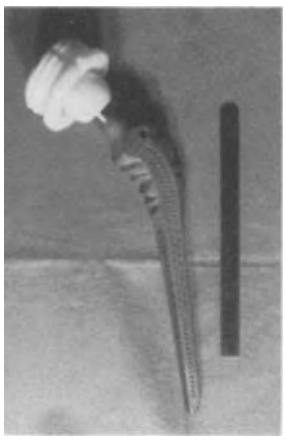


Fig. 4. Frialit Total Hip Replacement System: the cylindrical socket is made of the alumina ceramic as specified in the last column of Table 2. Its threads with asymmetrical cross section are designed for load transmission predominately by pressure. The BMO (biomechanically optimized) stepped stem is made of a TiAlFe alloy.

fixation of joint replacements and other load bearing implants. As the instability of the glasses and glass-ceramic under shear loading was already realized in the late 1970's, much hope concentrated on more or less dense hydroxylapatite coatings. However, here too, the lack of stability of this material in body environment is a fundamental problem, and all experts in this field agreed nearly unanimously during the 3rd World Biomaterials Congress in Kyoto, Japan, in April 1988 that even the best coatings of this kind will not last for more than about six years. They might contribute to the early healing process, but such coatings cannot replace mechanical fixation means like those shown in Figure 4 in long term implants.

The clinical applications of these bioactive materials are, therefore, confined to load-free or nearly load-free situations such as alveolar ridge augmentations, filling of periodontal defects, filling of cysts and other cavities, or corrections in the field of maxillofacial surgery.

The highly dense and pure alumina ceramic has been used in several high load-bearing applications for nearly two decades. No other ceramic has such a favorable combination of properties. The high-strength zirconia ceramics are multiphased, with at least one phase having reduced corrosion resistance. The essential properties of the medical-grade versions of the alumina material had been standardized during the 1970's (ISO 6474, ASTM F 603-83, DIN 58835). Extended clinical experiences have shown, however, that further improvements are necessary to extend the safety margin. The combination of properties that has been reached with a specially tailored material is shown in Table 2 and compared to the standard values.

Table 2. Properties of medical-grade alumina ceramics.

Property	Ceramic according to ISO 6474 ASTM F603-83 DIN 58835	Frialit Bioceramic
Density [g cm^{-3}]	> 3.9	> 3.98
Alumina content [%]	> 99.5	> 99.9
SiO_2 and alkali metal oxides [%]	< 0.1	< 0.05
Microstructure, average grain size [μm]	< 7	< 2.5
Microhardness [MPa]	23000	23000
Compressional strength [MPa]	4000	4000
Flexural strength [MPa]	> 400	> 450
Young's modulus [MPa]	380000	380000
Impact strength [cm MPa]	> 40	> 40
Wear resistance [mm^3 h^{-1}]	0.01	0.001
Corrosion resistance [mg m^{-2} d^{-1}]	< 0.1	< 0.1

4.1. Applications in Orthopedic Surgery

In orthopedic surgery the first ceramic implants whose design takes full account of the stress and strain field controlled bone reactions are the cylindrical sockets of the Frialit Total Hip Replacement system shown in the upper part of Figure 4. They are combined with a ball of the same ceramic fixed on a metal stem. Their clinical trial commenced in 1974. They have now stood the test of more than 14 years of clinical application. The first generation of these sockets and balls had been combined with metal stems which are still anchored with bone cement. Extended further animal experiments led to the design of stems with specially shaped steps and lacunae,[16] shown in the lower part of Figure 4. These stems are made of a vanadium-free high strength TiAlFe alloy tailor-made for medical applications.[17] This now completely cement-free implantable system has stood the test of more than six years of applications in many clinics.

One other hip replacement system with alumina ceramic sockets which also takes approximate account of the design rules mentioned above was introduced into clinical trials shortly afterwards. These ceramic sockets have also proved to be satisfactory.[18]

As already mentioned, some years earlier *Boutin* had commenced the application of alumina ceramic in hip surgery.[8] His design, however, closely followed the shape of plastic cups designed for cement fixation and did not take account of the design rules discussed above. Some years later *Chiari* et al. tested such sockets experimentally and *Plenk* found them to be separated from the bone by a soft tissue layer along most of the interface.[19]

Relatively early alumina ceramic implants were used in tumor surgery of the proximal femur and in the upper arm, but without convincing results.[20] Similarly, early attempts to introduce alumina ceramic components in knee surgery have not led to large scale applications.[21] Extended experiments with ceramic on ceramic articulating knee replacements never reached the state of clinical trials.[22] It was not until the introduction of total knee replacements with anchoring portions and femoral condyles of alumina ceramic and an articulating tibia plateau layer of polyethylene, and of ankle joints with a similar material combination, that ceramic components found clinical application in this part of the lower extremities.[23]

The discovery of a considerable reduction of the polyethylene wear debris in the combination of alumina ceramic balls with polyethylene sockets,[24] as compared to metal balls in the same application, led to large scale uses of this combination in Europe. Long term follow-up studies in many clinics have confirmed that this combination results in a reduction of the polyethylene wear debris by a factor of two.

4.2. Alumina Ceramics in Dentistry

The application of Degussit, a dense alumina ceramic, to dental implantology and other fields of medicine was suggested by *Sandhaus* as early as 1964.[25] The first ceramic dental implant system fully taking into account the remodeling ability of bony tissue was designed by *Schulte* and *Heimke* in 1975 and subsequently tested on a strictly

experimental basis with a detailed follow-up of each single implant. In 1977, following the presentation of the early, two years' results, eleven other clinics of the German speaking countries participated in this clinical study. In 1980 the results achieved were summarized in a special symposium. It was not until this survey was undertaken that these implants were made available to the dental practitioners. A detailed interim report has been prepared.[26]

This implant system (an example of such an implant is shown in Figure 3) allows immediate replacement of an extracted tooth, thus preventing the atrophy of the alveolar ridge with all its later difficulties. It can also be used as a so-called late implant in the already healed and even partially atrophied jaw. A variation of the original design takes special account of this application.[27]

Scientifically, all the different studies (e.g. histology) on retrieved implants, different types of mobility tests, and detailed studies of the gingival attachment either confirmed the initial design rules or, like the discovery of the load-line-shadow effect, even contributed to a more detailed understanding of the load-pattern-controlled tissue reactions around bioinert implants. In addition, the observation of full preservation of the shape of the alveolar ridge around such immediate implants after more than twelve years opens a new regime of dental care with the possibility of considerably improving public health.

A surprising point of view is also worth mentioning, amplifying the statement about dental care. From the definition of the term "bioinert" given in Table 1, mentioning the adsorption properties for body molecules, one would have expected a tendency for increased plaque formation with such ceramic implants. However, experience has shown beyond any doubt that the opposite is true: these implants cause much less plaque formation than metal implants or natural teeth.

The follow-up of all implants inserted in the Tübingen clinic (now more than 1000) has yielded more than one million items of data, which have been computerized and evaluated after five and ten years from all relevant points of view. The average success rate of these implants, if applied within their regime of indications, was 92.5% after five years, and remained so in the ten year analysis.[28]

Besides the *Sandhaus* implant already mentioned, there are other dental implant systems utilizing either alumina ceramic or alumina single crystals. None, however, meet the biomechanical requirements for osseo-integration of bioinert implants. Rather, all of them merely duplicate more or less the shape of the previous metallic implant designs. Therefore, many of these implants are separated from the surrounding bony tissue by soft tissue interlayers having different thicknesses. This soft interlayer, of course, results in implant mobility which, in turn, creates some mechanical irritation of the gingiva surrounding it and increases the probability of infection and implant loss.[5] There exists, however, no large-scale or long-term statistical evaluation on any of these implant systems.

4.3. Applications of Ceramics in ENT and Maxillofacial-Surgery

In the field of ears, nose and throat (ENT) surgery the transmission of forces is of minor importance for most of the large-scale applications. Thus, the bioactive ceramics have found some applications here.

Middle-ear implants of alumina ceramic replacing all or part of the ossicular chain (see Fig. 5) were tested and introduced clinically by *Plester* and *Jahnke*.[29] Almost simultaneously, *Reck*[30] evaluated a Ca-phosphate containing glass-ceramic for the same purpose and reported the formation of a thin bony membrane between the plate of these implants and the tympanic membrane. However, some concern exists about the building of a bony bridge between the bone around the oval window and the shaft of the implant because of its bioactivity. This same danger exists for hydroxylapatite implants suggested for this application.[31] The alumina and the glass ceramic ossicular chain replacements have now stood the test of up to nine years of clinical use.

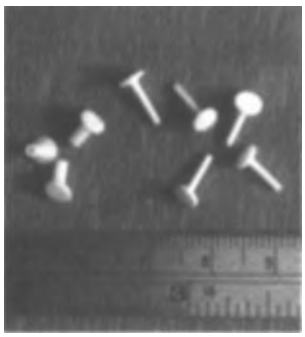


Fig. 5. Frialit middle ear implants of different shapes for easy adjustment to the individual situation.

Porous tricalciumphosphate ceramics were considered as filling material for different kinds of bone defects by many authors. *Zöllner* et al. used a relative stable material of this kind for the reconstruction of the mastoid and adjacent bone walls.[32] They confirmed the good bone bonding ability of this material, gave indications about its slow degradation, and demonstrated that such materials must not be used in positions immediately below the skin because of the danger of dehiscences.

The same group designed, tested clinically and introduced the alumina ceramic trachea supporting ring shown in Figure 6.[33] It is to replace the cartilage around the trachea if it has to be removed in tumor surgery.

Orbital support plates of alumina ceramic have been tested and clinically introduced by *Frenkel* et al. in the late 1970's.[34]

Many attempts have been made to improve the results of some branches of plastic surgery by the insertion of ceramic spacers. Examples are the attempts of *Swart* and *de*

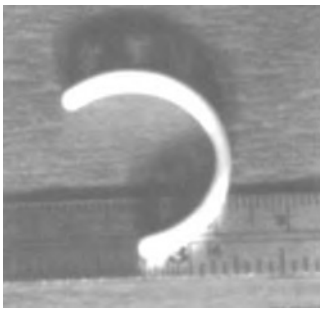


Fig. 6. Frialit trachea supporting ring.

Groot to change the jaw bone geometry with hydroxylapatite ceramic[35] and of *Wilson* with a bioactive glass.[36]

5. Final Remarks

Of all the ceramic materials considered for implant applications, only a few were found to meet the very severe requirements. The highly dense and pure alumina ceramic has stood the test of more than a decade of clinical use in different fields of surgery, and could eventually find large scale applications in several areas. Only one of the bioactive glasses has reached the state of routine application as ossicular chain replacement. Several Ca-phosphate ceramics have stood the test of nearly ten years of application in dentistry, in particular in alveolar ridge augmentations to improve the stabilization of total dentures.

In spite of the basic, still unsolved problem of its limited stability in the body environment, many attempts are still being made to elicit the favorable biological response to the Ca-phosphate ceramics for the fixation of bone replacements. Increasingly sophisticated composites and multilayer systems are being designed and tested. However, the more complicated the systems become, the higher the probability of failure and the greater the effort necessary to arrive at a well founded decision to commence clinical trials.

One more point needs to be considered: the present day success rates achieved with the already well established systems are to be regarded as the standard that any new system must surpass. Because one is dealing with humans, extremely strong evidence must exist and clearly indicate a high probability of a considerable improvement over existing systems before any clinical trial can be considered at all. Furthermore, any judgement about the success of an intended improvement cannot be given until at least five years of a closely controlled clinical series have been completed.

Received: October 26, 1988

[1] S. F. Hulbert, F. A. Young, R. A. Mathews, J. J. Klawitter, C. D. Talbert, F. H. Stelling, *J. Biomed. Mater. Res. 4* (1970) 433.
[2] L. L. Hench, R. J. Splinter, T. K. Greenlee, W. C. Allen, *J. Biomed. Mater. Res. Symp. 2* (1971) 117.
[3] J. Charnley, *Lancet* (1961) 1129.
[4] H. G. Willert, G. Puls, *Arch. Orthop. Unfall-Chir. 72* (1972) 33.
[5] H. Spiekermann in G. Heimke (Ed.): *Dental Implants*, Hanser, München 1980, p. 49.
[6] P. Griss, E. Werner, G. Heimke in G. W. Hastings, D. F. Williams (Eds.): *Mechanical Properties of Biomaterials*. Wiley, New York 1980, p. 217.
[7] H. A. McKellop, W. Phillips, I. C. Clark, H. C. Amstutz, *Trans. 10th Annu. Int. Biomater. Symp.*, Soc. for Biomater., San Antonio, TX, USA 1978, p. 153.
[8] P. Boutin, *Revue de chirurgie orthopédique et réparatrice de l'appareil moteur (Paris) 58* (1972) 229.
[9] P. Griss, G. Heimke in D. F. Williams (Ed.): *Biocompatibility of Clinical Materials*, CRC Press, Boca Raton, FL, USA 1981, p. 155.
[10] C. M. Büsing, G. Heimke, W. Schulte, W. Linn, *Der Pathologe 1* (1979) 61.
[11] B. A. Blenke, E. Pfeil, H. Brömer, *Z. Orthop. 112* (1974) 978.
[12] M. Jarchow, *Clin. Orthop. 157* (1981) 259.
[13] K. de Groot: *Bioceramics of Calcium Phosphate*, CRC Press, Boca Raton, FL, USA 1983.
[14] J. F. Osborn: *Implant Material Hydroxylapatite Ceramic. Basic Considerations and Clinical Applications*, Quintessenz-Verlags GmbH, Berlin 1985.
[15] T. Kokubo, S. Ito, M. Shigematsu, S. Sakka, T. Yamamuro, *J. Mater. Sci. 22* (1987) 4067.
[16] D. Stock, J. Gottstein, P. Griss, M. Winter, G. Heimke, C. M. Büsing, *Z. Orthop. 121* (1983) 640.
[17] J. Breme, G. Heimke in G. Lutjering, U. Zwicker, W. Bunk (Eds.): *Titanium. Science and Technology*, Dtsch. Ges. Metallkd. Oberursel 1985, p. 1351.
[18] H. Mittelmeier, *Med. Orthop. Tech. (MOT) 100* (1980) 19.
[19] H. Plenk in D. F. Williams (Ed.): *Biocompatibility of Orthopedic Implants*, CRC Press, Boca Raton, FL, USA 1982, p. 269.
[20] M. Slazer, K. Zweymüller, H. Locke, H. Plenk, G. Punzet, *Med. Orthop. Techn. 95* (1975) 40.
[21] W. Glien, G. Langer, P. Zinner, *Silikattechnik 28* (1977) 236.
[22] D. Geduldig, R. Lade, P. Prüssner, H. G. Willert, L. Zichner, E. Dörre in M. Schaldach, D. Hohmann (Eds.): *Artificial Hip and Knee Joint Technology*, Springer, Berlin 1976, p. 434.
[23] H. Oonishi, T. Hamaguchi, N. Okabe, T. Nabeshima, T. Hasegawa, Y. Kitamura, *Adv. Biomater. 5* (1983) 850.
[24] M. Semlitsch, M. Lehmann, H. Weber, E. Dörre, H.-G. Willert, *J. Biomed. Mater. Res. 11* (1977) 537.
[25] S. Sandhaus, Br. Pat. 1083769 (1967).
[26] W. Schulte, *Quintessence Int. 15* (1984) Report 226.
[27] G. H. Nentwig, *Die Quintessenz 36* (1985) Report 6772.
[28] B. d'Hoedt, D. Lukas, W. Schulte, *Dtsch. Zahnärztl. Z. 41* (1986) 1068.
[29] D. Plester, K. Jahnke, *Am. J. Otology 3* (1981) 104.
[30] R. Reck, *Clin. Otolaryngol. 6* (1981) 63.
[31] J. J. Grote in J. J. Grote (Ed.): *Biomaterials in Otology*, Martinus Nijhoff, The Hague 1984, p. 274.
[32] C. Zöllner, J. Strutz, C. Beck, C. M. Büsing in J. J. Grote (Ed.): *Biomaterials in Otology*, Martinus Nijhoff, The Hague 1984, p. 262.
[33] C. Zöllner, H. Weerda, J. Strutz, *Arch. Oto-Laryngology, Suppl. 1983/II* (1983) 214.
[34] R. Frenkel, J. Reuther, E. Dörre, *Dtsch. Z. Mund-Kiefer-Gesichts Chir. 4* (1980) 253.
[35] J. G. N. Swart, K. de Groot in G. Heimke (Ed.): *Dental Implants*, Hanser, München 1980, p. 97.
[36] J. Wilson, G. Merwin, L. Rodgers, D. Spilman in P. Christel, M. Meunier, A. J. C. Lee (Eds.): *Biological and Biomechanical Performance of Biomaterials*, Elsevier, Amsterdam 1986, p. 93.

Surface Chemistry with the Scanning Tunneling Microscope

Surface Imaging
Surface Spectroscopy
Surface Modification
Nanolithography

By Jürgen P. Rabe*

1. Introduction

The Scanning Tunneling Microscope (STM) is a new tool in surface science, which allows for a variety of very local investigations on a preselected area of the sample. Its essential feature is a fine tip which is brought into close proximity to the sample (gap ≤ 1 nm) and whose position normal as well as parallel to the surface is controlled very accurately on an atomic length scale, i.e. ≤ 0.1 nm. The particularly precise control of the normal coordinate is accomplished by the accurate measurement of the gap width by means of the electron tunneling current between tip and sample. With this original concept[1,2] semiconductor surfaces have been imaged in ultra high vacuum (UHV) with unprecedented resolution,[3-5] local work function images have been obtained,[6] and soon it was realized that one can also get important local electron spectroscopic information with the STM,[5,7-10] including, e.g., the superconducting energy gap.[11,12]

The requirements for a sample to be investigated are sufficient electrical conductivity, sufficient flatness, and limited mobility of surface atoms or molecules. There is no requirement for any degree of order, rendering the method applicable to the study of individual defects or, e.g., metallic glasses.[13] Important for the general applicability of STM to materials science and surface chemistry is the fact that the method itself does not require UHV. Indeed, atomic resolution images have been obtained in fluid environments such as cryogenic liquids,[14,15] air,[16] water[17] and electrolytes.[18] Also solvents, oils and even greases have been used.[19,20] The only condition is that neither the electrical conductivity nor the viscosity of the fluid is too large. The advantages of the fluid environment include protection of air sensitive materials like GaAs, increased stability of the tunneling gap and a higher experimentally accessible tip voltage range.[19] Moreover, surfaces can be imaged under chemically active solutions such as electroplating solutions[18] or etchants.[21]

The STM can, however, not only be used for the characterization of surfaces but with the same instrument one can also manipulate surfaces on a scale as small as subnanometers.[22-24] Of possible technological relevance in this context is nanolithography with the STM[25-27] and, possibly, even the ability to write and read information into and from single molecules.

Other types of imaging based on related concepts have also been introduced, having in common that a fine tip is scanned across the surface and some strongly distance dependent interaction is measured while scanning. Examples of these "Scanning Tip Microscopies" are Surface Potentiometry,[28,29] Atomic Force Microscopy[30] and Scanning Thermal Profilometry,[31] the latter two being also applicable to nonconducting surfaces. However, these methods will not be discussed here any further.

While most of the early STM work was performed on clean semiconductor surfaces in UHV, this field will only be briefly mentioned here. The interested reader is referred to other reviews[32-34] and the proceedings of the three International Conferences on Scanning Tunneling Microscopy.[35-37] Also the application of STM to nonconducting samples, either coated with an ultrathin conducting film[38-40] or replicated[41] will not be discussed in detail here. This review will, however, cover surface chemistry, imaging of organic molecules at surfaces and surface modifications with the STM.

2. The Method

Electron tunneling is a common phenomenon on the atomic scale, which allows electrons to penetrate into classically forbidden regions in space. The probability of finding an electron at increasing distances away from a nucleus decreases exponentially outside an atom. If one brings an atomically sharp metallic tip close (≤ 1 nm) to an electrically conducting surface a tunneling current will flow when a small potential difference (of the order of 1 V or less) is applied between the two. To a first approximation, the current depends exponentially on the gap width, decreasing by about one order of magnitude for every Ångstrom of increase in gap spacing. It is this very high sensitivity to the gap width which makes the tunneling current a suitable signal to control the gap by means of a feedback loop. The accuracy can be better than 0.01 nm.

If the tip is now scanned across the surface while the current is sensed, a topograph of the surface can be obtained in two ways. In the constant current mode[1,2] the tip height is adjusted with the feedback loop maintaining a constant current. The image is obtained as a map of the tip height $z(x, y)$ versus the lateral coordinates x and y (Fig. 1). Alternatively, in the constant height mode[42] the tip is

[*] Dr. J. P. Rabe
Max-Planck-Institut für Polymerforschung
Postfach 3148, D-6500 Mainz (FRG)

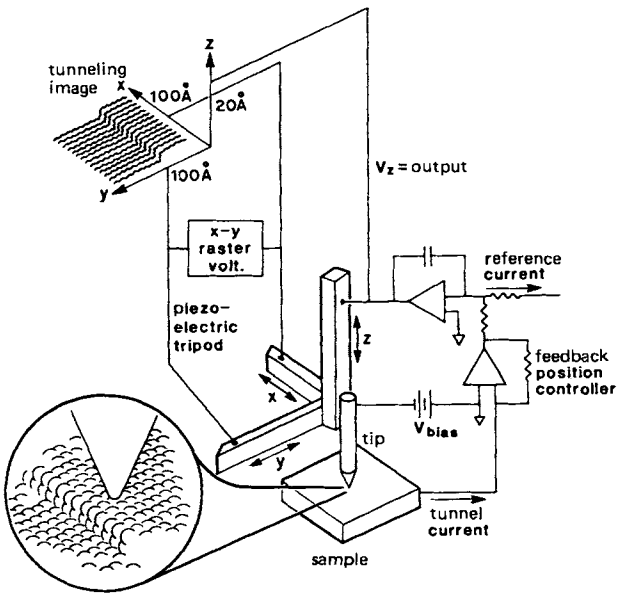


Fig. 1. Schematic illustration of the Scanning Tunneling Microscope [32]. The tunnel current from tip to sample, induced by V_{bias}, is maintained constant by an electronic feedback system (right), which controls the tip position normal to the sample surface via the z-leg of the piezoelectric tripod. A record of the z-leg feedback voltage, as the x-y tripod legs raster scan the tip laterally, constitutes a tunneling image, which is a form of replica of the sample surface (inset at bottom).

scanned at constant height and the current $I(x, y)$ is recorded as a function of x and y. In the latter case the limiting frequency of the feedback loop must be smaller than the frequency of current variations due to atomic structure. The feedback loop serves only to maintain the average current constant.

Common to all the published instrument designs are piezoelectric elements as x-, y- and z-translators. After the initially devised tripod[1,2] the simpler single tube[43] arrangement became widely used as a compact and fast scanner. Sample positioning, originally achieved with a piezoelectric walker ("louse")[1,2] has been simplified by differential springs, levers[44] or, elegantly, with a piezoelectric translator relying on the moment of inertia.[45] While external vibration isolation was essential in the earlier instruments, newer designs are often so small and rigid that it became less important or even obsolete.[46] Also the operating temperature range has been increased to extend from 4.2 K to 350 K.[11,46]

An essential feature of the STM is the tip. Different materials have been used, including W, Pt/Ir, Au and carbon. Also, tips have been prepared according to different procedures, e.g. mechanically ground or electrochemically etched. For use under liquid, they have been coated with glass or polymer, leaving only the last few microns bare. However, it appears that many results are fairly independent of the particular tip preparation recipe. On the other hand, since the formation of the outermost cluster of atoms on a macroscopic tip is usually not well controlled, some variation in instrumental resolution is observed even with equal tip preparation. Also the tip may change during scanning. In an attempt to obtain tips controlled to an atomic level, they have been reproducibly prepared and subsequently characterized in a field ion microscope.[47]

A theory of the STM[48,49] has been developed, based on the transfer Hamiltonian of *Bardeen*.[50] Assuming an ideal tunneling geometry (tip on flat) the tunneling current was found to be proportional to the local density of states (LDOS) of the surface at the center of curvature of the tip and at the Fermi energy. In the constant current mode the STM image then represents simply a contour of constant LDOS. In the usual case of an extended Fermi surface the image gives basically the contour of constant total charge density. In an attempt to determine how the LDOS is reflected in STM images the apparent size of an adsorbed atom has been studied as a function of bias for several different atoms.[51–53]

3. Conductor Surfaces

Gold was one of the first surfaces studied with the STM.[1,2,54–57] While the early studies in UHV revealed monoatomic steps and corrugation due to surface reconstructions, later also atomic corrugation of the close packed Au (111) surface was reported in both UHV and air.[58] Furthermore, hills on evaporated gold films, typically about 2 nm high, have been observed under a number of fluids, including glycerol, silicone- and paraffin-oil as well as several greases.[20]

The hexagonal reconstruction of Pt (100) has been imaged in UHV at terraces and domain boundaries.[59,60] Silver films on mica, exhibiting (111) surfaces, can be atomically flat across terraces several tens of in diameter. Atomic resolution images in air reveal, however, not the silver lattice but a larger lattice, possibly from a semiconducting surface layer of about monolayer thickness.[61]

While aluminum in air forms too insulating an oxide for STM imaging, niobium, on the other hand, forms a surface oxide layer which is sufficiently conducting for stable tunneling. Films prepared by vapor deposition at room temperature are fairly rough, but deposition at elevated substrate temperature gives considerably smoother films.[62]

Highly oriented pyrolytic graphite (HOPG) is a semimetal, which has been imaged at atomic resolution in UHV[63] and in a variety of fluids, e.g., air,[16] water,[17] electrolytes[18] and liquid helium.[15] It forms large (diameter ≈ 1 μm) atomically perfect, flat terraces, which are chemically inert; moreover, the spatial variation of the LDOS is very pronounced, resulting in high contrast images with a resolution of about 0.2 nm. However, attempts to use HOPG as a well characterized substrate to image monomolecular adsorbates on it with the STM suffered from its excessive inertness. In this context, defects may be of importance and have therefore been investigated in some de-

ADVANCED MATERIALS

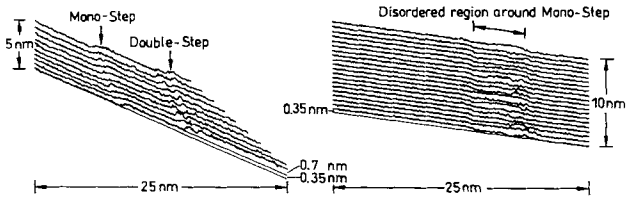


Fig. 2. STM images of mono- and bilayer steps on graphite in the constant current mode [64].

tail[64] (Fig. 2 and 3). Amorphous carbon, on the other hand, forms very flat films with grain sizes of the order of some nanometers[40,65] The problem of adhesion of adsorbates (e.g. a polymer) to graphite is also of interest in carbon fiber composites technology. Interestingly, carbon fiber surfaces can be imaged with the STM at atomic resolution.[64]

The first atomic resolution STM images were obtained on a silicon (111) surface in UHV with its 7×7 reconstruction ,[3] and it was also this surface which gave early electron spectroscopic results.[5,8-10] Experiments on freshly prepared silicon surfaces in air are, however, only possible for a limited time due to the formation of an insulating oxide surface layer.[66] In an attempt to avoid the oxide formation under ambient conditions a chemical preparation is required, which terminates dangling silicon bonds. For hydrogen terminated silicon atomically flat surfaces have been observed.[67] Other semiconductor surfaces investigated in detail include GaAs (110)[68] and, e.g., several low index faces of the group IV semiconductors Si, Ge and Sn.[69]

While direct local electron spectroscopic studies with the STM proved very successful in UHV, they appear more difficult in air or under liquids. Nevertheless, there also it is the electronic surface structure which is sensitively probed. An example of this is charge density waves in TaS_2. While STM images of native TaS_2 are dominated by a charge density wave state,[14,70] titanium doping systematically perturbs this electronic feature so that the surface structure can be imaged directly (Fig. 4).[71,72] It is expected that systematic studies of chemically modified surfaces will also lead to a better understanding of STM images.

Generally speaking, it appears easier to obtain atomic resolution images of semimetals or semiconductors than of simple metals. This has been attributed to the smeared-out electronic wavefunction in the case of metals

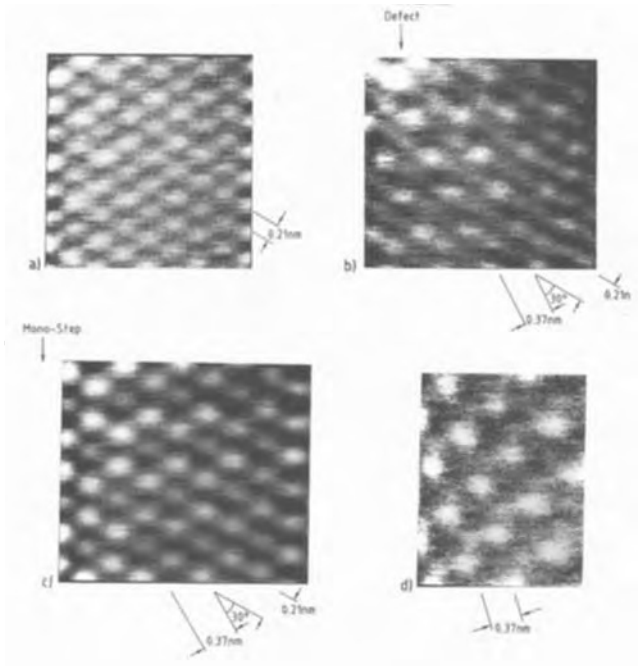


Fig. 3. STM images in the constant height mode [64]. a) Highly oriented pyrolytic graphite (HOPG). b) $\sqrt{3} \times \sqrt{3}$ R 30° superstructure near localized defect on graphite. c) Inverse $\sqrt{3} \times \sqrt{3}$ R 30° structure next to graphite step. d) $\sqrt{3} \times \sqrt{3}$ R 30° structure dominating STM image close to a defect. Intensity of superstructure relative to graphite image decays away from the defect over some 3 nm.

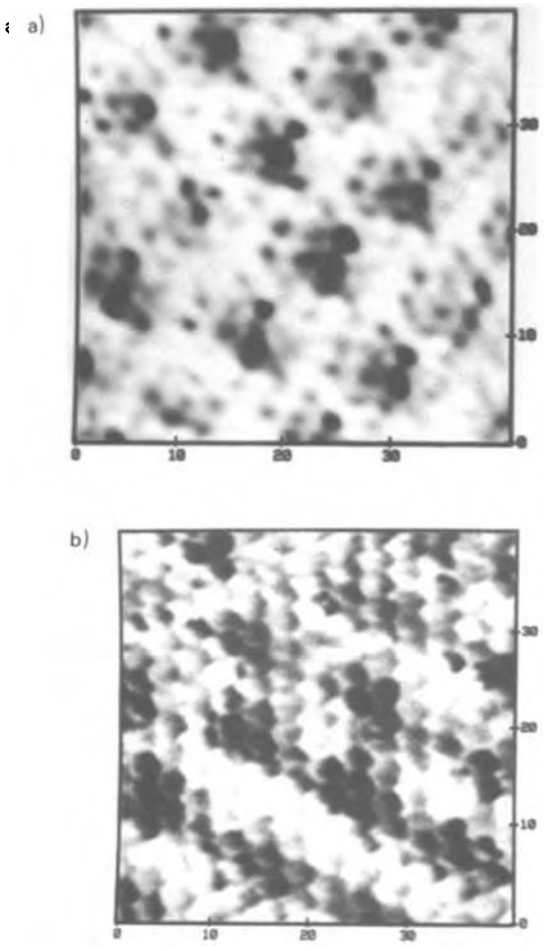


Fig. 4. Gray scale image of $Ti_xTa_{1-x}S_2$ recorded in the constant current mode [72]. The sample surfaces were covered with oil to improve the image stability. a) $x = 0.06$; The gray scale in this image (black minimum to white maximum) is 0.43 nm. b) $x = 0.1$; The gray scale in this image, 0.29 nm, is significantly smaller than in (a). The tip bias voltages are +8 mV and +9 mV, respectively, the tunneling current is 2.1 nA. x- and y-axes markings are in 0.1 nm.

and the large spatial variation of the LDOS of semiconductors, where higher contrast, higher resolution images and also more detailed spectroscopic information are obtained. In fact, the fairly high contrast in the atomic resolution images of the noble metals is difficult to interpret. Clearly, semiconductor surface studies in UHV have to date made by far the largest contribution of STM to high resolution microscopy and spectroscopy, partly since STM is well suited for these studies and partly since these surfaces had already been extensively investigated by other techniques.

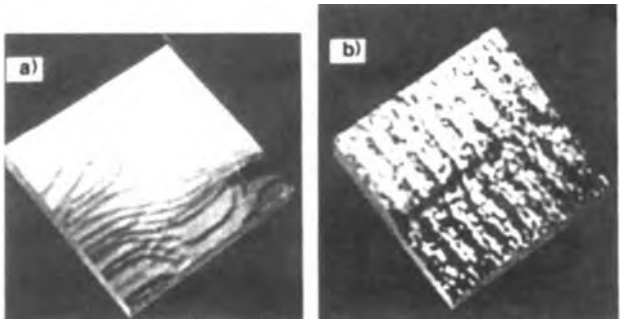


Fig. 5. STM images of the TTF-TCNQ surface [73]. a) A 200×200 nm^2 area. The surface is terraced, with steps approximately 1 nm high. b) A 10×10 nm^2 area in which rows of molecules are seen at a step.

The first molecularly resolved image of an organic conductor has been obtained on tetrathiafulvalene tetracyanoquinodimethane (TTF-TCNQ) crystals,[73] revealing monomolecular steps and the unit cell on the crystal surface (Fig. 5). Also some features in the STM image could be reproduced by simulations in which contours of constant electron density were calculated from the molecular orbitals that are involved in conduction (Fig. 6). These results suggest that the STM will also be a useful tool for the investigation of the electronic properties of organic conductors.

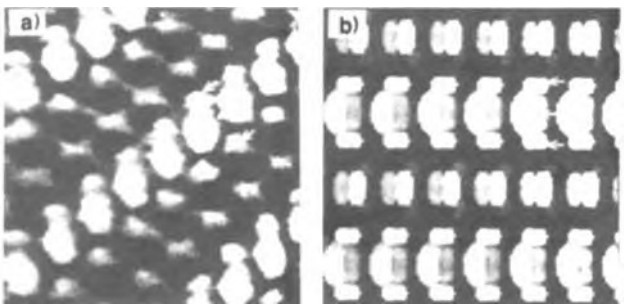


Fig. 6. Comparison of an experimental STM image and a theoretical simulation of the TTF-TCNQ surface [73]. a) A 2.5×2.5 nm^2 scan with a total height range of 0.9 nm. Lighter regions are higher. Arrows indicate a row of triplets of balls assigned to individual TCNQ molecules. b) A 2.5×2.5 nm^2 simulated image. Arrows indicate a row of TCNQ molecules along the *b* direction.

4. Organic Adsorbates

For an adsorbate to be imaged with the STM it is necessary that 1) the underlying substrate is sufficiently flat, 2) molecular mobility is not too high, and 3) the current through the molecule is sufficient. A number of atomically flat substrates such as graphite, suitably prepared gold and silver or silicon are available. However, the fact that some of these substrates can be imaged at atomic resolution in a variety of fluid environments indicates that in these cases the mobility of the environments adsorbates is too high for them to appear on the images in any way other than noise. On the other hand, adsorbates bonded chemically to a surface can be imaged. Moreover, their interaction with the substrate can be studied by imaging the electronic structure of the substrate close to the adsorbate. An example is the band bending around oxygen adsorbed on GaAs (110),[74] which reaches as far as 5 nm away from the adsorbate. Another example is a defect such as an adsorbate on graphite, which results in a superlattice appearing superimposed on the STM image of graphite and decaying away from the defect.[64, 75]

Clear examples of atom resolved surface chemistry are the imaging of chemical bond formation after adsorption of NH_3 on Si (001)[76] and a mapping of the reactivity of dangling bond states on Si (111)-(7 × 7).[77] For NH_3 as an adsorbate it was found that Si rest atoms are more reactive than Si adatoms and that center adatoms are more reactive than corner adatoms. Probing dangling bond states on both clean and NH_3-exposed surfaces revealed interactions and charge transfer between sites, influencing surface reactivity (Fig. 7).[77]

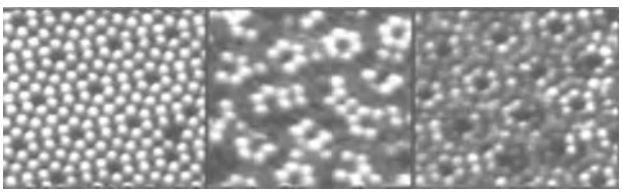


Fig. 7. Topographs [77] of the unoccupied states of a) a clean Si (111)-(7 × 7) surface (tip voltage = 0.8 V), b) partially reacted surface (tip voltage = 0.8 V), and c) partially reacted surface (tip voltage = 3.0 V).

Highly resolved images of organic adsorbates have been obtained on an ordered (3 × 3) superlattice of coadsorbed benzene and carbon monoxide on a rhodium (111) surface (Fig. 8).[78] While images on the close packed monolayer are very stable, for submonolayer coverage diffusion increases and it is observed that an individual molecule changes places during the STM scan of one image.

A similar situation is encountered for phthalocyanines on copper (100). While it appeared difficult to image a single phthalocyanine molecule on silver,[79] regular arrays of these molecules on Cu (100) could be observed and under

ADVANCED MATERIALS

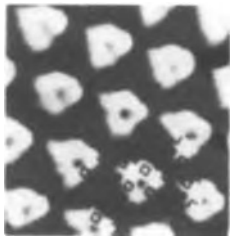


Fig. 8. STM image of an ordered (3 × 3) superlattice of coadsorbed benzene and carbon monoxide on rhodium (111) [78]. At tip voltage < 0.5 V a nominally threefold structure with a depression in the center is observed. According to the superimposed mesh based on the LEED model, the lobes appear to be localized between, rather than over, the underlying metal atoms.

some circumstances atomic scale features were observed, which agree well with Hückel molecular orbital calculations.[80] Attempts to image multilayers gave neither regular structures nor very high resolution, indicating that in this case the conductivity of the layer may be too small to allow for a nondestructive observation.

Studies on larger organic molecules have also been reported, including a whole single virus,[81] fatty acid salts,[82] lipid/protein membranes,[83] DNA,[84] several synthetic polymers such as phthalocyaninato-polysiloxane[64], poly-octadecylmethacrylate and poly-methylmethacrylate[85] and a liquid crystalline material,[86] all on graphite.

However, the interpretation of these experiments is difficult, since the tunneling distances are rather large and also the intrinsic conductivities often appear too small to explain the current densities used in the experiments. Here there may be significant surface conductivity due to adsorbed water and salts, which are always present in biological preparations. As a matter of fact, molecularly resolved images of macroscopically thick paraffin have been reported to be of varying quality, depending on the ambient humidity.[84] Another issue is the notoriously poor adhesion of adsorbates to graphite. While it may be enhanced around defects in the substrate, it is necessary to distinguish those defects carefully from an adsorbate.[64] It appears that this has not always been done. The interpretation is further complicated if one takes into account a deformation of the molecule during scanning.[87] In conclusion, while apparently several polymers have been imaged with the STM, clearly more work is necessary to understand the situation as well as in the case of the inorganic conductors.

5. Surface Modification with the STM

The STM setup also provides a means of modifying surfaces on an atomic scale and imaging the effect immediately afterwards. This is achieved by raising the tip voltage for a short time (e.g. 100 ns) to a value of the order of 4 V. However, the processes involved are not fully understood. For a germanium surface it was suggested that a transfer of tip material to the sample may occur.[22] For graphite immersed in an organic liquid (phthalates) it was argued that individual organic molecules had become selectively attached to the substrate.[23] On the other hand it was observed that similar modifications could be obtained without these specific molecules (Fig. 9).[24] For metallic glasses it has been suggested that local melting is responsible.[88] Though lithography on a nanometer scale has been shown to be possible,[25-27] more understanding is necessary to control the modifications better. This includes their dimensions as well as their stability, which, e.g. due to diffusion, can be limited to a time scale of hours.[24, 89]

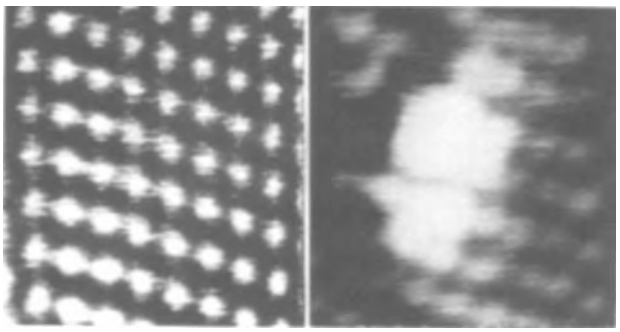


Fig. 9. STM images of highly oriented pyrolytic graphite (HOPG) in air in the constant height mode [24]. Tip voltage 100 mV, tunneling current 2 nA. Left: Atomic resolution image, representing for a flat terrace of about 1 μm diameter, before applying a voltage pulse. Right: Same area after applying a 100 ns pulse of 3.5 V. The surface has been modified on an area of about 0.5×1.0 nm^2.

6. Outlook

The STM is not only a microscope, local electron spectrometer and lithographer, it quite generally provides very locally injected low energy electrons for analytical or manipulative purposes. For example, the tunneling electrons can cause local excitations which then may decay radiatively. The corresponding light can be analyzed spectroscopically, leading to an optical spectroscopy with molecular spatial resolution.[90] Indeed, the STM appears to be close to what *R. P. Feynman* had asked for in 1960:[91] A machine, capable of storing and reading information on a small scale, say 100 atoms. Today it is envisioned that the miniaturization of computing may lead to a molecular electronics: single molecules acting as diodes, switches or molecular wires. Here the STM may provide the means to address the particular molecule.

Received: November 7, 1988

[1] G. Binnig, H. Rohrer, *Helv. Phys. Acta 55* (1982) 726.
[2] G. Binnig, H. Rohrer, C. Gerber, E. Weibel, *Phys. Rev. Lett. 49* (1982) 57.
[3] G. Binnig, H. Rohrer, C. Gerber, E. Weibel, *Phys. Rev. Lett. 50* (1983) 120.
[4] R. S. Becker, J. A. Golovchenko, E. G. McRae, B. S. Swartzentruber, *Phys. Rev. Lett. 55* (1985) 2028.

[5] R. M. Tromp, R. J. Hamers, J. E. Demuth, *Phys. Rev. B34* (1986) 1388.
[6] G. Binnig, H. Rohrer, *Surf. Sci. 126* (1983) 236.
[7] G. Binnig, K. H. Frank, H. Fuchs, N. Garcia, B. Reihl, H. Rohrer, F. Salvan, A. R. Williams, *Phys. Rev. Lett. 55* (1985) 991.
[8] R. S. Becker, J. A. Golovchenko, D. R. Hamann, B. S. Swartzentruber, *Phys. Rev. Lett. 55* (1985) 2032.
[9] R. S. Becker, J. A. Golovchenko, B. S. Swartzentruber, *Phys. Rev. Lett. 55* (1985) 987.
[10] R. J. Hamers, R. M. Tromp, J. E. Demuth, *Phys. Rev. Lett. 56* (1986) 1972.
[11] S. A. Elrod, A. L. de Lozanne, C. F. Quate, *Appl. Phys. Lett. 45* (1984) 1240.
[12] A. L. Lozanne, S. A. Elrod, C. F. Quate, *Phys. Rev. Lett. 54* (1985) 2433.
[13] R. Wiesendanger, M. Ringger, L. Rosenthaler, H. R. Hidber, P. Oelhafen, H. Rudin, H. J. Güntherodt, *Surf. Sci. 181* (1987) 46.
[14] R. V. Coleman, B. Drake, P. K. Hansma, C. G. Slough, *Phys. Rev. Lett. 55* (1985) 394.
[15] D. P. E. Smith, G. Binnig, *Rev. Sci. Instrum. 57* (1986) 2630.
[16] S. Park, C. F. Quate, *Appl. Phys. Lett. 48* (1986) 112.
[17] R. Sonnenfeld, P. K. Hansma, *Science (Washington) 232* (1986) 211.
[18] R. Sonnenfeld, B. C. Schardt, *Appl. Phys. Lett. 49* (1986) 1172.
[19] J. Schneir, P. K. Hansma, *Langmuir 3* (1987) 1025.
[20] B. Giambattista, W. W. McNairy, C. G. Slough, A. Johnson, L. D. Bell, R. V. Coleman, J. Schneir, R. Sonnenfeld, B. Drake, P. K. Hansma, *Proc. Natl. Acad. Sci. USA 84* (1987) 4671.
[21] R. Sonnenfeld, J. Schneir, B. Drake, P. K. Hansma, D. E. Aspnes, *Appl. Phys. Lett. 50* (1987) 1742.
[22] R. S. Becker, J. A. Golovchenko, B. S. Swartzentruber, *Nature (London) 235* (1987) 419.
[23] J. S. Foster, J. E. Frommer, P. C. Arnett, *Nature (London) 331* (1988) 324.
[24] J. P. Rabe, unpublished.
[25] M. Ringger, H. R. Hidber, R. Schlögl, P. Oelhafen, H. J. Güntherodt, *Appl. Phys. Lett. 46* (1985) 832.
[26] M. A. McCord, R. F. W. Pease, *J. Vac. Sci. Technol. B4* (1986) 86.
[27] M. A. McCord, R. F. W. Pease, *J. Vac. Sci. Technol. B6* (1988) 293.
[28] P. Muralt, D. W. Pohl, *Appl. Phys. Lett. 48* (1986) 514.
[29] J. R. Kirtley, S. Washburn, M. J. Brady, *Phys. Rev. Lett. 60* (1988) 1456.
[30] G. Binnig, C. F. Quate, C. Gerber, *Phys. Rev. Lett. 56* (1986) 930.
[31] C. C. Williams, H. K. Wickramsinghe, *Appl. Phys. Lett. 49* (1987) 1587.
[32] J. A. Golovchenko, *Science (Washington) 232* (1986) 48.
[33] G. Binnig, H. Rohrer, *Angew. Chem. 99* (1987) 622; *Angew. Chem. Int. Ed. Engl. 26* (1987) 606.
[34] P. K. Hansma, J. Tersoff, *J. Appl. Phys. 61* (1987) R1.
[35] Proc. 1st Int. Conf. Scanning Tunneling Microscopy, *Surf. Sci. 181* (1987).
[36] Proc. 2nd Int. Conf. Scanning Tunneling Microscopy, *J. Vac. Sci. Technol. A6* (1988) 257.
[37] Proc. 3rd Int. Conf. Scanning Tunneling Microscopy, *J. Microsc. (Oxford)*, in press.
[38] R. C. Jaklevic, L. Elie, W. Shen, J. T. Chen, *J. Vac. Sci. Technol. A6* (1988) 488.
[39] M. Amrein, A. Stasiak, H. Gross, E. Stoll, G. Travaglini, *Science (Washington) 240* (1988) 514.
[40] R. Guckenberger, C. Kösslinger, R. Gatz, H. Breu, N. Levai, W. Baumeister, *Ultramicroscopy 25* (1988) 111.
[41] J. A. N. Zasadzinski, J. Schneir, J. Gurley, V. Elings, P. K. Hansma, *Science (Washington) 239* (1988) 1013.
[42] A. Bryant, D. P. E. Smith, C. F. Quate, *Appl. Phys. Lett. 48* (1986) 832.
[43] G. Binnig, D. P. E. Smith, *Rev. Sci. Instrum. 57* (1986) 1688.
[44] J. E. Demuth, R. J. Hamers, R. M. Tromp, M. E. Welland, *J. Vac. Sci. Technol. A4* (1986) 1320.
[45] K. Besocke, *Surf. Sci. 181* (1987) 145.
[46] J. W. Lyding, S. Skala, J. S. Hubacek, R. Brockenbrough, G. Gammie, *Rev. Sci. Instrum.*, in press.
[47] H.-W. Fink, *IBM J. Res. Dev. 30* (1986) 460.
[48] J. Tersoff, D. R. Hamann, *Phys. Rev. Lett. 50* (1983) 1998.
[49] J. Tersoff, D. R. Hamann, *Phys. Rev. B31* (1985) 805.
[50] J. Bardeen, *Phys. Rev. Lett. 6* (1961) 57.
[51] N. D. Lang, *Phys. Rev. Lett. 56* (1986) 1164.
[52] N. D. Lang, *Phys. Rev. B34* (1986) 5947.
[53] N. D. Lang, *Phys. Rev. Lett. 58* (1987) 45.
[54] G. Binnig, H. Rohrer, C. Gerber, E. Weibel, *Surf. Sci. 131* (1983) L379.
[55] G. Binnig, H. Rohrer, C. Gerber, E. Stoll, *Surf. Sci. 144* (1984) 321.
[56] W. J. Kaiser, R. C. Jaklevic, *Surf. Sci. 181* (1987) 55.
[57] W. J. Kaiser, R. C. Jaklevic, *Surf. Sci. 182* (1987) L227.
[58] V. M. Hallmark, S. Chiang, J. F. Rabolt, J. D. Swalen, R. J. Wilson, *Phys. Rev. Lett. 59* (1987) 2879.
[59] R. J. Behm, W. Hoesler, E. Ritter, G. Binnig, *Phys. Rev. Lett. 56* (1986) 228.
[60] E. Ritter, R. J. Behm, G. Potsche, J. Wintterlin, *Surf. Sci. 181* (1987) 403.
[61] J. P. Rabe, H. Fuchs, unpublished.
[62] D. G. Walmsley, R. J. Turner, H. P. Hagan, N. Garcia, A. Baró, L. Vazquez, R. Paganini, *J. Vac. Sci. Technol. A6* (1988) 404.
[63] G. Binnig, H. Fuchs, C. Gerber, H. Rohrer, E. Stoll, E. Tosatti, *Europhys. Lett. 1* (1986) 31.
[64] J. P. Rabe, M. Sano, D. Batchelder, A. A. Kalatchev, *J. Microsc. (Oxford) 152* (1988) in press.
[65] A. Stemmer, A. Engel, R. Häring, R. Reichelt, U. Aebi, *Ultramicroscopy 25* (1988) 171.
[66] K. H. Besocke, M. Teske, J. Frohn, *J. Vac. Sci. Technol. A6* (1988) 408.
[67] W. J. Kaiser, L. D. Bell, M. H. Hecht, F. J. Grunthaner, *J. Vac. Sci. Technol. A6* (1988) 519.
[68] R. M. Feenstra, J. A. Stroscio, J. Tersoff, A. P. Fein, *Phys. Rev. Lett. 58* (1987) 1192.
[69] R. S. Becker, B. S. Swartzentruber, J. S. Vickers, *J. Vac. Sci. Technol. A6* (1988) 472.
[70] C. G. Slough, W. W. McNairy, R. V. Coleman, B. Drake, P. K. Hansma, *Phys. Rev. B34* (1986) 994.
[71] X.-L. Wu, C. M. Lieber, *J. Am. Chem. Soc. 110* (1988) 5200.
[72] X.-L. Wu, P. Zhou, C. M. Lieber, *Nature (London) 335* (1988) 55.
[73] T. Sleator, R. Tycko, *Phys. Rev. Lett. 60* (1988) 1418.
[74] J. A. Stroscio, R. M. Feenstra, A. P. Fein, *Phys. Rev. Lett. 58* (1987) 1668.
[75] H. Mizes, J. S. Foster, unpublished.
[76] R. J. Hamers, Ph. Avouris, F. Boszo, *Phys. Rev. Lett. 59* (1987) 2071.
[77] R. Wolkow, Ph. Avouris, *Phys. Rev. Lett. 60* (1988) 1049.
[78] H. Ohtani, R. J. Wilson, S. Chiang, C. M. Mate, *Phys. Rev. Lett. 60* (1988) 2398.
[79] J. K. Gimzewski, E. Stoll, R. R. Schlittler, *Surf. Sci. 181* (1987) 267.
[80] P. H. Lippel, R. J. Wilson, M. D. Miller, Ch. Wöll, S. Chiang, unpublished.
[81] A. M. Baró, R. Miranda, J. Alaman, N. Garcia, G. Binnig, H. Rohrer, C. Gerber, J. L. Carrascosa, *Nature (London) 315* (1985) 253.
[82] D. P. E. Smith, A. Bryant, C. F. Quate, J. P. Rabe, C. Gerber, J. D. Swalen, *Proc. Natl. Acad. Sci. USA 84* (1987) 969.
[83] J. K. H. Hörber, C. A. Lang, T. W. Hänsch, W. M. Heckl, M. Möhwald, *Chem. Phys. Lett. 145* (1988) 151.
[84] M. Amrein, G. Travaglini, R. Dürr, A. Stasiak, H. Gross, H. Rohrer, *3rd Int. Conf. Scanning Tunneling Microscopy*, Oxford 1988.
[85] T. R. Albrecht, M. M. Dovek, C. A. Lang, P. Grütter, C. F. Quate, S. W. J. Kuan, C. W. Frank, R. F. W. Pease, *J. Appl. Phys. 64* (1988) 1178.
[86] J. S. Foster, J. E. Frommer, *Nature (London) 333* (1988) 542.
[87] S. M. Lindsay, T. Thundat, L. A. Nagahara, *J. Microsc. (Oxford)*, in press.
[88] U. Staufer, R. Wiesendanger, L. Eng, L. Rosenthaler, H.-R. Hidber, H.-J. Güntherodt, *J. Vac. Sci. Technol. A6* (1988) 537.
[89] J. Schneir, O. Marti, G. Remmers, D. Gläser, R. Sonnenfeld, B. Drake, P. K. Hansma, *J. Vac. Sci. Technol. A6* (1988) 283.
[90] J. H. Coombs, J. K. Gimzewski, B. Reihl, J. K. Sass, R. R. Schlittler, *J. Microsc. (Oxford)*, in press.
[91] R. P. Feynman, *Engin. Sci. 1960*, February issue, p. 22.

Research News

Aluminum-rich Metallic Glasses

An enormous variety of metallic liquid solutions have been converted by rapid quenching from the melt into metallic glasses. They fall into two large groupings: (1) M + m, where M is a metal and m a metalloid, and (2) M + M', where only metals are present. In both categories, one or both M's most commonly are transition metals. Group-1 glasses often contain two or more distinct metalloids, whereas up to now studies of group-2 glasses have been restricted to binary systems. The total solute content has rarely been less than 15 at.%, and ≈20 at.% is more common.

Of the many hundreds of alloy systems in which melt-quenched metallic glasses have been recorded since the sport was invented in 1959, none include aluminum, although a few instances have been recorded of *partial* vitrification of rapidly quenched aluminum melts containing Si, Ge, Cu, Ni, Cr or Pd as solute—i.e., a small amount of glassy phase coexisted with a larger amount of metastable crystalline phase. Aluminum has always been regarded as a solvent inimical to glass formation.

It is therefore an occasion for surprise that within a few months, two teams in different countries, working quite independently of each other, have discovered similar families of aluminum-rich alloys that can be completely vitrified by rapid quenching from the melt. *Inoue, Ohtera, Tsai* and *Masumoto* in Sendai, Japan, were the first to publish;[1] they were followed five months later by *He, Poon* and *Shiflet*[2] in Charlottesville, Virginia. Both teams used single-roller melt-spinning (the most usual method used for research purposes nowadays): in this technique, a jet of molten alloy is directed at an angle at the circumference of a rapidly spinning copper wheel, and a narrow quenched ribbon is generated. In thework discussed here, the ribbons were 15–30 μm thick and 1–2 mm wide.

The two groups both made glasses always containing *two* solutes, one being a rare earth metal and the other a transition metal. The Japanese effort was entirely concentrated on the Al-Y-Ni system: the investigators found that *both* solutes were necessary to make a glass. Figure 1 shows the range of compositions in this system which gave fully amorphous ribbons: one Al-Y-Ni alloy examined by the American investigators is also included in this figure (in the lower left part). The Americans also studied a variety of other ternary aluminum alloys, in all of which the solutes were combinations of a rare earth and a transition metal. these included individual compositions in the Al-Ce-Fe, Al-Gd-Fe, Al-Ce-Ni, Al-Ce-Co, Al-Y-Co, Al-Ce-Rh and Al-Y-Ni systems. All of these had total solute contents of only 10–13 at.%, and it is noteworthy that the most interesting mechanical properties in the American study were found for the most dilute alloy, $Al_{90}Ce_5Fe_5$.

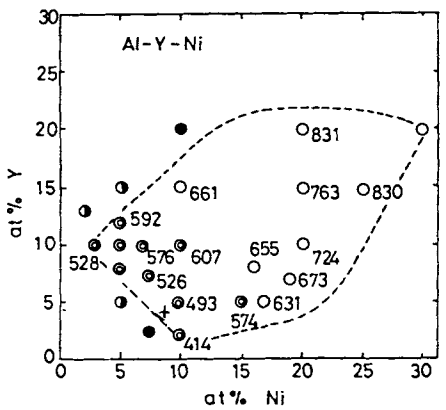


Fig. 1. Compositional range of melt-spun Al-Y-Ni alloys: ◎ amorphous, ductile; ○ amorphous, brittle; ◑ amorphous plus crystalline; ● crystalline. The numbers give the crystallization temperatures [°C] (from reference [1]). The cross in the lower left part gives a composition of an amorphous Al-Y-Ni alloy found by *He* et al. [2].

None of the numerous theoretical criteria which have been proposed to interpret glass-forming ability (GFA) of different alloy combinations and compositions[3] will help us here: for some of them (e.g., a criterion based upon the volume change on melting) we lack the experimental information that would enable us to check their applicability; for others we are faced by the difficulty that the criteria are applicable only to binary alloys. However, a very recent study[4] from the Virginia group, on Al-Fe-Gd glasses, has established that there is no deep eutectic anywhere in the glass-forming region and that the reduced glass-forming temperatures, $T_r > T_x/T_m$ (where T_x, T_m are crystallization and melting temperatures, respectively) are abnormally high (0.65–0.70); the reason is unknown. High T_r always favors glass formation, but the normal route to a high T_r is via depression of T_m at deep eutectics. These glasses, therefore, are anomalous.

The most thoroughly researched criterion for high GFA is undoubtedly the degree of mismatch in atomic size between solvent andsolute, and this criterion also appears to have the widest applicability.[3] For binary alloys, this criterion was studied in great detail by *Egami* and *Waseda*,[5] who established a functional relationship between the disparity in atomic volumes and the minimum solute concentration needed for a glass to be made in that alloy system: the larger the disparity, the smaller the minimum solute concentration needed. This quantified the well established

principle that crystallization of a melt is inhibited if it contains atoms differing widely in size.

Egami and *Waseda*'s analysis is not directly applicable to ternary alloys, but it is interesting to note that the rare earth solute atoms are always larger than the aluminum solvent, while the transition metal atoms are smaller. By way of example, atomic volumes for two of the new aluminum glasses (in Å^3) are: Al 16.6, Ce 34.4, Fe 11.8;—,Y 33.0, Ni 10.9. The implication is that a mixture of small and large solute atoms is particularly favorable for stabilizing a liquid/amorphous structure and discouraging crystallization. This conclusion is consistent with one of the few earlier studies that looked systematically at ternary glasses: *Ohnuma* et al.[6] examined a range of Co-B-TM alloys, where various transition metals were partially substituted for boron. It was found that the total solute content needed to achieve vitrification was the smaller, the larger the size of the transition metal atom: in general, the larger the disparity between the size of the solvent (cobalt) atom and the sizes of the (larger) transition metal and (smaller) boron solutes, the easier it was to make a glass.

The practical interest of the new glasses lies in their strength. *He* et al. found tensile strengths in the range 670–940 MPa, while *Inoue* et al. reported values in the range 730–1140 MPa for various compositions in their single alloy system. These strengths greatly exceed the strengths of even the best precipitation-hardened crystalline aluminum alloys (300–500 MPa) and the possibility of using ribbons of some of the new alloys as reinforcing fibers in composites at once presents itself. Advantages include in particular the low density of the fibers, their ductility which offers the prospect of enhanced intrinsic ductility in composites incorporating them, as well as good corrosion resistance. Drawbacks include a relatively low Young's modulus (up to 71 GPa), somewhat lower than for crystalline aluminum alloys, and rather low crystallization temperatures, 250–370°C for the compositions of greatest interest. However, this is still higher than the limiting temperature of use for organic fibers such as Kevlar.—The *Wall Street Journal* for October 6 carried a report of an interview with a staff scientist of Allied-Signal Corporation which is the principal commercial manufacturer of metallic glasses. This scientist very reasonably doubted whether the new glasses could be used as massive constructional materials, but made no reference to use in composites. The Virginia authors, also interviewed, expressed the belief that the aluminum glasses have a rosy future in the aerospace industry.

Research on metallic glasses, which excited a steadily high level of interest during the 1970s and early 1980s,[7] has shown signs of abating recently. Perhaps the new aluminum glasses will inject a new vitality into this field: certainly many questions related to the formation, properties and crystallization of these glasses deserve to be addressed.

Robert W. Cahn
Department of Materials Science and Metallurgy
University of Cambridge (UK)

[1] A. Inoue, K. Ohtera, A.-P. Tsai, T. Masumoto, *Jpn. J. Appl. Physics 27* (1988) L479.
[2] Y. He, S. J. Poon, G. J. Shiflet, *Science (Washington) 241* (1988) 1640.
[3] R. W. Cahn in P. R. Sahm, H. Jones, C. M. Adams (Eds.): *Science and Technology of the Undercooled Melt*, Martinus Nijhoff, Dordrecht 1986, p. 73–87.
[4] Y. He, S. J. Poon, G. J. Shiflet, *Scr. Metall. 22* (1988) 1813.
[5] T. Egami, Y. Waseda, *J. Non-Cryst. Solids 64* (1984) 113.
[6] S. Ohnuma, J. Kanehira, K. Shirakawa, T. Egami, T. Masumoto in T. Masumoto, K. Suzuki (Eds.): *Rapidly Quenched Metals (Proc. 4th Int. Conf., 1982)* Japan Institute of Metals, Sendai, Vol. 2, p. 1047.
[7] F. E. Luborsky (Ed.): *Amorphous Metallic Alloys*, Butterworths, London 1983.

Conference Reports

High-Temperature Superconductors in Strasbourg ...

The symposium on preparation and applications of high-temperature superconductors at the European Materials Research Society (E-MRS) conference on November 8–10, 1988 in Strasbourg, France attracted more than 200 scientists from Europe and overseas. Thirty-eight lectures, 15 of which were invited, and over 100 posters were presented in ten sessions. Most presentations discussed the structure of $YBa_2Cu_3O_7$ and Bi- and Tl-based superconductors, including the effect of substitutions and impurities. Other areas of interest were the preparation and characterization of thin film superconductors as well as bulk and thin film properties and their measurement by a variety of techniques such as X-ray photoelectron spectroscopy, Raman spectroscopy, nuclear magnetic resonance, etc. In addition, practical applications such as a Meissner-Ochsenfeld motor constructed by AEG engineers were presented during one of the two poster sessions.

A new phase in the Y-Ba-Cu-O system, namely $Y_2Ba_4Cu_8O_{16}$, which was reported at the Interlaken meeting earlier this year to be present in some thin films, can

now be prepared in bulk form, as *E. Kaldis* (ETH Zürich) explained during his presentation. This so-called 248-phase has a T_c of 80 K. The critical current density is comparable to that in the 123-phase, but the 248-phase shows a significantly improved oxygen stability.

A number of presentations discussed the preparation and properties of Bi-Sr-Ca-Cu-O and Tl-Ba-Ca-Cu-O superconductors. In both systems two superconducting phases with $T_c > 77$ K exist. While in the Tl-system it is possible to isolate the high-T_c and low-T_c phases, this is not so in the Bi-based system. The formation of the low-T_c phase apparently proceeds much faster here than the high-T_c phase. Larger fractions of the high-T_c phase are observed after reaction times of 50 to 100 hours, while the low-T_c phase appears after only a few hours of sintering. In several presentations the stabilizing effect of Pb doping on the high-T_c phase in Bi-Sr-Ca-Cu-O was discussed. From X-ray spectra it would appear that the Pb enters the structure on the Bi sites, as *S. Amelinckx* (Univ. of Antwerp) reported. Other dopants, e.g. Nd, Sm or Gd, seem to reduce the amount of high-T_c phase in the Bi-Sr-La-Cu-O system, as shown on a poster by *M. Raveau* et al. (Univ. of Caen).

H. J. Scheel (Univ. of Geneva) summarized the activities on crystal growth of oxide superconductors. Impurities at a level as low as 0.1 wt.% interfere significantly with crystal growth, so the starting materials should be at least of 99.99% purity. Even though many groups are working on crystal growth of high-T_c superconductors, there are still no large untwinned single crystals of good quality available. One reason for this is insufficient knowledge of the phase diagrams under certain conditions, such as oxygen partial pressure, CO_2 content, etc. Even at this symposium dominated by materials scientists, a conspicuous lack of phase equilibria studies was apparent.

While the current carrying capability in sintered bulk high-T_c superconductors remains a problem because of small coherence lengths, anisotropy and granularity (*R. Flükiger*, Kernforschungszentrum Karlsruhe), the situation with thin film superconductors looks more promising. A large number of groups presented papers on the preparation and characterization of high-T_c superconducting thin films. A wide variety of methods, such as sputtering, thermal- and laser-evaporation, molecular beam epitaxy, etc., were employed to produce superconducting films, and a general distinction was made between in-situ processing and post-anneal processing. In-situ processing takes place in the presence of activated oxygen at relatively high pressures during deposition. Post-anneal processing requires additional oxygen annealing to crystallize the films following deposition. The primary advantage of in-situ processing over post-anneal processing, in addition to the fact that no additional oxygen annealing is necessary, is the lower substrate temperature (500 to 700 °C as compared to 800 to 900 °C, respectively), which helps to avoid film-substrate reactions. A further problem with films made by post-anneal processing is their high surface roughness which makes electronic applications of these films difficult or impossible (*A. Kapitulnik*, Stanford Univ.). An interesting approach was presented by *H.-U. Habermeier* (Max-Planck-Institut für Festkörperforschung, Stuttgart). He exposed his films to an oxygen plasma during deposition as an alternative to furnace annealing and showed it to be an excellent tool to restore the oxygen content of the films, even at temperatures as low as 300 °C. The most commonly used substrates were single crystalline $SrTiO_3$ and MgO, but also films deposited on yttria-stabilized zirconia, Al_2O_3, sapphire, $LiNbO_3$, and Si were discussed. In view of potential applications, in particular applications in connection with semiconductor devices, these substrates are of primary interest.

In conclusion, there were no sensational reports, and no spectacular new T_c records were announced; the fax machine in the conference office certainly did not run hot as it did at the Interlaken meeting at the beginning of the year. However, this does not mean that no progress was made in the field of high-T_c superconductors, only that the hectic phase of the research and development disappeared —at least for the time being. The dust of previous stampedes towards higher T_c has settled to make room for serious, systematic work towards a more complete understanding of these novel materials.

... and Colorado Springs

After the conference on Critical Currents in High-T_c Superconductors held in Snowmass Village in August of last year, Colorado was, once again, the site of a major superconductivity conference. This time it was the Conference on the Science and Technology of Thin Film Superconductors that took place on November 14–18, 1988 in Colorado Springs, Colorado, USA. Over 200 scientists and engineers from around the world attended this conference, which was organized by the U. S. Department of Energy (DOE), the Solar Energy Research Institute (SERI), the National Institute of Standards and Technology (NIST) (formerly National Bureau of Standards, NBS), The Naval Research Laboratory (NRL), and the Lawrence Berkeley Laboratory (LBL). Thirty-six invited and contributed papers, and more than 40 posters were presented on thin film deposition techniques, characterization, theory, device design and ap-

plications as well as bulk material studies related to thin films. In addition to the technical presentations, a set of short courses was offered during the first day of the conference to bring the audience up to date with current research in the area. The courses, organized by Lawrence Berkeley Laboratory's Superconductivity Research Center for Thin Film Applications, were given by such prominent scientists as *S. Wolf* (NRL), *J. R. Kwo* (AT&T Bell Labs.), *J. Clarke* (UC Berkeley), and others. The topics ranged from an introduction to superconductivity, through fabrication and characterization of superconducting thin films, to superconducting electronics applications. These short courses were quite a success, since they offered the scientists involved in the preparation of films some insight into the problems engineers encounter when designing devices based on these films.

The technical presentations started off with representatives of DOE, NRL, and NIST giving overviews of the activities at their respective government agencies. Especially impressive was the budget increase for basic energy science at the DOE from \$ 12.4 million in the fiscal year 1987 to \$ 36.7 million in 1989.

Presentations during the first two days of the conference focused on film preparation and characterization. Among methods commonly used to deposit superconducting films were thermal and electron beam co-evaporation, laser ablation, dc- and magnetron sputtering, including multitarget sputtering, molecular beam epitaxy (MBE), metalorganic chemical vapor deposition, etc. A much discussed preparation technique was the laser ablation or laser enhanced deposition technique. A pulsed excimer laser beam is directed on a target mounted in a vacuum chamber under the heated substrate. The emitted atoms or molecules from the target collect on the substrate and form the film. Laser fluxes in the range of 0.1 to 5 J cm^{-2} were reported. The advantage of this method is quite obvious: a relatively simple arrangement is sufficient to produce films of 0.1 μm thickness in only a few minutes. The not very uniform coverage of the substrate by this method is an inherent problem which could be overcome, e.g. by a scanning set-up or a similar technique. A post-deposit oxygen annealing step can be avoided by plasma-assisted laser deposition, as *H. S. Kwok* (State Univ. of New York (SUNY), Buffalo) reported. The plasma between target and substrate is produced by a low pressure dc oxygen discharge. In addition to being a "one-step" process, this method is compatible with semiconductor processing since substrate temperatures as low as 400°C are sufficient. *J. R. Kwo* (AT&T Bell Labs.) used her MBE apparatus with a reactive oxygen species excited by a microwave plasma contained in a flow tube reactor. In this case, the substrate temperature was 550°C. *R. H. Hammond* (Stanford Univ.) also used a microwave cavity to produce atomic oxygen during film deposition. Using an oxygen partial pressure versus temperature diagram determined by *R. Bormann* (Univ. of Göttingen), he compared the film deposition and cooling conditions which he used with the data published by other groups.

Preparation of superconducting thin films made by a new method, electron beam flash evaporation, was discussed during the short courses as well as in several talks and posters. As with the laser ablation method, the flash evaporation process convinces by its simple approach. Small pellets (approx. 0.2–0.5 g) of the oxide components are evaporated to completion by a high-intensity electron beam from a water cooled copper hearth. It takes 30 to 40 s to completely evaporate a 0.3 g pellet, as reported by *P. R. Broussard* (NRL), and depending on the experimental set-up, the evaporation of one pellet results in a film thickness contribution of about 20 nm according to the information on the poster of *M. F. Davis* et al. (Univ. of Houston). No deposition-rate measuring schemes and complex feed-back circuits are required for this method. The stoichiometry of the films is very close to that of the pellet, even when large substrates are coated. The method has been used successfully for the preparation of both $YBa_2Cu_3O_x$ and $Bi_2Sr_2CaCu_2O_y$ superconducting films. Best results were obtained with Bi-based films deposited on MgO substrates, showing zero resistance critical temperatures of 85 K after short post-deposition annealing at 865°C in oxygen. Reproducibility of the films varies considerably among the different groups and the methods employed. Very reproducible films, however, resulted from the so-called "BaF_2 process", first used by *P. M. Mankiewich* (AT&T Bell Labs.). In this process, metallic Y and Cu together with BaF_2 are co-deposited in the presence of oxygen. The films are amorphous and insulating. Post-deposition annealing in wet oxygen is required to convert the films into superconductors with critical temperatures near 90 K. Even though post-deposition annealing is necessary to obtain superconductive films, these films are highly reproducible and are very robust and generally withstand the rough treatments with water and solvents during lift-off lithography. Many researchers reported on efforts to produce films by a one-step or in-situ process, i.e. a deposition procedure not requiring post-deposition oxygen annealing to produce a superconducting film. Common to all reported procedures are the relatively low substrate temperatures of 500 to 700°C as compared to conventional multistep processing requiring post-deposition annealing at 800 to 900°C. A development towards lower deposition temperatures is of course favorable in view of electronic applications that might require common processing steps for superconductors and semiconductors.

Throughout the entire meeting the issue of the determination of the substrate temperature came up repeatedly. The substrate temperature is one of the most crucial deposition parameters for all film preparation methods, yet in many cases not very accurate statements as to the real substrate temperature could be made, since many experimenters measure the temperature of the heating block rather than that of the substrate itself. According to one study,

ADVANCED MATERIALS

however, there can be a temperature difference of as much as 30 K between heater block and substrate surface, which led *R. H. Hammond* to conclude that the thermal contact between heater and substrate is of extreme importance.

Substrate materials commonly used in the preparation of superconducting films were $SrTiO_3$, MgO, cubic ZrO_2 (YSZ), and sapphire, all dielectric materials. Single crystalline $SrTiO_3$, which has only a 0.5% lattice mismatch with $YBa_2Cu_3O_7$, is the preferred substrate for achieving epitaxial films exhibiting the highest critical current density measured to date (of order 10^6 A cm^{-2} in zero field at 77 K). Because of their high dielectric losses, neither $SrTiO_3$ nor MgO is a suitable substrate material for microwave applications. Here the recently discovered $LaGaO_3$ and $LaAlO_3$ provide excellent microwave properties (low dielectric constant, low loss tangent) and are easier and less expensive to produce than $SrTiO_3$. Structure and lattice constants are favorable for growing epitaxial films of perovskite related superconductors. *R. W. Simon* (TRW) showed dielectric measurements confirming the desirable microwave properties of $LaAlO_3$ substrates. He speculated that $BaZrO_3$ might also turn out to be a good substrate material; an indication thereof could be the successful use of ZrO_2 buffer layers used on some $YBa_2Cu_3O_7$ films. *Simon* encouraged researchers to focus on new substrate materials; there is "no reason to be married to $SrTiO_3$", as he put it, "since this material has nothing to offer except high prices and bad high frequency properties". *H. S. Kwok* described films made by plasma-assisted laser deposition on dielectric, semiconducting, and metallic substrates. Especially interesting were his critical current measurements of films deposited on stainless steel. J_c of these flexible films decreased by as much as 20% from an initial value of about 1000 A cm^{-2} by repeated bending. *J. Tate* (Technische Universität München) showed that the films deposited by thermal co-evaporation on Si substrates had a 100 Å amorphous SiO_2 layer between substrate and $YBa_2Cu_3O_7$ film. The motivation for depositing films on semiconducting substrates was, of course, with a view to potential electronics applications, but the Munich group also argued that "if you can make films on Si, you can make them on anything".

The critical current density of superconducting films, apart from T_c the single most important parameter for any application, was most often measured by the four-point method. *S. Wolf* emphasized the need for a uniform standard in determining the critical current density. The ASTM standard of 1 μV cm^{-1} now used in many publications was really designed for long wires. As a better standard for short samples, the $\varrho < 10^{-11}\Omega$ cm specific resistivity criterion was suggested. The even more stringent criterion of $\varrho < 10^{-14}\Omega$ cm is being used by the Fermilab for their magnet wire. Since in many cases the critical current density is measured by less stringent criteria due to small samples and insufficient measurement resolution, it is important for comparison toinclude the measurement criterion along with the value of the critical current density.

Talks presented during the third day of the conference centered around Josephson junctions as well as electronics and microwave applications of thin film superconductors. *J. Przybysz* (Westinghouse R&D Center, Pittsburgh) gave an excellent overview of his group's effort to build Josephson shift registers. These and other digital elements are required for high speed signal processing, e.g. in microwave electronics, radar technology etc. There are essentially two ways to obtain superconducting digital circuits. One approach consists of using persistent current loops that are coupled to shift a single bit to the next loop; the other approach is first building logic gates from Josephson switches and then assembling shift registers and other circuits with these gates. The fastest Josephson shift register to date is a Fujitsu one-bit shift register operating at 2.3 GHz—still slower than the current state of the art GaAs technology. However, the Josephson shift register has the potential to reach 60 to 100 GHz clock frequencies, much higher than can be hoped for with GaAs circuits. One drawback with Josephson electronics is that in many cases the semiconductor-based measuring equipment stops working well before the limit of the former is reached.

R. Koch (IBM, Yorktown Heights) showed recent developments on SQUIDS made by magnetron sputtering Tl-Ba-Ca-Cu-O films on cubic zirconia and $SrTiO_3$ substrates, followed by annealing and patterning by photolithography. In addition he reported on voltage noise power measurements in thin film stripes. He showed that voltage noise power does not follow a square law, as would be expected for resistive noise, but varies almost linearly with the voltage. Such a behavior suggests that the noise is created by the motion of thermally excited flux vortices across the sample. Among other applications discussed were photodetectors for visible and infrared wavelengths, superconducting transmission lines for analog signal processing, voltage standards and an analog-to-digital converter based on a high-speed superconducting counter.

Interesting thoughts on the benefits of using the proximity effect with high-T_c superconductors were presented by *V. Z. Kresin* (LBL). A combination of an A 15 superconductor with a high-T_c superconductor would effectively raise T_c of the A 15 material. This combination could be useful in utilizing the good current carrying capabilities of metallic superconductors at higher temperatures. The T_c in the high-T_c superconductor of such a combination is lowered by the same token; but that can be useful in some cases, e.g. measuring normal state properties at low temperatures as done in fermiology. There is no experimental evidence for the proximity effect in high-T_c superconductors since very good quality films are required for these studies.

The last conference day was devoted to the "Colorado Superconductivity Shootout", an opportunity to compare thallium versus bismuth versus yttrium superconducting compounds. The basis for the "shootout" was a series of talks given by six speakers who then formed a panel to lead the subsequent discussion. The best aspects of

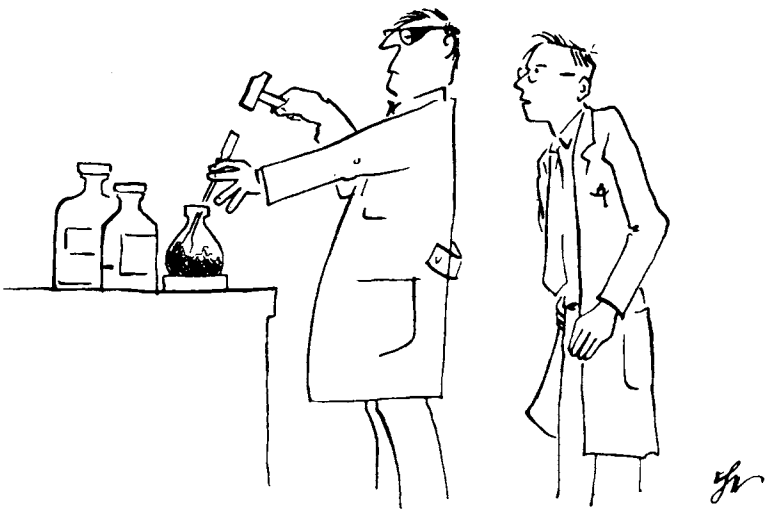
Tl-superconductors were presented by the inventor himself, *A. M. Hermann* (Univ. of Arkansas, Fayetteville). He pointed out the high current density in both bulk and thin films of Tl-based superconductors, as well as their excellent thermal and chemical stability. Bi-superconductors were defended by *R. J. Soulen* (NRL) and *N. G. Dhere* (SERI). Finally, *R. Simon* (TRW) presented a line-up of the three classes of high-T_c superconductors together with Nb as the representative for the conventional superconductors, much in the style of Consumer Report Charts on VCRs or automobiles. Although each material has advantages in specific areas, there were no overall winners or losers. The common consensus was that more effort is necessary to tame and understand these materials more thoroughly before selecting the superior superconductor.

During the following panel discussion, the toxicity of Tl-compounds was a prominent topic. *D. S. Ginley* (Sandia National Laboratories) stressed, as he had done during his talk on Tl-films earlier in the conference, that Tl is not exceptionally toxic. The problem is not the toxicity but the question of how to handle the substances. Tl, which accumulates in soft tissues, has a half-life of 20 to 30 days in the body; however $BaCO_3$, which is about 100 times less toxic than Tl, accumulates in bone marrow and thus remains inside the body considerably longer than Tl. The toxicity of Tl is quite well documented in a Johnson & Matthey summary sheet that includes data on skin absorption, lethal doses, etc.

The Conference on the Science and Technology of Thin Film Superconductors was in fact an exciting and important meeting, just as the organizers promised in their announcement. As a result of the very specialized focus on thin film superconductors, the number of attendees was manageable and it was not necessary to organize concurrent sessions, certainly a point that increased the efficiency of this meeting. The conference provided an excellent opportunity to meet researchers from industry as well as national laboratories and academic institutions, and to discuss a wide spectrum of problems ranging from preparation techniques through methods of characterization to circuit design using superconducting switching elements. In today's over-abundance of superconductivity conferences, this conference was well worth attending.

Herbert Jaeger
Max-Planck-Institut für Metallforschung
Pulvermetallurgisches Laboratorium
Stuttgart (FRG)

Call for Short Communications · Call for Short Communications · Call for Short Communications



... doesn't melt, won't dissolve, just can't be broken down — let's send it to ADVANCED MATERIALS!

ADVANCED MATERIALS from now on welcomes short communications from all over the world, from academia and from industry, from chemists, physicists and materials scientists, provided they are in keeping with the program outlined in the editorial on page 107. Authors who are interested in submitting short communications (up to six pages of doublespaced manuscript together with an appropriate number of figures and/or formulas) should prepare their manuscripts in accordance with the "Notice to Authors" (see page 109).

Call for Short Communications · Call for Short Communications · Call for Short Communications

Conference Calendar

February 1989

13–17 **Plasma Processing in Semiconductor Materials**
Bristol (United Kingdom)
Contact: Dr. S. Pringle, Dept. of Extramural Studies, The Univ., Queens Rd., Bristol BS8 1HR, UK

15–17 **Solid-State Circuits,**
36th IEEE Int. Conf.
New York (USA)
Contact: L. Winner, 301 Almeria Ave., Coral Gables, FL 33134, USA

19–22 **Adhesion,**
12th. Annu. Mtg.
Hilton Head Island (USA)
Contact: D. Hunston, NBS, Polym. Div., Gaithersburg, MD 20899, USA

21–24 **Recent Advances in Drug Delivery**
Salt Lake City (USA)
Contact: K. Knutson, Univ. of Utath, Dept. of Pharmaceutics, CCCD, 421 Wakara Way, Suite 318, Salt Lake City, UT 84108, USA

21–26 **Optical Fibers and their Applications,**
5th Symp.
Warsaw (Poland)
Contact: R. S. Romaniuk, IPI Warsaw Univ. of Technol., Nowowiepska 15–19, PL-00-665, Warsaw, Poland

26–3 **Microlithography,**
Symp. and Exhibition (Micro '89)
Santa Clara (USA)
Contact: Soc. of Photo-Optical Instrumentation Eng. (SPIE), P.O. Box 10, Bellingham, WA 98227, USA

27–1 **Microphysics of Surfaces, Beams and Adsorbates,**
3rd Top. Mtg.
Salt Lake City (USA)
Contact: R. B. Hall, Exxon Research & Eng., Rt. 22E, Annandale, NJ 08801, USA

27–3 **Superconductivity,**
Gordon Conf.
West Coast (USA)
Contact: A. Sleight, E. I. Du Pont de Nemours, Experimental Station 356/301, Wilmington, DE 19898, USA

27–3 **High-Temperature Superconducting Oxides: Processing & Related Properties,**
TMS Annu. Mtg.
Las Vegas (USA)
Contact: The Metallurgical Soc., 420 Commonwealth Dr., Warrendale, PA 15086, USA

March 1989

1–3 **Technical Ceramics,**
2nd Int. Congr. and Exhibit. (Techkeram 2)
Wiesbaden (Fed. Rep. Germany)
Contact: Demat Exposition Managing, P.O. Box 110611, D-6000 Frankfurt, FRG

5–10 **Liquid Crystals,**
6th Eur. Winter Conf.
Schladming (Austria)
Contact: P. Laggner, Inst. für Röntgenfeinstrukturforschung of the Austrian Acad. of Sci., Steyrergasse 17, A-8010 Graz, Austria

6–8 **Crystal Structure, Microstructure and Properties of Minerals and Ceramic Materials,**
Int. Colloq.
Bochum (Fed. Rep. Germany)
Contact: Prof. O. W. Flörke, Ruhr-Univ. Bochum, Inst. für Mineralogie, P.O. Box 102148, D-4630 Bochum, FRG

6–8 **Lithium Battery Technology & Applications,**
4th Int. Seminar
Deerfield Beach (USA)
Contact: S. P. Wolsky, Ansum Enterprises Inc., 950 De Soto Rd., Suite 3B, Boca Raton, FL 33432, USA

6–9 **Advanced Materials**
MRS Industry-Univ. Conf.
Denver (USA)
Contact: Dr. Fred Smith, Adv. Mater. Inst., Colorado School of Mines, 1500 Illinois, Golden, CO 80401, USA

6–9 **Condensed Matter Division,**
Eur. Phys. Soc.,
9th Gen. Conf.
Nice (France)
Contact: J. P. Latteuorte, Lab. de la Metiere Condensee, Univ. de Nice, F-06034 Nice, Cedex, France

6–10 **Quantum Wells for Optics and Optoelectronics; Picosecond Electronics and Optoelectronics,**
Top. Mtg.
Salt Lake City (USA)
Contact: Optical Soc. of America (OSA), 1816 Jefferson Pl. NW, Washington, DC 20036, USA

8–9 **Molecular Chemistry of Solid-State Electronics**
London (United Kingdom)
Contact: The Royal Society, 6 Carlton House Terrace, London SW1Y 5AG, UK

9–10 **The Martensitic Transformation in Science and Technology**
Bochum (Fed. Rep. Germany)
Contact: Dtsch. Ges. Metallkd., Adenauerallee 21, D-6370 Oberursel FRG

9–11 **Makromolekulares Kolloquium**
Freiburg (Fed. Rep. Germany)
Contact: Prof. H. Finkelmann, Inst. für Makromol. Chemie der Univ., Stefan-Meier-Str. 31, D-7800 Freiburg, FRG

11–14 **Surface Finishing '89**
Brighton (United Kingdom)
Contact: Inst. of Metal Finishing, Exeter House, 48 Holloway Head, Birmingham B1 1NQ, UK

12–14 **High-Tech-Materials and Finishing**
Berlin (West)
Contact: Technik + Kommunikation-Verlag GmbH, Ritterfelddamm 82 h + i, D-1000 Berlin 22

12–25 **Diffusion in Materials,**
NATO Adv. Study Inst.
Aussois (France)
Contact: A. L. Laskar, Phys. and Astron. Dept., Clemson Univ., Clemson, SC 29631, USA

13–14 **Regio Macro II**
Basel (Switzerland)
Contact: Prof. M. Mutter, Inst. für Org. Chem., Univ. Basel, St. Johanns-Ring 19, CH-4056 Basel, Switzerland

15–17 **Confocal Microscopy/3-D Image Processing in Microscopy,**
1st Int. Conf./2nd Int. Conf.
Amsterdam (Netherlands)
Contact: Bureau PAOG, Congr. Office, Tafelbergweg 25, NL-1105 BC, Amsterdam, Netherlands

15–17 **Intelligent Materials,**
Int. Workshop
Ibaraki (Japan)
Contact: T. Kurino, The Soc. of Nontraditional Technol., Toranomon Kotohira-Kaikan Bldg. 3F, 1-2-8 Toranomon, Minato-ku, Tokyo 105, Japan

20–22 **Mechanical Properties of Materials at High Rates of Strain,**
4th Int. Conf.
Oxford (United Kingdom)
Contact: J. Harding, Eng. Sci. Dept., Univ. of Oxford, Parks Rd., Oxford OX1 3PJ, UK

20–22 **Refractory Metals and Silicides**
Eur. Workshop
Houthalen (Belgium)
Contact: R. De Keersmaecker, IMBE, Kapeldreef 75, B-3030 Leuven, Belgium

20–23 **Surface Science,**
Interdisciplinary Conf.
Liverpool (United Kingdom)
Contact: P. Weightman, Liverpool Univ., Oliver Lodge Lab., Oxford St., P.O. Box 147, Liverpool L69 3BX, UK

27–31 **Aerospace Sensing,**
Tech. SPIE's Symp.
Orlando (USA)
Contact: Soc. of Photo-Optical Instrumentation Eng. (SPIE), Technical Program Committee, P.O. Box 10, Bellingham, WA 98227, USA

28–31 **Aluminum-Lithium**
5th Int. Conf.
Williamsburg (USA)
Contact: Al-Li-V, School of Eng. and Applied Sci., Thornton Hall, Univ. of Virginia, Charlottesville, VA 22901, USA

29–31 **Neutron and X-Ray Scattering: Complementary Techniques**
Canterbury (United Kingdom)
Contact: Dr. R. J. Newport, Univ. of Kent, Physics Dept., Canterbury, Kent CT2 7NR, UK

30–31 **Colorado Microelectronics**
Colorado Springs (USA)
Contact: CMC '89 Conf. Secretary, Microelectronics Research Lab., Univ. of Colorado, Colorado Springs, CO 80933-7150, USA

30–14 **High-T_c Superconductors,**
Exp. Workshop
Miramare (Italy)
Contact: Int. Ctr. for Theoretical Physics, P.O. Box 586, I-34100 Trieste, Italy

April 1989

1–6 **Superconductivity,**
2nd World Congr.
Houston (USA)
Contact: R. D. Kane, World Congr. on Superconductivity, P.O. Box 27805, Houston, TX 77227-7805, USA

3–5 **Modern Practice in Stress and Vibration Analysis**
Liverpool (United Kingdom)
Contact: Meetings Officer, Inst. of Physics, 47 Belgrave Sq., London SW1X 8QX, UK

3–6 **Low Energy Ion Beams,**
5th Conf.
Guildford (United Kingdom)
Contact: Meetings Officer, Inst. of Physics, 47 Belgrave Sq., London SW1X 8QX, UK

3–7 **Copolymerization and Copolymers in Dispersed Media**
Lyon (France)
Contact: I. Guillot/C. Pichot, Lab. des Materiaux Organiques, BP 24, F-69390 Vernaison, France

3–7 **High Temperature Materials '89**
Gaithersburg (USA)
Contact: J. W. Hastie, National Bureau of Standards, Gaithersburg, MD 20899, USA

4–7 **Electrochemical Processing of Semiconductors**
Berlin (West)
Contact: W. Pieth, Free Univ. of Berlin, Inst. of Phys. Chem., Takustraße 3, D-1000 Berlin 33

4–14 **Phase Transition in Soft Condensed Matter,**
NATO Adv. Study Inst.
Geilo (Norwegen)
Contact: G. Jarret, Inst. for Energy Technol., Dept. of Physics, P.O. Box 40, N-2007 Kjeller, Norwegen

6–7 **Modeling in Crystal Growth from the Melt,**
NATO Workshop
Parma (Italy)
Contact: G. Müller, Inst. für Werkstoffwissenschaften 6, Martensstraße 7, D-8520 Erlangen, FRG

10–12 **Bayreuther Polymer Symp.,**
Bayreuth (Fed. Rep. Germany)
Contact: BPS '89, Lehrstuhl Makromolekulare Chemie II, Univ. Bayreuth, Postfach 101251, D-8580 Bayreuth, FRG

10–13 **Microscopy of Semiconducting Materials,**
MRS 6th Oxford Conf.
Oxford (United Kingdom)
Contact: Administrator, Royal Microscopy Soc., 37/38 St. Clements, Oxford OX4 1AJ, UK

11–13 **Catalysis by Well Characterized Materials**
Liverpool (United Kingdom)
Contact: Prof. R. W. Joyner, Leverhulme Ctr. for Innovative Catalysts, Univ. of Liverpool, Grove St., P.O. Box 147, Liverpool L69 3BX, UK

17–26 **Ceramics and Composite Materials,**
Spring College in Mater. Sci.
Trieste (Italy)

Contact: Int. Ctr. for Theoretical Physics, Spring College in Mater. Sci. 1989, P.O. Box 586, I-34100 Trieste, Italy

18–19 **Industrial Water-Soluble and Water-Swellable Polymers**
Manchester (United Kingdom)
Contact: The Registar (Mid-Career Training), UMIST, P.O. Box 88, Manchester M60 1QD, UK

23–28 **Nondestructive Testing,**
12th World Conf. (WCNDT '89)
Amsterdam (Netherlands)
Contact: B. de Jong, RAI Organisatie Bureau Amsterdam bv, Europaplein 12, 1078 GZ Amsterdam, Netherlands

23–27 **American Ceramic Society,**
91st Annu. Mtg. and Expo.
Indianapolis (USA)
Contact: Dr. K. M. Nair, Electronics Dept., E.I. du Pont de Nemours Co., Inc., 3181 Buffalo Ave., Niagara Falls, NY 14302, USA

24–28 **Optical Science and Engineering,**
2nd Int. Congr.
Paris (France)
Contact: Soc. of Photo-Optical Instrumentation Eng. (SPIE), P.O. Box 10, Bellingham, WA 98227, USA

24–28 **Lasers and Electro-Optics,**
LEOS-IEEE-OSA Conf. (CLEO '89)
Baltimore (USA)
Contact: Optical Soc. of America (OSA), 1816 Jefferson Pl. NW, Washington, DC 20036, USA

24–28 **MRS Spring Mtg.**
San Diego (USA)
Contact: J. B. Ballance, MRS, 9800 McKnight Rd., Suite 327, Pittsburgh, PA 15237, USA

25–27 **Hot Isostatic Pressing of Materials**
Antwerpen (Belgium)
Contact: Hot Isostatic Pressing Conf., c/o K. VIV, Jan van Rijswijcklaan 58, B-2018 Antwerpen, Belgium

26–28 **Joining Ceramics, Glass and Metal**
3rd Int. Conf. (CGM '89)
Contact: Dtsch. Gesellsch. Metallkd., Adenauerallee 21, D-6370 Oberursel, FRG

May 1989

1–3 **Tunable Solid State Lasers,**
Top. Mtg.
North Falmouth (USA)
Contact: Optical Soc. of America (OSA), 1816 Jefferson Pl. NW, Washington, DC 20036, USA

1–5 **Scanning Microscopy,**
Salt Lake City (USA)
Contact: O. Johari, Scanning Microscopy Int., P.O. Box 66507, Chicago, IL 60666, USA

4–6 **The Solid State—Dynamics and Kinetics**
Annu. Mtg. Dtsch. Bunsen-Gesellsch. für Phys. Chem.
Siegen (Fed. Rep. Germany)
Contact: Dtsch. Bunsen-Gesellsch., Carl-Bosch-Haus, Varrentrappstr. 40/42, D-6000 Frankfurt am Main 90, FRG

7–12 **High-T_c Superconductor Technologies**
175th Mtg. Electrochem. Soc.
Los Angeles (USA)
Contact: S. Raider, IBM T. J. Watson Research Ctr., P.O. Box 218, York Town Heights, NY 10598, USA

7–12 **Fundamentals of Adsorption,**
3rd Int. Conf.
Nurrigen (Fed. Rep. Germany)
Contact: DECHEMA, Abt. Tagungen, P.O. Box 970146, Theodor Heuss-Allee 25, D-6000 Frankfurt am Main 97, FRG

8–12 **High Temperature and Wear Resistant Materials in a World of Changing Technology**
12th Int. Plansee Seminar
Plansee (Austria)
Contact: Metallwerk Plansee, A-6600 Reutte, Austria

9–11 **Coatings and Sensors for Acoustic and Electromagnetic-Optical Applications**
Univ. Park. (USA)
Contact: V. K. Varadan, Dept. of Eng. Sci. and Mechanics, Penn. State Univ., 227 Hammond Bldg., Univ. Park, PA 16802, USA

10–11 **Polyimides**
Montpellier (France)
Contact: Prof. M. Abadie, LEMD/MAO-USTL, F-34060 Montpellier Cedex 1, France

16–19 **Modern Developments in Materials Science and Technology,**
Annu. Mtg. Dtsch. Gesellsch. Metallkd.
Karlsruhe (Fed. Rep. Germany)
Contact: Dtsch. Gesellsch. Metallkd., Adenauerallee 21, D-6370 Oberursel, FRG

22–24 **Werkstoffanalytik,**
Wien (Austria)
Contact: Prof. Dr. M. Grasserbauer, Inst. für Analytische Chem. der Tech. Univ. Wien, Getreidemarkt 9, A-1060 Wien, Austria

22–24 **Glastechnische Tagung**
Stuttgart (Fed. Rep. Germany)
Contact: Dtsch. Glastechn. Gesellsch., Mendelssohnstr. 75–77, D-6000 Frankfurt am Main, FRG

22–25 **Clustering and Aggregated State of Matter**
Strasbourg (France)
Contact: Prof. E. Constantin, Groupe de Recherche de Spectrométrie de Masse Interlab., Dept. de Chim., 1 rue Blaise Pascal, 67008 Strasbourg Cedex, France

22–25 **Graphite Intercalation Compounds,**
5th Int. Symp. (ISGIC-5)
Berlin (West)
Contact: Dr. F. W. Froben, Fachbereich Physik, Freie Univ. Berlin, Arnimallee 14, D-1000 Berlin 33

24–26 **Advances in the Stabilization and Controlled Degradation of Polymers,**
11th Int. Conf.
Luzern (Switzerland)

Contact: Dr. A. V. Patsis, Inst. in Materials Sci, State Univ. of New York, New Paltz, NY 12561, USA

25–26 **Quantitative Methods in Assessment of Structural Defects**
Kansas City (USA)
Contact: A. P. Berens, Univ. of Dayton, Research Inst., 300 College Park Ave., Dayton, OH 45469, USA

29–31 **Cross-linked Polymers,**
3rd Int. Conf.
Luzern (Switzerland)
Contact: Dr. A. V. Patsis, Inst. in Materials Sci, State Univ. of New York, New Paltz, NY 12561, USA

29–2 **Molecular Beams**
Perugia (Italy)
Contact: V. Aquilanti, Univ. di Perugia, Dipt. di Chimica, I-06100 Perugia, Italy

30–2 **E-MRS Spring Mtg.**
Strasbourg (France)
Contact: P. Siffert, Ctr. de Recherches Nuclèaîre, Lab. PHASE, F-67037 Strasbourg, Cedex, France

31–2 **Applied Surface Analysis,**
11th Symp.
Cleveland (USA)
Contact: J. Grant, Research Inst., 300 College Park, Dayton, OH 45469-0001, USA

31–2 **Thermogravimmetry and Thermal Engineering,**
6th Biennial Conf.
Budapest (Hungary)
Contact: I. Benko, MATE, House of Technol. III. 318, P.O. Box 451, H-1372 Budapest, Hungary

June 1989

6–9 **Chemistry of Functional Dyes,**
Int. Symp. (ESTech '89)
Osaka (Japan)
Contact: Prof. T. Kitao, General Secretary of the Symp., Kinki Chem. Soc., Japan 1-8-4, Utsubo honmachi, Nishi-ku, Osaka 550, Japan

12–14 **Rubber,**
Int. Conf. 90 IRC Exhibition Paris (France)
Contact: Soc. de Chimie Industrielle, 28, rue Saint-Dominique, F-75007 Paris, France

12–15 **Narrow-Gap Semiconductors and Related Materials,**
Int. Conf.
Ogunquit (USA)
Contact: D. G. Seiler, Phys. Dept., Univ. of North Texas, P.O. Box 5368, Denton, TX 76203, USA

18–21 **Colloid & Surface Science,**
63rd ACS Div. of Colloid & Surface Chem. Symp.
Seattle (USA)
Contact: J. Berg, Dept. of Chemical Eng. BF-10, Univ. of Washington, Seattle, WA 98105, USA

19–21 **Composites**
Asia-Pacific 89
Adelaide (Australia)
Contact: The Secretariat, Techsearch, Composites Asia-Pacific '89, P.O. Box 2471, Adelaide S.A. 5001, Australia

19–21 **SAMPE-Electronics,**
3rd Int. Conf.
Los Angeles (USA)
Contact: M. Smith, Business Director, SAMPE, P.O. Box 2459, Covina, CA 91722, USA

21–23 **Chemically Modified Surfaces,**
Midland (USA)
Contact: W. T. Collins, Dow Corning Corp., Mail Stop C41C00, Midland, MI 48686, USA

21–23 **Electronic Materials**
Cambridge (USA)
Contact: The Metallurgical Soc., 420 Commonwealth Dr., Warrendale, PA 15086, USA

22–25 **Optics Asia '89**
Singapore (Singapore)
Contact: Asia '89, 994 Bendemeer Rd., N° 04-03, Singapore 1233, Singapore

25–30 **Solid State Sensors and Actuators (Transducers-5)/ Eurosensors III**
Montreux (Switzerland)
Contact: COMST S.A., P.O. Box 415, CH-1001 Lausanne 1, Switzerland

26–28 **Molecular Design of Functional Polymers,**
IUPAC Int. Symp.
Seoul (Korea)
Contact: IUPAC Int. Symp., c/o Polymer Soc. of Korea, Rm. 601, Hyecheon Bldg., 831 Yeoksam-dong, Kangnam-ku, Seoul 135-792, Korea

26–30 **Solid State Chemistry,**
2nd Int. Symp.
Pardubice (Czechoslovakia)
Contact: Dr. L. Koudelka, Inst. of Chem. Technol., Leninovo nam., 565, CS-53210 Pardubice, Czechoslovakia

26–30 **Supermembranes**
Trieste (Italy)
Contact: Int. Ctr. for Theoretical Physics, P.O. Box 586, I-34100 Trieste, Italy

27–28 **Polymer Latex III**
London (United Kingdom)
Contact: Miss M. Peacock, Plastics and Rubber Inst., 11 Hobart Place, London SW1W 0HL, UK

28–30 **Oxide Surfaces**
Midland (USA)
Contact: W. T. Collins, Mail Stop C41C00, Dow Corning Corp., Midland, MI 48686-0994, USA

July 1989

2–7 **Solid State Organic Materials,**
9th Int. Conf.
Como (Italy)
Contact: Centro di Cultura Scientifica, "A. Volta", Villa Olmo, Via Cantoni 1, I-22100 Como, Italy

3–6 **Conduction and Breakdown in Solid Dielectrics**
3rd Int. Conf. (ICSD '89)
Trondheim (Norway)
Contact: Prof. Sletbak, ICSD '89, The Norwegian Inst. of Technol., Sem Sælands V 13, N-7034 Trondheim, Norway

3–28 **Liquids, Freezing and the Glass Transition**
NATO Adv. Study Inst.
Les Houches (France)

Contact: École d'Été de Physique Théorique, F-74310 Les Houches, France

4–7 **Nonlinear and Electro-optics**
Int. Conf.
Cambridge (United Kingdom)
Contact: The Meetings Officer, The Inst. of Physics, 47 Belgrave Square, London SW1X 8QX, UK

9–14 **Scanning Tunneling Microscopy/Spectroscopy,**
4th Int. Conf.
Oarai (Japan)
Contact: O. Nishikawa, The Graduate School of Nagatsuta, Tokyo Inst. of Technol., 4259 Nagatsuta, Midori-ku, Yokohama 227, Japan

9–14 **Zeolites,**
8th Int. Conf.
Amsterdam (Netherlands)
Contact: M. Laboushere, 792 Keizersgracht, 1017 EC, Amsterdam, The Netherlands

10–12 **Applied Organometallic Chemistry: an Entry to the New Technology**
The Pines Resort (Australia)
Contact: Dr. A. F. Masters, School of Chemistry, Univ. of Sydney, Sydney, N. S. W. 2006, Australia

10–13 **Magnetic Resonance in Polymers,**
9th Spec. Colloq. Ámpere
Prague (Czechoslovakia)
Contact: P. M. M. Secretariat, c/o. Inst. of Macromol. Chem., Czech. Acad. of Sci., 16206 Prague, Czechoslovakia

10–14 **Electron Spectroscopy,**
4th Int. Conf.
Honolulu (USA)
Contact: G. E. McGuire, Microelectronics Ctr. of North Carolina, P.O. Box 12889, Research Triangle Park, NC 27709, USA

10–14 **Organic Coatings Science and Technology,**
15th Int. Conf.
Athens (Greece)
Contact: Dr. A. V. Patsis, Inst. in Materials Sci, State Univ. of New York, New Paltz, NY 12561, USA

11–14 **Numerical Analysis of Semiconductor Devices and Integrated Circuits,**
6th Int. Conf.
Dublin (Ireland)
Contact: J. J. H. Miller, Nase-Code Conf., INCA, P.O. Box 2, Dun Laoghaire, Ireland

12–14 **Solid-State Laser/Optical Fiber Science and Electromagnetic Theory '89,**
Top. Mtg./Sino-Japanese Joint Mtg.
Beijing (Peoples' Rep. China)
Contact: Optical Soc. of America (OSA), 1816 Jefferson Pl. NW, Washington, DC 20036, USA

16–21 **Catalysis,**
Eur. Conf.
Berlin (West)
Contact: Prof. G. Ertl, Fritz-Haber-Inst. der Max-Planck-Gesellsch., Faradayweg 4–6, D-1000 Berlin

17–20 **Polymer Blends**
Prague (Czechoslovakia)
Contact: P. M. M. Secretariat, c/o. Inst. of Macromol. Chem., Czech. Acad. of Sci., 16206 Prague, Czechoslovakia

18–20 **Polymer Chemistry: Aspects of Radical Polymerization**
Lancaster (United Kingdom)
Contact: Dr. J. R. Ebdon, Dept. of Chemistry, Univ. of Lancaster, Lancaster LA1 4YA, UK

18–21 **Integrated Optics and Optical Fiber Communications,**
7th Int. Conf. (IOOC-7)
Kobe (Japan)
Contact: P. W. Shumate, Jr., Bell Communications Research, 435 S St., Morristown, NJ 07960, USA

23–28 **Materials and Mechanisms of Superconductivity: High-Temperature Superconductors,**
Int. Conf. (HTSC-M^{2}S)
Stanford (USA)
Contact: Dr. T. H. Geballe, Dept. of Applied Phys., Stanford Univ., Stanford, CA 94305, USA

24–26 **Micro-Optics/Gradient-Index Optical Imaging Systems,**
2nd Conf./8th Top. Mtg.
Tokyo (Japan)
Contact: K. Iga, Tokyo Inst. of Technol., Research Lab. of Precision Machinery and Electronics, 4259 Nagasuta, Midori-ku, Yokohama 227, Japan

24–26 **Composite Structures,**
5th Int. Conf.
Paisley (United Kingdom)
Contact: Dr. I. H. Marshall, Dept. of Mechanical and Production Eng., Paisley College of Technol., High St., Paisley PA 12BE, UK

31–2 **Biologically-Engineered Polymers**
Cambridge (United Kingdom)
Contact: Royal Soc. of Chemistry, Burlington House, London W1V 0BN, UK

August 1989

2–7 **Pure and Applied Chemistry,**
32nd IUPAC Congr.
Stockholm (Sweden)
Contact: Stockholm Convention Bureau, P.O. Box 6911, S-10239 Stockholm, Sweden

13–26 **High-T_c Superconductors,**
NATO Adv. Study Inst.
Bad Windsheim (Fed. Rep. Germany)
Contact: R. Kossowsky, Applied Res. Lab., Pennsylvania State Univ., P.O. Box 30, State College, PA 16804, USA

14–17 **Shock Compression of Condensed Matter,**
APS Top. Conf.
Albuquerque (USA)
Contact: A. Roach, MS-P 915, Los Alamos Nat. Lab., Los Alamos, NM 87545, USA

14–18 **Hopping Transport,**
8th Conf.
Chapel Hill (USA)
Contact: M. Pollak, Dept. of Phys., Univ. of California, Riverside, CA 92521, USA

20–24 **Imaging Systems – 150 Years of Photography,**
Int. Symp. (ISIS '89)
Dresden (German Dem. Rep.)

Contact: Conf. Secretary, ISIS '89, Technische Univ. Dresden, Sektion Physik, Wissenschaftsbereich Photophysik, Mommsenstr. 13, DDR-8027 Dresden, GDR

20–25 **Crystal Growth: Progress in Science and Technology,** 9th Int. Conf. Sendai (Japan) Contact: Prof. T. Nishinaga, Inter Group Corp., Akasaka Yamakatsu Bldg., 8-5-32, Akasaka Minato-ku, Tokyo 107, Japan

21–24 **Amorphous and Liquid Semiconductors,** 13th Int. Conf. Asheville (USA) Contact: D. E. Sayers, P.O. Box 8202, North Carolina State Univ., Raleigh, NC 27695-8202, USA

21–26 **Photochemistry,** Int. Conf. Beijin (People's Rep. China) Contact: Prof. S. Wu, Inst. of Photographic Chem., Academia Sinica, Beijing, People's Rep. China

28–31 **Dynamical Processes in Excited States of Solids,** 7th Int. Conf. (DPC '89) Athens (USA) Contact: DPC '89, Prof. J. E. Rives, Dept. of Physics and Astronomy, Univ. of Georgia, Athens, GA 30602, USA

28–1 **Ferroelectricity,** 7th Int. Mtg. (IMF-7) Saarbrücken (Fed. Rep. Germany) Contact: Dr. J. Albers, Univ. des Saarlandes, Fachbereich Physik, D-6600 Saarbrücken, FRG

28–1 **Sintering,** 7th World Round Table Conf. Herceg-Novi (Yugoslavia) Contact: Dr. D. P. Uskoković, Serbian Academy of Sci. and Arts, Knez-Mihailova 35, 11000 Beograd, Yugoslavia

28–1 **X-Ray Optics and Microanalysis,** 12th Int. Congr. Cracow (Poland) Contact: S. Jasienska, Academy of Mining and Metallurgy, Inst. of Metallurgy, 30-059 Cracow, Poland

28–2 **Photochemistry for High Technology,** Int. Summer School Leuna-Merseburg (German Dem. Rep.) Contact: Prof. H.-J. Timpe, Sektion Chemie, Technische Hochschule für Chemie, Leuna-Merseburg, Gensaerstr., DDR-42 Merseburg, GDR

29–2 **Innovation and Perspectives in Solid Phase Synthesis,** Int. Symp. Oxford (United Kingdom) Contact: R. Epton, School of Appl. Sci., Wolverhampton Polytech., Wolverhampton WV1 1SB, UK

Materials Related Gordon Research Conferences

General Information

Contact: Dr. A. M. Cruickshank, Director, Gordon Research Conf., Gordon Res. Ctr., Univ. of Rhode Island, Kingston, RI 02881-0801, USA
Locations: Colby-Sawyer College (N), (S): New London, NH;
New Hampton School: New Hampton, NH;
Kimball Union Academy: Meriden, NH
Tilton School: Tilton, NH

June 1989

19–23 **Catalysis** Colby-Sawyer College (N) Chairman: L. D. Schmidt

26–30 **Polymers** Colby-Sawyer College (N) Chairman: J. P. Kennedy

July 1989

3–7 **Fiber Science** Colby-Sawyer College (N) Chairman: B. C. Goswami

3–7 **Thermosetting Polymers** Colby-Sawyer College (S) Chairman: N. J. Johnston

10–14 **Elastomers** Colby-Sawyer College (N) Chairman: G. Ver Strate

10–14 **Metal Hydrides** Tilton School Chairman: F. D. Manchester

17–21 **Corrosion** Colby-Sawyer College (N) Chairman: H. J. Grabke

17–21 **Chemistry at Interfaces** Kimball Union Academy Chairman: R. Johnson

17–21 **Superconducting Films** Tilton School Chairman: D. Gubser

31–4 **Ion-Containing Polymers** Colby-Sawyer College (S) Chairman: G. Wilkes

August 1989

7–11 **Physical Metallurgy** Tilton School Chairman: J. C. Williams

14–18 **Studies in Solid-State Ceramics** Colby-Sawyer College Chairman: U. Chowdhry

14–18 **Science of Adhesion** New Hampton School Chairman: R. A. Pike

ANGEWANDTE CHEMIE
International Edition in English
Volume 28 · Number 2
February 1989
Pages 135–252

Reaction Mechanisms in Heterogeneous Catalysis; C–H Activation as a Case Study

By Wilhelm F. Maier*

Heterogeneous catalysis is changing from an empirical art to an exact science. The various methods for the analysis of solids and surfaces, constantly refined by materials science and surface science, seem to be almost unlimited. The increasing availability of atomic resolution microscopy as well as synchrotron radiation allows the characterization of catalyst particles, surface structures, surface processes and surface intermediates. We have learned to determine the surface structure sensitivity of catalytic reactions. Thermodynamic and kinetic data of catalytic reactions are now determined routinely. Isotopic exchange and labeling experiments provide information about reactant-catalyst interactions. How much have we learned through these techniques about the nature or mechanism of heterogeneously catalyzed reactions? The following article attempts to summarize the progress and the problems encountered in mechanistic studies of C–H bond formation and activation in a hydrogen atmosphere as an example for the present state of the understanding of reaction mechanisms in heterogeneous catalysis.

1. Introduction

The activation and formation of carbon–hydrogen (C–H) bonds on surfaces are fundamental processes in heterogeneously catalyzed reactions. C–H activation is most commonly associated with functionalization and refining of hydrocarbons. The reverse process, C–H bond formation, is a central step in dihydrogen addition and hydrogenolysis reactions. Although C–H activation and hydrogenation are connected by microscopic reversibility, they have traditionally been treated separately. The astronomical number of publications concerned with these reactions prevents a comprehensive review. Secondary literature represents the most helpful source of information for the chemist.[1–3]

[*] Prof. Dr. W. F. Maier
Fachbereich 8 Chemie der Universität/Gesamthochschule
Schützenbahn 70, D-4300 Essen 1 (FRG)

2. General Aspects

Heterogeneously catalyzed reactions with hydrogen are surface reactions with three principal reaction partners: the organic molecule, hydrogen, and the catalyst surface. Although the effects of the structure of the organic molecule and of the reaction and process conditions[4] on the catalytic process are understood, empirical procedures still dominate in catalyst preparation and development.[5] Process catalysts, prepared by empirical recipes of a proprietary nature, often contain multiple additives of unknown function. The catalytic reaction, however, is still a molecular process and it is unlikely that all the additives participate in the catalytic process itself. More likely is that additives and pretreatment procedures chemically or morphologically modify the catalyst to provide a maximum concentration of active sites.[6] An understanding of the effect of modifiers on the surface and bulk structure of a catalyst

 © VCH Verlagsgesellschaft mbH, D-6940 Weinheim, 1989 0570-0833/89/0202-0135 $ 02.50/0

may therefore go hand in hand in hand with a molecular understanding of the active site structure.

It was hoped that organometallic chemistry would bring about this molecular understanding through the synthesis of well defined homogeneous analogues of the active site. Well known examples of homogeneous catalysts are Wilkinson's catalyst and its analogues for olefin hydrogenation. Deuteration reactions of olefins with Wilkinson type catalysts cleanly produce [D_2]alkanes,[7] in contrast to the mixture of isotopic isomers generated by heterogeneous catalysis.[2] Despite a wide range of applications and catalyst variations, there is no indication of a strong impact of this homogeneous catalyst upon the understanding of heterogeneous hydrogenation catalysis.[8] Mild, homogeneous activation of C–H bonds in alkanes[9] is achieved by reactive organometallic intermediates. Despite some theoretical insight into the mechanism of the homogeneous processes,[10] there is no evidence for an analogy with heterogeneously catalyzed C–H activation reactions. Organometallic chemistry has become a distinct field of chemical research which has opened up new avenues in heterogeneous catalysis, such as heterogenized homogeneous catalysis. This apparent lack of correlation between heterogeneous and homogeneous catalysis may largely be attributed to the dominating mononuclearity of organometallic compounds, which is in strong contrast to the rather large metal clusters encountered in heterogeneous catalysis. However, an analogy between homogeneous and heterogeneous catalysis is perhaps possible in the area of metal cluster chemistry. *Schmid* et al. observed not only the preferred formation of clusters of 13 and 55 atoms, they also obtained evidence for the formation of structured super clusters via the combination of 13 atom clusters (Fig. 1b).[11] Pd super clusters of this type might be present in heterogeneous Pd-catalysts.[6] Some structural order, similar to that found in Schmid's clusters, is recognizable in the TEM-picture of the Pd super clusters of a heterogeneous catalyst (Fig. 1a). The distance between the layers in these clusters is about 50 Å, which corresponds to a particle diameter of about 60 Å. We have observed similar super clusters on various Pd catalysts, such as Pd on SiO_2, TiO_2 and Al_2O_3, indicating that super cluster formation may be a general phenomenon for certain metals. These analogies between homogeneous clusters and heterogeneous catalysts suggest that metal cluster chemistry may eventually redeem the promises of organometallic chemistry with respect to heterogeneous catalysis. At present, however, we have to recognize that organometallic chemistry has not yet contributed significantly to the understanding of classical heterogeneous catalysis.

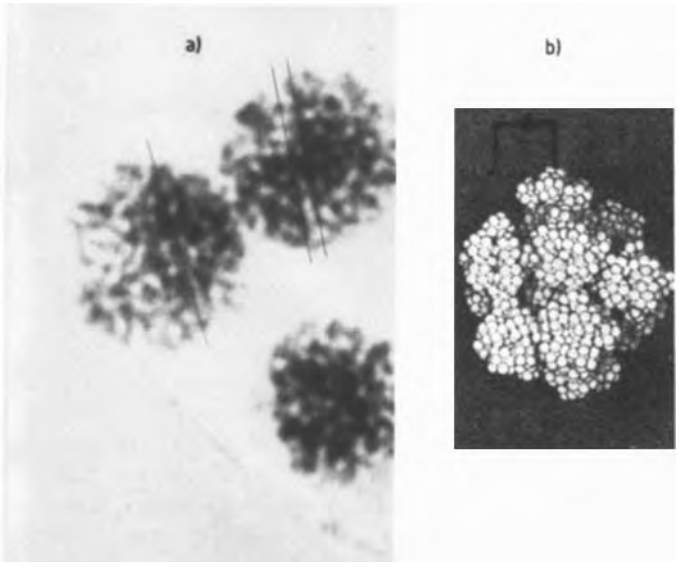
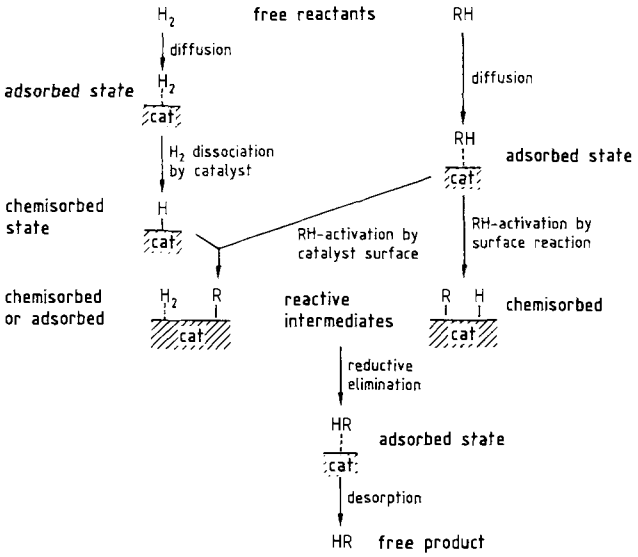


Fig. 1. a) TEM picture of Pd super clusters of a Pd/Al_2O_3 catalyst (magnification from Fig. 1B in [6]), b) postulated super cluster from homogeneous cluster chemistry [11]. Recognizable orientation in a) is marked with lines.

3. Reaction Conditions—Thermodynamic and Kinetic Aspects

Understanding of heterogeneously catalyzed reactions must be based on mechanistic studies of heterogeneous catalysis. Mechanistic studies in heterogeneous catalysis commonly determine thermodynamic and kinetic data as well as investigate isotopic exchange. Despite many decades of such research there is still little precise knowledge about the catalytic process itself. A problem in such mechanistic studies is that the reaction conditions chosen have to be examined carefully before meaningful conclusions can be drawn. Scheme 1 shows a simplified summary



Scheme 1. Summary of the processes involved in heterogeneously catalyzed reactions of hydrocarbons with hydrogen.

of the processes involved in C–H activations of alkanes with heterogeneous catalysts.

Depending on reaction conditions, any one of the steps in Scheme 1 may be rate determining. Activation barriers for C–H activation, commonly determined without knowledge of identity of the rate determining step, have contributed little to our mechanistic understanding. It is commonly accepted that activation barriers below 3 kcal mol^{-1} are indicative of diffusion control or hydrogen activation as the rate limiting step, conditions which do not contribute to the understanding of the reaction. Useful

data for mechanistic studies therefore require reaction conditions, under which the hydrocarbon itself is involved in the rate determining step, which is often indicated by higher activation barriers (>3 kcal mol^{-1}) and first and zero order reactions in hydrocarbon and hydrogen respectively. Such conditions ensure minimal residence time of the organic reactant on the catalyst surface and little interference by secondary surface processes. Appropriate reaction conditions can be readily achieved in gas phase flow reactors by using high hydrogen and low hydrocarbon partial pressures. The importance of controlling the reaction conditions is demonstrated by the dependence of the isotopic distribution of the products upon the concentration of adsorbed hydrogen and upon whether the reaction proceeds with a reaction-controlled or diffusion-controlled rate limiting step.[12]

Higher activation barriers (>3 kcal mol^{-1}) and positive and zero reaction orders in reactant and hydrogen, respectively, indicate that oxidative addition (chemisorption or adsorption of the hydrocarbon) or reductive elimination (desorption) is the rate determining step. Evidence for oxidative addition as the rate determining step has been found in the H/D exchange of 2,2-dimethylpentane on Rh.[13]

However, high activation barriers do not guarantee reaction rate control. First order reaction rates in hydrogen with activation barriers comparable to the condensation enthalpies of the reactant, the solvent, or water (commonly between 6 and 15 kcal mol^{-1}) are consistent with desorption of "surface-condensed" molecules being rate determining.[14] In this model the rate is determined by the formation of free surface sites for hydrogen chemisorption by desorption of adsorbed material (monolayers of water, solvent, or reactant).[14]

In addition to these problems of interpretation, kinetic studies, especially of olefin hydrogenation reactions, are often plagued by catalyst poisoning of still unknown origin.[15] Further difficulties result from lack of knowledge of the actual reaction temperature, since the temperature at the catalytically active center can exceed the average reactor temperature by up to several hundred degrees.[16]

The H/D exchange reactivity of those alkanes which are capable of forming olefinic or allylic intermediates (linear and cyclic alkanes) on Pt is inversely proportional to the vapor pressure, indicating a dependence on the concentration of adsorbed hydrocarbon.[17] Such a dependence of the C–H activation rate on the surface concentration of adsorbed hydrocarbons is supported by the vapor pressure dependent adsorption of saturated and unsaturated hydrocarbons on Rh-black (nonporous) under H/D exchange conditions.[13] Since adsorption is a purely physical process, this reaction follows the Langmuir/Hinshelwood formalism with physisorbed and not chemisorbed reactants.

4. Which Catalyst Properties are Important for Catalysis?

4.1. Surface Interactions

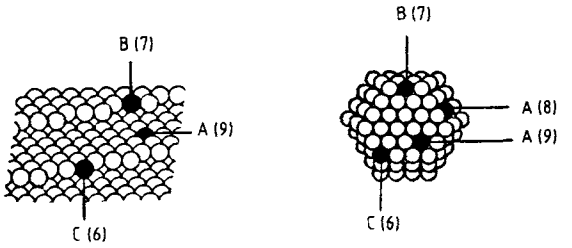
The chemical nature of the metal catalyst affects the activity and the selectivity of hydrogenation[2] and C–H activation reactions. However, the exact function of the metal catalyst in these reactions is still unclear. It was found that hydrogenation, dehydrogenation, and exchange reactions occur with spillover hydrogen (migration of dissociated hydrogen from the catalyst metal particle onto the support)[18] indicating that the metal is not necessarily part of the actual reaction. What then is the function of the noble metal particles in the catalytic reaction?

4.2. Surface Carbonization

Before we can address the metal surface itself, we have to consider surface carbonization. Carbonaceous residues rapidly form on catalyst surfaces during the catalytic reaction and cause variable deactivation due to surface blocking. It was never clear whether the catalytic reactions are happening on the exposed metal surface or on top of a rapidly forming carbonaceous overlayer. In 1950, *Beek* concluded that surface deposits are not involved in the reaction.[19] Carbonaceous residues were found to be catalytically inactive for hydrogen reactions.[20] Such insensitivity of the catalytic reaction to carbonaceous residues is observed in practice, where lower levels of carbonization on process catalysts do not seem to affect catalytic activity or selectivity. Cyclohexene and ethylene hydrogenation occur despite a rapid buildup of a carbonaceous overlayer so dense that direct interaction of the reactant with the Pt surface is essentially impossible.[21,22] It was suggested that the reaction occurs on top of the overlayer and that the carbonaceous overlayer material is part of the catalytically active site.[21] In the case of ethylene hydrogenation, the carbonaceous layer was shown to consist mainly of alkylidynes, which were proposed as direct mediators of the catalytic activity. This view was opposed by later studies on Pd catalysts, where the buildup and removal of surface alkylidynes is unrelated to the catalytic reaction itself and the carbonaceous materials, such as alkylidynes, were considered to be uninvolved bystanders in the catalytic process.[23] Similar insensitivity to carbonaceous buildup was found in the activity and selectivity of H/D exchange reactions of hydrocarbons on Rh black.[24] It was concluded that carbonaceous surface species are not required as part of the catalytically active site on catalyst surfaces. Catalytic reactions seem to be insensitive to the presence of carbonaceous deposits indicating that the reactions might not differentiate between an exposed metal surface and a carbon covered surface.[13] Only catalyst deactivation by extensive carbonization can be considered to be a true effect of carbonaceous material.

4.3. Surface Structure

There are only a few principally different sites on the surface of a face centered cubic crystal: terrace atoms on (111) or (100) surfaces (characterized by nine or eight nearest neighbors respectively); all surfaces with higher Miller Indices contain additional surface steps and kinks (characterized by seven or six nearest neighbors respectively). The same type of surface atoms are also present on metal particles (Scheme 2). A principal difference between step or



Scheme 2. Similar surface atom types on flat surfaces and particles of FCC metals. Atom types are characterized by the numbers of nearest neighbors in parentheses. A = on (111) or (100) terraces; B = on steps or edges; C = on kinks or corners.

kink atoms on plane surfaces and on metal particles is the degree of surface curvature. Especially for small particles surface curvature can be expected to affect the electronic and steric interaction of the surface with the reactant. Surface reactions which are influenced by the types of surface atoms are termed surface structure sensitive. Such sensitivity of catalytic reactions to the surface structure of the metal particles of the catalyst suggests that the ideal catalyst would be a material with the right surface structure rather than an empirical mixture of ingredients.

4.3.1. Analysis

Although surfaces of well defined structure are routinely prepared for surface science studies by the cutting of single crystals, their direct use in catalysis would be costly and unpractical. Whereas heterogeneous catalysts have metal surface areas of several $m^2\ g^{-1}$, single crystal surfaces have only a few cm^2 of surface area and their use outside of UHV-chambers is hampered by surface contamination and rearrangement in the first atomic layer. Direct application of the insights achieved by surface science studies to catalysis is also limited by the idealized conditions required for single crystal studies, which usually differ greatly from the conditions used in catalysis. Although the number of exposed surface atoms can be measured by various adsorption techniques, there is no relationship between this number and the number of active sites on the catalyst surface. There is general agreement that the catalytic intermediates are very unstable and very few in number.[25] An upper limit of 10^{-4} active sites/surface atom (steady state concentration) can be estimated based on data obtained during the study presented in ref. [13]. Whether the concentration of reactive intermediates is controlled by unique arrangements of the surface atoms or simply controlled by thermodynamic factors with all surface atoms as potential active sites is not clear. The direct study of catalytic reactions by surface science techniques[26] is therefore also limited by the low steady state concentration of reactive intermediates, which is orders of magnitude below the accuracy attainable in the preparation of defined surfaces. (The commonly attainable precision in the cutting angle leads to a concentration of defect sites of > 1% on the single crystal surface.) The importance of such surface imperfections has recently been demonstrated by *Poelsema, Lenz* et al. on nearly defect-free surfaces.[27] They found that H_2 dissociation occurs on the step atoms of Pt-surfaces, H_2 activation on terrace surfaces is therefore directly dependent on the defect concentration. This evidence for the high structure sensitivity of hydrogen activation on Pt seems to question the results of all previous structure sensitivity studies.

In spite of the mentioned difficulties, there are practical methods for generating catalysts with preferred surface orientations. The preparation of oriented Pd-catalysts of high catalytic selectivity has been achieved by epitaxial growth of Pd on a suitable support. Figure 2 shows the (111) orientation of a Pd film on sapphire and the (100) orientation of a Pd film on tungsten foils. As expected, these oriented Pd film catalysts show high *cis*- and semi-hydrogenation selectivities for the reduction of alkynes.[28]

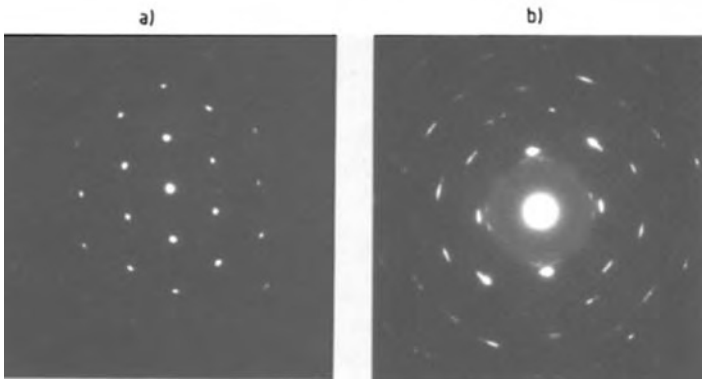


Fig. 2. Electron diffraction pattern of epitaxial Pd-films (thickness 100 nm) show a) the preferred (100) orientation of Pd on W foil and b) its preferred (111) orientation on sapphire.

Sophisticated transmission electron microscopy (TEM) studies allow the characterization of supported metal particles on practical catalysts,[29] but the wide distribution of particle sizes and shapes on a supported metal catalyst renders a detailed analysis of the surface composition of "real" catalysts impractical. Tunneling electron microscopy does allow the atomic characterization of selected portions of the surface, but there is still too little experience with this method for it to have an impact on our understanding of heterogeneous catalysis.

Nevertheless, simple geometric considerations predict that with increasing particle size the number of terrace type surface atoms increases while the number of step and especially kink type sites decreases.[17] The surface of idealized particles has a maximum step atom concentration for particles having an intermediate dispersion (= ratio of surface atoms to total number of atoms) of 30–60%,[30] while the surface of smaller metal particles is dominated by kink-type atoms. Investigations on the influence of catalyst dispersion on catalytic activity and selectivity are not only worthwhile, but are also the only methods currently available which give information about the surface structure sensitivities of catalytic reactions under real reaction conditions. These studies are normally conducted under standardized conditions using several, well characterized catalysts with widely differing dispersions. Additional complications in the interpretation of results are caused by the dependence of the work function on metal particle size, especially for very small particles. It is not yet possible to separate the effect of surface structure from particle size

effects. The increasingly metallic character of larger metal particles may affect catalytic reactions just as much as the changes in surface structure associated with these size changes. Further complications are caused by the morphological instability of supported or dispersed metal particles under the reaction conditions with respect to particle migration, fusion, reconstruction and crystallization processes. Pd and Ni based catalysts[31] are, because of their tendency to form β-hydride phases, especially prone to such morphological changes, which make conclusive analyses of particle size or surface structural effects difficult. The improved selectivity of Rosenmund,[32] Lindlar,[28,33] and other Pd catalysts[6] after empirical catalyst pretreatment with a modifier has been explained in terms of morphology changes caused by the modification process.

Figure 3 shows how the size of the Pd crystallites of a Pd/C catalyst in its untreated form increases after catalyst modification with the Rosenmund treatment and after

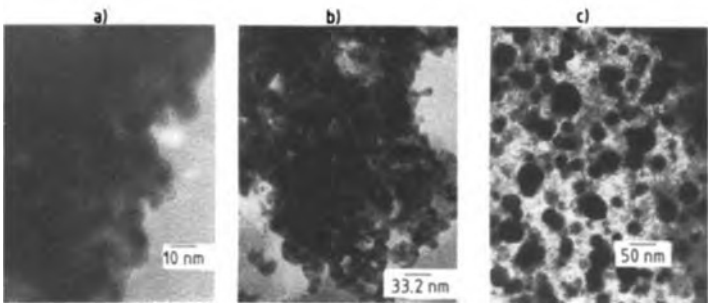


Fig. 3. TEM pictures showing the increase of Pd-particle size of a Pd/C catalyst. a) Untreated catalyst. b) Catalyst after Rosenmund treatment. c) Deactivated catalyst.

deactivation.[28] In this case deactivation can be attributed to loss of metal surface area and not catalyst poisoning. The problems of morphological instability, associated with heterogeneous Pd catalysts, were overcome by the use of epitaxial Pd-film catalysts on tungsten foil (see Fig. 2). The orientation of these Pd film catalysts increases with use, an effect associated with the orienting influence of the tungsten carrier material.[28]

4.3.2. Surface Structure Sensitive Reactions

The surface structure sensitivity of a catalytic reaction is commonly determined as the dependence of the reaction rate or selectivity on catalyst dispersion. Knowledge of the sensitivity of catalytic reactions to surface orientation[34] or particle size can be used for the rational improvement of heterogeneous catalysts.[28] Many examples of reactions exhibiting sensitivity to the surface structure of single crystals are known.[26] Based on several studies, *Boudart* et al. classified C–H bond breaking and forming as surface structure insensitive reactions and C–C bond forming and breaking as surface structure sensitive reactions.[35] However, many of the studies upon which the conclusions are based must be interpreted with caution; they neither cover the whole dispersion range from bulk metal to 100% dispersion nor do they report that reaction conditions have been applied which assure that the catalytic reaction is the rate determining step as discussed in Section 3. Hydrogenation reactions best illustrate the controversial nature of this new field. In spite of reaction rates that are zero order in reactant and first order in hydrogen, sensitivity of the rate of hydrogenation to metal dispersion was reported for supported Pd catalysts.[36,37] A moderate structure sensitivity was detected for propene hydrogenation on silica supported Pd catalysts.[36b] 1-Butyne hydrogenation is most rapid on low dispersed Pd catalysts while 1-butene hydrogenation is rather insensitive to Pd dispersion.[37a] On the basis of Pd particle size analysis, edge (step) type surface atoms seem to correlate with the isomerization of (+)-apopinene on dispersed Pd and Pt catalysts.[37b] These observations are in contrast with the generally accepted surface structure insensitivity of hydrogenation reactions. Structure insensitivity was observed in studies of cyclohexene hydrogenation over a limited dispersion range[38] as well as in the hydrogenation of ethylene on defined single crystal surfaces.[39] These discrepancies may be due to experimental conditions as well as to the special nature of ethylene or cyclohexene, which are not at all representative for the conformationally demanding higher olefins. A generalization of surface structure classifications of hydrogenation reactions in the absence of more reliable data seems premature.

There have been few studies on the structure sensitivity of H/D exchange of saturated alkanes. C–H activation of *n*-hexane is most effective on low dispersed (< 10%) Rh[24] and Pt[17] catalysts, and there is little change in turnover frequency at higher dispersions (> 10%). Although it was concluded that terrace surfaces are most effective for C–H activation, a simple particle size effect (e.g. work function) cannot be excluded. Structure sensitivity of rate and isotopic distribution of *n*-hexane exchange on Rh has been observed.[24] H/D exchange of *n*-hexane on Pt single crystal surfaces of (111) and (10,8,7) orientation shows no sensitivity of the reaction rate or isotopic distribution to the surface structure.[40] This was interpreted as structure insensitivity of the exchange reaction,[40] although the data are also consistent with terrace atoms being the active sites,[17] since terrace type surface atoms dominate on both crystal faces (see Section 4.3.1).

5. Hydrogen

While chemisorbed hydrogen on most group 8–10 metal surfaces is dissociated and located in the threefold hollow between the surface atoms,[41] little is known about the nature of the hydrogen in the catalytically active site. Nothing is known about the reactivity of this 'stable' surface hydrogen relative to "top on" bound or bridging hydrogen atoms for surface reactions with organic reactants.

6. Isotopic Exchange Reactions of Hydrocarbons

The structure of the organic reactant is known to influence both the rate and selectivity of C–H bond formation and activation. The most useful tool for probing C–H bond activation and formation mechanisms have been isotopic exchange experiments with deuterium [Eq. (a)].[42]

$$C_nH_m + q\,D_2 \xrightarrow{\text{catalyst}} C_nH_{m-q}D_q + q\,HD \qquad (a)$$

Here the number of deuterium atoms introduced into the hydrocarbon and their distribution are believed to be characteristic of the type of interaction (i.e. type of surface intermediate) between the catalyst and the hydrocarbon. Such experiments are carried out under low conversion conditions to ensure a single interaction of the reactant molecule with the catalyst. Large D_2/hydrocarbon ratios minimize hydrogen dilution (reintroduction of already exchanged H-atoms). Suitable reaction conditions are most readily attained in gas phase flow experiments. Analysis of the products by GC-MS provides information about the total conversion (reaction rate) and the isotopic distribution of the exchanged hydrocarbon.

Branched alkanes are less reactive than linear and cyclic alkanes.[17] Within these classes, the extent of conversion of an alkane correlates with its boiling point and the amount adsorbed with its vapor pressure.[13,17] This indicates that the overall conversion is largely controlled by the steady state surface concentration, while the relative reactivity of different classes of alkanes depends on the ease of formation of reactive surface intermediates (Scheme 4).

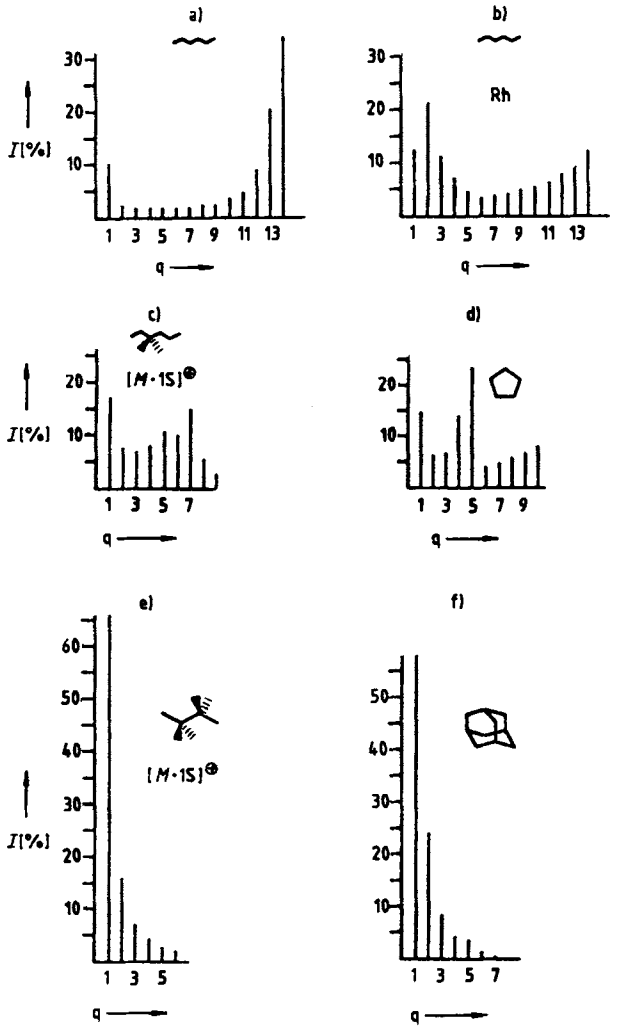


Fig. 4. Representative isotopic distributions ($M^{\oplus}$-peak) from H/D exchange experiments on group 8–10 catalysts at low hydrocarbon conversion. a) *n*-Hexane, b) *n*-hexane on Rh, c) 3,3-dimethylhexane, d) cyclopentane, e) 2,2,3,3-tetramethylbutane, f) adamantane. The distribution b) is typical for Rh. I = relative intensity, q = number of deuterium atoms in the hydrocarbon [cf. Eq. (a)].

The isotopic distribution of alkanes after exchange with deuterium, are obtained from the corrected MS pattern of the parent ion. There are some distinct and reproducible exchange patterns (Fig. 4) attributable to certain structural features of the hydrocarbon or the chemical nature of the catalyst. These patterns seems to provide direct information about the catalyst-hydrocarbon interaction.

6.1. Mono and Perdeuteration Maxima

H/D exchange reactions of straight chain hydrocarbons on various group 8–10 metal catalysts produce an isotopic distribution which is characterized by distinct mono and perdeuteration maxima (Fig. 4a).[17,24,43] This type of exchange selectivity has been studied in detail with *n*-hexane and other hydrocarbons on Pt catalysts.[17] In monodeuterated *n*-hexanes the deuterium was located at the terminal position as shown by high resolution ^2H NMR.[17] This assignment is also in agreement with the decreasing relative concentration of the D_1-maximum from *n*-pentane to *n*-heptane found in simple competition experiments, which correlates with the decreasing concentration of terminal C–H bonds.[17] It has been postulated that the activation of terminal C–H bonds leads to surface alkyl ligands which are more likely to reductively eliminate than to undergo additional C–H activations. Secondary C–H bond activation must therefore be the initiator of the multiple exchange processes leading to poly- and perdeuterated products, an interpretation which is also supported by steric arguments.[17] Earlier studies had already shown that the polydeuteration of quaternary centers does not proceed very effectively.[44] Perdeuteration maxima in side chains with three or more adjacent C–H bonds point to the formation of allylic intermediates. For example, the H/D exchange of 3,3-dimethylhexane (Fig. 4c) produces a D_7-maximum localized in the propyl side chain, while the methyl groups show only little D_1-exchange and the ethyl group a statistical distribution for D_1–D_5.[45] A rapidly converting olefin-allyl intermediate, postulated earlier as the most effective mechanism for polydeuteration of alkanes,[17] seems to be confirmed.

Polydeuteration via quaternary centers appears to proceed through metallocyclic α,γ- or α,δ-bound intermediates.[46] These intermediates seem to form more readily if the C–H-bonds activated are secondary rather than primary.[17] In compounds such as 2,2-dimethylbutane or 3,3-dimethylpentane, where allylic intermediates can not form due to the hydrocarbon structure, indications of the formation of vinyl-type intermediates have been obtained.[17] The presumably facile interconversion of σ- and π-vinyl groups in α,α,β-intermediates (see Scheme 4) is believed to be responsible for the direct formation of *trans*-hydrogenation products from alkynes.[2,14] Further evidence for vinylic intermediates has been obtained from mechanistic studies of olefin hydrogenation reactions.[47]

Competition experiments of *n*-hexane with various amounts of 4-methyl-2-pentene provide further evidence for the importance of π-olefin intermediates in polydeuter-

ation reactions. At very low olefin concentrations the 2-methylpentane produced shows a perdeuteration maximum while for *n*-hexane perdeuteration decreases with increasing olefin concentration.[17] Further evidence for olefinic intermediates was provided by high resolution ^2H NMR studies of the H/D exchange product of cyclopentane.[48]

The dominance of a D_1-product with a lack of significant formation of D_2- and higher deuterated isomers after exchange of compounds such as methane, tetramethylbutane (Fig. 4e) and adamantane (Fig. 4f) also support this mechanism.[24] The lack of polydeuteration in adamantane shows that the propagation of C–H activation requires the presence of planar π-bonded intermediates. Further evidence for the importance of planar π-bonded intermediates is provided by the D_2-product formed in H/D exchange experiments of norbornane,[44] where the formation of planar allylic intermediates is impossible due to the rigid structure.

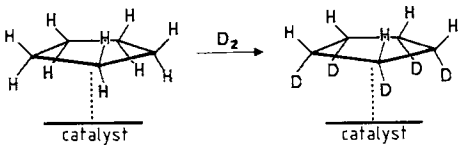
6.2. Dideuteration Maxima

The selective formation of D_2-maxima in the H/D exchange of saturated hydrocarbons on Rh catalysts is attributed to the chemical nature of the metal catalyst (Fig. 4b). A ^2H NMR study indicates that this D_2-maximum in *n*-alkanes is due to the formation of olefinic intermediates and not α,α-adsorbed species.[24] The same conclusion was arrived at independently by *Kemball* et al. for the origin of the D_2-maximum in cyclopentane exchange on Ni[48] and Rh[49] catalysts. It points to a high preference of Rh over other metals to form surface olefins as reactive intermediates in alkane exchange reactions. This preferred formation of D_2-alkanes is temperature and surface structure sensitive, particularly at low temperatures and low dispersions.[24] A decrease in the activation barrier for H/D exchange of *n*-alkanes was found for Rh-foil relative to dispersed Rh. Hydrocarbons which are not capable of forming olefinic intermediates (such as adamantane and tetramethylbutane) show no dependence of the activation barrier on dispersion. This has been interpreted as evidence for a concerted activation of adjacent C–H bonds with formation of olefinic intermediates on the surfaces of low dispersed Rh particles.[24]

6.3. Semideuteration Maxima

Another deuteration selectivity is the formation of semideuteration maxima for cyclic hydrocarbons, a selectivity observed on various metal catalysts (Fig. 4d). Semideuteration is most prominent in cyclopentane but still detectable in cyclohexane and cycloheptane.[17,50] These partial deuteration maxima are attributed to selective exchange on one side of the ring (Scheme 3).[51]

While rapid exchange on one ring side may proceed through the olefin-allyl conversion (see Section 6.1), there must also be an activation barrier for the ring flip. There is increasing perdeuteration with increasing temperature which is indicative of a higher energy intermediate or transition state. A vinylic intermediate has been suggested[17]



Scheme 3. Model to explain the preferred semideuteration in H/D-exchange reactions of cycloalkanes.

rather than the previously proposed roll-over mechanism.[44]

6.4. Olefin Deuteration

Many of the peculiar aspects of olefin deuteration have been discussed elsewhere.[2] For the content of this article it is important to recognize that deuteration of terminal olefins does not give the simple D_2-hydrocarbon expected from a *cis* addition of deuterium to the double bond, but results, in addition to varying amounts of polydeuterated isomers,[2] in a distribution of D_1, D_2 and D_3 isomers in a ratio of about 1:2:1 (Fig. 5). Since this ratio is not influenced by the extent of conversion or by the partial pressure of deuterium, intermolecular hydrogen exchange and C–H activation must be involved in the hydrogenation mechanism. ^2H NMR spectroscopy has provided evidence for the preferred allylic activation of adsorbed olefins as the origin of the D_1 and the D_3 products supporting the preference, postulated in Section 6.1, for allylic over vinylic intermediate formation in the catalytic process.[17] There appears to be only a small difference in the relative stability of allylic and vinylic intermediates. Allylic intermediates seem to form more readily if secondary C–H bonds are involved. The higher C–H bond energy of the methyl group may be responsible for the more facile exchange of the internal vinyl hydrogen (preferred formation of a vinyl or α,α,β-intermediate, see Scheme 4) in the H/D-exchange of propene.[47]

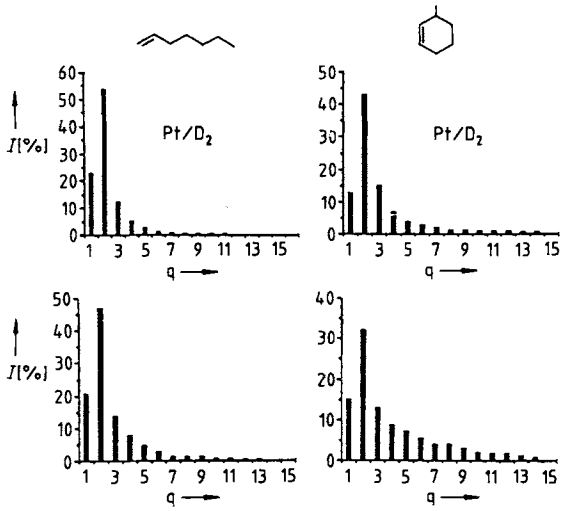
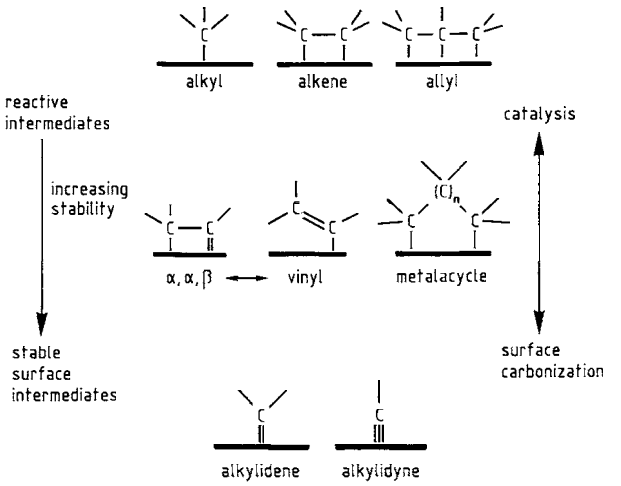


Fig. 5. Isotopic distribution ($M^{\oplus}$ ion) for alkanes obtained from the deuteration of 1-heptene (left) and 3-methylcyclohexene (right). Above: on a heterogeneous Pt catalyst: below: deuterium atoms in the gas phase after reaction with microwave plasma generated in a microwave discharge. (For a more detailed discussion of Figure 5 see Section 8.)

6.5. Reactive Intermediates, A Summary

It can be concluded that surface alkyl, olefin, and allyl ligands are catalytic intermediates in efficient H/D exchange processes. Vinylic and metallocyclic intermediates are also formed but apparently dominate only when the formation of allylic or olefinic intermediates is hindered. Alkylidenes and alkylidynes are not important intermediates in the catalytic exchange processes. This is most likely due to their higher kinetic or thermodynamic stability. Scheme 4 shows the relative importance of these reactive surface species.



Scheme 4. Surface intermediates ordered according to relative stability

Although there is some mechanistic understanding of C–H bond activation and formation processes, the desired molecular understanding of these heterogeneously catalyzed reactions has not been attained. There is still no convincing evidence for the successful identification and characterization of the above mentioned reactive intermediates in heterogeneously catalyzed reactions. Stable surface intermediates such as alkylidynes have been characterized with appropriate techniques but, as explained above, they are not involved in the catalytic process. Interpretations of reaction mechanism are therefore still speculative in nature and have increasingly been based on homogeneous organometallic analogues with an emphasis on covalent bonding. Multiple functionality is thus attributed to the transition metal surface. It is believed to simultaneously activate C–H and H–H bonds, and to serve as a mediator for the reactive intermediates determining the product composition. Although there is little doubt that hydrocarbon conversion on catalysts like zeolites is controlled by carbocations as reactive intermediates,[52] the question of whether radicals, charged, or covalently bonded species are the reactive intermediates in metal catalyzed reactions has not been resolved. This question may be ambiguous considering the change in electronic nature of such intermediates when interacting with the band structure of the metal surface. In fact, the catalytic activity of overlayers of carbonaceous material,[21] of gold films on platinum single crystal surfaces[53] and of spillover hydrogen,[18] suggests that catalysis may not require the presence of exposed catalyst metal surfaces.

7. Catalysis on Silica Overlayers

To investigate the true function of exposed transition metal surfaces in the catalytic reaction, transition metal film catalysts with and without a silica overlayer were compared.[54,55] It was expected that D_2 or H_2 would diffuse through the overlayer and become activated at the transition metal surface (see Scheme 5). The activated hydrogen could then diffuse back to the gas-surface interface in a process similar to hydrogen spillover.[18] Activated hydrogen on the oxide surface was expected to exhibit characteristic catalytic properties different from those of hydrogen on the exposed transition metal surface. Identification of such differences would allow the characterization of metal and of hydrogen spillover catalysis.



Scheme 5. Schematic representation of an overlayer catalyst with the related reaction processes.

The catalysts for these investigations were prepared by thin film deposition techniques on catalytically inactive single crystal silicon wafers. While the Pt/Si as well as the SiO_2/Pt/Si films were found to be catalytically active, SiO_2/Si films were catalytically inactive confirming the importance of Pt. The thin film catalysts were analyzed for composition and trace metal exposure using depth profiling procedures with secondary ion mass spectrometry (SIMS), Rutherford backscattering spectrometry (RBS), and Auger electron spectrometry (AES). All analytical techniques indicated that the silicon dioxide film is continuous, of uniform thickness, and uncontaminated by platinum. Impregnation of the SiO_2 surface of the catalytically inactive SiO_2/Si film with allyl platinum at readily detected concentrations of 10^8–10^{14} Pt atoms per cm^2 led to catalytically inactive materials. This excludes activity due to undetectable trace contamination of the SiO_2 surface with Pt. To exclude other alternative explanations for the observed catalytic activity such as cracks or pores in the silica overlayer, the following control experiments were conducted:

1. A 19 nm Pt layer was deposited on a Si surface through a mask so that the Pt surface was surrounded on all sides by a narrow frame of uncovered Si. The complete surface was then layered with silica. Since the catalytic activity per cm^2 Pt of the masked film was the same as that of an unmasked film, it could be excluded that the activity is purely due to edge effects.
2. Scanning electron microscope pictures show no visible cracks or pores.
3. The relative conversions in competitive deuterations of *n*-hexane and *n*-octane are independent of the presence and thickness of the silica overlayer and correlate with vapour pressure and not with hydrocarbon diffusion rates which supports the absence of small cracks or pores.

4. Subsequent deposition of SiO_2 or Au to fill cracks and pores does not decrease the catalytic activity.
5. SIMS does not show an increase in carbon content at the Pt-SiO_2 interface in used films; a carbon layer is normally formed immediately on the surface of Pt catalysts.

All these data suggest that there is no exposed Pt on the thin film catalysts indicating that the catalysis is happening on the silica surface itself. It was reported that H/D exchange reactions on overlayer catalysts show isotopic exchange patterns very similar to those on catalysts with exposed transition metal surfaces.[54] Activation barriers for these reactions are also very similar on both catalysts, while the catalytic activity decreases exponentially with increasing thickness of the silica overlayer. Similar catalysis on overlayered and exposed Pt films was also observed in hydrogenation-dehydrogenation studies with cyclohexene.[55]

Although all reaction and analytical data were consistent with catalysis on the outer silica surface, there was still a chance that cracks may be opening at higher reaction temperatures due to the different expansion coefficients of the individual layers. Since the analyses of the catalyst films are performed at room temperature, such temperature dependent crack openings would not be detected. *Cis*-semihydrogenation of 2-hexyne, a reaction most selective on Pd, was chosen to examine this possibility. While 2-hexyne hydrogenation on Pd under gas phase flow conditions produces *cis*-2-hexene with a selectivity of greater than 90%, the selectivity decreases to 68% *cis*-hexene on silica covered Pd films at lower temperatures. However, upon raising the temperature above 200 °C these silica covered Pd films gave the >90% *cis*-hydrogenation selectivity indicative of exposed Pd.[56] Control experiments with exposed Pd films showed high *cis*-semihydrogenation selectivity (>90%) over the whole temperature range studied. It must therefore be concluded, that on SiO_2/Pd/Si cracks are opening at higher temperatures and closing again at lower temperatures. Consequently it cannot be excluded that the observed catalysis at elevated temperatures is fully or partly due to direct metal hydrocarbon contacts. However, the fact that catalysis is still observed at lower temperatures on the SiO_2/Pd/Si films still supports the hypothesis that a transition metal hydrocarbon interaction is not required to achieve catalysis.

8. The Connection between Deuterium Atom Reactions and Catalysis

If the transition metal is not accessible to the organic reagent, then the following explanation is the only one consistent with the data presented. Deuterium or hydrogen diffuse through the silica overlayer and are activated (dissociated) at the transition metal surface. The hydrogen atoms diffuse back through the overlayer to the silica surface where they act as catalytically active sites. Such an interpretation is not unreasonable. Spillover hydrogen on silica and alumina has been shown to react with alkanes and olefins;[18] atomic hydrogen on alumina converts benzene to cyclohexane.[57] As early as 1912, *Langmuir* had noted that hydrogen atoms adsorbed on glass surfaces have a long-lived reactivity.[58] Surface diffusion of deuterium atoms on SiO_2 has an activation energy of ca. 15.0 kcal mol^{-1} [61] to 25 kcal/mol[60], on Al_2O_3 28 kcal/mol;[61] while the adsorption energy for H and D atoms on quartz is 12 kcal mol^{-1}.[62] This indicates significant bonding between the hydrogen atom and the silica surface. *Chen* and *White* obtained evidence for 4 states of spillover deuterium on Al_2O_3.[63] The active sites of these overlayer catalysts may therefore be similar, but not necessarily identical with adsorbed hydrogen atoms on silica surfaces.

Further support for such interpretations was obtained in a study which compared the isotopic distributions of hydrocarbons after gas phase and surface reactions with dissociated deuterium atoms generated by a microwave discharge.[64] On heterogeneous catalysts, deuteration of olefins is dominated by a D_2 maximum with varying amounts of polydeuterated isomers (see Fig. 5). It was found that the isotopic distribution of saturated hydrocarbons obtained from the reaction of mono-, di-, tri- and tetrasubstituted alkenes with deuterium atoms in the gas phase is identical to that obtained in deuteration reactions of olefins on Pt, while a slightly higher tendency to polydeuteration was observed on Pd catalysts.[64] The data suggest that the reactive intermediates in heterogeneously catalyzed olefin hydrogenation reactions behave like gas phase radicals, which supports the unimportance of distinct surface metal bonds in the reactive intermediates in such catalytic processes.

However, when saturated hydrocarbons such as *n*-alkanes or cycloalkanes are reacted with the deuterium atoms in the gas phase the polydeuteration maxima observed with Pt catalysts are not reproduced. A distinct D_1 maximum is observed in all cases with statistical fall-off to higher deuteration. No trace of the D_{14} maximum for *n*-hexane, the D_5 and D_{10} maxima for cyclopentane, or the D_7 maximum for 3,3-dimethylhexane was found in the gas phase reactions indicating that these maxima require either the presence of an exposed transition metal surface or at least the presence of a surface per se. However, the lack of a D_5 maximum for cyclopentane after exchange on atomically dispersed Pt (Fig. 6) indicates that this semi-

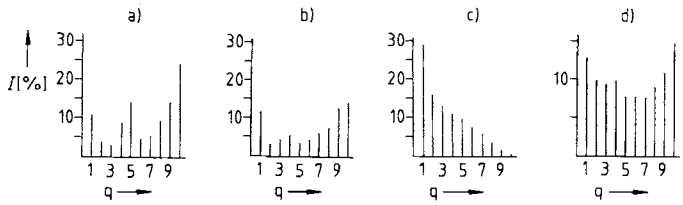


Fig. 6. Isotopic distribution ($M^{\oplus}$ ion) of cyclopentane after exchange with deuterium which was activated as follows: a) on a Pt film; b) on highly dispersed Pt; c) by microwave plasma in the gas phase; d) by microwave plasma in the gas phase in the presence of Al_2O_3.

deuteration maximum may be surface structure sensitive and require the presence of metal clusters. Figure 6 shows how different approaches to the activation of the deuterium for the reaction with cyclopentane affect the isotopic product distribution.

To test for the influence of the surface on the isotopic product distribution, the gas phase reactions were carried out in the presence of inert-membranes separating the deuterium atom flow from the hydrocarbon flow. It was hoped that deuterium atoms would diffuse through the membrane and react with the alkanes on the other side to form exchanged alkanes with per- or polydeuteration maxima.[64]

The expected perdeuteration maxima were obtained for cyclopentane and cyclohexane when a membrane of inert alumina or silica was placed between the gas phase streams of D atoms and cyclic alkanes. Increased polydeuteration was also observed in H/D exchange reactions of acyclic hydrocarbons, although no perdeuteration maxima were observed. Control experiments in the absence of the hydrogen-dissociating plasma showed no exchange.[64] Therefore, perdeuteration maxima in hydrocarbons are not useful as mechanistic tracers for the interaction of metal surface atoms with the substrate.

9. Summary and Outlook

Despite the obvious importance of catalytic C–H bond formation and activation, an understanding of such catalytic processes on the molecular level has not been reached. However, several important findings can be summarized. An exposed transition metal surface is not required for the hydrogenation of olefins or the C–H activation of alkanes. The primary function of group 8–10 transition metals in the catalysis of hydrogen reactions with C–H bond formation and activation is to dissociate (activate) hydrogen, the secondary function is to provide metal specific selectivity. The dissociated hydrogen seems to represent the catalytically active site. Since the concentration of dissociated hydrogen is highest at the hydrogen dissociation sources, i.e. the metal particles, exposed transition metal surfaces are the most effective catalyst surface for these types of reaction. The similar product distributions from the reactions of gas phase deuterium atoms and from heterogeneous catalysis in a deuterium atmosphere suggests a chemistry arising from surface radicals.

In spite of its complexity, heterogeneous catalysis is slowly changing from an empirical art to an understandable science. Modern analytical techniques are largely responsible for this transition. One of the most urgent problems in heterogeneous catalysis is the development of methods which allow the determination of the surface concentration of active sites and the identification and characterization of true reactive intermediates in catalytic processes. Solid state chemistry, materials science and surface science are important related areas for heterogeneous catalysis as are the empirical knowledge collected in catalysis research and chemical engineering and the mechanistic understanding of organic chemistry. A molecular understanding of heterogeneous catalysis requires a multidisciplinary approach and future progress will largely depend on the ability of the scientists to select the right combination of methods. Only such a molecular understanding of catalytic processes will provide insight into the controlling factors of chemical processes on heterogeneous surfaces.

This article was only made possible through the experimental contributions of my graduate students. Work on C–H activation was started with Carlito B. Lebrilla with contributions by Gene C. Lau and Susan B. Chettle. Major breakthroughs were achieved by the work of Jeffrey M. Cogen, Alan B. McEwen, and Judith G. Ulan with contributions from Felicia A. Etzkorn. I owe much to the continuing enthusiasm, engagement, skills, and many creative as well as aggressive discussions of these coworkers. I am also grateful to the invaluable contributions of materials scientists, who are coauthors of many of our papers.

Submitted: January 18, 1988 [A 708 IE]
Revised: October 26, 1988
German version: *Angew. Chem. 101* (1989) 135

[1] H. Pines: *The Chemistry of Catalytic Hydrocarbon Conversions*, Academic Press, New York 1981; P. N. Rylander: *Catalytic Hydrogenation over Platinum Metals*, Academic Press, New York 1967.
[2] G. C. Bond, P. B. Wells, *Adv. Catal. 15* (1964) 91.
[3] S. Siegel, *Adv. Catal. 16* (1966) 123; J. K. A. Clarke, J. J. Rooney, *ibid. 25* (1976) 125; F. G. Gault, *Gazz. Chim. Ital. 109* (1979) 255.
[4] M. Baerns, H. Hofmann, A. Renken: *Chemische Reaktionstechnik*, Thieme, Stuttgart 1987; J. J. Carberry, *Chem. Eng. Prog. 84*, No. 2 (1988) 51.
[5] G. Poncelet, P. Grange, P. A. Jacobs (Eds.): *Preparation of Catalysts*, Elsevier, Amsterdam 1983.
[6] W. F. Maier in R. N. Rylander, H. Greenfield, R. L. Augustine (Eds.): *Catalysis of Organic Reactions*, Marcel Dekker Inc., New York 1988, p. 211.
[7] B. R. James: *Homogeneous Hydrogenation*, Wiley-Interscience, New York 1973; A. I. Mikaya, V. G. Zaikin, V. M. Vdovin, *J. Mol. Catal. 32* (1985) 353.
[8] M. Hudlicky: *Reductions in Organic Chemistry*, Ellis Horwood, New York 1984; M. Bartók: *Stereochemistry of Heterogeneous Metal Catalysis*, Wiley, New York 1985.
[9] M. Ephritikhine, *Nouv. J. Chim. 10* (1986) 9; M. L. H. Greene, D. O'Hare, *Pure Appl. Chem. 57* (1985) 1897; R. H. Crabtree, *Chem. Rev. 85* (1985) 245; J. Halpern, *Inorg. Chim. Acta 100* (1985) 41; R. B. Bergman, *Science (Washington) 223* (1984) 902.
[10] P. Hofmann, H. Heiss, G. Müller, *Z. Naturforsch. B42* (1987) 395; J.-Y. Saillard, R. Hoffmann, *J. Am. Chem. Soc. 106* (1984) 2006.
[11] a) G. Schmid, N. Klein, *Angew. Chem. 98* (1986) 910; *Angew. Chem. Int. Ed. Engl. 25* (1986) 922; b) G. Schmid, *Chem. Unserer Zeit 22* (1988) 85.
[12] T. M. Miller, T. J. McCarthy, G. M. Whitesides, *J. Am. Chem. Soc. 110* (1988) 3156; S. Naito, M. Tanimoto, *J. Catal. 102* (1986) 377.
[13] J. M. Cogen, W. F. Maier, *Langmuir 3* (1987) 830.
[14] J. G. Ulan, W. F. Maier, *J. Mol. Catal.*, in press.
[15] A. S. Hussey, G. W. Keulks, G. P. Nowack, R. H. Baker, *J. Org. Chem. 33* (1968) 610.
[16] G. Georgiades, V. A. Self, P. A. Sermon, *Angew. Chem. 99* (1987) 1050; *Angew. Chem. Int. Ed. Engl. 26* (1987) 1042; S. B. Sharma, J. McClay, D. Böcker, R. D. Gonzales, *Tenth North Am. Meet. Catal. Soc. 1987.*
[17] C. B. Lebrilla, W. F. Maier, *J. Am. Chem. Soc. 108* (1986) 1606.
[18] W. C. Conner, Jr., G. M. Pajonk, S. J. Teichner, *Adv. Catal. 34* (1986) 1.
[19] O. Beek, *Discuss. Faraday Soc. 8* (1950) 118.
[20] T. Hattori, R. L. Burwell, Jr., *J. Phys. Chem. 83* (1979) 241; A. Takeuchi, J. R. Katzer, *J. Catal. 82* (1983) 351.
[21] S. M. Davis, F. Zaera, G. A. Somorjai, *J. Catal. 77* (1982) 439.
[22] S. M. Davis, G. A. Somorjai, *J. Catal. 65* (1980) 78.
[23] T. P. Beebe, J. T. Yates, Jr., *J. Am. Chem. Soc. 108* (1986) 663.
[24] J. M. Cogen, W. F. Maier, *J. Am. Chem. Soc. 108* (1986) 7752.
[25] J. J. Rooney, *J. Mol. Catal. 31* (1985) 147.
[26] G. A. Somorjai: *Chemistry in Two Dimensions*, Cornell University Press, New York 1981.
[27] B. Poelsema, L. S. Brown, K. Lenz, L. K. Verheij, G. Comsa, *Surf. Sci. 171* (1986) L395; K. Lenz, *Ber. KFA Jülich 1987*, No. 2141.
[28] J. G. Ulan, W. F. Maier, D. A. Smith, *J. Org. Chem. 52* (1987) 3132.
[29] M. J. Yacamán, A. Gómez, *Appl. Surf. Sci. 19* (1984) 348; P. J. F. Harris, *Surf. Sci. 185* (1987) L459.
[30] R. Van Hardeveld, A. Van Montfoort, *Surf. Sci. 4* (1966) 396; O. M. Poltorak, V. S. Boronin, *Russ. J. Phys. Chem. 40* (1966) 1437.
[31] R. Christoph, M. Baerns, *Chem. Ing. Tech. 57* (1985) 775; R. D. Kelley, G. A. Candela, T. E. Madey, D. E. Newbury, R. R. Schehl, *J. Catal. 80* (1983) 235.
[32] W. F. Maier, S. J. Chettle, R. S. Rai, G. Thomas, *J. Am. Chem. Soc. 108* (1986) 2608.

[33] J. G. Ulan, W. F. Maier, R. S. Rai, G. Thomas, *J. Org. Chem. 52* (1987) 3126.
[34] M. Boudart, *Adv. Catal. 20* (1969) 153; A. Frennet, G. Lienard, L. Degois, A. Crucq, *Bull. Soc. Chim. Belg. 88* (1979) 621; W. H. Manogue, J. R. Katzer, *J. Catal. 32* (1974) 166; G. A. Somorjai, J. Carrazza, *Ind. Eng. Chem. Fundam. 25* (1986) 63.
[35] M. Boudart, G. Djéga-Mariadassou: *Cinetique des Réactions en Catalyse Hétérogene*, Masson, Paris 1982; M. Boudart, *J. Mol. Catal. 30* (1985) 27.
[36] a) H. H. Kung, R. J. Pellet, R. L. Burwell, Jr., *J. Am. Chem. Soc. 98* (1976) 5603; b) E. Rorris, J. B. Butt, R. L. Burwell, Jr., J. B. Cohen, *Proc. 8th Int. Cong. Catal. Vol. 4* (Berlin 1984), p. 321.
[37] a) J. P. Boitiaux, J. Cosyns, S. Vasudevan, *Appl. Catal. 6* (1983) 41; b) F. Notheisz, M. Bartok, D. Ostgard, G. V. Smith, *J. Catal. 101* (1986) 212.
[38] E. Segal, R. J. Madon, M. Boudart, *J. Catal. 52* (1978) 45; E. E. Gonzo, M. Boudart, *ibid. 52* (1978) 462.
[39] A. Wieckowski, S. D. Rosasco, G. N. Salaita, A. Hubbard, B. E. Bent, F. Zaera, D. Godbey, G. A. Somorjai, *J. Am. Chem. Soc. 107* (1985) 5910; F. Zaera, G. A. Somorjai, *ibid. 106* (1984) 2288.
[40] S. M. Davis, G. A. Somorjai, *J. Phys. Chem. 87* (1983) 1545.
[41] H. Conrad, G. Ertl, E. E. Latta, *Surf. Sci. 41* (1974) 435.
[42] C. Kemball, *Adv. Catal. 11* (1959) 223; P. H. Emmet, *Catal. Rev. 7* (1972) 1; R. L. Burwell, Jr., *ibid. 7* (1972) 25; J. R. Anderson, *Rev. Pure Appl. Chem. 7* (1957) 165.
[43] F. G. Gault, C. Kemball, *Trans. Faraday Soc. 57* (1961) 178; J. A. Oliver, C. Kemball, R. Brown, E. W. Jamieson, *J. Chem. Soc. Faraday Trans. 1 81* (1985) 1871; M. A. Long, R. B. Moyes, P. B. Wells, J. L. Garnett, *J. Catal. 52* (1978) 206; R. S. Dowie, D. A. Whan, C. Kemball, *J. Chem. Soc. Faraday Trans. 1 68* (1973) 2150.
[44] R. L. Burwell, Jr., *Acc. Chem. Res. 2* (1969) 289.
[45] A. B. McEwen, W. F. Maier, D. A. Smith, *10th Symp. North Am. Catal. Conf. 1987*, 823.
[46] C. Kemball, R. Brown, *J. Chem. Soc. Chem. Commun. 1987*, 771.
[47] V. Mintsa-Eya, L. Hilaire, A. Choplin, R. Touroude, F. G. Gault, *J. Catal. 82* (1983) 267; S. Naito, M. Tanimoto, *ibid. 102* (1986) 377.
[48] R. Brown, C. Kemball, *J. Catal. 104* (1987) 480.
[49] A. C. Faro, C. Kemball, *J. Chem. Res. Miniprint 1982*, 3721; *ibid. 1984*, 3208.
[50] J. R. Anderson, C. Kemball, *Proc. R. Soc. London A 226* (1954) 472.
[51] R. L. Burwell, Jr., B. K. C. Shim, H. C. Rowlinson, *J. Am. Chem. Soc. 79* (1957) 5142; Y. Inoue, J. M. Herrmann, H. Schmidt, R. L. Burwell, Jr., J. B. Butt, J. B. Cohen, *J. Catal. 53* (1978) 401.
[52] G. C. Lau, W. F. Maier, *Langmuir 3* (1987) 164.
[53] J. W. A. Sachtler, M. A. VanHove, J. P. Biberan, G. A. Somorjai, *Phys. Rev. Lett. 45* (1980) 1601.
[54] A. B. McEwen, W. F. Maier, R. H. Fleming, S. M. Baumann, *Nature (London) 329* (1987) 531; A. B. McEwan, *Ph.D. thesis*. U. C. Berkley 1987.
[55] J. M. Cogen, K. Ezaz-Nikpay, R. H. Fleming, S. M. Baumann, W. F. Maier, *Angew. Chem. 99* (1987) 1222; *Angew. Chem. Int. Ed. Engl. 26* (1987) 1182.
[56] J. M. Cogen, W. F. Maier, *Appl. Catal.*, in press.
[57] P. Antonucci, N. Truong, N. Giordano, R. Maggiore, *J. Catal. 75* (1982) 140.
[58] I. J. Langmuir, *J. Am. Chem. Soc. 34* (1912) 1310.
[59] T. Fleisch, R. Abermann, *J. Catal. 50* (1977) 268.
[60] N. E. Lobashina, N. N. Savvin, I. A. Myasnikov, *Kinet. Katal. 25* (1984) 420; *ibid. 24* (1983) 634.
[61] R. Kramer, M. Andre, *J. Catal. 58* (1979) 287.
[62] G. Blyth, A. A. Clifford, P. Gray, J. I. Waddicor, *Int. J. Chem. Kinet. 18* (1986) 861.
[63] H.-W. Chen, J. M. White, *J. Mol. Catal. 35* (1986) 355.
[64] A. B. McEwen, F. A. Etzkorn, W. F. Maier, *Chimia 41* (1987) 293.
[65] J. M. Thomas, *Angew. Chem. 100* (1988) 1735; *Angew. Chem. Int. Ed. Engl. 27* (1988) 1673.

Biosynthetic Studies on Antibiotics

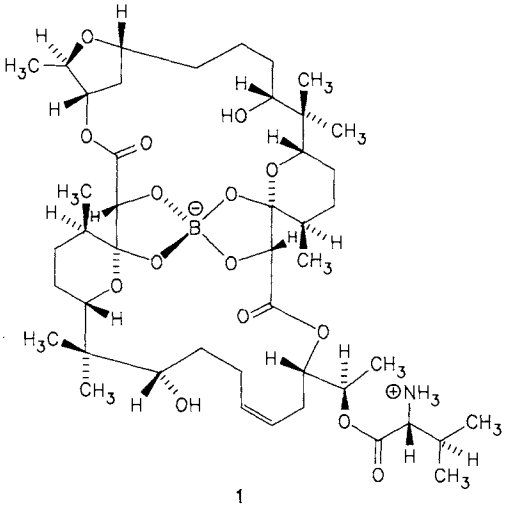
By Heinz G. Floss* and John M. Beale*

The intricacies of the synthetic chemistry executed by living cells in the assembly of complex organic natural products can be probed in great detail by stable-isotope labeling in conjunction with sophisticated 2D and multiple-quantum NMR methods of analysis. Mechanistic details are revealed by unraveling the "cryptic" stereochemistry of biosynthetic reactions with the aid of stereospecific isotope labeling. Analysis of blocked mutants and cloning of biosynthetic genes provides new tools for the study of biosynthetic pathways and for the exploitation of the chemical capabilities of living organisms.

1. Introduction

Living cells manage to elaborate a bewildering variety of organic molecules. Many of these are of ubiquitous or widespread occurrence in living organisms and are essential to the "conduct of business" of living cells. These are often called "primary metabolites"; they make up or are involved in the formation of the structural, functional, energy-producing, or information-containing molecules of living cells. Many other organic compounds are found in nature which are produced by a more limited range of organisms, sometimes only a few species. These are often called "secondary metabolites", a term which unfortunately has suggested to many biochemists that these compounds are secondary in importance. Some of these compounds serve more subtle and specialized functions in the survival of an organism in its overall environment, often relating to communication with other organisms, maintenance of symbiotic relationships, or defense against predators, but for the majority of these compounds no functions are (as yet) known. Many of these natural products are useful to man, for example, as drugs (antibiotics, alkaloids) or as flavoring or coloring agents; others may be detrimental, like toxins, poisons, or irritants.

The structures of organic natural products range from extremely simple ones, like formic acid, the defense and protective agent of certain ants and nettles, to very complex structures, like boromycin **1** (Fig. 1),[1,2] a boron-containing antibiotic produced by *Streptomyces antibioticus* containing 45 carbon atoms and 16 chiral centers. The synthetic prowess of living cells has been a challenge to generations of synthetic organic chemists; the desire to duplicate in the laboratory some of the chemistry carried out by nature has been one of the major driving forces for the development of new synthetic methodology. The chemistry executed by living cells in the course of such natural product syntheses is even more remarkable when one considers the constraints under which it has to be carried out: all reactions have to take place at room temperature, at neutral pH, at normal pressure, and in an aqueous environment! The desire to unravel the secrets of this chemistry has been the motivation of many bioorganic chemists who



1

Fig. 1. Boromycin **1**.

study the biosynthesis of such organic natural products. Beyond suggesting new approaches to the chemical total synthesis of complex organic molecules (biomimetic chemistry), the insights gained from such biosynthetic studies may lead to improved methods for the production of natural products which are of commercial value. They may suggest means of interfering with the formation of natural products which are detrimental to man, and they may allow the structural modification of natural products, for example, by diverting the biosynthetic machinery into producing analogues of the normal natural products from analogues of the biosynthetic precursors or intermediates, and by exchange of genetic information between different organisms. However, quite apart from these potential practical payoffs, biosynthetic studies on natural products generate fundamental knowledge which helps us understand how living organisms have evolved to become highly refined synthetic organic chemists and how the products of these synthetic labors help the organism maintain and improve its position within a particular ecosystem.

2. Experimental Approaches to Biosynthetic Studies

A multitude of different approaches are used to study the biosynthesis of natural products.[3] The majority of these involve the feeding of variously isotope-labeled pre-

[*] Prof. H. G. Floss, Prof. J. M. Beale
Department of Chemistry, University of Washington
Seattle, WA 98195 (USA)

cursors or intermediates to an intact organism to assess the role of the compound tested in a biosynthetic pathway. Such studies may be complemented or followed up by experiments with cell-free systems or, ultimately, purified enzymes. An alternative line of attack on biosynthetic problems involves the use of blocked mutants and, more recently, techniques of molecular genetics (e.g., the cloning of biosynthetic and regulatory genes).

In a classical tracer experiment[4] the putative precursor or intermediate is labeled with a radioactive isotope (e.g., ^{14}C or tritium) and administered to the biological system producing the metabolite under investigation. The proximity of the precursor–product relationship is assessed by examining the percentage incorporation, the percentage specific incorporation, or the dilution factor. Unless the values are very low (less than 0.01% incorporation) or very high (over 10% incorporation), it is often difficult to draw definitive conclusions from these values alone. Therefore, such experiments usually have to be followed up by a chemical degradation of the metabolite under investigation in order to determine whether the radioactivity is located specifically in the expected position.[5] An alternative is the labeling of the precursor in remote positions with two radioactive isotopes (e.g., ^{14}C and tritium) followed by an assessment of whether the ratio of the two isotopes remains constant during the metabolic transformation. Multiple labeling with two radioactive isotopes can also be used to probe specifically for the retention of certain hydrogen atoms relative to the backbone of the molecule in the transformation of a precursor to a product. However, most of these questions can now be probed more easily and/or more definitively by stable-isotope labeling followed by analysis of the product by mass spectrometry or NMR spectroscopy. The unique advantage of radioactive tracer experiments is their great sensitivity; this makes them the method of choice in those cases where the rate of synthesis of a metabolite is very low (e.g., in many experiments with intact higher plants) or where the amounts of metabolite produced are very small (e.g., in studies on the biosynthesis of many vitamins, cofactors, hormones, or pheromones). However, more often in contemporary natural products biosynthesis work, studies with radioactive tracers are used as a prelude to stable-isotope feeding experiments.

The use of stable-isotope labeling in conjunction with mass spectrometry and particularly high-field NMR spectroscopy has become one of the most incisive tools of research in natural products biosynthesis.[6] The power of this approach stems from the fact that the analytical methodology not only indicates the presence or absence of the isotope, but also reveals its distribution within a molecule and between individual molecules of a population. Thus, potentially, an enormous amount of metabolic information can be extracted with sophisticated spectroscopic techniques from the products of such stable-isotope labeling experiments. Tagging of a precursor with a single stable-isotope label (e.g., ^{13}C in a single position of a molecule) allows the fate of the labeled atom to be traced through a metabolic reaction sequence. The ^{13}C NMR signals corresponding to the atom or atoms in the product that originate(s) from the labeled atom of the precursor will show an increased intensity in the ^{13}C NMR spectrum. The fate of bonds can be traced through a metabolic reaction sequence by placing two stable isotopes at the two ends of the bond (e.g., two ^{13}C atoms at the two ends of a carbon–carbon bond) such that the ^{13}C NMR signal for each of the carbons is split into a doublet by coupling to the neighboring ^{13}C nucleus. The administered precursor is diluted by unlabeled material either synthesized endogenously from the available nutrients or administered externally together with the labeled sample. If the bond between the two stable isotopes is broken during the metabolic conversion, the stable isotope in each terminus will be diluted with a large excess of unlabeled material. If a bond is subsequently reformed, the probability of reconnecting the two stable isotopes in the same molecules becomes very small. Hence, the coupling between the two nuclei is lost. Retention of the coupling in the final product indicates that the two nuclei must have originated from the same molecule, strongly suggesting that the bond between them has never been broken.

Multiple stable-isotope labeling, first introduced into studies of natural products biosynthesis by *Seto* et al.[7] and by *Battersby* et al.[8] can also be used to distinguish between intra- and intermolecular processes in group-transfer and rearrangement reactions. In relatively simple cases, mass spectrometry may serve as the analytical tool to distinguish between intra- and intermolecular labeling, but with more complex molecules, NMR spectroscopy is usually the method of choice. In addition to the coupling analysis, which can be used with two magnetically active nuclei, intramolecular double labeling with two isotopes can also be detected if one isotope is magnetically active and the other exerts an isotopic shift on its NMR signal. In this way, the presence of deuterium can be detected by the α- or β-deuterium isotope shift on a ^{13}C NMR signal[9] and the presence of ^{18}O can be detected by the (smaller) α-^{18}O effect.[10] With these techniques, the retention of specific oxygen, hydrogen, or nitrogen atoms relative to the backbone of the precursor molecule can be probed definitively.

Key precursors, like glucose[11,12] or glycerol,[13] labeled uniformly with ^{13}C (90–99% enrichment in every carbon) can be used for mapping of metabolic pathways to a product in cases where it is not evident from the structure or from simple specific feeding experiments which metabolic route(s) is (are) involved in the construction of a particular metabolite. Extensive analysis of the homonuclear coupling patterns of the product from such a feeding experiment reveals which assemblies of carbon atoms in the product have been derived intact from the precursor molecule. Since the various pathways of primary metabolism lead to predictable coupling patterns, the involvement of certain metabolic routes (e.g., shikimate pathway, pentose phosphate shunt, Krebs cycle) can be inferred. Such experiments, particularly when applied to complex molecules, require the detailed analysis of often very complex second-order and/or overlapping coupling patterns, necessitating the extensive use of modern 2D and multiple-quantum NMR techniques. The amount of metabolic information that can be extracted from such experiments is usually proportional to the degree of sophistication of the

NMR analysis of the product. Hence, it is not surprising that many state-of-the-art 2D NMR techniques have been quickly adopted or modified for biosynthetic experiments (e.g., INADEQUATE,[14,15] triple-quantum INADEQUATE,[16] COSY,[17] and 2D heteronuclear correlation).[18] 2D NMR techniques have also been developed for the stereochemical analysis of stereospecifically deuterium-labeled natural products, as exemplified by the work of *Vederas* et al.[19] and *Gould* et al.[20]

Once the basic building blocks of a natural product have been identified, the studies often turn to a more detailed analysis of the biosynthetic reaction sequence and mechanistic aspects of biosynthetic transformations. Analysis of the stereochemistry of these transformations often provides mechanistic information, allows a discrimination between alternative pathways, or sometimes provides evidence for or against the involvement of a particular enzyme.[21] Since the majority of biochemical reactions take place at centers, usually carbon atoms, that are not a priori chiral, these studies usually rely on the synthesis of stereospecifically isotope-labeled substrates and the evaluation of their fate in the biosynthetic reaction sequence. Again, the isotope used in such studies may be radioactive (e.g., tritium) or stable (e.g., deuterium).

More detailed information is obtained by further studies with crude cell-free extracts or, eventually, individual purified enzymes. Even the use of a crude cell-free system has an advantage over that of whole cells in that one can be reasonably certain that an administered precursor will reach the site of synthesis. In a whole-cell experiment, nonincorporation of an administered compound may be due to permeability barriers which prevent its uptake by the cell. Studies with purified individual enzymes ultimately provide definitive mechanistic information on specific reaction steps. They also may shed light on the regulation of a biosynthetic pathway. However, one has to realize that studies at the enzymatic level can be quite involved and labor-intensive; therefore, many biosynthetic investigations are not carried all the way to this stage.

An altogether different approach to biosynthetic studies involves the use of genetic techniques. The preparation of mutants blocked in the synthesis of the metabolite under investigation in conjunction with assays for cosynthesis, in vivo or in vitro complementation, may reveal the minimum number of steps involved in a biosynthetic sequence. Chemical analysis of these mutants can establish the structures of intermediates, thus ultimately allowing the construction of a biosynthetic pathway. This approach has been extensively used to unravel the routes of primary metabolism. Its application to the study of secondary metabolites is more difficult because loss of the biosynthetic ability in this case does not result in a nutritional requirement. Thus, the selection of blocked mutants is more difficult, having to rely usually on the analysis of large numbers of colonies for some identifiable marker (e.g., loss of a pigment or loss of antibiotic activity). Nevertheless, the approach has been used successfully in natural products biosynthesis, particularly in the study of various antibiotics.[22-24] With the further development of systems for the genetic manipulation of organisms producing secondary metabolites, we are now beginning to see the impact of modern methods of molecular biology on such biosynthetic studies. Already, a number of antibiotic biosynthesis genes have been cloned, including those for entire pathways,[25] and a few have been sequenced. These genes are used to study the regulation and genetic control of antibiotic biosynthesis, to isolate biosynthetic genes from other organisms[26] and to construct genetically engineered organisms producing new hybrid antibiotics.[27,28] The next few years are likely to see a dramatic increase in the use of genetic approaches to the study of natural products biosynthesis, and these can be expected to be very incisive, particularly when combined with more traditional chemical and biochemical approaches.

In the following we will highlight some of these methods and approaches used in the study of natural products as we discuss various projects, most of which have been or are being conducted in our laboratory in the field of antibiotic biosynthesis.

3. Hydroaromatic Compounds—The Formation of Cyclohexane Rings

A number of antibiotics contain partially or fully reduced benzene rings which are evidently derived via the shikimate (**2**, Fig. 2) pathway, raising the question how a metabolic pathway designed to produce aromatic systems has been diverted into generating hydroaromatic struc-

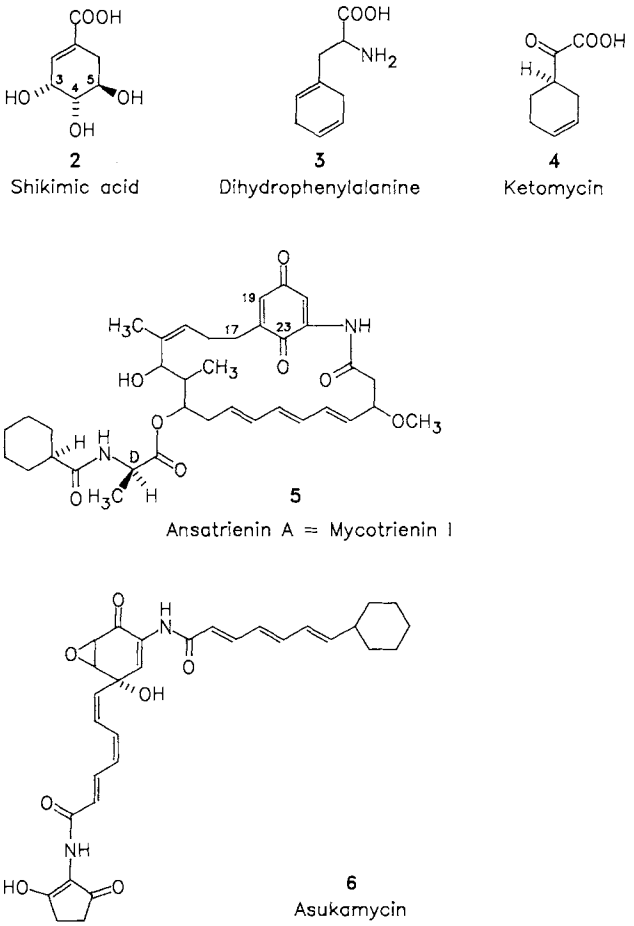


Fig. 2. Shikimic acid **2** and some of its hydroaromatic metabolites.

tures To obtain information on the mode of formation of these reduced aromatic ring systems, we have studied a number of examples (see Fig. 2) including the unconjugated cyclohexadiene system in dihydrophenylalanine **3**[29] and the cyclohexene ring in ketomycin **4**.[30]

Cyclohexane rings are found in two antibiotics, ansatrienin (mycotrienin) **5**, isolated from *Streptomyces collinus*[31-33] and *S. rishiriensis*,[34-36] and asukamycin **6**, isolated from *S. nodosus* var. *asukaensis*[37,38] (Fig. 2). Shikimate-derived cyclohexane rings are also found in the ω-cyclohexyl fatty acids of thermophilic acid bacteria and other bacteria,[39-42] e.g., ω-cyclohexylundecanoic acid **12** (see Fig. 4). In ansatrienin **5** the cyclohexane ring is present as a cyclohexanecarboxylic acid which is linked via a D-alanine residue to the macrocyclic lactam ring, whereas in asukamycin **6**, as in the ω-cyclohexyl fatty acids, the cyclohexane ring is attached to the end of a hydrocarbon chain. It seemed likely that in both the latter cases the cyclohexane ring also originates from cyclohexanecarboxylic acid which, in the form of its CoA ester, serves as the starter unit for a polyketide chain. The experimental evidence supports this notion, both in the case of the ω-cyclohexyl fatty acids and in that of asukamycin **6**. For example, feeding experiments with ^{13}C-labeled acetate and malonate clearly established the polyketide origin of the two olefinic hydrocarbon chains in **6**.[43] Cyclohexane[*carboxy*-^{14}C]carboxylic acid was incorporated into both asukamycin **6**[43] and ansatrienin **5**;[44] degradation of labeled **5** showed that essentially all the label was confined to the cyclohexylcarbonyl moiety. Further studies showed that the cyclohexane rings in both **5** and **6** are derived via the shikimate pathway and not by reduction of a benzene ring (no incorporation of labeled phenylalanine or benzoic acid).[43,44] Degradation of ansatrienin **5** derived from [U-^{14}C]shikimic acid showed that all seven carbon atoms of the precursor are incorporated to give rise to the seven carbon atoms of cyclohexanecarboxylic acid (Fig. 3). Consistent with this finding was the inefficient incorporation of labeled **3** into **5**.[44]

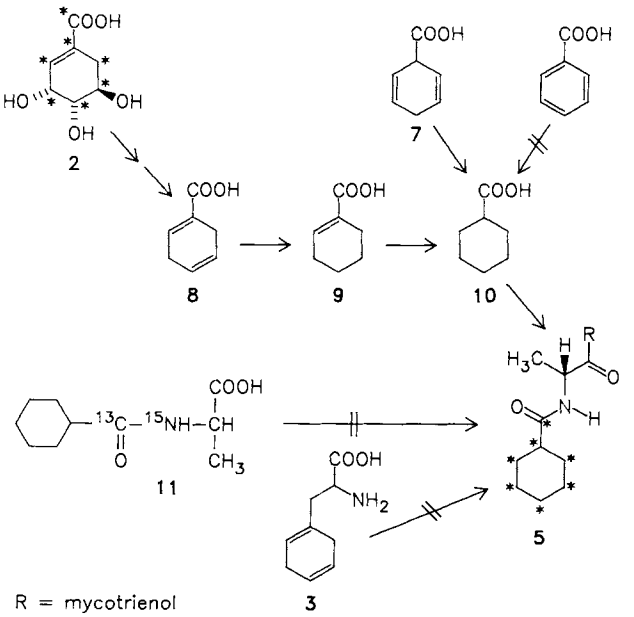


Fig. 3. Formation of the *N*-(cyclohexylcarbonyl)alanine moiety of ansatrienin **5** (mycotrienin) from shikimic acid **2**.

To obtain further information on the steps leading from shikimic acid **2** to cyclohexanecarboxylic acid, we have started to trace this sequence backwards. Good incorporation of 1,4-cyclohexadiene[*carboxy*-^{14}C]carboxylic acid (^{14}C-labeled **8**) into both ansatrienin **5**[44] and asukamycin **6**[43] suggested conversion of **2** to this unconjugated diene followed by sequential reduction of the two carbon-carbon double bonds. However, this conclusion was rendered questionable when it was observed that 2,5-cyclohexadiene[*carboxy*-^{14}C]carboxylic acid (^{14}C-labeled **7**) was incorporated into both antibiotics with comparable efficiency. Obviously, *Streptomyces* species have the ability to reduce carbon-carbon double bonds somewhat indiscriminately. The case for the intermediacy of the 1,4-diene **8** was strengthened, however, by the finding that ansatrienin A **5** is accompanied in the fermentation by a small amount (2 to 3%) of an analogue containing the 1-cyclohexenecarboxylic acid moiety (**9**) in place of cyclohexanecarboxylic acid.[44] The late steps in the reaction sequence from shikimic acid **2** to the cyclohexylcarbonyl moiety of **5** can therefore be written as shown in Figure 3.

Feeding experiments with ^{15}N-labeled D- and L-alanine showed that the D isomer was the more immediate precursor of the D-alanine moiety in ansatrienin **5**. It was also concluded that the incorporation of cyclohexanecarboxylic acid **10** into **5** involves the stepwise attachment of first alanine and then the acid moiety to the macrocycle rather than preassembly of cyclohexylcarbonylalanine **11**. The latter, doubly labeled with ^{13}C and ^{15}N in the amide linkage, gave incorporation of the components but no incorporation of the intact compound.[44]

The biosynthesis of cyclohexanecarboxylic acid raises the question of the stereochemistry of processing of intermediates in the pathway from shikimic acid **2**, i.e., the cryptic stereochemistry of formation of the symmetrical cyclohexane ring. This problem was addressed by two groups, that of *Okuda* in Tokyo and our own. Both laboratories used the same basic principle, asymmetric labeling of the cyclohexanecarboxylic acid moiety via a precursor carrying a stable isotope and conversion to a derivative containing an auxiliary chiral center followed by NMR analysis. Investigating the biosynthesis of ω-cyclohexylundecanoic acid **12** (Fig. 4), *Furukawa* et al. fed D-[6-^{2}H$_2$]glucose to *Curtobacterium pusilum*.[45] The resulting fatty acid was degraded by microbial oxidation with *Candida tropicalis* to cyclohexanecarboxylic acid **10**, which was further derivatized by reaction with phenyllithium to give cyclohexyl phenyl ketone **13**, followed by asymmetric reduction with (−)-*N*-methylephedrine/*N*-ethylaniline/$LiAlH_4$ to give (*S*)-α-cyclohexylbenzyl alcohol **14**. NMR analysis of **14** in the presence of a lanthanide shift reagent allowed the determination of the deuterium distribution between the hydrogens at C-2 and C-6 as well as between the equatorial and axial positions. The results of this analysis established the axial hydrogen at C-2 (as defined by the authors; C-6 of **10** in Fig. 7) as the primary site of labeling with 66% deuterium enrichment. The two hydrogens at C-6 each contained 5% deuterium and the remaining positions less than 2% each. The authors interpreted this result to indi-

cate reduction of the carbon-carbon double bond of shikimic acid by *syn* addition of hydrogen on the *Re-Re* face.[45] Implicit in this interpretation is the assumption that the primary site of labeling in shikimic acid **2** is at C-2.

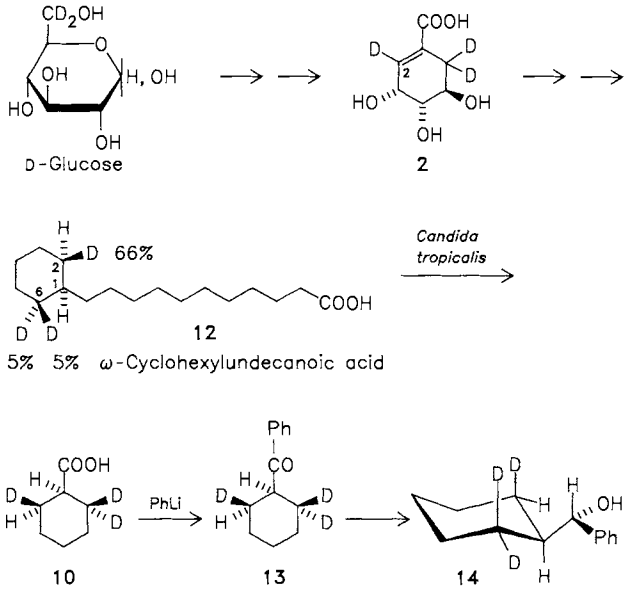


Fig. 4. Stereochemical analysis of cyclohexane ring formation in ω-cyclohexylundecanoic acid (**12**) biosynthesis [45].

In our own approach,[46] we synthesized a sample of [2-^{13}C]shikimic acid by the procedure of *Fleet* et al.[47] Starting from 10 g of D-[1-^{13}C]mannose, optically active D-(−)-[2-^{13}C]shikimic acid was obtained in 17–18% yield. A sample of this material was fed to *S. collinus* and the resulting ansatrienin **5**, showing one labeled position in the cyclohexane ring, was degraded to cyclohexylmethanol **15**, which was then derivatized with (*S*)-mandelic acid to give **16** (Fig. 5). The ^{13}C NMR spectrum of this derivative showed a chemical shift difference of $\Delta\delta = 0.05$ ppm between the signals for C-2 and C-6 of the cyclohexane ring, only one of which was enriched. An unambiguous assignment of these ^{13}C NMR signals, as well as of the ^{1}H NMR signals at these two carbon atoms, was made by synthesizing an authentic sample of (1*R*,2*R*)-[2-^{2}H]cyclohexylmethanol **15** (systematic numbering) by the route shown in Figure 6. Analysis of the (*R*)- and (*S*)-mandelate esters of this sample revealed that in the (*S*)-mandelate derivative C-2 (the *pro-R* carbon) resonates at higher and C-6 (the *pro-S* carbon) at lower field. A deuterium-decoupled 2D ^{1}H,^{13}C correlation spectrum[19] of the same samples revealed the proton assignments at these carbon atoms. Based on this analysis it was concluded that the ^{13}C in the biosynthetic sample resided exclusively in the *pro*-6*S* position. Hence, the steric course of the processing of shikimic acid **2** to cyclohexanecarboxylic acid **10** in the biosynthesis of ansatrienin **5** is the same as in the biosynthesis of cyclohexyl fatty acids such as **12**.[46] However, it was also found that the small amount of the 1-cyclohexenecarboxylic acid **9** accompanying the cyclohexanecarboxylic acid **10** in the hydrolysis of this biosynthetic sample of **5** carried the ^{13}C label not at C-2 but at C-6 (see **9**, Fig. 5). Hence, the process is more complex than a direct *Re-Re* reduction of the carbon-carbon double bond of **2**. By the route of *Fleet* et al.,[47] we also synthesized samples of **2** deuterated at C-2 and stereoselectively deuterated at C-6, and fed these to *S. collinus*.[48] Deuterium from C-2 was effectively incorporated and occupies the 6*R* (axial) position in the resulting cyclohexanecarboxylic acid, consistent with the results of *Furukawa* et al.[45] However, absolutely no deuterium from C-6 of **2** was incorporated; hence, the reaction sequence must include two steps involving hydrogen abstraction from C-6. A hypothetical pathway rationalizing these results is shown in Figure 7.

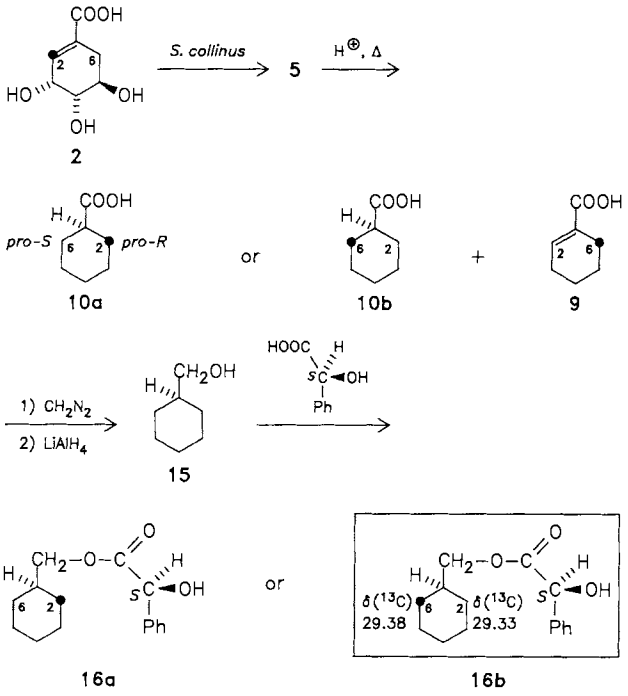


Fig. 5. Stereochemical analysis of cyclohexanecarboxylic acid (**10**) formation in ansatrienin biosynthesis [46]. The ester **16b** was obtained.

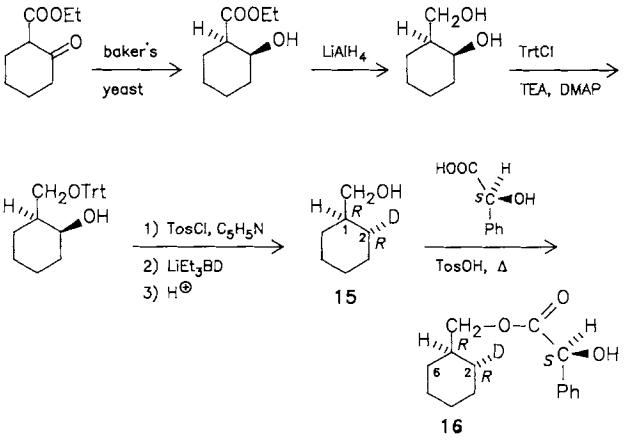


Fig. 6. Synthesis of (1*R*,2*R*)-[2-^{2}H]cyclohexylmethanol **15** for configurational assignment of its (*S*)-mandelate ester **16**. TEA = triethylamine, DMAP = 4-dimethylaminopyridine.

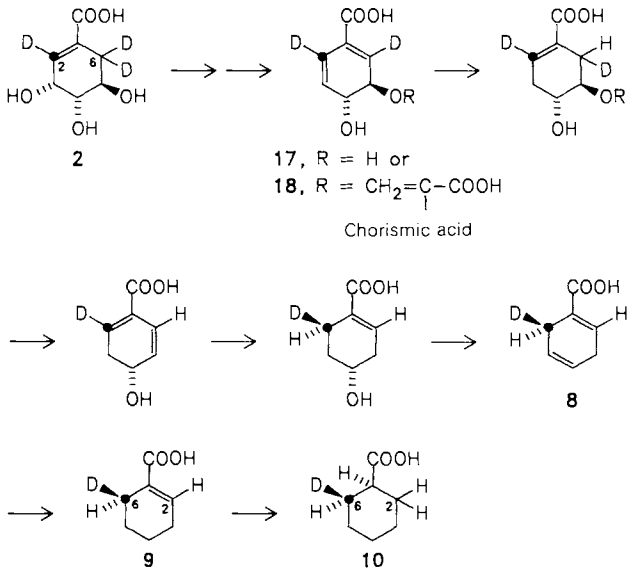


Fig. 7. Hypothetical pathway to the cyclohexanecarboxylic acid moiety of ansatrienin **5**.

4. Formation of Antibiotic Sugar Components

4.1. 2,6-Dideoxyhexoses

2,6-Dideoxyhexoses are found as sugar components of a wide variety of antibiotics. Two examples, studied in our laboratory, are chlorothricin **20** (see also Fig. 12)[49-53] and granaticin **19** (see also Fig. 28).[54-60] Chlorothricin is an unusual macrolide (see Section 5.1) containing two glycosidically linked 2-deoxy-D-rhamnose moieties **22**, to one of which is attached a modified 6-methylsalicylic acid. Granaticin, a member of the benzoisochromane quinone family (see Section 7), contains a 2,6-dideoxyhexose in a rather unusual double linkage to the aromatic aglycone (**21**). In both instances the origin of the deoxyhexose moiety was readily traced to glucose.

Feeding experiments with [3,4-^{14}C,1-^{3}H]- and [3,4-^{14}C,2-^{3}H]glucose and *S. violaceoruber* gave granaticin **19** without a decrease in the $^{3}H/^{14}C$ ratio,[61] pointing to intact incorporation of glucose and retention of both H-1 and H-2 in the process. In contrast, H-3 and H-5 are eliminated in the conversion, as shown by feeding experiments with correspondingly double-labeled glucose samples. Tritium from C-6 of glucose is incorporated into granaticin, with 80% residing in one or both of the *C*-methyl groups. Notably, tritium from C-4 of glucose is also efficiently incorporated and resides again almost exclusively in one or both of the *C*-methyl groups, as evidenced by recovery of 90% of the tritium in the acetic acid obtained by a Kuhn-Roth oxidation. Taken together, these results leave little doubt that the intact glucose molecule, with the exception of H-3 and H-5, gives rise to the deoxyhexose moiety **21** of granaticin **19** (Fig. 8). This conversion must involve removal of the oxygen functions from C-6 and C-2 of glucose and is accompanied by migration of H-4 to C-6 of the sugar.

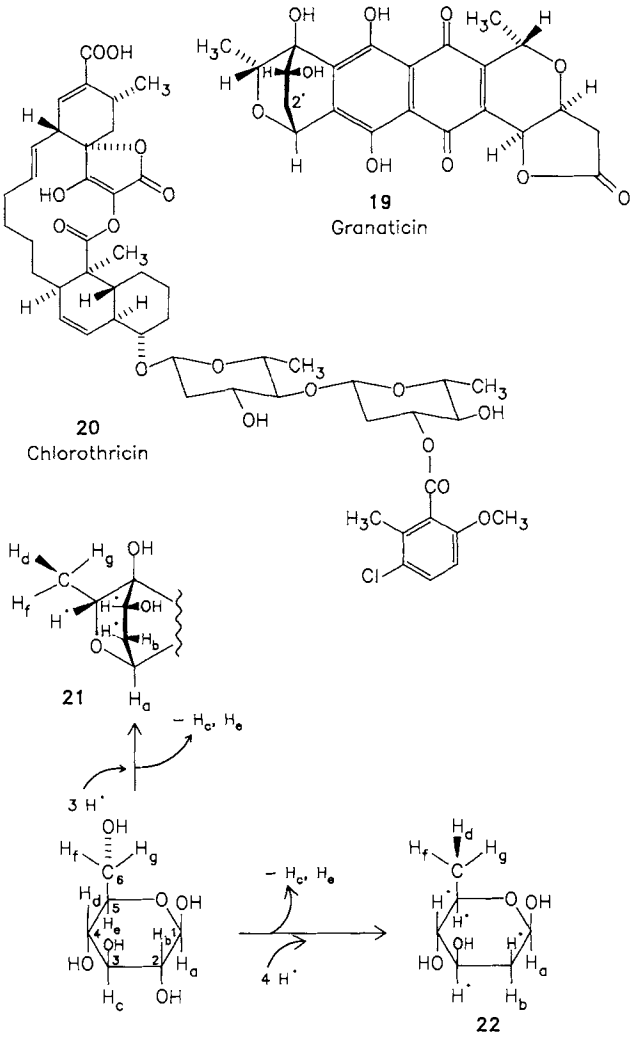


Fig. 8. Fate of glucose hydrogens in the conversion to the 2,6-dideoxyhexose moieties **21** and **22** of granaticin **19** and chlorothricin **20**, respectively.

Analogous results were obtained on formation of the two deoxyhexose moieties **22** of chlorothricin **20**. Early radiotracer experiments[62] had shown significant incorporation of ^{14}C-labeled D-glucose into **20** with about 30-35% of the total radioactivity of the antibiotic located in the two sugars. In further experiments,[63] glucose labeled with ^{14}C at C-6 and with tritium in various positions was fed to *S. antibioticus* and the resulting chlorothricin was degraded by methanolysis and alkaline hydrolysis to methyl 2-deoxy-α-D-rhamnoside,[49] which was analyzed for the change in $^{3}H/^{14}C$ ratio relative to the precursor. The results (Fig. 8) showed complete retention of the hydrogens in positions 2 and 6 and predominant retention of the hydrogen from C-1 (67%). The hydrogens at C-3 and C-5 were almost completely lost. About one-third of the tritium from C-4 of glucose was retained, but was shown by a Kuhn-Roth oxidation to be located not at C-4 but rather at C-6 of the deoxy sugar.

Loss of H-5 of the hexose and transfer of H-4 to C-6 as a hydride are typical of the reaction catalyzed by TDP-glucose oxidoreductase,[64] which converts TDP-D-glucose into TDP-4-oxo-6-deoxy-D-glucose. To probe further for the involvement of this enzyme in the first step of the

transformation of the glucose skeleton to that of 2,6-dideoxyhexoses, we elucidated the steric course of the hydrogen transfer from C-4 to C-6 of the hexose moiety. We had earlier determined the steric course of this reaction with the partially purified enzyme from *E. coli* using as substrate a mixture of unlabeled TDP-D-glucose and (6*R*)- or (6*S*)-TDP-D-[4-^{2}H,6-^{3}H]glucose.[65] The precursor was labeled in such a way that every tritiated molecule also contained deuterium. If the migration of deuterium from C-4 to C-6 is intramolecular, a chiral methyl group will be formed at C-6, and if the process is stereospecific, one enantiomer of the chiral methyl group will result predominantly or exclusively. Degradation of the resulting TDP-4-oxo-6-deoxyglucose by Kuhn-Roth oxidation followed by chirality analysis of the acetic acid generated from C-6 and C-5 of the sugar by the method of *Cornforth* et al.[66] and *Arigoni* et al.,[67] using an adapted procedure,[68] showed that the methyl group was indeed chiral. The precursor of 6*S* configuration had produced predominantly a methyl group of *R* configuration and the 6*R* isomer had produced predominantly an *S* methyl group,[65] showing that H-4 replaces the 6-hydroxyl group with inversion of configuration at C-6 (Fig. 8).

The stereochemical results on the TDP-glucose oxidoreductase reaction led to the proposal of a plausible model for the events in the active site of this enzyme during the catalytic process (Fig. 9). The carbohydrate moiety must be bound in a conformation placing H-5 and the 6-hydroxyl group in a *syn* orientation. A sandwich-like arrangement of the carbohydrate ring and the pyridine nucleotide cofactor, with the C-4 atoms of both moieties juxtaposed on each other, aided by two bases mediating proton transfers, one near the 4-hydroxyl group and one near H-5 and the 6-hydroxyl group, allows for transfer of H-4 to C-6 via the pyridine nucleotide with a minimum of motion.

Intramolecularity and migration of H-4 with the same stereochemistry was demonstrated for the formation of the methyl group in the 2-deoxy-D-rhamnoside moieties **22** of chlorothricin **20**[63] and in the deoxyhexose portion **21** of granaticin **19**[61] (Fig. 8). In these cases, (6*R*)- and (6*S*)-D-[6-^{14}C,4-^{2}H,6-^{3}H]glucose were fed to cultures of *S. antibioticus* and *S. violaceoruber*, respectively. Chlorothricin **20** was degraded to methyl 2-deoxy-α-D-rhamnoside, which was then subjected to Kuhn-Roth oxidation to carve out the methyl group and the attached carbon as acetic acid for chirality analysis, whereas granaticin **19** was subjected directly to Kuhn-Roth oxidation. The results leave little doubt as to the role of TDP-glucose oxidoreductase as the key enzyme in the formation of the deoxyhexose moieties of **19** and **20**. We have since demonstrated the presence of TDP-glucose oxidoreductase in cell-free extracts from both organisms and have shown that the enzyme activity is low during the growth phase and rises dramatically at the beginning of the antibiotic production phase.[69]

While in all the features examined so far the pathways to the 2,6-dideoxyhexose moieties of **19** and **20** were found to be identical, a difference was seen when we examined the steric course of replacement of the 2-hydroxyl group of glucose by hydrogen. This was done by feeding D-[2-^{2}H]glucose to *S. antibioticus* and to *S. violaceoruber*. Again, the resulting chlorothricin was degraded to methyl 2-deoxy-α-D-rhamnoside, which was then analyzed by deuterium NMR spectroscopy. The single signal in the spectrum appeared at the chemical shift of the equatorial hydrogen at C-2. Hence, deuterium occupies the 2*R* position and the replacement of the 2-hydroxyl group of glucose by a hydrogen occurs with inversion of configuration at C-2[70] (Fig. 8). The resulting granaticin was analyzed by ^{1}H NMR spectroscopy and found to be deuterated exclusively in the *pro*-2′*S* position. Hence, the newly introduced hydrogen occupies the *pro*-2′*R* position, having replaced the oxygen from C-2 of glucose with retention of configuration[61] (Fig. 8). It therefore appears that different pathways may be involved in the formation of the 2,6-dideoxyhexose moieties **21** and **22**, which differ in stereochemistry and thus perhaps also in mechanism.

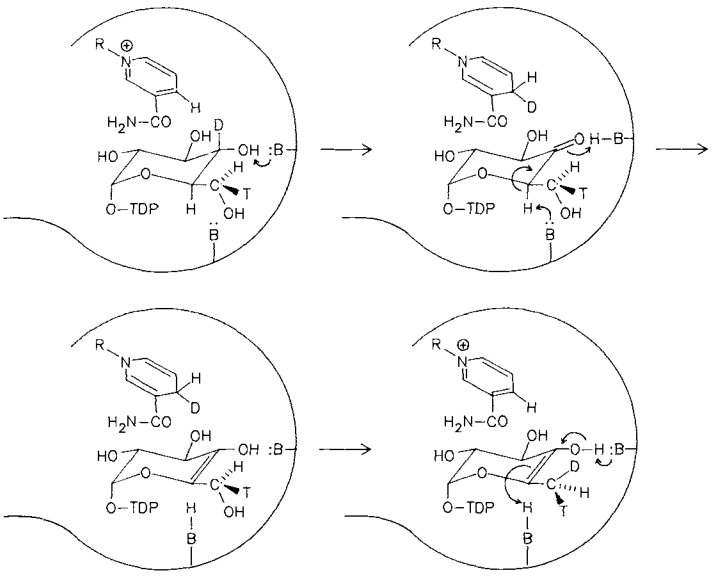


Fig. 9. Proposed stereochemical mechanism of the TDP-glucose oxidoreductase reaction [61, 65].

4.2. Spectinomycin and the Stereochemistry of the Inositol 1-Phosphate Synthase Reaction

Having available in (6*R*)- and (6*S*)-[4-^{2}H,6-^{3}H]glucose **23** a rather sophisticatedly labeled precursor designed specifically to probe for the stereochemistry and mechanism of the TDP-glucose oxidoreductase reaction, we decided to examine the formation of one more antibiotic, spectinomycin **24** (Fig. 10).[71,72] This unusual aminoglycoside, a metabolite of several *Streptomyces* species,[73,74] inhibits protein synthesis at the ribosomal level by selectively inhibiting initiating ribosomes.[75] The compound is used clinically for the treatment of gonorrhea as well as for veterinary purposes. Spectinomycin was chosen as a target because, as shown by earlier workers, it arises from two molecules of glucose,[76,77] both of which undergo stereochemical changes at C-6. One molecule of glucose gives rise to the 4,6-dideoxyhexose moiety making up ring C of the antibiotic, whereas the other is cyclized to *myo*-inositol, which is subsequently incorporated into the actinamine moiety (**25**) making up ring A of the antibiotic. In the

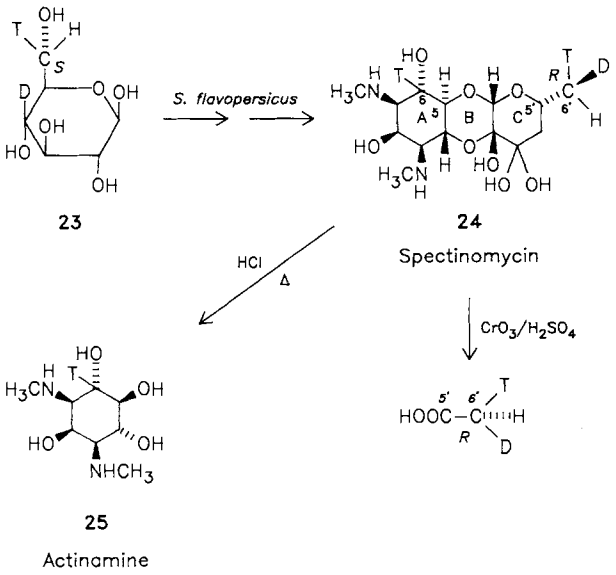


Fig. 10. Biosynthesis and chemical degradation of spectinomycin **24**.

latter conversion, C-1 and C-6 of glucose ultimately give rise to C-5 and C-6, respectively, of spectinomycin **24**.[77,78]

A high degree of incorporation of tritium from C-4 of glucose into the 6'-methyl group of spectinomycin suggested the involvement of the TDP-glucose oxidoreductase reaction in the formation of the 4,6-dideoxyhexose moiety of **24** as well.[78] Feeding experiments with (6*R*)- and (6*S*)-[6-^{14}C,4-^{2}H,6-^{3}H]glucose followed by Kuhn–Roth oxidation of **24** then showed that, as in all the other cases examined, the oxidoreductase reaction involves intramolecular transfer of H-4 to C-6, replacing the 6-hydroxyl group with inversion of configuration (Fig. 10).

Degradation of another aliquot of the samples of **24** from these two feeding experiments showed that the actinamine moiety of this antibiotic had been formed with predominant retention of the pro-6*S* hydrogen and loss of the pro-6*R* hydrogen of glucose (Fig. 10). This result was surprising because the stereochemistry of the cyclization of glucose 6-phosphate **26** to *myo*-inositol 1-phosphate **29** with the enzymes from rat testes and rat mammary gland had been studied earlier by *Kirkwood* et al.,[79] who reported that the reaction proceeds with loss of the pro-*S* hydrogen. Since *myo*-inositol has been firmly established as a precursor of the actinamine moiety of spectinomycin, this observation suggested that either the earlier results were incorrect or the stereochemistry of the *myo*-inositol synthase reaction is not uniform in different organisms. In collaboration with *Frank* and *Mary Loewus* of Washington State University, we therefore examined the steric course of the reaction catalyzed by the enzymes from beef testes and from pollen of *Lilium longiflorum*.[80] In both cases the cyclization proceeded with the same stereochemistry as observed for spectinomycin biosynthesis in *Streptomyces flavopersicus*, that is, with predominant loss of the pro-*R* and predominant retention of the pro-*S* hydrogen. The observed stereochemistry is consistent with the mechanistic classification of this enzyme as an aldolase[81] and with the general stereochemistry deduced for enzymatic aldol condensations.[82] Based on these stereochemical results, a mechanism was proposed in which a single basic group on the enzyme, positioned near C-1 and O-5 (in the substrate) and C-6 (in the product) mediates sequentially four proton transfers (Fig. 11). The first of these is abstraction of a hydrogen from the 1-OH group and subsequent addition of the hydrogen to O-5, thereby mediating the hemiacetal ring opening of glucose 6-phosphate **26**. Rotation around the C-4/C-5 axis, placing C-6 in proximity to C-1, is followed by dehydrogenation at C-5 to ketone **27**. Inspection of models indicates that binding of the substrate in a conformation that places the phosphorus of the phosphate group in an extension of the C-4/C-5 axis allows for this conformational reorientation without detaching the molecule from its essential binding sites on the enzyme. Abstraction of the pro-*R* hydrogen from C-6 by the same base followed by transfer of this hydrogen to the carbonyl oxygen at C-1 then sets the stage for the aldol condensation to form the C-6/C-1 bond in **28**. Reduction of the C-5 carbonyl group completes the sequence. This mechanism makes one prediction, namely that the enzyme should utilize the β rather than the α anomer of glucose 6-phosphate **26**. This prediction has recently been confirmed by *Sherman* et al.[83]

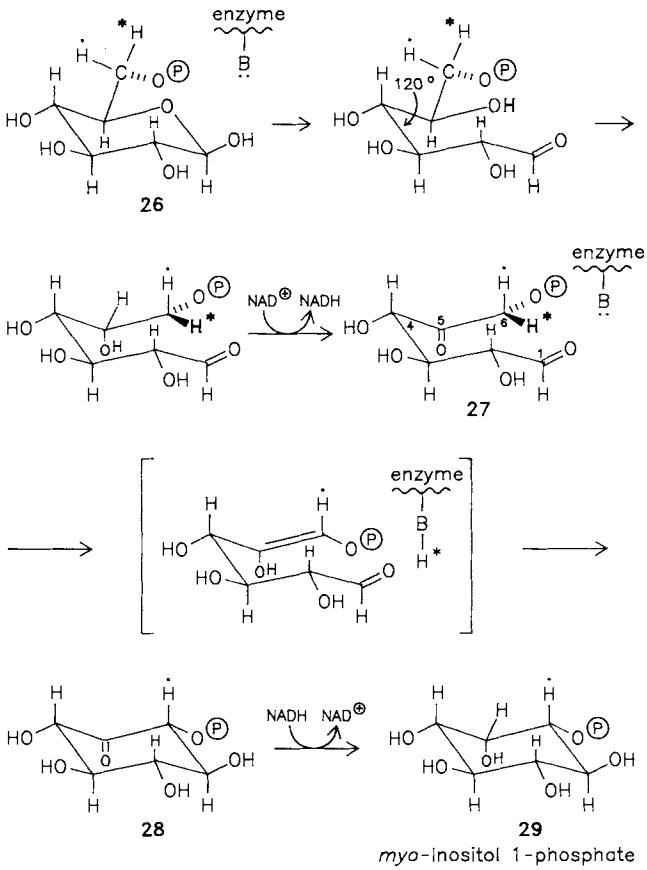


Fig. 11. Proposed stereochemical mechanism of the *myo*-inositol 1-phosphate synthase reaction [80].

5. Unusual Macrolides

In addition to the classical macrolide antibiotics,[84] exemplified by the 14-membered macrocyclic lactone tylosin

and the 16-membered erythromycin, Streptomycetes elaborate a number of "unusual" macrolides, which do not fit the standard structural, and therefore presumably biosynthetic, pattern of the classical compounds. Three of these, chlorothricin **20**, boromycin **1**, and aplasmomycin **31**, were the subject of biosynthetic studies in our laboratory.

5.1. Chlorothricin

Chlorothricin **20** (Fig. 12), isolated from cultures of *Streptomyces antibioticus*,[49] is an antibiotic inhibiting the anaplerotic CO_2 fixation catalyzed by pyruvate carboxylase.[85] Moreover, mode-of-action studies have pointed to an interaction between chlorothricin and the membrane phospholipids of *Bacillus subtilis*.[86] The mechanism of action of chlorothricin is clearly quite different from that of other macrolide antibiotics. Its structure is also quite different.[50–53] The aglycone of chlorothricin (chlorothricolide) represents a novel macrocyclic ring system incorporating a *trans*-octahydronaphthalene structure and a tetronic acid moiety spiro-linked to a cyclohexene ring.

Early radioactive tracer experiments carried out both in our laboratory and in that of *Pape* in Münster clearly established incorporation of acetate into both the aglycone and the acyl moiety, consistent with a polyketide origin of both these structural elements (see Fig. 12).[62] The distribution of the label between these two moieties was determined by methanolysis of **20**,[49] which produced the aglycone as its methyl ester as well as methyl 2-deoxy-D-rhamnoside and its derivative containing the 3-acyl moiety of **20**. The acyl moiety, but not the aglycone, was also efficiently labeled by the methyl group of methionine. The aglycone, on the other hand, was significantly labeled by propionate carrying ^{14}C in any of the three carbon atoms.[62]

Complete analysis of the ^{13}C NMR spectrum of chlorothricin[87] was followed by feeding experiments with specifically ^{13}C-labeled precursors.[63] These studies demonstrated unequivocally the origin of the acyl moiety from four acetate units and one methyl group of methionine, the latter providing the methoxy carbon. Formation of this portion of the molecule presumably proceeds via 6-methylsalicylic acid, which is further modified by chlorination and methylation. The 29 carbon atoms of the aglycone moiety represent ten acetate and two propionate units arranged in a contiguous chain starting with an acetate unit (C-29 and C-21) (Fig. 12). The two propionate units occupy positions 1, 2, 27 and 19, 20, 28 in the chain, and in one of these the branching methyl group has been oxidized to a carboxyl group (C-28).

It was not evident from the initial results with single-labeled acetate samples that C-25 and C-26 were also acetate-derived. However, chlorothricolide derived from [1,2-$^{13}C_2$]acetate showed coupling between the signals for C-25 and C-26 with $^1J_{C,C}=91.5$ Hz, typical of carbons in a tetronic acid structure. Thus, C-25 and C-26 arise from a single acetate unit. We propose that C-25 was initially directly linked to C-1 (**30**), belonging to the terminal unit of the polyketide chain.[63] In the subsequent processing of the polyketide, a Baeyer–Villiger oxidation then converts the C–C bond into an ester linkage (Fig. 13). Support for this proposal comes from the subsequent isolation of antibiotics, the tetrocarcins[88,89] and the kijanimycins,[90–92] in which the original C–C bond is retained in the form of an acyltetronic acid structure.

These results left the origin of three carbon atoms, C-22, C-23, and C-24 of the aglycone moiety, unaccounted for. Among a number of radioactive potential precursors tested,[63] succinic acid showed good incorporation into the aglycone; in particular, the two center carbon atoms were

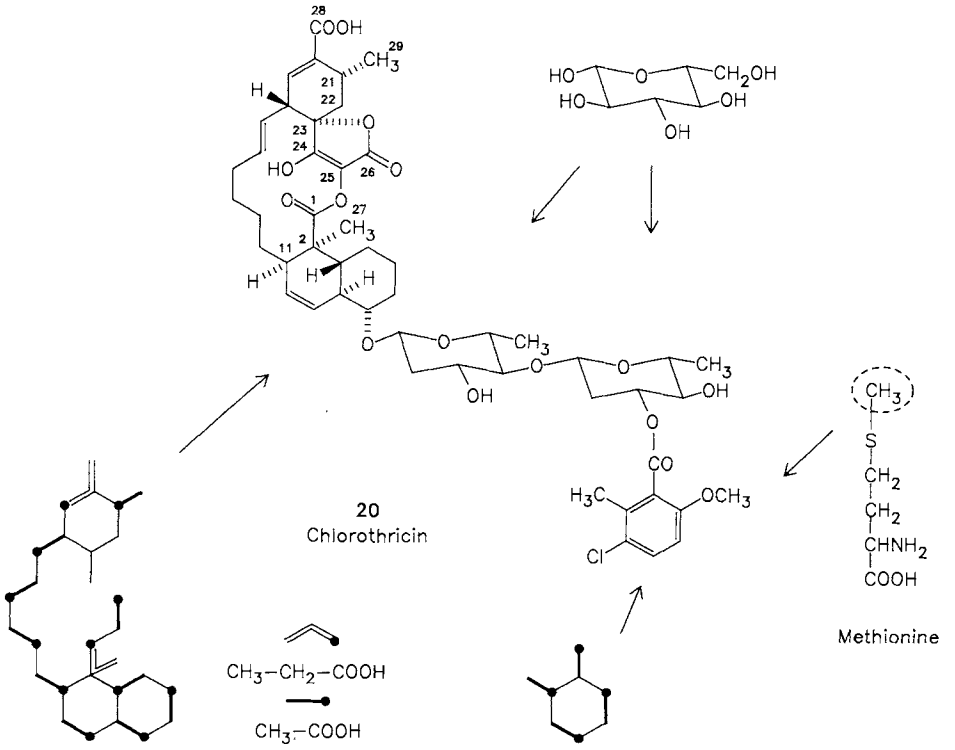


Fig. 12. Biosynthetic origin of chlorothricin **20**.

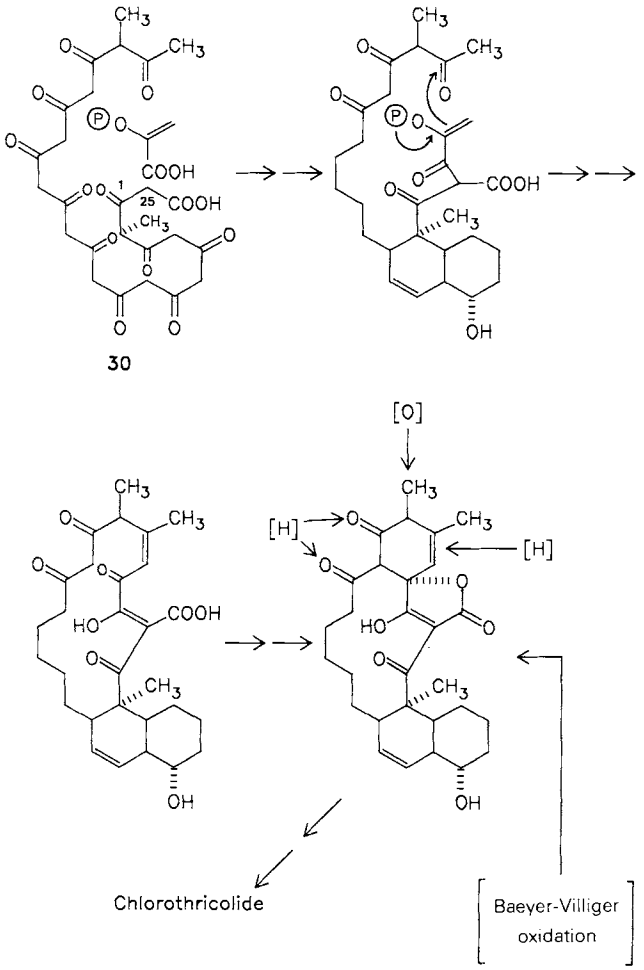


Fig. 13. Proposed biosynthesis of the chlorothricin aglycone, chlorothricolide.

used very efficiently. This led us to speculate that C-22, C-23, and C-24 may arise from the Krebs cycle intermediate oxalacetic acid, which would be incorporated with loss of the β-carboxyl group. However, this mechanistically attractive idea was quickly disproved when it was found that [1,4-$^{13}C_2$]succinic acid labeled exclusively the two carbon atoms arising from C-1 of propionate, but not C-24.[63] Following detailed scrutiny of a number of further compounds it was concluded that [2-^{14}C]glycerol might be a specific precursor. This notion was confirmed unequivocally by synthesizing and feeding [U-$^{13}C_3$]glycerol containing 99 atom% ^{13}C in each carbon atom. Extensive analysis of the coupling pattern of the resulting chlorothricolide showed the expected incorporation via acetyl-CoA into the acetate-derived carbons as well as some incorporation into the propionate-derived units, reflecting entry of acetyl-CoA into the Krebs cycle. Most importantly, however, C-22, C-23, and C-24 were all labeled and showed the expected coupling pattern for incorporation of an intact glycerol molecule. C-23 was coupled to both C-22 and C-24 as confirmed by a carbon-carbon decoupling experiment.[70] Glycerol is a symmetrical molecule in which the two hydroxymethyl groups are in an enantiotopic relationship and therefore distinguishable by an enzyme. Glycerol kinase, the enzyme mediating entry of glycerol into cellular metabolism, phosphorylates the pro-*R* hydroxymethyl group, which thus gives rise to C-3 of triose phosphates, phosphoglycerate, phosphoenolpyruvate, and ultimately pyruvate and lactate. To determine the "orientation" in which glycerol is incorporated into the three-carbon moiety of chlorothricolide, we synthesized and carried out feeding experiments with (2*R*)-[1-$^2H_2$]glycerol. The deuterium NMR spectrum of the resulting chlorothricolide methyl ester cleanly showed two signals, corresponding to the hydrogen of the propionate-derived methyl group, C-27, and to the *pro-R* hydrogen at C-22. Consequently, C-3 of glycerol gives rise to C-24 of chlorothricin and C-1 to C-22. The stereospecific retention of only one hydrogen at C-22 is consistent with intermediate formation of a double bond between C-21 and C-22 which is then reduced stereospecifically. The compound actually condensing with the polyketide portion to give the tetronic acid structure is almost certainly not glycerol itself, but rather a metabolite of it. On mechanistic grounds, we propose that the actual substrate is phosphoenolpyruvate. A plausible mechanism for the formation of chlorothricolide is shown in Figure 13.

An attempt was made to probe further the proposed mechanism by tracing the fate of the methyl hydrogens of acetate into chlorothricolide. This is commonly done by feeding experiments with sodium [2-^{13}C,$^2H_3$]acetate and analysis of the product by ^{13}C NMR spectroscopy for the deuterium-induced isotope shifts of the ^{13}C NMR signals. The α-deuterium shift is best observed with simultaneous ^{1}H and ^{2}H broadband decoupling to remove splitting by deuterium.[93] Alternatively, one may label the precursor with ^{13}C in the adjacent carbon position and detect deuterium through the β-deuterium shift which is relayed through two bonds.[9] Since the deuterium isotope shifts are additive, they allow not only detection of the presence of deuterium in a given position, but also determination of how many atoms of deuterium are attached to a particular carbon. Surprisingly, the chlorothricolide derived from sodium [2-^{13}C,$^2H_3$]acetate showed no deuterium in any of the acetate-derived positions. The only deuterated carbon was the propionate-derived methyl group, C-27, which carried two atoms of deuterium. Therefore, complete washout of deuterium from the methyl group of acetate must occur during the incorporation of the acetate units into the polyketide, possibly by extensive carboxylation/decarboxylation of acetyl-CoA.

On the other hand, acetyl-CoA seems to enter the Krebs cycle with retention of the deuterium to produce propionate units containing dideuterated methyl groups. From proffered [2-^{13}C,$^2H_3$]acetyl-CoA, one turn of the Krebs cycle will produce succinyl-CoA containing two atoms of deuterium at C-3, which upon rearrangement in the methylmalonyl-CoA mutase reaction will produce methylmalonyl-CoA monodeuterated at C-2. Further turns of the cycle will introduce at most one atom of deuterium into C-3 of the propionate units. The observed presence of two atoms of deuterium in this position can be explained in two ways. If succinyl-CoA and free succinate are in equilibrium, then one-half of the succinyl-CoA molecules will end up dideuterated at C-2, producing methylmalonyl-CoA with two deuterium atoms in the methyl group. Alternatively, a new, heretofore unsuspected pathway may op-

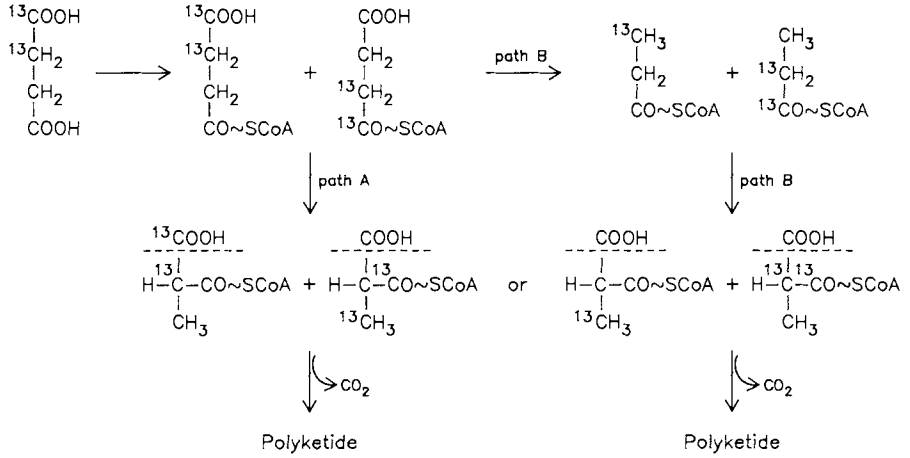


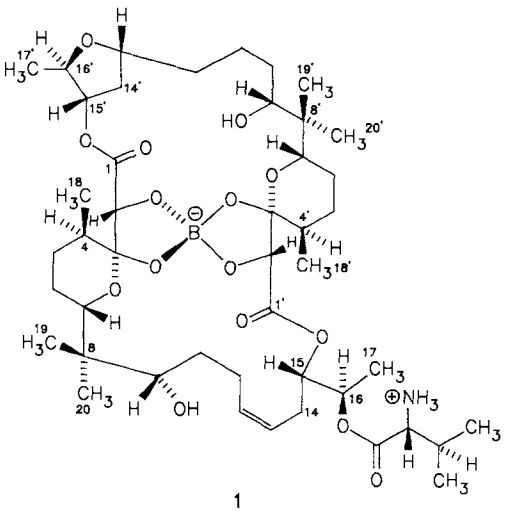
Fig. 14. Use of [1,2-$^{13}C_2$]succinic acid to distinguish two possible pathways to propionate units in polyketides. Prediction for path A: no ^{13}C-^{13}C one-bond coupling. Prediction for path B: ^{13}C-^{13}C one-bond coupling, C-1/C-2 and C-19/C-20.

erate, in which succinyl-CoA is directly decarboxylated to propionyl-CoA followed by carboxylation to methylmalonyl-CoA. As a probe to distinguish between these two possibilities, we synthesized a sample of [1,2-$^{13}C_2$]succinic acid. In the cell, this compound is metabolized to a 1:1 mixture of [1,2-$^{13}C_2$]- and [3,4-$^{13}C_2$]succinyl-CoA. Via the direct decarboxylation pathway (path B, Fig. 14), these would produce propionate units labeled in all three carbon atoms and showing coupling between C-1 and C-2. On the other hand, via the methylmalonyl-CoA mutase reaction (path A) the result would be propionate units which are also labeled in every carbon but show no one-bond coupling. Feeding of this precursor to the chlorothricin fermentation gave chlorothricolide in which the propionate-derived carbons were enriched but clearly showed no one-bond coupling. Therefore, direct decarboxylation of succinyl-CoA does not contribute significantly to the formation of propionate units in this polyketide synthesis.

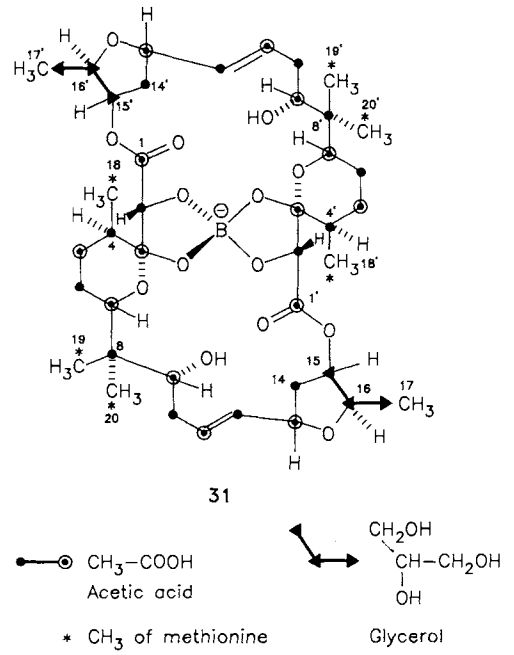
5.2. Boromycin and Aplasmomycin

Among the thousands of organic natural products there are only a handful which contain boron. The first of these to be discovered was the ionophoric antibiotic boromycin **1** (Figs. 1 and 15), a metabolite of *Streptomyces antibioticus*.[1,94] Its structure, elucidated by chemical degradations and an X-ray analysis[1,2] is that of a macrocyclic dilactone consisting of two carbon chains of identical carbon-carbon connectivities folded around a boron atom. In addition, a D-valine moiety is attached to one of the chains through an ester linkage. The antibiotic activity of boromycin **1** against gram-positive bacteria, certain fungi, and protozoa[95] is due to interaction with the cytoplasmic membrane resulting in the breakdown of the permeability barrier for potassium ions.

A second boron-containing ionophore, aplasmomycin **31** (Fig. 15), was isolated from a strain of *Streptomyces griseus* obtained from a sample of sea mud from the Sea of Japan.[96] Its structure[97-99] is similar to that of boromycin but lacks the D-valine moiety. In addition, the two macrolide chains in aplasmomycin have identical structure and the same configuration at every pair of chiral centers. Thus,



1



31

Fig. 15. Biosynthetic building blocks of aplasmomycin **31**. For comparison: boromycin **1**.

the ^{13}C NMR spectrum of this compound of 40 carbon atoms shows only 20 signals, which were readily assigned.[100] The conformations of **1** and **31** both in the crystal[97, 101] and in solution[100, 102, 103] are similar and, interestingly, they change little upon removal of the boron.

The biosynthesis of boromycin **1** and aplasmomycin **31** naturally has to be viewed in the context of that of classical macrolide antibiotics. The latter are formed by a version of the polyketide pathway in which one-carbon or two-carbon branches arise by substitution of propionate or butyrate units in place of acetate chain-extension units (cf. Ref. [84]). Based on this precedent, one would predict that the four methyl branches at C-4, C-4′, C-16, and C-16′ arise by incorporation of propionate units and the two geminal dimethyl branches at carbons 8 and 8′ arise by substitution of isobutyrate for acetate units. However, an alternate mode of biosynthesis was proposed by *Birch* et al.[104] at the time the first classical macrolide antibiotics were discovered. This envisioned construction of the contiguous polyketide carbon chain entirely from acetate units and introduction of the methyl branches by *C*-methylations (i.e., by transfer of methyl groups from *S*-adenosylmethionine). Feeding experiments with ^{13}C-labeled acetate or malonate and with [*methyl*-^{13}C]methionine immediately revealed that the origin of the carbon framework of both **1** and **31** follows the model of *Birch* rather than the path of classical macrolide biosynthesis (Fig. 15). C-1/C-1′ through C-14/C-14′ of each chain represent seven acetate units; three methyl groups in each chain, C-18/C-18′, C-19/C-19′, and C-20/C-20′, are derived from the methyl group of methionine; and the starter units, C-15/C-15′, C-16/C-16′, and C-17/C-17′ are not labeled by either acetate, methionine, or propionate.[105, 107] Complementary results on the biosynthesis of boromycin **1** were obtained by *Pape* et al. in Münster.[108]

The D-valine moiety of **1** was found to originate from D-valine as the immediate precursor. L-Valine is incorporated, but only via conversion to the D form with loss of the α-hydrogen. This was demonstrated unequivocally by showing predominant retention of deuterium in the incorporation of D-[2-^{2}H]valine and complete loss of deuterium from the corresponding L isomer.[105] This finding was surprising in view of the fact that the D-amino acid moieties of various peptide antibiotics originate from the free L-amino acid rather than the D-amino acid as the immediate precursor.[109–111] In those cases epimerization at the α-carbon occurs only after binding of the amino acid to the synthase at some stage during product assembly.[109–112] A different mechanism is evident in boromycin biosynthesis. An attempt was made[113] to achieve the directed biosynthesis of analogues of boromycin containing different amino acids in place of D-valine by feeding other D-amino acids in labeled form. However, except for a minimal incorporation of radioactivity from D-leucine, no formation of amino acid analogues of boromycin was evident.

Since the boromycin fermentation gave poor yields and inefficient incorporation of labeled precursors and since the NMR spectra of **1** are rather complex, we turned to the simpler system aplasmomycin **31** in order to unravel further details of the biosynthesis of this unusual macrodiolide system. Feeding experiments with ^{14}C-labeled pyruvate and lactate suggested that these compounds were only incorporated via metabolism to acetate. Glycerol was a very efficient precursor, which, as shown by a feeding experiment with [1,3-$^{13}C_2$]glycerol, not only labels both the acetate units (via metabolism to pyruvate and acetyl-CoA) and the methionine-derived methyl groups (via phosphoglyceric acid, serine, and the tetrahydrofolate system), but also specifically the starter unit (Fig. 15). A 3.5-Hz two-bond coupling between the signals for the highly enriched carbon atoms 15 and 17 unequivocally demonstrated that the three carbon atoms of the starter unit arise from an intact molecule of glycerol.[107]

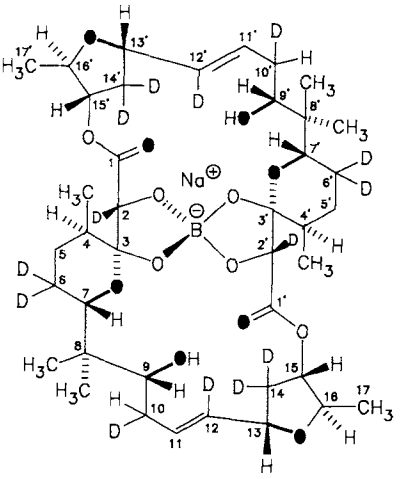
Starter units for the initiation of polyketide chains are generally thioesters of carboxylic acids; hence, instead of glycerol itself, a closely related metabolite is a likely candidate. Since the starter unit apparently is not formed via lactic or pyruvic acid, lactaldehyde or methylglyoxal were considered as possible intermediates because they could give rise to thioesters of pyruvic or lactic acid without going through the free acid. However, both compounds were ruled out by the stereochemical experiments discussed below and by the fact that [3-^{13}C]lactaldehyde and [3-^{13}C]methylglyoxal were incorporated exclusively into the carbon atoms derived from C-2 of acetate, but not into the starter unit.[114] The possibility was examined that serine might be the starter unit or a more immediate precursor of it. However, a feeding experiment with D,L-[3-^{13}C]serine gave incorporation only into the methionine-derived methyl groups (via the tetrahydrofolate system) and into the carbon atoms derived from C-2 of acetate (via acetyl-CoA).

We then decided to determine how the glycerol molecule is oriented in the starter unit and which hydrogens are retained in the transformation by feeding experiments with [1,1,3,3-$^{2}H_4$]-, (2*R*)-[1,1-$^{2}H_2$]-, and [2-$^{2}H_1$]glycerol. The aplasmomycin **31** from [2-$^{2}H_1$]glycerol contained no deuterium at all as revealed by mass spectrometry. The other two aplasmomycin samples showed nearly identical deuterium NMR spectra, revealing predominant labeling (38–39% enrichment) at C-17/C-17′, but no significant deuterium enrichment at C-15/C-15′. Hence, C-1 of glycerol, the *pro-R* hydroxymethyl group, which is phosphorylated by glycerol kinase, gives rise to C-17/C-17′ of aplasmomycin **31** whereas C-3 gives rise to C-15/C-15′. Only the hydrogens from C-1 of glycerol are retained and become part of the methyl group of the starter unit.[114] In addition, deuterium is incorporated into the methionine-derived methyl groups and to a very small extent into the acetate-derived portion of the molecule.

The above results set the stage for some further experiments on stereochemical aspects of the formation of the methyl groups of aplasmomycin **31**. All four methyl groups of each polyketide chain are labeled by C-1 of glycerol; C-17/C-17′ by direct incorporation of glycerol, C-18/C-18′, C-19/C-19′, and C-20/C-20′ via conversion of C-1 of glycerol to C-3 of serine and then to the methyl group of methionine. The steric course of the transfer of the latter to the polyketide backbone was probed by feeding experiments with (*methyl-R*)- and (*methyl-S*)-[*methyl*-$^{2}H_1$,^{3}H]methionine.[115] Kuhn–Roth oxidation of the resulting aplasmomycin samples gave radioactive acetic acid containing the chiral methyl groups from C-18/C-18′, C-19/C-19′,

and C-20/C-20′. Chirality analysis of these acetic acid samples[66-68] showed that the methyl group of methionine had been transferred to the polyketide chain with inversion of configuration. This result conforms to the steric course established for the majority of *S*-adenosylmethionine-dependent methyltransferases studied to date[116,117] and suggests a direct transfer of the methyl group from the sulfur of the substrate to the acceptor carbon in an S_N2 process. However, when serine stereospecifically labeled with deuterium and tritium at C-3 was used in feeding experiments, both the 3*R* and the 3*S* isomer produced aplasmomycin containing racemic methyl groups. Thus, the conversion of the methylene group of serine to the methyl group of methionine must be accompanied by complete racemization. Therefore, if a sample of glycerol chirally tritiated and deuterated at C-1 is fed to the cultures and the resulting aplasmomycin degraded by Kuhn-Roth oxidation, any chirality observed in the resulting acetic acid should be due entirely to C-17/C-17′, whereas the methionine-derived methyl groups would only contribute racemic acetic acid. When this experiment was carried out with (1*R*,2*R*)-[1-$^2H_1$,^3H]glycerol, the acetic acid from the degradation showed an *F* value of 35,[*] corresponding to *S* configuration with 52% *ee*. That the methionine-derived methyl groups were indeed racemic was confirmed by degradation of another sample to give a fragment containing only the latter methyl groups, but not C-17/C-17′. Kuhn-Roth oxidation of this material produced racemic acetic acid. The contribution of the methionine-derived racemic methyl groups to the chirality of the acetic acid from the Kuhn-Roth oxidation of aplasmomycin **31** can be estimated based on the earlier experiments with deuterated glycerol, and correction for this contribution indicates that the C-17/C-17′ methyl groups have *S* configurations with 84% *ee*.[114] The finding that the methyl group of the starter unit generated from (1*R*,2*R*)-[1-^2H,^3H]glycerol has high chiral purity and *S* configuration again rules out the involvement of the methylglyoxal synthase reaction as well as the pyruvate kinase reaction in the formation of the starter unit from glycerol. Pyruvate kinase would have generated a methyl group of *R* configuration,[118] whereas methylglyoxal synthase would have produced a racemic methyl group.[119]

Further information on the mode of assembly and modification of the polyketide chain of aplasmomycin **31** was obtained by determining the fate of the methyl hydrogen and carboxyl oxygen atoms of acetate during the biosynthesis. This was done using the isotope-shift methodology[9,10,93] and precursors intramolecularly double labeled with ^{13}C and ^2H or ^{13}C and ^{18}O. Aplasmomycin derived from [2-^{13}C,$^2H_3$]acetate was analyzed by ^{13}C NMR spectroscopy with simultaneous ^1H and ^2H broadband decoupling. The results, summarized in Figure 16, showed the incorporation of one atom of deuterium each at C-2/C-2′, C-10/C-10′, and C-12/C-12′ and two atoms of deuterium each at C-6/C-6′ and C-14/C-14′. Notably, no deuterium was present at C-4/C-4′ and only one deuterium atom at C-10/C-10′. The origin of the oxygen atoms was similarly probed with [1-^{13}C,$^{18}O_2$]acetate. The ^{13}C NMR spectrum of the aplasmomycin derived from this precursor showed isotopically shifted satellites for the signals at C-1/C-1′, C-7/C-7′, C-9/C-9′, and C-13/C-13′. Notably, C-3/C-3′ showed no isotopically shifted signal, indicating that the oxygen of the pyran ring is contributed by C-7/C-7′ and that, surprisingly, the other oxygen at C-3/C-3′ does not originate from the carboxyl group of acetate.[114]



31

Fig. 16. Origin of hydrogen and oxygen atoms of aplasmomycin **31** from acetate and glycerol. D = deuterium from [2-^{13}C,$^2H_3$]acetate; ● = ^{18}O from [1-^{13}C,$^{18}O_2$]acetate. Heavy lines connect the ^{18}O to the carbon from which it originated. C-17 and C-17′ are deuterated from (2*R*)-[1,1-$^2H_2$]glycerol.

A number of conclusions can be drawn from these results. The ^{18}O enrichment at C-1/C-1′ is as high as in the other labeled positions, suggesting that the lactone functions are formed directly from a carboxyl-activated derivative rather than from a carboxyl group obtained by hydrolysis of an activated intermediate (e.g., a thioester). In the latter case only half as much ^{18}O should have been retained at C-1/C-1′ as in the other positions. Methylation of the polyketide chain (both at C-4/C-4′ and C-8/C-8′) at the β-diketone stage seems plausible on mechanistic grounds. Methylation at C-4/C-4′ prior to removal of the C-5/C-5′ oxygen via a 4,5-ene intermediate would account for the lack of deuterium retention at C-4/C-4′. For the C-10/C-10′ to C-14/C-14′ segment, the retention of only one atom of deuterium at C-10/C-10′ implies removal of the C-11/C-11′ oxygen function via a 10,11-ene intermediate. Since the final product contains an 11,12 double bond and C-13/C-13′ initially is at the carbonyl oxidation level, a double bond shift seems a plausible possibility.

By process of elimination, the choice of the polyketide starter unit is narrowed down to phosphoglyceric acid or phosphoenolpyruvate as the two most likely candidates. These compounds have not been encountered before as polyketide starter units or, for that matter, as thioesters, and further verification of this tentative conclusion is highly desirable. Unfortunately, in view of the impermeability of cell membranes to phosphate esters this cannot be done by in vivo feeding experiments, but has to await the availability of a cell-free system. The finding that the oxygen of the tetrahydrofuran ring originates from C-13/C-13′

[*] The F value (see Ref. [68]) is an experimental measure of the configuration and optical purity of a chiral methyl group: F = 79 corresponds to 100% *ee R*; F = 50 to a racemate; F = 21 to 100% *ee S*.

rather than C-16/C-16′ is intriguing; it points to a displacement of the original oxygen at the center carbon of the starter unit. A plausible sequence of events is outlined in Figure 17, implying phosphoenolpyruvate as the starter moiety, but alternatives are certainly conceivable.[114]

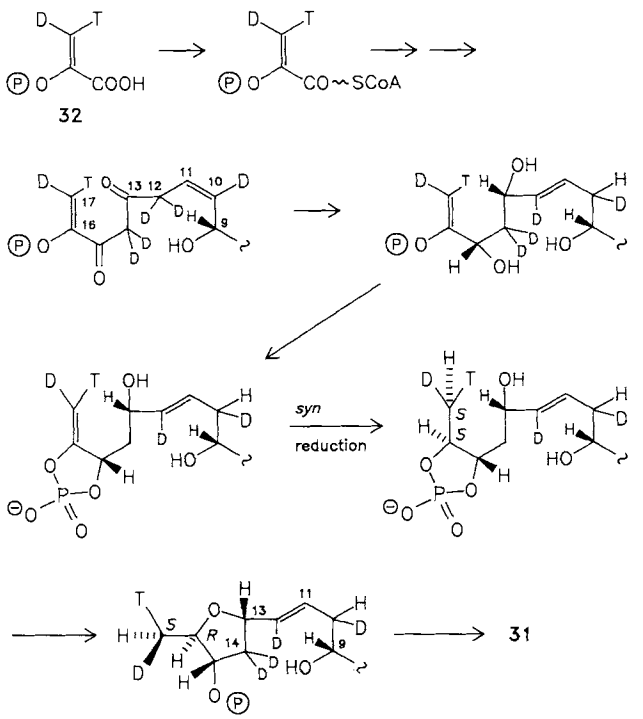


Fig. 17. Hypothetical mechanism for the formation of the C-9 to C-17 moiety of aplasmomycin **31**.

6. Formation of Some Unique Structural Elements in Antibiotics—mC_7N and C_5N Units

6.1. Background

The antibiotic asukamycin **6**[37,38] (Fig. 2), in addition to the cyclohexane ring, contains two other unique structural elements. One is a C_5N unit in the form of a molecule of 2-amino-3-hydroxycylopent-2-enone amide-linked to a short polyketide chain. The same structural unit is present in the closely related manumycin **44**[120,121] (see Fig. 24) and in reductiomycin **46**[122] (see Fig. 26) as well as in a number of other recently discovered antibiotics.[123-127] Until recently, nothing was known about its biosynthesis.

The other unique structural element present in asukamycin **6** as well as manumycin **44** and ansatrienin **5** (Fig. 2) consists of a six-membered carbocyclic ring, usually aromatic or quinoid, carrying an additional carbon and a nitrogen substituent in a 1,3 (*meta*) arrangement. This so-called mC_7N unit was first recognized as a structural element of the ansamycin antibiotic rifamycin B **35** (Fig. 18), not derived by the polyketide pathway.[128,129] It is present in all the ansamycins and in ansamitocin **34** (Fig. 18) as well as in structurally quite different antibiotics such as the mitomycins (see **36**, Fig. 18).[130] Other compounds contain mC_7N units which were proposed to be of similar biosyn-

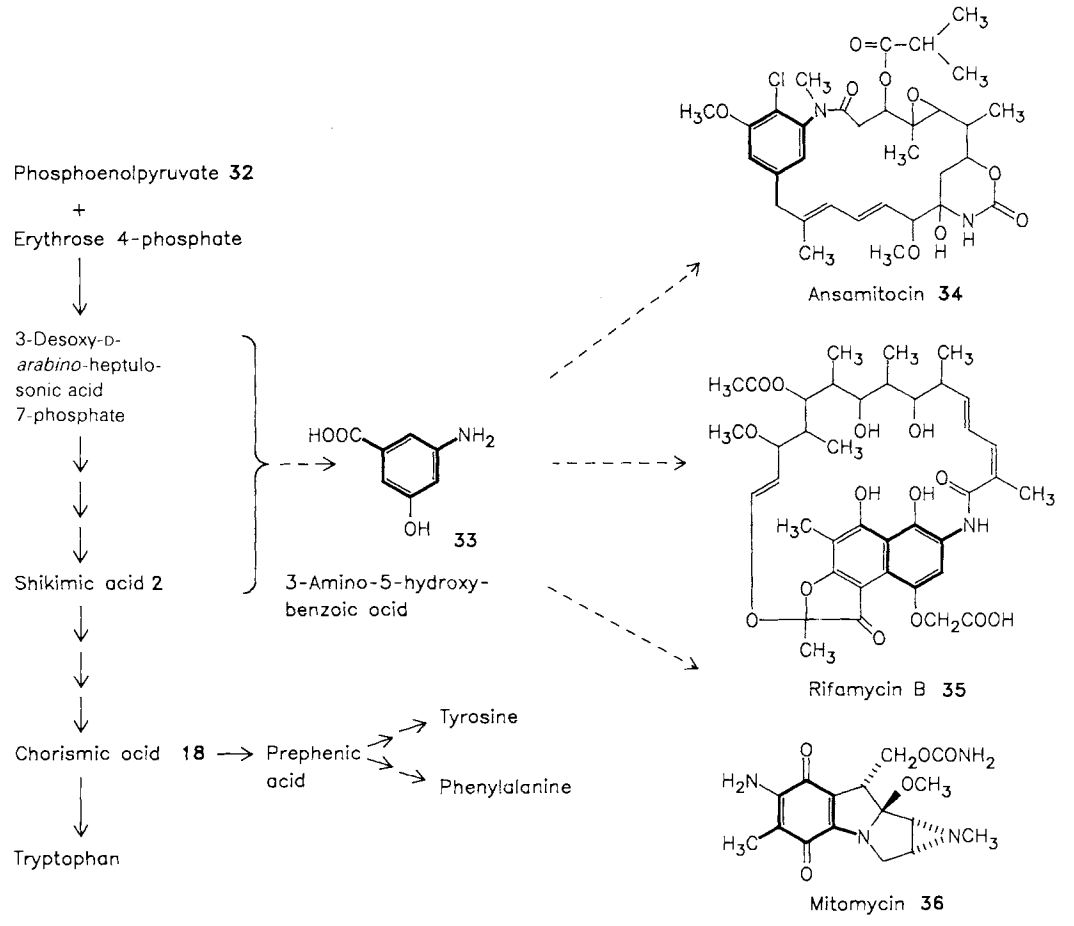


Fig. 18. Origin of the mC_7N units in rifamycin B **35**, ansamitocin **34**, and mitomycin **36**. The framework of the mC_7N unit is shown in heavy lines.

thetic origin:[131] e.g., the aminocyclitol valienamine, which is present in validamycin[132] and in the β-glucosidase inhibitor acarbose **42**[133] (see Fig. 22).

Feeding experiments with a variety of labeled precursors[130, 134–137] established a labeling pattern in the mC_7N unit of ansamycins and mitomycin **36** closely resembling that for shikimic acid. Yet, all attempts to demonstrate incorporation of labeled shikimic acid[134, 136, 138] or, in the case of mitomycin, also of dehydroquinic acid[137] were unsuccessful. These negative results may either reflect poor uptake of shikimic acid or indicate that the branch-off point for formation of the mC_7N unit is earlier in the shikimate pathway.

An important breakthrough was the demonstration by *Nüesch* and *Ghisalba* through genetic studies and by *Rickards* and co-workers through feeding experiments that 3-amino-5-hydroxybenzoic acid is a specific and proximate precursor of the mC_7N unit in rifamycin **35**[139] and its relative actamycin,[140] ansamitocin **34**,[141] and mitomycin **36**.[142] However, this leaves still unexplained how 3-amino-5-hydroxybenzoic acid is formed via the shikimate pathway. *Hornemann* et al.[137] established by degradation of mitomycin samples from various specifically labeled precursors that the nitrogen is attached to the carbon atom corresponding to C-5 of shikimic acid rather than to that corresponding to C-3. This finding was rather surprising, since it ruled out a straightforward transamination of 3-dehydroshikimic acid. This was confirmed by *Rinehart* et al.[143] who analyzed the ^{13}C–^{13}C coupling pattern in the mC_7N unit of geldanamycin **39**, an ansamycin antibiotic, biosynthesized from D-[U-$^{13}C_6$]glucose (Fig. 19). In contrast, the same experiment with pactamycin **38**[144] (Fig. 19), which contains a structurally more unusual mC_7N unit, revealed attachment of the nitrogen to the carbon corresponding to C-3 of shikimic acid or dehydroshikimic acid **37**,[12] indicating different pathways to the mC_7N units in these two compounds.[143] Consistent with this difference, the mC_7N unit of pactamycin **38** is formed via 3-aminobenzoic acid rather than 3-amino-5-hydroxybenzoic acid **33**. *Rinehart* et al. proposed (Fig. 19) that the mC_7N unit of pactamycin **38** is formed via transamination of dehydroshikimic acid **37** at C-3, whereas **33**, which gives rise to the other mC_7N units, is formed by oxidation of dehydroshikimic acid to the 5-oxo analogue followed by transamination at C-5.[143]

6.2. Naphthomycin and Ansatrienin

In our own studies on the biosynthesis of mC_7N units, we first focused on two ansamycin antibiotics, ansatrienin **5** (cf. Fig. 2) and naphthomycin A **40**, also a metabolite of *Streptomyces collinus*[145] (Fig. 20). The naphthomycins represent a small group of closely related antibiotics, whose structures were elucidated by chemical and spectroscopic means[146–150] and whose antibiotic activity is due to vitamin K antagonism.[145] As would be expected, the ansa chains of both types of compounds are derived from acetate and propionate units by the polyketide pathway.[148, 151, 152] Consistent with the results of *Rickards* and co-workers[140, 142] was our observation of very efficient and specific incorporation of 3-amino-5-hydroxy[*carboxy*-^{13}C]-benzoic acid into naphthomycin A **40** (64% enrichment at C-27)[152] as well as ansatrienin **5** (48% enrichment at C-17).[44, 152]

The site of attachment of the nitrogen to the shikimate-pathway-derived carbon skeleton was determined by feeding experiments with [U-$^{13}C_3$]glycerol and ^{13}C–^{13}C coupling analysis of the products.[153, 154] Glycerol as substrate has the advantage over D-[U-$^{13}C_6$]glucose that it is more

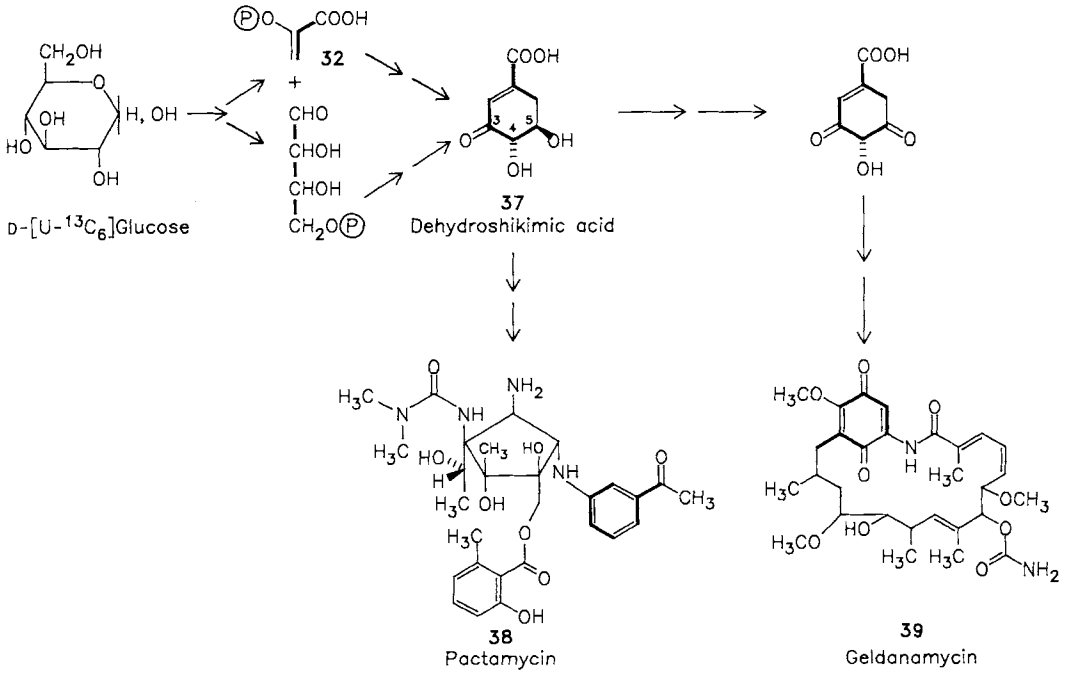
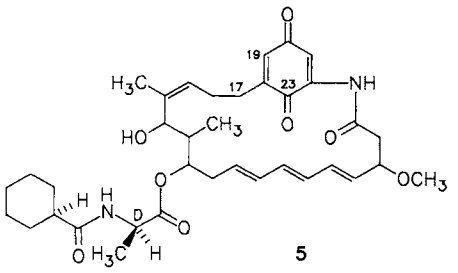
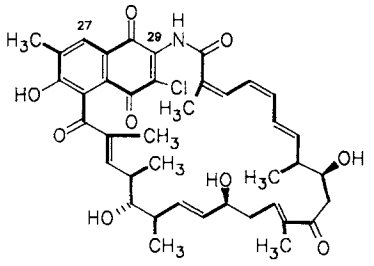


Fig. 19. Pactamycin **38** and geldanamycin **39**, the ^{13}C–^{13}C coupling patterns in their mC_7N units after feeding experiments with D-[U-$^{13}C_6$]glucose [12, 143], and a hypothesis for the formation of their mC_7N units via the shikimate pathway [143]. ^{13}C–^{13}C coupling is indicated by heavy lines connecting carbons.



5

Ansatrienin A = Mycotrienin



40

Naphthomycin A

Fig. 20. Naphthomycin A **40** and the enrichment and ^{13}C-^{13}C coupling pattern in a sample biosynthesized from [U-$^{13}C_3$]glycerol (cf. caption to Fig. 19).

efficiently utilized, even in the presence of other carbohydrates as carbon source; in addition, the coupling pattern of the products is not altered by metabolism of the substrate through the glycolytic pathway. Nevertheless, the products from feeding experiments with this precursor usually show very complex coupling patterns which require extensive use of 2D NMR techniques for analysis. Particularly useful is a triple-quantum version of the 2D INADEQUATE experiment which we developed for this purpose.[155] This experiment specifically detects assemblies of three directly coupled ^{13}C nuclei which share a unique triple-quantum-coherence frequency (see Section 6.3 and Fig. 23). The naphthomycin A **40** derived from [U-$^{13}C_3$]glycerol (Fig. 20) showed the expected couplings in the polyketide moiety; in addition, the mC_7N moiety contained two three-carbon assemblies derived intact from glycerol and one aromatic carbon, C-29, carrying the nitrogen, which was enriched but did not show significant coupling to neighboring carbons. Completely analogous results were obtained for ansatrienin **5**. This identifies the assembly of the mC_7N unit in **40** and **5** as being identical to that in mitomycin **36** and geldanamycin **39**; i.e., the nitrogen is attached to the carbon corresponding to C-5 of a shikimic acid molecule.

The presence in ansatrienin **5** of a shikimate-derived cyclohexanecarboxylic acid moiety in addition to the mC_7N unit offered the unique opportunity to test the proposition that the lack of incorporation of shikimic acid **2** into the mC_7N unit is due to impermeability of the cells. Conclusive evidence that shikimic acid labels only the cyclohexanecarboxylic acid moiety but not the mC_7N unit came from an experiment in which D-[2-^{13}C]shikimic acid was fed to *S. collinus*. The ^{13}C NMR spectra of the resulting **5** revealed approximately 5% enrichment in C-6 of the cyclohexane ring, but no significant enrichment (less than 0.2%) in C-19 or C-23, the two possible sites of labeling in the mC_7N unit.[46] It is therefore clear that, at least in the case of ansatrienin biosynthesis, the lack of incorporation of shikimic acid into the mC_7N unit is not due to permeability problems.

We conclude that the formation of 3-amino-5-hydroxybenzoic acid **33** must branch off at a much earlier stage in the shikimate pathway. To accommodate all the known facts about the biosynthesis of the mC_7N unit of the mitomycin, ansamycin, and ansamitocin antibiotics, we propose the pathway for the formation of 3-amino-5-hydroxybenzoic acid **3** shown in Figure 21. It had already been

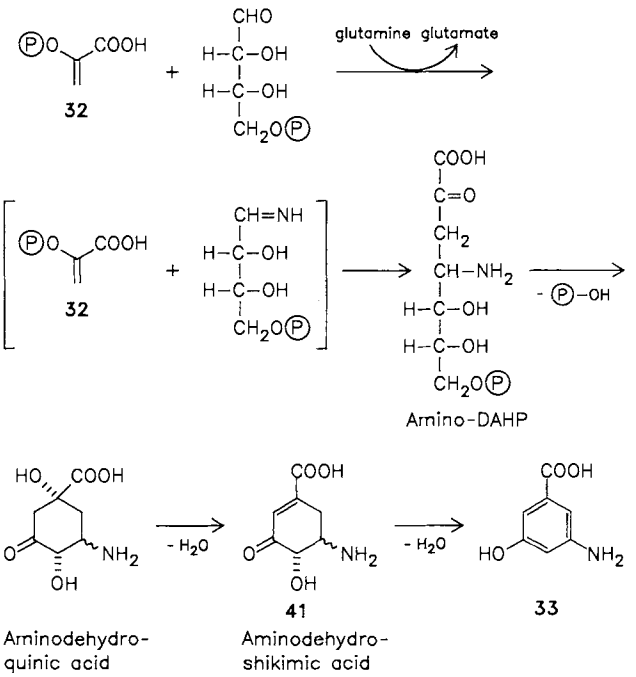


Fig. 21. Proposed mode of formation of 3-amino-5-hydroxybenzoic acid **33**, the precursor of mC_7N units.

suggested by *Hornemann* et al.[137] that the 4-deoxy-4-amino analogue of 3-deoxy-D-*arabino*-heptulosonic acid 7-phosphate (DAHP) is the precursor of the mC_7N unit. We are proposing that this compound ("amino-DAHP") is formed by an enzyme similar to DAHP synthase, but carrying an additional subunit which can hydrolyze glutamine. The nascent ammonia thereby produced reacts with the aldehyde group of erythrose 4-phosphate to form an imine. Condensation of the imine with phosphoenolpyruvate would then produce the amino analogue of DAHP. This notion is supported by the finding of *Jiao* et al.[156] that the most efficient source of the nitrogen of rifamycin is the amide nitrogen of glutamine. The amino analogue could then be carried through the next two stages of the shikimate pathway, possibly by the normal enzymes, to give the 5-amino analogue of 3-dehydroshikimic acid, which by enolization and dehydration would produce 3-amino-5-hydroxybenzoic acid. Obviously, this scheme is at the moment entirely speculative and awaits experimental scrutiny.

6.3. Acarbose

The α-D-glucosidase inhibitor acarbose **42** (Fig. 22)[133,157] is a pseudotetrasaccharide containing an unsaturated cyclitol moiety, valienamine, and a 6-deoxy sugar attached to a molecule of maltose. Valienamine is also a component of the antibiotic validamycin A;[132,158,159] it represents an mC_7N unit which had been proposed to arise in the same manner as the mC_7N unit of the ansamycins and mitomycins.[131] On the other hand, the substitution pattern of valienamine differs substantially from that of other mC_7N units, suggesting the possibility of a different biosynthetic origin. In collaboration with the group of *Pape* we examined this question by feeding [*carboxy*-^{13}C]-3-amino-5-hydroxybenzoic acid and 3-aminobenzoic acid to cultures of *Actinoplanes sp.* SN 23/29. NMR analysis of the resulting **42** showed no detectable incorporation of label from either precursor.[160] Hence, it does indeed appear that a different pathway is operating in the formation of the mC_7N unit of acarbose. To obtain more information, we carried out a feeding experiment with [U-$^{13}C_3$]glycerol. The analysis of the resulting **42** by a variety of multiple-quantum 2D NMR techniques revealed the labeling and coupling pattern shown in Figure 22. Particularly informative was the triple-quantum 2D INADEQUATE spectrum (Fig. 23). A strong signal indicated the presence of a contiguous array of three ^{13}C nuclei representing C-6, C-1, and C-2 of the valienamine moiety. The remaining four carbon atoms of this mC_7N unit are derived from glycerol as two C_2 units. This coupling pattern is in accord with formation of the valienamine moiety by cyclization of a heptulose which, in turn, arises by two successive transfers of C_2 units by transketolase onto a triose phosphate (Fig. 22). *Rinehart* et al.[161] have independently demonstrated the same mode of formation for the valienamine moiety of the antibiotic validamycin.

6.4. Asukamycin and Manumycin

Manumycin **44** (Fig. 24), a metabolite of *Streptomyces parvulus*,[120,121,162] and asukamycin **6** (cf. Fig. 2)[37,38] both contain an mC_7N unit and a C_5N unit connected by short polyene chains ending in carboxyl groups which are amide-linked to the nitrogens of the mC_7N and C_5N units. The polyketide origin of these polyene chains has been demonstrated for manumycin **44** by *Thiericke* and *Zeeck*[163] and for asukamycin **6** in our laboratory.[43] As shown in Figure 24, one polyketide chain in both antibiotics is initiated by the exocyclic carbon of the mC_7N unit, which presumably therefore at one point must have had the oxidation state of a carboxyl group. The other polyketide chain in manumycin is initiated by an acetate unit and in asukamycin by cyclohexanecarboxylic acid (see Section 3), both presumably in the form of their coenzyme A esters.

6.4.1. Origin of the mC_7N Unit

In light of the origin of the mC_7N units of the ansamycin and mitomycin antibiotics from 3-amino-5-hydroxybenzoic acid **33**, we fed this compound, labeled with ^{13}C in the carboxyl group, both to *Streptomyces nodosus* subspecies *asukaensis* and to *Streptomyces parvulus*. No significant incorporation of ^{13}C was seen into either asukamycin **6** or manumycin **44**.[164] Similarly, 3-amino[*carboxy*-^{13}C]-benzoic acid **43** was not significantly incorporated into manumycin, although addition of larger quantities of 3-aminobenzoic acid to the fermentation resulted in the formation of a new compound containing a simple benzene ring in place of the six-membered ring of **44**.[165] Feeding experiments with ^{13}C-labeled acetate indicated specific incorporation of two molecules of acetate into the mC_7N units of **6** and **44** in a tail-to-tail fashion (Fig. 24), labeling four of the seven carbon atoms of this moie-

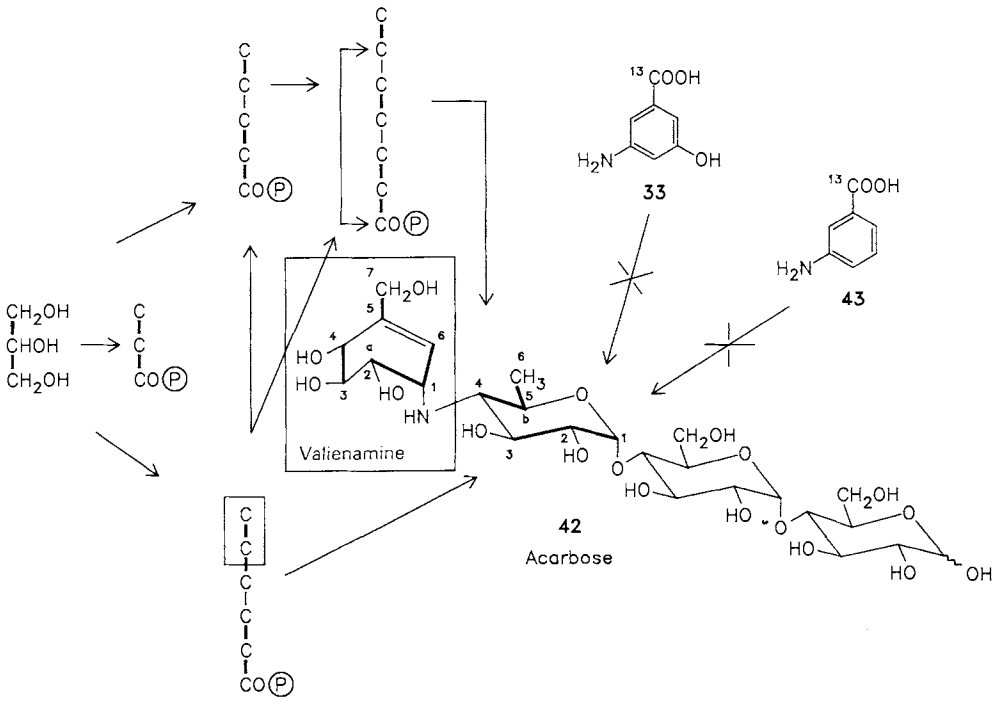


Fig. 22. Acarbose **42** and its ^{13}C-^{13}C coupling pattern and mode of formation from [U-$^{13}C_3$]glycerol.

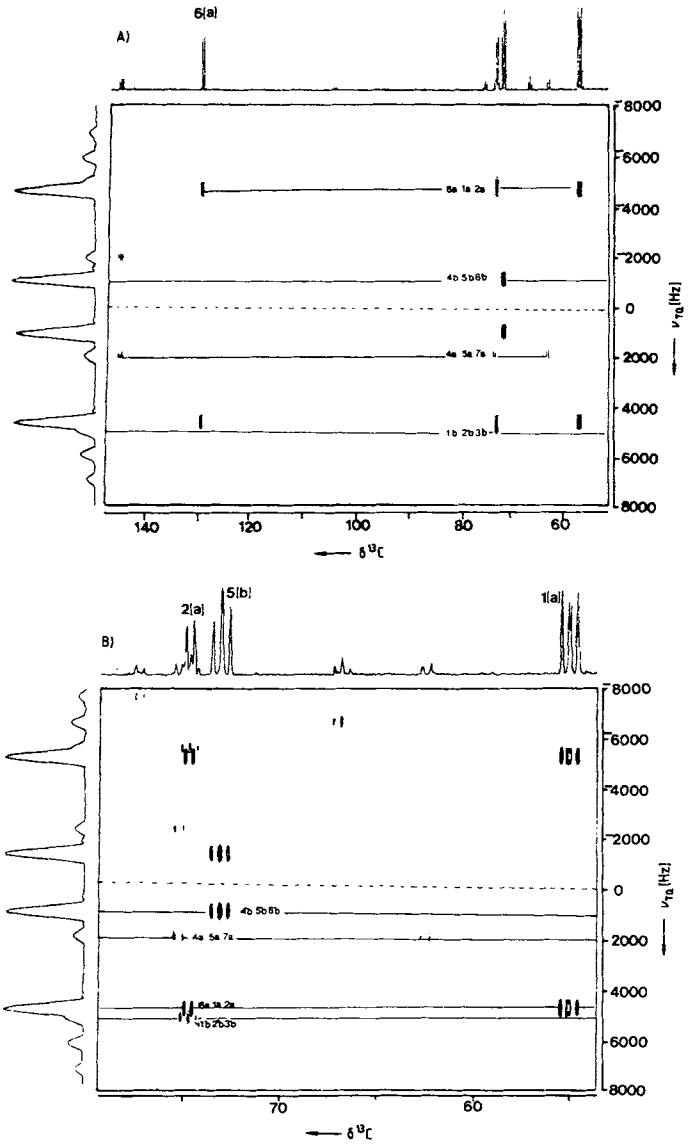


Fig. 23. Triple-quantum 2D INADEQUATE spectrum of acarbose **42** biosynthesized from [U-$^{13}C_3$]glycerol. A) Full 121.5-MHz spectrum. B) F2 expanded spectrum. The spectra are symmetrical around the $\nu_{TQ} = 0$ axis (dotted line). Signals sharing the same TQ frequency arise from contiguously coupled arrays of three ^{13}C nuclei. Some of the weaker signals, e.g., 4(a)5(a)7(a), arise from statistical coupling across one of the bonds, as confirmed by the double-quantum 2D INADEQUATE spectrum. The carbons in the valienamine moiety are indicated by "a", those in the 6-deoxy sugar moiety by "b".

ty.[163, 164] No such incorporation of acetate into the mC_7N unit is predicted via the shikimate pathway; hence, these results suggest a completely different origin of these mC_7N units. To probe for the origin of the remaining three carbon atoms, we again carried out experiments with [U-$^{13}C_3$]glycerol. Extensive analysis of the coupling patterns in the resulting **6** and **44** revealed that an intact glycerol molecule is incorporated into C-1, C-2, and C-3, albeit at somewhat lower enrichment than the incorporation of acetate into the other four carbon atoms of the mC_7N unit.[164] This pattern is indeed different from that predicted for glycerol incorporation via the shikimate pathway (i.e., two contiguously coupled three-carbon segments plus one enriched carbon atom without significant ^{13}C–^{13}C coupling). The latter pattern was, however, seen in the cyclohexane ring and the attached carbon of asukamycin **6**.

The tail-to-tail connection of two molecules of acetate in the mC_7N unit of asukamycin and manumycin suggests origin of those four carbon atoms from a four-carbon dicarboxylic acid generated via the Krebs cycle. This notion is supported by a feeding experiment with [1,4-$^{13}C_2$]succinic acid which gave low but specific incorporation into C-6 and C-7 of asukamycin.[166] The relatively low enrichment obtained with this precursor is in all likelihood due to extensive metabolism of succinate via the Krebs cycle. A more proximate precursor of the three glycerol-derived carbon atoms of the mC_7N unit has not yet been identified. However, a feeding experiment with D,L-[1-^{13}C]serine gave no detectable incorporation into either C-1 or C-3 of **6**. Similar results have been obtained with **44**.[167]

It is evident from the results described here that, again, the pathway operating in the formation of the mC_7N unit of these antibiotics is entirely different from that leading to the biosynthesis of the ansamycin and mitomycin antibiotics on the one hand and the valienamine moiety of acarbose **42** and validamycin on the other. However, considerable additional work is necessary to unravel the detailed features of this new pathway. The origin of another mC_7N unit, a structural element of the antibiotic kinamycin, has been studied by *Gould* et al. In this case the mC_7N unit was found to originate from acetate by the polyketide pathway.[168] All these studies taken together clearly indicate that the biosynthetic similarities among the various mC_7N units do not extend as far as some of the structural comparisons had originally suggested.

6.4.2. Origin of the C_5N Unit

Inspection of the structure of the C_5N unit of manumycin **44** and asukamycin **6**, the 2-amino-3-hydroxycyclopent-2-enone moiety, immediately reveals that it contains all the carbon, hydrogen, nitrogen, and oxygen atoms of 5-aminolevulinic acid **45** minus one molecule of water. Working with the asukamycin fermentation, we therefore tested the notion that the C_5N moiety arises by an intramolecular cyclization of **45**.[169]

In agreement with this idea, [2-^{14}C]glycine gave specific incorporation of up to 20% whereas [1-^{14}C]glycine gave nine times lower incorporation under comparable conditions. Intact incorporation of C-2 of glycine with the attached nitrogen was demonstrated by feeding [2-^{13}C,^{15}N]glycine and observing splitting of the ^{13}C NMR signal for C-2 of the 2-amino-3-hydroxycyclopent-2-enone moiety at $\delta = 115.4$ into a doublet by the attached ^{15}N. [1,4-$^{14}C_2$]Succinic acid was incorporated rather poorly (specific incorporation 0.3 to 0.6%), possibly reflecting the Krebs cycle activity in this organism, but the feeding experiments with [1,2-$^{13}C_2$]acetate and [U-$^{13}C_3$]glycerol (Fig. 24) support the notion that C-3, C-4, C-5, and C-1 of the C_5N unit arise from succinic acid. Two molecules of acetate are incorporated into these four carbon atoms in a tail-to-tail fashion, the carboxyl groups giving rise to C-1 and C-3. Finally, feeding experiments with 5-amino-[5-^{14}C]levulinic acid showed significant incorporation (specific incorpora-

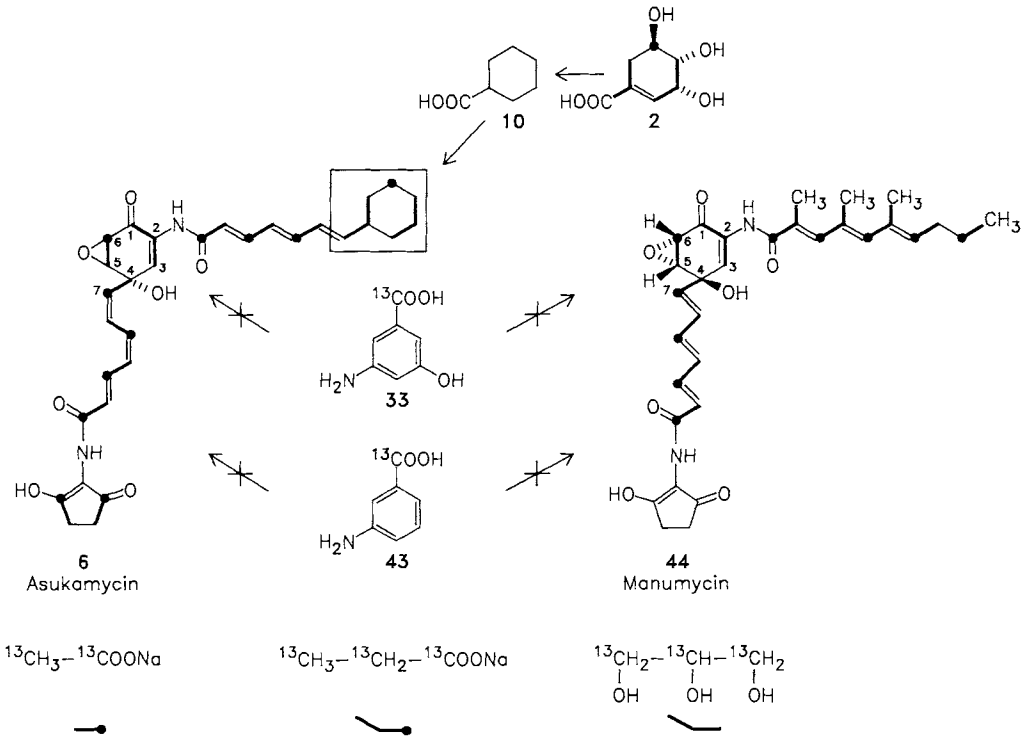


Fig. 24. Biosynthetic labeling patterns of asukamycin **6** and manumycin **44**.

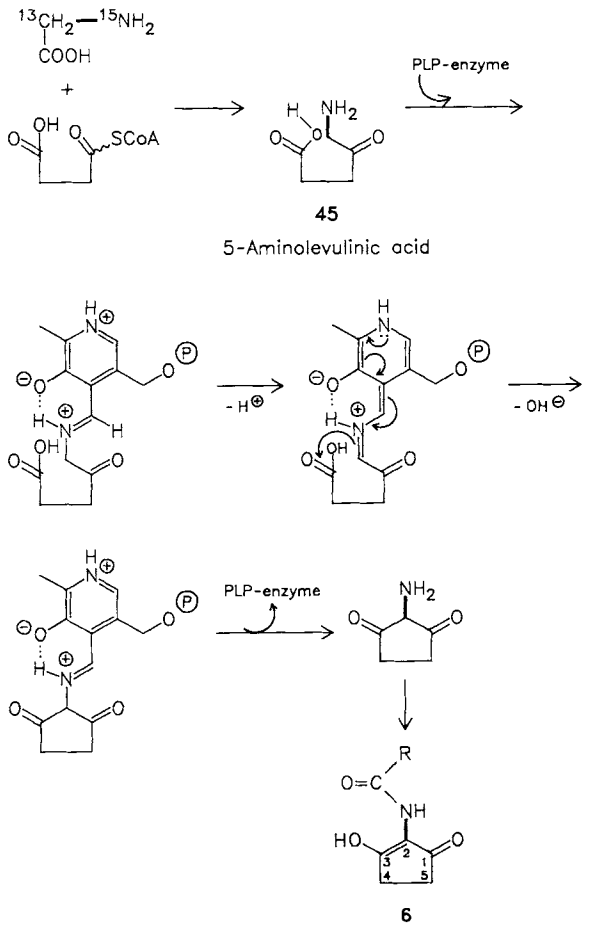


Fig. 25. Proposed mechanism for the formation of the C_5N unit in asukamycin **6** from 5-aminolevulinic acid **45**.

tion of 0.2 to 2.2%) despite the fact that this compound inhibited asukamycin formation and underwent extensive decomposition during the fermentation.

On the basis of these results, we suggested[169] that the 2-amino-3-hydroxycyclopent-2-enone moiety is formed from one molecule each of succinyl-CoA and glycine, with decarboxylation of the latter, via 5-aminolevulinic acid **45**, which then undergoes an intramolecular cyclization. Figure 25 shows a plausible mechanism for this reaction, invoking pyridoxal phosphate (PLP) catalysis to generate a carbanion at C-5 which attacks the carboxyl carbon.

6.5. Reductiomycin

We wanted to verify the biosynthetic origin of the C_5N unit established in asukamycin **6** in another example and we chose for this the antibiotic reductiomycin **46** (Fig. 26). The structure of this antibiotic, a metabolite of *Streptomyces xanthochromogenus*, was the subject of some controversy,[122,170,171] which was settled in favor of structure **46** by total synthesis.[172] Feeding experiments with ^{14}C-labeled precursors gave results similar to those obtained on the C_5N unit of asukamycin **6**.[173] [2-^{14}C]Glycine, but not [1-^{14}C]glycine, was efficiently incorporated into **46**, and both [1,4-$^{14}C_2$]succinic acid and 5-amino-[5-^{14}C]levulinic acid were incorporated significantly but less efficiently than [2-^{14}C]glycine. Unequivocal proof for the direct origin of the 2-amino-3-hydroxycyclopent-2-enone moiety from an intact molecule of 5-aminolevulinic acid **45** was ascertained by feeding experiments with a sample of the latter doubly labeled with ^{13}C in positions 4 and 5. The ^{13}C NMR spectrum of the resulting sample of **46** showed labeling exclusively in C-1, C-2, and C-3 of the

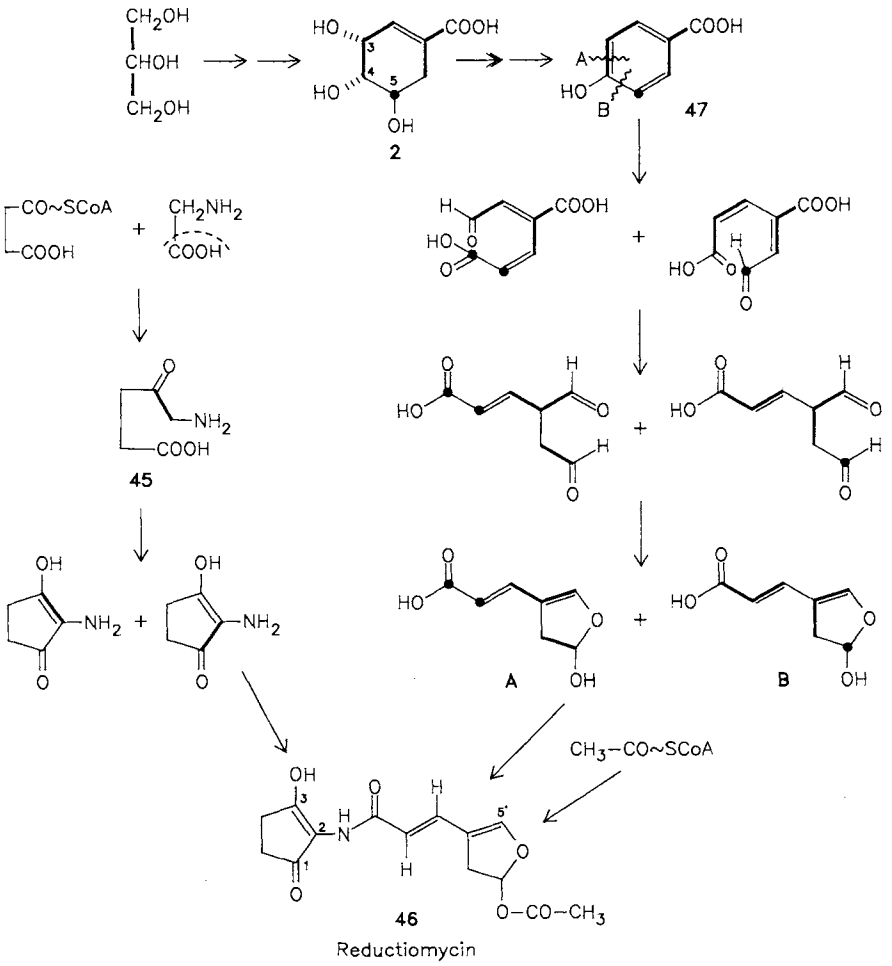


Fig. 26. Biosynthesis of the antibiotic reductiomycin **46**. **A** and **B** are the products formed by cleavage of **47** at A and B, respectively.

C_5N moiety. C-2 was twice as heavily enriched as C-1 and C-3; in half of the labeled molecules, C-2 was coupled to C-1 and in the other half to C-3. The patterns of incorporation of [1,2-$^{13}C_2$]acetate and [U-$^{13}C_3$]glycerol are fully in accord with formation of the C_5N unit by intramolecular cyclization of 5-aminolevulinic acid **45**.[173]

The origin of the remaining nine carbon atoms of **46** was less obvious. Inspection of the structure suggested the possibility that the entire nine-carbon assembly, including the acetoxy group, could be derived by a ring cleavage of tyrosine or a derivative thereof followed by a Baeyer–Villiger oxidation. However, this notion was quickly dismissed when it was found that [1-^{14}C]tyrosine was not at all incorporated and that [1,2-$^{13}C_2$]acetate gave high enrichment and coupling in the acetoxy group. The origin of the remaining seven carbon atoms making up the dihydrofuranylacrylic acid moiety was again probed in a feeding experiment with [U-$^{13}C_3$]glycerol.[173] The incorporation of three C_2 units from glycerol into the three acetate/succinate-derived portions of the molecule was readily detected. However, the seven carbon atoms of the dihydrofuranylacrylic acid moiety showed a very complex coupling pattern. By a 2D INADEQUATE experiment and subsequent spectral simulation, this was unraveled as a superimposition of two coupling patterns, each present in half of the labeled molecules (Fig. 26). One (cf. **B**) contained two intact molecules of glycerol and a single enriched but not coupled carbon and the other (cf. **A**) contained one C_3 segment, one C_2 segment, and two single enriched, but not coupled, carbon atoms. The coupling pattern in **B** is immediately reminiscent of a biosynthesis via the shikimate pathway. Cleavage of a molecule of shikimic acid **2** between C-4 and C-5 would give the observed pattern. Pattern **A** would result from a cleavage of shikimic acid between C-3 and C-4. The results thus suggested that the dihydrofuranylacrylic acid moiety might arise by aromatic ring cleavage of a symmetrical compound formed from shikimic acid **2**. A logical candidate would be 4-hydroxybenzoic acid **47** or the corresponding aldehyde. When this notion was tested by feeding 4-hydroxy-[*carboxy*-^{13}C]benzoic acid to *Streptomyces xanthochromogenus*, **46** was obtained which contained 64% ^{13}C exclusively in the expected position, C-5'.[173] Further experiments suggest that the ring cleavage occurs at the stage of the corresponding aldehyde.

7. Benzoisochromane Quinone Antibiotics

7.1. Background

In 1947 *Brockmann* and *Pini*[174] reported the isolation of a deep red, crystalline pigment from cultures of an Actinomycete. This compound, actinorhodin **55**, was the first

member of a sizable family of antibiotics sharing the common structural element of a disubstituted tricyclic benzoisochromane skeleton **48** (Fig. 27).[175] Additional common structural features are oxygen functions at C-11 and C-13, a quinone function in one of the aromatic rings and the absence of an oxygen function at C-9. The hydrogens at the two common chiral centers, C-3 and C-15, are in a *trans* relationship. Streptomycetes can elaborate either compounds of 15*R* (A series, actinorhodin, kalafungin) or 15*S* configuration (G series, granaticin, the nanaomycins, and the naphthocyclinones). At least in one case[176] the same culture has been observed to produce members of both enantiomeric series.

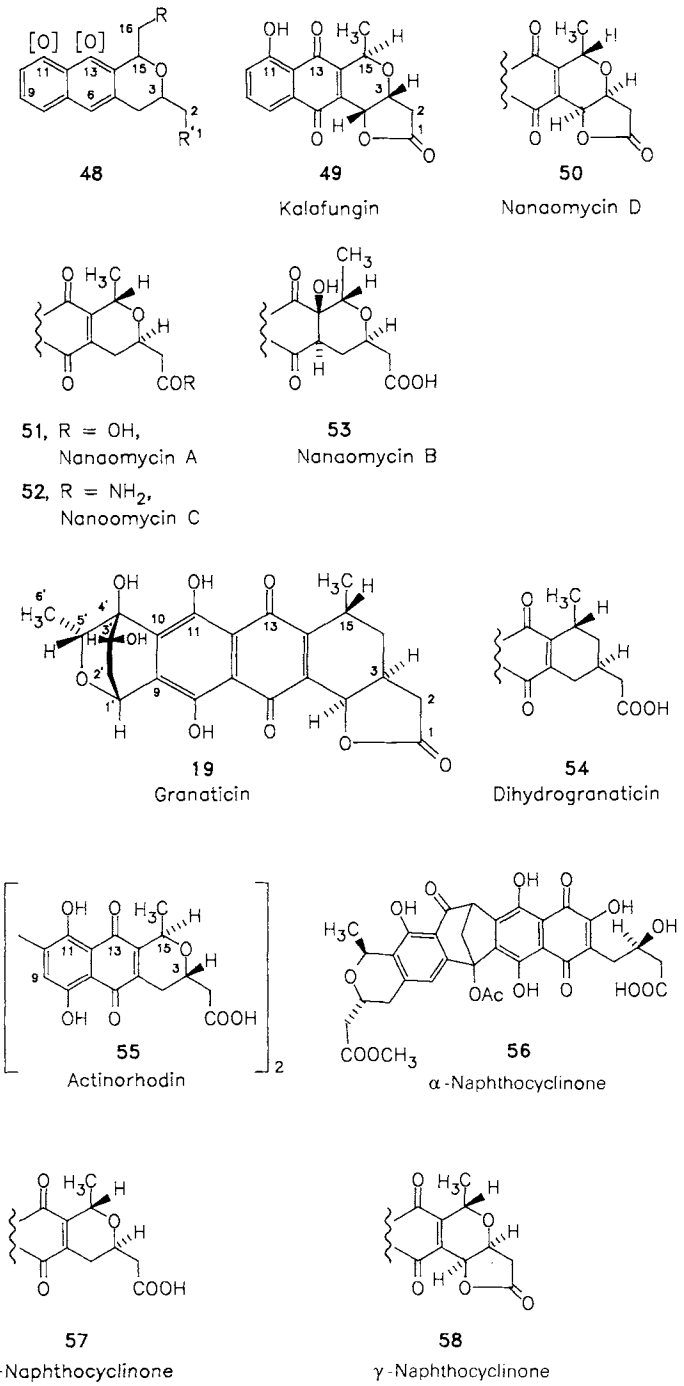


Fig. 27. Some benzoisochromane quinone antibiotics, sharing the common structural element **48**.

As reviewed earlier,[177] the benzoisochromane quinone antibiotics can be categorized into simple monomers, C-16-modified monomers, carbohydrate-modified monomers, and dimers. The simple monomers are represented by kalafungin **44**, a metabolite of *Streptomyces tanashiensis*,[178,179] and the nanaomycins **50**–**53** isolated from *S. rosa* var. *notoensis* (Fig. 27).[180–186] Most of these compounds show pronounced activity against gram-positive bacteria and mycoplasmas, as well as good antifungal activity;[181] nanaomycin A **51** has been approved for use in Japan as an anti-ringworm agent in cattle. Carbohydrate-modified monomers are represented by granaticin **19** and its congeners. These were first isolated from *S. olivaceus*,[54] but have also been obtained from various other *Streptomyces* species.[55–58] The structure of granaticin **19** (Fig. 27) was determined by spectroscopic methods[59] and by a single-crystal X-ray analysis.[60] Granaticin co-occurs with, among other congeners, its analogue dihydrogranaticin **54**, which does not contain a lactone ring.[57]

The simplest of the dimeric benzoisochromane quinones, actinorhodin **55** (Fig. 27)[187–189] from *S. coelicolor*, is a very deeply colored pH indicator, red in acid, blue at an alkaline pH. More highly modified dimers are the naphthocyclinones, which were isolated from cultures of *S. arenae* and whose structures were deduced by extensive spectroscopic studies[190–192] and by an X-ray analysis.[193] The quantitatively prevalent compound is α-naphthocyclinone **56** (Fig. 27) which lacks two carbon atoms in the "eastern" portion of the molecule compared to all the other naphthocyclinones.

7.2. Formation of the Polyketide Backbone

Feeding experiments with ^{13}C-labeled acetate and malonate have demonstrated unequivocally that the basic skeleton of the benzoisochromane quinone antibiotics is constructed from eight acetate/malonate units via the polyketide pathway, giving rise to the labeling patterns shown in Figure 28 for nanaomycin A **51**,[182] actinorhodin **55**,[194] and granaticin **19**.[61,195] The biosynthetic labeling pattern has been used in two instances to settle subtle structural uncertainties. *Ōmura* and co-workers placed the hydroxyl group in nanaomycin A at C-11 rather than C-8, because it is attached to a carbon enriched by [1-^{13}C]acetate,[182] and we showed that the two monomeric units in actinorhodin **55** are connected through C-10 labeled by the methyl group of acetate.[194] A feeding experiment with [1,2-$^{13}C_2$]acetate also established that all eight acetate units of **55** are incorporated intact into each monomer unit.[194] In the case of α-naphthocyclinone **56**, ^{13}C-labeled acetate and malonate gave the enrichment pattern shown in Figure 29, clearly indicating origin of this molecule from two polyketide chains plus one additional acetate moiety giving rise to the acetoxy group.[196] The involvement of two polyketide chains follows in particular from the finding that two directly connected carbons in the center of the molecule are both derived from C-2 of acetate.

Further information on the mode of polyketide assembly was sought in the case of granaticin **19** by following the fate of the methyl hydrogens and the carboxyl oxygens of acetate through the biosynthetic sequence.[197] Analysis of

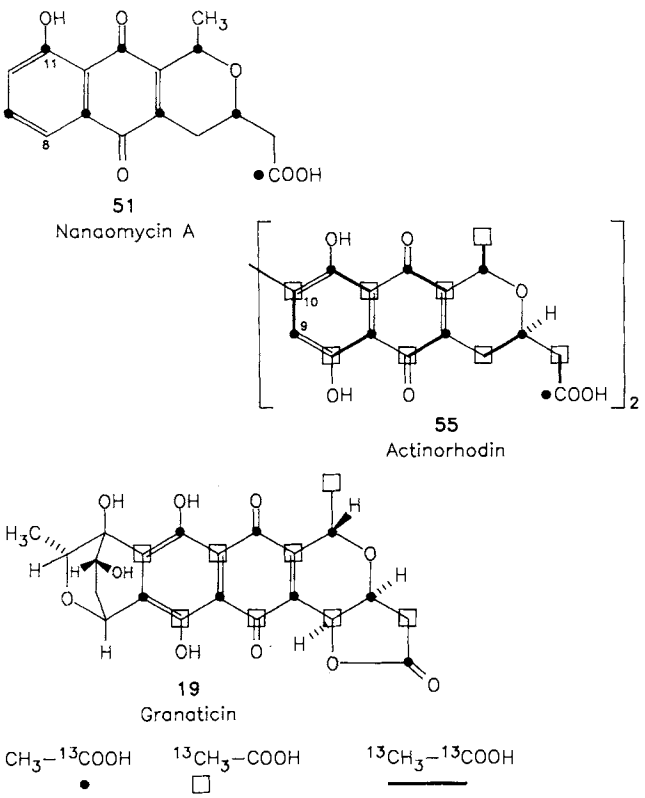


Fig. 28. Labeling and coupling pattern in benzoisochromane quinones after feeding experiments with ^{13}C-labeled acetate.

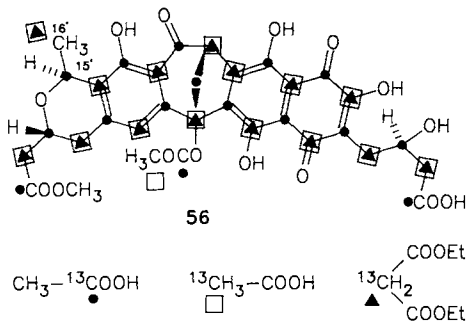


Fig. 29. Labeling pattern of α-naphthocyclinone **56** after feeding experiments with ^{13}C-labeled acetate and malonate.

a sample of **19** biosynthesized from [2-^{13}C,$^{2}H_3$]acetate by $^{13}C\{^{1}H,^{2}H\}$ triple-resonance spectroscopy showed the incorporation of one atom of deuterium each at C-2 and C-4 (Fig. 30). C-16 carried a maximum of two, not three, atoms of deuterium. These findings suggest that C-2 of the polyketide chain goes through the intermediate stage of a methine carbon, resulting in replacement of one of the original deuterium atoms by a normal hydrogen atom. The finding of only two rather than three atoms of deuterium in the methyl group of the starter unit is intriguing. It could have a trivial explanation—e.g., rapid equilibration between acetyl-CoA and malonyl-CoA—but it also would be consistent with the idea that the starter unit might be malonyl-CoA rather than acetyl-CoA. The resulting polyketide would have to be decarboxylated stereospecifically prior to release from the synthase.

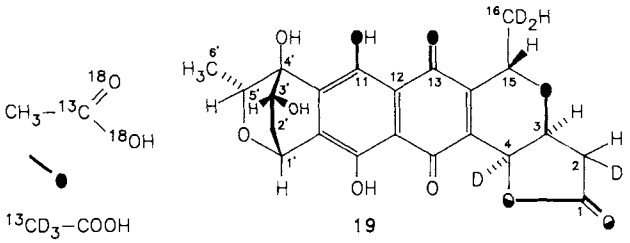


Fig. 30. Fate of the methyl hydrogens and the carboxyl oxygens of acetate in the biosynthesis of granaticin **19**.

The fate of the acetate oxygens was probed in an experiment with [1-^{13}C,$^{18}O_2$]acetate followed by ^{13}C NMR analysis of the product by the ^{18}O shift method. This experiment showed incorporation of ^{18}O at C-1, C-11, and C-13 and into the oxygen of the pyran ring (Fig. 30). The ^{18}O shift from the pyran ring oxygen was only observed on the ^{13}C NMR signal for C-3, not that for C-15, demonstrating that this oxygen is provided by the C-3 carbonyl group of the polyketide. The ^{18}O distribution between the carbonyl and the lactone oxygen at C-1 was not determined, because the granaticin sample was derivatized to the methyl ester of dihydrogranaticin **55** (Fig. 27) for NMR analysis. The ^{18}O enrichment at C-1 of this derivative was about half that in the other three positions, consistent with loss of half the ^{18}O during esterification. This result indicates the retention of only one atom of oxygen at the original C-1 of granaticin **19**. Hence, the formation of the lactone ring of granaticin from a free carboxyl group involves no loss of ^{18}O.[197]

7.3. Formation of the Sugar Moiety of Granaticin

In granaticin **19** the basic polyketide-derived skeleton is modified by the attachment of a six-carbon moiety to the aromatic system in an unusual, rigid [2.2.2] arrangement. Structural inspection of this additional six-carbon moiety identifies it as a 2,6-dideoxyhexose, and, in accord with this view, its origin was readily traced to glucose.[61] Details of the conversion of glucose to this dideoxyhexose moiety were discussed in Section 4.1.

An interesting problem is posed by the attachment of the sugar moiety, presumably in the form of TDP-4-oxo-2,6-dideoxyhexose **59**, to the aromatic ring system, since the process is completely regiospecific. This regiospecificity may be due to recognition of the substitution pattern at the opposite end of the aromatic moiety by the enzyme generating the first C–C bond to the sugar moiety. In this case the first bond formed may be the *C*-glycosidic linkage between C-1 of the sugar and C-9 of the aglycone (path A, Fig. 31). Alternatively, the first bond to the sugar moiety may be formed at the stage of an aromatic precursor not yet oxygenated at C-8 (path B, Fig. 31). This would imply that the first bond is formed by an aldol condensation between C-4 of the sugar and C-10 (activated by the 11-hydroxyl group) of the aromatic precursor. Hydroxylation at C-8 and closure of the *C*-glycosidic bond then completes the structure. In view of findings (see Section 7.6) that the stereochemistry in the pyran ring can be altered without

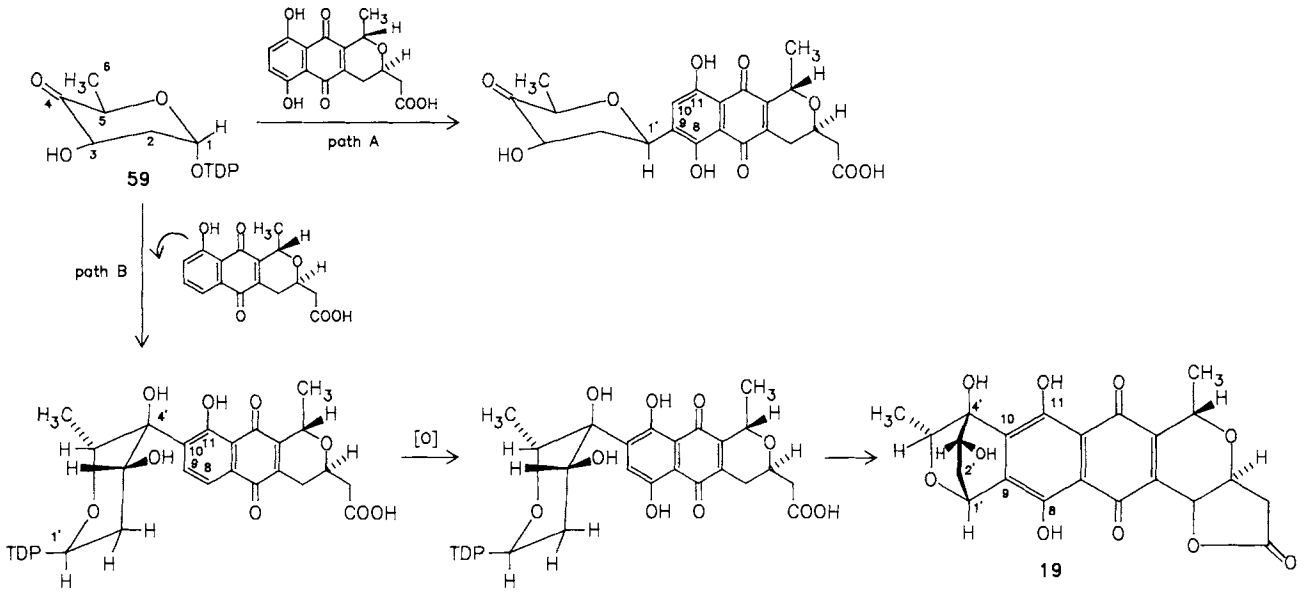


Fig. 31. Possible mechanisms for the attachment of the sugar moiety to the aromatic core of granaticin **19**.

losing the regiospecificity of sugar attachment, we favor the second possibility (path B).

7.4. Biosynthetic Interrelations among Benzoisochromane Quinone Antibiotics

Biosynthetic relations among the various nanaomycins were studied by *Ōmura* et al.[198] Using the fatty acid synthase inhibitor cerulenin[199] to inhibit de novo polyketide formation, they incubated cultures of *S. rosa* var. *notoensis* with individual nanaomycins and monitored their transformation, or lack thereof, to other nanaomycins. These experiments revealed that the biosynthetic reaction sequence was conversion of nanaomycin D to A to E to B (Fig. 32). All three conversions were also demonstrated in cell-free systems[201,202] and the enzyme catalyzing the first of these, nanaomycin D reductase, was purified and studied in some detail.[201,202] The epoxidation of nanaomycin A to E is catalyzed by a mixed function oxygenase requiring NADPH and oxygen.[200] Nanaomycin B synthase, catalyzing the reductive epoxide opening of nanaomycin E to B requires NADH or NADPH and is the first example of an enzyme catalyzing a reductive epoxide ring opening.[200] Nanaomycin D reductase, catalyzing the conversion of nanaomycin D to A, is a flavoprotein of molecular weight 68000 daltons containing FAD. It requires NADH as the reducing agent.[225] The reaction as catalyzed by this enzyme is essentially irreversible and a number of other benzoisochromane quinones, but not granaticin, can serve as substrate in place of nanaomycin D. It is well known[57,61,184,203] that the lactone forms of benzoisochromane quinone antibiotics and their ring-open dihydro forms are readily interconverted chemically under either reducing (lactone to dihydro) or oxidizing (dihydro to lactone) conditions. A likely mechanism for this interconversion is shown in Figure 33. The only redox reaction in the system is the interconversion of the quinone and the hydroquinone form. The hydroquinone of the lactone is then in equilibrium with the quinone of the ring-open dihydro form. *Ōmura* et al.[202] presented evidence, consistent with this view, that nanaomycin D reductase is in fact an NADH dehydrogenase using quinones as facultative electron acceptors.

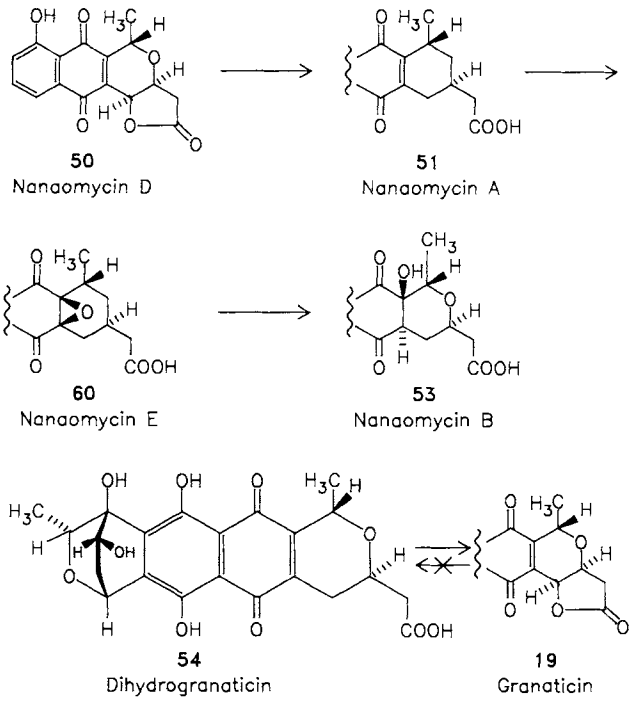


Fig. 32. Biosynthetic interrelations in the nanaomycin and granaticin series.

The finding that in the nanaomycin series the biosynthetic sequence proceeds from the lactone **50** to the ring-open dihydro form **51** is in marked contrast to the situation in the granaticin series. Here the biosynthetic se-

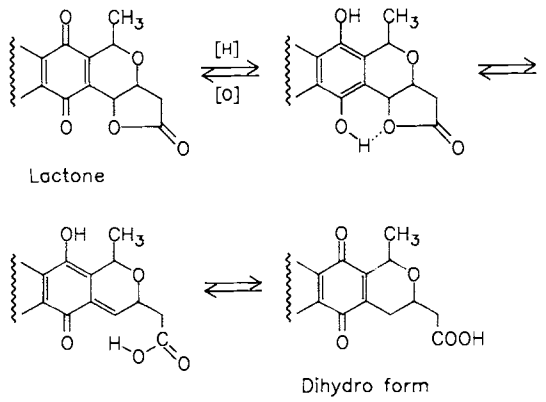


Fig. 33. Mechanism of the interconversion of benzoisochromane quinone lactones and their ring-open dihydro forms.

quence clearly proceeds from dihydrogranaticin **54** to granaticin **19** (Fig. 32). This was established by following the time course of the appearance of the two compounds in the fermentation[57,61] and by observing unidirectional conversion of **54** to **19** in cerulenin-inhibited cultures[197] and in cell-free extracts of *S. violaceoruber*.[61] Consistent with the mechanism shown in Figure 33, the enzymatic reaction is dependent on oxygen but no ^{18}O is incorporated into the product when the conversion is carried out in an atmosphere of $^{18}O_2$ gas.[61]

A detailed study has been made of the interconversions among naphthocyclinones in *S. arenae*.[204] The individual naphthocyclinones were prepared in ^{14}C-labeled form by biosynthesis from sodium [1-^{14}C]acetate and were then fed individually to cultures of *S. arenae*. The distribution of radioactivity among the various naphthocyclinones was analyzed after 6 h and 24 h of metabolism. The biosynthetic relationships established by these experiments are summarized in Figure 34. The main biosynthetic reaction sequence (**58** → **57** → **64** → **56**) parallels that seen in the nanaomycin series (**50** → **51** → **60** → **53**, Fig. 32) rather than that found for granaticin (**54** → **19**, Fig. 32). The lactone, γ-naphthocyclinone **58**, undergoes reductive ring opening to β-naphthocyclinone **57**, which is then epoxidized to **64**. Side reactions lead to δ-naphthocyclinone **62** and to the chlorohydrin **63** of β-naphthocyclinone. However, the main route of metabolism involves conversion of the epoxide and/or chlorohydrin of β-naphthocyclinone to α-naphthocyclinone **56** and further to α-naphthocyclinone acid, the end product of the pathway. This reaction has chemical precedent; both β-naphthocyclinone epoxide **64** and the chlorohydrin **63**, upon photolysis and hydrolysis of the product, give α-naphthocyclinone **56**. A likely mechanism, involving extrusion of C-15′ and C-16′ as acetaldehyde has been proposed.[192,204] The conversion of **57** to **62** is rather obscure, and nothing is known about the source of the additional three carbon atoms. Finally, the "monomer" **61** (Fig. 34), a degradation product of the naphthocyclinones,[190,191] and the corresponding "dimer" **65** were fed in radiolabeled form. The monomer was incorporated into the naphthocyclinones about four times more efficiently than the dimer. This suggests that **61** may serve as a precursor of the "western half" of the naphthocyclinones and

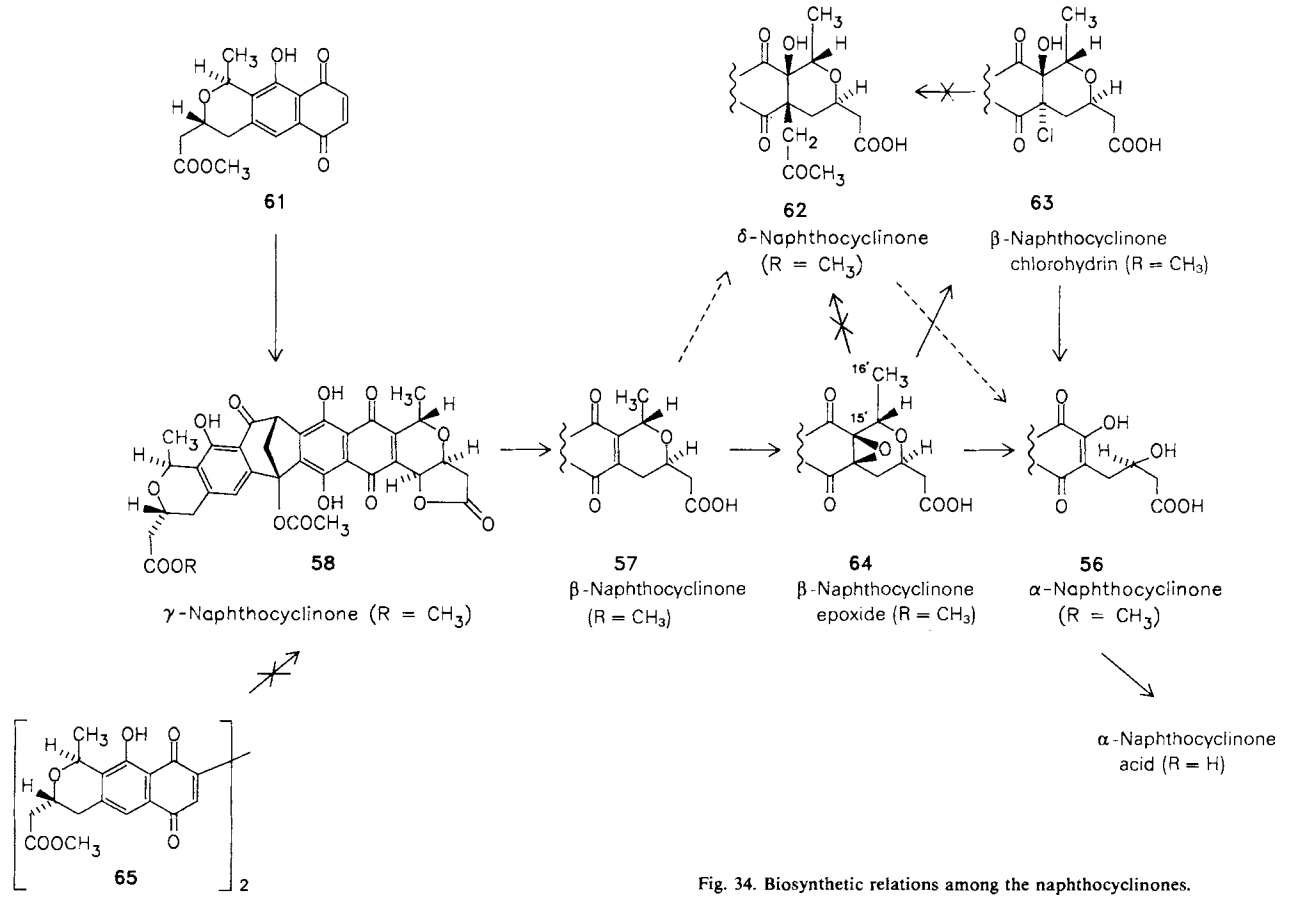


Fig. 34. Biosynthetic relations among the naphthocyclinones.

that the dimerization occurs either at the stage of a product derived from **61** or involves **61** and another monomeric unit to give an unsymmetrical dimer unit. However, more data are needed to draw definitive conclusions on this point.

7.5. Mapping of the Actinorhodin Biosynthetic Pathway by Analysis of Blocked Mutants

As a result of the extensive studies of *Hopwood* et al.,[205] *Streptomyces coelicolor* is today the genetically best-characterized member of the genus *Streptomyces*. Following the establishment of an extensive gene map for this organism, *Rudd* and *Hopwood*[206] isolated 76 mutants of *S. coelicolor* blocked in the biosynthesis of the antibiotic actinorhodin **55**. To select for these mutants, they exposed the colonies briefly to ammonia vapor, making use of the fact that **55** turns dark blue at an alkaline pH; nonproducing mutant colonies do not show this color change. Genetic mapping of these blocked mutants (*act* mutants) showed that all the biosynthetic genes are located in a narrow cluster on the *S. coelicolor* chromosome. The 76 *act* mutants were ordered into seven classes based on several criteria, primarily a cosynthesis assay. This assay involves growing two different mutant colonies next to each other on an agar plate; a mutant blocked late in the biosynthetic pathway (a "secretor" will accumulate a biosynthetic intermediate which diffuses into the surrounding agar and can be converted by a mutant blocked earlier in the pathway (a "converter") into **55**, giving rise to a blue zone in the converter colony where it borders the secretor.[206] The cosynthesis assay allowed ordering of the seven mutant classes in the following biosynthetic sequence:

$$\xrightarrow{\text{I}} \xrightarrow{\text{III}} \xrightarrow{\text{VII}} \xrightarrow{\text{IV}} \xrightarrow{\text{VI}} \xrightarrow{\text{V}} \text{actinorhodin } \mathbf{55}$$

The class *II* mutants cannot be assigned a position in the sequence; in all likelihood they are regulatory mutants. Mutants of classes I and III do not secrete diffusible intermediates; hence, they must be blocked very early in the biosynthetic pathway.

Mutants in classes VII, IV, VI, and V served as secretors in the cosynthesis assay, and our laboratory set out to isolate the biosynthetic intermediates from mutants representing these four classes (Fig. 35). The fractionation of culture extracts was guided by a modification of the cosynthesis assay, in which filter paper discs carrying fractions to be tested were placed on a lawn of a converter mutant. The intermediates in members of two classes (VII and VI) could be detected in the crude extract but were too unstable for isolation.[207] Class V, a very large mutant class, turned out to be genetically heterogeneous and yielded, from members of two subclasses, two compounds which were active in the cosynthesis assay, **70** and **49** (kalafungin) (Fig. 35).[208,209] Based on these structures as well as

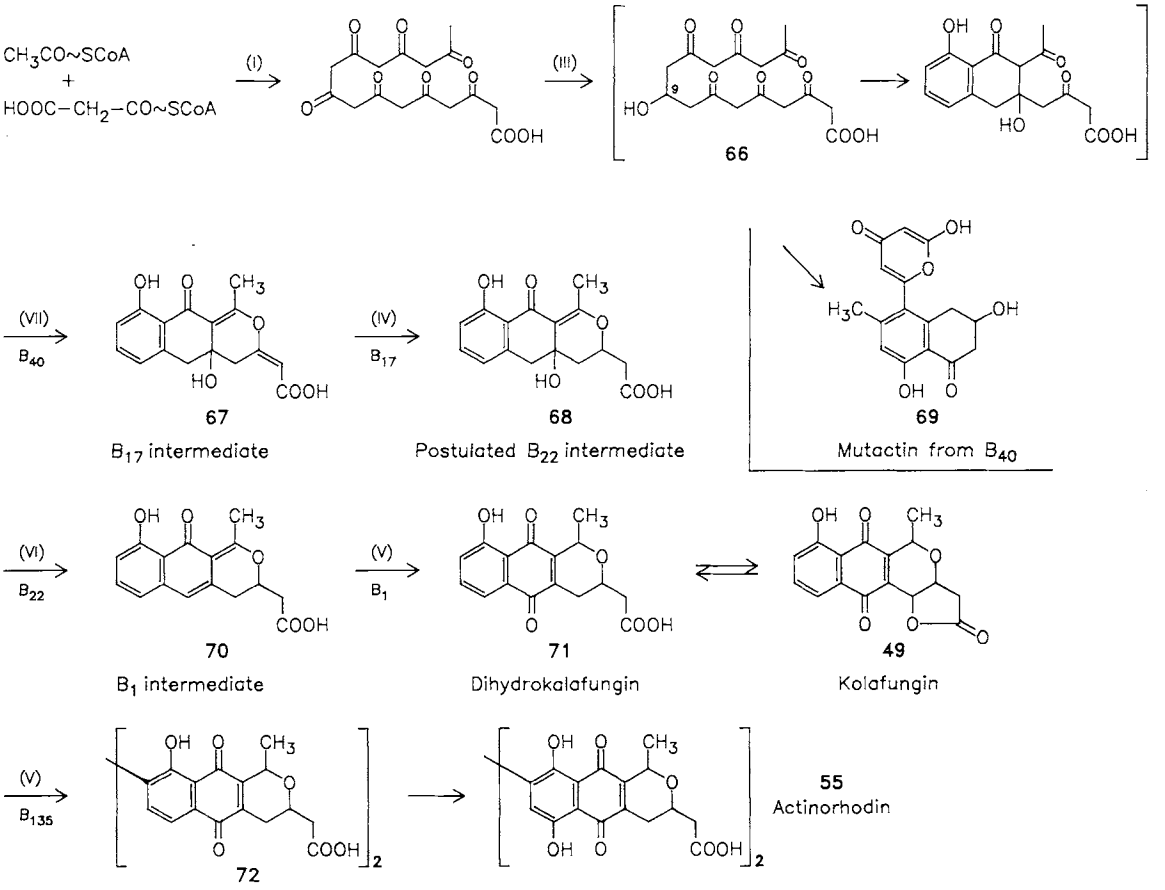


Fig. 35. Actinorhodin (**55**) biosynthesis intermediates isolated from blocked mutants, and their arrangement in a hypothetical pathway of actinorhodin formation.

that of compound **67** from mutant B_{17} (class IV), on the feeding experiments discussed earlier, and on mechanistic extrapolations, the hypothetical pathway for actinorhodin biosynthesis shown in Figure 35 was postulated. In particular, it is proposed that the dimerization occurs at the stage of dihydrokalafungin **71** or kalafungin **49** and that the introduction of the 8-hydroxyl groups is the terminal step of the reaction sequence. This accounts for the complete regiospecificity of the process without the need for an enzyme which is very discriminating as to the exact structure and stereochemistry at a remote site of its substrate.

The class VII mutant, B_{40}, produced copious amounts of a novel 16-carbon compound, mutactin **69** (Fig. 35), which, although not a precursor of **55**, is clearly related to the biosynthetic pathway. Its structure, established by X-ray crystallography and spectroscopic analysis,[210] can result from a different mode of cyclization of the presumed open-chain polyketide precursor **66** of actinorhodin after its reduction at C-9. Remarkably, mutactin **69** may be present as the racemate as suggested by both the X-ray structure and the absence of an optical rotation. A feeding experiment with [1,2-$^{13}C_2$]acetate revealed formation of **69** from eight intact molecules of acetate with a coupling pattern corresponding entirely to that seen in actinorhodin **55**. It is not at all obvious how the enzymatic reduction of a carbonyl group in a nonsymmetrical molecule can ultimately lead to a racemic product or how the resulting chiral center, if formed stereospecifically, can be racemized in a subsequent reaction. Mutactin **69** is also formed in traces by wild-type *S. coelicolor*, but not by *act* I and *act* III mutants, which lack the polyketide synthase and polyketide reductase, respectively, suggesting that mutactin formation shares these two enzymes with the actinorhodin biosynthetic pathway.

7.6. New Hybrid Antibiotics

Following the isolation and characterization of the *act* mutants and the finding that all the actinorhodin biosynthetic genes are contained in a cluster, *Malpartida* and *Hopwood*[211] succeeded in cloning the entire pathway. They constructed a plasmid, pIJ2303, carrying a DNA insert containing all the actinorhodin biosynthetic genes as evidenced by the fact that introduction of this plasmid restored synthesis of **55** in all *act* mutant classes and conferred the ability to synthesize **55** on a different organism, *S. parvulus*, which does not normally produce the compound. Further subcloning led to the construction of a series of plasmids containing various segments of the actinorhodin biosynthetic gene cluster.

Availability of the actinorhodin biosynthetic genes made it possible to examine whether new natural products could be generated by gene transfer between different *Streptomyces* strains producing different antibiotics. Obviously, to maximize chances of success one wants to start with strains producing relatively similar compounds. Therefore, in collaboration with the group of *Ōmura*, *Hopwood* and coworkers transformed the medermycin-producing *Streptomyces* AM-7161 (wild-type) with plasmids carrying some or all of the actinorhodin biosynthetic genes. Three transformants, each a recipient of a plasmid containing a gene which is lacking in class V *act* mutants of *S. coelicolor*, produced, in addition to medermycin **73**, one or two new compounds, mederrhodin A **74** and its ring-open dihydro derivative, mederrhodin B **75** (Fig. 36).[212,213] Mederrhodin A **74** has the same structure as medermycin **73** but carries the additional hydroxyl group at C-8 characteristic of actinorhodin **55**. In a similar collaboration with our laboratory, *Hopwood* and co-workers transformed the wild-type of the granaticin-producing *S. violaceoruber* and a nonproducing mutant with plasmids carrying some or all of the actinorhodin biosynthetic genes. A new compound, dihydrogranatirhodin **76** (Fig. 36), was produced by the transformant of the wild-type carrying pIJ2303. This compound has the same structure as dihydrogranaticin **54** (see Fig. 27) but the opposite configuration (actinorhodin stereochemistry) at either C-3 or C-15.[212]

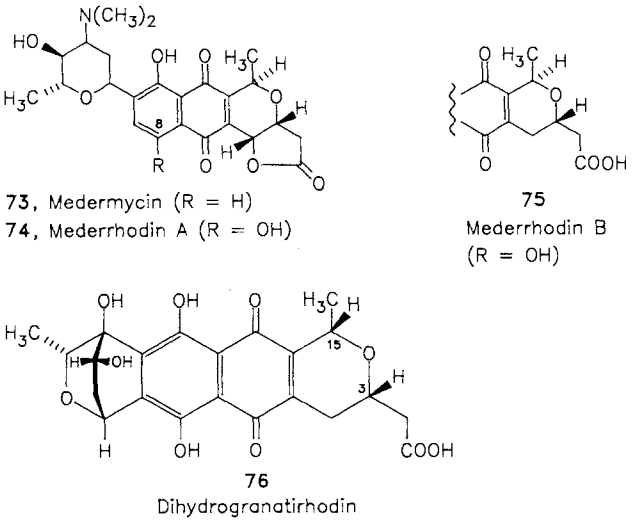
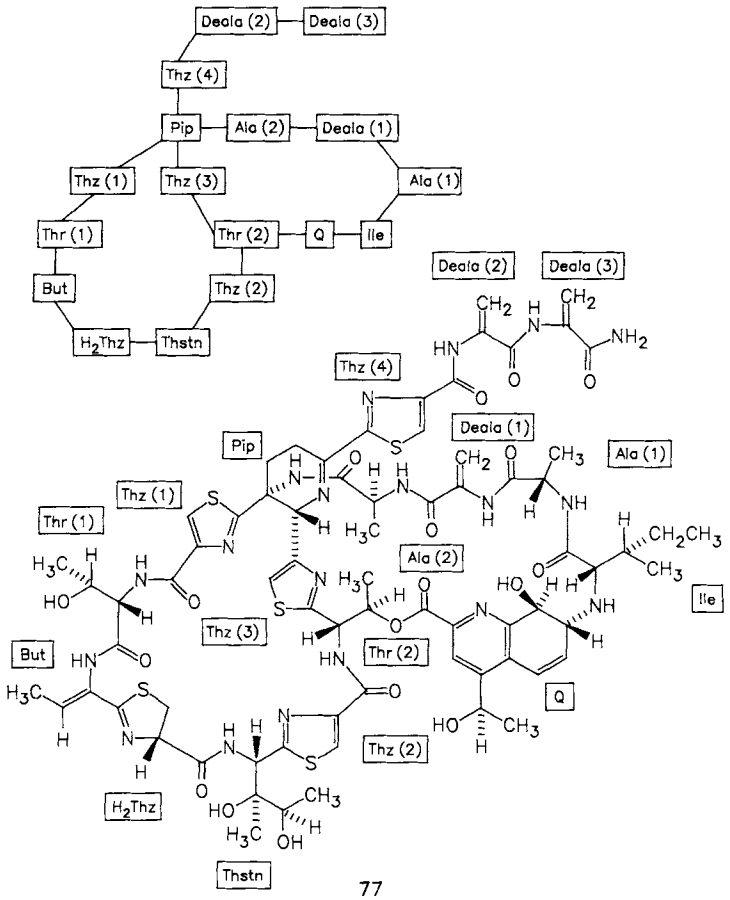


Fig. 36. Medermycin **73** and some new hybrid antibiotics in the benzoisochromane quinone series generated by genetic engineering.

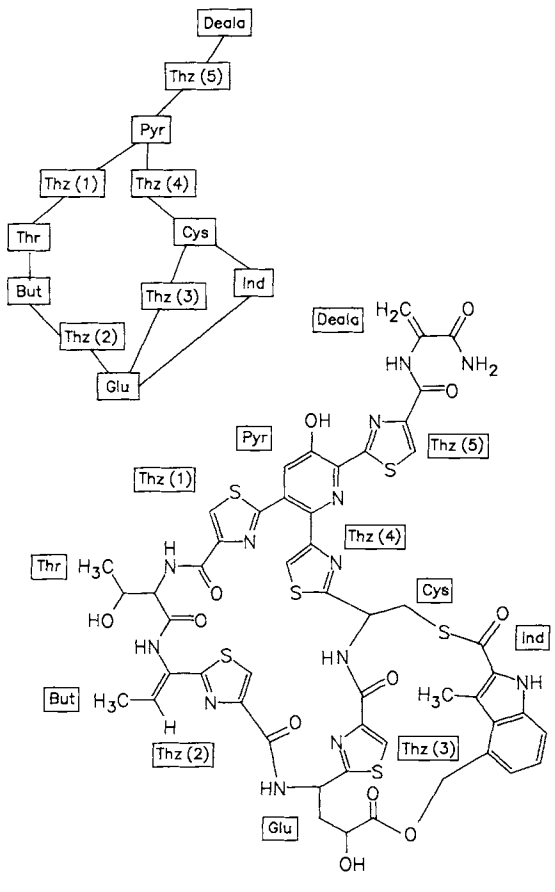
Dihydrogranatirhodin and the mederrhodins represent the first examples of the formation of new hybrid antibiotics by specific interspecies gene cloning. Although the structural modifications achieved are small, they demonstrate the feasibility of this approach; its potential and scope remain to be explored in further work.

8. Thiopeptide Antibiotics

Thiostrepton **77** (Fig. 37)[214–217] and nosiheptide **78**, also called multhiomycin,[218–220] are highly modified sulfur-rich peptide antibiotics. They belong to a family of about 20 known structures containing thiazole rings, which are called thiopeptide antibiotics. Their structures were elucidated by a combination of chemical degradations and X-ray crystallography. Most compounds in this family share a common architecture characterized by a macrocycle incorporating four thiazole and one pyridine or reduced pyridine ring, a side chain consisting of another thiazole and one or two dehydroalanine moieties, and an extra loop of more variable structure. Consistent with this common architecture, **77** and **78** share a common mode of



77



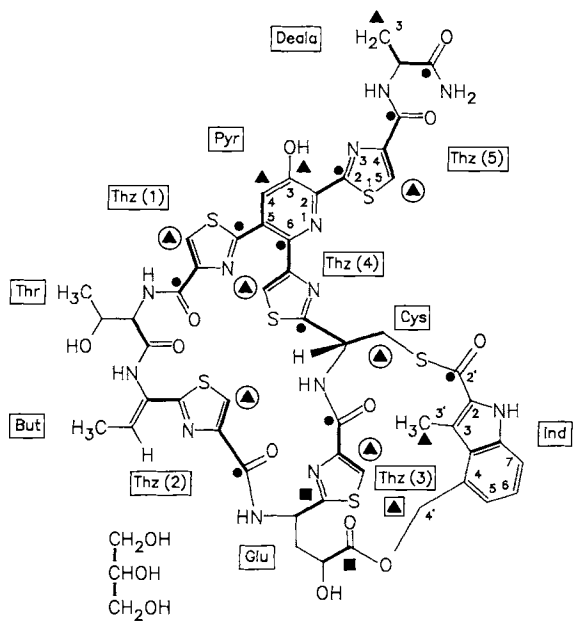
78

Fig. 37. Thiostrepton **77** and nosiheptide **78**. Thstn = thiostreptine residue, Q = quinaldic acid precursor, Cys = thiazoline residue, Thz = thiazole ring, Pip = dehydropiperidine ring.

action in their activity against gram-positive bacteria; both bind to the 50S ribosomal subunits,[221,222] thereby inhibiting the functions of elongation factors Tu and G.[222] Resistance to these antibiotics is due to methylation of a distinct site on the 23S rRNA by a specific methylase, resulting in the inhibition of antibiotic binding.[222] Nosiheptide **78** is used commercially in Europe and has been approved for use in Japan as a feed additive to increase weight gains in chickens;[223] thiostrepton **77** is not used commercially but is employed extensively as a research tool in molecular biology. Both **77** and **78** contain a number of unusual structural features which caused us to investigate their biosynthesis.

8.1. Biosynthesis of Nosiheptide

Since nosiheptide **78** is evidently a modified peptide, the incorporation of a variety of ^{14}C-labeled amino acids was tested in a series of preliminary feeding experiments with *S. actuosus*. These showed efficient incorporation of L-[U-^{14}C]threonine, L-[U-^{14}C]cysteine, L-[U-^{14}C]serine, L-[*methyl*-^{14}C]methionine, and L-[3'-^{14}C]- and D,L-[7a-^{14}C]tryptophan, but not of L-[U-^{14}C]alanine and L-[1'-^{14}C]phenylalanine.[224] In preparation for further, definitive experiments with ^{13}C-labeled precursors, the 51 signals in the ^{13}C NMR spectrum of nosiheptide **78** were unambiguously assigned. The signal assignments started from the earlier work of *Lukacs* and co-workers[218] and are based on chemical shift theory, multiplicity, ^{1}H-^{13}C correlations, long-range couplings, NOE effects, and multiple-quantum spectroscopy on multiply ^{13}C-enriched samples.[225-227]



78

L-[1,5-$^{13}C_2$]glutamate: ■ DL-[1-^{13}C]serine: ●
DL-[3-^{13}C]cysteine: ○ L-[3-^{13}C]serine: ▲
L-[*methyl*-^{13}C]methionine: □

Fig. 38. Labeling and coupling pattern in nosiheptide **78** after feeding experiments with various stable-isotope-labeled precursors.

The labeling and coupling patterns observed in **78** after feeding experiments with various ^{13}C-labeled precursors are shown in Figure 38. Specific labeling of the dehydroalanine moiety by L-[3-^{13}C]serine and D,L-[1-^{13}C]serine but not by D,L-[3-^{13}C]cysteine indicates that the dehydroalanine moiety specifically arises by dehydration of serine.[228] This parallels the origin of the dehydroalanine moieties of berninamycin as demonstrated by *Pearce* and *Rinehart* et al.[229,230] The five thiazole rings would be predicted to arise from a molecule of cysteine plus the carboxyl group of another acid or amino acid. This expectation is confirmed by the finding that D,L-[3-^{13}C]cysteine labels C-5 in all the thiazole rings as well as C-3 in the cysteine moiety. C-1 of the cysteine precursor serine, fed as the racemate, labeled the carbon atoms attached to C-4 of the five thiazole rings as well as C-2 of thiazole-4 (see Fig. 38). The same carbons that were enriched by C-3 of cysteine were also labeled by L-[3-^{13}C]serine.[224,228]

The two biosynthetically most unusual structural elements of **78** are the pyridine moiety and the indolecarboxylic acid moiety (Fig. 38). C-6 of the pyridine moiety is provided by the cysteine making up thiazole-4. The remaining four carbon atoms come from two molecules of serine which are connected tail-to-tail (i.e., through their C-3 atoms). This follows from the specific labeling of C-3 and C-4 of the pyridine ring by C-3 of serine and of the C-2 atoms of thiazole-1 and thiazole-5 by C-1 of serine.[224,228] The two serine moieties could be incorporated into the pyridine ring either intact or in the form of glycine and a C-1 unit following breakdown by serine hydroxymethyltransferase. An attempt to distinguish between these two possibilities by feeding experiments with [U-$^{13}C_3$]glycerol followed by coupling analysis gave incomplete results. Figure 38 shows the ^{13}C–^{13}C connectivities that were definitively established; however, a number of expected couplings were not seen, presumably due to the low enrichment of the sample.[224] On the other hand, recent experiments with L-[1,2-$^{13}C_2$]- and L-[2,3-$^{13}C_2$]serine have shown unequivocally that the two serine moieties are incorporated intact.[227] This would be consistent with a mechanism proposed by *Bycroft* et al.[231] which postulates that the pyridine ring arises from two molecules of dehydroalanine.

The incorporation of radioactive tryptophan into **78** suggested origin of the indolecarboxylic acid moiety in some way from that amino acid. It was found that C-3 of serine labeled both C-3′ and C-4′ of the indolecarboxylic acid moiety. Serine can give rise to the methyl group of methionine via the tetrahydrofolate pathway. However, feeding experiments with [*methyl*-^{13}C]methionine enriched nosiheptide **78** in only one carbon, C-4′, and C-1 of serine specifically labeled C-2′, the carboxyl group of the indolecarboxylic acid moiety. This led to the formulation of a specific hypothesis (Fig. 39) for the formation of the indolecarboxylic acid moiety through cyclization of tryptophan by bond formation between the carboxyl carbon and C-2 of the indole ring, followed by excision of the α carbon and the nitrogen of the side chain, methylation at the 4 position of the indole, and hydroxylation of the methyl group.[228] To test this postulate, we prepared a sample of L-tryptophan carrying ^{13}C at 50% enrichment in the 2 position of the indole ring and at 90% enrichment in the carboxyl group. The labeled indole was prepared by chemical synthesis and was then condensed with [1-^{13}C]serine using tryptophan synthase as the catalyst. ^{13}C NMR analysis of the nosiheptide resulting from the feeding of this precursor showed enrichment exclusively in C-2 and C-2′ of the indolecarboxylic acid moiety and coupling of these two signals to each other with the expected intensity ratios of the coupled and noncoupled signals. This result demonstrates unequivocally that the indolecarboxylic acid moiety arises by a rather unusual rearrangement of tryptophan (Fig. 39). In this process the two hydrogens of the side-chain methylene group of tryptophan are retained, as was demonstrated in a feeding experiment with D,L-[3-^{13}C,$^{2}H_2$]tryptophan.[227] Nonincorporation of ^{14}C- and ^{13}C-labeled 4-methyltryptophan into nosiheptide indicates that methylation of tryptophan is not the first step in the reaction sequence leading to the indolecarboxylic acid moiety.[224,227,228]

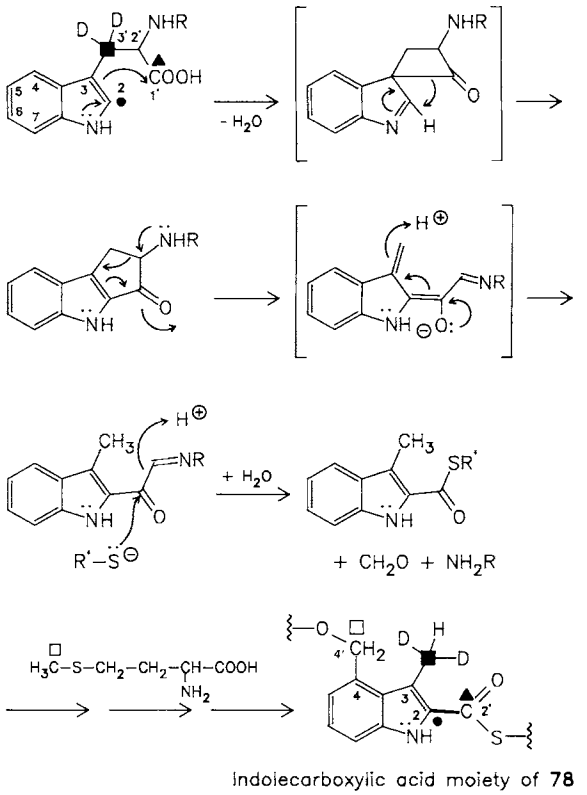


Fig. 39. Formation of the indolecarboxylic acid moiety of nosiheptide **78** from tryptophan, and a possible mechanism of this transformation. ■, ▲, ●, □: ^{13}C label.

The results obtained so far are consistent with formation of nosiheptide **78** by extensive modification of a primary peptide precursor which should have the following sequence:

H_2N-Ser-Cys-Thr-Thr-Cys-Glu-Cys-Cys-Cys-Ser-Cys-Ser-OH

Closure of the macrocycle by formation of the pyridine ring would involve connecting Ser-1 and Ser-10. Whether the tryptophan residue giving rise to the indolecarboxylic acid moiety is also part of the primary peptide, and how it would be linked to this, or whether it is attached at a later

stage remains to be established. Inhibition experiments with chloramphenicol suggest that the assembly of the primary peptide precursor is a nonribosomal process[227] and should thus be mediated by an enzyme as template in analogy to the biosynthesis of other peptide antibiotics.[232]

8.2. Biosynthesis of Thiostrepton

The biosynthesis of thiostrepton **77** in *S. azureus* largely follows similar lines as that of nosiheptide **78** (Fig. 40). In the studies on **77** we were greatly aided by the detailed ^{1}H and ^{13}C NMR analysis of this compound carried out by *Hensens* et al.,[233,234] although, based on the analysis of multiply labeled samples, several signal assignments had to be changed.[227] D,L-[3-^{13}C]Cysteine labeled five sites corresponding to the C-5 of the thiazole and dihydrothiazole rings (Fig. 40). The same carbon atoms were labeled by C-3 of serine. In addition, the latter compound labeled C-3 of the three dehydroalanine moieties, C-3 and C-4 of the piperidine ring, and C-3 as well as the methyl group of the quinaldic acid moiety. The latter methyl group was also the only position labeled by L-[*methyl*-^{13}C]methionine.

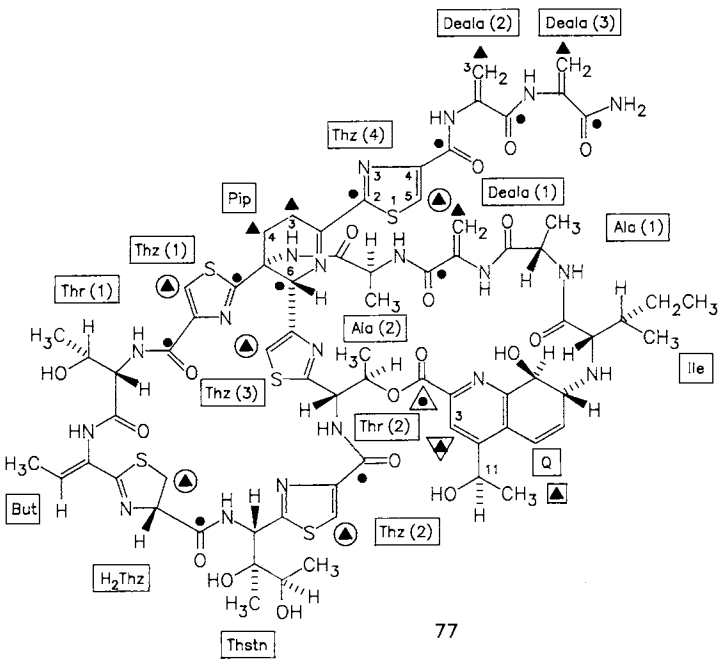


Fig. 40. Labeling pattern in thiostrepton **77** after feeding experiments with various stable-isotope-labeled precursors.

D,L-[1-^{13}C]serine labeled eleven sites, namely all the carbonyl groups attached to the thiazole and dihydrothiazole rings and the carbonyl groups of the dehydroalanine and quinaldic acid moieties as well as C-6 of the piperidine ring and C-2 of thiazole-1.[235] Experiments with L-[1,2-$^{13}C_2$]- and L-[2,3-$^{13}C_2$]serine demonstrated intact incorporation of all the serine molecules, except for the labeling of the quinaldic acid methyl group.[227,236] Finally, L-[*carboxy*-^{13}C]tryptophan labeled exclusively the carbonyl group of the quinaldic acid moiety.[235] It follows that in all likelihood the dehydroalanine moieties, the thiazole rings, and the piperidine ring in thiostrepton have the same origin as in nosiheptide.

The quinaldic acid moiety evidently arises by an expansion of the indole ring of tryptophan. The carbon skeleton of tryptophan can account for all the carbons of the quinaldic acid moiety except the methionine-derived methyl group. The ring expansion resembles that established for the formation of quinine-type alkaloids from tryptophan in higher plants;[237] i.e., C-3 of the tryptophan side chain (see Fig. 39 for numbering) should give rise to C-3 of the quinaldic acid and C-2 of the indole ring should give rise to C-11 of the quinaldic acid. Interestingly, D,L-2-methyl-[3'-^{13}C]tryptophan was efficiently incorporated and specifically labeled C-3 of the quinaldic acid moiety.[236] Hence, in this case methylation of tryptophan seems to take place before its further modification and/or incorporation into the peptide. In accord with this notion, we have demonstrated formation of 2-methyltryptophan in *S. azureus* both by trapping experiments and in a cell-free system.[238]

The steric course of the incorporation of the methionine methyl group into the quinaldic acid moiety in **77** was examined by feeding experiments with samples of methionine carrying a chiral methyl group. The resulting thiostrepton **77** was subjected to Kuhn–Roth oxidation and the tritiated acetic acid was analyzed for its chirality. Surprisingly, (*methyl-R*)-methionine produced a methyl group of *R* configuration and (*methyl-S*)-methionine gave a methyl group of *S* configuration in **77**.[239] It was also shown with [methyl-$^{13}C^{2}H_3$]methionine that all three methyl hydrogens are retained.[238] Thus it appears that the transfer of the methyl group proceeds with net retention of configuration. This is in contrast to the majority of methyltransferases studied so far (see Section 5.2). However, we have recently encountered another example of a methyl transfer with net retention of configuration in the biosynthesis of the antibiotic thienamycin which also contains a methyl group in the form of a hydroxyethyl function.[240] It seems likely that methyl transfer with net retention of configuration involves a two-step process.

8.3. Genetics of Nosiheptide and Thiostrepton Biosynthesis

Our longer term goal in the studies on nosiheptide and thiostrepton biosynthesis is to develop in parallel both the bioorganic chemistry and the genetics of formation of these antibiotics. This may eventually allow the production of new hybrid structures based on the knowledge and methods developed in these studies. The rationale for choosing this group of compounds for such studies is that they represent biologically very potent molecules and are therefore obvious targets for structure modification. However, their complexity severely limits the possibility of structure modification by chemical means. On the other hand, they should be ideal subjects for biological structure modification: they share the same overall architecture but are made up of somewhat different building blocks which one might be able to exchange. Also, they share a common

mode of action, reducing the likelihood that newly created hybrid antibiotics would kill the producing organism.

The genetic studies on *S. actuosus* and *S. azureus* are being carried out in collaboration with the laboratory of *W. R. Strohl* at Ohio State University. The overall strategy is based on the observation that in the cases examined the cluster of antibiotic biosynthesis genes also contains the resistance gene.[241-243] Hence, we are cloning size-fractionated partial digests of the parent DNA into a suitable plasmid, which is used to transform a sensitive organism. Selection for thiostrepton or nosiheptide resistance and for an additional marker on the plasmid then isolates the resistance gene plus additional biosynthetic genes from the cluster surrounding the resistance gene. The DNA inserts in the reisolated plasmids can be used to probe further into the biosynthetic gene cluster of the parent DNA. Biosynthetic genes from *S. azureus* will be used to transform *S. actuosus* and vice versa and the transformants will be analyzed for the appearance of new compounds. Hopefully, as more information develops about the biosynthetic pathway, it can also be used to select more directly for specific biosynthetic genes.

9. Conclusion and Outlook

The foregoing review of our work on the biosynthesis of antibiotics has given a glimpse of the multitude of different approaches and techniques that are used today in unraveling the metabolic pathways leading to secondary metabolite formation. The study of natural products biosynthesis has undergone several dramatic changes over the last few decades. The ready availability of isotopically labeled compounds starting in the late 1940s opened up the possibility of undertaking biosynthetic studies. The advent of Fourier transform NMR spectroscopy dramatically expanded the scope of such investigations by providing a tool with which far more definitive information could be gained with much greater ease than was possible before. Another revolution of the field is clearly in the making with the rapid development of the molecular biology of secondary metabolite formation. The incorporation of genetic approaches into biosynthetic studies promises to add yet another dimension to this field. It has the potential of bringing us closer to an understanding of fundamental questions as to how nature manages to elaborate this bewildering array of organic chemicals, and why. In addition, it may lead to exciting practical advances in the formation and production of commercially important natural products.

We acknowledge with pleasure the contributions of a large number of enthusiastic and dedicated co-workers, whose names are mentioned in the appropriate references. Our studies were made possible by financial support from the National Institutes of Health (Grant AI 20264), and we were greatly aided by the services of the Los Alamos Stable Isotope Resource (supported by NIH grant RR 02231 and by the Department of Energy), by the Purdue University Biological Magnetic Resonance Laboratory (supported by NIH grant RR 01077), and by the Ohio State University Campus Chemical Instrument Center. Finally, we thank Kay B. Kampsen for her skill and patience in typing this manuscript.

Received: November 11, 1987 [A 707 IE]
German version: *Angew. Chem. 101* (1989) 147

[1] R. Hütter, W. Keller-Schierlein, F. Knüsel, V. Prelog, G. C. Rodgers, P. Suter, G. Vogel, W. Voser, H. Zähner, *Helv. Chim. Acta 50* (1967) 1533.
[2] J. D. Dunitz, D. M. Hawley, D. Miklos, D. N. J. White, Y. Berlin, R. Marusic, V. Prelog, *Helv. Chim. Acta 54* (1971) 1709.
[3] For some reviews see: a) S. A. Brown, *Biosynthesis 1* (1972) 1-39; b) U. Sequin, A. I. Scott, *Science (Washington) 186* (1974) 101.
[4] H. G. Floss in E. A. Evans, M. Muramatsu (Eds.): *Radiotracer Techniques and Applications, Vol. 2*, Dekker, N.Y. 1977, pp. 689-732.
[5] H. Simon, H. G. Floss: *Bestimmung der Isotopenverteilung in markierten Verbindungen*, Springer, Berlin 1967.
[6] M. Tanabe, *Biosynthesis 2* (1973) 241-299; *3* (1974) 247-285; *4* (1976) 204-247.
[7] H. Seto, T. Sato, H. Yonehara, *J. Am. Chem. Soc. 95* (1973) 8461.
[8] A. R. Battersby, E. Hunt, E. McDonald, *J. Chem. Soc. Chem. Commun. 1973*, 442.
[9] M. J. Garson, J. Staunton, *Chem. Soc. Rev. 8* (1979) 59.
[10] J. C. Vederas, *Can. J. Chem. 60* (1982) 1637.
[11] D. E. Cane, T. Rossi, A. M. Tillman, J. P. Pachlatko, *J. Am. Chem. Soc. 103* (1981) 1838.
[12] K. L. Rinehart, M. Potgieter, D. L. Delaware, H. Seto, *J. Am. Chem. Soc. 103* (1981) 2099.
[13] J. M. Beale, J. P. Lee, A. Nakagawa, S. Ômura, H. G. Floss, *J. Am. Chem. Soc. 108* (1986) 331.
[14] N. E. Mackenzie, R. L. Baxter, A. I. Scott, P. E. Fagerness, *J. Chem. Soc. Chem. Commun. 1982*, 145.
[15] P. J. Keller, Q. Le Van, A. Bacher, J. P. Kozlowski, H. G. Floss, *J. Am. Chem. Soc. 105* (1983) 2505.
[16] J. M. Beale, C. E. Cottrell, P. J. Keller, H. G. Floss, *J. Magn. Reson. 72* (1987) 574.
[17] A. Bax, R. Freeman, *J. Magn. Reson. 44* (1981) 542.
[18] a) A. Bax, G. Morris, *J. Magn. Reson. 42* (1981) 164; b) M. R. Bendall, D. T. Pegg, D. M. Doddrell, D. M. Thomas, *ibid. 46* (1982) 43.
[19] L. A. Trimble, P. B. Reese, J. C. Vederas, *J. Am. Chem. Soc. 107* (1985) 2175.
[20] S. J. Gould, V. A. Palaniswamy, H. Bleich, J. Wilde, *J. Chem. Soc. Chem. Commun. 1984*, 1075.
[21] H. G. Floss in P. K. Stumpf, E. E. Conn (Eds.): *The Biochemistry of Plants, Vol. 7*, Academic Press, N.Y. 1981, pp. 177-214.
[22] K. F. Chater, D. A. Hopwood in M. Goodfellow, M. Mordarski, S. T. Williams (Eds.): *Biology of the Actinomycetes*, Academic Press, New York 1984, p. 229.
[23] C. R. Hutchinson, *Nat. Prod. Rep. 3* (1986) 133.
[24] K. L. Cox, S. E. Fishman, J. L. Larson, R. Stanzak, P. A. Reynolds, W. K. Yeh, R. M. van Frank, V. A. Birmingham, C. L. Hershberger, E. T. Seno, *J. Nat. Prod. 49* (1986) 971.
[25] F. Malpartida, D. A. Hopwood, *Nature (London) 309* (1984) 462.
[26] F. Malpartida, S. E. Hallam, H. M. Kieser, H. Motamedi, C. R. Hutchinson, M. J. Butler, S. A. Sugden, M. Warren, C. McKillop, C. R. Bailey, G. O. Humphreys, D. A. Hopwood, *Nature (London) 325* (1987) 818.
[27] D. A. Hopwood, F. Malpartida, H. M. Kieser, H. Ikeda, J. Duncan, I. Fujii, B. A. M. Rudd, H. G. Floss, S. Ômura, *Nature (London) 314* (1985) 642.
[28] H. G. Floss, *Trends Biotechnol. 5* (1987) 111.
[29] K. Shimada, D. J. Hook, G. F. Warner, H. G. Floss, *Biochemistry 17* (1978) 3054.
[30] Y. Takeda, V. Mak, C.-C. Chang, C.-j. Chang, H. G. Floss, *J. Antibiot. 37* (1984) 868.
[31] M. Damberg, P. Russ, A. Zeeck, *Tetrahedron Lett. 23* (1982) 59.
[32] W. Weber, H. Zähner, M. Damberg, P. Russ, A. Zeeck, *Zentralbl. Bakteriol. Mikrobiol. Hyg. Abt. 1 Orig. C2* (1981) 122.
[33] G. Lazar, H. Zähner, M. Damberg, A. Zeeck, *J. Antibiot. 36* (1983) 187.
[34] M. Sugita, K. Furihata, H. Seto, N. Ôtake, T. Sasaki, *Agr. Biol. Chem. 46* (1982) 1111.
[35] M. Sugita, Y. Natori, T. Sasaki, K. Furihata, A. Shimazu, H. Seto, N. Ôtake, *J. Antibiot. 35* (1982) 1460.
[36] M. Sugita, T. Sasaki, K. Furihata, H. Seto, N. Ôtake, *J. Antibiot. 35* (1982) 1467.
[37] K. Kakinuma, N. Ikekawa, A. Nakagawa, S. Ômura, *J. Am. Chem. Soc. 101* (1979) 3402.
[38] S. Ômura, C. Kitao, H. Tanaka, R. Oiwa, Y. Takahashi, A. Nakagawa, M. Shimada, Y. Iwai, *J. Antibiot. 29* (1976) 876.
[39] M. DeRosa, A. Gambacorta, L. Minale, J. D. Bu'lock, *Biochem. J. 128* (1972) 751.
[40] M. DeRosa, A. Gambacorta, J. D. Bu'lock, *J. Bacteriol. 117* (1974) 212; *Phytochemistry 13* (1974) 905, 1793.

[41] M. Oshima, T. Ariga, *J. Biol. Chem. 250* (1975) 6963.
[42] K. Suzuki, K. Saito, A. Kawaguchi, S. Okuda, K. Komagata, *J. Gen. Appl. Microbiol. 27* (1981) 261.
[43] T. S. Wu, A. Nakagawa, J. M. Beale, P. J. Keller, H. G. Floss, unpublished results.
[44] T. S. Wu, J. Duncan, S. W. Tsao, C.-j. Chang, P. J. Keller, H. G. Floss, *J. Nat. Prod. 50* (1987) 108.
[45] J. Furukawa, T. Tsuyuki, N. Morisaki, N. Uemura, Y. Koiso, B. Umezawa, A. Kawaguchi, S. Iwasaki, S. Okuda, *Chem. Pharm. Bull. 34* (1986) 5176.
[46] R. Casati, J. M. Beale, H. G. Floss, *J. Am. Chem. Soc. 109* (1987) 8102.
[47] G. W. J. Fleet, T. K. M. Shing, S. M. Warr, *J. Chem. Soc. Perkin Trans. 1 1984*, 905.
[48] R. Casati, H. Cho, J. M. Beale, H. G. Floss, unpublished results.
[49] W. Keller-Schierlein, R. Muntwyler, W. Pache, H. Zähner, *Helv. Chim. Acta 52* (1969) 127.
[50] R. Muntwyler, W. Keller-Schierlein, *Helv. Chim. Acta 55* (1972) 2071.
[51] M. Brufani, S. Cerrini, W. Fedeli, F. Mazza, R. Muntwyler, *Helv. Chim. Acta 55* (1972) 2094.
[52] R. Muntwyler, J. Widmer, W. Keller-Schierlein, *Helv. Chim. Acta 53* (1970) 1544.
[53] A. Gerhard, R. Muntwyler, W. Keller-Schierlein, *Helv. Chim. Acta 58* (1975) 1323.
[54] R. Corbaz, L. Ettlinger, E. Gäumann, J. Kalvoda, W. Keller-Schierlein, F. Kradolfer, B. K. Manukian, L. Neipp, V. Prelog, F. Reusser, H. Zähner, *Helv. Chim. Acta 40* (1957) 1262.
[55] S. Barcza, M. Brufani, W. Keller-Schierlein, H. Zähner, *Helv. Chim. Acta 49* (1966) 1736.
[56] C.-j. Chang, H. G. Floss, P. Soong, C.-T. Chang, *J. Antibiot. 28* (1975) 156.
[57] J. S. Pyrek, O. Achmatowicz, A. Zamojski, *Tetrahedron 33* (1977) 673.
[58] W. F. Fleck, D. G. Strauss, H. Prauser, *Z. Allg. Mikrobiol. 20* (1980) 543.
[59] W. Keller-Schierlein, M. Brufani, W. Barcza, *Helv. Chim. Acta 51* (1968) 1257.
[60] M. Brufani, M. Dobler, *Helv. Chim. Acta 51* (1968) 1269.
[61] C. E. Snipes, C.-j. Chang, H. G. Floss, *J. Am. Chem. Soc. 101* (1979) 701.
[62] R. Holzbach, H. Pape, D. Hook, E. F. Kreutzer, C.-j. Chang, H. G. Floss, *Biochemistry 17* (1978) 556.
[63] O. A. Mascaretti, C.-j. Chang, D. Hook, H. Otsuka, E. F. Kreutzer, H. G. Floss, *Biochemistry 20* (1981) 919.
[64] O. Gabriel, *Adv. Chem. Ser. 117* (1973) 387.
[65] C. E. Snipes, G.-U. Brillinger, L. Sellers, L. Mascaro, H. G. Floss, *J. Biol. Chem. 252* (1977) 8113.
[66] J. W. Cornforth, J. W. Redmond, H. Eggerer, W. Buckel, C. Gutschow, *Eur. J. Biochem. 14* (1970) 1.
[67] J. Lüthy, J. Rétey, D. Arigoni, *Nature (London) 221* (1969) 1213.
[68] H. G. Floss, M. D. Tsai, *Adv. Enzymol. 50* (1979) 243.
[69] K. Goeke, R. M. Mayer, H. G. Floss, unpublished results.
[70] J. J. Lee, J. P. Lee, P. J. Keller, C. E. Cottrell, C.-j. Chang, H. Zähner, H. G. Floss, *J. Antibiot. 39* (1986) 1123.
[71] P. F. Wiley, A. D. Argoudelis, H. Hoeksema, *J. Am. Chem. Soc. 85* (1963) 2652.
[72] T. G. Cochran, D. J. Abraham, L. L. Martin, *J. Chem. Soc. Chem. Commun. 1972*, 494.
[73] D. J. Mason, A. Dietz, R. M. Smith, *Antibiot. Chemother. (Washington) 11* (1961) 118.
[74] T. J. Oliver, A. Goldstein, R. R. Bower, J. C. Holper, R. H. Otto, *Antimicrob. Agents Chemother. 1961*, 495.
[75] B. J. Wallace, P.-C. Tai, B. D. Davis, *Proc. Natl. Acad. Sci. USA 71* (1974) 1634.
[76] L. A. Mitscher, L. L. Martin, D. R. Feller, J. R. Martin, A. W. Goldstein, *J. Chem. Soc. Chem. Commun. 1971*, 1541.
[77] R. M. Stroshane, M. Taniguchi, K. L. Rinehart, J. P. Rolls, W. J. Haak, B. A. Ruff, *J. Am. Chem. Soc. 98* (1976) 3024.
[78] H. Otsuka, O. A. Mascaretti, L. H. Hurley, H. G. Floss, *J. Am. Chem. Soc. 102* (1980) 6817.
[79] S. M. Byun, R. Jenness, W. P. Ridley, S. Kirkwood, *Biochem. Biophys. Res. Commun. 54* (1973) 961.
[80] M. W. Loewus, F. A. Loewus, G.-U. Brillinger, H. Otsuka, H. G. Floss, *J. Biol. Chem. 255* (1980) 11710.
[81] M. W. Loewus, *J. Biol. Chem. 252* (1977) 7221.
[82] K. R. Hanson, I. A. Rose, *Acc. Chem. Res. 8* (1975) 1.
[83] Y.-H. H. Wong, W. R. Sherman, *J. Biol. Chem. 260* (1985) 11083.
[84] S. Ōmura: *Macrolide Antibiotics. Chemistry, Biology and Practice*, Academic Press, New York 1984.
[85] P. W. Schindler, M. C. Scrutton, *Eur. J. Biochem. 55* (1975) 543.
[86] W. Pache, D. Chapman, *Biochim. Biophys. Acta 255* (1972) 348.
[87] O. A. Mascaretti, C.-j. Chang, H. G. Floss, *J. Nat. Prod. 42* (1979) 455.
[88] F. Tomita, T. Tamaoki, *J. Antibiot. 33* (1980) 940.
[89] N. Hirayama, M. Kasai, K. Shirahata, Y. Ohashi, Y. Sasada, *Tetrahedron Lett. 21* (1980) 2559.
[90] A. K. Mallams, M. S. Puar, R. R. Rossman, *J. Am. Chem. Soc. 103* (1981) 3938.
[91] A. K. Mallams, M. S. Puar, R. R. Rossman, A. T. McPhail, R. D. McFarlane, *J. Am. Chem. Soc. 103* (1981) 3940.
[92] A. K. Mallams, M. S. Puar, R. R. Rossman, A. T. McPhail, R. D. MacFarlane, R. L. Stephens, *J. Chem. Soc. Perkin Trans. 1 1983*, 1497.
[93] A. G. McInnes, J. A. Walter, J. L. C. Wright, *Tetrahedron Lett. 1979*, 3245.
[94] B. M. Miller, R. W. Burg, US Patent 3864479 (February 4, 1975).
[95] W. Pache in J. W. Corcoran, F. E. Hahn (Eds.): *Antibiotics, Vol. 3*, Springer, N.Y. 1975, p. 585.
[96] Y. Okami, T. Okazaki, T. Kitahara, H. Umezawa, *J. Antibiot. 29* (1976) 1019.
[97] H. Nakamura, Y. Iitaka, T. Kitahara, T. Okazaki, Y. Okami, *J. Antibiot. 30* (1977) 714.
[98] E. J. Corey, D. M. Hua, B.-C. Pan, S. P. Seitz, *J. Am. Chem. Soc. 104* (1982) 6818.
[99] J. D. White, T. R. Vendananda, M.-c. Kang, S. C. Choudhry, *J. Am. Chem. Soc. 108* (1986) 8105.
[100] T. S. S. Chen, C.-j. Chang, H. G. Floss, *J. Antibiot. 33* (1980) 1316.
[101] W. Marsch, J. D. Dunitz, D. M. J. White, *Helv. Chim. Acta 57* (1974) 10.
[102] T. C. Somers, J. D. White, J. J. Lee, P. J. Keller, C.-j. Chang, H. G. Floss, *J. Org. Chem. 51* (1986) 464.
[103] J. J. Lee, *Ph. D. Thesis*, Purdue University, West Lafayette, IN (USA) 1984.
[104] A. J. Birch, R. J. English, R. A. Massy-Westropp, M. Slaytor, H. J. Smith, *J. Chem. Soc. 1956*, 356.
[105] T. S. S. Chen, C.-j. Chang, H. G. Floss, *J. Org. Chem. 46* (1981) 2661.
[106] T. S. S. Chen, C.-j. Chang, H. G. Floss, *J. Am. Chem. Soc. 101* (1979) 5826.
[107] T. S. S. Chen, C.-j. Chang, H. G. Floss, *J. Am. Chem. Soc. 103* (1981) 4565.
[108] H.-G. Kirk, H. Pape, paper presented at the International Meeting on Medicinal Plant Research, Münster (FRG), May 1978.
[109] F. Lipmann, *Acc. Chem. Res. 6* (1973) 361.
[110] K. Kurahashi, *Annu. Rev. Biochem. 43* (1974) 445.
[111] E. Katz, A. L. Demain, *Bacteriol. Rev. 44* (1976) 449.
[112] E. Adams, *Adv. Enzymol. 44* (1976) 69.
[113] C. P. Gorst-Allman, C.-j. Chang, H. G. Floss, unpublished results.
[114] J. J. Lee, P. M. Dewick, C. P. Gorst-Allman, F. Spreafico, C. Kowal, C.-j. Chang, A. G. McInnes, J. A. Walter, P. J. Keller, H. G. Floss, *J. Am. Chem. Soc. 109* (1987) 5426.
[115] R. W. Woodard, L. Mascaro, R. Hörhammer, S. Eisenstein, H. G. Floss, *J. Am. Chem. Soc. 102* (1980) 6314.
[116] D. Arigoni, *Ciba Found. Symp. 60* (1978) 243.
[117] H. G. Floss in P. A. Frey (Ed.): *Mechanisms of Enzymatic Reactions: Stereochemistry*, Elsevier, Amsterdam 1986, pp. 71–88.
[118] I. A. Rose, *J. Biol. Chem. 245* (1970) 6052.
[119] M. Summers, I. A. Rose, *J. Am. Chem. Soc. 99* (1977) 4475.
[120] K. Schröder, A. Zeeck, *Tetrahedron Lett. 1973*, 4995.
[121] A. Zeeck, K. Schröder, K. Frobel, R. Grote, R. Thiericke, *J. Antibiot. 40* (1987) 1530.
[122] Y. Konda, K. Onda, K. Hinotozawa, S. Ōmura, *J. Antibiot. 34* (1981) 1222.
[123] P. Welzel, F.-J. Witteler, D. Müller, W. Reimer, *Angew. Chem. 93* (1981) 130; *Angew. Chem. Int. Ed. Engl. 20* (1981) 121.
[124] H. Nakano, M. Yoshia, K. Shirahata, S. Ishii, Y. Arai, M. Morimoto, F. Tomita, *J. Antibiot. 35* (1982) 760.
[125] S. Ōmura, N. Inamura, K. Hinotozawa, K. Otogura, G. Lukacs, R. Faghih, R. Tolmann, R. H. Arison, J. L. Smith, *J. Antibiot. 36* (1983) 1783.
[126] G. Werner, H. Hagenmaier, H. Drautz, A. Baumgartner, H. Zähner, *J. Antibiot. 37* (1984) 110.
[127] M. A. Goetz, P. A. McCormick, R. L. Monaghan, D. A. Ostlind, O. D. Hensens, J. M. Liesch, G. Albers-Schönberg, *J. Antibiot. 38* (1985) 161.
[128] R. J. White, E. Martinelli, G. G. Gallo, G. Lancini, P. Beynon, *Nature (London) 243* (1973) 273.
[129] M. Brufani, D. Kluepfel, G. C. Lancini, J. Leitich, A. S. Mesentsev, V. Prelog, F. P. Schmook, P. Sensi, *Helv. Chim. Acta 56* (1973) 2315.
[130] U. Hornemann, J. P. Kehrer, J. H. Eggert, *J. Chem. Soc. Chem. Commun. 1974*, 1045.
[131] U. Hornemann, J. P. Kehrer, C. S. Nunez, R. L. Ranieri, *J. Am. Chem. Soc. 96* (1974) 320.
[132] S. Horii, Y. Kameda, *J. Chem. Soc. Chem. Commun. 1972*, 747.
[133] E. Truscheit, W. Frommer, B. Junge, L. Müller, D. D. Schmidt, W. W. Wingender, *Angew. Chem. 93* (1981) 738; *Angew. Chem. Int. Ed. Engl. 20* (1981) 744.
[134] A. Karlsson, G. Sartori, R. J. White, *Eur. J. Biochem. 47* (1974) 251.
[135] R. J. White, E. Martinelli, *FEBS Lett. 49* (1974) 233.
[136] A. Haber, R. D. Johnson, K. L. Rinehart, *J. Am. Chem. Soc. 99* (1977) 3541.
[137] U. Hornemann, J. H. Eggert, D. P. Honor, *J. Chem. Soc. Chem. Commun. 1980*, 11.
[138] G. S. Bezanson, L. C. Vining, *Can. J. Biochem. 49* (1971) 911.
[139] O. Ghisalba, J. Nüesch, *J. Antibiot. 34* (1981) 64.
[140] J. J. Kibby, I. A. McDonald, R. W. Rickards, *J. Chem. Soc. Chem. Commun. 1980*, 768.
[141] K. Hatano, S. Akiyama, M. Asai, R. W. Rickards, *J. Antibiot. 35* (1982) 1415.
[142] M. G. Anderson, J. J. Kibby, R. W. Rickards, J. M. Rothschild, *J. Chem. Soc. Chem. Commun. 1980*, 1277.
[143] K. L. Rinehart, M. Potgieter, D. A. Wright, *J. Am. Chem. Soc. 104* (1982) 2649.

[144] D. D. Weller, K. L. Rinehart, *J. Am. Chem. Soc. 100* (1978) 6757.
[145] M. Balerna, W. Keller-Schierlein, C. Martius, H. Wolf, H. Zähner, *Arch. Mikrobiol. 65* (1969) 303.
[146] T. H. Williams, *J. Antibiot. 28* (1975) 85.
[147] M. Brufani, L. Cellai, W. Keller-Schierlein, *J. Antibiot. 32* (1979) 167.
[148] J. A. McDonald, R. W. Rickards, *Tetrahedron Lett. 22* (1981) 1149.
[149] W. Keller-Schierlein, M. Meyer, A. Zeeck, M. Damberg, R. Machinek, H. Zähner, G. Lazar, *J. Antibiot. 36* (1983) 484.
[150] W. Keller-Schierlein, M. Meyer, L. Cellai, S. Cerrini, D. Lamba, A. Segre, W. Fedeli, M. Brufani, *J. Antibiot. 37* (1984) 1357.
[151] M. Sugita, Y. Natori, N. Sueda, K. Furihata, H. Seto, N. Ōtake, *J. Antibiot. 35* (1982) 1474.
[152] S. W. Lee, *Ph. D. Thesis,* Purdue University, West Lafayette, IN (USA) 1983.
[153] X.-G. He, J. P. Lee, J. M. Beale, P. J. Keller, H. G. Floss, unpublished results; cf. J. P. Lee, *Ph. D. Thesis,* Ohio State University, Columbus, OH (USA) 1987.
[154] J. J. Wang, J. M. Beale, H. G. Floss, unpublished results.
[155] J. M. Beale, C. E. Cottrell, P. J. Keller, H. G. Floss, *J. Magn. Reson. 72* (1987) 574.
[156] R. Jiao, C. Liu, Z. Jin, X. Zhang, L. Ni, Z. Lu, *Sci. Sin. Ser B (Engl. Ed.) 27* (1984) 380.
[157] B. Junge, F.-R. Heiker, J. Kurz, L. Müller, D. D. Schmidt, C. Wünsche, *Carbohydr. Res. 128* (1984) 235.
[158] T. Iwasa, H. Yamamoto, M. Shibata, *J. Antibiot. 23* (1970) 595.
[159] S. Ogawa, T. Nose, T. Ogawa, T. Toyokuni, Y. Iwasawa, T. Suami, *J. Chem. Soc. Perkin Trans. 1 1985,* 2369.
[160] U. Degwert, R. von Hülst, H. Pape, R. E. Herrold, J. M. Beale, P. J. Keller, J. P. Lee, H. G. Floss, *J. Antibiot. 40* (1987) 855.
[161] T. Toyokuni, W.-Z. Jin, K. L. Rinehart, *J. Am. Chem. Soc. 109* (1987) 3481.
[162] R. Thiericke, M. Stellwaag, A. Zeeck, G. Snatzke, *J. Antibiot. 40* (1987) 1549.
[163] R. Thiericke, A. Zeeck, *J. Antibiot. 41* (1988) 694.
[164] J. M. Beale, R. E. Herrold, H. G. Floss, R. Thiericke, A. Zeeck, A. Nakagawa, S. Ōmura, *J. Am. Chem. Soc. 110* (1988) 4435.
[165] R. Thiericke, A. Zeeck, *J. Chem. Soc. Perkin Trans. 1 1988,* 2123.
[166] R. E. Herrold, J. M. Beale, A. Nakagawa, P. J. Keller, S. Ōmura, H. G. Floss, unpublished results.
[167] R. Thiericke, J. M. Beale, P. J. Keller, A. Zeeck, H. G. Floss, unpublished results.
[168] Y. Sato, S. J. Gould, *J. Am. Chem. Soc. 108* (1986) 4625.
[169] A. Nakagawa, T.-S. Wu, P. J. Keller, J. P. Lee, S. Ōmura, H. G. Floss, *J. Chem. Soc. Chem. Commun. 1985,* 519.
[170] K. Shimizu, G. Tamura, *J. Antibiot. 34* (1981) 649, 654.
[171] Y. Shizuri, M. Ojika, K. Yamada, *Tetrahedron Lett. 22* (1981) 4291.
[172] M. Ojika, H. Niwa, Y. Shizuri, K. Yamada, *J. Chem. Soc. Chem. Commun. 1982,* 628.
[173] J. M. Beale, J. P. Lee, A. Nakagawa, S. Ōmura, H. G. Floss, *J. Am. Chem. Soc. 108* (1986) 331.
[174] H. Brockmann, H. Pini, *Naturwissenschaften 34* (1947) 190.
[175] For convenience in comparing different members of the family we use a biosynthetic numbering, as in Fig. 27, rather than the systematic IUPAC numbering.
[176] K. Tsuzuki, Y. Iwai, S. Ōmura, H. Shimizu, N. Kitajima, *J. Antibiot. 39* (1986) 1343.
[177] H. G. Floss in J. W. Corcoran (Ed.): *Antibiotics, Vol. 4,* Springer, Berlin 1981, pp. 215–235.
[178] M. E. Bergy, *J. Antibiot. 21* (1968) 454.
[179] H. Hoeksema, W. C. Krueger, *J. Antibiot. 29* (1976) 704.
[180] S. Ōmura, H. Tanaka, Y. Koyama, R. Oiwa, M. Katagiri, T. Hata, *J. Antibiot. 27* (1974) 363.
[181] H. Tanaka, Y. Koyama, J. Awaya, R. Oiwa, M. Katagiri, T. Nagai, S. Ōmura, *J. Antibiot. 28* (1975) 860.
[182] H. Tanaka, Y. Koyama, T. Nagai, H. Marumo, S. Ōmura, *J. Antibiot. 28* (1975) 868.
[183] H. Tanaka, H. Marumo, T. Nagai, M. Okada, K. Taniguchi, S. Ōmura, *J. Antibiot. 28* (1975) 925.
[184] S. Ōmura, H. Tanaka, Y. Okada, H. Marumo, *J. Chem. Soc. Chem. Commun. 1976,* 320.
[185] M. Kasai, K. Shirahata, S. Ishii, K. Mineura, H. Marumo, H. Tanaka, S. Ōmura, *J. Antibiot. 32* (1979) 442.
[186] Y. Iwai, K. Kimura, Y. Takahashi, K. Hinotozawa, H. Shimizu, H. Tanaka, S. Ōmura, *J. Antibiot. 36* (1983) 1268.
[187] H. Brockmann, A. Zeeck, K. van der Merwe, W. Müller, *Justus Liebigs Ann. Chem. 698* (1966) 209, and references cited therein.
[188] A. Zeeck, P. Christiansen, *Justus Liebigs Ann. Chem. 724* (1969) 172.
[189] B. Krone, A. Zeeck, *Liebigs Ann. Chem. 1983,* 510.
[190] A. Zeeck, M. Mardin, *Liebigs Ann. Chem. 1974,* 1063.
[191] A. Zeeck, H. Zähner, M. Mardin, *Liebigs Ann. Chem. 1974,* 1100.
[192] B. Krone, A. Zeeck, *Liebigs Ann. Chem. 1983,* 471.
[193] E. Egert, M. Noltemeyer, G. M. Sheldrick, W. Saenger, H. Brand, A. Zeeck, *Liebigs Ann. Chem. 1983,* 503.
[194] C. P. Gorst-Allman, B. A. M. Rudd, C.-j. Chang, H. G. Floss, *J. Org. Chem. 46* (1981) 455.
[195] A. Arnone, L. Camarda, R. Cardillo, G. Fronza, L. Merlini, R. Mondelli, G. Nasini, J. S. Pyrek, *Helv. Chim. Acta 62* (1979) 30.
[196] K. Schröder, H. G. Floss, *J. Org. Chem. 43* (1978) 1438.
[197] X.-G. He, C.-C. Chang, C.-j. Chang, J. C. Vederas, A. G. McInnes, J. A. Walter, H. G. Floss, *Z. Naturforsch. C41* (1986) 215.
[198] C. Kitao, H. Tanaka, S. Minami, S. Ōmura, *J. Antibiot. 33* (1980) 711.
[199] S. Ōmura, *Bacteriol. Rev. 40* (1976) 681.
[200] S. Ōmura, S. Minami, H. Tanaka, *J. Biochem. (Tokyo) 90* (1981) 291.
[201] S. Ōmura, H. Tanaka, S. Minami, I. Takahashi, *J. Biochem. (Tokyo) 90* (1981) 355.
[202] H. Tanaka, S. Minami-Kakinuma, S. Ōmura, *J. Antibiot. 35* (1982) 1565.
[203] N. Tsuji, M. Kobayashi, Y. Terui, K. Tori, *Tetrahedron 32* (1976) 2207.
[204] B. Krone, A. Zeeck, H. G. Floss, *J. Org. Chem. 47* (1982) 4721.
[205] D. A. Hopwood, K. F. Chater, J. B. Dowding, A. Vivian, *Bacteriol. Rev. 37* (1973) 371.
[206] B. A. M. Rudd, D. A. Hopwood, *J. Gen. Microbiol. 114* (1979) 35.
[207] S. P. Cole, *Ph. D. Thesis,* Purdue University, West Lafayette, IN (USA) 1985.
[208] H. G. Floss, S. P. Cole, X.-G. He, B. A. M. Rudd, J. Duncan, I. Fujii, C.-j. Chang, P. J. Keller in H. Kleinkauf, H. von Döhren, G. Nesemann, H. Dornauer (Eds.): *Regulation of Secondary Metabolite Formation,* VCH Verlagsgesellschaft, Weinheim 1985, pp. 283–304.
[209] S. P. Cole, B. A. M. Rudd, D. A. Hopwood, C.-j. Chang, H. G. Floss, *J. Antibiot. 40* (1987) 340.
[210] H.-L. Zhang, J. M. Beale, J. Gallucci, X.-G. He, A. A. Adeferati, S. P. Cole, P. J. Keller, C.-j. Chang, H. G. Floss, unpublished results.
[211] F. Malpartida, D. A. Hopwood, *Nature (London) 209* (1984) 462.
[212] D. A. Hopwood, F. Malpartida, H. M. Kieser, H. Ikeda, J. Duncan, I. Fujii, B. A. M. Rudd, H. G. Floss, S. Ōmura, *Nature (London) 314* (1985) 642.
[213] S. Ōmura, H. Ikeda, F. Malpartida, H. M. Kieser, D. A. Hopwood, *Antimicrob. Agents Chemother. 29* (1986) 13.
[214] D. F. W. Gross, G. W. Kenner, R. C. Sheppard, C. E. Stehr, *J. Chem. Soc. 1963,* 2143.
[215] M. Bodansky, J. Fried, J. T. Sheehan, N. J. Williams, J. Alicino, P. I. Cohen, B. T. Keeler, C. A. Birkheimer, *J. Am. Chem. Soc. 86* (1964) 2478.
[216] M. Bodansky, J. A. Scozzie, I. Muramatsu, *J. Antibiot. 23* (1970) 9.
[217] B. Anderson, D. Crowfoot Hodgkin, M. A. Viswamitra, *Nature (London) 225* (1970) 233.
[218] H. Depair, J. P. Thomas, A. Brun, A. Olesker, G. Lukacs, *Tetrahedron Lett. 1977,* 1397, 1403, and references cited therein.
[219] C. Pascard, A. Ducruix, J. Lunel, T. Prange, *J. Am. Chem. Soc. 99* (1977) 6418.
[220] T. Endo, H. Yonehara, *J. Antibiot. 31* (1978) 623.
[221] S. Pestka, J. W. Bodley, *Antibiotics (N. Y.) 3* (1975) 551–573.
[222] E. Cundliffe, J. Thompson, *J. Gen. Microbiol. 126* (1981) 185.
[223] F. Benazet, M. Cartier, J. Florent, C. Godard, G. Jung, J. Lunel, D. Mancy, C. Pascal, J. Renaut, P. Tarridec, J. Theilleux, R. Tissier, M. Dubost, L. Ninet, *Experientia 36* (1980) 414.
[224] D. R. Houck, L.-C. Chen, P. J. Keller, J. M. Beale, H. G. Floss, *J. Am. Chem. Soc. 110* (1988) 5800.
[225] L. C. Chen, *Master Thesis,* Ohio State University, Columbus, OH (USA) 1985.
[226] D. R. Houck, *Ph. D. Thesis,* Ohio State University, Columbus, OH (USA) 1986.
[227] U. Mocek, J. M. Beale, C. Unkefer, H. G. Floss, unpublished results.
[228] D. R. Houck, L.-C. Chen, P. J. Keller, J. M. Beale, H. G. Floss, *J. Am. Chem. Soc. 109* (1987) 1250.
[229] C. J. Pearce, K. L. Rinehart, *J. Am. Chem. Soc. 101* (1979) 5069.
[230] K. L. Rinehart, D. D. Weller, C. J. Pearce, *J. Nat. Prod. 43* (1980) 1.
[231] B. W. Bycroft, M. S. Gowland, *J. Chem. Soc. Chem. Commun. 1978,* 256.
[232] H. Kleinkauf, H. von Döhren (Eds.): *Peptide Antibiotics. Biosynthesis and Function,* De Gruyter, Berlin 1982.
[233] O. D. Hensens, G. Albers-Schönberg, B. F. Anderson, *J. Antibiot. 36* (1983) 799.
[234] O. D. Hensens, G. Albers-Schöneberg, B. F. Anderson, *J. Antibiot. 36* (1983) 832.
[235] D. O'Hagan, J. M. Beale, H. G. Floss, unpublished results.
[236] P. Zhou, U. Mocek, J. M. Beale, H. G. Floss, unpublished results.
[237] E. Leete, J. N. Wemple, *J. Am. Chem. Soc. 91* (1969) 2698.
[238] P. Zhou, T. Frenzel, J. M. Beale, H. G. Floss, unpublished results.
[239] L.-D. Yuen, P. Zhou, J. M. Beale, H. G. Floss, unpublished results.
[240] D. R. Houck, K. Kobayashi, J. M. Williamson, H. G. Floss, *J. Am. Chem. Soc. 108* (1986) 5365.
[241] F. Malpartida, D. A. Hopwood, *John Innes Report 1983–1984* (1984) 90.
[242] K. F. Chater, C. J. Bruton, *Gene 26* (1983) 67; *EMBO J. 4* (1985) 1893.
[243] T. Ohnuki, T. Imanaka, S. Aiba, *J. Bacteriol. 164* (1985) 85.

When submitting manuscripts, authors of articles intended for publication as "Communications" are requested to read the "Notice to Authors" reproduced in the January issue of the journal following the list of contents; upon request, a copy can be obtained from the editorial office.

Gas Chromatographic Determination of the Enantiomeric Composition of Epoxy Alcohols**

By *Wilfried A. König,* Sabine Lutz, Gerhard Wenz, Günther Görgen, Christoph Neumann, Andreas Gäbler,* and *Wilhelm Boland*

Dedicated to Professor Kurt Heyns on the occasion of his 80th birthday

Chiral 2,3-epoxy alcohols, which are extremely useful building blocks in organic synthesis, are especially attractive since they are readily accessible by enzyme- and transition-metal-catalyzed processes from simple precursors[1,2] and by EPC syntheses (EPC = enantiomerically pure compounds) from natural products.[3] Of particular interest is the preparation of smaller functionalized epoxy alcohols (C_3–C_{10}) since these can be converted regio- and stereospecifically into important natural products.[4]

Ring-opening reactions of 2,3-epoxy alcohols with nucleophiles (also hydrides) have S_N2 character and proceed under mild conditions; they count among the best methods for the synthesis of two adjacent, stereochemically uniform sp^3 carbon centers.

However, the problem of an accurate determination of the enantiomeric excess (*ee*) of 2,3-epoxy alcohols has not yet been resolved satisfactorily, at least in the range of *ee* > 97%. The most commonly used method, the preparation of the diastereomeric esters with α-methoxy-α-trifluoromethylphenylacetic acid (MTPA ester, "Mosher ester")[5] is relatively insensitive[6] and, like all derivatizations with chiral reagents, involves the danger of falsifying the results by kinetic resolution or insufficient enantiomeric purity.

We now report on the gas chromatographic separation of enantiomeric epoxy alcohols using glass capillary columns coated with peralkylated α-cyclodextrins as stationary phase.[7] Perpentylated and perhexylated α-cyclodextrin[8] proved to be exceptionally enantioselective towards trifluoroacetylated hydroxy compounds.[8] The trifluoroacetylation, which is achieved in a few minutes at room temperature,[9] leads, in the case of epoxy alcohols, without racemization to highly volatile derivatives which are eluted with short retention times from the columns (Figs. 1 and 2). The separation results for a selection of epoxy alcohols are given in Table 1. In all cases where optically active

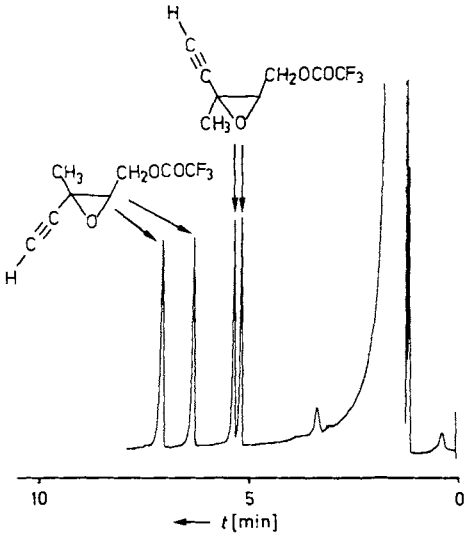


Fig. 1. Separation of the enantiomers of (*E*)- and (*Z*)-2,3-epoxy-3-methyl-4-pentyn-1-ol after trifluoroacetylation on a 38-m glass capillary coated with perhexylated α-cyclodextrin at 60°C and hydrogen (1 bar) as carrier gas.

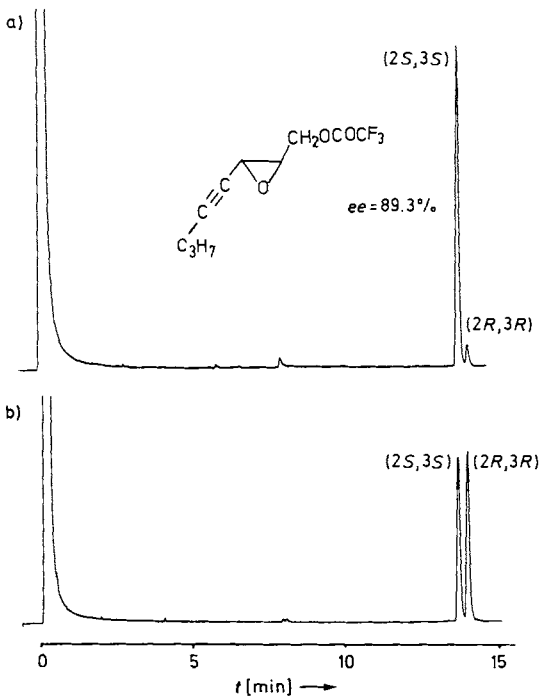


Fig. 2. a) Determination of the enantiomeric excess after trifluoroacetylation of a sample of (*E*)-2,3-epoxy-4-octyn-1-ol prepared by asymmetric epoxidation with L-diethyl tartrate as chiral reagent [2]. 40-m glass capillary coated with perpentylated α-cyclodextrin, at 80°C and hydrogen (1 bar) as carrier gas. b) Chromatogram of the racemate for comparison. *ee* value determined by electronic integration.

[*] Prof. Dr. W. A. König, Dipl.-Chem. S. Lutz
Institut für Organische Chemie der Universität
Martin-Luther-King-Platz 6, D-2000 Hamburg 13 (FRG)
Dr. G. Wenz
Max-Planck-Institut für Polymerforschung
Jakob-Welder-Weg 11, D-6500 Mainz (FRG)
Dipl.-Chem. G. Görgen, Dipl.-Chem. C. Neumann,
Dipl.-Biol. A. Gäbler, Prof. Dr. W. Boland
Institut für Organische Chemie der Universität
Richard-Willstätter-Allee, D-7500 Karlsruhe 1 (FRG)

[**] This work was supported by the Bundesminister für Forschung und Technologie (Research program "Polysaccharidforschung", Project No. 0319134A) and by the Fonds der Chemischen Industrie.

Table 1. Separation factors α for some gas chromatographic separations of epoxy alcohol enantiomers on hexakis-2,3,6-tris-*O*-pentyl)-α-cyclodextrin (I; 40-m glass capillary) and hexakis(2,3,6-tris-*O*-hexyl)-α-cyclodextrin (II, 38-m glass capillary).

Epoxy alcohol (trifluoroacetyl derivative)	α	Column	Column temp. [°C]
2,3-Epoxypropan-1-ol	1.110	I	45
2,3-Epoxy-2-methylpropan-1-ol	1.130	II	50
3,4-Epoxybutan-2-ol [a]	1.04/1.02	II	40
(*Z*)-2,3-Epoxypentan-1-ol	1.075	II	60
(*Z*)-3,4-Epoxyhexan-1-ol	1.139	II	60
(*E*)-3,4-Epoxyhexan-1-ol	1.096	II	60
(*E*)-2,3-Epoxy-3-methyl-4-pentyn-1-ol	1.121	II	60
(*Z*)-2,3-Epoxy-3-methyl-4-pentyn-1-ol	1.029	II	60
(*E*)-Epoxycinnamyl alcohol	1.103	II	100
(*Z*)-Epoxycinnamyl alcohol	1.020	II	100
(*E*)-4,5-Epoxyhexan-1-ol	1.030	I	60
(*E*)-2,3-Epoxyheptan-1-ol	1.020	II	60
(*E*)-2,3-Epoxy-4-octyn-1-ol	1.019	I	60

[a] Four stereoisomers.

epoxy alcohols are separated (2,3-epoxypropan-1-ol, (*E*)-2,3-epoxyheptan-1-ol, (*E*)-2,3-epoxy-4-octyn-1-ol (Fig. 2)), the (2*S*)-isomers were eluted before the (2*R*)-isomers. A remarkable finding is that not only the epoxy derivatives of allyl alcohols can be resolved but also compounds in which epoxy function and hydroxy function are separated by up to three carbon atoms.

Thus, a simple and reliable method is now available for checking the enantiomeric composition in asymmetric epoxidations even for enantiomeric excesses >98%.[10]

Received: September 5, 1988 [Z 2956 IE]
German version: *Angew. Chem. 101* (1989) 180

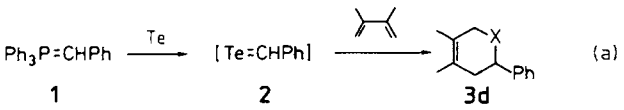
[1] W. E. Ladner, G. M. Whitesides, *J. Am. Chem. Soc. 106* (1984) 7250.
[2] a) T. Katsuki, K. B. Sharpless, *J. Am. Chem. Soc. 102* (1980) 5974; b) R. M. Hanson, K. B. Sharpless, *J. Org. Chem. 51* (1986) 1922.
[3] D. Seebach, E. Hungerbühler, *Mod. Synth. Methods 2* (1980) 91.
[4] A. Pfenninger, *Synthesis 1986*, 89.
[5] J. A. Dale, D. L. Dull, H. S. Mosher, *J. Org. Chem. 34* (1969) 2543.
[6] V. Schurig, *Kontakte (Darmstadt) 1985*, No. 2, p. 22.
[7] Coating by the static method: J. Bouche, M. Verzele, *J. Gas Chromatogr. 6* (1968) 501; see also W. A. König, K. Ernst, *J. Chromatogr. 280* (1983) 135.
[8] a) W. A. König, S. Lutz, G. Wenz, *Angew. Chem. 100* (1988) 989; *Angew. Chem. Int. Ed. Engl. 27* (1988) 979; b) W. A. König, S. Lutz, P. Mischnick-Lübbecke, B. Brassat, G. Wenz, *J. Chromatogr. 447* (1988) 193; c) W. A. König, P. Mischnick-Lübbecke, B. Brassat, S. Lutz, G. Wenz, *Carbohydr. Res. 183* (1988) 11.
[9] Approx. 0.1 mg of the sample was dissolved in 0.2 mL of dichloromethane. After addition of 0.05 mL of trifluoroacetic anhydride the solution was allowed to stand at room temperature for 10 min. The anhydride was then removed in a stream of nitrogen and the sample taken up in dichloromethane.
[10] Capillary columns with perpentylated α-cyclodextrin will be commercially available in the near future from Macherey-Nagel (Düren).

Tellurobenzaldehyde by Staudinger-Chalcogenation of the Ylide Benzylidenetriphenylphosphorane**

By *Gerhard Erker** and *Regina Hock*

The heavier analogues of ketones and aldehydes $R^1R^2C{=}X$ (X = Se, Se, Te) are characterized by enhanced π- and n-donor properties as well as increased π-acceptor ability.[1] Because of the resulting changes in chemical reactivity, these chalcogenocarbonyl compounds are of fundamental interest. In order to study systematic variations of characteristic properties, it is important that $R^1R^2C{=}X$ compounds be available for all the chalcogen elements X. Synthetic routes to thioketones and (sometimes extremely reactive) thioaldehydes have long been known.[2–4] Recently, several simple methods were described for preparing highly reactive selenoaldehydes.[3c, 5] To our knowledge, free telluroaldehydes, which are probably even less stable, have not yet been generated and characterized by subsequent chemical reactions.[6] For the generation of a telluroaldehyde, we have now successfully employed a synthetic method that has in the past been very useful for a preparation of selenoaldehydes.[3c]

Non-stabilized phosphorus ylides $Ph_3P{=}CHR$ react with elemental selenium to furnish selenoaldehydes [RCH=Se], which, for example, can be trapped in situ with 2,3-dimethylbutadiene to give 3,6-dihydro-2*H*-selenapyrans (e.g., **3c**). We have now prepared the 3,6-dihydro-2*H*-thiopyran derivative **3b**[7b] analogously, via intermediate thiobenzaldehyde generated from $Ph_3P{=}CHPh$ **1** and sulfur at 50°C. This reaction can be used to synthesize tellurobenzaldehyde as well [Eq. (a)], provided that the



(a)

3a, X = O; **b**, X = S; **c**, X = Se; **d**, X = Te

chalcogen has first been activated. Tellurium powder (99.0%, Merck) was treated with triphenylphosphine in toluene for 12 h at 105°C. Then, 2,3-dimethylbutadiene was added. Finally, a solution of the ylide **1** in toluene was added dropwise at 105°C. The reaction mixture was fil-

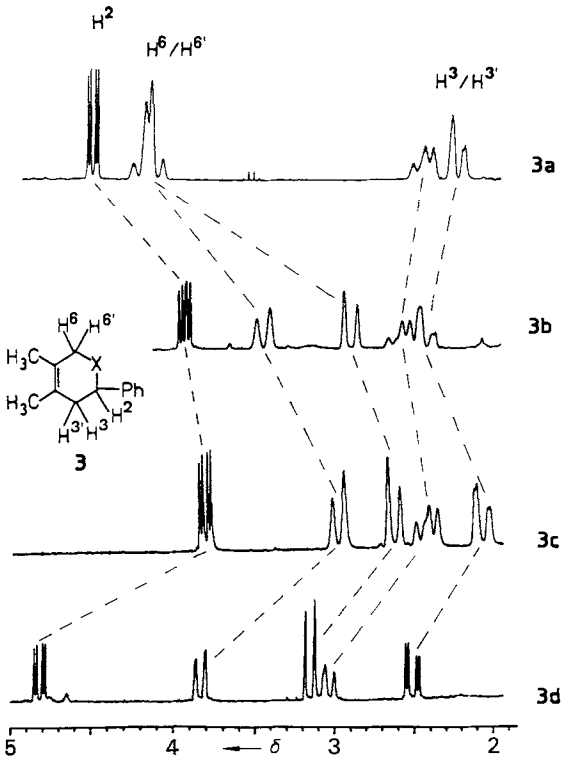


Fig. 1. Comparison of characteristic sections from the 200-MHz ^{1}H NMR spectra of the compounds **3a–d** [7].

[*] Prof. Dr. G. Erker, Dipl.-Chem. R. Hock
Institut für Organische Chemie der Universität
Am Hubland, D-8700 Würzburg (FRG)

[**] This work was supported by the Fonds der Chemischen Industrie, the Deutsche Forschungsgemeinschaft, and the Alfried Krupp-Stiftung.

tered, the solvent was removed in vacuo, and the residue extracted with hexane. 3,6-Dihydro-4,5-dimethyl-2-phenyl-2*H*-tellurapyran **3d** was separated from triphenylphosphane and stilbene (see below) by chromatography (silica gel/hexane). The "Diels-Alder adduct" **3d** of the in situ generated tellurobenzaldehyde **2** was isolated in 11% yield.

The rather sensitive tellurium compound **3d** was characterized by MS and NMR spectroscopy.[7d] Figure 1 shows, for comparison, characteristic sections of the ^{1}H NMR spectra of the four 3,6-dihydro-2*H*-chalcogenapyrans **3a–d**.

In the absence of an added scavenger, **2** reacts with **1** to give stilbene [Eq. (b)]. Due to the low thermal stability of

$$\underset{\mathbf{1}}{2\,Ph_3P{=}CHPh} \xrightarrow[100\,^\circ C]{Te_{cat}} 2\,Ph_3P + PhHC{=}CHPh \qquad (b)$$

the resulting Ph_3PTe[8] product, the stepwise ylide-alkylidene coupling reaction can also be achieved using a catalytic amount of tellurium. In a typical experiment, 5 g (14 mmol) of **1** and 0.18 g (1.4 mmol) Te in 100 mL toluene were heated for 6 hours at 100 °C. Chromatographic analysis of a sample revealed the formation of *cis*- and *trans*-stilbene in a 1:9 molar ratio. Fractional crystallization from acetone/methanol (1/7) yielded *trans*-stilbene (61%) and triphenylphosphane (70%).[9]

Received: October 11, 1988 [Z 3001 IE]
German version: *Angew. Chem. 101* (1989) 181

CAS Registry numbers:
1, 16721-45-2; **2**, 118399-76-1; **3d**, 118399-77-2; PhHC=CHPh, 103-30-0; Te, 13494-80-9; 2,3-dimethylbutadiene, 513-81-5.

[1] E. Vedejs, D. A. Perry, K. N. Houk, N. G. Rondan, *J. Am. Chem. Soc. 105* (1983) 6999; V. P. Rao, J. Chandrasekhar, V. Ramamurthy, *J. Chem. Soc. Perkin Trans. 2 1988*, 647, and references cited therein.

[2] In 1919, *H. Staudinger* prepared thiobenzophenone by reaction of $Ph_3P{=}CPh_2$ with sulfur [H. Staudinger, J. Meyer, *Helv. Chim. Acta 2* (1919) 635]. It now appears that this reaction can be applied quite generally. We therefore propose the term "Staudinger chalcogenation" for this type of reaction.

[3] Examples of reactions of phosphorus ylides a) with oxygen: H. J. Bestmann, O. Kratzer, *Chem. Ber. 96* (1963) 1899; b) with sulfur: H. Tokunaga, K. Akiba, N. Inamoto, *Bull. Chem. Soc. Jpn. 45* (1972) 506; c) with selenium: K. Okuma, J. Sakato, Y. Tachibana, T. Honda, H. Ohta, *Tetrahedron Lett. 28* (1987) 6649; G. Erker, R. Hock, R. Nolte, *J. Am. Chem. Soc. 110* (1988) 624.

[4] E. Vedejs, J. S. Stults, R. G. Wilde, *J. Am. Chem. Soc. 110* (1988) 5452; E. Vedejs, T. H. Eberlein, R. G. Wilde, *J. Org. Chem. 53* (1988) 2220; S. S.-M. Choi, G. W. Kirby, *J. Chem. Soc. Chem. Commun. 1988*, 177; H. J. Reich, C. P. Jasperse, *J. Am. Chem. Soc. 109* (1987) 5549; R. Okazaki, A. Ishii, N. Inamoto, *ibid. 109* (1987) 279; E. Vedejs, D. A. Perry, R. G. Wilde, *ibid. 108* (1986) 2985, and references cited therein.

[5] a) H. Bock, S. Aygen, P. Rosmus, B. Solouki, E. Weissflog, *Chem. Ber. 117* (1984) 187; R. H. Judge, D. C. Moule, *J. Am. Chem. Soc. 106* (1984) 5406; b) G. W. Kirby, A. N. Tretheway, *J. Chem. Soc. Chem. Commun. 1986*, 1152; R. Okazaki, A. Ishii, N. Inamoto, *ibid. 1986*, 71; G. A. Krafft, P. T. Meinke, *J. Am. Chem. Soc. 108* (1986) 1314; M. Segi, T. Nakajima, S. Suga, *ibid. 110* (1988) 1976; c) Selenoketones: Y. Nishiyama, S. Hamanaka, A. Ogawa, N. Kambe, N. Sonoda, *J. Org. Chem. 53* (1988) 1326; A. Ishii, R. Okazaki, N. Inamoto, *Bull. Chem. Soc. Jpn. 61* (1988) 861; J. Nakayama, K. Akimoto, J. Niijima, M. Hoshino, *Tetrahedron Lett. 28* (1987) 4423; P. T. Meinke, G. A. Krafft, J. T. Spencer, *ibid. 28* (1987) 3887; T. G. Back, D. H. R. Barton, M. R. Britten-Kelly, F. S. Guziec, Jr., *J. Chem. Soc. Perkin Trans. 1 1976*, 2079.

[6] a) R. E. Lyons, E. D. Scudder, *Chem. Ber. 64* (1931) 503; b) Metal complexes: H. Fischer, S. Zeuner, *J. Organomet. Chem. 252* (1983) C 63; H. Fischer, U. Gerbing, *ibid. 299* (1986) C 7; H. Fischer, I. Pahshalidis, *ibid. 348* (1988) C 1; A. F. Hill, W. R. Roper, J. M. Waters, A. H. Wright, *J. Am. Chem. Soc. 105* (1983) 5939; C. E. L. Headford, W. R. Roper, *J. Organomet. Chem. 244* (1983) C 53; W. Paul, H. Werner, *Angew. Chem. 95* (1983) 333; *Angew. Chem. Int. Ed. Engl. 22* (1983) 316; J. Wolf, R. Zolk, U. Schubert, H. Werner, *J. Organomet. Chem. 340* (1988) 161, and references cited therein.

[7] a) **3a**: H. Griengl, K. P. Geppert, *Mh. Chem. 107* (1976) 675; b) **3b**: J. E. Baldwin, R. C. G. Lopez, *Tetrahedron 39* (1983) 1487; B. F. Bonini, G. Mazzanti, P. Zani, G. Maccagnani, G. Barbaro, A. Battaglia, P. Giorgianni, *J. Chem. Soc. Chem. Commun. 1986*, 964; ^{13}C NMR ($CDCl_3$): δ = 19.3, 20.2 (CH_3), 32.8 (C6), 39.9 (C3), 43.4 (C2); c) **3c**: see [3c]; ^{13}C NMR ($CDCl_3$): δ = 19.9, 20.7 (CH_3), 24.1 (C6), 38.5 (C2), 40.8 (C3); d) **3d**: MS (EI, 70 eV); $M^{\oplus}$: m/z = 303–296, rel. intensities found (calcd.): 0.13 (0.14)/1.00 (1.00) /0.12 (0.13)/0.95 (0.93)/0.06 (0.08)/0.55 (0.58)/0.21 (0.23)/0.12 (0.14); exact mass, 302.0314 (302.0313); m/z ($M^{\oplus} - C_6H_{10}$ (=PhCH=Te)): 221–212, rel. intensities found (calcd.): 0.08 (0.08)/1.00 (1.00)/0.11 (0.07)/0.91 (0.94)/0.08 (0.04)/0.54 (0.58)/0.23 (0.22)/0.13 (0.14)/0.03 (0.03)/0.07 (0.08); exact mass, 219.9531 (calcd. and found.). ^{1}H NMR ($CDCl_3$): δ = 1.80, 1.83 (each 3H, CH_3), 2.41, 2.97, 4.80 (3H, ABX, ^2J = 13.8, ^3J = 10.9, 3.5 Hz), 3.07, 3.77 (2H, AX, ^2J = 11.8 Hz), 7.10–7.35 (5H, m, Ph). ^{13}C NMR ($CDCl_3$): δ = 18.2, 20.4 (CH_3), 4.3 (C6), 34.6 (C2), 42.7 (C3).

[8] R. A. Zingaro, B. H. Steeves, K. Irgolic, *J. Organomet. Chem. 4* (1965) 320; W.-W. du Mont, H.-J. Kroth, *ibid. 113* (1976) C 35.

[9] For examples of formally similar olefin formations see a) T. Severengiz, W.-W. du Mont, D. Lenoir, H. Voss, *Angew. Chem. 97* (1985) 1051; *Angew. Chem. Int. Ed. Engl. 24* (1985) 1041 [thermally-induced decomposition of $H_3CC(=Te)OSiMe_3$ to $Me_3SiO(CH_3)C{=}C(CH_3)OSiMe_3$]; b) G. Wittig, W. Böll, *Chem. Ber. 95* (1962) 2529 [formation of PPh_3 and $C_4H_9OCH{=}CHOC_4H_9$ from $Ph_3P{=}CHOC_4H_9$]; see also: E. Anders, T. Clark, T. Gassner, *ibid. 119* (1986) 1350.

The Solid-State Structure of $Me_2B-O-BMe_2$**

By *Horst Borrmann, Arndt Simon,* and *Heinrich Vahrenkamp**

Diboroxanes R_2BOBR_2 **1** are isoelectronic with allenes R_2CCR_2. The question of whether this isoelectronic relationship also results in isosterism, i.e., whether diboroxanes can have a linearly coordinated oxygen atom, has not yet been answered. Electron diffraction and X-ray structural analyses of three monomeric diboroxanes gave bond angles at oxygen of 144–166°,[1] with the larger bond angles presumably being due to steric rather than electronic effects, as is also found for the disiloxanes. In contrast, the results of complete IR spectroscopic analyses for diboroxanes with R = vinyl (in all three states) and R = Me (**1a**, in the solid-state) are in agreement with a linear B-O-B arrangement.[2]

$Me_2B-O-BMe_2$ **1a**

Compound **1a**, which crystallizes at −16 °C, thus offered the chance, via a structure determination, to finally clarify the situation. The X-ray structural analysis[3] was carried out at −160 °C on crystals which had been grown in glass capillaries on the diffractometer using the Bridgman method.[4] The surprising result is shown in Figure 1.

1a is, as predicted, centrosymmetric, however not so because of the presence of a linear B-O-B skeleton but because it is dimeric in the solid state. **1a** therefore appears to be the first boron-oxygen compound for which aggregation through formation of a BOBO four-membered ring has been observed.[5] The two B-O bond lengths are very different. The bond length within the ring (158 pm) is longer than all those which have been found for BX_4 compounds (143–156 pm),[6,7] while the exocyclic bond length (138 pm) is almost identical with those of BX_3 compounds (137 pm)[7] or monomeric diboroxanes (136 pm).[11] Figure 1

[*] Prof. Dr. H. Vahrenkamp
Institut für Anorganische und Analytische Chemie der Universität
Albertstrasse 21, D-7800 Freiburg (FRG)
Dipl.-Chem. H. Borrmann, Prof. Dr. A. Simon
Max-Planck-Institut für Festkörperforschung
Heisenbergstrasse 1, D-7000 Stuttgart 80 (FRG)

[**] We wish to thank Mr. *P. Behrens* for valuable assistance.

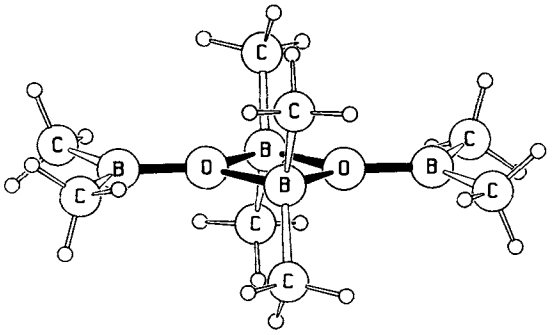
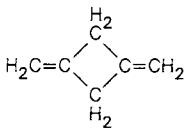


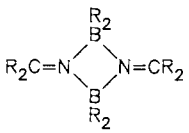
Fig. 1. Molecular structure of dimeric **1a** (small circles = H atoms). Bond lengths [pm]: B-O 158.0(1) (endocyclic), 137.7(1) (exocyclic), B-C 156.3-159.5(1); bond angles [°]: in the ring: O-B-O 86.1(1), B-O-B 93.9(1); external: B-O-B 133.2(1), O-B-C 119.8(1).

shows not only the centrosymmetry but also the two mutually perpendicular major planes of the molecule, whose aesthetically appealing form more than compensates for the nonappearance of a linear monomer.

Despite being dimeric, solid **1a** still represents an interesting example of isosterism since allene also forms a dimer **2**, the molecular geometry of which, as determined by STO-3G calculations,[8] corresponds in all details with that of dimeric **1a** (C-C distances 131 and 154 pm, angles in ring 87 and 93°). The same is true for dimeric alkylideneiminoboranes **3**, of which $[Me_2BNCHPh_2]_2$[9] has structural parameters which are almost identical with those of **1a** (B-N 159 pm, N-C 127 pm, angles in ring 87 and 93°).



2



3

The fact that **1a** is monomeric in the liquid and gas phases indicates that the enthalpy of formation for the dimer is low. The low temperature ^1H NMR spectrum of **1a** in solution shows a splitting of the signals, which was originally attributed to the bent form of the molecule.[10] This result must now be reinterpreted as being due to dimer formation at low temperature in solution. As shown in Figure 1, the monomer conformation,[1a] as determined by electron diffraction, remains almost unchanged upon formation of the dimer;[11] only one B-O bond is lengthened to a considerable extent.

The greater tendency of the diboroxane to dimerize, as compared to other R_2B-O compounds could perhaps be explained by a synergic effect. The formation of the B-O-B linkage means, firstly, that the electronic saturation of the two boron atoms through p_π-p_π interaction with the one oxygen atom is insufficient, and secondly that more negative charge is localized on the oxygen atom due to the inductive effect of the two boron atoms. The diboroxane is therefore both a stronger Lewis base and a stronger Lewis acid than a simple alkoxyborane. If the substituents are small enough, as in the title compound, an energetically favorable intermolecular saturation of the Lewis basicity and acidity is possible.

Received: August 31, 1988 [Z 2950 IE]
German version: *Angew. Chem. 101* (1989) 182

[1] a) G. Gundersen, H. Vahrenkamp, *J. Mol. Struct. 33* (1976) 97; b) L. Cynkier, N. Furmanova, *Cryst. Struct. Commun. 9* (1980) 307; c) C. J. Cardin, H. E. Parge, J. W. Wilson, *J. Chem. Res. Synop. 1983*, 93; *J. Chem. Res. Miniprint 1983*, 0801.

[2] a) J. D. Odom, A. J. Zozulin, S. A. Johnston, J. Durig, S. Riethmiller, E. J. Stampf, *J. Organomet. Chem. 201* (1980) 351; b) J. R. Durig, M. J. Flanagan, E. J. Stampf, J. D. Odom, *J. Mol. Struct. 42* (1977) 13.

[3] Monoclinic, $P2_1/c$, $Z=4$, $a=740.8(2)$, $b=819.9(2)$, $c=1105.6(3)$ pm, $\beta=96.70(2)°$; $\rho_{calcd}=0.79$ g cm^{-3} at the measurement temperature -160 ± 2°C; $(\omega/2\theta)$-scan in the range $3°<2\theta<56°$; 1624 symmetry-independent reflections, 1501 with $F>3\sigma(F)$; empirical absorption and extinction corrections. Calculations with SHELXTL-PLUS from *G. M. Sheldrick*, Göttingen 1987. $R=0.039$ ($R'=0.043$ for all reflections), $R_w=0.060$ (0.061); goodness of fit 2.474. The final Fourier difference map showed no features greater than 0.4 e Å^{-3}. Further details of the crystal structure investigation can be obtained from the Fachinformationszentrum Energie, Physik, Mathematik GmbH, D-7514 Eggenstein-Leopoldshafen 2 (FRG), on quoting the depository number CSD-53277, the names of the authors, and the journal citation.

[4] A. Simon, H. J. Deiseroth, E. Westerbeck, B. Hillenkötter, *Z. Anorg. Allg. Chem. 423* (1976) 203.

[5] The compounds $(RO)_2BX$, $ROBR_2$ and $ROBCl_2$ are monomeric; $ROBF_2$ and $ROBH_2$ have been reported to be trimeric or polymeric: H. Steinberg: *Organoboron Chemistry*, Wiley, New York 1964.

[6] a) S. J. Rettig, J. Trotter, *Can. J. Chem. 55* (1977) 958; *ibid. 56* (1978) 1676; b) R. Boese, R. Köster, M. Yalpani, *Chem. Ber. 118* (1985) 670.

[7] J. B. Farmer, *Adv. Inorg. Chem. Radiochem. 25* (1982) 187.

[8] P. Hemmersbach, M. Klessinger, P. Bruckmann, *J. Am. Chem. Soc. 100* (1978) 6344.

[9] J. R. Jennings, R. Snaith, M. M. Mahmoud, S. C. Wallwork, S. J. Bryan, J. Halfpenny, E. A. Petch, K. Wade, *J. Organomet. Chem. 249* (1983) C1.

[10] G. F. Lanthier, W. A. G. Graham, *Chem. Commun. 1968*, 715.

[11] The B-O-B angle decreases from 144 to 133° and the C-B-C angle from 122 to 112°; the angle between the two BC_2 planes increases from 72 to 90°.

Ethynol: Photochemical Generation in an Argon Matrix, IR Spectrum, and Photoisomerization to Ketene**

By *Remo Hochstrasser* and *Jakob Wirz**

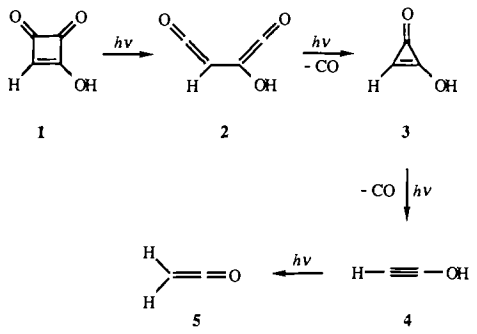
Ethynol (hydroxyacetylene) has been considered as a possible constituent of flames, planetary atmospheres, and interstellar clouds.[1a] Several quantum mechanical calculations have led to the prediction that the isolated molecule is kinetically stable with respect to the highly exothermic tautomerization to ketene.[1] Recently, *Schwarz* and coworkers provided the first experimental proof for the existence of ethynol[2] and related molecules[3] by tandem mass spectrometry. Further evidence for ynols is limited to rather tentative assignments of some IR bands observed after cryogenic trapping of products formed by flash vacuum pyrolysis.[4] Several unsuccessful attempts to generate matrix-isolated ethynol have been reported recently.[5] Acetylene diolate salts are well-known as products of oxocarbon chemistry[6a] and have been characterized recently by matrix IR spectroscopy.[6b] Ynolate ions are gaining interest as reactive species for synthesis.[7]

In the course of our investigations of keto-enol tautomerism,[8] we were searching for photochemical methods to generate ethynol under conditions suitable for its spectroscopic identification as well as for the study of its reaction kinetics in solution. We found that irradiation of 3-hydroxycyclobutene-1,2-dione (semisquaric acid) **1** in an argon

[*] Prof. Dr. J. Wirz, Dipl.-Math. R. Hochstrasser
Institut für Physikalische Chemie der Universität
Klingelbergstrasse 80, CH-4056 Basel (Switzerland)

[**] This work was supported by the Swiss National Science Foundation (part of project No. 2.034-0.86), Ciba-Geigy SA, Sandoz SA, F. Hoffmann-La Roche & Cie SA and the Ciba-Stiftung.

matrix cleanly yields ethynol **4** in three photochemical steps.



Semisquaric acid **1** was synthesized by the procedure of *Serratosa* et al.[9] Deuterated samples were obtained by exchange in D_2O. Selective isotopic enrichment was achieved by exploiting the different exchange rates; exchange at carbon required several days. A sample of **1** was sublimed from a small quartz container at ca. 100 °C, while a steady stream of argon was condensed on a CsI sample window at a temperature of 23 K. The resulting matrix was cooled to 12 K and irradiated with pulses from a KrF excimer laser (248 nm, 20 ns, ca. 10 mJ cm^{-2}).[10] The irradiation was interrupted repeatedly in order to monitor the progress of the reaction by IR spectroscopy. Usually, 15 to 25 spectra were recorded in the range from 3630 to 630 cm^{-1} for each sample. With an instrumental resolution of 0.2 cm^{-1}, the peaks were generally well separated and sufficiently sharp for a base-line correction by graphical interpolation to be carried out with negligible ambiguity to obtain the absolute absorbances of the bands.

In the initial stages of the irradiation, complex product mixtures formed, which were analyzed as follows. Peaks belonging to the same compound were identified on the basis that their absorbance ratio remained constant throughout the sequence of spectra. This could best be determined graphically by a pairwise comparison of peak intensities. Curved lines resulted, if the selected bands were due to different compounds. Smaller, but still quite pronounced deviations from linearity were observed when a pair of bands belonged to the same compound, but to different sites in the matrix; it is well-known that IR-bands of matrix-isolated molecules often exhibit site splitting. Finally, if the chosen pair of peaks corresponded to the same compound in the same site, the points accurately followed a straight line through the origin. Other criteria, such as the band splitting patterns and changes of site population observed upon slight warming of the matrix, were used to distinguish between independent components and different matrix sites for a single component. In this way, five independent reaction components were identified. Figure 1 shows the change in intensity of one characteristic peak of each of the five components with increasing irradiation time. The curves represent concentration profiles with arbitrary units, since the extinction coefficients are unknown. The different induction periods and the corresponding displacements of the concentration maxima of the intermediate products indicates that the components are formed sequentially.

The first photolysis product of **1**, 2-hydroxy-1,3-butadiene-1,4-dione (hydroxybiketenyl) **2**, exhibits two very strong, relatively broad carbonyl bands at 2112 and 2135 cm^{-1}. The strongest bands of the next product, 2-hydroxy-

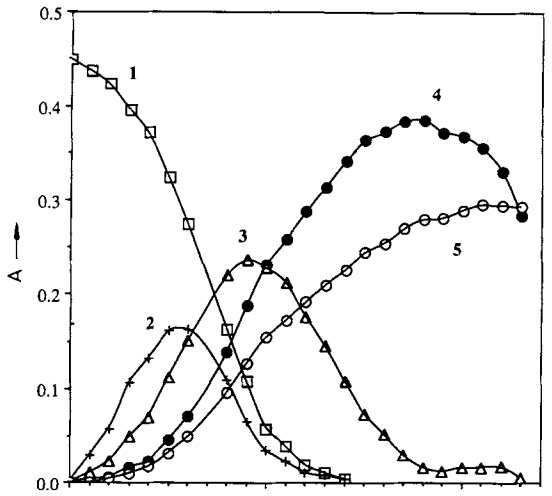


Fig. 1. Concentration profiles of the components **1** to **5**, plotted as the absorbance (A) of one characteristic band each: **1**, 1351.8; **2**, 2112.2; **3**, 1857.2; **4**, 3501.3; **5**, 2147.1 cm^{-1}. The abscissa orders the spectra chronologically, but approximately represents a logarithmic scale of the irradiation dose, as the irradiation times were increased considerably towards the end of the reaction. The full abscissa range corresponds to a dose of ca. 10^4 laser pulses (100 J cm^{-1}).

cyclopropenone **3**, are the C=O stretch at 1857 cm^{-1} and the C=C stretch at 1650 cm^{-1}. Ethynol **4** and its deuterium-substituted isotopomers each exhibit five bands above 630 cm^{-1} (Table 1). Work to determine the bending vibrations ν_6 to ν_9 in the spectral range below 630 cm^{-1} is in progress; the values 599, 523, 383, and 346 cm^{-1} may be quoted as preliminary results for HCCOH. The IR spectra of matrix-isolated ketene **5** and its mono- and dideutero derivatives are well-known.[11]

The photochemical valence isomerization and decarbonylation of cyclobutenediones[12] to cyclopropenones[13] and of the latter to yield acetylenes[14] are well-known reactions. We have obtained an authentic precedent for a reaction sequence of the type **1**→**2**→**3**→**4** under our conditions of matrix isolation by photolyzing 3,4-dimethylcyclobutenedione.[15] Analysis of the sequential spectra gave results analogous to those obtained with **1**. In this case two of the three expected intermediates, dimethylcyclopropenone[15] and 2-butyne, are known compounds which we identified unambiguously by independent synthesis and matrix isolation.

The observed IR bands leave no doubt that compound **4** retains both the OH/D and the CH/D groups of **1**; moreover, the band at 2198 cm^{-1} is characteristic for an unsymmetrically substituted alkyne. The stretching bands of **4**, apart from the OH-stretch, lie at much the same frequencies as those of fluoroacetylene.[17] A heuristic approach would be to consider the OH-stretching vibration as localized and to treat **4** as a quasilinear isotopomer of fluoroacetylene (OH ≙ ^{17}F, OD ≙ ^{18}F). This very simple model works amazingly well. The wave numbers of the H/D–C, C≡C, and C–O stretching bands (Table 1) obey both the Redlich-Teller product rule[18a] and the Decius-Wilson sum rule[18b] quite well and are reproduced within ±5 cm^{-1} by the following force field (f/N m^{-1}): 580 (H/D–C), 1400 (C≡C), 920 (C–O), and −40 for the cross terms H/D–C≡C and C≡C–O. The agreement with the frequencies and intensities predicted for ethynol by recent ab initio calculations[1a,5] is as good as can be expected.[19]

The spectrum of the matrix after the disappearance of components **1** to **3** is shown in Figure 2. Apart from bands

Table 1. Wavenumbers ($\tilde{\nu}$/cm^{-1}) and relative intensities (%) of the fundamental bands of **4** and its mono- and dideuterated derivatives in the range 3630 to 630 cm^{-1}.

HCCOH **4**	HCCOD	DCCOH	DCCOD	Description
3501.3 (60)	2587.5 (55)	3501.7 (75)	2586.8 (*100*)	ν_1(a'), OH/D stretching
3339.6 (25)	3339.6 (25)	2620.8 (*100*)	2620.4 (90)	ν_2(a'), CH/D stretching
2198.3 (*100*)	2196.2 (*100*)	2037.4 (55)	2035.1 (50)	ν_3(a'), CC stretching
1232.1 (25)	946.8 (10)	1230.9 (25)	944.5 (20)	ν_4(a'), COH/D bending
1072.1 (25)	1069.2 (15)	1050.5 (50)	1046.9 (15)	ν_5(a'), CO stretching

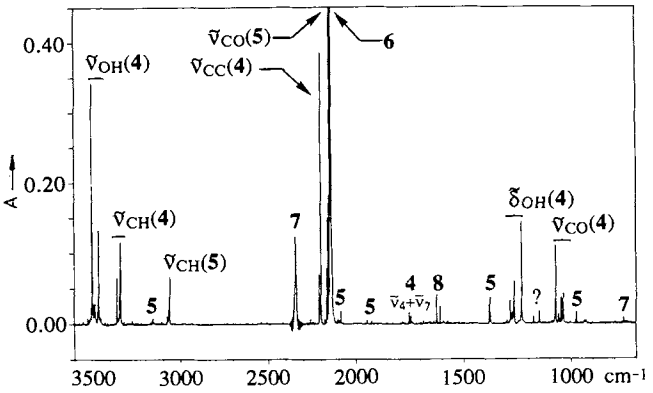


Fig. 2. Base-line corrected IR absorption spectrum of a mixture of ethynol **4** and ketene **5**. Other components: CO **6**, CO_2 **7**, H_2O **8**.

due to CO, CO_2, and H_2O, all significant absorptions can be assigned to either the intermediate ethynol **4** or the final product ketene **5**. The final reaction is very slow; presumably ethynol exhibits very little absorption at the irradiation wavelength of 248 nm.[10] Nevertheless, we maintain that the conversion to ketene is a photo-induced reaction of isolated ethynol. The rate of the isomerization **4**→**5** was independent of the water content of the matrix, which varied greatly from sample to sample. Furthermore, in deuterated samples the isotopic purity was retained through to the end product **5**. This excludes the possibility that the isomerization **4**→**5** is caused by a reaction with adventitious water in the matrix.

This work has provided conclusive evidence for the identification of ethynol and suggests that hydroxycyclopropenones could be suitable precursors for the photochemical generation of hydroxyacetylenes in solution. The two weak IR bands at 2230 and 1155 cm^{-1}, which were tentatively assigned to ethynol by *Lasne* and *Ripoll*,[4a] do not agree with our data, but we cannot exclude the possibility that the discrepancy is due to the different media.

Received: August 30, 1988;
revised: October 28, 1988 [Z 2948 IE]
German version: *Angew. Chem. 101* (1989) 183

[1] a) D. J. DeFrees, A. D. McLean, *J. Phys. Chem. 86* (1982) 2835 and references cited therein; b) K. Tanaka, M. Yoshimine, *J. Am. Chem. Soc. 102* (1980) 7655 and references cited therein; c) W. J. Bouma, R. H. Nobes, L. Radom, C. E. Woodward, *J. Org. Chem. 47* (1982) 1869; d) H. Huber, J. Vogt, *J. Chem. Phys. 64* (1982) 399; e) S. Schröder, W. Thiel, *J. Am. Chem. Soc. 108* (1986) 7985; f) B. L. M. van Baar, N. Heinrich, W. Koch, R. Postma, J. K. Terlouw, H. Schwarz, *Angew. Chem. 99* (1987) 153; *Angew. Chem. Int. Ed. Engl. 26* (1987) 140.

[2] B. van Baar, T. Weiske, J. K. Terlouw, H. Schwarz, *Angew. Chem. 98* (1986) 275; *Angew. Chem. Int. Ed. Engl. 25* (1986) 282.

[3] a) J. K. Terlouw, P. C. Burgers, B. L. M. van Baar, T. Weiske, H. Schwarz, *Chimia 40* (1986) 357; b) J. K. Terlouw, H. Schwarz, *Angew. Chem. 99* (1987) 829; *Angew. Chem. Int. Ed. Engl. 26* (1987) 805.

[4] a) M.-C. Lasne, J.-L. Ripoll, *Bull. Soc. Chim. Fr. 1986*, 766; b) Z. Jabry, M.-C. Lasne, J.-L. Ripoll, *J. Chem. Res. Synop. 1986*, 188; c) C. Wentrup, P. Lorenčak, *J. Am. Chem. Soc. 110* (1988) 1880.

[5] J. Dommen, M. Rodler, T.-K. Ha, *Chem. Phys. 117* (1987) 65.

[6] a) W. Büchner, *Helv. Chim. Acta 49* (1966) 907; b) O. Ayed, L. Manceron, B. Silvi, *J. Phys. Chem. 92* (1988) 37.

[7] P. J. Stang, K. A. Roberts, *J. Am. Chem. Soc. 108* (1986) 7125; C. J. Kowalski, G. S. Lal, M. S. Haque, *ibid. 108* (1986) 7127.

[8] M. Capponi, I. Gut, J. Wirz, *Angew. Chem. 98* (1986) 358; *Angew. Chem. Int. Ed. Engl. 25* (1986) 344; Y. Chiang, M. Hojatti, J. R. Keeffe, A. J. Kresge, N. P. Schepp, J. Wirz, *J. Am. Chem. Soc. 109* (1987) 4000 and references cited therein.

[9] A. Bou, M. A. Pericàs, F. Serratosa, *Tetrahedron Lett. 23* (1982) 361.

[10] Similar results were obtained upon irradiation with a low-pressure mercury lamp through a cut-off filter ($\lambda > 220$ nm). Without the filter ethynol was not accumulated in detectable quantity.

[11] C. B. Moore, G. C. Pimentel, *J. Chem. Phys. 38* (1963) 2816; J. L. Duncan, B. Munro, *J. Mol. Struct. 161* (1987) 311.

[12] D. Belluš, B. Ernst, *Angew. Chem. 100* (1988) 820; *Angew. Chem. Int. Ed. Engl. 27* (1988) 797.

[13] E. V. Dehmlow, *Tetrahedron Lett. 13* (1972) 1271; D. Eggerding, R. West, *J. Am. Chem. Soc. 98* (1976) 3641; E. V. Dehmlow, R. Neuhaus, H. G. Schell, *Chem. Ber. 121* (1988) 569.

[14] W. Sander, O. L. Chapman, *Angew. Chem. 100* (1988) 402; *Angew. Chem. Int. Ed. Engl. 27* (1988) 398.

[15] A. Treibs, K. Jacob, R. Tribollet, *Justus Liebigs Ann. Chem. 741* (1970) 101.

[16] R. Breslow, L. J. Altman, *J. Am. Chem. Soc. 88* (1966) 504.

[17] G. R. Hunt, M. K. Wilson, *J. Chem. Phys. 34* (1961) 1301.

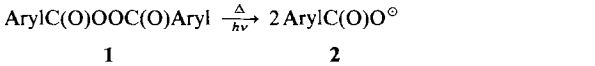
[18] E. B. Wilson, J. C. Decius, P. C. Cross; *Molecular Vibrations*, McGraw-Hill, New York 1955, a) p. 183, b) p. 186.

[19] B. A. Hess, L. J. Schaad, P. Čársky, R. Zahradník, *Chem. Rev. 86* (1986) 709.

Well-Resolved ESR Spectra of Arenecarboxyl Radicals in Solution**

By *Hans-Gert Korth,* Wolfgang Müller, Janusz Lusztyk,* and *Keith U. Ingold*

Dibenzoyl peroxide and related bis(arenecarbonyl) peroxides **1** are the most widely used initiators of free-radical processes. Their thermal and photochemical decomposition yields primarily arenecarboxyl radicals (arenecarbonyloxyl radicals) **2**.[1] The molecular and electronic struc-



1 **2**

a, Aryl = C_6H_5

tures of these radicals are currently under active investigation[2] as are the kinetics of their reactions.[3] Elucidation of the structures of the radicals **2** would be greatly aided if high resolution ESR spectra could be obtained. Benzoyloxyl **2a** has been observed by ESR in the solid state at very low temperatures[4,5] and this radical along with two *para*-substituted derivatives have been detected in solution at room temperature using time-resolved ESR spectroscopy.[6] In all these cases, the spectra were too poorly resolved to reveal any hyperfine splittings (HFS) by ring substituents. Earlier attempts to detect benzoyloxyl radicals by conventional ESR spectroscopy using continuous UV photolysis of dibenzoyl peroxide in suitable solvents have met

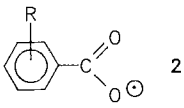
[*] Dr. H.-G. Korth [+], Dipl.-Chem. W. Müller
Institut für Organische Chemie der Universität—GHS
Universitätsstr. 5, D-4300 Essen 1 (FRG)
Dr. J. Lusztyk, Dr. K. U. Ingold
Division of Chemistry, National Research Council of Canada
Ottawa, Ontario K1A OR6 (Canada)
[+] NRCC/Summit Postdoctoral Fellow 1987–1988.

[**] Issued as NRCC No. 29827.

with no success,[7] presumably because of the high reactivity of the radicals[3] and/or other experimental problems.

We have recently reported[8] that carbonyloxyl radicals of the type $ROCO_2^{\circ}$, $RCH{=}CHCO_2^{\circ}$, and $RC{\equiv}CCO_2^{\circ}$, which we had earlier found to be relatively resistant to decarboxylation using UV/VIS absorption spectroscopy,[8,9] gave well-resolved ESR spectra in solution at low temperatures. The observations encouraged us to reevaluate the continuous UV photolysis of bis(arenecarbonyl) peroxides in solution as a source of $ArylCO_2^{\circ}$ radicals **2** that would be detectable by ESR spectroscopy. Once the critical conditions were worked out,[10] good first-derivative ESR spectra of $ArylCO_2^{\circ}$ were obtained for a wide variety of peroxides **1**[11] (see Table 1 and Fig. 1).

Table 1. ESR parameters for the radicals **2** in cyclopropane solution [a].



2

2	R	T [°C]	g	Hyperfine splitting [mT] a(o-H)	a(others) [b]
a	H	−120	2.01210(4) [c]	0.065(2) (2H)	
b	H	−125	2.01209(4)	0.065(2) (2H)	1.333(6) (^{13}C) [d]
c	4-*t*Bu	−121	2.01204(3)	0.063(2) (2H)	
d	4-F	−122	2.01220(9)	0.065(2) (2H)	
e	4-CF_3	−121	2.0124(1)	0.07(1) (2H)	
f	3-Cl	−120	2.01236(4)	0.065(2) (2H)	
g	2-F	−124	2.01164(4)	0.081(3) (1H)	0.840(5) (1F)
h	2-Cl	−120	2.01093	0.123(3) (1H)	0.390(5) (1Cl)

[a] Numbers in parentheses indicate the probable error in the last digit. [b] Experimental line widths were 0.02–0.03 mT. The upper limit for any additional, unresolved HFS was ≤0.02 mT. [c] g = 2.0117 [4], 2.0123 [6]. [d] From carbonyl-[^{13}C]-labeled peroxide, **1a**.

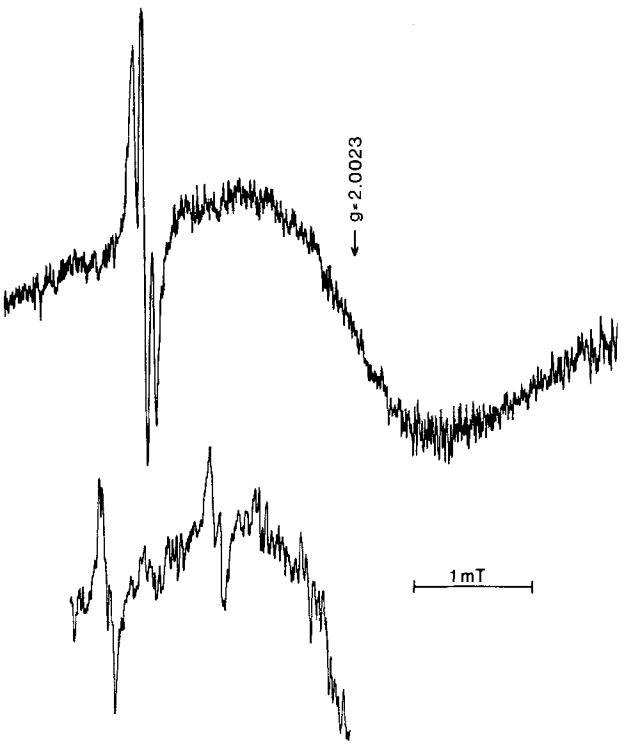
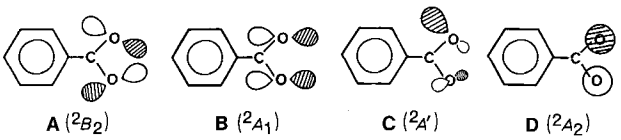


Fig. 1. ESR spectra of the benzoyloxyl radical **2a** at −120°C (top) and the 2-fluorobenzoyloxyl radical **2f** at −124°C (bottom) in cyclopropane. Microwave power: 15 mW.

The g-factors of our radicals **2** vary between 2.0109 and 2.0124 and thus lie in the range characteristic for carbonyloxyl radicals[4–6,8] and, in the only case where a direct comparison is possible, there is satisfactory agreement with the literature data.[6] The ESR signal of the benzoyloxyl radical **2a** (Fig. 1, top) shows HFS by just two equivalent hydrogen atoms in a 1:2:1 pattern. The same triplet pattern with virtually identical HFS is observed also with the *para*-substituted radicals, **2b**, **2c**, and **2d** and with the *meta*-substituted radical **2e**, which clearly indicates that the interaction of the unpaired electron with the two *ortho* protons is responsible for the triplet splitting. This is further confirmed by the spectra of the two *ortho*-substituted radicals **2f** (Fig. 1, bottom) and **2g**, which exhibit a doublet splitting by the *ortho* hydrogen and doublet and quartet splittings by the fluorine and chlorine substituents, respectively.

The lower energy states of the benzoyloxyl radical are the coplanar structures **A**–**D**, in which the unpaired electron resides almost exclusively in oxygen p-type orbitals; both theoretical[2] and experimental[4,5] evidence favor the



$^2B_2$ electronic configuration **A** as the ground state. Our observation of a coupling between the unpaired electron and the two *ortho* hydrogen atoms, or an *ortho* hydrogen and *ortho* halogen atom, support an in-plane orientation of the SOMO with the interaction occurring by a through-space mechanism. That is, our results are consistent with the σ-electronic structures **A**–**C** but inconsistent with the π-structure **D**.[12]

The ^{13}C HFS of 1.33 mT found for the carboxyl-[^{13}C]-labeled benzoyloxyl radical **2a** confirms the minor contribution of this carbon atom (ca. 1% 2s spin density) to the SOMO. Virtually the same ^{13}C HFS has been found for this radical in single crystals[13] and for the $Me_3CC{\equiv}C^{13}CO_2^{\circ}$ radical in solution.[8]

INDO calculations using AM1-UHF-optimized geometries are in accord with the experimental findings (see Fig. 2). The ground state appears to have a planar configuration with unequal C–O bond lengths. There is little spin density on either the carboxyl carbon or in the aromatic ring, with the highest spin density being found at the *ortho* positions. The INDO calculations overestimate the ^{13}C

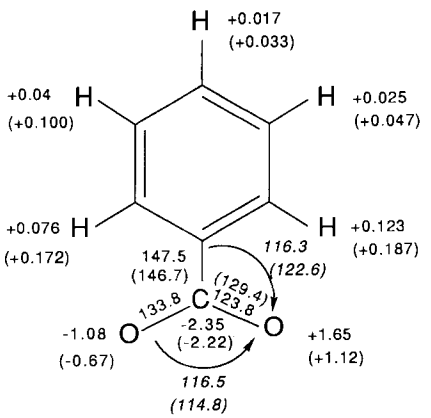


Fig. 2. Optimized AM1-UHF geometry (bond lengths in [pm], bond angles in [°]) and INDO hyperfine splittings ([mT]) of the benzoyloxyl radical **2a**. Data for C_{2v} geometry are given in parentheses.

HFS of the carboxyl carbon but they underestimate the ^{17}O HFS (the calculated isotropic ^{17}O HFS is 3.35 ± 0.5 mT, based on measurements for single crystals[5]). If the $CO_2^{\ominus}$ moiety is forced to adopt a C_{2v} geometry with equal C-O bond lengths, the INDO calculated ^1H HFS values increase while the ^{17}O HFS values decrease, thus moving these HFS values further from their experimental values. This behavior[14] may indicate an unsymmetrical equilibrium structure like **C** for this and other carbonyloxyl radicals.[15] However, because there is very little s-spin density on all the atoms of these radicals, the semiempirical calculations may not be adequate for a reliable assignment of a symmetrical or an unsymmetrical ground state structure.[16]

Received: September 8, 1988 [Z 2959 IE]
German version: *Angew. Chem. 101* (1989) 186

[1] R. Hiatt in D. Swern (Ed.): *Organic Peroxides, Vol. 2*, Wiley, New York 1971, p. 815; J. K. Kochi in J. K. Kochi (Ed.): *Free Radicals, Vol. 2*, Wiley, New York 1973, p. 699; S. Patai (Ed.): *The Chemistry of Peroxides*, Wiley-Interscience, New York 1983.
[2] See ref. [3] for leading references.
[3] J. Chateauneuf, J. Lusztyk, K. U. Ingold, *J. Am. Chem. Soc. 110* (1988) 2877, 2886.
[4] N. J. Karch, E. T. Koh, B. L. Whitsel, J. M. McBride, *J. Am. Chem. Soc. 97* (1975) 6729.
[5] J. M. McBride, R. A. Merrill, *J. Am. Chem. Soc. 102* (1980) 1723.
[6] S. Yamauchi, N. Hirota, S. Takahara, H. Sakuragai, K. Tokumaru, *J. Am. Chem. Soc. 107* (1985) 5021. The arenecarboxyl radicals were generated by laser flash photolysis of their parent peroxides and were detected in the absorption mode.
[7] Statements to this effect can be found in several reviews [1] but there appears to be only one explicit description of the experimental conditions employed: D. J. Edge, J. K. Kochi, *J. Am. Chem. Soc. 95* (1973) 2635.
[8] H. G. Korth, J. Chateauneuf, J. Lusztyk, K. U. Ingold, *J. Am. Chem. Soc. 110* (1988) 5929.
[9] J. Chateauneuf, J. Lusztyk, B. Maillard, K. U. Ingold, *J. Am. Chem. Soc. 110* (1988) 6727.
[10] Very dilute solutions of **1** (typically 1-3 mg, to avoid crystallization) in cyclopropane (ca. 0.5 mL) were sealed in 4 mm o.d. quartz tubes and photolyzed directly in the cavity of a Varian E-104 EPR spectrometer with the focused UV light from a 1 kW Hg/Xe lamp at ca. -120°C, using microwave power levels of 10-20 mW. We failed to detect any ESR spectra of radicals **2** on photolysis of **1**, Aryl = 4-$MeOC_6H_4$, 4-PhC_6H_4 and C_6F_5.
[11] We thank Dr. *J. Chateauneuf* for providing us with some of the bis(arenecarbonyl) peroxides **1**.
[12] A σ-electronic structure is further supported by the fact that the *g*-values for the 2-halobenzoyloxyl radicals **2f** and **2g** are lower than those of the other radicals **2**. The *g*-values of benzyl radicals, which have a π-electronic structure, are increased by *ortho* halogenation; see A. Berndt in H. Fischer (Ed.): *Landolt-Börnstein, New Series*, Springer, Berlin 1977, Vol. II/9b, p. 543; 1988, Vol. II/17c, p. 173.
[13] R. A. Merrill, *Ph. D. Thesis*, Yale University 1986. We thank Professor *J. M. McBride* for bringing this work to our attention.
[14] INDO calculations on other carbonyloxyls yield the same result.
[15] The experimental evidence which favors the symmetrical (C_{2v}) $^2B_2$ configuration **A** was obtained from the anisotropic ^{17}O HFS of $C_6H_5CO_2^{\ominus}/CD_3^{\ominus}$ radical pairs in a single crystal of $C_6H_5CO_3CD_3$ at 7-25 K [5, 13].
[16] High-level ab initio calculations on various carbonyloxyl radicals are in progress.

Octabromocyclohexaarsenate, $[As_6Br_8]^{2\ominus}$**

By *Ulrich Müller** and *Heike Sinning*

Organocyclopolyarsanes $(RAs)_n$ with various ring sizes have been known for some time (see, e.g., Refs. [1-4]). We have now prepared the first halogeno-cyclopolyarsane $[As_6Br_8]^{2\ominus}$.

With the intention of binding the $Cr(CO)_5$ fragment to the ion $[As_2SBr_5]^{\ominus}$,[5] we added solid $PPh_4[As_2SBr_5]$ to a solution of $[Cr(CO)_5(THF)]$ in THF (molar ratio 2.6 : 1). As the reaction mixture was stirred, $PPh_4[As_2SBr_5]$ slowly dissolved with gas evolution and a yellow powder precipitated, which contained, apart from sulfur, some chromium, very little carbon, and no bromine. The powder was removed by filtration and the filtrate cooled to -5°C to afford yellow crystals of $(PPh_4)_2[As_6Br_8]$. The first of the three crystal fractions also contained some $Cr(CO)_6$; yield 80%. We are currently investigating whether other halogen substituted polyarsanes can be synthesized by this method.[15] The carbonylchromium compound apparently acts as a reducing agent in the reaction. Further knowledge about the course of the reaction and about the other products will require more detailed studies. Although cyclopolyarsane complexes such as $[(PhAs)_6Mo(CO)_4]$[6] and $[(PhAs)_nMo_2(CO)_6]$ (n = 8, 9, 10)[7] are known, we have, up to now, not detected a corresponding complex with the $Cr(CO)_5$ fragment.

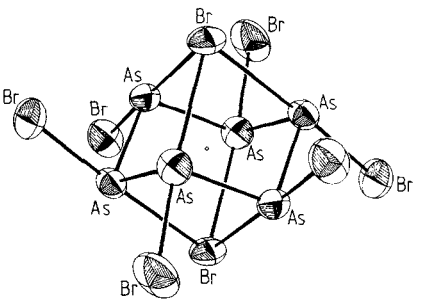


Fig. 1. Molecular structure of the anion of $(PPh_4)_2[As_6Br_8]$ (with 50% probability thermal motion ellipsoids at 20°C). Bond lengths [pm] and angles [°]: As-As 243.0 to 246.5(3), As-Br(terminal) 243.2 to 248.4(4), As-(μ_3-Br) 293.6 to 299.4(3); As-As-As 97.7 to 100.5(1), As-As-Br 87.2 to 89.9(1), Br-As-(μ_3-Br) 174.4 to 176.7(1).

The X-ray structural analysis[8] showed that $(PPh_4)_2[As_6Br_8]$ contains the $[As_6Br_8]^{2\ominus}$ ion, the structure of which is shown in Figure 1. The ion can be regarded as being an As_6Br_6 molecule with two additional $Br^{\ominus}$ ions. The As_6 ring has a chair conformation with the bromine atoms in equatorial positions. As_6Br_6 thus has the same structure as As_6Ph_6.[4] The average As-As bond length of 245.2 pm lies in the range found for polyarsanes[3,4,6,7,9] and polyarsenides.[10,11] The two other $Br^{\ominus}$ ions lie above and below the As_6 ring, each being bonded to three As atoms. The coordination geometry of each As atom can be described as a trigonal bipyramid in which one equatorial position is occupied by a lone pair of electrons and the axial positions by bromine atoms.

The separations between the $[As_6Br_8]^{2\ominus}$ ions are large because of the bulky cations; there are no intermolecular As···Br contacts. The IR and Raman spectra are consistent with the mutual exclusion rule for the point group D_{3d}. Seven IR and seven Raman bands were observed in the region between 100 and 300 cm^{-1}[12] (expected numbers: ten IR and eleven Raman bands[13]). Because of the near correspondence of the As-As and As-Br stretching frequencies at 270 cm^{-1},[14] considerable vibrational coupling is to be expected so that an exact assignment of the individual bands can only be achieved with difficulty.

Received: September 13, 1988 [Z 2966 IE]
German version: *Angew. Chem. 101* (1989) 187

[*] Prof. Dr. U. Müller, Dr. H. Sinning
Fachbereich Chemie der Universität
Hans-Meerwein-Strasse, D-3550 Marburg (FRG)

[**] This work was supported by the Deutsche Forschungsgemeinschaft and the Fonds der Chemischen Industrie. We thank Prof. *J. Strähle* for recording the Raman spectrum.

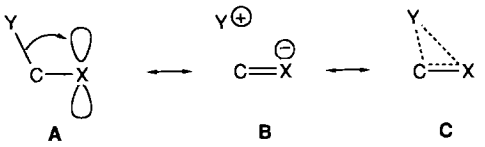
[1] L. R. Smith, J. L. Mills, *J. Organomet. Chem. 84* (1975) 1.

[2] M. Baudler, P. Bachmann, *Z. Anorg. Allg. Chem. 485* (1982) 129.
[3] O. Mundt, G. Becker, H. J. Wessely, H. J. Breunig, H. Kischkel, *Z. Anorg. Allg. Chem. 486* (1982) 70.
[4] A. L. Rheingold, P. J. Sullivan, *Organometallics 2* (1983) 327.
[5] U. Müller, A. Mohammed, *Z. Anorg. Allg. Chem. 533* (1986) 65.
[6] A. L. Rheingold, M. E. Fountain, *Organometallics 5* (1986) 2410.
[7] A. L. Rheingold, M. E. Fountain, A. J. DiMaio, *J. Am. Chem. Soc. 109* (1987) 141.
[8] X-ray structural analysis using 1517 observed ($F>2\sigma(F)$) independent reflections ($Mo_{K\alpha}$ radiation, Enraf-Nonius CAD4 four-circle diffractometer, empirical absorption correction, 1929 reflections measured in the range $\theta<18°$), $R=0.077$, $wR=0.028$. $a=1171.6(5)$, $b=1181.1(6)$, $c=1186.3(4)$ pm, $\alpha=62.87(3)$, $\beta=78.63(3)$, $\gamma=75.65(4)°$; space group $P\bar{1}$, $Z=2$. Further details of the crystal structure investigation can be obtained from the Fachinformationszentrum Energie, Physik, Mathematik GmbH, D-7514 Eggenstein-Leopoldshafen 2, on quoting the depository number CSD-53475, the names of the authors, and the journal citation.
[9] M. Baudler, J. Hellmann, P. Bachmann, K. F. Tebbe, R. Fröhlich, M. Feher, *Angew. Chem. 93* (1981) 415; *Angew. Chem. Int. Ed. Engl. 20* (1981) 406.
[10] W. Schmettow, H. G. von Schnering, *Angew. Chem. 89* (1977) 895; *Angew. Chem. Int. Ed. Engl. 16* (1977) 857.
[11] C. H. E. Belin, *J. Am. Chem. Soc. 102* (1980) 6036.
[12] IR bands in the solid state (in the range $\tilde{\nu}=100$–$400\ cm^{-1}$): 292 w, 270 w, 258 w, 228 s, 203 sh, 193 vs, 114 m. Raman bands (50–400 cm^{-1}): 290 vw, 262 w, 249 vw, 224 m, 204 s, 195 s, 120 vw, 90 m, 68 s.
[13] J. Weidlein, U. Müller, K. Dehnicke: *Schwingungsspektroskopie*, 2. Aufl., Thieme, Stuttgart 1988, p. 112.
[14] J. Weidlein, U. Müller, K. Dehnicke: *Schwingungsfrequenzen I*, Thieme, Stuttgart 1981, p. 60, 204.
[15] Note added in proof (January 16, 1989): Recently, another synthetic route and the structure of $[As_6I_8]^{2\oplus}$ have been described: C. A. Ghilardi, S. Midollini, S. Moneti, A. Orlandini, *J. Chem. Soc. Chem. Comm. 1988*, 1241.

The Structure of a *C*-Borylborirene with Strong C–B Hyperconjugation**

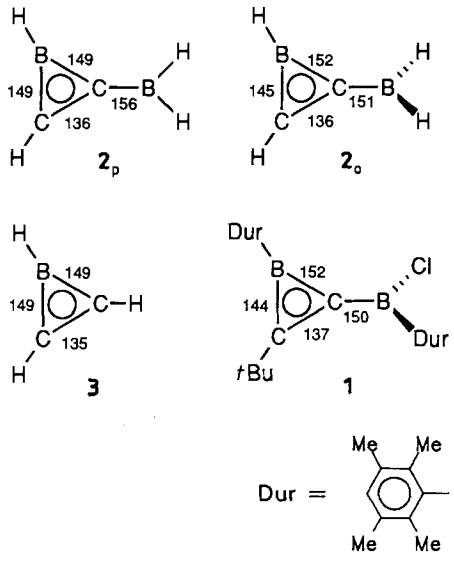
By *Andrea Höfner, Bernd Ziegler, Werner Massa,* and *Armin Berndt**

C–Y hyperconjugation in **A** leads, as illustrated by the resonance formulas **B** and **C**,[1] to shortening of the CX bond, lengthening of the CY bond and a decrease in the YCX angle.



The geometrical consequences of C–C hyperconjugation for carbocations were recently verified on the basis of the crystal structure of the 3,5,7-trimethyl-1-adamantyl cation.[3,4] The results of a crystal structure analysis of the *C*-borylborirene **1** presented here confirm the geometrical consequences of C–B hyperconjugation in a neutral molecule, which were predicted by ab-initio calculations.[5]

According to ab-initio calculations by *von Schleyer* et al.[5] (3-21G//3-21G), the bond lengths in the planar *C*-borylborirene $\mathbf{2}_p$ are very similar to those of the unsubstituted borirene **3**,[6,7] whereas those in the orthogonal *C*-borylborirene $\mathbf{2}_o$ differ greatly from those of $\mathbf{2}_p$ and **3** (compare the bond lengths [pm] in the structural formulas). The BCB angle in $\mathbf{2}_o$ is 11.5° smaller than in $\mathbf{2}_p$.[8] The



reason for this structural distortion[9] is C–B hyperconjugation, which according to the calculations[5] also leads to a stabilization of ca. 10 kcal mol^{-1} for $\mathbf{2}_o$ with respect to $\mathbf{2}_p$.

With the X-ray structural analysis of the *C*-borylborirene **1**, we have found an almost orthogonal conformation and structural parameters which are in good agreement with those calculated for $\mathbf{2}_o$.

1[10] was synthesized from *tert*-butyl(trimethylstannyl)acetylene and 1,2-dichloro-1,2-diduryldiborane(4).[12] A similar procedure has been used to prepare the (liquid) *tert*-butyl substituted analogue of **1**.[11] The result of an X-ray structural analysis[14] of **1** is shown in Figure 1.

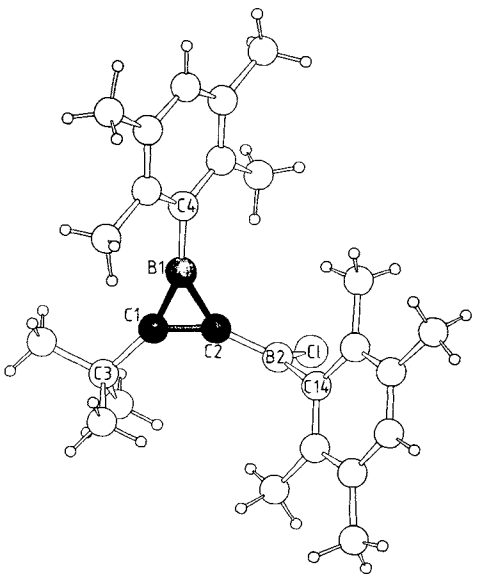


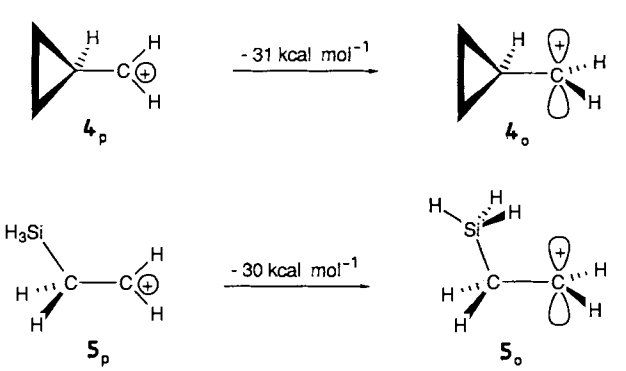
Fig. 1. Molecular structure (SCHAKAL program) of **1** projected approximately on the plane B1,C1,C2. Important bond lengths [Å] and angles [°]: C1-B1 144.3(4), C1-C2 136.7(4), C2-B1 151.6(4), C2-B2 149.8(5), C1-C3 150.6(4), B1-C4 154.8(4), B2-Cl 178.4(4), B2-C14 156.3(4); C1-B1-C2 54.9(2), B1-C1-C2 65.3(2), B1-C2-C1 59.8(2), C1-B1-C4 157.1(3), C2-B1-C4 147.9(3), B1-C1-C3 159.0(3), C2-C1-C3 135.7(3), B1-C2-B2 146.3(3), C1-C2-B2 153.8(3), C2-B2-C14 124.6(3), C2-B2-Cl 116.7(2), C14-B2-Cl 118.3(2); C1-C2-B2-C14 −95.5(6), C1-C2-B2-Cl 91.1(6).

[*] Prof. Dr. A. Berndt, Dipl.-Chem. A. Höfner, Dipl.-Chem. B. Ziegler, Prof. Dr. W. Massa
Fachbereich Chemie der Universität
Hans-Meerwein-Strasse, D-3550 Marburg (FRG)

[**] This work was supported by the Deutsche Forschungsgemeinschaft and the Fonds der Chemischen Industrie.

The B1,C1,C2 plane forms an angle of 85° with the C1,B2,C14 plane. The duryl rings are twisted by 49 and 88° with respect to the B1,C1,C2 and C2,B2,C1 planes. The C1C2 bond of 137 pm in the three-membered ring is considerably longer than the CC double bonds in cyclopropenes (130 pm[15]) but the same as that in the tri-*tert*-butylcyclopropenium ion.[16] The BC bond lengths in the three-membered ring of 144 and 152 (av. 148) pm are markedly shorter than the value of 155 pm calculated for the BC single bond in borirane.[6] The bond lengths in the borirene indicate delocalization of the two π-electrons.

The B1,C2,B2 angle in **1** (146.3°) is very similar to that calculated for $\mathbf{2}_o$ (145.7°),[5] unlike that for $\mathbf{2}_p$ (157.2°).[5] The different BC bond lengths in the ring of **1** and the exocyclic BC bond length of 150 pm, which is very short for a BC single bond, are in good agreement with the data calculated for $\mathbf{2}_o$, and therefore represent evidence for pronounced hyperconjugative interaction in orthogonal *C*-borylborirenes. Hyperconjugation is normally found only in charged systems.[17] The strong hyperconjugation in neutral *C*-borylborirenes is due to a combination of structural units which are most effective in this interaction, i.e., a strained three-membered ring (cf. **4**[18]) and atoms of low electronegativity (cf. **5**;[19] in **1** and **2** it is the boron atom with negative π-charge).



$\mathbf{4}_p$ $\mathbf{4}_o$ $\mathbf{5}_p$ $\mathbf{5}_o$

Received: September 15, 1988 [Z 2968 IE]
German version: *Angew. Chem. 101* (1989) 188

CAS Registry numbers:
1, 118376-38-8; *tert*-butyl(trimethylstannyl)acetylene, 34664-54-5; 1,2-dichloro-1,2-diduryldiborane, 118376-39-9.

[1] The mesomeric form **B**, which is usually used to represent hyperconjugation gives no indication of the YCX angle. The mesomeric form **C** represents asymmetric bridging, a stronger variation of hyperconjugation [2], and illustrates clearly *all* of the geometric consequences of hyperconjugation.

[2] P. von R. Schleyer, D. Lenoir, P. Mison, G. Liang, G. K. S. Prakash, G. A. Olah, *J. Am. Chem. Soc. 102* (1980) 683.

[3] T. Laube, *Angew. Chem. 98* (1986) 368; *Angew. Chem. Int. Ed. Engl. 25* (1986) 349.

[4] Impressive examples of the geometrical consequences of negative hyperconjugation: W. B. Farnham, D. A. Dixon, J. C. Calabrese, *J. Am. Chem. Soc. 110* (1988) 2607, and references cited therein.

[5] P. H. M. Budzelaar, K. Krogh-Jespersen, T. Clark, P. von R. Schleyer, *J. Am. Chem. Soc. 107* (1985) 2773, and references cited therein.

[6] P. H. M. Budzelaar, A. J. Kos, T. Clark, P. von R. Schleyer, *Organometallics 4* (1985) 429; when electron correlation is taken into account using MP2(FU)/6-31G*, bond lengths of 136 (C-C) and 147 (B-C) are obtained for **3**: P. von R. Schleyer, seminar at the 6th IMEBORON symposium, Bechyne, CSSR 1987.

[7] The bond lengths calculated for **3** have recently been confirmed experimentally: J. J. Eisch, *EUCHEM Conf. PSIBLOCS* (Paris 1988).

[8] The BCB angles are 157.2 ($\mathbf{2}_p$) and 145.7 ($\mathbf{2}_o$); P. von R. Schleyer (Erlangen), private communication.

[9] The shortening of the BC bond opposite to the exocyclic B atom can be explained using the Walsh orbitals of the three-membered ring.

[10] **1**: colorless crystals, m.p. 112°C, yield (NMR) ca. 95%, NMR spectra ($CDCl_3$): 300.1-MHz ^{1}H NMR: $\delta = 1.48$ (s, 9H; $C(CH_3)_3$), 2.24, 2.30, 2.36, 2.39 (4 s, each 6H; *o*- and *m*-CH_3), 7.06, 7.10 (2 s, each 1H; *p*-H); 100.6-MHz ^{13}C NMR (−40°C): $\delta = 19.5$ (q, 2C; *o*- or *m*-CH_3), 19.9 (q, 4C; *o*- or *m*-CH_3), 20.3 (q, 2C; *o*- or *m*-CH_3), 29.3 (q, 3C; $C(CH_3)_3$), 35.6 (s, 1C; $C(CH_3)_3$), 132.0, 132.2 (2 d, each 1C; *p*-C), 133.0, 133.1 (2 s, each 2C; *m*-C), 133.8, 136.1 (2 s, each 2C; *o*-C), 139.4 (s, 2C; *ipso*-C), 183.0 (s, 1C; =C−B), 189.2 (s, 1C; CB_2); 96.3-MHz ^{11}B NMR: $\delta = 66$ ($\nu_{1/2} \approx 1870$ Hz), 40 ($\nu_{1/2} \approx 850$ Hz).

[11] C. Pues, A. Berndt, *Angew. Chem. 96* (1984) 306; *Angew. Chem. Int. Ed. Engl. 23* (1984) 313.

[12] 1,2-dichloro-1,2-diduryldiborane(4) can be obtained from duryllithium and 1,2-dichloro-1,2-bis(dimethylamino)diborane(4) using a method similar to that described for 1,2-dichloro-1,2-dimesityldiborane(4) [13].

[13] R. Hunold, J. Allwohn, G. Baum, W. Massa, A. Berndt, *Angew. Chem. 100* (1988) 961; *Angew. Chem. Int. Ed. Engl. 27* (1988) 961.

[14] X-ray structural analysis of **1**: space group *C2/c*, $Z = 8$, $a = 2282.2(2)$, $b = 1190.5(2)$, $c = 2045.9(1)$ pm, $\beta = 113.65(1)°$, $\rho_{calcd} = 1.08$ g cm^{-3}; 2455 reflections were measured on a four-circle diffractometer (CAD4, Enraf-Nonius) with $Cu_{K\alpha}$ radiation at 220 K; from 2381 independent reflections, 2274 with $F_o > 2\sigma(F_o)$ were used in the structure determination; structure solved with direct methods, refined to $R = 0.042$, $wR = 0.040$ (weighting $w = 1/\sigma^2(F_o)$); no absorption correction ($\mu = 13.2$ cm^{-1}); Cl and C atoms refined with anisotropic temperature factors, H atoms with grouped common isotropic temperature factors (371 parameters); refinement of the B atoms with anisotropic temperature factors was possible without problems. Since, however, very little anisotropy was found, this refinement was dispensed with in order to improve the ratio of the number of parameters to the number of reflections. Further details of the X-ray structural analysis may be obtained from the Fachinformationszentrum Energie, Physik, Mathematik GmbH, D-7514 Eggenstein-Leopoldshafen 2, on quoting the depository number CSD-53358, the names of the authors, and the journal citation.

[15] P. H. Kasai, R. J. Myers, D. F. Eggers, K. B. Wiberg, *J. Chem. Phys. 30* (1959) 512.

[16] R. Boese, N. Augart, *Z. Kristallogr. 182* (1988) 32.

[17] R. Hoffmann, L. Radom, J. A. Pople, P. von R. Schleyer, W. J. Hehre, L. Salem, *J. Am. Chem. Soc. 94* (1972) 6221.

[18] M. Saunders, K. E. Laidig, K. B. Wiberg, P. von R. Schleyer, *J. Am. Chem. Soc. 110* (1988) 7652.

[19] S. G. Wierschke, J. Chandrasekhar, W. L. Jorgensen, *J. Am. Chem. Soc. 107* (1985) 1496.

Bromoselenates(II,IV), a Novel Type of Mixed Valence Compounds**

By *Bernt Krebs,** *Erhard Lühers,* and *Frank-Peter Ahlers*

Compounds of the chalcogens in the oxidation state +2 with chlorine, bromine and iodine are markedly less stable than the corresponding Se^{IV}- and Te^{IV}-compounds. Thus, the dominating species among the haloselenium and -tellurium anions were hitherto the long known hexahaloselenates(IV) and -tellurates(IV) $[XY_6]^{2\ominus}$ and the polynuclear species $[X_3Y_{13}]^{\ominus}$, $[X_2Y_{10}]^{2\ominus}$ and $[X_2Y_9]^{\ominus}$ (X = Se; Y = Cl, Br and X = Te; Y = Cl, Br, I), which are formed as degradation products of the tetrameric molecular halides X_4Y_{16}.[1,4e] Only recently was it also possible to prepare pure haloselenate(II) and -tellurate(II) anions and to isolate them in the form of the crystalline salts. The anions $[SeBr_4]^{2\ominus}$, $[Se_2Br_6]^{2\ominus}$, $[TeCl_4]^{2\ominus}$, $[TeBr_4]^{2\ominus}$ and $[TeI_4]^{2\ominus}$ could be characterized by structural analyses.[2-5] The same holds for further novel anions such as $[Se_3Br_8]^{2\ominus}$,[4b,c,6] $[Se_4Br_{14}]^{2\ominus}$,[6,7] $[Se_5Br_{12}]^{2\ominus}$,[4b,c,6] and $[Te_4I_{14}]^{2\ominus}$.[4b,c,6]

Exploiting the dissociation equilibria (a) and (b) already shown to be effective in the synthesis of pure haloselen-

$$\tfrac{1}{4}\,Se_4Br_{16} \rightleftharpoons SeBr_4 \rightleftharpoons SeBr_2 + Br_2 \qquad (a)$$

$$2\,SeBr_2 \rightleftharpoons Se_2Br_2 + Br_2 \qquad (b)$$

[*] Prof. Dr. B. Krebs, Dr. E. Lühers, Dipl.-Chem. F.-P. Ahlers
Anorganisch-chemisches Institut der Universität
Wilhelm-Klemm-Strasse 8, D-4400 Münster (FRG)

[**] This work was supported by the Deutsche Forschungsgemeinschaft, the Minister für Forschung des Landes Nordrhein-Westfalen, and the Fonds der Chemischen Industrie.

ates(II) in organic solvents we have now found access to a remarkable new class of mixed valence compounds in which selenium is present in the oxidation states +2 and +4. The anions **1**–**3** have been prepared and isolated in the form of the deep-red to reddish-black crystalline salts **1a**–**3a**, and have been characterized by X-ray structure analyses and vibrational spectra.

$[Se^{II}Se^{IV}Br_8]^{2\ominus}$ **1** $[Se^{II}_2Se^{IV}Br_{10}]^{2\ominus}$ **2** $[Se^{II}_3Se^{IV}Br_{12}]^{2\ominus}$ **3**

$[(C_2H_5)_4N]_2[Se_2Br_8]$ **1a** $[(nC_3H_8)_4N]_2[Se_3Br_{10}]$ **2a**
$[(C_6H_5)_4P]_2[Se_4Br_{12}]\cdot CH_2Cl_2$ **3a**

When bromides are added to the solutions of $SeBr_4$ in weakly polar organic solvents, nucleophilic addition reactions lead to the formation of complex reaction mixtures from which the mixed valence bromoselenates can be isolated. Of importance for their formation is the presence of $Br_3^{\ominus}$, since, on the one hand, it leads (with "neutralization" of the oxidation potential of Br_2) to a shift of the $SeBr_4$/$SeBr_2$ equilibrium (a) to the right, and, on the other, catalyzes the $Br^{\ominus}$-transfer (cf. Ref. [2]). Possible formal modes of reaction are the addition of $Br^{\ominus}$ to $SeBr_4$ to give bromoselenates(IV) followed by addition of $SeBr_2$ molecules to the selenate(IV) (or the substitution of $SeBr_4$ groups by $SeBr_2$ groups) or, conversely, the addition of $SeBr_4$ to initially formed bromoselenates(II). The reaction conditions

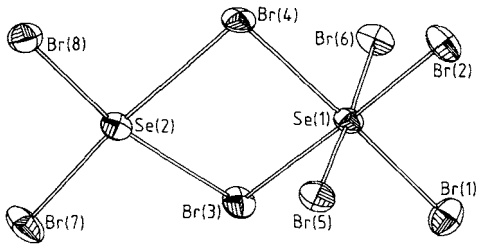


Fig. 1. Structure of **1** in the crystal of **1a** [8]. Important bond lengths [Å] and angles [°]: Se(1)-Br(1) 2.496(2), Se(1)-Br(2) 2.471(3), Se(1)-Br(3) 2.706(3), Se(1)-Br(4) 2.648(2), Se(1)-Br(5) 2.535(4), Se(1)-Br(6) 2.596(4), Se(2)-Br(3) 2.817(2), Se(2)-Br(4) 2.889(2), Se(2)-Br(7) 2.379(3), Se(2)-Br(8) 2.435(2), Se(1)···Se(2) 4.044(3); Br(1)-Se(1)-Br(2) 92.6(1), Br(7)-Se(2)-Br(8) 96.1(1), Br(3)-Se(1)-Br(4) 86.8(1), Br(3)-Se(2)-Br(4) 80.2(1) (cf. also [4c, 7]).

for reproducible synthesis of pure products by precipitation can be optimized by variation of reaction time, solvent, concentration, temperature, and counterion. As shown by an X-ray structure analysis,[8] **1** (Fig. 1) consists of a $Se^{IV}Br_6$ octahedral moiety and a square planar $Se^{II}Br_4$ moiety coupled via a common edge. As in all other haloselenates(II) the Se electron pairs not participating in bonding are stereochemically active in the sense of a ψ^2-octahedral $Se^{II}Br_4E_2$ coordination geometry. The Se^{II}–Br bridge bonds (average 2.853 Å) are very much longer than the terminal bonds (2.407 Å). The dihedral angle between the planar $Se^{II}Br_4$ moiety and the basal plane of the $Se^{IV}Br_6$ octahedron is 34°. In the $[Et_4N]_2[Se_2Br_8]$ salt prepared independently by *Hauge* et al.[7] the anion is much more strongly folded: the corresponding dihedral angle is 57°.

In the exactly centrosymmetric **2** (Fig. 2) the asymmetry of the $Se^{II}Br_4$ structural unit is even more pronounced ($Se-Br_{bridge}$ 2.970, $Se-Br_{term}$ 2.349 Å). Here we have the first example of a second $SeBr_2$ molecule being added to the $Se^{IV}Br_6$ octahedron in the *trans* position, and the resulting equatorial planes subtend an angle of 22°.

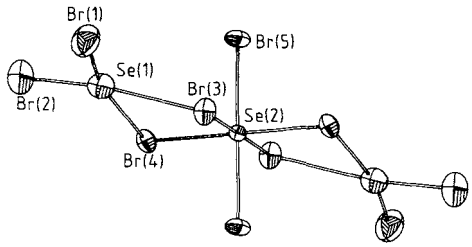


Fig. 2. Structure of **2** in crystals of **2a** [8]. Important bond lengths [Å] and angles [°]: Se(1)-Br(1) 2.338(2), Se(1)-Br(2) 2.360(2), Se(1)-Br(3) 2.943(2), Se(1)-Br(4) 2.997(2), Se(2)-Br(3) 2.557(1), Se(2)-Br(4) 2.570(1), Se(2)-Br(5) 2.549(1), Se(1)···Se(2) 4.042(3); Br(1)-Se(1)-Br(2) 99.5(1), Br(3)-Se(1)-Br(4) 76.7(1), Br(3)-Se(2)-Br(4) 91.9(1).

The structure of **3** (Fig. 3) is particularly noteworthy. In the first place, two $SeBr_2$ molecules are coordinated via *cis*-edges to the central $Se^{IV}Br_6$ octahedron; a third $SeBr_2$ unit bridges one of the $Se^{IV}BrSe^{II}$ four-membered rings such that a short Se–Se distance of 3.335 Å results between Se(4) and Se(2), indicating a bonding interaction. Se(2) thereby completes the square planar coordination geometry of Se(4). The $[Se_4Br_{12}]^{2\ominus}$ ions in **3a** are linked via unusually short Br–Br contacts of 3.116 Å between Br(6) and Br(9) to give polymeric associates.

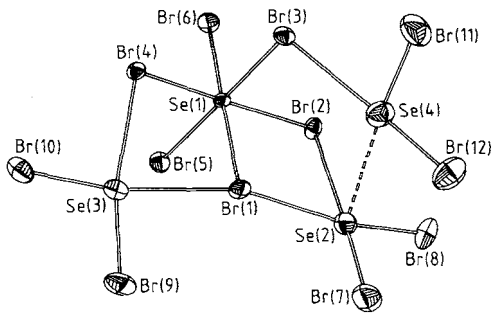


Fig. 3. Structure of **3** in crystals of **3a** [8]. Important bond lengths [Å] (all standard errors 0.003 Å): Se(1)-Br(1) 2.756, Se(1)-Br(2) 2.592, Se(1)-Br(3) 2.575, Se(1)-Br(4) 2.515, Se(1)-Br(5) 2.512, Se(1)-Br(6) 2.396, Se(2)-Br(1) 2.898, Se(2)-Br(2) 2.981, Se(2)-Br(7) 2.355, Se(2)-Br(8) 2.348, Se(3)-Br(1) 2.982, Se(3)-Br(4) 3.036, Se(3)-Br(9) 2.327, Se(3)-Br(10) 2.339, Se(4)-Br(3) 3.056, Se(4)-Br(11) 2.293, Se(4)-Br(12) 2.332, Se(1)···Se(2) 4.146, Se(1)···Se(3) 4.051, Se(2)-Se(4) 3.335.

The average Se–Br bond lengths (Figs. 1, 2 and 3) are significantly longer than those of two-electron two-center bonds, both in the case of Se^{II} as well as Se^{IV} (cf., e.g., Ref. [2]). This is consistent with a three-center four-electron model (with only one bonding MO per linear Br–Se–Br unit). As in other halochalcogenates a clear correlation between the *trans* oriented bonds is, in agreement with this model, also recognizable in **1**, **2** and **3**.[9]

The structural data of the diamagnetic compounds indicate that they belong to the Class I compounds of the Robin-Day classification,[10] i.e. that no significant valence exchange takes place. The different coordination geometries are clear indications of the different selenium valencies; as in the pure bromoselenates(II) the Se···Se distances are greater than 4 Å and thus rule out direct exchange contacts. The colors of the anions, which are darker with increasing degree of condensation, differ very little from those of the pure Se^{II} and Se^{IV} compounds; the exact measurement of the UV-VIS spectra, which presents diffi-

culties because of the equilibria present in solution, is currently being investigated.

Due to the reversibility of formation of the mixed valence bromoselenates, i.e. of their decomposition into stable $[SeBr_6]^{2\ominus}$ and $SeBr_2$, their preparative application as source material for the rather labile $SeBr_2$ in the pure state is conceivable.

Experimental

1a: A solution of $SeBr_4$ (0.88 g, 2.2 mmol) and Et_4NBr (0.46 g, 2.2 mmol) in CH_2Cl_2 (50 mL) was heated under reflux for 45 min. After cooling to 5°C, orange-red $[Et_4N]_2[Se_2Br_{10}]$ precipitated out, which, after a few hours' contact with the mother liquor, underwent decomposition, leading thereby to formation of deep-orange-red, crystalline **1a**. This is stable in moist air for a few days. Yield 22%; correct C,H,N analysis. M.p. 130°C. Raman: $\tilde{\nu}$=249 (s), 215 (vs), 153 (s), 111 (w) cm^{-1}; IR: 198 (vs) cm^{-1}.

2a: 0.98 g (2.45 mmol) of $SeBr_4$ and 0.65 g (2.45 mmol) of nPr_4NBr were dissolved at 40°C in 60 mL of CH_2Cl_2, and the solution kept at this temperature for 30 min, and then cooled to −20°C. After 2 h, reddish-black $[nPr_4N]_2[Se_5Br_{12}]$ began to precipitate which, after 2 d at −20°C, redissolved. Deep dark-red crystalline **2a** was then formed. This is air-stable for a few days. Yield 24%, correct C,H,N analysis. M.p. 121°C. Raman: $\tilde{\nu}$=265 (vs), 190 (s), 175 (s), 153 (m), 125 (s) cm^{-1}; IR: 264 (s), 206 (vs), 115 (m) cm^{-1}.

3a: 1.0 g (2.5 mmol) of $SeBr_4$ and 1.05 g (2.5 mmol) of Ph_4PBr were dissolved in 45 mL of CH_3CN at 35°C. After cooling to 20°C the solution was evaporated down under vacuum to 25 mL; after a few hours, deep-dark red **3a** crystallized at 20°C. Yield 18%; correct C,H analysis. M.p. 168°C (decomp.). Raman: $\tilde{\nu}$=255 (m), 226 (s), 163 (vs) cm^{-1}; IR: 176 (s) cm^{-1}.

Received: September 16, 1988 [Z 2970 IE]
German version: *Angew. Chem. 101* (1989) 190

[1] a) B. Krebs, V. Paulat, *Angew. Chem. 85* (1973) 662; *Angew. Chem. Int. Ed. Engl. 12* (1973) 666; b) *Z. Naturforsch. B34* (1979) 900; c) B. Krebs, K. Büscher, *Z. Anorg. Allg. Chem. 463* (1980) 56; d) B. Krebs, N. Rieskamp, A. Schäffer, *ibid. 532* (1986) 118; e) A. J. Privett, S. L. Craig, D. Y. Jeter, A. W. Cordes, R. T. Oakley, R. W. Reed, *Acta Crystallogr. Sect. C43* (1987) 2023; f) B. Krebs, K. Erpenstein, E. Lührs, unpublished.

[2] B. Krebs, A. Schäffer, S. Pohl, *Z. Naturforsch. B39* (1984) 1633.

[3] S. Pohl, W. Saak, B. Krebs, *Z. Naturforsch. B40* (1985) 251.

[4] a) S. Pohl, A. Schäffer, B. Krebs, *Z. Kristallogr. 162* (1983) 180; b) B. Krebs, E. Lührs, L. Stork, *ibid. 178* (1987) 127; c) B. Krebs, E. Lührs, L. Stork, R. Willmer, *Acta Crystallogr. Sect. A43* (1987) C-145; d) J. B. Milne, *Polyhedron 6* (1987) 849; e) cf. also B. Krebs, *Nova Acta Leopoldina 264* (1985) 131.

[5] Earlier spectroscopic evidence for haloselenates(II): K. J. Wynne, J. Golen, *Inorg. Chem. 13* (1974) 185; P. LaHaie, J. B. Milne, *ibid. 18* (1979) 632; J. B. Milne, P. LaHaie, *ibid. 22* (1983) 2425.

[6] B. Krebs, K. Erpenstein, E. Lührs, F.-P. Ahlers, unpublished.

[7] S. Hauge, K. Marøy, T. Ødegård, *Acta Chem. Scand. Ser. A42* (1988) 51, 56.

[8] Crystal data: Syntex $P2_1$ four-circle diffractometer, $Mo_{K\alpha}$ radiation, graphite monochromator, scintillation counter, $(2\theta$-$\theta)$ scan, T=143 K, empirical absorption corrections, EXTL- and SHELXTL programs, direct methods, least squares fit (Se, Br, P, Cl: anisotropic, C, N: isotropic, H: calculated coordinates, U(H)=1.2 U(C)): **1a**: orthorhombic, space group *Pnn*2, a=13.235(4), b=24.822(11), c=9.353(3) Å, V=3072.6 Å^3, Z=4, ρ_{calcd}=2.29 g cm^{-3}, $\mu(Mo_{K\alpha})$=127.0 cm^{-1}, $2\theta_{max}$=54°, 3810 independent reflections, R (R_w)=0.058 (0.050) for 2664 reflections with $I_0 > 1.96\sigma(I_0)$, 163 variables.—**2a**: monoclinic, space group $P2_1/n$, a=14.653(8), b=9.481(5), c=16.415(9) Å, β=110.09(3)°, V=2141.7 Å^3, Z=2, ρ_{calcd}=2.18 g cm^{-3}, $\mu(Mo_{K\alpha})$=118.1 cm^{-1}, $2\theta_{max}$=54°, 4995 independent reflections, R (R_w)=0.066 (0.059) for 3129 reflections with $I_0 > 1.96\sigma(I_0)$, 113 variables.—**3a**: monoclinic, space group $P2_1/c$, a=21.624(8), b=13.717(7), c=20.418(10) Å, β=95.77(3)°, V=6025.6 Å^3, Z=4, ρ_{calcd}=2.25 g cm^{-3}, $\mu(Mo_{K\alpha})$=104.7 cm^{-1}, $2\theta_{max}$=46°, 9441 unique reflections, R (R_w)=0.077 (0.057) for 4678 reflections with $I_0 > 1.96\sigma(I_0)$, 377 variables. Further details of the crystal structure investigations are available on request from the Fachinformationszentrum Energie, Physik, Mathematik GmbH, D-7514 Eggenstein-Leopoldshafen 2 (FRG), on quoting the depository number CSD-53416, the names of the authors, and the journal citation.

[9] Example: In 1 (Fig. 1) the shorter terminal bond (Se(2)-Br(7)) is opposite the longer bridge bond (Se(2)-Br(4)), and the longer terminal bond (Se(2)-Br(8)) is opposite the shorter bridge bond (Se(2)-Br(3)).

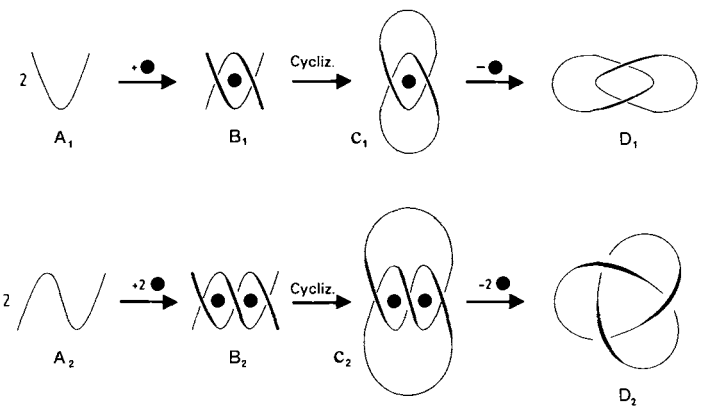
[10] M. B. Robin, P. Day, *Adv. Inorg. Chem. Radiochem. 10* (1967) 247.

A Synthetic Molecular Trefoil Knot**

By *Christiane O. Dietrich-Buchecker* and *Jean-Pierre Sauvage**

The synthesis of molecular knots has been a long-standing quest in chemistry.[1,2] Discussions about their hypothetical properties can be found in relatively old literature.[3] Such topologies are abundant in Nature since duplex circular DNA can be converted into highly knotted forms,[4] making the synthesis of knots an even more challenging problem for the chemist.

Recently, we have developed an efficient way of interlacing and interlocking molecular threads (formation of catenanes, Scheme 1, top) by taking advantage of a three-dimensional template effect around a transition metal.[5,6] We have now extended our synthetic concept to two transition metal centers connected by two bis-chelate molecular links (Scheme 1, bottom).



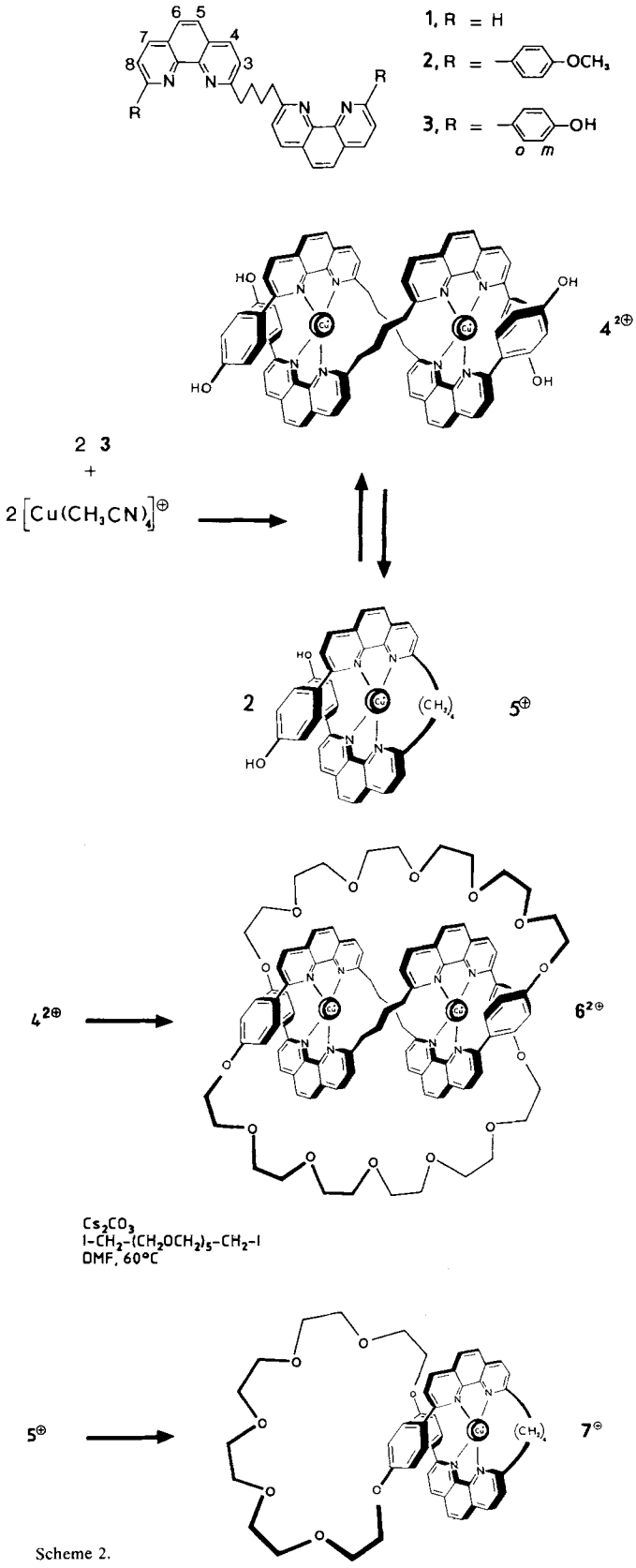
Scheme 1. Templated synthesis of interlocked macrocyclic ligands, the catenands. The function of the transition metal center is to gather two linear fragments $\mathbf{A}_1$ and to entwine them, leading to $\mathbf{B}_1$. After cyclization of $\mathbf{B}_1$ using the proper connections, $\mathbf{C}_1$ is formed. Its demetalation affords the catenand $\mathbf{D}_1$. Bottom: Strategy towards a trefoil knot using two transition metal centers as templating species. Two coordinating molecular threads $\mathbf{A}_2$ are interlaced on two transition metal centers, forming a double helix $\mathbf{B}_2$. After cyclization to $\mathbf{C}_2$ and demetalation, a knotted system $\mathbf{D}_2$ is obtained.

An important prerequisite for the success of such an approach is the formation of a helicoidal dinuclear complex. Of utmost importance is the stability of the double helix $\mathbf{B}_2$, which has to be stable under the conditions of the cyclization to $\mathbf{C}_2$. The choice of the chemical link between the two chelating subunits of each $\mathbf{A}_2$ fragment is thus crucial. Besides the chemical stability, steric parameters and flexibility are factors that also have to be examined. In particular, in the reaction of $\mathbf{A}_2$ and the transition metal ion (●), the formation of $\mathbf{B}_2$ has to be favored over that of polymeric complexes or that of the mononuclear complex by folding up of $\mathbf{A}_2$ on one metal center. Dinuclear helicoidal molecular architectures have been reported previously.[7-12] After many attempts with various linkers, we found that compounds with two 1,10-phenanthroline

[*] Dr. J.-P. Sauvage, Dr. C. O. Dietrich-Buchecker
Laboratoire de Chimie Organo-Minérale, UA 422 au CNRS,
Institut de Chimie, Université Louis Pasteur
1, rue Blaise Pascal, F-67000 Strasbourg (France)

[**] The work was supported by the CNRS. We express our gratitude to *A. Van Dorsselaer, F. Bitsch* and *R. Hueber*, for mass spectroscopy experiments and fruitful discussions. The important contribution of *J. P. Kintzinger* and *P. Maltese* to the NMR studies is also warmly acknowledged.

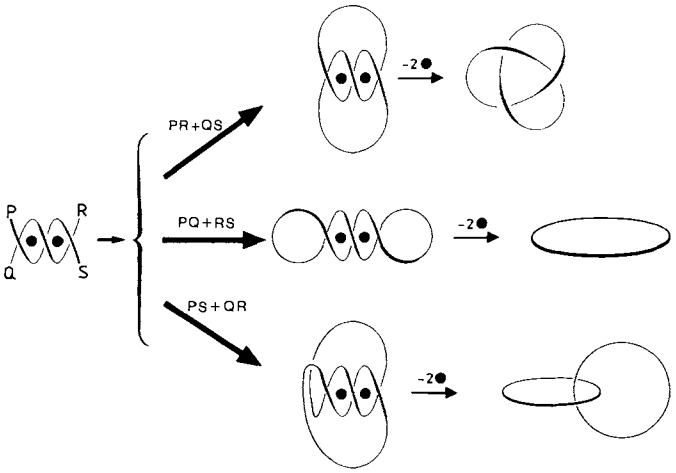
moieties connected via their 2-positions by a $-(CH_2)_4-$ tie, do indeed form a double helix when complexed to two copper(I) centers. Furthermore, by introducing appropriate functional groups at the 9-positions we have been able to make a molecular trefoil knot of the D_2 type according to the strategy depicted in Scheme 1 (bottom). The precursors used and the synthetic reactions are shown in Scheme 2.



Scheme 2.

1 was prepared in 86% yield by reaction of $Li(CH_2)_4Li$[13] with 1,10-phenanthroline (large excess) in diethyl ether at 0°C under experimental conditions resembling those previously reported for the preparation of 2,9-disubstituted-1,10-phenanthroline derivatives.[14] Addition of *p*-lithioanisole to a suspension of **1** in ether at +2°C followed by water hydrolysis and MnO_2 treatment led to **2** in 83% yield. Demethylation of **2** to **3** was carried out quantitatively under drastic conditions: HCl-pyridine at 210°C.[14b, 15] The double-helix complex $\mathbf{4}^{2\oplus}$ was prepared as a deep-red solid by addition of stoichiometric amounts of $[Cu(CH_3CN)_4]BF_4$ in CH_3CN to a solution of **3** in dimethylformamide (DMF). ^{1}H-NMR studies using the model compound **2** and copper(I) clearly show that the double-helix complex is formed together with considerable amounts of the mononuclear complex **2**-$Cu^{\oplus}$, indicating that crude $\mathbf{4}^{2\oplus}$ is probably contaminated by a large fraction of $\mathbf{5}^{\oplus}$. The complex mixture containing $\mathbf{4}^{2\oplus}$ was allowed to react under high dilution conditions[5] with two equivalents of the diiodo-derivative of hexaethyleneglycol, $ICH_2(CH_2OCH_2)_5CH_2I$,[16] in DMF at 60°C in the presence of Cs_2CO_3 (large excess). After work-up and repeated chromatographic purification (SiO_2; CH_2Cl_2/CH_3OH), the main compound isolated as its $BF_4^{\ominus}$ salt (24% yield) was shown to be the mononuclear complex $\mathbf{7}^{\oplus}$[17] formed by ring-closure of $\mathbf{5}^{\oplus}$, confirming that indeed the reaction between **3** and $[Cu(CH_3CN)_4]^{\oplus}$ leads mainly to $\mathbf{5}^{\oplus}$. In addition to $\mathbf{7}^{\oplus}$, a small amount (3% yield) of a slightly more polar copper(I) complex could be purified and isolated. This compound turned out to be the knotted system $\mathbf{6}^{2\oplus}$.

From a tetrafunctional double helicoidal precursor, several 2+2 connections are possible, the most probable ones being those depicted in Scheme 3.



Scheme 3. Some possible cyclization pathways for a tetrafunctionalized dinuclear helicoidal complex. With 1,10-phenanthrolinecopper(I) based systems, the most probable connections correspond to reaction PR + QS, leading to the desired knot.

$\mathbf{6}[BF_4]_2$ is a dark-red crystalline solid (needles) with a high resolution mass spectrum (FAB) showing a molecular peak at 1816.74 (calculated molecular weight for $\mathbf{6}^{2\oplus}$ = 1816). The ^{1}H-NMR spectrum of $\mathbf{6}^{2\oplus}$ is reproduced in Figure 1.[18]

Since $\mathbf{6}^{2\oplus}$ contains a double helix wound round two Cu^{I} ions, it is chiral. This can indeed be demonstrated in the presence of *Pirkle*'s reagent.[19] Clear splitting of peaks is observed for most aromatic signals even after addition of a small amount of chiral reagent.

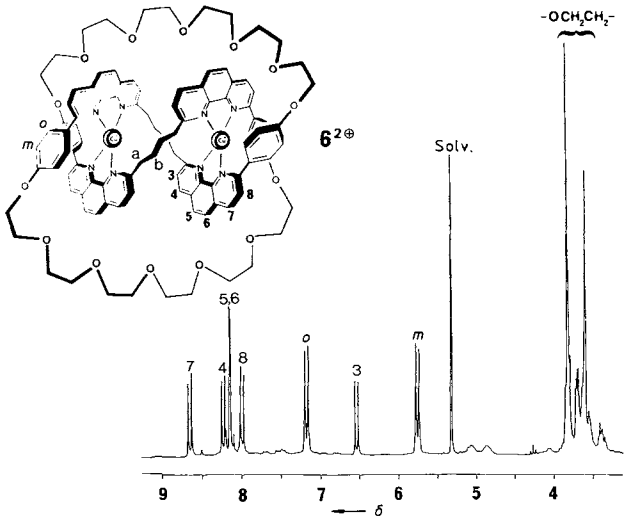
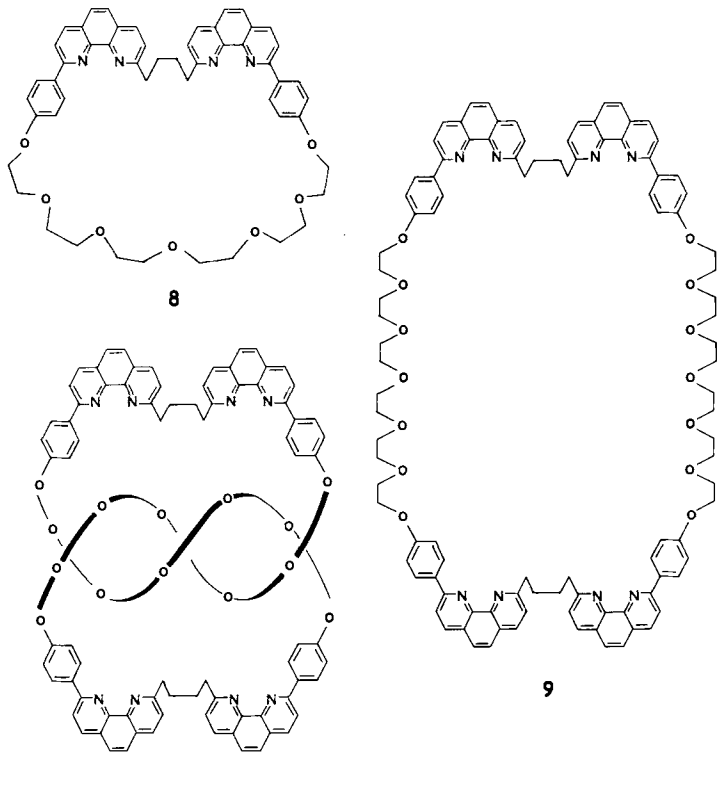


Fig. 1. ^{1}H-NMR spectrum (200 MHz) of $\mathbf{6}^{2\oplus}$ (5 mg $\mathbf{6}[BF_4]_2$ in 0.5 mL CD_2Cl_2. The $-(CH_2)_4-$ bridge shows two multiplets at $\delta = 0.5$ ($(CH_2)_b$) and 1.6 ($(CH_2)_a$).

Quantitative demetalation of the various copper(I) complexes by aqueous KCN leads to the corresponding free ligands (Scheme 4). A crystalline 43-membered ring **8** is obtained from $\mathbf{7}^{\oplus}$. It has been fully characterized. Demetalation of $\mathbf{6}^{2\oplus}$ affords the free trefoil knot **10** as a glass.

Very small amounts (ca. 0.5%) of **9**, the unraveled topological isomer of **10**, were isolated by careful chromatography of samples obtained by demetalating impure fractions from the chromatographic purification of $\mathbf{6}^{2\oplus}$. The comparison between the two isomers **9** and **10** is indeed a strong indication for the knotted topology of **10**. Both compounds have almost identical mass spectra (FAB): molecular peaks appear at nearly the same value (1690.9 for **10** and 1691.4 for **9**; calculated: 1690). Moreover, the general pattern and the various fragmentations of both compounds are strikingly similar.

By contrast, the ^{1}H-NMR spectra of **9** and **10** are remarkably different (Fig. 2). As expected, the spectra of **8** and **9** (Fig. 2a, b) are almost superimposable, whereas **10** leads to an extremely different spectrum with broad and



Scheme 4.

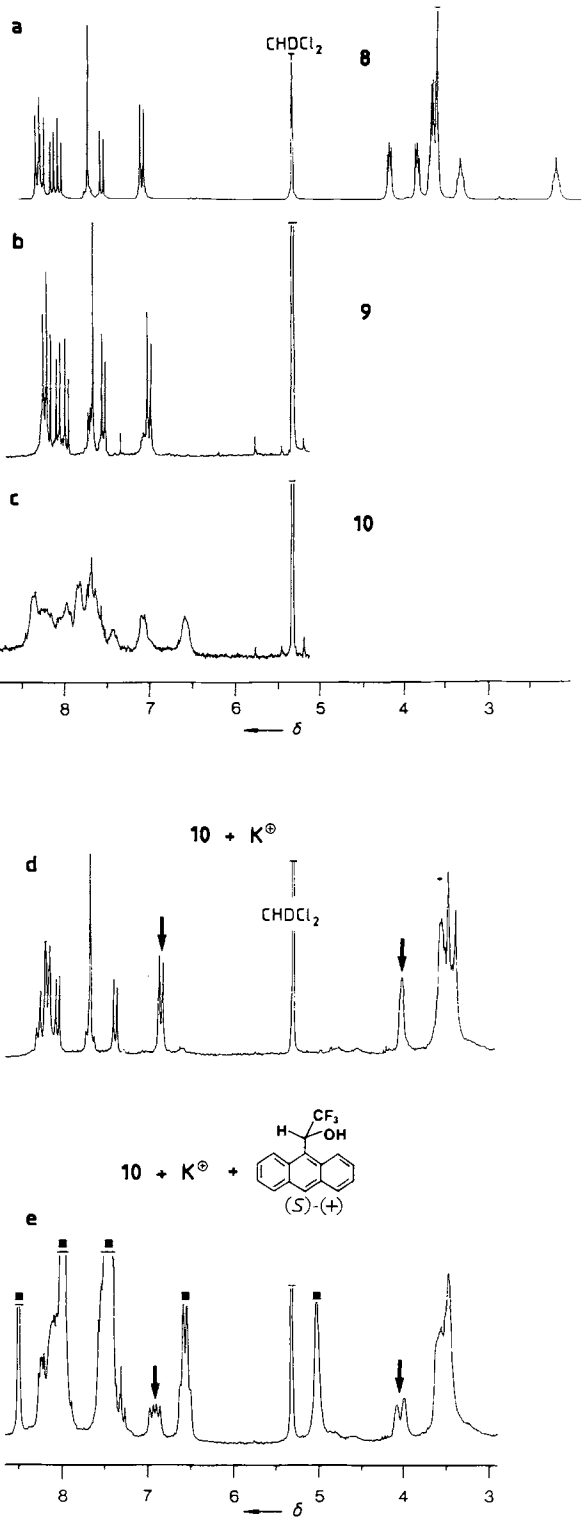


Fig. 2. a–c) 200-MHz ^{1}H-NMR spectra of **8**, **9** and **10**. d) ^{1}H-NMR spectrum of **10** after addition of KPF_6 (excess). e) Same spectrum as (d) but in the presence of *Pirkle*'s reagent; signals indicated by black squares.

poorly resolved signals spanning between $\delta = 6.5$ and 8.5 for the aromatic protons. The interconversion

$$6^{2\oplus} \underset{Cu^{+}}{\overset{CN^{\ominus}}{\rightleftharpoons}} \mathbf{10}$$

was shown to be perfectly reversible. It could be monitored by ^{1}H NMR spectroscopy and thin-layer chromatography, proving that the broad ^{1}H NMR spectrum of **10** was not due to the presence of impurities but rather that it reflects the raveled nature of its organic skeleton undergoing slow conformational changes.[20]

Unexpectedly, addition of KPF_6 to **10** leads to a drastic change in its ^{1}H NMR spectrum (Fig. 2c, d): both signal sharpening and chemical shift changes are observed. This is good evidence that $K^{\oplus}$ interacts with **10** via its O donor atoms. $K^{\oplus}$ complexation by either **8** or **9** was also detected under the same conditions, as indicated by chemical shift changes in the $-(CH_2O)-$ region in the presence of KPF_6. For the two latter complexes, no splitting of peaks was observed even after addition of large amounts of *Pirkle*'s reagent, in agreement with the achiral structure of **8** and **9**. In sharp contrast was the behavior of the $K^{\oplus}$ complex of **10**. Surprisingly large splitting of peaks was observed upon addition of *Pirkle*'s reagent, both for a $-(CH_2)-O-$ signal around $\delta = 4$ and in the aromatic region ($\delta H_m = 6.9$). This is indeed a clear demonstration that the molecular system is chiral, which is in agreement with the topological chirality of a trefoil knot.

Received: September 21, 1988 [Z 2972 IE]
German version: *Angew. Chem. 101* (1989) 192

[1] G. Schill: *Catenanes, Rotaxanes and Knots*, Academic Press, New York 1971. In particular, the last chapter contains interesting concepts and investigations of the synthesis of molecular knots.
[2] D. M. Walba, *Tetrahedron 41* (1985) 3161; D. M. Walba, J. D. Armstrong III, A. E. Perry, R. M. Richards, T. C. Homan, R. C. Haltiwanger, *ibid. 42* (1986) 1883.
[3] H. L. Frisch, E. Wasserman, *J. Am. Chem. Soc. 83* (1961) 3789; R. L. Kornegay, H. L. Frisch, E. Wasserman, *J. Org. Chem. 34* (1969) 2030; V. I. Sokolov, *Russ. Chem. Rev. (Engl. Transl.) 42* (1973) 452.
[4] K. N. Kreuzer, N. R. Cozzarelli, *Cell 20* (1980) 245; M. A. Krasnow, A. Stasiak, S. J. Spengler, F. Dean, T. Koller, N. R. Cozzarelli, *Nature 304* (1983) 559; J. D. Griffith, H. A. Nash, *Proc. Natl. Acad. Sci. USA 82* (1985) 3124.
[5] C. O. Dietrich-Buchecker, J. P. Sauvage, J. P. Kintzinger, *Tetrahedron Lett. 24* (1983) 5095; C. O. Dietrich-Buchecker, J. P. Sauvage, J. M. Kern, *J. Am. Chem. Soc. 106* (1984) 3043.
[6] J. P. Sauvage, *Nouv. J. Chim. 9* (1985) 299; C. O. Dietrich-Buchecker, J. P. Sauvage, *Chem. Rev. 87* (1987) 795, and references cited therein.
[7] G. Struckmeier, U. Thewalt, J. H. Furhop, *J. Am. Chem. Soc. 98* (1976) 278.
[8] W. S. Sheldrick, J. Engel, *Chem. Commun. 1980*, 5; *Acta Crystallogr. B 37* (1981) 250.
[9] G. C. van Stein, H. van der Poel, G. van Koten, A. L. Spek, A. J. M. Duisenberg, P. S. Pregosin, *J. Chem. Soc. Chem. Commun. 1980*, 1016; G. C. van Stein, G. van Koten, K. Vrieze, C. Brévard, A. L. Spek, *J. Am. Chem. Soc. 106* (1984) 4486.
[10] J. V. Bonfiglio, R. Bonnett, D. G. Buckley, D. Hamzetash, M. B. Hursthouse, K. M. A. Malik, A. F. McDonagh, J. Trotter, *Tetrahedron 39* (1983) 1865.
[11] J. M. Lehn, A. Rigault, J. Siegel, J. Harrowfield, B. Chevrier, D. Moras, *Proc. Natl. Acad. Sci. USA 84* (1987) 2565; see also: J.-M. Lehn, A. Rigault, *Angew. Chem. 100* (1988) 1121; *Angew. Chem. Int. Ed. Engl. 27* (1988) 1095.
[12] E. C. Constable, M. G. B. Drew, M. D. Ward, *Chem. Commun. 1987*, 1600.
[13] R. West, E. G. Rochow, *J. Org. Chem. 18* (1953) 1739; J. X. McDermott, J. F. White, G. M. Whitesides, *J. Am. Chem. Soc. 98* (1976) 6529.
[14] a) C. O. Dietrich-Buchecker, P. A. Marnot, J.-P. Sauvage, *Tetrahedron Lett. 23* (1982) 5291; b) C. O. Dietrich-Buchecker, J.-P. Sauvage, *ibid. 24* (1983) 5091; it was found as a general rule that mono-substitution occurred at low temperature (0–10°C) whereas disubstituted compounds were obtained at room temperature or above.
[15] T. J. Curphey, E. J. Hoffman, C. McDonald, *Chem. and Ind. (London) 1967*, 1138.
[16] The pure diiodo derivative of hexaethyleneglycol was obtained from PEG 300 (Fluka) following a procedure similar to that used for preparing the pentaethyleneglycol derivative: D. E. Fenton, D. Parkin, R. F. Newton, *J. Chem. Soc. Perkin Trans. 1 1981*, 449.
[17] The new compounds prepared were characterized by ^{1}H NMR (200 MHz) and mass spectroscopy (Fast Atom Bombardment = FAB). $7^{\oplus}$ has a ^{1}H NMR spectrum (CD_2Cl_2) and a mass spectrum consistent with its structure: $M_{calcd} = 908$; $M_{obs.} = 907.6$.
[18] The ^{1}H NMR spectrum of $6^{2\oplus}$ has been fully assigned by selective decoupling and by NOE and T_1 measurements. In addition, NOE measurements clearly show proximity between aromatic sites (4, 5 and 6) and some methylene groups of the hexaethyleneoxy fragment. This is in full agreement with the compactness of the system as expected from space-filling molecular models: J. P. Kintzinger, P. Maltese, private communication.
[19] W. Pirkle, M. S. Hoekstra, *J. Am. Chem. Soc. 98* (1976) 1832.
[20] High temperature ^{1}H NMR spectra recorded in [D$_6$]DMF. Indeed, the whole spectrum was well resolved with sharp signals at normal chemical shifts ($\delta = 7.3$ to 8.6) above 140°C.

Temperature Dependent Inversion of Elution Sequence in the Resolution of α-Amino Acid Enantiomers on Chiral Diamide Selectors

By *Katsunori Watabe, Rosita Charles,* and *Emanuel Gil-Av**

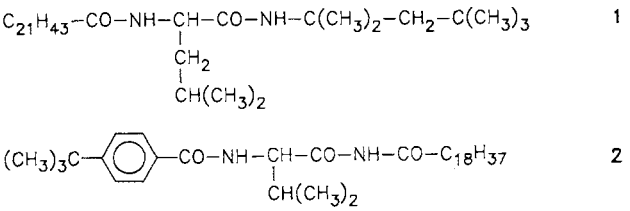
Stereoselectivity in chiral chromatography is measured by the resolution coefficient α, which also specifies the order of elution of a pair of enantiomers on a phase (selector) of given handedness.[1] On many selectors, the sequence of elution of the enantiomers of a given class of compounds was found to be consistently linked to their configuration.

In all studies carried out thus far, resolution has been found to decrease with increasing temperature. The Gibbs-Helmholtz relationship (a)[2] predicts, however, that if $\Delta\Delta H^0$ and $\Delta\Delta S^0$ are non-zero, have the same sign and are temperature independent (the general case), resolution will vanish ($\ln\alpha = 0$) at the isoenantioselective point $T_{iso} = \Delta\Delta H^0/\Delta\Delta S^0$. Thereafter, peak, reversal and improved resolution should result, as the temperature continues to be raised. This behaviour, which is known for achiral compounds,[3] had not been observed till now for enantiomers on chiral selectors.[4,5] The detection of such a peak inversion in chiral systems was of fundamental interest and of importance for understanding the influence of temperature, $\Delta\Delta H^0$ and $\Delta\Delta S^0$ on the stereoselectivity in the chromatographic separation of enantiomers.

$$\ln\alpha = \frac{\Delta\Delta S^0}{R} - \frac{\Delta\Delta H^0}{R}\frac{1}{T} \qquad \text{(a)}$$

It was observed in 1985[6] that the enantiomers of *N*-acetyl-valine-*tert*-butylamide were eluted at 170°C from a diamide phase in the reversed order as compared to a series of *N*-TFA-α-amino acid *tert*-butylamides, which had been studied previously.[7] Thereupon we investigated[8] the temperature dependence of the resolution coefficients for *N*-docosanoyl-L-leucine-(1,1,3,3-tetramethylbutyl)amide **1** (up to 220°C) and *N*-*para*-*tert*-butylbenzoyl-L-valine octadecylamide **2** (up to 200°C), coated on whisker-walled glass capillaries of 2–8 m length (up to 40000 plates). The selectands examined were optically enriched *N*-acyl-*tert*-butylamides of α-amino acids (Fig. 1), *N*-TFA isopropyl

[*] Prof. Dr. E. Gil-Av, Dr. K. Watabe, R. Charles
Department of Organic Chemistry, Weizmann Institute of Science
Rehovot 76100 (Israel)



1

2

esters of α- and γ-amino acids and *O*-pivaloyl *N*-TFA 2-amino alkan-1-ols (Fig. 2).

The plots in Figure 1 (for phase **1**) demonstrate that all curves for diamide selectands, except for the proline derivative, have a linear branch which crosses the $\ln\alpha = 0$ line and then shows inversion of the order of elution in agreement with the Gibbs–Helmholtz equation. The isoenantioselective points lie in the range 130–150 °C. Corresponding measurements on phase **2** confirmed these results. Re-examination of previous results[7] indicated similar behavior of diamide selectands on other diamide phases.[9] Recently, evidence for the occurrence of the inversion phenomenon for additional classes of compounds[10] and other selectors[11] was reported by other groups.

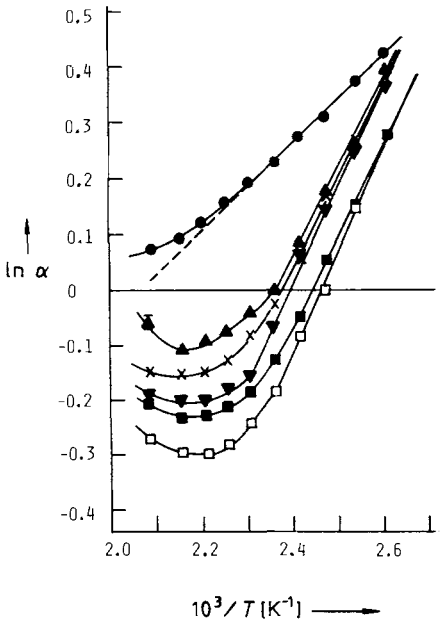


Fig. 1. Plots of $\ln\alpha$ versus $1/T$ for *N*-TFA-amino acid *tert*-butylamides on phase **1**. ● = proline, ▲ = alanine, × = α-aminobutyric acid, ▼ = leucine, ■ = valine, □ = *N*-acetylvaline *tert*-butylamide.

Previous failure to observe inversion would appear to be due largely to high T_{iso} values, at which the phase or the selectand might be unstable. In addition, the capacity ratios (k') decrease strongly with increasing temperature. Consequently, the term $k_2'/(k_2'+1)$ in the equation (b) for the peak resolution factor

$$R = \frac{\sqrt{N}}{4}\,\frac{\alpha-1}{\alpha}\,\frac{k_2'}{k_2'+1} \qquad \text{(b)}$$

becomes smaller so that for a detectable separation larger minimal α values are required. The dotted lines in Figure 2 delimit schematically the region which widens with rising temperature, in which, for a given plate number N, the peaks cannot be separated and the α values are undeterminable. Furthermore, the thermodynamic parameters might not remain constant at higher temperatures, leading to non-linearity of the Gibbs–Helmholtz plots.[2, 12]

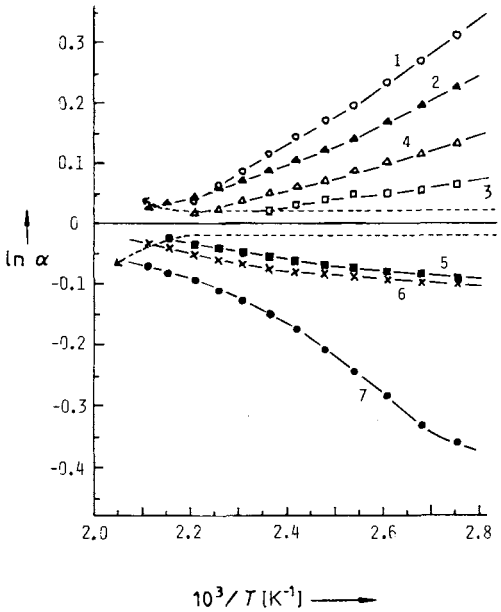
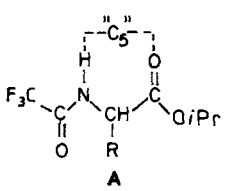


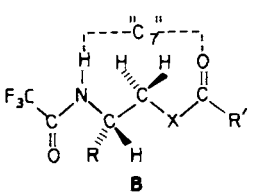
Fig. 2. Plots of $\ln\alpha$ versus $1/T$ for *N*-TFA-amino acid isopropylesters (1, 2, 3, 4, 6) and *O*-pivaloyl *N*-TFA-amino alcohols (5, 7) on phase **1**. 1 Alanine, 2 glutamic acid, 3 aspartic acid, 4 phenylglycines, 5 2-aminoheptan-1-ol, 6 γ-amino-δ-methylheptanoic acid, 7 leucinol. Separation is not possible in the region between the dotted lines.

A combination of these effects might explain the deviation from linearity of the curves in Figure 2 for *N*-TFA-amino acid esters and derivatives of 2-aminoalkan-1-ols on phase **1**. The corresponding plots show departures from linearity and merge into or approach the non-resolution zone at the maximum temperatures used.

The plots that exhibit inversion (Fig. 1) have a non-linear part with an inflexion point, after which the curve approaches the x-axis. The simultaneous occurrence of two resolution mechanisms with opposite enantioselectivities could explain the observed shape of the curves. It is known[14] that compounds that differ in the type of association which they form with the diamide phase can exhibit opposite orders of elution for the enantiomers. Thus, the *N*-TFA isopropyl esters of α-amino acids, which present a "C_5" moiety (**A**) to the phase, have $\alpha > 1$, whereas *N*-TFA-γ-amino acid esters and the 2-amino alkan-1-ol derivatives, which have a "C_7" moiety (**B**), have the opposite order of elution ($\alpha < 1$) (Fig. 2).



A

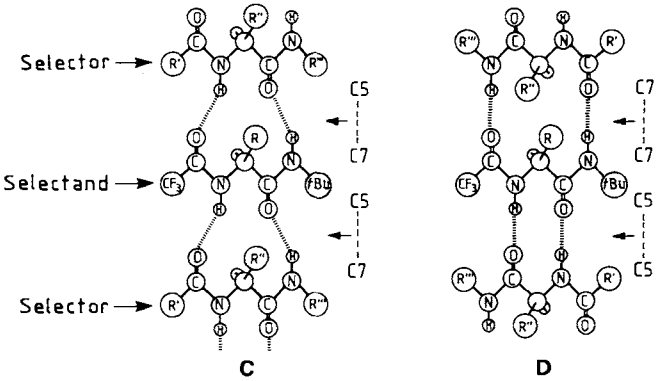


B

X = CH_2, R' = O*i*Pr
X = O, R' = *t*Bu

On the other hand, a phase may form associates of opposed stereoselectivity with the *same* selectand. Thus, the

N-TFA-*tert*-butyl amides of α-amino acids can intercalate between a diamide solvent in either a parallel (**C**) or an antiparallel (**D**) fashion (Scheme 1). The resulting hydrogen bonded structures and the orientation of the asymmetric centers towards each other are not the same. For each of these two modes of intercalation there should be a corresponding $\ln\alpha$ vs. $1/T$ plot analogous, respectively, to the curves with $\alpha > 1$ and $\alpha < 1$ of Figure 2. Superimposition of such individual contributions to the total resolution, if of appropriate magnitude, could lead to an overall curve, as found experimentally, i.e., a linear branch, inversion and an inflexion point.



R = CH_3, C_2H_5, $CH(CH_3)_2$, $CH_2CH(CH_3)_2$,

R' = n-$C_{21}H_{43}$, p-$(CH_3)_3C$-C_6H_4,

R'' = $CH_2CH(CH_3)_2$, $CH(CH_3)_2$

R''' = $C(CH_3)_2CH_2C(CH_3)_3$, n-$C_{18}H_{37}$,

Scheme 1. Parallel (**C**) and antiparallel (**D**) intercalation of an *N*-TFA-L-α-amino acid *tert*-butylamide in a diamide selector, with hydrogen bonding of type "C_5-C_7" (**C**) and "C_7-C_7" + "C_5-C_5" (**D**).

The proposed explanation is supported by the behavior of the *N*-TFA-*tert*-butyl amide of proline. This diamide selectand cannot intercalate between the phase molecules, as shown in Scheme 1, and indeed, behaves quite differently from the other diamide selectands (see Fig. 1). It should be emphasized that such a double mechanism of resolution (Scheme 1) is not a condition for the observation of inversion, but it might shift the T_{iso} point into a favorable range.

In conclusion, the sense of the stereoselectivity of a chiral selector-selectand system is not to be considered a constant property, but is temperature dependent. This is of particular importance for the determination of configuration from chromatographic data. In many cases, however, inversion of the order of elution cannot be observed, largely because of too high T_{iso} points. It is noteworthy that a temperature dependent inversion of the chirality of the products of certain stereoselective reactions has been observed[15, 16] and was interpreted analogously in terms of the Gibbs-Helmholtz relationship involving the thermodynamic parameters of the relevant transition states.[16]

Received: August 12, 1988 [Z 2924 IE]
German version: *Angew. Chem. 101* (1989) 194

[1] In this communication $\alpha = \alpha_{L/D}$, i.e., the ratio of the adjusted retention volumes of the L- and D enantiomers. For $\alpha > 1$, the D-isomer is eluted before the L-isomer. for $\alpha < 1$, the opposite applies.

[2] M. Lederer (*Proc. Int. Congr. Surf. Act. 2nd 1957*, p. 178) used the Gibbs-Helmholtz relationship to correlate the variation of R_f values with temperature.
[3] M. R. Hoare, Y. H. Purnell, J. H. Purnell, *Trans. Faraday Soc. 52* (1956) 222.
[4] B. Koppenhöfer, E. Bayer, *Chromatographia 19* (1984) 123.
[5] V. Schurig, R. Link, unpublished.
[6] R. Charles, E. Gil-Av, unpublished results.
[7] S.-C. Chang, R. Charles, E. Gil-Av, *J. Chromatogr. 202* (1980) 247.
[8] Preliminary communication; see K. Watabe, R. Charles, E. Gil-Av, *Int. Symp. Adv. Chromatogr. 23rd 1986* (Chiba, Japan), Abstracts p. 83.
[9] S.-C. Chang (University of Gainsville, Fl.), personal communication.
[10] B. Koppenhöfer, personal communication.
[11] We wish to thank Prof. *V. Schurig* for communicating his relevant observations in complexation gas chromatography prior to publication; see V. Schurig, J. Ossig, R. Link, *Angew. Chem. 101* (1989) 197; *Angew. Chem. Int. Ed. Engl. 28* (1989) 194.
[12] Dilution of diamide selectors by apolar solvents causes an increase of the resolution coefficients of the *N*-TFA α-amino acid esters [13]. This has been ascribed to dissociation of the hydrogen bonded network of the selector and to the higher stereoselectivity of the non-associated form. A similar change could occur on raising the temperature, leading to an upward curvature of the Gibbs-Helmholtz plot and implying that $\Delta\Delta H^0$ and/or $\Delta\Delta S^0$ depend on the temperature.
[13] T. Hobo, S. Suzuki, K. Watabe, E. Gil-Av, *Anal. Chem. 57* (1985) 364.
[14] B. Feibush, A. Balan, B. Altman, E. Gil-Av, *J. Chem. Soc. Perkin Trans. 2 1979*, 1230.
[15] H. Pracejus, A. Tille, *Chem. Ber. 96* (1963) 854.
[16] I. Ugi, *Chimia 40* (1986) 340.

Evidence for a Temperature Dependent Reversal of the Enantioselectivity in Complexation Gas Chromatography on Chiral Phases**

By *Volker Schurig,** *Joachim Ossig*, and *Rainer Link*

A temperature dependent reversal of the enantioselectivity (i.e., of the sign of $\Delta_{R,S}(\Delta G^0)$) of a defined, non-racemic stationary phase (selector) in the chromatographic separation of a chiral substrate (selectand) has been predicted on the basis of the temperature term in the Gibbs-Helmholtz relationship (a)[1]

$$RT\ln(K_R/K_S) = -\Delta_{R,S}(\Delta G^0) = -\Delta_{R,S}(\Delta H^0) + T\Delta_{R,S}(\Delta S^0) \quad (a)$$

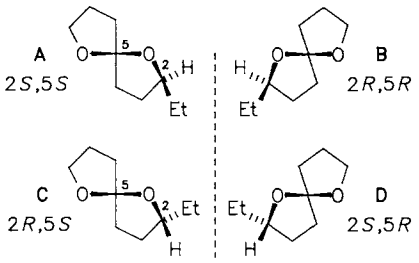
$$T_{iso} = \Delta_{R,S}(\Delta H^0)/\Delta_{R,S}(\Delta S^0) \quad (b)$$

(where **R** arbitrarily represents the enantiomer which is eluted after its **S** antipode from a chiral column). When $\Delta_{R,S}(\Delta G^0) = 0$ ($K_R = K_S$, no enantiomer separation), the isoenantioselective temperature T_{iso} [Eq. (b)] is reached. At T_{iso}, peak coalescence ('of the third kind'[2]) occurs; below it the order of elution is governed by $-\Delta_{R,S}(\Delta H^0)$ and above it by $\Delta_{R,S}(\Delta S^0)$). At the coalescence temperature T_{iso} (no enantiomer separation) the sign of enantioselectivity will change.[3]

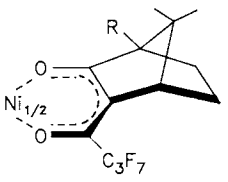
The first gas chromatographic evidence for a temperature dependent reversal of the enantioselectivity of a chiral stationary phase was obtained by *Watabe, Charles* and *Gil-Av* in a hydrogen-bonding selectand-selector system.[4] Here we report a further example which was observed by enantioselective coordination in complexation gas chromatography and is characterized by a low value of T_{iso}. In the gas chromatographic separation of the enantiomers of (*E*)-2-ethyl-1,6-dioxaspiro[4.4]nonane **1b** on nickel(II)-bis[3-(heptafluorobutanoyl)-(1*S*)-10-methylenecamphorate]

[*] Prof. Dr. V. Schurig, Dipl.-Chem. J. Ossig, Dr. R. Link
Institut für Organische Chemie der Universität
Auf der Morgenstelle 18, D-7400 Tübingen (FRG)

[**] This work was supported by the Deutsche Forschungsgemeinschaft and the Fonds der Chemischen Industrie. We wish to thank Prof. *E. Gil-Av*, Rehovoth, Israel, for communicating his results prior to publication.



1a = A + B
1b = C + D



2a, R = CH_3
2b, R = $CH{=}CH_2$

2b[5] the coordination interaction ($K_{mean}=(K_C+K_D)/2$) steadily decreases between 30°C and 150°C. No separation of the enantiomers **C** and **D** is observed between 70°C and 90°C. At 60°C **D** is eluted after **C** whereas at 140°C **C** is eluted after **D** (Fig. 1). Most important is the observation that enantiomer discrimination increases with increasing temperature above the coalescence region (Fig. 2), although the total coordination interaction decreases, as expected. Thus, the requirement of the Gibbs-Helmholtz equation of an increase of $+\Delta_{D,C}(\Delta G^0)$ above T_{iso} is fulfilled. Unfortunately, because of the decrease of the selectand-selector coordination at higher temperatures and the configurational lability of the chiral spirocenter of **1**, which causes characteristic interconversion profiles[2,6] (cf. Fig. 2), investigations could only be carried out up to 150°C.

The determination of the Gibbs-Helmholtz parameters of the enantioselective association between **1b** and **2b** from relative retention data[2,7] revealed a linear relationship between $R\cdot\ln(K_D/K_C)$ and 1/T (measured at five degree intervals between 50 and 65°C) with $-\Delta_{D,C}(\Delta H^0)=0.62$ kcal mol^{-1} and $\Delta_{D,C}(\Delta S^0)=-1.75$ cal mol^{-1} K^{-1},[8] from which $T_{iso}=354$ K (80°C) is calculated[9] (Fig. 3); this value is in agreement with the experiment (Fig. 2). Peak coalescence is observed for the enantiomers **A** and **B** of the (*Z*) diastereomer **1a** at 60°C.

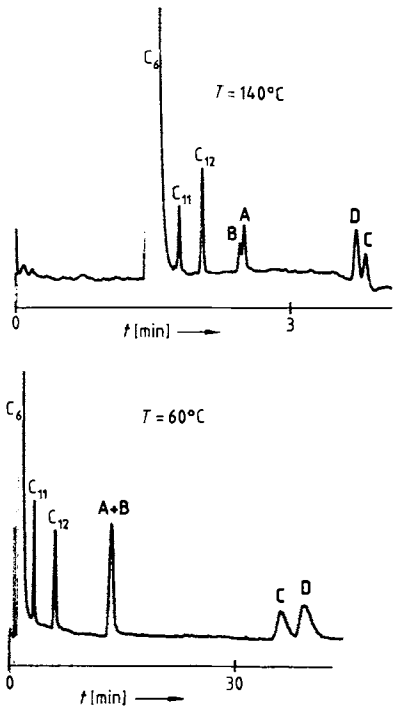


Fig. 1. Temperature dependent reversal of the enantioselectivity of **2b** (ca. 0.15 M in OV-101) in the separation of **1b** (enriched in the **D** enantiomer) by complexation gas chromatography. Column: 25 m × 0.25 mm fused silica capillary, 0.2 μ stationary phase, carrier gas: N_2. C_6 = *n*-hexane (solvent), C_{11} = *n*-undecane, C_{12} = *n*-dodecane.

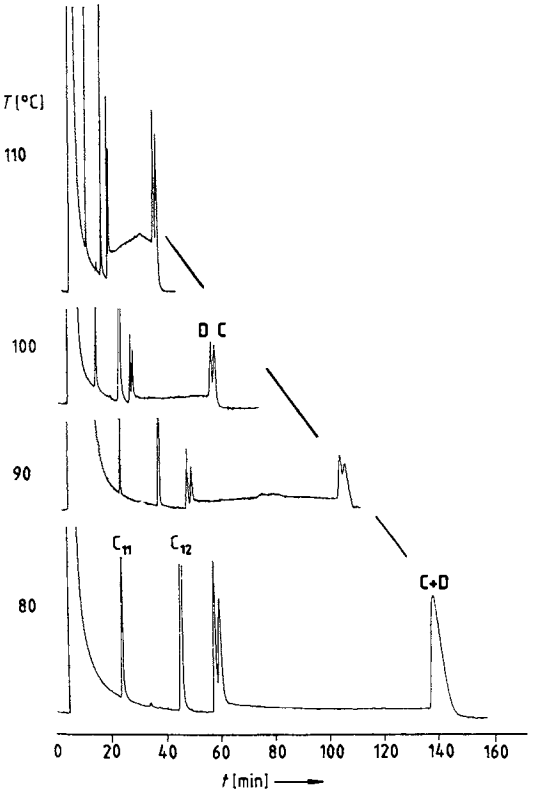


Fig. 2. Peak coalescence ('of the third kind') for the enantiomers **C** and **D** of **1b** (racemic) in complexation gas chromatography on **2b** (0.1 M in OV-101) at 80°C and increase of enantiomer discrimination with increasing temperature. Column: 34.2 m × 0.25 mm glass capillary, carrier gas: 1.0 bar N_2. C_{11} = *n*-undecane, C_{12} = *n*-dodecane.

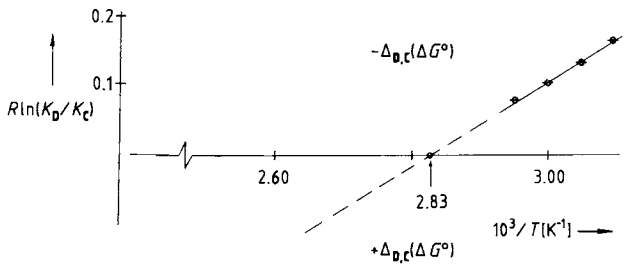


Fig. 3. Extrapolation to determine the isoenantioselective temperature T_{iso} for the separation of **1b** on **2b**. $R\cdot\ln(K_D/K_C)$ (T[°C]): 0.165 (50); 0.136 (55); 0.104 (60); 0.080[5] (65).

The findings could well be of considerable importance for the understanding of mechanistic aspects of enantioselectivity in chromatography, in particular, and of enantiomer recognition in chiral environments, in general. The influence of temperature on the discrimination of enantiomers will now have to be considered in rationalizing chiral recognition. In complexation gas chromatography, exceptions[2] to the rules correlating the absolute configurations of structurally closely related selectands with their

order of elution from chiral selectors[10] as well as unsatisfactory enantiomer separation for particular selectands[11] may well be due to the temperature dependence of the enantioselectivity, particularly for temperatures close to T_{iso}. It is intriguing to realize that above T_{iso}, preferential recognition of one enantiomer is not caused by stronger binding to a non-racemic matrix but is due to the higher degree of disorder in the resulting chemical interaction.

Received: August 23, 1988 [Z 2938 IE]
German version: *Angew. Chem. 101* (1989) 197

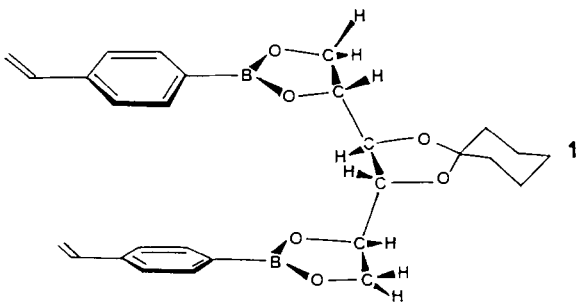
[1] a) B. Koppenhoefer, *Dissertation*, University of Tübingen 1980; b) B. Koppenhoefer, E. Bayer, *Chromatographia 19* (1984) 123; c) V. Schurig, *Angew. Chem. 96* (1984) 733; *Angew. Chem. Int. Ed. Engl. 23* (1984) 747.
[2] V. Schurig, W. Bürkle, *J. Am. Chem. Soc. 104* (1982) 7573.
[3] In principle, a temperature-dependent reversal of the enantioselectivity may also arise from structural or configurational changes in the non-racemic stationary phase upon heating or from changes of the individual contributions of competing mechanisms of chiral recognition.
[4] K. Watabe, R. Charles, E. Gil-Av: *23rd Int. Symp. Adv. of Chromatogr. 1986* (Chiba, Japan), Abstracts, p. 83; cf., *Angew. Chem. 101* (1989) 194; *Angew. Chem. Int. Ed. Engl. 28* (1989) 192.
[5] V. Schurig, A. Ossig, R. Link, *J. High Resolut. Chromatogr. Chromatogr. Commun. 11* (1988) 89.
[6] a) V. Schurig in J. D. Morrison (Ed.): *Asymmetric Synthesis, Vol. 1*, Academic Press, New York 1983, p. 59; b) V. Schurig, *J. Chromatogr. 441* (1988) 135.
[7] V. Schurig, R. Link in D. Stevenson, I. D. Wilson (Eds.): *Chiral Separations*, Plenum, London, in press.
[8] The enantioselective selectand-selector system **1b** and **2b** shows some unusual features which are not fully understood at present. Although the temperature-dependent reversal of the elution order of **1b** on **2b** is fully reproducible, $-\Delta_{D,C}(\Delta G^0) = RT \cdot \ln(K_D/K_C)$ almost doubled at, e.g., 60°C with increasing time of operation of the column, while K_{mean} remained essentially unchanged. Also, an excessive peak-broadening, reaching a maximum at T_{iso} has been observed both for the racemic mixture and the single enantiomers.
[9] Recently, in a careful study of the temperature dependence of the separation of **1a** and **1b** on **2a** (1*R*) in SE-54 polysiloxane in five degree intervals between 80 and 120°C, T_{iso} values as high as 200°C have been extrapolated for these *Z*/*E* isomers [7].
[10] V. Schurig, B. Koppenhöfer, W. Bürkle, *Angew. Chem. 90* (1978) 993; *Angew. Chem. Int. Ed. Engl. 12* (1978) 937.
[11] Thus, isopropyloxirane is not resolved on **2a** at 60°C (T_{iso}) [2]. Besides, it also shows a temperature dependent reversal of the elution sequence: V. Schurig, D. Wistuba, unpublished.

Can Polystyrene be Optically Active?**

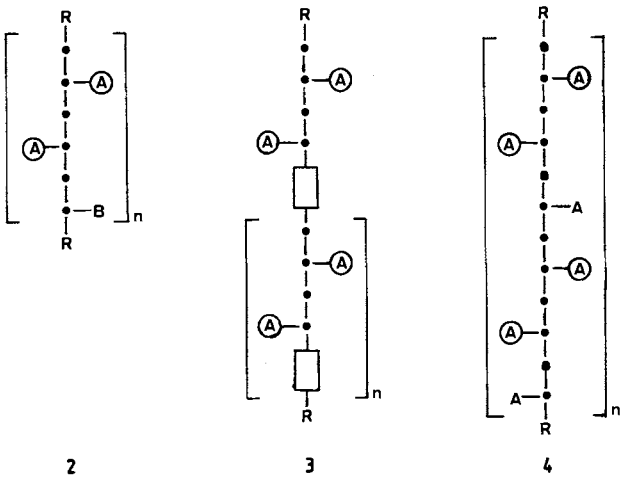
By *Günter Wulff** and *Pradeep K. Dhal*

Dedicated to Professor Kurt Heyns on the occasion of his 80th birthday

The question, as to whether polymers based on vinyl monomers can exhibit optical activity arising from a chiral configuration of the main chain (main chain chirality) has long been a subject of discussion. The conclusion of this debate, after consideration of all the commonly encountered and well-known structures of both homo- and copolymers, revealed that they are not expected to exhibit any such characteristics.[2] Careful symmetry considerations have shown recently that, particularly in the case of copolymers, several chiral structures are possible which should be able to exhibit optical activity.[1,3] By copolymerizing the mannitol derivative **1** with different comonomers and subsequent cleavage of the mannitol template, optically active copolymers (e.g., poly(4-vinylphenylboronic acid-co-styrene)) consisting of asymmetric triads of type **2** were obtained.[4-6]



1



2 **3** **4**

In this example, the diads having A substituents (4-vinylphenyl boronic acid residues incorporated via the mannitol derivative **1**) are decisive for chirality (in this case, the diad has the (*S*,*S*)-configuration).[6] The carbon atoms bearing B substituents do not represent stereogenic centers and essentially serve to separate the chiral diads from one another. Therefore, this spacer can also be composed of a relatively long chain fragment (stereoregular or atactic) of comonomer units (see **3**).[1,6] This gives rise to the question of whether a chain fragment consisting of an atactic sequence of homopolymer could fulfill the requirements of a spacer for the diads as well. If this were so, it would be possible to prepare, for the first time, optically active vinyl homopolymers possessing well-defined main chain chiral configurations.

In order to address this question, a systematic model study was carried out for all possible partial chain structures. We analyzed to what extent the asymmetric arrangement at the centers of the diad, which originally had a defined absolute configuration, is retained upon introduction of intermittent atactic units. The following essential simplifications were introduced:

a) Chain fragments consisting of one, two, or three monomer units with a statistical distribution of all possible configurations, were considered to serve as appropriate bridging groups between the diads in **3**.

[*] Prof. Dr. G. Wulff, Dr. P. K. Dhal
Institut für Organische Chemie und
Makromolekulare Chemie der Universität
Universitätsstrasse 1, D-4000 Düsseldorf (FRG)

[**] On the Chirality of Polyvinyl Compounds, Part 9. This work was supported by the Minister für Wissenschaft und Forschung des Landes Nordrhein-Westfalen and the Fonds der Chemischen Industrie. Part 8: [1].

b) Two stereocenters on each side of the investigated center were taken into account in determining the asymmetry of the centers in the tactic diads. Moreover, it was assumed that the arrangement of these four neighboring stereocenters would mainly govern the rotational contributions arising from the asymmetric center. The remaining parts of both chains were regarded as being identical (see Fig. 1).

c) It was assumed that identical partial structures within the chain would bring about optical rotations of the same sign for the entire molecule.

Although the introduction of these simplifications is not free from problems, in our opinion this approach is adequate for the assessment of possible effects.

Inspection of chain structures in the light of the above model reveals that, for a separating unit consisting of varying number of monomers, at least 25% of all the centers of the diads are stereogenic and chirotopic (asymmetric) and could contribute to the optical rotation. As an illustration, all possible partial structures for a polymer chain with two monomeric units in the spacer are shown in Figure 1. By taking the central carbon atom (one of the centers of the diad, in the box) as reference, it is evident that in formulas **c** and **e** this center is chirotopic but not stereogenic and that in formulas **d** and **f** it is stereogenic but not chirotopic (pseudo-asymmetric). In the arrangements **a**, **b**, **g**, and **h**, the central carbon atom is stereogenic and chirotopic (asymmetric). However, the structural arrangements in formulas **b** and **h** are mirror images of each other. Consequently, only the central stereogenic centers in the diastereomeric arrangements **a** and **g** (i.e., 25% of all centers) are expected to contribute appreciably to the optical rotation (same or opposite sign). Similar results are obtained when three or more monomeric units are present in the atactic part of the spacer. In contrast, if a single monomeric unit constitutes the separating component, half of the centers of the diads should be chirotopic and stereogenic (asymmetric). This type of chain configuration corresponds to the earlier discussed homopolymer type consisting of chiral hexads **4**.[1, 2c, 3]

From the above analysis, it appears that for chain structures of type **3** with separating units consisting of atactic homopolymer fragments, optical activity, albeit to a moderate extent, can be expected. The synthesis of this structure involved copolymerization of the monomer **1** with styrene in various molar ratios (see Table 1), whereby removal of the 3,4-*O*-cyclohexylidene-D-mannitol template yielded optically active copolymers with optical rotations in the range $[\alpha]_{365}^{30} = -28°$ to $-36°$ (Fig. 2). Quantitative deboronation using $AgNO_3/NH_3$ in acetone[6] resulted in the formation of the homopolymer **6a** containing distyryl

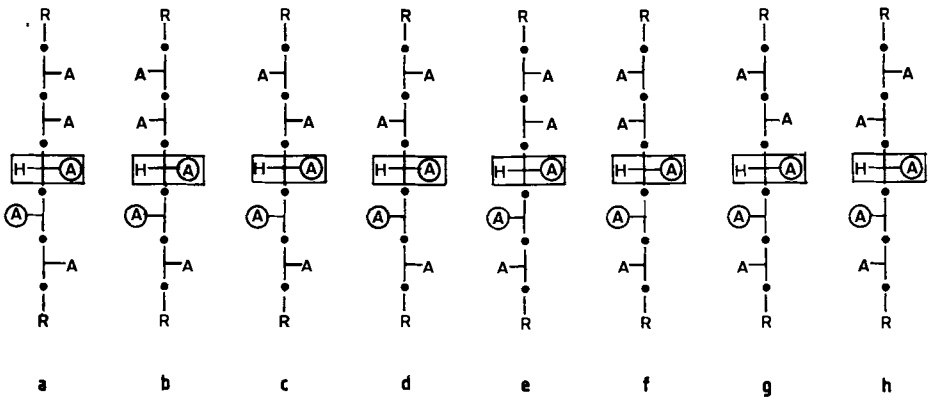


Fig. 1. Chain fragments consisting of a tactic diad of defined absolute configuration (in circles) with statistical distribution of all possible configurations in the atactic part. The center under consideration is indicated by a box. Two neighboring stereocenters on either side are taken into consideration. The separating atactic component consists of two or more monomeric units.

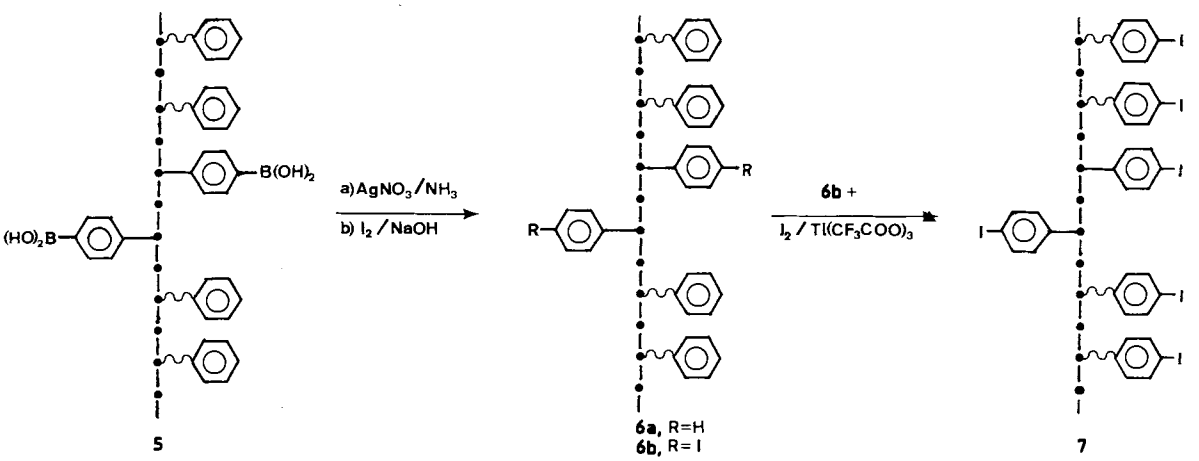


Fig. 2. Preparation of optically active homopolymers.

diads of known absolute configuration in an otherwise atactic polystyrene. As can be seen from Table 1, for certain compositions, distinct optical rotations were observed. Since the boric acid residues could be removed quantitatively, the possibility of any contribution from residual 4-(dihydroxyboryl)styryl diads to the observed optical activity can be ruled out. Furthermore, the circular dichroic (CD) spectrum of the polymer **6a** ($\lambda = 217$ nm, $[\Psi] = -245°$) does not resemble that typically found for 4-(dihydroxyboryl)-styryl diads[7] ($\lambda = 234$ nm, $[\Psi] = -2656°$) as in the case of **5**, but clearly resembles that of the distyryl diads ($\lambda = 217$ nm, $[\Psi] = -2395°$) present in the deboronated copolymers of **1** with methacrylonitrile.

Reduction in the optical activity of **6a** to one tenth of the value compared with the copolymer **5** could be explained in the following manner:

a) Approximately 25% of the total (S,S)-diads of **5** only contribute to the optical activity of **6a**.
b) The diastereomeric arrangements **a** and **g** might result in optical rotations of opposite sign.
c) The molar rotational contributions of chain segments bearing comonomer units are likely to be significantly higher than the corresponding homopolymers (**a** and **g**).

Using an analogous procedure, optically active poly(4-iodostyrene) was prepared. **5** was converted first to an optically active poly(styrene-co-4-iodostyrene) **6b** by replacing the boric acid residues with iodine.[8] This copolymer was subsequently subjected to thallium(III) trifluoroacetate catalyzed iodination[9] to produce the desired poly(4-iodostyrene). These homopolymers also showed distinct optical activity for particular compositions.

Table 1. Optical activity of co- and homopolymers (in THF). Polymer **5** was synthesized by radical copolymerization of **1** with styrene in various molar ratios followed by removal of the template [6]. Further details of the modification of **5** are outlined in the text and Fig. 2. The molecular weights of the polystyrene samples **6a**, as determined by GPC measurements using a polystyrene standard, were found to lie in the range $\overline{M} = 30000$–35000 [a].

Experiment No.	Mole fraction of **1** in monomer	in polymer	$[\alpha]_{365}^{20}$ [°] **5**	**6a**	**6b**	$[\alpha]_{436}^{20}$ [°] **7**
1	0.15	0.23	−31	−1	−36	−1
2	0.21	0.32	−36	−3.5	−44	−4.0
3	0.24	0.38	−34	−3.0	−37	−4.5
4	0.31	0.40	−33	−1.5	−34	0
5	0.35	0.47	−28	−0.5	−24	−1

[a] Representative physical data and elemental analyses for the polymers: polystyrene **6a** (No. 2): $\alpha_{measured} = -0.012 \pm 0.002°$ ($c = 0.32$), elemental analysis: calcd. C 92.26, H 7.74, found C 92.34, H 7.69; **6a** (No. 3): $\alpha_{meas.} = -0.011 \pm 0.002°$ ($c = 0.35$), found C 92.08, H 7.82; poly(4-iodstyrene) **7** (No. 2): $\alpha_{meas} = -0.015 \pm 0.002°$ ($c = 0.38$), calcd. C 41.77, H 3.06, found C 41.80, H 2.77; **7** (No. 3): $\alpha_{meas.} = -0.015 \pm 0.002°$ ($c = 0.33$), found C 41.88, H 2.70.

It has thus become possible, for the first time, to synthesize optically active homopolymers with well-defined structures based on 1-substituted olefins. The observed optical activity unequivocally originates from the chiral configurations in the main chain. Homopolymers with low optical activity, e.g., of the methacrylate type (for a concise survey see Ref. [1]) reported in the past have always remained ambiguous with respect to their structures and mechanisms of formation. As the possibility of a configurational chirality in the main chain was not conceivable, in some cases the optical activity of these polymers was attributed to a chiral conformation.

Received: August 29, 1988;
revised: October 4, 1988 [Z 2945 IE]
German version: *Angew. Chem. 101* (1989) 198

CAS Registry number:
(**1**) (styrene) (copolymers), 110590-46-0.

[1] G. Wulff, *Angew. Chem. 101* (1989) 22; *Angew. Chem. Int. Ed. Engl. 28* (1989) 21.
[2] General review articles dealing with optical activity of polymers: a) E. Selegny (Ed.): *Optically Active Polymers*, Reidel, Dordrecht 1979; b) M. Fontanille, A. Guyot (Eds.): *Recent Advances in Mechanistic and Synthetic Aspects of Polymerization*, Reidel, Dordrecht 1987, pp. 399–470; c) M. Farina, *Top. Stereochem. 17* (1987) I.
[3] Reviews: a) G. Wulff, *Nachr. Chem. Tech. Lab. 33* (1985) 956; b) in [2b], p. 399.
[4] G. Wulff, K. Zabrocki, J. Hohn, *Angew. Chem. 90* (1978) 567; *Angew. Chem. Int. Ed. Engl. 17* (1978) 535.
[5] G. Wulff, J. Hohn, *Macromolecules 15* (1982) 1255.
[6] G. Wulff, R. Kemmerer, B. Vogt, *J. Am. Chem. Soc. 109* (1987) 7449.
[7] G. Wulff, P. K. Dhal, *Macromolecules 21* (1988) 571.
[8] N. P. Bullen, P. Hodge, F. G. Thorpe, *J. Chem. Soc. Perkin Trans. 1 1981*, 1863.
[9] G. Wulff, P. K. Dhal, *Makromol. Chem. 188* (1987) 2847.

A Polyhedral Oligogermane: 4,8-Dibromo-octa-*tert*-butyltetracyclo[3.3.0.0^{2,7}.0^{3,6}]octagermane**

By *Manfred Weidenbruch**, *Fred-Thomas Grimm*, *Siegfried Pohl*, and *Wolfgang Saak*

In spite of much interest in inorganic rings and cages,[1] examples of these types of compound for the heavier elements of the fourth main group are restricted to the few bi- and polycyclic silicon compounds reported in the last few years. In addition to derivatives of bicyclo[1.1.0]tetrasilane[2] and bicyclo[2.2.0]hexasilane,[3] the first polycyclic oligosilanes have recently been reported.[4] Although an octasilacubane[5] has also been synthesized, it has yet to be structurally characterized.

In contrast, bi- and polycyclic oligogermanes have not previously been reported. In the early literature, the reductive dehalogenation of trichlorophenylgermane was reported to afford a compound of composition $(PhGe)_6$, which, at that time, was believed to be a hexagermabenzene derivative.[6] With the benefit of modern knowledge, a polyhedral germane would appear more likely.[7]

We now report the synthesis of a polycyclic oligogermane via a simple route. Treatment of germanium tetrabromide with *tert*-butyllithium gave a mixture of dibromodi-*tert*-butylgermane and 1,1,2,2-tetrabromo-1,2-di-*tert*-butyldigermane **1**[8] in 20% yield in each case. Reaction of the latter with excess naphthalene/lithium [Eq. (a)] afforded a

$$4\,t\mathrm{BuBr_2Ge{-}GeBr_2}t\mathrm{Bu} + 14\,\mathrm{C_{10}H_8/Li} \longrightarrow \underset{\mathbf{1}}{} \qquad \text{(a)}$$

$$t\mathrm{Bu_8Ge_8Br_2} + 14\,\mathrm{LiBr} + 14\,\mathrm{C_{10}H_8}$$

$$\mathbf{2}$$

[*] Prof. Dr. M. Weidenbruch, F.-T. Grimm, Prof. Dr. S. Pohl, Dipl.-Chem. W. Saak
Fachbereich Chemie der Universität
Carl-von-Ossietzky-Strasse 9-11, D-2900 Oldenburg (FRG)

[**] Compounds of Germanium and Tin, Part 4. This work was supported by the Deutsche Forschungsgemeinschaft and the Fonds der Chemischen Industrie. Part 3: M. Weidenbruch, K. Schäfers, S. Pohl, W. Saak, K. Peters, H. G. von Schnering, *Z. Anorg. Allg. Chem.* (in press).

mixture consisting of unreacted **1** and two other germanium compounds. The mass spectrum of the major product (crude yield 50%, HPLC) showed it to contain a skeleton of eight germanium atoms. The X-ray structural analysis[10] (Fig. 1) confirmed this, showing that **2** is 4,8-dibromo-octa-*tert*-butyltetracyclo[3.3.0.0^{2,7}.0^{3,6}]octagermane. Both enantiomers of the chiral molecule are present in pairs in the unit cell. Only four signals, instead of eight, were observed for the *tert*-butyl protons in the ^{1}H NMR spectrum[9] of **2**, which is in accord with the C_2 molecular symmetry. Not only does **2** exhibit exceptional thermal stability it is also air and moisture stable.

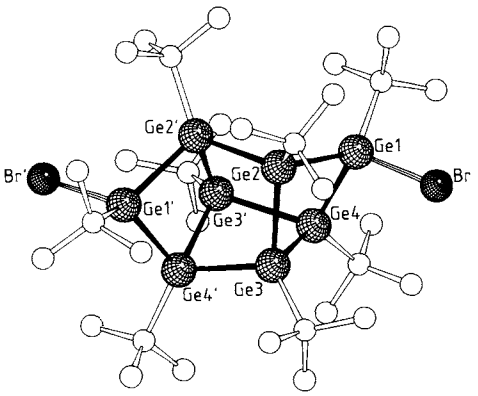


Fig. 1. Molecular structure of **2** (H atoms omitted). Selected bond lengths [pm] and angles [°] (standard deviations). The numbers marked with dashes indicate symmetry equivalent atoms. Ge1-Ge2 247.8(1), Ge1-Ge4 244.3(1), Ge2-Ge3 254.2(1), Ge2-Ge2' 246.1(1), Ge3-Ge4' 249.5(1), Ge-C 201.3 (ave.); Ge2-Ge1-Ge4 86.1(1), Ge1-Ge2-Ge3 87.9(1), Ge2-Ge3-Ge4 83.9(1), Ge1-Ge4-Ge3 90.1(1), Ge2'-Ge2-Ge3 94.3(1), Ge2-Ge3-Ge4' 103.8(1), Ge3-Ge4-Ge3' 82.5(1), Ge1-Ge4-Ge3' 103.6(1). Interplanar angles [°]: Ge2-Ge1-Ge4/Ge2-Ge3-Ge4 143.9, Ge4-Ge3-Ge4'/Ge4-Ge3'-Ge4' 141.8.

The absence of cyclotetragermanes in the reaction mixture suggests that these compounds, which are presumably the initial products of reaction (a), are subject to a spontaneous condensation reaction. The results reported here are in agreement with those of ab-initio calculations on bicyclo[2.2.0]hexagermane,[11] which predicted that the two fused four-membered rings are almost unstrained. The formation of an octagermacubane from **2** is not possible, since, in addition to the reductive elimination of the two bromine atoms, the cleavage and re-formation of a Ge–Ge bond is required.

Experimental procedure

Naphthalene/lithium (4.1 mmol) in THF (60 mL) was added to **1** (0.68 g, 1.18 mmol) in benzene (60 mL) and the resulting mixture stirred for 12 h at room temperature. The solvent was removed, the residue extracted with *n*-pentane, and the extract filtered to remove LiBr. Naphthalene was removed by vacuum sublimation. The resulting residue contained (HPLC analysis) 48% **2** and 15% **1**. Pure **2** was obtained by preparative HPLC (Nucleosil column, eluent *n*-hexane) followed by recrystallization from *n*-pentane.

Received: September 1988 [Z 2982 IE]
German version: *Angew. Chem. 101* (1989) 201

CAS Registry numbers:
1, 118437-11-9; **2**, 118437-12-0.

[1] I. Haiduc, D. B. Sowerby (Eds.): *The Chemistry of Inorganic Homo- and Heterocycles, Vol. 1, Vol. 2*, Academic Press, London 1987.

[2] S. Masamune, Y. Kabe, S. Collins, D. J. Williams, R. Jones, *J. Am. Chem. Soc. 107* (1985) 5552; R. Jones, D. J. Williams, Y. Kabe, S. Masamune, *Angew. Chem. 98* (1986) 176; *Angew. Chem. Int. Ed. Engl. 25* (1986) 173.

[3] H. Matsumoto, H. Miyamoto, N. Kojima, Y. Nagai, *J. Chem. Soc. Chem. Commun. 1987*, 1316; H. Matsumoto, H. Miyamoto, N. Kojima, Y. Nagai, M. Goto, *Chem. Lett. 1988*, 629.

[4] S. Masamune (Cambridge, MA, USA), personal communication; Editorial note: see Y. Kabe, M. Kuroda, Y. Honda, O. Yamashita, T. Kawase, S. Masamune, *Angew. Chem. 100* (1988) 1793; *Angew. Chem. Int. Ed. Engl. 27* (1988) 1725.

[5] H. Matsumoto, K. Higuchi, Y. Hoshino, H. Koike, Y. Naoi, Y. Nagai, *J. Chem. Soc. Chem. Commun. 1988*, 1083.

[6] R. Schwarz, M. Lewinsohn, *Ber. Dtsch. Chem. Ges. B64* (1931) 2352.

[7] Cf. A. Sekiguchi, C. Kabuto, H. Sakurai, *Angew. Chem. 101* (1989) 97; *Angew. Chem. Int. Ed. Engl. 28* (1989) 55.

[8] **1**: M.p. = 95–97 °C. ^{1}H NMR (C_6D_6): $\delta = 1.22$ (s). MS (70 eV): *m/z* 579 ($M^{\oplus}$, 5%), 522 ($M^{\oplus} - 57$, 12).

[9] **2**: Pale-yellow crystals, m.p. > 400 °C (decomp.). ^{1}H NMR: $\delta = 1.47$ (s, 18H), 1.52 (s, 18H), 1.54 (s, 18H), 1.56 (s, 18H). MS (CI, NH_3): *m/z* 1113 ($M^{\oplus} - 57 - 28$, 100%). MS (CI, isobutane): *m/z* 1113 (57%).

[10] Monoclinic, space group *C2/c* (No. 15), $a = 2062.0(2)$, $b = 1137.7(2)$, $c = 2077.1(4)$ pm, $\beta = 101.10(2)°$, $V = 4781.6 \times 10^6$ pm^3, $Z = 4$, $\rho_{calcd} = 1.66$ g cm^{-3}; 3750 independent reflections, 2817 observed ($I > 2\sigma(I)$), 190 variables, $R = 0.048$, $R_w = 0.044$. Further details of the X-ray structural analysis can be obtained from the Fachinformationszentrum Energie, Physik, Mathematik GmbH, D-7514 Eggenstein-Leopoldshafen 2, on quoting the depository number CSD-53421, the names of the authors, and the journal citation.

[11] S. Nagase, M. Nakano, *J. Chem. Soc. Chem. Commun. 1988*, 1077.

Residual Enantiomerism and Chromatographic Resolution of a 1,1,2-Triarylalkene**

By *Silvio E. Biali,* Zvi Rappoport,* Albrecht Mannschreck* and *Nikola Pustet*

1,1,2-Triarylalkenes exist in a chiral "propeller" conformation in which the three rings are twisted in the same sense.[1,2] The rotational behavior of molecular propellers is generally analyzed in terms of "flip" mechanisms involving correlated rotation of the rings and leading to helicity reversal.[3] In these mechanisms, as applied to alkene propellers,[4] the rings which flip pass through a plane perpendicular to the plane of the double bond, whereas those rings that do not flip pass through the plane of the double bond. According to the number of rings that flip, these mechanisms are dubbed three-, two-, one- or zero-ring flip. We have shown previously that the rotational mechanism of lowest activation energy (threshold mechanism) which leads to enantiomerization of the sterically hindered stable enol[5] 1,2,2-trimesitylethenol **1** and its acetate **2** is the three-ring flip.[4]

$Mes_2C{=}C(OH)Mes$ **1** $Mes_2C{=}C(OAc)Mes$ **2**

$Mes_2C{=}C(OAc)(2,4,6\text{-}Me_3\text{-}3\text{-}OMe\text{-}C_6H)$ **3**

Mes = 2,4,6-$Me_3C_6H_2$

The activation barriers for the three-ring flip of **1** and **2** are relatively low (77.0 and 79.5 kJ mol^{-1}, respectively)[4] and therefore the resolution of **1** and **2** at room temperature is precluded. Moreover, since the three-ring flip exchanges pairs of diastereotopic groups in all three rings, the higher energy flip processes cannot be followed by NMR spectroscopy. However, the preference for a low en-

[*] Dr. S. E. Biali, Prof. Dr. Z. Rappoport
Department of Organic Chemistry
The Hebrew University of Jerusalem
Jerusalem 91904 (Israel)
Prof. Dr. A. Mannschreck, N. Pustet
Institut für Organische Chemie der Universität
Universitätsstrasse 31, D-8400 Regensburg (FRG)

[**] This work was supported by the United States-Israel Binational Science Foundation (BSF) Jerusalem.

ergy enantiomerization via a three-ring flip raised an interesting possibility. If one of the mesityl rings is rendered dissymetric, e.g. by replacement of one of the mesityl protons by another substituent ("tag"), the compound should exist in four stereoisomeric forms (two enantiomeric pairs) due to the helicity and because the tag can lie either above or below the plane of the double bond. The three-ring flip will then result in *diastereomerization* (D) but not in enantiomerization (E), which requires both helicity reversal and "tag inversion" with respect to the C=C plane. Under conditions of fast three-ring flip the compound should exist in two residual enantiomeric forms (see Fig. 1)[6] which can

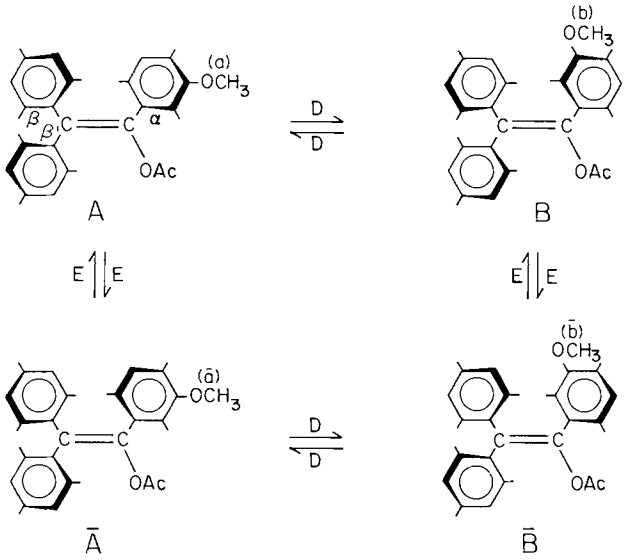


Fig. 1. Diastereomerization (D) and enantiomerization (E) of **3**. Dashes over capital letters denote enantiomers and over lowercase letters enantiotopic sites.

be interconverted only by a non-flip process, i.e., by passage of the tagged ring through the plane of the double bond. The barrier for this interconversion should be higher than that for the three-ring flip and, provided that it is sufficiently high, the lifetimes of the residual isomers should be long enough to enable resolution. The racemization barrier of a sample enriched in one enantiomer will then be the non-threshold rotational barrier for the process, in which the ring bearing the tag passes through the plane of the double bond. In order to investigate these possibilities, compound **3**, a derivative of **2** in which one aromatic proton of the α-ring is replaced by OMe, was chosen. The acetate group was chosen since we encountered difficulties in crystallization of its parent enol **4**. The choice of the *meta*-OMe substituent was based on three considerations. First, the height of the barriers are mainly determined by steric interactions between the *ortho*-methyl groups of the three rings in the ground and transition states, so that the presence of a *meta* substituent should not affect the barrier for the threshold mechanism in the absence of buttressing effects. Second, it is expected that the diastereomeric ratio will not differ appreciably from 1:1 and therefore both diastereomers could be detected in the NMR spectra under slow exchange conditions. Third, since the chemical shift of the OMe signal is very different from the other chemical shifts, this group should allow easy monitoring of the diastereomerization process.

Compound **3** was synthesized in two steps from dimesitylketene via the enol intermediate **4**[7] [Eq. (a)].

$$Mes_2C{=}C{=}O \xrightarrow[2)\ H^{\oplus}]{1)\ ArylMgBr} \underset{\mathbf{4}}{Mes_2C{=}C(OH)Aryl} \xrightarrow{Ac_2O/py} \mathbf{3} \qquad \text{(a)}$$

Aryl = 2,4,6-Me_3-3-OMe-C_6H

For a frozen propeller conformation, **3** should exist in four stereoisomeric forms. In Figure 1 the two diastereomeric forms (two pairs of enantiomers) are designated A and B; dash over a letter designates the other enantiomer. The OMe groups in A and B are designated a and b, respectively, and the corresponding enantiotopic sites in $\bar{A}$ and $\bar{B}$ are labelled ā and b̄. In the ^1H NMR spectrum ($C_6D_5NO_2$, room temperature), **3** displays 21 signals for the Me, AcO and Aryl-H groups and two OMe signals in the ratio of ca. 1.08, in agreement with the presence of two pairs of diastereomers in solution. This ratio increased to 1.15 upon raising the temperature to 378 K. In addition, some of the signals (including those for OMe) broadened and eventually coalesced. From the frequency difference between the two OMe signals ($\Delta\nu = 76$ Hz at 200 MHz) at slow exchange and the coalescence temperature ($T_c = 388$ K), a barrier of 79.5 kJ mol^{-1} was calculated for the diastereomerization of **3** using the Gutowsky–Holm approximation[8] and the Eyring equation. We ascribe this diastereomerization process, which exchanges the OMe groups a ⇌ b and ā ⇌ b̄, to a three-ring flip, by analogy with the isomerization of **2**. The equality of the rotational barriers for **2** and **3** indicates that the buttressing effect of the OMe substituent has little or no influence on the threshold barrier. The analogy with **2** suggests that the enantiomerization barrier must be higher than 79.5 kJ mol^{-1}. At 422 K (60 MHz) five Me, one AcO, one MeO and three Aryl-H signals are observed. The number of Me and Aryl-H signals is lower than expected for the residual isomers (nine Me and five Aryl-H signals). This high temperature spectrum can be explained either by a fast passage of both the β- and β′-rings through the plane of the double bond (a topomerization process), by a rapid rotation of the α-ring through the plane of the double bond (an enantiomerization process), or by simply assuming poor resolution of the pairs of *ortho* and *meta* signals for the β- and β′-rings at 60 MHz. Since the latter explanation seemed highly likely, we attempted the resolution of **3** by chromatography on an optically active column.

In principle, if the rotation of the rings is slow on the chromatographic time scale, *both* racemates should be resolved. In practice, using an optically active column of triacetylcellulose,[9] which has been used successfully for the separation of other helical compounds,[10] with EtOH/H_2O (96/4) as eluent, we observed rather erratic behavior; sometimes both racemates and sometimes a single (residual) racemate were resolved. As soon as an enriched solution was detected in the polarimetry cell, the flow through the column was stopped, the cell thermostated at 290 K and the racemization of the sample followed by polarimetry over the course of two half lives. The experimental racemization rate constant ($k = 2.4 \times 10^{-4}\ s^{-1}$) gives a racemization barrier $\Delta G^{\neq}$ of 91 kJ mol^{-1}. Since k(racemization) = $2k$(enantiomerization), the barrier for the enantiomerization process is 92.7 kJ mol^{-1} (at 290 K). This value most probably corresponds to a [β,β′]-two-ring flip process in which the α-ring passes through the plane of the double bond. Interestingly, the energy difference between

 © VCH Verlagsgesellschaft mbH, D-6940 Weinheim, 1989 0570-0833/89/0202-0200 $ 02.50/0

the three-ring flip and the enantiomerization barrier process is only 13.2 kJ mol^{-1}. This energy difference is reminiscent of the energy difference of 15.5 kJ mol^{-1} between the three-ring and the [α,β]-two-ring flip found for trimesitylethylene.[11] Not surprisingly, the energy required for the simultaneous introduction of two rings into the C=C plane is greater than twice that for one ring, as can be concluded from a calculation of the energy barrier for the zero-ring flip in the less crowded 1,1-diphenylethylene.[12] Finally, we would like to point out that, in retrospect, Adams' classical resolution of substituted styrenes[13] represents also the separation of residual enantiomers, provided that the twist angle Aryl–C=C differs from 90° in the ground state conformation of styrene.

In summary, we have shown that a suitably substituted triarylalkene propeller can be resolved into its residual enantiomers. Two rotational barriers were measured for **3**, a low energy diastereomerization barrier corresponding to a three-ring flip and a higher energy enantiomerization barrier corresponding probably to a [β,β']-two-ring flip.

Experimental Procedure

To a Grignard reagent prepared from 1-bromo-3-methoxy-2,4,6-trimethylbenzene [14] (2.45 g, 10.7 mmol) and magnesium (0.26 g, 10.8 mmol) in dry THF (35 mL) was added dropwise dimesitylketene[5,15] (3 g, 10.7 mmol) in dry THF (15 mL). After heating for 3 h at reflux, the mixture was poured onto HCl/ice and extracted with ether. The organic phase was separated, dried ($MgSO_4$) and the solvent was evaporated, leaving an oil, which according to NMR consisted mainly of **4**. Crude **4** was acetylated by refluxing for 5 h with Ac_2O (6 mL) in pyridine (21 mL). The mixture was poured into water and the resulting solid was treated with active charcoal and recrystallized three times from ethanol to afford analytically pure **3**, m.p. 122°C.

Received: July 5, 1988 [Z 2847 IE]
German version: *Angew. Chem. 101* (1989) 202

CAS Registry numbers:
3, 118042-67-4; **4**, 118042-68-5; $Mes_2C{=}C{=}O$, 87871-33-8; 1-bromo-3-methoxy-2,4,6-trimethylbenzene, 118042-66-3.

[1] M. Kaftory, S. E. Biali, Z. Rappoport, *J. Am. Chem. Soc. 107* (1985) 1701.
[2] For a review of helical compounds, including molecular propellers see: K. P. Meurer, F. Vögtle, *Top. Curr. Chem. 127* (1985) 1.
[3] R. J. Kurland, I. I. Schuster, A. K. Colter, *J. Am. Chem. Soc. 87* (1965) 2279; K. Mislow, *Acc. Chem. Res. 9* (1976) 26; R. Willem, M. Gielen, C. Hoogzand, H. Pepermans in M. Gielen (Ed.): *Advances in Dynamic Stereochemistry*, Freund, London 1985, p. 207.
[4] S. E. Biali, Z. Rappoport, *J. Am. Chem. Soc. 106* (1984) 477.
[5] Reviews of stable enols: H. Hart, *Chem. Rev. 79* (1979) 515; Z. Rappoport, S. E. Biali, *Acc. Chem. Res. 21* (1988), 442.
[6] P. Finocchiaro, D. Gust, K. Mislow, *J. Am. Chem. Soc. 96* (1974) 3198. See also H. Iwamura, K. Mislow, *Acc. Chem. Res. 21* (1988) 175, and references cited therein.
[7] Spectroscopic data for **3**: ^{1}H NMR ($C_6D_5NO_2$, room temperature (RT), 200 MHz): $\delta = 1.90$ (broad, OAc [4]), 1.92, 1.94, 2.01, 2.07, 2.08, 2.09, 2.12, 2.13, 2.16, 2.27, 2.43, 2.46, 2.51, 2.64 (Me), 3.32, 3.70 (OMe), 6.50, 6.54, 6.67, 6.69, 6.86, 6.99 (Ar–H); (422 K, 60 MHz): $\delta = 1.82$, 1.98, 2.06, 2.11, 2.20, 2.30, 3.48, 6.59, 6.69, 6.82. ^{13}C NMR ($C_6D_5NO_2$, RT, 50.33 MHz): $\delta = 13.70$, 14.44, 15.10, 19.68, 19.75, 19.93, 20.04, 20.43, 20.88, 20.98, 21.37, 21.63, 58.42, 58.53. UV (MeOH): $\lambda_{max}(\varepsilon) = 208$ (40300), 214 (40800), 241 nm (21150).
[8] H. S. Gutowsky, C. H. Holm, *J. Chem. Phys. 25* (1956) 1228.
[9] Separation conditions: sorbent 20–30 μm, column 2.5 × 30 cm, pressure 1.7 bar, flow-rate 3.5 mL min^{-1}, eluent EtOH/H_2O 96/4, column temperature 294 K.
[10] A. Mannschreck, D. Andert, A. Eiglsperger, E. Gmahl, H. Buchner, *Chromatographia 25* (1988) 182; M. A. Cuyegkeng, A. Mannschreck, *Chem. Ber. 120* (1987) 803.
[11] S. E. Biali, Z. Rappoport, *J. Org. Chem. 51* (1986) 2245.
[12] H. Stegemeyer, W. Rapp, *Ber. Bunsenges. Phys. Chem. 75* (1971) 1165.
[13] R. Adams, M. W. Miller, *J. Am. Chem. Soc. 62* (1940) 53; R. Adams, A. W. Anderson, M. W. Miller, *ibid. 63* (1941) 1589. See also: D. Cabaret, M. Maigrot, Z. Welvart, K. N. V. Duong, A. Gaudemer, *ibid. 106* (1984) 2870, and references cited therein.
[14] R. C. Fuson, J. Corse, D. B. Welldon, *J. Am. Chem. Soc. 63* (1941) 2645.
[15] R. C. Fuson, S. P. Rowland, *J. Am. Chem. Soc. 65* (1943) 992.

LiSrN—A Three Dimensional Structural Arrangement of Corner and Edge Sharing Orthorhombic Bipyramids, $NLi_{2/2}Sr_{4/4}$**

By *Gerhard Cordier, Axel Gudat, Rüdiger Kniep,* and *Albrecht Rabenau**

As part of our investigations related to the work of *Juza* et al.[1] on the phase relations and crystal structures of intermediate compounds in the lithium-metal-nitrogen ternary system,[2] we have prepared the compound LiSrN as metallically-lustrous single crystals. The product was obtained from the reaction of lithium nitride[3] with strontium (1 : 1 molar ratio) under a nitrogen atmosphere (1 atm) in a tantalum ampoule at 700°C; the melt was cooled to room temperature over a period of 12 hours. "LiSrN" was previously reported to have been prepared in 1970[4] and was indexed from X-ray powder diagrams as tetragonal ($a = 11.08$ Å, $c = 13.40$ Å). However, these powder diagrams have now been shown to actually correspond to a mixture of the phases LiSrN and Li_4SrN_2.[5] Our single crystal structure analysis of LiSrN reveals that it is in fact tetragonal but with $a = 3.924(3)$ Å and $c = 7.085(4)$ Å).[6]

The stoichiometric phase LiSrN is an isotype of the YCoC structural type which was first determined in 1986 by X-ray powder methods.[7] That the extent of occurrence of this very simple structural type is not restricted to the ternary transition metal carbides, but is also found in the realm of the main group elements, makes it of interest to examine more closely its structural features.

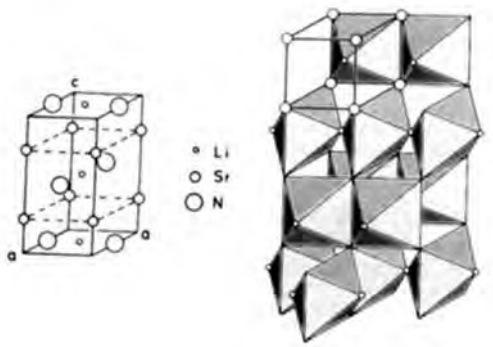


Fig. 1. LiSrN: unit cell (left) and a section of the structure assemblage (right, polyhedral representation). Explanation in text.

The metal cations (Fig. 1) are arranged as in the known cesium chloride structure. The anion occupies the center of two opposing faces of the cube (compressed here in one direction); along [001], the face centers are alternately occupied, each being turned 90° with respect to the other, thus resulting in the longer *c*-axis.[6] If one considers the crystal structure of LiSrN from the viewpoint of coordination polyhedra, then for each nitrogen atom an orthorhombic-bipyramidal environment (*mmm* symmetry) results. Lithium atoms occupy the apices of the flattened bipyra-

[*] Prof. Dr. A. Rabenau, Dr. G. Cordier [+], Dipl.-Chem. A. Gudat, Prof. Dr. R. Kniep [+]
Max-Planck-Institut für Festkörperforschung
Heisenbergstrasse I, D-7000 Stuttgart 80 (FRG)
[+] Permanent address:
Eduard-Zintl-Institut der Technischen Hochschule
Hochschulstrasse 4, D-6100 Darmstadt (FRG)

[**] We thank Dr. *L. M. Gelato* and Prof. *E. Parthé* for assistance with the use of the program STRUCTURE TIDY [9] and Prof. *H. G. von Schnering* for helpful discussions.

mids with a bond length (Li–N 1.962 Å) which is comparable with the axial bond distance (Li–N 1.938 Å) of the hexagonal-bipyramidally coordinated nitrogen atoms in Li_3N[8] and lies within the order of magnitude of the sum of the covalent single bond radii (Li–N 1.98 Å). In this way, extended chains of $[LiN]^{2-}$ result (cf. $[CoC]^{3-}$ in YCoC[7]) and are turned 90° with respect to one another in their sequence along [001]. The equatorial planes of the coordination bipyramids of the nitrogen atoms are composed of strontium atoms having tetrahedral coordination (Sr–N: 2.643 Å, Sr–N–Sr 95.85° and 84.15°).

The three-dimensional polyhedral framework (Fig. 1, right) consists of linear chains of lithium atom apex-shared bipyramids and linear chains of Sr–Sr edge-sharing bipyramids, which are bonded to each other through the common Sr corners without structural distortion. By this mode of connection ($NLi_{2/2}Sr_{4/4}$), the distance between the apical lithium atoms of the bipyramids (2×1.962 Å) corresponds exactly to the length of two unshared parallel edges (Sr···Sr) in the equatorial planes. One cannot generate this structural assembly with regular coordination octahedra, whereby the distance between two apical atoms is longer than the length of an edge by a factor of $\sqrt{2}$. A *c/a* ratio of 2.0 leads to a tetragonal-bipyramidal coordination (4/*mmm* symmetry) for the "interstitial" position; the *c/a* ratios of 1.880 and 1.804 for YCoC[7] and LiSrN, respectively, characterize their orthorhombic distortions.

Received: August 25, 1988 [Z 2941 IE]
German version: *Angew. Chem. 101* (1989) 204

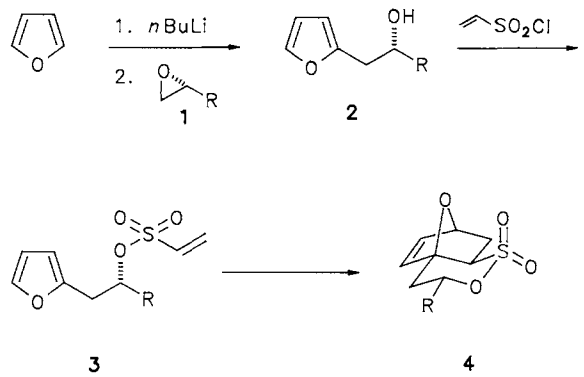
[1] R. Juza, K. Langer, K. von Benda, *Angew. Chem. 80* (1968) 373; *Angew. Chem. Int. Ed. Engl. 7* (1968) 360.
[2] A. Gudat, *Diplomarbeit*, Universität Düsseldorf 1987; A. Gudat, R. Kniep, A. Rabenau, 5th Vortragstagung GDCh-Fachgruppe Festkörperchemie, Erlangen, Sept. 28–30, 1988.
[3] A. Rabenau, *Solid State Ionics 6* (1982) 277.
[4] J.-F. Brice, J.-P. Motte, J. Aubry, *C. R. Hebd. Séances Acad. Sci. Ser. C270* (1970) 1658.
[5] G. Cordier, A. Gudat, R. Kniep, A. Rabenau, unpublished; Li_4SrN_2: tetragonal, $I4_1/amd$, $a = 3.822(2)$, $c = 27.042(9)$ Å.
[6] Crystallographic data: LiSrN, tetragonal, $I4_2/mmc$, $a = 3.924(3)$, $c = 7.085(4)$ Å, $Z = 2$; 111 independent reflections from 729 measured; $R = 0.035$; Philips PW 1100 single crystal diffractometer, $Mo_{K\alpha}$ radiation, 300 K. Further details of the crystal structure investigation can be obtained from the Fachinformationszentrum Energie, Physik, Mathematik GmbH, D-7514 Eggenstein-Leopoldshafen 2, on quoting the depository number CSD-53603, the names of the authors, and the journal citation.
[7] M. H. Gerss, W. Jeitschko, *Z. Naturforsch. B41* (1986) 946.
[8] A. Rabenau, H. Schulz, *J. Less Common Met. 50* (1976) 155.
[9] L. M. Gelato, E. Parthé, *J. Appl. Crystallogr. 20* (1987) 139.

Intramolecular Diels–Alder Reaction of Vinylsulfonic Acid Esters

By *Eva Bovenschulte, Peter Metz,** and *Gerald Henkel*

The intramolecularization of the Diels–Alder reaction has notably increased the synthetic potential of this cycloaddition, often making it easier to overcome reactivity, regiochemical, and stereochemical problems.[1] Moreover, the intramolecular variant makes it possible to control the configuration of up to four new chiral centers by an asymmetric center in the bridge which joins the diene and dienophile moieties.

As part of a project concerned with the enantioselective synthesis of both enantiomers of nonactic acid[2] and its homologues, the monomeric building blocks of the macrotetrolide antibiotics,[3] we have investigated the intramolecular Diels–Alder reaction of the vinylsulfonic acid esters **3**.



a, R = Me; **b**, R = Et; **c**, R = *i*Pr

The hydroxyalkylfurans **2** required for the synthesis of **3** are obtainable in good yields by lithiation of furan and subsequent alkylation with epoxides **1**.[4] With equimolar amounts of furan, *n*BuLi and **1**,[4] some double alkylation was observed; this side reaction can be completely suppressed by use of a slight excess of furan. **1a** and **1b** were employed as racemates; with (*R*)-**1c**[5] accessible in three steps from L-valine, the simple transition to an enantioselective synthesis should be demonstrated.

When the alcohols **2** are esterified with vinylsulfonic acid chloride,[6] the vinylsulfonates **3** are obtained which undergo a highly diastereoselective intramolecular Diels–Alder reaction already at room temperature to give the sultones **4**. No further diastereomers could be detected ^{1}H- or ^{13}C-NMR spectroscopically, even in the crude products. The sequence of the reaction steps—first, intermolecular esterification, and then intramolecular cycloaddition[7]—was confirmed for **4a** by spectroscopic characterization (^{1}H-, ^{13}C-NMR) of the labile intermediary sulfonate **3a**. The relative configurations of the tricyclic compounds **4** (*exo*-adduct, equatorial R) could be derived from the ^{1}H-NMR spectra, and in the case of **4a** unequivocally established by a crystal structure analysis.[8]

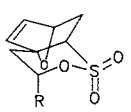
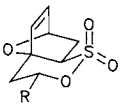
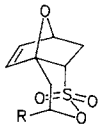
The high dienophilicity of vinyl sulfonates, which had already been observed in some intermolecular Diels–Alder reactions,[9] is underscored by the finding that the acrylate of **2a** (**2a** + acrylic acid chloride, Et_3N, THF 12 h, 25°C; 95% yield) does not cyclize even after heating in toluene at reflux for three days.

Results of MNDO[10,11] and MMPMI[10,12] calculations suggest a thermodynamic control of the relative configurations of **4** (Table 1).

If one assumes that the four possible diastereomers **4**–**7** are in equilibrium with one another by a reversible cycloaddition[9,13] of **3**, an almost exclusive formation of the *exo*-adduct **4** (**4** : **5** approx. 97 : 3) follows from the relative heats of formation listed in Table 1.

[*] Dr. P. Metz, E. Bovenschulte
Organisch-chemisches Institut der Universität
Corrensstrasse 40, D-4400 Münster (FRG)
Priv.-Doz. Dr. G. Henkel [†]
Anorganisch-chemisches Institut der Universität
Wilhelm-Klemm-Strasse 8, D-4400 Münster (FRG)
[†] Crystal structure analysis.

Table 1. Calculated heats of formation E_{rel} [kcal mol^{-1}] (relative to **4**) of the sultones **5**–**7** diastereomeric with **4** using MNDO [10, 11] (**a**, **b**) and MMPMI [10, 12] (**c**).

	 **5**	 **6**	 **7**
a	2.1	5.7	6.6
b	2.2	6.1	8.3
c	2.0	4.3	7.2

The conversion of the sultones **4** into actic acids and the extension of the title reaction to further 1,3-dienes are currently under investigation.

Experimental

2: The procedure given in Ref. [4a] was modified in that 1.4 equivalents of furan were employed.

1.20 g of (*R*)-**1c** [5] ($[\alpha]_D^{20} = +3.38$ (pure)) afforded, after Kugelrohr distillation at 60°C/0.5 mbar, 1.60 g (75%) of (*S*)-**2c** (correct MS high resolution) with $[\alpha]_D^{20} = -36.5$, $[\alpha]_{365}^{20} = -125.4$ (in each case $c = 0.54$ in $CHCl_3$). In an analogous way *rac*-**1a** furnished 65% *rac*-**2a** [4], while *rac*-**1b** afforded 74% *rac*-**2b** [4b].

4: A 0.24 M solution of the alcohol **2** in THF was treated with 2 equivalents of Et_3N. After cooling to 0°C, 1 equivalent of freshly distilled vinylsulfonic acid chloride **6** was added dropwise. After 1.5 h stirring at 0°C in the case of *rac*-**2a** and *rac*-**2b**, or 12 h stirring at room temperature in the case of the sterically stronger shielded alcohol (*S*)-**2c**, the reaction mixture was poured onto ice, saturated with NaCl and extracted three times with Et_2O. The combined organic phases were washed once with 2 N HCl and once with saturated $NaHCO_3$ solution, and then dried over $MgSO_4$. If the solvent is removed in vacuo at 0°C, the vinylsulfonic esters *rac*-**3a** and *rac*-**3b** can be isolated; their cyclization, however, already starts at room temperature and, is complete after maximally 3 h. If, the solvent is removed in vacuo at 40°C bath temperature, cycloaddition to give *rac*-**4a** and *rac*-**4b** takes place spontaneously. In the reaction of (*S*)-**2c**, no formation of (*S*)-**3c** was observed by thin-layer chromatography, and (+)-**4c** was isolated directly after removal of the solvent in vacuo even at 0°C. The crude sultones **4** were recrystallized from ether.—*rac*-**4a**: 3.69 g (90%) from 2.40 g *rac*-**2a**, m.p. 124°C; *rac*-**4b**: 2.00 g (92%) from 1.33 g *rac*-**2b**, m.p. 124°C; (+)-**4c**: 829 mg (87%) from 600 mg (*S*)-**2c**, m.p. 135°C, $[\alpha]_D^{20} = +17.3$, $[\alpha]_{365}^{20} = +38.7$ (in each case $c = 0.30$ in $CHCl_3$). Correct C,H analyses were obtained for **4a**–**c**.

Received: October 10, 1988 [Z 2998 IE]
German version: *Angew. Chem. 101* (1989) 204

[1] D. Craig, *Chem. Soc. Rev. 16* (1987) 187.
[2] A. Warm, P. Vogel, *Helv. Chim. Acta 70* (1987) 690, and references cited therein.
[3] W. Keller-Schierlein, H. Gerlach, *Fortschr. Chem. Org. Naturst. 26* (1968) 161.
[4] a) U. Schmidt, J. Gombos, E. Haslinger, H. Zak, *Chem. Ber. 109* (1976) 2628; b) M. J. Arco, M. H. Trammell, J. D. White, *J. Org. Chem. 41* (1976) 2075.
[5] B. Koppenhoefer, R. Weber, V. Schurig, *Synthesis 1982*, 316.
[6] E. F. Landau, *J. Am. Chem. Soc. 69* (1947) 1219.
[7] This sequence is not trivial, cf.: A. Pelter, B. Singaram, *J. Chem. Soc. Perkin Trans. 1 1983*, 1383.
[8] **4a** crystallizes in the space group $P2_1/n$ with $a = 5.990(2)$, $b = 9.421(3)$, $c = 18.280(5)$ Å, $\beta = 94.27(2)°$, $Z = 4$, $V = 1028.7$ Å^3, $\rho_{calcd} = 1.396$ g cm^{-3}, crystal dimensions $0.20 \times 0.15 \times 0.15$ mm^3. The diffraction data were collected with a single-crystal diffractometer Syntex $P2_1$ (graphite monochromator, scintillation counter, $Mo_{K\alpha}$-radiation, (θ-2θ)-scan, measuring rate 3–25° min^{-1}) at 150 K. 1514 reflections were obtained in the range $4° < 2\theta < 48°$, 1406 with $I > 1.96\sigma(I)$ considered as observed. Solution of structure by direct methods (SHELXS86); all calculations were carried out with the program system SHELXTL. The hydrogen atom positions were refined from difference Fourier syntheses. Anisotropic treatment of the non-hydrogen atoms gave $R = 0.031$ and $R_w = 0.033$ for the observed reflections. Further details of the crystal structure investigation are available on request from the Fachinformationszentrum Energie, Physik, Mathematik GmbH, D-7514 Eggenstein-Leopoldshafen 2 (FRG), on quoting the depository number CSD-53469, the names of the authors, and the journal citation.
[9] L. L. Klein, T. M. Deeb, *Tetrahedron Lett. 26* (1985) 3935.
[10] A chair conformation of the δ-sultone moiety was assumed in all calculations.
[11] QCPE No. 353 in the modification by *J. D. Bowden* (Atlanta University) and *G. S. Owen* (Georgia State University). The version used, which contained additional current parameters for sulfur (M. J. S. Dewar, C. H. Reynolds, *J. Comput. Chem. 7* (1986) 140) was kindly placed at our disposal by Professor *E. U. Würthwein* (Münster).
[12] MMPMI version 1.0 by *K. E. Gilbert* and *J. J. Gajewski* (Indiana University), Serena Software.
[13] L. A. Van Royen, R. Mijngheer, P. J. De Clercq, *Tetrahedron 41* (1985) 4667.

Identification of $[(OC)_4Fe{=}Si(CH_3)_2 \cdot \{(H_3C)_2N\}_3PO]$ as Intermediate in the Formation of Polysilanes from $(H_3C)_2SiCl_2$ and $[Na_2Fe(CO)_4]$**

By *Christian Zybill,* Dallas L. Wilkinson, Christian Leis,* and *Gerhard Müller*

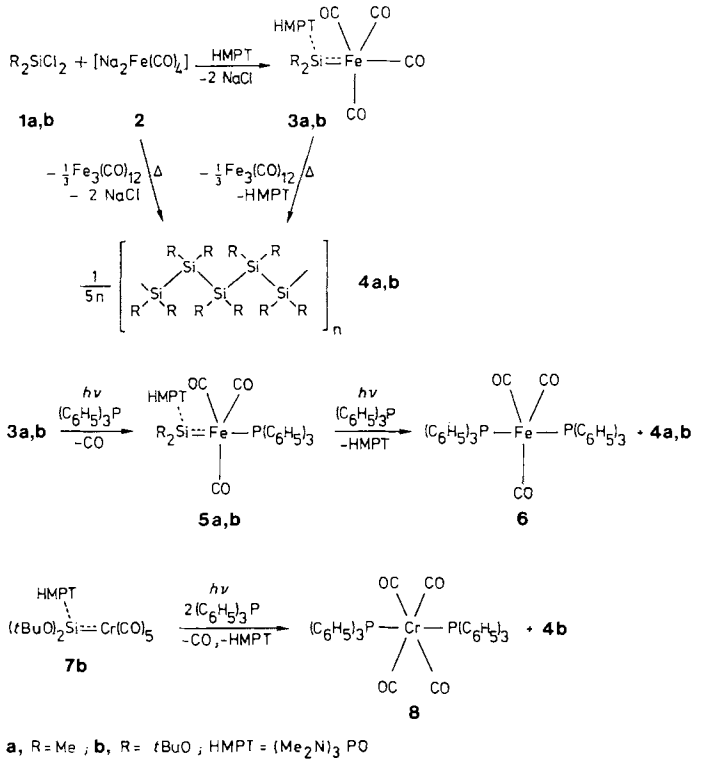
Polysilanes are being used to an increasing extent as precursors for semi-conductors in electronics and optics and also for the preparation of ceramics.[1] These polymers are synthesized conveniently by coupling reactions of dichlorosilanes with sodium. More recently, the reactions of suitable monomers in the presence of transition metal compounds have attracted growing interest. For example, $C_6H_5SiH_3$ is catalytically converted by $Cp_2Zr(CH_3)_2$ into chain polymers with molecular weights of ca. 1500.[2–4] Until now, however, the mechanism of this reaction has been a matter of controversy, particularly with regard to the role of silanediyl (silylene) complexes as possible intermediates.[5]

Using the system **1a/2**, we have now been able to prepare the polysilane **4a** and, via a trapping reaction with HMPT (hexamethyl phosphoric triamide) at −45°C, to isolate the silanediyl complex **3a**. The polysilane **4a** can also be prepared by thermal decomposition of **3a**. The photolysis of **3a** in the presence of $(C_6H_5)_3P$ proceeds stepwise, yielding first the mono(phosphane) complex **5a** and then the bis(phosphane) complex **6** with concomitant formation of polysilane. The latter reaction can also be successfully carried out for the analogous *tert*-butoxy compounds **3b** and **7b**. The polymerization products were spectroscopically characterized in each case. A cryoscopic molecular weight determination for a sample derived from the thermal decomposition of **3a** gave $M_n = 550 \pm 10$.

3a is a coordination compound of the dimethylsilanediyl ligand, which is of great interest, particularly with regard to its reactivity. This complex has been thoroughly investigated spectroscopically (^{29}Si NMR: $\delta = 92.4$); the CO ligands are fluctional at room temperature and rotation about the Fe–Si bond is unhindered. A single crystal X-ray structural analysis[6] showed an axial coordination of the silanediyl ligand to the $Fe(CO)_4$ fragments (Fig. 1), which can also be inferred from the IR data. The crystal contains two crystallographically independent molecules, which exhibit only slight structural differences. The silicon atom has a distorted tetrahedral coordination geometry

[*] Dr. C. Zybill, Dr. D. L. Wilkinson [+], C. Leis, Dr. G. Müller
Anorganisch-chemisches Institut
der Technischen Universität München
Lichtenbergstrasse 4, D-8046 Garching (FRG)
[+] Permanent adress:
Monash University, Clayton, Vic. (Australia)

[**] This work was supported by the Deutsche Forschungsgemeinschaft and a stipendium from the Alexander-von-Humboldt-Stiftung (*D. L. W.*). We thank Prof. *H. Schmidbaur* for support.



with the HMPT molecule being only weakly bound to silicon via the oxygen atom (Si-O, 1.731(4) and 1.736(4) Å for the two independent molecules). The Fe-Si bond lengths are 2.279(2)/2.292(2) Å (compare: Si-O 1.730(3), Fe-Si

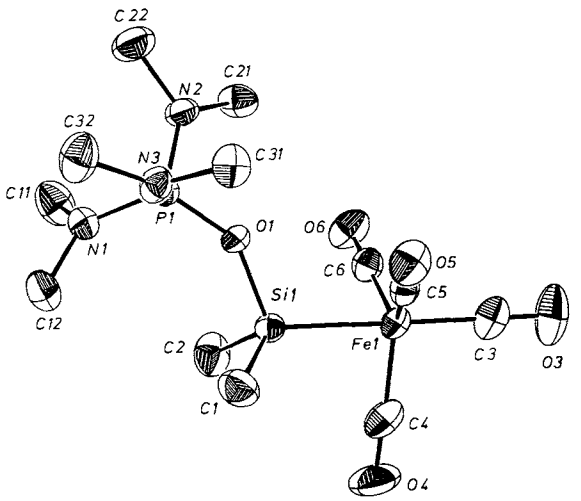


Fig. 1. Molecular structure of one of the crystallographically independent molecules of **3a** (ORTEP, 50% probability thermal motion ellipsoids, H atoms omitted). Important bond lengths [Å] and angles [°] for both molecules: Fe-Si 2.279(2)/2.292(2), Si-O 1.731(4)/1.736(4), Fe-C3 1.789(7)/1.782(7), Fe-C4 1.775(7)/1.734(7), Fe-C5 1.751(6)/1.762(7), Fe-C6 1.757(6)/1.743(6), Si-C1 1.871(6)/1.852(6), Si-C2 1.875(6)/1.862(6); Fe-Si-O1 110.4(1)/109.6(1), Fe-Si-C1 115.5(2)/116.8(2), Fe-Si-C2 115.4(2)/115.6(2), O1-Si-C1 103.8(2)/101.8(2), O1-Si-C2 102.7(2)/103.8(2), C1-Si-C2 107.7(3)/107.6(3).

2.289(3) Å in **3b**[5a]). Thus, replacing the *t*BuO substituents at silicon by methyl groups has surprisingly little effect on the structure of the silanediyl ligands. The results presented here provide evidence for the role of silanediyl complexes as intermediates in the polymerization of $(CH_3)_2Si$ units with the system **1a**/**2**. However, a more detailed understanding of this reaction, which can be both thermally and photochemically initiated, must await the results of further studies. Alternative mechanisms, are also plausible.[2-4, 7]

Experimental

3a: **1a** (0.75 g, 5.8 mmol) (distilled from K_2CO_3) was added dropwise to a solution of **2**·1,5 dioxane (2.0 g, 5.8 mmol) in THF (100 mL) at −45°C. After addition of HMPT (5 mL), the reaction mixture was stirred for a further 2 h, then filtered to remove NaCl. The solvent was removed in vacuo and the tarry residue re-extracted into THF (15 mL). Crystals of **3a** were obtained by cooling. **3a** can also be purified by column chromatography on a water cooled silica gel column with THF as eluent. The fast-moving, almost colorless fraction was collected. Yield 0.72 g (40%).

3a: ^{29}Si NMR (53.54 MHz, C_6D_6): $\delta = 92.4$ ($^2J(^{31}P,^{29}Si) = 17.5$ Hz); ^{1}H NMR (270.17 MHz, C_6D_6): $\delta = 0.77$ (s, 6H, H_3C–Si), 1.90 (d, 18H, $^3J(^{31}P,^1H) = 4.6$ Hz, H_3C–N); ^{13}C NMR (67.94 MHz, C_6D_6): $\delta = 11.00$ (H_3C–Si), 26.39 (d, $^2J(^{31}P,^{13}C) = 4.6$ Hz, H_3C–N), 218.87 (CO). Correct elemental analyses (C, H, N). **3b**: see [5a, c].

4 (from **1** and **2**): A mixture of **2**·1,5 dioxane (1.32 g, 3.8 mmol) and **1a** (5 mL) or **1b** (5 mL) in 50 mL THF was heated under reflux for 1 h. The reaction mixture was extracted into THF and the extract absorbed on a 10 cm Florisil column. $Fe_3(CO)_{12}$ was eluted with THF after which the Florisil was extracted with THF. Removing the solvent in vacuo afforded **4a** (121 mg) or **4b** (154 mg).

4a: ^{29}Si NMR (C_6D_6): $\delta = -22$ (br.); ^{1}H NMR (C_6D_6): $\delta = 0.2$ (br.); IR (KBr): no Si–O bands; MS (EI): masses up to *m/z* 420 observed, basis peak *m/z* 57; cryoscopic molecular weight determination in dioxane; $M_n = 550 \pm 10$. Correct elemental analyses (C, H). **4b**: ^{29}Si NMR (C_6D_6): $\delta = -91.2$ (br.); ^{1}H NMR (C_6D_6): $\delta = 1.2$ (br.).

4 (from **3**): 1 g of **3** was heated in 30 min to 120°C in vacuum and the temperature maintained at this value for 10 min. After cooling, the polysilane was extracted into THF. Yields: **4a**, 120 mg; **4b**, 80 mg.

5: A solution of **3a** (0.93 g, 3 mmol) or **3b** (1.54 g, 3 mmol) in THF (100 mL) was irradiated at −70°C in the presence of $(C_6H_5)_3P$ (787 mg, 3 mmol) for 2 h using a high-pressure Hg lamp. Removal of the solvent in vacuum afforded **5a** or **5b** in quantitative yield.

5a: ^{1}H NMR (C_6D_6): $\delta = 0.7$ (s, 6H, CH_3), 2.5 (d, $^3J(^{31}P,^1H) = 10.5$ Hz, H_3C–N), 7.0–7.3 (br, 15H, C_6H_5). **5b**: ^{1}H NMR (C_6D_6): $\delta = 1.7$ (s, 18H, *t*BuO), 2.5 (d, $^3J(^{31}P,^1H) = 10.5$ Hz, 18H, HMPT), 7.0–7.3 (br., 15H, C_6H_5); ^{31}P NMR (C_6D_6): $\delta = 87.8$.

6: Further irradiation of **5** at −40°C in the presence of $(C_6H_5)_3P$ (molar ratio 1:2) gave the phosphane complex **6** and the polysilane **4**, which was separated on Florisil as described above. Yield of **6**: 81%.

6: ^{1}H NMR (C_6D_6): $\delta = 7.1$ (br., 18H); 7.5–8.0 (m, 12H); ^{31}P NMR (C_6D_6): $\delta = 95.2$. Correct elemental analyses (C, H).

8: The synthesis of **8** from **7b** [5c] was carried out similarly to the synthesis of **6**: Yield: 79%.

8: ^{1}H NMR (C_6D_6): $\delta = 7.1$ (br., 18H), 7.5–8.0 (m, 12H); ^{31}P NMR (C_6D_6): $\delta = 79.6$. Correct elemental analyses (C, H).

Received: August 15, 1988 [Z 2926 IE]
German version: *Angew. Chem. 101* (1989) 206

[1] a) R. West, L. D. David, P. I. Djurovich, K. L. Stearley, K. S. V. Srinivasan, H. Yu, *J. Am. Chem. Soc. 103* (1981) 7352; b) *The XXI Organosilicon Symposium*, Montreal, June 3–4, 1988; c) R. D. Miller in [1b], Abstr. O9; d) N. Matsumoto in [1b], Abstr. O11; e) J. Maxka, T. Asuke, R. West in [1b], Abstr. P26; f) R. J. Weagley, K. McGrane, M. Abkowitz, F. Knier, M. Stolka in [1b], Abstr. P38; g) P. A. Bianconi, T. W. Weidman, *J. Am. Chem. Soc. 110* (1988) 2342; h) Y. Nagai, H. Matsumoto, K. Higuchi, Y. Hoshino, K. Kubota, H. Koike, Y. Naoi in [1b], Abstr. O34; i) J. Dunogués in [1b], Abstr. O5; j) R. M. Laine, K. A. Youngdahl, R. A. Kennish, T. R. Cronin in [1b], Abstr. P51.

[2] C. Aitken, J. F. Harrod, E. Samuel, *J. Organomet. Chem. 279* (1985) C11.

[3] K. A. Brown-Wensley in [1b], Abstr. O27.

[4] a) T. D. Tilley, J. Arnold, B. K. Campion, H. G. Woo, F. Elsner, R. H. Heyn, A. L. Rheingold, S. J. Geib, *Third Chemical Congress of North America*, June 5–10, 1988, Toronto, Abstr. INOR 62; b) J. Y. Corey, L. Chang, L. D. Lange in [1b], Abstr. P27.

[5] a) C. Zybill, G. Müller, *Angew. Chem. 99* (1987) 683; *Angew. Chem. Int. Ed. Engl. 26* (1987) 669; b) D. A. Straus, T. D. Tilley, A. L. Rheingold, S. J. Geib, *J. Am. Chem. Soc. 109* (1987) 5872; c) C. Zybill, G. Müller, *Organometallics 7* (1988) 1368; d) C. Zybill, D. L. Wilkinson, G. Müller, *Angew. Chem. 100* (1988) 574; *Angew. Chem. Int. Ed. Engl. 27* (1988) 583; e) C. Zybill, G. Müller in [1b], Abstr. O29.

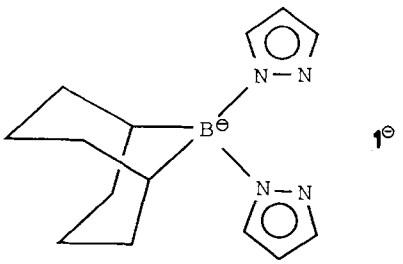
[6] Crystal structure data for **3a**: $C_{12}H_{24}FeN_3O_5PSi$, $M_r = 405.249$, monoclinic, space group $P2_1/c$ (No. 14), $a = 8.353(1)$, $b = 16.079(3)$, $c = 30.445(4)$ Å, $\beta = 106.74(1)°$, $V = 3915.7$ Å^3, $\rho_{calcd} = 1.375$ g cm^{-3} for $Z = 8$, $\mu(Mo_{K\alpha}) = 9.3$ cm^{-1}, $T = -40°C$. 9055 measured reflections, 6153 independent ($R_{int} = 0.038$) and 4539 observed with $F_0 \geq 4\sigma(F_0)$ ($(\sin\theta/\lambda)_{max} = 0.572$ Å^{-1}, $\pm h, +k, +l$, ω-scan, $\Delta\omega = 0.8°$, Syntex $P2_1$, $Mo_{K\alpha}$ radiation, $\lambda = 0.71069$ Å). Solution by direct methods (SHELXS-86), $R(R_w) = 0.053$ (0.051) for 415 refined parameters (anisotropic, H constant, SHELX-76). $\Delta\rho_{fin}$(max/min) = 0.44/−0.37 e Å^{-3}. Further details of the crystal structure investigation can be obtained from the Fachinformationszentrum Energie, Physik, Mathematik GmbH, D-7514 Eggenstein-Leopoldshafen 2 (FRG), on quoting the depository number CSD-53340, the names of the authors, and the journal citation.

[7] Earlier studies favor a radical mechanism for catalytic polymerization of $PhSiH_3$ with Cp_2ZrCl_2; see also: *ACS Monogr. 360* (1988) ("Inorganic and Organometallic Polymers").

Bis[(cyclooctane-1,5-diyl)di(pyrazol-1-yl)borato]cobalt: a Polypyrazolylborate Complex with Two Agostic Hydrogen Bonds**

By *Swiatoslaw Trofimenko, Joseph C. Calabrese,* and *Jeffery S. Thompson**

In this communication, we report on the synthesis and coordination chemistry of a novel polypyrazolylborate ligand, (cyclooctane-1,5-diyl)di(pyrazol-1-yl)borate $\mathbf{1}^{\ominus}$, prepared from 9-borabicyclo[3.3.1]nonane (BBN), pyrazole (Hpz), and potassium pyrazolide. This ligand is similar to the well-known dialkyl(pyrazol-1-yl)borate ligands $\mathbf{2}^{\ominus}$ in having two pyrazolyl groups bonded to the boron atom, but differs in that the alkyl substituents are part of a rigid bicyclic ring system. The results presented herein demonstrate that the Co^{II} coordination chemistry of $\mathbf{1}^{\ominus}$ is different from that of the ligands $\mathbf{2}^{\ominus}$[1-4] since it acts as a tridentate ligand binding through the two pyrazolyl nitrogen atoms and an agostic hydrogen bond to the metal ion.



$\mathbf{1}^{\ominus}$

$[R_2B(pz)_2]^{\ominus}$ $\mathbf{2}^{\ominus}$
$\mathbf{2a}^{\ominus}$, R = Me; $\mathbf{2b}^{\ominus}$, R = Et; $\mathbf{2c}^{\ominus}$, R = *n*Bu

Compounds containing agostic C-H-M bonds have been of great interest because of the proposed role of such interactions in addition/elimination reactions between alkanes and transition metal ions and in olefin polymerizations.[5-8] Although the ligand $\mathbf{2b}^{\ominus}$ provided some of the early examples of agostic hydrogen bonding in Mo chemistry, because of the scorpioid curling of its pseudoaxial ethyl group toward the metal ion, it has the disadvantage of exchange processes among the coordinated methylene hydrogen atoms and of inversion of the $B(pz)_2$-M ring at higher temperatures.[2-4] The new ligand $\mathbf{1}^{\ominus}$ has a single, fixed C-H bond directed towards the metal ion.

Metal complexes with $\mathbf{1}^{\ominus}$ were prepared in a straightforward manner, similar to the procedures used to prepare other polypyrazolylborate ligands and complexes.[1] Although the ligand is prepared as its potassium salt, it is more easily handled as the thallium salt Tl(**1**). Both the thallium salt and the cobalt complex **3**, have a sharp band in the IR spectrum indicative of an agostic bond:[5] 2766 cm^{-1} for Tl(**1**) and 2690 cm^{-1} for **3**. The color of **3** is not deep purple, like that of the known tetrahedral complexes **4**[2] and **5**,[3] but rather pale yellow-red, resembling, in that respect, the octahedral Co^{II} complexes.

$[Co(\mathbf{1})_2] \equiv [Co\{(Cyclooctanediyl)B(pz)_2\}_2]$
3

$[Co\{H_2B(pz)_2\}_2]$ **4** $[Co(\mathbf{2b})_2] \equiv [Co\{Et_2B(pz)_2\}_2]$ **5**

$K[Co(dacoda)(SO_3)] \cdot 5\,H_2O$
6

dacoda = 2,2′-(1,5-diazacyclooctane-1,5-diyl)diacetate

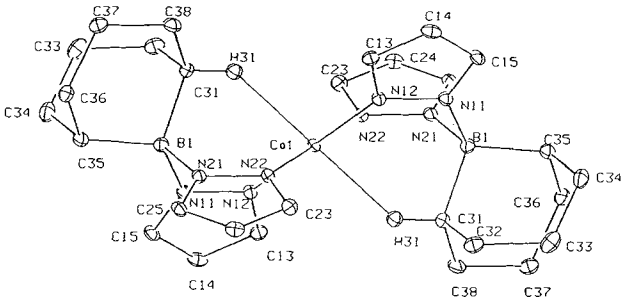


Fig. 1. Molecular structure of **3**. Selected bond lengths [Å]: Co-N12 1.925(3), Co-N22 1.920(3), Co-H31 2.166, Co-C31 2.942(4).

An X-ray structure determination[9] confirmed the pseudooctahedral structure involving two agostic C-H-M bonds (Fig. 1). The 2.166 Å Co-H distance compares well with the previously reported distance of 2.26 Å in the structually more complicated molecule **6**.[10] **3** contains a Co^{II} ion in a rare square planar arrangement with the four pyrazolyl groups, but also with apical agostic hydrogens. In solution, and especially on heating, **3** develops a reddish-purple color, that may be due to partial detachment of the C-H-M bonds and possibly a twist of the two $\mathbf{1}^{\ominus}$ ligands towards a tetrahedral geometry. However, on crystallization, the original material is recovered.

The ligand $\mathbf{1}^{\ominus}$ clearly imposes an unusual coordination geometry upon the Co^{II} ion, unlike that observed with other polypyrazolylborate ligands.[11] The present work, together with our other recent publications,[12] broadens the range of compounds that can be prepared with this growing class of polypyrazolylborate ligands through proper choice of substituents on both the pyrazole ring and the boron atom.

Experimental

K(**1**): Pyrazole (30.4 g, 0.44 mol) and dry KOH pellets (11.2 g, 0.2 mol) were stirred and refluxed in toluene (500 mL) in a 1 L flask. Water was removed by means of a Dean-Stark trap. When all of the water had been removed, 400 mL of a 0.5 M solution of 9-borabicyclo[3.3.1]nonane in THF was added

[*] Dr. J. S. Thompson, Dr. S. Trofimenko, Dr. J. C. Calabrese
E. I. du Pont de Nemours & Company
Central Research & Development Department
Experimental Station, Wilmington, DE 19880-0328 (USA)

[**] Contribution No. 4781 from the Central Research & Development Department, E. I. du Pont de Nemours and Company, Experimental Station, Wilmington, Delaware 19880-0328 (USA).

dropwise at such a rate that THF distilled over slowly. The evolution of hydrogen gas was followed by means of a wet-test meter. When the addition was complete and 5 L of hydrogen had evolved, the slurry was concentrated to approximately 400 mL, cooled slightly, and diluted with hexane to 1 L. A white precipitate formed. The solution was filtered while hot. The white precipitate was then washed with hexane and air-dried to afford K(**1**) as a white solid (54 g, 93% yield), which was used to prepare the other metal derivatives.

Tl(**1**) and [Co(**1**)$_2$] **3**: these compounds were prepared by adding an aqueous solution of $TlNO_3$ or $Co(NO_3)_2$ to a methanolic solution of K(**1**). The precipitated products were isolated by filtration, washed with water, then with methanol, and air-dried. The materials were recrystallized from toluene. Correct elemental analyses (C, H, N) were obtained.

Received: July 14, 1988 [Z 2860 IE]
German version: *Angew. Chem. 101* (1989) 207

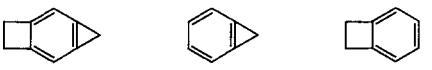
CAS Registry numbers:
K(**1**), 118398-68-8; Tl(**1**), 118398-69-9; **3**, 118398-70-2; BBN, 280-64-8; $TlNO_3$, 10102-45-1; $Co(NO_3)_2$, 10141-05-6; pyrazole, 288-13-1.

[1] S. Trofimenko, *Prog. Inorg. Chem. 34* (1986) 115.
[2] S. Trofimenko, *J. Am. Chem. Soc. 89* (1967) 3170; L. J. Guggenberger, C. T. Prewitt, P. Meakin, S. Trofimenko, J. P. Jesson, *Inorg. Chem. 12* (1973) 508.
[3] S. Trofimenko, *J. Am. Chem. Soc. 89* (1967) 6288.
[4] S. Trofimenko, *J. Am. Chem. Soc. 90* (1968) 4754; *Inorg. Chem. 9* (1970) 2493; F. A. Cotton, T. La Cour, A. G. Stanislowski, *J. Am. Chem. Soc. 96* (1974) 754; F. A. Cotton, V. W. Day, *J. Chem. Soc. Chem. Commun. 1974*, 415; F. A. Cotton, A. G. Stanislowski, *J. Am. Chem. Soc. 96* (1974) 5074.
[5] M. Brookhart, M. L. H. Green, *J. Organomet. Chem. 250* (1983) 395.
[6] A. Shiga, J. Kojima, T. Sasaki, Y. Kitazono, *Chem. Express 1986*, 623; Z. Dawoodi, M. L. H. Green, V. S. B. Mtetwa, K. Prout, A. J. Schultz, J. M. Williams, T. F. Koetzle, *J. Chem. Soc. Dalton Trans. 1986*, 1629; J. W. Park, P. B. Mackenzie, W. P. Schaefer, R. H. Grubbs, *J. Am. Chem. Soc. 108* (1986) 6402; M. Brookhart, S. K. Noh, F. J. Timmers, *Organometallics 6* (1987) 1829; J. R. Bleeke, J. J. Kotyk, D. A. Moore, D. J. Rauscher, *J. Am. Chem. Soc. 109* (1987) 417; F. Timmers, M. Brookhart, *Organometallics 4* (1985) 1365; J. C. Vites, G. Jacobsen, T. K. Dutta, T. P. Fehlner, *J. Am. Chem. Soc. 107* (1985) 5563; P. N. V. Pavankumar, B. Ashok, E. D. Jemmis, *J. Organomet. Chem. 315* (1986) 361.
[7] K. H. Den Haan, Y. Wielstra, J. H. Teuben, *Organometallics 6* (1987) 2053; K. H. Den Haan, J. L. De Boer, J. H. Teuben, A. L. Spek, B. Kojic-Prodic, G. R. Hays, R. Huis, *ibid. 5* (1986) 1726; W. J. Evans, D. K. Drummond, S. G. Bott, J. L. Atwood, *ibid. 5* (1986) 2389; J. Z. Cayias, E. A. Babaian, D. C. Hrncir, S. G. Bott, J. L. Atwood, *J. Chem. Soc. Dalton Trans. 1986*, 2743; G. Erker, W. Frömberg, K. Angermund, R. Schlund, C. Krüger, *J. Chem. Soc. Chem. Commun. 1986*, 372; B. Hessen, F. Van Bolhuis, J. Teuben, *Organometallics 6* (1987) 1352; R. Benn, S. Holle, P. W. Jolly, R. Mynott, C. C. Romao, *Angew. Chem. 98* (1986) 555; *Angew. Chem. Int. Ed. Engl. 25* (1986) 555; M. F. Asaro, S. R. Cooper, J. N. Cooper, *J. Am. Chem. Soc. 108* (1986) 5187; D. K. Bower, J. B. Keister, *J. Organomet. Chem. 312* (1986) C33; T. V. Ashworth, A. A. Chalmers, E. Meintjes, H. Oosthuizen, E. Singleton, *ibid. 276* (1984) C19; *286* (1985) 237; M. A. Bennett, T. I. McMahon, S. Pelling, G. B. Robertson, W. A. Wickramasinghe, *Organometallics 4* (1985) 754; R. H. Crabtree, E. M. Holt, M. Lavin, S. M. Morehouse, *Inorg. Chem. 24* (1985) 1986; G. Minghetti, M. A. Cinellu, A. L. Bandini, G. Banditelli, F. Demartin, M. Manassero, *J. Organomet. Chem. 315* (1986) 387; A. D. Horton, M. J. Mays, M. McPartlin, *J. Chem. Soc. Chem. Commun. 1987*, 424.
[8] B. E. Bursten, R. H. Cayton, *Organometallics 5* (1986) 1051; N. Koga, S. Obara, K. Kitaura, K. Morokuma, *J. Am. Chem. Soc. 107* (1985) 7109.
[9] **3**: triclinic, space group $P\bar{1}$ (No. 2), $a = 7.665(1)$, $b = 9.301(2)$, $c = 10.551(3)$ Å, $\alpha = 88.56(2)$, $\beta = 80.27(2)$, $\gamma = 66.26(2)°$, $V = 677.9$ Å^3; $Z = 1$, $\rho_{calcd} = 1.394$ g cm^{-3}, $3.9 < 2\theta < 55.0$ ($Mo_{K\alpha}$, $\lambda = 0.71069$ Å, $\mu = 6.63$ cm^{-1}, 4304 unique reflections collected, of which 2197 ($I > 3\sigma(I)$) were used to solve (heavy atom Patterson methods) and refine (full matrix, least squares) the structure. $R = 0.046$, $R_w = 0.066$. Further details of the crystal structure investigation can be obtained from the Director of the Cambridge Crystallographic Data Centre, Lensfield Road, Cambridge CB2 1EW (England), by quoting the full literature citation.
[10] K. Kanamori, W. E. Broderick, R. F. Jordan, R. D. Willett, J. I. Legg, *J. Am. Chem. Soc. 108* (1986) 7122.
[11] Neither [Ni(**2b**)$_2$], in which the C(H)–Ni distance is 2.5 Å (H. M. Echols, D. Dennis, *Acta Crystallogr. Sect. B 30* (1974) 2173), nor its Cr^{II} analog (F. A. Cotton, G. N. Motts, *Inorg. Chem. 22* (1983) 1136) show an agostic interaction.
[12] J. C. Calabrese, S. Trofimenko, J. S. Thompson, *J. Chem. Soc. Chem. Commun. 1986*, 1122; *Inorg. Chem. 26* (1987) 1507.

Structure, Deformation Electron Densities, Photoelectron Spectra, and Reactivity of 3,4-Dihydro-1*H*-cyclobuta[*a*]cyclopropa[*d*]benzene**

By *Dieter Bläser, Roland Boese,* Waldemar A. Brett, Paul Rademacher, Harald Schwager, Amnon Stanger,* and *K. Peter C. Vollhardt**

The title compound **1**[1] ranks among the most strained fused benzenes known.[2] Simple resonance pictures suggest increased double bond character[3] at the sites of ring fusion in **1** compared to that observed in 1*H*-cyclopropabenzene **2** and 1,2-dihydrocyclobutabenzene **3** and thus also suggest unusual reactivity in ring-opening transformations.



1 **2** **3**

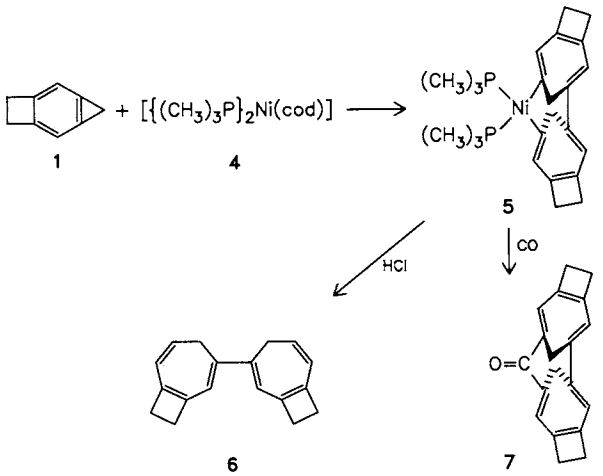
Interestingly, however, MNDO[4] calculations reveal that the energies of the frontier orbitals and the size of their coefficients at the sites of ring fusion in **1** are very similar to those found in the model systems **2** and **3**, indicating that, should attack by a metal be frontier-orbital-controlled, any observable rate differences may be attenuated. A theoretical estimation of the enthalpies of hydrogenation of the respective double bonds gave values of −48.6 (**2**), −22.3 (**3**), and −51.9 (cyclopropene bond in **1**) kcal mol^{-1}.[4c] Clearly (and not surprisingly) conversion of the cyclopropene (and not cyclobutene) carbons in **1** is favored thermodynamically, but (and in conflict with expectation) not much more than the cyclopropene bond of **2**.

Preliminary experiments showed that **3** is not attacked by (η^4-1,5-cyclooctadiene)[bis(trimethylphosphane)]nickel **4** (THF, 20–60 °C, 3 d); the only new products are metallic nickel and $Ni[P(CH_3)_3]_4$. In contrast, addition of **1** (2 equiv.)[5] to **4** (pentane, −78 to 20 °C, 3 h), resulted cleanly in the extremely air-sensitive metallacycle **5** (79%)[6]—a reaction that proceeded in a manner completely analogous to that of **2** to give **8**.[5a,f] The assignment of the *anti*-conformation of **5** is tentative and follows by analogy with the structure of the metallacycle **8** that has been proven by an X-ray analysis.[5f] Like **8**,[5a,f] compound **5** is hydrolyzed by HCl to **6** and carbonylated by CO to **7**.[7]

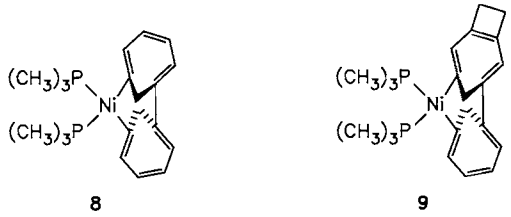
A competition experiment (**1** : **2** : **4** = 8 : 8 : 1, pentane in preparative, [D_8]THF in analytical ^{1}H-NMR runs carried out to 30% and 100% completion) gave results completely irreconcilable with a simple bond-fixation analysis but

[*] Dr. R. Boese, Dipl.-Ing. D. Bläser
Institut für Anorganische Chemie der Universität—GH
Universitätsstrasse 3-5, D-4300 Essen 1 (FRG)
Prof. Dr. P. Rademacher, Dipl.-Chem. W. A. Brett
Institut für Organische Chemie der Universität—GH
Essen (FRG)
Prof. Dr. K. P. C. Vollhardt, Dr. H. Schwager, Dr. A. Stanger
Department of Chemistry, University of California at Berkeley, and the Materials and Chemical Sciences Division
Lawrence Berkeley Laboratory
Berkeley, CA 94720 (USA)

[**] This work was supported by the Director, Office of Energy Research, Office of Basic Energy Sciences, Materials Science Division of the U.S. Department of Energy (Contract No. DE-AC03-76 SF 00098) and by the National Institutes of Health (CA 20713). *H. S.* was the recipient of an Otto-Hahn fellowship and a Max-Planck Institute for Coal Research (Mülheim) fellowship (1986–1987), *A. S.* acknowledges a Dr. Chaim Weizmann fellowship (1985–1987).



gratifyingly consistent with the calculations: not only were all possible coupling products **5**, **8**, an **9** formed, but incorporation of the less strained building block **2** was in fact dominant (in all cases, **5** : **8** : **9** = 1 : 4 : 4)! Assuming that the relative reactivity of **1** and **2**, respectively, is the same in the two consecutive (presumably η^2)[5c,8] metal complexation steps, its value would be approximately 1 : 2.



The reactions of the substrates **1** and **2** with **4**, with or without added ligands, are in excellent agreement with direct (perhaps HOMO controlled)[4b] attack of the arene on **4** (or its η^2-1,5-cyclooctadiene isomer bearing an open coordination site) followed by 1,5-cyclooctadiene dissociation, inhibited strongly at low concentrations of the aromatic substrate, less so when these are high. To shed light on the unexpectedly low reactivity of **1**, an X-ray analysis[10] was carried out at 100 K (Fig. 1) and the result compared with those for **2**[9a] and **3**.[9b]

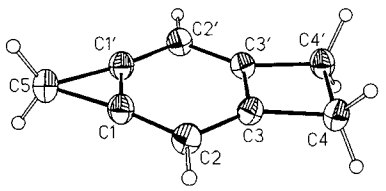


Fig. 1. Crystal structure of **1** (ellipsoids correspond to the 50% probability surface) [10] at 100 K. Distances [Å] and angles [°] (maximum standard deviations 0.001 Å and 0.1°, respectively), values after a libration correction [11] in parentheses: C1–C2 1.385 (1.388), C2–C3 1.405 (1.407), C3–C4 1.522 (1.524), C1–C5 1.508 (1.510), C1–C1′ 1.349 (1.353), C3–C3′ 1.402 (1.406), C4–C4′ 1.579 (1.583); C1–C2–C3 109.2, C1′–C1–C2 170.2, C1–C5–C1′ 53.2, C2–C3–C4 142.2, C3–C4–C4′ 86.7, C1′–C1–C2 126.3, C5–C1–C1′ 63.4, C2–C3–C3′ 124.4, C3′–C3–C4 93.3.

In **1**,[12] the bonds of the cyclopropene ring are 0.015–0.022 Å longer than those in **2**, and the bonds of the cyclobutene ring are 0.003–0.020 Å longer than in **3**. The largest differences in the bond distances of **1** and **2** are found for the bonds C1–C2 and C1′–C2′ (0.022 Å). The corresponding bond angle at C2 and C2′ is extremely small (109.2°), reduced by 4.0° and 6.8°, respectively, compared to those in **2** and **3**. Thus, there is an additive expansion effect of the double annelation in **1**, the reasons for which may be gleaned from the electron density maps (Fig. 2a).

Consistent with the assumption that the deviations of the electron density maxima from the direct C–C connections is a measure of strain (Fig. 2b), the cyclopropene ring pushes its electrons more strongly (0.27 Å) into the π-system than its cyclobutene counterpart (0.10 Å). The electron densities are moved into the exocyclic direction with respect to the bonds C1–C2 and C2–C3, a result of the intracyclic shifts of the annelated bonds. This shift is smaller with respect to C1–C2 (0.04 Å) than that with respect to C2–C3 (0.15 Å). The extent of this effect is also evident in the bond angles that can be assigned to the electron density maxima (Fig. 2b). In the cyclopropene moiety the "outside" angle is 98° instead of 53.2° for the nucleus–nucleus connection, that associated with the annelating carbon 170.2° instead of 141°; in the case of the four-membered ring the latter value is 130° instead of 142.2°. Even the smallest bond angle in the benzene nucleus is widened from 109.2° to 117°.

The X–X deformation electron density map perpendicular to the molecular plane in the C_2-axis reveals a π-contribution by its elliptical shape along the distances C1–C1′ and

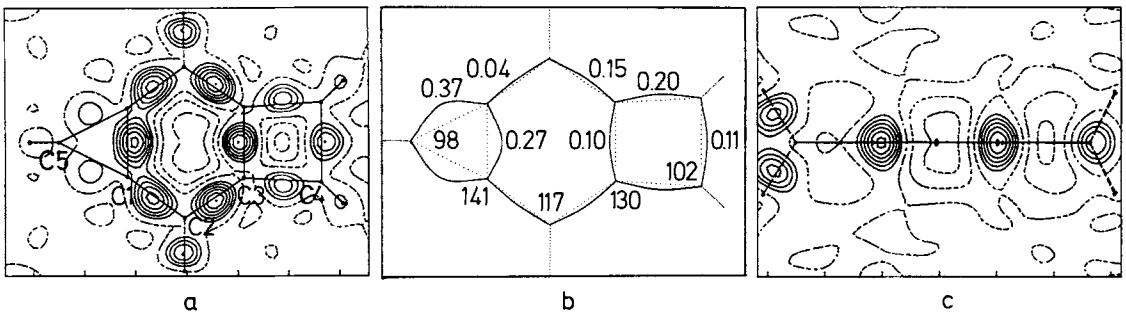


Fig. 2. a) Contour lines of the X–X deformation electron densities in the molecular plane of **1**. Unbroken lines: positive values and zero, distance 0.05 e/Å^3; broken lines: negative values, distance 0.1 e/Å^3. b) Electron density maxima shifts (decimal points in Å) of the internuclear distances (dotted); the unbroken lines lead in every case from nucleus to nucleus via the electron density maximum. The quoted angles [°] refer to the direct electron density maximum-nucleus-electron density maximum connections. The estimated standard deviations are 0.02 Å and 1°, respectively. c) Contour lines of the X–X deformation electron density lines perpendicular to the molecular plane in the C_2-axis of the molecule (edge view; left cyclopropene part, right cyclobutene part). Other details as in Fig. 2a.

C3–C3′, respectively, compared to the radial distribution along the single bond C4–C4′ (Fig. 2c). To counter the effects of the doubly induced strain, the system undergoes expansion, thus avoiding an even greater displacement of the electron density maxima from the direct internuclear connections.

That the structure of **1** is unusual is also reflected in its photoelectron spectrum.[13] Thus, not only are the first two ionization bands (π_2, π_3) shifted to lower energies, but their splitting (0.84 eV) is noticeably larger than those in **2** (0.66 eV) and **3** (0.54 eV).[14] Most importantly, and in contrast to 1,2,4,5-dicyclobutabenzene,[15] their average value (8.72 eV)[13] is ca. 0.1 eV lower than that estimated assuming a simple additive effect of the two annelated rings (C_6H_6 9.25 eV, **2** 9.15 eV, **3** 8.93 eV), consistent with the observed expansion of the aromatic ring. Ab initio calculations[16] indicate an overall stabilizing effect of this deformation, the sum of the heats of formation of benzene and **1** being lower than that of **2** and **3**.

Received: July 20, 1988;
revised: October 31, 1988 [Z 2873/2874 IE]
German version: *Angew. Chem. 101* (1989) 209

[1] a) C. J. Saward, K. P. C. Vollhardt, *Tetrahedron Lett. 1975*, 4539; b) D. Davalian, P. J. Garratt, W. Koller, M. M. Mansuri, *J. Org. Chem. 45* (1980) 4183.

[2] a) A. Greenberg, J. F. Liebman: *Strained Organic Molecules*, Academic Press, New York 1978; b) K. P. C. Vollhardt, *Pure Appl. Chem. 52* (1980) 1645; c) B. Halton, *Ind. Eng. Chem. Prod. Res. Dev. 19* (1980) 349; d) W. E. Billups, *Acc. Chem. Res. 11* (1978) 245; e) R. P. Thummel, *Isr. J. Chem. 22* (1982) 11; f) W. E. Billups, W. A. Rodin, M. M. Haley, *Tetrahedron 44* (1988) 1305.

[3] a) P. C. Hiberty, G. Ohanessian, F. Delbecq, *J. Am. Chem. Soc. 107* (1985) 3095; b) A. Stanger, K. P. C. Vollhardt, *J. Org. Chem. 53* (1988) 4889.

[4] a) M. J. S. Dewar, W. Thiel, *J. Am. Chem. Soc. 99* (1977) 4899, 4907; b) Y. Apeloig, D. Arad, *ibid. 108* (1986) 3241; c) these figures are in good agreement with strain energy values obtained using ab initio methods [16].

[5] a) R. Mynott, R. Neidlein, H. Schwager, G. Wilke, *Angew. Chem. 98* (1986) 374; *Angew. Chem. Int. Ed. Engl. 25* (1986) 367; b) R. Neidlein, A. Rufińska, H. Schwager, G. Wilke, *ibid. 98* (1986) 643 and *25* (1986) 640; c) H. Schwager, C. Krüger, R. Neidlein, G. Wilke, *ibid. 99* (1987) 72 and *26* (1987) 65; d) H. Schwager, R. Benn, G. Wilke, *ibid. 99* (1987) 73 and *26* (1987) 67; e) C. Krüger, K. Laakmann, G. Schroth, H. Schwager, G. Wilke, *Chem. Ber. 120* (1987) 471; f) H. Schwager, *Dissertation*, Universität Bochum 1986.

[6] **5**: orange-brown crystals, m.p. > 100 °C; IR (KBr): $\tilde{\nu}$ = 2952, 2902, 2821, 1483, 1459, 1429, 1414, 1378, 1345, 1299, 1255, 1237, 1226, 1183, 1166, 1116, 1067, 1049, 902, 780, 714, 662, 645, 614 cm^{-1}; ^1H NMR (500 MHz, [D$_8$]THF, 25 °C): δ = 6.18 (d, ^4J(H,P) = 3.6 Hz, 2H), 5.85 (s, 2H), 2.90 (br. d, ^2J(H,H′) = 8.8 Hz, 2H), 2.86–2.56 (m, 8H), 1.33 (dd, ^2J(H,H′) = 8.8 Hz, ^4J(H,P) = 3.9 Hz, 2H), 1.26 (d, ^2J(H,P) = 7 Hz, 18H); ^{13}C NMR (125 MHz, [D$_8$]THF, −30 °C): δ = 169.4, 144.1, 137.6, 129.4, 125.6, 115.9, 53.5, 30.3, 29.1, 16.7; ^{31}P NMR (125 MHz, [D$_8$]THF, 25 °C): δ = −17.9; MS (EI): *m/z* 234 (4%), 117 (4), 76 (71), 57 (100). — **6**: ^1H NMR (300 MHz, [D$_8$]THF, 25 °C): δ = 6.45 (s, 2H), 6.17 (d, J = 8.7 Hz, 2H), 5.17 (dt, J = 8.7, 15.2 Hz, 2H), 2.85 (m, 8H), 2.03 (d, J = 15.2 Hz, 4H). — **7**: stereochemistry tentative; ^1H NMR (300 MHz, [D$_8$]THF, 25 °C): δ = 6.50 (s, 2H), 6.42 (s, 2H), 2.94 (AA′BB′m, 8H), 2.92 (d, J = 11.1 Hz, 2H), 1.52 (d, J = 11.1 Hz, 2H). — **9**: ^1H NMR (300 MHz, [D$_8$]THF, 25 °C, obtained from the mixture with **5** and **8** by spectral subtraction): δ = 6.33 (dd, J = 6.10 Hz, 1H), 6.22 (m, 2H), 6.08 (dd, J = 6, 11 Hz, 1H), 5.96 (d, J = 6 Hz, 1H), 5.93 (br. s, 1H), 2.93 (br. d, J = 9 Hz, 1H), 2.84 (m, 3H), 2.64 (m, 2H), 1.32 (br. d, J = 9 Hz, 1H), 1.25 (d, J = 7 Hz, 18H), 0.94 (dd, J = 3 Hz, 9 Hz, 1H); ^{31}P NMR (125 MHz, [D$_8$]THF, 25 °C): δ = −17.8.

[7] The unexpected [5a, f] biscycloheptatriene structure of 7 is presumably a consequence of the cyclobutaannelation. a) F.-G. Klärner, E. K. G. Schmidt, M. A. Abdel Rahman, *Angew. Chem. 94* (1982) 136; *Angew. Chem. Int. Ed. Engl. 21* (1982) 138; *Angew. Chem. Suppl. 1982*, 331; b) F.-G. Klärner, E. K. G. Schmidt, M. A. Abdel Rahman, H. Kollmar, *ibid. 94* (1982) 137 and *21* (1982) 139; *Angew. Chem. Suppl. 1982*, 338; c) R. P. Thummel, P. Chayangkoon, *J. Org. Chem. 48* (1983) 596.

[8] a) E. Lindner, *Adv. Heterocycl. Chem. 39* (1986) 237; b) S. D. Chappell, D. J. Cole-Hamilton, *Polyhedron 1* (1982) 739.

[9] a) R. Neidlein, D. Christen, V. Poignee, R. Boese, D. Bläser, A. Gieren, C. Ruiz-Perez, T. Hübner, *Angew. Chem. 100* (1988) 292; *Angew. Chem. Int. Ed. Engl. 27* (1988) 294; b) R. Boese, D. Bläser, *ibid. 100* (1988) 293 and *27* (1988) 304.

[10] Crystal size 0.52 × 0.48 × 0.43 mm^3, monoclinic space group *C2/c*, a = 7.626(1), b = 8.566(1), c = 10.193(2) Å, β = 110.28(1)°, V = 624.6(2) Å^3, 100 K, $Mo_{K\alpha}$ radiation, ρ_{calcd} = 1.24 g cm^{-3}, measured data sets $\pm h \pm k \pm l$ to 60°, $\pm h + k + l$ to 90°, 3055 independent reflections, 1941 observed, R for $2\theta_{max}$ = 60°, 830 observed reflections, 59 parameters, extinction correction, R = 0.037, Rw = 0.044, $w^{-1} = \sigma^2(F_0) + 0.0005F^2$, R-values for high angle refinement ($60° \leq 2\theta \leq 90°$), C–H distances expanded to 1.08 Å and atomic positions as well as temperature factors of hydrogen atoms fixed to the values of the previous refinement, 1111 observed reflections, 42 parameters, R = 0.047, R_w = 0.045, $w^{-1} = \sigma^2(F_0) + 0.0005F^2$. Further details of the crystal structure investigation may be obtained from the Fachinformationszentrum Energie, Physik, Mathematik GmbH, D-7514 Eggenstein-Leopoldshafen 2 (FRG), by quoting the depository number CSD-53476, the names of the authors, and the journal citation.

[11] V. Schomaker, K. N. Trueblood, *Acta Crystallogr. Sect. B24* (1968) 63.

[12] The uncorrected data for **1**–**3** were used in this comparison [5].

[13] Measured at 23 °C on a Leybold-Heraeus UPG 200 spectrometer using He(I) radiation (21.21 eV). MNDO calculations allow the following assignments: 8.30 eV (π_3), 9.14 eV (π_2), 10.01 eV (ω_A cyclopropene ring), 10.84 eV (σ), 11.45 eV (π_1).

[14] F. Brogli, E. Giovannini, E. Heilbronner, R. Schurter, *Chem. Ber. 106* (1973) 961.

[15] C. Santiago, R. W. Gandour, K. N. Houk, W. Nutakul, W. E. Cravey, R. P. Thummel, *J. Am. Chem. Soc. 100* (1978) 3730.

[16] Y. Apeloig, *Proc. NATO Adv. Workshop on Stress and Strain*, Ratzeburg 1988, in press.

2,4,6-Triisopropylphenylcopper, a New Tetranuclear Organocopper Aggregate with Unsymmetrically Bridging σ–π Bonded Aryl Ligands**

By *Dominique Nobel, Gerard van Koten**, and *Anthony L. Spek*

In organic synthesis, there are many widely-used reactions which employ organocopper reagents or in which organocopper species are important intermediates; the Ullmann and Castro reactions are typical examples.[1] However, the available structural information for organocopper species is limited, owing to their high reactivity and to the difficulties encountered in preparing pure compounds and in growing single crystals.[2] Earlier results from this laboratory demonstrated that it was possible to isolate stable, well-defined aryl copper complexes when a coordinating function was introduced in the ring at the *ortho*-position(s). A similar stabilizing effect arises when steric hindrance is introduced near the metal–carbon bond. Representative structures are those of pentameric mesitylcopper **1**,[3] which contains three-center two-electron bonded mesityl ligands, and of monomeric 2,4,6-triphenylphenylcopper **2**,[4] which possesses a two-center two-electron σ-bonded aryl group.

[2,4,6-$Me_3C_6H_2Cu$]$_5$ **1** 2,4,6-$Ph_3C_6H_2Cu$ **2**

Herein, we report on the synthesis, characterization and reactivity of the new organocopper compound 2,4,6-triisopropylphenylcopper **3**, whose structure features an unsymmetrically bridging 2,4,6-triisopropylphenyl ligand, a novel

[*] Prof. Dr. G. van Koten, Dr. D. Nobel
Department of Metal-mediated Synthesis,
University of Utrecht
Padualaan 8, NL-3584 CH Utrecht (The Netherlands)
Dr. A. L. Spek
Department of Crystal and Structural Chemistry,
University of Utrecht
Padualaan 8, NL-3584 CH Utrecht (The Netherlands)

[**] This work was supported by the E.E.C. and SON/NWO.

bonding situation which provides the missing link between the two extremes represented by **1** and **2**.

[2,4,6-iPr$_3$C$_6$H$_2$Cu]$_4$ **3**

Compound **3** is conveniently prepared by the reaction of 2,4,6-iPr$_3$C$_6$H$_2$Li and CuBr in ether at 243 K, and can be isolated as a pale yellow, air and moisture sensitive solid. Crystals of **3** are thermally stable (decomp. 215°C) and dissolve readily in aprotic organic solvents including pentane. A cryoscopic molecular weight determination for **3** in benzene gave a concentration-independent molecular weight of 613 which is higher than that expected for the monomer (M = 266.9). This result, which indicates a degree of association of ca. 2.3, is good evidence for the presence of aggregated species in solution. At 198 K, the ^{1}H NMR spectrum of **1** ([D$_8$]toluene, 200 MHz) exhibits two equally intense sets of signals for the *ortho*-isopropyl substituents, with the CH resonances at δ = 4.47 and 3.50 and those of the CH$_3$ groups at δ = 1.79 and 1.04. At the same temperature, the ^{13}C NMR spectrum (50.32 MHz) shows not only signals attributable to two different *ortho*-isopropyl groups and a single *para*-isopropyl substituent, but also six separate signals for the carbon atoms of the aromatic rings. These ^{1}H and ^{13}C NMR data indicate that in **3**, although all the aryl ligands are equivalent, the molecular structure must possess a particular symmetry. On raising the temperature of the solution, spectral changes occur which are consistent with the occurrence of intermolecular exchange processes. For example, in the ^{1}H NMR spectrum, the sets of resonances attributed to the *ortho*-isopropyl groups coalesce at ca. 273 K, and at 293 K afford two broad signals at δ = 3.88 (CH) and 1.29 (CH$_3$).

A single crystal X-ray structural analysis[5] (Fig. 1a) showed that **1** exists in the solid state as a tetranuclear aggregate with (crystallographic point group $\bar{4}$) containing a slightly distorted square planar Cu$_4$ array (characterized by Cu–Cu distances of 2.445(1) Å and a Cu–Cu–Cu angle of 89.86(3)°) with each Cu–Cu edge bridged by the C_{ipso} of a 2,4,6-triisopropylphenyl unit.

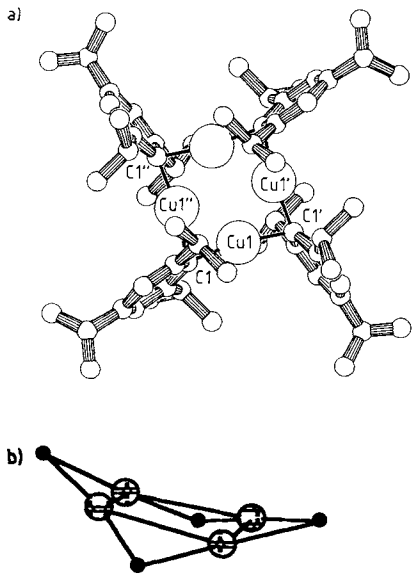


Fig. 1. a) Crystal structure of **3**. Selected bond lengths [Å] and angles [°]: Cu1–Cu1′ 2.445(1), Cu1–C1 1.958(7), Cu1″–C1 2.018(7); Cu1″–Cu1–Cu1′ 89.86(3), C1–Cu1–C1′ 169.8(3). b) Schematic representation of **3** showing the puckering of the Cu$_4$C$_4$ ring.

The resultant eight-membered Cu$_4$C$_4$ ring is distinctly puckered (Figure 1b) with the four Cu atoms and the four C_{ipso} atoms alternately situated ±0.0660(2) and ±0.578(7) Å, respectively, above and below the mean Cu$_4$ plane. The bridging mode of the aromatic rings is highly unsymmetrical, as illustrated both by the significant differences between the Cu1–C1 (1.958(7) Å) and Cu1″–C1 (2.018(7) Å) bond lengths and by the 67.4(3)° angle between the aromatic plane and the Cu1–Cu1″ vector.

A possible rationale for this geometry is that the aromatic C_{ipso} atom is σ-bonded to one copper center (Cu1) but π-bonded to the other (Cu1″); this is shown schematically in Figure 2. This bonding description is supported by

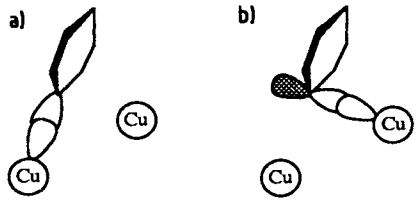
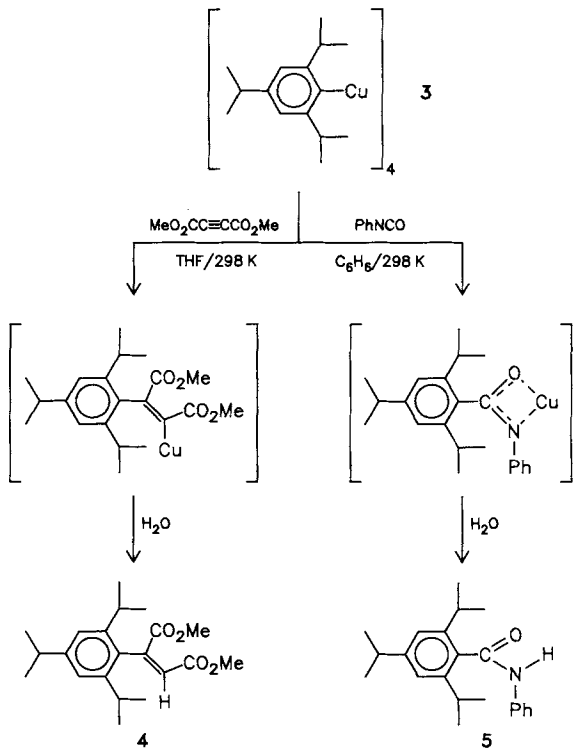


Fig. 2. Molecular orbitals involved in the σ- and π-interactions of **3**.

the almost linear C_{ipso}–Cu–C_{ipso} arrangement with an angle of 169.8(3)°. Consequently, the cluster might be best described as resulting from the association of four monomeric iPr$_3$C$_6$H$_2$Cu units having two-center two-electron bonds, whereby stabilization is provided by an interaction of the electron-rich π-orbital of C_{ipso}, perpendicular to the plane of the aryl ring, with an empty orbital of a neighboring copper atom.



These features in **3** and those found in complexes such as **1** and **2** confirm that steric factors can greatly affect the bonding mode of organic groups in organocopper com-

pounds: an increase of the steric requirements of the *ortho*-substituents (e.g., Ph > *i*Pr > Me) in arylcopper complexes results in an increased tendency to form two-center two-electron Cu-C bonds which are shielded by the *ortho*-substituents, thus hindering interactions with other mononuclear units (e.g. in **2**).

The peculiar bonding mode found in **3** is reflected in its unusual reactivity towards electrophilic substrates, such as dimethylacetylene dicarboxylate (DMADC) and phenyl isocyanate. At ambient temperature, both substrates insert into the Cu-C bond of **3** affording, after hydrolysis, the corresponding alkene **4** or amide **5** in quantitative yield.

The alkyne insertion reaction is normally only exhibited by hetero cuprate reagents (i.e., RCuMX species, M = Li, MgX),[6] while the isocyanate reaction is unprecedented for organocopper reagents. Preliminary experiments involving the *tert*-butyl analogue of **3** indicate a similar diverse reactivity. It can be anticipated that the sterically demanding *ortho-tert*-butyl groups would result in this compound being dimeric or even monomeric. However, its high instability has until now hampered the growth of crystals suitable for an X-ray analysis.

Experimental

3: A diethyl ether solution of triisopropylphenyllithium (1.0 M, 32 mL) was added at 233 K to a stirred suspension of CuBr (4.5 g, 31.3 mmol) in Et_2O. The reaction mixture was stirred for 1 h and the solvent removed in vacuo. The pale yellow residue was recrystallized from pentane to give **3** as yellow prisms in 50% yield. ^{1}H NMR (298 K, [D$_8$]toluene): $\delta = 1.21$ (d, 6H, *p*-CH(CH_3)$_2$, $^3J = 6.9$ Hz), 1.29 (d, 12H, *o*-CH(CH_3)$_2$, $^3J = 6.5$ Hz), 2.74 (sept., 1H, *p*-C*H*(CH$_3$)$_2$, $^3J = 6.9$ Hz), 3.88 (sept, 2H, *o*-C*H*(CH$_3$)$_2$, $^3J = 6.5$ Hz), 7.01 (s, 2H, Aryl-H). ^{13}C{^{1}H} NMR (298 K, [D$_8$]toluene): $\delta = 24.09$ (*p*-CH(*C*H$_3$)$_2$), 27.40 (*o*-CH(CH$_3$)$_2$), 34.96 (*p*-*C*H(CH$_3$)$_2$), 41.77 (*o*-*C*H(CH$_3$)$_2$), 120.86 (*m*-C), 136.17 (Cu-C), 152.58 (*p*-C), 167.00 (*o*-*C*H(CH$_3$)$_2$).

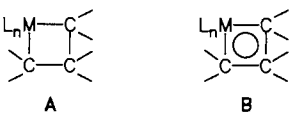
Reactions with DMADC and PhNCO: To a solution of **1** (0.26 g, 1 mmol) in benzene was added two equivalents of DMADC or PhNCO. After stirring for 1 h, the reaction mixture was poured into a 10% aqueous NH_4Cl solution. The organic layer was dried and the solvent removed in vacuo to afford a pale yellow solid which was recrystallized from pentane. **4**: m.p. 378 K. ^{1}H NMR ($CDCl_3$): $\delta = 1.16$ (d, 6H, *o*-CH(CH_3)$_2$, $^3J = 6.8$ Hz), 1.21 (d, 6H, *o*-CH(CH_3)$_2$, $^3J = 6.8$ Hz), 1.25 (d, 6H, *p*-CH(CH_3)$_2$, $^3J = 6.9$ Hz), 3.24 (sept, 1H, *p*-C*H*(CH$_3$)$_2$, $^3J = 6.9$ Hz), 3.89 (sept, 2H, *o*-C*H*(CH$_3$)$_2$, $^3J = 6.8$ Hz), 3.60 (s, 3H, OCH_3), 3.61 (s, 3H, OCH_3), 5.95 (s, 1H, HC=C), 7.03 (s, 2H, Aryl-H). FD-MS: *m/z* 346 (5%, $M^{\oplus}$), 331 (9, $M^{\oplus} - Me$), 286 (100, $M^{\oplus} - HCO_2Me$). **5**: m.p. 456 K. ^{1}H NMR ($CDCl_3$): $\delta = 1.26$ (d, 12H, *o*-CH(CH_3)$_2$, $^3J = 6.8$ Hz), 1.28 (d, 6H, *p*-CH(CH_3)$_2$, $^3J = 6.9$ Hz), 2.92 (sept, 1H, *p*-C*H*(CH$_3$)$_2$, $^3J = 6.9$ Hz), 3.10 (sept, 2H, *o*-C*H*(CH$_3$)$_2$, $^3J = 6.8$ Hz), 7.06-7.68 (8H, Aryl-H and NH). FD-MS: *m/z* 323 (5%, $M^{\oplus}$), 231 (100%, $M^{\oplus} - PhNH$).

Received: September 12, 1988 [Z 2963 IE]
German version: *Angew. Chem. 101* (1989) 211

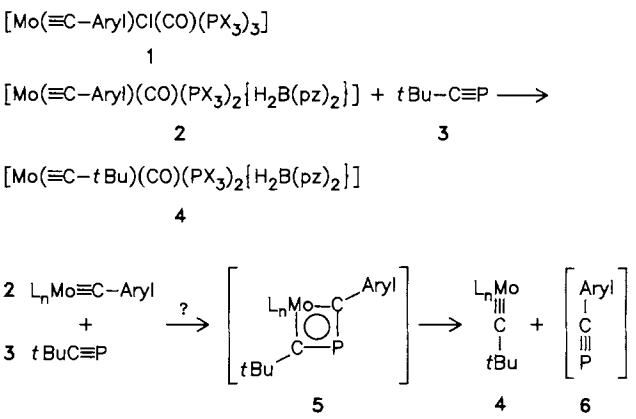
Reactions of Mono- and Dinuclear Metal-Alkylidyne Complexes with Phosphaalkynes: C≡P and C≡Mo Metathesis**

By *Anthony F. Hill, Judith A. K. Howard, Thomas P. Spaniol, F. Gordon A. Stone** and *Jürgen Szameitat*

Transition metal-mediated alkene- and alkyne-metathesis processes are considered to proceed via the cycloaddition of metal-carbon and carbon-carbon multiple bonds to form, often transiently, metallacyclobutanes **A** or metallacyclobutadienes **B**, respectively.[1,2] Guided by the isolobal analogy,[3] which relates the frontier orbitals and valence electrons of the fragments CR, P and d^5-ML_5 (M = Mo or W, L = ligand), we have addressed the question of cycloaddition and metathesis in reactions of a phosphaalkyne with both mononuclear and heterobinuclear metal-alkylidyne complexes.



Treating *t*BuC≡P **3**[4] with the alkylidynemolybdenum complex **2**, prepared from **1** and K[$H_2B(pz)_2$],[5] affords, in quantitative yield, the neopentylidynemolybdenum compound **4**. A plausible intermediate in this transformation is



Aryl = *o*-$H_3COC_6H_4$; X = OCH_3; pz = pyrazol-1-yl

the 1-phospha-3-molybdacyclobutadiene **5**, which may either retro-eliminate **3** or afford the phosphaalkyne **6**. The instability of the latter would then drive the process towards the observed quantitative formation of **4**.

We have so far been unable to isolate a mononuclear metal complex structurally akin to **B**. However, our extensive studies of the reactions of bi- and trinuclear metal-alkylidyne complexes with alkynes have led to the discovery of many dimetal compounds of type **7** which may be

[1] G. H. Posner: *An Introduction to Synthesis using Organocopper Reagents*, Wiley Interscience, New York 1980.

[2] G. van Koten, J. G. Noltes in G. Wilkinson, F. G. A. Stone, E. W. Abel (Eds.): *Comprehensive Organometallic Chemistry, Vol. II*, Pergamon Press, Oxford 1982, Chap. 14, p. 709.

[3] a) S. Gambarotta, C. Floriani, A. Chiesi-Villa, C. Guastini, *J. Chem. Soc. Chem. Commun. 1983*, 1156.

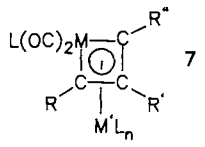
[4] R. Lingnau, J. Strähle, *Angew. Chem. 100* (1988) 409; *Angew. Chem. Int. Ed. Engl. 27* (1988) 436; according to the IUPAC rules the ligand should be referred to as a 5′-phenyl-*m*-terphenyl-2′-yl (Rule A-54-3).

[5] Tetragonal, space group $P\bar{4}2_1c$, $Z = 2$, $Mo_{K\alpha}$ radiation (Zr filtered), $a = b = 12.810(5)$, $c = 18.004(6)$ Å, $V = 2954(2)$ Å^3, $\rho_{calcd} = 1.200$ g cm^{-3}. 1623 independent reflections $I > 2.5\sigma(I)$, $(1.13° \leq \theta \leq 25.0°)$. The structure was solved using Patterson and Fourier methods and anisotropically refined to $R = 0.069$. Hydrogen atoms were located at calculated positions. Further details of the crystal structure investigation may be obtained from the Director of the Cambridge Crystallographic Data Centre, Lensfield Road, Cambridge CB2 1EW (England), on quoting the full literature citation.

[6] E. Wehman, G. van Koten, M. Knotter, H. H. Spelten, D. Heijdenrijk, A. N. S. Mak, C. H. Stam, *J. Organomet. Chem. 325* (1987) 293.

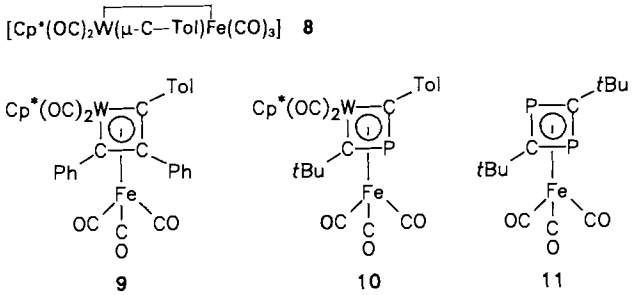
[*] Prof. Dr. F. G. A. Stone, Dr. J. A. K. Howard, Dr. J. Szameitat, Dr. A.. F. Hill, T. P. Spaniol
Department of Inorganic Chemistry, University of Bristol
Bristol BS8 1TS (U.K.)

[**] This work was supported by the U. K. Science and Engineering Research Council, the Deutsche Forschungsgemeinschaft and the Deutsche Bundesbahn. (Scholarship to T. P. S.)



7

regarded[6a,7] as metallacyclobutadienes stabilized by 'complexation' with metal–ligand fragments.[3,8] Accordingly, the bimetallic p-tolylmethylidyne complex **8**, which reacts with PhC≡CPh[7c] to yield such an 'Fe(CO)$_3$' coordinated tungstacyclobutadiene **9**, was treated with **3**. In this manner, complex **10** was isolated and fully characterized in-



8

9 **10** **11**

Cp* = η^5-$C_5(CH_3)_5$; Tol = p-$H_3CC_6H_4$

cluding an X-ray diffraction study.[9] The latter established the structure shown in Figure 1, which may be viewed as a 1-phospha-3-tungstacyclobutadiene moiety coordinated to an Fe(CO)$_3$ group.[6b]

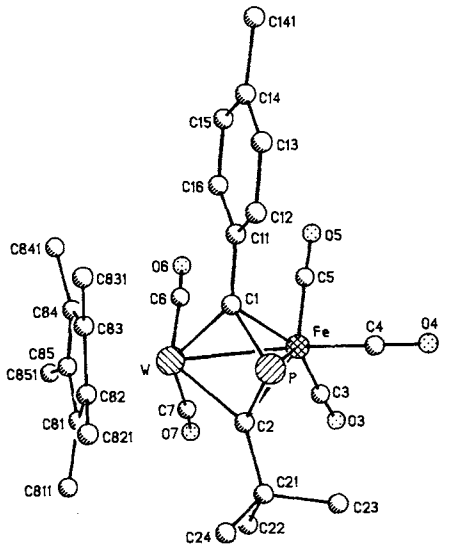


Fig. 1. Molecular structure of complex **10**. Bond lengths [Å]: C(1)-Fe 2.11(2), C(1)-P 1.76(2), C(1)-W 2.18(2), C(2)-Fe 2.14(1), C(2)-P 1.77(1), C(2)-W 2.22(1), Fe-P 2.34(1), W-Fe 2.720(2).

Despite the displacement (0.649 Å) of the W atom from the plane defined by C(1), C(2) and P, the close similarity between the bonds between P and C(1) [1.76(2)] and C(2) [1.77(1) Å], both clearly multiple in nature, indicates that considerable electron delocalization occurs within the ring. The gross structural features of **10** are directly comparable with those of **9** and attest to the validity of the isolobal replacement of RC≡CR and P≡CR units in **9** and **10**, or alternatively 'P' and d^5-ML$_5$ groups in relating **10** to the recently reported compound **11**.[10]

Experimental

2: A suspension of **1** (6.50 g, 10.0 mmol) and K[$H_2B(pz)_2$] (1.90 g, 1.02 mmol) in Et_2O (100 mL) was stirred for 3 h, filtered through a plug of alumina (3 × 3 cm) and then freed of solvent under reduced pressure to provide yellow microcrystals of **2** (5.04 g, 93%). IR (Et_2O): $\tilde{\nu}$(CO) = 1919 cm^{-1}; $^{13}C\{^1H\}$ NMR: δ = 281.3 (t, J(PC) = 26 Hz, C≡Mo), 235.6 (t, J(PC) = 16 Hz, CO); $^{31}P\{^1H\}$ NMR (85% H_3PO_4, external): δ = 161.2.

4: Diethyl ether (3 mL) and **3** (70 mg, 0.70 mmol) were condensed onto solid **2** (0.35 g, 0.55 mmol) at −78 °C. The mixture was warmed to room temperature, stirred for 18 h and freed of volatiles in vacuo. The residue was chromatographed on silica gel at −40 °C eluting with Et_2O. Removal of solvent from the major yellow eluate provided microcrystals of **4** (0.27 g, 84%). IR (Et_2O): $\tilde{\nu}_{max}$(CO) = 1912 cm^{-1}; $^{13}C\{^1H\}$ NMR: δ = 312.7 (t, J(PC) = 24 Hz, C≡Mo), 235.5 (t, J(PC) = 15 Hz, CO); $^{31}P\{^1H\}$ NMR: δ = 161.0.

10: A solution of **8** [7c] (0.21 g, 0.34 mmol) in THF at −78 °C was treated with **3** (60 mg, 0.60 mmol). The mixture was stirred at −5 °C for 10 min, and then freed of volatiles in vacuo. The residue was crystallized from toluene/hexane (1/3) to afford dark green crystals of **10** (0.13 g, 52%). IR (hexane): $\tilde{\nu}_{max}$(CO) = 2040vs, 1985 s, 1975 vs, 1911 m cm^{-1}; $^{13}C\{^1H\}$ NMR: δ = 222.9 (WCO, J(WC) = 142.3 Hz), 219.8 (WCO, J(WC) = 129.7 Hz), 214.3 (FeCO), 152.0 (CP, J(CP) = 61.8, J(WC) = 54.8 Hz), 123.0 (CP, J(PC) = 55.3, J(WC) = 51.1 Hz); $^{31}P\{^1H\}$ NMR: δ = 177.2.

Received: October 4, 1988 [Z 2989 IE]
German version: *Angew. Chem. 101* (1989) 213

[1] R. H. Grubbs in G. Wilkinson, F. G. A. Stone, E. W. Abel (Eds.): *Comprehensive Organometallic Chemistry, Vol. 8*, Pergamon Press, Oxford 1982, Chap. 54.

[2] R. R. Schrock, *J. Organomet. Chem. 300* (1986) 249.

[3] R. Hoffmann, *Angew. Chem. 94* (1982) 725; *Angew. Chem. Int. Ed. Engl. 21* (1982) 711.

[4] G. Becker, G. Gresser, W. Uhl, *Z. Naturforsch. B36* (1981) 16; review of phosphaalkyne chemistry: M. Regitz, P. Buiger, *Angew. Chem. 100* (1988) 1541; *Angew. Chem. Int. Ed. Engl. 27* (1988) 1484.

[5] Complex **1** was prepared using a procedure described by A. Mayr, A. M. Dorries, G. A. McDermott, D. Van Eugen (*Organometallics 5* (1986) 1504). The salt K[$H_2B(pz)_2$] was obtained as reported by S. Trofimenko (*Inorg. Synth. 12* (1970) 100).

[6] a) More conventionally, these compounds are formulated as heterobinuclear metal complexes in which the metal–metal bonds are spanned by μ-C(R)C(R′)C(R″) fragments (R, R′, R″ = alkyl or aryl groups). b) The WC_3- and WC_2P four-membered rings in **9** and **10** are necessarily nonplanar because of the relatively large radius of W compared with C or P. Hence the bonding of the Fe(CO)$_3$ group to these rings may be better described in terms of a σ bond involving the tungsten atom and η^3 coordination from the C_3 or C_2P fragments to the iron. However, the isolobal principle [3] is useful in relating the species concerned.

[7] In these species, M = Mo or W, L = η^5-C_5H_5 or η^5-C_5Me_5, and M′L$_n$ may be the groups Fe(CO)$_3$, Co(η^5-C_5Me_5), Rh(η^5-C_9H_7) (C_9H_7 = indenyl) or W(CO)(η-MeC_2Me)$_2$. See a) J. C. Jeffery, K. A. Mead, H. Razay, F. G. A. Stone, M. J. Went, P. Woodward, *J. Chem. Soc. Dalton Trans. 1984*, 1383; b) M. Green, J. A. K. Howard, S. J. Porter, F. G. A. Stone, D. C. Tyler, *ibid. 1984*, 2553; c) J. Hein, J. C. Jeffery, P. Sherwood, F. G. A. Stone, *ibid. 1987*, 2211; d) E. Delgado, M. E. Garcia, J. C. Jeffery, P. Sherwood, F. G. A. Stone, *ibid. 1988*, 207; e) M. E. Garcia, J. C. Jeffery, P. Sherwood, F. G. A. Stone, *ibid. 1988*, 2431, 2443. For complexes with M = Co, L = CO, and M′L$_n$ = W(CO)$_4$, see also I. J. Hart, F. G. A. Stone, *J. Chem. Soc. Dalton Trans. 1988*, 1899.

[8] F. G. A. Stone, *Angew. Chem. 96* (1984) 85; *Angew. Chem. Int. Ed. Engl. 23* (1984) 89.

[9] a) **10**: $C_{28}H_{31}O_5PFeW \cdot 0.5CD_2Cl_2$, M_r = 761.7, monoclinic, space group $P2_1/n$ (non-standard setting of $P2_1/c$, No. 14), Z = 4, a = 9.806(2), b = 16.899(3), c = 18.608(5) Å, β = 95.99(2)°, V = 3066(1) Å^3, ρ_{calcd} = 1.65 g cm^{-3}, $F(000)$ = 1500, $\mu(Mo_{K\alpha})$ = 44.7 cm^{-1}; $2\theta \leq 50°$ ($Mo_{K\alpha}$, λ = 0.71073 Å, ω-2θ scans, 293 K), 3179 absorption-corrected intensities ($F \geq 4\sigma(F)$). Refinement with anisotropic thermal parameters for all non-hydrogen atoms, and hydrogen atoms included in calculated positions, gave R_1 = 0.059 and R_2 = 0.055. b) Further details of the crystal structure investigation are available from the Director of the Cambridge Crystallographic Data Centre, Lensfield Road, Cambridge CB2 1EW (UK), on quoting the full literature citation. c) Computations were carried out on a D.E.C. micro-VAX II computer using the SHELXTLPLUS system of programs.

[10] R. Benn, H. Brenneke, A. Frings, H. Lehmkuhl, G. Mehler, A. Rufińska, T. Wildt, *J. Am. Chem. Soc. 110* (1988) 5661.

Hexaarsabenzene as Complex Ligand**

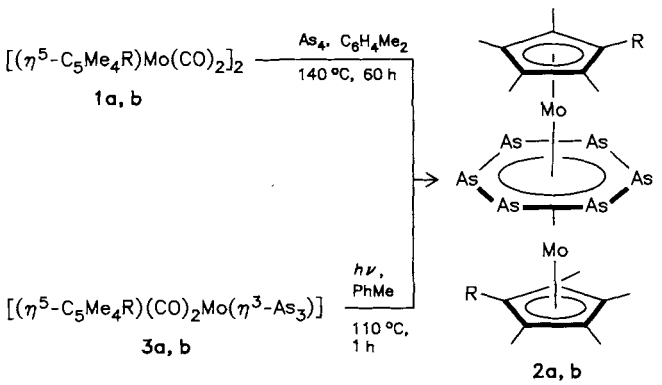
By *Otto J. Scherer,* Helmut Sitzmann,* and *Gotthelf Wolmershäuser*

The recently accomplished stabilization of *cyclo*-P_6 (hexaphosphabenzene) as middle deck of the triple decker complex **A**[1]

$[(\eta^5\text{-}C_5Me_5)Mo(\mu,\eta^6\text{-}P_6)Mo(\eta^5\text{-}C_5Me_5)]$ **A**

aroused hope that *cyclo*-As_6 (hexaarsabenzene) might possibly be stabilized in the same way.

Indeed, after initial difficulties[2] we have now been able to carry out such a stabilization. Complex-stabilized *cyclo*-As_6 (**2**) can be generated both thermally (**1** and As_4 as starting compounds) as well as photochemically[3] ($MoAs_3$-tetrahedranes **3** as starting compounds).



cis-$[(\eta^5\text{-}C_5Me_4R)(CO)Mo(\mu,\eta^2\text{-}As_2)]_2$ **4a, b**

a, R = Me; b, R = Et

In addition to the triple-decker complexes **2**, in the thermal process the complexes **3a**,[2,4] **3b** are formed, in the photochemical process the dinuclear complexes **4a**,[2] **4b**; the framework of **4** consists of two As_2Mo_2 tetrahedra with common Mo–Mo edge.[2,5] The complexes **2a, b** form brownish-red, air-stable crystals which are virtually insoluble in pentane, sparingly soluble in benzene, and only moderately soluble in dichloromethane (in all cases, however, **2b** dissolves better than **2a**). The ^1H NMR spectra[6] show, as in the case of **A**,[1] a distinct upfield shift for the CH_3 groups (ring current effect of *cyclo*-As_6?).

The crystal structure analysis of **2b**[7] shows that both five-membered rings and the As_6-ring are planar and parallel (Fig. 1). In contrast to the As_5-middle deck distorted by Jahn–Teller effects[8] (As–As = 2.389(2)–2.762(3) Å) in the 27 valence electron (VE) triple-decker **5**,[9] within the limits of error a regular arsenic hexagon is found in the 28 VE triple-decker **2b**. The mean As–As distance (2.35 Å) lies almost exactly between the values for an As–As single bond (e.g. As_4 = 2.44 Å[10]) and As=As double bond (ca. 2.24 Å[11]); in the case of **3a**[4] and Rb_4As_6 (planar six-membered ring),[12a] the mean value is 2.37 Å, in the case of **6**[13] it is 2.44 Å. The Mo–Mo distance[8] in **2b** (2.639(1) Å) is almost identical to that in **A** (2.647(1) Å)[1] and to other M–M distances in triple-decker complexes with a *cyclo*-P_6 middle deck.[1b] The same holds for the mean Mo–C distances and the mean As–As–Mo angle (64.2°; P–P–Mo = 64.8° in **A**[1]). The increase in size of the *cyclo*-E_6 middle deck on going from E = P (**A**[1]) to E = As leads to a decrease in the mean Mo–E–Mo angle in the $Mo(E_6)Mo$ framework (hexagonal bipyramid) (E = P: 62.8° in **A**[1]; E = As: 58.7° in **2b**).

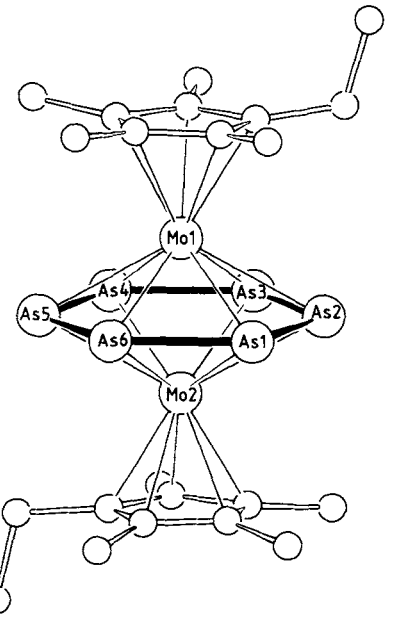


Fig. 1. Crystal structure of **2b**. Selected bond lengths [Å] and angles [°] (Cp′ = η^5-C_5Me_4Et): As1-As2 2.350(3), As2-As3 2.348(3), As3-As4 2.365(3), As4-As5 2.342(2), As5-As6 2.337(3), As1-As6 2.349(3), Mo1-Mo2 2.639(1); mean value: Mo-As 2.694, Mo-C 2.32, Mo1|Mo2-As_6(center) 1.32, Mo1|Mo2-Cp′(center) 1.98; As2-As1-As6 120.2(1), As1-As2-As3 119.7(1), As2-As3-As4 119.9(1), As3-As4-As5 119.9(1), As4-As5-As6 120.2(1), As1-As6-As5 120.1(1), Mo1-As_6(center)-Mo2 179.2; mean value: Mo1-As-Mo2 58.7, As-As-Mo1|Mo2 64.2.

$[\{(\eta^5\text{-}C_5H_5)Mo\}_2(As_5)]$ **5**

$[\{[MeC(CH_2PPh_2)_3]Co\}_2(\mu,\eta^3\text{-}As_3)]^{2\oplus}$ **6**

Experimental

Thermal procedure: A solution of 2.0 g (7.58 mmol) of $Mo(CO)_6$ in 80 mL of xylene was treated with an equivalent amount of HC_5Me_4R (R = Me, Et) and the mixture stirred under reflux for 24 h. The hot mixture was then treated with a hot solution of 3.5 g (11.7 mmol) As_4[2] (prepared in 350 mL of xylene under reflux). After 30 hours' refluxing, ca. 1/3 of the solvent was distilled off and the remaining mixture then treated with a freshly prepared hot solution of 1.5 g (5.0 mmol) of As_4 in 150 mL of xylene and stirred for a further 30 h under reflux. The reaction solution (containing small amounts of insoluble material) was evaporated down to ca. 50 mL (oil-pump vacuum), treated with 10 mL of silica gel (activity grade II), and dried under vacuum until freely flowing (black-brown powder). Upon subsequent chromatographic separation (35 × 3 cm column, filled with silica gel and petroleum ether (30–75 °C boiling range)), 497 mg (16%) of **3a** [517 mg (16%) of **3b**] was eluted as a yellow fraction with petroleum ether. With petroleum ether/toluene (10/1), 249 mg (9%) of **2a** [328 mg (12%) of **2b**] was eluted as a brownish-yellow fraction; finally, with petroleum ether/toluene (3/1), 10–20% of **1** was eluted. The yields quoted for **2** and **3** refer to 80% conversion.

Photochemical procedure: A solution of 0.28 mmol (143 mg) of **3a** [147 mg of **3b**] in 120 mL of toluene was heated to reflux in a Duran glass apparatus and irradiated with a 150-W mercury high-pressure lamp for 60 min with concomitant passage of N_2. After addition of ca. 3 mL of silica gel, the reaction mixture was evaporated to dryness and chromatographed (25 × 2 cm column). Elution with petroleum, to which toluene was added portionwise up to 20% by volume, afforded 67 mg (52%) of **2a** [66 mg (50%) of **2b**, recrystallizable from hot heptane] as a brownish-yellow fraction, which was followed

[*] Prof. Dr. O. J. Scherer, Dr. H. Sitzmann, Dr. G. Wolmershäuser [+]
Fachbereich Chemie der Universität
Erwin-Schrödinger-Strasse, D-6750 Kaiserslautern (FRG)
[+] X-ray structure analysis.

[**] This work was supported by the Fonds der Chemischen Industrie.

by the yellow fraction of **4a** [2], 47 mg (41%), [**4b**, 48 mg (41%)]. Irradiation of the isolated **4b** for 4 h in boiling toluene furnished ca. 10% **2b**.

Received: October 6, 1988 [Z 2994 IE]
German version: *Angew. Chem. 101* (1989) 214

[1] a) O. J. Scherer, H. Sitzmann, G. Wolmershäuser, *Angew. Chem. 97* (1985) 358; *Angew. Chem. Int. Ed. Engl. 24* (1985) 351; b) O. J. Scherer, J. Schwalb, H. Swarowsky, G. Wolmershäuser, W. Kaim, R. Gross, *Chem. Ber. 121* (1988) 443.

[2] O. J. Scherer, H. Sitzmann, G. Wolmershäuser, *J. Organomet. Chem. 309* (1986) 77.

[3] In analogy to *Jutzi*'s elegant synthesis of **A**: P. Jutzi, R. Kroos, *Chem. Ber. 121* (1988) 1399.

[4] I. Bernal, H. Brunner, W. Meier, H. Pfisterer, J. Wachter, M. L. Ziegler, *Angew. Chem. 96* (1984) 428; *Angew. Chem. Int. Ed. Engl. 23* (1984) 438.

[5] A.-J. Di Maio, A. L. Rheingold, *J. Chem. Soc. Chem. Commun. 1987*, 404.

[6] ^{1}H-NMR (200 MHz, C_6D_6, 293 K, TMS int.): **2a**: $\delta = -0.1$ (s, 30H) [2].—**2b**: $\delta = 0.01$ (s, 12H), −0.02 (s, 12H), 0.13 (q, ^3J(H,H) = 7.6 Hz, 4H), −0.4 (t, 6H).—**3a**|**4a** [2].—**3b**: $\delta = 1.66$ (s, 6H), 1.62 (s, 6H), 2.06 (q, ^3J(H,H) = 7.6 Hz, 2H), 0.68 (t, 3H).—**4b**: $\delta = 1.78$ (s, 12H), 1.75 (s, 12H), 2.20 (q, ^3J(H,H) = 7.6 Hz, 4H), 0.68 (t, 3H)—IR (*n*-heptane) of **3b**: $\tilde{\nu}$(CO) = 1981 (vs), 1924 (vs) cm^{-1}.—IR of **4b**: $\tilde{\nu}$(CO) = 1967 (vs), 1930 (m).—EI-MS (70 eV, 300°C) of **2a**: *m/z* 912 ($M^{\oplus}$, 73%), 837 ($M^{\oplus}$ − As, 100), 762 ($M^{\oplus}$ − 2 As, 22), 456 ($M^{\oplus}$/2, 33), 300 ($As_4^{\oplus}$, 32), 225 ($As_3^{\oplus}$, 5), 150 ($As_2^{\oplus}$, 10).

[7] **2b**: monoclinic, $P2_1/n$, $a = 9.174(1)$, $b = 19.854(3)$, $c = 15.174(5)$ Å, $\beta = 94.11(2)°$, $Z = 4$; 4610 independent reflections ($Mo_{K\alpha}$, $1.5° < \theta < 26°$), 3487 observed with $F_0^2 \geq 2.0\sigma(F_0^2)$, 301 parameters, $R = 0.057$, $R_w = 0.064$. One C_5Me_4Et ring is rotationally disordered. The two orientations differ by a 72° rotation in the ring plane with 50% population each. Further details of the crystal structure investigation are available on request from the Fachinformationszentrum Energie, Physik, Mathematik GmbH, D-7514 Eggenstein-Leopoldshafen 2 (FRG), on quoting the depository number CSD-53417, the names of the authors, and the journal citation.

[8] Theoretical studies: a) E. D. Jemmis, A. C. Reddy, *Organometallics 7* (1988) 1561; b) W. Tremel, R. Hoffmann, M. Kertesz, *J. Am. Chem. Soc.*, in press.

[9] A. L. Rheingold, M. J. Foley, P. J. Sullivan, *J. Am. Chem. Soc. 104* (1982) 4727.

[10] L. R. Maxwell, S. B. Hendricks, V. M. Mosley, *J. Chem. Phys. 3* (1935) 699.

[11] Review: A. H. Cowley, N. C. Norman, *Prog. Inorg. Chem. 34* (1986) I.

[12] a) H. G. von Schnering, *Angew. Chem. 93* (1981) 44; *Angew. Chem. Int. Ed. Engl. 20* (1981) 33; b) cf. also the equilibrium $As_6^{4\ominus}|As_4^{2\ominus}$ characterized by EXAFS studies: J. Rozière, A. Seigneurin, C. Belin, A. Michalowicz, *Inorg. Chem. 24* (1985) 3710.

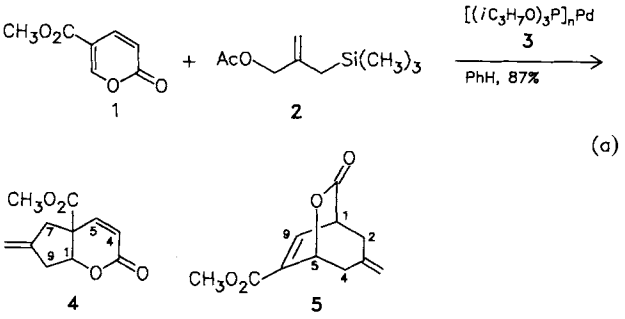
[13] M. Di Vaira, S. Midollini, L. Sacconi, *J. Am. Chem. Soc. 101* (1979) 1757.

Pyrones as Substrates for Palladium-Catalyzed [4+3] Cycloadditions**

By *Barry M. Trost** and *Stephan Schneider*

The schizophrenic behavior of pyrones is illustrated by their reacting as 4π electron partners towards olefins[1] and as 2π electron partners towards dienes.[2,3] The reactivity of trimethylenemethane-palladium complex as an equivalent of an electron-rich 4π-electron partner[4,5] (i.e., equivalent to an electron-rich diene) suggests that pyrones should participate as 2π-electron partners with this reactive intermediate. In contrast to such a prediction, we wish to report that either a [2+3] or a [4+3] cycloaddition may be observed depending upon the pyrone substitution, and that the latter represents the first example in which pyrone behaves as a 4π-electron substrate towards a 4π-electron reactant.

The commercially available methyl coumalate **1** reacts with 2-trimethylsilylmethylallyl acetate **2** in the presence of 5 mol% of the Pd^0 complex **3** formed in situ by reaction of one equivalent of palladium acetate with six equivalents of triisopropyl phosphite and two equivalents of *n*-butyllithium in *n*-hexane [Eq. (a)].[6] Surprisingly, an approximate



(a)

1:1-2 mixture of the [2+3] and [4+3] cycloadducts **4** and **5**,[7] respectively, are formed. Spectroscopic data provides ready structural assignment (Table 1). Most notably, the carbonyl bands in the IR spectrum and the positions of the ^{1}H-NMR signals of the olefinic protons (**4**: $\delta = 4.98$, 6.06,

Table 1. Spectral Data of **4**–**13** [a].

4: IR ($CDCl_3$): $\tilde{\nu}$(CO) = 1727. ^{1}H NMR: $\delta = 2.70$ and 3.02 (2 m; 2H each, 7- and 9-H), 3.79 (s; 3H, CH_3), 4.98 (m; 2H, exo-methylene H), 5.27 (dd, $J = 7.0$, 4.9; 1H, 1-H), 6.06 (d, $J = 5.9$; 1H, 4-H), 6.83 (d, $J = 5.9$; 1H, 5-H). MS: *m/z* ($M^{\oplus}$) 208.0735 (calcd. 208.0736)

5: IR: $\tilde{\nu}$(CO) = 1750, 1716. ^{1}H NMR: $\delta = 2.52$–2.79 (m; 4H, 2- and 4-H), 3.61 (ddd, $J = 6.8$, 6.4, 2.2; 1H, 1-H), 3.82 (s; 3H, CH_3), 4.88 (m; 2H, exo-methylene H), 5.47 (ddd, $J = 4.2$, 2.5, 1.7; 1H, 5-H), 7.22 (dd, $J = 6.8$, 1.7; 1H, 9-H). MS: *m/z* ($M^{\oplus}$) 208.0735 (calcd. 208.0736)

6: IR: $\tilde{\nu}$(CO) = 1760, 1735. ^{1}H NMR: $\delta = 2.22$ (ddd, $J = 16.6$, 9.2, 2.2; 1H, 7-H), 2.75 (ddd, $J = 16.6$, 8.0, 1.4; 1H, 7-H), 3.05, 3.25 (each m, AB-system: $J = 17.0$; 1H each, 9-H), 3.27 (m; 1H, 6-H), 3.78 (s; 3H, CH_3), 4.96 (m; 2H, exo-methylene H), 5.30 (t, $J = 5.6$; 1H, 5-H), 6.49 (d, $J = 5.6$; 1H, 4-H). MS: *m/z* ($M^{\oplus}$) 208.0730 (calcd. 208.0736)

7: IR: $\tilde{\nu}$(CO) = 1735. ^{1}H NMR: $\delta = 2.45$–2.77 (m; 4H, 2- and 4-H), 3.35 (m; 1H, 1-H), 4.84 (m; 2H, exo-methylene H), 5.01 (m; 1H, 5-H), 6.27 (m; 2H, 8- and 9-H). MS: *m/z* ($M^{\oplus}$) 150.0677 (calcd. 150.0681)

8: IR: $\tilde{\nu}$(CO) = 1730. ^{1}H NMR: $\delta = 0.99$ (t, $J = 7.6$; 3H, ethyl-CH_3), 1.74 (s; 3H, 8-CH_3), 2.14 (qd, $J = 7.6$, 1.4 (2H, ethyl-CH_2), 2.38–2.68 (m; 4H, 2- and 4-H), 3.18 (dd, $J = 6.2$, 2.3; 1H, 1-H), 4.67 (dd, $J = 4.0$, 2.8; 1H, 5-H), 4.78 (m; 2H, exo-methylene H). MS: *m/z* ($M^{\oplus}$) 192.1155 (calcd. 192.1150)

9: IR: $\tilde{\nu}$(CO) = 1725. ^{1}H NMR: $\delta = 1.50$ (s; 3H, CH_3), 1.95–2.10 (m; 2H), 1.37–1.68 (m; 8H), 3.32 (dd, $J = 5.8$, 2.5; 1H, 1-H), 4.74 (m; 2H, exo-methylene H). MS: *m/z* ($M^{\oplus}$) 204.1148 (calcd. 204.1150)

10: IR: $\tilde{\nu}$(CO) = 1735. ^{1}H NMR: $\delta = 1.62$ (m; 4H, 2'- and 3'-H), 2.03 (m; 4H, 1'- and 4'-H), 2.40–2.68 (m; 4H, 2- and 4-H), 3.02 (dd, $J = 5.8$, 2.7; 1H, 1-H), 4.64 (m; 1H, 5-H), 4.79 (m; 2H, exo-methylene H). MS: *m/z* ($M^{\oplus}$) 204.1152 (calcd. 204.1150)

11: IR: $\tilde{\nu}$(CO) = 1735. ^{1}H NMR: $\delta = 1.39$–1.85 (m; 6H, 2'-, 3'-, and 4'-H), 2.0–2.45 (m; 4H), 2.50–2.58 (m; 4H), 3.07 (dd, $J = 5.2$, 3.5; 1H, 1-H), 4.67 (m close to dd; 1H, 5-H), 4.81 (m; 1H, exo-methylene H). MS: *m/z* ($M^{\oplus}$) 218.1306 (calcd. 218.1307)

12: IR: $\tilde{\nu}$(CO) = 1730. ^{1}H NMR: $\delta = 1.25$–1.45 (m; 2H), 1.65–1.95 (m; 3H), 2.0–2.15 (m; 2H), 2.35–2.67 (m; 5H), 3.24 (td, $J = 6.2$, 2.4; 1H, 1-H), 4.80 (m; 2H, 3-CH_2), 5.75 (dd, $J = 6.2$, 2.7; 1H, 8-H). MS: *m/z* ($M^{\oplus}$) 204.1158 (calcd. 204.1150)

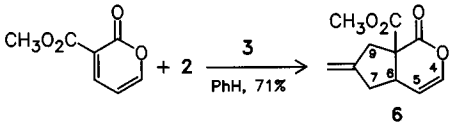
13: IR: $\tilde{\nu}$(CO) = 1735. ^{1}H NMR: $\delta = 2.32$–2.42 (m; 2H), 2.53–2.71 (m; 4H), 2.81–2.92 (m; 2H), 3.93 (dd, $J = 6.2$, 2.3; 1H, bridgehead next to carbonyl group), 4.74, 4.79 (2 m; 1H each, exo-methylene H), 4.93 (dd, $J = 4.2$, 2.3; 1H, bridgehead next to oxygen), 7.12–7.28 (m; 4H, aromatic H). MS: *m/z* ($M^{\oplus}$) 252.1149 (calcd. 252.1150)

[a] 200-MHz ^{1}H NMR and IR spectra in $CDCl_3$; $\tilde{\nu}$ in cm^{-1}, *J* in Hz.

[*] Prof. B. M. Trost, Dr. S. Schneider
Department of Chemistry, Stanford University
Stanford, CA 94305 (USA)

[**] We thank the National Science Foundation and the National Institutes of Health, the Institute of General Medical Sciences, and the Deutsche Forschungsgemeinschaft (postdoctoral fellowship for *S. S.*).

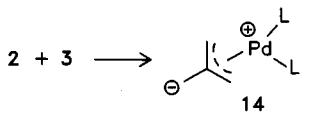
6.83; **5**: $\delta = 4.88$, 7.22), and of the proton adjacent to the ring oxygen atom (**4**: $\delta = 5.27$; **5**: $\delta = 5.47$) provide ready diagnosis of the structures of the cycloadducts. Placing the carbomethoxy group at the 3-position of the pyrone provides exclusive five-membered ring formation [Eq. (b)] to give cycloadduct **6** with a carbon skeleton reminiscent of the iridoids.[8]



(b)

6

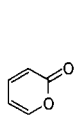
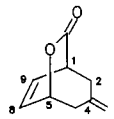
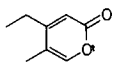
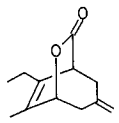
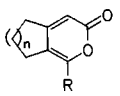
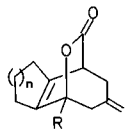
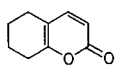
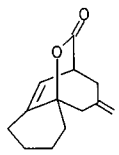
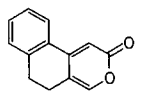
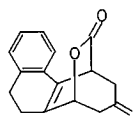
On the other hand, pyrone itself undergoes exclusive [4+3] cycloaddition to give **7** (see Table 2). Alkyl substituted and aryl substituted pyrones also lead only to [4+3] cycloadducts (**8**–**13**) normally in excellent yields. We attribute the low yield of **12** to the strain involved in bridging the positions 5 and 9 of the 3-methylene-6-oxa-7-oxobicyclo[3.2.2]non-8-ene nucleus by a $(CH_2)_4$-chain. Steric hindrance is a less likely cause for the low yield of **12**, for **9** is formed in excellent yield, even though the 4,5,6-trisubstituted pyrone starting compound is sterically more crowded. Pyrones bearing a 6-methylthio substituent[9] or a 4-methoxy substituent[10] failed to undergo cycloaddition.



14

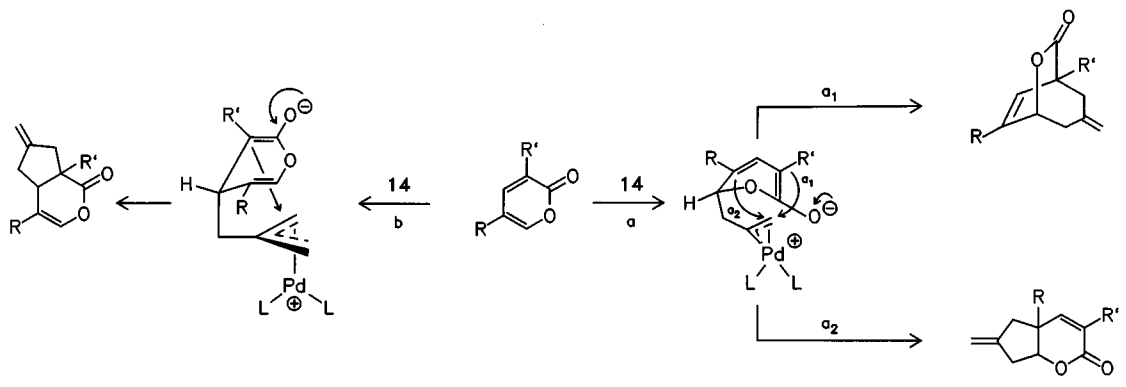
To understand why the trimethylenemethane–PdL_2 complex **14** (formed from **2** and **3**) diverges from its normal reactivity as an equivalent of an electron-rich diene, we suggest that this cycloaddition is a two step process[11] as depicted in Scheme 1. Nucleophilic attack by the TMM–PdL_2 complex at the 6-position is generally favored to generate the thermodynamically most stable dienolate (path a). The normal preference for such dienolates to react at the α-position then leads to the seven-membered ring products (path a_1). On the other hand, the incorporation of a strong anion stabilizing group at the 5-position ($R = CO_2CH_3$) increases the anionic nature of this carbon with the resultant partitioning along path a_2 becoming competitive with path a_1. When R′ is a strong electron-withdrawing group, charge effects appear to control the position of initial attack favoring path b which can only lead to [2+3] cycloadducts.

Table 2. [4+3] Cycloadditions [a].

Pyrone derivative	Cycloadduct [7]		Yield [%]
		7	70[b]
		8	89[b]
		n = 1, R = CH_3	9	86[c]
		n = 2, R = H	10	90[d]
		n = 3, R = H	11	92[e]
		12	23[b]
		13	90[b]

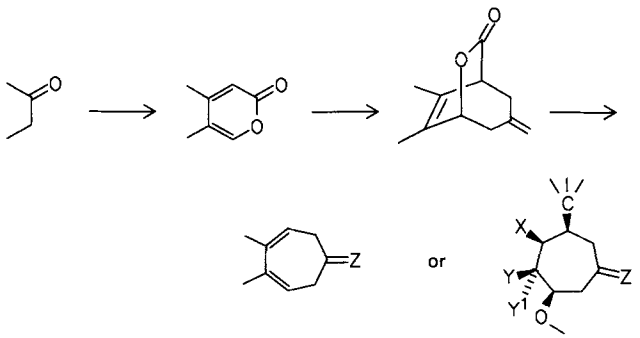
[a] General procedure: Reactions normally performed with 1 mmol of pyrone (1 M concentration in benzene) and 1.4 eq of 2-trimethylsilylmethylallyl acetate with 500 μl of the catalyst solution (generated by treating 0.25 mmol of palladium acetate in 1.8 ml of benzene with 1.50 mmol of triisopropyl phosphite and 320 μl of a 1.56 M hexane solution of *n*-butyllithium) at 80° in a sealed reaction vessel.

Synthetically, this [4+3] cycloaddition appears to be a most useful and general approach to seven-membered rings (see Scheme 2).[12, 13] The endocyclic double bond becomes a useful functional group for diastereocontrolled functionalization (such as a *cis*-hydroxylation) and the lactone bridge represents a *cis*-1,4-substitution of oxygen and carbon. Loss of carbon dioxide to form cycloheptadienes



Scheme 1. Proposed reaction routes to explain the products **4**–**13** obtained in the reactions according to Equation (a).

is also possible. The ready availability of the pyrones from ketones[14] enhances the value of this approach for the stereocontrolled construction of seven-membered rings.



Scheme 2. Seven-membered rings from ketones via pyrones and possible functionalizations.

Received: October 18, 1988 [Z 3014 IE]
German version: *Angew. Chem. 101* (1989) 215

[1] For some examples see: a) N. P. Shusherina, *Russ. Chem. Rev. 43* (1974) 851; b) H. Behringer, P. Heckmaier, *Chem. Ber. 102* (1969(2835; c) E. J. Corey, D. S. Watt, *J. Am. Chem. Soc. 95* (1973) 2303; d) D. Boger, M. D. Mullican, *J. Org. Chem. 49* (1984) 4033, 4045; e) G. H. Posner, W. Harrison, *J. Chem. Soc. Chem. Commun. 1985*, 1786; f) G. H. Posner, D. G. Wettlaufer, *Tetrahedron Lett. 27* (1986) 667; *J. Am. Chem. Soc. 108* (1986) 7373; g) M. E. Jung, L. J. Street, Y. Usui, *J. Am. Chem. Soc. 108* (1986) 6810; h) M. E. Jung, J. A. Hagenah, *J. Org. Chem. 52* (1987) 1889; i) M. E. Jung, Y. Usui, C. T. Vu, *Tetrahedron Lett. 28* (1987) 5977.

[2] For some examples see T. Imagawa, N. Sueda, M. Kawanisi, *Tetrahedron 30* (1974) 2227; T. Imagawa, T. Nakagawa, M. Kawanisi, K. Sisido, *Bull. Chem. Soc. Jpn. 52* (1979) 1506; Y. Nakahara, T. Tatsuno, *Chem. Pharm. Bull. 28* (1980) 1981; G. A. Kraus, K. Frazier, *J. Org. Chem. 45* (1980) 4820; G. A. Kraus, B. Roth, *ibid. 45* (1980) 4825; J. D. White, T. Matsui, J. A. Thomas, *ibid. 46* (1981) 3376; T. Matsui, T. Inoue, M. Nakayama, J. D. White, *Bull. Chem. Soc. Jpn. 56* (1983) 647; B. A. Brown, E. W. Colvin, *J. Chem. Soc. Chem. Commun. 1984*, 1514; M. Nakayama, J. Kuramoto, T. Matsui, J. D. White, *Bull. Chem. Soc. Jpn. 58* (1985) 3051; T. Matsui, S. Kitajima, M. Nakayama, *ibid. 61* (1988) 316.

[3] See also J. Staunton, *Compr. Org. Chem. 1979*, 629; J. Fried in R. C. Elderfield (Ed.): *Heterocyclic Compounds, Vol. 1*, Wiley, New York 1950, Chap. 7; L. F. Cavalieri, *Chem. Rev. 41* (1947) 525.

[4] B. M. Trost, *Angew. Chem. 98* (1986) 1; *Angew. Chem. Int. Ed. Engl. 25* (1986) 1.

[5] B. M. Trost, P. R. Seoane, *J. Am. Chem. Soc. 109* (1987) 615.

[6] B. M. Trost, T. N. Nanninga, *J. Am. Chem. Soc. 107* (1985) 1293; B. M. Trost, P. Renaut, *J. Am. Chem. Soc. 104* (1982) 6668.

[7] Compound characterized by spectral data and high resolution mass spectroscopy (see Table 1).

[8] Recent reviews: K. Buzogany, V. Cucu, *Farmacia (Bucharest) 31* (1983) 129; L. F. Tietze, *Angew. Chem. 95* (1983) 840; *Angew. Chem. Int. Ed. Engl. 22* (1983) 828; D. Sainty, F. Bailleul, P. Delaveau, H. Jacquemin, *J. Nat. Prod. 44* (1981) 576; L. J. El-Naggar, J. L. Beal, *ibid. 43* (1980) 649.

[9] Cf. R. K. Dieter, J. R. Fishpaugh, *Tetrahedron Lett. 27* (1986) 3823; *J. Org. Chem. 53* (1988) 2031.

[10] Commercially available 4-methoxy-6-methyl-2-pyrone was used.

[11] Cf. B. M. Trost, M. L. Miller, *J. Am. Chem. Soc. 110* (1988) 3687.

[12] Cf. B. M. Trost, D. T. MacPherson, *J. Am. Chem. Soc. 109* (1987) 3483.

[13] For a novel cycloaddition approach to seven-membered rings using cyclopropenone ketals and pyrones see ref. [1d] and D. L. Boger, C. E. Brotherton, *J. Am. Chem. Soc. 108* (1986) 6695, 6713. For other cycloadditions to seven-membered rings see R. Noyori, *Acc. Chem. Res. 12* (1979) 61; H. M. R. Hoffmann, *Angew. Chem. 96* (1984) 29; *Angew. Chem. Int. Ed. Engl. 23* (1984) 1; *ibid. 85* (1973) 877 and *12* (1973) 819.

[14] The 2-pyrones were synthesized first by classical formation of the 2-ethoxymethylene ketones followed by addition of ethyl lithioacetate and cyclization with 1–2% sulfuric acid in acetic acid. For some recent synthetic work, see Ref. [9] and H. Stetter, H. J. Kogelnick, *Synthesis 1986*, 140.

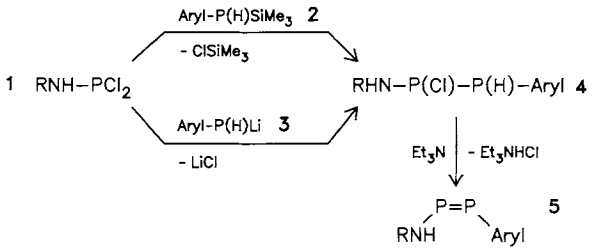
Synthesis, Structure, and Reactivity of Diphosphenes having a *cis*-Configuration

By *Edgar Niecke,* Berthold Kramer,* and *Martin Nieger*

In contrast to the diazene system (E = N), for which, depending on the substituents, both the *trans*-form **I** and the *cis*-form **II** may be thermodynamically favored,[1] stable[2] *cis*-diphosphenes **II** (E = P) were previously unknown.[3] We now report the synthesis of the first stable diphosphenes with a *cis*-configuration.



As has been shown by various synthetic studies, diphosphenes are accessible via β-elimination of hydrogen halides from suitably substituted diphosphane precursors.[4] We applied this synthetic method to diphosphanes having secondary amino substituents. Thus, reaction of the dichlorophosphanes **1a**[5] and **1b–d** with either the silylphosphane **2**[6] or the lithium phosphide **3** afforded the diphosphanes **4**. The base-induced elimination of hydrogen chloride from **4** gave the *cis*-diphosphenes **5**.



Aryl = $C_6H_2tBu_3$

R = *t*Bu (a), Adamantyl (b), CEt_3 (c), $C_6H_2iPr_3$ (d)

The structures and compositions of compounds **5a–d** and of the precursors **1b–d** have been determined on the basis of elemental analyses, mass and NMR spectral data, and X-ray structural analyses for **5a**, **b**. The intermediates **4a–d** were characterized by ^{31}P NMR spectroscopy.

The ^{31}P NMR signals of **5a–d** exhibit significant shifts to higher field ($\Delta\delta = 100$–200 ppm) compared with those of the known *trans*-1-aminodiphosphenes, $R'R''N–P=P–C_6H_2tBu_3$.[7] Conclusive proof of the *cis*-configuration was provided by X-ray structural analyses for **5a** and **5b** (Fig. 1).[8] The molecules, whose basic frameworks (without Me groups) have approximate C_s symmetry, have the *cis*-configuration with respect to the PP bond with the four atoms P(1), P(2), N(1) and C(11) lying in a plane (torsion angle N(1)-P(1)-P(2)-C(11) 0.6(2)° for **5a**, 0.5(2)° for **5b**).

The coplanarity of the substituents at the N atom makes possible a p–π interaction with the PP double bond, which might be responsible for the relatively short PN bond lengths (164.5(4) and 165.2(5) pm for **5a** and **5b**) and the large angles at P(1) (109.9(2) and 109.2(2)°, respectively). Unlike the amino group, the aryl substituent is twisted out

[*] Prof. Dr. E. Niecke, Dipl.-Chem. B. Kramer, M. Nieger
Anorganisch-chemisches Institut der Universität
Gerhard-Domagk-Strasse 1, D-5300 Bonn 1 (FRG)

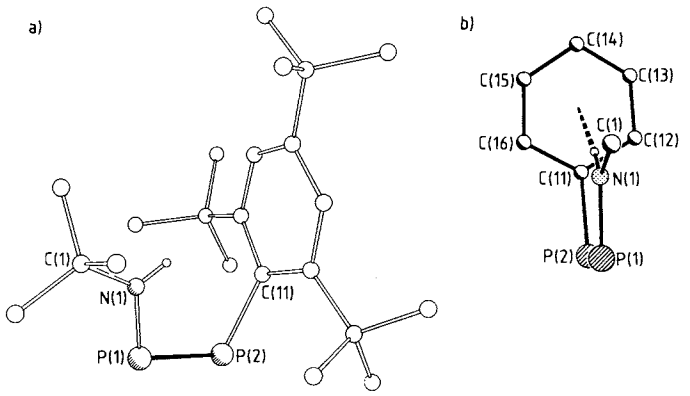
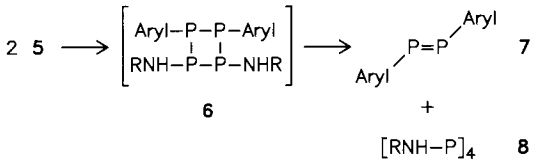


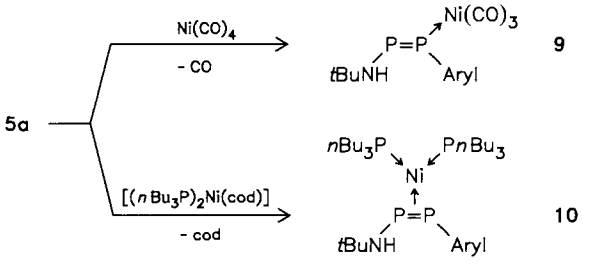
Fig. 1. a) Molecular structure of **5a**. Important bond lengths [pm] and angles [°] (for **5b** in parentheses): P(1)-N(1) 164.5(4) [165.2(5)], P(1)-P(2) 203.8(2) [204.4(2)], P(2)-C(11) 186.2(4) [185.5(5)]; N(1)-P(1)-P(2) 109.9(2) [109.2(2)], P(1)-P(2)-C(11) 102.0(2) [102.2(1)], C(1)-N(1)-P(1) 129.5(3) [127.8(3)]; torsion angle N(1)-P(1)-P(2)-C(11) 0.6(2) [0.5(2)]. b) View of the basis framework along the PP axis.

of the plane of the π-system with an angle between the PPN plane and the plane of the arene ring of 90°. The bond lengths P(2)-C(11) (186.2(4) and 185.5(5) pm for **5a** and **5b**), the angles at P(2) (102.0(2) and 102.2(1)°) and the PP bond lengths (203.8(2) and 204.4(2) pm) lie within the ranges normally found for diphosphenes.[3] Particularly noteworthy is the distance of the amino proton from the centroid of the arene ring (**5a**, 264 pm; **5b**, 270 pm) which suggests a weak attractive interaction between the proton and the aromatic π-system.[10] To what extent an interaction of this type is responsible for the stabilization of the *cis*-form of **5** with respect to the *trans*-form remains an open question.

The crystalline diphosphenes **5a-d** are practically indefinitely stable in the solid state under an inert atmosphere. In solution, they decompose within a few days at ambient temperature or a few hours at 60°C to give the *trans*-diphosphene **7**[2b] and the cyclotetraphosphane **8**. The latter two compounds can be regarded as being the products of the cycloreversion of the head to head dimer **6**.



Like their *trans*-analogues, the *cis*-diphosphenes react with transition metal compounds to furnish η^1- or η^2-complexes. This was demonstrated by the reaction of **5a** with nickel compounds to give the diphosphene complexes **9** and **10**.



Experimental

1b-d: 39 mL of 15% *n*BuLi solution in hexane (10% excess) was added dropwise to a solution of 50 mmol of adamantyl-NH_2, Et_3CNH_2 or $C_6H_2iPr_3NH_2$ in ether (20 mL). The reaction mixture was stirred for 1 h at 25°C after which it was added dropwise to a solution containing three molar equivalents of PCl_3 (14 mL) in ether (40 mL) at −60°C. The solution was allowed to warm to 25°C and the solvent removed in vacuum. The residue was extracted into pentane and LiCl was removed by filtration. The product was purified by distillation or recrystallization. **1b**: 9.4 g (74%), m.p. 25-27°C; **1c**: 9.7 g (61%), b.p. 56-57%/0.25 torr; **1d**: 11.9 g (74%), m.p. 48-50°C. MS: *m/z* 253 (**1b**$^{\oplus}$, 12%); 216 (**1c**$^{\oplus}$, 7%); 320 (**1d**$^{\oplus}$, 14%). ^{31}P NMR ($CDCl_3$): δ(**1b**) = 165.8; δ(**1c**) = 156.6; δ(**1d**) = 155.8.

5a, b: A solution of **2** (10 mmol) in *n*-hexane (30 mL) was reacted with 20 mmol of **1a** [5] or **1b** in *n*-hexane (20 mL) at 0°C. The solution was allowed to warm to 25°C and was stirred for a further 2 h. The diphosphanes **4a** and **4b** are formed as pairs of diastereomers. ^{31}P NMR (C_6D_6): δ(**4a**) = −60 (−49) (J(P,H) = 174 (213) Hz), 133 (122) (J(P,P) = 173 (263) Hz); δ(**4b**) = −59 (−49) (J(P,H) = 170 (212) Hz), 133 (121) (J(P,P) = 170 (260) Hz). The solution containing **4a** or **4b** was treated with one molar equivalent of Et_3N. After removal of the amine hydrochloride by filtration, the solution was cooled to 80°C to afford **5a** or **5b**. **5a**: 3.04 g (40%), m.p. 117-123°C; **5b**: 2.7 g (29%), m.p. 187-192°C. MS: *m/z* 379 (**5a**$^{\oplus}$, 30%); 457 (**5b**$^{\oplus}$, 1%). ^{31}P NMR (C_6D_6): δ(**5a**) = 377, 214 (J(P,P) = 526, J(P,H) = 12 Hz); δ(**5b**) = 375, 213 (J(P,P) = 524.5, J(P,H) = 12.7 Hz).

5c, d: To a solution of **1c** or **1d** in ether (30 mL) was added dropwise a solution containing an equimolar amount of **3** in ether (20 mL) at −50°C. The stirred solution was allowed to warm to room temperature and most of the solvent was removed under vacuum. The residue was extracted with hexane and LiCl removed by filtration to afford a solution containing **4c** or **4d** (mixtures of diastereomers). ^{31}P NMR: (C_6D_6): δ(**4c**) = −62.3 (−51.2) (J(P,H) = 178 (212.5) Hz), 136 (121.3) (J(P,P) = 175 (267) Hz); δ(**4d**) = −62.8 (−49.4) (J(P,H) = 180 (214) Hz), 142.1 (119.6) (J(P,P) = 179 (270) Hz). **4c** and **4d** were converted to the diphosphenes **5c** and **5d** as described for **4a, b**. **5c**: 0.85 g (20%), m.p. 134-137°C; **5d**: 1.85 g (35%), m.p. 112-115°C. MS: *m/z* 421 (**5c**$^{\oplus}$, 23%), 525 (**5d**$^{\oplus}$, 6%). ^{31}P NMR (C_6D_6): δ(**5c**) = 379.0, 212.3 (J(P,P) = 527.2, J(P,H) = 13.1 Hz); δ(**5d**) = 379.7, 209.3 (J(P,P) = 523, J(P,H) = 13.6 Hz).

9: $Ni(CO)_4$ (5 mmol) was added to a solution of **5a** (5 mmol) in toluene (50 mL). Gas evolved and the color of the solution changed from light-yellow to red-brown. After warming to 25°C, the solution was reduced to one quarter of its volume in vacuum. Addition of Et_2O (20 mL) and cooling to −30°C afforded the analytically pure complex **9**. Yield, 2.12 g (80%), m.p. 112-115°C (decomp.). MS: *m/z* 520 ($M^{\oplus}$, 5%). IR (C_6D_6): $\tilde{\nu}$ = 2085, 2040, 2012 cm^{-1}. ^{31}P NMR (C_6D_6): δ = 164, 341 (J(P,P) = 561 Hz).

10: A solution of **5a** (5 mmol) in toluene (30 mL) was treated with [(*n*$Bu_3P)_2$Ni(cod)] (5 mmol) (cod = 1,5-cyclooctadiene) and *n*Bu_3P (200 mg) dissolved in toluene (7 mL). The color became cherry-red. After the reaction was complete, the solution was cooled to −80°C to afford **10** as a deep-red solid. **10** decomposes in solution within a few hours at 25°C. ^{31}P NMR ([D_8]toluene, 203 K) Aryl$P^A P^K$NHCMe$_3$·Ni(*n*Bu_3P^M*n*Bu_3P^X): δ(A) = −55.1, δ(K) = 85.2, δ(M) = −3.9, δ(X) = 4.6; J(A,K) = 427, J(A,M) = 10, J(A,X) = 47.5, J(K,M) = 30.5, J(K,X) = 30.5, J(M,X) = 3.2 Hz.

Received: September 9, 1988 [Z 2962 IE]
German version: *Angew. Chem. 101* (1989) 217

[1] S. Patai: *The Chemistry of the Hydrazo, Azo and Azoxygroups*, Wiley, New York 1975.
[2] a) A.-M. Caminade, M. Verrier, C. Ades, N. Palillous, M. Koenig, *J. Chem. Soc. Chem. Commun. 1984*, 875; b) Stable *cis*-diphosphenes have been synthesized in the coordination sphere of a transition metal: M. Yoshifuji, T. Hashida, N. Inamoto, K. Hirotsu, T. Horiuchi, T. Higuchi, K. Ito, S. Nagase, *Angew. Chem. 97* (1985) 230; *Angew. Chem. Int. Ed. Engl. 24* (1985) 211.
[3] Review: A. H. Cowley, N. C. Norman, *Polyhedron 3* (1984) 389.
[4] E. Niecke, R. Rüger, *Angew. Chem. 95* (1983) 154; *Angew. Chem. Int. Ed. Engl. 22* (1983) 155; P. Jutzi, U. Meyer, B. Krebs, M. Dartmann, *ibid. 98* (1986) 894; *25* (1986) 919.
[5] O. J. Scherer, P. Klusmann, *Angew. Chem. 81* (1969) 743; *Angew. Chem. Int. Ed. Engl. 8* (1969) 752.
[6] W. Paulen, *Dissertation*, Universität Bonn 1984.
[7] L. N. Markovskii, V. D. Romanenko, A. V. Ruban, *Phosphorus Sulfur* **30** (1987) 447.
[8] X-ray structural analyses for **5a** ($C_{22}H_{39}NP_2$) [and **5b** ($C_{28}H_{45}NP_2$)]: M_r = 379.5 [457.6]; yellow crystals (0.3 × 0.3 × 0.4 [0.15 × 0.35 × 0.45] mm^3); space group $P2_1/c$ [*Pbca*], a = 10.441(7) [16.917(8)], b = 11.094(6) [17.026(7)], c = 21.165(7) [19.010(7)] Å, β = 90.52(4) [90]°, V = 2.451 [5.475] nm^3, Z = 4 [8], ρ_{calcd} = 1.03 [1.11] g cm^{-3}, $\mu(Mo_{K\alpha})$ = 0.18 [0.17] mm^{-1}; 4315 [4831] symmetry-independent reflections ($2\theta_{max}$ = 50°), of which 2293 [2567] with $|F| > 4\sigma(F)$ were used in the structure solution (direct methods) and refinement (258 [284] parameters); P, N and C atoms ani-

sotropic (unordered Me C atoms of the *para*-*t*Bu group of **5a** isotropic), H atoms (localized by electron density difference determination) refined with a "riding" model, amine H atoms refined free; $R = 0.076$ [0.076] ($R_w = 0.074$ [0.072], $w^{-1} = \sigma^2(F) + 0.0008F^2$). Further details of the crystal structure investigation may be obtained from the Fachinformationszentrum Energie, Physik, Mathematik GmbH, D-7514 Eggenstein-Leopoldshafen 2 (FRG), on quoting the depository numbers CSD-53329 (**5a**) and CSD-53407 (**5b**), the names of the authors, and the journal citation.

[9] The P–N bond length in diphosphenes with an orthogonal arrangement of the amino group with respect to the central π-system is 177 pm: E. Niecke, R. Rüger, M. Lysek, S. Pohl, W. W. Schoeller, *Angew. Chem. 95* (1983) 495; *Angew. Chem. Int. Ed. Engl. 22* (1983) 486.

[10] Cf. B. V. Cheney, M. W. Schulz, J. Cheney, W. G. Richards, *J. Am. Chem. Soc. 110* (1988) 4195, and references cited therein.

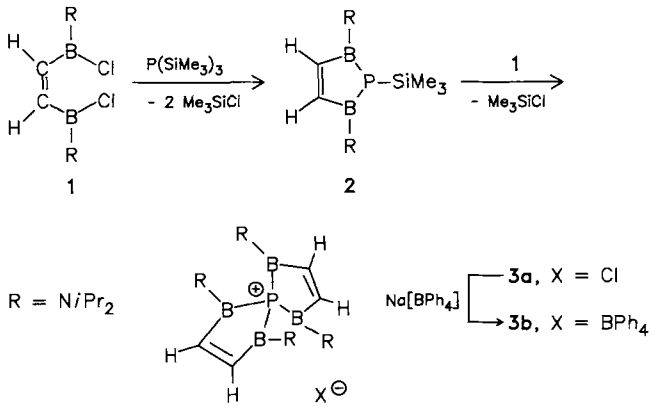
A Tetraborylphosphonium Ion with a Spiroheterocyclic Structure**

By *Matthias Driess, Pascal Frankhauser, Hans Pritzkow,* and *Walter Siebert**

Dedicated to Professor Ernst Otto Fischer on the occasion of his 70th birthday

Boron–phosphorus compounds with organic substituents have been far less thoroughly investigated than the corresponding boron–nitrogen compounds.[1] σ^3- or σ^4-coordinated boron and phosphorus atoms are present in phosphinoboranes $(R_2P-BR_2)_n$, n = 1–4.[2] Phosphonioborates, R_3P-BR_3 ("phosphaneboranes"), contain B and P atoms with coordination numbers of 4. To the best of our knowledge, examples of BP compounds with λ^5-phosphorus and λ^3,σ^3-boron atoms have not previously been reported. This category of compounds includes the *P*-borylphosphoranes R_2B-PR_4 and *P*-borylphosphonium ions $[R_2B-PR_3]^{\oplus}$.

We report here on the formation of the tetraborylphosphonium ions **3a**, **b** as the first compounds with λ^5,σ^4-phosphorus and λ^3,σ^3-boron atoms. The spirocyclic structure of the phosphonium ion, with tetrahedral coordination at the phosphorus atom, was determined by a crystal structure analysis of **3b**.



Compound **3a** was obtained for the first time as a colourless solid in 17% yield in the synthesis of the C_2B_2P derivative **2** from the diborylethene **1** and $P(SiMe_3)_3$.[3] By reacting **1** and $P(SiMe_3)_3$ in a ratio of 2:1 at 140°C, the yield of **3a** was increased to 64%. The use of bulky $N(iPr)_2$ groups on the boron atoms is essential for the kinetic stabilization of the spirocation of **3**. Other derivatives of **3**, for example with $R = NMe_2$ or NEt_2, could not be obtained.

3a is soluble in CH_2Cl_2 and $CHCl_3$, but not in toluene and THF. The ionic structure of **3a** was confirmed, following substitution of $Cl^{\ominus}$ with the non-coordinating $[BPh_4]^{\ominus}$ ion (→ **3b**), by comparison of the ^{31}P NMR chemical shifts: **3a** and **3b** have almost identical δ-values (−190.5 and −187.3, respectively).

The high field positions of the ^{31}P NMR signals of **3**, which are unusual for phosphonium salts, can be explained by the electropositive character of the boron atoms next to phosphorus. Other indications for this phenomenon were reported some time ago.[4] The electropositive character of the boron atoms in **3** is comparable to that of hydrogen atom substituents $[MePH_3^{\oplus}Cl^{\ominus}: \delta(^{31}P) = -156]$.[5]

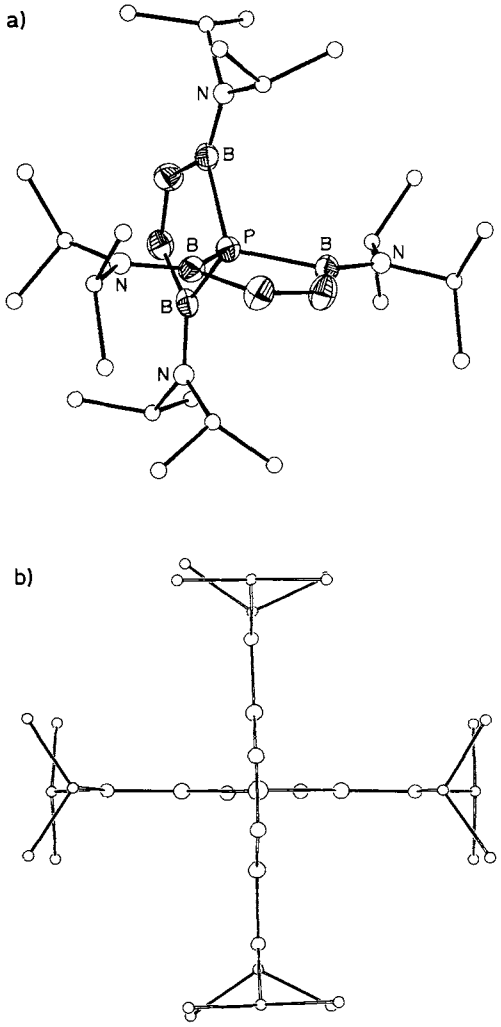


Fig. 1. Cation of **3b**. a) Structure in the crystal. Selected bond lengths [Å] and angles [°]: P-B 1.957–1.961(5), B-C 1.548–1.568(7), C-C 1.330, 1.334(6), B-N 1.357–1.374(7); B-P-B 93.0, 93.5, P-B-C 103.8–104.5(3), B-C-C 118.9–119.6(4). b) Projection in the direction of the S_4-axis.

In contrast, phosphorus atoms in tetraorganophosphonium compounds exhibit low field resonances.[6] For a phosphorane with a P–Cl bond, an even greater shielding

[*] Prof. Dr. W. Siebert, Dr. M. Driess, Dipl.-Chem. P. Frankhauser, Dr. H. Pritzkow
Anorganisch-chemisches Institut der Universität
Im Neuenheimer Feld 270, D-6900 Heidelberg (FRG)

[**] This work was supported by the Deutsche Forschungsgemeinschaft, the Fonds der Chemischen Industrie, and BASF AG.

of the ^{31}P nucleus can be anticipated. The ^{11}B spectra of **3a**, **b** show a signal at $\delta = 41.9$ ($b_{1/2} = 479$ Hz), and in addition, a signal at $\delta = -3.73$ in the spectrum of **3b** for $[BPh_4]^{\ominus}$. The ^1H NMR spectrum of **3a** exhibits a doublet at $\delta = 7.65$ for the olefinic protons, for which the coupling constant ($|^3J_{PH}| = 16.7$ Hz) is on average 11 Hz greater than for **2**.[3] This points to the greater s-character of the boron–phosphorus bond in **3**. Due to the BN π-bond, the two *i*Pr groups of the $N(iPr)_2$ unit are inequivalent.

An X-ray structural analysis also confirms the ionic structure of **3b** in the solid state (Fig. 1a).[8] The cation has approximately D_{2d} symmetry (Fig. 1b). The C_2B_2P rings are planar (maximum deviations from the best planes 0.008 and 0.019 Å) and lie perpendicular to each other (90.9°). The phosphorus atom has distorted tetrahedral coordination, for which the B-P-B angle inside the ring is considerably less (93–94°) than that between the rings (116–119°), but 4–5° larger than in 2,5-dihydro-2,5-bis(diisopropylamino)-1*H*,1,2,5-phosphadiborole.[9] The bond lengths are in good agreement with those of the *P*-phenyl substituted C_2B_2P derivatives,[9] although in these compounds the ring is not planar.

Experimental

3a (1,1'-Spirobi[2,5-bis(diisopropylamino)-2,5-dihydro-1*H*-1,2,5-phosphoniadiborole] chloride): A mixture of **1** (5.16 g, 16.17 mmol) [10] and $P(SiMe_3)_3$ (2.02 g, 8.08 mmol) was heated at 140°C for about 5 hours, until no more Me_3SiCl distilled over. The molten reaction mixture gradually solidified. The crude product was extracted twice with petrol ether then dissolved in CH_2Cl_2. After filtering off a yellow, insoluble compound, **3a** was obtained at −30°C as a colorless powder. Yield: 2.9 g (5.16 mmol, 64%); m.p. 273°C (decomp.).—^1H NMR (200 MHz, CD_2Cl_2): $\delta = 1.01$ (d, 24H, $J_{HH} = 6.9$ Hz), 1.28 (d, 24H), 3.27 (d sept, 4H, $^4J_{PH} \approx 1$ Hz), 3.40 (d sept., 4H, $^4J_{PH} = 2.9$ Hz), 7.65 (d, 4H, $^3J_{PH} = 16.7$ Hz). ^{13}C NMR (50 MHz): $\delta = 21.38$ (s, CH_3), 25.28 (s, CH_3), 47.13 (d, $^3J_{PC} = 6.5$ Hz, NCH), 60.20 (d, $^3J_{PC} = 11$ Hz, NCH), 159.3 (br., BC). MS (DCI (field desorption + chemical ionization), CH_4): *m/z* 562 (3%, $M^{\oplus}$), 546 (3%, $[M - Me - H]^{\oplus}$), 519 (6%, $[M - iPr]^{\oplus}$), 43 (100%, $iPr^{\oplus}$).

3b: A solution of **3a** (320 mg, 0.57 mmol) in CH_2Cl_2 (10 mL) was mixed with $Na[BPh_4]$ (340 mg, 0.99 mmol) and the reaction mixture stirred for 1 h. The insoluble components were filtered off and the solvent removed in a vacuum. **3b** was crystallized from a little acetonitrile at −30°C. Yield: 398 mg (0.47 mmol, 83%).

Received: August 10, 1988 [Z 2920 IE]
German version: *Angew. Chem. 101* (1989) 219

[1] a) *Gmelin, Handbuch der Anorganischen Chemie, Borverbindungen, Band 22/4, Erg.* 8th edit., Springer, Berlin 1975; b) P. I. Paetzold, *Adv. Inorg. Chem. 31* (1987) 123; c) D. B. Sowerby in I. Haiduc, D. B. Sowerby (Eds.): *The Chemistry of Inorganic Homo- and Heterocycles, Vol. 1*, Academic Press, New York 1987, p. 103.

[2] J. R. Wasson in: *Gmelin, Handbuch der Anorganischen Chemie, Borverbindungen Band 19/3*, 8th edit., Springer, Berlin 1975, p. 93.

[3] M. Driess, *Dissertation*, Universität Heidelberg 1988.

[4] H. Nöth, W. Schrägle, *Z. Naturforsch. B 16* (1961) 473.

[5] E. Fluck, J. Svara, B. Neumüller, H. Riffel, H. Thurn, *Z. Anorg. Allg. Chem. 536* (1986) 129.

[6] J. C. Tebby: *Phosphorus-31 NMR Spectroscopy in Stereochemical Analysis* (*Methods Stereochem. Anal. 8* (1987) 26).

[7] W. Kutzelnigg (Bochum), private communication.

[8] Crystal structure analysis of **3b**: space group $P2_1/n$, $a = 11.340(3)$, $b = 21.901(6)$, $c = 22.638(5)$ Å, $\beta = 104.30(2)°$, $V = 5448$ Å^3, $Z = 4$. 3199 observed reflections ($I \geq 2\sigma_I$), four-circle diffractometer. $Mo_{K\alpha}$ radiation, ω-scan. Non-hydrogen atoms anisotropic, phenyl rings and methyl groups as fixed groups (C-C 1.395 Å, C-H 0.95 Å). H atoms refined with common isotropic temperature factors, $R = 0.067$. Further details of the crystal structure investigation may be obtained from the Fachinformationszentrum Energie, Physik, Mathematik GmbH, D-7514 Eggenstein-Leopoldshafen 2 (FRG), on quoting the depository number CSD-53377, the names of the authors, and the journal citation.

[9] M. Driess, H. Pritzkow, W. Siebert, *Angew. Chem. 99* (1987) 789; *Angew. Chem. Int. Ed. Engl. 26* (1987) 781.

[10] M. Hildenbrand, H. Pritzkow, W.Siebert, *Angew. Chem. 97* (1985) 769; *Angew. Chem. Int. Ed. Engl. 24* (1985) 759.

$LiBH_4(NaBH_4)/Me_3SiCl$, an Unusually Strong and Versatile Reducing Agent**

By *Athanassios Giannis** and *Konrad Sandhoff*

Metal borohydrides MBH_4 (M = Li, Na, 1/2 Ca, 1/2 Zn) are amongst the most important reducing agents in organic chemistry.[1,2] Their reactivity is strongly influenced by the following factors: a) the solvent,[2] b) the metal ion M,[2] and c) the presence of catalysts such as $B(OMe)_3$,[3] *B*-methoxy-9-borabicyclononane,[3] or halides[4,5] of cobalt, nickel, iridium, osmium, copper, platinum and titanium. Despite the variation of these parameters, the range of functional groups that can be reduced by metal borohydrides is very limited. We now report a method which makes it possible also to reduce amino acids, carboxylic acids, amides, nitriles, nitroalkenes, and sulfoxides with alkali metal borohydrides in good yields.

We found that the addition of Me_3SiCl makes possible the reduction of α-amino acids with $LiBH_4$ in THF (Nos. 1–4 in Table 1). When optically pure α-amino acids were used, optically pure β-amino alcohols were obtained. This inspired us to investigate the use of $LiBH_4/Me_3SiCl$ as a reducing agent for other functional groups. Thus, simple carboxylic acids are reduced to alcohols (No. 5), while primary, secondary and tertiary amides (Nos. 6–8) and nitriles (Nos. 10–12) afford the corresponding amines. High yields were obtained in all cases. Dimethyl sulfoxide was reduced to dimethyl sulfide (No. 9), the dipeptide derivative Fmoc-L-Phe-L-Ala-OMe (No. 14) gave the corresponding amino alcohol, and *N*-benzyloxycarbonyl-6-amino-1-hexanol was converted into 6-amino-1-hexanol (No. 15). Similar results were obtained with $NaBH_4$ (Nos. 6, 8, 9, 11, 12, 14 and 15 in Table 1). Because of its good solubility in THF and the milder reaction conditions, $LiBH_4$[6] is, however, the reducing agent of choice.

The strength of this new system is demonstrated by the smooth reduction of the nitrostyrene derivative (No. 13) on a preparative scale (100 mmol) to afford the corresponding amine. Other methods for the reduction of conjugated nitroalkenes, such as $LiAlH_4$ reduction or catalytic hydrogenation, are unsatisfactory; far better results have been obtained using diborane in the presence of $NaBH_4$[7] or $BF_3 \cdot OEt_2$.[8]

We suggest that in reductions using $LiBH_4(NaBH_4)/Me_3SiCl$ in THF, a borane THF complex is formed [Eq. (a)] which, with the assistance of excess Me_3SiCl, acts as the reducing agent.

$$LiBH_4 + Me_3SiCl \xrightarrow{THF} LiCl + Me_3SiH + BH_3 \cdot THF \qquad (a)$$

The addition of Me_3SiCl makes it possible to carry out reductions with $LiBH_4$ or $NaBH_4$ which are either very slow or do not occur in its absence. The reaction mechanism, the use of other alkylhalogenosilanes,[9] and the suitability of the method for other functional groups remain to be investigated.

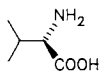
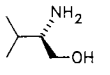
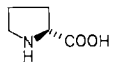
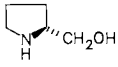
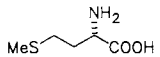
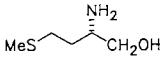
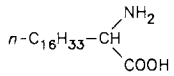
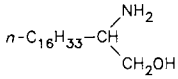
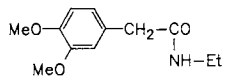
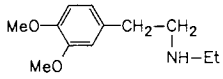
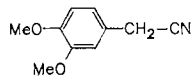
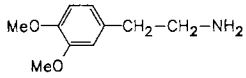
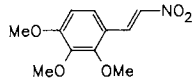
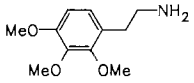
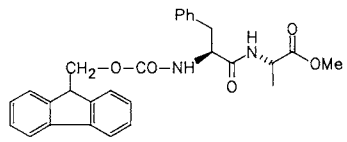
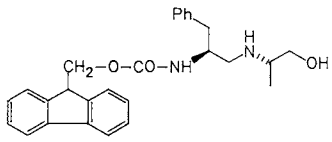
Typical procedures

Me_3SiH is formed in all reactions. It should therefore be ensured that this volatile silane (b.p. ~ 10°C) can escape from the reaction vessel.[10]

[*] Dr. A. Giannis, Prof. Dr. K. Sandhoff
Institut für Organische Chemie und Biochemie der Universität
Gerhard-Domagk-Strasse 1, D-5300 Bonn 1 (FRG)

[**] This work was supported by the Bundesministerium für Forschung und Technologie and the Deutsche Forschungsgemeinschaft. We thank Dr. *R. Kirstgen*, Dr. *S. Hilger* and Prof. Dr. *W. Steglich* for the starting materials for reactions **13** and **14**.

Table 1. Reductions with $LiBH_4(NaBH_4)/Me_3SiCl$.

No.	Starting material	Product [a]	Method [b]	Yield [%]
1			A	91
2			A	88
3			A	94
4			A	85
5	Ph–COOH	Ph–CH_2OH	A	92
6	Ph–CO–NH_2	Ph–CH_2–NH_2	A B	91 89
7			A	90
8	HCO–NMe_2	Me_3N	A B	72 [c] 71
9	Me–SO–Me	Me–S–Me	B	60
10	Ph–CN	Ph–CH_2–NH_2	A	90
11			B	90
12	Me–CN	Me–CH_2–NH_2	A B	75 [c] 70
13			A	91
14			A [d] B	60 55
15	Ph–CH_2–O–CO–NH–$(CH_2)_6$–OH	H_2N–$(CH_2)_6$–OH	A B	95 88

[a] All new compounds gave satisfactory C,H analyses and appropriate spectra. [b] A: $LiBH_4$ as reducing agent; B: $NaBH_4$ as reducing agent. [c] Isolated as the hydrochloride. [d] Purified by flash chromatography (silica gel, chloroform/methanol).

Reaction 1 in Table 1: A solution of Me_3SiCl (8.64 g, 80 mmol) was added under argon to a solution of $LiBH_4$ (0.87 g, 40 mmol) in THF (20 mL) over the course of 2 min. A precipitate of LiCl formed. L-valine (2.34 g, 20 mmol) was added portionwise to the mixture within 5 min. After stirring for 24 h at room temperature, 30 mL of MeOH were cautiously added and the volatiles removed by distillation. The residue was treated with 20% KOH solution and extracted three times with 50 mL portions of CH_2Cl_2. The organic phases were combined, dried over Na_2SO_4, and the solvent evaporated to afford L-valinol which was spectroscopically pure (^1H NMR). Yield after Kugelrohr distillation 1.87 g (91%), $[\alpha]_D^{24} = +14.7$ (neat).

Reaction 11 in Table 1: $NaBH_4$ (4.56 g, 120 mmol) was added to a solution of Me_3SiCl (26.04 g, 240 mmol) in THF (100 mL) and the mixture refluxed for 3 h under argon. A solution of 3,4-dimethoxybenzylcyanide (10 g, 56.4 mmol) in THF (50 mL) was then added over the course of 10 min. The solution was refluxed for a further 10 h. After cooling, 100 mL MeOH were cautiously added and the volatiles removed in vacuo. The residue was taken up in dilute HCl and washed with ether. The aqueous solution was treated with excess dilute NaOH and then repeatedly extracted with CH_2Cl_2. The organic extracts were combined, dried over Na_2SO_4, and the solvent evaporated to afford 2-(3,4-dimethoxyphenyl)ethylamine (pure by ^1H NMR). Yield after kugelrohr distillation 9.16 g (90%).

Received: September 26, 1988 [Z 2977 IE]
German version: *Angew. Chem. 101* (1989) 220

CAS Registry numbers:
PhCN, 100-47-0; MeCN, 75-05-8; Me_2S, 75-18-3; ClTMS, 75-77-4; $LiBH_4$, 16949-15-8; $NaBH_4$, 16940-66-2; Me_2SO, 67-68-5; Me_3N, 75-50-3; $EtNH_2$, 75-04-7; $PhCO_2H$, 65-85-0; $PhCONH_2$, 55-21-0; Me_2NCHO, 68-12-2; $PhCH_2OH$, 100-51-6; $PhCH_2NH_2$, 100-46-9; $Me_3N \cdot HCl$, 593-81-7; $EtNH_2 \cdot HCl$, 557-66-4; $HO(CH_2)_6NH_2$, 4048-33-3; $HO(CH_2)_6NHCO_2CH_2Ph$, 17996-12-2; $CH_3(CH_2)_{15}CH(NH_2)CO_2H$, 2187-07-7; (*L*)-*i*-PrCH(NH_2)CO_2H, 72-18-4; (*S*)-*i*-PrCH(NH_2)CH_2OH, 2026-48-4; 3,4-$(MeO)_2C_6H_3CH_2CN$, 93-17-4; (*L*)-$MeS(CH_2)_2CH(NH_2)CO_2H$, 63-68-3; $CH_3(CH_2)_{15}CH(NH_2)CH_2OH$, 23356-96-9; (*S*)-$MeS(CH_2)_2CH(NH_2)CH_2OH$, 2899-37-8; 3,4-$(MeO)_2C_6H_3(CH_2)_2NH_2$, 120-20-7; 3,4-$(MeO)_2C_6H_3CH_2CONHEt$, 118474-93-4; 2,3,4-$(MeO)_2C_6H_2(CH_2)_2NH_2$, 3937-16-4; 3,4-$(MeO)_2C_6H_3(CH_2)_2NHEt$, 39792-99-9; (*E*)-2,3,4-$(MeO)_3C_6H_2CH{=}CHNO_2$, 118474-94-5; methyl [*N*-(9*H*-fluoren-q-ylmethyloxycarbonyl)phenylalanyl]alanine, 118474-95-6; 9*H*-fluoren-q-ylmethyl 1-(1-hydroxy-2-propylamino)-3-phenyl-2-propylcarbamate, 118474-96-7; (*L*)-Proline, 147-85-3; (*L*)-Prolinol, 23356-96-9.

[1] A. Hajos in: *Houben-Weyl-Müller, Methoden der organischen Chemie, Band IV/1d*, Thieme, Stuttgart 1981, p. 1.

[2] E. R. H. Walker, *Chem. Soc. Rev. 5* (1976) 23.
[3] H. C. Brown, S. Narasimhan, *J. Org. Chem. 49* (1984) 3891.
[4] T. Sato, S. Suzuki, Y. Suzuki, Y. Miyaji, Z. Imai, *Tetrahedron Lett. 1969*, 4555.
[5] S. W. Heinzman, B. Ganem, *J. Am. Chem. Soc. 104* (1982) 6801.
[6] Obtainable from Aldrich or easily prepared according to H. C. Brown, Y. M. Choi, S. Narasimhan, *Inorg. Chem. 20* (1981) 4456.
[7] M. S. Mourad, R. S. Varma, G. W. Kabalka, *Synth. Commun. 14* (1984) 1099.
[8] R. S. Varma, G. W. Kabalka, *Synth. Commun. 15* (1985) 843.
[9] Using $NaBH_4/Me_2SiCl_2$, we were able to reduce benzyl cyanide to 2-phenylethylamine in 86% yield.
[10] O. W. Steward, O. R. Pierce, *J. Am. Chem. Soc. 83* (1961) 1916.

Enzymatic Synthesis of Selectively Protected Glycals**

By *E. Wolfgang Holla**

Glycals and their esters are versatile chiral building blocks.[1] They can be obtained in good yields from the corresponding saturated carbohydrates;[2] however, because of their overfunctionalization with hydroxyl groups and because of the absence of strategically valuable functional groups such as C=C and C=O bonds, these are in many cases unsuitable for direct conversion into the target molecules. The directed chemical linkage or transformation of glycals such as **1a** and **1b** at the hydroxyl groups usually requires tedious, multistep protection and deprotection procedures. Regioselective acetylations of D-glucal **1a** and D-galactal **1b** and deacetylations of the triacetates **5c**, **5d** have so far never been reported.[3] This prompted us to investigate lipase-catalyzed acetyl transfer reactions [Eq. (a)–(c)].[4]

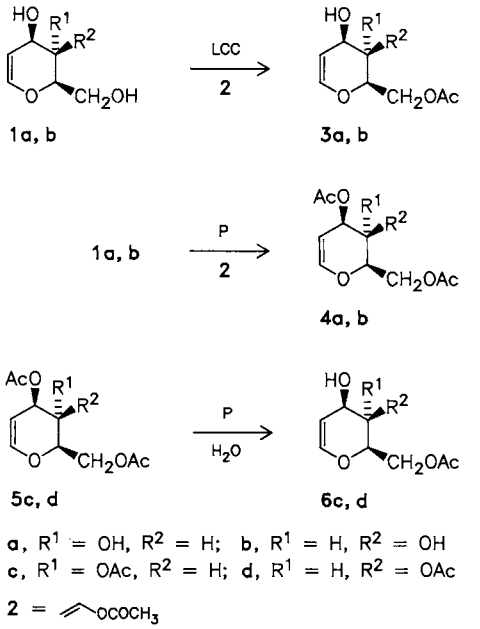
$$Gly(OCOR')_{n+x} + x\,H_2O \rightleftharpoons Gly(OCOR')_n(OH)_x + x\,R'COOH \quad (a)$$

$$Gly(OH)_{m+y} + y\,R'COOR'' \rightleftharpoons Gly(OH)_m(OCOR')_y + y\,R''OH \quad (b)$$

$$Gly(OH)_{m+y} + y\,R'COOCH{=}CH_2 \longrightarrow Gly(OH)_m(OCOR')_y + y\,CH_3CHO \quad (c)$$

In the present communication we report some novel, efficient and facile enzymatic syntheses of partially protected as well as fully hydroxyl-differentiated glucals and galactals.

Of primary interest was the realization of enzymatic transacetylations in nonaqueous organic media. Reversible transesterifications [Eq. (b)], however, generally result in unsatisfactory conversions. This problem can be overcome by using vinyl esters[5] [Eq. (c)]. An especially suitable reagent for irreversible enzymatic acetyl transfer is the inexpensive vinyl acetate **2**. For carrying out the reactions the glycals are either stirred with the enzyme in pure **2** at room temperature or are previously taken up in small amounts of a cosolvent and finally treated with **2** and the lipase (Table 1). The enzymes employed are commercially available lipases from *Candida cylindracea* (LCC) and *Pseudomonas fluorescens* (P).[6] Especially suitable for the selective acetylation of the primary hydroxyl groups of **1a** and **1b** are the *Candida lipases* (Scheme 1, Table 1). Thus, the reaction of **1a** in **2**/ethyl acetate in presence of the lipase OF afforded, in 24 hours, 6-*O*-acetyl-D-glucal **3a** in 90% yield. The galactal derivative **3b** was obtained by dissolving **1b** in a little water, addition of **2** and lipase S-VII, and stirring the resulting mixture for 45 minutes. With lipase P, on the other hand, the 3,6-di-*O*-acetyl derivatives **4a** and **4b** were obtained in 92% and 75% yield, respectively.



Scheme 1. Lipase-catalyzed acetylations and deacetylations.

Table 1. Enzymatic acetyl transfer reactions with D-glucal **1a**, D-galactal **1b** and 3,4,6-tri-*O*-acetyl-D-glucal **5c**.

Starting Cpd.	Enzyme [6] [a]	Reaction conditions [b]	Product	Isolated Yield [%] [c]
1a	OF, 0.4 g	**2** [d], 24 h	**3a**	90
1b	S-VII, 0.8 g	**2** [e], 45 min	**3b**	93
1a	P, 0.25 g	**2** [d], 48 h	**4a**	92
1b	P, 1.0 g	**2** [e], 20 h	**4b**	75 [f]
5c	P, 1.0 g	buffer [g], 5–7 h	**6c**	90

[a] The quoted amounts of enzyme refer to 1.0 g of starting compound; the enzymes can be used several times. [b] All reactions at room temperature. [c] After flash chromatography. [d] 20–25 vol-% ethyl acetate. [e] 1–4 vol-% water, 2 g of powdered molecular sieve 4 Å. [f] Approx. 10% of regioisomer found. [g] 10 mL 0.25 M potassium phosphate buffer, pH = 7.

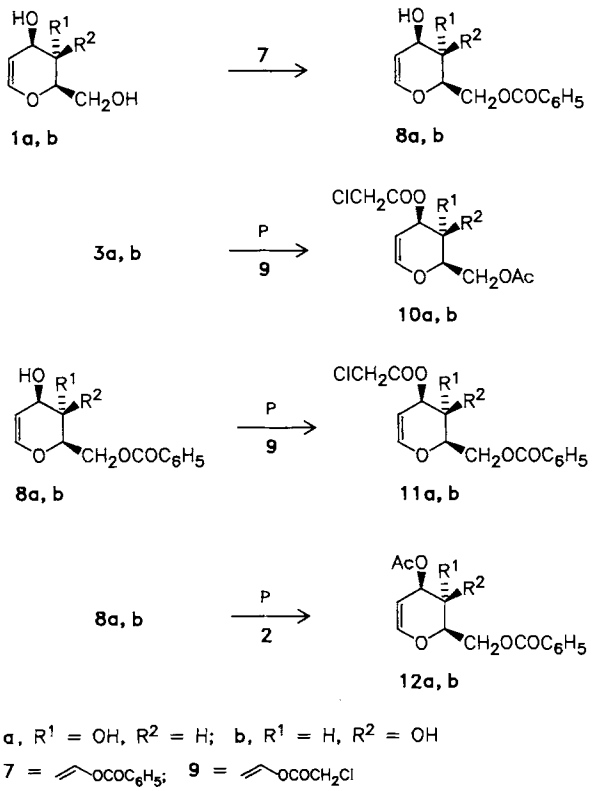
After completion of the reactions the insoluble enzymes can be recovered by membrane filtration and used again in further transformations.[7]

Especially interesting with regard to the regiochemistry is the deacetylation of tri-*O*-acetyl-D-glucal **5c**. The lipase-P-catalyzed ester cleavage in weakly buffered solution without pH-control affords 4,6-di-*O*-acetyl-D-glucal **6c** in 90% yield. In the case of the tri-*O*-acetyl-D-galactal **5d**, on the other hand, the formation of a complex mixture of **6d** and several di- and monoacetates is observed.

For the synthesis of completely hydroxyl-differentiated glycals we investigated the enzymatic transfer of benzoyl and chloroacetyl groups[8] by using vinyl esters **7** and **9**, respectively (Scheme 2, Table 2). Lipase AY-20 and, contrary to expectation, lipase P are suitable for the selective benzoylation of the 6-hydroxy groups of **1a** and **1b** with **7**. With tetrahydrofuran or water as cosolvent, the monobenzoates **8a,b** are obtained in about 70% yield.[9] Regioselective chloroacetylation of **3a,b** and **8a,b** with **9**/lipase P and acetylation of **8a,b** with **2**/lipase P gave the completely differentiated glycals **10a,b**, **11a,b**, and **12a,b** in good yields.[10]

[*] Dr. E. W. Holla
Hoechst Aktiengesellschaft
Postfach 800320, D-6230 Frankfurt am Main 80 (FRG)

[**] I am grateful to Frau *A. Weber* for carrying out some of the preparative work.



Scheme 2. Lipase-catalyzed synthesis of completely hydroxyl-differentiated glycals.

Table 2. Enzymatic acylations (benzoylation, chloroacetylation and acetylation) of glycals.

Starting Cpd.	Enzyme [6] [a]	Reaction conditions [b]	Product	Isolated yield [c] [%]
1a	AY-20	**7** [d], 6 h	**8a**	70 [e]
1b	AY-20	**7** [f], 8 h	**8b**	67
1b	P	**7** [f], 10 h	**8b**	66
3a	P	**9** [g], 2–3 h	**10a**	83 [e]
3b	P	**9** [g], 6 h	**10b**	80 [e]
8a	P	**9** [g], 1–2 h	**11a**	82
8b	P	**9** [g], 6 h	**11b**	80
8a	P	**2**, 5 h	**12a**	92
8b	P	**2** [g], 8 h	**12b**	80

[a] One gram of enzyme used per gram of starting compound; the enzymes can be used several times. [b] All reactions at room temperature. [c] After flash chromatography. [d] 30–40 vol-% tetrahydrofuran. [e] 5–10 vol-% regioisomer found. [f] 5–10 vol-% water, 3 g of powdered molecular sieve 4 Å. [g] 20–30 vol-% dimethoxyethane.

Our results show that the enzymatic acetylations and chloroacetylations of glucal **1a** and galactal **1b** as well as the lipase-catalyzed benzoylations first described by us provide versatile and efficient routes to useful monosaccharide synthetic building blocks.

Received: August 28, 1988 [Z 2934 IE]
German version: *Angew. Chem. 101* (1989) 222

[1] S. Hanessian: *Total Synthesis of Natural Products: The 'Chiron Approach'*, Pergamon, Oxford 1983; N. L. Holder, *Chem. Rev. 82* (1982) 287; T. D. Inch, *Tetrahedron 40* (1984) 3161.
[2] W. Roth, W. Pigman, *Methods Carbohydr. Chem. 2* (1963) 405.
[3] Concerning the problems of the regioselective acetylation and deacetylation of carbohydrates see a) A. H. Haines, *Adv. Carbohydr. Chem. 33* (1976) 11; b) *ibid. 39* (1981) 13; for differentiation of the OH groups of **1a** and **1b** see c) I. D. Blackburne, P. M. Fredericks, R. D. Guthrie, *Aust. J. Chem. 29* (1976) 381; d) W. Kinzy, R. R. Schmidt, *Tetrahedron Lett. 28* (1987) 1981; e) T. Maki, S. Tejima, *Chem. Pharm. Bull. 15* (1967) 1367.
[4] Lipase-catalyzed acetyl transfer reactions of saturated monosaccharides according to Equations (a) and (b) have already been described; see a) J.-F. Shaw, A. M. Klibanov, *Biotechnol. Bioeng. 29* (1987) 648; b) A. L. Fink, G. W. Hay, *Can. J. Biochem. 47* (1969) 353; c) J. Zemek, S. Kucar, D. Anderle, *Collect. Czech. Chem. Commun. 52* (1987) 2347; d) H. M. Sweers, C.-H. Wong, *J. Am. Chem. Soc. 108* (1986) 6421; e) M. Kloostermann, E. W. J. Mosmuller, H. E. Schoemaker, E. M. Meijer, *Tetrahedron Lett. 28* (1987) 2989; f) M. Therisod, A. M. Klibanov, *J. Am. Chem. Soc. 108* (1986) 5638.
[5] a) M. Degueil-Castaing, B. De Jeso, S. Drouillard, B. Maillard, *Tetrahedron Lett. 28* (1987) 953; b) Y.-F. Wang, C.-H. Wong, *J. Org. Chem. 53* (1988) 3127.
[6] The following lipases from *Candida cylindracea* (LCC) were employed: L-1754 Type VII from Sigma Chemie GmbH ("S-VII"), lipase AY-20 from Amano Pharmaceutical Co.; lipase OF from Meito Sangyo Co., Ltd.; lipase P from *Pseudomonas fluorescens* was supplied by Amano Pharmaceutical Co.
[7] The lipases were used up to ten times; the decrease in enzymatic activity is dependent on the type of lipase and reaction. The retention of enzymatic activity is currently under investigation.
[8] For the chemoselective cleavage of acetates, benzoates and chloroacetates see T. W. Greene: *Protective Groups in Organic Synthesis*, Wiley, New York 1981.
[9] For comparison: Treatment of **1a** with 1 equivalent of C_6H_5COCl/pyridine at 0°C gave **8a** in only 29% yield [3c].
[10] Acyl-group migrations were not observed in any of the reactions. All the given structures are consistent with the spectroscopic data.

Bis(trifluoromethyl)sulfene $(CF_3)_2C{=}SO_2$, Isolated as Adduct

By *Uwe Hartwig, Hans Pritzkow, Klaus Rall,* and *Wolfgang Sundermeyer**

Dedicated to Professor Heinrich Nöth on the occasion of his 60th birthday

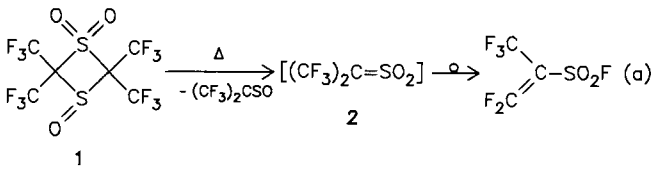
Sulfenes $R_2C{=}SO_2$ (thione *S,S*-dioxides) have so far not been isolated but only detected as unstable intermediates by (in most cases) cycloaddition reactions.[1] Of particular interest for investigations on the synthesis and stabilization of small reactive molecules are compounds with double bonds between main group elements of the second and third periods. Such species containing, for example, C=Si,[2] N=Si[3] and $C{=}SF_4$ bonds[4] have been isolated or stabilized as adducts[2,3] and characterized by structural analyses.

In reactions previously carried out with α-H-sulfonyl chlorides in the presence of suitable tertiary amines no symmetrically substituted sulfenes $R_2C{=}SO_2$ could be isolated, but, after further reaction, only sulfonylsulfenes,[1] as was recently demonstrated by us with the isolation of the amine-stabilized species **A**.[5,6]

$XCH_2{-}SO_2{-}C(X){=}SO_2{\leftarrow}N(CH_2CH_2)_3CH$ **A**,
X = H, Cl, Br, CF_3

A completely different route now led to the successful synthesis of bis(trifluoromethyl)sulfene **2**, namely via the symmetrical cleavage of 1,3-dithietane *S*-oxides.[7] The thermolysis of tetrakis(trifluoromethyl)-1,3-dithietane 1,1,3-trioxide **1**[8] already gave an indication of the existence of **2** [Eq. (a)], as did also the reaction of the corre-

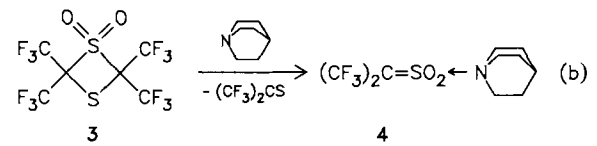
[*] Prof. Dr. W. Sundermeyer, Dr. U. Hartwig, Dr. H. Pritzkow, Dipl.-Chem. K. Rall
Anorganisch-chemisches Institut der Universität
Im Neuenheimer Feld 270, D-6900 Heidelberg 1 (FRG)



1 2

sponding 1,1,3,3-tetroxide with tertiary amines[9] and the isolation of cycloaddition products of **2** generated in situ.[10]

On the other hand, when tetrakis(trifluoromethyl)-1,3-dithietane 1,1-dioxide **3** is allowed to react with quinuclidine as tertiary amine in acetonitrile [Eq. (b)] not only is the dimer of hexafluoroacetone formed but also the bis(trifluoromethyl)sulfene-quinuclidine adduct **4**, which precipitates as colorless crystals in 74% yield [m.p. 181°C (de-



3 4

comp.)]. The 90 MHz ^{19}F NMR spectrum shows the same unusual shift [$\delta = -47.8$ (s) in CD_3CN] typical for the $F_3C-C=SO_2$-group with partial negative charge on the sulfene C-atom, as was already observed for the product of the reaction of the 1,1,3,3-tetroxide analogue of **3** with tertiary amines[9] and in the case of the (2,2,2-trifluoromethylsulfonyl)trifluoromethylsulfene-quinuclidine adduct.[6]

An X-ray structure analysis of **4**[11] showed that **2** was stabilized by coordination of a quinuclidine molecule to the SO_2-group (Fig. 1). The S–N distance (1.91 Å) is longer

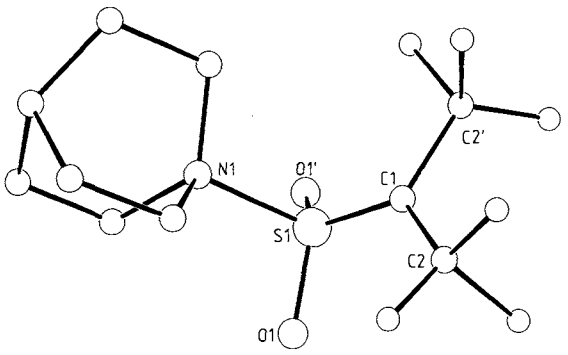


Fig. 1. Structure of **4** in the crystal. Important bond lengths [Å] and angles [°]: S1-N1 1.907(7), S1-C1 1.663(9), S1-O1 1.429(5), C1-C2 1.445(12); S1-C1-C2 120.2(5), C2-C1-C2' 118.5(9), O1-S1-O1' 118.3(4), N1-S1-O1 100.3(2), N1-S1-C1 107.0(4), O1-S1-C1 114.1(2).

than an S–N single bond, whereas the C–S distance (1.66 Å) is only slightly longer than an isolated C=S double bond. The mass spectrum, elemental analysis and the product of hydrolysis quinuclidinium-1,1,1,3,3,3-hexafluoropropane-2-sulfonate[12] likewise confirm the constitution of this first symmetrically substituted sulfene adduct **4**.

The analogous reaction with tetrafluoro-1,3-dithietane 1,1-dioxide **5** [Eq. (c)] proceeds completely differently. Instead of the expected difluorosulfene-quinuclidine adduct which, like **4**, should be soluble in polar aprotic solvents, only a product soluble in water and methanol is formed, the ^{19}F NMR spectrum of which shows two triplets at $\delta = -65.7$ and -78.8 of equal intensity and with the same coupling constant. The product, which formed colorless crystals (m.p. 124°C), was finally unequivocally identified as (quinuclidinodifluoromethylthio)difluoromethanesulfinate **6** by an X-ray structural analysis (Fig. 2).[13]

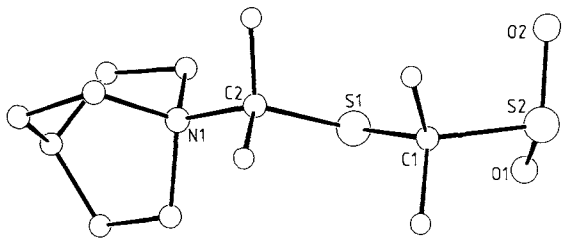


Fig. 2. Structure of **6** in the crystal. Important bond lengths [Å] and angles [°] (the values for each of the independent molecules are given): S1-C1 1.810(4), 1.820(4), S1-C2 1.798(4), 1.821(4), S2-C1 1.884(4), 1.897(4), S2-O1 1.476(3), 1.467(4), S2-O2 1.465(3), 1.441(4), C2-N1 1.514(5), 1.505(5); C1-S1-C2 98.3(1), 98.0(1), C1-S2-O1 97.2(1), 97.7(2), C1-S2-O2 101.9(2), 101.3(2), O1-S2-O2 111.5(1), 112.9(2), S1-C1-S2 108.2(2), 107.8(2), S1-C2-N1 112.1(2), 111.7(2).

The C–N distance corresponds to a single bond, so that one can speak here of an internal tetraalkylammonium salt in which the charges are separated by five bonds, whereas in the "inverse" fluorosulfene-trimethylamine adduct[14] only three bonds separate the positively and negatively charged centers.

Other than in the case of **3**, in the case of **5** the nucleophilic attack of the amine did not take place at the sulfur atom but at the carbon atom. As was expected, but hitherto not confirmed experimentally, the $C-SO_2$ bond is ruptured thereby, and not the electron-richer C–S bond.—The apparently nonpolar $C=SO_2$ bond (in sulfenes) is first polarized by steric and electronic effects of the substituents: usually as $R_2\overset{\ominus}{C}-\overset{\oplus}{S}O_2$, so that nucleophiles attack at the sulfur atom; if however the polarization is $R_2\overset{\oplus}{C}-\overset{\ominus}{S}O_2$, the nucleophilic attack takes place "inversely" at the carbon atom.[14–16]

Received: October 12, 1988 [3006 IE]
German version: *Angew. Chem. 101* (1989) 224

CAS Registry numbers:
3, 795-31-3; **4**, 118724-94-0; **5**, 767-45-3; **6**, 118724-95-1; quinuclidine, 100-76-5.

[1] B. G. Lenz, B. Zwanenburg in *Houben-Weyl-Müller: Methoden der organischen Chemie, Vol. E11*, Thieme, Stuttgart 1985, p. 1326.
[2] N. Wiberg, G. Wagner, G. Müller, J. Riede, *J. Organomet. Chem. 271* (1984) 381.
[3] N. Wiberg, K. Schurz, G. Müller, J. Riede, *Angew. Chem. 100* (1988) 979; *Angew. Chem. Int. Ed. Engl. 27* (1988) 935.
[4] T. Krügerke, J. Buschmann, G. Kleemann, P. Luger, K. Seppelt, *Angew. Chem. 99* (1987) 808; *Angew. Chem. Int. Ed. Engl. 26* (1987) 799.
[5] U. Hartwig, H. Pritzkow, W. Sundermeyer, J. Waldi, *Z. Naturforsch. B43* (1988) 271.
[6] U. Hartwig, H. Pritzkow, W. Sundermeyer, *Chem. Ber. 121* (1988) 1435.
[7] W. Sundermeyer, *Synthesis 1988*, 349.
[8] A. Elsässer, W. Sundermeyer, D. S. Stephenson, *Chem. Ber. 118* (1985) 116.
[9] U. Hartwig, *Dissertation*, Universität Heidelberg 1988.
[10] B. E. Smart, W. J. Middleton, *J. Am. Chem. Soc. 109* (1987) 4982.
[11] **4** crystallizes in the space group $P2_1/m$; $a = 7.432(4)$, $b = 10.610(9)$, $c = 8.249(5)$ Å, $\beta = 98.75(6)°$, $V = 643$ Å^3, $Z = 2$. 971 observed reflections ($I \geq 2\sigma(I)$, four-circle diffractometer, $Mo_{K\alpha}$ radiation, ω scan). The CF_3 group rotates or is disordered. The refinement (S, F, O, N, C anisotropic, H in calculated positions with a common temperature factor for all H atoms) gave $R = 0.104$, $R_w = 0.087$ [17].

[12] M.p. 166°C; 90 MHz ^{19}F NMR: $\delta = -61.5$.
[13] 6 crystallizes in the space group $Pc2_1n$; $a = 8.057(1)$, $b = 11.443(1)$, $c = 26.738(2)$ Å, $V = 2465$ Å^3, $Z = 8$ (two crystallographically independent molecules). 2102 observed reflections ($I \geq \sigma(I)$, two-circle diffractometer, ω scan). The refinement (S, F, O, N, C anisotropic, six H atoms fixed in calculated positions, the rest in observed positions refined isotropically) gave $R = 0.040$, $R_w = 0.038$ [17].
[14] U. Rheude, W. Sundermeyer, *Chem. Ber. 118* (1985) 2208.
[15] T. Kempe, T. Norin, *Acta Chem. Scand. Ser. B28* (1974) 609.
[16] R. Allmann, W. Hanefeld, M. Krestel, B. Spangenberg, *Angew. Chem. 99* (1987) 1175; *Angew. Chem. Int. Ed. Engl. 26* (1987) 1133.
[17] Further details of the crystal structure investigations are available on request from the Fachinformationszentrum Energie, Physik, Mathematik GmbH, D-7514 Eggenstein-Leopoldshafen 2 (FRG), on quoting the depository number CSD-53391, the names of the authors, and the journal citation.

Highly Selective Oxidations of $Fe(CO)_3$-Cyclohexadiene Complexes: Synthesis of 4b,8a-Dihydrocarbazol-3-ones and the First Total Synthesis of Carbazomycin A**

By *Hans-Joachim Knölker*, Michael Bauermeister, Dieter Bläser, Roland Boese,* and *Jörn-Bernd Pannek*

Tricarbonyl(η^5-cyclohexadienylium)iron cations $\mathbf{1}^{\oplus}$ are very useful reagents for regio- and stereoselective C–C bond formation. They afford a wide range of 5-*exo*-substituted tricarbonyl(η^4-cyclohexadiene)iron complexes[1] in the electrophilic substitution of electron-rich aromatic systems such as indole, pyrrole, furan, and aniline.[2,3] Furthermore, some 5-*exo*-substituted cyclohexadiene iron complexes bearing a hydroxy or an amino group in the side chain have been observed to undergo oxidative cyclizations to give fused ring systems.[3,4]

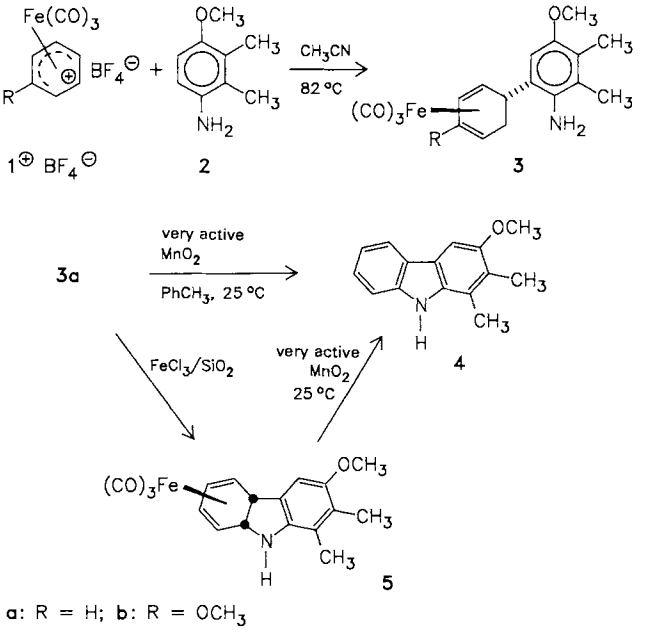
Our intention is to use a methodology of consecutive iron-induced C–C and C–N bond formation for the total synthesis of pharmacologically active heterocyclic natural products. Here we report a very direct route to tricyclic carbazole alkaloids and a stereoselective access to various metal-complexed dihydrocarbazole derivatives including the hitherto unknown 4b,8a-dihydrocarbazol-3-one **7**.

The iron complexes **3** were prepared stereoselectively from the cations $\mathbf{1}^{\oplus}$ and the amine **2** by modified literature procedures[3] (**3a**, 95%; **3b**, 64%) (Scheme 1). However, the described cyclization procedure (reaction with iodine in pyridine)[3] was ineffective for our highly donor substituted compounds. We found that employment of milder oxidizing agents leads to a very reagent-sensitive and selective reaction furnishing either the aromatized cyclization products (e.g., **4**) or the corresponding iron-complexed dihydro derivatives (e.g., **5**) depending on the reaction conditions. This method opens up the way to a very direct synthesis of many naturally occurring carbazole alkaloids which are oxygenated in the 3- or in the 2- and 6-position.[5] We envisaged an application in the total synthesis of the carbazomycins, which are the first antibiotics with a carbazole skeleton.[6]

[*] Dr. H.-J. Knölker, Dipl.-Chem. M. Bauermeister, J.-B. Pannek
Institut für Organische Chemie der Universität
Schneiderberg 1B, D-3000 Hannover 1(FRG)
Dr. R. Boese, Dipl.-Ing. D. Bläser
Institut für Anorganische Chemie der Universität
Universitätsstrasse 5-7, D-4300 Essen 1(FRG)

[**] Transition Metal-Diene Complexes in Organic Synthesis, Part 1. This work was supported by the Deutsche Forschungsgemeinschaft. We wish to thank Dr. *V. Wray*, Gesellschaft für Biotechnologische Forschung (GBF), Braunschweig-Stöckheim, for recording the COSY spectra and Dr. *K.-H. Geiss*, BASF Aktiengesellschaft, Ludwigshafen, for nonacarbonyldiiron.

Using the methodology described above, 4-deoxycarbazomycin B **4** has been synthesized in two steps from the cation $\mathbf{1a}^{\oplus}$ (Scheme 1). Reaction of **3a** (see above) with



Scheme 1.

very active manganese dioxide[7] afforded, in 28% yield, **4**, whose spectral data were identical with those reported by *Nakamura* et al. for the natural product.[6,8] An extensive investigation of the oxidative cyclization of **3a** showed that the scope of this reaction is much larger than originally anticipated. The one-pot transformation of **3a** to the carbazole **4** involves cyclizing dehydrogenation, aromatizing dehydrogenation and demetalation. This mechanism is supported by the isolation of the intermediate iron-complexed 4a,9a-dihydro-9*H*-carbazole **5** as a by-product in the cyclization of **3a** to **4** using $FeCl_3$ supported on silica gel[9] or 10% Pd/C at 80°C (Scheme 1). This strategy thus provides access to the interesting 4a,9a-dihydro-9*H*-carbazole skeleton[10] without additional annelated rings. The structure of **5** has been confirmed by an X-ray analysis (Fig. 1).[11] Single crystals of **5** exhibit optical anisotro-

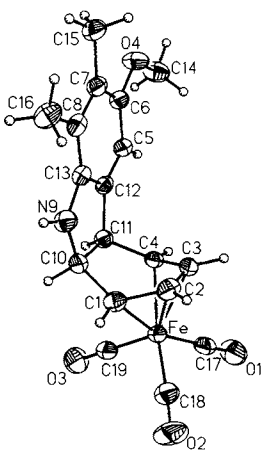


Fig. 1. Molecular structure of **5** [11]. Selected bond lengths [Å]: Fe-C1 2.106(3), Fe-C2 2.060(3), Fe-C3 2.063(2), Fe-C4 2.111(2), C1-C2 1.426(4), C2-C3 1.398(4), C3-C4 1.423(3), C4-C11 1.512(3), C1-C10 1.515(3).

pism. Rotation of these columnar crystals by 90° about the longitudinal axis results in a colour change from red to yellow. This interesting feature can be explained by the crystal packing (Fig. 2). When looking at the plane of the aromatic rings (Fig. 2a), which are arranged in parallel layers, the crystals appear red. Orthogonal to this direction (Fig. 2b) the crystals appear yellow. With very active manganese dioxide[7] **5** is smoothly converted into **4** (Scheme 1).

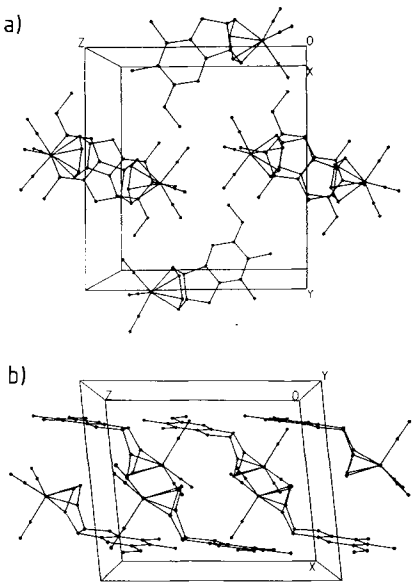
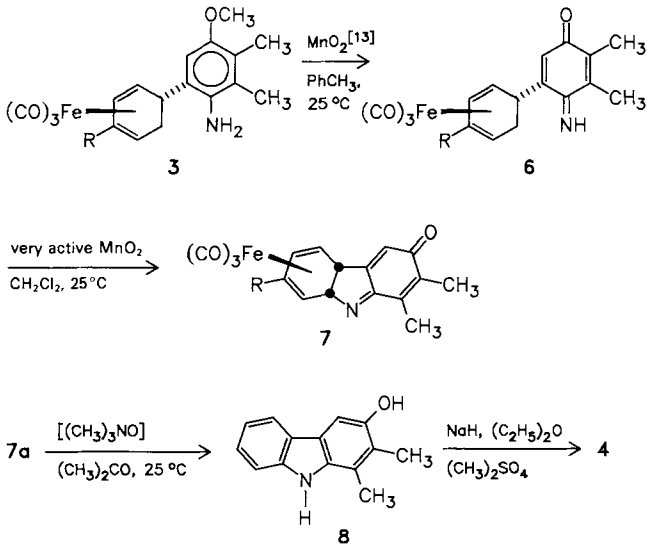
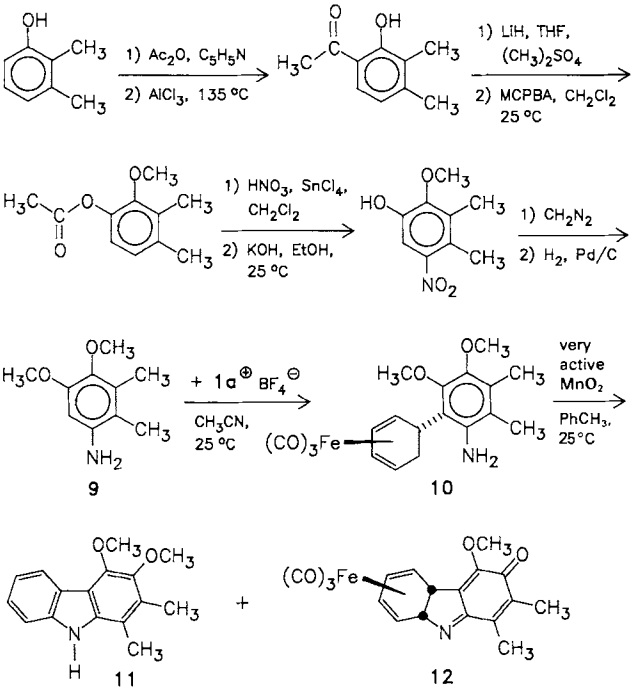


Fig. 2. The unit cell in crystals of **5** [11]. a) View perpendicular to the aromatic rings, b) side view (rotated by 90° about the *z* axis.

An even more striking example for the synthetic flexibility of these cyclizations is the first synthesis of the 4b,8a-dihydrocarbazol-3-ones **7** (Scheme 2). Selective oxidation of the complexes **3** using commercial MnO_2[13] gave the non-cyclized iminoquinones **6a** (60%) and **6b** (67%). The iminoquinones **6** are readily cyclized in a regio- and stereoselective manner to afford the novel iron-complexed 4b,8a-dihydrocarbazol-3-ones **7a** (90%) and **7b** (71%) again using very active manganese dioxide.[7] Structural assignments for **7** are based on ^1H, ^{13}C and COSY NMR spectra, and an X-ray crystal structure determination for **7a**.[1] The complexes **7** are stable at room temperature for at least several months, in contrast to the analogous 2,3-dihydroindol-5-ones, which are reported to undergo immediate ismerization to the 5-indolyl alcohols.[15] Upon demetalation of **7a**, however, rearrangement to the 3-carbazolyl alcohol **8** (93% yield) occurs instantaneously (Scheme 2). Methylation of **8** yields again 4-deoxycarbazomycin B **4** (96%). Due to the cleaner course of the iminoquinone-cyclization this route to the aromatized carbazoles is much better (48% overall yield of **4**) than the direct oxidative cyclization of the complexed amine **3a** (28% yield). Taking advantage of the tricarbonyliron fragment as a protecting group for the diene should allow exploitation of the iminoquinone reactivity in Michael and cycloaddition reactions.



Scheme 2.



Scheme 3.

Finally, to demonstrate the utility of these reactions in alkaloid synthesis, we completed the first total synthesis of the antibiotic carbazomycin A **11** (Scheme 3). The required amine **9** was prepared in eight steps from 2,3-dimethylphenol (28% overall yield). Subsequent C–C bond formation with **1a** to give the complex **10** (84% yield) and cyclization using very active manganese dioxide[7] (25% yield) afforded carbazomycin A **11**, the spectral data of which (UV, IR, ^1H NMR, ^{13}C NMR) are in full agreement with those of the natural product.[6] The isolation of the iron-complexed iminoquinone **12** as a byproduct in 17% yield indicates that the imonoquinone-cyclization could also be used for the synthesis of **11**.

Received: September 16, 1988 [Z 2969 IE]
German version: *Angew. Chem. 101* (1989) 225

[1] A. J. Pearson, *Acc. Chem. Res. 13* (1980) 463; A. J. Pearson in G. Wilkinson, F. G. A. Stone, E. W. Abel (Eds.): *Comprehensive Organometallic Chemistry, Vol. 8*, Pergamon, Oxford 1982, Chap. 58, p. 939.

[2] L. A. P. Kane-Maguire, C. A. Mansfield, *J. Chem. Soc. Chem. Commun. 1973*, 540.
[3] A. J. Birch, A. J. Liepa, G. R. Stephenson, *Tetrahedron Lett. 1979*, 3565.
[4] A. J. Birch, K. B. Chamberlain, D. J. Thompson, *J. Chem. Soc. Perkin Trans. 1 1973*, 1900; A. J. Pearson, M. Chandler, *ibid. 1982*, 2641.
[5] D. P. Chakraborty, *Prog. Chem. Org. Nat. Prod. 34* (1977) 299.
[6] K. Sakano, K. Ishimaru, S. Nakamura, *J. Antibiot. 33* (1980) 683; K. Sakano, S. Nakamura, *ibid. 33* (1980) 961; M. Kaneda, K. Sakano, S. Nakamura, Y. Kushi, Y. Iitaka, *Heterocycles 15* (1981) 993.
[7] A. J. Fatiadi, *Synthesis 1976*, 65.
[8] U. Pindur, L. Pfeuffer, *Heterocycles 26* (1987) 325.
[9] E. Keinan, Y. Mazur, *J. Org. Chem. 43* (1978) 1020; C. W. Ong, A. J. Pearson, *Tetrahedron Lett. 21* (1980) 2349.
[10] D. B. Grotjahn, K. P. C. Vollhardt, *J. Am. Chem. Soc. 108* (1986) 2091.
[11] **5**: monoclinic, $P2_1/c$, $a=10.105(1)$, $b=13.336(2)$, $c=12.297(2)$ Å, $\beta=96.27(1)°$, $V=1647.3(4)$ Å^3, $Z=4$, $\rho_{calcd}=1.485$ g cm^{-3}, $\mu=9.30$ cm^{-1}; $Mo_{K\alpha}$ radiation (graphite monochromator); scan range $3°\leq 2\theta\leq 45°$; 2915 independent reflections, observed 2572 with $F_0\geq 4\sigma(F)$, $R=0.037$, $R_w=0.045$ [12].
[12] Further details of the crystal structure investigation may be obtained from the Fachinformationszentrum Energie, Physik, Mathematik GmbH, D-7514 Eggenstein-Leopoldshafen 2 (FRG), on quoting the depository number CSD-53429, the names of the authors, and the journal citation.
[13] Manganese dioxide (precipitated active) from Merck-Schuchardt, (art. 805958).
[14] **7a**: triclinic, $P\bar{1}$, $a=7.697(4)$, $b=9.305(5)$, $C=11.467(6)$ Å, $\alpha=107.92(4)$, $\beta=100.53(4)$, $\gamma=100.32(4)°$, $V=743.5(7)$ Å^3, $Z=2$, $\rho_{calcd}=1.58$ g cm^{-3}; $\mu=10.3$ cm^{-1}; $Mo_{K\alpha}$ radiation (graphite monochromator); scan range $3°\leq 2\theta\leq 52°$; 2390 independent reflections, observed 2073 ($F_0\geq 4\sigma(F)$), $R=0.053$, $R_w=0.051$ [12].
[15] H.-J. Teuber, G. Staiger, *Chem. Ber. 87* (1954) 1251.

2-Chloro-2*H*-phosphirene/1-Chloro-1*H*-phosphirene Isomerization by [1,3]-Chlorine Shift**

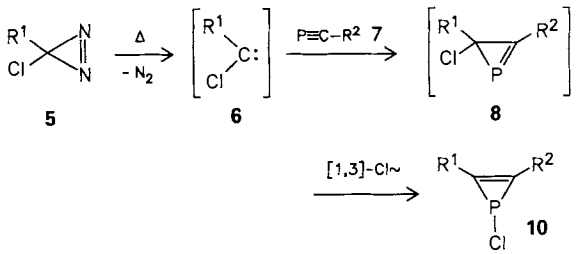
By *Oliver Wagner, Michael Ehle,* and *Manfred Regitz**

2*H*-Azirines **1** are stable and useful building blocks in heterocyclic synthesis.[1] In contrast, the 1*H*-azirines **2** are antiaromatic and short-lived, and consequently their existence could hitherto only be demonstrated by trapping reactions.[2] The energy gradient between the two azirine systems clearly manifests itself in unidirectional isomerizations (**2**→**1**).[3] We have now found exactly the opposite situation in the case of unsaturated three-membered ring systems with phosphorus as heteroatom: 2*H*-phosphirenes **3**[4] are converted by a substituent-shift from carbon to phosphorus into 1*H*-phosphirenes **4**.[5]



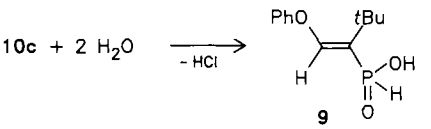
1 **2** **3** **4**

When chlorocarbenes **6** are generated from diazirines **5**[6] by thermal elimination of N_2 in presence of phosphaalkynes **7**,[7] subsequent work-up by distillation affords the 1-chloro-1*H*-phosphirenes **10** as stable, colorless oils.[13] Their constitution was confirmed by elemental analyses, the relatively high-field position of the ^{31}P-NMR signals and the occurrence of two ^{13}C-NMR signals characteristic for olefinic three-membered ring carbon nuclei (Table 1).



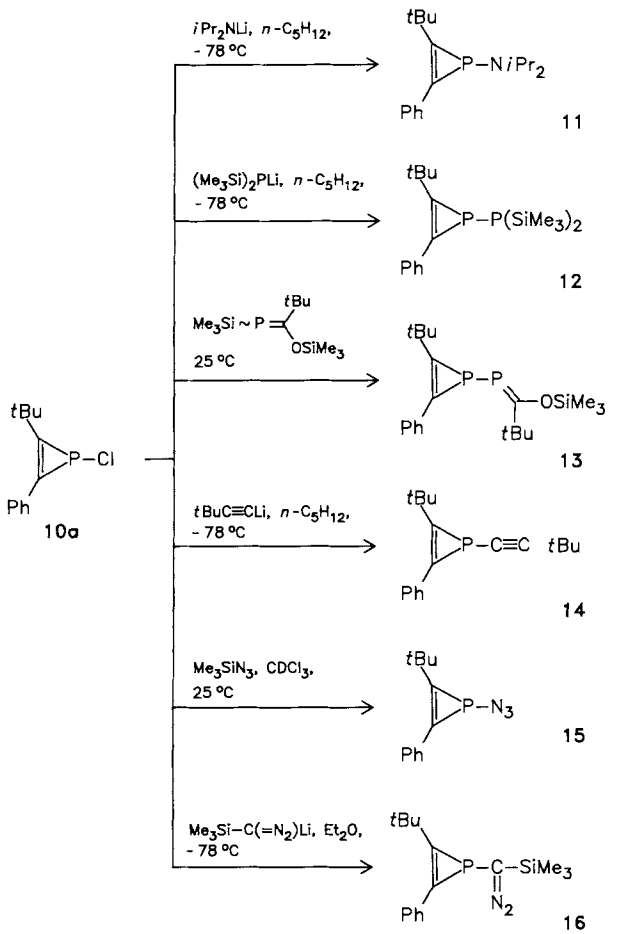
5 **6** **8** **10**

The constitution of **10c** was additionally confirmed by the result of hydrolysis in aqueous ether, which led with ring-opening and cleavage of the P-Cl bond to the phosphonous acid **9** [colorless crystals, m.p. 87 °C; IR (KBr): $\tilde{\nu}=2900$ (POH), 2400 cm^{-1} (PH); ^{1}H NMR ($CDCl_3$): $\delta=1.39$ (s, 9H, *t*Bu), 7.21 (m, 6H, phenyl- and olefin-H), 7.35 (d, $^1J_{PH}=568$ Hz, PH), 9.88 (br., 1H, POH); ^{13}C NMR ($CDCl_3$): $\delta=29.8$ [d, $^3J_{PC}=4.5$ Hz, $C(CH_3)_3$], 34.2 [d, $^2J_{PC}=6.9$ Hz, $C(CH_3)_3$], 119.5 (d, $^1J_{PC}=125.8$ Hz, C*t*Bu), 153.9 (d, $^2J_{PC}=31.3$ Hz, COPh); ^{31}P NMR ($CDCl_3$): $\delta=29.2$].



9

As primary products of the previously unknown intermolecular carbene addition to P-C triple bonds[8,9] only the 2-chloro-2*H*-phosphirenes **8** are conceivable; but these



Scheme 1. Nucleophilic substitutions of **10a**. For data of the products see Table 2.

[*] Prof. Dr. M. Regitz, Dipl.-Chem. O. Wagner, M. Ehle
Fachbereich Chemie der Universität
Erwin-Schrödinger-Strasse, D-6750 Kaiserslautern (FRG)

[**] Phosphorus Compounds of Unusual Coordination, Part 33. This work was supported by the Deutsche Forschungsgemeinschaft, the Fonds der Chemischen Industrie, and the Landesregierung von Rheinland-Pfalz.—Part 32: F. Zurmühlen, M. Regitz, *New J. Chem. 1988*, in press.

Table 1. Reaction conditions of the synthesis, boiling points, yields and NMR data of the 1-chloro-1*H*-phosphirenes **10a–g**.

Starting compounds	Product	R^1 (from **5**)	R^2 (from **7**)	Reaction conditions [a]	B.p. [°C] [b]/ *p* [mbar]	Yield [%]	$\delta(^{31}P)$ [c]	$\delta(^{13}C)$ ($^1J(P,C)$ [Hz]) [d] R^1-C	R^2-C
5a, **7a**	**10a**	Ph	*t*Bu	—, 30 min, 80°C	$150/10^{-2}$	63	−73.4	132.6 (69.4)	148.8 (70.6)
5b, **7a**	**10b**	*t*Bu	*t*Bu	—, 30 min, 150°C	$120/10^{-2}$	33	−67.2	145.6 (67.6)	
5c, **7a**	**10c**	PhO	*t*Bu	—, 48 h, 25°C	$150/10^{-2}$	40	−32.9	148.6 (78.8)	119.9 (53.2)
5d, **7a**	**10d**	MeO	*t*Bu	—, 48 h, 25°C	$60/10^{-2}$	35	−35.8	151.3 (75.2)	117.5 (54.9)
5a, **7b**	**10e**	Ph	1-adamantyl	benzene, 1 h, 90°C	$180/10^{-2}$	24	−77.6	133.2 (64.0)	147.6 (68.9)
5a, **7c**	**10f**	Ph	$C(Me)_2Et$	$(Me_3Si)_2O$, 1.5 h, 90°C	$150/10^{-2}$	39	−75.5	134.8 (63.9)	148.4 (70.5)
5c, **7c**	**10g**	PhO	$C(Me)_2Et$	$(Me_3Si)_2O$, 100 h, 25°C	$150/10^{-2}$	26	−28.8	—	—

[a] **10a–d** were prepared in a tenfold excess of **7a**; in the case of **10f, g** the hexamethyldisiloxane arising from the synthesis of the phosphaalkyne serves as solvent. The different reaction temperatures are determined by the decomposition temperatures of the diazirines **5**. [b] Furnace temperature in the Kugelrohr distillation. [c] $CDCl_3$, 85% H_3PO_4 (ext), 80.8 MHz. [d] $CDCl_3$, TMS (int), 50.2 MHz.

Table 2. Some physical data of the 1*H*-phosphirenes **11–16** [a].

11: colorless oil, b.p. 150°C/10^{-2}mbar; ^1H NMR: $\delta = 1.13$ [d, $^3J(H,H) = 7.5$ Hz, 12H, $CH(CH_3)_2$], 1.38 (s, 9H, *t*Bu), 3.15 [m, 2H, $CH(CH_3)_2$]; ^{13}C NMR: $\delta = 23.9$ [d, $^3J(P,C) = 7.3$ Hz, $CH(CH_3)_2$], 24.0 [d, $^3J(P,C) = 6.2$ Hz, $CH(CH_3)_2$], 29.9 [s, $C(CH_3)_3$], 34.1 [d, $^2J(P,C) = 6.4$ Hz, $C(CH_3)_3$], 43.2 [d, $^2J(P,C) = 5.7$ Hz, $CH(CH_3)_2$], 130.8 (d, $^1J(P,C) = 48.2$ Hz, =CPh), 149.5 (d, $^1J(P,C) = 58.6$ Hz, =C*t*Bu); ^{31}P NMR: $\delta = -127.2$

12: colorless oil, b.p. 180°C/10^{-2}mbar; ^{13}C NMR (C_6D_6): $\delta = 2.5$, 2.7 [each d, each $^2J(P,C) = 2.8$ Hz, $Si(CH_3)_3$], 29.5 [s, $C(CH_3)_3$], 34.4 [d, $^2J(P,C) = 5.2$ Hz, $C(CH_3)_3$], 116.2 (d, $^1J(P,C) = 47.7$ Hz, =CPh), 137.6 (d, $^1J(P,C) = 47.4$ Hz, =C*t*Bu); ^{31}P NMR: $\delta = -167.2$, −172.6 (each d, each $^1J(P,P) = 261$ Hz)

13 (*E* isomer): yellow powder, m.p. 49°C; ^1H NMR (C_6D_6): $\delta = 0.69$ (d, $^5J(P,H) = 1.4$ Hz, 9H, $Si(CH_3)_3$), 1.35 (d, $^4J(P,H) = 1.8$ Hz, 9H, *t*Bu on phosphaalkene), 1.48 (s, 9H, *t*Bu on ring); ^{13}C NMR (C_6D_6): $\delta = 1.59$ [d, $^4J(P,C) = 10.4$ Hz, $Si(CH_3)_3$], 29.5 [d, $^3J(P,C) = 8.6$ Hz, $C(CH_3)_3$ on phosphaalkene], 29.6 [s, $C(CH_3)_3$ on ring], 34.2 [d, $^2J(P,C) = 6.1$ Hz, $C(CH_3)_3$ on ring], 44.5 [d, $^2J(P,C) = 18.8$ Hz, $C(CH_3)_3$ on phosphaalkene], 112.9 (dd, $^1J(P,C) = 44.9$, $^2J(P,C) = 6.1$ Hz, =CPh), 131.1 (dd, $^1J(P,C) = 52.3$, $^2J(P,C) = 3.7$ Hz, =C*t*Bu), 226.2 (dd, $^1J(P,C) = 83.4$, $^2J(P,C) = 6.6$ Hz, P=C); ^{31}P NMR: $\delta = 166.7$, −176.8 (each d, each $^1J(P,P) = 263.5$ Hz)

14: colorless oil, b.p. 120°C/10^{-2}mbar; IR: $\tilde{\nu} = 2160$ cm^{-1} (C≡C); ^1H NMR: $\delta = 1.08$ (s, 9H, *t*Bu on acetylene), 1.42 (s, 9H, *t*Bu on ring); ^{13}C NMR: $\delta = 27.9$ [s, $C(CH_3)_3$ on acetylene], 29.4, 30.9 [each s, each $C(CH_3)_3$], 34.3 [d, $^2J(P,C) = 6.9$ Hz, $C(CH_3)_3$-ring], 83.8 (d, $^1J(P,C) = 110.2$ Hz, P–C≡C), 96.9 (d, $^2J(P,C) = 20.6$ Hz, P–C≡C), 116.2 (d, $^1J(P,C) = 43.1$ Hz, =CPh), 133.5 (d, $^1J(P,C) = 49.1$ Hz, =C*t*Bu); ^{31}P NMR: $\delta = -228$

15: colorless oil, not distilled; IR: $\tilde{\nu} = 2090$ cm^{-1} (N_3); ^{13}C NMR: $\delta = 29.4$ [s, $C(CH_3)_3$], 33.5 [d, $^2J(P,C) = 6.2$ Hz, $C(CH_3)_3$], 130.5 (d, $^1J(P,C) = 66.3$ Hz, =CPh), 146.6 (d, $^1J(P,C) = 62.8$ Hz, =C*t*Bu); ^{31}P NMR: $\delta = -106.7$

16: yellow oil, not distilled; IR: $\tilde{\nu} = 2040$ cm^{-1} (C=N_2); ^1H NMR (C_6D_6): $\delta = 0.27$ (s, 9H, $Si(CH_3)_3$), 1.39 (s, 9H, *t*Bu); ^{13}C NMR (C_6D_6): $\delta = -1.1$ [d, $^3J(P,C) = 3.0$ Hz, $Si(CH_3)_3$], 29.1 [s, $C(CH_3)_3$], 30.3 (d, $^1J(P,C) = 63.5$ Hz, P–C=N_2), 32.8 [d, $^2J(P,C) = 6.5$ Hz, $C(CH_3)_3$], 120.6 (d, $^1J(P,C) = 48.9$ Hz, =CPh), 138.4 (d, $^1J(P,C) = 56.2$ Hz, =C*t*Bu); ^{31}P NMR (C_6D_6): $\delta = -178.8$

[a] Unless otherwise stated IR spectra as film, ^1H- (200 MHz), ^{13}C- (50.2 Hz) and ^{31}P-NMR spectra (80.8 MHz) in $CDCl_3$ [TMS (int) and 85% H_3PO_4 (ext), respectively with b.p. data from Kugelrohr distillations.

cannot be isolated because of a rapid 1,3 chlorine shift to give compounds **10**. Resolution of the P=C double bond in **8** in favor of the C=C double bond in **10** is only understandable if the latter have no antiaromatic character. This in turn requires that the halogen does not lie in the plane of the three-membered ring.[10]

The chlorine substituent in **10** readily undergoes nucleophilic replacement. Reactions of **10a** with a series of nucleophiles (Scheme 1)—some at 25°C, some at −78°C—led to a broad spectrum of novel, functionalized 1*H*-phosphirenes (**11–16**); like **10a–g** they are sensitive to hydrolysis.

That the unsaturated three-membered ring of **10a** remains intact in all substitution reactions is already shown by the positions of the ^{31}P- and ^{13}C-NMR signals of the products (Table 2), which are comparable with those of the signals of **10**. Investigation of the reactivity of **11–16** will show whether such compounds have similar synthetic potential as the corresponding substituted cyclopropenes.

Experimental

10a: The solution of **5a** (0.48 g, 2.5 mmol) [6] in excess **7a** (2.0 g, 20 mmol) [7] was heated to 80°C for 30 min in a pressure Schlenk tube (protective shield). The deep-brown reaction solution was cooled to room temperature, the excess pressure equalized, unconsumed **7a** removed at 25°C/10^{-2} mbar (and recovered in a cooling trap at −200°C), and the residue purified by Kugelrohr distillation [150°C (furnace temperature)/10^{-2} mbar]. Yield: 0.36 g (63%) of colorless oil.

13: The solution of **10a** (0.45 g, 2.0 mmol) in excess (2,2-dimethyl-1-trimethylsiloxy-1-propylidene)trimethylsilylphosphane [11] was stirred for 6 h at room temperature (^{31}P-NMR monitoring; the crude solution contained the *E*/*Z* isomers in the ratio 5:1) [12]. After addition of 3 mL of pentane and cooling to −78°C, (*E*)-**13** precipitated out. Yield: 0.37 g (49%) of yellow, amorphous powder, m.p. 49°C.

All the new compounds gave correct elemental analyses.

Received: August 19, 1988 [Z 2933 IE]
German version: *Angew. Chem. 101* (1989) 227

[1] A. Padwa, A. D. Wollhouse in A. R. Katritzky, C. W. Rees (Eds.): *Comprehensive Heterocyclic Chemistry. Vol. 7.* Pergamon, Oxford 1984, p. 47 ff.
[2] M. Regitz, B. Arnold, D. Danion, H. Schubert, G. Fusser, *Bull. Soc. Chim. Belg. 90* (1981) 615.
[3] Cf. Ref. [1], p. 87.
[4] A compound of type **3** was first described only recently: O. Wagner, G. Maas, M. Regitz, *Angew. Chem. 99* (1987) 1328; *Angew. Chem. Int. Ed. Engl. 26* (1987) 1257.
[5] Isomers of type **4** with alkyl and aryl substituents on the phosphorus have been known for some time: F. Mathey, *Angew. Chem. 99* (1987) 285; *Angew. Chem. Int. Ed. Engl. 26* (1987) 275, and references cited therein.
[6] **5a**: A. Padwa, M. J. Pulwer, T. J. Blacklock, *Org. Synth. 60* (1981) 54; **5b**: W. H. Graham, *J. Am. Chem. Soc. 87* (1965) 4396; **5c**: R. A. Moss, L. A. Perez, J. Wlostowska, W. Guo, K. Krogh-Jespersen, *J. Org. Chem. 47* (1982) 4177; **5d**: N. P. Smith, J. D. R. Stevens, *J. Chem. Soc. Perkin Trans. 2 1979*, 1298.
[7] **7a**: G. Becker, G. Gresser, W. Uhl, *Z. Naturforsch. B 36* (1981) 16; improved synthesis: W. Rösch, U. Hees, M. Regitz, *Chem. Ber. 120* (1987) 1645; **7b**: T. Allspach, M. Regitz, G. Becker, W. Becker, *Synthesis 1986*, 31; **7c**: W. Rösch, U. Vogelbacher, T. Allspach, M. Regitz, *J. Organomet. Chem. 306* (1986) 39.
[8] For the intramolecular ring closure of phosphaalkenylcarbenes see [4].
[9] Addition of a silanediyl to phosphaalkynes: A. Schäfer, M. Weidenbruch, W. Saak, S. Pohl, *Angew. Chem. 99* (1987) 806; *Angew. Chem. Int. Ed. Engl. 26* (1987) 776; addition of a germanediyl to **7a**: A. H. Cowley, S. W. Hall, C. M. Nunn, J. M. Power, *J. Chem. Soc. Chem. Commun. 1988*, 753.
[10] In the case of the *P*-phenyl residue in 1,2,3-triphenyl-1*H*-phosphirene this has been confirmed by a crystal structure analysis: A. Marinetti, F. Mathey, J. Fischer, A. Mitschler, *J. Chem. Soc. Chem. Commun. 1984*, 45.
[11] G. Becker, *Z. Anorg. Allg. Chem. 430* (1977) 66.
[12] For the assignment of configuration see G. Becker, M. Rössler, W. Uhl, *Z. Anorg. Allg. Chem. 473* (1981) 7; for further examples see references to **7b** and **7c** in [7].
[13] Note added in proof (December 30, 1988): (1-chloro-2,3-diphenyl-1*H*-phosphirene)pentacarbonyltungsten was recently synthesized independently by us. Upon detaching the metal, however, the expected chlorophosphirene is hydrolyzed to bis(2,3-diphenyl-1*H*-phosphiren-1-yl) ether: B. Dechamps, F. Mathey, *New. J. Chem. 1989*, in press.

Book reviews are written by invitation from the editor. Suggestions for books to be reviewed and for qualified book reviewers are welcome. Publishers should send prospects or (better) books to the following address: Redaktion Angewandte Chemie, Postfach 101161, D-6940 Weinheim, Bundesrepublik Deutschland. The editor reserves the right of selecting which books will be reviewed. Uninvited books not chosen for review will not be returned.

Organoselenium Chemistry I. Functional Group Transformations. By *A. Krief* and *L. Hevesi*. Springer, Berlin 1988. xi, 221 pp., hardback, DM 186.00.—ISBN 3-540-18629-8

Selenium, whose discovery is ascribed to *Berzelius* in 1817, was during the 19th century already being mentioned occasionally in reports of organic compounds and organic reactions. It moved into the limelight of organic synthesis in the early thirties of the present century, with the discovery by *H. L. Riley* that α-CH_2 groups in olefins and ketones can be oxidized using selenium dioxide. At about the same time *O. Diels, L. Ruzicka* and others observed the dehydrogenating effect of elemental selenium, which at that time was used especially for converting steroids to phenanthrene derivatives or chrysene. The mid-seventies saw the beginning of a blossoming of organoselenium chemistry which continues today. On the one hand more and more organic molecules possessing selenium-containing skeletons or functional groups became accessible, while on the other hand various selenium reagents for carrying out especially mild or highly specific transformations were discovered. This work is associated particularly with the names of *N. D. Jones* and *K. B. Sharpless*.

The present-day importance of organoselenium chemistry has naturally led to the publication of numerous reviews and monographs on selenium compounds, and to these is now being added the work by *Krief* and *Hevesi*, which is to consist of two volumes. The authors' aim is to give an account of the most common selenium reagents, and the breadth and limits of their usefulness in organic synthesis.

The first volume, published in 1988, deals with actually or formally possible single stage processes involving selenium-containing intermediates, which cannot or need not be isolated. The second volume will treat processes with two or more stages involving selenium-containing intermediates. In addition there is to be a section on the preparation of the most important selenium reagents.

The introduction to Volume I deals with the occurrence of selenium and its compounds in nature, and with toxicity, biochemical functions, and some industrial and ecological aspects. This is followed by ten chapters on selenium compounds in organic synthesis, arranged according to the different oxidation states of selenium (-2 to $+6$). The contents of the individual chapters are best summarized by listing the chapter headings: Reactions involving hydrogen selenide, selenols and related compounds; Reactions of metallic or amorphous selenium with organic molecules; Reactions involving selenium oxides and their derivatives; Reactions using selenenyl halides and related compounds; Reactions involving benzeneseleninic anhydride and related compounds; Reactions using benzeneseleninyl halides; Reactions using perseleninic acids; Selenium dioxide oxidations; Reactions of imidoselenium compounds; Reactions involving selenium oxychloride and selenium tetrahalides.

As well as the synthetic methods themselves, the mechanistic aspects necessary for understanding them are briefly covered. The style of the book combines fluency and brevity with a high information content; the clearly presented reaction schemes and a comprehensive keyword index are especially good features. However, in the descriptions of the syntheses one often feels the lack of a critical evaluation, and especially of comparisons with other known methods for carrying out the same transformations. The book is definitely not a substitute for a comprehensive review of organoselenium chemistry, such as is contained in the two volumes on selenium and tellurium compounds published in 1986 and 1987 in the series "The Chemistry of Functional Groups (editors *S. Patai* and *Z. Rappoport*), but it will nevertheless be a valuable aid to the preparative chemist, and especially to the natural products chemist.

Herbert Meier [NB 933 IE]
Institut für Organische Chemie
der Universität Mainz (FRG)

Nitrile Oxides, Nitrones and Nitronates in Organic Synthesis. Novel Strategies in Synthesis. By *K. B. G. Torssell*. VCH Verlagsgesellschaft, Weinheim/VCH Publishers, New York 1988. xii, 332 pp., hardback, DM 115.00.—ISBN 3-527-26641-0/0-89573-304-8

The second volume in the series "Organic Nitro Chemistry" treats some further functional N–O derivatives such as nitrile oxides, nitrones and alkyl and silyl nitronates with the isoxazoles derived from them and their hydrogenated forms. The synthesis, reactivities and applications of the compounds are described.

After an introductory discussion of general aspects (Chapter 1, pp. 1–47: dipolar character, 1,3-dipolar addition, physico-chemical properties of the isoxazoles, stereo- and regiochemical considerations, asymmetric induction), the first part of the book (Chapters 2 and 3, pp. 55–89) deals with the synthesis and chemistry of nitrile oxides and nitrones. Since there are already several excellent review articles covering this field, a condensed survey is given here. (However, for the nitrile oxides there is no mention of the elegant synthesis from nitromethyl derivatives and Ph_3P–CCl_4 reported in 1983 by *Furukawa, Hashimoto* and *Nishiko*). Next comes a review (Chapter 4, pp. 95–122) of the synthesis, properties and reactions of alkyl and silyl nitronates, which are of interest as reagents in the nitro-aldol reaction (Henry reaction) as well as 1,3-dipoles.

The largest part of the book is Chapter 5 (pp. 129–270), which is concerned with the use of nitrile oxides, nitrones

and nitronates, and of their cycloaddition intermediates the isoxazoles, isoxazolines and isoxazolidines, in the synthesis of a wide range of types of compounds. As the author emphasizes under "Concluding Remarks" (p. 255), this chapter is intended as an extension of *A. I. Meyers* classic work "Heterocycles in Organic Synthesis", published more than 13 years ago, in relation to the isoxazoles and their hydrogenated derivatives and precursors. Cycloaddition of nitrile oxides, nitrones and nitronates to olefins and acetylenes gives isoxazole derivatives, whose reductive reactivation offers a useful and generally applicable route to a wide variety of hydroxy, carbonyl and amino compounds, and also to alkylated hydrocarbons, which can then be used as versatile building blocks for syntheses. Syntheses described here include: 2-nitroalcohols, α-cyanoketones, 2-cyanoalcohols by 3-H abstraction from isoxazoles, the Woodward-Olofson peptide synthesis, ketone anellations, 1,3-carbonyl shifts, β-polyketones (polyketides), 2-isoxazolines as masked aldols, other α,β-unsaturated carbonyl compounds, β-acylated acrylic esters, 1,4-diones, furans, 3(2*H*)-furanones and pyrones, pyrrole and indole derivatives, aziridines and 1-azirines, pyrazoles, imidazoles, oxazoles and isothiazoles. Next the synthesis of further heterocycles by ring transformations via the side-chains of isoxazoles is described; heterocycles accessible by this method are pyridines, pyrimidines, pyridazines, oxazines, quinolines and quinoxalines, azetidines, and condensed heterocyclic systems. Other syntheses dealt with are those of cyclopentane derivatives (e.g. rethrolones, prostaglandin precursors, terpenoids), 1,3-aminoalcohols, alkaloids (including syntheses by intramolecular cycloaddition), glycosides, amino acids and macrocycles.

In order to include also the most recent publications in this rapidly developing field, an addendum (pp. 271–300) has been provided, covering the literature from December 1985 to August 1987. Topics here include MCSCF calculations on the mechanism of 1,3 dipolar cycloadditions, FMO theory of the addition of nitrones to cumulenes, and syntheses of *D*-2-desoxyriboses, numerous alkaloids, diterpenes (e.g. Forskolin), flavonoids, ring strained nitrones, pheromones, and aryl- and heteroaryl-*C*-glycosides.

The book contains a total of 1806 literature citations, and a bibliography in Chapter 1 lists all relevant review articles covering the different subject areas dealt with. A large amount of information is collected together in the many tables. In a field where many excellent review articles have already been published, the author of this monograph has skilfully filled existing gaps in information on the synthesis and applications of nitrile oxides, nitrones and nitronates, and has at the same time provided a wide-ranging survey of new synthetic strategies based on the latent functional isoxazoles and their reduced forms obtained by these methods.

The high information content of this commendable monograph is, however, unfortunately reduced by the fact that some of the structural formulas are of poor quality (most of them are too lightly drawn, heteroatoms are badly placed, double bonds are depicted too narrowly, bonds are crooked, in stereochemical representations the arrowed bonds can scarcely be made out; consequently some of the reaction schemes lose much of their clarity, e.g. on pages 27, 56, 66, 77, 112, 178, 184, 209, 216, 226, 245, 276, 277 and 281). Despite these inadequacies in the formulas, the monograph can be thoroughly recommended to chemists with interests in synthesis, heterocyclic compounds and natural products as a rich source of information.

Heinrich Wamhoff [NB 938 IE]
Institut für Organische Chemie und Biochemie
der Universität Bonn (FRG)

Corrigendum

In the communication entitled "Disilene *versus* Silanediyl ("Silylene") Additions to CN and NCO Bonds" by M. Weidenbruch, B. Flintjer, S. Pohl, and W. Saal *(Angew. Chem. Int. Ed. Engl. 28* (1989) 95...97) the second line of the caption to Figure 1 on page 96 should read ... and angles [°] (standard deviations): Si1-Si2 243.5(1), Si1-N 179.8(2), C1-N 130.4(3), C1-Si2 ..., and not as printed.

Registered names, trademarks, etc. used in this journal, even when not marked as such, are not to be considered unprotected by law.

© VCH Verlagsgesellschaft mbH, D-6940 Weinheim, 1989.

Printed in the Federal Republic of Germany by Zechnersche Buchdruckerei, Speyer/Rhein.

All rights reserved (including those of translation into foreign languages). No part of this issue may be be reproduced in any form – by photoprint, microfilm, or any other means – nor transmitted or translated into a machine language without written permission from the publishers. Only single copies of contributions, or parts thereof, may be made for personal use. This journal was carefully produced in all its parts. Nevertheless, authors, editors and publisher do not warrant the information contained therein to be free of errors. Readers are advised to keep in mind that statements, data, illustrations, procedural details or other items may inadvertently be inaccurate.

Valid for users in the USA: The appearance of the code at the bottom of the first page of an article in this journal (serial) indicates the copyright owner's consent that copies of the article may be made for personal or internal use, or for the personal or internal use of specific clients. This consent is given on the condition, however, that the copier pay the stated per-copy fee through the Copyright Clearance Center, Inc., for copying beyond that permitted by Sections 107 or 108 of the U.S. Copyright Law. This consent does not extend to other kinds of copying, such as copying for general distribution, for advertising or promotional purposes, for creating new collective works, or for resale. For copying from back volumes of this journal see 'Permissions to Photo-Copy: Publisher's Fee List' of the CCC.

ADVANCED MATERIALS

Advanced Materials R & D—Planning for the Future

Editorial Essay

By James Economy*

1. Introduction

One of the major questions confronting materials scientists concerns their future role with respect to the emerging technologies of the 21st century. Today, we hear of many activities among the various nations of the world directed at achieving leadership in future industrial technologies through major commitments in advanced materials R&D. In Japan, seven specific areas in materials R&D were identified by the Ministry of International Trade and Industry (MITI) in the early 1980's and large joint industrial programs were established to carry out leading edge research in these areas.[1] In the USA, emphasis is being placed on more effectively coupling the materials research efforts in the universities and the national laboratories to industry. In Europe a number of activities can be identified; e.g., in Germany the government is beginning to foster closer interactions between the large chemical giants and the Max Planck Institute for Polymer Research in Mainz, while in France close collaborations between CNRS and industry are in place. As a backdrop, a number of the global technology companies have been acquiring key materials industries such as composites fabricators or advanced metal alloys manufacturers with the intent of better participating in these obvious growth areas.

One might ask which of these approaches if any provides a reasonable probability of fulfilling the hopes and anticipations of the countries or organizations who have committed significant resources to these activities? Stated somewhat differently, can one predict future needs with sufficient accuracy to lay out and justify an advanced materials program with the necessary effort and continuity to address the future technologies of the 21st century? Clearly the track record of industry has not been very good in the past two decades in developing new materials let alone in addressing the short-term needs for those industries which are dependent on advanced materials for their new product lines. Part of the problem lies in the fact that the chemical and metal companies who traditionally have provided most of the initiative to new materials development have dramatically changed their posture in the past twenty years. Thus, most of the metal industries have either sharply reduced or eliminated their R&D and that which remains tends to focus on very near term goals. Much of the chemical industry has emphasized forward integration into high value added markets where their skills in materials may provide significant leverage. On the other hand, many of the major industries such as electronics, aerospace, automotive etc. who have critical needs for new or improved materials for the most part still depend on the traditional materials suppliers who are actively pursuing the above indicated goals. Unfortunately, many of the R&D managers in the materials dependent industries are trained more in the needs and opportunities of the particular industry rather than in the synthesis and development of the advanced materials upon which the future of their industry may depend. Hence, programs on new materials development may not be as readily supported in such environments. Other factors that may be cited which work against the successful pursuit of advanced matrials R&D in the USA include the preoccupation of high level management with potential takeovers and the demands on R&D management to demonstrate an early return on investment in materials research.

In this paper, I first look at the field of advanced materials from a historical perspective and then examine closely two industrial R&D efforts with which I was directly involved. In the first case, the research was directed at development of new materials for diversification of the company into new areas, while in the second example, work on new materials was aimed at meeting the internal

Contents

J. Economy
Advanced Materials R&D—Planning for the Future 229
F. J. A. M. Greidanus, S. Klahn
Magneto-Optical Recording and Data Storage Materials 235
Research News
M. P. Schmidt
A Novel Monolithic Thin-Film Electroluminescent Device with Extrinsic Memory 241
Conference Reports
G. Sauthoff
Intermetallic Phases 243
N. Hampp
Biomaterials, Bioelectronics ... 245
R. W. Cahn
The 1988 Fall Meeting of the Materials Research Society 246
Conference Calendar 247

[*] Dr. J. Economy
IBM Almaden Research Center
650 Harry Road, San Jose, CA 95120-6099 (USA)

needs of the corporation. These two approaches are discussed in terms of their respective risks and payoff and then a number of generalizations are drawn concerning future directions for advanced materials research.

2. Historical Perspective (early 1900's–1960)

In spite of the current enthusiasm for R&D on advanced materials, a strong perception exists among many industrial leaders that the field is mature and that there are very few new materials with significant commercial value remaining to be discovered. In addition, recent experiences with the time required for development of new materials suggest that it takes far too long and is too risky bringing a new material to the marked place. Although these views are undoubtedly correct for a number of materials categories, the danger lies in the tendency to generalize them to the whole field of advanced materials. In this section, I would like to explore some of the sources for these perceptions and also describe why industrial scientists of an earlier era were indeed more successful in the commercial development of advanced materials.

When one examines the development of new materials prior to 1960, one can identify certain distinct patterns to these discoveries. Thus in the early 1930's when *Carothers* and his team were laying the foundation for the field of condensation polymers, they came up with the unexpected discovery that melts of aliphatic polyesters could be melt-drawn into filaments and then cold-drawn to achieve much higher strengths. The implications were undoubtedly obvious to the researchers and especially management that they had an alternative to silk and within several years a material (Nylon) had been selected, optimized and scaled-up to a semi-works facility. This also was the first example of melt-spun filaments, and required significant innovation in the design of the spinning system.

In an earlier era, *Acheson*'s work on the reaction of SiO_2 with carbon may have yielded the anticipated SiC, however what was unexpected was the very high hardness of the material. Its potential use as an abrasive must have been immediately obvious and within a short period of time, *Acheson* proceeded to scale up the reaction for commercial development.

In the early 1950's, the discovery of linear polyethylene by several groups of workers in different laboratories appears again to have been fortitous, but at least two of the groups recognized the significance almost immediately and within five years one of them, Phillips Petroleum, had put a 50 million pounds per year facility on stream. In fact, Phillips sold the know-how for such a plant to a number of other companies and undoubtedly quickly recouped its initial investment. Certainly, the earlier development of high pressure, branched polyethylene permitted easy identification of markets for the linear polyethylene with its greatly improved thermal resistance and stiffness.

These three examples, although taken from quite different periods of time, have a number of points in common which appear to characterize many of the major developments in commodity materials such as polymers (see Table 1 for a listing of the major commodity polymers). In each of these cases, there were readily identifiable markets which could be addressed almost immediately. Potential existed for low cost routes to the product and high level management had the technical background to commit resources for rapid scale-up in a timely way. To a considerable extent, one can understand why investment in industrial R&D during the period of 1930 to 1960 proved to be highly profitable. However, by 1960, it was becoming clear that it was unlikely that there would be any new commodity polymers and greater attention was focussed on specialty polymers. In fact from our vantage point today, the commodity polymers listed in Table 1 can only be considered as a mature field since the last one was introduced over 30 years ago. It is noteworthy that a significant industrial R&D effort continues on these polymers but it is directed primarily at improvements in the product and/or process. This kind of incremental research appears to have had significant payoffs in recent years — witness the recent progress in the manufacture of polyolefins.



Dr. Economy received his BS from Wayne State University (1950), his PhD from the University of Maryland under Professor W. J. Bailey (1954) and was a research associate at the University of Illinois (1954–1956) with Professor C. S. Marvel. He worked at Allied Chemical as a general research leader on polyolefin research from 1956–1960. From 1960–1975 he was Manager of Chemistry and of the Research Branch in the R&D Division of the Carborundum Co. From 1975–1989, he was Manager of the Polymer Science and Technology Department in the Research Division of IBM. Just now, in February 1989, he joins the faculty of the University of Illinois as Professor and Head of the Materials Science and Engineering Department. He has carried out research on high temperature polymers, flame resistant materials, high performance composites and advanced materials for microelectronic devices. He has received a number of distinguished awards including the AIC Chemical Pioneer Award (1987), ACS Phillips Medal (1985), the Southern Research Burn Institute Award (1976), Schoelkopf Medal (1972), and 14 IR 100 Awards for Outstanding Technical Developments in American Industry. He has published over 150 technical papers and received more than 70 US patents. He has served on numerous government committees and was chairman of the Polymer Division of the American Chemical Society (1985). He is a member of the National Academy of Engineering, the National Materials Advisory Board (since 1984) and is the USA representative to IUPAC's Macromolecular Division (since 1985).

Table 1. Commodity polymers.

Nylon
Polyester (PET)
Polyacrylates
Low Density Polyethylene
High Density Polyethylene
Polypropylene
Polystyrene
Poly(vinylchloride) (PVC)
Acrylonitrile-Butadiene-Styrene Copolymer (ABS)
Phenolic Resins
Urea

During the late 1950's the US Government began to pursue a more aggressive role in stimulating R&D on advanced materials to fill specific needs such as advanced military hardware, aerospace applications and nuclear reactors. Incentives in the form of large government grants were made available to encourage industry and university scientists to pursue these goals.

Another phenomenon which could be traced back to that particular era was the desire of many companies to diversify from their traditional businesses into areas with high growth opportunities such as plastics. If done properly, this kind of diversification could be extremely effective at insuring the long term stability of a company. However, the chief executive officer (CEO) often lacked the technical expertise or intuitive skills necessary to manage these new businesses and in such an environment high level decision making could lead to disastrous consequences or at least to delays on critical decisions. In the late 1960's, this problem would be further exacerbated by a new generation of CEO's drawn primarily from the financial ranks.

Undoubtedly the most dramatic change during this period was the dominating role assumed by the US government in defining its advanced materials needs. From an industrial viewpoint it was easy to focus on these government needs with the expectation of financial support by the government followed by the potential for a wider commercial development. As shown in Table 2, the needs of the Department of Defense (DOD) encompassed a wide range of exciting materials opportunities. It was only natural that many of the best scientists from industry and academia would be attracted to these areas, especially with the added inducement of financial support. Thus, this intrusion by the US government into the traditional market driven R&D of the past tended to focus attention of industrial R&D toward developments where potential for commercialization either might not exist or was much further off in the future.

Table 2. Advanced materials thrusts in the 1960's.

High temperature polymers
Flame resistant fabrics
Superconducting filaments
High performance composites
Pollution control systems
Ultrahard shapes

In recent years another factor acting to further complicate development of new materials has been the increasing level of sophistication and complexity of the new specialty materials. This increased complexity has unfortunately been more than matched by the large number of advanced techniques available for characterizing these materials. However, the investment in such tools and skilled personnel can be prohibitive, particularly for mid-size industries.

3. R&D at Carborundum Co. (1960–75)

Let me now consider the research program that I managed at the Carborundum Company, since it illustrates effectively a number of the issues raised in the previous section. As described in a recent paper,[2] the R&D work on advanced materials at Carborundum was highly successful from a technical viewpoint. Over 30 new materials were

Table 3. New materials developed at the Carborundum Co. (1963–1973).

	Field Tested	Now being worked on	Commercially Available
Engineering Plastics			
Ekonol	×		×
Ekkcel C-1000	×	×	
Ekkcel I-2000	×		×
Crosslinkable pitch			
Flame Resistant Fibers			
Kynol	×		×
Acetylated phenolic	×	×	
Chlorinated polyethylene			
Superconductors			
NbCN multifilament yarn	×		
Reinforcing Agents			
B_4C multifilament yarn	×	×	
AlB_2 single crystal flakes	×	×	
BN yarn (high modulus)	×		
Ekonol fiber (high modulus)	×		×
Glassy carbon fiber	×		×
Composites			
AlB_2 flakes in Al		×	
B_4C fibers in SiC		×	
BN fibers in BN	×		
SiC whiskers (oriented yarn)			
Purification Systems			
Molten metal filter	×		
$BaCrO_4$ exhaust catalyst	×		
Ion exchange fibers	×		×
Activated carbon fibers	×		×
Hyperfilter (activated carbon film)			
Glass fabric filter (high-temp. coating)			
High Temperature Insulation			
BN fiber	×		×
Pitch fiber	×		
Bn/SiO_2 fiber			
Ceramic fiber			

discovered and brought to the level of scale-up and test marketing. In Table 3 is provided a partial list of the materials developed during my tenure at Carborundum. The success of the program is best illustrated by the fact that eight of the materials are commercially available today, while work continues on at least six of the others. Considering the relatively small size of the group (30–40 people) it is all the more remarkable that so many materials could be developed and marketed in such a short period of time. There were indeed many novel features with respect to the organization and operations and these are discussed in detail elsewhere.[2] I do not intend to review the achievements of the group, but rather to focus on those features which greatly complicated commercial development. One point that is immediately obvious from an examination of Table 3 is that most of the materials were developed primarily in response to the general goals defined by the US Government.

To better illustrate the problems confronting researchers during that era it is instructive to review one of the programs in Table 3, namely, that on the aromatic polyesters of *p*-hydroxybenzoic acid (PHBA). Today, this class of polymers is being pursued aggressively by a number of companies with the anticipation that their use as engineering plastics will provide a major advance over metals such as aluminum or steel. Of particular interest here is the examination of key decisions made that critically influenced the directions of the program.

As shown in the chronology in Table 4, this program had its beginnings in early 1963, when the homopolymer of PHBA was successfully prepared for the first time and shown to be processible by sintering or metal forming techniques. This was followed by the successful synthesis in 1966 of the copolymers of PHBA which could be melt-processed at about 400 °C but still retained their properties to well over 300 °C. Our studies were prompted by the rather large DOD effort on high-temperature polymers initiated in the late 1950's. At the time most of the DOD effort was directed at heterocyclic and related ladder-like polymers that could be processed from solution into coatings and fibers and might have use at temperatures up to 800 °C. In our approach we had realized from a study on carbon fibers that the thermal oxidative stability of carbon was limited to 400 °C. Hence, it was clear that no carbon based polymer would have utility much above that temperature. We therefore undertook to look at potentially low cost polymers that were fabricable by melt or solid state processing with the idea that such systems would have far broader utility.

In early 1970 we commercially introduced the homopolymer of PHBA (Ekonol) as a material which could be fabricated by metal forming techniques such as plasma spraying or high energy forging. This was followed in 1972 by the copolymer of PHBA with biphenol terephthalate (Ekkcel) which was commercialized as an injection molding grade polymer with a use temperature in excess of 300 °C.

Table 4. The aromatic polyester strategy.

1963–1966	Discovery of the homopolymer of PHBA (1963) Discovery of copolymers of PHBA/BPT (1966)
1970–1972	Introduction of Ekonol/Ekkcel to market
	• Also developed high modulus fiber • Purchased Three Plastics Co. • Far east joint venture with Sumitomo Chemical • Metco markets Ekonol as plasma spray powder
	however
	• Acquisitions don't work out • Market for Ekkcel develops too slowly
1974–1978	Carborundum comes under financial duress
	• Tries to decommit from Ekonol • Cuts back effort on Ekkcel • Fiber is forgotten • Is acquired by Kennecott
	however
	• Metco holds Carbo to Contract on Ekonol • Dartco licenses Ekkcel • Sumitomo continues work on fiber
Today Program is Highly Successful	
	• Carborundum still manufactures Ekonol—very profitable • Dartco has 20,000,000 lb/yr plant on stream—Xydar (Ekkcel) • Sumitomo introduces Ekonol fiber (1985) • Many companies poised to introduce similar polymers
	however
	• Large potential may lie elsewhere • Fundamental understanding lags

To help accelerate commercialization of these new materials the Carborundum Co. acquired several US plastics companies (total value ca. $ 30 million) and also established a joint venture with Sumitomo Chemical in the Far East on these new polymers. In the meantime, in 1971, we also demonstrated that the copolymer could be melt drawn into a high modulus filament with properties similar to the Aramid fibers. Of more immediate importance, the Metco Co. began to make significant progress in marketing the Ekonol resin as a plasma spray powder. However, other than for that application, the markets for these materials developed very slowly in the ensuing three or four years. As it turned out, the acquisitions were not particularly good fits and contributed little to the commercialization of these new polymers.

In the meantime, the CEO of Carborundum began to explore other more direct routes to diversification that did not require as much commitment in time and resources, and the momentum to the materials R&D effort began to disappear. In fact by the late 1970's, attempts were made to license the polyester technology and to decommit from prior sales agreements. Fortunately, the Dart Corporation had identified an important use for the injection moldable polyester, Ekkcel, for high temperature cookware, and went ahead and licensed the technology from the Carborundum Co. By 1983–1984 they had made sufficient pro-

ADVANCED MATERIALS

gress to justify putting a 20 million lb plant on stream to manufacture the polymer under the trade-name Xydar. In the case of Ekonol, although Carborundum tried to decommit from manufacturing the polymer. Metco held them to an earlier agreement to supply the powder. Fortunately, for Carborundum, the use of Ekonol became and has continued to be a highly profitable specialty polymer. Subsequently, the Carborundum Co. was purchased by Kennecott which was acquired by SOHIO which was then taken over by British Petroleum.

There are several lessons to be gleaned from this brief narrative. First of all, the discovery, optimization, scale-up and test marketing of these new polymers was readily achieved within five to seven years, and this was true for practically all of the materials listed in Table 3. The next step which involved a much larger commitment of financial resources required a high level management better skilled in the nuances of the new technology and able to make key decisions in a timely fashion. Certainly our CEO was sufficiently committed that he acquired several engineering plastics companies with the intent that they would accelerate the use of these new polymers. Since these were already profitable organizations the risk in the acquisitions was minimal and at least created a very desirable image. Unfortunately it turned out that the product lines and skills base of these acquisitions were far removed from the potential uses of our new materials. Undoubtedly, the most serious problem was the absence of a clear market need which typified the developments described earlier in the "Historical Perspective". In retrospect, it is clear now that we should have been able to distinguish the needs of the market place from the wish list of government agencies.

4. Polymer R&D at IBM (1975-present)

Let me turn now to consider in some detail a different approach to advanced materials research in industry and one with which I have been involved with since 1975 at IBM. Here, the primary goal is to develop new or improved materials for the advanced devices currently in development in the operating divisions. There is however, a unique constraint, namely, these materials must be developed, optimized and available in reproducible quantities from a vendor within two to four years. This relatively short time represents the lead time normally provided in the design and development of a new device.

It is instructive to reflect on the environment within IBM when I first jointed the company in 1975, since the attitude toward development of new materials and especially polymers was and is typical of many industries whose product lines depend on development of new or improved materials. The group that I inherited and which included a number of excellent scientists, was accustomed to working closely with the operating divisions in a response

Table 5. Advanced polymer requirements for the information industry.

Semiconductor devices	Submicron resists
	Low and insulating layers
	Etch barriers (RIE)
Packaging	Temporary binders
	Low TEC substrates
	Photosensitive insulators
	Encapsulants
Storage	Binders
	Optical substrate
	Moisture barrier
	Plastic lens
Printers	Fuser
	Photoconductors
	Toners
	Plastic hammer
	Rough ribbons
	Damping
	Inks

mode to solve problems with materials that were provided by various vendors. At the time it was clear that there were needs within IBM for advanced polymers for the many new devices under development within the company (see Table 5). It was equally apparent that the traditional suppliers of new polymers were not particularly motivated to develop such systems primarily because of the very small volumes needed for many of the applications (< 1000 kg/yr). Yet these new materials were critical for the next generation of devices planned for the 1980's.

Hence, through the late 1970's, the polymer group was restructured to include a much stronger component dedicated to polymer synthesis. And by the early 1980's, the group was positioned to begin to make significant contributions to the advanced technologies of IBM. In fact, from 1982 to the present, the polymer group has on average successfully transferred two new materials each year to the operating divisions for use in a wide range of advanced devices. Some of these developments represented modifications of existing materials while others were at the leading edge of advanced materials development. By closely coupling our synthetic scientists with the device designers in the divisions, we were able to make modifications in the material adjusting in real time to the frequent design changes. As can been seen in Figure 1, this kind of internal

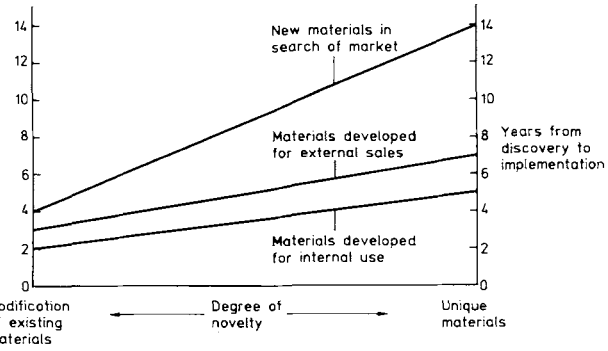


Fig. 1. Time scale for new materials development.

collaboration greatly reduces the time from conception to implementation as compared to similar research carried on by a typical vendor.

The need to conceive of, optimize and make available advanced materials within a two to four year time period has led us to challenge the scientists in our department in a unique fashion. First of all, it is essential that we pursue synthetic studies directed to what are perceived as the longer range needs. Toward that end, the scientists in the group are encouraged to spend ca. 50% of their time on basic studies in relevant areas. This aspect of their performance is measured primarily by the quality of their external publications and presentations. As specific needs emerge from the operating divisions, our scientists are able to draw upon this accumulated knowledge base to design solutions tailored to the specific needs. To further facilitate the transfer of advanced materials, we carry out studies to test the compatibility of these materials with device processing. Obviously, a critical part of the technology i.e., the design of the recipes used in device fabrication resides with the development groups in the divisions. We also have established a Synthetic Development Laboratory whose main role is to develop the optimum synthetic route, provide development quantities to the divisions and identify and work with vendors to provide commercial lots. Typically our involvement continues well into the development cycle and includes detailed characterization of the optimized material and establishment of materials specifications.

The success of the above approach is illustrated not only by the excellent track record in technology transfer to IBM's operating divisions over the past seven years, but also by the many scientific breakthroughs generated by our group (see Table 6). The scientific advances indicated here have either been cited as part of the five to six major scientific achievements of IBM's Almaden Research Center from the past three years or have been the basis for major external scientific awards.

Table 6. Significant polymer science and technology contributions from IBM's Almaden Research Center during the past three years.

Ordering in semiflexible polymers
Diffusion processes in the melt
Ageing/deageing processes
Nature of liquid crystalline polymers
Nature of monolayer films at surfaces
Mechanism of adhesion in polyimides
Measurement of attractive/repulsive forces at surfaces
Surface tunneling microscopy of gold atoms vs. organics on gold
FT Raman spectroscopy
Ab initio calculations of polymer conformations and properties
Polysilane conformations

An important component to the success of the polymer group in IBM has been the continuity of the effort over the past decade. To meet the increasing needs of the operating divisions the group has been increased from 25 people in 1975 to the present figure of ca. 60. In addition, we support between 24–27 post-doctoral scientists and host five to seven professors on sabbatical each year. The presence of these scientists greatly enhances our ability to address the basic aspects of a given problem while still focussing our attention on the short-term needs.

5. Conclusions and Recommendations

From the previous discussions in this paper, one can draw a number of conclusions concerning the future opportunities in advanced materials research.

1. The polymer materials research program at IBM represents a particularly effective model for industries which depend on the availability of advanced materials. In our group, requirements for a given application of the polymer are clearly understood and the scientist can make the incremental changes in a timely way to match the device needs. Obviously, other industries besides the information industry can greatly benefit from internal research groups whose charter includes designing the new materials which will be pivotal to their future product lines. This does not argue that joint efforts by major chemical companies and large users of polymers should not be pursued on optimizing polymers for specific uses. However, if the materials dependent industry has a core of scientists trained in the synthesis and processing of materials as relates to the company's need, then that group can take a leadership role in the interactions with the traditional materials suppliers.
2. The role of high level management is critical for those new materials programs which require significant investment. It is essential that such management be technically astute and be able to commit the resources of the company in a timely way. One can usually identify the presence of such management in those organizations which maintain an excellent track record on commercializing new materials. The converse hardly needs further discussion. It should be noted that in programs such as the one at IBM, the decision to scale-up a new material is not as expensive because of the smaller amounts involved and such decisions are made at an intermediate level of managements.
3. A number of companies are committing significant R&D resources to work in specific areas such as conducting polymers, non-linear optical materials, toughened ceramics, high-T_c superconductors, diamond films etc. with the expectation that the eventual payoff justifies the investment. Experience teaches us that programs which still require major technical breakthroughs can be stifled through early commitment of large resources. Typically, breakthroughs in these areas depend

on talented scientists working in small groups who understand and address the problem in its entirety. A commitment of larger resources aimed at increasing the likelihood of success often works in the opposite direction since the effort to be effectively managed is broken up into a series of interrelated tasks which are readily managed through PERT charts.

4. Recent attempts by the US Government to stimulate industrial R&D by building up efforts in universities and/or the National Laboratories does not address the critical problems confronting much of US industry. There is absolutely no substitute for industrial scientists who are effectively interfaced with the needs of the particular industry and its markets and have available to them the latest techniques to probe and address the future needs in materials.
5. It is essential that universities undertake to train high quality materials scientists skilled in synthesis and processing of new materials. It should be obvious that the development of new materials tailored to specific needs or-equally as important the unexpected discovery of materials with unique properties lies primarily within the purview of the clever scientists trained effectively in synthesis and processing of materials.

Finally, let me return to the question posed in the opening of this article; namely, can one organize an advanced materials R&D effort which addresses the opportunities of the 21st century? I would argue that for industry, the primary emphasis should be directed at fulfilling the perceived materials needs of the next two to five years as discussed in conclusion "1". Such an approach will not only impact the company's immediate needs, but hopefully would have sufficient latitude to permit for unexpected breakthroughs which address longer range opportunities. With respect to planning and implementing a materials R&D effort for the 21st century, past experience shows that it is extremely difficult to identify needs of the next five to seven years let alone 10–15 years from now. Thus, one must think in terms of national or even international programs to establish an infrastructure which 1) attracts talented young people into the science programs of our universities, 2) provides for continuity of high risk research in all sectors of the R&D establishment, and 3) places responsibility for commitment of funds and resources by the government and industry in the hands of technically astute leaders. In this way one can greatly increase the potential for successful development of advanced materials critical to high technology industries of the 21st century.

Received: November 23, 1988

[1] J. Economy (Chairman): *JTECH Panel Report on Advanced Materials in Japan*, JTECH-TAR-8502 (May 1986).
[2] J. Economy, *Chemist (Washington, D.C.)* 65 (1988) 8.

Magneto-Optical Recording and Data Storage Materials**

Rare-Earth Transition-Metal Alloys
Thermomagnetic Writing
Lorentz Microscopy

By Frans J. A. M. Greidanus* and Stefan Klahn

Amorphous rare-earth (RE) transition-metal (TM) alloys are used for magneto-optical (MO) recording a rapidly developing technology, which combines the possibility of achieving high bit densities with practically unlimited erasability and rewritability. During the last years new insights, relating material properties to recording performance, have been obtained. New experimental techniques, such as the observation of magnetic contrast in the electron microscope, have made a major contribution to the understanding of domain formation processes. The RE-TM alloys have been most successful in recording applications until now. In these materials the RE-TM composition determines both the compensation and Curie temperatures and has a strong impact on the recording characteristics. Improvements in deposition techniques and the application of dielectric layers resulted in carrier-to-noise ratios of 61 dB. Despite major improvements, problems related to corrosion and structural relaxation, which lead to long-term instabilities, have not yet been solved completely. Another important topic is the so-called direct-overwrite problem, which will be discussed in relation to the material properties.

[*] Dr. F. J. A. M. Greidanus
Philips Research Laboratories
P.O. Box 80000, 5600 JA Eindhoven (The Netherlands)
Dipl.-Phys. S. Klahn
Philips GmbH Forschungslaboratorium Hamburg
D-2000 Hamburg (FRG)

[**] We wish to thank our colleagues at the Philips Research Laboratories in Eindhoven and Hamburg, in particular *Ben Jacobs* and *Peter Hansen*, who have made a large contribution to our understanding of magneto-optical materials.

1. Introduction

In the past ten years the development of optical recording technology has led to products for various applications, such as the Compact Disc video and audio systems and the write-once DOR (Digital Optical Recording) system, which are now on the market. The availability of relatively cheap and mass-produced solid-state lasers made these developments possible. The driving forces behind these developments were the considerable advantages of optical recording over other storage techniques. Readout is done by a laser focussed through a substrate on the storage layer, providing a non-contact technique insensitive to dust and fine scratches on the substrate. A second advantage is the possibility of achieving high bit densities (10^8 bits cm^{-2}). This value compares favorably with other existing technologies, as can be seen in Figure 1.

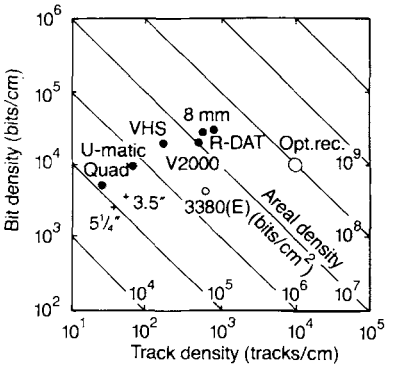


Fig. 1. Areal density for various recording systems. ●: helical scan, +: flexible disc, ○: rigid disc (courtesy of *S. B. Luitjens*).

In the history of optical recording three phases can be distinguished: 1) The oldest type of optical-storage systems are the replicated discs, used in the Compact Disc video and audio system. These are designed for the distribution of prerecorded information. 2) The second class is formed by write-once media. Here the writing process is based on the absorption of energy from a focussed laser beam, modulated according to the information to be recorded. The available commercial systems are based on the formation of holes in a reflective layer. 3) The latest class of optical systems, which is at present the subject of intensive research and development, employs media which can be erased and rewritten innumerable times. Here several different physical principles are being followed. Well known is the use of a reversible crystalline-to-amorphous phase transition in the recording film to store the information. A second method is based on a thermo-magnetic effect to write, and a magneto-optical (MO) effect to read out the information. In this review article we will focus our attention on the materials for this latter technique.

The principles behind MO recording have been known for years. However, it was not until the mid sixties that a record and playback system employing a laser beam was suggested. Writing of domains in a magnetic material by heating it locally above the Curie temperature was suggested in 1958 by *Mayer*,[1] long before an optical memory was envisioned. *Mayer* employed a focussed electron beam or the point of a heated needle. The first observation of an MO effect is even older and dates from 1846[2] when *Faraday* observed that polarized light passed through a fluid in a strong magnetic field changes its polarization state. Ever since this phenomenon has been designated as the Faraday effect when it refers to the transmitted beam, whereas it is called the Kerr effect when it refers to the reflected beam.

The first proposal for employing a laser both for writing (high power) and reading (low power) dates from 1965, when *Chang* et al.[3] discussed a memory based on $Gd_3Fe_5O_{12}$ (GdIG). Since then several other materials, such as MnBi, EuO, CoPt and $CoFe_2O_4$ have been suggested and investigated with respect to their applications as an MO memory layer. The most important development, however, was started by *Chaudhari* et al.[4] in 1973, with the observation that amorphous GdCo-layers possessing perpendicular anisotropy are suitable for MO recording. This discovery was the start of a series of exploratory studies in the rare-earth (RE) transition-metal (TM) binary and ternary alloy system with regard to their potential for MO data storage. These studies led, e.g., to the systems GdTbFe and TbFeCo which are the most suitable materials known today. To a large extent this is due to a steady increase in the signal-to-noise properties over the years as can be seen in Figure 2.

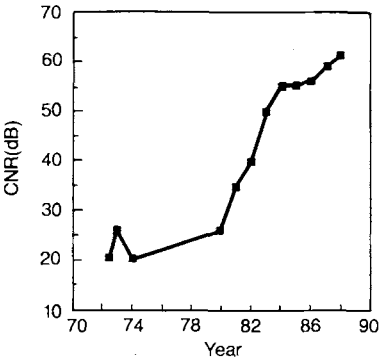


Fig. 2. Maximum reported carrier-to-noise ratio for MO recording (measured for a domain length of 1.5 μm at 1 MHz and 30 kHz bandwith) versus year of publication.

2. Magneto-Optical Recording

The principle of optical readout of domains in a perpendicular MO layer is shown in Figure 3a. The change of the polarization direction when linearly polarized light is reflected from a magnetic surface is shown here. Phenomenologically, MO effects can be described by assigning to

ADVANCED MATERIALS

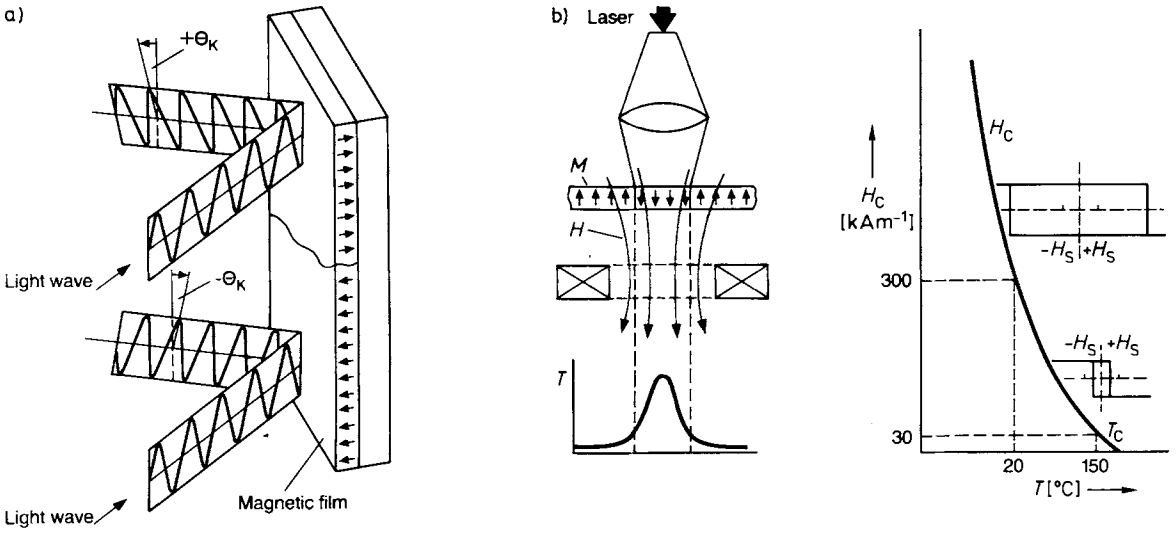


Fig. 3. a) Principle of MO reading. b) Principle of thermomagnetic writing.

the medium a dielectric tensor with non-zero off-diagonal elements. This is equivalent to introducing two different complex indices of refraction for right- and left-handed circulary polarized light. Microscopically these effects find their origin in the spin–orbit interaction, which couples the spin moment and the motion of the electron. The optical properties are influenced by the electron motion. The sign of the angle through which the polarization is rotated depends on the direction of the magnetization vector with respect to the propagation direction of the light. For practical materials the magnitude of the Kerr rotation is fairly small (typically 0.2–0.3°). Consequently the signals arising from the modulation of the polarization state of the reflected light are very small. Nevertheless, they can be detected with a good carrier-to-noise ratio (CNR) if sources of noise in the readout can be made sufficiently small.

Several schemes for thermomagnetic writing exist. With Curie point writing, the MO layer is heated above its Curie temperature and the magnetization is reversed in an applied magnetic field. A second method can be employed in materials in which the coercive field is a decreasing function of temperature. Upon heating, the magnetization can be reversed in an applied field larger than the coercive field of the layer at the elevated temperature, but smaller than the coercive fields in the remaining non-heated area of the film. In this way a domain can be written thermally, as illustrated in Figure 3b. This method is referred to as threshold writing when applied to ferromagnetic films and as compensation-point writing when applied to ferrimagnetic films. In general domains of the order of the diffraction limited diameter of the laser spot, which is about 1 μm, can be written, although it is possible to write substantially smaller domains, as will be discussed in Section 5.

The discs employed for MO recording consist of a glass or polycarbonate substrate coated with a photo-polymerized lacquer with pregrooves. On top of this a stack of optical layers containing the MO layer is deposited. Information can be written in a disc and read out with a special recorder using polarizing optics.[5]

3. Magneto-Optical Materials

In addition to a large Kerr rotation there are several other requirements a material has to satisfy in order to be suitable as a recording medium for thermomagnetic writing with optical readout. These requirements are:

1) Perpendicular magnetic anisotropy
2) High coercivity at room temperature
3) High magneto-optical figure of merit, $R\theta_k^2$, where θ_k is the Kerr rotation and R the reflectivity of the MO film
4) Switching characteristics matched to the available laser power ($T_c < 600$ K) and the available magnetic field strength (< 50 kA m^{-1})
5) Low media and write noise
6) Low deposition temperatures and high deposition rates
7) Long-term stability

The classes of materials which enable all these requirements to be fulfilled at the same time, are limited. The best candidates at present are the ferrimagnetic amorphous RE-TM alloys. Several compositions, mostly containing Gd and/or Tb as the RE atom and Fe and/or Co as the TM atom, were suggested and have been studied in the past. Among these, GdTbFe and TbFeCo are probably the most suitable materials. In the remaining part of this section we

will discuss how the requirements 1-7 can be fulfilled in the system $(Gd,Tb,Dy)_x(Fe,Co)_{100-x}$ with $(15 < x < 30)$.

1) Perpendicular anisotropy can be achieved by proper deposition conditions and composition. The origin of the perpendicular anisotropy in amorphous alloys is an anisotropic short-range ordering process during deposition. Mechanisms of magnetic anisotropy are magnetostriction, bond orientational anisotropy and single-ion (spin-orbit coupling) anisotropy.[6] Typical values for the anisotropy constant involved are $K_u = 10^4$ J m^{-3} for Gd based alloys and $K_u = 10^5$ J m^{-3} for Tb and Dy based alloys.

2) The absolute value of the magnetization of $Gd_{24}Tb_1Fe_{75}$ is shown in Figure 4 as a representative example. The RE and TM sublattices have opposite magnetization directions and the temperature dependence of the "sublattice" magnetizations differs as well. Because of this the resulting total magnetization becomes zero at a temperature which is called the compensation temperature, T_{comp}. At this temperature the coercive field, which is about proportional to $1/M_s$, diverges. The Kerr rotation is caused chiefly by the Fe sublattice and has a non-zero value at T_{comp}. By adjusting the position of T_{comp} a few tens of degrees below or above $T_{ambient}$, which can be achieved by choosing the proper composition, very high coercivity values, implying high domain stability, can be achieved.

3) The Kerr rotation for the RE-TM is only moderate, with typical values of 0.2–0.3°. However, the shot noise limited CNR measured during a recording experiment is not proportional to the Kerr rotation angle, θ_k, but to the MO figure of merit $R\theta_k^2$. By depositing a suitable optical enhancement layer, it is possible to increase the Kerr rotation at the expense of the reflectivity and thus increase the figure of merit. In this way a satisfactory CNR can be obtained.

4) The power necessary for switching the magnetization is determined both by the thermal properties of the MO layer stack and substrate and by the Curie temperature of the MO layer. As an example, T_c versus composition, x, is shown for the four binary systems GdFe, GdCo, TbFe and TbCo in Figure 5.[7] It can be seen that by a proper choice of composition, T_c can be adjusted. However, other requirements, such as a proper positioning of T_{comp}, should be achieved as well. Therefore it is necessary to use ternary systems in which T_c is adjustable by the Fe/Co ratio. In practical systems T_c is between 450 K and 500 K and T_{comp} is determined by the RE-TM ratio.

5) As the RE-TM-alloys are amorphous no crystal-grain boundaries are present. Therefore very low media-noise levels are achieved. By choosing proper RE-TM compositions, the write noise caused by imperfectly written domain patterns can be reduced to the level of the media noise.

6) The amorphous RE-TM alloys can conveniently be deposited with vapor deposition and sputtering techniques. In mass production lines, magnetron sputtering is preferred as it enables high deposition rates and does not necessitate substrate cooling.

The structure, and thus the magnetic properties, such as coercivity and anisotropy, as well as the stability against oxidation of the films, is very much dependent on the preparation parameters.[8] RE-TM films prepared with magnetron sputtering at low argon pressures (0.6 Pa) and short substrate-target distances (60 mm) are very dense and smooth, whereas films prepared at high argon pressures (2.5 Pa) and large substrate-target distances (120 mm) exhibit a porous microstructure with voids and a pronounced columnar structure. The films deposited under the latter conditions are much less stable against oxidation and show reduced anisotropy constants compared to the former. The target technology of RE-TM targets is a current is-

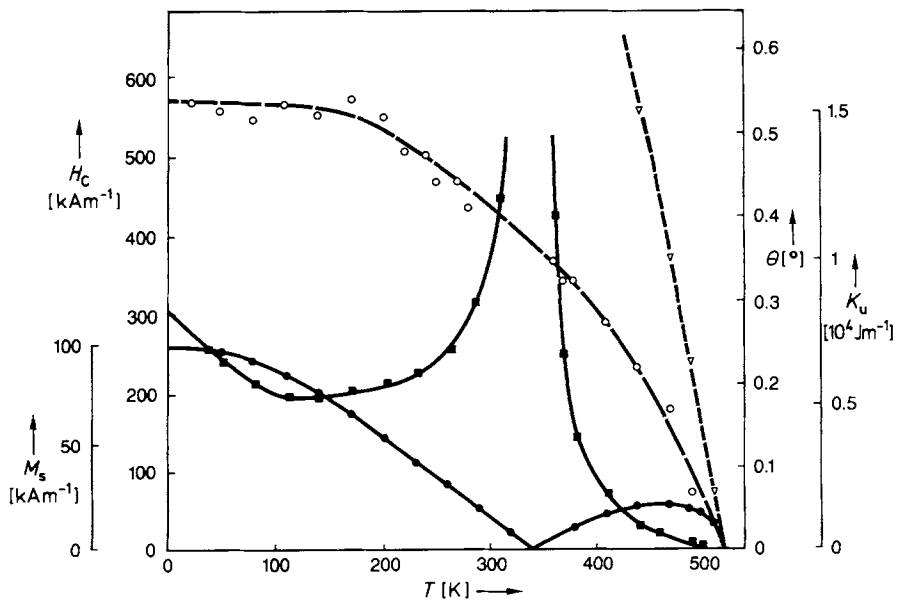


Fig. 4. Magnetic properties of a 50 nm thick $Gd_{24}Tb_1Fe_{75}$ layer versus temperature. The layer was protected with a 30 nm thick aluminum layer. ●: Saturation magnetization M_s, ■: Coercivity H_c, ○: Kerr rotation θ_k and ▽: Anisotropy K_u. The Kerr rotation is enhanced by the Al mirror.

ADVANCED MATERIALS

sue. One problem is the brittleness of the RE-TM alloys, another the homogeneity of the deposited films. The magnetic properties of the films are very dependent on the composition, e.g. the compensation temperatures change with 40 K to 100 K per atom percent RE. Therefore MO discs should have a homogeneity better than 0.5 atom percent, which requires homogeneous targets with almost equal distributions of the sputtered atoms. The distribution of the sputtered atoms depends on the preparation technique of the target, e.g. casting of an alloy or hot pressing of powders.

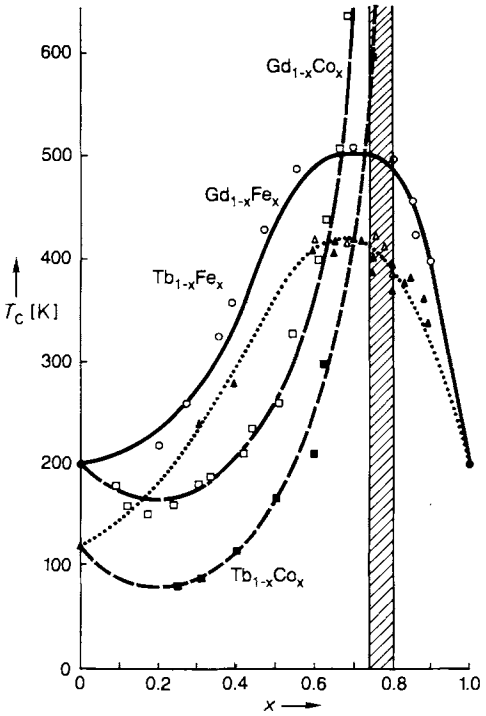


Fig. 5. Curie temperature versus composition for amorphous binary alloys (for references see *P. Hansen* [7], Fig. 2). The shaded area indicates the range of compensation temperatures in the vicinity of room temperature of these alloys.

7) One of the most serious disadvantages of the amorphous RE-TM alloys is their susceptibility to corrosion and oxidation.[9] Therefore long-term stability can only be achieved in a suitable multilayer structure in which the MO layer is covered by protection/passivation layers. Such a structure is shown in the inset of Figure 6. From the substrate side the MO layer is protected by means of a dielectric layer, which can be e.g. AlN or Si_3N_4. Apart from acting as a protection layer, this layer also serves as the optical enhancement layer discussed under 3). On the back side the MO layer is protected by means of a metallic layer, e.g. Al, which also serves as a reflector. Aging experiments on such a structure are also shown in Figure 6. In general several mechanisms contribute to the degradation of MO-layers: oxidation, corrosion, structural relaxation and crystallization. Degradation affects the following magnetic properties: magnetic anisotropy, saturation magnetization, coercive field, and compensation temperature.

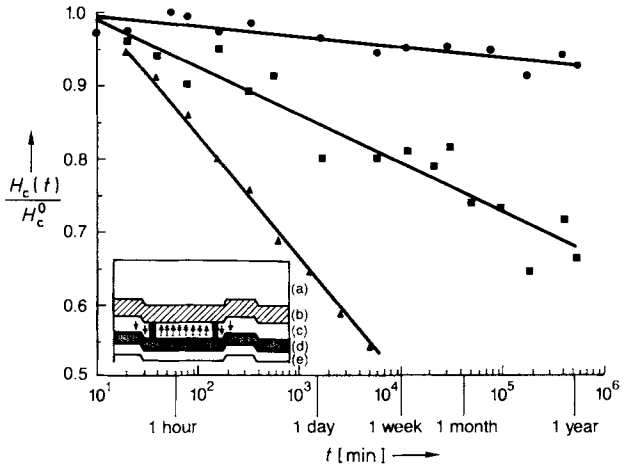


Fig. 6. Long-term stability of a GdTbFe MO layer. Measurements were performed at 80°C. ●: Structural relaxation, ▲: Oxidation of bare film, ■: Trilayer in dry atmosphere. The inset shows a typical trilayer stack. (a) substrate, (b) dielectric enhancement layer, (c) MO layer, (d) metal reflector, (e) organic protection layer.

4. Thermomagnetic Writing

It is of vital importance to have insight into the physics of the thermomagnetic writing process in amorphous RE-TM layers, since irregularities in the written domains cause the so-called write noise, which is often the main noise contribution in practice. For this reason, several recent theoretical papers dealing with the thermomagnetic writing process have appeared.[10–12] Several models have been worked out, starting from computer simulations,[10] or applying a "bubble-like" phenomenological description.[11,12] In the latter case the stability of the domain is given by the following equation:

$$F = \frac{\partial}{\partial r}(E_W + E_H + E_D) = F_W + F_H + F_D,$$

where E_W is the domain-wall energy, E_H the magnetic-field energy, E_D the demagnetizing energy, F_W, F_H and F_D the corresponding forces and r the domain radius. The resulting domain diameter can now be calculated by equating the total force, as given above, to the coercive force F_c. Of course, the proper temperature dependences of the magnetic properties, at the end of the laser pulse, have to be taken into account in the calculation.

Experimental observations of the dynamics of domain formation processes have been scarce hitherto.[13] However, very advanced techniques to study laser-written domains, using Lorentz microscopy, have recently become

available.[14, 15] An example is shown in Figure 7. In this case the MO layer was deposited on a specially prepared silicon wafer disc, with 100 μm by 100 μm windows with 10 nm thick Si_3N_4 membranes. On top of this Si_3N_4 layer the MO layer was deposited and protected with a thin Al/SiO_x layer. On this MO disc domains were written with a laser beam under various conditions. After recording, the silicon wafer was cut into pieces each containing a single window. These specimens were investigated in the electron microscope, using a special operation mode, called Lorentz microscopy. In this way it was possible to visualize magnetic contrast and to obtain images of the laser-written domains.

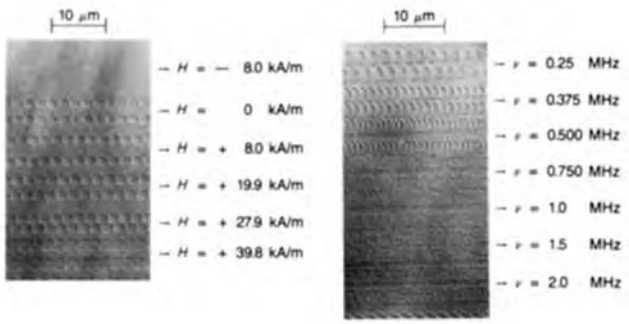


Fig. 7. Lorentz microscopy images of thermomagnetically written domains. Left: Dual tracks, written with laser modulation for various applied fields. Right: Dual tracks, written with magnetic-field modulation for various frequencies.

5. Direct Overwrite

The usual way to write data on an MO disc is to heat the MO layer locally in a fixed applied field. The information to be recorded is supplied by modulating the laser beam. The main drawback of this method is that information already recorded cannot be overwritten. Whole sectors or tracks have to be erased before new information can be recorded. Several solutions to this problem have been suggested. *Shieh* et al.[16] suggested a method for a direct-overwrite technique, utilizing the demagnetizing field of the MO layer itself. The use of exchange-coupled magnetic double layers may also offer interesting possibilities in this respect.[17] The most obvious and direct way to solve the direct-overwrite problem is to modulate the applied field.[18] Using this method, the MO layer is heated continuously by the laser, while the applied magnetic field is switched with a high frequency and modulated according to the information to be recorded. In this way old information can be overwritten, just as in conventional magnetic recording.

By switching the applied field while rotating the disc, overlapping domains of different polarity are written, leaving only a crescent. Because the dimensions of this crescent in the tangential track direction are only determined by the disc velocity and switching frequency of the applied field, domains much smaller than the laser spot can be written. In Figure 7 it can be seen that it is feasible to write domains as small as 0.25 μm in the writing direction in a $Gd_{15}Tb_{6.5}Fe_{78.5}$ layer. Apart from the direct overwrite feature and the possibility of obtaining very high recording densities, magnetic-field modulation offers two other advantages in MO recording. First the quality of the coded signals is improved, as the laser is on continuously and consequently there is no influence of a thermal history when writing a domain. Secondly, influences of compositional variations over the disc surface on the length of written domains, which is apparent in the case of laser modulation, are less critical when writing with magnetic-field modulation. This is due to the fact that the domain length in this case is only determined by the switching frequency of the applied field and the disc velocity.

The use of magnetic-field-modulation methods in MO recording requires the use of special magnetic heads which are capable of generating relatively high fields at large distances, which can be switched at high frequencies. It has recently been shown[19] that it is feasible to design heads which meet all the requirements.

6. Future Materials

Although it is possible to employ amorphous RE-TM compounds for MO recording there is a continuous search for materials with improved properties. The focus is mainly on an increased MO figure of merit and improved chemical stability. Another important development is the future availability of compact solid-state lasers operating at shorter wavelengths than 800 nm. A continuous shift towards blue wavelengths is expected in the future.

Giant MO effects have recently been found in uranium compounds at low temperatures.[20] It has not yet been possible to find room temperature ferromagnets with such high figures of merit, albeit that materials with higher Kerr rotations than the RE-TM materials are known. The material with the highest Kerr rotation at room temperature known today is the Heusler alloy PtMnSb discovered at our laboratories.[21] Despite several attempts, it has not yet been possible to induce perpendicular anisotropy in this material, which is essential for its applications. In PtMnSb the high Kerr rotation value is found at 720 nm. This could become a disadvantage in the future when recording at shorter wavelengths is expected.

Magnetic oxides, such as ferrites and garnets, show unsurpassed chemical stability. This can be combined with high MO figures of merit as has been shown e.g. by the work of *Martens* et al.[22] on Co-ferrite. One of the problems with the oxides is the presence of recording noise. CNR values comparable to those obtained for the RE-TM alloys have not been reported yet. Another drawback for the application of magnetic oxides is the necessity of using

high temperature deposition techniques. Nevertheless research is being continued at several laboratories and progress may be expected.

Very interesting MO effects have been found in metallic, artificially layered structures.[23,24] This is a new field but the possibility for "atomic engineering" in these materials may provide yet unknown and unexpected phenomena.

7. Summary and Outlook

In this article we have discussed materials for MO recording and their application in rewritable recording systems. After a long period of intensive research the RE-TM alloys can be adjusted to satisfy all the requirements for suitable MO materials. This has been made possible by new insights in the physics of the recording processes, combined with advanced preparation techniques. The requirement of direct overwrite, which is expected to be essential for practical applications, will have an impact on further developments in the RE-TM alloy system. Lorentz microscopy pictures show that extremely small domains can be written in a controlled way in these materials allowing for very high recording densities. Unfortunately the resolution during readout is limited by the spatial extent of the laser spot which is about 1 μm at the present wavelength of 800 nm.

The main disadvantage of the present materials is their moderate MO performance and chemical instability. Although some practical solutions to these problems have been found, these drawbacks are the driving force in the search for completely new classes of materials. Magnetic oxides and metallic multilayers offer some interesting prospects here. All these efforts are worth pursuing, because MO recording may develop as the future recording technology, combining the advantages of both magnetic and optical recording.

Received: December 15, 1988

[1] L. Mayer, *J. Appl. Phys. 29* (1958) 1003.
[2] M. Faraday, *Phil. Trans. R. Soc. 136* (1846) 1.
[3] J. T. Chang, J. F. Dillon, U. F. Gianola, *J. Appl. Phys. 36* (1965) 1110.
[4] P. Chaudhari, J. J. Cuomo, R. J. Gambino, *Appl. Phys. Lett. 22* (1973) 337.
[5] M. Hartmann, B. A. J. Jacobs, J. J. M. Braat, *Philips Tech. Rev. 42* (1985) 37.
[6] Y. Suzuki, S. Takayama, F. Kirino, N. Ohta, *IEEE Trans. Magn. MAG-23* (1987) 2275.
[7] P. Hansen, *J. Appl. Phys. 63* (1988) 2364.
[8] S. Klahn, H. Bentin, B. Knörr, H. Heitmann, H. Wilting, unpublished.
[9] H. Heitmann, M. Hartmann, S. Klahn, M. Rosenkranz, H. J. Tolle, P. Willich, *J. Appl. Phys. 61* (1987) 3331.
[10] M. Mansuripur, *J. Appl. Phys. 61* (1987) 1580.
[11] P. Hansen, *J. Appl. Phys. 62* (1987) 216.
[12] J. C. Suits, D. Rugar, C. J. Lin, *J. Appl. Phys. 64* (1988) 252.
[13] H.-P. D. Shieh, M. Kryder, *J. Appl. Phys. 61* (1987) 1108.
[14] J. C. Suits, R. H. Geiss, C. J. Lin, D. Rugar, A. E. Bell, *Appl. Phys. Lett. 49* (1986) 419.
[15] F. J. A. M. Greidanus, B. A. J. Jacobs, F. J. A. den Broeder, H. J. M. Spruit, M. Rosenkranz, unpublished.
[16] H-P. D. Shieh, M. H. Kryder, *Appl. Phys. Lett. 49* (1986) 473.
[17] J. Saito, M. Sato, H. Matsumoto, H. Akasaka, *Jpn. J. Appl. Phys. (S26-4)* (1987) 155.
[18] S. Araki, A. Asayama, H. Kobayashi, *IEEE Trans. J. Magn. Jpn. TJMJ-1* (1985) 691.
[19] J. J. M. Ruigrok, F. J. A. M. Greidanus, W. F. Godlieb, J. H. M. Spruit, *J. Appl. Phys. 63* (1988) 3847.
[20] W. Reim, *J. Magn. Magn. Mater. 58* (1986) 1.
[21] P. G. van Engen, K. H. J. Buschow, R. Jongebreur, M. Erman, *Appl. Phys. Lett. 42* (1983) 202.
[22] J. W. D. Martens, A. B. Voermans, *IEEE Trans. Magn. MAG-20* (1984) 1007.
[23] T. Katayama, H. Awano, Y. Nishihara, *J. Phys. Soc. Jpn. 55* (1986) 2539.
[24] W. B. Zeper, F. J. A. M. Greidanus, P. F. Carcia, C. R. Fincher, unpublished.

Research News

A Novel Monolithic Thin-Film Electroluminescent Device with Extrinsic Memory

Flat display panels are a part of many portable consumer products. Their visual performance is inferior to that of cathodic ray tubes: the luminance of liquid crystal displays (LCDs), the leading flat display technology, is very low, and, in the conventional line-by-line addressing mode, their contrast decreases with increasing panel size. Electroluminescent (EL) display devices are an interesting alternative to LCDs. Figure 1 shows the structure of a standard thin-film(TF) EL device. The active ZnS-Mn layer is sandwiched between two dielectric Y_2O_3 layers.[1,2] Electroluminescence is excited by an alternating field of some 10^6 V cm^{-1}, applied between the metallic and the transparent electrode.

In principle the visual performance of emissive display panels is independent of screen complexity and addressing mode. In practice, the average luminance decreases with

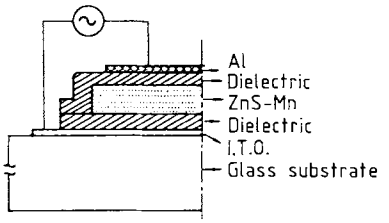


Fig. 1. Cross section of a standard TFEL structure (schematic). See also [7].

increasing screen size: in the line-by-line addressing mode, the time during which each pixel is excited is reduced to T/N, where the period T is determined by the operating frequency of the panel and N is the number of lines. This decrease in luminance can be compensated for by higher excitation currents, but the current density supported by the thin-film electrodes is limited. This practical limitation of screen size and complexity in EL panels can be overcome with the use of memory devices. An EL device with memory shows bistable behavior and remains in the ON or OFF state until the device is switched. Thus, for a static image on a display screen, no periodic refreshing of the screen is required. Standard ZnS-Mn EL devices have been shown to exhibit intrinsic bistability,[3] but the hysteresis margin is low and fades with aging of the device. Moreover, high EL efficiency and a large hysteresis margin cannot be obtained simultaneously. Consequently, this intrinsic memory effect cannot be used in display panels.

EL devices with extrinsic memory were proposed thirty years ago by *Kazan*.[4] The memory effect is produced by electrical coupling between a photoconductive (PC) layer and the EL device. A TFPCEL device can be switched ON either electrically (excitation of the EL layer) or optically (excitation of the PC layer). Due to the optical emission of the EL layer, the PC layer becomes photoconductive. The device remains thus in the ON state until the ac voltage which excites electroluminescence is switched OFF.

The first TFPCEL devices were developed ten years ago.[5] The photoconductive CdS layer was deposited on a separate transparent substrate, thus requiring an additional interconnecting step in producing a display panel. Moreover, due to the ohmic behavior of CdS layers, the dark switching voltage is inconveniently large and difficult to control. Electrical switching of such a TFPCEL display panel would be practically impossible.

Two french physicists, *P. Thioulouse* of the Centre National d'Etudes des Télécommunications (CNET, Bagneux) and *I. Solomon* of the Ecole Polytechnique (Palaiseau) have developed a device which solves both problems:[6–8] the TFEL device and PC layer are integrated on the same substrate, and the whole device can be switched ON electrically.

The original feature of this device is the choice of the PC-layer material, an amorphous hydrogenated silicon–carbon alloy (a-$Si_{1-x}C_x$:H), which can be deposited with high reproducibility in a conventional glow-discharge plasma reactor. Figure 2 shows the structure of the new TFPCEL device. Stoichiometric Ta_2O_5 is deposited by reactive magnetron sputtering on the ITO-coated glass substrate. Chlorine-free ZnS–Mn is deposited by electron beam evaporation. The photoconductive a-$Si_{1-x}C_x$:H layer has $n^{\oplus}$-i-$n^{\oplus}$ structure and can be grown in a single run. Due to carrier-injection from the $n^{\oplus}$ into the i-layer, the dark conductivity of the i-layer is strongly non-ohmic and governed by the density of states at the Fermi-level which can be adjusted by variation of the carbon content.[9]

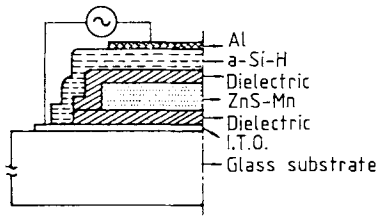


Fig. 2. Cross section of the new TFPCEL device (schematic). The photoconductive a-$Si_{1-x}C_x$:H layer has $n^{\oplus}$-i-$n^{\oplus}$ structure; its dark conductivity is therefore governed by space-charge limited conduction. This non-linear current–voltage characteristic favors electrical switching of the device [7].

The new device exhibits a combination of properties very favorable for application in display panels with high resolution: electrical switching is possible (Fig. 3) with a memory margin sufficiently large for large-size panel applications; the picture elements (pixels) have very sharp edges without the need for an additional photolithographic step; luminance (about 650 cd m^{-2}) and contrast are high, whereas the sensitivity of the PC layer to ambient light is rather low and can be adjusted by a proper choice of deposition conditions. No degradation of the memory effect was observed after more than 2000 hours of opera-

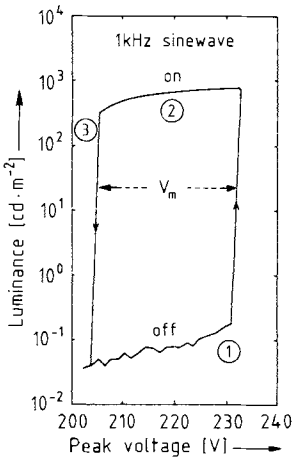


Fig. 3. Luminance vs. voltage characteristics of the new TFPCEL device operated in the dark with a 1 kHz sine waveform. The device is switched ON electrically (1) and remains in the ON (emitting) state (2) until the peak-to-peak voltage is decreased below the threshold value (3). The memory margin V_m is of the order of 25 V [7].

tion. The device is monolithic, and the addition of the PC layer to the conventional TFEL device requires only one additional step: the deposition of an amorphous silicon alloy using a well-known industrial deposition technique. The simplicity of the new device is an important difference to LCD panels driven by a-Si:H thin-film transistors, a very complex technology. The new TFPCEL structure, although still a prototype, clearly has the potential for use in highly complex display panels, and its high switching speed is compatible with TV applications.

Martin P. Schmidt
Palaiseau (France)

[1] M. J. Russ, D. I. Kennedy, *J. Electrochem. Soc. 114* (1967) 1066.
[2] T. Inoguchi, M. Takeda, Y. Kakihara, Y. Nakata, M. Yoshida, *Digest 1974 S.I.D. Int. Symp.* (Soc. for Inform. Display, Los Angeles 1974), p. 84.
[3] V. Marello, W. Rühle, A. Onton, *Appl. Phys. Lett. 31* (1977) 452.
[4] B. Kazan, *Proc. IRE 47* (1959) 12.
[5] G. Ollive, R. E. W. Lake, J. A. Bejar, *Thin Solid Films 41* (1977) 151.
[6] P. Thioulouse, I. Solomon, *IEEE Trans. Electron Devices ED-33* (1986) 1149.
[7] P. Thioulouse, C. Gonzalez, I. Solomon, *Appl. Phys. Lett. 50* (1987) 1203.
[8] P. Thioulouse, I. Solomon, Fr. Pat. Appl. 8614715 (1986); P. Thioulouse, Fr. Pat. Appl. 8419353 (1984).
[9] For a review see: J. Bullot, M. P. Schmidt, *Phys. Status Solidi (B) 143* (1987) 345.

Conference Reports

Intermetallic Phases

The first German symposium on intermetallics ("Intermetallische Phasen: Grundlagen—Einsatzmöglichkeiten—Herstellung") was held on November 24–25 in Bad Nauheim as a joint meeting of the Deutsche Gesellschaft für Metallkunde (DGM) and the Verein Deutscher Eisenhüttenleute (VDEh). It was attended by materials scientists and engineers—nearly half of them from industry—mostly from Germany, Switzerland and Austria. The symposium was composed of four main sessions:

- fundamentals
- structural materials for high-temperature applications and lightweight materials
- functional materials
- processing technology

and three workshop discussions dealing with the production of engine parts, the boundary conditions for intermetallic materials research, and the prospects of intermetallics for high-temperature applications. The aim was to bring together the various groups in research institutes and industry which are studying intermetallic phases, or are interested in applying intermetallics, in order to review the present situation, to assess the prospects and to define tasks for the future. In this symposium only invited lectures were given, and proceedings are not published.

The introductory lecture was given by *H. J. Engell* (Max-Planck-Institut für Eisenforschung, Düsseldorf) who explained that intermetallic phases occupy a position intermediate between metallic alloys and ceramics with respect to atom bonding and crystal structure. This results in the particular properties of intermetallics which make them promising for high-temperature applications and as functional materials. *E. Parthé* (Univ. of Geneva) discussed the crystal structures of intermetallics and showed that complex crystal structures—e.g. those of the Laves phases—result from the stacking of simple basic structures, planes or columns, which allows the prediction of new structures. The first paper by *J. Hünecke* and *H. Wever* (Tech. Univ. of Berlin) discussed constitutional disorder and its temperature dependence with respect to the β′-Hume-Rothery phases and the $B8_2$ phases NiSb and Ni_3Sn_2. The second paper by *J. Hünecke, H. Wever* and *G. Frohberg* outlined the diffusion mechanisms in intermetallics and applied the analysis to phases of types B2, DO_3, $B8_2$, $L1_2$ and A15. The session on fundamentals was concluded by a review by *P. A. Beaven* (GKSS-Forschungszentrum, Geesthacht) on the possibilities for the ductilization of intermetallics, and in particular the effects of composition, i.e. stoichiometry, macroalloying, microalloying, and of processing were discussed.

The session on structural materials for high-temperature applications was led off by an introductory lecture by *G. Sauthoff* (Max-Planck-Institut für Eisenforschung, Düsseldorf). First an overview was given on the criteria for the selection of phases for high-temperature applications, and on the nickel aluminides and titanium aluminides which are already a subject of materials developments, and are now beginning to be introduced commercially in the USA and Japan. Then some less common phases were described which are of special interest for applications at temperatures above 1000°C and are a subject of current research. Figure 1 shows some examples.

The oxidation and hot gas corrosion behavior was reviewed by *L. Singheiser* (Asea Brown Bovery, Mannheim). In particular the effects of alloying elements, of impurities

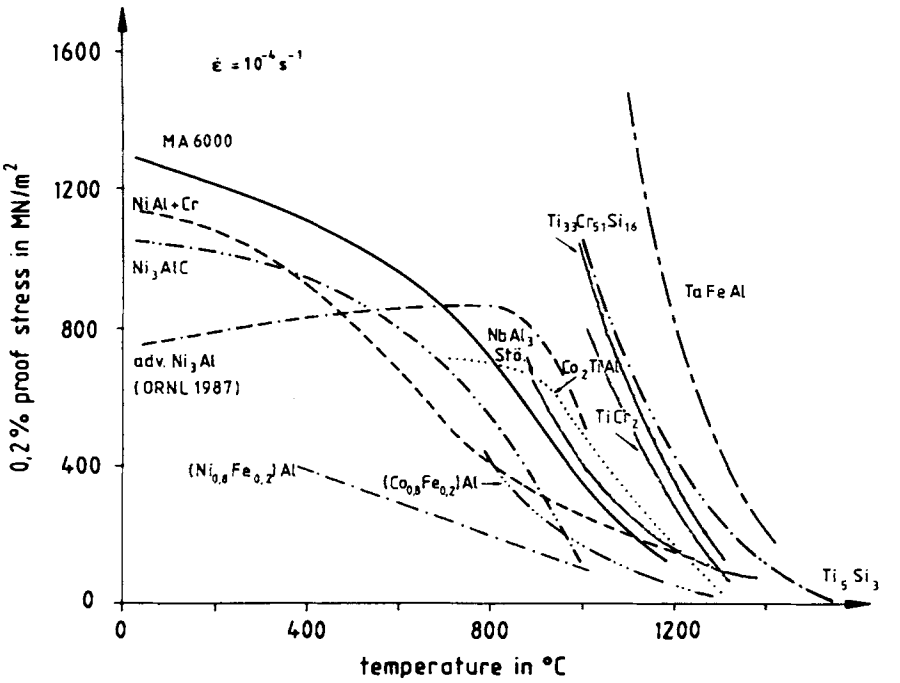


Fig. 1. 0.2% proof stress as a function of temperature for various phases and alloys (Machon, Sauthoff, Frommeyer et al., 1987).

in the atmosphere, and of evaporation of oxides were discussed, and the potential of various phases was evaluated. The creep behaviour of intermetallic phases was analyzed by *G. Sauthoff* and it was shown that the observed behavior can be described by the familiar constitutive equations. Then the possibilities for increasing the creep strengths were discussed, and examples were given with respect to B2 phases and other less common phases. The fatigue behavior was the subject of a paper by *A. Gysler, G. Lütjering* and *I.-G. Park* (Tech. Univ. of Hamburg-Harburg), who have studied the high-temperature fatigue of Al–Mn alloys with large volume fractions of Al_6Mn, in particular crack growth and the effects of atmosphere. As regards lightweight materials, *K.-H. Matucha* (Metallgesellschaft, Frankfurt) reported a current materials development based on Mg_2Si which aims at applications in conventional heat engines. *R. Wagner* (GKSS-Forschungszentrum, Geesthacht) reported work on intermetallic materials based on TiAl, Ti_3Al and Ti_5Si_3. In particular, metallurgical processing and the effects of alloying on microstructure and properties were discussed, and it was shown that both TiAl and the multiphase materials are promising for applications at temperatures up to 1000°C. Nickel aluminides were reviewed by *G. Frommeyer* (MPI für Eisenforschung, Düsseldorf). Ni_3Al and NiAl were discussed with respect to elasticity, plasticity, strengthening and alloying, and the resulting properties were shown.

The session on functional materials was led off by *H. Warlimont* (Vakuumschmelze, Hanau), who reviewed the various functional intermetallics—soft magnetic materials, hard magnetic materials, magnetostrictive materials, superconducting materials, shape-memory materials—with respects to processing and properties. In addition, the commercial importance and the economic potential of these intermetallics was emphasized. Magnetic rare-earth intermetallics were the subject of the paper by *W. Rodewald, W. Fernengel* and *B. Wall* (Vakuumschmelze, Hanau). In particular the properties were discussed and the production techniques were described. Superconducting A15 phases were discussed by *R. Flükiger* (Kernforschungszentrum Karlsruhe) with special reference to the effects of order and stoichiometry on the critial temperature, and a comparison was drawn to the Chevrel phases and the superconducting oxides.

The last session, on processing technology, began with a paper by *W. A. Kaysser* and *R. Laag* (MPI für Metallforschung, Stuttgart) on the fundamentals of powder metallurgy. Methods of powder production were described, the deformability and creep behavior of the powder particles was analyzed, and densification by hot isostatic pressing or hot extrusion was discussed. The report by *H. Grewe* and *W. Schlump* (Krupp Forschungsinstitut, Essen) dealt with the production of components of intermetallics by powder metallurgy. There is evidently a potential for near-net-shape-processed turbine components, the most promising phases being TiAl, Ti_3Al and related materials. The metallurgy of intermetallics was discussed by *G. Frommeyer* (MPI für Eisenforschung, Düsseldorf), with special reference to induction melting and electron-beam melting on the one hand and melt spinning and melt atomization on the other hand. The dependence of the process parameters on the thermodynamic properties of the respective systems was outlined, and examples were given. The thermo-mechanical treatment and forming of intermetallics was discussed by *C. Hartig* (Techn. Univ. of Hamburg-Harburg) with special reference to TiAl-based materials. The basic

principles were outlined and results from current research were presented.

The lectures gave rise to lively discussions which were continued during the breaks and the "Hessen Vesper" party. These many discussions and the workshop results were summarized by *H. Mecking* (Tech. Univ. Hamburg-Harburg) in his concluding remarks in the following way.

- The excellent and perfectly organized programme was a well-balanced presentation of the various aspects of intermetallics and offered a nice opportunity to "look over one's fences".
- This meeting is to be repeated, i.e. there should be a second symposium on intermetallics within two years, with more time for discussions.
- There are three stages of materials development. The first and traditional stage has been development by trial and error, with fundamental research lagging behind applications. The second stage is the optimization of existing materials on the basis of fundamental principles, e.g., as in the case of steels. The third stage is to derive concepts for the development of new materials, which is also the aim of this symposium, and which is supported by research programs of the Federal Ministry of Research and Technology (BMFT) and the German Research Society (DFG). However, the present projects for the development of new intermetallic materials have not been preceded by the necessary fundamental research, and in particular the physical mechanisms which control the plasticity and brittleness of the intermetallics have not yet been analyzed. Thus, much more fundamental research is necessary for achieving new materials developments.
- This fundamental research has to be concentrated on smaller groups of intermetallics, because the whole spectrum of intermetallics is much too broad and divergent. In view of high-temperature applications such a smaller group could be the aluminides and perhaps some silicides.
- Intermetallics have a wide-ranging potential for a variety of applications depending on the particular phases. Materials development on the basis of intermetallics is high tech—even though it may be less fascinating than space research—and must be continued.

Gerhard Sauthoff
Max-Planck-Institut für Eisenforschung
D-4000 Düsseldorf (FRG)

Biomaterials, Bioelectronics .

Only some months after its foundation the European Institute of Technology (EIT) held its first conference on biotechnology in Verona on 7–8 November 1988. In the opening session *J. M. Marcum,* the president of the EIT, outlined the goals for the EIT in general and for this conference in particular. One of the major tasks defined by the leading companies in chemistry and electronics which have set up the EIT is to act as a mediator between industry and university.

The strategy of the EIT, which is to support and monitor existing centers for the three areas of interest, information technology, materials technology and biotechnology, rather than to set up new groups, seems to be promising and flexible. The EIT will also foster liaison between different groups and catalyze contacts with potential industrial partners.

To define its own position and to initiate first contacts between industry and university the EIT invited more than 40 speakers to Verona. Nine topics, covering the broad range from basic research in biotechnology up to current scientific work with direct commercial applicability, were chosen for this conference, including a special session dealing with the organization and management of research. The first session ranged from the different possibilities for inducing overproduction in plant cell cultures (*G. Kochs* and *H. Grisebach,* University of Freiburg, FRG) up to transgenic plants (*S. Altenbach,* Plant Cell Research Institute, Dublin, USA), and gave an impression of the future importance of these methods. *K. Mosbach* (University of Lund, Sweden) presented interesting results on the production of synthetic enzyme complexes. The method he calls "molecular imprinting" offers a new promising practical approach for the synthesis of selective new materials for purification procedures. The use of enzymes from thermophilic bacteria (*M. Rossi,* University of Naples, Italy) which retain their activity even in mixtures with water-miscible organic solvents could soon become of industrial importance. The wide range of advanced techniques for the isolation of biotechnologically produced substances on a technical scale was described by *M. R. Kula* (KFA Jülich, FRG), *C. R. Lowe* (University of Cambridge, UK) and *M. A. Vijayalakami* (University of Compiègne, France). Concluding with the session on "Genetic and Plasmid Stabilization", the first day offered a program of high "information density" to all participants, covering all current problems in biotechnology.

The second day was devoted to more interdisciplinary sessions, on themes such as "protein engineering" and

"bioelectronics and biomaterials". Here I will focus attention especially on the latter topic. Biosensor research is clearly the dominant theme in this area. *I. J. Higgins* (Cranfield Institute of Technology, UK) reviewed the rapid development in the field of biosensors during the last few years. He expects protein engineering to make important advances in improving the stability of the biological components of biosensors, the most serious problem in current biosensor research. *Higgins* also reported on basic approaches to the development of biochips and biocomputers. He and others believe that bacteriorhodopsin will play an important role in that field. However, this work is still in its infancy, and it could take several more years to achieve a real breakthrough. *M. Thompson* (University of Toronto, Canada) gave a comprehensive overview of the problems of chemoreception and its role in biosensor development. The talk by *I. Karube* (Tokyo Institute of Technology, Yokohama, Japan) illustrated the steady progress being made in Japanese biosensor research and its industrial applications. This again reinforced the impression that Japanese leadership in the field of semiconductor-based biosensors is unchallenged. *M. T. Flanagan* (University College, London, UK) described the rapid evolution in the field of optical biosensors and the impressive achievements of his group in this technology. Thin films of trivalent metal phosphates have been developed by his group as new materials for optical waveguides. The cheap production of such films, their excellent structural integrity, and the ease of immobilizing proteins on their surfaces, could lead to wide use of such materials in the field of optical biosensors.

A special session of the conference was devoted to "research planning and training in biotechnology". National institutions such as the "Lund Science Park" (*S. J. Holm*, Lund, Sweden) provide a unique opportunity for scientists to offer their results to industry. Whereas such "technology parks" (usually in the neighbourhood of a university) work more on a local level, organizations such as GBF (*I. Klein*, Braunschweig, FRG, and EUREKA (*K. Draxler*, Vienna, Austria), aim to coordinate research projects on an international level. The EIT will also operate in this way. If the nearly perfect organization of this conference by *M. Chopplet* (EIT, Paris, France) can be extended into the EIT's work as mediator and communicator between industry and university, this institution will provide new leadership in this field.

Norbert Hampp
Institut für Physikalische Chemie
der Universität München (FRG)

The 1988 Fall Meeting of the Materials Research Society in Boston

The MRS held its Fall Meeting, approximately the 15th in its history, in Boston from 28 November to 3 December. 24 symposia, each lasting three or four days, incorporating more than 2000 papers in total, plus the traditional lunchtime symposium on 'Frontiers of Materials Research', constituted the main agenda. The printed program, incorporating abstracts to all papers, occupies 644 folio pages. The list of authors' names alone, just short of 5000, printed in very small type in three columns, fills 18 pages. In addition to the main programme, 27 short technical courses were on firm offer, at prices ranging from $ 320 to $ 770, with a further possible 23 courses on 'sale or return'. In addition, Prof. *Thurow* of the Massachusetts Institute of Technology delivered a lecture telling his compatriots what their country needed to do to maintain technological leadership, and Prof. *Jacques Friedel* of Paris gave a lecture of reminiscences to mark the occasion of his receipt of the MRS's annual award for distinguished materials scientists.

About 4000 participants crowded the two linked hotels which housed the Meeting (not all authors of multi-author papers were present), many spilling off at intervals to drink gallons of Coca-Cola, view the extensive exhibition of equipment and books or to consult the in-house employment exchange put on offer by the American Institute of Physics for the MRS. (This offers an indication of the type of jobs favored by MRS members.) The total membership of the MRS is now over 8000. Two peculiarities certainly help the MRS to recruit new members: all those who paid the $ 165 registration fee were automatically registered as MRS members for the coming year, and all (except students with their reduced fee) were entitled to a free subscription, not only to the Society's *Bulletin* but also to the *Journal of Materials Research* published by the Society.

The Society, which only twelve years ago was run on a part-time and shoestring basis by a single industrial scientist, now has 18 full-time headquarters staff, most of whom seemed to be in Boston being kept extremely busy. Certainly the symposia were faultlessly organized: timekeeping was so precise that it was possible, for those nippy on their feet, to run from one symposium to another to hear a particular paper. The Meeting as a whole was masterminded by a triumvirate of scientists; these selected the symposium topics (which are proposed by enthusiasts

among the membership), and each of the approved symposia was then organized by two, three or four scientists, aided by funds provided by several corporate and government sponsors, distinct for each symposium. (The funds provided are used, inter alia, to contribute to some of the costs of invited speakers and some others.) The MRS as a whole has also enrolled some 150 corporate sponsors who make it possible to keep the subscription at its modest level (US $ 50.00), so that many can afford to join.

Most of the symposia will be published in the form of volumes of camera-ready text. When this fall's publishing program is complete, the MRS will have published 144 full symposium proceedings in seven years. Some of the symposia publish only slim volumes of extended abstracts: this is entirely understandable with regard to the high-T_c superconductor symposium, which (as in previous years) will provide extended abstracts together (in due course) with an optional purchase of edited videotapes. It is less easy to understand why the symposium on 'Fractal Aspects of Materials' as in previus years only offers extended abstracts: perhaps the fractal dimension of the papers is such that an abbreviated view provides the same intellectual outline as a full paper would!

One third of the symposia were more or less closely linked to microelectronics concerns, though the titles did not always make this explicit: Advances in Materials, Processing and Devices in III-V Compound Semiconductors; Laser and Particle-Beam Modification of Chemical Processes on Surfaces; Chemical Perspectives of Microelectronic Materials; Thin Films—Stresses and Mechanical Properties ... and several others. Increasing attention to the chemical aspects of microelectronic technology has been noticeable in the last few Meetings, and this tendency has also extended to some other symposium fields (e.g., Graphite Intercalation Products—Science and Applications, which has been a favored field for several years). Generally speaking a new field is initially tried out in a first symposium; if the response is good, the topic may be repeated in a later Meeting, and some fields (such as Laser Annealing of Semiconductors, not represented this year) become hardy near-perennials.

After a slow start, polymers are moving into the limelight: in 1988, two symposia covered liquid-crystal polymers and rigid-rod polymers, and other topics such as diffusion in polymers were treated in earlier years. Some topics which cover a physics-chemistry spectrum are apt to be treated by a more physical approach: this is true, for instance, of the 1988 symposium on Pore Structure and Permeability of Cementitious Materials.—Metals have always been the poor relations at MRS Meetings, at least in their massive form (metallic thin films get plenty of attention!) In 1988, the third in a series of excellent symposia on High-Temperature Ordered Intermetallic Alloys was held; these alloys are of great longterm interest for aviation, both airframe and engine uses, and for some terrestrial uses as well. These symposia, like all MRS symposia, owe their inception to the advocacy of a few committed members. Perhaps in due course sufficient metallurgically inclined members will propose suitable symposium topics to improve the balance. But perhaps the apparent imbalance is as it ought to be, since MRS symposia have always tended to favor fields located in the gaps between the well established major sciences. Indeed, this sense of neglected interstices could be said to have been the reason for the creation of the MRS in the first instance.

Robert W. Cahn
Department of Materials Science and Metallurgy
University of Cambridge (UK)

Conference Calendar

March 1989

9-10 **The Martensitic Transformation in Science and Technology**
Bochum (Fed. Rep. Germany)
Contact: Dtsch. Ges. Metallkd., Adenauerallee 21, D-6370 Oberursel, FRG

9-11 **Makromolekulares Kolloquium**
Freiburg (Fed. Rep. Germany)
Contact: Prof. H. Finkelmann, Inst. für Makromol. Chemie der Univ., Stefan-Meier-Str. 31, D-7800 Freiburg, FRG

11-14 **Surface Finishing '89**
Brighton (United Kingdom)
Contact: Inst. of Metal Finishing, Exeter House, 48 Holloway Head, Birmingham B1 1NQ, UK

12-14 **High-Tech-Materials and Finishing**
Berlin (West)
Contact: Technik + Kommunikation-Verlag GmbH, Ritterfelddamm 82 h + i, D-1000 Berlin 22

12-25 **Diffusion in Materials,**
NATO Adv. Study Inst.
Aussois (France)
Contact: A. L. Laskar, Phys. and Astron. Dept., Clemson Univ., Clemson, SC 29631, USA

13-14 **Regio Macro II**
Basel (Switzerland)
Contact: Prof. M. Mutter, Inst. für Org. Chem., Univ. Basel, St. Johanns-Ring 19, CH-4056 Basel, Switzerland

13-15 **Mikroelektronik**
Baden-Baden (Fed. Rep. Germany)
Contact: VDE-Zentralstelle Tagungen, Stresemannallee 15, D-6000 Frankfurt 70, FRG

15–17 **Confocal Microscopy/3-D Image Processing in Microscopy,**
1st Int. Conf./2nd Int. Conf.
Amsterdam (Netherlands)
Contact: Bureau PAOG, Congr. Office, Tafelbergweg 25, NL-1105 BC, Amsterdam, Netherlands

15–17 **Intelligent Materials,**
Int. Workshop
Ibaraki (Japan)
Contact: T. Kurino, The Soc. of Nontraditional Technol., Toranomon Kotohira-Kaikan Bldg. 3F, 1-2-8 Toranomon, Minato-ku, Tokyo 105, Japan

20–22 **Mechanical Properties of Materials at High Rates of Strain,**
4th Int. Conf.
Oxford (United Kingdom)
Contact: J. Harding, Eng. Sci. Dept., Univ. of Oxford, Parks Rd., Oxford OX1 3PJ, UK

20–22 **Refractory Metals and Silicides**
Eur. Workshop
Houthalen (Belgium)
Contact: R. De Keersmaecker, IMBE, Kapeldreef 75, B-3030 Leuven, Belgium

20–23 **Eurocomposites and New Materials,**
Conf. and Exhib.
Bordeaux (France)
Contact: EACM, 2 Place de la Bourse, F-33076 Bordeaux Cedex, France

20–23 **Surface Science,**
Interdisciplinary Conf.
Liverpool (United Kingdom)
Contact: P. Weightman, Liverpool Univ., Oliver Lodge Lab., Oxford St., P.O. Box 147, Liverpool L69 3BX, UK

20–24 **Am. Phys. Soc. Mtg.**
St. Louis (USA)
Contact: W. W. Havens, Am. Phys. Soc., 335 E. 45th St., New York, NY, 10017; Tel. 212-6827341

27–31 **Aerospace Sensing,**
Tech. SPIE's Symp.
Orlando (USA)
Contact: Soc. of Photo-Optical Instrumentation Eng. (SPIE), Technical Program Committee, P.O. Box 10, Bellingham, WA 98227, USA

28–31 **Aluminum-Lithium**
5th Int. Conf.
Williamsburg (USA)
Contact: Al-Li-V, School of Eng. and Applied Sci., Thornton Hall, Univ. of Virginia, Charlottesville, VA 22901, USA

29–31 **Neutron and X-Ray Scattering: Complementary Techniques**
Canterbury (United Kingdom)
Contact: Dr. R. J. Newport, Univ. of Kent, Physics Dept., Canterbury, Kent CT2 7NR, UK

30–31 **Colorado Microelectronics**
Colorado Springs (USA)
Contact: CMC '89 Conf. Secretary, Microelectronics Research Lab., Univ. of Colorado, Colorado Springs, CO 80933-7150, USA

30–14 **High-T_c Superconductors,**
Exp. Workshop
Miramare (Italy)
Contact: Int. Ctr. for Theoretical Physics, P.O. Box 586, I-34100 Trieste, Italy

April 1989

1–6 **Superconductivity,**
2nd World Congr.
Houston (USA)
Contact: R. D. Kane, World Congr. on Superconductivity, P.O. Box 27805, Houston, TX 77227-7805, USA

2–4 **Solar Energy**
Int. Conf.
San Diego (USA)
Contact: Dept. of Mechanical Eng., San Diego State Univ., San Diego, CA 92182-0191, USA

3–5 **Molecular Electronics**
Bangor (Wales)
Contact: Prof. H. Block, Center for Molecular Electronics, School of Industrial Science, Cranfield Institute of Technology, Cranfield, Bedford MK43 OAL, UK

3–5 **Modern Practice in Stress and Vibration Analysis**
Liverpool (United Kingdom)
Contact: Meetings Officer, Inst. of Physics, 47 Belgrave Sq., London SW1X 8QX, UK

3–6 **Low Energy Ion Beams,**
5th Conf.
Guildford (United Kingdom)
Contact: Meetings Officer, Inst. of Physics, 47 Belgrave Sq., London SWIX 8QX, UK

3–7 **Copolymerization and Copolymers in Dispersed Media**
Lyon (France)
Contact: I. Guillot/C. Pichot, Lab. des Materiaux Organiques, BP 24, F-69390 Vernaison, France

3–7 **High Temperature Materials '89**
Gaithersburg (USA)
Contact: J. W. Hastie, National Bureau of Standards, Gaithersburg, MD 20899, USA

4–7 **Electrochemical Processing of Semiconductors**
Berlin (West)
Contact: W. Pieth, Free Univ. of Berlin, Inst. of Phys. Chem., Takustraße 3, D-1000 Berlin 33

4–7 **Refractories and High Temperature Materials**
Swansea (United Kingdom)
Contact: Inst. of Ceramics, Shelton House, Stoke Rd., Shelton, Stoke on Trent ST4 2DR, UK

4–14 **Phase Transition in Soft Condensed Matter,**
NATO Adv. Study Inst.
Geilo (Norwegen)
Contact: G. Jarret, Inst. for Energy Technol., Dept. of Physics, P.O. Box 40, N-2007 Kjeller, Norwegen

5–7 **Insulating Films on Semiconductors**
6th Int. Conf.
Garching (Fed. Rep. Germany)
Contact: F. Koch, Physik-Dept. E 16, Techn. Univ. München, D-8046 Garching, FRG

6-7 **Modeling in Crystal Growth from the Melt,**
NATO Workshop
Parma (Italy)
Contact: G. Müller, Inst. für Werkstoffwissenschaften 6, Martensstraße 7, D-8520 Erlangen, FRG

10-12 **Bayreuther Polymer Symp.,**
Bayreuth (Fed. Rep. Germany)
Contact: BPS '89, Lehrstuhl Makromolekulare Chemie II, Univ. Bayreuth, Postfach 101251, D-8580 Bayreuth, FRG

10-12 **British Liquid Crystal Society**
Annu. Conf. 1989
Sheffield (United Kingdom)
Contact: Dr. D. A. Dunmur, Dept. of Chemistry, Univ. of Sheffield, Sheffield S3 7HF, UK

10-12 **Microstructure of Materials in Packaging Technology**
51st WE-Heraeus-Seminar
Bad Honnef (Fed. Rep. Germany)
Contact: Dr. V. Schäfer, WE-Heraeus-Stift., Heraeusstr. 12-14, D-6450 Hanau, FRG

10-13 **Microscopy of Semiconducting Materials,**
MRS 6th Oxford Conf.
Oxford (United Kingdom)
Contact: Administrator, Royal Microscopy Soc., 37/38 St. Clements, Oxford OX4 1AJ, UK

11-13 **Catalysis by Well Characterized Materials**
Liverpool (United Kingdom)
Contact: Prof. R. W. Joyner, Leverhulme Ctr. for Innovative Catalysts, Univ. of Liverpool, Grove St., P.O. Box 147, Liverpool L69 3BX, UK

17-19 **Metals and Materials 89**
Guildford (United Kingdom)
Contact: Inst. of Metals, 1 Carlton House Terrace, London SW1Y 5DB, UK

17-20 **Rare Earth Materials**
5th Biliteral Symp. (FRG/USSR)
Bad Honnef (Fed. Rep. Germany)
Contact: Dr. J. Debrus, Physikzentrum, Hauptstr. 5, D-5340 Bad Honnef 1, FRG

17-21 **Metallurgical Coating**
Int. Conf.
San Diego (USA)
Contact: B. D. Sartwell, Naval Research Lab., Code 4675, Washington, DC 20375, USA, Tel. 202-767-4800, Fax 202-767-5301

17-26 **Ceramics and Composite Materials,**
Spring College in Mater. Sci.
Trieste (Italy)
Contact: Int. Ctr. for Theoretical Physics, Spring College in Mater. Sci. 1989, P.O. Box 586, I-34100 Trieste, Italy

17-29 **STM Basic Concepts and Applications**
NATO Adv. Study Inst.
Erice (Italy)
Contact: Dr. H. Rohrer, IBM Research Div., Zürich Research Lab., Saumerstr. 4, CH-8803 Rüschlikon, Switzerland

18-19 **Industrial Water-Soluble and Water-Swellable Polymers**
Manchester (United Kingdom)
Contact: The Registar (Mid-Career Training), UMIST, P.O. Box 88, Manchester M60 1QD, UK

19-21 **Particle Characterization**
4th Eur. Symp.
Nürnberg (Fed. Rep. Germany)
Contact: Prof. Dr. K. Leschonski, Techn. Univ. Clausthal, Inst. f. Mechan. Verfahrenstechn. u. Umweltverfahrenstechn., Leibnizstr. 15, D-3392 Clausthal-Zellerfeld, FRG

23-27 **American Ceramic Society,**
91st Annu. Mtg. and Expo.
Indianapolis (USA)
Contact: Dr. K. M. Nair, Electronics Dept., E.I. du Pont de Nemours Co., Inc., 3181 Buffalo Ave., Niagara Falls, NY 14302, USA

23-28 **Nondestructive Testing,**
12th World Conf.
(WCNDT '89)
Amsterdam (Netherlands)
Contact: B. de Jong, RAI Organisatie Bureau Amsterdam bv, Europaplein 12, 1078 GZ Amsterdam, Netherlands

24-28 **Optical Science and Engineering,**
2nd Int. Congr.
Paris (France)
Contact: Soc. of Photo-Optical Instrumentation Eng. (SPIE), P.O. Box 10, Bellingham, WA 98227, USA

24-28 **Lasers and Electro-Optics,**
LEOS-IEEE-OSA Conf.
(CLEO '89)
Baltimore (USA)
Contact: Optical Soc. of America (OSA), 1816 Jefferson Pl. NW, Washington, DC 20036, USA

24-28 **MRS Spring Mtg.**
San Diego (USA)
Contact: J. B. Ballance, MRS, 9800 McKnight Rd., Suite 327, Pittsburgh, PA 15237, USA

25-27 **Hot Isostatic Pressing of Materials**
Antwerpen (Belgium)
Contact: Hot Isostatic Pressing Conf., c/o K. VIV, Jan van Rijswijcklaan 58, B-2018 Antwerpen, Belgium

26-28 **Joining Ceramics, Glass and Metal**
3rd Int. Conf. (CGM '89)
Contact: Dtsch. Gesellsch. Metallkd., Adenauerallee 21, D-6370 Oberursel, FRG

26-28 **COAT TECH '89**
Int. Kongr. f. neue Beschichtungstechnologien
Wiesbaden (Fed. Rep. Germany)
Contact: Demat Exposition Managing, Fr. D. Schnabel, P.O. Box 110611, D-6000 Frankfurt 1, FRG

May 1989

1-3 **Tunable Solid State Lasers,**
Top. Mtg.
North Falmouth (USA)
Contact: Optical Soc. of America (OSA), 1816 Jefferson Pl. NW, Washington, DC 20036, USA

1-5 **Scanning Microscopy,**
Salt Lake City (USA)
Contact: O. Johari, Scanning Microscopy Int., P.O. Box 66507, Chicago, IL 60666, USA

4–6 **The Solid State—Dynamics and Kinetics**
Annu. Mtg. Dtsch. Bunsen-Gesellsch. für Phys. Chem.
Siegen (Fed. Rep. Germany)
Contact: Dtsch. Bunsen-Gesellsch., Carl-Bosch-Haus, Varrentrappstr. 40/42, D-6000 Frankfurt am Main 90, FRG

7–12 **High-T_c Superconductor Technologies**
175th Mtg. Electrochem. Soc.
Los Angeles (USA)
Contact: S. Raider, IBM T. J. Watson Research Ctr., P.O. Box 218, York Town Heights, NY 10598, USA

7–12 **Fundamentals of Adsorption,**
3rd Int. Conf.
Nurrigen (Fed. Rep. Germany)
Contact: DECHEMA, Abt. Tagungen, P.O. Box 970146, Theodor Heuss-Allee 25, D-6000 Frankfurt am Main 97, FRG

8–10 **Vakuumelektronik und Displays**
Garmisch-Partenkirchen (Fed. Rep. Germany)
Contact: VDE-Zentralstelle Tagungen, Stresemannallee 15, D-6000 Frankfurt 70, FRG

8–11 **SAMPE**
34th Int. Symp. and Exhib.
Reno (Italy)
Contact: SAMPE, 843 West Glentana, P.O. Box 2459, Covina, CA 91722, USA, Tel. 818-331-0616

8–12 **High Temperature and Wear Resistant Materials in a World of Changing Technology**
12th Int. Plansee Seminar
Plansee (Austria)
Contact: Metallwerk Plansee, A-6600 Reutte, Austria

9–11 **Coatings and Sensors for Acoustic and Electromagnetic-Optical Applications**
Univ. Park. (USA)
Contact: V. K. Varadan, Dept. of Eng. Sci. and Mechanics, Penn. State Univ., 227 Hammond Bldg., Univ. Park, PA 16802, USA

10–11 **Polyimides**
Montpellier (France)
Contact: Prof. M. Abadie, LEMD/MAO-USTL, F-34060 Montpellier Cedex 1, France

16–19 **Modern Developments in Materials Science and Technology,**
Annu. Mtg. Dtsch. Gesellsch. Metallkd.
Karlsruhe (Fed. Rep. Germany)
Contact: Dtsch. Gesellsch. Metallkd., Adenauerallee 21, D-6370 Oberursel, FRG

16–19 **Rare-Earth Magnets and Their Applications**
10th Int. Workshop
Kyoto (Japan)
Contact: Dr. C. Herget, Sparte Anorg. Chemie, Th. Goldschmidt AG, P.O. Box 101461, D-4300 Essen 1, FRG

22–24 **Sol-Gel-Gläser**
52nd WE-Heraeus-Seminar
Bad Honnef (Fed. Rep. Germany)
Contact: Dr. V. Schäfer, WE-Heraeus-Stift., Heraeusstr. 12–14, D-6450 Hanau, FRG

22–24 **Werkstoffanalytik,**
Wien (Austria)
Contact: Prof. Dr. M. Grasserbauer, Inst. für Analytische Chem. der Tech. Univ. Wien, Getreidemarkt 9, A-1060 Wien, Austria

22–24 **Glastechnische Tagung**
Stuttgart (Fed. Rep. Germany)
Contact: Dtsch. Glastechn. Gesellsch., Mendelssohnstr. 75–77, D-6000 Frankfurt am Main, FRG

22–25 **Clustering and Aggregated State of Matter**
Strasbourg (France)
Contact: Prof. E. Constantin, Groupe de Recherche de Spectrométrie de Masse Interlab., Dept. de Chim., 1 rue Blaise Pascal, 67008 Strasbourg Cedex, France

22–25 **Graphite Intercalation Compounds,**
5th Int. Symp. (ISGIC-5)
Berlin (West)
Contact: Dr. F. W. Froben, Fachbereich Physik, Freie Univ. Berlin, Arnimallee 14, D-1000 Berlin 33

24–26 **Advances in the Stabilization and Controlled Degradation of Polymers,**
11th Int. Conf.
Luzern (Switzerland)
Contact: Dr. A. V. Patsis, Inst. in Materials Sci, State Univ. of New York, New Paltz, NY 12561, USA

25–26 **Quantitative Methods in Assessment of Structural Defects**
Kansas City (USA)
Contact: A. P. Berens, Univ. of Dayton, Research Inst., 300 College Park Ave., Dayton, OH 45469, USA

29–31 **Cross-linked Polymers,**
3rd Int. Conf.
Luzern (Switzerland)
Contact: Dr. A. V. Patsis, Inst. in Materials Sci, State Univ. of New York, New Paltz, NY 12561, USA

30–2 **E-MRS Spring Mtg.**
Strasbourg (France)
Contact: P. Siffert, Ctr. de Recherches Nucléaire, Lab. PHASE, F-67037 Strasbourg, Cedex, France

31–2 **Applied Surface Analysis,**
11th Symp.
Cleveland (USA)
Contact: J. Grant, Research Inst., 300 College Park, Dayton, OH 45469-0001, USA

31-2 **Thermogravimetry and Thermal Engineering,**
6th Biennial Conf.
Budapest (Hungary)
Contact: I. Benko, MATE, House of Technol. III. 318, P.O. Box 451, H-1372 Budapest, Hungary

June 1989

5–7 **CONIMAT' 89**
1st Int. Convention for the Technology Transfer of New Materials
Strasbourg (France)
Contact: Adhesion Et Associes - CONIMAT', 9, rue de L'Ancienne Mairie, 92100 Boulogne, France, Tel. 48 25 26 04, Fax. 46 03 86 26

6–9 **Chemistry of Functional Dyes,** Int. Symp. (ESTech '89) Osaka (Japan) Contact: Prof. T. Kitao, General Secretary of the Symp., Kinki Chem. Soc., Japan 1-8-4, Utsubo honmachi, Nishi-ku, Osaka 550, Japan

12–15 **Narrow-Gap Semiconductors and Related Materials,** Int. Conf. Ogunquit (USA) Contact: D. G. Seiler, Phys. Dept., Univ. of North Texas, P.O. Box 5368, Denton, TX 76203, USA

18–21 **Colloid & Surface Science,** 63rd ACS Div. of Colloid & Surface Chem. Symp. Seattle (USA) Contact: J. Berg, Dept. of Chemical Eng. BF-10, Univ. of Washington, Seattle, WA 98105, USA

18–23 **Ceramic Materials and Production Methods** 1st Conf. of the Eur. Ceramic Soc. and Fair Maastricht (Netherlands) Contact: Mrs. L. M. J. Bos, P.O. Box 1630, 6201 BP Maastricht, Netherlands

19–21 **Composites** Asia-Pacific 89 Adelaide (Australia) Contact: The Secretariat, Techsearch, Composites Asia-Pacific '89, P.O. Box 2471, Adelaide S.A. 5001, Australia

20–22 **SAMPE** 3rd Int. Electronics Conf. Los Angeles (USA) Contact: M. Smith, Business Director, SAMPE, P.O. Box 2459, Covina, CA 91722, USA, Tel. 818-331-0616

21–23 **Chemically Modified Surfaces,** Midland (USA) Contact: W. T. Collins, Dow Corning Corp., Mail Stop C41C00, Midland, MI 48686, USA

21–23 **Electronic Materials** Cambridge (USA) Contact: The Metallurgical Soc., 420 Commonwealth Dr., Warrendale, PA 15086, USA

22–25 **Optics Asia '89** Singapore (Singapore) Contact: Asia '89, 994 Bendemeer Rd., N° 04-03, Singapore 1233, Singapore

25–29 **Composite Materials for High Temperature, Fundamental Principles and Performance** Jerusalem (Israel) Contact: Mrs. S. Cahana, Ministry of Sci. and Developm., P.O. Box 18195, 91181 Jerusalem, Israel

25–30 **Solid State Sensors and Actuators (Transducers-5)/ Eurosensors III** Montreux (Switzerland) Contact: COMST S.A., P.O. Box 415, CH-1001 Lausanne 1, Switzerland

26–28 **Molecular Design of Functional Polymers,** IUPAC Int. Symp. Seoul (Korea) Contact: IUPAC Int. Symp., c/o Polymer Soc. of Korea, Rm. 601, Hyecheon Bldg., 831 Yeoksam-dong, Kangnam-ku, Seoul 135-792, Korea

26–28 **Coherence and Quantum Optics** Conf. Rochester (USA) Contact: L. Mandel, Univ. of Rochester, Dept. of Physics, Rochester, NY 14627, USA, Tel. 716-275-4361

26–30 **Solid State Chemistry,** 2nd Int. Symp. Pardubice (Czechoslovakia) Contact: Dr. L. Koudelka, Inst. of Chem. Technol., Leninovo nam., 565, CS-53210 Pardubice, Czechoslovakia

26–30 **Supermembranes** Trieste (Italy) Contact: Int. Ctr. for Theoretical Physics, P.O. Box 586, I-34100 Trieste, Italy

27–28 **Polymer Latex III** London (United Kingdom) Contact: Miss M. Peacock, Plastics and Rubber Inst., 11 Hobart Place, London SW1W 0HL, UK

28–30 **Oxide Surfaces** Midland (USA) Contact: W. T. Collins, Mail Stop C41C00, Dow Corning Corp., Midland, MI 48686-0994, USA

July 1989

2–7 **Solid State Organic Materials,** 9th Int. Conf. Como (Italy) Contact: Centro di Cultura Scientifica, "A. Volta", Villa Olmo, Via Cantoni 1, I-22100 Como, Italy

3–6 **Conduction and Breakdown in Solid Dielectrics** 3rd Int. Conf. (ICSD '89) Trondheim (Norway) Contact: Prof. Sletbak, ICSD '89, The Norwegian Inst. of Technol., Sem Sælands V 13, N-7034 Trondheim, Norway

3–7 **Martensitic Transformations** Int. Conf. ICOMAT-89 Sydney (Australia) Contact: N. Kennon, Dept. of Metallurgy and Materials Eng., Univ. of Wollongong, Wollongong, NSW 2500, Australia

3–8 **Light-Sensitive and Conducting Polymers** Leipzig (German Dem. Rep.) Contact: Prof. H. K. Roth, TH Leipzig, Sekt. Naturwissenschaften, P.O. Box 66, DDR-7030 Leipzig, GDR

3–28 **Liquids, Freezing and the Glass Transition** NATO Adv. Study Inst. Les Houches (France) Contact: École d'Été de Physique Théorique, F-74310 Les Houches, France

4–7 **Nonlinear and Electro-optics** Int. Conf. Cambridge (United Kingdom) Contact: The Meetings Officer, The Inst. of Physics, 47 Belgrave Square, London SW1X 8QX, UK

9–14 **Scanning Tunneling Microscopy/Spectroscopy,** 4th Int. Conf. Oarai (Japan) Contact: O. Nishikawa, The Graduate School of Nagatsuta, Tokyo Inst. of Technol., 4259 Nagatsuta, Midori-ku, Yokohama 227, Japan

9–14 **Zeolites,**
8th Int. Conf.
Amsterdam (Netherlands)
Contact: M. Laboushere, 792 Keizersgracht, 1017 EC, Amsterdam, The Netherlands

10–12 **Appl. Organomet. Chemistry: an Entry to the New Technology**
The Pines Resort (Australia)
Contact: Dr. A. F. Masters, School of Chemistry, Univ. of Sydney, Sydney, N. S. W. 2006, Australia

10–13 **Magnetic Resonance in Polymers,**
9th Spec. Colloq. Ámpere
Prague (Czechoslovakia)
Contact: P. M. M. Secretariat, c/o. Inst. of Macromol. Chem., Czech. Acad. of Sci., 16206 Prague, Czechoslovakia

10–14 **Ion Sources**
Int. Conf.
Berkeley (USA)
Contact: W. O'Connor, Lawrence Berkeley Lab., 50B-2270, Berkeley, CA 94720, USA, Tel. 415-486-6386, Fax 415-486-7000

10–14 **Electron Spectroscopy,**
4th Int. Conf.
Honolulu (USA)
Contact: G. E. McGuire, Microelectronics Ctr. of North Carolina, P.O. Box 12889, Research Triangle Park, NC 27709, USA

10–14 **Organic Coatings Science and Technology,**
15th Int. Conf.
Athens (Greece)
Contact: Dr. A. V. Patsis, Inst. in Materials Sci, State Univ. of New York, New Paltz, NY 12561, USA

11–14 **Numerical Analysis of Semiconductor Devices and Integrated Circuits,**
6th Int. Conf.
Dublin (Ireland)
Contact: J. J. H. Miller, Nase-Code Conf., INCA, P.O. Box 2, Dún Laoghaire, Ireland

12–14 **Solid-State Laser/Optical Fiber Science and Electromagnetic Theory '89,**
Top. Mtg./Sino-Japanese Joint Mtg.
Beijing (Peoples' Rep. China)
Contact: Optical Soc. of America (OSA), 1816 Jefferson Pl. NW, Washington, DC 20036, USA

16–21 **Catalysis,**
Eur. Conf.
Berlin (West)
Contact: Prof. G. Ertl, Fritz-Haber-Inst. der Max-Planck-Gesellsch., Faradayweg 4–6, D-1000 Berlin

17–20 **Polymer Blends**
Prague (Czechoslovakia)
Contact: P. M. M. Secretariat, c/o. Inst. of Macromol. Chem., Czech. Acad. of Sci., 16206 Prague, Czechoslovakia

18–20 **Polymer Chemistry: Aspects of Radical Polymerization**
Lancaster (United Kingdom)
Contact: Dr. J. R. Ebdon, Dept. of Chemistry, Univ. of Lancaster, Lancaster LA1 4YA, UK

18–21 **Integrated Optics and Optical Fiber Communications,**
7th Int. Conf. (IOOC-7)
Kobe (Japan)
Contact: P. W. Shumate, Jr., Bell Communications Research, 435 S St., Morristown, NJ 07960, USA

23–24 **Computer-Aided Materials Characterization**
Int. Symp.
Charlotte (USA)
Contact: R. Biederman, Worcester Polytechn. Inst., Worcester, MA 01609, USA, Tel. 508-831-5453/5346

23–28 **Materials and Mechanisms of Superconductivity: High-Temperature Superconductors,**
Int. Conf. (HTSC-M^{2}S)
Stanford (USA)
Contact: Dr. T. H. Geballe, Dept. of Applied Phys., Stanford Univ., Stanford, CA 94305, USA

24–26 **Micro-Optics/Gradient-Index Optical Imaging Systems,**
2nd Conf./8th Top. Mtg.
Tokyo (Japan)
Contact: K. Iga, Tokyo Inst. of Technol., Research Lab. of Precision Machinery and Electronics, 4259 Nagasuta, Midori-ku, Yokohama 227, Japan

24–26 **Composite Structures,**
5th Int. Conf.
Paisley (United Kingdom)
Contact: Dr. I. H. Marshall, Dept. of Mechanical and Production Eng., Paisley College of Technol., High St., Paisley PA 12BE, UK

25–26 **Computer-Aided Microscopy and Quality Control**
Int. Conf.
Charlotte (USA)
Contact: J. Braun, EG+G Mound Appl. Technologies, Miamisburg, OH 45343-0987, USA, Tel. 513-865-3829

31–2 **Biologically-Engineered Polymers**
Cambridge (United Kingdom)
Contact: Royal Soc. of Chemistry, Burlington House, London W1V 0BN, UK

31–3 **Photoacoustic and Photothermal Phenomena**
6th Int. Mtg.
Baltimore (USA)
Contact: J. Murphy, Johns Hopkins Appl. Physics Lab., Johns Hopkins Rd., Laurel, MD 20707, USA, Tel. 301-953-6214

August 1989

2–7 **Pure and Applied Chemistry,**
32nd IUPAC Congr.
Stockholm (Sweden)
Contact: Stockholm Convention Bureau, P.O. Box 6911, S-10239 Stockholm, Sweden

13–26 **High-T_c Superconductors,**
NATO Adv. Study Inst.
Bad Windsheim (Fed. Rep. Germany)
Contact: R. Kossowsky, Applied Res. Lab., Pennsylvania State Univ., P.O. Box 30, State College, PA 16804, USA

14–17 **Shock Compression of Condensed Matter,**
APS Top. Conf.
Albuquerque (USA)
Contact: A. Roach, MS-P 915, Los Alamos Nat. Lab., Los Alamos, NM 87545, USA

ANGEWANDTE CHEMIE
International Edition in English
Volume 28 · Number 3
March 1989
Pages 253–396

Stiff-Chain Polymers—Structure, Phase Behavior, and Properties

By Matthias Ballauff*

Most of the industrial plastics used up to now consist of flexible macromolecules in which the repeat units are joined together in a nonlinear fashion by rotating bonds. Stiff-chain polymers, which in the ideal case have a rodlike shape, have received much less attention. The reason for this is that such polymers usually exhibit an exceedingly low solubility. Very often, they are absolutely insoluble and do not melt. However, in recent years these polymers have aroused technical interest because high-modulus fibers and moldings can be fabricated from them. These favorable mechanical properties are directly related to the nearly parallel arrangement of the rodlike macromolecules in the solid state which is achieved through spinning or extrusion from a liquid crystalline (nematic) state. It is therefore evident that a thorough understanding of the phase behavior and the structure is required for a universal technical utilization of these materials. The great variety of methods used in polymer science today has led to a deeper understanding of stiff-chain polymers. Experimental results together with theoretical modeling of the phase behavior have direct implications for the practical use of these macromolecular materials.

1. Introduction

Today, synthetic polymers represent a class of ubiquitous materials, for they may be molded easily into arbitrary shapes and used for a multitude of purposes. The almost inexhaustable varieties of molecular architecture constantly lead to new applications. However, the great potential of macromolecular materials has so far only been partially exploited, since mostly flexible polymers have been used, i.e. chain molecules in which the successive units are assembled by rotating bonds and form angles different from 180°. In contrast to this, stiff-chain polymers are derived from rigid monomer units connected in a collinear fashion. Their technical development and use has only just begun. This delay can be traced back to the low solubility of these polymers and to the necessity of using exotic solvents. In addition to this, the melting point is very high and in many cases the materials do not melt at all. This renders investigations in solution or in the melt by conventional physicochemical techniques a very difficult task. The processing of stiff-chain polymers is very often impossible for the same reasons. The ultimate cause for these problems lies in the rodlike shape of the macromolecules: because of their coil-like nature, flexible macromolecules may assume a vast number of conformations in the melt or in solution. Hence, melting or dissolving a flexible coil is accompanied by a substantial gain in entropy. In contrast, stiff-chain polymers experience no alteration in shape regardless of the state of their aggregation. Hence, dissolution in a solvent or melting requires cleavage of numerous intermolecular contacts, but leads only to a minor gain in entropy.

[*] Dr. Matthias Ballauff
Max-Planck-Institut für Polymerforschung
Postfach 3148, D-6500 Mainz (FRG)

 © VCH Verlagsgesellschaft mbH, D-6940 Weinheim, 1989 0570-0833/89/0303-0253 $ 02.50/0

This brief overview clearly demonstrates that great difficulties are encountered both in the processing and in the scientific investigation of stiff-chain polymers. Despite such unusual problems, this class of polymers has recently attracted unusual interest from the scientific and engineering communities. The underlying reasons for this development best emerge on comparing the phase behavior of stiff and of flexible macromolecules (Fig. 1).

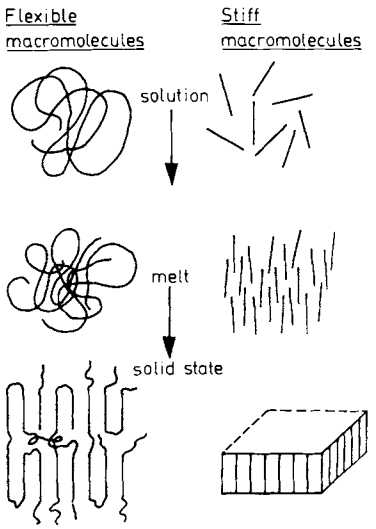
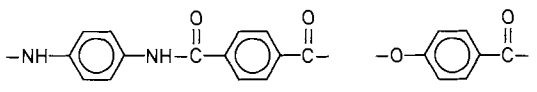


Fig. 1. Schematic comparison of the phase behavior of flexible and stiff macromolecules.

Flexible macromolecules assume a coiled conformation both in the melt as well as in solution. When the concentration of the dissolved macromolecules exceeds a critical value the coils overlap and form entanglements. If the degree of polymerization and the overlap are large enough these entanglements will govern the dynamics of such systems.[1] Furthermore, it is evident that solutions and melts from flexible macromolecules in equilibrium will be isotropic, i.e., there will be no preferred direction in the system. Complete crystallization from such a melt would require the disentanglement of all coils and adoption of a special conformation allowing the packing in the crystal. This qualitative argument already leads to the conclusion that flexible polymers can normally be transformed only into the semicrystalline state from the melt, if crystallization from the melt takes place at all. Figure 1 shows the typical lamellar morphology of the crystalline regions with the interdispersed amorphous phase. This arrangement has far-reaching consequences for the mechanical properties of these systems.

Stiff-chain polymers, depicted as rods in Figure 1, lead to an entirely different phase behavior. In contrast to flexible polymers there is no formation of entanglements. At higher concentrations, however, interaction between the rods leads to a constraint of rotation. The consequences of this effect on the dynamics of such a solution can be treated quantitatively.[1] Still higher concentrations are followed by an increase of parallel alignment of the rods due to steric effects. If the concentration exceeds a certain critical value that is a function of the axial ratio, i.e., the ratio of length to the diameter of the rods, a spontaneous transition to an ordered, liquid crystalline system takes place.[2,3] The ordered domains thus generated may be aligned by external fields or by flow processes, whereupon macroscopically oriented solutions or melts are formed. The strong steric interaction between the rods, which already causes partial alignment and liquid crystalline order in solution, will lead to a well-ordered, parallel arrangement of the macromolecules in the solid state. Under certain conditions, e.g., by spinning from liquid crystalline solutions, macroscopic order may be achieved in these systems and preserved upon transition to the solid state.

Thus, the discovery that poly-(*p*-phenyleneterephthalamide) **1** forms liquid crystalline solutions from which high modulus fibers may be spun was the major incentive for scientific and corporate research on stiff-chain polymers.[4,5] The unusual mechanical properties of these materials mainly derive from the high alignment of the rodlike molecules and the absence of an amorphous phase, which limits the mechanical strength of flexible polymers. A great number of stiff-chain polymers forming liquid crystalline melts or solutions[6,7] have now been synthesized and investigated. It is the goal of this review to demonstrate the interrelation of the phase behavior of stiff-chain polymers with their molecular architecture. The discussion is not restricted to liquid crystalline phases deriving from these systems (see Ref. [6] for a detailed discussion of liquid crystal polymers) but deals rather with the phase behavior in the entire accessible range of temperature. This requires first a discussion of how a rod-shaped structure of a macromolecule may be achieved. The typical phase behavior of stiff-chain polymers is discussed next using the polyester **2** of *p*-hydroxybenzoic acid as a well-investigated example. After this the molecular architecture necessary to lower the melting point below the temperature of thermal decomposition for the observation of liquid crystalline phases is discussed. The subsequent section is devoted to the experimental determination of chain stiffness. Then a short survey of the theory of the nematic phase is given. A central point of this discussion is the predictive power of theoretical models with regard to the phase behavior of stiff-chain macromolecules used in practice. A final section deals with the properties and possible applications of these materials.

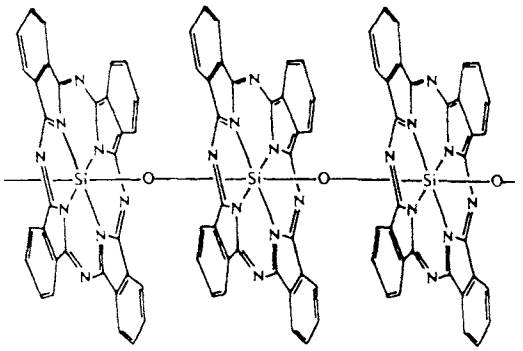


1 2

2. Molecular Architecture of Stiff-Chain Polymers

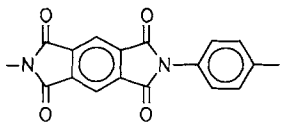
Already mentioned in Section 1, flexible polymers are usually built up by a sequence of nonlinearly linked units. Stiffness of the polymer chain is effected through building up the chain from anisometric groups. The rodlike shape may now be realized by a linear, rigid connection of these monomers or by the steric interaction of the neighboring

monomer. The polyphthalocyaninatosiloxanes **3** exampls of the latter building principle.[8]

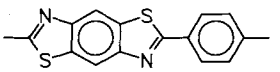


3

Here the flexible siloxane chain is forced into a stretched conformation by the steric repulsion of the densely packed phthalocyanine rings. In contrast to this the stiffness of the polyimide **4** follows from the molecular configuration of the repeat units in which planar rings are joined together by a C–N bond to a phenyl group.



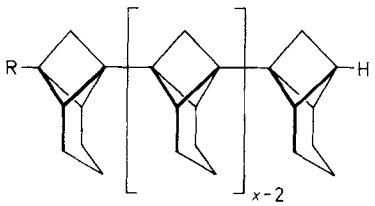
4



5

This bond is also located in the plane of the imide ring and parallel to the long axis of the polyimide molecule. Rotations about this C–N single bond do not affect the stiffness of the whole macromolecule. A similar, ladder-like structure is realized in the poly-*p*-phenylenebenzodithiazole **5**.[9]

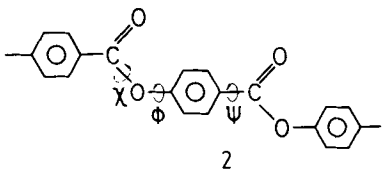
Chain stiffness can also be realized with cycloaliphatic structures of suitable geometry. The polypropellanes **6** recently introduced by *Schlüter*[10] may serve as examples. Here, as in the case of the polyimides **4**, the rotation around the C–C single bond connecting the repeat units does not result in a deviation from the rodlike shape.



6

In addition to this, chain stiffness can be introduced into flexible polymers by helical supramolecular structures. This building principle is very often found in biopolymers such as DNA,[11] Xanthan[12] or in a number of polypeptides. Here, extraordinary stiffness may be effected by winding up several helical strands.

In all the examples dealt with up to now, the extended shape is evident from the molecular architecture, whereas the discussion of chain stiffness in *p*-linked fully aromatic polyesters and polyamides is more complicated. Repeat units as in the polyester **2** (cf. Fig. 2) are only linear if there is no free rotation about the C(O)–O bond (angle χ),



2

Fig. 2. Definition of the torsion angles in the repeat unit of the polymer **2** for the calculation of the chain conformation within the framework of the rotational isomeric state model (cf. Fig. 14) [15–17, 87, 88].

i.e., if the ester group is planar. Rotations around the other framework bonds (torsion angle ϕ and ψ) do not lead to deviations from rodlike shape, since subsequent units may be assumed, to a first approximation, to be collinear. The analysis of the conformation of the polyester segment shown in Figure 2 by *Flory* et al.[15–17] indeed leads to the conclusion that the ester group (and also the amide group) is planar, and the oxybenzoyl unit and the analogous unit of the polyamides will exhibit a high stiffness. This analysis, however, does not take into account the influence of substituents in the *o*-position to the carboxy group[18] on the conformation. This point will be discussed further in Section 5.

3. Poly(4-oxybenzoate) as Example

In this section the polyester **2** of *p*-hydroxybenzoic acid (see Fig. 2) will be discussed as a well investigated example of a stiff-chain polymer. First experiments leading to the synthesis of this polymer were carried out as long ago as the end of the last century. Hence these investigations are among the oldest experiments in polymer science. *Schiff* in 1882[19] and *Klepl* in 1883[20] reported the isolation of oligomers from the products obtained upon reaction of *p*-hydroxybenzoic acid with $POCl_3$ or upon heating the monomer. *Emil Fischer* and *Karl Freudenberg*[21] synthesized the pure oligomers of *p*-hydroxybenzoic acid and of vanillic acid up to the tetramer. In the course of this work they found that the solubility of the products decreases strongly with increasing degree of polymerization. Starting from the acetoxybenzoic acids, *Gilkey* and *Caldwell*[22] succeeded in synthesizing the polymers of *m*- and *p*-hydroxybenzoic acid. The first systematic study of the polyester poly-(*p*-oxybenzoyl) **2** was conducted by *Economy* et al.,[23] who also investigated the structure by means of electron- and X-ray diffraction. A major improvement in the synthesis and subsequent characterization of the products with regard to their molecular weight was achieved by *Kricheldorf* and *Schwarz*.[24–26] On the basis of the latter works *Lieser*[27a] succeeded in 1983 in determining the phase behavior and the unit cells of the individual modifications of the polyester **2** by electron diffraction. According to *Lieser* **2** forms two orthorhombic modifications I and II at room temperature (see Fig. 3; cf. also Refs. [27b, c]).

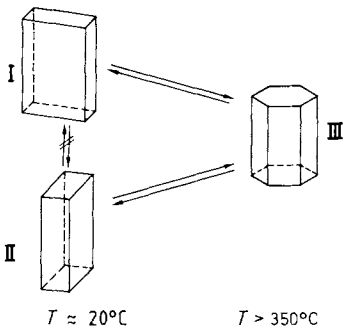


Fig. 3. Schematic representation of the unit cell of modifications I–III of the polyester **2** [27a]: The mixture of two orthorhombic modifications I and II at room temperature transforms reversibly into the pseudohexagonal modification III.

Both modifications are transformed through a first-order transition at 330°C into a pseudohexagonal phase III. Cooling down to room temperature again leads to a mixture of modifications I and II together with structures containing a number of defects.[27a] The fact that I cannot be transformed into II and vice versa suggests that the asymmetric macromolecules have different directions in the two phases.[27a] Since no macroscopically oriented samples suitable for X-ray scattering have been obtained up to now, this problem still remains unsolved. Investigations on the polycondensation with the help of small-angle X-ray scattering and electron microscopy show that the chains are sufficiently mobile even in the crystal structure, especially in phase III, and thus are sufficiently reactive, i.e. the macromolecules have enough reactivity that the polymerization will proceed mainly in the solid state.[28] A further point of interest is that poly(*p*-thiobenzoyl) exhibits the same phase behavior as poly-(*p*-oxybenzoyl) **2**.[29]

The absence of a melting process in the case of **2** renders the fabrication of this polymer by the usual methods employed in plastics technology impossible. Molding can be achieved only by high-energy forging. This problem, which is typical for stiff-chain polymers, may be circumvented in some cases, e.g. poly(*p*-phenyleneterephthalamide) **1**, which is sufficiently soluble in concentrated sulfuric acid. However, it is obvious that processing from such aggressive solvents gives rise to a number of technical problems. Molding directly from the melt is certainly the less costly alternative. An overview of the concepts for lowering the melting point of stiff-chain polymers, based on examples, is given in the next section.

4. Concepts for Improving the Solubility and for Lowering the Melting Points of Stiff-Chain Macromolecules

In principle the melting points of stiff-chain polymers can be lowered by the following modifications of the structure:

1) Insertion of flexible comonomer units ("spacers") like *n*-alkylene chains.[30,31] However, this strongly reduces the rigidity of the resulting macromolecules. These polymers are flexible coils in solution and will not be discussed in further detail here.

2) Inclusion of bent units of different size. This leads to a disturbance of the crystal structure and a lowering of the melting point.[32,33]

3) Appending of flexible side chains onto the stiff main chains. Here the side chains act like a bound solvent, which lowers the interaction between the main chains, and leads to a large increase in entropy when dissolving or melting the polymer.[34–38]

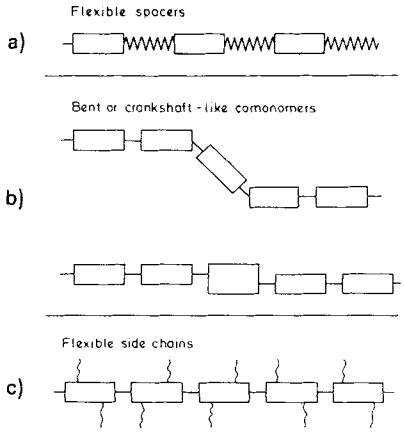
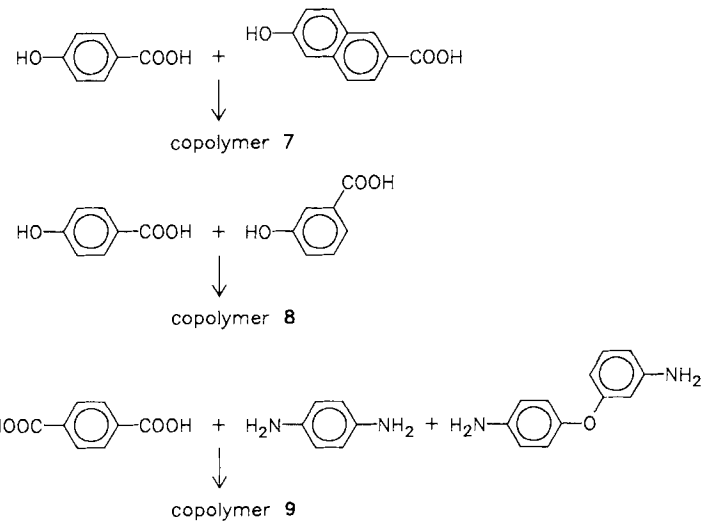


Fig. 4. Concepts for improving the solubility and meltability of stiff-chain polymers: a) insertion of flexible spacers between the rigid, mesogenic units; b) insertion of bent or crankshaft-like comonomers; c) appending of flexible side chains to the rigid, linear main chain.

4.1. Copolymers

Because of the increased interest being shown in stiff-chain macromolecules in industry for the fabrication of high-strength fibers, numerous copolyesters and copolyamides have been synthesized from relatively easily accessible fully aromatic hydroxycarboxylic acids and bisphenols and have been patented. Scheme 1 shows three selected examples which should serve as models for illustrating the main features of such polymers.

The first system shown, the copolyester **7** ("Vectra", Hoechst-Celanese)[39–41] consisting of 2-oxy-6-naphthoyl and *p*-oxybenzoyl units, exemplifies the disturbance of



Scheme 1. Selected copolymer systems.

crystallization by comonomer units of different size, which leads to a crankshaft-like structure along the polymer chain. The copolymer **8** of *p*- and *m*-hydroxybenzoic acids[24,42–46] consists of a sequence of linear and bent units of approximately equal size. It is especially suitable for structural investigations, since the phase behavior of poly(*p*-oxybenzoyl) **2** is already well-known (cf. Section 3). The third example, the copolyamide **9**[47–49] can assume a coiled or a stretched conformation. This is due to the 3,4′-linkage of the diaminodiphenyl ether, in which the 60° bend of the ether bond can be straightened out again by the *m*-linkage. Thus, the influence of intermolecular interactions on the conformation of the chain can be studied directly. A further example of technical importance is provided by the copolyester of *p*-hydroxybenzoic acid, terephthalic acid and 4,4′-biphenyldiol ("Xydar", Dartco).

The main problems concerning the synthesis and phase behavior of stiff-chain copolymers will now be discussed using results based on the second system (copolymer **8**) of Scheme 1. Later on, a comparison with the results of the other two systems will follow. Despite the inclusion of units along the chain which disrupt crystallization, the melting point of these materials may still exceed 300°C. This fact together with the low solubility leads to a number of problems during polycondensation in the melt. In general, two methods are used to circumvent these problems: the activation of the hydroxy groups by acetylation ("acetoxy method"; Fig. 5, top) or by silylation ("silyl method";

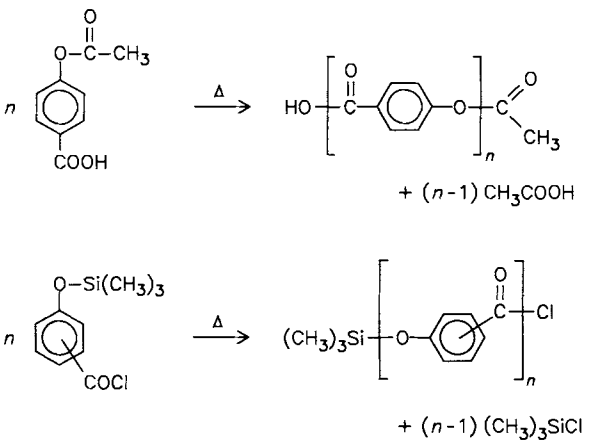


Fig. 5. Methods for polycondensation of aromatic polyesters: acetoxy method (above) and "silyl method" (below).

Fig. 5, bottom).[25,28] An important point during the polycondensation process is to maintain homogeneity at least in the early stage. Otherwise block copolymers instead of statistical copolymers may result. Since the copolymers **8** exhibit sufficient solubility in $CHCl_3$ up to a content of 40% of the linear *p*-component, a sequence analysis by means of ^{13}C NMR spectroscopy in solution is possible. This shows that the monomer units are distributed at random along the chain.[42,43] In the case of insoluble products a sequence analysis may be achieved in special cases by means of wide-angle X-ray scattering of solid oriented samples. This method of analysis has been developed by *Blackwell* et al.[49–51] and by *Bonart* et al.[52–54] and has been applied to a number of copolymer systems. In this treatment the intensity of the meridional reflections of samples with sufficient orientation[55] is compared to results of model calculations which explicitly simulate the deviation from a random sequence of the monomeric units. Using this method it has been shown that copolymer **7** is a statistical copolymer (see Ref. [51]). A similar analysis of the 3,4′-linked copolyamide **9** showed that it assumes a stretched conformation in the solid state.[49] This finding demonstrates the strong steric interaction of the chains in ordered systems which leads to a stiffening of systems which in themselves are flexible. Thus, the present results lead to the conclusion that statistical copolymers may be obtained if the conditions of polycondensation are well-defined. Also, the analysis shows the chains to adopt a stretched conformation in the solid state.

Another point of interest is the crystallinity of these copolyesters and -amides as well as the kind of distortion exerted by the bent or crankshaft-like comonomer onto the crystal lattice of the linear component. In principle, this poses the question of crystallization in random copolymers. A number of studies of this problem have been carried out on copolymer **7** by *Windle* et al.,[56] who have formulated the concept of "non-periodic layer crystallites" (NPL).[56–58]

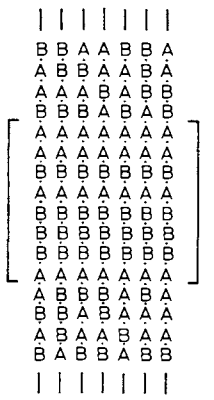


Fig. 6. "Non-periodic layer crystallite" (NPL) model of *Windle* et al. [56–58] for the crystallization of stiff-chain copolymers of the monomers A and B. The NPL crystallite marked in the figure by parentheses is built up by juxtaposition of parts of the chains having the same sequence of monomer units.

Here, the formation of small crystallites is modeled by putting together parts of the chains in the same sequence (see Fig. 6). In this model semicrystallinity thus may be brought about through lateral juxtaposition of parts of the chains having the same shape. The probability of finding a given fixed sequence of congruent units decreases strongly with the length of the sequence. Therefore these NPL crystallites will have a rather limited size. These ideas have been further developed by *Windle* et al.[57,58] A comparison with experimental results gave first hints that such ordered regions do indeed exist (cf. discussion of experimental findings in Refs. [57] and [58]).

The high crystallinity of copolyester **8** can be explained without the NPL concept, since investigations by X-ray[43] and electron diffraction[44] have shown that the modifications of the polyester **2** of *p*-hydroxybenzoic acid (see Section 3) can incorporate an appreciable number of bent *m*-

units. As is obvious from wide angle X-ray measurements[43] (cf. Fig. 7), even an amount of 10% hardly broadens the reflections. Electron diffraction studies[44] can supplement this information by more detailed information on the kind of defects. Only if the content of bent *m*-units is 30% or greater is the crystallinity disturbed considerably.

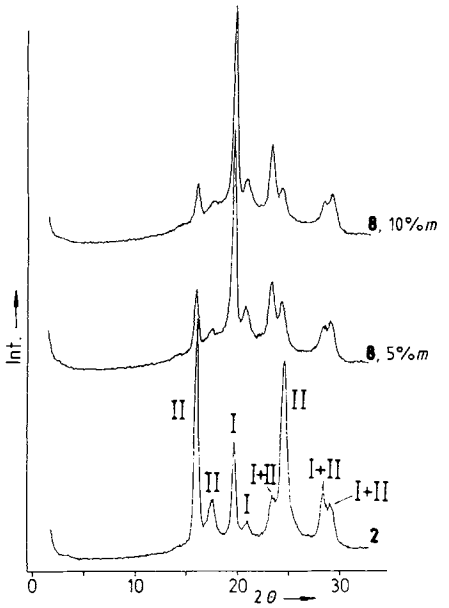


Fig. 7. X-ray diffractograms [43] of the polyester **2** of *p*-hydroxybenzoic acid and of the copolyester **8** containing 5% and 10% *m*-hydroxybenzoic acid at room temperature. The roman numerals I and II indicate the two orthorhombic low-temperature modifications I and II of **2** [27a] (cf. Fig. 3).

Having discussed the phase behavior of the materials at room temperature, the question now is how the disturbance of the comonomer units affects the phase behavior at elevated temperature. Figure 8 shows the diffractograms of copolymer **8** with 10% *m*-units at room temperature and above the temperature of the first order transition.[59,60] It is obvious that both modifications I and II have been transformed into modification III, the pseudohexagonal packing of the chains of which could be demonstrated with electron diffraction photographs[44] of oriented samples. Cooling the sample down to room temperature again leads to a mixture of I and II, as observed in the case of the homopolymer **2**. Rapid cooling, however, allows phase III to supercool down to room temperature if the disturbance by *m*-units ($\geq 30\%$) is strong enough.[59,60]

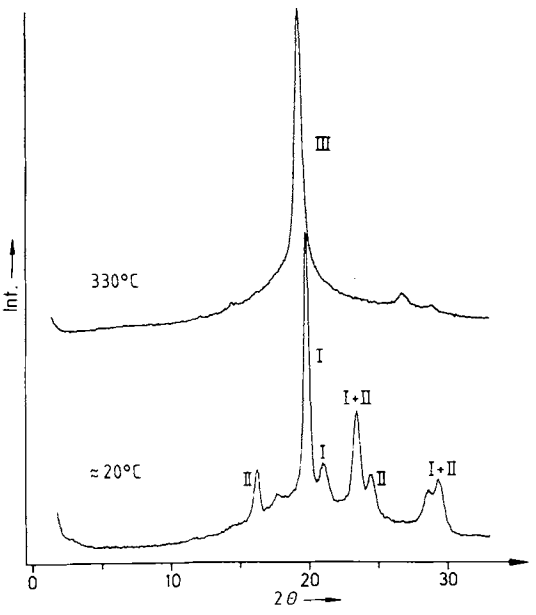


Fig. 8. X-ray diffractograms of copolyester **8** containing 10%. *m*-hydroxybenzoic acid at room temperature and at 330°C. The diffractograms demonstrate that both low-temperature modifications I and II (cf. Fig. 3) are transformed into the high temperature modification III.

All the results obtained on copolyester **7** up to now by X-ray studies (powder and fiber diagrams)[50,56,61] lead to the following conclusions: at room temperature there is a mixture of an amorphous phase and a strongly disturbed, probably pseudohexagonal phase.[61] The amount of the ordered phase, which could be compared with modification III of the polyester **2**, increases upon annealing. Raising the temperature diminishes the crystalline part and above 300°C there is only an amorphous melt. *Windle* et al.[56,62] investigated this phase by polarization microscopy and came to the conclusion that it is a biaxially nematic phase. Up to now only *Finkelman* et al.[63] have succeeded in providing direct evidence of a thermotropic biaxial nematic phase in liquid crystalline polymer with the mesogenic units in the side-chain. Similarly, *Ebert, Hermann-Schönherr Wendorff, Ringsdorf* and *Tschirner* have reported convincing evidence for a biaxial nematic phase in a stiff- chain polyester with flexible side chains.[64] Since there are no comparable conoscopic[*] observations on fully oriented samples of polyester 7, the above conclusion drawn by *Windle* et al. is only indirect and needs confirmation by further investigations.

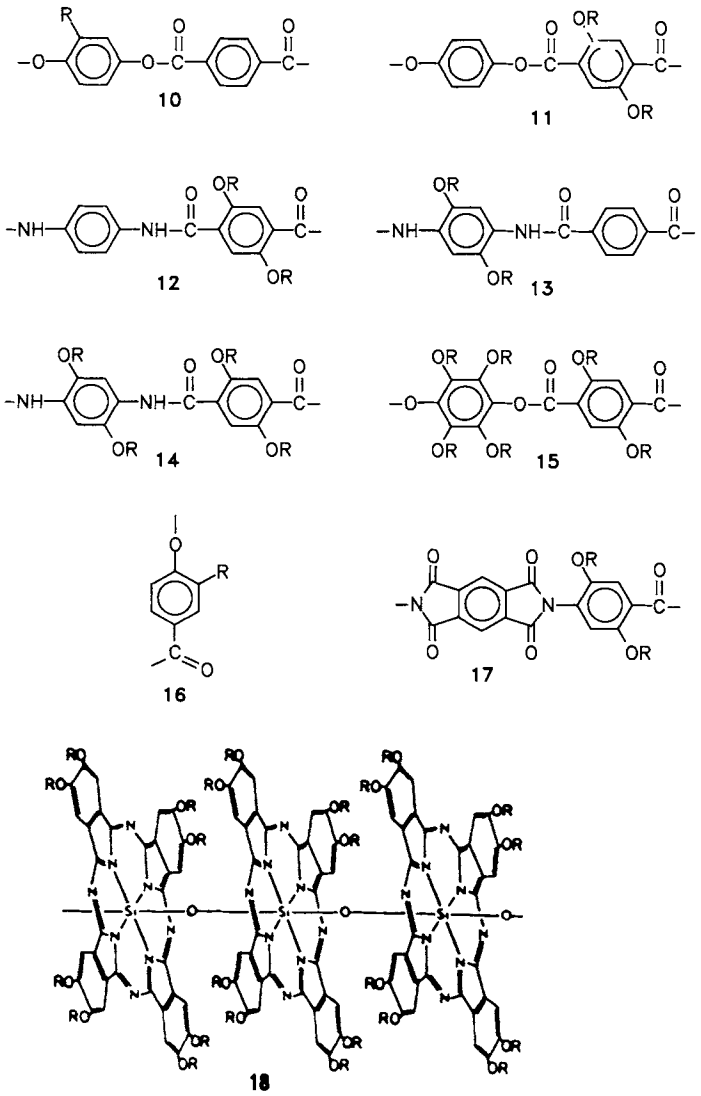
So far only a few measurements have been carried out on the glass transition in copolymers of the type **7**–**9**. Measurements of the glass transition temperature T_g of the copolyester **8** as a function of its composition show[43] that T_g does not increase but becomes smaller on increasing the amount of *p*-hydroxybenzoic acid. This unexpected result becomes plausible when the great number of defects in the orthorhombic or the pseudohexagonal structures is taken into account. Thus, at comparatively low temperatures a rotational motion of chain segments may be induced even if the free volume available is rather small, whereas an increase in mobility of non-linear segments would necessitate a much higher free volume. ^{2}H NMR spectroscopic investigations on the copolymers discussed here[65–67] would be very helpful, since the present results are not yet conclusive regarding the mechanism of motion. However, as already stated by *Wendorff* et al.,[68] this phase, especially the high-temperature modifications of the polyester **2** and of the copolymers of type **8**, may be compared with plastic crystals or highly ordered smectic phases, i.e., with systems characterized by positional long range order in which the molecules have certain rotational degrees of freedom above the glass temperature.

[*] Conoscopy: see E. Wahlstrom, *Optical Crystallography*, Wiley, New York 1979.

4.2. Stiff-Chain Macromolecules with Flexible Side Chains

The third concept delineated in Figure 4 for improving the solubility and lowering the melting point of stiff-chain polymers consists in the attachment of flexible side chains to rigid main chains. In contrast to the foregoing concepts, the stiffness of the main chain is fully preserved. During the process of melting or upon dissolution these side chains can adopt a vast number of configurations as in the case of flexible coils. To a first approximation these side chains act like a solvent bound to the main chain; by variation of the length and number of side chains per repeat unit the amount of "bound solvent" may be changed continuously.[37] The concept has already been realized in the case of helical polypeptides like poly(γ-benzylglutamate) and related polypeptides, where the phenyl group of the glutamic acid bears long *n*-alkyl substitutes.[13] In spite of the high degree of stiffness of the main chain these comb-like polymers are sufficiently soluble in organic solvents.

The first comb-like polymer of this kind based on stiff-chain polyesters was introduced by *Lenz* et al. in 1983.[34,69] It is the polyester **10** (Scheme 2) of terephthalic acid and 2-*n*-alkylhydroquinone. In accord with the above considerations the melting point decreases continuously with increasing length of the side chains. This enables the observation of liquid-crystalline phases over a conveniently accessible temperature range. In the meantime a series of these comb-like polymers[34,36,38,64,69-80] (see Scheme 2, systems **10**–**18**) have been studied, and in all cases a strong increase in solubility and a marked decrease in melting point have been reported. This enables polycondensation not only in the melt but also in solution. Furthermore, the materials obtained can be purified by precipitation from solution. In some cases the solubility is high enough to allow a characterization by the standard methods usually employed for flexible macromolecules.



Scheme 2. Stiff macromolecules with flexible side chains. R = $(CH_2)_nH$.

The most important results obtained with these systems will be discussed in the following using polyester **11** as example.[38,70,71] As is obvious from the wide angle X-ray patterns[71] measured at room temperature (see Fig. 9), polyesters **11** exhibit a high degree of crystallinity. Further-

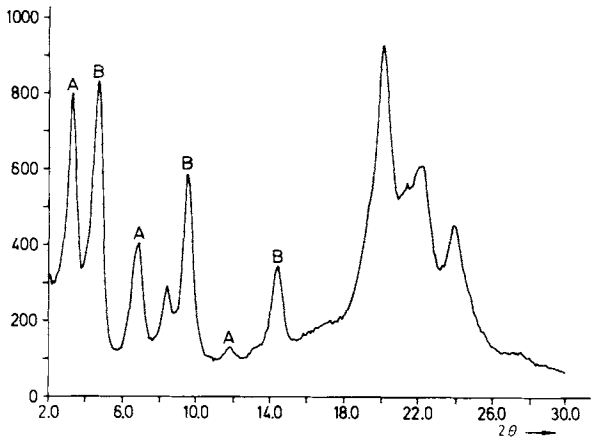


Fig. 9. X-ray diffractogram of the polyester **11**, R = $(CH_2)_{16}H$, at room temperature [71]. The reflections termed A and B originate from the layered structures A and B. Ordinate: Intensity.

more, the strong Bragg reflections marked A and B in the diffractogram in the region of small angles indicate, together with their higher orders, the formation of two layered modifications referred to in the following as A and B. A plot of the layer spacings for the modifications A and B versus the number of carbon atoms in the side chains (Fig. 10) demonstrates that the length of alkyl groups is decisive for the build-up of the structure.[71] For both modifications the intercept is, within the limits of error, the same. Its value approximately matches the diameter of the main chains; only the slope of the curve is different. In most of the systems presented in Scheme 2 three phase transitions of first order are observed:[38] at low temperatures there is an increase of disorder of the packing of the side chains which may be compared to the transition from the crystalline to the solute phase in the *n*-alkanes. Raising the temperature further leads to the mesophase and finally to the vanishing of liquid crystalline order and the formation of an isotropic melt. In the case of the polyester **11** one observes nematic mesophases for short side chains ($2 \leq n \leq 6$). If the side chains are long enough ($n \geq 8$), the modification A already present in the solid state (cf. Fig. 9)

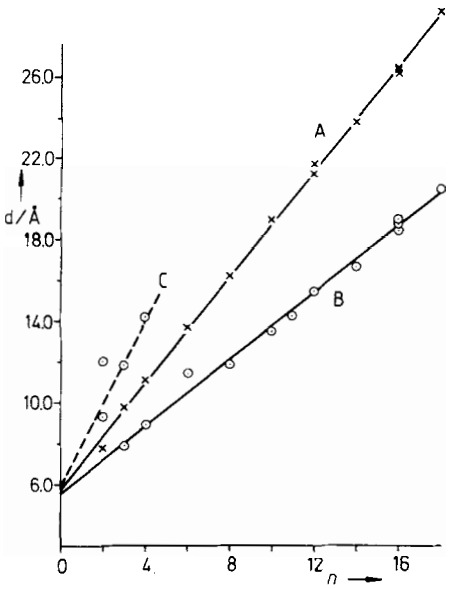


Fig. 10. Plot of the Bragg distances d calculated from the reflections A and B (see Fig. 9) versus n, the number of carbon atoms in the side chains of the polyester **11**. The modifications A and B differ with regard to the increment per CH_2 group. As expected the extrapolation to $n=0$ leads for both modifications to a value approximately corresponding to the diameter of the main chain. A third modification C is detectable only for short side chains [71].

remains stable also in the liquid crystalline phase. This is obvious from the strong Bragg reflections and their higher orders[38,70,71] (cf. Fig. 11).

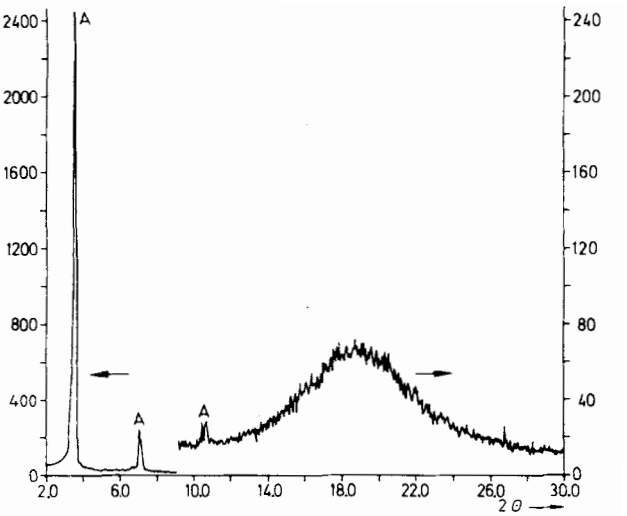


Fig. 11. X-ray diffractograms of the mesophase ($T=120$°C) of the polyester **11**, R = $(CH_2)_{16}H$ [71]. The strong Bragg reflection together with its higher orders is clearly visible. The halo in the wide angle region indicates liquid-like short-range order. Ordinate: Intensity.

This mesophase, first observed in the polyester **11**[38] also occurs in the polyamides **12**,[70,72] **13**[70,72] and **14**.[72] However, in contrast to the polyesters, in the case of these polyamides there is a strong correlation of the main chains through hydrogen bonding between amide bonds.[70,72,73]

Similarly to the systems discussed previously, the polyesters **10** form mesophases with a layered structure if the length of the chains is more than 12 C atoms; for shorter side chains, nematic mesophases are observed.[69] The polyimides **17**[75,76] can also be converted into layered mesophases whose Bragg distance lies near to that of the B modification of the polyester at high temperature.[76] Finally, the polyesters **16** of the 3-*n*-alkyl-4-hydroxybenzoic acid also form such layered structures in the mesophase if the side chains are long enough.[79] Hence, the formation of this mesophase is a general phenomenon that has not yet been observed in low molecular weight liquid crystals. The structural data available so far for the polyesters and amides **11**–**13** suggest an intercalated arrangement of the side chains,[70,71] since the layer spacings are much smaller than the overall breadth of the molecule:

Only when both phenyl rings of the repeat unit are substituted with side chains, as in the polyamides **14**, do the layer spacing and the breadth of the molecules (assuming a fully stretched conformation of the side chains) approximately coincide.[72] The model depicted in Figure 12 is nat-

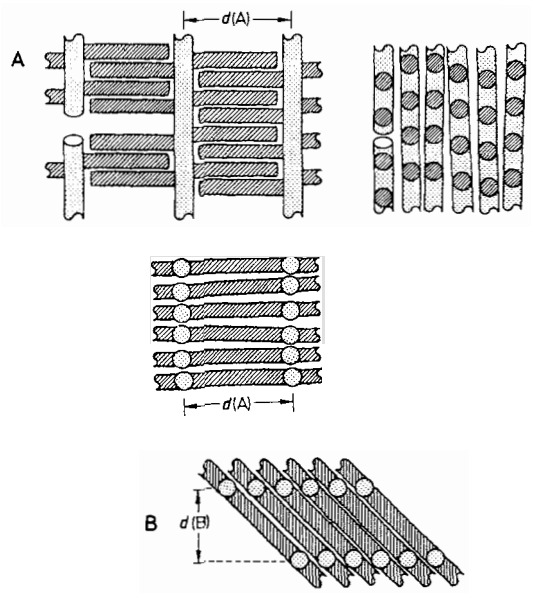


Fig. 12. Model [71] of the molecular structure of modifications A and B of the polyester **11**: The dependence of the layer spacing on the length of the side chains (see Fig. 10) leads to the proposition of an intercalated arrangement of the side chains. The absence of additional reflections in the diffractogram (Fig. 11) shows that there is no strict correlation of distances between main and side chains. The model is an idealized picture of the molecular arrangement of the side chains, the packing of which will exhibit an increasing number of defects with rising temperature [71].

urally idealized, for the packing of the side chains will exhibit an increasing number of defects with rising temperature. X-ray measurements conducted on polyimides **17** have shown that there are well-defined intermediate phases in this process. In these phases a part of the order of the side chains is preserved.[76] This becomes evident upon examining the X-ray diffractograms of the polyimide **17** at different temperatures[76] (Fig. 13).

The highly crystalline low-temperature modification is first transformed into an intermediate-temperature phase. The presence of only a few remnant reflections in the wide-angle region points to a high number of defects in the packing of the side chains. A further rise in temperature is finally followed by the formation of a mesophase in which

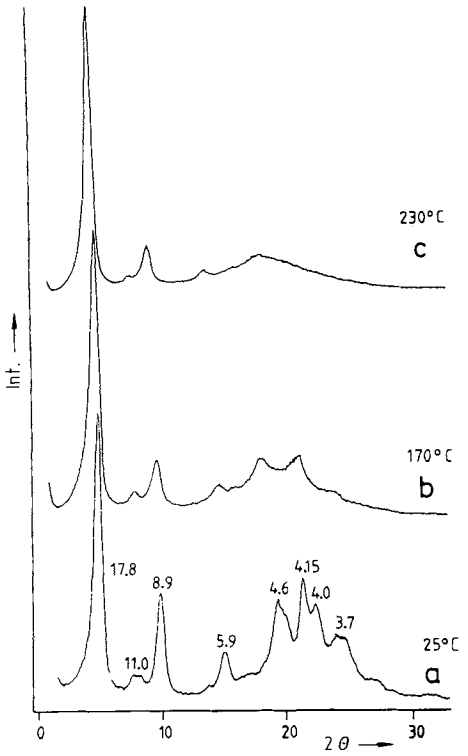


Fig. 13. X-ray diffractogram of polyimide **17**, R = $(CH_2)_{14}H$, as a function of the temperature [76]. a) Low-temperature modification; b) medium temperature modification with disarranged packing of the side chains; c) high-temperature modification (mesophase).

the long range order of the alkyl chains is no longer present. These conclusions are supported by results from ^2H NMR spectroscopic measurements on the polyimide **17**.[82]

The above mentioned organization of the rigid macromolecules with flexible side chains in the solid state and in the mesophase (liquid crystalline state phase) has important consequences for the dynamics of such systems. Thus, it could be shown by ^2H NMR experiments that the layered mesophase of the polyester **11** only partially aligns in magnet fields even if the field strength is very high (7 Tesla).[81,82] The result is corroborated by measurements of the diamagnetic susceptibility of such systems using a SQUID magnetometer.[83] This method utilizes the high sensitivity of a superconductivity coil with a semiconducting contact towards minute changes of the magnetic field in order to determine the magnetic susceptibility. If the tensor of the diamagnetic susceptibility of the polymer molecule is known, these measurements allow the determination of the degree of order and alignment present in the system.[84] Mesophases with layered structures of the polyester **11** orient only slowly whereas nematic phases (see above) of **11** bearing shorter side chains can be oriented to a high degree.[83]

These first experiments on orientation in a magnetic field reveal an important difference regarding the dynamics of nematic and smectic phases, which are also detected in low molecular weight liquid crystals: mesophases with layered structures have higher viscosities than the corresponding isotropic phases, whereas nematic liquid crystals generally exhibit a lower resistance to flow than the isotropic phase.[85] This can be demonstrated for polyester **11** by determination of the viscosity in the isotropic nematic and the layered mesophase.[86] The viscosity determined in the same system is thus unequivocally related to the microscopic organization of the macromolecules.

From the results discussed in this section concerning the structure of stiff macromolecules with flexible side chains it becomes obvious that the initial concept of the side chains being a "bound solvent" is indeed correct. For all the systems present in Scheme 2 there is a drastic decrease of the melting point and a marked increase of the solubility. For side chains of adequate lengths a new phenomenon, the formation of layered structures (see Fig. 12) occurs. By this peculiar arrangement an efficient packing of the molecules is achieved through separation of main and side chains.

5. Experimental Determination of Chain Stiffness

The determination of the shape, i.e. of the conformation of a macromolecule in the melt and in solution is one of the classical problems of polymer physics. Therefore, in the last 50 years a number of methods for determining the form of polymers have been developed. However, all these methods—except neutron scattering—require dissolution of the macromolecules. Due to their good solubility, flexible polymers could be studied by these methods with high precision. Hence, the shapes and conformations of flexible polymers are well known, whereas very little can be stated yet about the conformations of stiff macromolecules. This is due to the difficulties encountered in bringing stiff-chain polymers into solution. Before discussing these problems in more detail, an important chemical obstacle must first be mentioned.

The first requirement for chain stiffness is the correct structure of the chain, especially when the polymer has a ladder-like structure. A single open imide ring in the polyimide **17** would disrupt the rodlike character at this position and hence reduce chain stiffness considerably. Therefore polycondensation has to be conducted in such a manner that the formation of imide rings proceeds to practically 100% conversion, and open-structured intermediates like the polyamide acids in the preparation of the polyimides should be circumvented, if possible, in the case of polyimide **17** this can be achieved by reaction of pyromellitic anhydride with imidazole-blocked, substituted *p*-phenylene diisocyanates.[75,76] The synthesis of stiff-chain polymers with ladder-like structures thus requires a high standard regarding the completeness of reaction. In any case the degree of conversion should be checked by model reactions.

Once the problem of structure faults along the chains is solved, chain stiffness and conformation may be described in terms of three of the models presented schematically in Figure 14:

1) by *Flory*'s rotational isomeric state model (RIS),[87,88] in which the chain conformation and shape are described using molecular parameters (conformational energies, torsional angles) (cf. Fig. 2);

2) by the Kuhn model,[87,89] which idealizes the chain by a sequence of rods of length l_K (Kuhn length) held together by entirely flexible joints;
3) by the worm-like chain model of *Kratky* and *Porod*.[90] Here the chain is represented by a continuously bent stick or worm. Chain stiffness is characterized by the persistence length a; for very long chains[90] $2a = l_K$.

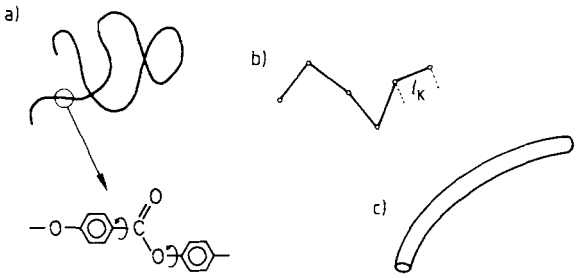


Fig. 14. Models for describing chain stiffness in polymers: a) RIS model (*Flory* [87, 88]); b) The Kuhn model [88, 89], l_K = Kuhn length; c) the —Kratky-Porod worm-like chain model [90] (see text).

The experimental determination of parameters necessary for the description in terms of the RIS model requires in most cases involved measurements of the depolarized light scattering of the electric and magnetic birefringence and the dipole moment of carefully chosen oligomers (cf. Refs. [15–17, 87, 88]). Very often these data are not available. Therefore in this context we only discuss methods for determining the Kuhn length or the persistence length of dissolved macromolecules. For this purpose the following methods are suitable:

1) Scattering methods[11,12,87,91–98] (light, X-ray, and neutron scattering)
2) Depolarized light scattering[87,98–101]
3) Electric and magnetic birefringence[87,101]
4) Flow induced birefringence[102]

Of these methods the scattering methods certainly give the most information with a minimum model assumptions. Therefore, a brief description of these methods and their data evaluation for assessment of chain stiffness will be given here. First the intensity of the light, X-ray, or neutron beam scattered by a solution of macromolecules is determined as a function of polymer concentration c_2 and the scattering angle θ. This experimental scattering intensity $I_{exp}(c_2, s)$ [$s = (4\pi/(\lambda)\sin(\theta/2)$] is then extrapolated to vanishing concentration.[93] Then the data are plotted in the following way:

$$\lim_{c_2 \to 0} \frac{Kc_2}{I_{exp}(s, c_2)} = \frac{1}{M_w I_n(s)} = \frac{1}{M_w}\left(1 + \frac{\langle R_g^2 \rangle}{3} s^2 + \cdots\right)$$

$$s\langle R_g^2 \rangle^{0.5} \ll 1$$

where M_w is the weight-average molecular weight, $\langle R_g^2 \rangle$ is the Z-average of the radius of gyration,[93] K is a constant depending on the radiation used and the system, and $I_n(s)$ is the structure or form factor of the single molecule.[103] The function $I_n(s)$ is normalized to 1 for $\theta = 0 : (I_n(0) = 1)$. The radius of gyration $\langle R_g^2 \rangle$ obtained from the slope of the above plot[93] in the region of small angles gives a measure of the spatial dimensions of the molecule. From the latter quantity the Kuhn length l_K may be calculated if the molecular weight distribution is known (see Ref. [11]).

If the polydispersity is not known with sufficient accuracy the determination of l_k becomes uncertain since the molecular weight distribution strongly influences this quantity.[91] As has been demonstrated by *Schmidt*[14] this problem may be overcome in an elegant way by combined measurements of the static and the dynamic light scattering, where the latter method yields additionally the hydrodynamic radius of the chain. Since this quantity only depends on the weight average of the degree of polymerization the polydispersity as well as the stiffness of the dissolved chains may be inferred in an unambiguous way.[14]

Further information is accessible from the form factor $I_n(s)$, the determination of which very often requires measurements of the X-ray and neutron scattering, since the range of s accessible in light scattering is too small in most cases. Figure 15 shows a reduced Kratky plot $I_n(s \cdot a)(s \cdot a)^2$ versus $s \cdot a$ for wormlike chains of differing stiffness.[11] For a better comparison the reduced variable $s \cdot a$ has been used instead of s. The parameter n indicated on the curve is the ratio of the length of the chain L to the persistence length a. Small length values of $n = L/a$ thus indicate high stiffness, whereas higher values of n characterize flexible macromolecules.

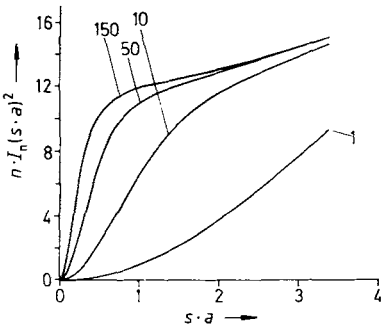


Fig. 15. Form factors of Kratky-Porod worm-like chains in a reduced plot (after [11]) a: persistence length, l: contour length of the macromolecule, $n = l/a$: number of persistence lengths per molecule is thus a measure of chain stiffness, i.e. $n \approx l$: great stiffness, $n \geq 100$: flexible coil (see detailed discussion in [11]).

In the case of flexible chains ($n = 200$) first a strong increase of $I_n(s)$ is observed, followed by a plateau-like region, and finally a practically linear region. Stiff chains, however, show only a weak upward curvature. A comparison of Figure 15 with experimentally obtained form factors may thus lead to an estimate of the chain stiffness. A problem in this comparison of experimental results with the above calculations is the finite diameter of the polymer chains leading to additional interferences not being taken into account in the above worm-like chain model of *Kratky* and *Porod*.[11] This effect is seen from a downward curvature of $I_n(s)s^2$ at higher values of s. The importance of this problem for a correct interpretation of $I_n(s)$ has been demonstrated recently by *Rawiso, Duplessix*, and *Picot*[104] using polystyrene as an example.

Whereas numerous measurements of the chain stiffness of polypeptides[24] and other biopolymers[12,92] have now been reported, only a few data are available on the synthetic systems discussed in Section 4. Thus, a compilation of persistence lengths obtained from typical polyamides in sulfuric acid[101] by methods 1)-4) (see above) contains results differing by one order of magnitude. This can be traced back mainly to the strong tendency for association of stiff chain macromolecules and the uncertainty regarding the molecular weight distribution. Consequently, there has been no quantitative study yet to assess the influence of fluctuations of the angle χ (cf. Fig. 2) on the RIS calculations of *Flory* et al.[15-17] *Birshtein*[105] has demonstrated theoretically that this effect may considerably reduce the persistence length. An experimental verification obtained from polydiacetylene in solution has been reported recently by *Allegra, Brückner, Schmidt* and *Wegner*.[106] First measurements on the soluble polyphthalocyaninatosiloxanes **18** unequivocally demonstrate the rodlike character of this polymer in agreement with the considerations given in Section 2.[107]

All the methods discussed above only allow the determination of chain stiffness and conformation of the single molecules in solution. The form factor of macromolecules in the melt or solid state can only be determined by neutron scattering on a mixture of protonated and deuterated molecules. Numerous such studies have been carried out on flexible macromolecules,[108] whereas to the best of the authors knowledge neutron scattering has not yet been applied to the systems discussed in Sections 4.1 and 4.2. The strong stiffening of chains through interactions with neighboring chains in the condensed phase has so far been demonstrated only by *Blackwell* et al.[49] on copolyamide **9** (Scheme 1, cf. Section 4.1).

6. On the Theory of Nematic Phases

As shown in Sections 4.1 and 4.2, stiff-chain macromolecules may form nematic as well as mesophases with a layered structure. In the course of this discussion it became evident that the arrangement of the chains is mainly determined by an efficient packing in space. In this section these considerations shall be discussed in more detail when dealing with the theory of nematic phases.

There are presently two fundamentally different approaches to the statistical mechanical description of nematic phases: 1) the Maier-Saupe theory[109] and its further development by *Luckhurst* et al.,[10] in which only the anisotropic attractive interactions between the rods are taken into account; 2) theories which are based on the repulsive interaction (excluded volume) and only introduce the attractive part of the potential afterwards.[111] Since it is well established today[112] that the structure of liquids is determined by repulsive interactions—i.e. by the form of the molecule—only theories which explicitly take this fact into account should come under discussion.

The statistical mechanics of ordered systems has been developed by the pioneering work of *Onsager*[113] and *Flory*.[114,115] Both authors were able to show by different methods that solutions of long rodlike molecules will spontaneously form nematic phases above a certain concentration. The fundamental concept of *Onsager* is depicted in Figure 16.[116] Consider a system of hard rods of length l and a square base with the length of the edges given by d. If the rods are aligned parallel to each other their volume is given by ld^2; this value coincides with the excluded volume of one molecule at dense packing. In dilute solution the excluded volume is of the order of l^2d. The volume fraction in solution at which the excluded volume of two rods is no longer negligible thus results in the ratio of d^2l to $l^2d = d/l$. Therefore it follows that the minimum volume fraction necessary for the formation of an ordered phase is proportional to the reciprocal axial ratio $x = l/d$ of the rods.

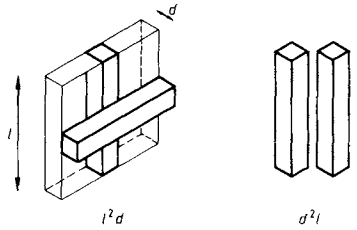


Fig. 16. Onsager theory of the isotropic to nematic phase transition: excluded volume of two rods in dilute solution (left) and in bulk (right).

This result can be quantitatively derived by the Onsager theory.[113] An important point of this statistical-mechanical treatment of a gas of long rods is the assumption that particles with different orientation may be treated as different thermodynamic components. Using this theory it was shown for the first time that systems without attractive interaction can only form ordered phases by steric repulsion. A major problem of Onsager's theory however, is the restriction of the calculation to purely binary interactions. Hence, the range of validity of this theory is confined to highly dilute solutions.[117] In addition to this shortcoming, the excluded volume per particle is overestimated in the frame of the Onsager theory. Hence the quantitative validity of the results derived therefrom has been doubted.[118]

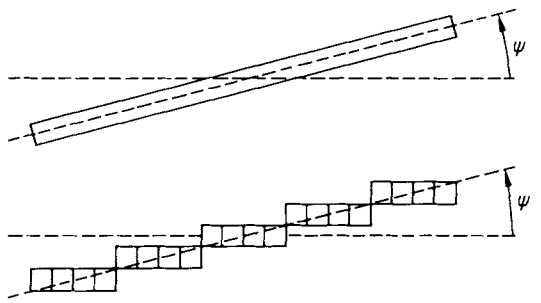


Fig. 17. Rendition of a rod in the lattice model of *Flory* [114, 115].

In contrast to Onsager's theory, the lattice model of *Flory* enables calculation over the entire range of concentration. The rod which forms an angle ψ with the preferred axis is represented in a cubic lattice by splitting up into submolecules[108] (see Fig. 17). By this artifice the partition

function can be calculated by the standard methods of lattice statistics. *Khokhlov* and *Semenov*[119] recently showed that the Flory theory reduces to the result of the so-called "decoupling approximation" by *Parsons*[120] at higher orientation; at vanishing concentration, the partition function of the Onsager theory is obtained.

The statistical-mechanical treatment of systems by rods over the entire range of concentration furthermore allows the calculation in the case of thermotropic nematic liquid crystals.[121-123] Thus, ordering transitions in condensed phases, in which attractive forces must also be taken into account may be dealt with in the framework of this model. Central to this extension of theory is the fact first put forward by *Flory* and *Ronca*[121] that only anisotropic dispersion forces matter. This can be explained in the following way: in dilute solution parallel alignment of two rods leads to more mutual contacts than a perpendicular arrangement; thus, ordering is favored if only binary interaction is considered. However, in condensed matter parallel alignment of molecules is not followed by an increase of interaction because cleavage of contacts between the two probe rods may be counteracted by formation of contacts with other rods. Hence, only anisotropic dispersion forces (Maier-Saupe interaction[109]) can directly promote ordering.

The above ideas are supported by a semiquantitative calculation of the so-called characteristic temperature of these anisotropic dispersion forces from optical and thermodynamic data.[124] Hence the nematic to isotropic transition temperatures of the homologous series of rod-shaped molecules[125, 126] can be described by a virtually constant characteristic temperature T^* which can be related directly to molecular parameters.[122, 123]

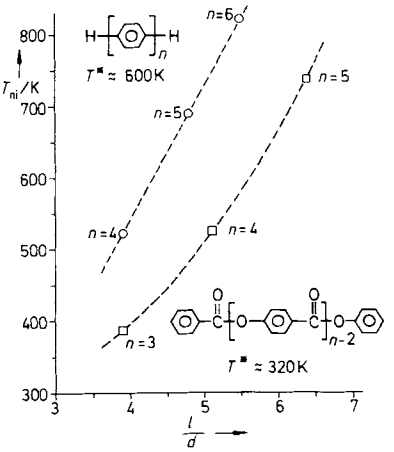


Fig. 18. Nematic-isotropic transition temperatures T_{ni} of two homologous series of rodlike molecules as a function of axial ratio l/d [122, 123]. The characteristic temperature T^* is a measure of the strength of the anisotropic dispersion forces [124].

Furthermore, the data in Figure 18 demonstrate the marked increase of the nematic-isotropic phase transition temperatures with increasing axial ratio, thus indicating directly and unambiguously the importance of the steric interactions between the rod-like molecule for the stability of the ordered phase.

A further advantage of the Flory theory lies in its applicability to a number of polymeric systems. This will be demonstrated in the following with flexible side chains already introduced in Section 4.2, while the second deals with mixtures of flexible and stiff macromolecules.

Stiff macromolecules with flexible side chains can be treated in the framework of the lattice model of *Flory* by introducing the main chain according to the Scheme shown in Figure 17 and appending the side chains in the sense of the Flory-Huggins statistics[127] for flexible chains. The details of this calculation have been described elsewhere[37] and will not be discussed here. The most important result of this theory is the finding that flexible side chains do indeed act to a good approximation like a "bound solvent" and shift the transition from the isotropic to the anisotropic solution to higher polymer concentrations.

An extension of this theory to thermotropic systems through introduction of anisotropic dispersion forces and free volume as indicated above[128] allows a direct comparison with the results obtained on stiff macromolecules with flexible side chains which form nematic phases (see Section 4.2). The experimental results on these systems again lead to the conclusion that flexible side chains are comparable to a solvent affixed to the rods. The above theory corroborates this concept also for the thermotropic systems under consideration here. The side chains weaken the steric as well as the attractive interaction between the main chains. These effects cause a continuous decrease of the transition temperature between nematic and isotropic phase, as observed experimentally on low molecular weight model systems[129] as well as on the polymers discussed in Section 4.2. Mesophases with layered structure observed in these systems with long side chains cannot be dealt with by this theory since the separation of main and side chains in the layers is not included in the model.

A further example for the broad applicability of the Flory model is given by the treatment of blends of stiff and flexible polymers, which is discussed in the following.

Mixtures of flexible polymers have been in use technologically for some time, and have been the subject of many scientific investigations in recent years.[130] The phase behavior and the compatibility of these systems can be described to a good approximation in terms of the Flory-Huggins theory,[127, 130, 131] which gives the following expression for the free energy of the mixture:

$$\Delta F_n/RT = \frac{\phi_1}{x_1}\ln\phi_1 + \frac{\phi_2}{x_2}\ln\phi_2 + \phi_1\phi_2\chi$$

The quantities ϕ_1 and ϕ_2 denote the volume fractions of the polymeric components and x_1 and x_2 their number of segments. The interaction parameter χ is a function of temperature and concentration in general.[131] However, this equation only holds true for isotropic systems. If there is liquid crystalline order in one phase the Flory-Huggins theory is no longer applicable. As has been demonstrated by *Flory*[132] demixing already occurs in purely athermal systems, i.e., when $\chi = 0$. Hence, the reason for this phase separation is of solely entropic nature. The ordered nematic phase formed during demixing excludes the flexible com-

ponent with high selectivity. This prediction could be fully verified for a number of ternary systems consisting of a flexible and a stiff polymer dissolved in a common solvent.[133]

An extension of the Flory model to include thermotropic mixtures of stiff and coiled macromolecules shows[134] that in this case incompatibility also results. This effect is more pronounced with increasing molecular weight of both compounds. Figure 19 illustrates this effect using as example the mixture of short-chain polystyrene and low molecular weight *p*-butyl-*N*-(*p*-ethoxybenzylidene)aniline, which typically forms thermotropic liquid crystals.[135]

In the isotropic phase both components are fully miscible. Cooling leads to an isotropic phase containing most of the polymer whereas the coexisting nematic phase has only a very small content thereof. The calculated phase diagram in Figure 19 (bold lines) shows that theory is in qualitative agreement with the experimental results of *Kronberg* et al.[134] All results given herein lead to the conclusion that mixtures of stiff and flexible polymers are incompatible upon formation of an ordered phase. For an isotropic mixture, however, the expression by *Flory* and *Huggins* is still valid, demixing is caused by an unfavorable enthalpic interaction. The realization of such a compatible mixture of a stiff chain and a flexible polymer (molecular composite) is of great technical interest since the favorable mechanical properties of composites could be obtained without having to tolerate internal surfaces as are formed by incorporation of glass and carbon fibers in conventional composite materials. Theoretical considerations[136] suggest that this goal may be achieved using the stiff macromolecules with flexible side chains introduced in Section 4.2.[136]

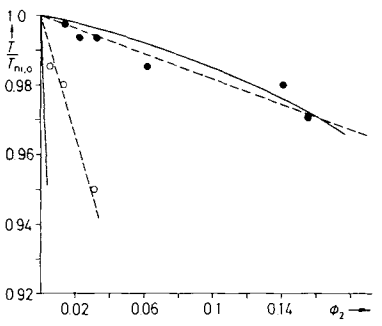


Fig. 19. Phase diagram of a mixture of oligomeric polystyrene (weight average molecular weight 4000) and the low molecular weight *p*-butyl-*N*-(*p*-ethoxybenzylidene)aniline, which forms nematic liquid crystals. Circles: experimental data of *Patterson* et al. [135] (open: nematic phase, filled: isotropic phase); bold curve: theoretical phase diagram [134].

7. Properties

The foregoing sections have shown that chain stiffness in macromolecular systems can cause the formation of highly ordered structures in solution, in the melt and in the solid state. The concepts introduced in Section 4 facilitate access to systems which are sufficiently soluble and melt undecomposed. In this section a brief overview of the technical application of such systems will be given.

As already mentioned in the introduction, the discovery of liquid crystalline order in solutions of poly-*p*-phenyleneterephthalamide **1** and the possibility of spinning this material from such solutions to high modulus fibers was the starting point for the intensive technical fabrication of stiff-chain macromolecules.[4,5,41,137,138] These fibers have a specific modulus higher than steel and exhibit a high thermal stability and a small thermal expansion coefficient.[138] The excellent mechanical properties are mainly traced back to the high orientation along the fiber axis. A short heat treatment at temperatures around 300 °C can even improve these mechanical properties. Since thermal polycondensation is rather slow in these systems the observed improvement must be mainly due to an increase of orientation and crystallinity. Fibers spun from poly-(*p*-phenylbenzodithiazole) **5** dissolved in polyphosphoric acid and subjected to a subsequent heat treatment[138] have an even higher modulus. All systems discussed up to this point require the use of strong mineral acids as solvent. In contrast, the copolyamide **9** (Scheme 1) can be spun from *N*-methylpyrrolidone (cf. Section 4.1,[47,48]) and obviates the use of mineral acids.

The aromatic polyesters introduced in Section 4 may be processed from the thermotropic mesophase if the content of disrupting units along the chains (Section 4.1) or the number of flexible side chains (Section 4.2) is high enough. Thus, aggressive or expensive solvents are no longer required making these materials interesting candidates for a wide spectrum of technical applications. Here also a heat treatment leads to considerable improvement in the mechanical properties.[139] In contrast to the polyamides, polycondensation in the solid-state plays an important role in this process.[138] Important copolyesters already produced in large-scale quantities are "Vectra" (Hoechst-Celanese) (cf. **7**) and "Xydar" (Dartco), which is the copolyester of terephthalic acid, *p*-hydroxybenzoic acid and 4,4'-biphenyldiol (cf. Section 4.1 and Ref. [138]). High-strength fibers can be spun from these materials. In addition to this the lower viscosity of the nematic phase[85] facilitates processing from the melt. The main areas of application of these stiff-chain polyamides and polyesters are as fibers for the fabrication of offshore cables, bullet resistant vests, rubber reinforcement tires, i.e., in all areas where high strength and light weight are required. Thermotropic polyesters have the advantage of being processable at temperatures below thermal decomposition. In addition to this they exhibit high flame resistance, small thermal expansion coefficients and small shrinkage upon cooling to room temperature, thus enabling the molding of intricate parts such as are needed for instance in microelectronics. Special properties such as the high transparency for microwaves and the high heat-deflection temperature make "Xydar" suitable for microwave ovenware. The insolubility in common organic solvents and the higher temperatures at which these materials can still be used allow their use in chemical equipment. This list, which is far from complete, already gives an idea of the numerous applications of these new materials. One problem, however, is the poor compressive strength. The mechanical properties measured perpendicular to the preferred direction are considerably poorer than those determined along the chain direction.

Fillers can improve these properties to a certain extent.[138] It seems, however, that a more fruitful way to solve this problem is a better control of structure and morphology in the solid state (see Section 4).

In conclusion, stiff-chain polymers are a very interesting class of new materials, both from the scientific point of view as well as from the point of view of possible applications. The potential of these promising polymers is still far from being exhausted and there will be more important developments in this field in the near future.

The author is indebted to Prof. Dr. G. Wegner and Dr. G. Lieser for stimulating discussions and critical revision of the manuscript. Financial support of the Bundesminister für Forschung und Technologie, Project "Steife Makromoleküle" is gratefully acknowledged.

Received: June 20, 1988 [A 711 IE]
German version: *Angew. Chem. 101* (1989) 261

[1] M. Doi, S. F. Edwards: *Theory of Polymer Dynamics*, Oxford University Press, Oxford 1986.
[2] S. Chandrasekhar: *Liquid Crystals*, Cambridge University Press, Cambridge 1974.
[3] P. G. de Gennes: *The Physics of Liquid Crystals*, Clarendon Press, Oxford 1974.
[4] P. W. Morgan, *Macromolecules 10* (1977) 1381.
[5] S. L. Kwolek, P. W. Morgan, J. R. Schaefer, L. W. Gulrich, *Macromolecules 10* (1977) 1390.
[6] H. Finkelmann, *Angew. Chem. 99* (1987) 840; *Angew. Chem. Int. Ed. Engl. 26* (1987) 816.
[7] See *Adv. Polym. Sci. 59-61* (1984) and *Faraday Discuss. Chem. Soc. 79* (1985).
[8] R. D. Joyner, M. E. Kennedy, *Inorg. Chem. 1* (1962) 717; M. Hartman, G. Meyer, D. Wöhrle, *Makromol. Chem. 176* (1975) 831; E. Orthmann, V. Enkelmann, G. Wegner, *Makromol. Chem. Rapid Commun. 4* (1983) 687.
[9] J. F. Wolfe, B. H. Loo, F. E. Arnold, *Macromolecules 14* (1981) 915.
[10] A.-D. Schlüter, *Macromolecules 21* (1988) 1208; *Angew. Chem. 100* (1988) 283; *Angew. Chem. Int. Ed. Engl. 27* (1988) 296.
[11] For the chain stiffness of DNA see R. G. Kirste, R. C. Oberthür in O. Glatter, O. Kratky (Eds.): *Small Angle X-ray Scattering*, Academic Press, London 1982, p. 387.
[12] T. Conielo, K. Kajiwara, W. Burchard, M. Bentini, N. Crescenzi, *Macromolecules 19* (1986) 2826, and references cited therein.
[13] I. Uematsu, Y. Uematsu, *Adv. Polym. Sci. 59* (1984) 37; H. Hanabusa, M. Sato, H. Shirai, K. Takemoto, E. Iizuka, *J. Polym. Sci. Polym. Lett. Ed. 22* (1984) 559.
[14] M. Schmidt, *Macromolecules 17* (1984) 553.
[15] P. A. Irvine, B. Erman, P. J. Flory, *J. Phys. Chem. 87* (1983) 2929.
[16] J. P. Hummel, P. J. Flory, *Macromolecules 13* (1980) 479.
[17] B. Erman, P. J. Flory, J. P. Hummel, *Macromolecules 13* (1980) 484. Concerning rotational barriers in amide and ester bonds, see: H. Kessler, *Angew. Chem. 82* (1970) 237; *Angew. Chem. Int. Ed. Engl. 9* (1970) 219; H. R. Kricheldorf, G. Schilling, *Makromol. Chem. 178* (1977) 3115.
[18] W. R. Krigbaum, *Faraday Discuss. Chem. Soc. 79* (1985) 133.
[19] H. Schiff, *Ber. Dtsch. Chem. Ges. 15* (1882) 2588.
[20] A. Klepl, *J. Prakt. Chem. 28* (1883) 194.
[21] E. Fischer, K. Freudenberg, *Justus Liebigs Ann. Chem. 372* (1910) 32.
[22] R. Gilkey, J. R. Caldwell, *J. Appl. Polym. Sci. 2* (1959) 198.
[23] J. Economy, R. S. Storm, V. I. Matkovich, S. G. Cottis, *J. Polym. Sci. Polym. Chem. Ed. 14* (1976) 2207.
[24] H. R. Kricheldorf, G. Schwarz, *Polym. Bull. 1* (1979) 383.
[25] H. R. Kricheldorf, G. Schwarz, *Makromol. Chem. 184* (1983) 475.
[26] H. R. Kricheldorf, G. Schwarz, *Polymer 25* (1984) 520.
[27] a) G. Lieser, *J. Polym. Sci. Polym. Phys. Ed. 21* (1983) 1611; b) S. Hanna, A. H. Windle, *Polymer 29* (1988) 236; c) *J. Economy* et al. have recently reported a second high temperature phase transition, which was identified through application of extreme heating rates (320 k/min) in the DSC: J. Economy, W. Volksen, C. Viney, R. Geiss, R. Siemens, T. Karis, *Macromolecules 21* (1988) 2777.
[28] G. Lieser, G. Schwarz, H. R. Kricheldorf, *J. Polym. Sci. Polym. Phys. Ed. 21* (1983) 1599.
[29] H. R. Kricheldorf, A. Conradi, *Macromolecules*, in press.
[30] For a review see: R. W. Lenz, *Faraday Discuss. Chem. Soc. 79* (1985) 21.
[31] A. Blumstein, M. Gauthier, O. Thomas, R. B. Blumstein, *Faraday Discuss. Chem. Soc. 79* (1985) 33.
[32] W. J. Jackson, Jr., *Br. Polym. J. 12* (1980) 154.
[33] B. P. Griffin, M. K. Cox, *Br. Polym. J. 12* (1980) 147.
[34] J. Majnusz, J. M. Catala, R. W. Lenz, *Eur. J. Polym. J. 19* (1983) 1043.
[35] H.-R. Dicke, R. W. Lenz, *J. Polym. Sci. Polym. Chem. Ed. 21* (1983) 2581.
[36] G. V. Laivins, D. G. Gray, *Macromolecules 18* (1985) 1783.
[37] M. Ballauff, *Macromolecules 19* (1986) 1366.
[38] M. Ballauff, *Makromol. Chem. Rapid Commun. 7* (1986) 407.
[39] G. W. Calundann, M. Jaffe, *Proc. Robert A. Welch Found. Conf. Chem. Res. 26* (1982) 247.
[40] G. W. Calundann, US-Pat. 4161470 (1974), Celanese.
[41] T.-S. Chung, *Polym. Eng. Sci. 26* (1986) 901.
[42] G. Schwarz, *Dissertation*, Universität Freiburg 1981.
[43] R. Rosenau-Eichin, M. Ballauff, J. Grebowicz, E. W. Fischer, *Polymer 29* (1988) 518.
[44] L.-S. Li, G. Lieser, R. Rosenau-Eichin, E. W. Fischer, *Makromol. Chem. Rapid Commun. 8* (1987) 159.
[45] H. R. Kricheldorf, A. Conradi, G. Schwarz, *Angew. Makromol. Chem. 145/146* (1986) 259.
[46] H. R. Kricheldorf, A. Conradi, R. Pakull, G. Schwarz, *Makromol. Chem. Symp.*, in press.
[47] S. Ozawa, Y. Nakagawa, K. Matsuda, T. Nishihara, H. Yuroki, Jpn. Pat. Doc. 52-37719 (1952); 53-32838 (1953).
[48] K. Matzuda, *Polym. Prepr. Am. Chem. Soc. Div. Polym. Chem. 20* (1979) 122.
[49] J. Blackwell, R. A. Cageao, A. Biswas, *Macromolecules 20* (1987) 667.
[50] J. Blackwell, A. Biswas, G. A. Gutierrez, R. A. Chivers, *Faraday Discuss. Chem. Soc. 79* (1985) 73, and references cited therein.
[51] A. Biswas, J. Blackwell, *Macromolecules 20* (1987) 2997.
[52] R. Bonart, G. Mulzer, J. Dietrich, *Makromol. Chem. 188* (1987) 637.
[53] R. Bonart, *Makromol. Chem. 188* (1987) 1187; R. Bonart, J. Dietrich, H. Zott, *ibid. 189* (1988) 227.
[54] R. Bonart, J. Blackwell, A. Biswas, *Makromol. Chem. Rapid Commun. 6* (1985) 353.
[55] L. A. Alexander: *X-ray Diffraction Methods in Polymer Science*, Krieger, Huntington, NY 1979.
[56] A. H. Windle, C. Viney, R. Golombok, A. M. Donald, G. R. Mitchell, *Faraday Discuss. Chem. Soc. 79* (1985) 55.
[57] S. Hanna, A. H. Windle, *Polymer 29* (1988) 207.
[58] R. Golombok, S. Hanna, A. H. Windle, *Mol. Cryst. Liq. Cryst. 155* (1988) 281.
[59] R. Rosenau-Eichin, *Dissertation*, Universität Mainz 1987.
[60] M. Ballauff, R. Rosenau-Eichin, E. W. Fischer, *Mol. Cryst. Liq. Cryst. 155* (1988) 211.
[61] D. J. Blundell, *Faraday Discuss. Chem. Soc. 79* (1985) 108.
[62] C. Viney, G. R. Mitchell, A. H. Windle, *Mol. Cryst. Liq. Cryst. 129* (1985) 75.
[63] F. Hessel, H. Finkelmann, *Polym. Bull. 15* (1986) 349; F. Hessel, R.-P. Herr, H. Finkelmann, *Makromol. Chem. 188* (1987) 1597.
[64] M. Ebert, O. Hermann-Schönherr, J. H. Wendorff, H. Ringsdorf, P. Tschirner, *Makromol. Chem. Rapid Commun. 9* (1988) 445.
[65] H. W. Spiess, *Adv. Polym. Sci. 66* (1985) 24.
[66] H. W. Spiess, *Colloid Polym. Sci. 261* (1983) 193.
[67] K. Müller, P. Meier, G. Kothe, *Prog. Nucl. Magn. Reson. Spectrosc. 17* (1985) 211.
[68] H. Bechtholdt, J. H. Wendorff, H. J. Zimmermann, *Makromol. Chem. 188* (1987) 651; T. H. Sauer, J. H. Wendorff, H. J. Zimmermann, *J. Polym. Sci. Polym. Phys. Ed. 25* (1987) 2471.
[69] K. Berger, M. Ballauff, *Mol. Cryst. Liq. Cryst. 157* (1988) 109.
[70] M. Ballauff, G. F. Schmidt, *Makromol. Chem. Rapid Commun. 8* (1987) 93.
[71] M. Ballauff, G. F. Schmidt, *Mol. Cryst. Liq. Cryst. 147* (1987) 163.
[72] M. Ballauff, *Makromol. Chem.*, in press.
[73] O. Hermann-Schönherr, J.-H. Wendorff, H. Ringsdorf, P. Tschirner, *Makromol. Chem. Rapid Commun. 7* (1986) 791.
[74] R. Stern, M. Ballauff, G. Wegner, *Makromol. Chem.*, in press.
[75] M. Bartmann, M. Dröscher, J. Finke, M. Wenzel, M. Ballauff, G. Wegner, Dtsch. Pat.-Anm. P370 1249.5.
[76] M. Wenzel, M. Ballauff, G. Wegner, *Makromol. Chem. 188* (1987) 2865.
[77] E. Orthmann, *Dissertation*, Universität Mainz 1986.
[78] H. Ringsdorf, P. Tschirner, O. Hermann-Schönherr, J. H. Wendorff, *Makromol. Chem. 188* (1987) 1431.
[79] T. Sauer, G. Wegner, *Mol. Cryst. Liq. Cryst.*, in press.
[80] C. Sirlin, L. Bosio, J. Simon, *J. Chem. Soc. Chem. Commun. 1987*, 379.
[81] U. Falk, B. Westermark, C. Boeffel, H. W. Spiess, *Mol. Cryst. Liq. Cryst. 153* (1988) 199.

[82] U. Falk, A. Adam, H. W. Spiess, unpublished; A. Whittaker, U. Falk, H. W. Spiess, *Makromol. Chem.*, in press.
[83] T. Dries, K. Fuhrmann, M. Ballauff, E. W. Fischer, unpublished.
[84] H. Gasparoux, B. Regaya, J. Prost, *C. R. Hebd. Séances Acad. Sci. Ser. B 272* (1971) 1168.
[85] K. F. Wissbrun, *Faraday Discuss. Chem. Soc. 79* (1985) 161, and references cited therein.
[86] C. Schrauwen, M. Ballauff, G. Wegner, unpublished.
[87] P. J. Flory: *Statistical Mechanics of Chain Molecules*, Interscience, New York 1969.
[88] P. J. Flory, *Macromolecules 7* (1974) 381.
[89] W. Kuhn, *Kolloid-Z. 68* (1934) 2.
[90] O. Kratky, G. Porod, *Recl. Trav. Chim. Pays-Bas 68* (1949) 1106; G. Porod, *Monatsh. Chem. 80* (1949) 251.
[91] M. Schmidt, G. Paradossi, W. Burchard, *Makromol. Chem. Rapid Commun. 6* (1985) 767.
[92] See summary by O. Kratky in O. Glatter, O. Kratky (Eds.): *Small Angle X-Ray Scattering*, Academic Press, London 1982, p. 3.
[93] See particularly Refs. [11], [14], and references cited therein.
[94] R. C. Oberthür, *Dissertation*, Universität Mainz 1974.
[95] P. Metzger-Cotts, G. C. Berry, *J. Polym. Sci. Polym. Phys. Ed. 21* (1983) 1255.
[96] C. C. Lee, S.-G. Chu, G. C. Berry, *J. Polym. Sci. Polym. Phys. Ed. 21* (1983) 1573.
[97] M. Arpin, C. Strazielle, *Makromol. Chem. 177* (1976) 581.
[98] W. R. Krigbaum, T. Tanaka, *Macromolecules 21* (1988) 743.
[99] Q. Ying, B. Chu, *Makromol. Chem. Rapid Commun. 5* (1984) 785.
[100] M. Arpin, C. Strazielle, G. Weill, H. Benoit, *Polymer 18* (1977) 262.
[101] K. Zero, S. M. Aharoni, *Macromolecules 20* (1987) 1957.
[102] V. N. Tsvetkov, L. N. Andreeva, *Adv. Polym. Sci. 39* (1981) 95.
[103] See also Rfs. [11] and [14].
[104] M. Rawiso, R. Duplessix, C. Picot, *Macromolecules 20* (1987) 630.
[105] T. M. Birshtein, *Polym. Sci. USSR (Engl. Transl.) 16* (1974) 60.
[106] G. Allegra, S. Brückner, M. Schmidt, G. Wegner, *Macromolecules 19* (1986) 399; cf. also Ref. [89].
[107] U. Caseri, T. Sauer, G. Wegner, *Makromol. Chem. Rapid Commun. 9* (1988) 651.
[108] See review by G. Wignall in H. F. Mark, N. M. Bikales, C. G. Overberger, G. Menges (Eds.): *Encyclopedia of Polymer Science and Engineering*, Wiley, New York 1987, Vol. 10, p. 112.
[109] W. Maier, A. Saupe, *Z. Naturforsch. A 13* (1958) 564; *A 14* (1959) 882; *A 15* (1960) 287.
[110] G. R. Luckhurst in G. R. Luckhurst (Ed.): *The Physics of Liquid Crystals*, Academic Press, London 1979, p. 85.
[111] M. A. Cotter, *Mol. Cryst. Liq. Cryst. 97* (1983) 29.
[112] H. C. Anderson, D. Chandler, J. D. Weeks, *Adv. Chem. Phys. 34* (1976) 105.
[113] L. A. Onsager, *Ann. N. Y. Acad. Sci. 51* (1949) 627.
[114] P. J. Flory, *Proc. R. Soc. London A 234* (1956) 73.
[115] P. J. Flory, *Adv. Polym. Sci. 59* (1984) 1; P. J. Flory, G. Ronca, *Mol. Cryst. Liq. Cryst. 54* (1979) 289.
[116] Cf. also Ref. [1].
[117] J. P. Straley, *Mol. Cryst. Liq. Cryst. 24* (1973) 7.
[118] A. Saupe, *J. Phys. (Orsay, Fr.) C 3 40* (1979) 207.
[119] A. R. Khokhlov, A. N. Semenov, *J. Statist. Physics 38* (1985) 161.
[120] J. D. Parsons, *Phys. Rev. A 19* (1979) 1225; see also S.-D. Lee, *J. Chem. Phys. 87* (1987) 4972.
[121] P. J. Flory, G. Ronca, *Mol. Cryst. Liq. Cryst. 54* (1979) 311.
[122] P. J. Flory, P. A. Irvine, *J. Chem. Soc. Faraday Trans. 1 80* (1984) 1807.
[123] M. Ballauff, P. J. Flory, *Ber. Bunsenges. Phys. Chem. 88* (1984) 530.
[124] P. A. Irvine, P. J. Flory, *J. Chem. Soc. Faraday Trans. 1 80* (1985) 1821; see also M. Warner, *J. Chem. Phys. 73* (1980) 5874.
[125] P. A. Irvine, P. J. Flory, D. Wu, *J. Chem. Soc. Faraday Trans. 1 80* (1984) 1795.
[126] M. Ballauff, D. Wu, P. J. Flory, E. M. Barrall II, *Ber. Bunsenges. Phys. Chem. 88* (1984) 524.
[127] P. J. Flory: *Principles of Polymer Chemistry*, Cornell University Press, Ithaca 1953.
[128] M. Ballauff, *Liq. Cryst. 2* (1987) 519.
[129] D. Demus, S. Diele, A. Hauser, I. Latif, C. Selbmann, W. Weissflog, *Cryst. Res. Technol. 20* (1985) 1547, and references cited therein.
[130] See summary by B. J. Schmitt, *Angew. Chem. 91* (1979) 286; *Angew. Chem. Int. Ed. Engl. 18* (1979) 273; *Ber. Bunsenges. Phys. Chem. 89* (1985) 1133.
[131] R. Koningsveld, L. A. Kleintjens, A. M. Leblans-Vinck, *Ber. Bunsenges. Phys. Chem. 89* (1985) 1234.
[132] P. J. Flory, *Macromolecules 11* (1978) 1138.
[133] E. Bianchi, A. Cifferi, G. Conio, E. Marsano, A. Tealdi, *Macromolecules 17* (1984) 1526, and references cited therein.
[134] M. Ballauff, *Ber. Bunsenges. Phys. Chem. 90* (1986) 1053.
[135] B. Kronberg, I. Bassignana, B. Patterson, *J. Phys. Chem. 82* (1978) 1714.
[136] M. Ballauff, *J. Polym. Sci. Polym. Phys. Ed. 25* (1987) 739.
[137] S. L. Kwolek, US-Pat. 3671542 (1972), E. I. duPont de Nemours & Co.
[138] S. L. Kwolek, P. W. Morgan, J. R. Schaefgen in H. F. Mark, N. M. Bikales, C. G. Overberger, G. Menges (Eds.): *Encyclopedia of Polymer Science and Engineering*, Wiley, New York 1987, Vol. 9, p. 1.
[139] R. R. Luise, US-Pat. 4183895 (1980), E. I. du Pont de Nemours & Co.

Theoretical Chemistry en route to a Theory of Chemistry

By Anton Amann* and Werner Gans*

Quantum mechanical and classical aspects are of equal importance in chemistry, and theoretical chemistry must be able to deal with this situation. Classical quantities with which a chemist has to deal include, for example, the temperature and the chemical potential of a substance, and chirality, knot-type and tertiary structures of molecules. Classical concepts of this type are no more consequences of traditional quantum chemistry than is the theory of complex chemical processes (for example adsorption, heterogeneous catalysis) and macroscopic systems. Algebraic quantum mechanics affords a general framework for the discussion of classical quantities and large systems. There are other independent approaches for the theoretical treatment of chemical problems; these can be summarized by using the keywords "fractals", "chaotic motion", "quasicrystals" and "knot theory". The relationships between these four research topics and their connection with algebraic quantum mechanics, as well as their importance for theoretical chemistry, were discussed at a NATO Workshop in 1987 (see Ref. [1]). In an extended theoretical chemistry, the notion of "molecules" will not play a role as central as it does in quantum chemistry. In the theory of large systems in particular, the introduction of complementary approaches appears to be appropriate; the term "molecule" as used by the chemist does not appear either in the description of disordered systems by means of fractals or in the thermodynamic limit of algebraic statistical mechanics.

1. Introduction

The last great advance in theoretical chemistry was due to the introduction of quantum mechanics; quantum chemistry, with the help of which it is now possible to carry out extremely accurate calculations of molecular properties, developed parallel to the development of computer technology. However, many other equally important aspects of chemistry have been forgotten by theoretical chemists; these include the term "substance", classes of compounds, and states of aggregation as well as attempts to understand chirality or macroscopic properties of large systems from a theoretical point of view. The contact with traditional theoretical areas of chemistry, such as thermodynamics and chemical kinetics, is very small; due to the great variety of chemical reactions the quantum-chemical treatment of kinetic problems is still in its infancy. In the course of time, quantum chemistry has seen the development of a large number of models (MO, VB, Hückel, "coupled electron pair approximation" (CEPA), and many others) which, although they all have a quantum-mechanical basis, are always adapted to a specific situation and often contain approximations which are dictated more by computational possibilities than by physical or chemical intuition. Important aspects of quantum mechanics are thus lost, and models are much less than a theory (and at best a good caricature) of a physical or chemical system. Models (e.g., the Ising model, the Debye-Hückel model for solvation shells of ions, electronegativity models) are useful or stimulating for the scientist's everyday work, but they are by definition never correct or incorrect.

A theory, however, makes a serious claim to represent the truth, and is characterized by three aspects:

- a mathematical formalism (guarantees the absence of contradictions)
- a clearly defined area within which it is valid ("universe of discourse", i.e., much more than a specific situation)
- an interpretation

In the case of quantum mechanics, these are the Hilbert space formalism, the restriction to the forms in which molecular matter is organized, and an interpretation which allows the chemist to deal in the same fashion with large and small systems.

Since quantum mechanics as a theory is highly developed, it has a considerable regulating influence; this refers generally to the formal requirements which a theory must fulfill. Above all however, other—as a rule classical—theories and observables should be compatible with quantum mechanics in a particular and well-specified sense. The development of theories takes place on many levels, so that in Section 3, four modern research areas which are of importance for theoretical chemistry will be presented. In Sections 2 and 4 we shall list reasons why numerical quantum chemistry, which with its molecular view of the world of chemistry is so successful in many ways, cannot deal with all those phenomena which require a theoretical explanation. The choice of topics dealt with in Section 3 is certainly not exhaustive, but it should indicate the direc-

[*] Dr. A. Amann
Laboratorium für Physikalische Chemie, ETH-Zentrum
CH-8092 Zürich (Switzerland)
Dr. W. Gans
Fachbereich Chemie der Freien Universität
Institut für Physikalische und Theoretische Chemie
Takustrasse 3, D-1000 Berlin 33

tion in which theoretical chemistry must progress if it is to create order and establish correlations in the rich area of chemical phenomenology.

2. Classical Quantities in Chemistry

Chemistry contains an enormous amount of empirical knowledge, which was originally collected and interpreted without the theoretical background of quantum mechanics. Most of the terms used by chemists are either related to terms from classical physical theories or are taken directly from these. Some examples are temperature, chemical potential, chirality, knot types in polymers (e.g., a DNA molecule) and nuclear frames of molecules.

Quantum mechanics in its original codification by *von Neumann* (Hilbert space quantum mechanics)[2] has only little in common with the terms mentioned above. It is not able to describe the quantities of classical physics (see the appendix to this section). However, in his later publications, dealing with the theory of operator algebras, *von Neumann* himself laid the foundations for the extension of the formalism of quantum mechanics.

Classical quantities or observables are characterized by the fact that they have dispersion-free expectation values in *each* state of the system under consideration. As is well-known, this is not true for the quantum mechanical observables (operators) position $\boldsymbol{Q}$ and momentum $\boldsymbol{P}$, whose properties are determined by Heisenberg's uncertainty principle: $[\boldsymbol{Q},\boldsymbol{P}] = \boldsymbol{QP} - \boldsymbol{PQ} = \mathrm{i}\hbar\boldsymbol{I}$, i.e., $\boldsymbol{Q}$ and $\boldsymbol{P}$ do not commute. Classical observables, however, commute not only with one another but also with all other observables which are present in the system. If the set of observables is extended on mathematical grounds to form an algebra, one says that the classical observables lie in the center of this algebra (for details see appendix). If an algebra of observables consists only of the center, the result is a completely classical theory; classical point mechanics, for example, can be thus described (the Koopman formalism[3]). Classical theories and quantum mechanics are of comparable importance in chemistry; the non-existence of classical quantities would in any case be contrary to the chemist's experience.

In general, chemical systems can be characterized by the observables (what do we see?) and their dynamics (what happens as time progresses?). We shall use the example of the chirality of molecules to show how it is possible by including systems with (infinitely) many degrees of freedom (and by a corresponding generalization of quantum mechanics: see appendix) to obtain classical observables, and also to show the consequences for the possible states of the system.

Chiral molecules, e.g., the amino acid alanine, are always dextro- or laevorotatory (D,L; *R*,*S*; +/− according to the preferred terminology). If $\boldsymbol{\Psi}_\mathrm{D}$ and $\boldsymbol{\Psi}_\mathrm{L}$ denote the corresponding ground state vectors, the rules of Hilbert space quantum mechanics also allow the existence of their superposition $\boldsymbol{\Psi}_0 \stackrel{\mathrm{def}}{=} 1/\sqrt{2}\,(\boldsymbol{\Psi}_\mathrm{D} + \boldsymbol{\Psi}_\mathrm{L})$. The totally symmetric (pure) ground state described by $\boldsymbol{\Psi}_0$ has, however, not been detected experimentally. It may exist, but if so it is short-lived and unstable. An experimental method for its detection has been suggested by *Quack*.[4] It must be remembered that $\boldsymbol{\Psi}_0$ has nothing to do with the clearly existent racemate, which is described by a density operator. A suggested solution to the problem presented here is as follows: the fiction of an isolated molecule should be discarded. Each molecule is in fact coupled to the radiation field, and the inclusion of the radiation field (a system consisting of an infinite number of bosons) leads to a qualitatively completely new discussion of the molecular system. An important keyword is the "infrared singularity". The conceptually clearly posed problems of this approach have not yet been solved in all mathematical details. The following (simplified) picture[5,6] results: if the energy difference of the two lowest eigenvalues of the molecular Hamiltonian operator is small enough (the corresponding eigenstates are then almost degenerate), two ground states exist for the complete system (molecule plus radiation field). These are interconvertible via space inversion and are thus chiral. The corresponding chiral state vectors lie in different sectors (see appendix) and thus may not be superposed. The condition of the near-degeneracy of the molecular eigenstates is important; it is fulfilled for alanine, but not, for example, for the potentially chiral ammonia isotopomer NHDT. The transition from alanine to NHDT thus represents a kind of qualitative jump. Alanine is characterized by a classical chirality observable, which commutes with all other observables and has the dispersion-free values of +1 or −1, depending on whether the state under study is laevo- or dextrorotatory. In contrast, NHDT and ammonia behave as isolated molecules, even when coupled to the radiation field, i.e., the totally symmetric state described by $\boldsymbol{\Psi}_0$ does exist. "Chiral" states for ammonia are not forbidden by the rules of quantum mechanics and have been prepared in the course of molecular beam experiments; they are non-stationary states corresponding to the chemist's "pyramid".

The instability of the totally symmetric ground state of a chiral molecule is perhaps also due to other effects, e.g. collisions with neighboring molecules. If the state described by $\boldsymbol{\Psi}_0$ is to be prepared experimentally, all effects of this type must be excluded. An interesting aspect of this discussion is provided by the non-inversion-invariant terms in the Hamiltonian operator, which correspond to the "weak neutral current in atomic nuclei" (cf. [4]). The coupling of molecules to their environment, and in particular to the radiation field, is, however, interesting and important in its own right, and not merely because of the chirality problem; it is responsible for the formation of the chemist's "quasi-molecules" with partially classical properties.

The chirality (of molecules) is an example of a classical observable; another is the temperature (of substances). Superpositions between thermal equilibrium states at different temperatures are thus forbidden.[7] The knot type of a (DNA) molecule is also conceptually a good example of a chemically relevant classical observable: superpositions of molecules with different knot patterns (see Section 3) are not observed experimentally. The knot type of a molecule is clearly and unequivocally determined (dispersion-free), but it is still completely unclear how to arrive at the corresponding classical observable. However, the examples of

chirality and temperature (among others) show that it is possible to derive classical observables with the help of the extended quantum-mechanical formalism even without resorting to ad hoc rules. In these two cases the large (infinite) number of degrees of freedom of the radiation field or of the macroscopic thermodynamic system plays a vital role in the emergence of the relevant classical observable.

Appendix

The basis for the following discussion is the Hilbert space $\mathscr{H}$ of the state vectors Ψ, on which a scalar product is defined. Observables such as the position Q and the momentum P are always described by (self-adjoint) linear operators, i.e., linear maps of the Hilbert space into itself. In the case of quantum mechanics it can be shown that to each non-trivial operator A on $\mathscr{H}$ there exists a state vector $\Psi \in \mathscr{H}$ such that the expectation value $\langle \Psi, A\Psi \rangle$ is not dispersion-free, i.e., $\langle \Psi, A^2\Psi \rangle \neq \langle \Psi, A\Psi \rangle^2$. (An operator is called nontrivial if it is not a scalar multiple of the unit operator I on $\mathscr{H}$). Traditional quantum mechanics, which allows all (bounded) linear operators on $\mathscr{H}$, thus has no room for dispersion-free (= classical) observables, and all operators have the remarkable property which is known from the Heisenberg uncertainty principle for position and momentum operators Q and P: $[Q,P] = QP - PQ = i\hbar I$, i.e., for each nontrivial operator A on $\mathscr{H}$, there is always an operator B, such that $[A,B] = AB - BA$ does not vanish, i.e. A and B do not commute.

A *-algebra of operators is closed under addition and multiplication of elements as well as multiplication by (complex) scalars and the formation of the adjoint of an operator, $A \rightarrow A^*$. The set $\mathscr{B}(\mathscr{H})$ of all linear (bounded) operators on a Hilbert space $\mathscr{H}$ is a *-algebra: this is the algebra of observables in traditional quantum mechanics. In generalized (algebraic) quantum mechanics, any possible *-sub-algebras of the algebra $\mathscr{B}(\mathscr{H})$ are permitted as algebras of observables. It is obvious that not all elements (operators) of an algebra of observables describe physically relevant quantities.[8-10]

If $\mathscr{M}$ is an algebra of observables of a physical system, its classical observables[8-12] are found in the so-called center $\mathscr{Z}(\mathscr{M})$ of $\mathscr{M}$, $\mathscr{Z}(\mathscr{M}) \stackrel{\text{def}}{=} \{A \in \mathscr{M} \mid AB = BA \text{ for all } B \in \mathscr{M}\}$. The center thus contains those operators of $\mathscr{M}$ which commute with *all* operators. $\mathscr{Z}(\mathscr{M})$ is usually only a part of $\mathscr{M}$, but if $\mathscr{Z}(\mathscr{M}) = \mathscr{M}$ the algebra $\mathscr{M}$ is referred to as commutative. Classical mechanics has such a commutative algebra of observables, and in particular there is no uncertainty principle for position and momentum.[8,9]

The existence of classical observables in an algebra of observables $\mathscr{M}$ has consequences for the structure of the Hilbert space: it splits up into sectors which are separated by a so-called superselection rule. The sectors are indexed by the possible dispersion-free values of the classical observables, and the superselection rule has the consequence that transition probabilities of the form $|\langle \Psi_l, A\Psi_k \rangle|^2$, $\Psi_l \in \mathscr{H}_l$, $\Psi_k \in \mathscr{H}_k$, $\mathscr{H}_l$, $\mathscr{H}_k$ = different sectors of $\mathscr{H}$, vanish for *all* observables $A \in \mathscr{M}$. Thus the state vector $\Psi = c_l\Psi_l + c_2\Psi_k$, c_1, $c_2 \in \mathbb{C}$ (after normalization) formed formally according to the normal superposition principle for states does not correspond to a pure state but to a mixture $\langle \Psi | A\Psi \rangle = |c_l|^2 \langle \Psi_l | A\Psi_l \rangle + |c_2|^2 \langle \Psi_k | A\Psi_k \rangle$, $A \in \mathscr{M}$. The vector Ψ describes for example a racemic mixture (an ensemble), but not a superposition of chiral states of a single molecule. In other words: classical observables restrict the universal validity of the superposition principle for state vectors.[9]

3. New Theoretical Concepts in Chemistry

The extension of quantum mechanics described in Section 2 thus offers the possibility of describing large systems and classical properties. However, various theoretical approaches for the description of macroscopic objects and systems with a large number of degrees of freedom have developed which are independent of quantum mechanics. As far as chemically relevant systems are concerned, considerable progress has been made recently through the introduction of theoretical concepts such as "fractals", "quasicrystals", and "chaotic motion for strongly coupled systems". These concepts are not completely independent of one another; the stochastic moment plays an important role, but not in the sense that symmetry is completely destroyed. Self-similarity and scaling invariance are the notions connecting these three areas, and there exist relations to the theory of critical exponents of phase transitions.[13,20]

In the following sections, these three areas will be described, together with examples of their application.

3.1. Fractals

Fractals have been known as mathematical objects for many years, though not under this name;[14] however, they were first introduced into science in the 1970's.[15-17] A characteristic of a fractal object is that the standard methods for determining its length and area fail; there exists no yardstick with which a fractal can be measured and which would give a finite value. When a fractal is enlarged or reduced in size, the same pattern is still found, so that we speak of scale- or dilation-invariance and refer to fractals as self-similar structures.

The properties described above can be seen very clearly from the so-called Sierpiński lattice (Fig. 1), in which the self-similarity is generated according to the following procedure: the starting point is an equilateral triangle whose sides are 2 units long, and this triangle contains three smaller upright triangles with sides of unit length. A further, smaller equilateral triangle standing on an apex is now placed into each of these upright triangles: thus the sides of the initial three smaller triangles are each divided into two, and the original pattern is obtained, but three

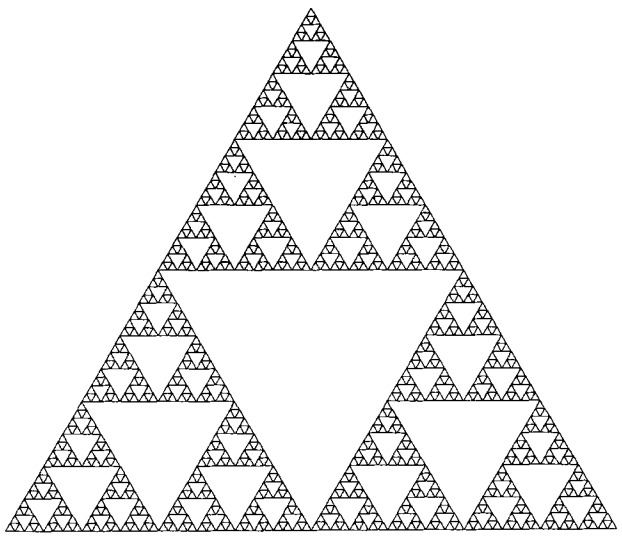


Fig. 1. The Sierpiński lattice after the sixth iteration.

times on half the scale. Iteration of this procedure N times gives the Nth stage of the Sierpiński lattice. The Sierpiński lattice itself is obtained by an infinite number of iterations and is to be understood as part of an infinite hierarchy of triangles of ever increasing size, since the same pattern must recur for each scale. In contrast to the so-called regular lattices, i.e., those with unit cells such as crystal lattices, the Sierpiński lattice is no longer translation-invariant. This has consequences: in the case of regular (two-dimensional) lattices the number of lattice points in a sphere of radius R is proportional to R^d with $d=2$. A similar power law, $N(R) \sim R^{\tilde{d}}$, applies for the Sierpiński lattice, but here $\tilde{d}=\ln 3/\ln 2=1.584$, i.e., it is smaller than the dimension d of the embedding space and is in particular non-integral. The number $\tilde{d}$ is called the *fractal dimension* of the lattice and is a universal characteristic of a given object. A second characteristic dimension of the Sierpiński lattice, to which we shall refer later, should be mentioned, namely its *spectral* dimension $\tilde{d}$. It is more difficult to derive than the fractal dimension determined from the self-similarity[18] and reflects the connectivity properties of the lattice. The inequality $\tilde{d} \leq \tilde{d} \leq d$ applies; only in the case of regular lattices are all dimensions equal.

The strict self-similarity, determined in the case of the Sierpiński lattice by the procedure followed in its construction, must be replaced by statistical self-similarity when natural objects are to be characterized by fractal dimensions. When such an object is enlarged or reduced in size, the structure obtained is not exactly the same but is similar, so that it is not possible solely on the basis of the structure observed to state the scale range concerned (scale-invariance). *Mandelbrot*[15] has listed many fractals observed in nature: coastlines, island archipelagos, lung alvaeoli, trees, mountains, etc. However, in contrast to the situation in mathematics, there are upper and lower bounds to self-similarity in nature, and scale invariance is present only within a certain range.

Chemically and physically interesting applications of fractals for the description of highly irregular structures have been described for aggregation phenomena,[19] percolation problems,[20] in heterogeneous catalysis,[21] for diffusion in disordered materials,[22] and for polymers.[23]

Aggregation clusters with fractal structures are known in particular for metal deposition under diffusion-controlled conditions or for aerosol formation (Fig. 2).

Figure 3 shows a percolation cluster. Such structures are formed in forest fires (at the time when the fire has just reached from one end of the forest to the other), in phase transitions in dilute magnets, in the transition liquid/glass, in polymer gel formation etc.[24] at a certain critical concentration p_c; a fractal is present at exactly this moment.

Extremely rough, fissured, and porous surfaces play an important role in heterogeneous catalysis. It is possible with the help of monolayers of adsorbed molecules of different (effective) diameters as yardsticks, to determine the fractal dimension of, for example, activated charcoal: $\tilde{d} \approx 2.78$. This indicates that many active centers lie close together, so that the surface becomes volume-like.[21,25]

Extremely disordered materials, e.g., glasses, can also be considered as fractals and simulated on a computer as deterministic fractals, since the fractal dimension $\tilde{d}$ is a statistical property. So-called anomalous time laws are found for chemical reactions in glasses; for long times t, the relaxation occurs according to a stretched exponential function (Kohlrausch-Williams-Watts law) [Eq. (a) for the "target annihilation" problem ($\phi(\tau)=1/e$)] or according to an algebraic decay law [eq. (b) for bimolecular reac-

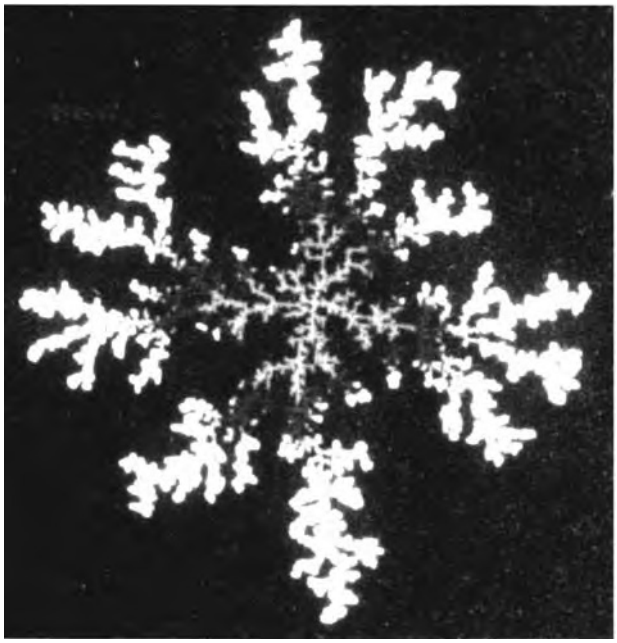


Fig. 2. Diffusion-controlled aggregate on a 600×600 square lattice. The different shadings show the development of the aggregate.

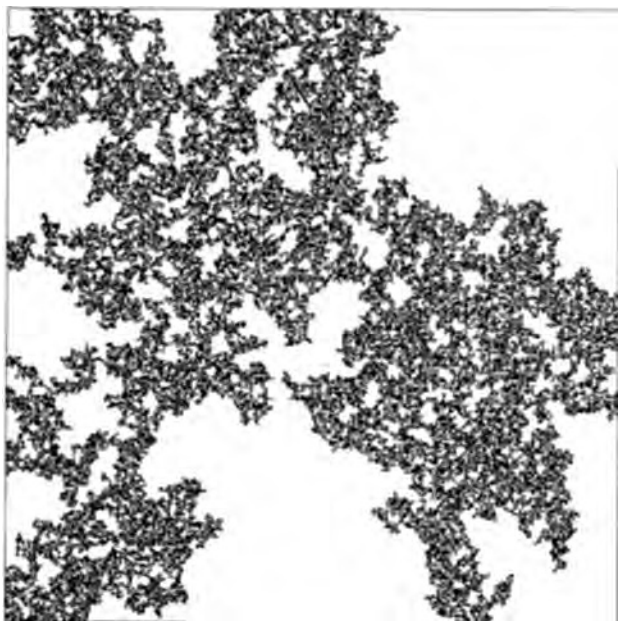


Fig. 3. Percolation cluster at the critical concentration $p_c \approx 0.593$ on a 500×500 square lattice.

$$\phi(t)=\exp[-(t/\tau)^{\alpha}] \qquad \alpha, \tau > 0, \qquad t > \tau \tag{a}$$

$$\phi(t) \sim t^{-\gamma} \qquad 0 < \gamma < 1 \tag{b}$$

tions].[22,26] The exponents α and γ in these decay functions ϕ are related to the spectral dimensions $\tilde{d}$ and not to the fractal dimension $\tilde{d}$; they reflect the connectivity of the lattice on which the particles follow their random paths. The second rate law (b) can in addition be interpreted as a temporal fractal, i.e., $\phi(bt)$ with $b>0$ behaves just as does $\phi(t)$ but on a different time scale determined by b, and there is no characteristic time for the process.

3.2. Spectra of Systems with Strongly Coupled Degrees of Freedom—Chaotic Motion in Molecules?

The rotatory, vibratory, and electronic degrees of freedom are strongly coupled in highly excited molecular states. The resulting spectra appear very "complicated", and the normal characterization of the energy levels by means of quantum numbers is impossible because of the coupling of the degrees of freedom. Although in principle the exact Hamiltonian operator incorporating all interactions could be written down, statistical methods are used in the analysis of such complex spectra, as in nuclear physics.[27] Of particular interest is the question as to whether the numerous, apparently randomly distributed energy levels form clusters for various values or whether they repel one another. A long sequence of random numbers within a certain interval, for example, forms a considerable number of clusters. If the distribution of the spacings S to the nearest neighbors are considered in units of D, the mean distance between the random numbers, the result is a Poisson distribution [Eq. (c), Fig. 4].

$$P_P(S)=(1/D)\exp(-S/D) \qquad (c)$$

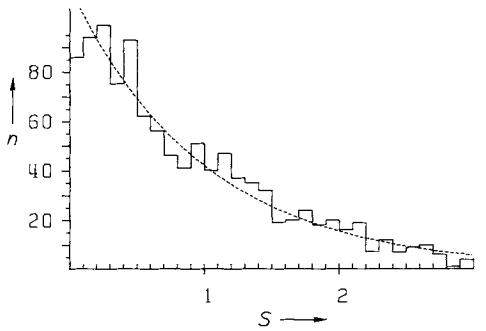


Fig. 4. Distribution of the energy level distances S for two uncoupled quartic oscillators [dotted line = Poisson distribution according to Eq. (c)]. n = number of cases with spacing S.

If this procedure is applied to "simple" spectra, i.e., low-energy spectra with quantum number characterization of the energy levels, a Poisson distribution of the nearest neighbor spacings is also obtained, i.e., smallest distances and cluster formation are allowed.

The Poisson distribution cannot, however, be fitted to the distribution of the distances to the nearest neighbor energy levels in the case of spectra from highly excited states with coupled degrees of freedom, since very small distances between the levels no longer occur. With the assumption of linear repulsion between the energy levels (see, e.g., Ref. [27]) a different distribution function is obtained, namely the Wigner distribution[28] [Eq. (d)].

$$P_W(S)=(\pi S/2D^2)\exp[-\pi S^2/4D^2] \qquad S\geq 0 \qquad (d)$$

In many cases, this function reproduces the distribution of the nearest neighbour spacings quite well (Fig. 5).

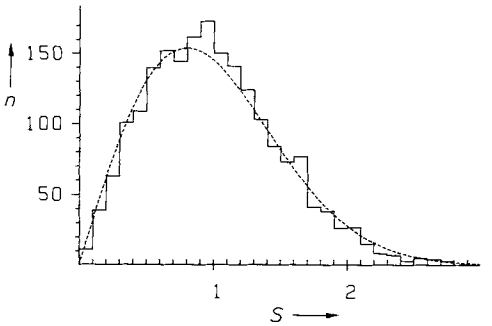


Fig. 5. Distribution of the energy level distances S for two strongly coupled quartic oscillators [dotted line = Wigner distribution according to Eq. (d)].

Between the extreme cases of Figures 4 and 5, there is a large transitional range, which will be of great interest to spectroscopists and theoreticians; it will hopefully be possible to use the spectra to obtain basic information on the dynamics of the systems under consideration.

The simplest systems in classical mechanics are integrable systems where the number of constants of the motion is equal to the number of degrees of freedom. However, when a non-integrable part is added to the Hamilton function (simple example: a rotator kicked periodically by a certain force) there no longer exist any constants of the motion (except for the energy). Integrable systems do not always possess periodic, closed orbits in phase space; it is possible that in the course of time a trajectory almost fills (in the sense of measure theory) an energy shell in phase space (ergodic behavior). Nevertheless, trajectories with neighboring initial conditions remain close together, and such a motion is referred to as regular. Non-integrable systems, in contrast, can exhibit so-called chaotic behavior, which means that trajectories which originally lay close together diverge exponentially; small variations of the initial conditions lead to a completely different behavior of the system, and such a motion is called chaotic or irregular.[29-31]

Regular and irregular systems differ however not only in their dynamic behavior but also in their relationship to quantum mechanics. Integrable systems can be quantized semiclassically;[32] the energy levels of the corresponding quantum system can be characterized by quantum numbers, and Poisson statistics governs their spectra. Model studies using harmonic or quartic oscillators have shown[33] that for the case of strong coupling in an approximate quantum treatment the energy levels of the spectrum repel one another, so that Wigner statistics must be used (fractal concepts can also be applied[34]). In this type of spectra, the semiclassical limit $\hbar\to 0$ yields a chaotic classical system. This does not however mean that one is al-

lowed to speak of "quantum chaos", since for quantum systems there is no criterium analogous to the difference between regular and chaotic trajectories in the classical case. However, one has become accustomed to speaking of regular and irregular spectra, in analogy to the dynamics of the corresponding classical systems.

Thus the difference between Poisson and Wigner distribution of the spacings between neighboring energy levels in spectra cannot serve as a measure for the chaotic behavior of quantum systems. *Kolmogorov* and *Sinaĭ*[35] have introduced an entropy, the Kolmogorov-Sinaĭ (KS) entropy, as a characteristic invariant for classical dynamical systems; it is strictly zero for regular motion, but has values >0 for chaotic motion; for completely random systems without a deterministic part, its value is ∞. Attempts to adapt this concept to dynamic systems of quantum mechanics have been made previously, in particular in connection with irregular spectra;[36,37] however, difficulties always occurred because of the intrinsic non-commutativity of the quantum mechanical algebra of the observables. A very promising approach to extending the KS entropy to the non-commutative, i.e., quantum mechanical, case has been made by *Connes, Størmer, Narnhofer* and *Thirring*.[38] It was shown that the KS entropy of a dynamics implemented by a Hamiltonian operator with a discrete spectrum vanishes; thus, from this point of view, Hamiltonian systems with discrete spectra are not chaotic. A non-vanishing KS entropy occurs, for example, in the dynamics on algebras which are encountered in algebraic statistical mechanics: these algebras, the so-called type-III W*-algebras,[39] are also non-commutative, but, for example, possess no smallest (one-dimensional) projectors, unlike the algebra of observables of standard quantum mechanics.

3.3. Quasicrystals

Translation invariance in planar and spatial structures implies that certain symmetry elements are excluded. For this reason, there are no fivefold rotation axes in the crystallographic groups of three-dimensional space. Thus, the discovery in 1984 by *Schechtman* et al.[40] of five- and tenfold symmetry axes in diffraction diagrams of aluminum-manganese alloys was even more sensational. As is often the case in science, mathematicians had already suggested a solution. *Penrose*,[41] *de Bruijn*,[42] and others had been studying so-called quasi-periodic lattices since the 1970's. These are lattices without translational symmetry, though they are not completely disordered patterns. Figure 6 shows a planar Penrose pattern which is built up from two different types of rhombus.

The sections of equal length are all parallel to the sides of a regular pentagon. As mentioned above, these patterns do not show translation invariance, but the pattern is self-similar in that an area (e.g., a pentagon with its surroundings) of diameter D occurs again with the same arrangement and a diameter somewhat larger than $2D$.[41]

Quasicrystalline structures are non-translation-invariant images of translation-invariant structures in spaces with a Euclidean dimension greater than three. They can be obtained by projection of a translation-invariant regular lattice in a higher-dimensional space. A three-dimensional quasicrystal is constructed by placing a three-dimensional (hyper)plane in a higher-dimensional (e.g., six-dimensional) lattice and projecting all those lattice points which lie at a certain distance T (where T is, for example, the length of the unit cell of the regular lattice) from the plane onto this plane. According to the position of the plane (rational or irrational slope) in the higher-dimensional space, one obtains a regular or quasi-periodic lattice in three dimensions. The compatibility of the fivefold symmetry with that of the higher-dimensional lattice determines whether fivefold point symmetries can occur in the quasicrystal. Representations Δ higher than three-dimensional of point groups G, which are not compatible with the translational symmetry of three-dimensional lattices, can be induced by subgroups of G according to the well-known Frobenius procedure.[43] The hyperplane (i.e. the three-dimensional space) must be situated in the higher-dimensional lattice in such a way that the representation Δ leaves the hyperplane invariant.[44]

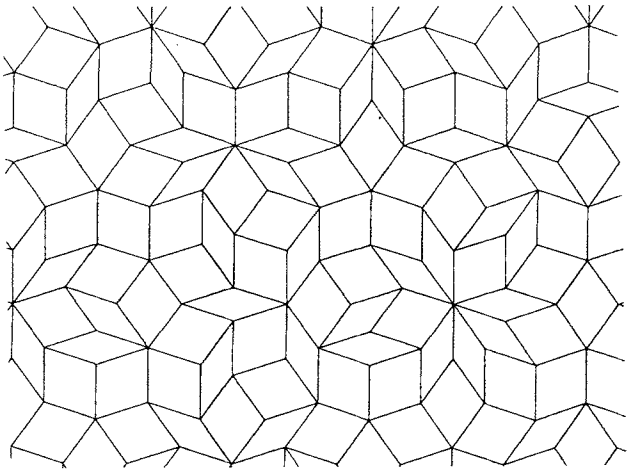


Fig. 6. Planar Penrose built up from two different types of rhombus.

In the alloy system Al-Mn-Si, there exists a normal crystalline phase which can be converted into a quasicrystalline phase by means of a small deformation. This phase transition corresponds to a change in the position of the hyperplane in higher-dimensional space.[44]

3.4. Knot Theory

The final topic is not so closely related to physical chemistry as are the three previous ones, but it has led to discussions between biochemists and mathematicians; some aspects of knot theory also make this field an interesting one for theoretical chemistry.

DNA molecules can be knotted under the influence of topoisomerases and by recombination. The first evidence of the existence of various types of knot was found on electrophoresis plates: differently knotted DNA molecules with the same nucleotide sequence wander at different rates. It is now possible to obtain excellent electron microscope pictures of knotted DNA molecules. This is made possible by coating the DNA strand by a layer of RecA protein.[45] In this way, the strand thickness is increased

from 10 Å to 100 Å, and the manner in which the strands cross each other can be clearly determined (Fig. 7).

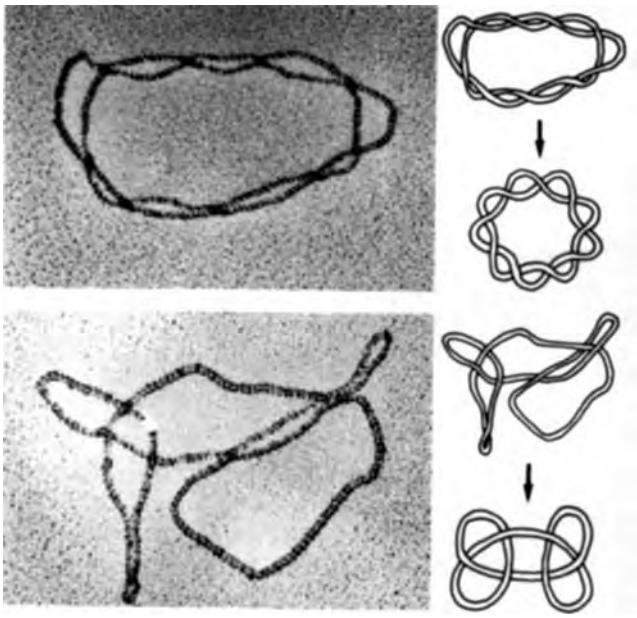


Fig. 7. Left: electron microscope pictures of knotted DNA strands; right: schematic diagrams of the real and ideal knots.

Knot theory, in mathematics, is a part of topology, i.e., one can deform knots without their undergoing any "essential" change (see Fig. 8). The study of knots was initiated by the physicist *P. G. Tait*,[46] he was interested in smoke rings and the Thomson (Kelvin) atomic theory. The main mathematical task is to find the characteristic topological invariants for knots and, because of the number of forms which a knot can assume, to define a notion of equivalence. Two knots which can be interconverted by means of an invertible differentiable map, which leaves the orientation of the space invariant, are said to be equivalent ("ambient isotopic").[47] For example, the two knots in Figure 8 are equivalent.

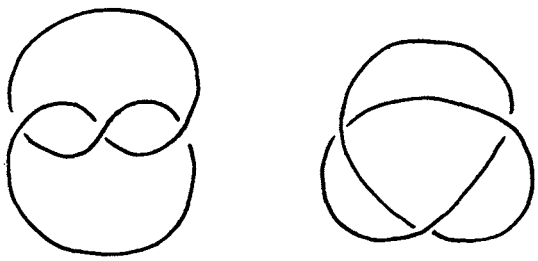


Fig. 8. Two different representations of the trefoil knot [55].

The question of equivalence becomes more difficult, however, as the number of crossing-points in the knot increases.

An invariant for knots, the so-called Alexander-Conway polynomial Δ_K, was introduced in 1928. A finite polynomial with integral coefficients in the variables $t^{1/2}$ and $t^{-1/2}$ is assigned to each oriented knot; equivalent knots lead to the same polynomial. The polynomial corresponding to the trefoil knot in Figure 8 is given by Equation (e).

$$\Delta_K(t) = t - 1 + t^{-1},\ t \in \mathbb{R} \qquad \text{(e)}$$

However, the Alexander-Conway polynomials very often assign the same invariant to inequivalent knots, e.g. the mirror images of the chiral trefoil knot. This problem was first solved only a few years ago by *Jones*,[48] who introduced new polynomials, which can distinguish between the "antipodes" of chiral knots, as invariants. *Interestingly, the Jones polynomials were discovered in the course of studies of a particular type of operator algebras which occur in algebraic quantum mechanics.* In addition, there was found to be a direct relationship between knot theory and mathematical structures in lattice models of algebraic statistical mechanics (Ising-like models, Yang–Baxter equation, see, e.g., Ref. [49]) and with group theory (braid groups).

There are several review articles on the present role of knot theory in chemistry which are worth reading, including those written by *Walba*,[50] *Wasserman* and *Cozzarelli*,[51] *Sumners*,[52] and the corresponding articles in Ref. [1]. Enzymes can be classified according to the type of knot and the chirality they produce from unknotted circular molecules, and the modes of reaction of differently knotted DNA molecules also differ. The knot type of a molecule is a classical observable in the sense of Section 2. As indicated above, there are indeed mathematical connections with quantum-mechanical structures, but at present there is no concrete indication as to how an observable "knot type" could be obtained in the center of an observable algebra.

All the concepts presented here are relevant to chemistry; the relationship between them can be seen from the importance of the terms "self-similarity", "random processes", and "operator-algebraic methods", and "large" systems are often studied. Numerical quantum chemistry is in the process of treating clusters, defect crystals, and polymers, since, thanks to the new generation of computers, the required calculation capacity is now available. However, theoretical chemistry is not bound to the molecular picture and must in future take much more account of very different levels of description, because both the language of the chemist and the theoretical foundation provided by quantum mechanics must be taken seriously. The following section will describe the relationship between the purely molecular and other, just as legitimate, points of view.

4. Do Molecules Exist?

The molecular viewpoint which is dominant in chemistry today has its roots in the period at the beginning of this century when, for example, *Wilhelm Ostwald* underwent "conversion" to atomism and thus to the molecular picture. The idea that it is possible and necessary to relate *all* the phenomena of chemistry to the properties of elementary entities is one shared by very many natural scientists. This way of thinking has resulted in great achievements and in much practical insight. In addition, the contribution of quantum chemistry to the confirmation of the "correctness" of quantum mechanics should not be underestimated

(e.g., the exact calculation of the dissociation energy of the H_2 molecule[53]). However, both quantum mechanics, on the one hand and chemical phenomenology, on the other, make it clear that the molecular point of view is *not the only possible one*:

- Quantum-mechanics is a holistic theory; thus coupled systems (e.g., electrons and nuclei in a molecule) form an inseparable unit. The state of the whole system cannot be reconstructed from the states of the partial systems. Thus, for example, in a discussion of macroscopic systems which consist of many molecules the restriction of the global state to one single molecule is no longer a pure state (but a mixed state represented by a density operator). Since, however, only pure states describe individual single molecules, the usual notion of "molecule" disappears in this case. In addition "molecules" in a macroscopic system are so strongly coupled via Einstein-Podolsky-Rosen correlations[9, 54] that also from this point of view it is no longer possible to speak of discrete molecules.
- According to chemical intuition, molecules contain a nuclear framework, i.e., the positions of the nuclei relative to one another are fixed. This intuition is taken into account in quantum chemistry by the Born-Oppenheimer "approximation". A superselection rule in the sense of Section 2 (with the classical observable "nuclear framework") applies to molecules with different frameworks, though it is by no means as strict as, for example, the superselection rules for charge or chirality. The Born-Oppenheimer picture of a molecule is often sufficient for the chemist's purposes, but cannot be maintained in precision spectroscopy. For a molecule such as ammonia the fiction of the nuclear framework collapses.[5, 6] Experiment (microwave spectroscopy) and quantum chemistry are in agreement, yielding a totally symmetric ground state for NH_3. A conventional rationalization of this fact is that the molecule exists in two pyramidal forms which interconvert by means of "tunneling". However, neither theory nor experiment support this rationalization: ground states in quantum mechanics are stationary and do not vary with time. Pyramidal states of NH_3 can be prepared experimentally, but are not eigenstates of the Hamiltonian operator and are thus not stationary.
- If an object, e.g., the surface of a heterogeneous catalyst or a disordered solid, is described as a fractal, the molecular picture has been left behind, since molecules are not self-similar or scale-invariant. Ordered crystal structures always possess a smallest unit, the unit cell, from which the crystal is built up by translation. The scale-invariance of fractal structures does not permit the occurrence of such smallest units. That both descriptions, the fractal and the molecular, are mutually exclusive but complementary is thus not only a question of magnitude but becomes evident through the completely different symmetry laws of the two points of view.

"Matter consists of molecules, and molecules consist of the nuclear framework and electrons": this idea is of great value for chemistry, but it is not universally applicable. There are situations in which completely different theoretical concepts and approaches must be applied.

5. What is Theoretical Chemistry and What is Its Purpose?

The most important aspects of theoretical chemistry, as they have been presented here, can be summarized by the following theses:

1. The theory of chemistry must be much more than a collection of models. Models are useful or useless according to the situation, but can never be right or wrong.
2. Theoretical chemistry takes its concepts from various sources. The contribution of quantum chemistry is important, but is by no means the only one.
3. Theoretical research cannot orient itself *solely* to the molecular picture of matter. Complementary approaches exist, for example, for scale-invariant fractal structures or in algebraic quantum mechanics of large systems.
4. Theoretical chemistry naturally has good contacts with applications. The actual purpose of the theory is, however, to understand phenomena and interrelationships in a qualitative manner. This qualitative understanding is just as "exact" as quantitative (numerical) statements.

A theory which is intended to help the science of chemistry, which is so rich in phenomenology, must be extended on various levels of knowledge; it must provide clear, universally valid concepts which are of sufficient clarity and longevity that chemists in laboratories can also profit from them.

For kindly providing the Figures for this article, we wish to thank: A. Blumen, J. Klafter, G. Zumofen (Figs. 1-3), T. Zimmermann (Figs. 4, 5), P. Kramer (Fig. 6) and A. Stasiak (Fig. 7). Special thanks are due to K. Lendi for critically reading the manuscript.

Received: April 12, 1988 [A 710 IE]
German version: *Angew. Chem. 101* (1989) 277
Translated by Professor *T. N. Mitchell*, Dortmund (FRG)

[1] A. Amann, L. S. Cederbaum, W. Gans (Eds.): *Fractals, Quasicrystals, Chaos, Knots and Algebraic Quantum Mechanics (Proc. NATO Adv. Res. Workshop New Theor. Concepts Phys. Chem. 1987*, Kluver Dordrecht 1988.
[2] J. von Neumann: *Mathematische Grundlagen der Quantenmechanik*, Springer, Berlin 1932.
[3] B. O. Koopman, *Proc. Symp. Appl. Math. Vol. 7 1957*, 97.
[4] M. Quack, *Chem. Phys. Lett. 132* (1986) 147.
[5] P. Pfeifer, *Dissertation*, Eidgenössische Technische Hochschule, Zürich 1980 (No. 6551).
[6] A. Amann in [1].
[7] M. Takesaki, *Commun. Math. Phys. 17* (1970) 33.
[8] J. M. Jauch: *Foundations of Quantum Mechanics*, Addison-Wesley, Reading, MA, USA 1968.
[9] H. Primas: *Chemistry, Quantum Mechanics and Reductionism*, Springer, Berlin 1983.
[10] A. Amann, *Fortschr. Phys. 34* (1986) 167.
[11] A. Amann, U. Müller-Herold, *Helv. Phys. Acta 59* (1986) 1311.
[12] A. Amann, *Helv. Phys. Acta 60* (1987) 384.
[13] G. L. Sewell: *Quantum Theory of Collective Phenomena*, Clarendon, Oxford 1968.
[14] F. Hausdorff, *Math. Ann. 79* (1919) 157.
[15] B. B. Mandelbrot: *The Fractal Geometry of Nature*, Freeman, San Francisco, USA 1982.
[16] P. Pfeifer, *Chimia 39* (1985) 120.
[17] G. Zumofen in [1].
[18] R. Rammal, G. Toulouse, *J. Phys. Lett. (Orsay, Fr.) 44* (1983) L 13.

[19] R. Jullien, *Contemp. Phys. 28* (1987) 477.
[20] D. Stauffer: *Introduction to Percolation Theory*, Taylor & Francis, London 1985.
[21] D. Avnir, P. Pfeifer, *Nouv. J. Chim. 7* (1983) 71.
[22] A. Blumen, J. Klafter, G. Zumofen in I. Zschokke (Eds.): *Optical Spectroscopy of Glasses*, Reidel, Dordrecht 1986, p. 199.
[23] P. G. de Gennes: *Scaling Concepts in Polymer Physics*, Cornell University, Ithaca, NY, USA 1985.
[24] R. Zallen in G. Deutscher, R. Zallen, J. Adler (Eds.): *Percolation Structures and Processes (Ann. Isr. Phys. Soc. 5* (1983), p. 3.
[25] D. Avnir, D. Farin, P. Pfeifer, *Nature (London) 308* (1984) 261.
[26] A. Blumen in [1].
[27] M. Carmeli: *Statistical Theory and Random Matrices*, Dekker, New York 1983.
[28] E. P. Wigner, *Oak Ridge Nat. Lab. Rep. ORNL (US) 2309* (1957) 59.
[29] A. J. Lichtenberg, M. A. Liebermann: *Regular and Stochastic Motion*, Springer, New York 1983.
[30] H. G. Schuster: *Deterministic Chaos*, VCH Verlagsgesellschaft, Weinheim 1988.
[31] A. Kunick, W. H. Steeb: *Chaos in dynamischen Systemen*, Bibliographisches Institut, Zürich 1986.
[32] I. C. Percival, *Adv. Chem. Phys. 36* (1977) 1.
[33] T. Zimmermann, L. S. Cederbaum, H.-D. Meyer, H. Köppel, *J. Phys. Chem. 91* (1987) 4446.
[34] L. S. Cederbaum, E. Haller, P. Pfeifer, *Phys. Rev. A 31* (1985) 1869.
[35] a) A. N. Kolmogorov, *Dokl. Akad. Nauk SSSR 119* (1958) 861; b) Ya. G. Sinaĭ, *ibid. 124* (1959) 768.
[36] P. Pechukas, *J. Phys. Chem. 86* (1982) 2239.
[37] J. W. Helton, M. Tabor, *J. Phys. A 18* (1985) 2743.
[38] A. Connes, H. Narnhofer, W. Thirring, *Commun. Math. Phys. 112* (1987) 691.
[39] O. Bratteli, P. W. Robinson: *Operator Algebras and Quantum Statistical Mechanics 1*, Springer, New York 1979.
[40] D. Shechtman, I. Blech, D. Gratias, J. W. Cahn, *Phys. Rev. Lett. 53* (1984) 1951.
[41] R. Penrose, *The Mathematical Intelligencer 2* (1979) 32.
[42] N. G. de Bruijn, *Proc. K. Ned. Akad. Wet. Ser. A 84* (1981) 38, 53.
[43] J. P. Serre: *Représentations Linéaires des Groupes Finis*, Hermann, Paris 1967.
[44] a) P. Kramer in [1]; b) A. Janner in [1]; c) D. Gratias in [1].
[45] M. A. Krasnow, A. Stasiak, S. J. Spengler, F. Dean, T. Koller, N. T. Cozzarelli, *Nature (London) 304* (1983) 559.
[46] P. G. Tait, *Sci. Pap. 1* (1898) 273.
[47] P. de la Harpe in [1], p. 10.
[48] V. F. R. Jones, *Bull. Am. Math. Soc. 12* (1985) 239.
[49] R. J. Baxter: *Exactly Solved Models in Statistical Mechanics*, Academic Press, London 1982.
[50] D. M. Walba, *Tetrahedron 41* (1985) 3161.
[51] S. A. Wasserman, N. R. Cozzarelli, *Science (Washington) 232* (1986) 951.
[52] D. W. Sumners, *J. Math. Chem. 1* (1987) 1.
[53] W. Kołos, L. Wolniewicz, *J. Chem. Phys. 49* (1968) 404.
[54] A. Einstein, B. Podolsky, N. Rosen, *Phys. Rev. 47* (1935) 777.
[55] Editorial note: the synthesis of a molecule with trefoil knot structure has been described recently: C. O. Dietrich-Buchecker, J.-P. Sauvage, *Angew. Chem. 101* (1989) 192; *Angew. Chem. Int. Ed. Engl. 28* (1989) 189.

The Structure of Lithium Compounds of Sulfones, Sulfoximides, Sulfoxides, Thioethers and 1,3-Dithianes, Nitriles, Nitro Compounds and Hydrazones

By Gernot Boche*

Acceptor-substituted lithio compounds $LiA-CR^1R^2$, in which the acceptor A is an RC(O), $N\equiv C$, RSO_2, RS(O)NR, RSO, RS, O_2N, or $RC(N-NR_2)$ group, have long played an important role in organic synthesis. Their significance has grown still further in the last fifteen years, as one has increasingly learnt to employ them successfully in chemo-, regio-, diastereo- and enantioselective reactions. Remarkably, little if anything was known of the structures of these compounds. It is therefore not surprising that interest in the structures of this class of compounds has greatly increased in recent years. In the following review, we shall summarize recent research into the structures of the lithio compounds of sulfones, sulfoximides, sulfoxides, thioethers and 1,3-dithianes, nitriles, nitro compounds, and hydrazones. Crystal structure determinations from recent years are central to this study. They are supplemented by solution studies and by calculations of structures. Structural similarities and differences between the individual states of aggregation are pointed out wherever possible, as is also the relationship between structure and reactivity.

1. Introduction

There can be no class of compounds for which a greater discrepancy exists between their importance in modern organic synthesis and the lack of knowledge about their structures than organometallic compounds. A new synthesis using these reagents can be found in practically every issue of any of the respected journals and is usually characterized by high chemo-, regio-, diastereo- or enantioselectivity. At the same time, the course of the reaction can often only be understood by the IOC method ("intuition of the organic chemist"). This state of affairs is unacceptable in the long term; firstly, because of the fundamental interest in knowing the structure of organometallic compounds, and secondly, because a knowledge of the structure-reactivity relationships for this class of compounds could well be of further help to the synthetic chemist.

It is therefore pleasing that in recent years structural aspects of organometallic chemistry, especially of organolithium compounds, have become the subject of growing interest, along with purely synthetic aspects.[1] Solution NMR spectroscopic studies by *Jackman* et al.,[2] and X-ray structural analyses by the groups of *Seebach* and *Dunitz*, have contributed substantially to an understanding of the structures of synthetically important enolates, ester-enolates and amide-enolates;[3] part of this work has been the subject of a review.[3a]

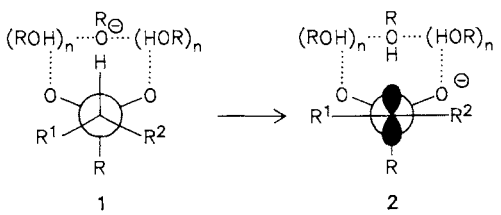
The following sections will report on the progress that has been made in recent years for lithio compounds of sulfones, sulfoximides, sulfoxides, thioethers and 1,3-dithianes, nitriles, nitro compounds and hydrazones, largely with the aid of X-ray structure determinations. The question as to what extent the results of solid-state investigations agree with those for solutions and with calculations ("gas-phase") will be given particular consideration. Additionally, we shall discuss the extent to which a knowledge of the structure allows the reactivity (selectivity) to be understood.

[*] Prof. Dr. G. Boche
Fachbereich Chemie der Universität
Hans-Meerwein-Strasse, D-3550 Marburg (FRG)

2. Monolithium and Dilithium Compounds of Sulfones

2.1. Monolithium Compounds

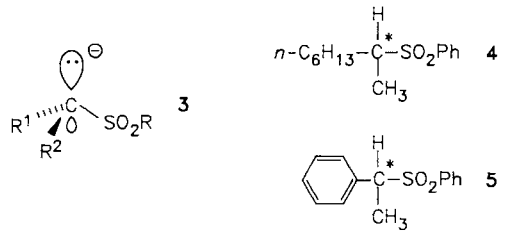
The remarkable fact that acyclic sulfones having a chiral α-carbon atom largely retain their configuration upon H/D exchange has led to numerous experimental[4-37] and theoretical[38-43] studies of the structures of the intermediate α-sulfonyl "carbanions". As early as the sixties, e.g., *Corey* et al.[15,19,20] concluded from their elegant studies of the deprotonation (and also decarboxylation and retro-aldol reactions) of chiral acyclic sulfones that the reaction should occur as outlined in Scheme 1.



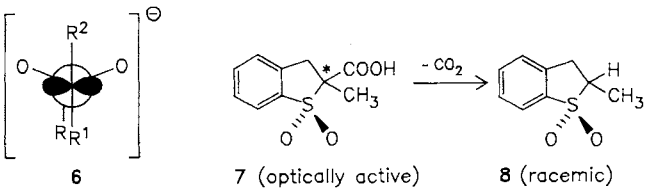
Scheme 1.

The leaving group (a proton in **1**) adopts a *gauche* orientation with respect to the two O atoms of the sulfone group. Cleavage of the proton then leads to a planar, chiral "carbanion" **2** (if $R^1 \neq R^2$), in which the lone pair of electrons on the anionic α-carbon atom is *gauche* to the two sulfonyl O atoms. Therefore, the chirality of an α-sulfonyl "carbanion" should not be due to the tetrahedral configuration at the α-C atom, as would be the case in **3**. If the anionic C atom were non-planar (or nearly planar, and

rapidly inverting), then upon H/D exchange of the optically active sulfones **4** and **5** the two $k_{exchange}/k_{racemization}$ ratios (k_e/k_r) should not be approximately equal (41 and 44 respectively), since the phenyl ring in **5** favors a planar α-carbon atom far more than does the *n*-hexyl group of **4**.[20] In this case, the achiral conformation **6** can be excluded. In contrast, decarboxylation of the optically active carboxylic acid **7** affords racemic **8**. Since the sulfone group is incorporated in a five-membered ring, the only intermediate "anion" that can be formed is an achiral one of type **6**.[20]



3 **4** **5**



6 **7** (optically active) **8** (racemic)

Corey and *Lowry*[19] were also able to show that protonation or deuteration of the "anion" **2** occurs from the same side as deprotonation. From their results, these authors also inferred an increased barrier to rotation about the C_α–S bond in α-sulfonyl "carbanions".[15,19,20]

Extensive spectroscopic investigations have been carried out by *Chassaing*, *Marquet* et al.[29,30,32] including a ^{13}C NMR study of lithium compounds **9**–**13**,[29,30] which gave the following results (Table 1):

Table 1. C,H coupling constants [Hz] for the α-C atom of **9**–**13** [29, 30].

	^1J(C,H)	Δ^1J("anion"–sulfone)
$PhSO_2CHPhLi$ **9**	168	+30
$CH_3SO_2CHPhLi$ **10**	163	+23
$tBuSO_2CHPhLi$ **11**	160	+21
$tBuSO_2CHLi$ **12**	142	+ 4
$PhSO_2CHLi$ **13**	139	0

In the benzylic "anions" **9**–**11**, the coupling constants $^1J_{C-H}$ for C_α are very large, in agreement with a nearly planar configuration at this C atom, and the authors assume a "very loose" C–Li bond.[29] By contrast, in the non-benzylic "anions" **12** and **13**, and in others of this type, the change in the coupling constant relative to that of the corresponding sulfone is considerably smaller, so that hybridization "between sp^2 and sp^3" is proposed, and with it a non-planar α-C atom.

These results lead to the interesting conclusion that for a sulfone group it appears to be irrelevant whether the negative charge to be stabilized is situated on a planar or on a pyramidalized α-C atom.

IR spectroscopic studies of $PhSO_2CH_2Li$[32] indicated an increase in the S–C_α and a decrease in the S–O force constants relative to the corresponding values for methylphenyl sulfone. The S–C_α bond should therefore be shortened in the "anion", and the S–O bond lengthened.

The results of 3-21G and 3-21G* (with consideration of the d-orbitals of sulfur) calculations carried out by *Wolfe* et al.[41] on α-sulfonyl carbanions (without a counterion) are in accord with the *gauche* conformation **2**. In **2**, the decisive interaction for stabilization, i.e., that between the n_C-orbital and the σ^*_{S-R}-orbital, is conformationally especially favorable.

Bond lengths (pm) for dimethyl sulfone $CH_3SO_2CH_3$ **14** and its anion **15** were calculated using 3-21G*,[41] and are presented in Table 2. The experimental values for **14** are given in parentheses.[44]

Table 2. 3-21G* bond lengths [pm] in **14** and **15** [41]; experimental values in parentheses [44].

	$H_2\overset{\ominus}{C}$–S	H_3C–S	S–O
$CH_3SO_2CH_3$ **14**	—	175.6 (177.1)	143.8 (143.5)
$CH_3SO_2\overset{\ominus}{C}H_2$ **15**	161.8	179.7	146.2

Thus, calculations for anion **15** also show a marked shortening of the S–C_α bond relative to the S–CH_3 bond of sulfone **14**, while the S–O bond is only negligibly lengthened.

For further elucidation of α-sulfonyl "carbanion" structures the following questions must be answered, and to do so requires the results of X-ray structure investigations.

1. What are the bond lengths and angles in the carbanion moiety? In particular, which is more favored, a chiral conformation as in **2**, with a planar α-C atom, or one with a pyramidalized α-C atom?

2. Where is the Li atom located? Although this question has been ignored in most studies to date, the IR spectroscopic investigations mentioned above[32] were interpreted in terms of lithium being bound simultaneously to the two oxygen atoms and to the anionic α-C atom. 3-21G* calculations for $LiCH_2S(H)O_2$,[42] however, gave a four-membered (C–S–O–Li) ring as the only energy minimum. We shall now show how a series of crystal structure investigations has led to a unified picture of the structure of "α"-lithiosulfones.

The first X-ray structure determination of an α-sulfonyl "carbanion",[45] that of α-(phenylsulfonyl)benzyllithium-tetramethylethylenediamine **16** was published by *Boche* et al.[46] Shortly afterwards, and independently, a paper by *Gais* appeared,[47] on (phenylsulfonyl)methyllithium-tetramethylethylenediamine **17**.

$[PhSO_2CHPhLi \cdot TMEDA]_2$ **16** $[PhSO_2CH_2Li \cdot TMEDA]_2$ **17**

TMEDA = tetramethylethylenediamine

Since the solid-state structures of **16** and **17** concur in their fundamental details, only that of **16** is shown in Figure 1.

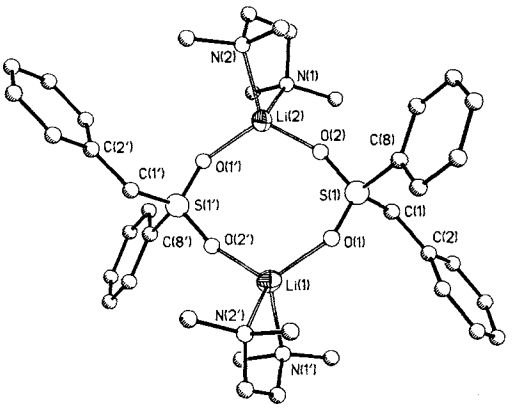


Fig. 1. Crystal structure of **16** [46].

16 and **17** crystallize as dimers, with the Li, S, and O atoms forming a flat, chair-like eight-membered ring. The sulfur atoms lie above and below the plane of the Li and O atoms. Thus, there is no Li–C bond, so that, in the solid state at least, these compounds cannot be called α-lithio sulfones![48]

The C(1)–S(1) distance of 164.1 (161.0) pm in **16** (**17**) is considerably shorter than the corresponding bond length in sulfones (mean value of 58 bond lengths: 180.6 pm[51]). This agrees with the qualitative evidence from the IR analysis,[32] and also with the results of calculations[41] (see Table 2). In sulfene and in thioformaldehyde, in which CS double bonds occur, the CS distances are 161.0(4)[52] and 161.08 pm,[53] respectively. However, in contrast to the IR spectroscopic evidence, the S–O bond lengths of 146.5 and 146.0 pm in **16** and **17**, respectively are only marginally longer than those found in sulfones (mean value of 53 bond lengths: 143.4 pm;[51] methyl phenyl sulfone 145.9 pm;[54] dimethyl sulfone 143.5 pm[44]). This agrees with the results of 3-21G* calculations (see Table 2).

The X-ray structures of lithiosulfones **18**–**22**, also determined in the groups of *Boche* and *Gais*, corroborate the picture found in **16** and **17**. Dimers are formed, independent of the complex ligands TMEDA or diglyme, linked together by an eight-membered (S–O–Li–O–S–O–Li–O) ring; no bond is formed between the Li atom and C_α; the C_α–S bond is shortened considerably, and the S–O bond slightly lengthened.

$[PhSO_2CH(CH{=}CH_2)Li \cdot Diglyme]_2$ **18**[55]

$[PhSO_2CH(SiMe_3)Li \cdot TMEDA]_2$ **19**[56]

$[PhSO_2C(CH_3)_2Li \cdot Diglyme]_2$ **20**[57]

$[PhSO_2C(CH_3)PhLi \cdot TMEDA]_2$ **21**[57]

$[CH_3SO_2CHPhLi \cdot TMEDA]_2$ **22**[58]

The conformation around the C_α–S bond and the configuration of the anionic α-C atom deserve special attention, because of their relevance to the solution stereochemical studies mentioned previously. Table 3 lists the torsion angles α(β) between the A(B) substituent on C_α and the R substituent on the neighboring S atom, for lithiosulfones **16**–**22**. The sum of the angles $|\alpha|+|\beta|$ is a measure of the pyramidalization of C_α, while the γ-values[59a] express the divergence of the unshared electron pair on C_α from the ideal *gauche* conformation. In the Newman projection **A**, the molecule is viewed from the α-C towards the S atom.

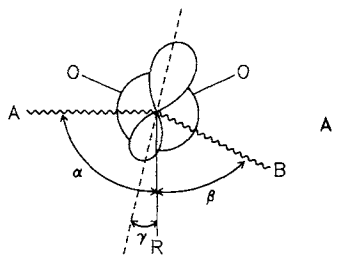


Table 3. Torsion angles α (β) [°] between the substituents A (B) on C_α and R on S; the sum of the angles $|\alpha|+|\beta|$ [°], and γ-values [59a] for lithiosulfones **16**–**22**. For definition of the angles see **A**.

α-Lithiosulfone	A	α	B	β	$\lvert\alpha\rvert+\lvert\beta\rvert$	γ [59a]
16 [a]	H	—	Ph	70	180 (?)	20 (?)
22	H	−109	Ph	73	182	18
19 [59b]	H	−76	$SiMe_3$	94	170	9
21	CH_3	−89	Ph	80	169	4.5
17	H	−81	H	81	162	0
18	H	−78	$CH{=}CH_2$	76	154	1
20	CH_3	−66	CH_3	73	139	3.5

[a] In **16**, the position of the benzylic H atom (A) could not be located sufficiently accurately [46].

From the numerical values of α and β in the individual compounds, it can be deduced that the substituents A and B are arranged by and large such that the lone pair of electrons adopts a *gauche* conformation to the two O atoms on sulfur. The solid-state structural data for α-sulfonyl "carbanions" **17**–**22** thus confirm that this conformation is the most thermodynamically stable, a conclusion which had also been reached on the basis of kinetic studies on chiral sulfones, such as **4** and **5**, in solution. Calculations ("gas phase") for **15** have also revealed a preferred *gauche* conformation.

Remarkably, however, apart from the Me_3Si substituted lithiosulfone **19**, only the phenyl substituted compounds **21** and **22** (and presumably also **16**) are largely planar. **17**, **18**, and especially **20** have a pyramidalized α-C atom (see the $|\alpha|+|\beta|$ values in Table 3). That this should be so for **18** is particularly surprising, considering the allylic position of the α-C atom. In (**16**), **19**,[59b] **21**, and **22**, a larger deviation from the ideal *gauche* conformation than in **17**, **18** and **20** is also observed (see the γ-values in Table 3).

How is the configuration at C_α and the conformation around the C_α–S bond of these α-sulfonyl "carbanions" to be understood? In the phenyl-substituted compounds (**16**), **21** and **22**, the flattening is doubtless connected with partial stabilization of the negative charge by p_π–p_π interactions with the phenyl ring. The conformation around the C_α–S axis is thought to be caused by van der Waals repul-

sion between the phenyl ring and the neighboring oxygen atom. Van der Waals interaction with the oxygen atoms is also thought to be responsible for the increase in pyramidalization observed between the CH_2 compound **17** and the $C(CH_3)_2$ compound **20**. The ease with which the configuration changes in **16**–**22** can therefore only mean that the energy difference between planar and pyramidalized α-C atoms in lithiosulfones is small.

Bors and *Streitwieser* came to exactly this conclusion in a comprehensive theoretical study of the structures of $CH_3SO_2CH_2^{\ominus}$, $CH_3SO_2CH_2Li$ and $LiCH_2SO_2CH_2Li$.[43] They used the 3-21G*+ basis set, which is extended relative to 3-21G*[41] and thus better describes the situation of the electrons on the anionic α-C atom. In order to test whether stabilization of a negative charge by a neighboring sulfonyl group could possibly be due to a p_π–d_π interaction, the 3-21G+ basis set was also used; this program neglects the d-orbitals on sulfur.

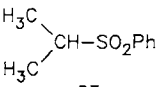
As far as the configuration at the anionic α-C atom in $CH_3SO_2CH_2^{\ominus}$ is concerned, 3-21G*+ led to a planar configuration, while 3-21G+ yielded a pyramidalized C_α in which the H atoms are bent out of the plane by 18.3°. Nevertheless, the energy difference between a planar and a pyramidalized α-C atom is not very large as shown by the energy of $CH_3SO_2CH_2^{\ominus}$ (3-21G*+), in which the H atoms on C_α are each bent out of the plane by 20° (away from the O atoms); it is a mere 0.57 kcal mol^{-1} less stable than the planar form! These calculations also show that from an *energetic* point of view, there is no reason to assume p_π–d_π conjugation between the lone pair of electrons on C_α and the sulfonyl group. Calculations of bond lengths, proton affinities, and electron densities gave the same result, which can only mean that the n_{C^-}–σ^*_{S-R} interaction is crucial for stabilization of the negative charge.[43]

The increased barrier to rotation about the C_α–S bond in α-sulfonyl "carbanions",[15,19,20] which *Corey* and coworkers deduced from the results of H/D exchange experiments, has also been verified by calculations.[43] The *gauche* conformation corresponding to **2**, with the lone pair on C_α lying between the O atoms of the RSO_2 group, represents a minimum on the potential hypersurface of $CH_3SO_2CH_2^{\ominus}$. Upon rotation through 90°, the energy rises by 14.33 kcal mol^{-1}; optimization of this "90°-conformation", assuming C_S-symmetry, yields a value that is increased by 9.31 kcal mol^{-1}.

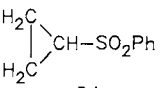
The question of whether a negative charge is better stabilized by an acceptor substituent X when the α-C atom is planar, or when it is pyramidalized, was first investigated with the aid of the "cyclopropyl effect". If stabilization occurs predominantly by delocalization and π-bond formation, a cyclopropyl compound C_3H_5–X should be less acidic than the corresponding isopropyl compound iC_3H_7–X, despite the fact that cyclopropane itself is more acidic than propane.[60] This is because the exocyclic "π-bond" in the three-membered ring "anion" confers additional strain on the latter; methylenecyclopropane is 13.5 kcal mol^{-1} more strained than cyclopropane.[61] Indeed, cyclopropyl ketones and other cyclopropylcarbonyl compounds show considerably reduced kinetic[25] and thermodynamic[31] acidity compared to the corresponding isopropyl compounds. The planarity of enolates as well as the double bond character of their C–C bonds, and the single bond character of the C–O bonds have been confirmed by X-ray structural data.[3]

Remarkably, with cyclopropyl and isopropyl sulfones application of this criterion led to contradictory results. *Zimmerman* et al.[8] (measurements in ether and hydrocarbons), and *Cram* et al.[21] (measurements in DMSO) reported that the equilibrium acidities of **23** and **24**, for instance, are approximately equal.

In H/D exchange experiments ($k_{H,rel}$ for exchange of 30% RH in CH_3OH/CH_3ONa (0.22 M) at 53.2°C), *De Boer* et al.[25] found cyclopropyl sulfone **24** to have a 34-fold higher acidity than **23**. Similar observations were made by



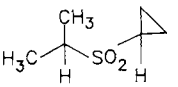
23



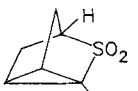
24

Kirmse et al.:[35] in *intra*molecular competitive H/D exchange of **25** (D_2O, 0.5 M NaOD, 74°C), the cyclopropyl H is 213 times more acidic than the isopropyl H.

In **26**, the cyclopropyl H adjacent to the SO_2 functionality is 145 times more acidic than the other H atom adjacent to the sulfone group (at 35°C).[35]



25



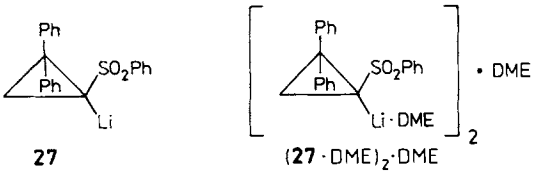
26

Completely different results have been reported by *Bordwell* et al.[28,31] As shown by Table 4, methyl sulfones, and the related methylsulfoximide and methyloxosulfonium ion, are more acidic than the corresponding cyclopropane derivatives. In addition, a comparison of cyclopropyl sulfones with the appropriate isopropyl sulfones shows that the latter are the more acidic.[31]

Table 4. The cyclopropyl effect on the equilibrium acidities K_a of sulfones and related compounds in DMSO [28, 31].

X	pK_a (H_3C-X)	pK_a (C_3H_5-X)	ΔpK_a
$\overset{\oplus}{S}(O)(NMe_2)Ph$	14.4	20.9 ± 0.3	6.5 ± 0.3
SO_2CF_3	18.8	26.6	7.8
$S(O)(NSO_2Ph)Tol$	24.5	28.8 ± 0.2	4.3 ± 0.2
SO_2Ph	29.0	> 32	> 3

The causes of this discrepancy for sulfones and related compounds are not known at present. One could deduce from the data in Table 4 that, "like enolate and nitronate ions, α-sulfonyl carbanions are planar",[31] but this has been repeatedly disproved by the structural studies on α-sulfonyl "anions" described above. The tetrahedral configuration of the α-C atom in 2,2-diphenyl-1-(phenylsulfonyl)cyclopropyllithium **27**, is utterly contrary to the data in Table 4, and to their interpretation. **27** crystallizes as a dimer with three molecules of dimethoxyethane (DME), (**27**·DME)$_2$·DME[62] (Fig. 2).



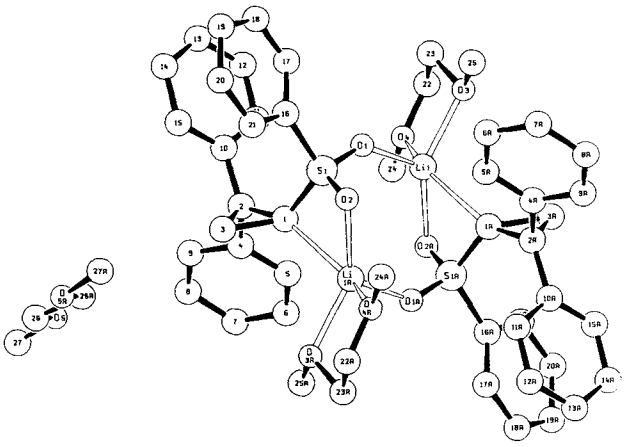


Fig. 2. Crystal structure of (**27**·DME)$_2$·DME [62].

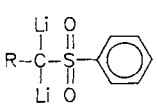
As in the crystal structures of the lithiosulfones **16**–**22**, the Li and sulfonyl O atoms are linked in such a way as to produce the typical (S-O-Li-O-S-O-Li-O) eight-membered ring. Each Li atom is bound to one DME molecule, with an additional molecule of DME cocrystallizing outside the "dimer". The most striking feature is that the $PhSO_2$ group is bent 61.7(5)° out of the plane of the cyclopropane ring. The bond between the Li atom and C_α (C1–Li1A 244.0(14) pm) is unique for lithiosulfones, and may be attributable to the high charge density in the exocyclic "anion" orbital. The bond axis C1–Li1A forms an angle of 24.9(6)° with the plane of the three-membered ring. Compared with the n_C–$\sigma^*_{S\text{-}C}$ interaction, a p_π–d_π interaction (delocalization) should therefore be of secondary importance in the stabilization of α-sulfonyl "anions".[34,63]

A glance at the literature shows how different **27** is from other cyclopropyl "anions" in which the charge is stabilized by delocalization. Because of the additional strain exerted by the double bond, cyclopropyl ester-enolates, for example, are highly reactive compounds even at −78°C, and can only be handled using special techniques.[64–66] The nitronate of nitrocyclopropane cannot be trapped with an electrophile (except in H/D exchange reactions), let alone be analyzed spectroscopically.[67] In contrast, 2,2-dimethyl-1-(phenylsulfonyl)cyclopropyllithium is—quite in accordance with the findings quoted above—stable even at 80°C in THF/DMSO.[21] Remarkably, we also found a tetrahedral α-C atom in the cyanocyclopropyl "anion" **64**. This agrees with the observation that, nitrile groups stabilize a negative charge predominantly by induction, and like the sulfone group not by delocalization (see Section 6).

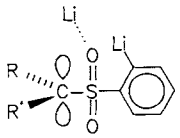
Thus, the X-ray crystal structures of lithiosulfones **16**–**22** and **27** published in the last three years, quantum mechanical calculations, and earlier kinetic and NMR spectroscopic studies provide a largely consistent picture of the structures of this class of compounds. The structure of a monomeric lithiosulfone is not known to date. It would also be interesting to know the C_α–S and S–O bond lengths in a lithiosulfone forced to adopt a conformation around the C_α–S axis which is rotated 90° from the optimum *gauche* conformation, e.g., that derived from **8**.

2.2. Dilithium Compounds

Dilithium derivatives[68] of sulfones have also been known for some time, and play a role in synthetic chemistry.[69] In systematic studies using reactions and NMR spectroscopy, *Gais* et al.[70] were the first to show that on synthesis of these compounds from sulfones or lithiosulfones and *n*-butyllithium the α,α-dilithio compounds **28** are not the only possible products.



28a: R = $CH{=}CH_2$
28b: R = Ph
28c: R = $SiMe_3$



29a: R = $CH{=}CH_2$, R' = H
29b: R = Ph, R' = H
29c: R = $SiMe_3$, R' = H
29d: R R' = $CH{=}CH{-}CH_2{-}CH_2$
29e: R = R' = $SiMe_3$

Reactions of phenyl sulfones, for instance, lead to the formation of α,*o*-dilithiosulfones **29** as well; in addition, the transformation **29** → **28** is observed. Thus, the α,α-"dianion" **28a** is only formed from the α,*o*-"dianion" **29a**, which is the initial product,[70a] upon raising the temperature. **29b** and **28b** behave similarly.[70c] The α,*o*-"dianion" **29c** is not formed; only the α,α-isomer **28c** is observed.[70b] In the case of **29d** and **29e** the α,α-compounds cannot be formed.[70c]

The most notable aspect of NMR studies of the α,*o*-dilithium compounds **29a**, **29d** and **29e** is the spectroscopic similarity of their α-C atoms to those of the corresponding α-monolithiosulfones. As X-ray structure determinations on monolithiosulfones **16**–**22** have shown, the Li atom is bound to the sulfonyl O atoms, not, however, to the α-C atom. *Boche* et al.[71] have also found exactly this bonding situation in **29e**, which crystallizes as an ether solvated, dimeric α,*o*-dilithium compound (Fig. 3).

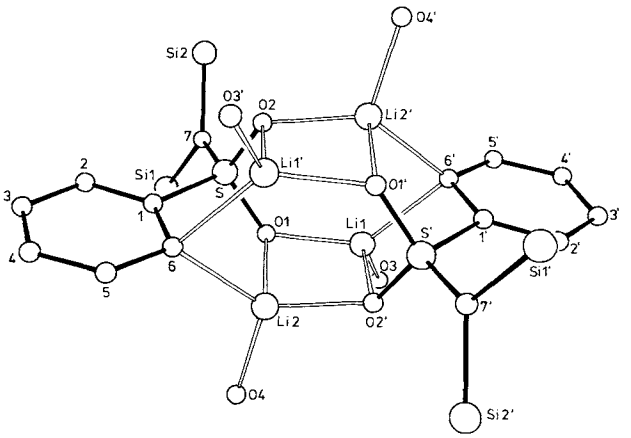


Fig. 3. Crystal structure of (**29e**)$_2$·4 Et_2O [71].

Figure 3 shows the characteristic (S-O-Li-O-S-O-Li-O) eight-membered ring of monolithiosulfones. The C_α-S bond is shortened to 163.7 pm, the lone pair of electrons on C_α adopts a *gauche* conformation with respect to the sulfonyl O atoms (rotated by ca. 18.5°), and the α-C atom is slightly pyramidalized.

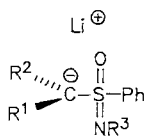
Additionally, **29e** represents an example of an *ortho*-lithium compound that is stabilized by coordination of an RSO_2 group. This type of structure was previously unknown.[72] Each Li atom is bound to an anionic phenyl C atom and to a sulfone O atom, giving rise to a five-membered (C-C-S-O-Li) ring, which is favorable for complex formation. A further coordination site on the lithium is occupied by an O atom of the sulfone group of the second "molecule", leaving a fourth coordination site vacant for the O atom of an ether molecule.

Regio- and stereocontrolled reactions of organolithium compounds, e.g., *ortho* lithiation and other reactions in which "complex-induced proximity effects" play a role, are currently of much synthetic significance.[73] RSO_2 substituents act as strongly directing groups in these reactions.[73b]

Recently, *Gais, Günther, Lindner* et al. have reported[74] the X-ray structure and the results of NMR spectroscopic studies for the α,α-dilithium compound dilithiotrimethyl(phenylsulfonylmethyl)silane **28c**. The crystal structure differs from those of the monolithium compounds **16**-**22** and **27** and from that of the α,*o*-dilithium compound **29e** in several respects. In **28c**, six "dianions" are aggregated to form $(\mathbf{28c})_6 \cdot Li_2O \cdot 10\,THF$. Most importantly, however, there are three different dianionic α-C atoms, each of which is bound to at least two Li atoms; obviously, the double negative charge on C_α must also be stabilized by Li-C bonds! (A similar bonding situation has also been observed for a dilithiated nitrile, see Section 10.2.) In the absence of Li_2O, **28c** crystallizes as $(\mathbf{28c})_4 \cdot 7\,THF$, whose structure has also been determined. Because of its solubility in THF, $(\mathbf{28c})_4 \cdot 7\,THF$ is amenable to multinuclear NMR spectroscopic studies. ^1H, ^{13}C, and ^6Li NMR data showed that also in solution one C atom is bound to two different Li atoms.

3. Lithium Compounds of Sulfoximides

Far less information is available on the structures of lithium compounds of sulfoximides (e.g., **30**) than for the related lithiosulfones, despite the fact that the former are of interest in asymmetric synthesis,[75] on account of the chiral center at sulfur.



30a: $R^1 = R^2 = H$, $R^3 = Me$
30b: $R^1 = R^2 = [^{13}C]Me$, $R^3 = Me$
30c: $R^1 = H$, $R^2 = R^3 = SiMe_3$

The first structural clues came from a ^{13}C NMR spectroscopic study by *Chassaing* and *Marquet*.[30a] On the basis of the $^1J_{CH}$ coupling constants of **30a** in THF, they concluded that the configuration of the α-C atom is pyramidalized, as in the corresponding α-sulfonyl "carbanion". The sulfoximide acidity measurements made by *Bordwell* and coworkers[28,31] are summarized in Table 4, together with the sulfone acidity measurements that were discussed in detail previously (see Section 2.1). As will be shown below, it can be assumed that an $RS(O)(NSO_2R')$ substituent, like an RSO_2 group, stabilizes a negative charge by n_C-σ^*_{S-C} interaction. For both the $RS(O)(NSO_2R')$ and RSO_2 groups, however, it remains unclear how the data in Table 4 and the conclusions drawn from them can be reconciled with this fact.

Detailed structural information was provided by the X-ray structure analysis of the sulfonimidoyl compound $((S)\text{-}\mathbf{30a})_4 \cdot 2\,TMEDA$, which was published by *Gais* et al. (Fig. 4).[76]

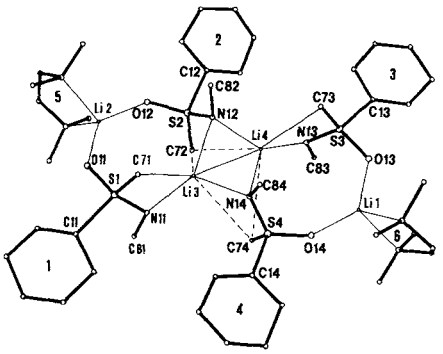
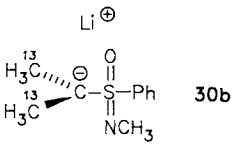


Fig. 4. Crystal structure of $((S)\text{-}\mathbf{30a})_4 \cdot 2\,TMEDA$ [76].

In contrast to the α-sulfonyl "carbanions" described in Section 2.1, **30a** does not crystallize as a dimer, but rather as a tetramer. The Li atom and the (*S*)-(*N*-methyl-*S*-phenylsulfonimidoyl)methanide moiety each occur in two different coordination environments. Li1 and Li2 are each coordinated to TMEDA and to the O atoms of two different "carbanions" (O13,O14 and O11,O12, respectively), a pattern equivalent to that found in α-sulfonyl "carbanions". Each of the other two Li atoms (Li3 and Li4), which are separated by only 278(5) pm, is coordinated to three N atoms of a sulfoximide group (N11,N12,N14 and N12, N13,N14, respectively), and to an "anionic" C atom (C71 or C73) with a mean Li-C distance of 249(5) pm). Thus, the Li-C bond in $((S)\text{-}\mathbf{30a})_4 \cdot 2\,TMEDA$ fundamentally differentiates this structure from those of the α-sulfonyl "carbanions" **16**-**22**, in which only Li-O bonds were observed!

The authors also discern a contact between the other two "anionic" C atoms (C72 and C74) and Li3 and Li4, respectively. The mean Li-C distance of 323(4) pm is, however, so large that it can hardly represent a bonding interaction. The S-CH_2 distances (mean value 164(2) pm) are shortened relative to the S-C distances in *S*-methylsulfoximides (mean value for nine compounds: 174 pm), though not to the same extent as in α-sulfonyl "carbanions" (see Section 2.1). Since the position of the H atoms on the "anionic" C atom could not be determined, nothing can be said about the configuration of this carbon, or about the conformation about the C-S axis.

Some information concerning the structure in solution ([D_8]-THF) was obtained using the ^{13}C-labeled compound **30b**.



30b

A diastereotopomerization of the two $^{13}CH_3$ groups was observed, caused either by rotation around the C–S bond, if the configuration of the "anionic" C atom is planar, or by rotation and inversion if it is pyramidal. The $\Delta G^{\neq}_{70°C}$ value for the topomerization is 9.2 ± 0.2 kcal mol^{-1}. It was, however, not possible to determine which mechanism is responsible for the topomerization. Preparatively, it is significant that even at $-70°C$ α-sulfonimidoyl "carbanions" of type **30**, $R^1 \neq R^2$, are not configurationally stable. It is interesting that an asymmetric elimination, with which 1-alkenylsulfoximides have been synthesized with a high degree of induction, was explained in terms of this configurational lability.[77]

30c could be crystallized without donor ligands, as the tetramer $(\mathbf{30c})_4 \cdot 2C_6H_{12}$.[78] The crystal structure is depicted in Figure 5 together with a partial structure showing the atom numbering scheme.

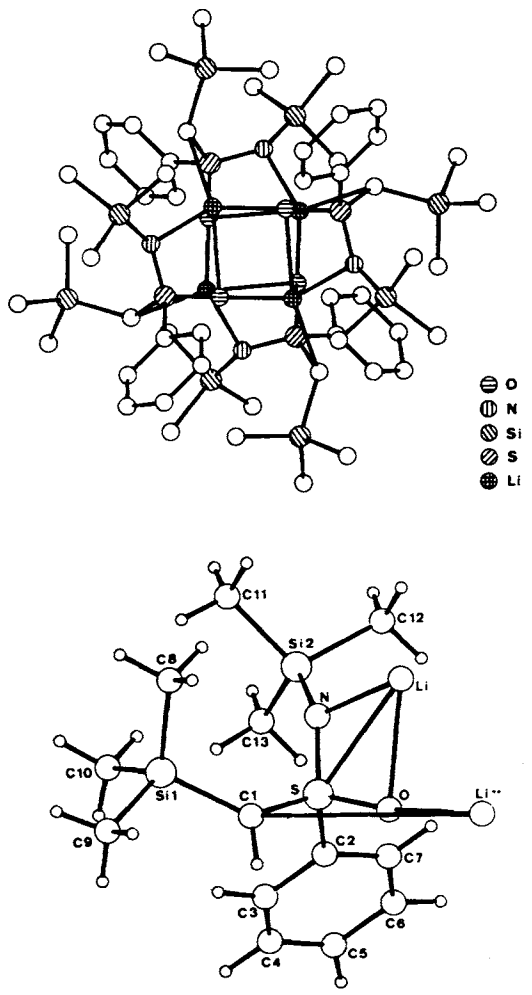


Fig. 5. Top: crystal structure of $(\mathbf{30c})_4 \cdot 2C_6H_{12}$; bottom: partial structure of $(\mathbf{30c})_4 \cdot 2C_6H_{12}$ with numbering scheme [78].

$(\mathbf{30c})_4 \cdot 2C_6H_{12}$ is composed of two *R,R*- and two *S,S*-**30c** diastereomers. A Li_4O_4 cube forms its center. Each Li atom is pentacoordinated to the O and C (!) atoms of one sulfonimidoyl anion, to the N and O atoms of a second, and to the O atom of a third. Two molecules of cyclohexane, derived from the solvent, are also present in the crystal lattice. $(\mathbf{30c})_4 \cdot 2C_6H_{12}$ is readily soluble in hydrocarbons, undoubtedly because the polar core, with its Li and C, N, and O atoms, is well-shielded by the eight trimethylsilyl and four phenyl groups. The configuration at C1 is of particular interest. C1 projects 17 pm out of the plane defined by its substituents S, Si1, and H1, so that C1 is markedly pyramidalized—in accordance with the results of the ^{13}C NMR spectroscopic studies on α-sulfonimidoyl "carbanions" mentioned above.[30] The conformation about the C1–S bond is such that the S–C2 bond lies approximately *anti* to the 243.08 pm long C1–Li** bond. The C1–S bond is—as in $((S)\text{-}\mathbf{30a})_4 \cdot 2$TMEDA—shortened relative to that in the sulfoximide, in this case to 163.7(4) pm.

Here, too, it is likely that a stabilization by n_C–σ^*_{S-C} interactions, in a way similar to that in α-sulfonyl "carbanions",[41,43] is responsible for the observed configuration and conformation. In contrast to the α-sulfonyl case, however, α-sulfonimidoyl "anions" also exhibit bonding between the Li atoms and the "anionic" C atoms. This could be connected with the lower acceptor ability of the sulfonimidoyl group compared to the sulfone group, and with the greater donor character of the O atoms in α-sulfonyl "carbanions" compared to the O and N atoms in α-sulfonimidoyl "carbanions".

The $^1J_{CH}$ coupling constant for the anionic C atom in $(\mathbf{30c})_4 \cdot 2C_6H_{12}$ (in $[D_{12}]$cyclohexane) is 5 Hz larger than that for the corresponding non-lithiated sulfoximide. This points to a hybridization between sp^2 and sp^3 in solution as well, a finding which is in agreement with the crystal structure of $(\mathbf{30c})_4 \cdot 2C_6H_{12}$, and with earlier NMR spectroscopic studies.[30] In THF, which has better solvating properties, Δ^1J_{CH} is significantly larger (15.0 Hz). A different, THF-solvated aggregate must be responsible for this, with a nearly planar "anionic" C-atom and perhaps with no contact to the Li lithium.

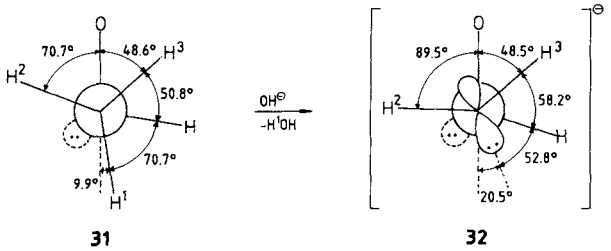
It is clear that, in contrast to the lithiosulfones, quite some work still remains to be done to better understand the structures of lithiosulfoximides and their reactions, particularly with respect to chiral induction.

4. Lithium Compounds of Sulfoxides

Because they contain a chiral $R^3S(O)$ group, α-sulfinyl "carbanions" $R^1R^2C{-}S(O)R^3M$ have in recent years proved to be important synthetic building blocks, as is demonstrated by a wealth of publications.[79,80] Almost all of these are also concerned to some extent with the structures of the "α"-lithiosulfoxide reagents.

The first clues to the structures of α-sulfinyl "carbanions" were provided by *Wolfe*, *Buncel* et al., who observed selectivity in the H/D exchange of the diastereotopic methylene protons of benzyl methyl sulfoxide (0.25 M NaOD in D_2O, 75°C).[81a,d] This study has been confirmed several

times, and applied to other sulfoxides,[81b] and was corroborated by *Wolfe* et al. using 3-21G* calculations. The quintessence of these studies is summarized in Figure 6.



31 **32**

Fig. 6. Newman projections of the energetically most favorable conformations of $H_3C-S(O)H$ **31** and its anion $H_2\overset{\ominus}{C}-S(O)H$ **32**, formed by reaction with $OH^{\ominus}$ [81b, c].

H^1, which has a virtually antiperiplanar arrangement with respect to the S-O bond, is cleaved from the sulfoxide $H_3C-S(O)H$ **31**, because the α-sulfinyl carbanion which is thus formed most closely resembles the optimum structure of $H_2\overset{\ominus}{C}-S(O)H$ **32**. The conformation about the C-S axis in **32**, in which the lone pair of electrons on the α-C atom is rotated 20.5° away from the position antiperiplanar to the S-O bond, represents a compromise between maximization of the $n_C-\sigma^*_{S-O}$ and $n_C-\sigma^*_{S-H}$ stabilization as well as minimization of lone pair repulsion.[81d] The configuration of the "anionic" C atom is strongly pyramidalized, with the substituents (H^2 and H^3) bent *towards* the O atom. A counter ion was not included in these calculations.

Further clues to the structures of α-sulfinyl "carbanions", particularly with regard to the position of the counter ion (usually lithium) were derived from reactions with electrophiles.[32, 79a, 82–86] Electrophiles containing oxygen (H_2O, D_2O, CO_2, RCHO, R_2CO and $(CH_3O)_3PO$) react with "α"-lithiosulfoxides in THF with retention of configuration, while CH_3I reacts with inversion (though an exception to this inversion with CH_3I has recently been observed[87]). *Biellmann* et al.,[83] *Durst* et al.,[84] and *Chassaing* and *Marquet*[85] concluded from this that the Li atom in the "α"-lithiosulfoxide is bound to the sulfoxide O and to the α-C atom, and that the stereoselectivity is connected with the ability of the electrophile to form a complex with lithium (Fig. 7).

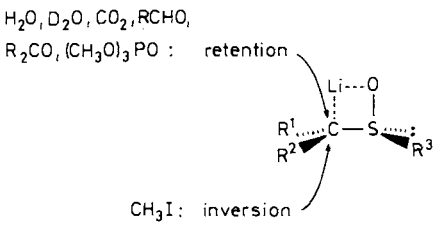


Fig. 7. "Ion-pair" model of "α"-lithiosulfoxides, and diastereofacial differentiation [83–85].

The *n*-BuLi in THF required to form the "α"-lithiosulfoxide is also led to the sulfoxide through complexation of the lithium with the sulfoxide O atom.[87]

Extensive IR, Raman, and ^{13}C NMR spectroscopic studies of lithiosulfoxides have been published by *Chassaing* and *Marquet*.[29, 30, 32] From the C,H coupling constants in **33**, **34** and **35**, they concluded that the α-C atoms in the benzylic anions **33** and **34** are largely planar, while the α-C atom in **35** is hybridized "between sp^2 and sp^3" (see Table 5).

Table 5. C,H coupling constants for the α-C atom of **33**, **34** and **35** [29, 30].

	^1J(C,H)	Δ^1J("anion"-sulfoxide)
$CH_3SOCHPhLi$ **33**	160	+20
*t*BuSOCHPhLi **34**	161	+23
*t*BuSOCH$_2$Li **35**	147.5	+10

According to a similar study, "α"-lithiothiacyclohexane 1-oxides are planar at C_α.[90] Finally, the topomerization of the α-H atoms in **36a–c** (Table 6) showed that these compounds are configurationally stable only at low temperatures, and that the counter ion has an influence on the rate of topomerization.

Table 6. Coalescence temperature of the signals of the two H atoms on C_α, and ΔG^+ values for the topomerization, for **36a–c** [32].

	$T_{coal.}$ [°C]	ΔG^+ ($T_{coal.}$) [kcal mol^{-1}]
$PhSOCH_2Li$ **36a**	−5	13.6
$PhSOCH_2K$ **36b**	−47.5	10.7
$PhSOCH_2K$ + [2.2.2]Cryptand **36c**	−66	10.7

The force constants derived from the vibrational spectra indicate a shortening of the C-S bond and a lengthening of the S-O bond.[32] A chelate structure, as depicted in Figure 7, was deduced from the presence of C-Li and O-Li stretching vibrations.[32] However, on the basis of ^{13}C NMR spectroscopic studies of fluoro(phenylsulfinyl)methyllithium, *Seebach* suggested that the Li atom might be bound only to the sulfinyl O atom.[91]

The first crystal structure of an α-sulfinyl "carbanion", that of (**38b**)$_2$·2TMEDA, was published by *Boche* et al.[92] The dimer is linked together through a (Li-O-Li-O) four-membered ring (Fig. 8).

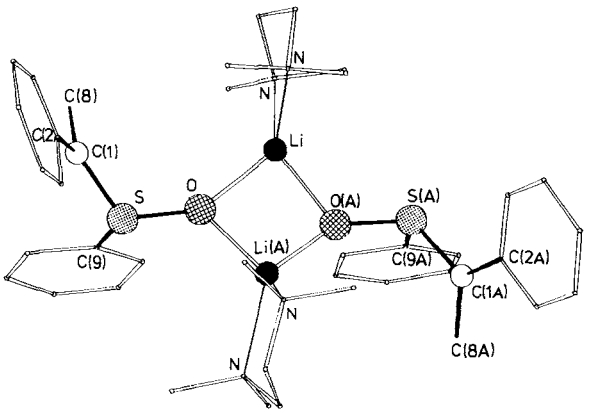
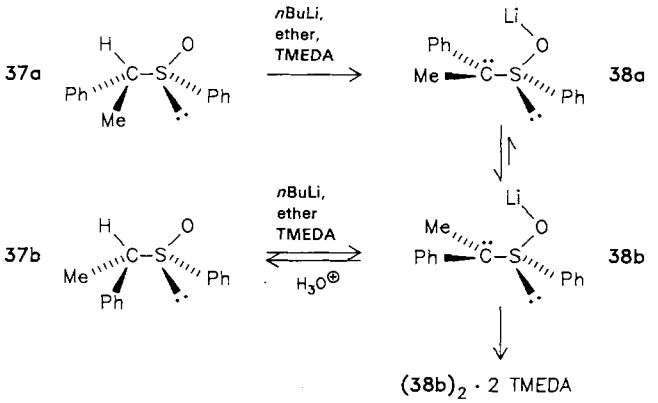


Fig. 8. Crystal structure of dimeric (**38b**)$_2$·2TMEDA [92].

The diastereomer $(\mathbf{38b})_2 \cdot 2$TMEDA is produced from a *ca.* 1:1 mixture of the two diastereomeric α-methylbenzyl sulfoxides **37a**, **b** with *n*-BuLi in ether/TMEDA. The phenyl rings at C1 and S are oriented *trans* to one another (torsion angle C2,C1,S,C9 = 152(1)°). Since protonation of **38** in ether solution yields only **37b**, and since the protonation of α-sulfinyl "carbanions" proceeds stereoselectively (see above), then presumably only one diastereomer is present in solution, i.e., that also observed in the crystalline state, **38b**. From the stereoselectivity of sulfoxide deprotonation with *n*-BuLi in ethereal solvents (see above), one might also have expected formation of the isomeric lithio sulfoxide **38a**. The topomerization data (see Table 6) suggest, however, that in solution at room temperature, **38a** will be rapidly converted into the obviously more thermodynamically stable **38b**.



The C1–S distance of 163(1) pm is distinctly shorter, and the S–O distance of 158(1) pm is somewhat longer than the corresponding bonds in sulfoxides (dimethyl sulfoxide 180 pm and 147 pm, respectively)[93]—a quantification of the vibrational spectral data.[32] Since the torsional angle C1,S,O,Li is 12(2)°, the Li atom does not lie exactly in the C1,S,O plane. The C1–Li distance is extraordinarily large, (400(3) pm), so that one can no longer speak of a C–Li bond (C–Li bonds are shorter than *ca.* 250 pm).[1] This distinguishes the bonding situation of the Li atom found in $(\mathbf{38b})_2 \cdot 2$TMEDA from that which is expected (see Fig. 7). Little can be said about the role of the TMEDA ligands here, since no other lithiosulfoxide structures are known at present.[164] But $(\mathbf{38b})_2 \cdot 2$TMEDA, at least, is not an α-lithiosulfoxide!

The configuration of the anionic C1 atom and the conformation about the C1–S axis of $(\mathbf{38b})_2 \cdot 2$TMEDA deserve particular attention (Fig. 9).

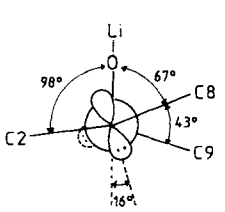
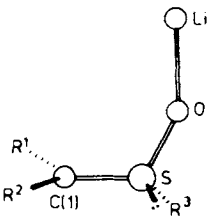


Fig. 9. Configuration of C1 and conformation along the C1–S bond in $(\mathbf{38b})_2 \cdot 2$TMEDA [92].

As can be seen, C1 is non-planar and projects 12(1) pm out of the S–C2–C8 plane; the substituents at C1 are bent *towards* the O atom (and thus also towards the Li atom). A planar benzylic α-C atom had been predicted on the basis of ^{13}C NMR spectroscopic data (see Table 5). The lone pair of electrons at C1 is bent *ca.* 16° away from the antiperiplanar position to the S–O bond, thus reducing repulsion between the two unshared pairs of electrons. The benzylic C1 atom in $(\mathbf{38b})_2 \cdot 2$TMEDA must be more nearly planar than the nonbenzylic C_α of the system $H_2\overset{\ominus}{C}-S(O)H$ **32** used in model calculations (Fig. 6), and should bear less charge. After allowing for this, the calculated structure[81b,c] of the α-sulfinyl anion moiety and that found in the solid state agree surprisingly well, especially considering that the calculations dispense with the Li atom. It is possible that the crystal structure of $(\mathbf{38b})_2 \cdot 2$TMEDA may even offer an explanation of why it is possible to disregard Li in the calculations. Since there is no C–Li bond in $(\mathbf{38b})_2 \cdot 2$TMEDA, the configuration of C_α and the conformation about C_α–S can hardly be significantly affected by the counter ion.

It would be presumptuous, on the basis of a single crystal structure of one α-sulfinyl "carbanion",[164] to attempt to deduce the structures of the entire class of compounds in a variety of media (the molecular weight has yet to be determined). Neither can one explain the observed diastereofacial differentiation, nor the diastereoselectivity of reactions with electrophiles, especially since these are not very pronounced, and exceptions have already been referred to.[87] Nonetheless, some insights can be attained, which—with all due caution—are discussed below.



38b–43

	R^1	R^2	R^3
38b	CH_3	Ph	Ph
39	H	Ph	CH_3
40	H	Ph	*t*Bu
41	H	S-*p*-Tolyl	*p*-Tolyl
42	H	H	*p*-Tolyl
43	H(Ph)	Ph(H)	Ph

Fig. 10. Bonding relationships of C1, S, O and Li in $(\mathbf{38b})_2 \cdot 2$TMEDA [92], and their extrapolation to the structures of **39**–**43**.

1. It can be seen from Figure 10 that the diastereofacial differentiation found in many cases, which had led to the "ion-pair" model (Fig. 7), is also in accord with the crystal structure of $(\mathbf{38b})_2 \cdot 2$TMEDA. Thus, for O-containing electrophiles, there exists the possibility of forming a complex with lithium with the reaction therefore occurring from the corresponding side.

2. If one assumes that, as in **38b**, the "large" substituents in lithiobenzylmethyl sulfoxide **39** and lithiobenzyl-*tert*-butyl sulfoxide **40** avoid one another, so that the configurations and conformations in these compounds are comparable with those in $(\mathbf{38b})_2 \cdot 2$TMEDA (Fig. 10), then the findings of *Ohno* et al.[80e,87] can be understood as follows. Methyl iodide approaches the methyl compound **39** from the face *away* from O and Li, as is normal, but with the *tert*-butyl compound **40**, steric hindrance from the *tert*-

butyl group is so great that CH_3I favors the otherwise unusual face with the O-Li bond.[164] The fact that lithiobenzylphenyl sulfoxide reacts with CH_3I to form a 1 : 1 diastereomeric mixture agrees with this; apparently when R^3 = Ph, both faces are equally favored.[92]

3. If **41** has the assumed structure, then the diastereoselectivity upon reaction with benzaldehyde found by *Gennari, Scolastico* et al.[94] can also be understood; the O···Li coordinated benzaldehyde approaches in such a manner as to undergo minimal interaction with the *p*-tolyl-S group. Similarly, it is clear why **42**, which is unsubstituted at the anionic C atom, does not react diastereoselectively,[95] although why a certain selectivity is found for the corresponding ZnCl compound is unclear.[96] The fact that the products of the reaction of **43** with benzaldehyde suggest the presence of various diastereomeric lithiosulfoxides could be due to the experimentally proven reversibility of this addition reaction.[97]

Conclusion: just as one swallow does not make a summer, one can not, of course, draw a complete picture of this class of compounds from *one*[164] crystal structure of a lithiosulfoxide. We are further still from understanding the stereoselective reactivity of lithiosulfoxides with electrophiles. It is pleasing, however, that the crystal structure of (**38b**)$_2$·2TMEDA is in overall agreement with the models derived from calculations as well as from selective reactions and spectroscopic data. It remains to be seen if and how structural studies on further lithiosulfoxides will consolidate and refine the current picture.[164]

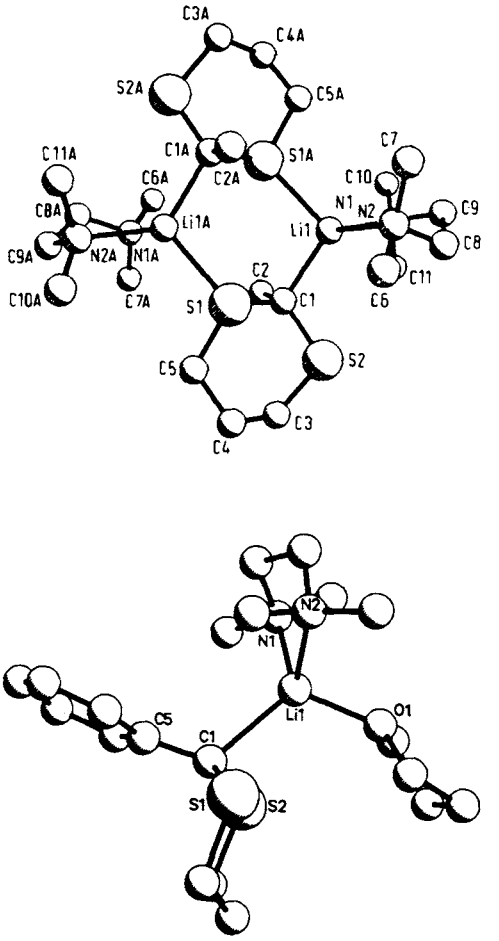
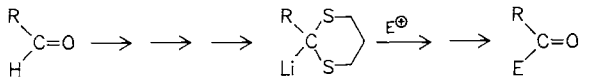


Fig. 11. Crystal structures of (**44a**)$_2$·2TMEDA [99] (top) and **44b**·TMEDA·THF [50a] (bottom).

5. Lithium Compounds of 1,3-Dithianes and Thioethers

5.1. Lithium Compounds of 1,3-Dithianes

Even in the early stages of the "carbanion era", lithiodithianes **44** found extensive use as Umpolung reagents.[98]



44a: R = CH_3
44b: R = Ph

It is therefore not surprising that even at the beginning of the eighties *Amstutz, Dunitz, Seebach* et al. had already carried out X-ray structure determinations of 2-lithio-2-methyl-1,3-dithiane **44a**, which crystallizes as (**44a**)$_2$·2TMEDA,[99] and of 2-lithio-2-phenyl-1,3-dithiane **44b**, which crystallizes as **44b**·THF·TMEDA[50] (Fig. 11).

(**44a**)$_2$·2TMEDA consists of three *trans*-linked six-membered chairs and two Li-TMEDA five-membered rings. The 33 pm difference between the C-Li and S-Li bond lengths corresponds approximately to the difference in the covalent radii of C and S (27 pm). The lithium atom therefore exhibits comparable interactions with the α-C atom of one dithiane ring and the S atom of the other. It is not entirely clear whether the equatorial position of lithium has steric grounds or whether it is due to electronic factors, as was assumed earlier;[100] however, since the methyl group is the smallest of the three substituents on the dithiane ring, it should occupy an axial position for steric reasons.[99] With THF instead of TMEDA, lithiodithiane **44a** also exists as a dimer (**44a**)$_2$·4THF in the solid state.[101] However, there is chemical evidence for a temperature-dependent monomer-dimer equilibrium in THF solution. According to cryoscopic measurements, monomeric **44a** is the major component in THF at low temperatures. Interestingly, TMEDA in THF associates with **44a** only to a small extent, as is also demonstrated by the melting point.[101] The ^{13}C NMR spectrum confirmed the dominant presence of monomeric **44a** at low temperatures.[102]

In contrast to (**44a**)$_2$·2TMEDA, **44b**·THF·TMEDA occurs as a monomer in the solid state. The Li atom is coordinated to the α-C atom, and also to one TMEDA and one THF molecule. The phenyl group in the unmetalated dithiane occupies an equatorial position, but in **44b**·THF·TMEDA it is axially oriented, as was also shown by trapping experiments in solution. At the same time, the plane of the benzene ring is twisted through 90°, whereby the optimum conformation for conjugative charge stabilization is attained. The benzylic α-C atom is, nevertheless, clearly pyramidalized (Fig. 12).

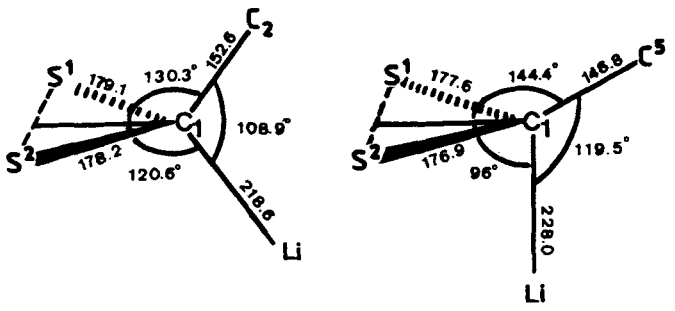


Fig. 12. Bond lengths and configuration at C1 for $(\mathbf{44a})_2 \cdot 2$TMEDA (left) and **44b**·THF·TMEDA [50a] (right).

As shown in Figure 12, the angle of 130.3° between the S1-C1-S2 bisector and the C1-C2 axis in $(\mathbf{44a})_2 \cdot 2$TMEDA changes to "only" 144.4° in **44b**·THF·TMEDA (here the C1-C5 axis). Together with the change in the C-Li bond length and in the angle of the C-Li bond to the bisector (see Fig. 12), this seems to indicate a transition towards a π-complex structure[49] for **44b**·THF·TMEDA. Compared to the differences in reactivity, however, and to the pK_a difference of eight units between the corresponding acids,[50a] these changes appear minor. The conclusions originally drawn[50a] from deformation density distributions about the nature of the C-Li bonds in $(\mathbf{44a})_2 \cdot 2$TMEDA and **44b**·THF·TMEDA were corrected in a later publication.[50b] The crystal structure data leave the question of the ionic nature of the C-Li bond open. On this point the authors adopt the viewpoint of *Streitwieser* et al.:[103] "operational criteria to distinguish charge transfer from polarization effects are difficult to devise, particularly within the limitations of working with real compounds".

5.2. Lithium Compounds of Thioethers

Up till now, crystal structure data have been obtained for the following α-lithiothioethers (Fig. 13): (phenylthio)methyllithium **45** as $(\mathbf{45})_2 \cdot 2$TMEDA,[50b] (methylthio)methyllithium **46** as $(\mathbf{46})_2 \cdot 2$TMEDA,[50b] and (*E*)-1-(*tert*-butylthio)-2-butenyllithium **47** as the monomeric TMEDA complex, **47**·TMEDA.[104]

$(\mathbf{45})_2 \cdot 2$TMEDA displays similarities to the lithiodithiane $(\mathbf{44a})_2 \cdot 2$TMEDA, but shows differences as well. Both form dimers with a six-membered ring, but in $(\mathbf{45})_2 \cdot 2$TMEDA the Li-C distance, for instance, is shorter than in $(\mathbf{44a})_2 \cdot 2$TMEDA (213.0, compared with 218.6 pm), while the Li-S bond length is longer (255.4, compared with 251.9 pm). Since the phenyl rings in $(\mathbf{45})_2 \cdot 2$TMEDA occupy equatorial positions, each S-phenyl bond lies antiperiplanar to the C-Li bond. If, as in the anomeric effect, this results from an interaction involving the lone pair of electrons on C_α and the $\sigma^*_{S\text{-phenyl}}$ orbital, then $C_{methylene}$-S (175.9 pm) should be shorter and C_{phenyl}-S (179.2 pm) longer than the corresponding bonds in CH_3-S-aryl molecules. Indeed, the Cambridge Structural Database gives mean values of 182.1 and 176.8 pm, respectively, which confirm these expectations.

Strangely, methylthiomethyllithium **46** dimerizes through a (Li-C-Li-C) four-membered ring to give $(\mathbf{46})_2 \cdot 2$TMEDA. There is no obvious explanation for the difference between this and $(\mathbf{45})_2 \cdot 2$TMEDA. The difference in energy between the six- and four-membered rings is probably only small. Although this difference "will doubtless soon be explained using semi-empirical or ab initio calculations",[50b] this has not yet happened.

The four-membered ring in $(\mathbf{46})_2 \cdot 2$TMEDA is folded along the Li-Li axis by 22°. Each C atom in the ring is five-fold coordinated, to two H atoms, two Li atoms and one S atom. The H-C-H and H-C-S bond angles are all close to the tetrahedral angle (between 103.3 and 109.2°), so that C_α can be described as sp^3-hybridized.

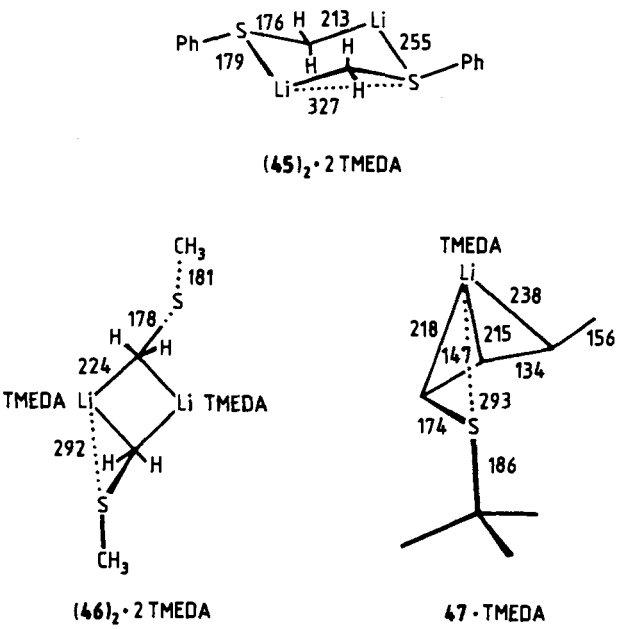
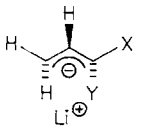


Fig. 13. Crystal structures of lithiothioethers.

The structure of lithiated 2-butenyl-*tert*-butyl sulfide **47**·TMEDA is of particular importance, since organometallic compounds of this type (i.e., also those with heteroatoms other than sulfur) are important as heterosubstituted allyl anion synthons.[105] Its reactions suggest a *cis* (*syn*) configuration for the "6π-electron, 4 atom" system.[106] The structure of such an "anion" was until now, however, unknown.

The following structural features are characteristic. The Li atom is bound to all three C atoms of the allyl moiety, as well as to the TMEDA N atoms (see Fig. 13). On the basis of the distance between Li and S (293 pm), there appears to be no interaction between them. The S atom lies in the plane of the allyl C atoms, and adopts a *cis* (*syn*) configuration, in agreement with the conclusions reached from trapping experiments.[106] The Li atom lies above and the *tert*-butyl group below the plane of the allyl C atoms. The *t*Bu-S bond is exceptionally long; at 186 pm, it is the longest known to date. The cause of this is again probably the n-σ* interaction mentioned above for **45**. The bond lengths in the allyl moiety are not appreciably different from those in allyl thioethers: C2-C3 134 (134 pm), and C1-C2 147 (149) pm.

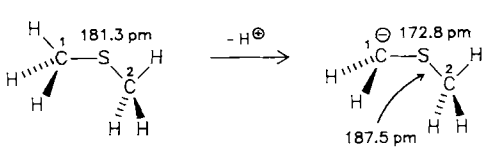
Can we use this structure to say anything about the α/γ-selectivity in reactions of such compounds with electrophiles? If **47**·TMEDA is a model of the reactive species, then the position of the Li atom, more or less in the center of the allyl group, shows that the counter ion cannot be crucial for α/γ selectivity. The structure accords far better with a situation in which all possible parameters, such as solvent, counter ion, coordination partner, temperature, electrophile, etc., are able to influence the course of the reaction.[105] Understanding such complexity is at present beyond the capabilities of the chemist.



48a: X = H, Y = SH
48b: X = SH, Y = H

The crystal structure of **47**·TMEDA was also compared with model calculations for *cis*(*syn*)-**48a** and *trans*(*anti*)-**48b**. The *cis*(*syn*) isomer is the more stable. Using 3-21G this extra stability amounts to 6.8 kcal mol^{-1}, while with 3-21+G‖3-21G it is 6.5 kcal mol^{-1}. The C1-C2-C3-Li moiety largely corresponds with that calculated for allyllithium,[107] with the allyl group as an η^3-ligand, and with an ionic bond to lithium. Interestingly, in both isomers the position of the Li atom is affected only negligibly by the position of the S atom, indicating the absence of a covalent Li-S bond; however, electrostatic interactions are also conceivable. Like the H atoms in allyllithium, the substituents are bent out of the C1-C2-C3 plane;[107] the inner ones away from lithium, the outer ones remaining largely in the plane, and H2 towards lithium. The most notable difference between the crystal structure of **47**·TMEDA and the calculated ("gas-phase") structure of **48** is the greater asymmetry in the coordination sphere of the Li atom in **47**·TMEDA. In the solid state, the difference between C1-Li and C3-Li distances is 20 pm, while the calculated values differ by only 10 pm. The C-C bonds also differ considerably between the two structures. While in **47**·TMEDA they amount to 147 and 134 pm, in **48a** they lie only 1.4 pm apart. Although it is not clear at present what determines these differences, the "reproduction" of the solid state structure by the calculations is on the whole satisfying and encouraging.

The question of how an RS group stabilizes an adjacent negative charge was first studied by *Wolfe* et al.[41, 108] On moving from dimethyl sulfide **49** to the anion **50**, their calculations show a shortening of the C1-S bond and a lengthening of the S-C2 bond, in keeping with the experimental data for lithiosulfides (see above).



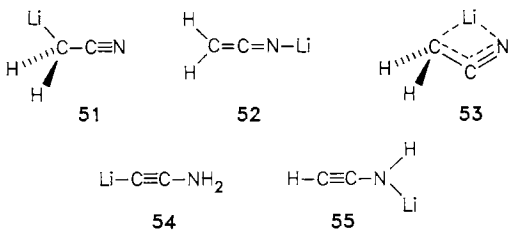
49 **50**

According to *Wolfe*, the participation of a sulfur d-orbital plays an important role here. Renewed investigations by *von Schleyer, Houk* et al.[109] concluded, however, that d-orbitals are only important in determining the geometry, and not the energy.

6. Lithio Compounds of Nitriles

There is no doubt that the extent of application of cyano-stabilized "carbanions" in synthesis[110] is inversely related to the knowledge of their structures. Only recently have these compounds become known in more detail. A comprehensive article by *von Schleyer, Moffatt* et al., which appeared in 1986, is concerned with structural calculations for monomeric, dimeric, tetrameric, solvated and non-solvated, lithium (and also sodium and magnesium) compounds of this type.[111] Calculations were also carried out for anions without counter ions. Some of the earlier experimental results, which are summarized in Ref. [111], and some of the calculated data will now be briefly discussed.

In principle, metalated monomeric nitriles can occur as *C*-metalated species **51**, *N*-metalated species (ketenimine derivatives) **52**, bridged compounds **53**, and in the case of acetonitrile also as the acetylene derivatives **54** and **55**. These alternatives were originally inferred from IR and NMR spectroscopic studies,[112] but were later revised in favor of ion-pair equilibria.[113]



51 **52** **53**

54 **55**

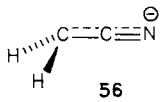
As well as these structural variants, one must—as always with organometallic compounds—take aggregation into consideration. *Das* and *Wilkie*,[114] for example, found that $LiCH_2CN$ is tetrameric in DMSO, and that LiCH(Ph)CN is dimeric in DMSO and in dimethoxyethane. In contrast, *Bauer* and *Seebach* observed dimeric $LiCH_2CN$ in THF between −108 °C and room temperature, and monomeric LiCH(Ph)CN at −108 °C.[101b, 115]

According to calculations at the (MP2/6-31+G*//6-31+G*) level, the anion $CH_2CN^{\ominus}$ **56** has a non-planar α-C atom, although the inversion barrier of 0.3 kcal mol^{-1} is minimal.

It is remarkable that on going from CH_3CN to $CH_2CN^{\ominus}$ **56**, the CN bond is only negligibly lengthened (Table 7).

Of the lithiated monomers, the most stable is the bridged species **53**, followed by the ketenimine derivative **52**, which is higher in energy by 9.7 kcal mol^{-1} (MP2/6-31G*//6-31G*) or 5.8 kcal mol^{-1} (6-31G*//6-31G*). Table 7 lists important bond lengths for both molecules.

Here, too, the comparatively short C-N bonds are clearly apparent.



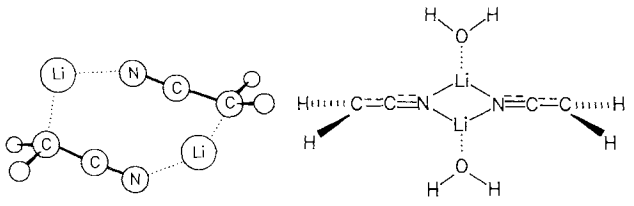
56

Table 7. Calculated bond lengths [pm] for CH_3CN, **56**, **53**, and **52**.

	CH_3CN [a]	**56** [a]	**53** [b]	**52** [b]
CN	113.55	116.22	116.5	118.0
CC	146.87	139.27	139.8	133.0

[a] 6-31+G*//6-31+G*. [b] 3-21G//3-21G.

Finally, the molecular weight determinations mentioned above also prompted calculations for dimeric structures; because of the size of the molecules, this had to be carried out using MNDO. Various considerations[111] led to the conclusion that in the absence of solvation the eight-membered ring dimer **57** ought to be most favored, while in ethereal solvents, and in the solid state, the di-solvated four-membered ring dimer **58** (with H_2O as the proven[107b] model for ethereal solvents) should occur.



57 58

What does the structure look like in reality? The first answer to this question was provided by the structure of α-cyanobenzyllithium, which crystallizes as $(\mathbf{59})_2 \cdot 2\text{TMEDA} \cdot C_6H_6$ (Fig. 14).[116]

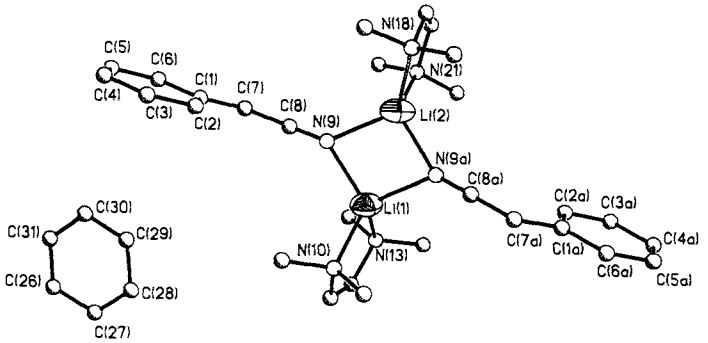
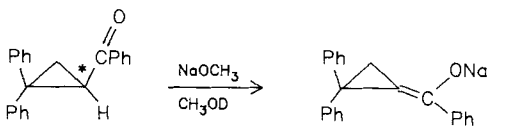


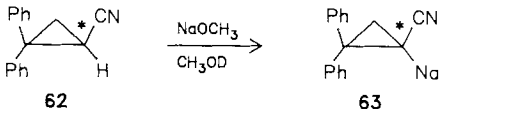
Fig. 14. Crystal structure of $(\mathbf{59})_2 \cdot 2\text{TMEDA} \cdot C_6H_6$ [116].

59 is the first lithionitrile to have yielded crystals that could be examined by X-ray crystallography. The co-crystallization of benzene (closest distance to the lithium compound: 378 pm) appears to be decisive here, since $LiCH_2CN$ and LiCH(Ph)CN have long been known as solids. The structure found in the solid state and that determined by MNDO-calculations[111,117] should therefore be the same as that indicated by the molecular weight determination[114,115] in solution at room temperature. Furthermore, the small difference in the heats of formation between $(\mathbf{59})_2 \cdot 4NH_3$ and $2\,[\mathbf{59} \cdot 3NH_3]$ $(-2NH_3)$ of only ca. 5 kcal mol^{-1} (MNDO)[117] suggests that **59** is a monomer[101b,115] in THF at −108 °C for entropy reasons. It is interesting that in lithionitrile **59**, too, the Li atom has no contact with the "anionic" C_α-atom, so that this is not an α-lithio compound either! To what extent the TMEDA ligands are responsible for this cannot be said at present. However, it appears that they are not important, as indicated by the crystal structure of the lithioaminonitrile **83**, in whose case the Li atoms are complexed with the O atoms of ether molecules (see Section 10.1). At −35 °C, the hydrogen atoms at C-7 and C-7a of $(\mathbf{59})_2 \cdot 2\text{TMEDA} \cdot C_6H_6$ could be located, and the sum of the bond angles at C7 (360°) and C7a (359.5°) determined. These atoms are therefore planar, which on the basis of their benzyl "anion" character and the inversion barrier in anion **56** of only 0.3 kcal mol^{-1}, is quite plausible.

The bonding situation in the almost linear C-C-N unit of **59** ($\sphericalangle$ = 178.4(1.0)°) is of particular interest. The C7-C8 and C8-N9 distances are 137.8(8) and 117.9(8) pm, respectively (mean values). The C-N distances calculated for **56** (116.22), **53** (116.5) and **52** (118.0 pm) therefore agree satisfactorily with those found in **59**. In nitriles, such as acetonitrile,[118] the C-N distance (115.7 pm) is only slightly shorter; in comparable ketenimines such as $Ph_2C{=}C{=}N{-}C_6H_4{-}p\text{-Br}$, by contrast, one finds shorter C-C, and above all significantly longer C-N bonds (133.0 and 124.0 pm, respectively),[119] in accordance with IR spectroscopic data.[116] The structural similarity of the lithium "keteniminate" **59** to normal ketenimines is hence considerably less than that of a lithium enolate to enol ethers, for which the pairs of C=C and C-O distances are almost identical.[120] The reason for this is probably a different mode of stabilization of the negative charge. While a carbonyl group acts predominantly via delocalization, in the nitrile group the (inductive) field effect also plays a considerable part. The "cyclopropyl effect" illustrates this difference splendidly. The comparatively less acidic (−)-(*R*)-(2,2-diphenylcyclopropyl)phenyl ketone **60**, for example, shows a k_R/k_E value of 1, on H/D exchange (0.1 M $NaOCH_3$ in CH_3OD).[121] The low acidity and complete racemization result from the additional strain that the planar enolate **61** introduces into the three-membered ring.



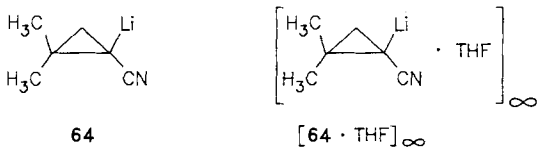
60 61



62 63

In the optically active nitrile **62**, a comparable experiment (1.0 M $NaOCH_3$ in CH_3OD) gives a contrasting k_R/k_E value of 1.2×10^{-4}, corresponding to 99.9 percent retention of the therefore at least strongly pyramidalized cyclopropyl "anion" **63**.[122,123] It was left to an X-ray structure determination to show that a nitrile group can also stabil-

ize a negative charge when the anionic α-C atom has a fully tetrahedral configuration. Figure 15 shows the structure of 1-cyano-2,2-dimethylcyclopropyllithium **64**, which crystallizes as $[\mathbf{64}\cdot THF]_\infty$.[124]



64 $[\mathbf{64}\cdot THF]_\infty$

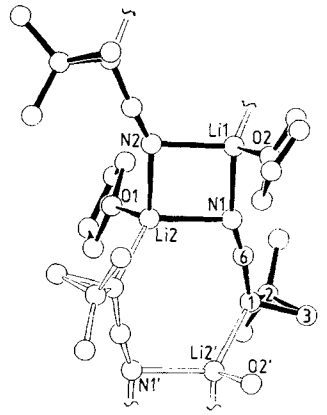


Fig. 15. Crystal structure of $[\mathbf{64}\cdot THF]_\infty$ [124].

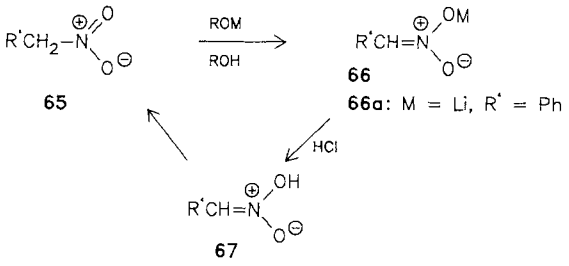
First, one observes that each Li atom is bound to the N atoms of two nitrile groups, producing the (Li-N-Li-N) four-membered ring also found in **59** (and calculated for **58**). The CN group, however, is no longer situated on a planar α-C atom, but on a tetrahedral one; it lies at an angle of 57.6° to the plane of the three-membered ring. At the same time, the anionic C atom possesses a short (214.3 pm) C-Li bond. This coordination, which leads to a genuine α-lithionitrile, is probably due to the high electron density in the exocyclic, "anionic", three-membered ring orbital, as is the case in the cyclopropylsulfonyl "anion" $(\mathbf{27}\cdot DME)_2\cdot DME$. The consequence of this is that, in addition to the (Li-N-Li-N) four-membered ring, one observes the (C-C-N-Li-C-C-N-Li) eight-membered aggregation pattern that was also predicted (see **57**). The C-Li axis is severely bent (51.8°) out of the plane of the cyclopropyl ring. The C1-C6 (140.0 pm) and C6-N1 (117.8 pm) bond lengths are not very different from those in cyclopropanecarbonitriles (e.g., cyclopropane-1,1,2,2-tetratetracarbonitrile: CC, 144.2 pm; CN, 115.0 pm).[125] This, together with the marked displacement of the nitrile group out of the plane of the three-membered ring, accords well with the importance of the (inductive) field effect in the stabilization of a negative charge by this acceptor substituent.[34]

It is also remarkable that the C2-C3 bond opposite to the nitrile group is shorter (147.3 pm) than either of the two adjacent bonds (C1-C2 150.0 pm; C1-C3 152.2 pm). This situation is expected for acceptor-substituted cyclopropanes if the 3*e'* Walsh-orbital can interact with an acceptor π*-orbital.[126, 127] This seems, therefore, still to be the case, even for the cyanocyclopropyl anion **64**.[128]

Conclusion: Although only two crystal structures of lithiated nitriles are available,[159] these, together with the solution studies, give a unified picture of the nature of lithionitrile structures, and of how a nitrile group stabilizes a negative charge. The (inductive) field effect is of great importance here. Once again, the agreement between calculations and solid-state structures should be particularly stressed, since not only the correct C-N bond lengths, but also the tetrahedral configuration of the cyanocyclopropyl "anion"[129] and the four- and eight-membered coordination rings were found both theoretically and experimentally.[159, 165]

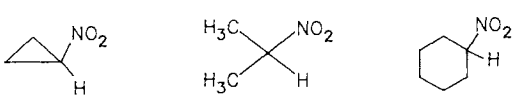
7. Lithiated Nitro Compounds

Although the "nitronate" structure **66** of nitro-"carbanions" is not really in question, until recently no simple member of this class of compounds had been structurally characterized. The formation of nitronates[130-132] has, however, been known since the end of last century, as has their protonation to give nitronic acids **67**,[133] which isomerize to the more stable nitro compounds **65**.



65 **66** **66a**: M = Li, R' = Ph **67**

Recent NMR investigations by *Bradamante, Pagani* et al.[34] are in agreement with the supposed structure of nitronates. Extensive information concerning their applications in synthesis is also available.[134] Nitro compounds and nitronates are of particular importance in substitution reactions that proceed with electron transfer.[135] The kinetic and thermodynamic acidity of nitro compounds has been intensively researched, since nitro compounds are deprotonated astonishingly slowly, given their high acidity.[136, 137] The much greater acidity of nitro compounds in hydroxylic solvents, such as alcohol and water, compared with that in non-hydroxylic solvents such as dimethyl sulfoxide is also noteworthy, as is the extraordinarily low acidity of nitrocyclopropane **68** as compared to **69** and **70**[138] (Table 8).



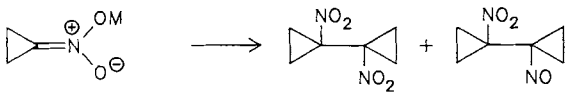
68 **69** **70**

Table 8. Equilibrium acidities pK_a of the nitro compounds **68**, **69**, and **70** in CH_3OH/H_2O (1/1) and in DMSO [137b].

	CH_3OH/H_2O (1/1)	DMSO
68	> 18	26.9 ± 0.2
69	8.85 ± 0.02	16.89 ± 0.05
70	10.07 ± 0.01	17.90 ± 0.05

The generally higher acidity of nitro compounds in hydroxylic solvents is attributed to stabilization of the nitronate by hydrogen bonding.[137a-c,e]

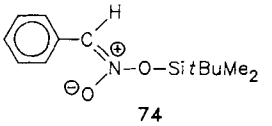
The lower acidity of the cyclopropane derivative **68** corroborates the assumption of a "nitronate" structure **71** for the corresponding "anion", in which an exocyclic C=N double bond gives rise to additional strain.[137b] However, except for H/D exchange, the nitronate **71**, which was generated using a wide variety of bases, could not be trapped by any of the many electrophiles tried.[67] Instead, under the reaction conditions used, **71** rapidly "dimerizes" to furnish **72** and **73**.[67] Therefore, several possible explanations for the reactivity and for the structure of **71** have been discussed.[67,139] The calculated acidity of nitrocyclopropane also does not conform to the pattern found for other CH-acids.[140]



71 **72** **73**

Boche et al. have recently reported the crystal structure of α-nitrobenzyllithium **66a**, which was synthesized from phenylnitromethane **65a** and lithium ethanolate in ethanol, and which crystallizes with ethanol as a polymeric aggregate [**66a**·EtOH]$_\infty$ (Fig. 16).[141] Each Li atom is bound to an O atom of three different nitronates and to an ethanol O atom. This gives rise to six-membered (Li-O-N-O-Li-O) rings, which are annelated through common Li and O atoms to form an endless, ribbon-like structure, which is additionally stabilized by hydrogen bonding. Once again, then, this is not an α-lithio compound! The best plane through C7, N8, O9 and O10 in the nitronate moiety is rotated by 15.2° with respect to the plane through C1-C6. This twisting, and the marked increase in the C1-C6-C7 (126.8(5)°), C6-C7-N8 (126.5(5)°) and C7-N8-O10 (124.7(5)°) bond angles beyond 120°, ensure weaker van der Waals repulsion between H1 and O10 (separation 236 pm). Similar bond angles were found in **74**.[142]

The C7-N8 bond in the nitronate [**66a**·EtOH]$_\infty$ (129 pm) is much shorter than the corresponding bond in uncharged nitro compounds, while the N8-O9 and N8-O10 bonds (133 and 130 pm) are longer. In 1,2-diphenyl-3-nitrocyclopropene, for example, CN 151.8, NO 121.4 and 121.7 pm are found.[143] The C7-N8 bond length in [**66a**·EtOH]$_\infty$ is approximately the same as that in the silyl nitronate **74** (130.2 pm).[142] If and how this finding can be applied to cyclopropyl nitronate **71** is not at present clear,[67,139] but the low acidity of nitrocyclopropane **68** and the high reactivity of nitronate **71** are probably connected with it.



74

The ethanol included in the crystal, and its hydrogen bonds to the nitronate O atoms (see Fig. 16b), confirm the explanation proposed for the increased acidity of nitro compounds in hydroxylic solvents.[137] As in the solid state, hydrogen bonding should also stabilize the nitronate in solution.

The solid-state structure of [**66a**·EtOH]$_\infty$ could perhaps serve as a model for the protonation of nitronates in solution to give nitronic acids. It is tempting to regard the hydrogen bonds, in the sense of the correlation principle,[144] as representing the initial stage in this reaction, and the structure of the fragment composed of phenylmethyl nitronate and ethanol as one point on the reaction pathway.[145] However, structural correlations of this type gain reliability only after statistical evaluation of a large number of structures containing a comparable structural fragment, so that the single finding in [**66a**·EtOH]$_\infty$ must be corroborated by further examples.

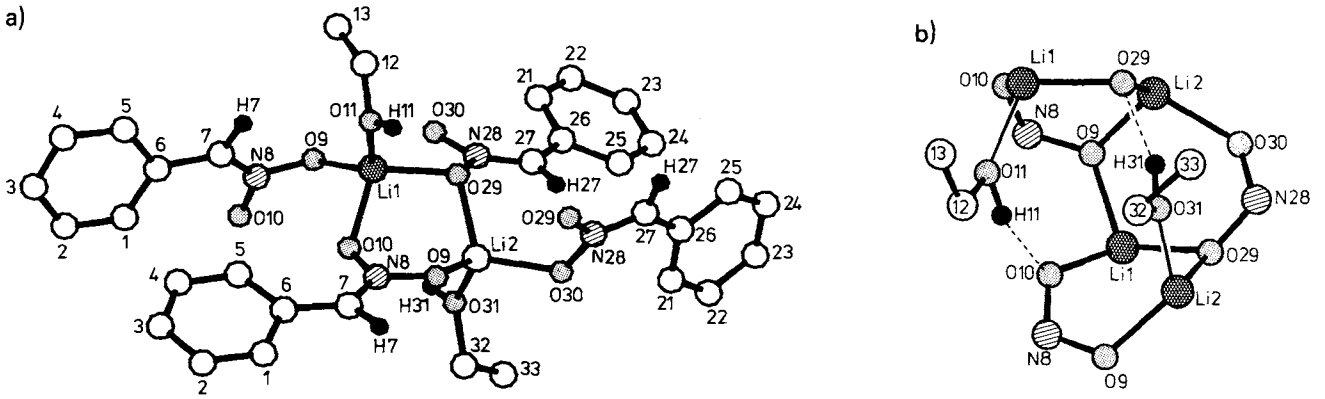
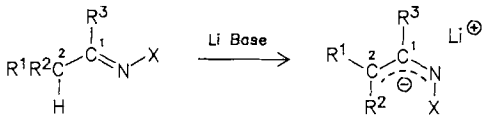


Fig. 16. a) Section of the crystal structure of [**66a**·EtOH]$_\infty$. b) Partial structure showing the hydrogen bonds.

8. Lithium Compounds of Hydrazones

Lithiohydrazones **76a** belong to the large group of 1-azaallyl "anions" **76** (metalloenamines, alkylidenamine-"anions", aza-enolates).

They are prepared from hydrazones **75a** (where X can also be an N-heterocycle) by deprotonation with lithium bases. Metalated alkylidenamines **76b**, oximes **76c**, and



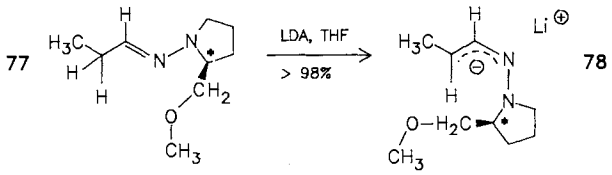
75 76

a: X = NR^4R^5; b: X = R; c: X = OH; d: X = OR

oxime ethers **76d** are obtained in an analogous manner from **75b**, **75c**, and **75d**, respectively. These 1-azaallyl "anions" are all of great importance in modern organic synthesis.[146] Numerous experimental[146-148] and theoretical[149] investigations into both the structures of 1-azaallyl "anions" **76** and their selective reactions with electrophiles E-X have been carried out, prompted by the practically quantitative asymmetric inductions that have been obtained using chiral 1-azaallylmetal reagents in the past fifteen years.[146-148] An excellent review of research into the structures of 1-azaallyl "anions" up to 1987 has been published by *Collum* and *Kallman*.[150] For reasons of space we have to limit ourselves here to structural studies on lithio compounds of hydrazones **76a**, with occasional references to the general situation in 1-azaallyl "anions", especially since the most recent results concern the former.

A great variety of possible structures exists for lithiohydrazones **76a**. The Li atom can be η^1-N bound, for example, whereby the lithium can interact either with the sp^2-orbital, in the plane of the azaallyl atoms, or perpendicular to them, with the p-orbital. In addition, η^1-C^2, η^3-C^2C^1N, and η^4 bonding with the Li ion are also conceivable; in the last of these the second N atom is also bound to Li. As far as the 1-azaallyl atoms C^2, C^1 and N are concerned, *E* and *Z* configurations are possible at both C^2C^1 and C^1N.

In a systematic study of the stereochemistry of lithiohydrazones **76a**, using ^1H NMR spectroscopy and trapping reactions with electrophiles E-X, *Enders, Newcomb, Bergbreiter* et al.[151] found a clear preference for the E_{CC} and Z_{CN} configurations. The stereochemistry does, however, depend on the solvent. Thus, deprotonation of the chiral propionaldehyde-SAMP (= (*S*)-1-amino-2-(methoxymethyl)pyrrolidine)hydrazone **77** with lithium diisopropylamide (LDA) in THF leads to the E_{CC}-Z_{CN}-lithiohydrazone **78** in >98% yield.



77 78

In the presence of HMPT, both configurations are altered. While the CC configuration could be determined by ^1H NMR spectroscopy, the only evidence for the CN configuration came from trapping reactions with electrophiles E-X. Very little can be said about the conformation(s) around the N-N bond, or about the position of the Li atom, and its mode of bonding to the 1-azaallyl anion moiety. In terms of these findings, the model **79** (Fig. 17) would appear to be most appropriate. Lithium is η^3-bound to the 1-azaallyl anion atoms, and also intramolecularly chelated to the ether oxygen.

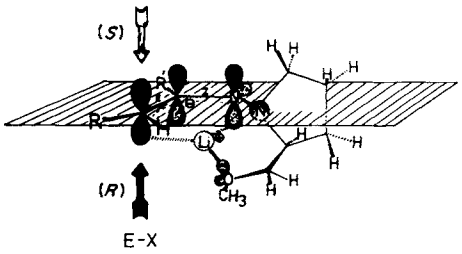


Fig. 17. Model structure **79** of a lithio-SAMP-hydrazone [146f, 151].

The first crystal structure[152] of a lithiohydrazone was published by *Collum, Clardy* et al.[153] in 1984. The lithiated cyclohexanone dimethylhydrazone **80** crystallizes as the polymer $[\mathbf{80}]_\infty$; the solvent (THF) is not incorporated into the crystal. Figure 18 shows a section of the structure.

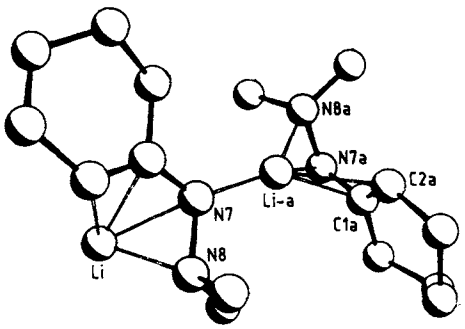
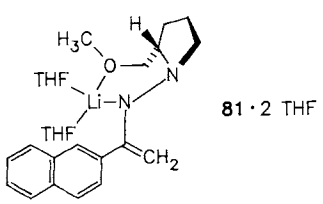


Fig. 18. Crystal structure of the asymmetric unit of lithiated cyclohexanone dimethylhydrazone $[\mathbf{80}]_\infty$ [153].

Remarkably, Li displays two different modes of bonding to the neighboring anions; to one it is bound in an η^1-N manner (N7), while to the other an η^4 bonding mode (N8a, N7a, C1a, C2a) is observed. An osmometric molecular weight determination in THF indicated a degree of aggregation of three or four. In a later paper,[154] the initial assumption that aggregates of **80** reacted with electrophiles E-X was revised in favor of reaction of a bis-solvated monomer. Kinetic studies had revealed the presence of an equilibrium tetramer $\rightleftharpoons$ 4[monomer·2solvent].

According to NMR studies, the crystals of lithiated, chiral 2-acetylnaphthalene-SAMP-hydrazone **81** contain two molecules of THF per molecule **81**;[155] a molecular weight determination in THF revealed the presence of a monomer.[101b]



81·2 THF

Recently, an X-ray structure determination of **81**·2THF was carried out.[156] As Figure 19 shows, **81**·2THF occurs

as a monomer in the solid state so that one can assume the situation in the solid to be a useful model for that in THF solution.

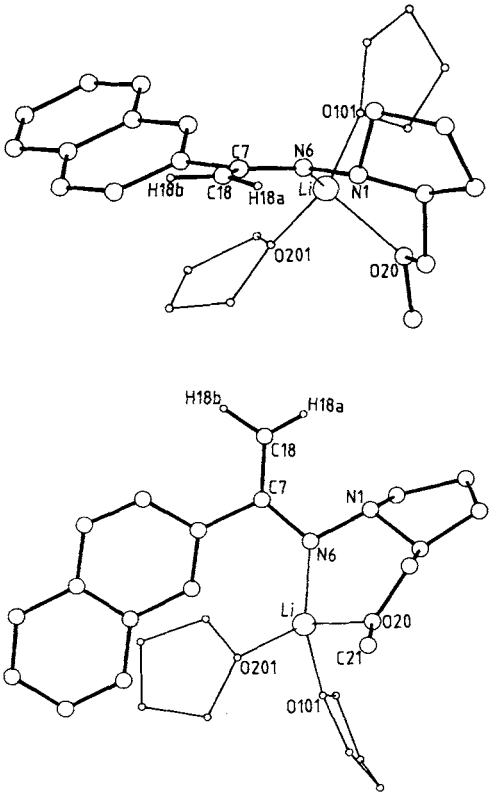


Fig. 19. Two views of the crystal structure of **81**·2THF [156].

In **81**·2THF, the N1–N6–C7–C18 atoms are almost planar (torsion angle −0.52(0.41)°), with the N–N bond lying *syn*-periplanar to the C–C "double bond" (C7–C18 137.2(2) pm). Theoretical[149] and solution[151] studies also show the *syn* configuration to be favored. The N6–N7 bond (136.9(2) pm) is somewhat shortened relative to that in enamines (138–142 pm).[157] The sum of the angles at N6 is 356.4°, indicating slight pyramidalization and therefore a high degree of sp^2 character. As Figure 19 bottom, in particular, shows, the lithium atom is η^1-bound to this nitrogen atom; intramolecular chelation to the methoxy group bends it 17.5(4)° out of the 1-azaallyl plane, so that it lies 59(4) pm below this plane (see Fig. 19, top). The structure of **81**·2THF thus agrees with the models of related compounds put forward by *Whitesell* et al.[158] and *Meyers* et al.[147] One can imagine asymmetric electrophilic substitutions of E–X with this and other chiral 1-azaenolates proceeding, as suggested,[146f] by a lithioretentive S_E2' mechanism; the actual course of the reaction is at present, however, unclear.

9. Summary and Prospects

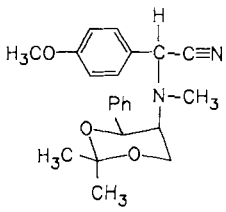
The structural studies presented in this article are based largely on X-ray structure investigations carried out in the last five years. This report can not, therefore, be more than an instantaneous picture of a field that is being intensively researched. A first review was justified, however, by the wealth of new results already now available.

It is necessary to be aware of the limitations introduced by the fact that the new data are derived predominantly from crystal structures, and that TMEDA is frequently involved as a complex ligand. In addition, one must also realize that there is no *one* structure for organolithium compounds anyway, since in solution, i.e., in various solvents, at least some deviation from a given crystal structure must be expected. Furthermore, solid state structures of "anions" can not be identical if the "ligands" (solvent molecules, TMEDA etc.) are different. Nonetheless, it is encouraging to realize that the crystal data often agree very well with those in solution and with calculated structures. Thus, a unified picture of lithiated sulfones can now be drawn, to which some ten X-ray structure determinations have made an important contribution. With lithiated nitriles, too, the situation is now somewhat better understood, even though only two crystal structures are known at present. With lithiated, chiral sulfoximides and sulfoxides,[164] several more crystal structure determinations will have to be performed. Because of their importance in reactions exhibiting chiral induction, it is natural to wish to understand this induction in terms of the structures of the lithium compounds. As with lithiated hydrazones, however, there are at present only the beginnings of an understanding of the structures; we are still very far away from understanding the often very selective reactions that occur with chiral induction. (Indeed, this is the case for reactions of organometallic reagents with electrophiles in general.) This is a field which will occupy chemists for some time to come. With lithiated 1,3-dithianes and thioethers, too, open questions remain, while lithiated nitro compounds show how much just one structure can explain, where there had previously only been strong indications.

10. Supplement

10.1. Structure of the Lithium Compound of Aminonitrile 82

Figure 20 shows the structure of the lithio compound **83** of aminonitrile **82**; **83** crystallizes as $[(\mathbf{83})_2 \cdot OEt_2]_\infty$.[160]



Without going into the details of the structure of $[(\mathbf{83})_2 \cdot OEt_2]_\infty$,[161] it should be emphasized that the (Li–N–Li–N) four-membered ring that is found in the lithionitriles $(\mathbf{59})_2 \cdot 2TMEDA \cdot C_6H_6$ (Fig. 14) and $[\mathbf{64} \cdot THF]_\infty$ (Fig. 15), is present here as well. This clearly shows that the "complex ligands" TMEDA, THF, and diethyl ether do not have a critical influence on the formation of this characteristic structural feature of lithionitriles. The

structural elements in $[(\mathbf{83})_2 \cdot 2OEt_2]_\infty$, i.e., ether, ketal, and amine, obviously do not disturb formation of the (Li-N-Li-N) four-membered ring in the solid state

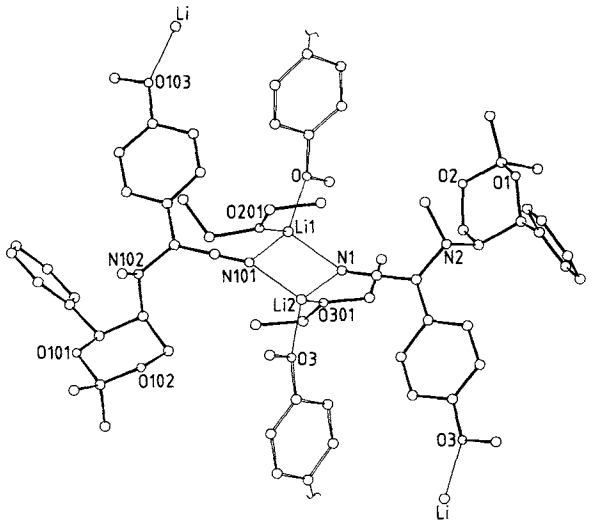


Fig. 20. Crystal structure of $[(\mathbf{83})_2 \cdot OEt_2]_\infty$ [160].

either.[165] Since Li1 and Li2 of $[(\mathbf{83})_2 \cdot 2OEt_2]_\infty$ are coordinated to the *p*-methoxyphenyl oxygen atoms of two further "anions", the dimer becomes a polymer.

10.2. The Structure of the Dilithium Compound of Trimethylsilylacetonitrile 84

Figure 21 shows the structure of the dilithium compound **84** of trimethylsilylacetonitrile, which crystallizes as $(\mathbf{84})_{12} \cdot 6OEt_2 \cdot C_6H_{14}$ from ether hexane.[162]

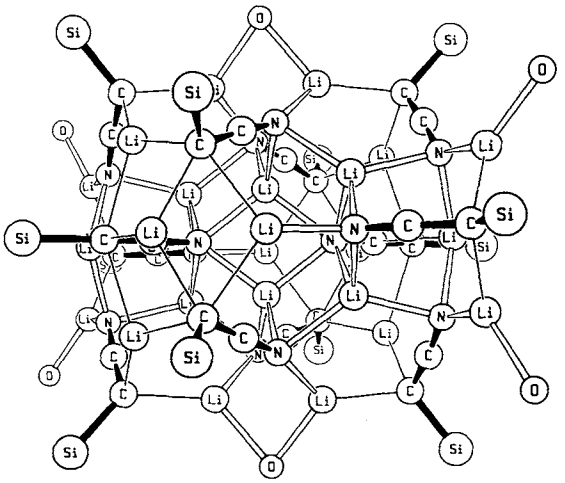


Fig. 21. Crystal structure of $(\mathbf{84})_{12} \cdot 6OEt_2$ · hexane (hexane, methyl and ethyl groups omitted) [162].

The dilithio compound **84** (as $(\mathbf{84})_{12} \cdot 6OEt_2 \cdot C_6H_{14}$) has a structure that is completely different from those of the monolithio compounds $(\mathbf{59})_2 \cdot 2TMEDA \cdot C_6H_6$, $[\mathbf{64} \cdot THF]_\infty$ and $[(\mathbf{83})_2 \cdot 2OEt_2]_\infty$. In **84**, 12 "dianions" are bound together with 24 Li atoms and six diethyl ether molecules to form an aggregate of unusual size (hexane lies outside of this unit). In the interior, one finds primarily N and Li atoms, while a hydrophobic shell composed of the C_2H_5 groups of the ether molecules and the CH_3 groups of the Me_3Si groups surrounds the whole (for reasons of clarity, these 12 C_2H_5 and 36 CH_3 groups are omitted in Figure 21). In contrast to the monolithio compounds (with the exception of $[\mathbf{64} \cdot THF]_\infty$, for which the cyanocyclopropyl "anion" represents a special case; see Section 6), in $(\mathbf{84})_{12} \cdot 6OEt_2 \cdot C_6H_{14}$ there are strong interactions between the α-C and Li atoms. Thus, there are three groups of Me_3Si-C-CN dianions. The α-C atom of the first group binds to two lithium atoms, while those of the second and third groups bind three; the third group is distinguished from the second by the cyano C atom also being bound to a Li atom. There is therefore an unmistakeable structural relationship between the dilithionitrile **84** and the dilithiosulfone $(\mathbf{28c})_6 \cdot Li_2O \cdot 10THF$ (see Section 2.2),[74] at least as far as the high degree of aggregation and the C-Li bonds are concerned.

The author offers his warmest thanks to the coworkers named in the literature references, for their patient and skilful handling of the sensitive crystals synthesized and investigated in Marburg. Representative of them all are Michael Marsch, who has an exceedingly skillful and fortunate hand with crystallizations and insertion of the crystals into the X-ray capillary tubes, and Dr. Klaus Harms, who carried out the measurements and calculations. Special thanks are due to the Deutsche Forschungsgemeinschaft, who supported our research as part of the Schwerpunktsprogramm "Reaction control by non-covalent interactions: quantification of the influence on structure, reactivity and selectivity", and in the Sonderforschungsbereich 260, "Organometallic compounds as selective reagents in organic chemistry". Without this support, our research would not have been possible.

Received: June 28, 1988 [A 709 IE]
German version: *Angew. Chem. 101* (1989) 286
Translated by Dr. *Michael Kertesz*, Burwood, Australia

[1] A review of the crystal structures of organolithium compounds can be found in W. Setzer, P. von R. Schleyer, *Adv. Organomet. Chem. 24* (1985) 353.
[2] a) L. M. Jackman, N. M. Szeverenyi, *J. Am. Chem. Soc. 99* (1977) 4954; b) L. M. Jackman, B. C. Lange, *Tetrahedron 33* (1977) 2737; c) *J. Am. Chem. Soc. 103* (1981) 4494; d) L. M. Jackman, C. W. De Brosse, *ibid. 105* (1983) 4177.
[3] a) A summary of the work of the Zürich groups and others, up to 1984, can be found in D. Seebach, *Proc. Robert A. Welch Found. Conf. Chem. Res. 27* (1984) 93; more recent work: b) D. Seebach, W. Bauer, J. Hansen, T. Laube, W. B. Schweizer, J. D. Dunitz, *J. Chem. Soc. Chem. Commun. 1984*, 853; c) W. Bauer, T. Laube, D. Seebach, *Chem. Ber. 118* (1985) 764; d) D. Seebach, R. Amstutz, T. Laube, W. B. Schweizer, J. D. Dunitz, *J. Am. Chem. Soc. 107* (1985) 5403; e) T. Laube, J. D. Dunitz, D. Seebach, *Helv. Chim. Acta 68* (1985) 1373; f) R. Amstutz, J. D. Dunitz, T. Laube, W. B. Schweizer, D. Seebach, *Chem. Ber. 119* (1986) 434; g) P. G. Williard, G. B. Carpenter, *J. Am. Chem. Soc. 108* (1986) 462.
[4] W. von E. Doering, L. K. Levy, *J. Am. Chem. Soc. 77* (1955) 509.
[5] F. G. Bordwell, P. J. Boutan, *J. Am. Chem. Soc. 79* (1957) 717.
[6] H. E. Zimmerman, B. S. Thyagarajan, *J. Am. Chem. Soc. 80* (1958) 3060.
[7] J. E. Taylor, F. H. Verhock, *J. Am. Chem. Soc. 81* (1959) 4537.
[8] H. E. Zimmerman, B. S. Thyagarajan, *J. Am. Chem. Soc. 82* (1960) 2505.
[9] D. J. Cram, W. D. Nielsen, B. Rickborn, *J. Am. Chem. Soc. 82* (1960) 6415.

[10] E. J. Corey, E. T. Kaiser, *J. Am. Chem. Soc. 83* (1961) 490.
[11] D. J. Cram, D. A. Scott, W. D. Nielsen, *J. Am. Chem. Soc. 83* (1961) 3696.
[12] R. Breslow, E. Mohacsi, *J. Am. Chem. Soc. 83* (1961) 4100.
[13] R. Breslow, E. Mohacsi, *J. Am. Chem. Soc. 84* (1962) 684.
[14] H. L. Goering, D. L. Towns, B. Dittmar, *J. Org. Chem. 27* (1962) 736.
[15] E. J. Corey, H. König, T. H. Lowry, *Tetrahedron Lett. 1962,* 515.
[16] D. J. Cram, A. S. Wingrove, *J. Am. Chem. Soc. 84* (1962) 1496.
[17] C. Y. Meyers, *Tetrahedron Lett. 1962,* 1125.
[18] D. J. Cram, A. S. Wingrove, *J. Am. Chem. Soc. 85* (1963) 1100.
[19] E. J. Corey, T. H. Lowry, *Tetrahedron Lett. 1965,* 793.
[20] E. J. Corey, T. H. Lowry, *Tetrahedron Lett. 1965,* 803.
[21] A. Ratajczak, F. A. L. Anet, D. J. Cram, *J. Am. Chem. Soc. 89* (1967) 2072.
[22] T. Durst, R. Viau, R. Van Den Elzen, C. H. Nguyen, *Chem. Commun. 1971,* 1334.
[23] L. A. Paquette, J. P. Freeman, M. J. Wyvratt, *J. Am. Chem. Soc. 93* (1971) 3216.
[24] J. N. Roitman, D. J. Cram, *J. Am. Chem. Soc. 93* (1971) 2225.
[25] W. T. van Wijnen, H. Steinberg, T. J. De Boer, *Tetrahedron 28* (1972) 5423, and references cited therein.
[26] J. W. Henderson, *Q. Rev. Chem. Soc. 2* (1973) 392.
[27] G. Barbarella, A. Garbesi, A. Fava, *J. Am. Chem. Soc. 97* (1975) 5883.
[28] F. G. Bordwell, N. R. Vanier, M. S. Matthews, J. B. Hendrickson, P. L. Skipper, *J. Am. Chem. Soc. 97* (1975) 7160.
[29] R. Lett, G. Chassaing, A. Marquet, *J. Organomet. Chem. 111* (1976) C17.
[30] a) G. Chassaing, A. Marquet, *Tetrahedron 34* (1978) 1399; b) W. Zarges, *Diplomarbeit,* Universität Marburg 1987.
[31] F. G. Bordwell, J. C. Branca, C. R. Johnson, N. R. Vanier, *J. Org. Chem. 45* (1980) 3884.
[32] G. Chassaing, A. Marquet, J. Corset, F. Froment, *J. Organomet. Chem. 232* (1982) 293.
[33] B. M. Trost, N. R. Schmuff, *J. Am. Chem. Soc. 107* (1985) 396.
[34] a) A. Berlin, S. Bradamante, R. Ferraccioli, G. A. Pagani, *J. Chem. Soc. Chem. Commun. 1986,* 1191; b) S. Bradamante, G. A. Pagani, *J. Chem. Soc. Perkin Trans. 2,* 1986, 1035.
[35] W. Kirmse, U. Mrotzeck, *J. Chem. Soc. Chem. Commun. 1987,* 710.
[36] Reviews: a) D. J. Cram: *Fundamentals of Carbanion Chemistry,* Academic Press, New York 1965, Chap. 2 and 3. It is always a pleasure to read this early review on the structure of acceptor-substituted "carbanions" with its many insights mostly received from H/D exchange reactions; b) P. D. Magnus, *Tetrahedron 33* (1977) 2019; c) E. Block: *Reactions of Organosulfur Compounds,* Academic Press, New York 1978, Chap. 2.5; d) J. C. Stowell: *Carbanions in Organic Synthesis,* Wiley, New York 1979; e) G. Boche, H. M. Walborsky in Z. Rappoport (Ed.): *The Chemistry of the Cyclopropyl Group,* Wiley, Chichester 1987, Chap. 12, p. 701; see also ref. [41].
[37] Ramberg-Bäcklund reaction: L. A. Paquette, *Acc. Chem. Res. 1* (1968) 209.
[38] T. Jordan, H. W. Smith, L. L. Lohr, Jr., W. N. Lipscomb, *J. Am. Chem. Soc. 85* (1963) 846.
[39] S. Wolfe, A. Rauk, I. G. Csizmadia, *J. Am. Chem. Soc. 91* (1969) 1567.
[40] S. Wolfe, A. Rauk, L. M. Tel, I. G. Csizmadia, *Chem. Commun. 1970,* 96.
[41] S. Wolfe, A. Stolow, L. A. La John, *Tetrahedron Lett. 24* (1983) 4071. An excellent review of "Sulfur-Containing Carbanions and Related Species" is given by *S. Wolfe* in F. Bernardi, I. G. Csizmadia, A. Mangini (Eds.): *Stud. Org. Chem. (Amsterdam) 19* (1985) 133.
[42] S. Wolfe, L. A. La John, D. F. Weaver, *Tetrahedron Lett. 25* (1984) 2863.
[43] D. A. Bors, A. Streitwieser, Jr., *J. Am. Chem. Soc. 108* (1986) 1397.
[44] a) H. Hargittai, I. Hargittai, *J. Mol. Struct. 20* (1974) 283; b) W. J. Pietro, M. M. France, W. J. Hehre, D. J. De Frees, J. A. Pople, J. S. Binkley, *J. Am. Chem. Soc. 104* (1982) 5039, and references cited therein.
[45] a) An X-ray structure analysis of $[(CH_3SO_2)_3C]^{\ominus}NH_4^{\oplus}$ was carried out at quite an early date: K. Hoogsteen, *Dissertation,* University of Groningen 1957; b) $[CH(SO_2CF_3)_2]^{\ominus}Rb^{\oplus}$: K. T. Davoy, T. Granstad, S. Husebye, *Acta Chem. Scand. Ser. A 33* (1979) 359; c) see also P. H. Laur, *Sulfur Org. Inorg. Chem. 3* (1972) 235.
[46] G. Boche, M. Marsch, K. Harms, G. M. Sheldrick, *Angew. Chem. 97* (1985) 577; *Angew. Chem. Int. Ed. Engl. 24* (1985) 573.
[47] H.-J. Gais, H. J. Lindner, J. Vollhardt, *Angew. Chem. 97* (1985) 865; *Angew. Chem. Int. Ed. Engl. 24* (1985) 859.
[48] Li-C bonds are in fact found in other "benzyllithium" compounds. Thus, for example, the Li atom in the polymeric benzyllithium-triethylenediamine complex bridges three C atoms (corresponding to C1, C2, and C3 in Fig. 1) [49], while in the monomeric dithiane·**44b**·THF·TMEDA (see Fig. 11) one finds a C-Li bond to the benzylic C atom [50]. As in other benzyllithium compounds with strong acceptor substituents A ((**38b**)·2TMEDA, A = –(O)SPh, Fig. 8; (**59**)$_2$·2TMEDA C_6H_6, A = –C≡N, Fig. 14; **66a** C_2H_5OH, A = NO_2, Fig. 16), the absence of a C-Li bond in **14** is therefore probably the result of the coordination saturation of the $Li^{\oplus}$ ion by heteroatoms of the acceptor substituent, and of the lower electron density at the benzylic, anionic C atom.
[49] S. P. Patterman, I. L. Karle, G. D. Stucky, *J. Am. Chem. Soc. 92* (1970) 1150.
[50] a) R. Amstutz, J. D. Dunitz, D. Seebach, *Angew. Chem. 93* (1981) 487; *Angew. Chem. Int. Ed. Engl. 20* (1981) 465; b) R. Amstutz, T. Laube, W. B. Schweizer, D. Seebach, J. D. Dunitz, *Helv. Chim. Acta 67* (1984) 224.
[51] *Cambridge Crystallographic Data Base* (updating 7/84), Cambridge Crystallographic Data Center, University Chemical Laboratory, Cambridge, England.
[52] R. E. Penn, R. J. Olson, *J. Mol. Spectrosc. 61* (1976) 21.
[53] a) D. R. Johnson, F. X. Powell, W. H. Kirchhoff, *J. Mol. Spectrosc. 39* (1971) 136; b) J. W. C. Johns, W. B. Olson, *ibid. 39* (1971) 479; c) M. E. Jacox, D. E. Milligan, *ibid. 58* (1975) 142.
[54] L. G. Norontsova, *Sov. Phys. Crystallogr. (Engl. Transl.) 10* (1965) 139.
[55] H.-J. Gais, J. Vollhardt, H. J. Lindner, *Angew. Chem. 98* (1986) 916; *Angew. Chem. Int. Ed. Engl. 25* (1986) 939.
[56] W. Hollstein, *Dissertation,* Universität Marburg 1988.
[57] H.-J. Gais, J. Vollhardt, G. Hellmann, H. Paulus, H. J. Lindner, *Tetrahedron Lett. 29* (1988) 1259.
[58] C. Zimmermann, *Diplomarbeit,* Universität Marburg 1988.
[59] a) In order to determine the γ value, it was assumed that the lone pair of electrons at C_α lies on the bisector of angle $|\alpha| + |\beta|$. The angle γ is then the torsion angle between this bisector and the substituent R on the S atom; b) the conformation of the trimethylsilyl compound **19** is possibly brought about by an attractive interaction between the Si and O atoms.
[60] A. Streitwieser, Jr., W. R. Young, *J. Am. Chem. Soc. 103* (1981) 5604.
[61] K. B. Wiberg, R. A. Fenoglio, *J. Am. Chem. Soc. 90* (1968) 3395.
[62] W. Hollstein, K. Harms, M. Marsch, G. Boche, *Angew. Chem. 100* (1988) 868; *Angew. Chem. Int. Ed. Engl. 27* (1988) 846.
[63] In triphenylphosphoniocyclopropanide the triphenylphosphane group is also bent severely (58°) out of the plane defined by the C atoms of three-membered ring: H. Schmidbaur, A. Schier, B. Milewski-Mahrla, U. Schubert, *Chem. Ber. 115* (1982) 722.
[64] I. Reichelt, H.-U. Reissig, *Liebigs Ann. Chem. 1984,* 531, and references cited therein.
[65] R. Häner, T. Maetzke, D. Seebach, *Helv. Chim. Acta 69* (1986) 1655, and references cited therein.
[66] Important literature dealing with this topic is summarized in [36e].
[67] J. Kai, P. Knochel, S. Kwiatkowski, J. D. Dunitz, J. F. M. Oth, D. Seebach, H.-O. Kalinowski, *Helv. Chim. Acta 65* (1982) 137.
[68] Review on dilithium compounds: A. Maercker, M. Theis, *Top. Curr. Chem. 138* (1987) 1.
[69] A summary of the publications dealing with the use of dilithiosulfones in synthesis can be found in [70].
[70] a) J. Vollhardt, H.-J. Gais, K. L. Lukas, *Angew. Chem. 97* (1985) 607; *Angew. Chem. Int. Ed. Engl. 24* (1985) 610; b) J. Vollhardt, H.-J. Gais, K. L. Lukas, *Angew. Chem. 97* (1985) 695; *Angew. Chem. Int. Ed. Engl. 24* (1985) 696; c) H.-J. Gais, J. Vollhardt, *Tetrahedron Lett. 29* (1988) 1529.
[71] W. Hollstein, K. Harms, M. Marsch, G. Boche, *Angew. Chem. 99* (1987) 1279; *Angew. Chem. Int. Ed. Engl. 26* (1987) 1287.
[72] Structural data for *ortho*-lithiated aromatics in which the Li atom is intramolecularly coordinated to an Me_2N or MeO group, can be found in a) J. T. B. H. Jastrzebski, G. van Koten, M. Konijn, C. H. Stam, *J. Am. Chem. Soc. 104* (1982) 5490; b) I. R. Butler, W. R. Cullen, J. Reglinski, S. J. Rettig, *J. Organomet. Chem. 249* (1983) 183; c) J. T. B. H. Jastrzebski, G. van Koten, K. Goubitz, C. Arlen, M. Pfeffer, *ibid. 246* (1983) C79; d) H. Dietrich, D. Rewicki, *ibid. 205* (1981) 281; e) see also W. Neugebauer, A. J. Kos, P. von R. Schleyer, *ibid. 228* (1982) 107; f) in 1,2,3,4-tetrahydro-1-magnesio-2-pivaloylisoquinoline, the magnesium atom bound to the "benzylic" C atom also forms a five-membered ring with the carbonyl O atom of the amide group: D. Seebach, J. Hansen, P. Seiler, J. M. Gromek, *J. Organomet. Chem. 285* (1985) 1; g) chelate controlled reactions: M. T. Reetz, *Angew. Chem. 96* (1984) 542; *Angew. Chem. Int. Ed. Engl. 23* (1984) 556.
[73] The importance of these selective reactions is demonstrated by a series of recent reviews: a) P. Beak, D. B. Reitz, *Chem. Rev. 78* (1978) 275; b) H. W. Gschwend, H. R. Rodriguez, *Org. React. (NY) 26* (1979) 1; c) P. Beak, V. Snieckus, *Acc. Chem. Res. 15* (1982) 306; d) P. Beak, A. I. Meyers, *ibid. 19* (1986) 356; e) G. W. Klumpp, *Recl. J. R. Neth. Chem. Soc. 105* (1986) 1.
[74] H.-J. Gais, J. Vollhardt, H. Günther, D. Moskau, H. J. Lindner, S. Braun, *J. Am. Chem. Soc. 110* (1988) 978.
[75] a) C. R. Johnson, J. R. Zeller, *Tetrahedron 40* (1984) 1225; b) C. R. Johnson, *Aldrichimica Acta 18* (1985) 3, and references cited therein.
[76] H.-J. Gais, I. Erdelmeier, H. J. Lindner, J. Vollhardt, *Angew. Chem. 98* (1986) 914; *Angew. Chem. Int. Ed. Engl. 25* (1986) 938.

[77] I. Erdelmeier, H.-J. Gais, H. J. Lindner, *Angew. Chem. 98* (1986) 912; *Angew. Chem. Int. Ed. Engl. 25* (1986) 935.

[78] H.-J. Gais, U. Dingerdissen, C. Krüger, K. Angermund, *J. Am. Chem. Soc. 109* (1987) 3775.

[79] Reviews: a) G. Solladié, *Synthesis 1981,* 185; b) *Asymmetric Synth. 2* (1983) 157; c) G. H. Posner, *ibid. 2* (1983) 225; d) M. R. Barbachyn, C. R. Johnson, *ibid. 4* (1985) 227; e) M. Venet, *Janssen Chimica Acta 3* (1985) Nr. 2, p. 18; f) K. Krohn, *Nachr. Chem. Tech. Lab. 35* (1987) 22; g) E. Block: *Reactions of Organosulfur Compounds,* Academic Press, New York 1978, Chap. 2.6.

[80] Several more recent articles: a) V. Cerè, C. Paolucci, S. Pollicino, E. Sandri, A. Fava, *J. Chem. Soc. Chem. Commun. 1986,* 223; b) R. Annunziata, M. Cinquini, F. Cozzi, L. Raimondi, *ibid. 1986,* 367; c) S. G. Pyne, S. L. Chapman, *ibid. 1986,* 1688; d) M. Braun, W. Hild, *Chem. Ber. 117* (1984) 413; e) K. Nakamura, M. Higaki, S. Adachi, S. Oka, A. Ohno, *J. Org. Chem. 52* (1987) 1414.

[81] a) A. Rank, E. Buncel, R. Y. Moir, S. Wolfe, *J. Am. Chem. Soc. 87* (1965) 5498; b) S. Wolfe, A. Stolow, L. A. La John, *Can. J. Chem. 62* (1984) 1470; This article contains a summary of all the relevant publications on stereoelectronic effects and kinetic acidities of diastereotopic hydrogen atoms in sulfoxides; c) see also [41, 42] and references cited therein; d) S. Wolfe, *Acc. Chem. Res. 5* (1972) 102.

[82] K. Nishihata, M. Nishio, *Tetrahedron Lett. 1976,* 1695, and references cited therein.

[83] a) J. F. Biellmann, J. J. Vicens, *Tetrahedron Lett. 1974,* 2915; b) *ibid. 1978,* 467.

[84] T. Durst, M. Molin, *Tetrahedron Lett. 1975,* 63, and references cited therein.

[85] G. Chassaing, R. Lett, A. Marquet, *Tetrahedron Lett. 1978,* 471.

[86] B. J. Hutchinson, K. K. Andersen, A. R. Katritzky, *J. Am. Chem. Soc. 91* (1969) 3839.

[87] This can be inferred from a recent article on benzylmethyl sulfoxide and benzyl *tert*-butylsulfoxide by *Ohno* et al. [80e], which contains a critical examination and a detailed discussion of the stereochemistry of H/D exchange and of deprotonation with *n*-BuLi in THF, as well as the reaction of lithium derivatives of methyl or benzyl *tert*-butylsulfoxide with D_2O, R_2CO, or CH_3I. It was found that in the methylation reaction, the lithio compounds of the two sulfoxides in THF exhibit different diastereofacial selectivities. In lithio-*tert*-butylsulfoxide, CH_3I attacks from the *same* side as D_2O and R_2CO! The role of the medium, which had been recognized earlier [88, 89], is emphasized as well. In THF, D_2O attacks from the same face as e.g., R_2CO but upon H/D exchange ($OD^{\ominus}$, D_2O, CH_3OD) it does so from the opposite face. This has been explained in terms of $OH^{\ominus}$ in D_2O/CH_3OD approaching from the side away from the sulfoxide atom, where rapid deuteration (protonation) then also occurs. Complexation of the base, $OH^{\ominus}$; with the sulfoxide atom via the counter ion, $M^{\oplus}$ in D_2O is less important than that of *n*-BuLi in THF.

[88] J. E. Baldwin, R. E. Hackler, R. M. Scott, *Chem. Commun. 1969,* 1415.

[89] T. Durst, R. R. Fraser, M. R. McClory, R. B. Swingle, R. Viau, Y. Y. Wigfield, *Can. J. Chem. 48* (1970) 2148.

[90] R. Lett, G. Chassaing, *Tetrahedron 34* (1978) 2705.

[91] C. Najera, M. Yus, R. Hässig, D. Seebach, *Helv. Chim. Acta 67* (1984) 1100.

[92] M. Marsch, W. Massa, K. Harms, G. Baum, G. Boche, *Angew. Chem. 98* (1986) 1004; *Angew. Chem. Int. Ed. Engl. 25* (1986) 1011.

[93] a) M. A. Viswamitra, K. K. Kannan, *Nature (London) 209* (1966) 2016; b) R. Thomas, C. B. Shoemaker, K. Eriks, *Acta Crystallogr. 21* (1966) 12.

[94] L. Colombo, C. Gennari, C. Scolastico, G. Guanti, E. Narisano, *J. Chem. Soc. Chem. Commun. 1979,* 591; *J. Chem. Soc. Perkin Trans. 1 1981,* 1278.

[95] G. I. Tsuchihashi, S. Iriuchijima, M. Ishibashi, *Tetrahedron Lett. 1977,* 4009.

[96] M. Braun, W. Wild, *Chem. Ber. 117* (1984) 413.

[97] C. A. Kingsbury, *J. Org. Chem. 37* (1972) 102.

[98] a) D. Seebach, K.-H. Gais, *J. Organomet. Chem. Libr. 1* (1976) 1; b) D. Seebach, *Synthesis 1969,* 17; c) D. Seebach, E. J. Corey, *J. Org. Chem. 40* (1975) 231; d) B.-T. Gröbel, *Synthesis 1977,* 357.

[99] R. Amstutz, D. Seebach, P. Seiler, B. Schweizer, J. D. Dunitz, *Angew. Chem. 92* (1980) 59; *Angew. Chem. Int. Ed. Engl. 19* (1980) 53.

[100] a) A. G. Abatjoglan, E. L. Eliel, L. F. Kuyper, *J. Am. Chem. Soc. 99* (1977) 8262; b) J.-M. Lehn, G. Wipff, *ibid. 98* (1976) 7498; c) J.-M. Lehn, G. Wipff, K. Demuynk, *Helv. Chim. Acta 60* (1977) 1239; d) N. D. Epiotis, R. L. Yates, F. Bernardi, S. Wolfe, *J. Am. Chem. Soc. 98* (1976) 5435.

[101] a) R. Amstutz, *Dissertatin No. 7210,* Eidgenössische Technische Hochschule Zürich 1983, cited in b) W. Bauer, D. Seebach, *Helv. Chim. Acta 67* (1984) 1972.

[102] D. Seebach, J. Gabriel, R. Hässig, *Helv. Chim. Acta 67* (1984) 1083.

[103] A. Streitwieser, D. L. Grier, B. A. B. Kohler, E. R. Vorpagel, G. W. Schriver in P. Coppers, M. B. Hall (Eds.): *Electron Distribution and Chemical Bond,* Plenum, New York, London 1982, p. 445.

[104] D. Seebach, T. Maetzke, R. K. Haynes, M. N. Paddon-Row, S. S. Wong, *Helv. Chim. Acta 71* (1988) 299.

[105] a) Review: J. F. Biellmann, J.-B. Ducep, *Org. React. (NY) 27* (1982) 1; RS compounds: b) E. J. Corey, B. W. Erickson, R. Noyori, *J. Am. Chem. Soc. 93* (1971) 1724, and references cited therein; c) D. Seebach, *Synthesis 1969,* 17.

[106] M. Pohmakotr, K.-H. Geiss, D. Seebach, *Chem. Ber. 112* (1979) 1420.

[107] a) T. Clark, C. Rhode, P. von R. Schleyer, *Organometallics 2* (1983) 1344; b) G. Decher, G. Boche, *J. Organomet. Chem. 259* (1983) 31.

[108] a) S. Wolfe, L. A. LaJohn, F. Bernardi, A. Mangini, G. Tonachini, *Tetrahedron Lett. 24* (1983) 3789; b) T. H. Dunning, Jr., P. J. Hay in H. F. Schaefer III (Ed.): *Methods of Electronic Structure Theory,* Plenum, New York 1977.

[109] P. von R. Schleyer, T. Clark, A. J. Kos, G. W. Spitznagel, C. Rhode, D. Arad, K. N. Houk, N. G. Rondan, *J. Am. Chem. Soc. 106* (1984) 6467.

[110] a) S. Arseniyadis, K. S. Kyler, D. S. Watt, *Org. React. (N.Y.) 31* (1984) 1; b) *Houben-Weyl: Methoden der Organischen Chemie, Vol. XIII/1, XIII/2a,* Thieme, Stuttgart 1970; c) E. Ciganek, W. J. Linn, O. W. Webster in Z. Rappoport (Ed.): *The Chemistry of the Cyano Group,* Wiley, New York 1970, p. 589; d) U. Schöllkopf, *Angew. Chem. 89* (1977) 351; *Angew. Chem. Int. Ed. Engl. 16* (1977) 339; e) *Pure Appl. Chem. 51* (1979) 1347; f) H. M. Walborsky, M. P. Periasamy in S. Patai, Z. Rappoport (Eds.): *The Chemistry of Triple-bonded Functional Groups, Suppl. C,* Wiley, New York 1983, p. 835; g) M. Charton, *ibid.,* p. 288; h) J. C. Stowell: *Carbanions in Organic Synthesis,* Wiley, New York 1979, p. 164.

[111] J. Kaneti, P. von R. Schleyer, T. Clark, A. J. Kos, G. W. Spitznagel, J. G. Andrade, J. B. Moffat, *J. Am. Chem. Soc. 108* (1986) 1481.

[112] a) C. Krüger, *J. Organomet. Chem. 9* (1967) 125; b) G. A. Gornowicz, R. West, *J. Am. Chem. Soc. 93* (1971) 1714.

[113] J. Kaneti, A. I. Nazir, I. G. Binev, V. B. Radomirska, I. N. Jochnovski, *J. Mol. Struct. 68* (1980) 11, and references cited therein.

[114] R. Das, C. A. Wilkie, *J. Am. Chem. Soc. 94* (1972) 4555.

[115] a) D. Seebach (Zürich), personal communication; b) see also footnote 11 in [111].

[116] G. Boche, M. Marsch, K. Harms, *Angew. Chem. 98* (1986) 373; *Angew. Chem. Int. Ed. Engl. 25* (1986) 373.

[117] According to MNDO calculations, the dimer $[PhCH(CN)Li \cdot 2\,NH_3]_2$ has a structure corresponding to **59**. It is ca. 5 kcal mol^{-1} more stable than $2\,PhCH(CN)Li \cdot 3\,NH_3 - 2\,NH_3$: S. Schröder, Universität Marburg 1986.

[118] C. C. Costain, *J. Chem. Phys. 29* (1958) 864. Interestingly, in nitrile complexes such as CH_3CN-BF_3, the C–N bond length is shortened to 113.5 pm (B. Swanson, D. F. Skriver, J. A. Ibers, *Inorg. Chem. 8* (1969) 2182), so that in **59**, in which the nitrile nitrogen atom is coordinated to two Li atoms a similar effect could be partly responsible for the short C–N bond length.

[119] a) J. J. Daly, *J. Chem. Soc. 1961,* 2801; b) R. R. Naqvi, P. J. Wheatley, *J. Chem. Soc. A 1970,* 2053; c) J. Lambrecht, B. Gambke, J. von Seyerl, G. Huttner, S. Kollmannsberger-von Nell, S. Herzberger, J. C. Jochims, *Chem. Ber. 114* (1981) 3751; d) abnormally short C-N bonds are found in ketenimines $(CH_3SO_2)_2\overset{\ominus}{C}-C\equiv\overset{\oplus}{N}-CH_3$ [119a, b]; see also e) J. Lambrecht, L. Zsolnai, G. Huttner, J. C. Jochims, *ibid. 114* (1981) 3655.

[120] One of many examples from the groups in Zürich: $H_2C{=}C(t\mathrm{Bu})OLi$: (C=C) $\delta = 134$, (C–O) 135 pm; enol ether: (C=C) $\delta = 132$, (C–O) 136 pm (R. Amstutz, W. B. Schweitzer, D. Seebach, J. D. Dunitz, *Helv. Chim. Acta 64* (1981) 2617).

[121] a) J. M. Motes, H. M. Walborsky, *J. Am. Chem. Soc. 92* (1970) 3697; b) J.-O. Levin, C. Rappe, *Chem. Scr. 1* (1971) 233.

[122] H. M. Walborsky, J. M. Motes, *J. Am. Chem. Soc. 92* (1970) 2445.

[123] A summary of the properties and reactions of cyano- and RC(O)-substituted cyclopropyl "anions" is given in [36e].

[124] G. Boche, K. Harms, M. Marsch, *J. Am. Chem. Soc. 110* (1988) 6925.

[125] F. H. Allen, *Acta Crystallogr. Sect. B 36* (1980) 81.

[126] R. Hoffmann, *Tetrahedron Lett. 1970,* 2907.

[127] H. Günther, *Tetrahedron Lett. 1970,* 5173.

[128] Accordingly, in the rearrangement of the 9-cyano-*cis*-bicyclo[6.1.0]nona-2,4,6-trien-9-yl "anion" an adjacent bond is broken: G. Boche, D. Martens, *Chem. Ber. 112* (1979) 175.

[129] a) H.-U. Wagner, G. Boche, *Z. Naturforsch. B 37* (1982) 1339; b) M. H. Lien, A. C. Hopkinson, M. A. McKinney, *J. Mol. Struct. 105* (1983) 37; c) A. C. Hopkinson, M. A. McKinney, M. H. Lien, *J. Comput. Chem. 4* (1983) 513.

[130] The crystal structures of nitronates having various acceptor substituents are known, see e.g. a) $2\,K^{\oplus}[O_2CCHNO_2]^{2\ominus}$: D. J. Sutor, F. J. Llewellyn, H. S. Maslen, *Acta Crystallogr. 7* (1954) 145; b) $(NH_4^{\oplus}, K^{\oplus})[(H_2NCO)_2CNO_2]^{\ominus}$: O. Simonsen, *Acta Crystallogr. Sect. B 37* (1981)

344; c) $2Rb^{\oplus}[(O_2N)_2C-C(NO_2)_2]^{2\ominus}$: B. Klewe, *Acta Chem. Scand. 26* (1972) 1049; d) $K^{\oplus}(Rb^{\oplus},Cs^{\oplus})$ $[(O_2N)_2CH]^{\ominus}$: N. V. Grigor'eva, N. V. Margolis, I. N. Shokor, I. V. Tselinski, V. V. Mel'nikov, *J. Struct. Chem. (Engl. Transl.) 9* (1968) 475; e) $K^{\oplus}(Rb^{\oplus}, Cs^{\oplus})$ $[(O_2N)_3C]^{\ominus}$: N. V. Grigor'eva, N. V. Margolis, I. N. Shokor, V. V. Mel'nikov, I. V. Tselinski, *ibid. 7* (1966) 272.

[131] Review: A. T. Nielsen, *Chem. Nitro Nitroso Groups 1* (1969) 349.

[132] First synthesis: A. F. Holleman, *Recl. Trav. Chim. Pays-Bas 13* (1894) 403.

[133] A. Hantzsch, O. W. Schultze, *Ber. Dtsch. Chem. Ges. 29* (1896) 699.

[134] a) D. Seebach, E. W. Colvin, F. Lehr, T. Weller, *Chimia 33* (1979) 1; b) M. Eyer, D. Seebach, *J. Am. Chem. Soc. 107* (1985) 3601; c) M. Braun, *Nachr. Chem. Tech. Lab. 33* (1985) 598.

[135] a) N. Kornblum, R. E. Michel, R. C. Kerber, *J. Am. Chem. Soc. 88* (1966) 5660, 5662; b) G. A. Russell, W. C. Danen, *ibid. 88* (1966) 5663; c) N. Kornblum, *Angew. Chem. 87* (1975) 797; *Angew. Chem. Int. Ed. Engl. 14* (1975) 734.

[136] D. J. Cram: *Fundamentals of Carbanion Chemistry*, Academic Press, New York 1965, Chap. 1.

[137] a) F. G. Bordwell, J. E. Bartmess, J. A. Hautala, *J. Org. Chem. 43* (1978) 3107; b) *ibid. 43* (1978) 3113; c) F. G. Bordwell, J. A. Hautala, *ibid. 43* (1978) 3116; d) F. G. Bordwell, J. C. Branca, D. L. Hughes, W. N. Olmstead, *ibid. 45* (1980) 3305; e) F. G. Bordwell, *Pure Appl. Chem. 49* (1977) 963.

[138] For nitrocyclopropane acidity see also P. W. K. Flanagan, H. W. Amburn, H. W. Stone, J. G. Traynham, H. Shechter, *J. Am. Chem. Soc. 91* (1969) 2797, and [36e].

[139] H.-U. Wagner, G. Boche, *Helv. Chim. Acta 66* (1983) 842.

[140] A. J. Gushurst, W. C. Jorgensen, *J. Org. Chem. 51* (1986) 3513; calculations of the potential hypersurface of $CH_3NO_2^-$: M. L. McKee, *J. Am. Chem. Soc. 108* (1986) 5784.

[141] G. Klebe, K. H. Böhn, M. Marsch, G. Boche, *Angew. Chem. 99* (1987) 62; *Angew. Chem. Int. Ed. Engl. 26* (1987) 78.

[142] E. W. Colvin, A. K. Beck, B. Bastiani, D. Seebach, Y. Kai, J. D. Dunitz, *Helv. Chim. Acta 63* (1980) 697.

[143] a) M. Marsch, W. Massa, G. Boche, unpublished; b) C. J. Cheer, D. Bernstein, A. Greenberg, P.-C. Lyu, *J. Am. Chem. Soc. 110* (1988) 226.

[144] H. B. Bürgi, J. D. Dunitz, *Acc. Chem. Res. 16* (1983) 153.

[145] T. Laube, J. D. Dunitz, D. Seebach, *Helv. Chim. Acta 68* (1985) 1373, have reported on the interaction between lithium enolates and secondary amines in the solid state (and in solution).

[146] Reviews: a) P. W. Hickmott, *Tetrahedron 38* (1982) 1975; b) D. Enders in H. Nozaki (Ed.): *Current Trends in Organic Synthesis*, Pergamon, Oxford 1983, p. 151; J. K. Whitesell, M. A. Whitesell, *Synthesis 1983*, 517; d) D. E. Bergbreiter, M. Newcomb, *Asymmetric Synth. 2* (1983) 243; e) R. R. Fraser, *Stud. Org. Chem. (Amsterdam) B* (1984) 65; f) D. Enders, *Asymmetric Synth. 3* (1984) 275.

[147] K. A. Kutomski, A. I. Meyers, *Asymmetric Synth. 3* (1984) 213, and references cited therein.

[148] K. Tomioka, K. Koga, *Asymmetric Synth. 2* (1983) 201, and references cited therein.

[149] a) K. N. Houk, R. W. Strozier, N. G. Roudan, R. R. Fraser, N. Chuaqui-Offermanns, *J. Am. Chem. Soc. 102* (1980) 1426, and references cited therein; b) R. Glaser, A. Streitwieser, Jr., *ibid. 109* (1987) 1258.

[150] N. Kallman, D. B. Collum, *J. Am. Chem. Soc. 109* (1987) 7466; see also A. S. Galiano-Roth, E. M. Michaelides, D. B. Collum, *ibid. 110* (1988) 2658, and the excellent NMR spectroscopic studies by *Jackman* et al., e.g. L. M. Jackman, L. M. Scarmoutzos, *ibid. 109* (1987) 5348.

[151] K. G. Davenport, H. Eichenauer, D. Enders, M. Newcomb, D. E. Bergbreiter, *J. Am. Chem. Soc. 101* (1979) 5654.

[152] Many examples of crystal structures of monomeric and dimeric 1-azaallyllithium compounds, which are not lithiohydrazones, have been published: a) D. Seebach, W. Bauer, J. Hansen, T. Laube, W. B. Schweizer, J. D. Dunitz, *J. Chem. Soc. Chem. Commun. 1984*, 853; b) R. A. Wanat, D. B. Collum, G. Van Dyne, J. Clardy, R. T. DePue, *J. Am. Chem. Soc. 108* (1986) 3415; c) H. Dietrich, W. Mahdi, R. Knorr, *ibid. 108* (1986) 2462; d) D. Colgan, R. I. Papasergio, C. L. Raston, A. H. White, *J. Chem. Soc. Chem. Commun. 1984*, 1708; e) R. I. Papasergio, C. L. Raston, A. H. White, *ibid. 1983*, 1419; f) T. Fjeldberg, P. B. Hitchcock, M. F. Lappert, A. J. Thorne, *ibid. 1984*, 822; g) B. Cetinkaya, P. B. Hitchcock, M. F. Lappert, M. Misra, A. J. Thorne, *ibid. 1984*, 148; h) R. A. Bartlett, H. V. R. Dias, H. Hope, B. D. Murray, M. M. Olmstead, P. P. Power, *J. Am. Chem. Soc. 108* (1986) 6921; i) P. von R. Schleyer, R. Hacker, H. Dietrich, W. J. Mahdi, *J. Chem. Soc. Chem. Commun. 1985*, 622; j) D. Barr, W. Clegg, R. E. Mulvey, R. Snaith, *ibid. 1984*, 469, 700.

[153] D. B. Collum, D. Kahne, S. A. Gut, R. T. DePue, F. Mohamadi, R. A. Wanat, J. Clardy, G. Van Dyne, *J. Am. Chem. Soc. 106* (1984) 4865.

[154] R. A. Wanat, D. B. Collum, *J. Am. Chem. Soc. 107* (1985) 2078.

[155] D. Enders, K. A. M. Kremer, unpublished results.

[156] D. Enders, G. Bachstädter, K. A. M. Kremer, M. Marsch, K. Harms, G. Boche, *Angew. Chem. 100* (1988) 1580; *Angew. Chem. Int. Ed. Engl. 27* (1988) 1522.

[157] K. L. Brown, L. Damm, J. D. Dunitz, A. Eschenmoser, R. Hobi, C. Kratky, *Helv. Chim. Acta 61* (1978) 3108.

[158] J. K. Whitesell, M. A. Whitesell, *J. Org. Chem. 42* (1977) 377.

[159] The crystal structure of a third lithionitrile, i.e., that of $[\mathbf{83})_2 \cdot 2OEt]_\infty$, is reproduced in Section 10, and fits into this picture.

[160] M. Marsch, K. Harms, G. Boche, P. Gerdes, D. Enders, unpublished.

[161] In connection with the structure of $[(\mathbf{83})_2 \cdot 2OEt_2]_\infty$, it is interesting that in reactions of **83** with α,β-unsaturated carbonyl compounds (Michael addition), one isomer is formed preferentially (*de* between 82 and >98%), so that high diastereofacial differentiation and diastereoselectivity are present.

[162] W. Zarges, M. Marsch, K. Harms, G. Boche, *Chem. Ber. 122* (1989), in press.

[163] Recent review: D. Seebach, *Angew. Chem. 100* (1988) 1685; *Angew. Chem. Int. Ed. Engl. 27* (1988) 1624.

[164] If the solid state structure of α-(*tert*-butylsulfinyl)-α-methylbenzyllithium-pentamethyldiethylenetriamine is a model for the reacting species in solution one easily recognizes the difficulties for an electrophile like CH_3I to approach the anionic C atom from the side opposite to the -OLi bond (M. Marsch, K. Harms, G. Boche, unpublished results, Universität Marburg, 1989).

[165] In contrast to the structures of $(\mathbf{59})_2 \cdot 2TMEDA \cdot C_6H_6$, $[(\mathbf{83})_2 \cdot 2OEt_2]_\infty$ and also $[\mathbf{64} \cdot THF]_\infty$ in the case of $[LiCH(CN)_2 \cdot HMPA]_\infty$ instead of the (Li-N-Li-N) four-membered ring a (Li-O-Li-O) ring is formed. Each Li atom is additionally bound to two N atoms of two malonodinitrile anions, K. Jens, J. Kopf, N. P. Lorenzen, E. Weiss, *Chem. Ber. 121* (1988) 1201. HMPA with its strong oxygen donor atom apparently makes the difference.

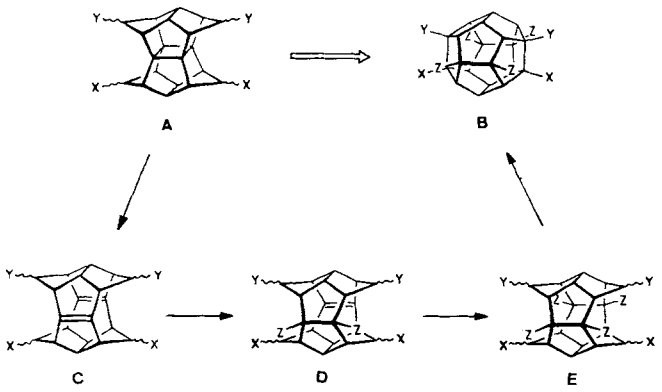
[166] A monomeric potassiosulfone has been described recently, H.-J. Gais, J. Vollhardt, C. Krüger, *Angew. Chem. 100* (1988) 1108; *Angew. Chem. Int. Ed. Engl. 27* (1988) 1092. Monomeric lithiosulfones should exist, e.g., in very dilute THF solutions, M. J. Kaufman, S. Gronert, D. A. Bors, A. Streitwieser, Jr., *J. Am. Chem. Soc. 109* (1987) 602.

When submitting manuscripts, authors of articles intended for publication as "Communications" are requested to read the "Notice to Authors" reproduced in the January issue of the journal following the list of contents; upon request, a copy can be obtained from the editorial office.

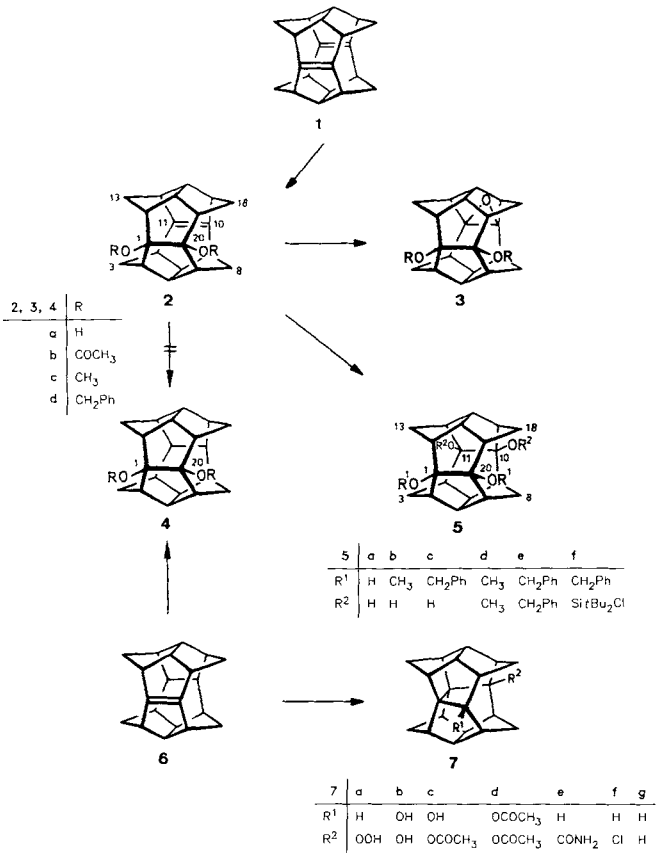
The Pagodane Route to Dodecahedranes: Chemistry and Structure of Bissecododecahedranes**

By *Georg Lutz, Dieter Hunkler, Grety Rihs,* and *Horst Prinzbach**

The energy-rich $C_{20}H_{20}$ hydrocarbon [1.1.1.1]pagodane **A** (X = Y = H)[1] can be converted into dodecahedrane **B** (X = Y = Z = H) catalytically[2] as well as stepwise (via **C**, **D** and **E**).[3] The yields of these procedures, yet encouraging in view of the ready availability of the starting materials, remain unsatisfactory for several reasons:[1] persistence of intermediates (e.g. **7**; cf. **13**, **14**),[4] "hyperstability",[3,5] particularly at the mono-ene step **D**, and the conditions necessary for the final dehydrogenative C–C bond formation **E** → **B**.[3,6] Limits drawn by this step **E** → **B** regarding a variable substitution of the pagodane and (seco)dodecahedrane frameworks[4] are the subject of this communication. Several promising ways out of this dilemma by functionalization of the four methylene positions (X, Y) are conceivable, and will be outlined in the two directly following communications.[7,8]



According to force-field (MM2) calculations, the unsaturated bissecododecahedranes **1** and **6** have olefin strains (OS)[5] of −11.4 and −13.9 kcal mol^{-1}, respectively.[3] However, whereas the diene **1** can be smoothly hydrogenated to the mono-ene **6**, the latter resists all attempts at hydrogenation, but can be epoxidized and cyclopropanated. The check remained to be made, whether bisseco intermediates **E** (X, Y = H) with four and two Z-substituents, respectively, can be prepared from **1** and **6**, and whether such Z-substituents survive dehydrogenative C–C bond formation[6] to give **B**.



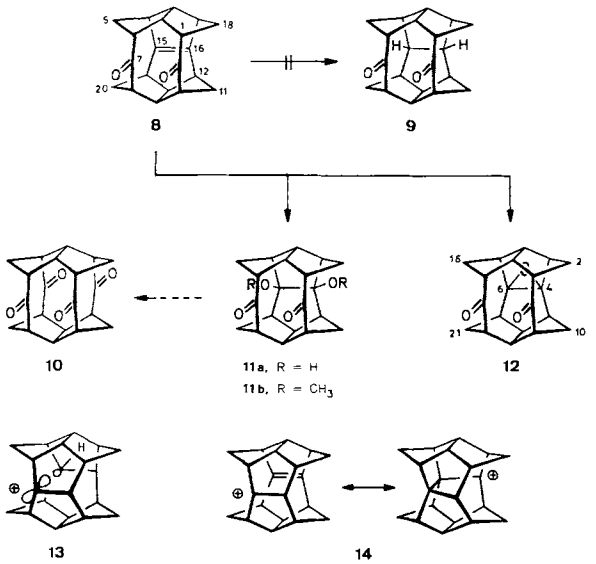
Diene **1** is rapidly oxidized by $KMnO_4$ (homogeneous solution in acetone/H_2O/CH_2Cl_2, −35 to 0°C, 2 h); with excess reagent the only product, according to thin-layer chromatographic monitoring formed in almost quantitative yield, is not the ene-diol **2a** or the tetrol **5a** but the octacyclic ene-dione **8**.[9] Under more drastic conditions, **8** reacts slowly with further reagent (to give, inter alia, lactones; besides the hydroperoxide **7a**), without tetrol **5a**, diol-dione **11a** or tetrone **10** being detectable (TLC, ^{1}H NMR, MS monitoring). The ene-diol **2a** is, however, obtainable selectively (>80%) by reaction of **1** with OsO_4 (1.2 equivs.) in benzene, since the very slowly formed osmate half-ester, identified ^{1}H-NMR spectroscopically, precipitates (total conversion after 2 d at 20°C). **2a** can be liberated from the latter with $LiAlH_4$; it is acid-labile: even traces of HCl catalyze rapid isomerization to give mainly **7b**.[1] This tendency for transannular C–C bond formation also manifests itself upon treatment with acetic anhydride/pyridine (20°C) with preferential formation of **7c,d** (together with some **2b**). Double etherification leading to **2c,d** (NaH, CH_3I or $PhCH_2Br$, 20°C, 1 d) is slow but unproblematical (>90%). The double bond in **2a** cannot be

[*] Prof. Dr. H. Prinzbach, Dipl.-Chem. G. Lutz, Dr. D. Hunkler
Chemisches Laboratorium der Universität
Institut für Organische Chemie und Biochemie
Albertstrasse 21, D-7800 Freiburg (FRG)
G. Rihs
Ciba-Geigy AG
CH-4002 Basel (Switzerland)

[**] This work was supported by the Deutsche Forschungsgemeinschaft, the Fonds der Chemischen Industrie, and BASF AG.

hydrogenated (to give **4a**) (Pd/C, Pt or N_2H_2), but can be epoxidized with *m*-chloroperbenzoic acid to give **3a** (95%). Both $KMnO_4$ (acetone/CH_2Cl_2, 20°C) and RuO_4 (CCl_4, 20°C) effect uniform glycol-cleavage of **2a** to give the enedione **8** (>95%). Hydroxylation of **2c,d** to the fourfold substituted bisseco compounds **5b,c**, on the other hand, is again selective (80–85%) via the osmate half-ester sparingly soluble in benzene (2 equiv. OsO_4, 20°C). Analogously to **2a**, **5b,c** can be converted into the more soluble D_{2h} symmetric tetraalkoxybisseco compounds **5d,e**. In the case of **5b,c** acid-catalyzed acetalization with 2,2-dimethoxypropane is again not possible without noticeable competition by transannular processes; in contrast, the reaction of **5c** with di-*tert*-butyldichlorosilane (1.5 equiv. 50°C, 2 d) in the presence of the BEMP-iminophosphorane base (2-*tert*-butylimino-2-diethylamino-1,3-dimethylperhydro-1,3,2-diazaphosphinane)[10] to give **5f** proceeds rather selectively (85–90%).

Not unexpectedly, the hyperstable bisseco-ene **6** is not oxidized by $KMnO_4$ (under various conditions); as in the case of **2a**, *cis*-hydroxylation (to **4a**) can only be achieved with OsO_4 in benzene, followed by $LiAlH_4$-reduction of the sparingly soluble osmate half-ester (>90%). Rather surprising and preparatively disadvantageous is the sensitivity of the saturated diol **4a** to transannular reactions, as known for **2a** and manifested, inter alia, in the very low-yield esterification to **4b** (25%); double alkylation to **4c,d** is practically quantitative, as in the case of **5b,c**. Thus, the prevailing transannular C–C bond formation to give nonacycles **7** in the case of the highly homoconjugated diene **1** is obviously a dominating process not only in the bisseco-enes **2** and **6**, but also in the saturated bisseco-compounds **4** and **5** (in the reaction of **6** with chlorosulfonyl isocyanate, e.g., **7e** is formed (ca. 60%)—presumably favored by the effective overlap between the empty p orbital and the opposite bridgehead C,H sp^3 orbital in cations of the type **13**.[11] A plausible intermediate is the cation **14** stabilized by hyperconjugation and generated from **1** by protonation and from **7f** by hydrolysis under superacidic conditions;[12] it is stable at room temperature for several hours.



The enedione **8** is another hyperstable olefin (*OS* according to MM2 calculations: −14.7 kcal mol^{-1}); even under drastic conditions it is not hydrogenated to **9**, but is smoothly oxidized to **12** by *m*-chloroperbenzoic acid. The dihydroxydione **11a**, sought for as precursor for the tetraketone **10**, and not observed in the oxidation of **8** with RuO_4 or $^1O_2$, is isolated in the form of the derivative **11b** (in moderate yield) from **5b** and RuO_4.

The tetrabenzyloxy derivative **5e** allowed an X-ray crystallographic examination of a first saturated bissecododecahedrane (Fig. 1).[14] In the crystal, the four substituents are arranged in such a way that a center of symmetry is preserved; their strain contribution is manifested, inter alia, in the length (1.614(4) Å) of the C–C bonds flanked by (almost orthogonally oriented) benzyloxy groups, and

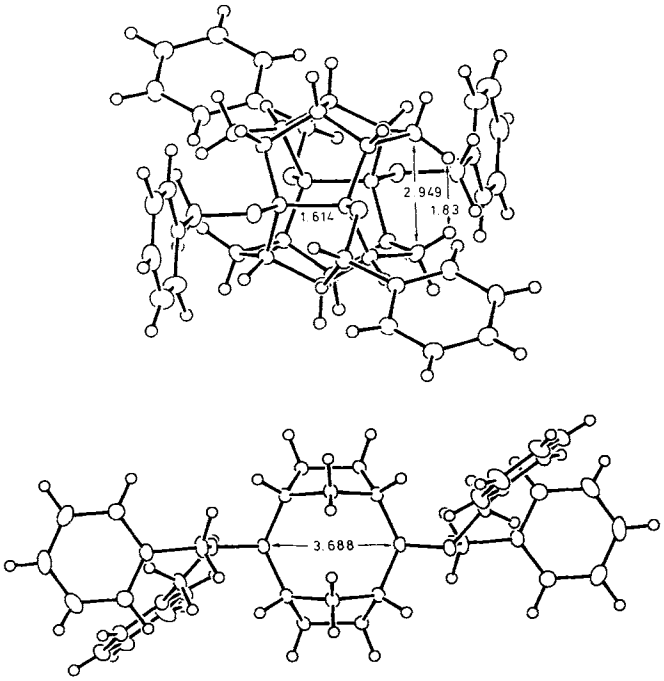
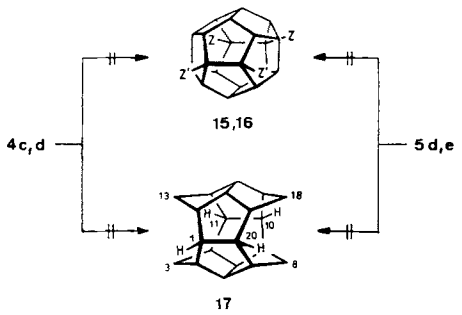


Fig. 1. Crystal structure of **5e** (distances in Å).

the torsional angle O-C1-C20-O of 4.2°. Considering the degree of substitution, there is a good overall agreement with the results of force field calculations.[3] Thus it is demonstrated that, with the bulging of the framework to 3.688 Å, the internal hydrogen atoms of the methylene positions are compressed to a distance (1.83 Å) considerably (ca. 0.5 Å) smaller than twice their van-der-Waals radius. As expected on the basis of force field calculations,[3, 15] this H–H distance is also smaller (ca. 0.1 Å) than in a dimethylsecododecahedrane.[16]

The hope that the OR substituents in the bissecododecahedranes **4** and **5** would survive the drastic conditions of dehydrogenation to the doubly and quadruply substituted dodecahedranes **15** (Z = H, Z′ = OR) and **16** (Z = Z′ = OR), respectively, through steric protection by the vicinal hydrogen atoms, was not realized: under multiple sets of dehydrogenative and hydrogenative conditions (Pd/C mixtures, 1–15 atm H_2, 170–250°C) the $C_{20}H_{22}$ nonacycle **7g**,[1] known to be stable under these conditions, is formed in consistently high yields (90%). That even in the case of the benzyl ethers **2d** and **5e** the respective glycols **2a** and **5a** and also the diol **7b** were not isolable, emphasizes the significance of heterolysis in these bridgehead positions;[13] that also the still unknown, saturated bisseco parent hydrocarbon **17** was not obtained is once more an indication for the high rate of the dehydrogenative olefina-

tion (formation of **2**, **6**) relative to the dehydrogenative C–C bond formation in such bisseco intermediates (**4**, **17**).



Under mild hydrogenative conditions (CH_2Cl_2, room temperature, Pd/C ca. 4 d), the very sparingly soluble tetrol **5a** arises from **5c**.

Received: August 18, 1988 [Z 2930 IE]
German version: *Angew. Chem. 101* (1989) 307
Publication delayed at authors' request

[1] W.-D. Fessner, G. Sedelmeier, P. R. Spurr, G. Rihs, H. Prinzbach, *J. Am. Chem. Soc. 109* (1987) 4626; W.-D. Fessner, H. Prinzbach in O. Chizhov (Ed.): *Organic Synthesis: Modern Trends*, Blackwell, Oxford 1987, p. 23.

[2] W.-D. Fessner, Bulusu A. R. C. Murty, J. Wörth, D. Hunkler, H. Fritz, H. Prinzbach, W. D. Roth, P. von R. Schleyer, A. B. McEwen, W. F. Maier, *Angew. Chem. 99* (1987) 484; *Angew. Chem. Int. Ed. Engl. 26* (1987) 452.

[3] P. R. Spurr, Bulusu A. R. C. Murty, W.-D. Fessner, H. Fritz, H. Prinzbach, *Angew. Chem. 99* (1987) 486; *Angew. Chem. Int. Ed. Engl. 26* (1987) 455.

[4] G. K. S. Prakash, V. V. Krishnamurthy, R. Herges, R. Bau, H. Yuan, G. A. Olah, W.-D. Fessner, H. Prinzbach, *J. Am. Chem. Soc. 108* (1986) 836. *Paquette* et al. have recently reported on mono- and 1,16-difunctionalizations: L. A. Paquette, J. C. Weber, T. Kobayashi, *ibid. 110* (1988) 1303; G. A. Olah, G. K. S. Prakash, T. Kobayashi, L. A. Paquette, *ibid. 110* (1988) 1304.

[5] W. F. Maier, P. von R. Schleyer, *J. Am. Chem. Soc. 103* (1981) 1891.

[6] L. A. Paquette, Y. Miyahara, C. W. Doecke, *J. Am. Chem. Soc. 108* (1986) 1716.

[7] R. Pinkos, G. Rihs, H. Prinzbach, *Angew. Chem. 101* (1989) 312; *Angew. Chem. Int. Ed. Engl. 28* (1989) 303.

[8] J.-P. Melder, H. Fritz, H. Prinzbach, *Angew. Chem. 101* (1989) 309; *Angew. Chem. Int. Ed. Engl. 28* (1989) 300.

[9] The new compounds have been characterized by elemental analyses and spectra (^1H and ^{13}C NMR, IR, MS). For example 1,20-dimethoxy-nonacyclo[12.6.0.0^{2,6}.0^{4,11}.0^{5,9}.0^{7,20}.0^{10,17}.0^{12,16}.0^{15,19}]eicos-10(11)-ene **2b**: m.p. 162–164°C. ^1H NMR ($CDCl_3$, 250 MHz): $\delta = 3.35$ (s, 2 OCH_3), 3.09 (d, 3*s*-, 8*s*-, 13*s*-, 18*s*-H), 2.99 (m, 6-, 15-H), 2.91 (m, 4-, 9-, 12-, 17-H), 2.89 (m, 2-, 7-, 14-, 19-H), 2.77 (m, 5-, 16-H), 1.72 (m, 3*a*-, 8*a*-, 13*a*-, 18*a*-H); $J_{2,3a} = 7.0$, $J_{2,3s} = 0$, $J_{3a,3s} = 13.5$, $J_{3a,4} = 4.5$, $J_{4,5} = 4.0$, $J_{5,6} = 10.0$, $J_{6,7} = 10.0$ Hz. ^{13}C NMR ($CDCl_3$, 100.6 MHz): $\delta = 150.6$ (C-10, -11), 106.9 (C-1, -20), 60.2 (C-5, -16), 58.5 (C-6, -15), 52.1 (C-2, -7, -14, -19), 51.1 (2 OCH_3), 45.8 (C-4, -9, -12, -17), 37.6 (C-3, -8, -13, -18).—1,10,11,20-Tetramethoxy-nonacyclo[12.6.0.0^{2,6}.0^{4,11}.0^{5,9}.0^{7,20}.0^{10,17}.0^{12,16}.0^{15,19}]eicosane **5d**: m.p. 249–250°C. ^1H NMR ($CDCl_3$, 250 MHz): $\delta = 3.40$ (d, 3*s*-, 8*s*-, 13*s*-, 18*s*-H), 3.36 (s, 4 OCH_3), 3.16 (m, 5-, 6-, 15-, 16-H), 2.99 (m, 2-, 4-, 7-, 9-, 12-, 14-, 17-, 19-H), 1.86 (dt, 3*a*-, 8*a*-, 13*a*-, 18*a*-H); $J_{2,3s} = 0$, $J_{2,3a} = 7.5$, $J_{3a,3s} = 15.0$, $J_{2,6} = 10.0$ Hz. ^{13}C NMR ($CDCl_3$, 100.6 MHz): $\delta = 104.3$ (C-1, -10, -11, -20), 59.4 (C-5, -6, -15, -16), 52.6 (C-2, -4, -7, -9, -12, -14, -17, -19), 50.9 (4 CH_3), 36.7 (C-3, -8, -13, -18).—5-Oxanonacyclo-[9.8.1.1.1^{7,18}.0^{3,18}.0^{4,6}.0^{4,9}.0^{6,17}.0^{8,12}.0^{15,19}]heneicosa-14,20-dione **12**: m.p. >330°C. ^1H NMR ($CDCl_3$, 250 MHz): $\delta = 3.50$ (m, 1-, 11-, 13-, 15-H), 3.38 (m, 12-, 19-H), 3.03 (d, 2*s*-, 10*s*-, 16*s*-, 21*s*-H), 2.97 (m, 8-, 18-H), 2.66 (t, 3-, 7-, 9-, 17-H), 1.86 (m, 2*a*-, 10*a*-, 16*a*-, 21*a*-H); $J_{1,2a} = 9.0$, $J_{1,19} = 11.5$, $J_{2a,2s} = 15.0$, $J_{2a,3} = 5.5$, $J_{3,18} = 5.5$, $J_{8,12} = 11.0$ Hz. ^{13}C NMR ($CDCl_3$, 100.6 MHz): $\delta = 212.4$ (C-14, -20), 82.6 (C-4, -6), 67.6 (C-8, -18), 55.5 (C-1, -11, -13, -15), 51.3 (C-12, -19), 46.0 (C-3, -7, -9, -17), 34.5 (C-2, -10, -16, -21). MS (EI): *m/z* 309 ($M^{\oplus}+1$, 100%). *s* = *syn*, *a* = *anti*.

[10] R. Schwesinger, *Chimia 39* (1985) 269; R. Schwesinger, H. Schlemper, *Angew. Chem. 99* (1987) 1212; *Angew. Chem. Int. Ed. Engl. 26* (1987) 1167.

[11] G. A. Olah, G. K. S. Prakash, J. G. Shih, V. V. Krishnamurthy, G. D. Mateescu, G. Liang, G. Sipos, V. Buss, T. M. Gund, P. von R. Schleyer, *J. Am. Chem. Soc. 107* (1985) 2764; E. W. Della, G. M. Elsey, *Tetrahedron Lett. 29* (1988) 1299.

[12] H. Prinzbach, Bulusu A. R. C. Murty, W.-D. Fessner, J. Mortensen, J. Heinze, G. Gescheidt, F. Gerson, *Angew. Chem. 99* (1987) 488; *Angew. Chem. Int. Ed. Engl. 26* (1987) 457.

[13] G. K. S. Prakash, W.-D. Fessner, G. Olah, G. Lutz, H. Prinzbach, *J. Am. Chem. Soc. 111* (1989) 746.

[14] Crystal data of **5e** (25°C, 0.6 × 0.5 × 0.2 mm^3); triclinic, space group *P1*, $a = 8.710(3)$, $b = 10.982(4)$, $c = 11.086(4)$ Å; $Z = 1$; reflections with $I > 2\sigma(I) = 3291$. Further details of the crystal structure investigation are available on request from the Fachinformationszentrum Energie, Physik, Mathematik GmbH, D-7514 Eggenstein-Leopoldshafen 2 (FRG), on quoting the depository number CSD-53282, the names of the authors, and the journal citation.

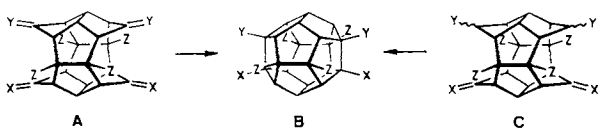
[15] W.-D. Fessner, *Dissertation*, Universität Freiburg 1986.

[16] G. G. Christoph, P. Engel, R. Usha, D. W. Balogh, L. A. Paquette, *J. Am. Chem. Soc. 104* (1982) 784.

The Pagodane Route to Dodecahedranes: Total Synthesis and Chemistry of 4,9,14,19-Tetrasubstituted [1.1.1.1]Pagodanes**

By *Johann-Peter Melder, Hans Fritz,* and *Horst Prinzbach**

Dehydrogenative C–C bond formation en route from pagodanes to dodecahedranes via bisseco- or secododecahedranes necessitates conditions which previously incorporated functional groups cannot survive.[1] A broad spectrum of such substituents would, on the other hand, tolerate a variety of methods established for the formation of C–C bonds between sp^2- or sp^2- and activated sp^3-C centers (**A** → **B** and **C** → **B**, respectively).[2] In close analogy to

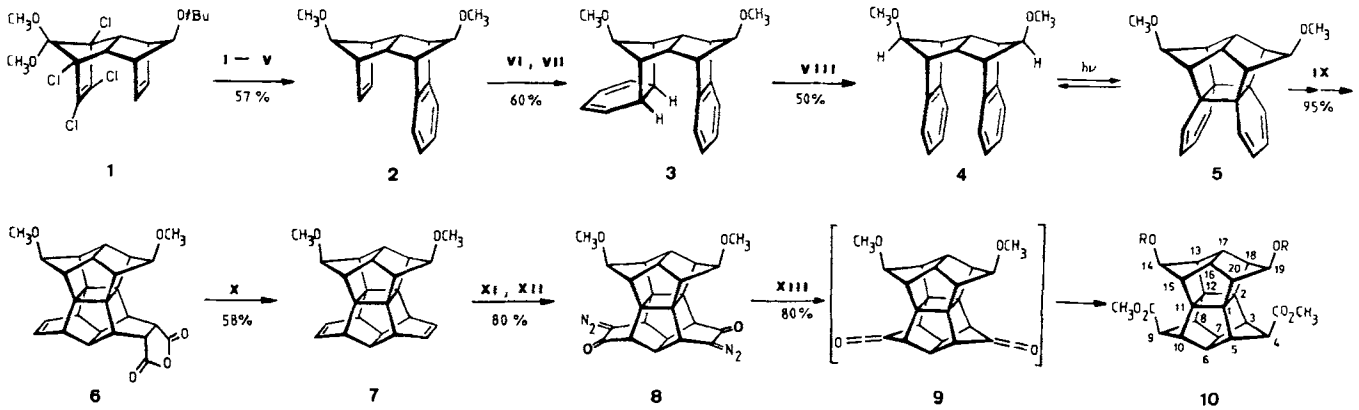


the preparation of the unsubstituted $C_{20}H_{20}$-pagodane (and of 4-*syn*,9-*syn*-disubstituted precursors[3]), we have developed the syntheses outlined in Schemes 1 and 2 for pagodanes appropriately functionalized in the four methylene positions (C-4, C-9, C-14, C-19).[4] An alternative protocol based on intramolecular functionalization is described in the directly following communication.[5,6]

Starting compound for the total synthesis is the C_{12}-diene **1**, an isodrin analogue, which is prepared in a ca. 40% yield from molar amounts of 7-*tert*-butoxynorbornadiene and tetrachlorocyclopentadienone-dimethyl ketal.[7] In this route to the *anti,anti*-dimethoxy-*syn,syn*-diester **10a**, condensed to 17 one-pot reactions (for ca. 40 functional changes), but not yet optimized in all individual steps (yield ca. 6% based on **1**; 85% per one-pot reaction!), an increased loss of material must be tolerated in the dehydrogenating aromatization **3** → **4** because of cleavage of etheral bonds in addition to the usual C—C homolysis. The steric shielding of the "inner" hydrogen atoms in **3** is presumably intensified by a "buttressing effect" of the CH_3O groups—which, however, influences only insignificantly the UV absorption of the face-to-face dibenzo com-

[*] Prof. Dr. H. Prinzbach, Dipl.-Chem. J.-P. Melder, Prof. Dr. H. Fritz
Chemisches Laboratorium der Universität
Institut für Organische Chemie und Biochemie
Albertstrasse 21, D-7800 Freiburg (FRG)

[**] This work was supported by the Deutsche Forschungsgemeinschaft, the Fonds der Chemischen Industrie, and BASF AG.



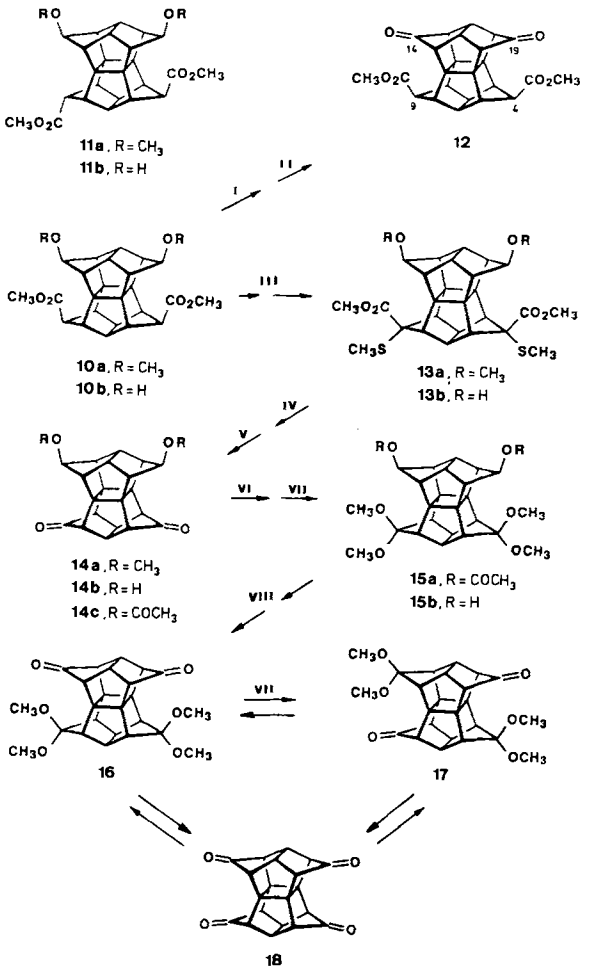
a, R = CH_3; b, R = H; c, R = $COCH_3$

Scheme 1. I: $C_4Cl_4O_2S$/toluene, Δ. II: Na/*t*BuOH/THF. III: HOAc/Ac_2O/$HClO_4$. IV: Li[HAl(O*t*Bu)$_3$]/THF. V: NaH/CH_3I. VI: $C_5Cl_4(OCH_3)_2$/toluene, Δ; Na/*t*BuOH/THF. VII: $C_4H_{10}O$/*p*-TosylOH/Δ. VIII: Pd/C, 190°C, 30 min. IX: MSA/toluene; 100°C. X: KOH/H_2O/CH_3OH, Δ; Cu_2O/2,2'-bipyridyl/quinoline, 200°C. XI: BH_3·THF/30% H_2O_2/NaOH; CrO_3/H_2O/H_2SO_4/acetone. XII: NaH/HCO_2CH_3/THF; *p*-TosylN$_3$/Et_3N/THF. XIII: CH_3OH, *hν*.

pound **4**[8] [(isooctane): $\lambda_{max}(\varepsilon)=287$ (330), 264 (1230), 257 (910), 228 (3440) nm] and the photoequilibrium established (ca. 3:1)[3,10] with the "*o,o-syn*-dibenzene" **5** [(isooctane): $\lambda_{max}(\varepsilon)=290$ (2400), 255 (2350), 215 (1830) nm] on irradiation at 254 nm. The CH_3O residues sterically hinder the domino-Diels–Alder addition **5**→**6**: the reaction with maleic anhyride (MA) requires rather drastic conditions (100°C), but without posing problems by thermal retrocleavage to give **4** [$t_{1/2}$(150°C)=30 min].[11] Despite this drawback for *exo* attack, *endo* addition still cannot compete.[12] The relatively low yield in the oxidative degradation **6**→**7** under similar drastic conditions as in **3**→**4** presumably has the same causes (C–O as well as C–C cleavage). The stereoselectivity of the addition of methanol to the ketene intermediates (**9**) is reduced: the photolysis of the bis(diazo)diketone mixture of C_2-**8** and C_s isomer (not shown here) in methanol furnished a 9:1 mixture of the *syn,syn*- and *syn,anti*-dimethyl esters **10a** and **11a**, respectively, in better than 90% yield; the products were separated by crystallization. The methyl ether groups in **10a** and **11a** can be readily cleaved with iodotrimethylsilane (TMSI). The quantitatively isolated, sparingly soluble dihydroxy diester **10b** is oxidized to the *syn,syn*-diketo diester **12** by pyridinium chlorochromate (PCC) with only minute loss of material.

Pagodane-4,9,14,19-tetrone **18**, the prototype of [1.1.1.1]pagodanes with four sp^2-hybridized bridge atoms, was obtained via the route depicted in Scheme 2: the mixture **10a/11a** can be converted into the *anti,anti*-dimethoxydione **14a** in 70% overall yield according to the method of *Trost* et al.,[13] whereby **11a** reacts much slower and only the bisthiomethylated intermediate **13a** needs to be isolated. In the case of **14a** the ether cleavage with TMSI (as carried out in the case of **10a**) to give the diol-dione **14b** turned out to be problematic. The diacetate **14c** is therefore prepared by treatment of **14a** with HBr/glacial acetic acid/acetic anhydride (110°C) (yield ca. 50%). Subsequent acetalization (**15a**), acetate hydrolysis (**15b**) and oxidation affords the D_{2h}-symmetrical, very sparingly soluble and extremely hygroscopic tetrone **18**. Upon heating in methanol/*p*-tosylOH, **16** equilibrates with **17** (ratio 2:3). From **18**, under the same conditions, the same mixture of **16**/**17** is formed.

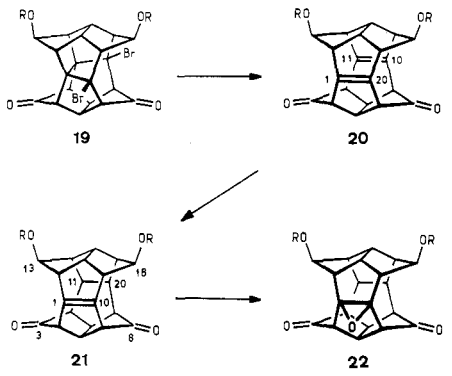
Concerning the opening of the four-membered ring and the stability of the functional groups under the conditions required[1,5] preliminary results for **14a** can be quoted: the



Scheme 2. I: TMSI/$CHCl_3$, 95%. II: PCC/CH_2Cl_2, 90%. III: LiN(*i*Pr)$_2$/CH_3SSCH_3/THF, −78°C, 88%. IV: KOH/$HO(CH_2)_2OH$, reflux; NCS/MeOH, 100%. V: conc. HCl/CH_2Cl_2, 88%. VI: HBr/HOAc/Ac_2O, reflux, 52%. VII: MeOH/*p*-TosylOH, 92%. VIII: PCC/CH_2Cl_2, 89%.

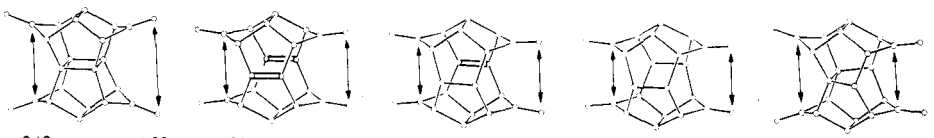
photoaddition of bromine to give **19a** is achieved in at least 80% yield, while the bromine elimination to give **20a** is almost quantitative. Bisseco-diene **20a** upon irradiation ($\lambda=254$ nm) undergoes a rapid [2+2] cycloaddition (**14a**), rapidly adds bromine (**19a**), and is slowly hydrogenated by N_2H_2 (**21a**). Not unexpectedly, the latter is stable towards

further hydrogenation, but is oxidized under standard conditions to the bisseco epoxide **22a**. The reactivity of the carbonyl groups in bisseco-frameworks is reduced:[14] In contrast to **14a**, compounds **20a–22a** cannot be condensed with phenylhydrazine or hydroxylamine. This cage effect can even be useful, e.g., in that the preparatively important cleavage of the two protecting methyl groups in **21a** with TMSI to give the diol **21b** is achieved without interference by the side reactions observed in the case of **14**, thus opening up an efficient entry to bisseco-tetrones.



a, R = CH_3; b, R = H

Force field (MM2) calculations[15] for **18**, the bisseco-dodecahedrane-tetrones **23–25**, and the hydrogenolysis product **26** (Scheme 3), reveal the following differences compared to the respective hydrocarbons (values in parentheses) of possibly preparative importance:[16] 1) the cleavage **18** → **23** is considerably exothermic; 2) the olefin strain in **23** (+9.7 kcal mol^{-1}) and **24** (+8.7 kcal mol^{-1}) is distinctly positive, and 3) ΔH_f^0 is more negative for **24** than for **26**. Accordingly, the four sp^2-hybridized bridge atoms should facilitate the thermal cleavage **18** → **23** as well as hydrogenation to **25**, and on the other hand should impair the detrimental competition by transannular C–C bond formation (**26**) frequently observed in the parent frameworks.

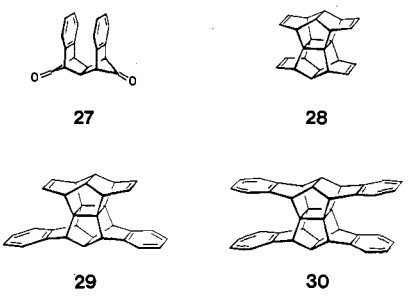


	18	**23**	**24**	**25**	**26**
ΔH_f° [kcal/mol]	- 22.1 (64.4)	- 48.6 (62.0)	- 62.6 (49.4)	- 77.7 (39.3)	- 58.2 (37.4)
E_{str} [kcal/mol]	132.8 (115.0)	68.1 (73.9)	77.8 (85.4)	86.5 (99.2)	101.3 (92.7)

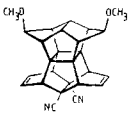
Scheme 3.

Received: August 18, 1988 [Z 2931 IE]
German version: *Angew. Chem. 101* (1989) 309
Publication delayed at authers' request

[1] G. Lutz, D. Hunkler, G. Rihs, H. Prinzbach, *Angew. Chem. 101* (1989) 307; *Angew. Chem. Int. Ed. Engl. 28* (1989) 298, and references cited therein.
[2] W. Carruthers: *Some Modern Methods of Organic Synthesis*, Cambridge University Press, Cambridge 1986, 3rd edit., p. 1.
[3] W.-D. Fessner, G. Sedelmeier, P. R. Spurr, G. Rihs, H. Prinzbach, *J. Am. Chem. Soc. 109* (1987) 4626.
[4] The new compounds have been characterized by their spectra (^{1}H and ^{13}C NMR, IR, MS) and elemental analyses. For example 15-*anti*,19-*anti*-dimethoxy-octacyclo[12.5.1.$0^{2,7}$.$0^{2,13}$.$0^{7,18}$.$0^{8,13}$.$0^{8,16}$.$0^{17,20}$]icosa-3,5,9,11-tetraene **5a**: m.p. 171 °C. ^{1}H NMR ($CDCl_3$, 250 MHz): δ = 5.74 (AA'BB', 4-, 5-, 10-, 11-H), 5.21 (AA'BB', 3-, 6-, 9-, 12-H), 4.19 (m, 15-, 19-H), 3.36 (s, 2 OCH_3), 3.15 (m, 17-, 20-H), 2.32 (m, 1-, 14-, 16-, 18-H); ^{13}C NMR ($CDCl_3$, 100.6 MHz): δ = 125.5 (C-4, -5, -10, -11), 123.8 (C-3, -6, -9, -12), 91.7 (C-15, -19), 61.2 (C-2, -7, -8, -13), 57.4 (2 OCH_3), 56.5 (C-1, -14, -16, -18), 51.7 (C-17, -20); UV (isooctane): $\lambda_{max}(\varepsilon)$ = 290 (2400), 255 (2350), 215 (1830) nm.—Dimethyl 14-*anti*,19-*anti*-dimethoxy-undecacyclo[9.9.0.$0^{1,5}$.$0^{2,12}$.$0^{2,18}$.$0^{3,7}$.$0^{6,10}$.$0^{8,12}$.$0^{11,15}$.$0^{13,17}$.$0^{16,20}$]icosane-4-*syn*,9-*syn*-dicarboxylate **10a**: m.p. 276 °C. ^{1}H NMR ($CDCl_3$, 400 MHz): δ = 3.64 (s, 2 CO_2CH_3), 3.50 (m, 14-, 19-H), 3.23 (s, 2 OCH_3), 3.19 (m, 16-, 17-H), 2.85 (m, 4-, 9-H), 2.81 (m, 6-, 7-H), 2.67 (m, 3-, 5-, 8-, 10-H), 2.33 (m, 13-, 15-, 18-, 20-H); ^{13}C NMR ($CDCl_3$, 100.6 MHz): δ = 173.2 (2 C=O), 93.2 (C-14, -19), 61.6 (C-1, -2, -11, -12), 58.1 (C-6, -7), 57.5 (C-4, -9), 57.1 (2 OCH_3), 55.6 (C-16, -17), 51.4 (2 CO_2CH_3), 44.2 (C-13, -15, -18, -20), 43.8 (C-2, -5, -8, -10); MS (EI): *m/z* 436 ($M^\oplus$, 79%), 75 (100).—14-*anti*,19-*anti*-Dimethoxy-undecacyclo[9.9.0.$0^{1,5}$.$0^{2,12}$.$0^{2,18}$.$0^{3,7}$.$0^{6,10}$.$0^{8,12}$.$0^{11,15}$.$0^{13,17}$.$0^{16,20}$]icosane-4,9-dione **14a**: m.p. 220 °C. IR: $\tilde{\nu}_{CO}$ = 1763 cm^{-1}; ^{1}H NMR ($CDCl_3$, 400 MHz): δ = 3.85 (m, 14-, 19-H), 3.52 (m, 16-, 17-H), 3.35 (m, 6-, 7-H), 3.30 (s, 2 OCH_3), 2.52 (m, 13-, 15-, 18-, 20-H), 2.25 (m, 3-, 5-, 8-, 10-H); ^{13}C NMR ($CDCl_3$, 100.6 MHz): δ = 210.2 (C-4, -9), 93.0 (C-14, -19), 60.0 (C-1, -2, -11, -12), 57.5 (2 OCH_3), 57.1 (C-16, -17), 47.7 (C-6, -7), 45.8 (C-3, -5, -8, -10), 44.6 (C-13, -15, -18, -20); MS (EI): *m/z* 348 ($M^\oplus$, 49%), 75 (100).—Undecacyclo[9.9.0.$0^{1,5}$.$0^{2,12}$.$0^{2,18}$.$0^{3,7}$.$0^{6,10}$.$0^{8,12}$.$0^{11,15}$.$0^{13,17}$.$0^{16,20}$]icosane-4,9,14,19-tetrone **18**: m.p. > 300 °C. IR: $\tilde{\nu}_{CO}$ = 1770 cm^{-1}; ^{1}H NMR ($CDCl_3$, 250 MHz): δ = 3.27 (4H), 2.28 (8H).—13-*anti*,18-*anti*-Dimethoxy-nonacyclo[12.6.0.0^{2,6}.$0^{4,11}$.$0^{5,9}$.$0^{7,20}$.$0^{10,17}$.$0^{12,16}$.$0^{15,19}$]icos-1(20)-ene-3,8-dione **21a**: m.p. 253–254 °C. IR: $\tilde{\nu}_{C=O}$ = 1714 cm^{-1}; ^{1}H NMR ($CDCl_3$, 400 MHz): δ = 4.41 (m, 13-, 18-H), 3.64 (m, 10-, 11-H), 3.44 (m, 15-H)*, 3.42 (m, 16-H)*, 3.33 (m, 2-, 7-H), 3.28 (2 OCH_3), 3.20 (m, 6-H), 3.20 (m, 14-, 19-H), 3.17 (m, 5-H), 2.88 (m, 4-, 9-H), 2.73 (m, 12-, 17-H); ^{13}C NMR ($CDCl_3$, 100.6 MHz): δ = 216.6 (C-3, -8), 148.7 (C-1, -20), 87.2 (C-13, -18), 60.3 (C-16), 59.6 (C-15), 56.4 (2 OCH_3), 56.3 (C-2, -7), 55.3 (C-10, -11), 54.9 (C-4, -9), 50.3 (C-12, -17), 49.4 (C-14, -19), 48.7 (C-5), 45.1 (C-6); MS (EI): *m/z* 350 ($M^\oplus$, 40%), 75 (100). *: assignment not certain.
[5] R. Pinkos, G. Rihs, H. Prinzbach, *Angew. Chem. 101* (1989) 312; *Angew. Chem. Int. Ed. Engl. 28* (1989) 303.
[6] Attempts to hydroxylate various 4,9-disubstituted pagodanes microbiologically have thus far failed: T. Pracht, K. Kieslich, H. Prinzbach, unpublished results.
[7] J.-P. Melder, F. Wahl, H. Fritz, H. Prinzbach, *Chimia 41* (1987) 426, and references cited therein.
[8] The diol **4**, H instead of CH_3, is also a suitable starting compound for the preparation of the dione **27** [7] and [2.2.2.2]pagodatetraene **28**. The di- and tetrabenzo derivatives **29** and **30** have already been prepared [9].



[9] C. Grund, H. Prinzbach, unpublished results.
[10] G. Sedelmeier, W.-D. Fessner, C. Grund, P. R. Spurr, H. Fritz, H. Prinzbach, *Tetrahedron Lett. 27* (1986) 1277; G. Sedelmeier, W.-D. Fessner, R. Pinkos, C. Grund, Bulusu A. R. C. Murty, D. Hunkler, G. Rihs, H. Fritz, C. Krüger, H. Prinzbach, *Chem. Ber. 119* (1986) 3442; Bulusu A. R. C. Murty, P. R. Spurr, R. Pinkos, C. Grund, W.-D. Fessner, D. Hunkler, H. Fritz, W. R. Roth, H. Prinzbach, *Chimia 41* (1987) 32.
[11] W. von E. Doering, W. R. Roth, R. Breuckmann, L. Figge, H.-W. Lennartz, W.-D. Fessner, H. Prinzbach, *Chem. Ber. 121* (1988) 1.
[12] Under high pressure (14 kbar, 16 h, 20°C), dicyanoacetylene preferentially adds (87 : 13) to **31** from the inner side (pincer); thus, there is an additional possibility of selective functionalization of the pagodane and (seco)dodecahedrane frameworks (F. G. Klärner, U. Artschwager-Perl, J.-P. Melder, G. Lutz, R. Pinkos, C. Grund, W.-D. Fessner, H. Prinzbach, unpublished results.



31

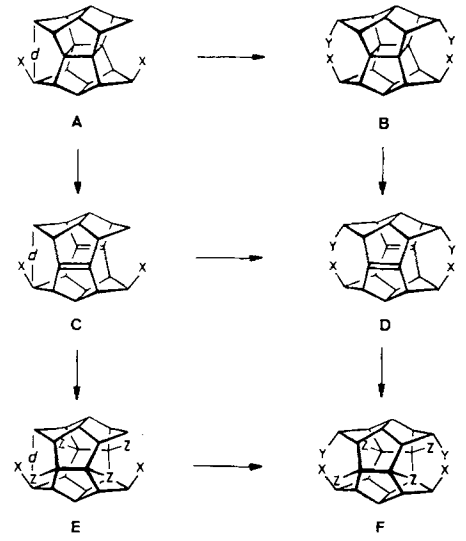
[13] B. M. Trost, Y. Tamaru, *J. Am. Chem. Soc. 99* (1977) 3101.
[14] W.-D. Fessner, H. Prinzbach in O. Chizhov (Ed.): *Organic Synthesis: Modern Trends*, Blackwell, Oxford 1987, p. 23.
[15] N. L. Allinger, *J. Am. Chem. Soc. 99* (1977) 8127; E. Keller, *Chem. Unserer Zeit 14* (1980) 56.
[16] P. R. Spurr, Bulusu A. R. C. Murty, W.-D. Fessner, H. Fritz, H. Prinzbach, *Angew. Chem. 99* (1987) 486; *Angew. Chem. Int. Ed. Engl. 26* (1987) 455.

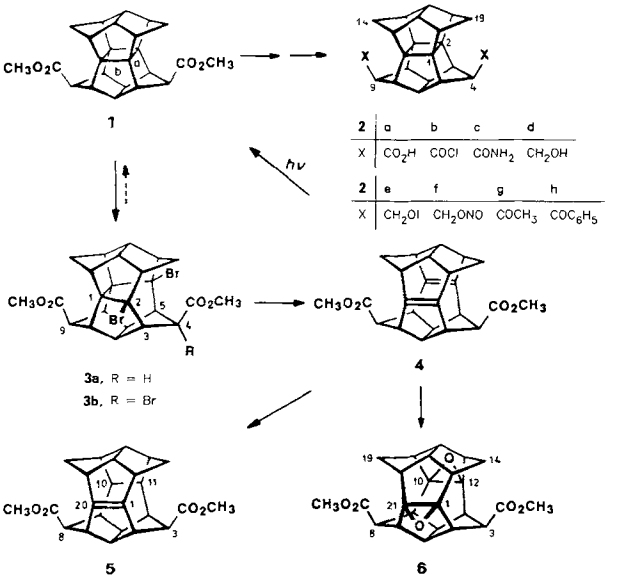
The Pagodane Route to Dodecahedranes: 4,9,14,19-Tetrasubstituted [1.1.1.1]Pagodanes by Intramolecular Functionalization**

By *Rolf Pinkos, Grety Rihs,* and *Horst Prinzbach**

Functionalization of the pagodane framework at the secondary positions 4, 9, 14 and 19 should open up a productive route to symmetrically highly functionalized pentagonal dodecahedranes. Concomitant with the development of a total synthesis,[1] our activities have been directed to the use of *syn,syn*-substituents X, selectively incorporated into readily accessible pagodanes **A** and bissecododecahedranes **C** and **E**, for the functionalization (Y) of the respective opposite methylene groups (**B**, **D**, **F**). In view of the limitations for the type of substitution (X, Y) as caused by the ring-opening conditions **B** → **D**,[2] a protocol with four-membered ring opening preceding functionalization (**A** → **C** → **D** → **F** or **A** → **C** → **E** → **F**) was to be followed. Depending on the transannular distance *d*, a functionalization via seven- or eight-membered transition states should be advantageous.

Fundamental limitations of this procedure are exemplified for the *syn,syn*-diester **1**: the opening of the lateral four-membered ring bonds a to give the bisseco-diene **4**[3] (**B** → **D**) according to the proven procedure[2] becomes complicated in so far as the α-ester position on the open side of the dibromide **3a** is brominated relatively rapidly (**3b**). In addition, during the 1,4-bromine elimination **1** is partly re-formed from **3a** (yield of **4** ca. 75% based on conversion of **1**). The diimide-reduction of **4** proceeds much more slowly than in the case of the ester-free diene,[2,4] but furnishes selectively the ene diester **5**. In the epoxidation of **4** with peracids under normal conditions, side reactions occur, which, however, can be avoided by the use of benzoylperoxycarbamic acid (100% **6**).





With increasing bulging of the carbon skeleton in going from **1** ($a = 1.583$ Å) via **4** (2.59 Å) to **5** (2.96 Å), the transannular distances *d* between methylene and ester-bearing C atoms decreases from 3.60 to 3.30 and 3.22 Å, respectively (MM2 calculations; cf. Scheme 3 in Ref. [1] and the distance of 2.949 Å for **5e** in Fig. 1 of Ref. [4])—with drastic consequences for the reactivity of the *syn*-ester groups: transformations, which in the case of **1** (to **2a**–**2h**[5]) were generally unproblematical and highly efficient, are, in the case of **4**, **5** and **6**, extremely retarded and unselective or even impossible without previous epimerization at the α-C atoms—due to steric interactions and poor solvation of the tetrahedral intermediates. Very informative in this context is the X-ray structure analysis[6] of the *syn,syn*-diepoxy diester **6** (Fig. 1). Unlike **1**,[5] **6** crystallized in the C_s symmetrical ester conformation. With a molecular diameter of

[*] Prof. Dr. H. Prinzbach, Dipl.-Chem. R. Pinkos
Chemisches Laboratorium der Universität
Institut für Organische Chemie und Biochemie
Albertstr. 21, D-7800 Freiburg (FRG)
G. Rihs
Ciba-Geigy AG
CH-4002 Basel (Switzerland)

[**] This work was supported by the Deutsche Forschungsgemeinschaft, the Fonds der Chemischen Industrie, and BASF AG.

2.935 Å, the distance between substituted and opposite methylene C atoms (3.611 Å in **1**) is now only 3.228 Å; the distance between the carbonyl C atoms and the respective

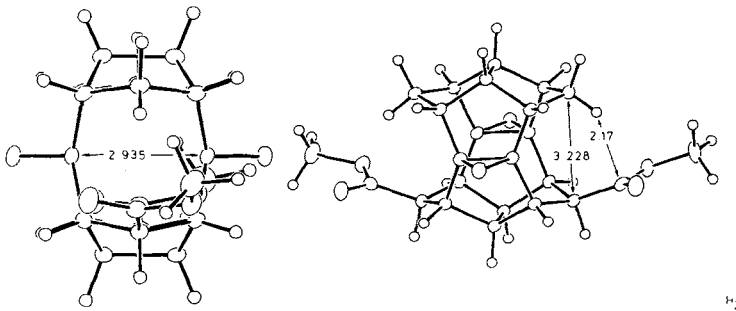


Fig. 1. Crystal structure of **6** (distances in Å).

syn-H atoms (2.17 Å; average 2.41 Å in **1**) is considerably less than the sum of the van-der-Waals radii.[7]

The extent of steric compression associated with the tetragonalization of the carbonyl centers in the diesters **4**–**6** becomes evident in the simulated structure (MM2) of the bishydrate **7** (Fig. 2) derived from the ene-diester **5**: the increase in strain of 36.6 kcal mol^{-1} compared to that in **5** reflects the extreme steric pressure between the *syn*-methylene hydrogen atoms and the opposite oxygen atoms located at a distance (2.27 and 2.31 Å) much smaller than the sum of their van-der-Waals radii.

7

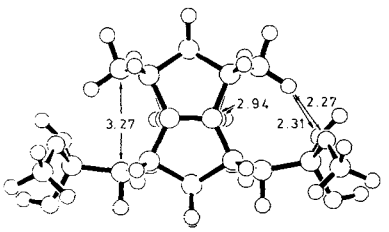
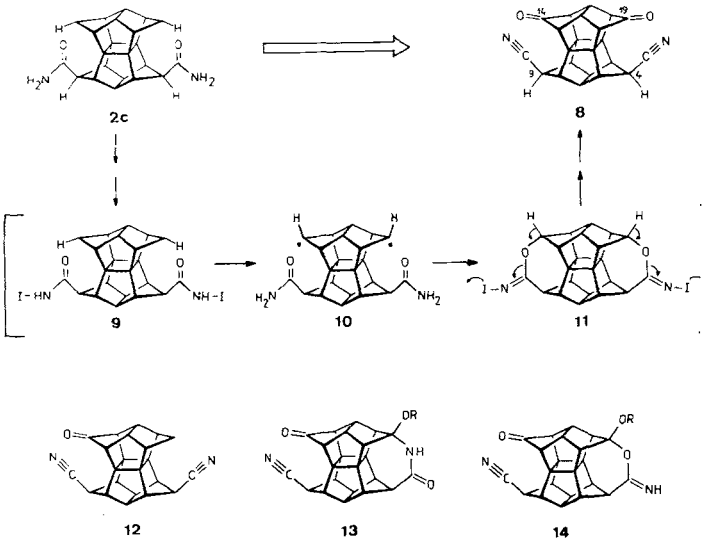


Fig. 2. MM2-simulated structure (SCHAKAL) of the bis-ester hydrate **7** (distances in Å).

A consequence of this drastically reduced reactivity of *syn*-oriented substituents in bisseco pagodanes with regard to the above schematized alternatives for methylene functionalization implies that the variation of the X residues required for the introduction of the Y functions is not possible at the stage of the bisseco structures **C** or **E** but must be brought about at the stage of the pagodanes **A**. Thus only such X residues can be considered which are stable or are appropriately modified under the conditions of the opening reactions **A**→**C** or **B**→**D**.

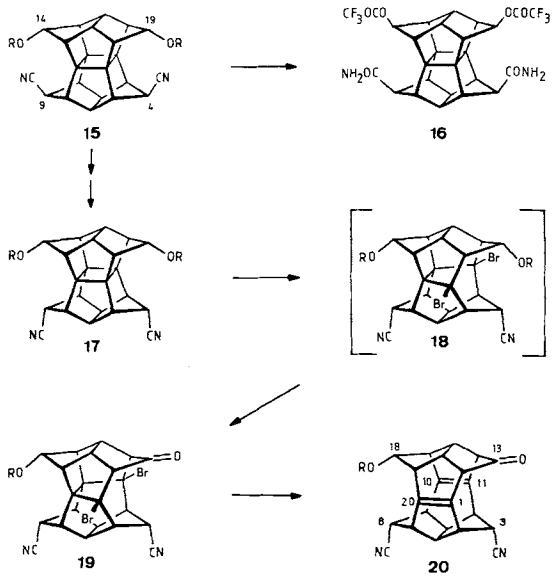
A twofold intramolecular, mechanistically remarkable functionalization of the type **A**→**B**, which proved highly valuable for the entire program, was realized—after unsatisfactory results with *inter alia*, the bishypoiodide **2e** and the dinitrite **2f**[8]—in a variant of the Barton reaction[10] with the *syn,syn*-dicarboxamide **2c**. By irradiation of a ca. 10^{-3} M solution of **2c** in CH_2Cl_2 in the presence of 12 equiv. I_2, after complete conversion and simple work-up (crystallization), the C_s-symmetrical 14,19-dioxopagodane-4-*syn*,9-*syn*-dicarbonitrile **8** can be reproducibly isolated in over 90% yield (for 2 mmol quantities; ca. 95% per function). From the mother liquor, two additional products can be separated chromatographically in variable amounts from other components and identified as ketodinitrile **12** and lactam **13**; the latter is differentiated from iminolactone **14** mainly by ^{13}C-NMR data. The sequence of the numerous intermediates in going from **2c** to **8** is not yet clear; the bisiodamide **9**, the diradical **10** and the bisiodoiminolactone **11** are merely guides. The unusual efficiency of both abstraction of ε-hydrogen atoms and ketone formation[10] is understood in terms of the rigid structure and the very favorable atomic distances.[11]



Starting from **8**, the functional groups and the stereochemistry at positions 4(9) and 14(19) in the [1.1.1.1]pagodane framework can be varied selectively. By twofold, acid-catalyzed nitrile hydrolysis of **8** (HCl/HOAc, reflux, 12 h), the previously reported[1] 4-*syn*,9-*syn*-pagodanedicarboxylic acid is obtained, by twofold *exo*-specific reduction with $NaBH_4$ (ethanol, 20°C) the all-*syn*-dihydroxydinitrile **15a** in quantitative yield. The spanning of the C4(19)- and/or C9(14)-positions by diatomic bridges as postulated in **11** as well as **13** and **14**—striven for en route to homologous dodecahedranes and according to force field calculations with increasing bulging of the skeletal frameworks (**B**→**D**→**F**) accompanied by decreasing strain—sets the scene for twofold epimerization at C14(19) in **15a**: the product isolated quantitatively from its solution in $CF_3CO_2H/CHCl_3$ (1:1, 20°C, 3 d) and, according to ^{1}H-NMR monitoring formed via several intermediates, is (tentatively) assigned the structure as *anti,anti*-bis(trifluoroacetoxy)-*syn,syn*-dicarboxamide **16**. The double epimerization at C-4(9) in **15a** to give the thermodynamically more stable 14-*syn*,19-*syn*-dihydroxy-4-*anti*,9-*anti*-dinitrile **17a** proceeds slowly because of strong kinetic preference for *exo*-protonation of the carbanions and is accomplished quantitatively by heating in *t*BuOH/*t*BuONa in a sealed tube (160°C, 1 h).

The effects of specific framework substitution upon the two-step opening of the four-membered ring (**B**→**D**), essential for advancement of the project,[12] have also been checked on **15b** and **17b**.[1] In the case of all-*syn*-**15b** the photoaddition of bromine under various conditions was so slow relative to several competing processes that a complex product mixture is present already after minimal conversion. **17b** under standard conditions (CH_2Cl_2/CH_3CN

(10:1), 15 equiv. Br_2), selectively furnishes the dibromoketone **19b** (yield ca. 85%); a preparatively very useful[13] stereofacial selectivity manifests itself in the regiospecific cleavage of the *syn*-ether on the "open" side of the dibromide **18b**. The elimination of bromine from **19b** to give the bisseco-diene **20b** proceeds almost without competition.



a, R = H; **b**, R = CH_3; **c**, R = $COCH_3$

Received: August 18, 1988 [Z 2932 IE]
German version: *Angew. Chem. 101* (1989) 312
Publication delayed at authors' request

[1] J.-P. Melder, H. Fritz, H. Prinzbach, *Angew. Chem. 101* (1989) 309; *Angew. Chem. Int. Ed. Engl. 28* (1989) 300.

[2] P. R. Spurr, Bulusu A. R. C. Murty, W.-D. Fessner, H. Fritz, H. Prinzbach, *Angew. Chem. 99* (1987) 486; *Angew. Chem. Int. Ed. Engl. 26* (1987) 455; R. Pinkos, *Diplomarbeit*, Universität Freiburg 1986.

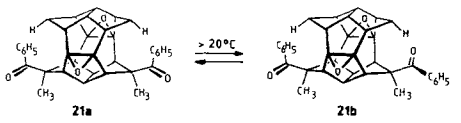
[3] The new compounds have been characterized by elemental analyses and spectra (^1H and ^{13}C NMR, IR, MS). For example dimethyl nonacyclo[12.6.0.0^{2,6}.0^{4,11}.0^{5,9}.0^{7,20}.0^{10,17}.0^{12,16}.0^{15,19}]icosa-1(20),10-diene-3-*syn*,8-*syn*-dicarboxylate **4**: m.p. 253–257°C. ^1H NMR ($CDCl_3$, 250 MHz): δ = 3.76 (s, 2 OCH_3), 3.45 (m, 2-, 4-, 7-, 9-H), 3.39 (m, 5-, 6-H), 3.31 (m, 15-, 16-H), 3.01 (m, 12-, 14-, 17-, 19-H), 2.56 (m, 3*a*-, 8*a*-H), 1.97 (d, 13*s*-, 18*s*-H), 1.32 (dt, 13*a*-, 18*a*-H); $J_{13a,13s}$ = 14.2 Hz. — Dimethyl 11,22-dioxaundecacyclo[13.7.0.0^{1,21}.0^{2,6}.0^{4,12}.0^{5,9}.0^{7,21}.0^{10,12}.0^{10,18}.0^{13,17}.0^{16,20}]docosane-3-*syn*,8-*syn*-dicarboxylate **6**: m.p. 215–218°C. ^1H NMR ($CDCl_3$, 250 MHz): δ = 3.78 (s, 2 OCH_3), 2.92–2.95 (m, 2-, 3*a*-, 4-, 7-, 8*a*-, 9-H), 2.87 (m, 5-, 6-H), 2.72 (m, 16-, 17-H), 2.50 (m, 13-, 15-, 18-, 20-H), 2.07 (d, 14*s*-, 19*s*-H), 1.49 (dt, 14*a*-, 19*a*-H); $J_{14s,14a}$ = 15.0 Hz; ^{13}C NMR ($CDCl_3$, 100.6 MHz): δ = 172.8 (2 C=O), 85.2 (C-1, -10, -12, -21), 64.5 (C-16, -17), 62.3 (C-5, -6), 52.1 (2 OCH_3), 50.5 (C-3, -8), 44.4 (C-2, -4, -7, -9, -13, -15, -18, -20), 32.1 (C-14, -19). — 14,19-Dioxo-undecacyclo[9.9.0.0^{1,5}.0^{2,12}.0^{2,18}.0^{3,7}.0^{6,10}.0^{8,12}.0^{11,15}.0^{13,17}.0^{16,20}]icosane-4-*syn*,9-*syn*-dicarbonitrile **8**: m.p. > 320°C. IR: $\tilde{\nu}_{CN}$ = 2225, $\tilde{\nu}_{CO}$ = 1765 cm^{-1}; ^1H NMR ($CDCl_3$, 400 MHz): δ = 3.34 (m, 16-, 17-H), 3.15 (m, 6-, 7-H), 3.02 (m, 3-, 5-, 8-, 10-H), 2.97 (m, 4*a*-, 9*a*-H), 2.53 (m, 13-, 15-, 18-, 20-H); ^{13}C NMR ($CDCl_3$, 100.6 MHz): δ = 206.8 (2 C=O), 118.2 (2 CN), 62.9 (C-1, -2, -11, -12), 58.5 (C-6, -7), 46.9 (C-16, -17), 46.8 (C-3, -5, -8, -10), 45.3 (C-13, -15, -18, -20), 40.6 (C-4, -9). — 14-*syn*,19-*syn*-Dimethoxy-undecacyclo[9.9.0.0^{1,5}.0^{2,12}.0^{2,18}.0^{3,7}.0^{6,10}.0^{8,12}.0^{11,15}.0^{13,17}.0^{16,20}]icosane-4-*anti*,9-*anti*-dicarbonitrile **17b**: m.p. 232–235°C. IR: $\tilde{\nu}_{CN}$ = 2230 cm^{-1}; ^1H NMR ($CDCl_3$, 250 MHz): δ = 3.74 (m, 14*a*-, 19*a*-H), 3.67 (m, 4*s*-, 9*s*-H), 3.55 (m, 6-, 7-H), 3.22 (s, 2 OCH_3), 2.68 (m, 3-, 5-, 8-, 10-H), 2.62 (m, 16-, 17-H), 2.40 (m, 13-, 15-, 18-, 20-H). — 20-*syn*-Methoxy-13-oxo-nonacyclo[12.6.0.0^{2,6}.0^{4,11}.0^{5,9}.0^{7,20}.0^{10,17}.0^{12,16}.0^{15,19}]icosa-1(20),10-diene-3-*anti*,8-*anti*-dicarbonitrile **20**: m.p. 235°C (CH_2Cl_2/ether). IR: $\tilde{\nu}_{CN}$ = 2230, $\tilde{\nu}_{CO}$ = 1725 cm^{-1}; ^1H NMR ($CDCl_3$, 400 MHz): δ = 5.08 (m, 8*s*-H), 3.81 (m, 5-, 6-H), 3.51 (m, 3*s*-H), 3.02 (s, OCH_3), 3.01 (m, 2-, 4-, 7-, 9-H), 2.92 (m, 17-, 19-, 18*a*-H), 2.80 (m, 15-, 16-H), 2.74 (m, 12-, 14-H); ^{13}C NMR ($CDCl_3$/C_6D_6, 100.6 MHz): δ = 211.4 (C=O), 122.1 (CN), 120.5 (CN), 158.3 (C-1, -11)*, 157.3 (C-10, -20)*, 79.9 (C-18), 60.3 (C-5, -6), 57.5 (OCH_3), 54.7 (C-12, -14), 50.6 (C-2, -4), 49.1 (C-7, -9), 48.8 (C-15, -16), 48.0 (C-17, -19), 33.8 (C-3), 31.6 (C-8). *s* = *syn*, *a* = *anti*; *: assignment not certain.

[4] G. Lutz, D. Hunkler, G. Rihs, H. Prinzbach, *Angew. Chem. 101* (1989) 307; *Angew. Chem. Int. Ed. Engl. 28* (1989) 298.

[5] W.-D. Fessner, G. Sedelmeier, P. R. Spurr, G. Rihs, H. Prinzbach, *J. Am. Chem. Soc. 109* (1987) 4626; W.-D. Fessner, *Dissertation*, Universität Freiburg 1986.

[6] Crystal data of **6** (25°C, 0.8 × 0.8 × 0.1 mm^3); orthorhombic, space group P_{bca}, a = 34.800(6), b = 13.616(4), c = 7.657(3) Å; Z = 8; reflections with $I > 2\sigma(I)$ = 2422; R = 0.051. Further details of the crystal structure investigation are available on request from the Fachinformationszentrum Energie, Physik, Mathematik GmbH, D-7514 Eggenstein-Leopoldshafen 2 (FRG), on quoting the depository number CSD-53283, the names of the authors, and the journal citation.

[7] In 4-*anti*,9-*anti*-dimethyl derivatives of **6** the mobility of *syn*-substituents is greatly restricted; the atropisomers **21a**, **b** can be separated at room temperature.



21a **21b**

[8] Homo-Norrish functionalization in the diketones **22**, **23** and **2h** was not achieved; it possibly failed because of unfavorable orientation of the carbonyl-n- and the C-H-orbitals involved [9].

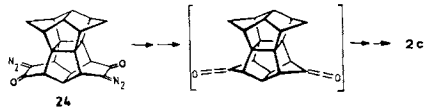


22 **23**

[9] P. J. Wagner in W. H. Watson (Ed.): *Stereochemistry and Reactivity of Systems Containing π-Electrons*, Verlag Chemie Int., Deerfield Beach, FL, USA 1983, p. 373.

[10] D. H. R. Barton, A. L. J. Beckwith, A. Goosen, *J. Chem. Soc. 1965*, 181; J. E. Baldwin, D. H. R. Barton, I. Dainis, J. L. C. Pereira, *J. Chem. Soc. C1968*, 2283; W. Carruthers: *Some Modern Methods of Organic Synthesis*, Cambridge University Press, Cambridge 1986, 3rd edit., p. 263.

[11] The efficiency of this entry to **8** can be improved further by no longer preparing the dicarboxamide **2c** via the diester **1**, but directly by photolysis of the bisdiazodiketone mixture **24** (and C_s isomer) in CH_2Cl_2/NH_3 (1:3, ca. 10^{-2} M solution, Hg high-pressure lamp, pyrex filter, −78°C) in over 80% yield (besides ca. 10% *syn.anti*-isomer).



24

[12] H.-P. Melder, R. Pinkos, H. Fritz, H. Prinzbach, *Angew. Chem. 101* (1989) 314; *Angew. Chem. Int. Ed. Engl. 28* (1989) 305.

[13] R. Pinkos, H.-P. Melder, H. Fritz, H. Prinzbach, *Angew. Chem. 101* (1989) 319; *Angew. Chem. Int. Ed. Engl. 28* (1989) 310.

The Pagodane Route to Dodecahedranes: Polyfunctionalized Pentagonal Dodecahedranes and Dodecahedrenes**

By *Johann-Peter Melder, Rolf Pinkos, Hans Fritz,* and *Horst Prinzbach**

An early defined goal in our quest for pentagonal dodecahedranes with pagodanes as central intermediates[1] is the modification of the outer dodecahedrane sphere with diverse substitution patterns.[2] Single and, in some cases, double and triple substitution of the parent dodecahedrane

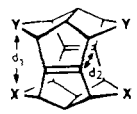
[*] Prof. Dr. H. Prinzbach, Dipl.-Chem. J.-P. Melder, Dipl.-Chem. R. Pinkos, Prof. Dr. H. Fritz
Chemisches Laboratorium der Universität
Institut für Organische Chemie und Biochemie
Albertstrasse 21, D-7800 Freiburg (FRG)

[**] This work was supported by the Deutsche Forschungsgemeinschaft, the Fonds der Chemischen Industrie and BASF AG. We thank Dr. *D. Hunkler* for NMR analyses, Dr. *J. Wörth* for MS analyses, Mrs. *M. Lutterbeck* and *M. Froom*, *G. Leonhardt* and *J. Leonhardt* for supplying starting materials, *G. Fehrenbach* for graphical work, and Dr. *W.-D. Fessner* and Dr. *L. Knothe* for helpful discussions.

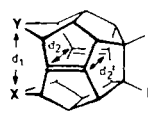
hydrocarbon has been reported by the *Paquette* group.[3] With the elaboration of highly efficient protocols for the activation of the 4,9,14,19-positions in the pagodane precursors, the scene was set for the preparation of pentagonal dodecahedranes **N**–**S** (Scheme 1) with four to eight skeletal positions being substituted.[4,5] The reliability of the force-field calculations[6] as to structural details is well established by X-ray analyses of relevant frameworks,[5,7,8] whilst the ΔH_f^0-, E_{str}- and olefin strain (*OS*)-data have to be taken as merely qualitative. The following points are essential: 1) the X–Y distances (d_1) of 2.8–3.0 Å in the bisseco- and monoseco-frameworks are favorable for *p/p* overlap; 2) the C–C bond formations bisseco→seco and seco→dodecahedrane are exothermic—except in the case of the dienes (**A**, **G**) and three-membered ring-enes (**D**, **K**); 3) the olefin strain for the monoseco-olefins **G**, **H** and **K** is positive, the hydrogenations **H**→**I** and **K**→**M** should therefore be possible; 4) the pyramidalization at the sp^2 centers in the case of the dodecahedrenes **N**, **O** and **Q** is of considerable but preparatively not necessarily limiting[9,10] order of magnitude. A general prerequisite for the realization of the individual projects is that the $2\sigma \rightarrow 2\pi$ cleavage of the respective pagodanes to give the bisseco-dienes **A** and the conversion of the latter into the differently saturated bisseco compounds **B**–**F** can be achieved with sufficient selectivity. For a given choice of X and Y in **A**–**F**, C–C bond formation methods can be employed (inter alia a–e) which require (and tolerate) quite different functional groups and, conducted irreversibly, should also overcome thermodynamically more or less unfavorable situations (e.g. **A**→**G**→**N**, **D**→**K**→**Q**).

Here we report a first preparative entry to four-, six- and eightfold functionalized pentagonal dodecahedranes of types **P** (**12a**–**d**, **13**), **R** (**15a**–**d**, **16**) and **S** (**18a**, **b**) and of dodecahedrenes of type **O** (**19a**, **b**) as highly versatile representatives using the Aldol variant (a). Homologous dodecahedranes are a subject of the following communication.[11]

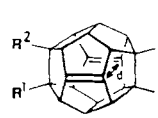
Starting material for all dodecahedranes presented here is the readily accessible dimethyl dioxopagodane-*syn,syn*-dicarboxylate **1**[4,5] or the bisseco-diene **4** derived from **1**. The opening of the four-membered ring in **1** leading to **4** via photobromination to give **2** and subsequent elimination of bromine was a priori not unproblematical: the addition of Br_2, already retarded by two keto[12] or two ester residues, proceeds so slowly under the concerted influence of these four functional groups, that (faster) subsequent bromination on the seco side of the dibromide **2** to give the tribromide **3** cannot be avoided.[13] This complication, however, has been satisfactorily solved: **3** can be obtained almost exclusively from **1**, when conversion is restricted to ca. 50% (yield ca. 95%; with increasing conversion, additional bromination products are formed) and can be separated easily and practically free of losses from **1** by filtration over silica (due to the high degree of substitution, **3** is not very susceptible to hydrolysis). Furthermore, the bromine substituent on C-4 is also eliminated (largely with retention) under the conditions of diene formation (Zn, NaI, Na_2SO_3, dimethylformamide (DMF), 140°C, 10 min);[5] besides diene **4** (ca. 90% isolated as crystals), at most traces of **1** are formed. Considerable steric compression on the seco side of **3** becomes evident, inter alia, from the hindered rotation of the *syn*-ester group on C-4; C_s symmetry is already destroyed at room temperature (cf. footnote [7] in Ref. [5]). The $[\pi_2+\pi_2]$ photocycloaddition, usually rapid in besseco-dienes, is not tangled by the C=O functions



	A	B	C	D	E	F
ΔH_f° :	2.7	-11.1	-24.4	1.6	2.1	-11.0
E_{str} :	67.0	77.1	87.7	88.9	112.4	100.2
OS :	-10.1	-10.6		-12.3		
d_1 :	3.0	2.9	2.8	3.0	2.9	2.9
d_2 :	2.7	3.1	3.6	3.6	3.4	3.5
Pyr. :	11.7	10.3		9.7		



	G	H	I	K	L	M
ΔH_f° :	15.1	-14.1	-44.1	7.1	-0.9	-22.4
E_{str} :	89.3	84.0	78.0	104.0	118.8	98.5
OS :	5.3	6.1		5.5		
d_1 :	3.0	2.9	2.8	3.0	2.9	2.9
$d_2(d_2')$:	2.9(3.1)	3.3(3.5)	3.7(3.9)	3.2(3.4)	3.5(3.7)	3.6(3.8)

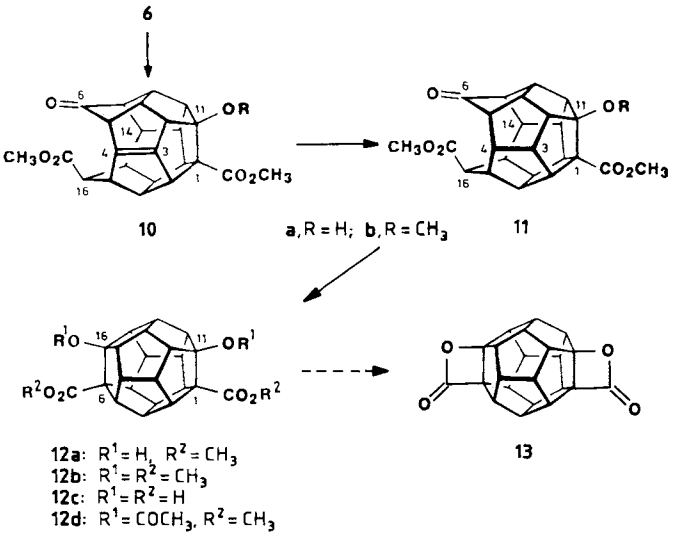


	N	O	P	Q	R	S
ΔH_f° :	21.0	-20.5	-62.4	8.3	-4.4	-33.4
E_{str} :	105.0	87.4	69.6	114.9	124.7	97.7
OS :	17.6	17.8		17.2		
d :	3.5	3.8	4.0	3.7	3.8	3.9
Pyr. :	45.2	46.2		45.6		

Scheme 1. Energy and structure data of model frameworks calculated for X = CH_2, Y = CO, Z = CH_2, R^1 = H, R^2 = OH; ΔH_f^0, E_{str}, *OS* [kcal mol^{-1}]; *d* [Å]; pyramidalization at the olefinic centers (pyr) [°].—The following methodologies are considered for the ultimate bond formations: a) Aldol addition (X = CHA, Y = C=O); b) pinacol addition (X = Y = C=O); c) Michael addition (X = CHA, Y = C=CHA); d) nucleophilic substitution (X = CHA; Y = CHL); e) oxidation (X = Y = CA$^{\oplus}$). A = acceptor group, L = leaving group.

in **4** (π/π distance ≥ 2.7 Å; $\lambda_{max}(CH_3CN) = 216$ nm ($\varepsilon =$ 1300), 270 (sh, 90), 314 (sh, 60)); upon acetone-sensitized excitation, **1** is formed quantitatively. For the unsaturated ε-ketoesters **5** and **6** differences compared to the diketo[12] and diester analogues[5] are manifest in the lability of the products derived from epoxidation and hydrogenation. The oxidation of **4** with *m*-chloroperbenzoic acid (*m*-CPB) (1.5 equiv., room temperature, CH_2Cl_2) leads selectively to the epoxyene **5**; oxidation of the latter to the diepoxide **7** (3.0 equiv., yield at least 80%) necessitates considerable thermal activation (rapid at 80°C), but is complicated in that **7** undergoes changes under the given conditions (as also on the TLC silica plates; acid catalysis). The hydrogenation of **4** with a large excess of diimide (hydrazine, HgO, 25 equiv., 0°C) ends with the hyperstable monoene **6**, which, however, after ca. 50% conversion is increasingly accompanied by secondary products (not **9**). Epoxidation of **6** furnishes **8**, which reacts further when *m*-CPB is used. That **4** is more reactive than **5** and **6** (cf. *OS* of −10.1, −10.6 and −12.3 kcal mol^{-1} for **A**, **B** and **D**, respectively) may reflect partial compensation of the hyperstability by destabilizing π/π interaction in **4**.[12]

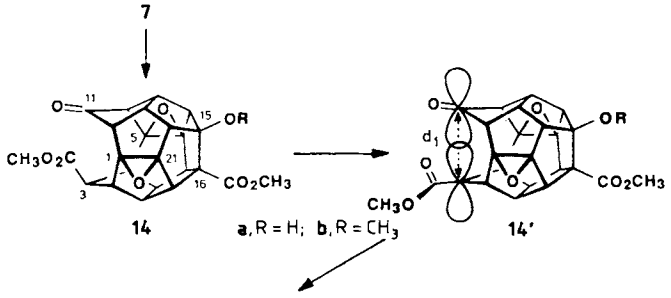
With the bisseco ε-ketoesters **4**–**8**, five substrates of the series **A**–**F** are available. For **P**-dodecahedranes initially sought after (e.g. **12a**), the appropriate precursor (**9**) is lacking. A detour is, however, offered by the reaction sequence **B**→**H**→**I**→**P**. In the case of the ε-keto ester **6** a



small enthalpy gain with moderate increase in strain is expected from model considerations for transannular bonding leading to β-hydroxyester **10a** (**B**→**H**, $\Delta\Delta H_f^0 = -3.0$ kcal mol^{-1}, $\Delta E_{str} = +6.9$ kcal mol^{-1}). Other than the hyperstable **6**, **10a** should undergo hydrogenation to give **11a** (cf. **H**→**I**, $OS = +6.1$ kcal mol^{-1}). The transformation of **11a** to the fourfold functionalized dodecahedrane **12a** (cf. **I**→**P**, $\Delta\Delta H_f^0 = -18.3$, $\Delta E_{str} = -8.4$ kcal mol^{-1}) is especially advantageous from energetic and stereoelectronic arguments. Indeed, this sequence from **6** to **12a** can be effected in a one-pot reaction not yet analyzed in detail: after prolonged reaction of **6** with hydrazine/HgO in large excess (25 equiv.) at 60°C, **12a** (dimethyl 11,16-dihydroxyundecacyclo[9.9.0.0^{2,0}.0^{3,7}.0^{4,20}.0^{5,18}.0^{6,16}.0^{8,15}.0^{10,14}.0^{12,19}.0^{13,17}]icosane-1,6-dicarboxylate) arises in 30–40% yield; it can be separated chromatographically from further, in part not yet fully characterized components (inter alia, **10a**, **11a**, **19a**) and crystallized from CH_2Cl_2/CH_3OH (colorless crystals, m.p. >320°C). Dimethyl ether **12b**, dicarboxylic acid **12c** and diacetate **12d** are first derivatives.[14] **10a** in the meantime (see below) has been selectively prepared from **6** under acid-catalysis conditions. An entry to **12a** almost free of losses (yield >90% based on **6**) is now opened up via hydrogenation to **11a** (Pd/C, CH_3OH, 20°C). The elimination of the OR- or CO_2R-functionalities in **12a**—exemplary also for **15a,b**, **18a,b** and **19a,b**—is now intensively studied as entry to 1,6-disubstituted dodecahedranes, their variation primarily under the aspect of olefin formation. The bislactone **13**, for example, is a potential precursor of a dodecahedradiene (cf. **21**) and prototype of annelated dodecahedranes.

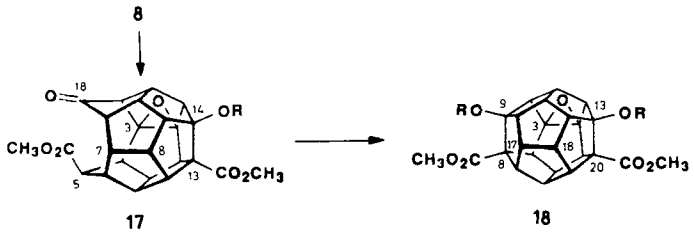
A gain in enthalpy with moderate increase in strain is likewise predicted for the cyclization of the bisseco-diepoxide **7** via the seco-diepoxide **14a** to the diepoxydodecahedrane **15a** (dimethyl 9,13-dihydroxy-2,18-dioxatridecacyclo[10.10.0.0^{1,3}.0^{3,10}.0^{4,8}.0^{5,22}.0^{6,20}.0^{7,17}.0^{9,16}.0^{11,15}.0^{13,21}.0^{14,19}.0^{17,19}]docosane-8,21-dicarboxylate) (cf. **E**→**L**→**R**): $\Delta\Delta H_f^0$ (ΔE_{str}) **E**→**L**/**L**→**R** = −3.0 (+6.4)/−3.5 (+5.9) kcal mol^{-1}. Our expectations were again fulfilled: Upon acid

catalysis (stirring over silica, CH_2Cl_2, 25 °C) from **7** dodecacycle **14a** slowly emerges (yield ca. 80%) and from the latter—with sufficient kinetic distinction for selective isolation of **14a**—the eightfold functionalized dodecahedrane **15a**, which crystallizes from CH_2Cl_2/CH_3OH as colorless crystals (m.p. > 320 °C, yield ca. 20%). The dimethyl ether **15b** is exclusively formed on addition of NaH (excess) and 3 equiv. CH_3I to a solution of **7** in anhydrous THF (room temperature). The β-hydroxy ester **15a** was converted into **15c**, **d**. The bislactone **16** is valuable, inter alia, as intermediate en route to the diepoxydodecahedradiene (cf. **23**).

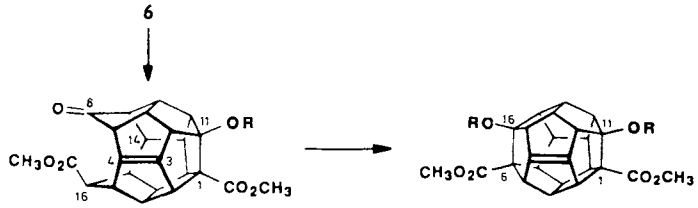


15a: $R^1 = H$, $R^2 = CH_3$
15b: $R^1 = R^2 = CH_3$
15c: $R^1 = R^2 = H$
15d: $R^1 = COCH_3$, $R^2 = CH_3$

The formation of the two C–C bonds in going from the bisseco-epoxide **8** via **17a** to the epoxydodecahedrane **18a** (dimethyl 9,13-dihydroxy-2-oxadodecacyclo[10.9.0.0^{1,3}.0^{3,10}.0^{4,8}.0^{5,21}.0^{6,19}.0^{7,17}.0^{9,16}.0^{11,15}.0^{13,20}.0^{14,18}]heneicosane-8,20-dicarboxylate) should profit from considerable driving force (cf. **F**→**S**: $\Delta\Delta H_f^0 = -22.4$, $\Delta E_{str} = -2.5$ kcal mol^{-1}). Indeed, **8** reacts slowly on SiO_2 (CH_2Cl_2, 25 °C) to give **17a** and then further to give **18a**, and reacts very rapidly with NaH/CH_3I (THF, 25 °C) to give **18b** (in each case colorless crystals from CH_2Cl_2/CH_3OH, m.p. > 320 °C.



The preparation of the dodecahedrenes **19** from the bisseco-ene **6** via **10** as intermediates was considered promising on the basis of energy criteria (cf. **H**→**O**: $\Delta\Delta H_f^0 = -6.4$, $\Delta E_{str} = +3.4$ kcal mol^{-1}). Such highly pyramidalized olefins are normally extremely reactive. Here the chances for isolation should, however, be improved by the special steric situation on the outer molecular sphere and by the type of substitution.[9] **6** changes only very slowly (ca. 50% conversion after 3 d) on SiO_2 (CH_2Cl_2, exclusion of oxygen, 25 °C); the steps leading to **10a** and to **19a** are kinetically so different that the comparably little oxygen-sensitive **10a** can be highly enriched and isolated by chromatography/crystallization in a yield of 95% based on conversion. Stirring of **6** over NaH (anhydrous THF, exclusion of oxygen, 25 °C) leads, after a few minutes, quantitatively to the Na_2-salt **19c** (with not absolutely water-free THF to the diol **19a**), while stirring over NaH/CH_3I (anhydrous THF, 25 °C) leads to the dimethyl ether **19b**. Ca. 10^{-2} M THF solutions of **19a** remain unchanged for days at room temperature; on heating under reflux, oligomeric (dimeric?) material separates out. The dodecahedrene **19a** (dimethyl 11,16-dihydroxy-undecacyclo[9.9.0.0^{2,9}.0^{3,7}.0^{4,20}.0^{5,18}.0^{6,16}.0^{8,15}.0^{10,14}.0^{12,19}.0^{13,17}]icosa-8-ene-1,6-dicarboxylate crystallized from CH_2Cl_2/CH_3OH is, as expected, sensitive towards oxygen; it is oxidized to **18a** with *m*-CPB, and is hydrogenated to **12a** over Pd/C.



C_{2v} symmetry is established for **12a** by five ^{1}H and seven ^{13}C, for **15a** by four ^{1}H and seven ^{13}C NMR framework signals, C_s symmetry for **18a** and **19a** by nine ^{1}H and twelve ^{13}C NMR framework signals each, all having appropriate intensities (Fig. 1); the assignment of the signals is confirmed by COSY, NOE and selective decoupling experiments. In the case of **18a** and **19a** the vicinal H,H coupling constants on the epoxide and ene sides, respectively, are 7–8 Hz, on the opposite sides 10–11 Hz. The ^{13}C NMR signals of the substituted quaternary C atoms generally

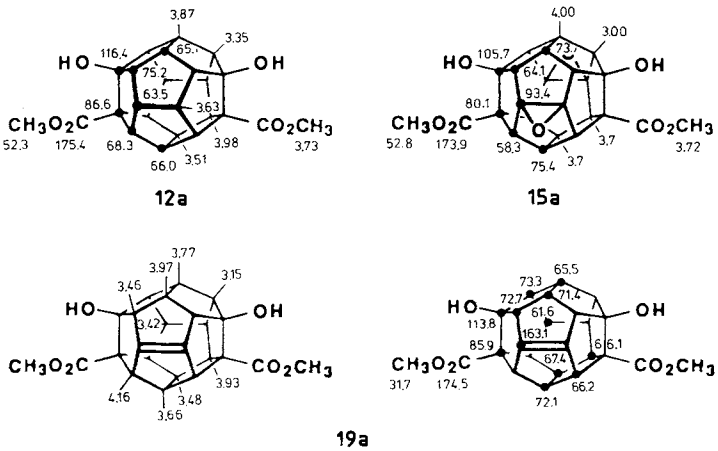
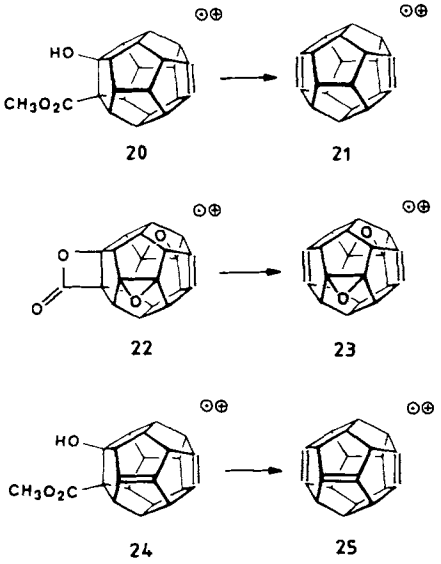


Fig. 1. ^{1}H and ^{13}C NMR data of **12a**, **15a** ($CDCl_3$) and **19a** ([D_8]THF).

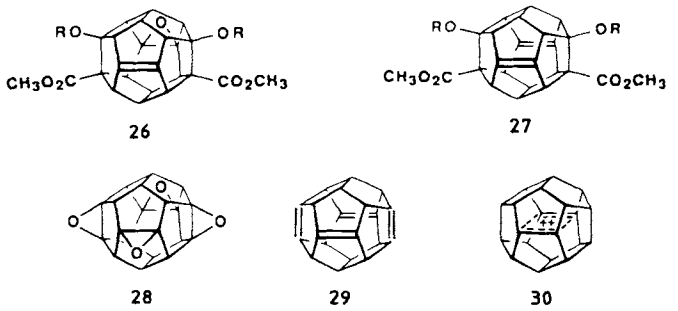
have similar chemical shifts as the signals in singly OH/CO_2R substituted dodecahedranes ($\delta = 116.0$ for C–OH, $\delta = 84.5$ for C–CO_2R[3]); those of the olefinic C atoms in **19a** are, partly also due to the substituents, shifted downfield compared to those in the planar bicyclo[3.3.0]octa-

1(5)-ene[15] (146.0 ppm) and those in the highly strained 10-selenatricyclo[3.3.3.$0^{3,7}$]undec-3(7)-ene[16]) ($\delta = 150.7$, cf. **10a**: $\delta_{C-4} = 145.2$, $\delta_{C-3} = 163.4$). In line with comparatively low strain in the saturated dodecahedranes are the C,H coupling constants (e.g. 134–140 Hz in the case of **12a**).

Information with regard to the stability of even multiply unsaturated dodecahedranes (cf. **27/29**) is provided by the EI mass spectra for **12**, **15**, **18** and **19**. The singly and doubly—and with limitations triply—unsaturated dodecahedrane radical cations resulting from elimination of the vicinal substituents are generally represented by relatively intense signals. Typical examples are the following: The ene radical cation **20** (*m/z* 332, 100%), which is formed from **12a**$^{\odot\oplus}$ (*m/z* 408, $M^{\oplus}$, 8%) via the successive expulsion of H_2O (*m/z* 390, 14%), CO (*m/z* 362, 42%) and CH_2O, and the diene radical cation **21** (*m/z* 256, 45%) from **20** via the same type of fragmentation. **15a**$^{\odot\oplus}$ (*m/z* 436, 9%, $M^{\oplus}$) first eliminates CH_4O from both sides (*m/z* 404 (100%), 372 (52%), cf. bislactone **16**), then CO_2 (diepoxyene **22**, *m/z* 328, 30%, and diepoxydiene **23**, *m/z* 284, 42%). **19a**$^{\odot\oplus}$ (*m/z* 406, 10%, $M^{\oplus}$) decays to the diene radical cation **24** (*m/z* 330, 74%) and triene radical cation **25** (*m/z* 254, 25%). Primarily subtle conformational differences between the ecliptically fixed vicinal pairs of substituents in **12**, **15**, **18** and **19** might be responsible for the varying degradation of the substituents.



Fourteen of the eighteen model frameworks depicted in Scheme 1, including four of the six dodecahedrane types, are represented by fully characterized compounds. Good



chances are seen for the now imminent thermodynamically unfavorable conversions of the type **D** → **Q** (**5** → **26**) and even **A** → **N** (**4** → **27**) whereby complexation of the vicinal hydroxy/ester functions can possibly be helpful. Such thermodynamically critical cases will also be explored in the meantime by S_N2 substitution in *syn,syn*-bisseco-diesters and -dinitriles with very good *anti,anti* leaving groups (Scheme 1, d, X = $CHCO_2CH_3$, CHCN; Y = CHI, $CHOCOCF_3$). Speculations are allowed on the stability and the bonding situation of rather exotic representatives such as the D_{2h} species **28** and **29** and the dication **30**.[7]

Received: November 15, 1988 [Z 3051 IE]
German version: *Angew. Chem. 101* (1989) 314

[1] The pioneering work of this route constitutes part of the Dissertation by *W.-D. Fessner*, Universität Freiburg 1986.

[2] W.-D. Fessner, Bulusu A. R. C. Murty, H. Prinzbach, *Angew. Chem. 99* (1987) 482; *Angew. Chem. Int. Ed. Engl. 26* (1987) 451; W.-D. Fessner, Bulusu A. R. C. Murty, J. Wörth, D. Hunkler, H. Fritz, H. Prinzbach, W. D. Roth, P. von R. Schleyer, A. B. McEwen, W. F. Maier, *ibid. 99* (1987) 484 and *26* (1987) 452; H. Prinzbach, W.-D. Fessner in O. Chizhov (Ed.): *Organic Synthesis: Modern Trends*, Blackwell, Oxford 1987, p. 23.

[3] L. A. Paquette, J. C. Weber, T. Kobayashi, *J. Am. Chem. Soc. 110* (1988) 1303; G. A. Olah, G. K. S. Prakash, T. Kobayashi, L. A. Paquette, *ibid. 110* (1988) 1304; L. A. Paquette, T. Kobayashi, J. C. Gallucci, *ibid. 110* (1988) 1305; J. C. Weber, L. A. Paquette, *J. Org. Chem. 53* (1988) 5315.

[4] J.-P. Melder, H. Fritz, H. Prinzbach, *Angew. Chem. 101* (1989) 309; *Angew. Chem. Int. Ed. Engl. 28* (1989) 300.

[5] R. Pinkos, G. Rihs, H. Prinzbach, *Angew. Chem. 101* (1989) 312; *Angew. Chem. Int. Ed. Engl. 28* (1989) 303.

[6] N. L. Allinger, *J. Am. Chem. Soc. 99* (1977) 8127; W. F. Maier, P. von R. Schleyer, *ibid. 103* (1981) 1891; MMP2-Calculations for unsaturated dodecahedranes as well as MM2 and ab initio calculations for bridged bicyclo[3.3.0]oct-1(5)-ene structures have been published recently: A. B. Mc. Ewen, P. von R. Schleyer, *J. Org. Chem. 51* (1986) 4357; D. A. Hrovat, W. T. Borden, *J. Am. Chem. Soc. 110* (1988) 4710, and references cited therein.

[7] W.-D. Fessner, G. Sedelmeier, P. R. Spurr, G. Rihs, H. Prinzbach, *J. Am. Chem. Soc. 109* (1987) 4626; G. K. S. Prakash, V. V. Krishnamurthy, R. Herges, R. Bau, H. Yuan, G. A. Olah, W.-D. Fessner, H. Prinzbach, *ibid. 110* (1988) 7764.

[8] J. C. Gallucci, C. W. Doecke, L. A. Paquette, *J. Am. Chem. Soc. 108* (1986) 1343; G. Lutz, D. Hunkler, G. Rihs, H. Prinzbach, *Angew. Chem. 101* (1989) 307; *Angew. Chem. Int. Ed. Engl. 28* (1989) 298.

[9] According to MM2 predictions the CC double bonds in the parent systems dodecahedrene **O** and dodecahedradiene **N** ($R^1 = R^2 = H$) respectively are strongly pyramidalized towards tetrahedral coordination with angles of 46.5° and 45.6° (for comparison: 63.4° for edges of the dodecahedrane **P**), but still flat enough that their reactivity ought to be kinetically reduced by the flanking methine groups. According to the olefin strain criteria reported by *Maier* and *Schleyer* [6], with calculated *OS* values of 18.3 and 18.0 (diene strain = 36.3 kcal mol^{-1}) these species should be manageable at low temperature.

[10] R. L. Viavattene, F. D. Green, L. D. Cheung, R. Majeste, L. M. Trefonas, *J. Am. Chem. Soc. 96* (1974) 4342; K. B. Wiberg, R. D. Adams, P. J. Okarma, M. G. Matturo, B. Segmüller, *ibid. 106* (1984) 2200; A.-D. Schlüter, H. Harnisch, J. Harnisch, U. Szeimies-Seebach, G. Szeimies, *Chem. Ber. 118* (1985) 3513; D. A. Hrovat, W. T. Borden, *J. Am. Chem. Soc. 110* (1988) 7229; P. E. Eaton, M. Maggini, *ibid. 110* (1988) 7230; K. Okada, H. Kawai, K. Okubo, T. Uesugi, M. Oda, *Tetrahedron Lett. 29* (1988) 2333; J. Schäfer, G. Szeimies, *ibid. 29* (1988) 5253.

[11] R. Pinkos, J.-P. Melder, H. Fritz, H. Prinzbach, *Angew. Chem. 101* (1989) 319; *Angew. Chem. Int. Ed. Engl. 28* (1989) 310.

[12] P. R. Spurr, Bulusu A. R. C. Murty, W.-D. Fessner, H. Fritz, H. Prinzbach, *Angew. Chem. 99* (1987) 486; *Angew. Chem. Int. Ed. Engl. 26* (1987) 455.

[13] The reactions leading to the diene **4** were carried out on a gram scale, all subsequent reactions on a 25–50 mg scale. The new compounds are characterized by spectra (^1H (400 MHz), ^{13}C NMR (100.6 MHz), IR, MS) and elemental analyses. For example: dimethyl 2,4-*anti*,12-tribromo-14,19-dioxo-decacyclo[9.9.0.0^{1,8}.0^{2,15}.0^{3,7}.0^{5,12}.0^{6,10}.0^{11,18}.0^{13,17}.0^{16,20}]-icosane-4-*syn*,9-*syn*-dicarboxylate **3**: colorless crystals, m.p. >320 °C. IR (KBr): $\tilde{\nu}$ = 1767, 1733 cm^{-1}. ^1H NMR ($CDCl_3$): δ = 4.17 (m, 3-H)*, 4.05 (m, 5-H)*, 3.89 (s, OCH_3), 3.72 (s, OCH_3), 3.72 (m, 6-H)*, 3.66 (m, 7-H)*, 3.54 (m, 8-, 10-H), 3.47 (m, 13-H)*, 3.41 (m, 15-H)*, 3.19 (m, 16-, 17-H), 2.95 (m, 18-, 20-H), 2.88 (m, 9-H). ^{13}C NMR ($CDCl_3$): δ = 205.4 (C-19)*. 202.5 (C-14)*, 170.5 (CO_2R)*, 168.3 (CO_2R)*, 88.3 (C-2, -12),

78.4 (C-1, -11), 70.7 (C-4), 61.0 (C-3)*, 60.9 (C-5)*, 59.7 (C-13)*, 59.4 (C-15)*, 59.1 (C-6)*, 57.6 (C-7)*, 54.3 (OCH_3(4)), 52.7 (OCH_3(9)). *: assignment uncertain.—Dimethyl 13,18-dioxo-nonacyclo[12.6.0.0^{2,6}.0^{4,11}.0^{5,9}.0^{7,20}.0^{10,17}.0^{12,16}.0^{15,19}]icosa-1(20),10-diene-3-*syn*,8-*syn*-dicarboxylate **4**: colorless crystals, m.p. >320°C. IR (KBr): $\tilde{\nu}$ = 1739 cm^{-1}. ^{1}H NMR ($CDCl_3$): δ = 3.77 (s, 2 OCH_3), 3.69 (m, 2-, 4-, 7-, 9-H), 3.56 (m, 5-, 6-H), 3.49 (m, 15-, 16-H), 3.30 (m, 12-, 14-, 17-, 19-H), 2.63 (t, 3-, 8-H, J = 5 Hz). ^{13}C NMR ($CDCl_3$): δ = 207.6 (C-13, -18), 171.8 (2 CO_2R), 160.4 (C-1, -10, -11, -20), 59.9 (C-5, -6), 55.3 (C-12, -14, -17, -19), 52.7 (2 OCH_3), 45.7 (C-3, -8), 45.5 (C-2, -4, -7, -9), 44.8 (C-15, -16).—Dimethyl 14,19-dioxo-11,22-dioxaundecacyclo[14.7.0.0.0^{1,21}.0^{2,6}.0^{4,12}.0^{5,9}.0^{7,21}.0^{10,12}.0^{10,18}.0^{13,17}.0^{16,20}]docosane-3-*syn*,8-*syn*-dicarboxylate **7**: colorless crystals, m.p. >320°C. IR (KBr): $\tilde{\nu}$ = 1732 cm^{-1}. ^{1}H NMR ($CDCl_3$): δ = 3.79 (s, 2 OCH_3), 3.14 (m, 5-, 6-H), 3.11 (m, 2-, 4-, 7-, 9-H), 3.02 (m, 16-, 17-H), 2.93 (m, 13-, 15-, 18-, 20-H), 2.93 (t, 3-, 8-H, J = 5.8 Hz). ^{13}C NMR ($CDCl_3$): δ = 204.7 (C-14, -19), 170.6 (2 CO_2CH_3), 85.1 (C-1, -10, -12, -21), 63.1 (C-5, -6), 53.7 (C-13, -15, -18, -20), 52.9 (2 OCH_3), 50.0 (C-3, -8), 48.8 (C-16, -17), 44.7 (C-2, -4, -7, -9).—Dimethyl 11-hydroxy-6-oxo-decacyclo[9.9.0.0^{2,18}.0^{3,10}.0^{4,17}.0^{5,9}.0^{7,14}.0^{8,12}.0^{13,20}.0^{15,19}]icosane-1,16-*syn*-dicarboxylate **11a**: colorless crystals, m.p. >320°C. ^{1}H NMR ($CDCl_3$): δ = 3.89 (m, 3-, 13-H), 3.86 (m, 2-, 20-H), 3.76 (s, OCH_3), 3.75 (s, OCH_3), 3.63 (m, 4-, 14-H), 3.49 (m, 8-, 9-H), 3.48 (m, 10-, 12-H), 3.36 (18-, 19-H), 3.35 (m, 5-, 17-H), 3.11 (t, 16-H, J = 6.5 Hz), 2.94 (m, 5-, 7-H). ^{13}C NMR ($CDCl_3$): δ = 221.4 (C-6), 175.7 (CO), 172.9 (CO), 115.9 (C-11), 87.2 (C-1), 74.5 (C-10, -12), 66.0 (C-2, -20), 63.9 (C-18, -19), 63.4 (C-3, -13), 58.6 (C-5, -7), 56.5 (C-8, -9), 55.0 (C-4, -14), 52.4 (C-16), 52.5 (OCH_3), 52.3 (OCH_3), 49.2 (C-15, -17).—Dimethyl 15-hydroxy-11-oxo-6,22-dioxadodecacyclo[10.10.0.0.0^{1,21}.0^{2,19}.0^{4,18}.0^{5,7}.0^{5,10}.0^{7,17}.0^{8,15}.0^{9,13}.0^{14,21}.0^{16,20}]docosane-3-*syn*,16-dicarboxylate **14a**: colorless crystals, m.p. p>320°C.—IR (KBr): $\tilde{\nu}$ = 1727 cm^{-1}. ^{1}H NMR ($CDCl_3$): δ = 3.83 (s, OCH_3), 3.78 (s, OCH_3), 3.57 (m, 9-, 13-H), 3.55 (m, 4-, 17-H), 3.48 (m, 18-, 19-H), 3.10 (m, 8-, 14-H), 3.19 (m, 2-, 4-H), 2.94 (m, 10-, 12-H), 2.93 (m, 3-H). ^{13}C NMR ($CDCl_3$): δ = 207.3 (C-11), 173.4 (CO), 170.7 (CO), 103.9 (C-15), 94.3 (C-7, -21), 81.3 (C-1, -5), 78.2 (C-16), 69.4 (C-18, -19), 61.9 (C-9, -13), 61.5 (C-8, -14), 56.7 (C-10, -12), 54.2 (C-17, -20), 53.0 (OCH_3), 52.9 (OCH_3), 50.0 (C-3), 48.8 (C-2, -4). MS (EI): *m/z* 436 ($M^{\oplus}$, 10%), 404 ($M^{\oplus}-CH_4O$, 100%).—Dimethyl 9,13-dimethoxy-2-oxadodecacyclo[10.9.0.0^{1,3}.0^{3,10}.0^{4,8}.0^{5,21}.0^{6,19}.0^{7,17}.0^{9,16}.0^{11,15}.0^{13,20}.0^{14,18}]henicosane-8,20-dicarboxylate **18b**: colorless crystals, m.p. >320°C.—^{1}H NMR ($CDCl_3$): δ = 4.12 (m, 7-, 19-H), 3.75–3.55 (m, 10-H), 3.69 (s, 2 CO_2CH_3), 3.16 (s, 2 OCH_3), 3.16 (m, 10-, 12-H); (C_6D_6/$CDCl_3$ (9/1)): δ = 4.08 (m, 7-, 19-H), 3.82 (m, 4-, 21-H), 3.50 (s, 2 CO_2CH_3), 3.41 (m, 17-, 18-H), 3.33 (m, 5-H), 3.28 (m, 14-, 16-H), 3.23 (m, 6-H), 3.17 (m, 10-H), 3.08 (m, 15-H), 3.02 (m, 10-, 12-H), 2.89 (s, 2 OCH_3). ^{13}C NMR ($CDCl_3$): δ = 173.9 (2 C=O), 116.9 (C-9, -13), 93.4 (C-1, -3), 85.5 (C-8, -20), 74.2 (C-5), 72.5 (C-11), 67.4 (C-14, -16), 67.0 (C-7, -19), 66.0 (C-6), 64.1 (C-15), 63.1 (C-17, -18), 58.6 (C-4, -21), 58.1 (C-10, -12), 52.2 (2 $COCH_3$), 3.16 (2 OCH_3). MS (EI): *m/z* 450 ($M^{\oplus}$, 55%), 422 (100%), 390 (36%), 360 (37%), 330 (48%), 270 (16%).

[14] H. Prinzbach, J.-P. Melder, unpublished.

[15] K. B. Becker, *Helv. Chim. Acta 60* (1977) 68.

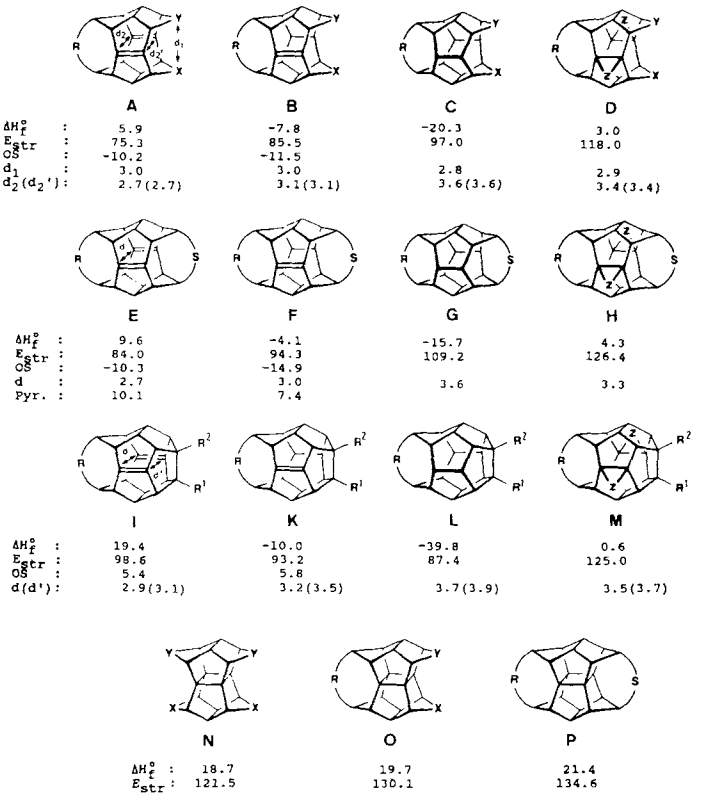
[16] D. A. Hrovat, F. Miyake, G. Trammell, K. E. Gilbert, J. Mitchell, J. Clardy, W. T. Borden, *J. Am. Chem. Soc. 109* (1987) 5524.

The Pagodane Route to Dodecahedranes: Polyfunctionalized Homologous Dodecahedranes and Dodecahedrenes**

By *Rolf Pinkos, Johann-Peter Melder, Hans Fritz,* and *Horst Prinzbach**

In memoriam Hans Musso

Our route to functionalized dodecahedranes[1] can be utilized for the homologization of the pentagonal framework by one,[2] two (or more) similar or different "bridges" and thus for the construction of novel poly(hetero)cyclic skeletons featuring more or less spherical surfaces and varying molecular diameters (cf. Fig. 29 in Ref. [3]). For a series of model frameworks with diatomic bridges—selected for their correspondence with the skeletons in Ref. [1]—energy and structure data are presented in Scheme 1. In spite of the deficiencies of such MM2 calculations[4] several preparatively significant conclusions are realistic in comparison with the non-homologous counterparts.[1] 1) The trends in energy and structure parameters within and between the seco-monohomologous (**A**–**D**) and the bishomologous dodecahedranes (**E**–**H**) resemble very closely that of the bisseco series in Ref. [1]; 2) for the mono-homologues (**I**–**M**) the consequences of the CH_2CO bridge are only minor when set gainst the seco analogues in Ref. [1]; 3) in the seco-series **A**–**D** the steric requirements for X-Y connecting bond formation (to give **I**–**M**) are therefore favorable; 4) for the homologous dodecahedradienes **E** and **I** strong transannular π/π interactions but different reactivities are to be expected.[5]

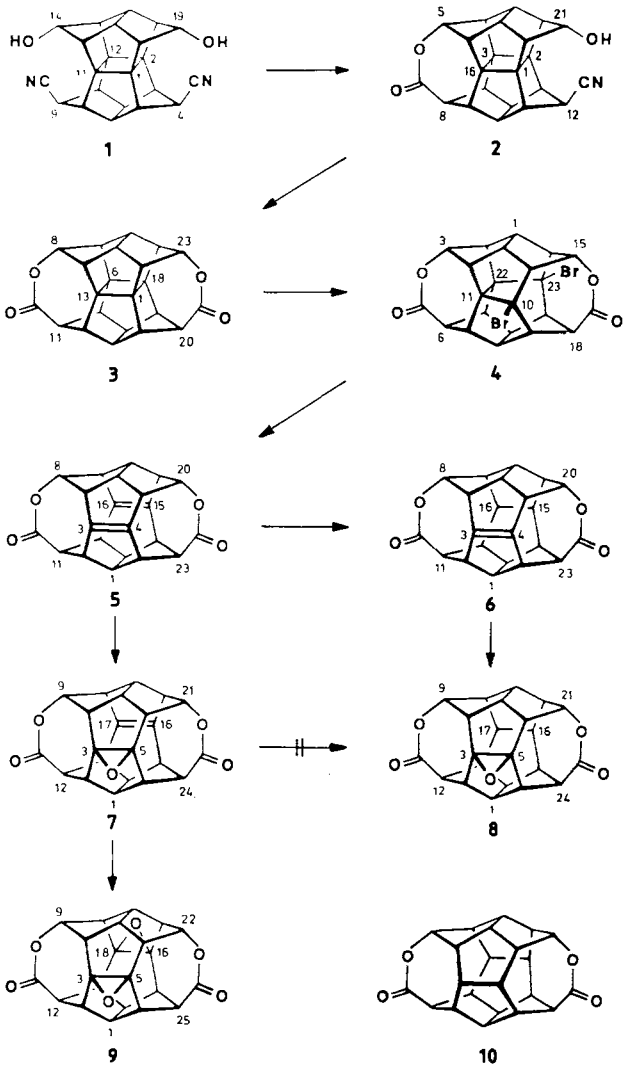


Scheme 1. Energy and structure data of model frameworks, calculated for R = S = CH_2CO, X = CH_2, Y = CO; ΔH_f^0, E_{str}, olefin strain (OS) [kcal mol^{-1}]; *d* [Å]; pyramidalization at the olefinic centers (pyr) [°].

In this communication we present bis- and monohomologous dodecahedranes of types **E**, **F**, **H** and **I**–**M**,[6] with COO units as diatomic bridges. Four and two five-membered rings, respectively, of the pentagonal dodecahedrane skeletons are herein replaced by seven-membered lactone rings. From previous work it could be inferred that tetrafunctionalized pagodanes **N** can be singly or doubly bridged to give **O** and **P**, respectively, and that the latter could be converted into the dienes **A** and **E**, respectively, by proven methodology.[7]

[*] Prof. Dr. H. Prinzbach, Dipl.-Chem. R. Pinkos, Dipl.-Chem. J.-P. Melder, Prof. Dr. H. Fritz
Chemisches Laboratorium der Universität
Institut für Organische Chemie und Biochemie
Albertstrasse 21, D-7800 Freiburg (FRG)

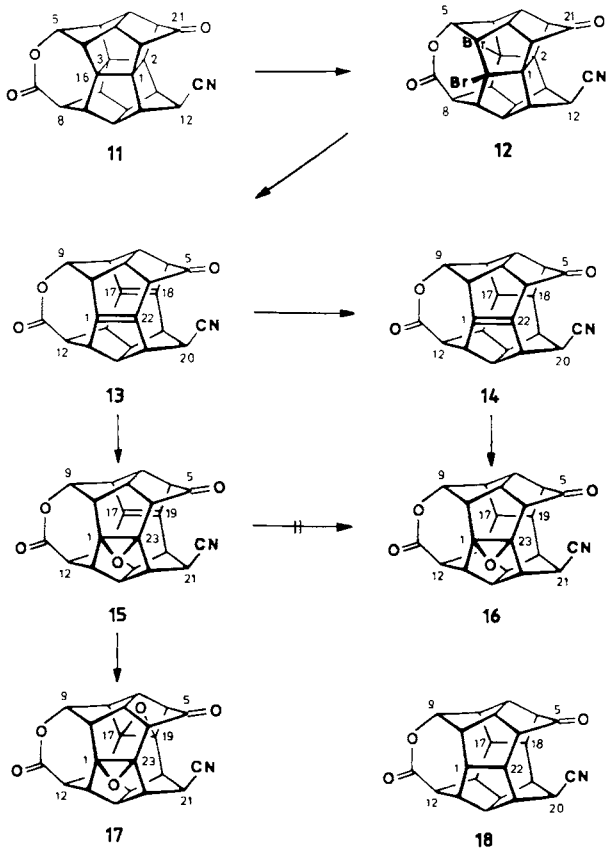
[**] This work was supported by the Deutsche Forschungsgemeinschaft, the Fonds der Chemischen Industrie and BASF AG. We thank Dr. *D. Hunkler* for NMR analyses, Dr. *J. Wörth* for MS analyses, Mrs. *M. Lutterbeck* and *M. Froom*, *G. Leonhardt* and *J. Leonhardt* for supplying starting materials, *G. Fehrenbach* for graphical work, and Dr. *W.-D. Fessner* and Dr. *L. Knothe* for helpful discussions.



Starting material is generally the dioxo-pagodane-*syn,syn*-dicarbonitrile (**N**, X = CHCN, Y = CO) or the all-*syn*-14,19-dihydroxy-4,9-dicarbonitrile **1** obtained therefrom in quantitative yield.[8] The latter is converted rapidly and uniformly into the monolactone **2** (**O**) on treatment with conc. acetic acid under reflux;[9] the cyclization to the more highly strained bislactone **3** (**P**) is relatively slow and unselective: after ca. 70% conversion (based on **2**, 40 min) the yield of **3** is ca. 40% (as alternative, double dehydration of the all-*syn*-dihydroxydicarboxylic acid prepared via **1** is investigated[10]).

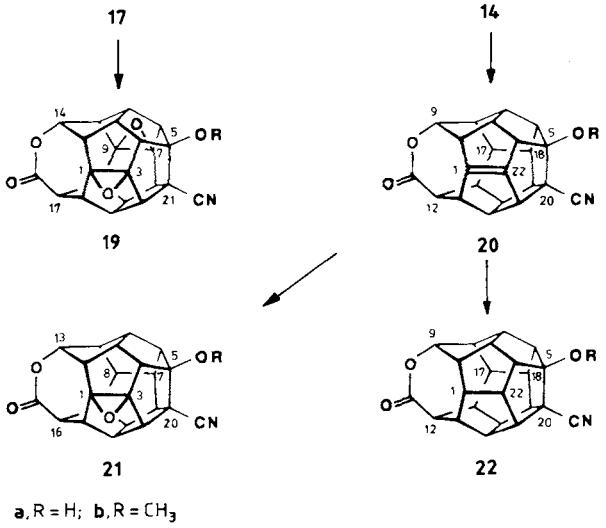
The conversion of bislactone **3** into the bishomologous dodecahedradiene **5** turned out to be straightforward: photobromination **3**→**4** under standard conditions[7] furnished dibromide **4** almost exclusively (ca. 95% isolated) even after quantitative conversion. The absence of competing bromination at the 11(20) positions can be attributed to only slight stabilization of the potential radical centers by the—for this purpose unfavorably oriented—α-carbonyl groups. Elimination of Br_2 to give **5** (**E**), in principle in competition to the re-formation of **3**, is also rapid and quantitative under proven conditions (Zn/NaI, Na_2SO_3, dimethylformamide (DMF), 150°C). The dodecahedradiene **5** (9,21-dioxaundecacyclo[11.11.0.0^{2,11}.0^{3,7}.0^{4,24}.0^{5,20}.0^{6,18}.0^{8,17}.0^{12,16}.0^{14,23}.0^{15,19}]tetracosa-3,15-diene-10,22-dione), with only slight pyramidalization of the olefinic centers, is quite persistent towards oxygen and can be crystallized from CH_2Cl_2 (m.p. >320°C; $\tilde{\nu}_{C=O}$ = 1720 cm^{-1}). The strong transannular π/π interaction expected for a transannular distance of (possibly somewhat more than) 2.7 Å manifests itself in a long wavelength UV absorption (CH_3CN, λ_{max} = 255 nm (sh, ε = 110)), in a quantitative [$\pi_2+\pi_2$]-photocycloaddition (leading to **3**) and quantitative bromine addition (leading to **4**). Also typical for structure **5**, which is rather similar to that of the bissecododecahedradienes, is the electrochemical oxidation to a radical cation and a dication.[11] The behavior of this "flattened" dodecahedradiene under diverse hydrogenation conditions is consistent with expectations based on calculations: with diimide the reaction always comes to an end at the stage of the dodecahedrene **6** (**F**); the saturated, clearly more strained bishomododecahedrane **10** (**G**) is not attained even under drastic conditions. Oxidation of **5** with *m*-chloroperbenzoic acid or peroxycarbamic acid is surprising in that the second oxidation step is so rapid that even with equivalent amounts of oxidizing agent considerable amounts of diepoxide **9** (**H**) are found besides monoepoxide **7** (TLC, ^{1}H NMR). Oxidation of **6** to **8** with peroxycarbamic acid at 40°C (CH_2Cl_2) is rapid and free of competition. **7** cannot be hydrogenated to **8**.

The ε-ketonitrile **11**, which is obtained in quantitative yield from the monolactone **2**, was an obvious precursor for monohomologous dodecahedranes (**I**–**M**) (Aldol-route[11]). The conversion of **11** into the secohomododecahedradiene **13** (**A**) is more laborius insofar as **12**, the product of a regiospecific addition of bromine on the lactone side of **11**, undergoes further unselective bromination. The loss of material remains limited, however, if the bromination is stopped at ca. 50% conversion, whereupon **12** can be cleanly separated by chromatography (>90%). Dehalogenation to **13** is quantitative. In **13**, with its almost parallel CC double bonds ($d \geq 2.7$ Å, λ_{max}(CH_3CN) = 306 nm (ε = 70), 271 (sh, 220), 260 (sh, 250), 223 (1040)),

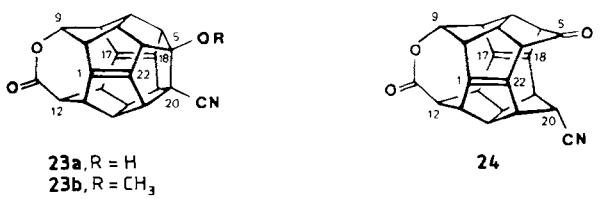


$[\pi_2+\pi_2]$-photocycloaddition (acetone, to give **11**) and bromination (to **12**) again proceed uniformly. Qualitative differences compared to the diene **5** are manifest in the analogous derivatization reactions: under the hydrogenation conditions effective in the case of **5**, **13** reacts only extremely slowly; with a very large excess of diimide ($N_2(CO_2K)_2$, CH_3CO_2H, CH_2Cl_2/CH_3OH, 0°C, 14 h), however, **14** (**B**) is formed quantitatively. The latter proves to be hyperstable—no **18** (**C**)—but is oxidized by peroxycarbamic acid ($CHCl_3$, 60°C) to **16**. At room temperature, the diene **13** is converted quantitatively into the monoepoxide **15**, which, at 70°C, is further oxidized very slowly to the diepoxide **17** (**D**) (>80% isolated). Presumably, with increasing bulging of the molecular framework, i.e., with decreasing (increasing) d_1 (d_2) distances, destabilizing interactions between C=O and C≡N become effective. Hydrogenation of **15** to **16** cannot be achieved.

As in the case of the analogous pentagonal dodecahedranes the prognosis for cyclization of the seco precursors (**14**→**20** (**B**→**K**), **16**→**21** and **17**→**19** (**D**→**M**)) was promising. First examples have been realized: under reversible (I, *tert*-butyl alcohol, potassium *tert*-butoxide, THF, 20°C) as well as irreversible (II, NaH/CH_3I, THF, 40°C) reaction conditions, **17** was uniformly transformed (>95% isolated) into homologous diepoxydodecahedranes **19a** (**b**), and **14**, equally selectively, into the homologous dodecahedranes **20a** (**b**). The latter, inspite of (presumably) considerable pyramidalization of the olefinic C atoms, are virtually insensitive to oxygen and can be isolated in the crystalline state. As expected, the olefin **20a** (5-hydroxy-11-oxo-10-oxaundecacyclo[11.9.0.0^{2,9}.0^{3,7}.0^{4,22}.0^{5,20}.0^{6,18}.0^{8,17}.0^{12,16}.0^{14,21}.0^{15,19}]dodeca-1(22)-ene-20-carbonitrile) is hydrogenated to **22a** (**L**); peracid oxidation leads quantitatively to **21a**.



The cyclization **13**→**23** (**A**→**I**) should be considerably endothermic. In preliminary experiments carried out reversibly (conditions I) as well as irreversibly (II), neither **23a** nor **23b**, but only *anti*-nitrile **24**, i.e. rapid and quantitative epimerization at C-20, was observed. That no H/D exchange takes place in **24** under analogous conditions underscores the importance of *syn*-orientation for the CN or COOR substituents in the (bis)seco substrates—possibly an essential for the preparation of the pentagonal dodecahedranes.[1]



Exemplary for the diverse (bis)homologous dodecahedranes, the ^1H and ^{13}C NMR data of **5** (C_{2v}), **19a** (C_s) and **20a** (C_1) are given in Figure 1. COSY, NOE and selective decoupling experiments have allowed complete assignment of all signals. Inter alia, the geometrical consequences of the homologization of the dodecahedrane framework, indicated by the d (d') distances (Scheme 1), are reflected in chemical shifts, especially of the olefinic signals. Besides the generally intense $M^{\oplus}$ signals, the EI mass spectra feature no significant signals for pentagonal dodecahedranes that could result from CO_2 eliminations; with **22a** as so far singular exception: *m/z* 345 ($M^{\oplus}$, 85%), 302 ($M^{\oplus}-HOCN$, 100%), 274 ($M^{\oplus}-HOCN-CO$, 86%), 258 ($M^{\oplus}-HOCN-CO_2$, 32%).

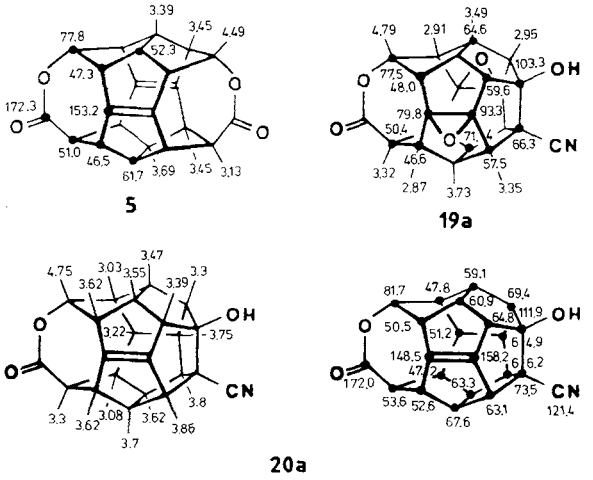


Fig. 1. ^1H and ^{13}C NMR data of **5**, **19a** ($CDCl_3$) and **20a** ($CDCl_3$/[D_6]dimethyl sulfoxide.

The results of this and the preceding communication open up a preparative entry to variously modified, saturated and unsaturated dodecahedranes: Our routes to tetrafunctionalized pagodanes[1] are efficient, the mode of substitution can be deliberately varied, and the methods for the ultimate C–C bond formations can be adjusted to the respective thermodynamic situation. The first steps of our pagodane synthesis[14] have already been performed on the kg scale[15] and we hope that appropriately equipped institutions will assist us in lifting subsequent steps to this scale.

Received: November 15, 1988 [Z 3052 IE]
German version: *Angew. Chem. 101* (1989) 319

[1] J.-P. Melder, R. Pinkos, H. Fritz, H. Prinzbach, *Angew. Chem. 101* (1989) 314; *Angew. Chem. Int. Ed. Engl. 28* (1989) 305, and references cited therein.

[2] The preparation of mono (hetero)homologous dodecahedranes has been reported recently: L. A. Paquette, T. Kobayashi, M. A. Kesselmayer, *J. Am. Chem. Soc. 110* (1988) 6568; J. C. Weber, L. A. Paquette, *J. Org. Chem. 53* (1988) 5315.

[3] H. Prinzbach, W.-D. Fessner in O. Chizhov (Ed.): *Organic Synthesis: Modern Trends*, Blackwell, Oxford 1986, p. 23.

[4] N. L. Allinger, *J. Am. Chem. Soc. 99* (1977) 8127.

[5] The energetic and structural consequences of the incorporation of two monoatomic bridges (R = S = CH_2) are documented for two examples:

diene E: $\Delta H_f^0 = 64.0$, $E_{str} = 74.3$ kcal mol^{-1}, $d = 2.8$ Å, pyramidalization = 17.8°. pagodane P: $\Delta H_f^0 = 104.1$, $E_{str} = 153.1$ kcal mol^{-1} (W.-D. Fessner, *Dissertation*, Universität Freiburg 1986). The formation of such monoatomic bridges is apparently only feasible after opening of the pagodane four-membered ring.

[6] H. Prinzbach, R. Pinkos, unpublished.

[7] P. R. Spurr, Bulusu A. R. C. Murty, W.-D. Fessner, H. Fritz, H. Prinzbach, *Angew. Chem. 99* (1987) 486; *Angew. Chem. Int. Ed. Engl. 26* (1987) 455.

[8] R. Pinkos, G. Rihs, H. Prinzbach, *Angew. Chem. 101* (1989) 312; *Angew. Chem. Int. Ed. Engl. 28* (1989) 303.

[9] The reactions leading to the dienes **5/13** were carried out on the gram scale, all subsequent reactions thus far on the 25–50 mg scale. The new compounds are characterized by spectra (^{1}H NMR (400 MHz), ^{13}C NMR (100.6 MHz), IR, MS) and elemental analyses. For example 21-*syn*-hydroxy-7-oxo-6-oxadodecacyclo[11.9.0.0^{1,16}.0^{2,11}.0^{2,20}.0^{3,9}.0^{3,16}.0^{4,19}.0^{5,17}.0^{8,15}.0^{10,14}.0^{18,22}]docosane-12-*syn*-carbonitrile **2**: colorless crystals, m.p. 290°C. IR (KBr): $\tilde{\nu}$ = 3420, 2960, 2225, 1760, 1695 cm^{-1}. ^{1}H NMR ($CDCl_3$): δ = 4.77 (m, 5-H), 4.30 (m, 21*a*-H), 3.32 (m, 8-H), 3.07 (m, 12*a*-H), 3.03 (m, 10-, 11-, 13-, 14-H), 2.81 (m, 18-, 19-H), 2.63 (m, 20-, 22-H), 2.46 (m, 9-, 15-H), 2.41 (m, 4-, 17-H). ^{13}C NMR ($CDCl_3$): δ = 174.0 (C-7), 120.3 (CN), 92.5 (C-5), 81.7 (C-21), 63.9 (C-1, -2)*, 62.1 (C-3, -16)*, 61.2 (C-8), 59.4 (C-10, -14), 51.5 (C-18, -19), 51.0 (C-20, -22), 48.6 (C-11, -13), 44.6 (C-4, -17), 42.1 (C-12), 42.0 (C-9, -15).—9,22-Dioxatridecacyclo-[11.11.0.0^{1,18}.0^{2,20}.0^{3,12}.0^{4,19}.0^{5,11}.0^{6,13}.0^{6,18}.0^{7,16}.0^{8,14}.0^{15,24}.0^{17,23}]tetracosane-10,21-dione **3**: colorless crystals, m.p. > 320°C. IR (KBr): $\tilde{\nu}$ = 2960, 1700 cm^{-1}. ^{1}H NMR ($CDCl_3$): δ = 4.93 (m, 8-, 23-H), 3.47 (m, 11-, 20-H), 3.22 (m, 15-, 16-H), 3.00 (m, 3-, 4-H), 2.70 (m, 7-, 14-, 17-, 24-H), 2.65 (m, 2-, 5-, 12-, 19-H). ^{13}C NMR ($CDCl_3$): δ = 173.8 (C-10, -21), 94.0 (C-8, -23), 63.9 (C-11, -20), 61.8 (C-1, -6, -13, -18), 59.5 (C-15, -16), 52.4 (C-3, -4), 47.1 (C-2, -5, -7, -12, -14, -17, -19, -24).—4,10,17,23-Tetroxatridecacyclo[12.12.0.0^{2,12}.0^{3,5}.0^{3,8}.0^{5,25}.0^{6,22}.0^{7,20}.0^{9,19}.0^{13,18}.0^{15,25}.0^{16,18}.0^{16,21}]hexacosane-11,24-dione **9**: colorless crystals, m.p. > 320°C. IR (KBr): $\tilde{\nu}$ = 2940, 1725 cm^{-1}. ^{1}H NMR ($CDCl_3$): δ = 4.69 (t, 4-, 22-H, J = 7.3 Hz), 3.39 (m, 1-, 14-H), 3.37 (t, 12-, 25-H, J = 6.9 Hz), 3.05 (m, 7-, 20-H), 2.97 (m, 6-, 8-, 19-, 21-H), 2.93 (m, 2-, 13-, 15-, 26-H). ^{13}C NMR ($CDCl_3$): δ = 170.8 (C-11, -24), 84.0 (C-3, -5, -16, -18), 77.9 (C-9, -22), 66.1 (C-1, -14), 56.1 (C-7, -20), 51.3 (C-12, -24), 45.7 (C-6, -8, -19, -21)*, 44.5 (C-2, -13, -15, -26)*.—7,21-Dioxo-6-oxadodecacyclo[11.9.0.0^{1,16}.0^{2,11}.0^{2,20}.0^{3,9}.0^{3,16}.0^{4,19}.0^{5,17}.0^{8,15}.0^{10,14}.0^{18,22}]docosane-12-*syn*-carbonitrile **11**: colorless crystals, m.p. > 320°C. IR (KBr): $\tilde{\nu}$ = 2965, 2230, 1765, 1695 cm^{-1}. ^{1}H NMR ($CDCl_3$): δ = 4.97 (m, 5-H), 3.39 (m, 8-H), 3.18 (m, 18-, 19-H), 3.13 (m, 10-, 14-H), 3.07 (m, 11-, 13-H), 3.03 (m, 12*a*-H), 2.68 (m, 4-, 17-H), 2.62 (m, 9-, 15-H), 2.58 (m, 20-, 22-H). ^{13}C NMR ($CDCl_3$): δ = 209.7 (C-21), 173.0 (C-7), 119.0 (CN), 90.2 (C-5), 66.4 (C-1, -2)*, 61.4 (C-3, -16)*, 59.1 (C-10, -14), 49.5 (C-18, -19), 48.8 (C-8), 46.6 (C-11, -13)*, 46.2 (C-20, -22)*, 42.8 (C-15, -19), 42.4 (C-12).—5,11-Dioxo-10-oxadecacyclo-[11.9.0.0^{2,9}.0^{3,7}.0^{4,22}.0^{6,18}.0^{8,17}.0^{12,16}.0^{14,21}.0^{15,19}]docosa-1(22),17-diene-20-*syn*-carbonitrile **13**: colorless crystals, m.p. > 320°C. IR (KBr): $\tilde{\nu}$ = 2910, 2240, 1715, 1230 cm^{-1}. ^{1}H NMR ($CDCl_3$): δ = 4.52 (t, 9-H, J = 6.5 Hz), 3.64 (m, 2H), 3.63 (m, 2H), 3.56 (m, 2-, 8-H), 3.50 (m, 4H), 3.42 (m, 4-, 6-H), 3.03 (t, 12-H, J = 6.0 Hz), 2.88 (t, 20-H, J = 4.5 Hz). ^{13}C NMR ($CDCl_3$): δ = 157.2 (C-1, -17)*, 154.9 (C-18, -22)*, 119.2 (CN), 76.2 (C-9), 61.0 (C-14, -15), 54.8 (C-3, -7), 49.3, 48.6, 47.9, 46.7, 45.1, 31.7 (C-20). *a* = *anti*. *: assignment uncertain.

[10] J.-P. Melder, H. Fritz, H. Prinzbach, *Angew. Chem. 101* (1989) 309; *Angew. Chem. Int. Ed. Engl. 28* (1989) 300.

[11] For **5** a first reversible oxidation step with + 1.39 V (vs. Ag/AgCl) and a second irreversible step with ca. + 1.7 V were measured cyclovoltametrically (G. Lutz, M. Dietrich, J. Heinze, H. Prinzbach, unpublished). The dication is much less stable than the radical cation: ESR [12] and NMR spectroscopic [13] characterization of these ions (presumably **i**, **ii**) is under way.



i



ii

[12] H. Prinzbach, Bulusu A. R. C. Murty, W.-D. Fessner, J. Mortensen, J. Heinze, G. Gescheidt, F. Gerson, *Angew. Chem. 99* (1987) 488; *Angew. Chem. Int. Ed. Engl. 26* (1987) 457.

[13] G. K. S. Prakash, V. V. Krishnamurthy, R. Herges, R. Bau, H. Yuan, G. Olah, W.-D. Fessner, H. Prinzbach, *J. Am. Chem. Soc. 110* (1988) 7764.

[14] W.-D. Fessner, G. Sedelmeier, P. R. Spurr, G. Rihs, H. Prinzbach, *J. Am. Chem. Soc. 109* (1987) 4626.

[15] Thanks are due to Dr. *K. Schenker* and Dr. *D. Beck*, Ciba-Geigy AG, Basel, for their kind mediation.

Do Any AB_n Molecules Have Anomalous Shapes? ν_3 of TiF_4 and TiF_3 and Their Relevance to the Shape of TiF_2**

By *Ian R. Beattie,* Peter J. Jones,* and *Nigel A. Young*

Recent experimental work suggests that all discrete molecular first-row transition-element dichlorides are linear in the ground electronic state. We now find that an IR band previously assigned to matrix-isolated TiF_3 is due to TiF_4. Further, the band assigned to TiF_2 is due to TiF_3. The reported bond angle of 120° for "TiF_2" can thus be explained by the presence of trigonal-planar TiF_3. "TiF_2" was a key molecule in the proposals for nonlinearity of AB_2 species. We question whether there is unambiguous evidence of anomalous shape for any high-temperature AB_n molecule.

In 1979 *Drake* and *Rosenblatt*[1] summarized the experimental data on the structures of metal dihalide and trihalide molecules. The dichlorides (MCl_2) of the first-row transition series and calcium were assigned a linear configuration, which is in agreement with recent work.[2,3] For the difluorides (MF_2), those of Ca, Sc, Ti, and V were assigned as nonlinear, the remainder as linear. For ScF_2 and VF_2 (which are both monoisotopic) the bond angles were estimated[4] by analogy with those of neighboring molecules. Thus CaF_2[5] and TiF_2[6] represent key experimental points in the assignment of nonlinear structures to these MX_2 species.

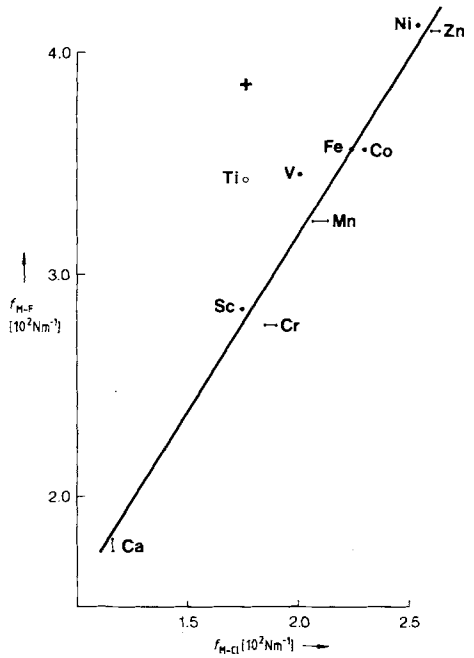


Fig. 1. Plot of f_{M-F} versus f_{M-Cl} for MX_2 molecules in argon matrices.

In Figure 1 we plot the Simple Valence Force Field bond-stretching force constants f_{M-F} and f_{M-Cl} for the MX_2 molecules isolated in argon matrices. The calcula-

[*] Prof. I. R. Beattie, P. J. Jones, Dr. N. A. Young
Chemistry Department, Southampton University
Southampton SO9 5NH (UK)

[**] We thank the Scientific and Engineering Research Council for financial support for this work.

tions are based on the reported experimental[2-7] values of ν_3 and assume that the MX_2 molecule is linear and symmetrical. If the molecule is nonlinear, our calculation will yield an apparently lower force constant than that which would be obtained using the correct molecular geometry. This rather crude approach to the bonding in these molecules leads to a roughly linear relationship between f_{M-F} and f_{M-Cl}. The straight line on the graph is based on a least-squares plot *including the origin* but omitting the titanium point, which is well removed from the line.

Matrix isolation studies of lower-valent fluorides are fraught with difficulty (notably the occurrence of ^{19}F in 100% abundance, which makes even the *formula* of the species isolated open to question). Figure 1 suggests the force constant value for TiF_2 may be in error. Allowing the molecule to bend to 120° moves TiF_2 even further from the line, to the point designated + in Figure 1. In view of the importance of TiF_2 in valence theory we have studied the vapors over heated TiF_3 and TiF_4.

In our experiment, vaporization of TiF_4 (prepared from titanium and fluoride) at ca. 100°C followed by cocondensation of the vapors with argon or neon (Fig. 2) gave IR spectra almost identical in frequency and intensity pattern to those assigned to TiF_3.[6] Using a Perkin Elmer 983 G infrared spectrometer at 0.5-cm^{-1} resolution, we did not observe any additional bands in the 1000- to 200-cm^{-1} region. Similar results were obtained by heating TiF_3 (Alfa Inorganics).

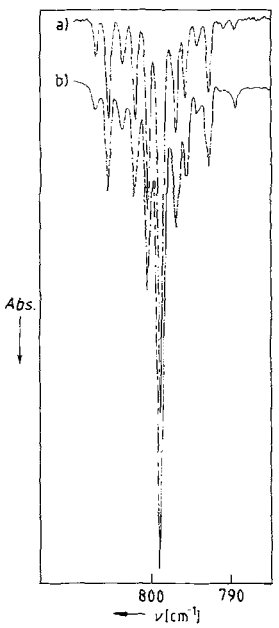


Fig. 2. Comparison of the IR spectra of a) TiF_4 in neon and b) TiF_3 in neon [6].

A mass spectrometric study[8] has shown that TiF_4 sublimes unchanged. Further, TiF_4 was the *only* vapor species identified from the initial heating of commercial TiF_3 at 708 K. If the TiF_3 was held at 848 K for sufficient time to avoid "swamping the mass spectrometer with TiF_4,"[8] some TiF_3 could be observed. The authors also report univariant vaporization for the two-phase region $Ti+TiF_2$, again with *only TiF_3 and TiF_4 identified as vapor species.*

We conclude that the band originally assigned to TiF_3[6] was ν_3 of TiF_4. The reported spectrum of TiF_2 was generated by heating "commercially available" TiF_3 and passing the vapors (i.e., TiF_4) into a cell containing elemental titanium at 940 or 1100°C. By contrast, the mass spectrometric studies[8] show that up to 1025 K (the limit of these experiments) the vapors would contain *only* TiF_4 and TiF_3. In our experiment, passing TiF_4 vapor (from commercial TiF_3) over titanium metal at ca. 800–850°C, followed by matrix isolation in argon, led to an IR spectrum showing a sharp, intense new band at 740 cm^{-1} (together with the band at 792 cm^{-1} due to TiF_4). *There were no other intense bands in this region of the IR spectrum.* The 740-cm^{-1} band was ca. 60% of the intensity of the TiF_4 band. Under high resolution this band showed titanium-isotope fine structure, the frequencies agreeing to better than 1 cm^{-1} with those assigned[6] to TiF_2. *Our results, combined with the earlier mass spectrometric data, identify the 740-cm^{-1} band as due to TiF_3, not TiF_2.*

We further find that matrix isolation of the vapors from recently sublimed TiF_3 (heated rapidly to ca. 850°C) gave bands at 740 cm^{-1} (TiF_3) and 792 cm^{-1} (TiF_4) in roughly equal proportions. It is thus clear that TiF_3 both disproportionates and sublimes unchanged on heating, a not unexpected behavior for halides in this region of the periodic table.[9]

For trigonal-planar TiF_3 the isotope intensity and frequency pattern calculated for ν_3 (neglecting the in-plane deformation) is *identical* to that calculated for TiF_2 with a bond angle of 120°. The angle calculated[6] for "TiF_2" in an argon matrix is 119.5°, while in neon, where there are at least two sites, angles of 125.4° and 123.4° are given.

There are many theories of why certain high-temperature molecules adopt anomalous geometries. However, the evidence for such distortions is in many cases not definitive. Electron-diffraction molecular-scattering patterns are averaged over all thermal vibrations *and* all species in the vapor; the precise interpretation of electric deflection data on such molecules is open to question, as is that derived from ESR measurements in matrices.[10] IR isotope shift data for matrix-isolated species become insensitive as the mass of the central atom increases. For "TiF_2" the isotope shift between ^{46}Ti and ^{50}Ti in argon was 2.1 cm^{-1} *less* than that calculated for a linear molecule (which was why it represented a key observation). CaF_2 is another key molecule, but here the difference between the observed isotope shift (^{40}Ca, ^{44}Ca in krypton) and the calculated shift for a linear molecule is less than 1 cm^{-1}.[15]

Observation of the totally symmetric stretching vibration in the IR spectrum has been used as a criterion of geometry, notably for compounds of the heavier elements where the symmetric stretch and the antisymmetric stretch approach one another in frequency. In such cases *partial* isotopic substitution ($^{16}O/^{18}O$; $^{35}Cl/^{37}Cl$) can lead to unambiguous identification of both ν_1 and ν_3.[11] Even in these cases, however, great caution is necessary, as may be seen by reference to elegant papers by *Lesiecki* and *Nibler* et al.[12]

Where a lowering of symmetry results in the resolution of a degeneracy (T_d to *any* lower symmetry; D_{3h}, with loss of the C_3 axis, e.g., to C_{2v}), the observation of additional bands coupled with partial isotopic substitution can lead to assignment of the point group. However, *Beattie* et al.[13] produced evidence that $ThCl_4$ had T_d symmetry in neon, but a lower symmetry in krypton, illustrating the possibility that matrix gases may cause a change of geometry. In the case of T-shaped UO_3[14] one could imagine a trigonal-

planar gas-phase molecule being distorted along a coordinate towards $UO_2^{2\oplus}O^{2\ominus}$ in a matrix.

There are many careful and very difficult experiments in the literature. The purpose of this communication is to question how many of the results on high-temperature molecules lead to *unambiguous* determination of the shape of the *free molecule*.

Received: July 14, 1988;
revised version: November 10, 1988 [Z 2858 IE]
German version: *Angew. Chem. 101* (1989) 322

[1] M. C. Drake, G. M. Rosenblatt, *J. Electrochem. Soc. 126* (1979) 1387.
[2] I. R. Beattie, P. J. Jones, A. D. Willson, N. A. Young, *High Temp. Sci.*, in press.
[3] J. S. Ogden, R. S. Wyatt, *J. Chem. Soc. Dalton Trans. 1987*, 859.
[4] J. W. Hastie, R. H. Hauge, J. L. Margrave, *Chem. Commun. 1969*, 1452; *High Temp. Sci. 1* (1969) 76.
[5] V. Calder, D. E. Mann, K. S. Seshadri, M. Allavena, D. White, *J. Chem. Phys. 51* (1969) 2093.
[6] J. W. Hastie, R. H. Hauge, J. L. Margrave, *J. Chem. Phys. 51* (1969) 2648.
[7] J. W. Hastie, R. H. Hauge, J. L. Margrave, *High Temp. Sci. 3* (1971) 257; D. White, G. V. Calder, S. Hemple, D. E. Mann, *J. Chem. Phys. 59* (1973) 6645; C. W. De Kock, D. A. Van Leirsberg, *J. Am. Chem. Soc. 94* (1972) 3235; *J. Phys. Chem. 78* (1974) 134; D. W. Green, D. P. McDermott, A. Bergman, *J. Mol. Spectrosc. 98* (1983) 111; A. Snelson, *J. Phys. Chem. 70* (1966) 3208; R. S. Wyatt, *Ph. D. Thesis*, Southampton University 1983; K. R. Millington, *Ph. D. Thesis*, Southampton University 1987; K. R. Thompson, K. D. Carlson, *J. Chem. Phys. 49* (1968) 4379.
[8] N. D. Potter, M. H. Boyer, F. Ju, D. L. Hildenbrand, E. Murad: *Thermodynamic Properties of Propellant Combustion Products*, U. S. Clearinghouse Fed. Sci. Tech. Inform. AD, No. 715567 (1971).
[9] P. Ehrlich, G. Pietzka, *Z. Anorg. Allg. Chem. 275* (1954) 121.
[10] ESR work on TiF_2: T. C. De Vore, W. Weltner, *J. Am. Chem. Soc. 99* (1977) 4700.
[11] See, for example: I. R. Beattie, J. S. Ogden, R. S. Wyatt, *J. Chem. Soc. Dalton 1983*, 2343; S. D. Gabelnick, G. T. Reedy, M. G. Chasanov, *J. Chem. Phys. 60* (1974) 1167; D. W. Green, K. M. Ervin, *J. Mol. Spectrosc. 89* (1981) 145.
[12] M. L. Lesiecki, J. W. Nibler, *J. Chem. Phys. 64* (1976) 871; M. Lesiecki, J. W. Nibler, C. W. De Kock, *ibid. 57* (1972) 1352.
[13] I. R. Beattie, P. J. Jones, K. R. Millington, A. D. Willson, *J. Chem. Soc. Dalton 1988*, 2759.
[14] See, for example: S. D. Gabelnick, G. T. Reedy, M. G. Chasanov, *J. Chem. Phys. 59* (1973) 6397.
[15] All calculations neglect anharmonicity.

tBu$_2$P–P=PBrtBu$_2$ · LiBr and the Formation of tBu$_2$P–$\ddot{\text{P}}$

By *Gerhard Fritz,* Tilo Vaahs, Holm Fleischer,* and *Eberhard Matern*

Although complexes having terminal phosphanediyl (phosphinidene) ligands—formed via phosphole complexes—are well-known,[1] all efforts to isolate a free phosphinidene have been unsuccessful up to now. Thus, for example, free phosphinidenes could not be detected in the thermolysis of 7-phosphanorbornadienes or of $(PMe)_5$.[2] Attempts to form free phosphinidenes via decomplexation of terminal phosphinidene complexes have also failed.[2] Apparently, what is lacking is a suitable precursor, from which phosphinidenes can be generated at sufficiently low temperatures.

We have now found that the reaction of **1**[3] with **2** affords yellow, toluene-soluble crystals of **3**.[4] The formulation of **3** as the LiBr adduct of a P–P ylide took into account the ^{31}P NMR spectroscopic data, which were consistent with multiple bond character for the P^2–P^3 bond, and the increased coordination number at P^3.

$$(t\text{Bu}_2\text{P})_2\text{PLi} + \text{Br–CH}_2\text{–CH}_2\text{–Br} \longrightarrow$$

1 **2**

$$t\text{Bu}_2\text{P}^1\text{–P}^2\!=\!\text{P}^3\text{Br}t\text{Bu}_2\cdot\text{LiBr} \xrightarrow{20\,^\circ\text{C}} \text{P}_n(\text{P}t\text{Bu}_2)_n$$

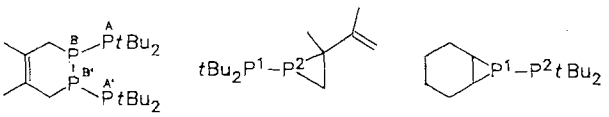
3 **4, 5**

The LiX adduct of a C–P ylide $Ph_3\overset{\oplus}{P}\text{–}\overset{\ominus}{\ddot{C}}RR'\cdots LiX$ can be understood in analogous terms.[5] **3** resembles the lithiated ylides $(R_2CLi\text{–}PR_3)X$ of *H. Schmidbaur* and *W. Tronich*[6] and the 1,1,3,3-tetraphenyl-1λ^5,2λ^3,3λ^5-triphosphenyl cation[8] and triphosphenium ions[7] described by *A. Schmidpeter* et al. A crystal structure analysis of **3** was, until now, not possible.

Compound **3** decomposes upon warming to 20 °C with quantitative formation of tBu$_2$PBr, LiBr, and the cyclophosphanes **4** ($n=3$) and **5** ($n=4$).[9] The formation of these compounds suggests that 2,2-di-*tert*-butyl-1,1-diphosphanediyl, **6**, is the intermediate in this reaction. Therefore, we attempted to obtain evidence for the intermediacy of **6** by trapping reactions. Decomposition of **3** in 2,3-

$t\text{Bu}_2\text{P–}\ddot{\text{P}}$ **6**

dimethyl-1,3-butadiene at ambient temperature gives rise to the compounds **7** and **8**; the cyclophosphanes **4** and **5** are no longer formed. The formation of **7** is favored with respect to **6** and suggests the presence of $t\text{Bu}_2\text{P–P=P–P}t\text{Bu}_2$ as a reactive intermediate.[10] The decomposition of **3** in cyclohexene led to **9**,[10] but in this case, the major products were the cyclophosphanes **4** and **5**.



7 **8** **9**

The reaction of **3** with dimethylbutadiene to give **8** is analogous to the conversion of terminal phosphinidene complexes to vinylphosphirane complexes.[1] The formation of **9** from **3** and cyclohexene is directly comparable to the reaction of phosphinidene complexes with olefins.[1]

Received: July 21, 1988;
revised: November 24, 1988 [Z 2876 IE]
German version: *Angew. Chem. 101* (1989) 324

CAS Registry numbers:
1, 118201-82-4; **2**, 106-93-4; **3**, 118631-50-8; **4**, 118281-67-7; **5**, 118281-66-6; **6**, 118655-68-8; **7**, 118631-51-9; **8**, 118631-52-0; **9**, 118631-53-1; 2,3-dimethyl-1,3-butadiene, 513-81-5; cyclohexene, 110-83-8.

[*] Prof. Dr. G. Fritz, Dr. T. Vaahs, Dipl.-Chem. H. Fleischer, Dr. E. Matern
Institut für Anorganische Chemie der Universität
Engesserstrasse, D-7500 Karlsruhe (FRG)

[1] Review: F. Mathey, *Angew. Chem. 99* (1987) 285; *Angew. Chem. Int. Ed. Engl. 26* (1987) 275.
[2] K. C. Caster, L. D. Quin, *Tetrahedron Lett. 24* (1983) 5831.
[3] G. Fritz, T. Vaahs, *Z. Anorg. Allg. Chem. 552* (1987) 18.
[4] 1.3 g (3.2 mmol) of **1**·THF was stirred in 15 mL of THF and treated at 0 °C with 0.6 g (3.2 mmol) of **2**. After the evolution of gas (C_2H_4) had ceased, the solution was stirred for 2 h at −40 °C; during this time the color changed from orange to yellow. The solution was cooled to −78 °C. After 2 d, **3** precipitated as a yellow, microcrystalline powder, which was recrystallized from toluene. Yield: 0.5 g (31%). ^{31}P NMR:

$\delta = 20.6$ (dd, P^1), -88.9 (dd, P^2), 175.6 (dd, P^3); $J_{12} = -252$, $J_{13} = 40$, $J_{23} = -683$ Hz.

[5] M. Schlosser, K. F. Christmann, *Justus Liebigs Ann. Chem. 708* (1967) 1.

[6] H. Schmidbaur, W. Tronich, *Chem. Ber. 101* (1968) 3545, 3556.

[7] A. Schmidpeter, S. Lochschmidt, W. S. Sheldrick, *Angew. Chem. 97* (1985) 214; *Angew. Chem. Int. Ed. Engl. 24* (1985) 226.

[8] A. Schmidpeter, S. Lochschmidt, W. S. Sheldrick, *Angew. Chem. 94* (1982) 72; *Angew. Chem. Int. Ed. Engl. 21* (1982) 63.

[9] Since one of the $PtBu_2$ groups in **4** is *trans* to the others, only three signals, rather than four, are observed in the ^{31}P NMR spectrum. $\delta = 67$ (1P), 47 (2P). The signal at $\delta = -163$ (3P, high field shift typical for three-membered ring compounds) consists of two overlapping signal patterns for the three exocyclic P atoms. MS: *m/z* 528.2631 ($M^{\oplus}$), 471.1945 ($M^{\oplus} - t$Bu). **5** crystallizes from the reaction mixture at -20°C. ^{31}P NMR: $\delta = 63$ (P_{subst}), -43 (P_{ring}), $^1J_{PP} = -329$ Hz. MS: *m/z* 708.3562 ($M^{\oplus}$), 559.2389 ($M^{\oplus} - P$tBu), 533.1407 ($M^{\oplus} - 3t$Bu). Compounds **4** and **5** are known from the decomposition of $tBu_2P-P(SiMe_3)-P(SiMe_3)_2$ [G. Fritz, T. Vaahs, *Z. Anorg. Allg. Chem. 553* (1987) 85]. They are formed at 65 °C (15 h) with preferred cleavage of $P(SiMe_3)_3$ [side product, $tBuP(SiMe_3)_2$] suggesting the intermediacy of **6**.

[10] For the trapping reactions, **1** was dissolved in 2,3-dimethyl-1,3-butadiene or cyclohexene. **2** was then added at 0°C and the solution stirred at 20°C for 5 d. In each case, a clear orange solution formed which gradually became cloudy as LiBr precipitated. Quantities for **7** and **8**: 0.5 g (1.21 mmol) **1**, 0.22 g (1.21 mmol) **2**, 10 mL 2,3-dimethyl-1,3-butadiene; for **9**: 1.0 g (2.42 mmol) **1**, 0.44 g (2.42 mmol) **2**, 15 mL cyclohexene. ^{31}P NMR (spectrum of the reaction solution): **7**: $\delta = 45.3$ (P^A), -48.7 (P^B), $J_{BB'} = -277$, $J_{AB} = -329$, $J_{AB'} = 65$, $|J_{AA'}| \leq 1$ Hz. **8**: $\delta = 34.5$ (d, P^1), -189.0 (d, P^2); $J_{12} = -233$ Hz. **9**: $\delta = 65.5$ (d, P^2), -225.0 (d, P^1), $J_{12} = -220$ Hz. The formation of **7** can be compared with the reaction of $tBuP=P-SiMe_3$ [from $tBuClP-P(SiMe_3)_2$] with 2,3-dimethyl-1,3-butadiene [G. Fritz, H. Fleischer, *Z. Anorg. Allg. Chem.*, in press] as well as the reactions of $tBu_2P-P=PtBu$ [from $tBu_2P-P(SiMe_3)-PCltBu$] and $tBu_2P-P=P-SiMe_3$ [from $tBu_2P-P(Cl)-P(SiMe_3)_2$] with cyclopentadiene [G. Fritz, T. Vaahs, *Z. Anorg. Allg. Chem. 552* (1987) 34].

$[M(NMesBMes_2)_2]$ (M = Cr, Ni): Stable, Distorted, Two-Coordinate d^4 and d^8 Complexes**

By *Ruth A. Bartlett, Hong Chen,* and *Philip P. Power**

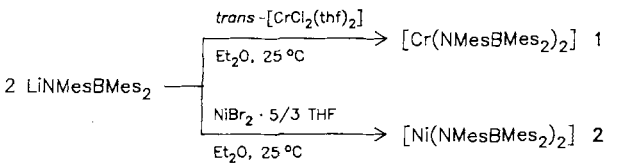
Many three-coordinate complexes are now known for a wide range of transition metals.[1,2] However, except for d^{10} complexes, stable, two-coordinate transition-metal species are extremely rare. Currently, the range of such compounds is confined to the metals Mn,[3-6] Fe,[6,7] and Co[6,7] involving a few bulky alkyl[3,4] and amide[5,6] groups for Mn and silylamide ligands only for Fe and Co.[6,7] Divalent nickel silylamides such as $[Ni\{N(SiMe_3)_2\}_2]$ appear to be unstable,[8] and homoleptic Ni^{II} alkyls appear to be unknown. Similarly, no homoleptic, monomeric amide or alkyl derivatives have been described for Cr^{II}, although higher-coordinate base-stabilized Cr^{II} alkyls and amides have been reported.[9]

Recently, we have shown that borylamide ligands, $^{\ominus}NRBMes_2$ (R = Ph or Mes), are effective in achieving a low coordination number in Mn by preventing association.[5] This is a consequence of both the large ligand size and the significantly reduced nitrogen lone pair availability for bridging. We now describe the synthesis and structural characterization of the complexes $[M(NMesBMes_2)_2]$ (**1**, M = Cr; **2**, M = Ni), the first[10] neutral two-coordinate derivatives of Cr^{II} and Ni^{II}.

[*] Prof. P. P. Power, R. A. Bartlett, H. Chen
Department of Chemistry, University of California
Davis, CA 95616 (USA)

[**] This work was supported by the National Science Foundation and the Petroleum Research Fund.

The complexes **1** and **2** were synthesized in moderate yield by reaction of the lithium borylamide $LiNMesBMes_2$[5] and *trans*-$[CrCl_2(thf)_2]$ or $NiBr_2 \cdot 5/3\,THF$ (Scheme 1).[11]



Scheme 1. Mes = 2,4,6-trimethylphenyl.

The chromium complex, **1**, was obtained as green crystals (m.p. 195 °C) from hexane and has the X-ray crystal structure[12] shown in Figure 1. A key feature is the N1-Cr-N2 angle of 112.3(3)°, which is far from the expected linear or near-linear configuration. There are Cr···C10 and Cr···C37 contacts of about 2.39 Å, which are much shorter than that previously observed (2.536(5) Å) in the manganese analogue, $[Mn(NMesBMes_2)_2]$ **3**, even though Cr and Mn have similar metallic radii.[5] In addition, the angles between the B1-C10 and B2-C37 bonds and the respective mesityl planes (10.2 and 15.2°, respectively) indicate moderately strong Cr···C interactions. The asymmetry of the B-C bonds and the N-B-C angles within each ligand support this view. Two other structural

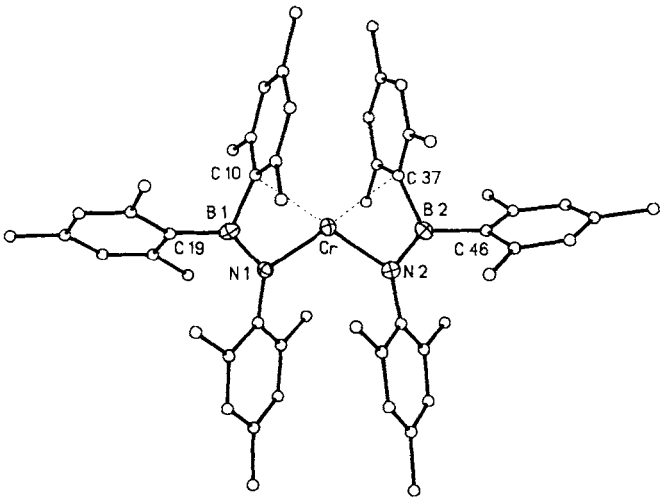


Fig. 1. Crystal structure of **1** [12]. The hydrogen atoms and solvent hexane molecule have been omitted for clarity. Selected bond distances [Å] and angles [°]: Cr-N1 1.980(7), Cr-N2 1.988(7), N1-B1 1.373(13), N2-B2 1.381(12), B1-C10 1.647(14), B1-C19 1.598(14), B2-C37 1.646(14), B2-C46 1.624(14), Cr···C10 2.383(15), Cr···C37 2.391(15); N1-Cr-N2 112.3(3), Cr-N1-B1 98.8(6), Cr-N2-B2 96.8(6), N1-B1-C10 113.1(8), N1-B1-C19 128.7(9), C10-B1-C19 118.1(8), N2-B2-C37 115.4(8), N2-B2-C46 129.4(9). Angle between Cr-N1-C10 plane and Cr-N2-C37 plane = 18.7°.

features merit comment. First, the twist angles between the boron and nitrogen planes are 11.1° for both ligands. This, together with the average B-N distance of 1.377(13) Å, shows that both B-N bonds have an undiminished p-p π interaction.[5] Second, the dihedral angle between the Cr-N1-C10 and Cr-N2-C37 planes is 18.7° whereas an angle closer to 90° might be expected for a quasi-tetrahedral

configuration. Thus, the structure of **1** is nearer to distorted square planar than it is to the distorted tetrahedral type seen in **3** or the almost linear geometry seen in **2**. Square-planar coordination is, of course, known for a number of d^4 complexes, for example, *trans*-$[Cr\{N(SiMe_3)_2\}_2(thf)_2]$.[9]

The structure of the dark red nickel complex **2** (m.p. 165 °C) is shown in Figure 2. The main features of interest are the wide, almost linear, N1-Ni-N2 angle of 167.9(1)° and a possible Ni···C19 interaction at 2.611(3) Å. These two parameters are in sharp contrast to the deviations found in **1**. The relatively minor distortions from linearity could be due to crystal packing. Nevertheless, some asymmetry is evident in the B-C bonds and the N-B-C angles. The asymmetries, however, do not mirror the wide N-Ni-N angle or the long Ni···C contacts. The short B-N distances and the low (13.5°) twist angles between the B and N planes indicate that the B-N double bond is preserved.

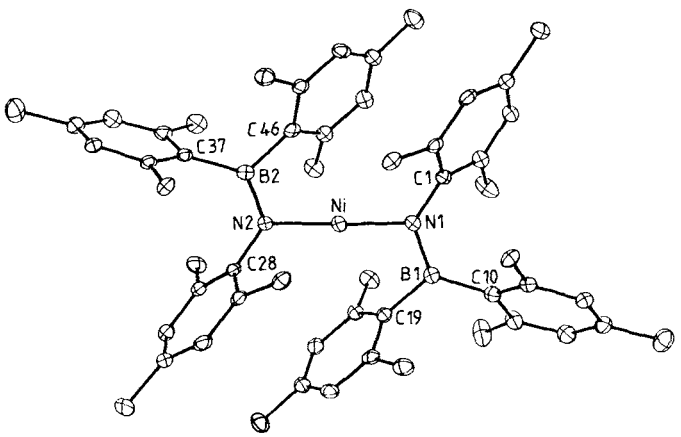


Fig. 2. Crystal structure of **2** [12]. Hydrogen atoms omitted for clarity. Selected bond distances [Å] and angles [°]: Ni-N1 1.867(2), Ni-N2 1.865(2), N1-B1 1.411(4), N2-B2 1.412(4), B1-C10 1.595(3), B1-C19 1.617(4), B2-C37 1.596(3), B2-C46 1.619(4), N1-C1 1.424(4), N2-C28 1.428(3), Ni···C19 2.611(3), Ni···C46 2.703(3); N1-Ni-N2 167.9(1), N1-B1-C10 125.6(3), N1-B1-C19 111.9(2), N2-B2-C37 126.0(3), N2-B2-C46 112.8(2).

The differences between the structures of **1** and **2** are probably both steric[13] and electronic in origin. The smaller size of nickel favors a wide N-M-N angle. The large size of chromium permits closure of this angle and the d^4 electron configuration is probably responsible for the quasi-square-planar geometry. Also, the nickel center is more electron rich than chromium and has less tendency to achieve a higher electron density through structural distortion. Possible supporting evidence comes from a comparison of the average B-N distances in **1** (1.377(12) Å) and **2** (1.412(4) Å). It can be argued that the value for **2** is longer because the more electron-rich nickel center can donate electron density more effectively into the B-N π* orbital than chromium. More conclusive evidence awaits the synthesis and spectroscopic characterization of complexes involving a wider variety of ligands and transition metals. An alternative explanation is that, owing to the larger size of Cr, the ionic character of the Cr-N bond in **1** is greater than that of the Ni-N bond in **2**. Thus, the negative charge on the nitrogens in **1** is greater, which leads to a stronger B-N π interaction.

The absorption spectra of **1** and **2** were recorded in toluene at ambient temperature. For **1**, two absorptions were seen at $\lambda = 16030$ ($\varepsilon = 252$) and 12530 cm^{-1} (77). This result is consistent with the X-ray structure but does not rule out other conformations in solution. The more intensely colored **2** has three absorptions at $\lambda = 28985$ ($\varepsilon = 1200$), 23060 (1100), 17480 cm^{-1} (914). In the absence of comparative data for other complexes it is difficult to draw many structural conclusions from these spectra. Magnetic measurements (using the Evans method)[14] for **1** and **2** at 25 °C support a high-spin configuration for **1**. No paramagnetically shifted peaks could be detected for **2** nor could different environments for the mesityl groups be distinguished.

Received: August 26, 1988;
revised: October 1, 1988 [Z 2943 IE]
German version: *Angew. Chem. 101* (1989) 325

CAS Registry numbers:
1·(hexane), 119038-80-1; **2**, 119011-38-0; *trans*-$[CrCl_2(thf)_2]$, 15604-50-9.

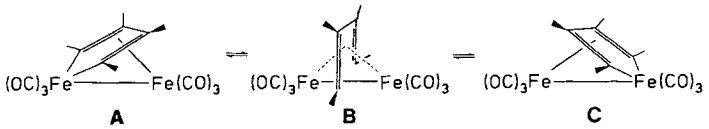
[1] P. G. Eller, D. C. Bradley, M. B. Hursthouse, D. W. Meek, *Coord. Chem. Rev. 24* (1977) 1; D. C. Bradley, *Chem. Br. 11* (1975) 393.
[2] M. F. Lappert, P. P. Power, A. R. Sanger, R. C. Srivastava: *Metal and Metalloid Amides*, Ellis-Horwood, Chichester 1980; G. K. Barker, M. F. Lappert, J. A. K. Howard, *J. Chem. Soc. Dalton Trans. 1978*, 734.
[3] N. H. Buttrus, C. Eaborn, P. B. Hitchcock, J. D. Smith, A. C. Sullivan, *J. Chem. Soc. Chem. Commun. 1985*, 1380.
[4] R. A. Andersen, A. Haaland, K. Rypdal, H. V. Volden, *J. Chem. Soc. Chem. Commun. 1985*, 1807.
[5] R. A. Bartlett, X. Feng, M. M. Olmstead, P. P. Power, K. J. Weese, *J. Am. Chem. Soc. 109* (1987) 4851. Other examples of lithium borylamides have also been structurally characterized: P. Paetzold, C. Pelzer, R. Boese, *Chem. Ber. 121* (1988) 51. In addition, the transition-metal complexes $[M\{NB(Et)C(Et)C(Me)SiMe_2\}_2]$ (M = Fe, Co) have been reported: R. Köster, G. Seidel, R. Boese, B. Wrackmeyer, *ibid. 120* (1987) 669. In this case, however, the borylamide group does not prevent association through amide bridging.
[6] R. A. Bartlett, P. P. Power, *J. Am. Chem. Soc. 109* (1987) 7563. No stable Cr^{II} or Ni^{II} complexes of the $^{\ominus}N(SiMePh_2)_2$ ligand have been isolated so far.
[7] R. A. Andersen, J. C. Green, M. F. Lappert, W.-P. Leung, K. Faegri, A. Haaland, K. Rypdal, *Inorg. Chem. 27* (1988) 1782. $[Co\{N(SiMe_3)_2\}_2]$ is also known to be monomeric in solution: D. C. Bradley, K. J. Fisher, *J. Am. Chem. Soc. 93* (1971) 2058.
[8] $[Ni\{N(SiMe_3)_2\}_2]$ and apparently other nickel(II) silylamides are unstable at room temperature: H. Bürger, U. Wannagat, *Monatsh. Chem. 95* (1964) 1099; cf. [6]. However, the dimer $[\{Ni(NPh_2)_2\}_2]$ is stable: H. Hope, M. M. Olmstead, B. D. Murray, P. P. Power, *J. Am. Chem. Soc. 107* (1985) 712.
[9] D. C. Bradley, M. B. Hursthouse, C. W. Newing, A. J. Welch, *J. Chem. Soc. Chem. Commun. 1972*, 567.
[10] A linear coordination for nickel has been observed in the ion $[NiO_2]^{2\ominus}$: B. Nowitzki, R. Hoppe, *Croat. Chem. Acta 57* (1984) 537. Also, the high-temperature gas-phase electron diffraction structure of $CrCl_2$ at ca. 1100 K indicates that it may have a bent structure as a monomer, although, at present, the evidence appears to be inconclusive: M. Hargittai, O. V. Dorofeeva, J. Tremmel, *Inorg. Chem. 24* (1985) 3963.
[11] Both starting materials, which have been structurally characterized, were synthesized by Soxhlet extraction of the anhydrous metal dihalide with THF. The structure of pale blue *trans*-$[CrCl_2(thf)_2]$ is square planar with long axial metal-halide interactions. The structure of salmon-pink $NiBr_2 \cdot 5/3\,THF$ consists of infinite chains of edge-bridged *trans*-$[NiBr_4(thf)_2]$ octahedra with every third nickel missing an axial THF.
[12] Crystal data at 130 K with $Mo_{K\alpha}$ radiation ($\lambda = 0.71069$ Å). **1**: $a = 16.496(4)$, $b = 16.286(4)$, $c = 19.335(7)$ Å, $\beta = 91.31(2)°$, $Z = 4$, monoclinic, space group $P2_1/a$, $R = 0.09$. **2**: $a = 11.447(5)$, $b = 13.720(6)$, $c = 15.896(7)$ Å, $\alpha = 103.46(3)$, $\beta = 101.61(3)$, $\gamma = 100.04(3)°$, $Z = 2$, triclinic, space group $P\bar{1}$, $R = 0.046$. Further details of the crystal structure investigation may be obtained from the Fachinformationszentrum Energie, Physik, Mathematik GmbH, D-7514 Eggenstein-Leopoldshafen 2 (FRG), on quoting the depository number CSD-53425, the names of the authors, and the journal citation.
[13] The X-ray crystal structure of $[Ni(NPhBMes_2)_2]$ has also been solved in this laboratory. It has a much diminished N-Ni-N angle of 135.7(1)°. This observation emphasizes the importance of the ligand size in influencing the structure of these complexes.
[14] D. F. Evans, *J. Chem. Soc. 1959*, 2005.

 © VCH Verlagsgesellschaft mbH, D-6940 Weinheim, 1989 0570-0833/89/0303-0317 $ 02.50/0

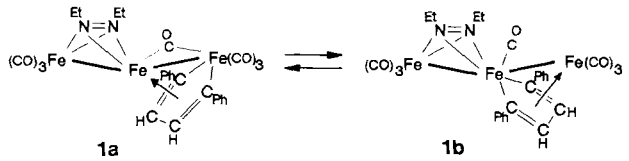
Two Ferrole Isomers in Equilibrium: Experimental Confirmation of an Old Hypothesis**

By *Miklos Tasi, Anne K. Powell,* and *Heinrich Vahrenkamp**

After 30 years of extensive investigations of the chemistry of alkyne iron carbonyl compounds, almost 100 ferracyclopentadienyl iron complexes are now known.[1] Numerous structural and spectroscopic studies have confirmed the idea that in diiron complexes of type **A** the ferracyclopentadienyl unit acts as a π-ligand towards the $Fe(CO)_3$ fragment.[1,2] On the basis of these investigations, it was also assumed that only a low energy barrier exists for the site exchange of the ferrole ring (**A** ⇄ **C**) and that this process passes through a transition state **B** of C_{2v} symmetry.[3] The only evidence for a dynamic behavior of ferroles until now was, however, the earlier observation[3a] that optically active oxy- and hydroxy-substituted ferroles racemize at higher temperatures.



We have now been able to detect the reversible interconversion of two isomeric ferrole complexes. Heating the μ_3-azoalkane-bridged triiron cluster $[Fe_3(CO)_9(N_2Et_2)]$[4] in the presence of excess phenylacetylene in petrol ether at 110°C for 10 min afforded the two isomers **1a** and **1b** in 18 and 57% yield, respectively. Brown **1a** and red **1b** were separated by chromatography with hexane on silica gel and were characterized spectroscopically[5] and by crystal structure analyses.[6] Both clusters contain an almost linear triiron skeleton (Fe–Fe–Fe angles 162 and 167°). The central iron atom is bound to both the μ-azoalkane and the μ-butadienediyl ligands, which adopt the most favorable arrangement with respect to each other whereby they are located on opposite sides of the clusters. The FeC_4 rings in both compounds are almost planar (largest deviations from the best plane being 9 and 11 pm, respectively). Characteristically, the bonding mode of the CO group on the central iron atom—bridging in **1a** and terminal in **1b**—adapts itself to the location of the butadienediyl ligand.



Since the two iron atoms bound to the butadienediyl ligand in **1** are located in different environments (without taking the C_4 ligand into account), a flip-flop process for the ferrole rings as in **A** ⇄ **C** should be readily detectable. The thermal treatment of **1a** and **1b** shows that this process does in fact occur. Heating the pure isomers in solution led to equilibrium mixtures of **1a** and **1b**; at 90°C, the ratio **1a**/**1b** was ca. 3/7 and at 110°C, 1/10. From the temperature dependence of the equilibrium constants, an isomerization enthalpy of 90±20 kJ mol^{-1} could be estimated. The uncertainty in this value is largely due to the fact that the compounds slowly decompose above 90°C. For the same reason, an accurate kinetic study of the isomerization reaction was also not possible.[7]

Although a large number of ferrole complexes having the two iron atoms in different environments are known,[1] for none of them was an isomerization as in **A** ⇄ **C** observed.[8] Apparently, one of the isomers is always decidedly favored with respect to the other, since the bonding situation in these complexes calls for a π-interaction between the more electron-rich iron atom and the ferracyclopentadienyl ring.[1,3b] The occurrence of the isomerization for **1a** and **1b** may be regarded as a further demonstration of the ability of polymetallic compounds to undergo charge delocalization. Thus, in the ferrole-like clusters **1**, two of the carbonyl ligands of the basic ferrole structure (see **A** and **C**) have been replaced by the $Fe(CO)_3(N_2Et_2)$ group, which is bound to the ferrole unit through iron–iron and iron–nitrogen bonds. Since systems with metal–metal bonds are known to be capable of delocalizing electron density,[9] and since the azo ligand is also known to act as an electron reservoir,[10] it is possible that these two factors contribute to a balancing of the charge in the ferrole unit, whereby the isomerization process becomes more facile.

Our observations are in accord with the arguments for the possible isomerization of ferrole compounds.[3b] In particular, the data are in agreement with the proposed transition state **B** with C_{2v} symmetry and also with a stepwise folding over of the two ends of the butadienediyl moiety (flyover bridge, C_2 symmetry). The fact that in **1a** as in **1b**, the phenyl groups are bound to the iron-complexed inner C atoms of the C_4 ligand suggests that the butadienediyl unit migrates without intermediate C–C bond-making and bond-breaking, which rules out, for example, a transition state with a μ_2-η^4-cyclobutadiene ligand.

The chemical objective of this investigation, which led to the complexes **1**, is the construction of organic molecules within the ligand spheres of clusters. In this respect, the controlled elimination of CO or $Fe(CO)_n$ groups from **1** might offer access to new C–N bond-forming reactions.

Received: August 31, 1988 [Z 2951 IE]
German version: *Angew. Chem. 101* (1989) 327

CAS Registry numbers:
1a, 118682-16-9; **1b**, 118682-17-0; $Fe_3(CO)_9(N_2Et_2)$, 107556-56-9; phenylacetylene, 536-74-3.

[*] Prof. Dr. H. Vahrenkamp, Dr. M. Tasi, Dr. A. K. Powell
Institut für Anorganische und Analytische Chemie der Universität
Albertstrasse 21, D-7800 Freiburg (FRG)

[**] This work was supported by the Stiftung Volkswagenwerk and the Rechenzentrum der Universität Freiburg.

[1] a) *Gmelins Handbuch der Anorganischen Chemie, Band Fe, C3,* Springer, Berlin 1980, p. 24; b) W. P. Fehlhammer, H. Stolzenberg in G. Wilkinson, F. G. A. Stone, E. W. Abel (Eds.): *Comprehensive Organometallic Chemistry, Vol. 4,* Pergamon, Oxford 1982, p. 548.

[2] a) A. A. Hock, O. S. Mills, *Acta Crystallogr. 14* (1961) 139; b) G. Dettlaff, E. Weiss, *J. Organomet. Chem. 108* (1976) 213.

[3] a) R. Case, E. R. H. Jones, N. V. Schwarz, M. C. Whiting, *Proc. Chem. Soc. London 1962.* 256; b) D. L. Thorn, R. Hoffmann, *Inorg. Chem. 17* (1978) 126.

[4] E. J. Wucherer, H. Vahrenkamp, *Angew. Chem. 99* (1987) 353; *Angew. Chem. Int. Ed. Engl. 26* (1987) 355.

[5] IR (pentane): **1a**: $\tilde{\nu}$=2069 (m), 2045 (vs), 2034 (sh), 2000 (s), 1996 (s), 1971 (m), 1959 (s), 1822 (m) cm^{-1}; **1b**: $\tilde{\nu}$=2062 (w), 2043 (vs), 2033 (sh), 1992 (m), 1987 (m), 1965 (m), 1947 (w), 1893 (w) cm^{-1}. ^{1}H NMR (room temperature, $CDCl_3$, int. TMS): **1a**: δ=7.30–7.19 (m, 10H), 6.99 (s, 2H),

3.57 (q, J=7.0 Hz, 2H), 2.67 (q, J=7.0 Hz, 2H), 1.06 (t, J=7.0 Hz, 6H); **1b**: δ=7.28–7.18 (m, 10H), 5.82 (s, 2H), 3.32 (q, J=7.1 Hz, 2H), 2.94 (q, J=7.1 Hz, 2H), 0.81 (t, J=7.1 Hz, 6H).

[6] **1a**: monoclinic, $P2_1/c$, a=1734.7(4), b=797.9(7), c=2023.7(5) pm, β=93.16(2)°, Z=4; 2683 reflections, R=0.048. **1b**: monoclinic, $P2_1/c$, a=1460.0(2), b=844.1(7), c=2240.2(5) pm, β=91.87(1)°, Z=4; 3509 reflections, R=0.031. Further details of the crystal structure investigations can be obtained from the Fachinformationszentrum Energie, Physik, Mathematik GmbH, D-7514 Eggenstein-Leopoldshafen 2, on quoting the depository number CSD-53297, the names of the authors, and the journal citation.

[7] UV spectroscopic monitoring of the equilibration shows an isosbestic point during the first 10–15 min. Thereafter, the system becomes unclean due to decomposition. This decomposition also makes a quantitative interpretation of the IR data impossible.

[8] Cf. L. J. Todd, J. P. Hickley, J. R. Wilkinson, J. C. Huffman, K. Foltig, *J. Organomet. Chem. 112* (1976) 167.

[9] H. Vahrenkamp, *Adv. Organomet. Chem. 22* (1983) 169.

[10] A. Albini, H. Kisch, *Top. Curr. Chem. 65* (1976) 105.

The 30-Electron Rule for Triple-Decker Complexes —Vanadium, Niobium and Tantalum Complexes as Illustrative Examples**

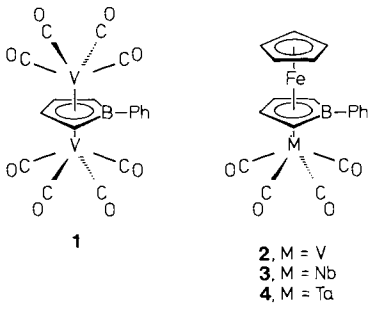
By *Gerhard E. Herberich,* Ingeborg Hausmann,* and *Norbert Klaff*

The number of valence electrons in the triple-decker complexes thus far isolated[2] lies between 26 in $[(\mu\text{-}\eta^6\text{-}C_6H_6)(VCp)_2]$[3] and 34 in $[(\mu\text{-Cp})(NiCp)_2]^{\oplus}$.[4] *R. Hoffmann* et al. have demonstrated in a definitive treatise on the MO scheme of triple-decker complexes that closed electron shells are achieved with 30 and 34 valence electrons;[5a] this conclusion has often been cited as the 30/34e rule. Wade's cluster rules[5b] lead to a narrower statement for triple-decker complexes: the magic number of valence electrons is 30.[5c]

The many triple-decker sandwich complexes with one or two outer Cp ligands often have a valence electron count deviating from 30.[2] For instance, in the case of vanadium the 26e systems $[(\mu\text{-}\eta^6\text{-}C_6H_6)(VCp)_2]$[3] and $[(\mu\text{-}\eta^6\text{-}P_6)\text{-}\{V(C_5Me_4R)_2\}_2]$ (R = Me, Et)[3] are known, but no 30e systems. On the other hand, it can be seen from the general MO scheme for triple-decker complexes that: a rigid 30e rule should apply when strong σ-donor-π-acceptor ligands such as carbon monoxide are present in the outer complex fragments. As illustrative examples for this assertion, we describe here some 30e complexes containing $M(CO)_4$ fragments, where M is an element of the fifth subgroup (vanadium, niobium, tantalum).

1-Phenyl-2,5-dihydro-1*H*-borole reacts with $V(CO)_6$ in hexane with dehydrogenative complexation to give red, crystalline **1**. The electrophilic stacking of the hydride **5**[6] with $V(CO)_6$ in hexane affords red needles of **2**. The complexes **1** and **2** are the first 30e triple-decker complexes of vanadium. The higher homologues **3** and **4** are obtained as deep-red needles by electrophilic stacking of sodium borataferrocene **6**[6] with **7** or **8**, respectively[7] in THF; they are the first triple-decker complexes of niobium and tantalum.

The new complexes[8] are sensitive to light and extremely sensitive to nucleophilic degradation.[1] In the IR spectrum they show the typical pattern of three CO bands for $M(CO)_4$ groups with highly perturbed local C_{4v} symmetry (Table 1). Their NMR data, with ^{11}B and ^{13}C NMR signals



1

2, M = V
3, M = Nb
4, M = Ta

$[CpFeH(\eta^5\text{-}C_4H_4BPh)]$ **5**
$Na[CpFe(\eta^5\text{-}C_4H_4BPh)]$ **6**
$Na[(\mu\text{-Cl})_3\{M(CO)_4\}_2]$
7, M = Nb; **8**, M = Ta

Table 1. $\tilde{\nu}$(CO) values in hexane.

Compound	$\tilde{\nu}$(CO) [cm^{-1}]
1	2022 m, 1974 w, 1943 s
2	2030 m, 1964 w, 1932 s
3	2033 m, 1949 w, 1929 s
4	2035 m, 1939 w, 1920 s

at comparatively high field, confirm the presence of a bridging 1*H*-borole ligand; the AA'BB' system in the ^1H NMR spectrum shows the small coupling constant $N = {}^3J_{23} + {}^4J_{24}$ of only 3.9–4.2 Hz which is typical for the triple-decker structure.[9] The closely related triple-decker

$[NMe_3Ph][(\mu\text{-}\eta^5\text{-}C_4H_4BPh)\{Cr(CO)_3\}(FeCp)]$ **9**

complex **9** has been characterized by X-ray crystallography;[10a] here again, as in the case of the molybdenum and tungsten homologues,[10b] the outer carbonyl ligands enforce a 30e configuration.

Experimental

1: A mixture of 1-phenyl-2,5-dihydro-1*H*-borole (2.0 g, 14 mmol) and $V(CO)_6$ (1.00 g, 4.6 mmol) in hexane (20 mL) was heated to 55°C for 16 h. Filtration and chromatographic work-up (silica gel, −20°C) of the hexane filtrate afforded a yellow zone containing 7.3 mg (32 μmol; 0.7%) of $[V(CO)_4Cp]$ and a second, carmine-red zone, from which 9.6 mg (21 μmol; 0.9%) of red crystals of **1** were obtained by threefold crystallization. M.p. 68°C, decomp. 74°C, soluble even in pentane, light-sensitive in solution.—^1H NMR (80 MHz, [D$_6$]acetone): δ=7.66 (m, 2H$_o$), 7.36 (m, 2H$_m$+H$_p$), 5.72 (m, H-3,4), 4.29 (m, H-2,5); $N = {}^3J_{23} + {}^4J_{24}$=4.2 Hz. ^{11}B NMR (32.08 MHz, $CDCl_3$, ext. $BF_3 \cdot OEt_2$): δ=21.

2: A solution of **5** (345 mg, 1.32 mmol) [6] in hexane (100 mL) was treated with a solution of $V(CO)_6$ (361 mg, 1.65 mmol) in hexane (25 mL) at −25°C and the mixture stirred for 7 d at room temperature. Chromatographic work-up (Al_2O_3 with 7% water, −35°C) afforded a first runnings of $V(CO)_6$ with pentane, then a red zone with pentane/toluene (1/1), from which 228 mg (0.54 mmol; 41%) of red needles of **2** were obtained after removal of the eluent and crystallization from hexane at −30°C. M.p. 140°C (decomp.), light- and air-sensitive, soluble even in pentane.—^1H NMR (80 MHz, $CDCl_3$, int. TMS): δ=7.72 (m, 2H$_o$), 7.34 (m, 2H$_m$+H$_p$), 4.08 (s, Cp), 4.48 (m, H-3,4), 3.43 (m, H-2,5); $N = {}^3J_{23} + {}^4J_{24}$=4.0 Hz. ^{11}B NMR (32.08 MHz, $CDCl_3$, ext. $BF_3 \cdot OEt_2$): δ=11.4. ^{13}C-NMR (67.88 MHz, $CDCl_3$, −70°C): δ=255 (br., CO), 140.9 (s, C$_i$), 132.5 (dm, $^1J_{CH}$=155 Hz, C$_o$), 127.4 (dd, $^1J_{CH}$=158 Hz, C$_m$), 126.9 (dt, $^1J_{CH}$=159 Hz, C$_p$), 68.6 (dm, $^1J_{CH}$=177 Hz, Cp), 66.6 (d, $^1J_{CH}$=165 Hz, C-2,5), 65.0 (d, $^1J_{CH}$=183 Hz, C-3,4).

3: A solution of the salt 7 (prepared from 2.00 g (3.62 mmol) of $[Na\{O(CH_2CH_2OMe)_2\}_2][Nb(CO)_6]$ and 0.72 g (7.3 mmol) of CuCl [7]) in 250 mL of Et_2O was treated dropwise at −70°C with a solution of **6** (prepared from 0.85 g (3.25 mmol) of **5** by deprotonation with NaH [6]) in 120 mL of Et_2O and the mixture stirred for ca. 12 h at room temperature. Filtration,

[*] Prof. Dr. G. E. Herberich, Dr. I. Hausmann, Dipl.-Chem. N. Klaff
Institut für Anorganische Chemie der Technischen Hochschule
Professor-Pirlet-Strasse 1, D-5100 Aachen (FRG)

[**] Triple-Decker Complexes, Part 6. This work was supported by the Deutsche Forschungsgemeinschaft and the Fonds der Chemischen Industrie.—Part 5: [1].

drying under vacuum, extraction with hexane and crystallization at −30°C afforded 300 mg (0.64 mmol; 20% referred to **5**) of deep-red, light- and air-sensitive needles of **3**. M.p. 143°C (decomp.), soluble even in pentane.—^{1}H NMR (80 MHz, $CDCl_3$, int. TMS): δ=7.67 (m, 2 H_o), 7.35 (m, 2 H_m + H_p), 4.18 (s, Cp), 4.93 (m, H-3,4), 3.72 (m, H-2,5); $N = {}^3J_{23} + {}^4J_{24}$ = 3.9 Hz. ^{11}B NMR (32.08 MHz, $CDCl_3$, ext. $BF_3 \cdot OEt_2$): δ = 13.8. ^{13}C NMR (67.88 MHz, $CDCl_3$, −70°C): δ = 251.6 (s, CO), 141.4 (s, C_i), 132.9 (dm, $^1J_{CH}$ = 157 Hz, C_o), 127.7 (dd, $^1J_{CH}$ = 154 Hz, C_m), 127.2 (dt, $^1J_{CH}$ = 160 Hz, C_p), 69.9 (dm, $^1J_{CH}$ = 177 Hz, Cp), 66.4 (d, $^1J_{CH}$ = 167 Hz, C-2,5), 66.2 (d, $^1J_{CH}$ = 183 Hz, C-3,4).

4: Synthesis and work-up as described for **3**; 1.95 g (3.05 mmol) $[Na\{O(CH_2CH_2OMe)_2\}_2][Ta(CO)_6]$, 0.60 g (6.1 mmol) CuCl and 0.79 g (3.02 mmol) **5** give 430 mg (0.78 mmol; 26% referred to **5**) deep-red, almost air-stable needles of **4**. M.p. 164°C (decomp.), soluble even in pentane.—^{1}H NMR (80 MHz, $CDCl_3$, int. TMS): δ = 7.66 (m, 2 H_o), 7.34 (m, 2 H_m + H_p), 4.21 (s, Cp), 4.85 (m, H-3,4), 3.63 (m, H-2,5); $N = {}^3J_{23} + {}^4J_{24}$ = 3.9 Hz. ^{11}B NMR (32.08 MHz, $CDCl_3$, ext. $BF_3 \cdot OEt_2$): δ = 12.8. ^{13}C NMR (67.88 MHz, $CDCl_3$, −70°C): δ = 246.7 (s, CO), 140.6 (s, C_i), 133.0 (dm, $^1J_{CH}$ = 157 Hz, C_o), 127.8 (dd, $^1J_{CH}$ = 160 Hz, C_m), 127.4 (dt, $^1J_{CH}$ = 154 Hz, C_p), 70.9 (dm, $^1J_{CH}$ = 178 Hz, Cp), 64.3 (d, $^1J_{CH}$ = 156 Hz, C-2,5), 64.7 (d, $^1J_{CH}$ = 190 Hz, C-3,4).

Received: September 6, 1988;
revised: November 28, 1988 [Z 2957 IE]
German version: *Angew. Chem. 101* (1989) 328

CAS Registry numbers:
1, 118657-21-9; **2**, 118657-22-0; **3**, 118657-23-1; **4**, 118657-24-2; **5**, 103432-55-9; **6**, 118657-25-3; **7**, 84821-59-0; **8**, 118657-26-4; $V(CO)_6$, 14024-00-1; $[Na\{O(CH_2CH_2OMe)_2\}_2][Nb(CO)_6]$, 12189-43-4; $[Na\{O(CH_2CH_2OMe)_2\}_2][Ta(CO)_6]$, 12189-44-5; 1-phenyl-2,5-dihydro-1*H*-borole, 84017-49-2.

[1] G. E. Herberich, U. Büschges, *Chem. Ber.*, in press.
[2] For further references see: a) W. Siebert, *Angew. Chem. 97* (1985) 924; *Angew. Chem. Int. Ed. Engl. 24* (1985) 943; b) O. J. Scherer, J. Schwalb, H. Swarowsky, G. Wolmershäuser, W. Kaim, R. Gross, *Chem. Ber. 121* (1988) 443.
[3] a) A. W. Duff, K. Jonas, *J. Am. Chem. Soc. 105* (1983) 547; b) P. T. Chesky, M. B. Hall, *ibid. 106* (1984) 5186; c) K. Angermund, K. H. Claus, R. Goddard, C. Krüger, *Angew. Chem. 97* (1985) 241; *Angew. Chem. Int. Ed. Engl. 24* (1985) 237; d) K. Jonas, W. Rüsseler, K. Angermund, C. Krüger, *ibid. 98* (1986) 904 and *25* (1986) 927.
[4] H. Werner, A. Salzer, *Synth. Inorg. Met. Org. Chem. 2* (1972) 239; A. Salzer, H. Werner, *Angew. Chem. 84* (1972) 949; *Angew. Chem. Int. Ed. Engl. 11* (1972) 930; *Synth. Inorg. Met. Org. Chem. 2* (1972) 249; H. Werner, B. Ulrich, A. Salzer, *J. Organomet. Chem. 141* (1977) 339; E. Dubler, M. Textor, H. R. Oswald, G. B. Jameson, *Acta Crystallogr. Sect. B 39* (1983) 607.
[5] a) J. W. Lauher, M. Elian, R. H. Summerville, R. Hoffmann, *J. Am. Chem. Soc. 98* (1976) 3219; b) K. Wade, *Adv. Inorg. Chem. Radiochem. 18* (1976) 1; c) further theoretical studies: [3b]; E. D. Jemmis, A. C. Reddy, *Organometallics 7* (1988) 1561.
[6] G. E. Herberich, B. Hessner, D. P. J. Köffer, *J. Organomet. Chem. 362* (1989) 243.
[7] F. Calderazzo, G. Pampaloni, *J. Organomet. Chem. 303* (1986) 111.
[8] Correct C,H analyses. The molecular ions and successive cleavage of 8 (in the case of **1**) and 4 (in the case of **2**-**4**) CO groups are observed in the mass spectra.
[9] G. E. Herberich, B. Hessner, R. Saive, *Organomet. Chem. 319* (1987) 9.
[10] a) G. E. Herberich, B. Hessner, J. A. K. Howard, D. P. J. Köffer, R. Saive, *Angew. Chem. 98* (1986) 177; *Angew. Chem. Int. Ed. Engl. 25* (1986) 165; b) G. E. Herberich, K. Peters, unpublished.

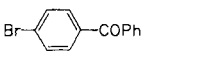
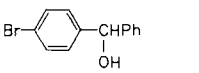
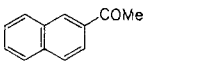
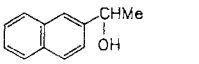
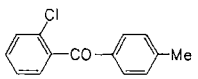
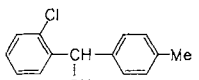
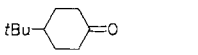
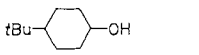
$NaBH_4$ Reduction of Ketones in the Solid State

By *Fumio Toda,* Koji Kiyoshige,* and *Minoru Yagi*

Previously we reported that Baeyer-Villiger oxidations of ketones with *m*-chloroperbenzoic acid proceed much faster in the solid state than in solution.[1] We have now found that reductions of ketones with $NaBH_4$ also proceed in the solid state (Table 1). In addition, the formation of 1 : 1 inclusion complexes can be exploited to carry out regio- and enantioselective reductions leading to products such as **2a** and **4**, which are of interest as synthetic building blocks but only accessible with difficulty by other routes.

A mixture of the ketone and a tenfold molar amount of $NaBH_4$ was finely powdered using an agate mortar and pestle and kept in a dry box at room temperature for five days, being stirred once a day. The reaction mixture was extracted with ether, and the dried ether solution was evaporated to give the corresponding alcohol in the yields shown in Table 1. Almost the same results were obtained by shaking the mixture for a day using a test-tube shaker.

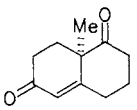
Table 1. Reduction of simple ketones in the solid state by $NaBH_4$.

Ketone	Alcohol	Yield [%]
Ph_2CO	Ph_2CH-OH	100
trans-PhCH=CHCOPh	*trans*-PhCH=CHCHPh (OH) + $PhCH_2CH_2CHPh$ (OH)	100 (1 : 1)
		100
		53
PhCHCOPh (OH)	*meso*-PhCH–CHPh (OH OH)	62
$PhCH_2COPh$	$PhCH_2CHPh$ (OH)	63
		21
		92
$PhCOCONiPr_2$	$PhCHCONiPr_2$ (OH)	24

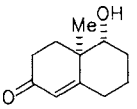
Treatment of a 1 : 1 inclusion complex[2,3] of (*R*)-**1** and (*R,R*)-**5** with $NaBH_4$ in the solid state for 3 days gave (*R,R*)-**2a** of 100% *ee* ($[\alpha]_D$ −192.8 (c = 0.24, benzene)) in 54% yield. The corresponding reaction of a 1 : 1 complex of (*S*)-**1** and (*S,S*)-**5** gave (*S,S*)-**2a** of 100% *ee*. Treatment of the racemic diketone **1** with (*R,R*)-**5** results in selective formation of an inclusion complex with (*R*)-**1**; decomposition of the complex gives (*R*)-**1** of 100% *ee*. Since the hydride attacks the carbonyl carbon at the 7-position from the side opposite the methyl group,[4] (*R*)-**1** should give (*R,R*)-**2a** of 100% *ee*, as was found. The IR spectrum and $[\alpha]_D$ value of the product were comparable to those of an authentic sample ($[\alpha]_D$ −203 (c = 1.545, benzene)) prepared by biological reduction of *rac*-**1**.[5]

The enone moiety of (*R*)-**1** is presumably masked by forming a hydrogen bond with the hydroxyl group of (*R,R*)-**5**, so that the other carbonyl group is reduced selectively. When the reduction of (*R*)-**1** is carried out in the presence of (*R,R*)-**5** in a suspension in water, the diol **2b** is obtained as a mixture of diastereomers.

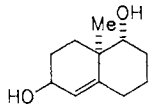
[*] Prof. F. Toda, K. Kiyoshige, M. Yagi
Department of Industrial Chemistry, Faculty of Engineering
Ehime University, Matsuyama 790 (Japan)



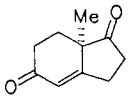
(R)-(−)-1



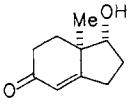
(R,R)-(−)-2a



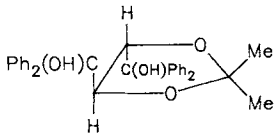
2b



(R)-(−)-3



(R,R)-(−)-4



(R,R)-(−)-5

It is not easy to prepare even racemic alcohol *rac*-**2a**. Recently, a preparative synthesis of *rac*-**2a** by selective reduction of *rac*-**1** with $NaBH_4$ in $MeOH/ClCH_2CH_2Cl$ (1:1) at −78 °C was reported.[4] A more complicated preparative method is the MnO_2 oxidation of *rac*-**2b**, prepared by reduction of *rac*-**1**.[6] The above-mentioned biological method is also complicated.[5]

Similar reduction of a 1:1 complex[3] of (*R*)-**3** and (*R,R*)-**5** with $NaBH_4$ in the solid state gave (*R,R*)-**4** of 100% *ee* ($[\alpha]_D$ −98.2 (c = 0.3, benzene) in 55% yield. The $[\alpha]_D$ value is comparable to that recorded for an authentic sample ($[\alpha]_D$ −97 (c = 1.415, benzene) prepared by a biological method.[7]

Received: September 14, 1988;
supplemented: November 17, 1988 [Z 2967 IE]
German version: *Angew. Chem. 101* (1989) 329

[1] F. Toda, M. Yagi, K. Kiyoshige, *J. Chem. Soc. Chem. Commun. 1988*, 958.
[2] Some alcohol host compounds such as **5** form inclusion complexes with a wide variety of guest compounds and form crystalline inclusion compounds with a stoichiometric host:guest ratio: F. Toda, *Top. Curr. Chem. 140* (1987) 43, *149* (1988) 211.
[3] F. Toda, K. Tanaka, *Tetrahedron Lett. 29* (1988) 551.
[4] D. E. Ward, C. K. Rhee, W. M. Zoghaib, *Tetrahedron Lett. 29* (1988) 517.
[5] V. Prelog, W. Acklin, *Helv. Chim. Acta 39* (1956) 748.
[6] F. Sondheimer, D. Elad, *J. Am. Chem. Soc. 79* (1957) 5542.
[7] W. Acklin, V. Prelog, A. P. Prieto, *Helv. Chim. Acta 41* (1958) 1416.

Formation of a Phosphaferracyclopentadiene Ring by Coupling of a Phosphaalkyne with Two Fluoromethylidyne Ligands**

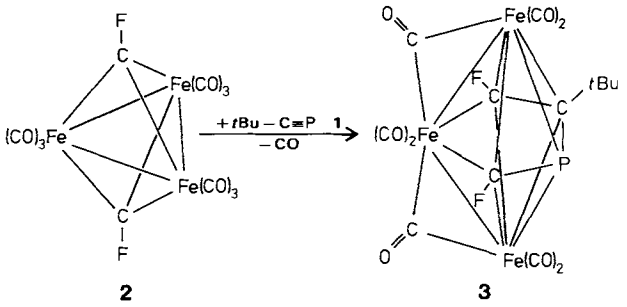
By *Dieter Lentz** and *Heike Michael*

The coordination chemistry of the phosphaalkyne *t*BuC≡P **1**[1] has been extensively investigated in the last few years.[2] Other reactions that have been reported recently for **1** include its cyclodimerization and cyclotrimerization,[3] [2+2]-, [3+2]- and [4+2]-cycloadditions,[4] dimerization with insertion of CO,[5] as well as a reaction with a Fischer-type carbene complex.[6]

[*] Priv.-Doz. Dr. D. Lentz, Dipl.-Chem. H. Michael
Institut für Anorganische und Analytische Chemie
der Freien Universität
Fabeckstrasse 34-36, D-1000 Berlin 33

[**] This work was supported by the Fonds der Chemischen Industrie, the Deutsche Forschungsgemeinschaft and the BASF AG (donation of pentacarbonyliron). We thank Prof. *J. Fuchs* for assistance with the crystal structure investigation and Dipl.-Chem. *L. Turowsky* for providing the compound *t*BuC≡P.

In the course of our investigations of the reactivity of $[Fe_3(CO)_9(\mu_3\text{-}CF)_2]$ **2**[7] towards alkynes,[8] we have discovered a novel type of reaction. Thus, reaction of **1** with **2** proceeds with coupling of both CF ligands to the phosphaalkyne to afford the five-membered phosphaferra heterocycle of complex **3**.



2 **3**

The ^{19}F NMR spectrum of **3** exhibits two doublets and the ^{31}P NMR spectrum contains a doublet of doublets (Table 1).

Table 1. Spectroscopic data for the compounds **3** and **5a-c**.

3: IR (*n*-pentane): $\tilde{\nu}$ = 2078 (s), 2033 (vs), 1994 (s), 1877 (m), 1861 (m) cm^{-1}; ^{19}F NMR ($CDCl_3$, $CFCl_3$ ext. standard): δ = −68.7 ($^3J_{PF}$ = 24 Hz), −99.5 ($^2J_{PF}$ = 61 Hz); ^{31}P NMR ($CDCl_3$, H_3PO_4 ext. standard): δ = 2.9 (dd); MS (80 eV): *m/z* 554 ($M^{\oplus}$), successive CO cleavage and further smaller fragment ions, high resolution of the molecular ion peak: calcd. 553.8051, found 553.8046

5a: IR (*n*-pentane): $\tilde{\nu}$ = 2071 (w), 2038 (w), 2010 (w), 1986 (vs), 1956 (m) cm^{-1}; ^{19}F NMR ($CDCl_3$, $CFCl_3$ ext. standard): δ = −67.6 ($^3J_{PF}$ = 17 Hz), −100.4 ($^2J_{PF}$ = 34 Hz); ^{31}P NMR ($CDCl_3$, H_3PO_4 ext. standard): δ = 74.0 (dd); MS (80 eV): *m/z* 746 ($M^{\oplus}$), successive CO cleavage and additional smaller fragment ions, high resolution of the peak $M^{\oplus}$ − CO: calcd. 717.7253, found 717.7224

5b: IR (*n*-hexane): $\tilde{\nu}$ = 2076 (s), 2039 (s), 2035 (m), 2026 (vs), 2001 (m), 1999 (m), 1993 (w), 1983 (m), 1979 (m), 1976 (m), 1933 (m), 1929 (m), 1880 (m), 1868 (m) cm^{-1}; ^1H NMR (CD_2Cl_2): δ = 1.82 (CH_3, $^5J_{HF}$ = 2.4 Hz), 4.99 (C_5H_5, $J_{PH} \approx 2$ Hz); ^{19}F NMR (CD_2Cl_2, $CFCl_3$ ext. standard): δ = −64.9 ($^3J_{PF}$ = 17.1, $^5J_{HF}$ = 2.4 Hz), −101.6 ($^2J_{PF}$ = 30.5 Hz, $^4J_{FF}$ = 3.1 Hz); ^{31}P NMR (CD_2Cl_2, H_3PO_4 ext. standard): δ = 116 (br); MS (80 eV): *m/z* 730 ($M^{\oplus}$), successive CO cleavage and further smaller fragment ions, high resolution of the molecular ion peak: calcd. 729.7721, found 729.7726

5c: IR (*n*-pentane): $\tilde{\nu}$ = 2074 (s), 2038 (s), 2023 (vs), 1996 (m), 1979 (m), 1961 (w), 1913 (m), 1876 (m), 1863 (m) cm^{-1}; ^1H NMR (CD_2Cl_2): δ = 1.76 (CH_3, $^5J_{HF}$ = 2.4 Hz), 2.03 (Cp*); ^{19}F NMR (CD_2Cl_2, $CFCl_3$ ext. standard): δ = −65.7 ($^3J_{PF}$ = 21.4, $^5J_{HF}$ = 2.4 Hz), −96.6 ($^2J_{PF}$ = 29.9 Hz, $^4J_{FF}$ = 3.1 Hz); ^{31}P NMR (CD_2Cl_2, H_3PO_4 ext. standard): δ = 110 (br); MS (80 eV): *m/z* 800 ($M^{\oplus}$), successive CO cleavage and further smaller fragment ions, high resolution of the molecular ion peak: calcd. 799.8504, found 799.8516

An X-ray structure analysis[9] showed that **3** has a pentagonal bipyramidal cluster skeleton (Fig. 1a). The five-membered Fe-C-P-C-C ring is completely planar (maximum deviation 0.4 pm) with the two F atoms and the central C atom of the *t*Bu group also lying in this plane (maximum deviation 0.8 pm). The near equality of the two C-P bond lengths indicates extensive delocalization of the electrons in the five-membered ring. Assuming that the phosphorus atom contributes three skeletal electrons, the cluster **3** conforms with the Wade rules,[10] which predict this type of *closo* structure for 16 skeletal electrons. A carbon analogue of **3**, $Fe_2(CO)_8[Fe(CPh)_4]$ (i.e., with CPh instead of P) was synthesized by *Hübel* et al. in 1959[11a] and was structurally characterized[11b] some years later.

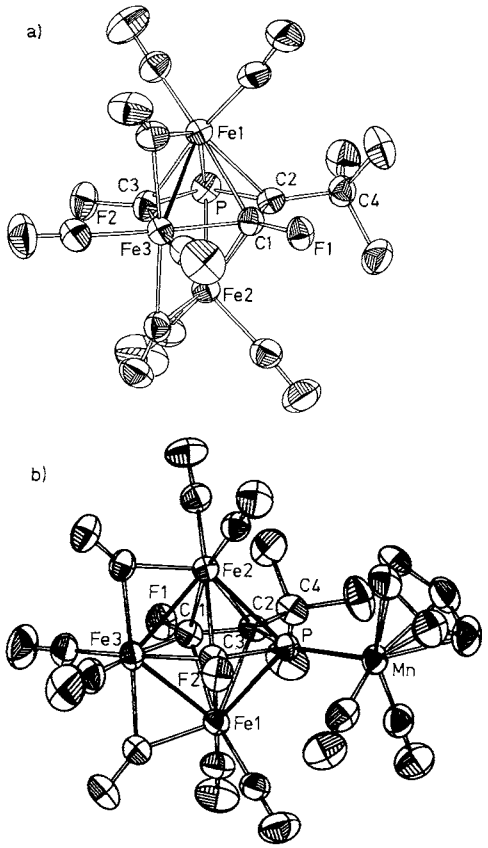
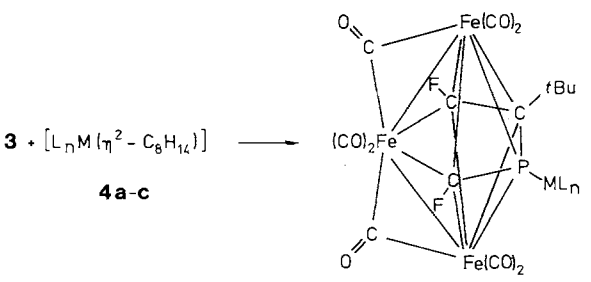


Fig. 1. a) Molecular structure of **3**. b) Molecular structure of **5b**. Important bond lengths [pm] and angles [°] for **3/5a**. Fe2-Fe3 245.13(7)/245.3(1), Fe1-Fe3 245.35(6)/245.9(1), Fe3-C1 199.9(4)/200.4(4), Fe3-C3 196.9(3)/196.1(5), Fe2-C1 212.4(4)/212.1(5), Fe2-C3 209.7(4)/208.9(5), Fe2-C2 230.0(4)/226.7(4), Fe2-P 242.9(1)/244.5(2), Fe1-C1 215.1(4)/211.6(5), Fe1-C3 209.7(4)/210.7(4), Fe1-C2 224.2(4)/229.9(4), Fe1-P 241.8(2)/241.6(2), C1-C2 143.4(5)/143.4(6), C1-F1 137.9(4)/138.2(5), C3-P 180.8(4)/180.1(5), C3-F2 138.5(4)/139.0(5), C2-P 180.2(3)/181.1(4), C2-C4 155.0(5)/155.7(6), Fe-CO_{term} 178.1(4)-181.8(4)/177.2(5)-180.8(5), Fe3-μ-CO 205.5(5), 205.9(4)/203.5(5), 207.2(5), Fe2-μ-CO 188.7(4)/189.2(5), Fe1-μ-CO 188.4(4)/187.6(5), Mn-P —/217.2(2), Mn-CO —/178.0(5), 178.5(5), Mn-C_{Cp} —/213.1(6)-215.2(6); Fe2-Fe3-Fe1 87.48(3)/87.48(4), C1-Fe3-C3 77.8(2)/76.7(2), Fe3-C1-C2 127.5(3)/129.3(3), C1-C2-P 114.7(3)/112.7(3), C2-P-C3 91.3(2)/91.5(2), P-C3-Fe3 128.7(2)/129.6(3), Fe2-P-Fe1 88.79(4)/88.64(5), Mn-P-C2 —/141.8(2), Mn-P-C3 —/126.6(2), Mn-P-Fe1 —/130.97(6), Mn-P-Fe2 —/137.54(6), P-Mn-CO —/91.1(2), 93.6(2).

Since the phosphorus atom in **3** occupiés the apex of a distorted square based pyramid (Fig. 1a), it should be possible to coordinate a further metal ligand fragment (ML_n) in this position provided that the P atom possesses a nonbonding pair of electrons. Thereupon, we reacted **3** with the chromium compound **4a** and with the manganese complexes **4b** and **4c** (Cp* = C_5Me_5) to afford the clusters **5a**-**c**, in which **3** is bound as a ligand to the ML_n fragment of **4**. This bonding situation results in a marked low field shift for the ^{31}P resonances and a decrease in the magnitude of the F-P coupling constants.



a, $L_nM = (CO)_5Cr$; **b**, $L_nM = Cp(CO)_2Mn$; **c**, $L_nM = Cp^*(CO)_2Mn$

The crystal structure of **5b**[9] showed that the cluster skeleton of **3** hardly changes upon coordination to the $MnCp(CO)_2$ fragment (Fig. 1b). Without exception, the differences between the bond lengths and angles of **3** and **5b** are very small. Like **3**, **5b** has a planar Fe-C-P-C-C ring (maximum deviation 2.5 pm) with the ring substituents lying in the plane (maximum deviation 12 pm).

Experimental

3: **1** (120 mg, 1.2 mmol) and **2** (300 mg, 0.62 mmol) were dissolved in *n*-pentane (250 mL) in a photolysis apparatus under an Argon atmosphere. The solution was irradiated for 30 min using a high pressure mercury lamp (Philipps HPK 125 W, pyrex glass filter), then filtered through a thin layer of silica gel (Woelm 63-200 μm). After removal of the solvent under vacuum, the product was dissolved in the minimum volume of pentane and the solution cooled to −20°C to afford deep-green crystals of **2**. Yield: 220 mg (64% based on **2**), m.p. 142-143°C.

5a: **3** (30 mg, 0.06 mmol) was stirred with **4a** (37 mg, 0.12 mmol) in *n*-pentane (20 mL) for 2 h at room temperature. The reaction solution was filtered through a thin layer of silica gel (Woelm 63-200 μm). After removal of unreacted starting material by elution with pentane, **5a** was eluted with CH_2Cl_2. Hexane (50 mL) was added to the eluate and the solution was concentrated on a rotary evaporator until the onset of crystallization. Cooling to −78°C afforded **5a** as yellow-green crystals. Yield: 13 mg (30% based on **3**), dec. >70°C.

5b: A solution of **3** (112 mg, 0.2 mmol) and **4b** (58 mg, 0.2 mmol) in *n*-hexane (50 mL) was heated under reflux for 3 h. The reaction solution was filtered through a thin layer of silica gel (Woelm 63-200 μm). Unreacted starting material was eluted with hexane. **5b** was obtained by elution with CH_2Cl_2. The solvent was removed using a rotary evaporator and the residue extracted into *n*-pentane. Cooling to −20°C afforded dark-green crystals of **5b**. Yield: 57 mg (40%), m.p. 138-139°C.

5c: Analogous to **5b**. Yield: 26 mg (18%), dark green crystals, m.p. 162-163°C.

Received: September 9, 1988 [Z 2961 IE]
German version: *Angew. Chem. 101* (1989) 330

CAS Registry numbers:
1, 78129-68-7; **2**, 94621-00-8; **3**, 119208-83-2; **4a**, 92889-73-1; **4b**, 49716-47-4; **4c**, 119322-87-1; **5a**, 119208-84-3; **5b**, 119208-85-4; **5c**, 119208-86-5.

[1] G. Becker, G. Gresser, W. Uhl, *Z. Naturforsch. B36* (1981) 16; review: M. Regitz, P. Binger, *Angew. Chem. 100* (1988) 1541; *Angew. Chem. Int. Ed. Engl. 27* (1988) 1484.

[2] O. J. Scherer, *Angew. Chem. 97* (1985) 905; *Angew. Chem. Int. Ed. Engl. 24* (1985) 924, and references cited therein; M. L. Ziegler, R. Balles, B. Nuber, G. Becker, H. Schmidt, B. Kanellakopulus, B. Powietzka, *ibid. 99* (1987) 929 and *26* (1987) 900; S. I. Al-Resayes, P. B. Hitchcock, M. F. Meidine, J. F. Nixon, *J. Organomet. Chem. 341* (1987) 457.

[3] P. Binger, R. Milczarek, R. Mynott, M. Regitz, W. Rösch, *Angew. Chem. 98* (1986) 645; *Angew. Chem. Int. Ed. Engl. 25* (1986) 644; P. B. Hitchcock, M. J. Maah, J. F. Nixon, *J. Chem. Soc. Chem. Commun. 1986*, 737; A. R. Barron, A. F. Cowley, *Angew. Chem. 99* (1987) 956; *Angew. Chem. Int. Ed. Engl. 26* (1987) 907; R. Milczarek, W. Rüsseler, P. Binger, K. Jonas, K. Angermund, C. Krüger, M. Regitz, *ibid. 99* (1987) 957 and *26* (1987) 908; P. Binger, R. Milczarek, R. Mynott, M. Regitz, *J. Organomet. Chem. 323* (1987) C35; M. Driess, D. Hu, H. Pritzkow, H. Schäufele, U. Zenneck, M. Regitz, W. Rösch, *ibid. 334* (1987) C35; P. Binger, R. Milczarek, R. Mynott, C. Krüger, Y.-H. Tsay, E. Raabe, M. Regitz, *Chem. Ber. 121* (1988) 637.

[4] W. Rösch, H. Richter, M. Regitz, *Chem. Ber. 120* (1987) 1809; W. Rösch, U. Hess, M. Regitz, *ibid. 120* (1987) 1645 and earlier work in this series; A. H. Cowley, S. W. Hall, C. M. Nunn, J. M. Power, *Angew. Chem. 100* (1988) 874; *Angew. Chem. Int. Ed. Engl. 27* (1988) 838.

[5] A. R. Barron, A. H. Cowley, S. W. Hall, C. M. Nunn, *Angew. Chem. 100* (1988) 873; *Angew. Chem. Int. Ed. Engl. 27* (1988) 837.

[6] K. H. Dötz, A. Tiriliomis, K. Harms, M. Regitz, U. Annen, *Angew. Chem. 100* (1988) 725; *Angew. Chem. Int. Ed. Engl. 27* (1988) 713.

[7] D. Lentz, I. Brüdgam, H. Hartl, *Angew. Chem. 97* (1985) 115; *Angew. Chem. Int. Ed. Engl. 24* (1985) 119.

[8] D. Lentz, H. Michael, *Chem. Ber. 121* (1988) 1413 and unpublished results.

[9] **3**: $P2_1/n$, $a=1242.1(2)$, $b=1877.2(3)$, $c=864.1(2)$ pm, $\beta=109.95(2)°$, $Z=4$, $\rho_{calcd}=1.94$ g cm^{-3}; $R=0.026$ ($Mo_{K\alpha}=71.069$ pm, 3356 reflections, 3044 with $I>2\sigma(I)$, anisotropic temperature factors for Fe, P, F, C; H atoms isotropic; 299 refined parameters). **5b**: $P2_1/c$, $a=967.3(3)$, $b=1459.2(4)$, $c=1851.9(5)$ pm, $\beta=90.20(3)°$, $Z=4$, $\rho_{calcd}=1.85$ g cm^{-3}; $R=0.035$ ($Mo_{K\alpha}=71.069$ pm, 4607 reflections, 3962 with $I>2\sigma(I)$, anisotropic temperature factors for Fe, Mn, P, F, C; H atoms isotropic; 409 refined parameters, empirical absorption correction with the program DIFABS from *D. Stuart* and *N. Walker* [12]. Further details of the crystal structure investigations can be obtained from the Fachinformationszentrum Energie, Physik, Mathematik GmbH, D-7514 Eggenstein-Leopoldshafen 2, on quoting the depository number CSD-53426, the names of the authors, and the journal citation.

[10] K. Wade, *Adv. Inorg. Chem. Radiochem. 18* (1976) 1.

[11] a) W. Hübel, E. H. Braye, *J. Inorg. Nucl. Chem. 10* (1959) 250; b) R. P. Dodge, V. Schomaker, *J. Organomet. Chem. 3* (1965) 274; A. A. Hock, O. S. Mills, *Acta Crystallogr. 14* (1961) 139.

[12] N. Walker, D. Stuart, *Acta Crystallogr. Sect. A39* (1983) 158.

Microstructure of a Discotic Polymer as Revealed by Electron Diffraction and High-Resolution Imaging

By *Ingrid Gisela Voigt-Martin,* Heinz Durst, Volker Brzezinski, Herbert Krug, Willi Kreuder,* and *Helmut Ringsdorf*

Electron microscopy has become a powerful tool to obtain atomic-level as well as molecular-level information.[1] It has recently been applied to study the microstructure and defects in smectic liquid crystals[2–5] without resorting to staining methods which are liable to cause artifacts.

Polymeric liquid crystals are well suited for such investigations because they are nonvolatile and their mesophases can be frozen in below their glass transition temperatures.[6] This allows detailed structural investigations because both the microstructure and defects in polymeric liquid crystals are retained in the glassy state. The smectic layers exhibit well-defined undulations and contain single and multiple dislocations.[5]

Recently, polymers with disclike mesogens as side groups[7] or in the main chain[8,9] have been described. They exhibit a discotic columnar structure as elucidated by X-ray investigations.[10] For low-molecular-weight compounds such liquid-crystalline microstructures have been known since 1977.[11] These compounds contain flat, rigid discs (e.g., triphenylene) and several flexible alkyl chains.[12] In discotic main-chain polymers[8] around ten to one hundred of such molecular discs are linked via flexible alkyl spacers (Fig. 1).

The polymer **1a**[8] shows an ordered, hexagonal columnar mesophase (D_{ho}) in complete analogy to its low-molecular-weight model compound **1b**. The mesophase width is even broader than for the hexakis(pentyloxy)triphenylene **1b**.[13] In contrast to **1b**, which crystallizes on cooling, the D_{ho} microstructure of the polymer can be frozen in below the glass transition temperature $T_g=60$ °C (Fig. 2).

The electron diffraction pattern (primary diffraction) indicates a hexagonal microstructure. The diffraction spots are sharp and show both first- and second-order reflections (Fig. 3). The measured lattice spacing is $d=18.1$ Å, from which a hexagonal lattice constant of $a=20.9$ Å could be calculated in agreement with the values obtained by X-ray studies (17.7 Å and 20.4 Å, respectively[10]).

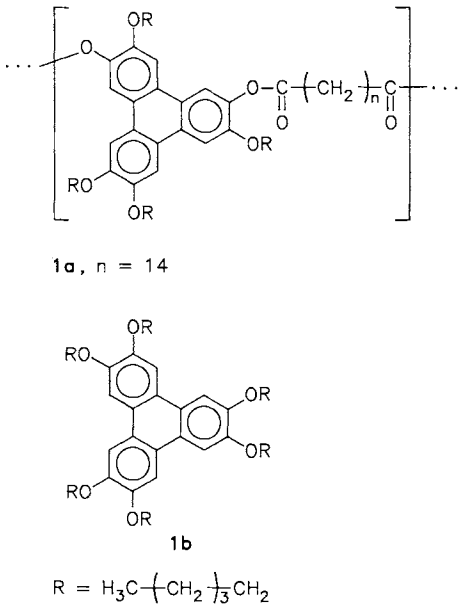


Fig. 1. Schematic representation of a repeating unit of the discotic polymer **1a** and structure of the model compound **1b**.

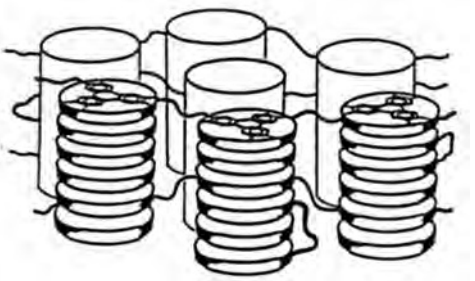


Fig. 2. Schematic representation of the D_{ho} mesophase of the polymeric triphenylene derivative **1a**.

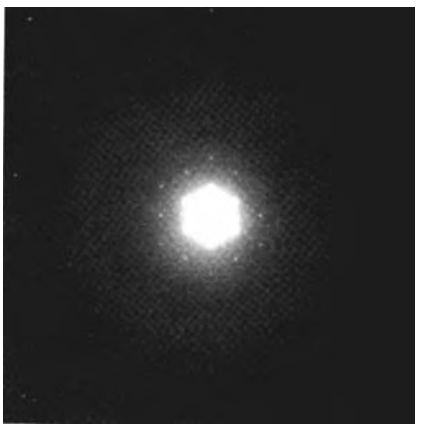


Fig. 3. Electron diffraction of the discotic polymer **1a**; D_{ho} phase viewed along the column axis.

The spots are arranged in a hexagon, but they are not arced as in the X-ray pattern of the same polymer.[10] Two explanations can be put forward. Firstly, the electron beam probes a very small area of about 2 μm in diameter, within which the orientation is apparently almost perfect. In contrast to this, X-rays probe about 1 mm^2, so that an average orientation is obtained. Secondly, the thickness of the film

[*] Dr. I. G. Voigt-Martin, H. Durst, V. Brzezinski, H. Krug
Institut für Physikalische Chemie der Universität
Welder-Weg 15, D-6500 Mainz (FRG)
Dr. W. Kreuder, Prof. Dr. H. Ringsdorf
Institut für Organische Chemie der Universität Mainz (FRG)

for electron microscopy is of the order of several hundred angstroms only. This corresponds roughly to one hundred molecular triphenylene discs stacked on top of one another (see Fig. 2). This, in turn, is the typical correlation length within the columns of discotic liquid crystals.[17] The thin-film technique enables almost undisturbed columns to be observed which extend through the whole thickness of the polymer films.

While diffraction techniques give important general information regarding molecular packing, it is difficult and often impossible to elicit details regarding defects and correlation distances from them without making massive assumptions. The reason is that phase information is always lost in a diffraction pattern so that the Fourier transform contains amplitude information only. Phases can be reintroduced mathematically but this involves assumptions or additional information. An alternative approach is to apply high-resolution direct imaging. This method allows the observation of molecular structures. In Figure 4 the two-

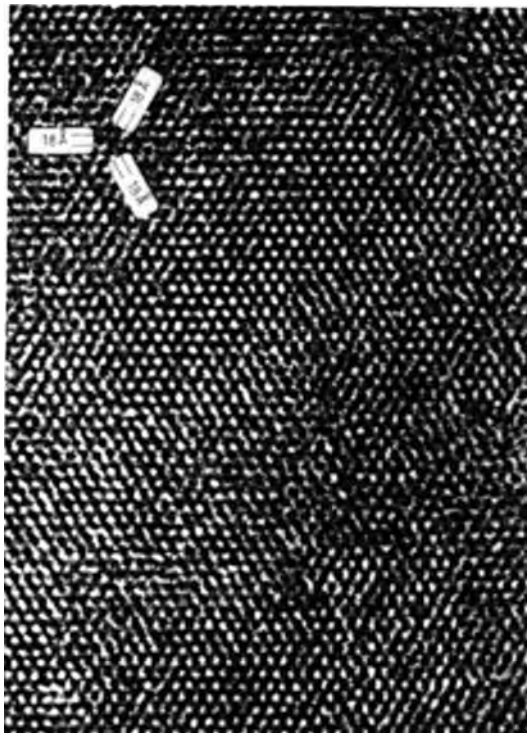


Fig. 4. Bright-field high-resolution electron micrograph of the discotic polymer **1a**. Middle: D_{ho} phase viewed along the column axis. Lower half: Tilted domain.

dimensional hexagonal packing of the molecular columns of the discotic liquid-crystalline polymer **1a** is shown for the first time. The single columns of the packed triphenylene discs (cf. Fig. 2) can be resolved and their distance (ca. 18 Å) is in agreement with the values obtained from electron diffraction (see Fig. 3) and X-ray diffraction.[10] In the same specimen other domains were observed with a slight tilt angle between the local column axis and the beam axis. This high-resolution direct imaging involves special techniques and is—in contrast to inorganic materials—difficult to apply to beam-sensitive samples like this polymer. For comparison, the computer-treated image is shown in Figure 5.[16] In the context of investigations of ultrathin films[18] these electron-microscopic images stimu-

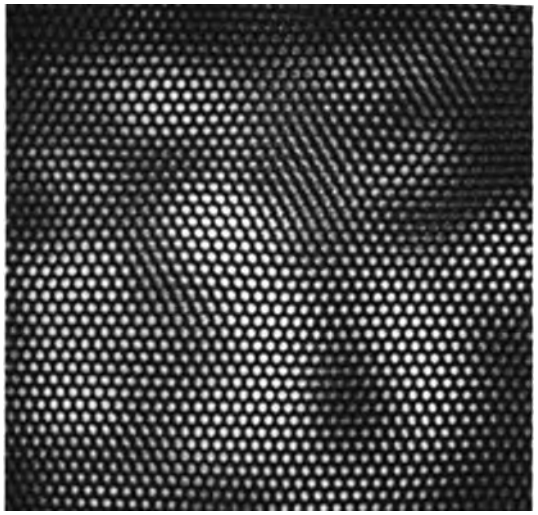


Fig. 5. Computer-treated high-resolution electron micrograph of discotic polymer **1a** (cf. Fig. 4).

late provocative ideas regarding applications in the fields of electronics and optoelectronics.[19] The submicrometer structures in the systems applied so far are still roughly a hundred times larger than those in the discotic polymer **1a**. For instance, in the field of information storage one can envisage addressing such regularly ordered nanometer structures. Configurations similar to scanning tunnel electron microscopy could be applied for implanting electrons into single columns of ordered discotic polymers. Furthermore, these columns are densely stacked π systems surrounded by paraffinic chains, which give an insulation against the six columns in the immediate neighborhood, so that they might act as molecular conductors. The predominant conductivity[20] across the thin film might be further increased by doping with electron-acceptor molecules.[21]

Experimental Procedure

In order to study the mesophase of polymer **1a** by electron microscopy, 400-Å films were prepared by spreading a polymer solution in chloroform (30/100 w/v) on a water surface. The dried film was sandwiched between two carbon films and transferred onto copper grids for electron microscopy. Orientation was obtained by annealing in a magnetic field of 1.5 T just below the D_{ho}→isotropic phase transition temperature. The magnetic field direction was chosen to be in the film plane, so that the columns are oriented perpendicular to the film, as is to be expected from the known anisotropy of the magnetic susceptibility of a similar low-molecular-weight discotic compound [17]. Finally, the film was cooled to ambient temperature and thus the orientation was frozen in. The production and interpretation of a high-resolution electron micrograph is not a trivial matter. It is particularly difficult in the case of beam-sensitive samples, where special cryogenic methods combined with the low-dose technique have to be developed and applied [3]. In order to understand the difficulties regarding interpretation of the electron micrographs, it is necessary to explain the physics involved without detailed reference to the mathematics, which is related elsewhere [15].

Imaging involves a two-stage process, mathematically expressed by two Fourier transforms. The first involves the production of an electron diffraction pattern (primary diffraction) in reciprocal space from the object in real space (first Fourier transform). Subsequently, in a second Fourier transformation, an image is produced from the diffraction pattern. It is important to realize that the objective lens of the microscope produces a phase shift so that the expression for the phases and amplitudes in reciprocal space is modified by an oscillating microscope transfer function which depends on the defocus value [4], as well as on manipulations in reciprocal space involving the objective aperture. In order to image objective details having certain spatial frequencies, therefore, a very specific transfer function must be chosen. In the low-angle range which is relevant for these samples, the band width is very narrow and only a very small range of frequencies is transferred. Furthermore, because of the rapidly oscillating transfer function, higher-order re-

flections may have suffered a phase change so that the information in the appropriate frequency range is transferred with reversed contrast.

The second stage in image analysis involves image reconstruction, where the electron micrograph now serves as object. Filtering of Fourier frequencies in reciprocal space (secondary diffraction pattern) is performed generally with the aid of a computer. The various stages of frequency filtering are very complex and must be treated with careful consideration of the physics involved. Otherwise, artifacts can easily be introduced. The safest way to guard against this is to compare the original image (which must be of very high quality) with the computer-treated image, and to ensure that defects have not been introduced which were not in the original. Details regarding these procedures will be published elsewhere [16].

Received: September 22, 1988;
supplemented: December 2, 1988 [Z 2974 IE]
German version: *Angew. Chem. 101* (1989) 332

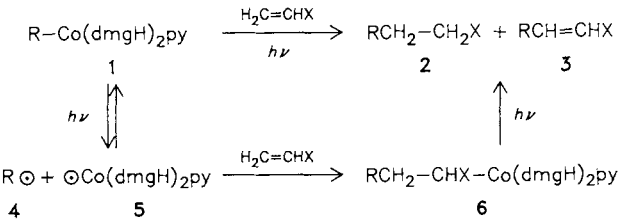
CAS Registry numbers:
1a, 118891-82-0; **1b**, 69079-52-3.

[1] L. D. Marks, D. J. Smith, *Nature (London) 303* (1983) 316; J.-O. Malm, J.-O. Bovin, A. Petford-Long, D. J. Smith, G. Schmid, N. Klein, *Angew. Chem. 100* (1988) 580; *Angew. Chem. Int. Ed. Engl. 27* (1988) 555.
[2] H. Durst, I. G. Voigt-Martin, *Makromol. Chem. Rapid Commun. 7* (1986) 785; I. G. Voigt-Martin, H. Durst, *Liq. Cryst. 2* (1987) 585; I. G. Voigt-Martin, H. Durst, H. Krug, *Macromolecules*, in press.
[3] I. G. Voigt-Martin, H. Durst, *Liq. Cryst. 2* (1987) 601.
[4] I. G. Voigt-Martin, H. Durst, B. Reck, H. Ringsdorf, *Macromolecules 21* (1988) 1620.
[5] I. G. Voigt-Martin, H. Durst, *Macromolecules 22* (1989) 168.
[6] H. Finkelmann, *Angew. Chem. 99* (1987) 840; *Angew. Chem. Int. Ed. Engl. 26* (1987) 816; H. Finkelman, G. Rehage, *Adv. Polym. Sci. 60/61* (1984) 174.
[7] W. Kreuder, H. Ringsdorf, *Makromol. Chem. Rapid Commun. 4* (1983) 807.
[8] Synthesis and characterization of **1**: W. Kreuder, H. Ringsdorf, P. Tschirner, *Makromol. Chem. Rapid Commun. 6* (1985) 367.
[9] G. Wenz, *Makromol. Chem. Rapid Commun. 6* (1985) 577.
[10] O. Hermann-Schönherr, J. H. Wendorff, W. Kreuder, H. Ringsdorf, *Makromol. Chem. Rapid Commun. 7* (1986) 97.
[11] S. Chandrasekhar, B. K. Sadashiva, K. A. Suresh, *Pramana 9* (1977) 471; *Chem. Abstr. 88* (1978) 30566y.
[12] J. Billard, J. C. Dubois, Nguyen Huu Tinh, A. Zann, *Nouv. J. Chim. 2* (1978) 535; C. Destrade, P. Foucher, H. Gasparoux, Nguyen Huu Tinh, A. M. Levelut, J. Malthete, *Mol. Cryst. Liq. Cryst. 106* (1984) 121.
[13] A. M. Levelut, *J. Phys. Lett. 40* (1979) 81.
[14] D. Goldfarb, R. Poupko, Z. Luz, H. Zimmermann, *J. Chem. Phys. 79* (1983) 4035.
[15] J. Amoros, M. Amoros: *Molecular Crystals: Their Transform and Diffuse Scattering*, Wiley, New York 1983; J. Cowley: *Diffraction Physics*, North Holland, Amsterdam 1986.
[16] I. G. Voigt-Martin, H. Durst, H. Krug, *Macromolecules*, in press.
[17] M. Gharbia, M. Cagnon, G. Durand, *J. Phys. Lett. 46* (1985) 683; cf. A. M. Levelut, *J. Chem. Phys. 80* (1983) 149.
[18] H. Ringsdorf, B. Schlarb, J. Venzmer, *Angew. Chem. 100* (1988) 117; *Angew. Chem. Int. Ed. Engl. 27* (1988) 113; H. Ringsdorf, G. Schmidt, J. Schneider, *Thin Solid Films 152* (1987) 207.
[19] T. Iwayanagi, T. Ueno, S. Nonogaki, H. Ito, C. G. Willson: "*Materials and Processes for Deep U. V. Lithography*", *Adv. Chem. Ser.*, in press.
[20] L. Y. Chiang, J. P. Stokes, C. R. Safinya, A. N. Bloch, *Mol. Cryst. Liq. Cryst. 125* (1985) 279; B. Mourey, J. N. Perbet, M. Hareng, S. Le Berre, *ibid. 84* (1982) 193.
[21] P. Davidson, A. M. Levelut, H. Strzelecki, V. Gionis, *J. Phys. Lett. 44* (1983) 823.

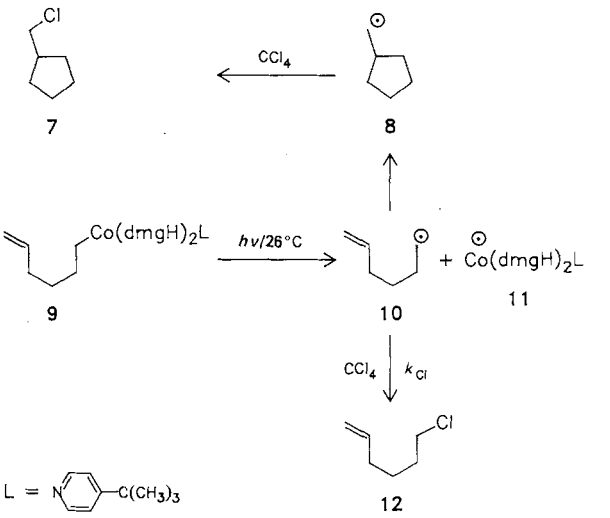
On the Formation of "Free Radicals" from Alkylcobalt Complexes**

By *Bernd Giese,* Jens Hartung, Jianing He, Ottmar Hüter,* and *Andreas Koch*

Alkylcobaloximes of type **1** are becoming of increasing importance in organic synthesis, since their photolysis generates radicals which can be used for both carbon-carbon[1] and carbon-heteroatom bond-forming reactions.[1c,2] Preparatively useful reactions include cyclizations[1a] and intermolecular additions to olefins,[1b-d] which, depending on the reaction conditions and the substituents, afford alkanes **2** and/or alkenes **3** (H_2dmg = 2,3-butanedionedioxime).



On the basis of ESR measurements, it has been concluded that alkyl radicals generated from alkylcobaloximes in a matrix still undergo an interaction with the Co^{II} complex **5**.[3] By carrying out reactivity and selectivity studies on alkylcobaloximes in organic solvents, we have now been able to show that C-C bond formation involves the reaction of free radicals that do not differ from those generated from other radical sources.



In order to determine the reactivity, the hexenylcobaloxime **9** was photolyzed in the presence of various quantities of CCl_4 at 26°C using a 300 W sun lamp. From the ratio of the products **12** and **7** and the known rate of cyclization of the hexenyl radical **10**,[4] the rate of abtraction of chlorine from CCl_4 could be determined as $6.9 \times 10^3\ M^{-1}\ s^{-1}$. This value agrees remarkably well with the literature value for the hexenyl radical, which was generated from the corresponding azo compound.[5]For intermolecular addition reactions with the alkene **16**, the reaction rates for the intermediates generated by reduction of the cyclohexylmercury salt **13**[6] and by photolysis of the cyclohexylcobaloxime **14** were also identical within the limits of experimental error (Table 1). Since the mercury salt gives rise to uncomplexed radicals, these reactivity experiments lead to the conclusion that free radicals are formed in the photolysis of cobaloximes.

These findings were supported by stereochemical studies. Thus, in the cyclization of the 1-methylhexenylcobal-

[*] Prof. Dr. B. Giese, Dipl.-Ing. J. Hartung, Dipl.-Ing. J. He, Dipl.-Ing. O. Hüter, Dipl.-Ing. A. Koch
Institut für Organische Chemie der Technischen Hochschule
Petersenstrasse 22, D-6100 Darmstadt (FRG)

[**] This work was supported by the Stiftung Volkswagenwerk.

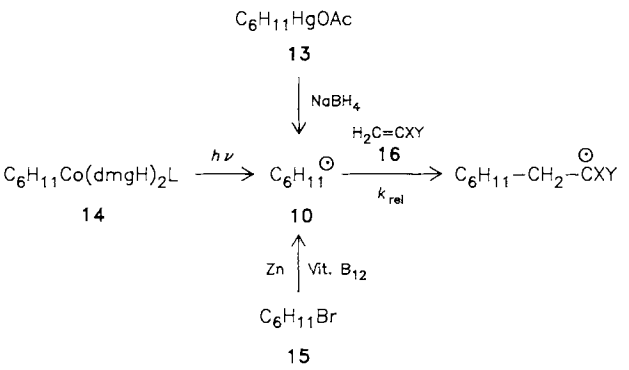
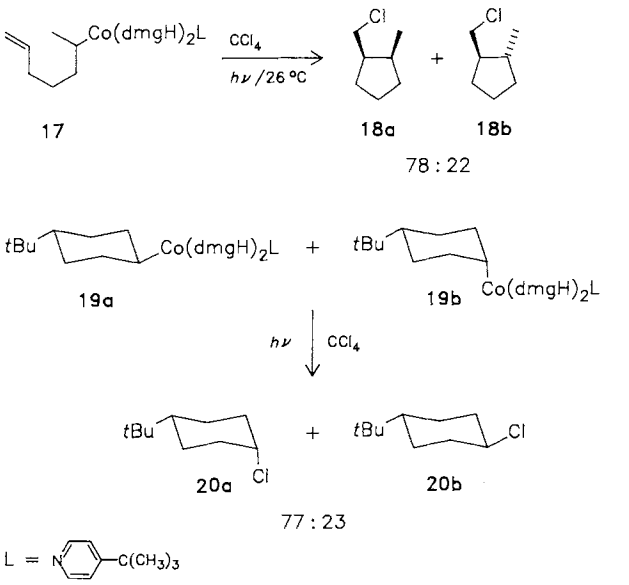


Table 1. Reactivity k_{rel} (20°C) of the alkenes **16** in C–C coupling with the cyclohexyl radical **10** which was generated from different precursors. L in **14** = pyridine.

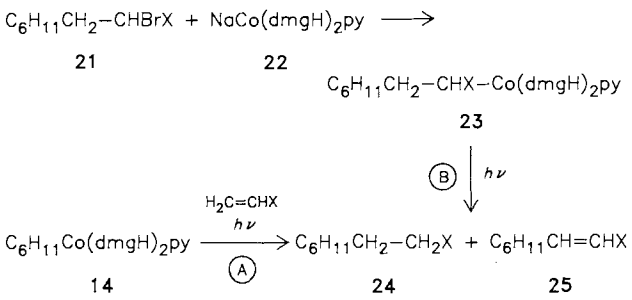
Alkene 16		k_{rel} with different radical sources		
X	Y	**13** ($NaBH_4$) [a]	**14** ($h\nu$) [a]	**15** (Zn/Vit. B_{12}) [b]
CH_3	C_6H_5	0.04	—	0.04
EtO	CN	0.14	0.13	—
CH_3	CO_2Et	0.21	—	0.22
H	CO_2Et	0.27	—	0.27
CH_3	CN	0.58	—	0.61
H	CN	≡1.00	≡1.00	≡1.00
Cl	CO_2Et	3.1	2.6	—
Cl	CN	8.8	11	—

[a] Solvent: CH_2Cl_2. [b] Solvent: DMF.

oxime **17**, formation of the *cis*-disubstituted cyclopentane is favored (**18a** : **18b** = 78 : 22, 26°C) and, independent of their configuration, the *tert*-butylcyclohexylcobaloximes **19a** and **19b** react with CCl_4 to afford the chlorides **20a** and **20b** in the ratio 77 : 23. These stereoselectivities correspond with those of free, uncomplexed radicals.[7]



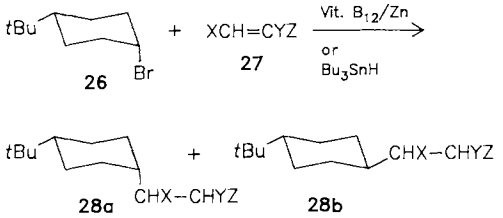
According to these results, the C–C coupling products **2** and **3** are formed via the free radical **4** in the photolysis of the cobaloxime **1**. The question remains as to whether the "adduct cobaloxime" **6** is an intermediate in this reaction. In order to answer this question, we prepared independently the cobaloximes **23** from the corresponding bromides **21** and the Co^I complex **22**.[8] Photolysis of **23** affords the alkanes **24** and the alkenes **25** in a ratio which depends on the substituent X and the solvent. The data show that the photochemical reaction of the cobaloxime **14** (≅ **1**) with alkenes (Reaction Ⓐ) and the irradiation of the adduct cobaloxime **23** (≅ **6**) (Reaction Ⓑ) have identical product ratios. The amount of alkanes **24** in the product mixture increases with increasing electron withdrawing character of the substituent X and upon changing from an aprotic to a protic solvent. Furthermore, when the experiments were carried out in CH_3OD a deuterium atom was incorporated. This indicates an ionic cleavage of the cobalt–carbon bond in the formation of alkanes. The alkenes **25** are formed by elimination of hydridocobaloxime from the cobaloxime **23**.[9]



X	Solvent	Reaction Ⓐ **24** : **25**	Reaction Ⓐ *E* : *Z* (**25**)	Reaction Ⓑ **24** : **25**	Reaction Ⓑ *E* : *Z* (**25**)
CO_2Et	CH_2Cl_2	0 : 100	20 : 1	0 : 100	20 : 1
	CH_3CO_2H	58 : 42	20 : 1	58 : 42	20 : 1
CN	CH_2Cl_2	29 : 71	1.4 : 1	23 : 77	1.1 : 1
	CH_3CO_2H	90 : 10	2.4 : 1	88 : 12	2.0 : 1

Uncomplexed free radicals are also involved in the vitamin B_{12} catalyzed C–C coupling of alkyl halides with alkenes. This is shown by the reaction rates of the alkenes **16** when the cyclohexyl radical is generated by the method of *Scheffold* et al.[10] from cyclohexyl bromide **15**, vitamin B_{12}, and Zn (Table 1). Furthermore, the stereoselectivity is independent of whether the radical intermediate is prepared from *tert*-butylcyclohexyl bromide with vitamin B_{12} or with tributylstannane.

The proof of the occurrence of uncomplexed radicals presented here is important for the design of syntheses us-



X	Alkene 27 Y	Z	Vit. B_{12} **28a** : **28b**	Bu_3SnH **28a** : **28b**
H	CO_2Et	CO_2Et	61 : 39	56 : 44
CN	H	CN	44 : 56	40 : 60
Me	H	CN	30 : 70	27 : 73
Me	CO_2Et	CO_2Et	30 : 70	27 : 73
*i*Pr	CO_2Et	CO_2Et	11 : 89	12 : 88

ing cobaloximes and has implications for the discussion of vitamin B_{12} catalyzed reactions in living organisms.[11]

Received: October 20, 1988 [Z 3018 IE]
German version: *Angew. Chem. 101* (1989) 334

[1] a) M. Tada, M. Okabe, *Chem. Lett. 1980*, 201; b) B. P. Branchaud, M. S. Meier, Y. Choi, *Tetrahedron Lett. 29* (1988) 167; c) A. Ghosez, T. Göbel, B. Giese, *Chem. Ber. 121* (1988) 1807; d) Salophen Co complexes have also been used: V. F. Patel, G. Pattenden, *J. Chem. Soc. Chem. Commun. 1987*, 871.

[2] a) B. P. Branchaud, M. S. Meier, M. N. Malekzadeh, *J. Org. Chem. 52* (1987) 212; b) V. F. Patel, G. Pattenden, *Tetrahedron Lett. 28* (1987) 1451.

[3] a) P. Maillard, C. Gianotti, *Can. J. Chem. 60* (1982) 1402; b) D. W. R. Rao, M. C. R. Symons, *J. Chem. Soc. Faraday Trans. 1 1984*, 423.

[4] C. Chatgilialoglu, K. U. Ingold, J. C. Scaiano, *J. Am. Chem. Soc. 103* (1981) 7739.

[5] D. R. Jewell, L. Mathew, J. Warkentin, *Can. J. Chem. 65* (1987) 311.

[6] B. Giese, *Angew. Chem. 95* (1983) 771; *Angew. Chem. Int. Ed. Engl. 22* (1983) 753.

[7] a) A. L. J. Beckwith, I. A. Blair, G. Phillipou, *J. Am. Chem. Soc. 96* (1974) 1613; b) F. D. Greene, C. C. Chu, J. Walia, *J. Org. Chem. 29* (1964) 728.

[8] The structures of the cobaloximes **23** (X = CO_2Et, CN) were confirmed by elemental analyses and IR and NMR spectroscopy. The ^1H NMR data (300 MHz, $CDCl_3$) are particularly characteristic: **23** (X = CO_2Et): δ = 0.55–1.17 (m, 8H, cyclohexyl + CH_2), 1.22 (t, 3H, J = 7.5 Hz, CH_3, ethylester), 1.50–1.64 (m, 5H, cyclohexyl + CH_2), 2.09–2.13 (m, 1H, Co–CH), 2.18 (s, 6H, CH_3, Hdmg), 2.21 (s, 6H, CH_3, Hdmg), 3.89–3.91 (m, 2H, CH_2, ethyl ester), 7.27–7.30 (m, 2H, pyridine), 7.68–7.73 (m, 1H, pyridine), 8.49–8.51 (m, 2H, pyridine), 17.89 (s, 2H, OH).—**23** (X = CN): δ = 0.48–2.20 (m, 14H), 2.23 (s, 6H, CH_3), 2.26 (s, 6H, CH_3), 7.28–7.34 (m, 2H, pyridine), 7.71–7.77 (m, 1H, pyridine), 8.45–8.49 (m, 2H, pyridine), 18.05 (s, 2H, OH).

[9] For the elimination mechanism see S. Derenne, A. Gaudemer, M. D. Johnson, *J. Organomet. Chem. 322* (1987) 22.

[10] R. Scheffold, M. Dike, S. Dike, T. Herold, L. Walder, *J. Am. Chem. Soc. 102* (1980) 3642; R. Scheffold, L. Walder, C. Weymuth, *Pure Appl. Chem. 59* (1987) 363; R. Scheffold, *Nachr. Chem. Tech. Lab. 36* (1988) 261.

[11] In enzyme reactions, both the position and the conformation of the radical may be determined by the enzyme, see J. Retey, J. A. Robinson: *Stereospecificity in Organic Chemistry and Enzymology*, Verlag Chemie, Weinheim 1982; J. Halpern, *Science (Washington, D.C.) 227* (1985) 869.

Correlation of the Dynamic Behavior of *n*-Alkyl Ligands of the Stationary Phase with the Retention Times of Paracelsin Peptides in Reversed Phase HPLC

By *Bettina Pfleiderer, Klaus Albert, Klaus D. Lork, Klaus K. Unger, Hans Brückner,* and *Ernst Bayer**

In reversed phase high performance liquid chromatography (RP-HPLC), the retention of substances and the selectivity of the separation are influenced by the following properties of the basis gel: chemical structure and surface of the basis gel, and the nature, chain length, and density of the hydrophobic ligands. In this study, we have determined the mobility of *n*-alkyl ligands on silica gel using ^{13}C CP/MAS NMR spectroscopy and have correlated this with the unusual retention behavior of paracelsin peptides on these RP carriers. The natural mixture of sequence-analogous eicosapeptides (Scheme 1) which was used is of great interest because of its antibiotic and membrane active properties, such as hemolysis of erythrocytes and voltage dependent ionic conductivity in liquid bilayer membranes.[1–3]

1	2	3	4	5	6	7	8	9	10	11	12	13	14	15	16	17	18	19	20	
Ac-	Aib-	Ala-	Aib-	Ala-	Aib-	**Ala**-	Gln-	Aib-	**Val**-	Aib-	Gly-	Aib-	Aib-	Pro-	Val-	Aib-	Aib-	Gln-	Gln-	Pheol **A**
Ac-	Aib-	Ala-	Aib-	Ala-	Aib-	**Ala**-	Gln-	Aib-	**Leu**-	Aib-	Gly-	Aib-	Aib-	Pro-	Val-	Aib-	Aib-	Gln-	Gln-	Pheol **B**
Ac-	Aib-	Ala-	Aib-	Ala-	Aib-	**Aib**-	Gln-	Aib-	**Val**-	Aib-	Gly-	Aib-	Aib-	Pro-	Val-	Aib-	Aib-	Gln-	Gln-	Pheol **C**
Ac-	Aib-	Ala-	Aib-	Ala-	Aib-	**Aib**-	Gln-	Aib-	**Leu**	Aib-	Gly-	Aib-	Aib-	Pro-	Val-	Aib-	Aib-	Gln-	Gln-	Pheol **D**

Scheme 1. Structure of the paracelsin peptides **A**–**D**. Ac = Acetyl; Aib = α-aminobutyric acid (2-methylalanine), Pheol = phenylalaninol; all chiral components have the L configuration.

RP materials with *n*-alkyl chain lengths $1 < n < 20$ were prepared by reacting LiChrospher (Si 100, 10 μm) with the appropriate *n*-alkyldimethylchlorosilane.[4] The ligand density was 3.5 ± 0.2 mol m^{-2}.

Since changes in the mobility of *n*-alkyl groups are revealed by the relaxation behavior of the carbon atoms, they can be characterized through determination of the spin-lattice relaxation times T_1[5] or the relaxation times in the rotating coordinate system $T_{1\rho H}$.[6] We chose the $T_{1\rho H}$ values of the protons as a measure of the mobility of the alkyl chains, since $T_{1\rho H}$ gives information about rates of motion in the kHz range,[6] and because relatively small changes in the mobility result in large changes in the $T_{1\rho H}$ times. In contrast, the T_1 times, which are sensitive in the MHz range, exhibit only small differences.[7] In the range of slow molecular motions, the $T_{1\rho H}$ values are averaged completely by ^{13}C-^1H dipolar interactions.[8] However, the high mobility of the alkyl chains, which exhibit liquid-like behavior, and the additional rapid rotation of the probe at the magic angle (MAS, $\nu_{rot} = 4000$–5000 Hz) lead to a drastic reduction in the dipolar interactions, so that averaging by spin diffusion does not occur in these systems. This phenomenon has been observed by *Alemany* et al. for highly mobile molecules.[9, 10]

Solid-state NMR spectroscopy on C_8 and C_{18} phases has shown that the total mobility of the C_{18} chain is smaller than that of the C_8 chain.[11] For a more thorough investigation, materials with n = 4, 5, 6, 8, 10, 12, 14, and 18 were selected for $T_{1\rho H}$ measurements using ^{13}C CP/MAS NMR spectroscopy. Figure 1 shows the dependence of the relaxation times $T_{1\rho H}$ of the terminal methyl groups of the stationary phase upon the alkyl chain length n. Analogous behavior was observed for the (n − 1) and (n − 2) methylene groups of the respective *n*-alkyl ligands. Surprisingly, a maximum in the $T_{1\rho H}$ value of ca. 80 ms occurs for a chain length of n = 6–8. The $T_{1\rho H}$ values of the alkyl chain carbon atoms of the C_4 and C_8 phases are given for comparison in Table 1. In the case of the C_8 phase (and also the C_5 and C_6 phases), they increase in the direction of the terminal methyl group, whereas in the C_4 phase they are practically identical for all positions.

The temperature dependence of the relaxation times revealed that an increase in the $T_{1\rho H}$ values corresponds to a higher mobility of the *n*-alkyl chain. Thus, the relatively small $T_{1\rho H}$ values of the C_4 phase indicate a low motional

[*] Prof. Dr. E. Bayer, Dipl.-Chem. B. Pfleiderer, Dr. K. Albert
Institut für Organische Chemie der Universität
Auf der Morgenstelle 18, D-7400 Tübingen (FRG)
Dr. K. D. Lork, Prof. Dr. K. K. Unger
Institut für Anorganische Chemie und Analytische Chemie der Universität
J.-J.-Becher-Weg 24, D-6500 Mainz (FRG)
Prov.-Doz. Dr. H. Brückner
Institut für Lebensmitteltechnologie der Universität Hohenheim
Postfach 700562, D-7000 Stuttgart 70 (FRG)

 © VCH Verlagsgesellschaft mbH, D-6940 Weinheim, 1989 0570-0833/89/0303-0327 $ 02.50/0

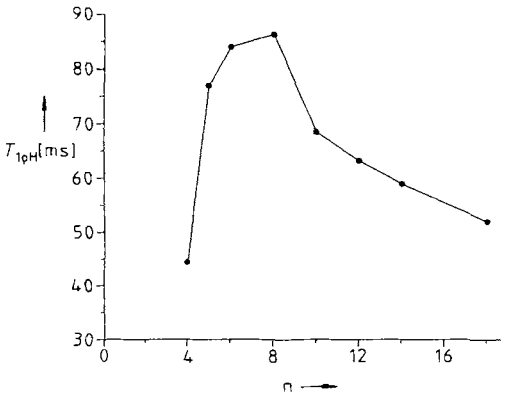


Fig. 1. Dependence of the $T_{1\rho H}$ values of the terminal methyl groups on the chain length n of the *n*-alkyl ligands.

Table 1. $T_{1\rho H}$ values [ms] of the alkyl chain carbon atoms of the C_4 and C_8 phases.

	C-1	C-2	C-3	C-4	C-5	C-6	C-7	C-8
C_4 phase	37.0	41.0	42.5	44.4				
C_8 phase	56.2	62.5	61.8	71.8	71.8	64.7	78.0	86.3

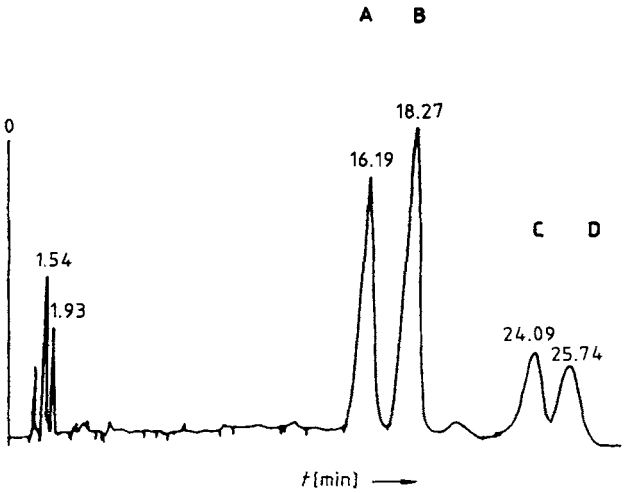


Fig. 2. HPLC chromatogram of the natural mixture of paracelsin peptides **A**, **B**, **C**, and **D**; t = retention time. Chromatographic conditions: column: 250 mm × 4.6 mm; stationary phase: LiChrospher RP-8, Si 100 (Merck), 5 μm; eluent: acetonitrile/methanol/water (39/39/22); UV detection at $\lambda = 206$ nm; $T = 303$ K; flow rate: 1 mL min^{-1}; quantity injected: ca. 20 μg peptide mixture in 20 μL methanol.

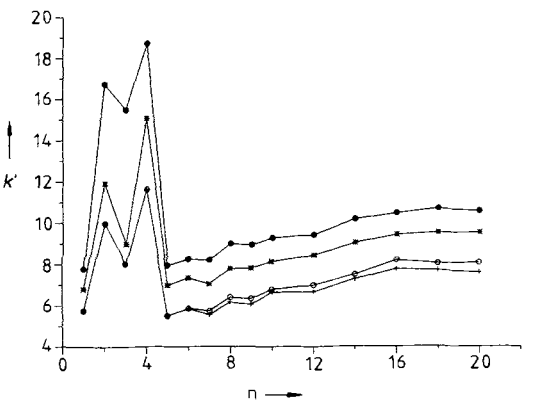


Fig. 3. Dependence of the capacity factors k' of the paracelsin peptides **A** (+), **B** (○), **C** (*), and **D** (●) on the alkyl chain length n; k' is defined as $(t - t_0)/t_0$, where t_0 = retention time of water. Chromatographic conditions as in Fig. 2, but with LiChrospher, Si 100 (Merck), 5 μm, chemically modified with *n*-alkyldimethylchlorosilanes, n = 2–20, as stationary phase.

freedom for all the carbon atoms of this phase, and the maximum of the methyl $T_{1\rho H}$ value at n = 6–8 means that the mobility of the terminal methyl group is highest for chains of these lengths. The mobility becomes increasingly restricted for chains with n > 10 and approaches that found for n = 4. A similar behavior, albeit without a pronounced maximum, has been found in relaxation time measurements on RP phases in suspension.[12] The strength of the dependence of the mobility upon the chain length is influenced by the solvating ability of the suspending liquid.[13, 14]

The mobility of the *n*-alkyl ligands reflects their conformational behavior. Suitable sensors for the determination of conformation are, for example, peptides and proteins, for which the conformation influences the interaction with the stationary phase. A connection between the retention of peptides in RP-HPLC and their conformational behavior has been found by *Houghten* and *Ostrech*.[15] The HPLC elution profile of the paracelsin peptides **A**–**D** (see Scheme 1) on a C_8 phase showed that a complete separation of the compounds is possible, in spite of the extremely small structural differences (only one CH_2 group more from **A** to **B** and from **C** to **D**).

This finding led to a systematic investigation of the dependence of the retention of paracelsin peptides on the alkyl chain length n. In this manner, an unusual behavior was detected (Fig. 3). Maxima in the retention, and therefore also in the capacity factors k', occur for n = 2 and 4. Beyond n = 5, the retention times increase only slightly and are comparable with that retained for a C_1 phase. The same behavior, although less pronounced, was observed also when binary eluents (methanol/water 85/15 *v/v*) were used. It was also found that the retention times of the peptides decrease on going from n to (n + 1) when n is an even number.

Comparing the dependence of the methyl $T_{1\rho H}$ values of the stationary phase and of the capacity factors k' of the paracelsin peptides upon the chain length n shows that a maximum in the retention corresponds to a minimum in the mobility of the *n*-alkyl chain. This can be explained by the assumption that the low mobility of the alkyl chains of the C_4 phase reflects a conformation (preferably a *trans-gauche* conformation) which facilitates a maximum steric interaction with the paracelsin peptides.

A comparison of the parcelsin components **B** and **C** is illustrative for the separation behavior. The replacement of Ala by Aib in position 6 and of Leu by Val in position 9 (cf. Scheme 1) leads to isobaric peptides of nominal atomic mass 1921. Nevertheless, the k' values of **C** are considerably larger than those of **B**. This can be explained by the fact that the (formal) removal of a CH_2 group from position 9 of **B** (replacement of Leu by Val) and its introduction in position 6 (replacement of Ala by Aib) leads to a more lipophilic peptide which interacts more strongly with the RP phase. The interaction with the stationary phase is favored by the remarkably stable helical conformation of the paracelsin peptides, which has been detected by circular dichroic measurements and by temperature dependent ^{13}C NMR spectroscopy.[1] A predominantly α-helical structure is assumed, in analogy with the crystal structure of the paracelsin analogue alamethicin.[16] In contrast, protected homopeptides of Aib have 3_{10} helical structures.[17–19]

From the α-helical projection[20] of the paracelsin peptides, it can be seen that the amino acids in positions 6 and 9 lie on the same side of the helix. If a horizontal interaction of the peptide helix with the stationary phase is assumed, the alkyl side chains of these amino acids point directly towards the relatively rigid alkyl chains of the C_4 phase; this leads to optimum interaction and thus to maximum k' values for the paracelsin peptides on the C_4 phase.

Received: September 22, 1988 [Z 2975 1E]
German version: *Angew. Chem. 101* (1989) 336

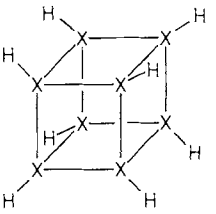
[1] H. Brückner, H. Graf, M. Bokel, *Experientia 40* (1984) 1189.
[2] M. Przybylski, I. Dietrich, I. Manz, H. Brückner, *Biomed. Mass Spectrom. 11* (1984) 569.
[3] G. Boheim, W. Hanke, G. Jung, *Biophys. Struct. Mech. 8* (1983) 181.
[4] K.-D. Lork, K. K. Unger, J. N. Kinkel, *J. Chromatogr. 352* (1986) 199.
[5] M. Gangoda, R. K. Gilpin, B. M. Fung, *J. Magn. Reson. 74* (1987) 134.
[6] G. E. Maciel, D. W. Sindorf, *J. Am. Chem. Soc. 102* (1980) 7606.
[7] J. Schäfer, M. D. Sefcik, E. O. Stejskal, R. A. McKay, *Macromolecules 14* (1981) 275.
[8] P. Caravetti, J. A. Deli, G. Bodenhausen, R. R. Ernst, *J. Am. Chem. Soc. 104* (1982) 5506.
[9] L. B. Alemany, D. B. Grant, R. J. Pugmire, T. D. Alger, K. W. Zilm, *J. Am. Chem. Soc. 105* (1983) 2133.
[10] L. B. Alemany, D. B. Grant, R. J. Pugmire, T. D. Alger, K. W. Zilm, *J. Am. Chem. Soc. 105* (1983) 2142.
[11] D. W. Sindorf, G. E. Maciel, *J. Am. Chem. Soc. 105* (1983) 1848.
[12] R. K. Gilpin, *Anal. Chem. 57* (1985) 1465.
[13] K. Albert, B. Evers, E. Bayer, *J. Magn. Reson. 62* (1985) 428.
[14] E. Bayer, A. Paulus, B. Peters, G. Laupp, K. Albert, *J. Chromatogr. 364* (1986) 25.
[15] R. A. Houghten, J. M. Ostresh, *Biochromatography 2* (1986) 80.
[16] R. O. Fox, F. M. Richards, *Nature (London) 300* (1982) 325.
[17] R.-P. Hummel, C. Toniolo, G. Jung, *Angew. Chem. 99* (1987) 1180; *Angew. Chem. Int. Ed. Engl. 26* (1987) 1150.
[18] G. Jung, R.-P. Hummel, K. P. Voges, K. Albert, C. Toniolo in G. R. Marshall (Eds.): *Peptides, Chemistry and Biology*, Escom, Leiden 1988, p. 37.
[19] H. Brückner in W. A. König, W. Voelter (Eds.): *Chemistry of Peptides and Proteins, Vol. 4*, Attempto Verlag, Tübingen 1988, in press.
[20] M. Schiffer, A. B. Edmundson, *Biophys. J. 7* (1967) 1219.

Much Less Strained Cubane Analogues with Si, Ge, Sn, and Pb Skeletons**

By *Shigeru Nagase**

Polyhedral carbon compounds such as tetrahedrane (C_4H_4), prismane (C_6H_6), and cubane (C_8H_8) have long formed interesting synthetic targets in organic chemistry;[1] among these, cubane is especially intriguing because of its high O_h symmetry and high strain.[2] There is currently considerable interest in replacing the carbons in these compounds by heavier homologues such as silicon in the expectation of unprecedented physical and chemical properties.[3]

As we have demonstrated in a recent theoretical study on persilatetrahedrane,[4] polyhedral silicon compounds consisting of only fused three-membered rings possess high strain and are subject to "bond stretch" isomerism.[5,6] In contrast, we have shown that they become significantly less strained than the corresponding carbon compounds as the number of fused four-membered rings increases.[7] Thus, persilacubane **1**, having six fused four-membered Si rings, is much less strained than cubane.[7,8] Indeed, the first polyhedral silicon compound, a persilacubane derivative (**1** with tBuMe$_2$Si instead of H) was recently synthesized and its novel properties were investigated.[9]



1, X = Si
2, X = Ge
3, X = Sn
4, X = Pb

We report now ab initio calculations of the structures and strain of still heavier cubane homologues, pergermacubane **2**, perstannacubane **3**, and perplumbacubane **4**. Geometries were fully optimized at the Hartree-Fock (HF) level with the GAUSSIAN 82 program[10] by using the ab initio effective core potentials[11] and the double-zeta (DZ) basis sets[12] augmented by a set of six d-type polarization functions[13] on each heavy atom.

Table 1. Optimized bond lengths and ionization potentials (I_p) of cubane and its homologues **1**–**4** of O_h symmetry [a].

	C_8H_8 [b]	**1**	**2**	**3**	**4**
d_{X-X} [Å]	1.559	2.382	2.527	2.887	2.949
d_{X-H} [Å]	1.081	1.477	1.542	1.714	1.744
I_p [eV] [c]	10.4	8.3	7.7	7.1	6.6

[a] The total energies are −34.78608 (**1**), −33.85480 (**2**), −30.72293 (**3**), and −31.25989 (**4**) a.u. [b] HF/6-31G* values taken from [7]. For the electron diffraction values of d_{C-C} (1.575 Å) and d_{C-H} (1.100), see A. Almenningen, T. Jonvik, H. D. Martin, T. Urbanek, *J. Mol. Struct. 128* (1985) 239. [c] Based on Koopmans' theorem.

Table 1 shows the optimized structures of **1**–**4** together with the ionization potentials. The Si–Si, Ge–Ge, Sn–Sn, and Pb–Pb bond distances in the cubic skeletons are only ca. 0.02–0.04 Å longer at the HF/DZ+d level than those in the four-membered rings of cyclotetrasilane (2.363 Å), cyclotetragermane (2.508), cyclotetrastannane (2.867), and cyclotetraplumbane (2.908). The bond distances in the strain-free molecules X_2H_6 were calculated to be 2.344 (Si), 2.480 (Ge), 2.839 (Sn). and 2.868 (Pb) Å.

The Si–Si bond distances of 2.382 Å in **1** compare favorably with the values of 2.38–2.45 Å in the X-ray structure of the derivative Si_8R_8 synthesized recently:[9] the somewhat longer bond distances and slightly distorted cubic structure (∢SiSiSi = 87–92°) in this derivative are most likely ascribable to the presence of the bulky tBuMe$_2$Si groups.

$$X_8H_8 + 12\,H_3X{-}XH_3 \longrightarrow 8\,HX(XH_3)_3 \qquad \text{(a)}$$

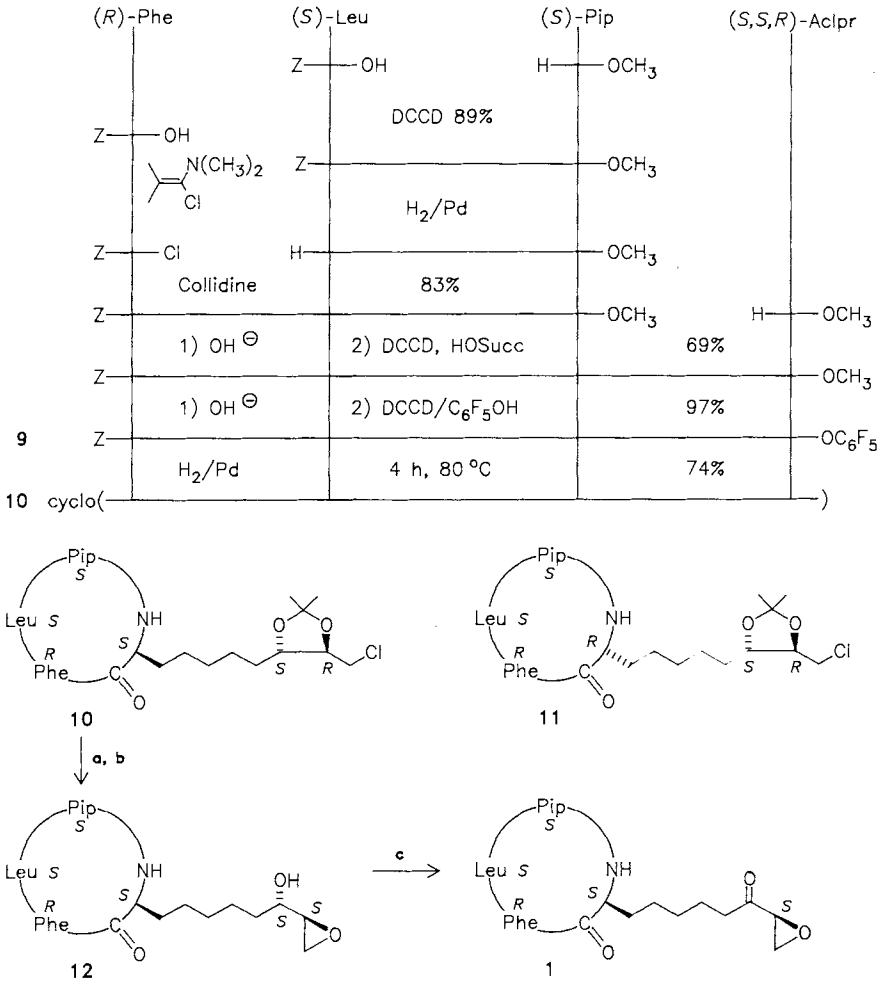
1–**4**

X = Si, Ge, Sn, Pb

Table 2 summarizes the strain energies calculated from the so-called homodesmotic reactions (a).[14,15] It should be noted that the strain energy of 99.1 kcal mol^{-1} calculated for **1** agrees reasonably well with our previous HF/6-31G* value of 93.5 kcal mol^{-1}.[7]

[*] Prof. S. Nagase
Department of Chemistry, Faculty of Education
Yokohama National University, Yokohama 240 (Japan)

[**] This work was supported in part by a grant from the Ministry of Education, Science, and Culture in Japan. Calculations were carried out at the Computer Center of the Institute of Molecular Science.



Scheme 2. (*S,S,R*)-Aclpr = 8,9-*O*-isopropylidene-protected amino-10-chloro-8,9-dihydroxydecanoic acid. a) oxalic acid/dioxane/H_2O, 80°C, 12 h; b) K_2CO_3/CH_3OH, RT, 4 h; c) DCCD/DMSO/dichloroacetic acid.

on the other hand—which is also catalyzed by 4-pyrrolidinopyridine—this inversion of configuration is of secondary importance,[12] because the configurationally stable ring is quickly closed. Hydrolysis of the isopropylidene compound **10** and epoxide formation yielded **12**, which reacts with DMSO/DCCD to give the epoxyketone **1**. The NMR spectrum, mass spectrum and α_D^{20} value were identical with those of the natural product.

Received: October 10, 1988 [Z 3000 IE]
German version: *Angew. Chem. 101* (1989) 344

CAS Registry numbers:
1, 86402-37-1; **9**, 118891-72-8; **10**, 118891-73-9; **11**, 119006-95-0; **12**, 118891-74-0; Z-(*S*)-Leu-OH, 2018-66-8; H-(*S*)-Pip-OCH_3, 90710-04-6; Z-(*R*)-Phe-OH, 2448-45-5; H-(*S,S,R*)-Aclpr-OCH_3, 118891-77-3; Z-(*R*)-Phe-Cl, 118234-98-3; Z-(*S*)-Leu-(*S*)-Pip-OCH_3, 118891-75-1; H-(*S*)-Leu-(*S*)-Pip-OCH_3, 118891-76-2; Z-(*R*)-Phe-(*S*)-Leu-(*S*)-Pip-OCH_3, 118333-11-2; Z-(*R*)-Phe-(*S*)-Leu-(*S*)-Pip-(*S,S,R*)-AclprOC_6F_5, 118891-78-4.

[1] K. Umehara, K. Nakahara, S. Kiyoto, M. Iwami, M. Okamoto, H. Tanaka, M. Kohsaka, H. Aoki, H. Imanaka, *J. Antibiot. 36* (1983) 478.
[2] M. Kawai, R. S. Pottorf, D. H. Rich, *J. Med. Chem. 29* (1986) 2409.
[3] A. Closse, R. Huguenin, *Helv. Chim. Acta 57* (1974) 533.
[4] M. Kawai, D. H. Rich, J. D. Walton, *Biochem. Biophys. Res. Commun. 111* (1983) 398.
[5] S.-D. Kim, H. W. Knoche, L. D. Dunkle, D. A. McCrery, K. B. Tomer, *Tetrahedron Lett. 26* (1985) 969.
[6] S. P. Tanis, B. A. Horenstein, R. P. Scheffer, J. B. Rasmussen, *Heterocycles 24* (1986) 3423.
[7] S. Takayama, A. Isogai, M. Nakata, H. Suzuki, A. Suzuki, *Agric. Biol. Chem. 48* (1984) 839.
[8] A. Hirota, A. Suzuki, K. Aizawa, S. Tamura, *Agric. Biol. Chem. 37* (1973) 955.
[9] U. Schmidt, A. Lieberknecht, H. Griesser, F. Bartkowiak, *Angew. Chem. 96* (1984) 310; *Angew. Chem. Int. Ed. Engl. 23* (1984) 318.
[10] R. Jacquier, R. Lazaro, H. Ranirisehena, Ph. Viallefont, *Tetrahedron Lett. 27* (1986) 4735.
[11] M. Kawai, J. H. Gardner, D. H. Rich, *Tetrahedron Lett. 27* (1986) 1877.
[12] All attempts to isomerize the cyclopeptide **10** by prolonged heating to 80°C with 1,8-diazabicyclo[5.4.0]undec-7-ene or 4-pyrrolidinopyridine failed.

Alkyl and Alkylidyne Complexes of Rhenium**

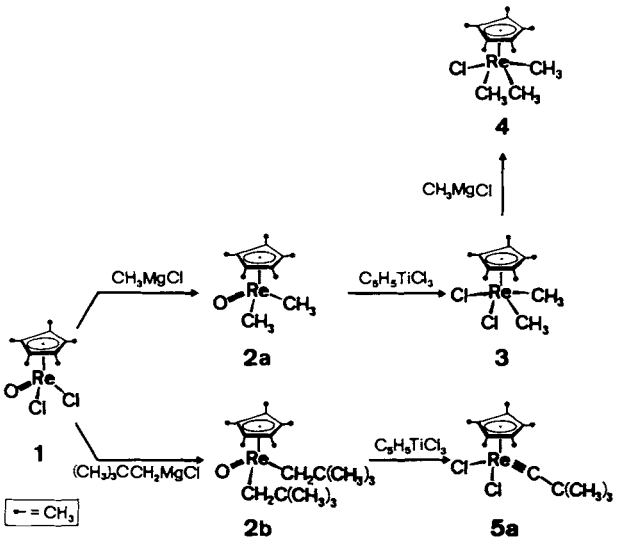
By *Josef K. Felixberger, Paul Kiprof, Eberhardt Herdtweck, Wolfgang A. Herrmann,* Ralf Jakobi,* and *Philipp Gütlich**

Because of its great variety of oxidation states, the element rhenium allows the fixation of many different types of ligand in stable complexes, and the catalytic activity of some rhenium complexes is based on the readily achieved,

[*] Prof. Dr. W. A. Herrmann, J. K. Felixberger, P. Kiprof, Dr. E. Herdtweck
Anorganisch-chemisches Institut der Technischen Universität München
Lichtenbergstrasse 4, D-8046 Garching (FRG)
Prof. Dr. P. Gütlich, R. Jakobi
Institut für Anorganische Chemie und Analytische Chemie der Universität
Staudinger-Weg 9, D-6500 Mainz (FRG)

[**] Multiple Bonds between Main Group Elements and Transition Metals, Part 63. This work was supported by the Deutsche Forschungsgemeinschaft, the Merck'sche Stiftung für Kunst und Wissenschaft e.V. (Stipendium for *J. K. F.*), the Fonds der Chemischen Industrie, and Degussa AG. Part 62: W. A. Herrmann, R. A. Fischer, E. Herdtweck, *J. Am. Chem. Soc.*, in press.

reversible change in the metal oxidation state.[1] Whereas methylrhenium(VII) oxide CH_3ReO_3[2] is an effective catalyst for the metathesis of olefins,[3] the sterically less readily accessible d^0-Re^{VII} complex $(\eta^5\text{-}C_5Me_5)ReO_3$, and in particular its reduced derivative **1** (d^2-Re^V), are suitable precursors for the preparation of model compounds for these reactions. We now report on stepwise alkylation and halogenation reactions, which afford new alkylidyne complexes of rhenium in high oxidation states, and which can be expected to be applicable to other organometallic oxides.



Scheme 1.

As shown in Scheme 1, the oxodichloride **1** can be converted into the known dimethyl derivative **2**[1] using methylmagnesium chloride (75% yield). The selectivity of the reaction is demonstrated by the fact that methylation at the ReO group does not occur. A less direct route involving a chlorination step allowed the synthesis of alkyl(halogen) derivatives without changing the metal oxidation state. Thus, reaction of the oxophilic chlorinating agent trichloro(η^5-cyclopentadienyl)titanium(IV) with **2a** yields the isolable intermediate *dimethyl* product **3**, which can be selectively methylated to afford the otherwise inaccessible *trimethyl* derivative **4** (Scheme 1). The analogous *tetramethyl* compound can be obtained by further reaction with the Grignard reagent, but is more easily prepared by exhaustive methylation of $(\eta^5\text{-}C_5Me_5)ReCl_4$.[4] Thus, the complete series of compounds $(\eta^5\text{-}C_5Me_5)Re(CH_3)_nCl_{4-n}$ (n = 0–4) is now available.

Although the alkylation and chlorination of **1** and **2** described here can in general be extended to higher alkyl derivatives, further, special reactions of the products cannot be excluded. An example with interesting preparative consequences is provided by the neopentyl compound **2b**. Once again, the organotitanium(IV) reagent proved to be suitable for the intended oxygen-chlorine exchange, but this reaction was followed by oxidation of the metal center with concomitant elimination of neopentane (GC and ^1H NMR detection). The isolable final product, obtained in 65% yield, was the blue, paramagnetic alkylidyne-Re^{VI} complex **5a** (Scheme 1), whose identity was confirmed by elemental analysis, vapor pressure osmometry, mass spectroscopy, and ESR spectroscopy. The ESR spectrum of **5a** (toluene solution) exhibits a sextet signal pattern ($I = 5/2$; $^{185}Re/^{187}Re$, $\langle g\rangle = 2.050$, $\langle A\rangle = 233 \times 10^{-4}$ cm^{-1}; **5b**, $\langle g\rangle =$ 2.074, $\langle A\rangle = 196 \times 10^{-4}$ cm^{-1}; **5c**, $\langle g\rangle = 2.104$) and thus corresponds with that expected for a d^1 spin system of hexavalent rhenium. Unlike those of **5a** and **5b**, the ESR spectrum of **5c** shows a singlet. Obviously the unpaired electron in this complex does not couple with the rhenium atom. The paramagnetic nature of **5a** was confirmed by magnetic measurements. The complex follows almost precisely the Curie law (Fig. 1a) and the effective magnetic moment closely approaches the theoretical value for a d^1 system of 1.73 B.M. (Fig. 1b). This means that the central atom is indeed present in a higher oxidation state (Re^{VI}) and that the electron density at the carbyne carbon atom (formally a trianion) is very high.[5]

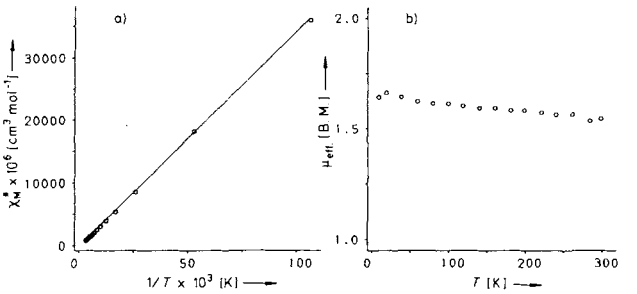
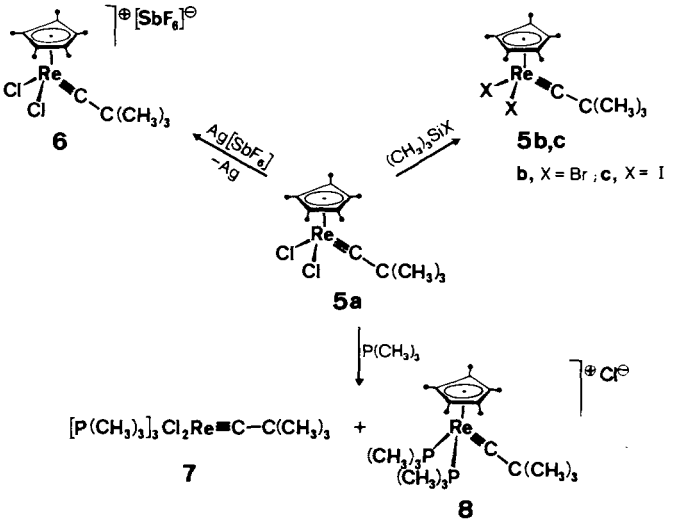


Fig. 1. Results of magnetic measurements on **5a**. a) χ_M^* as a function of reciprocal temperature. **5a** closely follows the Curie law ($\chi_M^* = C/T$, C = Curie konstant = 0.344(1) cm^3 mol^{-1}). b) Effective magnetic moment μ_{eff} as a function of temperature (cf. text).

As shown in Scheme 2, **5a** is converted by trimethylsilyl halides $(CH_3)_3SiX$ (X = Br, I) into the thermally stable, paramagnetic derivatives **5b** (green) and **5c** (brown). A structural assignment for the solid state was based on a single crystal X-ray analysis of the bromo compound **5b**[6] (Fig. 2). The Re–Cl distance of 167(1) pm is extremely short, as is typical for a rhenium–carbon triple bond length of ca. 173 pm.[7] The sequence of atoms Re≡C–C is almost linear (173(1)°). Two bromine atoms and the centrally coordinated C_5Me_5 ligand complete the distorted tetrahedral coordination geometry (Fig. 2).



Scheme 2.

The new alkylidyne complexes **5a–c** undergo reversible one-electron oxidations (**5a**: $E_{1/2} = 0.71$ V, CH_2Cl_2 solution, vs. Ag/AgCl). As would be expected from the cyclo-

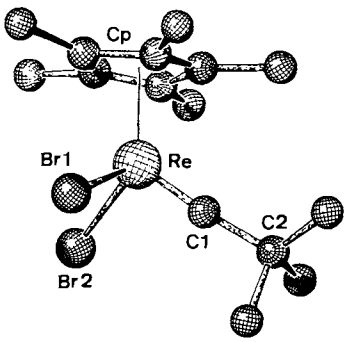


Fig. 2. Molecular structure (SCHAKAL) of the paramagnetic alkylidyne complex **5b** at 23°C. The complex crystallizes from *n*-hexane in the orthorhombic space group $P2_12_12_1$. Selected bond lengths [pm] and angles [°]: Re-C1 167(1), Re-Br1 248.9(1), Re-Br2 248.7(1), Re-Cp* 205; Br1-Re-Br2 93.50(5), C1-Re-Br1 98.0(3), C1-Re-Cp 125, Re-C1-C2 173(1) [Cp: center of ligand $C_5(CH_3)_5$].

voltammetric data, **5a**, for example, is oxidized by silver hexafluoroantimonate ($E^0 \approx 1.00$ V) in dichloromethane to afford the cationic, diamagnetic alkylidyne complex **6** with formation of silver. Apart from signals for the *tert*-butyl group and the ring ligands, the ^{13}C NMR spectrum of **6** (Table 1) shows the particularly characteristic alkylidyne resonance at $\delta = 338.0$ ($CDCl_3$).[8]

In addition to the oxidation of **5a** to **6**, which formally contains heptavalent rhenium, its reduction to give rhenium(V) complexes is also possible. The addition of a threefold molar amount of trimethylphosphane to the intense blue solution of **5a** in toluene furnishes the complexes **7** (15% yield, orange crystals) and **8** (50%, yellow, fluffy precipitate); see Scheme 2. The elemental analysis and spectral data of **7** are consistent with the formula shown in Scheme 2. The ^1H and ^{31}P NMR spectra are in accord with a meridional arrangement of the PMe_3 ligands, which can give rise to two structural isomers. The ^{13}C NMR spectrum (Table 1), which exhibits a quartet for the carbyne carbon atom ($^2J_{C,P} = 13.5$ Hz), shows that the three phosphane ligands have a *cis* arrangement with respect to the carbyne moiety. The ^1H NMR spectrum of **8** shows, besides the resonances of the $(\eta^5\text{-}C_5Me_5)Re{\equiv}CCMe_3$ fragment, signals for two chemically equivalent PMe_3 ligands. Elemental analysis, NMR data, and electrical conductivity ($\Lambda = 57.0$ S cm^2 mol^{-1}; $c = 0.22$ mmol L^{-1}, CH_2Cl_2, 20°C) corroborate the formulation of **8** as an ionic alkylidyne complex of pentavalent rhenium. The oxidation product of the reaction is a methylphosphorus(V) chloride (NMR detection).

Upon passing oxygen through a solution of **5a**, cleavage and derivatization of the alkylidyne ligand occurs affording **1**, its dimer, and, as organic products, pivalic anhydride and pivaloyl chloride (GC/MS/IR detection).

Compounds **5** and **6** represent the first examples of alkylidyne cyclopentadienyl complexes of rhenium in high oxidation states; analogous complexes having rhenium in low oxidation states have been known for some time.[7a,9] The complexes **5** are also the first monomeric 17-electron carbyne complexes, which were previously thought of as unstable molecules.[10] Because of its free coordination site and high oxidation state of the central atom as well as the resulting electrophilicity of the metal, the coordinatively unsaturated alkylidyne complex **6** in particular appears to be a promising model for investigations of alkyne metathesis. Some data for the new compounds are collected in Table 1.

Experimental Procedure

2b: A suspension of **1** (3.50 g, 8.6 mmol) in THF (50 mL) was added dropwise to a solution of $(CH_3)_3CCH_2MgCl$ (25 mmol) in THF (50 mL) at −70°C. After stirring for 15 min, the solution was allowed to warm to room temperature and then stirred for a further 1 h. 1,4-Dioxane (2.20 mL, 25 mmol) was added and the solvent removed under vacuum. The resulting residue was extracted into *n*-hexane and the solution filtered to remove $MgCl_2 \cdot$ 1,4-dioxane. **2b** was purified by column chromatography on silylated kieselgel at 15°C with *n*-hexane as eluent. Yield: 3.30 g (80%); brown needles.

3: A solution of **2a** (368 mg, 1.00 mmol) and $(\eta^5\text{-}C_5H_5)TiCl_3$ (220 mg, 1.00 mmol) in toluene (20 mL) was stirred at room temperature for 15 h. After removing the solvent in vacuum, the residue was suspended in CH_2Cl_2

Table 1. Spectroscopic data for the new organorhenium complexes **2b** and **3**–**8** [a, b].

Compound	IR $\tilde{\nu}$ [cm^{-1}]	NMR (δ values, J in Hz) ^1H NMR	^{13}C NMR	^{31}P NMR [c]
2b	966 vs (νReO)	1.46 [s, 15H, C_5Me_5], 1.48 [s, 18H, CMe_3], 2.42, 3.39 [2 × d, ^2J(H,H) = 11.9, 2 × 2H, 2 × CH_2]	11.3 [C_5Me_5], 32.4 [CH_2], 33.5 [CMe_3], 36.7 [CMe_3], 98.7 [C_5Me_5]	
3	325 vs, 287 m (νReCl)	1.93 [s, 15H, C_5Me_5], 4.69 [s, 6H, $Re(CH_3)_2$]	11.8 [C_5Me_5], 41.2 [$Re(CH_3)_2$], 100.0 [C_5Me_5]	
4		3.26 [s, 15H, C_5Me_5], 56.4 [s, 3H, $ReCH_3$], 58.7 [s, 6H, $Re(CH_3)_2$]		
5a	322 s, 310 s (νReCl)	−5.3 [br, paramagnetism!]		
6	660 vs, 640 vs (νSbF), 265 vs (νReCl)	1.41 [s, 9H, CMe_3], 2.44 [s, 15H, C_5Me_5]	12.4 [C_5Me_5], 28.8 [CMe_3], 55.0 [CMe_3], 127.3 [C_5Me_5], 338.0 [Re≡C]	
7	951 vs (νPC), 302 s (νReCl)	1.13 [s, 9H, CMe], 1.69 [vt, J = 7.7, 18H, 2 × PMe_3], 1.73 [d, 9H, ^2J(H,P) = 8.8, PMe_3]	18.9 [vt, J = 31.4, 2 × PMe_3], 25.6 [d, J(C,P) = 34.2, PMe_3], 27.7 [s, CMe_3], 52.6 [s, CMe_3], 279.3 [q, ^2J(C,P) = 13.5; Re≡C]	−19.7 [d, ^2J(P,P) = 12.7, 2P], −21.9 [t, ^2J(P,P) = 12.7, 1P]
8		1.05 [s, 9H, CMe_3], 1.75 [vd, 18H, J = 18.3, PMe_3], 1.99 [s, 15H, C_5Me_5]	12.2 [s, C_5Me_5], 25.5 [dd, ^1J(C,P) = 41.3, ^3J(C,P) = 2.5, 2 × PMe_3], 27.3 [s, CMe_3], 55.3 [s, CMe_3], 101.3 [s, C_5Me_5], 304.1 [t, ^2J(C,P) = 10.0, Re≡C]	−32.0 [s, 2 × PMe_3]

[a] Correct elemental analyses and isotopically exact mass spectra were obtained for all compounds. Molecular weight determination for **5a** (vapor pressure osmometry, benzene): found 434, calcd 461.5. [b] Solvent: C_6D_6 (**2b**, **4**), CD_2Cl_2 (**3**), $C_6D_5CD_3$ (**5**), $CDCl_3$ (**6**, **7**, **8**); spectra at +25°C. The ^1H NMR spectra of **3** and **4** show strong temperature dependence (singlet/triplet spin equilibria, d^2 configuration). ^1H NMR: 400 MHz, ^{13}C NMR: 100 MHz, ^{31}P NMR: 109.4 MHz. [c] H_3PO_4 as external standard.

and then adsorbed on silylated kieselgel 60. **3** was eluted with toluene as a brown band. Yield: 225 mg (60%), red-brown crystals.

4: A suspension of **3** (422 mg, 1.00 mmol) in toluene (10 mL) was added dropwise to a solution of CH_3MgCl (1.00 mmol) in THF (20 mL) at −70°C. The reaction mixture was allowed to warm to room temperature and stirred for 1 h to afford a brown solution, which was chromatographed on silylated kieselgel 60 at 15°C with *n*-hexane as eluent. Yield: 200 mg (40%), brown crystals.

5a: A solution of **2b** (2.40 g, 5.00 mmol) and $(\eta^5\text{-}C_5H_5)TiCl_3$ (2.20 g, 10.0 mmol) in toluene (75 mL) was heated under reflux for 18 h. After removal of the solvent in vacuum, the crude product was purified by column chromatography on silylated kieselgel. **5a** was eluted with *n*-hexane as a broad, blue band. The eluate (ca. 500 mL) was concentrated to ca. 150 mL and cooled to −78°C to afford crystals of **5a**. Yield: 1.50 g (65%), blue needles.

5b/5c: A stirred solution of **5a** (462 mg, 1.00 mmol) in CH_2Cl_2 (5 mL) was reacted with 4.0 mmol of $(CH_3)_3SiX$ (X = Br, I) at room temperature for 20 h. The solution was adsorbed on silylated kieselgel and purified by column chromatography on the same material (25 × 1 cm, 15°C). **5b** and **5c** were eluted with *n*-hexane as green and brown bands, respectively. Yields: 210 mg (40%) **5b**, green needles and 225 mg (40%) **5c**, brown needles, after recrystallization from *n*-hexane.

6: A solution of **5a** (230 mg, 0.50 mmol) in CH_2Cl_2 (5 mL) was combined with a solution of $Ag[SbF_6]$ (150 mg,. 0.50 mmol) in CH_2Cl_2 (5 mL) at −78°C. After stirring for 30 min at room temperature, a green-blue solution had formed. Yield 260 mg (75%) after filtration and recrystallization of the soluble components from $CHCl_3$.

7/8: A solution of **5a** (462 mg, 1.00 mmol) in toluene (10 mL) was reacted with $P(CH_3)_3$ (310 µL, 3.00 mmol) at −78°C. Warming to 25°C furnished a brown solution of **7** and a white precipitate of **8**. After stirring for 1 h at 25°C, the solution of **7** was filtered and then purified by chromatography on silylated kieselgel (30 × 1 cm, 15°C). **7** was eluted with toluene as a narrow brown band. Yield: 85 mg (15%), orange crystals (from *n*-hexane/ether). **8** was extracted from the residue with THF as a yellow solid. Yield: 290 mg (50%).

Received: October 13, 1988;
revised version: January 2, 1989 [Z 3007 IE]
German version: *Angew. Chem. 101* (1989) 346

CAS Registry numbers:
1, 104349-81-7; **2a**, 91129-18-9; **2b**, 118799-55-6; **3**, 118799-48-7; **4**, 118799-49-8; **5a**, 118799-50-1; **5b**, 118799-56-7; **5c**, 118799-57-8; **6**, 118799-52-3; **7**, 118799-53-4; **8**, 118799-54-5; $(\eta^5\text{-}C_5H_5)TiCl_3$, 1270-98-0.

[1] Reviews: a) W. A. Herrmann, *Comments Inorg. Chem. 7* (1988) 73; b) W. A. Herrmann, *Angew. Chem. 100* (1988) 1269; *Angew. Chem. Int. Ed. Engl. 27* (1988) 1297.

[2] W. A. Herrmann, J. Kuchler, J. K. Felixberger, E. Herdtweck, W. Wagner, *Angew. Chem. 100* (1988) 420; *Angew. Chem. Int. Ed. Engl. 27* (1988) 394.

[3] W. A. Herrmann, W. Wagner, unpublished results 1987/88.

[4] M. Flöel, E. Herdtweck, W. Wagner, J. Kulpe, P. Härter, W. A. Herrmann, *Angew. Chem. 99* (1987) 787; *Angew. Chem. Int. Ed. Engl. 26* (1987) 787.

[5] Foner magnetometer, $B = 1.8$ T; probe temperature variation using a helium flow-cryostat, calibration with $Hg[Co(SCN)_4]$. χ_G = measured susceptibility [cm³]; χ_M = molar susceptibility [cm³ mol⁻¹]; χ_M^{corr} = corrected molar susceptibility [cm³ mol⁻¹]; $\chi_{M,dia}$ = diamagnetic correction, determined from the Pascal constants; μ_{eff} = effective magnetic moment [B.M.]; M = molar mass [g mol⁻¹]. $X_{M,dia} = 210 \times 10^{-6}$ cm³ mol⁻¹; $\chi_M = \chi_G \cdot M$; $\chi_M^{corr} = \chi_M + \chi_{M,dia}$; $\mu_{eff} = [\chi_M^{corr} \cdot T]^{1/2}$.

[6] **5b**: Dark-green, *temperature-sensitive* needles; orthorhombic, $P2_12_12_1$ (Int. Tab. No. 19); $a = 1456.9(9)$, $b = 1448.8(9)$, $c = 865.5(3)$ pm, $V = 1827 \times 10^6$ pm³, $Z = 4$; $M_r = 550.4$; $\rho_{calcd} = 2.00$ g cm⁻³; $F_{000} = 1036$; CAD4 (Enraf-Nonius), graphite monochromator, $\lambda = 0.71073$ Å ($Mo_{K\alpha}$), measurement range: $2° \le \theta \le 25°$, t(max) = 60 s, $h(0/17)$, $k(0/17)$, $l(0/10)$; 1856 measured reflections, 117 suppressed, 1739 independent reflections, 1380 independent reflections with $I > 5\sigma(I)$ used in the refinement; structure solution by direct methods, 88 parameters, full-matrix least-squares refinement; all carbon atoms isotropic, all other non-hydrogen atoms anisotropic, hydrogen atoms not found or not calculated; empirical absorption correction, $\mu = 110.6$ cm⁻¹, crystal form not determined; transmission factors 0.844 to 1.000. $R = \Sigma(||F_0| - |F_c||)/\Sigma|F_0| = 0.054$; $R_w = [\Sigma w(|F_0| - |F_c|)^2/\Sigma w F_0^2]^{1/2} = 0.061$; $GOF = [\Sigma w(|F_0| - |F_c|)^2/(NO - NV)]^{1/2} = 7.565$ ($w = 1/\sigma^2[F_0]$); $\Delta e_0/Å^3 = 1.28$ (1.1 Å away from heavy atom Re); shift/err = 0.01. The quality of the structure determination was influenced by decomposition of the crystal (50%) during the measurement. Refinement of the enantiomers made no difference. Recrystallization of **5b**, and of the isostructural iodine derivative, always gave *temperature-stable* crystals with orthorhombic metric, but with fourfold cell volume. The X-ray analyses of these phases are in progress. Further details of the crystal structure investigation may be obtained from the Fachinformationszentrum Energie, Physik, Mathematik GmbH, D-7514 Eggenstein-Leopoldshafen 2 (FRG), on quoting the depository number CSD-53375, the names of the authors, and the journal citation.

[7] a) Recent review: J. S. Murdzek, R. R. Schrock in H. Fischer, P. Hofmann, F. R. Kreissl, R. R. Schrock, U. Schubert, K. Weiss (Eds.): *Carbyne Complexes*, VCH Verlagsgesellschaft, Weinheim 1988, p. 147ff. b) More recent work: P. D. Savage, G. Wilkinson, M. Motevalli, M. B. Hursthouse, *Polyhedron 6* (1987) 1599.

[8] H. P. Kim, R. J. Angelici, *Adv. Organomet. Chem. 27* (1987) 51.

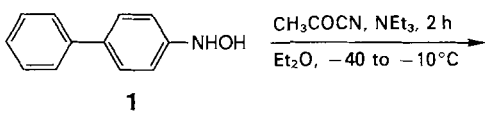
[9] a) E. O. Fischer, R. C. Clough, P. Stückler, *J. Organomet. Chem. 120* (1976) C6; b) E. O. Fischer, P. Rustemeyer, D. Neugebauer, *Z. Naturforsch. B35* (1980) 1083.

[10] C. J. Leep, K. B. Kingsbury, L. McElwee-White, *J. Am. Chem. Soc. 110* (1988) 7535.

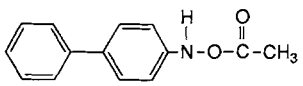
Synthesis of *O*-Acetyl-*N*-(4-biphenylyl)hydroxylamine ("N-Acetoxy-4-aminobiphenyl"), an Ultimate Metabolite of Carcinogenic 4-Aminobiphenyl, and Its Reaction with Deoxyguanosine**

By *Michael Famulok, Ferdinand Bosold,* and *Gernot Boche**

One possibility for the conversion of mutagenic and carcinogenic amines such as 4-aminobiphenyl[1] into an ultimate carcinogen consists in *N*-oxidation to *N*-(4-biphenylyl)hydroxyl amine ("*N*-hydroxy-4-aminobiphenyl") **1**[2] followed by *O*-acetylation to the title compound **2** ("*N*-acetoxy-4-aminobiphenyl").[3] Although the carcinogenicity of aromatic amines has been known since 1895,[4] **2** is the first metabolite of a mutagenic and carcinogenic aromatic amine activated by an *N*-acetoxy group,[5] which was isolated. Herein we report on the synthesis of **2** and its reaction with deoxyguanosine **3**.



1



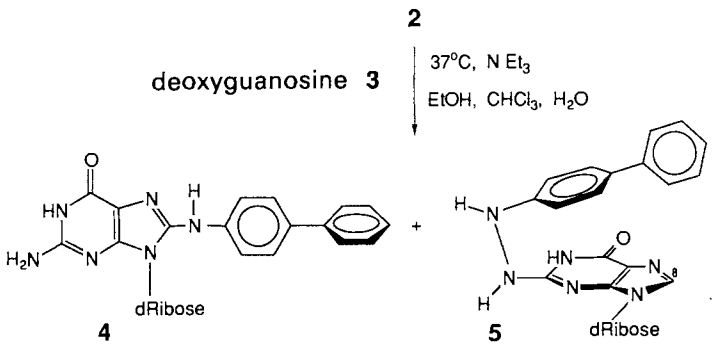
2

Although **2** is thermally labile and decomposes within an hour above 10°C it can be subjected to an elemental analysis (C,H,N) and ^{13}C NMR spectroscopic characterization. Proof for the *O*-acetyl structure is afforded in particular by the carbonyl band at $\tilde{\nu} = 1755$ cm⁻¹; in contrast, the isomeric *N*-acetyl compound (hydroxamic acid) absorbs at 1642 cm⁻¹.

Reaction of **2** with deoxyguanosine **3** in ethanol/chloroform/water at 37°C leads to the two adducts **4** and **5** in 6% and 3% yield respectively.[6] The isolation of **4** and **5** is therefore important, because **4** and (very small amounts of) **5** were also found upon feeding dogs with 4-aminobiphenyl (ABP) and subsequent enzymatic cleavage of the DNA (from the epithelium of the bladder). The yield of **5** was apparently too small to be able to quote experimental data which unequivocally confirm its structure.[7] **4** has also been obtained together with two unidentified products upon reaction of *O*-acetyl-*N*-(4-biphenylyl)-*N*-trifluoroacetylhydroxylamine with **3** in sodium citrate buffer (pH

[*] Prof. Dr. G. Boche, Dipl.-Chem. M. Famulok, F. Bosold
Fachbereich Chemie der Universität
Hans-Meerwein-Strasse, D-3550 Marburg (FRG)

[**] This work was supported by the Fonds der Chemischen Industrie, by the Deutsche Forschungsgemeinschaft, and by BASF AG.



7.0) and ethanol at 50°C.[8] The assumption that **2** is the reactive species in this reaction is confirmed by our findings.[9]

Experimental

2: A suspension of 4.00 g (21.6 mmol) of **1** in diethyl ether (50 mL) and triethylamine (2.9 mL, 21.6 mmol) cooled to −40°C was treated with a solution of acetyl cyanide [10] (1.50 g, 21.6 mmol) in diethyl ether (30 mL) and the mixture vigorously stirred for 2 h between −40° and −10°C. After extraction with ice-water the aqueous phase was extracted at 0°C with 50 mL of CH_2Cl_2, the organic phases combined, dried with $MgSO_4$, and the solvent removed in a rotary evaporator at 0°C. The residue was rapidly dissolved at room temperature in 100 mL of ether/petroleum ether (1/1) and 20 mL of CH_2Cl_2 and recrystallized at −30°C. The bright yellow crystals of **2** were dried at −20°C. Yield 3.98 g (81%); correct elemental analysis (C,H,N). ^{1}H NMR (400 MHz, $CDCl_3$, 230 K): δ = 2.27 (s, 3H), 7.15 (d, 2H), 7.38 (t, 1H), 7.47 (t, 2H), 7.58 (2d, 4H), 8.90 (N−H, 1H). ^{13}C NMR (400 MHz, $CDCl_3$, 230 K): δ = 19.3, 116.9, 126.7, 127.0, 127.7, 128.7, 136.7, 140.1, 145.4, 170.8. IR (Nujol): $\tilde{\nu}$ = 3245, 1755, 1223 cm^{-1}.

Reaction of **2** with **3**: **2** (909 mg, 4.00 mmol) was treated with a solution of **3** (1.07 g, 4.00 mmol) and triethylamine (455 mg, 4.50 mmol) in 70 mL of ethanol/$CHCl_3$/water (7/3/4) at 37°C. After 1 h the solvent was removed; the adducts **4** and **5** were first separated over a silica gel column with $CHCl_3$/ethanol (7/3) and then by preparative HPLC [11]. Yield (after silica gel chromatography): **4**: 112 mg (6%); ^{1}H NMR ([D$_6$]DMSO, 400 MHz: the data agree with those quoted in Ref. [7a]. ^{13}C NMR: δ = 38.4, 61.2, 71.2, 82.8, 87.2, 112.1, 117.6, 125.9, 126.5, 126.6, 128.7, 132.2, 140.0, 140.3, 143.1, 149.5, 153.0, 155.9. MS (FD): *m/z* 434 (100%, $M^{\oplus}$), 318 (61%, $M^{\oplus}$ − dRibose + H). IR (KBr): $\tilde{\nu}$ = 3329, 2927, 1680, 1562, 1356, 1024, 960, 764, 698 cm^{-1}; **5**: 55 mg (3%); ^{1}H NMR ([D$_6$]DMSO, 400 MHz): δ = 2.12 (m, 1H), 2.42 (m, 1H), 3.47 (m, 2H), 3.76 (m, 1H), 4.28 (m, 1H), 4.91 (s, OH), 5.21 (s, OH), 5.95 (dd, 1H), 6.35 (s, 2H, −NH−NH−), 7.37 (d, 2H), 7.37 (t, 1H), 7.40 (s, 1H), 7.48 (t, 2H), 7.65, 7.66 (2d, 4H), 8.24 (s, 1H, NH); the singlet of H-8 of the deoxyguanosine part of **5** (δ = 7.40) is shifted markedly upfield compared to that of **3** ([D$_6$]DMSO, 300 MHz, δ = 7.94) and other purine nucleosides and nucleotides (see C. J. Pouchert, J. R. Campbell: *The Aldrich Library of NMR Spectra, Vol. 8*, Aldrich Chemical Company, Milwaukee 1974). This suggests a folded conformation for **5** in which the biphenyl moiety lies above the guanine part of the molecule and thus provides for the shielding of H-8. A similar folded conformation was found for methotextrate in an unpolar solvent (P. Faupel, V. Buss, *Angew. Chem. 100* (1988) 422; *Angew. Chem. Int. Ed. Engl. 27* (1988) 423). ^{13}C NMR: δ = 61.8 (t, ^1J(C-H) = 140.0 Hz), 70.7 (d, ^1J(C-H) = 149.9 Hz), 82.0 (d, ^1J(C-H) = 163.5 Hz), 87.2 (d, ^1J(C-H) = 147.2 Hz), 125.0 (s), 126.5 (d, ^1J(C-H) = 159.5 Hz), 126.6 (d, ^1J(C-H) = 159.7 Hz), 127.0 (s), 127.4 (d, ^1J(C-H) = 212.6 Hz), 127.4 (d, ^1J(C-H) = 162.6 Hz), 128.3 (d, ^1J(C-H) = 162.4 Hz), 128.9 (d, ^1J(C-H) = 161.7 Hz), 138.3 (s), 139.0 (s), 139.6 (s), 148.8 (s), 155.4 (s); the C-2 signal of the dRibose moiety is covered by DMSO signals. MS (FD): *m/z* 434 (100%, $M^{\oplus}$), 318 (78%, $M^{\oplus}$ − dRibose + H); IR (KBr): $\tilde{\nu}$ = 3334, 2924, 1658, 1522, 1487, 1333, 1086, 1049, 764, 698 cm^{-1}. UV: λ_{max} = 251, 216 nm.

Received: October 14, 1988;
revised: November 28, 1988 [Z 3010 IE]
German version: *Angew. Chem. 101* (1989) 349

CAS Registry numbers:
1, 6810-26-0; **2**, 119273-47-1; **3**, 961-07-9; **4**, 84283-08-9; **5**, 117205-56-8; CH_3COCN, 631-57-2; *N*-(4-biphenylyl)-*O*-pivaloylhydroxylamine, 119273-48-2.

[1] T. S. Scott: *Carcinogenic and Chronic Toxic Hazards of Aromatic Amines*, Elsevier, Amsterdam 1962.

[2] J. W. Gorrod, L. A. Damani: *Biological Oxidation of Nitrogen in Organic Molecules*, VCH Verlagsgesellschaft, Weinheim 1985.

[3] a) H. Bartsch, M. Dworkin, J. A. Miller, E. C. Miller, *Biochim. Biophys. Acta 286* (1972) 272; see also b) E. Kriek, *ibid. 335* (1974) 177; c) C. M. King, *Cancer Res. 34* (1974) 1403; d) E. C. Miller, *ibid. 38* (1978) 1479; e) F. A. Beland, W. T. Allaban, F. E. Evans, *ibid. 40* (1980) 834; f) E. C. Miller, J. A. Miller, *Cancer (Amsterdam) 47* (1981) 2327; g) I. B. Glowinski, L. Savage, M.-S. Lee, C. M. King, *Carcinogenesis 4* (1983) 67; h) S. S. Thorgeirsson in H. Greim, R. Jung, M. Kramer, H. Marquardt, F. Oesch (Eds.): *Biochemical Basis of Chemical Carcinogenesis*, Raven Press, New York 1984, p. 47; i) T. J. Flammang, F. F. Kadlubar, *Carcinogenesis 7* (1986) 919; j) C.-C. Lai, E. C. Miller, J. A. Miller, A. Liem, *ibid. 9* (1988) 1295.

[4] L. Rehn, *Arch. Klin. Chir. 50* (1895) 588.

[5] *N*-Acetoxy compounds of other mutagenic and carcinogenic aromatic amines which were prepared in solution but not isolated and characterized: a) Y. Hashimoto, K. Shudo, T. Okamoto, *J. Am. Chem. Soc. 104* (1982) 7636; *Biochem. Biophys. Res. Commun. 96* (1980) 355; *92* (1980) 971; b) K. B. Delclos, W. G. Tarpley, E. C. Miller, J. A. Miller, *Cancer Res. 44* (1984) 2540; c) A. M. Lobo, M. M. Marques, S. Prabhakar, H. S. Rzepa, *J. Chem. Soc. Chem. Commun. 1985*, 1113; *J. Org. Chem. 52* (1987) 2925. Prepared in solution, characterized, but not isolated: 4-(acetoxyamino)quinoline 1-oxide: d) Y. Kawazoe, O. Ogawa, G.-F. Huang, *Tetrahedron 36* (1980) 2933; e) M. Demeunynck, N. Thome, M.-F. Lhomme, J. M. Mellon, J. Lhomme, *J. Am. Chem. Soc. 108* (1986) 3539, and references cited therein. Obtained in substance and characterized *O*-acetyl-*N*-arylhydroxylamines: f) W. Borsche, *Ber. Dtsch. Chem. Ges. 56* (1923) 1494; g) A. C. Huggett, J. L. Cone, S. S. Thorgeirsson, P. P. Roller, *J. Org. Chem. 52* (1987) 4933; h) G. Boche, F. Bosold, S. Schröder, *Angew. Chem. 100* (1988) 965; *Angew. Chem. Int. Ed. Engl. 27* (1988) 973; i) *O*-acetyl-*N*-(2-naphthyl)hydroxylamine: M. Famulok, F. Bosold, G. Boche, *Tetrahedron Lett.*, in press. We have also allowed **2** to react with *N*-methylaniline in analogy to the results described in Refs. [5h, i]: M. Famulok, F. Bosold, G. Boche, unpublished.

[6] Analogously to **2**, we have prepared and characterized *N*-(4-biphenylyl)-*O*-pivaloylhydroxylamine and allowed it to react with **3**; **4** and **5** were obtained in similar yields as in the case of **2**; M. Famulok, F. Bosold, G. Boche, unpublished.

[7] a) F. F. Kadlubar, F. A. Beland, D. T. Beranek, K. L. Dooley, R. H. Heflich, F. E. Evans in T. Sugimura, S. Kondo, H. Takebe (Eds.): *Environmental Mutagens and Carcinogens*, A. R. Liss, New York 1982, p. 385; b) F. A. Beland, D. T. Beranek, K. L. Dooley, R. H. Heflich, F. F. Kadlubar, *EHP Environ. Health Perspect. 49* (1983) 125; the authors assume hydroxylamine **1** as reactive metabolite which is formed from the *N*-glucuronide of **1** in the acid medium of the urine and reacts further after protonation at the oxygen; c) a review of "DNA adducts of aromatic amines" is given in H.-G. Neumann, *J. Cancer Res. Clin. Oncol. 111* (1986) 100.

[8] a) R. Shapiro, G. R. Underwood, H. Zawadzka, S. Broyde, B. E. Hingerty, *Biochemistry 25* (1986) 2198. These authors also allowed *O*-acetyl-*N*-(4-biphenylyl)-*N*-trifluoroacetylhydroxylamine to react with the dinucleotide d(CpG) under the same conditions at 37°C and obtained the adduct d(CpG$^{8\text{-ABP}}$); b) with the tetranucleotide 5′-d(TpGpCpA)-3′, the adduct 5′-d(TpG$^{8\text{-ABP}}$pCpA)-3′ was found: D. D. Lasko, A. K. Basu, F. F. Kadlubar, F. E. Evans, J. O. Lay, Jr., J. M. Essigmann, *ibid. 26* (1987) 3072.

[9] **4** and **5** were also obtained when the hydroxylamine **1** was allowed to react with DNA at pH 5 and the DNA finally cleaved enzymatically [7]; upon feeding rats with *N*-acetyl-*N*-(4-biphenylyl)hydroxylamine, **4** was detected with the help of a ^{32}P-post-labeling assay: R. C. Gupta, N. R. Dighe, *Carcinogenesis 5* (1984) 343.

[10] Acyl cyanides were used successfully for the first time for the *O*-acylation of *N*-arylhydroxylamines by S. Prabhakar, A. M. Lobo, M. M. Marques, *Tetrahedron Lett. 23* (1982) 1391.

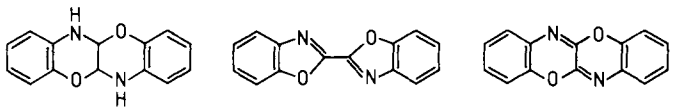
[11] LiChrosorb RP 18, 7 μm, preparative HPLC column (20 × 230 mm), isocratic elution with methanol/water (1/1).

Photochemical Formation of a Stable Oxalic Acid Orthoamide with a Propellane Structure

By *Erich Tauer,* Karl-Heinz Grellmann, Mathias Noltemeyer,* and *George M. Sheldrick*

We have recently reported[1] that the condensation of glyoxal with 2-aminophenol does not give 2,2′,3,3′-tetrahy-

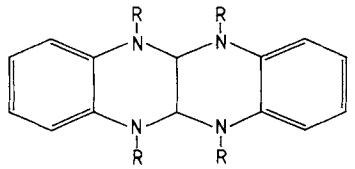
[*] Dr. E. Tauer, Dr. K. H. Grellmann
Max-Planck-Institut für Biophysikalische Chemie,
Abt. Spektroskopie
Am Fassberg, D-3400 Göttingen (FRG)
Dr. M. Noltemeyer, Prof. G. M. Sheldrick
Institut für Anorganische Chemie der Universität
Tammannstrasse 4, D-3400 Göttingen (FRG)



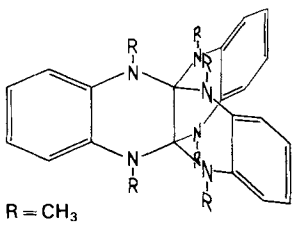
1 2 3

dro-2,2'-bibenzoxazole as was previously assumed, but affords, instead, 5a,6,11a,12-tetrahydro[1,4]benzoxazino[3,2-*b*][1,4]benzoxazine **1**. Exposure of an air-saturated solution of **1** in an inert solvent (e.g., cyclohexane) to long wavelength light ($\lambda \geq 260$ nm) leads to the formation of 2,2'-bibenzoxazole **2**; when the photolysis is performed with short wavelength light ($\lambda < 260$ nm), [1,4]benzoxazino[3,2-*b*][1,4]benzoxazine **3** is formed additionally.

In order to study the mechanism of this photooxidation reaction in more detail, we prepared derivatives and analogues of **1**, for example, the compound 5,5a,6,11,11a,12-hexahydro-5,6,11,12-tetramethyl-quinoxalino[2,3-*b*]quinoxaline **4** which has not yet been described in the literature.



4



5

R = CH_3

Compound **4** exhibits very surprising photochemical properties. Irradiation of a nitrogen-purged solution of **4** in cyclohexane with light of wavelength $\lambda = 254$ nm yields the oxalic acid orthoamide **5** in 11% chemical yield along with other, as yet uncharacterized photoproducts. **5** is a stable compound and can be recrystallized from ethanol. It absorbs similarly to **4** in the UV and has an unstructured fluorescence spectrum. An X-ray structure analysis[2] (Fig. 1) showed that **5** has a [4,4,4]-propellane structure with the molecule lying with C1 and C10 on a crystallographically exact threefold symmetry axis (symmetry position x,x,x); the molecular symmetry is D_3. The difference electron density map showed additional maxima which were assigned to a disordered solvent molecule (ethanol), whose presence was also indicated by the elemental analysis.

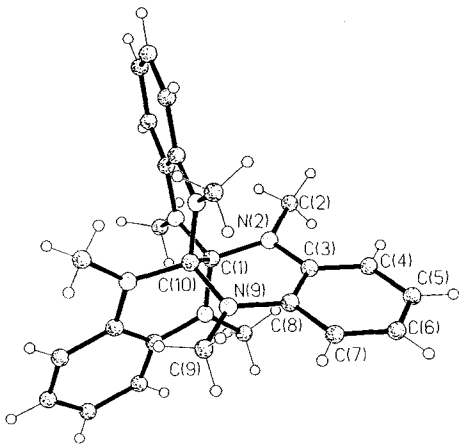


Fig. 1. Molecular structure of **5**. Selected bond lengths [pm] and angles [°]: C1-C10 157.9(7), C1-N2 144.5(3), C10-N9 145.1(3), C2-N2 145.0(5), C3-C4 138.9(5), C4-C5 138.5(7), C5-C6 134.8(8), C6-C7 137.8(6), C3-C8 141.7(5); N2-C1-C10 107.2(2), C1-N2-C2 121.6(3), N2-C3-C8 120.0(3), C1-C10-N9 107.4(2).

Nothing is known about the mechanism of the photoreaction **4** → **5**. To the best of our knowledge, **5** is the first orthoamide derivative of oxalic acid with the substitution pattern of a hexaminoethane.

Experimental Procedure

4: *N,N'*-dimethyl-N,N'-ditosyl-*o*-phenylenediamine [3] (88 g, 0.2 mol) was heated in a mixture of H_2SO_4 (80 mL) and H_2O (8 mL) for 5 h, after which the solution was poured into 300 mL of ice water [4]. The resulting solution was allowed to flow under N_2 into 1 L of NaOH (6 M) and the free amine was steam distilled under N_2 into a light-protected receiving flask. After ca. 3 L of liquid had been collected, 19.2 g of a 30% aqueous solution of glyoxal (0.1 mol) was added to the amine-water emulsion with rapid stirring. After stirring for a further 48 h, the crude product was collected by filtration, washed with H_2O, and dried. Yield: 19 g (65%), m.p. 160–164°C. Recrystallizing three times from 2-propanol (1 g/50 mL) under N_2 afforded colorless crystals of **4** (14.3 g, m.p. 167–169°C). ^{1}H NMR (80 MHz, $CDCl_3$): $\delta = 2.98$ (s, 12H, CH_3), 4.28 (s, 2H, CH), 6.5 (m, 8H, arylH); UV (C_6H_{12}): λ_{max}/nm (logε) = 312 (4.11), 257 (4.14), 227 (4.81). Correct elemental analysis.

5: A solution of **4** (1 g) in p.a. cyclohexane (1.3 L) was photolyzed (48 h) in a Rayonet reactor under N_2 using 16 lamps ($\lambda = 254$ nm). After removal of the solvent on a rotary evaporator, the mixture was separated chromatographically (Al_2O_3, cyclohexane/diisopropyl ether 3/1). It yielded 520 mg of unreacted **4** and, after recrystallization from ethanol, 53 mg (11%) of **5** as colorless crystals, m.p. 272–273°C. MS: $m/z = 426$ ($M^{\oplus}$); ^{1}H NMR (80 MHz, $CDCl_3$): $\delta = 2.7$ (s, 18H, CH_3), 6.5–6.85 (m, 12H, arylH); UV (C_6H_{12}): λ_{max}/nm (logε) = 316 (4.38), 310 (4.34), 250 (4.33, sh), 227 (4.99); fluorescence: $\lambda_{max} = 347$ nm (line width 50 nm). Correct elemental analysis.

Received: October 17, 1988 [Z 3012 IE]
German version: *Angew. Chem. 101* (1989) 350

CAS Registry numbers:
4, 13784-23-1; **5**, 118894-97-6; *N,N'*-dimethyl-*N,N'*-ditosyl-*o*-phenylenediamine, 29627-62-1; glyoxal, 107-22-2.

[1] E. Tauer, K. H. Grellmann, E. Kaufmann, M. Noltemeyer, *Chem. Ber. 119* (1986) 3316.

[2] **5**·0.5EtOH: cubic, space group $Pa\bar{3}$, $a = 1677.6(5)$ pm, $V = 4.7213$ nm^3, $Z = 8$, $\rho_{calcd} = 1.299$ g cm^{-3}, $\mu = 0.08$ mm^{-1} ($Mo_{K\alpha}$); 6934 intensities measured to $2\theta = 45°$, 968 symmetry independent reflections with $F > 3\sigma(F)$ used in the structure solution (SHELXS-86) and refinement (SHELX-76), non-hydrogen atoms anisotropic and H atoms as rider model, $R = 0.090$, $wR = 0.092$, $w^{-1} = \sigma^2 + 0.0008F^2$. Further details of the crystal structure investigation may be obtained from the Fachinformationszentrum Energie, Physik, Mathematik GmbH, D-7514 Eggenstein-Leopoldshafen 2 (FRG), on quoting the depository number CSD-53369, the names of the authors, and the journal citation.

[3] Synthesis according to H. Stetter, *Chem. Ber. 86* (1953) 161.

[4] Hydrolysis according to G. W. H. Cheeseman, *J. Chem. Soc. 1955*, 3308.

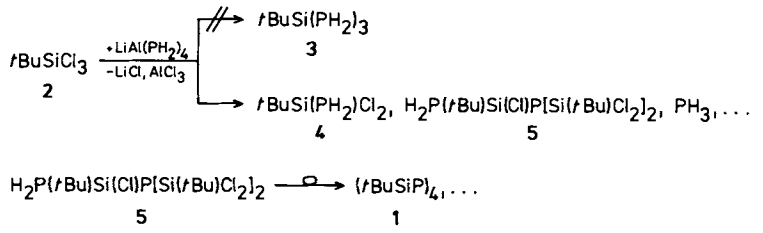
(*t*BuSiP)$_4$—The First Silaphosphacubane**

By *Marianne Baudler,* Guido Scholz, Karl-Friedrich Tebbe,* and *Magda Fehér*

Although a large number of phosphorus-silicon heterocycles having various molecular frameworks are already known,[1,2] a silaphosphane with a cubane structure has yet to be reported. We have now prepared the first silaphosphacubane, *closo*-tetrakis(*tert*-butylsilylphosphane) **1**, and

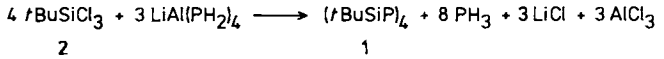
[*] Prof. Dr. M. Baudler, G. Scholz, Prof. Dr. K.-F. Tebbe, Dr. M. Fehér
Institut für Anorganische Chemie der Universität
Greinstrasse 6, D-5000 Köln 41 (FRG)

[**] Contributions to the Chemistry of Phosphorus, Part 192. This work was supported by the Minister für Wissenschaft und Forschung des Landes Nordrhein-Westfalen and the Fonds der Chemischen Industrie. Part 191: M. Baudler, C. Block, H. Budzikiewicz, H. Münster, *Z. Anorg. Allg. Chem.*, in press.



wish to report here on its unexpected formation and remarkable molecular structure.

After having successfully synthesized several organotris(phosphino)silanes $RSi(PH_2)_3$ (R = Me, Et, *i*Pr, Ph),[3] we found that phosphination of the trichlorosilane **2** with $LiAl(PH_2)_4$[4] (1,2-dimethoxyethane (DME), −40 °C) does not lead to the *tert*-butyl compound **3**, but instead affords **4**, **5**,[5] PH_3, and small quantities of other compounds which were not further characterized. The course of the reaction is obviously determined by the bulky *tert*-butyl group. In contrast to **4**, compound **5** is not stable in the reaction mixture at room temperature and upon removal of the solvent. Under these conditions it undergoes rearrangement to afford a mixture of more highly condensed Si–P compounds, from which **1** may be obtained in analytically pure form by extraction with *n*-hexane; the reaction can be described in an idealized manner by the following equation: [6]



The silaphosphane **1** forms colorless, tetrahedral, or platelike crystals (m.p. 323–324 °C, dec., sealed tube) which are stable under an inert atmosphere and moderately soluble in hydrocarbons, THF, and monoglyme. Compound **1** is sensitive to oxidation and hydrolysis, particularly in solution. Apart from the signal group for the $M^{\oplus}$ ion (*m/z* 464–469), the mass spectrum (15 eV, 100 °C) shows only a low-intensity signal group for the ion $(M-t\mathrm{Bu}+\mathrm{H})^{\oplus}$. The ^{31}P NMR spectrum (*n*-hexane, 25 °C, 121.497 MHz) exhibits a singlet at $\delta = -177.0$ with ^{29}Si satellites and the $^{1}H\{^{31}P\}$ NMR spectrum (300.135 MHz) a singlet at $\delta = 1.01$. The ^{29}Si DEPT NMR spectrum (THF/[D_8]THF, 25 °C, 59.628 MHz) consists of an AX_3Y system with $\delta = -28.5$ and the calculated coupling constants $^{1}J_{SiP} = +37.6(1)$ Hz, $^{3}J_{SiP} = -12.6(3)$ Hz, and $^{2}J_{HP} = +23.8(1)$ Hz. One band is observed in the IR spectrum at 413 (s) with a shoulder at 380 cm^{-1} and in the Raman spectrum three bands (with splittings) appear at 375 (s), 402 (m), and 439 (vs), which can be assigned to the stretching vibrations of the Si–P skeleton. All these findings are consistent only with the presence of the symmetrical cage compound 2,4,6,8-tetra-*tert*-butyl-1,3,5,7-tetraphospha-2,4,6,8-tetrasilapentacyclo-[4.2.0.$0^{2,5}$.$0^{3,8}$.$0^{4,7}$]octane **1**. The exact molecular parameters were obtained from an X-ray structure analysis[7] (Fig. 1).

Two different molecules of symmetry $\bar{4}$ (S_4) and 23 (*T*) are present in the crystal in the ratio 6:2; their structural parameters differ only slightly (Table 1). The cage, which is highly distorted compared with a cube, is composed of a larger P_4 tetrahedron and a smaller Si_4 tetrahedron. The bond angle at silicon is considerably larger than that of a corner of a cube, while that at phosphorus is correspondingly smaller, which results in the phosphorus atoms being displaced outwards. The *tert*-butyl substituents have a staggered arrangement. The silicon–carbon bonds in the molecule of $\bar{4}$ symmetry point almost exactly in the direction of the diagonal of the phosphorus–silicon cage, while those of the molecule with symmetry 23 lie precisely in this orientation.

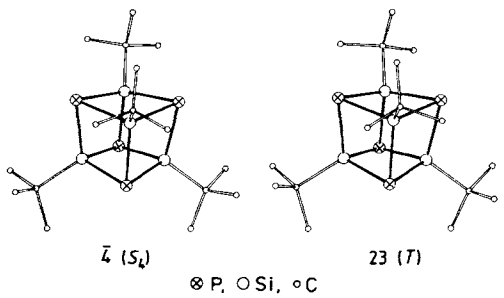


Fig. 1. Molecular structures of **1** in the crystal.

Table 1. Selected interatomic distances [pm] and angles [°] for the two different molecules of **1** [mean values (S_4) and values (*T*)].

Distance	S_4	*T*	Angle	S_4	*T*
P-Si	228.1(2)	227.8(3)	P-Si-P	101.61(7)	101.62(9)
P···P	353.6(3)	353.1(4)	Si-P-Si	77.03(31)	77.02(9)
Si···Si	284.1(8)	283.6(4)	P-Si-C	116.5(15)	116.5(2)
Si-C	189.4(6)	190.3(7)	Si-C-C	109.6(7)	106.2(5)
C-C	151.8(19)	155.6(10)	C-C-C	109.3(8)	112.5(5)
			P-Si-C-C	−174.9(5)	−173.2(4)
				− 56.1(5)	
				+ 63.5(5)	

Compound **1** is most likely formed by intermolecular condensation of four-membered ring compounds with alternating Si and P atoms and reactive PH and SiCl groups, which can be detected as intermediates using ^{31}P NMR spectroscopy. The remarkable thermal stability of **1** compared to the related heterophosphacubane $(PhSnP)_4$[9] can be attributed to the similar covalent radii of phosphorus and silicon and to the bulky *tert*-butyl substituents.

Received: October 20, 1988 [Z 3017 IE]
German version: *Angew. Chem. 101* (1989) 352

CAS Registry numbers:
1, 118762-11-1; **2**, 18171-74-9; **4**, 118762-12-2; **5**, 118762-13-3; $LiAl(PH_2)_4$, 25248-80-0; PH_3, 7803-51-2.

[1] Review: G. Fritz, *Adv. Inorg. Chem. 31* (1987) 171.
[2] a) M. Baudler, H. Jongebloed, *Z. Anorg. Allg. Chem. 458* (1979) 9; b) M. Baudler, T. Pontzen, *ibid. 491* (1982) 27; c) M. Baudler, T. Pontzen, U. Schings, K.-F. Tebbe, M. Fehér, *Angew. Chem. 95* (1983) 803; *Angew. Chem. Int. Ed. Engl. 22* (1983) 775.
[3] M. Baudler, G. Scholz, W. Oehlert, *Z. Naturforsch. B*, in press.
[4] a) A. E. Finholt, C. Helling, V. Imhof, L. Nielsen, E. Jacobson, *Inorg. Chem. 2* (1963) 504; b) A. D. Norman, D. C. Wingeleth, *ibid. 9* (1970) 98; c) A. D. Norman, *ibid. 9* (1970) 870.

[5] **4**: ^{31}P NMR (36.434 MHz, DME, −60°C): $\delta = -240.1$ (t with ^{29}Si satellites, $^1J(PH) = +195.2$ Hz, $^1J(PSi) = +48.1$ Hz).—**5**: $^{31}P\{^1H\}$ NMR (121.497 MHz, DME, −60°C): AB system with $\delta(A) = -214.6$, $\delta(B) = -237.5$, $^2J(AB) = \pm 12.5$ Hz; ^{1}H NMR (300.135 MHz, DME/[D$_8$]THF, −60°C): $\delta = 1.36$ (m, $^1J(P_AH) = +186$ Hz, 2H; PH_2), 1.03 (s, 9H; tBuSi$_x$), 0.86 (s, $^3J(HSi_y) = \pm 6.5$ Hz, 9H; tBuSi$_y$), 0.84 (s, $^3J(HSi_z) = \pm 6.7$ Hz, 9H; tBuSi$_z$); $^{29}Si\{^1H\}$ NMR (59.628 MHz, DME/[D$_8$]THF, −60°C): $\delta = +50.1$ (dd, $^1J(Si_xP_A) = +49.5$ Hz, $^1J(Si_xP_B) = +131.5$ Hz, 1 Si; $H_2P_ASi_x(t\text{Bu})Cl$), +48.9 (dd, $^1J(Si_{y/z}P_B) = +160.2$ Hz, $^3J(Si_{y/z}P_A) = \pm 3.5$ Hz, 2 Si; $P_B(Si_{y/z}(t\text{Bu})Cl_2)_2$).

[6] **1**: A solution of **2** (19.2 g, 100 mmol) in DME (40 mL) was added dropwise to 188.7 mL (50 mmol) of a stirred 0.265 M solution of $LiAl(PH_2)_4$ in DME within 20 min. After stirring for an additional 1 h at −40°C, PH_3 was removed at room temperature and the solvent pumped off completely under water-pump vacuum within 2 h. The pale yellow residue was dried for 30 min at 0.1 torr and then extracted with four 100-mL portions of hexane. The extracts were combined and concentrated to 100 mL. Cooling to −35°C for 12 h to 5 d afforded crystals of pure **1**, which were washed with cold hexane (−35°C, 3 × 4 mL). Yield: 0.54 g (7% based on $LiAl(PH_2)_4$).

[7] Crystal structure analysis of **1**: space group $P\bar{4}3n$ (No. 218); $a = 1740.9(4)$ pm, $V = 5276.2 \times 10^6$ pm^3, $Z = 8$, $\rho_{X\text{-ray}} = 1.1698$ g cm^{-3}, $F(000) = 1984$; $\mu(Mo_{K\alpha}) = 0.4595$ mm^{-1}. CAD4 diffractometer (Enraf-Nonius), room temperature, $Mo_{K\alpha}$ radiation, $2\theta \leq 54°$; 1066 independent reflections, 578 with $|F_0| \geq 4\sigma(F_0)$. Solution with direct methods (SHELX 86); refinement: P, Si, C anisotropic, H in fixed methyl groups with d(C-H) = 108 pm (SHELX76); $R = 0.026$, $R_w = 0.035$. For further details of the structure determination see [8].

[8] K.-F. Tebbe, M. Fehér, *Acta Crystallogr. C*, in press.

[9] H. Schumann, H. Benda, *Angew. Chem. 80* (1968) 846; *Angew. Chem. Int. Ed. Engl. 7* (1968) 813.

A Novel Trimeric Chiral Copper(I) Thiophenolate with Intramolecular Coordination**

By *D. Martin Knotter, Gerard van Koten,* Hendrik L. van Maanen, David M. Grove,* and *Anthony L. Spek*

To date only a few structures of copper(I) thiophenolates, either with or without discrete donor ligands, have been elucidated and none of these structures have a potentially chelating group on the thiophenolate ring.[1] Here, we wish to present results concerning the synthesis, structural characterization, and unusual properties of a copper(I) thiophenolate, **1**, whose thiophenolate ligands have a 1-(dimethylamino)ethyl group in the *ortho* position. In this type of thiophenolate we can anticipate formation of a six-membered metallacycle through intramolecular chelation of the chiral CH(Me)NMe$_2$ group. Consequently, the complex may exhibit new and interesting behavior.

The 2:1 reaction of optically pure, chiral 2-[(*R*)-1-(dimethylamino)ethyl]thiophenol with Cu_2O in ethanol affords in high yield the copper(I) thiophenolate **1**.

$$6\,HSC_6H_4\{CH(Me)NMe_2\}\text{-}o + 3\,Cu_2O \xrightarrow{\text{ethanol, reflux}} 2[CuSC_6H_4\{CH(Me)NMe_2\}\text{-}o]_3 + 3\,H_2O$$

1

[*] Prof. Dr. G. van Koten, Drs. D. M. Knotter, H. L. van Maanen, Dr. D. M. Grove
Laboratory of Organic Chemistry, Department of Metal-Mediated Synthesis, University of Utrecht
Padualaan 8, NL-3584 CH Utrecht (The Netherlands)
Dr. A. L. Spek
Laboratory for Crystal and Structural Chemistry, University of Utrecht
Padualaan 8, NL-3584 CH Utrecht (The Netherlands)

[**] This work was supported in part (*A. L. S.*) by the Netherlands Foundation for Chemical Research (SON) with financial aid from the Netherlands Organization for Scientific Research (NWO).

Compound **1** is a yellow, air-sensitive solid which is readily soluble in most organic solvents and which was found by cryoscopy to be trimeric. Recrystallization from THF affords the crystalline solvate **1**·THF, which has a melting point of 148°C with no visible decomposition.

Spectroscopic characterization of **1** included IR (absence of the SH band at 2600 cm^{-1} found in the parent thiophenol), UV/VIS, and ^{1}H NMR spectroscopy. In its electronic spectrum, **1** (solid) shows an absorption maximum at 400 nm. Furthermore, **1**·THF shows an emission maximum at 556 nm and the crystals show intense triboluminescence when mechanically disrupted; green flashes are clearly visible even in broad daylight.

The 200.13-MHz ^{1}H and 50.32-MHz ^{13}C NMR spectra of **1** (solvent free) in [D$_8$]toluene are temperature dependent. At 358 K the ^{1}H NMR spectrum of **1** shows only one thiophenolate ligand pattern with chemical shifts that are consistent with a noncoordinated amine substituent.[2] At a lower temperature (233 K) four ligand patterns are present in a 9:2:2:2 ratio, ascribable to the presence of two trimeric species in a 3:2 ratio: a major symmetric one with ligand pattern intensity 9 and a minor asymmetric one with three separate ligand patterns with 2:2:2 intensity. The number of methyl groups present in this ^{1}H NMR spectrum and the corresponding ^{13}C NMR spectrum at 233 K is clear evidence for coordination of nitrogen to copper in both species.

To help elucidate the structural aspects and geometry of trimeric **1** in solution, a single-crystal X-ray analysis of **1**, obtained from THF solution, was carried out[3] (Fig. 1a).

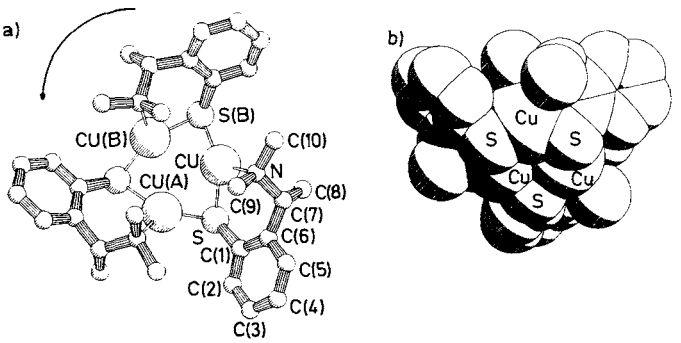


Fig. 1. a) Structure of **1** in the crystal (excluding disordered THF). Important bond lengths [Å] and angles [°]: Cu-S 2.231(2), Cu-S(B) 2.186(2), Cu-N 2.077(7), Cu-Cu(A) 2.828(1); N-Cu-S 101.6(2), S(B)-Cu-N 129.3(2), S-Cu-S(B) 128.4(1), C1-S-Cu 107.5(3), Cu(A)-S-C1 109.9(3), Cu-S-Cu(A) 79.63(7). The molecule has a crystallographic threefold rotation axis. Arrow indicates the "left-hand turn" of the chelating arms. b) Space-filling model of compound **1** showing the "open" S_3 side.

The crystal structure of **1** shows a unit cell containing two independent trimeric molecules and two disordered THF molecules. Each trimeric molecule has a central Cu_3S_3 six-membered ring of chair conformation and C_3 symmetry, comprising alternate copper and sulfur atoms; the amine substituent of each thiophenolate ligand is *N*-coordinated to a neighboring copper atom. In this way each copper atom is trigonally coordinated (2 S, 1 N) and each sulfur is tetrahedrally coordinated (2 Cu, 1 C_{aryl}, lone pair). All aromatic groups are equatorially bound to sulfur with respect to the Cu_3S_3 ring. Furthermore, all chelate rings are identical. The copper–sulfur bond lengths and the distance between copper atoms are typical for bridged copper–sulfur compounds.[4] The Cu–N distance is short, though in the expected range.

One striking result of the C_3 symmetry of this molecule and the equatorial coordination of the aryl groups is that the Cu_3S_3 ring has an S_3 side which is "open" and a Cu_3 side, with Cu···Cu distances of 2.828(1) Å, which is shielded by the organic groups (Fig. 1b). The whole molecule is chiral and the CH(Me)NMe_2 group of the chelating ligand shows a left-hand turn in which the *C*-methyl group is positioned axially with respect to the aromatic ring.[5] The alternative "right-hand turn" conformation was not detected by NMR and we assume that this conformation, which places the *C*-methyl group in an equatorial position is sterically unfavorable.

This solid-state structure of **1** in which all ligands are equivalent appears to correspond to the major species present in solution at low temperature. The minor asymmetric species, with which the major species is interconvertible at higher temperatures, is almost certainly also a trimer. We believe this trimer to be derived from the symmetric form by inversion of one S atom whereby one aromatic ring assumes an axial position with respect to the Cu_3S_3 ring. The interconversion of these two isomers, as seen in the ^1H NMR spectra is probably an intramolecular process; there is no concentration dependence either of the cryoscopic molecular weight in benzene or of the isomer ratio determined from low-temperature ^1H NMR spectra. The postulated S inversion is well known for thioethers[6] but is new for d^{10} metal thiolates, and the proposed asymmetric structure bears analogy to that of $[B_3(SR)_3]$.[7]

Compound **1** is the first characterized metal thiophenolate with a chelating group in the *ortho* position. Due to this chelating group we have been able to isolate a trimeric, neutral copper(I) thiophenolate—this is quite remarkable since neutral species in this type of chemistry are rare and trimers were until now unknown.[1] Because the sulfur and nitrogen atoms are in fixed positions with respect to one another, compound **1** may be used as a chiral tridentate sulfur ligand in the way thio-[9]crown-3 ethers have been used.[8] Another direction we are exploring is the use of **1** as a chiral template for the synthesis of higher-order cuprates.[9]

Experimental Procedure

1: A mixture of Cu_2O (4.38 g, 30.6 mmol) and 2-[(*R*)-1-(dimethylamino)ethyl]thiophenol (7.73 g, 42.6 mmol) in 100 mL of ethanol was refluxed for 20 h under a nitrogen atmosphere. Excess Cu_2O was removed by filtration and the clear yellow ethanol solution evaporated in vacuo to afford the yellow solid product. Recrystallization from a saturated THF solution was carried out by slow cooling over two days from 68 to 14°C in a 3-L Dewar flask initially filled with 68°C water. **1**·THF was obtained as pale yellow needles (m.p. 148°C). Yield: 8.03 g (78%). Crystals of the solvate were dissolved in pentane and the solvent removed in vacuo to afford solvent-free **1**.

Received: October 19, 1988 [Z 3016 IE]
German version: *Angew. Chem. 101* (1989) 351

[1] J. R. Nicholson, I. L. Abrahams, W. Clegg, C. D. Garner, *Inorg. Chem. 24* (1985) 1092, and references cited therein.

[2] **1**: ^1H NMR (200.13 MHz, $C_6D_5CD_3$, 358 K): $\delta = 7.53$ (d, $J = 7$ Hz, 1H; *o*-H_{ar}), 6.5–6.9 (m; 3H, H_{ar}), 3.10 (q, $J = 6$ Hz, 1H; CH), 2.02 (s, 6H; $N(CH_3)_2$), 1.35 (d, $J = 6$ Hz, 3H; α-CH_3). ^1H NMR (200.13 MHz, $C_6D_5CD_3$, 223 K); C_3 conformer: $\delta = 7.62$ (d, $J = 7$ Hz, 1H; *o*-H_{ar}), 6.80 (dd, 1H; *m*-H_{ar}), 2.57 (q, $J = 6$ Hz, 1H; CH), 1.86 (d, $J = 6$ Hz, 3H; α-CH_3); C_1 conformer: $\delta = 8.04$ (d, $J = 7$ Hz, 1H; *o*-H_{ar}), 7.63 (d, $J = 7$ Hz, 1H; *o*-H_{ar}), 7.49 (d, $J = 7$ Hz, 1H; *o*-H_{ar}), 6.76 (dd, 1H; *m*-H_{ar}), 6.87 (dd, 1H; *m*-H_{ar}), 6.65 (dd, 1H; *m*-H_{ar}), 4.48 (q, $J = 6$ Hz, 1H; CH), 0.63 (d, $J = 6$ Hz, 3H; α-CH_3), 2.63 (q, $J = 6$ Hz, 1H; CH), 1.76 (d, $J = 6$ Hz, 3H; α-CH_3), 2.50 (q, $J = 6$ Hz, 1H; CH), 0.72 (d, $J = 6$ Hz, 3H; α-CH_3). Irrespective of the symmetry of the whole molecule and provided that the Cu^I–N coordination is stable on the NMR time scale, the NMe groups are diastereotopic owing to the presence of the chiral benzylic center [10].

[3] **1**, $C_{34}H_{50}Cu_3N_3OS_3$: space group $P6_3$, $a = b = 13.743(1)$, $c = 11.248(1)$ Å, $V = 1839.8(3)$ Å^3, 100 K, $Z = 2$, $\rho_{calcd} = 1.451$ g cm^{-3}, $\mu = 19.8$ cm^{-1}; Enraf-Nonius CAD4 ($Mo_{K\alpha}$, Zr filtered); 1448 reflections with $I \geq 2.5\sigma(I)$ used. The structure was solved by standard Patterson and Fourier techniques (SHELXS-86) and refined with full-matrix least-squares methods (SHELX76). Final $R = 0.054$, $R_w = 0.067$ [$w = 1/\sigma^2(F)$; 140 parameters]. The THF molecule was refined with a disordered model. Further details concerning the structure are available on request from the Director of the Cambridge Crystallographic Data Centre, University Chemical Laboratory, Lensfield Road, Cambridge CB2 1EW (England).

[4] I. G. Dance, M. L. Scudder, L. J. Fitzpatrick, *Inorg. Chem. 24* (1985) 2547.

[5] G. van Koten, J. G. Noltes, *J. Am. Chem. Soc. 101* (1979) 6593.

[6] a) K. G. Orrell, V. Šik, C. H. Brubaker, B. McCulloch, *J. Organomet. Chem. 276* (1984) 267; b) E. W. Abel, S. K. Bhargava, K. G. Orrell, A. W. G. Platt, V. Šik, T. S. Cameron, *J. Chem. Soc. Dalton Trans. 1985*, 345.

[7] S. Pollitz, F. Zettler, D. Forst, H. Hess, *Z. Naturforsch. B31* (1976) 897.

[8] H. J. Küppers, A. Neves, C. Pomp, D. Ventur, K. Wieghardt, B. Nuber, J. Weiss, *Inorg. Chem. 25* (1986) 2400; M. T. Ashby, D. L. Lichtenberger, *ibid. 24* (1985) 636.

[9] Preliminary studies show that the novel complex MeLi·**1** is able to enantioselectively transfer the methyl group in a 1,4 addition to PhCH=CHC(O)Ph (30% *ee*). The first example of a mixed organo thiolatocopper compound obtained from $[CuSC_6H_4\{CH_2NMe_2\}\text{-}o]_3$ and $[CuC{\equiv}CtBu]_n$, namely, $[Cu_6(SC_6H_4\{CH_2NMe_2\}\text{-}o)_4(C{\equiv}CtBu)_2]$, has recently been characterized.

[10] G. van Koten, J. T. B. H. Jastrzebski, J. G. Noltes, W. M. G. F. Pontenagel, J. Kroon, A. L. Spek, *J. Am. Chem. Soc. 100* (1978) 5021.

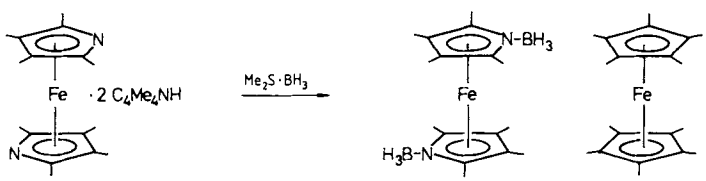
$(C_4Me_4NBH_3)_2Fe$—a Metal Complex Isosteric with Decamethylferrocene with Characteristic Metallocene Disorder**

By *Norbert Kuhn,* Eva-Maria Horn, Roland Boese,** and *Norbert Augart*

The coordination chemistry of the dihydro-1,2-azaborolides **1**[1,2] is based on a productive application of the isosteric principle, since these ligands can be formally prepared from the cyclopentadienide ion **2** by replacement of



1 **2** **3** **4a**, R = H; **4b**, R = CH_3



5 **6** **7**

[*] Prof. Dr. N. Kuhn, Dipl.-Chem. E.-M. Horn
Fachbereich 6 (Chemie) der Universität—Gesamthochschule
Lotharstrasse 1, D-4100 Duisburg 1 (FRG)
Dr. R. Boese, Dipl.-Chem. N. Augart
Institut für Anorganische Chemie der Universität—Gesamthochschule
EARN ID: CAN010 at DE0HRZ1A
Universitätsstrasse 3–5, Postfach 103764, D-4300 Essen (FRG)

[**] Heterocycles as Ligands, Part 4. This work was supported by the Deutsche Forschungsgemeinschaft and the Fonds der Chemischen Industrie. We thank Prof. Dr. *P. Sartori* for helpful discussions and support.—Part 3: [7].

a C_2 fragment by a BN unit. In contrast to the borole dianions[1,3] and pyrroles,[4] which are closely related through similar ring structures, the exocyclic BN compounds **3** and **4a** have so far not been used as ligands; the reason for this may be connected with unsolved problems in their synthesis.[5]

The synthesis of the trihydro(tetramethylpyrrolyl)borate ligand **4b** at the complex center by borylation of the corresponding azacyclopentadienyl complex is conceivable. For the synthesis of the decamethylferrocene analogue iron(II) trihydro(tetramethylpyrrolyl)borate **6** we allowed the tetramethylpyrrole adduct **5**[7] instead of the inaccessible 1,1'-diazaferrocene to react with $Me_2S \cdot BH_3$. The sandwich compound **6** thus obtainable in good yields is readily soluble in dipolar aprotic solvents and is air-stable in the solid state. As expected, the ^{13}C NMR shift of the coordinated C atoms in **6** ($\delta = 98.56$, 86.97) differs very little from the corresponding values of the starting compound **5**;[7] the ^{11}B NMR spectrum ($\delta = -20.23$ (q), $^1J_{B,H} = 94.84$ Hz) shows the analogy between the ligands **4b** and the pyridine-borane adducts.[8] Stepwise cleavage of the BH_3 groups of **6** to give bis(tetramethylpyrrolyl)iron, visible in the mass spectrum as most intense peak, could not be reproduced preparatively.

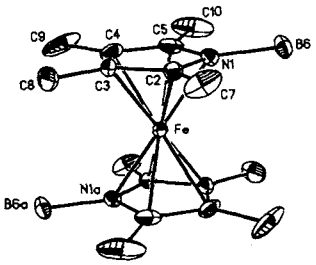


Fig. 1. Molecular structure of **6** with thermal ellipsoids drawn at the 50% probability level (without hydrogen).

Upon determination of the crystal structure of **6**[9] disorders similar to those already established by *Seiler* and *Dunitz* for ferrocene,[10a,b] nickelocene[10c] and ruthenocene[10d] were observed. Cobaltocene is also disordered in the crystal, so that disorders can be regarded as a characteristic feature of the metallocenes. Upon refinement with anisotropic temperature factors (Fig. 1), better referred to here as anisotropic displacement parameters (ADPs),[13] the displacements are neither compatible with a temperature oscillation nor with a rotational disorder, even in lower symmetries. Rather, on assuming centrosymmetry, there are disorders in which the rings are each arranged around a shifted and rotated C_5 axis. This is illustrated for **6** in Figure 2; all atoms were freely refined with good convergence and with the same R value, using in each case

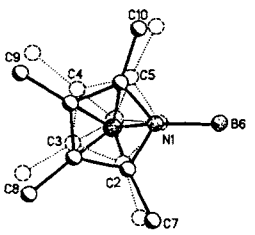


Fig. 2. Presentation of the disorder of **6**; the atoms drawn in unbroken and in broken lines are each refined with 50% occupation factors.

isotropic displacement factors and 50% occupation factors. Therefore an analysis of the ADPs with the THMA program[14] was not necessary. The bond lengths within each of the "half molecules" are comparable with those that were also obtained in the refinement with ADPs, which will be discussed further.

On the basis of the isosteric principle **6** could also be isostructural with decamethylferrocene **7**.[15] In the crystal, **7** has D_{5d} symmetry in the space group *Cmca*, whereby the fivefold axes of the molecules are orthogonal. This could also be true in the case of **6** if boron and nitrogen lie on the crystallographic mirror plane. We found, however, that **6** is monoclinic (Laue symmetry $2/m$) and has the space group $P2_1/n$. The fivefold axes in the refinement with ADPs are tilted at 85.1°, thus resulting in the lower symmetry of **6**. The molecular geometry of **6** is changed slightly compared to that of **7**,[15] despite the isosteric relationship of the two compounds, since the exocyclic BH_3 group in the ligand **4b** does not compensate the smaller radius of the nitrogen atom compared to the carbon. Thus, the projection of the coordination center onto the ring plane is shifted in the direction of the nitrogen atom relative to the geometrical center of the ring. Hereby, the bonds to C2 and C5 ($\bar{d}$(Fe-C2,5) = 2.029 Å) as well as the iron-nitrogen bond (d(Fe-N1) = 2.004(1) Å) are shorter than the mean value of the Fe-C bond in **7** ($\bar{d}$(Fe-C) = 2.050 Å); this is compensated by the marked expansion of the bonds to C3 and C4 ($\bar{d}$(Fe-C3,4) = 2.077 Å) in the sense of a distance lying in the expected range d (Fe-C_4N(center)) of 1.655 Å. In a similar way, the relative expansion of the C3-C4 bond (1.432(3) Å) essentially equals the shortening of the C-N bonds ($\bar{d}$(N1-C2,3) = 1.398 Å), so that the mean value of the ring bonds in **6** ($\bar{d}$ = 1.41 Å) almost agrees with that in **7** ($\bar{d}$ = 1.42 Å). The B-N bond (d(N1-B6) = 1.599(2) Å) is noticeably longer than the mean value of the exocyclic C-C distances both in **6** ($\bar{d}$ = 1.49 Å) and in **7** ($\bar{d}$ = 1.50 Å); this makes the BH_3 groups protrude out more from the ring plane of the ligand in the direction away from the coordination center. Hereby, the mean plane of the atoms C(7-10)B6 forms an angle of 1.8° with the mean ring plane C(2-5)N1.

The shift of the ligand **4b** relative to the molecular axis of **6** thus corresponds to that of the borole dianion.[16] However, due to the ratio of the radii, this ligand is shifted in the opposite direction, which is probably also true in the case of the hitherto unknown ligand **3**. In contrast, in the diazaborolide complexes of iron[17] the proximity of the heteroatoms in the ring leads to an equalization of the difference in the radii and to central coordination. The structure of iron(II) trihydro(tetramethylpyrrolyl)borate **6** thus demonstrates possibilities and limitations of the use of the isosteric principle in the construction of sandwich complexes.

Experimental

6: A mixture of **5** (0.63 g, 1.15 mmol) and $Me_2S \cdot BH_3$ (0.05 mL, 6.9 mmol) in benzene (20 mL) was stirred for 10 min. After addition of 40 mL of pentane the resulting precipitate was purified by recrystallization from CH_2Cl_2/ether. Yield 301 mg (80%), bright orange crystals.—^1H NMR (60 MHz, [D_6]benzene, TMS int.): $\delta = 2.0$ (s, 12H; C(2,5)-CH_3), 1.38 (s, 12H, C(3,4)-CH_3), BH_3 not ovserved.—^{11}B NMR (25.71 MHz, CD_2Cl_2, $BF_3 \cdot Et_2O$ ext.): $\delta = -20.23$ (q, $^1J(^{11}B,^1H) = 94.84$ Hz).—$^{13}C\{^1H\}$ NMR (75.43 MHz, CD_2Cl_2, TMS int.): $\delta = 98.56$ (C2,5), 86.97 (C3,4), 10.18 (C2,5-CH_3), 7.97 (C3,4-CH_3).—MS (70 eV): m/z 328 ($M^{\oplus}$, 15%), 314 ($M^{\oplus} - BH_3$, 54), 300 ($M^{\oplus} - 2BH_3$, 100), 285 ($M^{\oplus} - 2BH_3 - CH_3$, 23) and further fragments.

Received: November 4, 1988 [Z 3037 IE]
German version: *Angew. Chem. 101* (1989) 354

[1] Review of earlier works: G. Schmid, R. Köster in *Houben-Weyl-Müller: Methoden der Organischen Chemie Band 13/3*, Thieme, Stuttgart 1984, p. 1.
[2] G. Schmid, *Comments Inorg. Chem. 4* (1985) 17; G. Schmid, F. Schmidt, *Chem. Ber. 119* (1986) 1766; G. Schmid, G. Barbenheim, *ibid. 120* (1987) 401, and references cited therein.
[3] G. E. Herberich, M. Negele, *J. Organomet. Chem. 350* (1988) 81; G. E. Herberich, B. Hessner, H. Ohst, I. A. Raap, *ibid. 348* (1988) 305, and references cited therein.
[4] N. Kuhn, E. M. Horn, E. Zauder, D. Bläser, R. Boese, *Angew. Chem. 100* (1988) 572; *Angew. Chem. Int. Ed. Engl. 27* (1988) 579, and references cited therein.
[5] On attempting to repeat a synthesis of $Na(C_4H_8O_2)^{\oplus}C_4H_4NBH_3^{\ominus}$ [6] we obtained a mixture of the anions $BH_4^{\ominus}$, $pyBH_3^{\ominus}$, $py_2BH_2^{\ominus}$, $py_3BH^{\ominus}$.
[6] B. Györi, J. Emri, P. Szarvas, *Acta Chim. Acad. Sci. Hung. 86* (1975) 235.
[7] N. Kuhn, E. M. Horn, R. Boese, N. Augart, *Angew. Chem. 100* (1988) 1433; *Angew. Chem. Int. Ed. Engl. 27* (1988) 1368.
[8] H. Nöth, B. Wrackmeyer, *Chem. Ber. 107* (1974) 3070.
[9] Cell data (130 K): $a=9.183(3)$, $b=9.743(2)$, $c=9.774(3)$ Å, $\beta=101.73(2)°$, $P2_1/n$, $Z=2$, 3116 independent reflections, 2908 observed ($F_0 \geq 4\sigma(F)$), ω data collection on a Nicolet R3m/V X-ray four-circle diffractometer, $2\theta_{max}=65°$, $Mo_{K\alpha}$ radiation, empirical absorption correction in the 2θ range of 3°–50°, min/max transmission: 0.955/0.984; all non-hydrogen atoms with anisotropic displacement factors: 113 parameters, $R=0.0485$, $R_w=0.0695$, $w^{-1}=(\sigma^2(F_0)+0.00133F_0^2)$, maximum residual electron density 0.892 e/Å^3. Further bond lengths [Å] and angles [°]: C2-C7 1.485(3), C3-C8 1.484(4), C4-C9 1.497(4), C5-C10 1.489(3); C2-N1-C5 108.4(1), C2-N1-B6 125.7(1), C5-N1-B6 125.4(1), N1-C2-C3 108.7(1), C2-C3-C4 106.9(2), C3-C4-C5 107.5(2), C4-C5-N1 108.5(1).—Further details of the crystal structure investigation are available on request from the Fachinformationszentrum Energie, Physik, Mathematik GmbH, D-7514 Eggenstein-Leopoldshafen 2 (FRG), on quoting the depository number CSD-53652, the names of the authors, and the journal citation.
[10] a) P. Seiler, J. D. Dunitz, *Acta Crystallogr. Sect. B 25* (1979) 1068, and references cited therein; b) *ibid. Sect. B 25* (1979) 2020; c) *ibid. Sect. B 26* (1980) 2255; d) *ibid. Sect. B 26* (1980) 2946.
[11] *Seiler* and *Dunitz* have already established [10a] that the determination of the structure of the cobaltocene by *Bünder* and *Weiss* [12] contained temperature factors which point to disorders. We were able to confirm this by low-temperature structure analyses; we also established that disorders of the cyclopentadienyl rings similar to those in ferrocene occur in ferrocinium tetrafluoroborate and in cobaltocinium hexafluorophosphate.
[12] W. Bünder, E. Weiss, *J. Organomet. Chem. 92* (1975) 65.
[13] a) J. D. Dunitz, V. Schomaker, K. N. Trueblood, *J. Phys. Chem. 92* (1988) 856; b) J. D. Dunitz, C. Krüger, H. Irngartinger, E. F. Maverick, Y. Wang, N. Nixdorf, *Angew. Chem. 100* (1988) 415; *Angew. Chem. Int. Ed. Engl. 27* (1988) 387.
[14] K. N. Trueblood, *Acta Crystallogr. Sect. A 34* (1978) 950; the most recent version is the Program THMA11.
[15] D. P. Freyberg, J. L. Robbins, K. N. Raymond, J. C. Smart, *J. Am. Chem. Soc. 101* (1979) 892.
[16] G. E. Herberich, W. Boveleth, B. Hessner, D. P. J. Köffer, M. Negele, R. Saive, *J. Organomet. Chem. 308* (1986) 153.
[17] a) G. Schmid, S. Amirkhalili, U. Höhner, R. Boese, *Chem. Ber. 115* (1982) 3850; b) G. Schmid, U. Höhner, D. Kampmann, D. Zaika, R. Boese, *ibid. 116* (1983) 951; c) G. Schmid, G. Barbenheim, R. Boese, *Z. Naturforsch. B 40* (1985) 787.

Structural Diversity in Iodoantimonates; the Anions $Sb_3I_{11}^{2\ominus}$, $Sb_5I_{18}^{3\ominus}$ and $Sb_6I_{22}^{4\ominus}$**

By *Siegfried Pohl,* Rainer Lotz, Wolfgang Saak,* and *Detlev Haase*

The trihalides of the heavy elements of the fifth main group can react as Lewis acids with halide ions to give anions of various degrees of condensation (see, e.g., Ref. [1]). Thus, on reaction with iodide, SbI_3 forms iodoantimonates in which Sb^{III} is generally coordinated with distorted octahedral geometry.

[*] Prof. Dr. S. Pohl, Dipl.-Chem. R. Lotz, Dipl.-Chem. W. Saak, Dipl.-Ing. D. Haase
Fachbereich Chemie der Universität
Postfach 2503, D-2900 Oldenburg (FRG)

[**] This work was supported by the Fonds der Chemischen Industrie.

Besides the antimonates $Sb_2I_9^{3\ominus}$ and $[SbI_4^{\ominus}]_\infty$ mentioned in Ref. [2], the SbI_3-rich anions $Sb_6I_{22}^{4\ominus}$,[3] $Sb_8I_{28}^{4\ominus}$,[4,5] $[Sb_2I_7^{\ominus}]_\infty$,[5] and $[Sb_3I_{10}^{\ominus}]_\infty$[4,6] have recently been prepared, some of them having the same formula but different structures. We have now been able to isolate three novel iodoantimonates, namely salts **1**–**3**:

$[Cu(CH_3CN)_4]_2Sb_3I_{11}$ **1** $(Me_4N)_3Sb_5I_{18}$ **2** $[(C_5H_5)_2Fe]_4Sb_6I_{22}$ **3**

The compounds **1** and **2** are obtained upon reaction of CuI and Me_4NI respectively with SbI_3 in acetonitrile. **3** is prepared according to equation (a), likewise in acetonitrile; the ferrocene employed in this reaction is not oxidized completely.

$$6(C_5H_5)_2Fe + 3I_2 + 6SbI_3 \longrightarrow [(C_5H_5)_2Fe]_4Sb_6I_{22} + 2/3(C_5H_5)_2FeI_3 + 4/3(C_5H_5)_2Fe \quad \text{(a)}$$

3

All three compounds were characterized by X-ray structure analyses.[7] The $Sb_3I_{11}^{2\ominus}$ ion of **1** forms three face-sharing octahedra (Fig. 1), comparable in this respect to the suboxide $Cs_{11}O_3$.[8] The anions $Sb_5I_{18}^{3\ominus}$ (Fig. 2) and $Sb_6I_{22}^{4\ominus}$ (Fig. 3), on the other hand, consist of edge-sharing octahedra. The anion of **3**, like other iodoantimonates,[4] corresponds to a section from a layer of the CdI_2 structure. It thus has a structure other than the ion of the same composition in **4**[3] (see below).

$[Fe(1,10\text{-phen})_3]_2Sb_6I_{22}\cdot 2CH_3CN$ **4**

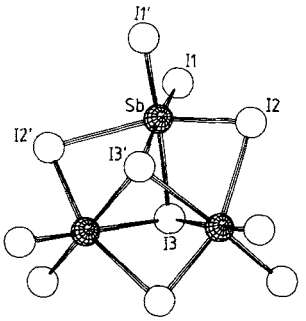


Fig. 1. Structure of the anion of **1** in the crystal. Distances [pm]: Sb-I1 278.2(2), Sb-I2 297.7(3), Sb-I2' 346.4(3), Sb-I3 335.6(2). The disorder of I2 derived from the crystallographic point symmetry (D_3) is not shown here for sake of clarity (I2 lies next to the twofold axis of rotation).

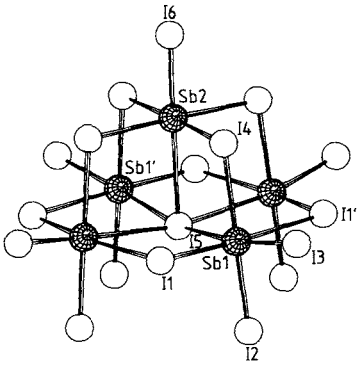


Fig. 2. Structure of the anion of **2** in the crystal (C_s symmetry). Distances [pm]: Sb1-I1 281.0(2), Sb1-I1' 354.8(2), Sb1-I2 289.1(2), Sb1-I3 277.0(2), Sb1-I4 316.9(2), Sb1-I5 341.8(1), Sb2-I4 302.8(2), Sb2-I5 354.7(4), Sb2-I6 272.4(5).

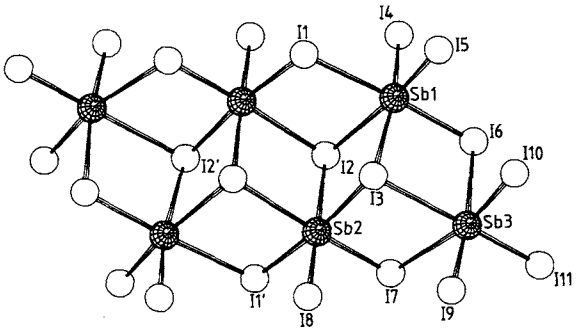


Fig. 3. Structure of the anion of **3** in the crystal (C_i symmetry). Distances [pm]: Sb1-I1 326.3(1), Sb1-I2 331.1(1), Sb1-I3 346.9(1), Sb1-I4 278.4(1), Sb1-I5 281.2(1), Sb1-I6 288.0(1), Sb2-I1' 298.0(1), Sb2-I2 336.9(1), Sb2-I2' 327.9(1), Sb2-I3 311.6(1), Sb2-I7 284.8(1), Sb2-I8 280.7(2), Sb3-I3 336.5(2), Sb3-I6 348.9(2), Sb3-I7 352.9(2), Sb3-I9 276.4(2), Sb3-I10 279.0(2), Sb3-I11 278.6(2).

The stereochemistry of the individual Sb^{III} atoms is similar in all three compounds: in the distorted SbI_6 octahedra the almost linear I-Sb-I units oriented perpendicular to each other can, according to *Rundle*[9] be described by four-electron three-center bonds. Within such a three-center bond the distances, as a measure of the bond strengths, can in some cases be very different. Thus, they vary from symmetric arrangements (I-Sb in each case 302.8 pm, see I4-Sb-I4' in **2**) through to strongly asymmetric groups (e.g. I5-Sb2-I6 in **2** with 354.7 and 272.2 pm). These variations are accompanied by deviations of the I-Sb-I angle from 180° by up to 20° (I2-Sb-I2' angle in **1**: 159.0°). Possibly a slight stereochemical influence of the non-bonding electron pair of antimony(III) is also reflected in these distortions. The structure of $Sb_5I_{18}^{3\ominus}$ also contains approximately linear Sb-I-Sb units (see Sb1-I5-Sb1' in Fig. 2). Comparable groupings have already been found in the anion $(PhSbI_2)_4I^{\ominus}$[10] and in the central Sb_6I_6 twin cube of **4**.[3] In all cases the Sb-I distances indicate that iodine, in contrast to Sb as central atom in linear units, forms only weak, almost symmetrical bonds with the two neighboring atoms. Due to the flexibility of the Sb-I bonds, a large number of different linkages are possible for the SbI_6 octahedra, thus enabling an optimal fit of the anions to the "spatial requirements" of the respective cations. The result is the observed structural diversity, which is not limited to the iodoantimonates—and not even to the fifth main group elements. Thus, the different forms of Te_4I_{16}[11] correspond in the coupling of the octahedra to the different $Sb_6I_{22}^{4\ominus}$ ions (see above). Such a conformity of the structures can be an indication that the species $Te_3I_{11}^{\oplus}$, $Te_5I_{18}^{2\oplus}$ and $Te_6I_{22}^{2\oplus}$ isoelectronic with $Sb_3I_{22}^{2\ominus}$, $Sb_5I_{18}^{3\ominus}$ and $Sb_6I_{22}^{4\ominus}$ respectively are likewise stable and isolable with suitable anions.

Experimental

1: 0.19 g (1 mmol) of CuI and 0.75 g (1.5 mmol) of SbI_3 were dissolved with heating in 80 mL of CH_3CN. Within ca. 6 days at −18°C bright red prisms of **1** crystallized out in ca. 85% yield. The compound rapidly loses acetonitrile. The elemental analysis was therefore only satisfactory regarding the ratio Cu : I : Sb.

2: The compound (orange-red prisms) was always obtained in admixture with $(Me_4N)_3Sb_2I_9$ and $(Me_4N)_4Sb_8I_{28}$ upon using the same procedure as for **1**; see also Ref. [5].

3: 0.09 g (0.5 mmol) of ferrocene, 0.06 g (0.25 mmol) of I_2 and 0.25 g (0.5 mmol) of SbI_3 were successively dissolved with heating in 150 mL of CH_3CN. Within 1 day at room temperature black compact crystals separated out in 82% yield; satisfactory C,H,Fe,I analysis.

Received: October 21, 1988 [Z 3021 IE]
German version: *Angew. Chem. 101* (1989) 355

[1] K. B. Dillon, A. W. G. Platt, A. Schmidpeter, F. Zwaschka, W. S. Sheldrick, *Z. Anorg. Allg. Chem. 488* (1982) 7; W. Willing, U. Müller, J. Eicher, K. Dehnicke, *ibid. 537* (1986) 145; W. S. Sheldrick, H.-J. Häusler, J. Kaub, *Z. Naturforsch. B43* (1988) 789; A. T. Mohammed, U. Müller, *ibid. 40* (1985) 562; U. Ensinger, W. Schwarz, A. Schmidt, *ibid. 37* (1982) 1584; A. L. Rheingold, A. D. Uhler, A. G. Lauders, *Inorg. Chem. 22* (1983) 3255.

[2] A. F. Wells: *Structural Inorganic Chemistry*, 5th Edit., Clarendon Press, Oxford 1984, p. 465f, 884ff.

[3] S. Pohl, D. Haase, R. Lotz, W. Saak, *Z. Naturforsch. B43* (1988) 1033.

[4] S. Pohl, W. Saak, D. Haase, *Z. Naturforsch. B42* (1987) 1493.

[5] S. Pohl, R. Lotz, D. Haase, W. Saak, *Z. Naturforsch. B43* (1988) 1144.

[6] S. Pohl, W. Saak, P. Mayer, A. Schmidpeter, *Angew. Chem. 98* (1986) 813; *Angew. Chem. Int. Ed. Engl. 25* (1986) 825.

[7] **1**: trigonal, $P\bar{3}c1$, $a = 1199.7(1)$, $c = 2015.1(1)$ pm, $Z = 2$. 1254 independent reflections, 820 with $I > 2\sigma(I)$; $R = 0.057$, $R_w = 0.052$. I2 (see Fig. 1) is also disordered on assuming the space group $P3c1$; in $P6_3/mcm$ the cation would *also* be disordered (two half-occupied sites), so that $P3c1$ was chosen as space group.—**2**: tetragonal, $P4/nnc$, $a = 1252.1(1)$, $c = 3779.7(2)$ pm, $Z = 4$. 2141 independent reflections, 1158 with $I > 2\sigma(I)$; $R = 0.048$, $R_w = 0.044$.—**3**: monoclinic, $P2_1/n$, $a = 1277.5(1)$, $b = 1746.7(1)$, $c = 1973.2(1)$ pm, $\beta = 103.2(1)°$, $Z = 2$. 6475 independent reflections, 4549 with $I > 2\sigma(I)$; $R = 0.051$, $R_w = 0.045$.—Solution and refinement: G. M. Sheldrick, SHELXS-86, Göttingen 1986; G. M. Sheldrick, SHELX-76 *(Program for Crystal Structure Determination)*, University of Cambridge, England 1976. Plots: E. Keller, SCHAKAL 86 *(Program for the Graphic Representation of Molecular and Crystallographic Models)*, Freiburg 1986. Further details of the crystal structure investigations are available on request from the Fachinformationszentrum Energie, Physik, Mathematik GmbH, D-7514 Eggenstein-Leopoldshafen 2 (FRG), on quoting the depository number CSD-53468, the names of the authors, and the journal citation.

[8] A. Simon, *Struct. Bonding (Berlin) 36* (1979) 81.

[9] R. E. Rundle, *J. Am. Chem. Soc. 85* (1963) 112.

[10] J. von Seyerl, O. Scheidsteger, H. Berke, G. Huttner, *J. Organomet. Chem. 311* (1986) 85.

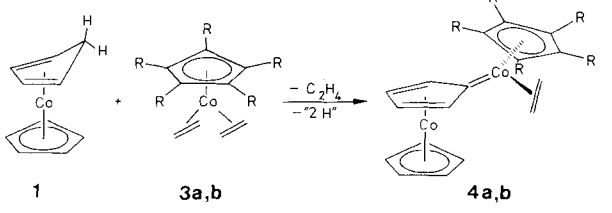
[11] B. Krebs, V. Paulat, *Acta Crystallogr. Sect. B32* (1976) 1470; R. Kniep, H. J. Beister, D. Wald, *Z. Naturforsch. B43* (1988) 966.

Synthesis and Structure of a Binuclear *syn*-Coordinated μ-Cycloheptatrienyl Hydrido Complex with Hindered C_7H_7 Rotation**

By *Hubert Wadepohl,* Wolfgang Galm,* and *Hans Pritzkow*

Dedicated to Professor E. O. Fischer on the occasion of his 70th birthday

(η^6-Cycloheptatriene)metal complexes, like the (η^4-cyclopentadiene) compounds[1] with two fewer ring carbons, have an activated methylene *exo*-CH bond.[2,3] In such compounds, the *endo*-hydrogen also exhibits enhanced reactivity: at elevated temperature a shift from the methylene group to a vinylic ring position is observed. Whereas the unsubstituted η^4-C_5H_6 complex **1** does not rearrange at 100°C,[3] $[(\eta^6\text{-}C_7H_8)Cr(CO)_3]$ **2** displays a [1,5]-sigmatropic shift of the *endo*-hydrogen atom.[4] We have already ex-



1 **3a,b** **4a,b**

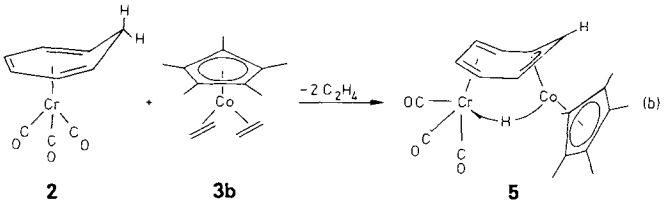
a, R = H; b, R = Me

[*] Dr. H. Wadepohl, Dipl.-Chem. W. Galm, Dr. H. Pritzkow
Anorganisch-chemisches Institut der Universität
Im Neuenheimer Feld 270, D-6900 Heidelberg (FRG)

[**] This work was supported by the Land Baden-Württemberg, (Forschungsschwerpunkt No. 40, "The Chemistry of Isolated and Complexed π Systems").

ploited the activation of the *exo*-CH bond in **1** in the synthesis of the (μ-η^4:η^1-cyclopentadi*enylidene*) complexes **4a**, **4b**, following reaction (a).[5,6]

Whereas both methylene CH bonds were finally cleaved in this reaction, the analogous reaction of **2** with **3b** led to the heterodimetallic complex *syn*-(μ-η^4:η^3-cycloheptatri*enyl*)(μ-hydrido)(tricarbonyl)chromium(η-pentamethylcyclopentadienyl)cobalt **5** [Eq. (b)].



2 **3b** **5**

$[Cp^*Co(CO)]_2$ ($Cp^* = \eta^5$-C_5Me_5) was formed in a side reaction; thus the yield of red-brown **5** amounted to only 15–25%. In contrast to the reaction of complex **1**, the formation of **5** from **2** cannot be explained by an attack of the incoming reagent[7] at the *exo*-CH bond of the methylene group. Instead, attack at the chromium atom leads to a change in the hapticity of the seven-membered ring. Loss of ethene and a hydrogen shift then leads to **5**. The hydrogen shift is reversible; thus, complex **2**, together with $[Cp^*Co(CO)_2]$, was formed upon reaction of **5** with CO (1 bar, room temperature, THF).

An X-ray crystal structure was obtained of **5** to clarify the coordination geometry of the cycloheptatrienyl ring.[8] Complex **5** has approximately C_s symmetry (Fig. 1). The

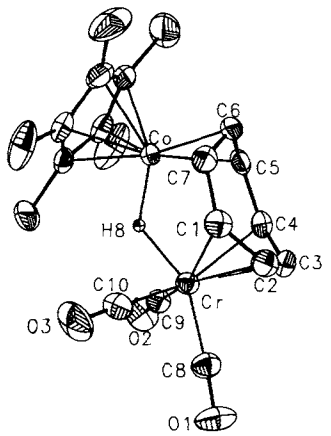


Fig. 1. Molecular structure of **5**. Selected bond lengths [Å] and angles [°] with standard deviations in parentheses: Cr-Co 2.899(1), Cr-H8 1.69(2), Cr-C1/4 2.300(4), Cr-C2/3 2.166(3), Cr-C8 1.817(3), Cr-C9 1.841(3), Cr-C10 1.857(4), Co-H8 1.54(3), Co-C6 1.945(3), Co-C5/7 2.071(4), Co-C(Cp*) 2.052(4)···2.089(3), C1/4-C2/3 1.393(5), C1/4-C7/5 1.447(5), C5/7-C6 1.408(6); Co-Cr-C8 174.3(1), Cr-H8-Co 127(1), C8-Cr-H8 150.0(8).

noncrystallographic mirror plane is comprised of both metal atoms, the hydrido ligand (H8), a carbonyl group (C8–O1), and the carbon atom C6 of the C_7H_7 ligand. On the distorted pseudo-octahedral-coordinated chromium atom there are two carbonyl groups in *cis* positions and one in a *trans* position to Co and thus to the CrHCo bond. The bond lengths in the C_7 ring can be interpreted in terms of (η^4-diene)chromium and (η^3-enyl)cobalt units, joined to each other by relatively long (1.45 Å) C–C bonds. The cycloheptatrienyl ring has a boat conformation (the dihedral angle between the η^4-diene and the η^3-enyl planes is 59°). The chromium, the cobalt, and the bridging hydrogen atom (H8) make up a 3c-2e MHM′ system.[9] Thus, both metals attain an 18-valence-electron configuration. Until now, CrHCo three-center bonds had not been investigated by structural analysis. In contrast to other complexes with a *syn*-M(μ-η^4:η^3-C_7H_7)M′ structure,[10] **5** has a large metal–metal distance (2.899 Å). This is attained by a shift of the chromium atom towards C2 and C3, rather than by a more pronounced folding of the C_7H_7 ring. Hence, Cr–C2/C3 bonds are shorter than Cr–C4/C5 bonds.

To our knowledge, until now it had not been possible to freeze out the rotation of the cycloheptatrienyl ring in *syn*-M(μ-C_7H_7)M′ complexes on the NMR time scale,[10,11] although this has been achieved with *anti*-M(μ-C_7H_7)M′ structures. However, in the ^1H and ^{13}C NMR spectra of **5**, measured at temperatures of approximately 200 K, we observed the expected signal patterns for a rigid μ-η^4:η^3-C_7H_7 structure. The ^1H resonance of the central proton (H6) of the enyl unit of the bridging ligand is shifted upfield of the outer protons H5 and H7 by $\Delta\delta \approx 1$. Normally, the reverse order is observed in η^3-allyl complexes,[12] which is also the case for *anti*-[$(CO)_3Fe(\mu$-η^4:η^3-$C_7H_7)Mo(CO)_2Cp$] **6**.[13a] Similar high-field shifts in $[Cp(CO)_2Mo(\eta^3$-$C_7H_7)]$ and $[(CO)_3Co(\eta^3$-$C_7H_7)]$ ($\Delta\delta \approx 1.5$) have been attributed to the boat conformation of the seven-membered ring.[14] An analogous explanation for *syn*-M(μ-η^4:η^3-C_7H_7)M′ complexes like **5** seems reasonable. In numerous examples with a similar folding of the ligand, however, the average ^1H NMR shifts of fluxional μ-η^4:η^3 cycloheptatrienyl ligands are at a lower field ($\delta(C_7H_7)_{mean} \approx 4.2$ to 3.5)[10,11] than in **5** ($\delta(C_7H_7)_{mean} = 2.92$).

In the literature[10b] the different rotational energy barriers for *anti*- and *syn*-M(μ-1-4-η^4:5-7-η^3-C_7H_7)M′ complexes have been explained by the p_π–p_π orbital overlap between the localized η^4-diene and η^3-enyl ring fragments. Thus, measurements of the bond lengths between these fragments and the torsion angles C3-C4-C5-C6 and C2-C1-C7-C6 should provide useful evidence for this overlap. For instance, these come to 1.49 Å and 61°, respectively, in **6**[13b] (*anti* structure, high rotational barrier), 1.43 Å and 0/34°, respectively, in *syn*-[(μ-CO)(μ-η^4:η^3-C_7H_7)-$\{Fe(CO)_2\}_2]^\ominus$,[10a] and 1.45 Å and 22/24°, respectively, in *syn*-$[(CO)_2Rh(\mu$-η^4:η^3-$C_7H_7)Fe(CO)_3]$[10b] (both low rotational barriers). However, the observed geometry of **5** (C1/4-C7/5 1.45 Å, torsion angles 0, 8.7°) shows that the mentioned structural parameters in the solid state cannot be correlated with the molecular dynamics in solution without further evidence.

Experimental Procedure

A solution of **2** (280 mg, 1.23 mmol) and **3b** (320 mg, 1.28 mmol) in 40 mL of petroleum ether was heated at 60–80°C for 6 h. The solvent was removed from the resulting green solution in vacuo, and the dark residue was redissolved in 20 mL of toluene. Red-brown crystals of **5** were obtained from solution at −25°C, which were recrystallized from toluene several times. Yield: 80 mg (15%) of red-brown prismatic crystals, dec. > 180°C. By further solvent concentration and cooling (−25°C), unreacted **2** and $[Cp^*Co(CO)]_2$ could be isolated.

5: IR (THF): $\tilde{\nu}$(CO) = 1957.5 (vs), 1878 (vs) cm^{-1}. ^1H NMR (200.1 MHz, [D_8]toluene), T = 350 K: δ = 2.92 (s, 7H, C_7H_7), 1.54 (s, 15H, Cp^*), −10.18 (s, 1H, bridging H); T = 200 K: δ = 4.07 (br. s, 2H, H2,3), 2.68 and 2.58 (each br. s, 2H, H1,4 and H5,7), 1.55 (br. s, 1H, H6), 1.38 (s, 15H, Cp^*), −10.13 (s, 1H, bridging H). $^{13}C\{^1H\}$ NMR (50.3 MHz, [D_8]toluene), T = 300 K: δ = 237.9 (CO), 93.7 (C_5Me_5), 68.2 (br, C_7H_7), 8.9 (C_5Me_5); T = 190 K: δ = 238.2 and 238.4 (CO), 93.2 (C_5Me_5), 83.6, 66.6, 59.5, 56.5 (C_7H_7), 8.7 (C_5Me_5). EI-MS (70 eV): m/z (%) 422 (9, $M^\oplus$), 394 (5, $[M-CO]^\oplus$), 366 (6, $[M-2CO]^\oplus$), 336 (92, $[M-3CO-2H]^\oplus$), 250 (27, $[Cp^*Co(CO)_2]^\oplus$), 222 (18, $[Cp^*Co(CO)]^\oplus$),

194 (100, $[Cp^*Co]^{\oplus}$), 193 (10), 192 (60), 133 (36), 92 (35, $[C_7H_8]^{\oplus}$), 91 (80, $[C_7H_7]^{\oplus}$), 59 (16, $Co^{\oplus}$), 52 (38, $Cr^{\oplus}$). Correct C,H analysis.

Received: October 24, 1988 [Z 3024 IE]
German version: *Angew. Chem. 101* (1989) 357

CAS Registry numbers:
2, 12125-72-3; **3b**, 80848-36-8; **5**, 118921-07-6.

[1] E. O. Fischer, G. E. Herberich, *Chem. Ber. 94* (1961) 1517.
[2] J. D. Munro, P. L. Pauson, *J. Chem. Soc. 1961*, 3475.
[3] G. R. Knox, M. Nutley, P. L. Pauson, S. Toma, W. E. Watts, P. A. Elder, R. Griffiths, *J. Chem. Res. (M) 1981*, 1901.
[4] M. I. Foreman, G. R. Knox, P. L. Pauson, K. H. Todd, W. E. Watts, *J. Chem. Soc. Perkin Trans. 2 1972*, 1141.
[5] H. Wadepohl, H. Pritzkow, *Angew. Chem. 99* (1987) 132; *Angew. Chem. Int. Ed. Engl. 26* (1987) 127; W. Galm, *Diplomarbeit*, Universität Heidelberg 1988.
[6] The *exo*-alkyl-substituted derivatives of **1** do not react.
[7] Presumably, a 16-VE fragment, either $[(\eta^5\text{-}Cp^*)Co(C_2H_4)]$ or $[(\eta^3\text{-}Cp^*)Co(C_2H_4)_2]$.
[8] **5**: triclinic, space group $P\bar{1}$, $a=8.463(2)$, $b=9.656(3)$, $c=12.586(3)$ Å, $\alpha=71.67(2)$, $\beta=83.53(2)$, $\gamma=73.84(2)°$, $V=937.4$ Å^3, $Z=2$, $\mu=14.6$ cm^{-1}, Stoe/Siemens four-circle diffractometer ($Mo_{K\alpha}$ radiation, ω-scan, empirical absorption correction), 3066 independent reflections with $I \geq 2\sigma(I)$, all non-hydrogen atoms anisotropic, all H atoms localized in difference Fourier syntheses and refined isotropically, $R=0.036$; $R_w=0.023$, $w=1/\sigma^2(F)$. Further details of the crystal structure investigation can be obtained from the Fachinformationszentrum Energie, Physik, Mathematik GmbH, D-7514 Eggenstein-Leopoldshafen 2 (FRG), on quoting the depository number CSD-53443, the names of the authors, and the journal citation.
[9] R. Bau, R. G. Teller, S. W. Kirtley, T. F. Koetzle, *Acc. Chem. Res. 12* (1979) 176; R. G. Teller, R. Bau, *Struct. Bonding (Berlin) 44* (1981) 1.
[10] a) M. Moll, H. Behrens, W. Popp, G. Liehr, W. P. Fehlhammer, *Z. Naturforsch. B 38* (1983) 1446; b) M. J. Bennett, J. L. Pratt, K. A. Simpson, L. K. K. LiShingMan, J. Takats, *J. Am. Chem. Soc. 98* (1976) 4810; c) R. G. Ball, F. Edelmann, G.-Y. Kiel, J. Takats, R. Drews, *Organometallics 5* (1986) 829.
[11] a) G. Deganello: *Transition Metal Complexes of Cyclic Polyolefins*, Academic Press, London 1979, Chap. 1; b) A. Salzer, T. Egolf, W. von Philipsborn, *Helv. Chim. Acta 65* (1982) 1145, and references cited therein; c) F. Edelmann, J. Takats, *J. Organomet. Chem. 344* (1988) 351; d) F. Edelmann, G.-Y. Kiel, J. Takats, A. Vasudevamurthy, M.-Y. Yeung, *J. Chem. Soc. Chem. Commun. 1988*, 296.
[12] M. L. H. Green, P. L. I. Nagy, *Adv. Organomet. Chem. 2* (1964) 325.
[13] a) F. A. Cotton, C. R. Reich, *J. Am. Chem. Soc. 91* (1969) 847; b) F. A. Cotton, B. G. DeBoer, M. D. LaPrade, *Proc. 23rd Int. Congr. Pure Appl. Chem. Boston 1971, Vol. 6;* cited in [10b].
[14] a) J. W. Faller, *Inorg. Chem. 8* (1969) 767; b) M. A. Bennett, R. Bramley, R. Watt, *J. Am. Chem. Soc. 91* (1969) 3089.

Selective Hydrogenation of Esters to Alcohols with a Catalyst Prepared from Rh_2O_3, $Sn(n\text{-}C_4H_9)_4$, and SiO_2: Evidence for Site Isolation**

By *Abdellah El Mansour, Jean P. Candy,* Jean P. Bournonville, Osmar A. Ferretti,* and *Jean-Marie Basset**

A new generation of bimetallic catalysts exhibiting unusual activities and/or selectivities can be obtained via the reaction of organometallic compounds of main-group elements, in particular group IV, with supported group VIII transition metals.[1] We report here that the reaction of $Sn(n\text{-}C_4H_9)_4$ with Rh_2O_3/SiO_2 results in a $Rh/Sn/SiO_2$ catalyst which is more active and much more selective than Rh/SiO_2 for the hydrogenation of ethyl acetate to ethanol. Our results indicate the ability of tin atoms to isolate rhodium atoms from their neighbors. The concept of real (or apparent) site isolation of rhodium by zinc atoms has been recently advanced by *Ichikawa* et al.[2] to explain the selective hydroformylation of ethylene on a $Rh/Zn/SiO_2$ catalyst.

Catalyst **B** (Rh_2O_3/SiO_2),[3] obtained by oxidation of catalyst **A** (Rh/SiO_2), reacts with $Sn(n\text{-}C_4H_9)_4$ to give catalyst **C** in a two-step process (Table 1). Between 25 and 150 °C

Table 1. Amount of gases evolved (mol C_4/mol Sn) during the preparation of catalyst **C** from $Sn(n\text{-}C_4H_9)_4$ and catalyst **B** (Sn/Rh = 2/1).

T[°C]	1-C_4H_8	2-(*E*)-C_4H_8	2-(*Z*)-C_4H_8	$\sum C_4H_8$	$\sum C_4H_{10}$	H_2O
50	0.12	0.05	0.02	0.19	0.20	–
100	0.56	0.24	0.14	0.94	0.74	–
150	0.70	0.30	0.20	1.20	1.07	–
200	1.44	0.42	0.48	2.34	1.35	+
300	1.45	0.60	0.44	2.49	1.42	+

ca. 1 mole of butane and 1 mole of butene are evolved per mole of stannane. Above 150 °C, mostly butenes and water are produced. The amount of butenes and butane evolved at 300 °C is close to the expected value of four C_4 molecules per tin atom, indicating that the surface does not contain any significant amount of hydrocarbon residue. This result was confirmed by the IR spectra of the catalyst taken in situ at various temperatures. The $\nu_{C\text{-}H}$ and $\delta_{C\text{-}H}$ bands centered at ca. 2800–3200 and 1200–1600 cm^{-1}, respectively, which are intense at 25 °C, almost disappear under vacuum at ca. 200 °C. At the end of the reaction the final ratio butane/butenes is close to 0.5/1 which agrees fairly well with reaction (a).

$$Rh_2O_3 + 4\,Sn(n\text{-}C_4H_9)_4 \longrightarrow Rh_2Sn_4 + 11\,C_4H_8 + 5\,C_4H_{10} + 3\,H_2O \quad (a)$$

The mass balance data (Table 1) suggests that the reaction occurs in two steps: below ca. 150 °C rhodium(III) would not be reduced since equimolar amounts of *n*-butenes and *n*-butane are formed. At this stage the presence of a partially alkylated Sn–Rh bimetallic complex, $[(Rh^{III}\text{-}O)_xSnBu_y]$ ($x+y=4$), can be postulated. Above ca. 150 °C this complex would decompose under partial vacuum with concomitant reduction of Rh^{III} and Sn^{IV} to give Rh^0 and Sn^0 (catalyst **C**). After treatment of **C** under H_2 at 500 °C, X-ray photoelectron spectroscopic measurements confirmed the presence of Rh^0 and Sn^0 (Table 2).

Table 2. Binding energies [eV] of Rh($3d_{5/2}$, $3d_{3/2}$) and Sn($3d_{5/2}$, $3d_{3/2}$) electrons in various rhodium, tin, and rhodium-tin samples.

Sample	Rh		Sn		Ref.
	$3d_{3/2}$	$3d_{5/2}$	$3d_{3/2}$	$3d_{5/2}$	
Rh_2O_3	313.2	308.5 ± 0.5			[4a, b]
Rh metal	311.7	307.0 ± 0.3			[4a–d]
SnO_2			494.9	486.4	[4a]
Sn metal			493.15	484.7	[4a]
$Rh/Sn/SiO_2$	311.6	306.9	493.5	485.0	[4e]

[*] Dr. J. P. Candy, Dr. J.-M. Basset, Dr. A. El Mansour
Institut de Recherches sur la Catalyse
2 Avenue Albert Einstein, F-69626 Villeurbanne Cédex (France)
Dr. J. P. Bournonville
Institut Français du Pétrole
2-4 Avenue de Bois-Préau, F-92506 Rueil-Malmaison Cédex (France)
Dr. O. A. Ferretti
CINDECA (UNLP-CONICET)
47 n° 257, 1900 La Plata (Argentina)

[**] The authors would like to express their thanks to Dr. *J. C. Bertolini, R. Gallezot, J. L. Duvaux*, and *I. Mutin* for helpful discussions regarding X-ray photoelectron spectroscopy and STEM experiments. *J.-M. B.* would like to express his best thanks to Prof. *W. A. Herrmann* for his kind hospitality in Munich and for helpful discussions.

The particles obtained in **C** are bimetallic as demonstrated by STEM (scanning transmission electron microscopy). Their Sn/Rh ratio was the same as that of the starting materials, at least for Sn/Rh < 2. (The tin X-ray emission peak was always associated with that of rhodium.) The chemisorption properties of these bimetallic particles are drastically modified with respect to those of supported rhodium. Whereas Rh/SiO_2 chemisorbs ca. 1 mole of CO and 0.53 mole of H_2 per mole of rhodium atoms (25 °C, 100 mbar of CO or H_2), the bimetallic Rh/Sn (1/1) chemisorbs only 0.4 mole of CO and 0.05 mole of H_2 per mole of rhodium atoms (under the same conditions). IR spectroscopy of CO chemisorbed on catalyst **C** brings supplementary information. With Rh/SiO_2 two strong bands at 2055 and 1878 cm^{-1} are reasonably assigned to the terminal carbonyl and bridging carbonyl, respectively[5] (Fig. 1). With $Rh/Sn/SiO_2$ only one band is observed at 2000 cm^{-1}, which is also reasonably assigned to a linear carbonyl; the band ascribed to a bridging carbonyl is no longer present (only an extremely small shoulder at ca. 1850 cm^{-1} is observed possibly due to traces of bridging CO on $Rh/Sn/SiO_2$).

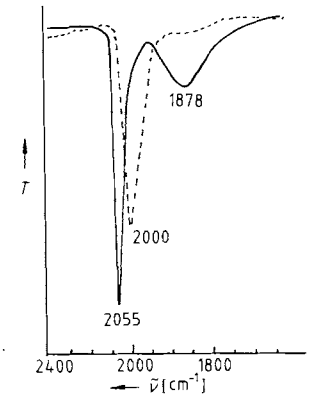
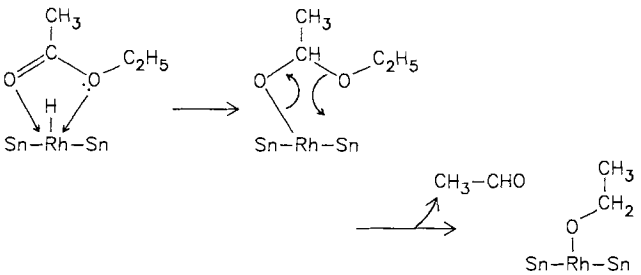


Fig. 1. IR spectrum of CO adsorbed on Rh/SiO_2 (—) and $Rh/Sn/SiO_2$ (---). T = transmission.

The new catalyst **C** exhibits a very high chemoselectivity in the hydrogenation of ethyl acetate to ethanol (Table 3). As the ratio Sn/Rh increases from 0/1 to 0.2/1, the conversion of ethyl acetate decreases sharply, whereas the selectivity of ethanol formation increases significantly. Above an Sn/Rh ratio of 0.2/1 both the conversion of ethyl acetate and the selectivity of ethanol formation increase with tin content to reach values higher than 95% for an Sn/Rh ratio higher than unity, whereas Rh/SiO_2 gives CH_4, C_2H_6, CO, and CO_2, corresponding to a completely unselective C–C or C–O bond cleavage. $Rh/Sn/SiO_2$ with Sn/Rh = 1.7/1 exhibits a very high chemoselectivity for the C(O)–O bond cleavage of the ester group (Table 3). The drastic difference in the nature of the catalysts **A** and **C** is also evident from the variation of apparent activation energy, which decreases from 75.2 kJ mol^{-1} for pure Rh/SiO_2 to 46 kJ mol^{-1} for $Rh/Sn/SiO_2$. The concept of site isolation accounts quite well for a mechanism where the ester could be coordinated to a single rhodium atom; H transfer to the carbon atom of the carbonyl group is followed by a kind of concerted reaction leading to acetaldehyde[6] and rhodium alkoxide (Scheme 1). In agreement with this concept is the absence of C–C bond breakage, which is known to occur on metallic ensembles.[7]

Table 3. Catalytic activity r and selectivity S_i of various $Rh/Sn/SiO_2$ catalysts in the hydrogenation of ethyl acetate to ethanol. $T = 543$ K; H_2/AcOEt = 9/1; $p = 5$ MPa.

Sn/Rh	Contact time [h^{-1}]	Conversion [%]	S_i EtOH	Et_2O	MeCHO	C_2H_6	CH_4 + CO	$r \times 10^3$ [mol h^{-1} g^{-1}]
0/1	40	1.32	57.2	—	—	9.7	33.1	6.0
0.2/1	40	0.11	66.0	—	—	14.2	19.8	0.5
0.7/1	40	1.12	94.9	—	—	3.9	1.2	5.1
1.0/1	40	2.42	95.2	—	—	4.0	0.8	11.0
1.4/1	40	3.76	95.6	—	—	3.7	0.7	17.1
1.7/1	40	4.66	97.2	—	—	2.5	0.3	21.2
1.7/1	18.5	10	91.0	1.5	1.5	5.5	0.5	21
1.7/1	7.4	25	88.5	1.0	2.5	7.0	1.0	21
1.7/1	3.7	50	85.0	0.8	4.0	9.0	1.2	21
1.7/1	2.2	85	80.0	0.8	5.2	12.2	1.8	21



Scheme 1. Proposed mechanism of hydrogenation of ethyl acetate on catalyst **C**.

In conclusion, the concept of rhodium site isolation by tin atoms, which may account for the high chemoselectivity of **C**, is supported by three experimental facts: Tin decreases sharply the amount of H_2 and CO chemisorbed on rhodium in agreement with the partial coverage (or poisoning) of catalytically active rhodium atoms by inactive tin atoms. Tin suppresses the presence of bridging carbonyls, in agreement with a possible isolation of rhodium atoms from their neighbors. It is possible that other factors may be superimposed, such as an electronic effect of tin which increases slightly the electron density on rhodium.

Experimental Procedure

Rhodium was grafted on silica (Aerosil, 350 m^2 g^{-1}) by cationic exchange between $[RhCl(NH_3)_5]^{2\oplus}$ ions and $Si-O^{\ominus}NH_4^{\oplus}$ groups at pH 10. The $Si-O^{\ominus}NH_4^{\oplus}$ groups were obtained by exchange between $Si-O^{\ominus}H^{\oplus}$ groups and $NH_4^{\oplus}$ ions in ammonia solution. $[RhCl(NH_3)_5](OH)_2$ was obtained by contact of $[RhCl(NH_3)_5]Cl_2$ with an anionic exchange resin (IRA 400) in aqueous solution. The surface complex obtained by this route was decomposed by calcination at 300 °C in flowing dry air and then reduced in flowing hydrogen at 300 °C to give catalyst **A**. This catalyst contains 1 wt% of rhodium. **A** could be transformed into **B** by treatment with dry O_2 at 25 °C for 1 h. The particle size of **B** was in the range of 1.0–1.5 nm as determined by electron microscopy.

Adsorption of a given amount of $Sn(n\text{-}C_4H_9)_4$ in *n*-heptane on **B** [3] was achieved at 25 °C for 15 min. Various concentrations of $Sn(n\text{-}C_4H_9)_4$ at this stage could govern the final Sn/Rh ratio, at least for Sn/Rh ratios lower than 1.7/1. After removal of the solvent under vacuum (10^{-4} torr, 16 h), the solid was progressively heated in a closed vessel at 50, 100, 150, 200, and 300 °C. Qualitative and quantitative analysis of the gas phase was carried out after each plateau. Blank experiments carried out under the same conditions between $Sn(n\text{-}C_4H_9)_4$ and a silica pretreated at 25 or 200 °C did not show any significant reaction. The amount of tin that could react with **B** was proportional to the rhodium content up to an Sn/Rh ratio of ca. 1.7/1. $Rh/Sn/SiO_2$ catalysts with various tin contents were prepared (Table 3). Prior to catalytic measurements, the samples were treated "in situ" under flowing hydrogen (5 MPa, 8 mole of H_2 per gram of catalyst per hour at 100 °C (1 h), 250 °C (1 h), and 450 °C (2 h)). The hydrogenation of ethyl acetate was carried out in a conventional fixed-bed flow-differential reactor at 270 °C under 4.5 MPa of H_2 and 0.5 MPa of ethyl acetate. The contact time was varied between 2.2 and 40 h^{-1}. Activity (r) can be defined as the number of moles of ethyl acetate transformed per gram of catalyst per hour. Selectivity (S_i) can be defined

as the ratio of the carbon weight in product i to the total carbon weight in all the products.

Received: July 28, 1988;
revised: November 23, 1988 [Z 2893 IE]
German version: *Angew. Chem. 101* (1989) 361

[1] Y. A. Ryndin in J. M. Basset, B. C. Gates, J. P. Candy, A. Choplin, M. Leconte, F. Quignard, C. Santini (Eds.): *Surface Organometallic Chemistry, Molecular Approaches to Surface Catalysis* (NATO-Workshop), Kluwer, Dordrecht 1988, p. 127.

[2] M. Ichikawa, A. J. Lang, D. T. Shriver, W. M. H. Sachtler, *J. Am. Chem. Soc. 107* (1985) 7216.

[3] J. P. Candy, O. Ferretti, G. Mabillon, J. P. Bournonville, A. El Mansour, J. M. Basset, G. Martino, *J. Catal. 112* (1988) 201.

[4] a) C. D. Wagner, W. M. Riggs, L. E. Davis, J. F. Moulder, G. E. Muilenberg: *Handbook of X-ray Photoelectron Spectroscopy*, Perkin Elmer, Eden, MN, USA; b) J. P. Contour, G. Mouvier, M. Hoogewys, C. Leclere, *J. Catal. 44* (1977) 293; c) L. T. Anderson, M. S. Scurell, *ibid. 59* (1979) 340; d) L. W. Kenneth, F. H. Russel, *ibid. 69* (1981) 212; e) this work: $Rh/Sn/SiO_2$ (Sn = 4.0 wt%, Rh = 2.6 wt%) treated under flowing hydrogen for 5 h at 500°C.

[5] a) J. T. Yates, J. M. Duncan, S. D. Worley, R. W. Vaughan, *J. Chem. Phys. 70* (1979) 1219; b) M. Primet, *J. Chem. Soc. Faraday Trans. 1 74* (1978) 2570; c) J. L. Bilhou, V. Bilhou-Bougnol, W. F. Graydon, J. M. Basset, A. K. Smith, G. M. Zanderighi, R. Ugo, *J. Organomet. Chem. 153* (1978) 73.

[6] With this kind of catalyst, acetaldehyde is hydrogenated much faster to ethanol than ethyl acetate.

[7] J. A. Dalmon, G. A. Martin, *J. Catal. 66* (1981) 214; J. Sinfelt: *Bimetallic Catalysts; Discovery, Concepts and Applications*, Wiley, New York 1983.

Flexible Syntheses of Optically Active Isocarbacyclins**

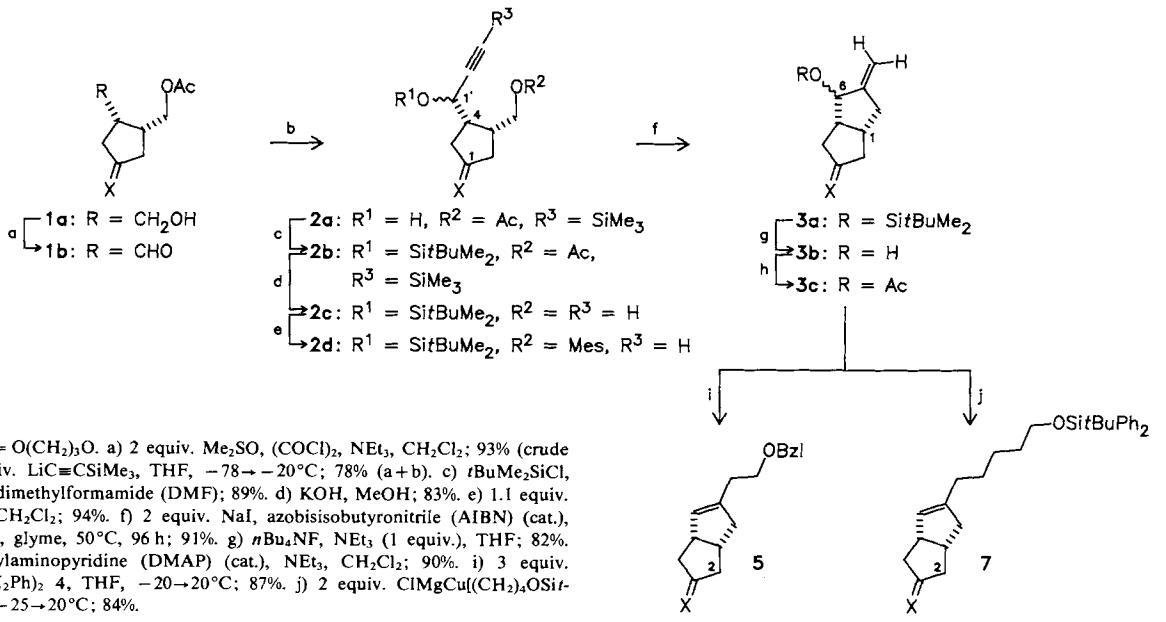
By *Horst Hemmerle* and *Hans-Joachim Gais**

Great hopes are placed on stable analogues of the hemostase regulator prostacyclin[1a] for the therapy of vascular diseases.[1b] The most promising compound aside from carbacyclin[1b] is isocarbacyclin **15a**[2] (see Scheme 3). Its biological activity is determined not only by the sense of chirality but also the structure of both side chains. For example, the derivative **15b** is characterized by strong inhibition of platelet aggregation *and* oral activity;[3b] its analogue with a triple bond between C13 and C14 and an ethyl instead of a methyl group on the alkyne C of R is possibly even more potent.[4a] Syntheses appropriate for the attainment of compounds of the type **15** must therefore be enantioselective and flexible with regard to *both* side chains.[3] We now describe two novel entries to **15** which fulfill these conditions.

The skeletal framework, the upper side chain and the 6,9α double bond of **15** are established starting from **1** or **8** by radical 5-*exo*-*dig*-cyclization[3f,5] and γ-substitution with cuprates[6] (see Schemes 1 and 2).[7] The lower side chain is then generated by proven methods[1b,3,4] (see Scheme 3); one central building block, **10c**, already contains the requisite hydroxymethyl group, in the case of the other, **3c**, it is missing and must be incorporated at a later stage. We have already described optimized routes with enzyme-catalyzed asymmetric key steps for the synthesis of the starting compounds (−)-**1a**[8] and (+)-**8a**.[9–11]

The synthesis of the allylic acetate **3c** begins with the oxidation of the alcohol **1a** to the aldehyde **1b** and its addition to lithium(trimethylsilyl)acetylide (Scheme 1). The alkynol **2a** is obtained as a diastereomeric mixture ((1′*R*)-**2a** : (1′*S*)-**2a** = 3 : 1); C-4 epimers were not formed. Silylation, selective cleavage of the trimethylsilyl and acetyl groups and subsequent mesylation furnished the mesylate **2d**. The primary iodide[12] generated in situ from **2d** was cyclized in a radical reaction by the tin method[13] to give **3a** in 91% yield. This was then converted into **3c**.

3c reacts smoothly with the cuprates **4** and **6** to give the bicyclic alkenes **5** and **7**, respectively, which were isolated in yields of 87% and 84%, respectively. The transformation **3c** → **5** can also be achieved with stable benzyloxymethylmagnesium chloride[15] in the presence of 10 mol-% CuI.

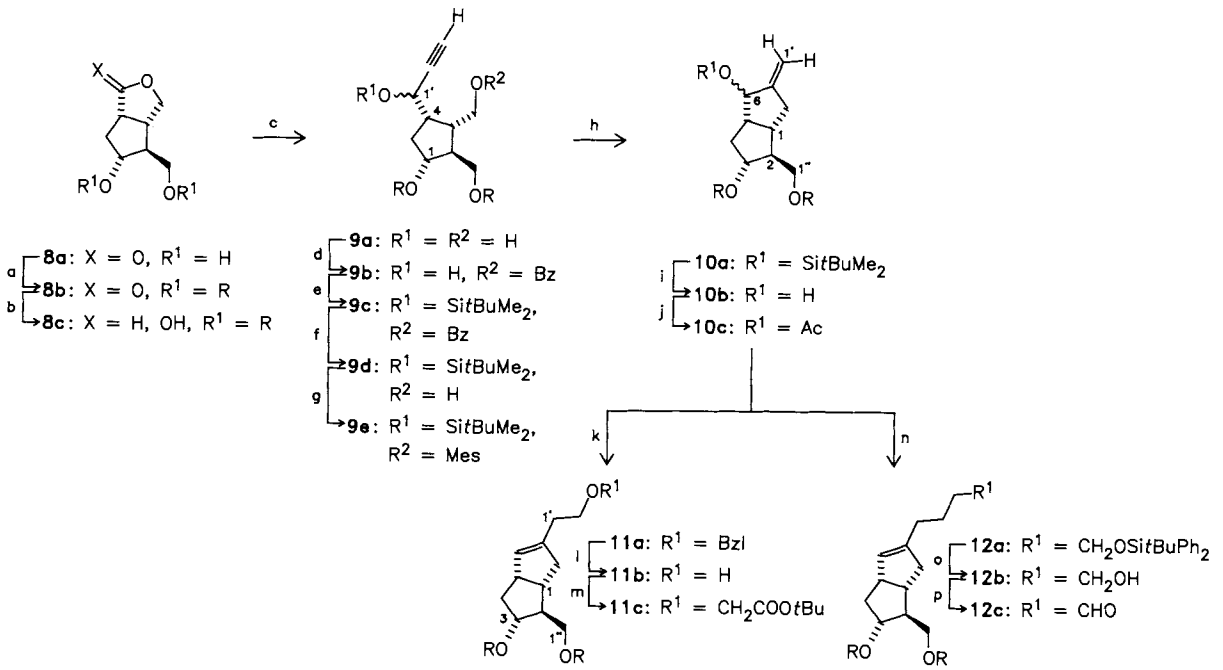


Scheme 1 [14]. X = $O(CH_2)_3O$. a) 2 equiv. Me_2SO, $(COCl)_2$, NEt_3, CH_2Cl_2; 93% (crude yield). b) 1.1 equiv. $LiC{\equiv}CSiMe_3$, THF, −78 → −20°C; 78% (a+b). c) $tBuMe_2SiCl$, imidazole (ImH), dimethylformamide (DMF); 89%. d) KOH, MeOH; 83%. e) 1.1 equiv. $MeSO_2Cl$, NEt_3, CH_2Cl_2; 94%. f) 2 equiv. NaI, azobisisobutyronitrile (AIBN) (cat.), 2 equiv. nBu_3SnH, glyme, 50°C, 96 h; 91%. g) nBu_4NF, NEt_3 (1 equiv.), THF; 82%. h) Ac_2O, dimethylaminopyridine (DMAP) (cat.), NEt_3, CH_2Cl_2; 90%. i) 3 equiv. $ClMgCu(CH_2OCH_2Ph)_2$ **4**, THF, −20 → 20°C; 87%. j) 2 equiv. $ClMgCu[(CH_2)_4OSitBuPh_2]_2$ **6**, ether, −25 → 20°C; 84%.

Racemates of bicyclic compounds of the type **5** and **7** have already been converted into *rac*-**15b** and *rac*-**15a** (R = *n*-C_5H_{11}), respectively.[3b,c] The attachment of the lower side chain would be shortened still further by a selective deprotonation of **5** and **7** (X = O) at C-2 with chiral bases.[16]

[*] Prof. Dr. H.-J. Gais, Dipl.-Chem. H. Hemmerle
Institut für Organische Chemie und Biochemie
der Universität
Albertstrasse 21, D-7800 Freiburg (FRG)

[**] This work was supported by the Deutsche Forschungsgemeinschaft, Schering AG, Berlin, and Merck AG, Darmstadt (FRG). We thank *H. Müller* for valuable assistance and Dr. *D. Hunkler* for NMR experiments.



Scheme 2 [14]. R = tetrahydropyranyl (THP). a) Dihydropyran, THF, pyridinium *p*-toluenesulfonate (PPTS) (cat.); 95%. b) 1.1 equiv. iBu_2AlH, THF, $-78\rightarrow-20$°C; 95%. c) 3 equiv. BrMgC≡CH, THF; 96%. d) 1.1 equiv. BzCl, pyridine, −30°C; 74%. e) $tBuMe_2SiCl$, ImH, DMF; 97%. f) KOH, MeOH, 0°C; 71%. g) 1.1 equiv. $MeSO_2Cl$, NEt_3, CH_2Cl_2, −30°C; 95%. h) 2 equiv. NaI, AIBN (cat.), 2 equiv. nBu_3SnH, glyme, 50°C, 96 h; 82%. i) nBu_4NF, NEt_3 (1 equiv.), THF; 87%. j) Ac_2O, DMAP (cat.), NEt_3, CH_2Cl_2; 91%. k) 2 equiv. **4**, THF, $-25\rightarrow20$°C; 92%. l) Na, EtOH, NH_3, THF, −78°C; 82%. m) 10 equiv. $BrCH_2COOtBu$, nBu_4NHSO_4, NaOH; 74%. n) 3 equiv. **6**, ether, $-25\rightarrow20$°C; 95%. o) nBu_4NF, NEt_3 (1 equiv.), THF; 92%. p) SO_3·pyridine, Me_2SO, NEt_3; 94%.

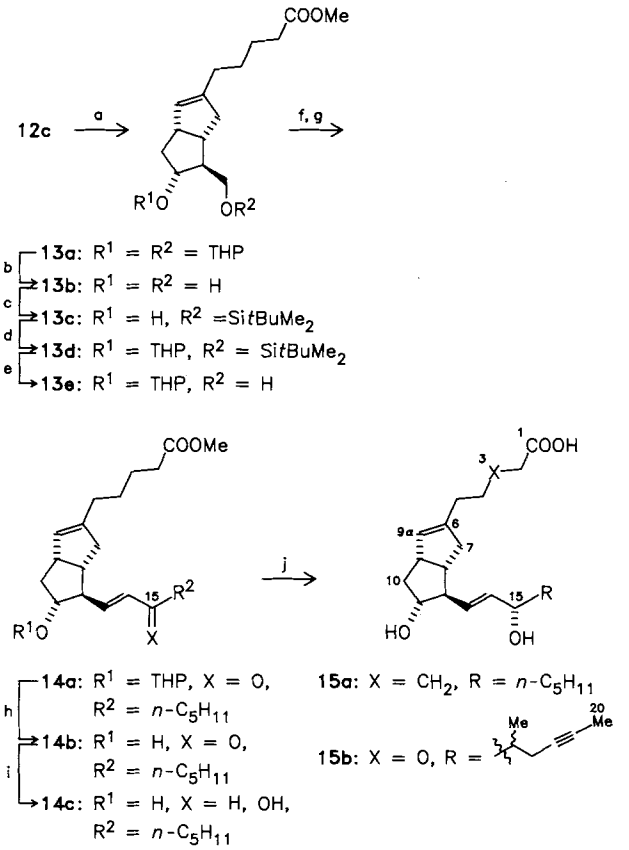
For the synthesis of the allylic acetate **10c** functionalized on C-2 (Table 1), the lactone **8a** was converted into the hemiacetal **8c**, from which the diastereomeric alkynediols **9a** ((1′*S*)-**9a** :(1′*R*)-**9a** = 6 : 1) were prepared by reaction with three equivalents of bromomagnesium acetylide (Scheme 2); C-4 epimers were not found. The diastereomeric ratios of **2a** and **9a** indicate opposite asymmetric inductions for the acetylide additions to **1b** and to the aldehyde in equilibrium with deprotonated **8a**. The mesylate **9e** was then obtained from **9a** by protective group manipulations and mesylation in the way shown in Scheme 2. The radical ring closure of the primary iodide generated in situ from **9e** leads smoothly to the formation of **10a** in 82% yield.

The flexibility of our concept for the generation of upper side chains is demonstrated by the reactions of **10c** with the cuprates **4** and **6** to give the two alkenes **11a** (92%) and **12a** (95%), respectively, with the double bond in the correct position for **15**.

The following findings for the synthesis of the alkenes **5** (**11a**) and **7** (**12a**) are still important: Despite greater steric hindrance, the intermediary alkyl radical generated from (1′*S*)-**2d** [(1′*S*)-**9e**] cyclizes in the same way as its epimer formed from (1′*R*)-**2d** [(1′*R*)-**9e**], *and* both C-6 epimeric acetates **3c** (**10c**)[17] react with the cuprates **4** and **6** with substitution, whereby regiomers were not detectable NMR spectroscopically in any of the cases.

In order to obtain the intermediate compound **11c** with the upper side chain of **15b**, the benzyl ether **11a** was cleaved in the usual way to give the alcohol **11b**, which was then treated with *tert*-butyl bromoacetate to give **11c**.[4] The compound **13a** with the upper side chain of **15a** was obtained from **12a** via the alcohol **12b** and the aldehyde **12c** (Schemes 2 and 3).

Scheme 3 outlines by way of example the routine path leading to the linking of the lower side chain of **15a** to



Scheme 3 [14]. a) Ag_2O, NaOH, EtOH, H_2O; $H_3O^{\oplus}$; CH_2N_2; 85%. b) MeOH, PPTS (cat.); 93%. c) $tBuMe_2SiCl$, ImH, DMF; 86%. d) Dihydropyran, PPTS (cat.); 91%. e) nBu_4NF, NEt_3 (1 equiv.), THF; 92%. f) SO_3·pyridine, Me_2SO, NEt_3; 93% (crude yield). g) 3 equiv. $(MeO)_2PO-CH_2-CO-(CH_2)_4Me$, NaH, glyme, 0°C; 65% (f+g). h) MeOH, PPTS (cat.); 92%. i) 10 equiv. 2,6-*t*Bu-4-Me-$C_6H_2OAliBu_2$, toluene, $-78\rightarrow-10$°C; 87%. j) NaOH, MeOH, H_2O; $H_3O^{\oplus}$; 95%.

Table 1. Selected physical data of (6*S*)-**10c**, **11a**, **11c**, **13b**, and **15a**.

(6*S*)-**10c** (R = H): m.p. 84°C, $[\alpha]_{365}^{20} = +228.7$ ($c = 0.52$, CH_2Cl_2); ^1H NMR (400 MHz, $CDCl_3$): $\delta = 1.48$ ($J_{4\alpha,4\beta} = 13.0$, $J_{4\alpha,3\beta} = 9.5$, $J_{4\alpha,5\beta} = 9.0$ Hz, 4-H^{α}, 1H), 1.62 ($J_{2\alpha,1\beta} = 9.0$, $J_{2\alpha,3\beta} = 9.0$, $J_{2\alpha,1''} = 9.0$, $J_{2\alpha,1'''} = 5.0$ Hz, 2-H^{α}, 1H), 1.87 (ddd, $J_{4\beta,4\alpha} = 13.0$, $J_{4\beta,5\beta} = 9.0$, $J_{4\beta,3\beta} = 6.0$ Hz, 4-H^{β}, 1H), 2.01–2.18 (m, 1-H^{β}, 8-H^{α}, Ac, 5H), 2.46 (m, 8-H^{β}, 1H), 2.78 ($J_{5\beta,6\beta} = 8.3$, $J_{5\beta,1\beta} = 9.0$, $J_{5\beta,4\alpha} = 9.0$, $J_{5\beta,4\beta} = 9.0$ Hz, 5-H^{β}, 1H), 3.68 (dd, $J_{1''',1'''} = 10.5$, $J_{1''',2\alpha} = 9.0$, 1‴-H, 1H), 3.87 (dd, $J_{1''',1'''} = 10.5$, $J_{1''',2\alpha} = 5.0$, 1‴-H, 1H), 3.92 ($J_{3\beta,2\alpha} = 9.0$, $J_{3\beta,4\beta} = 6.0$, $J_{3\beta,4\alpha} = 9.0$ Hz, 3-H^{β}, 1H), 5.02–5.06 (m, 1′-H, 2H), 5.32–5.37 (m, $J_{6\beta,5\beta} = 8.3$ Hz, 6-H^{β}, 1H)

11a (R = H): $[\alpha]_{365}^{20} = -19.6$ ($c = 0.5$, CH_2Cl_2); ^1H NMR (400 MHz, $CDCl_3$): $\delta = 1.35$ ($J_{4\beta,4\alpha} = 13.5$, $J_{4\beta,5\alpha} = 9.0$, $J_{4\beta,3\alpha} = 9.0$ Hz, 4-H^{β}, 1H), 1.69 ($J_{2\beta,1\alpha} = 9.0$, $J_{2\beta,3\alpha} = 9.0$, $J_{2\beta,1''} = 9.0$, $J_{2\beta,1'''} = 5.0$ Hz, 2-H^{β}, 1H), 1.82–2.40 (m, OH, 8-H^{β}, 4-H^{α}, 1′-H, 1-H^{α}, 6H), 2.50 (m, 8-H^{α}, 1H), 3.01 (m, 5-H^{α}, 1H), 3.55 (t, $J_{2',1'} = 6.8$ Hz, 2′-H, 2H), 3.50–3.69 (m, 1″-H, 2H), 3.79–3.99 (m, OH, 3-H^{α}, 2H), 4.50 (s, CH_2Ph, 2H), 5.36 (m, 6-H, 1H), 7.22–7.39 (m, Ph, 5H)

11c (R = H): $[\alpha]_D^{20} = +3.8$ ($c = 0.51$, CH_2Cl_2)

13b: m.p. 51°C, $[\alpha]_D^{20} = -11.5$ ($c = 0.21$, CH_2Cl_2)

15a: m.p. 76–78°C; $[\alpha]_D^{20} = +15.2$ ($c = 0.5$, MeOH); ^1H-NMR (400 MHz, $CDCl_3$): $\delta = 0.81$–0.92 (m, 20-H, 3H), 1.18–1.70 (m, 13H), 1.84–2.09 (m, 4H), 2.20–2.40 (m, 5H), 2.96 (m, 9-H, 1H), 3.68–4.60 (m, 5H), 5.26 (m, 9α-H, 1H), 4.90–5.50 (m, 13-H, 14-H, 2H); ^{13}C NMR (100 MHz, $CDCl_3$): $\delta = 14.10$ (q), 22.69 (t), 24.38 (t), 25.30 (t), 26.96 (t), 30.32 (t), 31.76 (t), 33.99 (t), 37.00 (t), 39.13 (t), 39.51 (t), 44.38 (d), 56.57 (d), 58.00 (d), 73.52 (d), 77.30 (d), 129.02 (d), 133.40 (d), 135.68 (d), 141.16 (s), 178.20 (s)

13a. Stereoselective reduction of the hydroxy-enone **14b**, which is obtained in 40% yield based on **13a**, with the Yamamoto reagent[18] afforded the epimeric allylic alcohols **14c** ((15*S*)-**14c** : (15*R*)-**14c** = 9 : 1), which could be easily separated chromatographically and, according to HPLC were free of isomeric carbacyclins. Hydrolysis of (15*S*)-**14c** afforded (+)-isocarbacyclin **15a**, whose 400-MHz ^1H NMR spectrum contains no evidence of an isomer with the double bond between C-6 and C-7.

Received: October 28, 1988 [Z 3030 IE]
German version: *Angew. Chem. 101* (1989) 363

[1] a) J. R. Vane, *Angew. Chem. 95* (1983) 782; *Angew. Chem. Int. Ed. Engl. 22* (1983) 741; b) R. C. Nickolson, M. H. Town, H. Vorbrügger, *Med. Res. Rev. 5* (1985) 1.

[2] M. Shibasaki, Y. Torisawa, S. Ikegami, *Tetrahedron Lett. 24* (1983) 3493.

[3] Previous syntheses of **15**: a) [2]; b) K. Kojima, K. Koyama, S. Amemiya, S. Saito, *Chem. Pharm. Bull. 35* (1987) 948, and references cited therein; c) K. Kojima, S. Amemiya, K. Koyama, S. Saito, T. Oshima, T. Ito, *ibid. 35* (1987) 4000; d) K. Bannai, T. Tanaka, N. Okamura, A. Hazato, S. Sugiura, K. Manabe, K. Tomimori, S. Kurozumi, *Tetrahedron Lett. 27* (1986) 6353; e) Y. Nagao, T. Nakamura, M. Kume, M. Ochiai, K. Fuji, E. Fujita, *J. Chem. Soc. Chem. Commun. 1987*, 269; f) M. Suzuki, H. Koyano, R. Noyori, *J. Org. Chem. 52* (1987) 5583, and references cited therein; g) S. Hashimoto, T. Shinoda, S. Ikegami, *J. Chem. Soc. Chem. Commun. 1988*, 1137.

[4] a) Such side chains and those of **15b** were developed by the Schering group for highly active carbacyclins, see: W. Skuballa, E. Schillinger, C.-S. Stürzebecher, H. Vorbrüggen, *J. Med. Chem. 29* (1986) 313, and references cited therein; b) A. Takahashi, M. Shibasaki, *J. Org. Chem. 53* (1988) 1227.

[5] M. Julia, C. James, *C. R. Hebd. Séances Acad. Sci. 255* (1962) 959; T. Ohnuki, M. Yoshida, O. Simamura, *Chem. Lett. 1972*, 797; J.-K. Choi, D. J. Hart, Y.-M. Tsai, *Tetrahedron Lett. 23* (1982) 4765; G. Stork, R. Mook, Jr., *J. Am. Chem. Soc. 105* (1983) 3720; E. J. Corey, S. G. Pyne, *Tetrahedron Lett. 24* (1983) 2821; D. J. Clive, P. L. Beaulieu, L. Set, *J. Org. Chem. 49* (1984) 1313.

[6] H. L. Goering, S. S. Kanter, E. P. Seitz, Jr., *J. Org. Chem. 50* (1985) 5495.

[7] "Three-component coupling" syntheses of **15a** with Murahashi reaction or radical cyclization: [3d, f].

[8] H. Hemmerle, H.-J. Gais, *Tetrahedron Lett. 28* (1987) 3471.

[9] a) H.-J. Gais, K. L. Lukas, W. A. Ball, S. Braun, H. J. Lindner, *Liebigs Ann. Chem. 1986*, 687; b) H.-J. Gais, H. J. Lindner, T. Lied, K. L. Lukas, W. A. Ball, B. Rosenstock, H. Sliwa, *ibid. 1986*, 1179.

[10] Carbacyclin syntheses with (+)-**8a**: a) H.-J. Gais, W. A. Ball, J. Bund, *Tetrahedron Lett. 29* (1988) 781; b) H.-J. Gais, G. Schmiedl, W. A. Ball, J. Bund, I. Erdelmeier, *ibid. 29* (1988) 1773; I. Erdelmeier, H.-J. Gais, *J. Am. Chem. Soc. 111* (1989) 1125.

[11] B. Riefling, W. P. Brümmer, H.-J. Gais, *NATO ASI Ser. C178* (1986) 347.

[12] Y. Ueno, C. Tanaka, M. Okawara, *Chem. Lett. 1983*, 795.

[13] B. Giese: *Radicals in Organic Synthesis: Formation of Carbon-Carbon Bonds*, Pergamon, Oxford 1986.

[14] Mes = SO_2Me, Bzl = CH_2Ph, Bz = COPh.

[15] B. Castro, *Bull. Soc. Chim. Fr. 1967*, 1533.

[16] We have prepared the corresponding *cis*-(1*R*)-trimethylsilyl enol ether (80% *ee*, 80%) of *cis*-bicyclo[3.3.0]octane-3,7-dione mononeopentylacetal via enantioselective deprotonation with *N*-lithiumbis[(*S*)-1-phenylethyl)]amide: N. Reuter, *Diplomarbeit*, Technische Hochschule Darmstadt 1988.

[17] The configurations at C-6 of **3c** and C-6 of **10c** were determined by decoupling and NOE experiments.

[18] S. Iguchi, H. Nakai, M. Hayashi, H. Yamamoto, K. Maruoka, *Bull. Chem. Soc. Jpn. 54* (1981) 3033.

Copper(I)-Promoted Michael-Addition Reaction of Organozincs of Esters, Nitriles, and α-Amino Acids**

By *Yoshinao Tamaru,* Hiroto Tanigawa, Tetsuji Yamamoto,* and *Zen-ichi Yoshida**

The Michael addition reaction is one of the most important methods to construct desired molecules. Classically it is the reaction of soft α-carbonyl carbanions with electron-deficient olefins.[1] Development of copper-promoted 1,4-addition of hydrocarbon groups has greatly expanded the scope of this reaction.[2] Although we are still short of a general method to conduct Michael addition with such carbanions as those remote from carbonyls by more than two carbons, two precedents have been reported. One is the reaction of β-zinc esters[3a] and the other is that of β-, γ-, and δ-zinc nitriles and esters,[3b,c] the latter being reported very recently during preparation of this manuscript.

Here we report that organozincs[3d-f] bearing electrophilic functionalities (ester,[4] nitrile, α-amino acid) essentially at any positions more remote than the β-position serve as Michael donors and add to α,β-unsaturated aldehydes, ketones, and esters in the presence of trimethylsilyl chloride[5] and cuprous cyanide.[6]

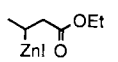
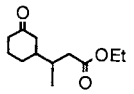
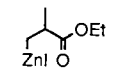
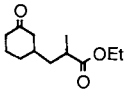
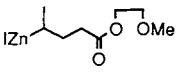
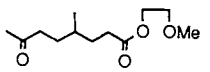
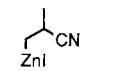
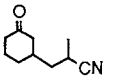
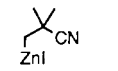
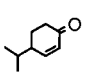
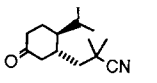
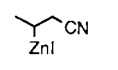
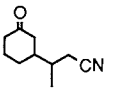
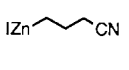
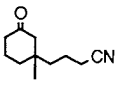
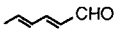
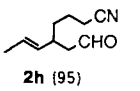
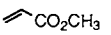
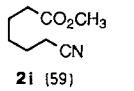
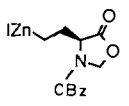
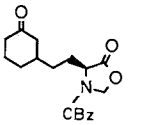
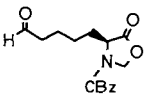
Some representative results are summarized in Table 1 and Scheme 1. The following points deserve comment:

1. The results of runs 1 and 2 indicate that the position of the methyl group of the starting iodoesters does not change during the reaction. This regiochemistry is in sharp contrast to the Michael addition reaction of β-zinc esters developed by *Kuwajima* et al.[3a] and also to our previous observation on the reaction of **1a** and **1b** with aldehydes.[4d] These two reactions only provide 3-substituted 2-methylpropionic esters (e.g., a product like **2b**) through a rearrangement via a common intermediate **3** (Scheme 2).[7] The same is valid in the reactions of the nitrile series (runs

[*] Dr. Y. Tamaru, Prof. Z. Yoshida, H. Tanigawa, T. Yamamoto
Department of Synthetic Chemistry, Faculty of Engineering
Kyoto University, Yoshida, Kyoto 606 (Japan)

[**] This work was supported by the Ministry of Education, Science and Culture (Japan). It was presented at the 56th Annual Meeting of the Chemical Society of Japan (April 1988). Abstract II, p. 1758. We are indebted to Dr. *Y. Ito* and Dr. *T. Hayashi* and to *Y. Matsumoto* (Kyoto University) for the determination of *ee* values and helpful discussion.

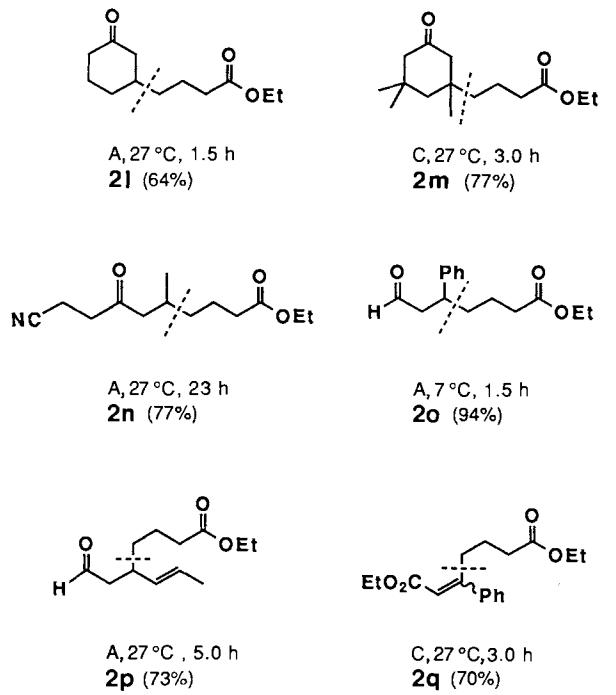
Table 1. Michael addition of organozincs of esters, nitriles, and α-amino acids.

Run	Michael donor [a]	Acceptor	Reaction conditions [b]	Product (yield [%]) [c]
1	 **1a**		B, 7 °C, 1.5 h	 **2a** (78) [d]
2	 **1b**		B, 7 °C, 1.5 h	 **2b** (70) [d]
3	 **1d**		A, 27 °C, 4.0 h	 **2c** (76)
4	 **1e**		B, 7 °C, 10 h	 **2d** (70) [d]
5	 **1f**		B, 0 °C, 40 h	 **2e** (54)
6	 **1g**		B, 7 °C, 5.0 h	 **2f** (62) [e]
7	 **1h**		B, 7 °C, 19 h	 **2g** (70)
8	**1h**		B, 27 °C, 4.0 h	 **2h** (95)
9	**1h**		C, 0 °C, 16 h	 **2i** (59)
10	 **1i** [f]		B, 0 °C, 15 h	 **2j** (71) [d]
11	**1i** [f]		B, 7 °C, 6.0 h	 **2k** (70) [g]

[a] For the generation of **1**, see [6]. [b] CuCN/HMPA ratio in equivalents: A, 0.05/1.0); B, 0.35/1.5; C, 1.0/1.5. [c] Yields are for the homogeneous products purified by column chromatography over silica gel and based on the unsaturated carbonyl compounds. [d] Diastereomeric ratio was not determined. [e] Diastereomeric mixture (1 : 1) was obtained. [f] The starting iodide was prepared according to the literature procedure: D. H. R. Barton, Y. Hervé, P. Potier, J. Thierry, *J. Chem. Soc. Chem. Commun. 1984*, 1298. CBz = benzyloxycarbonyl. [g] $[\alpha]_D^{20} = +101$ ($c = 0.34$, $CHCl_3$).

4–6) in which no isomerization via **4** (Scheme 2) is observed.

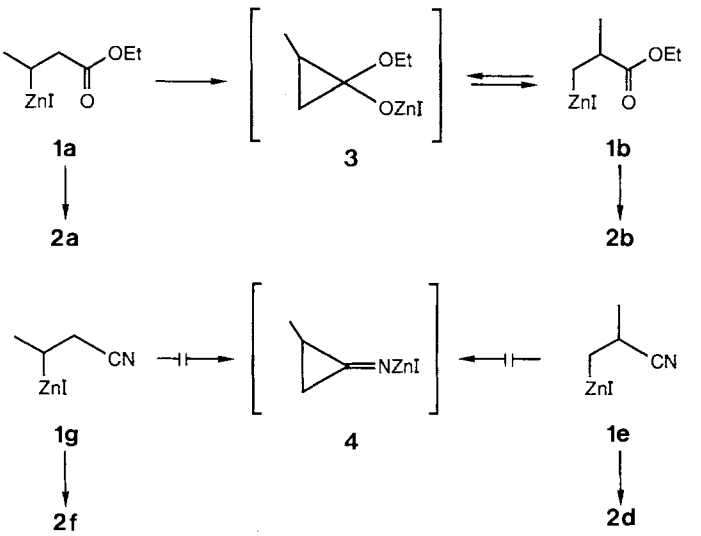
2. The reaction of the present organozinc-Cu^I system with 2,4-hexadienal results in specific 1,4-addition. The sole products were **2h** and **2p** without any traces of 1,2- or 1,6-addition products. The formation of **2g** and **2m** in reasonable yields from highly substituted and hence unreactive ketones as well as a highly *trans*-selective addition (run 5) may be valuable aspects of the reaction. Furthermore, the successful reactions with olefinic (run 9) and acetylenic esters (e.g., to give **2q**) clearly indicate the wide scope of the reaction.



Scheme 1. Reaction of ethyl 4-(iodozinca)butyrate **1c** with α,β-unsaturated ketones, esters, and aldehydes. For the reaction conditions (A, B, C) and yields, see footnotes [b] and [c] in Table 1.

3. The reaction is not confined to β- and γ-esters and nitriles. Their higher homologues react with similar effectiveness.[8] Among these, the β-zinc esters and nitriles proved to be by far the least reactive.[4d,9] For example, neither **1e** nor **1g** reacts with 3-methyl-2-cyclohexenone even under forcing conditions (C: 7 °C, 20 h; cf. run 7).

4. Most importantly, the results in runs 10 and 11 suggest that the reaction opens a new and efficient route to the



Scheme 2. Possible isomerizations of organozinc compounds.

syntheses of chiral amino acid derivatives. The product **2k** was obtained in more than 99% *ee*.[10]

Received: September 13, 1988 [Z 2965 IE]
German version: *Angew. Chem. 101* (1989) 358

CAS Registry numbers:
2a (isomer 1), 118762-78-0; **2a** (isomer 2), 118762-88-2; **2b** (isomer 1), 118762-79-1; **2b** (isomer 2), 118762-89-3; **2c**, 118762-80-4; **2d** (isomer 1), 118762-81-5; **2d** (isomer 2), 118762-90-6; **2e**, 118762-82-6; **2f** (isomer 1), 118762-83-7; **2f** (isomer 2), 118762-91-7; **2g**, 118762-84-8; **2h**, 118762-85-9; **2i**, 17592-25-5; **2j** (isomer 1), 118762-86-0; **2j** (isomer 2), 118762-92-8; **2k**, 118762-87-1; CuCN, 544-92-3; ethyl 3-iodobutanoate, 7425-50-5; ethyl 3-iodo-2-methylpropionate, 118762-74-6; methoxyethyl 5-iodo-4-methylpentanoate, 118762-75-9; 3-iodo-2-methylpropiononitrile, 80279-14-7; 3-iodo-2,2-dimethylpropiononitrile, 118762-76-8; 3-iodobutyronitrile, 6727-72-6; 4-iodobutyronitrile, 6727-73-7; 3-benzyloxycarbonyl-4(*S*)-(2-iodoethyl)-oxazolidin-5-one, 118762-77-9; 2-cyclohexen-1-one, 930-68-7; 3-buten-2-one, 78-94-4; 4-isopropyl-2-cyclohexen-1-one, 500-02-7; 3-methyl-2-cyclohexen-1-one, 1193-18-6; 2,4-hexadienal 80466-34-8; methyl acrylate, 96-33-3; acrolein, 107-02-8; trimethylsilyl chloride, 75-77-4.

[1] E. D. Bergmann, D. Ginsburg, R. Pappo, *Org. React. (NY) 10* (1959) 179.
[2] G. H. Posner, *Org. React. (NY) 19* (1972) 1.
[3] a) E. Nakamura, I. Kuwajima, *J. Am. Chem. Soc. 106* (1984) 3368; b) M. C. P. Yeh, P. Knochel, *Tetrahedron Lett. 29* (1988) 2395; c) P. Knochel, M. C. P. Yeh, S. C. Berk, J. Talbert, *J. Org. Chem. 53* (1988) 2392. For Michael reaction of alkylzincs, see: d) R. A. Watson, R. A. Kjonaas, *Tetrahedron Lett. 27* (1986) 1437; e) C. Petrier, C. Dupuy, J. L. Luche, *ibid. 27* (1986) 3149; f) P. Knochel, J. F. Normant, *ibid. 27* (1986) 4431.
[4] a) Y. Tamaru, H. Ochiai, T. Nakamura, Z. Yoshida, *Tetrahedron Lett. 27* (1986) 955; b) H. Ochiai, Y. Tamaru, K. Tsubaki, Z. Yoshida, *J. Org. Chem. 52* (1987) 4418; c) Y. Tamaru, H. Ochiai, T. Nakamura, Z. Yoshida, *Org. Synth.*, in press; d) Y. Tamaru, T. Nakamura, M. Sakaguchi, H. Ochiai, Z. Yoshida, *J. Chem. Soc. Chem. Commun. 1988*, 610.
[5] a) E. J. Corey, N. W. Boaz, *Tetrahedron Lett. 26* (1985) 6015, 6019; b) Y. Horiguchi, S. Matsuzawa, E. Nakamura, I. Kuwajima, *ibid. 27* (1986) 4025, 4029.
[6] The zinc iodides **1a–i**, prepared in situ by the reaction of the corresponding iodide with 1.05–1.10 equivalents of Zn–Cu couple in dioxane/HMPA (60°C, 3–5 h) [4], were successively treated at the temperature indicated in Table 1 and Scheme 1 with CuCN and trimethylsilyl chloride (2 equivalents) and then with an α,β-unsaturated carbonyl compound (0.7 equivalents). The reaction was monitored by gas chromatography using biphenyl as an internal standard. For the stoichiometries of CuCN and HMPA and the reaction conditions for Michael addition, see Table 1.
[7] The cyclization of **1a** and **1b** to **3** seems to proceed only at higher temperatures and in the presence of a silylating agent. As a matter of fact, 1-ethoxy-1-(*tert*-butyldimethylsiloxy)cyclopropane was obtained in 65–70% isolated yield by heating a mixture of *tert*-butyldimethylsilyl chloride and ethyl 3-(iodozinca)propionate in tetrahydrofuran/*N*,*N*-dimethylacetamide at 60°C for ca. 12 h (unpublished results). Note that in the present reaction **1a** and **1b** were exposed to trimethylsilyl chloride at ambient temperature or below, while the reactions of **1a** and **1b** with aldehydes only proceed in the presence of trimethylsilyl chloride at higher temperatures (ca. 60°C) [4d].
[8] Under conditions B (7°C, 3 h), δ- and ε-zinc nitriles reacted with 2-cyclohexenone to furnish the corresponding 1,4-addition products in 70 and 92% isolated yields, respectively.
[9] The low reactivity of these β-zinc esters and nitriles may primarily be ascribed to the electron-withdrawing effect of the carbonyl and cyano groups.
[10] The *ee* values were determined by means of HPLC with a chiral stationary phase column (Sumipax OA-1100, *n*-hexane/1,2-dichloroethane/ethanol = 100/20/1), using racemic **2k** as a reference.

BOOK REVIEWS

Book reviews are written by invitation from the editor. Suggestions for books to be reviewed and for qualified book reviewers are welcome. Publishers should send prospects or (better) books to the following address: Redaktion Angewandte Chemie, Postfach 101161, D-6940 Weinheim, Bundesrepublik Deutschland. The editor reserves the right of selecting which books will be reviewed. Uninvited books not chosen for review will not be returned.

Introduction to Microscale High-Performance Liquid Chromatography. Edited by *D. Ishii*. VCH Verlagsgesellschaft, Weinheim/VCH Publishers, New York 1988. xiv, 208 pp., bound, DM 118.00.—ISBN 3-527-26636-4; 0-89573-309-5

The editor of this book and author of several of the chapters is amongst the leading advocates of microcolumn techniques in HPLC. Although several monographs on the use of narrow bore columns have already appeared in the last few years, this technique still generates only marginal interest, despite the continuing growth in the application of HPLC with columns of 2 to 5 mm internal diameter. The advantages of narrowing the cross-section are a reduction in the amount of eluent needed, an increase in the solute concentration at the peak maximum, the possibility of more easily combining HPLC with mass spectrometry, and an increase of 30 times in permeability when open capillaries are used, allowing the use of longer columns. Even for LC it can be shown theoretically that with capillary columns several hundred thousand plates can be achieved. However, with the narrow capillary columns, of the order of 10 μm diameter, which theory indicates are needed for LC, the sample injection volumes are limited to a few nL. Furthermore, the peak volumes are so small (1 to 10 nL) that when using photometric detectors it does not appear possible to achieve high detection sensitivities. "Thus, the apparatus must be designed by each laboratory." This quotation from the book sums up the whole range of problems.

The book gives a good overview of the capabilities and problems of microcolumn techniques using open or irregular packed capillaries, and "semimicro" columns with diameters of less than 1.5 mm. The problems of choosing a suitable sample introduction system, detector and connection methods (eliminating dead volume so far as possible) are explained, and various solutions to these problems are described and amplified by examples of the chromatograms obtained (effects of time constants, etc.). Regrettably, in one of the most important figures (Fig. 2-3), which is intended to illustrate the advantages of microcolumns, such as enhanced detection sensitivity, the curves do not agree with the legends. It is sufficient here to point out that

columns with larger diameters can be more heavily loaded (in volume *and* mass), resulting in similar trace detection sensitivities. Consequently it only makes sense to use columns with smaller diameters to improve the detection sensitivity when the amount of sample available is very limited.

Examples of applications are included so as to illustrate the capabilities of microcolumn techniques. The critical reader will notice that many of the compounds in the separation examples are condensed arenes, chlorinated biphenyls, phthalic acid esters, tocopherols, etc.—all of which are compounds with very large molar extinction coefficients. In other examples (Figs. 7-58 to 7-66) columns with internal diameters in the conventional range (2.1 to 4.6 mm), packed with very small particles (average diameter $<5\,\mu m$), have been used. In English-speaking usage (and in this book) columns such as these are also often referred to as "microcolumns". However, in the introduction a clear distinction is made between the two sorts of microcolumns, namely those with small column diameters, and those that have normal diameters but are packed with small particles. This book is concerned only with techniques using small diameter microcolumns. It is recommended as reading for anyone interested in these techniques and wishing to put them to practical use.

Heinz Engelhardt [NB 912 IE]
Institut für Angewandte Physikalische Chemie
der Universität Saarbrücken (FRG)

Borane Reagents. Series: Best Synthetic Methods. By *A. Pelter, K. Smith,* and *H. C. Brown*. Academic Press, New York 1988. xxxi, 503 pp., hardback, $ 55.00.—ISBN 0-12-549875-6

The basic philosophy of the series "Best Synthetic Methods" has already been discussed at some length in the review of the first three volumes.[*] To summarize briefly, it sets out to provide the practical chemist with the best preparative method for each case, giving all the details needed. This laudable aim has only been partly translated into reality in the volumes that have appeared up to now. Can the new title "Borane Reagents" turn out to be more satisfactory in this respect? The authors appear to have had their doubts about this, expressed in the preface as follows: "For a field as varied as the use of borane reagents this presents a considerable challenge, since literally hundreds of conceptually different important synthetic reactions are involved...". In order to adequately cover the large amount of material, the book has been divided into four sections. Section 1 describes how particular classes of compounds can be prepared using borane reagents, Section 2 describes reductions using boranes and complex boron hydrides, Section 3 deals with the different variants of hydroboration reactions, and Section 4 with the applications of organoboron compounds in synthesis. Sections 2 to 4 are generously furnished with laboratory recipes in the style of "Organic Syntheses". Regrettably, however, there is no tabulated survey of reaction examples, including conditions and yields.

The first impression is confusing; in common with other authors in this series *Pelter, Smith* and *Brown* have a tendency towards the encyclopedic. A critical selection, or an impartial comparison with alternative methods, which is after all the declared aim of the series, does not occur anywhere in the book. It is undeniable that synthesis without the help of hydroboration and reduction by boron hydrides is nowadays unthinkable, but is this also true of the many different CC bond-forming reactions of organoboranes? The addition reactions of allyl boron esters *(R. W. Hoffmann* and *W. R. Roush)* or of boroenolates *(S. Masamune* and *D. A. Evans)* to aldehydes have certainly extended synthetic capability in useful directions, but it remains to be seen how far this will be true of the Matteson reaction (dichloromethyllithium + alkyldialkoxyboranes) or of the "boron-Wittig" reaction. In general, though, it appears that synthetic chemists who happily use hydroboration or reduction by boron hydrides have not been so ready to use boranes for forming CC linkages, despite many efforts at making this attractive to them.

The division of the book into four sections has meant that much information has been delocalized all over the book and is hard to retrieve. For example, on page 59 one learns that alcohols can in general be prepared by oxidation of organoboron compounds using hydrogen peroxide, but to find synthetic methods for organoboranes one has to thumb through many pages before discovering the required information on pages 165ff. of Chapter 3. This chapter does not, however, include details of the oxidation; the necessary information on the conversion using hydrogen peroxide etc. does not appear until page 251, but the relevant laboratory procedure is on page 346. Thus, despite the very useful details which the book contains, it turns out to be a maze. In view of the fact that *H. C. Brown* has already publicized "his" reaction through numerous review articles and *three* books ("Hydroboration", Benjamin 1962; "Boranes in Organic Chemistry", Cornell University Press 1972; "Organic Synthesis via Boranes", Wiley 1975), the question arises whether there is a need for a further lengthy description. As the proportion of really new methods in the book is not very great, one is inclined to answer no to this question, especially since the days of generous library budgets are long past.

Johann Mulzer [NB 941 IE]
Institut für Organische Chemie
der Freien Universität Berlin

Carbyne Complexes. By *H. Fischer, P. Hofmann, F. R. Kreissl, R. R. Schrock, U. Schubert,* and *K. Weiss*. VCH Verlagsgesellschaft, Weinheim/VCH Publishers, New York 1988. xviii, 235 pp., bound, DM 120.00.—ISBN 3-527-26948-7/0-89573-849-X

This volume, dedicated to Prof. *E. O. Fischer,* was issued in celebration of his 70th birthday on 10 November 1988. Five of Prof. *Fischer*'s former co-workers have contributed articles on the synthesis, molecular and electronic structure, reactivity, and catalysis of the "Fischer-type" carbyne complexes, joined by *R. R. Schrock* who (with *J. S. Murdzek*) has reviewed high oxidation state alkylidyne complexes, i.e. those of the "Schrock-type". This work, taken together with a previous dedicatory volume "Transition

[*] *Angew. Chem. Int. Ed. Engl. 26* (1987) 593.

[1] a) Alkylidynetricobalt nonacarbonyl cluster complexes: D. Seyferth, *Adv. Organometal. Chem. 14* (1976) 97-144; μ_2- and μ_3-carbyne complexes with different transition metal centers: b) F. G. A. Stone, *Angew. Chem. 96* (1984) 85-108; *Angew. Chem. Int. Ed. Engl. 23* (1984) 89-112; c) H. P. Kim, R. J. Angelici, *Adv. Organomet. Chem. 27* (1987) 51-112.

Metal Carbene Complexes" by the same five former coworkers with *K.-H. Dötz* (VCH Verlagsgesellschaft, Weinheim/VCH Publishers, New York 1983), serves as a remarkable tribute to the legacy of organometallic chemistry originated by Prof. *E. O. Fischer* and this students, over and above the contributions to the metallocenes and π-aromatic complexes for which *Fischer* was recognized by the 1973 Nobel Prize in Chemistry (jointly with *G. Wilkinson*).

The scope of the work under review is limited to mononuclear complexes containing the chemistry of the terminally bonded ≡CR group. As a matter of general information, it should be noted that the carbyne group is also observed in edge- or face-bridging positions in cluster complexes of dimetallic or higher nuclearity,[1a-c] reference to which is made in the introduction to the article by *P. Hofmann* (see below). The syntheses and chemical and structural properties of these polynuclear carbyne complexes are sufficiently different, however, to justify the decision to consider these outside the scope of the present volume.

The literature is covered to late 1987, starting with the report in 1973 of the first carbyne complex (E. O. Fischer, G. Kreis, C. G. Kreiter, J. Müller, G. Huttner, H. Lorenz, *Angew. Chem. 85* (1973) 618-620; *Angew. Chem. Int. Ed. Engl. 12* (1973) 564-565). The articles are preceded by a foreword by *W. A. Herrmann* describing some personal characteristics of Prof. *E. O. Fischer* and reviewing highlights of his scientific career. Among other things we learn that Prof. *Fischer* has an abiding interest in the history of art, one of the few diversions he has permitted himself in an otherwise absorbing career in science.

The first article in the volume is by *H. Fischer* on the synthesis of Fischer-type carbyne complexes of Group VI to VIII transition metals. Some 18 to 20 twenty methods are reviewed, starting from the original synthesis in which a nucleophile is abstracted from a Fischer-carbene in the reaction of its complex with a Lewis acid. Methods involving the abstraction of $O^{2\ominus}$ from acyl metallates, or conversion of other groups containing an sp^2-hybridized carbon, are also included, as are the conversions of complexes already containing an sp-hybridized carbon (such as CS or CNR).

The second article was contributed by *U. Schubert* and covers the reports of some eighty structures of carbyne complexes. Of these, 80% are of Group VI metal (Cr, Mo, or W) complexes. Only two of these, namely the complexes $Cp(CO)_2Cr{\equiv}C{-}CPh{=}CPh{-}C{\equiv}Cr(CO)_2Cp$, and $(t\mathrm{BuO})_3W{\equiv}CPh$, consist of an $L_nM{\equiv}CR$ unit for which structures of both the corresponding acetylene, $RC{\equiv}CR$, and the dinuclear metal fragment, $L_nM{\equiv}ML_n$, are known. The bond distances, $d(Cr{\equiv}C) = 170.7(2)$ pm and $d(W{\equiv}C) = 175.8(5)$ pm respectively, are those obtained by adding together one half of the M≡M and C≡C distances in the reference compounds. The M−C(carbyne) bond lengths for first row transition metals (Cr, Mn or Fe) are found in the range 165-175 pm, while whose for second or third row transition metals (Mo, W, Os or Ta) are in the range 175-190 pm; these constitute the shortest known metal-carbon distances.

The third article is by *P. Hofmann* on electronic structure. Analyses of ≡CR and various $\equiv ML_n$ fragments using the extended Hückel method are first presented. These are followed by summaries of results of calculations as they have appeared in the literature, including some based on other methods such as the Fenske-Hall SCF approximation or *ab initio* SCF-MO. The available theoretical work provides qualitatively consistent results explaining the important aspects of the chemistry of these complexes. Comparisons with experimental studies such as electronic absorption spectra and high resolution X-ray (X−X) determinations are also included.

The fourth article consists of a selected review by *F. R. Kreissl* of reactions of the Fischer-carbyne complexes. In these the carbyne carbon is generally found to be electrophilic, in contrast to that of the Schrock-alkylidynes in which the carbyne carbon is nucleophilic; the division is not rigid however, as some Fischer-carbyne complexes such as $C_5H_5(CO)_2M{\equiv}CR$ (M = Mo or W) reveal nucleophilic behavior at the carbyne carbon. The various chemical properties discussed for complexes of the general formula $X(CO)_nM{\equiv}CR$ are: substitution of X or CO, modification of the carbyne side chain at R, addition of a nucleophile or an electrophile at C, transfer of the carbyne ligand, and oxidation or reduction of the metal.

The article on high oxidation state alkylidyne complexes follows next. These are known for Nb, Ta, Mo, W, and Re, in which the metal is in its highest possible oxidation state, i.e. d^0, counting the alkylidyne as a trianion. The first such complex was the salt $[Li(dmp)][Ta(\equiv CCMe_3)(CH_2CMe_3)_3]$, obtained by removing the alkylidene α-proton in $Ta(=CHCMe_3)(CH_2CMe_3)_3$ with butyllithium in the presence of dmp (N,N′-dimethylpiperazine). The same general strategy proves successful for other metals, e.g. $W(OMe)_3Cl_3 + 6\,Me_3CCH_2MgCl$ (in diethyl ether at 0°C) → $W(\equiv CCMe_3)(CH_2CMe_3)_3$ (50% yield), or $MoO_2Cl_2 + 6\,Me_3CCH_2MgCl$ (in diethyl ether at −78°C) → $Mo(\equiv CCMe_3)(CH_2CMe_3)_3$ (ca. 35% yield). Additionally, complexes of other alkylidyne groups may be accessed through metathetical reactions with alkynes, or by reactions of alkynes (or, in a few cases, nitriles) with complexes containing metal-metal triple bonds. Schrock-type carbyne complexes have also been obtained by halogenation of Fischer-type carbyne complexes (*A. Mayr*), which results may explain the role of oxidizing co-catalysts in the olefin metathesis by Fischer-carbyne complexes (see below). Metallocyclobutadiene complexes and their role in alkyne metathesis, along with other reactions of alkylidyne complexes, are also reviewed. The structural properties ($M{\equiv}C_\alpha$ bond length and $M{-}C_\alpha{-}C_\beta$ bond angle) of some 16 d^0 alkylidyne complexes are tabulated, as are also some ^{13}C NMR data (C_α chemical shift $^2J(CP)$, where applicable) for over 250 alkylidyne complexes. The article concludes with a brief section on rhenium complexes. At Prof. *Schrock*'s invited lecture at the recent E. O. Fischer Festkolloquium in Garching, however, emphasis was placed on the growing importance of the d^0-alkylidyne chemistry of this metal.

The volume concludes with an article by *K. Weiss* reviewing the catalytic reactions of carbyne complexes. This begins with a section on alkene metathesis and ring opening polymerizations by carbyne complexes in the presence of Lewis acid co-catalysts; cationic complexes are believed to be the active catalysts. For the complex $Br(CO)_4W{\equiv}CPh$, the tautomeric 16-electron halogeno-carbene form $(CO)_4W{=}C(Br)Ph$ has been proposed (by *T. J. Katz*) to be the active form. Alkyne metathesis and alkyne polymerization are also reviewed, resulting in a small but not significant overlap with some material in the immediately preceding article.

All in all, I have found this work to be uniformly well written, well balanced in its coverage, and free of errors. I highly recommend it to every chemist interested in organometallic chemistry and the applications of organometallic compounds to catalysis. For the benefit and encourage-

ment of younger chemists, in the spirit of Prof. *E. O. Fischer* to whom this work is dedicated, I also recommend to the publishers that they should produce a paperback student edition.

Herbert D. Kaesz [NB 946 IE]
Department of Chemistry and Biochemistry
University of California, Los Angeles, CA (USA)
[1988–89 Humboldt Senior US Fellow
Institut für Anorganische und Analytische Chemie
der Universität Freiburg (FRG)]

From CA to CAS Online. By *H. Schulz.* VCH Verlagsgesellschaft, Weinheim 1988. xii, 227 pp., hardcover, DM 56.00.—ISBN 3-527-26866-9

The book comprises two parts; the first by *Hedda Schulz* is principally concerned with the hard copy services available from Chemical Abstracts, while the second, largely written by *H. R. Pichler,* deals with CAS Online.

After a brief introduction, the first part of the book is devoted to explaining the organization of the material within Chemical Abstracts. It starts by illustrating the differences in the information provided in abstracts of journal articles, patents, books, dissertations, etc. Unfortunately, unnecessary repetition of pointers to CA volume number and abstract number, language indicator and the like, has tended to obscure the useful guidance given here.

However, the larger part of this section of the book is devoted to illustrating (a) the indexes provided with each issue of Chemical Abstracts, (b) the volume indexes, and (c) the collective indexes. The approach is very thorough and the use of examples of searches to highlight the different informational content of the indexes is very helpful. Great emphasis is placed on the need to consult the Index Guide, which is so often overlooked even by experienced searchers.

The section ends with a brief mention of the various computer readable services produced by Chemical Abstracts and with an introduction to CAS Online. Whilst mention is made of the other hosts providing online access to Chemical Abstracts files, prominence is given to the CAS Online service, but some of the statements made are open to debate.

In Chapter 8, Mr. *Pichler* follows the elementary approach favored by *Hedda Schulz* but in this case most of the information provided is readily available in publications produced by Chemical Abstracts themselves. The "official" Chemical Abstracts guides to CAS Online are quite outstanding, being very informative and illustrated with many examples, and the availability of these, together with the excellent training and instruction manuals provided by all the Online vendors, seriously reduces the value of this part of the book.

In the last chapter an attempt has been made to compare conventional searches through hard copy with online searching, by repeating some of the searches set out in Part 1. Unfortunately, since the online part of this comparison appears to have been carried out by inexperienced searchers and no attempt has been made to check the relevance of the answers, this section adds nothing to the debate.

Thus the Fischer–Tropsch search illustrated in Part 1 using hard copy indexes was repeated online using an almost identical approach, to give 895 references from six months of Chemical Abstracts. It would have been much more interesting to see if the 71 references found immediately with the first simple strategy represented the total available from that particular volume. This would have illustrated the great advantage of online searching for such subjects, and established the cost effectiveness or otherwise of using online in preference to conventional methods.

When repeating the search for DOS, a plasticizer, the searcher misinterpreted the online search output, which showed that references were available in CAOLD, and failed to notice that the manual search had given identical results.

Recent advances in online search facilities, for example training packages such as the STN Mentor series, and front-end packages such as STN Express, have further changed the overall picture with regard to instruction books such as this.

However, whilst the book is somewhat eulogistic about CAS Online and STN, the first part by *Hedda Schulz* is sufficiently useful to make it worth consideration, especially for academic institutions with limited online facilities.

James F. Sibley [NB 934 IE]
Shell International Petroleum Company Ltd.
London (Great Britain)

Registered names, trademarks, etc. used in this journal, even when not marked as such, are not to be considered unprotected by law.

© VCH Verlagsgesellschaft mbH, D-6940 Weinheim, 1989.

Printed in the Federal Republic of Germany by Zechnersche Buchdruckerei, Speyer/Rhein.

All rights reserved (including those of translation into foreign languages). No part of this issue may be be reproduced in any form – by photoprint, microfilm, or any other means – nor transmitted or translated into a machine language without written permission from the publishers. Only single copies of contributions, or parts thereof, may be made for personal use. This journal was carefully produced in all its parts. Nevertheless, authors, editors and publisher do not warrant the information contained therein to be free of errors. Readers are advised to keep in mind that statements, data, illustrations, procedural details or other items may inadvertently be inaccurate.

Valid for users in the USA: The appearance of the code at the bottom of the first page of an article in this journal (serial) indicates the copyright owner's consent that copies of the article may be made for personal or internal use, or for the personal or internal use of specific clients. This consent is given on the condition, however, that the copier pay the stated per-copy fee through the Copyright Clearance Center, Inc., for copying beyond that permitted by Sections 107 or 108 of the U.S. Copyright Law. This consent does not extend to other kinds of copying, such as copying for general distribution, for advertising or promotional purposes, for creating new collective works, or for resale. For copying from back volumes of this journal see 'Permissions to Photo-Copy: Publisher's Fee List' of the CCC.

European Materials Societies

Editorial Essay

By Robert Lallement*

It is well known that many major changes in human history have coincided with the mastering of the technology of new materials, so that we read of the Stone Age, then the Bronze Age, followed by the Iron Age. Each breakthrough in materials technology has brought about a modification in the habits of men and their ways of life. Whether the changes have been good or bad is another question ... Nevertheless, it is a fact that the peoples or nations who achieved such breakthroughs usually also gained political power. This applies equally to the Hyksos, who conquered Egypt 4000 years ago through their mastery of the use of horses, metals, and war chariots, and to the nations which today have the technology for using nuclear materials.

What label can be applied to the age we now live in?—perhaps the steel and concrete age, or the plastics age? Are we now entering the era of titanium, carbon and plutonium?

The current worldwide interest in materials R & D has as its background the clear relationship that exists between technological progress and the discovery and mastering of new materials. This is not merely a passing fashion of the eighties, even though the fascination which the topic has for the media and for technical and political official bodies may sometimes appear exaggerated and irritating.

Leaving aside the materials mania, the facts which concern us as scientists are that, in the first place, advances in materials science have an essential role in the future of mankind, and secondly, the last ten or fifteen years have seen a scientific revolution in the approach to materials science. Before this, the subject was treated essentially through a *categorial* approach, with distinct sciences of ferrous materials, ceramics, plastics, etc., which were rigidly separated and did not interact very much. That approach has become less and less valid, and nowadays the optimum use of materials requires an *integrated* approach. The only effective way to prepare students and researchers for real life in our universities or laboratories is to teach them the *science of materials*, which is a cocktail of chemistry, physics, metallurgy, mechanics, and even other sciences. Our old categories are exploding and fading away:

Come teachers and searchers
Throughout the land
And keep your eyes wide open
The chance won't come again
Your old road is rapidly ageing
For the times they are a-changing.

Adapted from a song by *Bob Dylan*

The metallurgical societies, which were established according to the old categories, must adapt themselves, and these changes are already beginning. For example, the (UK) Institute of Metals has now become the Institute of Materials, the (US) Metallurgical Society is now the Minerals, Metals and Materials Society, and the Société Française de Metallurgie may soon become the Société Française de Métallurgie et des Matériaux.

Along with these trends towards increasing integration between the different aspects of materials science, we are also beginning to see moves towards growing European integration, where the long-established national scientific societies are now finding that they need to adjust to the de-

[*] Dr. R. Lallement
Commissariat a L'Énergie Atomique (CEA)
31-33 Rue de la Fédération, 75752 Paris Cedex 15 (France)

Contents

R. Lallement
European Materials Societies 357
G. A. Ozin, A. Kuperman, A. Stein
Advanced Zeolite Materials Science 359
Research News
J. M. McBride
Symmetry Reduction in Solid Solutions: A New Method for Materials Design 377
H. Büttner, A. Bussmann-Holder
Ferroelectricity and Superconductivity 379
Book Reviews 381
Conference Calendar 388

veloping European Physical Society, a Federation of European Chemical Societies, a European Polymer Federation and similar societies for other disciplines, and it seems likely that eventually we shall have a European Materials Society. At present, though, we are far from that goal. Many of the national societies in European countries are fighting for survival. They suffer financial difficulties, they sometimes find it a struggle to organize meetings that come up to the best international standards, and they compete with difficulty against the well organized US and Japanese scientific bodies.

Recognizing these problems, the Institute of Materials (IOM), Deutsche Gesellschaft für Metallkunde (DGM) and Société Française de Métallurgie (SFM) decided early in 1988 to join together and create the Federation of European Materials Societies (FEMS). I have the honor of being elected as the first acting president of FEMS. It is satisfying to report that many national bodies in Europe have responded positively to our invitation to join the Federation. We have already launched a first European Technical Conference, EUROMAT 89, to be held in Aachen in November 1989, and further European conferences are in preparation. In addition we have already signed an agreement with the Minerals, Metals and Materials Society for future collaboration. This is a significant step towards an effective and cordial relationship with the US scientific community. These and our other activities are expected to make a major contribution towards improving international communication in the world of materials science and engineering.



Dr. Robert Lallement, born in 1934, graduated from Ecole des Mines de Paris in 1955. He received a Master of Science from Caltech, Pasadena, CA in 1959 and an Ingénieur Docteur from Paris University in 1963. In 1969 he became Head of the Metallurgy and Fuel Division in the French Atomic Energy Commission (CEA); since 1982 he has been in charge of the nuclear programs in the French CEA. Dr. Lallement has been Acting Chairman of the French Metallurgical Society since 1987 and he is the first president of the Federation of European Materials Societies.

The following review articles will appear in future issues:

G. M. Whitesides, C. D. Bain: Modeling Organic Surfaces with Self-Assembled Monolayers

F. Garnier: Functionalized Conducting Polymers—Towards Intelligent Materials

D. W. McCall: Materials Issues in Electronic Systems

W. Michaeli: Material Processing—a Key Factor

B. R. Philips, D. Tanner, J. A. Fitzgerald: The Kevlar Story—An Advanced Materials Case Study

M. Salkind: Aerospace Materials Research Opportunities

D. F. Williams: Challenges in Materials for Health Care Applications



From March 1st, the editorial team of Advanced Materials will be strengthened by the appointment of Dr. Peter Gregory as Associate Editor. Peter Gregory studied chemistry at University College London, England, gaining a B.Sc. in 1983 and a Ph.D. working in the research group of Alwyn Davies in 1986. His doctoral work included a study of the radical and radical ion chemistry of polyacetylenes and other industrially utilized polymers along with research into the single electron transfer reactions of organic molecules in general. He then moved to West Germany, working for just over two years in the interdisciplinary research group of Paul Schleyer at the University of Erlangen-Nürnberg. Here he gained experience in a number of areas, ranging from spectroscopy and crystallography, through the development of high density materials, to the application of computers in chemistry. With this broad background he will help make Advanced Materials the journal which best serves the needs of the materials science community.

ADVANCED MATERIALS

Advanced Zeolite Materials Science**

By Geoffrey A. Ozin,* Alex Kuperman, and Andreas Stein

Molecular Electronics
Quantum Dots/Chains
Zeolite Electrodes, Batteries and Membranes
Nonlinear Optical Materials
Chemical Sensors
Zeolite-Polymer Composites

1. Introduction

In today's search for smaller, faster, more selective and efficient products and processes, the ability to engineer well defined spatial microarrangements of pure substances and composite materials is becoming pivotal in creating new molecular level electronic, optical and magnetic devices. One attractive method for assembling and maintaining controlled microstructures is to use solid host lattices that serve as templates within which a guest stucture of nanometer architecture can be assembled. It is the thesis of this paper that zeolites as microporous molecular electronic materials with nanometer dimension window, channel and cavity architecture represent a "New Frontier" of solid state chemistry with great opportunities for innovative research and development.

Since the first synthetic preparation of zeolites by *Barrer* in the 1940's[1] these aluminosilicate materials have been used in large quantities for hydrocarbon conversion, size/shape selective heterogeneous catalysis, gas separation and purification, as well as for ion exchange, dessication and sorbing processes.[2] Although only few zeolite compositions are used in large scale processes, the number of specifically tailored zeolite structures and modifications has increased immensely within the last decade, along with the number of publications concerning new physicochemical characterization techniques for these framework materials. In zeolite characterization X-ray and neutron diffraction, solid state magic angle spinning (MAS) NMR and FT mid and far infrared spectroscopy have proven particularly useful.[3] Combined, these methods provide comprehensive information about zeolite physicochemical properties and allow one to monitor transformations of and within the zeolite lattice.

Much zeolite research and development is still aimed at the traditional uses mentioned above. However, within the last few years considerable effort has been directed at new uses of zeolites as advanced materials. For example, in the field of solar energy conversion technology a spatially well organized molecular system is required that models photosynthetic mechanisms, thereby allowing redox reactions to proceed efficiently along desired paths. Other potential applications include zeolite electrodes and electron relays, zeolite batteries, zeolite fast ion conductors, intrazeolite semiconductors, zeolite chemical sensors, zeolite imaging and data storage materials, zeolite lasers and displays, as well as zeolite composites to form permselective membranes or thin films.

Most of the traditional and advanced applications for zeolites are based on the ability of these open crystalline structures to selectively incorporate and exchange both charged and neutral species within the void spaces and interconnecting channels on a molecular scale. In order to appreciate the unique features of zeolites it is necessary to take a brief look at their structures and compositions. Conventional zeolite structures are composed of three dimensional networks of SiO_4 and AlO_4 tetrahedra in which a unit negative charge is associated with each AlO_4 tetrahedron. This charge must be counter-balanced by a positive inorganic or organic ion. Depending on the type of connection between tetrahedral building blocks, linear or pseudo-linear channels may be formed with diameters ranging from 4.2 to 7.4 Å. In other structural types cages are formed with diameters of 6.4 to 12 Å and window sizes from 2.3 Å (6-ring) to 13 Å (18-ring). Figure 1 illustrates some typical examples of commonly encountered zeolite structures.

Isomorphous replacement of framework $Al^{3\oplus}$ and $Si^{4\oplus}$ by other elements such as $Ga^{3\oplus}$, $Ge^{4\oplus}$, $B^{3\oplus}$, $P^{5\oplus}$ as well as enrichment in framework $Si^{4\oplus}$ can be readily achieved. Most notable in this context are synthetic strategies that lead to highly or completely siliceous zeolites like ZSM-5 and silicalite as well as a new generation of molecular sieves exemplified by the aluminophosphates (ALPO's), silicoaluminophosphates (SAPO's) and their metal doped analogues denoted MAPO's and MAPSO's, where, for example, M = Li, Be, Mg, Cr, Mn, Fe, Co or Zn. The lattice of silicalite is neutral in contrast to the positively charged SAPO lattice which is negatively charged when $P^{5\oplus}$ has been partially replaced by $Si^{4\oplus}$, allowing for cation exchange. Recently a novel positively charged SAPO lattice has been synthesized in which $Al^{3\oplus}$ has been partially re-

[*] Prof. G. A. Ozin, A. Kuperman, A. Stein
Lash Miller Chemistry Department
University of Toronto
80 St. George Street, Toronto, Ontario M5S 1A1 (Canada)

[**] The generous financial support of the Natural Science and Engineering Research Council of Canada's Operating and Strategic Programmes, Union Carbide, Tarrytown, NY, USA, and Alcan, Canada, is gratefully appreciated. *A. S.* is deeply indebted to NSERC for a science graduate scholarship. Preprints of manuscripts from Professors *Tom Mallouk* and *Thomas Bein* assisted us greatly in the writing of this review paper. We also thank all our coworkers at the University of Toronto for many enlightening suggestions and discussions during the course of our research in advanced zeolite materials science.

placed by $P^{5\oplus}$, now permitting the less common mode of anion exchange.[4] The majority of the new generation molecular sieves crystallize with an encapsulated organic template, usually a charge balancing alkylammonium ion. The template can be effectively removed by controlled calcination procedures to yield the protonated analogue of the sieve which can often be subsequently ion-exchanged for other cationic guests. A wide variety of guests have been encapsulated in zeolites ranging from atoms, ions, metal clusters and salts to coordination complexes and organometallics. Until very recently this kind of inclusion chemistry has been driven mainly by the science and technology of specific molecule adsorption and diffusion, molecular sieving and chemical/catalytic transformations, usually taking advantage of restricted geometry environments.

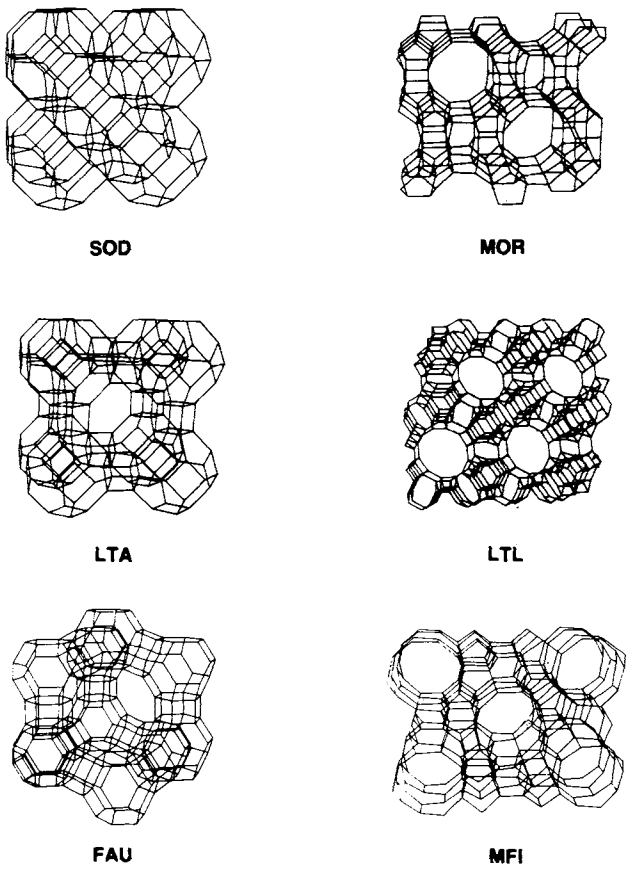


Fig. 1. Some typical zeolite structures: (SOD) sodalite, (LTA) Linde type A zeolite, (FAU) faujasite: zeolites X or Y, (MOR) mordenite, (LTL) Linde type L zeolite, and (MFI) ZSM-5 [49].

In view of the impressive range of zeolite framework structures and element substitution, rich extraframework cation modification, variety of encapsulated guests, tunable Brønsted acidity and lattice oxygen basicity, as well as the controllable hydrophobic/hydrophilic character, one can envisage that future innovations in the field will likely occur at the interface between zeolite science, solid state chemistry and molecular electronics.

2. Intrazeolitic Semiconductors

While the physical properties of materials are fairly well understood on both the molecular and bulk levels, the quantum size regime encompassing microscopically structured solids from 5 to 100 Å is the subject of much current research.[5] Particles of this size display electrical, optical and magnetic properties that are essentially independent of their chemical composition, but are related instead to their extremely small dimensions.

The tremendous present interest in ultrasmall semiconductor particles can be considered to derive from the original notion of artificially layered structures known as semiconductor superlattices, and from the exciting optical and electrical properties that such quasi-two dimensional (2D) electron systems offer. The formation of modulated chemical composition layers of this kind with a periodicity larger than the natural lattice spacing but smaller than the de Broglie wavelength of electrons of the semiconductor components, allows the realization of band gap engineering, heterojunctions, composition and doping superlattices, multiple quantum well (MQW) lasers, high electron mobility transistors, (HEMT's) non-linear optical (NLO) superlattices and optical transistors (transphasors) to name just a few applications.[6a]

Theoretical considerations have indicated that quantum size effects are significantly enhanced when the dimensionality of a quasi-2D semiconductor is further reduced. For example, strongly enhanced electron mobilities and resonant tunneling have been predicted and recently observed in the case of quantum wires and quantum boxes. Fundamental alterations in their electronic/optical properties are expected by the novel 1D and 0D quantum confinement of excitons and the modified density of states.[6b]

A major challenge in the synthesis of spatially resolved materials is the reproducible fabrication of microscopically organized semiconducting solids having quasi-1D and quasi-0D electronic/optical properties. Common methods for producing quantum microstructures include molecular beam epitaxy (MBE), metal-organic chemical vapor deposition (MOCVD), electron beam lithography and reactive ion etching.[6b, 7] As a way to avoid the minimum size limitations of electron-beam lithography, which are typically ca. 0.02 μm,[6b, 8] quantum size particles have been prepared and studied in liquid suspensions, micelles, glasses, and zeolites.[9] Host matrices like zeolites reduce the interchain and interlayer perturbation often encountered in other low dimensional solids.[10] Zeolites have an advantage over the other matrices listed, because they permit the ordered inclusion of particles with very small dimensions and a very uniform size distribution. By using zeolites of different architecture the spatial arrangement of

ADVANCED MATERIALS

the quantum size particles can be controlled and cluster growth constrained to molecular dimensions. At the same time the zeolite lattice provides a stabilizing medium because of kinetic impediments imposed on further agglomeration processes. Modification of framework charge density and electric field gradients provides extra flexibility for designed perturbation of the entrapped semiconductor characteristics (i.e. a semiconductor-support effect).

In what follows we describe some pioneering experiments aimed at producing well defined semiconductor quantum dots and semiconductor superlattices in various zeolite hosts.

3. Quantum Dots and Semiconductor Superlattices

An intriguing new avenue of advanced zeolite materials science involves the synthesis and stabilization of isolated sub-colloidal dimension intrazeolite semiconductor aggregates. As the pore filling of the zeolite is increased a percolation threshold is reached. At this point a semiconductor supercluster lattice is created by the 3D interconnection of intrazeolite quantum dots to yield materials with properties intermediate between those of discrete, "molecule-like" semiconductor clusters and bulk semiconductors. Experiments of this kind have been reported for narrow band gap semiconductors like CdS, CdSe and PbS.

Herron et al.[11, 12] have recently succeeded in incorporating semiconductor materials inside zeolites X, Y, and A. Such particles are referred to as "quantum dots" in the terminology of finely divided semiconductors. Excitons in these materials are confined in three dimensions. Due to the small size and reduced dimensionality of the occluded semiconductors, their electronic properties are altered. Absorption edge energies of confined CdS microcrystals are larger than in the bulk semiconductor,[8] so that spatial confinement of these materials allows for band gap adjustment. As the semiconductor cluster size decreases the excited-state relaxation dynamics are also influenced considerably by the host and its interface with the semiconductor.[11]

CdS particles were synthesized inside the zeolite A, X or Y framework by exposing the calcined $Cd^{2\oplus}$ ion exchanged zeolite to flowing hydrogen sulfide at 100°C. X-ray diffraction (XRD) and extended X-ray absorption fine structure (EXAFS) results revealed that discrete, cubic $(CdS)_4$ clusters (interpenetrating Cd and S tetrahedra) with a Cd-S bond length of 2.47 Å were formed strictly inside the smaller sodalite cages, where a stabilizing interaction between the cluster and framework oxygen of the double 6-rings was possible (Fig. 2). At low $Cd^{2\oplus}$ loading these clusters were isolated but formed an interconnecting extended supercluster structure as the cluster concentration increased. In this case the Cd-Cd separation between adjacent sodalite cages was ca. 6 Å, allowing for long-range interactions. It has been suggested that the supercluster was formed by a percolative process with a percolation threshold of 4 ± 1 wt%. At higher loading $(CdS)_4$ clusters must populate adjacent sodalite units. The highest CdS loading that was achieved (ca. 23 wt%) filled nearly all sodalite cages. The CdS clusters, as well as PbS clusters encapsulated in zeolites[13] were stable for at least six months in a dry, oxygen-free environment.

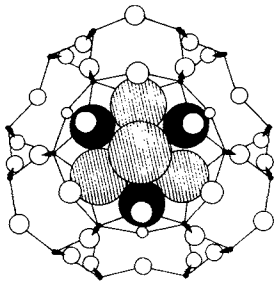


Fig. 2. Representation of the Cd_4S_4 cube inside the sodalite unit [12, 14].

Optical absorption near 290 nm characterized these ultrasmall semiconductor aggregates. Discrete $(CdS)_4$ cubes began to interconnect at higher loading densities to create a supercluster structure displaying optical absorption near 350 nm. The latter absorption is likely due to an exciton transition similar to that found in 25–30 Å colloidal CdS particles. Above the percolation threshold the absorption spectra became independent of the CdS concentration. *Wang* and *Herron*[11] studied the photoluminescence and relaxation dynamics of the superclusters. The three different emission bands observed were attributed to defect luminescence: a yellow/green band due to Cd atoms, a red band caused by sulfur vacancies, and a blue band due to shallow donors, which was probably also sulfur related. Defects like these break up the supercluster into smaller units of irregular sizes. The authors believe that the effect of the surrounding matrix on the absorption spectra of the semiconductor clusters was small, and did not alter the conclusions drawn about quantum size effects.

It has been found that partial occupancy of zeolite sites by $Cd^{2\oplus}$ produces CdS supercluster size distributions in the zeolite lattice rather than the possibly more desirable homogeneous semiconductor superlattice. Only in the case of zeolite X with the highest ion-exchange capacity, can the maximum loading of 25 wt% CdS be achieved which is close to the 27 wt% required for filling available sodalite cages. A similar investigation by *Moller* et al.[14] involved the incorporation of quantum size CdSe clusters in zeolite Y, which are of interest in the study of photosensitized electron-transfer reactions utilized for solar energy conversion and photocatalysis. A mixture of CdSe and probably helical Se chains was obtained.

The early results from these systems support the idea that semiconductor loaded zeolites have the potential to be tuned from 0D quantum dot type structures to 3D superlattice structures, the spatial arrangement and distribution of which are controlled by the templating action and framework architecture of the zeolite host.

4. Silver Sodalites: Novel, Optically Responsive, Packaged Silver Salts

β-Cages are the building blocks for several classes of zeolites. The zeolites composed exclusively of β-cages, called sodalites, have been studied mainly as model compounds for larger zeolite systems. Because of their small entrance windows (2.3 Å diameter) which block the passage of most molecules, sodalites have not been used in applications involving catalysis or gas separation. However, closer inspection leads to the realization that the sodalite lattice forms a convenient matrix for encapsulation of a variety of guests. By controlling the loading of the trapped species, it is possible to form cluster and extended supercluster structures in the quantum size regime, similar to the semiconductor superclusters described in the previous section. One important advantage of sodalites is that the lattice is comprised entirely of close-packed sodalite cages, rather than the coexisting sodalite and supercages of other zeolite hosts, thereby permitting direct or through-bond interaction between guests in *all* cages. In addition, the presence of guest-anions make sodalites unique. These can be used as internal reagents (e.g. for intra-sodalite cage redox reactions) and provide great flexibility in the composition of trapped species. By judicious selection of the anion and cation one can form packaged insulators and semiconductors as well as metals within the sodalite framework. Control of the guest-concentration in sodalites facilitates the transition above a percolation threshold (PT) from molecular type species to expanded bulk materials, as illustrated in Figure 3.

One facet of Figure 3 has recently been studied in our laboratory.[15] A range of novel silver sodalites have been synthesized. These solid state microstructures are viewed as "packaged" silver salts comprised of nanoassemblies of silver cations tetrahedrally organized with various charge balancing anions. A collection of physicochemical characterization techniques have been employed to interrogate the structure and properties of the parent silver sodalites, as well as the chemical and physical transformations of the encapsulated silver salts that relate to a number of transducer effects. An interesting question in these materials concerns intercavity communication between aggregates of the entrapped silver salt and the connection of their properties with those of the analogous bulk phase material (such as electronic transport, photoconductivity, photoaggregation and photoluminescence). Intracavity redox processes that produce encapsulated silver clusters and expanded-metal-superlattice phenomena above the PT loading level are also intriguing avenues of enquiry within the silver sodalite family of materials. In this section we will briefly describe the synthesis and characterization of a few key silver sodalites and examine their possible utilization in high resolution imaging/printing and high density data storage applications. A summary of some of the attractive features of silver sodalites in solid state chemistry is presented schematically in Figure 4.

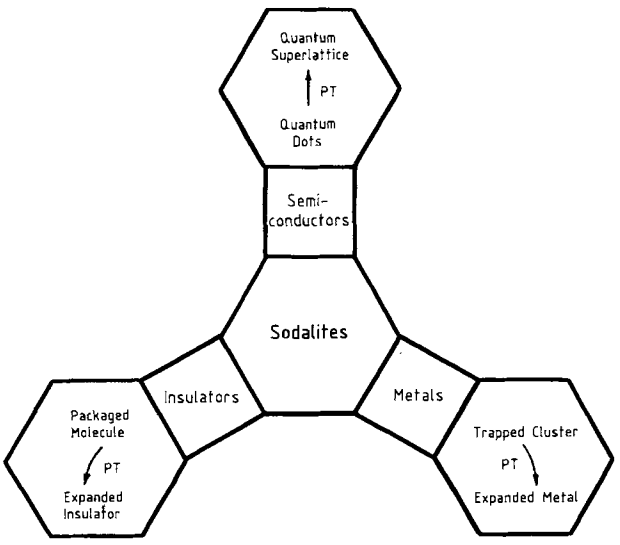


Fig. 3. Origami diagram showing the transitions between isolated and expanded insulators, semiconductors and metals that can potentially be formed within sodalites (PT = percolation threshold) [15].

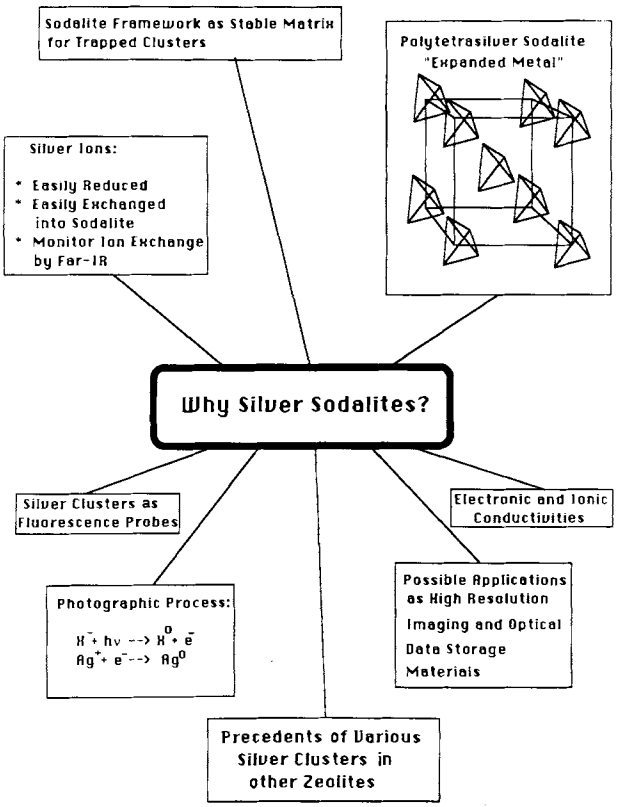


Fig. 4. Summary of the attractive features of silver sodalites in solid state chemistry [15].

ADVANCED MATERIALS

Sodalites with sodium cation guests are readily synthesized by hydrothermal reactions of silicate and aluminate sources (e.g. kaolin; or silica gel and sodium aluminate) with the appropriate anion salt in concentrated NaOH solutions. Sodium ions are exchanged for silver ions in a silver salt melt, or in some instances, in a silver salt aqueous solution. The framework structure is generally maintained after exchange, as confirmed by powder X-ray diffraction studies and mid-IR spectroscopy of the framework vibrations. The silver sodalites prepared to-date in our laboratory are listed in Table 1. The silver exchange process is conveniently monitored by the accompanying intensity changes of diagnostic sodium and silver ion translatory modes in the far-IR as well as by shifts in the frequencies of far-IR anion translations.

Table 1. Silver sodalites [15, 48].

Sodalite Type	Reason for Study
Ag, Cl–SOD	Analogues to photochromic and cathodochromic sodalites
Ag, Br–SOD	Similarities with photographic process
Ag, I–SOD	Occluded guest species are photoconductors, semiconductors, fast-ion conductors Study variation in properties down a group
Ag, S–SOD	Sensitization
Ag, Br, S–SOD	Photographic imaging
Ag, OH–SOD	Some hydroxide present in most hydrothermally prepared sodalites
Ag_6–SOD	Cages contain only three silver ions and no anion Occluded metal clusters Expanded metal Quantum size effects
Ag, CO_3–SOD	Intracage anion decomposition possible
Ag, HCO_2–SOD ≡ Ag, Fo–SOD Ag, C_2O_4–SOD ≡ Ag, Ox–SOD Ag, ClO_4–SOD Ag, SO_x–SOD	Redox switching
Na, Ag, X–SOD	Mixed cation systems to study silver concentration effects Tunable insulators /semiconductors (NaX: insulators; AgX: semiconductors, ion conductors)

Many of the silver sodalites prepared in these studies are novel materials. Interesting responses in color as well as luminescence properties were observed upon exposing several compositions to a variety of physical stimuli, including heat, light, pressure, moisture, X-rays and e-beams (Table 2). Some of the changes were reversible or semi-reversible.

The observed effects are related to the ease of silver reduction and the ability of the silver to form small clusters or expanded superclusters within the sodalite framework. In silver hydroxo-, formato- and oxalato sodalites this is facilitated by the intrazeolitic redox reactions (1)–(4). Reaction (4) can be effected both thermally and photolytically. Depending on the level of silver exchange, aggregates of the type $(Ag_nNa_{4-n})^{q\oplus}$, $n=0$ to 4, may be formed within the cages, where charge variations of q in the range $q=(4-n)$ to 4 can lead to the observed optical responses.

$$2\,Ag^{\oplus}(Z) + H_2O(Z) \longrightarrow 2\,Ag^0(Z) + 1/2\,O_2 + 2\,H^{\oplus}(Z) \quad (1)$$

$$2\,Ag^{\oplus}(Z) + OH^{\ominus}(Z) \longrightarrow 2\,Ag^0(Z) + 1/2\,O_2 + H^{\oplus}(Z) \quad (2)$$

$$2\,Ag^{\oplus}(Z) + HCO_2^{\ominus}(Z) \longrightarrow 2\,Ag^0(Z) + CO_2(Z) + H^{\oplus}(Z) \quad (3)$$

$$2\,Ag^{\oplus}(Z) + C_2O_4^{2\ominus}(Z) \longrightarrow 2\,Ag^0(Z) + 2\,CO_2 \quad (4)$$

The silver, oxalato-sodalite (Ag, Ox–SOD) system will be used as an illustrative example. The results of a full-profile Rietveld analysis of X-ray powder diffraction data for completely silver ion-exchanged Ag, Ox–SOD showed that the intracage Ag-Ag distances varied from 4.5 Å to ca. 6 Å, and intercage Ag-Ag distances from 4.5 to 4.9 Å, depending on the cage contents. These interatomic distances are too long for direct overlap of the silver orbitals but they are well within the range of through-bond interaction involving the sodalite framework. Such long range interactions would allow the formation of an expanded silver supercluster. From a unit cell size study of Na,Ag,Ox-sodalites with various silver loadings, together with transmission electron microscopy (TEM) and powder XRD data, it was determined that β-cage encapsulated $Na_n^{\oplus}Ag_{4-n}^{\oplus}$ moieties were distributed statistically throughout the sodalite lattice, in a solid-solution like manner as a function of n.

After aqueous silver exchange, Na,Ag,Ox-sodalites are white. Following thermal treatment at a temperature allowing for intrazeolite oxalate redox reaction (4), the materials

Table 2. Qualitative responses of silver sodalites to various physical stimuli [15, 48].

Barochromic:

White Ag, OH–SOD or Ag, HCO_2–SOD samples darken upon application of pressure.

Hydrochromic:

Ag, OH–SOD undergoes a reversible color change upon dehydration.

Photochromic:

Color changes and/or sample darkening can be produced by irradiation of Ag, Ox–SOD, Ag, OH–SOD, $AgCO_3$–SOD, Ag, HCO_2–SOD and sulfur-doped silver sodalites with various light sources.

Thermochromic:

Na, Ag, Ox–SOD, Ag, OH–SOD and sulfur-doped silver sodalites undergo various color changes upon heat treatment.

X-ray sensitivity:

White Ag, Ox–SOD turns yellowish green upon exposure to X-rays.

Fluorescence changes:

Heat, light and X-rays can induce Na, Ag, Ox–SOD samples to fluorescence under UV-light.

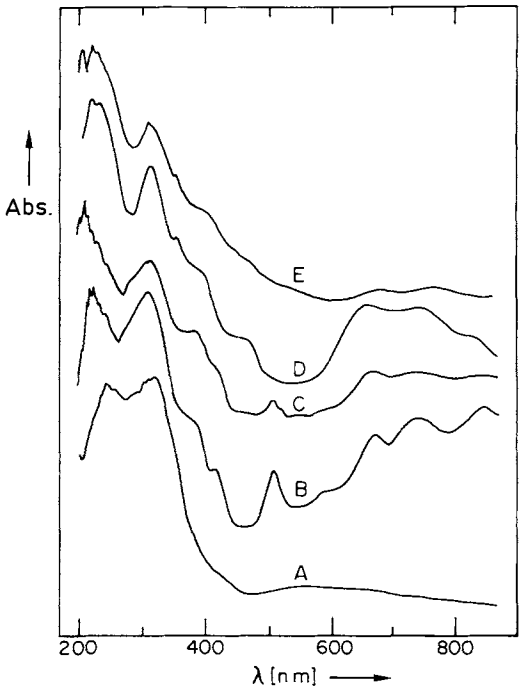


Fig. 5. UV-visible reflectance spectra of oxalato sodalites. A) Na,Ox-SOD (white); B) Na,Ag,Ox-SOD (1 Ag/unit cell), (light grey); C) Na,Ag,Ox-SOD (2 Ag/unit cell), (bluish grey); D) Ag,Ox-SOD (green); E) Ag,Ox-SOD, exposed to sunlight for four days (pale yellowish green). Samples B–E had been synthesized by $AgNO_3$-melt exchange at 230°C [15, 48].

absorb light in the UV and visible regions, the absorption spectrum depending on the silver concentration (Fig. 5). Concentration effects are also exhibited by the position of the most intense emission bands. Variations in both the identities of trapped silver clusters and the unit cell sizes could be responsible for the shifts in transition energies.

The fate of the oxalate ion during thermal treatment was followed by thermogravimetric analysis coupled with mass spectrometry (TGA-MS), mid-IR spectroscopy and powder X-ray diffraction. A comparison of the results for sodium oxalato-sodalite and silver oxalato-sodalite indicated that the reduction potential of the cation directs the reaction mechanism. While in the silver oxalate sodalite the anion is oxidized to CO_2 with concomitant reduction of the silver ions, oxalate ion decomposition in the sodium oxalate sodalite produces CO and $CO_3^{2\ominus}$, with no redox reaction occurring. In Na,Ag,Ox-sodalites the degree of silver exchange can thus be used to control not only the optical and structural properties, but also the thermal behavior of the sodalite.

Although the number of electron equivalents involved in intracavity silver ion reduction was shown to be relatively small, the alterations in silver cluster optical properties that ensue are quite spectacular. As a result, the silver sodalites lend themselves to applications in high resolution imaging and optical data storage, because the regular close-packed framework structure can trap and stabilize clusters formed inside. During a write cycle these clusters can be manipulated by the physical or chemical treatments described above (Table 2) to change their optical properties and produce a mark on the sodalite samples. The presence or absence of an optically absorbing or fluorescing mark defines a binary state. The size of the mark is affected mainly by the silver distribution, the sodalite particle size and the writing mechanism employed. The sodalite may be in the form of a self-supporting pressed disk, suspended in another material (e.g. glass or polymer), or supported on a substrate as a thin film.[15]

5. Quantum Chains

The isolation of selenium chains with controlled lengths and conformations in a zeolite host provides an interesting opportunity to probe quantum size effects in a 1D semiconductor. This type of selenium falls into the category of a "quantum chain", and may comprise a system that can exhibit discrete energy levels within the bulk semiconductor band structure with quantization of electronic properties in one dimension. One can expect isolated selenium chains to bridge the behavior between atomic/molecular forms of selenium and the bulk semiconductor trigonal form. In this regard, some interesting structure-property questions arise concerning the effects of interchain interactions, spatial restrictions and confinement on chain conformation. Selenium is of interest, because it has an intermediate electrical conductivity with a negative coefficient of resistivity in the dark. It is markedly photoconductive and has uses in, for example, photoelectric devices and xerography.

Bogomolov et al.[16] stabilized single selenium and tellurium chains in the unidimensional mordenite channels by injecting Se or Te into the zeolite from a melt under pressure or by incorporating the chalcogenide in the mordenite channels by vapor phase absorption. Isolated Se chains in mordenite channels are strongly photosensitive.[17] Results from a quantitative X-ray microprobe analysis indicated that one trigonal (helical) Se or Te chain was present in each channel with a period multiple with that of mordenite. The important question of whether the Se chains were actually *included and isolated* within the zeolite was addressed by *Tamura* et al.[17] The Se uptake (23%) in mordenite agreed with an estimate based on the assumption that the bond length of a single occluded Se chain is 2.32 Å and that the chain forms the same helical structure as in the crystalline trigonal Se. High-resolution electron micrographs of mordenite, into which Se had been inserted[10] provided further evidence of the inclusion of Se chains. This analytical technique, together with EXAFS, ^{77}Se MAS-NMR, and optical spectroscopy has provided impressive details on the distribution and form of channel confined selenium, intrachain bond length and conformational information as well as a preliminary insight into quantum size effects in one dimension. From inspection of

Figure 6a, one can determine that only one Se chain is capable of being accommodated in the large channel of mordenite. Occupied mordenite channels could be distinguished from empty channels in high resolution micrographs of Se_n/MOR (Fig. 6d). Here the white bands show white dots for the main and subsidiary channels devoid of selenium, whereas the dark bands show black main channels and white small channels. This confirms that the selenium is indeed incorporated into the large channels of mordenite.

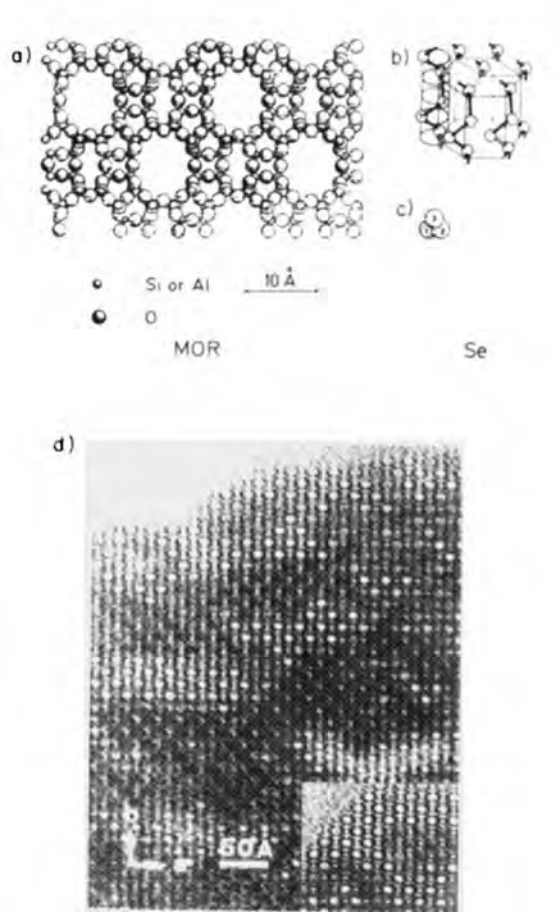


Fig. 6. a) Schematic drawing of the framework structure of mordenite (along [001]). b) The structure of crystalline Se, shown in elevation. c) A projection of the chain of Se along the *c*-axis. d) High-resolution electron micrograph of mordenite into which Se has been inserted. The regions of light contrast are seen to be indistinguishable from mordenite devoid of any guest species. At the regions of dark contrast, caused by uptake of Se the small channels are still empty as indicated by the small white dots [10].

Parise et al.[18] extended the incorporation of selenium chains to other molecular sieves, including zeolites A, X, Y, AlPO-5 and mordenite. Their study showed how the zeolite framework structure can be used to direct the growth of the occluded selenium to its various allotropes. In all samples the band gaps blue-shifted from the respective band gaps of the bulk trigonal and monoclinic forms. While only Se_8 crown rings formed inside zeolite A (band gap close to the value for monoclinic Se: Se_8 rings), helical chains predominated in the other zeolites (band gap-energy close to that for trigonal Se). In the X and Y samples the framework system was occupied by a mixture of selenium allotropes and helical chains. Mordenite and AlPO-5 resulted in the highest degree of order, having single helical chains in the 12-ring channels, with a Se-Se distance (2.34 Å) ca. 2% shorter than in crystalline trigonal Se (2.373 Å).

The particle size dependence of the band gap of semiconductor materials like ZnS, CdS, PbS is now well documented. Their optical properties have been reasonably described by the "electron-hole in a sphere" model of *Brus* and the increase in band gap follows as a result of the 3D spatial confinement of the electron-hole pair. Unlike these isotropic semiconductor particles, selenium is structurally unique in its ability to exist as helical chains and Se_8, Se_7, Se_6 puckered rings, with intraatomic chain and ring bonding being much stronger than inter-chain and inter-ring interactions. It is noteworthy that the theoretical models for size quantization effects in the optical absorption spectra of layered semiconductor colloidal particles involve modifications of the electron-in-a-cubic-box model to account for charge confinement in a rectangular box with an infinite potential barrier, which can be thinned to include the case of a single-layer 2D sheet. Thus it is likely that a different approach will be required to explain the 0.2 eV blue shift observed in the band gap of the intrazeolite Se helical chain, relative to the bulk trigonal phase. A possible contribution to the widened band gaps in the chain form arises from a reduced selenium chain length, and 1D quantum size effects. However, it is difficult to evaluate the role of chain-chain interactions on the 0.2 eV blue shift. A 0.3 eV blue shift observed in intrazeolite Se_8 appears to have its origin in the loss of ring-ring interactions. One should keep in mind that small changes in Se-Se bond lengths, together with alterations in helical pitch and dihedral angle could all contribute to the small differences observed among the optical spectra of intrazeolite selenium and their bulk analogues.

6. Molecular Wires—Conducting Polymers in Zeolites

An intriguing new direction in zeolite science focusses attention on synthetic strategies for the encapsulation of so called molecular wires", composed of "isolated" strands of conducting and semiconducting chain structures like those found in polythiazyl, polypyrrole, and polyaniline, for example, in the unidimensional channel structures of mordenite, L-zeolite and ALPO-5 hosts.

Quite often, the anisotropic electronic, magnetic and optical properties of so-called one-dimensional materials in the bulk solid phase are influenced to some degree by interchain interactions. For example, polythiazyl $(SN)_x$ is a room temperature metallic conductor, which does not un-

dergo a metal insulator Peierls distortion on cooling and, moreover, becomes superconducting at low temperatures. Tunable band filling in 1D solids is often achieved by chemical doping with electron donors or acceptors, or by electrochemical oxidation/reduction. The resulting cation/anion pair interactions are thought to play a role in the properties of the 1D material. Thus "isolated" conducting chains confined to a 1D zeolite channel provide an interesting situation for comparison with "interacting" chains in the bulk.

A recent study by *Bein* and *Enzel*[19] gives an example of the utility of zeolites in such developments. These workers allowed pyrrole (vapor and solution phase) to diffuse into Fe^{III}-containing faujasite (Y) or mordenite (M). The pyrrole polymerized within the channel system where the extraframework Fe^{III} ions served as an oxidant. The polypyrrole chains formed are expected to be 1D molecular conductors. The host pore and channel structure was anticipated to affect the polymer chain length and thus the transport properties of the molecular wires. Using the diagnostic 2.7 eV and 2.0 eV $\pi \rightarrow \pi^*$ absorptions as indicators of the degree of polymerization it was concluded that vapor phase treated $Fe^{III}Y$ contains *shorter* polypyrrole chains than those encapsulated in $Fe^{III}M$. Because of the insolubility of bulk polypyrrole, solvent extraction experiments were incapable of establishing the location (internal vs. external) of the polymerization product. However, indirect evidence provided a case for internal imbibement of the polypyrrole chain. This evidence included a) the inability to form polypyrrole in Na^{I} or Fe^{II} forms of the zeolites compared to the Fe^{III} form, b) the superior UV-visible transmission properties and narrower FT-Raman line widths of zeolite polymerized pyrrole inclusion compared to the bulk form and c) the lesser encapsulation quality of the polymer in the mordenite compared to the Y zeolite host where the former has the smaller free pore volume.

Another material of great interest for the formation of intrazeolitic molecular wires is polyaniline encapsulated in zeolite hosts. Here the possibility exists of obtaining isolated structurally defined chains whose electronic transport behavior can be switched from insulating to conducting by electrochemical oxidation and/or chemical protonation. The selection of acid versus alkali metal ion-exchanged zeolite hosts is therefore crucial in terms of synthetic strategy, details of intrazeolite polymerization, and properties of the resulting encapsulated polymer.

Polyaniline is a novel conducting polymer, salts of which have been synthesized with electrical conductivities up to $10\ \Omega^{-1}\ cm^{-1}$. In contrast to polypyrrole, which contains nitrogens as pendant groups attached to a polyacetylene like backbone, polyaniline exists with amine and imine nitrogen atoms (the relative amounts dependent on the degree of oxidation) occupying bridging positions in the backbone-structure which, furthermore, can be protonated and deprotonated by an appropriate choice of pH.[20]

Key questions are: What is the state of protonation/oxidation when aniline is polymerized and encapsulated in different zeolite host lattices, and, what are the structure-property relationships between the "isolated" polyaniline chains so formed and their connection (if any) to the bulk polyaniline analogues?

In the first study to address such questions concerning isolated polyaniline chains, the host structures examined were the sodium and Brønsted acid forms of zeolite Y and mordenite.[21] Polyaniline (PANI) was synthesized intrazeolitically via the oxidative polymerization of preloaded anilinium ion. Although ca. 30–50% extractable PANI was probably formed on the external surface, supporting evidence was given for the stabilization of polyaniline *inside* the zeolite channel system. The electronic spectrum of the various zeolite samples indicates that both the oxidized insulating (590 nm) and the conductive (800 nm) forms of PANI had been encapsulated. Polymerization appeared to be favored in the larger pore network of zeolite Y in comparison to mordenite as indicated by the red shift of the 800 nm absorption of the former relative to the latter.

Clearly these studies represent only the beginning of a large and fascinating enquiry on the synthesis, characterization and structure-property relationships of "molecular wires" comprised of isolated conducting polymeric chains in zeolite hosts. Future work will undoubtedly focus attention on other synthetic pathways to intrazeolite "molecular wires", such as electropolymerization, as well as host control over polymer chain length, definition of degree of polymerization and the intriguing question of the transport properties of "isolated" conducting chains.

7. Intrazeolite Multicomponent Electron-Transfer Chains

The utilization of zeolites in the assembly of molecular structures is demonstrated in an elegant experiment by *Mallouk* et al.[22] These workers used zeolite Y to form a molecular chain of three redox-active molecules at a reactive SnO_2 electrode surface. This self-assembly reaction overcame the great difficulty of direct synthesis. The SnO_2-covered electrode surface was allowed to react with the cationic silane (Fig. 7 top) to produce a coating a few monolayers thick. A dense single layer of zeolite particles was formed on the surface, linked to the silane coating by Si-O-Si bridges at free silanol groups. By immersing this electrode-zeolite assembly in a solution, anions and cations were incorporated at three specific ion binding sites: 1) a multiply charged anion (e.g. $[Fe(CN)_6]^{4\ominus}$) on the bridging silane; 2) a large cation (e.g. a substitution-inert metal polypyridyl complex) size-excluded on the outer zeolite surface; and 3) a small cation (e.g. cationic metallocene) that can enter the zeolite framework. The resulting structure shown in Figure 7 (bottom) was characterized electrochemically, by optical spectroscopy and by scanning elec-

ADVANCED MATERIALS

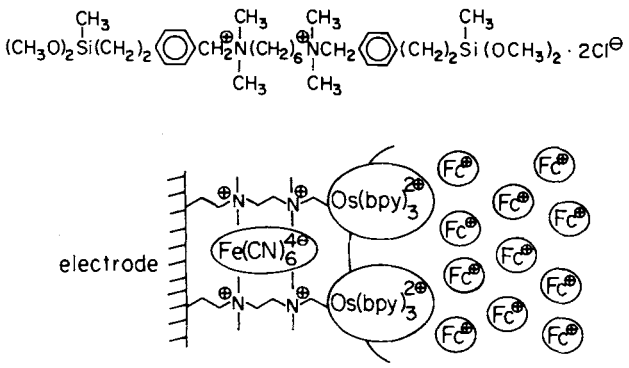


Fig. 7. Top: Cationic silane, used to functionalize the SnO_2 electrode surface before the reaction with zeolite particles. Bottom: Scheme showing the self-assembled redox chains at the zeolite Y-modified electrode. $Fc^{\oplus}$ refers to intrazeolitic cationic metallocenes. The $Os(bpy)_3^{2\oplus}$ complex is size-excluded from the anionic zeolite framework [22].

tron microscopy (SEM). The system functioned as a redox active vectorial chain only when all three components were anchored at their specific sites. Molecular microstructures of this type may serve as models for natural photosynthetic systems.

In another study *Mallouk* et al. have recently achieved long-lived light-induced charge separation in a self-assembling zeolite-based molecular triad.[23] This multicomponent system is composed of a zeolite L or Y surface-bound $RuL_3^{2\oplus}$ sensitizer, an attached $2\,DQ^{2\oplus}$ acceptor (*N,N'*-dialkyl-2,2'-bipyridinium) oriented into the open anionic structure of the zeolite and a secondary acceptor, benzylviologen ($BV^{2\oplus}$), contained within the zeolite framework (Fig. 8). Transient diffuse reflectance and luminescence lifetime measurements on this organized assembly show that intramolecular electron-transfer quenching from $Ru^{2\oplus}$ to the $2\,DQ^{2\oplus}$ moiety occurs within 5 ns or less and that the formation of the $Ru^{3\oplus}$-$BV^{\oplus}$ charge-separated state occurs in about 100 ns; this indicates that electron transfer from

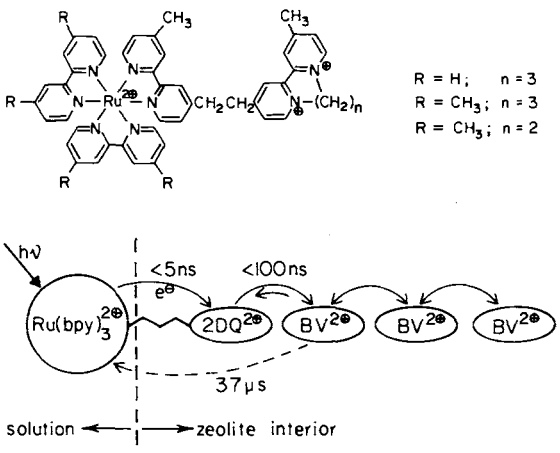


Fig. 8. Possible spatial arrangement of the $RuL_3^{2\oplus}$-$2\,DQ^{2\oplus}$ complex and $BV^{2\oplus}$ at the aqueous solution/zeolite interface. The structure of the $RuL_3^{2\oplus}$-$n\,DQ^{2\oplus}$ complex is also shown [23].

$2\,DQ^{\oplus}$ to $BV^{2\oplus}$ is complete within ≤ 100 ns. Of particular note is the long-lived nature of the $Ru^{3\oplus}$-$BV^{\oplus}$ charge-separated state, which decays via first-order kinetics with a lifetime of 37 ± 5 μs. The quantum yield for its formation is $17 \pm 5\%$.

The kind of spatial arrangement of the molecular triad shown in Figure 8 is considered to provide close contact of $BV^{2\oplus}$ contained in the zeolite with transiently formed $2\,DQ^{\oplus}$. This permits fast and efficient formation of $BV^{\oplus}$. The long lifetime of the charge-separated $Ru^{3\oplus}$-$BV^{\oplus}$ state has been attributed to a favorable spatial separation of $Ru^{3\oplus}$ and $BV^{\oplus}$ and the possibility of isoenergetic electron-exchange along the $BV^{2\oplus}$ chain depicted in Figure 8.

The work of *Mallouk* et al. has relevance to electron-transfer reactions in photosynthetic chains and light-to-chemical energy conversion systems. Of special note is the fact that the zeolite-based triad spatially resembles and behaves like the membrane-bound special pair-pheophytin-quinone triad in the reaction center of photosynthetic bacteria, which has two extremely fast forward electron-transfer steps and a long-lived charge-separated state.

8. Zeolite Electrodes—Zeolite-Modified Electrodes

Zeolites are essentially cationic conductors with the same temperature dependence typically displayed by solid ionic conductors (higher mobility of ions at higher temperature). However, some indications of partial electronic conductivity exist, for example in silver exchanged zeolite A.[24] By appropriate modifications of the zeolite composition the conductivity properties of zeolites can be altered to allow their use as solid electrolytes, membranes in ion-selective electrodes and as host structures for cathode materials in battery systems.[25]

Two types of applications exist for zeolites as part of electrode systems. In zeolite-modified electrodes the zeolite acts as a charge, size and shape selective membrane to impart a chemically specific environment for absorbed molecules at an electrode surface.[26] High product selectivities can be obtained with zeolite-modified electrodes in electrosynthetic reactions.[27] The second type, an ultramicroelectrode utilizes the zeolite framework as a matrix for intrazeolitically generated electrode components. Typically metals or metal oxides serve as electrode microstructures in and/or on the zeolite support, but organometallic or organic components, such as the polypyrrole quantum wires mentioned above can also be utilized. Organic molecular ultramicroelectrodes allow the study of conductivity and electrochemical reactivity on very small scales, as well as electrode processes at shorter times, in restricted environments and unconventional media.[26] They have potential relevance to photosynthetic systems and molecular electronics (e.g. sensors, solid state devices).

The zeolite electrode systems to be briefly described in this section include: a) encapsulated Pt_n clusters; b)

$M(bpy)_3^{2\oplus}/M(CpR)_2^{\oplus}$; c) $EDTA/MV^{2\oplus}/ZnTMPyP^{4\oplus}/Pt_n$; d) $MV^{2\oplus}/CoTMPyP^{4\oplus}$; e) $MnTMPyP^{5\oplus}$; f) composite zeolite electrodes.

An important question in all these systems is that of making electrical contacts. Some commonly used methods include 1) spring loaded contacts or coatings such as silver paint with zeolite pellets; 2) molecular attachments such as in the methylviologen-porphyrin studies described in the previous section; and 3) a method developed by *Pons* et al.[28] that avoids fixed electrical contacts altogether. The latter method consists of applying bipolar electrolytic conditions to dispersions of ultramicroelectrodes using feeder electrodes. The zeolite-supported ultramicroelectrode acts both as a mobile electrode and an electrolyte. A wide range of ultramicroelectrodes can then be accessed. This technique was applied in the study of zeolite encapsulated metal clusters for dispersion electrolyses,[26,29] as outlined below.

In practice one finds that zeolite supported platinum clusters permit dispersion electrolyses under low ionic strength conditions where microelectrodes could not function. Pt_n/zeolite Y has been shown to be a much more effective ultramicroelectrode system than $Pt_n/\gamma\text{-}Al_2O_3$ for aqueous electrolyses.[29] Control experiments showed that, although an increase in the conductivity of aqueous media did ensue from ions exchanged from the virgin zeolite, the higher ohmic background was dwarfed by the electrochemical response obtained in the presence of platinum supported in the zeolite.

Gallezot's procedures for the formation, location and sizing of Pt_n in zeolite Y were employed in the fabrication of the Pt-Y electrodes. After $[Pt(NH_3)_4]^{2\oplus}$ ion-exchange for $Na^{\oplus}$ in Na-Y, the zeolite was dried at 135°C and then heated in flowing oxygen to promote H_2O/NH_3 loss and autoreduction of Pt^{II} to Pt^0 via NH_3. The details of the activation step were crucial in determining the state and distribution of Pt_n within the zeolite microstructure. At 300°C, 6–13 Å Pt_n remained in the supercages while at 600°C, 15–20 Pt_n formed throughout the bulk of the crystal.

Typical results for the two-phase system C_6H_6/H_2O showed markedly enhanced currents at a given voltage for 1% Pt-Y (with mainly internally sited platinum), compared to 1% $Pt\text{-}Al_2O_3$, and essentially zero response for the feeder electrodes alone. The current-voltage responses of different Pt-Y loaded samples for the electrolysis of water showed that the electrolytic effectiveness followed the order: 1% Pt-Y > 5% Pt-Y > 10% Pt-Y = 1% $Pt\text{-}Al_2O_3$. Comparisons between the electrolyte response of Pt-Y samples, implied that the internally confined particles did not contribute to the electrolyses. This was rationalized by the inability to achieve electric fields high enough for bipolar electrolysis to occur on intracrystalline sited platinum particles at the voltages employed. By contrast, externally sited particles could be physically charged at the feeder electrode or via other previously charged supported platinum sites. Similar effects have been experienced for dispersion electrolysis of ferrocene/CH_3CN and a substituted ferrocene/CH_3CN too bulky to enter the Pt-Y sample, thereby supporting the proposal of externally active platinum sites in Pt-Y. In the dispersion electrolysis the zeolite support yielded a more effective material than the alumina. Based on XPS determined platinum particle sizes and associated surface areas these results suggest that the electrode processes may be affected by particle size in the submicron range.

Recently the preparation and electrochemical behavior of simple, self-assembly vectorial electron transport chains on zeolite Y modified SnO_2 electrodes have been described.[27] These involve a Y zeolite which has been ion exchanged with a tris(bipyridyl) metal complex $M(bpy)_3^{2\oplus}$ (M = Ru, Os), and a metallocene cation $M(CpR)_2^{\oplus}$ and $M(Cp)(CpR)^{\oplus}$ (M = Co, Fe; Cp = η^5-C_5H_5 and R = H, CH_3, NH_2, CO_2CH_3, $CH_2N(CH_3)_2$). Matching of the potentials of externally sited $M(bpy)_3^{2\oplus}$ and intrazeolite $M(CpR)_2^{\oplus}$ ensures facile redox reactions, an order of magnitude enhanced over the situation when $M(bpy)_3^{2\oplus}$ is absent from the system. Rapid electron-transfer cross reactions between the two complexes are proposed to explain this behavior.

Electrodes were prepared from conductive SnO_2 coated glass squares contacted to copper wire via colloidal silver paint. The electrode was dipped into a suspension containing the ion-exchanged zeolite and polystyrene in THF, and was allowed to dry in air. Scanning transmission electron microscopy and electron diffraction (STEM) experiments on freshly cleaved electrodes showed a film thickness of about 60 μm with most of the polystyrene forming a porous layer at the outer surface of the film. The metal guest was located in the ca. 1 μm zeolite particles which formed a porous compact layer tightly adhering to the SnO_2 substrate.

Reduction and oxidation peaks of the surface bound couple $Ru(bpy)_3^{2\oplus/1\oplus}/ZY/SnO_2$ occurred at −0.76 and −0.55 V vs. the saturated calomel electrode (SCE). It is interesting that the $E_{1/2}$ of this couple ($E_0 = -0.66$ V vs. SCE) was shifted about 600 mV positive of its value in polar organic solvents (−1.24 V vs. SCE), pointing to the stabilizing effect of adsorption of $Ru(bpy)_3^{1\oplus}$ relative to $Ru(bpy)_3^{2\oplus}$ on the zeolite. The quantity of charge passed in the $Ru(bpy)_3^{2\oplus}$ reduction wave indicated that only the surface $Ru(bpy)_3^{2\oplus}$ contacting the SnO_2 electrode was electrochemically accessible. In the case of a $Co(CpCH_3)_2^{1\oplus}/ZY/SnO_2$ electrode only a small fraction of the intrazeolite $Co(CpCH_3)_2^{\oplus}$ was reduced or oxidized. The $E_{1/2}$ of $Co(CpCH_3)_2^{1\oplus/0}$ also shifted to a more positive value (−0.66 V vs. SCE) compared to its solution phase value (−1.10 V vs. SCE). A tenfold increase in the height of the cathodic wave for an $Ru(bpy)_3^{2\oplus}/Co(CpCH_3)_2^{1\oplus}/ZY/SnO_2$ electrode was observed compared to the case when surface bound $Ru(bpy)_3^{2\oplus}$ was absent. Similar current enhancements were obtained for a number of substituted

ADVANCED MATERIALS

$Co(CpR)_2^{1\oplus}$ species provided that the respective $E_{1/2}$ was positive or coincident with the $Ru(bpy)_3^{2\oplus}$ wave. The mechanism shown in Figure 9a was proposed to rationalize the observation of current enhancement, where the large cathodic wave represents the reduction of bulk $Co(CpR)_2^{1\oplus}$ mediated by surface adsorbed $Ru(bpy)_3^{2\oplus}$. The observed enhanced anodic wave was ascribed to the reverse electrocatalytic reaction shown in Figure 9b. The key finding of this study is that rapid vectorial electron transfer from the electrode to the bulk materials occurs almost entirely through the $M(bpy)_3^{2\oplus}$ complex.

a) *Cathodic process:*

$$Ru(bpy)_3^{2\oplus}(surf.) + e^{\ominus}(electrode) \longrightarrow Ru(bpy)_3^{\oplus}(surf.)$$
$$\uparrow$$
$$Ru(bpy)_3^{2\oplus}(surf.) + Co(CpCH_3)_2^{0}(bulk) \longleftarrow Co(CpCH_3)_2^{\oplus}(bulk)$$

b) *Anodic process:*

$$Ru(bpy)_3^{2\oplus}(surf.) + Co(CpCH_3)_2^{0}(bulk) \longrightarrow Co(CpCH_3)_2^{\oplus}(bulk)$$
$$\uparrow \qquad\qquad +$$
$$Ru(bpy)_3^{2\oplus}(surf.) + e^{\ominus}(electrode) \longleftarrow Ru(bpy)_3^{\oplus}(surf.)$$

Fig. 9. Proposed mechanisms for the cathodic and anodic reactions at a $Co(CpCH_3)_2^{\oplus}/ZY/SnO_2$ electrode [27].

Experiments of this kind stimulated research on more sophisticated intrazeolite molecular electron transport chains composed of porphyrins and viologens. Two fascinating new systems will be referred to, one involving photochemical H_2 evolution via singlet-state electron-transfer quenching of zinc tetra(*N*-methyl-4-pyridyl) porphyrin cations ($ZnTMPy^{4\oplus}$) using internally platinized zeolite L particles (Fig. 10a),[30] the other involving current rectification and electron trapping by surface bound monomolecular metalloporphyrin layers on zeolite Y containing intrazeolite viologens (Fig. 10b).[31]

The first zeolite electrode concerns a metalloporphyrin-based electron-transport chain which self-assembles by virtue of ion-exchange and steric interactions with a zeolite L particle. The microstructure imposed by the zeolite permits $ZnTMPyP^{4\oplus}$ to be held in sufficient proximity to a $MV^{2\oplus}$ cation so that singlet-state electron-transfer quenching occurs on the sub-nanosecond time scale. With $EDTA^{2\ominus}$ added as a sacrificial electron donor, H_2 is evolved from water under illumination with visible light at the internal platinized zeolite L-containing $ZnTMPyP^{4\oplus}$ and $MV^{2\oplus}$. Figure 10a displays the fabrication and operating details of this compartmentalized photochemical system. The linear channels which run through zeolite L and bind $MV^{2\oplus}$ are shown as idealized hexagonal prisms. The zeolite outer surface strongly binds the $ZnTMPyP^{4\oplus}$ cation as it is size excluded from the bulk. When a more sterically hindered porphyrin replaces $ZnTMPyP^{4\oplus}$, a system results which is inactive for both H_2 evolution and singlet state quenching by $MV^{2\oplus}$. These observations are rationalized in terms of closely assembled and organized triads of molecules

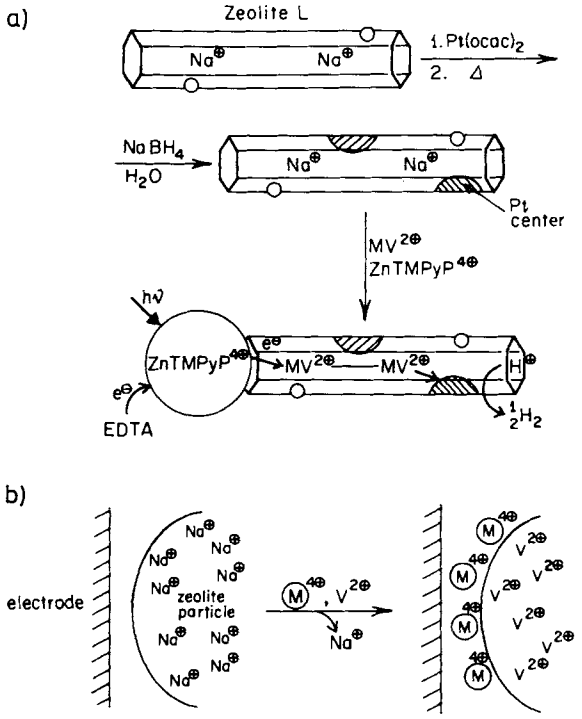


Fig. 10. a) Preparation and operation of the compartmentalized photochemical system, composed of platinized zeolite L containing $ZnTMPyP^{4\oplus}$ and $MV^{2\oplus}$ [30]. b) Preparation of metalloporphyrin/viologen($V^{2\oplus}$)-exchanged zeolite Y particles and zeolite-modified electrodes [31].

$EDTA^{2\ominus}$, $ZnTMPyP^{4\oplus}$, $MV^{2\oplus}$ located at the zeolite/solution interface.

This elegant study demonstrates that molecular level organization of electron donor, metalloporphyrin and quencher in zeolite L is feasible. Such integrated, highly ordered systems can sustain photochemical production of H_2 from water via singlet state electron transfer quenching of the porphyrin molecule. An attractive feature of the system is its self-assembly by ion-exchange from simple commercially available components. Considerable scope clearly exists for maximizing quantum yields for electron-hole separation through the clever design of more complex interfacial assemblies.

Li et al.[31] exchanged zeolite Y with viologen cations which diffused into the bulk and attached monolayers of larger cobalt or zinc porphyrin cations to the outer surface of the zeolite. The porphyrin molecules sealed the zeolite against rapid exchange of viologen molecules and facilitated the electron transfer between the encapsulated viologen ions and the surroundings of the microstructure. The porphyrin tends to remain attached to the zeolite surface because its ionic charge is high enough to avoid exchange with the ionic species of the solution, even in reduced forms of complexed metal.[32]

Another zeolite electrode system of this type was fabricated using $Mn^{III}TMPyP^{5\oplus}$ fixed onto the outer surface of zeolite Y (ZY) in contact with a controlled potential metal-

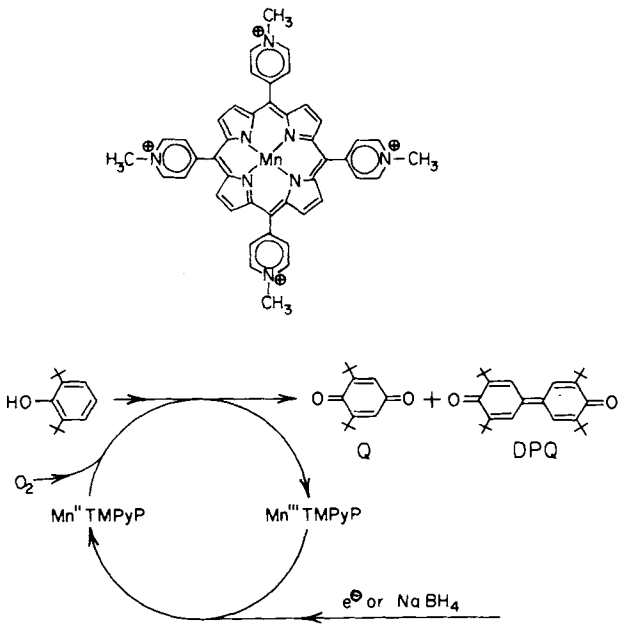


Fig. 11. Catalytic oxidation of 2,6-di-*tert*-butylphenol using a controlled potential metallic electrode (Pt grid) composed of $Mn^{III}TMPyP^{5\oplus}$ fixed onto the outer surface of zeolite Y [32].

lic electrode (Pt grid).[32] The test reaction was the oxidation of 2,6-di-*tert*-butylphenol to produce 2,6-di-*tert*-butyl-*p*-benzoquinone (Q) and diphenoquinone (DPQ). The overall catalytic process is summarized in Figure 11, where the catalytic species is $Mn^{II}TMPyP^{4\oplus}$. The study proves that $Mn^{III}TMPyP^{5\oplus}/ZY$ participates in the heterogeneous catalyzed O_2 oxidation of di-*tert*-butylphenol with quantitative conversion of the phenol to the quinone products and electrochemical regeneration of the catalyst.

The response of zeolite electrodes can be optimized by preparing a composite electrode with carbon paste. For example, *Creasy* and *Shaw*[33] constructed electrodes of methyl viologen exchanged zeolites Y and A mixed with carbon paste for the electroreduction of oxygen. The results showed that the electroreduction of oxygen by methyl viologen proceeded more efficiently upon incorporation of zeolite Y into a carbon paste electrode and that efficient mediation required the zeolite to be in close proximity to the conducting carbon particles. An optimum current was obtained when the zeolite was saturated with methylviologen.

Other zeolite composite electrodes have been formed by codepositing zeolites with organic salts or polystyrene, mixing them with conductive carbon powder or pressing them into pellets coated with doped tin oxide.[34]

9. Zeolite Solid State Batteries

In the context of advanced zeolite materials science and battery research, it is especially humbling to learn that solid state, multiple-layer zeolite batteries, having excellent high temperature (500°C) and low temperature (−78°C) operating characteristics, were developed by *Freeman* as early as 1965.[35]

The feasibility of fabricating a battery utilizing zeolite materials relates to the fact that zeolites are fairly good solid state ionic conductors with relatively small activation energies for conduction (e.g., dehydrated NaX, $\sigma(Na, 300°C) = 10^{-4}$ to $10^{-5}\ \Omega^{-1}\ cm^{-1}$). Experimentally, two types of ion motion in zeolites have been detected: a) cation jumps from site to site, b) ionic relaxation or restricted local motions of cations. These phenomena in A, X, and Y zeolites are believed to be due to cation mobility in supercages and sodalite cages. The non-monotonic ionic radius dependence of the activation energies for conduction of alkaline metal cations in faujasite has been explained in terms of a model involving coulombic interactions of the cation with the lattice and a repulsive term between cations. Some illustrative data are given in Table 3.[36]

Table 3. Activation energies [kJ mol^{-1}] for cation conduction in faujasite.

Si/Al	1.25	1.7	2.5	2.9
$Li^{\oplus}$	303	—	378	—
$Na^{\oplus}$	219	231	310	332
$K^{\oplus}$	229	226	230	271
$Rb^{\oplus}$	282	282	282	295
$Cs^{\oplus}$	232	243	—	—

Thus the activation energies tend to be larger for small cations and higher Si/Al ratios. Intercation repulsion effects appear to be responsible for the deviation of $Rb^{\oplus}$ and $Cs^{\oplus}$ from this scheme as well as the unexpected Si/Al ordering scheme. When polyvalent cations are exchanged for $Na^{\oplus}$, the activation energy for $Na^{\oplus}$ migration in the supercages, compared to the parent $Na^{\oplus}$ form decreases significantly as seen from Table 4.[36] At low $Ca^{2\oplus}$ loadings, occupancy of sodalite cages with the divalent cation is favored. Thus charge density is localized more in the sodalite cages, resulting in a decreased activation energy for $Na^{\oplus}$ migration in the supercages.

Table 4. Activation energies [kJ mol^{-1}] for cation conduction in faujasite.

Si/Al	1.25		2.5
$Ca_{42}Na_2$	247	$Ca_{26}Na_3$	172
$Ca_{40}Na_6$	192	$Ca_{22}Na_9$	163
$Ca_{35}Na_{16}$	167	$Ca_{20}Na_{15}$	180

Summarizing a large amount of conductivity data, a picture has been advanced for the motion of exchangeable cations in zeolites. It is based on the concept of highly correlated cation jumps and the idea of local cation jumps in, for example, the sodalite cages, usually from AC, DC conductivity and NMR relaxation time measurements.

With the above background material on ionic conduction of extraframework cations in zeolites, let us briefly

turn our attention to *Freeman*'s pioneering studies of zeolite batteries. Using the original notation of *Freeman* to describe a zeolite multiple layer cell composition:

$|Au|Cu^{II}X|NaX|Zn|$

one speaks of a gold catholyte contact, a copper-exchanged zeolite X catholyte, a sodium zeolite X separator and a zinc anode. The operation of the cell appears to be zinc oxidation at the anode with the liberation of electrons and concomitant reduction of Cu^{II}. This must be accompanied by the necessary ionic charge transfer of Zn^{II} liberated from the anode passing through the NaX separator lattice, to find a cation vacancy probably in the $Cu^{II}X$ lattice. Open circuit voltages for cells fabricated by pressed pellet techniques were found to be surprisingly reproducible and fell in the range 1.36–1.40 V with $Ag^{I}X$ as zeolite catholyte and calcium exchanged zeolite A (CaA) as separator, or 1.17–1.25 V with a $Hg^{II}X$ catholyte. The $|Au|Hg^{II}X|NaX|Zn|$ cell is particularly outstanding in that an appreciable current could be drawn with only a 23% drop in voltage as the load was applied.

Since most zeolites are thermally stable to at least 750 °C, zeolite cells are operable at unusually high temperatures, providing the contacts, electrodes, and intrazeolite metals are stable. In $Au|Cu^{II}X|NaX|Zn|$ an exponential increase in current with temperature is found over the range from 260 °C (3×10^{-7} A output current) to 500 °C (2.8×10^{-5} A).

The $|Au|Ag^{I}X|CaA|Mg|$ cells with magnesium anodes displayed the highest open circuit voltages obtained from single zeolite cells (1.95–2.10 V, for four different cells). It is remarkable that a $|Au|Hg^{II}X|CaA|Zn|$ cell could be operated at −78 °C with an open circuit voltage of about 1.0 V compared to 1.1 V at room temperature.

In a more recent vein, *Andersen* et al.[37] have used AC conductivity measurements on $NH_4^{\oplus}$ and $H_3O^{\oplus}$ zeolites A, X, Y and have established that $NH_4^{\oplus}$ and $H_3O^{\oplus}$ cations are mobile with conductivities dependent on the degree of hydration of the zeolite. Cell reactions have been developed for these zeolites which exploit the mobilities of the proton and ammonium ions. Cells were constructed from porous platinum blocking electrodes deposited onto pressed zeolite wafers as illustrated below:

$H_2|Pt|H_3O^{\oplus}Z|Pt|H_2$

Here the half reactions at the porous platinum electrodes involve:

$1/2\,H_2 \longrightarrow H^{\oplus} + e^{\ominus}$ anode

$H^{\oplus} + e^{\ominus} \longrightarrow 1/2\,H_2$ cathode

where the proton conductivity involves $H_3O^{\oplus}$ transfer across the solid zeolite electrolyte layer. An interesting extension of this idea involves an NH_4Z solid state electrolyte cell:

$H_2|Pt|NH_4^{\oplus}Z^{\ominus}|Pt|H_2$

where in a similar arrangement $NH_4^{\oplus}$ is gradually replaced by $H_3O^{\oplus}$ with NH_3 evolved at the cathode according to the following cell reactions:

$H_2O + 1/2\,H_2 \longrightarrow H_3O^{\oplus} + e^{\ominus}$ anode

$H_3O^{\oplus} + NH_4^{\oplus}Z \longrightarrow H_3O^{\oplus}Z + NH_4^{\oplus}$ zeolite electrolyte

$NH_4^{\oplus} + e^{\ominus} \longrightarrow NH_3 + 1/2\,H_2$ cathode

These results are quite fascinating and clearly have ramifications in advanced battery and fuel cell applications, as well as in electrochromic zeolite and molecular size/shape selective ionic-conductivity sensor elements.

Another interesting solid state zeolite cell involves the concept of utilizing dehydrated zeolite crystals as host structures for liquid and volatile electrochemically active species. *Coetzer* et al.[38] have employed this idea to investigate the performance of zeolite/iodine and zeolite/sulfur cathodes in solid state cells. For example, dehydrated sodium exchanged zeolite A (NaA) impregnated with I_2 has been used as a cathode material in a silver/I_2 solid state cell as shown in Figure 12.

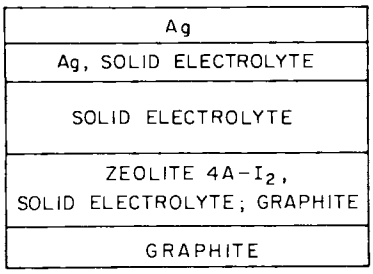


Fig. 12. A diagrammatic sketch of a Ag/zeolite 4A–I_2 cell [38].

Two quaternary amine iodide/AgI solid electrolytes, namely $Ag_{44}I_{53}(C_{11}H_{30}N_3)_3$ and $Ag_{21}I_{25}(C_9H_{24}N_2)_2$ having room temperature ionic conductivities of ca. $3 \times 10^{-2}\ \Omega^{-1}\ cm^{-1}$ are used in these cells instead of well known $Ag^{\oplus}$ conductors like $RbAg_4I_5$, as the latter is electrolytically unstable in the presence of elemental iodine. Thus it is advantageous to complex the iodine in the cathode in some way at reduced activity, as found in RbI_3, Me_4NI_5 and Me_4NI_9. The NaA/I_2 cathode is another way of achieving the goal of controlled iodine release for the cell reaction $2\,Ag + I_2 \rightarrow 2\,AgI$.

The NaA/I_2 complex used contained 38.9 wt% I_2 giving the formula $Na_{12}Al_{12}Si_{12}O_{48} \cdot 4.3\,I_2$ for the zeolite/I_2 storage cathode. A multilayer, 20 mm diameter cell construction was employed. Anode and cathode components contained finely ground electrolyte material to enhance elec-

trode-electrolyte interfacial contacts and disc binding qualities, while the cathode was mixed with finely divided graphite to enhance the electronic conductivity as the zeolites are electronic insulators.

The formation of resistive AgI ($\sigma_{25°C} \approx 10^{-4}\ \Omega^{-1}\ cm^{-1}$) as the only discharge product in the $NaA/I_2/Ag$ cell caused the internal resistance to rise and the load voltage to drop accordingly with time. This necessitates the use of relatively thin cathodes for this type of cell (cf. the Li/2-polyvinylpyridine-I_2 heart pacemaker[39]).

In summary, these results illustrate the intriguing possibility of immobilizing volatile electrochemically active species in zeolites for use as cathodes in ambient temperature cells. The immense flexibility in the choice of a zeolite host offers great opportunities for optimizing an electroactive guest molecule. One might remark on concluding this section, that it is rather surprising that the literature on zeolite batteries has been quite sparse since *Freeman*'s early pioneering work. It is expected that this situation will change rapidly as research in zeolite materials science gathers momentum in the late 1980's.

10. Optozeolite Chemical Sensors

A sensor can be defined as a small device that converts any microchange of temperature, pressure, concentration or other property into a detectable signal. The success of a chemical sensor is determined by its sensitivity and reproducible performance. The sensing element is expected to incorporate at least the following attributes: selectivity and site reversibility with respect to guest binding, fast response, small size, ruggedness, low cost, and the potential for facile integration into an automated system. With respect to sensor architecture most devices today employ a union between a selective chemireceptor and a transducer which is capable of translating the resulting physicochemical perturbation into a usable signal. Gas-sensitive metal gate semiconductor devices, chemically sensitive field effect transistors, Schottky diodes, chemiresistors and surface acoustic wave sensors represent just a few of the emerging technologies with promise in the chemical sensor field.

The concept of using zeolites as size and shape selective chemical sensors was at the basis of our research efforts to elicit from such materials an optical response such as intensity and lifetime modification due to intrusion of an adsorbate into the pore system of a zeolite. It is noteworthy that the recent patent literature mentions zeolites in applications ranging from moisture sensing,[40] oxygen monitoring,[41] and carbon monoxide detection[42] to the selective detection of ethylene, ethane and propylene.[43]

Luminescent centers housed in various zeolites were selected mainly from $Eu^{3\oplus}$, $Mn^{2\oplus}$ and $Ag^{\oplus}$ which have an extensive photochemical/photophysical solid-state literature for a range of hosts. These include single crystals, glasses, layered materials and oxide supports. Although the optical absorption and luminescence properties of certain intrazeolite metal guests are quite well understood, little is known about their excited state lifetime properties. Even less information is available on the response of these properties to specific molecule absorption and luminescence quenching in the time domain. An attractive feature of intrazeolite luminescent metal probes (ILMP's) is that one can fine-tune their optical characteristics over useful ranges of frequency and, as has been discovered recently, in time. Parameters that can be varied include the zeolite type, co-cations, Si/Al ratio and loading of the ILMP. A useful example of loading and co-cation effects stems from luminescence lifetime data obtained from the study of

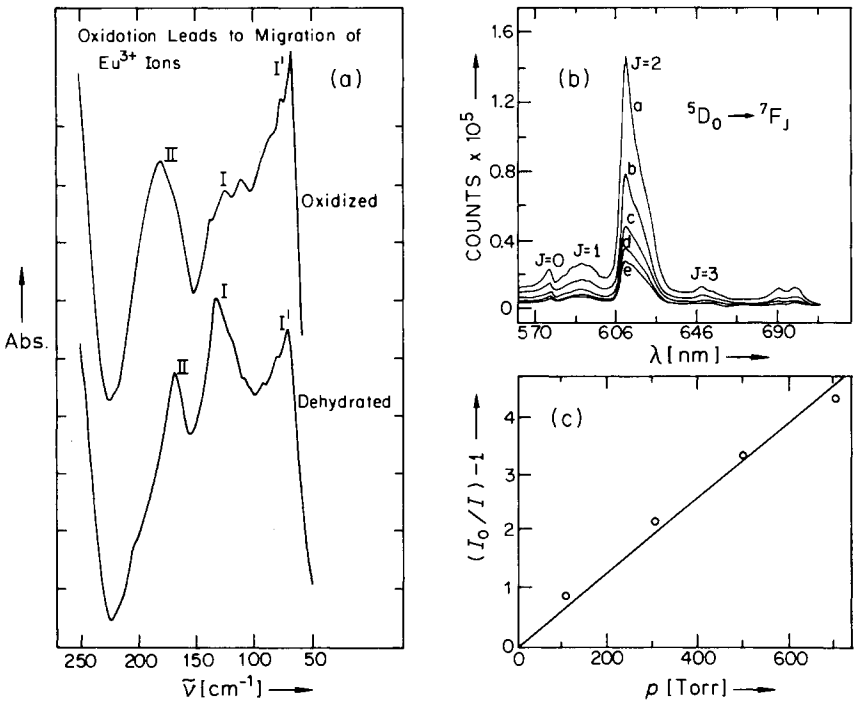


Fig. 13. a) Far infrared spectra of $Eu^{3\oplus}Y$. b) The quenching of $Eu^{3\oplus}$ luminescence at various oxygen pressures: a: vacuum, b: 105 Torr, c: 500 Torr, d: 700 Torr, e: 760 Torr. c) Stern–Volmer plot for the $J=2$ luminescence quenching depicted in b) [44].

ADVANCED MATERIALS

silver faujasites.[44a,b] The observed long-lived emissions have been associated with a spin-forbidden phosphorescence of intrazeolite $Ag_2^{\oplus}$.

The impetus for the study of $Eu^{3\oplus}$-ZY was the intrinsic very bright fluorescence of $Eu^{3\oplus}$ and the well understood luminescence spectroscopy in other solids. $Eu^{3\oplus}$ cation site locations within zeolite Y were established by far infrared spectroscopy that conveniently pinpoints cation translatory modes (Fig. 13a). The fluorescence intensity of $Eu^{3\oplus}$ was quenched upon admission of oxygen (Fig. 13b). A study of the O_2-concentration effect showed that the quenching kinetics were Stern-Volmer in nature (Fig. 13c). The lifetime decays of $Eu^{3\oplus}$-ZY also showed sensitivity to oxygen (Fig. 14). These O_2 quenching effects were found to be completely reversible at room temperature. These results demonstrate that the concept of a time-domain zeolite sensor is valid.

The sensing of NH_3 by $Eu^{3\oplus}$-ZY is noteworthy (Fig. 14b). The response was rather different to that given by O_2. While the $Eu^{3\oplus}$ $J=2$ transition decreased in intensity the $J=0$ transition was enhanced as the pressure of NH_3 was increased. The behavior was reversible upon heating the zeolite to 200°C. This is indeed a unique response. None of the adsorbates screened so far (H_2, N_2, CO, C_2H_4, O_2) produced this signature. The unusual NH_3 effect is believed to originate from a dramatic change in symmetry at the $Eu^{3\oplus}$ ion, possibly due to complexation of $Eu^{3\oplus}$ by NH_3 or the presence of $NH_4^{\oplus}$ ions formed by the interaction of NH_3 with the lattice hydroxy groups, the latter being formed from the hydrolysis of H_2O by $Eu^{3\oplus}$.[44a,b]

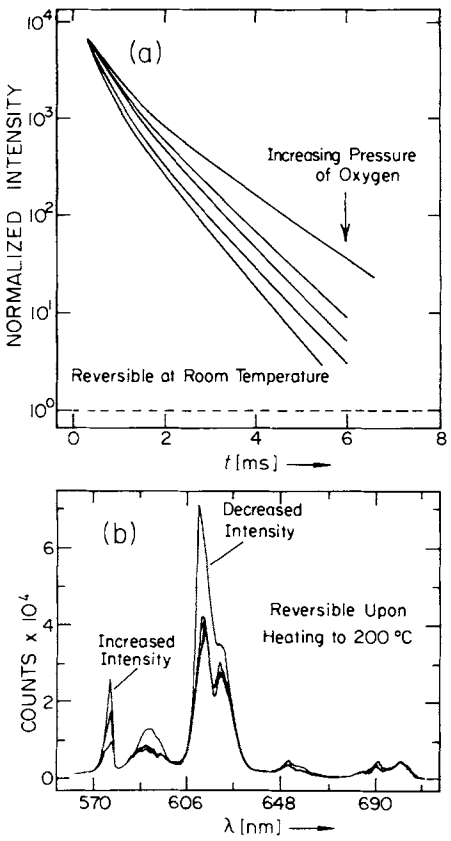


Fig. 14. a) Lifetime quenching of $Eu^{3\oplus}$-ZY luminescence by oxygen. b) The quenching of $Eu^{3\oplus}$ luminescence in zeolite X by ammonia [44].

The new generation MnAPO and MnAPSO molecular sieves provide a unique opportunity for studying the photophysical behavior of a luminescent $Mn^{2\oplus}$ framework probe. Most detailed results have been obtained so far with the MnAPSO-31 and 44 template-containing and template-free materials.[44c] Detailed EPR, steady state and time resolved optical reflectance/emission spectroscopic studies of these materials have yielded evidence for magnetic and electric dipole-coupled $Mn^{2\oplus}$ framework centers, some sites experiencing detectable interactions with neighboring template molecules.[44c]

Laser induced fluorescence studies aimed at exploring specific adsorbate quenching effects in template free MnAPSO-44 have been performed. N_2O, CO, N_2 and O_2 show reversible intensity quenching responses. Whether these are dynamic and/or static and molecule specific has yet to be quantified. It is notable that Ar, CH_4, C_3H_6 and CH_3COOCH_3 display no intensity quenching effects under similar conditions while quenching with NH_3 is irreversible. These results are encouraging as they suggest that framework metal luminescent centers might be susceptible to selective adsorbate quenching. Clearly these early studies represent just a modest beginning. Much fascinating work remains to be done in the search for a molecule size/shape discriminating optozeolite chemical sensor.

11. Tunable Non-Linear Optical Zeolites

The development of new non-linear optical (NLO) materials, which allow frequency multiplication and mixing of UV-VIS-IR radiation for laser and electrooptics applications (optical processing/computing, image analysis, switches, modulators) has recently been extended into the world of zeolites. *Cox* et al.[45] have given the first report of a non-linear optical material, fabricated by the confinement of an organic guest in an acentric zeolite host with a one-dimensional channel structure.

NLO effects are usually obtained by the polarization of a medium by an incident electric field:

$$P = \chi_1 E + \chi_2 E^2 + \chi_3 E^3 + \cdots$$

χ_1 = first order susceptibility tensor (linear optical properties, refraction, absorption); χ_2 = second order susceptibility tensor (zero for centrosymmetrical materials; non-zero values yield frequency doubling, frequency mixing effects); χ_3 = third order susceptibility tensor (non-zero for all materials, provides access to the Kerr effect, self focussing, degenerate four wave mixing, third harmonic generation).

The connection of electric susceptibilities to NLO effects derives from the polarization induced by an oscillating dipole which radiates energy. The electric field associated with the radiating dipole is proportional to the polarization:

$$E_{rad} \propto P(\omega) \quad \text{or} \quad P(2\omega) \quad \text{or} \quad P(3\omega)$$

Therefore the intensity of the radiating signal is given by

$$I \propto |E_{rad}|^2$$

and for second harmonic generation

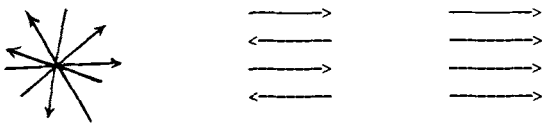
$$I(2\omega) \propto |\chi_2|^2 I^2(\omega).$$

In order to relate microscopic to macroscopic susceptibilities one considers first the molecular response to electric fields:

$$\mu = \mu_0 + \alpha E + \beta E^2 + \gamma E^2 + \cdots$$

μ_0 = permanent GS dipole moment, α = linear polarizability (2nd rank tensor, proportional to χ_1), β = second order polarizability (3rd rank tensor, proportional to χ_2), γ = third order polarizability (4th rank tensor, proportional to χ_3).

Each component molecule of a material acts as a source of non-linear polarization and so the macroscopic response is the sum of the macroscopic responses averaged over all orientations. For second harmonic generation (SHG), χ_2 must be non-zero. To achieve this objective it is mandatory that all molecular dipoles point in the same direction on average, that is:



Random	Alignment	Orientation
$\chi_2 = 0$	$\chi_2 = 0$	$\chi_2 \neq 0$

It is difficult to orient small molecules by electric or magnetic fields, because of their small dipole moments and magnetic susceptibilities. Thus it is clearly beneficial to incorporate such molecules into larger host structures to enhance orientation and alignment in addition to other properties such as mechanical stability and processibility etc. The non-centrosymmetric structural features required for SHG may be imposed on a guest species by an acentric zeolite host. In some cases synergistic sorbate-host interactions between two centric species yield a non-centrosymmetric product with very different NLO properties from either guest or host. *Cox* et al.[45] have incorporated *p*-nitroaniline (NA) and 2-methyl-*p*-nitroaniline (MNA) in zeolites Y, Omega, Mordenite and AlPO-5 in order to study changes in SHG. Note that NA has a large hyperpolarizability β but crystallizes centrosymmetrically giving $\chi_2 = 0$. To overcome the problem of relative orientation of molecules in a solid various kinds of molecular engineering approaches have been investigated, such as simple chemical modification to induce non-centrosymmetric crystallization or inclusion tuning of the organic guest by encapsulation into an acentric inorganic or organic host lattice.

NA in the centrosymmetric molecular sieves zeolite Y, Omega and Mordenite showed no SHG. For the case of NA in the acentric zeolite ALPO-5, a loading dependence of the SHG signal was observed with a maximum SHG of 630 relative to quartz at 13 wt% NA loading when all the pores were filled (Fig. 15) a magnitude *ten* times larger

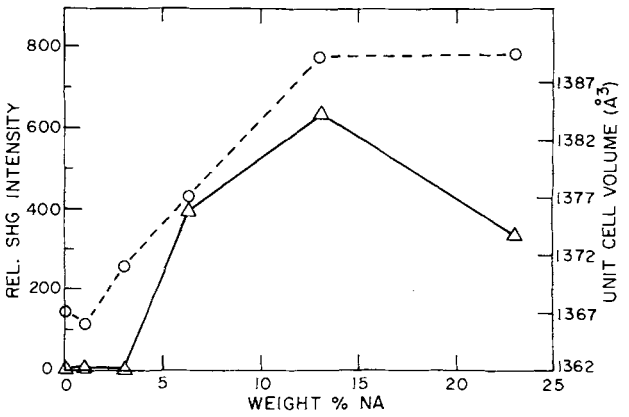


Fig. 15. *p*-Nitroaniline (NA) in ALPO-5. Loading level (weight % NA) versus SHG intensity relative to quartz (solid line) and unit cell volume in Å³ (dashed line) [45].

than that of any previously reported organic or inorganic inclusion complex. The observation of a maximum SHG at full loading implies encapsulation of NA within the pores of the ALPO-5 molecular sieve. MNA, which has a SHG by itself, loses its SHG upon inclusion in ALPO-5. The authors attributed subtle steric, symmetry and host-guest interaction effects to the ability of ALPO-5 to switch the SHG of NA on and that of MNA off. Future work concerning SHG in molecular sieves will focus attention on the effects of loading levels, other acentric hosts, host-guest interactions, and the nature of the guests.

12. Zeolite Membranes and Thin Films

In this section, a brief description will be presented of the recent development of a new generation of zeolite composite films and well-defined inorganic membrane structures that offer controlled porosity in the 10 Å range. The ultimate goal is to employ these microstructures as

ADVANCED MATERIALS

"molecular sieve" elements in chemical sensors, so that only those molecules that are able to pass through the membrane are detected at the sensor surface. The methodology employed to create such a molecule size/shape discriminating inorganic membrane structure involves the incorporation of zeolite crystals into a glass or ceramic matrix. The key objective here is to allow only passage of specific molecules through the zeolite channels while the matrix support remains impermeable.

Synthesis of the inorganic matrix derives from well established sol-gel processing technology based on the controlled hydrolysis of tetraethylorthosilicate (TEO), usually in an alcoholic solvent:

$$Si(OEt)_4 + 4\,H_2O \xrightarrow[\text{base}]{\text{acid or}} Si(OH)_4 + 4\,EtOH$$

$$n\,Si(OH)_4 \longrightarrow (SiO_2)_n + 2n\,H_2O$$

Depending on the conditions employed (pH, concentrations, temperature, solvent, etc.) condensation and polymerization of silicate species via Si-O-Si bonds can be biased towards either weakly branched "fractal" structures and microporous gels, or compact, fully polymerized colloidal particles and macroporous gels. Acid hydrolysis leads to the former, while base hydrolysis favors the latter. Incorporation of zeolite microcrystals into the sol-gel process followed by viscous sintering can provide a microcomposite thin film, composed of an impermeable silica matrix with "molecular sieving" capabilities determined by the channel architecture of the embedded zeolite.

One step in the development of thin films is the functionalization of the zeolite surface to improve the adherence properties of the zeolite on a substrate material or to use the zeolite itself as a substrate. *Bein* et al.[46] have addressed this question by studying the reactions of mono- and polyfunctional silanes (functional groups OR, Cl, NR_2, H) with zeolite Y surfaces. Although these workers were mainly interested in the possibility of anchoring molecules to the *internal* surface of zeolite pore systems, their conclusions apply similarly to the external surfaces. At moderate reaction temperatures the functional groups at the silane were lost to form bridges to the zeolite framework. As the reaction continued, Si-C bonds were broken at elevated temperatures and more highly substituted siloxane species were anchored to the zeolite framework. As expected, bridged hydroxy groups were found to be far more reactive than terminal hydroxy groups.

Early zeolite membrane experiments by *Bein* et al.[47] focussed attention on silica embedded faujasite and ZSM-5 zeolites. SEM studies revealed a fairly homogeneous dispersion of zeolite crystals in the membrane. Protrusion of single layers of zeolite crystals out of the amorphous matrix made them accessible to probe molecules adsorbing from the gas phase. This feature of these membranes is vital for sensor coatings.

The central issue of molecular access to the membrane-embedded zeolite crystals was addressed by using a surface acoustic wave device in selective adsorption experiments and mid-IR spectroscopy. A thin film of the membrane on a quartz crystal microbalance showed that in the absence of zeolite crystals, acid-catalyzed gel based films did not adsorb even nitrogen. However, gas uptake was observed when the zeolite was incorporated into the silica membrane.

In the mid-IR experiments, the Brønsted acid protons (hydroxy groups) located on the external surface of the zeolite crystals (3720–3750 cm^{-1}) were readily distinguished from internally located zeolite structural hydroxy groups (3640–3540 cm^{-1}). The gel-derived surface OH groups were characterized in the absence of zeolite by broad, weak IR bands with a sharp onset at 3750 cm^{-1} down to ca. 3200 cm^{-1}.

The key experiment involved the behavior of these differently located hydroxy groups to the adsorption of probe organic molecules whose reaction or interaction with hydroxy groups was determined by size/shape (kinetic diameter) and chemical considerations (pyridine, 5.9 Å; $(C_4H_9)_3N$, 8.1 Å; 2,2,4-trimethylpentane, 6.2 Å; NH_3, 2.6 Å; $(C_4F_9)_3N$, 10.2 Å). The results of these size/shape selective adsorption/reaction experiments provided fairly convincing evidence that, in most membranes studied, the zeolites were completely accessible from the gas phase. The membranes excluded molecules which were larger than the pore openings of the zeolite embedded in the composite. This type of microcomposite membrane is envisaged to offer great opportunities in the development of size/shape discriminating chemical sensors.

A different approach to producing thin zeolite-containing coatings used electrodeposition at a Pt or glassy carbon containing rotating disk electrode (RDE).[25] *Murray* et al. prepared the zeolite-coated RDE by spinning a Pt or glassy carbon RDE in a solution containing powdered zeolite A, Et_4NClO_4/CH_3CN and an oxidant species (1,3-dinitrobenzene, 1,4-dinitrobenzene or tetracyanoquinodimethane). A coating was formed upon repetitive scanning through the reduction waves of the oxidant. The embedded zeolite particles retained their molecular sieving properties. The coating thickness could be increased for organic oxidants by cycling through the second reduction wave and generating a dianion.

In order to use silver sodalites as optical data storage materials, *Stein*[48] embedded sodalites in a polymethylmethacrylate (PMMA) matrix and prepared thin films of the zeolite/polymer composite. This application differs from the above examples in the fact that direct access of gases or other chemicals to the zeolite is *not* required, nor even desirable. The sodalite was ground, sieved and stirred into a toluene/PMMA mixture to achieve a uniform distribution. A thin film was applied on a fused silica disk or similar support and was allowed to dry and cure at room temperature, before being treated near the glass temperature

of PMMA. The hard, highly transparent amorphous polymer PMMA was chosen because its refractive index matched that of sodalite very closely, so that light scattering was minimized. Although individual particles remained visible in many samples, greater control over the mixing and the sodalite particle size should yield fairly homogeneous films.

13. Conclusion

The unique advantages of zeolites are obvious. The stage is therefore set for some rapid and significant developments involving the synthesis, characterization and structure-property relationships of zeolite based electronic, optical, magnetic and dielectric materials. Zeolites, like any other solid state materials, have their limitations. Those specific to zeolites include pore plugging, poisoning, structural defects, the difficulties of growing large single crystals, and interfacing a zeolite device with the outside world. Many of these problems can however, be solved and are deemed to be interesting research projects.

Much of the research involving new applications for zeolite materials is still at a fairly early stage, but one can extrapolate from the present trends to make the following conjectures: the recent discovery of all-silica zeolites will pave the way to zeolite semiconductors; the marked proton conductivity of certain acid zeolites makes possible the fabrication of electrochromic zeolites; the unveiling of acentric zeolites allows the design of zeolite piezoelectric devices; the molecule size pore and channel structure of zeolites provides a novel medium in which to create ultrahigh resolution images and package and process information at high storage densities; the unidimensional channel architecture of certain zeolites permits the assembly of low dimensional zeolite conductors and the control of energy transfer and energy migration in restricted dimensions. All of this implies that innovation in zeolite materials science is likely to burgeon and flourish in the near future.

Received: December 20, 1988

[1] R. M. Barrer: *Hydrothermal Chemistry of Zeolites*, Academic Press, New York 1972.
[2] J. M. Newsam, *Science 231* (1986) 1093; J. M. Thomas, *Angew. Chem. 100* (1988) 1735; *Angew. Chem. Int. Ed. Engl. 27* (1988) 1673.
[3] M. D. Baker, G. A. Ozin, J Godber, *Catal. Rev.-Sci. Eng. 27* (1985) 591; G. Engelhardt, D. Michel: *High Resolution Solid-State NMR of Silicates and Zeolites*, Wiley, Chichester 1987; C. Baerlocher, *Zeolites 6* (1986) 325.
[4] A. Dyer, S. A. Malik, A. Araya, T. J. McConville in P. A. Williams, M. J. Hudson (Eds.): *Recent Developments in Ion Exchange*, Elsevier, Amsterdam 1987, p. 257.
[5] W. P. Halperin, *Rev. Mod. Phys. 58* (1986) 533.
[6] a) V. Narayanamurti, *Science 235* (1987) 1023; K. Ploog, *Angew. Chem. 100* (1988) 611; *Angew. Chem. Int. Ed. Engl. 27* (1988) 593; b) M. Tsuchiya, J. M. Gaines, R. H. Yan, R. J. Sinies, P. O. Holtz, L. A. Coldren, P. M. Petroff, *Phys. Rev. Lett. 1989*, 466; M. A. Reed, J. N. Randall, R. J. Aggarwal, R. J. Motyi, T. M. Moore, A. E. Wetsel, *Phys. Rev. Lett. 1988*, 535.
[7] J. N. Randall, M. A. Reed, T. M. Moore, R. J. Matyi, J. W. Lee, *J. Vac. Sci. Technol. B6* (1988) 302.
[8] H. Temkin, G. J. Dolan, M. B. Panish, S. N. G. Chu, *Appl. Phys. Lett. 50* (1987) 413.
[9] L. Brus, *J. Phys. Chem. 90* (1986) 2555.
[10] O. Terasaki, K. Yamazaki, J. M. Thomas, T. Ohsuna, D. Watanabe, J. V. Sanders, J. C. Barry, *Nature 330* (1987) 58.
[11] Y. Wang, N. Herron, *J. Phys. Chem. 92* (1988) 4988.
[12] N. Herron, Y. Wang, M. M. Eddy, G. D. Stucky, D. E. Cox, K. Moller, T. Bein, *J. Am. Chem. Soc.* 111 (1989) 530.
[13] Y. Wang, N. Herron, *J. Phys. Chem. 91* (1987) 257.
[14] K. Moller, M. Eddy, G. D. Stucky, N. Herron, T. Bein, *J. Am. Chem. Soc.*, submitted.
[15] G. A. Ozin, A. Stein, G. D. Stucky, J. P. Godber, *J. Inclusion Phenom.*, in press; G. A. Ozin, J. P. Godber, A. Stein, *U. S. Pat.*, Filed August 1988.
[16] V. N. Bogomolov, S. V. Kholodkevich, S. G. Romanov, L. S. Agroskin, *Solid State Commun. 47* (1983) 181.
[17] K. Tamura, S. Hosokawa, H. Endo, S. Yamasaki, H. Oyanagi, *J. Phys. Soc. Jpn. 55* (1986) 528.
[18] J. B. Parise, J. E. MacDougall, N. Herron, R. Farlee, A. W. Sleight, Y. Wang, T. Bein, K. Moller, L. M. Moroney, *Inorg. Chem. 27* (1988) 221.
[19] T. Bein, P. Enzel, *Nature*, submitted.
[20] P. M. McManus, R. J. Cushman, S. C. Yang, *J. Phys. Chem. 91* (1987) 744.
[21] T. Bein, P. Enzel, *Synth. Metals*, in press.
[22] Z. Li, C. Lai, T. E. Mallouk, *Inorg. Chem. 28 (1989)* 178.
[23] J. S. Krueger, J. E. Mayer, T. E. Mallouk, *J. Am. Chem. Soc. 110* (1988) 8232.
[24] N. Petranovic, M. Susic, *Zeolites 3* (1983) 271.
[25] C. G. Murray, R. J. Nowak, D. R. Rolison, *J. Electroanal. Chem. 164* (1984) 205.
[26] D. R. Rolison, E. A. Hayes, R. J. Nowak, S. Pons, M. Fleischmann, *J. Phys. Chem.*, in press.
[27] Z. Li, T. E. Mallouk, *J. Phys. Chem. 91* (1987) 643.
[28] M. Fleischmann, J. Ghoroghchian, S. Pons, *J. Phys. Chem. 89* (1985) 5530; M. Fleischmann, J. Ghoroghchian, D. R. Rolison, S. Pons, *J. Phys. Chem. 90* (1986) 6392.
[29] D. R. Rolison, R. J. Nowak, S. Pons, J. Ghoroghchian, M. Fleischmann, *J. Phys. Chem.*, in press.
[30] L. Persaud, A. J. Bard, A. Campion, M. A. Fox, T. E. Mallouk, S. E. Webber, J. M. White, *J. Am. Chem. Soc. 109* (1987) 7309.
[31] Z. Li, C. M. Wang, L. Persaud, T. E. Mallouk, *J. Phys. Chem. 92* (1988) 2592.
[32] B. De Vismes, F. Bedioni, J. Devynck, C. Bied-Charreton, *J. Electroanal. Chem. 187* (1985) 197; B. De Vismes, F. Bedioni, J. Devynck, C. Bied-Charreton, M. Perrée-Fauvet, *Nouv. J. Chim. 10* (1986) 81.
[33] K. E. Creasy, B. R. Shaw, *Electrochim. Acta 33* (1988) 551.
[34] B. R. Shaw, K. E. Creasy, *J. Electroanal. Chem. 243* (1988) 209.
[35] D. C. Freeman, Jr., US-Pat. 3 186 875, 1965.
[36] W. J. Mortier, R. A. Schoonheydt, *Prog. Solid State Chem. 16* (1985) 1.
[37] E. Krogh Anderson, I. G. Krogh Anderson, E. Skou, S. Yde-Andersen, *Solid State Ionics 18/19* (1986) 1170.
[38] M. M. Thackeray, J. Coetzer, *Solid State Ionics 6* (1982) 135.
[39] M. D. Ingram, C. A. Vincent, *Chem. Br. 20* (1984) 235.
[40] Y. Masumoto, *Jpn. Pat.*, Application May 1985.
[41] B. Sulzberger, G. Calzaferri, *J. Photochem. 19* (1982) 321.
[42] H. Otsuki, M. Kobayashi, Y. Usami, *Jpn. Pat.*, Application August 1985.
[43] A. Bellomo, A. DeRobertis, D. DeMarco, *Inquinamento 22* (1980) 47.
[44] a) G. A. Ozin, M. Baker, A. Kuperman, H. Wiggenhauser, M. M. Olken, E. Flanigen, P. Caughlin, W. Mercer, *U. S. Pat.*, Filed August 1988; b) M. Baker, M. M. Olken, G. A. Ozin, G. A. Ozin, *J. Am. Chem. Soc. 110* (1988) 5709; c) G. A. Ozin, A. Kuperman, E. Flanigen, H. Wiggenhauser, W. Mercer, P. Caughlin, Final Report "Zeolite Chemical Sensors", Union Carbide, Tarrytown 1988.
[45] S. D. Cox, T. E. Gier, G. D. Stucky, J. Bierlein, *J. Am. Chem. Soc. 110* (1988) 2986.
[46] T. Bein, R. F. Carver, R. D. Farlee, G. D. Stucky, *J. Am. Chem. Soc. 110* (1988) 4546.
[47] T. Bein, K. Brown, P. Enzel, C. J. Brinker in *Better Ceramics Through Chemistry III*, MRS Proceedings, in press.
[48] A. Stein, *M. Sc. Thesis*, University of Toronto 1988.
[49] W. M. Meier, D. H. Olson, *Atlas of Zeolite Structure Types*, Structure Commission of the International Zeolite Association 1978.

Research News

Symmetry Reduction in Solid Solutions: A New Method for Materials Design

Since 1808 Proust's Law of Definite Proportions has played a key role in the development of modern chemistry, but by focussing attention on "pure" substances it has subtly tended to discourage chemists from studying solid solutions. Recently they are rediscovering what metallurgists have long known, that solid solutions offer exceptional opportunities for tailoring the physical and chemical properties of materials.

Most chemists would probably view a molecular solid solution as the analogue of a fluid solution, envisioning a lattice of host molecules replaced at random by guest molecules. For a more detailed understanding of the system's properties they would probably consult its phase diagram. This vision suffers from two serious errors which illustrate the maxim that casual application of valid concepts can be more misleading than simple ignorance.

The first error is to assume equilibrium. Most crystals are kinetic, not thermodynamic, phenomena. The distribution of solute molecules, like a crystal's overall shape, is controlled more by the dynamics of crystal growth than by the system's equilibrium stability. Once a molecule is built into the lattice, it is usually slow to change position or orientation. Local equilibration at the solid-fluid interface is probably faster than in the bulk, but even crystal surfaces rarely display the equilibrated, symmetrical form in which the shape and area of each facet is adjusted to minimize surface free energy. The failure of crystals to equilibrate has long been recognized as important both in theory and in technology. A key factor in increasing the sensitivity of photographic emulsions was learning to influence the dynamics of silver halide crystallization so as to obtain a tabular crystal habit.

The presence of a second error in the naive view of solid solutions was recognized only quite recently. Its recognition has fundamental implications both for technology and for our understanding of crystallization. This error is the assumption that guest molecules are randomly oriented, that is, that unit cell sites which are related to one another by symmetry operations of the host's crystal space group should have equal probabilities of occupancy by guest molecules. If occupancy were random, a guest molecule would disturb local symmetry in its immediate vicinity, but the average guest population for each type of lattice site would still reflect the overall symmetry of the host. Thus bulk properties of macroscopic crystal fragments would display the same symmetry as the pure host.

Such retention of symmetry makes good thermodynamic sense, but crystals are not equilibrium systems. Twenty years ago *Kitaigorodsky* cautioned that "Formally speaking, (retention of symmetry) does not necessarily occur."[1] Nonetheless he asserted on intuitive and empirical grounds, "If a substitution of A molecules for B is possible in which the B crystal retains its symmetry, we shall find that this is the substitution that actually occurs." This point of view seemed so natural that few scientists took seriously his "formal" warning that selective substitution might destroy crystal symmetry.

In a series of publications that began last summer *Lahav* and *Leiserowitz* of the Weizmann Institute and their collaborators have challenged the assumption of symmetrical substitution.[2] On the basis of this and other recent work,[3,4] it now seems that solid solutions should routinely show lower symmetry than the pure host, and that this reduction will provide a new level of control over solid-state properties.

The Weizmann studies began with efforts to control crystal growth by inhibiting molecular deposition on particular facets through selective adsorption of additives. Additive molecules were designed so that the portion in contact with the crystal facet closely resembled the host molecule, while the portion away from the crystal surface differed in structure. Thus the additive would adsorb strongly to a chosen crystal face, become trapped within the surface layer, and by protruding prevent deposition of further layers of host molecules on that face. Deposition would continue unhindered on faces to which the additive did not adhere.

To visualize this process, consider the packing of "ducks" in Figure 1. The guest ducks have a projection be-

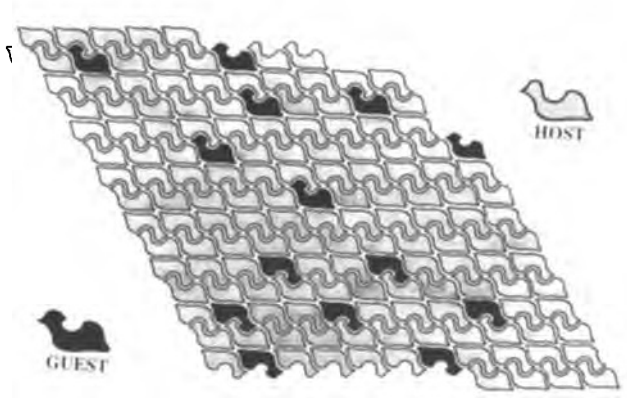


Fig. 1. Schematic solid solution of ducks with pointed heads in a *P*2 lattice of ducks with rounded heads. Note how diagonals of the crystal divide it into sectors with different symmetry properties. This shows that crystal growth nucleated at the center.

hind their heads which makes it difficult to continue deposition of host molecules in the top and bottom rows. Ultimately the head of a host duck may deform enough for it to occupy the unfavorable site where a guest's head protrudes, but the addition will be slower than normal because more energy is required.

One might imagine that the same problem would retard completion of the column at the right border of Figure 1. Here, however, the retardation would be modest, because the guest will soon leave the surface spontaneously, removing the obstacle to column growth. On the top and bottom surfaces the offending guests are locked in by a row of hosts. Many hosts would have to depart in order to allow the guest to escape, and this would take time under conditions of supersaturation. One would expect duck crystals grown in the presence of these guests to be wider than normal in comparison to their height.

In practice, appropriately chosen additives have proven useful for controlling the shape of individual crystals. They have also allowed resolution of racemic mixtures by selectively inhibiting the growth of one of the two enantiomeric crystal forms.[2e] Naturally, additives that were particularly effective in preventing crystal growth were not easily found beneath the crystal surface. Although guest molecules could sometimes be detected by spectroscopic or chromatographic techniques, their concentration was usually too low for diffraction studies that would reveal their orientation. This made it difficult to confirm a clear prediction of the proposed mechanism of growth inhibition, namely, that adsorption of additive molecules should be selective not only for certain faces, but also for certain additive orientations on those faces.

As host molecules deposit on a given face, they must assume all the symmetry-related orientations of the unit cell. At the crystal surface most bulk symmetry operations do not apply, so usually each "symmetry-related" orientation shows a different type of contact with any one crystal surface. This poses no problem for new host molecules, but for the additives some orientations will not fit to the surface. Thus only certain orientations of additive should be included through a given face, and the position of the crystal resulting from growth through that face should have lower symmetry than the pure host lattice.

In the case of Figure 1 hosts must be able to add to the top surface both head-up and head-down, but guests may add only head-up. This results in a division of the crystal into four triangular sectors, separated by diagonal lines which intersect in the region where growth began. The right and left sectors consist of molecules which were deposited through lateral faces as the crystal grew. They contain no guests, except for the one on the right border that will be rejected as the crystal continues to grow. Both top and bottom sectors include guests, but in opposite orientations. In the top all guests are oriented head-up; in the bottom, head-down. Although the crystal as a whole retains a statistical two-fold symmetry axis through its center, the top and bottom sectors considered individually have lost the axial symmetry of pure host.

Two types of diffraction studies now confirm these predictions. In both cases the additives were designed to favor high levels of incorporation and to maximize diffraction contrast. In one case, cinnamamide/thienylacrylamide, the additive differed from host only by replacement of a phenyl ring by a thienyl ring, whose sulfur provided good X-ray contrast.[2a] In the other, asparagine/aspartic acid, an NH_2 group of the host was replaced by OH, and neutron diffraction contrast was supplied by deuterating the guest molecule.[2a,b] Despite the similarity of guests to hosts, individual sectors from both solid solutions show reduction of symmetry ($P2_1/c$ to $P1$ and $P2_12_12_1$ to $P2_1$, respectively) and substantial differences in guest population among "symmetrically equivalent" sites (as much as 15% vs. 2%).

In the 99 : 1 cinnamamide/cinnamic acid system where low contrast and low additive incorporation made diffraction useless, symmetry reduction through selective incorporation was demonstrated by photochemistry.[2a,c] Although pure cinnamamide is centrosymmetric and thus achiral, unsymmetric incorporation of cinnamic acid makes opposite ends of a solid-solution crystal enantiomeric. Photocycloadducts between host and guest from one end of a crystal were optically active with enantiomeric excesses near 50% in the predicted direction. Cycloadducts from the other end of the same crystal showed the opposite stereochemistry, as expected.

Nonlinear optics may represent the most important application of symmetry lowering in solid solutions. These properties depend both on molecular features and on crystal packing. Crystals of many promising molecules have proven unsuitable because their symmetry pairs molecules in offsetting, antiparallel orientations. Cancellation can be avoided by replacing molecules in one of the orientations by additives, or by including the candidate molecule selectively as a guest in a centrosymmetric host. Second harmonic generation has now been used to demonstrate symmetry lowering in solid solutions containing as little as 0.01% guest.[2d] Solid solutions should provide a much greater number and variety of materials displaying second harmonic generation and other phenomena which require crystal polarity, such as piezo- or pyroelectricity.

Bertman and *McBride* have demonstrated another manifestation of symmetry lowering in solid solutions.[3] Host crystals of fatty acid diacyl peroxides viewed along their nominal tetragonal symmetry axes were birefringent, when they were grown so as to incorporate 5–15% of an additive. Diffraction studies on crystal segments showed complete loss of symmetry ($P4_12_12$ to $P1$). Using a polarizing microscope it was possible to trace the growth history of each crystal through differing interference colors in adjacent crystal sectors. These differences resulted from differing orientation of the polarizability tensors of guest molecules.

From one point of view this simple technique uses the additives as "indicators" to provide a new means for studying crystal growth. From another, it provides a new way to study molecular recognition by showing whether the growth site on a crystal surface can distinguish certain structural features of the additive. For example, a particular surface was shown to distinguish chlorine from iodine, but not from bromine.

If symmetry lowering in solid solutions is so general, it seems surprising that it was not recognized long ago, particularly in optical mineralogy, where solid solutions have been studied so extensively. Over the years anomalies have indeed been noted in which high symmetry minerals show division into sectors with lowered symmetry, but this phenomenon was usually attributed to strain fields or gross chemical segregation. By careful optical and X-ray studies *Allen* and *Buseck* recently established that sectoring in optically anisotropic grossular garnets is due to differing ratios of $Al^{3\oplus}$ to $Fe^{3\oplus}$ in octahedral sites which are nominally related by symmetry.[4] To explain this desymmetrization they independently postulated the type of selection during crystal growth that was proposed by *Lahav, Leiserowitz*, and their collaborators.

For all its aesthetic appeal, crystal symmetry can become a liability for designing new materials, e.g. for nonlinear optics, when it results in cancellation of desired properties between symmetry-related molecules. The generality of symmetry lowering during crystallization of solid solutions provides a promising new approach for circumventing this obstacle.

[1] A. I. Kitaigorodskii: *Organic Chemical Crystallography*, Consultants Bureau, New York 1961, p. 233.

[2] a) M. Vaida, L. J. W. Shimon, Y. Weisinger-Lewin, F. Frolow, M. Lahav, L. Leiserowitz, R. K. McMullan, *Science (Washington D.C.) 241* (1988) 1475–1479; b) Y. Weisinger-Lewin, F. Frolow, R. M. McMullan, T. F. Koetzle, M. Lahav, L. Leiserowitz, *J. Am. Chem. Soc. 111* (1989) 1035; c) M. Vaida, L. J. W. Shimon, J. van Mil, K. Ernst-Cabrera, L. Addadi, L. Leiserowitz, M. Lahav, *ibid. 111* (1989) 1029; d) I. Weissbuch, M. Lahav, L. Leiserowitz, G. R. Meredith, H. Vanherzeele, *Chem. Mater. 1* (1989) 114; e) L. Addadi, Z. Berkovitch-Yellin, I. Weissbuch, M. Lahav, L. Leiserowitz, *Top. Stereochem. 16* (1986) 1–85.

[3] J. M. McBride, S. B. Bertman, *Angew. Chem. 101* (1989) 342 *Angew. Chem. Int. Ed. Engl. 28* (1989) 330.

[4] F. M. Allen, P. R. Buseck, *Am. Mineral. 73* (1988) 568–584.

J. Michael McBride
Department of Chemistry, Yale University
New Haven, CT 06511 (USA)

Ferroelectricity and Superconductivity

Some time ago the editor of this journal asked one of us *(H. B.)* to give, every now and then, comments on recent research news, of course, mainly concerned with materials science. Since most of the materials described in this journal are by far too complicated for basic theoretical investigations I wondered, being a theoretical physicist, what the editors really want to see in my comments. I decided that they probably want to have some founded speculations, some educated guesses, and perhaps a personal view on basic problems and ideas. Here is a first try; it is written under the impression that progress in modern materials science is mainly achieved under a broad view of various mechanical, electromagnetic or thermal properties of complex materials.

As an example, I want to discuss some theoretical considerations of the relationship between ferroelectricity and high-temperature superconductivity. This first comment is somewhat courageous as up to now there are many open questions since the pioneering ideas of *B. T. Matthias*[1] who suggested that there must be a mutual exclusion of these two properties. I don't want to give a full account of the historical aspects of the following discussion but would like to point to another paper discussing the coexistence of both effects.[2] (Experimentally, for example, it is very difficult to measure a reversable polarization in good conductors, but it seems to have been established that the superconductor GeTe is also ferroelectric.) Today we know that ferroelectricity is inherently related to the local electron–phonon coupling resulting in a soft-mode behavior for displacive ferroelectrics.[3] In recent years the late *H. Bilz* and his coworkers suggested a shell-model description of the lattice-dynamics of ferroelectrics where the main nonlinearity is locally centered at the lattice site of the chalcogen-ion (preferably oxygen) of representative ferroelectric materials.[4] The microscopic origin of the lattice instability is the nonlinear polarizability of the electron cloud around the oxygen ion, resulting in a dynamic hybridization of the corresponding p-orbitals with the orbitals of the metal-ion ("dynamic covalency").

Recently (but before the discovery of the new high-temperature superconductors), discussion of a possible connection of both phenomena was taken up again. Within the shell-model the point was stressed that a dynamic covalency induces phonon anomalies.[5] That might be thought of as the origin of both, ferroelectricity and superconductivity. Contrary to this, it was argued that pure static polar-

izabilities or static hybridizations are not favorable for these anomalies.

The spectacular discovery by *J. G. Bednorz* and *K. A. Müller*[6] of the perovskite $La_{2-x}BaCuO_4$ as a high-temperature superconductor opens up again the discussion of the relationship between ferroelectricity and superconductivity. These materials and the later ones with even higher transition temperatures (the Y-Ba-Cu-O compounds as well as the Bi-Sr-Ca-Cu-O materials), not only show structural instabilities but are also structurally closely related to many ferroelectric oxides.[7] There is even a ferroelectric-like instability in the Y-Ba-Cu-O compound at high temperatures inferred experimentally from a large dielectric constant.[8] Here it should be pointed out that in spite of the structural similarity of both compounds additional doping and other defects destroy ferroelectricity, but simultaneously are necessary ingredients for superconductivity. This may yield some kind of material recipe to construct both kinds of properties. (Obviously *K. A. Müller* is by no accident also a highly respected expert in the fields of ferroelectric materials and structural phase transitions.)

In this new class of materials one should also consider the Ba-K(Pb)-Bi-O compound[9] where Bi plays the role of the copper ion, not only allowing for a dynamic polarization of the oxygen but also giving rise to charge fluctuations at the metal site. All these facts are discussed in detail elsewhere[10] where the original shell-model is extended and compared to other models. This point of view has now been taken up by several groups and becomes more and more popular. Recently it was shown[11] that in the classical strong coupling formalism an increase in the transition temperature might occur if there is an anharmonic double-well interatomic potential. Such anharmonicities simultaneously, of course, must lead to lattice instabilities and its origin might be the dynamic covalency discussed above. In an interesting paper, *Villars* et al.[12] systematically looked for chemical trends in both high-temperature superconducting materials and high-temperature ferroelectrics. They showed that three relevant parameters, namely the averaged valence electron number, the orbital radii of the ions and the electronegativity, determine the characteristic properties of both classes of materials. All these results together indicate the possibility of a common origin of both phenomena. While in ferroelectrics the instability of the oxygen ion triggers the high macroscopic polarizability, in superconductors we deal with a metal-ion with variable valencies. This discussion, mainly originating from a lattice-dynamical point of view, can also be carried out in the context of systems with correlated electrons. In this respect, *Callaway* et al.[13] introduced their polarization induced pairing model. In an extended Hubbard system they calculated a phase diagram where, for reasonable interaction parameters, the possibility of electron pairing exists (whether this gives rise to long-range order superconductivity is still an open question). Quite recently *Varma*[14] studied a similar effect for the superconducting state resulting from an effective negative intra-atomic electron-electron interaction (especially for the Bi-ion). The origin of this negative interaction is an electron-transfer from the oxygen to the Bi-ion together with sp-hybridization. The same line of thought can be attributed to a paper by *Tesanovic* et al.[15] in which a "unified" picture of the high-temperature superconductors is presented and, in addition to the above ideas, the importance of the various anisotropic geometries of the Cu(Bi)-O arrangements are discussed in detail. With these arguments we are back at the starting point where a mutual exclusion of ferroelectricity and superconductivity was supposed to be based upon geometrical reasons. Probably it is this anisotropy which favors high-temperature superconductivity, as it is also most important for ferroelectricity.

What do we learn from this interpretation of a common origin of ferroelectricity and high-temperature superconductivity? In both cases there is the possibility of a structural instability and therefore it might be worthwhile to look for noncrystalline, that is glassy or even fractal structures[16], to further enhance the transition temperature. Furthermore, the proper choice of highly polarizable anions and valence fluctuating cations with the proper orbitals for hybridization may point to classes of other superconductors. But be cautious, this is a comment on some theoretical ideas of ferroelectricity and superconductivity. Nature might be more elegant.

[1] B. T. Matthias, *Mater. Res. Bull. 5* (1970) 665.
[2] J. Birman, *Ferroelectrics 16* (1977) 171.
[3] J. F. Scott, *Rev. Mod. Phys. 46* (1974) 83; G. Shirane, *ibid. 46* (1974) 437.
[4] R. G. Migoni, H. Bilz, D. Bäuerle, *Phys. Rev. Lett. 37* (1978) 1155; H. Bilz, H. Büttner, A. Bussmann-Holder, W. Kress, U. Schröder, *ibid. 48* (1982) 264; H. Bilz, G. Benedek, A. Bussmann-Holder, *Phys. Rev. B35* (1987) 4840.
[5] H. Bilz, H. Büttner, A. Bussmann-Holder, P. Vogl, *Ferroelectrics 73* (1987) 498.
[6] J. G. Bednorz, K. A. Müller, *Z. Phys. B64* (1986) 188; Nobel Lecture: *Angew. Chem.* [Adv. Mater.] *100* (1988) 757; *Angew. Chem. Int. Ed. Engl.* [Adv. Mater.] *27* (1988) 735.
[7] For a broad overview of recent results see: J. Müller, J. L. Olsen (Eds.): *Proc. Interlaken Conf. High-T_c Superconductors*, North-Holland, Amsterdam 1988.
[8] L. R. Testardi, W. G. Moulton, H. Mathias, N. K. Ng, C. M. Rey, *Phys. Rev. B37* (1988) 2324.
[9] R. J. Cava, B. Batlogg, J. J. Krajewski, R. Farrow, L. W. Rupp, Jr., A. E. White, K. Short, W. F. Peck, T. Kometani, *Nature (London) 332* (1988) 814.
[10] A. Bussmann-Holder, A. Simon, H. Büttner, *Phys. Rev. B39* (1989) 207.
[11] J. R. Hardy, J. W. Flocken, *Phys. Rev. Lett. 60* (1988) 2191.
[12] P. Villars, J. C. Phillips, K. Rabe, I. D. Brown, unpublished preprint. (We thank *J. C. Phillips* for sending us the manuscript before publication.)
[13] J. Callaway, D. G. Kanhere, J. K. Misra, *Phys. Rev. B36* (1987) 7174.
[14] C. M. Varma, *Phys. Rev. Lett. 61* (1988) 2713.
[15] Z. Tesanovic, A. R. Bishop, R. L. Martin, K. A. Müller, unpublished preprint. (We thank *A. R. Bishop* for sending us the manuscript before publication.)
[16] H. Büttner, A. Blumen, *Nature (London) 329* (1987) 700.

Helmut Büttner, A. Bussmann-Holder
Physikalisches Institut der Universität Bayreuth (FRG)

Book Reviews

Zeolites, Crystal Growth, Polymers and Miscellanea

Catalysis on Zeolites. Edited by *D. Kalló* and *Kh. M. Minachev*. Akadémiai Kiadó, Budapest 1988. xi, 583 pp., bound, DM 115.00.—ISBN 963 05 4559 x

During recent decades zeolites and related molecular sieve materials have proved remarkably successful in various branches of chemistry and chemical engineering. Perhaps the most striking progress has been achieved in the application of zeolites as catalysts. Important advantages of zeolites over more conventional porous solids are their high density and strength of acid sites, the availability of numerous techniques for chemical modifications, and their thermal stability. Moreover, with the advent of molecular sieve materials, the door was opened to shape-selective catalysis, which led to a number of new catalytic processes. Today, zeolites can be tailored for a wide variety of catalytic applications. It is therefore not surprising that catalysis on zeolites is among the major research topics in almost all industrialized countries. About 15 years ago, the European socialist countries, in an attempt to coordinate and intensify their efforts in the field of zeolite catalysis, founded a coordination council, and this book is a state-of-the-art report on the achievements of this multinational cooperation.

The book contains 17 chapters written by experts from Bulgaria, Czechoslovakia, the German Democratic Republic, Hungary, Poland and the Soviet Union. About two-thirds of these chapters focus on non-catalytic aspects of zeolite science, e.g., quantum chemical studies, hydrothermal synthesis, spectroscopic characterization, and chemical procedures for modifying zeolites such as ultrastabilization and dealumination at high temperatures by gaseous reactants such as $SiCl_4$, or isomorphous substitution of silicon and aluminum by transition metals. An excellent chapter by *Wichterlová* et al. deals with the introduction of trivalent cations such as $Al^{3\oplus}$, $Fe^{3\oplus}$ and $Cr^{3\oplus}$ into zeolites, and the catalytic properties of the resulting materials. The six catalytic chapters focus around the preparation or transformation of hydrocarbons, e.g., the disproportionation of alkylaromatics, the Fischer–Tropsch synthesis, the dehydration of methanol, and the oligomerization and hydrogenation of alkenes. In one chapter the concept of hard and soft acids or bases is applied to zeolites. The final chapter reviews industrial applications of zeolites in the German Democratic Republic: catalysts were developed at Leuna for hydrocracking of vacuum gas oil, isomerization of light gasoline, isomerization of C_8-aromatics, and shape-selective hydrocracking of n-alkanes in reformer gasoline.

This is a very valuable book which contains a number of outstanding chapters prepared with great care and expertise. Among these are the chapter by *Shpiro* et al. on the application of SIMS, XPS and related spectroscopic techniques to zeolites, the chapter by *Wichterlová* et al. mentioned above, and the review by *Becker* et al. on industrial zeolite catalysts developed in the GDR, to mention only a few. The value of the book is further enhanced by the long lists of references given at the end of each chapter and the thoroughly prepared subject index.

The contributions collected in this volume also prove that the joint endeavor of the socialist countries led to a very high level of research in zeolite materials science. Given this high level, one wonders why the book pays hardly any attention to the more recent molecular sieves, i.e., zeolites of the newer generations, crystalline aluminophosphates, and materials derived from the latter, such as silicoaluminophosphates. It is also surprising that there is no chapter on the use of zeolite catalysts for the manufacture of organic intermediates containing oxygen, nitrogen, sulfur and other heteroatoms. Nevertheless, in view of the high quality of the contributions and the well-arranged layout, the book can be recommended to everybody who is involved with zeolites and zeolite-like molecular sieve materials.

Jens Weitkamp
Institut für Technische Chemie I
der Universität Stuttgart (FRG)

Crystals in Gels and Liesegang Rings. By *H. K. Henisch*. Cambridge University Press, Cambridge 1988. xiii, 197 pp., bound, $ 35.00.—ISBN 0-521-34503-0

Although, in general, large crystals are not obtained in gels, the use of gels opens the door to the search for crystals with new and interesting optical or electronic properties. Moreover, the techniques are incomparably cheap and may lead to crystals of high perfection. Since the physical and chemical processes in gels are very complex, and inadequate understanding often results in poor crystal growth, this comprehensive review of the techniques of crystal growth in gels will be greatly appreciated.

This instructive presentation reveals the extensive practical experience of the author and his group. The book is divided into five chapters, the first four of which have already been published by the author in the monograph "Crystal Growth in Gels" (Pennsylvania State University

Press 1970), essentially in the present form. With 475 references up to 1986, the new presentation is excellently documented and completely covers the field of crystal growth in gels.

The first chapter gives a review of the early work on the growth of crystals in gels, and introduces the basic growth procedures, in which the gel is in contact with either one reagent reservoir or two separate reagent reservoirs. The operation of the techniques is instructively explained with examples of their application to various materials. Doping possibilities and difficulties that may be encountered are discussed for the first time in this book.

The second chapter deals with the preparation and properties of various gels. Their formation, structure, handling and properties, such as density and porosity, are described in great detail for silica hydrogels. A new contribution deals with the one-dimensional diffusion of one or two counter-diffusing reagents in gels. The diffusion is investigated by numerical method as a function of position and time. According to the two basic growth systems, solutions are determined for gels of finite and semi-infinite lengths with a single diffusant, and for finite gels with two species having equal diffusion coefficients. Constant or time-dependent concentrations are prescribed at the boundaries. Unfortunately the initial distributions are not mentioned.

The influence of reagent distribution on growth rate and crystal perfection is investigated in the third chapter. Growth models of crystals and the importance of diffusive transport are discussed. In addition, sophisticated growth methods and special treatments of growth systems such as reimplantation of crystals are described. In the fourth chapter nucleation and crystal growth are treated by the usual phenomenological theory and illustrated with experimental examples.

The last chapter presents the history of Liesegang rings, numerous instructive examples of Liesegang structures, and many numerical solutions on the formation and spreading of particular precipitation structures for the two basic growth systems. For the calculations the author considers diffusive transport, and assumes two conditions for precipitation, i.e., that the local concentration of the reacting species is nearly uniform, and that the reaction product concentration exceeds a critical value. The detailed presentation of numerical results for various parameters are very helpful in understanding the complex physical and chemical processes in gels. The interesting software used by the author is available for IBM-compatible personal computers. The chapter ends with two reference lists of crystals grown in gels and of growth rate measurements.

From this book the interested crystal grower can find much useful advice on the procedures of crystal growth in gels. In addition it provides the reader with simple theoretical models which are useful in understanding the basic processes such as diffusion, nucleation and crystal growth in gels. The book is easily readable and gives a full and up-to-date coverage of the literature. It will be of great interest to scientists who are involved in crystal growth or materials syntheses.

Erich Schönherr
Max-Planck-Institut für Festkörperforschung
Stuttgart (FRG)

Polymer Science in the Next Decade, an International Symposium Honoring Hermann F. Mark on his 90th Birthday. Edited by *O. Vogl* and *E. W. Immergut*. Wiley, Chichester 1987. x, 284 pp., paperback, £ 90.00.—ISBN 0-471-63239-2

The above book contains the proceedings of the symposium "Polymer Science in the Next Decade", which was held in New York in 1985 to honor *Hermann F. Mark*. Subdivided into four sections, it consists of a series of short reviews on a wide variety of subjects relating to contemporary polymer science. At first one might be inclined towards the view that this is one of the numerous books put together after a symposium without much editing, and hence of rather limited use. However, closer inspection reveals that the present book is indeed an interesting contribution to the literature of polymer science. First of all, the man being honored is *Hermann F. Mark*, who can certainly be counted among the great scientists of this century. Born in 1895, he has contributed greatly to physical chemistry and to polymer science. He still continues a very active schedule of travelling and lecturing around the world. So it seems rather appropriate that on the occasion of his 90th birthday a symposium on opportunities and future trends in polymer science has taken place.

The list of speakers includes renowned names such as *Paul Flory* and *Linus Pauling*. The multitude of topics reflects modern polymeric science in a very lively fashion. The short articles are useful for gaining a first insight into the present status of certain fields. Noteworthy is the contribution of *M. F. Perutz* on the design and engineering of proteins. Another well-written review by *Katchalski-Katzir*, *Wilchek* and *Patchornik* deals with chemically active and biologically specific polymers. An article of particular interest by *F. R. Eirich* gives a very personal view on macromolecules and evolution. A number of other reviews are much shorter, but still quite useful to get an idea of present trends in polymer science. In addition to these purely scientific reviews, the book contains many personal recollections concerning *H. F. Mark* and the early days of polymer science. Both the scientific part and the more personal statements are useful for anyone who wants an overview of contemporary polymer science and how it came into being. Thus, the book is certainly recommended for libraries of departments of chemistry and biology.

Matthias Ballauff
Max-Planck-Institut für Polymerforschung
Mainz (FRG)

Thermotropic Liquid Crystals, Fundamentals. By *G. Vertogen* und *V. A. de Jeu*. Springer-Verlag, Berlin 1988. xi, 324 pp., hard cover, DM 134.00.—ISBN 3-540-17946-1

The chemistry and physics of liquid crystals is certainly one of the most fruitful areas of modern materials science. However, despite the enormously growing literature there are only a few books available treating this subject. The classical treatise by *de Gennes* ("The Physics of Liquid Crystals", Oxford 1974) is no longer up-to-date, despite the clarity of presentation. The book by *Vertogen* and *de Jeu* aims to fill this gap. It is the clear intention of the authors to focus solely on fundamental aspects of thermotropic liquid crystals.

The book is organized in four sections. Part I is devoted to an introduction of the subject, and gives a very clear descriptive account of the various liquid crystalline phases. Here the reader finds an overview of some more recent developments, such as smectics with bond orientational order. However, other topics of interest such as discotic or polymeric liquid crystals are dealt with in a very brief manner. Part II deals with continuum theory, introduced entirely in tensor notation. Experiments relating to the orientational behavior of liquid crystals are described from a theoretical point of view in Part III. The final part outlines the present state of the theories of liquid crystalline order.

In all chapters the material is treated in a rigorous mathematical way. This makes the book rather tedious reading for the beginner, but is very useful for those who are more advanced in this field. A very thorough introduction of the Landau theory, and the treatment of molecular statistical theories starting from the theory of simple liquids, is certainly of particular interest, since it may not be found in other books. However, the choice of experimental examples has been restricted to only a few selected samples. Consequently the book is not a guide to current experimental work in this field. One wonders if a treatise on thermotropic liquid crystals can virtually omit areas such as polymer liquid crystals or discotics without being regarded as incomplete. Nevertheless, the consistent and vigorous presentation of the selected topics makes this treatise a highly useful and indispensable book for everyone working seriously in the field of liquid crystals.

Matthias Ballauff
Max-Planck-Institut für Polymerforschung
Mainz (FRG)

Synthesis and Separations Using Functional Polymers. By *D. C. Sherrington* and *P. Hodge*. Wiley, Chichester 1988. x, 454 pp., bound, £ 52.50.—ISBN 0-471-91848-2

Coming into prominence some 25 years ago as supports for solid phase peptide synthesis, synthetic functional polymers have emerged as a class of novel materials with a multitude of applications, such as supports for biotechnology, solid phase organic synthesis, and separation techniques, as well as for several other purposes. The obvious advantages of these heterogeneous systems (ease of separation, recycling etc.) have stimulated a great deal of research interest in this area, which is evident from the many research papers and review articles on these topics. During the development of the field it became evident that the technique is far more complex than was initially thought; this warrants careful consideration of the chemical and physical properties of the polymeric supports used, and of optimizing the specific reaction conditions necessary with these systems. To apply them correctly requires a thorough understanding from the standpoints of organic chemistry (or biochemistry) and polymer chemistry.

In bringing out this volume to provide researchers with an in-depth and up-dated overview covering all these aspects, *D. C. Sherrington* and *P. Hodge* have done a commendable job with the help of a group of well-known scientists. By summarizing the published work of many leading practitioners of polymer supported chemistry, this book provides a critical review of some of the most important aspects. The present volume is a sequel to the first book on this topic ("Polymer-supported Reactions in Organic Synthesis") by the same editors, published nearly a decade ago. While some of the chapters of the earlier book have merely been updated since 1979, others are new additions.

The book is divided into eleven chapters dealing with several interesting aspects of the applications of functional polymers in chemical operations (syntheses and separations). It appears that the chapter authors were persuaded to cover the entire story instead of highlighting their own scientific accomplishments. Thus, with the exception of one chapter, a wide and balanced coverage of the specific topics has been achieved.

The book begins with a chapter by *Guyot*, which gives an authoritative and comprehensive account of the design and structural characterization of polymeric supports. Support design appears to be critically important for success in this field. The second chapter by *Hodge* provides a detailed review of the applications of functional polymers in synthetic organic chemistry. Further interesting aspects of the applications of functional polymers covered in this book include: "Polymeric Phase Transfer Catalysts" (*Tomoi* and *Ford*); "Polymeric Models of Reactive Biological Systems" (*Challa* and *van den Berg*); "Polymers in Affinity Chromatography" (*Jervis*); "Polymeric Ligands in Hydrometallurgy" (*Warshawsky*); "Polymer Bound Transition Metal Complex Catalysts" (*Garrou* and *Gates*) and "Use of Chiral Polymers for the Separation of Enantiomers" (*Pirkle* and *Mohler*), which provide valuable information on the state of the art in these research topics. Somewhat more specialized applications are dealt with in the chapters on "Design and Industrial Applications of Polymeric Acid Catalysts" (*Widdecke*), and "Properties of Polymeric Rose Bengals—Polymers as Photochemical Reagents" (*Neckers*). The last chapter of the book, "A Wider Perspective of Polymeric Supports and Reactive Polymers"

by *Sherrington*, deals with broader aspects of this field, covering new types of supports, polymeric vesicles, microcapsules, polymeric drugs, photoresists, etc. This clearly demonstrates the interdisciplinary aspects of functional polymers, and should stimulate further research interest.

One would have wished to find additional chapters on the applications of functional polymers for immobilization of enzymes and microorganisms, as well as on polymer-supported synthesis of oligonucleotides, which are likely to be some of the more rapidly expanding areas of research involving polymer supports. Nevertheless, this book serves as an excellent source of information on the applications of functional polymers. The bibliography is extensive (over 1500 citations) and up-to-date. In one particular chapter, citations are sometimes given for less accessible periodicals, even though the same results have also been published in more generally available journals. Figures and formulas are quite clear and the presentation of the book is excellent, with a colorful waterproof cover. It should find its place in all chemical libraries, and is highly recommended to all scientists working with polymeric supports, as well as to aspiring newcomers to this field. It is likely to serve as the standard monograph for some years to come.

Günter Wulff, Pradeep K. Dhal
Institut für Organische Chemie
und Makromolekulare Chemie
der Universität Düsseldorf (FRG)

Polymer Modified Textile Materials. By *J. Wypych*, Wiley, New York 1988. xiii, 317 pp., bound, £ 70.00.—ISBN 0-471-83959-0

Composites have been treated frequently in reviews and monographs; polymer-coated textile fibers, however, have been considered to a much lesser degree in the literature, although the materials and their interactions are similar. It is true that in the latter materials the polymer constitutes only a small fraction of the total mass, but it plays a key role in the often highly sophisticated applications of these textile materials.

The raw materials for coating polymers, textile materials and release papers are treated in the first chapter. In particular, solutions, emulsions/dispersions and plastisols are discussed. The second chapter deals with machines and equipment for compounding, coating, heating and finishing. Six commonly used processes, namely spreading, dipping, spraying, immersion, melt coating and lamination are treated in detail. Many photographs and diagrams of machines giving useful information are included, particularly in conjunction with examples of applications, cost analysis and ecological aspects. Production lines are described in Chapter 5, in a manner similar to that in Chapter 2, but it is incomprehensible why these two chapters were not kept together in their logical sequence.

"The scope of application of coating methods", with emphasis on end-use, type of resins, and technical demands, is discussed in Chapter 3. Topics included are consumer items, industrial uses, technical products, geotextiles and -membranes, special yarns, and PTFE-coated glass fibers. Chapter 4 describes some interesting developments, including products with advanced mechanical, thermal, and optical properties, textiles with improved dimensional stability, permeability to water and air, and special properties with regard to burning, abrasion, cleaning and ageing behavior, to give only a few examples.

Chapters 6–8 treat the rheology of the coating processes and the most important factors affecting the processes. Numerous scanning electron micrographs showing the structure of the coated materials are included. Heat and mass transfer in coating processes are discussed in relation to recent achievements of chemical engineering.

The last two chapters are concerned with toxicity (LD_{50} values, smoke production, water pollution) and waste aspects, with particular consideration of recycling and separation methods, topics which have become increasingly important.

The organization of the material in the monograph is not entirely convincing. Furthermore, the presentation is strong in some chapters and weak in others – as is to be expected for a book written by a single author and covering such a broad field. Finally, some editorial effort would certainly have improved the text.

Nevertheless, the book gives a most valuable review of the state of the art of applying polymers to textile materials to improve their properties and make them suitable for special applications.

Hartwig Höcker
Deutsches Wollforschungsinstitut
an der Technischen Hochschule Aachen (FRG)

Foams and Biliquid Foams—Aphrons. By *F. Sebba*. Wiley, Chichester 1987. vii, 236 pp., bound, £ 29.59.—ISBN 0-471-91685-4

It is not easy to assign this book to a specific category. On the one hand it is intended as a textbook on foam systems, while on the other hand it contains a number of sections which are more in the nature of popular scientific writing. The author tends very much towards a simplified style of presentation. This is certainly an advantage for readers who are not specialists in colloid chemistry. In the diagrams too one finds that only the essential relationships are outlined. The illustrations look as though they have been taken from a set of lecture notes. Furthermore the whole book makes a similar impression.

The most important of the 13 chapters have the following titles: Forces Operating at Interfaces; Thin Liquid Films; Polyhedral Gas Foams; Colloidal Gas Aphrons;

Spreading of Lenses on Water; Biliquid Foams; Polyaphrons; Applications of Polyaphrons; Invert Aphrons; Unusual Forms of Aphrons.

The Greek-derived word "aphrons" is used by the author to describe those systems which are known in general scientific usage as "concentrated emulsions". The work of *Princen* and *Lissant* and their colleagues has unfortunately been ignored, which is especially regrettable in view of the fact that modern theories on the flow behavior of foam systems originate from this group.

While the book's treatment of theoretical aspects is rather elementary, and even incomplete, the reader nevertheless finds here an extensive and hitherto unique compendium of interesting observations which the author, as an expert on this topic, has collected together. This constitutes the real worth of the book, despite some other serious shortcomings.

Gerhard Platz
Institut für Physikalische Chemie
der Universität Bayreuth (FRG)

Dispersing Powders in Liquids. By *R. D. Nelson*. Elsevier, Amsterdam 1988. xviii, 246 pp., bound, US $ 84.25.—ISBN 0-444-43004-0

This book is published as Volume 7 in the series "Handbook of Powder Technology" and comprises 245 pages, divided into eight well-arranged chapters. These describe the fundamental characteristics that play a role in the dispersion of inorganic materials in powder form. Unfortunately, certain materials of technical importance, for example synthetic silicas and carbon blacks, are not dealt with here. This is rather a pity, since these substances have very high specific surface areas which generally render them difficult to disperse. The reviewer also feels that the book lacks two chapters which would be of relevance for practical purposes—one about dispersers and one on the correct choice of mill base compositions. In the appendices the list of "liquids" includes only chemically pure solvents, but not, for instance, a selection of liquid binders, which are of technical importance in different fields of industry. This book is therefore not so much intended for experimentalists and technologists, but is more suited to the needs of readers with educational objectives, particularly since it deals with numerous basic physical principles. In this context, it is encouraging that the HLB value is also considered here; the fact that this value was established phenomenologically has often led to it being overlooked in scientific articles.

All in all, this small book is an ideal reference source for anyone who is not familiar with the problems relating to the surface science of materials in powder form.

Horst Ferch
Degussa, Hanau (FRG)

A Guide to Materials Characterization and Chemical Analysis. Edited by *J. P. Sibilia*. VCH Verlagsgesellschaft, Weinheim 1988. x, 318 pp., bound, DM 75.00.—ISBN 3-527-26867-7

This book represents a survey of state-of-the-art techniques for modern materials characterization and analysis. The book covers approximately 75 techniques that are used in characterization of chemicals, polymers, ceramics, metals and composites. The first chapter provides an introduction to how one might utilize the techniques that follow in practical problem-solving applications. Each of the following chapters describes one or more techniques, with the presentation organized according to the use of the technique, sample preparation, underlying physical and chemical principles, applications, and limitations. Due to the breadth of coverage, only a limited amount of space is devoted to each technique. However, this is adequate to introduce the technique; several references are listed after each section, providing in-depth detailed information for the reader who is interested in a more rigorous treatment.

This is a valuable book for materials laboratories and general industrial laboratories where characterization and analysis of many different substances may require several different techniques. It serves as a good review for established scientists as well as a useful resource for beginners.

J. Wayne Rabalais
Department of Chemistry
University of Houston (USA)

DECHEMA Corrosion Handbook, Vol. 2. Edited by *D. Behrens*. VCH Verlagsgesellschaft, Weinheim 1988. x, 340 pp., bound, DM 775.00.—ISBN 3-527-26653-4

The DECHEMA Corrosion Handbook—a series of at least twelve volumes is planned—is a completely new English edition of the DECHEMA Werkstoff-Tabelle.

The second volume (340 pages) describes the corrosion properties of metallic, non-metallic inorganic, and organic materials in corrosive media of aliphatic aldehydes, ammonia and ammonium hydroxide, sodium hydroxide and the underground corrosion in soil. The largest parts of this volume are devoted to sodium hydroxide (154 pages) and soil (90 pages).

Some errors of the first volume which had earlier been criticized by the reviewer have been corrected in Volume 2. As an example, some electrochemical reference systems are now mentioned in the introductory part of some chapters, but in addition to these many others are mentioned in the detailed descriptions of the corrosion behavior of the different materials. In subsequent volumes a list of all these reference systems should be included in the introduction, citing also their potentials versus the Standard Hydrogen Electrode.

In general, the clearly arranged layout of the first volume is continued in the second volume. Much valuable in-

formation concerning the corrosion behaviour of widely different materials has been carefully collected, taking into account the literature up to approximately 1985.

The first chapter, which discusses the corrosion properties in solutions of aliphatic aldehydes, contains a very well written introduction which describes the most important technical processes in which aliphatic aldehydes are used, and gives a summary of the most important corrosion problems. The different aldehydes are then described in detail, including a short summary of the corrosion problems that may arise for the given aldehyde in a given technical application. This descriptive part is more informative than the short summary table, which gives only general ratings for the different materials.

The same is true for the second chapter, which describes the corrosion behavior of materials in ammonia and ammonium hydroxide. Again, the introduction is well written, summarizing technical processes in which ammonia participates, and discussing major corrosion problems such as H-embrittlement in these solutions. The detailed description of the individual corrosion properties of the different materials is accurate and careful. In some cases, however, the electrochemical background of the corrosion process in electrolytes should have been presented more clearly, e.g. in the discussion of the activation of the corrosion process by O_2 (p. 58), or in the description of the "chemical conversion process" of the corrosion induced by O_2 (p. 55). Reference should have been made here to the electrochemical nature of the corrosion process, the O_2-reduction being the cathodic reaction.

Chapter 3 is devoted to corrosion in alkaline environments. In contrast to Chapters 1 and 2 the introduction is rather short, and presents only limited information on the technical processes in which NaOH is used, the practical corrosion problems, etc. The introduction provides some general information concerning pitting corrosion, pitting potentials and stress corrosion cracking. However, this information is rather limited, and should have been incorporated into a chapter devoted to basic corrosion mechanisms, which is missing from the Corrosion Handbook. The corrosion properties of the individual materials are discussed in great detail, with special emphasis on the corrosion of metals under conditions of stress corrosion cracking. After discussing the individual metallic, non-metallic inorganic, and organic materials, tables are presented which summarize the corrosion properties of these materials in different NaOH solutions at different temperatures, etc. These tables are quite informative to the reader. A point of criticism to the reviewer is the rather frequent statement of electrode potential without any reference system (Figs. 11, 20, 22, 23, ..., Table 11 ...). As an example, Fig. 19 shows the lifetime of an unalloyed steel in 33% NaOH as a function of the electrode potential. The result of this technically important figure is that stress corrosion cracking is observed only in a very limited potential range. However, the potential axis is given in "Volt" without any reference, and consequently the figure could be quite misleading to inexpert readers. The number of reference systems used in the Corrosion Handbook is quite large (Ag/AgCl, $Cu/CuSO_4$, Hg/HgO, SME? page 112) and these should be summarized in the introduction.

The last chapter is concerned with the underground corrosion in soil. The introduction covers about 30 pages and describes the chemical composition of different soils, their corrosivity, corrosion due to microorganisms in soil, and the possibilities for protecting metallic materials in soil, e.g. by cathodic protection. In general, this part is well written and quite informative, but the electrochemical aspects of cathodic protection could have been presented in more detail, in a better arranged and more compressed form, without repeating the same facts—e.g. the correlation between organic coating and cathodic protection—in many places throughout the text. Some techniques which are used to measure the correct protection potential—e.g. switch-off potentials—are mentioned later in this chapter, and these too should have been incorporated into the introduction. The rest of the chapter is well written and, for example, clearly shows the importance of correctly chosen organic coatings for the corrosion protection of steel pipes which are polarized cathodically.

In summary, the second volume of the DECHEMA Corrosion Handbook is a highly valuable reference book for all engineers working in the area of corrosion, provided the user has a thorough knowledge of the basic physical concepts in corrosion science.

Martin Stratmann
Max-Planck-Institut für Eisenforschung
Düsseldorf (FRG)

Semiconductor Electrodes. Edited by *H. O. Finklea*. Elsevier, Amsterdam 1988. xxii, 520 pp., bound, DFl. 340.00.—ISBN 0-444-42926-3

Continuing the series "Studies in Physical and Theoretical Chemistry" (Elsevier) a new edition entitled "Semiconductor Electrodes" is now available (Vol. 55). The ten chapters by different authors are devoted to particular semiconductor electrode materials. Following a concise and well written introduction by *H. Finklea*, Chapter 2 describes the photoelectrochemistry of the large band gap oxides TiO_2 and $SrTiO_3$. A wealth of information on physical and photoelectrochemical properties is presented in this chapter. The inclusion of basic experimental aspects such as ohmic contacts, electrode preparation and sample mounting is definitely an advantage for the interested reader. Chapters 3 and 4 deal with other less intensively investigated semiconducting metal oxides (Fe_2O_3, SnO_2, In_2O_3 and WO_3). Here, too, valuable information on electrode preparation and growth methods is given, in addition to the detailed analysis of the photoelectrochemical behavior.

ADVANCED MATERIALS

In Chapter 5, Si and Ge are treated, including an important section on etching procedures which are of general relevance for those working with Si. *N. S. Lewis* and *A. B. Bocarsly* review the photoelectrode properties of these materials in aqueous and non-aqueous solutions, and include very specific topics such as derivatized surfaces (attaching mediators for improved redox activity). The following chapter on II-VI semiconductor electrodes reviews the fundamental photoelectrochemical observations on CdS, CdSe and CdTe. This chapter contains a section on thin film electrodes, including ceramic, vacuum deposited, electroplated, painted, sprayed and immersion-plated electrodes.

The next chapter treats GaP electrode behavior, and contains an interesting but somewhat speculative section on surface luminescence. Chapter 8 is a thorough and sound description of photoelectrochemical processes occurring on GaAs electrodes. Thermodynamic and kinetic aspects of electrode stability are dealt with, and expressions for the stabilization efficiency for three cases are given. Here *K. W. Frese,* Jr. also reviews CO_2 reduction at GaAs surfaces and includes data on light-to-electricity regenerative solar energy conversion. In Chapter 9 *L. F. Schneemeyer, A. Heller* and *B. Miller* review the many properties of InP electrodes. Eleven growth methods are briefly described including chemical vapor deposition, and liquid encapsulated Czochralski and molecular beam epitaxy. A short overview on solid state photovoltaic InP-based systems provides the background for the electrochemical sections that follow.

Photoanodes and -cathodes in aqueous and non-aqueous regenerative cells are thoroughly described, followed by a very intriguing section on hydrogen-evolving InP photocathodes covered by quasi-transparent metal catalysts. In addition, CO_2 and SO_2 reduction are treated. The chapter ends with a section on polycrystalline InP electrodes, including grain boundary passivation and hot carrier injection. The last chapter is devoted to the layered type transition metal dichalcogenides MoX_2 and WX_2, X = S, Se. Here *B. Scrosati* gives a thorough review of the solid state and photoelectrochemical characteristics of these materials. The section on surface morphology and its influence on the photoelectrochemistry is especially carefully written, and is followed by sections on photointercalation, behavior in non-aqueous electrolytes, and polycrystalline samples.

In summary the book contains a wealth of information on the most relevant semiconductor electrodes to date, written by some of the leading researchers in the field. There are only a few critical points to be addressed. A chapter on the intensively studied ternary chalcopyrites would have completed this volume. In addition, it would have been desirable to include also some authors from outside the United States, in accordance with the development and history of research in this area. The price of DFl. 340 appears too high for a book made by photographic reproduction.

Hans-Joachim Lewerenz
Hahn-Meitner-Institut
Berlin (FRG)

Call for Short Communications · Call for Short Communications · Call for Short Communications



... doesn't melt, won't dissolve, just can't be broken down — let's send it to ADVANCED MATERIALS!

ADVANCED MATERIALS welcomes short communications. Peer review, a wide circulation and short publication times are guaranteed. For instructions for authors please write to:
ADVANCED MATERIALS · Editorial Office · P.O. Box 101161 · D-6940 Weinheim · Federal Republic of Germany

Call for Short Communications · Call for Short Communications · Call for Short Communications

Conference Calendar

April 1989

10–12 **Bayreuther Polymer Symp.,**
Bayreuth (Fed. Rep. Germany)
Contact: BPS '89, Lehrstuhl Makromolekulare Chemie II, Univ. Bayreuth, Postfach 101251, D-8580 Bayreuth, FRG

10–12 **British Liquid Crystal Society**
Annu. Conf. 1989
Sheffield (United Kingdom)
Contact: Dr. D. A. Dunmur, Dept. of Chemistry, Univ. of Sheffield, Sheffield S3 7HF, UK

10–12 **Microstructure of Materials in Packaging Technology**
51st WE-Heraeus-Seminar
Bad Honnef (Fed. Rep. Germany)
Contact: Dr. V. Schäfer, WE-Heraeus-Stift., Heraeusstr. 12–14, D-6450 Hanau, FRG

10–13 **Microscopy of Semiconducting Materials,**
MRS 6th Oxford Conf.
Oxford (United Kingdom)
Contact: Administrator, Royal Microscopy Soc., 37/38 St. Clements, Oxford OX4 1AJ, UK

11–13 **Catalysis by Well Characterized Materials**
Liverpool (United Kingdom)
Contact: Prof. R. W. Joyner, Leverhulme Ctr. for Innovative Catalysts, Univ. of Liverpool, Grove St., P.O. Box 147, Liverpool L69 3BX, UK

17–19 **Metals and Materials 89**
Guildford (United Kingdom)
Contact: Inst. of Metals, 1 Carlton House Terrace, London SW1Y 5DB, UK

17–20 **Rare Earth Materials**
5th Biliteral Symp. (FRG/USSR)
Bad Honnef (Fed. Rep. Germany)
Contact: Dr. J. Debrus, Physikzentrum, Hauptstr. 5, D-5340 Bad Honnef 1, FRG

17–21 **Metallurgical Coating**
Int. Conf.
San Diego (USA)
Contact: B. D. Sartwell, Naval Research Lab., Code 4675, Washington, DC 20375, USA, Tel. 202-767-4800, Fax 202-767-5301

17–26 **Ceramics and Composite Materials,**
Spring College in Mater. Sci.
Trieste (Italy)
Contact: Int. Ctr. for Theoretical Physics, Spring College in Mater. Sci. 1989, P.O. Box 586, I-34100 Trieste, Italy

17–29 **STM Basic Concepts and Applications**
NATO Adv. Study Inst.
Erice (Italy)
Contact: Dr. H. Rohrer, IBM Research Div., Zürich Research Lab., Saumerstr. 4, CH-8803 Rüschlikon, Switzerland

18–19 **Industrial Water-Soluble and Water-Swellable Polymers**
Manchester (United Kingdom)
Contact: The Registar (Mid-Career Training), UMIST, P.O. Box 88, Manchester M60 1QD, UK

19–21 **Particle Characterization**
4th Eur. Symp.
Nürnberg (Fed. Rep. Germany)
Contact: Prof. Dr. K. Leschonski, Techn. Univ. Clausthal, Inst. f. Mechan. Verfahrenstechn. u. Umweltverfahrenstechn., Leibnizstr. 15, D-3392 Clausthal-Zellerfeld, FRG

23–27 **American Ceramic Society,**
91st Annu. Mtg. and Expo.
Indianapolis (USA)
Contact: Dr. K. M. Nair, Electronics Dept., E.I. du Pont de Nemours Co., Inc., 3181 Buffalo Ave., Niagara Falls, NY 14302, USA

23–28 **Nondestructive Testing,**
12th World Conf. (WCNDT '89)
Amsterdam (Netherlands)
Contact: B. de Jong, RAI Organisatie Bureau Amsterdam bv, Europaplein 12, 1078 GZ Amsterdam, Netherlands

24–28 **Optical Science and Engineering,**
2nd Int. Congr.
Paris (France)
Contact: Soc. of Photo-Optical Instrumentation Eng. (SPIE), P.O. Box 10, Bellingham, WA 98227, USA

24–28 **Lasers and Electro-Optics,**
LEOS-IEEE-OSA Conf. (CLEO '89)
Baltimore (USA)
Contact: Optical Soc. of America (OSA), 1816 Jefferson Pl. NW, Washington, DC 20036, USA

24–28 **MRS Spring Mtg.**
San Diego (USA)
Contact: J. B. Ballance, MRS, 9800 McKnight Rd., Suite 327, Pittsburgh, PA 15237, USA

25–27 **Hot Isostatic Pressing of Materials**
Antwerpen (Belgium)
Contact: Hot Isostatic Pressing Conf., c/o K. VIV, Jan van Rijswijcklaan 58, B-2018 Antwerpen, Belgium

26–28 **Joining Ceramics, Glass and Metal**
3rd Int. Conf. (CGM '89)
Contact: Dtsch. Gesellsch. Metallkd., Adenauerallee 21, D-6370 Oberursel, FRG

26–28 **COAT TECH '89**
Int. Kongr. f. neue Beschichtungstechnologien
Wiesbaden (Fed. Rep. Germany)
Contact: Demat Exposition Managing, Fr. D. Schnabel, P.O. Box 110611, D-6000 Frankfurt 1, FRG

May 1989

1–3 **Tunable Solid State Lasers,**
Top. Mtg.
North Falmouth (USA)
Contact: Optical Soc. of America (OSA), 1816 Jefferson Pl. NW, Washington, DC 20036, USA

1–5 **Scanning Microscopy,**
Salt Lake City (USA)
Contact: O. Johari, Scanning Microscopy Int., P.O. Box 66507, Chicago, IL 60666, USA

4–6 **The Solid State—Dynamics and Kinetics**
Annu. Mtg. Dtsch. Bunsen-Gesellsch. für Phys. Chem.
Siegen (Fed. Rep. Germany)
Contact: Dtsch. Bunsen-Gesellsch., Carl-Bosch-Haus, Varrentrappstr. 40/42, D-6000 Frankfurt am Main 90, FRG

7–12 **High-T_c Superconductor Technologies**
175th Mtg. Electrochem. Soc.
Los Angeles (USA)
Contact: S. Raider, IBM T. J. Watson Research Ctr., P.O. Box 218, York Town Heights, NY 10598, USA

7–12 **Fundamentals of Adsorption,**
3rd Int. Conf.
Nurrigen (Fed. Rep. Germany)
Contact: DECHEMA, Abt. Tagungen, P.O. Box 970146, Theodor Heuss-Allee 25, D-6000 Frankfurt am Main 97, FRG

8–10 **Vakuumelektronik und Displays**
Garmisch-Partenkirchen (Fed. Rep. Germany)
Contact: VDE-Zentralstelle Tagungen, Stresemannallee 15, D-6000 Frankfurt 70, FRG

8–11 **SAMPE**
34th Int. Symp. and Exhib.
Reno (Italy)
Contact: SAMPE, 843 West Glentana, P.O. Box 2459, Covina, CA 91722, USA, Tel. 818-331-0616

8–12 **High Temperature and Wear Resistant Materials in a World of Changing Technology**
12th Int. Plansee Seminar
Plansee (Austria)
Contact: Metallwerk Plansee, A-6600 Reutte, Austria

9–11 **Coatings and Sensors for Acoustic and Electromagnetic-Optical Applications**
Univ. Park. (USA)
Contact: V. K. Varadan, Dept. of Eng. Sci. and Mechanics, Penn. State Univ., 227 Hammond Bldg., Univ. Park, PA 16802, USA

10–11 **Polyimides**
Montpellier (France)
Contact: Prof. M. Abadie, LEMD/MAO-USTL, F-34060 Montpellier Cedex 1, France

16–17 **Reinforcement of Elastomers**
Akron Polymer Conf.
Akron (OH, USA)
Contact: P. Francik, Materials Chemistry, Technical Ctr., Goodyear, Akron, OH 44316, USA

16–19 **Modern Developments in Materials Science and Technology,**
Annu. Mtg. Dtsch. Gesellsch. Metallkd.
Karlsruhe (Fed. Rep. Germany)
Contact: Dtsch. Gesellsch. Metallkd., Adenauerallee 21, D-6370 Oberursel, FRG

16–19 **Rare-Earth Magnets and Their Applications**
10th Int. Workshop
Kyoto (Japan)
Contact: Dr. C. Herget, Sparte Anorg. Chemie, Th. Goldschmidt AG, P.O. Box 101461, D-4300 Essen 1, FRG

22–24 **Sol-Gel-Gläser**
52nd WE-Heraeus-Seminar
Bad Honnef (Fed. Rep. Germany)
Contact: Dr. V. Schäfer, WE-Heraeus-Stift., Heraeusstr. 12–14, D-6450 Hanau, FRG

22–24 **Werkstoffanalytik,**
Wien (Austria)
Contact: Prof. Dr. M. Grasserbauer, Inst. für Analytische Chem. der Tech. Univ. Wien, Getreidemarkt 9, A-1060 Wien, Austria

22–24 **Glastechnische Tagung**
Stuttgart (Fed. Rep. Germany)
Contact: Dtsch. Glastechn. Gesellsch., Mendelssohnstr. 75–77, D-6000 Frankfurt am Main, FRG

22–25 **Clustering and Aggregated State of Matter**
Strasbourg (France)
Contact: Prof. E. Constantin, Groupe de Recherche de Spectrométrie de Masse Interlab., Dept. de Chim., 1 rue Blaise Pascal, 67008 Strasbourg Cedex, France

22–25 **Graphite Intercalation Compounds,**
5th Int. Symp. (ISGIC-5)
Berlin (West)
Contact: Dr. F. W. Froben, Fachbereich Physik, Freie Univ. Berlin, Arnimallee 14, D-1000 Berlin 33

24–26 **Advances in the Stabilization and Controlled Degradation of Polymers,**
11th Int. Conf.
Luzern (Switzerland)
Contact: Dr. A. V. Patsis, Inst. in Materials Sci, State Univ. of New York, New Paltz, NY 12561, USA

25–26 **Quantitative Methods in Assessment of Structural Defects**
Kansas City (USA)
Contact: A. P. Berens, Univ. of Dayton, Research Inst., 300 College Park Ave., Dayton, OH 45469, USA

29–30 **TriboCeram 89**
2. Fachsymp.
Frankfurt (Fed. Rep. Germany)
Contact: TCI Techn. + Kommunik. Verlags GmbH, Tagungssekretariat, Ritterfeldamm 82 h+i, 1000 Berlin 22, Tel. 030/3653640, Fax 030/36588 40

29–31 **Cross-linked Polymers,**
3rd Int. Conf.
Luzern (Switzerland)
Contact: Dr. A. V. Patsis, Inst. in Materials Sci, State Univ. of New York, New Paltz, NY 12561, USA

30–2 **E-MRS Spring Mtg.**
Strasbourg (France)
Contact: P. Siffert, Ctr. de Recherches Nucléaire, Lab. PHASE, F-67037 Strasbourg, Cedex, France

31–2 **Applied Surface Analysis,**
11th Symp.
Cleveland (USA)
Contact: J. Grant, Research Inst., 300 College Park, Dayton, OH 45469-0001, USA

31-2 **Thermogravimetry and Thermal Engineering,**
6th Biennial Conf.
Budapest (Hungary)
Contact: I. Benko, MATE, House of Technol. III. 318, P.O. Box 451, H-1372 Budapest, Hungary

June 1989

5–6 **Test Methods for Composite Materials**
Seminar
Basel (Switzerland)
Contact: Technomic Publishing AG, Elisabethenstr. 15, CH-4051 Basel, Switzerland, Tel. 061/237011, Fax. 061/233978

5–7 **CONIMAT' 89**
1st Int. Convention for the Technology Transfer of New Materials
Strasbourg (France)
Contact: Adhesion Et Associes - CONIMAT', 9, rue de L'Ancienne Mairie, 92100 Boulogne, France, Tel. 48252604, Fax. 46038626

6–9 **Chemistry of Functional Dyes,**
Int. Symp. (ESTech '89)
Osaka (Japan)
Contact: Prof. T. Kitao, General Secretary of the Symp., Kinki Chem. Soc., Japan 1-8-4, Utsubo honmachi, Nishi-ku, Osaka 550, Japan

7–8 **Micromechanical Analysis of Composite Materials**
Seminar
Basel (Switzerland)
Contact: Technomic Publishing AG, Elisabethenstr. 15, CH-4051 Basel, Switzerland, Tel. 061/237011, Fax. 061/233978

7–9 **Hot Isostatic Pressing**
2nd. Int. Conf.
Gaithersburg (MD, USA)
Contact: Robert Schaefer, A 153 Materials Building, NIST, Gaithersburg, MD 20899, USA

12–15 **Narrow-Gap Semiconductors and Related Materials,**
Int. Conf.
Ogunquit (USA)
Contact: D. G. Seiler, Phys. Dept., Univ. of North Texas, P.O. Box 5368, Denton, TX 76203, USA

12–16 **Advanced Materials Chemistry Conf.**
St. Augustine (FL, USA)
Contact: Prof. R. S. Drago, Dept. of Chem., Univ. of Florida, Gainesville, FL 32611, USA

13–14 **Nonlinear Optical Polymers for Soldier Survivability**
Science Symp.
Natick (USA)
Contact: Th. Sklarsky, US Army Natick RD+E Center, Attn: STRNC-EMP, Natick, MA 01760-5014, USA, Tel. 508-651-4687

18–21 **Colloid & Surface Science,**
63rd ACS Div. of Colloid & Surface Chem. Symp.
Seattle (USA)
Contact: J. Berg, Dept. of Chemical Eng. BF-10, Univ. of Washington, Seattle, WA 98105, USA

18–23 **Ceramic Materials and Production Methods**
1st Conf. of the Eur. Ceramic Soc. and Fair
Maastricht (Netherlands)
Contact: Mrs. L. M. J. Bos, P.O. Box 1630, 6201 BP Maastricht, Netherlands

19–21 **Composites**
Asia-Pacific 89
Adelaide (Australia)
Contact: The Secretariat, Techsearch, Composites Asia-Pacific '89, P.O. Box 2471, Adelaide S.A. 5001, Australia

20–22 **SAMPE**
3rd Int. Electronics Conf.
Los Angeles (USA)
Contact: M. Smith, Business Director, SAMPE, P.O. Box 2459, Covina, CA 91722, USA, Tel. 818-331-0616

21–23 **Chemically Modified Surfaces,**
Midland (USA)
Contact: W. T. Collins, Dow Corning Corp., Mail Stop C41C00, Midland, MI 48686, USA

21–23 **Electronic Materials**
Cambridge (USA)
Contact: The Metallurgical Soc., 420 Commonwealth Dr., Warrendale, PA 15086, USA

22–25 **Optics Asia '89**
Singapore (Singapore)
Contact: Asia '89, 994 Bendemeer Rd., N° 04-03, Singapore 1233, Singapore

25–29 **Composite Materials for High Temperature, Fundamental Principles and Performance**
Jerusalem (Israel)
Contact: Mrs. S. Cahana, Ministry of Sci. and Developm., P.O. Box 18195, 91181 Jerusalem, Israel

25–30 **Solid State Sensors and Actuators (Transducers-5)/ Eurosensors III**
Montreux (Switzerland)
Contact: COMST S.A., P.O. Box 415, CH-1001 Lausanne 1, Switzerland

26–28 **Molecular Design of Functional Polymers,**
IUPAC Int. Symp.
Seoul (Korea)
Contact: IUPAC Int. Symp., c/o Polymer Soc. of Korea, Rm. 601, Hyecheon Bldg., 831 Yeoksam-dong, Kangnam-ku, Seoul 135-792, Korea

26–28 **Coherence and Quantum Optics**
Conf.
Rochester (USA)
Contact: L. Mandel, Univ. of Rochester, Dept. of Physics, Rochester, NY 14627, USA, Tel. 716-275-4361

26–30 **Solid State Chemistry,**
2nd Int. Symp.
Pardubice (Czechoslovakia)
Contact: Dr. L. Koudelka, Inst. of Chem. Technol., Leninovo nam., 565, CS-53210 Pardubice, Czechoslovakia

26–30 **Supermembranes**
Trieste (Italy)
Contact: Int. Ctr. for Theoretical Physics, P.O. Box 586, I-34100 Trieste, Italy

27–28 **Polymer Latex III**
London (United Kingdom)
Contact: Miss M. Peacock, Plastics and Rubber Inst., 11 Hobart Place, London SW1W 0HL, UK

28–30 **Chemically Modified Oxide Surfaces**
Midland (USA)
Contact: W. T. Collins, Mail Stop C41C00, Dow Corning Corp., Midland, MI 48686-0994, USA

July 1989

2–7 **Solid State Organic Materials,**
9th Int. Conf.
Como (Italy)
Contact: Centro di Cultura Scientifica, "A. Volta", Villa Olmo, Via Cantoni 1, I-22100 Como, Italy

3–6 **Conduction and Breakdown in Solid Dielectrics**
3rd Int. Conf. (ICSD '89)
Trondheim (Norway)
Contact: Prof. Sletbak, ICSD '89, The Norwegian Inst. of Technol., Sem Sælands V 13, N-7034 Trondheim, Norway

Materials Related Gordon Research Conferences

General Information

Contact: Dr. A. M. Cruickshank, Director, Gordon Research Conf., Gordon Res. Ctr., Univ. of Rhode Island, Kingston, RI 02881-0801, USA
Locations: Colby-Sawyer College (N), (S): New London, NH;
New Hampton School: New Hampton, NH;
Kimball Union Academy: Meriden, NH
Tilton School: Tilton, NH

June 1989

19–23 **Catalysis**
Colby-Sawyer College (N)
Chairman: L. D. Schmidt

26–30 **Polymers**
Colby-Sawyer College (N)
Chairman: J. P. Kennedy

July 1989

3–7 **Fiber Science**
Colby-Sawyer College (N)
Chairman: B. C. Goswami

3–7 **Thermosetting Polymers**
Colby-Sawyer College (S)
Chairman: N. J. Johnston

10–14 **Elastomers**
Colby-Sawyer College (N)
Chairman: G. Ver Strate

10–14 **Metal Hydrides**
Tilton School
Chairman: F. D. Manchester

17–21 **Corrosion**
Colby-Sawyer College (N)
Chairman: H. J. Grabke

17–21 **Chemistry at Interfaces**
Kimball Union Academy
Chairman: R. Johnson

17–21 **Superconducting Films**
Tilton School
Chairman: D. Gubser

31–4 **Ion-Containing Polymers**
Colby-Sawyer College (S)
Chairman: G. Wilkes

August 1989

7–11 **Physical Metallurgy**
Tilton School
Chairman: J. C. Williams

14–18 **Studies in Solid-State Ceramics**
Colby-Sawyer College
Chairman: U. Chowdhry

14–18 **Science of Adhesion**
New Hampton School
Chairman: R. A. Pike

3–7 **Martensitic Transformations**
Int. Conf. ICOMAT-89
Sydney (Australia)
Contact: N. Kennon, Dept. of Metallurgy and Materials Eng., Univ. of Wollongong, Wollongong, NSW 2500, Australia

3–8 **Light-Sensitive and Conducting Polymers**
Leipzig (German Dem. Rep.)
Contact: Prof. H. K. Roth, TH Leipzig, Sekt. Naturwissenschaften, P.O. Box 66, DDR-7030 Leipzig, GDR

3–28 **Liquids, Freezing and the Glass Transition**
NATO Adv. Study Inst.
Les Houches (France)
Contact: École d'Été de Physique Théorique, F-74310 Les Houches, France

4–7 **Nonlinear and Electro-Optics**
Int. Conf.
Cambridge (United Kingdom)
Contact: The Meetings Officer, The Inst. of Physics, 47 Belgrave Square, London SW1X 8QX, UK

9–14 **Scanning Tunneling Microscopy/Spectroscopy,**
4th Int. Conf.
Oarai (Japan)
Contact: O. Nishikawa, The Graduate School of Nagatsuta, Tokyo Inst. of Technol., 4259 Nagatsuta, Midori-ku, Yokohama 227, Japan

9–14 **Zeolites,**
8th Int. Conf.
Amsterdam (Netherlands)
Contact: M. Laboushere, 792 Keizersgracht, 1017 EC, Amsterdam, The Netherlands

10 **Bonding and Repair of Composite Materials**
Birmingham (United Kingdom)
Contact: John Herriot, Butterworth, P.O. Box 63, Westbury House, Bury St., Guildford GU2 5BH, UK

10–12 **Appl. Organomet. Chem.: an Entry to the New Technology**
The Pines Resort (Australia)
Contact: Dr. A. F. Masters, School of Chemistry, Univ. of Sydney, Sydney, N. S. W. 2006, Australia

10–13 **Magnetic Resonance in Polymers,**
9th Spec. Colloq. Ámpere
Prague (Czechoslovakia)
Contact: P. M. M. Secretariat, c/o. Inst. of Macromol. Chem., Czech. Acad. of Sci., 16206 Prague, Czechoslovakia

10–14 **Ion Sources**
Int. Conf.
Berkeley (USA)
Contact: W. O'Connor, Lawrence Berkeley Lab., 50B-2270, Berkeley, CA 94720, USA, Tel. 415-486-6386, Fax 415-486-7000

10–14 **Electron Spectroscopy,**
4th Int. Conf.
Honolulu (USA)
Contact: G. E. McGuire, Microelectronics Ctr. of North Carolina, P.O. Box 12889, Research Triangle Park, NC 27709, USA

10–14 **Organic Coatings Science and Technology,**
15th Int. Conf.
Athens (Greece)
Contact: Dr. A. V. Patsis, Inst. in Materials Sci, State Univ. of New York, New Paltz, NY 12561, USA

11–14 **Numerical Analysis of Semiconductor Devices and Integrated Circuits,**
6th Int. Conf.
Dublin (Ireland)
Contact: J. J. H. Miller, Nase-Code Conf., INCA, P.O. Box 2, Dún Laoghaire, Ireland

12–14 **Solid-State Laser/Optical Fiber Science and Electromagnetic Theory '89,**
Top. Mtg./Sino-Japanese Joint Mtg.
Beijing (Peoples' Rep. China)
Contact: Optical Soc. of America (OSA), 1816 Jefferson Pl. NW, Washington, DC 20036, USA

16–21 **Catalysis,**
Eur. Conf.
Berlin (West)
Contact: Prof. G. Ertl, Fritz-Haber-Inst. der Max-Planck-Gesellsch., Faradayweg 4-6, D-1000 Berlin

17–20 **Polymer Blends**
Prague (Czechoslovakia)
Contact: P. M. M. Secretariat, c/o. Inst. of Macromol. Chem., Czech. Acad. of Sci., 16206 Prague, Czechoslovakia

18–20 **Polymer Chemistry: Aspects of Radical Polymerization**
Lancaster (United Kingdom)
Contact: Dr. J. R. Ebdon, Dept. of Chemistry, Univ. of Lancaster, Lancaster LA1 4YA, UK

18–21 **Integrated Optics and Optical Fiber Communications,**
7th Int. Conf. (IOOC-7)
Kobe (Japan)
Contact: P. W. Shumate, Jr., Bell Communications Research, 435 S St., Morristown, NJ 07960, USA

23–24 **Computer-Aided Materials Characterization**
Int. Symp.
Charlotte (USA)
Contact: R. Biederman, Worcester Polytechn. Inst., Worcester, MA 01609, USA, Tel. 508-831-5453/5346

23–28 **Materials and Mechanisms of Superconductivity: High-Temperature Superconductors,**
Int. Conf. (HTSC-M^{2}S)
Stanford (USA)
Contact: Dr. T. H. Geballe, Dept. of Applied Phys., Stanford Univ., Stanford, CA 94305, USA

24–26 **Micro-Optics/Gradient-Index Optical Imaging Systems,**
2nd Conf./8th Top. Mtg.
Tokyo (Japan)
Contact: K. Iga, Tokyo Inst. of Technol., Research Lab. of Precision Machinery and Electronics, 4259 Nagasuta, Midori-ku, Yokohama 227, Japan

24–26 **Composite Structures,**
5th Int. Conf.
Paisley (United Kingdom)
Contact: Dr. I. H. Marshall, Dept. of Mechanical and Production Eng., Paisley College of Technol., High St., Paisley PA 12BE, UK

25–26 **Computer-Aided Microscopy and Quality Control**
Int. Conf.
Charlotte (USA)
Contact: J. Braun, EG+G Mound Appl. Technologies, Miamisburg, OH 45343-0987, USA, Tel. 513-865-3829

31–2 **Biologically-Engineered Polymers**
Cambridge (United Kingdom)
Contact: Royal Soc. of Chemistry, Burlington House, London W1V 0BN, UK

31–3 **Photoacoustic and Photothermal Phenomena**
6th Int. Mtg.
Baltimore (USA)
Contact: J. Murphy, Johns Hopkins Appl. Physics Lab., Johns Hopkins Rd., Laurel, MD 20707, USA, Tel. 301-953-6214

August 1989

2–7 **Pure and Applied Chemistry,**
32nd IUPAC Congr.
Stockholm (Sweden)
Contact: Stockholm Convention Bureau, P.O. Box 6911, S-10239 Stockholm, Sweden

13–26 **High-T_c Superconductors,**
NATO Adv. Study Inst.
Bad Windsheim (Fed. Rep. Germany)
Contact: R. Kossowsky, Applied Res. Lab., Pennsylvania State Univ., P.O. Box 30, State College, PA 16804, USA

14–17 **Shock Compression of Condensed Matter,**
APS Top. Conf.
Albuquerque (USA)
Contact: A. Roach, MS-P 915, Los Alamos Nat. Lab., Los Alamos, NM 87545, USA

14–18 **Hopping Transport,**
8th Conf.
Chapel Hill (USA)
Contact: M. Pollak, Dept. of Phys., Univ. of California, Riverside, CA 92521, USA

16–18 **Properties Through Processing**
Amherst (USA)
Contact: H. H. Winter, Dept. Chem. Eng., Univ. of Massachusetts, Amherst, MA 01003, USA

20–24 **Imaging Systems — 150 Years of Photography,**
Int. Symp. (ISIS '89)
Dresden (German Dem. Rep.)
Contact: Conf. Secretary, ISIS '89, Technische Univ. Dresden, Sektion Physik, Wissenschaftsbereich Photophysik, Mommsenstr. 13, DDR-8027 Dresden, GDR

20–25 **Crystal Growth: Progress in Science and Technology,**
9th Int. Conf.
Sendai (Japan)
Contact: Prof. T. Nishinaga, Inter Group Corp., Akasaka Yamakatsu Bldg., 8-5-32, Akasaka Minato-ku, Tokyo 107, Japan

21–24 **Amorphous and Liquid Semiconductors,**
13th Int. Conf.
Asheville (USA)
Contact: D. E. Sayers, P.O. Box 8202, North Carolina State Univ., Raleigh, NC 27695-8202, USA

21–25 **Phonons 89**
Heidelberg (Fed. Rep. Germany)
Contact: Inst. f. Angew. Physik II, Univ. of Heidelberg, Albert-Überle-Str. 3–5, D-6900 Heidelberg, FRG

21–26 **Photochemistry,**
Int. Conf.
Beijin (People's Rep. China)
Contact: Prof. S. Wu, Inst. of Photographic Chem., Academia Sinica, Beijing, People's Rep. China

27–1 **Supramolecular Organic Chemistry and Photochemistry**
Workshop
Saarbrücken (Fed. Rep. Germany)
Contact: Prof. Dr. H.-J. Schneider, FR Organ. Chem., Univ. des Saarlandes, D-6600 Saarbrücken, FRG

28–31 **Dynamical Processes in Excited States of Solids,**
7th Int. Conf. (DPC '89)
Athens (USA)
Contact: DPC '89, Prof. J. E. Rives, Dept. of Physics and Astronomy, Univ. of Georgia, Athens, GA 30602, USA

28–1 **Surface Modification Technologies**
3rd Int. Conf.
Neuchatel (Switzerland)
Contact: The Metallurgical Soc., 420 Commonwealth Dr., Warrendale, PA 15086, USA, Tel. 412-776-9050

28–1 **Ferroelectricity,**
7th Int. Mtg. (IMF-7)
Saarbrücken (Fed. Rep. Germany)
Contact: Dr. J. Albers, Univ. des Saarlandes, Fachbereich Physik, D-6600 Saarbrücken, FRG

28–1 **Sintering,**
7th World Round Table Conf.
Herceg-Novi (Yugoslavia)
Contact: Dr. D. P. Uskoković, Serbian Academy of Sci. and Arts, Knez-Mihailova 35, 11000 Beograd, Yugoslavia

28–1 **X-Ray Optics and Microanalysis,**
12th Int. Congr.
Cracow (Poland)
Contact: S. Jasienska, Academy of Mining and Metallurgy,
Inst. of Metallurgy,
30-059 Cracow, Poland

28–2 **Photochemistry for High Technology,**
Int. Summer School
Leuna-Merseburg (German Dem. Rep.)
Contact: Prof. H.-J. Timpe, Sektion Chemie, Technische Hochschule für Chemie, Leuna-Merseburg, Gensaerstr., DDR-42 Merseburg, GDR

29–2 **Innovation and Perspectives in Solid Phase Synthesis,**
Int. Symp.
Oxford (United Kingdom)
Contact: R. Epton, School of Appl. Sci., Wolverhampton Polytech., Wolverhampton WV1 1SB, UK

September 1989

3–5 **Advanced Ceramics and P/M Materials, Development and Applications**
Int. New Business and High Tech Conf.
Jyväskylä (Finland)

Contact: EAMI, Ms. R. Hänninen, Reumantie 4, 18100 Heinola, Finland, Tel. 358-10-57062, Fax 358-10-57161

4–8 **Electrically and Optically Active Polymers,**
21st Europhysics Conf.
Lodz (Poland)
Contact: Dr. J. Ulanski, Polymer Inst., Tech. Univ. of Lodz, Zwirki 36, 90-924 Lodz, Poland

4–8 **Macromolecules 89,**
Eur.-Am. Conf. on Functional Polymers and Biopolymers
Oxford (United Kingdom)
Contact: Prof. R. Epton, School of Appl. Sci., The Polytechnic, Wolverhampton WV1 1SB, UK

4–8 **Olefin Metathesis and Polymerization,**
8th Int. Symp.
Bayreuth (Fed. Rep. Germany)
Contact: Office ISOM 8, Lab. für Anorg. Chem., Univ. Bayreuth, Postfach 101251, D-8580 Bayreuth, FRG

5–7 **Interfacial Phenomena in Composite Materials,**
Int. Conf.
Sheffield (United Kingdom)
Contact: J. Herriot, Butterworth, P.O. Box 63, Westbury House, Bury St., Guildford GU2 5BH, UK

5–8 **Optical, Electrical and Acoustic Properties**
Kent (United Kingdom)
Contact: M. D. Shuttleworth, Plastics and Rubber Inst., 11 Hobart Pl., London SW1W 0HL, UK

5–8 **Polymers, Laminations and Coatings**
TAPPI Conf.
Orlando (FL, USA)
Contact: Mtg. Dept., TAPPI Technology Park, P.O. Box 105113, Atlanta, GA 30348-5113, USA

5–9 **Accelerators in Appl. Res. Technology**
1st Eur. Conf.
Frankfurt (Fed. Rep. Germany)
Contact: K. Bethge, Inst. f. Kernphysik, August-Euler-Str. 6, D-6000 Frankfurt 90, FRG

6–9 **Magnetic Materials and Applications (EMMA '89)**
Rimini (Italy)
Contact: L. Pareti, EMMA '89, Istituto Maspec, Via Chiavari 18/A, I-43100 Parma, Italy, Phone 521-95811, Fax 521-96315

7–9 **Biomaterials**
8th Eur. Congr.
Heidelberg (Fed. Rep. Germany)
Contact: Dr. U. Soltesz, Fraunhofer-Institut für Werkstoffmechanik, Wöhlerstr. 11, D-7800 Freiburg, FRG

10–11 **Ceramics in Medicine**
2nd Int. Symp.
Heidelberg (Fed. Rep. Germany)
Contact: Dtsch. Keram. Gesellsch., Frankfurter Str. 196, D-5000 Köln 90, FRG

10–12 **Colloidal Dispersions**
Faraday Discussion 90
Bristol (United Kingdom)
Contact: Prof. R. H. Ottewill, School of Chemistry, Univ. of Bristol, Bristol BS8 1TS, UK

10–14 **Optical Communications,**
15th Eur. Conf.
Gothenburg (Sweden)
Contact: P. A. Andrekson, Dept. of Optoelectronics, Chalmers Univ. of Technol., S-41296 Gothenburg, Sweden

10–23 **Molecular Dynamics of Liquid Crystals**
NATO Adv. Study Inst.
Il Ciocco, Lucca (Italy)
Contact: Prof. C. A. Veracini, Dipartimento di Chimica, Universita di Pisa, Viale Risorgimento 35, I-56100 Pisa, Italy

11–13 **Charge Transfer in Polymeric Systems,**
RSC, Faraday Div.
Contact: Dr. J. F. Gibson, Royal Soc. of Chemistry, Burlington House, Piccadilly, London W1V 0BN, UK

11–13 **Holographic Systems, Components and Applications,**
2nd Int. Conf.
Bath (United Kingdom)
Contact: Inst. of Electronic and Radio Eng., Conf. Dept., Savoy Hill House, London WC2R 0JD, UK

11–13 **Surface Analysis Techniques and Applications**
Manchester (United Kingdom)
Contact: E. Wellingham, Conf. Secretariat, Field End House, Bude Close, Nailsea, Bristol BS19 2FQ, UK

13–15 **Microscopy,**
150th Anniversary Commemorative Mtg.
Oxford (United Kingdom)
Contact: Microscopical Soc., 37–38 St. Clements, Oxford OX4 1AJ, UK

17–22 **Defect Recognition and Image Processing in Semiconductors,**
3rd Mtg. (DRIP-3)
Yokohama (Japan)
Contact: Prof. T. Ogawa, Gakushuin Univ., Dept. of Physics, 1-5-1 Mejiro, Toshima-ku, Tokyo 171, Japan

17–22 **Optics and Optical Engineering,**
Cambridge Symp.
Cambridge (USA)
Contact: Soc. of Photo-Optical Instrumentation Eng. (SPIE), P.O. Box 10, Bellingham WA 98227, USA

18–22 **Quantum Electronics**
9th Natl. Conf.
Oxford (United Kingdom)
Contact: Mrs. M. Sherwen, Rutherford Appleton Lab., Chilton, Didcot, Oxon OX11 OQX, UK

20–22 **Structural Adhesives in Engineering**
SAE II '89
Bristol (United Kingdom)
Contact: J. Herriot, SAE II '89, Butterworth Scientific Ltd., PO Box 63, Westbury House, Bury St., Guildford, Surrey GU2 5BH, UK

20–22 **Manmade Fibers**
Int. Congr.
Dornbirn (Austria)
Contact: Austrian Manmade Fibers Inst., Plossigasse 8, A-1041 Vienna, Austria

21–22 **Fire Retardant Polymers**
Torino (Italy)
Contact: Prof. L. Costa, Dipt. di Chim. dell'Università di Torino, Via P. Giuria, 7, 10125 Torino, Italy

24–28 **Metallization of Polymers**
Int. Colloquium
Montreal (Canada)
Contact: Ed. Sacher, Ecole Polytechnique, Université de Montreal, Quebec H3C 3A7, Canada

25–26 **Additive Approaches to Improved Polymer Performance**
Toronto (Canada)
Contact: Jeff Hood, Stochem. Inc., 106 Summerlea Rd., Brampton, Ontario L6T 4X3, Canada

25–27 **Surface Engineering with High Energy Beams,**
2nd Int. Seminar
Lisbon (Portugal)
Contact: Secretariat of ISHT '89 Seminar, Ctr. of Mech. and Mater. of the Tech. Univ. Lisbon (CEMUL), 1096 Lisboa Codex, Portugal

25–29 **Vacuum Solid Surfaces**
IVC-11/CSS-7
11th Int. Conf./7th Int. Conf.
Cologne (Fed. Rep. Germany)
Contact: D. A. Benninghoven, Physikalisches Inst. der Univ. Münster, Wilhelm-Klemm-Str. 10, D-4000 Münster, FRG

26–28 **Optical Memory,**
Int. Symp. (ISOM '89)
Kobe (Japan)
Contact: ISOM '89 Secretariat, Business Ctr. for Academic Soc. Japan, 3-23-1 Hongo, Bunkyo-ku, Tokyo 113, Japan

26–28 **SAMPE**
21st Int. Techn. Conf.
Atlantic City (USA)
Contact: SAMPE, 843 W. Glentana, P.O. Box 2459, Covina, CA 91722, USA, Tel. 818-331-0616

26–29 **Structure and Dynamics of Colloidal Systems**
3rd Eur. Colloid and Interface Conf.
Basel (Switzerland)
Contact: Dr. M. Zulauf, F. Hoffmann-La Roche & Co, ZFE 65-509, CH-4002 Basel, Switzerland

27–29 **Polymer Reaction Engineering**
3rd Berlin Int. Workshop
Berlin (West)
Contact: Prof. Dr. K.-H. Reichert, Inst. f. Techn. Chemie, TU Berlin, Straße des 17. Juni 135, D-1000 Berlin 10

27–29 **New Polymers**
1st Materials Symp.
Regensburg (Fed. Rep. Germany)
Contact: OTTI-Fortbildung, Martin-Luther-Straße 10, D-8400 Regensburg, FRG

30–4 **High-T_c Thin Films and Single Crystals**
Int. Conf.
Ustron (Poland)
Contact: M. W. Gutowski, Inst. of Physics, ON-3 Polish Acad. of Sci., Al. Lotnikow 32/46, PL-02668 Warszawa, Poland

October 1989

1–4 **Grenzflächen in kondensierten Systemen – Gleichgewicht und dynamische Phänomene**
Kolloid-Gesellsch. Hauptvers.
Bochum (Fed. Rep. Germany)
Contact: Prof. Dr. G. H. Findenegg, Physikal. Chem. II, Ruhr-Univ., P. O. Box 102148, D-4630 Bochum 1, FRG, Tel. 0234/7004229

1–5 **The Metallurgical Society,**
Fall Mtg.
Indianapolis (USA)
Contact: Mtgs. Dept., TMS, 420 Commonwealth Dr., Warrendale, PA 15086, USA

1–5 **Halide Glasses,**
6th Int. Symp.
Clausthal (Fed. Rep. Germany)
Contact: Prof. G. Frischat, Tech. Univ. Clausthal, Fak. für Bergbau, Hütten- und Maschinenwesen, Adolf-Römer-Str. 2A, D-3392 Clausthal-Zellerfeld, FRG

2–4 **Electron and Optical Beam Testing of Integrated Circuits,**
2nd Eur. Conf.
Duisburg (Fed. Rep. Germany)
Contact: E. Kubalek, Werkstoffe der Elektronik, Univ. Duisburg, Kommandanten-Str. 60, D-4100 Duisburg 1, FRG

2–4 **High Temperature Polymers**
Cleveland (USA)
Contact: Vivian E. Malpass, Ferro Corp., Technical Ctr., 7500 East Pleasant Valley Rd., Independence, OH 44131, USA

2–5 **Materials Week**
Technical Conf.
Indianapolis (IN, USA)
Contact: Technicol Dept. Marketing, ASM Int., Metals Park, OH 44073, USA

9–10 **Quasikristalle**
DFG-Rundgespräch
Bad Honnef (Fed. Rep. Germany)
Contact: Dr. J. Tobolski, Dtsch. Forschungsgem., Bad Godesberg, Kennedyallee 40, D-5300 Bonn 2, FRG

9–11 **Dtsch. Keramische Gesellsch. Jahrestagung 1989**
Koblenz (Fed. Rep. Germany)
Contact: Dtsch. Keramische Gesellsch., Frankfurter Str. 196, D-5000 Köln 90, FRG, Tel. 02203-69069, Fax 02203-69301

11–13 **Materials for Electrochemistry**
Stuttgart (Fed. Rep. Germany)
Contact: Prof. F. von Sturm, Jahnstr. 26, D-8901 Biberbach, FRG

11–13 **Surface Technology Forum**
SURTEC '89
Berlin (West)
Contact: AMK Berlin, M 3/Surtec, Messedamm 22, D-1000 Berlin 19

15–18 **Unconventional Photoactive Solids,**
4th Int. Conf.
San Jose (USA)
Contact: Dr. C. G. Willson, IBM Almaden Research Ctr., 650 Harry Road, San Jose, CA 95120, USA

16–19 **High-Tech-Coating,**
Congr. and Exhibition
Wiesbaden (Fed. Rep. Germany)
Contact: Demat Exposition Managing, P.O. Box 110611, D-6000 Frankfurt, FRG

17–19 **Optical Storage for Large Systems**
4th Annu. Conf.
New York, NY
Contact: Rothchild Consult., 256 Laguna Honda Blvd., San Francisco, CA 94116-1496, USA

22–28 **Solid-State and Integrated Circuit Technology,**
2nd Int. Conf.
Beijing (Peoples' Rep. China)
Contact: Continuing Education in Eng., Univ. Extension, Univ. of California, 2223 Fulton St., Berkeley CA 94720, USA

23–24 **Hochtemperatur-Supraleiter und Kristallchemie III**
Bad Honnef (Fed. Rep. Germany)
Contact: Dr. J. Debrus, Physikzentrum, Hauptstr. 5, D-5340 Bad Honnef 1, FRG

24–29 **Applications of Surface and Interface Analysis,**
Eur. Conf. (ECASIA '89)
Antibes (France)
Contact: J. Fauvet, Soc. Français du Vide, 19, rue du Renard, F-75004 Paris, France

November 1989

5–8 **Solid State Ionics,**
7th Int. Conf.
Hakone (Japan)
Contact: Dr. Y. Saito, Res. Lab. of Engineering Materials, Tokyo Inst. of Technol., 4259 Nagatsuta-cho, Midori-ku, Yokohama 227, Japan

14–15 **Polypropylene**
Madrid (Spain)
Contact: D. Varley, Plastics and Rubber Inst., 11 Hobart Place, London SW1W 0HL, UK

22–24 **Euromat '89**
Eur. Conf. on Materials
Aachen (Fed. Rep. Germany)
Contact: Dtsch. Gesellsch. Metallkd., Adenauerallee 21, D-6370 Oberursel, FRG

27–29 **Electronic Packaging**
55th WE-Heraeus-Seminar
Bad Honnef (Fed. Rep. Germany)
Contact: Dr. V. Schäfer, WE-Heraeus-Stift., Heraeusstr. 12–14, D-6450 Hanau, FRG

27–2 **MRS Fall Mtg.**
Boston (USA)
Contact: A. Wagner, Materials Research Soc. (MRS), 9800 McKnight Rd., Suite 327, Pittsburgh, PA 15237, USA

December 1989

12–15 **Pacific Polymer**
Hawaii (USA)
Contact: J. C. Vogl, Pacific Polym. Federation, Polytechnic Univ., 333 Jay St., Brooklyn, NY 11201, USA

ANGEWANDTE CHEMIE

International Edition in English

Volume 28 · Number 4
April 1989
Pages 397–534

Metallocene Carbene Complexes and Related Compounds of Titanium, Zirconium, and Hafnium

By Gerhard Erker*

The structure and reactivity spectrum of transition-metal carbene complexes has been widened significantly by the bent metallocenes of titanium, zirconium, and hafnium. Proceeding from metal carbonyls and reactive (butadiene)-, (aryne)-, or (olefin)MCp_2 complexes, many new Fischer-type metaloxycarbene complexes of Zr, Hf, V, Nb, Cr, Mo, W, Mn, Re, Fe, Ru, Os, Co, Ni, and Rh have been synthesized. The incorporation of titanocene, zirconocene, or hafnocene fragments allows new types of carbene complexes to be prepared. For the (alkylidenamido)metallocene complexes $[Cp_2M(X)(\equiv N=CRR')]$, metallocene ylides $[Cp_2M(R)(\equiv CHPPh_3)]$, and binuclear (μ-alkynyl)metallocene compounds, some metal–ligand π bonding is indicated. Metallocene complexes with metallaoxirane units, $Cp_2\overline{M-CH_2-O}$, show similar chemical behavior to that of binuclear (μ-methylene)complexes $L_n\overline{M-CH_2-M}L_n$. The methylene groups of zirconaoxirane complexes, which are derived from carbon monoxide, may be expelled as ethylene by thermally induced CC coupling. With metal hydrides, CH_2 transfer with insertion into the metal–hydride bond occurs. In one case, methylene insertion into a metal–carbon bond can even be observed. These reactions of Ti-group metallaoxiranes could be models for postulated intermediates in the Fischer–Tropsch synthesis.

1. Introduction

Carbene complexes are among the most important organometallic compounds. The discovery of heteroatom-stabilized carbene complexes $[L_nM=CR(OR)]$ by *E. O. Fischer* et al.[1] and of heteroatom-free metal alkylidene complexes $[L_nM=CR_2]$ by *R. R. Schrock* et al.[2] laid the foundation for the recognition of reactive carbene complexes as decisive intermediates for many metal-catalyzed transformations of organic substrates.[3] Carbene complexes are becoming increasingly important as reagents in organic synthesis. The nucleophilic Schrock-type carbene complexes, obtained from the early transition metals, have ylide character and have proved useful as selective Wittig reagents.[4] The CR(OR) units of Fischer-type carbene complexes are being employed very successfully as C_1 synthons in template-controlled CC-coupling sequences.[5] The $-C(=M)OR'$ unit can activate a neighboring R group, in a manner similar to that of ester groups $-C(=O)OR'$.[6] Last but not least, the carbene complexes are significant as the simplest organometallic complexes with a metal–carbon π bond.[7]

New developments have broadened considerably the preparative routes to and applications of transition-metal car-

[*] Prof. Dr. G. Erker
Institut für Organische Chemie der Universität
Am Hubland, D-8700 Würzburg (FRG)

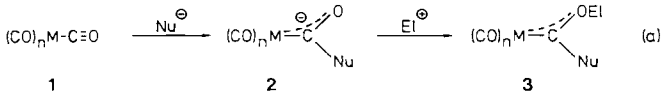
 © VCH Verlagsgesellschaft mbH, D-6940 Weinheim, 1989 0570-0833/89/0404-0397 $ 02.50/0

bene complexes. The bent metallocenes of group 4 transition metals[8, 9] have played an important role in this. The chemistry of titanocene, zirconocene, and hafnocene complexes has erupted with a range of new kinds of organometallic compounds that resemble the traditional mono- or multinuclear carbene complexes in their bonding properties and reactions. Consequently, the structure and reactivity spectrum of this class of compounds has been significantly widened. Selected examples illustrating these developments will be discussed in this article.

2. Synthesis and Properties of Metaloxycarbene Complexes

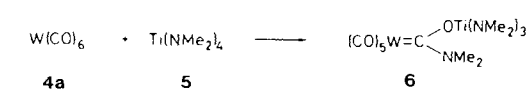
2.1. The Fischer Route

In the two-step conversion of metal carbonyls to metal carbene complexes developed by *E. O. Fischer* et al. [Eq. (a)], a carbon nucleophile is added to the M–C≡O unit of **1** in the first step to form an acylmetalate complex **2**.[1, 10] The product **3** results from further reaction with an electrophile. Organometallic compounds (e.g., from elements of the Ti group) can also function as the electrophile. As an example, the complexes $[(CO)_5Cr=C(CH_3)OTiClCp_2]$ and $[\{(CO)_5Cr=C(CH_3)O\}_2TiCp_2]$ are obtained from Cp_2TiCl_2.[11]



1 **2** **3**

This route to carbene complexes is quite general. The limits of this method are determined by the balance of reactivity at the acylmetalate intermediate **2**. On the one hand, an adequate stabilization of **2** is required, without which it would not form at all. On the other hand, the success of the second part of the reaction path can be adversely affected by overly strong localization of the negative charge at the $(CO)_nM$ group. If the intermediate **2** is too stable, it frequently resists the *O*-alkylation in the following step. Metal alkylation or reaction at another ligand affords acyl complexes rather than the desired Fischer-type carbene complex.[12] The simplest way to bypass the limitations of the Fischer synthesis would seem to be to reverse the order of the reaction steps in Equation (a). Titanium and zirconium compounds having a Lewis acidic metal center and nucleophilic ligands have proven themselves very successful as reagents for this procedure. Thus, the reaction of $[Ti(NMe_2)_4]$ **5** with $[W(CO)_6]$ **4a** affords the carbene complexes **6**. Other metal carbonyls (M = Mo, Fe, Ni) react similarly. The bis(pentamethylcyclopentadienyl)zirconium dihydride reagent **7** was used to convert metal carbonyls (M = Zr, Nb, Cr, Mo, W, Rh) into zirconiumoxycarbene complexes (e.g., **4b** → **8**). In several cases, the addition of the monomeric **7** is reversible.[13]



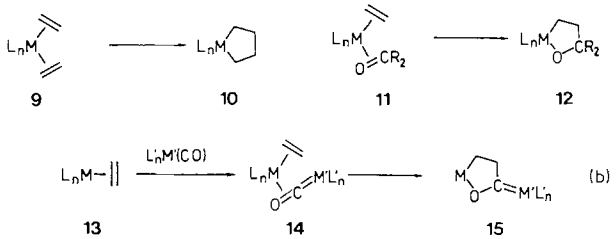
4a **5** **6**



4b **7** **8**

2.2. Synthesis of Metaloxycarbene Complexes without Nucleophilic Addition

Heteroatom-stabilized carbene complexes can be prepared by routes avoiding nucleophilic addition to metal carbonyls. Examples are the L_nM-induced cleavage of electron-rich olefins $(R_2N)_2C=C(NR_2)_2$[14] and reactions of metalate complexes, Na_2ML_n, with Vilsmeier salts, $(RClC=NR_2)^{\oplus}Cl^{\ominus}$, to give the carbene complexes $[L_nM=CR(NR_2)]$,[15] both developed by *Lappert* et al. Metal carbonyls can be converted into carbene complexes by reaction with very reactive η^2-olefin complexes of titanocene, zirconocene, or hafnocene. Although these reactions formally resemble the original reaction sequence of *E. O. Fischer*, they are probably mechanistically quite different [Eq. (b)] and complement the "classical" reaction in Equation (a). They are reminiscent of a frequently observed organometallic reaction, namely, the (presumably) concerted ring-closure of bis(olefin)metal complexes **9** to give metallacyclopentanes **10**.[16] The oxametallacyclopentanes **12** ($L_nM = Cp_2Ti$, Cp_2Zr, Cp_2Hf) are formed analogously from (η^2-ketone)(η^2-olefin)metal complexes **11**. If the side-on-coordinated organic carbonyl compound is replaced in **11** by a metal carbonyl complex, an analogous ring-closure reaction affords the metallacyclic metaloxycarbene complex **15** (**13** → **14** → **15**).



9 **10** **11** **12**

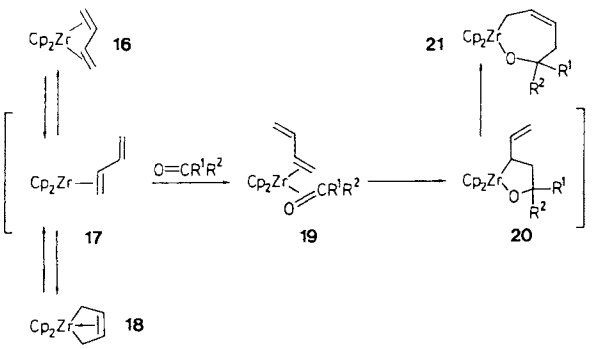
13 **14** **15**

For this reaction, the few known isolable mono(olefin)-metallocene complexes of the Ti group are obvious candidates, e.g., (ethylene)bis(η-pentamethylcyclopentadienyl)titanium or (ethylene)bis(indenyl)titanium.[17] We have used (butadiene)bis(cyclopentadienyl)zirconium and related compounds for carbene complex syntheses by Equation (b). They are available as easily accessible starting materials on a large scale.

2.2.1. Carbene Complexes from (η^4-Diene)metallocenes

(Butadiene)zirconocene exists at room temperature as two isolable isomers, (*s-trans*-η^4-butadiene)- and (*s-cis*-η^4-butadiene)zirconocene **16** and **18**, respectively.[18] The equilibration (**16**:**18** ≈ 1:1 at 25 °C; $\Delta G^{\ddagger}_{10.5\,°C}$ (**16** → **18**) = 22.7 kcal mol^{-1}) presumably occurs through the coordinatively unsaturated intermediate (η^2-butadiene)zirconocene **17**. The isomers **16** and **18** have very different reactivities.[19, 20] The (*s-cis*-η^4-diene)metallocene has metal alkyl character and adds to organic carbonyl compounds, behaving as a typical carbon nucleophile. By comparison, the CC-coupling reactions of the non-nucleophilic, coordinatively saturated (*s-trans*-η^4-diene)metallocene species proceed via the easily obtainable (η^2-diene)metallocene intermediate **17**. Surprisingly, several ketones have been shown to react faster via this reaction path (**17**) than by direct nucleophilic addi-

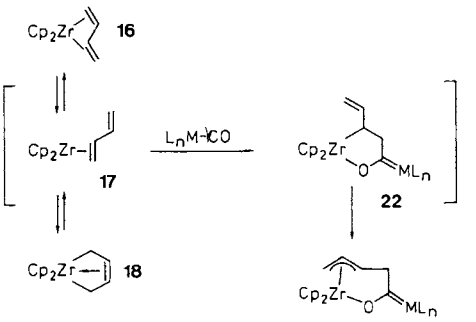
tion: under kinetic control, the only observed reaction of a **16/18** mixture with excess ketones is that of the (*s-trans*-η^4-butadiene)zirconocene. The heterocycle **21** is thereby formed via **19** and **20**. The (*s-cis*-η^4-diene)$ZrCp_2$ isomer does not react until the temperature is increased sufficiently to allow the **18** → **16** isomerization to occur.[21]



Hexacarbonylchromium reacts slowly at room temperature (12 h) with the equilibrium mixture of (*s-cis*-/*s-trans*-η^4-butadiene)zirconocene **16/18** to form the (η^3-allyl)zirconiumoxycarbene complex **23a**. Reaction of **16/18** with $Mo(CO)_6$ or $W(CO)_6$ affords the analogous **23b,c**.[22] Between −20 °C and 0 °C, the isomerization **16** ⇄ **18** is frozen out, and only the (*s-trans*-η^4-butadiene)zirconocene **16** reacts (quickly) with [$Fe(CO)_5$]. The metallacyclic (η^3-allyl)zirconiumoxycarbene complex **24a** is formed as the sole product, since the expected intermediate with (σ-allyl)metallocene structure rearranges very quickly to the more stable π-allyl form **24a**. The reaction of [$(CO)_4Fe(PPh_3)$] with the **16/18** mixture leads just as easily to the formation of the phosphane-substituted iron carbene complex **24b**.[23] Under the usual conditions of the Fischer synthesis, the *O*-alkylation step gives carbene complexes with negligible amounts of side products *only* with the use of nitrosyl ligands or very strong alkylating agents. Carbene transfer reactions (e.g., from [Cp(CO)(NO)Mo=CRPh] to photochemically generated [$Fe(CO_4)$]) represent alternative routes to simple tetracarbonyl(carbene)iron complexes.[24]

The synthesis of cobalt and rhodium carbene complexes by the route in Equation (a) requires the presence of ligands to stabilize the acylmetalate intermediate.[25,26] Carbene complexes with the (η-cyclopentadienyl)cobalt or -rhodium fragments have thus far been prepared by alternative reaction paths.[13c,15] $CpRh(CO)_2$ reacts at room temperature with the **16/18** equilibrium mixture to give the carbene complex **25a**. At lower temperatures, only the *s-trans* isomer **16** reacts.[27]

The metallacyclic (η^3-allyl)zirconiumoxycarbene complex **25b** crystallizes on cooling the $CpCo(CO)_2$/(butadiene)zirconocene reaction mixture. At room temperature in solution, a fast equilibrium between the carbene complex and the starting materials is established. In the reverse reaction with CC bond cleavage, only (*s-trans*-η^4-butadiene)zirconocene **16** is formed together with $CpCo(CO)_2$ under kinetic control. This complex then isomerizes to the *s-cis* isomer **18**. The equilibrium position between metaloxycarbene complex and starting complexes is influenced by the introduction of substituents at the Co-bound Cp ligands. The zirconiumoxycarbene complex **25c** was obtained from [(η-C_5H_4Cl)$Co(CO)_2$] by reaction with the Zr reagent. The

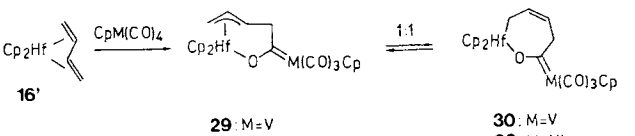


ML_n = $Cr(CO)_5$, $Mo(CO)_5$, $W(CO)_5$ (**23a,b,c**);
$Fe(CO)_4$, $Fe(CO)_3PPh_3$ (**24a,b**);
Rh(CO)Cp, Co(CO)Cp, Co(CO)(η-C_5H_4Cl) (**25a,b,c**);
$Ni(CO)_3$ (**26**);
$Zr(CO)Cp_2$, $Hf(CO)Cp_2$ (**27a,b**);
$V(CO)_3Cp$ (**28**)

equilibrium position for this reaction at room temperature is such that no starting materials could be detected (^1H NMR spectroscopy).[28]

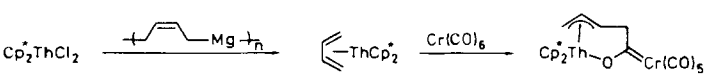
The isolation of the nickel carbene complex **26** was complicated by the fast equilibrium with the reactants $Ni(CO)_4$ and (*s-trans*-η^4-butadiene)zirconocene **16**. In solution, **26** is stabilized by the presence of excess tetracarbonylnickel.[29a,b] Under the usual conditions, $Cp_2Zr(CO)_2$ and $Cp_2Hf(CO)_2$ were converted into the metaloxycarbene complexes **27a** and **27b**, respectively.[29]

Carbene complexes of vanadium are rare, although it is possible that they play an important role in vanadium-catalyzed reactions.[15a,30] Reaction of $CpV(CO)_4$ with (butadiene)zirconocene affords the vanadium carbene complex **28**. When **28** is dissolved in benzene at room temperature, equilibrium between **28** and the starting materials is established immediately (**28**: starting materials ca. 1:1 at 25 °C).[31] The equilibrium position is shifted advantageously by the use of (butadiene)hafnocene **16'**. Reaction of $CpV(CO)_4$ with **16'**[19,20] at room temperature affords the (η^3-allyl)-metaloxycarbene complex **29**. In solution, **29** does not equilibrate with the mononuclear starting materials, but instead slowly transforms into the isomeric seven-membered ring (σ-allyl)metaloxycarbene complex **30**,[31] eventually establishing an equilibrium (1:1 at 25 °C). The niobium carbene complex **31**, obtained from **16'** and $CpNb(CO)_4$ behaves analogously.[29a,32] Few heteroatom-stabilized carbene complexes of niobium have been reported[13b,d,33] thus far.



29: M=V
31: M=Nb
30: M=V
32: M=Nb

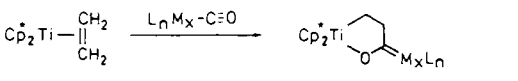
The very reactive η^4-diene complexes of the actinide element thorium can likewise function as reagents for carbene syntheses. (η^4-Butadiene)$ThCp_2^*$ **34** reacts at 0 °C with hexacarbonylchromium to afford the thoriumoxycarbene complex **35**. With [$Mo(CO)_6$] and [$W(CO)_6$], **34** afforded corresponding products.[34]



33 **34** **35**

2.2.2. *Carbene Complexes from (η^2-Olefin)- and (η^2-Aryne)metallocenes*

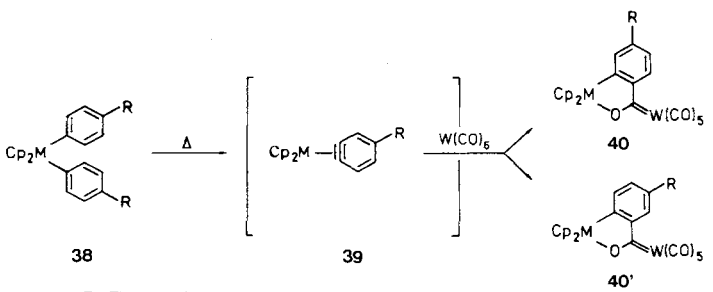
Takaya et al. used (η^2-ethylene)bis(η-pentamethylcyclopentadienyl)titanium **36** (originally reported by *Bercaw* et al.[17a]) as a reagent for carbene complex syntheses. The titaniumoxycarbene complexes **37a–c** were formed by reaction of **36** with the hexacarbonyl complexes of chromium, molybdenum, and tungsten at $-20\,^{\circ}C$. The titaniumoxycarbene complexes **37d** and **37e**, respectively, are formed analogously by addition of **36** to the carbonyl ligands of $Mn_2(CO)_{10}$ and $Re_2(CO)_{10}$. From the X-ray analysis of the rhenium carbene complex **37e**, it can be seen that the metallacyclic carbene ligand occupies the *trans* position at the binuclear metal carbonyl. Application of the Fischer synthesis [Eq. (a)] to $Mn_2(CO)_{10}$ and $Re_2(CO)_{10}$ normally affords *cis*-configurated monocarbene complexes.[10]



36

37a $M_xL_n = Cr(CO)_5$
37b $M_xL_n = Mo(CO)_5$
37c $M_xL_n = W(CO)_5$
37d $M_xL_n = trans\text{-}Mn_2(CO)_9$
37e $M_xL_n = trans\text{-}Re_2(CO)_9$

(η^2-1,2-Didehydrobenzene)zirconocene and -titanocene **39** (M = Zr, R = H and M = Ti, R = H, respectively) are easily generated by thermolysis of the diphenylmetallocenes **38**. In the absence of other reagents, they react with aromatic hydrocarbons by C–H activation, in a reversal of the reaction leading to their formation. The (aryne)metallocenes **39** add a broad palette of organic compounds having reactive π systems, with formation of five-membered benzannelated metallacycles. Thus $(C_6H_4)ZrCp_2$, thermally generated in situ at 90 °C from diphenylzirconocene, reacts with the stilbene isomers stereospecifically to give *cis*- or *trans*-1,1-bis(cyclopentadienyl)-2,3-diphenylzirconaindan.[36] Reaction between hexacarbonyltungsten and the zirconocene **38** (M = Zr, R = H) at 90 °C affords the five-membered metallacyclic benzannelated zirconiumoxycarbene complex **40**. A labeling experiment showed that this carbene complex is formed from the (aryne)metallocene intermediate **39**. Similarly, bis(*p*-tolyl)zirconocene **38** (M = Zr, R = CH_3) reacts with $W(CO)_6$ to afford the zirconiumoxycarbene complexes **40** and **40'** in the ratio 60:40. Thermally generated (η^2-aryne)titanocene also reacts with $Mo(CO)_6$ or $W(CO)_6$ immediately to afford analogous compounds.



38 **39** **40** **40'**

M = Zr, Ti; R = H, CH_3

2.3. Structures of Metallacyclic Zirconiumoxycarbene Complexes

There are many X-ray structural analyses of zirconiumoxycarbene complexes.[13, 22, 27, 28, 31, 37] By comparison, only a few metaloxycarbene complexes of titanium[35] or hafnium[32] have been crystallographically characterized (see Table 1). These complexes all belong to the same metallacyclic (η^3-allyl)metaloxycarbene structural type. This is true even when the equilibrium position in solution favors the σ-allyl isomer. The ZrCr and ZrW complexes **23a** and **23c**, respectively, are typical examples.[22] Both compounds exhibit an unsymmetrical Zr-bound η^3-allyl group. The bonds to the terminal allyl carbons are short and distances to C-2 and C-3 of the chain increasingly longer (**23a/23c**: Zr-C1 = 2.420(6)/2.421(14); Zr-C2 = 2.491(6)/2.497(12); Zr-C3 = 2.624(7)/2.621(15) Å). The very short carbon–oxygen bond in the carbene ligand is particularly striking. A comparison of the O–C carbonyl distances in the metallacyclic zirconiumoxycarbene complexes with those in traditional acyclic Fischer-type carbene complexes demonstrates this general effect very clearly: $d(O\text{-}C_{carbene}) = 1.254(5)$ Å for **23a** vs. 1.314(1) Å for $[H_5C_2O-C(CH_3)=Cr(CO)_5]$.[10] Together with the relatively long $M\text{–}C_{carbene}$ and Zr–O bonds, the short $O\text{–}C_{carbene}$ bond lengths clearly indicate acylmetalate character for these zirconiumoxycarbene complexes[39] (**A** ↔ **B**).



A **B**

All examples known thus far of the $[Cp_2M(X)OC\{=M'L_n\}R]$ complex type (M = Ti, Zr, Hf) have significant acyl character. Substitution of the *O*-bound alkyl group in Fischer-type carbene complexes by a very oxophilic metal complex fragment with strong σ-donor properties leads to a considerable polarization of the $[M-OC(R)=M(CO)_n]$ unit (see **B**).[39]

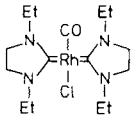
Fischer-type carbene complexes can be described as compounds with weak transition-metal–carbon π bonding. Experimental criteria for such π bonding include a short M=C bond, a higher activation barrier for rotation about the M=C bond axis, and a more stable preferred geometry for the $-O-C(R)=ML_n$ system. The composition of many

Table 1. Selected bond lengths *d* and ^{13}C NMR chemical shifts δ of the carbene carbon for metaloxycarbene complexes $[\{M^1\}O-C(R)=M^2L_n(CO)_m]$[a].

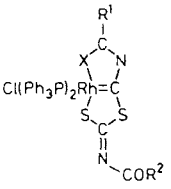
Compound	$M^2L_n(CO)_m$	$d(O\text{–}C)$ [Å]	$d(C\text{-}M^2)$ [Å]	δ [b]	Ref.
23a	$Cr(CO)_5$	1.254(5)	2.063(4)	363.7	[22]
23c	$W(CO)_5$	1.262(11)	2.198(10)	342.2	[22, 29c]
40a	$W(CO)_5$	1.21(2) [c]	2.250(8) [c]	329.7	[37]
		1.36(2) [c]	2.25(1) [c]		
25c	Co(CpCl)CO	1.286(6)	1.829(5)	311.9	[28b]
25b	Co(Cp)CO	1.287(4)	1.815(4)	311.8	[28a]
25a	Rh(Cp)CO	1.278(4)	1.925(3)	300.8	[27]
28	$V(CO)_3Cp$	1.270(4)	2.102(3)	–	[31]
31	$Nb(CO)_3Cp$	1.247(7)	2.216(6)	–	[32]

[a] $[M^1] = Cp_2Zr$ except for **31** (Cp_2Hf), R = C_4H_6 (π-allyl form) except for **40a** (R = C_6H_4). [b] Standard: TMS in C_6D_6. [c] Crystallographically independent units.

Fischer-type carbene complexes complicates or hinders the estimation of the M=C bond strength using such criteria. Thus, the high local symmetry of the $[M(CO)_5]$ fragment generally leads to low M–C rotational barriers in $[R'O-C(R)=M(CO)_5]$ carbene complexes.[40] *Lappert* et al. determined a Rh=C rotational barrier of $\Delta G^{\ddagger}_{55\,°C} \approx 16$ kcal mol^{-1} for the heteroatom-stabilized carbene complex **41**, for which such symmetry-related effects are negligible.[41] Similar rhodium carbene complexes have very short $Rh-C_{carbene}$ bond lengths (**42a**, 1.930(6) Å; **42b**, 1.930(11) Å). The rhodium–carbon bond in the acyclic rhodium carbene complex $[Cl_2(Et_2P)_2Rh=C(H)NMe_2]$ is considerably longer (1.961(11) Å).[42]



41



42a: X = O, $R^1 = R^2$ = Ph
42b: X = S, $R^1 = N(CO_2Et)_2$, R^2 = OEt

Although the carbene carbon in the rhodium carbene complex **25a** has only one heteroatom substituent, the $Rh-C_{carbene}$ bond length determined by X-ray diffraction (1.925(3) Å) is even shorter than those of **42a, b**. The metal carbene unit in **25a** has the geometry expected for a heteroolefin system. The four substituents O1, C12, C16 and D3 (= center of the Cp ring C17-C21; atom numbering analogous to the cobalt carbene complex **25c**, Fig. 1) are arranged coplanar with the central Rh=C unit (maximum deviation from the best plane: −0.09 Å for C12). Only one geometric isomer was found in the crystal. The bulky Cp substituent at rhodium has *Z* geometry with respect to the OZr group at the carbene carbon atom.[27] The cobalt carbene complex **25b** has an analogous structure in the crystal. The Co=C bond (1.815(4) Å) is much shorter than those in the open-chain cobalt carbene complexes $[(CO)_3(GePh_3)Co=C(C_2H_5)OC_2H_5]$ (1.913(11) Å),[25] $[Cp(PhS)Co=C(C_4H_{10}N_2)]$ (1.902(3) Å), or $[(PPh_3)(NO)(CO)Co=C(C_5H_{12}N_2)]$ (1.974(15) Å).[43] Complex **25b** also exhibits only one "double-bond isomer"

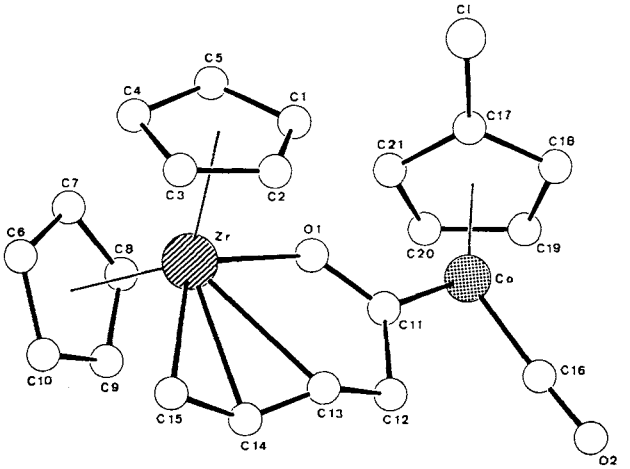


Fig. 1. Molecular structure of **25c** [28b].

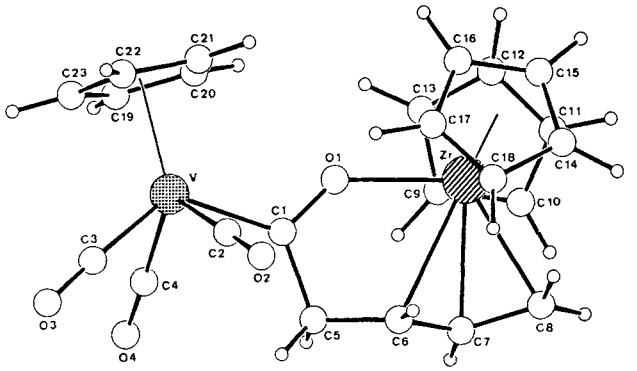


Fig. 2. Molecular structure of **28** [31].

in the crystal. The CO ligand bound to Co is *E*-oriented to the OZr group at the carbene carbon.

Compound **28** is the first vanadium carbene complex for which an X-ray structural analysis was carried out (Fig. 2). The bonding in the metallacyclic ring system is typical for complexes of this type. The η^3-allyl unit is distorted in the direction of a $(\sigma,\pi$-allyl)$ZrCp_2$ structure. The C–O bond of the carbene ligand is short [d(C1-O1) = 1.270(4) Å]; thus, **28** shows considerable acylmetal complex character. The vanadium–$C_{carbene}$ bond length of 2.102(3) Å is clearly longer than $d(V-C_{CO})$ ($\approx$ 1.90 Å). For the analogous niobium carbene complex **31**, the $Nb-C_{carbene}$ distance is 2.216(6) Å.

The tungsten carbene complex **40a** also has a very short $C_{carbene}$–O bond length (1.21(2) Å) and hence significant acylmetal complex character. The peculiarity with **40a**, however, is that in the crystal it exists as an organometallic oligomer (Fig. 3). The molecular units are joined by the carbonyl group lying *trans* to the carbene ligand. The carbonyl oxygen O6 functions as a donor ligand in the oligomer, connecting one monomeric unit with the next unit through

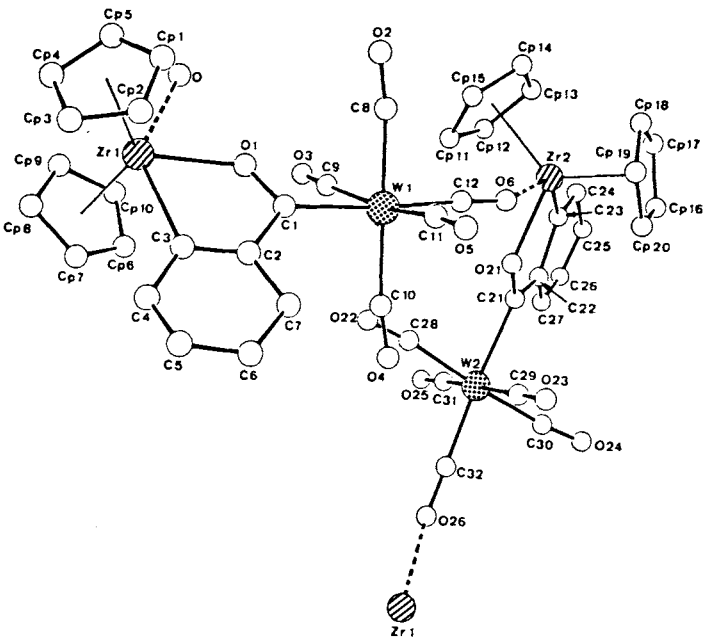


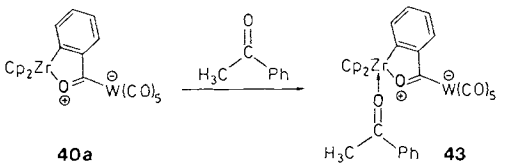
Fig. 3. Molecular structure of **40a**: the asymmetric unit with the two crystallographically independent molecules. Intermolecular interactions between Zr2 and O6 as well as Zr1 and O26 are indicated [37].

Zr. In this way, the zirconium attains an 18-electron configuration. A helical organometallic oligomeric chain is obtained from these "intermolecular" bonds, which are weak [d(Zr2-O6) = 2.49(2) Å; d(Zr1-O26) = 2.40(2) Å] compared with the Zr–O bond in the five-membered ring [d(Zr1-O1) = 2.16(2) Å].[37]

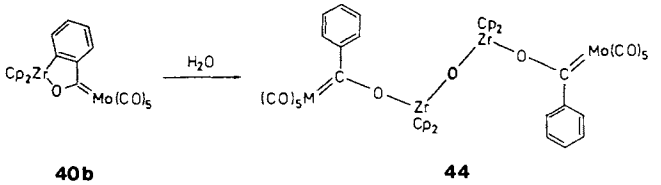
2.4. Reactivity of Metaloxycarbene Complexes

The synthesis of metaloxycarbene complexes from metallocenes is a useful extension of the classical synthesis developed by *E. O. Fischer* et al. Many reactions undergone by Fischer-type carbene complexes should also occur with the metallacyclic metaloxycarbene complexes. However, from the results thus far, it has become clear that the bonding of the electropositive early transition metal to the carbene oxygen can lead to a very specific and to some extent unexpected chemistry (e.g., of the zirconiumoxycarbene complexes).

The solid-state structure of the zirconiumoxycarbene complex **40a**, for example, is unexpected. The monomeric carbene complex unit functions as an organometallic Lewis acid in the crystal.[44] Complex **40a** even adds suitable donor ligands (e.g., methylamine) in solution. Dynamic ^{1}H NMR spectroscopy shows a fast exchange of the coordinated amine ligands with the free base in solution.[28a] Organic carbonyl compounds were added to **40a** to form 1:1 adducts: reaction with acetophenone gave complex **43** (IR: $\tilde{\nu}$(CO) = 1647 cm^{-1} vs. 1684 cm^{-1} for the free ketone[38,45]). Dynamic ^{13}C NMR spectroscopy revealed the rapid exchange of the organic carbonyl ligand [^{13}C carbonyl resonance of the bound/free acetophenone (−80 °C in CD_2Cl_2): δ = 208.4 and 198.2, respectively].



Open-chain multinuclear M−O−M-bridged bis(carbene) complexes have been obtained from the extremely moisture-sensitive metallacyclic carbene complexes and H_2O (e.g., **40b** → **44**). In the crystal, complex **44** shows an unexpected antiperiplanar arrangement of the bulky O−C(Ph)=Mo(CO)$_5$ substituents relative to the linear central (μ-oxo)bis(zirconocene) unit.[46]



The tungsten carbene complex **23c** reacts with ketones under mild conditions to give CC coupling at the η^3-allyl group. Regioselective addition of the terminal allyl carbon was observed with benzophenone, acetone, acetophenone, and pinacolone. The resulting nine-membered metallacyclic

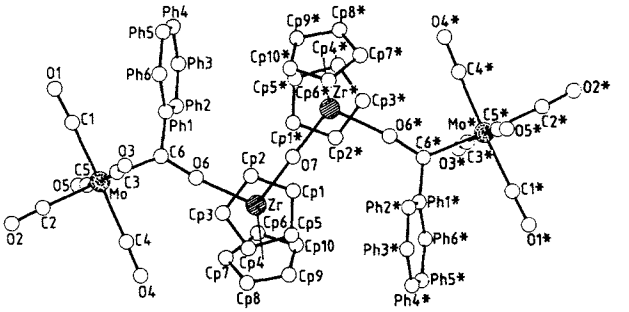
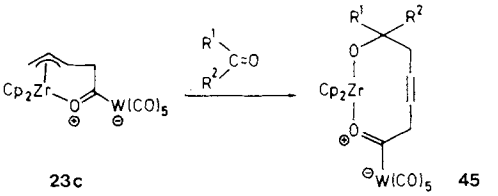


Fig. 4. Molecular structure of the bis(carbene) complex **44** [46].

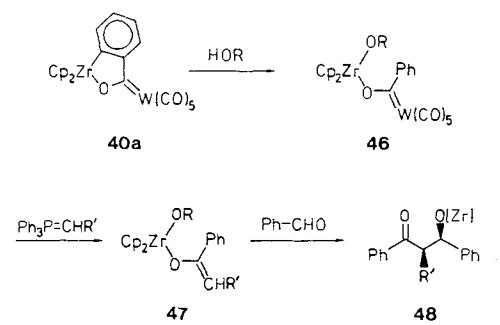
system **45** has a chiral ring conformation. When these rings were formed from prochiral ketones, diastereomeric products were observed.[47]



The C=ML$_n$ group in a Fischer-type carbene complex is similar to the C=O group in an organic carbonyl compound.[5,6] *Casey* et al. have shown that [(CO)$_5$W=C(Ph)OCH$_3$] reacts with non-stabilized phosphorous ylides in a reaction formally analogous to Wittig olefination (although probably different mechanistically); thus, reaction with $Ph_3P{=}CH_2$ gave $H_2C{=}C(Ph)OCH_3$ and [(CO)$_5$W(PPh$_3$)].[48]

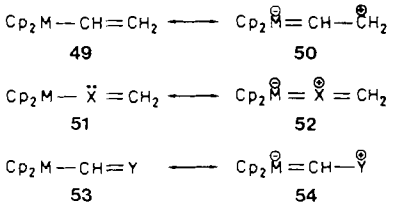
The *ortho*-hydrogen atom very effectively shields the Zr–C σ bond in **40a** against attack by electrophiles.[36] Thus far, this bond could only be broken by protic reagents. With alcohols, one obtains (alkoxy)zirconiumoxycarbene complexes **46**. Carbene complexes with chiral auxiliaries at zirconium can be prepared in this way.

The carbene complex **46** reacts quickly with $Ph_3P{=}CH_2$ at room temperature to form the corresponding zirconium enolate **47** (R′ = H). Phosphorus ylides with only one alkyl group at the ylide carbon react in the same way.[38] This reaction can be seen as the synthetic equivalent of a Wittig olefination of a carboxylate salt—a reaction that cannot be directly realized because of the reduced carbonyl activity of carboxylate salts. The zirconium enolates obtained (**47**) react readily at room temperature with benzaldehyde in a *syn*-selective aldol reaction to give **48**.[49]



3. Complexes with Metallocene–Ligand π Bonding

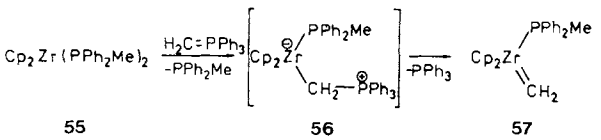
The metallocene units in the carbene complexes described in the preceding Section performed important roles as auxiliaries. Their presence facilitated (or even made possible) the synthesis of the carbene complexes and to some extent modified the properties of these carbene complexes compared with ordinary Fischer-type carbene complexes. On the other hand, the central metal atom of the bent metallocene unit can itself be bound to a carbene ligand. The formation of simple alkylidene units at titanocene Cp_2Ti or zirconocene Cp_2Zr can lead to compounds with considerable M=C π-bond character.[7] In principle, complexes with $Cp_2M=L$ π-bond character can also result through combination of the metallocene unit with organic ligands capable of metal–carbon π conjugation. Thus far, no evidence for a significant π interaction exists in (σ-alkenyl)- or (σ-alkynyl)metallocene compounds.[50] It is possible that for simple mononuclear complexes **49**, the resulting charge separation is too disadvantageous (resonance structure **50**). These unfavorable effects can be decreased by the introduction of suitable heteroatoms in the α- or β positions to the metal. In a series of systems with the general formulas **51** or **53**, a considerable π character of the $Cp_2M=L$ bond was demonstrated.



49 **50** **51** **52** **53** **54**

3.1. (Alkylidene)metallocene Complexes

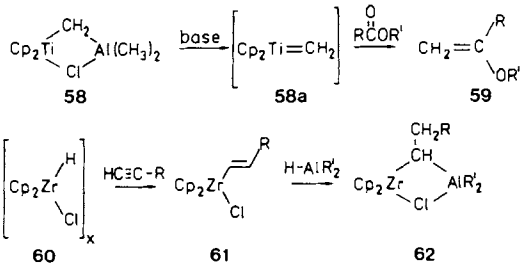
The valence orbitals of the bent metallocene that extend into the "ligand plane" can interact with the sp^2 and p orbitals of alkylidene ligands.[8] Calculations performed on model compounds attribute metallaolefin character to the $X_2Ti=CH_2$ group.[51] The $Cp_2M=CR_2$ complexes have a very electrophilic metal center. Stabilization can be achieved by occupation of the available acceptor orbital at the metal (e.g., by a phosphane). This hinders the dimerization of the (alkylidene)zirconocene to the stable 1,3-dimetallacyclobutane system. The phosphane-stabilized (carbene)zirconocene complex **57** was obtained from reaction between bis(cyclopentadienyl)bis(phosphane)zirconium(II) **55** and an ylide.[52]



55 **56** **57**

Far more significant, though, is the stabilization of the coordinatively unsaturated $Cp_2M=CHR$ unit by 1:1 complex formation with aluminum halide compounds as in **58** ("Tebbe's reagent") or **62**.[53]

The (alkylidene)metallocene complexes released from these adducts have a nucleophilic carbene carbon atom.



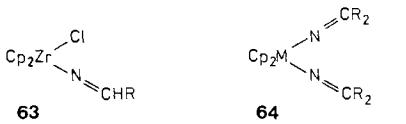
58 **58a** **59** **60** **61** **62**

They function as selective Wittig olefination reagents with organic carbonyl compounds (e.g., **58a** → **59**).[54] On reaction with olefins, **58a** affords metallacyclobutanes, which can form other (alkylidene)metallocene complexes by a formal [2 + 2] cycloreversion.[55]

3.2. π Conjugation in Metallocene Complexes

3.2.1. (Alkylidenamido)metallocene Complexes

Alkylidenamido complexes $[M]-N=CR_2$ with some M–N π character have been prepared for a range of transition metals.[56] The zirconocene complexes **63** are obtained by hydrozirconation of nitriles.[57] Bis(alkylidenamido) metallocene complexes **64** are prepared from the reaction between metallocene dihalides and lithium alkylidenamides.[58] Zirconocene, generated in situ, oxidatively adds benzophenone azine in a reaction involving N–N cleavage.[59] The X-ray structure analysis of **63a** shows a nearly linear Zr–N=CHPh unit (Zr-N-C = 170.5(5)°).[57b] This compound has the shortest reported Zr–N bond thus far [d(Zr–N) = 2.013(5) Å]. Complex **63a** exhibits the stereochemical properties of a heteroallene system.[57b]



63 **63a**: R=Ph **64** **64a**: M=Zr, R=Ph

The bis(alkylidenamido) complex **64a** adopts a similar structure. The Zr–N distances (Zr-N1 = 2.058(2) Å and Zr-N2 = 2.063(2)° Å) are only slightly longer than in **63a**. The Zr-N1-C1 angle (173.7(2)°) is somewhat greater than the Zr-N2-C2 angle (164.1(2)°) and could point to an easier rearrangement to a purely σ-bound ligand in this compound. Fast equilibration between the "inward" and "outward" oriented aryl groups at the terminal carbon atoms of the alkylidene moieties in **64a** takes place in solution.[59]

3.2.2. Metallocene Ylides

Metallocene ylides **66**–**69** are examples of compounds **53** with $X=PR_3$.[60] *Kaska* et al. obtained the zirconocene ylide **66** and its hafnium analogue by reacting metallocene dichlorides with excess methylenetriphenylphosphorane.[61] Intramolecular transylidation makes metal-substituted ylides with at least one alkyl group (usually methyl) at phosphorus readily available.[62]

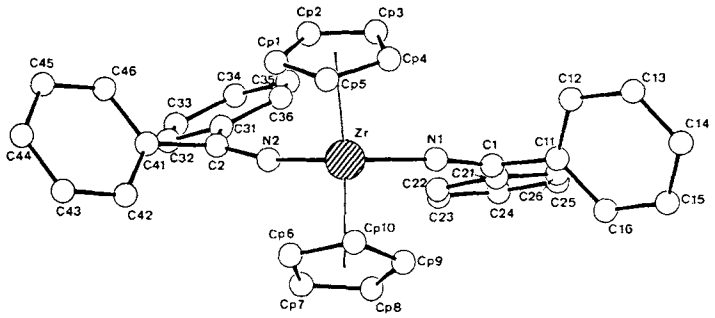
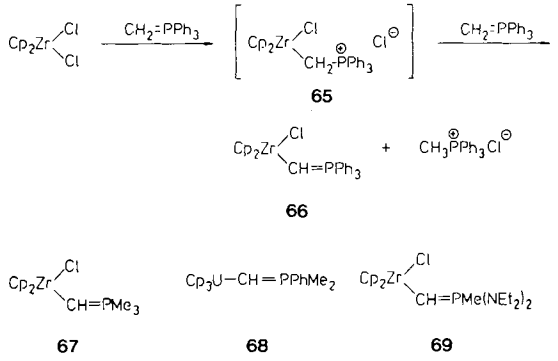
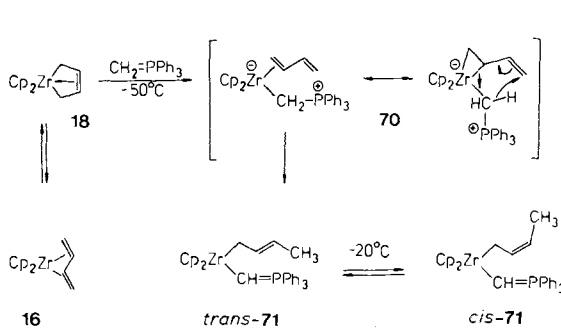


Fig. 5. Molecular structure of **64a** [59].

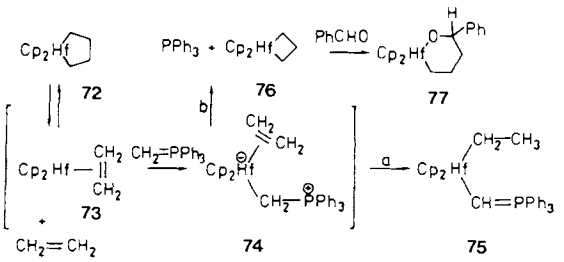


Compounds of the type $[Cp_2M(R)(CH=PPh_3)]$ (R = alkyl or aryl) can be obtained from methylenetriphenylphosphorane and (olefin)metallocene complexes in a reaction involving C–H activation and hydrogen migration.[63] From a 1:1 mixture of (*s-cis*-/*s-trans*-η^4-butadiene)hafnocene only the *s-trans* isomer reacts with the ylide under kinetic control at 0 °C. Cleavage of a C–H bond at the ylide carbon and hydrogen migration to the end of the diene chain takes place. Stereoselective formation of (*trans*-σ-2-butenyl)$Cp_2Hf(-CH=PPh_3)$ was observed. Equilibration with the *cis* isomer only occurs above 35 °C. Further stereochemical information is obtained from the reaction of the (*s-cis*-/*s-trans*-η^4-butadiene)zirconocene mixture **16/18** with $CH_2=PPh_3$. The *s-cis* isomer reacts selectively at −50 °C to give the (*trans*-σ-2-butenyl)metallocene ylide *trans*-**71**. This result possibly points to a concerted hydrogen shift in an organometallic system that occurs analogously to the homo-1,5-hydrogen shift in the purely organic methylvinylcyclopropane → hexadiene rearrangement. At −20 °C, *trans*-**71** equilibrates with *cis*-**71**.

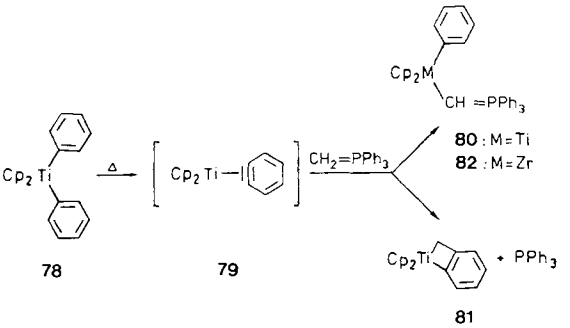
A mixture of bis(cyclopentadienyl)zirconacyclopentane and $CH_2=PPh_3$ at room temperature affords $[Cp_2Zr(C_2H_5)(CHPPh_3)]$ after expulsion of ethylene. The



analogous reaction of (η^2-benzophenone)zirconocene gives $[Cp_2Zr(OCHPh_2)(CHPPh_3)]$. From bis(cyclopentadienyl)hafnacyclopentane **72**, (η^2-ethylene)hafnocene **73** was generated (reversibly) at 90 °C by liberation of ethylene. Intermediate **73** can react with the ylide in two different ways. Addition and intramolecular hydrogen shift affords $[Cp_2Hf(C_2H_5)(CHPPh_3)]$ **75** (path a). In a competitive reaction, transfer of the whole methylene group from the ylide to the reactive organometallic intermediate and release of a molar equivalent of triphenylphosphane gives bis(cyclopentadienyl)hafnacyclobutane **76** (path b; relative product ratios a:b ≈ 2). At elevated temperature, hafnacyclobutane **76** is stable with respect to cleavage to (methylene)hafnocene and ethylene, in contrast to the titanacyclobutane analogue. In the presence of benzaldehyde, no Wittig olefination product was observed but rather the formation of the aldehyde insertion product **77**.[64]



(η^2-1,2-Didehydrobenzene)titanocene **79**, generated thermally from diphenyltitanocene **78**, reacts with methylenetriphenylphosphorane to form the products **80** and **81** competitively (70:30 at 80 °C).[63e, 65] In contrast, (aryne)zirconocene and $CH_2=PPh_3$ afford only the zirconocene ylide **82**.



For these metallocene ylides, a clearly observable increase in carbene complex character is apparent on going from hafnium through zirconium to the titanium compound. The growing π character of the $M-C_{ylide}$ bond in the series **75**, **82**, **80** is discernible from the resonances of the CH group moving to increasingly lower field in the NMR spectra [$^1H/^{13}C$: δ = 3.72/91.6 (**75**); 5.65/106.2 (**82**); 8.78/165.2 (**80**).[63d] All metallocene ylides characterized by X-ray structure analysis have nearly coplanar arrangements of the four substituents (two Cp ligands, hydrogen, and PPh_3) at the central [M]–C_{ylide} unit (see Fig. 6). The dynamic NMR spectra (coalescence of the signals of the diastereotopic Cp ligands) showed that variation of the metal resulted in different $\Delta G^{\neq}_{rot}$ for the hindered rotation about the M–$CHPPh_3$ bond. This rotational barrier increases on going from Hf (**75**) to Zr (**82**) and then Ti (**80** (see Table 2). In addition, a clear progressive

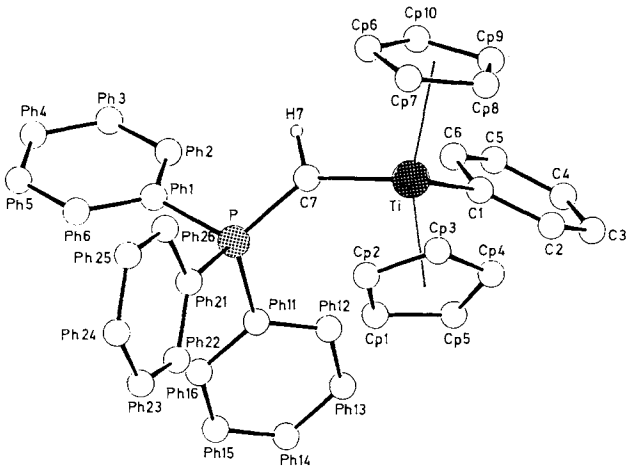


Fig. 6. Molecular structure of the titanocene ylide **80**.

Table 2. Characteristic data for the M–C(ylide) bonds in metallocene ylides **75**, **82**, and **80** [63].

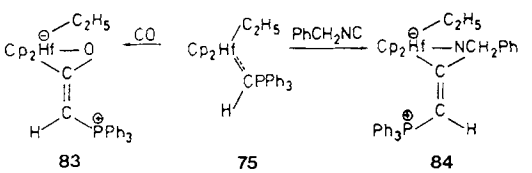
	75 (M = Hf)	**82** (M = Zr)	**80** (M = Ti)
dM–C(ylide) [Å]	2.149(6)	2.157(4)	2.033(6)
Δd [Å] [a]	0.10	0.18	0.22
$\Delta G^{\ddagger}_{rot}$ (T) [kcal mol^{-1}]	<8 (< −100 °C)	8.4 (−102 °C)	12.0 (−34 °C)

[a] Shortening of the M–C(ylide) bond owing to π interaction given relative to an adjacent M–C σ bond used as an internal standard.

shortening of the M–C_{ylide} bond length (referred to a suitable intramolecular standard) can be seen from the X-ray structure analyses of these compounds.

These data imply that the hafnium compound **75** has a comparatively small π component of the M–C_{ylide} bond; in the zirconium ylide **82** this π component is significantly greater. The titanium ylides have pronounced carbene complex character. A description of their bonding must therefore involve resonance form **54** (M = TiPh; Y = PPh_3).

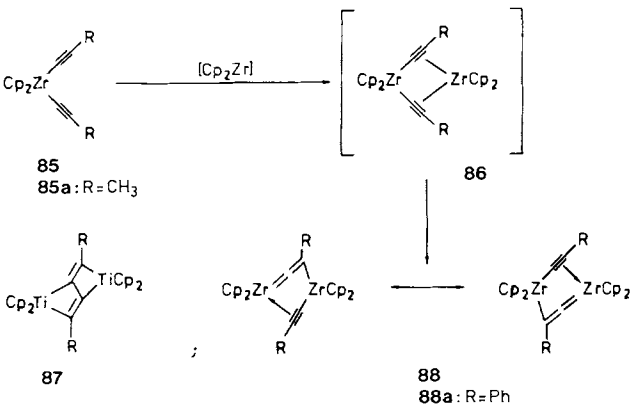
This gradually changing carbene complex character is reflected in the reactivity of the metallocene ylides. Under standard conditions, the "carbene complex" **80** does not convert acetophenone, for example, into the enolate form nor reacts with carbon monoxide or benzyl isocyanide. It behaves as a coordinatively saturated compound. By contrast, the Ph_3PCH ligands of the zirconocene and, particularly, the hafnocene ylides function as carbon bases. With CO or $PhCH_2NC$, both **82** and the more reactive **75** undergo insertion exclusively into the formally stronger M–$CHPPh_3$ bond.[61, 63g]



3.2.3. π Conjugation at Binuclear (Alkynyl)metallocene Complexes

The X-ray structure analysis of the bis(propynyl)zirconocene **85a** reveals no conjugative interaction between the π systems of the σ-bound ligands and the available acceptor orbital at zirconium. The geometry of **85a** is that of a "normal" pseudo-tetrahedrally coordinated zirconium(IV) compound with a Cp–Zr–Cp angle of 132°. The linear σ-propynyl ligands subtend an angle at Zr of 103.6(1)°. The CC triple bond length is normal (1.206(4) Å). The Zr–C σ bonds to the alkynyl ligands are not shortened (2.249(3) Å).[50, 66]

The formally d^1-configurated [$Cp_2M-C\equiv CR$] complexes are different. The reaction between $(Cp_2TiCl)_2$ and $NaC\equiv CPh$ affords the binuclear diamagnetic titanium compound **87** by CC coupling of the σ-alkynyl groups to give a bridging substituted butadiene.[67] Replacement of the titanocene group by zirconocene or hafnocene gives a completely different binuclear structural type (without CC coupling) of general formula $[Cp_2M(CCR)]_2$. Thus, compound **88** was obtained by reaction of the mononuclear bis(alkynyl)metallocene complexes **85** with a zirconocene source, either [Cp_2Zr(butadiene)] or [$Cp_2Zr(CO)_2$]. Addition to give **86** is followed by rearrangement involving σ-alkynyl ligand migration to afford **88**. Hafnium analogues of **88** may be synthesized similarly.



In contrast to the mononuclear bis(alkynyl)zirconocene **85**, complex **88a** clearly shows lengthening of the C≡C bond of the alkynyl ligand (d(C1-C2) = 1.261(2) Å). The Zr–C bond is very short (2.188(2) Å) and the bond distances Zr–C1* and Zr–C2* are 2.407(2) and 2.431(2) Å, respectively. The large Zr···Zr separation (3.506(1) Å) excludes a direct metal–metal interaction.[68] These data justify a description of these diamagnetic complexes by equivalent resonance forms involving partial carbene character of the alkynyl ligands.

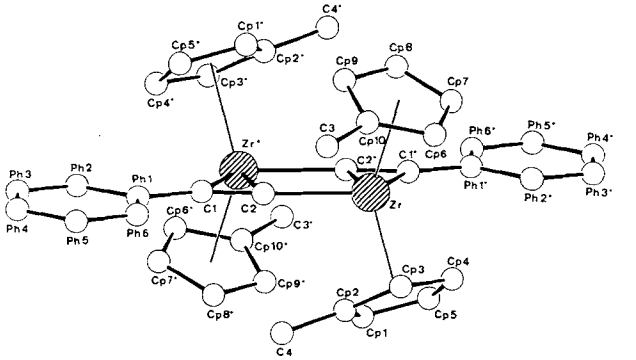


Fig. 7. Molecular structure of **88a** [68].

It seems, then, that metal–carbon π conjugation is significant in (alkynyl)metallocene compounds if the resulting unfavorable charge distribution can be compensated for. In the binuclear bis(alkynylmetallocene) complexes **88** this occurred by head-to-tail coupling of two identical mononuclear metallocene complex units.[69]

The X-ray structure analysis of $[Cp_2Zr(\mu\text{-}CH=CHPh)(\mu\text{-}Cl)ZrCp_2]$ also reveals a very short Zr–C distance (2.194(7) Å). A participation of the resonance form with metal carbene complex character should probably be used here to describe the structural properties of the binuclear (alkenyl)metallocene compound.[70]

4. Metallocene Compounds with a Metallaoxirane Structure

In the Fischer–Tropsch synthesis of hydrocarbons from CO and H_2, methylene groups on the surface of the active catalyst seem to play an important role. In particular, a series of simple experiments by *R. Pettit* et al. appears to confirm the original mechanistic proposal,[71] despite many other formulations of the reaction pathway.[72] These results demonstrate that, under various conditions, diazomethane can influence an active Fischer–Tropsch catalyst. Expulsion of N_2 possibly leads to the formation of a methylene complex at the catalyst surface. In the absence of hydrogen, the fast formation of ethylene as the sole product was observed. On addition of molecular hydrogen, the dimerization of methylene does not occur. Instead, CH_2 inserts into the M–H bonds formed on the surface. The growth of the alkyl chains occurs on the resulting surface-bound methyl groups. After removal of the catalyst, the product mixture of hydrocarbons was found to be very similar to that obtained from the Fischer–Tropsch synthesis. A detailed product analysis has shown that surface-bound methylene groups participate in this process both at the initiation and at the chain-growth steps. A schematic depiction is shown in Section 4.4.[73]

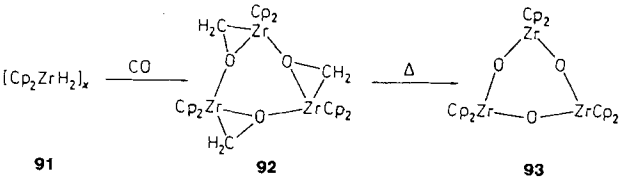
Models for this chemistry on a molecular basis have been developed. In many cases, multinuclear metal complexes with direct metal–metal bonds bridged by methylene ligands have been investigated as analogues of parts of a metal surface. Bi- and multinuclear μ-methylene complexes, "dimetallacyclopropanes", have been prepared in large numbers. A number of the reactions of these complexes show similarities to proposed steps of the Fischer–Tropsch synthesis.[74, 75] Critically, though, it has not been unambiguously established that *Pettit*'s experiments investigating parts of the Fischer–Tropsch synthesis really model the chemistry of the methylenes at the metal surface. The additional presence of a not easily reducible metal oxide (thorium oxide, zirconium oxide, titanium oxide) together with the reductive components (usually iron or cobalt) is essential for Fischer–Tropsch catalysts.[72b] Therefore, the CH_2-transforming steps might well take place at a metal oxide surface. Molecular models for this exhibit the metallaoxirane group **90** rather than the dimetallacyclopropane unit **89**.



89

90

Metallaoxiranes can be constructed stepwise by the use of hydrogen and carbon monoxide. Metallocene dihydrides can be obtained from Cp_2M precursors and H_2.[76] The reaction of $(Cp_2ZrH_2)_x$ **91** with CO affords trimeric (η^2-formaldehyde)zirconocene **92**, a compound with a metallaoxirane structure. Thermolysis of this complex leads to the expulsion of all three methylene groups and the formation of the "metal oxide" fragment $(Cp_2ZrO)_3$ **93**. This example shows that there are aspects in the chemical behavior of zirconocene-derived metallaoxiranes that are related to Fischer–Tropsch type chemistry.[77]



91 **92** **93**

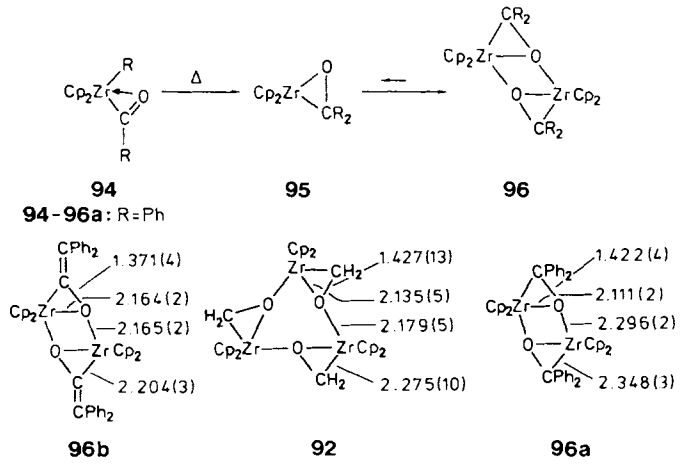
4.1. Formation of Metallaoxiranes

4.1.1. (η^2-Ketone)- and (η^2-Aldehyde)metallocene Complexes

Many metals from the right-hand side of the periodic table form complexes containing side-on–bonded ketone or aldehyde ligands; these complexes are obtained by reaction of a coordinatively unsaturated metal complex fragment with the organic carbonyl compounds. This method cannot usually be used for the synthesis of (η^2-ketone)- or (η^2-aldehyde)-complexes (metallaoxiranes) of titanocene, zirconocene, or hafnocene, since the resulting metallacyclic three-membered ring compounds are too reactive. They often add a further $R^1R^2C=O$ molecule very readily, followed by ring expansion via CC coupling.

Metallaoxiranes of zirconocene can be prepared from (η^2-acyl)zirconocene complexes **94**. The three-membered ring structure is formed easily by this route. Proceeding from (η^2-acetyl)zirconocene chloride, the ketene complex $[Cp_2Zr(\eta^2\text{-}O=C=CH_2)]$ (isolated as a dimer) was obtained after α-deprotonation.[78] (η^2-Ketone)metallocene complexes are frequently obtained by addition of a carbon nucleophile at the carbonyl group of an (η^2-acyl)metallocene. An existing σ-bonded alkyl or aryl group in a metal complex can be used in this way, via an intramolecular nucleophilic addition. The formation of (η^2-benzophenone)zirconocene **95a** (isolated at room temperature as the dimer **96a**) is a typical example (Scheme 1).[63f, 79]

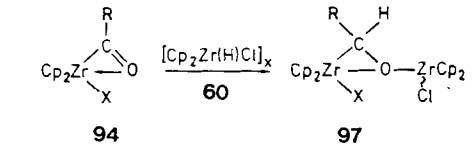
Metallaoxiranes containing the bis(cyclopentadienyl)-zirconocene fragment are characterized by oligomer formation, which occurs by coupling of the three-membered rings by bridge formation between the metallaoxirane oxygen (donor) and the metal (acceptor) in the ring plane.[80] Through this coupling, dimers or trimers with planar $(\overline{M-O-C})_n$ frameworks were obtained. The bonding between the monomeric units can be very different in strength. In the cyclodimeric (η^2-diphenylketene)zirconocene **96b**, for example, there is a central Zr_2O_2 four-membered ring with four equally short metal–oxygen distances,[78b] whereas in the cyclotrimeric (η^2-formaldehyde)zirconocene **92** the bonds between the monomers are significantly longer.[77]

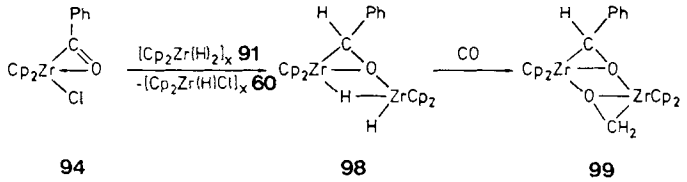


Scheme 1. Formation and structural properties of (η^2-ketone)- and (η^2-aldehyde)zirconocene complexes (bond lengths in Å).

Cyclodimeric (η^2-benzophenone)zirconocene **96a** is an even more loosely bound adduct. At high temperatures a considerable amount of the monomeric metallaoxirane **95a** is present in equilibrium.[63f, 79]

Similarly, metallaoxiranes are obtained from intermolecular addition of nucleophiles to an (η^2-acyl)metallocene. (Hydrido)metallocenes have proven particularly suitable as reagents in the formation of (η^2-RCHO)MCp_2 complexes. In general, they directly afford multinuclear metallocenes with bridging $Cp_2\overline{M-O-CHR}$ units. Typical examples are the reactions of (η^2-acyl)alkyl- or (η^2-acyl)halozirconocene complexes **94** (X = alkyl or Cl) with the hydrozirconation reagent **60**, which leads to aldehyde-bridged binuclear metallaoxiranes **97**. Analogous products were isolated in most cases from further reaction, arising from **97** by rearrangement (e.g., intramolecular alkylidene shift, see Section 4.2) and/or halide/hydride ligand exchange with **60**.[81]

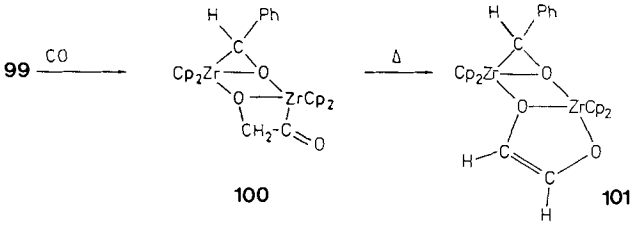




The synthesis of compounds with the $Cp_2\overline{M-O-CH_2}$ unit is a special case. They cannot be made using mononuclear formyl complexes of the Ti group as starting materials. (η^2-HCHO)MCp_2 complexes can, however, be obtained by direct carbonylation of several (hydrido)metallocenes. *Floriani* et al. showed in 1978 that the carbonylation of the oligomeric **60** leads to the binuclear (μ-η^1:η^2-formaldehyde)zirconocene complex **97a** (X = Cl, R = H), containing a metallaoxirane structural unit. The carbonylation of oligomeric **91** affords in a similar manner the cyclotrimeric **92** described above.[77]

An (η^2-benzaldehyde)Cp_2Zr/(η^2-formaldehyde)Cp_2Zr 1:1 adduct is obtained from (η^2-benzoyl)zirconocene chloride **94** in a reaction sequence involving hydrozirconation, Cl/H ligand exchange, and carbonylation. The binuclear intermediate, (η^2-benzaldehyde)zirconocene/dihydridozirconocene **98**, was isolated.[81]

In some cases, the methylene-bridged Zr–O unit appears to show a carbonylation chemistry similar to that of several binuclear μ-methylene complexes. Thus, **99** reacts at high temperature with CO at elevated pressure to give the insertion product **100**. Thermolysis of **100** affords the binuclear enediolate complex **101**. Starting from **98**, two molecules of carbon monoxide have thus been reductively coupled via a metallaoxirane intermediate.[81b]



The formation of enediolate complexes from metal alkyls also occurs via intermediates with metallaoxirane character (i.e., (η^2-ketone)metallocenes). Thus, exactly 1.5 molar equivalents of CO are taken up by the very reactive alkylmetallocene 1,1-bis(cyclopentadienyl)hafnacyclobutane **76** under ambient conditions. This affords compound **102** (Fig. 8), a 1:1 adduct of mono- and biscarbonylation products; in this case, the proposed intermediate, an (η^2-ketone)hafnocene, forms a complex with the enediolate before further reaction with carbon monoxide occurs.[83]

4.1.2. α-Metalated Ethers with Metallaoxirane Structures

(α-Metallocenyl)-substituted ethers exhibit three local minima on the (Cp_2MX)–CH_2OCH_3 hypersurface, similar to (η^2-acyl)metallocene complexes[84] [orientation of the CH_3OCH_2 ligands: η^1-O outside (**103**), η^2-O outside (**104a**), and η^2-O inside (**104b**)].

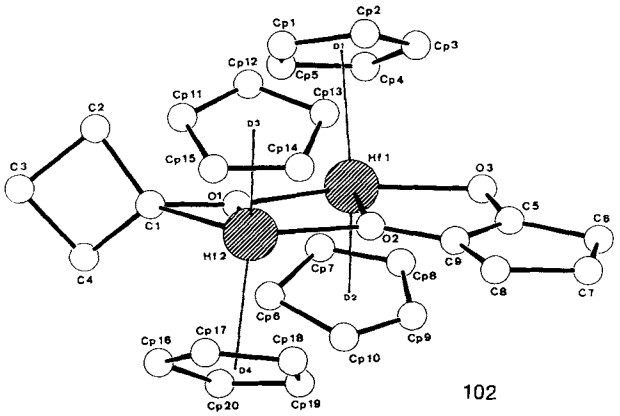


Fig. 8. Molecular structure of the (η^2-ketone)hafnocene/(enediolato)MCp_2 1:1 adduct **102**.

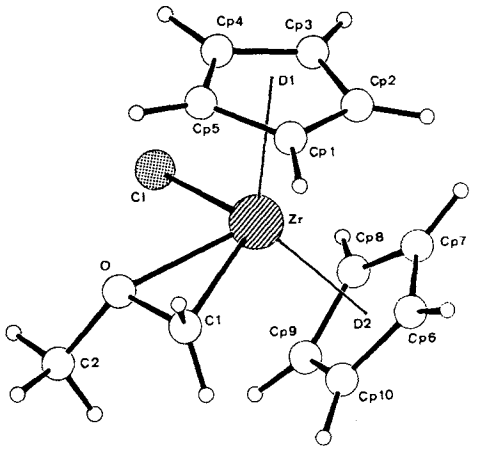
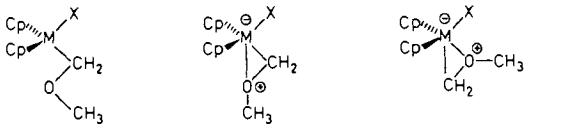


Fig. 9. Molecular structure of **106**.

The reaction of titanocene dichloride with $ClMgCH_2OCH_3$ affords the η^1 complex **105**, having the η^1-O-outside structure. In contrast to this, the reaction of zirconocene dichloride with the same Grignard reagent gives the η^2-complex **106** with η^2-O-inside orientation [d(Zr-C1) = 2.271 (5) Å; d(Zr-O) = 2.204 (3) Å; d(C1-O) = 1.414 (6) Å] (Fig. 9).[85]

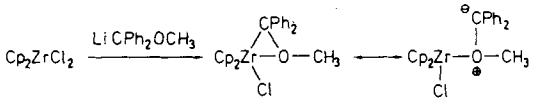


103
105: X = Cl, M = Ti

104a

104b
106: X = Cl, M = Zr

An analogous complex, **107**, is obtained by reacting Cp_2ZrCl_2 with lithiated benzhydryl methyl ether. In this case, the Zr–C bond in the three-membered ring (2.395 (6) Å) is considerably longer than the Zr–O bond (2.215 (4) Å). This can be described in terms of a contribution by the oxonium ylide resonance structure. Compounds of the type $[Cp_2\overline{Zr(X)CR_2OR}]$ can be understood as oxonium ylides internally stabilized by metallaoxirane formation.[86] The binuclear (μ-η^1:η^2-formaldehyde)zirconocene complex **97a** is a further example of this type of compound.

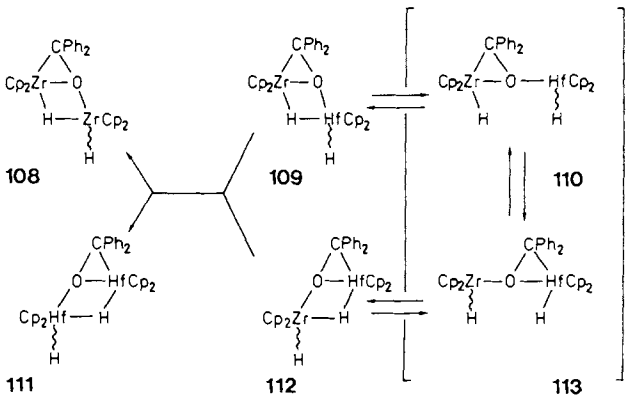


107

4.2. Dynamic Behavior of the Metallaoxiranes—Intramolecular Alkylidene Migration

A necessary requirement for CC coupling reactions of methylene units at the heterogeneous Fischer–Tropsch catalyst is the mobility of these groups on the surface. It is difficult to model this important dynamic property with simple molecular compounds. A larger molecular framework is required. The smallest possible segment of a metal oxide matrix at which such a migratory reaction can still occur is the M–O–M unit. (μ-η^1:η^2-O=CR'R^2)Metallocenes (e.g., **95**, **97**, and **98**; cf. Section 4.1.1) result from saturating this unit with ligands and bridging an M–O bond with an alkylidene moiety.

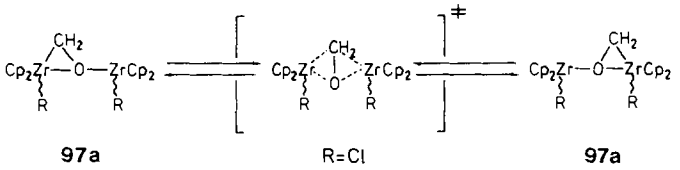
Fast, thermally induced intramolecular alkylidene shifts along the M–O–M framework are the rule with complexes containing the $\overline{Zr\text{-}CR^1R^2\text{-}O\text{-}Zr}$ group. For example, the reaction of the dimeric (η^2-benzophenone)zirconocene **96** (R = Ph) with $(Cp_2HfH_2)_x$ at room temperature affords the binuclear (μ-η^1:η^2-O=CPh$_2$) hydride-bridged Zr/Hf compound **109**. At 60 °C this complex is in equilibrium with its isomer **112**, in which the metal atoms have formally exchanged positions. Above 80 °C, subsequent statistical distribution (**108**, **109**, **111**, **112**) of metal centers is observed. The rearrangement **109** $\rightleftharpoons$ **112** requires initial opening of the hydride bridge (formation of **110**). Fast migration of the diphenylcarbene group along the Zr–O–Zr framework can then take place. Closure of the hydride bridge in the rearranged product **113** affords the isomer **112**.[63f]



108 **109** **110**

111 **112** **113**

This alkylidene migratory rearrangement occurs much faster if there is no hydride bridge at the participating metal centers that needs to be broken in the rate-determining step. This is shown by the dynamic NMR spectra of the open-chain (μ-η^1:η^2-formaldehyde)zirconocene complex **97a**. From the coalescence of the ^{1}H NMR cyclopentadienyl resonances at −140 °C, an activation barrier of $\Delta G^{\neq}_{-140\,°C} \approx$ 7 kcal mol^{-1} was estimated for the migration of the CH_2 group along the Zr–O–Zr moiety.



97a R=Cl **97a**

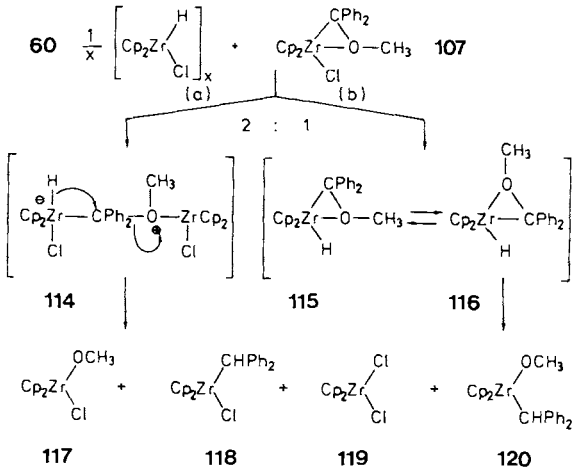
This fast automerization reaction appears to be quite general for μ-η^1:η^2-aldehyde complexes of this particular structural type (e.g., $[Cp_2\overline{ZrPh(CH_2-O)}ZrPhCp_2]$, $\Delta G^{\neq}_{-80\,°C} \approx 10$ kcal mol^{-1}; $[Cp_2\overline{ZrCl(CHMe-O)}ZrClCp_2]$, $\Delta G^{\neq}_{-8\,°C} \approx 13$ kcal mol^{-1}). Experimental studies aimed at explaining the reaction mechanism of the alkylidene migration at these binuclear metallocene complexes[81, 87] suggest a concerted "dyotropic" rearrangement.[88] Fast dyotropic

rearrangements in molecular compounds may possibly serve as models for migratory reactions on surfaces.

4.3. Alkylidene Transfer Reactions

Several metallocene complexes with metallaoxirane structural units undergo thermally induced alkylidene-coupling reactions. Thus, the compound **107** decomposes at 40 °C with formal cleavage of the diphenylcarbene moiety to give $[Cp_2Zr(Cl)OCH_3]$ and tetraphenylethylene. The methylene-bridged complex **106** is thermally more stable. It requires a temperature of ca. 200 °C to decompose to give $[Cp_2Zr(Cl)OCH_3]$ and $CH_2=CH_2$.[85]

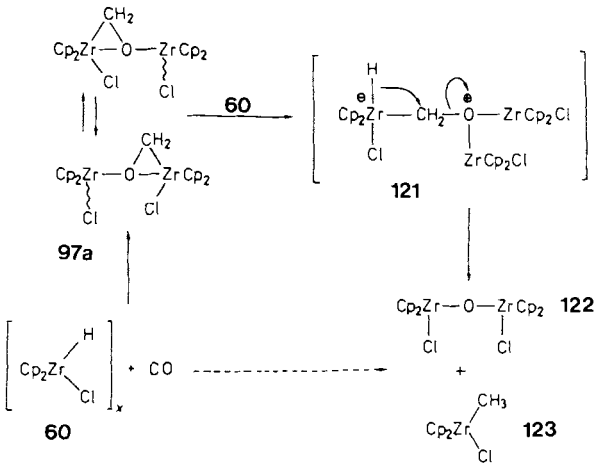
Alkylidene moieties of metallaoxiranes can be transferred to hydrido complexes and insert into the M–H bond. Thus, **107** reacts with **60** at 40 °C, transferring the CPh_2 unit to give the insertion product benzhydrylzirconocene chloride **118** and **117** [path (a)]. The nucleophilicity of the alkylidene carbon in **107** (the oxonium ylide character of this compound was confirmed by X-ray structure analysis; see Section 4.1.2) assists the formation of the intermediate **114**, which can then undergo hydride migration. The side products of this reaction, **119** and **120**, can be rationalized as resulting from intramolecular variants of this alkylidene insertion reaction occurring after Cl/H ligand exchange [path (b)].



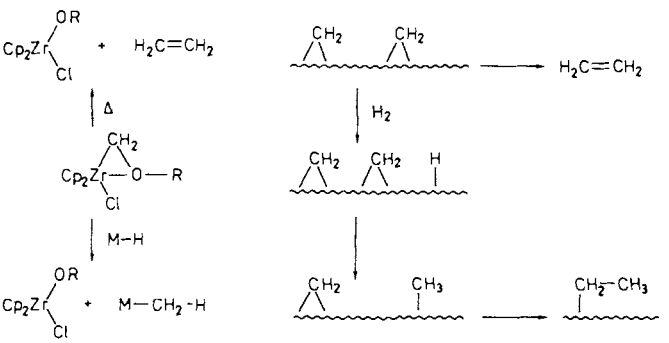
Methylene transfer from the metallaoxirane **106** to $(Cp_2Zr(H)Cl)_x$ **60** to give methylzirconocene chloride **123** is equally facile. The binuclear complex **97a**, in which the Zr–O unit is bridged by a CH_2 group stemming from CO and H_2, also reacts in this way. At 40 °C in a slow reaction, **123** and the "metal oxide" **122** are formed very cleanly.[86a]

4.4. Do Aspects of the Chemistry of Zirconocene Metallaoxiranes Have Relevance to Fischer–Tropsch Chemistry?

As far as the formation of methylene groups from CO and H_2 at an active heterogeneous Fischer–Tropsch catalyst is concerned, the question should be answered in the negative. The surface-bound CH_2 moieties there presumably result from carbon monoxide, after dissociative adsorption and

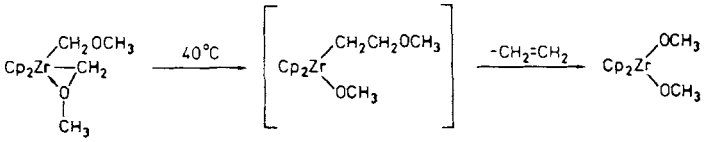


hydrogenation of carbide intermediates.[72b] The characteristic series of reactions of the surface methylenes in Fischer–Tropsch catalysis, generally accepted after the experiments of *Pettit* et al.,[73] are reflected to some extent in the chemistry of molecular metallaoxiranes. The dimerization to give olefins and the alkylidene insertion into metal–hydride bonds are particularly noteworthy. These reactions correspond, at least formally, to two important reaction steps of methylene at the catalyst (Scheme 2).



Scheme 2. A comparison between metallaoxirane reactions (left) and proposed steps in methylene chemistry at a catalyst surface (right).

The chemistry of metallaoxiranes thus far offers no simple molecular examples modeling the C–C bond-forming steps of methylene inserting into metal–carbon bonds at the catalyst. Possibly, such a reaction step takes place during the thermally induced intramolecular formation of ethylene from **124**. Further growth of alkane chains by intermolecular CH_2 insertion in this case is prohibited by fast β-OCH_3 elimination, with release of ethylene.



The thermal decomposition of metalated thioether complexes $[Cp_2Zr(CR_2SCR')_2]$ to give $[Cp_2Zr(SR')_2]$ and $R_2C=CR_2$ may also possibly occur by this pathway.[90]

5. Outlook

Very few areas of research have so consistently produced such new and interesting results over the years as the chemistry of carbene complexes. As many examples in this article show, structural features first found with "classical" Fischer-type carbene complexes are increasingly being found for other types of organometallic compounds as well. It is expected that typical carbene complex reactions will be found for related compounds with some degree of carbene complex character. Transition-metal carbene complexes are firmly established in organic synthesis with many applications. They are now helping to make accessible experimental studies at the borderline between homogeneous and heterogeneous catalysis. Mechanistically oriented studies on the chemistry of metallaoxirane compounds as described above represent one of many possible starting points.

The work described here was carried out by a group of talented co-workers whose names appear in the list of references. To them go my particular thanks for a stimulating time working together that has given me much pleasure. Part of these results were obtained during time spent at the Max-Planck-Institut für Kohlenforschung in Mülheim a. d. Ruhr. I wish to thank Professor Dr. G. Wilke for his very generous support. I am grateful to the leaders and co-workers of many groups of the Institute for help and many stimulating discussions. Financial support from the Deutsche Forschungsgemeinschaft, the Fonds der Chemischen Industrie, the Minister für Wissenschaft und Forschung des Landes Nordrhein-Westfalen, the Fritz-Thyssen-Stiftung, the Stiftung Volkswagenwerk, and the Alfried Krupp von Bohlen und Halbach-Stiftung is gratefully acknowledged.

Received: February 16, 1988;
revised: June 22, 1988 [A 712 IE]
German version: *Angew. Chem. 101* (1989) 411
Translated by Dr. *Mark G. Humphrey*

[1] E. O. Fischer, A. Maasböl, *Angew. Chem. 76* (1964) 645; *Angew. Chem. Int. Ed. Engl. 3* (1964) 580; *Chem. Ber. 100* (1967) 2445; *Adv. Organomet. Chem. 14* (1976) 1.

[2] R. R. Schrock, *J. Am. Chem. Soc. 96* (1974) 6796; R. R. Schrock, J. D. Fellmann, *ibid. 100* (1978) 3359.

[3] T. J. Katz, *Adv. Organomet. Chem. 16* (1977) 283; N. Calderon, J. P. Lawrence, E. A. Ofstead, *ibid. 17* (1979) 449; H. W. Turner, R. R. Schrock, J. D. Feldmann, S. J. Holmes, *J. Am. Chem. Soc. 105* (1983) 4942; K. J. Ivin: *Olefin-Metathesis*, Academic Press, London 1983; R. H. Grubbs in G. Wilkinson, F. G. A. Stone, E. W. Abel (Eds.): *Comprehensive Organometallic Chemistry, Vol. 8*, Pergamon Press, Oxford 1982, p. 499.

[4] R. R. Schrock, *Acc. Chem. Res. 12* (1979) 98; T. Kauffmann, R. Abeln, S. Welke, D. Wingbermühle, *Angew. Chem. 98* (1986) 927; *Angew. Chem. Int. Ed. Engl. 25* (1986) 909.

[5] C. P. Casey in H. Alper (Ed.): *Transition Metal Organometallics in Organic Synthesis, Vol. 1*, Academic Press, New York 1976, 190; F. J. Brown, *Prog. Inorg. Chem. 27* (1980) 1; K. H. Dötz, *Angew. Chem. 96* (1984) 573; *Angew. Chem. Int. Ed. Engl. 23* (1984) 587; W. D. Wulff, P.-C. Tang, *J. Am. Chem. Soc. 106* (1984) 434, 1132; C. P. Casey, N. L. Hornung, W. P. Kosar, *ibid. 109* (1987) 4908; M. Brookhart, W. B. Studabaker, *Chem. Rev. 87* (1987) 411; R. Aumann, H. Heinen, C. Krüger, *Chem. Ber. 120* (1987) 1287; A. Parlier, H. Rudler, N. Platzer, M. Fontanille, A. Soum, *J. Chem. Soc. Dalton Trans. 1987*, 1041.

[6] K. S. Chan, W. D. Wulff, *J. Am. Chem. Soc. 108* (1986) 5229; Y.-C. Xu, W. D. Wulff, *J. Org. Chem. 52* (1987) 3263.

[7] C. N. Wilker, R. Hoffmann, O. Eisenstein, *Nouv. J. Chim. 7* (1983) 535; *J. Am. Chem. Soc. 104* (1982) 632; J. Ushio, H. Nakatsuji, T. Yonezawa, *ibid. 106* (1984) 5892; E. A. Carter, W. A. Goddard III, *ibid. 108* (1986) 4746.

[8] J. W. Lauher, R. Hoffmann, *J. Am. Chem. Soc. 98* (1976) 1729.

[9] J. L. Petersen, L. F. Dahl, *J. Am. Chem. Soc. 96* (1974) 2248; *ibid. 97* (1975) 6416, 6422; J. L. Petersen, D. L. Lichtenberger, R. F. Fenske, L. F. Dahl, *ibid. 97* (1975) 6433; H. H. Brintzinger, L. S. Bartell, *ibid. 92* (1970) 1105; H. H. Brintzinger, L. L. Lohr, Jr., K. L. Tang Wong, *ibid. 97* (1975) 5146; J. H. Osborne, A. L. Rheingold, W. C. Trogler, *ibid. 107* (1985) 7945; L. Zhu, N. M. Kostić, *J. Organomet. Chem. 335* (1987) 395.

[10] Review: U. Schubert, H. Fischer, P. Hofmann, K. Weiss, K. H. Dötz, F. R. Kreissl: *Transition Metal Carbene Complexes*, Verlag Chemie, Weinheim 1983.

[11] E. O. Fischer, S. Fontana, *J. Organomet. Chem. 40* (1972) 159; H. G. Raubenheimer, E. O. Fischer, *ibid. 91* (1975) C23; see also C. P. Casey, R. E. Palermo, A. L. Rheingold, *J. Am. Chem. Soc. 108* (1986) 549.

[12] C. M. Jensen, C. B. Knobler, H. D. Kaesz, *J. Am. Chem. Soc. 106* (1984) 5926; E. O. Fischer, V. Kiener, D. S. P. Bunbury, E. Frank, P. F. Lindley, O. S. Mills, *Chem. Commun. 1968*, 1378; W. Wong, K. W. Chiu, G. Wilkinson, A. M. R. Galas, M. Thornton-Pett, M. B. Hursthouse, *J. Chem. Soc. 1983*, 1557; A. W. Parkins, E. O. Fischer, G. Huttner, D. Regler, *Angew. Chem. 82* (1970) 635; *Angew. Chem. Int. Ed. Engl. 9* (1970) 633.

[13] a) W. Petz, *J. Organomet. Chem. 72* (1974) 369; J. Pebler, W. Petz, *Z. Naturforsch. B29* (1974) 658; b) R. S. Threlkel, J. E. Bercaw, *J. Am. Chem. Soc. 103* (1981) 2650; c) P. T. Barger, J. E. Bercaw, *Organometallics 3* (1984) 278; *J. Organomet. Chem. 201* (1980) C39; G. S. Ferguson, P. T. Wolczanski, *J. Am. Chem. Soc. 108* (1986) 8293; d) P. T. Wolczanski, R. S. Threlkel, J. E. Bercaw, *ibid. 101* (1979) 218; e) P. T. Barger, B. D. Santarsiero, J. Armantrout, J. E. Bercaw, *ibid. 106* (1984) 5178.

[14] M. F. Lappert, A. J. Oliver, *J. Chem. Soc. Dalton Trans. 1974*, 65; M. F. Lappert, P. L. Pyl, *ibid. 1977*, 2172.

[15] a) A. J. Hartshorn, M. F. Lappert, K. Turner, *J. Chem. Soc. Dalton Trans. 1978*, 348; M. J. Doyle, M. F. Lappert, P. L. Pyl, P. Terreros, *ibid. 1984*, 2355, and references cited therein; b) M. F. Lappert, A. J. Oliver, *J. Chem. Soc. Chem. Commun. 1972*, 274; c) *J. Chem. Soc. Dalton Trans. 1974*, 65; d) P. B. Hitchcock, M. F. Lappert, G. M. McLaughlin, A. J. Oliver, *ibid. 1974*, 68.

[16] A. Stockis, R. Hoffmann, *J. Am. Chem. Soc. 102* (1980) 2952; Recent articles: E. Negishi, S. J. Holmes, J. M. Tour, J. A. Miller, *ibid. 107* (1985) 2568; G. Erker, U. Dorf, A. L. Rheingold, *Organometallics 7* (1988) 138; S. L. Buchwald, B. T. Watson, J. C. Huffman, *J. Am. Chem. Soc. 109* (1987) 2544; W. A. Nugent, D. L. Thorn, R. L. Harlow, *ibid. 109* (1987) 2788, and references cited therein.

[17] a) S. A. Cohen, P. R. Auburn, J. E. Bercaw, *J. Am. Chem. Soc. 105* (1983) 1136; b) H. Lehmkuhl, R. Schwickardi, *J. Organomet. Chem. 303* (1986) C43.

[18] G. Erker, J. Wicher, K. Engel, F. Rosenfeldt, W. Dietrich, C. Krüger, *J. Am. Chem. Soc. 102* (1980) 6344.

[19] a) G. Erker, J. Wicher, K. Engel, C. Krüger, *Chem. Ber. 115* (1982) 3300; G. Erker, K. Engel, C. Krüger, A.-P. Chiang, *ibid. 115* (1982) 3311; U. Dorf, K. Engel, G. Erker, *Organometallics 2* (1983) 462; G. Erker, K. Engel, C. Krüger, G. Müller, *ibid. 3* (1984) 128; C. Krüger, G. Müller, G. Erker, U. Dorf, K. Engel, *ibid. 4* (1985) 215; G. Erker, K. Engel, U. Korek, P. Czisch, H. Berke, P. Caubere, P. Vanderesse, *ibid. 4* (1985) 1531; G. Erker, T. Mühlenbernd, R. Benn, A. Rufinska, Y.-H. Tsay, C. Krüger, *Angew. Chem. 97* (1985) 336; *Angew. Chem. Int. Ed. Engl. 24* (1985) 321; G. Erker, T. Mühlenbernd, A. Rufinska, R. Benn, *Chem. Ber. 120* (1987) 507; b) H. Yasuda, Y. Kajihara, K. Mashima, K. Nagasuna, K. Lee, A. Nakamura, *Organometallics 1* (1982) 388; Y. Kai, N. Kanehisha, K. Miki, N. Kasai, K. Mashima, K. Nagasuna, H. Yasuda, A. Nakamura, *J. Chem. Soc. Chem. Comm. 1982*, 191; c) R. Bechthaus, K.-H. Thiele, *J. Organomet. Chem. 268* (1987) C7; d) R. Benn, G. Schroth, *ibid. 228* (1982) 71.

[20] Reviews: a) G. Erker, C. Krüger, G. Müller, *Adv. Organomet. Chem. 24* (1985) 1; b) H. Yasuda, K. Tatsumi, A. Nakamura, *Acc. Chem. Res. 18* (1985) 120; H. Yasuda, A. Nakamura, *Angew. Chem. 99* (1987) 745; *Angew. Chem. Int. Ed. Engl. 26* (1987) 723.

[21] a) G. Erker, K. Engel, J. L. Atwood, W. E. Hunter, *Angew. Chem. 95* (1983) 506; *Angew. Chem. Int. Ed. Engl. 22* (1983) 494, 675; G. Erker, U. Dorf, *Angew. Chem. 95* (1983) 800; *Angew. Chem. Int. Ed. Engl. 22* (1983) 777, 1066; b) H. Yasuda, Y. Kajihara, K. Mashima, K. Nagasuna, A. Nakamura, *Chem. Lett. 1981*, 671; M. Akita, H. Yasuda, A. Nakamura, *ibid. 1983*, 217.

[22] G. Erker, U. Dorf, R. Benn, R.-D. Reinhardt, J. L. Petersen, *J. Am. Chem. Soc. 106* (1984) 7649.

[23] G. Erker, R. Lecht, *J. Organomet. Chem. 311* (1986) 45.

[24] a) E. O. Fischer, F. R. Kreißl, E. Winkler, C. G. Kreiter, *Chem. Ber. 105* (1972) 588; b) M. F. Semmelhack, R. Tamura, *J. Am. Chem. Soc. 105* (1983) 4099, and references cited therein; E. O. Fischer, H. J. Beck, C. G. Kreiter, J. Lynch, J. Müller, E. Winkler, *Chem. Ber. 105* (1972) 162.

[25] Cf. [24a]; D. J. Darensbourg, M. Y. Darensbourg, *Inorg. Chem. 9* (1970) 1691; F. Carre, G. Cerveau, E. Colomer, R. J. P. Corriu, J. C. Young, *J. Organomet. Chem. 179* (1979) 215; *ibid. 205* (1981) 31; Y. Yamamoto, H. Yamazaki, *Bill. Chem. Soc. Jpn. 48* (1975) 3691.

[26] H. Werner, W. Paul, R. Feser, R. Zolk, P. Thometzek, *Chem. Ber. 118* (1985) 261; D. B. Jacobson, B. S. Freiser, *J. Am. Chem. Soc. 107* (1985) 5870; H. C. Clark, K. J. Reimer, *Inorg. Chem. 14* (1975) 2133; P. J. Fraser, W. R. Roper, F. G. A. Stone, *J. Chem. Soc. Dalton Trans. 1974*, 760; P. R. Branson, R. A. Cable, M. Green, M. K. Lloyd, *J. Chem. Soc. Chem. Commun. 1974*, 364; P. Hong, N. Nishii, K. Sonogashira, N. Hagihara, *ibid. 1972*, 993.

[27] G. Erker, R. Lecht, Y.-H. Tsay, C. Krüger, *Chem. Ber. 120* (1987) 1763.

[28] a) G. Erker, R. Lecht, J. L. Petersen, H. Bönnemann, *Organometallics 6* (1987) 1962; b) G. Erker, R. Lecht, C. Krüger, Y.-H. Tsay, H. Bönnemann, *J. Organomet. Chem. 326* (1987) C75.

[29] a) R. Lecht, *Dissertation*, Universität Würzburg 1987; b) J. L. Simunic, A. R. Pinhas, *Organometallics 6* (1987) 1358; c) U. Dorf, *Dissertation*, Universität Bochum 1985.

[30] J. Martin, C. Moise, J. Tirouflet, *C. R. Seances Acad. Sci. Ser. 2, 292* (1981) 1143.

[31] G. Erker, R. Lecht, R. Schlund, K. Angermund, C. Krüger, *Angew. Chem. 99* (1987) 708; *Angew. Chem. Int. Ed. Engl. 26* (1987) 666.

[32] X-ray crystal structure analysis: E. Herdtweck, unpublished.

[33] Cf. M. F. Lappert, C. R. C. Milne, *J. Chem. Soc. Chem. Commun. 1978*, 925.

[34] G. Erker, T. Mühlenbernd, R. Benn, A. Rufinska, *Organometallics 5* (1986) 402.

[35] K. Mashima, K. Jyodoi, A. Ohyoshi, H. Takaya, *J. Chem. Soc. Chem. Commun. 1986*, 1145; K. Mashima, K. Jyodoi, A. Ohyoshi, H. Takaya, *Organometallics 6* (1987) 885.

[36] a) K. Kropp, G. Erker, *Organometallics 1* (1982) 1246; b) G. Erker, K. Kropp, *J. Am. Chem. Soc. 101* (1979) 3659; *J. Organomet. Chem. 194* (1980) 45; c) S. L. Buchwald, B. T. Watson, J. C. Huffman, *J. Am. Chem. Soc. 108* (1986) 7411.

[37] G. Erker, U. Dorf, R. Mynott, Y.-H. Tsay, C. Krüger, *Angew. Chem. 97* (1985) 572; *Angew. Chem. Int. Ed. Engl. 24* (1985) 584.

[38] G. Erker, in A. de Meijere, H. tom Dieck (Eds.): *Organometallics in Organic Synthesis*, Springer Verlag, Berlin 1987, p. 143; *Polyhedron 7* (1988) 2451.

[39] P. M. Fritz, M. Steimann, W. Beck, *Chem. Ber. 120* (1987) 253, and references cited therein.

[40] C. G. Kreiter, V. Formacek, *Angew. Chem. 84* (1972) 155; *Angew. Chem. Int. Ed. Engl. 11* (1972) 141; E. O. Fischer, H. Hollfelder, P. Friedrich, F. R. Kreißl, G. Huttner, *Chem. Ber. 110* (1977) 3467.

[41] M. J. Doyle, M. F. Lappert, *J. Chem. Soc. Chem. Commun. 1974*, 679.

[42] M. Cowie, J. A. Ibers, *Inorg. Chem. 15* (1976) 552; K. Itoh, I. Matsuda, F. Ueda, Y. Ishii, J. A. Ibers, *J. Am. Chem. Soc. 99* (1977) 2118; M. J. Doyle, M. F. Lappert, G. M. McLaughlin, J. McMeeking, *J. Chem. Soc. Dalton Trans. 1974*, 1494; A. W. Coleman, P. B. Hitchcock, M. F. Lappert, R. K. Maskell, H. J. Müller, *J. Organomet. Chem. 296* (1985) 173; C. Bianchini, C. Mealli, A. Meli, M. Sabat, J. Silvestre, R. Hoffmann, *Organometallics 5* (1986) 1733; P. B. Hitchcock, M. F. Lappert, G. M. McLaughlin, A. J. Oliver, *J. Chem. Soc. Dalton Trans. 1974*, 68; B. Cetinkaya, M. F. Lappert, G. M. McLaughlin, K. Turner, *ibid. 1974*, 1591.

[43] D. W. Macomber, R. D. Rogers, *Organometallics 4* (1985) 1485; A. W. Coleman, P. B. Hitchcock, M. F. Lappert, R. K. Maskell, H. J. Müller, *J. Organomet. Chem. 250* (1983) C9.

[44] a) M. Appel, W. Sacher, W. Beck, *J. Organomet. Chem. 333* (1987) 237; 322 (1987) 351; M. Appel, W. Beck, *ibid. 319* (1987) C1; b) S. F. Pedersen, J. C. Dewan, R. R. Eckman, K. B. Sharpless, *J. Am. Chem. Soc. 109* (1987) 1279; M. T. Reetz, M. Hüllmann, T. Seitz, *Angew. Chem. 99* (1987) 478; *Angew. Chem. Int. Ed. Engl. 26* (1987) 477; H. Hartmann, A. F. Abdel Hady, K. Sartor, J. Weetman, G. Helmchen, *ibid. 99* (1987) 1188 and *26* (1987) 1143; T. Poll, J. O. Metter, G. Helmchen, *ibid. 97* (1985) 116 and *24* (1985) 112; c) T. R. Kelly, A. Whiting, N. S. Chandrakumar, *J. Am. Chem. Soc. 108* (1986) 3510; S. Danishefsky, J. F. Kerwin, Jr., S. Kobayashi, *ibid. 104* (1982) 358.

[45] G. Erker, M. T. Ashby, M. Aulbach, unpublished; cf. B. P. Susz, P. Chalandon, *Helv. Chim. Acta 41* (1958) 1332.

[46] G. Erker, U. Dorf, C. Krüger, Y.-H. Tsay, *Organometallics 6* (1987) 680.

[47] G. Erker, F. Sosna, unpublished.

[48] T. J. Burkhardt, C. P. Casey, *J. Am. Chem. Soc. 94* (1972) 6543.

[49] G. Erker, P. Czisch, unpublished; cf. Y. Yamamoto, K. Maruyama, *Tetrahedron Lett. 21* (1980) 4607; D. A. Evans, L. R. McGee, *ibid. 21* (1980) 3975; M. T. Reetz, R. Peter, *ibid. 22* (1981) 4691.

[50] D. J. Cardin, M. F. Lappert, C. L. Raston: *Chemistry of Organo-Zirconium and -Hafnium Compounds*. Wiley, New York 1986; P. C. Wailes, R. S. P. Coutts, H. Weigold: *Organometallic Chemistry of Titanium, Zirconium and Hafnium*, Academic Press, New York 1974.

[51] R. J. Goddard, R. Hoffmann, E. D. Jemmis, *J. Am. Chem. Soc. 102* (1980) 7667; A. K. Rappé, W. A. Goddard III, *ibid. 104* (1982) 297; M. M. Francl, W. J. Pietro, R. F. Hout, Jr., W. J. Hehre, *Organometallics 2* (1983) 281, 815; M. M. Francl, W. J. Hehre, *ibid. 2* (1983) 457; T. E. Taylor, M. B. Hall, *J. Am. Chem. Soc. 106* (1984) 1576; D. S. Marynick, C. M. Kirkpatrick, *ibid. 107* (1985) 1993; A. R. Gregory, E. A. Mintz, *ibid. 107* (1985) 2179.

[52] J. Schwartz, K. I. Gell, *J. Organomet. Chem. 184* (1980) C1.

[53] F. N. Tebbe, G. W. Parshall, G. S. Reddy, *J. Am. Chem. Soc. 100* (1978) 3611; E. V. Anslyn, R. H. Grubbs, *ibid. 109* (1987) 4880; S. M. Clift, J. Schwartz, *ibid. 106* (1984) 8300; F. M. Hartner, Jr., S. M. Clift, J. Schwartz, T. H. Tulip, *Organometallics 6* (1987) 1346.

[54] K. A. Brown-Wensley, S. L. Buchwald, L. F. Cannizzo, L. E. Clawson, S. Ho, J. D. Meinhart, J. R. Stille, D. Strauss, R. H. Grubbs, *Pure Appl. Chem. 55* (1983) 1733; S. H. Pine, R. Zahler, D. A. Evans, R. H. Grubbs, *J. Am. Chem. Soc. 102* (1980) 3270; S. H. Pine, R. J. Pettit, G. Geib, S. G. Cruz, C. H. Gallego, T. Tijerina, R. D. Pine, *J. Org. Chem. 50* (1985) 1212; W. A. Kinney, M. J. Coghlan, L. A. Paquette, *J. Am. Chem. Soc. 107* (1985) 7352; T. Okazoe, K. Takai, K. Oshima, K. Utimoto, *J. Org. Chem. 52* (1987) 4410; see also G. M. Smith, M. Sabat, T. J. Marks, *J. Am. Chem. Soc. 109* (1987) 1854.

[55] F. Bickelhaupt, *Angew. Chem. 99* (1987) 1020; *Angew. Chem. Int. Ed. Engl. 26* (1987) 990.

[56] a) M. Kilner, *Adv. Organomet. Chem. 10* (1972) 162; b) Selected examples: R. E. Cramer, K. Panchanatheswaran, J. W. Gilje, *J. Am. Chem. Soc. 106* (1984) 1853; M. Green, R. J. Mercer, C. E. Morton, A. G. Orpen, *Angew. Chem. 97* (1985) 422; *Angew. Chem. Int. Ed. Engl. 24* (1985) 422; J. E. Bercaw, D. L. Davies, P. T. Wolczanski, *Organometallics 5* (1986) 443; I. A. Latham, G. J. Leigh, G. Huttner, I. Jibril, *J. Chem. Soc. Dalton Trans. 1986*, 377; M. Bochmann, L. M. Wilson, *J. Chem. Soc. Chem. Commun. 1986*, 1610; H. Werner, W. Knaup, M. Dziallas, *Angew. Chem. 99* (1987) 277; *Angew. Chem. Int. Ed. Engl. 26* (1987) 248; R. F. Jordan, C. S. Bajgur, W. E. Dasher, A. L. Rheingold, *Organometallics 6* (1987) 1041; E. J. Roskamp, S. F. Pedersen, *J. Am. Chem. Soc. 109* (1987) 3152; D. S. Richeson, J. F. Mitchell, K. H. Theopold, *ibid. 109* (1987) 5868.

[57] a) P. Etievant, G. Tainturier, G. Gautheron, *C. R. Seances Acad. Sci. Ser. C283* (1976) 233; *Bull. Soc. Chim. Fr. 1978*, 292; b) G. Erker, W. Frömberg, J. L. Atwood, W. E. Hunter, *Angew. Chem. 96* (1984) 72; *Angew. Chem. Int. Ed. Engl. 23* (1984) 68; W. Frömberg, G. Erker, *J. Organomet. Chem. 280* (1985) 343.

[58] a) K. Farmery, M. Kilner, *J. Organomet. Chem. 16* (1969) P51; H. R. Keable, M. Kilner, *Chem. Commun. 1971*, 349; W. Clegg, R. Snaith, H. M. M. Shearer, K. Wade, G. Whitehead, *J. Chem. Soc. Dalton Trans. 1983*, 1309; b) M. R. Collier, M. F. Lappert, J. McMeeking, *Inorg. Nucl. Chem. Lett. 7* (1971) 689.

[59] G. Erker, W. Frömberg, C. Krüger, E. Raabe, *J. Am. Chem. Soc. 110* (1988) 2400.

[60] W. C. Kaska, *Coord. Chem. Rev. 48* (1983) 1.

[61] J. C. Baldwin, N. L. Keder, C. E. Strouse, W. C. Kaska, *Z. Naturforsch. B35* (1980) 1289.

[62] H. Schmidbaur, W. Scharf, H.-J. Füller, *Z. Naturforsch. B32* (1977) 858; W. Scharf, D. Neugebauer, U. Schubert, H. Schmidbaur, *Angew. Chem. 90* (1978) 628; *Angew. Chem. Int. Ed. Engl. 17* (1978) 601; K. I. Gell, J. Schwartz, *Inorg. Chem. 19* (1980) 3207; G. W. Rice, G. B. Ansell, M. A. Modrick, S. Zentz, *Organometallics 2* (1983) 154; H. Schmidbaur, R. Pichl, *Z. Naturforsch. B40* (1985) 352; H. Schmidbaur, R. Pichl, G. Müller, *ibid. B41* (1986) 395; *Angew. Chem. 98* (1986) 572; *Angew. Chem. Int. Ed. Engl. 25* (1986) 574; *Chem. Ber. 120* (1987) 39.

[63] a) G. Erker, P. Czisch, R. Mynott, *Z. Naturforsch. B40* (1985) 1177; b) G. Erker, P. Czisch, C. Krüger, J. M. Wallis, *Organometallics 4* (1985) 2059; c) G. Erker, P. Czisch, R. Mynott, Y.-H. Tsay, C. Krüger, *ibid. 4* (1985) 1310; d) G. Erker, P. Czisch, R. Mynott, *J. Organomet. Chem. 334* (1987) 91; d) H. J. R. de Boer, O. S. Akkerman, F. Bickelhaupt, G. Erker, P. Czisch, R. Mynott, J. M. Wallis, C. Krüger, *Angew. Chem. 98* (1986) 641; *Angew. Chem. Int. Ed. Engl. 25* (1986) 639; f) G. Erker, U. Dorf, P. Czisch, J. L. Petersen, *Organometallics 5* (1986) 668; g) G. Erker, U. Korek, J. L. Petersen, *J. Organomet. Chem. 355* (1988) 121.

[64] Cf. W. R. Tikkanen, J. L. Petersen, *Organometallics 3* (1984) 1651.

[65] Cf. R. Neidlein, A. Rufinska, H. Schwager, G. Wilke, *Angew. Chem. 98* (1986) 643; *Angew. Chem. Int. Ed. Engl. 25* (1986) 640; C. Krüger, K. Laakmann, G. Schroth, H. Schwager, G. Wilke, *Chem. Ber. 120* (1987) 471; A. R. Bulls, W. P. Schaefer, M. Serfas, J. E. Bercaw, *Organometallics 6* (1987) 1219.

[66] W. Frömberg, *Dissertation*, Universität Bochum 1986; X-ray crystal structure analysis: C. Krüger, E. Raabe, W. Frömberg, unpublished.

[67] J. H. Teuben, H. J. de Liefde Meijer, *J. Organomet. Chem. 17* (1969) 87; D. G. Sekutowski, G. D. Stucky, *J. Am. Chem. Soc. 98* (1976) 1376.

[68] G. Erker, W. Frömberg, R. Mynott, B. Gabor, C. Krüger, *Angew. Chem. 98* (1986) 456; *Angew. Chem. Int. Ed. Engl. 25* (1986) 463; G. Erker, *Jahrb. Akad. Wiss. Göttingen 1985*, 19.

[69] J. L. Atwood, W. E. Hunter, A. L. Wyada, W. J. Evans, *Inorg. Chem. 20* (1981) 4115; W. J. Evans, I. Bloom, W. E. Hunter, J. L. Atwood, *Organometallics 2* (1983) 709; B. Schubert, E. Weiss, *Chem. Ber. 116* (1983) 3212; N. A. Bell, I. W. Nowell, G. E. Coates, H. M. M. Shearer, *J. Organomet. Chem. 273* (1984) 179; P. N. V. P. Kumar, E. D. Jemmis, *J. Am. Chem. Soc. 110* (1988) 125.

[70] G. Erker, K. Kropp, J. L. Atwood, W. E. Hunter, *Organometallics 2* (1983) 1555.

[71] F. Fischer, H. Tropsch, *Brennst. Chem. 7* (1926) 97; *Chem. Ber. 59* (1926) 830.

[72] a) J. Kummer, P. H. Emmett, *J. Am. Chem. Soc. 75* (1953) 5177; H. Pichler, H. Schultz, *Chem. Ing. Tech. 42* (1970) 1160; b) H. H. Storch, N. Goulombic, R. B. Anderson; *The Fischer-Tropsch and Related Syntheses*, Wiley, New York 1951; R. Eisenberg, D. E. Hendriksen, *Adv. Catal. 28*(1979) 79; E. L. Mutterties, J. Stein, *Chem. Rev. 79* (1979) 479; W. A. Herrmann, *Angew. Chem. 94* (1982) 118; *Angew. Chem. Int. Ed. Engl. 21* (1982) 117; C. K. Rofer-DePoorter, *Chem. Rev. 81* (1981) 447; C. Masters, *Adv. Organomet. Chem. 17* (1979) 61; G. Henrici-Olivé, S. Olivé, *Angew. Chem. 88* (1976) 144; *Angew. Chem. Int. Ed. Engl. 15* (1976) 136; J. Falbe

(Ed.): *New Syntheses with Carbon Monoxide*, Springer Verlag, Berlin 1980; E. L. Kugler, F. W. Steffgen (Eds.): *Hydrocarbon Synthesis from Carbon Monoxide and Hydrogen, Adv. Chem. Ser. 178* (1979).

[73] R. C. Brady III, R. Pettit, *J. Am. Chem. Soc. 102* (1980) 6181; *ibid. 103* (1981) 1287.

[74] C. E. Sumner, Jr., P. E. Riley, R. E. Davis, R. Pettit, *J. Am. Chem. Soc. 102* (1980) 1754; W. A. Herrmann, *Adv. Organomet. Chem. 20* (1982) 159; *J. Organomet. Chem. 250* (1983) 319; K. H. Theopold, R. G. Bergman, *J. Am. Chem. Soc. 105* (1983) 464; M. Cooke, N. J. Forrow, S. A. R. Knox, *J. Chem. Soc. Dalton Trans. 1983,* 2435; J. Holton, M. F. Lappert, R. Pearce, P. I. W. Yarrow, *Chem. Rev. 83* (1983) 135; P. M. George, N. R. Avery, W. H. Weinberg, F. N. Tebbe, *J. Am. Chem. Soc. 105* (1983) 1393; J. E. Hahn, *Prog. Inorg. Chem. 31* (1984) 205; H. Fischer, S. Zeuner, K. Ackermann, J. Schmid, *Chem. Ber. 119* (1986) 1546; I. M. Saez, N. J. Meanwell, A. Nutton, K. Isobe, A. Vázquez de Miguel, D. W. Bruce, S. Okeya, D. G. Andrews, P. R. Ashton, I. R. Johnstone, P. M. Maitlis, *J. Chem. Soc. Dalton Trans. 1986,* 1565.

[75] G.-W. Wang, H. Hattori, H. Itoh, K. Tanabe, *J. Chem. Soc. Chem. Commun. 1982,* 1256; D. R. Fahey, *J. Am. Chem. Soc. 103* (1981) 136; S.-S. Sung, R. Hoffmann, *ibid. 107* (1985) 578; K. Maruya, A. Inaba, T. Maehashi, K. Domen, T. Onishi, *J. Chem. Soc. Chem. Commun. 1985,* 487; M. H. Chisholm, *J. Organomet. Chem. 334* (1987) 77; I. M. Saez, P. M. Maitlis, *ibid. 234* (1987) C14; cf. J. C. Hayes, G. D. N. Pearson, N. J. Cooper, *J. Am. Chem. Soc. 103* (1981) 4648; R. Köster, M. Yalpani, *Angew. Chem. 97* (1985) 600; *Angew. Chem. Int. Ed. Engl. 24* (1985) 572; H. Werner, H. Kletzin, A. Höhn, W. Paul, W. Knaup, M. L. Ziegler, O. Serhadli, *J. Organomet. Chem. 306* (1986) 227; R. McCrindle, G. J. Arsenault, R. Farwaha, M. J. Hampden-Smith, A. J. McAlees, *J. Chem. Soc. Chem. Commun. 1986,* 943; P. M. Loggenberg, L. Carlton, R. G. Copperthwaite, G. J. Hutchings, *ibid. 1987,* 541.

[76] S. Couturier, B. Gautheron, *J. Organomet. Chem. 157* (1978) C61; J. M. Manriquez, D. R. McAlister, R. D. Sanner, J. E. Bercaw, *J. Am. Chem. Soc. 98* (1976) 6733.

[77] K. Kropp, V. Skibbe, G. Erker, C. Krüger, *J. Am. Chem. Soc. 105* (1983) 3353.

[78] a) R. M. Waymouth, B. D. Santarsiero, R. J. Coots, M. J. Bronikowski, R. H. Grubbs, *J. Am. Chem. Soc. 108* (1986) 1427; b) G. S. Bristow, P. B. Hitchcook, M. F. Lappert, *J. Chem. Soc. Chem. Comm. 1982,* 162.

[79] F. Rosenfeldt, G. Erker, *Tetrahedron Lett. 21* (1980) 1637; G. Erker, F. Rosenfeldt, *J. Organomet. Chem. 224* (1982) 29; *Tetrahedron 38* (1982) 1285.

[80] H. Takaya, M. Yamakawa, K. Mashima, *J. Chem. Soc. Chem. Commun. 1983,* 1283; S. Stella, C. Floriani, *ibid. 1986,* 1053; B. M. Martin, S. A. Matchett, J. R. Norton, O. P. Anderson, *J. Am. Chem. Soc. 107* (1985) 7952.,

[81] a) G. Erker, K. Kropp, C. Krüger, A.-P. Chiang, *Chem. Ber. 115* (1982) 2447; b) G. Erker, *Acc. Chem. Res. 17* (1984) 103; P. T. Wolczanski, J. E. Bercaw, *ibid. 13* (1980) 121.

[82] G. Fachinetti, C. Floriani, A. Roselli, S. Pucci, *J. Chem. Soc. Chem. Commun. 1978,* 269; X-ray crystal structure analysis: S. Gambarotta, C. Floriani, A. Chiesi-Villa, C. Guastini, *J. Am. Chem. Soc. 105* (1983) 1690.

[83] a) J. M. Manriquez, D. R. McAlister, R. D. Sanner, J. E. Bercaw, *J. Am. Chem. Soc. 100* (1978) 2716; F. Rosenfeldt, *Dissertation,* Universität Bochum 1981; P. Hofmann, M. Frede, P. Stauffert, W. Lasser, U. Thewalt, *Angew. Chem. 97* (1985) 693; *Angew. Chem. Int. Ed. Engl. 24* (1985) 712; see also C. D. Wood, R. R. Schrock, *J. Am. Chem. Soc. 101* (1979) 5422; b) G. Erker, P. Czisch, R. Schlund, K. Angermund, C. Krüger, *Angew. Chem. 98* (1986) 356; *Angew. Chem. Int. Ed. Engl. 25* (1986) 364; c) J. D. Meinhart, B. D. Santarsiero, R. H. Grubbs, *J. Am. Chem. Soc. 108* (1986) 3318.

[84] P. Hofmann, P. Stauffert, K. Tatsumi, A. Nakamura, R. Hoffmann, *Organometallics 4* (1985) 404; *J. Am. Chem. Soc. 107* (1985) 4440.

[85] a) G. Erker, C. Krüger, R. Schlund, *Z. Naturforsch. B42* (1987) 1009; G. Erker, R. Schlund, C. Krüger, *J. Organomet. Chem. 338* (1988) C4; b) *J. Chem. Soc. Chem. Commun. 1986,* 1403.

[86] a) G. Erker, U. Dorf, J. L. Atwood, W. E. Hunter, *J. Am. Chem. Soc. 108* (1986) 2251; b) G. Erker, F. Rosenfeldt, *Tetrahedron Lett. 22* (1981) 1379.

[87] a) G. Erker, K. Kropp, *Chem. Ber. 115* (1982) 2437; b) K. I. Gell, G. M. Williams, J. Schwartz, *J. Chem. Soc. Chem. Commun. 1980,* 550.

[88] Review: M. T. Reetz, *Adv. Organomet. Chem. 16* (1977) 33.

[89] G. Erker, R. Schlund, unpublished.

[90] A. S. Ward, E. A. Mintz, M. R. Ayers, *Organometallics 5* (1986) 1585; A. S. Ward, E. A. Mintz, M. P. Kramer, *ibid. 7* (1988) 8.

Perspectives in Photochromism: A Novel System Based on the 1,5-Electrocyclization of Heteroanalogous Pentadienyl Anions

By Heinz Dürr*

Dedicated to Professor Emanuel Vogel and Professor Klaus Hafner on the occasion of their 60th birthdays

The molecular process whereby light induces color changes in certain substances, namely photochromism, is currently a topic of active research. Many reactions—mainly monomolecular—have been reexamined in greater detail from the standpoint of photochromism. Those found to be especially suitable for such studies include *cis-trans* isomerizations, pericyclic reactions, tautomerizations and dissociations. The most important in this group are undoubtedly the electrocyclization reactions. In this paper we present spiro[fluorene-9,1'-[1,8a]-dihydroindolizine] and its bis- and tris-aza analogues as examples of a promising new system with a wide range of variability. Not only the classical uses, but also those in new fields such as frequency doubling of laser radiation, holography or molecular microcircuit chips can now be considered.

1. Introduction

Light and color—two directly interrelated concepts—have fascinated mankind since early times, with ever more novel aspects emerging. The term photochromism involves both these phenomena. The earliest scientific studies were those of *ter Meer*,[1] *Marckwald*[2a] (who was one of the first to use the expression "phototropy"[2b]), and more recently *Hirshberg*.[3] Photochromism[4] is a reversible transformation of a single chemical species between two states whose absorption spectra are recognizably different, the transformation in at least one direction being induced by electromagnetic radiation [Eq. (a)].

$$A(\lambda_1) \underset{h\nu_2,\,\Delta}{\overset{h\nu_1}{\rightleftharpoons}} B(\lambda_2) \qquad (a)$$

Species A is transformed into the higher energy form B as a result of irradiation with light. The reverse reaction to A usually occurs as a spontaneous thermal process, but may also be light-induced. Equation (a) holds true only for unimolecular reactions. More recently bimolecular photochromic systems, based on a cycloaddition or cycloreversion, have also been discovered [Eq. (b)].

$$A + B \underset{h\nu_2,\,\Delta}{\overset{h\nu_1}{\rightleftharpoons}} C \qquad (b)$$

Photochromic systems[4, 5] according to Equation (a) can be classified into several groups on the basis of the photochemically induced primary step:

1) photoreversible systems, in which the colored form B undergoes a light-induced reaction back to the form A,
2) thermoreversible systems, in which the colored form B reverts thermally to A,
3) photo- and thermoreversible systems,
4) inverse photochromic systems, in which the initial form A absorbs at the longer wavelength and form B at the shorter wavelength,
5) multiphotochromic systems, in which more than two forms undergo photochemical and/or thermochemical interconversion.

This review begins with a brief survey of the most important photochromic compounds—mainly organic. This is followed by an outline of the development of a new photochromic system based on a 1,5-electrocyclization, and the possibilities which it offers. The review finally deals with some typical applications of common photochromic materials.

2. Common Photochromic Systems

Photochromic systems[4, 5] may be classified into six major groups according to reaction types, which are discussed in Sections 2.1 to 2.6.

2.1. Triplet-Triplet Absorption

The simplest photochromic system is one which contains molecules in the stable ground state and in a metastable, photochemically excited state. Examples are fluorescein in a boric acid matrix,[6] and picene in polymer films.[7] The triplet-triplet excitation in coronene also belongs to this class.[8]

2.2. *cis-trans* Isomerization

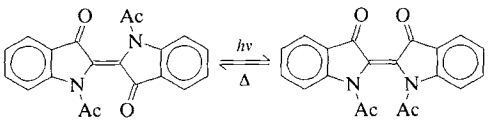
When the double bonds of alkenes, azomethines or azo compounds are excited either directly or via spectral sensitiz-

[*] Prof. Dr. H. Dürr
Fachbereich 13—Organische Chemie der Universität
D-6600 Saarbrücken (FRG)

 © VCH Verlagsgesellschaft mbH, D-6940 Weinheim, 1989 0570-0833/89/0404-0413 $ 02.50/0

ers, a reversible *cis-trans* isomerization is observed. The two configurational isomers usually differ in the positions and intensities of their UV absorption maxima.

N,N'-disubstituted indigo derivatives such as **1** have been suggested as combined solar energy storage and conversion systems.[9, 10] Here a small proportion of the energy is stored in the *cis* isomer **2**; the greater part, however, is converted into molecular motion (Scheme 1).



1 (*trans*) **2** (*cis*)

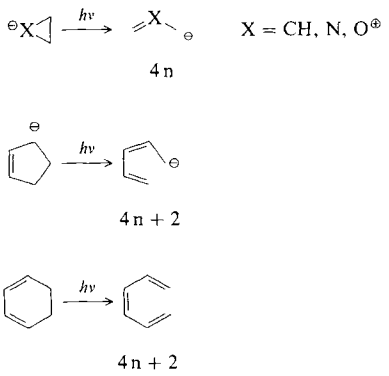
Scheme 1.

The advantages of this system lie in the absorption spectrum of **1**, which coincides very well with the photochemically active region of the solar spectrum, in the well known light fastness of indigo dyes, and in the fact that the reverse reaction **2** → **1** is strictly quantitative. Similar results have also been obtained with thioindigo derivatives.[11] A disadvantage is that in all cases the specific energy storage capacity is low owing to the high molecular weights of the indigo derivatives. The absorption maxima for the colored variants formed on irradiation of various compounds are shown in Figure 6.

Cis-trans isomerizations also have an important role in simpler compounds such as stilbenes,[12, 13] benzylidene anilines[14a] and azobenzenes,[14b, 15] and in biological systems such as retinal in the human eye.[4] More recently so-called "photoresponsive crown ethers" have also been prepared; in these too, the light-sensitive behavior is based on *cis-trans* isomerization.[14b]

2.3. Pericyclic Reactions

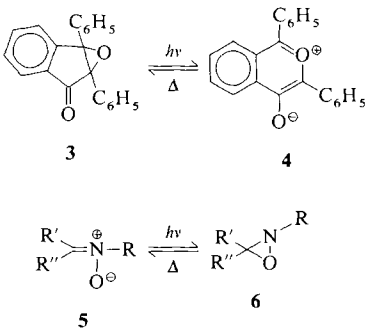
Of the different classes of pericyclic reactions, the electrocyclic reactions have proved to be especially suitable as a basis for photochromic systems. Scheme 2 shows three dif-



Scheme 2.

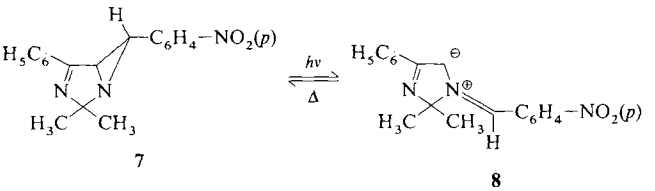
ferent types of ring-opening reactions. However, only a few of the many possible electrocyclization reactions are important.

For example, irradiation of the epoxyindanones with the general structure **3** leads to opening of the three-membered ring followed by rearrangement to give pyrylio-oxides **4**[16]. The most important representatives of this series have been studied in detail by *Ullman* et al.[17, 18] (Scheme 3).



Scheme 3.

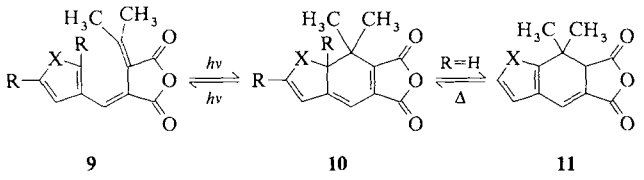
In an analogous way, the nitrones **5** can be converted by irradiation into the oxaziridines **6** (Scheme 3). These are powerful oxidizing agents, highly reactive, and in most cases cannot be isolated.[19] The reverse reaction takes place upon heating. Interesting photochromic molecules of the aziridine type have been found by *Do Minh* and *Trozzolo* et al.[20–22] These show photochromic behavior even in the crystalline state, whereas many other systems are photochromic only in solution. An especially efficient photochromic system is found in the bicyclic aziridine **7**, which undergoes a light-induced reaction according to Scheme 4 to give monocyclic **8**.[20–22]



Scheme 4.

The butadiene-cyclobutene isomerization, although extremely important from a theoretical and preparative point of view, is of no significance as a photochromic system, as the shifting absorption maxima in these derivatives are nearly all in the UV rather than in the visible region. This limitation does not, however, apply to $4n + 2$ systems (6π), whose photochromism results from the electrocyclic 1,3,5-hexatriene/1,3-cyclohexadiene interconversion. This group includes the fulgides **9**, which have been developed for specific technological uses. In this class of bis(methylene)succinic anhydride derivatives, which were first synthesized by *Stobbe*,[23b] *Heller* et al.[23a, 24–27] showed that the 1,5 hydrogen shift to structure **11**, following the photochemical valence isomerization reaction **9** → **10**, could be suppressed by substituting methyl groups in place of hydrogen atoms (Scheme 5).

Derivatives such as Aberochrome 540 **9a** and Aberochrome 999 **9b** are used as actinometric substances in the UV and visible regions (see Section 4). The photochromic pyrene

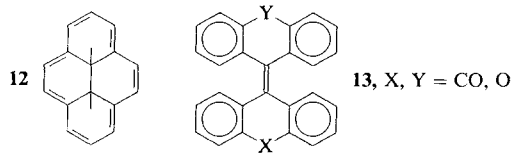


9 **10** **11**

9a, X = O, R = CH_3 (Aberochrome 540)
9b, X = S, R = C_6H_5 (Aberochrome 999)

Scheme 5.

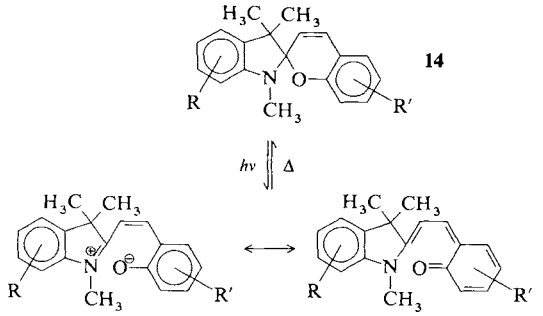
derivative **12**[28, 29] and the hexacycles **13**[30, 31] are other 6π systems which undergo analogous electrocyclic reactions (Scheme 6).



12 **13**, X, Y = CO, O

Scheme 6.

An electrocyclic $(4n + 2)$-reaction ($n = 1$) is also found in the spiropyrans **14**,[32–35] as shown in Scheme 7. UV irradi-



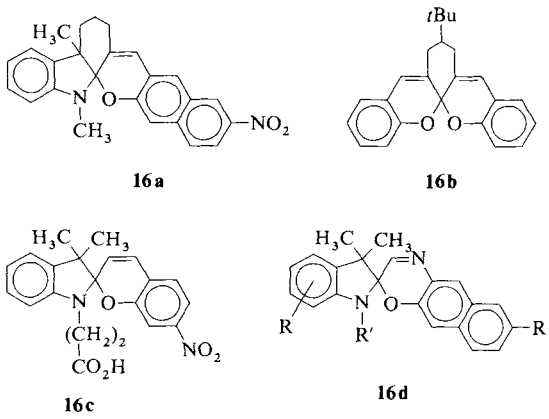
14 **15**

Scheme 7. R and R' can be a large number of organic groups; each ring can also contain several substituents (see Ref. [4]).

ation of the colorless spiro compounds **14** leads to cleavage of the C–O bond to give the open chain compounds **15**, which absorb strongly in the visible region. These highly interesting photochromic spiropyran derivatives have been studied very intensively,[32–49] and the literature up to 1970 is very well covered by *Brown*.[4] This system too has led to quite a number of practical applications (see Section 4).

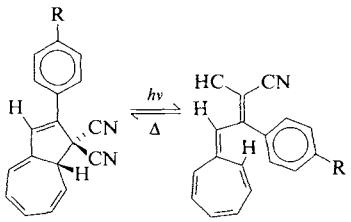
Bräuchle et al. have shown that an unstable intermediate with an orthogonally bridged structure is formed during ring-opening of spirodihydroindoles at 4.2 K.[46] Bridged compounds of this kind, such as **16a**[47] and analogues such as **16b**[48] and the spiro compounds **16c**[49a] and **16d** (Scheme 8), have been synthesized.

16c is a fatigue resistant spiropyran.[49a] According to most recent findings replacement of a CH group by N affords various spirooxazines.[49b] Another important system belonging to this class is that of the phytochromes, which have been studied by *Schaffner* and *Braslavsky* et al.; these have an important biochemical role in regulating plant growth.[49c] An electrocyclic reaction involving a $4n + 2$ π-electron ($n = 2$) system has been observed in the vinylheptafulvene derivative **18** (Scheme 9).[50]



16a **16b** **16c** **16d**

Scheme 8. Indolinospiropyrans **16**; photostable spiropyrans **16c,d.**

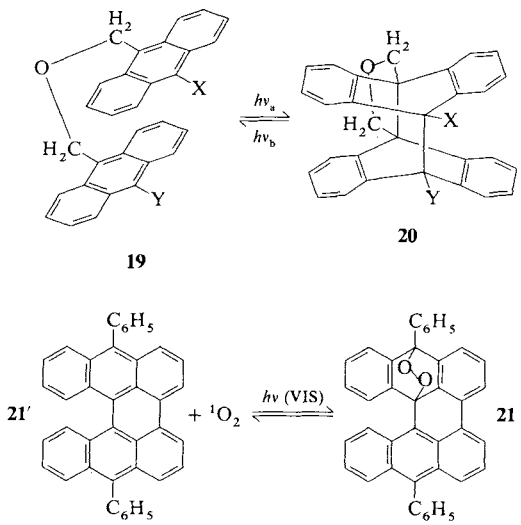


17 **18**

a, R = OCH_3; **b**, R = NO_2

Scheme 9. Photochromic system based on a 10π-electrocyclization.

Cycloadditions are another important class of pericyclic reactions which provide a basis for photochromic molecules. Examples are the [4 + 4] cycloadditions of "bracketed" dianthracene derivatives **19** (Scheme 10); *Bouas-Laurent* was able to demonstrate photochromic behavior in the system **19** → **20**, and to clarify the details of the reaction sequence in a series of elegant studies.[51, 52]



19 **20** **21'** **21**

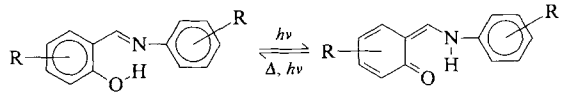
	X	Y		X	Y		X	Y
a	H	H	**b**	CH_3	H	**c**	C_6H_5	H
d	Br	H	**e**	CH_3	CN	**f**	C_6H_5	CN
g	CH_3	Br	**h**	Br	Br	**i**	C_6H_5	C_6H_5

Scheme 10. Photochromic systems based on bimolecular reactions. Reaction **19** → **20**: solvent ether or methylcyclohexane, $\lambda = 335$ nm; reaction **20** → **19**: $\lambda = 254$ nm. Yield of **20a–i**: 20–90%.

Brauer et al.[53, 54] have described a cycloreversion which occurs in *endo*-peroxides such as **21** (Scheme 10). The reaction releases singlet oxygen, $^1O_2$, which then recombines reversibly with **21'**. We thus have here a bimolecular photochromic system contrasting with the intramolecular cycloaddition **19** → **20**. In the latter case, however, the effectiveness of the photocycloaddition results from the bridges between the rings.—Sigmatropic reactions do not yet appear to have been used as a basis for photochromic systems.

2.4. Tautomerization

Light-induced tautomerizations can occur in the form of prototropic rearrangements such as **22** → **23** for the case of salicylidene-anilines (Scheme 11);[55-60] similar behavior is found in 2-, 3- or 4-(salicylidenamino)pyridines.[61]



22 **23**

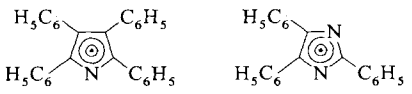
Scheme 11. R can be any group, e.g. aryl, methyl.

Such prototropic processes may be either thermally or photochemically activated. In the above example the prototropic behavior is responsible for the observed photochromism. Light-fastness of dyes is often the result of photochemically induced prototropy of this kind.

2.5. Dissociation

2.5.1. Homolytic Cleavage of Bonds

Typical examples of this type are the cleavage reactions of octaphenyl-1,1'-bipyrrolyl and of hexaphenyl-1,1'-biimidazolyl, which on exposure to light yield the colored free radicals **24a** and **24b** respectively (Scheme 12). These reactions too form the basis of a photochromic system.[62]

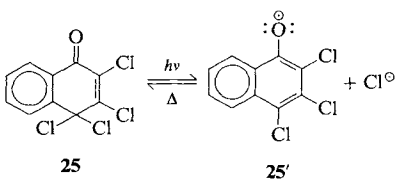


24a **24b**

Scheme 12.

2.5.2. Heterolytic Cleavage of Bonds

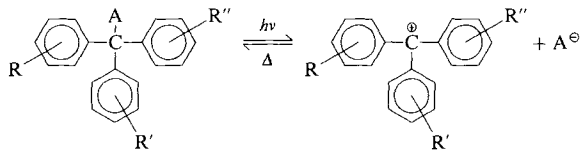
An example of this class is the loss of a Cl atom from **25**,[63] followed by recombination to give the original compound. This reaction was first formulated as in Scheme 13. More recent work[64] has shown that instead of a radical pair[63] this cleavage gives a carbenium ion.



25 **25'**

Scheme 13.

The same holds true for triarylmethane derivatives **26**, whose photochromic behavior was observed as long ago as the turn of the century by *Hantzsch* et al.[65] Irradiation of the colorless (leuco) form **26** gives the strongly colored triarylmethyl cations **27**, with release of an anion $A^{\ominus}$; the thermally induced decoloration of the cation depends critically on the solvent and the anion concentration (Scheme 14).[65-67]



26 **27**

Scheme 14. R = R' = R'' = $N(CH_3)_2$; A = CN, SO_3H.

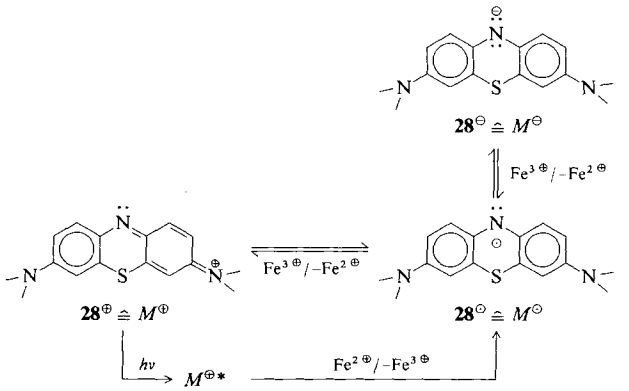
Triarylmethane derivatives whose leuco form is a spiro compound have been studied by *Gleiter* et al.[41b] In these compounds the reaction of the colored form with other anions or with the solvent, as can occur in **27**, is prevented (cf. also Ref. [68]).

2.6. Electron Transfer/Redox Photochromism

The best known photochromic system based on an electron transfer reaction is undoubtedly that of AgCl, which is decomposed by light according to Equation (c)

$$AgCl \underset{\Delta}{\overset{h\nu}{\rightleftharpoons}} Ag^0 + Cl^{\odot} \qquad (c)$$

This electron transfer reaction is of great practical importance in photochromic spectacle lenses based on silicate glass.[69] An example of a photochromic electron transfer reaction in organic chemistry is the methylene blue system which has been investigated by *Parker* (Scheme 15).[70]



Scheme 15.

3. The Development of a New Photochromic System

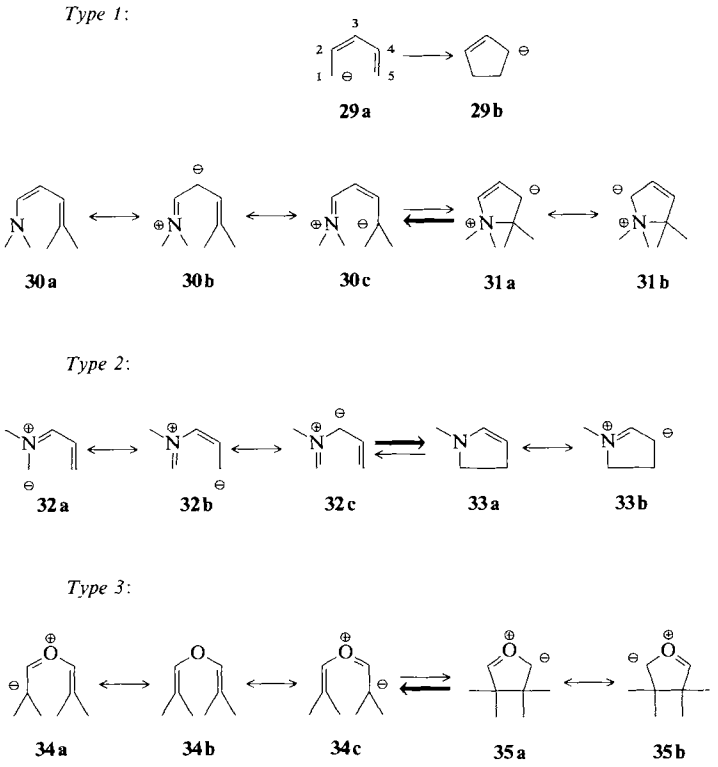
Pericyclic reactions, and electrocyclic reactions especially, belong to a class of rearrangements[71] which can cause photochromic behavior. The 1,5-electrocyclization reac-

tions[72, 73] of the pentadienyl anion and of its heterocyclic analogs appeared to offer attractive possibilities for this purpose.

3.1. The 1,5-Electrocyclization Reaction

The 1,5-electrocyclization reaction can in principle proceed thermally as a disrotatory process and photochemically as a conrotatory process.

According to *Huisgen*[72] one can in addition distinguish three different cases for those hetero-analogs of the pentadienyl **29a** or cyclopentenyl anions **29b** in which a carbanion C atom is replaced "isoelectronically" by a heteroatom[72] (Scheme 16).



Scheme 16. Substituents not shown for clarity.

In type 1 (heteroatom in position 1) **30a** is a formally uncharged mesomeric structure, whereas the cyclic form **31** must be formulated as a resonance hybrid of dipolar structures. In this case, therefore, in the equilibrium **30** ⇌ **31** the ring-opened species **30** predominates. If the heteroatom is in the 2-position (type 2), an uncharged ring structure **33a** becomes possible, with the result that the equilibrium **32** ⇌ **33** is shifted towards the cyclic form **33**. In type 3 (heteroatom in the 3-position), only formula **34b** is uncharged, and the dominant species is therefore **34**, i.e. the ring-opening is favored.

If we now wish to design a photochromic system based on a 1,5-electrocyclization, the molecular structures need to be such that equilibrium mixtures are possible in each of the types 1 to 3. The individual ring-opened or cyclic systems can therefore only be allowed to have small values of ΔG_0 and $\Delta G^{\#}$. In order to synthesize tailor-made photochromic molecules one must ensure that this condition is satisfied. In the following, new systems and synthetic methods for photochromic molecules of types 1, 2 and 3 are described.

3.2. Synthetic Routes

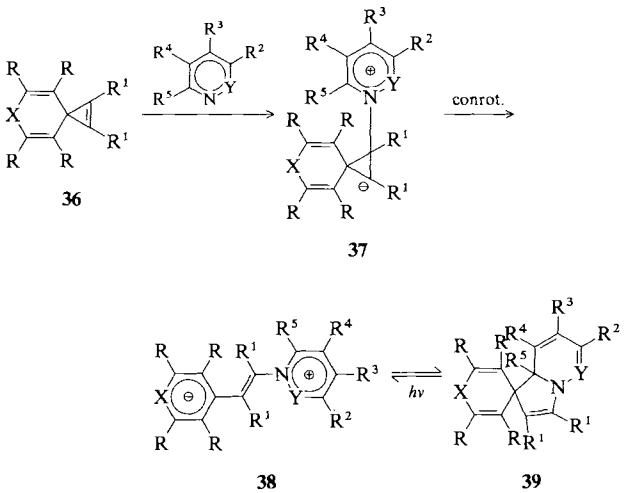
3.2.1. *Type 1 Systems*

No photochromic systems of type 1 have so far been discovered (cf. Ref. [72]).

3.2.2. *Type 2 Systems*

Systems of type 2 can be regarded as "1,3-dipoles of allylic type".[72] The organic chemist's entire armory has been brought to bear on the study of 1,3-dipolar cycloadditions,[73] but despite this it is only quite recently that the reaction has been successfully used in an effective photochromic system.

Cyclopropene route: When spirocyclopropenes with the general structure **36**[74] are allowed to react with pyridine or pyridazine derivatives, or spiro [4a,5]dihydropyrrolo-[1,2-*b*]pyridazines, photochromic spiro[1,8-a]dihydroindolizines **39**, Y = CH, **39**, Y = N, respectively, are formed. Some representative examples of these, synthesized according to Scheme 17, are listed in Table 1.[75–77]



Scheme 17. Cyclopropene route to **38** and **39**. Solvent: CH_2Cl_2/ether, temp.: 20–25 °C, yield: 12–89% (see Table 1).

The reaction mechanism leading to the formation of **39** may be described as follows: the pyridine derivative attaches itself to the electron-deficient cyclopropene ring in **36** by nucleophilic addition. The resulting cyclopropyl anion undergoes a ring-opening to give an allyl anion, in this case the betaine derivative **38**; the process **37** → **38** is a cooperative reaction which, according to the *Woodward-Hoffmann* rules, is a conrotatory ring-opening. The betaine derivative **38** can undergo 1,5-electrocyclization to give **39**. The action of light on **39** gives **38**, and the transformation **38** ⇌ **39** thus constitutes a new photochromic system.

Compounds with a very wide range of absorption wavelengths can be synthesized using this cyclopropene route (see

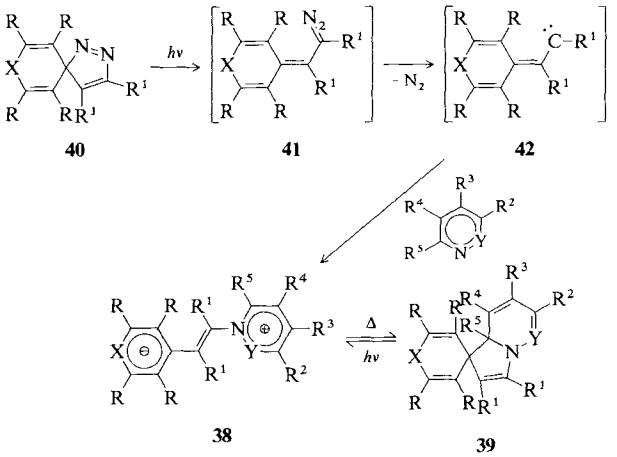
Table 1. Some data for the betaines **38** and the spiro[1,8a-dihydroindolizines] (and their N-analogues) **39**. $-R-R- = -(CH=CH)_2-$ (benzoannelation). $R^1 = CO_2CH_3$. Of the betaines, **38k** and **38s** (see Table 5) could be isolated. UV data determined at 20 °C in $CHCl_3$

	X [a]	Y	R^2	R^3	R^4	R^5	**39** M.p. [°C]	**39** Yield [%]	**39** λ_{max} [nm](ε)	**38** λ_{max} [nm]	**38** $k_{38\rightarrow 39}$ [s^{-1}]
a	–	CH	H	H	H	H	135	63	384 (10500)	586	4.88×10^{-3}
b	–	CD	D	D	D	D	138	73	383	586	3.4×10^{-3}
c	–	CH	H	OCH_3	H	H	145–147	73	376 (7730)	552	11.0×10^{-3}
d	H;H	CH	H	$(CH=CH)_2$		H	162	52	385 (13380)	572	1.2×10^{-3}
e	–	CH	H	$(CH=CH)_2$		H	162	78	378 (14390)	600	40 [b]
f	–	CCH_3	H	H	H	H	130	31	383 (11100)	570	2.21×10^{-3}
g	–	N	H	H	H	H	146	74	389 (9480)	505	14×10^{-3}
h	–	$C(CH=CH)_2$		H	H	H	192	84	360 (15400)	724	2.7 [b]
i	–	$C(CH=CH)_2$		H	H	CH_4	36	40	363 (12250)	726	0.1 [b]
j [d]	–	CH	H	H	H	H	184	12	376 (10600)	694	832 [b]
k [e]	–	CH	H	H	H	H	194	89	392 (11300)	629	27.7 [b, c]
l	C=O	CH	H	H	H	H	183	61	388 (8260)		

[a] A dash signifies a zero bridge. [b] Determined flash photolytically by Dr. *H. Hermann*, Mülheim a. d. Ruhr (FRG). [c] Cyclization in two part steps; the value quoted refers to the rapid step, which is neither first order nor second order. [d] $R^1 = H$. [e] $R = C_6H_5$.

Table 1). Molecules with properties tailor-made for specific applications can be synthesized under very mild conditions in excellent yields.[74–78a] Novel materials of type **39** containing crown ether units have also been prepared.[78b]

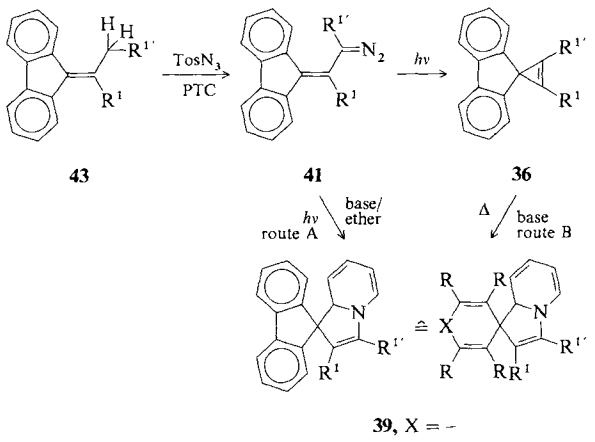
Pyrazole route: A problem was encountered, however, when attempts were made to adapt the above synthesis to prepare CN-substituted spirodihydroindolizines. Cyano-substituted spirocyclopropenes (**36**, with $R^1 = CN$) are unknown.[79] We therefore developed an alternative method, in which the spiropyrazole derivative **40** is irradiated directly (Scheme 18). This results in ring opening with in situ formation of the diazo compound **41**, which then loses nitrogen to give the fulvenecarbene **42**. This can then react with the diazine to form a betaine **38**. Cyclization then affords the spirodihydroindolizine or the N-analogues **39**. By this route it is also possible to prepare cyano-substituted species **39**, and to obtain derivatives containing low reactivity groups, e.g. R^1 = trifluoromethyl, in considerably better yields.[75, 80]



Scheme 18. Pyrazole route to **38** and **39**. $-R-R- = -(CH=CH)_2-$ (benzoannelation), R^1 = CN, CO_2CH_3 etc., X = – (zero bridge), C=O, S.

Diazo or vinylcarbene route: In both the above described methods, only symmetrical substitution at the 2,3 positions of **39** is possible, i.e., $R^1 = R^{1'}$. Since the photochromic properties of **39** are determined essentially by the double bond between C-2 and C-3 it became necessary to find a method for synthesizing asymmetrically substituted versions of **39**.

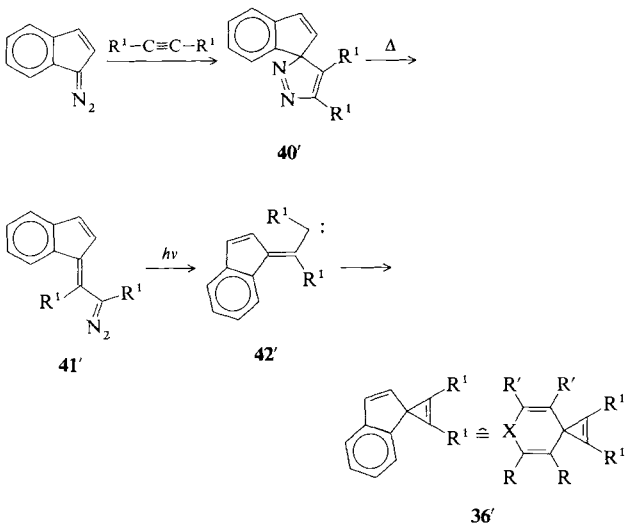
The already known fulvene derivative **43** is treated with $TosN_3$ in the presence of a phase transfer catalyst (PTC); this results in the formation of compound **41** by transfer of a diazo group[81] (Scheme 19, route B). The action of light on **41** then gives, via the vinylcarbene **42**, the spirocyclopropene derivative **36**. This reacts with suitable nucleophilic bases to give **39**. Alternatively **39** can be synthesized by direct photolysis of **41** in an ether solution of the base[82, 83a] (route A).



Scheme 19. Diazo- or vinylcarbene route to (**38** and) **39**. Route A: $R^1 = R^{1'} = CO_2CH_3$: yield 75%; $R^1 = CO_2CH_3$, $R^{1'}$ = CN: 12%; route B, see Table 1.

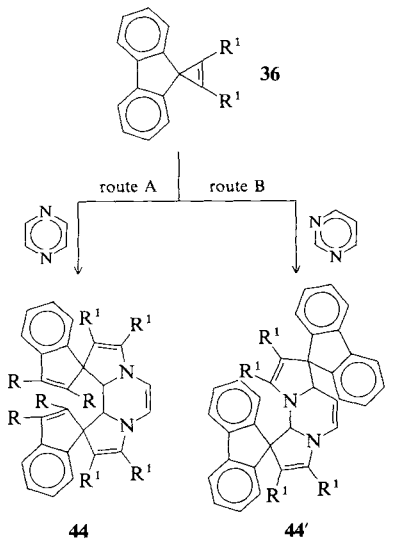
Retro-1,5-electrocyclization: Suitable spiropyrazole derivatives **40** undergo an interesting thermolysis. Thus, from the spiro[indene-1,3′-pyrrole] **40′** one obtains a vinyldiazoalkane **41′**.[82] By a route analogous to that in Scheme 19, **41** can then react to give the DHI derivative **39** (see Scheme 20) via **36′**.

Bichromophoric systems: For synthesizing bifunctional photochromic molecules (cf. also Section 1) of type 2, there are in principle two possible routes: 1) from a monofunctional unsaturated spiro compound and a bifunctional base, and 2) from a bifunctional unsaturated spiro compound and a



Scheme 20. $-R-R- = -(CH=CH)_2-$, $R' = H$, $R^1 = CO_2CH_3$ ($\equiv E$), X = – (zero bridge).

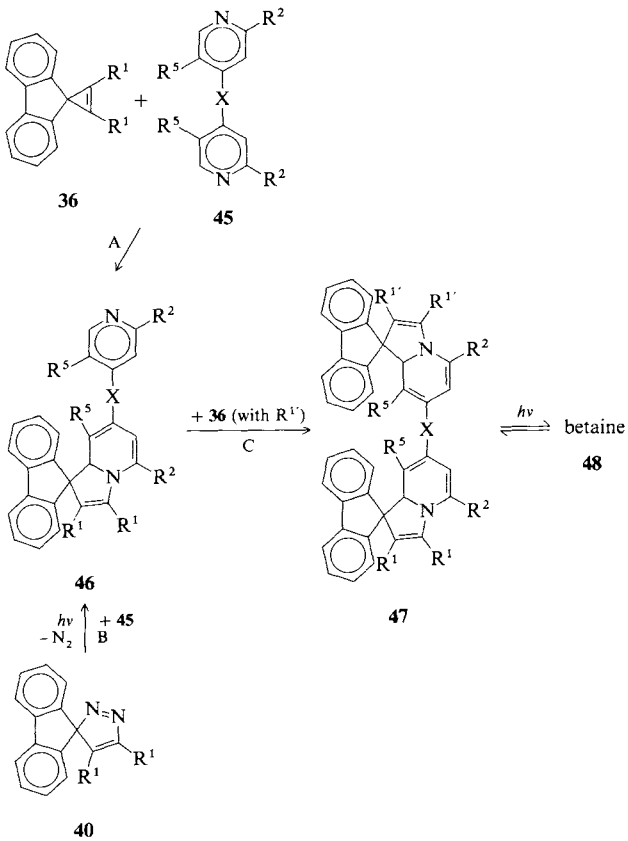
monofunctional base, the route to the bifunctional spiro compound being via either a bis(diazo) compound or a bis-alkyne.[83b]—As shown in Scheme 21, the reaction of **36** with



Scheme 21. $-R-R- = -(CH=CH)_2-$. Route A: $R^1 = CO_2CH_3$: yield 50%; $R^1 = CO_2tBu$: 30%. Route B: $R^1 = CO_2CH_3$: 24%; $R^1 = CO_2tBu$: 32%; $R^1 = COCH_3$: 28%.

pyrazine or pyrimidine (in contrast to the reaction with pyridazine derivatives) affords the very interesting bis-adducts **44** and **44'**, respectively (Route 1). However, only the compounds of type **44'** are photochromic.

If we separate the two nucleophilic centers of the azines, we have molecules of the bis(pyridine) type **45**. Reaction of such a bis-base **45** with spirocyclopropenes **36** gives first 1:1 adducts **46**. However, depending on the reaction conditions, one may also synthesize the 2:1 adduct **47** (Scheme 22, Table 2). By suitable sequencing of the individual steps of



Scheme 22. $R^1 = CO_2CH_3$, $COCH_3$ (see Table 2).

this reaction one can obtain both symmetrical and asymmetrical bichromophores[40, 84] (steps A, C or B, C).—Recently route 2, via a bis(diazo)compound, has also been realized.[84]

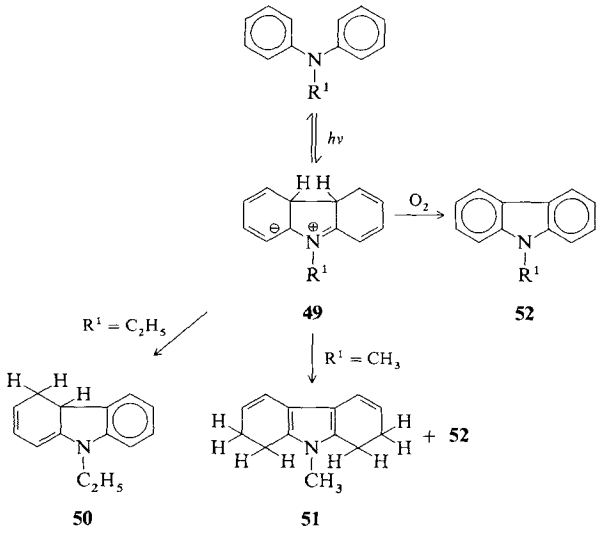
Table 2. Some data of the 2:1 adducts **47**. $E = CO_2CH_3$. UV data determined at 20 °C in CH_2Cl_2.

	R^1	$R^{1'}$	X [a]	R^2	R^5	**47**			**48**	
						M.p. [°C]	Yield [%]	λ_{max} [nm] (ε)	λ_{max} [nm]	$k_{48\rightarrow47}$ [s^{-1}]
a	E	E	–	H	H	218	39	396 (20400)	630	6.7×10^{-3}
b	Ac	Ac	–	H	H	160	48	420 (13600)	575	1.7×10^{-3}
c	E	E	–	Me	H	220	75	396 (20900)	628	2.1×10^{-3}
d	E	E	–	H	Me	192	69	399 (14500)	623	17.8×10^{-3}
e	E	E	$(CH_2)_2$	H	H	126	48	381 (24600)	596	6.9×10^{-3}
f	E	E	$(CH)_2$	H	H	186	73	394 (15100)	702	4.6×10^{-3}
g	E	Ac	–	H	H	188	37	407 (16700)	585	2.5×10^{-3}
h	E	Ac	–	Me	H	138	28	404 (22300)	590	9.0×10^{-3}
i	E	Ac	$(CH)_2$	H	H	162	58	401 (23800)	650	1.3×10^{-3}

[a] A dash signifies a zero bridge.

3.2.3. *Type 3 Systems*

Systems of this type have already been known for some time. However, owing to subsequent thermal reactions—mainly sigmatropic H-shifts (and possibly oxidations) at



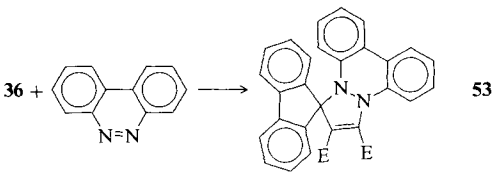
49 **52** **50** **51**

Scheme 23.

moderate or high temperatures—irreversible secondary reactions to **51** or **52** occur (Scheme 23), and the system cannot therefore be regarded as reversibly photochromic[85].

3.2.4. Mixed Systems

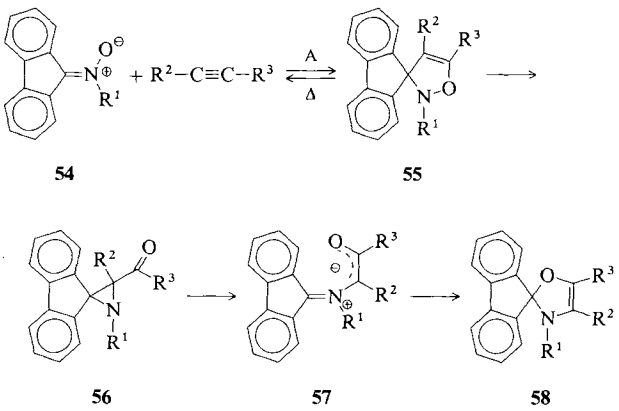
Type 1, 2 systems: If in the pyridazine derivatives, which normally give compounds **39**, one blocks the *o* or *o'* position by benzoannelation, the ring closing reaction in the betaine **38**—for example, starting from **36** and benzo[*c*]cinnoline—must proceed with the formation of a dihydropyrazoline ring rather than a dihydropyrroline ring (Scheme 24). This opens the way to an elegant route to **53**, the first type 1, 2 system.[86]



53

Scheme 24. E = CO_2CH_3.

Type 1, 2 aza-oxa systems: One expects that it should be possible to synthesize isoxazoles from nitrones and alkynes by 1,3 dipolar cycloaddition. It is in fact found that the appropriate spirodihydroisoxazolines **55** can be obtained by this method; however, these are no longer photochromic—instead they are thermochromic at moderate temperatures. At higher temperatures they are transformed irreversibly via **56** and **57** into spirodihydrooxazolines **58**[87a] (Scheme 25).

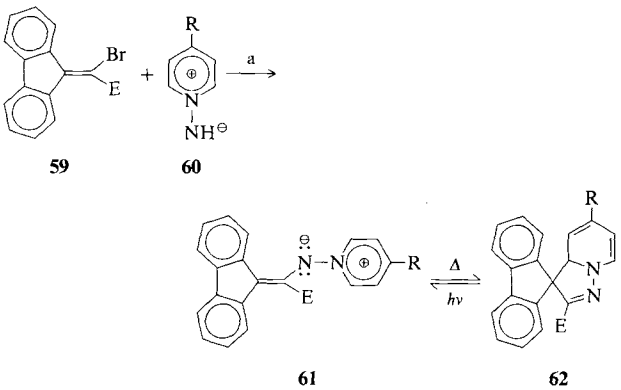


54 **55**

56 **57** **58**

Scheme 25. 0–10 °C; $R^1 = C_6H_5$, $R^2 = R^3 = CF_3$, yield of **55**: 89%; $R^1 = C_6H_5$, $R^2 = R^3 = COCH_3$: 80%.

Type 2, 3 diaza systems: The 1,3 dipolar cycloaddition reaction which is so effective as a method for synthesizing five-membered rings[72] can also be used to prepare spiroheterocyclic compounds of the 2, 3 type. If a suitable substituted dibenzopentafulvene[87b] is treated with pyridine-*N*-imine **60**[88] according to Scheme 26, the corresponding



59 **60**

61 **62**

Scheme 26. R = H: yield 67%; R = CH_3: 30%; R = CN: 35%; E = CO_2CH_3.

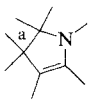
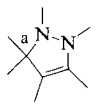
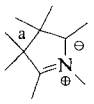
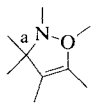
3,3a-dihydropyrazolo[1,5-*a*]pyridine **62** is formed. Compounds with the structure **62** are again photochromic, and thus constitute the first system of type 2, 3 with a dihydropyrazole ring as central unit.[40, 84, 89a]

3.3. Structure and Reactivity

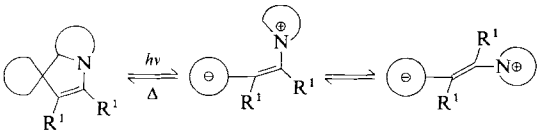
Does the reaction **39** → **38** mentioned previously involve a 1,5-electrocyclization, as has been postulated for the system pentadienyl anion-cyclopentenyl anion (**29a** → **29b**)? For a better comparison, in Table 3 **39** and related compounds are reduced to the central heterocycle, which becomes closed during the 1,5-electrocyclization.

In Table 3 the σ–bonds which undergo photochemical (or in a few cases thermochemical) cleavage are marked "a". These cases differ significantly from the ring-opening of the cyclopentenyl anion, since here no anion is formed. The photoinduced products from these electroneutral five-membered heterocycles are in all cases zwitterions or betaines;

Table 3. Classification and characteristic structural features of the new photochromic systems. a: σ bond formed upon 1,5-electrocyclization (cf. also [49c]).

Cpd	Type	Central five-membered ring	Cpd	Type	Central five-membered ring
39	1, 2		**53**	1, 2	
49	3		**55**	1, 2	
			62	2, 3	

Scheme 27 shows—greatly simplified—their *E*- and *Z*-isomers. This behavior is a characteristic feature of this class of photochromic molecules, distinguishing them from the electrocyclizations of 6-atom-6π systems described previously (cf. Scheme 2).



39 *E*-**38** *Z*-**38**

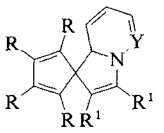
Scheme 27.

3.4. UV Spectra and $t_{1/2}$ Measurements

The UV spectra of the dihydroindolizines **39**, X = CH, and dihydropyrrolo[1,2-*b*]pyridazine **39**, X = N, usually have absorption maxima in the near UV between about 360 and 410 nm. The betaines **38** produced by photochemical action absorb at about 505 to 726 nm (Table 1). Similar results are found for the bichromophoric systems **47** and the corresponding betaines **48** (381–420 nm and 575–702 nm, resp.). **39** and **47** are therefore colorless and pale yellow, respectively, while the betaines **38** and **48** all show colors which vary from red to violet or blue-green. With regard to the possible applications, the colored forms (i.e. the betaines **38** or **48**) offer a range of colors covering virtually all possible shades. The compounds **39** and **47**, on the other hand, absorb in the short wavelength region of the solar spectrum (UVA). The thermally induced reverse reaction of the betaines **38** formed from **39** can be monitored by UV spectroscopy, thus allowing one to determine the reaction rate and the half-life $t_{1/2} = \ln 2/k$ for the colored betaine form **38**.

The activation parameters for the reaction **38** → **39** can be determined from measurements at different temperatures. Table 4 shows some typical examples of results obtained from such measurements. To analyze structure-reactivity relationships for these systems we may divide the molecule **39** into three regions A, B and C as indicated in Scheme 28.

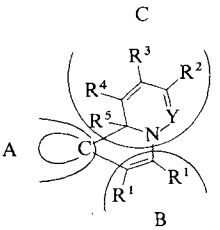
Table 4. Activation parameters for the cyclization of betaines **38** to dihydroindolizines (and N analogues) **39** (in CH_2Cl_2). –R–R– = –(CH=CH)$_2$–benzoannelation).



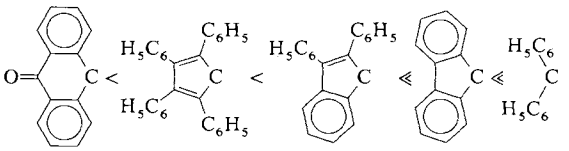
39

39	R^1	Y	$\Delta G^{\neq}$ [kcal mol^{-1}]	$\Delta H^{\neq}$ [kcal mol^{-1}]	$\Delta S^{\neq}$ [cal mol^{-1} K^{-1}]	$t_{1/2}$ [s]
a	CO_2CH_3	CH	20.1	15.9	–14.2	14.2
m	CN	CH	23.4	17.8	–18.6	16800
n	CN	N	22.4	15.3	–22.0	3375
o	CN	CCH_3	31.6	23.2	–24.9	113760

The data in Tables 1, 2 and 4 show that the half-life of the colored form **38** increases as certain changes are made in each of the three regions, as detailed below.



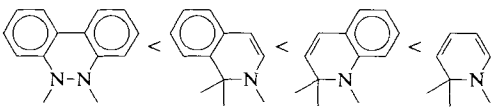
Region A:



Region B:

$$R^1 = H < CF_3 < C_6H_5CO < CH_3CO < CH_3CO_2 < CN$$

Region C:

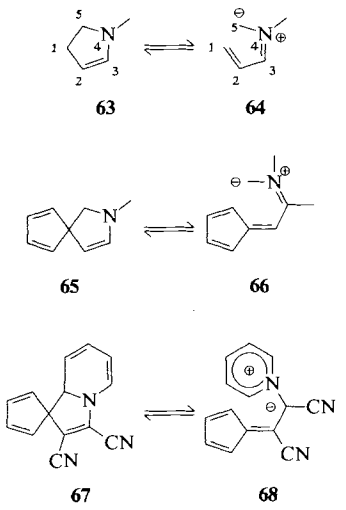


Scheme 28. The changes quoted in the regions A, B and C stabilize the colored form **38** (i.e. increase $t_{1/2}$).

Region A: increase in $t_{1/2}$ occurs in the sequence anthronyl, tetraphenylcyclopentadienyl, indenyl, fluorenyl and finally diphenyl groups.[89b]

Region B: With regard to the substituent R^1, replacement of hydrogen by trifluoromethyl, benzoyl, acetyl, acetoxy, or cyano groups similarly reduces the energy of the colored forms and thus stabilizes them. It thus appears that the stronger the electron-withdrawing effect of the double bond, the greater is the delocalization of the negative charge, and the consequent stabilizing effect of the substituent.

Region C: The half-life of the colored form is increased on going from a tricyclic azine (benzo[*c*]cinnoline) to a bicyclic azine isoquinoline (quinoline) through to a monocyclic azine. This can be explained by the increasing degree of resonance stabilization of the betaine **38** in this sequence of structures. For R^2 to R^5 the sequence $H < CH_3 < N(CH_3)_2$ applies. $t_{1/2}$ is generally increased by substituents R^5.



Scheme 29. Equilibrium between dihydropyrroles (**63, 65, 67**) and betaines (**64, 66, 68**). Arbitrary numbering of the atoms.

These structure-reactivity relationships[90, 91] can be understood on the basis of semiempirical MINDO/3 calculations (Fig. 1).[92] For these calculations the structure **65** was chosen as the model for the closed ring form (≙ **39**), and the structure **64** for the betaine form (≙ **38**) (Scheme 29).

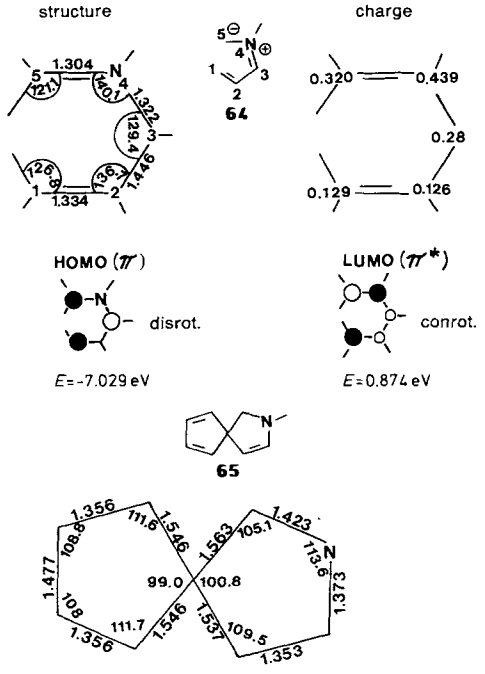


Fig. 1. Selected results of the MINDO/3 calculations on **64** (model for **38**) and **65** (model for **39**).

For the betaine **64** the following results were obtained:

1) The bond between C-2 and C-3 is to be regarded as a single bond, and all the others as double bonds (rotation about the C-2/C-3 bond therefore gives conformers).
2) The negative charges are localized preferentially on C-3 and C-5, and the positive charges mainly on the nitrogen. This means that electron acceptor substituents should have particular importance, mainly at C-3.

Analogous results are obtained from MINDO/3 calculations on more complex systems[92] of the types **67** and **68**, leading to conclusions similar to those above. The results of an X-ray structural analysis on **39** confirm the calculated geometry of the spirodihydroindolizine form **39**[91a] (Fig. 2).

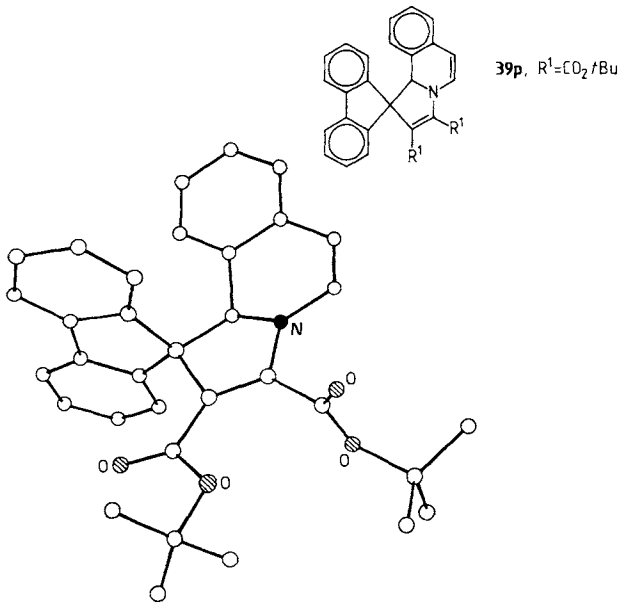


Fig. 2. Structure of **39p** in the crystal; for accurate values for bond lengths and bond angles see Ref. [91].

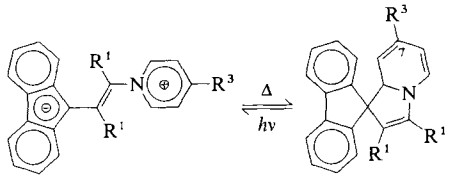
3.5. Hammett Studies of the Thermal Electrocyclization 38 → 39

In order to test the results from semi-empirical MINDO/3 calculations and to quantify electronic effects involved in the 1,5-electrocyclization **38** → **39**, LFER (= Linear Free Energy Relationship) studies were carried out. The first compounds to be investigated in this way were 7-substituted compounds **39**.

The substituents $R^1 = COOCH_3$, $COCH_3$ and CN were introduced into region B of the molecule[83, 93] (see Scheme 28). The ϱ-values obtained from a Hammett correlation of the cyclization rate constant $k_{38\rightarrow39}$ are slightly positive for the reaction R^3-**38m** → R^3-**39m**, while those for the reactions R^3-**38a** → R^3-**39a** and R^3-**38q** → R^3-**39q** are clearly negative (Fig. 3).

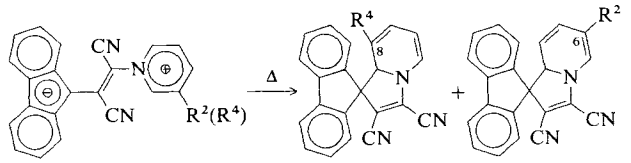
How can this effect be explained? Scheme 30 provides some answers. We shall consider only the partial structure α in the betaine structure; several resonating structures are conceivable.

If there is a strong electron acceptor such as CN at position 3, it is evident that a positive reaction center is present in the transition state. Strong acceptor substituents thus fa-



① R^3-**38** R^3-**39**

a, $R^1 = CO_2CH_3$; **q**, $R^1 = COCH_3$
R^3 = H, CH_3, OCH_3, Cl, CO_2CH_3, CN



② $R^2(R^4)$-**38m** R^4-**39m** R^2-**39m**

R^3-**38m** and R^3-**39m** see R^3-**38** and R^3-**39**, R^1 = CN

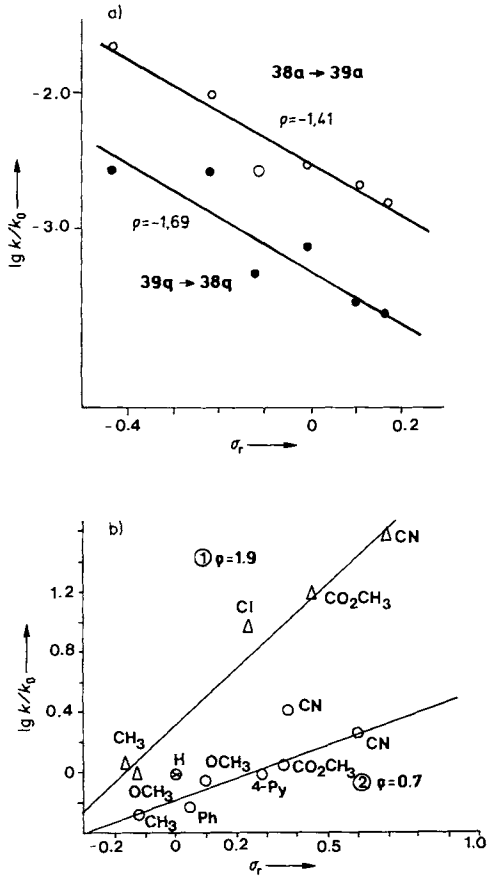
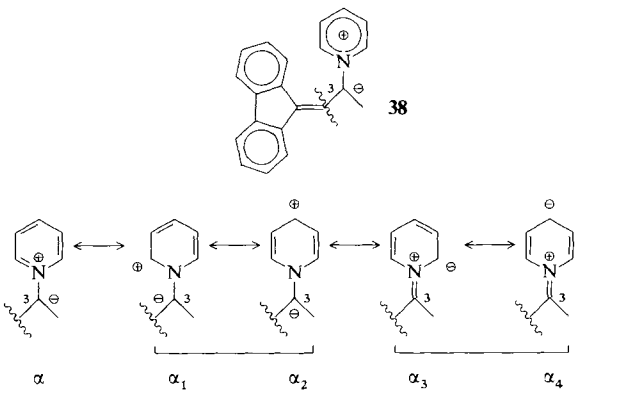


Fig. 3. Hammett correlations for the 1,5-electrocyclization of some betaines **38** to give spirodihydroindolizines **39**. a) Reactions **38a** → **39a** and **38q** → **39q** (r = 0.983 and 0.82); b) reactions of *m*- and *p*-substituted **38m** to give **39m** (r = 0.962 and 0.981, resp.).

vor the nucleophilic cyclization **38** → **39**, so that structures α_1 and α_2 have the greatest weighting. If, on the other hand, position 3 is occupied by a weak electron acceptor, the reaction center in the transition state is instead more negative in nature, and in this case, therefore, the electrocyclization should be regarded as electrophilic. The corresponding data for the effects of donor or acceptor groups in region C are summarized in Figure 3 b.



Scheme 30. Partial structures of the betaines **38**, whereby the localization of the charges in the hetero-ring is explained.

3.6. Regioselectivity

If the betaine **38m** is substituted at position 6 (cf. Fig. 3), then 1,5-electrocyclization should give regioisomers of the types R^2-**39m** and R^4-**39m**. One expects intuitively that of the two regioisomers, R^2-**39m** should predominate. However, a detailed investigation (Fig. 4), gives the wholly unexpected result that the sterically less favorable regioisomer

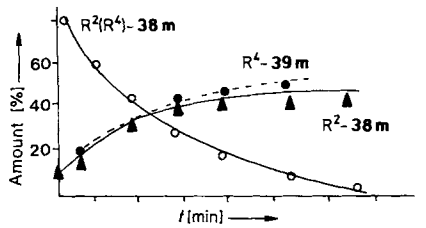


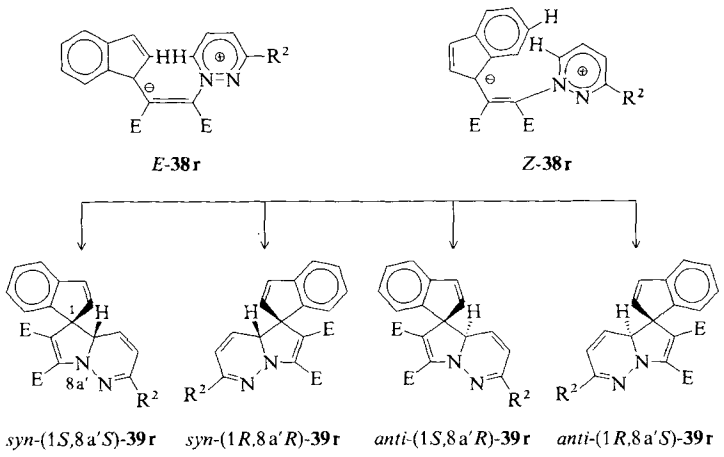
Fig. 4. Regioselectivity in the 1,5-electrocyclization of substituted betaines **38m** to the regioisomers R^4-**39m** and R^2-**39m**. The diagram is valid for $R^2 = R^4 = OCH_3$, CH_3, Cl, C_6H_5, CO_2CH_3, CN.

R^4-**39m** is formed. Moreover, in the cases where R is a donor substituent (OCH_3, CH_3, Cl) the reaction is regiospecific: in the case of the substituents C_6H_5, CO_2CH_3, and CN, the amounts of R^4-**39m** are 40, 58 and 75%, respectively.

This phenomenon is more characteristic of a pericyclic than of an ionic reaction.

3.7. Stereochemistry of the 1,5-Electrocyclization Reaction

The 1,5-electrocyclization of **39** is expected to occur photochemically as a conrotatory process and thermally as a disrotatory process (system with $(4n + 2)\pi$ electrons). Ring opening at bond "a" gives initially the *E* isomer of **38**, which can then undergo thermal conversion into the *Z* isomer. The stereochemistry of the ring closing reaction **38** → **39** can best be determined by choosing a compound that contains an asymmetrical spiro group; this results in the formation of diastereomers instead of enantiomers. For this purpose we synthesized the indenylspirene **39r**. The action of light on this molecule should give the achiral betaine **38r**. Electrocyclization of the latter should now furnish four enantiomers or two diastereomers (see Scheme 31).



E-38r *Z*-38r

syn-(1*S*,8a'*S*)-39r *syn*-(1*R*,8a'*R*)-39r *anti*-(1*S*,8a'*R*)-39r *anti*-(1*R*,8a'*S*)-39r

Scheme 31. Possible diastereomers **39r** in the 1,5-electrocyclization of **38r**, $R^2 = C_6H_5$; $E = CO_2CH_3$

According to an NMR analysis two isomer pairs were formed in the ratio 94:6. Exact analysis of the 400-MHz NOE difference spectrum showed that the *syn* diastereomeric pair had been isolated as the dominant components. The measured diastereomeric ratio also remained constant after several cycles, indicating that the reaction **38r** → **39r**, $R^2 = C_6H_5$, is *diastereoselective*.[82b] This is also true for the derivative with R^2 = styryl (*syn*:*anti* = 92:8). These results therefore demonstrate for the first time that in the 1,5-electrocyclization of a dihydropyrrole system the stereochemistry is preserved, and that the ring closing reaction **38** → **39** is therefore disrotatory.

For the 1,5-electrocyclization reaction **38** → **39** we find small values for $\Delta H^{\neq}$ and large negative values for $\Delta S^{\neq}$; depending on the substituents either electrophilic or nucleophilic cyclization can occur, and the HOMO has the correct orbital coefficients.

The reaction is regioselective and diastereoselective, and is therefore probably a pericyclic reaction.

3.8. The Photochemical Reaction 39 → 38

To obtain a deeper insight into the photochemical reaction **39** → **38**, it is necessary to determine firstly its multiplicity and secondly its kinetics. To do this, however, a quantitative determination of the competing photophysical processes is first needed, and the absorption and emission spectra must be known. Table 5 gives a summary of experimental data for selected spirodihydroindolizines (and N-analogues) **39**.

From the UV spectra (see Tables 1 and 2) one can further determine the natural lifetimes, and from the fluorescence spectra the fluorescence quantum yields Φ_F (Table 6). Owing to the low fluorescence quantum yields, it is not always possible to measure the lifetimes τ of **39** directly at room temperature, but measurements can be made at 77 K (Table 6).

As Table 5 shows, the compounds **39** can be divided into three groups:

A) compounds with a C_6-spiro bridge and cyano (or ester) substituents R^1 (**39s, t**),

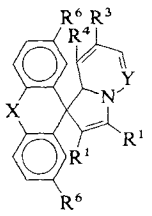
B) compounds with a C_5-spiro bridge and ester substituents R^1 (**39a, e, g, g(Cl$_2$), g(Br$_2$)**), and

C) compounds with a C_5-spiro bridge and cyano substituents R^1 (**39e, m, n**).

On going from group B to group A the UV absorption and fluorescence maxima undergo bathochromic shifts (i.e. to longer wavelengths). The fluorescence quantum yields are very small in all three groups. The singlet energies for groups B and C are 65–68 kcal mol^{-1}, and for group A 59–63 kcal mol^{-1}.[94]

The exact excitation energies of the compounds **39** made up of orthogonal structural units are likely to fall within region C (cf. Scheme 28). Pariser-Parr-Pople calculations[94] lend support to this assignment. It appears, therefore, that the effective chromophore in **39** may be the (aza)butadienylvinyl moiety. Intramolecular charge-transfer excitations appear less likely,[94] and the ^1A_g state from which emission occurs is not reached directly by absorption.

Table 5. Selected emission data of some dihydroindolizines (and N-analogues) **39**. $E = CO_2CH_3$.

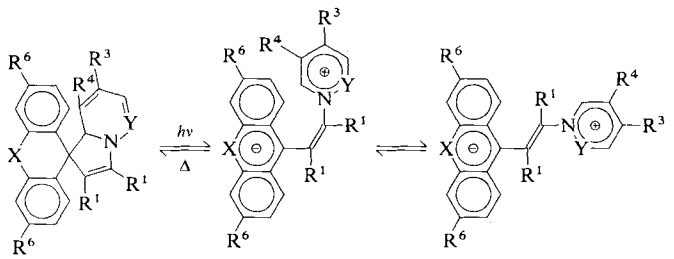


39

39	X	Y	R^1	R^3	R^4	R^6	λ_f(max) [nm] [a]	λ_{ex}(max) [nm] [b]	$E(S_1)$ [kcal mol^{-1}] [c]	$E(S_1)$ [kcal mol^{-1}] [d]
a	–	CH	E	H	H	H	460	335	68.2	67.6
e	–	CH	E	$(CH=CH)_2$		H	450	330	65.8	70.2
e'	–	CH	CN	$(CH=CH)_2$		H	460	410	65.0	64.0
g	–	N	E	H	H	H	493	340	66.5 (65.7) [e] 65.8	67.6
g(Cl$_2$)	–	N	E	H	H	Cl	462	395	66.5	66.5
g(Br$_2$)	–	N	E	H	H	Br	497	390	66.1	66.5
m	–	CH	CN	H	H	H	495	360	67.6	62.2
n	–	N	CN	H	H	H	454	370	66.6	67.1
s	C=O	N	CN	H	H	H	508	400	63.6	60.6
t	C=O	CH	CN	$(CH=CH)_2$		H	520	450	58.9	59.3

[a] Maximum at 25 °C (in CH_2Cl_2). [b] λ_{ex}(max), excitation wavelength. [c] From emission spectra. [d] From absorption spectra. [e] at 77 K.

Table 6. Fluorescence lifetime τ_s, fluorescence quantum yields Φ_F, reaction quantum yields Φ_R and rate constants k_{ic} and k_R for the photochemical ring-opening **39** → **38** at 25 °C.



39 *E*-**38** *Z*-**38**

39	X	Y	R^1	R^3	R^4	R^6	τ_S [ns]	Φ_F $\times 10^3$	k_F [s^{-1}]	Φ_{ic}	k_{ic} [s^{-1}]	Φ_R [a]	k_R [a] [s^{-1}]
a	–	CH	E	H	H	H	1.94	–	–	0.67	2.20×10^8	0.43	3.41×10^8
d	H, H	CH	E	$(CH=CH)_2$		H	0.50	–	–	0.20	1.63×10^9	0.80	4.04×10^8
d(Cl_2)	H, H	CH	E	$(CH=CH)_2$		Cl	0.15	1.0	3.12×10^6	0.29	4.67×10^9	0.70	1.93×10^9
g	–	N	E	H	H	H	0.68	–	–	0.65	5.12×10^8	0.35	9.61×10^8
n	–	N	CN	H	H	H	0.21	3.5	1.74×10^7	0.36	3.00×10^9	0.63	1.74×10^9
s'	C=O	N	E	H	H	H	0.42	2.2	5.24×10^6	0.41	1.38×10^9	0.58	9.76×10^8
u	H, H	N	E	H	H	H	0.43	2.3	5.40×10^6	0.43	1.30×10^9	0.56	1.00×10^9

[a] Determined at 77 K.

3.8.1. The Multiplicity of the Photochemical Reaction 39 → 38

Attempts to quench the triplet level of **39** using known quenching agents such as diacetyl or anthracene remained unsuccessful; formation of the betaine **38** was not affected at all. Another attempt had a similar result; when tetramethyl-1,2-dioxetane is decomposed thermally, triplet acetone is formed as a chemically induced species.[95, 96] If this experiment is carried out in the presence of **39**, formation of **38** via chemiexcitation is not observed. From this one must conclude that the excited state is a singlet or a fast reacting triplet which does not undergo bimolecular quenching (for details see Ref. [94]).

The determination of the quantum yield for ring opening is not a trivial problem. The general scheme can be formulated on the principle that the reaction is not only thermally but also photochemically reversible. This means that the reverse photochemical reaction (rate constant k_1) is superimposed on the reverse thermal reaction (rate constant k_2). The analysis must therefore be carried out using non-linear optimization methods (for details see Ref. [97]).

Table 6 lists the exact values. Table 7 also includes approximate values for Φ_R, determined by the classical method, neglecting the reverse thermal and photochemical reactions. The quantum yields are also wavelength-dependent (see Fig. 5). There exists as yet no simple explanation for these facts.

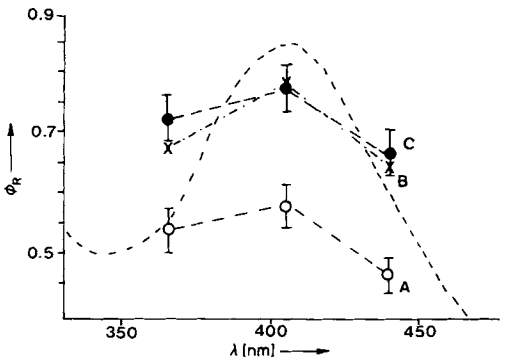


Fig. 5. Dependence of the quantum yield Φ_R on wavelength in the photoreaction of the spirodihydroindolizine **39m** to give the betaine **38m**. As derivatives of **39m** the following were used: **A**: $R^3=CH_3$; **B**: $R^3=CO_2CH_3$; **C**: $R^3=CN$ (see also Table 5).

Table 7. Reaction quantum yield Φ_R for the photoreactions **39n** → **38n** and **38n** → **39n** at 25 °C. For details see text. I_0 = intensity [Einstein s^{-1} cm^{-2}]. For substituents see Tables 1 and 5.

39n $\underset{\Phi_2}{\overset{\Phi_1}{\rightleftharpoons}}$ **38n**

I_0	k_2	Φ_1 [a]	Φ_1 [b]	Φ_2 [b]	Φ_2 [b]
3.6×10^{-11}	3.8×10^{-4}	1.32	0.94	0.84 ± 0.11	0.05 ± 0.12
4.5×10^{-11}	1.7×10^{-4}	1.11	0.02	0.81 ± 0.09	0.015 ± 0.11
8.0×10^{-10}	2.1×10^{-4}	0.86	0.002	0.87 ± 0.09	0.002 ± 0.10

[a] Uncorrected values. [b] Corrected values taking k_2 into consideration.

3.8.2. Kinetics

The kinetics of the photochemical ring opening can be determined from the measured data, using Equation (d):

$$\Phi_F + \Phi_R + F_{ic} + \Phi_{isc} = 1 \qquad \text{(d)}$$

where Φ_F, Φ_R, Φ_{ic} and Φ_{isc} are the quantum yields for fluorescence, reaction, internal conversion and intersystem crossing, respectively.

Since the reaction does not proceed via the triplet state of **39**,[194] we can insert the value $\Phi_{isc} = 0$. With this assumption

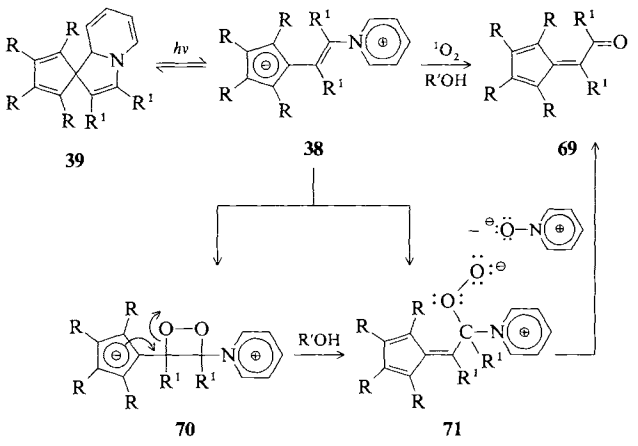
the reaction rate constant k_R can now be calculated (see Table 6).

The evaluation of k_R shows that the reaction rates decrease in the series **39d** (Cl_2) > **39n** > **39u** > **39s'** > **39g** > **39d** > **39a** (for formulas see Table 5).

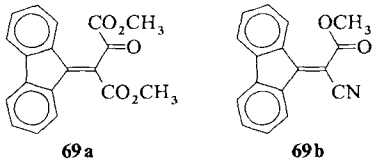
The conclusions reached are summarized as follows: Compounds **39** with electron-withdrawing CN groups in region B and electron-deficient dihydrodiazine groups in region C are evidently the fastest reacting systems in the photochemical reaction **39** → **38**. Laser flash photolysis studies of the kinetics of the process **39** → **38** indicate that, following the photoexcitation, the betaine **38** appears immediately in the *Z* form.[98] However, flash spectroscopic experiments on a spirotetrahydroindolizine with R^1 = benzoyl suggest the formation of an isomer which undergoes a first order conversion to the *Z* form.[99] In the chromophoric systems **47** the photochemical reaction is considerably more complex.

3.8.3. Photostability

When the spirodihydroindolizines (and *N*-analogues) **39** are irradiated with light it is found that the compounds decompose after some time. However, if oxygen is excluded by working with degassed samples, these systems are noticeably more stable. It is possible that in the presence of oxygen the betaine **38** acts as a sensitizer towards singlet oxygen. We have tried to clarify this problem by experiments in which singlet oxygen was deliberately generated, with hematoporphyrin as a sensitizer. Under these conditions the reaction of $^1O_2$ with **39** → **38** gave a base-free product, which in the case of the bis-ester **39a** was the fluorenylideneoxalacetic acid ester **69a**, and in the case of the bis-cyano compound was the cyanoacetic acid derivative **69b**. How could these products be formed? It is possible that the first stage is a photochemical ring-opening of the spirodihydroindolizine derivative **39**, with an electrocyclic reaction giving a betaine **38**. Oxygen could then add on to the betaine in a [2 + 2]cycloaddition, with formation of the dioxetane **70**. Ring opening and elimination of pyridine-*N*-oxide (identified by spectroscopy) should then give the products **69a** or **69b**. However, a possibility which now appears more likely is the direct action of $^1O_2$ on the betaine **38** to form a peroxide **71**, which then decomposes in the manner indicated, giving the appropriate product **69a** or **69b** (Scheme 32).[100a] Recently, it could be shown that the betaine **38** can indeed function as a singlet oxygen sensitizer.[100b]



product when $R^1 = CO_2CH_3$: **69a**; when R^1 = CN: **69b**



69a **69b**

Scheme 32. $-R-R- = -(CH_2=CH_2)_2-$; $E = CO_2CH_3$.

4. Possible Applications

The inherent properties of photochromic systems make them suitable for use in many different areas. Basically there are four main groups of possible applications, each making use of different special properties:

1) the control and measurement of radiation intensity,
2) visual contrast effects,
3) solar energy conversion,
4) information imaging and storage.

In the following, representative examples will be described for each of the four groups.

The physical (and chemical) characteristics which are important in applications of photochromic systems include:

- the spectral regions where absorption occurs, or the operating wavelengths
- sensitivity
- reversibility and useful life (number of cycles)
- properties as a storage medium.

The desirable properties for the application areas listed above sometimes overlap with each other to a considerable extent. Differences also arise according to whether the properties of the systems are measured in polar or non-polar solvents, or in the crystalline phase or in a polymeric matrix.

4.1. Absorption Region or Operating Wavelengths

The absorption region is subject to wide variation according to which class of materials is used. Figure 6 shows the

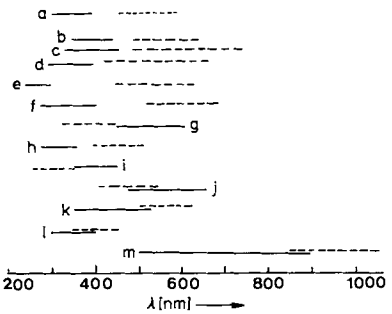


Fig. 6. Regions of the operative wavelengths of selected photochromic compounds before (——) and after (– – –) irradiation. a: fulgides (cf. **9**); b: spirodihydroindolizines (and N-analogues, cf. **39**); c: bis(spirodihydroindolizines) (cf. **47**); d: spiropyrans (cf. **14**, **16c**, **72**); e: triphenylmethane derivatives (cf. **26**); f: hexaarylbiimidazolyls (cf. **24b**); g: formazenes; h: hydrazones; i: stilbenes; j: indigoids (cf. **1**, **2**); k: azomethines (cf. **8**, **22**); l: azo compounds; m: cyanines.

absorption regions for commonly used photochromic compounds. It can be seen from the figure that in most cases the colorless form A absorbs in the near UV or visible region, while the colored form B absorbs in the range 450–600 nm. Only the bis-betaines **48** and the cyanines continue to show absorptions in the long-wave visible, or even the short-wave IR regions.[101, 102]

High extinction coefficients and conversion efficiencies are found especially for those compounds in which

- a conjugation blocking group is photolytically removed,
- a cyanine structure is formed,
- a polyene is formed,
- a charge-transfer complex is formed.

4.2. Sensitivity

The sensitivity of a photochromic system for information storage is given by the energy in joule per cm^2 of surface area which is needed to change the optical signal function (optical density (D)) by 0.1 compared with a suitable density standard. Photochromic systems are found to have maximum sensitivities of the order of $E_{max} \approx 10^{-3}$ J cm^{-2} dB^{-1}.

Semiempirical formulas exist for determining this quantity.[103] The main feature of the results is η, which depends on the position of the photochemical equilibrium and often has a value in the range 0.5–1.0.

4.3. Reversibility and Useful Life (Number of Cycles)

In nearly all the areas where photochromic substances can be used, the reversibility and the useful life in cycles are among the most important properties. The useful life in cycles, Z, is essentially limited by the relative incidence of reversible (and irreversible) side reactions. The irreversible reactions are known as fatigue processes. The matrix too can cause effects which limit the life. Some typical experimentally measured values Z_{exp} for various systems are listed in Table 8.

The intensively studied spiropyran derivatives[4] show very short lifetimes of $Z_{exp} = 10^1$–10^2 cycles. The newer systems based on the spirodihydroindolizines **39**, the thymines and the fulgides (e.g. Aberochrome 540, **9a**) give Z_{exp} values of 10^3–10^4. For Aberochrome 555 **9b** and the salicylideneanilines, Z_{exp} values as high as 10^4–10^5 are found. These newer photochromic systems are of great interest because of their long useful lifes.

Molecules whose photochromism is based on triplet-triplet absorption, e.g. coronene, should in principle be capable of giving an infinite number of cycles.

Table 8. Number of cycles E_{exp} achieved experimentally for some photochromic and some non-photochemical systems.

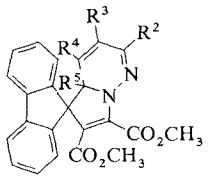
System	Working principle	$Z_{exp.}$	Ref.
Organic photochromic systems:			
Spirodihydroindolizines (*N*-analogues) **39**	Electrocyclic (Valence tautomerization)	$>10^3$	[40, 74–80, 82–84]
Fulgides, e.g.			
Aberochrome 999 (cf. **9b**)	Valence tautomerization	$\approx 10^3$	[23–27]
Aberochrome 540 (cf. **49a**)	Valence tautomerization	10^4 to 10^5	[23–27]
Spiropyrans in polymers	Valence tautomerization	10^1 to 10^2	[4, 32–47]
Anthracenes	Dimerization	10^3	[4]
Dinitrobenzylpyridines	Tautomerization	10^3	[4]
Thymine	Dimerization	10^3	[4]
α-Salicyclideneaniline	Tautomerization	10^4 to 10^5	[104a]
Acridizinium compounds	Dimerization in the crystalline phase	10^4	[104a]
Diisopropoxyindigo in epoxide resin	Isomerization	10^2	[104b]
Aziridines	Valence tautomerization	10^2	[101]
Inorganic photochromic systems:			
AgX glasses	Photolysis	3×10^5 to 10^6	[101]
Calcium fluoride, doped.	Electronic process	10^4	[101]
Strontium titanate, iron-doped	Electronic process	10^4	[101]
Non-photochemical systems:			
Magnetic tape	Magnetic process	10^5 to 10^6	[101]
MnBi-film	Magnetooptic process	10^4	[101]
FEPC devices	Photoconductor + ferroelectric	10^{11}	[101]
Photosensitive thermoplastic films	Electrostatic process	10^2 to 10^4	[101]
MNOS-CCD storage devices	Electronic process	10^{10} to 10^{12}	[101]

4.4. Photochemical Stability

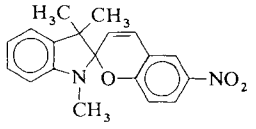
The photochemical stability (on which the potential useful life indirectly depends) can also be determined by a photochemical degradation experiment.

Table 9 gives some recent results from stability tests of this

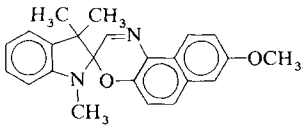
Table 9. Comparison of the photochemical stability of spirodihydroindolizine derivatives **39g, v–y** [105] and classical compounds **72** [4], **73** [49b, 108], **74** [109] of the spiropyran type. The decrease in depth of color with time (100% at $t = 0$) upon irradiation with a xenon high-pressure lamp (Sun-Test apparatus, light (irradiation) intensity 140000 Lux; on CR 39® glass, at ca. 40 °C). $t_{1/2}$ = half-life.



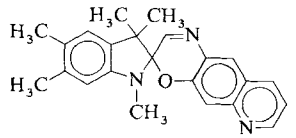
39



72



73



74

					Duration of xenon test					
	R^2	R^3	R^4	R^5	1 h	2 h	3 h	4 h	5 h	$t_{1/2}$
					Coloration [%]					
39g	H	H	H	H	72.9	58.4	34.6	25.5	16.5	2.2 h
39v	CH_3	H	H	H	47.7	12.1				57 min.
39w	CH_3	H	H	CH_3	85.3	73.5	60.3	55.8		4.34 h
39x	CH_3	CH_3	CH_3	CH_3	73.5	29.4	7.3			1.56 h
39y	CH_3	H	CH_3	CH_3	no coloration produced					
72										10 min
73										200 h
74										225 h [a]

[a] Under inert gas.

kind. The test conditions are in most cases those used in commercial "sun test" equipment (e.g., a high-pressure xenon lamp giving an illumination of 140000 Lux).

4.5. Information Storage Properties

Photochromic media which are to be used for display and storage applications must perform satisfactorily with regard to the properties discussed in Section 4. The operating wavelength range can nowadays be chosen to suit any specification quite accurately. Wavelengths of particular interest are those of the inexpensive He/Ne lasers ($\lambda = 633$ nm) and GaAs IR lasers ($\lambda = 830$ nm). Fast optical storage devices with rates of the order of 10^6 cycles per second are required here. For this application it will certainly be necessary to develop suitably modified versions of known photochromic systems. On the other hand, photochromic systems, as a result of their lack of graininess, have high storage densities and high image resolving power compared with AgX films. Their resolving power is in most cases about 1000 mm^{-1} [102] (see Table 10). The signal-to-noise ratio is very good.

4.6. Recent Developments

In the first group of applications, photochromic systems are used in controlling or measuring radiation intensity.

These applications make use of the change in color of photochromic materials, which is essentially caused by the action of sunlight. This property finds applications where

Table 10. Resolving powers (AV) and storage densities (D_F) of photochromic systems and other storage materials [101, 102].

System	AV [mm^{-1}]	D_F [bit cm^{-2}]
Organic photochromic systems:		
72 in polyvinylbutyral (5 μm layer)	≥ 1000	10^8
Inorganic photochromic systems:		
Photochromic glasses (AgX)	2100	4.4×10^8
Alkali metal halides	1000	10^8
Sodalite films	100	10^6
AgX materials:		
ORWO NP 55	91	8.3×10^5
ORWO PF 5	250	6.25×10^6
ORWO DK 5	600	3.6×10^7
ORWO LP 2	2500	6.25×10^8
Agfa-Gevaert 8 E 70	3000	9×10^8
Other light-sensitive materials:		
Diazo microfilm	1000	10^9
Dichromate films	2000–4000	4×10^8 to 1.6×10^9
PbI_2 films	1000	10^8
Dylux XP-503	500	2.5×10^7

optical filters are generally used, i.e. in spectacles, optical lenses, glass used in buildings, and windshields for automobiles and aircraft (cf. Table 11).

Silver halide spectacle lenses show fatigue effects and a slow (non-linear) fading behavior when they have been in use for some time,[4, 69] and organic photochromic substances have therefore been developed for this purpose and recently introduced onto the market. Instead of the aziridines previously used for this purpose,[106] which are photochromic only in the crystalline state, spiropyrans, such as **72**[107] have been introduced as substances having suitable properties for photochromic spectacle lenses. Systems showing virtually no fatigue have been discovered in the spirooxazines, and are being marketed by the American Optical Company (**73**),[108] PPG (**74**)[109] and Rodenstock.[110] (Systems which could be suitable for this application are described in Refs. [76, 77].)

Heller et al., whose conventional types of fulgides,[23–26] being inverse photochromic systems, are unsuitable for this application, has patented a new isomeric fulgide system known as Heliochrome, which should find applications as a photoreactive material for optical lenses or spectacles.[111]

Various types of actinometers based on photochromic substances have recently come onto the market, and are used to measure radiation intensities.

Of the systems used, only a few will be mentioned here. Aberochrome 540 **9a**[23–27, 103, 112] derived from the fulgides series and Aberochrome 999, **9b**, can be used in the UV and visible regions. The *endo* peroxides of the heterocoeranthrone (Actinochrome® 238/334 and 475/610)[53, 54] (cf. also **21**), whose photochromism is based on a bimolecular photoreaction, are also employed in these spectral regions. In a similar way the spiropyran **72** is used in lithography as a simple dosimeter.

Another important area of application is that of contrast effects. In this class of applications photochromic substances are efficient as active light filters, and in the production of printing plates and printed circuits.[101, 113, 114]

The third main field of application is in solar energy con-

Table 11. Applications of photochromic materials

Control & measurement of radiation intensities	Contrast effects	Recording and storage of information
a) Optical filters – Lenses – Glasses – Cuvettes	Masks for contrast equalization in photography – Film materials	a) Imaging – Instantaneous imaging materials – Office copying materials – Microfilm – Microfilm copying materials – Sprays
Radiation protection equipment – Glasses – Spectacles – Films – Containers	Amplifying contrast in projected images – Projection screens – Projection walls	b) Digital information – Slow storage – Bulk data storage (archives etc.)
Protection from sun	Production of printing plates and circuit boards – Photoresists – Photopolymers	Holography – Storage disks – Storage films – Crystals
Protection from flash exposure, lasers etc.	Solar energy conversion	Data display systems – Display screens (image screens)
Document preservation	Energy storage	Q-switches (for lasers)
Temperature indicators		Molecular electronics
b) Actinometry, dosimetry – Actinometer – Dosimeter		

version. The need here is for photochromic systems which absorb in the visible region and have a high energy storage capacity. In these systems, however, the solar energy is stored indirectly as heat. The most favorable system of this type is quadricyclane.[115] However, the merits of this approach to research on solar energy conversion are now being questioned.[9] Storage of solar energy in other forms, namely as chemical or electrical energy, appears to have advantages.[10]

A very interesting application of photochromic systems is in the area of information recording. Two particularly important systems are the Dylux process and the perhalide process. By evaluating image-forming properties it is possible to identify materials suitable for use in photocopying and instantaneous imaging,[102] though in these applications the necessary life is only one cycle ($Z = 1$).

These techniques found a useful application in the photochromic micro-imaging (PCMI) process developed by the National Cash Register Company.[116] Microimages are now generally produced using diazo microfilm or vesicular films (polyester/diazonium salts).[117]

Photochromic substances of the fulgide type, which can be employed for information recording and in holography have also been developed by *Heller* et al.[118] Also the photochromic 2,4,5-triphenylimidazolyl dimers (cf. **24b**) can be employed as photoinitiators for producing holograms.[119]

A promising future application in the production of optical recording materials is based on the *trans-cis* isomerization of azobenzenes in a liquid crystalline medium. Azobenzene fixed covalently to glass in a nematic or cholesteric phase gives stable images with excellent resolution on exposure to light. This process has also been used for the production of holograms.[120]

An extension of this principle is the coupling of photochromic molecules—such as azobenzene,[121] spiropyrans[122] or fulgides[121]—with polymers or liquid crystalline polymers. Such combinations have been employed in holography[117] or in non-destructive optical "read-out" systems.[121–123] Nonlinear optical recording processes are based on the excitation of photochromic molecules by two-photon processes. Spiropyrans have been employed under these conditions in non-destructively operating write- and read-out systems using He/Ne lasers.[124] Photochromic spiropyrans have also found use in the production of photoresists.[125]

A new application of tailor-made molecules of the spirodihydroindole type is in frequency doubling of laser radiation. The thread-like dipolar merocyanine-type molecules become aligned in an electric field. In the presence of two electric fields the quasi-crystalline dyestuff aggregates form an excellent frequency doubler.[120] A similar system based on spirodihydroindolizine derivatives has recently been patented.[127]

An interesting potential application has been proposed in the field of molecular electronics.[128–131] By using a one-dimensional conductor ("molecular wire") of the polyacetylene type in combination with suitable molecular switches—e.g. salicylideneanilines—it should be possible to make a molecular microchip whose information storing capacity is a factor of 10^6 greater than that of conventional microchips. Such a completely new technology would make it possible to design a new generation of high performance computers with memory elements of nanometer dimensions.

5. Summary and Future Prospects

The development of new photochromic systems which involve a 1,5-electrocyclization has been described. This reaction is in principle based on the cyclization of conjugated 1,3-dipoles of the allylic type. The 1,5-electrocyclization is formally the first intermediate stage envisaged for a "1,3-dipolar (non-cooperative) cycloaddition" as described by *Huisgen*.[72] It is therefore an elegant method for synthesizing five-membered ring systems, although in the case of photochromic systems there are additional restrictions with regard to photoreversibility (and thermoreversibility).

The new photochromic systems (see also Table 3) vary widely in their properties. They provide a useful extension to the palette of homologous series of photochromic systems. In the area of basic research this reaction offers the possibility of synthesizing new photochromic substances with:

- improved photostability, and thus longer useful life (number of cycles),
- higher sensitivity, especially for information recording,
- a wider choice of operating wavelengths, especially with regard to absorption in the IR region for use with IR lasers (e.g. GaAs),
- amplification capability, i.e. with quantum yields > 1,
- functional groups which confer solubility in water.

Important objectives for future research include modifying already known systems by incorporating them physically or chemically into liquid crystals or polymers, so as to obtain improved properties for specific applications, and developing an effective molecular electronics system based on photochromic molecules to produce new VLSI (very large scale integrated) computer chips.

My thanks are due to Frau Prof. S. E. Braslavsky, MPI Mülheim and Herrn Priv. Doz. Dr. A. M. Braun, EPFL Lausanne for carefully reading the manuscript. I also thank my coworkers V. Bach, J. Besse, C. Dorweiler, H. Gross, G. Hauck, M. Herrig, M. Holderbaum, R. Johann, H. P. Jönsson, S. Kenziora, H. Kilburg, G. Klauck, J. Mosbach, T. Münzmay, V. Port, P. Scheidhauer, C. Schommer, C. Shulz, P. Spang, A. Thome and K. Zils for their involvement and enthusiasm in this project. Last but not least, my thanks are due to the Deutsche Forschungsgemeinschaft and to the Fonds der Chemischen Industrie for financial support, and to BASF for providing many chemical compounds.

Received: January 21, 1987;
revised: November 2, 1987 [A 713 IE]
German version: Angew. Chem. 101 (1989) 427

[1] J. E. ter Meer, *Justus Liebigs Ann. Chem. 181* (1876) 1.
[2] a) W. Marckwald, *Z. Phys. Chem. Stoechiom. Verwandtschaftsl. 30* (1899) 140; b) The term *phototropy* is nowadays understood to mean the light-induced interactions occurring in biological systems, including the effects of light on the nutritional systems of plants or microorganisms, while *phototropism* is the tendency of plants to turn towards the source of light.
[3] Y. Hirshberg, *C. R. Hebd. Séances Acad. Sci. 231* (1950) 903.
[4] G. H. Brown: *Photochromism*, Wiley-Interscience, New York 1971.
[5] Review articles and books: a) R. D. Murray, *"Silverless Imaging Systems", Neblette's Handb. Photogr. Reprogr. 7th Ed. 1977*, p. 397; b) V. A. Barachevskii, G. I. Lashkov, V. A. Tsekhomskii: *Photochromism and its Use*, Izd. Khimiya, Moscow 1977; *Chem. Abstr. 89* (1978) B:14791h; c) H. G. Heller, *Chem. Ind. (London) 1978*, 193; d) A. S. Kholmanskii, A. V. Zubkov, K. M. Dyumaev, *Russ. Chem. Rev. 50* (1981) 305; e) A. V. El'tsov, V. A. Bren, Y. E. Gerasimenko: *Organic Photochromic Substances*, P. P. Khimiya, Leningradskoe Otdelenie, Leningrad 1982, p. 285; *Chem. Abstr. 99* (1983) B:4775y; f) G. Smets, *Adv. Polym. Sci. 50* (1983) 17; g) E. Fischer, *Rev. Chem. Intermed. 5* (1984) 393; h) L. H. Marcus, *Gov. Rep. Announce, Index (U.S.) 80* (1980) 5760; *Chem. Abstr. 94* (1981) 130192r, 130193s, 130196v; i) *Workshop on Photochromics, Xth IUPAC Symposium on Photochemistry*, Interlaken 1984.
[6] G. N. Lewis, D. Lipkin, T. T. Magel, *J. Am. Chem. Soc. 63* (1941) 3005.
[7] M. W. Windsor, US-Pat. 3214382 (1965), TRW Inc.; *Chem. Abstr. 76* (1971) 45277f.
[8] J. Kropp, M. W. Windsor, *U.S. Gov. Res. Dev. Rep. 68* (1968) 56; *Chem. Abstr. 70* (1968) 72511k.
[9] H. D. Scharf, J. Fleischhauer, H. Leismann, I. Ressler, W. Schlecker, R. Weitz, *Angew. Chem. 91* (1979) 696; *Angew. Chem. Int. Ed. Engl. 18* (1979) 652.
[10] E. Schumacher, *Chimia 32* (1978) 193.
[11] a) G. M. Wyman, W. R. Brode, *J. Am. Chem. Soc. 73* (1951) 1487; D. A. Rogers, J. D. Margerum, G. M. Wyman, *ibid. 79* (1957) 2464; b) D. L. Ross, *Appl. Opt. 10* (1971) 571; c) M. Irie, M. Kato, *J. Am. Chem. Soc. 107* (1985) 1024.
[12] a) D. Gegiou, K. A. Muszkat, E. Fischer, *J. Am. Chem. Soc. 90* (1968) 3907; b) review: E. Fischer, *Chem. Unserer Zeit 9* (1975) 85.
[13] a) F. B. Mallory, C. W. Mallory, S. E. Sen Loeb, *Tetrahedron Lett. 26* (1985) 3773; b) F. B. Mallory, C. W. Mallory, *Org. React. (NY) 30* (1984) 48; c) K. A. Muszkat in S. Patai, Z. Rapoport: *The Chemistry of Quinoid Compounds, Vol. 2*, Wiley, New York 1988.
[14] a) P. Ball, C. H. Nicholls, *Dyes Pigm. 6* (1985) 13; *Chem. Abstr. 102* (1985) 96938k; b) S. Shinkai, T. Okawa, Y. Kusano, O. Manabe, K. Kikukawa, T. Goto, T. Matsuda, *J. Am. Chem. Soc. 104* (1982) 1960.
[15] J. Labsky, F. Mikes, J. Kalal, *Polym. Bull. 4 (12)* (1981) 711.
[16] D. R. Arnold, L. A. Karnischky, *J. Am. Chem. Soc. 92* (1970) 1404.
[17] E. F. Ullman, J. E. Milks, *J. Am. Chem. Soc. 84* (1962) 1315.
[18] E. F. Ullman, W. A. Henderson, Jr., *J. Am. Chem. Soc. 88* (1966) 4942; *89* (1967) 4390.
[19] a) J. S. Splitter, M. Calvin, *J. Org. Chem. 23* (1958) 65; *30* (1965) 3427; b) W. D. Emmons, *J. Am. Chem. Soc. 78* (1956) 6208; *79* (1957) 5739.
[20] a) A. M. Trozzolo, W. Yager, G. Griffin, H. Kristinsson, I. Sarkar, *J. Am. Chem. Soc. 89* (1967) 3357; b) T. Do Minh, A. M. Trozzolo, *ibid. 94* (1972) 4046.
[21] A. M. Trozzolo, T. M. Leslie, A. S. Sarpotdar, R. D. Small, G. J. Ferraudi, T. Do Minh, R. L. Hartless, *Pure Appl. Chem. 51* (1979) 261.
[22] A. M. Trozzolo, A. S. Sarpotdar, T. M. Leslie, R. L. Hartless, T. Do Minh, *Mol. Cryst. Liq. Cryst. 50* (1979) 201.
[23] a) R. J. Hart, H. G. Heller, *J. Chem. Soc. Perkin Trans. 1 1972*, 1321; H. G. Heller, M. Szewczyk, *ibid. 1974*, 1487; b) cf. also H. Stobbe, *Ber. Dtsch. Chem. Ges. 38* (1905) 3893.
[24] a) P. J. Darcy, R. J. Hart, H. G. Heller, *J. Chem. Soc. Perkin Trans. 1, 1978*, 571; b) C. Oscar, H. G. Heller, S. Patharakorn, *ibid. 1986*, 1599; c) P. J. Darcy, H. G. Heller, S. Patharakorn, R. D. Pigott, J. Whittal, *ibid. 1986*, 315.
[25] H. G. Heller, J. R. Langan, *J. Chem. Soc. Perkin Trans. 2 1981*, 341.
[26] a) P. J. Darcy, H. G. Heller, P. J. Strydom, J. Whittall, *J. Chem. Soc. Perkin Trans. 1, 1981*, 202; b) H. D. Ilge, R. Paetzold, *J. Signalaufzeichnungsmater. 5* (1977) 57; *Z. Chem. 23* (1983) 221, see also earlier works cited therein.
[27] a) A. P. Glaze, S. A. Harris, H. G. Heller, W. Johncock, S. N. Oliver, P. J. Strydom, J. Whittall, *J. Chem. Soc. Perkin Trans. 1, 1985*, 957; b) cf. C. Lenoble, R. S. Becker, *J. Phys. Chem. 90* (1986) 2651.
[28] V. Boekelheide, J. B. Philips, *J. Am. Chem. Soc. 89* (1967) 1695.
[29] V. Boekelheide, W. Pepperdine, *J. Am. Chem. Soc. 92* (1970) 3684.
[30] Y. Hirshberg, E. Fischer, *J. Chem. Soc. 1953*, 629.
[31] a) K. A. Muszkat, *Top. Curr. Chem. 88* (1980) 91; b) T. Wismonski-Knittel, G. Fischer, E. Fischer, *J. Chem. Soc. Perkin Trans. 2, 1974*, 1930; c) E. Fischer, *Rev. Chem. Intermed. 5* (1984) 393.
[32] E. D. Bergmann, A. Weizmann, E. Fischer, *J. Am. Chem. Soc. 72* (1950) 5009.
[33] E. Fischer, Y. Hirshberg, *J. Chem. Soc. 1952*, 4522.
[34] Y. Hirshberg, E. Fischer, *J. Chem. Soc. 1954*, 297, 3129.
[35] T. Bercovici, R. Heiligman-Rim, E. Fischer, *Mol. Photochem. 1* (1969) 23, 189.
[36] R. Gautron, *Bull. Soc. Chim. Fr. 1970*, 4255.
[37] J. Gervais, R. Guglielmetti, *C. R. Séances Acad. Sci. Ser. C 271* (1970) 110.
[38] A. Samat, R. Guglielmetti, J. Metzger, *Helv. Chim. Acta 55* (1972) 1782.
[39] a) P. Appriou, J. Guillerez, F. Garnier, R. Guglielmetti, *Helv. Chim. Acta 58* (1975) 2553; b) M. Le Baccon, F. Garnier, R. Guglielmetti, *Bull. Soc. Chim. Fr. II 1979*, 315.
[40] M. A. Galbershtam, L. M. Mikheeva, N. P. Samilova, *Khim. Geterotsikl. Soedin. 11* (1972) 1534.
[41] a) J. Kolc, R. S. Becker, *Photochem. Photobiol. 12* (1970) 383; b) K. H. Knauer, R. Gleiter, *Angew. Chem. 89* (1977) 116; *Angew. Chem. Int. Ed. Engl. 16* (1977) 113.
[42] I. B. Lazarenko, N. M. Przhiyalgorskaya, M. A. Galbershtam, G. K. Bobyleva, N. N. Suvorov, *Khim. Geterotsikl. Soedin 10* (1982) 1363; *11* (1984) 1482.
[43] a) B. S. Lukyanov, L. E. Nivorozhikin, Y. E. Chernysh, V. I. Minkin, *Khim. Geterotsikl. Soedin. 8* (1985) 1031; b) Y. Kalysky, T. E. Orlowski, D. J. Williams, *J. Phys. Chem. 87* (1983) 26, 5333.
[44] E. Davin-Pretelli, M. Guilliano, G. Mille, J. Chouteau, R. Guglielmetti, *Helv. Chim. Acta 60* (1977) 215.
[45] N. D. Dimitrieva, R. M. Liberzon, Y. S. Ryabokobylko, *Zh. Org. Khim. 21* (1985) 1340.
[46] M. Gehrtz, C. Bräuchle, J. Voitländer, *J. Am. Chem. Soc. 104* (1982) 2094; cf. also C. Lenoble, R. S. Becker, *J. Phys. Chem. 90* (1986) 62.
[47] a) M. A. Galbershtam, A. P. Sidorov, N. M. Przhiyalgorskaya, Y. P.-Strockach, V. A. Barachevsky, I. V. Manakova, N. N. Suvorov, *Khim. Geterotsikl. Soedin 9* (1982) 1205; b) M. Kryzewski, B. Nadolski, *J. Chem. Soc. Faraday Trans. 2 76* (1980) 351.
[48] F. Feichtmayr, A. Oberlinner, *Liebigs Ann. Chem. 1979*, 1337.
[49] a) I. Karube, M. Yamazaki, H. Matsuoka, S. Suzuki, *Chem. Lett. 1983*, 691; b) US-Pat. 4215010 (1980); c) S. E. Braslavsky, A. R. Holzwarth, K. Schaffner, *Angew. Chem. 95* (1983) 670; *Angew. Chem Int. Ed. Engl. 22* (1983) 656.
[50] J. Daub, T. Knöchel, A. Mannschreck, *Angew. Chem. 96* (1984) 980; *Angew. Chem. Int. Ed. Engl. 23* (1984) 960; A. Bäumler, J. Daub, W. Pickl,

W. Rieger, *Chem. Ber. 118* (1985) 1857; J. Daub, S. Gierisch, U. Klement, T. Knöchel, G. Maas, U. Seitz, *ibid. 119* (1986) 2631.
[51] A. Castellan, J. M. Lacoste, H. Bouas-Laurent, *J. Chem. Soc. Perkin Trans. 2 1979*, 411.
[52] a) A. Castellan, J. P. Desvergne, H. Bouas-Laurent, *Nouv. J. Chim. 3* (1979) 231; b) see also H. D. Becker, K. Sandross, K. Anderson, *Chem. Phys. Lett. 77* (1981) 246.
[53] R. Schmidt, R. Drews, H. D. Brauer, *J. Phys. Chem. 86* (1982) 4909.
[54] H. D. Brauer, R. Schmidt, *Photochem. Photobiol. 37* (1983) 587; 39 (1984) 489; *41* (1985) 119.
[55] A. Senier, F. G. Shepheard, *J. Chem. Soc. 95* (1909) 1943; *101* (1912) 1950.
[56] V. de Gaouck, R. J. W. Le Fèvre, *J. Chem. Soc. 1939*, 1457.
[57] E. Hadjoudis, E. Hayon, *J. Phys. Chem. 74* (1970) 3184.
[58] T. Rosenfeld, M. Ottolenghi, A. Y. Meyer, *Mol. Photochem. 5* (1973) 39.
[59] a) L. J. Miller, D. J. Margerum, *Tech. Chem. (NY) 3* (1971) 557; b) P. Jacques, J. P. Biava, A. Gourso, J. Faure, *J. Chim. Phys. Phys. Chim. Biol. 76* (1979) 566; c) P. Jacques, *ibid. 79* (1982) 352; *Dyes Pigm. 5* (1984) 351.
[60] a) J. W. Lewis, J. W. Sandorfy, *Can. J. Chem. 60* (1982) 1738; b) R. S. Becker, C. Lenoble, A. Zein, *J. Phys. Chem. 91* (1987) 3509, 3517.
[61] a) E. Hadjoudis, I. Moustakali-Mavridis, J. Xexakis, *Isr. J. Chem. 18* (1979) 202; b) I. Moustakali-Mavridis, E. Hadjoudis, A. Mavridis, *Acta crystallogr. Sect. B36* (1980) 1126; c) E. Hadjoudis, *J. Photochem. 17* (1981) 355.
[62] S. M. Blinder, N. W. Lord, *J. Chem. Phys. 36* (1961) 540; K. Maeda, A. Chinone, T. Hayashi, *Bull. Chem. Soc. Jp. 43* (1970) 1431.
[63] F. Feichtmayr, G. Scheibe, *Z. Naturforsch. B 13* (1958) 51.
[64] E. P. A. Zweegers, C. A. G. Varma, *J. Phys. Chem. 83* (1979) 1821.
[65] A. Hantzsch, G. Osswald, *Ber. Dtsch. Chem. Ges. 33* (1900) 278.
[66] A. D. Little, *Appl. Opt. 8* (1969) 2285.
[67] M. W. Geiser, N. J. Turro, W. Wadell, H. Walter, *Photochem. Photobiol. 25* (1977) 15.
[68] M. Kuzuya, T. Usui, F. Miyake, K. Kamiya, T. Okuda, *Chem. Pharm. Bull. 30* (1982) 708; see also S. Gunzenhauser, H. Balli, *Helv. Chim. Acta 68* (1985) 56, 64.
[69] G. Gliemeroth, K. H. Mader, *Angew. Chem. 82* (1970) 421; *Angew. Chem. Int. Ed. Engl. 9* (1970) 434.
[70] C. A. Parker, *J. Chem. Phys. 63* (1959) 26.
[71] a) R. B. Woodward, R. Hoffmann, *Angew. Chem. 81* (1969) 797; *Angew. Chem. Int. Ed. Engl. 8* (1969) 781; b) K. Fukui, *Acc. Chem. Res. 4* (1971) 57.
[72] R. Huisgen, *Angew. Chem. 92* (1980) 979; *Angew. Chem. Int. Ed. Engl. 19* (1980) 947.
[73] Review: E. C. Taylor, I. J. Turchi, *Chem. Rev. 79* (1979) 181.
[74] G. Hauck, H. Dürr, *Angew. Chem. 91* (1979) 1010; *Angew. Chem. Int. Ed. Engl. 18* (1979) 945.
[75] H. Gross, H. Dürr, *Angew. Chem. 94* (1982) 204; *Angew. Chem. Int. Ed. Engl. 21* (1982) 216; *Angew. Chem. Suppl. 1982*, 559.
[76] H. Dürr, G. Hauck, DOS 29 06 193 (1980).
[77] H. Dürr, H. Gross, K. D. Zils, DOS 32 20 257 (1983).
[78] a) H. Dürr, H. Gross, G. Hauck, *Chem. Berg. 116* (1983) 856; b) H. Dürr, K. P. Janzen, A. Thome, B. Braun, DOS P 35 21 432.5 (1988).
[79] H. Dürr, W. Gombler, R. Sergio, *Angew. Chem. 84* (1972) 215; *Angew. Chem. Int. Ed. Engl. 11* (1972) 224.
[80] H. Gross, *Dissertation*, Universität Saarbrücken 1982.
[81] M. Regitz, *Angew. Chem. 78* (1966) 684; *Angew. Chem. Int. Ed. Engl. 5* (1966) 681.
[82] a) H. Dürr, H. P. Jönsson, P. Scheidhauer, T. Münzmay, P. Spang, DOS P 3521432.5 (1985); b) H. Dürr, P. Scheidhauer, J. Besse, *XIth IUPAC Symposium on Photochemistry*, Lissabon 1986, Abstr. 202; c) cf. also D. H. Hunter, S. K. Sim, *Can. J. Chem. 50* (1972) 669, 678.
[83] a) H. P. Jönsson, *Dissertation*, Universität Saarbrücken 1985; b) P. Spang, *Dissertation*, Universität Saarbrücken 1985.
[84] H. Dürr, P. Spang, *Angew. Chem. 96* (1984) 277; *Angew. Chem. Int. Ed. Engl. 23* (1984) 241; H. Dürr, C. Schommer, T. Münzmay, *ibid. 98* (1986) 565 and *25* (1986) 572.
[85] a) K. H. Grellmann, W. Kühnle, H. Weller, T. Wolff, *J. Am. Chem. Soc. 103* (1981) 6889; b) K. H. Grellmann, M. Schmitt, H. Weller, *J. Chem. Soc. Chem. Commun. 1982*, 591; c) A. G. Schultz, *Acc. Chem. Res. 16* (1983) 210.
[86] H. Dürr, A. Thome, U. Steiner, T. Ulrich, E. Rabe, C. Krüger, *J. Chem. Soc. Chem. Commun. 1988*, 338.
[87] a) V. Bach, *Diplomarbeit*, Universität Saarbrücken 1984; b) T. L. Gilchrist, C. W. Rees, *J. Chem. Soc. C 1968*, 779.
[88] A. Meuwsen, R. Gösl, *Chem. Ber. 92* (1959) 2521.
[89] a) C. Schommer, *Dissertation*, Universität Saarbrücken 1987; b) C. Dorweiler, T. Münzmay, P. Spang, M. Holderbaum, H. Dürr, E. Raabe, C. Krüger, *Chem. Ber. 121* (1988) 843.
[90] C. Dorweiler, *Dissertation*, Universität Saarbrücken 1986.
[91] a) C. Dorweiler, P. Spang, H. Dürr, K. Peters, H. G. von Schnering, *Isr. J. Chem. 25* (1985) 246; b) for the Hammett calculation see H. G. O. Becker: *Elektronentheorie organisch-chemischer Reaktionen*, H. Deutsch, Berlin 1974, p. 83.
[92] a) N. A. Garcia, G. Rossbroich, S. E. Braslavsky, H. Dürr, C. Dorweiler, *J. Photochem. 31* (1985) 297; b) C. Dorweiler, H. Dürr, H. P. Jönsson, *Xth IUPAC Symposium on Photochemistry*, Interlaken 1984, Abstr. 359.
[93] a) G. Klauck, *Dissertation*, Universität Saarbrücken 1983; b) A. Berkessel, *Diplomarbeit*, Universität Saarbrücken 1982.
[94] H. Gross, H. Dürr, W. Rettig, *J. Photochem. 26* (1984) 165.
[95] N. J. Turro, P. Lechtken, N. E. Schore, G. Schuster, H. Steinmetzer, A. Yekta, *Acc. Chem. Res. 7* (1974) 97.
[96] W. Adam, *Adv. Heterocycl. Chem. 21* (1977) 437.
[97] R. Bär, G. Gauglitz, R. Benz, J. Polster, P. Spang, H. Dürr, *Z. Naturforsch. A 39* (1984) 662.
[98] U. Steiner, Universität Konstanz, private communication.
[99] H. Dürr, H. Gross, K. D. Zils, G. Hauck, G. Klauck, H. Herrmann, *Chem. Ber. 116* (1983) 3915.
[100] a) H. Dürr, H. Gross, *Tetrahedron Lett. 22* (1981) 4679; b) T. Wegmann, *Diplomarbeit*, Universität des Saarlandes, 1989.
[101] a) J. Epperlein, B. Hofmann, K. S. Topperka, *J. Signalaufzeichnungsmater. 3* (1975) 173; b) J. Epperlein, B. Hofmann, K. S. Topperka, *ibid. 4* (1976) 155.
[102] H. Böttcher, J. Epperlein: *Moderne photographische Systeme*, VEB Deutscher Verlag für Grundstoffindustrie, Leipzig 1983.
[103] a) E. Fischer, *EPA Newslett. Nov. 1984*, 17; b) H. Rau, *ibid. July 1984*, 31; c) A. M. Braun, E. Oliveros, E. Moretti: *Technologie Photochimique*, Press Swiss Romande, Lausanne 1986, p. 62.
[104] a) D. S. Lo, D. M. Manikowski, M. M. Hanson, *Appl. Opt. 10* (1971) 978; b) D. L. Ross, *ibid. 10* (1971) 571.
[105] H. P. Jönsson, *Dissertation*, Universität Saarbrücken, see pp. 129, 132.
[106] a) D. L. Fanselow, DOS 28 28 965 (1979); b) A. M. Trozzolo, US-Pat. 39 64 823 (1979); US-Pat. 3 984 177 (1976); DOS 25 10 836 (1975).
[107] S. Seikosha Co., Jap. Pat. 59 78 721; Jap. Pat. 59 78 272 (1984).
[108] R. J. Hovey, C. H. Fuchsmann, P. G. Piusz, DOS 29 36 255 (1980).
[109] Dr. R. J. Hurditch, PPG Industries, Barberton, OH (USA), private communication.
[110] M. Melzig, DOS P 33 45 624; 33 45 625 (1985).
[111] H. G. Heller, Eur. Pat. 0 140 540 (1985).
[112] a) H. G. Heller, Br. Pat. 7/1464603 (1976); US-Pat. 9/719254; b) *Xth Symposium on Photochemistry*, Interlaken 1984, Abstr. 369.
[113] E. Reckziegel, *Chem.-Ztg. 10* (1972) 535; W. Frass, *Chem. Unserer Zeit 17* (1983) 33.
[114] G. A. Delzenne, *Adv. Photochem. 11* (1979) 2; F. Eplattenier, *Swiss Chem. 7* (1985) 19.
[115] T. Laird, *Chem. Ind. (London) 1978*, 186; K. Maruyama, K. Terada, Y. Yamamoto, *Chem. Lett. 1981*, 839.
[116] D. E. King, *Chem. Br. 4* (1968) 107.
[117] a) *Folienserie des Fonds der Chemischen Industrie*, p. 36, Frankfurt am Main 1986; b) E. J. Bargon (Ed.): *Methods and Materials in Microelectronic Technology*, IBM Res. Symp. Ser., Plenum Press, New York 1984.
[118] H. G. Heller, C. Goodman, Br. Pat. 2 104 539 A (1983); H. Goodman, D. J. Pearsons, Br. Pat. 2 142 011 A (1985); H. G. Heller, DOS 2 647 850 (1978).
[119] E. F. Haugh, US-Pat. 3 658 526 (1972); B. L. Booth, *Appl. Opt. 11* (1972) 2944; *14* (1975) 593.
[120] W. Haas, J. Adams, J. Wysocki, *Mol. Cryst. Liq. Cryst. 7* (1969) 371; K. Ichimura, Y. Suzuki, A. Hosoki, K. Aoki in H. Dürr, H. Bouas-Laurent (Ed.): *Photochromic Molecules and Systems*, Elsevier, Amsterdam 1989.
[121] M. Eich, J. H. Werndorff, B. Reck, H. Ringsdorf, *Makromol. Chem. Rapid Commun. 8* (1987) 59.
[122] a) Y. Suzuki, K. Ozawa, A. Hosoki, K. Ichimura, *Polym. Bull. 17* (1987) 285; b) I. Cabrera, V. Krongauz, H. Ringsdorf, *Angew. Chem. 99* (1987) 1204; *Angew. Chem. Int. Ed. Engl. 26* (1987) 1178.
[123] W. J. Tomlinson, *Appl. Opt. 23* (1984) 4609.
[124] K. Ichimura, M. Sakuragi, *J. Polym. Sci. Polym. Lett. Ed.*, in press.
[125] M. Irie, T. Iwayanagi, Y. Taniguchi, *Macromolecules 18* (1985) 2418.
[126] a) G. R. Meredith, D. J. Williams, S. N. Fishman, E. S. Goldburt, V. A. Krongauz, *J. Phys. Chem. 87* (1983) 1697; b) G. R. Meredith, V. A. Krongauz, D. J. Williams, *Chem. Phys. Lett. 87* (1982) 289; c) V. A. Krongauz, *Isr. J. Chem. 18* (1979) 304.
[127] H. Dürr, V. Bach, DOS P 37 10 889.1 (1987).
[128] a) H. Sixl, *Umschau 83* (1983) 474; b) W. P. Su, J. R. Schrieffer, A. J. Heeger, *Phys. Rev. Lett. 42* (1979) 1698.
[129] K. Menke, S. Roth, *Chem. Unserer Zeit 20* (1986) 1.
[130] F. L. Carter (Ed.): *Molecular Electronic Devices*, Dekker, New York 1982.
[131] C. C. Ku, R. Liepins: *Electrical Properties of Polymers*, Hanser, München 1987.

Alkoxide Clusters of Molybdenum and Tungsten as Templates for Organometallic Chemistry: Comparison with Carbonyl Clusters of the Later Transition Elements

By Malcolm H. Chisholm,* David L. Clark, Mark J. Hampden-Smith, and David H. Hoffman

Dedicated to Professor Donald C. Bradley

Alkoxide and carbonyl ligands complement each other because they both behave as "π buffers" to transition metals. Alkoxides, which are π donors, stabilize early transition metals in high oxidation states by donating electrons into vacant d_π orbitals, whereas carbonyls, which are π acceptors, stabilize later transition elements in their lower oxidation states by accepting electrons from filled d_π orbitals. Both ligands readily form bridges that span M–M bonds. In solution fluxional processes that involve bridge–terminal ligand exchange are common to both alkoxide and carbonyl ligands. The fragments $[W(OR)_3]$, $[CpW(CO)_2]$, $[Co(CO)_3]$, and CH are related by the isolobal analogy. Thus the compounds $[(RO)_3W\equiv W(OR)_3]$, $[Cp(CO)_2W\equiv W(CO)_2Cp]$, hypothetical $[(CO)_3Co\equiv Co(CO)_3]$, and $HC\equiv CH$ are isolobal. Alkoxide and carbonyl cluster compounds often exhibit striking similarities with respect to substrate binding—e.g., $[W_3(\mu_3\text{-}CR)(OR')_9]$ versus $[Co_3(\mu_3\text{-}CR)(CO)_9]$ and $[W_4(C)(NMe)(O\mathit{i}Pr)_{12}]$ versus $[Fe_4(C)(CO)_{13}]$—but differ with respect to M–M bonding. The carbonyl clusters use e_g-type orbitals for M–M bonding whereas the alkoxide clusters employ t_{2g}-type orbitals. Another point of difference involves electronic saturation. In general, each metal atom in a metal carbonyl cluster has an 18-electron count; thus, activation of the cluster often requires thermal or photochemical CO expulsion or M–M bond homolysis. Alkoxide clusters, on the other hand, behave as electronically unsaturated species because the π electrons are ligand-centered and the LUMO metal-centered. Also, access to the metal centers may be sterically controlled in metal alkoxide clusters by choice of alkoxide groups whereas ancillary ligands such as tertiary phosphanes or cyclopentadienes must be introduced if steric factors are to be modified in carbonyl clusters. A comparison of the reactivity of alkynes and ethylene with dinuclear alkoxide and carbonyl compounds is presented. For the carbonyl compounds CO ligand loss is a prerequisite for substrate uptake and subsequent activation. For $[M_2(OR)_6]$ compounds (M = Mo and W) the nature of substrate uptake and activation is dependent upon the choice of M and R, leading to a more diverse chemistry.

1. Introduction

In inorganic chemistry, the term *cluster* is used to describe an assemblage of two or more metal atoms held together, at least in part, by metal–metal bonds.[1b] There may or may not be bridging ligands. Some of the earliest examples of clusters were discovered in the field of transition-metal carbonyl chemistry and within recent years giant carbonyl clusters, either neutral or bearing an overall charge, e.g,

$[Rh_{15}(CO)_{27}]^{3\ominus}$ $[Ni_{16}(CO)_{23}(C_2)_2]^{2\ominus}$ $[Pt_{19}(CO)_{22}]^{4\ominus}$ $[Pt_{38}(CO)_{44}H_x]^{2\ominus}$

where the value of x is still uncertain,[2] have attracted attention. There is also an extensive group of gold phosphane clusters[3] and, for the early transition elements, the halide complexes $[M_6Cl_{12}]^{2\oplus}$, where M = Nb and Ta, and $[M_6Cl_8]^{4\oplus}$, where M = Mo and W, each containing an octahedron of metal atoms, have been known for over 20 years.[4] More recently, the recognition of cluster subunits in inorganic solids has become an increasingly important aspect of solid-state chemistry. For instance, the lower-valent (subvalent) halides,[5] oxides,[6] and sulfides[7] of a wide variety of metals have "cluster units" that are separated from one another by bridging atoms or are fused by common metal atoms at a vertex or along a common edge or face. Examples of these types of compounds include the Chevrel phases.[7, 8]

Homoleptic metal alkoxides[9] are a well-established group of compounds having empirical formulas $[M(OR)_x]$, where x also represents the formal oxidation state of the metal, M. In general, the empirical formula is not the molecular formula because the metal strives to attain its preferred coordination number by alkoxide bridge formation. Thus, oligomeric structures, $[M(OR)_x]_n$, where n represents the de-

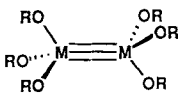
[*] Prof. M. H. Chisholm
Department of Chemistry, Indiana University
Bloomington, IN 47405 (USA)
Dr. D. L. Clark (J. Robert Oppenheimer Fellow)
INC-4, C346,
Los Alamos National Laboratory
Los Alamos, NM 87545 (USA)
Prof. M. J. Hampden-Smith
Department of Chemistry, University of New Mexico
Albuquerque, NM 87131 (USA)
Prof. D. M. Hoffman
Department of Chemistry, Harvard University
Cambridge, MA 02138 (USA)

 © VCH Verlagsgesellschaft mbH, D-6940 Weinheim, 1989 0570-0833/89/0404-0432 $ 02.50/0

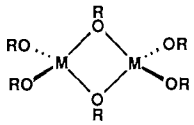
gree of oligomerization, are often found both in the solid state and in solution. The value of n is dependent on the nature of the metal and the steric properties of R. The species present in solution may not be the same as that found in the solid state and the nature of the solvent and temperature can lead to complex equilibria.

Bradley[10] formulated a structural theory for the oligomerization of metal alkoxides based on the premise that the observed structures represent a compromise of opposing forces—an enthalpic drive to form the maximum number of M–O bonds by alkoxide bridge formation and an entropic drive to minimize aggregration. In his pioneering studies, *Bradley*[11] was quick to recognize that the discrete oligomeric metal oxo alkoxides and metal oxo siloxanolates bridge the gap between polymeric alkoxides and the macromolecular solid-state structures of metal oxides and metal silicates. In all these compounds of formula $[M(OR)_x]_n$ or $[MO_a(OR)_b]_n$, however, the oligomerization involved the formation of bridges via oxo or alkoxide groups, and the term cluster is not appropriate because, as in polyoxometalate chemistry,[12] there are no metal–metal bonds.

Only within the last decade has the importance of metal–metal bonding become apparent in metal alkoxide chemistry. It was first unequivocally recognized with the structural characterization of $[Mo_2(OCH_2tBu)_6]$ **1a**, a member of an extensive class of $[Mo_2(OR)_6]$ compounds.[13] Compound **1a** adopts an ethane-like structure, **1**, rather than the common bridged dimer structure depicted by **2**. For the first time the dominant influence of a metal–metal bond was seen in the chemistry of metal alkoxides. In this instance the M–M bond is a triple bond of electronic configuration $\sigma^2\pi^4$.

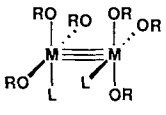


1a, M = Mo, R = CH_2tBu
1b, M = W, R = tBu



2

Following the discovery of $[Mo_2(OR)_6]$ compounds, related $[W_2(OR)_6]$ compounds were isolated, often with supporting Lewis bases as in **3a** (py = pyridine).[14] The latter compounds adopt a structure depicted by **3**. Again, the unbridged M–M triple bond is retained.



3a, M≡W, R = *i*Pr, L = py

In recent years a variety of cluster alkoxides of molybdenum and tungsten have been synthesized and characterized in which alkoxide bridges and metal–metal bonds are present. A new structural relationship between metal oxides and metal alkoxides has emerged. The molecular alkoxide-supported clusters of molybdenum and tungsten contain M_xO_y cores that are analogues of the cluster subunits found in the solid-state structures of reduced metal oxides. For example, the $[W_4(OEt)_{16}]$ cluster[15] contains the same $[M_4(\mu_3\text{-}O)_2(\mu\text{-}O)_4O_{10}]$ unit found in the $[Ba_{1.14}Mo_8O_{16}]$ structure (Fig. 1).[16]

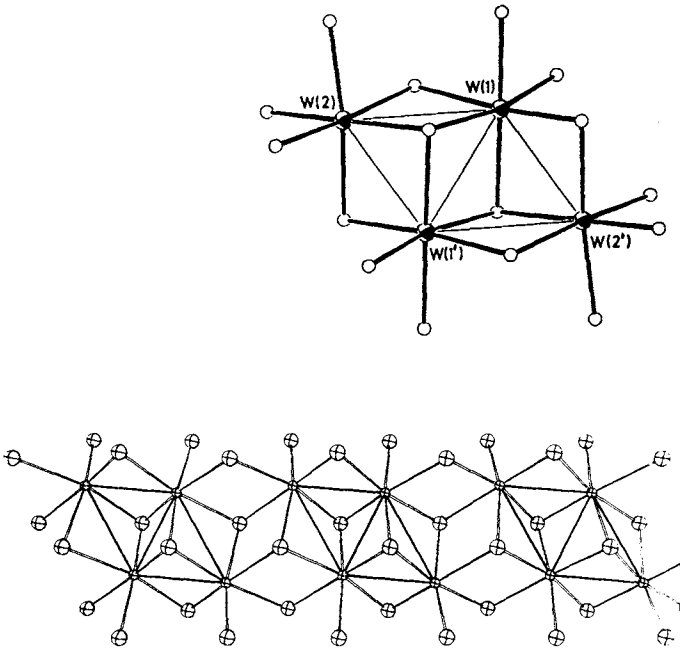


Fig. 1. The $[W_4(\mu_3\text{-}O)_2(\mu\text{-}O)_4(O)_{10}]$ unit in $[W_4(OEt)_{16}]$ (top) and a view of the similar Mo cluster linkages found in infinite chains within the solid-state structure of $[Ba_{1.14}Mo_8O_{16}]$ (bottom).

Because there are structural similarities between alkoxide clusters and reduced metal oxides, which serve as heterogeneous catalysts for a variety of reactions involving hydrocarbons and for small molecule activation, we set out to examine the organometallic chemistry of discrete molybdenum and tungsten alkoxide dimers and clusters. From our work a wide variety of dinuclear and cluster alkoxides are now known in which a hydrocarbon fragment or an atom such as H,[17] C,[18] or N[19] is attached to one or more metal atoms. As our work has progressed, we have come to recognize the similarities as well as differences between alkoxide and traditional carbonyl cluster chemistry. In this article we explore some of these relationships from the standpoint of synthesis, structure, bonding, and reactivity.

2. General Comparisons

2.1. Alkoxide and Carbonyl Ligands: Complementary Aspects of Metal–Ligand Bonding

Alkoxide and carbonyl ligands are both π buffers. The CO ligand acts as a π acceptor, stabilizing electron-rich metal atoms in their low-to-mid oxidation states. The extent of metal-to-CO ($d_\pi \rightarrow \pi^*$) back-bonding is reflected in the values of ν(CO) as, for example, in the $(t_{2g})^6$ $[M(CO)_6]^n$ ions: M = Mn, n = + 1, 2090 cm^{-1}; M = Cr, n = 0, 2000 cm^{-1}; M = V, n = − 1, 1860 cm^{-1}. Alkoxides are uninegative π donors, π^x, where $0 < x < 4$, and thus can stabilize high-oxidation-state metal centers in which vacant metal d_π orbitals are present: e.g., the d^0 metal complex $[Mo(OMe)_6]$.[20] The alkoxide ligand is electronically flexible in that π^x can vary as a function of the M–O–C angle; i.e.,

as the angle approaches 180°, x approaches 4 if the metal has available vacant d_π orbitals. The M–O–C angle is influenced by steric and electronic factors at the metal and may respond to substrate uptake or release from the metal center. Sterically demanding RO ligands will commonly have large M–O–C angles. If there are filled metal d_π orbitals, these will be raised in energy by the presence of alkoxide ancillary ligands.

Alkoxide and carbonyl ligands may take up bridging or semibridging positions and are often fluxional on the NMR time scale, showing rapid bridge–terminal exchange. The presence of bridging versus terminal OR groups does not necessarily change the total valence electron count at a metal center.

It is nearly always possible to arrive at an 18-valence-electron count for early-transition-metal alkoxide complexes by invoking d_π–p_π bonding, although it is important to note that the electrons involved in π bonding are ligand-centered. The LUMOs of metal alkoxide complexes are metal-centered (d orbitals) and therefore the compounds usually behave as coordinatively unsaturated species and are labile toward Lewis base uptake. By contrast, metal carbonyl complexes are generally coordinatively saturated and react either by nucleophilic attack on the carbon atom of a CO ligand (i.e., nucleophilic attack at the LUMO), or by initial dissociation of CO. The latter process can be induced thermally, photochemically, or by reaction with a reagent such as Me_3NO, which acts as an oxygen-atom transfer reagent generating CO_2 and either an unsaturated metal carbonyl cluster or a loosely ligated Me_3N adduct. Metal alkoxide complexes are inherently more substitutionally labile, being susceptible to both nucleophilic attack at the metal and electrophilic attack at oxygen, provided steric factors are not limiting. Dissociation of $OR^{\ominus}$ in nonpolar hydrocarbon solvents has never been established and does not present an important reaction pathway for alkoxide complexes.

Bulky OR ligands can stabilize unusually low coordination numbers and coordinative unsaturation can be tailored for substrate selectivity in binding to the metal centers by varying R. This parallels the common use of specific PR_3 or η^5-C_5R_5 ligands to control access to the metal coordination sphere in organometallic chemistry.[21]

2.2. Isolobal Relationships

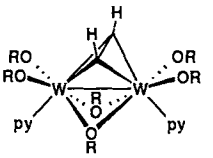
Important to the understanding of structure and reactivity patterns in organometallic chemistry has been the recognition of isolobal relationships between organometallic and organic fragments.[22] Two fragments are isolobal if the number, symmetry properties, occupation by electrons, and approximate energy of their frontier orbitals are similar. Thus methylene, CH_2, is isolobal with the 16-electron fragment $[Fe(CO)_4]$ and the trinuclear carbonyl cluster $[Fe_3(CO)_{12}]$ is an organometallic analogue of cyclopropane. Similarly, CH and $[CpM(CO)_2]$ (M = Mo, W) are isolobal, and the compounds HC≡CH, **4**, and **5**

$[Cp(CO)_2M{\equiv}M(CO)_2Cp]$ **4** $\qquad$ $[Cp(CO)_2M{\equiv}CR]$ **5**

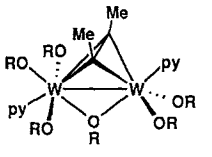
are isolobal analogues having C≡C, M≡M, and M≡C bonds, respectively. The $[PtL_2]$ fragment is also isolobal with CH_2, and the combination of $[PtL_2]$ with either ethylene or ethyne to give $[L_2Pt(C_2H_4)]$ or $[L_2Pt(C_2H_2)]$ provides a parallel with the formation of cyclopropane and cyclopropene, respectively. Limitations to the successful combination of isolobal fragments often arise because of a mismatch of orbital energies or steric factors. It has, for example, been stated that "a mouse and an elephant are isolobal in that they both have four legs and a tail. However, they do not mate, except with themselves."[23]

It is informative to examine some isolobal relationships for alkoxide complexes and fragments of molybdenum and tungsten complexes. For example, the $[M(OR)_3]$ unit may be viewed as a 15-electron fragment if the alkoxide ligands are each counted as 4-electron donors. Thus, the compounds **1** are inorganic analogues of alkynes and are alkoxide analogues of compounds **4** (M = Mo, W).[24] Likewise, the alkylidyne compounds $[(t\mathrm{BuO})_3M{\equiv}CR]$[25,26] and **5**[27] are isolobal.

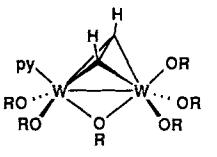
There are, however, some important differences between the alkoxide and carbonyl analogues that arise because of the different π-donor/acceptor properties of the ligands. The $[M_2(OR)_6]$ compounds can coordinate two neutral ligands to give $[M_2(OR)_6L_2]$ compounds with retention of the M≡M bond (see **3**); i.e., the $[M(OR)_3L]$ fragment is isolobal to $[M(OR)_3]$. Formation of the M–L σ bond occurs with loss of one M–OR π bond. In contrast, compounds **4** coordinate Lewis bases, L, to give M–M single-bond compounds



6, R = *i*Pr



7, R = CH_2*t*Bu



8, R = *t*Bu

$[Cp_2M_2(CO)_4(L)_2]$. The $[CpM(CO)_2L]$ unit is a 17-electron fragment and is isolobal with the methyl radical. Similarly, whereas $[Co(CO)_3]$ is isolobal with CH and the alkyne adduct $[Co_2(CO)_6(\mu\text{-}C_2H_2)]$ is a tetrahedrane analogue formed by the combination of a hypothetical $[(CO)_3Co{\equiv}Co(CO)_3]$ unit with HC≡CH, the alkyne adducts of **1** often have supporting Lewis base ligands and bridging alkoxides (e.g., **6–8**).[28] Again, the additional coordination in the alkoxide-supported alkyne adducts reflects the electronic flexibility of the alkoxide ligands: (1) RO-to-M d_π bonding may be sacrificed in favor of σ donation from Lewis bases. (2) The facile interchange between terminal and bridging positions allows for the optimization of metal–metal and metal–ligand bonding.

2.3. Cluster Syntheses

The dinuclear complexes **1**, or their Lewis base adducts, provide useful starting materials for the assembly of trinuclear and tetranuclear compounds. The reactions bear a striking resemblance to the metal carbonyl cluster-building reactions so ably employed by *Stone* and his co-workers.[29] For example, oxo-,[30,31] imido-,[32] and alkylidyne-capped triangles[33] can be formed according to reactions (a)–(c).

Mixed-metal M_2M' clusters (M, M' = Mo, W) can be synthesized similarly.

$$[M_2(OR)_6] + [MO(OR)_4] \rightarrow [M_3(\mu_3\text{-}O)(OR)_{10}] \quad (a)$$

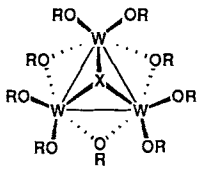
$$[M_2(OR)_6] + [M(NH)(OR)_4] \rightarrow [M_3(\mu_3\text{-}NH)(OR)_{10}] \quad (b)$$

$$[M_2(OR)_6] + [M(CR')(OR)_3] \rightarrow [M_3(\mu_3\text{-}CR')(OR)_9] \quad (c)$$

These comproportionation reactions have steric limitations based on the nature of R and, incidentally, may also be viewed as redox reactions:

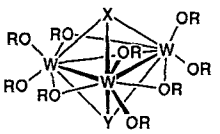
$$2\,M^{III} + M^{VI} \rightarrow 3\,M^{IV}$$

The product clusters adopt geometries that have bridging alkoxide ligands as shown in **9** and **10** below.



9

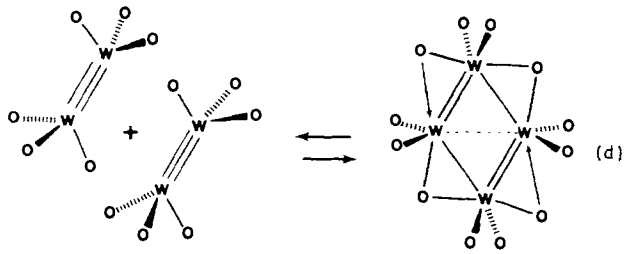
R = *i*Pr, CH_2*t*Bu
X = CMe, CEt, CPh



10

R = *i*Pr, CH_2*t*Bu
X = NH, O
Y = OR

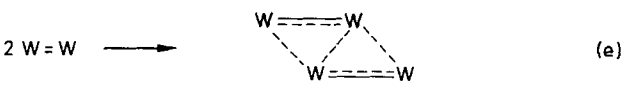
It is also possible to reversibly couple $[W_2(OR)_6]$ compounds to give $[W_4(OR)_{12}]$ [Eq. (d)].[34–36]



O = OR

(d)

In other cases the reaction path leading to alkoxide cluster formation is less well defined, as in the preparation of $[W_4(OR)_{16}]$ compounds from the reactions between $[W_2(NMe_2)_6]$ and ROH (R = Et, Me).[37] The W_4 unit in the $[W_4(OR)_{16}]$ compounds can be considered, formally at least, to arise from the coupling of two $[W_2(OR)_8]$ (M≡M) units [Eq. (e)].



(e)

The formation of the unique high-oxidation-state carbide cluster $[W_4(C)(NMe)(O\mathit{i}Pr)_{12}]$ in the alcoholysis of $[W_2(NMe_2)_6]$ with 2-propanol is also not understood in terms of a detailed reaction pathway.[38] This is often the case as well in metal carbonyl cluster chemistry when carbide or nitride ligands arise. Nevertheless, there is a formula analogy between several of these alkoxide- and carbonyl-supported clusters, as, for example, in the following:

$[W_3(\mu_3\text{-}CR')(OR)_9]$ $[Co_3(\mu_3\text{-}CR)(CO)_9]$
$[M_3(\mu_3\text{-}NH)(OR)_{10}]$ $[Fe_3(\mu\text{-}NH)(CO)_{10}]$
$[W_4(C)(\mu\text{-}X)(O\mathit{i}Pr)_{12}]$ (X = O, NR) $[Fe_4(C)(CO)_{13}]$
$[W_4(O\mathit{i}Pr)_{12}]$ $[Co_4(CO)_{12}]$

3. Electronic Structure Relationships in Selected Alkoxide and Carbonyl Clusters

To start our discussion of the complementary role of alkoxide and carbonyl ligands as π buffers, we draw specific attention to the nature of the frontier orbitals of the free ligands, CO and $OR^{\ominus}$, that are used in bonding to metals. These are shown schematically in Scheme 1.



Scheme 1. Frontier orbitals of CO (left) and $RO^{\ominus}$ (right).

The $RO^{\ominus}$ ligand has a low-lying sp-hybridized σ lone pair and higher-lying oxygen p_π lone pairs. In a complex with a linear M–O–C angle the higher-lying π orbitals are degenerate, but, as this angle becomes smaller, only one orbital retains its pure p character while the other mixes with oxygen s. This mixing lowers the energy of the orbital. The CO ligand has a filled σ orbital, containing the C lone pair, and vacant π* orbitals which are degenerate.

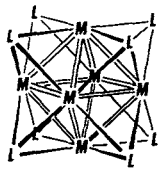
Thus, both $RO^{\ominus}$ and CO ligands have frontier orbitals of σ and π symmetry and, by symmetry, may have similar interactions with metal atoms. The primary difference between these ligands arises from the electron occupation of the π orbitals. The vacant π* orbitals of CO are well-suited for accepting electron density from electron-rich metals, whereas the filled p_π orbitals of the $RO^{\ominus}$ ligand can donate to electron-poor metal centers. There is also an important difference in the relative energies of the σ- and π-type orbitals. The electronegativity of oxygen places the filled oxygen lone pairs well below the metal orbitals of all but the most highly oxidized metal centers whereas the π* orbitals of CO are higher in energy than metal d_π atomic orbitals. As a consequence, in metal alkoxides the metal–oxygen π bonds will be ligand-centered MOs whereas in metal carbonyls the metal–carbonyl π bonds will be primarily metal d_π in character.

In some respects the alkoxide ligand with its flexible M–O–C angle is analogous to the nitrosyl ligand;[39] the geometry of the M–N–O moiety (linear or bent) also depends on the electronic requirements of the metal center. A bent M–O–C moiety generates a lone pair, having s and p character, that is poised for alkoxide bridge formation.

3.1. $[M_6(\mu_3\text{-}L)_8L_6]^{n\ominus}$ Clusters

The central $[M_6(\mu_3\text{-}L)_8]$ core (**11**) of the $[M_6(\mu_3\text{-}L)_8L_6]^{n\ominus}$ cluster consists of an octahedron of metal atoms inscribed

within a cube of ligands that cap each triangular face. The six terminal ligands (not shown in **11**) radiate from the vertices of the M_6 octahedron. This basic cluster geometry is found for both carbonyl- and alkoxide-supported clusters—e.g., $[Mo_6(\mu_3\text{-}OMe)_8(OMe)_6]^{2\ominus}$ [40] and $[Co_6(\mu_3\text{-}CO)_8(CO)_6]^{4\ominus}$ [2]—and serves as a good starting point for comparison of the clusters.



11

The bonding in these M_6 clusters has been the subject of numerous theoretical studies ranging in methodology from the d-orbital overlap model of *Cotton* and *Haas* to more sophisticated treatments employing the X_α-SW density functional technique.[41–48] Only recently, however, has interest focused on the role of π-donor versus π-acceptor ligands.[49–51]

The 30 primarily metal-d atomic orbitals of a "naked" M_6 octahedral cluster generate a manifold of thirteen metal–metal bonding MOs ($a_{1g} + a_{2u} + e_g + t_{1u} + t_{2u} + t_{2g}$) and seventeen weakly metal–metal anitbonding MOs ($a_{2g} + e_g + e_u + t_{1g} + t_{2g} + t_{1u} + t_{2u}$). The occupation of these cluster orbitals by electrons will depend on the metal. By symmetry, the interaction of ligand σ lone-pair orbitals with the M_6 cluster core will be identical for both carbonyl and alkoxide ligand sets. The six terminal ligand σ orbitals ($a_{1g} + e_g + t_{1u}$) can interact with radially directed M_6 cluster orbitals and the eight face-capping ligand σ orbitals ($a_{1g} + a_{2g} + t_{1u} + t_{2g}$) can interact with M_6 cluster orbitals derived predominantly from virtual metal s and p atomic orbitals.

The primary difference in metal–ligand bonding between carbonyl and alkoxide ligand sets arises from the nature of the π interaction of the eight face-capping ligands with the M_6 cluster core. For the eight face-capping ligands, the sixteen π orbitals ($e_g + e_u + t_{1g} + t_{2g} + t_{1u} + t_{2u}$) match the symmetry of sixteen of the seventeen weakly antibonding cluster MOs in the naked M_6 cluster. The a_{2g} M_6 cluster orbital has no symmetry match and is unaffected by interaction with the ligands. This is schematically illustrated in the interaction diagram in Figure 2, which is only meant to show in a qualitative fashion the difference in the face-capping ligand π interaction for octahedral M_6 clusters supported by carbonyl or alkoxide ligands. The blocks of M_6 cluster orbitals in the center of Figure 2 represent the number of symmetry-related cluster orbitals after taking into account the M–L σ bonding. Only the interaction of π orbitals is depicted.

For the carbonyl-supported cluster $[Co_6(\mu_3\text{-}CO)_8(CO)_6]^{4\ominus}$, the seventeen metal–metal cluster antibonding orbitals are occupied. Metal–carbonyl π back-bonding stabilizes sixteen cluster antibonding orbitals by transfer of electron density to the CO π* orbitals. As *Mingos* and *Johnston*[51] have pointed out, the removal of electron density from the cluster antibonding orbitals leads to a strengthening of the metal–metal bonding in the late-transition-metal

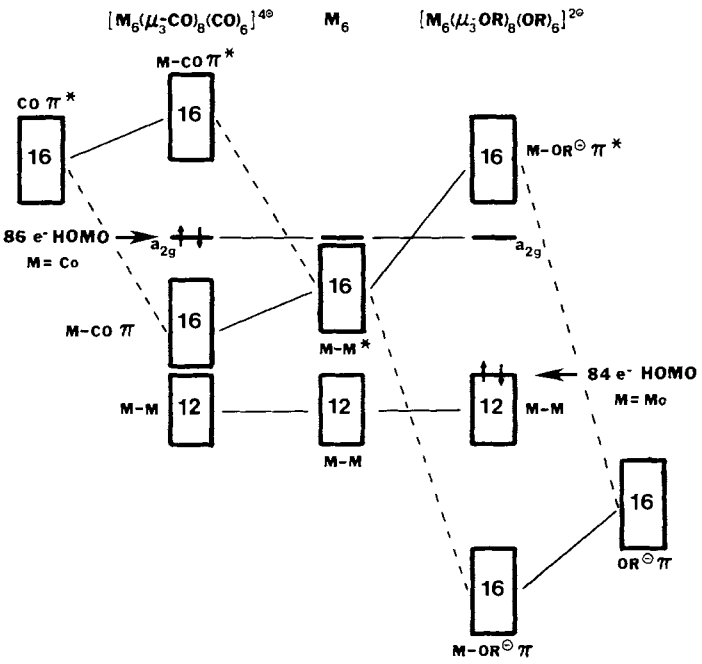
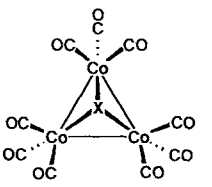


Fig. 2. Qualitative MO diagram illustrating the interaction of the sixteen π orbitals of the capping ligands with the weakly antibonding M_6 cluster MOs in $[M_6(\mu_3\text{-}L)_8L_6]$ compounds. In the center column are 12 M–M cluster bonding orbitals, 16 M–M cluster antibonding orbitals, and the noninteracting a_{2g} cluster orbital, after taking into account the M–L σ bonding. The left two columns illustrate the interaction of vacant CO π* orbitals with the 16 M–M antibonding cluster orbitals to generate an 86-electron cluster for M = Co. The right two columns illustrate the interaction of filled $OR^\ominus$ π orbitals with the 16 M–M antibonding cluster orbitals to generate an 84-electron cluster for M = Mo.

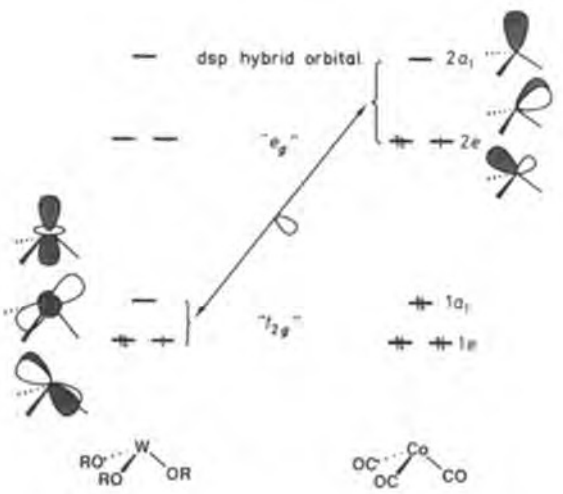
cluster. For the alkoxide-supported cluster $[Mo_6(\mu_3\text{-}OR)_8(OR)_6]^{2\ominus}$, where the corresponding cluster antibonding orbitals are empty, π donation from the alkoxide π lone-pair orbitals results in a destabilization of the cluster antibonding orbitals such that they are moved up and out of the frontier region. This effectively replaces sixteen metal–metal antibonding MOs with sixteen new ligand-based π-bonding orbitals. Finally, the difference in cluster electron count (86 electrons for $[Co_6(\mu_3\text{-}CO)_8(CO)_6]^{4\ominus}$ and 84 electrons for $[Mo_6(\mu_3\text{-}OR)_8(OR)_6]^{2\ominus}$) depends on the electron occupation of the nonbonding a_{2g} cluster MO.

3.2. Alkylidyne-Capped Clusters

Cobalt and tungsten form ethylidyne-capped clusters **12**[52–57] and **9** (X = CMe).[33] Aside from a similarity in formula, $[M_3(\mu_3\text{-}CMe)(L)_9]$, both compounds have approximate C_{3v} symmetry though the immediate coordination about the metal atoms is rather different.



12, X = CMe



Scheme 2. Frontier orbitals of the cluster fragments $W(OR)_3$ and $Co(CO)_3$.

Electronically, the clusters are related by a d^3–d^9 "hole formalism",[58] and the frontier orbitals of the ML_3 fragments that make up the clusters are isolobal (Scheme 2).

The frontier orbitals of a C_{3v} ML_3 fragment are well-known[59] and consist of low-lying $1a_1 + 1e$ orbitals, remnants of the octahedral t_{2g} set, and high-lying $2a_1 + 2e$ orbitals. The $2a_1$ orbital is a "dsp" hybrid and the 2e orbital is the remnant of the e_g octahedral set. With respect to bonding capability, the three valence electrons in a d^3 $[W(OR)_3]$ fragment formally reside in the lower $1a_1 + 1e$ orbitals, whereas in the d^9 $[Co(CO)_3]$ fragment three electrons reside in the upper $2a_1 + 2e$ set and the $1a_1$ and 1e are filled.

Orbital interaction diagrams for the combining of the $[W_3(OR)_9]^{3\oplus}$ and $[Co_3(CO)_9]^{3\oplus}$ frontier orbitals with $CMe^{3\ominus}$ are shown in Figures 3 and 4, respectively. The important metal-based fragment orbitals are drawn on the left of each interaction diagram.

Within each cluster the memory of the octahedral parentage of the ML_3 fragments persists. The C_{3v} molecular symmetry of **9** and **12** creates sets of orbitals with a and e symmetry. For the tungsten cluster the lower two sets are used in M–M and M–C alkylidyne bonding whereas for cobalt, with 24 metal-based electrons, the highest two a + e sets are used for M–M and M–C alkylidyne bonding. A similar relationship in both M–M and M–C (carbide) bonding is observed for the following cluster carbides:

$[W_4(\mu_4\text{-}C)(NMe)(O\mathit{i}Pr)_{12}]$ $[W_4(\mu_4\text{-}C)(O)(O\mathit{i}Pr)_{12}]$[18]
$[Fe_4(\mu_4\text{-}C)(CO)_{13}]$ $[Fe_4(\mu_4\text{-}C)(CO)_{12}]^{2\ominus}$[60]

One point of difference that is found in a comparison of the $M_3(\mu_3\text{-}CR)$ and $M_4(\mu_4\text{-}C)$ early- and late-transition-metal clusters arises from the different energies of the cluster frontier orbitals. Despite the higher formal oxidation state of the metal atoms in the early-transition-metal clusters, the tungsten orbitals are closer in energy to those of the carbide or alkylidyne carbon. Consequently, in the $W_4(\mu_4\text{-}C)$-containing clusters there is a significant bonding interaction between the carbon 2s atomic orbital and the metal atoms.[18] This is not observed in the $Fe_4(\mu_4\text{-}C)$ carbonyl clusters.[61, 62] For the alkylidyne-capped compounds the greater W_3-to-CR bonding manifests itself in what is tantamount to a rehybridization of the alkylidyne carbon;[58] that is, in **12** the alkylidyne carbon is essentially sp hybridized,[54–57] whereas in **9** (X = CMe) the alkylidyne carbon is sp^3 hybridized. Thus, in Figure 3, the carbon 2s character of the alkylidyne fragment orbital $3a_1$ is transferred to the $1a_1$ MO leaving the carbon $2p_z$ character entirely in the $3a_1$ MO.

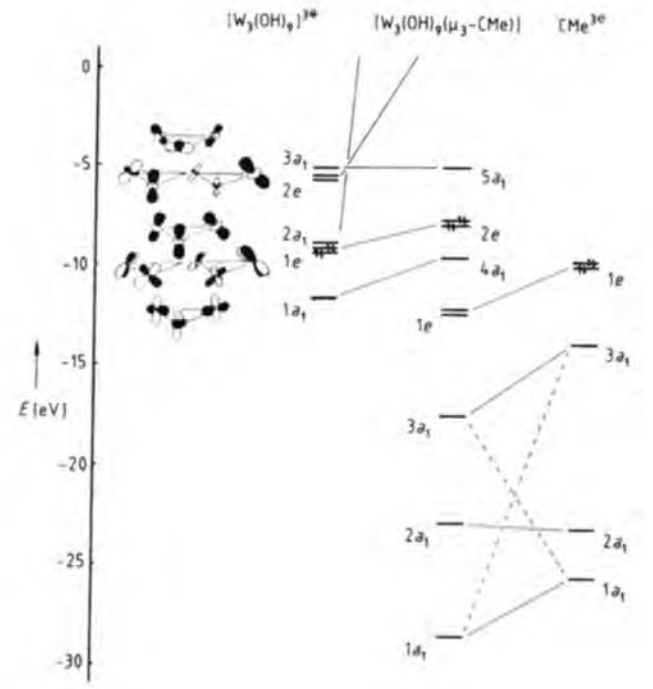


Fig. 3. An MO interaction diagram [58] showing the formation of the complex $[W_3(\mu_3\text{-}CMe)(OH)_9]$ from the fragments $[W_3(OH)_9]^{3\oplus}$ and $CMe^{3\ominus}$. The geometry of the cluster was taken from the crystal structure of **9** (X = CMe, R = *i*Pr).

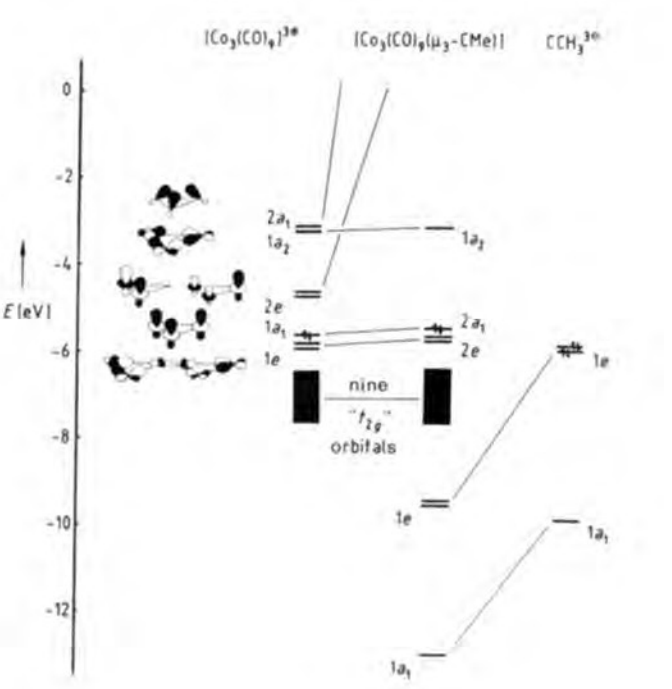
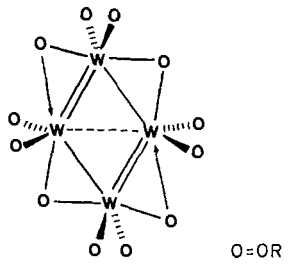


Fig. 4. An MO interaction diagram [58] showing the formation of **12** from the fragments $[Co_3(CO)_9]^{3\oplus}$ and $CMe^{3\ominus}$.

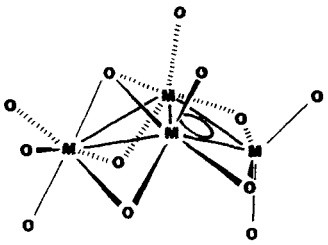
3.3. $[ML_3]_n$ Clusters

One final point of comparison between the d^3 $[M(OR)_3]$ and d^9 $[Co(CO)_3]$ fragments concerns the role of steric factors associated with the alkoxide ligands. The hypothetical molecule $[(CO)_3Co{\equiv}Co(CO)_3]$ is unstable with respect to $[Co_4(CO)_{12}]$, but $[(RO)_3M{\equiv}M(OR)_3]$ compounds can be stabilized by use of bulky R groups such as *t*Bu. As the bulk of R is decreased, the $[M_2(OR)_6]$ compounds couple to form $[M_4(OR)_{12}]$ compounds that, in contrast to $[Co_4(CO)_{12}]$, do not contain a tetrahedral M_4 core. The compounds $[W_4(OR)_{12}]$ (R = *i*Pr, cyclopentyl) adopt a distorted rhomboidal M_4 core **13** with alternating short (2.50 Å) and long (2.71 Å) M–M bonds corresponding formally to M–M double and single bonds.[34,35] This is, of course, a simplistic view and there is a significant M–M bonding interaction between the backbone tungsten atoms. The short diagonal M–M distance is 2.8 Å.



13

O=OR



14

Less sterically demanding OR ligands, such as R = CH_2*i*Pr, CH_2-cyclohexyl, CH_2-cyclopentyl, and CH_2-cyclobutyl, form $[M_4(OR)_{12}]$ compounds (M = Mo, W) with a butterfly of M atoms (**14**) in which one metal atom is octahedrally coordinated with respect to oxygen.[63]

These structures illustrate an important point: In the chemistry of alkoxide clusters involving molybdenum and tungsten the importance of metal–oxygen bonding is certainly as great as that of metal–metal bonding. The observed structures reveal a subtle balance between M–O and M–M bonding within the steric constraints imposed by the specific alkoxide ligand.

4. Alkoxide Clusters—Templates for Organometallic Chemistry

The alkoxide cluster compounds of molybdenum and tungsten offer many attractive features for the development of a rich organometallic chemistry:[64,65]

1. By suitable choice of alkoxide ligand, steric access to the metal may be made substrate-selective.
2. The metal atoms behave as Lewis acidic centers and the presence of M–M bonds provides reservoirs of electrons for π-acid substrates.
3. Alkoxide ligands are electronically flexible and readily move between terminal and bridging modes. Their electron-releasing property may be tuned by variation of R. Response to substrate uptake or release may involve a change in M–O–C angle or terminal–bridge site exchange.
4. Synthetic procedures have now been established to incorporate a variety of functional groups of interest into the alkoxide clusters. Examples for such clusters are:

$[W_3(O)(OR)_8(R')_2]$ (R' = aryl)[66]
$[W_4(p\text{-tolyl})_2(OR)_{10}]$[66]
$[W_4(H)_2(O{i}Pr)_{14}]$[17]
$[Mo_4(N)_2(O{i}Pr)_{12}]$[19]
$[W_3(CR)(CO)_2(O{i}Pr)_9]$[67]
$[W_2(H)(CR)(\mu\text{-}C_4Me_4)(O{i}Pr)_4]$[68]

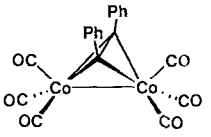
5. Unlike most organometallic systems it is not necessary to generate a reactive species by chemical or physicochemical means. For example, the fragments $[Cp^*_2M]$ (M = Ti, Zr, Hf, Mo, W), $[Co_2(CO)_6]$, [CpCo], $[PtL_2]$, and [Cp*IrL] have no known isolated existence (shelf-life)[69] and are prepared from precursor complexes, whereas the compounds **1** are isolable and have well-defined electronic structures involving metal-centered HOMOs and LUMOs.[70]

Elsewhere we have emphasized the importance of alkoxide ligands as ancillary ligands in organometallic chemistry of the early transition elements, lanthanides, and actinides.[65] We have also described in detail reactions involving $[M_2(OR)_6]$ compounds and C–O, C–C, and C–N triple bonds.[71–73] We shall restrict our discussion here to the reactions of alkynes and ethylene with $[W_2(OR)_6]$ compounds and a comparison with related reactions employing dinuclear or trinuclear carbonyl clusters.

4.1. Alkyne Derivatives

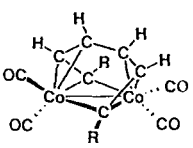
As long ago as 1968 it was written: "The sticky brown soups formed in the reactions between acetylenes and metal carbonyls yield an amazing variety of complexes including many of the organometallic exotica."[74] In these reactions, η^2- and μ-alkyne complexes and products derived from alkyne–alkyne and alkyne–carbonyl coupling are observed, including η^4-cyclobutadiene, μ-metallacyclopentadiene, and cyclopentadienone complexes.

The first structural characterization of an M_2(μ-alkyne) adduct (**15**) was undertaken by *Sly*[75] and reported in 1959. Compound **15** had been prepared earlier[76] in the reaction between $[Co_2(CO)_8]$ and diphenylacetylene.



15

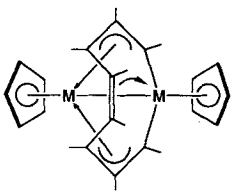
In 1964 *Mills* and *Robinson*[77] reported the structure of **16**. This was the first structural characterization of a product derived from the coupling of three alkynes, namely one acetylene and two tert-butylacetylene molecules, and featured a "flyover ligand".



16, R = *t*Bu

In reactions between $[Co_2(CO)_8]$ and alkynes the uptake of alkyne ligands is accompanied by loss of carbonyl ligands. Because a "μ-perpendicular" alkyne (see **15**) is a four-electron donor, two carbonyl ligands are lost, and the electron counts in $[Co_2(CO)_8]$ and compounds of type **15** are the same. Further alkyne uptake requires CO elimination unless alkyne–carbonyl coupling occurs.

The formation of **15** may be considered to arise from the formal addition of an alkyne to hypothetical $[(CO)_3Co \equiv Co(CO)_3]$. Though it is unlikely that this represents the mode of formation of compounds of type **15**, it has been shown that certain alkynes will add directly to compounds of type **4** to give related μ-perpendicular alkyne adducts, $[Cp_2(CO)_4M_2(\mu\text{-}C_2R_2)]$.[78, 79] The same compounds were first synthesized in the reactions between $[Cp(CO)_3M\text{-}M(CO)_3Cp]$ and alkynes under conditions in which carbonyl elimination was favored.[80] *Muetterties* and *Slater*[81, 82] subsequently showed that $[Cp_2(CO)_4Mo_2(\mu\text{-}C_2Et_2)]$ would react further with diethylacetylene under forcing conditions ($T > 100\,^{\circ}C$) to give, by successive elimination of carbon monoxide, $[Cp_2Mo_2(\mu\text{-}C_4Et_4)(CO)_3]$ and $[Cp_2Mo_2(\mu\text{-}C_4Et_4)(CO)]$. Finally, it is worth mentioning that compounds lacking any carbonyl ligands and containing a μ-C_8R_8 ligand derived from the coupling of four alkynes have been isolated (**17**).[83] Originally, these were isolated from



17

reactions involving alkynes and $[Cp_2Mo_2(CO)_4]$, but subsequently a high-yield synthesis from a mononuclear source was discovered.[84] This stepwise coupling of alkynes at a dimetal center is suggestive of an alkyne polymerization process. The elimination of the μ-C_xR_x ligand from the dimetal center, however, is not achieved catalytically. Because of the successive loss of CO ligands, elimination of C_xR_x would leave behind a coordinatively unsaturated and presumably highly energetic bimetallic species.

Reactions of alkynes with compounds of type **1** do not involve the elimination of alkoxide ligands. The latter act as electronic spectator ligands, but, by their steric demands, they influence greatly the course of the reaction. The bulky *t*BuO ligands prevent stable coordination of all but the least sterically demanding alkyne, C_2H_2. The compounds $[Mo_2(O\mathit{t}Bu)_6(C_2H_2)]$[85, 86] and **8**[28] have both been characterized in solution, and an X-ray crystallographic study has been carried out for **8**.[28] The C–C distance for the μ-C_2H_2 ligand in **8** is the longest reported (1.44(1) Å). This distance approaches that observed in the tetrahedral skeleton of $C_4(\mathit{t}Bu)_4$ (1.48(1) Å).[87]

A typical C–C distance for a μ-C_2R_2 ligand in carbonyl-supported dinuclear compounds is 1.34(2) Å.[88] Carbon–carbon distances determined in the proximity of heavy metal atoms, however, have estimated standard deviations in the range of one- to three-hundredths of an angstrom, which leads to problems in establishing meaningful differences in the various $M_2(\mu\text{-}C_2R_2)$-containing compounds. For this reason, we used NMR spectroscopy as a alternative probe of C–C bonding in $M_2(\mu\text{-}C_2H_2)$-containing compounds.

Table 1. C–C bond distances and ^{13}C–^{13}C coupling constants for $M_2(\mu\text{-}C_2H_2)$-containing compounds and tetra-*tert*-butyltetrahedrane.

Compound	d(C–C) [Å]	$^1J(^{13}C, ^{13}C)$ [Hz]	Ref.
$C_4(\mathit{t}Bu)_4$	1.48(1)	9.2	[87, 89]
$[W_2(O\mathit{t}Bu)_6(py)(C_2H_2)]$ **8**	1.44(1)	10.3	[28, 86]
$[W_2(O\mathit{i}Pr)_6(py)_2(C_2H_2)]$ **6**	1.39(2)	11.4	[28, 86]
$[W_2(OCH_2\mathit{t}Bu)_6(py)_2(C_2H_2)]$	1.39(2)	19.0	[28]
$[Mo_2(O\mathit{t}Bu)_6(C_2H_2)]$	–	23.2	[86]
$[Mo_2(O\mathit{i}Pr)_6(py)_2(C_2H_2)]$	1.368(6)	28.2	[101, 86]
$[Mo_2(Cp)_2(CO)_4(C_2H_2)]$	1.337(5)	43.4	[86]
$[Co_2(CO)_6(C_2H_2)]$	1.327(6)	56.0	[86][a]

[a] The distance quoted is for the closely related compound $[Co_2(CO)_4(PMe_3)_2(\mu\text{-}C_2H_2)]$: S. Aime, D. Osella, E. Giamello, G. Granozzi, *J. Organomet. Chem.* 262 (1984) C1.

The ^{13}C–^{13}C coupling constants for a number of compounds containing the μ-C_2H_2 ligand were determined by the simulation of the AA'XX' NMR spectra (^{13}C and ^1H) obtained for the μ-*C_2H_2 labeled compounds, where *C represents 90 mol% ^{13}C. As summarized in Table 1, there is an approximately inverse relationship between C–C distance and the magnitude of $^1J_{^{13}C,\,^{13}C}$. The value reported for $C_4(\mathit{t}Bu)_4$[89] is approached only by compound **8**.[28] Most importantly, the data in Table 1 reveal that the carbonyl-supported μ-perpendicular-C_2H_2 compounds have values of $^1J_{^{13}C,\,^{13}C}$ that are considerably greater than those found for the alkoxide-supported compounds. Also, for a given alkoxide ligand, the value of $^1J_{^{13}C,\,^{13}C}$ is greater for molybdenum than for tungsten complexes. From our X-ray crystallography and NMR studies we conclude that the alkoxide-supported complexes reduce coordinated alkynes more than their carbonyl analogues; i.e., the alkoxide-supported metal fragments π back-bond better.

We have investigated[86] the bonding in alkoxide- and carbonyl-supported $M_2(\mu\text{-}C_2H_2)$-containing compounds by the use of MO calculations employing the method of *Fenske* and *Hall*.[90] While the qualitative features of the bonding in the $M_2(\mu\text{-}C_2H_2)$-containing compounds are very similar for both alkoxide- and carbonyl-supported compounds, differences arise because of the relative orbital energies of the metal fragments. Despite the higher formal oxidation states of the metal atoms in the alkoxide-supported compounds, there is a more favorable match between metal d_π and C_2 π* orbitals. This is in the order of W > Mo and is assisted by the alkoxide p_π lone-pair orbitals because oxygen-to-metal p_π–d_π donation raises the energy of metal d_π electrons. The converse is true in the carbonyl-supported compounds in that d_π–π* interactions with CO lower the energy of the metal d_π orbitals.

A measure of the importance of alkoxide π donation is obtained from a calculational procedure that we have termed "the frozen π orbital approach".[91] In this procedure the Mulliken populations of the μ-C_2 moiety are determined in two separate calculations, one involving only the oxygen-to-metal σ interactions and the other employing oxygen σ and π orbitals. The effect of "turning on" the oxygen p_π donation is to increase the Mulliken population of the C_2 π* orbitals. The latter provides a measure of metal-to-C_2 d_π–π* back-bonding or, equivalently, alkyne reduction.

Perhaps the most obvious indication of the ability of the dimolybdenum and ditungsten center to back-bond to π-acceptor ligands is seen in the remarkably low values of $\tilde{\nu}$(CO) observed for $[M_2(OtBu)_6(\mu\text{-CO})]$ compounds: 1670 and 1580 cm^{-1} for M = Mo and W, respectively.[92] These values reflect the back-donation order W > Mo and are well below the $\tilde{\nu}$(CO) values reported for all known μ_2-CO carbonyl-supported compounds.[93]

The unique degree of M_2-to-substrate π* bonding is also illustrated by the reactions between alkynes and **1b**, in which there is a metathesis of the W≡W and C≡C bonds [Eq. (f)].[25, 94] This reaction has been extensively studied by *Schrock* and co-workers and some of the products **18** find use as alkyne metathesis catalysts.[95, 96]

$$[(t\text{BuO})_3\text{W}\equiv\text{W}(O t\text{Bu})_3] + \text{RC}\equiv\text{CR}' \longrightarrow$$
1b

$$[(t\text{BuO})_3\text{W}\equiv\text{CR}] + [(t\text{BuO})_3\text{W}\equiv\text{CR}'] \quad \text{(f)}$$
18

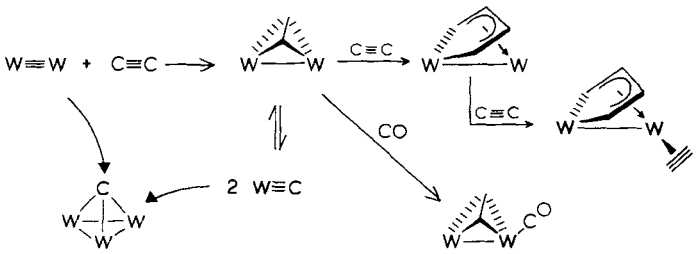
A clear connection between $W_2(\mu\text{-}C_2R_2)$-containing compounds and alkylidyne compounds was first observed for **8**, which is in equilibrium with **18** (R = H).[28] The latter is not isolable but may be stabilized and crystallized as the quinuclidine adduct, **18** · quinuclidine (R = H).[94] Subsequently, evidence has been gathered for related equilibria [Eq. (g)] involving other alkoxide ligands ($OCEt_3$, O*i*Pr, OCH_2tBu) and alkynes (C_2H_2, C_2Me_2, C_2Et_2).[72, 97, 98]

$$2\,[(\text{RO})_3\text{W}\equiv\text{CR}'] \rightleftharpoons [W_2(\text{OR})_6(\mu\text{-}C_2R'_2)] \quad \text{(g)}$$

The metathesis reaction (f) may be viewed as an oxidative cleavage of the M≡M bond. In this description two metal atoms in oxidation state +3 are oxidized to oxidation state +6 and the alkyne is reduced by six electrons to give two $RC^{3\ominus}$ ligands. Similarly, equilibrium (g) may be viewed as an internal redox reaction of the type well-documented in metal–sulfur chemistry.[99]

Strong Lewis bases, when added to an equilibrium mixture of W–alkylidyne and $W_2(\mu\text{-}C_2R_2)$-containing compounds [Eq. (g)], form adducts with the alkylidyne complexes. By contrast, π-acceptor ligands, such as CO or an alkyne, react preferentially with the $W_2(\mu\text{-}C_2R_2)$ compound and draw off equlibrium (g) to the right.[97, 98] Indeed, all $[W_2(OR)_6(\mu\text{-}C_2R'_2)]$ compounds react with alkynes to give alkyne–alkyne carbon–carbon coupling.[72, 100]

A summary of the reactions between alkynes and $[W_2(OR)_6]$ compounds is shown in Scheme 3. Note that the less sterically demanding alkoxide groups O*i*Pr and OCH_2tBu allow isolation of $[W_2(OR)_6(\mu\text{-}C_4R'_4)(\eta^2\text{-}C_2R'_2)]$ compounds (R′ = Me, Et).[100] The reaction sequence is suggestive of alkyne polymerization. In practice, however, tungsten is reluctant to give up the coordinated hydrocarbon ligands, though related $[Mo_2(OR)_6]$ compounds have been found to be alkyne trimerization catalysts and $[Mo_2(OR)_6(\mu\text{-}C_2R'_2]$ and $[Mo_2(OR)_6(\mu\text{-}C_4R'_4]$ compounds have been reliably identified as intermediates in the catalytic cycle.[101] This catalytic cycle contrasts with the alkyne–alkyne coupling reactions observed at carbonyl-supported dinuclear centers.



Scheme 3. Reactions of $[W_2(OR)_6]$ with alkynes.

4.2 Ethylene Activation

The classic example of ethylene activation at a metal carbonyl cluster is the reaction of C_2H_4 with $[Os_3(CO)_{12}]$.[102] Originally, the reaction was carried out at elevated temperatures (125 °C, 1 atm C_2H_4), leading to the isolation of a μ-vinylidene complex, **19**.[103] Under these conditions no intermediates were detected. Presumably the forcing conditions were required for CO dissociation, which was followed by ethylene coordination and C–H activation. Support for this reaction scheme was found in a variety of experiments. For instance, the substitutionally labile compound **20**[104] and ethylene were found to react under much milder conditions (25 °C) to give the first example of an ethylene adduct in carbonyl cluster chemistry, **21**. The likely hydrido-vinyl intermediate **22**[105, 106] was also prepared from reactions involving "unsaturated" $[H_2Os_3(CO)_{10}]$ and ethylene[107, 108] and acetylene.[107]

$[H_2Os_3(\mu\text{-}CCH_2)(CO)_9]$ **19**
$[Os_3(CO)_{11}(NCMe)]$ **20**
$[Os_3(\eta^2\text{-}C_2H_4)(CO)_{11}]$ **21**
$[HOs_3(\mu\text{-}CHCH_2)(CO)_9]$ **22**
$[Re_2(H)(\mu\text{-alkenyl})(CO)_8]$ **23**

The light-induced reactions between $[Re_2(CO)_{10}]$ and alkenes at 22 °C giving **23** provide excellent examples of photolytic alkene activation.[109] No intermediate was detected in the latter study, but presumably photolysis induces CO ligand expulsion, generating unsaturated species such as $[Re_2(CO)_9]$ that rapidly react with alkenes.

These reactions involving carbonyl complexes may be contrasted with our recent studies of the reactions between $[W_2(OR)_6]$ compounds and ethylene that are summarized in this article. The latter occur under mild conditions (− 78 to 0 °C, ≤ 1 atm C_2H_4) and reveal a remarkable sensitivity toward steric factors imposed by the alkoxide ligands. This is illustrated by the following experimental observations:[103] (1) $[W_2(OtBu)_6]$ **1b** and ethylene (1 atm) do not react in hydrocarbon solvents (benzene, toluene, hexane) at 22 °C; (2) $[W_2(O\text{-cyclohexyl})_6]$ and ethylene (1 atm) react slowly in hydrocarbon solvents at 22 °C to give **24** and ethane with no evidence for any intermediate; (3) $[W_2(OiPr)_6]$ and ethylene (1 atm) react in hydrocarbon solvents at 0 °C to give a "tris-ethylene adduct" **25**, which can be described *formally* as $[W_2(OiPr)_6(C_2H_4)_3]$;[110] (4) under similar conditions $[W_2(OCH_2t\text{Bu})_6]$ yields the bis-ethylene adduct **26**.[111]

$[W_2(\text{O-cylcohexyl})_6(\mu\text{-}CCH_2CH_2CH_2)]$ **24**
$[W_2(OCH_2t\text{Bu})_6(C_2H_4)_2]$ **26**

Compound **26** is formed reversibly [Eq. (h)] and there is no evidence by NMR spectroscopy for an intermediate mono-ethylene adduct $[W_2(OCH_2tBu)_6(C_2H_4)]$, which therefore must be a higher-energy species.[111]

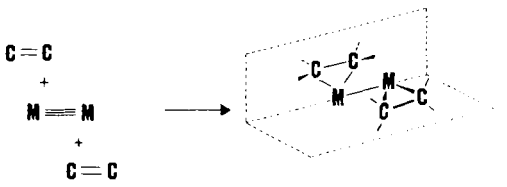
$$[W_2(OCH_2tBu)_6] + 2\,C_2H_4 \rightleftharpoons [W_2(OCH_2tBu)_6(C_2H_4)_2] \quad (h)$$
26

Although equilibrium (h) is established rapidly, it is not rapid on the NMR time scale and the ^1H and ^{13}C NMR spectra for **26** indicate that the molecule must have a virtual C_2 axis of symmetry. There are three types of OCH_2tBu ligands in the integral ratio 1:1:1 and each ligand has diastereotopic methylene protons. The proton signals for the η^2-C_2H_4 ligands represent an ABCD spin system which requires restricted rotation of the ethylene ligand about the C_2–W bond. The proton-decoupled ^{13}C NMR spectrum of **26** containing 99 mol% ^{13}C in the C_2H_4 ligand gives rise to an AB spectrum, which indicates the existence of two types of carbon atoms. The value of $^1J_{^{13}C,^{13}C}$ is 28 Hz, significantly smaller than that in ethylene (67 Hz[112]), which, together with the value of $^1J_{^{183}W,^{13}C}$ (36 Hz) suggests a significant rehybridization of the ethylene molecule upon coordination to the tungsten center. The relative intensities of the tungsten satellites due to coupling to ^{183}W, $I = 1/2$ (14.5% natural abundance), indicate that each ethylene is bound to only one tungsten atom.

Unfortunately, we have as yet been unable to obtain crystals of **26** that are suitable for an X-ray study; therefore, the detailed structure is not known. We can, however, assign a structure based on the NMR data and consideration of how a d^3–d^3 W≡W bond will interact with two C=C bonds (Scheme 4). In order for d_π-to-C_2 π^* back-bonding (W → C_2) to be effective, the C–C vectors would have to be aligned with the W–W axis. If the two WC_2 planes are at right angles, there can be a mixing of W–W π bonding and W-to-C_2 $d_\pi \rightarrow \pi^*$ back-bonding.

The $W_2(C_2)_2$ moiety shown in Scheme 4 is consistent with the observed restricted rotation about the olefin C_2-to-W axis and accounts for C_2 molecular symmetry. Based on NMR data, however, we cannot exclude the possibility of a structure in which W–W π bonding has been totally sacrificed in favor of W-to-C_2 $d_\pi \rightarrow \pi^*$ back-bonding.

One final point concerning the reversible formation of **26** that is worthy of mention arises from labeling studies employing *cis*-, *trans*-, and *gem*-$C_2H_2D_2$. The smaller gyromagnetic ratio of D ($I = 1$) leads to a simplification of the ABCD spin system because $J_{H\text{-}D} \approx 0$ Hz. Indeed, from these spectra it has been possible to extract the various H–H coupling constants and to satisfactorily simulate the ABCD spectrum of the ethylene signals associated with **26**. The coupling constants are markedly different from those of ethylene and comparable to those in phosphiranes, $RP(CH_2)_2$.[113] This supports the hypothesis that ethylene coordination to tungsten occurs with extensive rehybridization and suggests that the WC_2 moiety is best described as a metallacyclopropane. It is also significant that the spectra of the reversibly formed adducts [Eq. (h)] involving *cis*-, *trans*-, and *gem*-$C_2H_2D_2$ show no evidence of ethylene isomerization. This observation provides good evidence that both C–H bond activation and olefin metathesis reactions do no occur.



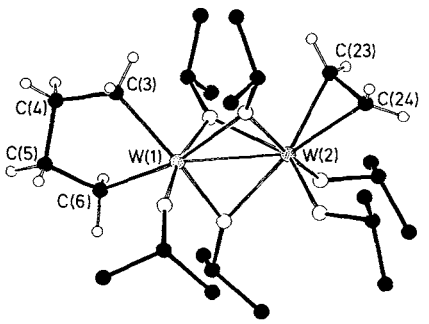
Scheme 4. Proposed structure of **26**.

In the reaction between $[W_2(OiPr)_6]$ and ethylene a "tris-ethylene" adduct is formed rapidly. This "tris-ethylene" adduct is, in fact, the dinuclear metallacyclopentane–ethylene complex **25**, which is formed reversibly [Eq. (i)].[110] There is no spectroscopic evidence that a bis-ethylene or mono-ethylene adduct is present in the equilibrium mixtures.

$$[W_2(OiPr)_6] + 3\,C_2H_4 \rightleftharpoons [W_2(OiPr)_6(CH_2)_4(\eta^2\text{-}C_2H_4)] \quad (i)$$
25

The molecular structure of **25** observed in the solid state is shown in Figure 5. Each tungsten atom is in a distorted octahedral environment if the η^2-C_2H_4 ligand is considered to occupy one coordination site. The W–W distance (2.64 Å) is intermediate between a W–W single (2.75 Å) and W–W double bond distance (2.50 Å). It is consistent with describing the $(CH_4)_4$ ligand as dianionic and the η^2-C_2H_4 ligand as either a neutral Lewis base donor or a metallacyclopropane, that is, a $C_2H_4^{2\ominus}$ ligand.

Compound **25** is fluxional in solution and shows rapid alkoxide group scrambling, presumably via a reversible opening and closing of O*i*Pr bridges. This fluxional process creates an apparent mirror plane of symmetry such that C_α is equivalent to C'_α and C_β to C'_β (Fig. 5, bottom). In addition, there is a lower-energy process that involves W–C_2 (ethylene) rotation which makes C_γ and C'_γ equivalent. Only at $-90\,^\circ C$ in [D_8]toluene are the ^1H and ^{13}C spectra consistent with the structure shown in Figure 5.



25

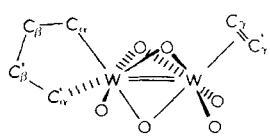


Fig. 5. Molecular structure of **25**. Top: Ball-and-stick drawing [110]. Selected bond lengths [Å]: W(1)-W(2) 2.643(1), W(1)-C(3) 2.191(12), W(1)-C(6) 2.173(12), W(2)-C(23) 2.151(11), W(2)-C(24) 2.179(12), C(23)-C(24) 1.428(17), C(3)-C(4) 1.523(17), C(4)-C(5) 1.522(20), C(5)-C(6) 1.524(18). Bottom: Schematic drawing.

Though **25** is formed reversibly [Eq. (i)], it reacts irreversibly in solution and in the solid-state above 0 °C according to the stoichiometry shown in Equation (j) to give **27**.

$$\underset{\mathbf{25}}{} \longrightarrow \underset{\mathbf{27}}{[W_2(O\mathit{i}Pr)_6(\mu\text{-}CCH_2CH_2CH_2)]} + C_2H_6 \quad (j)$$

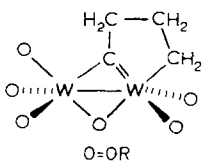
During studies of reaction (j) in [D_8]toluene, the formation of free ethylene and [$W_2(O\mathit{i}Pr)_6$] can be monitored by NMR spectroscopy. Reactions employing [$W_2(O\mathit{i}Pr)_6(CD_2)_4(\eta^2\text{-}C_2D_4)$] proceed to give the labeled alkylidyne-bridged compound [$W_2(O\mathit{i}Pr)_6(\mu\text{-}CCD_2CD_2CD_2)$] sufficiently slowly (because of a significant kinetic isotope effect) that [$W_4(O\mathit{i}Pr)_{12}$] can be detected in solution. The latter arises from the combination of the equilibria shown in Equations (d) and (i).

The bis-ethylene complex **26** and ethylene react further to give [$W_2(OCH_2\mathit{t}Bu)_6(\mu\text{-}CCH_2CH_2CH_2)$] and ethane but only slowly at ambient temperatures and pressure. In studies of these reactions the intermediate [$W_2(OCH_2\mathit{t}Bu)_6(CH_2)_4(\eta^2\text{-}C_2H_4)$] (structure type **25**, see Fig. 5) can be detected by NMR spectroscopy.[110]

In the reaction between [W_2(O-cyclohexyl)$_6$] and ethylene (> 3 equiv. 22 °C, [D_8]toluene or hexane), the alkylidyne-bridged compound **24** is formed, though no intermediate has been detected.[110] A similar reaction occurs for the complex containing O-cyclopentyl ligands. In this case, however, the metallacyclopentane–ethylene complex analogous to **25** can be detected by NMR spectroscopy studies.[110] The stoichiometric reaction shown in equation (k) is therefore operative for R = *i*Pr, $CH_2\mathit{t}Bu$, cyclopentyl, and cyclohexyl but not for R = *t*Bu, which fails to show any reactivity toward ethylene at 22 °C under comparable conditions.

$$[W_2(OR)_6] + 3\,C_2H_4 \longrightarrow [W_2(OR)_6(\mu\text{-}CCH_2CH_2CH_2)] + C_2H_6 \quad (k)$$

We have not as yet obtained crystals of any [$W_2(OR)_6(\mu$-$CCH_2CH_2CH_2)$] compound that are suitable for a single-crystal X-ray determination, but the 1:1 pyridine adduct **27** · py, obtained by crystallization from hexane/pyridine solvent mixtures, has been fully characterized (Fig. 6).[110] The pyridine molecule is only weakly bound, as evidenced by the long W–N bond distance (2.41 Å), and in [D_8]toluene solution the ^{13}C NMR spectra of unligated **27** and its pyridine adduct are the same except for the presence of free pyridine signals in the latter. Indeed, from NMR studies of the [$W_2(OR)_6(\mu$-$CCH_2CH_2CH_2)$] compounds, and the analogous labeled compounds derived from reactions employing $^*C_2H_4$, where *C represents 99 mol% ^{13}C, we can formulate a common structure (Scheme 5).[110, 114]



Scheme 5. Proposed structure of the alkoxide alkylidyne complexes [$W_2(OR)_6(\mu$-$CCH_2CH_2CH_2)$].

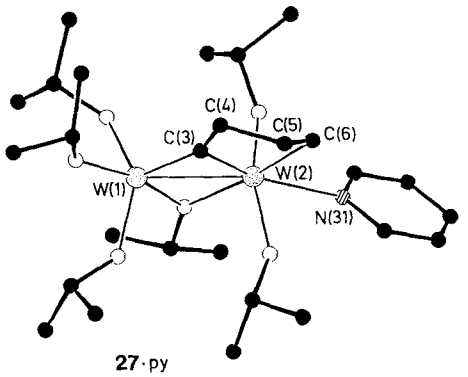
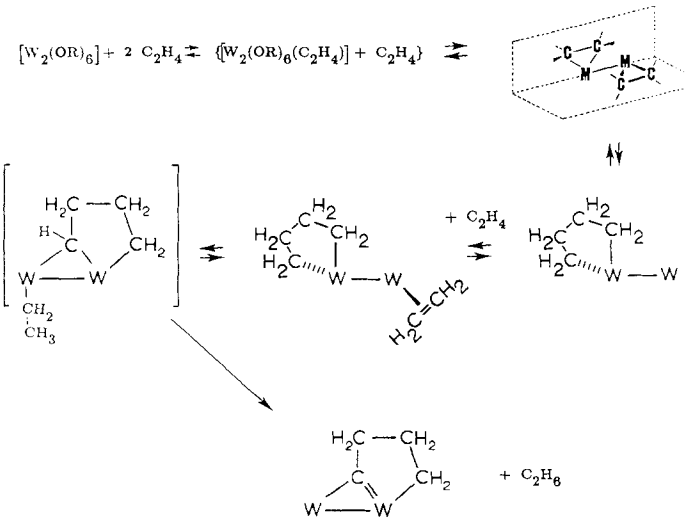


Fig. 6. A ball-and-stick drawing of the molecular structure of **27** [110]. Selected bond distances [Å]: W(1)-W(2) 2.6742(7), W(1)-C(3) 1.974(8), W(2)-C(3) 1.956(7), W(2)-C(6) 2.190(8), C(3)-C(4) 1.500(11), C(4)-C(5) 1.529(12), C(5)-C(6) 1.545(12), W(2)-N(31) 2.414(6).

Initially, we proposed[114] that the formation of the μ-$CCH_2CH_2CH_2$-containing compounds arose from a reaction sequence involving activation of a mono-ethylene adduct to give, by way of a hydrido-vinyl ligand, a μ-vinylidene ligand. This reaction path has a direct parallel with what has been observed in carbonyl dinuclear and cluster chemistry. Addition of ethylene to the μ-vinylidene ligand would then generate the μ-$CCH_2CH_2CH_2$ ligand. We can now dismiss this reaction pathway in favor of the one shown in Scheme 6.



Scheme 6. Proposed pathway for the formation of compounds having the structure shown in Scheme 5 from [$W_2(OR)_6$] and ethylene.

The intermediacy of compounds of type **25** is implicated by what we have described earlier but proof of their direct role in the formation of compounds of type **27** has come from kinetic and labeling studies.[110] What has been presented here sufficiently emphasizes the point that dinuclear alkoxides, [$W_2(OR)_6$], provide templates for C–C and C–H bond activation under mild conditions. All of the reactions described in Equations (h)–(k), which involve *reversible* ethylene binding as well as carbon–carbon and carbon–hydrogen bond activation, occur at or below room temperature.

5. Concluding Remarks

Alkoxide clusters of molybdenum and tungsten provide templates for an extensive organometallic chemistry. The choice of alkoxide ligand generates specific structural classes of clusters, which, in turn, are substrate-selective. For example, tungsten compounds of type **1** react with one equivalent of carbon monoxide to yield $[W_2(OR)_6(\mu\text{-}CO)]$ (R = *t*Bu) or $[W_4(\mu\text{-}CO)_2(OR)_{12}]$ (R = *i*Pr, CH_2tBu), whereas $[W_4(OR)_{12}]$ compounds of structural type **14** (R = CH_2iPr, CH_2-cyclopentyl, CH_2-cyclohexyl) and one equivalent of CO yield the carbido oxo cluster $[W_4(\mu_4\text{-}C)(\mu_3\text{-}O)(OR)_{12}]$.[92, 115] In contrast to carbonyl cluster chemistry, the alkoxide clusters of molybdenum and tungsten have HOMOs and LUMOs that are metal-centered and substrate activation occurs without the loss of alkoxide ligands, for instance in reactions of $[(RO)_3W\equiv W(OR)_3]$ with alkynes and ethylene. Obtaining insight into the nature of small-molecule activation by discrete alkoxide clusters promises to be an exciting endeavor.

We thank the Department of Energy, Office of Basic Sciences, Chemistry Division, for support of this work. M.H.C is indebted to all the talented co-workers cited in the references.

Received: August 30, 1988 [A 714 IE]
German version: *Angew. Chem. 101* (1989) 446

[1] a) F. A. Cotton, G. Wilkinson: *Advanced Inorganic Chemistry*, Wiley-Interscience, New York, 1988; b) [1a], p. 1053.
[2] J. Lewis, *Chem. Br. 24* (1988) 795; [1a], p. 1062–1078, and references cited therein.
[3] D. M. P. Mingos, *Progr. Inorg. Chem. 32* (1984) 237; *Polyhedron 3* (1984) 1289.
[4] L. Pauling: *The Nature of the Chemical Bond*, Cornell University Press, Ithaca, NY, USA 1960, p. 440.
[5] J. D. Corbett: *Solid State Chemistry: A Comprehensive Overview (Adv. Chem. Ser. 186* (1980) 329).
[6] R. E. McCarley, *Polyhedron 5* (1986) 51; *J. Solid State Chem. 57* (1985) 17.
[7] J. D. Corbett, *J. Solid State Chem. 39* (1981) 56.
[8] F. S. Delk, M. J. Sienko, *Inorg. Chem. 19* (1980) 1352.
[9] D. C. Bradley, R. C. Mehrotra, P. Gaur: *Metal Alkoxides*, Wiley, New York 1978.
[10] D. C. Bradley, *Nature (London) 182* (1958) 1211.
[11] D. C. Bradley, *Coord. Chem. Rev. 2* (1967) 299.
[12] M. T. Pope: *Heteropoly and Isopolymetallates*, Springer, New York 1983.
[13] M. H. Chisholm, F. A. Cotton, C. A. Murillo, W. W. Reichert, *Inorg. Chem. 16* (1977) 1801.
[14] M. Akiyama, M. H. Chisholm, F. A. Cotton, M. W. Extine, D. A. Haitko, D. Little, P. E. Fanwick, *Inorg. Chem. 18* (1979) 2266.
[15] M. H. Chisholm, J. C. Huffman, C. C. Kirkpatrick, J. Leonelli, K. Folting, *J. Am. Chem. Soc. 103* (1981) 6093.
[16] R. E. McCarley, M. H. Luly, T. R. Ryan, C. C. Torardi, *ACS Symp. Ser. 155* (1981) 41.
[17] M. H. Chisholm, J. C. Huffman, C. A. Smith, *J. Am. Chem. Soc. 108* (1986) 222.
[18] M. H. Chisholm, D. L. Clark, J. C. Huffman, C. A. Smith, *Organometallics 6* (1987) 1280.
[19] M. H. Chisholm, K. Folting, J. C. Huffman, J. Leonelli, N. S. Marchant, C. A. Smith, L. C. E. Taylor, *J. Am. Chem. Soc. 107* (1985) 3722.
[20] E. Jacob, *Angew. Chem. 94* (1982) 146; *Angew. Chem. Int. Ed. Engl. 21* (1982) 142.
[21] C. A. Tolman, *Chem. Rev. 77* (1977) 313.
[22] R. Hoffmann, *Angew. Chem. 94* (1982) 725; *Angew. Chem. Int. Ed. Engl. 21* (1982) 711.
[23] B. F. G. Johnson (Cambridge, England), personal communication.
[24] M. D. Curtis, *Polyhedron 6* (1987) 759.
[25] R. R. Schrock, M. L. Listemann, L. G. Sturgeoff, *J. Am. Chem. Soc. 104* (1982) 4291.
[26] M. H. Chisholm, D. M. Hoffman, J. C. Huffman, *Inorg. Chem. 22* (1983) 2903.
[27] E. O. Fischer, T. L. Lindner, G. Huttner, P. Friedrich, F. R. Kreissl, J. O. Besenhard, *Chem. Ber. 110* (1977) 3397.
[28] M. H. Chisholm, K. Folting, D. M. Hoffman, J. C. Huffman, *J. Am. Chem. Soc. 106* (1984) 6794.
[29] F. G. A. Stone, *Angew. Chem. 96* (1984) 85; *Angew. Chem. Int. Ed. Engl. 23* (1984) 89.
[30] M. H. Chisholm, K. Folting, J. C. Huffman, C. C. Kirkpatrick, *Inorg. Chem. 23* (1984) 1021.
[31] M. H. Chisholm, K. Folting, J. C. Huffman, E. M. Kober, *Inorg. Chem. 24* (1985) 241.
[32] M. H. Chisholm, D. M. Hoffman, J. C. Huffman, *Inorg. Chem. 24* (1985) 796.
[33] M. H. Chisholm, K. Folting, J. A. Heppert, D. M. Hoffman, J. C. Huffman, *J. Am. Chem. Soc. 107* (1985) 1234.
[34] M. H. Chisholm, D. L. Clark, K. Folting, J. C. Huffman, *Angew. Chem. 98* (1986) 1021; *Angew. Chem. Int. Ed. Engl. 25* (1986) 1014.
[35] M. H. Chisholm, D. L. Clark, K. Folting, J. C. Huffman, M. J. Hampden-Smith, *J. Am. Chem. Soc. 109* (1987) 7750.
[36] M. H. Chisholm, D. L. Clark, M. J. Hampden-Smith, unpublished.
[37] M. H. Chisholm, J. C. Huffman, C. C. Kirkpatrick, J. Leonelli, *J. Am. Chem. Soc. 103* (1981) 6093.
[38] M. H. Chisholm, D. L. Clark, J. C. Huffman, C. A. Smith, *Organometallics 6* (1987) 1280.
[39] [1a], pp. 63–64.
[40] M. H. Chisholm, J. A. Heppert, J. C. Huffman, *Polyhedron 3* (1984) 475.
[41] F. A. Cotton, T. E. Haas, *Inorg. Chem. 3* (1964) 10.
[42] L. J. Guggenberger, A. W. Sleight, *Inorg. Chem. 8* (1969) 2041.
[43] D. M. P. Mingos, *J. Chem. Soc. Dalton Trans. 1974*, 133.
[44] D. M. P. Mingos, M. I. Forsyth, *J. Chem. Soc. Dalton Trans. 1977*, 610.
[45] D. W. Bullet, *Phys. Rev. Lett. 39* (1977) 644.
[46] F. A. Cotton, G. G. Stanley, *Chem. Phys. Lett. 58* (1978) 450.
[47] B. E. Bursten, F. A. Cotton, G. G. Stanley, *Isr. J. Chem. 19* (1980) 132.
[48] T. Hughbanks, R. Hoffmann, *J. Am. Chem. Soc. 105* (1983) 1150.
[49] R. G. Wolley, *Inorg. Chem. 24* (1985) 3519.
[50] R. G. Wolley, *Inorg. Chem. 24* (1985) 3525.
[51] R. G. Johnston, D. M. P. Mingos, *Inorg. Chem. 25* (1986) 1661.
[52] R. Markby, I. Wender, R. A. Friedel, F. A. Cotton, H. W. Sternberg, *J. Am. Chem. Soc. 80* (1958) 6529.
[53] D. Seyferth, *Adv. Organomet. Chem. 14* (1976) 97.
[54] M. B. Hall, P. T. Chesky, *Inorg. Chem. 20* (1981) 4419.
[55] M. B. Hall, D. E. Sherwood, *Organometallics 1* (1982) 1519.
[56] M. B. Hall in: B. L. Shapiro (Hrsg.) *Organometallic Compounds: Synthesis, Structure and Theory*, Texas A&M University Press, College Station, TA, USA 1983, p. 334.
[57] B. E. R. Schilling, R. Hoffmann, *J. Am. Chem. Soc. 101* (1979) 3456.
[58] M. H. Chisholm, B. K. Conroy, J. D. Martin, unpublished.
[59] M. Elian, R. Hoffmann, *Inorg. Chem. 14* (1975) 1058.
[60] J. S. Bradley, *Adv. Organomet. Chem. 22* (1983) 1.
[61] S. Harris, J. S. Bradley, *Organometallics 3* (1984) 1086.
[62] R. Hoffmann, S. D. Wijeyesekera, C. N. Wilker, *Organometallics 3* (1984) 949, 962.
[63] M. H. Chisholm, J. C. Huffman, C. E. Hammond, M. J. Hampden-Smith, K. G. Moodley, *J. Am. Chem. Soc. 110* (1988) 3314.
[64] M. H. Chisholm, *Polyhedron 2* (1983) 681.
[65] W. E. Buhro, M. H. Chisholm, *Adv. Organomet. Chem. 27* (1987) 311.
[66] M. H. Chisholm, K. Folting, B. W. Eichhorn, J. C. Huffman, *J. Am. Chem. Soc. 109* (1987) 3146.
[67] M. H. Chisholm, K. Folting, J. Klang, *Organometallics 8* (1989) 89.
[68] M. H. Chisholm, B. W. Eichhorn, J. C. Huffman, *J. Chem. Soc. Chem. Commun. 1985*, 861; *Organometallics 8* (1989) 49, 67.
[69] J. P. Collman, L. S. Hegedus, J. R. Norton, R. G. Finke: *Principles and Applications of Organotransition Metal Chemistry*, University Science Books, Mill Valley, CA, USA 1987.
[70] M. H. Chisholm, *Angew. Chem. 98* (1986) 21; *Angew. Chem. Int. Ed. Engl. 25* (1986) 21.
[71] M. H. Chisholm, J. C. Huffman, D. M. Hoffman, *Chem. Soc. Rev. 14* (1985) 69.
[72] M. H. Chisholm, B. K. Conroy, B. W. Eichhorn, K. Folting, D. M. Hoffman, J. C. Huffman, N. S. Marchant, *Polyhedron 6* (1987) 783.
[73] M. H. Chisholm, *New J. Chem. 11* (1987) 459.
[74] G. E. Coates, M. L. H. Green, K. Wade: *Organometallic Compounds: The Transition Elements*, 3rd ed., 1968, Chap. 8.
[75] W. G. Sly, *J. Am. Chem. Soc. 81* (1959) 18.
[76] H. W. Sternberger, H. Greenfield, R. A. Friedel, J. Wotiz, H. R. Markby, I. Wender, *J. Am. Chem. Soc. 76* (1954) 1457.
[77] O. S. Mills, G. Robinson, *Proc. Chem. Soc. London 1964*, 187.
[78] R. J. Klingler, W. Butler, M. D. Curtis, *J. Am. Chem. Soc. 97* (1975) 3535.
[79] W. I. Bailey, Jr., M. H. Chisholm, F. A. Cotton, L. A. Rankel, *J. Am. Chem. Soc. 100* (1978) 5764.

[80] A. Nakamura, M. Hagihara, *Nippon Kagaku Zasshi 84* (1963) 344.
[81] S. Slater, E. L. Muetterties, *Inorg. Chem. 19* (1980) 3337.
[82] S. Slater, E. L. Muetterties, *Inorg. Chem. 20* (1981) 946.
[83] S. A. R. Knox, R. F. D. Stansfield, F. G. A. Stone, M. J. Winter, P. Woodward, *J. Chem. Soc. Chem. Commun. 1978*, 221.
[84] M. Green, N. C. Norman, A. G. Orpen, *J. Am. Chem. Soc. 103* (1981) 1269.
[85] R. R. Schrock, H. Strutz, *Organometallics 3* (1984) 1600.
[86] M. H. Chisholm, B. K. Conroy, D. L. Clark, J. C. Huffman, *Polyhedron 7* (1988) 903.
[87] H. Irngartinger, A. Goldmann, R. Jahn, M. Nixdorf, H. Rodewald, G. Maier, K.-D. Malsch, R. Emrich, *Angew. Chem. 96* (1984) 967; *Angew. Chem. Int. Ed. Engl. 23* (1984) 993.
[88] For a listing of C–C distances in perpendicular $M_2(\mu\text{-}C_2R_2)$ carbonyl-containing complexes, see D. M. Hoffman, R. Hoffmann, C. R. Fisel, *J. Am. Chem. Soc. 104* (1982) 3858.
[89] T. Loerzer, R. Machinek, W. Lüttke, L. H. Franz, K.-D. Malsch, G. Maier, *Angew. Chem. 95* (1983) 914; *Angew. Chem. Int. Ed. Engl. 22* (1983) 878.
[90] M. B. Hall, R. F. Fenske, *Inorg. Chem. 11* (1972) 768.
[91] M. H. Chisholm, D. L. Clark, *Comments Inorg. Chem. 6* (1987) 23.
[92] P. J. Blower, M. H. Chisholm, D. L. Clark, B. W. Eichhorn, *Organometallics 5* (1986) 2125.
[93] For neutral molecules, bridging CO groups absorb in the range 1700–1860 cm^{-1}: [1a], p. 1034.
[94] R. R. Schrock, M. L. Listemann, *Organometallics 4* (1985) 74.
[95] R. R. Schrock, J. H. Weingrovius, J. Sancho, *J. Am. Chem. Soc. 103* (1981) 3932.
[96] R. R. Schrock, J. Sancho, *J. Mol. Catal. 15* (1982) 75.
[97] M. H. Chisholm, B. K. Conroy, J. C. Huffman, N. S. Marchant, *Angew. Chem. 98* (1986) 448; *Angew. Chem. Int. Ed. Engl. 25* (1986) 446.
[98] M. H. Chisholm, B. K. Conroy, J. C. Huffman, *Organometallics 5* (1986) 2394.
[99] W. H. Pan, M. A. Harmer, T. R. Halbert, E. I. Stiefel, *J. Am. Chem. Soc. 106* (1984) 459.
[100] M. H. Chisholm, D. M. Hoffman, J. C. Huffman, *J. Am. Chem. Soc. 106* (1984) 6806.
[101] M. H. Chisholm, K. Folting, J. C. Huffman, I. P. Rothwell, *J. Am. Chem. Soc. 104* (1982) 4289.
[102] A. J. Deeming in: B. F. G. Johnson (Ed.): *Transition Metal Clusters*, Wiley, New York 1980, p. 321, and references cited therein.
[103] A. J. Deeming, M. Underhill, *J. Chem. Soc. Dalton Trans. 1974*, 1415.
[104] B. F. G. Johnson, J. Lewis, D. Pippard, *J. Organomet. Chem. 145* (1978) C4.
[105] A. G. Orpen, D. Pippard, G. M. Sheldrick, K. D. Rouse, *Acta Crystallogr. Sect. B34* (1978) 2466.
[106] J. J. Guy, B. E. Reichert, G. M. Sheldrick, *Acta Crystallogr. Sect. B32* (1976) 3319.
[107] A. J. Deeming, P. Hamo, M. Underhill, *J. Chem. Soc. Dalton Trans. 1975*, 1614.
[108] J. B. Keister, J. R. Shapley, *J. Organomet. Chem. 85* (1975) C29.
[109] P. O. Nubel, T. L. Brown, *J. Am. Chem. Soc. 104* (1982) 4955; *ibid. 106* (1984) 644.
[110] M. H. Chisholm, M. J. Hampden-Smith, J. C. Huffman, unpublished.
[111] M. H. Chisholm, M. J. Hampden-Smith, *Angew. Chem. 99* (1987) 936.; *Angew. Chem. Int. Ed. Engl. 26* (1987) 903.
[112] H. Günther, *Angew. Chem. 84* (1972) 907; *Angew. Chem. Int. Ed. Engl. 11* (1972) 861.
[113] H. Goldwhite, D. Rowsell, L. Vertal, M. T. Bowers, M. A. Cooper, p. L. Maratt, *Org. Magn. Reson. 21* (1983) 494.
[114] M. H. Chisholm, M. J. Hampden-Smith, *J. Am. Chem. Soc. 109* (1987) 5871.
[115] M. H. Chisholm, M. J. Hampden-Smith, unpublished.

When submitting manuscripts, authors of articles intended for publication as "Communications" are requested to read the "Notice to Authors" reproduced in the January issue of the journal following the list of contents; upon request, a copy can be obtained from the editorial office.

Reductive Dimerization of a Phosphaalkyne with Complexation to Samarium**

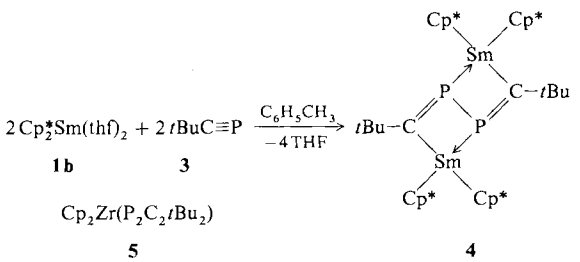
By *Anja Recknagel, Dietmar Stalke, Herbert W. Roesky* and *Frank T. Edelmann**

Of great importance for the organometallic chemistry of lanthanides in low formal oxidation states was the discovery of decamethylsamarocene **1a** by *Evans* et al.[1] Like the THF adduct **1b**, complex **1a** undergoes a number of interesting reactions;[2] for example, **2**,[3] the first dinitrogen complex of an f element was recently prepared. Noteworthy, however, is the complete absence of complexes containing phosphorus ligands.[2] Since phosphaalkynes exhibit an especially diverse reactivity toward organometallic complexes, we have investigated the reaction of 2-*tert*-butyl-1-phosphaethyne **3** with **1b**. This reaction results in reductive dimerization of the phosphaalkyne; the resulting new ligand remains coordinated to samarium.

Cp^*_2Sm **1a** $Cp^*_2Sm(thf)_2$ **1b** $[Cp^*_2Sm(\mu\text{-}\eta^2\text{:}\eta^2\text{-}N_2)SmCp^*_2]$ **2**

$Cp^* = (\eta^5\text{-}C_5Me_5)$

The adduct **1b**[4] reacts rapidly with the phosphaalkyne **3**[5] in toluene at room temperature, the reaction mixture displaying a striking color change from deep violet to orange-red. Recrystallization of the product from toluene affords bright red, air-sensitive crystals of composition $[Cp^*_2Sm(t\text{BuC}\equiv\text{P})]_2$ **4** (correct elemental analysis, molecular weight (EI-MS) 1042).



The ^{31}P NMR spectrum shows that the samarium complex **4** does not contain diphosphacyclobutadiene[6, 7] as ligand. The chemical shift (singlet at $\delta = -260.1$) lies in the same region as that found for the zirconium complex **5** ($\delta = -247$) recently described by *Binger* et al.[8] In that compound, $t\text{BuC}\equiv\text{P}$ is dimerized to a bent 1,3-diphosphabicyclo[1.1.0]butane. The ^1H NMR spectrum of **4** (in C_6D_6) shows a singlet for the C_5Me_5 groups ($\delta = 1.54$) and for the *tert*-butyl groups ($\delta = -2.61$). Thus, the spectroscopic data do not allow an unequivocal description of the bonding in the new ligand. The structure of **4** was therefore elucidated by X-ray structure analysis (Fig. 1),[9] which revealed a novel ligand in **4**, the dianion of a 2,3-diphosphabutadiene.

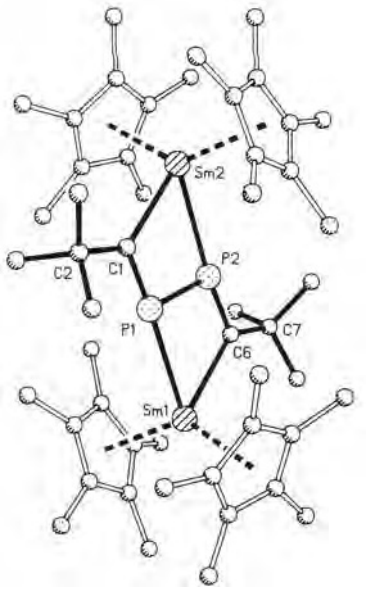


Fig. 1. Molecular structure of **1**. Selected bond lengths [pm]: Sm1-P1 295.2(2), Sm2-P2 294.5(2), Sm1-C6 255.7(6), Sm2-C1 255.6(6) (see also text).

As in the neutral species,[10] the P–C double bonds have a *trans* arrangement. The P=C bond lengths are 169.4(7) (P1-C1) and 169.8(7) (P2-C6). The P1–P2 distance of 220.7(2) is in agreement with a single bond. Each samarium bridges a phosphorus and a carbon atom. All samarium and phosphorus atoms lie in a common plane with C1, C2, C6, and C7 (largest deviation from the plane: 1.5 pm). The mean distance of the samarium atoms from the center of the Cp* ring is 247 pm.

The reductive dimerization of the phosphaalkyne is not fully surprising in view of the reduction potential of **1b**, which is similar to that of alkali metals. The result presented here should encourage the use of reactive phosphorus ligands in the organometallic chemistry of f elements.

Experimental Procedure

Compound **3** (0.4 g, 4.0 mmol) was added to a solution of **1b** (1.7 g, 3.0 mmol) in toluene (20 mL) and the reaction mixture was stirred for 12 h at room temperature. The orange-red solution was filtered and the filtrate was concentrated to ca. 10 mL and then cooled to −25 °C. After 48 h, 1.2 g (40%) of **4** was isolated as red crystals, m.p. 215 °C.

Received: November 3, 1988 [Z 3035 IE]
German version: *Angew. Chem. 101* (1989) 496

CAS Registry numbers:
1b, 79372-14-8; **3**, 78129-68-7; **4**, 119325-99-4; **4** · $C_6H_5CH_3$, 119326-00-0.

[*] Dr. F. T. Edelmann, A. Recknagel, Dr. D. Stalke, Prof. Dr. H. W. Roesky
Institut für Anorganische Chemie der Universität
Tammannstrasse 4, D-3400 Göttingen (FRG)

[**] This work was supported by the Deutsche Forschungsgemeinschaft, the Stiftung Volkswagenwerk and the Fonds der Chemischen Industrie.

[1] W. J. Evans, L. A. Hughes, T. P. Hanusa, *J. Am. Chem. Soc. 106* (1984) 4270.
[2] W. J. Evans, *Polyhedron 6* (1987) 803.
[3] W. J. Evans, T. A. Ulibarri, J. W. Ziller, *J. Am. Chem. Soc. 110* (1988) 6877.

[4] W. J. Evans, J. W. Grate, H. W. Choi, I. Bloom, W. E. Hunter, J. L. Atwood, *J. Am. Chem. Soc. 107* (1985) 941.
[5] a) G. Becker, G. Gressner, U. Uhl, *Z. Naturforsch. B 36* (1981) 16; b) M. Regitz, P. Binger, *Angew. Chem. 100* (1988) 1541; *Angew. Chem. Int. Ed. Engl. 27* (1988) 1484.
[6] P. Binger, R. Milczarek, R. Mynott, M. Regitz, W. Rösch, *Angew. Chem. 98* (1986) 645; *Angew. Chem. Int. Ed. Engl. 25* (1986) 644.
[7] P. B. Hitchcock, M. J. Maah, J. F. Nixon, *J. Chem. Soc. Chem. Comun. 1986*, 737.
[8] P. Binger, B. Biedenbach, C. Krüger, M. Regitz, *Angew. Chem. 99* (1987) 798; *Angew. Chem. Int. Ed. Engl. 26* (1987) 764.
[9] **4** · toluene: $C_{50}H_{78}P_2Sm_2 \cdot C_7H_8$, monoclinic, $C2/c$, $a = 2143.1(2)$, $b = 1520.2(3)$, $c = 3359.6(3)$ pm, $\beta = 93.04(2)^\circ$, $V = 10.93$ nm^3, $\rho_{calcd} = 1.38$ g cm^{-3}, $Z = 8$, $\mu(Mo_{K\alpha})$, graphite monochromator) = 2.23 mm^{-1}, 10281 measured reflections, of which 7096 were independent and 6165 observed with $F \geq 3\sigma F$, $2\theta_{max} = 45^\circ$. Data collected on a Stoe-Siemens AED at -85 °C, structure solution and refinement with SHELX 86, refinement of 550 parameters, all non-hydrogen atoms refined anisotropically. All hydrogen atoms were placed at ideal geometric positions and included in the calculation as rigid groups according to a riding model. $R = 0.043$, $R_w = 0.062$, $w^{-1} = \sigma(F) + 0.0008\,F^2$, maximal residual electron density 9.0×10^2 e nm^{-3}. Further details of the crystal structure investigation may be obtained from the Fachinformationszentrum Energie, Physik, Mathematik GmbH, D-7514 Eggenstein-Leopoldshafen 2 (FRG), an quoting the depository number CSD-51414, the names of the authors, and the journal citation.
[10] R. Appel, V. Barth, F. Knoch, *Chem. Ber. 116* (1983) 938.

$[\{Cp(CO)_2Mn\}_2(\mu\text{-}H)]^{\ominus}$: A New, Versatile Reagent**

By *Karl Plößl, Gottfried Huttner,** and *Laszlo Zsolnai*

Dedicated to Professor Hans Bock on the occasion of his 60th birthday

The $Cp(CO)_2Mn$ fragment is one of the most versatile 16-electron species. $Cp(CO)_2Mn$ derivatives are usually obtained by substitution of weakly bound ligands L in $Cp(CO)_2MnL$ (e.g., L = THF).[1, 2] Anionic starting complexes for the formation of $Cp(CO)_2Mn$ complexes were not available previously and there have been no reports so far on the use of the recently reported anions **1**–**3** for the preparation of unusual ligands of the nitrogen group.[5]

$[Cp(CO)_2Mn]^{2\ominus}$ **1** $[Cp(CO)_2MnH]^{\ominus}$ [3] **2**

$[(MeC_5H_4)(CO)_2MnSiR_3]^{\ominus}$ [4] **3**

We have now found that the novel title compound **4** is a versatile reagent for carrying out this kind of chemistry. $Cp(CO)_2Mn(thf)$ reacts with $NaBH_4$ to give **4**, which could be obtained as a crystalline $[Na(crypt)]^{\oplus}$ salt.[6]

$$Cp(CO_2)Mn(thf) \xrightarrow[2)\ (crypt)]{1)\ NaBH_4} [Na(crypt)]^{\oplus}\left[Cp(CO)_2Mn(H)Mn(CO_2)Cp\right]^{\ominus}$$

4

$Cp = (\eta^5\text{-}C_5H_5)$

The anion **4** has a hydride-bridged Mn–Mn bond,[7] whereas the isoelectronic compound $[\{Cr_2(CO)_{10}\}(\mu\text{-}H)]^{\ominus}$ is "open" (i.e., without direct metal–metal contact).[8] Complex **4** reacts with halides of elements of the nitrogen group in the ways already found for $Na_2[M_2(CO)_{10}]$ (M = Cr, Mo, W).[9] Reaction of **4** with $AsCl_3$ gives the chloroarsanediyl complex **5**, which is also accessible by a different route;[10] with $SbCl_3$ the analogous antimony complex **6** is formed.[11] The non-optimized yields (**5**, 24%; **6**, 39%) are appreciably better than those obtained by previous synthetic methods (**5**, 6.6%; **6**, 18%). These syntheses and the reactions of **4** described here can be extended to its MeC_5H_4 and Me_5C_5 analogues.[12]

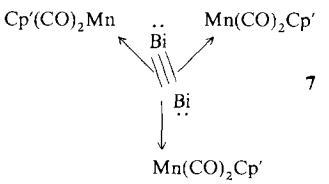
$$\left[Cp(CO)_2Mn(H)Mn(CO_2)Cp\right]^{\ominus} \xrightarrow{ECl_3} Cp(CO)_2Mn(Cl)(E)Mn(CO)_2Cp$$

4 **5**, E = As; **6**, E = Sb

Complex **4a**, prepared analogously to **4**, and $BiCl_3$ react to give **7**,[7] the first derivative of dibismuth coordinated side-on by three 3d L_nM fragments[13].

$$\left[Cp'(CO)_2Mn(H)Mn(CO_2)Cp'\right]^{\ominus} \xrightarrow{BiCl_3}$$

4a



7

$Cp' = (\eta^5\text{-}C_5H_4CH_3)$

Complex **7** displays the starlike structure typical of threefold side-on-coordinated Bi_2 (Fig. 1).[13] The Bi_2Mn_3 framework has D_{3h} symmetry; the arrangement of the $(MeC_5H_4)(CO)_2Mn$ fragments also approximates this symmetry (Fig. 1). The Bi–Bi distance in **7** (281.3 pm) has the value expected for side-on-coordinated Bi_2.[13] The Bi–Mn distances (289.7–295.0 pm) have a mean value of 293.2 pm. Bi–Mn distances of similar length were found previously only in sterically crowded molecules such as $Bi[Mn(CO)_5]_3$[14] (288.4–291.6 pm). This lengthening of the M–X bonds is typical of molecules of the type $(L_nM)_3X_2$ (X = Bi, Sb, As, L_nM = 16-electron fragment).[13, 15, 16]

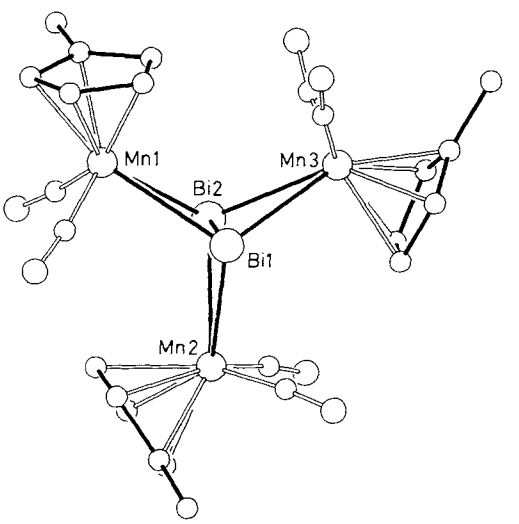


Fig. 1. Molecular structure of **7**[7].

[*] Prof. Dr. G. Huttner, Dipl.-Chem. K. Plößl, Dr. L. Zsolnai
Anorganisch-chemisches Institut der Universität
Im Neuenheimer Feld 270, D-6900 Heidelberg (FRG)

[**] This work was supported by the Fonds der Chemischen Industrie and the Deutsche Forschungsgemeinschaft.

Experimental Procedure

All reactions were performed under nitrogen with freshly prepared dried solvents. ^{1}H NMR, Bruker AC 200; IR, Perkin-Elmer 983 G; UV/VIS, Perkin-Elmer Lambda 9.

Na(crypt) · **4**: A solution of $CpMn(CO)_3$ (4.5 g, 22 mmol) in 400 mL of THF was irradiated for 3.5 h. The resulting wine-red soltion was treated with $NaBH_4$ (1 g, 26.3 mmol) and [2.2.2]cryptand (1 g, 2.6 mmol) [6] and then stirred in the dark at 25 °C for 12 h. The resulting brown suspension was filtered through 3 cm of diatomaceous earth, the filtrate was evaporated to dryness at 25 °C and 10^{-2} mbar, and the brown residue was washed with *n*-pentane until the IR spectrum no longer showed the presence of $CpMn(CO)_3$ (2.2 g of $CpMn(CO)_3$ was recovered). The red-brown powder was recrystallized from THF/*n*-pentane at − 30 C. The salts of **4** are air-sensitive to different degrees depending on the cation [17]. Yield: 2.0 g Na(crypt) · **4** (24% based on the amount of $CpMn(CO)_3$ employed, 48% based on the amount recovered). Correct C, H, N analysis; $C_{32}H_{47}Mn_2N_2NaO_{10}$ (752). IR (THF): $\tilde{\nu}_{CO}$ = 1901 (m), 1875 (vs), 1825 (vs), 1810 (m) cm^{-1}. ^{1}H NMR ([D$_6$]acetone, 293 K): δ = 4.18 (s, 10H), 3.65 (m, 24H), 2.71 (t, 12H), − 26.9 (s, br., 1H). UV/VIS (THF): λ_{max} (ε) = 405 (3090) and 508 (800) nm (L mol^{-1} cm^{-1}) [18].

7: Na · **4a** (1 g, 2.5 mmol) [12] was dissolved in 30 mL of THF · $BiCl_3$ (0.9 g, 2.9 mmol) was then added to this solution at 25 °C, resulting in foaming and the formation of a dark precipitate. The suspension was stirred for 30 min at 25 °C and then transferred directly to silylated silica gel. Chromatography on a silica gel column (30 × 1.5 cm, − 20 °C) gave a yellow forerun upon elution with *n*-pentane. Elution with CH_2Cl_2 afforded a long yellow-brown band, which, upon removing the solvent and recrystallizing the residue from 10 mL of CH_2Cl_2 at − 30 °C, gave brown needle-shaped crystals of **7**: Yield: 240 mg of **7** (15% based on $BiCl_3$). IR (CH_2Cl_2): $\tilde{\nu}_{CO}$ = 1908 (vs) and 1864 (s) cm^{-1}. ^{1}H NMR ($CDCl_3$): δ = 4.38 (m), 4.3 (m) (total 12H), 2.13 (s, 9H).

Received: November 3, 1988;
supplemented: December 27, 1988 [Z 3036 IE]
German version: *Angew. Chem. 101* (1989) 482

CAS Registry numbers:
4 · Na$^{\oplus}$, 119366-71-1; **4** · Na(crypt)$^{\oplus}$, 119366-67-5; **4** · $Me_4N^{\oplus}$, 119366-68-6; **4** · $Bu_4N^{\oplus}$, 119366-69-7; **4a** · Na$^{\oplus}$, 119391-00-3; **7**, 119366-70-0; $BiCl_3$, 7787-60-2; $CpMn(CO)_3$, 12079-65-1; crypt, 23978-09-8.

[1] E. O. Fischer, M. Herberhold: *"Essays in Coordination Chemistry", Experientia Supplement IX*, Birkhäuser, Basel 1964, pp. 259–305.
[2] W. Strohmeier, *Angew. Chem. 76* (1964) 873; *Angew. Chem. Int. Ed. Engl. 3* (1964) 749.
[3] V. S. Leong, N. J. Cooper, *Organometallics 7* (1988) 2080.
[4] a) U. Kirchgässner, U. Schubert, *Organometallics 7* (1988) 784; b) E. Kunz, M. Knorr, J. Willnecker, U. Schubert, *New J. Chem. 12* (1988) 467.
[5] $[(MeC_5H_4)(CO)_2MnSiR_3]^{\ominus}$ is apparently suitable for such syntheses: U. Schubert, personal communication.
[6] crypt = 4,7,13,16,21, 24-hexaoxa-1,10-diazabicyclo[8.8.8]hexacosane, $N(C_2H_4OC_2H_4OC_2H_4)_3N$.
[7] Na(crypt) · **4**: a = 1803.2 (7), b = 1434.6 (7), c = 1719.6 (8) pm, β = 126.32 (3), space group $C2/c$, Z = 4. Solution and refinement of the structure (SHELX 76 and SHELX 86, G. Sheldrick, Universität Göttingen) led to R_1 = 0.071; R_2 = 0.064. $d_{Mn\text{-}Mn}$ = 298.3 (1), $d_{Mn\text{-}H}$ = 167.1 pm. **7**: a = 1081.6 (4), b = 1162.1 (5), c = 1249.5 (3) pm, α = 114.24 (3), β = 96.68 (3), γ = 109.46 (3)°, space group $P\bar{1}$, Z = 2. Solution and refinement of the structure (see Na(crypt) · **4**) led to R_1 = 0.041; R_2 = 0.036. $d_{Bi\text{-}Bi}$ = 281.3 (0), $d_{Bi\text{-}Mn}$ = 289.7 (2)–295.0 (2) pm. Further details of the crystal structure investigation may be obtained from the Fachinformationszentrum Energie, Physik, Mathematik GmbH, D-7514 Eggenstein-Leopoldshafen 2 (FRG), on quoting the depository number CSD-53411, the names of the authors, and the journal citation.
[8] J. Roziers, J. M. Williams, R. P. Stewart, Jr., J. L. Petersen, L. F. Dahl, *J. Am. Chem. Soc. 99* (1977) 4497.
[9] G. Huttner, K. Evertz, *Acc. Chem. Res. 19* (1986) 406.
[10] J. von Seyerl, U. Moering, A. Wagner, A. Frank, G. Huttner, *Angew. Chem. 90* (1978) 912; *Angew. Chem. Int. Ed. Engl. 17* (1978) 844.
[11] U. Weber, L. Zsolnai, G. Huttner, *J. Organomet. Chem. 260* (1984) 281.
[12] K. Plößl, A. Strube, G. Huttner, unpublished.
[13] Cf. $Bi_2[M(CO)_5]_3$: G. Huttner, U. Weber, L. Zsolnai, *Z. Naturforsch. B 37* (1982) 707; A. M. Arif, A. H. Cowley, N. C. Norman, M. Pakulski, *Inorg. Chem. 25* (1986) 4836.
[14] J. M. Wallis, G. Müller, H. Schmidbaur, *Inorg. Chem. 26* (1987) 458.
[15] G. Huttner, U. Weber, B. Sigwarth, O. Scheidsteger, *Angew. Chem. 94* (1982) 210; *Angew. Chem. Int. Ed. Engl. 21* (1982) 411.
[16] B. Sigwarth, L. Zsolnai, H. Berke, G. Huttner, *J. Organomet. Chem. 226* (1982) C5.
[17] The anion **4** can also be isolated as a pyrophoric powder containing naked Na$^{\oplus}$ or, by metathesis, as the $Me_4N^{\oplus}$ or $Bu_4N^{\oplus}$ salt.
[18] The given ε values are lower limits owing to the tendency of the compounds to decompose.

Chiral Building Blocks for the Synthesis of Triquinane Sesquiterpenes: Derivatives of 2-Methylbicyclo[3.3.0]octan-3-ol from Catalpol**

By *Klaus Weinges*,* *Helene Iatridou*, *Hans-Georg Stammler*, and *Johannes Weiss*

An increasing number of natural products with angular or linear triquinane carbon frameworks have been isolated in recent years and have encouraged the development of general approaches to their synthesis.[1] Because of the special biological activity often exhibited by triquinane sesquiterpenes, we are interested in synthesizing them in enantiomerically pure form. This goal can be realized by transformation of the ketoenol ether **1**[2a] to chiral compounds that display suitable structural features for the synthesis of triquinane sesquiterpenes. Compound **1** can be prepared in 93% yield from the naturally occurring catalpol according to a published procedure[2b] that has since been improved. Cuprate addition to the enone of silyl ether **2** (Scheme 1) introduces the methyl substituent at C-2, which is characteristic of a series of angular and linear triquinanes.[1]

Ramberg–Bäcklund reaction of **9** resulted in ring contraction[3] to give the pentalene derivative **10**, which was converted into 8-*tert*-butyldimethylsiloxy-2-methylbicyclo[3.3.0]octan-3-ol **11**[4] by stereoselective hydroboration. The two hydroxyl substituents at C-8 and C-3, which were selectively protected in **11** and **13**, respectively, allowed, after oxidation, a variety of alkylation reactions to be carried out at the neighboring C atoms. As in analogous compounds,[1,5] five-membered ring annelation at C1-C2 and C2-C3 gives frameworks of the angular and linear triquinanes, respectively. Furthermore, variation of the substituents at C-7[6a] or C-4[6b] offers a direct route to specific members of this class of compounds.

The C-7 geminal methyl substituents of **15**, which are introduced by a simple methylation reaction, are also found in the carbon skeletons of the antibiotically active (−)-hypnophilin[7] and (−)-coriolin **20**, which, in addition, exhibits antitumor activity.[8] Compound **15** was used to easily prepare (1*R*, 2*R*, 3*R*, 5*R*, 8*R*)-(+)-benzoyloxy-

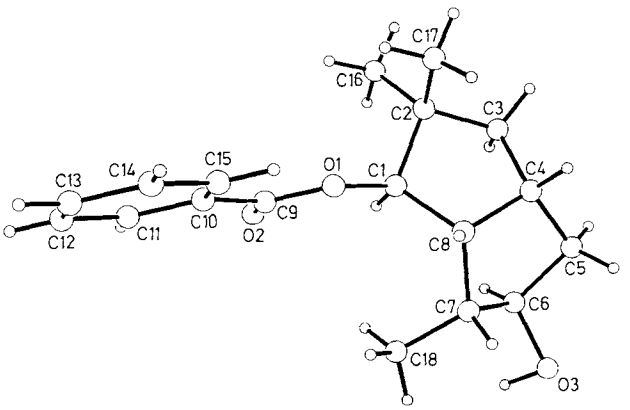
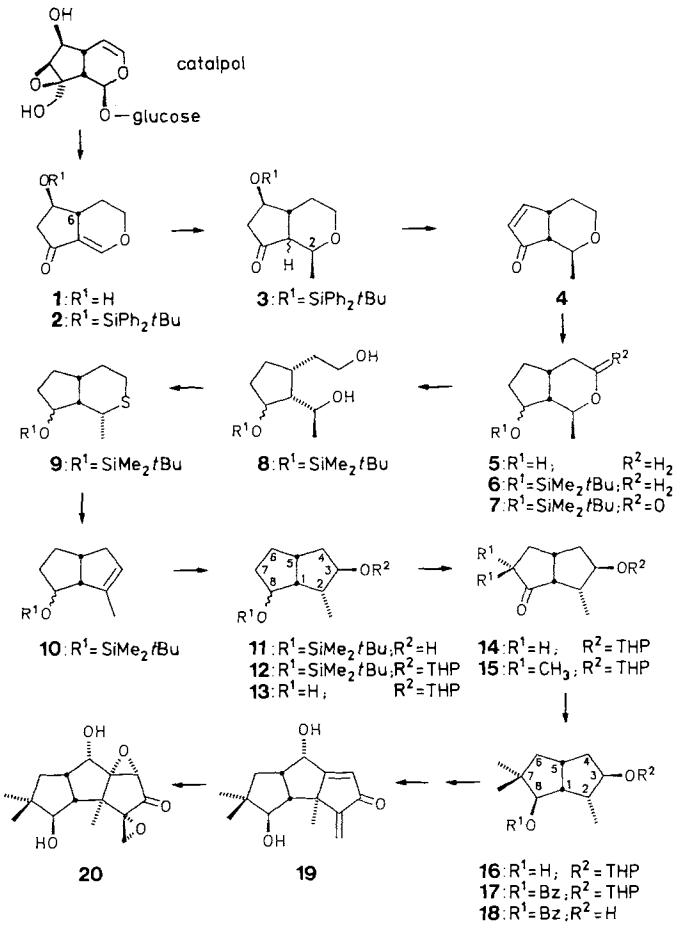


Fig. 1. Molecular structure of **18** [12]. The numbering is unsystematic.

[*] Prof. Dr. K. Weinges, Dipl.-Chem. H. Iatridou
Organisch-chemisches Institut der Universität
Im Neuenheimer Feld 270, D-6900 Heidelberg 1 (FRG)
Prof. Dr. J. Weiss [+], Dipl.-Chem. H.-G. Stammler [+]
Anorganisch-chemisches Institut der Universität Heidelberg
[+] X-ray structure analysis.
[**] Chemistry and Stereochemistry of the Iridoids, Part 11. This work was supported by the Deutsche Forschungsgemeinschaft. Part 10: [3].



Scheme 1. Reaction conditions: **1** → **2**: *t*BuPh$_2$SiCl, imidazole, DMF, RT (room temperature), 5 h, 71%; **2** → **3**: Me$_2$CuLi, ether, − 75 °C, 1 h; sat. NH$_4$Cl solution, − 75 °C → 20 °C, 87% *cis-/trans-***3** (3:2), no separation; **3** → **4**: KOH in THF/MeOH, − 50 °C, 4 h, 83%; **4** → **5**: NaBH$_4$, EtOH, − 10 °C, 1.5 h, 88% *endo/exo*-alcohol (93:7); **5** → **6**: *t*BuMe$_2$SiCl, imidazole, DMF, RT, 2 h, 90%; **6** → **7**: $RuO_2 \cdot xH_2O$, $NaIO_4$, $H_2O/CCl_4/CH_3CN$, 16 h, RT, 79%; **7** → **8**: $LiAlH_4$, THF, − 10 °C, 1 h, 94%; **8** → **9**: 1) CH_3SO_2Cl, pyridine, − 15 °C → RT, 2.5 h, 2) $Na_2S \cdot xH_2O$, EtOH, 80 °C, 2 h, 88%; **9** → **10**: 1) *m*-chloroperbenzoic acid, CH_2Cl_2, − 15 °C → RT, 1 h, 65%, 2) K_2CO_3, *N*-chlorosuccinimide, CH_2Cl_2, RT, max. 72 h, 3) *m*-chloroperbenzoic acid, CH_2Cl_2, 24 h, RT, 81%, 4) *t*BuOK, THF, 0 °C → RT, 1 h, 64%; **10** → **11**: 1 M $BH_3 \cdot$ THF in THF, 0 °C, 1 h; 2 N NaOH, 30% H_2O_2, 30 min, 95%; **11** → **12**: 3,4-dihydro-2*H*-pyran, *p*-toluenesulfonic acid in THF, CH_2Cl_2, RT, 1 h, 93%; **12** → **13**: $(n\text{Bu})_4NF \cdot 3\,H_2O$, THF, RT, 72 h, 95%; **13** → **14**: pyridinum dichromate, DMF, RT, 2 h, 76%; **14** → **15**: *t*BuOK, THF, − 75 °C, 20 min; MeI, − 75 °C → 0 °C, 15 min, 65%; **15** → **16**: Li, NH_3, THF, *t*BuOH, − 75 °C, 20 min, 48% after chromatographic separation (flash) of the *endo*-alcohol (37%), which can be reoxidized to the ketone **15** in 70% yield; **16** → **17**: PhCOCl, pyridine, − 10 °C → RT, 16 h, 86%; **17** → **18**: $CH_3COOH/H_2O/$THF, RT, 16 h, 84%.

2,7,7-trimethylbicyclo[3.3.0]octan-3-ol **18**, which *Matsumoto* et al. used in racemic form to synthesize the coriolin precursor **19**.[9a] Racemic **18**, slightly modified, was also employed by other authors[9b-e] as a coriolin precursor. The synthesis of optically active **20** has only been achieved so far by *Demuth* et al.[10] via racemate resolution of a racemic bicyclic intermediate. Enantiomerically pure (+)-**18** can be prepared on a gram scale from **1** according to the reactions shown in Scheme 1[11] (ca. 4.5 g of **18** was obtained from 170 g of **1**). Unlike racemic **18**,[9a] (+)-**18** is a crystalline product (m.p. 87 °C; $[\alpha]_\lambda^{20}$: $\lambda = 589$, + 1.06; 578, + 1.19; 546, + 1.59; 436, + 3.18; 365, + 6.55 ($c = 1.13$ in acetone)), the constitution and configuration of which were confirmed by X-ray diffraction (Fig. 1).[12]

Received: November 10, 1988 [Z 3045 IE]
German version: *Angew. Chem. 101* (1989) 485

[1] a) L. A. Paquette, *Top. Curr. Chem. 119* (1984) 1; b) B. M. Trost, *Chem. Soc. Rev. 11* (1982) 141.
[2] a) K. Weinges, H. von der Eltz, *Angew. Chem. 92* (1980) 639; *Angew. Chem. Int. Ed. Engl. 19* (1980) 628; b) K. Weinges, S. Haremsa, U. Huber-Patz, R. Jahn, H. Rodewald, H. Irngartinger, H. Jaggy, E. Melzer, *Liebigs Ann. Chem. 1986*, 46.
[3] K. Weinges, S. Haremsa, *Liebigs Ann. Chem. 1987*, 679.
[4] *endo*-**11**: (1*R*,2*R*,3*R*,5*R*,8*R*)-(−)-8-*tert*-butyldimethylsilyloxy-2-methylbicyclo[3.3.0]octan-3-ol: m.p. 37–38 °C; $[\alpha]_\lambda^{20}$: $\lambda = 589$, − 353.9; 578, − 356.6; 546, − 366.4; 436, − 420.3; 365, − 489.2 ($c = 1.03$ in acetone).
[5] Review: M. Ramaiah, *Synthesis 1984*, 529.
[6] Examples: a) hirsutic acid C: F. W. Comer, J. Trotter, *J. Chem. Soc. B 1966*, 11; complicatic acid: G. Mellows, P. G. Mantle, T. C. Feline, D. J. Williams, *Phytochemistry 12* (1973) 2717; hypnophilin: [7]; coriolin: [8]; b) silphines: F. Bohlmann, J. Jakupovic, *ibid. 19* (1980) 259; laurenenes: R. E. Corbett, C. M. Couldwell, D. R. Lauren, R. T. Weavers, *J. Chem. Soc. Perkin Trans. 1, 1979*, 1791; isocomenes: R. N. Harris III, D. Van Derveer, J. A. Bertrand, *J. Chem. Soc. Chem. Commun. 1977*, 456.
[7] B. M. Gianneti, B. Steffan, W. Steglich, *Tetrahedron 42* (1986) 3587.
[8] T. Takeuchi, H. Iinuma, J. Iwanaga, S. Takahashi, T. Takita, H. Umezawa, *J. Antibiot. 22* (1969) 215; S. Takahashi, N. Naganawa, H. Iinuma, T. Takita, K. Maeda, H. Umezawa, *Tetrahedron Lett. 1971*, 1955; H. Nakamura, T. Takita, H. Umezawa, M. Kunishima, Y. Nakayama, Y. Iitaka, *J. Antibiot. 27* (1974) 301.
[9] a) T. Ito, N. Tomiyoshi, K. Nakamura, S. Azuma, M. Izawa, F. Maruyama, M. Yanagiya, H. Shirahama, T. Matsumoto, *Tetrahedron 40* (1984) 241; b) K. Iseki, M. Yamazaki, M. Shibashaki, S. Ikegami, *ibid. 37* (1981) 4411; c) S. Knapp, A. F. Trope, M. S. Theodore, N. Hirata, J. J. Barchi, *J. Org. Chem. 49* (1984) 608; d) F. P. Schuda, M. R. Heimann, *Tetrahedron 40* (1984) 2365; e) P. Magnus, C. Exon, P. Albaugh-Robertson, *ibid 41* (1985) 5861.
[10] M. Demuth, P. Ritterskamp, E. Weight, K. Schaffner, *J. Am. Chem. Soc. 108* (1986) 4149.
[11] Compounds **2**–**5**, **18**, and the corresponding *endo* isomers of **6**–**13** were characterized by elemental analysis and spectroscopy (IR, ^{1}H, ^{13}C NMR). Optical rotations {$[\alpha]_D^{20}$ (*c* in acetone)}: *cis*-**3**, + 14.4 (1.11); *endo*-**6**, − 13.7 (1.07); *endo*-**7**, − 106.4 (1.10); *endo*-**8**, − 5.0 (1.01); *endo*-**10**, + 22.3 (1.01); *endo*-**11**, − 353.9 (1.03); *endo*-**13**, + 87.0 (1.03); **18**, + 1.06 (1.13).
[12] Since the absolute configuration of **1** at C-6 is known [2b] and no reaction is performed at this C atom, the absolute configuration of **18** can also be determined by X-ray structure analysis. Crystal dimensions 0.8 × 0.6 × 0.5 mm^3, orthorhombic, $P2_12_12_1$, $Z = 4$, $a = 9.885$ (5), $b = 12.776$ (5), $c = 13.395$ (7) Å, $V = 1692.7$ Å^3, $\varrho_{calcd} = 1.13$ g cm^{-3}, $\mu = 0.17$ cm^{-1}. Siemens-Stoe diffractometer, $Mo_{K\alpha}$ radiation, graphite monochromator, $2\theta \cdot \omega$ scan with $2\theta \leq 55°$, empirical absorption correction (ψ scans of 7 reflections, min. transmission 0.715, max. transmission 0.855). 2240 independent reflections, 876 with $I > 2.5\,\sigma(I)$. Structure solution: direct methods (SHELXTL program). Structure refinement: "cascade matrix" procedure, which is based on F_w with $w = 1/\sigma^2(F)$. All C and O atoms refined anisotropically, H atoms refined isotropically. Hydrogen atoms on C atoms refined at calculated positions, hydrogen-atom position of the hydroxyl group refined from difference Fourier syntheses with a fixed O–H distance of 0.92 Å. 191 parameters; $R = 0.054$ ($R_w = 0.043$), maximal residual electron density 0.13 eÅ^{-3}, minimal residual electron density − 0.2 eÅ^{-3}. Further details of the crystal structure investigation may be obtained from the Fachinformationszentrum Energie, Physik, Mathematik GmbH, D-7514 Eggenstein-Leopoldshafen 2 (FRG), on quoting the depository number CSD-53487, the names of the authors, and the journal citation.

New Intermediates in the Cyclocotrimerization of Thioxophosphorus(v) Cations with Alkynes**

By *Ekkehard Lindner*,* *Volker Käss*, *Wolfgang Hiller*, and *Riad Fawzi*

Alkyne cyclotrimerization is an important and extensively investigated route to benzene derivatives.[1] The introduction of heteroatoms such as N, O, P, or S considerably ex-

[*] Prof. Dr. E. Lindner, Dipl.-Chem V. Käss, Dr. W. Hiller, Dr. R. Fawzi
Institut für Anorganische Chemie der Universität
Auf der Morgenstelle 18, D-7400 Tübingen 1 (FRG)

[**] Synthesis and Properties of Metal-Containing Heterocycles and Their Reactions, Part 62. This work was supported by the Deutsche Forschungsgemeinschaft and the Fonds der Chemischen Industrie. *V. K.* thanks the Studienstiftung des deutschen Volkes for a fellowship. Part 61: E. Lindner, K. E. Frick, M. Stängle, R. Fawzi, W. Hiller, *Chem. Ber. 122*, (1989) 53.

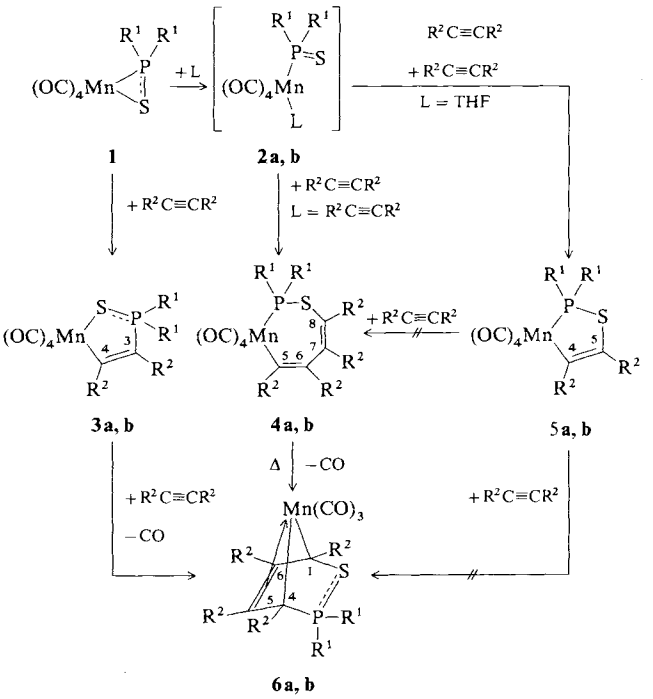
pands the palette of available products.[2] The cyclotrimerization of alkynes on transition-metal complexes proceeds via bisalkyne complexes, which undergo C–C bond formation to give metallacyclopentadienes.[3] These products can react in two ways with an additional alkyne present in the coordination sphere of the metal: either formal insertion of the alkyne into an M–C bond to give metallacycloheptatrienes or cycloaddition to give metallabicycloheptadienes.[4] Another possibility is the direct Diels-Alder cycloaddition of the alkyne without prior coordination to the metal. This reaction is especially important when strongly activated alkynes are employed.[5]

The cyclocotrimerization of $R_2P{=}S$ cations with alkynes can only be carried out on 3d metals; this reaction is not observed for higher homologues.[6] In the case of manganese, only thiaphosphametallacyclopentadienes and -bicycloheptadienes have so far been observed as intermediates. The latter species have made accessible highly substituted thiophenes, phospholes, and their complexes, which are otherwise difficult to obtain.[2b] We have now succeeded in isolating two further intermediates which are important for understanding the mechanism of this mixed cyclotrimerization.

Reaction of $[BrMn(CO)_5]$ with $R^1_2P(S)H$ in the presence of a base leads to formation of **1**, the first (η^2-diorganothioxophosphorus)manganese complex (Scheme 1); the kinetic stabilization of **1** is due to the bulky cyclohexyl groups on the phosphorus. Smaller substituents (R^1 = Me, Et, Ph) result in immediate dimerization to give $[(OC)_4Mn(\mu\text{-}S{=}PR^1_2)]_2$. These dimers are in equilibrium with the monomers $[(OC)_4Mn(\eta^2\text{-}S{=}PR^1_2)]$, which can be trapped with alkynes.

Reaction of **1** with the acetylene dicarboxylates $R^2C{\equiv}CR^2$ in THF under mild conditions gives initially the manganacyclopentadienes **3a, b**, which then yield the manganabicycloheptadienes **6a, b**.[7] In addition, the P-isomeric metallacyclopentenes **5a, b** and, in lower yield, the P-isomeric metallacycloheptadienes **4a, b** were obtained for the first time. In contrast, **4a, b** precipitate as the main products from hexane solution; in refluxing THF, they rearrange quantitatively with loss of CO to give **6a, b.** Surprisingly, neither **4a, b** nor **6a, b** can be prepared from the P-isomeric metallacyclopentenes **5a, b** and free alkyne.

The metallabicycloheptadienes **6a, b** are thus formed via two parallel routes. Free alkyne inserts into the Mn–P bond of **1** to give **3**, which, in turn, affords **6**. Alternatively, the Mn–S bond of **1** opens—this step has been confirmed for the analogous cobalt complexes by CO addition[8]—and the resulting 16-electron species is stabilized by addition of a donor ligand L. If the coordination site is blocked by a solvent molecule L, only a small amount of **4** is formed, since a [2 + 2 + 2] cycloaddition can only occur after displacement of L by an alkyne. In noncoordinating solvents such as hexane, the 16-electron complex fragment can only be stabilized by the alkyne. Therefore, the reaction occurs much faster and the main product is **4**, which is transformed into **6** upon warming of the THF solution.



Scheme 1. R^1 = cyclohexyl, L = THF, $R^2C{\equiv}CR^2$: **a**, $R^2 = CO_2CH_3$; **b**, $R^2 = CO_2C_2H_5$. The numbering of the ring carbon atoms is for assignment of the NMR signals.

Compounds **1** and **3**–**6** were characterized by complete elemental analyses as well as by mass, IR, and NMR spectra (Table 1). In addition, X-ray crystal structures were obtained for **1** and **4a** (Fig. 1).[9]

Whereas the P–S distance in **1** is in agreement with that of other (η^2-thioxophosphorus)metal complexes,[6, 8, 10] it is considerably longer in **4a** owing to the Mn–P–S–C arrangement. The seven-membered ring of **4a** exists in boat conformation; its folding is determined by the orientation of the three planes Mn-P-C5, P-S-C5-C6 (± 14 pm), and S-C6-C7-

Table 1. Spectroscopic data, R_f values, and melting points for **1** and **3a**–**6a**.

	1	**3a**	**4a**	**5a**	**6a**
IR [cm^{-1}]: ν(CO) [a]	2071 m	2079 m	2080 m	2074 m	2018 vs
	2000 s	2001 vs	2020 s	2001 sh	1950 s
	1986 vs	1996 sh	1996 vs	1995 vs	1943 sh
	1958 s	1950 s	1970 s	1958 s	
ν(PS) [b]	535	534	517	534	537
$^{31}P(^1H)$ NMR [c]	81.1	101.6	166.8	126.0	92.0
$^{13}C(^1H)$ NMR [d]		159.61 (C3) [e]	133.05 (C5) [f]	134.02 (C4) [g]	52.93 (C1)
		130.77 (C4)	131.09 (C6) [h]	160.54 (C5) [i]	51.90 (C4) [j]
			145.02 (C7)		103.97 (C5) [k]
			193.15 (C8) [l]		101.58 (C6)
$M^{\oplus}$ [m]	396	538	680	538	652
R_f [n]	0.83	0.33	0.11	0.30	0.14
Dec. [°C]	128	137	157	148	169

[a] In CCl_4. [b] In KBr. [c] In THF, δ values relative to 85% H_3PO_4 in [D_6]acetone ext., −40 °C. [d] In $CDCl_3$, δ values relative to TMS, only ring carbon atoms. [e] d, $^1J_{PC}$ = 27.3 Hz. [f] d, $^2J_{PC}$ = 5.2 Hz. [g] d, $^2J_{PC}$ = 14.1 Hz. [h] d, $^3J_{PC}$ = 3.5 Hz. [i] d, $^2J_{PC}$ = 8.0 Hz. [j] d, $^1J_{PC}$ = 36.1 Hz. [k] d, $^2J_{PC}$ = 2.0 Hz. [l] d, $^2J_{PC}$ = 21.9 Hz. [m] From field-desorption mass spectra. [n] On silica with petroleum ether (60–90 °C)/ethyl acetate (10/1).

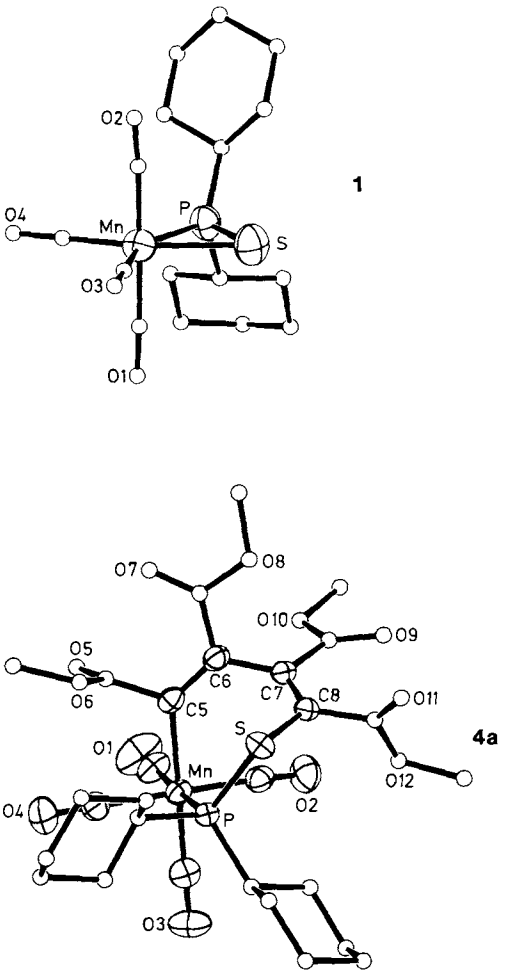


Fig. 1. Molecular structures of **1** (top) and **4a** (bottom). Important bond lengths [Å] and bond angles [°]: **1**: Mn-S 244.0 (2), Mn-P 226.1 (2), S-P 200.6 (2); S-Mn-P 50.4 (1), Mn-S-P 60.2 (1), Mn-P-S 69.5 (1). **4a**: Mn-P 233.3 (1), S-P 212.9 (1), Mn-C5 208.4 (4), C5-C6 135.2 (6), C6-C7 148.3 (6), C7-C8 132.8 (5), S-C8 177.7 (4); Mn-P-S 116.4 (1), P-Mn-C5 87.1 (2), P-S-C8 105.6 (1).

C8 (± 0.5 pm) (interplanar angle 145° and 119°) with respect to one another. As expected, the C–C bond lengths alternate.[4]

Experimental Procedure

1: $R^1_2P(S)H$ and $N(C_2H_5)(i\text{-}C_3H_7)_2$ (3.0 mmol each) in 50 mL of diisopropyl ether were added dropwise to a solution of $[BrMn(CO)_5]$ in 50 mL of diisopropyl ether at 60 °C. After stirring for 1 h, the solvent was removed in vacuo. The residue was suspended in 10 mL of methanol, filtered off (P4), and washed with methanol. Yield: 1.01 g (85%).

4: $R^2C{\equiv}CR^2$ (2.0 mmol) was added to a solution of **1** (0.5 mmol) in 25 mL of hexane and the resulting solution was stirred for 12 h. The precipitate was filtered off (P4), washed with hexane, and dissolved in ether. Addition of hexane resulted in precipitation of **4.** Yield: 0.238 g (70%) **4a**; 0.213 g (58%) **4b.**

3a–6a: $H_3CO_2C{\equiv}CCO_2CH_3$ (4.0 mmol) was added to a solution of **1** (1.0 mmol) in 50 mL of THF and the resulting mixture was stirred at 25 °C for 4 d. The solvent was then removed in vacuo and the crude product was purified by medium-pressure column chromatography (Merck-Lobar-Fertigsäule Gr. B LiChroprep Si 60, 40–63 μm) with petroleum ether (60–90 °C)/ethyl acetate (10/1) as eluent (cf. R_f values in Table 1). Yields: 69 mg (13%) **3a**; 27 mg (4%) **4a**; 102 mg (19%) **5a**; 182 mg (28%) **6a**.

Received: October 20, 1988 [Z 3019 IE]
German version: *Angew. Chem. 101* (1989) 460

CAS Registry numbers: **1**, 119208-87-6; **3a**, 119208-89-8; **4a**, 119208-90-1; **4b**, 119208-88-7; **5a**, 119208-91-2; **6a**, 119208-92-3; $H_3CO_2CC{\equiv}CCO_2CH_3$, 762-42-5; $H_5C_2O_2CC{\equiv}CCO_2C_2H_5$, 762-21-0; $(cyclo\text{-}C_6H_{11})_2P(S)H$, 14610-03-8; $BrMn(CO)_5$, 14516-54-2.

[1] a) E. Lindner, *Adv. Heterocycl. Chem. 39* (1986) 237 and references cited therein; b) R. G. Bergman, *Pure Appl. Chem. 53* (1981) 161.
[2] a) H. Bönnemann, *Angew. Chem. 97* (1985) 264; *Angew. Chem. Int. Ed. Engl. 24* (1985) 248; b) E. Lindner, A. Rau, S. Hoehne, *ibid. 93* (1981) 822 and **20** (1981) 788.
[3] Y. Wakatsuki, O. Nomura, K. Kitaura, K. Morokuma, H. Yamazaki, *J. Am. Chem. Soc. 105* (1983) 1907.
[4] H. Hoberg, D. Schaefer, G. Burkhart, C. Krüger, M. J. Romao, *J. Organomet. Chem. 266* (1984) 203.
[5] D. R. McAllister, J. E. Bercaw, R. G. Bergman, *J. Am. Chem. Soc. 99* (1977) 1666.
[6] D. H. M. W. Thewissen, *J. Organomet. Chem. 192* (1980) 115; H. P. M. M. Ambrosius, J. N. Noordik, G. J. A. Ariaans, *J. Chem. Soc. Chem. Commun. 1980*, 832; D. S. Bohle, C. E. F. Rickard, W. R. Roper, *Angew. Chem. 100* (1988) 308; *Angew. Chem. Int. Ed. Engl. 27* (1988) 302.
[7] E. Lindner, A. Rau, S. Hoehne, *Angew. Chem. 93* (1981) 821; *Angew. Chem. Int. Ed. Engl. 20* (1981) 787.
[8] E. Lindner, K. E. Frick, R. Fawzi, W. Hiller, M. Stängle, *Chem. Ber. 121* (1988) 1075.
[9] *Crystal data*: **1** crystallizes from methanol (233 K): triclinic $P\bar{1}$, lattice constants $a = 1064.1(4)$, $b = 1226.6(6)$, $c = 854.3(3)$ pm, $\alpha = 95.48(3)$, $\beta = 112.86(3)$, $\gamma = 67.51(3)°$, $V = 947.5 \times 10^6$ pm^3, $\rho_{calcd} = 1.389$ g cm^{-3}, $Z = 2$, $Mo_{K\alpha}$ radiation, (graphite monochromator), measuring range $\theta_{max} = 24°$, total number of reflections 3183, number of symmetry-independent reflections with $I \geq 3\,\sigma(I)$ 2360, refined parameters 208, empirical absorption correction (DIFABS), $R = 0.045$, $R_w = 0.045$. The structure was solved by direct methods (SHELXS). **4a** crystallizes from methanol (233 K): triclinic $P\bar{1}$, lattice constants $a = 1286.4(5)$, $b = 1393.0(5)$, $c = 984.0(3)$ pm, $\alpha = 110.51(4)$, $\beta = 103.11(4)$, $\gamma = 83.82(4)°$, $V = 1607.7 \times 10^6$ pm^3, $\rho_{calcd} = 1.406$ g cm^3, $Z = 2$. $Mo_{K\alpha}$ radiation, (graphite monochromator), measuring range $\theta_{max} = 24°$, total number of reflections 5328, number of symmetry-independent reflections with $I \geq 3\,\sigma(I)$ 3389, refined parameters 388, empirical absorption correction (DIFABS), $R = 0.041$, $R_w = 0.046$. The structure was solved by direct methods (SHELXS). Further details of the crystal structure investigations may be obtained from the Fachinformationszentrum Energie, Physik, Mathematik GmbH, D-7514 Eggenstein-Leopoldshafen 2 (FRG), on quoting the depository number CSD-53 332, the names of the authors, and the journal citation.
[10] a) E. Lindner, C.-P. Krieg, W. Hiller, R. Fawzi, *Angew. Chem. 96* (1984) 508; *Angew. Chem. Int. Ed. Engl. 23* (1984) 523; b) E. Lindner, K. Auch, W. Hiller, R. Fawzi, *ibid. 96* (1984) 287 and *23* (1984) 320.

Discovery of a D-Stereospecific Aminopeptidase and Its Use as a Catalyst in Organic Synthesis

By *Yasuhisa Asano,* Akiko Nakazawa, Yasuo Kato,* and *Kiyosi Kondo*

Enzymatic reaction has increasingly been applied to organic synthesis.[1] Several attempts have recently been reported on the in vitro synthesis of D-amino-acid–containing peptides and amides.[2] Naturally, however, these enzymatic reactions have the inevitable drawback that they are not stereospecific for substrates with D-configurations. To the best of our knowledge, there has been no report of an aminopeptidase catalyzing the stereospecific hydrolysis of D-amino-acid–containing peptides,[3] although such peptides do exist in nature.[4]

An enrichment culture technique was used for the selection of a desirable microorganism and resulted in the isolation of *Achromobacter* sp. SCRC C1-38 from a soil sample. The enzyme hydrolyzing D-alanine amide was purified about 2800-fold with a 17% yield from a cell-free extract of the bacterium. The molecular weight of the native enzyme was estimated to be approximately 122 000, with two identical subunits having molecular weights of about 59 000. Figure 1 shows a typical course of D-stereospecific hydrolysis of D,L-alanine amide to yield D-alanine. The rate of the hydrolysis

[*] Dr. Y. Asano, A. Nakazawa, Y. Kato, Dr. K. Kondo
Sagami Chemical Research Center
Nishi-Ohnuma 4-4-1 Sagamihara, Kanagawa 229 (Japan)

of L-alanine amide was less than 0.01% that of D-alanine amide. The identity of the D-alanine thus formed was confirmed by its isolation (correct elemental analysis: $[\alpha]_D^{20}$ −14.15 (c = 6.6, 1 N HCl)). Substrates of the enzyme included D-alanine amide (relative velocity, 100%: K_m value, 0.65 mM), glycine amide (44%, 22.3 mM), D-α-aminobutyric acid amide (30%, 18.3 mM), D-serine amide (29%, 27.0 mM), D-alanine 3-aminopentane amide (32%, 2.27 mM), D-alanine *p*-nitroanilide (96%, 0.51 mM), D-alanine methyl ester (75%), the dimer (21%, 10.2 mM), trimer (92%, 0.57 mM), and tetramer (89%, 0.32 mM) of D-alanine, D-alanylglycine (95%, 0.98 mM), D-alanylglycylglycine (45%, 0.37 mM), and D-alanyl-L-alanyl-L-alanine (100%, 0.65 mM). These results show that the enzyme has higher affinity toward peptide substrates than toward amino acid amides. The enzyme showed neither endopeptidase nor carboxypeptidase activity. When the release of amino acids from D-alanylglycylglycine was followed with time, the enzyme exhibited a mode of action typical of aminopeptidases (EC 3.4.11).[5] The effect of various compounds and metal ions on the enzyme activity indicated that the enzyme is a thiol-peptidase. Thus, we tentatively named the enzyme as "D-alanine aminopeptidase".

For enzyme-catalyzed D-stereospecific aminolysis of amino acid esters, the enzyme was immobilized by urethane prepolymer PU-6[7] and was incubated in water-saturated organic solvents (benzene, butyl acetate, 1,1,1-trichloroethane; Table 1). D-Alanine 3-aminopentane amide was quantitatively synthesized from D-alanine methyl ester and 3-aminopentane in 1 h. The catalytic activity (k_{cat}) was calculated to be as high as 7700 min^{-1}, which is several hundred to ten thousand times greater than those in α-chymotrypsin-[2a] or subtilisin[2b]-catalyzed peptide syntheses, respectively. D-Alanine 3-aminopentane amide was synthesized in 46% yield from D,L-alanine methyl ester, while no product was formed from L-alanine methyl ester. The aminolysis reaction also progressed well with D-alanine amide. The substrate specificity for the acyl donor part in this aminolysis reaction was reflected in the hydrolytic reaction. However, the substrate specificity for the nucleophile part differed: no formation of D-alanine polymer was observed when D-alanine methyl ester alone was incubated with the immobilized enzyme, but D-alanine *N*-alkylamides of *n*-butylamine, benzylamine, and neopentylamine could be synthesized in high yields.

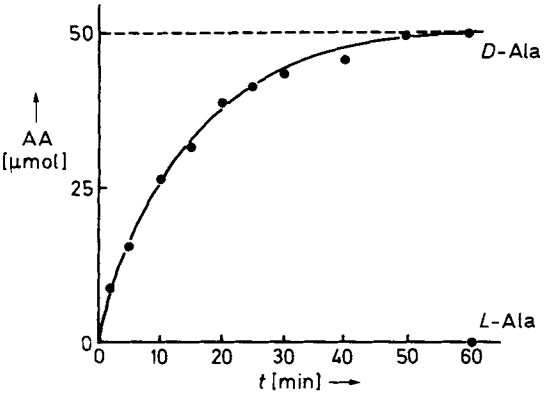


Fig. 1. Kinetic resolution of D,L-alanine amide by *Achromobacter* D-alanine aminopeptidase. *Achromobacter* sp. SCRC C1-38 was cultivated aerobically at 190 °C for 18 h in a TGY medium [8]. The enzyme was purified from cells (about 190 g wet weight) from 20 liters of culture by a procedure involving protamine sulfate treatment, ammonium sulfate fractionation, column chromatography on DEAE-Toyopearl and Butyl-Toyopearl, and gel filtration on Sephadex G-200. The activity of D-alanine aminopeptidase was routinely assayed at 30 °C by measuring the production of D-alanine from D-alanine amide, and D-alanine was determined with D-amino acid oxidase [9]. One unit of enzyme activity was defined as the amount of enzyme that catalyzed the formation of 1 μmol of D-alanine per minute. The enzyme was judged to be homogeneous based on the results of native and SDS-polyacrylamide gel electrophoresis, HPLC on a TSK Gel G-3000 SW column, and isoelectric focusing (pI = 4.2), since all of the results gave a single band or a single peak. The specific activity of the homogeneous enzyme was 596 units mg^{-1} at 30 °C and pH 8.0 with D-alanine amide as the substrate. A reaction mixture containing 0.5 mmol Tris hydrochloride (pH 8.0), 0.1 mmol D,L-alanine amide hydrochloride, and 5 units of the purified enzyme in a total volume of 5.0 mL was incubated at 30 °C. The content of L-alanine was measured with L-alanine dehydrogenase. AA = amount of amino acid.

Table 1. Aminolysis of alanine methyl ester with 3-aminopentane catalyzed by *Achromobacter* D-alanine aminopeptidase [a].

Acyl donor	Solvent	Yield [%] [b]
D-alanine methyl ester HCl	butyl acetate	98
D,L-alanine methyl ester HCl	butyl acetate	48
L-alanine methyl ester HCl	butyl acetate	0
D-alanine methyl ester HCl	benzene	98
D-alanine methyl ester HCl	trichloroethane	91
D-alanine methyl ester HCl	toluene	67

[a] A reaction mixture containing PU-6-immobilized D-alanine aminopeptidase (7.5 units of partially purified enzyme of 210 units mg^{-1}), 0.1 mmol of alanine methyl ester hydrochloride, and 0.5 mmol of 3-aminopentane in water-saturated organic solvent (1 mL) was incubated at 30 °C for 1 h. [b] The yield was calibrated with chemically synthesized authentic products with ninhydrin.

The discovery of this new D-alanine aminopeptidase could bring about a new methodology in the kinetic resolution of amino acid amides, as well as in the formation of peptide bonds between racemic amino acid esters to yield D-amino acid *N*-alkylamides,[7] with extremely high D stereoselectivities.

Received: October 31, 1988 [Z 3031 IE]
German version: *Angew. Chem. 101* (1989) 511

CAS Registry numbers:
D-alanine aminopeptidase, 119413-52-4; 3-aminopentane, 616-24-0; D-alanine methyl ester HCl, 14316-06-4; D,L-alanine methyl ester HCl, 13515-97-4; L-alanine methyl ester HCl, 2491-20-5; D-alanine 3-aminopentanamide, 119337-32-5; D,L-alanine amide, 20108-77-4; glycine amide, 598-41-4; D-α-aminobutyric acid amide, 104652-77-9; D-serine amide, 104714-52-5; D-alanine *p*-nitroanilide, 77286-89-6; D-alanine methyl ester, 21705-13-5; D-alanine dimer, 923-16-0; D-alanine trimer, 1114-94-9; D-alanine tetramer, 926-78-3; D-alanylglycine, 3997-90-8; D-alanylglycylglycine, 77286-90-9; D-alanyl-L-alanyl-L-alanine 5874-89-5; D-alanine amide 35320-22-0; D-alanine 338-69-2.

[1] G. M. Whitesides, C.-H. Wong, *Angew. Chem. 97* (1985) 617; *Angew. Chem. Int. Ed. Engl. 24* (1985) 617; C. Laane, J. Tramper, M. D. Lilly (Eds.): *Biocatalysts in Organic Media*, Elsevier, Amsterdam 1987; H. Yamada, S. Shimizu, *Angew. Chem. 100* (1988) 640; *Angew. Chem. Int. Ed. Engl. 27* (1988) 622.

[2] a) J. B. West, C.-H. Wong, *J. Org. Chem. 51* (1986) 2728; b) A. L. Margolin, D.-F. Tai, A. M. Klibanov, *J. Am. Chem. Soc. 109* (1987) 7885; c) K. Kato, K. Kawahara, T. Takahashi, S. Igarashi, *Agric. Biol. Chem. 44* (1980) 821; I. B. Stoineva, D. D. Petkov, *FEBS Lett. 183* (1985) 103; H. Nakajima, S. Kitabatake, R. Tsurutani, K. Yamamoto, I. Tomioka, K. Imahori, *Int. J. Pept. Protein Res. 28* (1986) 179; A. L. Margolin, A. M. Klibanov, *J. Am. Chem. Soc. 109* (1987) 3802; C. F. Barbas III, C.-H. Wong, *J. Chem. Soc. Chem. Commun. 1987* 533.

[3] M. Sugie, H. Suzuki, *Agric. Biol. Chem. 50* (1986) 1397; Y.-C. Tsai, C.-P. Tseng, K.-M. Hsiao, L.-Y. Chen, *Appl. Environ. Microbiol. 54* (1988) 984.

[4] K. H. Schleifer, O. Kandler, *Bacteriol. Rev. 36* (1972) 407; H. Manabe, *Phytochemistry 25* (1986) 2233; H. Kleinkauf, H. von Döhren, *Curr. Top. Microbiol. Immunol. 91* (1981) 129; K. Richter, R. Egger, G. Krell, *Science 238* (Washington) (1987) 200.

[5] Nomenclature Committee of the International Union of Biochemistry: *Enzyme Nomenclature*, Academic Press, New York 1984, p. 332.

[6] S. Fukui, A. Tanaka, *Adv. Biochem. Eng. Biotechnol. 29* (1984) 1.

[7] Pfizer Inc. has synthesized various synthetic sweeteners containing the D-alanine *N*-alkylamide moiety: US Pat. 4411925 (1983).

[8] Y. Asano, T. Sekigawa, H. Inukai, A. Nakazawa, *J. Bacteriol. 170* (1988) 3189.

[9] C. C. Allain, L. S. Poon, C. C. G. Chan, W. Richmond, P. C. Fu, *Clin. Chem. 20* (1974) 470.

Selenium-Catalyzed Synthesis of *S*-Alkyl Thiocarbamates from Amines, Carbon Monoxide, Sulfur, and Alkyl Halides

By *Noboru Sonoda,* Takumi Mizuno, Sinkichi Murakami, Kiyoshi Kondo, Akiya Ogawa, Ilhyong Ryu,* and *Nobuaki Kambe*

Development of synthetic reactions utilizing the characteristics of heteroatoms is of great importance. In particular, organoselenium chemistry and its synthetic applications have been growing quite rapidly.[1, 2] About ten years ago, we found a convenient method for preparing carbonyl selenide **2** by acid decomposition of amine salts of selenocarbamates (**1**) [Eq. (a)], readily available by reaction of elemental selenium with carbon monoxide and a secondary amine under mild conditions [Eq. (b)].[3]

$$\underset{\mathbf{1}}{[R^1R^2NH_2]^{\oplus}\,[R^1R^2NC(=O)Se]^{\ominus}} \xrightarrow{+\,H^{\oplus},\ -78\,^{\circ}C} Se{=}C{=}O + 2\,R^1R^2NH_2^{\oplus} \qquad (a)$$

$$\underset{\mathbf{2}}{}$$

$$2\,R^1R^2NH + CO + Se \xrightarrow{20\,^{\circ}C,\ 1\ atm} \mathbf{1} \qquad (b)$$

This has enabled us to examine the properties and reactivity of **2**.[4, 5] Thus, we have discovered a facile exchange reaction of **2** with elemental sulfur [Eq. (c)]. Treatment of **2**

$$\underset{\mathbf{2}}{Se{=}C{=}O} + S \xrightarrow[-45\,^{\circ}C]{Et_3N,\ THF} \underset{\mathbf{3}}{S{=}C{=}O} + Se \qquad (c)$$

(535 mg, 5 mmol) in 5.0 mL of THF with a THF solution (5.0 mL) of elemental sulfur (160 mg, 5 mmol) and triethylamine (0.14 mL, 1 mmol)[6] over the range of -45 to 5 °C for 1 h gave carbonyl sulfide **3** (88% yield)[7] and metallic selenium.

We also observed that amine salts of selenocarbamates **1** can react with secondary amines to give a mixture of both amine salts **1** and **1'**,[8] suggesting an equilibrium with **2** as intermediate [Eq. (d)].[9] This finding and exchange reaction

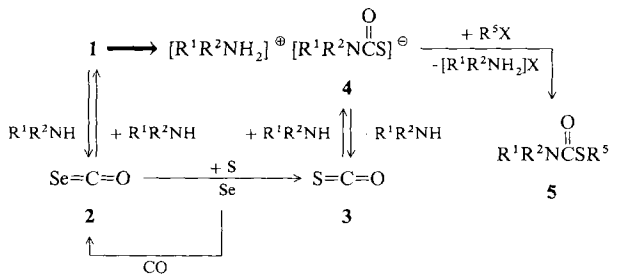
$$\begin{array}{l} \xrightarrow{-\,R^1R^2NH} \\ \xleftarrow{+\,R^1R^2NH} \end{array} [R^1R^2NH_2]^{\oplus}\,[R^1R^2NC(=O)Se]^{\ominus} \quad \mathbf{1}$$

$$\mathbf{2} \qquad (d)$$

$$\begin{array}{l} \xrightarrow{+\,R^3R^4NH} \\ \xleftarrow{-\,R^3R^4NH} \end{array} [R^3R^4NH_2]^{\oplus}\,[R^3R^4NC(=O)Se]^{\ominus} \quad \mathbf{1'}$$

(c) led us to develop a new selenium-catalyzed synthesis of thiocarbamates **4** from elemental sulfur, carbon monoxide, and amines under mild conditions[10–12] (Scheme 1).

The reaction of elemental sulfur (20 mmol) with carbon monoxide (1 atm) and diethylamine (50 mmol) at ambient temperature *in the presence of a catalytic amount of selenium (10 mol%)*[14] proceeded smoothly, accompanied by carbon monoxide uptake to yield **4** ($R^1 = R^2 = Et$). Treatment of the product with methyl iodide gave *S*-methyl *N,N*-diethylthiocarbamate **5a** ($R^1 = R^2 = Et$, $R^5 = Me$) in 79



Scheme 1. Synthesis of **4** by Se–S exchange.

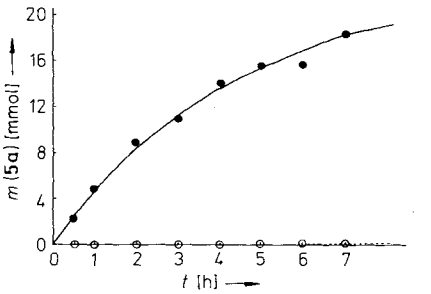


Fig. 1. Yields of **5a** versus reaction time t in the presence and absence of selenium catalyst. The solid line indicates yields of **5a** in the reaction of diethylamine (50 mmol) with carbon monoxide (1 atm) and sulfur (20 mmol) in the presence of selenium (10 mol%) at 30 °C; the dotted line shows the yields obtained without catalyst.

Table 1. Results of selenium-catalyzed synthesis of *S*-alkyl thiocarbamates **5a–i** by the route shown in Scheme 1.

Compound	R^1	R^2	R^5X	Yield [%]
5a	Et	Et	MeI	79
5b	Et	Et	$PhCH_2Br$	100
5c	Et	Et	4-Cl-C_6H_4-CH_2Cl	90
5d	*n*Pr	*n*Pr	MeI	87
5e	*n*Pr	*n*Pr	EtI	82
5f	*n*Bu	*n*Bu	MeI	87
5g	$-(CH_2)_5-$		MeI	92
5h	*n*Bu	H	MeI	69
5i	Ph	H [a]	MeI	41

[a] Triethylamine (50 mmol) and prolonged reaction time (20 h) were required.

(91)% isolated (GLC) yield. Use of a smaller amount of selenium (2.5 mol%) was also effective with prolonged reaction time (20 h) to give **5a** without decrease in the yield (85%). The yields of **5a** versus reaction time in both the presence and absence of selenium catalyst are given in Figure 1, which clearly shows the excellent catalytic activity of selenium.

A variety of *S*-alkyl thiocarbamates (**5b–i**), including the important agrochemicals **5c** and **5e**,[15] were prepared in good to excellent yields under similar reaction conditions (Table 1).

Experimental Procedure

5a: Elemental sulfur (0.32 g, 10 mmol) and selenium (79 mg, 1 mmol) were added to a THF solution (20 mL) of diethylamine (2.1 mL, 20 mmol), and the solution was vigorously stirred at 30 °C for 7 h under carbon monoxide (1 atm). After evacuation of carbon monoxide, sulfur (32 mg, 1 mmol) was added to the resulting transparent yellow solution, thereby resulting in the precipitation of metallic selenium [19]. Methyl iodide (1.0 mL, 16 mmol) was then added at 0 °C, and the mixture was stirred at room temperature for 2 h. Removal of the selenium-containing precipitate, followed by evaporation and distillation, gave **5a** in 79% yield (1.16 g) as a colorless oil; b.p. = 112 °C/14 torr (in [11a] 132.5–133.0 °C/87 torr); IR (neat): $\tilde{\nu} = 1645\ cm^{-1}$ (C=O); ^1H NMR ($CDCl_3$): $\delta = 1.17$ (t, $J = 7.1$ Hz, 6H), 2.31 (s, 3H), 3.38 (q, $J = 7.1$ Hz, 4H); MS: m/z 147 ($M^{\oplus}$). Correct C, H, N, S analysis.

[*] Prof. Dr. N. Sonoda, T. Mizuno, S. Murakami, Dr. K. Kondo, Dr. A. Ogawa, Dr. I. Ryu, Dr. N. Kambe
Department of Applied Chemistry, Faculty of Engineering
Osaka University, Suita, Osaka 565 (Japan)

Received: November 14, 1988 [Z 3049 IE]
German version: *Angew. Chem. 101* (1989) 476

[1] C. Paulmier (Ed.): *Selenium Reagents and Intermediates in Organic Synthesis*, Pergamon, Oxford 1986.
[2] S. Patai, Z. Rappoport (Eds.): *The Chemistry of Organic Selenium and Tellurium Compounds*, Wiley, Chichester 1986.
[3] K. Kondo, S. Yokoyama, N. Miyoshi, S. Murai, N. Sonoda, *Angew. Chem. 91* (1979) 760; *Angew. Chem. Int. Ed. Engl. 18* (1979) 691.
[4] For the reaction of **2** with amines, see: K. Kondo, S. Yokoyama, N. Miyoshi, S. Murai, N. Sonoda, *Angew. Chem. 91* (1979) 761; *Angew. Chem. Int. Ed. Engl. 18* (1979) 692.
[5] Compound **2** can be stored at $-30\,^{\circ}C$ in THF solution under acidic conditions for a few months and then gradually decomposes to carbon monoxide and selenium.
[6] In the absence of triethylamine, this Se–S exchange reaction was quite slow. A possible pathway is given by Equation (e).

$$2 + {}^{\ominus}S{-}S_x{-}\overset{\oplus}{N}R_3 \longrightarrow {}^{\ominus}Se{-}C{=}O \longrightarrow S{=}C{=}O + {}^{\ominus}Se{-}S_x{-}\overset{\oplus}{N}R_3 \qquad (e)$$

$$R_3\overset{\oplus}{N}{-}S_{x-1}{-}S \qquad \mathbf{3}$$

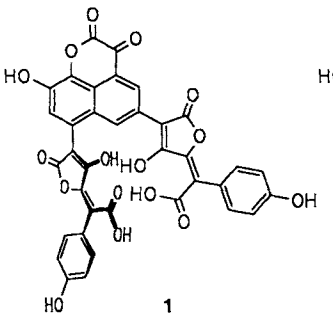
[7] Generated **3** was introduced into a THF solution of diethylamine at $-90\,^{\circ}C$, and the solution was stirred for 1 h at below $-20\,^{\circ}C$. The **4** ($R^1 = R^2 = Et$) thereby formed was esterified by methyl iodide to give **5a**. The yield of **3** was determined by GLC analysis of **5a** (88%).
[8] A THF solution of **1** ($R^1 = R^2 = Et$), prepared by reaction of diethylamine (5 mmol) and selenium (1 mmol) with carbon monoxide, and di-*n*-propylamine (5 mmol) was stirred at $20\,^{\circ}C$ for 30 min. Quenching the reaction mixture with methyl iodide (15 mmol) gave a 46:54 mixture of *Se*-methyl *N,N*-diethylselenocarbamate **6a** and *Se*-methyl *N,N*-di-*n*-propylselenocarbamate **6b**. A similar reaction of **1**, $R^1 = R^2 = n$-propyl, with diethylamine gave a 48:52 mixture of **6a** and **6b**. These results strongly suggest that an equilibrium, as shown in Equation (d) is set up.
[9] A direct nucleophilic attack of amine at the carbonyl carbon of **1** is not likely because of the steric hindrance of the alkyl group: see K. Kondo, N. Sonoda, K. Yoshida, M. Koishi, S. Tsutsumi, *Chem. Lett. 1972*, 401.
[10] Direct reaction of amines with elemental sulfur and carbon monoxide requires severe conditions (90–120 °C, 13–27 atm CO, 60–62%); see D. W. Grisley, Jr., J. A. Stephens, *J. Org. Chem. 26* (1961) 3568.
[11] For other preparative methods for *S*-alkyl thiocarbamates **5**, see a) H. Tilles, *J. Am. Chem. Soc. 81* (1959) 714; b) H. Eilingsfeld, L. Möbius, *Chem. Ber. 98* (1965) 1293; c) K. Akiba, N. Inamoto, *J. Chem. Soc. Chem. Commun. 1973*, 13; d) R. Riemschneider, *J. Am. Soc. Chem. 78* (1956) 844.
[12] The selenium-catalyzed synthesis of *S*-alkyl thiocarbamates **5** from primary amines, carbon monoxide, and organic disulfides has been reported by *P. Koch* [13].
[13] P. Koch, *Tetrahedron Lett. 1975*, 2087.
[14] The reaction without selenium catalyst under similar conditions was very sluggish and gave only a trace amount of **5a**.
[15] Compound **5c** (Benthiocarb) is an important herbicide for rice crops and is produced industrially on a large scale [16, 17]; **5e** (EPTC) possesses outstanding effectiveness and selectivity for control of annual grasses and many broadleaved weeds [11a, 18].
[16] W. Chin-Hsien, *Synthesis 1981*, 622.
[17] H. Sugiyama, *J. Synth. Org. Chem. Jpn. 38* (1980) 555.
[18] H. J. Sanders, *Chem. Eng. News 59* (1981) No. 31, p. 20.
[19] Compound **1**, $R^1 = R^2 = Et$, was completely decomposed by addition of elemental sulfur, and metallic selenium was recovered. GLC analysis after addition of MeI showed that the product **5a** was pure; *Se*-methyl *N,N*-diethylselenocarbamate **6a** was not detected (< 0.01%).

Complexation of Cesium 137 by the Cap Pigments of the Bay Boletus (*Xerocomus badius*)

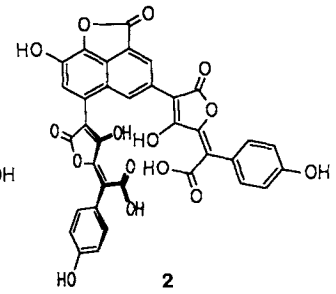
By *Dieter C. Aumann, Gabriele Clooth, Bert Steffan,* and *Wolfgang Steglich**

Investigations of the amount of radionuclides present in fungi after the reactor accident at Chernobyl have repeatedly shown high amounts of cesium 137 in the bay boletus (*Xerocomus badius*).[1–4] By contrast, cepe (*Boletus edulis*), a closely related edible mushroom, concentrates this radionuclide to only a small extent.

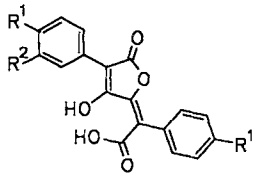
We reported earlier that the brown pileus of the bay boletus contains the unusual pulvinic acid derivatives badione A **1** and norbadione A **2**, which are absent in cepe.[5] Since **1** and **2** are present in the fungus as potassium complexes,[5–7] we examined whether these pigments play a role in the concentration of ^{137}Cs by bay boletus.



1



2



	R^1	R^2
3a	OH	H
3b	OH	OH
3c	H	H

To this end, the brown pileus of fresh bay boletus[8] was peeled off and, like the rest of the fungus, measured in a gamma spectrometer[9] (Table 1). The ratio of the specific activities gives an enrichment factor of 3.4 for ^{137}Cs in the pileus.[3] An analogous experiment with cepe gave an enrichment factor of only 0.6.

The weight ratio of pileus pigment to the rest of the fungus is very difficult to determine precisely by peeling the fruiting body. In a further experiment, therefore, the outsides of the pilei of three fresh bay boleti were carefully washed with dimethyl sulfoxide (DMSO), resulting in nearly complete dissolution of the pigment. Chromatographic purification on Sephadex LH-20 (eluant: methanol containing 5% DMSO) afforded 12 mg of a mixture of complexes **1** and **2** (according to NMR spectroscopy), which was measured in the gamma spectrometer. An enrichment factor of 87 ± 10 for ^{137}Cs in the pileus pigments was derived from the specific activity of the pigments ($11\,316 \pm 1184$ Bq/kg) and that of the "washed" fungi (130 ± 7 Bq/kg fresh weight). Interestingly, an even larger enrichment factor (138 ± 18) was obtained for the "normal" complexing metal ^{40}K.[10] This is also revealed by a comparison of the X-ray emission spectra of the pileus and the isolated pigment complex (Fig. 1).[6]

The binding of cesium to norbadione **2** is corroborated by an independent experiment using a standard solution of

Table 1. Enrichment of ^{137}Cs in the pileus of bay boletus.

	Activity: pileus A_p [Bq/kg] [a]	Activity: fruiting body A_f [Bq/kg] [a]	Enrichment factor A_p/A_f
X. badius	340 ± 50	100 ± 20	3.4 ± 0.8
B. edulis	53 ± 7	87 ± 12	0.6 ± 0.1
B. erythropus	23 ± 10	8.8 ± 3.3	2.6 ± 1.5

[a] Based on fresh weight: collected near Bonn in September 1987.

[*] Prof. Dr. W. Steglich, Dr. B. Steffan
Institut für Organische Chemie und Biochemie der Universität
Gerhard-Domagk-Strasse 1, D-5300 Bonn 1 (FRG)
Prof. Dr. D. C. Aumann, Dr. G. Clooth
Institut für Physikalische Chemie der Universität,
Abteilung Nuklearchemie
Wegelerstrasse 12, D-5300 Bonn 1 (FRG)

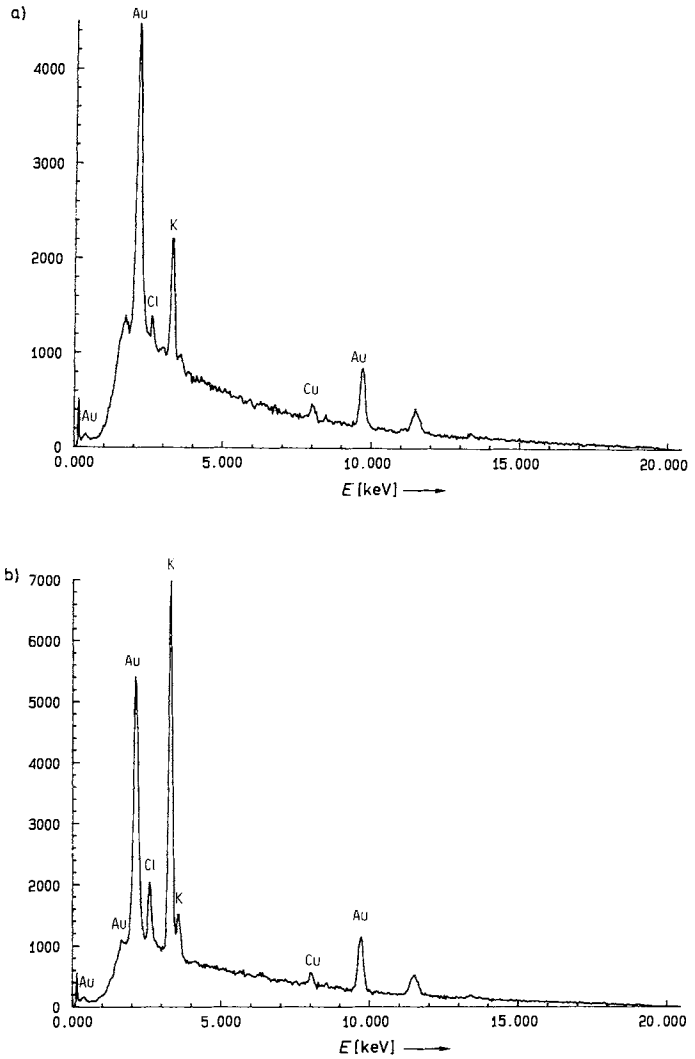


Fig. 1. X-ray emission spectrum of a) the pileus of bay boletus and b) the pigment complex isolated with DMSO. Ordinate: counts.

^{137}CsCl (31 Bq/100 μL). Assuming that cesium chloride is bound by **2** in a molar ratio of 1:1, 100 μL of this solution corresponds to approximately 5 mg of **2**. When 100 μL of this solution is treated with 2.5 mg of **2** and the reaction mixture is separated by column chromatography on Sephadex LH-20 (eluant: MeOH), a forerun containing 15 ± 1.7 Bq and a norbadione fraction containing 14.5 ± 1.5 Bq are obtained. The column retains 0.1 Bq. After filtration of the norbadione fraction through a column containing the cationic exchange resin Dowex 50-W X4, the radioactivity of the eluate is below the limits of detection, whereas the exchange resin now contains all the radioactivity. Thus, norbadione forms a 1:1 complex with cesium chloride,[11] which undergoes decomposition upon exposure to the strongly acidic cation exchanger.

In addition to **1** and **2**, simple pulvinic acids such as atromentic acid **3a** and xerocomic acid **3b**[12] may be responsible for binding cesium in fungi. When the complexation experiments described above are carried out with **3a** followed by chromatography on Sephadex LH-20, half of the radioactivity is found in the atromentic acid fraction. The same holds for methyl atromentate. On the other hand, the permethyl derivative of atromentic acid displays no binding of cesium chloride. When a molar equivalent of the ^{137}CsCl standard solution is added to a mixture containing molar equivalents of **2** and **3a**, all the radioactivity is found in the norbadione fraction after chromatography on Sephadex LH-20. Thus, norbadione is a much better ligand for cesium compared with simple pulvinic acids.[13] We ascribe this to the presence of two pulvinic acid chains in **1** and **2**, which, according to models, offer good spatial prerequisites for the complexation of a potassium or cesium ion. The detailed structure of the complexes, as well as the determination of the complexation constants, is the goal of further investigations.

Other mushrooms that contain pigments of the badione or norbadione type in their pilei[14] can also strongly concentrate ^{137}Cs. An example is *Boletus erythropus*,[5] which exhibits an enrichment factor of 2.6 ± 1.5 (Table 1). Surprisingly, the pileus of the American boletus *Boletus mirabilis* collected on Vancouver Island in September 1987 contains twice as much ^{137}Cs as the bay boletus fungi collected near Bonn, although no significant fall-out from Chernobyl was recorded in western Canada. Since *B. mirabilis* shows high values for ^{137}Cs and particularly low values for ^{134}Cs, the contamination in this case must have occurred earlier.[15] In an older sample of *B. erythropus* (Bonn, 1982), the amount of ^{134}Cs was below the limits of detection.

The results presented here show that bay boletus and *B. erythropus*, in contrast to cepe, contain pileus pigments that bind potassium and cesium ions absorbed from the environment by the mycelia and transported to the fruiting body. These findings explain the different enrichment factors found for these fungi.

Received: December 29, 1988;
supplemented: January 17, 1989 [Z 3093 IE]
German version: *Angew. Chem. 101* (1989) 495

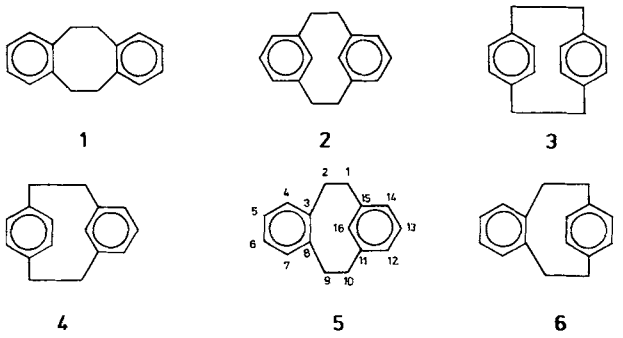
[1] Cf., e.g., the report of the Bayerische Staatsministerium für Landesentwicklung und Umweltfragen: *Auswirkungen des Unfalls im Kernkraftwerk Tschernobyl auf Bayern*, February 1987; radioactivity report (nuclide-specific analysis), TÜV Bayern, issue IX/87.
[2] E. F. Elstner, R. Fink, W. Höll, E. Lengfelder, H. Ziegler, *Oecologia 73* (1987) 553.
[3] D. Molzahn, D. Reinen, H. Behr, P. Kocksholt, P. Patzelt, *Z. Mykologie*, in press.
[4] R. Seeger in Arbeitsgemeinschaft Mykologie Ostwürttemberg (AMO) der Deutschen Gesellschaft für Mykologie: *Beiträge zur Kenntnis der Pilze Mitteleuropas, Band 3*, Einhorn Verlag, Schwäbisch Gmünd 1987, p. 289.
[5] B. Steffan, W. Steglich, *Angew. Chem. 96* (1984) 435; *Angew. Chem. Int. Ed. Engl. 23* (1984) 445.
[6] We thank *M. Kesten*, DFVLR Köln-Porz, for recording the spectra.
[7] Compound **2** is also present as a potassium complex in *Pisolithus tinctorius*: M. Gill, D. A. Lally, *Phytochemistry 24* (1985) 1351.
[8] Collected in autumn 1988 in the Kottenforst near Bonn. Pilei collected in 1986 and 1987 show comparable contents of ^{40}K, ^{134}Cs, and ^{137}Cs.
[9] ORTEC high-purity germanium-well detector, type GWL 110240-S.
[10] ^{40}K: pileus pigments 20526 ± 2167 Bq/kg; remaining fungus 149 ± 12 Bq/kg fresh weight.
[11] The norbadione–cesium chloride (1:1) complex gave a correct C, H, O, Cl analysis; the amount of Cs was determined by atomic absorption.
[12] W. Steglich, W. Furtner, A. Prox, *Z. Naturforsch. B 23* (1968) 1044.
[13] Involvement of the pulvinic acid moieties in the complexation is indicated by ^{1}H NMR investigations on **3c**. In [D$_6$]acetone, the carboxyl protons of **3c** appear, only upon cooling to 200 K, as a broad signal at $\delta = 17.2$, whereas in the cesium chloride complex the corresponding proton gives a sharp singlet ($\delta = 17.6$) even at 270 K.
[14] Review: M. Gill, W. Steglich, *Prog. Chem. Org. Nat. Prod. 51* (1987) 59.
[15] Pilei: *B. mirabilis* (Bamfield, Vancouver Island (Canada), September 1987): ^{137}Cs 760 ± 40 Bq/kg fresh weight, ^{134}Cs 40 ± 10; *X. badius* (Bonn, September 1988): ^{137}Cs 340 ± 50, ^{134}Cs 90 ± 30; *X. badius* (Regensburg, October 1986): ^{137}Cs 1373 ± 126, ^{134}Cs 457 ± 80 (half-lives: ^{134}Cs 2.06 a, ^{137}Cs 30.14 a). We thank Dr. *H. Besl*, Regensburg, for sending us *X. badius*.

syn- and *anti*-[2.2]Orthometacyclophane **

By *Graham Bodwell, Ludger Ernst, Matthias W. Haenel,* and *Henning Hopf**

Dedicated to Professor D. J. Cram on the occasion of his 70th birthday

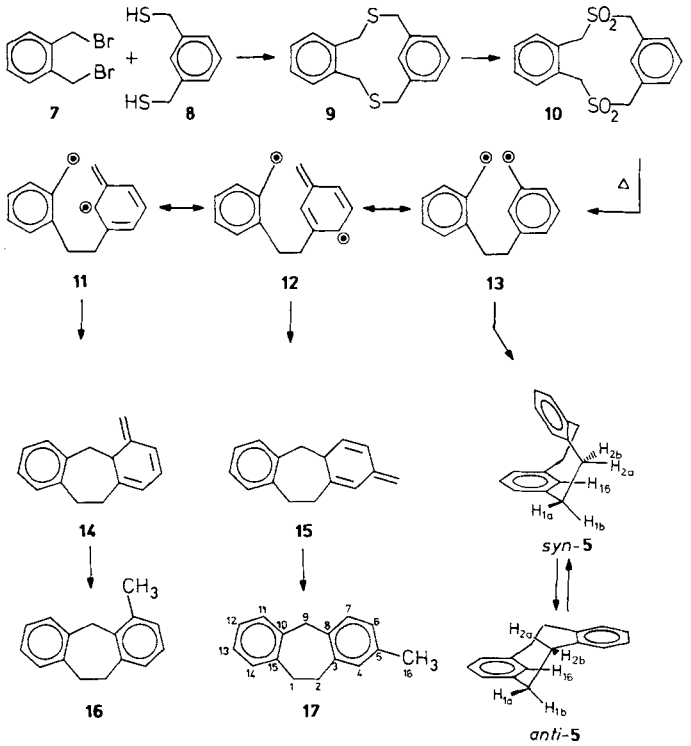
In [2.2]orthocyclophane **1** (tetrahydrodibenzocyclooctene) as well as in [2.2]meta- **2** and [2.2]paracyclophane **3**, the two ethano bridges connect equivalent positions of the two benzene rings. These hydrocarbons have long been known and their chemical and spectroscopic properties have been well investigated.[1] In addition to these three isomers, however, three other [2.2]cyclophanes are conceivable, whose bridges link nonequivalent carbon atoms of the benzene rings. Whereas [2.2]metaparacyclophane **4** was prepared long ago by Lewis acid–catalyzed rearrangement of **3**,[2] the synthesis of [2.2]orthoparacyclophane **6** has not yet been achieved. The route to [2,2]orthometacyclophane **5**[3] described here extends the series of available "unsymmetrical cyclophanes".[4]



1 **2** **3** **4** **5** **6**

The synthesis follows conventional routes of paracyclophane chemistry (Scheme 1).[1] Addition of a dilute solution of **7** and **8** in a 1:1 ratio in benzene to a dilute, vigorously stirred solution of sodium hydroxide (ethanol:water 4:1) afforded the dithiacyclophane **9** in 79% yield.[5] Oxidation of **9** with 30% hydrogen peroxide in the presence of 1% acetic acid yielded the expected bissulfone **10** (93%).[5]

Sulfone pyrolysis[6] at 535 °C and 10^{-2} torr gave, after column chromatography (silica gel, dichloromethane:ethyl acetate 1:1), a yellow oil (71%), which did not crystallize even after addition of pentane. Whereas the thin layer chromatogram showed only one spot, the 400-MHz ^{1}H NMR spectrum revealed that at least three products had been formed in the reaction. Although it was possible to separate analytical amounts of the product mixture by HPLC (RP-8, 7 μm, 10 × 250 mm), attempts to carry out separations on a preparative scale, as well as gas-chromatographic separation on XE-60 (strong decomposition at 180–260 °C), were



Scheme 1.

unsuccessful. Only the use of SE-30 as stationary phase (column temperature 180 °C) brought success; two fractions were obtained. The first fraction (16% of the product) contained the desired [2](1,2)[2](1,3)cyclophane **5** as a *syn*/*anti* mixture (ratio ca. 4:1),[5] as shown, in particular, by the NMR spectra (Table 1). In both isomers, the aromatic protons give rise to an AA'BB' pattern for the *ortho*-disubstituted benzene moiety and an A_2MX pattern for the *meta*-disubstituted moiety. The chemical shifts of *syn*-**5** and *anti*-**5** are characteristically different.

Except for 16-H, all aromatic protons in *syn*-**5** are more strongly shielded ($\Delta\delta$ between -0.4 and -0.7) than the corresponding protons in *anti*-**5**. This is due to the magnetic anisotropy of the opposite benzene ring.[9] However, since the rings in *syn*-**5** are not parallel to each other but rather mutually inclined (see below), 16-H lies in the deshielding region of the *ortho*-substituted ring ($\Delta\delta = +0.71$). Whereas the intraannular aromatic protons are strongly shielded in *anti*-[2.2]metacyclophanes (see **2**),[10] this is not observed in *anti*-**5**, since the aromatic rings of *anti*-**5** do not lie over each other as much as they do for double *meta* bridging.

The bridge protons in *syn*-**5** give a first-order spectrum, whose coupling constants are in good agreement with the values calculated for the torsional angles obtained from force-field calculations (MMX87[11]) (Table 1).[12] The ^{1}H NMR signals of the bridges of *anti*-**5** could not be analyzed in detail, since three of the four protons have very similar shifts according to C,H-COSY and their signals are partially overlapped by those of the main component. Striking is the strong upfield shift of 2-H_a, which extends far into the shielding region of the *meta*-substituted ring. When the measuring temperature is raised to over 100 °C (solvent: [D_6]DMSO), the ^{1}H NMR signals of the isomers of **5** are increasingly broadened; however, no coalescence of the signals is observed up to the maximum attainable temperature of 150 °C. Since the smallest frequency difference between corresponding protons is 200 Hz, the interconversion barrier (ΔG^*) must be greater than 20 kcal mol^{-1} at 150 °C. Presumably, however, the value is below 24 kcal mol^{-1}, so that

[*] Prof. Dr. H. Hopf, Dr. G. Bodwell
Institut für Organische Chemie der Technischen Universität
Hagenring 30, D-3300 Braunschweig (FRG)
Prof. Dr. L. Ernst [+]
NMR-Laboratorium der Chemischen Institute der Technischen Universität Braunschweig
Prof. Dr. M. W. Haenel
Max-Planck-Institut für Kohlenforschung
Kaiser-Wilhelm-Platz 1, D-4330 Mülheim a. d. Ruhr (FRG)

[+] NMR spectroscopy and force-field calculations

[**] Cyclophanes, Part 28. This work was supported by the Fonds der Chemischen Industrie and the Deutsche Forschungsgemeinschaft. We thank *D. Stoffels* and Dr. *G. Schomburg*, Max-Planck-Institut für Kohlenforschung, Mülheim a. d. Ruhr, for their help in carrying out the gas-chromatographic separations. Part 27: R. Frim, M. Rabinovitz, G. Bodwell, F.-W. Raulfs, H. Hopf, *Chem. Ber.*, in press.

Table 1. NMR data for the isomers of **5** [a].

Position	*syn*-**5**		*anti*-**5**	
	$\delta(^{13}C)$	$\delta(^{1}H)$	$\delta(^{13}C)$	$\delta(^{1}H)$
1, 10	36.6	2.42 (a), 3.53 (b)	40.8	2.96 (a), 2.83 (b)
2, 9	36.1	2.78 (a), 3.15 (b)	39.4	1.47 (a), 2.87 (b)
3, 8	140.1	–	142.8	–
4, 7	130.8	6.75	132.5	7.22
5, 6	125.0	6.84	126.9	7.27
11, 15	143.6	–	145.6	–
12, 14	124.7	6.31	123.3	6.88
13	127.4	6.55	130.3	7.23
16	138.3	7.79	129.9	7.08

Coupling constants of *syn*-**5** :

J(H,H)	exp.	calcd [b]	(θ)	J(H,H)	exp.	calcd [b]	(θ)
1a,1b	−13.7	–		1b,2a	1.0	0.7	(−77°)
1a,2a	6.0	6.2	(44°)	1b,2b	7.1	8.4	(34°)
1a,2b	11.9	12.0	(155°)	2a,2b	−13.2	–	

[a] 400 MHz, $CDCl_3$/TMS; $\delta(^{13}C)$ values relative to $CDCl_3$, $\delta = 77.05$. Assignments by 2D techniques [7] (H,H-COSY and its variant for long-range couplings, C,H-COSY and C,H-COLOC) and by a selective $^{13}C\{^{1}H\}$ NOE experiment [8]. [b] Calculated according to [12] using the torsional angle θ from our MMX87 calculation [11].

it does not appear reasonable to attempt a separation of the isomers at room temperature. For the "mononuclear" (3*Z*)-3,4-didehydro[6]metacyclophane, ΔG^{*} was found to be 16.5 kcal mol^{-1} for flipping of the bridge from one side of the ring to the other.[13] Thus, the replacement of the rigid *ortho*-phenylene unit of **5** by the more flexible *cis*-ethylene unit considerably facilitates the conformational transformation.

Particularly noteworthy in the ^{13}C NMR spectrum is the deshielding of C-16 in *syn*-**5** relative to the *anti* isomer. Such deshielding has also been found for C-8 in *anti*-**2**,[14] for C-11 in [5]metacyclophane,[15a] and, to a lesser extent, for C-12 in [6]metacyclophane;[15b] in the latter two compounds, the deshielding correlates with the degree of nonplanarity of the aromatic ring.[15a] Our data do not fit this picture, since we observed no deshielding of C-16 in *anti*-**5**, even though the geometries of the *meta*-substituted rings of *syn*- and *anti*-**5** are calculated to be practically identical. According to the MMX87 calculations, in both isomers C-16 is bent by 14° and C-13 by 6° toward the *exo* side from the plane formed by C-11, C-12, C-14, and C-15. To reduce the strain, the bonds C1-C2, C2-C3, and C3-C8 are lengthened, the angles C1-C2-C3 and C2-C3-C8 in the "*ortho* half" of the molecule increased, and the angles C2-C1-C15 and C1-C15-C16 in the "*meta* half" decreased compared with the normal values. The *ortho*-substituted rings are practically planar and form an angle of 54° (*syn*-**5**) and 5° (*anti*-**5**) with the plane C11-C12-C14-C15 of the *meta*-substituted ring.[16] A very small distance of 2.1 Å was calculated for the separation of 16-H and 2-H_b in *syn*-**5**. Indeed, 2-H_b does show a large nuclear Overhauser effect (16%) when the resonance of 16-H is saturated, although the geminal 2-H_a strongly competes with 16-H in the dipolar relaxation of 2-H_b. In accord with the NMR finding that *syn*-**5** predominates at equilibrium, a lower strain energy is calculated for *syn*-**5** compared with *anti*-**5** ($\Delta H = -1.75$ kcal mol^{-1}); however, this should be treated as only a rough value.

The main fraction consisted of a mixture of dibenzoannelated cycloheptadienes **16** (4%) and **17** (77%), as shown, in particular, by the NMR spectra.[5, 17] The formation of the isomeric hydrocarbons **16, 17,** and **5** can be explained most simply as proceeding via the diradicals **11**–**13**. Whereas C–C bond formation in **13** directly gives *syn*- and *anti*-**5**, compounds **16** and **17** must have been formed via **14** and **15**, respectively. Examples of the required hydrogen shift are known from the literature.[18]

Received: November 21, 1988 [Z 3061 IE]
German version: *Angew. Chem. 101* (1989) 509

CAS Registry numbers:
syn-**5**, 119392-52-8; *anti*-**5**, 119477-47-3; **7**, 91-13-4; **8**, 41563-69-3; **9**, 23144-82-3; **10**, 119392-53-9; **16**, 119392-50-6; **17**, 119392-51-7.

[1] Review in P. M. Keehn, S. M. Rosenfeld (Eds.): *Cyclophanes, Vol. 1 and 2*, Academic Press, New York 1983.
[2] D. J. Cram, R. C. Helgeson, D. Lock, L. A. Singer, *J. Am. Chem. Soc. 88* (1966) 1324.
[3] An unsuccessful attempt 18 years ago to prepare **5** by sulfone pyrolysis was also reported: F. Vögtle, P. Neumann, *Tetrahedron 26* (1970) 5847 (footnote on p. 5867).
[4] V. Boekelheide, *Acc. Chem. Res. 13* (1980) 65; cf. M. Nakazaki, Y. Yamamoto, Y. Miura, *J. Org. Chem. 43* (1978) 1041.
[5] All new compounds were characterized by the usual spectroscopic methods, mass spectra, and elemental analyses; the dithia[3.3]orthometacyclophane **9** was prepared earlier by *Vögtle* et al. (*F. Vögtle*, personal communication).
[6] F. Vögtle, L. Rossa, *Angew. Chem. 91* (1979) 534; *Angew. Chem. Int. Ed. Engl. 18* (1979) 514.
[7] Summary of new NMR techniques: a) J. K. M. Sanders, B. K. Hunter: *Modern NMR Spectroscopy*, Oxford University Press, Oxford 1987; b) A. E. Derome: *Modern NMR Techniques for Chemistry Research*, Pergamon Press, Oxford 1987.
[8] See, e.g., P. Bigler, M. Kamber, *Angew. Chem. 97* (1985) 701; *Angew. Chem. Int. Ed. Engl. 24* (1985) 705; *Magn. Reson. Chem. 24* (1986) 972. We thank Dr. *P. Bigler*, Institut für Organische Chemie der Universität Bern, for his microprogram for the selective measurement of hetero-NOEs.
[9] C. E. Johnson, F. A. Bovey, *J. Chem. Phys. 29* (1958) 1012.
[10] D. J. Wilson, V. Boekelheide, R. W. Griffin, Jr., *J. Am. Chem. Soc. 82* (1960) 6302.
[11] MMX87: Serena Software, Bloomington, IN 47402 (USA).
[12] C. A. G. Haasnoot, F. A. A. M. de Leeuw, C. Altona, *Tetrahedron 36* (1980) 2783.
[13] J. L. Goodman, J. A. Berson, *J. Am. Chem. Soc. 107* (1985) 5424.
[14] T. Sato, T. Takemura, M. Kainosho, *J. Chem. Soc. Chem. Commun. 1974*, 97.
[15] a) L. W. Jenneskens, F. J. J. de Kanter, W. H. de Wolf, F. Bickelhaupt, *Magn. Reson. Chem. 24* (1986) 308; b) Y. Tobe, personal communication, cited in [15a].
[16] In *anti*-**5**, C-13 and the midpoint of the C3–C8 bond lie on the open side of the angle.
[17] The main isomer **17** was enriched with preparative gas chromatography (20 mm × 1.5 m stainless steel tubes, 20% SE-30 on volasphere A 4, 100–120 mesh, 180 °C (6% **16**, 94% **17**) and identified by NMR spectroscopy. ^{1}H NMR (400 MHz, $CDCl_3$/TMS): $\delta = 7.14$ (d, $J = 7$ Hz, 1H, 11-H), 7.10–7.06 (m, 3H, 12,13,14-H), 7.04 (d, $J = 8$ Hz, 1H, 7-H), 6.90 (br. s, 1H, 4-H), 6.88 (d, $J = 8$ Hz, 1H, 6-H), 4.05 (s, 2H, 9-H), 3.16–3.07 (m, 4H, 1,2-H), 2.25 (s, 3H, CH_3). ^{13}C NMR (101 MHz, $CDCl_3$/TMS): $\delta = 139.32$, 139.28, 138.9 (all s, C-3,10,15), 136.0, 135.9 (both s, C-5,8), 130.4 (d, C-4), 129.4 (d, C-14), 129.0 (d, C-7), 128.8 (d, C-11), 126.6 (d, C-6), 126.5, 126.0 (both d, C-12,13), 40.5 (t, C-9), 32.49, 32.48 (both t, C-1,2), 20.9 (q, CH_3). Assignment by H,H- and C,H-COSY, degree of substitution of the C atoms by DEPT. On the basis of the following data, we propose structure **16** for the component formed only in traces: $\delta(^{1}H) = 4.10$ (s, 9-H), 2.39 (s, CH_3); $\delta(^{13}C) = 130.7$, 129.8 (both d, C-11,14(?)), 128.2 (d, C-4(?)), 126.35, 126.32, 126.2, 125.6 (all d, C-5,6,12,13), 35.0 (t, C-9), 33.0, 32.0 (both t, C-1,2), 20.1 (q, CH_3).
[18] a) H. Plieninger, W. Maier-Borst, *Angew. Chem. 75* (1963) 1177; *Angew. Chem. Int. Ed. Engl. 3* (1964) 62; b) W. J. Bailey, R. A. Baylouny, *J. Org. Chem. 27* (1962) 3476.

2-Pentyltricyclo[1.1.1.0^{1,3}]pentane and Its Homopolymer, a Soluble Poly([1.1.1]propellane)**

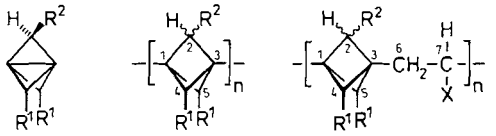
By *Klaus Opitz* and *Arnulf-Dieter Schlüter**

The [1.1.1]propellanes **1a,b** are interesting and versatile building blocks for the synthesis of homo- and copolymers

[*] Dr. A.-D. Schlüter, K. Opitz
Max-Planck-Institut für Polymerforschung
Postfach 31 48, D-6500 Mainz (FRG)

[**] We thank Prof. Dr. *G. Wegner*, Mainz, for support of this work.

having novel structures.[1] The homopolymers **2a,b**[1a-e] and the alternating 1:1 copolymers **3a,b**[1c,f] have been obtained, in some cases with high molecular weights, by both anionically initiated and spontaneous polymerization. They have a common structural feature, the highly strained bicyclo[1.1.1]pentane unit. The poly([1.1.1]propellanes) **2a,b** are rigid rods, which explains their failure to dissolve or melt, even for low degrees of polymerization ($\bar{P}_n$).

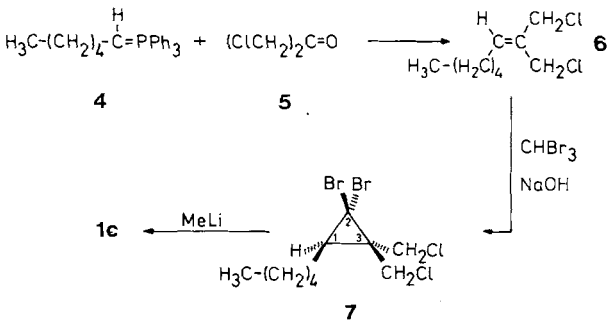


1 **2** **3**

a, $R^1=H, R^2=H$; **b**, $R^1,R^1=-(CH_2)_3-$, $R^2=H$; **c**, $R^1=H, R^2=(CH_2)_4-CH_3$

Macromolecules with rigid main chains are of theoretical and practical interest,[2] because of their tendency toward self-organization in solution on the one hand and their material properties (rigidity, tensile strength) on the other. The synthesis of soluble poly([1.1.1]propellanes) is important for the investigation and exploitation of these features. We describe here a simple synthesis of 2-pentyltricyclo[1.1.1.$0^{1,3}$]pentane **1c**[3,4] on a 5-g scale as well as its anionically initiated polymerization.[5]

We synthesized the propellane **1c** in analogy to the route used by *Szeimies* et al. to prepare the unsubstituted [1.1.1]propellane **1a**.[6] Reaction of the ylide **4**[7] with 1,3-dichloroacetone **5** yielded the olefin **6**, which, in turn, smoothly gave the dibromocarbene adduct **7**. Reaction of **7** with methyllithium afforded, after recondensation under high vacuum, compound **1c** as a solvent-free, colorless and distillable (b.p. 72 °C/12 torr, partial decomposition) liquid (20–25% based on **5**). NMR spectroscopic data for the compounds **1c**, **6**, and **7** are given in Table 1. The IR spectrum of **1c** displays a very intense absorption band at $\nu = 610\ cm^{-1}$, which is typical of small-ring propellanes;[8] exposure of **1c** to air leads to immediate disappearance of this band.



Treatment of **1c** with a small amount of a solution of *tert*-butyllithium in pentane results in an appreciable increase in viscosity. After standard workup (precipitation from toluene by addition of methanol, lyophilizing with benzene), the poly([1.1.1]propellane) **2c** was obtained as a colorless, fibrous material, along with unreacted starting material and oligomers. Polymer **2c** is soluble in toluene, as well as in chloroform, tetrahydrofuran, and petroleum ether (weight ratio **1c**:oligomer:**2c** = 1:1.3:2).

The structural assignment of the polymer **2c** is based mainly on its ^{13}C NMR spectrum (Table 1). This shows four

Table 1. ^1H ($CDCl_3$, 300 MHz) und ^{13}C NMR data ($CDCl_3$, 75 MHz) for **1c**, **2c**, **3c**, **6**, und **7**.

1c: ^1H NMR: $\delta = 2.60$ (m, 1H), 2.50 (m, 1H), 2.17 (m, 1H), 1.76 (m, 2H), 1.40–1.20 (m, 8H), 0.88 (m, 3H). ^{13}C NMR: $\delta = 91.17$ (C-2), 71.94 (C-4 or C-5), 69.24 (C-5 or C-4), 31.40, 29.29, 24.21, 22.47 (4 CH_2), 13.95 (CH_3), 5.26 (C-1,3)

2c: ^1H NMR (broad, unstructured signals, not baseline separated): $\delta = 2.12$, 1.87, 1.66, 1.55–1.05, 0.91, 0.78 (*t*Bu end group). ^{13}C NMR: $\delta = 61.7$ (C-2), 48.7 (C-4 or C-5), 44.3 (C-5 or C-4), 41.6 (C-1,3), 32.5, 29.8 (2 CH_2), 26.5 (*t*Bu end group; very low intensity) 25.3, 22.7 (2 CH_2), 14.1 (CH_3)

3c (X = CN): ^1H NMR (broad, unstructured signals, not baseline separated): $\delta = 2.46$, 2.12, 2.01, 1.88–1.15, 0.89 (CH_3). ^{13}C NMR: $\delta = 119.8$ (CN), 60.5 (very broad, C-4,5), 41.5 (C-1 or C-3), 40.4 (C-3 or C-1), 32.2 (CH_2), 29.5 (very broad, C-2), 48.5 (very broad, C-4 or C-5), 45.0 (very broad, C-4 or C-5), 28.9, 24.2, 22.5 (3 CH_2), 14.0 (CH_3)

6: ^1H NMR: $\delta = 5.75$ (t, 1H; 3-H), 4.22 (s, 2H; CH_2Cl), 4.18 (s, 2H; CH_2CL), 2.13 (dt, 2H; 4-H), 1.45–1.25 (m, 6H; 5-, 6-, 7-H), 0.88 (t, 3H; 8-H). ^{13}C NMR: $\delta = 136.67$ (C-3), 132-42 (C-2), 47.51, 39.01 (2 CH_2Cl), 31.35, 28.63, 27.88, 22.42 (4 CH_2), 13.91 (CH_3)

7: ^1H NMR: $\delta = 4.10–3.80$ (m, 4H; CH_2Cl), 1.65–1.20 (m, 9H; CH, 4 CH_2), 0.91 (t, 3H; CH_3). ^{13}C NMR: $\delta = 49.59$, 44.10 (2 CH_2 Cl), 41.45 (C-3), 40.30 (C-1 or C-2), 36.75 (C-2 or C-1), 31.39, 27.85, 27.38, 22.44 (4 CH_2), 13.94 (CH_3)

signals at $\delta = 41.59$, 44.28, 48.72, and 61.70, as expected for the monosubstituted bicyclic repeating unit (**2a**: $\delta = 39$ (C-1,3), 49 (C-2,4,5)[1c-e]). The signal of the methylene group (C-4 or C-5) at $\delta = 44.28$ consists of three lines in an intensity ratio of 1:2:1. This splitting is a possible indication that the monomer adds to the growing chain with no preferred orientation[9] and that **2c** is present as an atactic polymer. The average degree of polymerization of **2c** was determined by ^1H NMR spectroscopy from the ratio of the signal intensities of the terminal *tert*-butyl group at $\delta = 0.78$ and the methyl group of the pentyl chain at $\delta = 0.91$ to be $\bar{P}_n \approx 40$.

Preliminary investigations show that the properties of **2c** are considerably different from those of the unsubstituted polymer **2a**. For instance, **2a** is insoluble in refluxing toluene, whereas **2c**, despite the presumably higher $\bar{P}_n$ value (40[10]), dissolves completely in several organic solvents at room temperature. Unusually sharp and nearly complete weight loss is observed in thermogravimetric investigations of **2a** at 300 °C;[1e] by contrast, the polymer **2c** suffers continuous weight loss to ca. 5% of the initial weight at 300–450 °C (N_2; rate of heating 3 K/min). Pure **2c** under gentle pressure or from solution forms transparent films, which, however, exhibit only low mechanical strength. Preliminary viscosity measurements in chloroform at 25 °C gave a Staudinger index of $[\eta] = 0.34\ dLg^{-1}$ for **2c**.

The positive effect of the pentyl chain on solubility is also shown by the copolymers, which are easily prepared from the propellane **1c** and acceptor-substituted olefins. Thus, reaction of **1c** with two equivalents of acrylonitrile, without addition of an initiator, gave the alternating copolymer **3c** (X = CN), which, in contrast to the corresponding copolymer from **2a** and acrylonitrile,[1c] is readily soluble. The structure of **3c** was confirmed by spectroscopic data [Table 1; gel permeation chromatography (GPC) (*o*-dichlorobenzene; standard, polystyrene): $M_w = 530\,000$; $M_n = 176\,000$; $M_w/M_n = 3.02$; viscosity ($CHCl_3$, 20 °C): $[\eta] = 6.4\ dL\,g^{-1}$].

Experimental Procedure

1c: A solution of **7** (38 g, 0.10 mol) in 100 mL of diethyl ether was added dropwise over 30 min to 130 mL of a 1.6 M solution of methyllithium in ether (0.21 mol) at −45 °C. After stirring for 1 h at 20 °C, **1c** was condensed under vacuum (1 Pa) into a trap cooled to −30 °C (5.9 g, 43%) and then further purified by recondensation from a vessel cooled to 0 °C into a dry-ice trap (yield: 4.75 g, 34%). For smaller runs (10–15 g of **7**) the yields of **1c** can be

increased up to 60%; similar yields are obtained by adding methyllithium to **7**. Compound **1c** is storable under nitrogen at $-20\,^{\circ}C$.

6: A 1.6 M solution of *n*BuLi in hexane (310 mL) was added to hexyl(triphenyl)phosphonium chloride (215 g, 0.50 mol, Aldrich) in 1 L of diethyl ether at 20 °C. The clear, dark red solution was cooled to $-65\,^{\circ}C$ and treated over 2 h with a solution of **5** (65 g, 0.50 mol) in 1 L of ether. The resulting precipitate was filtered off under suction at low temperature, the solvent was removed, and the residue was distilled (b.p. 50 °C/0.1 Pa; yield 50–60 g, 51–61%).

7: A solution of **6** (48 g, 0.25 mol) and bromoform (80 g, 0.3 mol) in 80 mL of dichloromethane was treated at room temperature with 0.8 g of trimethyl(phenyl)ammonium chloride and 0.8 mL of ethanol. A 50% solution of sodium hydroxide (80 mL) was then added dropwise to the stirred solution. After stirring for 3 d, the reaction mixture was subjected to aqueous workup. Vacuum distillation (0.1 Pa, bath at 110 °C) afforded reusable starting material and **7** as a colorless liquid (b.p. 95 °C/0.1 Pa; yield 42 g, 46%; yield when **6** was reused, 90%).

Received: November 9, 1988 [Z 3044 IE]
German version: *Angew. Chem. 101* (1989) 513

CAS Registry numbers:
1c, 119298-85-0; **2c**, (homopolymer) 119298-86-1; **3c**, 119298-87-2; **4**, 16666-79-8; **5**, 534-07-6; **6b**, 119326-88-4; **7**, 119326-89-5; $CHBr_3$, 75-25-2; MeLi, 917-54-4; NaOH, 1310-73-2; $H_3C(CH_2)_3Li$, 594-19-4.

[1] a) A.-D. Schlüter, *Angew. Chem. 100* (1988) 283; *Angew. Chem. Int. Ed. Engl. 27* (1988) 296; b) *Macromolecules 21* (1988) 1208; c) H. Bothe, A.-D. Schlüter, *196th ACS National Meeting*, Los Angeles 1988; *Polym. Prepr. Am. Chem. Soc. Div. Polym. Chem. 29* (1988) 412; d) P. Kaszynski, J. Michl, *J. Am. Chem. Soc. 110* (1988) 5225; e) A.-D. Schlüter, *Polym. Commun. 30* (1989) 34; f) H. Bothe, A.-D. Schlüter, *Makromol. Chem. Rapid Commun. 9* (1988) 529.

[2] a) P. W. Morgan, *Macromolecules 10* (1977) 1381; b) S. L. Kwolek, P. W. Morgan, J. R. Schäfer, L. W. Gulrich, *ibid. 10* (1977) 1390; c) H. Finkelmann, *Angew. Chem. 99* (1987) 840; *Angew. Chem. Int. Ed. Engl. 26* (1987) 816.

[3] For the positive effect of alkyl chains on solubility, see a) W. Heitz, *Chem.-Ztg. 110* (1986) 385, and references cited therein; b) J. Majnusz, J. M. Catala, R. W. Lenz, *Eur. Polym. J. 19* (1983) 1043; c) M. Ballauff, G. F. Schmidt, *Mol. Cryst. Liq. Cryst. 147* (1987) 163; d) M. Rehahn, A.-D. Schlüter, G. Wegner, W. J. Feast, *Polymer*, in press.

[4] The pentyl chain should be long enough to increase significantly the solubility of the polymer and short enough to allow distillative purification of the monomer at low temperatures.

[5] Preliminary results show that **1c** also undergoes radical-initiated polymerization.

[6] a) K. Semmler, G. Szeimies, J. Belzner, *J. Am. Chem. Soc. 107* (1985) 6410; b) J. Belzner, U. Bunz, K. Semmler, G. Szeimies, K. Opitz, A.-D. Schlüter, *Chem. Ber.* 122 (1989) 397.

[7] Hexyl(triphenyl)phosphonium bromide is available commercially.

[8] K. B. Wiberg, *Acc. Chem. Res. 17* (1984) 379.

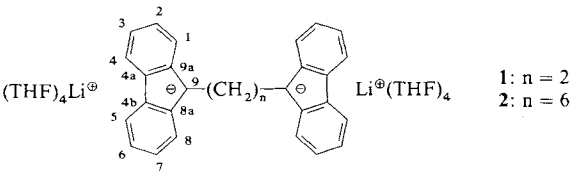
[9] B. Vollmert: *Grundriß der Makromolekularen Chemie, Bd. 1*, Vollmert-Verlag, Karlsruhe 1982, p. 227.

[10] The $\bar{P}_n$ value of **2a** could not be determined [1e]; the $\bar{P}_n$ value of **2b** was estimated to be 20 [1a, b]. Presumably, $\bar{P}_n$ of **2a** is similar.

The Structures of 1,n-Bis(9-lithio-9-fluorenyl)ethane · 8 THF and -hexane · 8 THF as Models for Solvent-Separated Ion Pairs**

By *Bardo Becker, Volker Enkelmann,* and *Klaus Müllen**

The rate of an intramolecular electron transfer depends, apart from geometric factors, on the ion-pair structure of the charged π systems involved.[1–3] Thus, for the alkali-metal derivatives of various radical anions, the rate of intramolecular electron transfer is increased on going from contact ion pairs to solvent-separated ion pairs[3, 4] as well as when the counterion is arranged between the charged units.[5] Spectroscopic investigations of biselectrophoric systems in solution often provide only indirect information on the relevant structures involved in electron transfer.[3, 5] Crystal structure investigations of carbanions have been carried out mostly for salts containing heteroatom bases as ligands to promote crystallization or stabilize the salt and have revealed contact ion pairs.[6] Removal of the counterion from the carbanion has been achieved by using crown ethers,[7] tetramethylethylenediamine,[8] and ethylenediamine[9] as ligands. We have now succeeded in crystallizing the diionic systems 1,n-bis(9-lithio-9-fluorenyl)ethane and -hexane as adducts with eight THF molecules (**1** and **2**, respectively) from pure THF. Their molecular structures, which are models for solvent-separated ion pairs, show that each lithium atom is surrounded tetrahedrally by four THF molecules and that there are minimal interactions between the fluorenyl moieties.



Compound **1** was prepared by treating 1,2-di(9-fluorenyl)ethane (0.2 g, 0.56 mmol) in 40 mL of dry THF at $-20\,^{\circ}C$ with highly active lithium.[10] The dark red solution thereby obtained afforded a microcrystalline precipitate. Heating of the solution to redissolve the product and slow cooling (48 h) from 25 °C to $-25\,^{\circ}C$ yielded **1** as long red needles. The hexane analogue **2** (pale red plates) was prepared similarly.[11] When **1** (or **2**) was transferred under inert gas to an NMR tube and solvolyzed with [D_4]methanol, the relative intensities of the ^1H NMR signals revealed the presence of eight THF ligands per molecule (for ^1H and ^{13}C NMR data of **1** and **2**, see Table 1).

The crystal structures of **1** and **2** (Fig. 1)[12] display the following features: (1) The chains have all-*trans* conformation, and the fluorenyl moieties, which are planar within the

Table 1. ^1H and ^{13}C NMR chemical shifts of **1** and **2** ([D_8]THF).

Position	δH		δC	
	1 [a]	**2** [a]	**1** [a]	**2** [b]
Aryl				
1(8)	7.65	7.18	114.77	114.13
3(6)	6.35	6.24	107.15	106.98
2(7)	6.85	6.69	118.90	118.69
4(5)	7.90	7.74	118.90	118.69
9	–	–	98.30	95.01
8a(9a)	–	–	135.85	135.54
4a(4b)	–	–	123.39	121.91
Alkyl				
1′	3.37	3.02	30.31	34.22,
2′	–	1.65	–	32.32,
3′	–	1.46	–	27.89 [c]

[a] $-30\,^{\circ}C$. [b] $-20\,^{\circ}C$; Variation of δC of the unsaturated center of **2** between -70 and $+20\,^{\circ}C$ less than 0.3. [c] The assignment of the signals was not confirmed experimentally.

[*] Prof. Dr. K. Müllen, Dipl.-Chem. B. Becker
Institut für Organische Chemie der Universität
J.-J.-Becher-Weg 18–20, D-6500 Mainz 1 (FRG)
Dr. V. Enkelmann
Max-Planck-Institut für Polymerforschung
Postfach 3148, D-6500 Mainz 1 (FRG)

[**] This work was supported by the Stiftung Volkswagenwerk and the Fonds der Chemischen Industrie.

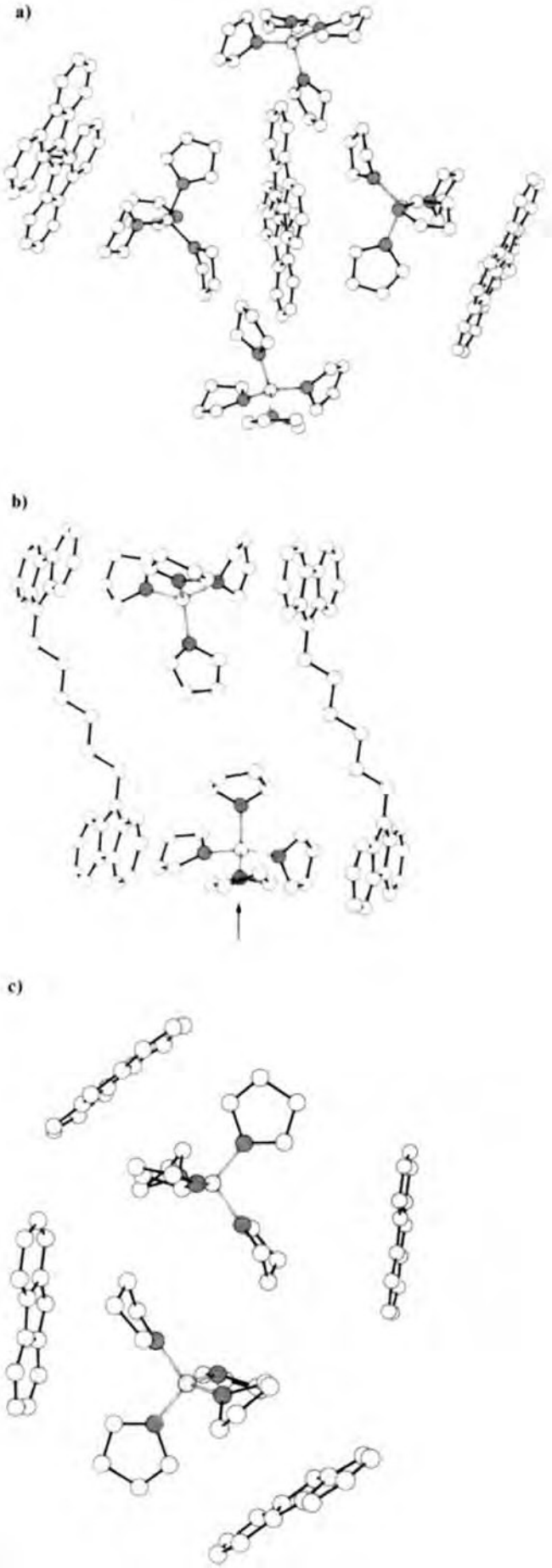


Fig. 1. a) Molecular structure of **1**. b) Molecular structure of **2**. c) Projection of the structure of **2** in the direction shown in Fig. 1 b. ○ = Li, ● = O.

limits of experimental error, lie parallel to each other. (2) In both cases, two crystallographically independent molecules are present; i.e., the asymmetric unit comprises two molecules of the type [fluorenyl$(CH_2)_{n/2}$(Li$(THF)_4$)]. Each lithium ion is surrounded by four THF molecules, the oxygen atoms of which approximate a regular tetrahedron [d(Li-O) ca. 190 pm, $\sphericalangle$ (O-Li-O) 104–114°, d(O-O) 299–317 pm, $\sphericalangle$ (O-O-O) 56.6–62.8°]. (3) No contacts smaller than the van der Waals distances are found between lithium ions and carbon centers of the fluorenyl moieties. The shortest distances d(Li-C) are 436 pm in **1** and 442 pm in **2**. (4) In the crystal lattice of **2**, the Li–Li distances (less than 1000 pm) are 756, 852, and 870 pm, the intramolecular C9–C9 distances 888 and 896 pm, and the intermolecular C9–C9 distances 770 pm. Thus, these values are of a similar magnitude as the C9–Li distances, which are between 563 and 895 pm.

A comparison with the structures of fluorenyllithium adducts[9, 13] and larger π-delocalized carbanions containing fluorenyl units[14–16] is very informative. For fluorenyllithium · 2 quinuclidine, contact ion pairs are found in which the metal lies above the plane of the π system[13] and the distance d(C9–Li) is 233 pm. The structure is explained in terms of electrostatic effects.[10, 13, 17, 18] The formation of a "solvent-separated" ion pair in the case of fluorenyllithium · 2 ethylenediamine is due to the stabilizing effect of NH hydrogen bonds to the carbanion.[9] In larger systems[14, 15] a Li center can interact with the fluorenyl moieties of two molecules to form a double-layer structure.

The salts **1** and **2** clearly differ from the cases known so far. The crowded coordination spheres of the metals, each of which is surrounded by four tetrahedrally arranged solvent molecules, prevent close Li–C contacts. Further, there are neither intra- nor intermolecular fluorenyl–fluorenyl interactions. Thus, no assignment of a carbanion to "its" counterion can be made. Instead, the Li and the C9 centers are arranged with equal separations in a quasi-ionic lattice. Since the rings in the two crystallographically different molecules are not oriented parallel to one another, no stacked structures with particularly strong Li–fluorenyl interactions in the stacking planes are found. On the contrary, comparison of Figures 1 b and 1 c reveals that a three-dimensional saltlike packing arises owing to the presence of cavities containing the Li$(THF)_4$ units next to the fluorenyl rings. Special geometric assignments (e.g., between Li$(THF)_4$ and the central cyclopentadienide ring) of the shortest Li–C distances given are not apparent.

The fluorenyllithium system is one of the best-investigated carbanion systems. The crystal structures of the derivatives **1** and **2** are good models for solvent-separated ion pairs in THF and may facilitate a deeper theoretical understanding of these species, which have been postulated mainly on the basis of spectroscopic data. Further, there is no evidence for an "aggregation" of the carbanion subunits.

Received: October 17, 1988 [Z 3011 IE]
German version: *Angew. Chem. 101* (1989) 501

CAS Registry numbers:
1, 119366-94-8; **2**, 119391-03-6; 1,2-di(9-fluorenyl)ethane, 3747-24-8.

[1] F. Gerson, W. Huber, W. B. Martin, Jr., P. Caluwe, T. Pepper, M. Szwarc, *Helv. Chim. Acta 67* (1984) 416.
[2] W. Irmen, W. Huber, J. Lex, K. Müllen, *Angew. Chem. 96* (1984) 800; *Angew. Chem. Int. Ed. Engl. 23* (1984) 818.
[3] W. Huber, H. Unterberg, K. Müllen, *Angew. Chem. 95* (1983) 239; *Angew. Chem. Int. Ed. Engl. 22* (1983) 242.

[4] J. Fiedler, W. Huber, K. Müllen, *Angew. Chem. 98* (1986) 444; *Angew. Chem. Int. Ed. Engl. 25* (1986) 443.
[5] S. Mazur, V. M. Dixit, F. Gerson, *J. Am. Chem. Soc. 102* (1980) 5343.
[6] W. N. Setzer, P. von R. Schleyer, *Adv. Organomet. Chem. 24* (1985) 353; C. Schade, P. von R. Schleyer, *ibid. 27* (1987) 169.
[7] M. M. Olmstead, P. P. Power, *J. Am. Chem. Soc. 107* (1985) 2174; R. A. Bartlett, P. P. Power, *Organometallics 5* (1986) 1916; M. M. Olmstead, P. P. Power, K. J. Weese, R. J. Doedens, *J. Am. Chem. Soc. 109* (1987) 2541; P. P. Power, *Acc. Chem. Res. 21* (1988) 147.
[8] H. Schmidbaur, E. Weiß, B. Zimmer-Gasser, *Angew. Chem. 91* (1979) 848; *Angew. Chem. Int. Ed. Engl. 18* (1979) 782; K. R. Pörschke, C. Krüger, Y.-H. Tsay, *ibid. 88* (1976) 682 bzw. *15* (1976) 621.
[9] S. Buchholz, K. Harms, G. Boche, *9th IUPAC Conf. Phys. Org. Chem.* (Regensburg 1988), Abstracts p. 54; S. Buchholz, K. Harms, M. Marsch, W. Massa, G. Boche, *Angew. Chem. 101* (1989) 57; *Angew. Chem. Int. Ed. Engl. 28* (1989) 72.
[10] U. Jakaki, G. L. Collins, J. Smid, *J. Organomet. Chem. 145* (1978) 139; L. L. Chan, J. Smid, *J. Am. Chem. Soc. 90* (1968) 4654.
[11] Under these experimental conditions, UV spectroscopic investigations [10] have revealed that **1** and **2** are present as solvent-separated ion pairs. The NMR chemical shifts of **1** and **2** (Table 1) largely correspond to those of simple fluorenyllithium systems [19]. The differences in the δH and δC values observed for **1** and **2** provide no evidence of an interaction between the fluorenyl moieties.
[12] Crystal structure analyses of **1** and **2**: Enraf-Nonius CAD 4 diffractometer, $Cu_{K\alpha}$ radiation, $\lambda = 1.5405$ Å, graphite monochromator. The structures were solved by direct methods (DIRDIF). Empirical absorption correction, anisotropic temperature factors for O, C, Li, refinement of the H atoms in the "riding mode" with fixed isotropic temperature factors. **1**: $T = 120$ K, triclinic, space group $P\bar{1}$, $a = 17.350(2)$, $b = 10.091(6)$, $c = 17.870(1)$ Å, $\alpha = 104.91(5)$, $\beta = 66.24(6)$, $\gamma = 105.33(7)°$, $V = 2721$ Å^3, $Z = 2$, $\rho_{calcd} = 1.16$ g cm^{-3}, $\mu(Cu_{K\alpha}) = 5.477$ cm^{-1}. 5984 reflections, of which 3564 were observed [$I > 3\,\sigma(I)$]. $R = 0.068$, $R_w = 0.065$. **2**: $T = 150$ K, triclinic, space group $P\bar{1}$, $a = 18.610(3)$, $b = 18.836(3)$, $c = 9.751(1)$ Å, $\alpha = 100.07(1)$, $\beta = 104.52(1)$, $\gamma = 63.12(2)°$, $V = 2942$ Å^3, $Z = 2$, $\rho_{calcd} = 1.13$ g cm^{-3}, $\mu(Cu_{K\alpha}) = 5.274$ cm^{-1}. 4879 reflections, of which 3235 were observed [$I > 3\,\sigma(I)$]. $R = 0.094$, $R_w = 0.096$. Further details of the crystal structure investigations may be obtained from the Fachinformationszentrum Energie, Physik, Mathematik GmbH, D-7514 Eggenstein-Leopoldshafen 2 (FRG), on quoting the depository number CSD-53726, the names of the authors, and the journal citation.
[13] M. Walczak, G. D. Stucky, *J. Organomet. Chem. 97* (1975) 313.
[14] D. Bladauski, H. Dietrich, H.-J. Hecht, D. Rewicki, *Angew. Chem. 89* (1977) 490; *Angew. Chem. Int. Ed. Engl. 16* (1977) 474.
[15] D. Bladauski, D. Rewicki, *Chem. Ber. 110* (1977) 3920.
[16] J. J. Brooks, W. Rhine, G. D. Stucky, *J. Am. Chem. Soc. 94* (1972) 7339.
[17] T. A. Albright, P. Hofmann, R. Hoffmann, C. P. Lillya, P. A. Dobosh, *J. Am. Chem. Soc. 105* (1983) 3396.
[18] R. J. Bushby, M. P. Tytko, *J. Organomet. Chem. 270* (1984) 265.
[19] J. A. Dixon, P. A. Gwinner, D. C. Lini, *J. Am. Chem. Soc. 87* (1965) 1379; R. H. Cox, *J. Phys. Chem. 73* (1969) 2649; U. Edlund, *Org. Magn. Reson. 12* (1979) 661.

17- to 19-Electron Pentamethylcyclopentadienyl Iron Dithiocarbamate Complexes. Formation of a Cp*Fe^{IV} Complex

By *Marie-Hélène Desbois* and *Didier Astruc* *

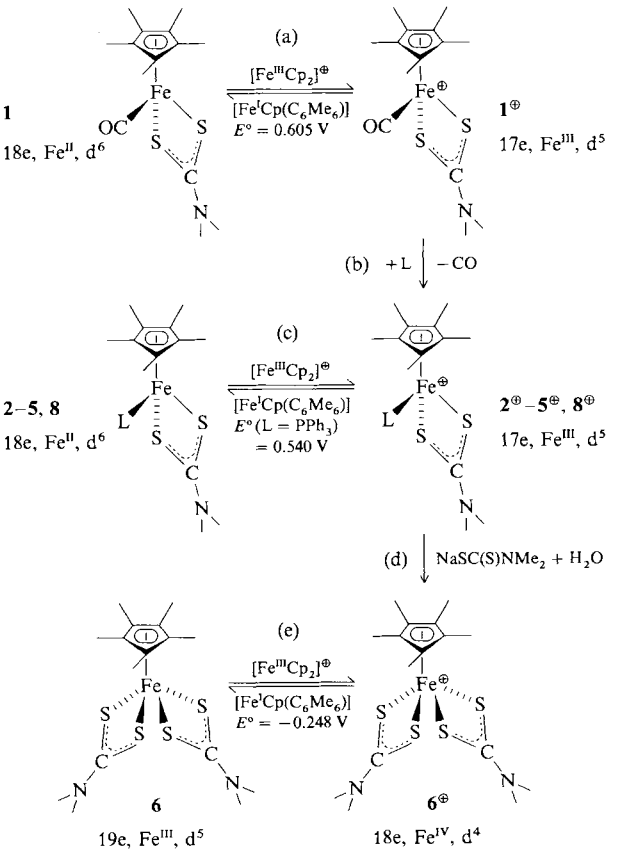
The chemistry of inorganic and organometallic radicals[1] has attracted much attention recently because of their involvement in electron-transfer-catalyzed (ET-catalyzed) reactions[2] and energy conversion.[3] We wish to report a series of kinetically very labile but thermally stable 17e complexes of general formula **A** (Cp* = η^5-C_5Me_5; counterion $PF_6^\ominus$), their oxidation to $\mathbf{6}^\oplus$, and several new redox couples.

$[Fe^{III}Cp^*(\eta^2\text{-}SC(S)NMe_2)(L)]^\oplus$ **A**
$\mathbf{1}^\oplus$, L = CO
$\mathbf{2}^\oplus$, L = MeCN
$\mathbf{3}^\oplus$, L = Me_2CO
$\mathbf{4}^\oplus$, L = CH_2Cl_2
$\mathbf{5}^\oplus$, L = THF
$[Fe^{IV}Cp^*(\eta^2\text{-}SC(S)NMe_2)_2]^\oplus$ $\mathbf{6}^\oplus$

Oxidation of the red precursor complexes **1**[4] or $[Fe^{II}Cp^*(\eta^1\text{-}SC(S)NMe_2)(CO)_2]$ **7**[4] by one equivalent of $[FeCp_2]^\oplus$ in THF gives green $\mathbf{1}^\oplus$ and $FeCp_2$ in 85% yield each [Eq. (a)]. The new 17e complex $\mathbf{1}^\oplus$ was characterized by elemental analysis as well as by IR, ESR, and Mössbauer spectroscopy and compares with other 17e complexes of the type $[FeCp^*(L^1)(L^2)(CH_3)]^\oplus$ (L^1, L^2 = CO, phosphane).[5] It can be reduced back to **1** in 81% yield using $[Fe^ICp(C_6Me_6)]$[6] in THF [Eq. (a) in Scheme 1].

The chemistry of $\mathbf{1}^\oplus$ is of interest since this species was proposed to be an intermediate in the ET-catalyzed conversion of **7** to **1**.[7] The complex $\mathbf{1}^\oplus$ is insoluble in THF, but its CO ligand is extremely labile in polar solvents such as MeCN, Me_2CO, and CH_2Cl_2. When $\mathbf{1}^\oplus$ is dissolved in any of these solvents at 20 °C, its green color rapidly turns red, the color of $\mathbf{2}^\oplus$, $\mathbf{3}^\oplus$, and $\mathbf{4}^\oplus$, respectively, and CO evolves [Eq. (b)]. The reaction $\mathbf{1}^\oplus \rightarrow \mathbf{2}^\oplus + CO$ could be followed by visible spectroscopy at 5 °C (Fig. 1) and two isosbestic points (λ = 488 and 600 nm) were observed.

The complexes $\mathbf{2}^\oplus$–$\mathbf{4}^\oplus$ could also be characterized by their ESR spectra in solution, which are characteristic of 17e Fe^{III}



Scheme 1. The counterion is always $PF_6^\ominus$. $E°$ is given relative to the standard calomel electrode (SCE).

[*] Prof. D. Astruc, Dr. M.-H. Desbois
Laboratoire de Chimie Organique et Organométallique
U.A. C.N.R.S. N°. 35, Université de Bordeaux I
351 cours de la Libération, 33405 Talence Cedex (France)

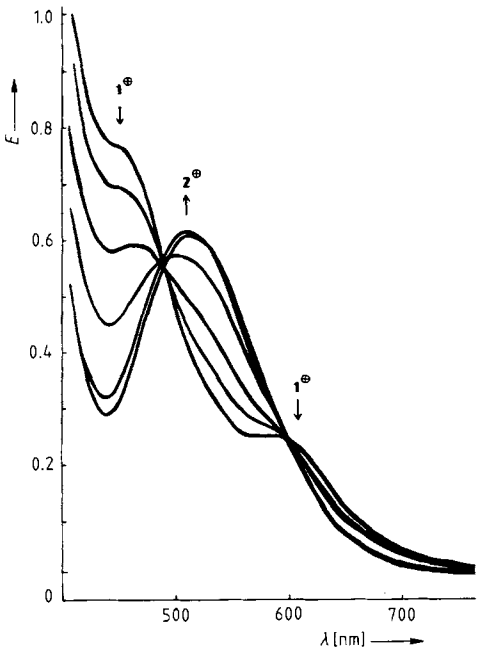


Fig. 1. Visible spectroscopy of the conversion of $\mathbf{1}^{\oplus}$ ($c = 3.2 \times 10^{-3}$ mol L^{-1}) to **2** in CH_3CN at 5 °C. E = extinction coefficient.

Table 1. Physical data for the cations $\mathbf{1}^{\oplus}$–$\mathbf{4}^{\oplus}$ and $\mathbf{6}^{\oplus}$ as $PF_6^{\ominus}$ salts.

$\mathbf{1}^{\oplus}$: Mössbauer data (mm s^{-1} vs Fe; 298 K, 77 K): $IS = 0.518$, $QS = 0.686$. IR (KBr pellet): $\tilde{\nu}$[cm^{-1}] = 2030, 1985 (CO), 1550 (CN), 1015 (CS). ESR (solid sample, 10 K): $g_1 = 2.239$, $g_2 = 2.107$, $g_3 = 2.049$; orthorhombic transition at 200 K: $g_1 = 2.237$, $g_{2,3} = 2.071$. Visible spectrum (MeCN): λ[nm] (ε [L mol^{-1} cm^{-1}]) = 584 (811), 452 (2451). Elemental analysis calcd for $C_{14}H_{21}FeNOPS_2F_6$: C 34.72, H 4.37, Fe 11.53, N 2.89; found: C 34.19, H 4.36, Fe 12.11, N 2.77.

$\mathbf{2}^{\oplus}$: Mössbauer data (mm s^{-1} vs Fe; 298 K): $IS = 0.550$, $QS = 0.620$. IR (MeCN, 298 K): $\tilde{\nu}$[cm^{-1}] = 1535 (CN), 1035 (CS). ESR (CH_3CN, 20 K): $g_1 = 2.611$, $g_2 = 2.184$, $g_3 = 2.001$. Visible spectrum (MeCN, 5 °C): λ[nm] (ε [L mol^{-1} cm^{-1}]) = 514 (1823). Elemental analysis calcd for $C_{15}H_{24}FeS_2N_2PF_6$: C 36.23, H 4.86, N 5.63; found: C 36.48, H 4.63, N 5.08

$\mathbf{3}^{\oplus}$: IR (Me_2CO, 298 K): $\tilde{\nu}$[cm^{-1}] = 1510 (CN), 1015 (CS). ESR (Me_2CO, 20 K): $g_1 = 2.453$, $g_2 = 2.035$, $g_3 = 1.995$

$\mathbf{4}^{\oplus}$: IR (CH_2Cl_2): $\tilde{\nu}$[cm^{-1}] = 1520 (CN), 1015 (CS). ESR (CH_2Cl_2, 20 K): $g_1 = 2.571$, $g_2 = 2.135$, $g_3 = 1.990$

$\mathbf{6}^{\oplus}$: ^{1}H NMR (CD_3CN, 20 °C, TMS): $\delta = 3.228$ (s, 12H; NMe), 1.279 (s, 15H; Me). ^{13}C NMR (CD_3CN): $\delta = 200.56$ (CN), 106.04 (C_5Me_5), 38.42 (NMe), 9.75 ($C_5(CH_3)_5$). IR (KBr pellet, 298 K): $\tilde{\nu}$[cm^{-1}] 1540 (CN), 1005 (CS). Mössbauer data (mm s^{-1} vs Fe 298 K, 77 K): $IS = 0.460$, $QS = 0.220$. Cyclic voltammetry (dimethylformamide, 0.1 M $nBu_4N^{\oplus}BF_4^{\ominus}$, 298 K, $v = 400$ mV s^{-1}, Pt): E°[V] vs SCE = -0.248 ($\Delta E_p = 135$ mV, $i_a/i_c = 0.89$, $\alpha = 0.67$, $D = 1.07 \times 10^{-5}$ cm^2 s^{-1}, $k_s = 4 \times 10^{-3}$ cm s^{-1}; $\Delta G^{\neq} = 5.88$ kcal mol^{-1}), -0.765 ($\Delta E_p = 210$ mV, $i_a/i_c = 0.88$, $\alpha = 0.60$, $D = 1.46 \times 10^{-5}$ cm^2 s^{-1}, $k_s = 2.3 \times 10^{-3}$ cm s^{-1}; $\Delta G^{\neq} = 5.62$ kcal mol^{-1}). Elemental analysis calcd for $C_{16}H_{27}S_4N_2FePF_6$: C 33.33, H 4.72, N 4.85; found: C 33.59, H 4.71, N 4.65

piano-stool complexes (Table 1).[5] Their IR spectra show the absence of carbonyl groups. The homogeneous reaction of $\mathbf{4}^{\oplus}$ with a CH_2Cl_2/THF mixture (3/1) slowly gives $\mathbf{5}^{\oplus}$ (4 h, 20 °C).

The 17e complexes $\mathbf{2}^{\oplus}$–$\mathbf{5}^{\oplus}$ can be reduced by [$Fe^{I}Cp(C_6Me_6)$] to **2**–**5**, which, in turn, can be reoxidized back to $\mathbf{2}^{\oplus}$–$\mathbf{5}^{\oplus}$ using $[FeCp_2]^{\oplus}$ [Eq. (c)], all the redox reactions being performed in THF at 20 °C. Reaction (b) follows pseudo-first-order kinetics and its rate depends on L ($t_{1/2}$: 57 min in CH_2Cl_2, 25 °C; 13.5 min in Me_2CO, 5 °C; 5 min in MeCN, 5 °C), suggesting an associative mechanism via the formation of 19e intermediates or transition states as the rate-limiting step. Reaction of $\mathbf{2}^{\oplus}$–$\mathbf{4}^{\oplus}$ with one equivalent of PPh_3 in situ cleanly gives the known complex $\mathbf{8}^{\oplus}$.[7]

$[Fe^{III}Cp^*(\eta^2\text{-}SC(S)NMe_2)(PPh_3)]^{\oplus}$ $\mathbf{8}^{\oplus}$

Reaction of one equivalent of $Na^{\oplus}{}^{\ominus}SC(S)NMe_2 \cdot 2\,H_2O$ with $\mathbf{1}^{\oplus}$ in CH_2Cl_2 at 20 °C gives initially the red complex $\mathbf{4}^{\oplus}$, which is transformed into the green complex $\mathbf{6}^{\oplus}$ within 1.5 h [Eq. (d)]. The complex $\mathbf{6}^{\oplus}$ crystallized in 75% yield (0.2-mmol scale) and was characterized as an 18e Fe^{IV} complex by ^{1}H and ^{13}C NMR, IR, and Mössbauer spectroscopy. The NaOH formed in this reaction was titrated by a 0.01 N solution of HCl; its amount agreed with the stoichiometry of Equation (f). Further H_2 was detected by gas chromatography. Thus water is reduced in this reaction:

$$[Fe^{III}Cp^*(SC(S)NMe_2)(L)][PF_6] + NaSC(S)NMe_2 + H_2O \rightarrow [Fe^{IV}Cp^*(SC(S)NMe_2)][PF_6] + NaOH + 1/2\,H_2 + L \quad (f)$$

$L = CO, CH_2Cl_2$

We propose that the 19e intermediate **6** is formed in reaction (f) and reduces H_2O. Cyclic voltammetry of $\mathbf{6}^{\oplus}$ shows a quasi-reversible redox system, $\mathbf{6}^{\oplus}/\mathbf{6}$, with $E^{\circ} = -0.248$ V vs SCE [Eq. (e)]. The complex $\mathbf{6}^{\oplus}$ is also formed in lower yields (30–40%) by disproportionation of the 17e complexes $\mathbf{1}^{\oplus}$–$\mathbf{5}^{\oplus}$ and $\mathbf{8}^{\oplus}$ at 20 °C in the absence of $Na^{\oplus}{}^{\ominus}SC(S)NMe_2$ but in the presence of water. Reduction of $\mathbf{6}^{\oplus}$ to **6** can be rapidly effected at 20 °C using one equivalent of [$Fe^{I}Cp(C_6Me_6)$] in THF. The birefringent purple/blue-turquoise 19e Fe^{III} complex **6** is soluble in ether and shows an ESR spectrum typical[8] of 19e Fe species (20 K, solid state: $g = 2.268$, 2.126, 2.035).

In summary, access to the 17e complexes of general formula **A** opens a route to several new redox couples for which both forms were isolated and characterized. This chemistry demonstrates the good electron-reservoir properties of the $SC(S)NMe_2$ ligand and the intermediacy of 19e species in the reactions of 17e complexes with various ligands.

Received: October 14, 1988 [Z 3009 IE]
German version: *Angew. Chem. 101* (1989) 459

CAS Registry numbers:
1, 84541-24-2; $\mathbf{1}^{\oplus}PF_6^{\ominus}$, 119366-46-0; **2**, 119366-39-1; $\mathbf{2}^{\oplus}PF_6^{\ominus}$, 119366-47-1; **3**, 119366-40-4; $\mathbf{3}^{\oplus}PF_6^{\ominus}$, 119366-49-3; **4**, 119366-41-5; $\mathbf{4}^{\oplus}PF_6^{\ominus}$, 119366-51-7; **5**, 119366-42-6; $\mathbf{5}^{\oplus}PF_6^{\ominus}$, 119366-53-9; **6**, 119366-43-7; $\mathbf{6}^{\oplus}PF_6^{\ominus}$, 119366-55-1; **7**, 89875-07-0; **8**, 119366-44-8; $\mathbf{8}^{\oplus}PF_6^{\ominus}$, 118228-79-8; $(FeCp_2)^{\oplus}PF_6^{\ominus}$, 11077-24-0; $Fe^{I}Cp(C_6Me_6)$, 70414-92-5; $Na^{\oplus}{}^{\ominus}SC(S)NMe_2$, 128-04-1; $[FeCp^*(CO)_2]$ dimer, 35344-11-7.

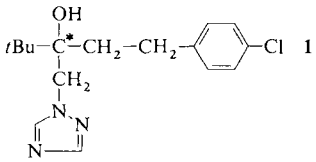
[1] a) H. Bock, *Angew. Chem. 89* (1977) 631; *Angew. Chem. Int. Ed. Engl. 16* (1977) 613; b) W. Kaim, *Coord. Chem. Rev. 76* (1987) 187; c) T. L. Brown, *Ann. N.Y. Acad. Sci. 331* (1980) 80; d) D. Astruc, *Chem. Rev. 88* (1988) 1189.
[2] a) M. Chanon, *Acc. Chem. Res. 20* (1987) 214; b) J. K. Kochi, *J. Organomet. Chem. 300* (1986) 139; c) D. Astruc, *Angew. Chem. 100* (1988) 662; *Angew. Chem. Int. Ed. Engl. 27* (1988) 643.
[3] J.-M. Lehn, J.-P. Sauvage, R. Ziessel, *Nouv. J. Chim. 3* (1979) 423.
[4] a) D. Catheline, D. Astruc, *Organometallics 3* (1984) 1094; b) D. Catheline, E. Román, D. Astruc, *Inorg. Chem. 23* (1984) 4508.
[5] J. Morrow, J. Ruiz, M.-H. Desbois, J.-M. Manriquez, D. Astruc, *Organometallics 6* (1987) 2605.
[6] D. Astruc, J.-R. Hamon, M. Lacoste, M.-H. Desbois, A. Madonik, E. Roman in R. B. King, J. S. Eisch (Eds.): *Organometallic Synthesis, Vol. IV*, Elsevier, Amsterdam 1988, p. 172.
[7] C. Amatore, J.-N. Verpeaux, A. Madonik, M.-H. Desbois, D. Astruc, *J. Chem. Soc. Chem. Commun. 1988*, 200.
[8] M. V. Rajasekharan, S. Giezynski, J. H. Ammeter, N. Ostwald, J.-R. Hamon, P. Michaud, D. Astruc, *J. Am. Chem. Soc. 104* (1982) 2400.

The Enantiomers of the Azole Fungicide HWG-1608—Asymmetric Synthesis of a 2-Hydroxyethyl Azole Fungicide**

By *Johannes Kaulen**

Dedicated to Professor Hans Rudolph on the occasion of his 60th birthday

The azole fungicide HWG-1608 **1** (commercial name Folicur®, Raxil®), first synthesized by *Holmwood* et al., is a new, highly effective fungicide belonging to the class of ergosterol-biosynthesis inhibitors.[1] Compound **1** has an asymmetric center and is therefore prepared commercially as a racemate. However, the pure enantiomers were required for more detailed biological and biochemical investigations. We report here the synthesis of the enantiomers of **1** via a reaction sequence in which both enantiomers can be obtained—either by asymmetric synthesis or by separation of diastereomers—using the same chiral auxiliary.



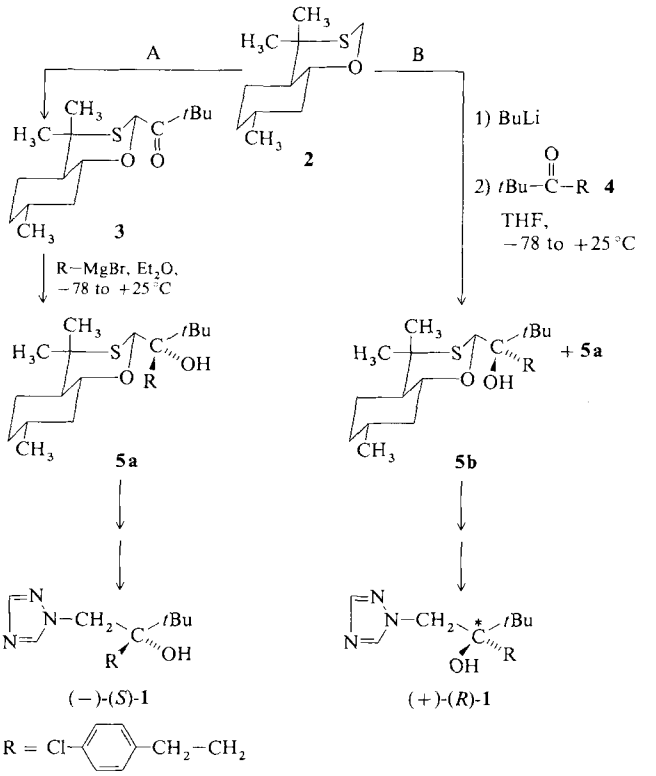
The synthesis of the enantiomers was achieved by extending the oxathiane method developed by *Eliel* et al. to azole chemistry, starting from the chiral oxathiane derivatives **2** and **3**[2] (Scheme 1), which are readily accessible from (+)-pulegone.

Grignard addition of *p*-chlorophenethylmagnesium bromide to **3** (path A) afforded **5a**,[3] the precursor of (−)-(*S*)-**1**, with excellent diastereoselectivity (*de* > 95%). Addition of lithiated **2** to the *tert*-butyl ketone **4**, an intermediate in the commercial synthesis of racemic **1**, gave primarily **5b** (*de* = 48%,[4] path B), which was surprisingly easy to separate from **5a** (SiO_2, petroleum ether:diethyl ether 5:1; R_F values: **5b**, 0.43; **5a**, 0.31). This route provided easy access to large quantities of pure **5b**, the precursor of (+)-(*R*)-**1**.[5]

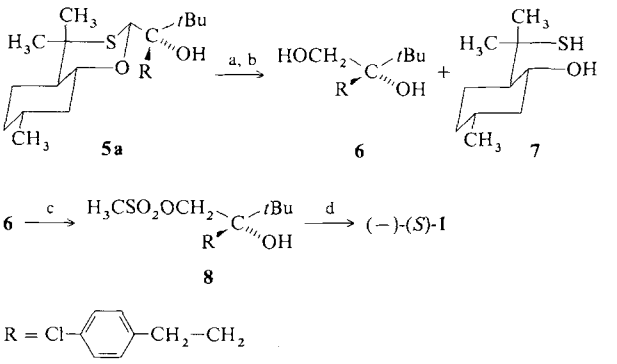
The diastereoselectivity observed for path B is appreciably higher than that usually found for addition of **2** to ketones,[2a] presumably because the *tert*-butyl group is more sterically demanding than the phenethyl moiety.

Mild cleavage of the oxathiane moiety of **5a** with *N*-chlorosuccinimide (NCS)/silver nitrate[2, 6] and in situ reduction of the liberated aldehyde with $LiAlH_4$[7] affords the diol **6**. The oxathiane chiral auxiliary is thereby recovered in the form of the mercapto alcohol **7**.[2] Selective mesylation of **6** to give **8** and nucleophilic replacement of the mesyloxy group by a triazole group leads to the desired (−)-(*S*)-**1** (95% *ee*, Scheme 2). Compound **5b** reacts in a similar fashion to give (+)-(*R*)-**1**. The overall yield of (−)-(*S*)-**1** in this five-step synthesis starting from **3** is 37%.

The absolute configurations of the intermediate and end products were confirmed by X-ray structure analysis of (−)-(*S*)-**1**[1b] and support the rules established earlier by *Eliel* et al.[2a]



Scheme 1.



Scheme 2. NCS, $AgNO_3$, CH_3CN, 15 min 40–50 °C [2, 6]. b) $LiAlH_4$, Et_2O, 3 h, 35 °C [7] (85% crude yield for two steps). c) CH_3SO_2Cl, Et_3N, CH_2Cl_2, 4 h 25 °C (89% crude yield). d) Sodium salt of triazole, DMF, 6 h 120 °C, 37% overall yield from **3**.

The novel combination of the complementary paths A and B allows both enantiomers of HWG-1608 **1** to be prepared using the same chiral auxiliary. The active (−)-(*S*) enantiomer is obtained by an asymmetric synthesis, the less active (+)-(*R*) enantiomer by intervening separation of diastereomers. Thus, as exemplified by (−)-(*S*)-**1**, we have accomplished the asymmetric total synthesis of a 2-hydroxyethyl azole fungicide.[8]

Experimental Procedure

The structures of all new compounds were confirmed by ^1H NMR, IR, and mass spectra (Table 1) as well as by C, H analyses. The diastereomeric excesses were determined by capillary chromatography, HPLC, and ^1H NMR spectroscopy. The enantiomeric purity of the end products was determined by high-pressure liquid chromatography on chiral columns.

5a: A solution of **3** (31.3 g, 0.11 mol) [2a] in 200 mL of anhydrous diethyl ether was added to a solution of the Grignard reagent prepared from 4-chlorophenethyl bromide (48.3 g, 0.22 mol) in 100 mL of anhydrous diethyl ether at −78 °C. The bath was allowed to warm slowly to room temperature and the reaction mixture was then heated at reflux for 3 h. Workup was carried out by

[*] Dr. J. Kaulen
Bayer AG,
Zentrale Forschung ZF-FGF
D-5090 Leverkusen (FRG)

[**] We thank Dr. *L. Born* (X-ray structure analysis), Dr. *R. Grosser* (determination of optical purity), and Dr. *T. Werner* (structure elucidation), Bayer AG, Zentrale Forschung, for their assistance in carrying out this work.

Table 1. Characteristic spectroscopic data for the diastereomers **5a** and **5b**: ^{1}H NMR: 360 MHz ($CDCl_3$); MS: 70 eV; IR: neat (NaCl).

5a: ^{1}H NMR: δ = 0.93 (d, J = 6.7 Hz, 3H, CH_3-CH), 1.02 (s, 9H, *t*Bu); 1.29 and 1.42 (each s, each 3H, CH_3-C-CH_3); 2.75 and 3.05 (each d of t, J = 4.9, 12.8 Hz, each 1 H, $HO-C-CH_2-$), 2.06 (s, 1H, *OH*), 3.36 (d of t, J = 4.0, 10.7 Hz, 1H, $>CH-OR$), 5.29 (s, 1H, $-S-CH-O$), 7.15–7.28 (m, 4H, arom. H)

5b: ^{1}H NMR: δ = 0.92 (d, J = 6.4 Hz, 3H, CH_3-CH); 1.03 (s, 9H, *t*Bu); 1.29 and 1.44 (each s, je 3H, CH_3-C-CH_3); 2.59 and 3.09 (each d of t, J = 5.0, 13.1 Hz, each 1H, $HO-C-CH_2$); 3.37 (s, 1H, *OH*); 3.41 (d of t, J = 4.3, 10.7 Hz, 1H, $>CH-OR$); 5.05 (s, 1H, $-S-CH-O$); 7.17–7.30 (m, 4H, arom. H)

MS (identical for **5a** and **5b** ($M^{\oplus}$ absent): m/z 367 ($M^{\oplus}-t$Bu, 4%); 199 ($C_{11}H_{19}SO$, oxathiane fragment, 100%)

IR (identical for **5a** and **5b**): $\tilde{\nu}$ = 3550 cm^{-1} (OH)

pouring the reaction mixture into 200 mL of a saturated NH_4Cl solution, separating the ether phase, extracting three times with dichloromethane, and drying the combined organic phases over Na_2SO_4, then concentrating the solution in a rotary evaporator and removing low-boiling impurities in vacuo (0.1 mbar, bath temperature 140 °C). Yield: 40.2 g (86%) **5**. Ratio **5a:5b** = 97.7:2.3 (95.4% *de*). The product was used without further purification (for spectroscopic data see Table 1).

5b: A solution of butyllithium (1.98 M, 45.5 mL, 90 mmol) in hexane was added under N_2 to a solution of **2** (18.0 g, 90 mmol) [2c, d] in 100 mL of dry THF at −78 °C. The reaction mixture was warmed briefly to 0 °C and then cooled again to −78 °C. Compound **4** (20.2 g, 90 mmol) [1a] in 50 mL of dry THF was added dropwise at this temperature. The resulting reaction mixture was warmed slowly in the bath to room temperature and then stirred for 30 min at 25 °C. Workup was carried out as for **5a**. Yield: 37.6 g (98%) crude product. Ratio **5a:5b** = 26:74 (48% *de*). Chromatography on 1 kg of silica (petroleum ether:ether 5:1 as eluent) gave, as the first fraction, 20.5 g (54%) of **5b**, followed by a second fraction containing 4.04 g (18%) of **5a**, both compounds being isolated as colorless oils (for spectroscopic data see Table 1).

(−)-(*S*)-**1**: Crude **8** (27.3 g, 81.5 mmol) was stirred with the sodium salt of triazole (22.3 g, 0.24 mol, 3 equiv.) in 100 mL of dry dimethylformamide (DMF) under N_2 for 6 h at 120 °C. The DMF was removed in a rotary evaporator and the residue was dissolved in water/dichloromethane. The organic phase was separated and the aqueous phase was extracted twice with CH_2Cl_2. The combined organic phases were dried over Na_2SO_4, and concentrated in a rotary evaporator. The entire crude product was purified by chromatography on 1 kg of SiO_2 (CH_2Cl_2:MeOH 95:5 as eluent). Yield: 12.4 g (49%, 37% overall yield starting from **3**) (−)-(*S*)-**1**: $[\alpha]_D^{20} = -34.0$ (c = 1, $CHCl_3$); enantiomeric purity determined by HPLC to be ≥ 95%; spectroscopic data identical with that of racemic reference compound.

Received: September 18, 1988 [Z 2981 IE]
German version: *Angew. Chem. 101* (1989) 507

CAS Registry numbers:
(*S*)-**1**, 119364-85-1; **2**, 79618-03-4; **3**, 92572-79-7; **4**, 66346-01-8; **5a**, 119298-82-7; **5b**, 119364-84-0; **6**, 119298-83-8; **8**, 119298-84-9; 4-chlorophenethyl bromide, 6529-53-9; triazole sodium salt, 41253-21-8.

[1] a) G. Holmwood, K. H. Büchel, K. Lürssen, P. E. Frohberger, W. Brandes, *Eur. Pat.* 40345 (1981), Bayer AG; b) D. Berg, L. Born, K. H. Büchel, G. Holmwood, J. Kaulen, *Pflanzenschutz-Nachr. Bayer Ger. Ed. 40* (1987) 111; *Pflanzenschutz-Nachr. 40* (1987) 111; c) Review on ergosterol-biosynthesis inhibitors; W. Krämer in W. S. Bowers (Ed.): *Chemistry of Plant Protection, Vol. 1*, Springer, Berlin 1986, pp. 26–64; d) Whereas (−)-(*S*)-**1** is appreciably more effective than its enantiomer in in-vitro studies, the difference in the green house—especially with azole-resistant fungi—is less pronounced [1b].

[2] a) E. L. Eliel, S. Morris-Natschke, *J. Am. Chem. Soc. 106* (1984) 2937; b) *ibid. 106* (1984) 2943; c) *Tetrahedron Lett. 22* (1981) 2855; d) E. L. Eliel, J. E. Lynch, F. Kunze, S. V. Freye, *Org. Synth. 65* (1987) 215; e) Reviews: E. L. Eliel, *Phosphorus Sulfur 24* (1985) 453; E. L. Eliel, J. K. Koskimies, B. Lohri, W. J. Frazec, S. Morris-Natschke, J. E. Lynch, K. Soai in E. L. Eliel (Ed.): *Asymmetric Reactions and Processes in Chemistry, ACS Symp. Ser. 185* (1982) 37–53.

[3] The diastereomeric excess determined by capillary gas chromatography was practically independent of the solvent used (diethyl ether or THF) and of the nature of the Grignard reagent (bromide or iodide).

[4] Attempts to increase the diastereoselectivity by transmetalation (reaction of lithiated **2** with $ClTi(OiPr)_3$, $MgBr_2$, or $ZnCl_2$) were unsuccessful, since the metalated oxathianes thus formed did not add to **4**.

[5] Reversal of the order of addition of reagent and substrate (i.e., addition of *tert*-butylmagnesium bromide to **3**, with 4-chlorophenethyl instead of *t*Bu), a commonly used trick in asymmetric synthesis, did not lead to **5b**; in addition to unchanged starting material, the secondary alcohol (Grignard reduction of the ketone) was found.

[6] E. J. Corey, B. W. Erickson, *J. Org. Chem. 36* (1971) 3553.

[7] Reduction with $NaBH_4$ gave, besides **6** (20% yield), a very stable boron chelate complex containing two units of **6** as main product (40%). This complex could be isolated by chromatography, but could not be converted into **6** under mild conditions.

[8] Azole fungicides with secondary hydroxyl groups at the stereogenic center have been obtained in special cases by asymmetric reduction of ketones, cf. U. Kraatz, P. Feyen, Eur. Pat. 196504 (1986), Bayer AG; Y. Yoneyoshi, G. Gohfu, K. Mamada, T. Nishioka, Eur. Pat. 170350 (1986), Sumitomo; Y. Funaki, Y. Yoneyoshi, Y. Ishiguri, K. Izami, Eur. Pat. 175278 (1986), Sumitomo.

Synthesis, Structure, and Bonding of the Cation $[\{(C_6H_5)_3PAu\}_5C]^{\oplus}$ **

By *Franz Scherbaum, Andreas Grohmann, Gerhard Müller,* and *Hubert Schmidbaur**

The diverse observations of unexpectedly strong metal–metal interactions in polynuclear gold(I) compounds, which lead to molecular conformations with close Au···Au contacts on the one hand[1–3] and discrete Au–Au bonds on the other,[4–6] have recently focused attention especially on polyaurated organogold compounds. The aggregation of gold atoms at a single carbon atom in these compounds results in particularly striking examples of the phenomenon of "secondary" Au···Au bonding, which is only partly understood. This is above all true for the recently reported dication $[\{(C_6H_5)_3PAu\}_6C]^{2\oplus}$, in which the central C atom is surrounded octahedrally by six gold atoms.[7] Owing to their high formation tendency and stability, the salts of this dication are surprisingly easy to prepare in high yields. A polyauriomethane compound with a coordination number of 5 at the C atom is exemplified by a (triauriomethyl)oxazoline complex with a complicated structure:[8] The first coordination sphere, which is tetragonal-pyramidal, contains an organic group in addition to four gold atoms. Supported by structure analyses, plausible descriptions of the bonding in both electron-deficient species were given on the basis of simple MO diagrams. In continuation of these studies, we have now synthesized and structurally characterized a second homoleptic cation, $[\{(C_6H_5)_3PAu\}_5C]^{\oplus}$, in which the central C atom is surrounded by five gold atoms.

The starting material for this new cation is bis(dimethoxyboryl)methane **1**,[9] which reacted in the expected way[7,8] with triphenylphosphanegold(I) chloride in the presence of cesium fluoride in hexamethylphosphoric triamide. Whereas the stoichiometry in earlier examples was more or less straightforward,[7] it is largely ambiguous here owing to the formation of several side products. Therefore, Equation (a) does not completely balance.

$$\underset{\mathbf{1}}{CH_2[B(OCH_3)_2]_2} \xrightarrow[\text{HMPA, 24 h, 20 °C}]{[(C_6H_5)_3PAuCl]/CsF} \underset{\mathbf{2}}{[\{(C_6H_5)_3PAu\}_5C]^{\oplus}BF_4^{\ominus}} \quad (a)$$

[*] Prof. Dr. H. Schmidbaur, Dipl.-Chem. F. Scherbaum, Dipl.-Chem. A. Grohmann[+], Dr. G. Müller[+]
Anorganisch-chemisches Institut der Technischen Universität München
Lichtenbergstrasse 4, D-8046 Garching (FRG)

[**] This work was supported by the Deutsche Forschungsgemeinschaft (Leibniz-Programm), the Fonds der Chemischen Industrie, and Degussa AG. We thank *J. Riede* for preparing the crystallographic data set.

[+] X-ray structure analysis

The yield of **2** (84%!), however, is very satisfactory. The dication $[\{(C_6H_5)_3PAu\}_6C]^{2\oplus}$ is also present in small amounts in the reaction mixture. Only for very long reaction times does it eventually become the main product.

Compound **2** precipitates as yellow, rhombic crystals (with three molecules of dichloromethane per formula unit) from CH_2Cl_2/benzene or CH_2Cl_2/diethyl ether. The compound is readily soluble in halogenated hydrocarbons, slightly soluble in benzene, and insoluble in both diethyl ether and petroleum ether. The substance turns brown above 202 °C and melts at 243–245 °C. Between − 45 and + 45 °C, the solutions of **2** in CD_2Cl_2 show only one sharp $^{31}P\{^1H\}$ NMR signal, the chemical shift of which ($\delta = 32.1$) is distinct from that of the $[(LAu)_6C]^{2\oplus}$ ion (L = Ph_3P: $\delta = 27.7$). The ^1H NMR spectrum of **2** only shows a multiplet at $\delta = 7.0$–7.6, but the $^{13}C\{^1H\}$ NMR spectrum is so well resolved that particularly the resonances of C_{ipso} ($\delta = 132.4$, $^1J = 50.4$ Hz) and C_{ortho} ($\delta = 134.4$, $N = 14.7$) reveal a higher-order splitting, which indicates a $^4J(PP')$ long-range coupling. Similar observations were made earlier for $[(LAu)_6C]^{2\oplus}$, where an AXX'_4X'' spin system was found. As in the previous cases (above), the NMR signal of the central C atom of **2** could not be localized. The anion $BF_4^{\ominus}$ is identified by its known resonances. All NMR spectra indicate diamagnetism in the samples.

The X-ray structure analysis[10] confirmed that the composition corresponds to the cations $[\{(C_6H_5)_3PAu\}_5C]^{\oplus}$ and the anions $BF_4^{\ominus}$; in addition, it showed the presence of three CH_2Cl_2 solvate molecules per formula unit for the rhombic crystals (space group $R\bar{3}$) grown from CH_2Cl_2/diethyl ether. The cation has crystallographic C_3 symmetry. The five gold atoms occupy the corners of a slightly distorted, carbon-centered trigonal bipyramid (Fig. 1). This framework is characterized by close axial–equatorial contacts ($Au_{ax}\cdots Au_{eq}$) of 2.987(1) and 2.903(1) Å and longer $Au_{eq}\cdots Au_{eq}$ distances of 3.600(1) Å. The distances Au-C1 (2.079(5), 2.080(5), and 2.093(5) Å) hardly differ. Each gold atom is bonded to a $(C_6H_5)_3P$ ligand. The angles C1-Au-P are 173.0(3)° for Au_{eq} and 180° for Au_{ax} for the given symmetry.

A simple MO diagram can also be used to describe the bonding in the cation of **2** (Fig. 2). Assuming the idealized point group D_{3h}, the five C1-directed gold orbitals (sp hybrid orbitals) and the C1 atomic orbitals give rise to four bonding MOs according to symmetry criteria; these bonding MOs can be exactly filled by the eight valence electrons available, thereby giving a diamagnetic ground state. The LUMO is a nonbonding orbital; its relatively small separation in energy from the HOMO presumably causes the light absorption in the visible region. The scheme in Figure 2 ignores the energy contributions expected for Au···Au interactions, which are probably responsible for the stability of the species $[(LAu)_5C]^{\oplus}$ and for the spontaneous addition of a fifth $LAu^{\oplus}$ fragment to the tetraauriomethane unit $(LAu)_4C$ ("aurophilicity").[11] The importance of relativistic effects has already been discussed elsewhere.[12] For systems whose binding can be described according to Figure 2, a reduction in energy is expected when the symmetry is lowered from D_{3h} to C_{3v}. It remains an open question whether the slight distortion found in the cation of **2** can be interpreted in these terms or whether simple ligand–ligand repulsion or packing effects determine the symmetry lowering.

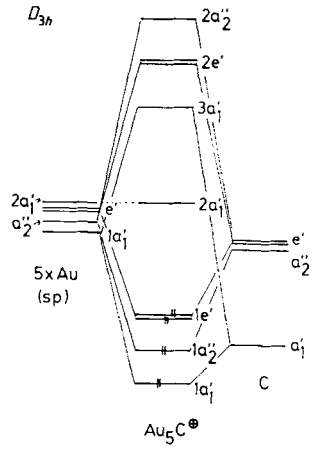


Fig. 2. MO diagram for describing the bonding in the cation $[\{(C_6H_5)_3PAu\}_5C]^{\oplus}$. Assuming the idealized point group D_{3h}, the orbitals of the central C atom and the five σ orbitals (sp hybrid orbitals) of the Au atoms are ordered according to symmetry.

Ab initio calculations, assuming a trigonal-bipyramidal structure, have predicted a "global" stability for $Li_5C^{\oplus}$; in fact, this species has been observed by mass spectrometry.[13] For $H_5C^{\oplus}$, on the other hand, the calculations indicate that a low-symmetry structure is favored (point group C_s). It should be noted that the cations $[(LAu)_5C]^{\oplus}$, $Li_5C^{\oplus}$, and $H_5C^{\oplus}$ do not belong to the class of compounds with "hypervalent" atoms,[14] but rather to the electron-deficient systems, since the Au–C bonds of **2** have a bond order of $4/5 = 0.8$ according to the MO scheme. Therefore, the Au···Au interactions should indeed strongly determine the stability of such species.

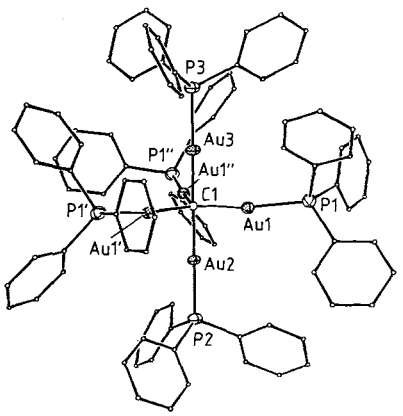


Fig. 1. Molecular structure of the cation of **2** with numbered atoms. Selected distances [Å] and angles [°]: Au1-Au2 2.987(1), Au1-Au3 2.903(1), Au1-Au1' 3.600(1), C1-Au1 2.079(5), C1-Au2 2.080(5), C1-Au3 2.093(5), Au1-P1 2.290(2), Au2-P2 2.264(3), Au3-P3 2.261(3); Au1-C1-Au2 91.8(3), Au1-C1-Au3 88.2(3), Au1-C1-Au1' 119.9(1); P1-Au1-C1 173.0(3).

Experimental Procedure

A solution of **1** (0.3 g, 1.88 mmol) in 10 mL of HMPA was slowly added dropwise to a stirred suspension of CsF (7.4 g, 48.7 mmol) in a solution of $[Ph_3PAuCl]$ (1.87 g, 3.78 mmol) in 40 mL of HMPA at room temperature. After stirring for 24 h at 20 °C, the reaction mixture was filtered and the filter cake was washed with 5 mL of CH_2Cl_2. The combined filtrates were then diluted with 20 mL of benzene. Addition of pentane resulted in formation of a yellow precipitate which was reprecipitated twice from CH_2Cl_2/benzene and three times from CH_2Cl_2/diethyl ether. Yield 1.52 g (84% based on $[Ph_3AuCl]$), m.p. 243–245 °C; correct elemental analysis.

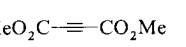
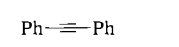
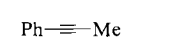
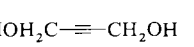
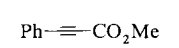
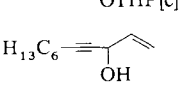
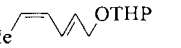
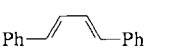
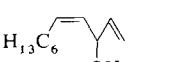
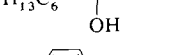
Received: December 19, 1988 [Z 3091 IE]
German version: *Angew. Chem. 101* (1989) 464

[1] H. Schmidbaur in: *Gmelin Handbuch der Anorganischen Chemie, Organogold Compounds*, Springer, Berlin 1980; P. G. Jones, *Gold Bull. 19* (1986) 46; R. J. Puddephatt: *The Chemistry of Gold*, Elsevier, Amsterdam 1979.

[2] H. Schmidbaur, W. Graf, G. Müller, *Angew. Chem. 100* (1988) 439; *Angew. Chem. Int. Ed. Engl. 27* (1988) 417; *Helv. Chim. Acta 69* (1986)

1748; H. Schmidbaur, A. Schier, G. Reber, G. Müller, *Inorg. Chim. Acta 147* (1988) 143.
[3] H. Schmidbaur, C. Hartmann, G. Reber, G. Müller, *Angew. Chem. 99* (1987) 1189; *Angew. Chem. Int. Ed. Engl. 26* (1987) 1146, and references cited therein.
[4] H. Schmidbaur, R. Franke, *Inorg. Chim. Acta 13* (1975) 84; H. Schmidbaur, J. R. Mandl, A. Frank, G. Huttner, *Chem. Ber. 109* (1976) 466.
[5] H. Schmidbaur, A. Wohlleben, F. E. Wagner, D. F. van de Vondel, G. P. van der Kelen, *Chem. Ber. 110* (1977) 2758.
[6] H. Schmidbaur, C. Hartmann, J. Riede, B. Huber, G. Müller, *Organometallics 5* (1986) 1652.
[7] F. Scherbaum, A. Grohmann, B. Huber, C. Krüger, H. Schmidbaur, *Angew. Chem. 100* (1988) 1602; *Angew. Chem. Int. Ed. Engl. 27* (1988) 1544.
[8] F. Scherbaum, B. Huber, G. Müller, H. Schmidbaur, *Angew. Chem. 100* (1988) 1600; *Angew. Chem. Int. Ed. Engl. 27* (1988) 1542.
[9] D. S. Matteson, R. B. Castle, *J. Am. Chem. Soc. 92* (1970) 231, and earlier work.
[10] Crystal structure data: $C_{91}H_{75}Au_5PF_4P_5 \cdot 3\,CH_2Cl_2$, $M_r = 2649.92$, rhombohedral, space group $R\bar{3}$ (Nr. 148), $a = b = 18.469(2)$, $c = 46.090(4)$ Å, $\alpha = \beta = 90$, $\gamma = 120°$ (in hexagonal placement), $V = 13615.2$ Å^3, $Z = 6$, $\rho_{calcd} = 1.939$ g cm^{-3}, $\mu(Mo_{K\alpha}) = 83.5$ cm^{-1}, $F(000) = 7620$, $T = -50$ °C. 4719 unique reflections to $(\sin\theta/\lambda)_{max} = 0.572$ Å^{-1}, 3997 with $F_o \geq 4.0\,\sigma(F_o)$ "observed". Empirical absorption correction (rel. transmission: 0.55–1.00), $R(R_w) = 0.035$ (0.031), $w = 1/\sigma^2(F_o)$ (346 refined parameters, anisotropic, H constant). The residual electron density showed no special features ($\Delta\rho_{fin} = +1.05/-0.92\,e$Å^{-3}, maxima at CH_2Cl_2). Further details of the crystal structure investigation may be obtained from the Fachinformationszentrum Energie, Physik, Mathematik GmbH, D-7514 Eggenstein-Leopoldshafen 2 (FRG), on quoting the depository number CSD-53707, the names of the authors, and the journal citation.
[11] Cf. [11]. Aurophilicity refers to the tendency of $LAu^{\oplus}$ to aggregate at polynuclear gold(I) compounds. It is fundamentally different from the aggregation of zerovalent or low-valent gold atoms at gold clusters with average oxidation states less than +1.
[12] P. Pyykkö, *Chem. Rev. 88* (1988) 563; R. Arriata-Perez, G. L. Malli, *Chem. Phys. Lett. 125* (1986) 143; cf. also [2, 3, 7, 8].
[13] E. D. Jammis, J. Chandrasekhar, E.-U. Würthwein, P. von R. Schleyer, J. W. Chinn, Jr., F. J. Landro, R. J. Lagow, B. Luke, J. A. Pople, *J. Am. Chem. Soc. 104* (1982) 4275.
[14] "Hypervalent" molecules (*J. I. Musher*) usually have a central atom with 2-center 2-electron bonds.

Table 1. Stereoselective hydrogenation of alkynes, alkenynes, and alkadienes.

Starting material	Product	Yield [%] [a]
Alkynes		
$MeO_2C{-}{\equiv}{-}CO_2Me$		98
Ph–≡–Ph		98 (99)[b]
Ph–≡–Me		98 (99)[b]
$HOH_2C{-}{\equiv}{-}CH_2OH$		98
Ph–≡–CO_2Me		97
Alkenes		
		95
		96
Alkadienes		
		96
		96
		95
		97
		97

[a] Yields at 100% conversion. [b] Yields determined by gas chromatography. [c] THP = tetrahydropyranyl, R = Me or CH_2OTHP.

A Highly Selective Montmorillonite Catalyst for Hydrogenation of Alkynes, Alkenynes, and Alkadienes**

By *Boyapati Manoranjan Choudary,** *Gangavaram Vasantha Madhava Sharma,* and *Patibandla Bharathi*

Transition-metal complexes immobilized on a montmorillonite support, a class of smectite clay, are known to induce enhanced selectivity towards terminal alkynes and alkenes in hydrogenation reactions.[1, 2] Recently, we reported the synthesis and characterization of a montmorillonite-supported bipyridinepalladium(II) acetate complex[3] which was found to hydrogenate alkynes and alkenes more effectively than analogous polymer-anchored bipyridinepalladium(II) complexes.[4]

We report here that the montmorillonite-supported complex (see Experimental Procedure) catalyzes the *cis*-selective hydrogenation of the C–C triple bond in alkynes and alkenynes and the regioselective hydrogenation of alkadienes to alkenes.

Hydrogenation of triple bonds, irrespective of their position, always precedes that of double bonds. The high *cis*-selectivity in the hydrogenation of triple bonds in variously substituted alkynes and in conjugated and unconjugated alkenynes (Table 1) demonstrates the versatility of this catalytic system.

By contrast, the effectiveness of the widely used Lindlar catalyst and *Osborn*'s cationic rhodium complex catalyst strongly depends on the compound being hydrogenated. Lindlar catalyst and the recently reported Pd/W system rarely exceed 92% *cis*-selectivity in the semihydrogenation of triple bonds in simple alkynes.[5] A striking failure of the Lindlar catalyst is observed in the semihydrogenation of ethyl phenylpropiolate, which primarily gave totally hydrogenated product.[6] Similarly, a rhodium cationic complex afforded poor selectivity in the semihydrogenation of 1,4-butynediol, although the *cis*-selectivity exhibited by the complex is as high as 99% in most cases.[6] Further, the recovery of the complex from the reaction medium is difficult.

The most impressive and unusual finding in the present study is the totally regioselective 1,2 addition in the hydrogenation of 1,4-substituted, 1,3-butadienes by the catalytic system described here. The selectivity includes the hydrogenation of the less hindered double bond in unsymmetrical dienes and of the *trans* in preference to the *cis* double bond in symmetrical dienes. Selective 1,2 additions in the hydrogenation of butadienes can be ascribed to η^2 coordination of the diene at the palladium center. This selective η^2 coordination may be due to the restricted space available in montmorillonite for η^4 coordination.

The bipyridinepalladium complex is a near-inactive homogeneous catalyst, and the polymer-bound complex[4] is known for its poor *cis* selectivity and regioselectivity in the hydrogenation of diphenylacetylene and sorbic acid, respectively. The selectivity of the montmorillonite-supported catalyst may be due to the preferred orientation of the substrate,

[*] Dr. B. M. Choudary, Dr. G. V. M. Sharma, P. Bharathi
Regional Research Laboratory
Hyderabad 500007 (India)

governed by the least possible repulsion with the oxygens of the silicate layers of the support, and to the spatial requirements of the substrate–Pd^{II} adduct.

The stereoselectivity displayed by the montmorillonite–Pd^{II} catalyst offers a useful tool for organic synthesis, especially of biologically active compounds such as carbohydrates, leukotrienes, prostaglandins, and pheromones.

Experimental Procedure

All operations were carried out under inert atmosphere unless specified otherwise.

Preparation of the catalyst: H-montmorillonite, prepared from natural montmorillonite K 10 (Fluka, surface area 232 $m^2 g^{-1}$; surface acidity, 0.85 mmol NH_3 adsorbed per gram of support; mesh size < 200) by treatment with saturated sodium chloride solution followed by 0.1 N HCl, was allowed to react with excess $SOCl_2$ in dry benzene under reflux for 24 h to give chloromontmorillonite. The chloromontmorillonite (5 g) was suspended in dry THF and cooled to $-80\,^{\circ}C$ and excess *n*-butyllithium (6.25 mL, 10 mmol, 1.6 M in hexane) was added to the stirred suspension. The solution was stirred at $0\,^{\circ}C$ for 4 h and then allowed to warm to room temperature. After the solution was stirred for 1 h at room temperature, bipyridine (3 g, 19 mmol) was added as a solid and the solution was brought to reflux for 4 h. The reaction mixture turned purple during refluxing. It was allowed to cool to room temperature and air was bubbled through the solution until the entire solution had become yellow. The resulting montmorillonite bipyridine was thoroughly washed with THF, ethyl acetate, and benzene and was subjected to Soxhlet extraction for 24 h with THF to remove any adhering bipyridine. Reaction with $Pd(OAc)_2$ (0.11 g, 0.5 mmol) in benzene under stirring for 6 h gave the catalyst, which was thoroughly washed with benzene and THF (nitrogen content, 0.4 mmol g^{-1}; Pd, 0.2 mmol g^{-1}; surface area, 10.7 $m^2 g^{-1}$; surface acidity, 0.445 mmol NH_3 adsorbed per gram of catalyst; mesh size < 200).

Hydrogenation: The hydrogenation reactions were conducted under very mild conditions, at room temperature and atmospheric pressure in 100-mL flasks. The catalyst (0.048 mmol) was pretreated in THF (6 mL) with hydrogen in a classical hydrogenation apparatus; then the substrate (4.8 mmol) was introduced and hydrogenation was continued until the theoretical volume of hydrogen had been absorbed. The catalyst was removed by simple filtration and the reaction mixture was purified by column chromatography. All the products were characterized by spectral data.

Received: October 19, 1988 [Z 3015 IE]
German version: *Angew. Chem. 101* (1989) 506

[1] B. M. Choudary, K. Ravi Kumar, Zafar Jamil, G. Thyagarajan, *J. Chem. Soc. Chem. Commun. 1985*, 931.
[2] T. J. Pinnavia, *Science (Washington) 220* (1983) 365.
[3] B. M. Choudary, P. Bharathi, *J. Chem. Soc. Chem. Commun. 1987*, 1505.
[4] R. J. Card, C. E. Liesner, D. C. Neckers, *J. Org. Chem. 44* (1979) 1095; R. J. Card, D. C. Neckers, *Inorg. Chem. 17* (1978) 2345.
[5] J. G. Ulan, W. F. Maier, *J. Org. Chem. 52* (1987) 3132.
[6] R. R. Schrock, J. A. Osborn, *J. Am. Chem. Soc. 98* (1976) 2143.

A Structure for the H-Bonded Complex of Nylon-66 with Perfluoroglutaric Acid

By *Michal Harel, Meir Lahav,* Leslie Leiserowitz,* Jan van Mil*, and *E. Wasserman**

Crystalline complexes of biopolymers with small molecules are being reported with increasing frequency.[1] Yet reports of such combinations with man-made polymers have been rare.[2] Among the few examples are the adducts of nylon-66, nylon-6, and Kevlar with perfluoroglutaric, -adipic, and -succinic acid.[3] These complexes are also unusual in that hydrogen bonds involving the acid functionalities cause hydrocarbon and fluorocarbon components to mix on the molecular level despite the phase separation often found with such combinations. However, only speculations have been available as to their structures. Here we summarize a multifaceted approach which has yielded an unusual arrangement for one such complex, the crystalline phase of nylon-66 with perfluoroglutaric acid **1**. The techniques employed were X-ray powder diffraction, crystal density measurements, molecular packing considerations, and solid-state ^{13}C NMR spectroscopy.

$HO_2C(CF_2)_3CO_2H$ **1**

A crystalline complex was obtained by stirring a chloroform solution of **1** (0.1 M) with solid nylon-66 at room temperature. Elemental analysis indicated the presence of two molecules of **1** per C_{12} repeat unit of nylon-66. Decomposition of the complex by stirring in water and titrating the dissolved acid yielded the same polyamide/acid ratio.

The solid-state NMR spectrum of the complex had a sharp singlet at $\delta \approx 178$ for the polyamide carbonyl and a broad multiplet at $\delta \approx 162$ for the acid carbonyl. This broadening suggested either disorder or nonequivalent acid units.[4] The latter alternative is consistent with the stoichiometry of two diacids per C_{12} repeat. Only one molecule of **1** per nylon C_{12} is required for saturation of the hydrogen-bonding capabilities of an amide group.

The analysis of the crystal structure was based on the peaks in an X-ray powder scan using $Co_{K\alpha}$ radiation. A triclinic cell was selected and refined by *Visser*'s automated method.[5] The fit between observed and calculated $d(hkl)$ spacings is given in Table 1. The cell constants are: $a = 8.54$, $b = 17.75$, $c = 4.73$ Å, $\alpha = 92.2$, $\beta = 98.7$, $\gamma = 93.7\,^{\circ}$, $V = 707.4$ Å^3; $\rho_{calcd} = 1.67\ g\,cm^{-3}$ for $Z = 2$ with molecular formula (nylon, **1**) $C_6H_{11}NO$, $C_5H_2O_4F_6$, $\rho_{obs.} = 1.59\ g\,cm^{-3}$.

The packing of the nylon chains is essentially determined from the cell constants. The *a,b* layer of the nylon is depicted in Figure 1a. The 17.7-Å axis closely matches the axial length of 17.2 Å in uncomplexed nylon-66,[6] an all-*trans* extended structure. The conformation of nylon in the adduct approximates that of the neat polymer. The length of the chain is increased from 17.2 to 17.7 Å by holding the C–C bond length at 1.54 Å and increasing the C–C–C angle to 114.5°. The nylon molecules are thus parallel to the *b* axis and stacked along *c* forming *b,c* layers. With these extended polymer chains the orientation of the diacid is effectively con-

Table 1. Experimental and calculated $d(hkl)$ spacings (in Å) determined from the refined unit cell parameters.

h	*k*	*l*	$d_{exp.}$	d_{calcd}	*h*	*k*	*l*	$d_{exp.}$	d_{calcd}
1	0	0	8.423	8.422	0	4	−1	3.292	3.294
−1	2	0	6.333	6.326	−1	4	1	3.101	3.101
			5.304		−3	1	0	2.803	2.803
0	0	1	4.670	4.676	1	4	1		2.804
1	3	0		4.679	3	0	−1	2.589	2.589
0	4	0	4.423	4.423	3	1	−1	2.550	2.548
0	2	−1	4.227	4.219	0	6	−1		2.550
2	1	0	4.032	4.033	0	1	−2	2.332	2.333
−1	4	0		4.034	3	0	1	2.258	2.258
−1	1	−1	3.809	3.814	1	1	2	2.138	2.136
1	4	0		3.807	−1	2	−2		2.137
2	0	−1	3.403	3.401	0	3	2		2.138

[*] Dr. E. Wasserman, Dr. J. van Mil [+]
E.I. du Pont de Nemours and Company
Central Research and Development Department, Experimental Station
Wilmington, DE 19898 (USA)
[**] Dr. M. Harel, Prof. M. Lahav, Prof. L. Leiserowitz
Department of Structural Chemistry
Rehovot 76100 (Israel)
[+] Present addresses:
AT&T Laboratories
POB 900, Princeton, NJ 08540 (USA)

strained to parallel that of the polyamide. Indeed, the *a* axis of 8.5 Å is compatible with adjacent nylon layers interleaved by *b,c* layers of **1** (Fig. 1a). The ratio of nylon amide to acid carboxyl groups is 1:2. We have assumed that the molecules are arranged so that the maximum number of O–H and N–H proton donors and oxygen proton acceptors participate in hydrogen bonds. The conformation and orientation of the molecules of **1** were adjusted so that the greatest stabilization by two- or three-center hydrogen bonds was realized (Fig. 1).

The pseudo space group symmetry of the *a,b* layer structure of the nylon component is monoclinic $P112/m$; i.e., the layer contains a twofold axis perpendicular to the *a,b* plane and a mirror plane within the layer. The pseudo twofold symmetry of the *a,b* nylon layer suggests that the two "crystallographically independent" molecules of **1** are centered on the pseudo twofold axes at $x,y \approx (1/2, 0)$ and $(1/2, 1/2)$. The diacid[7] centered on (1/2, 0) **A** (Fig. 1), can span the nylon amides separated by 7.6 Å, since the intramolecular distance between the carboxyl groups is ca 7.2 Å for a coplanar extended carbon skeleton. The two carboxyls of **A** each adopt an antiplanar conformation to form O–H · · · O(amide) bonds and bridge the nylon chains separated by the 8.5-Å *a* axis. This antiplanar O=C–O–H conformation, albeit rare in carboxylic acids,[9] has been found in a derivative of proline[10] and in 1,4-cubanedicarboxylic acid.[11] To form the O–H · · · O(amide) bonds, the plane of each carboxyl becomes perpendicular to that of the glutaric carbon chain. The molecule **A** forms hydrogen bonds along the *b* axis with the carboxyl groups of the two straddling **B** molecules centered on the pseudo twofold axes at $x,y \approx (1/2, 1/2)$ and $(1/2, -1/2)$. The carboxyls of **B** adopt the more frequently observed synplanar O=C–O–H conformations to form the O–H · · · O(acid) hydrogen bonds. The ensembles of acid molecules **A** and **B** may be related either by pseudo translation or by a pseudo glide plane along *b*. The latter would appear to be preferred, as shown in Figure 1b, to allow the carboxyl groups to form linear O–H · · · O bonds and coplanar O–H · · · O=C groups. The different environments of acids **A** and **B** are consistent with the broad ^{13}C NMR signal at $\delta = 162$.

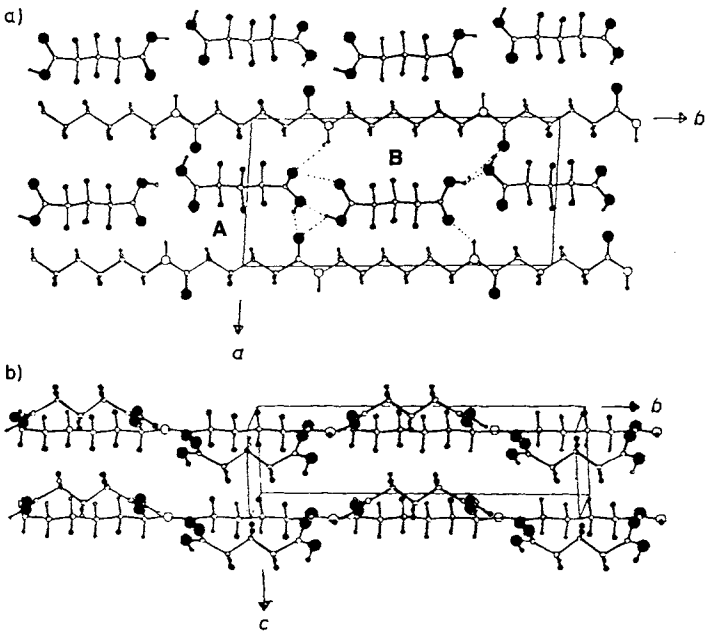


Fig. 1. Packing arrangement of nylon-66/1 viewed along the *c* axis (a) and the *a* axis (b). ● = H,F; ○ = C; ● = O; ○ = N.

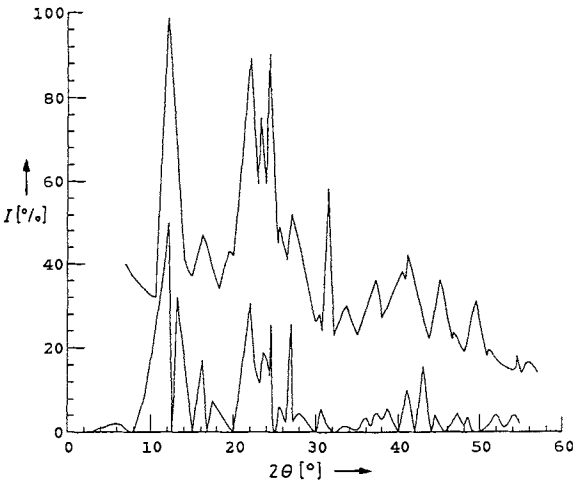


Fig. 2. Experimental (upper curve) and calculated (lower curve) X-ray diffraction powder intensity patterns as a function of Bragg angle 2θ (for $Co_{K\alpha}$ radiation) of nylon-66/1.

The X-ray powder pattern, calculated from the above coordinates, is in good agreement with experiment below $2\theta \approx 25°$ (Fig. 2), indicating the validity of the large-scale features of the model. The deviations at higher Bragg angles (as well as the lower observed density $\rho_{exp.}$ above) may arise from local disorder and "amorphous" regions.[12]

The network of hydrogen bonds can explain why the formation of an adduct between the diacid and nylon-66 is sensitive to the length of the diacid. Shorter and longer acids will not match the spacing between the hydrogen-bond-forming amides of the polymer; neither perfluorosuccinic nor perfluoroadipic acid forms an adduct with nylon-66.[3, 13] The conformation and orientation of **1** also leads to efficient packing of the fluorocarbon chains along the 4.7-Å *c* axis. An analogous array would be more open with the nonfluorinated glutaric acid, which does not form an adduct with nylon-66.[3, 14]

The reasonable F · · · F contacts between molecules of **1** separated by the 4.7-Å axis is achieved by stacking CF_2 arrays. A similar arrangement is found in the high-pressure form of polytetrafluoroethylene, whose chains, with a planar carbon backbone, are stacked along a 5-Å axis.[15] In the nylon/**1** complex the hydrocarbon and fluorocarbon groups can each pack efficiently along the 4.7-Å axis because the planes of their carbon backbones are almost perpendicular. The proximity of the fluorines of the diacid to hydrogens of the nylon is noteworthy, suggesting some compatibility of these often disparate components. The attraction of negative fluorine to slightly positive hydrogens may be a contributing factor.

Received: June 22, 1988;
revised: December 23, 1988 [Z 2820 IE]
German version: *Angew. Chem. 101* (1989) 515

[1] a) S. Susaki, S. Tukiyawa, *Polym. J. (Tokyo) 19* (1987) 1081; b) D. Lee, J. Blackwell, *J. Polym. Sci. Polym. Phys. Ed. 19* (1981) 459; c) J. Kraut in P. Boyer (Ed.): *The Enzymes, Vol. III*, Academic Press, New York 1971, pp. 547–560; d) L. N. Johnson, D. C. Philips, *Nature 206* (1965) 761.

[2] a) M. M. Iuvleva, S. P. Popkov, *Polym. Sci. USSR (Engl. Transl.) 24* (1982) 236; b) K. H. Gardner, R. R. Matheson, P. Avakian, Y. T. Chiu, T. D. Gierke, *ACS Symp. Ser. 260* (1984) 91; c) Y. Chatani, S. Okamura, *Polymer 28* (1982) 1815.

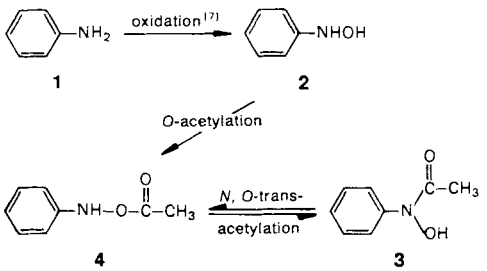
[3] a) S. M. Aharoni, E. Wasserman, US Pat. 4 362 851 (1982), Allied Corp.; b) *Macromolecules 15* (1982) 20.

[4] In the molecular complex of nylon-6 with **1** the carbonyl of perfluoroglutaric acid appears as a sharp singlet in the ^{13}C NMR spectrum.
[5] J. W. Visser, *J. Appl. Crystallogr. 2* (1969) 89.
[6] C. W. Bunn, E. V. Garner, *Proc. R. Soc. London A189* (1947) 39.
[7] Bond lengths and bond angles for perfluoroglutaric acid were taken from the native glutaric acid structure [8]. Fluorine atoms were added with C–F bond lengths of 1.3 Å.
[8] J. D. Morrison, J. M. Robertson, *J. Chem. Soc. 1949*, 1001.
[9] L. Leiserowitz, *Acta Crystallogr. Sect. B32* (1976) 775.
[10] M. Fujinaga, M. N. G. James, *Acta Crystallogr. Sect. B36* (1980) 3196.
[11] O. Ermer, J. Lex, 99 (1987) 455; *Angew. Chem. Int. Ed. Engl. 26* (1987) 447.
[12] Rotations of the planes of carbon atoms and *syn–anti* interconversion of a carboxyl may contribute to the deviations. These have appeared in molecular dynamic simulations by Dr. *J. J. Wendoloski*, personal communication.
[13] This is in contrast to the formation of stable complexes between nylon-6 and perfluorosuccinic, -adipic, and -glutaric acids.
[14] Other structural variations might occur if, in order to effect better packing of chains along the 4.7-Å *c* axis, the nylon adopts a helical conformation, as in γ-nylon. Then, the alternate amide groups are interlinked by N-H · · · O (amide) bonds along the *c* axis. Furthermore, the interleaving carboxyl groups, adjacent to such amide groups, could still form O-H · · · O (amide) bonds, although distorted as in the crystal structure of urea.
[15] H. D. Flack, *J. Polym. Sci. Part A-2 10* (1972) 1799.

Formation of *N*-(Deoxyguanosin-8-yl)aniline in the in vitro Reaction of *N*-Acetoxyaniline with Deoxyguanosine and DNA**

By *Michael Famulok* and *Gernot Boche**

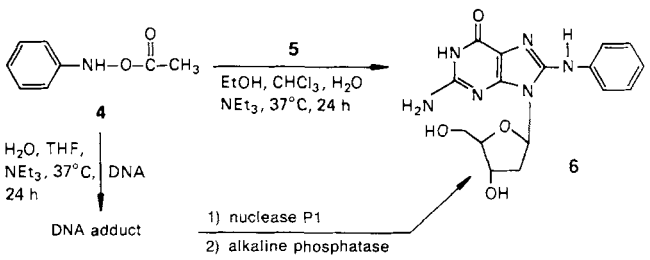
The acute toxicity of aniline **1** is due to the formation of methemoglobin; the metabolite phenylhydroxylamine **2** appears to play the crucial role in this process.[1, 2] In the Ames test,[3a] **1** and **2** exhibit mutagenicity in the *S. typhimurium* TA 98 strain only in the presence of norharmane (H-pyrido-[4,3-*b*]indole = β-carboline) and rat liver homogenate.[3b, c] In animal experiments, no tumor induction in $B6C3F_1$ mice was observed even after feeding them high doses of aniline hydrochloride (6000 and 12000 ppm) for long periods (103 weeks). By contrast, half of that amount of aniline hydrochloride (3000 and 6000 ppm, respectively, 103 weeks) caused Fischer 344 rats to develop sarcomas in the spleen.[4] Of interest, therefore, is the observation that ^{14}C-labeled aniline binds to DNA in the kidneys, colon, and spleen of rats, whereas practically no DNA binding could be detected in mice.[5] Both recent[6a] and earlier investigations[6b] have further shown that *N*-acetoxyarylamines are key metabolites in the carcinogenesis of aromatic amines. They are formed by *O*-acetylation of arylhydroxylamines or by *N,O*-transacetylation of the corresponding hydroxamic acids[6] (Scheme 1).



Scheme 1.

[*] Prof. Dr. G. Boche, Dipl.-Chem. M. Famulok
Fachbereich Chemie der Universität
Hans-Meerwein-Strasse, D-3550 Marburg (FRG)

[**] This work was supported by the Deutsche Forschungsgemeinschaft, the Fonds der Chemischen Industrie, and BASF AG.



Scheme 2.

We recently showed that *O*-acetyl-*N*-(4-biphenylyl)hydroxylamine (*N*-acetoxy-4-aminobiphenyl)[8a] and *O*-acetyl-*N*-(2-naphthyl)hydroxylamine("*N*-acetoxy-2-naphthylamine")[8b] react with deoxyguanosine **5** to give adducts that have been isolated by other authors[9] from the DNA of the bladder epithelium of dogs after they were treated with 4-biphenylamine and 2-naphthylamine, respectively. Here we report that a corresponding metabolite of **1**, compound **4**, which can form in vivo from **2** and **3**,[6] reacts with **5** to give an adduct, *N*-(deoxyguanosin-8-yl)aniline **6**. Further, we were able to show that **6** is also formed in the in vitro reaction of **4** with DNA (Scheme 2).

Adduct **6** is a new compound; previous attempts using "activated aniline derivatives" to prepare an adduct of aniline **1** and **5** by in vitro electrophilic substitution failed.[10] Only adducts of **5** with aromatic amines known to be strong carcinogens have been known so far.[8, 11]

To show that **4** also reacts with DNA, the DNA was cleaved hydrolytically after reaction and the DNA hydrolysate was analyzed by HPLC. Figure 1a shows the HPLC profile of the adduct **6**; Figure 1b shows that of the hydrolysate after reaction of **4** with DNA under the same conditions. A concentration determination[13] revealed that 0.26% of the deoxyguanosine molecules present in the DNA had undergone amination by **4** to form the deoxyguanosine C8 adduct of the DNA.

In conclusion, **4**, a potential metabolite and ultimate carcinogen of aniline **1** covalently binds in vitro to deoxyguanosine **5** and DNA to form the deoxyguanosine C8 adduct **6**.

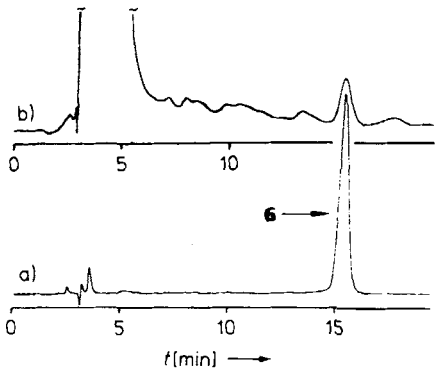


Fig. 1. a) HPLC profile of **6**. b) HPLC profile of the DNA hydrolysate after reaction of **4** with DNA. HPLC conditions: Nucleosil RP 18, 7 μm, 230- × 6-mm column, UV absorption at 260 nm, 35% CH_3OH, flow rate 0.7 mL min^{-1}, retention time of **6**, 15.4 min [12].

Experimental Procedure

Preparation of **4**: Compound **4** was first prepared in solution by *A. M. Lobo* et al. [14]; we have now isolated and completely characterized **4**. AcCN (2.07 g, 30.0 mmol) in 20 mL of Et_2O was added to a solution of **2** (3.27 g, 30.0 mmol) and NEt_3 (3.54 g, 35.0 mmol) in 50 mL of Et_2O (−40 °C, 20 min). The solution was stirred for 3 h at −15 °C, dried with $MgSO_4$ at 0 °C, and filtered. The oil

remaining after removal of the solvent in vacuo was dissolved in 10 mL of CH_2Cl_2, and 120 mL of petroleum ether (40–60 °C) was than added. The solution was concentrated to 70 mL and cooled for 3 h at −30 °C. The crystals that formed were collected and dried at −20 °C. Yield: 2.95 g (65%); m.p. 27–29 °C (not corrected); correct C,H,N elemental analysis (the sample was weighed and maintained at −78 °C until combustion). NMR (400 MHz, $CDCl_3$, 230 K): $\delta(^1H)$ = 2.24 (s, 3H), 7.07 (d, 2H), 7.11 (t, 1H), 7.35 (t, 2H), 8.86 (s, 1H, NH); $\delta(^{13}C)$ = 19.22, 116.36, 123.89, 129.00, 146.08, 170.78; IR (Nujol): $\tilde{\nu}$[cm^{-1}] = 3253, 1758, 1603, 1494, 1378, 1220, 723.

Reaction of **4** with **5** to give **6**: Compounds **4** (605 mg, 4.00 mmol) and **5** (1.07 g, 4.00 mmol) and NEt_3 (455 mg, 4.50 mmol) were stirred in a 7:3:4 mixture (70 mL) of EtOH, $CHCl_3$, and H_2O under N_2 for 24 h at 37 °C. After removal of the solvent, the residue was dissolved in 400 mL of H_2O and the resulting solution was extracted with 150 mL of Et_2O (6 ×) and 100 mL of *n*BuOH (5 ×). After removal of the *n*BuOH, the residue was dissolved in 10 mL of 50% CH_3OH and **6** was purified by HPLC (30% CH_3OH, 230 × 20 mm), LiChrosorb, RP 18, 7 μm, 1400 psi = 98 bar). Yield: 6%. NMR (400 MHz, [D_6]DMSO): $\delta(^1H)$ = 2.02 (m, 1H), 3.76 (m, 2H), 3.93 (m, 1H), 4.43 (m, 1H), 5.36 (s, 1H, OH), 5.98 (s, 1H, OH), 6.33 (q, 1H), 6.45 (s, 2H, NH_2), 6.90 (t, 1H), 7.25 (t, 2H), 7.73 (d, 2H), 8.63 (s, 1H, NH), 10.83 (s, 1H, NH), a sugar H is overlapped by DMSO signals; $\delta(^{13}C)$ (^1J(C, H)[Hz]) = 38.39 (t, 131.28), 61.20 (t, 141.33), 71.14 (d, 150.52), 82.72 (d, 163.03), 87.08 (d, 146.00), 112.14 (s), 117.21 (d, 162.10), 120.44 (d, 160.00), 128.39 (d, 158.10), 140.77 (s), 143.11 (s), 149.39 (s), 153.01 (s), 156.03 (s); IR (KBr): $\tilde{\nu}$[cm^{-1}] = 3343, 3206, 1681, 1600, 1562, 1498, 1355, 1099, 751; UV (CH_3OH): λ_{max}[nm] = 283.0, 204.0; FD-MS: *m/z* 358 ($M^{\oplus}$, 26.1%), 359 ($M^{\oplus}$ + H, 100), 381 ($M^{\oplus}$ + Na, 33.5).

Reaction of **4** with DNA to give **6**: A solution of calf thymus DNA (30 mg), **4** (30 mg, 0.2 mmol), and NEt_3 (17 mg, 0.17 mmol) in 20 mL of H_2O/THF (1/1) was kept for 20 h at 37 °C. After removal of the THF, extraction with 25 mL of Et_2O (3 ×), and addition of 10 mL of H_2O, the H_2O phase was treated with 2 mL of a 3 M NaOAc solution and 50 mL of EtOH. The DNA was precipitated at −20 °C, centrifuged at 10000 rpm for 10 min, and washed twice with 70% EtOH. After addition of 30 mL of H_2O, 1 mL of the solution contained 0.95 mg of DNA (UV determination of concentration). Following the literature procedure [15], 0.95 mg of DNA was hydrolyzed with nuclease P1 and alkaline phosphatase and the enzymes were then precipitated by addition of 800 μL of 3 M NaOAc solution and 20 mL of EtOH at −20 °C and removed by centrifugation. The solvent was removed from the supernatant and the residue was dissolved in 1 mL of 35% CH_3OH and analyzed by HPLC.

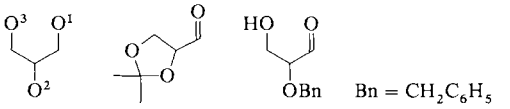
Received: November 28, 1988 [Z 3067 IE]
German version: *Angew. Chem. 101* (1989) 470

[1] M. Kiese: *Ferrihemoglobinemia: A Comprehensive Treatise*. CRC Press, Cleveland, OH, USA 1974, pp. 3ff.
[2] D. Henschler (Ed.): *Gesundheitsschädliche Arbeitsstoffe*, 1st–4th issue, VCH Verlagsgesellschaft, Weinheim 1987, Aniline (Supplement 1983).
[3] a) D. M. Maron, B. N. Ames, *Mutat. Res. 113* (1983) 173; b) M. Nagao, M. Yahagi, Y. Honda, T. Senio, T. Matsushima, T. Sugimura, *Proc. Jpn. Acad. 53* (1977) 34; c) J. Suzuki, N. Takahashi, Y. Kobayashi, R. Miyamae, M. Ohsawa, S. Suzuki, *Mutat. Res. 178* (1987) 187.
[4] *Bioassay of Aniline Hydrochloride for Possible Carcinogenicity*, Publication NCI CG TR 130, Washington, DC, National Cancer Institute, NIH, US PHS, Department of Health and Human Services 1978, pp. 1–53.
[5] D. J. McCarthy, W. R. Waud, R. F. Struck, D. L. Hill, *Cancer Res. 45* (1985) 174.
[6] a) C.-C. Lai, E. C. Miller, J. A. Miller, A. Liem, *Carcoinogenesis (London) 9* (1988) 1295; b) Review: D. W. Hein, *Biochim. Biophys. Acta 948* (1988) 37.
[7] a) J. W. Gorrod, L. A. Damani (Eds.): *Biological Oxidation of Nitrogen in Organic Molecules*, Ellis Horwood, Chichester 1985; b) J. W. Gorrod, D. Manson, *Xenobiotica 16* (1986) 933.
[8] a) M. Famulok, F. Bosold, G. Boche, *Angew. Chem. 101* (1989) 349; *Angew. Chem. Int. Ed. Engl. 28* (1989) 337, and references cited therein; b) *Tetrahedron Lett. 30* (1989) 321, in press, and references cited therein.
[9] a) F.F. Kadlubar, F. A. Beland, D. T. Beranek, K. L. Dooley, R. H. Heflich, F. E. Evans in T. Sugimura, S. Kondo, H. Takebe (Eds.): *Environmental Mutagens and Carcinogens*, A. R. Liss, New York 1982, 385; b) F. A. Beland, D. T. Beranek, K. L. Dooley, R. H. Heflich, F. F. Kadlubar, *EHP Environ. Health Perspect. 49* (1983) 125.
[10] M. D. Jacobson, R. Shapiro, G. R. Underwood, S. Broyde, L. Verna, B. E. Hingerty, *Chem. Res. Toxicol. 1* (1988) 152.
[11] Review: H.-G. Neumann, *J. Cancer Res. Clin. Oncol. 112* (1986) 100.
[12] Variation of the HPLC conditions (30% CH_3OH, flow rate 0.7 mL min^{-1}, [retention time of **6**: 26.3 min]), as well as addition of authentic **6** to the DNA hydrolysate, confirmed the presence of **6** in the DNA hydrolysate.
[13] The concentration of **6** in the DNA hydrolysate was determined from the area below the HPLC profiles.
[14] A. M. Lobo, M. M. Marques, S. Prabhakar, H. S. Rzepa, *J. Org. Chem. 52* (1987) 2925.
[15] C. W. Gehrke, R. A. McCune, M. A. Gama-Sosa, M. Ehrlich, K. C. Kuo, *J. Chromatogr. 301* (1984) 199.

2-*O*-Benzylglyceraldehyde: A Synthetic Building Block Available in Both Enantiomeric Forms and Configurationally Stable Owing to Rapid Oligomerization**

By *Volker Jäger** and *Volkmar Wehner*

Optically active C_3 building blocks of type **1** are of great importance in organic synthesis.[1] Thus far, the key part is taken by 2,3-*O*-isopropylideneglyceraldehyde **2**, whose two enantiomers are readily accessible[1, 2] and which finds highly diverse uses due to the free aldehyde and the protected diol function. However, **2** is not stable as a monomer and undergoes racemization on storage.[3]



1 **2** **3**

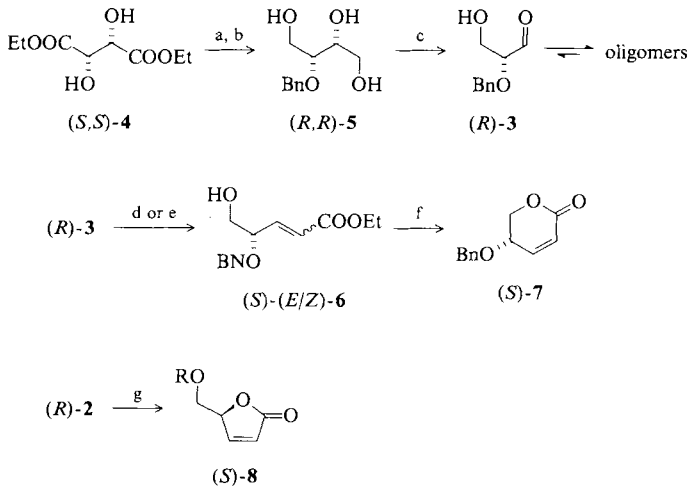
In principle, glyceraldehyde derivatives with one free and one protected hydroxyl group could offer new applications, since O^2/O^3 are more strongly differentiated and regio- and stereoselectivities may be altered by action of the free hydroxyl group in the first or subsequent steps. We report here a new, simple synthesis of both enantiomers of such a compound, namely, **3**, as well as some transformations that confirm this and which, in addition, prove **3** to be configurationally stable at room temperature.

(*R*)-2-*O*-Benzylglyceraldehyde, (*R*)-**3**, was prepared earlier from D-mannitol (four steps, ca. 5% overall yield) or D-glucose (six steps, ca. 50%) and used directly without further analysis.[4] Both enantiomers, (*R*)-**3** and (*S*)-**3**, are now readily obtained, as shown in Scheme 1, from the corresponding tartrates **4** via the known 2-*O*-benzylthreitols **5**[5] (three steps, ca. 70% overall yield). The freshly prepared aldehyde **3**, obtained as a colorless oil upon distillation, initially has a fruitlike odor; upon standing, it turns sirupy, then becomes a waxy, odorless solid. This behavior is reminiscent of the oligomerization and polymerization known for similar hydroxyaldehydes.[6] Indeed, neat **3** evolves into a mixture of at least ten oligo-/stereoisomers. The ^{13}C NMR spectrum of a sample recorded after 17 h showed a small peak at δ = 202.4 (*C*HO), but at least 32 signals in the region δ = 60–100 where three are expected for the monomeric aldehyde **3**.

What about the configurational stability (C-2) of **3**, the crucial factor determining its preparative utility? The rapid oligomerization [to (hemi)acetals] gave fair promise that the racemization observed for *monomeric* relatives such as **2** might be obviated. The optical rotation of freshly distilled (*R*)-**3** in ethanol was found to be + 21.7 (c = 1.23), which decreased rapidly (+ 16.1 after 6 h), but later increased slowly and finally remained constant at + 30.3 (± 0.8) after 19 d!

[*] Prof. Dr. V. Jäger, Dipl.-Chem. V. Wehner
Institut für Organische Chemie der Universität
Am Hubland, D-8700 Würzburg (FRG)

[**] This work was supported by the Fonds der Chemischen Industrie, the Deutsche Forschungsgemeinschaft, and Bayer AG, Wuppertal-Elberfeld. We thank the state of Bavaria for a Graduiertenförderungsstipendium (*V. W.*), Dr. *C. Hubschwerlen* (Hoffmann-La Roche, Basel), Dr. *A. Kleemann*, and Dr. *K. Drauz* (Degussa AG, Hanau) for donation of chemicals, and *H. Sattler* for experimental assistance.



Scheme 1. Preparation and Horner/Wittig products of **3**. The formulas give starting materials and products with respect to (*R*)-**3**; all reactions were carried out in both series of enantiomers. The structures of **6** and **7** were confirmed by spectroscopic data (IR, ^1H, ^{13}C NMR) and correct elemental analyses. a, b) According to *Seebach* et al. [5]: PhCHO, TosOH · H_2O (cat.), C_6H_6, reflux; m.p. 45 °C; then $LiAlH_4$, $AlCl_3$, CH_2Cl_2, − 40 °C to reflux temperature; overall yield ca. 75% **5**. c) $NaIO_4$, H_2O, 20 °C; 90–96% **3**; b.p. ca. 140 °C/0.005 torr (short-path distillation); 5–50-mmol scale. d) $(EtO)_2P(O)CH_2COOEt$, NaH, THF, 0 °C; addition of **3** at − 78 °C, then allowed to warm to room temperature; 76–78% **6** (colorless oil) with $E:Z = > 97:3$, enantiomer ratio > 97:3 according to NMR analysis with 5.8% (+)-Eu(hfc)$_3$ and comparison with (*S*):(*R*) mixtures (86:14 and 33:67); boiling range 150–180 °C (bath temperature, kugelrohr)/0.08 torr; (*S*)-(*E*)-**6**: $[\alpha]_D^{22}$ + 73.8 (*c* = 0.90, $CHCl_3$), (*R*)-(*E*)-**6**: $[\alpha]_D^{22}$ − 74.4 (*c* = 0.90, $CHCl_3$). e) $Ph_3P=CH-COOEt$, MeOH, 0 °C, 94% (*S*)-**6** or (*R*)-**6** with $Z:E = 76:24$ (according to ^1H, ^{13}C NMR) and a small amount of **7** (3–5%), which increases at the expense of (*Z*)-**6** on standing. f) TosOH · H_2O (0.1 equiv.), toluene, 20 °C; MPLC (LiChroprep Si-60, petroleum ether/ethyl acetate 2:1, detection of 254 nm); colorless crystals, m.p. 71–71.5 °C, 53–55% yield; (*S*)-**7**: $[\alpha]_D^{21}$ + 121.6 (*c* = 0.852, $CHCl_3$); (*R*)-**7**: $[\alpha]_D^{21}$ − 120.9 (*c* = 0.852, $CHCl_3$); enantiomeric ratio > 96:4 according to NMR analysis with 8.5 mol% (+)-Eu(hfc)$_3$ and comparison with a 71:29 mixture [9]. g) see [2b].

Similar behavior ("mutarotation") is known for (*R*)- and (*S*)-glyceraldehyde.[6]

Next: Is it possible to preserve this presumed configurational stability (with respect to C-2) of the oligomeric mixture formed from **3** in subsequent reactions, in particular with respect to C–C bond formation? In order to answer this, we converted **3** into the pentenoic esters **6**: analogous Horner and Wittig reactions with **2** had earlier led to popular C_5 building blocks with *E* and *Z* selectivity, respectively.[2b, 7] Starting from (*R*)-**3** and using potassium carbonate as base,[8a] the Horner phosphonate procedure afforded, after 45 h at room temperature, 49% of the "pure" (^1H NMR) *E*-ester **6**. However, on addition of the optically active shift reagent (+)-Eu(hfc)$_3$, this turned out to be a 73:27 mixture of the (*S*)/(*R*) enantiomers. When the sodium phosphonate was prepared prior to use, the reaction occurred appreciably faster;[8b] **6** was formed with an *E*/*Z* ratio of > 97:3 in high enantiomeric purity (see Scheme 1).

The *Z*-selective Wittig reaction with ethoxycarbonylmethylenetriphenylphosphorane in absolute, acid-free methanol (according to the "Kishi footnote"[7]) gave a 94% yield of pentenoic esters **6** as a 24:76 mixture of *E*/*Z* isomers starting from either (*R*)- or (*S*)-**3**. The *Z* compounds readily undergo acid-catalyzed lactonization to give the penten-5-olides **7**, which, according to NMR analysis, are also enantiomerically "pure" (i.e., enantiomeric ratio > 96:4; see Scheme 1).[9] Fully analogous results were obtained for samples of (*R*)- and (*S*)-**3** that had been stored for eight weeks at room temperature and had turned into waxlike solids.

The cyclization of (*Z*)-**6** to the six-membered lactone **7** demonstrates that the use of benzylglyceraldehyde **3** offers new possibilities that are complementary to those given by the acetonides **2**. The analogous sequence, starting from (*S*)-**2**, had earlier led to the five-membered lactone (*S*)-**8**[2b] (see Scheme 1); recently, this route was employed as part of an efficient synthesis of 3′-azidothymidine (AZT or ZDV).[10]

We expect the benzylglyceraldehydes **3** and the new building blocks **6** and **7** derived therefrom to find manifold uses in organic synthesis.

Received: November 28, 1988 [Z 3069 IE]
German version: *Angew. Chem. 101* (1989) 512

CAS Registry numbers:
(*R*)-**3**, 76227-09-3; (*S*,*S*)-**4**, 13811-71-7; (*R*,*R*)-**5**, 84379-52-2; (*S*)-(*E*)-**6**, 119770-82-0; (*S*)-(*Z*)-**6**, 119770-83-1; (*R*)-(*E*)-**6**, 119770-84-2; (*R*)-(*Z*)-**6**, 119770-88-6; (*S*)-**7**, 119770-85-3; (*R*)-**7**, 119770-86-4; PhCHO, 100-52-7; $(EtO)_2P(O)CH_2COOEt$, 867-13-0; $Ph_3P=CH-COOEt$, 1099-45-2; diethyl 3-benzyloxy-2-hydroxybutanedioate, 119770-87-5.

[1] a) G. J. McGarvey, M. Kimura, T. Oh, J. M. Williams, *J. Carbohydr. Chem. 3* (1984) 125; b) T. D. Inch, *Tetrahedron 40* (1984) 3161; c) J. Jurczak, S. Pikul, T. Bauer, *ibid. 42* (1986) 447; d) J. Mulzer, *Nachr. Chem. Tech. Lab. 32* (1984) 146; e) H.-J. Altenbach, *ibid. 36* (1988) 33; f) S. Takano, *Pure Appl. Chem. 59* (1987) 353.

[2] According to our experience, the best procedures are: a) (*R*)-**2**: R. Dumont, H. Pfander, *Helv. Chim. Acta 66* (1983) 814; b) cf. B. Häfele, V. Jäger, *Liebigs Ann. Chem. 1987*, 85; c) (*S*)-**2**: C. Hubschwerlen, *Synthesis 1986*, 962.

[3] For example, storage as a frozen solution in benzene and redistillation prior to use is recommended (cf. [1c]). The 2,3-*O*-cyclohexylidene derivatives (analogous to **2**) can be preserved in the deep freezer: M. Grauert, *Diplomarbeit*, Universität Göttingen 1984, p. 54; cf. M. Grauert, U. Schöllkopf, *Liebigs Ann. Chem. 1985*, 1817. We thank Prof. *U. Schöllkopf* and Prof. *D. Hoppe* for this suggestion.

[4] C. E. Ballou, H. O. L. Fischer, *J. Am. Chem. Soc. 77* (1955) 3329; D. Charon, L. Szabó, *J. Chem. Soc. Perkin Trans 1, 1980*, 1970; cf. 2-*O*-methyl-D-glyceraldehyde from D-mannitol (4 steps, ca. 5%): N. Bischofberger, H. Waldmann, T. Saito, E. S. Simon, W. Lees, M. D. Bednarski, G. M. Whitesides, *J. Org. Chem. 53* (1988) 3457. For a widely applicable route to 2-*O*-substituted *D*-glyceraldehydes, see T. Schubert, F. Kunisch, P. Welzel, *Tetrahedron 39* (1983) 2211; cf. U. Peters, W. Bankova, P. Welzel, *ibid. 43* (1987) 3803. We thank Prof. *P. Welzel* for useful discussions.

[5] D. Seebach, E. Hungerbühler, *Mod. Synth. Methods 2* (1980) 152; see also references in [1e].

[6] S. Coffey (Ed.): *Rodd's Chemistry of Carbon Compounds, Vol. 1D*, p. 48, 2nd ed. 1965; *Vol. 1E, Suppl.*, 2nd ed. 1983, Elsevier, Amsterdam; E. Baer, H. O. L. Fischer, *J. Am. Chem. Soc. 61* (1939) 761.

[7] N. Minami, S. S. Ko, Y. Kishi, *J. Am. Chem. Soc. 104* (1982) 1109; T. Katsuki, A. W. M. Lee, P. Ma, V. S. Martin, S. Masamune, K. B. Sharpless, D. Tuddenham, E. J. Walker, *J. Org. Chem. 47* (1982) 1373; J. Mulzer, M. Kappert, *Angew. Chem. 95* (1983) 60; *Angew. Chem. Int. Ed. Engl. 22* (1983) 63; *Angew. Chem. Suppl. 1983*, 23; see also references in [1] and [2b].

[8] Adapted from S. Takano, A. Kurotaki, M. Takahashi, K. Ogasawara, *Synthesis 1986*, 403; b) Procedure analogous to J. R. Luly, J. F. Dellaria, J. J. Plattner, J. L. Soderquist, N. Yi, *J. Org. Chem. 52* (1987) 1487.

[9] *Note added in proof* (11 March 1989): According to HPLC on triacetyl cellulose, (*S*)-**7** is obtained with an enantiomeric ratio > 99.8:0.2. We thank Dipl.-Chem. *N. Klaunzer*, Universität Würzburg, for carrying out these analyses; cf. U. Gerlach, T. Haubenreich, S. Hünig, N. Klaunzer, *Liebigs Ann. Chem. 1989*, 103.

[10] C. K. Chu, J. W. Beach, G. V. Ullas, Y. Kosugi, *Tetrahedron Lett. 29* (1988) 5349.

Stabilization of Niobium(0) and Tantalum(0) in Mixed Metal Clusters containing Silver Atoms**

By *Fausto Calderazzo,** *Guido Pampaloni, Ullrich Englert,* and *Joachim Strähle*

Clusters with supporting bridge ligands are rare among Group 5 metals, the only crystallographically established example being $[Cp_3Nb_3(CO)_7]$[1] ($Cp = \eta^5$-C_5H_5). On the other hand, halo-, oxo-, and sulfido-bridged clusters of vanadium, niobium and tantalum in oxidation states higher than I are well documented in the literature.[2] Vanadium(0) compounds are readily accessible,[3] whereas niobium(0) and tantalum(0) complexes mostly have to be prepared by metal vaporization.[4] Among the mixed metal clusters $[\{(PPh_3)Au\}_3V(CO)_5]$ has been prepared and structurally characterized,[5] while a positive oxidation state for niobium has been found[6] in $[\{(PPh_3)Au\}_2Nb(C_5H_4R)_2]^{\oplus}$.

We now wish to report the first structurally characterized carbonyl clusters containing niobium and tantalum in the formal zero oxidation state.

The reactions of **1** (dmpe = 1,2-bis(dimethylphosphino)ethane) with silver salts of poorly coordinating anions, namely $AgNO_2$ and $AgBF_4$, in THF at room temperature afford compounds of analytical composition **2** [Eq. (a)].

$$3\ NEt_4[M(CO)_4(dmpe)] + 3\ AgNO_2 \longrightarrow \underset{\mathbf{1}}{} \quad \underset{\mathbf{2}}{[AgM(CO)_4(dmpe)]_3} + 3\ NEt_4NO_2 \quad (a)$$

a, M = Nb; **b**, M = Ta

The solid state structures of **2** were established by single crystal X-ray diffraction methods.[7] Both compounds are isotypic, as shown by Gandolfi photographs of the single crystals used for subsequent intensity measurements.

The complexes **2** are structurally related to the osmium[12] and iron-platinum[13] raft-like clusters. The ten non-hydrogen atoms in the asymmetric unit are arranged around the intersection of a crystallographic threefold axis with three twofold axes, i.e. the point symmetry of the resulting molecule is D_3, the three silver atoms and the three Group 5 metal atoms lying in the plane containing the twofold axes (Fig. 1).

The arrangement of the metal atoms in almost equilateral triangles corresponds to that of a (111) plane in a close-packed metal structure, the intermetallic angles being all close to 60°. The almost identical Ag–Ag distances of 2.842 Å in **2a** and **2b** are shorter than in silver metal (2.883 Å).[14] In the intermetallic cubic Laves phase $NaAg_2$, which contains a network of corner-connected Ag_4 tetrahedra, the Ag–Ag distances are 2.810 Å.[15] Moreover, a Ag–Ag distance of 2.994(6) Å has been found[16] in the heterometallic cluster $[Pt_2Ag_2Cl_4(C_6F_5)_4]^{2\ominus}$. The distances between Ag and Nb or Ta in **2a** and **2b** are also very similar (2.888 Å) and might be compared with the sum of the metallic radii (2.91 Å[14]).

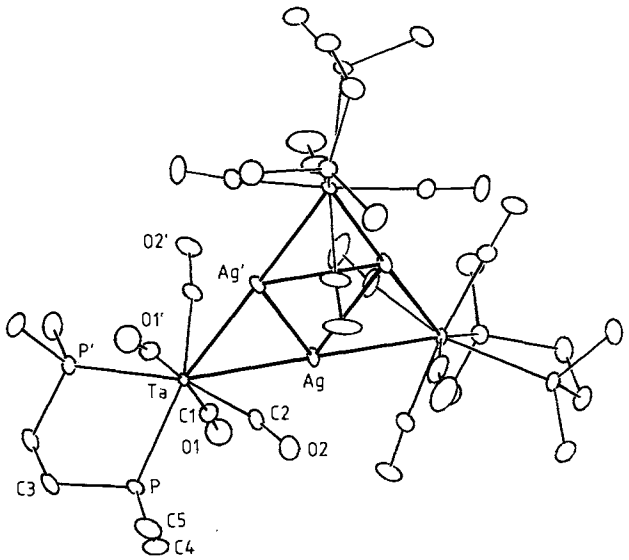


Fig. 1. ORTEP view of **2b** (thermal ellipsoids are drawn at the 10% probability level). Selected interatomic distances [Å] and angles [°]: **2a**; Ag-Nb 2.8879(2), Ag-Ag' 2.8424(5), Nb-C1 2.079(4), Nb-C2 2.103(4), Ag-C1 2.768(4), Ag-C2 2.593(4), Ag-Nb-Ag' 58.96(1), Nb-C1-O1 175.6(3), Nb-C2-O2 169.4(3); **2b**: Ag-Ta 2.8884(2), Ag-Ag' 2.8418(8), Ta-C1 2.049(4), Ta-C2 2.082(5), Ag-C1 2.784(4), Ag-C2 2.614(5), Ag-Ta-Ag' 58.93(2), Ta-C1-O1 177.6(4), Ta-C2-O2 172.1(4).

The coordination polyhedron for the Group 5 metal atom in **2**, for which 84 cluster electrons have been calculated, may be regarded as a distorted square antiprism. Bonding in raft-like clusters has been discussed by *Mingos* and *Evans*[17] and it has been shown that the known examples, containing both axial and equatorial ligands[12] or equatorial ligands only[13] on the metal atom occupying the central position on the edge of the equilateral triangle, contain 90 or 86 electrons, respectively.

The reactivity of these clusters is now under investigation.

Experimental

Only the preparation of **2b** is described in detail, since **2a** can be obtained analogously.

A solution **1b** [18] (0.471 g, 0.82 mmol) in THF (300 ml) was treated at room temperature with $AgNO_2$ [19] (0.257 g, 1.67 mmol) under an argon atmosphere. The reaction mixture was warmed at 45 °C for 30 minutes, cooled to room temperature and filtered. The solvent was partially removed in vacuo at 0 °C until some red-orange solid began to separate. When the volume of the solvent was reduced to ca. 30 ml, the solid was filtered and dried in vacuo at room temperature (0.164 g). The filtered solution was cooled to −30 °C affording a second crop (0.02 g) of **2b** (40% total yield with respect to tantalum) as red-orange crystals [20]. $\chi_M^{corr} = +1.1 \times 10^{-8}$ m^3 mol^{-1} at 20 °C; diamagnetic correction $= -1.1 \times 10^{-8}$ m^3 mol^{-1}.—Compound **2b** was also obtained upon reaction of **1b** with $AgBF_4$ in THF at −60 °C (identification via IR spectrum and element analysis.

Received: November 28, 1988 [Z 3068 IE]
German version: *Angew. Chem. 101* (1989) 469

CAS Registry numbers:
1a, 119998-94-6; **1b**, 119998-96-8; **2a**, 119998-97-9; **2b**, 119998-98-0; Ta, 7440-25-7; Nb, 7440-03-1; 7440-22-4

[*] Prof. F. Calderazzo, Dr. G. Pampaloni, Dr. U. Englert
Dipartimento di Chimica e Chimica Industriale
Sezione di Chimica Inorganica
Via Risorgimento 35, I-56100 Pisa (Italy)
Prof. Dr. J. Strähle
Institut für Anorganische Chemie der Universität
Auf der Morgenstelle 18, D-7400 Tübingen (FRG)

[**] This work was supported by the Consiglio Nazionale delle Ricerche (C.N.R., Roma) and the Commission of the European Communities (C.E.C., Bruxelles, award of a grant to *U. Englert* in the framework of the Science Programme).

[1] W. A. Herrmann, H. Biersack, M. L. Ziegler, K. Weidenhammer, R. Siegel, D. Rehder, *J. Am. Chem. Soc. 103* (1981) 1692. Other cases are possibly represented by $[VCpCo_3(CO)_9]$ [H. J. Haustein, K. E.

Schwarzhans, *Z. Naturforsch. B 33* (1978) 1108] and by [$VCp_4(CO)_4$] [W. A. Herrmann, J. Plank, B. Reiter, *J. Organomet. Chem. 164* (1979) C25].

[2] E. L. Muetterties, *J. Organomet. Chem. 200* (1980) 177; F. Stollmaier, A. Simon, *Inorg. Chem. 24* (1985) 168; C. M. Bolinger, J. Darkwa, G. Gammie, S. D. Gammon, J. W. Lyding, T. B. Rauchfuss, S. R. Wilson, *Organometallics 5* (1986) 2386; F. Bottomley, D. F. Drummond, D. E. Paez, P. S. White, *J. Chem. Soc. Chem. Commun. 1986*, 1752; F. A. Cotton, G. Wilkinson: *Advanced Inorganic Chemistry*, 5th Edition, J. Wiley, New York 1988, p. 802–803.

[3] F. Calderazzo, G. Pampaloni, *J. Organomet. Chem. 303* (1986) 111 and references therein; F. Calderazzo, G. Pampaloni, G. Pelizzi, F. Vitali, *Organometallics 7* (1988) 1083.

[4] F. G. N. Cloke, M. L. H. Gree, *J. Chem. Soc. Dalton Trans. 1981*, 1938; F. G. N. Cloke, P. J. Fyne, V. C. Gibson, M. L. H. Green, M. J. Dedouc, R. M. Perutz, A. Dix, A. Gourdon, K. Prout, *J. Organomet. Chem. 277* (1984) 61.

[5] J. E. Ellis, *J. Am. Chem. Soc. 103* (1981) 6106; the corresponding tantalum derivative has been isolated: G. F. P. Warnock, J. E. Ellis, *ibid. 106* (1984) 5016.

[6] M. Fajardo, M. P. Gomez-Sal, P. Royo, S. Martinez Carrera, S. Garcia Blanco, *J. Organomet. Chem. 312* (1986) C44.

[7] a) Structure determination of **2a**: Enraf Nonius CAD4, graphite monochromator, $Cu_{K\alpha}$ radiation ($\lambda = 1.5418$ Å); red rhombohedrons, $R\bar{3}c$, hexagonal setting, No. 167 [8]; $a = 14.323(1)$, $c = 44.772(4)$ Å, $V = 7954.6$ Å^3, $Z = 6$, $\varrho_{calc} = 1.739$ g cm^{-3}, $\mu(Cu_{K\alpha}) = 162.93$ cm^{-1}, $F(000) = 4068$, 20 °C. 7946 measured and 5091 observed intensities, ω-scan, $\theta_{max} = 69°$, empirical absorption correction (Ψ-scan method [9]; 1211 symmetrically independent reflections [$I > 3.5\,\sigma(I)$] in structure solution [10] (Patterson and Fourier methods) and refinement (full matrix) for 84 parameters; anisotropic refinement for non-hydrogen atoms, hydrogen atoms included in structure factor calculations, correction for secondary extinction [11] applied on F_c, $R = 0.044$, $R_w = 0.057$ [$w = 1/\sigma^2(F_0)$]; b) Structure determination of **2b**: Enraf Nonius CAD4, graphite monochromator, $Mo_{K\alpha}$ radiation ($\lambda = 0.7107$ Å); red rhombohedrons, $R\bar{3}c$, hexagonal setting, No. 167 [8]; $a = 14.274(5)$, $c = 44.55(3)$ Å, $V = 7860.6$ Å^3, $Z = 6$, $\varrho_{calc} = 2.095$ g cm^{-3}, $\mu(Mo_{K\alpha}) = 78.82$ cm^{-1}, $F(000) = 4644$, 20 °C. 6411 measured and 3372 observed intensities, ω-scan, $\theta_{max} = 25°$, empirical absorption correction (Ψ-scan method [9]); 984 symmetrically independent reflections [$I > 3.5\,\sigma(I)$] in structure solution [10] (atom coordinates of **2a** as model) and refinement (full matrix) for 84 parameters; anisotropic refinement for non-hydrogen atoms, hydrogen atoms included in structure factor calculations, correction for secondary extinction [11] applied on F_c, $R = 0.029$, $R_w = 0.037$ [$w = 1/\sigma^2(F_0)$]; c) Further details concerning the structure determinations are available on request from the Fachinformationszentrum Energie, Physik, Mathematik GmbH, D-7514 Eggenstein-Leopoldhafen (FRG), on quoting the depository number CSD-56631, the names of the authors, and the journal citation.

[8] T. Hahn (Ed.): *International Tables for Crystallography, Vol. A*, D. Reidel Publ. Comp., Dordrecht, 1983.

[9] A. C. T. North, D. Phillips, F. S. Mathews, *Acta Crystallogr. 24 A* (1968) 351.

[10] a) B. A. Frenz, *The ENRAF-NONIUS CAD4 SDP: A Real Time System for Concurrent X-Ray Data Collection and Crystal Structure Determination*, in H. Schenck, R. Olthof-Hazekamp, H. von Koningsveld and G. C. Bassi (Eds): *Computing in Crystallography*. Delft University Press 1978; SDP Plus, Version 1.1, 1984 and VAXSDP, Version 2.2, 1985.

[11] W. H. Zachariasen, *Acta Crystallogr. 16* (1963) 1139.

[12] R. J. Goudsmit, J. G. Jeffrey, B. F. G. Johnson, J. Lewis, R. C. S. McQueen, A. J. Sanders, J. C. Liu, *J. Chem. Soc. Chem. Commun. 1986*, 24.

[13] G. Longoni, M. Manassero, M. Sansoni, *J. Am. Chem. Soc. 102* (1980) 7973.

[14] A. F. Wells, *Structural Inorganic Chemistry*, 5th Edition, Clarendon, Oxford 1984.

[15] P. Feschotte, E. L. Spitz, *J. Less-Common Met. 138* (1988) 155.

[16] R. Usón, J. Forniés, B. Menjón, F. A. Cotton, R. Falvello, M. Tomás, *Inorg. Chem. 24* (1985) 4651.

[17] D. G. Evans, D. M. P. Mingos, *Organometallics 2* (1983) 435.

[18] The compounds **1** are obtained as red-orange microcrystalline solids by UV irradiation (medium pressure mercury lamp, 150 W; M = Nb, 2 h, M = Ta, 3 h in a slow stream of argon) of THF solutions of [Et_4N][$M(CO)_6$] in the presence of stoichiometric amounts of dmpe. Satisfactory elemental analyses were obtained for these compounds.

[19] G. Brauer, *Handbook of Preparative Inorganic Chemistry Vol. 2*, Academic Press, New York 1964, p. 1048.

[20] Correct-elemental analyses for **2a** and **2b**—IR spectra (ν in cm^{-1}): **2a** in nujol: 1935(s), 1840(vs); in THF: 1930(s), 1842(vs) cm^{-1}; **2b** in nujol: 1923(s), 1832(vs); in THF: 1928(s), 1843(vs).

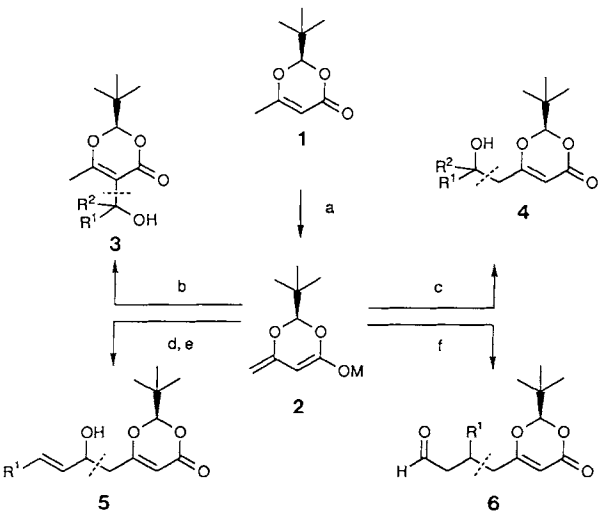
The Dienolate of (*R*)-2-*tert*-Butyl-6-methyl-1,3-dioxin-4(2*H*)-one—a Chiral Acetoacetic Ester d^4-Reagent**

By *Dieter Seebach,** *Ulf Misslitz*, and *Peter Uhlmann*

We recently reported[1] an efficient conversion of (*R*)-3-hydroxybutanoic acid into the title compound **1**, which has emerged as a valuable building block for the synthesis of enantiomerically pure compounds (EPC syntheses):[2] cuprates, Cu(I)-doped Grignard reagents, thiolates and catalytically activated hydrogen add to C-6 of the heterocycle exclusively with relative topicity *ul*.[3]

In view of the fact that there are hardly any *chiral* synthetic equivalents[4a] of the acetoacetic ester dianion,[4b] it appeared promising to study the reactivity of the dienolate derivatives **2** generated from the dioxinone **1** and Li, Na, or K hexamethyldisilazide, as well as of the corresponding silyldienol ethers [**2**, M = $SiMe_3$, Si(*t*Bu)Me_2].

The Li dienolate reacts with acetaldehyde at the C-5 ring position to give essentially one[5] diastereoisomer **3a** (20:1). In contrast, products **4a–h** of hydroxybenzylation at the exocyclic C-1 position are formed highly regioselectively with aromatic aldehydes and ketones (modest stereoselectivity, $\leq 3:1$), substituents on the benzene ring influencing the yield more than the diastereodifferentiation.



Scheme 1. a) $MN(SiMe_3)_2$ (M = Li, Na, K), THF, −75 °C, 1 h. b) With M = Li; Alkyl-CHO, −105 °C, 1 h. c) With M = Li; R^1R^2CO, −105 °C (R^1 = Aryl, R^2 = H) or −75 °C (R^1 = Aryl, R^2 + H), 1 h. d) Me_3SiCl or Me_2(*t*Bu)SiCl, −75 to 0 °C, 16 h. e) Aryl-CH=CH-CHO, Lewis acid, CH_2Cl_2, −75 °C, (R^1 = Aryl), 6 h. f) With M = Li, Na or K, R^1-CH=CH-CHO, −105 °C, 1 h.

To our surprise, α,β-unsaturated aldehydes such as crotonaldehyde and cinnamaldehyde combine with the same Li dienolate in a Michael addition of the exocyclic nucleophilic center (a^3/d^4-coupling), with very high regio-[5] and stereoselectivity (ca. 20:1, products **6**). The 1,2-adducts **5**, on the other hand, were obtained from the reaction of the silylenol ethers **2**-$SiMe_3$ or -Si(*t*Bu)Me_2 with α,β-unsaturat-

[*] Prof. Dr. D. Seebach, Dr. U. Misslitz, Dipl.-Chem. P. Uhlmann
Laboratorium für Organische Chemie der
Eidgenössischen Technischen Hochschule
ETH-Zentrum
Universitätstrasse 16, CH-8092 Zürich (Switzerland)

[**] Part of the Master's thesis of *P. U.*, ETH-Zürich, 1988. We thank the Deutsche Forschungsgemeinschaft for a postdoctoral fellowship for *U. M.* (1987/1988).

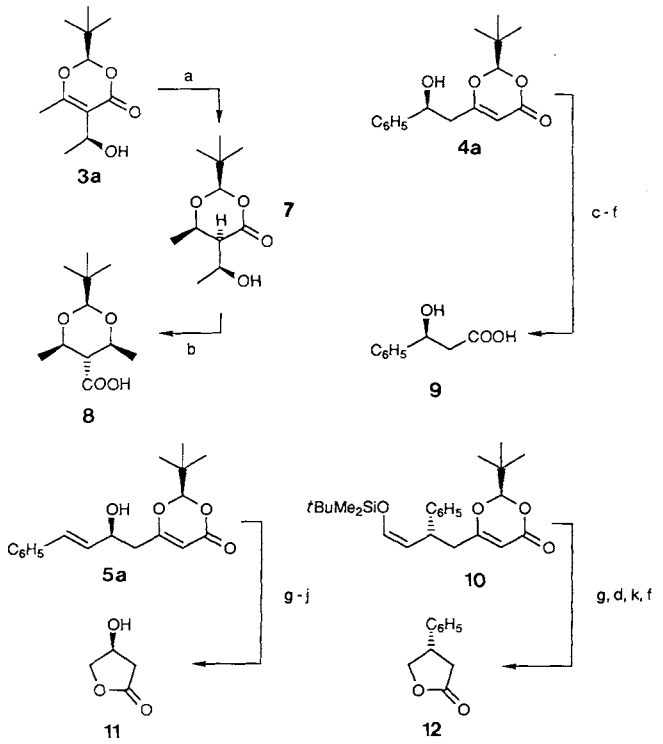
Table 1. Data of some products **3**–**6** from the dioxinone **1** and aldehydes or ketones.

Compound	R^1	R^2	M in **2**	Yield [%]	Diastereomeric ratio
3a	CH_3	H	Li	42	20:1 [a]
4a	Phenyl	H	Li	61	3:1 [b]
4b	Phenyl	CH_3	Li	6	3:1
4c	Phenyl	CF_3	Li	95	2:1 [c]
4d	*p*-Nitrophenyl	H	Li	72	3:2
4e	*p*-Nitrophenyl	CH_3	Li	50	3:2
4f	*p*Methoxyphenyl	H	Li	14	3:1
4g	Mesityl	H	Li	27	3:1
4h	1-Naphthyl	H	Li	60	3:1
5a	Phenyl		$Si(tBu)Me_2/TiCl_4$	47	3:2
5a	Phenyl		$SiMe_3/SnCl_4$	43	1:1
5a	Phenyl		$SiMe_3/BF_3 \cdot OET_2$	52	1:1
6a	Phenyl		Li	43	20:1 [d]
6a	Phenyl		Na	50	3:2
6a	Phenyl		K	46	6:1
6b	CH_3		Li	41	20:1 [e]

[a] M.p. 59–60 °C, $[\alpha]_D = -215$ ($c = 1.0$, EtOH). [b] Major diastereoisomer: m.p. 103–104 °C, $[\alpha]_D = -114$ ($c = 1.0$, EtOH). [c] Major diastereoisomer: m.p. 143–144 °C, $[\alpha]_D = -144$ ($c = 1.0$, EtOH). [d] $[\alpha]_D = -65.0$ ($c = 1.5$, CH_2Cl_2). [e] $[\alpha]_D = -132$ ($c = 2.4$, CH_2Cl_2).

ed β-arylaldehydes such as cinnamaldehyde in the presence of Lewis acids (see Scheme 1 and Table 1).

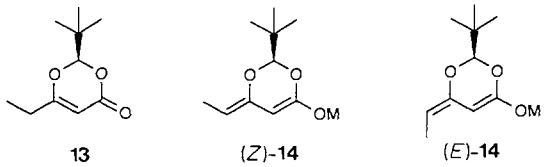
The configurations of the following products were determined by chemical correlations: **3a, 4a** and **5a**, as well as **10**, the (*Z*)-silyldienol ether derivative of **6a** (see Scheme 2). Thus, the acetaldehyde adduct **3a** was hydrogenated (→ **7**) and the product rearranged to the achiral (optically inactive) dioxanecarboxylic acid **8** with C_s-symmetry, under acid catalysis conditions (the substitution pattern of the six-membered rings in **7** and **8** being confirmed by NOE measurements). A diastereomerically pure sample of the major



Scheme 2. a) 5% Rh/Al_2O_3, EtOAc, 50 bar H_2, room temp., 24 h. b) $CHCl_3$, CF_3CO_2H, room temp., 48 h. c) O_3, CH_2Cl_2, CH_3OH, −75 °C. d) $P(OCH_3)_3$, −75 to +20 °C, 12 h. e) KOH, 6 h. f) HCl. g) O_3, CH_3OH, −75 °C. h) $P(OCH_3)_3$, −75 to +20 °C, 1 h. i) $NaBH_4$, −75 to +20 °C, 16 h. j) CF_3COOH, CH_2Cl_2, room temp., 48 h. k) $LiAlH_4$, THF, 0 °C, 2 h, then room temp., 48 h.

product **4a** was converted into the known (*S*)-3-hydroxy-3-phenylpropanoic acid[6] (**9**, > 95% *ee*) by ozonolysis of the dioxinone double bond. Similarly, treatment with ozone, reduction of the resulting aldehyde group and lactonization under acidic conditions converted the products **5a** and **10** into optically active samples of the known butyrolactones **11**[7] and **12**,[8] respectively.

Not having carried out any mechanistic investigations as yet, we refrain from speculating about possible reasons for the observed selectivities and leave more or less obvious explanations to the imagination of the reader.[9] We hope to gain some valuable relevant information in this connection from ongoing studies of the reactions of *E*/*Z*-dienol derivatives **14** (M = Li, Na, K, SiR_3) generated from the ethyl-substituted[1] heterocycle **13**.



13 (*Z*)-**14** (*E*)-**14**

Finally, it should be pointed out that structures of type **4** and **5**, and their conversion into 3,5-dihydroxycarboxylic acids are of interest with regard to the syntheses of compactin and its analogues.[10]

Received: November 18, 1988 [Z 3057 IE]
German version: *Angew. Chem. 101* (1989) 484

[1] D. Seebach, J. Zimmermann, *Helv. Chim. Acta 69* (1986) 1147; D. Seebach, S. Roggo, J. Zimmermann in W. Bartmann, K. B. Sharpless (Eds): *Stereochemistry of Organic and Bioorganic Transformations, Proceedings of the Seventeenth Workshop Conference Hoechst*, VCH-Verlagsgesellschaft, Weinheim, 1987, p. 85–126; J. Zimmermann, D. Seebach, *Helv. Chim. Acta 70* (1987) 1104.
[2] D. Seebach, J. Zimmermann, U. Gysel, R. Ziegler, T.-K. Ha, *J. Am. Chem. Soc. 110* (1988) 4763.
[3] D. Seebach, V. Prelog, *Angew. Chem. 94* (1982) 696; *Angew. Chem. Int. Ed. Engl. 21* (1982) 654.
[4] a) R. H. Schlessinger, E. J. Iwanowicz, J. P. Springer, *J. Org. Chem. 51* (1986) 3070; b) Dienolate of the achiral acetonide of acetoacetic acid enol: A. B. Smith, III, R. Scarborough, *Tetrahedron Lett. 1978*, 4193.
[5] Unidentified side products < 10%.
[6] C. Schöpf, W. Wüst, *Justus Liebigs Ann. Chem. 626* (1959) 150.
[7] R. E. Moore, A. J. Blackman, C. E. Cheuk, J. S. Mynderse, *J. Org. Chem. 49* (1984) 2484.
[8] I. W. Lawston, T. D. Inch, *J. Chem. Soc. Perkin Trans. 1*, 1983, 2629.
[9] What is the configuration of the primary adduct with two new stereogenic centers and an exocyclic double bond, leading to the formation of **3**?—Is the *Z*-configuration of the enolate leading to the isolation of **10** an indication of a primary 1,2-addition of C-5 of the heterocycle to the unsaturated aldehyde, followed by an oxido-Cope rearrangement? Is **3** a product of kinetic control and **4** of thermodynamic control?
[10] T. Rosen, C. H. Heathcock, *Tetrahedron 42* (1986) 4909.

Shortened C–C Bonds in Coupled Bicyclo[1.1.0]butanes**

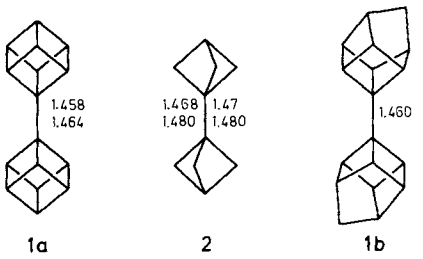
By *Otto Ermer,* Peter Bell, Jörg Schäfer* and *Günter Szeimies*

Bonds involved in widened bond angles are shortened. We have recently exemplified this for the case of 1,4-cubanedi-

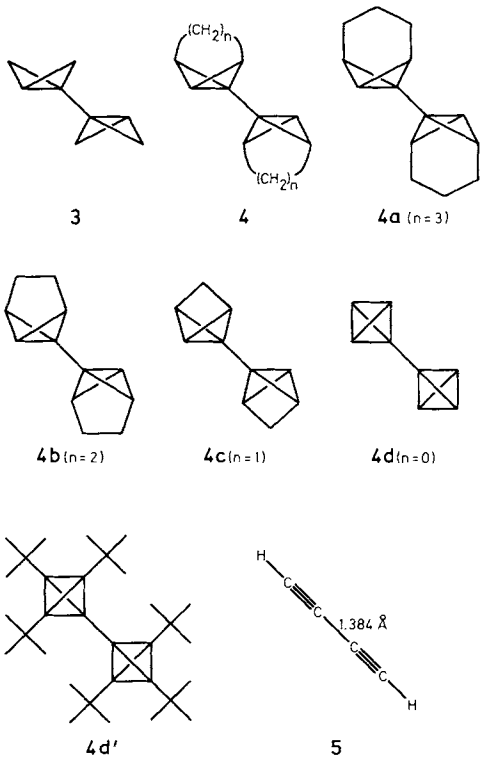
[*] Prof. Dr. O. Ermer, Dipl.-Chem. P. Bell
Institut für Organische Chemie der Universität
Greinstrasse 4, D-5000 Köln 41 (FRG)
Prof. Dr. G. Szeimies, Dipl.-Chem. J. Schäfer
Institut für Organische Chemie der Universität
Karlstrasse 23, D-8000 München 2 (FRG)

[**] This work was supported by the Fonds der Chemischen Industrie and the Deutsche Forschungsgemeinschaft.

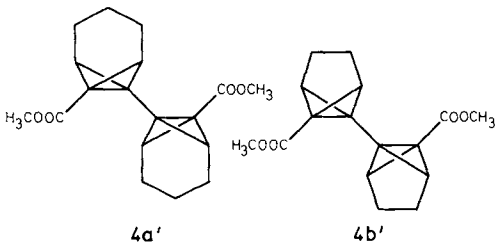
carboxylic acid, whose $C(sp^3)$–$C(sp^2)$ single bonds are shortened by ca. 0.04 Å, since they participate in three exocyclic CCC angles widened by 16.0° (average) beyond the tetrahedral value. This led us to the prediction that the central CC single bonds in the coupled cubane and bicyclo[1.1.1]pentane systems **1a** and **2**, respectively, should be shortened by about 0.08 Å to 1.46 Å, since they participate in six similarly widened CCC angles.[1] This prediction has now been confirmed experimentally several times, also for the similarly coupled homocubane **1b**; the respective bond lengths [Å] determined by X-ray analysis for parent systems and derivatives are reproduced in the formula diagrams.[2]



The central CC bond of the 1,1'-coupled bicyclo[1.1.0]butane **3** may be expected to be shortened still further, since the exocyclic angles at the tertiary carbon atoms of bicyclo[1.1.0]butane exceed the tetrahedral value, on average, by 20.2°,[3] and are thus larger than in cubane or bicyclo[1.1.1]pentane. The introduction of short bridges as in **4**, with $n \leq 2$, should lead to further shortenings; according to model considerations, **4a** ($n = 3$) is, in the present context, comparable with **3**.



Thus, in the series from **4a** (**3**) through **4b** and **4c** we are faced with further growing widenings of the angles at the central CC bond until, in the ultimate member bitetrahedryl **4d** ($n = 0$), values near arc $\cos(-\sqrt{2/3}) - 109.5 = 35.3°$ are reached. The latter extreme case of bitetrahedryl **4d** with a presumably ultrashort central CC bond is obviously hypothetical and hardly realizable; with due reference to tetra-*tert*-butyltetrahedrane,[4] the hexa-*tert*-butyl derivative **4d'** could be feasible and stable. As a rough estimate for the maximally conceivable bond shortening by angle widening, the length of the central CC single bond (1.384(2) Å) in diacetylene **5**[5] may eventually be used. Viewing acetylene as "bicyclo[0.0.0]ethane," formal angle widenings of $180 - 109.5 = 70.5°$[6] and a bond shortening of $1.54 - 1.38 = 0.16$ Å are obtained. Herein we describe the structure analyses of the two esters **4a'** and **4b'**,[7] which we have carried out in an attempt to "approach" the extreme bitetrahedryl **4d**. As expected, particularly short central CC bonds are observed in both cases.



Important findings of the crystal structure analyses[8] are summarized in Figure 1. Both coupled bicyclo[1.1.0]butane derivatives **4a'** and **4b'** are centrosymmetric in the crystal. Ignoring the ester groups, C_{2h} symmetry is closely approximated. Nonetheless, however, the conformation about the central CC bond is by no means ideally staggered, since, as a result of the relatively unsymmetric angle distortions at C(1) and C(1') not even approximate local C_3 symmetry is present about this bond: as the torsion angles and Newman projections of Figure 1 show, a plane may be drawn through C(1) and C(1') such that the four bonded C atoms lie on one side of this plane! The length of the central CC bond in **4a'** is 1.445(3) Å (librationally corrected 1.448 Å) and the adjacent bond angles are on average widened by 18.7° out to 128.2°. As expected, the central CC bond in **4b'** is shortened still somewhat further to 1.440(2) Å (libr. corrected 1.443 Å) in view of the adjacent angles being widened on average by 21.4° out to 130.9° (Fig. 1). To our knowledge this is the shortest non-cyclic (unbent) CC single bond between saturated, tetravalent C atoms observed so far.[9]

The CC bonds between the bicyclobutane skeletons and the ester groups in **4a'** and **4b'** are more severely shortened (by ca. 0.07 Å; Fig. 1) than would be expected on the grounds of the angle widenings alone. Presumably conjugation effects between the carbonyl group and the cyclopropane rings are responsible for this. Conversely, the CC bonds common to the annelated three-membered rings are remarkably long (1.547(3) Å in **4a'**, 1.532(2) Å in **4b'**; 1.497(3) Å in bicyclo[1.1.0]butane[3]). Consideration of comparable bicyclo[1.1.0]butane derivatives[10] shows that the conjugation between carbonyl group and three-membered ring may again be responsible.

The longest known single bonds between saturated, tetravalent C atoms are stretched by ca. 0.10 Å with respect to the normal value (1.54 Å).[11] In **4a'** and **4b'** the other extreme is reached, with the central bond shortened by just this amount, so that a variation of altogether ca. 0.20 Å is now recorded experimentally for such bonds. The length of the central CC bond in **4b'** (1.440(2) Å) may be regarded as an upper limit of that in bitetrahedryl **4d**. A narrower experimental delimitation would be possible by studying the cou-

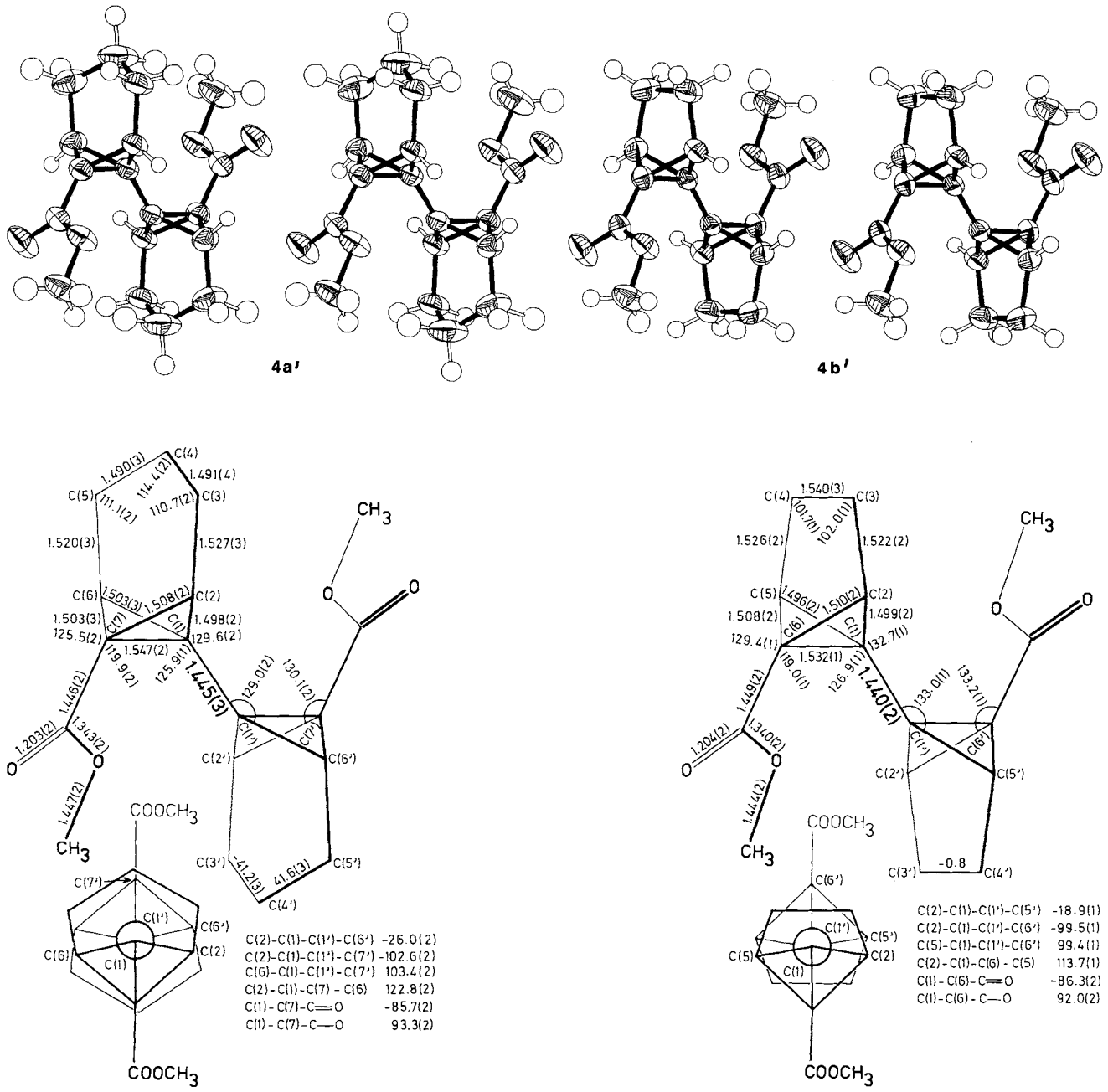


Fig. 1. Structures of **4a'** (left) and **4b'** (right) in the crystal. Top: stereoviews with vibrational ellipsoids at the 50% probability level; temperature factors of the H atoms trebled. Bottom: bond lengths [Å], selected bond and torsion angles [°], Newman projections along C(1)–C(1'), and atomic numbering.

pled homotetrahedrane **4c**, whose six internal CCC angles should be widened on average by about 28° to 138° (estimate based on structural data for tricyclo[2.1.0.0^{2,5}]pentane[10] itself). These angle openings approach those in **4d** already to within ca. 7°. (The system **4c** is unknown, but appears to have a fair chance of being turned into reality, so that the most extreme shortening of a CC bond thus seems experimentally attainable). In tetra-*tert*-butyltetrahedrane the CC bonds between the tetrahedrane skeleton and the *tert*-butyl groups are shortened on average by 0.05 Å to 1.49 Å.[12] Based on the successful extrapolation of the lengths of the central CC bonds in bicubyl **1a** and 1,1'-bi(bicyclo-[1.1.1]pentyl) **2** from 1,4-cubanedicarboxylic acid, a shortening of 0.10 Å would be expected for the central CC bond of bitetrahedryl **4d**. This estimate is not very reliable, however, since the corresponding three independent CC bond lengths in crystalline tetra-*tert*-butyltetrahedrane display substantial scatter and are not particularly precise (1.480–1.503 Å, $\sigma \approx 0.005$ Å[12]). In the light of the findings for **4a'** and **4b'** the estimated shortening indeed appears too low, presumably owing to some weak non-bonding H···H repulsions in tetra-*tert*-butyltetrahedrane which counteract the CC bond contractions.

Received: November 14, 1988 [Z 3047 IE]
German version: *Angew. Chem. 101* (1989) 503

CAS Registry numbers:
4a', 119337-45-0; **4b'**, 119337-46-1.

[1] O. Ermer, J. Lex, *Angew. Chem. 99* (1987) 455; *Angew. Chem. Int. Ed. Engl. 26* (1987) 447.

[2] a) Coupled Cubanes: R. Gilardi, M. Maggini, P. E. Eaton, *J. Am. Chem. Soc. 110* (1988) 7232. The authors discuss a central CC shortening of even 0.114 Å for **1a** and criticize our pre-estimate of 0.08 Å [1]. In doing so, they refer to a CC reference length of 1.572 Å based on bond lengths between quaternary C atoms in hydrocarbons, for example 1,1'-biadamantyl. This length, however, may not be regarded as a standard value for an unstrained CC single bond, yet is to be viewed as stretched due to nonbonding H ··· H repulsions. The $C(sp^3)$–$C(sp^2)$ shortening of 0.04 Å observed in 1,4-cubanedicarboxylic acid arises exclusively from angle widening without involvement of nonbonding interactions. Consequently, our predicted shortening of 0.08 Å in **1a** and **2** [1] could meaningfully only refer to the usual standard length of an unstrained CC single bond of 1.54 Å. The shortenings measured in the meantime for **1a** and **2** (and **1b**) thus agree very satisfactorily with our prognosis. b) Coupled bicyclo[1.1.1]pentanes: U. Bunz, K. Polborn, H.-U. Wagner, G. Szeimies, *Chem. Ber. 121* (1988) 1785; P. Kaszynski, J. Michl, *J. Am. Chem. Soc. 110* (1988) 5225; A. C. Friedli, P. Kaszynski, J. Michl, *Tetrahedron Lett. 30* (1989) 455. c) Coupled homocubane: J. Schäfer, K. Polborn, G. Szeimies, *Chem. Ber. 121* (1988) 2263.

[3] K. W. Cox, M. D. Harmony, G. Nelson, K. B. Wiberg, *J. Chem. Phys. 50* (1969) 1976.

[4] G. Maier, S. Pfriem, U. Schäfer, R. Matusch, *Angew. Chem. 90* (1978) 552; *Angew. Chem. Int. Ed. Engl. 17* (1978) 520; G. Maier, *ibid. 100* (1988) 317 and *27* (1988) 309.

[5] M. Tanimoto, K. Kuchitsu, Y. Morino, *Bull. Chem. Soc. Jpn. 44* (1971) 386.

[6] Compare the respective ideas of Baeyer in his strain theory: A. Baeyer: *Ber. Dtsch. Chem. Ges. 18* (1885) 2269.

[7] R. Römer, J. Harnisch, A. Röder, A. Schöffer, G. Szeimies, G. Germain, J. M. Arrieta, *Chem. Ber. 117* (1984) 925. Herein, the diethyl ester corresponding to **4a'** is described. For the present structure analyses, we have used the similarly prepared dimethyl esters since they have a higher melting point and crystallize better; see also A. Meyer, *Dissertation*, Universität München 1988.

[8] 1,1'-Bi(tricyclo[4.1.0.0^{2,7}]heptane-7,7'-dicarboxylic acid dimethyl ester) **4a'**: monoclinic crystals (from methanol/ether); m.p. 184 °C (decomp); space group $C2/c$, $Z = 4$, $a = 15.560(3)$, $b = 6.063(1)$, $c = 17.238(2)$ Å, $\beta = 103.68°$; $\varrho_{calcd} = 1.271$ g cm^{-3}; molecular symmetry C_i. Intensity measurements at room temperature on a four-circle diffractometer ($\lambda_{Mo} = 0.71069$ Å, $\theta_{max} = 30°$); direct methods; refinement (C,O anisotropic, H isotropic) with inclusion of 1756 reflections with $F_o > 3\sigma(F_o)$; $R = 0.069$, $R_w = 0.077$. —1,1'-Bi(tricyclo[3.1.0.0^{2,6}]hexane-6,6'-dicarboxylic acid dimethyl ester **4b'**: triclinic crystals (from methanol/ether): m.p. 119 °C; space group $P\bar{1}$, $Z = 1$, $a = 5.761(2)$, $b = 7.863(1)$, $c = 8.412(2)$ Å, $\alpha = 97.94(2)$, $\beta = 95.50(2)$, $\gamma = 107.39(3)°$; $\varrho_{calcd} = 1.278$ g cm^{-3}; molecular symmetry C_i. Measuring conditions, structure solution and refinement as for **4a'** (1716 reflections, $R = 0.046$, $R_w = 0.061$).—Further details of the crystal structure investigations are available on request from the Fachinformationszentrum Energie, Physik, Mathematik GmbH, D-7514 Eggenstein-Leopoldshafen 2 (FRG), on quoting the depository number CSD-53450, the names of the authors, and the journal citation.

[9] The *generally* shortest distances between single bonded, tetravalent C atoms probably occur in two tricyclo[2.1.0.0^{2,5}]pentan-3-one derivatives. For the distance between the two C atoms common to the three-membered rings, *Irngartinger* et al. have measured values of 1.417(1) [10a] and 1.416(2) Å [10b]. It should be noted, however, that these three-membered ring bonds, in contrast to the exocyclic central CC bond in the coupled systems discussed here, are severely bent and thus the bond length definition becomes problematic.

[10] a) H. Irngartinger, A. Goldmann, *Angew. Chem. 94* (1982) 786; *Angew. Chem. Int. Ed. Engl. 21* (1982) 769; H. Irngartinger, K. L. Lukas, *ibid. 91* (1979) 750 and *18* (1979) 694; b) P. Dowd, P. Garner, R. Schappert, H. Irngartinger, A. Goldmann, *J. Org. Chem. 47* (1982) 4240; H. Irngartinger, A. Goldmann, R. Schappert, P. Garner, P. Dowd, *J. Chem. Soc. Chem. Commun. 1981*, 455; c) H. Irngartinger, A. Goldmann, R. Schappert, P. Garner, C. L. Go, P. Dowd, *ibid.* 1985, 113; H. Irngartinger, R. Jahn, H. Rodewald, Y. H. Paik, P. Dowd, *J. Am. Chem. Soc. 109* (1987) 6547; H. Irngartinger, A. Goldmann, U. Huber-Patz, P. Garner, Y. H. Paik, P. Dowd, *Acta Crystallogr. C44* (1988) 1472.

[11] M. A. Flamm-ter Meer, H.-D. Beckhaus, K. Peters, H.-G. von Schnering, C. Rüchardt, *Chem. Ber. 118* (1985) 4665; C. Rüchardt, H.-D. Beckhaus, *Angew. Chem. 97* (1985) 531; *Angew. Chem. Int. Ed. Engl. 24* (1985) 529; N. Yannoni, B. Kahr, K. Mislow, *J. Am. Chem. Soc. 110* (1988) 6670.

[12] H. Irngartinger, A. Goldmann, R. Jahn, M. Nixdorf, H. Rodewald, G. Maier, K.-D. Malsch, R. Emrich, *Angew. Chem. 96* (1984) 967; *Angew. Chem. Int. Ed. Engl. 23* (1984) 993; H. Irngartinger, R. Jahn, G. Maier, R. Emrich, *ibid. 99* (1987) 356 and *26* (1987) 356.

Synthesis and Structure of a Phenylsodium Solvate, Bis[μ-phenyl(pentamethyldiethylenetriamine)-sodium] **

By *Uwe Schümann, Ulrich Behrens,* and *Erwin Weiss* *

Phenylsodium was known for quite some time before it could be prepared in a relatively pure form by reaction (a).

$$LiPh + NaO\mathit{t}Bu \rightarrow NaPh + LiO\mathit{t}Bu \quad (a)$$

As in the case of phenyllithium, single crystals were not obtainable; hence the structure of these important alkali-metal compounds have thus far remained unsolved. Phenyllithium has, however, already been investigated X-ray crystallographically in three different solvated forms and, depending upon the solvent, was found to be present as tetramer (**1**), dimer (**2**) or monomer (**3**).

$[PhLi(OEt_2)]_4$[3] **1** $[PhLi(tmeda)]_2$[4] **2** $[PhLi(pmdta)]$[5a, 6] **3**

tmeda = tetramethylethylenediamine
pmdta = pentamethyldiethylenetriamine

The complexes **1**–**3** are thus excellent models for demonstrating the influence of a solvent on the structure of organolithium compounds. The degree of association of the complexes decreases with increasing hapticity of the ligands. The tridentate ligand pmdta was found to be the most suitable ligand for the stabilization of the monomeric form, also in the case of alkyllithium compounds.[6] We therefore decided to employ it in our attempted synthesis of a phenylsodium solvate.

Reaction of NaPh with pmdta in hexane led indeed to a 1:1 adduct (**4**), from which crystals suitable enough for an X-ray structure analysis could be obtained. The structure is shown in Figure 1.[7]

$[PhNa(pmdta)]_2$ **4**

Contrary to what has been found in the case of LiPh, the solvate of NaPh with the tridentate ligand pmdta is not monomeric but dimeric, thus reflecting the larger ionic radius of $Na^{\oplus}$, i.e. $Li^{\oplus}$ favors the coordination number 4 in many of its solvates, whereas a higher coordination number is possible in the case of $Na^{\oplus}$.

The $Na^{\oplus}$ ions in **4** are coordinated in an extremely distorted trigonal-pyramidal geometry; the N–Na–N angles are only about 67.6°. The central N atom (N2) of the three N atoms is much more weakly bonded than the two terminal N atoms, since its lone pair cannot be optimally oriented towards the $Na^{\oplus}$ ion.

Comparative considerations[8] show that N–metal–N angles of 80–87° occur in organolithium compounds, and of 67–77° in organosodium compounds. According to *Stucky* et al.,[9] in agreement with this the N–M–N angle in tmeda complexes should be 85° for M = Li and 56° for M = K. As in other phenyl-metal compounds the phenyl rings in **4** are planar, but the C–C–C angles deviate from 120°; for the C atom (C1) directly adjacent to the metal atom the angle is only 111.7°.

[*] Prof. Dr. E. Weiss, Dr. U. Schümann, Prof. Dr. U. Behrens
Institut für Anorganische und Angewandte Chemie der Universität
Martin-Luther-King-Platz 6, D-2000 Hamburg 13 (FRG)

[**] Metalalkyl and Metalaryl Compounds, Part 38. This work was supported by the Deutsche Forschungsgemeinschaft and the Fonds der Chemischen Industrie.—Part 37: E. Weiss, T. Lambertsen, B. Schubert, J. K. Cockcroft, *J. Organomet. Chem. 358* (1988) 1.

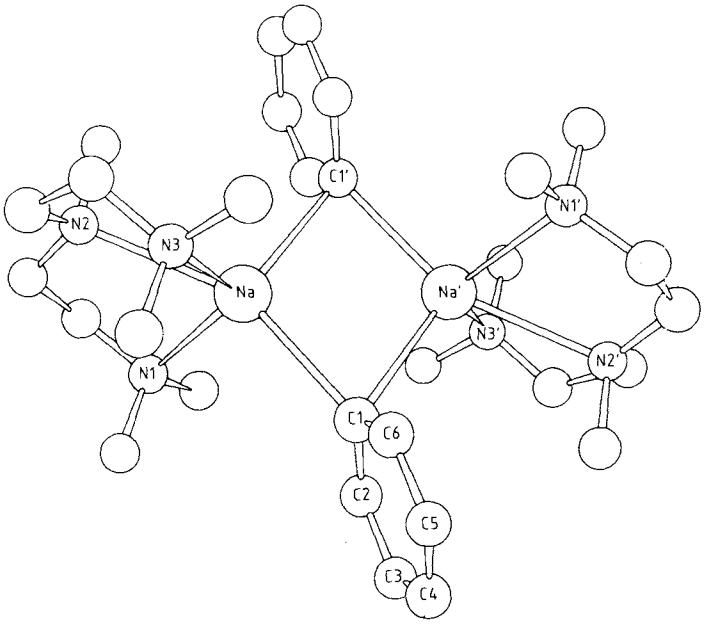


Fig. 1. Structure of **4** in the crystal. ORTEP plot of the centrosymmetric molecule. Important bond lengths [pm] and angles [°]: Na-C1 265.8(4), Na-C1' 268.2(6), Na-N1 264.6(3), Na-N2 271.2(3), Na-N3 260.9(3), Na-Na' 323.7(3), C-C (phenyl) 138.6 (mean value, min. 134.4, max. 141.0); N-C 145.3 (mean value, min. 142.9, max. 148.7); Na-C1-Na' 74.6, C1-Na-C1' 105.4, N1-Na-N2 67.6, N2-Na-N3 67.7, N1-Na-N3 119.1(1), C1-Na-N1 102.5(1), C1-Na-N3 99.7(1), C2-C1-C6 111.7(3), C1-C2-C3 124.3(4), C2-C3-C4 120.8(4), C3-C4-C5 119.3(5), C4-C5-C6 119.0(4), C5-C6-C1 124.9(4).

Experimental

All operations were carried out under an inert gas and with carefully dried solvents. For the synthesis of phenylsodium according to equation (a) [2], it is advisable to recrystallize the NaO*t*Bu before use; sublimation leads to considerable losses and less pure products. A suspension of 0.25 g (2.5 mmol) of NaPh (containing ca. 0.6 weight-% Li, corresponding to 7.3 mol-% LiPh) in 30 mL of hexane was brought into solution by addition of 1.2 mL (5.8 mmol) of anhydrous pmdta. Upon completion of the addition, a part of the phenylsodium already in solution re-precipitated as a white powder. The supernatant, intensely red solution was pipetted off and yielded, after cooling to $-30\,^{\circ}C$, 1.17 g (17%) of **4** in the form of coarsely crystalline light-brown, pyrophoric platelets (correct analysis for Na, C, H, N). Single crystals suitable for an X-ray structure analysis were obtained from the mother liquor.

Received: November 7, 1988 [Z 3040 IE]
German version: *Angew. Chem. 101* (1989) 481

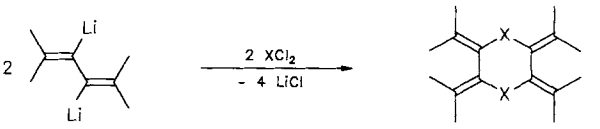
CAS Registry number:
4, 119503-02-5.

[1] F. S. Acree, *Ber. Dtsch. Chem. Ges. 37* (1904) 2753; W. Schlenk, J. Holtz, *ibid. 50* (1917) 262.
[2] G. Thirase, E. Weiss, *J. Organomet. Chem. 81* (1974) C1.
[3] H. Hope, P. P. Power, *J. Am. Chem. Soc. 105* (1983) 5320.
[4] D. Thönnes, E. Weiss, *Chem. Ber. 111* (1978) 3157.
[5] a) U. Schümann, J. Kopf, E. Weiss, *Angew. Chem. 97* (1985) 222; *Angew. Chem. Int. Ed. Engl. 24* (1985) 215; b) W. Bauer, W. R. Winchester, P. von R. Schleyer, *Organometallics 6* (1987) 2371.
[6] U. Schümann, E. Weiss, H. Dietrich, W. Mahdi, *J. Organomet. Chem. 322* (1987) 299.
[7] X-ray structure analysis of **4**: space group $P2_1/n$ (monoclinic), $a = 1001.6(4)$, $b = 1219.2(5)$, $c = 1476.7(6)$ pm, $\beta = 92.93(3)^{\circ}$, 293 K, $\varrho_{calcd} = 1.01\ g\,cm^{-3}$, $Z = 2$, $Mo_{K\alpha}$ radiation, structure determination by direct methods (SHELXS 84 [10]), refinement to $R = 0.052$ (unweighted), 1611 symmetry independent and significant reflections in the range $4^{\circ} < 2\theta < 50^{\circ}$ ($|F| > 5\,\sigma(F)$). Anisotropic temperature factors for Na, C, N, H atoms at calculated positions with common isotropic temperature factors. Number of refined parameters 173. Further details of the crystal structure investigation are available on request from the Fachinformationszentrum Energie, Physik, Mathematik GmbH, D-7514 Eggenstein-Leopoldshafen 2 (FRG), on quoting the depository number CSD-53692, the names of the authors, and the journal citation.
[8] U. Schümann, *Dissertation*, Universität Hamburg 1987.
[9] R. Zerger, W. Rhine, G. D. Stucky, *J. Am. Chem. Soc. 96* (1974) 5441.
[10] G. Sheldrick, SHELXS-84, Programs for Crystal Structure Solution, Göttingen 1984.

Tetraalkylidene-1,4-diboracyclohexanes from 3,4-Dilithio-2,5-dimethyl-2,4-hexadiene; the First "Hetero[6]radialene" with Chair Conformation**

By *Adalbert Maercker**, *Walter Brieden*, *Thomas Schmidt*, and *Heinz Dieter Lutz*

We recently reported the synthesis and structure of the first "dimetalla[6]radialene" **2a**.[1] In the crystalline state it has a twist conformation. Besides **2a**, only one further "hetero[6]radialene" has so far been reported in the literature, the corresponding sulfur compound **2b**, which was obtained—likewise with twist conformation—in a multistep synthesis.[2] In the meantime we have been able to prepare **2b** quite easily, and analogously to **2a**, from 3,4-dilithio-2,5-dimethyl-2,4-hexadiene **1**,[3] whereby it is advantageous to convert the sulfur dichloride into diimidazolyl sulfide prior to the reaction.[4]



1 **2**

a: X = Me_2Sn **c**: X = *t*BuB
b: X = S **d**: X = Ph_2NB

Since boraheterocycles are currently the subject of intensive studies—both theoretically and preparatively[5]—we have also tried to synthesize 1,4-dibora[6]radialenes by our method, particularly as these compounds can be expected to exhibit interesting properties with regard to their stereochemistry, NMR spectroscopy, and reactivity towards dienophiles.

Reaction of **1**[6, 7] with *tert*-butyldichloroborane in diethyl ether at $-50\,^{\circ}C$ leads to formation of a colorless, crystalline substance that is surprisingly stable towards air and hydrolysis, and which, according to the spectroscopic data,[8] is 1,4-di(*tert*-butyl)-2,3,5,6-tetra-2-propylidene-1,4-diboracyclohexane **2c** (yield 34%, not optimized, remainder presumably polymers). However, before any comments could be made about the conformation, an X-ray structure analysis[9] had to be carried out. It was established that **2c** is in fact the first "hetero[6]radialene" with chair conformation (Fig. 1).

Remarkable features of the structure of **2c** are, on the one hand, the large dihedral angles in the two butadiene units (with 74° and 73° they are only 10° smaller than in the analogous ditin compound **2a**, which has a twist conformation) and, on the other, that the central bonds of the butadiene units, which exhibit practically no double bond character, are, with lengths of 1.511(4) and 1.517(4) Å, identical with the corresponding distances in **2a**, i.e. there is no detectable influence of the heteroatoms on these bonds.

[*] Prof. Dr. A. Maercker, Dipl.-Chem. W. Brieden
Institut für Organische Chemie der Universität
Adolf-Reichwein-Strasse, D-5900 Siegen (FRG)
Dipl.-Chem. T. Schmidt[+], Prof. Dr. H. D. Lutz[+]
Institut für Anorganische Chemie der Universität
Adolf-Reichwein-Strasse, D-5900 Siegen (FRG)
[+] X-ray structure analysis.

[**] Polylithium Organic Compounds, Part 10. This work was supported by the Stiftung Volkswagenwerk and the Fonds der Chemischen Industrie.—Part 9: A. Maercker, K.-D. Klein, *Angew. Chem. 101* (1989) 63; *Angew. Chem. Int. Ed. Engl. 28* (1989) 83.

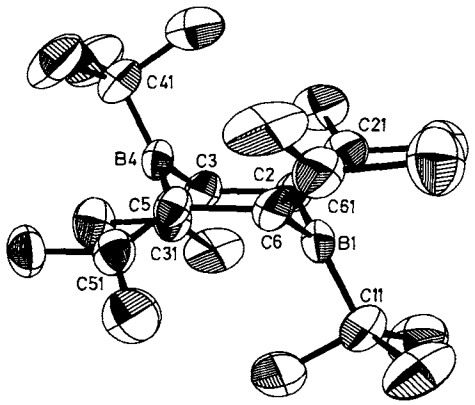
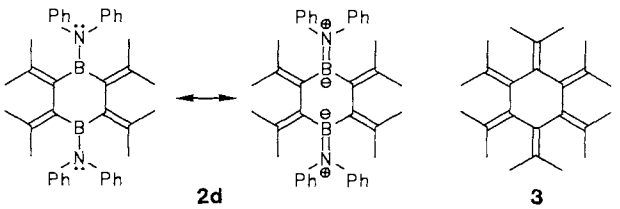


Fig. 1. Molecular structure of **2c** (thermal ellipsoids at the 50% probability level). Important bond lengths [Å] and angles [°]: B1-C2 1.566(4), C2-C3 1.511(4), C3-B4 1.572(5), B4-C5 1.568(4), C5-C6 1.517(4), C6-B1 1.567(4), B1-C11 1.590(5), B4-C41 1.586(5), C2-C21 1.338(4), C3-C31 1.344(4), C5-C51 1.343(4), C6-C61 1.341(4); C2-B1-C6 113.0(3), C2-B1-C11 122.5(3), C6-B1-C11 122.6(3), B1-C2-C3 110.2(2), B1-C2-C21 125.8(3), C3-C2-C21 123.2(3), C2-C3-B4 110.0(2), C2-C3-C31 123.0(3), B4-C3-C31 126.2(3), C3-B4-C5 112.8(3), C3-B4-C41 122.6(3), C5-B4-C41 122.6(3), B4-C5-C6 109.5(2), B4-C5-C51 126.6(3), C6-C5-C51 123.3(3), B1-C6-C5 110.3(2), B1-C6-C61 126.2(3), C5-C6-C61 122.7(3); dihedral angles C21-C2-C3-C31 74.0(2), C61-C6-C5-C51 73.4(2).

In contrast to the disulfur compound **2b**[2]—but in analogy to **2a**[1]—**2c** does not react with 4-phenyl-1,2,4-triazole-3,5-dione in a [4 + 2]-cycloaddition. Probably the coplanar attitude of the isopropylidene groups is additionally thwarted by the *tert*-butyl groups on the boron atoms.

A further 1,4-dibora[6]radialene, **2d**, could be prepared analogously in 38% yield by reaction of **1** with dichloro(*N,N*-diphenylamino)borane. **2d** is likewise a colorless, crystalline air-stable compound, whose structure was confirmed NMR spectroscopically and mass spectroscopically.[11]



Whether **2d**, like **2c**, has a chair conformation is not known. The relationship of **2d** with the isocyclic [6]radialene **3**, which is strikingly evident in the mesomeric resonance structure with B=N double bonds, leads us to presume, however, that **2d**, in analogy to **3**,[12] has a chair conformation. The importance of the ionic resonance structure in describing the bonding of **2d** manifests itself in the ^{11}B NMR spectrum: as expected[13] the resonance of **2d** ($\delta \approx 43$) absorbs at very much higher field than that of **2c** ($\delta \approx 77$).

Even knowing that **2c**, other than **2a, b**, assumes a chair conformation, it was not possible to discover any indications of this difference in the ^{1}H or ^{13}C NMR spectra. Furthermore, the spectra of the crude products also did not show any evidence of the presence of di-2-propylideneboracyclopropanes, which are conceivable as intermediates of the reaction of **1** with dihaloboranes.

Experimental

2c: A solution of *tert*-butyldichloroborane (7.0 g, 0.05 mol) [14] in diethyl ether (100 mL) was added dropwise within 2 h to a stirred 1.0 M solution of **1** (50 mL, 0.05 mol) [6, 7] in diethyl ether (diluted with 150 mL of diethyl ether) at −50 °C. After warming to room temperature and aqueous work-up the reaction mixture was evaporated down in a rotary evaporator and treated with a small amount of methanol. **2c** crystallized (3.0 g, 34%) [8]; m.p. 241–243 °C (from ethanol), correct elemental analysis (C, H, B).

2d: A 1.0 M solution of **1** (50 mL, 0.05 mol) [6, 7] in diethyl ether (diluted with 150 mL of diethyl ether) was added dropwise within 2 h to a stirred solution of dichloro(*N,N*-diphenylamino)borane [15] (12.5 g, 0.05 mol) in diethyl ether (200 mL) at −60 °C; work-up as in the case of **2c**. **2d** was obtained (5.4 g, 38%) [11]; m.p. 265–266 °C (from dichloromethane), correct elemental analysis (C, H, B).

Received: November 15, 1988 [Z 3054 IE]
German version: *Angew. Chem. 101* (1989) 477

[1] A. Maercker, F. Brauers, W. Brieden, M. Jung, H. D. Lutz, *Angew. Chem. 100* (1988) 413; *Angew. Chem. Int. Ed. Engl. 27* (1988) 404.
[2] W. Ando, Y. Hanyu, T. Takata, K. Ueno, *Tetrahedron Lett. 26* (1985) 3019.
[3] A. Maercker, W. Brieden, A. Groos, unpublished.
[4] A. Banerji, G. P. Kalena, *Tetrahedron Lett. 21* (1980) 3003.
[5] Review: W. Siebert, *Pure Appl. Chem. 59* (1987) 947.
[6] A. Maercker, R. Dujardin, *Angew. Chem. 97* (1985) 612; *Angew. Chem. Int. Ed. Engl. 24* (1985) 571.
[7] A. Maercker, R. Dujardin, F. Brauers, *Organomet. Synth. 4* (1988) 362.
[8] **2c**: ^{1}H-NMR (80 MHz, $CDCl_3$): $\delta = 0.98$ (s, 18 H; $2 \times C(CH_3)_3$), 1.57 (s, 12 H; $4 \times CH_3$), 1.65 (s, 12 H; $4 \times CH_3$).—^{13}C-NMR (100.6 MHz, $CDCl_3$): $\delta = 21.3$ (CH_3), 26.2 (CH_3), 28.7 (CH_3), 31.7 (CMe_3), 125.9 (CMe_2), 147.2 (BC).—^{11}B-NMR (128.4 MHz, $CDCl_3$): $\delta = 76.9$ ($\nu_{1/2} \approx 700$ Hz).—UV (*n*-hexane): $\lambda_{max} = 337$ nm ($\varepsilon = 12400$).—MS (70 eV): *m/z* 352 ($M^{\oplus}$, 33%), 295 ($M^{\oplus} - CMe_3$, 17%), 239 (30%), 41 (100%).
[9] **2c**: crystal dimensions 0.16 mm × 0.26 mm × 0.35 mm, space group $P\bar{1}$, $a = 16.385(3)$, $b = 14.106(3)$, $c = 9.672(3)$ Å, $\alpha = 98.34(2)$, $\beta = 119.69(2)$, $\gamma = 100.53(2)°$, $V = 1835.1$ Å^3, $Z = 3$, $\varrho_{calcd} = 0.956$ g cm^{-3}, $\varrho_{exp} = 0.94$ g cm^{-3}, $\mu(Mo_{K\alpha}) = 0.5$ cm^{-1}, $\theta_{max} = 25°$. 3068 independent reflections with $I > 2\sigma(I)$ were measured at 293 K on a four-circle diffractometer (CAD 4, Enraf-Nonius, $Mo_{K\alpha}$ radiation, graphite monochromator); structure solution by direct methods, protons located by difference Fourier analyses. Refinement by the full matrix method (B, C anisotropic, H isotropic) converged in the last cycle for 352 parameters at $R = 0.050$, $R_w = 0.035$ ($w = 1/\sigma^2(F_o)$). All calculations were carried out with the system NRCVAX [10]. Further details of the crystal structure investigation are available on request from the Fachinformationszentrum Energie, Physik, Mathematik GmbH, D-7514 Eggenstein-Leopoldshafen 2 (FRG), on quoting the depository number CSD-53427, the names of the authors, and the journal citation.
[10] The NRCVAX Crystal Structure System: E. J. Gabe, F. L. Lee, Y. Le Page, *Crystallogr. Comput. Data Collect. Struct. Determ. Proteins Databases Pap. Int. Summer Sch. 9th 1984* (1985) 167–174.
[11] **2d**: ^{1}H-NMR (80 MHz, $CDCl_3$): $\delta = 1.03$ (s, 12H; $4 \times CH_3$), 1.72 (s, 12H; $4 \times CH_3$), 7.10–7.20 (m, 20H; $4 \times C_6H_5$).—^{13}C-NMR (100.6 MHz, $CDCl_3$): $\delta = 22.0$ (CH_3), 26.1 (CH_3), 125.0 (*p*-C), 127.3 (CMe_2), 128.1 (*m*-C), 128.4 (*o*-C), 142.1 (BC), 149.7 (NC).—^{11}B-NMR (128.4 MHz, C_6D_6): $\delta = 42.5$ ($\nu_{1/2} \approx 950$ Hz).—UV (*n*-hexane): $\lambda_{max} = 228$ sh ($\varepsilon = 32800$), 276 nm (19100).—MS (70 eV); *m/z* 574 ($M^{\oplus}$, 100%), 234 (40%), 194 (90%), 165 (40%).
[12] G. Wilke, *Angew. Chem. 100* (1988) 189; *Angew. Chem. Int. Ed. Engl. 27* (1988) 185.
[13] Cf. B. Wrackmeyer, R. Köster in R. Köster (Ed.): *Houben-Weyl-Müller, Methoden der Organischen Chemie, XIII/3c*, Thieme, Stuttgart 1984, p. 377–611; H. Nöth, B. Wrackmeyer, *NMR Basic Princ. Prog. 14*, (1978) 29–61.
[14] P. A. McCusker, E. C. Ashby, H. S. Makowski, *J. Am. Chem. Soc. 79* (1957) 5179, 5182.
[15] H. J. Becher, *Z. Anorg. Allg. Chem. 289* (1957) 262.

The Influence of Packing Effects on the Solid-State Fluorescence of Diketopyrrolopyrroles**

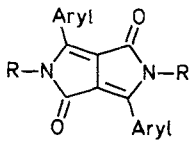
By *Heinz Langhals,* Thomas Potrawa, Heinrich Nöth*, and *Gerald Linti*

Very little is known about the influence of the crystal structure of a compound on its fluorescence quantum yield.[1]

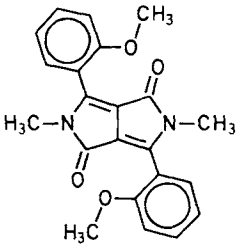
[*] Prof. Dr. H. Langhals, Dipl.-Chem. T. Potrawa
Institut für Organische Chemie der Universität
Karlstrasse 23, D-8000 München 2 (FRG)
Prof. Dr. H. Nöth [†], Dipl.-Chem. G. Linti [†]
Institut für Anorganische Chemie der Universität
Karlstrasse 23, D-8000 München 2 (FRG)
[†] X-ray structure analyses.

[**] This work was supported by the Deutsche Forschungsgemeinschaft and the Fonds der Chemischen Industrie.

This interrelationship will be examined more closely with the diketopyrrolopyrroles **1** as examples. Diketopyrrolopyrroles are important organic pigments.[2] It has recently been found that if they bear suitable substituents they can be used as light-fast fluorescent dyes, even in homogeneous solution,[4] and that they exhibit characteristically large Stokes shifts and high fluorescence quantum yields; consequently they are of interest for dye-lasers or fluorescence-solar collectors.[5]



1



2

It has been observed that some of the dyes, e.g. **1**, R = CH_3, aryl = 3,5-tBu$_2$C$_6$H$_3$, **1**, R = C_2H_5, aryl = 2-$CH_3C_6H_4$, or **1**, R = H, aryl = 2-$CH_3C_6H_4$ exhibit an intense solid-state fluorescence, whereas others, e.g. **1**, R = H, aryl = C_6H_5, fluoresce only weakly as solids. This difference disappears in solution. The dye **2** is an important link between these types, since it has two modifications: the thermodynamically stable yellow form **2a** shows an intense solid-state fluorescence, while the orange colored form **2b** fluoresces only weakly. To investigate the influence of packing effects on the solid-state fluorescence the crystal structures of each modification were determined by X-ray diffraction analysis (Fig. 1).[6, 7]

Both modifications crystallize monoclinically. Their crystallographically determined densities differ very little. In both crystal lattices the chromophores are similarly stacked, but differently ordered with respect to each other. No dimeric pairs are found, neither in **2a** nor in **2b**. Charge transfer (CT) interactions are not likely to be the reason for the low fluorescence quantum yields of **2b**, since in each case electron-rich molecular moieties are relatively far removed from electron-deficient moieties of the neighboring molecules (see Fig. 2; the shortest intermolecular distance between C=O and O–CH_3 is 4.38 Å for **2a** and 3.95 Å for **2b**).

Intramolecular CT interactions are also ruled out, since the electron-rich methoxy groups in both modifications are far apart from the carbonyl groups (4.16 Å in **2a** and 4.36 Å in **2b**) and the distances differ only negligibly. Furthermore, no significant dependence of the fluorescence quantum yield on the solvent polarity is observed in solution; the fluorescence quantum yield in chloroform and acetonitrile differ only very little.

A marked difference between the two modifications is, however, the distance between the chromophore planes in the crystal lattice. In the weakly fluorescing form **2b** the chromophores lie essentially under one another (Fig. 2 bottom) and are 3.81 Å apart. The concomitant strong interaction of the chromophores leads to a bathochromic shift of the orange colored absorption compared to the solution (cf. also J aggregates[8]). In the yellow modification **2a**, on the other hand, the chromophores are tightly compressed against each other. A chromophore-chromophore interaction can occur only with the next but one layer, and this is already at a distance of 6.18 Å; the interactions are therefore negligible.

We believe that the small distance of the chromophores in **2b** leads not only to a long-wavelength absorption, but also to a strong interaction of the electron system and lattice vibrations, since a periodic change of the chromophore distance gives rise to a periodic change in the UV/VIS absorption or fluorescence spectrum. The electronic excitation can flow into lattice vibrations via the coupling (cf. also Ref. [9]), and internal conversion (IC) is therefore required. The fluorescence deactivation is, however, of no importance in the case of the pigment **2a** because of the greater distance of the chromophores. The interactions are already weak and are hardly influenced by lattice vibrations—the chromophores are isolated in the crystal lattice just as they are in a dilute solution. This explains the strong solid-state fluorescence of the pigment.

Because of the special properties of the dye **2**, new optical memories could be developed in which the information is

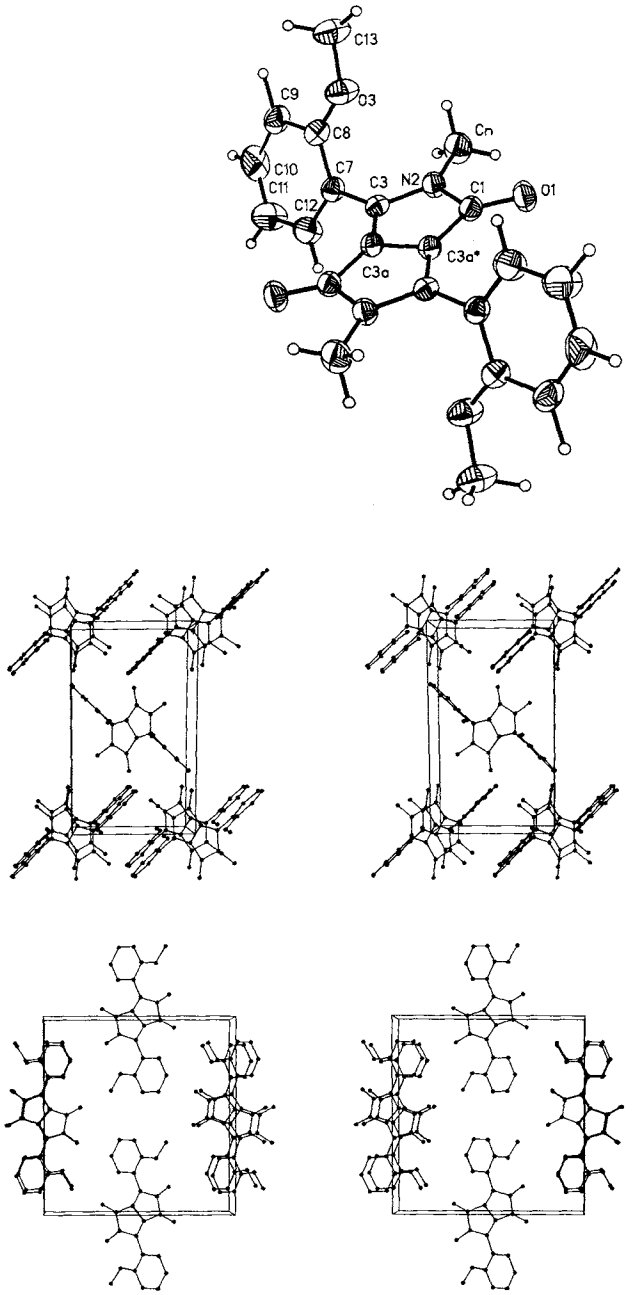


Fig. 1. Structure of **2** (top) and crystal lattices (stereoviews) of the two modifications **2a** (center) and **2b** (bottom).

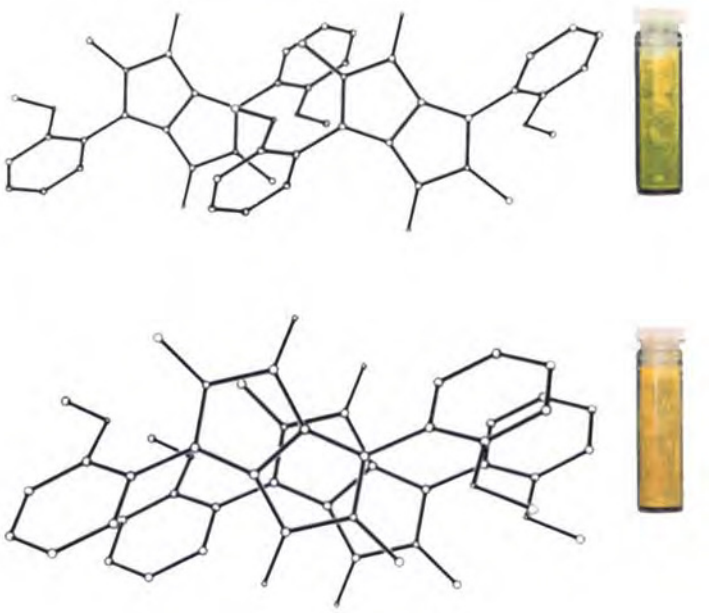


Fig. 2. Arrangement of the chromophores of **2a** (top) and **2b** (bottom) in the crystal lattice (view perpendicular to the chromophore plane). Alongside the structure diagrams, samples of the substances are shown as powders fixed on glass.

recorded by conversion of **2b** into **2a**. The read-out of the information is accomplished via the fluorescence and thus offers the advantage of simple, robust optics. Because of the great tendency of the dye to crystallize from homogeneous solution in the modification **2b**, an optical memory can also be erased. For this purpose, for example, **2b** is mixed in the ratio 1:5 with extra-pure anthracene. Conversion into the strongly fluorescing **2a** is induced by heating with a laser beam to just under 200 °C. For erasing this information the mixture is heated to just over the melting point of anthracene which then dissolves the pigment. Upon rapid cooling, anthracene crystallizes again, in admixture with **2b**.

For the synthesis of **2**, 2-methoxybenzonitrile is condensed with diisopropyl succinate, under usual reaction conditions,[3, 10] to give the corresponding diketopyrrolopyrrole, and then alkylated with methyl tosylate.[3, 11] Upon recrystallization the thermodynamically unstable modification **2b** is obtained, which is irreversibly converted at 195 °C into the stable yellow modification **2b**. The conversion enthalpy is -1.5 kcal mol^{-1}. Crystals of the yellow modification **2a** (in admixture with **2b**) can also be obtained by innoculation of a supersaturated dye solution.

Experimental

3,6-Bis(2-methoxyphenyl)-2,5-dihydropyrrolo[3,4-*c*]pyrrole-1,4-dione: A mixture of 2-methoxybenzonitrile (12.51 g, 93.95 mmol), KO*t*Bu (10.75 g) and isopropyl succinate (9.57 g, 46.8 mmol) was allowed to react as described in Refs. [3, 10] and then subjected to work-up. Yield: 400 mg (2.4%) of dark-red glimmering crystals, M.p. 336–337 °C (decomp., from toluene).—R_f (silica gel, toluene/acetone = 4:1) = 0.20. IR (KBr): $\tilde{\nu}$ = 3398 cm^{-1} (m), 3305 (m), 1641 (s), 1591 (s), 1563 (s), 1490 (m), 1256 (s), 1185 (m), 1119 (s), 832 (m), 750 (s), 651 (m), 575 (m). UV (DMF): λ_{max} (lg ε) = 525 nm (4.496), 489 (4.397), 460 (sh). Fluorescence (DMF): λ_{max} = 533 nm, 575. MS (70 eV) *m/z* = 348 (100%), 333 (3), 317 (4), 255 (6), 225 (4), 174 (10, $M^{2\oplus}$), 135 (9), 92 (33), 91 (39).

3,6-Bis(2-methoxyphenyl)-2,5-dimethyl-2,5-dihydropyrrolo[3,4-*c*]-pyrrole-1,4-dione (**2a**, **2b**): A mixture of the precursor (400 mg, 1.14 mmol) and *p*-toluenesulfonic acid methyl ester (2.08 g, 11.2 mmol) was allowed to react with a solution of K_2CO_3 (1.2 g) in DMF (5 mL) as described in Refs. [2, 11] and then subjected to work-up. Yield: 360 mg (84%) of orange crystals (**2b**). Transformation point 195 °C, m.p. 281–282 °C (from ethanol/chloroform 3:1).—R_f (*tert*-butyl methyl ether) = 0.44. IR (KBr): $\tilde{\nu}$ = 2940 cm^{-1} (w), 2835 (w), 1680 (s), 1616 (m), 1595 (m), 1488 (m), 1465 (m), 1437 (m), 1424 (w), 1252 (s), 1223 (w), 1033 (m), 756 (m), 744 (m), 636 (w). UV ($CHCl_3$): λ_{max} (lg ε) = 454 nm (4.206). Fluoroescence ($CHCl_3$): λ_{max} = 514 nm. Fluorescence quantum yield: $\Phi(CHCl_3)$ = 0.68, $\Phi(CH_3CN)$ = 0.59. ^{1}H-NMR ($CDCl_3$): δ = 3.00 (s, 6H), 3.83 (s, 6H), 6.84–7.12 (m, 4H), 7.28–7.60 (m, 4H). ^{13}C-NMR ($CDCl_3$): δ = 28.35 (q), 55.52 (q), 109.43 (s), 111.34 (d), 117.49 (s), 121.07 (d), 131.94 (d), 132.48 (d), 146.60 (s), 157.05 (s), 162.14 (s). MS (70 eV) *m/z* = 376 (100%, $M^{\oplus}$), 361 (4), 345 (6), 318 (5), 283 (10), 214 (9), 200 (8), 186 (9), 148 (52), 135 (21), 133 (34), 105 (18), 91 (12), 77 (7).—**2a**: UV (solid): absorption edge at 518 nm (point of inflection). Fluorescence (solid): λ_{max} = 525 nm.—**2b**: UV (solid): adsorption edge at 532 nm (point of inflection). Fluorescence (solid): λ_{max} = 555 nm (weak).

Received: October 27, 1988;
supplemented: December 27, 1988 [Z 3028 IE]
German version: *Angew. Chem. 101* (1989) 497

CAS Registry numbers:
2, 119273-55-1; 2-methoxybenzonitrile, 6609-56-9; diisopropyl succinate, 924-88-9; 3,6-bis(2-methoxyphenyl)-2,5-dihydropyrrolo[3,4-*c*]pyrrole-1,4-dione, 119273-54-0.

[1] F. H. Quina: "Photophysical Concepts in Condensed Media" in W. Adam, *Chemistry and Biology of the Generation of Excited States*, Academic Press, London 1982, p. 1–36.
[2] a) D. G. Farnum, G. Metha, G. G. I. Moore, F. P. Siegal, *Tetrahedron Lett. 1974*, 2549; b) Ciba-Geigy AG (A. Igbal, L. Cassar), Eur. Pat. 61426 A1 (September 29, 1982); *Chem. Abstr. 98* (1984) P73838n.
[3] T. Potrawa, H. Langhals, *Chem. Ber. 120* (1987) 1075.
[4] Ciba-Geigy AG (M. Jost, A. Iqbal, A. C. Rochat) Eur. Pat. 0133156 A2 (February 13, 1985); *Chem. Abstr. 102* (1985) P186667a.
[5] H. Langhals, *Nachr. Chem. Techn. Lab. 28* (1980) 716.
[6] X-ray structure analysis of **2a**: $C_{22}H_{20}N_2O_4$, M_r = 376.4, a = 8.285 (3), b = 8.272 (4), c = 14.585 (9) Å, β = 102.31 (3)°, V = 976.5 Å^3, Z = 2, ϱ_{calc} = 1.281 g cm^{-3}, μ = 0.79 cm^{-1}, space group $P2_1/c$.—Data collection: single crystal: 0.13 × 0.22 × 0.25 mm^3, ω-2θ scan, measured 2θ-range: 2–48° in $hk \pm l$, signal width < 0.9°, two standard reflections measured after each 48 intensity measurements, 1514 measured reflections, 1315 symmetry independent and 899 considered as observed ($I \geq 2\sigma(I)$). No absorption correction.—Solution of structure: direct methods, anisotropic description of the non-hydrogen atoms, isotropic description of the H-atoms. 157 parameters, R = 0.079; R_w = 0.082, $w^{-1} = \sigma^2 F + 0.0244\,F^2$, $\Delta/\sigma < 0.004$, $\varrho < 0.24$ e/Å^3. X-ray structure analysis of **2b**: $C_{22}H_{20}N_2O_4$, M_r = 376.4, a = 4.276 (2), b = 14.203 (10), c = 14.905 (10), β = 92.83 (5)°, V = 904.1 Å^3, Z = 2, ϱ_{calc} = 1.382 g cm^{-3}, μ = 0.94 cm^{-1}, space group $P2_1/n$.—Data collection: single crystal: 0.3 × 0.5 × 0.35 mm^3, 2θ scan, measured 2θ range: 2–48° in $hk \pm l$, signal width: 1.9° + 0.35 tg β, two standards after each 48 measurements; 1695 measured reflections, 1295 symmetry independent reflections, 1211 considered as observed ($I \geq 2.5\sigma(I)$9).—Solution of structure as described above: 157 parameters, R = 0.087, R_w = 0.098, $w^{-1} = \sigma F + 0.00105\,F^2$, $\Delta/\sigma < 0.003$, $\varrho \leq 0.34$ e/Å^3.—Further details of the crystal structure investigation are available on request from the Fachinformationszentrum Energie, Physik, Mathematik GmbH, D-7514 Eggenstein-Leopoldshafen 2 (FRG), on quoting the depository number CSD-53702, the names of the authors, and the journal citation.
[7] H. Langhals, T. Potrawa, D.O.S. P3901988.8 (July 29, 1988).
[8] T. Förster, *Naturwissenschaften 33* (1946) 166.
[9] H. Langhals, S. Demmig, H. Huber, *Spectrochim. Acta, 44A* (1988) 311.
[10] Ciba-Geigy AG (A. C. Rochat, A. Iqbal, L. Cassar), Eur. Pat. 94911 A2 (November 23, 1983); *Chem. Abstr. 100* (1984) P87260q.
[11] Ciba-Geigy AG (A. Iqbal, J. Pfenninger, A. C. Rochat, F. Bäbler), Eur. Pat. 181290 (November 7, 1984); *Chem. Abstr. 105* (1986) P210422b.

A Simple Synthesis of Dioxoisobacteriochlorins from Hematoporphyrin **

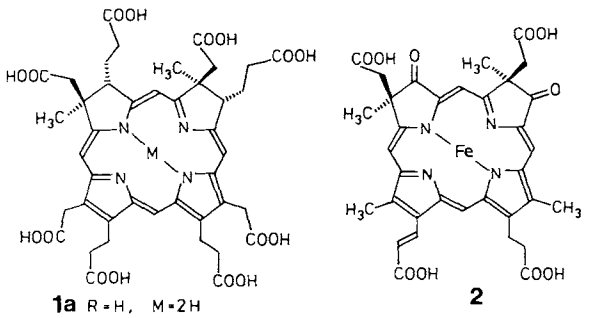
By *Franz-Peter Montforts,* Frank Romanowski,* and *Jan W. Bats*

Sirohydrochlorins **1a, b**,[1] siroheme **1c**[2] and heme d_1 **2**[3] are all porphinoid natural products containing the

[*] Prof. Dr. F.-P. Montforts, Dipl.-Chem. F. Romanowski
Institut für Organische Chemie, Fachbereich 2, der Universität
Leobener Strasse/NW 2, D-2800 Bremen 33 (FRG)
Dr. J. W. Bats
Institut für Organische Chemie der Universität
Niederurseler Hang, D-6000 Frankfurt am Main 50 (FRG)

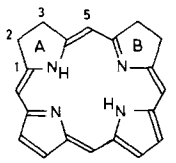
[**] This work was supported by the Deutsche Forschungsgemeinschaft and the Fonds der Chemischen Industrie. We thank Dr. *H. M. Schiebel* (Braunschweig) for recording the mass spectra.

isobacteriochlorin framework **3**. Partially hydrogenated derivatives of the metal-free macrocycles **1a, b** have been recognized as biosynthetic precursors for vitamin B_{12};[1,4] the iron-containing derivatives play a central role as cofactors in nitrile- and sulfite-reducing enzymes of bacteria and plants. Metal-free dioxoisobacteriochlorins could possibly also gain medical importance as photosentizers in photodynamic tumor therapy.



1a R = H, M = 2H
1b R = CH_3, M = 2H
1c R = H, M = Fe

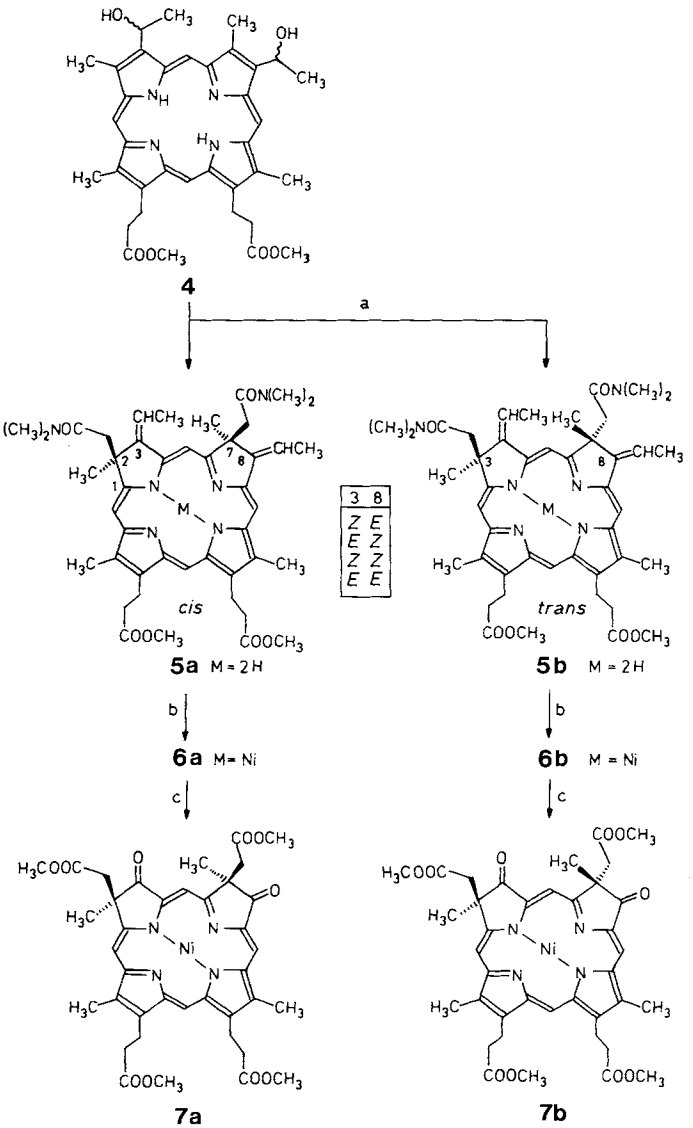
2



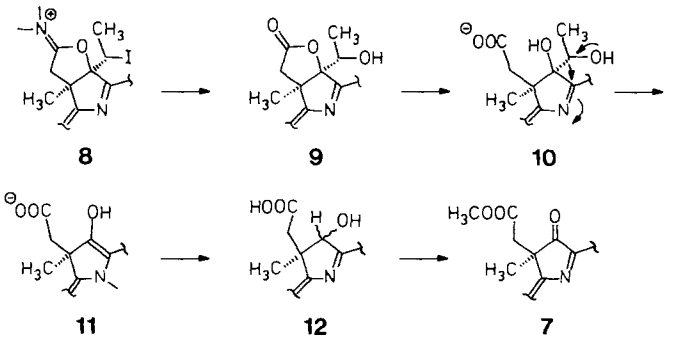
3

The biological and chemical importance of these natural products, which occur only in trace amounts, and the difficulty of isolating them, even on a very small scale, prompted the search for selective synthetic routes. Besides numerous syntheses of model compounds,[5] so far only one circuitous total synthesis of **1a**[6] and one unselective partial synthesis of **2**[5h] have been described. We now report a simple route for synthesizing the isobacteriochlorin skeleton by double amide acetal Claisen rearrangement from the inexpensive hematoporphyrin dimethyl ester **4**. Via this route, the geminally dialkylated structural elements in rings A and B are obtained at the same time. Cleavage of the incorporated amide groups and of the new exocyclic double bonds then leads directly to isobacteriochlorins **7** with the substitution pattern of **2** (Scheme 1).

The ester **4**[7] is available in any desired amount from slaughter-house wastes as direct transformation product of the red blood pigment heme and is thus an ideal economical and ecological starting material for the synthesis of compounds with complex porphinoid structures. The isobacteriochlorin chromophore with dialkylated 2 and 7 positions is formed upon double amide acetal Claisen rearrangement[8] at the hydroxyalkyl substituents of **4**. Since **4** is present as a binary diastereomeric mixture, the two stereoisomeric isobacteriochlorins of type **5a** and **5b** are formed with *cis*- and *trans* arrangement, respectively, of the newly introduced acetamide side chains. The *cis*/*trans* diastereomers can easily be separated chromatographically. In each of these *cis* and *trans* diastereoisomers there are four double-bond isomers, which originate from the newly formed exocyclic double bonds at the 3 and 8 positions. Owing to the stereoselective course of the Claisen rearrangement, the (*Z*,*Z*) isomers predominate.[8d] A clean chromatographic separation of the double-bond isomers is extremely difficult; fortunately it is not even necessary, because of the 3,8-oxo substitution in the target structures. The cleavage of the amide groups and of the double bonds, which is necessary for the further synthesis, could not be achieved under conventional hydrolysis and oxidation conditions even with the robust nickel complexes **6**, because of the lability of the chromophoric system. It can, however, be accomplished surprisingly easily, if both reactions are coupled with each other (Scheme 2). Iodolactonization leads via the immonium ester **8** to hydrolysis of the amide groups and oxidation of the double bonds.[9] The initially incorporated iodine is probably substituted by OH under the reaction conditions via neighboring group participation of the lactone oxygen. The resulting structures **9** containing a five-membered lactone ring, hydroxy substituents and the familiar isobacteriochlorin chromophore could be deduced unequivocally from the IR, mass and electron spectra. A more detailed characterization of the hydroxylactones **9** was not attempted because of the complex stereochemistry.



Scheme 1. Reaction conditions: a) $CH_3C(OCH_3)_2N(CH_3)_2$, *o*-xylene, 4-Å molecular sieve, argon, 160 °C, 2 h; flash chromatography, silica gel, CH_2Cl_2 + methyl acetate + MeOH (10 + 5 + 0.5), yield of **5** 50%. b) 2 equiv. Ni^{II} acetylacetonate, $CHCl_3$, reflux, chromatography Alox N III, CH_2Cl_2 + methyl acetate + MeOH (10 + 5 + 0.5), yield each 90%. c) 3 equiv. I_2, THF + H_2O (1 + 1), argon 25 °C, 6 h; flash chromatography, silica gel, CH_2Cl_2 + methyl acetate + MeOH (10 + 5 + 0.5); 2. 5 M KOH, MeOH, 60 °C, 24 h; 5 M HCl, 60 °C, 30 min; 3. CH_2N_2, Et_2O/MeOH, 25 °C, 2 h; flash chromatography, silica gel, CH_2Cl_2 + methyl acetate (10 + 1); yield after crystallization 47%.—All the compounds were prepared as enantiomeric mixtures. All new compounds, insofar as crystalline, are characterized by elemental analysis, UV/VIS, ^{1}H-NMR and mass spectra.



Scheme 2. Cleavage of the amide groups and the exocyclic double bonds of **6**, for access to **7**.

The alkaline hydrolysis of the lactones **9** is accompanied by retroaldol-type fragmentation, in the course of which the originally exocyclic double bonds at positions 3 and 8 are removed quite easily. Retroaldol-like processes of this type are well documented in porphyrin chemistry and have already been exploited synthetically.[10] Tautomerization, spontaneous subsequent oxidation of **12** to give the stable dioxoisobacteriochlorin-type structure, and esterification to **7** (Table 1) complete the synthesis.

Table 1. Selected spectroscopic data of **7a** and **7b**.

7a: UV/VIS ($CHCl_3$): λ_{max} (ε) = 386 (39 670), 437 (43 940), 585 (12 850), 619 nm (40 692); ^1H NMR ($CDCl_3$, 360 MHz): δ = 1.65, 1.71 (2s, each 3H, CH_3 an C-2 and C-7), 3.56 (s, 2H, 2- or 7-CH_2), 3.61 (d, ^2J = 3 Hz, 2H, 2- or 7-CH_2), 8.12, 8.17, 9.00, 9.07 (4s, je 1H, CH); MS (270 °C): *m/z* (rel. int. [%]) 770 (100, $M^{\oplus}$), 697 (45, $M^{\oplus} - CH_2CO_2CH_3$)
7b: UV/VIS ($CHCl_3$): λ_{max} (ε) = 385 (38 900), 436 (43 800), 586 (13 660), 617 nm (39 600); ^1H NMR ($CDCl_3$, 360 MHz): δ = 1.53, 1.57 (2s, each 3H, CH_3 an C-2 and C-7), 3.70 (AB system, J_{AB} = 17 Hz, 2- or 7-CH_2), 3.76 (AB system, J_{AB} = 17.5 Hz, 2- or 7-CH_2), 8.04, 8.12, 8.98, 9.03 (4s, each 1H, CH); MS (230 °C): *m/z* (rel. int. [%]) 770 (100, $M^{\oplus}$), 697 (68, $M^{\oplus} - CH_2CO_2CH_3$)

Assignment of the configurations of the pure crystalline diastereomers **7a** and **7b** is based on a crystal structure analysis[11] of **7a** (Fig. 1), in which the naturally occurring *cis*-configuration was found. The ligand system of the planar tetracoordinated nickel atom is, as expected, not planar in itself but deformed in a saddle-shaped fashion (ruffling). The carbon atoms of the methine bridges lie pairwise above and below the ring plane formed by the metal atom and its coordinated nitrogen atoms. The reasons for the deformation of the ligand system of metal-porphyrins have been investigated and discussed in detail.[12] A comparison with these findings shows that the dioxoisobacteriochlorin **7a** with its trigonal 3,8-carbon atoms deviates less from planarity than would be expected for tetrahydroporphyrins with tetrahedrally coordinated 3,8 centers.[13] In order to clarify whether the saddle-shaped structure is responsible for the biological function of heme d_1 **2** we are currently attempting the synthesis of this natural product according to the concept presented here.

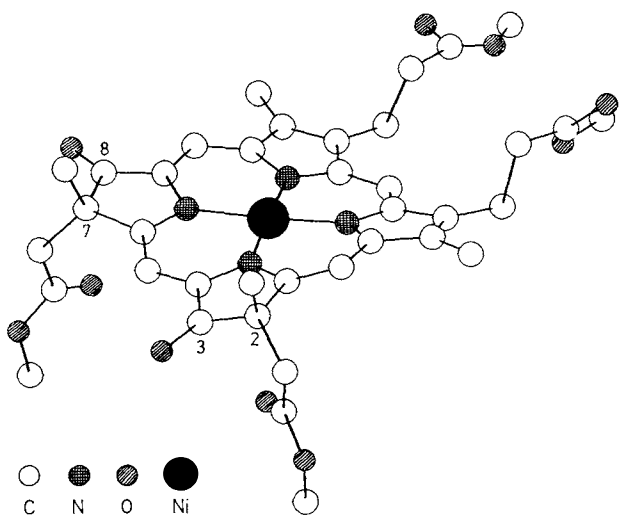


Fig. 1. Crystal structure of **7a**. Sideview showing the saddle-shaped deformation (ruffling) of the ligand system.

Received: November 7, 1988 [Z 3038 IE]
German version: *Angew. Chem. 101* (1989) 471

[1] a) V. Y. Bykhovsky, N. I. Zaitseva, V. N. Bukin, *Dokl. Akad. Nauk. SSR 224* (1975) 1431; b) A. R. Battersby, E. McDonald, H. R. Morris, M. Thompson, D. C. Williams, V. Y. Bykhovsky, N. I. Zaitseva, V. N. Bukin, *Tetrahedron Lett. 1977*, 2217; c) A. R. Battersby, K. Jones, E. McDonald, J. A. Robinson, H. R. Morris, *ibid. 1977*, 2213; d) R. Deeg, H. P. Kriemler, K. H. Bergmann, G. Müller, *Hoppe-Seylers Z. Physiol. Chem. 358* (1977) 339; e) A. I. Scott, A. J. Irwin, L. M. Siegel, J. M. Shoolery, *J. Am. Chem. Soc. 100* (1978) 316, 7987; f) K. H. Bergmann, R. Deeg, K. D. Gneuss, H. P. Kriemler, G. Müller, *Hoppe-Seylers Z. Physiol. Chem. 358* (1977) 1315; g) G. Müller, K. D. Gneuss, H. P. Kriemler, A. I. Scott, A. J. Irwin, *J. Am. Chem. Soc. 101* (1979) 3655.

[2] a) L. M. Siegel, M. J. Murphy, H. Kamin, *J. Biol. Chem. 248* (1973) 251; b) M. J. Murphy, L. M. Siegel, H. Kamin, D. Rosenthal, *ibid. 248* (1973) 2801; d) M. J. Murphy, L. M. Siegel, S. R. Tove, H. Kamin, *Proc. Natl. Acad. Sci. USA 71* (1974) 612.

[3] a) T. Kuronen, M. Ellfok, *Biochem. Biophys. Acta 275* (1972) 308; b) R. Timkovich, M. S. Cork, P. V. Taylor, *J. Biol. Chem. 259* (1984) 1577, 15089; c) W. Wu, C. K. Chang, *J. Am. Chem. Soc. 109* (1987) 3149, and references cited therein.

[4] a) A. R. Battersby, E. McDonald in D. Dolphin (Ed.): *Vitamin B_{12}, Vol. 1*, Wiley, New York 1982, p. 107; b) A. R. Battersby, *Acc. Chem. Res. 19* (1986) 147.

[5] a) F.-P. Montforts, S. Ofner, V. Rasetti, A. Eschenmoser, W. D. Woggon, K. Jones, A. R. Battersby, *Angew. Chem. 91* (1979) 752; *Angew. Chem. Int. Ed. Engl. 18* (1979) 675; b) P. Naab, R. Lattmann, C. Angst, A. Eschenmoser, *ibid. 92* (1980) 143 bzw. *19* (1980) 143; c) S. Ofner, V. Rasetti, B. Zehnder, A. Eschenmoser, *Helv. Chim. Acta 64* (1981) 1431; d) P. J. Harrison, C. J. R. Fookes, A. R. Battersby, *J. Chem. Soc. Chem. Commun. 1981*, 797; e) D. M. Arnott, A. R. Battersby, P. J. Harrison, G. B. Henderson, Z. C. Sheng, *ibid. 1984*, 525; f) A. R. Battersby, L. A. Reiter, *J. Chem. Soc. Perkin Trans. 1 1984*, 2743; g) H. M. Inhoffen, W. Nolte, *Justus Liebigs Ann. Chem. 725* (1969) 167; h) [3c].

[6] M. H. Block, S. C. Zimmerman, G. B. Henderson, S. P. D. Turner, S. W. Westwood, F. J. Leeper, A. R. Battersby, *J. Chem. Soc. Chem. Commun. 1985*, 1061.

[7] R. K. DiNello, C. K. Chang in D. Dolphin (Ed.): *The Porphyrins, Vol. 1*, Academic Press, New York 1978, p. 297.

[8] a) H. Meerwein, W. Florian, N. Schön, G. Stopp, *Justus Liebigs Ann. Chem. 641* (1961) 1; b) D. Felix, K. Gschwend-Steen, A. E. Wick, A. Eschenmoser, *Helv. Chim. Acta 52* (1969) 1030; c) A. E. Wick, D. Felix, K. Steen, A. Eschenmoser, *ibid. 47* (1964) 2425; d) F.-P. Montforts, G. Zimmermann, *Angew. Chem. 98* (1986) 451; *Angew. Chem. Int. Ed. Engl. 25* (1986) 458.

[9] a) G. W. J. Fleet, M. J. Gough, T. K. M. Shing, *Tetrahedron Lett. 24* (1983) 3661; b) Y. Tamura, M. Mizutani, Y. Furukawa, S. Kawamura, Z. Yoshida, Y. Yanagi, M. Minobe, *J. Am. Chem. Soc. 106* (1984) 1079.

[10] a) R. B. Woodward, W. A. Ayer, J. M. Beaton, F. Bickelhaupt, R. Bonett, P. Buchschacher, G. L. Closs, H. Dutler, J. Hannah, F. P. Hauck, S. Ito, A. Langemann, E. LeGoff, W. Leimgruber, W. Lwowski, J. Sauer, Z. Valenta, H. Volz, *J. Am. Chem. Soc. 82* (1960) 3800; b) R. B. Woodward, *Angew. Chem. 72* (1960) 651; c) R. Schwesinger, R. Waditschatka, J. Rigby, R. Nordmann, W. B. Schweizer, E. Zass, A. Eschenmoser, *Helv. Chim. Acta 65* (1982) 600.

[11] **7a**: tetragonal, space group $I4_1$, a = 31.190(4), c = 16.218(2) Å, V = 15 777(6) Å^3, Z = 16, ϱ_{calcd} = 1.300 g cm^{-3}, $\mu(Cu_{K\alpha})$ = 11.7 cm^{-1}. The structure was determined by direct methods. $R(F)$ = 0.073 for 4635 reflections with $I > 0$. Enraf-Nonius CAD4 diffractometer; SDP program system. Further details of the crystal structure investigation are available

on request from the Fachinformationszentrum Energie, Physik, Mathematik GmbH, D-7514 Eggenstein-Leopoldshafen 2 (FRG), on quoting the depository number CSD-53390, the names of the authors, and the journal citation.

[12] a) A. Eschenmoser, *Angew. Chem. 100* (1988) 5; *Angew. Chem. Int. Ed. Engl. 27* (1988) 5; b) C. Kratky, R. Waditschatka, C. Angst, J. E. Johansen, J. C. Plaquevent, J. Schreiber, A. Eschenmoser, *Helv. Chim. Acta 68* (1985) 1312.

[13] A parameter d_m has been defined [Ref. 12b] for the extent of deformation of a ligand by ruffling. In the porphinoid and corrinoid nickel complexes known so far the values for d_m lie between 0.738 for highly deformed nickelhexahydroporphyrins and 0.181 for almost planar nickeltetradehydrocorrins. The nickel isobacteriochlorin **7a** exhibits a slight deformation with a d_m parameter of 0.32.

Radical Anion Salts of Naphthalenetetracarboxylic Acid Derivatives—a Novel Class of Electrically Conducting Compounds**

By *Gerhard Heywang,* Liborius Born, Hans-Georg Fitzky, Tillmann Hassel, Jürgen Hocker, Hans-Klaus Müller, Bernd Pittel* and *Sigmar Roth*

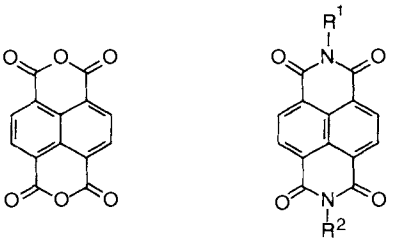
Dedicated to Professor Hans Rudolph on the occasion of his 60th birthday

In numerous studies[1, 2] of the charge-transfer complex of tetracyanoquinodimethane (TCNQ) and tetrathiafulvalene (TTF), general structural principles have been elaborated for electrically conducting molecular crystals. Since access to the charge-transfer complexes known so far is, in all cases relatively difficult, further, more readily variable radical anion salts are of special interest. We report herein on some new electrically conducting compounds based on naphthalenetetracarboxylic acid derivatives.

Nelson[3] detected a radical cation $\mathbf{1}^{\odot\ominus}$ ESR spectroscopically upon electroreduction of the naphthalenetetracarboxylic acid dianhydride **1** (NTDA). According to our calculations the electron affinity (EA) of **1** is comparable to that of TCNQ both according to the PPP method as well as the MNDO method: PPP: $EA_{TCNQ} = 4.30$, $EA_1 = 4.03$ eV; MNDO: vertical: $EA_{TCNQ} = 2.80$, $EA_1 = 2.87$ eV. Since the LCAO coefficients of the LUMO at the anhydride oxygen atoms of **1** are equal to zero, naphthalenetetracarboxylic acid diimides **2** should exhibit a comparable acceptor behavior.

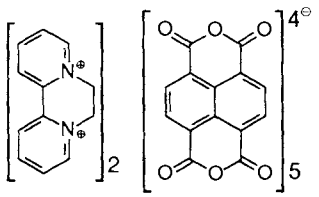
The electrochemical reduction of **1** in the presence of tetramethylammonium methyl sulfate leads to bluish-black needles with a metallic luster and the composition $[N(CH_3)_4]^{\oplus} \cdot \mathbf{1}^{\odot\ominus}$ (= **3a**) ($\sigma = 1.2 \times 10^{-4}$ S cm^{-1}). A number of other complex salts can be prepared analogously from **1** (Table 1).

Upon electrolysis in the presence of dication-methyl sulfates their anion is also incorporated into the complex salts (see **3e** and **3g**). Replacement of a $\mathbf{1}^{\odot\ominus}$ unit by a methyl sulfate ion gives rise to an increase in the conductivity by two powers of ten (cf. **3d**/**3e** and **3f**/**3g**). The complex salts **3h** and **3i** show an unusual stoichiometry and the best conductivities. The X-ray structure analysis[4] of **3h** (Fig. 1) supports the proposed stack-like structure and shows a lengthening of the CO double bond from approx. 1.185 to 1.200–1.212 Å for all NTDA units. From the stoichiometry of **3h** it follows that four electrons are shared by five molecules of **1**. The separation of the NTDA planes in **1**



1

2a, $R^1 = Ph$, $R^2 = Ph$
2b, $R^1 = CH_3$, $R^2 = CH_3$
2c, $R^1 = CH_2CH_2\overset{\oplus}{N}(CH_3)_3\ {}^{\ominus}OSO_2OCH_3$, $R^2 = CH_2CH_2\overset{\oplus}{N}(CH_3)_3\ {}^{\ominus}OSO_2OCH_3$
2d, $R^1 = CH_2CH_2CH_2\overset{\oplus}{N}(CH_3)_3\ {}^{\ominus}OSO_2OCH_3$, $R^2 = Ph$



3h

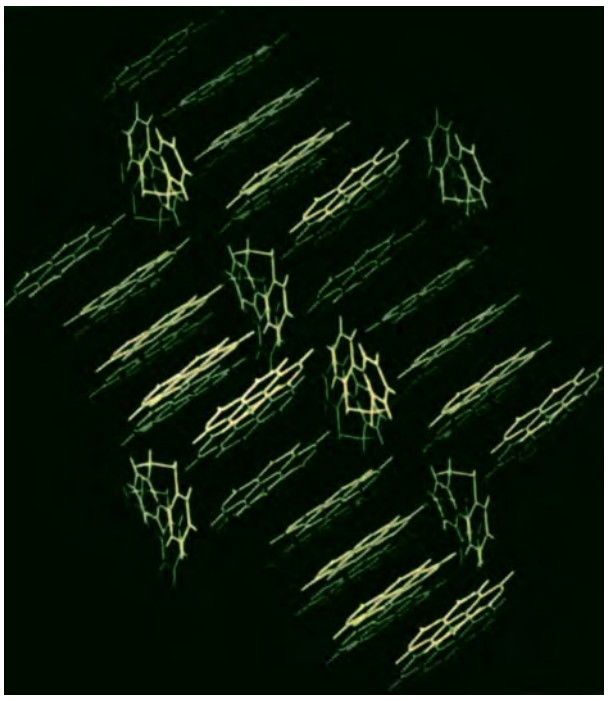


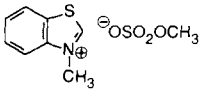
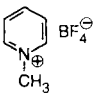
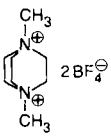
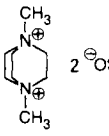
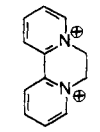
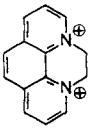
Fig. 1. SMART representation of the complex **3h** for demonstrating the stacking arrangement of the anionic units. Shown are two layers with the molecules **1** from each four unit cells.

[*] Dr. G. Heywang (ZF-FKH, Geb. Q18), Dr. L. Born, Dr. H.-G. Fitzky, Dr. T. Hassel, Dr. H.-K. Müller
Zentralbereich Zentrale Forschung
Dr. J. Hocker
Zentralbereich Personal
Dr. B. Pittel
Zentralbereich AG-Verwaltung
BAYER AG, D-5090 Leverkusen (FRG)
Dr. S. Roth
Max-Planck-Institut für Festkörperforschung
Heisenbergstr. 1, D-7000 Stuttgart 80 (FRG)

[**] This work was supported by the Bundesminister für Forschung und Technologie (O3C 203).

(3.21–3.36 Å) is comparable with the separation of the molecular planes in TCNQ complexes[5].

Table 1. Radical anion salts of NTDA **1**.

Cpd	Composition [a]	Supporting electrolyte XY or XY_2	Conductivity σ [S cm^{-1}] pellet [b] (crystal [c])
3a	$X^{\oplus}\,1^{\odot\ominus}$	$[N(CH_3)_4](OSO_2OCH_3)$	1.2×10^{-4}
3b	$X^{\odot}\,1^{\odot\ominus}$		5.7×10^{-4}
3c	$X^{\oplus}\,1^{\odot\ominus}$		4.0×10^{-3}
3d	$X^{2\oplus}\,2(1^{\odot\ominus})$	$A(BF_4)_2$[d]	3.0×10^{-5} (5.0×10^{-3})
3e	$X^{2\oplus}\,1^{\odot\ominus}\,Y^{\ominus}$	$A(OSO_2OCH_3)_2$[d]	4.0×10^{-3}
3f	$X^{2\oplus}\,2(1^{\odot\ominus})$		3.7×10^{-5}
3g	$X^{2\oplus}\,1^{\odot\ominus}\,Y^{\ominus}$		4.2×10^{-3} (5.0×10^{-1})
3h	$2X^{2\oplus}\,(5\,1)^{4\ominus}$		5.0×10^{-2} (7.5–10)
3i	$2X^{2\oplus}\,(5\,1)^{4\ominus}$		3.0×10^{-2}

[a] From elemental analyses which agree with the calculated values (± 0.3%). [b] Conductivity measurement under a pressure of 17.64 kN cm^{-2} by four-point contact. [c] Crystal needles of at least 1 mm in length were brought into contact with four annealed 20-μm gold wires via conducting silver and measured. [d] A = $(CH_3)_3NCH_2CH_2N(CH_3)_3$.

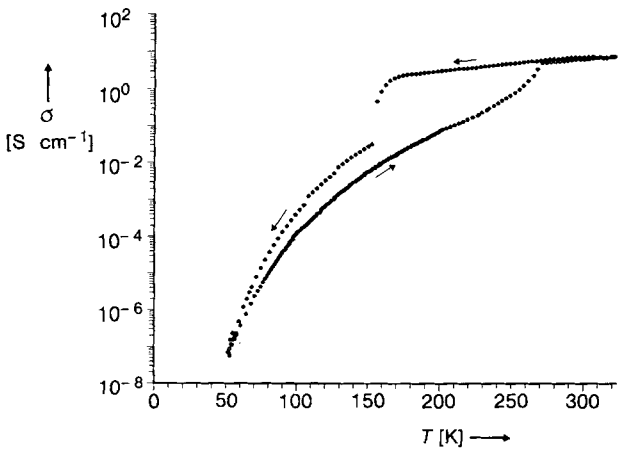
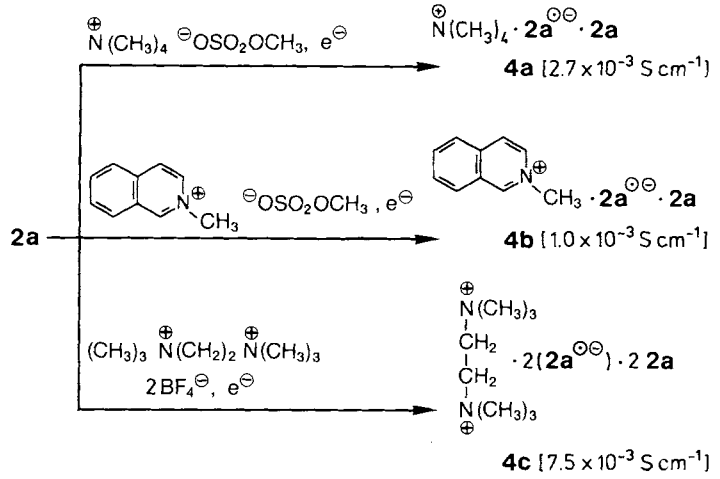
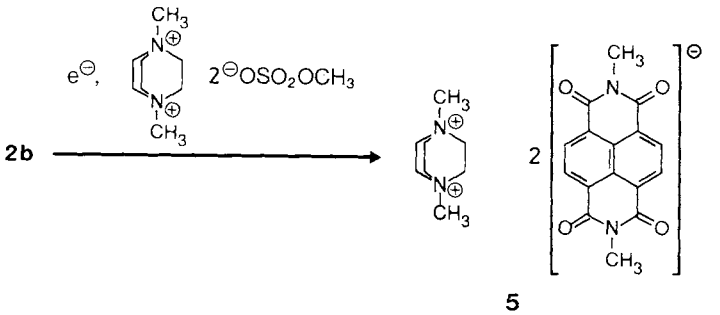


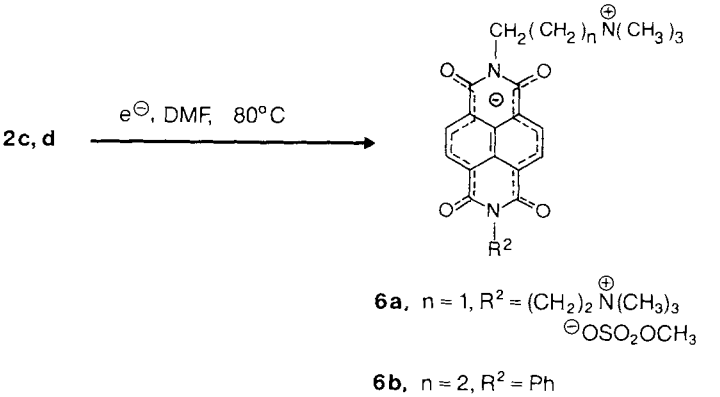
Fig. 2. Temperature dependence of the electrical conductivity σ of the complex **3h**, measured on a crystal needle of about 2 mm in length.

The electrical conductivity of **3h** (Fig. 2) is practically temperature-independent over a wide range. On cooling below 150 K, a phase transition, as is to be expected in the case of one-dimensional organic conductors,[6] is observed. The result is a rapid decrease in conductivity.

Electrochemical reduction of **2a** leads, independently of the supporting electrolyte employed, to the complex salts **4**, in which equal numbers of $\mathbf{2a}^{\odot\ominus}$ ions and **2a** molecules are present in each case.







6a, n = 1, $R^2 = (CH_2)_2\overset{\oplus}{N}(CH_3)_3\ \ominus OSO_2OCH_3$

6b, n = 2, R^2 = Ph

In contrast, the electrocrystallization of **2b** affords complex salts in which no neutral diimide molecules are present, e.g., **5** ($\sigma = 4.6\times10^{-6}$ S cm^{-1}). Despite their sparing solubility the naphthalenetetracarboxylic acid diimides **2c** and **2d** can be reduced to the complex salts **6a** and **6b**, respectively, in the absence of a supporting electrolyte.

The conductivities of the salts **6**, which because of the bulky trimethylammonium substituents do not necessarily

exhibit the planarity required for organic conductors, are surprisingly high (**6a**: $7 \times 10^{-3}\,S\,cm^{-1}$; **6b**: $3.5 \times 10^{-4}\,S\,cm^{-1}$).

Experimental

3h: A solution of **1** (268 mg, 1 mmol) and 5,6-dihydro-4a,6a-phenanthrolindionium bis(tetrafluoroborate) (1.77 g, 5 mmol) in 100 mL of dimethylformamide (DMF) was electrolyzed at 20 °C and a current of 1.5 mA for 21.5 h in a 100-mL electrolytic cell fitted with two 16 cm^2 platinum electrodes (separation 1 cm). A cell potential of 1.8 V was established. 249 mg of the radical anion salt were deposited at the cathode (73%, current yield 48.5%) in the form of bluish-black needles with a metallic luster, which decomposed without melting at 360 °C; satisfactory C, H, N analyses. IR spectrum: very broad bonds with low intensity, $\tilde{\nu}_{CO}$ = 1678, 1720 cm^{-1}; ESR spectrum: g = 2.0036, 0.6 spins/complex (reference standard "strong pitch" from Bruker).

Received: September 5, 1988 [Z 2955 IE]
German version: *Angew. Chem. 101* (1989) 462
Publication delayed at authors' request

CAS Registry numbers:
1, 81-30-1; **2a**, 24259-89-0; **2b**, 20958-66-1; **2c**, 30840-04-1; **2d**, 119298-32-7; **3a**, 119298-33-8; **3b**, 119298-34-9; **3c**, 111220-14-5; **3d**, 111220-09-8; **3e**, 119298-35-0; **3f**, 111220-10-1; **3g**, 111220-00-9; **3h**, 119298-37-2; **3i**, 119298-36-1; **4a**, 119298-39-4; **4b**, 119298-41-8; **4c**, 111220-07-6; **5**, 111220-16-7; **6a**, 119298-43-0; **6b**, 119326-15-7

[1] J. B. Torrance, *Acc. Chem. Res. 12* (1979) 79.
[2] W. E. Hatfield: *Molecular Metals*, Plenum, New York 1979.
[3] S. F. Nelson, *J. Am Chem. Soc. 89* (1967) 5925.
[4] Crystal structure data of **3h**: Enraf-Nonius CAD4 diffractometer, $Cu_{K\alpha}$ radiation, graphite monochromator, T = 296 K, triclinic, space group $P\bar{1}$, a = 8.935 (1), b = 12.785 (2), c = 15.995 (2) Å, α = 112.38 (2), β = 92.03 (1), γ = 93.68 (1)°, five molecules of **1** and two molecules of 5,6-dihydro-4a,6a-phenanthrolinium in the unit cell with one molecule of **1** at a symmetry center. ϱ_{calc} = 1.687 g cm^{-3}. R_1 (3192 reflections, 666 variable) = 0.032. A detailed description (methods of measurement and structure determination, atomic coordinates, bond data and further plots) will be published in *Z. Kristallogr.*
[5] a) TTF-TCNQ: T. J. Kistenmacher, T. E. Phillips, D. O. Cowan, *Acta Crystallogr. Sect. B30* (1974) 763; b) e.g. diphosphonium-TCNQ salts: P. Batail, L. Ouahab, J.-F. Halet, J. J. Padiou, M. Lequan, R. M. Lequan, *Synth Met. 10* (1985) 415.
[6] For example F. Denoyer, R. Comès, A. F. Garito, A. J. Heeger, *Phys. Rev. Lett. 35* (1975) 445.
[7] A. F. Garito, A. J. Heeger, *Acc. Chem. Res. 7* (1974) 232.

Sodium Pentaphosphacyclopentadienide (NaP_5) and the Pentaphosphacyclopentadienide Ion ($P_5^{\ominus}$): Theoretical Predictions of Molecular Structures, Infrared and Raman Spectra**

By *Tracy P. Hamilton* and *Henry F. Schaefer III**

A recent review[1] and a communication[2] to this journal have reported the synthesis and some properties of NaP_5 and $P_5^{\ominus}$. Sodium pentaphosphacyclopentadienide solutions are golden orange, extremely sensitive to oxidation, and stable for 7–10 days in concentrations of 10^{-2} M at room temperature. From the shape of the ultraviolet (electronic) spectrum *Baudler* and co-workers[2] concluded that $P_5^{\ominus}$ is aromatic, as might be suggested from the presence of six π-electrons. $P_5^{\ominus}$ has also been observed[3] (along with $P_n^{\ominus}$, n = 1–4, 6–9) in the negative ion mass spectrum of red phosphorus at 325 °C.

Baudler et al.[2] report features of the infrared and Raman spectra in their 1988 communication. Specifically they assign an intense IR band at 815 cm^{-1} and a medium-intense polarized Raman band at 463 cm^{-1} to the vibrational modes E_1' and A_1' of the planar, five-atom ring of D_{5h} symmetry. The IR fundamental assigned at 815 cm^{-1} appeared very suspicious to us, since even diatomic P_2 (with a formal triple bond) has a lower P–P stretching freqency, ω_e = 781 cm^{-1}.[4] $P_2^{\oplus}$ and $P_2^{\ominus}$, which both have higher formal bond orders (2 1/2) than expected for $P_5^{\ominus}$ with D_{5h} symmetry, have harmonic vibrational frequencies[3, 4] $\omega_e(P_2^{\oplus})$ = 672 cm^{-1} and $\omega_e(P_2^{\ominus}) = 640 \pm 50$ cm^{-1}. Thus a P–P stretching vibrational frequency as high as 815 cm^{-1} for $P_5^{\ominus}$ would appear counterintuitive to us.

We now report the use of ab initio molecular quantum mechanics in a study of the $P_5^{\ominus}$ and NaP_5 systems. Three basis sets of contracted gaussian functions were used in conjuction with the self-consistent-field (SCF) method. The smallest basis set was the 3-21G* set of *Pople* et al.,[5] the double zeta plus polarization (DZ + P) basis used here was that of *Huzinaga*[6] and *Dunning* and *Hay*.[7] The orbital exponent for the set of six d-like functions on each phosphorus atom was α = 0.5. The largest basis set appended diffuse s and p functions on P in order to better describe the anionic character of the $P_5^{\ominus}$ negative ion. In this DZ + P + diffuse basis set, the orbital exponents of the added primitive gaussian functions were[8] $\alpha_s(P) = 0.0348$ and $\alpha_p(P) = 0.0348$. For the $P_5^{\ominus}$ anion, the numbers of contracted gaussian functions were thus 95 (3-21G*), 120 (DZ + P) and 140 (DZ + P + diffuse).

The predicted SCF molecular structures for NaP_5 and $P_5^{\ominus}$ are shown in Figure 1. All geometrical parameters were optimized and each structure was proven to be a minimum. The P–P distances in the P_5 ring are 2.081 Å ($P_5^{\ominus}$, 3-21G*) and 2.093 Å (NaP_5, 3-21G*), i.e. the interaction of the $Na^{\oplus}$ ion with the $P_5^{\ominus}$ ring increases the ring bond distances by 0.013 Å, a result that should be reasonably independent of the basis set. In the isolated $P_5^{\ominus}$ anion, the bond distance changes very little as the basis set is increased in size from 3-21G* to DZ + P [r(P–P) increases by 0.012 Å] to DZ + P + diffuse (a further increase of 0.002 Å). Based on past experience,[9] one would expect the final predicted P–P distance in $P_5^{\ominus}$ (DZ + P + diffuse SCF; 2.095 Å) to be reliable to within ± 0.02 Å.

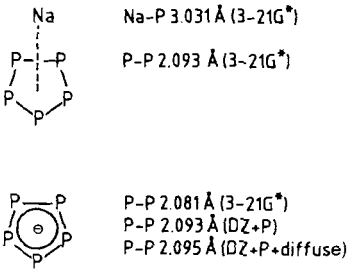


Fig. 1. Ab initio theoretical predictions of the molecular structures of $P_5^{\ominus}$ and NaP_5. All structures have been demonstrated to be true equilibrium geometries via harmonic vibrational analyses (see text).

Does our prediction of r_e(P–P) = 2.095 ± 0.02 Å for $P_5^{\ominus}$ make a statement about the aromaticity of this molecular ion? The two experimentally known P–P single bond distances in the gas phase are 2.219 Å (diphosphane P_2H_4[10]) and 2.223 Å (tetraphosphorus P_4[11]). Since the P–P bonds

[*] Prof. H. F. Schaefer III, T. P. Hamilton
Center for Computational Quantum Chemistry
School of Chemical Sciences
University of Georgia
Athens, Georgia 30602 (USA)
[**] Contribution CCQC No. 44. This work was supported by the US Air Force Office of Scientific Research under Grant AFOSR-88-0167. We thank Dr. *Brian Yates* for suggesting this problem.

in $P_5^{\ominus}$ are 0.12 Å shorter than these two classic P–P single bonds, we conclude that *on the basis of its molecular structure* (there may be other valid criteria[12]) conjugative effects are important for $P_5^{\ominus}$.

The predicted harmonic vibrational frequencies and infrared intensities for the isolated $P_5^{\ominus}$ anion are seen in Table 1.

Table 1. Predicted SCF total energies [hartree] and harmonic vibrational frequencies [cm^{-1}] for the $P_5^{\ominus}$ ion. Only the E_1' fundamental is allowed in the infrared, and the very weak E_1' IR intensities are given in km mol^{-1} in parentheses.

Basis set	3-21G*	DZ + P	DZ + P + diffuse
Total energy	−1695.55363	−1703.68491	−1703.70000
Fundamentals			
P–P stretch E_1'	575 (0.01)	568 (0.02)	564 (0.07)
P–P stretch E_2'	548	535	532
P–P stretch A_1'	523	514	509
In-plane ring deform. E_2'	349	341	336
Out-of-plane puckering E_2''	234	229	224

It is clear that these results are not concordant with *Baudler*'s assignment of an intense IR band at 815 cm^{-1} to the D_{5h} structure of $P_5^{\ominus}$. First, the predicted E_1' harmonic vibrational frequency is much lower, 564 cm^{-1} (DZ + P + diffuse SCF). Further corrections[13] for electron correlation and anharmonicity will only serve to lower the 564 cm^{-1} prediction. Second, the E_1' fundamental of $P_5^{\ominus}$ assigned by *Baudler* et al. is predicted here to have a very low IR intensity, namely 0.07 km mol^{-1}.

Could the attachment of $Na^{\oplus}$ to $P_5^{\ominus}$ radically change the predicted IR spectrum of $P_5^{\ominus}$? With the 3-21G* basis set, the SCF harmonic vibrational frequencies are 560 (E_1), 533 (E_2), 510 (A_1), 351 (E_2), 244 (E_2), 212 (A_1), and 122 cm^{-1} (E_1). Thus, the attachment of $Na^{\oplus}$ in a C_{5v} symmetrical arrangement (as suggested by *Baudler*) does shift the E_1' vibrational frequency, but downward and by only 15 cm^{-1} (from 575 to 560 cm^{-1}). Moreover, the IR intensity is increased, but only to 0.5 km mol^{-1}, still very weak. Thus, the feature observed by *Baudler* et al. at 815 cm^{-1} cannot be one of the fundamental vibrational frequencies of a NaP_5 molecule with C_{5v} symmetry.

The present theoretical study *is* in harmony with *Baudler*'s assignment of a medium-intense polarized Raman band at 463 cm^{-1} to the A_1' P–P stretching fundamental. The ab initio[14] 3-21G* A_1' Raman intensity is 63 $Å^4$ amu^{-1}, which value may be characterized as "medium-intense" by comparison with known Raman intensities[15] (cf. e.g. 302 $Å^4$ amu^{-1} for the strongest Raman band (A_{1g}) in ethane and 6 $Å^4$ amu^{-1} for the analogous weaker Raman band (A_g) in ethylene). Our DZ + P + diffuse SCF prediction places the harmonic vibrational frequency at 509 cm^{-1}, or 9.9% above experiment. This is just the sort of error one would expect[9] from the neglect of correlation effects and anharmonicity in the theoretical treatment. Thus, theory and experiment concur for the observed Raman band but conflict for the assigned intense IR band at 815 cm^{-1}.

Can we suggest a possible interpretation of the strong IR band observed by *Baudler* et al.[2]? Conceivably. The $P_3^{\ominus}$ ion, which is valence isoelectronic with N_2O, probably has a $D_{\infty h}$ structure with short P–P bonds (1.920 Å) and an asymmetric P–P stretch ω_3 = 886 cm^{-1} at the DZ + P SCF level of theory. This harmonic vibrational frequency lies 8.7% above that observed by *Baudler* et al. and has a very large IR intensity, 338 km mol^{-1}. Thus, the theoretical asymmetric P–P stretch for $P_3^{\ominus}$ fits the Baudler $P_5^{\ominus}$ assignment very closely. However, *Baudler* et al. present no evidence that the NaP_5 studied experimentally may have been contaminated by NaP_3.

Received: November 21, 1988 [Z 3063 IE]
German version: *Angew. Chem. 101* (1989) 500

CAS Registry numbers:
NaP_5, 113035-94-2; $P_5^{\ominus}$, 109660-04-0.

[1] M. Baudler, *Angew. Chem. 99* (1987) 429; *Angew. Chem. Int. Ed. Engl. 26* (1987) 419.
[2] M. Baudler, S. Akpapoglou, D. Ouzounis, F. Wasgestian, B. Meinigke, H. Budzikiewicz, H. Münster, *Angew. Chem. 100* (1988) 288; *Angew. Chem. Int. Ed. Engl. 27* (1988) 280.
[3] J. T. Snodgrass, J. V. Coe, C. B. Friedhoff, K. M. McHugh, K. H. Bowen, *Chem. Phys. Lett. 122* (1985) 352.
[4] K. P. Huber, G. Herzberg, *Constants of Diatomic Molecules*, Van Nostrand Reinhold, New York 1979.
[5] M. S. Gordon, J. S. Binkley, J. A. Pople, W. J. Pietro, W. J. Hehre, *J. Am. Chem. Soc. 104* (1982) 2797.
[6] S. Huzinaga: *Approximate Atomic Wavefunctions. II*, (Department of Chemistry Report). University of Alberta, Edmonton, Alberta, Canada 1971.
[7] T. H. Dunning, P. J. Hay in H. F. Schaefer III (Ed.): *Modern Theoretical Chemistry, Vol. 3*, Plenum, New York, 1977, pp. 1–27.
[8] M. J. Frisch, J. A. Pople, J. S. Binkley, *J. Chem. Phys. 80* (1984) 3265.
[9] See, for example, H. F. Schaefer III in D. R. Lide, M. A. Paul (Eds.): *Critical Evaluation of Chemical and Physical Structural Information*, National Academy of Sciences, Washington, DC, USA 1974, pp. 591–602.
[10] J. R. Durig, L. A. Carreira, J. D. Odom, *J. Am. Chem. Soc. 96* (1974) 2688.
[11] N. J. Brassington, H. G. M. Edwards, D. A. Long, *J. Raman Spectrosc. 11*, (1981) 346.
[12] J. E. Rice, T. J. Lee, R. B. Remington, W. D. Allen, D. A. Clabo, H. F. Schaefer III, *J. Am. Chem. Soc. 109* (1987) 2902.
[13] See, for example, B. H. Besler, G. E. Scuseria, A. C. Scheiner, H. F. Schaefer III, *J. Chem. Phys. 89* (1988) 360.
[14] M. J. Frisch, Y. Yamaguchi, J. F. Gaw, H. F. Schaefer III, J. S. Binkley, *J. Chem. Phys. 84* (1986) 531.
[15] M. Gussoni in W. B. Person, G. Zerbi (Eds.): *Vibrational Intensities in Infrared and Raman Spectroscopy*, Elsevier, Amsterdam, 1982, pp. 221–238.

2′-Aminomethylbiphenyl-2-carboxylic Acid as Component of a Cyclopeptide; Crystal Structure and Conformation in Solution**

By *Volker Brandmeier, Martin Feigel** and *Matthias Bremer*

One of the main objectives in peptide chemistry is to achieve a preferred conformation in a peptide unit by the incorporation of pseudo-amino acids.[1–3] Since relatively rigid natural peptides contain aromatic groups as spacers,[4] it is reasonable to assume that inflexibility may be realizable in the same way in syntheses with pseudo-amino acids. Even the fixation of antiparallel peptide chains to a β-pleated sheet seems possible with arenes, whereby the bridge molecules serve as substitute for the β-turn.[1d] We report here on the incorporation of 2′-aminomethylphenyl-2-carboxylic acid **1** in a cyclopeptide.

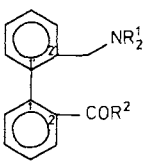
Formation of a cyclic array from two units of **1** and two L-amino acids affords, e.g., the compound **3**. If **1** is considered as substitute for the two central amino acids of a β-turn,

[*] Dr. M. Feigel, Dipl.-Chem. V. Brandmeier, Dipl.-Chem. M. Bremer
Institut für Organische Chemie der Universität
Henkestrasse 42, D-8520 Erlangen (FRG)

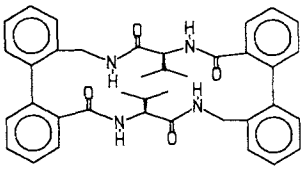
[**] This work was supported by the Deutsche Forschungsgemeinschaft. We thank Hoechst AG for carrying out the analyses.

then **3** is an analogue of a cyclohexapeptide. Cyclohexapeptides often have a structure determined by two β-turns which remains unchanged in the solid state and in solution.[5] Is a similar structure preferred with **1** in the ring?

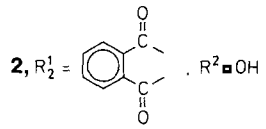
Three diastereomers which differ in the atropisomerism of the biphenyl moieties are expected for the cyclic compound **3**. The two isomers with biphenyl units of the same configuration (*R,R* or *S,S*) have C_2 symmetry, whereas the isomer with *R,S*-configurated biphenyl units is C_1 symmetric.



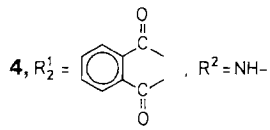
1, $R^1 = H, R^2 = OH$



3



2, $R^1_2 =$, $R^2 = OH$



4, $R^1_2 =$, $R^2 = NH\text{-}CH(iPr)\text{-}COOMe$

The pseudo-amino acid **1** is accessible as *N*-phthalimide-protected derivative **2** in 60% yield in two steps from diphenic anhydride.[6] Coupling of methyl valinate to **4**, cleavage of the protecting group with hydrazine, and cyclodimerization (azide method according to *Medzihradszky*, see Ref. [7]) affords **3** in moderate yield (22%) as a mixture of three isomers **3A**, **3B** and **3C**, which can be separated chromatographically (15% **3A**, 5% **3B**, 2% **3C**). The ^{1}H-NMR spectra show that **3A** and **3C** are isomers with C_2 symmetry (single set of signals), whereas **3B** has C_1 symmetry. When **3A** is dissolved in $CDCl_3$ and the solution is kept at 55 °C for 24 h a 1:1:1 mixture of the three isomers **3A**–**3C** is obtained. A mixture of all three isomers is also formed from **3A**, **3B** or **3C** in dimethyl sulfoxide (DMSO) after briefly heating to 80 °C. When the chromatographically separated isomers are crystallized from acetonitrile, **3A** is obtained in crystalline form from fraction 1 (= **3A**). **3C** (C_2 symmetry) crystallizes in both cases from fractions 2 (= **3B**) or 3 (= **3C**). **3B** could so far not be obtained in crystalline form.

This relatively rapid, reversible interconversion of the isomers (solvent, temperature, half-life (ca): $CDCl_3$, 55 °C, 10 h; DMSO, 80 °C, a few minutes) rules out any difference in the chirality of the amino acid valine in **3A**, **3B** and **3C**, for a much slower epimerization would be expected without base catalysis. The isomerization is thus apparently an atropisomerization of the biphenyl units. **3B** with C_1 symmetry contains *R*- and *S*-configurated biphenyl units, whereas **3A** and **3C** (each with C_2 symmetry) contain *R,R*- or *S,S*-configurated biphenyl units.

The X-ray structure analysis shows that **3A** has almost C_2 symmetry in the solid state (Fig. 1, because of the incorporation of one acetonitrile molecule per molecule of **3A** in the crystal, the isopropyl groups have different orientation, so that the actual symmetry is only C_1). Both valine units have identical configuration. The chirality analysis by hydrolysis and chiral gas chromatography showed the presence of L-valine; thus, the biphenyl moieties in **3A** have *S,S*-configuration, and in **3C**, correspondingly, *R,R*-configuration.

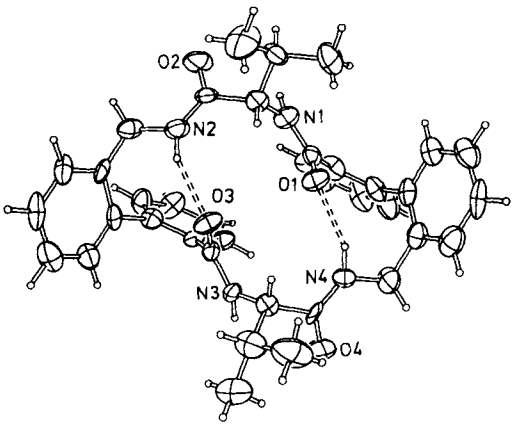


Fig. 1. Structure of **3A** in the crystal [13] (ORTEP).

All amide bonds of **3A** are *trans*-oriented in the solid state. The phenyl rings in the biphenyl units are twisted by torsion angles of 109 and 108° respectively. A striking feature is that each of the carbonyl groups on the biphenyl units is twisted about 40° from the ring plane of the arene in the direction of the amide proton of the same biphenyl unit. The C atoms of these carbonyl groups are located 10° outside of the ring planes. The two peptide torsion angles φ(−124.7, −118.9) and ψ(96.6, 98.6) at the valine units lie in the energetically flat region of the Ramachandran diagram (between the geometries of idealized β-pleated sheet and γ-loop).[14] Bond lengths and torsion angles of the isopropyl side chains are within the range of statistical variance of an analysis of the side chain conformations of valine units in crystal structures.[8] The bond angles in the lower valine unit in Figure 1 deviate up to 4° from the statistical mean, which is not unusual in strained systems.[8]

The O–N distances between CO (biphenyl) and CH_2NH are 2.87 (N4–O1) and 2.83 Å (N2–O3), respectively, and thus lie in a range typical for hydrogen bonded O and N atoms.[9] The reversal of the peptide chain is achieved by the pseudo-amino acid **1**, but the observed pattern cannot be compared very well with known peptide loop patterns. Under no circumstances is a pseudo β-turn present, since the NH and CO groups of the two valine units would then form hydrogen bonds between the chains. Rather, one can speak of a δ-turn; this, however, has thus far only been found with central *cis* amide bonds.[10, 3a]

Is the solid-state conformation **3A** also retained in solution? The ^{1}H NMR spectrum of **3A** shows only one set of signals, i.e. C_2 symmetry is observed, at least on a time average. The values determined from coupling constants (in $CDCl_3$) for the NH–CH dihedral angles are in good agreement with the angles in the solid state (Table 1). ^{1}H NMR data also confirm the presence of the two H bonds: both the temperature gradients ($\Delta\delta/\Delta T \times 10^3$ [K^{-1}] in DMSO: 3.2 (CH_2NH), 7.2 (*i*PrCHNH)) as well as the solvent dependence of the chemical shifts of the amide protons ($\delta_{DMSO} - \delta_{CDCl_3}$: 0.0 ($CH_2NH$), 1.6 (*i*PrCHNH) show that the amide protons, which form H bonds in the solid state, are shielded against the solvent in solution, not however the amide protons which are free in the solid state.

The spatial environment of the protons in the solid state is also retained in solution ($CDCl_3$): all cross signals in

Table 1. Comparison of the dihedral angles derived from vicinal coupling constants of **3A** in $CDCl_3$ [12] with the angles from the X-ray structure analysis. The coupling constants in DMSO deviate somewhat from those in $CDCl_3$ (see text).

Centers	$^3J(CDCl_3)$ [Hz]	$\theta(CDCl_3)$ [°]	θ(X-ray structure analysis) [°] [a]	^3J(DMSO) [Hz]
*i*PrCH, NH	10.3	160–180	174/174	8.8
$CH_2(H_a)$, NH	6.0	25–32/130–137	129/123	5.8
$CH_2(H_b)$, NH	2.5	55–60/110–116	109/117	3.9

[a] Two values per dihedral angle because of C_1 symmetry of the solid state conformation (see text and Fig. 1).

2D NOE NMR spectra (NOESY or ROESY[11]) correspond to short H–H distances in the solid state (Table 2). The converse, namely that each short H–H distance in the solid state gives a cross signal in the NMR spectrum in solution, also holds true.

Table 2. NOE effects in the ^1H NMR spectra of **3A** in $CDCl_3$ and corresponding proton–proton distances in the solid state. Cross signals between aryl protons are not taken into consideration.

Centers	NOE-intensity	*d* (X-ray structure analysis) [Å] [a]
$CH_2(H_b)$, CH_2NH	+	2.57/2.98
CH_2NH, *i*PrCH	+ +	2.53/2.42
$CH_2(H_a)$, H-3′	+ +	2.34/2.66
$CH_2(H_b)$, H-6	+	2.62/2.74
NH(Val), H-3	+ +	2.62/2.35
NH(Val), *i*PrCH	+	2.67/2.70

[a] Two values per proton pair because of the C_1 symmetry of the solid state conformation.

Thus, all NMR data suggest that the conformation determined by the X-ray structure analysis is retained in $CDCl_3$; in the polar solvent DMSO, however, the structure of **3A** is less rigid. DMSO solvates the polar amide bonds better, so that intramolecular interactions are no longer effective. This manifests itself in the faster transformation of the atropisomers in DMSO and in the coupling constants (Table 1), which are rather mean values of the coupling constants of several conformations.

With **3A** it has thus been possible for the first time to determine the influence of a biphenyl-containing pseudo-amino acid (**1**) on the conformation of a cyclopeptide (**3**), both in the solid state as well as in solution. The conformation of the atropisomer **3A** is identical in the crystal and in $CDCl_3$; in DMSO, deviations are possible. **1**, as part of the cyclopeptide, effects a reversal of the peptide chain and thereby generates a new type of peptide loop. Derivatives with other amino acids will show whether the cross-linking of the antiparallel peptide chains by hydrogen bridges also exists in longer chains.

Experimental

N-(2′-Phthalimidomethylbiphenyl-2-carbonyl)valine methyl ester **4**: A solution of **2** [6] (3.27 g, 9.2 mmol) and H-Val-OMe·HCl (1.53 g, 9.2 mmol) in CH_2Cl_2 (50 mL) was treated at −10 °C, first with 5.5 mL (50 mmol) of *N*-methylmorpholine (NMM) and then dropwise with 6.2 mL of a 50% solution of propylphosphonic acid anhydride (39 mmol). After removal of the solvent by evaporation the residue was taken up in ethyl acetate, washed with saturated $NaHCO_3$ solution, saturated NaCl solution and 5% $NaHSO_4$ solution, and dried over $MgSO_4$. The oily **4** obtained after removal of the ethyl acetate by evaporation was used in the next step of the synthesis without further purification (yield: 3.3 g, 77%).—^1H NMR (400 MHz, $CDCl_3$, 23 °C, 2 sets of signals because of biphenyl atropisomerism): δ = 7.90–7.25 (m, 12H; H_{aryl}), 7.66 (d, 1H; NH), 7.58 (d, 1H; NH), 4.93 (2 AB, 4H; CH_2), 4.50 (dd, 1H; *i*PrCH), 3.83 (dd, 1H; *i*PrCH), 3.70 (s, 3H; OMe), 3.37 (s, 3H; OMe), 2.02 (m, 1H; Me_2CH), 1.86 (m, 1H; Me_2CH), 0.78 (2d, 6H; 2 CH_3), 0.51 (d, 3H; CH_3), 0.37 (d, 3H; CH_3).—EI-MS: *m/z* (%) 470 (62, $M^{\oplus}$), 411 (21), 339 (61), 310 (100), 160 (99).

3: A solution of **4** (3.17 g, 6.7 mmol) in methanol (30 mL) was treated with 4.0 mL (80 mmol) of $N_2H_4 \cdot H_2O$ and the mixture stirred for 15 h at room temperature. The precipitated phthalhydrazide was filtered off and the filtrate evaporated down and dried. The residue (**1**, but R^2 = Val-hydrazide) was taken up in THF (50 mL) and the solution cooled to −20 °C. After addition of conc. HCl (5.6 mL) and a solution of 500 mg (7.2 mmol) of $NaNO_2$ in 5 mL of water the resulting suspension was stirred for 90 min. After dilution with 25 mL of THF (cooled to −10 °C) and addition of 11.0 mL (100 mmol) of NMM the mixture was warmed within ca. 12 h to 0 °C and allowed to stand at room temperature for 2 d. The solvent was then removed by evaporation and the residue was taken up in 300 mL of ethyl acetate and washed with $NaHCO_3$, NaCl, and $NaHSO_4$ solutions. The crude product obtained after drying and removal of the solvent was purified by column chromatography (silica gel 60, $CHCl_3$/THF = 5/1). Three fractions were collected (yields: fraction 1 (= **3A**): 330 mg, 15%; fraction 2 (= **3B**): 8 mg, 5%; fraction 3 (= **3C**): 29 mg, 2%). The three fractions were first characterized by ^1H NMR and DCI-MS and then recrystallized from acetonitrile. Crystalline fractions of **3A** and **3C**, after hydrolysis and derivatization as perfluoropropionylvaline isopropyl esters, were investigated by gas chromatography on a Chirasil-Val capillary column for their enantiomeric purity. The results were, in the case of **3A** 93.8% L-Val and 6.2% D-Val and in the case of **3C** 93.6% L-Val and 6.4 D-Val.—Selected data for **3A**: m.p. 207–220 °C. Satisfactory C, H, N analysis.—^1H NMR (400 MHz, $CDCl_3$, 23 °C): δ = 8.33 (b, 2H; CH_2NH), 7.53–6.93 (m, 16H; aryl), 6.12 (d, 2H; $CHNH$), 4.25 (AB, 4H; CH_2), 4.08 (t, 2H,; *i*PrCH), 2.03 (m, 2H; Me_2CH), 0.82 (d, 6H; CH_3), 0.72 (d, 6H; CH_3). $^{13}C\{^1H\}$ NMR (100.5 MHz, $CDCl_3$): δ = 170.2 (CH−C=O), 167.7 (Aryl-C=O), 141.4, 140.4, 134.1, 134.0, 130.9, 130.7, 130.4, 128.2, 128.1, 127.6, 127.5, 127.3 (C_{aryl}), 58.5 (*i*PrCH), 43.4 (Aryl-CH_2), 29.5 (Me_2CH), 19.3 (CH_3), 17.8 (CH_3). DCI-MS (NH_3, negative): *m/z* (%) 616 (100, $M^{\ominus}$), 426 (2), 408 (2), 241 (10), 162 (6).

Received: November 11, 1988;
revised: December 27, 1988 [Z 3046 IE]
German version: *Angew. Chem. 101* (1989) 466

CAS Registry numbers:
1 (R^2 = NH-CH*i*Pr-CO-$NHNH_2$ instead of OH), 119297-33-5; **2**, 119297-30-2; **3**, 119297-31-3; **4**, 119297-32-4; H-Val-OMe·HCl, 6306-52-1.

[1] For example synthetic β-loops: a) D. S. Kemp, P. E. McNamara, *J. Org. Chem. 50* (1985) 5834; b) U. Nagai, K. Sato, *Tetrahedron Lett. 26* (1985) 647; c) K. Sato, U. Nagai, *J. Chem. Soc. Perkin Trans. 1 1986*, 1231; d) M. Feigel, *J. Am. Chem. Soc. 108* (1986) 181; e) M. Kahn, S. Wilke, B. Chen, K. Fujita, *ibid. 110* (1988) 1638.

[2] Surrogates of peptide bonds: A. F. Spatola in B. Weinstein (Ed.): *Chemistry and Biochemistry of Amino Acids*, Marcel Dekker, New York 1983, p. 267–357.

[3] Examples of aromatic pseudo-amino acids: a) P. van der Elst, E. van den Berg, H. Papermans, L. van der Auwera, R. Zeeuws, D. Trouwe, G. van Binst, *Int. J. Pept. Protein Res. 29* (1987) 318; b) M. Feigel, G. Lugert, C. Heichert, *Liebigs Ann. Chem. 1987*, 367.

[4] a) S. D. Jolad, J. J. Hoffmann, S. J. Torrance, R. M. Wiedhopf, J. R. Cole, J. K. Arora, R. B. Bates, R. L. Gariulo, G. R. Kriek, *J. Am. Chem. Soc. 99* (1977) 8040; b) D. H. Williams, M. P. Williamson, D. W. Butcher, S. J. Hammond, *ibid. 105* (1983) 1332.

[5] Y. A. Ovchinnikov, V. T. Ivanov, *The Proteins Vol. V, Cyclic Peptides*, Academic Press, New York 1982, p. 308.

[6] V. Brandmeier, M. Feigel, *Tetrahedron 45* (1989), in press.

[7] Y. S. Klausner, M. Bodansky, *Synthesis 1974*, 549.

[8] R. O. Gould, A. M. Gray, P. Taylor, M. D. Walkinshaw, *J. Am. Chem. Soc. 107* (1985) 5921.

[9] C. Toniolo, *CRC Crit. Rev. Biochem. 9* (1980) 1.

[10] A. N. Stroup, A. L. Rockwell, A. L. Rheingold, L. M. Gierasch, *J. Am. Chem. Soc. 110* (1988) 5157.

[11] H. Kessler, C. Griesinger, R. Kerssebaum, K. Wagner, R. R. Ernst, *J. Am. Chem. Soc. 109* (1987) 607.

[12] V. F. Bystrov in J. W. Emsley, J. Feeney, L. H. Sutcliffe, *Prog. Nucl. Magn. Reson. Spectrosc. 10* (1976) 41.

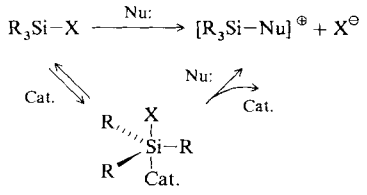
[13] **3A**: colorless rectangular platelets from acetonitrile, single crystal $0.4 \times 0.4 \times 0.2$ mm^3; monoclinic, space group $P2_1$, a = 791.2(3), b = 1708.0(11), c = 1387.2(6) pm, β = 103.23(3)°, $V = 1825 \times 10^6$ pm^3, Z = 2; 4850 reflections measured; asymmetric data set 4111 reflections, 2489 with $F > 2\sigma(F)$ observed. 401 refined parameters, R = 0.116, R_w = 0.086. Further details of the crystal structure investigation are available on request from the Fachinformationszentrum Energie, Physik, Mathematik GmbH, D-7514 Eggenstein-Leopoldshafen 2 (FRG), on quoting the depository number CSD-53482, the names of the authors, and the journal citation.

[14] See, e.g., A. L. Lehninger, *Biochemistry*, Worth, New York 1975, Chap. 6.

A Compound Containing Hexacoordinated Silicon —a Model for Nucleophilic Attack on Anionic, Pentacoordinated Silicon Species?

By *Francis Carré, Geneviève Cerveau, Claude Chuit, Robert J. P. Corriu,** and *Catherine Réyé*.

Species containing hexacoordinated silicon have been proposed as intermediates (or transition states) in the course of chemical reactions at silicon.[1, 6] Such species are uncharged when they are formed by nucleophilic solvents such as hexamethylphosphoric triamide (HMPA) dimethylformamide (DMF) or dimethyl sulfoxide; this is the case in the racemization,[1] hydrolysis or alcoholysis of chlorosilanes.[3] Anionic complexes result in the activation of SiH[4], SiO[4, 7, 8], SiN[9] and SiC[10, 11] bonds by fluoride anions; this provides a very useful catalytic procedure for organic syntheses. Recently, the role of such hypervalent silicon species (both penta- and hexacoordinated) has been most clearly demonstrated in the case of group transfer polymerization.[6] In all cases the mechanisms proposed[2] involve nucleophilic attack on an anionic or neutral pentacoordinated silicon species (Scheme 1).

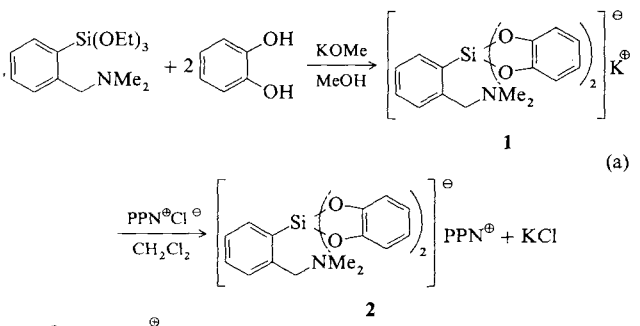


Scheme 1. Cat = $F^{\ominus}$, $RCO_2^{\ominus}$, HMPA, DMSO.

We have already reported on nucleophilic reactions at the anionic, pentacoordinated silicon center of catechol silicates[12] and shown the enhanced reactivity of pentavalent species (neutral[13] or anionic[14]) compared to that of the corresponding four-coordinate neutral species.

The concept developed by *Dunitz* et al.[15] that molecular interactions in the solid state provide an indication of preferred pathways in chemical reactions motivated our interest in attempting to synthesize an anionic pentacoordinated silicon complex which might become hexacoordinated through a dative Si ← N bond. Such a compound would provide a model for nucleophilic attack on an anionic, pentacoordinated silicon atom.

Herein, we wish to report on the structure of the (PPN)-silicate **2** (PPN = bis(triphenylphosphoranylidene)ammonium)[16] prepared according to equation (a).



(a)

$PPN^{\oplus} = Ph_3P{=}\overset{\oplus}{N}{=}PPh_3$

[*] Prof. R. J. P. Corriu, F. Carré, G. Cerveau, C. Chuit, C. Réyé
Institut de Chimie Fine
Université des Sciences et Techniques du Languedoc
Unité Associée C.N.R.S. UA n° 1097
Place E. Bataillon, 34060 Montpellier Cedex (France)

The molecular structure of **2** was determined by a crystal structure analysis.[17] The anion of the complex **2** tends to adopt an octahedral geometry (Fig. 1) with the atoms C91 and O4, O2 and N and O1 and O3 located opposite each other referred to the central silicon atom, giving bond angles of 167.3(4), 172.6(3) and 175.2(3)°, respectively. The remaining angles at the silicon atom are 80 to 96°. The silicon–

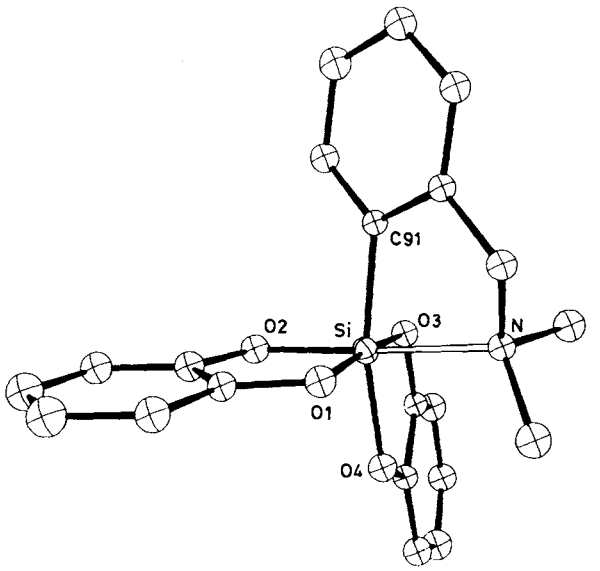
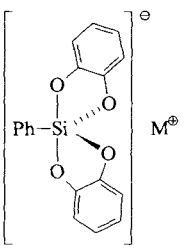
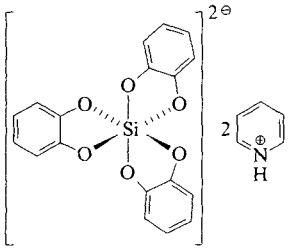


Fig. 1. Molecular structure of the anion of complex **2** (ORTEP, displacement spheres 20%, H atoms omitted for clarity). Selected bond lengths [Å] and bond angles [°] = Si-O1 1.779(7), Si-O2 1.785(7), Si-O3 1.785(6), Si-O4 1.776(7), Si-C91 1.917(9), Si-N 2.157(7); O1-Si-O3 175.2(3), O2-Si-N 172.6(3), O4-Si-C91 167.3(4), C91-Si-N 80.2(3), O1-Si-O2 89.6(3), O3-Si-O4 87.4(3).

carbon bond C91-Si, 1.917(9) Å, is exceptionally long (1.87 to 1.88 Å in Ph_4Si[18]). The four silicon–oxygen bond lengths are equal within the limits of experimental error (average 1.781(6) Å); noteworthy is that this value is significantly longer than that reported for the corresponding bonds in the anion of **3a** (average 1.747 Å[19]) and also longer than the values reported by *Holmes* et al.[20] for three related anions with pentacoordinated silicon (average of 1.744 Å). In contrast, the lengths of the six Si–O bonds in the anion of



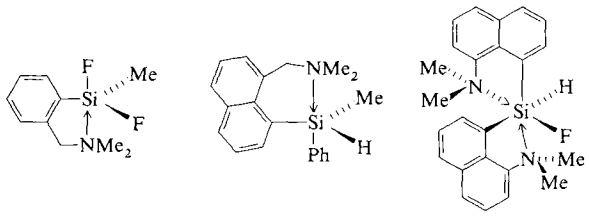
3a, M = Me_4N
3b, M = Na



4

4[21], a species with hexacoordinated silicon, are very similar to those in **2** (between 1.765 Å and 1.813(3) Å, average value 1.784 Å). We are therefore of the opinion that **2** more closely resembles a hexacoordinated species with formal doubly negatively charged silicon than a pentacoordinated species. This view is consistent with the short Si ← N distance: the length of the dative Si ← N bond (2.15 Å) is comparable to that observed in silatranes (5-aza-2,8,9-trioxa-1-silabicyclo[3.3.3]undecanes)[22] (2.0 to 2.4 Å), and shorter

than those in neutral compounds with pentacoordinated (e.g. **5**, **6**)[5, 23] and hexacoordinated silicon (e.g. **7**).[24]



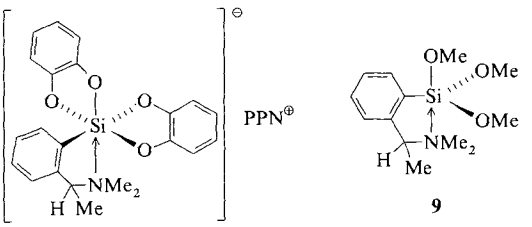
5 Si–N 2.35 Å

6 2.66 Å

7 2.68, 2.64 Å

In solution, the ^{29}Si chemical shift of **2** ($\delta = -121.2$) is similar to that of the hexacoordinated silicates of catechol,[25] while a shift of $\delta(^{29}Si) = -87.4$ is observed for the sodium salt **3b**.[12b] The ^1H NMR spectrum of **2** clearly shows the resonance of the NMe_2 groups as a sharp singlet even at low temperature (−100 °C). The lack of diastereotopism of the Me groups (NMe_2) can be explained either in terms of an intramolecular non-dissociative isomerization process such as a Bailar twist[26] or in terms of a rapid equilibrium between open and closed forms allowing rotation and inversion at the nitrogen center.

To clarify this point we synthesized the silicate **8**[27] in which, because of the chirality of the benzylic carbon, the NMe_2 group is rendered diastereotopic when the nitrogen atom is coordinated at silicon even when isomerization processes take place at the silicon. (The insertion of a chiral benzyl group had already allowed us to distinguish clearly between pseudorotation and ring opening-closing processes in the case of pentacoordinated silicon compounds.[28])



8

9

The ^1H NMR spectra of **8** recorded at several temperatures showed only one coalescence due to the chirality of the benzylic carbon (Fig. 2). This observation and that with the complex **2** (sharp singlet for the NMe_2 group) can be regarded as signs for an intramolecular non-dissociative isomerization process around silicon.

Moreover this ^1H NMR study (Fig. 2) allowed the evaluation of the free energy of activation of the Si ← N bond breaking: $\Delta G^* = 10.25$ kcal mol^{-1} ($T = -58$ °C). In the case of the trimethoxy compound **9**, ΔG^* was found to be 7.6 kcal mol ($T = -110$ °C).[29] This activation energy difference between the anionic compound and the neutral compound clearly indicates the high tendency of the anionic compound to undergo nucleophilic attack and confirms the increase in reactivity towards strong nucleophiles observed with anionic pentacoordinated silicon compounds, compared to that of the corresponding tetravalent neutral species.[13]

Thus, the hexacoordinate structure of **2** with almost regular octahedral angles and a short Si ← N bond (2.15 Å) provides strong support for the possibility of nucleophilic attack on an anionic pentacoordinated silicon species through a hexacoordinate intermediate, as postulated several years ago.[2] Furthermore, it is worth noting that the regular isomerization process around the silicon atom observed for **2** and **8** needs a very low activation energy since it persists even at very low temperatures.

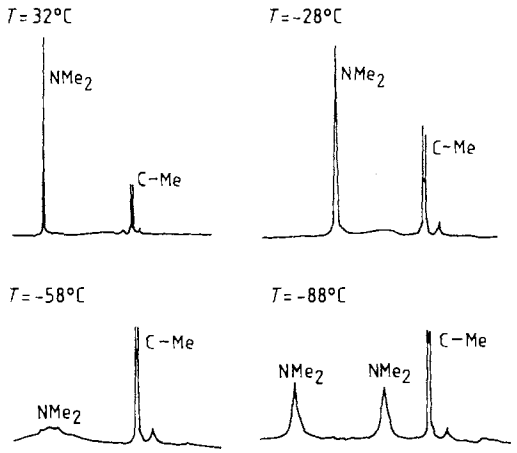


Fig. 2. ^1H NMR spectra of **8** at different temperatures, solvent CD_2Cl_2.

Received: November 24, 1988 [Z 3066 IE]
German version: *Angew. Chem. 101* (1989) 474

CAS Registry numbers:
1, 119596-24-6; **2**,119596-26-8; **2** · MeOH, 119596-29-1; **8**, 119596-28-0; ^{29}Si, 14304-87-1; catechol, 120-80-9; [2-(dimethylaminomethyl)phenyl]triethoxysilane, 87996-38-1; [2-(1-dimethylaminoethyl)phenyl]triethoxysilane, 119596-23-5.

[1] R. J. P. Corriu, M. Henner, *J. Organomet. Chem. 74* (1974) 1.
[2] R. J. P. Corriu, C. Guerin, J. J. E. Moreau, *Top Stereochem. 15* (1984) 158, and references cited therein.
[3] R. J. P. Corriu, G. Dabosi, M. Martineau, *J. Organomet. Chem. 150* (1978) 27; b) *ibid. 154* (1978) 33; c) *ibid. 186* (1980) 25.
[4] R. J. P. Corriu, R. Perz, C. Reyé, *Tetrahedron 39* (1983) 999, and references cited therein.
[5] R. J. P. Corriu, J. C. Young in S. Patai, Z. Rappoport (Eds.): *The Chemistry of Organic Silicon Compounds*, Wiley Interscience, New York 1988.
[6] D. Y. Sogah, W. B. Farnham in H. Sakurai (Ed.): *Organosilicon and Bioorganosilicon Chemistry*, Ellis Horwood, Chichester 1985, p. 219, and references therein.
[7] J. Boyer, R. J. P. Corriu, R. Perz, C., Reyé, *Tetrahedron 39* (1983) 117; R. J. P. Corriu, R. Perz, *Tetrahedron Lett. 26* (1985) 1311.
[8] I. Kuwajima, E. Nakamura, *J. Am. Chem. Soc. 97* (1975) 3257; I. Kuwajima, E. Nakamura, M. Shimizu, *ibid. 99* (1977) 1265.
[9] R. J. P. Corriu, V. Huynh, J. J. E. Moreau, M. Pataud-Sat, *Tetrahedron Lett. 23* (1982) 3257.
[10] E. Nakamura, T. Murofushi, M. Shimizu, I. Kuwajima, *J. Am. Chem. Soc. 98* (1976) 2346; A. Hosomi, A. Shirabata, H. Sakurai, *Tetrahedron Lett. 1978*, 3043; I. Kuwajima, E. Nakamura, K. Hashimoto, *Tetrahedron 39* (1983) 975.
[11] G. Cerveau, C. Chuit, R. J. P. Corriu, C. Reyé, *J. Organomet. Chem. 328* (1987) C17.
[12] a) A. Boudin, G. Cerveau, C. Chuit, R. J. P. Corriu, C. Reyé, *Angew. Chem. 98* (1986) 472; *Angew. Chem. Int. Ed. Engl. 25* (1986) 473; b) *Bull. Chem. Soc. Jpn 61* (1988) 101.
[13] J. Boyer, C. Breliere, R. J. P. Corriu, , A. Kpoton, M. Poirier, G. Royo, *J. Organomet. Chem. 311* (1986) C39.
[14] R. J. P. Corriu, C. Guerin, B. J. L. Henner, W. W. C. Wong Chi Man, *Organometallics 7* (1988) 237.
[15] D. Britton, J. D. Dunitz, *J. Am. Chem. Soc. 103* (1981) 2971.
[16] Bis(triphenylphosphoranylidene)ammonium bis(1,2-benzenediolato)[2-(dimethylaminomethyl)phenyl]silicate **2**: 6 mmol of catechol (0.66 g) and 3 mmol of [2-(dimethylaminomethyl)phenyl]triethoxysilane (0.89 g) were dissolved in 20 mL of methanol in a Schlenck tube under nitrogen; 3 mmol of KMeO in methanol (10 mL) was added dropwise at room temperature, and the resulting solution was then stirred for 4 hours at this temperature. After removal of the solvent under vacuum the residue was washed once with anhydrous ether. [PPN]Cl (3 mmol, 1.72 g) in CH_2Cl_2 (15 mL) was

then added dropwise to a suspension of the potassium complex in CH_2Cl_2 (15 mL) and the mixture stirred for 30 min. Removal of the KCl by filtration under nitrogen followed by removal of the solvent under vacuum afforded **2** as a white powder. After crystallization from MeOH, white crystals were obtained (67% yield, 1.84 g): mp 183–187 °C.—^{1}H NMR (CD_2Cl_2): δ = 2.35 (s, 6H, NMe_2), 3.71 (s, 2H, CH_2N), 6.2–6.6 (m, 8H), 6.84–7.0 (m, 4H), 7.2–7.75 (m, 30H); ^{29}Si NMR (CD_2Cl_2): δ = −121.2; negative-ion FAB MS m/z −378 ($[M-PPN]^{\ominus}$).

[17] Crystal structure data of **2** from CH_3OH: monoclinic, space group $P2_1$, a = 10.448(3), b = 25.150(7), c = 9.544(3) Å, β = 98.43(2)°, V = 2480.8 Å^3, ϱ_{calcd} = 1.270 g cm^{-3}, $\mu(Mo_{K\alpha})$ = 1.6 cm^{-1}, Z = 2. 3661 unique reflections up to (sin θ/λ) = 0.572, 2200 with $F_0 \geq 2.4\,\sigma(F_0)$. Enraf-Nonius CAD4 diffractometer, $Mo_{K\alpha}$ radiation, λ = 0.71069 Å. T = 20 °C). Solution by direct methods (MULTAN-80). $R(R_w)$ = 0.051 (0.053), $w = 1/(\sigma^2(F_0) + 0.011\,F^2)$ for 299 refined parameters (P and Si atoms anisotropic, all others isotropic, CH_3 as rigid groups, SHELX-76) $\Delta\varrho_{fin}$ = 0.38 e^- Å^{-3}. Further details of the crystal structure investigation may be obtained from the Cambridge Crystallographic Data Centre, University Chemical Laboratory, Lensfield Road, Cambridge CB2 1EW, England, on quoting the depository number, the names of the authors, and the journal citation.

[18] C. Glidewell, G. M. Sheldrick, *J. Chem. Soc. (A) 1971*, 3127.

[19] F. P. Boer, J. J. Flynn, J. W. Turley, *J. Am. Chem. Soc. 90* (1968) 6973.

[20] R. R. Holmes, R. O. Day, J. J. Harland, J. M. Holmes, *Organometallics 3* (1984) 347.

[21] J. J. Flynn, F. P. Boer, *J. Am. Chem. Soc. 91* (1969) 5756.

[22] M. G. Voronkov, V. M. D'Yakov, S. V. Kirpichenko, *J. Organomet. Chem. 233* (1982) 1.

[23] a) C. Breliere, F. Carre, R. J. P. Corriu, M. Poirier, G. Royo, *Organometallics 5* (1986) 388; b) G. Klebe, *J. Organomet. Chem. 332* (1987) 35.

[24] a) C. Breliere, F. Carre, R. J. P. Corriu, M. Poirier, G. Royo, J. Zwecker, *Organometallics*, in press; b) G. Sawitzki, H. G. von Schnering, *Chem. Ber. 109* (1976) 3728.

[25] J. A. Cella, J. D. Cargioli, E. A. Williams, *J. Organomet. Chem. 186* (1980) 13.

[26] J. C. Bailar, *J. Inorg. Nucl. Chem. 8* (1958) 165; R. S. Michalak, S. R. Wilson, J. C. Martin, *J. Am. Chem. Soc. 106* (1984) 7529; F. Carre, E. Colomer, R. J. P. Corriu, M. Lheureux, *J. Organomet. Chem. 331* (1987) 29.

[27] Complex **8** was prepared in exactly the same way as complex **2** [16]. After crystallization from MeOH, colorless crystals were obtained (69% yield) m.p. 143.5 °C; ^{1}H NMR (CD_2Cl_2): δ = 1.31 (d, 3H), 2.2 (s, 6H; NMe_2), 4.22 (q, 1H), 6.21–6.61 (m, 8H), 6.85–7.18 (m, 4H), 7.18–7.72 (m, 30H); ^{29}Si NMR (CD_2Cl_2): δ = −119.88; negative ion FAB-MS: m/z −392 ($[M-PPN]^{\ominus}$).

[28] R. J. P. Corriu, A. Kpoton, M. Poirier, G. Royo, J. Y. Corey, *J. Organomet. Chem. 277* (1984) C25.

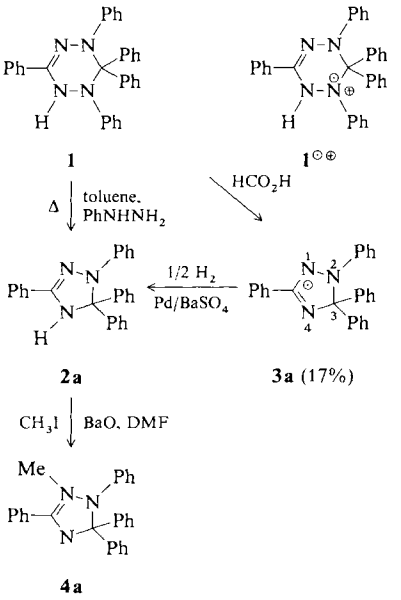
[29] R. J. P. Corriu et al., unpublished results.

2,3-Dihydro-1*H*-1,2,4-triazol-1-yls, a Novel Group of Stable Radicals**

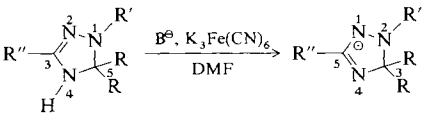
By *Franz A. Neugebauer,* Hans Fischer,* and *Claus Krieger*

After addition of tetracyanoethylene, $FeCl_3$ or BF_3-ether, solutions of leucoverdazyl **1** show a strong ESR signal. The partially resolved ESR spectrum was assigned to the leucoverdazyl radical cation $\mathbf{1}^{\odot\oplus}$.[1]

This surprising detection of a leucoverdazyl radical cation prompted us to check the observations. By chromatographic separation of the reaction mixtures, e.g. of the solution of **1** in formic acid, we were able to isolate a stable monomeric radical. The ESR spectrum of this radical (Fig. 1) is virtually the same as the ESR spectrum of the solution of **1** in 1,4-dioxane + BF_3-ether, regarding its spectral range and hyperfine structure. The constitution of the radical was deduced from chemical reactions and confirmed by X-ray structure analysis (Fig. 2). Accordingly the radical is 2,3-dihydro-2,3,3,5-tetraphenyl-1*H*-1,2,4-triazol-1-yl **3a**.[2] Hydrogenation of **3a** (0.5 mol H_2, $Pd/BaSO_4$) led to the leuco compound **2a**,[2] methylation of which afforded only the 1-methyl derivative **4a**,[2] obviously for steric reasons.—Evidence for the radical cation $\mathbf{1}^{\odot\oplus}$ was not found.



The 4,5-dihydro-1*H*-1,2,4-triazoles **2** were found to be suitable educts for the generation of radicals of type **3**. Compound **2a** (m.p. 192–193 °C, yield 72%) was prepared from **1** by thermal ring contraction. Reaction of *N*-phenylacetamidrazone with dichlorodiphenylmethane and BaO in dimethylformamide afforded **2b** (m.p. 179–180 °C, yield 41%). **2c** was obtained by reaction of *N*-phenyl-benzohydrazonyl chloride with 9-aminofluorene (m.p. 231–232 °C, yield 31%). All the compounds have been satisfactorily characterized.[2]



2 **3**

	R	R	R′	R″
a	Ph	Ph	Ph	Ph
b	Ph	Ph	Ph	Me
c	2,2′-biphenyldiyl			Ph
d	Me	Me	Me	Ph

The stable radicals **3a–c**[2] can be obtained from **2a–c** by dehydrogenation, e.g., with PbO_2, Ag_2O or $K_3Fe(CN)_6$. **3a** crystallizes from ethyl acetate in the form of black prisms (m.p. 162–163 °C, yield 90%). The ESR spectrum of **3a** is reproduced in Figure 1. **3b** crystallizes from cyclohexane/petrol ether (b.p. 40 °C) as dark-brown crystals (m.p. 77–78 °C, yield 51%), while **3c** separates from cyclohexane in the form of black crystals (m.p. 170–171 °C, yield 77%). The stability of the radicals decreases considerably when the phenyl substituents in positions 2 and 3 are replaced by methyl groups. It was not possible to isolate the radical **3d** obtained from **2d**.[3] All ENDOR/TRIPLE data are collected in Table 1.

[*] Prof. Dr. F. A. Neugebauer, H. Fischer, C. Krieger
Abteilung Organische Chemie,
Max-Planck-Institut für medizinische Forschung
Jahnstrasse 29, D-6900 Heidelberg 1 (FRG)

[**] This work was supported by the Deutsche Forschungsgemeinschaft and the Fonds der Chemischen Industrie.

Table 1. Isotropic HFS coupling constants [mT] of **3a–d** in toluene; ENDOR/TRIPLE at 230 K [a].

	3a	**3b**	**3c**	**3d**
$a(N^1)$	0.644	0.654	0.647	+0.642
$a(N^2)$	0.758	0.755	0.726	+1.049
$a(N^4)$	0.395	0.379	0.380	+0.398
a(H)(2-CH_3)				+0.953
a(H)(3,3-CH_3)				−0.051
a(H)(2,4,6-H von 2-Ph)	−0.196	−0.202	−0.200	
a(H)(3,5-H von 2-Ph)	+0.069	+0.068	+0.067	
a(H)(5-CH_3)		−0.090		
a(H)[b]	≈ +0.0017	0.020	+0.040	
a(H)[b]			+0.019	

[a] The tentative assignments of the $a(N^1)$ and $a(N^2)$ couplings have to be confirmed by ^{15}N-labeling; ENDOR data conversion 1 mT = 28.042 MHz. [b] The assignment of this proton coupling, apparently from the substituents R, is still open.

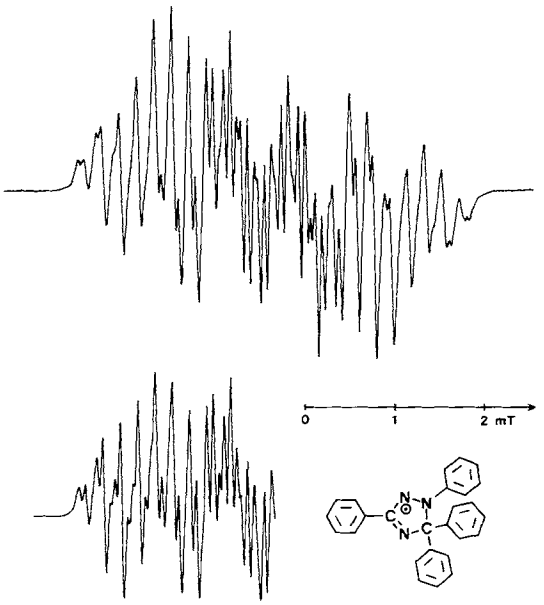


Fig. 1. ESR spectrum of **3a** in toluene (297 K); the lower half-spectrum is a simulation using the data $a(N^1) = 0.645$, $a(N^2) = 0.760$, $a(N^4) = 0.395$, a(H) (2,4,6-H of 2-Ph) = 0.195, a(H) (3,5-H of 2-Ph) = 0.070 mT.

The X-ray structure analysis of **3a**[4] reveals an almost planar 2,3-dihydro-1*H*-1,2,4-triazol-1-yl ring (Fig. 2), with the conjugated phenyl substituents in positions 2 and 5 almost coplanar. The N(1)–C(5) and N(1)–N(2) distances, which indicate considerable double-bond character (≈ 50%), correspond to the bond lengths of comparable hydrazyl partial structures; 1,3,5-triphenylverdazyl: C–N = 138, N–N = 135 pm,[5] 2,2-diphenyl-1-picrylhydrazyl: N–N = 133 pm.[6] The N–C_{Ph} bonds of these radicals are ≈ 142 pm long. The somewhat shorter N(2)–C(A1) distance (139.6 pm) in **3a** is a good indication that the unpaired electron is slightly more delocalized into the coplanar oriented *N*-phenyl ring. Consistent with this, relatively large couplings are found for the protons of the *N*-phenyl substituents by ESR. The C(5)–N(4) distance (130.5 pm) in **3a** almost corresponds to a C=N double bond (≈ 125 pm); the adjacent N(4)–C(3) bond is a perfect single bond (C–N ≈ 147 pm). The C(3)–N(2) distance is exceptionally large (150.6 pm). Most probably, this is a result of the steric repulsion of the three closely adjacent phenyl substituents on C(3) and N(2). According to the structure data of **3a** and the ESR-ENDOR results, the radicals **3a–d** have a π-SOMO which is mainly localized on N(1), N(2) and N(4). **3a–c** are

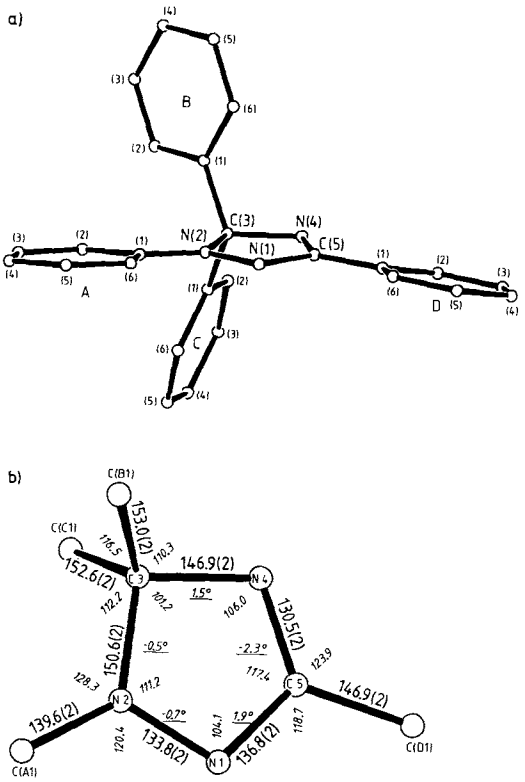


Fig. 2. Structure of **3a** in the crystal. a) Perspective drawing; b) bond lengths [pm], bond angles [°], and torsion angles [°] of the central 2,3-dihydro-1*H*-1,2,4-triazol-1-yl ring.

stable derivatives of the parent radical 2,3-dihydro-1*H*-1,2,4-triazol-1-yl, which has been observed by ENDOR (100 K) after ^{60}Co-γ-irradiation of 1,2,4-triazole single crystals:[7] $a[H^2(NH)] \approx -0.85$, $a(H^{3,3}) \approx +5.6$, $a(H^5) \approx -0.1$ mT; no a(N) data. The β-coupling of the protons in position 3 is one of the largest known proton couplings [H°: a(H) ≈ 50.6 mT]. This special case is a result of the binding of the methylene group to the two terminal atoms of a 5 π electron system (Whiffen rule[8]). Our synthesis of **3a–d** now provides the possibility of determining the comparative α- and β-^{13}C couplings in this system. This is currently being investigated.

Received: November 15, 1988 [Z 3053 IE]
German version: *Angew. Chem. 101* (1989) 486

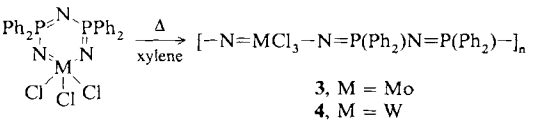
[1] A. M. Nesterenko, O. M. Polumbrik, L. N. Markovskii, *Zh. Org. Khim. 19* (1983) 1961; *J. Org. Chem. USSR (Engl. Transl.) 19* (1983) 1722.
[2] All the new compounds gave correct elemental analyses. UV, ^1H-NMR and mass spectra are in complete agreement with the described structures.
[3] K. N. Zelenin, V. A. Khrustalev, V. P. Sergutina, *Zh. Org. Khim. 16* (1980) 942; *J. Org. Chem. USSR (Engl. Transl.) 16* (1980) 822.
[4] **3a**: Black orthorhombic prisms from ethyl acetate, ca. 0.2 × 0.2 × 0.35 mm, $Pna2_1$, $a = 895.6(1)$, $b = 1515.9(2)$, $c = 1454.7(2)$ pm, $\varrho_{calcd} = 1.259$ g cm^{-3} for $Z = 4$. 2003 symmetry independent reflections measured (Nonius CAD4 diffractometer, MoK_α radiation). Solution of structure by direct methods. Refinement by full matrix least squares methods (non-H anisotropic, H isotropic) converged at $R = 0.028$ for 1625 observed reflections [$I > 2.0\,\sigma(I)$]. Further details of the crystal structure investigation are available on request from the Fachinformationszentrum Energie, Physik, Mathematik GmbH, D-7514 Eggenstein-Leopoldshafen 2 (FRG), on quoting the depository number CSD-53481, the names of the authors, and the journal citation.
[5] D. E. Williams, *J. Am. Chem. Soc. 91* (1969) 1243; *Acta Crystallogr. Sect. B 29* (1973) 96.
[6] D. E. Williams, *J. Am. Chem. Soc. 89* (1967) 4280.
[7] P. Gloux, B. Lamotte, *Mol. Phys. 25* (1973) 161; *24* (1972) 23; P. Gloux, *ibid. 21* (1971) 829.
[8] D. H. Whiffen, *Mol. Phys. 6* (1963) 223.

Synthesis and Analysis of Polymetallaphosphazenes**

By *Herbert W. Roesky** and *Michaela Lücke*

In the past few years increasing interest has been directed to an area of research that is not just confined to the traditional limits of inorganic chemistry. Thus, interactions between elements of the main- and sub-groups of the periodic table lead to novel catalysts and new precursors for ceramic and electronic materials.[1] *Allcock* et al. have recently reported the synthesis of polyphosphazenes containing metal complex fragments in the side chain, which they are now investigating with regard to their suitability as such catalytic systems etc.[2] We have now succeeded in incorporating transition metals directly into the polymer chain and thus in obtaining the first polymetallaphosphazenes.

In these novel polymers a phosphorus atom is replaced by a transition metal in each monomer unit; they are obtained via a ring-opening reaction[3] upon heating **1**[4] or **2**[5] in xylene.



1, M = Mo
2, M = W

3, M = Mo
4, M = W

The properties of **3** and **4** are noteworthy: they are virtually inert towards hydrolysis, even in boiling water, and they do not decompose below about 300 °C. Elemental analyses show that no eliminations occur as side reactions. The molecular weights of the fractions soluble in THF have been determined by HPLC[6] and viscometry[7] using polystyrene calibration standards.[8] Based on HPLC-measurements of the THF soluble fractions we have obtained molecular weights of 11 800 and 34 500 for **3** and 11 800, 34 500, and 68 000 for **4** (Table 1). The limiting viscosities obtained for the soluble fractions of **3** and **4** from the viscosity measurements were compared with those of the polystyrene calibration standards (Fig. 1).[9] The results yielded mean molecular weights of 24 000 for **3** and 37 000 for **4**.

Table 1. Molecular weights of the THF-soluble fractions of **3** and **4** and their percentage amounts.

Polymer	Mol.wt. [a]	Fraction of polymer with this mol.wt. [%]
3	11 800	41
	34 500	57
4	11 800	31
	34 500	40
	68 000	28

[a] The molecular weights determined by HPLC could be confirmed by GPC measurements.

Since **3** and **4** exhibit polyelectrolyte character, tetraethylammonium tetrafluoroborate had to be added as supporting electrolyte to ensure a normal run of these viscosity measurements.[10] We shall report elsewhere on the possible applications of these polymetallaphosphazenes.

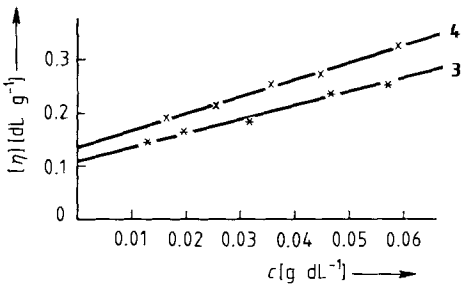


Fig. 1. Limiting viscosities of the polymer mixtures for the determination of the average molecular weights $\bar{M}$ of **3** and **4** (**3**: $[\eta]$ $(c \rightarrow 0) = 0.11$; $\bar{M} = 24000$; **4**: $[\eta]$ $(c \rightarrow 0) = 0.14$, $\bar{M} = 37000$).

Experimental:

3: A solution of **1** (0.2 g, 0.32 mmol) in dry xylene (50 mL) was stirred at room temperature under an atmosphere of N_2 for 1 h and then gradually warmed to 40 °C. After 1.5–2 h the temperature was raised to 80 °C. The reaction was complete after 12–16 h. After removal of the solvent (oil-pump vacuum, 10^{-3} torr) there remained a bright yellow, fine powder which was up to 55% soluble in xylene. This fraction was also soluble in THF, and inert to boiling water.—IR: $\tilde{\nu}$ = 1590 w, 1485 w, 1440 m, 1410 w, 1260 vs, 1220 w, 1170 m, 1100 s, 1040 s, 960 m, 940 m, 900 m, 860 m, 800 vs, 740 w, 730 m, 690 m, 580 w, 540 s, 510 m cm^{-1}.

4: A solution of **2** (0.2 g, 0.28 mmol) in dry xylene (50 mL) was stirred at room temperature under an atmosphere of N_2 for 1 h. The mixture was then heated for 1 h at 60 °C and a further 20 h at 110 °C. After removal of the solvent (oil-pump vacuum) there remained a light-brown solid which was up to 50% soluble in xylene. This fraction was also soluble in THF, and was inert towards boiling water.—IR: $\tilde{\nu}$ = 1590 w, 1480 w, 1435 vs, 1400 w, 1260 vs, 1175 w, 1150 w, 1120 s, 1060 m, 1035 m, 1020 m, 995 w, 970 m, 923 m, 800 s, 770 w, 750 m, 730 vs, 690 sh, 610 w, 550 s, 500 s cm^{-1}.

Received: September 29, 1988;
revised: December 12, 1988 [Z 2983 IE]
German version: *Angew. Chem. 101* (1989) 480

[*] Prof. Dr. H. W. Roesky, Dipl.-Chem. M. Lücke
Institut für Anorganische Chemie der Universität
Tammannstrasse 4, D-3400 Göttingen (FRG)

[**] This work was supported by the Deutsche Forschungsgemeinschaft and the Fonds der Chemischen Industrie. We thank Prof. Dr. *G. Wegner*, Mainz (FRG) for generous support.

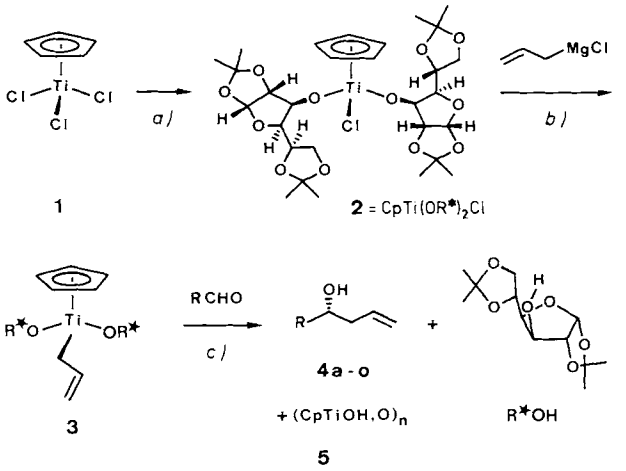
[1] F. L. Carter: *Molecular Electronic Devices*, Marcel Dekker, New York 1982; L. L. Hench, D. R. Ulrich: *Ultrastructure Processing of Ceramics, Glasses and Composites*, Wiley, New York 1984; H. W. Roesky, *Chem. Soc. Rev. 15* (1986) 309.
[2] H. R. Allcock, J. L. Desorcie, G. H. Riding, *Polyhedron 6* (1987) 119.
[3] R. H. Neilson, P. Wisian-Neilson, *Chem. Rev. 88* (1988) 541.
[4] H. W. Roesky, K. V. Katti, U. Seseke, H. G. Schmidt, E. Egert, R. Herbst, G. M. Sheldrick, *J. Chem. Soc. Dalton Trans. 1987*, 847.
[5] H. W. Roesky, K. V. Katti, U. Seseke, M. Witt, E. Egert, R. Herbst, G. M. Sheldrick, *Angew. Chem. 98* (1986) 447; *Angew. Chem. Int. Ed. Engl. 25* (1986) 477.
[6] Procedure for HPLC: LiChroCART® 250-4 column, LiChrospher® 1000 RP-8 (10 μm). Flow rate 0.5 mL/min, feed rate 10 mm/min, pressure 576 psi, temperature 25 °C. Solvent THF/methanol 1/99 or THF/water 55/45. Injection volume 1 μL. UV detection of **3** and **4** at 230 nm and of the polystyrene calibration standards 11 800, 34 500 and 68 000 [8] at 254 nm. Concentrations of **3** and **4** and the polystyrene calibration standard 1 μg/μL. After the analysis of the polymer mixtures of **3** and **4** the chromatograms obtained were compared with those of the polystyrene calibration standards.
[7] KPG® Ubbelohde viscometer Oa. 15 mL/25°C. **3** and **4** were dissolved as polymer mixture in 15 mL of THF, and, after addition of 20–30 mg of tetraethylammonium tetrafluoroborate, investigated viscometrically at 25 °C. The Staudinger index $[\eta]$ was determined by plotting the limiting viscosities against the concentration.
[8] Polystyrene calibration standard for lipophilic gel permeation chromatography from Merck AG, Darmstadt (FRG).
[9] The polystyrene calibration standards of molecular weights 11 800, 34 500, 68 000 and 127 000 were each measured in 15 mL of THF at 25 °C. The calibration curve was obtained by plotting the Staudinger indices $[\eta]$ versus the molecular weights.
[10] M. Hoffmann, H. Krämer, R. Ruhn, *Polymeranalytik I*, Thieme, Stuttgart 1977.

Enantioselective Allylation of Carbonyl Compounds with Titanium-Carbohydrate Complexes**

By *Martin Riediker** and *Rudolf O. Duthaler*

Among the stereoselective reactions reported so far the allylation of carbonyl compounds is unique in that several stereogenic centers can be generated in one step and the products exhibit versatile functionality.[1] High enantioselectivity and double stereocontrol are achieved with allylmetal compounds containing chiral ligands, especially good results being obtained with allylboron compounds,[2] allylstannanes[3] and allylsilanes.[4] Largely due to the pioneering work of *Seebach* et al.[5a] and *Reetz*,[5b] allyltitanium compounds and other organotitanates have been established as inexpensive, easily accessible and ecologically unobjectionable reagents. The chiral titanium complexes investigated so far, which have mainly been developed for asymmetric alkylation, were, however, not suited for the enantioselective transfer of allyl groups.[6, 7] The high diastereocontrol which can be achieved with such allyltitanium reagents[5, 8] would, nevertheless, lead one to expect that good enantioselectivity should also be realizable under suitable conditions. One of the first successes in this context was the high induction which was achieved in the transfer of chiral allyl groups to aldehydes.[9]

By reaction of cyclopentadienyltitanium(IV) trichloride **1**[10] with commercially available 1,2:5,6-di-*O*-isopropylidene-α-D-glucofuranose ("diacetone-glucose")/triethylamine we obtained the stable dialkoxy(chloro)cyclopentadienyl titanate **2**, which, in the absence of moisture, can be stored either as stock solution in ether (0.05–0.1 M) or toluene (0.1–0.2 M) or as crystalline solid after precipitation with hexane



Scheme 1. a) 1,2:5,6-Di-*O*-isopropylidene-α-D-glucofuranose/Et_3N/Et_2O, room temperature (RT); b) Et_2O, 0 °C; c) 1. −78 °C, 2. H_2O/THF, −30 °C to RT.

(Scheme 1). Highly stereoselective reagents can be prepared from this novel complex by exchange of the remaining chloro ligand for transferable groups.[11]

Thus, reaction of **2** with allylmagnesium chloride affords the allyltitanium complex **3**, which is brought to reaction in situ at −74 °C with aldehydes; addition at the *re*-side leads, with numerous substrates, to homoallyl alcohols **4** in good yields and with high enantiomeric purity (Scheme 1, Table 1). The temperature dependence of this reaction is astonishingly small; thus, reaction with benzaldehyde at 0 °C furnishes the product **4a** with 80% *ee*. By controlled hydrolysis the filterable titanate **5** can be precipitated and by treatment with HCl (g) reconverted into $CpTiCl_3$ **1**.[16] In the process the chiral auxiliary diisopropylideneglucose can either be recovered or, after hydrolysis with 0.1 N HCl, be separated by aqueous extraction.

Table 1. Enantioselective allylation of aldehydes with the reagent **3** (cf. Scheme 1).

R	Prod.	Yield [%] [a]	Config.	*ee* [%] [b]	Ref. [c]	$[\alpha]_D$ [°]	(*c*) [d]
Phenyl	**4a**	85	*R*	90	[2a]	+43.7	(6.7)
p-Nitrophenyl	**4b**	82	*R*	91	[3]	+23.6	(5.1)
2,3-Dihydro-1,4-Benzodioxin-6-yl	**4c**	78	*R* [e]	90		+23.5	(5.0)
1-Naphthyl	**4d**	83	*R*	88	[3]	+76.2	(9.6)
9-Anthryl	**4e**	80	*R* [e]	94		+19.9	(5.9)
9-Phenanthryl	**4f**	60	*R* [e]	92		+53.9	(5.0)
Vinyl	**4g**	61	*R*	86	[2a]	−13.8	(6.2) [f]
α-Styryl	**4h**	51	*R*	90	[2a]	−13.5	(9.7) [f]
Ethyl	**4i**	67	*S*	93	[2a]	− 3.8	(7.7)
n-Propyl	**4j**	78	*S*	93	[2a]	−11.7	(10.0)
n-Nonyl	**4k**	88	*S*	92	[2e]	−10.4	(6.7)
Isobutyl	**4l**	55	*R*	85	[15]	−22.4	(10) [f]
Isopropyl	**4m**	67	*R*	90	[2a]	+ 1.2	(9.9)
Cyclohexyl [g]	**4n**	78	*R*	92	[3]	+ 8.2	(0.6)
tert-Butyl	**4o**	58	*R*	88	[2a]	+10.3	(10.5)

[a] The yields are, in general, not optimized. [b] Determination of the enantiomeric excess by capillary GC (Chirasil-L-Val* [12]) after derivatization with isopropyl isocyanate (**4a, b, d, h, i, k–m, o**) or (*R*)-(+)-3,3,3-trifluoro-2-methoxy-2-phenylpropionyl chloride [13] (**4g, j, n**) or by HPLC on a "Baker-bond Chiral Ionic DNBPG Column" (**4c, f**) or on cellulose triacetate [14] (**4e**). [c] The signs of the rotations in benzene correspond to the configurational assignments in the cited works. [d] Concentration in benzene. [e] New compound; the configuration was assigned on the basis of analogies. [f] In Et_2O. [g] In EtOH.

As exemplified in Scheme 2 with the reactions of **6a, b**, titanates such as **7a–c** with substituted allyl groups are also highly enantioselective allylating reagents. These compounds are prepared from the corresponding lithium or Grignard reagents. As in the case of achiral allyltitanates[5, 8] the diastereomeric purity of the products **8b, c** is near the limit of detection (≥ 99%).[12]

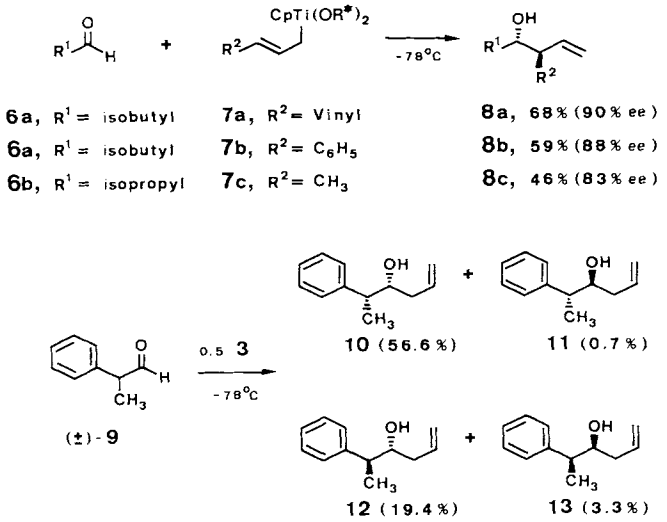
Reaction of racemic hydratopaldehyde **9** with 0.5 equivalents of allyl titanate **3** leads to formation of the stereoisomeric homoallyl alcohols **10–13** (80% based on **3**) in the ratio 70.8:0.9:24.2:4.1, whereby **10/11** are the products from (*R*)-**9** and **12/13** those from (*S*)-**9** (Scheme 2). The moderate differentiation of enantiomers (2.5:1) as well as the higher diastereoselectivity in the case of the more reactive enantiomer (*R*)-**9** (97% *de*, matched case) would indicate a certain Cram selectivity of the reagent **3**, which, however, is outweighed by the enantiofacial differentiation (71% *de* in the case of (*S*)-**9**, mismatched case).

The titanium reagent **3** exhibits the usual chemoselectivity:[5] at −74 °C it does not react with ketones. At 0 °C, however, aryl ketones are transferred smoothly into tertiary homoallyl alcohols, but the asymmetric induction is, as expected, small (ca. 50% *ee*; 80% *ee*, however, in the case of acetophenone). In contrast to the allyl compounds, analogous alkyl- and aryltitanates do not react with aldehydes, even at elevated temperatures.

[*] Dr. M. Riediker [+], Dr. R. O. Duthaler
Zentrale Forschungslaboratorien, Ciba-Geigy AG
Postfach, CH-4002 Basel (Switzerland)

[+] Present address:
Research Laboratories, Plastics Division, Ciba-Geigy Corporation
Ardsley, NY 10502 (USA)

[**] Enantioselective Syntheses with Titanium-Carbohydrate Complexes, Part 1.



Scheme 2.

With the chiral reagents **3** and **7a–c** the enantioselective allylation of aldehydes has been achieved for the first time with organotitanium compounds. Boron reagents[12] exhibit a similar stereoselectivity, but the advantage of titanium chemistry[5] must not be overlooked, e.g. simple preparation, chemoselectivity, inexpensive auxiliaries, as well as the possibility of recovering diisopropylideneglucose and $CpTiCl_3$ **1**. Still a drawback of this method is, however, that the high price of L-glucose impedes an equally good access to the other enantiomers of the homoallyl alcohols **4**. Concerted efforts are therefore currently directed at solving this problem with other ligands.

Experimental

Stock solution of **2** in ether: A solution/suspension of **1** (11.0 g, 50 mmol, freshly sublimed[10]) in Et_2O (400 mL, distilled over Na/benzophenone) was treated with 26.0 g (0.1 mol) of 1,2:5,6-di-*O*-isopropylidene-α-D-glucofuranose (R*OH, crystallized from cyclohexane) under argon in the absence of moisture. After 2 min at room temperature (RT) a solution of 15.2 mL (110 mmol) of Et_3N in 125 mL of Et_2O was added dropwise to the stirred mixture within 1 h. The resulting suspension was stirred for ca. 15 h; the $Et_3N \cdot HCl$ was then filtered off under argon and washed three times with ca. 50 mL of Et_2O (14.2 g of $Et_3N \cdot HCl$ vacuum dried). The content of **2** in the yellow filtrate (0.09 M) was calculated from the volume of the solution assuming a quantitative conversion.

(*R*)-1-Phenyl-3-buten-1-ol (**4a**): 7.2 mL of a 1.25 M solution of allylmagnesium chloride in THF (Aldrich, 9 mmol) was added dropwise within 10 min at 0 °C under argon to 110 mL of a ca. 0.09 M solution of **2** in Et_2O (9.9 mmol). After stirring for 1 h at 0 °C the orange suspension was cooled to −74 °C and treated within 5 min with 0.8 mL (8 mmol) of benzaldehyde. The mixture was stirred for 2 h at −74 °C, warmed to ca. −30 °C and hydrolyzed by addition of 16 mL of a ca. 5 M solution of H_2O in THF (1 h, RT). Filtration, washing with Et_2O and drying (high vacuum) yielded 4.2 g of **5** (yellowish solid). The filtrate was evaporated and the solid residue stirred with 100 mL of hexane. Subsequent filtration furnished 4.4 g of R*OH. Chromatography (80 g silica gel, hexane: AcOEt 3:1) finally afforded 1.01 g (85%) of **4a** (90% *ee*, determined as described in [12]).

Received: December 21, 1988 [Z 3095 IE]
German version: *Angew. Chem. 101* (1989) 488

[1] a) R. W. Hoffmann, *Angew. Chem. 94* (1982) 569; *Angew. Chem. Int. Ed. Engl. 21* (1982) 555; b) Y. Yamamoto, *Acc. Chem. Res. 20* (1987) 243.
[2] a) R. W. Hoffmann, T. Herold, *Chem. Ber. 114* (1981) 375; b) R. W. Hoffmann, *Pure Appl. Chem. 60* (1988) 123; c) H. C. Brown, P. K. Jadhav, *J. Am. Chem. Soc. 105* (1983) 2092; d) H. C. Brown, P. K. Jadhav, K. S. Bhat, *ibid. 110* (1988) 1535; e) W. R. Roush, A. E. Walts, L. K. Hoong, *ibid. 107* (1985) 8186; f) W. R. Roush, L. Banfi, *ibid. 110* (1988) 3979; g) W. R. Roush, K. Ando, D. B. Powers, R. L. Halterman, A. D. Palkowitz, *Tetrahedron Lett. 29* (1988) 5579; h) M. T. Reetz, T. Zierke, *Chem. Ind. (London) 1988*, 663.
[3] a) N. Minowa, T. Mukaiyama, *Bull. Chem. Soc. Jpn. 60* (1987) 3697; b) G. P. Boldrini, L. Lodi, E. Tagliavini, C. Tarasco, C. Trombini, A. Umani-Ronchi, *J. Org. Chem. 52* (1987) 5447.
[4] a) T. Hayashi, Y. Matsumoto, T. Kiyoi, Y. Ito, S. Kohra, Y. Tominaga, A. Hosomi, *Tetrahedron Lett. 29* (1988) 5667; b) R. Imwinkelried, D. Seebach, *Angew. Chem. 97* (1985) 781; *Angew. Chem. Int. Ed. Engl. 24* (1985) 765; c) A. Hosomi, *Acc. Chem. Res. 21* (1988) 200.
[5] a) D. Seebach, B. Weidmann, L. Widler in R. Scheffold (Ed.): *Modern Synthetic Methods, Vol. 3*, Salle, Frankfurt am Main, Sauerländer, Aarau 1983, p. 217; b) M. T. Reetz: *Organotitanium Reagents in Organic Synthesis*, Springer, Berlin 1986.
[6] D. Seebach, A. K. Beck, R. Imwinkelried, S. Roggo, A. Wonnacott, *Helv. Chim. Acta 70* (1987) 954.
[7] a) M. T. Reetz, S.-H. Kyung, J. Westermann, *Organometallics 3* (1984) 1716; b) H. Takahashi, A. Kawabata, K. Higashiyama, *Chem. Pharm. Bull. 35* (1987) 1604.
[8] a) F. Sato, K. Iida, S. Iijima, H. Moriya, M. Sato, *J. Chem. Soc. Chem. Commun. 1981*, 1140; b) M. T. Reetz, M. Sauerwald, *J. Org. Chem. 49* (1984) 2292; c) S. Collins, W. P. Dean, D. G. Ward, *Organometallics 7* (1988) 2289; d) D. Seebach, L. Widler, *Helv. Chim. Acta 65* (1982) 1972; e) M. T. Reetz, R. Steinbach, J. Westermann, R. Peter, B. Wenderoth, *Chem. Ber. 118* (1985) 1441.
[9] a) H. Roder, G. Helmchen, E. M. Peters, K. Peters, H.-G. von Schnering, *Angew. Chem. 96* (1984) 895; *Angew. Chem. Int. Ed. Engl. 23* (1984) 898; b) T. Krämer, D. Hoppe, *Tetrahedron Lett. 28* (1987) 5149.
[10] R. D. Gorsich, *J. Am. Chem. Soc. 82* (1960) 4211.
[11] M. Riediker, R. W. Lang, R. Duthaler, P. Herold, K. Oertle, G. Bold, Eur. Pat.-Anm. 0254 685 (27. Jan. 1988), Ciba-Geigy AG.
[12] H. Frank, G. J. Nicholson, E. Bayer, *Angew. Chem. 90* (1978) 396; *Angew. Chem. Int. Ed. Engl. 17* (1978) 363.
[13] J. A. Dale, H. S. Mosher, *J. Am. Chem. Soc. 95* (1973) 512.
[14] H. Koller, K.-H. Rimböck, A. Mannschreck, *J. Chromatogr. 282* (1983) 89.
[15] B. Cazes, C. Vernière, J. Goré, *Synth. Commun. 13* (1983) 73.
[16] With one equivalent of conc. HCl a crystalline tetramer is formed; A. C. Skapski, P. G. H. Troughton, *Acta Crystallogr. Sect. B 26* (1970) 716.

Enantioselective Aldol Reaction of *tert*-Butyl Acetate using Titanium-Carbohydrate Complexes**

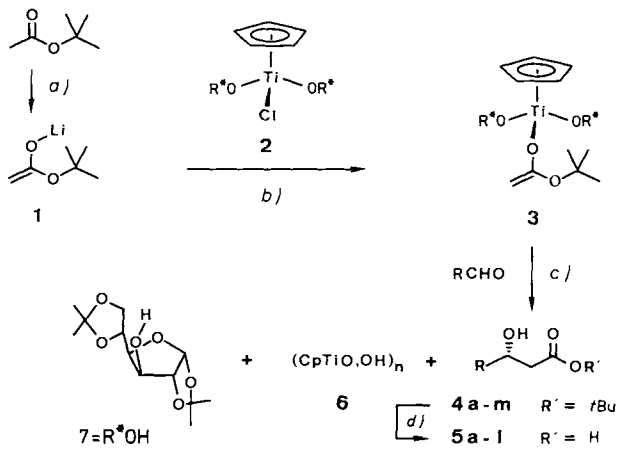
By *Rudolf O. Duthaler,* Peter Herold, Willy Lottenbach, Konrad Oertle,* and *Martin Riediker*

The Aldol reaction is one of the most important methods for the stereoselective construction of complex acyclic molecules.[1] Covalently bound chiral auxiliaries readily induce high stereoselectivity in the case of propionate enolates, whereas in the case of acetate enolates this could hitherto only be achieved via a circuitous route involving auxiliary substituents.[2] More recently, methods have been developed which enable the stereoselective addition of α-unsubstituted enolates.[3] A particularly efficient approach makes use of metal complexes with chiral ligands.[4] It should, however, be mentioned, that many β-hydroxy esters (such as **4**) are accessible by enantioselective reduction of the corresponding β-oxo esters as well.[5]

The successful asymmetric allylation of carbonyl compounds with novel cyclopentadienyltitanium-carbohydrate complexes[6] motivated us to apply this principle also to the acetate-Aldol reaction.[7] We have found that, in this way, a variety of β-hydroxycarboxylic acids are accessible in 90–95% optical purity (Scheme 1, Table 1).

[*] Dr. R. O. Duthaler, Dr. P. Herold, Dr. W. Lottenbach, Dr. K. Oertle, Dr. M. Riediker [+]
Zentrale Forschungslaboratorien, Ciba-Geigy AG
Postfach, CH-4002 Basel (Switzerland)
[+] Present address:
Research Laboratories, Plastics Division, Ciba-Geigy Corporation
Ardsley, NY 10502 (USA)

[**] Enantioselective Syntheses with Titanium-Carbohydrate Complexes, Part 2.—Part 1: [6].

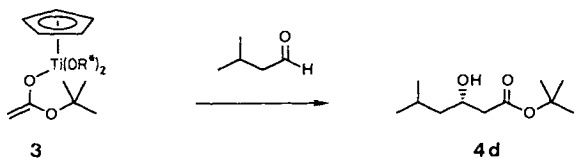


Scheme 1. a) Li-diisopropylamide, Li-cyclohexyl(isopropyl)amide or Li-dicyclohexylamide/Et_2O/−74 °C; b) 1 h −30 °C or 24 h −74 °C; c) 2 h −74 °C, H_2O; d) CF_3CO_2H/100 mbar/1–5 h (RT) or 2 N NaOH/16 h RT. (Residue R, see Table 1 below.)

Transmetalation of the relatively stable lithium enolate **1** of *tert*-butyl acetate with chloro(cyclopentadienyl)-bis(1,2:5,6-di-*O*-isopropylidene-α-D-glucofuranos-3-*O*-yl) titanate **2** as stock solution in toluene (0.09–0.2 M) or Et_2O (0.05–0.09 M[6] furnishes the titanium enolate **3**, which is brought to reaction in situ with aldehydes to give the hydroxy esters **4a–m**. In analogy to the allylation[6] the enolate preferably adds to the *re*-side of the aldehydes. With the exception of **4m**, the *tert*-butyl esters **4** can be converted into the acids **5a–l** either by cleavage with acid or by basic hydrolysis; in the case of crystalline compounds, crystallization from cyclohexane generally affords optically pure samples.

The titanium oxide complex **6** formed during hydrolytic work-up can be filtered off and reconverted into $CpTiCl_3$, the starting material for the complex **2**, by treatment with HCl.[6] The chiral auxiliary is either separated unchanged or, after acetal hydrolysis in 0.1 N HCl, extracted with water.

On optimization of the reaction conditions it was found that transmetalation of the lithium enolate **1** at −74 °C proceeds very slowly (24 h) and can be accelerated significantly by warming to ca. −30 °C (≈ 1 h). Since the lithium amide bases apparently do not react with the titanate **2**, it is even possible to add the *tert*-butyl acetate and the titanium reagent simultaneously to the base. The titanium enolate **3** tolerates elevated temperatures and, astonishingly, the enantioselectivity of the Aldol reaction is almost temperature independent, as shown in Scheme 2 for isovaleraldehyde; the reaction can even be carried out at room temperature without significant loss of optical induction.



Scheme 2.

T [°C]	**4d**, Yield [%]	**4d**, *ee* [%]
−74	81	94
−30	68	92
−15	72	95
0	68	95
+27	60	96

The chirally modified titanium reagent **3** is thus a novel acetate enolate, which adds with striking enantiofacial differentiation to the *re*-side of many aldehydes. The optical purity of the β-hydroxy acids **5** formed thereby is as high as in the best known methods.[3, 4] However, the reaction can be carried out at higher temperatures, and the tedious synthesis of a chiral auxiliary, the reaction steps for introduction and removal of the auxiliary reagent as well as the synthesis of special derivatives (cf. Ref. [4c]) are circumvented. Moreover, not only can the non-toxic titanium complex be recovered in a simple way via **6**, but, in most cases, also the inexpensive commercially available auxiliary **7** by crystallization. Since (L)-glucose is relatively expensive, work aimed at making the enantiomers of **4** and **5** accessible by the same principle is in progress.

Table 1. β-Hydroxy esters **4** and β-hydroxy acids **5** by enantioselective Aldol reaction of the titanium enolate **3** (cf. Scheme 1).

	R	Ester **4**				Acid **5**			
		Yield [%]	*ee* [%] [a]	$[\alpha]_D$ [°]	(*c*) in $CHCl_3$	Yield [%]	M.p. [°C]	$[\alpha]_D$ [b] [°]	(*c*) in $CHCl_3$
a	*n*-Propyl	51	94	+23.0	(1)	97	liq.	+28.3	(1)
b	*n*-Heptyl	87[c]	95	+18.7	(1)	99	47–48	+19.5[d]	(1)
c	*n*-Undecyl	70[c]	94[f]	+14.5	(1.1)	99	67.5–68.5	+14.0[d]	(1)
d	Isobutyl	81	94	+14.8	(1)	99	82–83 (±: 62[g]	+14.2[d]	(1.2)
e	Isopropyl	66	95	+35.0	(1.1)	81	liq.	+41.7	(1)
f	Cyclohexyl	70[c]	92	+26.8	(1.1)	97	71.5–72.5	+31.8[d]	(1.1)
g	*tert*-Butyl	80[c]	91	+42.2	(1.2)	95	88–89	+53.2[d]	(1)
h	(*E*)-1-Pentenyl	81	91	+14.5	(1)	94	liq.	+16.0	(0.9)
9	α-Styryl	64	96[f]	+10.2	(1.2)	99	116.5–117; ±: 102[g]	+16.2[d]	(1)
								−16.9[h]	(2.02)
j	2-Methyl-1-propenyl	58[c]	92[f]	+25.5	(1.2)	74[i]	53–54	+28.2	(0.1)
k	Isopropenyl	81	96	+27.9	(1)	92	liq.	+38	(1)
l	Phenyl	69	95[f]	+42.8	(2)	99	115–116; ±: 88[g]	+60.5[d]	(1)
m	2-Furyl	62	90[f]	+22.2	(1.5)	[i]			

[a] Determined by capillary GC (Chirasil L-Val*) of the *O*-(*N*-isopropylamino)carbonyl-*N*-isopropyl-substituted amide of the acid **5** [8]. [b] The configuration was assigned on the basis of a comparison of published rotation values (**5b, c** [5a]; **5a, e, g, l** [9]; **5i** [10]) or by analogy (rotation, sequence of elution upon capillary GC [8b]) (**5d, f, h, j, k, m**). [c] Simultaneous addition of *tert*-butyl acetate and **2** to the Li-dicyclohexylamide. [d] ≥ 99% *ee* after crystallization from cyclohexane. [e] Owing to solubility problems the Aldol reaction was carried out at −40 °C. [f] Determined by ^1H NMR spectroscopy of the (*R*)-(+)-3,3,3-trifluoro-2-metboxy-2-phenylpropionic acid esters [11] of **4c, i, j, l, m**. [g] The racemate crystallizes as conglomerate of the enantiomers (m.p. IR, cf. [12]). [h] In CH_3OH. [i] Unstable compound.

Experimental

A solution of dicyclohexylamine (14.5 g, 80 mmol) in absolute ether (150 mL) was treated at −25 °C with 43.7 mL (70 mmol) of 1.6 M butyllithium in hexane. After 30 min at −25 °C, the mixture was cooled to −74 °C and a solution of 6.96 g (60 mmol) of *tert*-butyl acetate in 40 mL of absolute ether was added dropwise within 35 min. After stirring for 30 min at −74 °C 842 mL (80 mmol) of a 0.095 M solution of **2** in toluene, precooled to −74 °C, was transferred within 40 min to this mixture via a cannula. After 1 h at −74 °C the mixture was warmed in 25 min to −30 °C, stirred at this temperature for 30 min and finally recooled to −74 °C. A solution of the aldehyde (60 mmol) in absolute ether (30 mL) was then added dropwise within 40 min and the mixture stirred for 2 h at −74 °C. After hydrolysis with 130 mL of a 5 M solution of H_2O in THF and stirring for 1 h at room temperature (RT), the titanium compounds were recovered by filtration (Celite®). The filtrate was washed with 100 mL of saturated NaCl solution, the aqueous phase extracted twice with ether. For hydrolysis of **7**, the residue of the dried ($MgSO_4$) organic phase was stirred with 1 L of 0.1 N HCl at RT. The β-hydroxy ester **4** was isolated by extraction with ether and purified by column chromatography (silica gel).

Received: December 21, 1988 [Z 3096 IE]
German version: *Angew. Chem. 101* (1989) 490

[1] a) C. H. Heathcock in J. D. Morrison (Ed.): *Asymmetric Synthesis, Vol. 3, Part B*, Academic Press, Orlando 1984, Chap. 2; b) D. A. Evans, J. V. Nelson, T. R. Taber, *Top. Stereochem. 13* (1982) 1; c) S. Masamune, W. Choy, J. S. Petersen, L. R. Sita, *Angew. Chem. 97* (1985) 1; *Angew. Chem. Int. Ed. Engl. 24* (1985) 1.

[2] a) D. A. Evans, J. Bartroli, T. L. Shih, *J. Am. Chem. Soc. 103* (1981) 2127; C. Mioskowski, G. Solladié, *Tetrahedron 36* (1980) 227.

[3] a) M. Braun, *Angew. Chem. 99* (1987) 24; *Angew. Chem. Int. Ed. Engl. 26* (1987) 24; b) M. Braun, R. Devant, *Tetrahedron Lett. 25* (1984) 5031; c) L. S. Liebeskind, M. E. Welker, *ibid. 25* (1984) 4341; d) St. G. Davies, I. M. Dordor, P. Warner, *J. Chem. Soc. Chem. Commun. 1984*, 956; e) I. Ojima, H. Boong Kwon, *J. Am. Chem. Soc. 110* (1988) 5617; f) G. Helmchen, U. Leikauf, I. Taufer-Knöpfel, *Angew. Chem. 97* (1985) 874; *Angew. Chem. Int. Ed. Engl. 24* (1985) 874; g) W. Oppolzer, J. Marco-Contelles, *Helv. Chim. Acta 69* (1986) 1699; h) J. D. Elliott, J. Steele, W. S. Johnson, *Tetrahedron Lett. 26* (1985) 2535.

[4] a) M. Guetté, J. Capillon, J.-P. Guetté, *Tetrahedron 29* (1973) 3659; b) N. Iwasawa, T. Mukaiyama, *Chem. Lett. 1983*, 297; c) S. Masamune, T. Sato, B.-M. Kim, T. A. Wollmann, *J. Am. Chem. Soc. 108* (1986) 8279; d) M. T. Reetz, F. Kunish, P. Heitman, *Tetrahedron Lett. 27* (1986) 4721; e) I. Paterson, *Chem. Ind. (London) 1988*, 390.

[5] a) M. Nakahata, M. Imaida, H. Ozaki, T. Harada, A. Tai, *Bull. Chem. Soc. Jpn. 55* (1982) 2186; b) R. Noyori, T. Ohkuma, M. Kitamura, H. Takaya, N. Sayo, H. Kumobayashi, S. Akutagawa, *J. Am. Chem. Soc. 109* (1987) 5856; c) D. F. Taber, P. B. Deker, M. D. Gaul, *ibid. 109* (1987) 7488.

[6] M. Riediker, R. O. Duthaler, *Angew. Chem. 101* (1989) 488; *Angew. Chem. Int. Ed. Engl. 28* (1989) 494.

[7] M. Riediker, R. W. Lang, R. Duthaler, P. Herold, K. Oertle, G. Bold. Eur. Pat.-Anm. 0254685 (January 27. 1988), Ciba-Geigy AG.

[8] a) H. Frank, G. J. Nicholson, E. Bayer, *Angew. Chem. 90* (1978) 396; *Angew. Chem. Int. Ed. Engl. 17* (1978) 363; b) W. A. König, I. Benecke, N. Lucht, E. Schmidt, J. Schulze, S. Sievers, *J. Chromatogr. 279* (1983) 555.

[9] R. Devant, M. Braun, *Chem. Ber. 119* (1986) 2191.

[10] H. H. Meyer, *Liebigs Ann. Chem. 1979*, 484.

[11] J. A. Dale, H. S. Mosher, *J. Am. Chem. Soc. 95* (1973) 512.

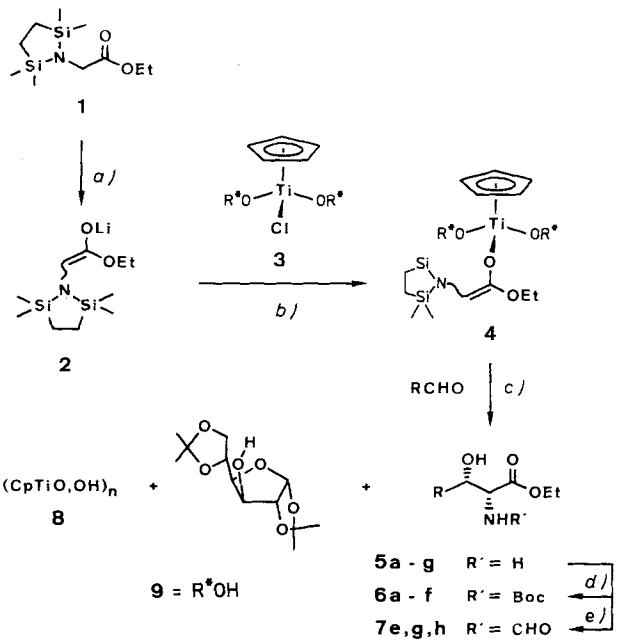
[12] A. Collet, J. Jacques, *Bull. Soc. Chim. Fr. 1972*, 3857.

Enantioselective Synthesis of D-*threo*-β-Hydroxy-α-amino Acids with Titanium-Carbohydrate Complexes**

By *Guido Bold,* Rudolf O. Duthaler,* and *Martin Riediker*

Stimulated by the successful isolation of structurally interesting, uncommon α-amino acids having remarkable biological properties[1] great progress has been made in recent years in the enantioselective synthesis of such compounds.[2] Diastereoselective reactions of chiral glycine derivatives have proven particular successful, whereby, aside from the alkylation of enolates,[3] the Aldol reaction plays an especially significant role, since this leads to the important class of β-hydroxy-α-amino acids.[4] However, the removal and separation of the chiral auxiliaries are usually tedious and, in some cases, limit the scope of application of these methods. In this respect the use of chiral metal complexes is more advantageous, particularly in catalytic processes such as the gold(I)-catalyzed addition of ethyl isocyanate to aldehydes, which affords β-hydroxy-α-amino acids with high stereoselectivity.[5]

We therefore decided to apply our novel titanium-carbohydrate complexes,[6] which have proven to be especially useful in enantioselective allylation[7a] and acetate-Aldol reactions,[7b] to reactions of substituted enolates. The lithium enolate **2** of ethyl (2-(2,2,5,5-tetramethyl-1-aza-2,5-disilacyclopent-1-yl)acetate **1**[8] can be transmetalated in a slow reaction with chloro(cyclopentadienyl)bis(1,2:5,6-di-*O*-isopropylidene-α-D-glucofuranos-3-yl) titanate **3**.[7] Subsequent Aldol reaction of the titanium enolate **4** yields D-*threo*-β-hydroxy-α-amino acid esters **5** with astonishingly high stereoselectivity (Scheme 1, Table 1). As previously in the allylation[7a] and acetate-Aldol reaction,[7b] the addition occurs preferentially from the *re*-side of the aldehydes. In comparison with the unselective reactions of the lithium enolates of *N*-bis-silylated glycine esters,[16] the high *syn*-selectivity of this reaction is remarkable as well. Although the free amino acid esters **5** can be isolated, it is advisable to protect the amino function, e.g. as *tert*-butyl carbamates **6** or as formamides **7**.



Scheme 1. a) Li-diisopropylamide or Li-cyclohexylisopropylamide/THF, −78 °C; b) THF/Et_2O, 17 h, −78 °C; c) inverse addition, −78 °C to room temperature (RT), hydrolysis; d) Boc_2O/$NaHCO_3$/dioxane/H_2O, 2.5 h RT; e) HCO_2Et, 5.5 h reflux.

The titanate **8** that precipitates upon hydrolysis can be separated by filtration and converted into $CpTiCl_3$, the starting material for the reagent **3**.[7] By extraction with solvents the chiral auxiliary **9** can also be separated from the polar, water-soluble products **5**.

[*] Dr. G. Bold, Dr. R. O. Duthaler, Dr. M. Riediker[+]
Zentrale Forschungslaboratorien, Ciba-Geigy AG
Postfach, CH-4002 Basel (Switzerland)

[+] Present address:
Research Laboratories, Plastics Division, Ciba-Geigy Corporation
Ardsley, NY 10502 (USA)

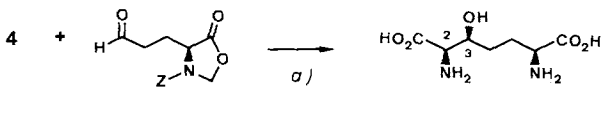
[**] Enantioselective Syntheses with Titanium-Carbohydrate Complexes, Part 3.—Part 2: [7b].

Table 1. D-*threo*-β-Hydroxy-α-amino acid derivatives **5**–**7** by Aldol reaction with the titanium enolate **4** (cf. Scheme 1).

R	R'	Prod.	Yield [%]	*de* [%] [a]	*ee* [%] [a]	$[\alpha]_D$ [°]	(*c*) in EtOH	Configuration
Methyl	Boc	**6a**	53	≥98	97	+18.8	(1.4)	[b]
n-Propyl	Boc	**6b**	66	≥98	98	+ 4.2	(1.0)	[c]
tert-Butyl	Boc	**6c**	43	≥96	96	+ 9.8	(0.7)	[e]
Vinyl	Boc	**6d**	48	≥97	97	−25.2	(1.5)	[f]
Isopropenyl	Boc	**6e**	57	99	98	−12.8	(0.7)	[e]
	CHO	**7e**	61	99	98 [g]	−14.9	(1.1)	[e]
	H	**5e**	45	99	98	+ 2.2	(1.0)	[e]
Phenyl	Boc	**6f**	60	≥96	97	+ 8.5	(1.1)	[h]
Methoxycarbonyl	CHO	**7g**	70	87	78 [j]	−50.6	(0.8)	[e]
tert-Butoxycarbonyl [k]	CHO	**7h**	66	≥96	87 [j]	−20.4	(1.05)	[e]

[a] Determination by capillary GC (Chirasil-L-Val)[R] [9], 90–180 °C, 2 °C min^{-1}, after derivatization with trifluoroacetic anhydride. The stereoisomeric mixture of the unselective reaction of the Li-enolate **2** served as reference. [b] Comparison with D-threonine (see [a]). [c] Hydrolysis to the free amino acid: $[\alpha]_D = -19.4°$ ($c = 1$, 5 N HCl) [10, 11] (^{1}H NMR). [d] 24 h RT for the Aldol reaction. [e] Assignment based on analogy [9b] (see [a]). [f] Conversion into methyl 2-*tert*-butoxycarbonylamino-3-(*tert*-butyldimethylsiloxy)-4-pentenoate or *tert*-butyl *N*-(2,2-dimethyl-4-vinyl-1,3-dioxan-5'-yl)carbamate, comparison with the literature data [12]. [g] Derivatization with Ac_2O/pyridine, otherwise as [a]. [h] Hydrolysis to phenylserine: $[\alpha]_D = +52°$ ($c = 0.8$, 6 N HCl) [13, 4b] (^{1}H NMR). [i] According to ^{1}H NMR. [j] Derivatization with *N,O*-bis(trimethylsilyl)acetamide, otherwise as [a]. [k] Aldehyde prepared by ozonolysis (O_3/CH_2Cl_2, −78 °C, Me_2S, 0 °C-RT, 19 h) of di-*tert*-butyl fumarate [14] (b.p. 50 °C/28 mbar). Ozonolysis in CH_3OH: CH_2Cl_2 3:1 [15] gives another product, presumably a (semi)acetal.

The titanium complex **4** is thus a novel, chirally modified glycine enolate which reacts with high stereoselectivity with a variety of aldehydes to give D-*threo*-β-hydroxy-α-amino acids. Noticeably lower selectivity has so far only been observed with methyl glyoxylate (→ **7g**).[17] A better result, however, is obtained with *tert*-butyl glyoxylate (→ **7h**). Advantages compared to other methods[4, 5] are the easily accessible, commercially available chiral auxiliary, the recoverability of the reagents, the flexibility in the choice of the *N*-protecting group in the product, and the ease of liberation of the amino acid merely by ester hydrolysis.



10, z = CO_2CH_2Ph **11** (49%)

Scheme 2. a) 1. −78 °C to RT, 2. Work-up, 3. 5 N HCl, 2 h 100 °C.

The reaction of **4** with the modified glutamic acid semialdehyde **10**[18] outlined in Scheme 2 shows that sensitive substrates are compatible with the reaction conditions. The product 2,6-diamino-3-hydroxy-heptane diacid **11** is a constituent of microbial cell walls.[19] According to the ^{13}C NMR spectrum, **11** is stereochemically pure; the (2*R*,3*S*)-configuration was assigned in analogy to the other examples and is thus not strictly proven.

Experimental

A solution of cyclohexylisopropylamine (2.26 mL, 13.5 mmol) in dry THF (60 mL) was treated at −20 °C with 7.6 mL (12.2 mmol) of a 1.6 M solution of butyllithium in hexane (argon). After 20 min the mixture was cooled to −78 °C and treated dropwise with a solution of ethyl(2,2,5,5-tetramethyl-1-aza-2,5-disilacyclopent-1-yl)acetate (3.0 g, 12.24 mmol) **1** [8] in 60 mL of THF. After 1 h, 142 mL (13.5 mmol) of a 0.095 M solution of **3** in ether [7] was added to the mixture, which, after stirring for 17 h at −78 °C, was transferred via a steel cannula under argon pressure into a solution of the aldehyde (13.5 mmol) in 15 mL of THF cooled to −78 °C. After 17 h at −78 °C the reaction mixture was allowed to warm slowly to room temperature (ca. 3 h), stirred for ca. 2 h (longer if necessary, cf. the reaction with pivaldehyde (→ **6c**)), and hydrolyzed with 1.5 mL of water. After ca. 2 h, **8** was collected by filtration. There are then several variants for the isolation of the product from the filtrate: a) After addition of a 10% NaCl solution the bis(silyl) derivative of the product can be extracted with ether together with **9**. A part of **9** can be separated by crystallization from cyclohexane (150 mL). For the *N*-desilylation, the residue from the mother liquor is stirred for 2 h in a mixture of 4.5 mL AcOH, 24 mL of H_2O and 120 mL of THF. After careful evaporation in a high vacuum the residue is either directly chromatographed (silica gel, CH_2Cl_2:EtOh 9:1, +1% of 25% NH_3) (→ **5**) or first derivatized: 5.3 g (24.5 mmol) of di-*tert*-butyl dicarbonate, $NaHCO_3$ (6.7 g) in dioxane:H_2O 1:1 (80 mL), 2 h RT (→ **6**) or ethyl formate, 5.5 h heating under reflux (→ **7**).

b) After the separation of **8**, the filtrate is treated with 24 mL H_2O and 4.5 mL AcOH and stirred for 2 h at RT. After evaporation to a third of the volume, **9** is extracted three times with 150 mL of ether. After washing three times with 100 mL 0.05 N HCl, the aqueous phase is adjusted to pH 4 and evaporated down under high vacuum. The subsequent steps are then as described under (a).

Received: December 21, 1988 [Z 3097 IE]
German version: *Angew. Chem. 101* (1989) 491

CAS Registry numbers:
1, 78605-23-9; **3**, 119528-80-2; **5a**, 3182-94-3; **5b**, 119717-11-2; **5c**, 119594-37-5; **5d**, 119594-38-6; **5e**, 119594-39-7; **5f**, 119677-35-9; **5g**, 119594-40-0; **5h**, 119594-41-1; **6a**, 119594-42-2; **6b**, 119594-43-3; **6c**, 119594-44-4; **6d**, 119594-45-5; **6e**, 119594-46-6; **6f**, 119594-47-7; **7e**, 119619-03-3; **7g**, 119594-48-8; **7h**, 119594-49-9; **10**, 89969-26-6; **11**, 10575-47-0.

[1] a) G. C. Barrett (Ed.): *Chemistry and Biochemistry of the Amino Acids*, Chapman and Hall, London 1985; b) *Amino Acids, Pept. Proteins* (Specialist Periodical Reports) *Vol. 1–19* (1969–1987); c) I. Wagner, H. Musso, *Angew. Chem. 95* (1983) 827; *Angew. Chem. Int. Ed. Engl. 22* (1983) 816; d) E. A. Bell, *Endeavour 4* (1980) 102; e) G. Nass, K. Poralla, H. Zähner, *Naturwissenschaften 58* (1971) 603.
[2] a) H.-J. Altenbach, *Nachr. Chem. Tech. Lab. 36* (1988) 999; b) K. A. Kochetkov, V. M. Belikov, *Russ. Chem. Rev. 56* (1987) 1045; c) α-Amino Acid Synthesis, Tetrahedron Symposia in Print No. 33, *Tetrahedron 44* (1988) 5253–5605.
[3] a) U. Schöllkopf, *Top. Curr. Chem. 109* (1983) 65; b) D. Seebach, D. D. Miller, S. Müller, T. Weber, *Helv. Chim. Acta 68* (1985) 949; c) R. M. Williams, P. J. Sinclair, D. Zhai, D. Chen, *J. Am. Chem. Soc. 110* (1988) 1547.
[4] a) U. Schöllkopf, J. Bardenhagen, *Liebigs Ann. Chem. 1987*, 393; b) D. Seebach, E. Juaristi, D. D. Miller, C. Schickli, T. Weber, *Helv. Chim. Acta 70* (1987) 237; c) D. Seebach, S. G. Müller, U. Gysel, J. Zimmermann, *ibid. 71* (1988) 1303; d) Y. N. Belokon', A. G. Bulychev, S. V. Vitt, Y. T. Struchkov, A. S. Batsanov, T. V. Timofeeva, V. A. Tsyryapkin, M. G. Ryzhov, L. A. Lysova, V. I. Bakhmutov, V. M. Belikov, *J. Am. Chem. Soc. 107* (1985) 4252; e) T. Owa, M. Otsuka, M. Ohno, *Chem. Lett. 1988*, 83; f) D. A. Evans, A. E. Weber, *J. Am. Chem. Soc. 108* (1986) 6757; g) *ibid. 109* (1987) 7151; h) H. Kuzuhara, N. Watanabe, M. Ando, *J. Chem. Soc. Chem. Commun. 1987*, 95.
[5] a) Y. Ito, M. Sawamura, T. Hayashi, *J. Am. Chem. Soc. 108* (1986) 6405; b) *Tetrahedron Lett. 28* (1987) 6215.
[6] M. Riediker, R. W. Lang, R. Duthaler, P. Herold, K. Oertle, G. Bold, Eur. Pat.-Anm. 0254685 (January 27, 1988), Ciba-Geigy AG.
[7] a) M. Riediker, R. O. Duthaler, *Angew. Chem. 101* (1989) 488; *Angew. Chem. Int. Ed. Engl. 28* (1989) 494; b) R. O. Duthaler, P. Herold, W. Lottenbach, K. Oertle, M. Riediker, *ibid. 101* (1989) 490 and *28* (1989) 495.
[8] S. Djuric, J. Venit, P. Magnus, *Tetrahedron Lett. 22* (1981) 1787.
[9] a) H. Frank, G. J. Nicholson, E. Bayer, *Angew. Chem. 90* (1978) 396; *Angew. Chem. Int. Ed. Engl. 17* (1978) 363; b) E. Bayer, *Z. Naturforsch. B38* (1983) 1281.
[10] T. T. Otani, M. R. Briley, *J. Pharm. Sci. 65* (1976) 534.
[11] Y. Ariyoshi, N. Sato, *Bull. Chem. Soc. Jpn. 44* (1971) 3435.
[12] Y. Ohfune, H. Nishio, *Tetrahedron Lett. 25* (1984) 4133.
[13] K. Vogler, *Helv. Chim. Acta 33* (1950) 2111.
[14] J. Blake, J. R. Tretter, G. J. Juhasz, W. Bonthrone, H. Rapoport, *J. Am. Chem. Soc. 88* (1966) 4061.
[15] A. Vasella, R. Voeffray, J. Pless, R. Huguenin, *Helv. Chim. Acta 66* (1983) 1241.
[16] K. Rühlmann, G. Kuhrt, *Angew. Chem. 80* (1968) 797; *Angew. Chem. Int. Ed. Engl. 7* (1968) 809.
[17] With the method of *Hayashi* et al. [5] an almost racemic mixture of diastereomers is formed with methyl glyoxylate as substrate; A. Togni, Ciba-Geigy AG, Basel, unpublished results.
[18] B. H. Lee, M. J. Miller, *Tetrahedron Lett.25* (1984) 927.
[19] a) H. R. Perkins, *Biochem. J. 115* (1969) 797; b) I. Kawamoto, T. Oka, T. Nara, *J. Bacteriol. 146* (1981) 527.

Structure of Chloro(cyclopentadienyl)bis(1,2:5,6-di-*O*-isopropylidene-α-D-glucofuranos-3-O-yl) Titanate, a Novel Titanium-Carbohydrate Complex**

By *Martin Riediker, Andreas Hafner,* Umberto Piantini, Grety Rihs,* and *Antonio Togni**

In the preceding communications[1] we have shown that complex **1** is of special importance as a precursor for enantioselective allyl and ester enolate additions to aldehydes. This novel Ti^{IV}-complex with monodentate "sugar ligands" is the first representative of a new class of compounds[2] and can be isolated as a yellowish powder, which is very sensitive to hydrolysis.[3] To throw some light on the mechanism of chirality transfer its structure has been determined, both in the solid state (X-ray analysis) and in solution (NMR spectroscopy).

$TiCp(OR^*)_2Cl$ **1**

$Cp = \eta^5\text{-}C_6H_5$; OR* = 1,2:5,6-Di-*O*-isopropylidene-α-D-glucofuranoso-3-*O*-yl

Figure 1 shows the crystal structure of **1**. Table 1 contains selected bond lengths, bond angles, and torsion angles.

The complex **1** is monomeric. The coordination geometry is best described as a three-legged piano stool arrangement. Additional Ti–O interactions can be ruled out, because the shortest non-bonding Ti–O distance (Ti1–038) is 414 pm. The Ti–O bond lengths of 180.9(8) and 178.6(8) pm are about 5 pm shorter than in **2** (185.5(2) pm)[7] and 10 pm shorter than in **3** (190.3(2) pm),[8] but ca. 5 pm longer than in **4** (175.0(2) pm).[7] The Ti–O–C bond angles (145.8(8)° und 153.1(9)°) reflect the double bond character of the Ti–O bond. Values of 133.2(2)°, 145.5° and 166.2(2)°, respectively, were measured for **2**,[7] **3**,[8] and **4**.[7]

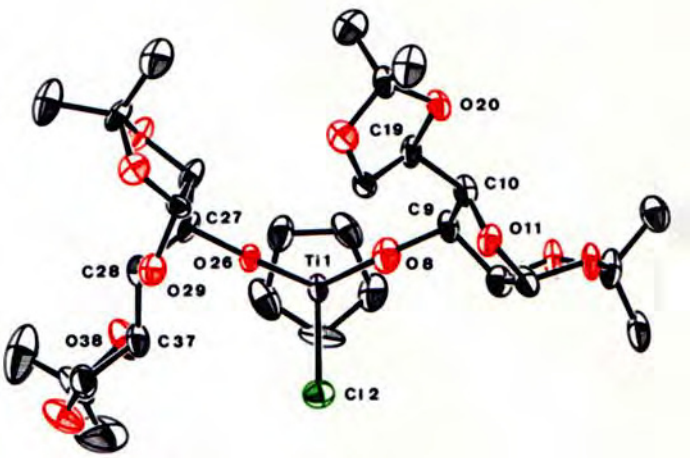


Fig. 1. ORTEP drawing of **1**. Projection along the Cp_{center}-Ti axis (vibration ellipsoids at the 20% probability level).

Table 1. Selected bond lengths, dihedral angles, and torsion angles of **1**.

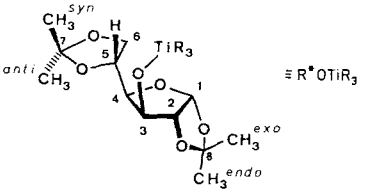
Bond lengths [pm]			
Ti1-Cl2	228.8(5)	$Ti1\text{-}Cp_{center}$	201.3(9)
Ti1-O8	180.9(8)	Ti1-O26	178.6(8)
O8-C9	143(1)	O26-C27	141(2)
$C_{Cp}\text{-}C_{Cp}^{mean}$	140(1)		
Bond angles [°]			
O8-Ti1-Cl2	102.0(4)	26-Ti1-Cl2	101.3(3)
Ti1-O8-C9	145.8(8)	Ti1-O26-C27	153.1(9)
$O8\text{-}Ti1\text{-}Cp_{center}$	117(1)	$026\text{-}Ti1\text{-}Cp_{center}$	118(1)
		O8-Ti1-O26	104.0(4)
Torsion angles [°]			
Cl2-Ti1-O8-O9	+115(2)	Cl2-Ti1-O26-C27	−124(2)
Ti1-O8-C9-C10	+162(2)	Ti1-O26-C27-C28	+120(2)
O11-C10-C19-O20	+79(1)	O29-C28-C37-O38	−179(1)

$[Cp_2Ti(OEt)Cl]$ **2** $[Cp_2Ti(OCH{=}CH_2)_2]$ **3**

$[CpTiCl_2O\text{-}CMe_2\text{-}CMe_2\text{-}OCl_2TiCp]$ **4**

The torsion angles of the freely rotating single bonds in the two carbohydrate ligands (cf. Table 1) differ considerably. The orientation of the ligands relative to the Cp ring is therefore completely different. The dioxolane ring (with C-5 and C-6 of the glucose) of one carbohydrate ligand is facing towards the Cp ring whereas in the other ligand it is situated opposite to the Cp ring. Due to this conformation the $Ti(OR^*)_2$ fragment forms a chiral cavity at the titanium atom. The Cp ligand borders the upper side of the cavity, while the chloro ligand borders the opposite side.

Different sets of signals are observed for the two carbohydrate ligands of complex **1**, both in the ^1H NMR and in the ^{13}C NMR spectrum (Table 2). The assignment of the ^1H resonances of the two ligands was possible with the aid of H, H–COSY and homonuclear difference NOE experiments. Measurements at variable temperatures (−100 to +100 °C)



1, $R_3 = Cp(OR^*)Cl$; **5**, $R_3 = Cp(OR^*)(CH_2\text{-}CH{=}CH_2)$

Table 2. NMR data of the complexes **1** and **5**.

1, ^1H-NMR (400 MHz, CD_2Cl_2): δ = 1.27 (q, *J* = 0.75 Hz, 3H, 8′-CH_3^{exo}), 1.28 (q, *J* = 0.75 Hz, 3H, 8-CH_3^{exo}), 1.38 (q, *J* = 0.75 Hz, 3H, 7-CH_3^{syn}), 1.40 (q, *J* = 0.75 Hz, 3H, 7′-CH_3^{syn}), 1.44 (q, *J* = 0.75 Hz, 3H, 7-CH_3^{anti}), 1.46 (m, 9H, 8-CH_3^{endo}, 8′-CH_3^{endo}, 7′-CH_3^{anti}), 3.86 (dxd, *J* = 8.5 Hz, 5.8 Hz, 1H, 6-H^{anti}), 3.97 (dxd, *J* = 8.5 Hz, 2.5 Hz, 1H, 4-H), 3.95–3.99 (m, 1H, 4′-H); 3.93–3.98 (m, 1H, 6′-H^{anti}), 4.05–4.12 (m, 2H, 5′-H, 6′-H^{syn}), 4.09 (dxd, *J* = 8.5 Hz, 6.1 Hz, 1H, 6-H^{syn}), 4.24 (dxdxd, *J* = 8.5 Hz, 6.1 Hz, 5.8 Hz, 1H, 5-H), 4.44 (dxd, *J* = 3.5 Hz, 0.5 Hz, 1H, 2′-H), 4.51 (dxd, *J* = 3.5 Hz, 0.5 Hz, 1H, 2-H), 5.10 (dxdxd, *J* = 2.5 Hz, 0.5 Hz, 1H, 3′-H), 5.11 (dxdxd, *J* = 2.5 Hz, 0.5 Hz, 0.5 Hz, 1H, 3-H); 5.81 (dxd, *J* = 3.5 Hz, 0.5 Hz, 1H, 1-H), 5.83 (dxd, *J* = 3.5 Hz, 0.5 Hz, 1H, 1′-H), 6.65 (s, 5H, Cp)

^{13}C-NMR (100 MHz, CD_2Cl_2): δ = 25.60(q), 25.85(q), 26.45(q), 26.50(q), 26.95(q), 27.00(q), 27.05(q) 27.10(q), 67.85(t), 67.95(t), 72.25(d), 72.75(d), 82.75(d), 83,55(d), 85.05(d), 85.35(d), 91.70(d), 92.10(d), 105.60(d), 105.70(d), 109.40(s), 109.50(s), 112.10(s), 112.20(s), 118.35(d)

^{13}C-NMR (100 MHz, $[D_8]THF$): δ = 25.80(q), 26.15(q), 26.55(q, 2c), 26.60(q), 27.10(q), 27.15(q, 2c), 67.85(t), 68.10(t), 73.05(d), 73.25(d), 83.45(d), 83.60(d), 86.29(d), 86,35(d), 88.77(d), 89.32(d), 92.10(d), 106.20(d), 106.25(d), 109.60(s), 109.65(s), 111.90(s), 112.10(s), 115.60(s), 144.80(d) [a]

[a] The signals of the two methylene carbon atoms could not be determined (not even at −80 °C), since they are very broad, presumable due to dynamic effects ($\eta^1 \rightarrow \eta^3 \rightarrow \eta^1$ equilibrium).

[*] Dr. A. Hafner, Dr. A. Togni, Dipl.-Chem. Dr. M. Riediker [+], G. Rihs
Zentrale Forschungslaboratorien, Ciba-Geigy AG
Postfach, CH-4002 Basel (Switzerland)
Dr. U. Piantini
Organisch-Chemisches Institut der Universität
Winterthurerstrasse 190, CH-8057 Zürich (Switzerland)
[+] Present address:
Research Laboratories, Plastics Division, Ciba-Geigy Corporation
Ardsley, NY 10502 (USA)

[**] Enantioselective Syntheses with Titanium-Carbohydrate Complexes, Part 4. - Part 3: [1c]

gave no indication of an inversion at the metal center or of a rapid ligand exchange. Furthermore, no further conformational isomers could be detected, even at $-100\,^{\circ}C$, so that it can be assumed that a relatively rigid conformation exists in solution. Since the H, H coupling constants of the ligands are practically identical to those of the free 1,2:5,6-di-*O*-isopropylidene-α-D-glucofuranose, greater deformations of the glucose skeleton due to complexation can be ruled out. However, no data on the H–C4′–C5′–H torsion angle is available, because $J_{4'\text{-}H,5'\text{-}H}$ coupling constants could not be determined. Since no NOEs are observed between protons that do not belong to the same carbohydrate unit, these two ligands must be spatially separated. A strong NOE with the Cp ligand is, however, exhibited by the 3-H and 3′-H protons. Due to the fact that the NOEs are practically identical, these two protons must lie approximately the same distance from the Cp ring. 7-CH_3^{syn} exhibits a weak NOE with the Cp ligand; this indicates that this methyl group is also located near to the Cp ring. Additional NOEs with the Cp ligand were not observed. These observations strongly suggest a similar conformation of the complex **1** in solution and in the solid state.

The chloro ligand can be replaced in a metathesis reaction, either by an η^1-allyl or an ester enolate ligand. These ligands can then be transferred with high enantioselectivity to aldehydes.[1] The reagent **5** used for the allylation could be isolated and characterized by ^{13}C-NMR (Table 2). From a comparison of the ^{13}C-T_1 relaxation times with those of **1** it could be concluded that the complex **5** is monomeric.

$[TiCp(OR^*)_2(CH_2-CH=CH_2)]$ **5**

The two 1,2:5,6-di-*O*-isopropylidene-α-D-glucofuranosyl ligands again show two different sets of signals, even at room temperature. There is no indication of a rapid ligand exchange or an inversion at the metal center taking place. The chiral cavity found in the complex **1** is apparently retained also in the complex **5**. The product enantioselectivities obtained for the reactions of **5** can be reasonably attributed to a coordination of the aldehyde in such a chiral cavity.

Received: December 21, 1988 [Z 3098 IE]
German version: *Angew. Chem. 101* (1989) 493

CAS Registry numbers:
1, 119528-80-2; **5**, 119503-26-3

[1] a) M. Riediker, R. O. Duthaler, *Angew. Chem. 101* (1989) 488; *Angew. Chem. Int. Ed. Engl. 28* (1989) 494; b) R. O. Duthaler, P. Herold, W. Lottenbach, K. Oertle, M. Riediker, *ibid. 101* (1989) 490 and *28* (1989) 495; c) G. Bold, R. O. Duthaler, M. Riediker, *ibid. 101* (1989) 491 and *28* (1989) 497.

[2] *D. Seebach* et al. have used titanium-complexed bidentate D-mannitol derivatives in asymmetric alkylation and Diels-Alder reactions; D. Seebach, A. K. Beck, R. Imwinkelried, S. Roggo, A. Wonnacott, *Helv. Chim. Acta 70* (1987) 954.

[3] Correct elemental analyses (C, H, Cl).

[4] Crystals of **1** can be grown at 233 K in an inert gas atmosphere from a THF solution of **1** by slow diffusion of pentane into this solution.

[5] Orthorhombic, $P2_12_12_1$, $a = 1081.6(3)$, $b = 1120.7(4)$, $c = 2656.1(6)$ pm, $V = 3.220 \times 10^9$ pm^3, $Z = 4$, $\varrho_{calcd} = 1.375$ g cm^3; intensity measurements at 193 + 3 K were carried out on a Philips PW-1100 diffractometer (graphite monochromator, $Mo_{K\alpha} = 70.926$ pm, $\theta/2\,\theta$ scan $6^\circ < 2\,\theta < 56^\circ$, reflection width 1.2°). Solution of structure with 3056 observed independent reflections by the classical heavy atom method. The refinement according to the least squares method [6] with anisotropic temperature factors converged at $R = 0.053$. The hydrogen atoms could not be located. Further details of the crystal structure investigation are available on request from the Director of the Cambridge Crystallographic Data Centre, University Chemical Laboratory, Lensfield Road, Cambridge CB2 1EW (England), on quoting the full citation of the journal.

[6] Enraf-Nonius: *Structure Determination Package*, Enraf-Nonius, Delft (The Netherlands) 1982.

[7] J. C. Huffmann, K. G. Moloy, J. A. Marsella, K. G. Caulton, *J. Am. Chem. Soc. 102* (1980) 3009.

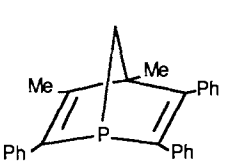
[8] M. D. Curtis, S. Thanedar, W. M. Butler, *Organometallics 3* (1984) 1855.

Phosphanorbornadienes as Ligands in the Transition Metal-Catalyzed Synthesis of Fine Chemicals**

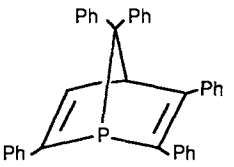
By *Denis Neibecker** and *Régis Réau*

Since *Wilkinson* et al.[1] demonstrated that rhodium-phosphane complexes are by far the best catalysts for the hydroformylation of α-olefins, many works have been devoted to improving the activity and selectivity of these catalytic systems by varying the phosphane.[2] In spite of the large number of phosphanes tested, the hydroformylation of olefins, especially functionalized ones, has not yet been accomplished with enough selectivity to become a valuable synthetic tool. As a consequence, new phosphanes are potentially of interest for the development of more efficient catalytic systems.

The phosphanorbornadienes **1** and **2**, first described by *Mathey* et al. in 1981, are now readily available compounds,[3] which, according to their Tolman's parameters,[4] are hindered and poor σ-donor ligands.[5]

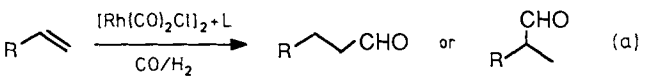


1



2

Since it is well established that phosphanes exhibiting such stereoelectronic properties enhance both the activity and selectivity of the rhodium catalyst in the hydroformylation of olefins,[6] we decided to investigate catalysts generated in situ from phosphanorbornadiene and $[Rh(CO)_2Cl]_2$ as catalyst precursors, a conventional method in hydroformylation chemistry[2] [Eq. (a); dppb = 1,4-bis(diphenylphosphino)butane].



(a)

3, R = *n*Bu **4**, R = Ph **5**, R = COOEt

L = PPh_3, dppb, **1**, **2**

At first, we compared the activities of the phosphanorbornadienes in the hydroformylation of 1-hexene under conventional conditions[2] with those of triphenylphosphane, the phosphane ligand used on an industrial scale[7] (Table 1).

The (phosphanorbornadiene)rhodium complexes exhibit the same stereoselectivity as the triphenylphosphane rhodium complex—predominantly *n*-heptanal, **3**, is formed—but

[*] Dr. D. Neibecker, Dr. R. Réau
Laboratoire de Chimie de Coordination du CNRS, Unité No. 8241, liée par conventions à l'Université Paul Sabatier et à l'Institut National Polytechnique
205 route de Narbonne, F-31077 Toulouse Cedex (France)

[**] The authors wish to thank the Centre National de la Recherche Scientifique (CNRS) for financial support and the Société Nationale des Poudres et Explosifs (SNPE) both for financial support and a fellowship to *R. R.* and for permission to publish this paper. They are also grateful to Dr. *F. Mathey* and *A. Breque* from the Ecole Polytechnique, Palaiseau (France) for providing the phosphanorbornadienes. Helpful discussions with Dr. *F. Mathey*, Dr. *S. Lecolier* (SNPE) and Dr. *I. Tkatchenko* (CNRS) are also gratefully acknowledged.

Table 1. Hydroformylation of 1-hexene. [a]

Phosphane	Conversion [%]	Yield of Aldehydes [%]	3 [%]	TOF [b] [h^{-1}]
PPh_3	6	100	71	39
1	27	100	68	204
2	62	100	68	402

[a] [Substrate]/[Rh] = 220, [phosphane]/[Rh] = 5, 80 °C, CO/H_2 (1/1) 20 bar, 20 min. [b] TOF turnover frequency defined as mol of substrate hydroformylated per mol of catalyst per hour.

they are much more active. No side reactions such as hydrogenation or isomerization of the substrate are observed. These findings led us to examine the hydroformylation of functionalized olefins, namely styrene and ethyl acrylate.

Preliminary runs performed with styrene at 40 °C revealed that only the rhodium complex of **2** provided an efficient catalytic system. It then was used under milder conditions for comparison with triphenylphosphane, which is reported to be the most efficient ligand for rhodium-catalyzed styrene hydroformylation[8] (Table 2).

Table 2. Hydroformylation of styrene [a].

Phosphane	Conversion [%]	Yield of Aldehydes [%]	4 [%]	TOF [b] [h^{-1}]
PPh_3	10	100	95	3.6
2	46	100	91	17

[a] [Substrate]/[Rh] = 220, [phosphane]/[Rh] = 5, 25 °C, CO/H_2 (1/1) 20 bar, 360 min. [b] See footnote in Table 1.

The results quoted in Table 2 show that phosphanorbornadiene **2** is a more efficient ligand than triphenylphosphane for the hydroformylation of styrene. This result is promising not only for the selective production of hydratropaldehyde **4** (a starting material for cosmetics, polymers and pharmaceuticals[9]) but also for the synthesis of 2-arylpropionaldehydes and therefore of the corresponding acids which are now commonly used as antiinflammatory drugs.[10]

Finally, the hydroformylation of ethyl acrylate was studied. It is reported that this reaction requires drastic conditions (typically 150 °C, 100 bar) and that only (diphosphane)rhodium complexes are catalytically active.[11] In spite of these results, the activity of the (phosphanorbornadiene)rhodium systems in the hydroformylation of ethyl acrylate at 25 °C was investigated. The (dppb)Rh system, which is the most active and selective catalyst system described so far[12] for this reaction, served for comparison.

The results (Table 3) show that the hydroformylation of ethyl acrylate does indeed proceed under mild conditions. Furthermore, it is shown for the first time that this reaction can be catalyzed effectively by (monophosphane)rhodium systems. Ethyl 2-formylpropionate **5** selectivity reaches 100%, and the phosphanorbornadienes **1** and **2** induce a better activity than the best diphosphane described so far.

Table 3. Hydroformylation of ethyl acrylate [a].

Phosphane	Conversion [%]	Yield of Aldehydes [%]	5 [%]	TOF [b] [h^{-1}]
dppb	56	100	100	11
2	71	100	100	14
1	70	100	100	15

[a] [Substrate]/[Rh] = 220, [phosphane]/[Rh] = 5, 25 °C, CO/H_2 (1/1) 20 bar, 720 min. [b] See footnote in Table 1.

In conclusion, this work demonstrates that phosphanorbornadienes are valuable ligands for rhodium catalysts for the hydroformylation of olefins. These original phosphanes lead to highly selective and active catalytic systems under very mild conditions. Considering the diversity of the investigated substrates, these new catalytic systems may be used for a large variety of olefins, especially functionalized ones.

Experimental

The hydroformylation reactions were performed in a home-made 100-mL Teflon-coated stainless steel autoclave, equipped with a magnetic stirrer, a safety valve, a ball valve for the introduction of liquids, a manometer and an argon/gas inlet-outlet valve. In a typical run, 0.02 mmol of $[Rh(CO)_2Cl]_2$ and 0.2 mmol of ligand were placed in the autoclave. The atmosphere was replaced by argon and a toluene solution (8 mL) containing the substrate (9 mmol) and NEt_3 (0.4 mmol) was introduced through the ball valve. This valve was closed and the autoclave was pressurized with CO (10 bar) and H_2 (10 bar) and thermostated at the required temperature in about 5 min. After the reaction time quoted in the Tables, the autoclave was cooled to −40 °C and vented in ca. 1 h in a well-ventilated hood. The reaction products were collected under argon into a Schlenk tube with toluene and analyzed by gas chromatography. Conversion of the substrates and stereoselectivity with respect to the aldehydes **3**, **4** and **5** were determined relative to internal standards.

Received: November 21, 1988 [Z 3062 IE]
German version: *Angew. Chem. 101* (1989) 479

CAS Registry numbers:
1, 79032-37-4; **2**, 79032-31-8; **3**, 111-71-7; **4**, 93-53-8; **5**, 27772-62-9; dppb, 7688-25-7; $[Rh(CO)_2Cl]_2$, 14523-22-9; PPh_3, 603-35-0; styrene, 100-42-5; 1-hexene, 592-41-6, ethyl acrylate, 140-88-5.

[1] D. Evans, J. A. Osborn, G. Wilkinson, *J. Chem. Soc. A 1968*, 3133.
[2] J. Falbe, *New Synthesis with Carbon Monoxide*, Springer, Berlin, 1980.
[3] F. Mathey, F. Mercier, C. Charrier, *J. Am. Chem. Soc. 103* (1981) 4595.
[4] C. A. Tolman, *Chem. Rev. 77* (1977) 313.
[5] For **1**, Tolman's steric parameter θ has been calculated to be 147° from its structural data and is comparable to that of triphenylphosphane (θ = 145°) [4]. Tolman's electronic parameters ν have been determined as 2070.4 cm^{-1} for compound **1** [between that of PPh_3 (ν = 2068.9 cm^{-1}) and that of tris(4-chlorophenyl)phosphane (ν = 2072.8 cm^{-1})] and as 2072.9 cm^{-1} for compound **2** [close to that of tris(4-chlorophenyl)phosphane] [4].
[6] J. D. Unruh, J. R. Christenson, *J. Mol. Catal. 14* (1982) 19; W. R. Moser, C. J. Papile, D. A. Brannon, R. A. Durwell, S. J. Weininger, *ibid. 41* (1987) 271.
[7] K. Weissermel, H. J. Arpe: *Industrial Organic Chemistry*, Verlag Chemie, Weinheim 1978; *Chimie Organique Industrielle*, Masson, Paris 1981.
[8] T. Hayashi, M. Tanaka, I. Ogata, *J. Mol. Catal. 6* (1979) 1; A. Cerriotti, L. Goulaschelli, G. Longoni, M. C. Malatesta, O. Strumolo, *ibid. 24* (1984) 309.
[9] H. Bönnemann, *Angew. Chem. 85* (1973) 1024; *Angew. Chem. Int. Ed. Engl. 12* (1973) 964.
[10] G. Paninello, J. K. Stille, *J. Am. Chem. Soc. 109* (1987) 7122; D. P. Riley, D. P. Getman, G. R. Beck, R. M. Heintz, *J. Org. Chem. 52* (1987) 287.
[11] M. Matsumoto, M. Tamura, *J. Mol. Catal. 16* (1982) 195.
[12] M. Tanaka, T. Hayashi, I. Ogata, *Bull. Chem. Soc. Jpn. 50* (1979) 2351.

Book reviews are written by invitation from the editor. Suggestions for books to be reviewed and for qualified book reviewers are welcome. Publishers should send prospects or (better) books to the following address: Redaktion Angewandte Chemie, Postfach 101161, D-6940 Weinheim, Bundesrepublik Deutschland. The editor reserves the right of selecting which books will be reviewed. Unlimited books not chosen for review will not be returned.

Intermolecular Complexes. (Series: Studies in Physical and Theoretical Chemistry, Vol. 52). By *P. Hobza* and *R. Zahradnik*. Elsevier, Amsterdam 1988. 308 pp., hard cover, HFl 245.00.—ISBN 0-444-98943-9

Experimental and theoretical studies of intermolecular complexes are becoming an ever more important part of physical chemistry, and many review articles on the topic have been published in the last few years. The authors of this volume have taken on the task of providing a more comprehensive overview of recent developments in the area of intermolecular interactions.

In a short introductory chapter the scope of the book is defined, the basic features of intermolecular interactions are summarized, and reference is made to earlier reviews of the topic. This is followed by a discussion of theoretical approaches to the problem, and the numerical methods that are now routinely used for calculations on intermolecular interactions. The methods covered range from those based on configuration interaction (CI) and perturbation theory, through self-consistent field (SCF) methods, to the completely empirical methods. Detailed derivations are not given. A knowledge of the necessary formalism for the various methods is generally assumed. On the other hand, the capabilities, and also the limitations, of the various methods are illustrated using examples taken from the literature. The third chapter consists of a very brief summary of experimental techniques.

The next chapter contains a detailed and systematic survey of quantum chemical calculations and experimental results concerning the structures and spectroscopic properties of isolated dimers (ranging from inert gas dimers through various hydrogen-bonded complexes to G–C base pairs. The final chapter is an interesting account of biochemical aspects, in which van der Waals complexes play an important role.

With such a wide range of topics it is understandable that they are often merely broached without a deeper analysis, and that the selection of systems for discussion and of methods of calculation is considerably influenced by the authors' own field of work on ab initio calculation methods. However, this in no way diminishes the worth of the book—on the contrary it is clearly and comprehensibly written, and with more than 1200 references it offers a comprehensive and unbiased coverage of the literature, although regrettably only up to 1984.

The book can be thoroughly recommended to all chemists as a source book for preparing lectures, and as an introduction to the field. For specialists working in the area of intermolecular interactions, especially hydrogen bonding, this book is essential reading; it is also an extremely useful work of reference by virtue of the large amount of tabulated data and literature references which it contains.

Alfred Karpfen [NB 960 IE]
Institut für Theoretische Chemie und Strahlenchemie
der Universität Wien (Austria)

Corrigendum

In the communication entitled "$(t\mathrm{BuSiP})_4$—The First Silaphosphacubane" by M. Baudler, G. Scholz, K.-F. Tebbe, and M. Fehér (*Angew. Chem. Int. Ed. Engl. 28* (1989) 339–341), the calculated coupling constants of the AX_3Y system in the ^{29}Si NMR spectrum of **1** should be $^1J_{SiP} = +37.6(1)$ Hz, $^3J_{SiP} = -12.6(3)$ Hz, and $^2J_{PP} = +23.8(1)$ Hz (the last coupling constant was printed incorrectly as $^2J_{HP}$).

Registered names, trademarks, etc. used in this journal, even when not marked as such, are not to be considered unprotected by law.

© VCH Verlagsgesellschaft mbH, D-6940 Weinheim, 1989. - Printed in the Federal Republic of Germany by Konrad Triltsch, Druck- und Verlagsanstalt Würzburg.

All rights reserved (including those of translation into foreign languages). No part of this issue may be reproduced in any form — by photoprint, microfilm, or any other means — nor transmitted or translated into a machine language without written permission from the publishers. Only single copies of contributions, or parts thereof, may be made for personal use. This journal was carefully produced in all its parts. Nevertheless, authors, editors and publisher do not warrant the information contained therein to be free of errors. Readers are advised to keep in mind that statements, data, illustrations, procedural details or other items may inadvertently be inaccurate.

Valid for users in the USA: The appearance of the code at the bottom of the first page of an article (serial) indicates the copyright owner's consent that copies of the article may be made for personal or internal use, or for the personal or internal use of specific clients. This consent is given on the condition, however, that the copier pay stated per-copy fee through the Copyright Clearance Center, Inc. (CCC), for copying beyond that permitted by Sections 107 or 108 of the U.S. Copyright Law. This consent does not extend to other kinds of copying, such as copying, for general distribution, for advertising or promotional purposes, for creating new collective works, or for resale. For copying from back volumes of this journal see 'Permissions to Photo-Copy: Publisher's Fee List' of the CCC.

Editorial office: Postfach 101161, D-6490 Weinheim, Federal Republic of Germany, Telephone (06201) 602255, Telex 465516 vchwh d, Telefax (06201) 602328.

Editor: *Peter Gölitz*

Associate editors: *D. I. Loewus, A. Stimson.* **Editorial assistant:** *E. Schweikart*

Publishers: VCH Verlagsgesellschaft mbH. (Managing Director: *Hans Dirk Köhler*), Pappelallee 3, D-6940 Weinheim, Federal Republic of Germany.

Advertising office (Advertising Manager *R. J. Roth*): Postfach 101161, D-6940 Weinheim, Federal Republic of Germany, Telephone (06201) 606130, Telex 467155, Telefax (06201) 606184.

ADVANCED MATERIALS

Polymers as Advanced Materials

Editorial Essay

By Claus D. Eisenbach* and Dietrich Haarer*

The bottleneck in the development of new technologies is often defined by the limitations of the available materials. Obvious examples for such limitations in materials parameters are a) that charge carrier mobilities can control the maximum frequency in semiconductors or b) that the read/write speeds and signal-to-noise ratios of possible optical stores depend on the sensitivity of the storage media. Progress in these and other fields has been mostly due to interdisciplinary efforts: The improved production of epitaxially grown semiconductor layers has contributed as much to the development of semiconductors as has the art of producing thin, sputtered films to the development of optical storage media, and polymer science is crucial to the success of many device applications. In the semiconductor industry, for instance, polymers play a crucial role as photoresists, dielectric layers, and packaging materials, or in the field of optical data stores, polymeric materials can be used as substrates as well as in the form of thin films as data carriers. In high performance polymers the combination of low weight, moderate thermal stability and high tensile strength, has further improved fiber reinforced materials, and has lead to major breakthroughs in aerospace technology.

Polymer science is a young discipline which has lately made large steps towards innovative materials and processes. This is a consequence of the almost unlimited scope for the molecular design of macromolecules, and of blending polymers with low or high molecular weight components. Polymer processing and molding, not to speak of composites, will also make major contributions to the further development of advanced materials. The field of "materials science" has increased in importance relative to physics and chemistry. This trend is documented by the increase in the representation of the "materials science" research faculty staff in the US program of the Interdisciplinary Laboratories (IDLs)/Materials Laboratories (MRLs) from 19% in 1970 to 35% in 1985.[1]

Polymers are ideal examples of structural and functional materials because of their versatility in practically all areas of modern life and technology. Some of their outstanding properties are high elasticity, stiffness, toughness, strength, good thermal resistance, and high chemical stability. Typical examples of their uses are high impact thermoplasts, thermoplastic elastomers, ultrahigh modulus fibers and temperature resistant polymers. An extension of the potential of engineering plastics beyond the organic multiphase polymer systems is given by the combination of polymers with non-polymeric and/or non-organic materials resulting in high performance composites. Progress in this area is favored by the growing research activity in interface phenomena and thin coatings and films. Finally, the electronic properties of polymers or macromolecular systems open up fascinating prospects for storing, processing and transmitting of data, as has been outlined by recent developments in the area of polymeric light waveguides, non-linear optics or conducting polymers.

It is a primary objective of basic materials science to develop a detailed knowledge of the structure-property relationships in macromolecular systems in order to understand how the molecular architecture of the individual polymer chain influences the morphology and superstructure of the polymeric materials. This goal can only be achieved by an interdisciplinary research and development effort, combining the natural sciences and engineering. As a result of the funding situation in West Germany, these considerations have resulted in an effort by researchers from different fields and from both academic and industrial laboratories to cooperate more closely, to participate in joint research programs and even in the establishment of new institutes supported through governmental and industrial research funds. This is reflected by the natural science activities of central research institutions and of universities such as those in Darmstadt and Kaiserslautern. Polymer materials science is especially strong in Freiburg, Mainz and Bayreuth, emphasized by the recent founding of the Max Planck Institute for Polymer Research (Mainz) and the Institute for Materials Science (Bayreuth).

The situation in Bayreuth, where both authors are working illustrates the general concept of the concerted efforts in materials science. Macromolecular topics have been highly emphasized in both the Chemistry and Physics departments leading to a great deal of interdepartmental research: Our program ranges from the synthesis of new macromolecular and micellar systems, through their extensive characterization to specific investigations, e.g. electronic processes in synthetic and biological macromolecular systems. The newly established Institute of Materials Science was conceived as a place of interaction between basic and applied research and is well situated within this environment to interact with the high temperature-geo scientists in the university as well as the local ceramics and electronics industries.

In order to promote this interdisciplinary approach to materials science a symposium was held in Bayreuth from 10.–12. April at which topics of current interest from the areas of polymeric, structural and functional materials were

[*] Prof. C. D. Eisenbach
Makromolekulare Chemie II
Universitätsstraße 30
D-8580 Bayreuth (FRG)

Prof. D. Haarer
Experimentalphysik IV
Universitätsstraße 30
D-8580 Bayreuth (FRG)

presented and discussed, complemented by contributions from the related fields of inorganic/organic polymers and ceramics. It is planned to integrate the inorganic non-metallic materials into the future symposium programs, corresponding to our wishes for the development of materials science in Bayreuth. A key issue and primary concern of this meeting was to discuss the different facets of fundamental and applied research and thus provide a platform for the dialogue between people working in academia and in industrial research institutions. The symposium focused on strategies and steps towards polymers with new and unusual properties, and experimental results and theoretical concepts of the structure-property relationship of organic polymeric materials. Furthermore, connections, similarities and analogies between polymeric materials, and ceramics or inorganic materials in general became visible. Also in this respect, first signs have become apparent at a recent materials science conference organized by the West German Ministry of Science and Technology (BMFT).[2] Among the subjects which were highlighted at this meeting, polymers have made remarkable progress in high-tech applications such as information technology, where tailor-made photoconductive media dominate the field of electro-photography and are finding application in modern techniques of offset-printing. The impact which non-linar optical polymeric materials will make on the advancement of integrated optics was assessed and without doubt the use of polymers as light fibers is a feasible and interesting application. Research into conductive polymeric materials has recently made progress in terms of an increased understanding of the basic processes, but applications for example, in the field of rechargeable batteries are still at an early stage and can therefore not be fully assessed. Liquid crystalline polymers will probably make significant progress in the near future, although it is not yet clear whether it will be the mechanical aspects, (flow viscosity during processing etc.) or the optical aspects of this new class of polymers which will carry the main impact. The mechanical properties of new polymeric materials like copolymers and polymer blends will, without doubt, be a field of active research, where new synthetic materials will be of eminent importance. A question to be answered is, whether or not reinforced polymeric materials can only be made through macroscopic reinforcement with carbon- or glass-fibers, or whether they can also be made by "molecular reinforcement", i.e. by synthesizing molecularly ordered macromolecules with rod-like elements which form structures with a higher degree of order.

Several of the long-term goals of materials research were compiled at a recent IUPAC-meeting in Japan.[3] One of these goals is the development of "molecular devices", for which the basic questions are still unanswered, namely how to manipulate data at a molecular level, but towards which steps have been taken in laser techniques like hole burning or electric techniques like tunnelling microscopy, where ultra-high frequency resolution or spatial resolution can be achieved. However, we have long to wait before the elegant schemes of dynamic biological systems can be incorporated into technical systems as the difficult task of tailoring macromolecules to mimic self-organization phenomena, and molecular reinforcement of macromolecular systems in synthetic polymeric materials has first to be mastered. Molecular schemes like those in nature also require systems which are far from thermodynamic equilibrium. Here we have to explore the largely unknown field of molecular assembly which is certainly different from most present synthetic procedures. If these and many other materials related problems are to be effectively solved it is clear that an interdisciplinary approach is needed, and we are sure that it is this approach which will lead us to new frontiers to the benefit of all.

[1] P. A. Psaras, H. D. Langford (Eds): *Advancing Materials Research*, National Academy Press, Washington D.C. 1987.

[2] *Symposium Materialforschung 1988 des Bundesministers für Forschung und Technologie (BMFT)*, 12.–14. September 1988, Vorträge und Poster, Band 1 and 2, Hamm/Westfalen 1988, KFA Jülich GmbH, 1988. See also: W. Faul, *Angew. Chem. Adv. Mater. 100* (1988) 1824; *Angew. Chem. Int. Ed. Engl. Adv. Mater. 27* (1988) 1754.

[3] K. Ohsima, K. Saito, M. Hirooka (Eds): *Advanced Materials for Innovations in Energy, Transportation & Communications. Perspectives and Recomendations.* The Chemical Society of Japan, Tokyo 1987.



Dr. Claus D. Eisenbach is Professor of Macromolecular Chemistry at the University of Bayreuth. He studied chemistry at the University of Mainz, where he obtained his Ph.D. in 1974. After two postdoctoral years at the University of Massachusetts in Amherst, USA, he started a university career in Freiburg. In 1984 he became a professor of Macromolecular Chemistry at the University of Karlsruhe, and in 1986 he moved to Bayreuth. His research activities cover polymer synthesis and photoreactions in polymers.



Dr. Dietrich Haarer is Professor of Physics at the University of Bayreuth. A physicist by training, he received his Ph.D. in 1969 from the University of Stuttgart. With short interruptions he then worked until 1980 at the IBM research laboratory in San Jose, California, which he left as manager of the Organic Solids Department taking up his current position. His research activities include laser spectroscopy and laser chemistry. He is an Editorial Advisor for Advanced Materials.

ADVANCED MATERIALS

Modeling Organic Surfaces with Self-Assembled Monolayers**

Interfacial Structure
Wettability
Long-Chain Thiols
on Gold

By Colin D. Bain* and George M. Whitesides*

The interfacial properties of organic materials are of critical importance in many applications, especially the control of wettability, adhesion, tribology, and corrosion. The relationships between the microscopic structure of an organic surface and its macroscopic physical properties are, however, only poorly understood. This short review presents a model system that has the ease of preparation and the structural definition required to provide a firm understanding of interfacial phenomena. Long-chain thiols, $HS(CH_2)_nX$, adsorb from solution onto gold and form densely packed, oriented monolayers. By varying the terminal functional group, X, of the thiol, organic surfaces can be created having a wide range of structures and properties. More complex systems can be constructed by coadsorbing two or more thiols with different terminal functional groups or with different chain lengths onto a common gold substrate. By these techniques, controlled degrees of disorder can be introduced into model surfaces. We have used these systems to explore the relationships between the microscopic structure of the monolayers on a molecular and supramolecular scale and their macroscopic properties. Wettability is a macroscopic interfacial property that has proven of particular interest.

1. Introduction

Much of modern materials science has been devoted to the discovery, development and production of materials with desired combinations of bulk mechanical, electrical or optical properties. In an increasing number of materials systems, however, performance is determined not only by the properties of the bulk but also by the characteristics of interfaces either within the material or between the material and the outside world. Examples abound: the strength and toughness of a carbon fiber composite is strongly influenced by the bond between the fiber and the polymer matrix; cracks may propagate rapidly along grain boundaries; the biological response to implanted materials is critically determined by the properties of their surfaces; surface states can pin the Fermi level in semiconductors; water and oil repellency are determined by the outermost few angströms of a material; optical losses occur through reflection, scattering and non-linear processes at interfaces. As trends towards miniaturization continue, the ratio of surface to volume increases and the importance of understanding and controlling interfacial properties grows commensurately.

The goal of relating the microscopic (atomic, molecular and supramolecular) structure of a surface to its macroscopic physical, chemical or biological properties (wettability, corrosion resistance, adhesive strength, biocompatibility) is not trivial, and may prove as great a challenge as the development of new materials. Attaining this goal is made more difficult by the complexity and inaccessibility of many interfaces of practical importance. Consequently, the ability to create model surfaces in which the structure is controlled on an atomic scale plays a vital role. Epitaxial growth techniques, such as molecular beam epitaxy (MBE) and vacuum pyrolysis epitaxy (VPE), have provided a way forward in the study of semiconductors and ceramics, but such techniques cannot easily be applied to the synthesis of model organic surfaces. Recently it has become clear that organic monolayer films offer the level of structural control required for detailed studies of organic surfaces. Of all the types of monolayer film studied since *Benjamin Franklin* first poured oil onto Clapham Pond, two systems appear particularly promising: monolayers prepared by adsorption of alkanethiols on gold,[1] silver, copper or platinum, and those generated by reaction of alkyltrichlorosilanes with silicon or glass.[2] In this review we will concentrate on monolayers of alkylsulfur compounds on gold, with the emphasis on our own research. First, we will discuss the difference between these self-assembled monolayers and films produced by the Langmuir–Blodgett (LB) technique. We will then summarize the structural properties of monolayers generated by adsorption of thiols on gold. The bulk of the review is devoted to explaining, with examples, how the structure of the monolayer–air or monolayer–liquid interface can be varied in a controlled manner, and to discussing the types of information that can be derived from studies of model organic surfaces.

[*] Dr. C. D. Bain
Department of Chemistry, University of Cambridge
Lensfield Road, Cambridge CB2 1EW (UK)
Prof. G. M. Whitesides
Chemical Laboratories, Harvard University
12 Oxford Street, Cambridge MA 02138 (USA)

[**] This work was funded in part by the Office of Naval Research, by (DARPA/URI), and by the National Science Foundation through grants to the Harvard University Materials Research Laboratory.

2. Langmuir–Blodgett and Self-Assembled Monolayers

The traditional means of forming an organic monolayer film is to spread an insoluble compound on an aqueous subphase, compress the film mechanically with a barrier until the molecules are densely packed and oriented approximately normal to the surface, and then to transfer this monolayer, if desired, to a solid substrate by "dipping" (Fig. 1 top). Much elegant work has been performed using these LB monolayers,[3] and the LB technique is particularly useful when multilayers are desired. LB monolayers, however, suffer several drawbacks as model systems for studying interfacial properties. First, they are only metastable and tend to relax into more stable structural forms. Surface properties of LB films are most easily studied after the film has been transferred to a solid substrate, a procedure that may be complicated by changes in the structure of the monolayer during the transfer process. Second, they are not normally chemically bonded to the substrate and hence are not robust. LB monolayers can often be removed from a substrate simply by rinsing with either aqueous or non-aqueous solvents. Third, one is restricted to compounds that form LB films on water and that can be transferred intact to a substrate. It is, in particular, difficult to generate surfaces exposing polar functional groups at the monolayer–air interface by this technique. It is also difficult to form highly crystalline monolayers since they tend to be brittle and crack easily upon compression or during transfer.

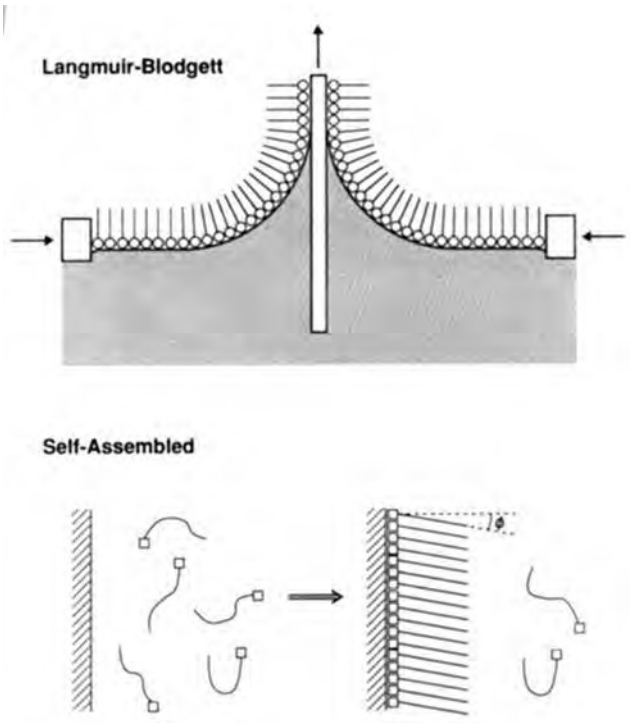


Fig. 1. Top: A Langmuir–Blodgett monolayer can be transferred from the surface of water to a hydrophilic solid by raising the substrate through the water–air interface while maintaining a constant surface pressure with movable barriers. Bottom: Self-assembled monolayers form spontaneously upon immersion of the substrate in a dilute solution of the adsorbate. Monolayer formation is driven by a strong, specific interaction between the head group (squares) and the surface of the substrate. One such system comprises thiols, RSH, adsorbed onto films of noble metals, such as gold, silver and copper. The cant (Φ) of the hydrocarbon chains varies with the choice of substrate.

Self-assembled monolayers rely on a strong specific interaction between an adsorbate and a substrate to drive the spontaneous formation of a monolayer film (Fig. 1 bottom).[4] To prepare a self-assembled monolayer, the substrate is simply immersed in a dilute (ca. 1 mM) solution of the adsorbate at room temperature for an interval varying from a few minutes to several days, depending on the system. The principal substrate in our studies has been a gold film (1000–2000 Å thick) evaporated onto a polished silicon wafer, and we have used long-chain organosulfur compounds, typically thiols, $HS(CH_2)_nX$, as adsorbates. The densely packed, oriented films that result are thermodynamically stable and mechanically robust. Monolayers of thiols on gold can be removed from the solutions from which they have been adsorbed and immersed in aqueous or non-aqueous solvents, in acid or in base, without apparent adverse effects. The range of organic species that can be incorporated into these monolayers is large: few ligands compete effectively with a thiol in coordinating to the gold, and the thiol group is sufficiently unreactive to be compatible with most other functional groups. A variety of chemical reactions can also be performed on the monolayers in order to interrogate the structure or to modify the surface. Self-assembled monolayers of thiols adsorbed on gold are thus well suited for our studies.

We,[5] and others,[2, 6] have also used alkyltrichlorosilanes as precursors to monolayers of alkylsiloxanes on glass or silicon. These monolayers exhibit greater thermal, chemical (except in the presence of aqueous base) and mechanical stability than thiols adsorbed on gold: they can even be heated in boiling water or scrubbed vigorously without degradation. The high reactivity of the $SiCl_3$ group limits the chemistry of surfaces that can be created directly by adsorption of alkyltrichlorosilanes on silicon. The thermal and chemical stability of the monolayers does, however, allow extensive synthetic modification of pre-formed films. *Ulman* et al.[6] using a modification of a technique proposed by *Sagiv* et al.[7] have recently demonstrated the feasibility of monolayer-by-monolayer synthesis of high-quality multilayer films with alkyltrichlorosilanes. These multilayers have great potential for controlling the bulk optical and electrical properties of thin films, but are beyond the scope of this review.

3. Structure of Monolayers of Thiols on Gold

Our investigations have centered on the adsorption onto gold of linear thiols, $HS(CH_2)_nX$, where $n \geq 10$ and X is any one of a wide range of functional groups that are compatible with thiols and that do not disrupt the packing of the hydrocarbon chains. We and others have characterized the result-

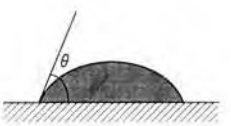
ing films by a range of techniques including ellipsometry, transmission electron microscopy (TEM), contact angle determination, reflection adsorption infrared spectroscopy (RAIRS), X-ray photoelectron spectroscopy (XPS) and electrochemistry.[8–13] The picture that emerges is of a pin-hole-free, monolayer film comprising a densely packed array of *trans*-extended hydrocarbon chains, strongly anchored to the gold surface through the sulfur atom, and tilted approximately 30° from the normal to the surface. The nature of the bonding between sulfur and gold has not yet been established incontrovertibly, but available evidence points to both alkanethiols and dialkyl disulfides generating gold thiolates (Au—SR) upon adsorption. (For clarity we will use terms such as "monolayer of alkanethiol" in this review to indicate the molecular precursor, even though the actual species on the surface is probably a thiolate). The tail group, X, is the predominant chemical functionality exposed at the surface. The essential structure of the monolayer appears to be preserved for a number of tail groups exhibiting a range of intermolecular interactions.[11] Except for short chains ($n < 10$), the structure of the monolayer and the properties of the monolayer–liquid or monolayer–air interface appear to be largely independent of the length of the hydrocarbon chain.[9]

This last observation is significant. If we are to use monolayers of thiols on gold as models for other surfaces, or to study interfacial phenomena in general, it is important that the gold substrate and the sulfur–gold interface do not affect the measured properties at the monolayer–ambient interface. The gold does have an indirect effect on the properties of the monolayer through its influence on the cant of the hydrocarbon chains and hence on the orientation of the tail group at the surface of the monolayer. (If the organic monolayer is very thin, the polarizability of the gold substrate will also influence the wetting of the surface.) Small changes in the orientation of functional groups at the surface can lead to measurable changes in interfacial properties. For example, the chain tilt of monolayers of thiols adsorbed on silver is approximately zero, compared with ca. 30° on gold; the contact angle of water on a monolayer terminated by hydroxy groups on silver (X = OH) is 20°,[6] whereas on gold angles of < 15° are observed. This residual influence of the substrate is not necessarily a disadvantage: the fact that we can even ask questions about the influence of the orientation of a functional group on the macroscopic properties of an interface is a testimony to the power of the technique of self-assembly.

4. Effect of the Chemical Structure of an Interface on Wettability

Wettability is a representative macroscopic physical property of surfaces that we have studied extensively. An understanding of the microscopic basis of wettability is important for two reasons: first, many technologies rely on controlling wettability; and second, the wettability of a flat surface is determined by interfacial free energies and hence reflects intermolecular interactions at the solid–liquid and solid–vapor interfaces.[14] In fact, wettability appears to be an extremely sensitive analytical tool for elucidating the structure of surfaces. Wettability is quantified by the measurement of the contact angle, θ, between the tangent to a drop of liquid where it meets the surface and the surface itself. Different liquids probe different molecular forces. Water senses primarily polar functional groups in the substrate, whereas a hydrocarbon, such as hexadecane, interacts purely by dispersive forces. Different values of the contact angle may be observed for drop edges that have advanced or receded across the surface prior to measurement. Although this hysteresis in the contact angle undoubtedly carries a wealth of structural information about the surface, no microscopic theory yet exists that explains the origin of hysteresis.

Table 1. Advancing contact angles θ_a of water and hexadecane on monolayers of representative thiols on gold



Thiol	$\theta_a(H_2O)$ [°]	$\theta_a(C_{16}H_{34})$ [°]
$HS(CH_2)_2(CF_2)_5CF_3$	118	71
$HS(CH_2)_{17}CH_3$	112	47
$HS(CH_2)_{17}CH=CH_2$	107	39
$HS(CH_2)_{19}Br$ [a]	97	< 5
$HS(CH_2)_{11}OCOCF_3$ [d]	96	62
$HS(CH_2)_{19}F$ [a]	95	< 5
$HS(CH_2)_{19}Cl$ [a]	83	< 5
$HS(CH_2)_{16}OCH_3$	75	41
$HS(CH_2)_{10}CO_2CH_3$	67	28
$HS(CH_2)_{11}CN$ [b]	63	< 5
$HS(CH_2)_{10}CONH_2$ [c]	13	< 5
$HS(CH_2)_{15}CO_2H$	< 10	< 5
$HS(CH_2)_{11}OH$	< 10	< 5

From [1], except [a] *B. Burbaum*, unpublished results, [b] *P. Laibinis*, unpublished result, [c] *L. Janes*, unpublished result. [d] By reaction of a monolayer formed from $HS(CH_2)_{11}OH$ with trifluoroacetic anhydride.

A large range of functional groups can be expressed at the surface of a monolayer of a thiol on gold. Thiols with highly polar tail groups, such as carboxylic acids, form monolayers that are wetted by water and by all non-reactive organic liquids. Fluorinated thiols form monolayers that are more water- and oil-repellent than Teflon. The hydrophobicity and oleophobicity of the surface can be varied almost independently between these two extremes (Table 1). In general, the lower the surface tension, γ_{lv}, of the probe liquid, the smaller the contact angle. By judicious choice of tail group, this relationship can be reversed. For example, a monolayer of $HS(CH_2)CO_2CH_3$ is wetted by acetonitrile (γ_{lv} = 29.3 mN m^{-1}; $\theta \approx 0°$) but not by hexadecane (γ_{lv} = 27.2 mN m^{-1}; $\theta = 28°$). We have, however, not yet succeeded in mimicking the unusual properties of the surface of

water itself, which is wetted by water (since any pure liquid wets itself) but not by hexadecane.

One of the key questions that we have sought to answer is how wettability is influenced by the depth of a species beneath the solid–liquid interface. The strength of the interaction between two bodies separated by a third medium can be calculated from bulk optical properties by Lifshitz theory. Given the short range of the intermolecular interactions that determine the wetting of organic surfaces, such continuum theories can at best provide only an approximate answer. Using monolayers we can tackle this problem from a molecular perspective.[4] Figure 2 plots the contact angles of

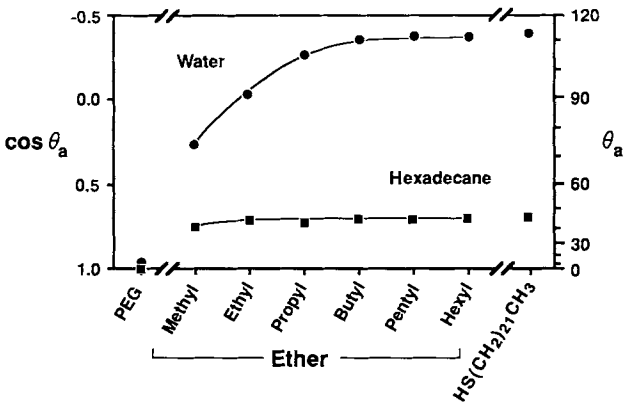


Fig. 2. ω-Mercaptoethers, $HS(CH_2)_{16}O(CH_2)_nCH_3$, adsorb from ethanol onto gold and form monolayers in which the depth of the polar ether group beneath the outer surface of the monolayer increases with increasing n. The advancing contact angles θ_a of water and hexadecane are shown as a function of the length of the terminal alkyl chain. Also shown are the contact angles on polyethylene glycol (PEG) and on a monolayer of docosanethiol on gold, models of surfaces in which ether groups are, respectively, fully exposed to the contacting liquid, and completely buried.

water and hexadecane on monolayers of ether-terminated alkanethiols, $HS(CH_2)_{16}O(CH_2)_nCH_3$, n = 0–5. In this study[15] the polar ether group was buried progressively deeper beneath the monolayer–liquid interface by increasing the length of the terminal alkyl chain. The contact angles of hexadecane confirm that the dispersion interaction between the ether group and hexadecane is very short range, dropping to essentially zero when a 2 Å thickness of hydrocarbon material intervenes. Water was able to sense the polar ether group at greater depths beneath the monolayer–water interface: a butyl group was required to screen the ether oxygen fully from the supernatant drop. Similar results have been obtained using amides in place of ethers.[16] Thus we see that one only needs to control the structure of the outermost few angströms of a smooth solid in order to determine its wetting properties. Furthermore, as an analytical technique, wettability approaches the best UHV spectroscopies in terms of surface sensitivity.

5. Construction of Complex Interfaces

5.1. Multiple Functional Groups

The ability to synthesize surfaces containing a unique functional group helps us to understand the contributions of individual chemical species to interfacial properties. Real surfaces, however, are complex both chemically and structurally. There is no a priori reason to assume that the different chemical components in an interface behave independently and hence that the properties of a multi-component surface can be inferred with confidence from the properties of surfaces composed of structured arrays of the pure components. The first step in extending our model to approximate real surfaces more closely is to introduce more than one functional group into the monolayer. To a certain extent this end can be achieved by performing reactions on the monolayer after formation. More generally, we can generate polyfunctional surfaces by coadsorbing two or more thiols on gold.

In interpreting coadsorption experiments, two questions immediately present themselves. First, does the composition of the monolayer reflect the relative concentrations of the two components in solution? Second, do the different components in the monolayer phase segregate into macroscopic domains? The answer to both questions appears to be no. The composition of the monolayer is strongly influenced by interactions between the adsorbates and the solvent and among the tail groups within the monolayer. Changing the nature of the solvent, from ethanol to isooctane for example,[11] can dramatically alter the composition of a monolayer even when the concentrations in solution remain unchanged. If the adsorption components have different chain lengths, cohesive interactions between crystalline hydrocarbon chains favor incorporation of the longer chain into the monolayer. Far from merely being an inconvenience, the relationships between the composition of the monolayer and the concentrations of the adsorbates provide a handle on the molecular interactions present in the monolayer, and offer valuable insights into other processes of self-assembly, such as membrane and micelle formation.

The question of the distribution of components within the monolayer is more difficult to resolve. Although numerous pieces of evidence militate against the formation of macroscopic islands ($\geq$ 1000 Å across), the components are almost certainly not randomly dispersed, but form small clusters, as they do in solution (if by doing so the free energy is lowered). A better knowledge of the pair distribution function in these "mixed monolayers" would improve our understanding of real surfaces which, too, reconstruct to minimize their free energy.

A simple example of a mixed monolayer which displays the essential features of a coadsorption experiment is $HS(CH_2)_{11}OH/HS(CH_2)_{10}CH_3$ adsorbed from ethanol onto gold.[17] Figure 3A displays the relationship between the mole fraction χ^{OH} of $HS(CH_2)_{11}OH$ in the adsorption solu-

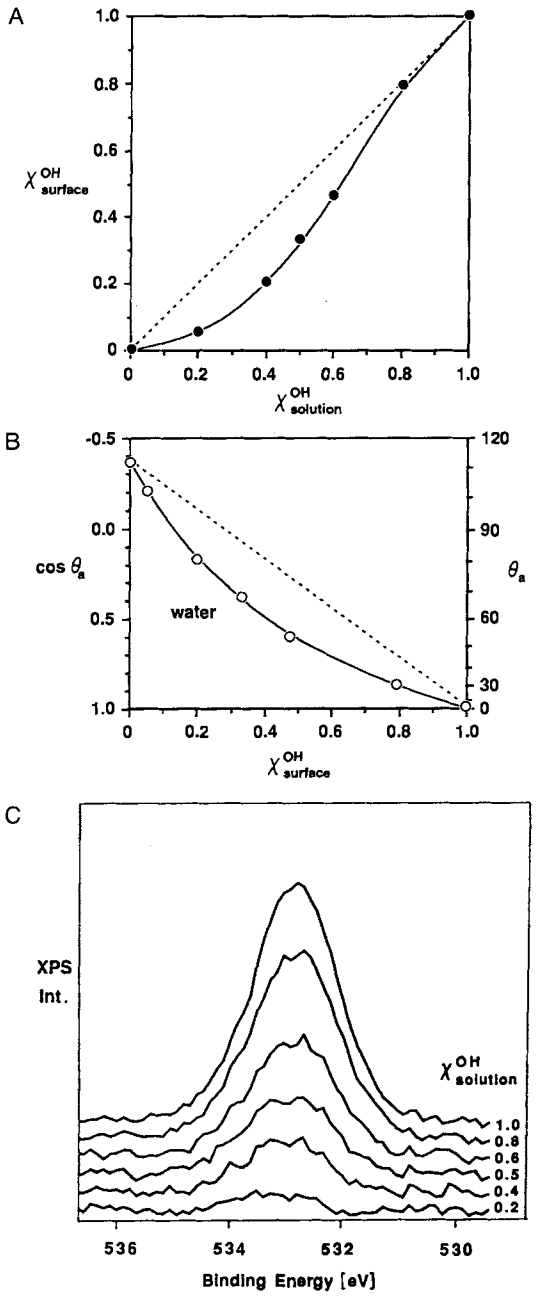


Fig. 3. Monolayers exposing both methyl and hydroxy groups at the surface of the monolayer may be formed by adsorption from solutions containing mixtures of $HS(CH_2)_{11}OH$ and $HS(CH_2)_{10}CH_3$. A) Plots of the mole fraction of the hydroxy-terminated chain in the monolayer as a function of the mole fraction in solution. For clarity, the calculation of the mole fraction in solution included only the thiol species; B) plot of the advancing contact angle of water as a function of the composition of the monolayer; C) the oxygen (1s) region of the XPS spectra of the monolayers (XPS intensity in arbitrary units). The areas under these peaks were used to calculate the compositions of the monolayers.

tion and in the monolayer. The compositions of the monolayers were determined from the intensity of the O(1s) peak obtained by XPS (Fig. 3C). From solutions in ethanol there is a preference for adsorption of the methyl-terminated thiol. Adsorption of $HS(CH_2)_{11}OH$ is particularly disfavored at low concentrations, possibly due to incomplete hydrogen-bonding of the terminal hydroxy groups in the nonpolar environment provided by the surrounding methyl groups at the surface of the monolayer. The advancing contact angle of water is shown in Figure 3B as a function of the mole fraction, χ^{OH}, of the hydroxy-terminated component in the monolayer. If the wettability of a mixed monolayer were simply a linear combination of the wetting properties of the constituent components, we would expect a linear relationship between $\cos\theta_a$ and χ^{OH}. The actual graph is concave: the hydroxy groups at the surface of the monolayer are more hydrophilic at low χ^{OH}, when they are in a nonpolar environment, than at high χ^{OH}, when they are surrounded by other OH groups to which they can hydrogen bond. This result is consistent with the observed bias against adsorption of hydroxy groups at low χ^{OH}.

Although mixed monolayers such as these may seem simple, the correlations between wettability and structure derived from such systems have proved invaluable in improving our understanding of a complex organic surface—chromic-acid-oxidized polyethylene—which contains a mixture of polar and nonpolar functionality.[18] Comparison of the polymer with mixed monolayers supported the hypothesis that the polyethylene surface was composed of domains comprising largely polar or largely nonpolar groups, rather than containing a homogeneous distribution throughout the functionalized interphase.

The principles established for simple systems composed of two thiols are readily generalizable to cases in which both thiols are terminated by complex functional groups or in which there are more than two components in the monolayer.

5.2. Control over Surface Disorder

Many real surfaces differ from the model monolayers discussed so far in another important respect: they are disordered. The chains and tail groups in the densely packed, oriented monolayers presented above do not have the degrees of freedom available in an amorphous polymer or a fluid biological surface. As a consequence, the monolayer cannot reconstruct in response to changes in its environment, and we cannot easily use these monolayers to study dynamic processes at interfaces. We can introduce free volume, with the conformational freedom that entails, into the outer part of the monolayer by coadsorbing two thiols with different chain lengths.[1,19,20] We expect the resulting mixed monolayers to have two distinct phases: the inner part, adjacent to the gold surface, remains densely packed (and hence insulates the monolayer–liquid or monolayer–air interface from the influence of the substrate), but the outer part of the monolayer contains fewer hydrocarbon chains per unit area and is free to become disordered (Fig. 4). By placing functional groups at the ends of the shorter chains, in the transition region between the ordered and disordered phases of the monolayer,[20] we can also introduce a degree

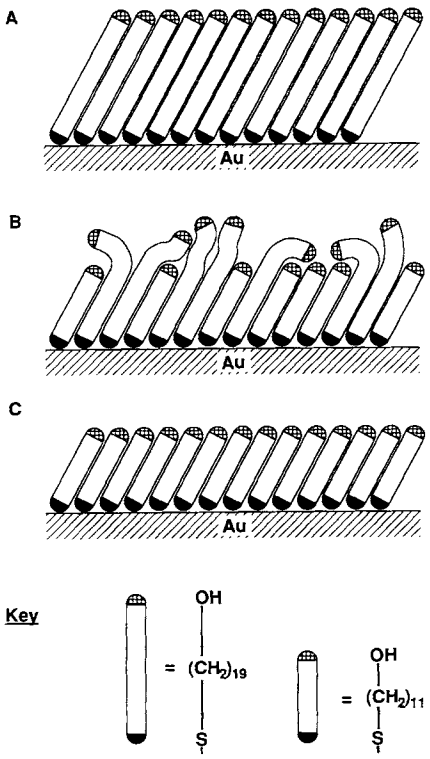


Fig. 4. Schematic illustration of monolayers of hydroxy-terminated thiols on gold. A) Pure monolayer of $HS(CH_2)_{19}OH$; B) monolayer containing equal amounts of $HS(CH_2)_{19}OH$ and $HS(CH_2)_{11}OH$. The inner part of the monolayer is densely packed, the outer part loosely packed and disordered; C) pure monolayer of $HS(CH_2)_{11}OH$.

of three-dimensionality beyond that achievable simply by varying the position of a functional group in a polymethylene chain.

The consequences of introducing disorder into the outer part of the monolayer can be seen clearly in monolayers composed of mixtures of $HS(CH_2)_{11}OH$ and $HS(CH_2)_{19}OH$ (Fig. 5).[19] Pure monolayers of either species expose only polar hydroxy groups at the monolayer–liquid interface and hence yield very low contact angles with water ($\theta < 15°$). In a mixed monolayer, however, the last eight carbons of the longer chains can form a disordered, liquid-like layer on top of the densely-packed lower phase of the monolayer. Since this disordered region exposes nonpolar polymethylene chains to the water drop, we expect to see a sharp increase in the contact angle (Fig. 5). The observation of just such a maximum confirms our model and rules out the formation of large, single-component domains within the monolayer: each of these domains would expose only hydroxy groups at the surface and hence the mixed monolayers would be wetted by water, independent of composition. Comparison of the contact angles in Figure 5 with those shown in Figure 3 suggests that even the most disordered mixed monolayer still exposes an approximately 2:1 ratio of polar hydroxy to nonpolar methylene groups to a water drop. This ratio is not

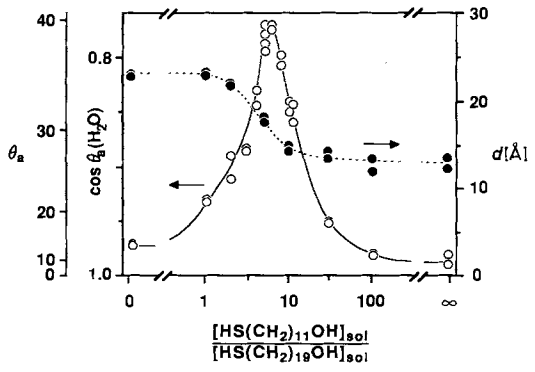


Fig. 5. Ellipsometric thickness d and advancing contact angles θ_a of water for mixed monolayers of $HS(CH_2)_{19}OH$ and $HS(CH_2)_{11}OH$. The abscissa represents the ratio of concentrations of $HS(CH_2)_{19}OH$ to $HS(CH_2)_{11}OH$ in solution. The maximum in contact angle correlates approximately with the monolayer shown schematically in Figure 4B.

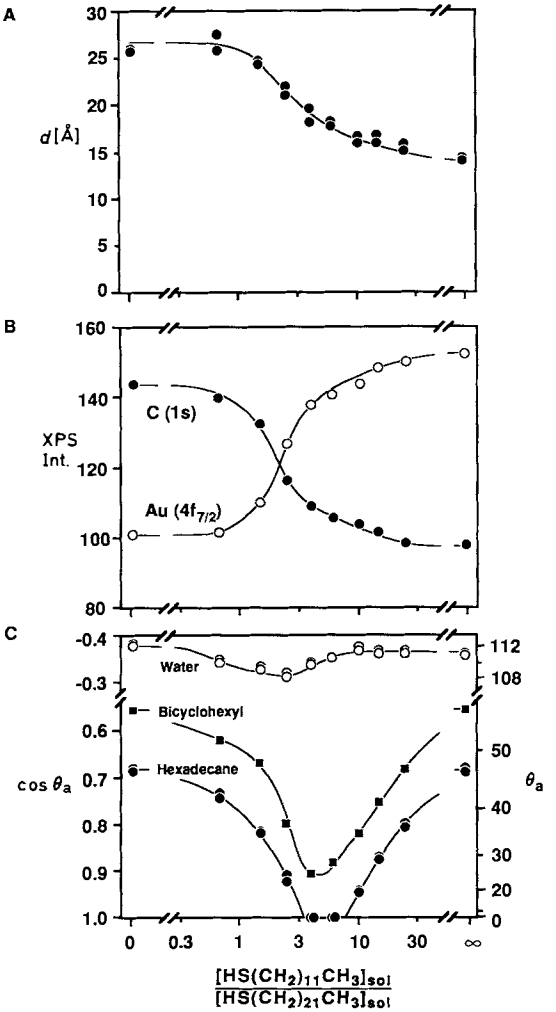


Fig. 6. Mixed monolayers formed by coadsorption of $HS(CH_2)_{21}CH_3$ and $HS(CH_2)_{11}CH_3$ from isooctane. The abscissa represents the ratio of concentrations of $HS(CH_2)_{21}CH_3$ to $HS(CH_2)_{11}CH_3$ in solution. A) Ellipsometric thickness of the monolayers; B) intensity of the C (1s) and Au ($4f_{7/2}$) peaks obtained by XPS (arbitrary units): The compositions of the monolayers can be calculated from the intensities of these peaks. C) Advancing contact angles of water, hexadecane and bicyclohexyl.

unreasonable. We would expect the monolayer to reconstruct to maximize hydrogen-bonding and to minimize the number of hydrophobic contacts.

If the two thiols are terminated by methyl groups instead of hydroxy groups, then the resulting mixed monolayers allow us to probe the effect of local structure on dispersive interactions and on the hydrophobic effect. Figure 6 shows the ellipsometric thickness d, XPS intensities and contact angles θ_a for monolayers adsorbed from mixtures of $HS(CH_2)_{11}CH_3$ and $HS(CH_2)_{21}CH_3$ in isooctane. (The first two techniques serve to establish the composition of the monolayer.) Pure monolayers of either component expose a densely packed array of methyl groups at the surface of the monolayer, and are both hydrophobic and oleophobic. The surface of a monolayer containing an approximately equal mixture of the two components resembles a liquid, linear hydrocarbon. The advancing contact angle of water θ_a is insensitive to the detailed structure of the hydrocarbon surface. On the other hand, hydrocarbon liquids, such as bicyclohexyl and hexadecane, show large changes in contact angle in response to variations in the structure of the surface. A corollary of these observations is that variations in the strength of the hydrophobic effect arise largely from hydrocarbon–hydrocarbon interactions rather than hydrocarbon–water interactions. There is also some evidence[11] that decane can penetrate into holes left in a monolayer of $HS(CH_2)_{21}CH_3$ by the presence of molecules of $HS(CH_2)_{11}CH_3$—a primitive type of molecular recognition.

6. Concluding Remarks

We can only arrive at a detailed understanding of the complex physical and chemical properties of surfaces through the study of well-defined model systems. Phenomena such as wetting, adhesion, and friction are all functions (albeit complicated ones) of the microscopic chemical structure of a surface. Self-assembled monolayer films of thiols on gold are model systems in which the microscopic structural attributes of an organic surface can be varied independently and the influence on interfacial properties determined. We believe that they, and other related systems, will provide the bridge between the physical-organic chemistry of solutions and the materials science of organic solids. The research presented here is only a first step towards developing an understanding of organic surfaces. We still have to learn more about measuring and controlling the lateral distribution of functional groups. Many interesting features of wetting—especially the influence of roughness and chemical heterogeneity, and the origin of hysteresis—are still not understood. We have barely touched upon interfacial properties other than wetting, such as adhesion, friction and electrochemistry. Much remains to be learned about the physical-organic chemistry of condensed interphases.

Self-assembled monolayers are more than mere model systems for the surfaces of materials. They provide a starting point for practical technologies to solve interfacial problems. Two examples are the use of monolayers of alkylsiloxanes to promote adhesion or, with the opposite intent, to prevent catalyst particles from sticking to the walls of reactors. The intermolecular interactions controlling the structure of self-assembled monolayers are also acting in other spontaneously assembling systems. In studying them we will learn more about membranes, micelles and microemulsions.

Received: February 2, 1989

[1] C. D. Bain, *PhD Thesis*, Harvard University 1988. G. S. Ferguson, G. M. Whitesides, *Chemtracts 1* (1988) 171.
[2] J. Sagiv, *J. Am. Chem. Soc. 102* (1980) 92.
[3] See, for example, a recent review: H. Möhwald, *Angew. Chem. Adv. Mater. 100* (1988) 750; *Angew. Chem. Int. Ed. Engl. Adv. Mater. 27* (1988) 728.
[4] For a review of early work on self-assembled monolayers, see W. A. Zisman in F. M. Fowkes (Ed.): *Contact Angles, Wettability, and Adhesion (Adv. Chem. 43)* American Chemical Society, Washington, DC 1964, pp. 1–51.
[5] S. R. Wasserman, G. M. Whitesides, I. M. Tidswell, B. M. Ocko, P. S. Pershan, J. D. Axe, *J. Am. Chem. Soc.*, in press; S. R. Wasserman, Y.-T. Tao, G. M. Whitesides, *Langmuir*, in press.
[6] N. Tillman, A. Ulman, T. L. Penner, *Langmuir*, in press.
[7] L. Netzer, R. Iscovici, J. Sagiv, *Thin Solid Films 99* (1982) 235.
[8] R. G. Nuzzo, D. L. Allara, *J. Am. Chem. Soc. 105* (1983) 4481.
[9] C. D. Bain, E. B. Troughton, Y.-T. Tao, J. Evall, G. M. Whitesides, R. G. Nuzzo, *J. Am. Chem. Soc. 111* (1989) 321.
[10] M. D. Porter, T. B. Bright, D. L. Allara, C. E. D. Chidsey, *J. Am. Chem. Soc. 109* (1987) 3559.
[11] R. G. Nuzzo, L. H. Dubois, D. L. Allara, *J. Am. Chem. Soc.*, in press.
[12] L. Strong, G. M. Whitesides, *Langmuir 4* (1988) 546.
[13] C. D. Bain, G. M. Whitesides, *J. Phys. Chem.*, in press.
[14] P. G. DeGennes, *Rev. Mod. Phys. 57* (1985) 827; J. N. Israelachvili: *Intermolecular and Surface Forces*, Academic Press, London 1985.
[15] C. D. Bain, G. M. Whitesides, *J. Am. Chem. Soc. 110* (1988) 5897.
[16] B. Burbaum, L. Janes, G. M. Whitesides, unpublished results.
[17] C. D. Bain, G. M. Whitesides, *J. Am. Chem. Soc. 110* (1988) 6560.
[18] S. R. Holmes-Farley, C. D. Bain, G. M. Whitesides, *Langmuir 4* (1988) 921.
[19] C. D. Bain, G. M. Whitesides, *Science (Washington, D.C.) 240* (1988) 62.
[20] C. D. Bain, G. M. Whitesides, *J. Am. Chem. Soc. 110* (1988) 3665.

The following review articles will appear in future issues:

D. W. McCall: Materials Issues in Electronic Systems. *W. Michaeli:* Material Processing—a Key Factor. *B. R. Philips, D. Tanner, J. A. Fitzgerald:* The Kevlar Story—An Advanced Materials Case Study. *M. Salkind:* Aerospace Materials Research Opportunities. *D. F. Williams:* Challenges in Materials for Health Care Applications. *T. Kodas:* Aerosol/Processing of Complex Metal Oxides. *H. Warlimont:* Rapidly Quenched Materials. *H.-W. Schmidt:* Dichroic Dyes and Liquid Crystalline Side Chain Polymers.

Functionalized Conducting Polymers—Towards Intelligent Materials

Molecular Electronics
Wires, Sensors, Transducers
Polymer Modified Electrodes

By Francis Garnier*

Organic conjugated polymers and oligomers constitute a three-dimensional network of molecular wires, in which all monomeric units can be functionalized with various prosthetic groups. By varying the nature of these groups, specific interactions with external physical or chemical phenomena can be developed in these materials, leading to molecular devices such as sensors, transducers, memories and logic operators. Chemists have already mastered the realization of many of these functional elements, which mimic those existing in organized beings. The further assembly of these elements in multifunctionalized organic conducting polymers and oligomers will represent the next step towards intelligent materials.

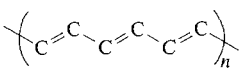
1. Introduction

Inter (between, within), *legere* (to read, to bring together, to choose). The study of all the functions that underlie *intelligence* has long been one of the major goals of science. The analysis of the elements that define organized beings has up to now been the privileged sphere of biology, which has aimed at the understanding, down to the molecular level, of the fundamental processes associated with the faculties of sensing and controlling the environment. On the physical sciences side, electronics is one of the methods developed by men for imitating some of these basic functions in macroscopic devices such as sensors, memories and logic circuits. In these research areas chemistry has mainly had a supporting role, whether conceptual, for explaining the chemical processes involved, or experimental, in the synthesis of model molecules mimicking such biological functions, and also in making the materials needed for electronic devices.

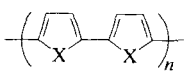
Chemistry has, however, recently developed methods for the a priori control of molecular properties,[1] and a fascinating challenge has now emerged: is it now conceivable to progress beyond the macroscopic approach used in conventional electronics, and also to bypass the inherent complexity of biological systems, in order to build new materials able to perform at a molecular level the basic functions, i.e. recognition, control of chemical processes, memory and logic, which define intelligent structures? Ideas that were regarded a few years ago as long term speculation,[2] are now approaching reality, based on the fact that chemists have learned how to build molecular wires and incorporate into them various types of functions. These new materials are functionalized organic conducting polymers and oligomers, and this article reports on the advances in research which will lead to such molecular devices being constructed in the near future.

2. Molecular Wires

The concept of molecular wires stems from about ten years ago, when it was shown that the individual macromolecular chains of organic conjugated polymers possess a high intrinsic electrical conductivity.[3] These organic conducting polymers have since aroused much interest, and a deep knowledge has been gathered on their physical and chemical properties. The macromolecular chains of these polymers show a regular alternation of single and double bonds, in the manner of the prototype polyacetylene.[4] Other classes of conducting polymers were later synthesized, including polypyrrole,[5] polythiophene,[6] and polyaniline.[7]



Polyacetylene



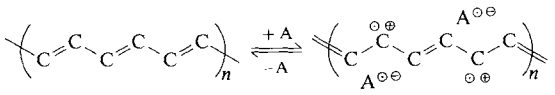
Polypyrrole (X = NH)
Polythiophene (X = S)

The conjugation of the π-electron system creates a molecular orbital which extends throughout the polymer chain. Using the concept of the one-electron model as a first approximation, these low dimensional materials can be described by a fully occupied valence band and an empty conduction band, formed by the conjugated π and π* systems, respectively. In this state these polymers show semiconducting properties associated with a band gap of about 2 eV. The injection of holes or electrons into these chains, by p-type or n-type doping respectively, leads to electrical conduction, due to the creation of soliton or polaron states in the gap. This doping is performed by the inclusion of electron acceptors, such as halogens, or electron donors, such as alkaline metals, which intercalate between the conjugated polymer chains and lead to their oxidation or reduction, respectively. It must be pointed out that this term of doping is employed

[*] Dr. F. Garnier
Laboratoire de Matériaux Moléculaires
CNRS
2 rue Dunant, F-94320 Thiais (France)

here in a chemical sense and not in the commonly accepted one in solid state physics. The conductivity values depend on the amount of electrons or holes created in the polymer chains, which is determined by the concentration of dopant in the polymer. Very high concentrations of dopants A can be achieved: up to one dopant species for every two or three units of monomer M contained in the polymer, corresponding to $[A]/[M] \approx 0.3-0.5$. The conductivity can reach values as high as that of metals such as Pt or Fe, $\sigma = 2 \times 10^5\ S\ cm^{-1}$, as was recently demonstrated by *Naarmann* et al. in the case of polyacetylene;[8] however, a real metallic state has not yet been obtained as shown by the behavior as a function of temperature.

This doping reaction, which is reversible and can be electrochemically driven, confers on these polymers interesting electroactive properties. It has been shown that even for polymer layers up to hundreds of microns thick the whole polymer is entirely electroactive, implying that the polymer chains stretch throughout these layers. Some defects evidently exist in these chains, such as interruption of conjugation and branching, but interchain hopping of charges allows all the chains to be electroactive. The doping process thus involves every two or three monomer units along all polymer chains, and it can be considered as operating at the molecular level of these conducting polymers (Scheme 1).



Scheme 1. Reversible doping of polyacetylene with an electron acceptor A.

Films of organic conducting polymers behave as organic electrodes, which can be charged and discharged with large amounts of dopants, and this characteristic has been the starting point for numerous studies on "organic batteries",[3] mainly based on polypyrrole and polyaniline and already commercialized, and also on some electrochromic devices.[9] In these applications, the electroactive polymer chains are considered as playing only the passive role of a conducting network for hosting incoming dopant anions, and their potential has thus been largely underestimated. As a matter of fact, these macromolecular conjugated chains, formed by the theoretically infinite coupling of monomer units, possess an intrinsic electrical conduction, and thus represent true molecular wires, i.e. wires consisting of just a one molecule sequence. Furthermore, the fact that every second or third monomer unit along all these wires is involved in the doping–undoping process means that all these monomer units can in theory be individually electrically addressed in the whole polymer layer. This interaction at a molecular level thus opens up the field of molecular devices.

3. Molecular Sensors and Transducers

These molecular wires form unique routes for the reversible transfer of electronic information between an electrode, onto which these polymer chains are grafted, and various prosthetic groups R, which can be covalently bonded as side groups all along the conducting chains (Fig. 1). Depending on the nature of R, these structures can act as molecular sensors or molecular transducers.

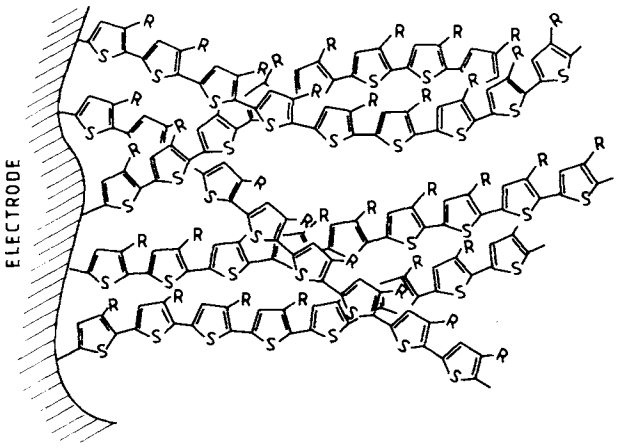


Fig. 1 Three-dimensional distribution of prosthetic groups R along ideally conjugated polythiophene chains grafted onto an electrode.

Owing to the richness of chemical synthesis, a large variety of functions can theoretically be incorporated into these conducting polymers by the initial synthesis of a functionalized monomer. This second generation of organic conducting polymers, obtained by their functionalization, has recently excited much interest in view of its great potential, and many experiments have been proposed. This functionalization is experimentally difficult since the steric and electronic properties of most of the interesting substituents on monomers are not easily compatible with the synthesis of a conducting polymer. Thus the electrical conduction in these macromolecular chains requires the stereoregular alternation of single and double bonds, and any structural defect, such as an sp^3 carbon atom or a chain end, is known to result in the interruption of conjugation and hence of conduction. The polymerization reaction is difficult to control, and it has been observed that the more sterically demanding a substituted monomer is, the higher is the concentration of defects in its corresponding polymer. Thus, most of the examples which will be described in the following suffer from a very low electrical conductivity ($\sigma \approx 10^{-4}\ S\ cm^{-1}$). Recently, however, by carefully analyzing the steric and electronic factors which, for a given substituent on a monomer, control the conducting and electroactive properties of the corresponding polymer, we have developed the concept of a "functionalization environment" which allows these problems to be overcome.[10]

Provided that these criteria are fulfilled, substituents can now be envisaged that will give specific interactions with almost any kind of external physical or chemical phenomenon. Examples of *physical quantities* that can be sensed

by the use of appropriate R groups are photon fluxes, electric fields and magnetic fields.

The principle of photon sensing has already been demonstrated by the bonding of the well known photoactive metal complex $Ru(bpy)_3^{2\oplus}$ to the monomeric units of polypyrrole.[11] This functionalized polymer has indeed shown a photoresponse, although its intrinsic electronic conduction has not yet been mastered due to the large steric constraints of the metal complex ($\sigma \approx 10^{-4}$ S cm^{-1}). The principle of sensitivity to a magnetic field B has also been proposed recently,[12] using a nitroxide radical grafted on polydiacetylene; the results are, however, a subject of controversy. Even if not yet experimentally demonstrated, the sensitivity to an electric field E is within reach, by substituting a highly polarizable group as already envisioned.[2] The application of an electric field will induce a large dipole moment on the side chain of the conducting system and create electron sinks or electron reservoirs which will lead to a modification of the charge transport properties of the main conducting chain.

Selective chemical interactions with the environment can also be developed in these electroactive polymers by appropriate functionalization. The most significant features which govern fundamental processes in biological systems involve recognition, whether of ions, as in transmembranous transfers, or of optically active species. Both of these recognition phenomena have already been imitated at the molecular level by appropriate functionalization of conducting polymers. Thus, ionic selectivity has been demonstrated in the case of a new class of polymers, the poly(dibenzo crown ethers), which contain crown ethers of variable size.[13] Owing to the well known specific complexation of cations by crown ethers, a highly selective uptake of various cations in solution has been observed with these polymers. A second example relates to the covalent binding of a polyether substituent onto the monomeric units of polypyrrole, which also induce selective complexation of cations such as $Li^{\oplus}$.[14] These last two ion selective materials, however, still suffer from a low electronic conductivity of the polymer backbone, due to the fact that the polymerization reaction is not yet well controlled. On the other hand, by applying the concept of functionalization environment, we were recently able to synthesize polythiophene derivatives substituted with polyether groups, showing both a high electrical conductivity ($\sigma = 10$ S cm^{-1}) and ionic selectivity.[10] The interest in controlling these two properties at the same time arises from the possibility of new materials having both an electronic and an ionic conductivity, which mimic membrane processes and thus open up a large potential in the realization of ion selective electrochemically controlled membranes.

Perhaps the most challenging recognition property concerns enantioselectivity, i.e. the ability to discriminate between optically active substrates. We have recently succeeded in achieving this ultimate type of recognition, by the controlled functionalization of polythiophenes. Thiophene monomers bearing large chiral groups such as R* = (2 *S*)-(+)-$(CH_2)_3OCH(Et)C_6H_5$ were first synthesized, and then electropolymerized as thin films on an electrode. The characterization of the resulting polymer has confirmed that it is chiral (specific rotation = + 3000°), and still conducting ($\sigma = 12$ S cm^{-1}) and electroactive, despite having such bulky substituents. When used as an organic electrode in an electrolytic medium with $ClO_4^{\ominus}$ anions, a reversible, electrochemically driven doping–undoping process is observed. If an optically active anion such as (1 *S*)-(+)-10- or (1 *R*)-(−)-10-camphorsulfonate is used instead of $ClO_4^{\ominus}$, this chiral organic electrode shows a different response depending on the camphorsulfonate enantiomer used (Fig. 2). A ratio of about two has been observed for the oxidation rates at comparable doping levels of the chiral doping matrix, thus defining its selectivity towards these enantiomers.[15] We have also confirmed that when the enantiomer R* = (2 *R*)-(−)-$(CH_2)_3OCH(Et)C_6H_5$ is used as side group on the polythiophene chain, a reverse selectivity is observed for the camphorsulfonate enantiomers.

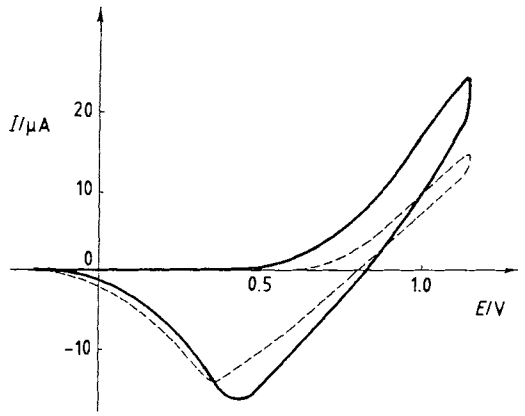


Fig. 2. Cyclic voltammogram of chiral polythiophene using optically active chiral anion as doping agent: (——), (– – –): (+)- and (−)-10-camphorsulfonate, respectively. E vs. saturated calomel electrode.

This effect has been interpreted on the basis of the chiral environment created by the bulky R* groups around the polythiophene conducting chains. During the doping process, the anions have to percolate through this chiral environment in order to reach the thiophene rings and produce the electronic doping interaction. These results are the first unambiguous evidence that electroactive functionalized polymers are capable of molecular recognition of enantiomers during the electrochemical doping process. This configurational selectivity imposed by the chiral environment appears to mimic the structural control in enzymes caused by the protein subunits surrounding their active site.

4. Molecular Catalysts

The functionalized polymer–enzyme analogy can be carried further, since functionalized conducting polymers are not only able to act as molecular sensors and transducers, but also allow the control of chemical reactions by the incorporation of redox centers or of metallic submicroaggregates able to induce electrocatalytic processes. Thus, many types

of redox centers such as metalloporphyrins,[16] ferrocene,[17] metal complexes of bipyridines,[18] and nickel cyclames[19] have already been either covalently bonded or electrostatically included in polypyrrole. Various submicroaggregates of metals such as Pt, Pd, Cu, Ni, Ag have also been incorporated in polythiophenes by an electrochemical deposition method which allows precise control of the size and spatial distribution of these aggregates (Fig. 3).[20] Pt and Cu for instance have been shown by Extended X-Ray Absorption Fine Structure (EXAFS) to exist as coordinated atoms or as small clusters along the individual conducting chains.[21] When the size of the metal particles is increased, aggregates can be visualized by scanning electron microscopy (SEM), appearing then as deposits (size ca. 20 nm) on polymer fibers (diameter ca. 10 nm), in which the disposition of the individual polymer chains is not yet well understood.

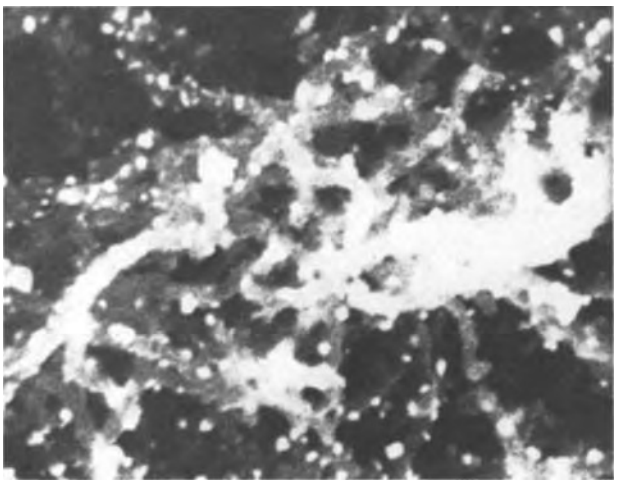


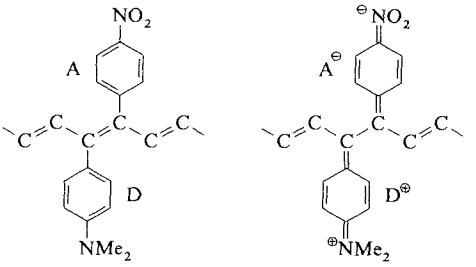
Fig. 3. Scanning electron micrograph of silver aggregates deposited along the conducting fibers of polymethylthiophene. Enlargement: 30 000 ×.

These redox and metal centers can be electrochemically addressed through the conducting chains of the polymer, allowing the controlled triggering of fundamental chemical processes such as the reduction of $H^{\oplus}$,[20] CO_2[19] or O_2,[20] or the oxidation of H_2O[22] or ROH.[23] High catalytic activity has been demonstrated,[20] resulting from the molecular distribution of these catalytic centers in three-dimensional materials of hundreds of microns in thickness. Furthermore, the regioselectivity observed, e.g. in the catalytic hydrogenation of unsaturated compounds with substituted polypyrroles,[24] indicates that the reactions proceed under a stereochemical control exerted by the environment of the catalytic centers in the conducting polymers. This result is very promising in relation to the possibility of using conducting polymers with chiral substituents such as those described in the previous section, for inducing asymmetry during these catalytic reactions through a template effect, although such an effect has still to be experimentally demonstrated.

These few examples show how far chemists have already gone in the realization of molecular materials capable to perform physical and chemical recognition, to transfer molecular signals, and to induce electrocatalytic reactions. Of course, the phenomena of molecular recognition, signal transfer and catalytic control are also known for individual molecules and supramolecules in homogeneous phases.[1] The important step achieved with functionalized conducting polymers is the assembly of these functional elements in a three-dimensional architecture based on a network of molecular wires able to carry electronic information to and from these elements. There is still a long way to go before these elaborate structures can be addressed at a molecular level.

5. Molecular Electronics

The introduction of memory effects and logic functions in these materials is the field of molecular electronics. In molecular wires switching, gating and amplification functions result from the ability to modulate their charge transfer properties, and memory effects are directly related to bistability phenomena. For example, donor (D)–acceptor(A) systems in which a charge separation can be photochemically induced can be covalently bonded as side groups along the conducting chains; by altering the amount of charge transfer between D and A the extent of conjugation, and thus the charge transport properties of the chains, can be modified. Such a type of "push-pull" mechanism[2] is depicted in Scheme 2.



Scheme 2. Left: conjugated conducting chain of polyacetylene; right: interruption of conjugation and conduction due to charge transfer D → A.

If we use a D–A system in which the extent of charge transfer is controlled by an external variable such as light intensity, the charge transport properties of the conducting polymer chains can be modulated ("molecular modulation" of a signal). If a very large variation of this charge transfer is imposed, electron sinks will be created along the conducting chains which will hinder any conduction, thus leading to molecular switches. Considerable knowledge of such D–A systems is already available, e.g. in dye chemistry. As a consequence of the very short time scale associated with light excitation phenomena, which typically lies in the order of 10^{-15} s for reaching Franck–Condon states, ultra-fast modulation and switching can be expected with these new molecular structures.

Memory effects will be obtained if bistable structures showing some hysteresis can be produced. Bistability is al-

ready a well studied phenomenon, and molecular systems exhibiting this effect have been proposed, based, for example, on an antiferroelectric to ferroelectric transition induced by the application of an external field,[25] on a ferrimagnetic to ferromagnetic transition in heterobimetallic complexes,[26] or on the more familiar modification of optical properties that occurs in photochromic molecules following a light pulse.

Unlike inorganic semiconductors, where the semiconducting properties are associated with a macroscopic solid state, whether crystalline or amorphous, in organic molecules the properties are intrinsic to the molecules. The new concept of molecular semiconductors opens up a new field, both theoretically and with regard to applications.[27] The semiconducting properties of undoped conjugated polymers such as polyacetylene and polythiophene have been used in various devices, such as Schottky junctions,[29] homo- and heterojunctions,[29] organic–inorganic junctions,[30] and field-effect transistors.[31] Although the results are promising, it has been acknowledged in all these investigations that the devices suffer from the very poor semiconducting properties of these conjugated polymers. As already observed for most organic semiconductors, these materials have large concentrations of structural defects and impurities, which create efficient traps and recombination centers. Thus the carrier mobility which is one of the most important characteristics for a semiconductor, is very low, rarely exceeding $10^{-5}\,cm^2\,V^{-1}\,s^{-1}$, a value which has to be compared with about $1\,cm^2\,V^{-1}\,s^{-1}$ for a classical amorphous inorganic semiconductor such as Si, and more than $10^2\,cm^2\,V^{-1}\,s^{-1}$ for monocrystalline Si. A large improvement in the semiconducting properties of these organic materials thus appeared essential in order to consider them for electronics applications. An important achievement has been the use of conjugated oligomers instead of the corresponding polymers. Oligomers can be synthesized as chemical compounds with a well defined structure and a much lower concentration of defects and impurities than the corresponding polymers. By controlling the conjugation length, it is possible to prepare oligomers showing almost the same band-gap energy as the parent polymers, and their solubility and low molecular weight allow them to be easily processed by vacuum or by Langmuir–Blodgett techniques. The most important advantage is their structural homogeneity, which leads to carrier mobility values as high as $2\times10^{-2}\,cm^2\,V^{-1}\,s^{-1}$ in the case of thiophene oligomers.[32] This spectacular increase in mobility underlines the major role played by structural defects for limiting the charge transport properties in polymer chains. Thus, conjugated oligomers, which can be functionalized in the same way with prosthetic groups R, appear to be promising in meeting the requirements for applications in electronics.

A last important aspect which deserves attention concerns the tunability of the electronic properties of these organic semiconductors compared to inorganic semiconductors. Indeed, the characteristics of electronic devices, junctions and transistors, are mainly determined by the intrinsic electronic properties of their n- and p-type semiconducting components. The common inorganic semiconductors, such as Si, GaAs and InP, have discrete band energy values, which impose limits on the characteristics of the corresponding devices. On the other hand, in organic materials which are capable of either large or subtle chemical modifications, these band energy values can be controlled over a wide range, and can thus be tuned in order to achieve almost any desired characteristic. Functionalized organic conjugated polymers and oligomers will thus be able to perform memory and logic functions. Compared to conventional inorganic materials, the easy tuning of their electronic properties offers a promise as great as the first proposals, some decades ago, for using polymers instead of metals.

Received: November 21, 1988

[1] J. M. Lehn, *Angew. Chem. 100* (1988) 91; *Angew. Chem. Int. Ed. Engl. 27* (1988) 89; D. J. Cram, *ibid. 100* (1988) 1041 and *27* (1988) 1009; C. J. Pedersen, *ibid. 100* (1988) 1053 and *27* (1988) 1021.
[2] F. Carter (Ed.): *Molecular Electronic Devices*, Marcel Dekker, New York 1982.
[3] T. A. Skotheim (Ed.): *Handbook of Conducting Polymers*, Marcel Dekker, New York 1986.
[4] H. Shirakawa, E. Louis, A. MacDiarmid, C. Chiang, A. J. Heeger, *J. Chem. Soc. Chem. Commun. 1977*, 758.
[5] A. F. Diaz, K. K. Kanazawa, J. P. Gardini, *J. Chem. Soc. Chem. Commun. 1979*, 635.
[6] G. Tourillon, F. Garnier, *J. Electroanal. Chem. 135* (1982) 173.
[7] A. G. MacDiarmid, J. C. Chiang, M. Halpern, W. S. Huang, S. L. Mu, N. D. L. Somasiri, W. Wu, S. Yaniger, *Mol. Cryst. Liq. Cryst. 121* (1985) 173.
[8] N. Basescu, Z. X. Liu, D. Moses, A. J. Heeger, H. Naarmann, H. Teophilou, *Nature (London) 327* (1987) 403.
[9] F. Garnier, G. Tourillon, M. Garzard, J. C. Dubois, *J. Electroanal. Chem. 148* (1983) 299.
[10] J. Roncali, R. Garreau, D. Delabouglise, F. Garnier, M. Lemaire, *Synth. Met. 28* (1989) C341.
[11] G. Bidan, A. Deronzier, J. C. Moutet, *Nouv. J. Chim. 8* (1984) 501.
[12] Y. K. Korshak, T. V. Medvedeva, A. A. Ovchinnikov, V. N. Spector, *Nature (London) 326* (1987) 370.
[13] V. Leberre, L. Angely, N. Simonet-Gueguen, J. Simonet, *J. Electroanal. Chem. 206* (1986) 115.
[14] M. G. Minett, J., R. Owen, *Synth. Met. 28* (1989) C211.
[15] J. Roncali, R. Garreau, D. Delabouglise, F. Garnier, M. Lemaire, *Makromol. Chem. Makromol. Symp. 20* (1988) 601.
[16] A. Bettelheim, B. A. White, S. A. Ratbuck, R. W. Murray, *Inorg. Chem. 26* (1987) 1009.
[17] J. G. Eaves, H. S. Munro, D. Parker, *Synth. Met. 26* (1986) 123.
[18] F. Daire, F. Bedioui, J. Devynck, C. Bied Charreton, *J. Electroanal. Chem. 205* (1986) 309; R. A. Bull, F. R. Fan, A. J. Bard, *J. Electrochem. Soc. 131* (1984) 687.
[19] J. P. Collin, J. P. Sauvage, *J. Chem. Soc. Chem. Commun. 1987*, 1075.
[20] G. Tourillon, F. Garnier, *J. Phys. Chem. 88* (1984) 5281; A. Yassar, J. Roncali, F. Garnier, *J. Electroanal. Chem. 255* (1988) 53.
[21] D. Gourier, G. Tourillon, *J. Phys. Chem. 90* (1986) 5561.
[22] D. Gningue, H. Horowitz, F. Garnier, *J. Electrochem. Soc. 135* (1988) 1695.
[23] A. Deronzier, L. Coche, J. C. Moutet, *J. Electroanal. Chem. 198* (1986) 187.
[24] L. Coche, J. C. Moutet, *J. Am. Chem. Soc. 109* (1987) 6887.
[25] J. Malthete, A. Collet, *J. Am. Chem. Soc. 109* (1987) 7544.
[26] O. Kahn, Y. Pei, M. Verdaguer, J. P. Renard, J. Sletten, *J. Am. Chem. Soc. 110* (1988) 782.
[27] J. Simon, J. J. André: *Molecular Semiconductors*, Springer, Berlin 1985.
[28] S. Glenis, G. Tourillon, F. Garnier, *Thin Solid Films 139* (1986) 221.
[29] T. Wada, A. Takeno, M. Iwaki, H. Sasabe, Y. Kobayashi, *J. Chem. Soc. Chem. Commun. 1985*, 1194.
[30] G. Horowitz, F. Garnier, *Chemtronics 1* (1986) 80.
[31] A. Tsumura, H. Koezuka, S. Tsunada, T. Ando, *Chem. Lett. 1986*, 863.
[32] F. Garnier, G. Horowitz, D. Fichou, *Synth. Met. 28* (1988) 705.

Biomaterials Highlights

Materials for Biomedical Applications—Bone and Joint Replacements

By Günther Heimke*

This contribution is the first of a sequence of reports on the recent developments in the field of the so-called "biomaterials", which, of course, are not at all "bio" or living materials but, rather, replace those living materials which have ceased to serve their purpose.

The science of biomaterials can be regarded as another prototype of the many interdisciplinary fields of research which have emerged during the last decades. It gained general recognition about the mid nineteen seventies as evidenced by the foundation of societies for biomaterials or similar organizations in most of the industrialized nations of the world. In 1980 the European Society for Biomaterials organized the 1st World Congress on Biomaterials in Vienna, Austria, while the 3rd World Biomaterials Congress in Kyoto, Japan, in April 1988 attracted more than 1000 participants. The 4th Congress of this type will again be organized by the European Society and is scheduled for 1992 in Berlin. Besides these world congresses, individual biomaterials societies organize meetings in their own particular areas. The next US conference will be held in Orlando, Florida towards the end of April 1989, and the 8th European Conference on Biomaterials will be in Heidelberg, Germany, from the 7th to the 9th of September 1989, immediately followed by a more specialized symposium entitled "Ceramics in Medicine".

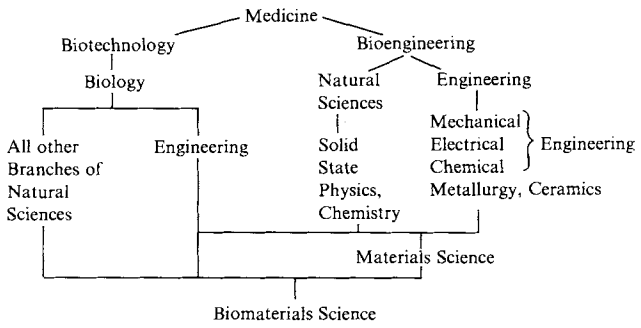
The field of biomaterials is, of course, one branch of the large area of contact between medicine and the natural sciences and engineering disciplines. Actually, there are two such contact areas; biotechnology and bioengineering. The term biotechnology is now mostly used to describe all activities related to the application of modern biology, in particular the possibility of genetic manipulation of micro organisms, to medicine, chemistry, and all other fields of natural science and engineering. The term bioengineering comprises all other contact areas of the natural sciences and engineering to medicine. Scheme 1 is an attempt to express these correlations and to define the position of biomaterials within such a framework.

In most reports on biomaterials in the different fields of medicine, much more emphasis is placed on the different kinds of tissue reactions the materials stimulate or avoid, than to the materials themselves. The reason is obvious: Most of the presently used implant materials have already acquired bulk properties which satisfy the requirements of their particular applications, and therefore, interest is focussed on the reaction along the interface between the biological tissue and the material. At an early stage of biomaterials development the first approximation was that both

[*] Prof. G. Heimke
Department of Bioengineering
Clemson University
Clemson, SC 29634 (USA)



From now on, Professor Günther Heimke (Clemson University, S.C., USA) will be providing a quarterly report on various aspects of biomaterials research and development which will be published as the Biomaterials Highlights column of Advanced Materials. Günther Heimke was educated as a physicist with emphasis on solid state physics at the University of Heidelberg and at the Martin-Luther-Universität, Halle, where he gained an M.Sc. and a D.Sc. After several years of university teaching and research into magnetic materials, in particular ceramic magnets, he moved to the industrial sector continuing work on magnets in both West Germany and in the USA before joining Friedrichsfeld GmbH, taking responsibility for the research and development of oxide ceramics. It was here that he became involved with biomaterials, introducing the use of alumina ceramic materials in medical devices, such as joint replacements and dental implants. After his retirement he recieved an invitation to be a guest professor at the Department of Bioengineering, School of Engineering, Clemson University, where he is now a research professor. He has authored and co-authored more than 150 publications and two books, and holds more than 40 German patents on which many international patents are based.



Scheme 1. The position of the science of biomaterials within the branches of biotechnology and bioengineering.

sides of this interface were required to remain in their original state for as long as possible. But it was soon realized that this was a severe oversimplification if looked at from both sides of the interface.

The tissue adjacent to the implant has, because of this implantation, been separated from those portions which have just been replaced by the implant, and has therefore been deprived of about half of its nutrition pathway. In addition, most of the remaining blood vessels meeting this interface have been blocked by blood clots. Cells have been damaged, and their remnants together with other disrupted materials like collagen stimulate defence processes mainly aimed at their removal.

On the materials side, the electrolytic environment can cause many reactions, starting with the removal of the layers originally absorbed in air or during sterilization, and continuing via, for example, the formation of metal organic complexes, to cell mediated processes. These reactions vary from tissue to tissue and also from material to material.

The knowledge about these interfacial processes has not yet been summarized and generalized in a manner which allows sufficiently reliable predictions about the degree of compatibility of a new candidate implant material to be made. This statement already points to one difficulty; there is no general biocompatibility. The kind of tissue reaction to an implant depends not only on the type of surrounding tissue (e.g. muscle, bone, blood, skin) but also on many more parameters, like the degree of vascularization, stresses and strains, or relative motion.

The dense, highly pure alumina ceramic can be used to demonstrate this problem: This oxide ceramic is now widely regarded as the prototype of a bioinert material as nearly nothing goes into solution, and densely adsorbed body molecules even "camouflage" such an implant against the body's immune system. Thus, if implanted in connective tissue (muscle, bone) all reactions have been shown to be essentially controlled by the stress and strain field created in the surrounding tissue and the relative motions resulting from them. As this stress and strain field can be controlled by the shape of the implant, a reliable osseo-integration of such implants can be achieved in bony tissue, as has been documented by the clinical success rates of dental implants and acetabular components of total hip replacements in long term follow-up studies.[1-4] This same material cannot be used in the cardiovascular system because of its blood clotting potential.[5] The reasons for this behavior have not yet been fully understood. Some attempts to correlate the initial process of clot formation to surface properties like the work function or the band gap and width have not yet led to conclusive results.[6]

Because of this lack of a sufficiently general set of rules for the selection or tailoring of implant materials, it will be the task of this series to present the most recent knowledge and developments in a sequence of contributions, each devoted to the most recent achievements in one particular field of implantology. Observations made at the combined meeting of the American Orthopedic Research Society and the American Academy of Orthopedic Surgeons (AAOS) in Las Vegas in February 1989 are the motivation behind these reports in the field of bone and joint replacements. In comparing the topics of the papers presented during these meetings with those presented on similar occasions in the early and even in the mid eighties, some shift can be seen as expressed in Table 1.

Table 1. The shift of emphasis in research on bone and joint replacement materials during the last decade.

Time period	Basic materials related research	Clinical studies
Late seventies and early eighties	Description of the results of interface reactions to potential new implant materials	Relatively short term follow-up studies with essentially phenomenologic description of results
Late eighties	Nearly no new materials; studies on causes for different kinds of interface reactions, e.g. from immunological points of view	Eight to more than ten years follow-up studies with attempts to statistically analyse results.

In basic materials related research it appears that the ceramics explored essentially during the seventies (see the recent survey in this journal[7]) have been the last large, unique group of solids introduced into the field of implant materials. Now, some hopes for further improvements rest with different kinds of material combinations like fiber reinforced plastics, e.g. for bone plates in order to avoid the stress shielding which is assumed to compromise the results of metal plates.

One means for implant fixation, porous coatings consisting of beads sintered or otherwise attached to the surfaces of the anchoring portions of joint replacements, have become widely used, particularly in the USA since the late seventies. Now, longer term clinical follow-up studies increasingly reveal that the success rates are not much better or more predictable than with implants anchored via the polymethylmethacrylate bone cement. This has even resulted in recommendations to abandon such coatings completely and return to the cementing technique.[8]

In order to overcome these problems much interest is presently focused on bioactive coatings (hydroxyapatite [HA] ceramics, Ca-phosphate containing glasses or glass-ceramics). Nearly all experts in this field agreed at last years biomaterials meeting in Kyoto, Japan, that dissolution of at least the HA coatings occurs within about four to six years in the body environment, and that only their combination with undulating surfaces will provide the reliable mechanical interlocking with the surrounding bony tissue necessary to yield some improvements.

The multivariant statistical evaluations of the more recent follow-up studies gave further details on the influence of different implant shapes and sizes as well as operational procedures. There was even the recommendation to abandon the use of conically shaped acetabular components (*D. A. Fisher*, Indianapolis, IN, USA and *T. H. Mallory*, Columbus, OH, USA, paper no. 9 of the AAOS Meeting). A marked detrimental influence of medication by making interface remodeling necessary for osseo-integration was demonstrated for indomethacin and ibuprofen and, to a lesser degree, aspirin (*T. M. Trancik* and *M. Mills*, Trans. 35th Meeting ORS, Las Vegas, 1989, p. 338).

Besides the overview already given in Table 1, it appears that the now nearly 30 years (since *Charnley*'s introduction of the PMMA bone cement) of large scale clinical experience with implants in orthopedic surgery allow for a much more detailed understanding of implant related responses and many of the side effects. Their feedback in the application of implants, however, will become more and more difficult to judge because of the relatively high success rates already achieved.

[1] B. d'Hoedt, *Dtsch. Z. Zahnärztl. Implantologie 2* (1986) 6.
[2] B. d'Hoedt, C. M. Büsing, *Fortschr. Zahnärztl. Implantol. 1* (1985) 150.
[3] B. d'Hoedt, D. Lukas, W. Schulte, *Dtsch. Zahnärztl. Z. 41* (1986) 1068.
[4] G. Heimke, D. Stock, W. Seiwert, C. M. Büsing, J. Gottstein in S. M. Perren, E. Schneider (Eds.): *Biomechanics: Current Interdisciplinary Research*, Matinus Nijhoff Publishers, Dordrecht 1985, p. 141.
[5] A. J. Mountvala, *Am. Ceram. Soc. Bull. 52* (1973) 479.
[6] R. Ebert, M. Schaldach, Paper presented at the 12th Int. Conf. Medical and Biological Engineering/5th Int. Conf. Medical Physics, Jerusalem, Israel 1979.
[7] G. Heimke, *Adv. Mater. 1989*, 7; *Angew. Chem. 101* (1989) 111; *Angew. Chem. Int. Ed. Engl. 28* (1989) 111.
[8] R. G. Volz, J. K. Nisbet, R. W. Lee, M. G. McMurtry, *Clin. Orthop. Relat. Res. 226* (1988) 38.

Conference Reports

Molecular Electronics—Science and Technology

By Ari Aviram*

The conference on molecular electronics took place during the week of February 19. to 24. 1989 on the island of Hawaii in Kona, under the sponsorship of the Engineering Foundation. Seventy scientists took part in the program that consisted of 34 invited talks, 16 contributed talks and 10 posters.

Molecular Electronics is the study of molecular properties that may lead to signal processing. Though the name of the field implies technological applications, the state of the art is at a stage that requires considerable basic science groundwork to foster a solid foundation for building future technology. In essence this is an exciting aspect of the field, since it provides an opportunity to break new ground in our understanding of the molecular universe and to develop new techniques for interaction with single molecules or small groups of molecules.

Recent advances in nanolithography and scanning tunneling microscopy have given a boost to the field of molecular electronics. As such, the conference program was organized around these developments as well as several other themes that represent the multidisciplinary facets of this young science. The organizers prepared the program to probe the following questions: What are the limits of current solid state technology? What is the status of nanolithography? What are the current approaches to molecular signal processing and the theoretical basis for those approaches? What are the current methods that will permit interaction between the macrocosm and the molecular world?

The trend for miniaturization and compaction in current solid state technology for microchip fabrication may stall

[*] Dr. A. Aviram
IBM Research Division
T. J. Watson, Research Center
Yorktown Hts., N.Y. 10598 (USA)

when the dimensions of individual conventional devices reach a few hundred Angstroms. This was the assessment presented by Dr. *Robert Keyes* of IBM. These dimensions are still large when molecules are considered since molecules are on a scale of tens of Angstroms. Therefore, it is expected that molecular electronics will only become more desirable when lithography dimensions of about one hundred Angstroms are reached. Nanolithography, the art and technology responsible for fabrication of the fine patterns which are the essence of the microchip, has already reached dimensions in laboratory demonstrations that permit interaction with molecules. This was reported by four leading scientists in the field; Professor *Pease* of Stanford, Professor *Smith* of MIT, Professor *Wilkinson* of Glasgow University and Dr. *Chang* of IBM.

The advances reported, offer exciting possibilities for the fabrication of molecular electronic components. Fabrication of microstructures with linewidths in the 10 nm to 100 nm region is now well established. Not only simple structures for quantum transport studies have been fabricated, but complex circuits and chips for silicon field effect transistors (FET's) and GaAs high electron mobility transistors (HEMTs) with gate lengths down to 70 nm have also been successfully fabricated and perform well. While the electron beam method remains the key lithography approach, focused ion beam and X-ray proximity printing techniques are now available with resolution down to 30 nm. Very thin resist material based on Langmuir–Blodgett films suitable for nanolithography have been developed with defect density almost as low as conventional resists now used in the integrated circuit manufacturing. The use of the scanning tunneling microscope (STM) as a nanofarbrication tool with the capability of directly manipulating molecules and selectively pinning and unpinning molecules with feature sizes as small as 0.4 nm was also shown. These represent the smallest man-made structures ever reported, and the STM may well prove to be a key technique for the fabrication of the sub-10 nm structures needed for molecular electronics in the future. However, it was pointed out by Dr. *Chang* and by Professor *Smith* that although it is possible to produce today the patterns needed for molecular electronics, mass-producing them is something else altogether. The electron beam method currently employed is too slow for commercial applications at the one hundred Angstrom level and a significant amount of development work has to be invested in order to produce a satisfactory commercial nanolithography technology for molecular electronics.

Following these insights on nanolithography, the program focused on current techniques that enable interaction with molecules. Attention centered on applications of STM. Among the participants was Nobel Laureate Dr. *Heinrich Rohrer* of IBM, co-inventor of the STM. Dr. *Rohrer* discussed a new technique of molecular electrochemistry with the STM. This technique permits electrochemical alteration of single molecules or groups of molecules that are addressed with the STM tip. The whole spectrum of current achievements with the STM was presented in a lecture presented by Professor *Calvin Quate* of Stanford University. He showed the ability of this instrument to disclose detailed aspects of molecular activity, such as the sequence of molecular interactions that leads to blood clotting.

The core of the program consisted of presentations regarding various approaches to molecular electronics. Three basic approaches emerged as the dominant representatives of current thinking. One is molecular photonics, also termed "Optical Computing". This approach was outlined by a number of speakers who discussed theoretical aspects as well as the preparation and properties of new materials. Professor *Robert Munn* from UMIST, Manchester, described new computational techniques to calculate linear and nonlinear optical and dielectric properties of molecular crystals, and Professor *David Bloor* from Queen Mary College, described optical studies of the third-order optical non-linearities of polydiacetylenes, and progress towards nonlinear optical devices using these materials.

Another approach was that of Professor *John Barker* from Glasgow, who presented arguments that the best architecture of a molecular computer would require departure from current von Neumann architecture and development of cellular automata. He presented molecular structures that form the proper logic for this architecture.

The third approach outlined was the new theory for molecular electronics that describes molecular switches and a blueprint for future molecular electronic devices. This concept was presented by Dr. *Ari Aviram* of IBM. The theory describes cross-structured molecules that can be employed in a planar technology to fabricate memory cells, logic gates and other components that are needed to form complete molecular integrated circuits.

The conference devoted a large portion of the program to theoretical papers that give justification to the field. Theories were presented for intramolecular electron transfer and the formalism for computing such events. The two presentations by Professor *Mark Ratner* from Northwestern and Professor *Noel Hush* from University of Sydney were important in this respect. Also, the formalism of computing the efficiency of molecular switches was presented in a paper by Dr. *Christian Joachim* of CNRS, France.

Contributions of special interest included electrochemical enzyme control, by Professor *Masuo Aizawa* of Tokyo Institute of Technology, and a synthetic approach to molecular switches outlined by Professor *Jean-Pierre Launay* of Pierre et Marie Curie University in Paris. Also significant was the talk by Professor *Gareth Roberts* of Oxford University who described novel applications of organic thin films to a variety of devices including night vision telescopes.

The conference Molecular Electronics – Science and Technology was a very exciting and important meeting. It produced the recognition that molecular electronics is not just a gleam in the margins of theoretical papers but rather a new and important field of science that is nourished by many supporting sciences and technologies.

Ceramics in Bologna

By Suk-Joong L. Kang*

The 7th International Symposium on Ceramics (7th SIMCER) was held from December 14–17, 1988 in Bologna, Italy. The meeting was organized by the Centro Ceramico in Bologna as part of the 900th anniversary celebrations of Bologna University, and about 730 participants from nearly 30 countries throughout the world attended. Two sessions were organized to run in parallel, one for advanced ceramics, and the other for more traditional ceramics. Approximately 100 papers and posters were presented in the advanced ceramics sessions and about 50 in the traditional ceramics sessions.

The advanced ceramics meeting consisted of six sessions: 1) Superconductivity, 2) Composites, 3) Ceramics on Duty, 4) Processing of High Tech Ceramics, 5) Electronic Ceramics and 6) Structural Ceramics, each being opened by one or two plenary lectures and lasting for half a day.

In the first lecture, *D. R. Clarke* (U.S.A.) presented "Ceramic Superconductors; Relationships between Processing, Microstructure and Properties", emphasizing state-of-the-art research in oxide superconductors and future tasks. The lecture was followed by several contributed papers and a general discussion on the future prospects for these materials. Compared to their bright future in micro-electronics, their application in power transmission systems was thought to be much more difficult.

The afternoon session began with two lectures: "Principles of Design with Ceramic Matrix Composites" (*A. G. Evans*, U.S.A.) and "Whisker Reinforced Ceramics; Toughening Behavior and Properties" (*P. Becker*, U.S.A.). The first described the design principles of composite materials based on fracture mechanics and experimental observations at interfaces and the second gave an overview of recent experimental results.

On the second day, in the session entitled "Ceramics on Duty", microstructure development and the dependence of mechanical properties upon the sintering and environmental conditions were discussed for various materials, ranging from structural ceramics, such as SiC and Si_3N_4, to electronic ceramics, such as $SrTiO_3$. In the afternoon session, "Processing of High Tech Ceramics", *G. Onoda* (U.S.A.) discussed "Basic Phenomena in Ceramic Forming Processes", pointing out the volume expansion of powder mixtures caused by shearing and the problems this brings in powder processing.

On the morning of the 16th, in the "Electronic Ceramics" session *R. E. Newnham* (U.S.A.) lectured on "Electro-Ceramics; the Age of Integration and Miniaturization", and emphasized an important trend in electroceramics research, that of integration and miniaturization of sensors and actuators, after which about ten papers on various materials were presented. The lecture on "Structural Ceramics" given by *F. Thümmler* (FRG), summerizing the range of ceramic materials and components used as structural parts and presenting future trends in the field, was followed in the afternoon by eight other papers.

The last day was separated in the program and devoted to a special meeting "Zirconia 88". *D. Broussand* (France) gave a talk on the "Effect of Powder Characteristics on Forming and Microstructure Development of ZrO_2-Y_2O_3 Ceramics", presenting test results on four kinds of commercial powders. Among the subsequent contributed papers, the paper on "Numerical Methods for the Calculation of Stress Intensity Factors" (*W. Müller*, FRG) provided a relaxed and pleasant time for the audience by demonstrating the toughening effect of ZrO_2 particles by using a movie film, which in fact could be used effectively for demonstration purposes in university courses.

In addition to invited lectures and the presentation of papers, poster presentations were also made in the afternoons of the 14th and 16th, and, although approximately one third of the posters were missing, those that were presented were informative and of high quality.

The success of this small conference, which can boast the participation of numerous representative people, may well be due to the good opportunity given for the discussion of the problems and advances in high-tech ceramics lead by leading scientists in the relevant fields. Despite the small number of papers presented the conference covered an almost unlimited number of topics in advanced ceramics. The materials dealt with were also so multivarious that many of them were mentioned only once or twice during the whole meeting. This was advantageous for the people who wanted to get a general view of the current topics and latest results, but disadvantageous to those who were more interested in specific areas. On the whole, it was an informative and agreeable meeting and the organizers should be congratulated.

[*] Dr. S.-J. L. Kang
Max-Planck-Institut für Metallforschung
Heisenbergstraße 5, D-7000 Stuttgart 80 (FRG)

Atomic Steps on Surfaces

By Martin Henzler *

A special workshop on atomic steps at surfaces and interfaces (organized by *M. Henzler, W. Ranke* and *M. Scheffler*) was held at the Ringberg Castle in Rottach-Egern, FRG, from January 15–18, 1989. Due to the hospitality of the Max-Planck-Gesellschaft the participants from Germany (West and East), other European countries and the USA had an ideal meeting place for extensive discussions on an exciting topic.

In surface science in the past, surfaces have been frequently dealt with as if they were free of defects. This simplification was mainly due to the lack of reliable measurements of the defects and a lack of theory concerning deviations from periodicity. However, over the last twenty years, a few groups have developed defect analysis via profile analysis of diffraction spots. Other techniques, especially microscopy have contributed a lot, so that now the atomic step is the best investigated defect at surfaces. It was therefore worthwhile to put together all available information on steps with respect to verification, theory and properties into one workshop.

It was very helpful to have all the powerful structure elucidation methods reviewed, such as the various microscopies (transmission electron microscopy by *H. Bethge* and *H. Höche*, both Halle, GDR; low energy electron microscopy by *E. G. Bauer*, Clausthal, FRG; scanning tunnel microscopy by *R. M. Feenstra*, Yorktown Heights, USA, and *R. J. Behm*, München, FRG) which reveal many details and beautiful images. The diffraction techniques (low energy electron diffraction by *M. G. Lagally*, Madison, USA, and *W. Moritz*, München, FRG; helium atom scattering by *J. P. Toennies*, Göttingen, FRG; X-ray scattering by *E. Vlieg*, Amsterdam, Netherlands) are complementary due to their ability to supply quantitative information.

If the existence of steps, their shape, density, and distribution on a surface is known, it is of interest, which kind of properties may be influenced or even determined by those steps. Some theoretical reviews on total energy calculations for semiconductors (*J. Chadi*, Palo Alto, USA) and for metals (*P. M. Marcus*, Yorktown Heights, USA) showed atom arrangements at steps to be quite different from ideal lattice sites. There are now a wide variety of well established and quantitatively measured properties due to the presence of steps. Some properties are inherently coupled with steps, like crystal growth, which was discussed experimentally (*E. Bauser*, Stuttgart, FRG, and *H. Höche*, Halle, GDR) and theoretically with quite different methods and aspects (*E. V. Albano*, Mainz, FRG, and *G. Stoyanov*, Sofia, Bulgaria). Of course, many studies on adsorption, desorption and reaction clearly show the quite different effects of steps (*K. Wandelt*, Bonn, FRG; *C. Benndorf*, Hamburg, FRG, and *G. A. Somorjai*, Berkeley, USA). Over twenty posters exhibited many details of important new developments.

All these results demonstrated, that atomic steps are not just unknown or disliked disturbances of an otherwise well-defined experiment. Including steps in all considerations brings the investigated surface closer to reality and to reproducibility. It is clear that the experiments on the best, defect free surfaces are better described and discussed when defects like steps are included. This extension is needed, since many properties are strongly influenced, e.g. for adsorption, the edge sites have a different binding energy and different vibrational modes. Due to this knowledge, many high index faces are under investigation, since they provide two or more very different surface sites. Although these faces are not yet known in as much detail as the low index phases, both microscopy and diffraction provide an increasing amount of detail. Finally a new field of properties becomes available by the inclusion of step properties. Any variation of the shape of a surface during the experiment requires the formation or variation of steps. There was an interesting discussion on the probability of crossing a step during surface diffusion. The roughening of a step during growth, due to heating is a more and more tractable phenomenon. The behavior of adsorbates at steps may change drastically and a study of this may lead to a detailed description of catalysis. Some adsorbates may even initiate a rearrangement of step atoms so that the surface forms new facets. Therefore the stability of surfaces is now to be studied taking into account processes at steps.

Of course, steps are not the only present and only important defects on surfaces. They are, however, the best investigated, and are therefore the model for all other defects. The workshop provided not just the state of the art information, but helped to combine the available information to form new ideas.

[*] Prof. Dr. M. Henzler
Institut für Festkörperphysik
Universität Hannover, Appelstraße 2
D-3000 Hannover 1 (FRG)

Book Reviews

Ternary Alloys

Ternary Alloys—A Comprehensive Compendium of Evaluated Constitutional Data and Phase Diagrams: Volumes 1 and 2, Ternary Silver Alloys. Edited by *G. Petzow* and *G. Effenberg*. Principal reviewer: *H. L. Lukas*. VCH Verlagsgesellschaft, Weinheim, Fed. Rep. Germany/VCH Publishers, New York, N.Y., U.S.A. 1988, Vol. 1, 612 pp. Vol. 2, 624 pp. £ 250 per volume (special arrangements for series subscribers). ISBN 3-527-26941-X and 3-527-26942-8

Metallurgists, like any other kind of scientist, have numerous useful tools of their trade, and a few indispensable ones. Prominent among the indispensable ones are phase diagrams. They are equally necessary to researchers who seek to develop new alloys or improve existing ones, and to producers who seek to optimize the properties of standard alloys by modifications to manufacture or heat-treatment. Modern metallurgy would simply not exist without them.

The first really accurate phase diagram (Cu–Sn) was determined by *Heycock* and *Neville*, two Cambridge chemists, and published in 1904. Only 32 years later, a notable German pioneer, *Max Hansen*, published *Der Aufbau der Zweistofflegierungen:* this reported on the phase constitution of 828 metallic systems and included 456 critically evaluated phase diagrams. After the war, three separate revisions and supplements of this work appeared and other critical compilations of binary phase diagrams were published subsequently. The key word is 'critical': somebody has to make judgements between conflicting data and interpretations. To organize and institutionalize, on a worldwide basis, the heavy task of assembling information, evaluating and reviewing it, an Alloy Phase Diagram International Commission (APDIC) was set up some years ago and a journal, *Bulletin of Alloy Phase Diagrams*, instituted.

One might suppose that the availability of so many binary phase diagrams would satisfy the needs of most metallurgists, but in fact alloys become ever more complex, and many contain at least three major constituents. Ternary diagrams have, therefore, become increasingly important in recent years, and many have been evaluated for, and published in, the *Bulletin*. In its last issue an editorial tells the reader that up to now, 635 binary systems have already been evaluated and published in the journal, its Indian sister journal, or in books, and over 400 more are in progress. In December 1988, the *Bulletin* informed the reader, 606 ternary systems had also been evaluated and published, and 408 had been evaluated but not yet published. As a proportion of possible ternary systems (bearing in mind that more than half of the elements are metals) this is still only modest, but it must be borne in mind that the effort involved in determining a ternary system is much greater than for a binary. (The great English metallurgist *R. S. Bradley*, for instance, spent over a decade of single-minded labor around the middle of the century on the determination of the Al-Fe-Ni diagram alone).

The ca. 2000 binary and ternary phase diagrams now reasonably well established (many others have only been cursorily surveyed) are a truly tiny fraction of the possible total. Figure 1 (note the logarithmic ordinate scale) was published recently by one of the editors, *G. Petzow*, of the volumes under review. Allowing for 100 elements (including a few transuranics) the number of possible 50-element systems exceeds by a large margin the age of the universe in seconds.

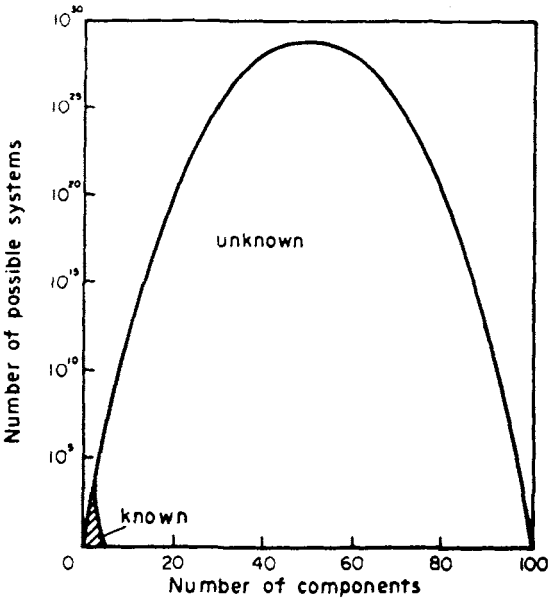


Fig. 1. Numbers of known and unknown heterogeneous systems.

Fortunately, 50ary phase diagrams run into such formidable problems of determination, evaluation and depiction that we can comfortably forget about them; even quaternary and quinary systems, which are occasionally published, are hard to determine and harder to understand when published. What really matters to practitioners is the availability of numerous reliable and conveniently available ternary systems. The new series on which the German evaluators and the publishers have now courageously embarked clearly will fulfil this need.

The two volumes under review incorporate critically evaluated data for 446 ternary systems containing silver, critically updated to January 1988 and based on over 1900 publications of experimental work, taken from the huge database maintained at the Max-Planck-Institut für Metallforschung in Stuttgart, with German Government support. Though

the calculation of phase diagrams from thermochemical data has made great strides recently, this approach is apparently not yet being used for these volumes, because of the very high standards of accuracy which are being adopted and because of the difficulty in securing adequately precise 'optimization' for the three constituent binaries of each ternary system, which is a prerequisite for ternary calculations. For many though not all of the 446 systems, ternary diagrams are included; evaluated binary diagrams are also included where these are not readily available in one of the standard volumes of binaries already published.

Each system is the responsibility of an individual evaluator, 20 of whom contributed to these two volumes and although half of these 20 are German, many nationalities are represented. Each evaluation was then critically reviewed by one of a small band of reviewers. This has become universal practice in all assessments of ternary diagrams under the broad aegis of APDIC as the present volumes are. The reviewers and the original evaluators, if need be, met to resolve their differences at one of the numerous editorial conferences held at a specially provided rural idyll.

The task of producing volumes like these is truly daunting, quite apart from the successive levels of evaluation and reviewing to which all the work is subject. Finding the original publications (many in exceedingly obscure periodicals); assessing their reliability; turning the diagrams into standard format; finding and assembling crystallographic information about the phases (structure types and lattice parameters are cited); creating isothermal and 'vertical' sections; in particular, drawing up the involved 'reaction schemes' for the more complex ternary systems which have become de rigueur for serious depictions of ternary diagrams, to render them more intelligible; computer-based creation of final drawings and checking of the final printed form... all this has called for a very large team of participants both in Stuttgart and elsewhere, and at the publishers a very long term commitment to a colossal task, as well as generous Government funding without which the (admittedly) high price of the volumes would have gone right through the roof.

The stated objective of the series is to have so much information not just cited but presented in the volumes that most users will never need to got to the original literature. In this reviewer's opinion, that objective has been achieved.

The next set of volumes, three in number, on ternaries containing aluminum, is at an advanced state of preparation and is due to be published this year. It should be noted that as the series progresses, the task will become gradually less onerous. This can be appreciated by noting that the two "Ag" volumes incorporate 28 Ag-Al-X systems, and none of these 28 need be repeated in the "Al" volumes. This 'reduction effect' will become more pronounced as successive volumes are published.

There have been other compilations of ternary phase diagrams in book form. First one should point out a publication entitled *Phase Diagrams for Ceramists,* published by the American Ceramic Society originally in 1964 and repeatedly updated since. This contains information on many binary, ternary, quaternary and even a few quinary systems of ceramics. The ceramists are entirely separate from the APDIC organization. (There are no compilations of phase diagrams of polymers, and indeed very few such diagrams exist. The concept of phase equilibria is only making slow headway in the polymer world, though both theorists and experimentalists are now working extensively on the concept of miscibility and separation of phases in 'polymer blends').

India has played a large part in the international metallurgical effort, and many evaluations have originated there; *Raghavan* in Delhi has published three volumes on Fe ternaries (the latest has just appeared) with one more to come. Even so, the four Indian volumes only scratch the surface of the enormous range of Fe ternaries! In America, a Cu-O-X volume is expected to appear soon (again, clearly, a small subset of Cu ternaries) while in Britain, as a result of work initiated years ago by that prince of evaluators, the late *Geoffrey Raynor,* a volume of Au ternaries is expected to be published soon by the Institute of Metals. The editor of this is *Alan Prince,* who is now the doyen of British evaluators and has played a substantial part in the two Ag volumes under review here. When the Stuttgart team gets to Au, which should not be long in view of its position in the alphabet, arrangements will undoubtedly be made to make full use of the British work, to avoid needless duplication, but presumably the information in the British volume will all be included in the VCH series, which is intended to be as comprehensive as is humanly possible.

It is entirely appropriate that the massive international effort which has created this first fruit, the silver volumes, should be centered in Stuttgart. Many of the early phase diagrams were determined by the German pioneer, *Gustav Tammann.* Germany has long had an indigenous tradition of high-class metallography, including a training program for metallographers which has no equal; metallography (and the ability to judge critically the results of metallographic investigations) is an essential constituent of phase diagram determination and evaluation. *Max Hansen,* the father of phase diagram evaluation, worked at the Stuttgart Institute, and as the editors of the silver volume indicate in their preface, they are seeking to create a sort of '*ternary Hansen*'. In this ambitious task, to judge from its first fruit, they have triumphantly succeeded, and the publishers also deserve every credit for their courage and long-term commitment in bringing this venture to the public.

Robert W. Cahn
Department of Materials Science & Metallurgy
Cambridge University (UK)

Organic Conductors, Fibers, Thin Films...

One-Dimensional Conductors. (Springer Series in Solid State Science 72.) By *S. Kagoshima, H. Nagasawa* and *T. Sambongi*. Springer-Verlag Berlin 1988. xii, 235 pp., hard cover, DM 99.—ISBN 3-540-18154-7

This volume is a very good introduction to the physics and electronic properties of one-dimensional conductors. After a brief introduction describing the features of one-dimensional conductors the basic theoretical aspects of a one-dimensional electron system are explained. Thus the important concepts of the one-dimensional conduction band, the Peierls instability and transition, the electron-phonon coupling and Kohn anomaly, the nesting of the Fermi surface, charge density waves, fluctuations in one dimension, and the role of the Coulomb interaction are described and discussed. In addition, a comparison of the conditions in two and three dimensions is made. This chapter serves as an excellent introduction to the field for graduate and undergraduate students of physics and chemistry, as well as for researchers in other fields of solid state physics.

In Chapters III to VII the chemical and physical properties of typical one-dimensional conductors are reviewed. The review starts with TTF-TCNQ and related materials, giving a reasonably complete survey of their properties, starting with crystal growth, followed by the electrical and magnetic properties and the behavior of the charge density wave. This part is important because it was in crystals of TTF-TCNQ that more or less all the typical one-dimensional phenomena were first experimentally observed. In addition, this chapter contains descriptions of the properties of some other TTF salts, as well as of the Bechgaard salts $(TMTSF)_2X$. For the latter in particular the superconducting properties of the $(TMTSF)_2PF_6$ and $(TMTSF)_2AsF_6$ salts under pressure are explained. The superconductivity at ambient pressure in $(TMTSF)_2ClO_4$ is mentioned only briefly, and the properties of the many important BEDT-TTF radical salts discovered since 1982 are discussed only on one page, giving some cause for criticism. The original text was written in 1981 in Japan and printed there in 1982. The review on the various materials is therefore more or less complete up to 1980. In the preface the authors mention that in rewriting the volume for the Springer Series in Solid State Science they revised the contents and updated each chapter in the light of recent developments in this field. The updating of all the chapters is, however, by far too short and incomplete, so that in all cases the newest ideas and developments in the field are more or less lacking. In this sense the contents of the volume unfortunately do not represent the "state of the art".

In Chapters IV and V the properties of the inorganic materials MX_3 ($NbSe_3$, TaS_3, $TaSe_3$ etc.) and of the Krogmann salts KCP are described, with an emphasis on the important concept of charge density waves. The optical and magnetic properties, as well as some structural aspects of one-dimensional systems, are also discussed with an account of some experimental results. In the next very short chapter the properties of the linear chain polymers $(CH)_x$ and $(SN)_x$ are presented. Here again the latest experimental results and theoretical ideas on polyacetylene are missing, but the reader is certainly introduced to the problems, and especially to the concept of solitons in polymers. In the last chapter the synthesis, structure, conductivity and superconductivity of the linear chain mercury compounds are discussed.

Despite some criticism, mainly regarding the scant coverage of experimental results since 1980, the volume certainly achieves its aim of providing an introduction to the field of one-dimensional conductors, and it was high time that such a survey was written.

Dieter Schweitzer
Max-Planck-Institut für Medizinische Forschung
Heidelberg (FRG)

Graphite Fibers and Filaments. Springer Series in Materials Science, Vol. 5. By *M. S. Dresselhaus, G. Dresselhaus, K. Sugihara, I. L. Spain* and *H. A. Goldberg*. Springer, Berlin/Heidelberg 1988. x, 382 pp., hard cover, DM 122.00.—ISBN 3-540-18938-6

News of the publication of "Graphite Fibers and Filaments" might lead one to ask whether it is really necessary or desirable to add yet another volume to the already existing monographs and review articles on carbon fibers. However, after looking more closely through the contents of this book one can answer yes to the question. One important reason is the topicality of this progress report, as the whole field is certainly still undergoing rapid development; an additional reason of even more crucial importance is that the book concentrates on the physical properties of the fibers.

The idea of writing this book arose at a specialist conference, and the names of the team of authors, from MIT, Colorado State University and Hoechst Celanese, were a guarantee that the material would be competently covered. In doing so the authors have not hesitated to include their original contributions to fill gaps in the literature that became apparent.

Following a brief description of the existing types of fibers, their manufacture is treated in the second chapter. The synthesis of the types of carbon fibers derived from rayon, polyacrylonitrile and mesophase pitch as precursors is briefly covered. More space is given to the preparation and the mechanism of growth of carbon filaments produced by

thermal decomposition of hydrocarbons in the presence of metallic catalysts, the so-called CCVD (catalytic chemical vapor-deposited) filaments.

In the chapter "Structure" a basis is laid down for all the discussions that follow concerning the properties of the fibers. Starting from the crystal structure of graphite and the structural defects that are observed, the different types of filaments with partially graphitic structure are described, as well as highly disordered fibers. The picture thus developed is supported by results from X-ray diffraction, small angle scattering and electron microscopy.

The chapter "Lattice Properties" begins with a description of the lattice dynamics of single crystal graphite and the related elastic constants, and goes on to develop models for the fibers, taking into account the effects of defects. Techniques for structural characterization are described, in particular Raman spectroscopy which provides a sensitive method for non-destructive analysis of the spatial distribution of lattice disorder in carbon fibers.

After the preparatory treatment of fundamentals, the central theme of the book is reached, namely the thermal, mechanical, electronic, magnetic and high-temperature properties of carbon fibers (138 pp.). The anomalous temperature dependence of the in-plane lattice constants and the corresponding temperature dependence of the thermal expansion coefficient are taken as a basis for understanding the experimental behavior of fibers from different sources. The mechanical properties are of crucial importance for technological applications. Although the theoretical tensile strength and elastic modulus of an ideal graphite lattice are not fully realized in practice, the strength-to-mass ratios of fibers and fiber-resin composites are superior to those of metals. The degree of orientation, nature of defects, stacking arrangement of the fibrils, and uniformity of stress within the fiber influence the models and are shown to determine the experimental properties of the technical fibers.

The high degree of ordering in CCVD fibers ensures that, in every chapter of the book, this type is given preferential treatment compared with the fibers based on pitch and polyacrylonitrile which are currently used in engineering applications. The authors expect the production costs of vapor-grown fibers to fall to comparable levels in the future, with market penetration into all areas of application where the short fiber length is adequate.

Special chapters are devoted to intercalation and ion implantation. The intercalation reaction starts at the free ends of the fibers and is facilitated by a high degree of structural order, so here again vapor-grown fibers dominate the discussion. The applications of fibers and composites receive only a condensed treatment in the last chapter (35 pp.).

Of the 500 literature references listed, a large proportion are for the years 1984 to 1987. The detailed subject index (22 pp.) greatly facilitates using the book as a work of reference. However, it would have been desirable to include a summary of the numerical properties of fibers and filaments made by different processes and after-treatments in the form of an appendix table. This well produced book can be recommended without reservation, and has the potential to become a standard work on the physical properties of carbon fibers, especially if the authors are also prepared to take on the job of updating the treatment in the future.

Ferdinand von Sturm
Biberbach (FRG)

Thin Liquid Films. Edited by *I. B. Ivanov*. Marcel Dekker Inc, New York 1988. 1160 pp., bound, US $ 295.— ISBN 0-8247-7763-8

The editor has undertaken the tremendous task of bringing together 23 leading experts in the field of liquid films, to contribute to this volume which is intended to cover comprehensively and systematically the major aspects of this rapidly developing field.

Thin liquid films are very important in many technological and biological areas such as oil recovery, coating, the etching or protection of microelectronic elements and cell communication in biology, but these subjects are not covered by this book. Instead it considers basic principles and processes, and there is definitely a need for a well-founded collection and critical evaluation of the status of research in this fundamental area.

The book is organized into 15 chapters with the first six arranged in a logical way whereas the others are important but could partly be presented in a different order. At the beginning there are two chapters on thermodynamics followed by one on the statistical mechanics of inhomogeneous films. Then van der Waals interactions, electrostatic interactions and steric interactions are analyzed and described in consecutive chapters. Very important for the theoretical understanding are the problems of drainage and hydrodynamic stability and this is presumably the reason why these specialized areas are presented following the fundamental theory.

Then a separate chapter is devoted to quasielastic light scattering from liquid films, because this technique shows great promise in the study of dynamic properties. The coalescence of dispersions is then considered theoretically for various practical situations and the results are compared extensively with experimental data. The same holds for the chapter on equilibrium properties of free films and the stability of foams and emulsions. The section on interfacial rheological properties of surfactant films then presents experimental data and briefly relates them with theoretical models.

The next chapter then considers ordering processes and forces in liquid crystalline films, comparing theory and experiment. A long chapter on black lipid membranes then mostly concentrates on electrochemical and photochemical studies displaying relevant theories and drawing many conclusions about biological processes (bioenergetics and physiology). In the final chapter the electrical breakdown of bilayer lipid membranes is analyzed theoretically. This process

has been of high theoretical interest for years but is also of biological relevance for processes like cell fusion.

The editor has managed to smoothly connect these chapters avoiding much duplication of information from the different contributors. The contributions are very thoroughly written and edited, and the illustrations are well conceived. The book contains numerous important references which are complete up to about 1984 but are fewer in number for the following years, depending on the subject and on the insight of the corresponding authors into recent literature.

The book is highly recommended for those scientists looking for a detailed, in depth treatment and understanding of the principal mechanisms since theoretical questions are discussed exhaustively. It contains extended and critical reviews of specialized topics and is thus very valuable. However, I do not think that the book will find a broad readership, despite the fact that the field is expanding: It contains more than 1100 pages and is too demanding for the student or non-expert. Thus, I am afraid it will not contribute as much as intended to a cross-disciplinary discussion.

In criticizing the large volume of the book it is very daring to list subjects which I had wished to be included. However, since in my view progress in the field has to a large extend been due to the availability of new characterization techniques there should have been one contribution on these new methods. Examples of these techniques are evanescent wave techniques applied in optical and Raman spectroscopy or in X-ray and neutron scattering, and nonlinear optical techniques and IR spectroscopy which are useful in the study of the structure of liquid films. Various classical techniques like optical microscopy have gained new importance through developments of affordable image analysis systems. There are also several groups involved in computer simulations of the behavior of surfactants at interfaces and these studies, started in the last decade, will gain considerable value in the near future. These things are unfortunately not mentioned in the book. Despite these deficiencies, this is a very important work for those wanting to specialize in some aspects and for those that need an in depth coverage of thin films but I am skeptical, despite personal wishes, that it will find a broad readership.

Helmuth Möhwald
Institut für Physikalische Chemie
der Universität Mainz (FRG)

Inorganic and Organometallic Polymers (ACS Symposium Series 360). Edited by *M. Zeldin, K. J. Wynne* and *H. R. Allcock*. American Chemical Society, Washington 1988. xii, 512 pp., bound, US $ 119.95.—ISBN 0-8412-1442-5

This book reviews the field of inorganic-organic polymers—polysilanes, polysilazanes, polysiloxanes, polyphosphazene, boron-containing polymers and other related polymers—both from a fundamental point of view and with regard to their uses in advanced materials (if such a distinction is still necessary). Such a book was needed since this field is in rapid development. The origin of the book was a symposium held on this topic in Denver in April 1987, which accounts for the very large number of authors involved. A serious effort seems to have been made to avoid the inconsistancies and overlapping inherent in this type of publication. The scientific content is of high quality throughout the book, the presentation is well harmonized, and the indexes (authors, affiliation, subject) are useful guidelines for finding the topics of interest. Only a few typographical errors have been noticed. The drawings are of good quality and accompanied by explicit captions. The book is divided into seven sections, with special emphasis on the chemistry of polysilanes.

A brief preface and an introduction are given before the various fields are reviewed. The part devoted to polysilanes and polycarbosilanes constitutes one fourth of the book. It is justified by the high level of activity on this topic. The historical parts of most chapters overlap each other and, more than once, the chemical pathways shown and the types of synthesis described are repeated. Apart from these minor points, this section is well documented and presented and very informative. It should be read by anyone who intends to begin work in this area. It is also very useful for the specialist who wants to find fairly recent references in this burgeoning field. *F. S. Kipping* is usefully cited as the grandfather of this organosilicon chemistry. This was necessary since many other pioneers in other disciplines have been forgotten. All aspects of the polysilane field are treated: synthesis, characterization, spectroscopic data (absorption and fluorescence) structures, computational information, new synthetic routes, kinetic experiments and mechanisms.

The second section is related to polysilazanes and also suffers from the overlapping of certain chapters. However, as previously, the quality of each section more than compensates for this minor inconvenience. This part is of appropriate length (40 pages) for as are all the other sections of this book.

The chapter treating polysiloxanes is more conventional, since this field is well documented and most readers are familiar with the chemistry of the siloxane group, the various derivatives which can be formed, and the expected properties of the materials. The amphipathic nature of the polysiloxane derivatives is usefully recalled and related to some specific properties: biocompability, resistance to atomic oxygen, adhesiveness, etc. The chapter devoted to molecular metals is not altogether consistent with the previous sections, and relevant pioneering work is not mentioned. The brief section concerned with chemical routes which avoid the use of elemental silicon for making alkyl silicates would have been better inserted into another chapter.

The section on polyphosphazene is written by leading experts in the field, as are most of the other sections. All the latest developments in this now firmly established field are covered.

The use of sol-gel processes for making materials is usefully treated, with special emphasis on SiO_2 and TiO_2 based

materials. The first of these chapters (*C. J. Brinter* et al.) is a good and simple introduction to the field. The possibility of making new devices (field effect transistors with sensor properties) is briefly, perhaps too briefly, mentioned in the next chapter. The use of TiO_2 films as photoanodes for the decomposition of water is treated in another section (*S. Sakka* et al.). It is regrettable that their potential usefulness is not compared with that of single crystal devices.

The section on boron-containing polymers is more speculative, but an interest in them as precursors to boron-nitrogen oligomers is mentioned (*S. Y. Shaw*) and the postulated mechanisms involved in the fabrication of preceramics are described (*K. J. Panorek* et al.).

Finally, a few miscellaneous metal and metalloid containing polymers are treated in the final section: metallo-tetraphenylporphyrins, poly(trisbipyridine) metal complexes, oligomeric organotin compounds, etc.

In conclusion, this book will very probably serve both as a reference book for readers familiar with this area, and as an introduction for engineers wishing to acquire a basic knowledge in this important field.

Jacques Simon
École Supérieure de Physique
et Chimie Industrielles
Paris (France)

Solid/Liquid Dispersions. Edited by *Th. F. Tadros*. Academic Press, London 1987. xii, 331 pp., bound, £ 25.—ISBN 0-12-682178-X

This book deals with the preparation, stabilization and flocculation of dispersions, and also describes their rheological properties. The material is divided into 13 chapters written by experts in the field as follows:

Chapter 1: Introduction (*T. F. Tadros*). This introductory chapter gives a short overview of the technological importance of dispersions. The reader is referred to the appropriate later chapters for further details, and a few of the results from these chapters are summarized in advance.

Chapter 2: The preparation of solid/liquid dispersions (*D. J. Walbridge*). This chapter is concerned with the preparation and stabilization of dispersions. Methods for preparing both polymeric latexes and inorganic colloids, by means of precipitation reactions or by comminution of large particles, are discussed. The basic principles of dispersing agents for aqueous and non-aqueous systems are described.

Chapter 3: The structure of the liquid/solid interface and the electrical double layer (*J. Lyklema*). This chapter deals mainly with the electrical double layer at interfaces between solid bodies and liquid media.

Chapter 4: The stability of solid/liquid dispersions (*B. H.-Bijsterbosch*). This chapter is concerned with the DVLO theory, repulsive and attractive interactions between two particles, and the kinetic aspects of coagulation.

Chapter 5: Adsorption of surface-active agents at the solid/liquid interface (*E. Aveyard*). In this chapter the adsorption of surface-active agents at interfaces between solids and liquids is discussed. In particular the importance of the role played by the surface electrical charge on the particles is considered in more detail.

Chapter 6: Adsorption of polymers at the solid/liquid interface (*T. Cosgrove*). This chapter is concerned with the adsorption of polymers at the interfaces between solids and liquids. The discussion here deals mainly with the conformations of the polymers and the thickness of the adsorbed layer.

Chapter 7: The stability of solid/liquid dispersions in the presence of polymers (*B. Vincent*). In this chapter the author emphasizes the effects of adsorption on the aggregation of the dispersed particles and on the stability of dispersions.

Chapter 8: Flocculation by polymers and polyelectrolytes (*J. Gregory*). This chapter is devoted to the flocculation of dispersions by polymers and polyelectrolytes, including also a brief discussion of the thermodynamics and kinetics of flocculation.

Chapter 9: The properties of concentrated dispersions (*R. H. Ottewill*). In this chapter the author briefly describes how, on the basis of small angle neutron scattering studies, information can be obtained about the structures of concentrated dispersions; the relationship between the structure and the shear modulus of the system is also discussed.

Chapter 10: Rheology of colloidal dispersions (*J. W. Goodwin*). This chapter deals with the fundamentals of the rheological behavior of concentrated dispersions. A short overview of the various rheological phenomena is given. In addition the various measurement techniques used for characterizing the rheological behavior of concentrated dispersions are discussed in more detail.

Chapter 11: The sedimentation of suspensions and methods for preventing the formation of dilatant sediments (*T. F. Tadros*). This chapter deals with the sedimentation of dispersions and the formation or avoidance of sediments.

Chapter 12: The use of spectroscopic pK_a probes for determining electrostatic boundary potentials (*T. W. Healy, B. Lovelock* and *F. Grieser*). The specialized title of this chapter sets it aside from the pattern of the preceding chapters. The authors here describe how spectroscopic probes can be used to determine electrostatic boundary potentials.

Chapter 13: Summary of the properties of suspensions (*T. F. Tadros*). In this final chapter the editor summarizes the topics covered in the preceding chapters, drawing together the various macroscopic properties of dispersions.

In almost all the chapters the treatment is virtually limited to presenting the theoretical basis for the processes and phenomena described. These basic principles are often only supported by schematic diagrams. Only in comparatively rare cases is the opportunity taken to illustrate the theory by giving actual experimental results. The book is especially suitable for anyone wishing to begin work in the area of dispersions. The chapters are written clearly and simply; they do not break any new ground, i.e. almost everything

contained here can also be found in other textbooks of colloid chemistry or electrochemistry. Nevertheless, it is useful to have these fundamentals, which are essential to the theoretical understanding of dispersions, collected together in a compact form, and the book fulfills this requirement to a large extent. There is a small disadvantage arising from the fact that the individual chapters have been written by different authors; this means that one often finds repetitions of material which is not strictly necessary for the understanding of the discussion.

Heinz Hoffmann
Physikalische Chemie I
Universität Bayreuth (FRG)

Conference Calendar

May 1989

16–19 **Materials Science and Technology**
Annu. Mtg. Dtsch. Gesellsch. Metallkd.
Karlsruhe (Fed. Rep. Germany)
Contact: Dtsch. Gesellsch. Metallkd., Adenauerallee 21, D-6370 Oberursel, FRG

16–19 **Rare-Earth Magnets and Their Applications**
10th Int. Workshop
Kyoto (Japan)
Contact: Dr. C. Herget, Sparte Anorg. Chemie, Th. Goldschmidt AG, P.O. Box 101461, D-4300 Essen 1, FRG

22–23 **Biosensors**
Int. Workshop
Braunschweig-Stöckheim (Fed. Rep. Germany)
Contact: Prof. R. Schmid, GBF–Bereich ETN, Mascheroder Weg 1, D-3300 Braunschweig, FRG

22–24 **Sol-Gel-Glasses**
52nd WE-Heraeus-Seminar
Bad Honnef (Fed. Rep. Germany)
Contact: Dr. V. Schäfer, WE-Heraeus-Stift., Heraeusstr. 12–14, D-6450 Hanau, FRG

22–24 **Materials Analysis**
Vienna (Austria)
Contact: Prof. Dr. M. Grasserbauer, Inst. für Analytische Chem. der Techn. Univ. Wien, Getreidemarkt 9, A-1060 Wien, Austria

22–24 **Glass Technology**
Stuttgart (Fed. Rep. Germany)
Contact: Dtsch. Glastechn. Gesellsch., Mendelssohnstr. 75–77, D-6000 Frankfurt am Main, FRG



22–24 **Reinforced Plastics**
Int. Conf.
Mainz (Fed. Rep. Germany)
Contact: Dr. J.-P. Schik, Arbeitsgemeinschaft Verstärkte Kunststoffe, Am Hauptbahnhof 12, D-6000 Frankfurt am Main, FRG, Tel. (069) 27105-34, Fax (069) 232799

22–25 **Clustering and Aggregated State of Matter**
Strasbourg (France)
Contact: Prof. E. Constantin, Groupe de Recherche de Spectrométrie de Masse Interlab., Dept. de Chim., 1 rue Blaise Pascal, 67008 Strasbourg Cedex, France

22–25 **Graphite Intercalation Compounds**
5th Int. Symp. (ISGIC-5)
Berlin (West)
Contact: Dr. F. W. Froben, Fachbereich Physik, Freie Univ. Berlin, Arnimallee 14, D-1000 Berlin 33

23–25 **High-T_c Superconductivity**
Workshop
Alabama (USA)
Contact: Dr. F. Madarasz, Center for Appl. Optics, Univ. of Alabama, Huntsville, AL 35899, USA, Tel. 205/895-6030, Fax 205/895-6618

24–26 **Stabilization and Controlled Degradation of Polymers**
11th Int. Conf.
Lucerne (Switzerland)
Contact: Dr. A. V. Patsis, Inst. in Materials Sci, State Univ. of New York, New Paltz, NY 12561, USA

25–26 **Quantitative Methods in Assessment of Structural Defects**
Kansas City (USA)
Contact: A. P. Berens, Univ. of Dayton, Research Inst., 300 College Park Ave., Dayton, OH 45469, USA

29–30 **TriboCeram 89**
2. Fachsymp.
Frankfurt (Fed. Rep. Germany)
Contact: TCI Techn. + Kommunik. Verlags-GmbH, Tagungssekretariat, Ritterfelddamm 82 h + i, 1000 Berlin 22, Tel. 030/3653640, Fax 030/3658840

29–31 **Cross-linked Polymers**
3rd Int. Conf.
Lucerne (Switzerland)
Contact: Dr. A. V. Patsis, Inst. in Materials Sci., State Univ. of New York, New Paltz, NY 12561, USA

30–2 **E-MRS Spring Mtg.**
Strasbourg (France)
Contact: P. Siffert, Ctr. de Recherches Nucléaire, Lab. PHASE, F-67037 Strasbourg, Cedex, France

31–2 **Applied Surface Analysis**
11th Symp.
Cleveland (USA)
Contact: J. Grant, Research Inst., 300 College Park, Dayton, OH 45469-0001, USA

31–2 **Thermogravimetry and Thermal Engineering**
6th Biennial Conf.
Budapest (Hungary)
Contact: I. Benko, MATE, House of Technol. III 318, P.O. Box 451, H-1372 Budapest, Hungary

June 1989

5–6 **Test Methods for Composite Materials**
Seminar
Basel (Switzerland)
Contact: Technomic Publishing AG, Elisabethenstr. 15, CH-4051 Basel, Switzerland, Tel. 061/237011, Fax 061/233978

5–7 **CONIMAT' 89**
1st Int. Convention for the Technology Transfer of New Materials
Strasbourg (France)
Contact: Adhesion Et Associes–CONIMAT', 9, rue de L'Ancienne Mairie, 92100 Boulogne, France, Tel. 48252604, Fax 46038626

6–9 **Chemistry of Functional Dyes**
Int. Symp. (ESTech '89)
Osaka (Japan)
Contact: Prof. T. Kitao, General Secretary of the Symp., Kinki Chem. Soc., Japan 1-8-4, Utsubo honmachi, Nishi-ku, Osaka 550, Japan

7–8 **Micromechanical Analysis of Composite Materials**
Seminar
Basel (Switzerland)
Contact: Technomic Publishing AG, Elisabethenstr. 15, CH-4051 Basel, Switzerland, Tel. 061/237011, Fax 061/233978

7–9 **Hot Isostatic Pressing**
2nd Int. Conf.
Gaithersburg (MD, USA)
Contact: Robert Schaefer, A 153 Materials Building, NIST, Gaithersburg, MD 20899, USA

12–15 **Narrow-Gap Semiconductors and Related Materials**
Int. Conf.
Ogunquit (USA)
Contact: D. G. Seiler, Phys. Dept., Univ. of North Texas, P.O. Box 5368, Denton, TX 76203, USA

12–16 **Advanced Materials Chemistry Conf.**
St. Augustine (FL, USA)
Contact: Prof. R. S. Drago, Dept. of Chem., Univ. of Florida, Gainesville, FL 32611, USA

13–14 **Nonlinear Optical Polymers for Soldier Survivability**
Science Symp.
Natick (USA)
Contact: Th. Sklarsky, US Army Natick RD + E Center, Attn: STRNC-EMP, Natick, MA 01760-5014, USA, Tel. 508-651-4687

18–21 **Colloid & Surface Science**
63rd ACS Div. of Colloid & Surface Chem. Symp.
Seattle (USA)
Contact: J. Berg, Dept. of Chemical Eng. BF-10, Univ. of Washington, Seattle, WA 98105, USA

18–23 **Ceramic Materials and Production Methods**
1st Conf. of the Eur. Ceramic Soc. and Fair
Maastricht (Netherlands)
Contact: Mrs. L. M. J. Bos, P.O. Box 1630, 6201 BP Maastricht, Netherlands

19–21 **Composites**
Asia-Pacific 89
Adelaide (Australia)
Contact: The Secretariat, Techsearch, Composites Asia-Pacific '89, P.O. Box 2471, Adelaide S.A. 5001, Australia

20–22 **SAMPE**
3rd Int. Electronics Conf.
Los Angeles (USA)
Contact: M. Smith, Business Director, SAMPE, P.O. Box 2459, Covina, CA 91722, USA, Tel. 818-331-0616

21–23 **Chemically Modified Surfaces**
Midland (USA)
Contact: W. T. Collins, Dow Corning Corp., Mail Stop C41C00, Midland, MI 48686, USA

21–23 **Electronic Materials**
Cambridge (USA)
Contact: The Metallurgical Soc., 420 Commonwealth Dr., Warrendale, PA 15086, USA

22–25 **Optics Asia '89**
Singapore (Singapore)
Contact: Asia '89, 994 Bendemeer Rd., N° 04-03, Singapore 1233, Singapore

25–29 **Composite Materials for High Temperature, Fundamental Principles and Performance**
Jerusalem (Israel)
Contact: Mrs. S. Cahana, Ministry of Sci. and Developm., P.O. Box 18195, 91181 Jerusalem, Israel

25–30 **Solid State Sensors and Actuators (Transducers-5)/ Eurosensors III**
Montreux (Switzerland)
Contact: COMST S.A., P.O. Box 415, CH-1001 Lausanne 1, Switzerland

26–28 **Molecular Design of Functional Polymers**
IUPAC Int. Symp.
Seoul (Korea)
Contact: IUPAC Int. Symp., c/o Polymer Soc. of Korea, Rm. 601, Hyecheon Bldg., 831 Yeoksam-dong, Kangnam-ku, Seoul 135-792, Korea

26–28 **Coherence and Quantum Optics**
Conf.
Rochester (USA)
Contact: L. Mandel, Univ. of Rochester, Dept. of Physics, Rochester, NY 14627, USA, Tel. 716-275-4361

26–30 **Solid State Chemistry**
2nd Int. Symp.
Pardubice (Czechoslovakia)
Contact: Dr. L. Koudelka, Inst. of Chem. Technol., Leninovo nam., 565, CS-53210 Pardubice, Czechoslovakia

Materials Related Gordon Research Conferences

General Information

Contact: Dr. A. M. Cruickshank, Director, Gordon Research Conf., Gordon Res. Ctr., Univ. of Rhode Island, Kingston, RI 02881-0801, USA
Locations: Colby-Sawyer College (N), (S): New London, NH;
New Hampton School: New Hampton, NH;
Kimball Union Academy: Meriden, NH;
Tilton School: Tilton, NH

June 1989

19–23 **Catalysis**
Colby-Sawyer College (N)
Chairman: L. D. Schmidt

26–30 **Polymers**
Colby-Sawyer College (N)
Chairman: J. P. Kennedy

July 1989

3–7 **Fiber Science**
Colby-Sawyer College (N)
Chairman: B. C. Goswami

3–7 **Thermosetting Polymers**
Colby-Sawyer College (S)
Chairman: N. J. Johnston

10–14 **Elastomers**
Colby-Sawyer College (N)
Chairman: G. Ver Strate

10–14 **Metal Hydrides**
Tilton School
Chairman: F. D. Manchester

17–21 **Corrosion**
Colby-Sawyer College (N)
Chairman: H. J. Grabke

17–21 **Chemistry at Interfaces**
Kimball Union Academy
Chairman: R. Johnson

17–21 **Superconducting Films**
Tilton School
Chairman: D. Gubser

31–4 **Ion-Containing Polymers**
Colby-Sawyer College (S)
Chairman: G. Wilkes

August 1989

7–11 **Physical Metallurgy**
Tilton School
Chairman: J. C. Williams

14–18 **Studies in Solid-State Ceramics**
Colby-Sawyer College
Chairman: U. Chowdhry

14–18 **Science of Adhesion**
New Hampton School
Chairman: R. A. Pike

26–30 **Supermembranes**
Trieste (Italy)
Contact: Int. Ctr. for Theoretical Physics, P.O. Box 586, I-34100 Trieste, Italy

27–28 **Polymer Latex III**
London (United Kingdom)
Contact: Miss M. Peacock, Plastics and Rubber Inst., 11 Hobart Place, London SW1W 0HL, UK

28–30 **Chemically Modified Oxide Surfaces**
Midland (USA)
Contact: W. T. Collins, Mail Stop C41C00, Dow Corning Corp., Midland, MI 48686-0994, USA

July 1989

2–7 **Solid State Organic Materials**
9th Int. Conf.
Como (Italy)
Contact: Centro di Cultura Scientifica, "A. Volta", Villa Olmo, Via Cantoni 1, I-22100 Como, Italy

3–6 **Conduction and Breakdown in Solid Dielectrics**
3rd Int. Conf. (ICSD '89)
Trondheim (Norway)
Contact: Prof. Sletbak, ICSD '89, The Norwegian Inst. of Technol., Sem Sælands V 13, N-7034 Trondheim, Norway

3–7 **Martensitic Transformations**
Int. Conf. ICOMAT-89
Sydney (Australia)
Contact: N. Kennon, Dept. of Metallurgy and Materials Eng., Univ. of Wollongong, Wollongong, NSW 2500, Australia

3–8 **Light-Sensitive and Conducting Polymers**
Leipzig (German Dem. Rep.)
Contact: Prof. H. K. Roth, TH Leipzig, Sekt. Naturwissenschaften, P.O. Box 66, DDR-7030 Leipzig, GDR

3–28 **Liquids, Freezing and the Glass Transition**
NATO Adv. Study Inst.
Les Houches (France)
Contact: École d'Été de Physique Théorique, F-74310 Les Houches, France

4–7 **Nonlinear and Electro-Optics**
Int. Conf.
Cambridge (United Kingdom)
Contact: The Meetings Officer, The Inst. of Physics, 47 Belgrave Square, London SW1X 8QX, UK

9–14 **Scanning Tunneling Microscopy/Spectroscopy**
4th Int. Conf.
Oarai (Japan)
Contact: O. Nishikawa, The Graduate School of Nagatsuta, Tokyo Inst. of Technol., 4259 Nagatsuta, Midori-ku, Yokohama 227, Japan

9–14 **Zeolites**
8th Int. Conf.
Amsterdam (Netherlands)
Contact: M. Laboushere, 792 Keizersgracht, 1017 EC, Amsterdam, The Netherlands

10 **Bonding and Repair of Composite Materials**
Birmingham (United Kingdom)
Contact: John Herriot, Butterworth, P.O. Box 63, Westbury House, Bury St., Guildford GU2 5BH, UK

10–12 **Appl. Organomet. Chem.: an Entry to the New Technology**
The Pines Resort (Australia)
Contact: Dr. A. F. Masters, School of Chemistry, Univ. of Sydney, Sydney, N.S.W. 2006, Australia

10–13 **Magnetic Resonance in Polymers**
9th Spec. Colloq. Ámpere
Prague (Czechoslovakia)
Contact: P. M. M. Secretariat, c/o. Inst. of Macromol. Chem., Czech. Acad. of Sci., 16206 Prague, Czechoslovakia

10–14 **Ion Sources**
Int. Conf.
Berkeley (USA)
Contact: W. O'Connor, Lawrence Berkeley Lab., 50B-2270, Berkeley, CA 94720, USA, Tel. 415-486-6386, Fax 415-486-7000

10–14 **Electron Spectroscopy**
4th Int. Conf.
Honolulu (USA)
Contact: G. E. McGuire, Microelectronics Ctr. of North Carolina, P.O. Box 12889, Research Triangle Park, NC 27709, USA

10–14 **Organic Coatings Science and Technology**
15th Int. Conf.
Athens (Greece)
Contact: Dr. A. V. Patsis, Inst. in Materials Sci., State Univ. of New York, New Paltz, NY 12561, USA

11–14 **Numerical Analysis of Semiconductor Devices and Integrated Circuits**
6th Int. Conf.
Dublin (Ireland)
Contact: J. J. H. Miller, Nase-Code Conf., INCA, P.O. Box 2, Dún Laoghaire, Ireland

12–14 **Solid-State Laser/Optical Fiber Science and Electromagnetic Theory '89**
Top. Mtg./Sino-Japanese Joint Mtg.
Beijing (People's Rep. China)
Contact: Optical Soc. of America (OSA), 1816 Jefferson Pl. NW, Washington, DC 20036, USA

16–21 **Catalysis**
Eur. Conf.
Berlin (West)
Contact: Prof. G. Ertl, Fritz-Haber-Inst. der Max-Planck-Gesellsch., Faradayweg 4–6, D-1000 Berlin

17–20 **Polymer Blends**
Prague (Czechoslovakia)
Contact: P. M. M. Secretariat, c/o. Inst. of Macromol. Chem., Czech. Acad. of Sci., 16206 Prague, Czechoslovakia

18–20 **Polymer Chemistry: Aspects of Radical Polymerization**
Lancaster (United Kingdom)
Contact: Dr. J. R. Ebdon, Dept. of Chemistry, Univ. of Lancaster, Lancaster LA1 4YA, UK

18–21 **Integrated Optics and Optical Fiber Communications**
7th Int. Conf. (IOOC-7)
Kobe (Japan)
Contact: P. W. Shumate, Jr., Bell Communications Research, 435 S St., Morristown, NJ 07960, USA

23–24 **Computer-Aided Materials Characterization**
Int. Symp.
Charlotte (USA)
Contact: R. Biederman, Worcester Polytechn. Inst., Worcester, MA 01609, USA, Tel. 508-831-5453/5346

23–28 **Materials and Mechanisms of Superconductivity: High-T_c Superconductors**
Int. Conf. (HTSC-M^{2}S)
Stanford (USA)
Contact: Dr. T. H. Geballe, Dept. of Applied Phys., Stanford Univ., Stanford, CA 94305, USA

24–26 **Micro-Optics/Gradient-Index Optical Imaging Systems**
2nd Conf./8th Top. Mtg.
Tokyo (Japan)
Contact: K. Iga, Tokyo Inst. of Technol., Research Lab. of Precision Machinery and Electronics, 4259 Nagasuta, Midori-ku, Yokohama 227, Japan

24–26 **Composite Structures**
5th Int. Conf.
Paisley (United Kingdom)
Contact: Dr. I. H. Marshall, Dept. of Mechanical and Production Eng., Paisley College of Technol., High St., Paisley PA 12BE, UK

25–26 **Computer-Aided Microscopy and Quality Control**
Int. Conf.
Charlotte (USA)
Contact: J. Braun, EG + G Mound Appl. Technologies, Miamisburg, OH 45343-0987, USA, Tel. 513-865-3829

31–2 **Biologically-Engineered Polymers**
Cambridge (United Kingdom)
Contact: Royal Soc. of Chemistry, Burlington House, London W1V 0BN, UK

31–3 **Photoacoustic and Photothermal Phenomena**
6th Int. Mtg.
Baltimore (USA)
Contact: J. Murphy, Johns Hopkins Appl. Physics Lab., Johns Hopkins Rd., Laurel, MD 20707, USA, Tel. 301-953-6214

August 1989

2–7 **Pure and Applied Chemistry**
32nd IUPAC Congr.
Stockholm (Sweden)
Contact: Stockholm Convention Bureau, P.O. Box 6911, S-10239 Stockholm, Sweden

13–26 **High-T_c Superconductors**
NATO Adv. Study Inst.
Bad Windsheim (Fed. Rep. Germany)
Contact: R. Kossowsky, Applied Res. Lab., Pennsylvania State Univ., P.O. Box 30, State College, PA 16804, USA

14–17 **Shock Compression of Condensed Matter**
APS Top. Conf.
Albuquerque (USA)
Contact: A. Roach, MS-P 915, Los Alamos Nat. Lab., Los Alamos, NM 87545, USA

14–18 **Hopping Transport**
8th Conf.
Chapel Hill (USA)
Contact: M. Pollak, Dept. of Phys., Univ. of California, Riverside, CA 92521, USA

16–18 **Properties Through Processing**
Amherst (USA)
Contact: H. H. Winter, Dept. Chem. Eng., Univ. of Massachusetts, Amherst, MA 01003, USA

20–24 **Imaging Systems—150 Years of Photography**
Int. Symp. (ISIS '89)
Dresden (German Dem. Rep.)
Contact: Conf. Secretary, ISIS '89, Technische Univ. Dresden, Sektion Physik, Wissenschaftsbereich Photophysik, Mommsenstr. 13, DDR-8027 Dresden, GDR

20–25 **Crystal Growth: Progress in Science and Technology**
9th Int. Conf.
Sendai (Japan)
Contact: Prof. T. Nishinaga, Inter Group Corp., Akasaka Yamakatsu Bldg., 8-5-32, Akasaka Minato-ku, Tokyo 107, Japan

21–24 **Amorphous and Liquid Semiconductors**
13th Int. Conf.
Asheville (USA)
Contact: D. E. Sayers, P.O. Box 8202, North Carolina State Univ., Raleigh, NC 27695-8202, USA

21–25 **Phonons 89**
Heidelberg (Fed. Rep. Germany)
Contact: Inst. f. Angew. Physik II, Univ. of Heidelberg, Albert-Überle-Str. 3–5, D-6900 Heidelberg, FRG

21–26 **Photochemistry**
Int. Conf.
Beijing (People's Rep. China)
Contact: Prof. S. Wu, Inst. of Photographic Chem., Academia Sinica, Beijing, People's Rep. China

27–1 **Supramolecular Organic Chemistry and Photochemistry**
Workshop
Saarbrücken (Fed. Rep. Germany)
Contact: Prof. Dr. H.-J. Schneider, FR Organ. Chem., Univ. des Saarlandes, D-6600 Saarbrücken, FRG

28–31 **Dynamical Processes in Excited States of Solids**
7th Int. Conf. (DPC '89)
Athens (USA)
Contact: DPC '89, Prof. J. E. Rives, Dept. of Physics and Astronomy, Univ. of Georgia, Athens, GA 30602, USA

28–1 **Surface Modification Technologies**
3rd Int. Conf.
Neuchatel (Switzerland)
Contact: The Metallurgical Soc., 420 Commonwealth Dr., Warrendale, PA 15086, USA, Tel. 412-776-9050

Registered names, trademarks, etc. used in this journal, even when not marked as such, are not to be considered unprotected by law.

© VCH Verlagsgesellschaft mbH, D-6940 Weinheim, 1989. – Printed in the Federal Republic of Germany by Konrad Triltsch Druck- und Verlagsanstalt Würzburg.

All rights reserved (including those of translation into foreign languages). No part of this issue may be reproduced in any form — by photoprint, microfilm, or any other means — nor transmitted or translated into a machine language without written permission from the publishers. Only single copies of contributions, or parts thereof, may be made for personal use. This journal was carefully produced in all its parts. Nevertheless, authors, editors and publisher do not warrant the information contained therein to be free of errors. Readers are advised to keep in mind that statements, data, illustrations, procedural details or other items may inadvertently be inaccurate.

Valid for users in the USA: The appearance of the code at the bottom of the first page of an article (serial) indicates the copyright owner's consent that copies of the article may be made for personal or internal use, or for the personal or internal use of specific clients. This consent is given on the condition, however, that the copier pay stated per-copy fee through the Copyright Clearance Center, Inc. (CCC), for copying beyond that permitted by Sections 107 or 108 of the U.S. Copyright Law. This consent does not extend to other kinds of copying, such as copying, for general distribution, for advertising or promotional purposes, for creating new collective works, or for resale. For copying from back volumes of this journal see 'Permissions to Photo-Copy: Publisher's Fee List' of the CCC.

Editorial office: Postfach 10 11 61, D-6490 Weinheim, Federal Republic of Germany, Telephone (06201) 60 22 55, Telex 465 516 vchwh d, Telefax (06201) 602 328.

Editor: *Peter Gölitz*

Associate Editor: *Peter Gregory*

Publishers: VCH Verlagsgesellschaft mbH. (Managing Director: *Hans Dirk Köhler*), Pappelallee 3, D-6940 Weinheim, Federal Republic of Germany.

Advertising office (Advertising Manager *R. J. Roth*): Postfach 10 11 61, D-6940 Weinheim, Federal Republic of Germany, Telephone (0 62 01) 60 61 30, Telex 467 155 vchwh d, Telefax (0 62 01) 606 184.

ANGEWANDTE CHEMIE
International Edition in English
Volume 28 · Number 5
May 1989
Pages 535–676

A Chemical Approach to Protein Design— Template-Assembled Synthetic Proteins (TASP)

By Manfred Mutter* and Stéphane Vuilleumier

In memoriam Emil Thomas Kaiser

Advances in methodology in both chemistry and molecular biology allow us to take a fresh look at protein science. Chemical synthesis of peptides and site-directed mutagenesis are now standard research tools, paving the way for the construction of new proteins with tailor-made structural and functional properties. The decisive hurdle on the way lies not in the synthesis of the molecules proper but rather in a better understanding of the complex folding pathways of polypeptide chains into spatially well-defined structures. Can the chemist use his synthetic tools to *bypass* the notorious "folding problem?" In this article, we present a new approach developed in our laboratory, which opens a chemical route to artificial proteins with predetermined three-dimensional structures, allowing a first step towards the synthesis of new proteins with functional properties.

Synthetic analogs of globular proteins are unknown. The capability of adopting a dense globular configuration stabilized by self-interactions and of transforming reversibly to the random coil are characteristics peculiar to the chain molecules of globular proteins alone.
P. J. Flory[1]

1. Introduction

Over the last few years, vigorous research efforts and advances in peptide and protein synthesis, modification, and analysis have led us to believe that a thorough understanding of the "big questions" of protein chemistry[2, 3] lies within reach. Dealing with the flood of data they are now in a position to produce easily and quickly, chemists and molecular biologists have attempted to pinpoint the molecular determinants of protein folding, structure, and function. Their ultimate ambition is the creation of new proteins ("protein design") with tailor-made structural and functional properties.[4] How distant is this fascinating goal? The purpose of the present article is to give an answer to this question, by reviewing the advances in the field of protein design that have occurred since our last review article.[4] We shall first consider the aspects of protein structure relevant to the design of new proteins and show that the modification of natural proteins by recombinant DNA methods ("protein engineering") and the construction of new polypeptide chains designed to fold in specific ways ("protein de novo design") are complementary and convergent methods that yield valuable insights into the prospects and limitations of protein design. In the second part of this article, we shall

[*] Prof. Dr. M. Mutter[+], Dipl.-Natw. S. Vuilleumier
Institute of Organic Chemistry, University of Basel
St. Johanns-Ring 19, CH-4056 Basel (Switzerland)
[+] Present address:
Institut für Organische Chemie der Freien Universität
Takustrasse 3, D-1000 Berlin 33

 © *VCH Verlagsgesellschaft mbH, D-6940 Weinheim, 1989* *0570-0833/89/0505-0535 $ 02.50/0*

concentrate on a new general approach we have developed for the construction of artificial proteins that relies on the potential of synthetic chemistry, emphasizing the role the chemist may play in the interdisciplinary adventure of protein design.

1.1. Proteins and Chemists

The advent of gene technology[5] has made possible the identification, gene cloning and sequencing, expression, and isolation of virtually any protein. As a result, proteins will play an increasingly important role in tomorrow's pharmaceuticals.[6] Therefore, chemists have shown increasing interest in understanding proteins in molecular and atomic detail.

Protein chemistry has been a challenge for chemists ever since *Emil Fischer* attempted the synthesis of polypeptides[7] into "... the longest possible chain, in order to compare the obtained products with natural proteins ".[8] We now know that natural evolution has been most restrictive in the selection of sequences. For example, in a polypeptide chain of 100 amino acids, the 20 proteinogenic amino acids allow 20^{100} different proteins (a number greater than the estimate of atoms in the universe) to be constructed. Humans, in comparison, possess a mere 10^4-10^5 different genes suited to code for proteins. Sequences, however, are hardly the whole story: natural proteins are unique in the world of polymers in that they adopt a dense, well-defined, globular conformation,[1] an additional and essential feature probably unanticipated by *Fischer*. The same structural type is adopted by many different sequences,[9] but short identical sequences may adopt different conformations in different proteins.[10] Most human-designed polypeptide chains do not fold and present themselves as flexible coils in solution, indicating strict requirements for globularity. This is where the protein designer meets the "famous" folding problem.[11, 12]

1.2. The Protein Knows How to Fold[13]

So have we really learned how the protein does it, as *Edsall* proposed twenty years ago? The classical work of *Anfinsen* and co-workers[14] on ribonuclease A has shown that, for at least some proteins, the amino acid sequence contains the full information needed to determine the correct conformation of the protein and that the protein can be denatured and renatured without loss of enzymatic activity. In other words, the free energy of folding determines the reversible transition between the unfolded and the folded state. However, it is still unclear if thermodynamic stability, as implied above, is the sole determinant of protein conformation. The question whether the global minimum of the conformational energy surface of a polypeptide chain, rather than a local one, is reached upon folding is still an open one. Sampling of all possible chain conformations would take an impossibly long time,[15] implying that kinetics also plays a role in folding. However, this is only valid for the unrealistic case where there are no restrictions by long-range interactions in the conformational space of the chain. Neither kinetic limitations nor metastability need to be assumed to account for the native structure of proteins if the volume of the chain excluded upon folding and the fact that the possible conformations are not all of equal energy are taken into consideration.[16]

1.3. Ball and Chain

The complexity of protein folding has always been a source of encouragement for hypotheses and speculation. It is perhaps sensible, therefore, to summarize what is known about the basics of protein structure.

Natural proteins are linear chains of amino acids linked by amide (peptide) bonds. The amino acid residues along the chain form a sequence, the *primary structure*. The polypeptide chain is intrinsically flexible owing to rotational freedom around the N–C_α and C_α-CO bonds of each amino acid unit, defined by the backbone dihedral angles ϕ and ψ, respectively.[2, 3] Limitations on the range of these rotation angles, and hence on the conformational space of the chain, arise from unfavorable interactions.[17] Even so, the number of possible conformers for a chain of the length of a typical protein is astronomical, since an unfolded ("random coil") polypeptide chain has virtually complete conformational freedom.[18] The native state of a protein is a tightly packed,[19] highly ordered structure. Thus, conformational entropy is a significant term in the energy balance between folded and unfolded states,[16] although the estimation of its magnitude is still very difficult. The important constraints of tight packing give rise to regular structural motifs, called *secondary-structure* elements.[2, 3, 9, 16] The α-helix,[20] β-sheet,[21] and β-turns[22] are well-known examples and some of the aspects relevant to protein design will be discussed in more detail in Section 3.2. These secondary-structure elements are assembled in compact arrangements that constitute the three-dimensional structure of the protein, the *tertiary structure*.

It has been proposed that the folding process follows the logic of protein structural hierarchy. Hydrogen-bonded secondary structures have been thought to act as seeds[23] for folding, since they may form early on and direct rapid and efficient folding. However, experimental study of pathways and structural characterization of folding intermediates,[11, 12, 23] while proving difficult owing to the high cooperativity of the folding transition, point to "nativelike" intermediates. A presently popular model is that the refolding chain rapidly collapses to a compact state where secondary structure is present ("the molten globule"), to then rearrange into the final structure.[24] Significantly, it is still discussed whether or not there is only one folding pathway for a given polypeptide chain.[25]

Finally, it should be emphasized here that the situation in vivo does not have to be that of the test-tube. For example, enzymes have been found which can catalyze disulfide bond rearrangement and peptidyl-prolyl *cis–trans* isomerization,[26] as well as prevent formation of improperly folded structures and assist in refolding.[27]

1.4. The Complex Interplay of Different Energy Contributions Determines Protein Stability

What are, then, the intrinsic factors in the polypeptide chain that stabilize it in a defined three-dimensional confor-

mation? The unfavorable conformational entropy term[16] (see Section 1.3) is compensated for by many different factors in folded proteins (Fig. 1, Table 1).

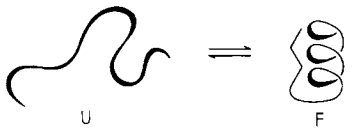


Fig. 1. The energy equation for the folding of a short polypeptide chain into a folding unit. ΔG, the Gibbs free energy of folding, is the sum of enthalpy terms (ΔH) and solvation entropy (ΔS_{solv}) and chain entropy (ΔS_{chain}) terms. The small absolute value of this ΔG originates in the small difference between the energies of the folded (F) and unfolded (U) states (see Table 1). Therefore, an accurate prediction of protein stability is difficult.

$$\Delta G_{F-U} = \Delta H - T\Delta S_{solv} - T\Delta S_{chain}$$

Table 1. An estimation of the various energy contributions which determine protein stability (from [2]).

Energy contributions	ΔG_{F-U} [kcal mol^{-1}]
Conformation entropy	+330 to +1000
Unfavorable interactions in F	+200
Hydrophobic interactions	−264
Van der Waals interactions	−227
Required hydrogen bonds, other	− 49 to −719
Observed ΔG_{F-U}	− 5 to −10

Interactions of the chain with the solvent surroundings cause nonpolar side chains to cluster together in the protein interior, while hydrophilic, charged groups tend to be at the protein surface. This *"hydrophobic interaction"* effect was first predicted and discussed by *Kauzmann*[28] before any protein structure had been solved by X-ray analysis. It has since been intensively studied in terms of the tendency of amino acid derivatives to partition between a polar and an apolar phase[29] and in terms of the contributions of different atom types to solvation free energy of the protein.[30]

The two main secondary-structure types, the α-helix and the β-sheet, are maintained by an extensive *H-bond* network.[2, 3, 9] Most groups capable of hydrogen bonding in proteins appear to be hydrogen-bonded.[31] It is still unclear in what way H-bonds inside a protein are more stable than those between solvent and protein. Whereas the energetic contribution of an isolated H-bond to the overall stability of a protein is probably very small, the cooperative formation of H-bonds most certainly has an important role in protein folding and stability.

The relative importance of *electrostatic forces* depends very much on the estimation of the value of the dielectric constant ε. It is unclear just where and when polarity at the protein surface will be similar to that of water ($\varepsilon \approx 81$) and which ε value best describes the situation inside a given protein (see Ref. [32] for a commentary). *Ion-pair interactions* stabilize tertiary rather than secondary structure and are mostly found at the protein's surface.[33] Dipole interactions[34, 35] have been intensively studied in the case of α-helices. The helix dipole is parallel to the helix axis and points to the N-terminus of the helix, yielding a net partial positive charge at the N-terminus and a net partial negative charge at the C-terminus; this fact has been put forward to explain the occurrence of *antiparallel*, rather than parallel, helical bundles in proteins.

Other forces, such as covalent forces, attractive dispersion forces, and van der Waals repulsion forces,[2, 3] contribute to the energies of both the folded and unfolded state. They may be regarded as less important in influencing the folding in a particular three-dimensional structure, although they have to be taken into account in computations.

The disulfide bond between two cysteines acts as a special structure-stabilizing device. It behaves, in effect, as a *cross-link* which "holds" the structure together. Cross-links constrain the unfolded state to a much smaller collection of conformers, reducing its conformational entropy and making the native state[36, 37] more favorable energetically.

By focusing on the "static" elements of protein structure, we may have created the impression that proteins are rigid, motionless macromolecules. This, naturally, is not true, since flexibility plays an important role at all levels of protein structure and function.[38] A protein may be described as consisting of a collection of substates.[39] There is a whole branch of protein science which is concerned with protein dynamics.[40]

There is one main lesson to be learned from studies on the stability of proteins. The overall energy difference between unfolded and folded states of a protein is *small*[2, 3, 18, 28, 41] (on the order of 5–10 kcal mol^{-1}) in comparison to the total stabilizing and destabilizing energy contributions involved, making protein stability difficult to estimate or calculate.

2. From Structural Prediction to Structure Design

Computations of peptide and protein structure[42] are hampered by numerous pitfalls. Energy minimization of macromolecular systems requires extensive computer time because of the many variables involved. The energy functions in use are still dependent on each researcher's estimation of the relative importance of the different energy terms. This can make comparisons of modeled structures difficult. Moreover, the problem of taking solvent and entropy factors into account in the calculations has, in spite of significant advances,[43] still not been definitely resolved.

Because it is not yet possible to predict the structure from the sequence,[44] we must still rely on more or less elaborate guesswork. This remains an important yet unsatisfactory aspect of protein science. Computers, which have become indispensable to interpret the sequence data produced by gene technology,[45] are now a standard tool in the laboratory. Commercial software packages offering numerous prediction algorithms and "sequence crunching" facilities[46] are available. These semiempirical methods of structure prediction have a long history. The most widely used prediction code is still probably that of *Chou* and *Fasman*,[47] which assigns to each amino acid a probability to be part of an α-helix, β-turn, or β-sheet, based on the statistical analysis of the occurrence of each amino acid in each type of secondary structure of protein X-ray structures known at high-resolution. Other methods include the method of *Garnier* et al.,[48] based on information theory, the statistical mechanical approach of *Tanaka* and *Scheraga*,[49] and methods based on stereochemical considerations. These can range from simple, visual aids such as the helical wheel[50] (Fig. 2) and net[51] representations to the sophisticated set of rules of *Lim*.[52]

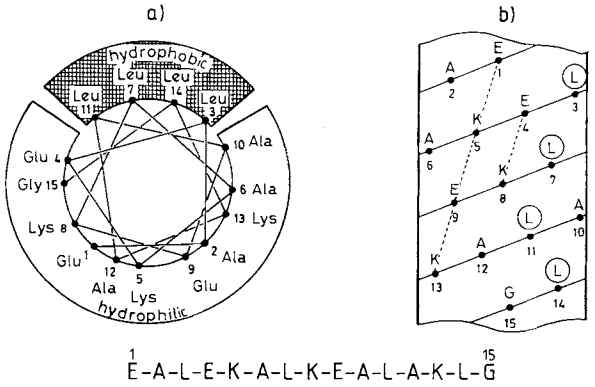


Fig. 2. The helical wheel [50] (a) and net [51] (b) representations, emphasizing amphiphilicity and favorable electrostatic interactions, respectively [35], in the sequence Glu-Ala-Leu-Glu-Lys-Ala-Leu-Lys-Glu-Ala-Leu-Ala-Lys-Leu-Gly [53].

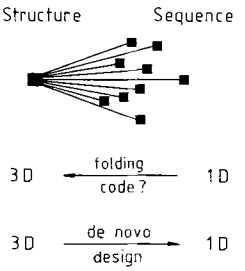


Fig. 4. We are still unable to predict if and how a given polypeptide sequence will fold into a (unique) three-dimensional conformation. In protein de novo design, an opposite approach is taken by trying to find a new sequence (primary structure) which is compatible with an initially chosen three-dimensional structure and folds into this structure under adequate conditions. The rationale for this approach lies in the knowledge, gained from solved X-ray structures, that different polypeptide sequences can have the same structural fold (the "degenerate folding code").

Recently, various combinatorial, pattern-matching approaches have been introduced[54] based on modern computing languages and technology. These bring some improvement at the price of introducing more variables derived from solved X-ray structures. These structural prediction schemes, despite all refinements, have not fared better than 60% in a three-state (α, β, random coil) model.[55] This is because they all rely on sequence (i.e., on local interactions) and cannot take into account the *long-range interactions* that significantly determine the final conformation of a polypeptide chain[44] in the absence of a solved X-ray structure from a related sequence (for detailed recent discussions of structure prediction, see Refs. [54–56]).

In summary, we have to admit that in spite of decades of research on protein folding[11,12] and structure,[2,3,9] our knowledge is not adequate to predict if a given polypeptide sequence will fold and, if so, what its structure will be. We have gained important insights into the rules that determine protein topology (Fig. 3), particularly by X-ray crystallography, and it can be anticipated that the systematic search of data bases will uncover yet more "hidden" motifs of protein structure; however, we still know very little about any rules of folding.[57] Here lies the main obstacle to be overcome on the way to protein design. The fact that an arbitrarily conceived polypeptide sequence will probably have little tendency to fold in a three-dimensional conformation strongly supports this view. This unsatisfactory state of affairs has led to the idea (Fig. 4) of finding all sequences compatible with a given structure (a *"prefolded backbone"*[57]). First expressed in this form by *Drexler*,[58] it has since been given a computational treatment.[59] This development is only one example illustrating the increasing "symbiosis" between biological and computer science. Until now, protein design has very much been the domain of molecular modeling[64] and knowledge-based protein design,[65] and has had the tendency to confine itself to the colorful world of computer screens. Of course, experimental work with the designed molecules will always be necessary to assess the adequacy of our ideas and representations about protein structure and folding.

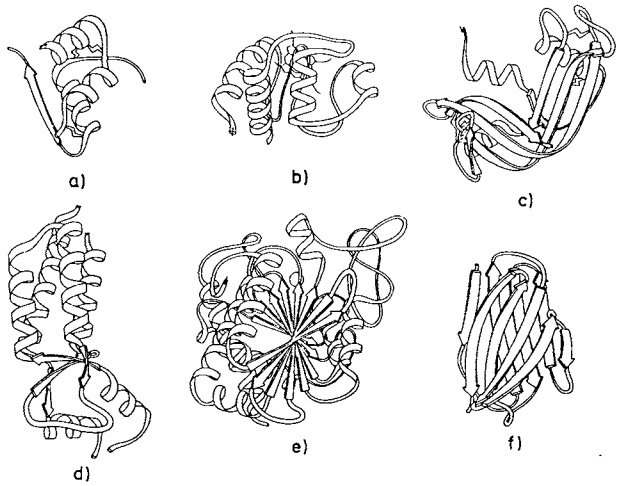


Fig. 3. Examples of protein packing arrangements, as drawn by *J. S. Richardson* [9] based on the solved X-ray structures. a) Insulin (small, disulfide-rich); b) cytochrome C (small, metal-rich); c) ribonuclease A (antiparallel β structure); d) tobacco mosaic virus protein (antiparallel up-and-down α-helix bundle); e) carboxypeptidase (parallel α/β structure); f) immunoglobulin V_L domain (antiparallel β greek key β-barrel structure). The drawings are not on the same scale.

3. Protein Design: A Scientific Challenge with Important Implications

One might ask what sense it makes to redesign what already exists in nature. Has it not always been the ultimate goal of the synthetic chemist to devise and synthesize new molecules with well-defined and interesting properties? Most of all, would the construction of new proteins unknown by nature not show convincingly that we really do understand in some way the complex interplay of primary, secondary, and tertiary structure of natural proteins? From this point of view, the construction of artificial proteins plays a role in protein chemistry similar to that of total synthesis in natural products chemistry.

Apart from the scientifically satisfying goal of being capable of synthesizing new and interesting macromolecules, there is a real need in research and industry for tailor-made molecules that accomplish tasks similar to those of naturally occurring proteins or enzymes, but under different conditions and with different specificities.

Will we succeed in becoming chemical *architects*? In the absence of clear rules which would allow the construction of a building from the ground up (de novo design), it seems

more promising to first transform existing ones (natural proteins) step by step. This is the approach of "protein engineering", which is discussed in Section 3.1 in view of its potential for the construction of new proteins.

3.1. Protein Engineering: Manipulating a Natural Tertiary Structure

Among the tools of genetic engineering,[62] the new technique of site-directed mutagenesis[63] has had an enormous impact in the few years since its introduction (see Ref. [64]). This approach allows one to alter the amino acid sequence of a protein by introducing an appropriately mismatched synthetic oligonucleotide into the protein gene (Fig. 5a). The "non-invasiveness" and selectivity of the technique has decisively expanded the classical approach of chemical modification of proteins.[65] Although unusual for the "traditional" chemist, it constitutes a relatively "safe" approach to protein design, because the starting point is an amino acid sequence

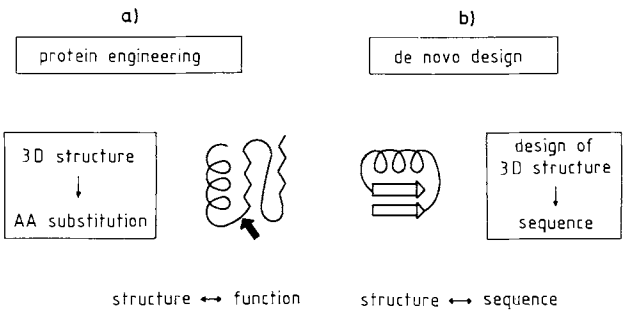


Fig. 5. Protein engineering and de novo design are two convergent approaches for the construction of new proteins. In protein engineering (a), point mutations are made by site-directed mutagenesis in the sequence of a natural protein, allowing for detailed studies on the relationship between sequence, structure, and function (AA = amino acid). In de novo design (b), the target three-dimensional conformation is designed from first principles. Here, the major hurdle is to find a sequence that will fold in the predetermined three-dimensional conformation.

which is *known to fold* in a tertiary structure. On the other hand, only limited modifications may be undertaken if one is to preserve the structural or functional integrity of the system under study. This is a direct consequence of the subtle equilibrium between the folded and unfolded form of a protein (see Section 1.4).

It would be presumptuous to review here the achievements and possibilities of "protein engineering", especially since there is already an excellent introductory monograph on the subject.[66] However, we would like to mention briefly some of the recent achievements which illustrate the potential of the technique in guiding us towards a better understanding of important features of protein stability and folding, a preliminary condition of efficient protein design.

The work dealing with the stabilization of enzymatic catalysts is of direct industrial relevance: T4 lysozyme has been temperature-stabilized by the introduction of a disulfide bond;[37,67] the stability of the protease subtilisin has been improved with respect to oxidation, heat, and alkali,[68] and its substrate specificity has been modified by alteration of steric, hydrophobic, and electrostatic complementarity at the binding site.[68]

Site-directed mutagenesis studies on enzymology classics such as trypsin[69] and carboxypeptidase[70] have caused reassessment and refinement of our description of the catalytic mechanisms involved. For Tyr-tRNA synthetase, site-directed mutagenesis has led to a description of the mechanism of catalysis[71] at a level of detail which could not have been reached before the introduction of this technique.

Site-directed mutagenesis has also afforded new insights into protein structure and folding. Owing to the wealth of data recently published on this subject, we can only mention a few representative examples. It was shown that secondary-structure elements play an important role in the folding and structural stability of dihydrofolate reductase.[72] A lysine-to-leucine mutation in an amphipathic helix sequence of bovine growth hormone slows the folding process and causes increased precipitation in refolding experiments, pointing to the stabilization of an associated folding intermediate by the aggregation of amphiphilic helices.[73]

A proline-to-alanine mutation in thioredoxin suppresses the slowest phase of folding, demonstrating the essential role of the proline residue in the process.[74] Another study of proline isomerization with staphylococcal nuclease suggests that this phenomenon could be relevant to both the folded and unfolded states.[75] In this same model system, the changes observed upon mutation in the enthalpy and entropy of reversible denaturation have been explained by changes in the solvation and/or the conformation of the denatured state.[76]

Systematic changes in the sequence of the N-terminal domain of the phage λ repressor reveal the nonuniformity of structural information: while some positions along the sequence are critical, with changes capable of tipping the balance between folding and unfolding, others are relatively unimportant in a structural sense and a wide range of substitutions and modifications at these positions are possible.[77] Intensive studies with the T4-lysozyme system have led to significant insights into protein stability.[78] This protein has been found to be surprisingly tolerant of mutations made at its surface, while mutations that make it more temperature-sensitive occur in regions of rather low mobility and low solvent accessibility in the folded protein. Numerous replacements of a proline located at the C-terminus of a T4-lysozyme helix extend this helix without increasing protein stability.[79] This implies either that the intrahelical H-bonds are not more stable than protein–solvent H-bonds or that the resultant helix does not interact with the rest of the protein as well as it does in the wild-type enzyme.

Further experiments with T4 lysozyme[80] have permitted the experimental study of side-chain hydrophobicity in protein systems, making a comparison of the results with the various hydrophobicity scales for amino acid derivatives possible.[29] Another study of hydrophobic interactions has been initiated for the packing of amphiphilic α-helices and β-sheets with ribonuclease as a model.[81] Also, first experimental insights on the contribution of the helix dipole[35] to protein stability have been gained.[82] Finally, site-directed mutagenesis is leading us to a quantitative understanding of hydrogen bonding.[83] Selected aspects of this rapidly growing field have recently been reviewed.[84]

The important results just mentioned make it clear that protein de novo design will strongly benefit from a deeper

understanding of tertiary-structure formation emerging from this technique. Site-directed mutagenesis allows the study of exquisitely specific and systematic modifications in protein-size systems. However, the very complexity of the effects of the introduced change is often difficult to understand, analyze, and quantitate.

This suggests that synthetic peptide chemistry can be an approach of choice in helping us to understand the relevant forces in protein structure, by permitting us to study them in model systems of lower complexity. In this sense, protein engineering and de novo design by chemical methods represent *convergent* approaches for the construction of novel proteins (cf. Fig. 5).

3.2. Protein de novo Design: The Construction of a Predetermined Three-Dimensional Conformation from Elementary Building Blocks

The complexity of protein folding makes it difficult to synthesize a new sequence that will adopt the designed conformation (Fig. 5b). Is there any way to bypass the problem? The patterns and regularities, presented above, that are to be found in protein structure lend credit to this somewhat optimistic view. Examples include:

1. the *limited diversity* of structural topologies[9, 85] observed in natural proteins (Fig. 3);
2. the *degeneracy* of the folding code (many different sequences being able to adopt a given structure, Fig. 4);
3. improved knowledge of the relation between sequence and secondary structure (model studies with synthetic peptides, see below) and of the factors influencing protein folding and stability (site-directed mutagenesis, see Section 3.1).

The working strategy in protein de novo design is based on the current ideas of folding and structure already described. The tertiary structure of a protein is considered in terms of the assembly of secondary-structure[9, 85, 86] elements joined by turns,[22] bulges, loops,[87] or less ordered chain segments (Fig. 6).

Sequence blocks are designed that have a high propensity to adopt defined conformations based on experimentally or semiempirically determined conformational parameters of the amino acid residues; they are then assembled into small "globular tertiary structures", so-called *folding units*. Of course, both gene-technological and chemical approaches to de novo design of proteins are possible. However, attempts to design new proteins *directly* by the use of DNA recombinant methods have not to our knowledge been described in the literature. As mentioned above, the complexity of the protein-size systems that can be studied by gene-technological methods can often make clear-cut answers difficult to obtain.

In de novo design with chemical methods, the topic we will concentrate on for the remainder of this article, only small proteins seem to lie within reach due to practical limitations in synthesis and purification (see below). The folding of such short polypeptides into compact, globular structures is particularly unfavorable[4, 89] due to the following factors:

1. the high flexibility of linear polypeptides (small excluded volume effects);

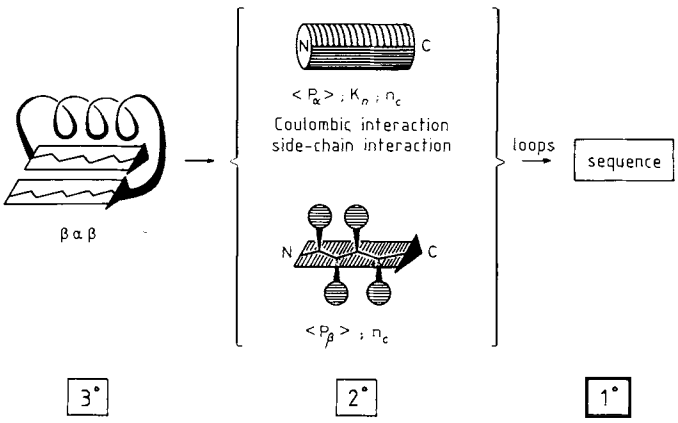


Fig. 6. The analysis of tertiary structure (3°) is based on current ideas on protein folding and topology, shown here for the case of a βαβ folding unit. The tertiary structure is considered in terms of assembly of secondary-structure (2°) elements joined by short peptide segments (turns, loops). Application of prediction parameters such as Chou–Fasman [47] propensities for an amino acid to be in an α-helix ($\langle P_\alpha \rangle$) or β-sheet ($\langle P_\beta \rangle$, the Zimm–Bragg [88] coefficient for helix elongation (K_n), or the experimentally determined critical chain lengths for α-helix or β-sheet formation (n_c), as well as consideration of favorable Coulombic and side-chain interactions [35], leads to the design of sequences (primary structure, 1°) with potential for adopting amphiphilic structures compatible with the chosen structural fold.

2. the small volume-to-surface ratio, which limits the number of possible hydrophobic interactions (S_{solv} in Fig. 1, the major driving force for folding);
3. the lack of the long-range interactions found in natural proteins, which contribute to the stabilization of secondary structures.

These detrimental factors can be compensated for by amphiphilic secondary-structure blocks,[4, 90] which can provide a contribution to intramolecular folding by interacting to form an energetically favorable structure with a proteinlike hydrophobic core and a hydrophilic surface (Fig. 7).

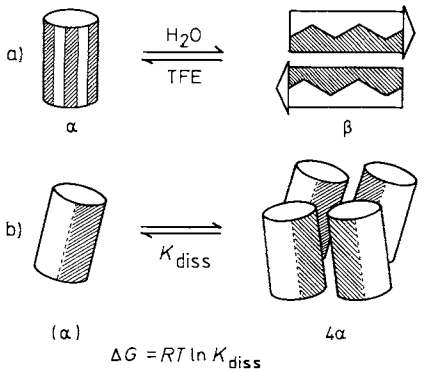


Fig. 7. The amphiphilicity of secondary-structure building blocks is the driving force for self-assembly. a) Amphiphilic sequences of the type $(A-B)_n$, where A and B denote hydrophobic (e.g., Leu, Val) and hydrophilic (e.g., Glu, Lys) amino acids, respectively, have a high tendency to associate in aqueous medium, possibly in a β-conformation-forming bilayer with hydrophobic core and hydrophilic surface [91]. 2,2,2-Trifluoroethanol (TFE) can shift the conformational equilibrium towards α-helix formation. b) Amphiphilic helices have a strong tendency to self-assemble into more or less defined multimeric complexes. For example, primary sequences of the type $(A\text{-}A\text{-}B\text{-}B)_n$ seem to have a tendency for preferentially forming four-helix-bundle (4α) structures. In one instance, the free energy of tetramerization (ΔG) has been estimated to be 20 kcal mol^{-1} for helices of medium size [92].

3.2.1. *Designing the Secondary-Structure Blocks*

Systematic experimental studies with synthetic model peptides have proved to be very useful in the design of peptide blocks, providing a sound experimental alternative to the prediction and energy calculation algorithms. This is of particular relevance for protein design, the ultimate goal of structure prediction and design being the experimental confirmation of its adequacy.

The first systematic studies on defined peptide models were initiated more than 20 years ago with homooligopeptides. These yielded valuable experimental insights into the fundamental phenomenon of secondary-structure formation, in particular the critical chain length for α-helix and β-sheet formation as a function of amino acid residue and experimental conditions.[93, 94] These studies were expanded by the use of "host–guest" cooligopeptides.[95] This idea originates from macrocyclic organic chemistry[96] and was successfully applied to polypeptides for the derivation of the Zimm–Bragg σ,s parameters[91] describing the α-helix-to-random-coil transition.[97] By measuring the influence of a given residue (guest) on the conformational properties of the homopolymer host peptide, the helical potential of the guest residue could be indirectly determined. Detailed studies of secondary structure succeeded through the synthesis of well-defined synthetic host–guest peptides; eventually, the importance of neighboring-residue effects on the stability of β-sheet and α-helix structures could be assessed for the first time.[94, 98–101] The tentative, experimental conformational propensities that could be defined for many amino acids showed that the conformational preferences derived from a statistical analysis of protein X-ray structures do not necessarily apply to small peptides, as has also been noted by other workers.[102] A valuable "spin-off" of these results was the study of the impact of conformation-dependent physicochemical features of peptides on peptide synthesis.[98, 99, 103]

Homooligopeptides and cooligopeptides, of course, are a far cry from the peptide sequences encountered in natural proteins, but ideally lend themselves to the design of secondary-structure blocks with predetermined properties such as block length and hydrophobicity. With regard to protein design, amphiphilic structures are of particular importance.

The synthesis of cooligopeptides consisting of alternating hydrophilic and hydrophobic amino acids with chain lengths between 6 and 10 residues allowed the assessment of the *β-structure-forming* potential[100] of such amphiphilic structures (Table 2). Solubility problems, which usually make a conformational analysis difficult, could be avoided by the use of polyethylene glycol as a solubilizing C-terminal protecting group.[104] In this manner, β-structure-forming oligopeptides, whose insolubility is notorious,[105] could also be studied in aqueous solution. As can be seen from Table 2, the critical chain length for β-structure formation (6–11 residues) is in the range observed for β-structure blocks in proteins.[106] The surprisingly high propensity of this type of amphiphilic peptide for β-structure formation in aqueous solution (comparable to the behavior of hydrophobic homooligopeptides[107]) is best explained by the formation of a peptide bilayer-sheet[91] (Fig. 7), in which the hydrophilic residues are oriented towards the aqueous phase. Sequence-specific effects, as well as sufficient overall hydrophobicity

Table 2. Experimentally determined critical number of dipeptide units n_c necessary for β-structure formation in amphiphilic oligopeptides of different sequences (PEG = polyethylene glycol as C-terminal protecting group).

Peptide	Solvent	n_c	Chain length
$(Ile\text{-}Gln)_n$-Ile-Gly-PEG	H_2O	2	6
$(Ile\text{-}Thr)_n$-Gly-OH	CF_3CH_2OH	3	7
$(Thr\text{-}Val)_n$-Gly-OH	H_2O	4	9
$(Ser\text{-}Leu)_n$-Gly-PEG	H_2O	4	9
$(Ser\text{-}Ala)_n$-Ser-PEG	H_2O	>4	> 9
$(Val\text{-}Lys)_n$-Gly-PEG	H_2O, pH 10	>5	>11

(in order to increase the solvation entropy S_{solv}) also seem to influence the stability of this type of structure.[108]

The critical chain length for *α-helix* formation[110] was found to be in the range of 10–15 residues in helix-supporting media like 2,2,2-trifluoroethanol, depending on the helix-forming potential of the individual residues. A dramatic reduction of the critical chain length can be achieved by the incorporation of α-aminoisobutyric acid (Aib), which has a strong helix-inducing effect.[113] The large number of helical Aib-containing peptides described[110–112] allow some guidelines for the design of helical building blocks to be formulated. The helix stability increases with increasing number of Aib residues; i.e., the critical chain length is reduced. Incorporation of Aib should allow the formation of an amphiphilic α-helix when the sequence is displayed in the helical-wheel representation (cf. Fig. 2). As shown in Figure 8, an amphiphilic Aib-containing peptide of 18 residues

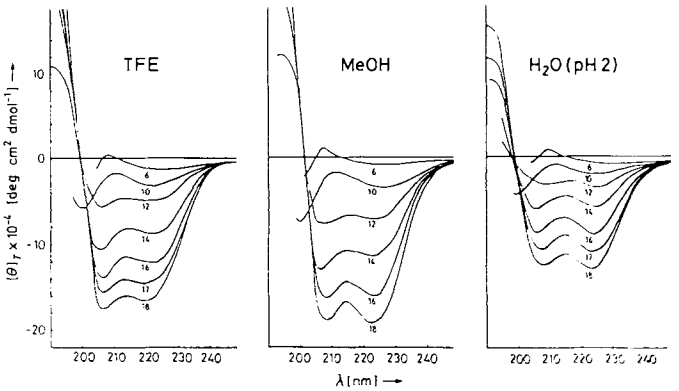


Fig. 8. Chain-length dependence of α-helix formation for the sequence Pro-Glu-[Ala-Aib-Glu-Aib]$_{1-4}$ [109], as found by circular dichroism (CD), in trifluoroethanol, methanol, and water (pH 2) at a concentration of 1 mg mL^{-1}. It is possible to estimate the helical content of the peptide from the total ellipticities $[\theta]_T$ shown on the ordinate axis. Introduction of the non-proteinogenic amino acid α-aminobutyric acid (Aib) favors helix formation [109–112]. The numbers under the curves give the number of amino acid esters per peptide. For example, the sequence with 12 amino acid residues is: Pro-Glu-(Ala-Aib-Glu-Aib)$_2$-Ala-Aib.

displays a well-developed helix in a number of solvents and particularly in water;[109–112] replacement of Aib by Ala in such peptides leads to a significant reduction in the helical content of the peptide.[112] Recently, a number of elegant strategies for the synthesis of α-methyl derivatives of amino acids have been described,[114] so that it is to be expected that these will become valuable building blocks for the conformational stabilization of helical sequences.[115]

3.2.2. *What Can Peptides Teach Us about Proteins and vice versa?*

In view of the notable advances in the conformational analysis of natural peptides made possible by modern spectroscopic techniques of NMR,[116] CD,[117] and IR,[118] the experimental study and optimization of secondary-structure formation is no longer a fundamental problem. Indeed, conformational aspects of peptides have become the focus of much interest in their relation to biological function. In turn, this has led to some general insights into the role and occurrence of secondary structure in natural proteins. Detailed studies on the conditions for secondary-structure formation in "natural" sequences[35, 119] have already caused an unanticipated expansion of the Zimm–Bragg theory of helix formation,[120] since the experimentally observed helical content in these short peptides is significantly higher than predicted by theory. This supports models of protein folding where secondary structures form early on during folding.[23, 24] Very recently, synthetic peptide models have been used to study protein folding pathways.[121]

Synthetic peptide models may also be used to try to mimic certain properties of macromolecular systems (e.g., protein surfaces). In such instances, the flexibility of a peptide can be deliberately reduced by the introduction of some kind of restriction (chemical or physicochemical) in its conformational space. Along with the pioneering studies of *E. T. Kaiser* with amphiphilic helical peptide hormones and toxins,[90] representative examples have included experiments with peptides for calmodulin binding,[122] zinc-binding peptides with zinc-finger conformation,[123] protein ion-channel models,[124] receptor mimics,[125] DNA-binding peptides,[126] and antigenic peptides with conformational features of protein-immunogen epitopes.[127]

Model peptides will continue to be useful in the future for the design of polypeptides of defined tertiary structure, and perhaps, ultimately, for the prediction of structure from sequence. They may also prove helpful in correlating physicochemical properties with sequence and sequence with conformation. The main hurdle in de novo design does not reside in the formation of secondary structure itself, but rather in the assembly of secondary structures to a tertiary structure. The experimental gap between secondary and tertiary structure will be a most important aspect of research in the field of peptide and protein structure.

3.2.3. *From Secondary to Tertiary Structure: The Long Journey of "de novo" Designed Proteins from the Computer Screen to the Test-tube.*

Significantly, experimental feedback at this higher structural level has been sparse until now, if one considers the few attempts in this direction that have been described in the literature. Examples include a 34-residue ββα peptide designed to bind nucleic acids,[128] a four-stranded antiparallel β-pleated sheet that binds DDT,[129, 130] a synthetic model of tropomyosin designed to form a two-stranded α-helical structure (coiled coils),[131] a study of repeating peptides designed to adopt a cross β-conformation,[132] two folding units with βαβ packing arrangement of 38- and 35-residue length,[133] and the chemical synthesis of a 66-residue protein with antiparallel β-structure ("betabellin").[134, 135] In what seems to be the most successful achievement to date, a four-helix bundle was assembled step by step. First, it could be shown that amphiphilic helical sequences associated predominantly to a tetramer in aqueous solution.[136] The chemical synthesis of the corresponding dimer[92] (a 35-mer consisting of two helices linked by a turn) resulted in increased stability of the four-helix bundle formed by self-association. Finally, the physicochemical and conformational properties of the designed proteins were used to design and synthesize by recombinant DNA techniques a single-chain four-helix-bundle protein.[137, 138] Preliminary results indicate that the postulated four-helix bundle is indeed formed. However, it must be noted that in the absence of X-ray structure or detailed NMR studies for any of the "artificial proteins" described, it has not yet been possible to bring unequivocal proof for the designed structures.

In our view, the paucity of published research in this area reflects the unfavorable solution properties of designed peptides. This gives rise to a twofold problem: the insolubility of fully protected, growing peptide chains causes difficulties during synthesis, and the deprotected, unfolded peptide product tends to aggregate and so to be insoluble as well. The propensity for intermolecular aggregation—as a competing process to intramolecular folding—seems to be a central, intrinsic problem in the design of artificial proteins. This is actually something to be expected if one considers the energetic contributions to protein stability (Fig. 1, Table 1) and their consequences for de novo design.

1. In order to fold in a globular structure, a polypeptide chain must be hydrophobic enough so that the *entropy of solvation*, S_{solv}, gained upon folding more than compensates for the loss of chain entropy, S_{chain} (Table 1).
2. In order to *reduce the chain entropy*, S_{chain}, of the unfolded state (i.e., to "destabilize" it), as well as to "seed" folding, the secondary-structure blocks must be partially folded even in the absence of long-range interactions. Strictly amphipathic α-helices and β-sheets may be used to achieve this. On the other hand, the pronounced amphiphilicity in the unfolded block makes these molecules sensitive to *intermolecular aggregation*.

Clearly, an adequate balance between hydrophobicity and hydrophilicity of the target molecule is very difficult to achieve. Of course, this "two-step" strategy of first designing secondary-structure blocks and then connecting them by loops and turns to obtain folding units may very well turn out to be too gross an approximation of folding pathways. A better understanding of the importance of loops and turns for structure and folding[92, 137, 138] could bring some improvements. In any case, the "perfect" design ("overdesign"[135]) of three-dimensional conformations is presently neither sufficient nor adequate to compensate for our still imperfect knowledge of folding mechanisms. Here lie "big open spaces" for research in protein design.

These difficulties do not exclude the occasional "single hit", as the examples cited above can testify. But one main question for future, *rational* protein design will be: Can we, following a *general* strategy, design proteins of defined three-dimensional conformation in a first step and introduce functional properties into these structures in a second step?

In this regard, it is our conviction that synthetic chemistry has novel and important contributions to make to some of the most basic problems of de novo design. Before we engage in a discussion of protein design with "chemical tools", we first take a critical look at the craft of the peptide chemist, the chemical synthesis of peptides and proteins.

4. Chemical Peptide and Protein Synthesis: Art or Handicraft?

The chemical synthesis of peptides reflects an effort which spans over a century. To attempt an exhaustive overview would be an affront to the contributors who would inevitably be passed over in the process. Rather, we will try to discuss the achievements, problems, and prospects in the field relevant to protein design and refer the interested reader to leading monographs[139-141] and recent symposia reports[142] for more comprehensive background information.

Peptide synthesis appears to have become routine. First, peptide synthesis can be performed with the help of fully automated "synthesizers" which deliver primary sequences of up to 50 amino acids in a short time and on a variable scale. Second, DNA recombinant techniques allow, in principle, the synthesis of any amino acid sequence; even large-scale production has been made possible in a few instances.[6] In view of this situation, one is tempted to conclude that peptide and protein synthesis no longer are subjects for scientific investigation. In fact, there is no doubt that the progress and achievements in peptide synthesis, mainly stimulated by *Merrifield*'s method of solid-phase synthesis[143] and, more recently, by DNA recombinant methods applied to peptide synthesis,[5,6,123,130,137,138,144,145] have overshadowed some unsolved and longstanding problems in peptide and protein chemistry. In spite of the success of these synthetic methods, there is no unique, generally applicable procedure for building up a peptide or a protein. As shown in Table 3, every method has its characteristic scope and limitations. The ultimate use of the synthetic product must determine the synthetic strategy.

It is indisputable that the advent of solid-phase peptide synthesis[143] has helped chemical synthesis to become an important tool in the study of this class of biopolymers.[147] However, owing to the great expectations held for future achievements in peptide and protein chemistry, it is perhaps appropriate to pause and reconsider its possibilities and its limitations in order to evaluate the kind of answers we can expect in the future. In 1971, *E. Wünsch*[160] summarized the achievements of peptide chemistry at the time. Classical peptide chemistry in solution had already reached its golden age. The methods for amino acid protection, activation, and coupling and for peptide purification and analysis constituted an impressive body of knowledge. By contrast, some fundamental limitations of solid-phase peptide synthesis, which was in its eighth year of existence, were becoming evident, which *Wünsch* described as the "inborn errors" ("Geburtsfehler") of the solid-phase method:

1. the absolute necessity of quantitative coupling in each step due to the impossibility of purification of intermediates;
2. the large excess of *N*-protected amino acid derivatives necessary to ensure quantitative coupling;
3. the hazardous effect of side reactions that can occur during amino acid activation, coupling, and deprotection stages due to the impossibility of intermediate purification;
4. the critical analytical controls for quantitative coupling (which also are chemical reactions) are submitted to the same limitations as the coupling reaction itself;

Table 3. Comparison of the different methods in use today for peptide and protein synthesis (AA = amino acid).

Method	Main features	Advantages	Shortcomings	References[a]
Synthesis in solution [b]	< 100 AA residues	purification of intermediates; high purity	know-how; time-intensive; solubility problems	[139*, 146]
Solid-phase synthesis [b]	< 50 AA residues (although > 100 often attempted)	simple, fast screening, automatic	purification problems; analytical controls	[147*, 148*, 92, 129, 133, 149, 150]
Condensation of fragments obtained by solid-phase synthesis [b]	< 100 AA residues	use of purified fragments	low solubility and yield; racemization	[151]
Polyethylene glycol-supported synthesis [b]	< 30 AA residues	solubilization; homogeneous reaction conditions	difficult automation; isolation of peptide	[104*, 133]
Semisynthesis [b]	protein fragments, proteins	minimal protection	optimization; no routine	[152*, 153]
Enzymatic synthesis [b]	AA's → proteins	selectivity, no racemization aqueous media, solubility	optimization; no routine	[154*, 155]
Recombinant techniques [c]	DNA protein-size	"nature pure" "endless supply"	gene expression, product isolation, gene product renaturation	[5*, 6*, 144*, 123, 130, 137, 138, 145, 156]

[a] Selected references; an asterisk indicates a review article. [b] Chemical methods allowing the incorporation of non-proteinogenic amino acids [133, 150], peptidomimetics [157], turn mimetics [158], or α- and β-secondary-structure mimetics [159] or the selective introduction of spectroscopic probes. [c] Genetic methods, limited to natural sequences.

5. the solubility problems of protected amino acid derivatives; swelling problems of the peptide resin due to aggregation effects during chain elongation and the related problems of hindered reactant diffusion;
6. the often harsh deprotection conditions after completion of synthesis.

Have we made progress in resolving these problems? There have been a number of important methodological improvements. For example, we now have a better knowledge of side-chain protection chemistry and possess better methods for anchoring peptides on polymeric supports.[148] The side reactions that occur during coupling and deprotection of the different protecting groups are now better known.[161] An important renewal occurred with the introduction of an alternative synthetic strategy to the acid-labile Boc/Bzl standard combination for main/side-chain protection, namely, the milder base-labile Fmoc/*t*Bu combination[162] for which new polymer supports have been developed.[163] But the decisive impulse for the enormous expansion of automated peptide synthesis has probably been due to advances in purification procedures, notably reverse-phase HPLC. Unfortunately, it is perhaps just the unanticipated usefulness of synthetic peptides in modern biology[164] (and hence the increased popularity of the solid-phase method despite the major shortcomings listed above) that has made more research in the methodology somewhat unattractive.

Indeed, it should not be forgotten that there are some pending problems in chemical peptide synthesis, such as the impact of conformational effects on solvation properties and coupling kinetics. Systematic studies in our laboratory on secondary structure formation in solution and on polymer-bound peptides showed that conformational transitions during chain elongation (e.g., from random-coil to β-sheet conformation) may result in a dramatic reduction in the rate of the coupling step.[98, 99] Since we still know little about secondary-structure formation of fully protected peptides, we can make only limited predictions on the influence of these conformational effects on the course of synthesis.[98, 99, 103] Each peptide displays some characteristic properties and is therefore a unique, complex entity. This is the reason why there can be no general standard procedure for peptide synthesis.

What are the perspectives for chemical peptide and protein synthesis? Can it establish itself as a valuable complement, or even alternative, to DNA recombinant techniques? Clearly, the incorporation of nonproteinogenic amino acids and unnatural building blocks remains the privilege of the chemist and represents an increasingly valuable asset in modern drug design, as well as in investigations on peptide and protein conformation, structure–activitiy relationships, or macromolecular recognition.

Perhaps the most fascinating prospect of chemical synthesis of peptides and proteins is offered by de novo design of proteins, a research area still very much in its infancy. The efficient and reliable synthesis of even small protein domains (folding units of 50–100 residues) will require in most cases the combination of different synthetic strategies. Methods involving the condensation of fully protected fragments either in solution or on the insoluble support (see Table 3 for references) are now finding increasing popularity. In the long term, the combined use of the chemical and biochemical techniques presented in Table 3 will be essential for a full exploitation of the potential of synthesis for the construction of new proteins (Fig. 9).

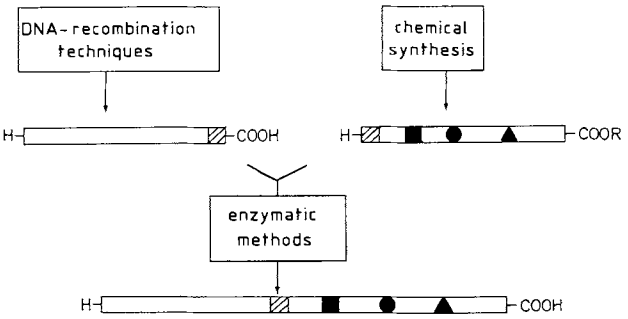


Fig. 9. A hypothetical scheme illustrating the potential of the combination of different methods for the synthesis of proteins. A polypeptide fragment produced by DNA recombination techniques (left) is coupled enzymatically (minimal side-chain protection) to a chemically synthesized fragment (right) containing non-proteinogenic amino acids, mimetics, or spectroscopic probes (solid symbols).

In this respect, synthesis itself does not seem to constitute the most difficult problem along the way. Indeed, one might even consider the fundamental synthetic problems to be essentially solved, since the tools of gene technology make it in principle possible to build up any amino acid sequence, and the chemical methods of peptide and protein synthesis, invaluable for their unlimited potential for structural modification, are more restricted by the necessary time and know-how expense than by the methodology itself.

5. The Use of Chemical Tools in Protein Design

The major question for protein de novo design lies in the search for polypeptide sequences that fold in a certain three-dimensional conformation, rather than in the chemical establishment of the sequence. However, the chances for solving this "folding problem" in the near future are low. The results of protein engineering have shown just how complex a relation there is between the primary sequence and tertiary structure in natural proteins. Indeed, it seems almost hopeless to try to get a grasp of the patterns of evolutionary selection and optimization in order to derive some general rules for the construction of new proteins.

In this context, the question as to whether linear polypeptide chains have the most suitable structural features to form globular structures seems justified. Although this can only be a mere speculation, it might be that Mother Nature had no other choice. Once the ribosomal synthesis "plant" yielding linear polypeptides from genetic information in linear form had been developed, she had to "learn", in an evolutionary process of optimization, how to fold sequences into biologically useful conformations. Along these lines, a newly formulated hypothesis[137] proposes that protein sequences have evolved not only to fold into unique three-dimensional conformations, but also to exclude alternative conformations. Could this be a very exclusive and unusual property of natural proteins? The fact that the number of proteins occur-

ring in nature only represents a vanishingly small percentage of all the possible polypeptide sequences is in support of this idea.

Can the chemist circumvent the long and difficult pathway of evolution by making use of the synthetic tools at his disposal?[89] Is it possible to construct peptidic architectures with a higher propensity for folding into a globular conformation than linear polypeptides? The construction of peptide chains with an *unnatural connectivity* (for example, branched structures, Fig. 10) could represent an example of this. Surprisingly, peptide chemists involved in protein design have made little use of what may be their most powerful tool.



Fig. 10. Strategies for protein de novo design. The construction of tertiary structures from secondary-structure elements can occur by two different approaches, as shown here for a four-helix-bundle protein. In order to reach the designed tetrameric structure (middle, see Fig. 7b), which arises through self-association of the amphiphilic helix blocks, the helices may be linked by loops to yield a polypeptide chain (left, see [138]) with the linear connectivity found in natural proteins. In contrast, the same packing arrangement may be reached by grafting the individual helix blocks onto a carrier molecule (template). These template-assembled synthetic proteins (TASP) have an unnatural, branched connectivity of the peptide chains, and thus are accessible only by synthetic chemistry.

A number of research groups have been involved in the construction of artificial proteinlike structures. We proposed that peptide blocks be assembled on a multifunctional carrier molecule, for example in the construction of enzyme models.[4, 165] A similar concept was applied by *Heidemann* et al.[166] for the study of triple-helix formation in collagen models. The use of multifunctional linkers in the construction of a β-barrel-forming protein ("betabellin") by solid-phase synthesis[134, 135, 167] and, very recently, of a disulfide bridge cross-link for the design of parallel two-stranded coiled coils in tropomyosin models[168] have also been reported.

5.1. Template-Assembled Synthetic Proteins (TASP)

We have recently taken these ideas further into a general, novel strategy for the construction of proteinlike tertiary structures, in an attempt to merge the possibilities of synthetic organic chemistry with the features of protein structure.[169] Amphiphilic secondary-structure-forming peptide blocks are fixed on a tailor-made template molecule, which directs the peptide chains into proteinlike packing arrangements. Accordingly, we termed the resulting macromolecules template-assembled synthetic proteins (TASP, Fig. 11).

Thus, rather than being linked by loops to a linear polypeptide chain, secondary-structure-forming peptide blocks are assembled by covalent attachment to a carrier molecule, resulting in a branched structure (Fig. 10). This difference in connectivity of the chain has important consequences with respect to the adoption of a globular conformation: while the linear assembly of β-sheet and α-helical peptide blocks necessitates a specific folding process to achieve formation of the postulated folding unit, the branched molecule can more directly adopt a compact structure. The multifunctional carrier molecule plays a determining role in this respect by (1) favoring intramolecular interactions between the covalently fixed peptide blocks and (2) predetermining the packing topology of the TASP molecule (Fig. 12) by the number, type, and spatial arrangement of its functional groups (peptide block "anchoring points"). Hence, the carrier is not merely a structure-stabilizing cross-link but can be considered as a *template* for the onset of the three-dimensional conformation of the designed molecule.

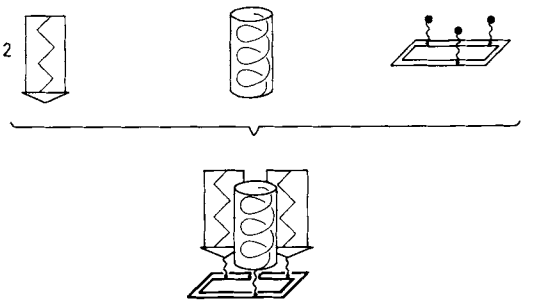


Fig. 11. Template-assembled synthetic proteins (TASP) as a new concept for the construction of artificial proteins. Amphiphilic secondary-structure-forming peptide blocks (α-helices, β-sheets) are grafted onto an adequate carrier molecule (template). In this example, two β-sheet blocks and an α-helix block are assembled on a trifunctional template molecule to a βαβ-like folding unit.

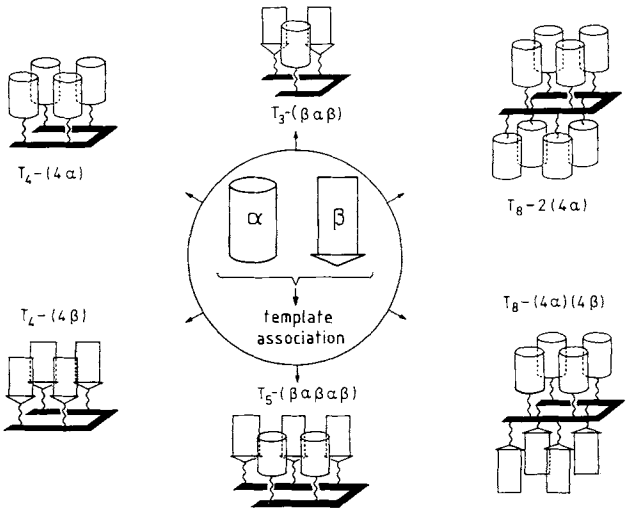


Fig. 12. Schematic representation of different possible packing arrangements (topologies) in TASP molecules (T_n, T = template molecule, n = number of attachment sites on T; α, β, amphiphilic peptide blocks with tendency for helix (α) and β-sheet (β) secondary-structure formation). The number, nature, and spatial orientation of the attachment sites in the carrier molecule predetermine the topological features of the TASP molecule and thus act as a *template* for the folding of the molecule in the predetermined structure.

5.2. TASP Molecules: The Chemist's Escape from the Folding Problem?

The conceptual simplicity of this strategy enables us to discuss some fundamental aspects of the energetics (with respect to folding) of TASP molecules. The template molecule induces intramolecular interactions between covalently bound peptide chains, so that the unfolded molecule has a

high coil density (to be compared, perhaps, to the "collapsed state" of a linear polypeptide chain). The amphiphilicity of the secondary structure that forms under adequate (renaturing) conditions leads to the self-association of these template-bound peptides to a compact structure ("intramolecular collapse") as hydrophobic interactions are optimized. Hence, the formation of secondary structures (nucleation step) becomes the rate-limiting step for folding (Fig. 13).

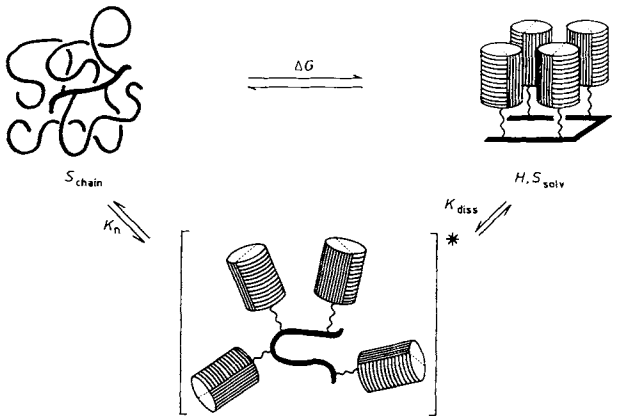
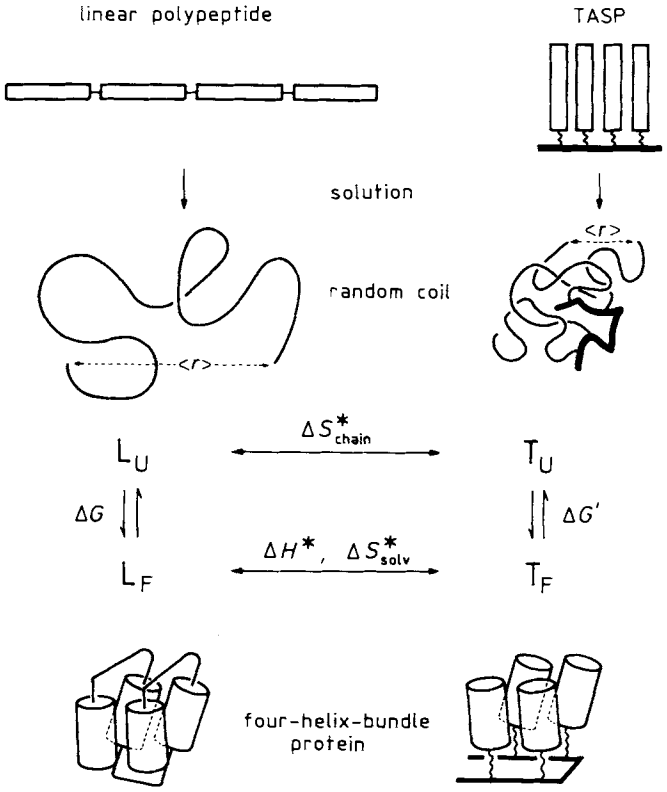


Fig. 13. Hypothetical folding pathway of TASP molecules, shown for the four-helix-bundle arrangement. The unordered, branched "compact" molecule is thought to reach a globular-like state through a rate-limiting nucleation step in which secondary structure is formed and the chain entropy, S_{chain}, decreases in comparison to the unfolded state. This process can be described by the Zimm–Bragg equation $K_n = \sigma s^n$ (σ and s denote the helix nucleation and growth parameters, respectively, for every amino acid; n, chain length [88]). In the intramolecular association of amphiphilic peptide blocks, increase in the solvation entropy, S_{solv}, (release of associated water molecules in the formation of a hydrophobic core), determines the greater part of the driving force for folding. The free energy of tetramerization may be described by $K_{diss} = [\alpha]^4/[4\alpha]$. In the hypothetical intermediate, indicated by an asterisk, intramolecular interactions are forced by the covalent bonds between peptide blocks and template, so that the propensity of intermolecular aggregation typical of amphiphilic peptide chains is significantly reduced.

Owing to this simple mechanism of "folding", the assembly of secondary-structure blocks in TASP molecules should not encounter the substantial energy barriers postulated for the folding pathway of linear peptide chains (Fig. 14).

From an experimental point of view, the phenomenon of self-association is very important. The short-range interactions induced by the template between amphiphilic peptides make intermolecular aggregation less likely than intramolecular contacts. This means that the susceptibility towards aggregation should be reduced in TASP molecules in comparison to linear polypeptides.

The branched structure of TASP molecules causes high volume density and therefore significant "excluded volume effects" in the random-coil state of the molecule. Consequently, the chain entropy (S_{chain}) of the "unfolded" state is decreased, resulting in a potentially larger value of ΔG_{F-U} (cf. Fig. 1).[89] A qualitative comparison (Fig. 14) of linear (L) and branched (T) polypeptides further illustrates this point. The destabilization of the unfolded state in branched molecules (supplying, ΔS^*_{chain}, Fig. 14) represents a source of increased thermodynamic stability (ΔG^*_{L-T}) for the folded TASP molecule (T_F) compared to the corresponding linear polypeptide (L_F) (provided the packing, and hence the enthalpies, H, and solvation entropies, S_{solv}, of the folded



$$\Delta G^*_{L-T} = \Delta G' - \Delta G \approx \Delta S^*_{chain}$$

Fig. 14. Schematic representation of thermodynamic aspects of the folding of linear (L) and branched (T) polypeptides. While the unordered (U) conformation of both molecules under poorly solvating conditions (near the so-called theta point) is exclusively determined by short-range interactions, extensive "excluded volume effects" [1] arise as a consequence of long-range interactions, when the chain enjoys good solvation. This can be expressed in terms of an increase of the end-to-end vector $\langle r \rangle$. Due to the higher coil density in the branched molecule, the number of accessible conformations is smaller than in the linear molecule, causing a decrease in the chain entropy, S_{chain}. This, in turn, leads to a destabilization of the unfolded state T_U of the branched molecule. Under the assumption that the intramolecular interactions in the folded state (F) are similar in both linear and branched molecules (i.e., $\Delta H^*, \Delta S^* \approx 0$), the branched molecule will be stabilized relative to the linear by a difference in free energy $\Delta G^*_{L-T} = \Delta S^*_{chain}$, as can be taken from the figure. TASP molecules should therefore be more stable thermodynamically than linear polypeptides of equivalent packing arrangement (here, a four-helix-bundle structure). This aspect of the energetics is of great importance with respect to subsequent modification of the structure in order, for example, to introduce functionality into the molecular structure.

molecules L_F and T_F are of comparable magnitude). Therefore, we predict that TASP molecules will be more stable thermodynamically than their linear counterparts. The energetic aspects of TASP molecules are of importance when considering the final goals of protein design, namely, the incorporation of functional properties in predetermined three-dimensional structures (Section 6).

5.3. The Design and Construction of TASP Molecules

The most noteworthy feature of the present approach is its application to the design of proteins having different packing arrangements (topologies) (cf. Fig. 12). The computer-assisted design of TASP molecules proceeds in four steps:

1. design of amphiphilic peptide blocks according to the rules of secondary-structure formation (Fig. 15a);

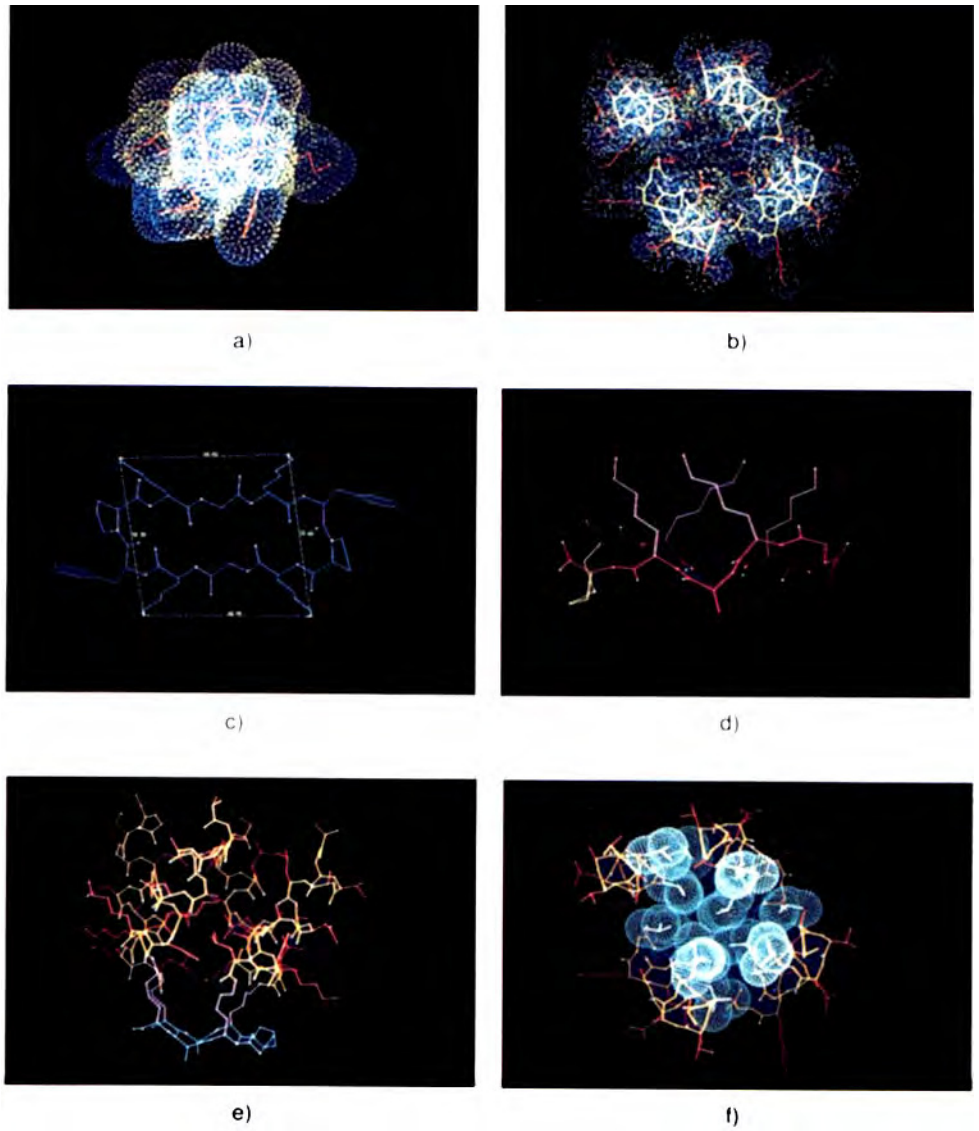


Fig. 15. TASP design by computer-assisted molecular modeling (using the "Roche interactive molecular graphic system" (RIMG) [170], taking a "four-helix-bundle" TASP as an example (T_4-(4α) in Fig. 12). a) The design of secondary-structure blocks. Computer-generated standard helix (seen from the end of the helix cylinder) for the sequence Glu-Ala-Leu-Glu-Lys-Ala-Leu-Lys-Glu-Ala-Leu-Ala-Lys-Leu (cf. Fig. 2). The dotted van der Waals surfaces of hydrophobic (yellow) and hydrophilic (blue) residue side chains highlight the amphiphilic nature of the sequence. b) "Self-association" of the helices into a four-helix-bundle arrangement, with the hydrophobic side chains (Leu) on the inside and the hydrophilic groups (Lys, Glu) on the outside surface. (c) Design of an adequate template: the cyclic decapeptide of sequence *cyclo*(-Pro-Lys-Ala-Lys-(D)Phe-)$_2$ (an analogue of gramicidine S [171]). The relative distance between ε-amino groups of the lysine side chains is about 10–11 Å (dotted square, yellow) in this energetically favored conformation (two antiparallel β-strands (Lys-Ala-Lys) joined by two type-II β-turns (D-Phe-Pro)). The tetrafunctional molecule is therefore ideally suited to act as a template in directing the formation of a four-helix-bundle structure (see Fig. 15e, f). d) Side view of the cyclic template molecule *cyclo*(-Cys-Lys-Ala-Lys-Pro-Gly-Lys-Ala-Lys-Cys-). Ring closure occurs through a disulfide bond (yellow) between the cysteines (peptide backbone red, lysine side chains magenta). e) Side view of a template-assembled four-helix-bundle protein [172]. The C-terminal carboxyls of the four helices (Fig. 15b) are linked to the four ε-amino groups of the template lysines by amide bond formation (the template is an open-chain variant of the one shown in Fig. 15d). While the template backbone is held in place, the lysine side chains (magenta) and the covalently bound helices (yellow and red) are left to undergo conformational relaxation, free rotation around all their bonds being allowed. This results in a strain-free, energetically favorable conformation. f) The same molecule as in Fig. 15e, seen in an end-on view, from the N-terminal end of the four-helix cylinder. The formation of a hydrophobic core in the inside of the four-helix bundle is emphasized by the van der Waals surfaces of the leucine side chains. The helix axes in this favorable conformation are tilted towards each other in a manner reminiscent of four-helix bundles in natural proteins (helix backbone in yellow, hydrophilic side chains in red).

2. self-association of the peptide blocks to multimer systems having predefined packing arrangements so that favorable interactions arise ("conformational relaxation") (Fig. 15b);
3. design of an adequate template and attachment of the peptide block assembly to the template functional groups (Fig. 15c and 15d);
4. conformational energy minimization of the template-assembled protein to obtain a modeled (hypothetical conformation of the TASP molecule (Fig. 15e and 15f).

In principle, any multifunctional molecule (e.g., cyclic peptides, peptides with conformational constraints, saccharides, and polycyclic, aliphatic, or aromatic systems) with adequate spatial arrangement of the attachment sites may serve as a template molecule (Fig. 16).

In our exploratory studies, we used oligopeptides as templates because the well-established orthogonal[173] main- and side-chain protection techniques of peptide chemistry provide the necessary flexibility for the synthesis of TASP molecules (Figs. 17, 18).

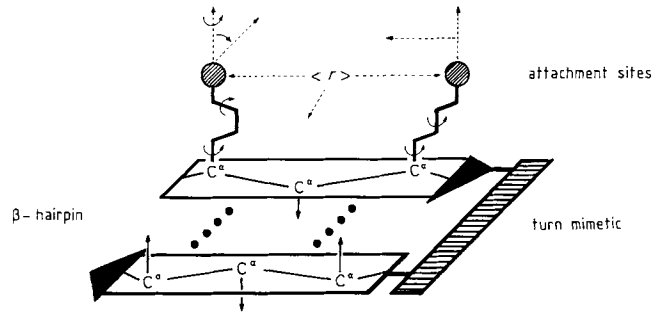


Fig. 16. Schematic representation of a template molecule for TASP design. On the right, incorporation of a turn mimetic [158] (here, a rigid bifunctional molecule matching the spatial requirements of a type-II β-turn) can stabilize the β-hairpin conformation required by design (see Fig. 15d). Rotational freedom around their C–C methylene bonds allow the lysine side chains to meet the requirements in average distances, $\langle r \rangle$, between the attachment sites (here the ε-amino groups of the lysines) suitable for the construction of TASP molecules with proteinlike packing arrangements.

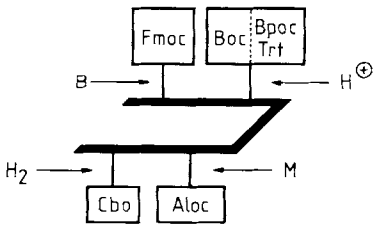


Fig. 17. The selective removal of one protecting group in the presence of many others (orthogonal protection[173]) is a prerequisite in order to fully exploit the potential of the TASP strategy. The protecting groups shown here as examples are Fmoc (9-fluorenylmethyloxycarbonyl), cleaved by base (B); Boc (*tert*-butyloxycarbonyl), Bpoc (biphenyl-*iso*-propyloxycarbonyl), and Trt (trityl), which are differentially sensitive to acids ($H^{\oplus}$); Cbo (benzyloxycarbonyl), cleaved by hydrogenation (H_2); and Aloc (allyloxycarbonyl), which can be cleaved by Pd^0 metal complexes (M). See also Figs. 18 and 19 for experimental examples.

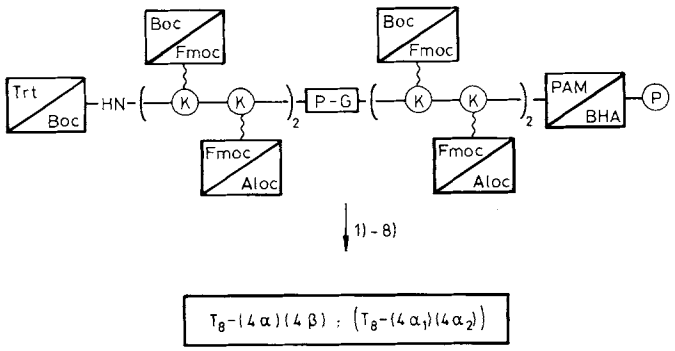


Fig. 18. Synthetic strategy for the synthesis of two-"domain" TASPs [174] of types T_8-(4α)(4β) and T_8-(4α_1)(4α_2) (Fig. 12). The template was assembled on a phenylacetamidomethyl (PAM) resin (P, cross-linked polystyrene) by stepwise addition of N^{α}-Trt (trityl) amino acids with N^{ε}-Fmoc (9-fluorenylmethyloxycarbonyl) and N^{ε}-Boc (*tert*-butyloxycarbonyl) side-chain protection of the lysine (K) ε-amino groups. In an alternative synthesis, the protecting-group combination N^{α}-Boc/N^{ε}-Fmoc/N^{ε}-Aloc (allyloxycarbonyl) was used on a benzhydrylamine (BHA) resin. Thus, as indicated, selective cleavage of the orthogonally protected ε-amino groups of the template lysines allows for the establishment of the two different "domains", 4α and 4β (see Fig. 24a) or 4α_1 and 4α_2. Steps: 1) Trt-(Boc) cleavage; 2) *N*-acylation; 3) Boc (Fmoc) cleavage; 4) 15(13) coupling cycles α(α_1); 5) Fmoc (Aloc) cleavage; 6) 9(15) coupling cycles β (α_2); 7) *N*-acyclation; 8) removal of protecting groups and cleavage from resin.

The model template shown in Fig. 15c is a cyclic decapeptide with two antiparallel β-sheet segments (Lys-Ala-Lys) linked by two β-turns, based on the gramicidin S structure.[171] Computer-assisted molecular modeling shows that the four ε-amino groups of the lysine side chains are properly spaced, in a low-energy conformation, for the construction of a four-helix-bundle tertiary structure (Fig. 15).

The construction of TASP molecules is achieved by the standard strategies of peptide synthesis (solution[139] and polymer-supported synthesis methods;[104, 148] an example is shown in Fig. 18). The applicability of the template approach is not restricted by synthetic considerations. Orthogonal protection techniques (Fig. 17), in combination with segment condensation strategies (Fig. 19), allow the chemical synthesis of a variety of TASP topologies. It is possible to link peptide blocks of different sequences and opposite orientation. For example, experimental evidence on the influence of the dipole as a function of the parallel or antiparallel arrangement of the chains[34] could be gained.

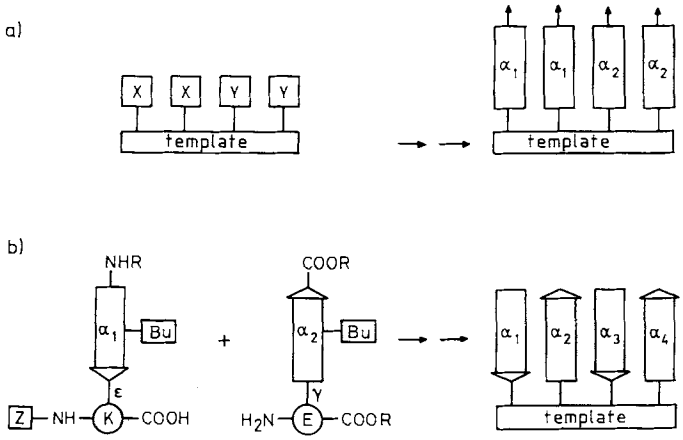


Fig. 19. Synthetic strategies in TASP design: the selective deprotection of protecting groups (see Figs. 17 and 18) allows for the synthesis of TASP molecules with secondary-structure blocks of different sequences. a) The *parallel* assembly of four-helices with two different sequences α_1 and α_2 after independent removal of the protecting groups X and Y, respectively. The synthesis can occur stepwise from the C-terminus or by fragment condensation. b) The block condensation of fully protected peptide sequences in solution allows the synthesis of TASPs with *antiparallel* arrangement of secondary-structure blocks (K, lysine; E, glutamic acid; Z-, Bu-, benzyloxycarbonyl and *tert*-butyl-based protecting groups, respectively).

Stepwise polymer-supported synthesis is the best strategy for rapid evaluation of the overall properties of a designed molecule, whereas segment condensation techniques in solution guarantee higher flexibility and of course better structural reliability (Fig. 19). Is is important to note that the establishment of the postulated tertiary structure only occurs after removal of all side-chain protecting groups at the end of the synthesis. Thus, the synthesis of TASP molecules does not suffer from any specific limitations in comparison to that of linear peptides.[98, 99, 103]

5.4. Properties of TASP Molecules

So far, we have described examples of TASP molecules with βαβ-,[175] 4α-,[172, 176] and 4α/4β-like topologies[174] (Fig. 12) following the methods described above (Fig. 20).

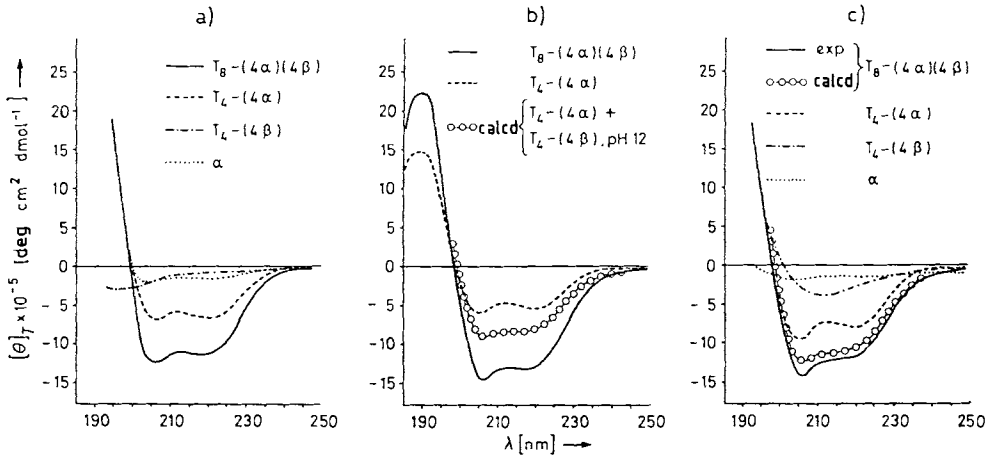


Fig. 20. CD spectra of T_8-(4α)(4β), a representative two-"domain" TASP in buffer at pH 5 (a), pH 7 (b), and pH 12 (c) at a concentration of 0.1 mM (taken from [174]). The sequences are: T_8: Ac-[Lys(α)-Lys(β)]$_2$-Pro-Gly-[Lys(β)-Lys(α)]$_2$-εCA-GlyOH (εCA = ε-amino caproic acid spacer). α: Ac-Glu-Ala-Leu-Glu-Lys-Ala-Leu-Lys-Glu-Ala-Leu-Ala-Leu-Ala-Lys-Leu-Gly-; β: Ac-[Val-Lys]$_4$-Gly-. The ellipticities of the two-"domain" TASP T_8-(4α)(4β) correspond to the experimentally determined values for the individual single "domains" T_4-(4α) and T_4-(4β) at pH 12; at pH 7, a considerable template-enhanced stabilization of the secondary structures is observed. Note that the single peptide block (α) does not show significant helix formation, pointing, again, to the structure-inducing effect of the template (see text).

These experimental studies already point to some characteristic properties of these molecules (Fig. 20), even if a more complete picture of their structural and dynamic properties can only be gained by further work, in particular detailed NMR studies.

1. TASP molecules show good solubility and occur as a rule as monomeric species in aqueous solution. With respect to the postulated structure and its hypothetical "folding mechanism", this finding is of great importance. Indeed, as already mentioned, the highly amphiphilic nature of the secondary-structure blocks explains their strong tendency for aggregation. This can be observed in linear amphiphilic polypeptides of similar size and amino acid composition (such as α-helix and β-sheet oligopeptide blocks joined by loops), where undirected interactions between the blocks often hinder the desired intramolecular folding. In contrast, the covalent grafting of these blocks to the template molecule leads to a forced spatial proximity of the amphiphilic peptide blocks, favoring intramolecular interactions. The intrinsic propensity for aggregation of such blocks can lead in the case of TASP molecules to the desired, compact monomeric species,[175] in which polar side chains point towards the solvent and impart good solubility to the TASP molecule.
2. Spectroscopic measurements (mostly CD and IR) show that the tendency for adopting secondary structure is higher in oligopeptides when they are template-associated. This "template-induced effect" is most striking when secondary-structure formation is observed at a chain length lower than the experimentally determined critical chain length of the same block on its own (Fig. 20).

These results can all be interpreted in terms of the model discussed above. The stabilization of amphiphilic secondary structures in TASP molecules is the consequence of interactions between neighboring peptide blocks on the template. In contrast to the situation met in "isolated" oligopeptides, the critical chain length for secondary structure formation in TASP molecules is comparable to the length of secondary-structure elements observed in natural globular proteins.[106] This stabilization of the blocks arises from the increase in solvation entropy due to release of associated water molecules to the solvent as a hydrophobic "core" is formed between them (through the "hydrophobic interaction"[28]), a process favored by the fixation of the peptide blocks on the template.

Current studies on the denaturation of TASP molecules confirm the above model. They suggest that TASP molecules could show higher stability than their linear polypeptide counterparts with a natural fold (see Section 5.1 and Fig. 14).

The main challenge now is to obtain information on the structural features of TASP molecules in the greatest possible detail. Efforts towards this goal are under way in our laboratory. We are presently synthesizing TASP molecules using different methods of conventional peptide synthesis in solution (Fig. 19) in an attempt to obtain crystallizable products.

6. Prospects and Challenges in Protein Design by Chemical Methods

As we learn an increasing amount about the redesign of secondary structural regions in molecules where tertiary structure is all important, we are moving closer to the time when it will be possible to put together what we have learned about building molecules in regions outside the active site with the work which we have done on the active sites so that we can consider the construction of whole enzymatic systems with new structural features and catalytic functions.

E. T. Kaiser[179]

TASP molecules are a new class of macromolecules, exhibiting structural features of both synthetic polymers (branched chains, graft polymers) and globular proteins (peptide building blocks, hydrophobic core, hydrophilic sur-

face). TASP design is a domain of synthetic organic chemistry. The possibilities for structural variation are limited only by the chemist's intuition (Fig. 21).

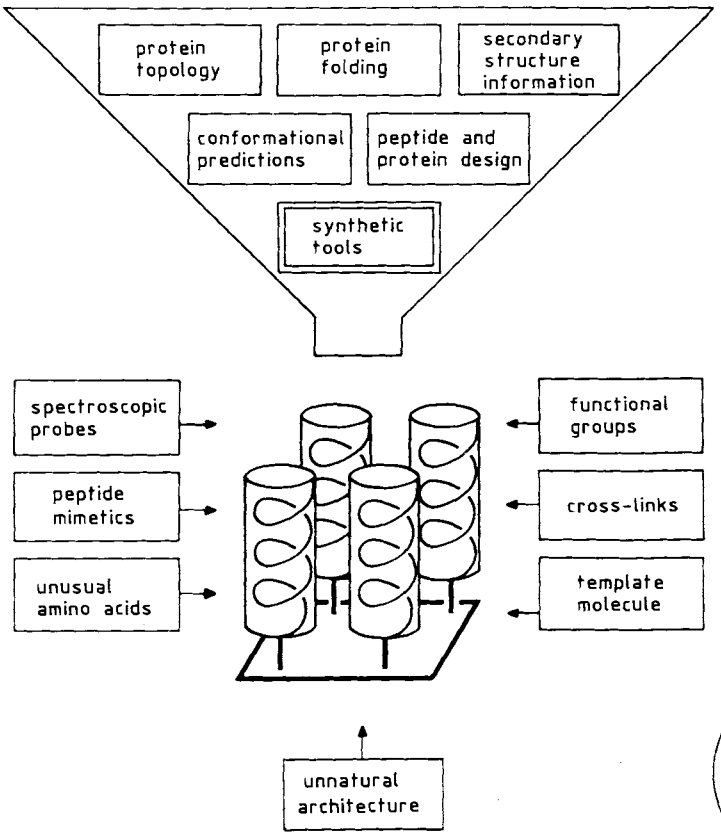


Fig. 21. Nature's rules and chemist's tools [89]: the unification of our knowledge about structure and function of natural proteins with the synthetic tools of the chemist possibly opens new perspectives for the resolution of the folding problem in the construction of new proteins. TASP molecules represent a new generation of macromolecules that exhibit features of both natural proteins (globular structure) and synthetic polymers (unnatural architecture).

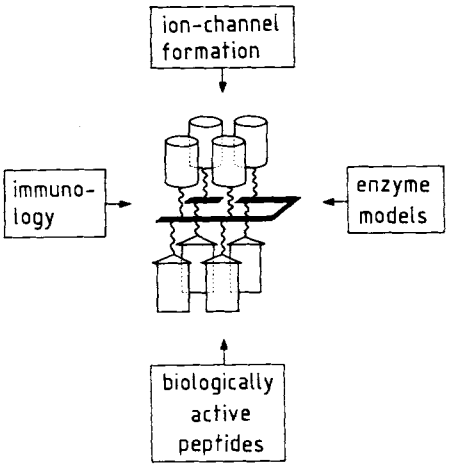


Fig. 22. Application of TASP. From the design of a tertiary structure to function: Once access to molecules with predetermined three-dimensional conformation has been gained, the incorporation of functional properties is the next step in protein design. (see also Figs. 23 and 24). *Sasaki* and *Kaiser* recently reported a molecule that was designed according to these principles and exhibited catalytic activity [176].

On the basis of the results presented in Section 5, we cannot resist proposing that the present approach may represent a generally applicable strategy for the construction of artificial proteins of a variety of structural types, thereby offering a surprising possible solution to the central problem in today's protein de novo design: the troublesome folding process of a linear polypeptide chain into a globular structure can be bypassed by the construction of molecules with an "inbuilt" driving force for folding ("template effect"). Once in a position to design molecules with a predetermined three-dimensional conformation, we will have made the critical step towards the incorporation of function in proteinlike macromolecules (Fig. 22). In this respect, it is encouraging to note that the energetics of such systems (see above, Fig. 14) indicate that TASP molecules may be more tolerant to structure modification than the corresponding linear polypeptides.

Happily enough, interdisciplinary approaches using the methods of both chemistry and molecular biology to study the fascinating questions of modern molecular biology have recently met with success. It seems worthwhile to consider attempts towards tailor-made protein models such as catalytic antibodies,[176, 177] "hybrid enzymes",[178] and enzymes with altered active sites[179] from the perspective of TASP design.

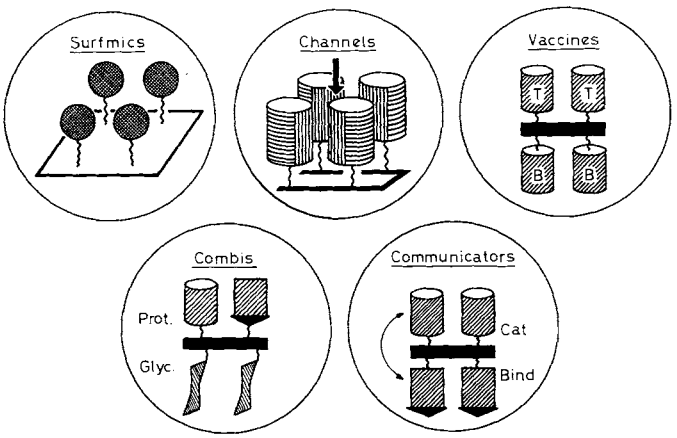


Fig. 23. Perspectives of protein design using the TASP approach. The "reconstruction" of receptor, catalytic, or antigenic sites from a natural protein or enzyme to a tailor-made TASP molecule is of great interest. "Surfmics" would be surface mimetics in which side chains of functionally relevant surface residues are assembled on a template matching the spatial requirements of the active site of the protein. "Communicators" could be molecules such as two-"domain" TASPs (for example, with both a catalytic and a binding site) and "vaccines" would be molecules containing both B and T cell epitopes. "Channels" of well-defined size could emerge from putting various numbers of amphiphilic, membrane-spanning helices (with formation of a hydrophilic core and a hydrophobic surface [184]) on a specially designed template. A "glycoprotein-like" molecule might be obtained by combining peptidic and glycosidic elements on a template ("combis") following the principles of TASP synthesis described in the text. Exploratory studies on the design and synthesis of such "functional" TASP molecules are in progress in our laboratory.

The schematically drawn TASP molecules shown in Figure 23 point to such possibilities. The design and synthesis of such systems will be a platform for interdisciplinary research in the near future. Perhaps the computer-created molecules shown in Figure 24 will not remain on the screen much longer.

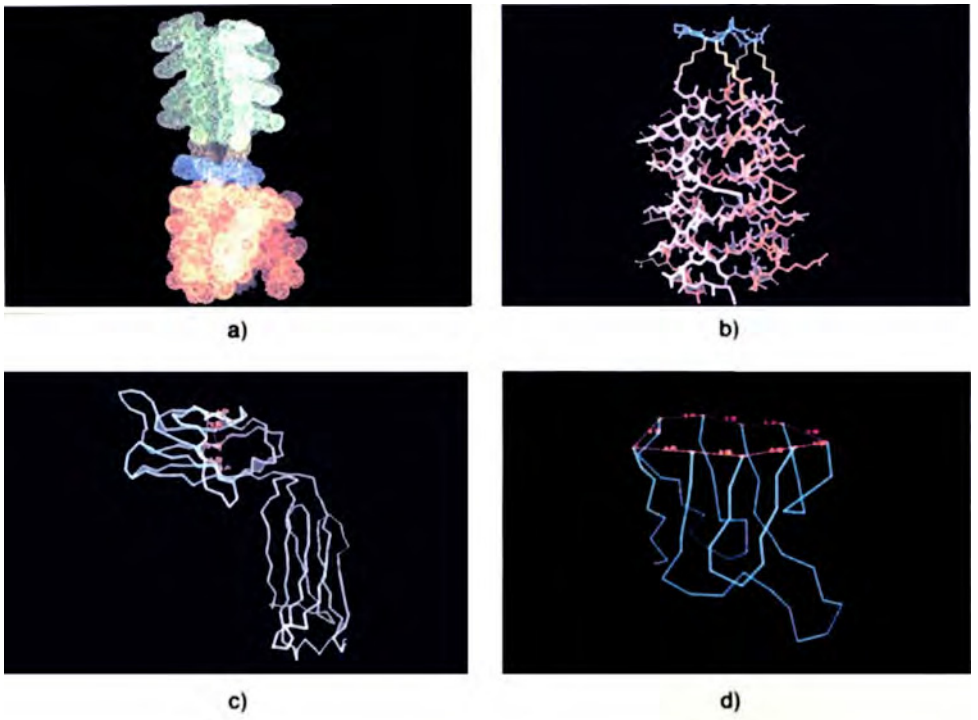


Fig. 24. Possible applications of the TASP approach for the design of functional artificial proteins. To date, most of these examples exist only on the computer screens they were designed on. Fortunately, we were able to take some pictures before the structures disappeared. We are now actively trying to find them again in the test-tube. a) Side view of a template-assembled "two-domain" protein model [174] (T_8-(4α)(4β) in Fig. 12) (template in blue, lysine side chains in yellow, four-helix-bundle structure in red, 4β structure in green). The independent functionalization of the two folding units opens a variety of possibilities (see Figs. 22 and 23). b) Template-assembled model of the ROP protein [180], a biologically relevant TASP molecule. The four-helix bundle protein ROP, which consists of a helix-turn-helix dimer was modeled so as to allow a covalent fixation of the four helices (white, red, magenta, ocher) on a tetrafunctional template (blue, lysine side chains in yellow). After conformational relaxation of the template, the TASP ROP model showed a strain-free three-dimensional conformation with a packing arrangement similar to that of the natural structure [181]. c) TASP molecules with binding properties: The variable domain of the phosphocholine-binding immunoglobulin McPC 603 Fab fragment [182] (left) was cut (red line) from the rest of the protein and grafted onto a tailor-made template (right). The synthetic accessibility of protein subdomains following this ideas [183] could extend the template concept still further.

The authors gratefully acknowledge the financial support of the Swiss National Science Foundation, the Hoffmann-La Roche Research Foundation, and the CIBA Foundation. S. V. thanks the "Stiftung der schweizerischen chemischen Industrie" for a doctoral grant. M. M. would like to express his thanks to all cited co-workers past and present, as well as to Priv.-Doz. Dr. K. Müller and Dr. K. Gubernator, Hoffmann-La Roche, Basel, for their essential collaboration in the molecular modeling work. We thank R. Bielmann for drawing the figures.

Received: October 4, 1988 [A 717 IE]
German version: *Angew. Chem. 101* (1989) 551

[1] P. J. Flory, *Statistical Mechanics of Chain Molecules*, Interscience, New York 1969.
[2] T. E. Creighton: *Proteins*, Freeman, New York 1983.
[3] G. E. Schulz, R. H. Schirmer: *Principles of Protein Structure*, Springer, Berlin 1979.
[4] M. Mutter, *Angew. Chem. 97* (1985) 639; *Angew. Chem. Int. Ed. Engl. 24* (1985) 639.
[5] Examples: a) J. E. Davies, H. G. Gassen, *Angew. Chem. 95* (1983) 26; *Angew. Chem. Int. Ed. Engl. 22* (1983) 13; b) E. Gross, J. Meienhofer (Eds.): *The Peptides: Analysis, Synthesis, Biology*, Academic Press, New York; c) R. Wetzel, D. V. Goeddel in [5b], *Vol. 5*, 1983, p. 2.
[6] D. Blohm, C. Bollschweiler, H. Hillen, *Angew. Chem. 100* (1988) 213; *Angew. Chem. Int. Ed. Engl. 27* (1988) 207.
[7] E. Fischer, *Ber. Dtsch. Chem. Ges. 39* (1906) 530.
[8] E. Fischer, *Ber. Dtsch. Chem. Ges. 40* (1907) 1754.
[9] a) J. S. Richardson, *Adv. Protein Chem. 34* (1981) 167; b) A. V. Finkelstein, O. B. Ptitsyn, *Prog. Biophys. Mol. Biol. 50* (1987) 171.
[10] a) W. Kabsch, C. Sander, *Proc. Natl. Acad. Sci. USA 81* (1984) 1075; b) I. A. Wilson, D. H. Haft, E. D. Getzoff, J. A. Tainer, R. A. Lerner, S. Brenner, *ibid. 82* (1985) 5255; c), P. Argos, *J. Mol. Biol. 197* (1987) 331.
[11] R. Jaenicke, *Prog. Biophys. Mol. Biol. 49* (1987) 117.
[12] T. E. Creighton, *Proc. Natl. Acad. Sci. USA 85* (1988) 3082.
[13] T. J. Edsall in R. Alexander (Ed.): *Structural Chemistry and Molecular Biology*, Freeman, San Francisco 1968, p. 88.
[14] C. B. Anfinsen, *Science (Washington, D.C.) 181* (1973) 223.
[15] C. Levinthal, *J. Chim. Phys. 65* (1968) 44.
[16] K. A. Dill, *Biochemistry 24* (1985) 1501.
[17] G. N. Ramachandran, V. Sasisekharan, *Adv. Protein Chem. 23* (1968) 283.
[18] C. Tanford, *Adv. Protein Chem. 23* (1968) 121.
[19] a) F. M. Richards, *Annu. Rev. Biophys. Bioeng. 6* (1977) 151; b) M. H. Zehfus, G. D. Rose, *Biochemistry 25* (1986) 5759.
[20] a) T. E. Creighton, *Nature (London) 326* (1987) 547; b) D. J. Barlow, J. M. Thornton, *J. Mol. Biol. 201* (1988) 601; c) L. G. Presta, G. D. Rose, *Science (Washington, D.C.) 240* (1988) 1632; d) J. S. Richardson, D. C. Richardson, *ibid. 240* (1988) 1640.
[21] F. R. Salemme, *Prog. Biophys. Mol. Biol. 42* (1983) 95.
[22] a) G. D. Rose, L. M. Gierasch, J. A. Smith, *Adv. Protein Chem. 37* (1985) 1; b) E. J. Milner-White, R. Poet, *Trends Biochem. Sci. Pers. Ed. 12* (1987) 189.
[23] a) R. L. Baldwin, *Trends Biochem. Sci. Pers. Ed. 11* (1986) 6; b) P. S. Kim, R. L. Baldwin, *Annu Rev. Biochem. 51* (1982) 459.
[24] See, e.g., a) R. Pain, *Trends Biochem. Sci. Pers. Ed. 12* (1987) 309; b) D. A. Dolgikh, R. I. Gilmanshin, E. V. Brazhnikov, V. E. Bychkova, G. V. Semisotnov, S. Y. Venyaminov, O. B. Ptitsyn, *FEBS Lett. 136* (1981) 311; c) M. Ohgushi, A. Wada, *ibid. 164* (1983) 21; d) K. Kuwajima, H. Yamaya, S. Miwa, S. Sugai, T. Nagamura, *ibid. 221* (1987) 115.
[25] S. C. Harrison, R. Durbin, *Proc. Natl. Acad. Sci. USA 82* (1985) 4028.
[26] R. Freedman, *Nature (London) 329* (1987) 196 and references cited therein.
[27] H. Pelham, *Nature (London) 332* (1988) 776 and references cited therein.
[28] W. Kauzmann, *Adv. Protein Chem. 14* (1959) 1.
[29] a) A. Radzicka, R. Wolfenden, *Biochemistry 27* (1988) 1664; b) J.-L. Fauchère, V. Pliska, *Eur. J. Med. Chem. Chim. Ther. 18* (1983) 369; c) G. D. Rose, A. R. Geselowitz, G. J. Lesser, R. H. Lee, M. H. Zehfus, *Science (Washington, D.C.) 229* (1985) 834 and references cited therein.
[30] D. Eisenberg, A. D. McLachlan, *Nature (London) 319* (1986) 199.
[31] E. N. Baker, R. E. Hubbard, *Prog. Biophys. Mol. Biol. 44* (1984) 97.

[32] A. Warshel, *Nature (London) 330* (1987) 15.
[33] a) D. J. Barlow, J. M. Thornton, *J. Mol. Biol. 168* (1983) 867; b) A. A. Rashin, B. Honig, *ibid. 173* (1984) 515.
[34] a) W. G. J. Hol, P. T. van Duijnen, H. J. C. Berendsen, *Nature (London) 273* (1978) 443; b) W. G. J. Hol, L. M. Halie, C. Sander, *ibid. 294* (1980) 532; c) R. M. Sheridan, R. M. Levy, F. R. Salemme, *Proc. Natl. Acad. Sci. USA 79* (1982) 4545; d) W. G. J. Hol, *Prog. Biophys. Mol. Biol. 45* (1985) 149; e) K.-C. Chou, G. M. Maggiora, G. Nemethy, H. A. Scheraga, *Proc. Natl. Acad. Sci. USA 85* (1988) 4295.
[35] a) K. R. Shoemaker, P. S. Kim, E. J. York, J. M. Stewart, R. L. Baldwin, *Nature (London) 326* (1987) 563; b) S. Marqusee, R. L. Baldwin, *Proc. Natl. Acad. Sci. USA 84* (1987) 8898.
[36] T. E. Creighton, *Prog. Biophys. Mol. Biol. 33* (1978) 231.
[37] R. Wetzel, *Trends Biochem. Sci. Pers. Ed. 12* (1987) 478.
[38] R. Huber, *Angew. Chem. 100* (1988) 79; *Angew. Chem. Int. Ed. Engl. 27* (1988) 79.
[39] H. Frauenfelder, F. Parak, R. D. Young, *Annu. Rev. Biophys. Biophys. Chem. 17* (1988) 451.
[40] J. A. McCammon, S. C. Harvey: *Dynamics of Proteins and Nucleic Acids*, Cambridge University Press, Cambridge 1987.
[41] P. L. Privalov, *Adv. Protein Chem. 33* (1979) 167.
[42] a) H. A. Scheraga, *Biopolymers 22* (1983) 1; b) V. J. Hruby (Ed.): *The Peptides: Analysis, Synthesis, Biology, Vol. 7*, Academic Press, Orlando 1985; c) S. S. Zimmermann in [42b], p. 165.
[43] a) A. T. Hagler in [42b], p. 213; b) W. L. Jorgensen, J. Tirado-Rives, *J. Am. Chem. Soc. 110* (1988) 1657; c) M. Levitt, R. Sharon, *Proc. Natl. Acad. Sci. USA 85* (1988) 7557.
[44] J. M. Thornton, *Nature (London) 335* (1988) 10.
[45] C. DeLisi, *Science (Washington, D.C.) 240* (1988) 47.
[46] G. von Heijne, *Nature (London) 333* (1988) 605.
[47] P. Y. Chou, G. D. Fasman, *Adv. Enzymol. 47* (1978) 45.
[48] J. Garnier, D. J. Osguthorpe, B. Robson, *J. Mol. Biol. 120* (1978) 97.
[49] S. Tanaka, H. A. Scheraga, *Macromolecules 10* (1977) 305, and references cited therein.
[50] M. Schiffer, A. B. Edmundson, *Biophys. J. 7* (1967) 121.
[51] P. Dunnill, *Biophys. J. 8* (1968) 865.
[52] a) V. I. Lim, *J. Mol. Biol. 88* (1974) 857; b) *ibid. 88* (1974) 873.
[53] One-letter code for amino acids: IUPAC-IUB Joint Commission on Biochemical Nomenclature (JCBN), *Biochem. J. 219* (1984) 345; *Eur. J. Biochem. 138* (1984) 9.
[54] W. R. Taylor, *Protein Eng. 2* (1988) 77, zit. Lit.
[55] a) W. Kabsch, C. Sander, *FEBS Lett. 155* (1983) 179; b) K. Nishikawa, *Biochim. Biophys. Acta 748* (1983) 285.
[56] a) G. E. Schulz, *Annu. Rev. Biophys. Biophys. Chem. 17* (1988) 1; b) R. Y. Yada, R. L. Jackman, S. Nakai, *Int. J. Pept. Protein Res. 31* (1988) 98; c) M. J. Rooman, S. J. Wodak, *Nature (London) 335* (1988) 45.
[57] C. Pabo, *Nature (London) 301* (1983) 200.
[58] K. E. Drexler, *Proc. Natl. Acad. Sci. USA 78* (1981) 5275.
[59] J. W. Ponder, F. M. Richards, *J. Mol. Biol. 193* (1987) 775.
[60] a) P. Kollman, *Annu. Rev. Phys. Chem. 38* (1987) 303; b) J. A. McCammon, *Science (Washington, D.C.) 238* (1987) 486; c) H. Frühbeis, R. Klein, H. Wallmeier, *Angew. Chem. 99* (1987) 413; *Angew. Chem. Int. Ed. Engl. 26* (1987) 403.
[61] a) T. Blundell, D. Carney, S. Gardner, F. Hayes, B. Howlin, T. Hubbard, J. Overington, D. A. Singh, B. L. Sibanda, M. Sutcliffe, *Eur. J. Biochem. 172* (1988) 513; b) W. G. J. Hol, *Angew. Chem. 98* (1986) 765; *Angew. Chem. Int. Ed. Engl. 25* (1986) 767.
[62] See, e.g.: D. Botstein, D. Shortle, *Science (Washington, D.C.) 229* (1985) 1193.
[63] a) R. J. Leatherbarrow, A. R. Fersht, *Protein Eng. 1* (1986) 1; b) J. R. Knowles, *Science (Washington, D.C.) 236* (1987) 1252; c) W. V. Shaw, *Biochem. J. 246* (1987) 1.
[64] A. R. Fersht, J.-P. Shi, A. J. Wilkinson, D. M. Blow, P. Carter, M. M. Y. Waye, G. P. Winter, *Angew. Chem. 96* (1984) 455; *Angew. Chem. Int. Ed. Engl. 23* (1984) 467.
[65] R. E. Feeney, *Int. J. Pept. Protein Res. 29* (1987) 145.
[66] Example: D. L. Oxender, C. F. Fox (Eds.): *Protein Engineering*, Alan R. Liss, New York 1987.
[67] L. J. Perry, R. Wetzel, *Science (Washington, D.C.) 226* (1984) 555.
[68] J. A. Wells, D. A. Estell, *Trends Biochem. Sci. Pers. Ed. 13* (1988) 291.
[69] C. S. Craik, S. Roczniak, C. Largman, W. J. Rutter, *Science (Washington, D.C.) 237* (1987) 909.
[70] S. J. Gardell, C. S. Craik, D. Hilvert, M. S. Urdea, W. J. Rutter, *Nature (London) 317* (1985) 551.
[71] W. H. J. Ward, A. R. Fersht in S. A. Benner (Ed.): *Redesigning the Molecules of Life*, Springer, Berlin 1988, p. 59.
[72] K. M. Perry, J. J. Onuffer, N. A. Touchette, C. S. Herndon, M. S. Gittelman, C. R. Matthews, J.-T. Chen, R. J. Mayer, K. Taira, S. J. Benkovic, E. E. Howell, J. Kraut, *Biochemistry 26* (1987) 2674.
[73] D. N. Brems, S. M. Plaisted, H. A. Harel, C.-S. C. Tomich, *Proc. Natl. Acad. Sci. USA 85* (1988) 3367.
[74] R. F. Kelley, F. M. Richards, *Biochemistry 26* (1987) 6765.
[75] P. A. Evans, C. M. Dobson, R. A. Kautz, G. Hatfull, R. O. Fox, *Nature (London) 329* (1987) 266.
[76] D. Shortle, A. K. Mieker, E. Freire, *Biochemistry 27* (1988) 4761.
[77] J. F. Reidhaar-Olson, R. T. Sauer, *Science (Washington, D.C.) 241* (1988) 53.
[78] a) B. W. Matthews, *Biochemistry 26* (1987) 6885 (review); b) T. Alber, S. Dao-Pin, K. Wilson, J. A. Wozniak, S. P. Cook, B. W. Matthews, *Nature (London) 330* (1987) 41; c) T. Alber, S. Dao-Pin, J. A. Nye, D. C. Muchmore, B. W. Matthews, *Biochemistry 26* (1987) 3754.
[79] T. Alber, J. A. Bell, S. Dao-Pin, H. Nicholson, J. A. Wozniak, S. Cook, B. W. Matthews, *Science (Washington, D.C.) 239* (1988) 631.
[80] M. Matsumura, W. J. Bechtel, B. W. Matthews, *Nature (London) 334* (1988) 406.
[81] J. T. Kellis, K. Nyberg, D. Sali, A. R. Fersht, *Nature (London) 333* (1988) 784.
[82] a) D. Sali, M. Bycroft, A. R. Fersht, *Nature (London) 335* (1988) 740; b) H. Nicholson, W. J. Becktel, B. W. Matthews, *ibid. 336* (1988) 651.
[83] A. R. Fersht, *Trends Biochem. Sci. Pers. Ed. 12* (1987) 301.
[84] D. P. Goldenberg, *Annu. Rev. Biophys. Biophys. Chem. 17* (1988) 481.
[85] M. G. Rossman, P. Argos, *Annu. Rev. Biochem. 50* (1981) 497.
[86] C. Chothia, *Annu. Rev. Biochem. 53* (1984) 537.
[87] J. F. Leszczynski, G. D. Rose, *Science (Washington, D.C.) 234* (1987) 849.
[88] B. H. Zimm, J. K. Bragg, *J. Chem. Phys. 31* (1959) 526.
[89] M. Mutter, *Trends Biochem. Sci. Pers. Ed. 13* (1988) 260.
[90] a) E. T. Kaiser, F. J. Kezdy, *Science (Washington, D.C.) 223* (1984) 249; b) E. T. Kaiser, *Trends Biochem. Sci. Pers. Ed. 12* (1987) 305; c) E. T. Kaiser, F. J. Kezdy, *Annu. Rev. Biophys. Biophys. Chem. 16* (1987) 561.
[91] a) G. Ebert, *Top. Curr. Chem. 128* (1985) 1; b) M. Mutter, R. Hersperger, unpublished.
[92] S. P. Ho, W. F. DeGrado, *J. Am. Chem. Soc. 109* (1987) 6751.
[93] M. Goodman, C. Toniolo, F. Naider in E. R. Blout, F. A. Bovey, M. Goodman, N. Lotan (Eds.): *Peptides and Proteins*, Wiley, New York 1974, p. 308.
[94] F. Maser, K. Bode, V. N. R. Pillai, M. Mutter, *Adv. Polym. Sci. 65* (1983) 177.
[95] a) J. M. Becker, F. Naider, *Biopolymers 17* (1978) 2189; b) F. Naider, J. M. Becker, A. Ribeiro, M. Goodman, *ibid. 17* (1978) 2213.
[96] D. J. Cram, K. N. Trueblood, *Top. Curr. Chem. 98* (1981) 43.
[97] a) H. A. Scheraga, *Pure Appl. Chem. 50* (1978) 315; b) M. Sueki, S. Lee, S. P. Powers, J. B. Denton, Y. Konishi, H. A. Scheraga, *Macromolecules 17* (1984) 148.
[98] a) M. Mutter, V. N. R. Pillai, H. Anzinger, E. Bayer, C. Toniolo in K. Brunfeldt (Ed.): *Peptides 1980*, Scriptor, Copenhagen 1981, p. 660; b) S. Abdel Rahman, H. Anzinger, M. Mutter, *Biopolymers 19* (1980) 173; c) V. N. R. Pillai, M. Mutter, *Acc. Chem. Res. 14* (1981) 122; d) C. M. Deber, V. J. Hruby, K. D. Kopple (Eds.): *Peptides Structure and Function*, Pierce Chemical Company, Rockford 1985; e) M. Mutter, K.-H. Altmann, D. Bellof, A. Flörsheimer, J. Herbert, M. Huber, B. Klein, L. Strauch, T. Vorherr, H.-U. Gremlich in [98d], p. 397.
[99] a) F. Maser, B. Klein, M. Mutter, C. Toniolo, G. M. Bonora, *Biopolymers 22* (1983) 233; b) M. Mutter, F. Maser, K.-H. Altmann, C. Toniolo, G. M. Bonora, *ibid. 24* (1985) 1057.
[100] a) K.-H. Altmann, M. Mutter, *Int. J. Pept. Protein Res. 26* (1985) 373; b) K.-H. Altmann, A. Flörsheimer, M. Mutter, *ibid. 27* (1986) 314.
[101] K. Bode, M. Mutter, M. Goodman, *Helv. Chim. Acta 68* (1985) 705.
[102] See, e.g., J. Murphy, W.-J. Zhang, W. Macaulay, G. Fasman, R. B. Merrifield, *J. Biol. Chem. 262* (1987) 17304.
[103] a) S. B. H. Kent in [98d], p. 407; b) E. Atherton, R. C. Sheppard in [98d], p. 415; c) A. G. Ludwick, L. W. Jelinski, D. Live, A. Kintanar, J. J. Dumais, *J. Am. Chem. Soc. 108* (1986) 6493; d) C. Toniolo, G. M. Bonora, E. P. Heimer, A. M. Felix, *Int. J. Pept. Protein Res. 30* (1987) 232.
[104] M. Mutter, E. Bayer in [5b], *Vol. 2*, 1980, p. 285.
[105] See, e.g., D. G. Osterman, E. T. Kaiser, *J. Cell. Biochem. 29* (1985) 57.
[106] W. R. Taylor, J. M. Thornton, *J. Mol. Biol. 173* (1984) 487.
[107] G. M. Bonora, M. Palumbo, C. Toniolo, M. Mutter, *Makromol. Chem. 180* (1979) 1293.
[108] M. Mutter, K.-H. Altmann, *Angew. Makromol. Chem. 145/146* (1986) 211.
[109] A. Flörsheimer, Ph. D. Thesis, Universität Basel 1986.
[110] M. Mutter, K.-H. Altmann, A. Flörsheimer, J. Herbert, *Helv. Chim. Acta 69* (1986) 786.
[111] See, e.g.: a) D. Leibfritz, E. Haupt, N. Dubischer, H. Lachmann, R. Oekonomopoulos, G. Jung, *Tetrahedron 38* (1982) 2165; b) C. Toniolo, G. M. Bonora, A. Bavoso, E. Benedetti, B. Di Blasio, V. Pavone, C. Pedone, *Biopolymers 22* (1983) 205; c) B. V. V. Prasad, P. Balaram, *CRC Crit. Rev. Biochem. 16* (1984) 307; d) G. Valle, M. Crisma, F. Formaggio, C. Toniolo, G. Jung, *Liebigs Ann. Chem. 1987*, 1055; e) E. K. S. Vijayakumar, T. S. Sudha, P. Balaram, *Biopolymers 23* (1984) 877; f) H. Schmitt, G. Jung, *Liebigs Ann. Chem. 1985*, 321; g) H. Balaram, M. Sukumar, P. Balaram, *Biopolymers 25* (1987) 2209; h) J. R. Cann, R. E. London, C. J. Unkefer, R. J. Vavrek, J. M. Stewart, *Int. J. Pept. Protein Res. 29* (1987) 486; i) G. E. Esposito, J. A. Caver, J. Boyd, I. D. Campbell, *Biochemistry 26* (1987) 1043; j) P. Wipf, H. Heimgartner, *Helv. Chim. Acta 71* (1988) 140; k) *ibid. 71* (1988) 258; l) I. L. Karle,

J. L. Flipper-Anderson, M. Sukumar, P. Balaram, *Int. J. Pept. Protein Res. 31* (1988) 567.
[112] M. Mutter, M. Huber, S. Vuilleumier, unpublished.
[113] A. W. Burgess, S. J. Leach, *Biopolymers 12* (1973) 2599.
[114] a) U. Schöllkopf, *Top. Curr. Chem. 109* (1983) 65; b) G. C. Barrett in G. C. Barrett (Ed.): *Chemistry and Biochemistry of the Amino Acids*, Chapman and Hall, London 1985, S. 246; c) D. Seebach, R. Imwinkelried, T. Weber in R. Scheffold (Ed.): *Modern Synthetic Methods, Vol. 4*, Springer, Berlin 1986, p. 125.
[115] a) E. Altmann, K.-H. Altmann, M. Mutter, *Angew. Chem. 100* (1988) 855; *Angew. Chem. Int. Ed. Engl. 27* (1988) 858; b) E. Altmann, K.-H. Altmann, K. Nebel, M. Mutter, *Int. J. Pept. Protein Res. 32* (1988) 344.
[116] a) K. Wüthrich: *NMR of Proteins and Nucleic Acids*, Wiley, New York 1986; b) H. Kessler, M. Gehrke, C. Griesinger, *Angew. Chem. 100* (1988) 507; *Angew. Chem. Int. Ed. Engl. 27* (1988) 490; c) M. Nilges, A. M. Gronenborn, A. T. Brünger, G. M. Clore, *Protein Eng. 2* (1988) 27; d) R. Kaptein, R. Boelens, R. M. Scheek, W. F. van Gunsteren, *Biochemistry 27* (1988) 5389.
[117] a) R. W. Woody in [42b], p. 15; b) W. C. Johnson, Jr, *Annu. Rev. Biophys. Biophys. Chem. 17* (1988) 145; c) A. M. Labhart, *Meth. Enzymol. 131* (1986) 126.
[118] a) S. Krimm, J. Bandekar, *Adv. Protein Chem. 38* (1986) 181; b) W. K. Surewicz, H. H. Mantsch, *Biochim. Biophys. Acta 952* (1988) 115; c) T. A.-Keiderling, *Nature (London) 322* (1986) 851.
[119] a) A. Bierzinski, P. S. Kim, R. L. Baldwin, *Proc. Natl. Acad. Sci. USA 79* (1982) 2470; b) P. S. Kim, R. L. Baldwin, *Nature (London) 307* (1984) 329; c) K. R. Shoemaker, P. S. Kim, D. N. Brems, S. Marqusee, E. J. York, I. M. Chaiken, J. M. Stewart, R. L. Baldwin, *Proc. Natl. Acad. Sci. USA 82* (1985) 2349.
[120] a) M. Vasquez, M. R. Pincus, H. A. Scheraga, *Biopolymers 26* (1987) 351; b) M. Vasquez, H. A. Scheraga, *ibid. 27* (1987) 41.
[121] a) T. G. Oas, P. S. Kim, *Nature (London) 336* (1988) 42; b) P. E. Wright, H. J. Dyson, R. A. Lerner, *Biochemistry 27* (1988) 7167.
[122] K. T. O'Neil, H. R. Wolfe, Jr., S. Erickson-Viitanen, W. F. DeGrado, *Science (Washington, D.C.) 236* (1987) 1454.
[123] A. D. Frenkel, J. M. Berg, C. O. Pabo, *Proc. Natl. Acad. Sci. USA 84* (1987) 4841.
[124] J. D. Lear, Z. R. Wasserman, W. F. DeGrado, *Science (Washington, D.C.) 240* (1988) 1177.
[125] W. J. Kullmann, *J. Med. Chem. 27* (1984) 106.
[126] See, e.g.: a) R. Mayer, G. Lancelot, C. Helene, *FEBS Lett. 153* (1983) 339; b) L. Walters, E. T. Kaiser, *J. Am. Chem. Soc. 107* (1985) 6422.
[127] a) E. Pfaff, M. Mussgay, H. O. Böhm, G. E. Schultz, H. Schaller, *EMBO J. 1* (1982) 869; b) H. J. Dyson, R. A. Lerner, P. E. Wright, *Annu. Rev. Biophys. Biophys. Chem. 17* (1988) 305; c) M. Mutter, K.-H. Altmann, K. Müller, S. Vuilleumier, T. Vorherr, *Helv. Chim. Acta 69* (1986) 985.
[128] a) B. Gutte, M. Däumigen, E. Wittschieber, *Nature (London) 281* (1979) 650; b) R. Jaenicke, B. Gutte, U. Glatter, W. Strassburger, A. Wollmer, *FEBS Lett. 114* (1980) 161.
[129] R. Moser, R. M. Thomas, B. Gutte, *FEBS Lett. 157* (1983) 247.
[130] R. Moser, J. Frey, K. Münger, T. Hehlgans, J. Klauser, H. Langen, E.-L. Winnacker, R. Mertz, B. Gutte, *Protein Eng. 1* (1987) 339.
[131] S. Y. M. Lau, A. K. Taneja, R. S. Hodges, *J. Biol. Chem. 259* (1984) 13253.
[132] a) F. R. Carbone, S. J. Leach, *Int. J. Pept. Protein Res. 26* (1985) 225; b) *ibid. 26* (1985) 498.
[133] M. Mutter, K.-H. Altmann, T. Vorherr, *Z. Naturforsch. B41* (1986) 1315.
[134] B. W. Erickson, S. B. Daniels, P. A. Reddy, C. G. Unson, J. S. Richardson, D. C. Richardson in R. Fletterick, M. Zoller (Eds.): *Current Communications in Molecular Biology, Computer Graphics and Molecular Modeling*, Cold Spring Harbor Laboratory, New York 1986, p. 53.
[135] J. S. Richardson, D. C. Richardson in [66], p. 149.
[136] D. Eisenberg, W. Wilcox, S. M. Eshita, P. M. Pryciak, S. P. Ho, W. F. DeGrado, *Proteins 1* (1986) 16.
[137] W. F. DeGrado, L. Regan, S. P. Ho, *Cold Spring Harbor Symp. Quant. Biol. 52* (1987) 521.
[138] L. Regan, W. F. DeGrado, *Science (Washington, D.C.) 241* (1988) 976.
[139] a) E. Wünsch (Ed.): *Methoden der Organischen Chemie (Houben-Weyl), Band XV*, Thieme, Stuttgart 1974; b) M. Bodansky: *Principles of Peptide Synthesis*, Springer, Berlin 1984; c) *The Practice of Peptide Synthesis*, Springer, Berlin 1984.
[140] a) C. Birr: *Aspects of the Merrifield Peptide Synthesis*, Springer, Berlin 1978; b) J. M. Stewart, J. D. Young: *Solid Phase Peptide Synthesis*, Pierce Chemical Company, Rockford 1984.
[141] J. Meienhofer et al. (Eds.): *The Peptides, Analysis, Synthesis, Biology, Vol. 1–9*, Academic Press, New York 1979–1987.
[142] a) D. Theodoropoulos (Ed.): *Peptides 1986, Proceedings of the 19th European Peptide Symposium*, W. de Gruyter, Berlin 1987; b) G. R. Marshall (Ed.): *Peptides Chemistry and Biology, Proceedings of the 10th American Peptide Symposium*, Escom, Leiden 1988.
[143] R. B. Merrifield, *J. Am. Chem. Soc. 85* (1963) 2149.
[144] S. Josephson, R. Bishop, *Trends Biotechnol. 6* (1988) 218.
[145] J. S. Huston, D. Levinson, M. Mudgett-Hunter, M.-S. Tai, J. Novotny, M. N. Margolies, R. J. Ridge, R. E. Bruccoleri, E. Haber, R. Crea, H. O. P. Permann, *Proc. Natl. Acad. Sci. USA 85* (1988) 5879.
[146] See, e.g.: a) S. Kiyama, N. Fujii, H. Yajima, M. Moriga, A. Takagi, *Int. J. Pept. Protein Res. 23* (1984) 174; b) H. Schmitt, G. Jung, *Liebigs Ann. Chem. 1985*, 321; c) A. M. Felix, E. P. Heimer, C. T. Wang, T. J. Lambros, J. S. Wistok, M. Roszkowski, M. Ahmad, A. Confalone, J. W. Scott, D. Parker, J. Meienhofer, A. Trzeciak, D. Gillessen, *Int. J. Pept. Protein Res. 26* (1985) 130; d) N. Fujii, M. Sakurai, K. Akaji, M. Nomisu, H. Yajima, K. Mizuta, M. Aono, M. Moriga, K. Inoue, R. Hosotani, T. Tobe, *Chem. Pharm. Bull. 34* (1986) 2397; e) K. Ando, K. Kitagawa, S. Kiyama, T. Kawamoto, T. Akita, I. Yamamoto, K. K. Torizuka, *ibid. 35* (1987) 60; f) E. Wünsch, L. Moroder, S. Göhring-Romani, H. J. Musiol, W. Göhring, G. Bovermann, *Int. J. Pept. Protein Res. 32* (1988) 368.
[147] S. B. H. Kent, *Annu. Rev. Biochem. 57* (1988) 957.
[148] a) G. Barany, R. B. Merrifield in [5b], *Vol. 2*, 1980, p. 3; b) G. Barany, N. Kneib-Cordonier, D. G. Mullen, *Int. J. Pept. Protein Res. 30* (1987) 705.
[149] a) I. Clark-Lewis, R. Aebersold, H. Ziltener, J. W. Schrader, L. E. Hood, S. B. H. Kent, *Science (Washington, D.C.) 231* (1986) 134; b) W. F. Heath, R. B. Merrifield, *Proc. Natl. Acad. Sci. USA 83* (1986) 6367; c) J. D. Wade, S. P. Fitzgerald, M. R. McDonald, J. G. McDougall, G. W. Tregear, *Biopolymers 25* (1986) S21; d) A. N. Eberle, E. Atherton, A. Dryland, R. C. Sheppard, *J. Chem. Soc. Perkin Trans. 1 1986*, 361; e) G.-S. Lu, S. Mojsov, R. B. Merrifield, *Int. J. Pept. Protein Res. 29* (1987) 545; f) J. Rivier, R. Galejean, L. Simon L. J. Cruz, B. M. Olivera, W. R. Gray, *Biochemistry 26* (1987) 8508; g) A. Fournier, C. T. Wang, A. M. Felix, *Int. J. Pept. Protein Res. 31* (1988) 1; h) C.-R. Wu, J. D. Wade, G. W. Tregear, *ibid. 31* (1988) 47; i) D. Hudson, *J. Org. Chem. 53* (1988) 617; j) Y.-Z. Lin, G. Caporoso, P.-Y. Chang, X.-H. Lee, J. P. Tam, *Biochemistry 27* (1988) 5640; k) K. Nokihara, T. Semba, *J. Am. Chem. Soc. 110* (1988) 7847; l) R. F. Nutt, S. F. Brady, P. L. Darke, T. M. Ciccarone, C. D. Colton, E. M. Nutt, J. A. Rodkey, C. D. Bennett, L. H. Waxman, I. S. Sigal, P. S. Anderson, D. F. Veber, *Proc. Natl. Acad. Sci. USA 85* (1988) 7129; m) I. Clark-Lewis, L. E. Hood, S. B. H. Kent, *ibid. 85* (1988) 7897; n) E. Atherton, J. L. Holder, R. C. Sheppard, R. M. Valerio, *J. Chem. Soc. Perkin Trans. 1 1988*, 2887; o) L. R. Cameron, J. L. Holder, M. Meldal, R. C. Sheppard, *ibid. 1 1988*, 2895.
[150] B. Rajashekar, E. T. Kaiser, *J. Biol. Chem. 261* (1986) 13617.
[151] a) S. H. Nakagawa, H. S. H. Lau, F. J. Kezdy, E. T. Kaiser, *J. Am. Chem. Soc. 107* (1985) 7087; b) J. Blake, D. Yamashiro, K. Ramasharma, C. H. Li, *Int. J. Pept. Protein Res. 28* (1986) 468; c) T. Kubiak, D. B. Whitney, R. B. Merrifield, *Biochemistry 26* (1987) 7849; d) R. E. Reid, *Int. J. Pept. Protein Res. 30* (1987) 613; e) M. Narita, S. Isokawa, S. Nagasawa, T. Ishijima, *Macromolecules 20* (1987) 2306; f) F. Albericio, E. Nicolas, J. Josa, A. Grandas, E. Pedroso, E. Giralt, C. Granier, J. van Rietschoten, *Tetrahedron 43* (1987) 5961; g) J.-M. Sabatier, M. Tessier-Rochat, C. Granier, J. van Rietschoten, E. Pedroso, A. Grandas, F. Albericio, E. Giralt, *ibid. 43* (1987) 5973; h) P. Sieber, *Tetrahedron Lett. 28* (1987) 2107; i) H. Rink, *ibid. 28* (1987) 3787; j) T. A. Lyle, S. F. Brady, T. M. Ciccarone, C. D. Colton, W. J. Paleveda, D. F. Veber, R. F. Nutt, *J. Org. Chem. 52* (1987) 3752; k) A. Ajayaghosh, V. N. R. Pillai, *Tetrahedron 44* (1988) 6661; l) B. Blankemeyer-Menge, R. Frank, *Tetrahedron Lett. 29* (1988) 5871.
[152] a) R. E. Offord; *Semisynthetic Proteins*, Wiley, Chichester 1980; b) I. M. Chaiken, *CRC Crit. Rev. Biochem. 11* (1981) 255; c) R. E. Offord, *Protein Eng. 1* (1987) 151.
[153] Examples: a) C. Mitchinson, R. L. Baldwin, *Proteins 1* (1986) 23; b) K. Rose, C. Herrero, A. E. I. Proudfoot, R. E. Offord, C. J. A. Wallace, *Biochem. J. 249* (1988) 83; c) T. L. Ciardelli, B. Landgraf, R. Gadski, J. Strnad, P. E. Cohen, K. A. Smith, *J. Mol. Recognit. 1* (1988) 42.
[154] See, e.g.: a) J. S. Fruton, *Adv. Enzymol. 53* (1982) 239; b) K. Morihara, *Trends Biotechnol. 5* (1987) 164; c) J. Meienhofer, S. Udenfriend (Eds.): *The Peptides: Analysis, Synthesis, Biology, Vol. 9*, Academic Press, Orlando 1987; d) H. D. Jakubke in [154c], p. 103.
[155] a) T. Nakatsuka, T. Sasaki, E. T. Kaiser, *J. Am. Chem. Soc. 109* (1987) 3808; b) C. F. Barbas III, J. R. Matos, J. B. West, C.-H. Wong, *ibid. 110* (1988) 5162.
[156] M. Ikekara, E. Ohtsuka, T. Tokunaga, S. Nishikawa, S. Uesegi, T. Tanaka, Y. Aoyama, S. Kikyodani, K. Fujimoto, K. Yanase, K. Fuchimura, H. Morioka, *Proc. Natl. Acad. Sci. USA 83* (1986) 4695.
[157] a) P. S. Farmer, *„Drug Design," Med. Chem. (Academic Press) 10* (1980) 119; b) A. F. Spatola, *Chem. Biochem. Amino Acids Pept. Proteins 7* (1983) 267.
[158] a) U. Nagai, K. Sato, *Tetrahedron Lett. 26* (1985) 647; b) M. Kahn, S. Wilke, B. Chen, K. Fujita, *J. Am. Chem. Soc. 110* (1988) 1638; c) D. S. Kemp, W. E. Stites, *Tetrahedron Lett. 29* (1988) 5057; d) M. G. Hinds, N. G. J. Richards, J. A. Robinson, *J. Chem. Soc. Chem. Commun. 1988*, 1447; e) I. Ernest, I. Kalvoda, M. Mutter, unpublished.
[159] a) D. S. Kemp, T. P. Curran, *Tetrahedron Lett. 29* (1988) 4931; b) *ibid. 29* (1988) 4935; c) D. S. Kemp, B. R. Bowen, *ibid. 29* (1988) 5077; d) *ibid. 29* (1988) 5081.

[160] E. Wünsch, *Angew. Chem. 83* (1971) 773; *Angew. Chem. Int. Ed. Engl. 10* (1971) 786.
[161] M. Bodansky, J. Martinez in [5b], *Vol. 5*, 1983, p. 111.
[162] E. Atherton, R. C. Sheppard in [154c], p. 1.
[163] A. Dryland, R. C. Sheppard, *J. Chem. Soc. Perkin Trans. 1 1986*, 125.
[164] R. A. Lerner, *Adv. Immunol. 36* (1984) 1.
[165] H. Anzinger, J. Schmitt, M. Mutter, *Makromol. Chem. Rapid Commun. 2* (1981) 637.
[166] a) W. Roth, E. Heidemann, *Adv. Polym. Sci. 43* (1982) 143; b) W. Germann, E. Heidemann, *Biopolymers 27* (1987) 157.
[167] a) C. G. Unson, B. W. Erickson, D. C. Richardson, J. S. Richardson, *Fed. Proc. Fed. Am. Soc. Exp. Biol. 43* (1984) 1837; b) J. S. Richardson, D. C. Richardson, B. W. Erickson, *Biophys. J. 45* (1984) 25a; c) B. W. Erickson, U.S. patent 4 515 920 (1985).
[168] R. S. Hodges, P. D. Semchuk, A. K. Taneja, C. M. Kay, J. M. R. Parker, C. T. Mant, *Peptide Research 1* (1988) 19.
[169] a) M. Mutter in [142b], p. 349; b) M. Mutter, E. Altmann, K.-H. Altmann, R. Hersperger, P. Koziej, K. Nebel, G. Tuchscherer, S. Vuilleumier, H.-U. Gremlich, K. Müller, *Helv. Chim. Acta 71* (1988) 835.
[170] K. Müller, H. J. Ammann, D. M. Doran, P. Gerber, G. Schräpfer in A. F. Harms (Ed.): *Innovative Approaches in Drug Research*, Elsevier, Amsterdam 1986, p. 125.
[171] S. E. Hull, R. Karlsson, P. Main, M. M. Woolfson, E. J. Dodson, *Nature (London) 275* (1978) 206.
[172] M. Mutter, G. Tuchscherer, *Makromol. Chem. Rapid Commun. 9* (1988) 437.
[173] G. Barany, F. Albericio, *J. Am. Chem. Soc. 107* (1985) 4936 and references cited therein.
[174] M. Mutter, R. Hersperger, K. Gubernator, K. Müller, *Proteins*, in press.
[175] M. Mutter, K.-H. Altmann, G. Tuchscherer, S. Vuilleumier, *Tetrahedron 44* (1988) 771.
[176] P. G. Schultz, *Science (Washington, D.C.) 240* (1988) 426.
[177] Examples: a) K. D. Janda, D. Schloeder, S. J. Benkovic, R. A. Lerner, *Science (Washington, D.C.) 241* (1988) 1188; b) S. J. Benkovic, A. D. Napper, R. A. Lerner, *Proc. Natl. Acad. Sci. USA 85* (1988) 5355.
[178] T. Sasaki, E. T. Kaiser, *J. Am. Chem. Soc. 111* (1989) 380.
[179] E. T. Kaiser, *Angew. Chem. 100* (1988) 945; *Angew. Chem. Int. Ed. Engl. 27* (1988) 913.
[180] D. Banner, M. Kokkinidis, *J. Mol. Biol. 196* (1987) 657.
[181] B. Dörner, K. Gubernator, M. Mutter, unpublished.
[182] Y. Satow, G. H. Cohen, E. A. Padlan, D. R. Davies, *J. Mol. Biol. 190* (1986) 593.
[183] K. Müller, M. Mutter, unpublished.
[184] W. F. DeGrado, Z. R. Wasserman, J. D. Lear, *Science (Washington D.C.) 243* (1989) 622.

Chemical Modifications of Biopolymers by Quinones and Quinone Methides

By Martin G. Peter*

Many quinones and their precursors, which are transformed oxidatively into quinones and/or quinone methides, are important natural products. As secondary metabolites, they frequently possess antibiotic and cytotoxic activities, in addition to acting sometimes as pathogens. Several plants and animals, especially insects, use quinonoid substances for defense, often with spectacular results. On the macromolecular level, quinone methides have a key role in the plant kingdom in lignin biosynthesis; the biosynthesis of melanoproteins exemplifies the reactions of *o*-quinones in the animal kingdom. In insects, cross-linking of structural proteins through quinones and quinone methides results in the construction of the sclerotized exoskeleton. For mankind, the reactivity of quinones in biological systems has far-reaching consequences of pharmaceutical, toxicological, and technical relevance. The examples in this review show that a common principle underlies these reactions, namely, the chemical modification of biopolymers. As demonstrated particularly well in a more detailed discussion of the chemical principles of insect cuticle sclerotization, several major and important new results have emerged from the development and applications of modern methods of sample separation and from solid-state NMR spectroscopy.

1. Introduction

Quinones, quinone methides, and often their phenolic precursors are widely distributed in nature. A large number of phenolic and quinonoid compounds occur as secondary metabolites,[1] and numerous examples are given in reviews on natural products of plants,[2, 3] marine organisms,[4] fungi,[5] and insects.[6] This review covers the irreversible reactions of quinonoids in biochemical environments. Thus, quinonoids that participate in reversible primary metabolic processes, such as electron transport, are not described here. The term "quinonoids" is meant to include *o*- and *p*-quinones in addition to any reactive intermediates that can form upon oxidation of a diphenol.

Quinonoids often show pronounced biological activities, such as antibiotic, cytotoxic, or allergenic actions, and they may serve the organism producing them as a weapon for defense. The biological activity of many quinonoids consists ultimately in chemical modification and denaturation of biopolymers, thereby damaging the exposed organism. When we look, however, at the organism that produces phenols together with the appropriate oxidative enzymes, interaction of quinones or quinone methides with macromolecules is usually beneficial, as exemplified by the biosynthesis of melanoproteins in animals, lignopolysaccharides in plants, and sclerotins in insects. One example of a useful technical application of protein–quinone interactions is the tanning of animal hides in the production of leather.

However, undesired and even deleterious results of protein–quinone interactions are exemplified by the toxicity of certain xenobiotic phenolic substances, which can eventually cause allergies, liver damage, or cancer. Aberrant metabolism of phenolic compounds may also have pathological consequences. Another unfavorable effect of quinonoid substances is the decrease in the nutritional value of vegetable and fruit foodstuffs in the presence of plant phenols or tannins.

An understanding of the chemical principles of quinone reactions in biological systems is of great importance, not only for finding new technical applications or developing methods for interfering to our benefit with undesired and deleterious effects of quinones, but also for gaining insight into fundamental processes of life.

Our views on the reactions of quinonoids in biological systems are mostly derived from the results of studies in preparative or mechanistic organic chemistry. A large variety of diphenols and oxidants as well as quinones and nucleophiles have been employed in organic synthesis for the construction of quinone derivatives, and the great preparative value of the various reactions is amply documented in several excellent reviews.[7–10]

In contrast, studies on the reactions of quinonoid compounds in biological systems have rarely led to an unambiguous structural characterization of the reaction products. One of the reasons is immediately obvious to the preparative organic chemist: the primary reaction products are unstable themselves. They readily undergo secondary reactions which are difficult, if not impossible, to control in an aqueous environment. Some ideas on the pathways of secondary reactions can be derived from the structures of new, unexpected products that again have been discovered during synthetic or mechanistic studies, and several examples will be discussed in this review. Besides this more classical approach, many significant discoveries have emerged from the availability of advanced methods of product separation and modern spectroscopic techniques including ESR as well as high-field and solid-state NMR spectroscopy.

An evaluation of our present knowledge on the reactions of quinones and quinone methides in biological systems will be useful for a critical assessment of the molecular aspects of

[*] Prof. Dr. M. G. Peter
Institut für Organische Chemie und Biochemie der Universität
Gerhard-Domagk-Strasse 1, D-5300 Bonn 1 (FRG)

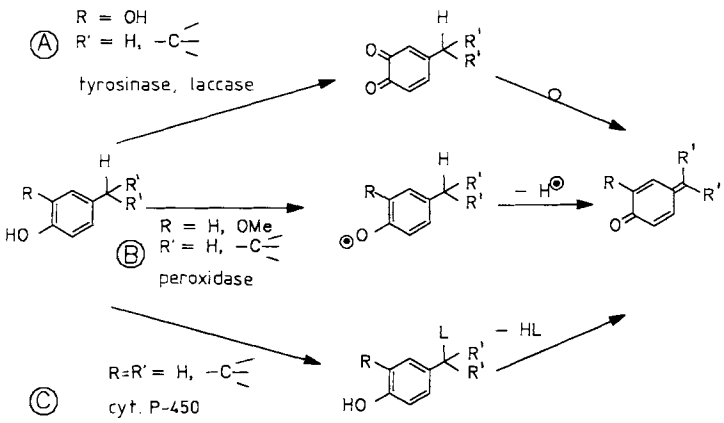
 © VCH Verlagsgesellschaft mbH, D-6940 Weinheim, 1989 0570-0833/89/0505-0535 $ 02.50/0

their biochemical behavior and may also help to clarify some of the remaining ambiguities. The first part of this review provides a general description of the reactions of quinones, including a few selected examples of obvious biological relevance. A brief review on polyphenol–biopolymer complexes is then followed by a critical evaluation of the structural and biological aspects of chemical modification of proteins, polysaccharides, and nucleic acids. Radical reactions are not treated separately. They will be mentioned when there is evidence for the participation of radical intermediates in biopolymer modifications. Finally, the mechanisms of insect cuticle sclerotization will be discussed as a particularly puzzling example of the fascinating roles of quinone–biopolymer interactions in nature.

2. General Principles

2.1. Biological Oxidation of Phenols

The enzyme-catalyzed oxidations that lead to quinones and quinone methides from 4-alkyl 1,2-diphenols and 4-alkyl monophenols are summarized in Scheme 1.[11,12] 2-Alkyl 1,4-diphenols react analogously.



Scheme 1. For Ⓐ, Ⓑ, Ⓒ see text.

The enzymes involved in the primary oxidation step are of three principal types. Tyrosinase (monophenol monooxygenase; EC 1.14.18.1) hydroxylates a monophenol in the *o*-position. This enzyme also has diphenoloxidase activity, transforming an *o*-diphenol into an *o*-quinone by two-electron transfer. Semiquinone radical anions are detectable by ESR spectroscopy in aqueous solution when the oxidation is performed in the presence of diamagnetic metal ions.[13,14] These radicals are generated by comproportionation of an *o*-quinone and excess *o*-diphenol.[13,15] Both *o*- and *p*-diphenols are also oxidized by diphenoloxidases of the laccase type, which catalyze one-electron transfers. Tautomerization of the alkylquinones leads to the corresponding quinone methides (Scheme 1, pathway Ⓐ).

Peroxidase/H_2O_2-catalyzed oxidation of monophenols yields phenoxyl radicals in a one-electron transfer. When the side chain of a 4-alkyl monophenol is unsaturated and in conjugation with the phenoxyl radical, a *p*-quinone methide radical is one of the possible resonance structures. When the side chain is saturated, radical abstraction is required for quinone methide formation (Scheme 1; pathway Ⓑ). Peroxidase/H_2O_2 oxidation of diphenols leads to semiquinone radicals, and the corresponding radical anions of *o*-diphenols have been observed by ESR spectroscopy, again as complexes with divalent metal ions.[13,16] Semiquinone radicals can also form through one-electron reductions of quinones by several flavoenzymes, such as NADPH-cytochrome P-450 reductase. Reduction of oxygen by semiquinone radicals yields superoxide anion radicals.[17] A quinone-mediated shuttle of electrons from superoxide to hydrogen peroxide then results in the formation of hydroxyl radicals.[18] A description of the mechanisms of protein modification by the highly cytotoxic and mutagenic oxygen radicals[19] is beyond the scope of this review.

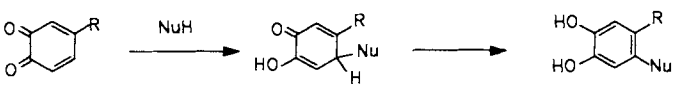
Finally, quinone methides may form through oxidative introduction of a leaving group into the side chain and subsequent elimination of HL (Scheme 1; pathway Ⓒ). This reaction sequence is important, for example, in the metabolism of certain monophenolic xenobiotics. It starts usually with a hydroxylation mediated by cytochrome P-450.

Quinones can form under physiological conditions also in nonenzymatic reactions. Autooxidation of a phenolic compound leads to a phenoxyl or to a semiquinone radical that can add molecular oxygen. The quinol hydroperoxide then decays to the corresponding quinone.[20,21]

Quinones and quinone methides are electrophilic species that will react with a variety of nucleophiles by vinylogous addition. Phenoxyl and semiquinone radicals, besides being intermediates in quinone methide formation, are likely to react further by phenolic coupling. Both nucleophilic addition and oxidative phenolic coupling are also fundamental processes in the polymerization of phenolic compounds.

2.2. Nucleophilic Addition

The vinylogous, Michael-type addition of a nucleophile to the α,β-unsaturated carbonyl system of a quinone is a well-known reaction (Scheme 2).

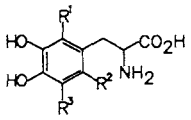


Scheme 2. R = H, alkyl.

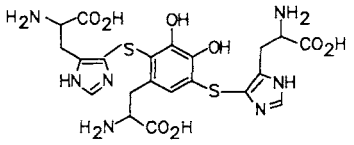
The primary addition product is a substituted *o*-diphenol which, in the presence of an oxidant (e.g., excess quinone) will yield a substituted *o*-quinone. Depending on the reaction conditions and the type of nucleophile, further reactions may follow; if R = H, for example, a second Michael addition followed by an oxidation may lead to a bis-substituted quinone. According to the terminology that has been created by *Wanzlick*,[7] such reaction sequences are classified as A-D-A-D, where A and D mean addition and dehydrogenation, respectively. The overall pathway applies to *p*-quinones and to quinone methides in analogous ways.

The addition of nucleophiles to quinones and quinone methides occurs in biological systems usually as a spontaneous, nonenzymatic reaction. The nucleophiles, available from functional groups of polypeptides, polysaccharides, and nucleic acids, are thiols, thioethers, primary and secondary amines, and hydroxyl groups. The biological relevance of Scheme 2 is illustrated in the following with a few examples of reactions which have led to structurally defined products.

Oxidation of Dopa by means of tyrosinase in the presence of cysteine yields a mixture of the 1,4- and 1,6-thiol-addition products **1–4**,[22] which are important intermediates in phaeomelanin biosynthesis (see Section 3). The main component (74%) is the 1,6-addition product 5-cysteinyl-Dopa **1**. However, *Kalyanamaran* et al.[23] observed by ESR spectroscopy only the 1,4-addition product of cysteine to 4-methyl-*o*-benzoquinone, generated by periodate oxidation of 4-methylcatechol at pH 3.0 in the presence of $Zn^{2\oplus}$ ions. Vinylogous thiol addition to 2-methyl-1,4-naphthoquinone (menadione) leads to semiquinone radical anions even in the absence of spin-stabilizing metal ions.[24]



1–4

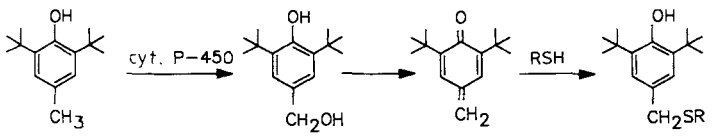


5

1: $R^1 = R^2 = H$, $R^3 = SCH_2CH(NH_3^{\oplus})COO^{\ominus}$
2: $R^1 = R^3 = H$, $R^2 = SCH_2CH(NH_3^{\oplus})COO^{\ominus}$
3: $R^1 = SCH_2CH(NH_3^{\oplus})COO^{\ominus}$, $R^2 = R^3 = H$
4: $R^1 = R^3 = SCH_2CH(NH_3^{\oplus})COO^{\ominus}$, $R^2 = H$

Biogenetically related to bis(cysteinyl)-Dopa **4** is the naturally occurring adenochromine **5**, which presumably is a precursor of adenochromes, the iron-binding pigments of *Octopus vulgaris*. Degradation of adenochrome revealed one of the components to be the unusual amino acid 5-mercaptohistidine linked to a Dopa moiety.[25]

Thiols may also add to quinone methides, as has been demonstrated conclusively through isolation of the adduct **6**, formed by addition of cysteine to the quinone methide generated from 2,6-di-*tert*-butyl-4-methylphenol (Scheme 3; cf. Scheme 1, pathway Ⓒ).[26]

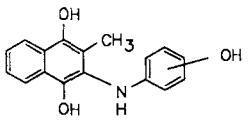


6

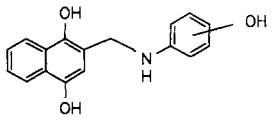
Scheme 3.

Primary and secondary amines yield, in general, addition products according to Scheme 2 (for reviews, see Refs. [7, 9, 10]). Owing to the basicity of the amino nitrogen, the reaction is strongly pH dependent. Reaction of aniline ($pK_a = 4.6$) with *o*-benzoquinone in glacial acetic acid to form the bis-addition product was first observed in 1913.[27] The same product is also obtained in aqueous buffer at physiological pH when catechol is oxidized in situ by means of tyrosinase in the presence of aniline.[28, 29] Semiquinone radical anions are generated in the presence of $Zn^{2\oplus}$ during addition of aniline to 4-methyl-*o*-benzoquinone.[23]

The addition of an aromatic amine to an *o*-quinone methide in tautomeric equilibrium with the corresponding *p*-quinone is exemplified in Scheme 4 (cf. Scheme 1, pathway Ⓐ). The reaction of 3- or 4-hydroxyaminophenol with menadione in methanol/acetic acid leads to the classical Michael-type addition product **7** and to the *o*-quinone methide adduct **8**.[30]



7



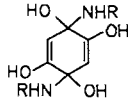
8

Scheme 4.

Under aprotic conditions, aliphatic amines ($pK_a = 9-11$) will also lead to A-D-A-D products in appreciable yields. A classical example is the preparation of 4,5-bis(dimethylamino)-1,2-benzoquinone in dry acetone.[31] Some related 1,4-addition products from the tyrosinase-catalyzed oxidation of 4-methylcatechol in the presence of β-alanine methyl ester have been isolated, along with Schiff bases, in rather low yields and characterized by spectroscopic methods.[32]

The *o*-quinone formed in the oxidation of dopamine can cyclize to 2,3-dihydroindole-5,6-diol. Determination of the relative rates of intramolecular and intermolecular additions of amines and thiols to electrochemically generated dopamine-quinone in aqueous buffer at pH 7.4[33] has revealed that the SH group of cysteine reacts ca. two times faster than that of glutathione and ca. 200 times faster than aniline, the addition of which is ca. ten times faster than the intramolecular cyclization of dopamine. This again is faster than the addition of α-amino groups of amino acids by a factor of about two. The preference for intramolecular cyclization as compared to intermolecular addition has also been demonstrated by conducting the oxidation of Dopa in the presence of *p*-benzoquinone.[34]

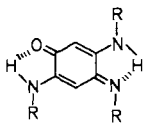
A fundamentally different reaction of amines is the nucleophilic 1,2 addition to a quinonoid carbonyl group. A recent example is the formation of the tetrols **9** from several biogenic amines and 2,5-dihydroxy-*p*-benzoquinone in ethanolic solution.[35] Under the same conditions, histamine adds with the primary amino rather than with the imidazole nitrogen. With *p*-benzoquinone, the usual 2,5-disubstituted products are generated through the A-D-A-D sequence.



9

R = $PhCH_2CH_2$, $p-HO-C_6H_4CH_2CH_2$, 4-imidazolyl-CH_2CH_2

The 1,2-carbonyl addition is usually followed by dehydration to the corresponding Schiff base. Thus, the A-D-A-D condensation product from aniline and *o*-benzoquinone has long been known.[27–29] The corresponding products **10** have been obtained from *o*-quinones and aliphatic amines in methanol[36] or glacial acetic acid,[32] although the reaction mixtures are extremely complex and the yields are sometimes exceedingly low.



10

R = Me, Et, *n*Bu [36], $CH_2CH_2COOCH_3$ [32]

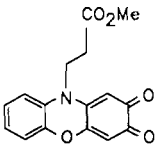
Another way of generating Schiff bases starts with vinylogous 1,4 addition to, for example, an *o*-quinone, followed by reoxidation and tautomerization to the 2-hydroxy-*p*-quinone imine. Schiff base formation with aliphatic amines, particularly α-amino acids, may be followed by Strecker degradation, that is, rearrangement and ultimately deamination.

2.3. Formation of Heterocyclic Compounds

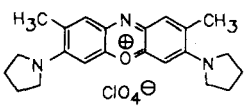
A considerable variety of heterocyclic compounds are known to arise from secondary transformations of the initial quinone and quinone methide addition products. The pertinent literature from the fields of biology and biochemistry documents that, with the exception of the intermediates in melanin biosynthesis (see Section 3), little attention has usually been paid to the idea that biopolymer modification may eventually also occur in such secondary reactions. Since we cannot a priori exclude the possibility that secondary reactions are biologically important, it is appropriate to present a few examples of the formation of heterocyclic derivatives from quinonoid compounds in reactions of possible biological relevance (for a review, see Ref. [37]).

Reaction of *p*-benzoquinone with *o*-aminophenol in glacial acetic acid yields 2-aminophenoxazin-3-one, in addition to higher-condensed heterocyclic ring systems.[38] 2-Aminophenoxazin-3-one is also generated upon oxidation of *o*-aminophenol mediated by oxyhemoglobin in human erythrocytes.[39] The phenoxazine ring system occurs in nature as a structural element in the actinomycin antibiotics and in certain insect pigments, the ommochromes. Their biomimetic preparation has been studied along with the enzymatic reactions involved in their biosynthesis (for reviews, see Refs. [7, 40, 41]). 2-Aminothiophenols yield the corresponding phenothiazinones in an analogous reaction.[42, 43]

Phenoxazinones may also form during the reaction of an *o*-quinone with an aliphatic amine. Compound **11** was isolated in low yield after oxidation of catechol in the presence of β-alanine methyl ester in glacial acetic acid.[32] An intermediate in this reaction is obviously the corresponding *N*-alkyl-*o*-aminophenol, which adds in an A-D-A-D sequence to a second molecule of *o*-benzoquinone. Similarly, the phenoxazine salt **12** is prepared from various α-amino acids and 5-methyl-4-pyrrolidino-1,2-benzoquinone in aqueous methanol.[44] In this case, the nitrogen atom is most likely derived from the α-amino acid, which loses its side chain in a Strecker-type degradation sequence.

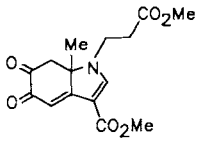


11

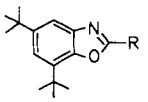


12

The rather unusual indole derivative **13** is formed in small amounts during oxidation of 4-methylcatechol in the presence of β-alanine methyl ester in acetic acid.[45] Apparently, Nenitzescu-type addition of the enamine that forms by a dehydrogenation of β-alanine methyl ester and nitrogen addition of another amino ester to the *o*-quinone in the usual 1,4 fashion is followed by cyclization and deamination.

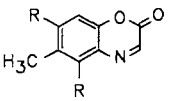


13

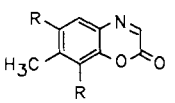


14

More highly substituted *o*-quinones, such as 3,5-di-*tert*-butyl-*o*-benzoquinone, react with primary amines of the type $R\text{-}CH_2\text{-}NH_2$ to yield stable addition/condensation products, such as the benzoxazole **14**.[46] In this case, Schiff base formation is followed by rearrangement and intramolecular oxidative cyclization. Likewise, the reaction of 3,5-di-*tert*-butyl-*o*-benzoquinone with α-amino acid esters leads to the corresponding benzoxazinones.[47] Addition-condensation of glycine ethyl ester with 4-methyl-*o*-quinone yields a product that has been described as either **15** or **16**.[48]



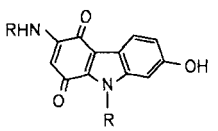
15



16

R = $NHCH_2COOEt$

Dimerization of 2-alkylamino-*p*-benzoquinones leads to the carbazole derivatives **17**, which have been found after reactions of primary alkylamines[49] or glycine ethyl ester[48] with *p*-benzoquinone.



17

R = alkyl, CH_2COOEt

3. On the Structures of Polyphenol–Biopolymer Complexes

Polyphenolic biopolymers are in general highly complex materials and our knowledge of their structures is rather fragmentary. A tremendous amount of work involving model reactions, degradation, and biosynthetic studies has led to recognition of partial structures from which overall constitutions have been derived. Though it is not the intention of this article to review the chemistry of polyphenolic polymers, it may be useful to recall first some basic facts before considering the interactions of these polymers with other biopolymers. An overview on the principal classes of polyphenolic polymers is given in Table 1.

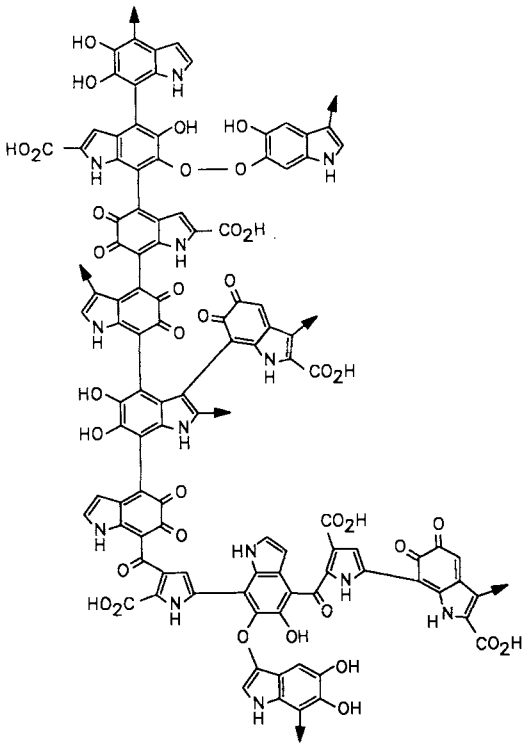
Table 1. Classes of polyphenolic biopolymers

Polymer	Phenolic monomer	Ref.
eumelanin	Dopa, dopamine, or noradrenaline	[50, 51]
phaeomelanin	Dopa and cysteine	[50, 52]
allomelanins	catechols containing no nitrogen	[50]
lignin	methoxy(propyl)phenols	[53, 54]
fungal lignin	styrylpyrones	[55]
brown algae tannins	phloroglucinol	[56, 57, 58]
condensed tannins	flavanols	[59, 60]
hydrolyzable tannins	gallic acid and glucose	[61]
humic acids	various	[62]

The binding interactions between polyphenolic polymerization products of quinonoids and other biopolymers—i.e., proteins, polysaccharides, and nucleic acids—are caused in principle by the following processes:

1. Covalent trapping of reactive intermediates, such as quinones, quinone methides, or radicals, during any stage of the polymerization process. In this case, the complex of the polyphenol and biopolymer is formed either by continuation of the polyphenolic polymerization or by addition of a functional group of the biopolymer to a reactive center of a polyphenol.
2. Noncovalent association between the biopolymer and the polyphenol. In this case, stabilization is achieved predominantly by a multiplicity of hydrogen bonds, in addition to electrostatic and hydrophobic interactions.
3. Cross-linking of biopolymers by a combination of covalent and noncovalent forces.

Tyrosinase-catalyzed oxidation of tyrosine or Dopa leads to a highly inhomogeneous black polymer, eumelanin (see Refs. [50, 51] for reviews and definition of various melanins and Ref. [63] for discussions of the mechanisms of melanin formation). An intermediate in the polymerization process is 2,3-dihydro-5,6-dihydroxyindole-2-carboxylic acid which arises from Dopa-quinone by an intramolecular 1,4 addition of the α-amino group. A generally accepted scheme for the structure of Dopa-melanin is depicted in Scheme 5.[50, 51] The polymer contains C–N, C–C, and C–O bonds which are formed through addition of the corresponding nucleophiles to intermediate *o*-quinonoid species or by oxidative phenolic coupling reactions. The structure is further complicated by the presence of pyrrolecarboxylic acid units that arise from degradation of indolic entities. ESR spectra of both synthetic and natural eumelanins reveal the presence of *o*-semiquinone radicals in these polymers.[64, 65] Quinone methides are not considered as significant intermediates in eumelanin biosynthesis.

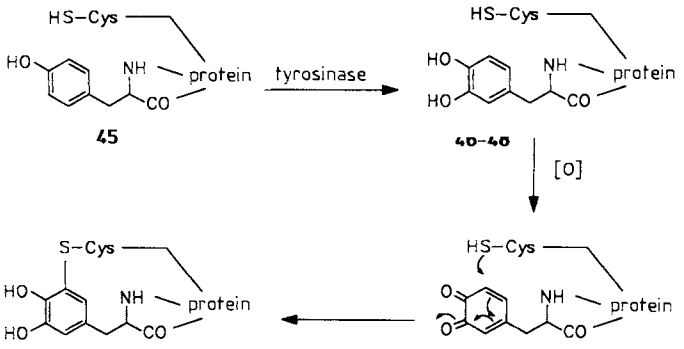


Scheme 5.

Low-molecular-weight tyrosine-containing peptides also polymerize upon oxidation with tyrosinase.[66] Depending on the position of the amino acid in the peptide sequence, different types of intermediates are distinguishable by UV spectroscopy: *N*-terminal tyrosine yields a Dopa-quinone residue, whereas tyrosine in the peptide chain or at the *C*-terminus leads to *N*-acyl Dopa-quinone units. In contrast to the eumelanins, which form by oxidative polymerization of free tyrosine, the polymers of peptidic tyrosine are soluble in water.

Natural eumelanin is always associated tightly with protein. When Dopa is oxidized by means of tyrosinase in the presence of various proteins, cysteinyl-Dopa residues are isolated after acid hydrolysis of the reaction product.[67] Recently, *Ito* et al. showed that peptide-bound 5-cysteinyl-Dopa residues are formed when proteins are subjected to oxidation with tyrosinase.[68] The mechanism of the reaction is understood as an enzyme-catalyzed hydroxylation of tyrosine residues followed by further oxidation of the resulting Dopa residues and nucleophilic addition of peptidic cysteinyl SH groups (Scheme 6).

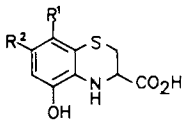
These results demonstrate conclusively that melanoprotein biosynthesis involves Michael-type 1,6 additions of cysteinyl SH groups to Dopa-quinone, generated by hydroxylation of either free or peptidic tyrosine and subsequent oxidation of the resulting Dopa residues.



Scheme 6.

It is assumed that the structure of dopamine melanin is similar to that of Dopa melanin. However, application of CP/MAS ^{13}C NMR spectroscopy has recently revealed that the polymer of dopamine contains high amounts of aliphatic carbon atoms.[69] Therefore, in contrast to the formation of Dopa melanin, the polymerization must occur largely via dihydroindole and dopamine units.

Oxidation of Dopa in the presence of cysteine leads to the brown phaeomelanins. The principal intermediates are the cysteinyl-Dopa derivatives **1**–**4** and the benzothiazines **18** and **19**, which are formed through intramolecular cyclization via the corresponding *o*-quinone imine.[52] Apparently, Schiff base formation and reduction by excess diphenol is favored over intramolecular 1,4 Michael addition of nitrogen in this case. Recent investigations by means of ^{13}C NMR spectroscopy indicate that the polymerization of 5-cysteinyl-Dopa occurs also with partial degradation of the side chains of the Dopa and the cysteinyl moieties.[70]

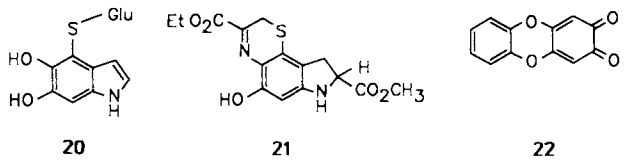


18, 19

18: $R^1 = H$, $R^2 = CH_2CH(NH_3^{\oplus})COO^{\ominus}$
19: $R^1 = CH_2CH(NH_3^{\oplus})COO^{\ominus}$, $R^2 = H$

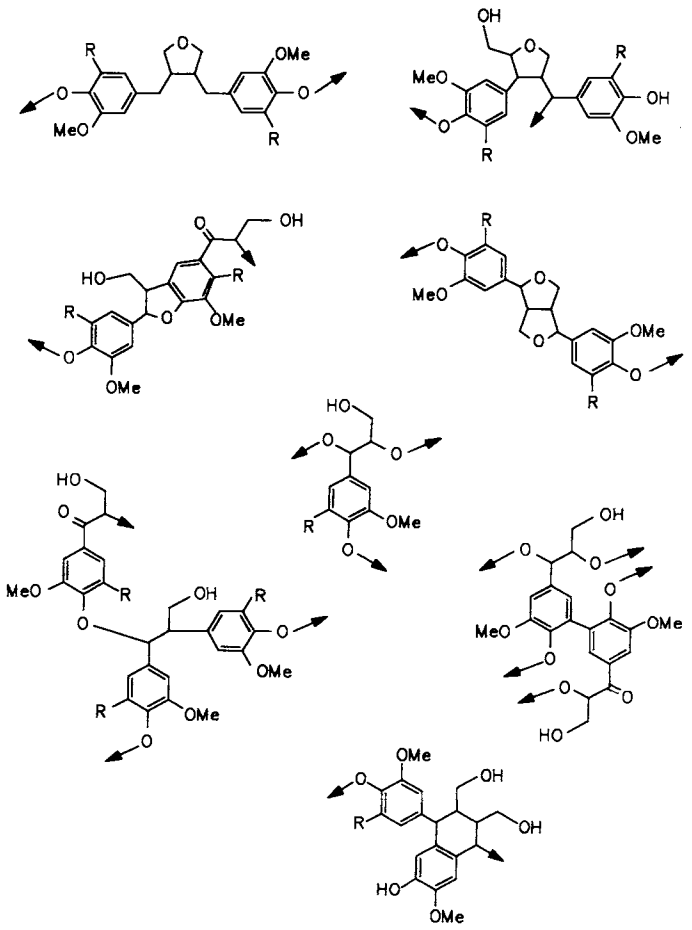
The distinction between eumelanins and phaeomelanins seems to be rather arbitrary. Though 5-cysteinyl-Dopa is a poor substrate of tyrosinase, its enzymatic oxidation is accelerated by Dopa. Thus, Dopa and 5-cysteinyl-Dopa will copolymerize under oxidative conditions, and the relative amounts of the two diphenols in the polymers are reflected by the sulfur contents.[71] Such mixed eumelanins/phaeomelanins can be characterized by ESR spectroscopy.[72]

Tyrosinase-catalyzed oxidation of 5,6-dihydroxyindole leads in the presence of glutathione to adduct **20**.[73] The tetrahydrothiazinoindole **21** was isolated from a reaction of dopachrome methyl ester with cysteine ethyl ester or glutathione.[74] The structures of these compounds are most interesting with respect to melanoprotein biosynthesis. They suggest that covalent linkages can form by SH addition not only to Dopa-quinone but also to reactive indolic intermediates.



Enzymatic oxidation of catechols that do not contain nucleophilic nitrogen leads to dark polymers, the allomelanins or catecholmelanins. Chemical investigations on their structure (reviewed in Ref. [50]) have only revealed that C–C and C–O bonds are formed. The latter may arise both by Michael-type addition of H_2O to an *o*-quinone and by addition of phenolic hydroxyl groups of unoxidized substrate. It is not always clear whether nucleophilic additions or radical reactions are involved. One of the reaction products in the enzymatic oxidation of catechol is the dibenzodioxinquinone **22**.[75] More recently, **22** was synthesized on a preparative scale from catechol.[76] The dibenzodioxin ring system is found in nature in the ecklonoquinones.[76]

Nitrogen has been found in various allomelanins (see Ref. [50] for a review). It is reasonable to assume that the nitrogen is introduced into these polymers in the form of amino acid residues, since the biosynthesis starts from nitrogen-free catechol precursors. The presence of nitrogen is not necessarily indicative of an intact amino acid–polyphenol linkage, since Strecker degradation may have occurred (cf. formula **12**).

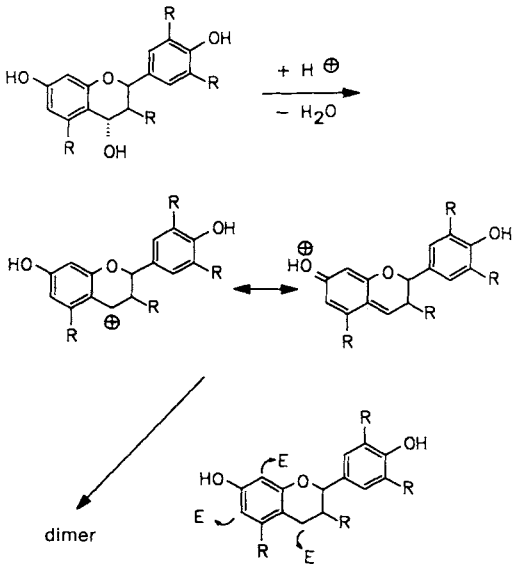


Scheme 7. R = H, OMe.

Freudenberg's classical work[53] revealed that lignins are formed by polymerization of *p*-hydroxy-*m*-methoxyphenylpropyl units. The initial one-electron oxidation is performed by a peroxidase, and intermediates are free radicals and *p*-quinone methides (cf. Scheme 1, pathway Ⓑ). Some principal structural elements of the polymer are depicted in Scheme 7.[54] Lignins do not contain detectable amounts of nitrogen.

The tannins of brown algae contain C–O and C–C linkages between adjacent phloroglucinol units.[57, 58] Their biosynthesis most likely follows oxidative coupling pathways between phenoxyl and aryl radicals. Covalent binding with amino acid residues of proteins could result from similar processes involving tyrosine. Indeed, nitrogen has been found in varying amounts in high-molecular-weight algal tannins.[56] Sulfur can be present in the form of sulfate.[58] Oligomeric phloroglucinols occur also in several fern species,[77] but their structure differs principally from that of the algal polymers by a linkage of the aromatic units via methylene bridges.

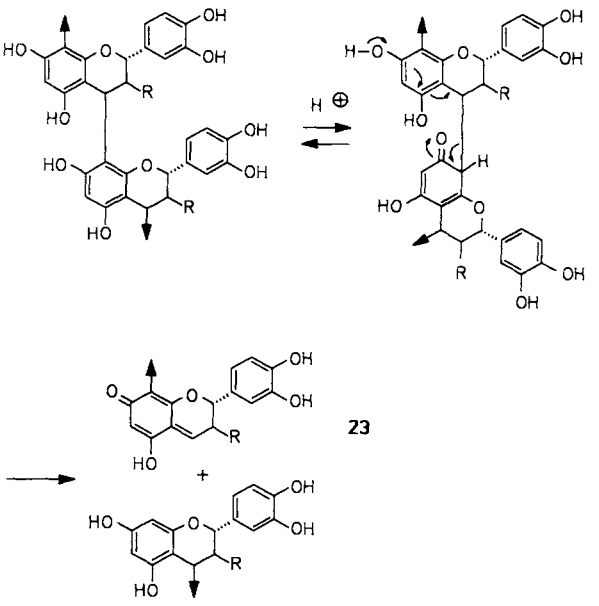
The vegetable tannins are grouped into two classes, the hydrolyzable and the condensed tannins. The hydrolyzable tannins are composed of glucose and oligomers of gallic acid which are combined by oxidative phenolic coupling.[61] The condensed tannins are generated from 3- and 4-hydroxyflavanols. The elegant studies of *Roux* and *Ferreira*[59] on the biomimetic synthesis of condensed tannins suggest that intermediates are either carbocations or quinone methides. Polymerization occurs via nucleophilic carbon addition (Scheme 8).



Scheme 8. R = H, OH.

binding is observed at pH values in the range 3–5. This has been taken as evidence for ionic interactions between positively charged lysine and arginine residues with acidic groups of the tannins.[79] Strong binding occurs also with synthetic polymers that do not contain basic functionalities, such as polyamides, polyvinylpyrrolidones, or urea–formaldehyde resins. In this case the polyphenol–polyamide complex must be stabilized by hydrogen bonds between phenolic hydroxyl and amide carbonyl groups. The degree of polymerization in condensed tannins must be ≥ 6 in order to effect denaturation of protein.[80] Quantitative analyses of noncovalent protein–polyphenol interactions have been published recently.[81]

Chaotropic reagents have varying effects on the stability of tannin–protein complexes. Thus, 8 M urea effectively strips hydrolyzable, but not condensed tannins, from collagen. Apparently, there are also covalent linkages in the aggregates of proteins and condensed tannins. For example, quinone methide **23**, formed from polymeric proanthocyanidin at pH 4.1 according to the hypothetical mechanism in Scheme 9, could react with nucleophilic functional groups of the protein.[82] Evidence for the formation of a quinone methide from 4,7-flavandiol in acidic solution has been obtained by UV spectroscopy in the presence of thiophenol.[83] Alternatively, the corresponding carbenium ion may be the reactive intermediate. Trapping of such intermediates by nitrogen or oxygen nucleophiles has so far not been reported.



Scheme 9. R = H, OH.

Owing to the technical applications in the tanning of leather and the undesired effects on vegetable foodstuffs, there is considerable interest in tannin–protein interactions. A comprehensive, though somewhat outdated, review on this subject is available in the classical book by *Gustavson*.[78] According to traditional views, both groups of tannins interact with collagen by noncovalent forces. A maximum of

Probably the most complex natural polymers are the humic acids, and an admirable compilation of their chemistry and biochemistry has been published.[62] It is well established that they arise inter alia from polyphenolic polymers and contain heteroelements of proteinaceous origin. They are sometimes considered as the end products of the decomposition of various biomaterials in the soil.

4. Reactions of Functional Groups of Biopolymers with Quinones and Quinone Methides

In Section 3, we have considered biologically important macromolecular polyphenol–biopolymer complexes with respect to the structural principles governing the association of the two components. We shall now discuss correlations of observed biological activities of quinonoids with structural modifications of the various cellular components.

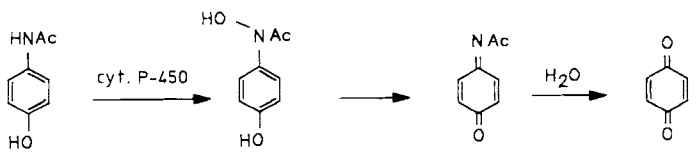
4.1. Reactions of Thiols and Sulfides

In the aqueous intracellular environment, the strongest nucleophiles are the cysteinyl SH groups. UV-spectroscopic evidence for the reaction between cysteine and various quinones was reported first by *Mason* and *Peterson*,[84] who studied models for melanoprotein biosynthesis, and later by *Pierpoint*[85] in an investigation of the enzymatic oxidation of chlorogenic and caffeic acids in the presence of amino acids. Actually, the first proof for the structure of the addition products of cysteine to an *o*-quinone was presented by *Ito* and *Prota*,[22] who isolated the cysteinyl-Dopa isomers **1**–**4**.

Besides the reactions occurring in melanoprotein biosynthesis, addition of the thiol group of cysteine-containing peptides is amply documented by isolation of glutathionyl-SH adducts from in vitro and in vivo transformations of several phenols and quinonoids.

Estradiol is converted by tyrosinase into a mixture of 2,3,17- and 3,4,17-estratriol; in the presence of $Zn^{2\oplus}$, semiquinone radicals are observed.[13] The catechol estrogens produce semiquinone radicals also upon autooxidation in alkaline solution or under the action of peroxidase/H_2O_2. The 3,4-catechol is presumably more cytotoxic than the 2,3-catechol.[13] Addition of glutathionyl SH to the *o*-quinone that results from oxidation of 17-ethynyl-3,4,17-estratriol has been discussed in the context of 17-ethynyl-2,17-estradiol binding to rat liver microsomes.[86]

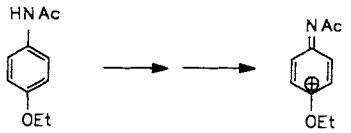
The analgetic drug 4-hydroxyacetanilide (paracetamol) **24** may cause liver necrosis when administered to mammals in high doses. The cytotoxic effects result from metabolic conversion of **24** to *N*-acetyl-*p*-benzoquinone imine **25** and hydrolysis of **25** to *p*-benzoquinone (Scheme 10). Oxidation of **24** is catalyzed by a cytochrome P-450-dependent monooxygenase[87] or by prostaglandin H synthetase.[88] Formation of 3-(glutathion-*S*-yl)-4-hydroxyacetanilide has been observed in vitro.[87, 88] After the cells are depleted of glutathione, liver damage results most likely from covalent binding of **25** to proteins. Besides SH addition, **25** undergoes extensive polymerization under physiological conditions.



24 **25**

Scheme 10.

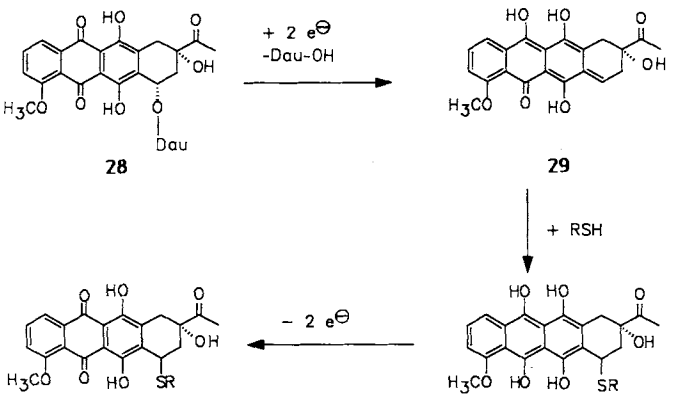
Replacement of the hydroxyl group of **24** by an ethoxy group leads to another analgetic, phenacetin **26**. In contrast to **24**, phenacetin is weakly carcinogenic. This difference has been ascribed to the oxidative formation of the nitrenium ion **27** rather than a *p*-quinone imine from **26**[89] (Scheme 11).



26 **27**

Scheme 11.

The antitumor activity of daunomycin **28** and related anthraquinone antibiotics has been associated with intercalation into DNA, cross-linking of double strands, and induction of single-strand breaking, either by interactions with oxygen radicals or by nucleophilic addition (for a review, see Ref. [90]). Biopolymer modification in the latter reaction is suggested by the isolation of the products **30** from model reactions in which the quinone methide **29** was generated by elimination of the sugar moiety from the enzymatically reduced anthraquinone (Scheme 12).[91]

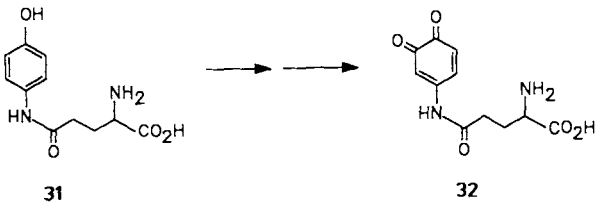


28 **29** **30**

Scheme 12. Dau = 1-β-3-amino-2,3,6-trideoxy-L-lyxohexosyl; R = $CH_2CH(NHCOCH_3)COOH$, β-D-glucosyl.

Some cysteinyl-Dopa compounds and cysteaminyl phenols show selective cytotoxic activity and inhibit growth of certain tumors.[92] It is thought that this biological activity rests on the quinonoid oxidation product (e.g., of **1**) which again may act as a scavenger for SH groups of enzymes involved in DNA biosynthesis.

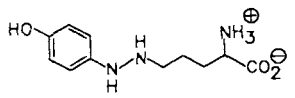
The glutaminyl derivative **31** is a natural product from the mushroom *Agraricus bisporus*.[93] Enzymatic oxidation of **31** leads to the corresponding benzoquinone **32** (Scheme 13), which is a powerful inhibitor of sulfhydryl-dependent respiratory enzymes[93] and shows antineoplastic activity in murine melanoma cells.[94]



31 32

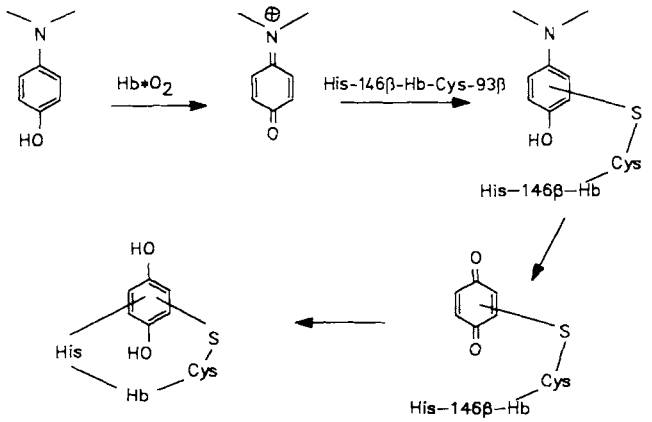
Scheme 13.

The unusual phenylhydrazine **33** occurs together with 4-diazocyclohexadienone in the related fungus *A. xanthoderma*, extracts of which possess strong antibiotic and cytotoxic activity.[95]



33

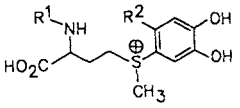
Oxidation of 4-(dimethylamino)phenol by oxyhemoglobin leads to loss of a cysteine and a histidine residue.[96] It has been postulated that cysteine-93β of hemoglobin adds to the *p*-quinone iminium ion, and autooxidation of the adduct is followed by hydrolysis and addition of histidine-146β to the substituted *p*-quinone (Scheme 14). Though the structure of the adduct has not been proven in detail, supporting evidence for this pathway was provided by tryptic digestion of the final product and subsequent amino acid analysis.



Scheme 14.

Aberrant metabolism of brain catecholamines may lead to severe neurological disorders. It has been suggested that the abnormal oxidation of certain neurotransmitters results in covalent modification of proteins in catecholaminergic neurons.[33] Supporting evidence was obtained by isolation of 6-(2-aminoethyl)-2,3,5-trihydroxyphenyl-glutathione from an in vitro oxidation of the highly neurotoxic 6-hydroxydopamine in the presence of glutathione as well as from an in vivo system.[97]

Vinylogous sulfide addition of peptidic methionine residues to *o*-benzoquinone at varying pH values was suggested as a tool for investigations on the structure and conformation of proteins.[98] Indirect evidence for the 1,4 addition of *N*-acetylmethionine to *o*-benzoquinone[99] or Dopa-quinone[100] was obtained from UV-spectroscopic investigations, which suggested the structures **34** and **35**, respectively. At physiological pH, however, failure to detect a sulfide–quinone addition product was reported.[23]



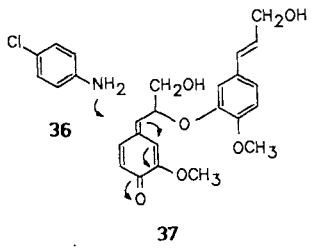
34,35

34: R^1 = Ac, R^2 = H
35: R^1 = H, R^2 = $CH_2CH(NH_3^{\oplus})COOH^{\ominus}$

Likewise, reaction of the rare amino acid selenomethionine (see Ref. [101] for a review) with *o*-benzoquinone in 1 N HCl has been studied.[102] The structure of the product was proposed to be analogous to **34**.

4.2. Reactions of Amino Groups

Incorporation of an aromatic amine into a synthetic lignin has been observed upon peroxidase/H_2O_2-catalyzed copolymerization of **36** with coniferyl alcohol at pH 7.5[103] (Scheme 15). Addition of **36** to the quinone methide **37** was evident from ^1H and ^{13}C NMR spectra of the product mixture.

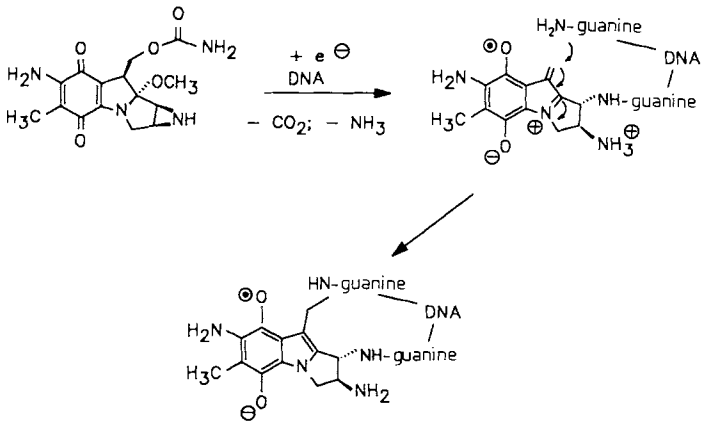


36 **37**

Scheme 15.

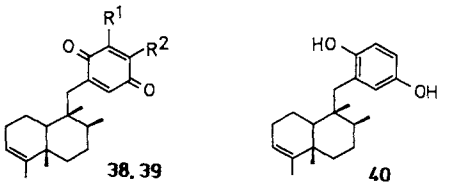
Heteroaromatic amines are very abundant in nucleic acids, and additions of base residues to quinones or quinone methides are conceivable. However, the corresponding addition products have apparently not been isolated. Though not related directly to the reactivity of a quinone according to Scheme 2, it is interesting to note that the antitumor agent mitomycin C cross-links DNA via addition of guanine residues, as depicted in Scheme 16.[104] The reaction proceeds probably via an iminium ion rather than the formerly postulated quinone methide.

Another group of biologically active quinonoid natural products should be mentioned here, though their mode of action has not yet been elucidated. The sesquiterpenoid monoaminoquinones **38** and **39** were isolated from the sponge *Dysidea avara*.[105] Most likely, they arise as artifacts



Scheme 16.

from the parent *p*-diphenol avarol **40** during the extraction procedure. Avarol **40** and the aminoquinones **38** and **39** show pronounced inhibition of sea-urchin egg development. Related compounds from the sponge *Smenospongia sp.* possess cytotoxic and antimicrobial activity.[106]



38, 39 **40**

38: $R^1 = H$; $R^2 = NHCH_3$
39: $R^1 = NHCH_3$, $R^2 = H$

Aliphatic amines ($pK_a = 9-11$) occur in biological systems in great variety. Primary amines include the catecholamines, the ε-amino groups of either free or peptidic lysine, and the α-amino groups of amino acids and *N*-terminal residues in polypeptides. Proline and hydroxyproline are secondary amines, and the imidazole nitrogen of histidine ($pK_a = 6.05$) occupies an intermediate position between aromatic and aliphatic amines.

Though leading usually to intractable complex mixtures, reactions of amino acids and proteins with enzymatically generated quinones have been studied in great detail by spectroscopic methods, such as UV[84, 85] and, more recently, ESR spectroscopy.[23] Isolation of a structurally defined reaction product was not attempted in these investigations. Thus, *Mason* and *Peterson*[84] described the absence of a reaction of 3-substituted indole and 4-substituted imidazole as well as of the serine hydroxyl group and amido, ureido, and guanidino nitrogen, with a variety of *o*-quinones generated from the parent diphenols with *o*-diphenol oxidase in aqueous buffer. The UV spectra indicated, however, some reactions with primary and secondary aliphatic amines and thiols. Similar results were obtained by *Pierpoint*,[85] who interpreted UV spectra of mixtures of phenoloxidase, amino acids, and chlorogenic or caffeic acid as an indication for the addition of primary α-amino groups and the ε-amino group of lysine to the *o*-quinones.

Absence of the reaction of a primary amine with the *o*-quinone of *N*-acetyldopamine at physiological pH has been reported from ESR studies conducted under conditions of spin stabilization with $Zn^{2\oplus}$.[14] *Kalyanamaran* et al.,[23] using a similar experimental protocol, have drawn the following conclusions: α-amino groups of amino acids form 1,4-addition products at pH ≥ 8; with lysine and histidine, addition occurs with the α-amino rather than with the ε-amino and imidazole nitrogen, respectively; the secondary amino group of hydroxyproline adds even at physiological pH; the *N*-terminal amino groups of peptides also react at lower pH values, owing to the decreasing basicity seen with increasing numbers of amino acids. The addition of proline nitrogen to 4-methyl-*o*-benzoquinone was first suggested by *Jackson* and *Kendal*[107] some 40 years ago in a study on the violet pigment formed upon exposure of crude extracts of potatoes or mushrooms to air. However, according to *Weaver* et al.,[93] this color is caused by the presence of γ-glutaminyl-3,4-benzoquinone **32**.

Poison ivy (*Toxicodendron radicans*, Anacardiaceae) contains urushiol, which consists of a mixture of the 3-hexadec(en)yl and 3-pentadec(en)yl catechols **41**. The urushiols act as potent allergens, causing severe skin irritation upon repeated contact with the plant. It is thought that the toxicity of the diphenolic compounds results from their oxidation to *o*-quinones, in addition to the presence of the lipophilic side chains. Their mechanism of action has been described as an oxidative addition to serum protein through mercapto or terminal amino groups according to Scheme 2. This results in chemically modified polypeptides which are allergenic. This view has been supported indirectly by isolation of corresponding derivatives in model experiments[108] as well as in studies on the binding of the oxidation products (presumably *o*-quinones) of various alkyl-substituted diphenols to proteins.[109] When γ-globulin was washed through a column cotaining quinone-coated Celite, binding of the protein was most extensive when the quinone was derived from 3-pentadecylcatechol, whereas 4-methyl-, 5-methyl-, or 6-methyl-3-pentadecyl-*o*-benzoquinone resulted in diminished binding of protein. The presence of more than one methyl group, such as in 4,5-dimethyl- or 4,5,6-trimethyl-3-pentadecyl-*o*-benzoquinone abolished protein binding nearly completely.[109]

More recently, cross-reactivity of urushiol analogues in urushiol-sensitized Guinea pigs has been demonstrated with compounds **42** and **43**.[110] Blocking of the amino group in **42** or **43** in the form of the methanesulfonamide resulted in loss of cross-reactivity in sensitized animals. Resorcinol derivatives did not cross-react with urushiol. It should be noted that the *p*-quinone primin **44** also shows pronounced allergenic activity (for a review, see Ref. [3]).



41-43 **44**

41: $R^1 = R^2 = OH$,
$R^3 = n\text{-}C_{15}H_{31}$, $n\text{-}C_{15}H_{29}$, $n\text{-}C_{16}H_{33}$, $n\text{-}C_{16}H_{31}$
42: $R^1 = OH$, $R^2 = NH_2$, $R^3 = C_nH_{2n+1}$ (n = 13, 15, 17)
43: $R^1 = NH_2$, $R^2 = OH$, $R^3 = C_nH_{2n+1}$ (n = 13, 15, 17)

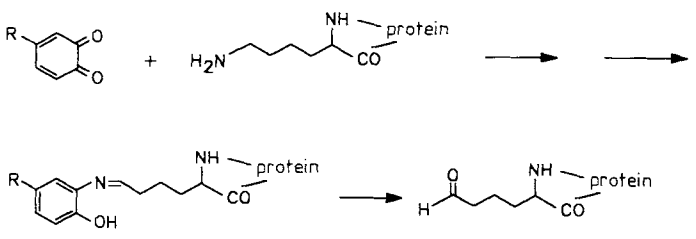
Plant materials often undergo extensive browning when wounded tissue is exposed to air. This browning reaction leads to a decrease in the nutritional value of vegetable food-

stuffs, and it is understood as an oxidative modification of lysine residues in proteins by plant phenolics. A novel approach towards the identification of quinonoid–lysine addition products is offered by high-resolution mass spectroscopy of degradation products of hydrogenated plant proteins.[111, 112] The results obtained upon analysis of the extremely complex product mixtures provided some, though not fully convincing, evidence for the presence of an addition product between lysine and caffeic acid.

A similar reaction between chlorogenic acid and the ε-amino group of lysine has been suggested in order to explain the partial inactivation of a potato virus upon exposure to chlorogenic acid and phenol oxidase.[113, 114] Cross-linking of protein subunits was observed, and digestion with trypsin (which cleaves peptide bonds adjacent to lysine residues) was less extensive with the cross-linked than with monomeric diphenol–protein reaction product. It was suggested that the mechanism of cross-linking involves a D-1,4-A-D-1,6-A sequence, resulting in a 3,5-diamino-4-alkyldiphenol. Alternatively, coupling of two catechol units via an aryl ether linkage was considered.[113] The stoichiometry of binding of chlorogenoquinone was dependent on the pH of the reaction mixture: at pH 7.0, there was a 1:1 ratio between chlorogenic acid and protein subunit, whereas a ratio of 2:1 was observed at pH 7.8.

A highly interesting example of the occurrence of 3,4-dihydroxyphenylalanine residues in a protein has been found in the periostracum[115] and in the phenol glands[116] of the mussel *Mytilus edulis*. The byssus of the same molluscs also contains a catechol oxidase,[117] and it is believed that the enzyme oxidizes peptidic Dopa units to the corresponding *o*-quinones, which then add ε-amino groups of lysine residues. Though cross-linking via cysteinyl SH groups is also a possibility (cf. Scheme 6), the protein contains no cysteine and only traces of methionine.[116] Thus, a unique type of natural glue is formed that enables the mussel to adhere tightly to the surface of a support. It is noteworthy in this context that the natural product primin **44** and some homologues possess molluscicidal activity.[118]

Sequential addition of two ε-amino groups of lysine residues to quinones must not necessarily represent the only pathway of protein cross-linking in biological systems that do not contain sulfur nucleophiles. When the addition reaction is followed by rearrangement and hydrolysis of the azomethine (Scheme 17), an aldehyde is generated in a Strecker-type reaction. The aldehyde is itself reactive as both an electrophilic amino-group acceptor and a component in aldol condensations. Further rearrangements and reactions can follow. They represent one of the principally possible structural modifications in collagen and related proteins (for a review, see Ref. [119].



Scheme 17.

α-Aminoadipic acid could be isolated after catechol/peroxidase/H_2O_2-mediated protein modification, followed by performic acid oxidation and hydrolysis.[120] Protein cross-linking by various catechols and peroxidase/H_2O_2 was also described[121, 122] but structures of the cross-links have not yet been determined. Treatment of proteins with peroxidase/H_2O_2 in the absence of catechols leads to oxidative coupling of tyrosine residues.[123]

Mechanism-based inactivation of tyrosinase during oxidation of catechol has long been known (for a review, see Ref. [124]). An earlier report, describing covalent attachment of radiolabeled catechol, presumably through nucleophilic groups of the enzyme,[125] is obviously not confirmed by the results of *Lerch*,[124, 126] who showed that, though a histidine residue at the active site was destroyed during catalysis, only insignificant amounts of substrate were bound covalently to the protein.

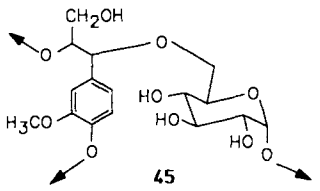
Addition products of amines to an intermediate *o*-quinone methide, which was derived from pyridoxol under rather harsh conditions, have been investigated in order to provide models for the neurotoxic action of certain vitamin B_6 derivatives.[127] Though possible in principle, an addition of amino acids or proteins to quinone methides in a biochemical environment has so far not been confirmed experimentally.

4.3. Reactions of Hydroxyl Groups

The most abundant oxygen nucleophile in biological systems is, of course, water. Other candidates for nucleophilic addition include carbohydrates and the hydroxyl groups of serine, threonine, and hydroxyproline residues. Furthermore, the phenolic hydroxyl groups of the substrates themselves can act as nucleophiles, and many examples for this type of C–O bond formation are found in the field of natural products chemistry. Reactions of alcohols with *p*-quinones are of considerable value in preparative organic chemistry.[10] The addition of carboxylates should be considered in this context also.

With respect to protein modification, no example of the addition of hydroxyl functions of serine, threonine, or hydroxyproline to a quinone has been reported so far. However, *p*-quinone has been used to immobilize enzymes on hydroxyalkyl methacrylate polymers[128] and on polysaccharides.[129] The nature of the reactions involved has not been determined in detail. Since the polymers are first activated by *p*-benzoquinones, formation of C–O bonds through nucleophilic addition is conceivable. After reoxidation, the protein is attached presumably via mercapto or amino group addition. Thus, the sequence is A(hydroxyl group to benzoquinone)-D-A(protein to quinone-modified polymer).

The addition of hydroxyl groups of polypeptides to intermediates in lignin biosynthesis has not yet been observed. However, lignin does contain C–O bonds from carbohydrates, as was first suggested by *Freudenberg*.[53] The structures of the linkages have been indirectly identified after digestion with cellulase followed by methylation analysis of a lignin–carbohydrate complex from *Pinus densiflora* wood.[130] A representative example is given in formula **45**. Other types of C–O bonds, namely, ether linkages to ferulic



45

acid and ester linkages to *p*-coumaric acid, exist in wheat straw.[131]

5. The Mechanisms of Insect Cuticle Sclerotization

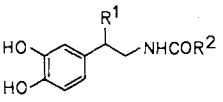
In the foregoing sections, we have seen that reactions of quinonoids with biopolymers result in a variety of types of covalent and noncovalent bonding, in addition to secondary modifications such as deamination or reactions with oxygen radicals. We shall now turn to a fascinating process in nature, namely, the hardening and darkening of the exoskeleton of insects. This subject has been studied quite vigorously in recent years and we shall ask ourselves to what extent the results of chemical investigations of other biological systems may also be valid for this process.

Arthropods in general require a stiff exoskeleton for maintaining such essential life functions as muscle attachment, body structure, and protection against chemical or mechanical threats from the environment. In insects, the process of hardening of the cuticle is termed "sclerotization", and it is often accompanied by darkening of the cuticle. The most prominent examples can be seen in the more or less dark brown cuticles of many insect pupae. In the larval stage, stiffening of the mandibles is necessary to provide the functionally intact organs for food intake. From a more practical viewpoint, the study of sclerotization might suggest new approaches in insect control, since inhibition of this process would be lethal to insects. One of the prerequisites for the development of new insecticides is, of course, some idea about their possible mode of action.

The molecular mechanisms of insect cuticle sclerotization have long attracted the attention of many researchers. However, the numerous attempts to elucidate the chemistry of this process have met with rather limited success. In fact, several hypotheses still exist concerning the nature of the interactions of polyphenols with structural proteins and chitin, and at least some experimental evidence has been obtained for nearly all of them.[132] It is generally assumed that structural proteins are covalently modified and cross-linked by *o*-quinones and *p*-quinone methides that are generated by enzymatic oxidation of *N*-acyl-3,4-dihydroxyphenethylamines. According to other hypotheses, sclerotization is effected by noncovalent polyphenol–protein interactions and by a decrease of water in the cuticle. Several reviews have appeared in the last few years,[132–135] and only the most conclusive results shall be included here together with some important historical observations.

The earliest investigation on the mechanism of sclerotization goes back to *Pryor*, who, in 1940, described the hardening of cockroach egg cases[136] and of insect cuticle[137] as a result of covalent cross-linking of proteins by *o*-quinones. He also suggested the name "sclerotin" for the brown protein–quinone complex. Reactions of peptidic amino groups was assumed after the observation that pretreatment of the proteins with formaldehyde prevented sclerotin formation. Very important is also *Pryor*'s assumption that the stiffness of the cuticle may increase owing to quinone polymerization in the "meshes of the protein network".[136]

The principal sclerotization substrate was identified in the classical work of *Karlson*'s group some 25 years ago; they isolated *N*-acetyldopamine **46** from larvae of the blowfly *Calliphora erythrocephala*[138] and, subsequently, from other insect species.[139] Another principal sclerotization agent is *N*-β-alanyldopamine **47**,[140] which, in contrast to **46**, contains a free primary amino group.



46–48

46: $R^1 = H$, $R^2 = CH_3$
47: $R^1 = H$, $R^2 = CH_2CH_2NH_2$
48: $R^1 = OH$, $R^2 = CH_3$

The fundamental role of the dopamine derivatives in sclerotization is now well established. Inhibition of Dopa decarboxylase by α-methyl-Dopa or carbidopa (deamino-α-hydrazino-α-methyl-Dopa) interferes with the biosynthesis of the sclerotization agents.[141, 142] Pupae of the fly *Lucilia cuprina* that were treated with such compounds during immature stages display a light color and die from dehydration.

The idea that enzymatic oxidation of the diphenols yields *o*-quinones, which cannot cyclize to indole derivatives and therefore react according to Scheme 2, has been presented many times in the literature. According to these hypotheses, cross-linking occurs between ε-amino groups of lysine residues through either a D-1,4-A-D-1,6-A or a D-1,4-A-D condensation sequence, followed by Schiff base formation. Since mercapto groups are present in cuticle proteins, if at all, only to a small extent,[143] participation of ε-lysine amino groups is likely.

Inhibition of the phenoloxidase in mosquitoes with 2,6-di-*tert*-butyl-4-(α,α-dimethylbenzyl)phenol prevents sclerotization of the pupal cuticle and the pupae die rapidly after the molt.[144] The cross-linking of tyrosine-rich proteins, which can be achieved with tyrosinase in the presence of **46** or **47**,[145b] is inhibited by the resorcinol analogue *N*-acetyl-2-hydroxytyramine by an as yet unknown mechanism.[146]

The isolation of a bis-lysine adduct from hardened insect material has been reported only once.[147] The original data have not been published so far, and therefore this most important result is not accessible to evaluation. Other indications for reactions of amino groups during sclerotization are derived indirectly from differences in the amounts of lysine in hydrolysates of sclerotized and soft cuticles.[133, 143, 148] The participation of histidine residues in protein modification has been demonstrated by application of CP/MAS NMR spectroscopy to cuticles of insect pupae that had been fed [1,3-$^{15}N_2$]histidine and [*phenyl*-^{13}C]dopamine.[149] The results revealed clearly the presence of ^{15}N–^{13}C linkages, but it is not possible to decide whether attachment of a dopamine metabolite to protein results in cross-linking. Participation

of histidine in sclerotization is also evident from comparative amino acid analysis.[150]

Several lines of evidence indicate that, besides cross-linking of insect cuticle proteins via basic amino acid residues and *o*-quinones, other mechanisms are involved in sclerotization. Racemic *N*-acetylnoradrenaline **48** was isolated from reaction mixtures containing **46** and powdered insect cuticle. Likewise, oxidation of 4-methylcatechol with cuticle from flies leads to 3,4-dihydroxybenzyl alcohol and to 3,4-dihydroxybenzaldehyde.[151] These results indicate a side-chain hydroxylation mechanism which is not consistent with an enzyme-controlled reaction.[152, 153] Since dopamine-β-hydroxylase is known to produce (*R*)-noradrenaline from dopamine, the occurrence of racemic **48** must be explained by a rearrangement of the *o*-quinone of *N*-acetyldopamine to the corresponding *p*-quinone methide and nonstereoselective addition of water to this electrophilic species. In analogy to the biosynthesis of lignin, the formation of racemic **48** is most likely a side reaction in the polymerization of **46** in insect cuticle (cf. Scheme 1, pathways Ⓑ and Ⓒ). The enzyme that catalyzes quinone methide formation has not yet been isolated. It is interesting to note that tyrosinase catalyzes the oxidative decarboxylation of 3,4-dihydroxymandelate to protocatechuic aldehyde, presumably via the *p*-quinone methide.[154] An impressive number of side-chain-oxidized derivatives and benzodioxin dimers of **46** and **47** have been isolated from cuticles of various insects (for reviews, see Refs. [132, 133]), but their functional role in sclerotization has not been elucidated in molecular terms.

The tan color of most sclerotized insect cuticles indicates extensive polymerization of the phenolic precursors. Dark cuticles contain eumelanin in varying amounts[40, 148, 155] besides polyphenolic polymers that arise from the oxidation of the sclerotization substrates via reactive *o*-quinones and *p*-quinone methides. The presence of melanin in sclerotized cuticle has also been demonstrated by ESR spectroscopy.[14, 64] Copolymerization of peptidic tyrosine residues with sclerotization substrates has been observed in a few instances.[156, 157] Investigation of insoluble materials by CP/MAS ^{13}C NMR spectroscopy provides a nondestructive method for the observation of polyphenolic polymers, and its application has revealed the presence of 1,2-diphenoxy carbon atoms in sclerotized insect cuticle.[158]

Melanization and sclerotization of insect cuticles are separate processes, as was first recognized by *Karlson* et al. in 1962,[159] who also discovered the presence of the nonproteinogenic amino acid β-alanine in sclerotized cuticle of the blowfly *Calliphora erythrocephala*.[160] It appears now that this amino acid is present in all sclerotized cuticles and that it plays an essential role in the regulation of the balance between melanin and sclerotin formation.[155] Mutants of the fruit fly *Drosophila melanogaster* that are unable to biosynthesize β-alanine or to transport the amino acid into the cuticle incorporate Dopa or dopamine into black eumelanin.[161] The stiffness of the cuticle is decreased in these cases.[162] Likewise, ethyl hydrazinoacetate, an inhibitor of β-alanine biosynthesis or transport, causes a black coloration of the pupae of *Manduca sexta*, which normally are brown.[163] Probably, β-alanine is necessary for acylation of dopamine, thus preventing intramolecular oxidative cyclization and facilitating protein cross-linking by intermolecular nucleophilic addition. Since *N*-β-alanyldopamine **47** is, in fact, a component of the sclerotization process, this hypothesis appears quite attractive. However, the question whether cross-linking occurs on the monomeric or on the polymeric level remains unanswered. According to another theory, binding of β-alanine to chitin is required for the correct packing of the macromolecular network in the cuticle.[162] The β-alanine-mediated browning of chitin[162] results most likely from Maillard-type reactions.[119, 164]

Chitin is not a necessary component for sclerotin formation, since *o*-quinones and protein are sufficient to harden and darken the egg cases of cockroaches which are devoid of chitin.[136] However, when chitin deposition is blocked by diflubenzuron, the cuticles may blacken[165] and sclerotization can be affected (for a review, see Ref. [166]). Noncovalent binding of *N*-acetyldopamine-derived polymer to chitin has been reported.[167]

Chitin appears to be tightly associated with protein, but the types of bonds are unknown. Again, covalent polysaccharide–protein linkages are in principle possible, either through acyl linkages between amino or hydroxyl groups or through glycosidic coupling of polypeptides with the reducing sugar unit. Attempts to isolate conjugates of amino sugar and amino acids have so far not been successful. Therefore, the question concerning the molecular architecture of chitin–protein–polyphenol complexes remains unanswered. If glycosidic bonds are formed between the reducing terminus of chitin and ε-amino groups of lysine, rearrangement and subsequent hydrolysis could eventually lead to allysine residues (cf. Scheme 17). This mechanism is analogous to that of the glucose-mediated covalent cross-linking of collagen.[168]

According to other theories, the importance of covalent interaction is generally overemphasized and sclerotization results from the reduction of the water content in the cuticle and from noncovalent binding of proteins to polymers of the *N*-acylcatecholamines.[152, 169] Those polymers do not contain appreciable amounts of indole units, since intramolecular cyclization of the quinones of *N*-acylcatecholamines is very slow. Therefore, despite their origin from dopamine derivatives, they are to be classified as allomelanins (see Section 3). In view of the possibility of quinone methide formation, one expects the properties of these polymers to be similar to those of condensed tannins and lignin. Their interaction with proteins would thus lead to noncovalent interactions as well as random covalent binding.

6. Summary and Prospect

Reactions of quinones and quinone methides have many important and often spectacular results in nature. In this article, we have considered defensive systems, toxic effects, and diminishing of the value of vegetable foodstuffs. We have also seen examples of the construction of macromolecular, highly complex polymers as essential prerequisites for the sustaining of life in various organisms. On the molecular level, the common principle is always a chemical modification of biopolymers, either covalent or noncovalent. Quite often, reactions of sulfur nucleophiles with quinones and quinone methides prevail. When sulfur is absent, modifications occur via nitrogen nucleophiles in proteins and via

oxygen nucleophiles in polysaccharides. Finally, biopolymer modifications can be induced indirectly, for example, through deamination or quinone-mediated electron-transfer processes which result in the formation of oxygen radicals.

Some of the past theories of covalent quinone–protein binding, which were derived from model systems, have to be revised. It appears that the role of ε-amino groups of lysine residues is less important for covalent binding than has been assumed previously. Certainly, there are decreases in the number of lysine residues after the reaction of a protein with quinones. However, lysine may also suffer oxidative deamination. Blocking of lysine with aldehydes also decreases binding of quinones. This does not prove covalent binding, since noncovalent interactions will also be impaired when the aldehyde reaction leads to deamination or to loss of positive charges. It appears that the imidazole nitrogens of histidine residues are much more important in nucleophilic addition than the ε-amino groups of lysine.

The most significant and spectacular advances in the direct observation of insoluble biopolymers have been achieved by applications of solid-state NMR spectroscopy.[69, 149, 158] However, not all speculations are resolved now and nature presents many variations, including noncovalent binding and C–C bond formation by oxidative coupling. A thorough experimental investigation is mandatory in any case if questions concerning molecular structure are raised.

Several issues may be raised at this point for future discussions: The study of protein–quinone interactions, such as those involved in natural defense mechanisms and sclerotization processes, provides a basis for seeking new pharmaceutical applications (cf. daunomycin) or avoiding toxic effects (cf. paracetamol). The knowledge of the biosynthesis and structural principles of macromolecular networks may help in the design of new compounds for medical use, such as those interfering with melanogenesis in melanoma cells, or for agricultural applications, such as those impairing the construction of a sclerotized exoskeleton in insect pests. Finally, new materials can be envisaged that share such properties as hardness with lignocellulose, or stiffness and low density with the exoskeleton of insects, or strength with the byssal threads of the common fouling mussel. The construction of new materials from chemically modified proteins has been suggested recently[170] and, with advancing techniques in protein design and engineering, the time may have arrived to look more closely into this matter. Thus, an understanding of the principles of the reactions of quinones in biological systems is important from a practical viewpoint. However, our desire to analyze the unknown in order to discover causal relationships and to unravel nature's molecular construction plans is motivated above all by sheer curiosity.

Much of the work cited from this laboratory was performed by a number of skilled students whose names appear in the references. I am indebted to them for their encouraging engagement and endurance. Quite a few of the ideas discussed in this article were born in stimulating discussions with many colleagues, and I am grateful especially to Prof. P. Karlson (Marburg), Prof. W. Steglich (Bonn), and Dr. G. F. Weirich (Beltsville). Several projects were only successful through the cooperativity of colleagues in zoology: Prof. A. Egelhaaf (Cologne), the late Prof. H. Emmerich (Darmstadt), Prof. K. Scheller (Würzburg), and Prof. R. Keller (Bonn). Most of the experimental work mentioned was funded generously by the Deutsche Forschungsgemeinschaft to whom I am particularly indebted for a Heisenberg Award. Further support from the Fonds der Chemischen Industrie is gratefully acknowledged.

Received: May 5, 1988 [A 715 IE]
German version: *Angew. Chem. 101* (1989) 572

[1] R. H. Thomson: *Naturally Occurring Quinones*, Academic Press, London 1971; *Naturally Occurring Quinones, Vol. 3*, Chapman and Hall, London 1987.
[2] R. H. Thomson, *Recent Adv. Phytochem. 12* (1979) 287.
[3] H. Schildknecht, *Angew. Chem. 93* (1981) 164; *Angew. Chem. Int. Ed. Engl. 20* (1981) 164.
[4] D. J. Faulkner, *Nat. Prod. Rep. 4* (1987) 539; *ibid. 3* (1986) 1; *ibid. 1* (1984) 551; T. Higa, *Mar. Nat. Prod. Chem. Biol. Perspect. 4* (1981) 93; J. T. Baker, V. Murphy in R. J. Moore (Ed.): *CRC Handbook of Marine Science, Vol. 2*, CRC Press, Boca Raton, FL, USA 1981, p. 7.
[5] W. B. Turner: *Fungal Metabolites*, Academic Press, London 1971; W. B. Turner, D. C. Aldridge: *Fungal Metabolites, Vol. 2*, Academic Press, London 1983; M. Gill, W. Steglich, *Prog. Chem. Org. Nat. Prod. 51* (1987) 1.
[6] H. Schildknecht, *Angew. Chem. 82* (1970) 17; *Angew. Chem. Int. Ed. Engl. 9* (1970) 1; M. S. Blum, *Annu. Rev. Entomol. 32* (1987) 381.
[7] H.-W. Wanzlick, *Angew. Chem. 76* (1964) 313; *Angew. Chem. Int. Ed. Engl. 3* (1964) 401.
[8] W. M. Horspool, *Q. Rev. Chem. Soc. 23* (1969) 204.
[9] a) S. Patai (Ed.): *The Chemistry of Quinonoid Compounds*, Wiley, London 1974; b) S. Patai, Z. Rappoport (Eds.): *ibid. Vol. 2*, Wiley, Chichester 1988.
[10] H. Ulrich, R. Richter in *Houben-Weyl-Müller: Methoden der Organischen Chemie, Bd. VII/3a*, Thieme, Stuttgart 1977, p. 1; C. Grundmann, *ibid. Bd. VII/3b*, 1979, p. 1.
[11] A. M. Mayer, E. Harel, *Phytochemistry 18* (1979) 193.
[12] A. B. Turner, *Q. Rev. Chem. Soc. 18* (1964) 347.
[13] B. Kalyanamaran, R. C. Sealy, K. Sivarajah, *J. Biol. Chem. 259* (1984) 14018.
[14] M. G. Peter, H. B. Stegmann, H. Dao-Ba, K. Scheffler, *Z. Naturforsch. C40* (1985) 535.
[15] M. J. Nilges, H. M. Swartz, A. Riley, *J. Biol. Chem. 259* (1984) 2446.
[16] B. Kalyanamaran, R. C. Sealy, *Biochem. Biophys. Res. Commun. 106* (1982) 1119.
[17] P. L. Chesis, D. E. Levin, M. T. Smith, L. Ernster, B. N. Ames, *Proc. Natl. Acad. Sci. USA 81* (1984) 1696; P. Nata in [9b], p. 879; M. C. Depew, J. K. S. Wan in [9b], p. 963.
[18] H. Nohl, W. Jordan, *Bioorg. Chem. 15* (1987) 374.
[19] K. J. A. Davies, *J. Biol. Chem. 262* (1987) 9895; K. J. A. Davies, M. E. Delsignore, S. W. Lin, *ibid. 262* (1987) 9902; K. J. A. Davies, M. E. Delsignore, *ibid. 262* (1987) 9908.
[20] H. Musso, D. Maaßen, *Justus Liebigs Ann. Chem. 689* (1965) 93.
[21] M. K. Manthey, S. G. Pyne, R. J. W. Truscott, *J. Org. Chem. 53* (1988) 1486.
[22] S. Ito, G. Prota, *Experientia 33* (1977) 1118.
[23] B. Kalyanamaran, P. I. Premovic, R. C. Sealy, *J. Biol. Chem. 262* (1987) 11080.
[24] N. Takahashi, J. Schreiber, V. Fischer, R. P. Mason, *Arch. Biochem. Biophys. 252* (1987) 41.
[25] A. Palumbo, S. Ito, G. Nardi, G. Prota, *Comp. Biochem. Physiol. B58* (1977) 353; S. Ito, G. Nardi, G. Prota, *J. Chem. Soc. Chem. Commun. 1976*, 1042.
[26] Y. Nakagawa, K. Hiraga, T. Suga, *Biochem. Pharmacol. 32* (1983) 1417.
[27] F. Kehrmann, M. Cordone, *Ber. Dtsch. Chem. Ges. 46* (1913) 3009.
[28] C. E. M. Pugh, H. S. Raper, *Biochem. J. 21* (1927) 1370.
[29] R. H. Hackman, A. R. Todd, *Biochem. J. 55* (1953) 631.
[30] H.-J. Kallmayer, *Arch. Pharm. (Weinheim Ger.) 312* (1979) 73, 230.
[31] L. Horner, H. Lang, *Chem. Ber. 89* (1956) 2768.
[32] M. G. Peter, *Z. Naturforsch. C33* (1978) 912.
[33] D. C. S. Tse, R. L. McCreery, R. N. Adams, *J. Med. Chem. 19* (1976) 37.
[34] A. Hikosaka, J. Kumanotani, *Bull. Chem. Soc. Jpn. 43* (1970) 2620.
[35] C. R. Tindale, *Aust. J. Chem. 37* (1984) 611.
[36] R. Davies, J. L. Frahn, *J. Chem. Soc. Perkin Trans. 1 1977*, 2295.
[37] Reviews on the use of quinones in the synthesis of heterocycles: K. T. Finley in [9b], p. 537; R. W. Middleton, J. Parrick in [9b], p. 1019.
[38] A. Bolognese, G. Scherillo, W. Schäfer, *J. Heterocycl. Chem. 23* (1986) 1003.
[39] A. Tomoda, J. Yamaguchi, H. Kojima, H. Amemiya, Y. Yoneyama, *FEBS Lett. 196* (1986) 44.
[40] H. Kayser, *Compr. Insect Physiol. Biochem. Pharmacol. 10* (1985) 367.
[41] E. Haslam: *The Shikimate Pathway*, Hallsted Press, New York 1974.

[42] S. Nan'ya, T. Tange, E. Maekawa, Y. Ueno, *J. Heterocycl. Chem. 23* (1986) 1267.
[43] N. E. Mackenzie, S. Surendrakumar, R. H. Thomson, H. J. Cowe, P. J. Cox, *J. Chem. Soc. Perkin Trans. 1 1986*, 2233.
[44] G. Prota, G. Curro, *Tetrahedron 30* (1974) 3627.
[45] M. G. Peter, F. Speckenbach, *Helv. Chim. Acta 65* (1982) 1279.
[46] E. J. Corey, K. Achiwa, *J. Am. Chem. Soc. 91* (1969) 1429.
[47] K. Köhler, *Dissertation*, Universität Bonn 1985.
[48] P. A. Cranwell, R. D. Haworth, *Tetrahedron 27* (1971) 1831.
[49] R. Ott, E. Pinter, P. Kajtna, *Monatsh. Chem. 110* (1979) 51.
[50] R. A. Nicolaus: *Melanins*, Hermann, Paris 1968.
[51] G. A. Swan, *Prog. Chem. Org. Nat. Prod. 31* (1974) 521.
[52] R. H. Thomson, *Angew. Chem. 86* (1974) 355; *Angew. Chem. Int. Ed. Engl. 13* (1974) 305.
[53] K. Freudenberg, A. C. Neish: *Constitution and Biosynthesis of Lignin*, Springer, Berlin 1968.
[54] H. Nimz, *Angew. Chem. 86* (1974) 336; *Angew. Chem. Int. Ed. Engl. 13* (1974) 313.
[55] C. K. Wat, G. H. N. Towers, *Recent Adv. Phytochem. 12* (1979) 371.
[56] A. G. McInnes, M. A. Ragan, D. G. Smith, J. A. Walter, *Hydrobiologia 116/117* (1984) 597.
[57] M. A. Ragan, *Phytochemistry 23* (1984) 2029.
[58] J. Peter-Katalinić, H. Egge, B. Deutscher, W. Knöß, K.-W. Glombitza, *Biomed. Environ. Mass Spectrom. 15* (1988) 595.
[59] D. G. Roux, D. Ferreira, *Prog. Chem. Org. Nat. Prod. 41* (1982) 47.
[60] L. Y. Foo, L. J. Porter, *Phytochemistry 19* (1980) 1747.
[61] E. Haslam, *Prog. Chem. Org. Nat. Prod. 41* (1982) 1.
[62] W. Ziechmann: *Huminstoffe*, Verlag Chemie, Weinheim 1980.
[63] A. Körner, J. Pawelek, *Science (Washington D.C.) 217* (1982) 1163; J. Pawelek, A. Körner, A. Bergstrom, J. Bologna, *Nature (London) 286* (1980) 617; J. Cabanes, F. García-Cánovas, J. A. Lozano, J. García-Carmona, *Biochim. Biophys. Acta 923* (1987) 187.
[64] H. S. Mason, D. J. E. Ingram, B. Allen, *Arch. Biochem. Biophys. 86* (1960) 225.
[65] R. C. Sealy, C. C. Felix, J. S. Hyde, H. M. Swartz, *Free Radicals Biol. 4* (1980) 209; M. Pasenkiewicz-Gierula, R. C. Sealy, *Biochim. Biophys. Acta 884* (1986) 510.
[66] K. T. Yasunobu, E. W. Peterson, H. S. Mason, *J. Biol. Chem. 234* (1959) 3291.
[67] T. Kato, S. Ito, K. Fujita, *Biochim. Biophys. Acta 881* (1986) 415.
[68] S. Ito, T. Kato, K. Shinpo, K. Fujita, *Biochem. J. 222* (1984) 407.
[69] M. G. Peter, H. Förster, *Angew. Chem. 101* (1989) No. 6; *Angew. Chem. Int. Ed. Engl. 28* (1989) No. 6.
[70] R. M. B. Deibel, M. R. Chedekel, *J. Am. Chem. Soc. 106* (1984) 5884; M. R. Chedekel, K. V. Subbarao, P. Bhan, T. M. Schultz, *Biochim. Biophys. Acta 912* (1987) 239.
[71] S. Ito, E. Novellino, F. Chioccara, G. Misuraca, G. Prota, *Experientia 36* (1980) 822.
[72] R. C. Sealy, J. S. Hyde, C. C. Felix, I. A. Menon, G. Prota, H. M. Swartz, S. Persad, H. F. Haberman, *Proc. Natl. Acad. Sci. USA 79* (1982) 2885; R. C. Sealy, J. S. Hyde, C. C. Felix, I. A. Menon, G. Prota, *Science (Washington D.C.) 217* (1982) 545.
[73] M. d'Ischia, A. Napolitano, G. Prota, *Tetrahedron 43* (1987) 5351.
[74] M. d'Ischia, A. Napolitano, G. Prota, *Tetrahedron 43* (1987) 5357.
[75] W. G. C. Forsythe, V. C. Quesnel, *Biochim. Biophys. Acta 25* (1957) 155.
[76] W. L. Lütolf, R. Prewo, J. H. Bieri, P. Rüedi, C. H. Eugster, *Helv. Chim. Acta 68* (1985) 860.
[77] J. von Euw, T. Reichstein, C.-J. Widén, *Helv. Chim. Acta 68* (1985) 1251; W. J. Richter, F. Raschdorf, J. von Euw, T. Reichstein, C.-J. Widén, *ibid. 70* (1987) 881.
[78] K. H. Gustavson: *The Chemistry of Tanning Processes*, Academic Press, New York 1956.
[79] K. M. Meek, J. B. Weiss, *Biochim. Biophys. Acta 587* (1979) 112.
[80] A. E. Hagerman, L. G. Butler, *J. Biol. Chem. 256* (1981) 4494.
[81] J. P. McManus, K. G. Davis, T. H. Lilley, E. Haslam, *J. Chem. Soc. Chem. Commun. 1981*, 309; J. P. McManus, K. G. Davis, J. E. Beart, S. H. Gaffney, T. H. Lilley, E. Haslam, *J. Chem. Soc. Perkin Trans. 2, 1985*, 1429.
[82] J. E. Beart, T. H. Lilley, E. Haslam, *J. Chem. Soc. Perkin Trans. 2, 1985*, 1439.
[83] M. R. Attwood, B. R. Brown, S. G. Lisseter, C. L. Torrero, P. M. Weaver, *J. Chem. Soc. Chem. Commun. 1984*, 177.
[84] H. S. Mason, E. W. Peterson, *Biochim. Biophys. Acta 111* (1965) 134.
[85] W. S. Pierpoint, *Biochem. J. 112* (1969) 609.
[86] J. L. Maggs, P. S. Grabowski, B. K. Park, *Biochem. Pharmacol. 32* (1983) 2793.
[87] D. C. Dahlin, G. T. Miwa, A. Y. H. Lu, S. D. Nelson, *Proc. Natl. Acad. Sci. USA 81* (1984) 1327.
[88] D. W. Potter, J. A. Hinson, *J. Biol. Chem. 262* (1987) 974.
[89] M. Novak, M. Pelecanou, L. Pollack, *J. Am. Chem. Soc. 108* (1986) 112.
[90] M. J. Waring, *Annu. Rev. Biochem. 50* (1981) 159.
[91] K. Ramakrishnan, J. Fisher, *J. Med. Chem. 29* (1986) 1215.
[92] S. Ito, S. Inoue, Y. Yamamoto, K. Fujita, *J. Med. Chem. 24* (1981) 673; S. Ito, T. Kato, K. Ishikawa, T. Kasuga, K. Jimbow, *Biochem. Pharmacol. 36* (1987) 2007.
[93] R. F. Weaver, K. V. Rajagopalan, P. Handler, P. Jeffs, W. L. Byrne, D. Rosenthal, *Proc. Natl. Acad. Sci. USA 67* (1970) 1050.
[94] A. Rosowski, M. Wick, S.-H. Kim, *Congr. Am. Chem. Soc.*, Honolulu 1979, Abstr. MEDI 36.
[95] S. Hilbig, T. Andries, W. Steglich, T. Anke, *Angew. Chem. 97* (1985) 1063; *Angew. Chem. Int. Ed. Engl. 24* (1985) 1063.
[96] P. Eyer, E. Lierheimer, M. Strosar, *Mol. Pharmacol. 23* (1983) 282.
[97] Y.-O. Liang, P. M. Plotsky, R. N. Adams, *J. Med. Chem. 20* (1977) 581.
[98] M. N. Gupta, G. S. Murthy, P. J. Vithayathil, *Int. J. Pept. Protein Res. 15* (1980) 243.
[99] P. J. Vithayathil, G. S. Murthy, *Nature (London) New Biol. 236* (1972) 101.
[100] M. N. Gupta, P. J. Vithayathil, *Bioorg. Chem. 11* (1982) 101.
[101] I. Wagner, H. Musso, *Angew. Chem. 95* (1983) 827; *Angew. Chem. Int. Ed. Engl. 22* (1983) 816.
[102] M. N. Gupta, R. Gopinath, K. Raju, *Anal. Biochem. 118* (1981) 227.
[103] K. T. von der Trenck, D. Hunkler, H. Sandermann, *Z. Naturforsch. C36* (1981) 714.
[104] M. Tomasz, R. Lipman, D. Chowdary, J. Pawlak, G. L. Verdine, K. Nakanishi, *Science (Washington D.C.) 235* (1987) 1204; M. Tomasz, R. Lipman, B. F. McGuinness, K. Nakanishi, *J. Am. Chem. Soc. 110* (1988) 5892.
[105] G. Cimino, S. De Rosa, S. De Stefano, L. Cariello, L. Zanetti, *Experientia 38* (1982) 896.
[106] M.-L. Kondracki, M. Guyot, *Tetrahedron Lett. 28* (1987) 5815.
[107] H. Jackson, L. P. Kendal, *Biochem. J. 44* (1949) 477.
[108] D. J. Liberato, V. S. Byers, R. G. Dennick, N. Castagnoli, *J. Med. Chem. 24* (1981) 28.
[109] J. S. Byck, C. R. Dawson, *Anal. Biochem. 25* (1968) 123.
[110] M. A. ElSohly, P. D. Adawadkar, D. E. Benigni, E. S. Watson, T. L. Little, *J. Med. Chem. 29* (1986) 606.
[111] R. Davies, W. M. Laird, R. L. M. Synge, *Phytochemistry 14* (1975) 1591.
[112] J. Eagles, J. F. March, R. L. M. Synge, *Phytochemistry 19* (1980) 1771.
[113] W. S. Pierpoint, R. J. Ireland, J. M. Carpenter, *Phytochemistry 16* (1977) 29.
[114] W. S. Pierpoint, *Phytochemistry 21* (1982) 91.
[115] J. H. Waite, S. O. Andersen, *Biochim. Biophys. Acta 541* (1978) 107.
[116] J. H. Waite, M. L. Tanzer, *Science (Washington D.C.) 212* (1981) 1038.
[117] J. H. Waite, *J. Mar. Biol. Assoc. UK 65* (1985) 359.
[118] H. Schildknecht, J. Lubosch, *Z. Naturforsch. C42* (1987) 31.
[119] J. J. Harding, *Adv. Protein Chem.* 37 (1985) 247.
[120] M. A. Stahmann, A. K. Spencer, *Biopolymers 16* (1977) 1299.
[121] M. A. Stahmann, A. K. Spencer, G. R. Honold, *Biopolymers 16* (1977) 1307.
[122] C. Hasson, M. Sugumaran, *Arch. Insect Biochem. Physiol. 5* (1987) 13.
[123] R. Aeschbach, R. Amado, H. Neukom, *Biochim. Biophys. Acta 439* (1976) 292.
[124] K. Lerch, *Mol. Cell. Biochem. 52* (1983) 125.
[125] B. J. B. Wood, L. L. Ingraham, *Nature (London) 205* (1965) 291.
[126] K. Lerch, *Proc. Natl. Acad. Sci. USA 75* (1978) 3635.
[127] M. Frater-Schröder, M. Mahrer-Busato, *Bioorg. Chem. 4* (1975) 332.
[128] N. Stambolieva, J. Turkova, *Collect. Czech. Chem. Commun. 45* (1980) 1137.
[129] J. Brandt, L.-O. Andersson, J. Porath, *Biochim. Biophys. Acta 386* (1975) 196.
[130] T. Watanabe, S. Kaizu, T. Koshijima, *Chem. Lett. 1986*, 1871.
[131] A. Scalbert, B. Monties, J.-Y. Lallemand, E. Guittet, C. Rolando, *Phytochemistry 24* (1985) 1359.
[132] P. C. J. Brunet, *Insect Biochem. 10* (1980) 467.
[133] S. O. Andersen, *Annu. Rev. Entomol. 24* (1979) 29.
[134] H. Lipke, M. Sugumaran, W. Henzel, *Adv. Insect Physiol. 17* (1983) 1.
[135] M. G. Peter, *Habilitationsschrift*, Universität Bonn 1982.
[136] M. G. M. Pryor, *Proc. R. Soc. (London) B128* (1940) 378.
[137] M. G. M. Pryor, *Proc. R. Soc. (London) B128* (1940) 393.
[138] P. Karlson, C. E. Sekeris, K. E. Sekeri, *Hoppe-Seylers Z. Physiol. Chem. 327* (1962) 86.
[139] P. Karlson, C. E. Sekeris, *Nature (London) 195* (1962) 183.
[140] T. L. Hopkins, T. D. Morgan, Y. Aso, K. J. Kramer, *Science (Washington D.C.) 217* (1982) 364.
[141] I. F. Turnbull, N. A. Pyliotis, A. J. Howells, *J. Insect Physiol. 26* (1980) 525.
[142] K. G. Raghavan, G. B. Nadkarni, *Insect Biochem. 8* (1978) 53.
[143] R. H. Hackman, M. Goldberg, *Insect Biochem. 7* (1977) 175.
[144] V. Semensi, M. Sugumaran, *Pestic. Biochem. Physiol. 26* (1986) 220.
[145] a) K. Scheller (Ed.): *The Larval Serum Proteins of Insects*, Thieme, Stuttgart 1983; b) L. Grün, M. G. Peter in [145a], p. 102.
[146] M. G. Peter, U. Grittke, L. Grün, D. Schäfer in A. Zabza, F. Sehnal, D. L. Denlinger (Eds.): *Endocrinological Frontiers in Physiological Insect Ecology*, Politechnika Wroclawska Poland, Wroclaw 1988, p. 519.
[147] A. C. Neville: *Biology of the Arthropod Cuticle*, Springer, Berlin 1975, p. 126.

[148] R. H. Hackman in M. Rockstein (Ed.): *The Physiology of Insecta, Vol. 6*, Academic Press, New York 1974, p. 215.
[149] J. Schaefer, K. J. Kramer, J. R. Garrow, G. S. Jacob, E. O. Stejskal, T. L. Hopkins, R. D. Speirs, *Science (Washington D.C.) 235* (1987) 1200.
[150] L. Grün, *Dissertation*, Universität Bonn 1986.
[151] M. Sugumaran, H. Lipke, *FEBS Lett. 155* (1983) 65.
[152] M. G. Peter, *Insect Biochem. 10* (1980) 221.
[153] M. G. Peter, W. Vaupel, *J. Chem. Soc. Chem. Commun. 1985*, 848.
[154] M. Sugumaran, *Biochemistry 25* (1986) 4489.
[155] I. Kayser-Wegmann, H. Kayser in [145a], p. 151.
[156] L. Grün, M. G. Peter, *Z. Naturforsch. C39* (1984) 1066.
[157] H. Lipke, W. J. Henzel, *Insect Biochem. 11* (1981) 445.
[158] M. G. Peter, L. Grün, H. Förster, *Angew. Chem. 96* (1984) 614; *Angew. Chem. Int. Ed. Engl. 23* (1984) 638.
[159] P. Karlson, I. Schlossberger-Raecke, *J. Insect Physiol. 8* (1962) 441.
[160] P. Karlson, K. E. Sekeri, V. I. Marmaras, *J. Insect Physiol. 15* (1969) 319.
[161] M. E. Jacobs, *Insect Biochem. 8* (1978) 37; A. F. Sherald, *Experientia 36* (1980) 143.
[162] M. E. Jacobs, *J. Insect Physiol. 31* (1985) 509.
[163] I. Ujváry, K. Hiruma, L. M. Riddiford, G. Matolcsy, C. R. Roseland, K. J. Kramer, *Insect Biochem. 17* (1987) 389.
[164] M. Angrick, D. Rewicki, *Chem. Unserer Zeit 14* (1980) 149.
[165] a) J. E. Wright, A. Retnakaran (Eds.): *Chitin and Benzoylphenyl Ureas*, Dr. W. Junk Publishers, Dordrecht 1987; b) B. Mauchamp, O. Perrineau in [165a], p. 101.
[166] E. Cohen in [165a], p. 43.
[167] M. G. Peter, R. Keller, G. Kegel in R. A. A. Muzzarelli, C. Jeuniaux, G. W. Gooday (Eds.): *Chitin in Nature and Technology*, Plenum, New York 1986, p. 21.
[168] M. J. C. Kent, N. D. Light, A. J. Bailey, *Biochem. J. 225* (1985) 745.
[169] J. F. V. Vincent, J. E. Hillerton, *J. Insect Physiol. 25* (1979) 653; J. E. Hillerton, J. F. V. Vincent, *ibid. 25* (1979) 957.
[170] K. Kaleem, F. Chertok, S. Erhan, *Nature (London) 325* (1987) 328.

Structure and Dynamics of Chiral Molecules**

By Martin Quack*

Could there be chiral methane? What is the characteristic structural feature (in a physicochemical sense) of a molecule? This question dates back to *Louis Pasteur*, the discoverer of molecular chirality, and since the work of *van't Hoff* and *Le Bel* is generally considered by chemists as solved. In the present article it is pointed out that there exist fundamentally conflicting theoretical views of the physical origin of molecular chirality. These views predict consequences that could, in principle, be distinguished experimentally, but at present there is no conclusive experimental evidence available. Possible experiments are suggested that test different hypotheses. The importance of the magnitude of the parity-violating energy difference ΔE_{PV} in molecules due to the weak nuclear force for both the structure and spectra of chiral molecules and for the kinetics of racemization is discussed. The chemical relaxation rate coefficient of chiral molecules with some appreciable energy of excitation is derived for several limiting cases of a simple statistical mechanical model, which takes ΔE_{PV} into account.

"Si les principes immédiats de la vie immédiate sont dissymétriques, c'est que, à leur élaboration, présidents des forces cosmiques dissymétriques; c'est là, suivant moi, un des liens entre la vie à la surface de la terre et le cosmos, c'est-à-dire l'ensemble des forces répandues dans l'univers".[***]
L. Pasteur[19]

1. Introduction

Since Pasteur's first separation of crystals of racemic organic compounds (such as the sodium ammonium salt of tartaric acid) into left- and right-handed, optically active compounds 140 years ago,[1] two major questions related to this observation of chirality have been addressed repeatedly:

1. What is the origin of chirality in *molecular physics* and thus the "nature" or intrinsic structural feature of a chiral molecule or chiral substance?
2. What is the origin of chirality in (molecular) *biology* (i.e. the *chiral bias* favoring some enantiomers over others)?

These two questions are quite distinct, although related to each other. The second question concerns one of the more obvious, major unsolved problems in biochemical research.[2-17] We shall concentrate here on the first question, which is considered by many to be solved. This is not so, as we shall demonstrate. It may be that proper consideration of the first question will help to solve the second.

Even today the "structure" of chiral molecules is discussed by most chemists in terms of *macroscopic molecular models* in three dimensional space in the framework of conventional stereochemistry.[1c, 3, 18-23] It was recognized by *Friedrich Hund*[24] that in the framework of quantum mechanics certain problems arise with classical stereochemistry due to the possibility of tunneling, which connects left- and right-handed structures. *Hund* provided an immediate apparent solution to these problems by considering the time scales for interconversion between enantiomers (see Section 2.2). *Primas*[25] pointed out, however, that this solution does not explain, why one cannot buy in a drug store the substance corresponding to the coherent superposition of left- and right-handed states of chiral molecules such as alanine. Of course the reason for this may be trivial, the superposition states may be unstable and thus difficult to store in bottles (one cannot buy free radicals such as CH_3 in bottles in a drug store, but there is good evidence for their existence). However, a *possible* solution of "Primas' paradox" is the nonexistence of these achiral states of chiral molecules, which leads to the more recent discussions of chirality.[26-32] These invoke either essential interactions with the radiation field, or else with other external agents in order to explain the physics of chiral molecules.

Finally, after the discovery of the chiral symmetry violating weak nuclear interaction[33-41] it would appear natural to assume that this force has also fundamental implications for the physics of chiral molecules.[10, 11, 17, 42-54] In contrast to the other three fundamental forces of physics (strong nuclear forces, electromagnetic interaction, and gravitation) this "weak interaction" is intrinsically chiral. It is responsible for the β-decay of the neutron. It has been shown to lead to a nonconservation of the quantum number "parity" in nuclear decay processes[34] and in atomic spectroscopy.[40] In chemistry it has a most striking, as yet hypothetical, consequence: Under appropriate conditions it leads to a parity-violating energy difference E_{PV}[10, 11] between two enantiomers **R** and **L**, in thermodynamic terms, i.e. to a thermodynamic reaction energy $\Delta_R U_0^0$ different from zero

[*] Professor Dr. M. Quack
Laboratorium für Physikalische Chemie der
Eidgenössischen Technischen Hochschule
ETH-Zentrum, Universitätsstrasse 22, CH-8092 Zürich (Switzerland)

[**] Based on the final part of the Hund/Klemm lecture ("Wie bewegen sich Moleküle?", October 27, 1986) at the Max-Planck Institut für Festkörperforschung, Stuttgart (FRG). The main, first part will be published separately. The first Hund/Klemm lecture forms the basis of a review by H. Bock and R. Dammel in *Angew. Chem.* 99 (1987) 518; *Angew. Chem. Int. Ed.* 26 (1987) 504.

[***] If the foundations of life are dissymmetric, then because of dissymmetric cosmic forces operating at their origin; this, I think, is one of the links between the life on this earth and the cosmos, that is the totality of forces in the universe.

for the racemization (a) (leaving the sign undetermined; see also appendix); $|\Delta_R U_0^0| \equiv |\Delta E_{PV}|$.

$$\mathbf{L} \rightleftharpoons \mathbf{R} \qquad \text{(a)}$$

All of the above mentioned discussions of molecular chirality result in differing views about the actual "structure" (in a general, physicochemical sense) of chiral molecules and substances. These differences should not be dismissed entirely as problems in the realm of bad terminology or philosophy. Rather, we shall demonstrate that the different views correspond to different theories of chirality with conflicting predictions concerning the outcome of certain experiments. To decide unequivoqually which theories must be dismissed, one must perform an experiment which discriminates between them. To date, there is essentially no experimental evidence available on some central questions and this aspect has been largely overlooked in the theoretical discussions of the problem. The present paper is intended to fill this gap. Some possible experiments[50] will be discussed.

2. A Critical Discussion of Different Points of View Concerning Molecular Chirality

In this section we shall summarize some of the general aspects and predictions of the various theories of chirality. Predictions for specific experiments will be given in Section 3.

2.1. Macroscopic Molecular Models and Classical Mechanics: "The Classical Hypothesis"

The original description of chiral molecules was given in terms of molecular models that are the microscopic analogue of macroscopic models satisfying the laws of classical mechanics of our everyday world.[1, 18-21] It is in essence also the starting point of the organic stereochemists models. In modern language one would take the approximate Born-Oppenheimer potentials as true effective potential functions for the essentially classical motion of the heavy nuclei. These potentials may then either be symmetrical with respect to space inversion or there may be a slight asymmetry if there is a parity-violating term. In the former case the occurrence of left- and right-handed enantiomers arises from the initial conditions of a given experiment. It would arise quite naturally and is *not* difficult to understand. Because of the experimentally established energetic equivalence (to within rather large experimental error!) this was the historically prevalent point of view.[18-21] *Pasteur* seems to have seriously considered also an intrinsic asymmetry. In this latter case enantiomerism would be rather similar to all other kinds of isomerism with a small $\Delta_R U_0^0$.

With the advent of quantum mechanics, governing also molecular vibrations and rotations, one might consider the classical point of view as irrelevant and superseded.[24] However, one might also take an extreme outsider's point of view along the following lines: The motion corresponding to the interconversion of enantiomers in complex organic molecules is of very low frequency. It may be that for such motions quantum mechanics becomes invalid, and classical mechanics (or something similar) is *intrinsically* valid (i.e. not just as an approximation to quantum mechanics). There is no computational test of sufficient accuracy in the quantum chemistry of enantiomers, which could disprove such a hypothesis. More interestingly, we are not aware *of any direct experimental test*. Such tests might search for either tunneling in the *symmetric* case (absent in classical mechanics) or look for direct violations of the quantum mechanical superposition principle, which is irrelevant for Newtonian mechanics both in the symmetric and asymmetric cases.

Before discussing specific experiments, it should be pointed out, that the "classical hypothesis" seems rather inconsistent and theoretically remote. There is no good reason for treating electrons and nuclei on a totally different footing, which is implied by taking the Born-Oppenheimer potentials as more than an approximate trick. In reality there is no good reason to assume that there are such potentials and one should consistently treat *both* electrons and nuclei by the same mechanics (quantum or classical). There *is* sufficient evidence for excluding a classical mechanical treatment for the electronic motions in enantiomers. One would thus be tempted to discard the classical hypothesis on theoretical grounds. In the absence of direct experimental tests, some might wish to resist this temptation.

2.2. The Quantum Mechanical Point of View with a Space Reflection Invariant Hamiltonian: "*Hund*'s Hypothesis"

Hund[24] recognized that in quantum mechanics there will be a small splitting $\Delta E_{\pm}$ due to tunneling between eigenstates of positive and negative overall parity, if the total hamiltonian $\boldsymbol{H}$ is invariant under space reflection for the potentially enantiomeric molecular system. The eigenfunctions of $\boldsymbol{H}$ would thus be achiral. Their superposition results in left- and right-handed enantiomers, which are *time dependent molecular states*. *Hund* estimated the time dependence for typical compounds and concluded that on ordinary time scales the tunneling contribution to interconversion would be negligible: The enantiomers are predicted to be kinetically stable.

In order to avoid certain confusions that sometimes arise, we should stress that there is no reason whatsoever to request that a molecule or chemical compound should correspond to an eigenstate of $\boldsymbol{H}$. Many molecules are known to exist as kinetically stable entities, often even as scattering resonances in the continuum far above the ground state of $\boldsymbol{H}$. A simple example is formaldehyde H_2CO, which is unstable with respect to decomposition into $H_2 + CO$, according to current thermodynamic data ($\Delta_R H_0^0 = -1.7 \pm 6$ kJ mol^{-1}, a more pronounced example is $N_2H_4 = N_2 + 2\,H_2$, $\Delta_R H_0^0 = -109$ kJ mol^{-1}). These molecules are kinetically stable. In this context it may be useful to provide some orders of magnitude. The racemization of aspartic acid is among the fastest for amino acids and is believed to occur unimolecularly under certain conditions.[56, 60] At 310 K the rate constant is $k_{rac} \simeq 2.7 \times 10^{-11}$ s, corresponding to a chemical relaxation time of about 1200 years. Most of the reaction occurs by thermal excitation over a barrier of about 125 kJ mol^{-1}.

Hund's hypothesis is perfectly consistent with all available experimental evidence. One may raise, however, some theoretical objections. The first, and certainly most serious one, concerns the influence of parity-violating perturbations due to the weak nuclear force. As this was only discovered in 1956,[33-35] *Hund* could not know about it. In 1927 it seemed apparently too remote to even hypothesize about this possibility. Today we must take it into account.[6, 10, 11, 42-55] However, this does not automatically invalidate *Hund*'s hypothesis for the fundamental structure and dynamics of enantiomers, whose properties depend critically on certain parameters, the splitting $\Delta E_{\pm}$ due to tunneling and the parity-violating splitting ΔE_{PV} (see appendix). Only when the inequality (1) holds will *Hund*'s hypothesis be valid. Current theory would seem to exclude the inequality (1) for a number of typical cases.[10, 11] However, from an experimental point of view the question is open.[50]

$$\Delta E_{\pm} \gg E_{PV} \tag{1}$$

The second objection was raised by *Pfeifer*.[26] He points out that *Hund*'s treatment neglects some interactions with the radiation field. If these are included, *Pfeifer* finds that the achiral eigenstates are removed and that the chiral states correspond to stable states of the system due to a superselection rule. Experimentally, this point also remains open.[50]

The third and perhaps least serious objection comes from a discussion of collisional effects by *Harris* and *Stodolsky*.[30] To the extent that at very low gas densities the idealization of a collision free molecule is adequate, this work complements *Hund*'s work but does not reject his hypothesis (for a discussion of crystallization see Ref. [57]).

2.3. Influence of the Radiation Field: *Pfeifer*'s "Superselection Rule Hypothesis"

Pfeifer pointed out two weaknesses of *Hund*'s treatment.[26, 58, 59] Firstly, *Hund* does not explicitly account for the *apparent* absence of "isomers of well defined parity".[50] These would thus seem to be unstable or nonexistent, in contrast to the established high stability of enantiomers. This objection may or may not be taken seriously. Certainly the repeated statement[58, 27] that "according to experiment space reflection invariant pure states for enantiomeric molecules do not exist" is incorrect, as to the best of our knowledge no experimental evidence has ever been presented for the *absence* of states of well defined parity (there is no evidence for their *existence* either, but that is a different matter, see Section 3.1). Thus, *Hund*'s treatment would seem to be somewhat incomplete but not necessarily incorrect. However, the first observation led *Pfeifer* to note that secondly, *Hund* omits to treat the interactions with the radiation field, which cannot be entirely removed. When *Pfeifer* includes these, he finds[58] within the framework of algebraic quantum mechanics (see also Ref. [27]) a superselection rule, which, indeed, excludes on theoretical grounds the existence of states of well defined parity under certain conditions for enantiomeric systems. Thus, even without parity violating terms in the hamiltonian, the stable ground state of enantiomeric systems corresponds to left- and right-handed isomers and not to the symmetric state of positive parity.

Pfeifer's superselection rule certainly constitutes a most striking theoretical finding. He also gives some numerical estimates for molecules.[26, 58] However, there is no direct experimental test of the superselection rule hypothesis as yet.[26, 50] On the theoretical side, some aspects of *Pfeifer*'s treatment have been revised or extended.[27] One might also raise at least two general theoretical objections to *Pfeifer*'s treatment:

1. *Maxwell*'s equations and quantum field theory have equations of motion that are space reflection invariant, as is the molecular hamiltonian in the approximation used by *Pfeifer*. Thus from general symmetry considerations his result would seem undesirable, if not impossible.

2. It is not clear whether the infinite boundary conditions for the field used by *Pfeifer*, excluding gravitation, can correspond to any real physical situation or are meaningful idealizations. The two objections are related and we realize, of course, that the symmetry breaking is the *essence* of *Pfeifer*'s theory. As the theoretical situation is not entirely clear, we would summarize that *experimentally* the question is definitely open.

2.4. The Stabilization of Enantiomers by Collision: "The Collision Hypothesis"

It has been suggested that interactions with some external medium, in particular also collisions in a gas, tend to stabilize enantiomers (**L** and **R**) and destabilize parity isomers (+ and −)[30, 31, 32] (see also Ref. [59]). In discussing a Bloch type relaxation equation for the density matrix $\boldsymbol{P}$ of a two level problem in the $|\mathbf{L}>$ and $|\mathbf{R}>$ basis, *Harris* and *Stodolsky* derive the equation (2) for the relaxation to equilibrium for the population difference Δp of **L** and **R** (if $p^e_{\mathbf{L}} \simeq p^e_{\mathbf{R}}$ for the equilibrium population p^e).

$$\Delta p(t) = \boldsymbol{P}_{\mathbf{LL}} - \boldsymbol{P}_{\mathbf{RR}} = \Delta p(0) \exp[-(\bar{\delta}^2/\bar{\lambda})\, t] \tag{2}$$

Here, one has $\bar{\lambda}^{-1} \approx T_2$, the phase relaxation rate constant that can be assumed to be proportional to the collision frequency in a gas, and $\Delta E_{\pm} = 2\,\bar{\delta}$, the tunneling splitting for the parity states, which can be related to the rate of racemization in the absence of collisions (Section 4). Equation (2) is assumed to hold in the case of strong damping, i.e. $(\bar{\lambda}/\bar{\delta}) \gg 1$. One has the seemingly paradoxical result that the *population relaxation rate* $T_1^{-1} \simeq \bar{\delta}^2/\bar{\lambda}$ and thus the racemization rate constant k_{rac} are inversely proportional to the collision rate. But, normally, in the low pressure range of unimolecular reactions (of which racemizations are special cases) one has $k \propto$ collision rate, i.e. just the opposite behavior. This results from the mechanism of an ordinary unimolecular reaction, which involves a collisional activation process to energized states with fast reaction.[60, 70] The model of *Harris* and *Stodolsky* applies to the "low temperature limit" two state model of racemization only.

It is this starting point which one may criticize: In real polyatomic molecules, the two state model would apply only at exceedingly low temperatures $T \ll 1$ K, where all molecules are in the rotational and vibrational ground state. This will be difficult to achieve. A second criticism of the model comes from its neglect of the radiation field. One can

estimate that under dilute beam conditions thermal radiative transitions between ground and vibrationally excited states may be at least as important if not more so than transitions by collisions.[50] Thirdly, as noted also by *Harris* and *Stodolsky*, there are cases of low collision rate and sufficiently fast inversion rate, where *Hund*'s model would be applicable. One might then ask for the "structure" of the isolated molecule.

Whether or not the *Harris* and *Stodolsky* model is relevant to the stabilization or existence of long-lived enantiomers in dilute gases for real molecules at ordinary temperatures could be decided only by the direct experimental determination of the molecular relaxation parameters. To our knowledge, there exists no experimental evidence either supporting or denying this hypothesis. Thus, the theory merits an experimental test, possibilities for which will be discussed in Section 3.

2.5. Weak Nuclear Interaction and Parity Violation in Molecules

The first new aspect (after quantum mechanics and *Hund*) in terms of the *physics* of molecular chirality was certainly the discovery of the parity-violating weak nuclear force.[33-35] Parity violation in physics in general and for chiral molecules in particular clearly was not foreseen by theoretical reasoning alone. Parity violation leads to a slight energy difference for the **L** and **R** isomers. Recent estimates on the basis of fairly detailed quantum chemical calculations place the parity-violating energy difference of enantiomers ΔE_{PV} in the range of 10^{-14} J mol^{-1} or about 10^{-4} to 10^{-5} Hz in frequency units.[10, 11] If this is accepted, the structure of enantiomers would be dominated by this energy difference. Tunneling from **L** to **R** would be quite negligible for typical molecules at low temperatures and the probability density for true molecular eigenstates associated mostly with one enantiomer (say **L**) would be negligible for that part of the configuration space associated with the other enantiomer (**R**). Optical isomers would then resemble ordinary isomers **A** and **B**, such as *cis-trans* isomers, separated by an energy difference ΔE_{AB} at the zero-point level. For these the eigenstates of the molecular hamiltonian are sufficiently well localized at low energies that they may be associated with one isomer only.

From the theoretical side this situation appears to be fairly well understood. However, there exists no experimental test yet. Clearly, a direct experimental measurement of the parity-violating energy difference would be in order.[50] If the experimentally measured ΔE_{PV} were to be much smaller than the theoretical prediction, it might be that there are many optically active molecules, for which parity violation would be dynamically unimportant.

From a fundamental point of view the structural hypothesis of enantiomers based upon parity violation is the most interesting one, as it is based on symmetry arguments[61] closely related to general conservation laws[71] following the thoughts of *A. E. Noether*. Understanding the structure of enantiomers in terms of the parity-violating energy difference by a quantitative measurement might have consequences beyond physical stereochemistry in the realm of the physics of fundamental symmetries.[50, 62]

2.6. Symmetry Breaking *de facto* or *de lege*

At this point it may be useful to distinguish the symmetry breaking through initial conditions in the ordinary classical (Section 2.1) or quantum (Section 2.2) theory from the symmetry breaking by *violation* of the fundamental symmetry law of parity conservation (Section 2.5).

If the initial conditions of a physical system can be chosen in different, but symmetrically equivalent ways, the symmetry of the *phenomena* or the actual state of motion will not necessarily reflect the underlying symmetry. A classical mass point moving in a symmetrical double well potential will be localized on one side, if it lies below the barrier of the double well. The direction of motion of the planets around the sun is well defined and does not reflect the symmetry of the law of motion or of space. The same is true for the **L** and **R** enantiomers in the classical situation or *Hund*'s hypothesis. And a cigarette without filter will be lit at *one end*, even if it is symmetrical.

The symmetry of the underlying law or structure is broken *de facto* by the chosen initial conditions. But the underlying symmetrical law allows also the opposite, *symmetrically equivalent* solution. In the quantum case (Section 2.2) one has then the interesting possibility of a symmetrical state of motion by the superposition principle, but such a symmetrical state is no more likely than the asymmetrical state. In classical mechanics this symmetrical state does not exist, as the superposition principle is lacking.

If, however, the symmetry is already broken in the underlying law of motion (asymmetrical double well for the classical mass point, parity violation for **L** and **R**, cigarette with a filter), then the two states of motion are not symmetrically equivalent, and we speak of symmetry breaking *de lege*. If the symmetry breaking *de lege* is small, then in quantum mechanics a very nearly symmetrical state can be generated by linear superposition, which will evolve slowly in time with respect to its symmetry properties (time-dependent symmetry violation).

These two situations of symmetry breaking *de facto* and *de lege* are obviously quite different and should be distinguished by appropriate terminology, as proposed. There is a third class of symmetry breaking, which is commonly named "*spontaneous*".[63] It arises with an intrinsically symmetrical dynamical structure and *Pfeifer*'s hypothesis is an example of this. One might add that one view of parity violation introduces this as a spontaneous symmetry breaking in a cosmological context. Thus, the parity-violating molecular hamiltonian of our present world arises as a particular solution out of a fundamentally symmetrical situation at the origin of our universe. It may be that the **L** isomer of a given molecule is more stable than the **R** isomer in our world; this view implies that another world may exist in which the reverse would be true. This view of parity violation is nevertheless consistent with the statement that the left-right symmetry-breaking in our world is *de lege*, as the laws of motion are now defined in the present context.

2.7. "Totaliter aliter"

Before discussing experiments discriminating between current hypotheses of the structure of chiral molecules, one should consider the possibility that the experimental result will contradict *all* current hypotheses and is thus "totally different" (totaliter aliter[64]). Such a discussion must necessarily be speculative, as otherwise we could have listed yet another, specific alternative. Effects that have not been considered so far and that may influence the structure of chiral molecules are time reversal symmetry violation and gravitation. Both are very small at the molecular level, but one is talking about small effects anyway. At the other end of the spectrum one has configuration interaction of the molecular low energy states with excited electronic states and dissociative states that are achiral. This might influence the $\Delta E_{\pm}$ in an unpredicted way, as it is usually calculated as a tunneling splitting in the electronic ground state. At still higher energies there are states, where the particle concept (electrons and nuclei) of molecular structure is no longer useful. The effects of configuration interaction with such high energy field states (including increasing numbers of positrons, antiprotons etc.) are small, but not easy to predict and may perhaps lead to surprising consequences for the very small energy effects that we consider in chiral molecules. Finally, there might be effects from an as yet unknown force.

Even this list is not complete. Together with the five specific alternatives mentioned before it should convince the reader, that no definite statement on the structure of chiral molecules will be possible without direct experimental tests, even if *some* of the theoretical alternatives may seem remote or might even be excluded as inconsistent with currently established facts by a sufficiently careful analysis.

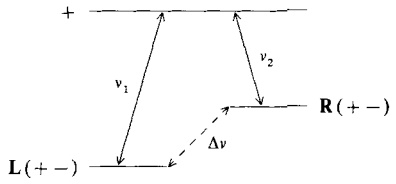
3. Experimental Tests

We shall discuss possible experimental tests of the hypotheses, labeled **1–5** following the order of Section 2. In each case we shall discuss the *principle* of the experiment, not the details of its realization, which are complex and often not obvious, and its capabilities to distinguish between the various hypotheses.

3.1. The Principles of the Experimental Testing of Various Hypotheses Concerning Molecular Chirality

1. The first class of experiments concerns the spectroscopy of separate enantiomers. Proposals and actual experiments of high accuracy have been communicated in the radiofrequency and infrared ranges. If the weak nuclear force has sufficient influence, the absorption frequencies for the individual **R** and **L** isomers will be slightly different. Measurements with CO_2 lasers have been attempted on CHFClBr by *Kompanets* et al.[43] but gave a null result. Experiments on camphor by *Arimondo* et al.[52] gave the same absorption frequencies for D and L to an accuracy $\Delta\nu/\nu$ of 10^{-8}, probably still far away from an expected effect, although no accurate calculations have been carried out. Calculations for NMR chemical shifts predict differences of about 1 mHz, which may be measurable but have not yet been proven experimentally.[47–49] If successful, these experiments are, in principle, able to discriminate the inversion symmetrical hypotheses **1–4** from the asymmetrical **5**. They do not give, however, a direct measure of the parity-violating energy difference of enantiomers ΔE_{PV}. We note that in atomic spectroscopy the search for effects from the weak nuclear force has been successful,[39–41] and for diatomic molecules there are some null results available in searches for both parity and time-reversal symmetry-violation.[51, 53, 54]

2. The second class of experiments concerns spectroscopic transitions *between* the **R** and **L** isomers. When ΔE_{PV} is much larger than the splitting due to tunneling, one-photon transitions (at mHz frequencies) are strictly forbidden. However, a two-photon transition with an intermediate state of well defined parity will be allowed according to the following scheme:



Scheme 1. Two-photon transfer between the enantiomers **R** and **L**.

Possible transitions in this case may involve an excited electronic state that is achiral and has rovibronic levels of well defined parity. The corresponding transitions would occur in the visible or UV part of the spectrum.

Stabilizing two lasers at the transition frequencies ν_1 and ν_2 of the **L** and **R** isomers one could measure the beating between them, which may occur on the time scale of hours. This experiment is technically very difficult as it requires long time stabilization of the frequency to within $\Delta\nu/\nu \approx 10^{-19}$, quite apart from other difficulties. A slightly more favorable situation would occur for special molecules, having a small tunneling splitting ($\Delta E_{\pm} \ll \Delta E_{PV}$) in the vibrational ground state and a large one ($\Delta E_{\pm} \geq \Delta E_{PV}$) in a vibrationally excited state of the electronic ground state. Scheme 1 would then allow a measurement in the IR with a gain of a factor of about ten concerning the required accuracy. In even more special cases, it may be possible to measure the highly forbidden transition $\mathbf{L} \leftrightarrow \mathbf{R}$ at the frequency $\Delta\nu$ directly. This will happen, when tunneling is just sufficient to mix the **L** and **R** wave functions slightly, still preserving the dominant asymmetry. The $\mathbf{L} \leftrightarrow \mathbf{R}$ transition will then be slightly allowed as it acquires a weak inversion transition character. Of course, such optical isomers are necessarily rather short-lived, and are not the most typical cases. The second class of experiments allows us to measure ΔE_{PV} and thus to decide to what extent inversion symmetry is violated *de lege* or not (i.e. preferring hypothesis **5** to the others).

3. A third class of experiments is somewhat speculative at present. It would be based on the kinetic selection of **L** and **R** isomers due to the asymmetric kinetics in the case of an appreciable ΔE_{PV}:

$$\mathbf{L} \underset{k_{LR}}{\overset{k_{RL}}{\rightleftharpoons}} \mathbf{R} \qquad \text{(b)}$$

$$\frac{k_{RL}}{k_{LR}} = 1 \pm \bar{A} \qquad (3)$$

with $\bar{A}$ of the order of 10^{-18}. This is not directly measurable, but in relation with nonequilibrium kinetic schemes in evolutionary times, mechanisms have been discussed that would lead to a measurable selection of **L** or **R**.[7-9, 12] *If* a mechanism of this kind could be found for a quantitatively well understood laboratory reaction, the measured selection rate for **L** or **R** could be interpreted in terms of $\bar{A}$ and finally ΔE_{PV}. Such an experiment would be an outstanding achievement in chemical kinetics, but at present there are no ideas as to how it could be realized. It might also be possible to unravel the mechanism of the natural selection of optical isomers in prebiotic times from fossil documents and thereby obtain the relevant parameters. Again this is at present a remote possibility. If ever such evaluations became possible they would discriminate hypothesis **5** against the others and, perhaps, provide a result for ΔE_{PV} in certain molecules.

4. Another experiment has been proposed, which is based on the generation of states of well defined parity and the observation of the time dependence of parity.[50] The principle of the experiment is based on three steps: a) Preparation of molecular states of well defined parity (for instance (+) from optically active molecules (**R** or **L**) of ill defined parity in the electronic ground state. b) Free evolution of the isolated molecule with initially well defined parity (+). Under this condition the probability for negative parity will increase quadratically with time; for short times Equation (4) holds.[50] For long times one has an oscillation with period τ [Eq. (5)].

$$p_- = (\pi \Delta E_{PV} t/h)^2 \tag{4}$$

$$\tau_\pm = h/\Delta E_{PV} \tag{5}$$

c) Spectroscopic observation of the population of states of the "forbidden" parity (for example p_-) as a function of time. According to Equations (4) or (5) one can evaluate ΔE_{PV} and again distinguish hypothesis **5** from the others. This experiment allows us, however, also to decide between hypothesis **2** and **1** or **3**. In the preparation step [Eq. (6)] of the experiment one generates a linear superposition state λ_+ [Eq. (6)],

$$\chi_+ = (\lambda + \varrho)/\sqrt{2} \tag{6}$$

where λ and ϱ are the eigenfunctions of the **L** and **R** isomers (cf. Appendix). According to the quantum mechanical superposition principle this is always possible whether or not there is a sizeable ΔE_{PV} (hypotheses **2** and **5**). According to the classical hypothesis **1** or the superselection rule hypothesis **3**[26] the preparation step will generate only **R** or **L** or mixtures of **R** and **L**. These can be distinguished experimentally from the χ_+ state by the dipole absorption spectrum. χ_+ has only strong electric dipole absorptions to states of negative parity whereas **L** and **R** and mixtures have strong electric dipole absorption to both positive and negative rovibronic states. Thus, in an appropriate electronic transition, for example,[50] hypotheses **1** and **3** would predict a spectrum with about twice as many lines than predicted by hypotheses **2** and **5**. The experiment provides a direct test of the superposition principle for enantiomers. It would not allow one to differentiate between hypotheses **1** and **3**, which both require violation of the quantum mechanical superposition principle. Hypothesis **1** is in a sense a very general hypothesis and **3** might be thought to be a special, precise formulation. In that sense a distinction between **1** and **3** would become meaningful only if precise alternatives were formulated. This class of experiments would be a test for all possible hypotheses except **4** and is thus very powerful. We have also discussed in detail[50] that the experiment should be practical, even if difficult and expensive in its setup. Although the experiment is subject to numerous obvious complications, the evidence presented in Ref. [50] and further investigations[65] all suggest that the experiment can be realized with a guarantee of a definite outcome, whichever this may be. Complications could arise if ΔE_{PV} is either very small or much larger than currently predicted. If ΔE_{PV} is very small, from the absence of parity evolution one could then only derive an upper *limit* on ΔE_{PV}. If ΔE_{PV} is very large, the oscillation of parity might be so fast that it would *simulate* an **L**–**R** mixture, leading to the incorrect conclusion that hypotheses **1** or **3** are appropriate. By increasing time resolution, it should be easy to avoid such an error. Also, a very large ΔE_{PV} would be easily measured by a class 2 experiment and if established, proper precautions could be taken. We might also mention that the technique of *Kukolich* et al.[68] could be useful in the realization of our experiment (see also the related discussion below). Another realization involving excited electronic states is sketched in Figure 1.[50]

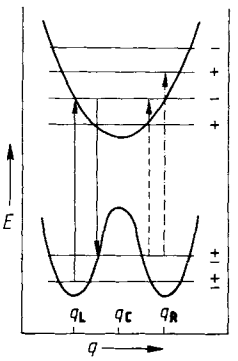
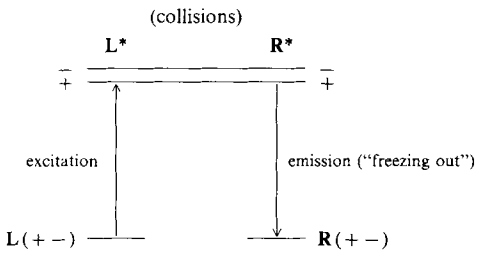


Fig. 1. Scheme for the generation of states of well defined parity (if possible) in a molecule that is chiral in the electronic ground state. The ground state potential has a high barrier for racemization, the excited state a low barrier or none as shown. q = inversion coordinate. In a first optical transition (↑) one generates a state of well defined parity (−) in the excited state, and in the second (↓) in the ground state. The dashed lines indicate the spectroscopic observation of the outcome of the experiment (after Ref. [50]).

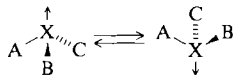
5. The final class of experiments would test the collisional hypothesis **4** perhaps by observation of the time dependence of optical activity.[30] A nontrivial time dependence will only be observed for rather quickly interconverting enantiomers, according to current estimates of ΔE_{PV}. A possible realization of the experiment would follow Scheme 2.

In a molecular beam of stable **L** and **R** isomers a pump laser would be used to excite the **L** isomer, for example, to an electronic or vibrational state in which the splitting due to tunneling is sufficient to allow interconversion at an observable rate, ideally complete inversion to **R** within a time of free flight in the beam. This transformation could be followed as a function of the length of flight along the beam by measuring the optical activity by Raman scattering[66] perhaps with CARS or Fourier transform techniques[67] in or-



Scheme 2. Experiment for testing the collision hypothesis **4** via the time dependence of the optical activity.

der to increase sensitivity (a serious problem in measuring optical activity). One might also increase sensitivity by freezing out the transformed molecules with a dump laser and collecting the stable "product" **R** for some time until sufficient material for the experimental sensitivity is available. In the free evolution stage of the experiment p_+ and p_- would remain constant and $p_{\mathbf{R}}$ and $p_{\mathbf{L}}$ would oscillate as suggested by *Harris* and *Stodolsky*. According to their prediction, this oscillation should *be slowed down* if we allow for collisions with some background gas in the molecular beam chamber. One needs just to investigate the $\mathbf{L} \rightarrow \mathbf{R}$ interconversion as a function of gas pressure, using Equation (2) for the evaluation of the relevant parameters. If the effect predicted by *Harris* and *Stodolsky* is observed, their hypothesis **4** would be confirmed for the molecular system in question, and one might, by systematic investigations, obtain an understanding of the circumstances in which the collisional stabilization of enantiomers is relevant (see also Section 4). A complication will arise in all these experiments, because a real molecule is not a two level system and even if the initial state is a coherent superposition of just two states, collisions will tend to transfer excitation to other states. It may also be useful to study the $\mathbf{L} \rightarrow \mathbf{R}$ oscillations by observations of quantities other than optical activity. A promising technique could be based upon the experiment of *Kukolich* et al.,[68] who studied collision cross sections of parity states (−) and of superposition states (+ −) in ammonia. They used the measurement of polarization in a microwave cavity (their case 2 experiment), which may be more sensitive than the measurement of optical activity. Indeed this experiment could be carried out in a very imaginative way in selected high *J, K* states of *near* symmetric tops with almost oriented molecules:



(c)

As indicated by the dipole moment arrows in Equation (c), the $\mathbf{L} \rightarrow \mathbf{R}$ interconversion in an oriented molecular beam will change the macroscopic electric dipole moment orientation and this could be detected. The dynamic situation can again become very complex with collisions.[69]

We have shown in this section that meaningful *real* experiments (as opposed to thought experiments) could test the different hypotheses on the structure of enantiomers. The hypotheses provide significantly different predictions for the various experiments. An appropriate combination of the different experiments discussed here would allow us to exclude all but one of the hypotheses, but we do not know which one would remain intact, even though intuition may suggest one. As discussed in Section 2.7, perhaps none of the hypotheses would survive the test, but this appears unlikely. At present, to the best of our knowledge, there is no definite experimental evidence available whatsoever. It should be obvious that the outcome of the experiments will depend in general also upon molecular parameters. Different hypotheses may therefore be correct for different molecules. It is then in order to discuss the scope of these hypotheses to make predictions concerning the influence of molecular parameters.

3.2. The Influence of Molecular Parameters

Molecular properties can influence considerably the nature of chirality in a given molecule. The most obvious case in question arises for *Hund*'s hypothesis and the parity-violation hypothesis. The inequality (1) determines which one applies. We have fairly standard techniques to estimate $\Delta E_{\pm}$, although it may sometimes be difficult to calculate the reaction path and barrier height for racemization by accurate ab initio techniques. The calculation of ΔE_{PV} by ab initio methods has just started.[10, 11] It is not clear yet (to the author) to what extent one can be certain that all the important effects have been included in the calculations. In this sense, too, an experimental test would be important. If current theoretical results are accepted, one would be able to calculate the relevant parameters in inequality (1) for simple molecules. More investigations of ΔE_{PV} are needed.

The classical hypothesis (**1**) is, at present, purely qualitative. *Pfeifer* has tried to make some estimates, for which molecular parameters his superselection rule should be applicable.[26, 58] The problem deserves more quantitative theoretical investigations.[27] The interested experimentalist would like to know from the theoretician, for which molecules and at what energies the symmetry breaking phase transition occurs, if it happens at all. Probably the isolated two-level approximation has to be abandoned for realistic estimates.

Harris and *Stodolsky*[30] have provided a collision theory formulation for their hypothesis. So far, no one has actually calculated quantitative cross sections for specific examples. Before planning experiments, such calculations would be helpful. The most serious problems will arise from the multistate nature of real molecules. That is, a large multichannel scattering calculation will be required, even if many channels are closed.

For the purpose of estimating collisional effects on the various doublet states of enantiomers, one may consider the results on ammonia inversion sublevels.[68] Here it is found that in the basis of parity states effective cross sections for T_1 and T_2 processes are somewhat larger than gas kinetic values and of about the same order of magnitude in inert gas collision partners, T_1 being shorter than T_2 with dipolar collision partners. This can be understood by a mechanism of dipolar relaxation connecting the parity sublevels but not the **R**–**L** sublevels. One can show that for a *degenerate* two-level problem, T_1 for the parity basis χ corresponds to T_2 for the ϱ–λ basis (see Appendix). Extrapolating from these results one would thus assume fast, approximately gas kinetic phase relaxation for the density matrix in the (ϱ, λ) basis and fast

Table 1. Some chiral molecules of particular theoretical or experimental interest.

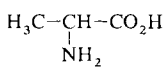
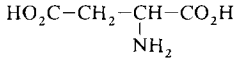
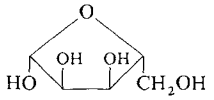
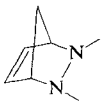
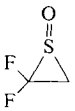
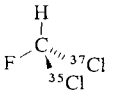
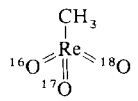
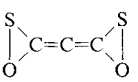
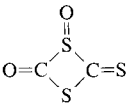
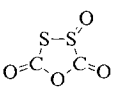
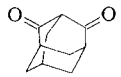
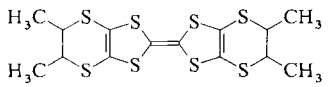
Molecule	Name	Remarks and references
		volatile, gas phase spectroscopy [43] possible: IR-laser chemistry
	camphor	(volatile) gas phase spectroscopy [52]
	alanine	theory: $\Delta E_{PV}^{max} \approx 10^{-13}$ J mol^{-1} (L more stable [10, 11])
	aspartate	theory: $\Delta E_{PV}^{max} \approx 8 \times 10^{-14}$ J mol^{-1} (L more stable [11]), well known racemization rate [56]
	ribose	theory: $\Delta E_{PV} \approx 2 \times 10^{-14}$ J mol^{-1} (D more stable [11])
H–Te–Te–H (hypothetical structure, twisted 90°)		relativistic theory $\Delta E_{PV} \approx 10^{-8}$ J mol^{-1} [49]
$Pt(C_2H_2)_2$ (hypothetical structure)		relativistic theory [49] $\Delta E_{PV} \approx 10^{-7}$ J mol^{-1}
$[CHCl_2CH_2TlH]^{\ominus}$ (hypothetical structure)		calculated difference in NMR chemical shift of enantiomers $\approx$ 1 mHz [47, 48]
		suitable for spectroscopy
	*N*,*N*′-dimethyl-2,3-diazabicyclo[2.2.1]hept-5-ene	modest barrier, NMR spectroscopy [91]
	1,2,2-trimethylaziridine (also 1*H*-aziridine and oxaziridines)	modest barrier [90], expected low barrier in excited electronic states vibrational and electronic spectroscopy. Higher barriers with NCl [92]
	(general sulfoxides)	modest barrier, laser chemistry and spectroscopy
	(general phosphanes)	intermediate barrier, spectroscopy and IR laser chemistry (similar also PX_5)
CHD=C=CHD	dideuterioallene	isotopic chirality, very small ΔE_{PV} expected
		isotopic chirality, suitable for spectroscopy in jets and overtones [93], very small ΔE_{PV} expected
		isotopic chirality with heavy atom, volatile compound for spectroscopy [94] and laser chemistry
		hypothetical spinless chiral molecule
		hypothetical spinless chiral molecule (also related derivatives)
		hypothetical spinless chiral molecule [96]
DFC=C=CH*H	allene (vibrationally twisted)	dynamic chirality [88] locally CH* excited dynamical chirality (Section 4)

Table 1. (Continued)

Molecule	Name	Remarks and references
	adamantanedione	proposed dynamical (electronic) chirality [86]
	methane	dynamic chirality of certain levels (Section 4)
		basis for chiral conductor [95], macroscopic electronic effects in ΔE_{PV}?

population relaxation in the χ_+, χ_- basis. On the other hand, by the same argument as for other isomerizations with high barriers, one would assume slow population relaxation T_1 in the (ϱ, λ) basis. This would easily explain why the "isomers of well defined parity" are not normally found in nature (*Primas*' paradox): They are collisionally unstable and equilibrate at about the gas kinetic collision rate. The arguments given above for collisions hold also for thermal background radiation, which will probably, via vibrationally excited states, quickly interconvert the + and − isomers but not **L** and **R**.[50] Quantitative experimental results on these cross sections are lacking, however, and would be obtained by a combination of experiments of type (4) and (5). Thus, some of the experiments discussed in Section 3.1 would provide information on molecular stationary state, collisional and radiative kinetic properties.

For carrying out spectroscopic experiments on the foundations of molecular chirality, it may be useful to choose from a list of suitable molecules. Criteria are: 1. Simplicity (few atoms); 2. volatile compounds; 3. heavy nuclei (for a large ΔE_{PV}); 4. a limited number of nuclei with spin (perhaps a "spinless" molecule, except for the NMR experiments) in order to remove close degeneracies in the spectra; 5. for some investigations molecules with modest energy barriers for racemization. Table 1 summarizes some molecules that may be considered, including a few for which ΔE_{PV} has been calculated. In a search, it transpired that "spinless" enantiomeric compounds are not known, and some are proposed to stimulate the imagination of the synthetic chemist.

4. The Kinetics of Racemization

Molecular structures are in general time dependent and thus an understanding of the dynamics of chiral molecules and of the kinetics of racemization is required in relation to their structural properties. Racemization reactions are a special class of isomerization reactions, which can be dealt within the framework of unimolecular rate theory.[70] Under ordinary "high temperature" conditions they can be discussed approximately in terms of a quasiclassical barrier crossing in the theory of reversible unimolecular reactions[72] or, even more simply by the kinetic scheme in Eqs. (b) and (3) with a very small $\bar{A}$. The rate constants will follow the Arrhenius law (7).

$$k_{RL} \simeq k_{LR} \simeq A \exp(-E_A/RT) \tag{7}$$

Another limit is the symmetrical two level tunneling model of racemization which does not lead to kinetic equations but to oscillatory motion.[24] The period of oscillation ($\Delta E_{PV} \simeq 0$) is given by Equation (8).

$$\tau = h/\Delta E_{\pm} \tag{8}$$

These descriptions are textbook material in the realm of kinetics[60] or of spectroscopy ("ammonia inversion").[73] The treatment of *Harris* and *Stodolsky*[30] extends the "low temperature" two-level tunneling model to cases involving parity violation and collisions. We shall not discuss these simplified models further but rather refer to the extensive literature on this subject.

Closer inspection of the dynamics of racemization shows, however, that it has certain very special features because of the *approximate* nonrigid molecular symmetry of space inversion and energy equivalence of **L** and **R** isomers.[71, 74–76] These special kinetic properties have not been discussed before for real chiral molecules at finite energies, where, in general, a very large number of quantum states renders statistical approximations useful.[77] We shall consider the strongly quantized case at energies below the classical energy barrier. Here, the reaction is dominated by quantum tunneling and quasiclassical barrier crossing is not a useful concept. In this case, the molecular spectrum shows close degeneracies associated with the interplay of ΔE_{PV} and $\Delta E_{\pm}$ and the average spacing of molecular states $\delta = \varrho^{-1}$ (ϱ = density of rovibronic or nurovibronic states subject to symmetry constraints[76]). This situation leads to very peculiar kinetic properties, depending on these three parameters. Similar behavior is expected for other isomerizations with a very small energy difference between reactant and product states, but in the case of chiral molecules it is essential for symmetry reasons and it thus reveals some of the fundamental properties of chiral molecules. We shall discuss some simple limiting cases of the kinetics of racemization in turn. We start by disregarding collisional and radiative transitions and give a phenomenological discussion of their effects at the end.

The experimental situation that one should have in mind in the following discussion of racemization of an ensemble of isolated molecules is a cold molecular beam in high vacuum, for instance a supersonic jet, excited to some energy $E \pm \Delta E$, for instance with a laser, such that $\Delta E \gg \delta$ but $\Delta E \ll E < E_0$ (classical threshold for racemization). We shall thus calculate the statistical, microcanonical racemization rate under these conditions. Thermal rate constants can be derived from this.

If an ordinary microcanonical equilibrium were obtained in these racemizations, it would be governed by the densities of states ϱ of the **R** and **L** enantiomers. In order to get an estimate for this we may use a semiclassical approximation for the harmonic density of states [Eqs. (9) and (10)][70] and neglect to a first approximation the differences between the frequencies $\nu_i^{\mathbf{L}}$ and $\nu_i^{\mathbf{R}}$ of the isomers (but not ΔE_{PV}).

$$\varrho_{\mathbf{L}} = \frac{(E + aE_Z^{\mathbf{L}})^{s-1}}{\prod_i h\nu_i^{\mathbf{L}}} \tag{9}$$

$$\varrho_{\mathbf{R}} = \frac{(E + aE_Z^{\mathbf{R}} + \Delta E_{PV})^{s-1}}{\prod_i h\nu_i^{\mathbf{R}}} \tag{10}$$

Hence, with s vibrational degrees of freedom, and with vibrational zero point energies $E_Z^{\mathbf{L}} \simeq E_Z^{\mathbf{R}}$ and vibration frequencies $\nu_i^{\mathbf{L}} \simeq \nu_i^{\mathbf{R}}$ one gets, setting $E' = E + aE_Z$ (with an energy dependent "constant" $0 \leq a \leq 1$) the Equations (11) and (12).

$$K_{micro} = \frac{k_{\mathbf{RL}}^{micro}}{k_{\mathbf{LR}}^{micro}} \simeq \left(\frac{E' + \Delta E_{PV}}{E'}\right)^{s-1} \tag{11}$$

$$\ln(K_{micro}) = (s-1)\ln\left(1 + \frac{\Delta E_{PV}}{E'}\right) \simeq (s-1)\frac{\Delta E_{PV}}{E'} \tag{12}$$

Thus, with $\Delta E_{PV} \ll E'$, K_{micro} will deviate very little from 1 (say, typically, by 10^{-18}). The actual situation is more complicated.

4.1. "Fast Tunneling" with Negligible Parity Violation and Small Densities of States

The time evolution for the isolated chiral molecule is governed by the differential equation (13) for the time evolution operator $\boldsymbol{U}$,[78] which solves the time-dependent Schrödinger equation for Ψ and the Liouville-von Neumann equation for P according to equations (14)–(16).

$$i\hbar\frac{\partial \boldsymbol{U}}{\partial t} = \boldsymbol{H}\,\boldsymbol{U} \tag{13}$$

$$\boldsymbol{U}(t) = \exp(-i\,\boldsymbol{H}t/\hbar) \tag{14}$$

$$\Psi(t) = \boldsymbol{U}(t)\,\Psi(0) \tag{15}$$

$$\boldsymbol{P}(t) = \boldsymbol{U}(t)\,\boldsymbol{P}(0)\,\boldsymbol{U}^{+}(t) \tag{16}$$

$\Psi(t)$ is the wave function of a molecule and $\boldsymbol{P}(t)$ the density operator of an ensemble, respectively. In order to consider racemization or the time dependence of optical activity, we could write these equations as matrix equations in the basis of molecular states of well defined handedness (ϱ_i and λ_i). These are not generally eigenstates of $\boldsymbol{H}$ and thus the matrix representation of $\boldsymbol{H}$ will contain off-diagonal contributions. One can calculate these off-diagonal contributions by means of the Born Oppenheimer approximation in terms of a tunneling through the potential barrier, but this is by no means a necessary or exact description of the problem and is given here only for visualization. If the rovibronic density ϱ of molecular states is low [inequality (17)],

$$\delta = \varrho^{-1} \gg \Delta E_{\pm},\ \Delta E_{PV} \tag{17}$$

the total hamiltonian matrix is approximately block diagonal, with two dimensional blocks of the form (18),

$$\boldsymbol{H}^{(2)} = \begin{pmatrix} \langle E_k\rangle - \Delta E_{PV}^{(k)}/2 & \Delta E_{\pm}^{(k)}/2 \\ \Delta E_{\pm}^{(k)}/2 & \langle E_k\rangle + \Delta E_{PV}^{k}/2 \end{pmatrix} \tag{18}$$

$\langle E_k\rangle$ is the average diagonal energy of the k th two-dimensional block. We shall make use of circular frequencies instead of energy parameters [Eqs. (12) and (20)].

$$D_k = 2\pi\Delta E_{\pm}^{(k)}/h \tag{19}$$

$$\Delta_k = 2\pi\Delta E_{PV}^{(k)}/h \tag{20}$$

Suppose we have an equal initial population in N quantum states of the pure **L** isomer [Eq. (21)].

$$p_{\mathbf{L}}(0) = \sum_{j=1}^{N} P_{jj(\mathbf{L})}(0) = 1 \tag{21}$$

The time evolution of the population of the **R** isomer is given by (22) (cf. Ref. [77] and Appendix).

$$p_{\mathbf{R}}(t) = N^{-1}\sum_{i=1}^{N}\frac{D_i^2}{D_i^2 + \Delta_i^2}\left[\sin\left(\frac{t}{2}\sqrt{D_i^2 + \Delta_i^2}\right)\right]^2 \tag{22}$$

We consider now the special case $D_k \gg \Delta_k \approx 0$. In practice this applies always at high energies, with large tunneling frequencies (say $10^6\ s^{-1}$ or more); one then obtains (23).

$$p_{\mathbf{R}}(t) \simeq N^{-1}\sum_{i=1}^{N}\left[\sin\left(\frac{tD_i}{2}\right)\right]^2 \tag{23}$$

The D_i at energy $E \pm \Delta E$ will vary widely. For states that are highly excited in the coordinate associated with the tunneling motion, D_i will be large, for other states it will be small. This situation is well known for the case of ammonia, where excitation of the NH stretching modes increases the inversion splitting only slightly.[73] Even if the coupling of vibrational modes is large, at high energies, the most reasonable assumption would be that the D_i are randomly distributed according to some distribution function $G(D)$ with the average $\langle D_i^2(E)\rangle$ increasing with molecular energy E. If N is very large, we can replace the sum in Eq. (23) by an integral, neglecting terms of the order 1/N [Eq. (24)].

$$p_{\mathbf{R}}(t) = \int_{-\infty}^{+\infty} dD\,G(D)[\sin tD/2]^2 \Big/ \int_{-\infty}^{+\infty} dD\,G(D) \tag{24}$$

In this description, the detailed rovibrational molecular dynamics is contained in the spectral distribution function $G(D)$. Little is known as to what this may be. We shall

consider two possible assumptions: (25) and the Lorentz function (27). From (25) we get (26), while (27) gives (28).

$$G(D) = \begin{cases} \text{constant}, & -D_{max} < D < D_{max} \\ 0 & \text{otherwise} \end{cases} \quad (25)$$

$$p_R(t) = \frac{1}{2}\left[1 - \frac{\sin(D_{max}t)}{D_{max}t}\right] \quad (26)$$

$$G(D) = D_L/[\pi(D^2 + D_L^2)] \quad (27)$$

$$p_R(t) = \tfrac{1}{2}[1 - \exp(-D_L t)] \quad (28)$$

Both approaches give an approximate relaxation to the expected microcanonical equilibrium $(t \to \infty)\ p_L \approx p_R \approx 1/2$ (for $\Delta E_{PV} \to 0$). Only in the second case is this relaxation truly exponential with a chemical relaxation time $\tau_R = 1/D_L$. Real distribution functions for D will probably be characterized by some maximum value D_{max} such as in Equation (26), corresponding to the one-dimensional model with a tunneling splitting D_{max} calculated with *all* the energy in the racemization mode. One can develop detailed models for $G(D)$. The main result here is that in real, excited molecules under the conditions discussed *one will observe relaxation to zero optical activity even without collisions*. This is in contrast with the two-level prediction of oscillatory optical activity. Before discussing other limiting cases we should give typical experimental conditions, in which the present case will apply. For a molecule SOFCl after IR multiphoton excitation or a molecule such as ($\overline{CF_2NClCH_2}$) after overtone laser excitation of CH modes one will expect such a behavior. The density of states is still quite small and the tunneling splitting can always be made sufficiently large ($D \gg \Delta$) by adequate excitation. Racemization in the beam can then be sufficiently fast (ns to ms time range) that both collisions and spontaneous and thermally induced radiative transitions are negligible: we are talking about conditions that may prevail in real experiments. In principle, one can also excite selectively one pair of tunneling levels and observe oscillatory dependence, but this is less important in practice.

4.2. Large Parity-Violating Energy Difference ΔE_{PV} and "Slow Tunneling", with a Small Density of States

Current calculations suggest that, at low energies, ΔE_{PV} will exceed $\Delta E_{\pm}$ in chiral molecules. As long as Equation (17) is satisfied, we still obtain the block diagonal structure of $\boldsymbol{H}$ as given by Equation (18). By the arguments given in Section 4.1 one obtains from Equation (22) with normalized distribution functions $F(\Delta)$ and $G(D)$ Equation (29).

$$p_R(t) = \int_{-\infty}^{+\infty} d\Delta F(\Delta) \int_{-\infty}^{+\infty} dD G(D) \frac{D^2}{D^2 + \Delta^2}\left[\sin\left(\frac{t}{2}\sqrt{D^2 + \Delta^2}\right)\right]^2 \quad (29)$$

ΔE_{PV} is essentially an electronic property depending upon the electronic wave function at the positions of the nuclei.[6, 10, 11, 45, 49] Although this certainly depends on the rovibrational state, it makes sense to take it as being constant, particularly for rigid molecules without large amplitude motions (except for racemization). The distribution function $F(\Delta)$ is thus approximately a Dirac delta distribution $\delta(\Delta - \Delta_c)$. On the other hand, D will vary in a wide range from D_a to D_b, as discussed before. In order to obtain a simple result we assume that (30) applies.

$$G(D) = \frac{\sqrt{D^2 + \Delta_c^2}}{N_0 D} \text{ for } D_a < D < D_b \quad (30)$$

with N_0 as normalization constant, so that $\int_{-\infty}^{+\infty} G(D)\,dD = 1$.

$$N_0 = \sqrt{D_b^2 + \Delta_c^2} - \sqrt{D_a^2 + \Delta_c^2} - \Delta \ln\left\{\frac{D_a(\Delta + \sqrt{D_b^2 + \Delta_c^2})}{D_b(\Delta + \sqrt{D_a^2 + \Delta_c^2})}\right\} \quad (31)$$

For $\Delta_c \ll D$ one obtains a constant distribution and results equivalent to Equation (26). For $\Delta_c \gg D$, $G(D)$ is proportional to $1/D$ (assuming positive D_a and D_b). One obtains Equation (32).

$$p_R(t) = \frac{1}{2N_0}\left\{(\sqrt{\Delta_c^2 + D_b^2} - \sqrt{\Delta_c^2 + D_a^2}) - \frac{1}{t}[\sin(t\sqrt{\Delta_c^2 + D_b^2} - \sin(t\sqrt{\Delta_c^2 + D_a^2})]\right\} \quad (32)$$

As $t \to \infty$ this relaxes, with some oscillations, to a stationary value [Eq. (33)].

$$p_R(\infty) = \frac{1}{2N_0}\{\sqrt{D_b^2 + \Delta_c^2} - \sqrt{D_a^2 + \Delta_c^2}\} \quad (33)$$

These expressions are valid for all ratios of Δ_c, D_a, and D_b. When we assume $\Delta_c \gg D_a, D_b$, we find the somewhat simpler result (34).

$$p_R(\infty) = \left\{1 + \frac{4\Delta_c^2}{D_b^2 - D_a^2}\ln\left(\frac{D_b}{D_a}\right)\right\}^{-1} \quad (34)$$

Only in Equation (34) have we made use of $\Delta_c \gg D_a, D_b$, thus that $p_R(\infty)$ remains small. *Again p_R does not oscillate as* $t \to \infty$ (neglecting terms of the order 1/N). Under these conditions an initial optical activity due to the condition $p_L(0) = 1$ will relax to a somewhat smaller than initial but still large value. In contrast to the result of Section 4.1, one cannot be sure that this result will be applicable in practice, neglecting collisional and radiative effects. This will only be true, if for some molecule the ΔE_{PV} is quite large. In this case we could learn about ΔE_{PV} from the kinetics of racemization. Fundamentally similar results are also obtained for the physically less likely case that ΔE_{PV} varies strongly with the rovibrational quantum state. Assuming for instance $F(\Delta)$ and $G(D)$ to be constant in the interval $-\Delta_m \le \Delta \le +\Delta_m$ and $-D_m \le D \le +D_m$ and zero outside, one finds a relaxed $(t \to \infty)$ population ($\Delta_m \gg D_m$) [Eq. (35)].

$$p_R(\infty) = \left(\frac{\pi D_m}{8\Delta_m}\right) + \frac{1}{4}\left[1 - \left(\frac{D_m^2 + \Delta_m^2}{D_m \Delta_m}\right)\arctan\left(\frac{D_m}{\Delta_m}\right)\right] \quad (35)$$

Separate forward and backward fluxes cannot be defined in any of these cases. Probability "appears" through tunnel-

ing across the boundary. Nevertheless, if one defines forward and backward rate coefficients in a kinetic relaxation scheme [Eq. (b) in Section 3.1], which is approximately possible, the rate coefficients depend upon the initial state and do not satisfy the detailed balance relationship Equations (3) or (11). This is an unusual situation in kinetics, which has, however, been encountered before.[77]

4.3. Very Large Densities of States: Pauli Equation for Racemization

For polyatomic molecules with more than 10 to 20 heavy atoms one can estimate with approximations such as Eq. (9) or by more accurate calculations[76] that the density of rovibronic states even at modest energies (≈ 50 kJ mol^{-1}) quickly becomes sufficiently large that (36) holds true.

$$\delta = \varrho^{-1} \ll \Delta E_{\pm}, (\Delta E_{\mathrm{PV}}) \tag{36}$$

The hamiltonian matrix can no longer be brought into the block diagonal structure as in Equation (18) and, in general, any level of the **R** isomer will be coupled to many levels of the **L** isomer and vice versa. A finite matrix expansion of Equations (13)–(16) would then require matrices of the order of at least many times $\Delta E_{\pm}\,\varrho$ or $\Delta E_{\mathrm{PV}}\,\varrho$, which will be large numbers. Making use of statistical assumptions that have been discussed in detail elsewhere[77, 79] one can derive a Pauli equation for the specific rate coefficients $k_{\mathbf{RL}}^{\mathrm{micro}}(E)$ and $k_{\mathbf{LR}}^{\mathrm{micro}}(E)$ as a function of excitation energy E [Eqs. (37) and (38)].

$$k_{\mathbf{RL}}^{\mathrm{micro}}(E) = 2\pi \langle D_{\mathbf{RL}}^2 \rangle \varrho_{\mathbf{R}}^{\omega} \tag{37}$$

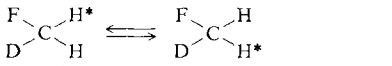
$$k_{\mathbf{LR}}^{\mathrm{micro}}(E) = 2\pi \langle D_{\mathbf{LR}}^2 \rangle \varrho_{\mathbf{L}}^{\omega} \tag{38}$$

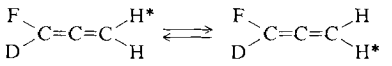
$\langle D_{\mathbf{LR}}^2 \rangle$ is the mean square "tunneling" coupling between all quantum states of **R** and **L** isomers at energy **E** in an interval ΔE which is large enough to render the average meaningful ($D_{\mathbf{RL}}$ *cannot* be calculated directly by a two-level tunneling model). The $\varrho^{\omega} = h\varrho/2\pi$ are the densities of states in circular frequency units. In contrast to the results of Section 4.2, Equations (37) and (38) satisfy the detailed balance relationship in Equations (11) and (12). The optical activity will relax to zero (practically) with a relaxation time $\tau_{\mathbf{R}} = 1/(k_{\mathbf{RL}} + k_{\mathbf{LR}})$. Again, it will not oscillate. The density of states ϱ that has to be considered in the inequality (36) is not the full density of states but rather only the density of those states that are effectively coupled (by matrix elements of the order $\sqrt{\langle D_{\mathbf{LR}}^2 \rangle}$). The transition between the situations in Sections 4.1 and 4.2 ("cases C" of Ref. [77]) and the Pauli equation ("case B" of Ref. [77]) will happen at values $\varrho^{-1} \simeq \Delta E_{\pm}$. From studying this transition experimentally one would thus learn about the coupling dynamics between the **R** and **L** isomers in real polyatomic molecules, beyond the two-level approximation. The experiment would simply use the rapid increase of both ϱ and $\Delta E_{\pm}$ with excitation energy. The infrared laser chemistry of racemization has recently been discussed in this context.[77b]

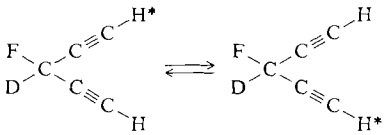
4.4. Dynamic Chirality and the Possible Existence of Chiral Methane

The common description of chiral molecules is based upon a Born-Oppenheimer potential with a double well and a barrier (such as in Fig. 1), which separates the two enantiomers. Racemization may occur in this description either by quantum tunneling through the barrier or by a quasiclassical barrier crossing above the barrier. We have stressed before that this description is unnecessary. This may appear obvious, because an observed *phenomenon* such as chirality, cannot depend on some arbitrary approximation that we use for its description. Atomic chirality is known to occur where this description would be meaningless.[41] It may be useful to complement these general observations with specific *molecular* examples of *dynamical chirality* beyond Born-Oppenheimer potentials.

Work by *Mecke*[80] and more recently by *Child* and *Lawton*[81] and others[82] suggests that high overtone excitation of high frequency modes in molecules with equivalent X–H modes may lead to long-lived localized vibrational excitations ("local modes"), in the following examples marked by asterisks.


(d)


(e)


(f)

Molecules with such localized vibrational excitations are chiral. The coupling including racemization is entirely vibrational (rotational) and unrelated to any electronic potential barriers. Although the lifetimes for localized states have probably been overestimated in early work,[81, 83] current evidence suggests that whereas the racemization (d) may occur on the subpicosecond time scale, the racemization (e) should be slower and in the case of acetylenic CH (or also alcoholic OH) stretching modes may exceed many picoseconds.[84] Such dynamic chirality could be studied by time resolved vibrational spectroscopy.[85] No direct experimental evidence has yet been presented, but one can be fairly certain from indirect evidence that the phenomenon exists.

Another kind of dynamic chirality has recently been proposed on the basis of localized *electronic* carbonyl excitation in an adamantanedione.[86] The chirality and its lifetime has not yet been established experimentally. Optical activity in vibrationally twisted allene has been discussed as well.[88] One should realize that also *rotation* may induce a dynamic asymmetry or chirality, for example by centrifugal distortion (for magnetic effects see Ref. [89]).

A particularly interesting case of dynamic chirality is methane, by tradition the prototype of an achiral, highly symmetric, tetrahedral molecule.[20] We shall discuss the consequences of parity violation and methane inversion from the present point of view. Figure 2 gives a rotational

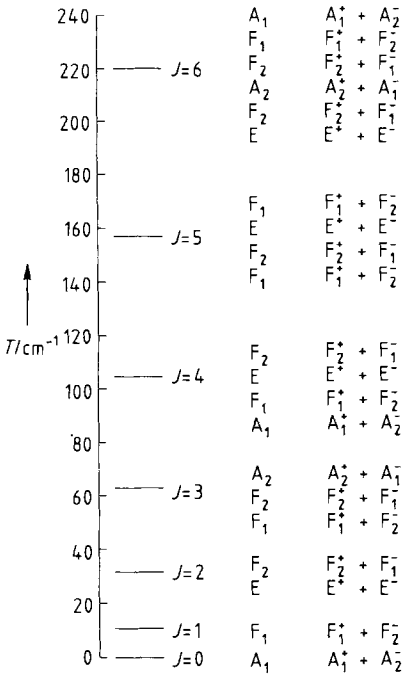


Fig. 2. Rotational energy level scheme for methane with symmetry assignments as explained in the text (after Ref. [100]). T = term value = $E/(hc)$ (for nomenclature cf. also Ref. [75]).

energy level scheme for methane. The zero order spherical top levels shown at the left-hand side are split by centrifugal distortion into sublevels, classified in the point group species (A_1, A_2, E, F_1, F_2) as shown in the middle. These strongly J-dependent splittings are large, of the order of 0.1 cm^{-1} here, and can be much larger. Each of these levels is further split by a very small amount into a sublevel of positive and negative parity (+, −) as indicated by the molecular symmetry group species notation on the right-hand side.[74, 75] (In Ref. [99] a different nomenclature has been used. According to the authors involved, the current nomenclature from Ref. [75] should be preferred.) It turns out that for CH_4 only the $A_2^{\pm}$ (combining with nuclear spin $I = 2$), the $F_1^{\pm}$ (combining with nuclear spin $I = 1$) and the $E^{\pm}$ (combining with nuclear spin $I = 0$) exist, because of the Pauli principle. Thus the $A_{1,2}$ and $F_{1,2}$ levels in T_D have all well defined parity (either + or −) and there is no inversion splitting for these. However, the $E^{\pm}$ pair does occur. Whereas in an asymmetrically substituted molecule with a high barrier the $\pm$ splitting due to tunneling must be very small for symmetry reasons, in a symmetrical molecule such as methane there are further contributions to this splitting, which are still very small but which are potentially much larger than the tunneling splitting. According to all current quantum chemical evidence the inversion splitting must be very small in methane.[97] There have also been experimental investigations on this question.[98, 99]

Nevertheless, for special dynamical reasons, or by using the influence of external fields as in atoms,[40, 41] the splitting may be made very small for some E^+, E^- level pair, so that $\Delta E_{\pm} \ll \Delta E_{PV}$. In this case ΔE_{PV} will generate new levels ϱ and λ (see Appendix), which have no well defined parity and are chiral: The probability density distribution $|\Psi_{\lambda,\varrho}(x,y,z)|^2$ for the four protons around the carbon nucleus will be asymmetric. This effect can be tested by a spectroscopic experiment (in principle also by diffraction methods, but accuracy will be too low there). It leads in any case to a fundamental revision of the stereochemical concepts introduced by *van't Hoff* and *Le Bel* some 100 years ago.[20]

4.5. Effects of Collisional and Radiative Processes

A complete treatment of collisional and radiative processes in a complex multilevel problem is beyond the scope of this article. However, we shall provide a phenomenological discussion of the effects expected in relation to the kinetic schemes in Sections 4.1. to 4.3. These complement the two-level treatment of collisions given by *Harris* and *Stodolsky*.[44]

Collisional and radiative effects can be introduced in general in a *reduced* density matrix equation of motion by adding non-Hamiltonian terms (cf. Eq. (16)). They can also be simulated approximately by phenomenologically adding contributions from a continuous spectrum to the molecular hamiltonian (Eqs. (13) and (18)), for instance in the form of complex energies $E_k - i\Gamma_k/2$ with a width Γ_k. The effect on kinetic schemes as described in Sections 4.1 to 4.3 is known. The width has the effect of changing the density of states from a Dirac δ-distribution to a more continuous function.[77] Then, by connecting the blocks of the effective hamiltonian instead of the relaxation [Eqs. (26), (28) or (32)] one has a transition to the Pauli equation rate coefficients (37) and (38). This changes somewhat the relaxation rate, but always leads to *complete racemization* at $t \to \infty$. In this sense collisions and spontaneous and thermal radiative processes *promote* racemization. This is somewhat in contrast to the result of *Harris* and *Stodolsky*,[44] not because their theoretical result would be subject to doubt, but because here we consider a complex multilevel problem at finite energy, whereas their result refers to the $T \to 0$, $E \to 0$ limit of a pure two-level problem. Of course, the present qualitative predictions can be tested by experiments similar to those we have proposed in Section 3. There is no evidence available on chiral molecules. However, in a dynamically very similar case of IR-multiphoton excitation, collisions were, indeed, found to enhance the corresponding equilibration process by the mechanism discussed above, which has also been established experimentally.[87]

5. Conclusions

We have demonstrated that different current hypotheses about the physical-chemical structure of chiral molecules lead to experimentally distinguishable consequences. Possible experiments using spectroscopic probes of molecular quantum state structure or probing the kinetics of racemization have been proposed. Although difficult and expensive (on the chemical, not particle physics scale) they would seem worthwhile in order to experimentally settle the questions posed.

It has been known to chemists and biologists for 140 years that chiral molecules carry a message for living beings: Chirality determines the fragrance of fruits, it can make all the

difference between bitter and sweet and it may distinguish healthy drug from deadly poison.[101] Chiral molecules recognize each other not just as key and lock but as hand and glove. It is also believed by many that chiral compounds in nature are messengers of the evolution of living beings.

It seems to be much less well known that molecular chirality may carry an as yet hidden message on the subtle physical forces governing molecular structure and dynamics and, perhaps, following the motto by *Pasteur*, on the structure of our universe.

I am most grateful to A. Ross and R. Marquardt, who kindly read and criticized the manuscript. Various aspects of the problem have been discussed with A. Amann, L. D. Barron, J. Dunitz, P. Pfeifer, V. Prelog, H. Primas, J. Robert, and P. von R. Schleyer. This work is financially supported by the Schweizerischer Nationalfonds and the Schweizerischer Schulrat.

Appendix: Some equations for the matrix representations of the two level problem with near degeneracies.

The hamiltonian matrix has the form (A 1). The eigenvalues for a hermitian operator $\boldsymbol{H}$ (A 2) follow from (A 3).

$$\boldsymbol{H} = \begin{pmatrix} H_{11} & H_{12} \\ H_{21} & H_{22} \end{pmatrix} \tag{A 1}$$

$$H_{12}H_{21} = H_{12}H_{12}^{*} = |H_{12}|^2 \tag{A 2}$$

$$E_{1,2} = \frac{H_{11} + H_{22}}{2} \pm \frac{1}{2}[(H_{11} - H_{22})^2 + 4|H_{12}|^2]^{\frac{1}{2}} \tag{A 3}$$

If we work in the basis $\chi_{\pm}$ of states of well defined parity and take ΔE_{PV} as perturbation one may identify (with real H_{12} and positive $\Delta E_{\pm}$) the expressions (A 4) and (A 5).

$$\Delta E_{PV} = 2H_{12} \tag{A 4}$$

$$H_{11} = -\Delta E_{\pm}/2 = -H_{22} \tag{A 5}$$

If we work in the basis of "left" and "right" handed states λ and ϱ, one has (positive ΔE_{PV}) the equations (A 6) and (A 7).

$$H'_{11} = -\Delta E_{PV}/2 = -H'_{22} \tag{A 6}$$

$$\Delta E_{\pm} = 2H'_{12} \tag{A 7}$$

The eigenvalues with respect to the average energy $(E_1 + E_2)/2 = \langle E \rangle \equiv 0$ are obviously the same ($\Delta E_{\pm}$ and ΔE_{PV} are defined real, positive) [(A 8)]. It is immaterial, whether ΔE_{PV} (Ref. [50]) or the tunneling $\Delta E_{\pm}$ (Section 4) is introduced as "perturbation".

$$E_{1,2} = \langle E \rangle \pm \frac{1}{2}(\Delta E_{\pm}^2 + \Delta E_{PV}^2)^{\frac{1}{2}} \tag{A 8}$$

Eigenvectors for the example of basis χ are given by (A 9) where x and y are defined via S [Eq. (A 10)] according to (A 11) and (A 12).

$$\boldsymbol{C} = \begin{pmatrix} x & y \\ -y & x \end{pmatrix} \tag{A 9}$$

$$S = (\Delta E_{\pm}^2 + \Delta E_{PV}^2)^{\frac{1}{2}} \tag{A 10}$$

$$x^2 = \frac{S + \Delta E_{\pm}}{2S} \tag{A 11}$$

$$y^2 = \frac{S - \Delta E_{\pm}}{2S} \tag{A 12}$$

The signs of the roots $\sqrt{x^2}$ and $\sqrt{y^2}$ can be taken in various combinations respecting $\boldsymbol{C}^{T}\boldsymbol{C} = \boldsymbol{I}$ (S is defined positive). One has by convention $E_1 < E_2$ and $H_{11} < H_{22}$. Some sign combinations in Ref. [50] were inconsistent with the correct figure ($E_{\lambda} < E_{\varrho}$). Figure 3 represents the situation ($x = y = 1/\sqrt{2}$ [Eq. (A 13)–(A 16)].

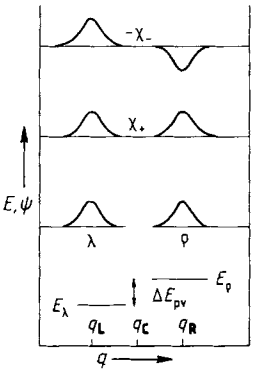


Fig. 3. Scheme for wave functions in a nearly degenerate situation ($\Delta E_{\pm} \approx 0$) in a chiral molecule (see text).

$$\lambda = \frac{1}{\sqrt{2}}(\chi_+ - \chi_-) \tag{A 13}$$

$$\varrho = \frac{1}{\sqrt{2}}(\chi_+ + \chi_-) \tag{A 14}$$

$$\chi_+ = \frac{1}{\sqrt{2}}(\lambda + \varrho) \tag{A 15}$$

$$-\chi_- = \frac{1}{\sqrt{2}}(\lambda + \varrho) \tag{A 16}$$

According to the superposition principle (if valid) these can always be generated by one of the methods of Section 3. The time evolution results from Equation (A 17) giving Equation (22) for $P_{RR} = p_R$, for example.

$$\boldsymbol{U} = \boldsymbol{C}\begin{pmatrix} \exp(-iE_1 t/\hbar) & 0 \\ 0 & \exp(-iE_2 t/\hbar) \end{pmatrix}\boldsymbol{C}^{T} \tag{A 17}$$

The density matrix with the elements $P_{ij} = \langle c_i c_j^* \rangle$ ($\langle\ \rangle$ = average over an appropriate ensemble) has the form (A 18) in the λ-ϱ basis and the form (A 19) in the $\chi_\pm$ basis.

$$\begin{pmatrix} P_{RR} & P_{RL} \\ P_{LR} & P_{LL} \end{pmatrix} = \boldsymbol{P}^{\lambda,\varrho} \tag{A 18}$$

$$\begin{pmatrix} P_{++} & P_{+-} \\ P_{-+} & P_{--} \end{pmatrix} = \boldsymbol{P}^{\chi_\pm} \tag{A 19}$$

For the degenerate system (or nearly degenerate system) at any temperature with $kT \gg S$ (A 10) Equation (A 20) holds.

$$\boldsymbol{P}^{\lambda,\varrho} = \boldsymbol{P}^{\chi_\pm} = \begin{pmatrix} \frac{1}{2} & 0 \\ 0 & \frac{1}{2} \end{pmatrix} \tag{A 20}$$

$\boldsymbol{P}$ is invariant under the basis transformation (as any other constant diagonal matrix), also in the many level case, if $\boldsymbol{H}$ is block diagonal as in Equation (18). A racemic mixture of **R** and **L** is identical to a mixture of + and − in terms of any observable ensemble property. A common model for $\boldsymbol{P}$, simplified for the degenerate case, considered as a reduced density matrix of the molecule interacting by collisions or otherwise with a thermal bath gives the expressions (A 21) and (A 22), from which the relationships (A 24) and (A 25) can be derived for the relaxation times given here by τ_1 and τ_2 with the basis transformation (A 23).

$$(P_{11} - P_{22}) = (P_{11}^0 - P_{22}^0)\exp(-t/\tau_1) \tag{A 21}$$

$$P_{12} = P_{12}^0 \exp(-t/\tau_2) \tag{A 22}$$

$$\boldsymbol{P}^{\chi_\pm} = \boldsymbol{C}\boldsymbol{P}^{\varrho,\lambda}\boldsymbol{C}^{\mathrm{T}} \tag{A 23}$$

$$\tau_1^{\chi_\pm} = \tau_2^{\varrho,\lambda} \tag{A 24}$$

$$\tau_2^{\chi_\pm} = \tau_1^{\varrho,\lambda} \tag{A 25}$$

Here we have made use of the reality of $\boldsymbol{P}$ in the case of a degenerate model, because $E_{1,2}$ can be set to zero without loss of generality. To within this approximation the assignment of "phase" or "population" relaxation times τ_1 and τ_2 is arbitrary in the two level problem (cf. Section 3).

Received: August 25, 1988 [A716 IE]
German version: *Angew. Chem. 101* (1989) 588

[1] a) L. Pasteur, *C.R. Hebd. Seances Acad. Sci. 26* (1848) 535; *ibid. 27* (1848) 401; b) *Ann. Chim. Phys. 24* (1848) 442; c) In simple terms chiral molecules are related to their mirror images like idealized left and right hands. This is the origin of the terminology, from greek $\tilde{\eta}$ $\chi\varepsilon\iota\varrho$ (the hand, with the interesting second meaning "power"). For an elementary introduction to some concepts of chirality see: C. Reichardt, *Chem. Uns. Zeit. 4* (1970) 188; H. Weyl: *Symmetry*, Princeton University Press, Princeton, NJ, USA 1952; H. Genz: *Symmetrie, Bauplan der Natur*, Piper, München 1987; E. Ruch, *Angew. Chem. 89* (1977) 67; *Angew. Chem. Int. Ed. Engl. 16* (1977) 65; R. Janoschek, *Naturwiss. Rundsch. 39* (1986) 327; K. Mainzer, *Symmetrien der Natur*, W de Gruyter, Berlin 1988.
[2] a) M. Eigen, R. Winkler: *Das Spiel*, Piper, München 1975; b) H. Kuhn, J. Waser in W. Hoppe (Ed.): *Biophysics*, Springer, Berlin 1983, p. 830.
[3] V. Prelog, *Science (Washington) 193* (1976) 17.
[4] L. D. Barron, *J. Am. Chem. Soc. 108* (1986) 5539; *Chem. Phys. Lett. 135* (1987) 1; *ibid. 123* (1986) 423.
[5] I. Gutman, V. Babovic, S. Jokic, *Chem. Phys. Lett. 144* (1988) 187.
[6] S. Mason, *Nature (London) 314* (1985) 400.
[7] A. Klemm, *Z. Naturforsch. A 40* (1985) 1231; I. Gutman, A. Klemm, *ibid. 42* (1987) 899.
[8] F. F. Seelig, *J. Theor. Biol. 34* (1972) 197.
[9] a) F. C. Frank, *Biochem. Biophys. Acta 11* (1953) 459; b) V. Babovic, I. Gutman, S. Jokic, *Z. Naturforsch. A 42* (1987) 1024.
[10] S. F. Mason, G. Tranter, *Chem. Phys. Lett. 94* (1983) 34; *Mol. Phys. 53* (1984) 1091.
[11] G. E. Tranter, *Chem. Phys. Lett. 120* (1985); *ibid. 121* (1985) 339; *Mol. Phys. 56* (1985) 825; *Chem. Phys. Lett. 135* (1987) 279; *Nachr. Chem. Tech. Lab. 34* (1986) 866; *Nature (London) 318* (1985) 172.
[12] D. Kondepudi in B. H. Weber, D. J. Depew, J. D. Smith (Eds.): *Entropy, Information and Evolution*, MIT Press, Cambridge, MA, USA 1988; D. K. Kondepudi, G. W. Nelson, *Nature (London) 314* (1985) 438.
[13] R. A. Hegstrom, *Nature (London) 297* (1982) 643; *315* (1985) 749.
[14] L. J. Dunne, *Chem. Phys. Lett. 121* (1985) 17.
[15] G. Wald, *Ann. N.Y. Acad. Sci. 69* (1957) 353.
[16] P. Schuster, *Adv. Chem. Phys. 55* (1983) 109.
[17] C. de Reyff, *J. Chim. Phys. 80* (1983) 563.
[18] L. Pasteur, *C. R. 51* (1860) 298.
[19] a) L. Pasteur in *Leçons de chimie professées en 1860 par MM. Pasteur, Cahours, Wurtz, Berthelot, Sainte-Claire Deville, Barral et Dumas*, Hachette, Paris 1861 (Recherches sur la dissymétrie moléculaire des produits organique naturels 1860–1883); b) reprinted in C. Bourgois (Ed.): Louis Pasteur, J. H. van't Hoff, A. Werner, *Sur la dissymétrie moléculaire*, Collection Epistème, Paris 1986; c) see also L. Pasteur, *Bull. Soc. Chim. Fr. 42* (1884) 215.
[20] J. H. van't Hoff: *Vorlesungen über theoretische und physikalische Chemie, Band 2*, Vieweg, Braunschweig 1899; *Die Lagerung der Atome im Raume*, Vieweg, Braunschweig 1876; in P. M. Bazendijk (Ed.): *La chimie dans l'espace*, Rotterdam 1887 (reprinted in [19b]).
[21] A. Werner: *Sur les Composés Métalliques a Dissymétrie Moléculaire* in *Conf. Soc. Chim. Fr. 1912*; reprinted in [19b].
[22] a) R. S. Cahn, C. Ingold, V. Prelog, *Experientia 12* (1956) 81; *Angew. Chem. 78* (1966) 413; *Angew. Chem. Int. Ed. Engl. 5* (1966) 385. b) For methods of assignment of absolute Configurations see: J. D. Dunitz: *X-ray Analysis and the Structure of Molecules*, Cornell University Press, Ithaca, NY, USA 1979; S. F. Mason: *Molecular Optical Activity and the Chiral Discrimination*, Cambridge University Press, Cambridge 1982; c) D. Arigoni, S. Eliel, *Top. Stereochem. 4* (1969) 127.
[23] E. Heilbronner, *Über die Symmetrie in der Chemie* in the book *Panta Rhei*, Verlag Hans Erni Stiftung, Luzern, Switzerland 1981.
[24] F. Hund, *Z. Phys. 43* (1927) 805.
[25] H. Primas: *Chemistry, Quantum Mechanics and Reductionism*, Springer, Berlin 1981.
[26] P. Pfeifer in J. Hinze (Ed.): *Energy Storage and Redistribution in Molecules (Proc. of Two Workshops, Bielefeld 1980)*, Plenum, New York 1983, p. 315.
[27] A. Amann in A. Amann (Ed.): *Fractals, Quasicrystals, Chaos, Knots and Algebraic Quantum Mechanics*, Kluwer, Dordrecht 1988, S. 305; see also A. Amann, W. Gans, *Angew. Chem. 101* (1989) 277; *Angew. Chem. Int. Ed. Engl. 28* (1989) 268.
[28] A. J. Leggett, S. Chakravarty, A. T. Dorsey, M. P. A. Fisher, A. Garg, W. Zwerger, *Rev. Mod. Phys. 59* (1987) 1.
[29] H. Spohn, R. Dumcke, *J. Stat. Phys. 41* (1985) 389.
[30] R. A. Harris, L. Stodolsky, *J. Chem. Phys. 74* (1981) 2145.
[31] M. Simonius, *Phys. Rev. Lett. 40* (1978) 980.
[32] E. B. Davies, *Commun. Math. Phys. 64* (1979) 191.
[33] T. D. Lee, C. N. Yang, *Phys. Rev. 104* (1956) 254.
[34] C. S. Wu, E. Ambler, R. W. Hayward, D. D. Hoppes, R. P. Hudson, *Phys. Rev. 105* (1957) 1413.
[35] R. L. Garwin, L. M. Lederman, M. Weinrich, *Phys. Rev. 105* (1957) 1415.
[36] J. H. Christenson, J. W. Cronin, V. L. Fitch, R. Turlay, *Phys. Rev. Lett. 13* (1964) 138.
[37] R. S. Casella, *Phys. Rev. Lett. 21* (1968) 1128; *ibid. 22* (1969) 554.
[38] a) R. Novick (Ed.): *Thirty years since parity nonconservation*, Birkhäuser, Basel, Switzerland 1986; b) Howard Georgi: *Weak interactions and modern particle theory*, Benjamin, Menlo Park, CA, USA 1984.
[39] M. A. Bouchiat, C. Bouchiat, *J. Phys. (Les Ulis Fr.) 35* (1974) 111.
[40] a) M. A. Bouchiat, J. Guena, L. Hunter, L. Pottier, *Phys. Lett. B 117* (1982) 358; b) C. Bouchiat, C. A. Piketty, *ibid. 128* (1983) 73.
[41] S. L. Gilbert, C. E. Wiemann, *Phys. Rev. A 34* (1986) 792; for further experiments see X. Chen, V. L. Telegdi, A. Weis, *J. Phys. B 20* (1987) 5653, and references cited therein.
[42] M. Karplus, *Rev. Mod. Phys. 32* (1960) 455.
[43] O. N. Kompanets, A. R. Kukudzhanov, V. S. Letokhov, L. L. Gervits, *Opt. Commun. 19* (1976) 414; V. S. Letokhov, *Phys. Lett. A 53* (1975) 275.
[44] R. A. Harris, L. N. Stodolsky, *J. Chem. Phys. 73* (1980) 3862.
[45] D. W. Rein, R. A. Hegstrom, P. G. H. Sanders, *Phys. Lett. A 71* (1979) 499.
[46] B. Ya Zel-dovich, D. B. Saakyan, I. I. Sobel-man, *Sov. Phys. JETP Lett. 25* (1977) 94.
[47] A. L. Barra, J. B. Robert, L. Wiesenfeld, *Phys. Lett. A 115* (1986) 443.
[48] A. L. Barra, J. B. Robert, L. Wiesenfeld, *BioSystems 20* (1987) 57; *Europhys. Lett. 5* (1988) 217.
[49] L. Wiesenfeld, *Mol. Phys. 64* (1988) 739.
[50] M. Quack, *Chem. Phys. Lett. 132* (1986) 147.
[51] O. P. Sushkov, V. V. Flambaum, *Sov. Phys. JETP (Engl. Transl.) 48* (1978) 608.
[52] E. Arimondo, P. Glorieux, T. Oka, *Opt. Commun. 23* (1977) 369.

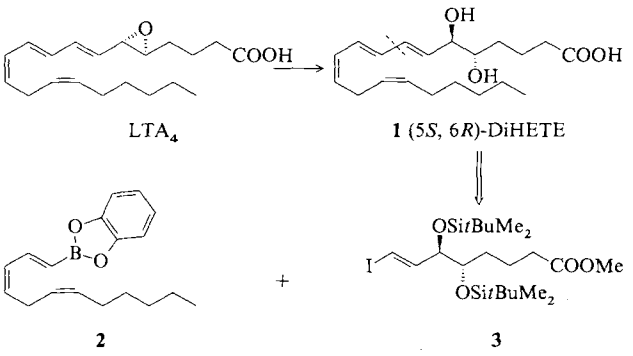
[53] D. A. Wilkening, N. F. Ramsey, D. J. Larson, *Phys. Rev. A 29* (1984) 425.
[54] L. M. Labzovskii, *Sov. Phys. JETP (Engl. Transl.) 48* (1978) 434.
[55] R. A. Harris in R. G. Wooley (Ed.): *Quantum Dynamics of Molecules*, Plenum, New York 1980, p. 357.
[56] J. L. Bada, *Adv. Chem. Ser. 106* (1971) 309; P. M. Masters, J. L. Bada, J. S. Ziegler, *Nature (London) 268* (1977) 71; A. Shimoyama, K. Harada, *Chem. Lett. 1984*, 1661; P. Masters Helman, J. L. Bada, *Proc. Natl. Acad. Sci. USA 72* (1975) 2892.
[57] I. Weissbuch, L. Addadi, Z. Berkovitch-Yellin, E. Gati, S. Weinstein, M. Lahav, L. Leiserowitz, *J. Am. Chem. Soc. 105* (1983) 6615.
[58] P. Pfeifer, *Dissertation*, Eidgenössische Technische Hochschule, Zürich 1980.
[59] E. B. Davies, *Ann. Inst. Henri Poincaré A 28* (1978) 91.
[60] M. Quack, S. Jans-Bürli: *Molekulare Thermodynamik und Kinetik*, Verlag der Fachvereine, Zürich, Switzerland 1986.
[61] L. D. Barron, *Chem. Soc. Rev. 15* (1986) 189.
[62] P. Bloch, P. Pavlopoulos, R. Klapisch (Eds.): *Fundamental Symmetries*, Plenum, New York 1987.
[63] F. Strocchi: *Elements of Quantum Mechanics of Infinite Systems*, World Scientific, Singapore 1985.
[64] This expression results from an apocryphical discussion of possible structures of the paradise: it was found to be "taliter aliter" (in somewhat distorted Latin, instead of the alternatives of either "taliter" or else "aliter").
[65] M. Quack, unpublished results.
[66] L. D. Barron: *Molecular Light Scattering and Optical Activity*, Cambridge University Press, Cambridge 1982.
[67] P. L. Polavarapu, *Chem. Phys. Lett. 148* (1988) 21.
[68] S. G. Kukolich, J. H. S. Wang, D. E. Oates, *Chem. Phys. Lett. 20* (1973) 519.
[69] H. Mäder, J. Ekkers, W. Hoke, W. H. Flygare, *J. Chem. Phys. 62* (1975) 4380; J. C. McGurk, H. Mäder, R. T. Hofmann, T. G. Schmalz, W. H. Flygare, *ibid. 61* (1974) 3759.
[70] M. Quack, J. Troe, *Int. Rev. Phys. Chem. 1* (1981) 97, and references cited therein.
[71] M. Quack, *Stud. Phys. Theor. Chem. 23* (1983) 355.
[72] M. Quack, *Ber. Bunsenges. Phys. Chem. 88* (1984) 94.
[73] G. Herzberg: *Molecular Spectra and Molecular Structure*, Van Nostrand, New York 1945, 1966.
[74] H. C. Longuet-Higgins, *Mol. Phys. 6* (1963) 445.
[75] M. Quack, *Mol. Phys. 34* (1977) 377.
[76] M. Quack, *J. Chem. Phys. 82* (1985) 3277.
[77] a) M. Quack, *Adv. Chem. Phys. 50* (1982) 395; b) *Infrared. Phys. 29* (1989), in press.
[78] A. Messiah: *Mécanique Quantique*, Dunod, Paris 1983.
[79] M. Quack, *Nuovo Cimento Soc. Ital. Fis. B 63* (1981) 358.
[80] R. Mecke, *Z. Elektrochem. Angew. Phys. Chem. 54* (1950) 38.
[81] M. S. Child, R. T. Lawton, *Faraday Discuss. Chem. Soc. 71* (1981) 273.
[82] W. Karlein, J. Manz, V. Mohan, H. J. Schreier, T. Spindler, *Mol. Phys. 64* (1988) 563.
[83] M. Quack, *Faraday Discuss. Chem. Soc. 71* (1981) 359.
[84] K. von Puttkamer, H. R. Dübal, M. Quack, *Faraday Discuss. Chem. Soc. 75* (1983) 197, 263.
[85] A. Lauberau, M. Stockburger (Eds.): *Time Resolved Vibrational Spectroscopy*, Springer, Berlin 1985.
[86] E. W. Meijer, H. Wynberg, *Angew. Chem. 100* (1988) 1004; *Angew. Chem. Int. Ed. Engl. 27* (1988) 975.
[87] M. Quack, *Ber. Bunsenges. Physik. Chem. 85* (1981) 318; D. W. Lupo, M. Quack, *Chem. Rev. 87* (1987) 181.
[88] Y. N. Chiu, *Isr. J. Chem. 26* (1985) 166.
[89] G. Wagnière, A. Meier, *Chem. Phys. Lett. 93* (1982) 78; G. Wagnière, *Z. Naturforsch. A 39* (1984) 254.
[90] J. M. Lehn, J. Wagner, *J. Chem. Soc. Chem. Comm. 1986*, 148.
[91] J. E. Anderson, J. M. Lehn, *J. Am. Chem. Soc. 89* (1967) 81.
[92] D. Felix, A. Eschenmoser, *Angew. Chem. 80* (1968) 197; *Angew. Chem. Int. Ed. Engl. 7* (1968) 224.
[93] H. R. Dübal, M. Quack, *Mol. Phys. 53* (1984) 257.
[94] J. K. Felixberger, J. G. Kuchter, E. Herdtweck, R. A. Paciello, W. A. Herrmann, *Angew. Chem. 100* (1988) 975; *Angew. Chem. Int. Ed. Engl. 27* (1988) 946.
[95] J. D. Wallis, A. Karrer, J. D. Dunitz, *Helv. Chim. Acta 69* (1986) 69.
[96] Suggested by *D. Seebach*, Zürich.
[97] P. von R. Schleyer, I. Shavitt, M. J. M. Pepper, R. Janoschek, M. Quack, to be published.
[98] I. Ozier, P. Yi, A. Kosha, N. F. Ramsey, *Phys. Rev. Lett. 24* (1971) 642.
[99] J. T. Hougen, *J. Chem. Phys. 55* (1971) 1122; P. R. Bunker: *Molecular Symmetry and Spectroscopy*, Academic Press, New York 1979.
[100] A. Amrein, M. Quack, U. Schmitt, *J. Phys. Chem. 92* (1988) 5455.
[101] *S*-asparagine has a bitter taste, whereas *R*-asparagine has a sweet taste; *S*-contergan® is teratogenic (with potential lethal consequences for the feti), *R*-contergan® seems to be harmless and a useful drug; *S*-penicillamine is an antiarthritic drug, *R*-penicilliamine is highly toxic; certain benzpyrene metabolites are extremely carcinogenic in one form and apparently harmless in the other.

When submitting manuscripts, authors of articles intended for publication as "Communications" are requested to read the "Notice to Authors" reproduced in the January issue of the journal following the list of contents; upon request, a copy can be obtained from the editorial office.

Stereocontrolled Total Synthesis of (5*S*,6*R*)-, (5*S*,6*S*)-, (5*R*,6*R*)-, and (5*R*,6*S*)-(7*E*,9*E*,11*Z*,14*Z*)-5,6-Dihydroxy-7,9,11,14-icosatetraenoic Acid (5,6-DiHETE) Methyl Esters**

By *K. C. Nicolaou,** *J. Y. Ramphal, J. M. Palazon,* and *R. A. Spanevello*

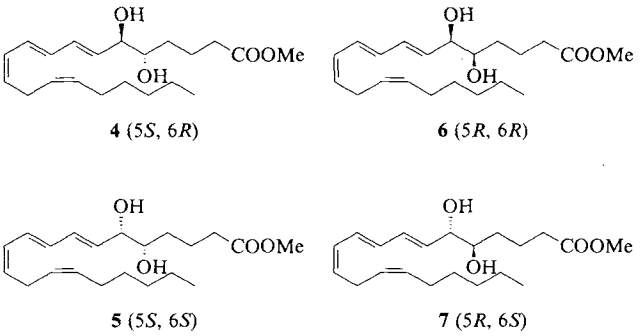
(5*S*,6*R*)-(7*E*,9*E*,11*Z*,14*Z*)-5,6-Ddihydroxy-7,9,11,14-icosatetraenoic acid (5,6-DiHETE) **1** is a naturally occurring and biologically active metabolite of arachidonic acid derived from leukotriene A_4 (LTA_4) by regio- and stereoselective hydrolysis (Scheme 1).[1]



Scheme 1. Biogenetic generation and retrosynthetic analysis of (5*S*,6*R*)-DiHETE **1**. LT_4 = leukotriene A_4.

Nonenzymatic hydrolysis of LTA_4 leads to the isomeric (5*R*,6*R*)-DiHETE. In order to render these compounds readily available for biological studies and to compare their actions with those of lipoxin A_4,[2] we embarked on a program directed towards the synthesis of all four 5,6-isomeric DiHETE methyl esters (**4**–**7**, Scheme 2) as well as their fully saturated derivatives **S4**–**S7**.

The general and flexible strategy for the construction of the targeted DiHETE derivatives was based on the retrosynthetic analysis shown in Scheme 1. Thus, disconnection of



Scheme 2. Structures of synthesized DiHETE methyl esters **4**–**7**.

the bond between C-8 and C-9 accompanied by suitable functional group manipulation led to intermediates **2** and **3** as potential precursors. The Pd^0–TlOH–catalyzed coupling reaction of vinyl borane derivatives with vinyl halides developed by *Kishi* et al.[3,4] was envisioned as the key synthetic step to produce the skeleton of **1** from fragments **2** and **3** (Scheme 1).

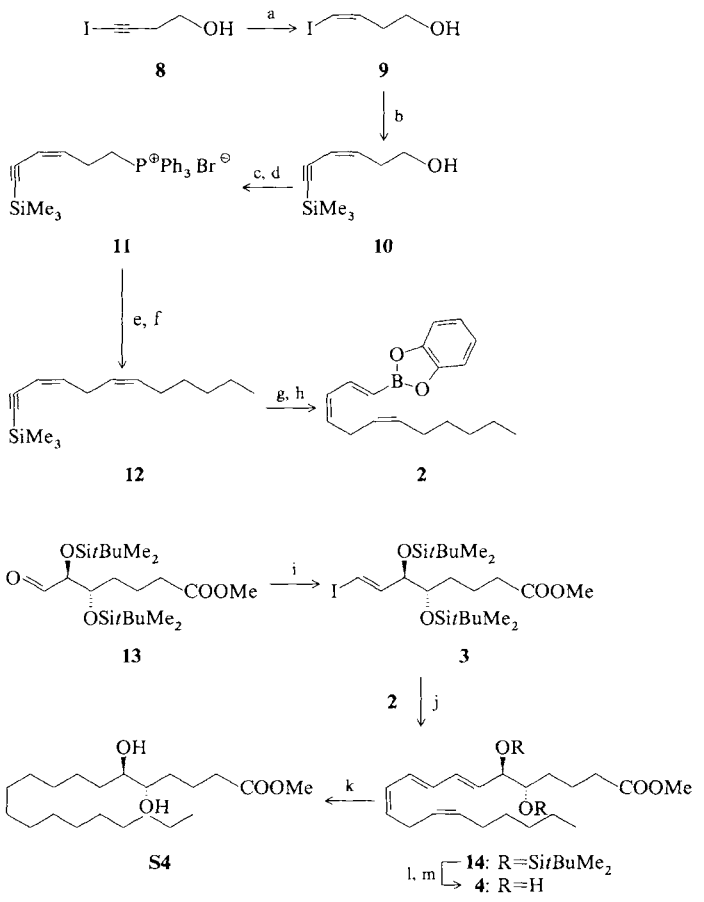
Scheme 3 details the synthesis of (5*S*,6*R*)-DiHETE methyl ester **4**. Thus, selective reduction of the alkynyl iodide **8** gave the vinyl iodide **9** in 54% yield. Coupling of **9** with trimethylsilylacetylene assisted with $Pd(PPh_3)_4$ and CuI as catalysts afforded enyne **10** in 90% yield.[5] Sequential treatment of **10** with Ph_3P/CBr_4 and then with PPh_3 gave phosphonium salt **11** (92%) via the corresponding bromide (91%). Generation of the ylide from **11** with $KN(SiMe_3)_2$ followed by addition of hexanal resulted in the formation of the dienyne **12** as the major product accompanied by its *trans* isomer at the newly formed double bond (82% total yield, *cis*:*trans* ca. 4:1). Chromatographic separation of **12** from its isomer, followed by desilylation (79%) and regioselective hydroboration[6] with benzodioxaborole gave the requisite vinyl boronate **2** (55%). Compound **2** was then coupled with the vinyl iodide **3** (synthesized from the previously known aldehyde **13**[5] by a $CrCl_2$-mediated[7] reaction with iodoform, 70% yield) under the Kishi conditions [$Pd(PPh_3)_4$–TlOH],[3] affording the DiHETE skeleton **14** (55%). Finally, fluoride-induced desilylation of **14**, followed by diazomethane treatment (to methylate varying amounts of carboxylic acid formed) gave (5*S*,6*R*)-DiHETE methyl ester **4** in 85% overall yield.[8] Exhaustive hydrogenation of **4** smoothly led to the saturated compound **S4** (80%).

The total synthesis of the remaining DiHETE methyl esters **5**–**7** (Scheme 2) and their saturated counterparts **S5**–**S7** proceeded along similar lines from vinyl boronate **2** and the appropriate stereoisomers of vinyl iodide **3**, readily available from the corresponding aldehydes[5] as mentioned above. The described chemistry simplifies the construction of these linear icosanoids[9] and makes them readily available for further studies.

Experimental Procedure

Coupling of 2 with 3 to give 14: To a 250-mL round-bottom flask equipped with a magnetic stirrer was added **2** (103 mg, 0.37 mmol) in 5 mL of THF followed by hexane (30 mL). The solution was degassed by bubbling argon for 15 min before adding a degassed solution of 10% aqueous TlOH (2.52 mL, 1.14 mmol) with vigorous stirring over a period of 3 min at room temperature (RT). A THF solution (1 mL) of **3** (143 mg, 0.26 mmol) was then added followed by immediate addition of $Pd(PPh_3)_4$ (75 mg, 0.065 mmol) in 3 mL of THF. The reaction mixture was stirred for 0.5 h (TLC monitoring) at 25 °C and then transferred to a separatory funnel, diluted with ether (150 mL), and washed with saturated

[*] Prof. K. C. Nicolaou, J. Y. Ramphal, Dr. J. M. Palazon [+], Dr. R. A. Spanevello [++]
University of Pennsylvania, Department of Chemistry
Philadelphia, PA 19104-6323 (USA)
[+] NATO fellowship (Spain), 1987–1988.
[++] CONICET (Consejo Nacional de Investigaciones Cientificas y Tecnicas) fellowship (Argentina), 1987–1988.
[**] We wish to acknowledge financial support of this work by the National Institutes of Health and Smith Kline and French (USA).



Scheme 3. Total synthesis of **4** and **S4**. a) $TosNHNH_2$ (2.0 eq.)/NaOAc (3.0 eq.), THF:H_2O (1:1), reflux, 4h, 54%. b) $HC{\equiv}C{-}SiMe_3$ (1.0 eq.), $Pd(PPh_3)_4$ (0.04 eq.)/CuI (0.16 eq)/Et_2NH, 0 °C, 1h, 90%. c) PPh_3 (1.3 eq.)/CBr_4 (1.3 eq.), CH_2Cl_2, −30 °C, 2.5 h, 91%. d) PPh_3 (1.2 eq.), CH_3CN, 36 h, reflux, 92%. e) $KN(SiMe_3)_2$ (1.05 eq.), THF, −78 → 0 °C, 1 h, then −78 °C, hexanal (1.2 eq.), 2 h, 82% (*cis:trans* ca. 4:1). f) Chromatography (SiO_2, petroleum ether). g) KCN (7.0 eq.)/$AgNO_3$ (4.0 eq.), THF:EtOH:H_2O (1:1:1), 0 °C, 2 h, 79%. h) 1,3,2-Benzodioxaborole ("catecholborane") (5.0 eq.), benzene, 75 °C, 28 h, 55%. i) $CrCl_2$ (6.0 eq.)/CH_3I (2.0 eq.), THF, 0 °C, 8 h, 70%. j) **2** (1.4 eq.), $Pd(PPh_3)_4$ (0.25 eq.)/TlOH (4.4 eq.), THF:hexane:H_2O, 25 °C; 1h, 55%. k) H_2-Pd/C, MeOH, 25 °C, 5 h, 80%. l) nBu_4NF (2.2 eq.), THF, 25 °C, 3 h. m) CH_2N_2, Et_2O, 0 °C, 0.5 h, 85%.

sodium chloride solution (15 mL). The organic phase was dried ($MgSO_4$) and filtered through a celite pad, concentrated, and subjected to flash column chromatography (silica, 3% ether in petroleum ether), furnishing **14** as a colorless oil (82 mg, 55%). **14**: $R_f = 0.31$ (silica, 3% ether in petroleum ether); $[\alpha]_D^{20}$ +2.93° ($c = 0.48$, $CHCl_3$). MS: calculated for $C_{33}H_{62}O_4Si_2$, 578.418; found, 579.426 ($M+1$). IR (neat): $\tilde{\nu}_{max}$ = 3010, 2940, 2860, 1755, 1470, 1440, 1358, 1267, 1170, 1112, 1000, 840, 780 cm^{-1}. UV (CH_3OH): λ_{max} = 205, 262 (sh), 274, 285 (sh) nm. ^1H NMR ($CDCl_3$, 500 MHz): $\delta = 6.45$ (t, $J = 12.59$ Hz, 1H, olefinic), 6.16 (m, 2H, olefinic), 6.01 (t, $J = 10.88$ Hz, 1H, olefinic), 5.61 (dd, $J = 15.38$, 7.49 Hz, 1H, olefinic), 5.39 (m, 3H, olefinic), 3.98 (t, $J = 4.32$ Hz, 1H, CH-OSi), 3.67 (s, 3H, $COOCH_3$), 3.56 (q, $J = 3.05$ Hz, 1H, CHOSi), 2.92 (t, $J = 7.30$ Hz, 2H, bis-allylic), 2.25 (t, $J = 7.52$ Hz, 2H, CH_2COOCH_3), 2.05 (q, $J = 6.92$ Hz, 2H, allylic), 1.55 (m, 2H, CH_2), 1.28 (m, 8H, CH_2), 0.88 (m, 21H, 2 × *Si*t*Bu*, CH_3), 0.04 (s, 12H, $SiMe_2$).

Desilylation of ***14*** *to give* ***4*****:** Compound **14** (76 mg, 0.13 mmol) was azeotropically dried with benzene and dissolved in dry THF (3.0 mL). The magnetically stirred solution was treated with tetra-*n*-butylammonium fluoride (*1 M* solution in THF, 300 µL, 0.300 mmol) at 25 °C. Stirring was continued for 3 h at RT while the reaction was monitored by TLC. The solution was then diluted with ether (100 mL) and washed with pH 6 phosphate buffer (1 mL). The organic layer was separated and washed with saturated sodium chloride solution (2 mL), dried ($MgSO_4$), and concentrated. Ether (25 mL) was added followed by cooling to 0 °C and diazomethane treatment to give, after concentration, the crude methyl ester, which was subjected to flash column chromatography (silica, ether), furnishing pure **4** as a colorless oil (38.6 mg, 85%). **4**: $R_f = 0.52$ (silica, ether); $[\alpha]_D^{20}$ +0.91° ($c = 0.44$, $CHCl_3$). MS: calculated for $C_{21}H_{34}O_4$, 350.246; found, 333.243 ($M-OH$). IR (neat): $\tilde{\nu}_{max}$ = 3385, 3000, 2910, 2825, 1728, 1425, 1240, 1156, 1072, 988, 905, 722 cm^{-1}. UV (CH_3OH): λ_{max} = 320, 283 (sh), 274, 261 (sh) 205 nm. ^1H NMR ($CDCl_3$, 500 MHz): $\delta = 6.52$ (dd, $J = 14.47$, 11.01 Hz, 1H, olefinic), 6.35 (dd, $J = 15.22$, 10.55 Hz, 1H, olefinic), 6.19 (dd, $J = 14.46$ Hz, 10.41 Hz, 1H, olefinic), 6.03 (t, $J = 10.90$ Hz, 1H, olefinic), 5.72 (dd, $J = 15.05$, 7.05 Hz, 1H, olefinic), 5.42 (m, 2H, olefinic), 5.39 (m, 1H, olefinic), 4.11 (m, 1H, $CH-OH$), 3.68 (m, 1H, $CH-OH$), 3.64 (s, 3H, $COOCH_3$), 2.91 (t, $J = 7.12$ Hz, 2H, bis-allylic), 2.33 (t, $J = 6.70$ Hz, 2H, CH_2COOCH_3), 2.15 (s, 2H, O*H*), 2.03 (q, $J = 7.02$ Hz, 2H, allylic), 1.23 (m, 10H, CH_2), 0.86 (t, $J = 6.47$ Hz, 3H, CH_3).

Hydrogenation of ***4*** *to give* ***S4*****:** To a 25-mL round-bottom flask equipped with a magnetic stirrer and filled with argon was placed a solution of **4** (40 mg, 0.069 mmol) in distilled methanol (2 mL) and 10% Pd/C (8 mg, 20% by weight). The argon was replaced with hydrogen and the reaction mixture was vigorously stirred under hydrogen for 18 h while monitored by TLC. The hydrogen was removed and the catalyst was filtered off through a celite pad. The solution was concentrated and subjected to flash column chromatography (silica, 10% petroleum ether in ether), furnishing saturated **4** as a white waxy solid (19.8 mg, 80%). 4: $R_f = 0.47$ (silica, ether); $[\alpha]_D^{20}$ + 0.55° ($c = 0.55$, $CHCl_3$). MS calculated for $C_{21}H_{42}O_4$, 358.131; found, 376.343 ($M + NH_4$): IR ($CHCl_3$): $\tilde{\nu}_{max}$ = 3420, 3020, 2930, 2858, 1730, 1467, 1440, 1218, 755, 670 cm^{-1}. ^1H NMR ($CDCl_3$, 500 MHz): $\delta = 3.65$ (s, 3H, $COOCH_3$), 3.57 (m, 2H, *CH*-OH), 2.35 (t, $J = 7.36$ Hz, 2H, CH_2COOCH_3), 1.84 (s, 1H, OH), 1.58 (s, 1H, OH), 1.47–1.42 (m, 5H, CH_2), 1.23 (s. 25H, CH_2), 0.86 (t, $J = 6.77$ Hz, 3H, CH_3).

Received: December 8, 1988;
revised: February 6, 1989 [Z 3081 IE]
German version: *Angew. Chem. 101* (1989) 621

[1] Isolation: a) J. Haeggstrom, J. Meijer, D. Radmark, *J. Biol. Chem. 261* (1986) 6332; b) P. Borgeat, B. Samuelsson, *ibid. 254* (1979) 7865; c) J. Haeggstrom, A. Wetterholm, M. Hamberg, J. Meijer, R. Zipkin, O. Radmark, *Biochim. Biophys. Acta 958* (1988), 469. Synthesis: d) J. Adams, B. J. Fitzsimmons, Y. Girard, J. F. Evans, J. Rokach, *J. Am. Chem. Soc. 107* (1985) 464.

[2] C. N. Serhan, M. Hamberg, B. Samuelsson, *Proc. Natl. Acad. Sci. USA 81* (1984) 5335.

[3] J. Uenishi, J.-M. Beau, R. W. Armstrong, Y. Kishi, *J. Am. Chem. Soc. 109* (1987) 4756, and references cited therein.

[4] For other examples of borane–vinyl iodide coupling, see: a) W. R. Roush, R. Riva, *J. Org. Chem. 53* (1988) 710; b) F. Haviv, J. D. Ratajczyk, R. W. DeNet, Y. C. Martin, R. D. Dyer, G. W. Carter, *J. Med. Chem. 30* (1987) 254; c) G. Cassani, P. Massardo, P. Piccardi, *Tetrahedron Lett. 24* (1983) 2513; d) N. Miyaura, A. Suzuki, *J. Organomet. Chem. 213* (1981) 653.

[5] K. C. Nicolaou, C. A. Veale, S. E. Webber, H. Katerinopoulos, *J. Am. Chem. Soc. 107* (1985) 7515, and references cited therein.

[6] N. Miyaura, H. Suginome, A. Suzuki, *Tetrahedron 39* (1983) 3271.

[7] T. Kazuhiko, K. Nitta, K. Utimoto, *J. Am. Chem. Soc. 108* (1986) 7408.

[8] Small amounts of the δ-lactone corresponding to **4** were also formed in this reaction. Conversion of this lactone to **4** was easily accomplished by exposure to Et_3N in methanol.

[9] All new compounds exhibited satisfactory spectroscopic and analytical and/or exact mass data. Yields refer to chromatographically and spectroscopically homogeneous materials.

Azonia Derivatives of Arenes: Synthesis and Properties of 10c-Azoniafluoranthene **

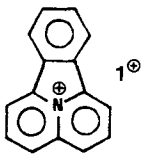
By *Marc Fourmigué,* Kamal Boubekeur, Patrick Batail,* and *Klaus Bechgaard*

Radical cation salts of arenes such as naphthalene and fluoranthene exhibit an extremely narrow solid-state EPR line (10–20 mG, compared to 1.35 G for DPPH[11]). This is believed to be due to the strongly one-dimensional nature of the conducting electrons and related to the metallic behavior arising from a strict 2:1 stoichiometry of the mixed-valent $(aryl)_2X$ salts.[2, 3] Promising applications of these compounds as magnetic field probes are restricted, however, because of their lack of stability.[4]

[*] Dr. M. Fourmigué, K. Boubekeur, Dr. P. Batail
Laboratoire de Physique des Solides associé au CNRS,
Université de Paris-Sud
F-91405 Orsay (France)
Prof. Dr. K. Bechgaard
H. C. Ørsted Institutet
DK-2100 København (Denmark)

[**] This work was supported by the University of Copenhagen, CNRS, and ANVAR (Paris).

Heteroatom substitution at appropriate positions in the carbon framework of the arene molecule is expected to enhance the stability of the corresponding radical species. We therefore investigated the closed-shell cation $\mathbf{1}^{\oplus}$, which is isoelectronic with fluoranthene. We report here the synthesis and characterization of $\mathbf{1}^{\oplus}$ and demonstrate that its reduction affords the neutral radical $\mathbf{1}^{\odot}$, which is isoelectronic with the fluoranthene radical anion and was characterized by EPR and cyclic voltammetry experiments.



The cation $\mathbf{1}^{\oplus}$ is especially attractive for the following reasons (Fig. 1): (1) the crisscross mode of overlap of 2:1 fluoranthenium salts, which actually minimizes the intradimer van der Waals interactions, should be preserved in $\mathbf{1}^{\odot}$ in the solid state and in $(\mathbf{1})_2X$ salts;[5, 6] (2) there is essentially no odd-electron density in the SOMO of $\mathbf{1}^{\odot}$ at the nitrogen atom. Therefore, the hyperfine interaction with the nitrogen atom ($S = 1$) is minimal and consequently no EPR line broadening should occur in the solid because of the replacement of C by N.

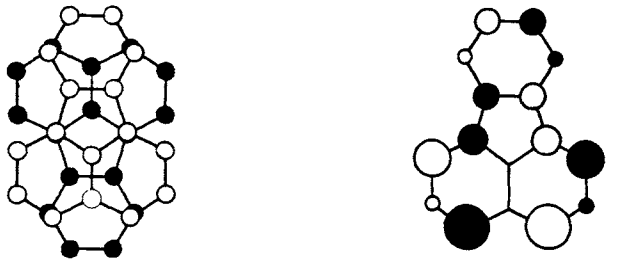
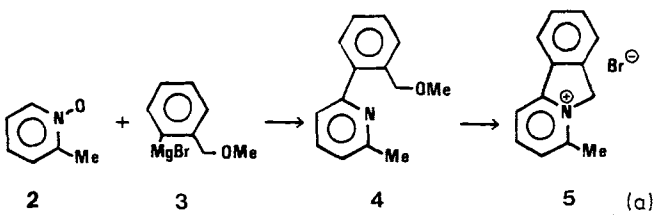


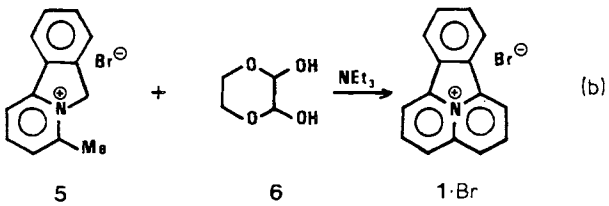
Fig. 1. Left: The overlap between adjacent molecules in the fluoranthenium salts [5]. Right: The electronic density in the fluoranthene LUMO. Radii are proportional to the coefficients of the LUMO [16].

The cation $\mathbf{1}^{\oplus}$ was synthesized as follows: The salt **5**, with two potentially nucleophilic sites available for a Westphal condensation with an α-dioxo compound, was selected as starting material for the synthesis of $\mathbf{1}^{\oplus}$.[6] Compound **5** was obtained in two steps [Eq. (a)],[7] starting with the known addition of alkyl or aryl Grignard reagents to pyridine *N*-oxide.[8]



2 **3** **4** **5** (a)

The use of the *ortho*-substituted bromobenzene **3** gives the pyridine **4**, isolated in 40% yield after a dehydration step with acetic anhydride. Hydrolysis of **4** in concentrated HBr, concomitant with the intramolecular quaternization, leads directly to the salt **5**. Reaction of **5** with the anhydrous glyoxal equivalent **6**[9] in the presence of an equimolar amount of triethylamine allows the double condensation and simultaneous elimination to give the fully aromatized bromide salt $\mathbf{1}^{\oplus}$ [Eq. (b)].



5 **6** **1**·Br (b)

Cyclic voltammetry experiments performed in acetonitrile (NBu_4PF_6, 0.1 M) demonstrate that $\mathbf{1}^{\oplus}$ is reduced at $E_{1/2} = -0.9$ V versus SCE. Sweep-rate dependance of the voltammogram indicates a quasi-reversible behavior.[10] This is in contrast to most of the pyridinium-like cations (e.g., *N*-methylpyridinium, -quinolinium, -acridinium, -quinolizinium, and acridizinium) in which reduction to the neutral radical is irreversible unless the cation carries an electron-attracting substituent at the position of highest electron density in the LUMO.[11]

The neutral radical generated by reduction of $\mathbf{1}^{\oplus}$ in acetonitrile solution on Na/Hg amalgam is persistent for several hours when kept under oxygen-free conditions. The EPR solution spectrum gives five equally spaced, rather broad lines with an apparent hyperfine splitting (a_H) of 5.17 G. This spectrum is similar to that of the isoelectronic fluoranthene radical anion ($a_{H3} = 5.24$, $a_{H1} = 3.93$, $a_{H8} = 1.2$ G[12]) when line broadening occurs. Attempts to isolate the neutral radical $\mathbf{1}^{\odot}$ in the solid state have been so far unsuccessful.

In order to characterize this new heterocyclic structure more completely, we also carried out an X-ray crystal structure investigation of $\mathbf{1} \cdot PF_6$. The cation is essentially planar. The single salient structural difference with fluoranthene is a significant contraction of the bond lengths around the nitrogen atom (Fig. 2).

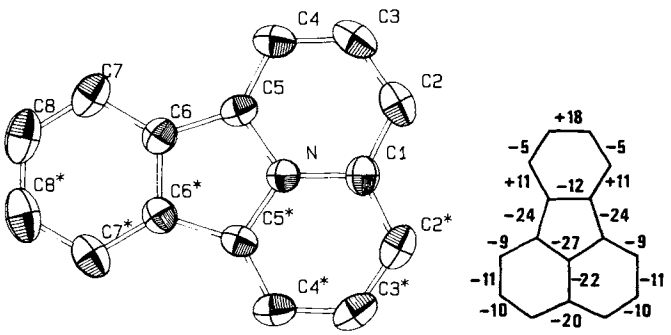


Fig. 2. Molecular structure of $\mathbf{1} \cdot PF_6$ [13]. Ellipsoids are scaled to enclose 50% of the electronic density. Significant bond distances [Å] and angles [°]: N-C1 1.378(5), N-C5 1.384(4), C1-C2 1.402(4), C2-C3 1.358(5), C3-C4 1.400(5), C4-C5 1.358(5), C5-C6 1.452(4), C6-C6* 1.402(5), C6-C7 1.395(5), C7-C8 1.381(5), C8-C8* 1.396(6); C1-N-C5 123.7(2), C5-N-C5* 112.6(3), N-C1-C2 115.8(2), C2-C1-C2* 128.3(4), C1-C2-C3 121.0(3), C2-C3-C4 121.7(3), C3-C4-C5 118.4(3), C4-C5-N 119.4(3), N-C5-C6 105.6(3), C4-C5-C6 135.0(3), C5-C6-C6* 108.1(3), C5-C6-C7 130.8(3), C6*-C6-C7 121.1(3), C6-C7-C8 117.4(3), C7-C8-C8* 121.5(3). Right: Bond-length variations from fluoranthene to $\mathbf{1}^{\oplus}$ (in 10^{-3} Å) [15].

Experimental Procedure

4: A THF solution of 2-methylpyridine N-oxide (75.3 g, 0.69 mol) [15] was added dropwise to a THF solution of **3**, prepared from the corresponding *ortho*-substituted bromobenzene (138.7 g, 0.69 mol, Mg (16.8 g, 0.69 mol), and EtBr (18.8 g, 0.17 mol) in dry THF. The mixture was stirred ca. 12 h. Hydrolysis yielded a pasty white precipitate. The THF solution was decanted and the precipitate washed with $CHCl_3$. The combined solutions were washed with 0.1 N NaOH followed by 0.1 N HCl and then evaporated. The neutral clear oil was boiled with 500 mL of acetic anhydride for 3 h. After evaporation of the anhydride, the dark residue was treated with 200 mL of 0.1 N NaOH and extracted with toluene three times. The combined solution was extracted with 2 N HCl and the acidic solution cooled and basified with concentrated NaOH. The supernatant oil was extracted with ether and the solution was dried with $MgSO_4$ and evaporated. Vacuum distillation yielded a slightly fluorescent oil (60 g; 41%), b.p. 114–116 °C (0.5 torr). ^{1}H NMR ($CDCl_3$, 60 MHz, TMS): δ = 2.55 (s, 3H, Me-C), 3.3 (3H, s, OMe), 4.55 (2H, s, CH_2), 7.0–7.7 (7H, m, aryl H). Correct C,H,N elemental analysis.

5: A solution of **4** (60 g, 0.28 mol) in 48% HBr (500 mL) and AcOH (500 mL) was refluxed for 4 h. Evaporation and recrystallization from EtOH yielded **5** as its bromide (47.4 g, 64%), m.p. 245–248 °C. ^{1}H NMR (CF_3CO_2H, 60 MHz, TMS): δ = 3.0 (3H, s, Me), 5.75 (2H, s, CH_2), 7.7–8.6 (7H, m, aryl H). UV/VIS (EtOH): λ [nm] = 252 (lg ε = 4.08), 318 (4.02). Correct C,H,N analysis.

1$^{\oplus}$: A solution of **5** (13 g, 0.05 mol), **6** (7 g, 0.05 mol), and Et_3N (7 mL, 0.05 mol) in EtOH was refluxed for 1 h, then cooled, evaporated, and precipitated by addition of Et_2O. The dark crystalline product was recrystallized twice from EtOH/AcOEt (1:1) and then from dimethyl sulfoxide (DMSO) (yield of **1** · Br: 4.7 g, 33%). Addition of 70% HPF_6 to an ethanolic solution of **1** · Br resulted in the precipitation of a $PF_6^{\ominus}$ salt, which was recrystallized from acetonitrile as transparent needles. ^{1}H NMR ([D$_6$]DMSO, 90 MHz, TMS): δ = 9.5 (2H, d), 8.7–9.2 (6H, m), 8.15 (2H, pseudo q). ^{13}C NMR ([D$_6$]DMSO, 22.6 MHz, TMS): δ = 139.17, 137.73, 136.43, 131.75, 129.80, 126.35, 123.04, 120.83. UV/VIS (EtOH): λ [nm] = 220 (lg ε = 4.58), 240 (4.15), 252 (4.16), 272 (4.4), 295 (3.96), 306 (sh, 3.89), 343 (sh, 3.77), 358 (3.92), 377 (3.86). Correct C,H,N analysis.

Received: December 7, 1988 [Z 3077 IE]
German version: *Angew. Chem. 101* (1989) 607

[1] DPPH = α,α'-diphenyl-β-picrylhydrazyl, a stable free radical used as an EPR reference.
[2] V. Enkelmann, *Adv. Chem. Ser. 217* (1988) 177.
[3] G. Sachs, E. Dormann, M. Schwœrer, *Solid State Commun. 53* (1985) 73.
[4] E. Dormann, G. Sachs, W. Stöcklein, B. Bail, M. Schwœrer, *Appl. Phys. A 30* (1983) 227.
[5] V. Enkelmann, B. S. Morra, C. Kröhnke, G. Wegner, J. Heinze, *Chem. Phys. 66* (1982) 303.
[6] M. Jørgensen, T. Bjørnholm, K. Bechgaard, *Proc. Int. Conf. Sci. Technol. Synth. Met.* (Santa Fe, NM, USA, 1988), *Synth. Met. 27* (1988) 159.
[7] The unsubstituted analogue of **5** has been synthesized by a very different route which could not be used for the synthesis of **5**: A. Fozard, C. K. Bradsher, *J. Org. Chem. 32* (1967) 2966.
[8] T. Kato, H. Yamanaka, *J. Org. Chem. 30* (1965) 910.
[9] M. C. Venuti, *Synthesis 1982*, 61.
[10] All electrochemical criteria for reversibility are satisfied for low sweep rates (typically below 100 mV s^{-1}); for details, see: A. J. Bard, L. R. Faulkner; *Electrochemical Methods*, Wiley, New York 1980, p. 224.
[11] P. Hanson, *Adv. Heterocyc. Chem. 25* (1979) 205.
[12] K. Möbius, M. Plato, *Z. Naturforsch. A 22* (1967) 929.
[13] **1** · PF_6: space group $P2_1/m$ with a = 6.280 (3), b = 11.338 (2), c = 9.736 (1) Å, β = 97.17 (3)°, V = 688.1 Å^3, Z = 2, ϱ_{calcd} = 1.68 g cm^{-3}, μ = 2.589 cm^{-1}, F_{000} = 176. Data were collected at room temperature using graphite-monochromated $Mo_{K\alpha}$ radiation (λ = 0.71073 Å) and an Enraf-Nonius CAD4-F diffractometer. The crystal structure was solved by direct methods using the Enraf-Nonius SDP program package. Hydrogen atoms with geometrically calculated positions were included in scale-factor calculation but not refined. 950 reflections ($I > 3\,\sigma(I)$) were used for 112 parameters, R = 0.045, R_w = 0.043, GOF = 0.671. Further details of the crystal structure investigation are available on request from the Fachinformationszentrum Energie, Physik, Mathematik GmbH, D-7514 Eggenstein-Leopoldshafen 2 (FRG), on quoting the depository number CSD-53732, the names of the authors, and the journal citation.
[14] A. C. Hazell, D. W. Jones, J. M. Sowden, *Acta Crystallogr. Sect. B 33* (1977) 1516.
[15] Aldrich reagent grade (98%) was used.
[16] E. Heibronner, P. A. Straub: *Hückel Molecular Orbitals*, Springer, Berlin 1966.

A Joint Structural Characterization of Colloidal Platinum by EXAFS and High-Resolution Electron Microscopy

By *Daniel G. Duff, Peter P. Edwards*, John Evans, J. Trevor Gauntlett, David A. Jefferson, Brian F. G. Johnson, Angus I. Kirkland,* and *David J. Smith*

The structures and morphologies adopted by small metal particles continue to attract widespread interest. Of particular importance in this regard are the structures of particles of metals such as Pd, Pt, Ru, and Cu, which find extensive application in commercial catalysis.

To date, the most successful techniques for probing the structure of such species have been bright- and dark-field transmission electron microscopy (TEM)[1, 2] to yield information about the morphology and surfaces in projection, coupled with electron diffraction data from larger particles to yield unit-cell dimensions and orientation, and high resolution electron microscopy (HREM) to yield precise information on the atomic arrangement and the nature of defect structures such as twin planes and stacking faults.[3–5] However, when faced with the task of characterizing particles from a colloidal solution, special problems arise. Although the homogeneity of the sol may be reliably ascertained by examining more than one specimen grid and a number of grid squares within each, there still remains the possibility that what is imaged in the electron microscope may not be the same as the species present in solution. Electron microscopy necessitates desiccation of the sample followed by electron irradiation: indeed, *Thomas, Millward,* and *Harriman*[6] have noted beam-induced reduction of iridium dioxide colloids, and preliminary results of our own suggest that for very small particles this may happen too quickly to be observed in some systems.

Hence we require an *ensemble* technique capable of operating on solutions to confirm the structural information provided by electron microscopy. Visible spectrophotometry provides only limited and qualitative information concerning particle size and degree of aggregation. However, EXAFS provides exactly the required information on the particle structure with limited perturbation of the system and, although not ideal where long-range order is concerned, is especially useful in the regime of small particle size (30-Å diameter and below). It is thus ideally complementary to an electron-microscopic study.

In this communication we therefore report a joint structural characterization of a platinum sol by EXAFS and HREM. Our results confirm that the HREM images obtained represent an accurate reflection of the structure of the particles present in solution in this case.

The synthesis is an adaptation of one previously described.[7, 8] A greater residual molar ratio of polymer to

[*] Dr. P. P. Edwards, D. G. Duff, Dr. D. A. Jefferson, Dr. B. F. G. Johnson, A. I. Kirkland
Department of Chemistry,
Lensfield Road, Cambridge CB2 1EW (England)
Prof. J. Evans, Dr. J. T. Gauntlett
Department of Chemistry, The University,
Southampton SO9 5NH (England)
Prof. D. J. Smith
Center for Solid State Science, Arizona State University
Tempe AZ 40587 (USA)

[**] The authors would like to thank the Science and Engineering Research Council (SERC), the Ernest Oppenheimer Foundation, British Alcan, and the B.P. Venture Research Unit for financial support. *D.A.J.* also acknowledges NSF grant DMR-8677609 for support at Arizona State University.

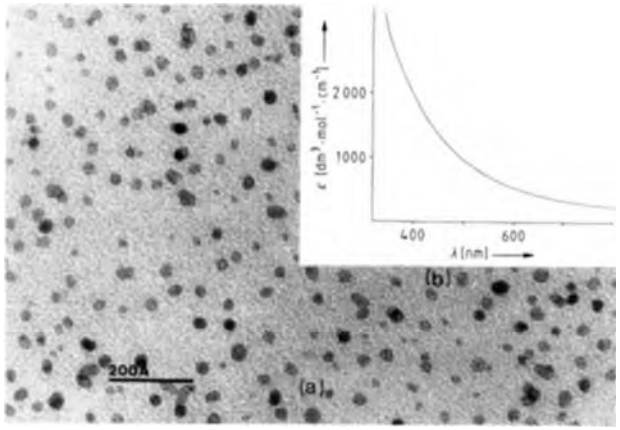


Fig. 1 a) A typical low-resolution transmission electron micrograph of particles from the platinum sol. b) The optical extinction of the sol in the visible region of the spectrum.

metal (54.05 versus 40.95) was used in a more concentrated preparation, and a concentration of metal of 10^{-2} M was employed. TEM of the dark brown sol (Fig. 1 a) reveals small particles with minimal aggregation on the grid. The optical spectrum (Fig. 1 b) shows the featureless absorbance decreasing to long wavelengths typical for platinum sols. As previously noted[9] for platinum colloids prepared by different routes, a double-log plot of absorbance against wavelength is linear over the wavelength range 400–600 nm. The gradient (−3.3) corresponds well with the values reported by *Furlong* et al.[9] for well-dispersed sols of small particles, aggregated sols displaying flatter spectral curves and consequently straight lines of shallower gradient in the double-log plot. These results confirm the genuinely well-dispersed nature of the sol as revealed by TEM. Syntheses performed at the concentrations used by *Hirai* et al.[7, 8] and those using a tenth of the metal and polymer concentrations employed here (10^{-3} M Pt and 0.3 g polyvinylpyrrolidone (PVP)) both showed a high frequency of aggregated particles.

A size-distribution histogram measured from 100 particles from the low-resolution micrographs is presented in Figure 2. The mean (equivalent circle) diameter of the measured particles is 26 Å with a standard deviation of 11 Å, yielding a coefficient of variation of 43%. The volume-weighted mean particle diameter is 31 Å.

High-resolution electron microscopy showed the majority of particles present to have structures based on apparently perfect fcc packing with the particles exhibiting roughly hexagonal outlines in projection when viewed down a ⟨110⟩ direction, suggesting an approximate cubeoctahedral morphology. Some images were also recorded of particles in

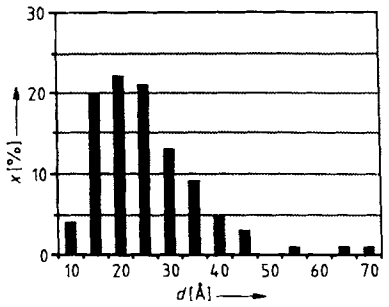


Fig. 2. A histogram of particle diameters measured from low-resolution electron micrographs. x = percentage of particles, d = equivalent circle diameter.

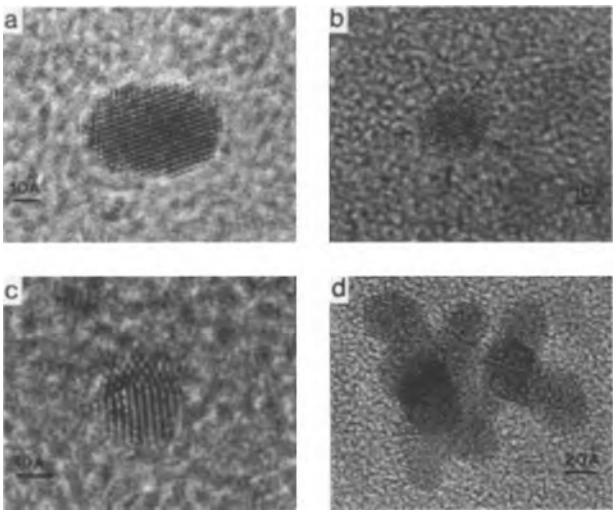


Fig. 3 a) A high-resolution image of an apparently perfect fcc Pt particle in a <110> orientation. b) An image of an apparently perfect decahedral particle viewed down the fivefold symmetry axis. c) A similar particle but tilted further from this axis. d) A <100>-oriented agglomerate of apparently perfect fcc particles as observed in the more dilute sols referred to in the text.

⟨100⟩ orientations. A typical image of a small particle is shown in Figure 3 a, clearly indicating the apparently perfect fcc lattice; while the particle possesses flat {111} surfaces, the {100} surfaces appear noticeably roughened. This second feature is similar to that observed by *Schmid* et al.[11] for small Pt particles prepared by electron-beam decomposition of the cluster $[Pt_{55}(AstBu_3)_{12}Cl_{20}]$.[12] However, the adatom growth processes on {100} faces observed by *Schmid* et al. were not observed here, even during real-time recording of the images via a video tape recorder (VTR) system. Furthermore, the well-defined surfaces present on these particles are in contrast to the more rounded surfaces observed for small Pt particles supported on carbon black.[13]

Although the majority of particles conformed to the above description, a significant percentage showed alternative structures. A very small number of decahedral multiply twinned particles were observed (Fig. 3 b, c) and, in addition to these, some particles apparently displayed single microtwins on {111} planes. Recent image simulation studies[14] have indicated that such decahedral particles tilted from the fivefold symmetry axis may give rise to images apparently containing single microtwins, and therefore these particles could also contribute to the multiply twinned fraction. Nonetheless, the vast majority of particles showed no obvious radial twinning. Complications could also arise from the specific concentrations employed: in particular, when sols prepared at different metal and polymer concentrations were examined, aggregates of particles were frequently observed on the specimen grid (Fig. 3d), although it is significant that the individual particles making up this aggregate are clearly perfect fcc crystals. Full details of these related sols will be published elsewhere.[15]

The acquired EXAFS data lends strong support to the assignment of the colloidal particles in solution as fcc platinum crystallites. Comparison of experimental EXAFS data for colloidal platinum and the bulk metal are shown in Figure 4 a. The similarity in the two structures is obvious from their k^3-weighted EXAFS spectra (Fig. 4 a). The close correlation of their Fourier transforms is also noteworthy (Fig. 4 b), the radius ratios in the radial distribution function being excellent evidence for fcc packing. However, there is a small difference in the frequency of the two spectra, notice

 © VCH Verlagsgesellschaft mbH, D-6940 Weinheim, 1989 0570-0833/89/0505-0591 $ 02.50/0

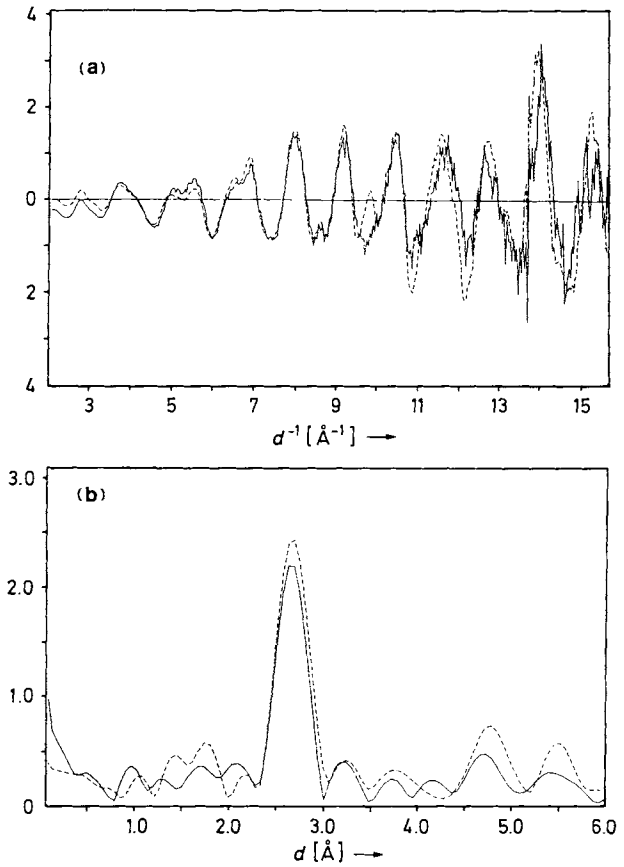


Fig. 4 a) k^3-weighted EXAFS spectra after background subtraction. b) Fourier transformations of the spectra in Fig. 4a. —— colloid, ----- bulk metal.

Table 1. Experimental EXAFS data for colloidal and bulk platinum.

	Pt metal	Pt colloid
E0	12.1(5)	12.7(8)
R1	2.748(1)	2.737(2)
A1	0.0104(1)	0.0115(2)
R	25.3	38.1

able at > 11 Å^{-1}. Fourier filtration around the first shells allows the major component of this difference to be identified. Refinement of E0, R1, and A1 (see *Experimental Procedure*) converges to minima listed in Table 1.

The source of the frequency difference between the spectra is the difference in the interatomic distance to the first coordination shell. This distance, in colloidal platinum, is 0.011(2) Å less than in the bulk metal, indicating relaxation of fcc packing in the colloid structure. The Debye–Waller factor for the first coordination shell in the colloid spectrum is given for an amended first-shell occupancy of 11.2. The following approximations were made in assuming this. From the particle size distribution an average spherical particle volume of 16470 Å^3 was calculated. Since the particle has close-packed structure, the actual volume occupied by metal atoms is 74% of this value or 12190 Å^3, which corresponds to 1110 atoms. Approximately 250 of these are on the surface with 9 or less nearest neighbors. These surface atoms were assumed to have 8.5 nearest neighbors each, giving an average coordination number throughout the particle of 11.2.

If the coordination number is allowed to refine freely with the other three parameters, a minimum is reached when N = 9.9(7). The interatomic distance and E0 are unaffected while A1 falls to 0.0108(5). A coordination number of ten is more reasonable for a nonspherical particle with a greater proportion of atoms at the surface, such as in the colloid. However, similar refinement of the same parameters for the bulk metal reaches an almost identical minimum (N1 = 9.7(5); A1 = 0.0092(3)), thus illustrating how refinement of two highly correlated parameters can lead to false minima. Therefore, calculated values of the first-shell occupancy were employed at all times.

Relaxation of the surface structure on certain faces of the colloidal particle, where the lower coordination number introduces distortions away from close packing, results in a higher Debye–Waller factor for the first coordination shell. A small fraction of non-fcc particles would also be expected to have a similar effect, and disorder due to larger-amplitude vibrations than in the bulk will also occur.

Lattice contractions in small platinum particles have previously been reported.[16–18] Our results show a lattice contraction of 0.4%, well within the limits of theoretical calculations[19] for this particle size. However, the electron diffraction results of *Solliard* and *Flueli*,[18] when extrapolated to a volume-weighted mean particle diameter of 31 Å, yielded a contraction of 0.6% (still concurring with the calculations). This difference possibly arises from surface adsorption on the sol particles by species such as oxygen, thereby changing the nature of the surface stresses (*Solliard* and *Flueli* worked on vacuum-evaporated particles and, presumably, cleaner surfaces than those present in this system). EXAFS has previously been used to measure relaxations in platinum clusters of 12-Å diameter in which a contraction of 4.3% was found,[17] but this contraction was very sensitive to gas adsorption, almost vanishing when the particles were exposed to hydrogen.

We have thus demonstrated the usefulness of a combined EXAFS/electron-microscopic investigation as a tool in the elucidation of small-particle structures. EXAFS is suited to the determination of accurate lattice parameters such as the observed contraction of the particles in solution. HREM, however, yields data on short-range defect and minority structures inaccessible to EXAFS. In particular, the potential of EXAFS for probing the nature of extremely small solution species cannot be overemphasized in view of the proposed importance of such species in the nucleation and growth processes operative in colloidal solution.

Experimental Procedure

The synthesis was performed in a 100-mL round-bottomed Pyrex flask, rigorously cleaned as follows. A cleaning mixture containing hydrofluoric acid, nitric acid, and a surfactant (Lipsol) was prepared following a method previously described in the literature [20]. The flask was filled with this mixture and left for 10 min. The cleaning fluid was decanted off and the flask rinsed ten times with hot tap water, five times with laboratory-supply distilled water, and three times with water distilled in a glass apparatus. Polytetrafluoroethylene (PTFE) stirring beads were cleaned of metal by soaking in aqua regia for several hours, followed by extensive rinsing as above. The flask was then arranged as for the reaction with the stirring bead added and glass-distilled water was boiled under reflux for 30 min therein and decanted.

A solution of H_2PtCl_4 (248 mg; Johnson Matthey Chemicals plc, 39.34% Pt) in glass-distilled water (25 mL) was added to a solution of PVP (3 g; Polysciences Inc., weight-average molecular weight 10000) in analytical reagent grade methanol (25 mL) with stirring (PTFE-coated magnetic stirring bead). The stirring bead was then removed and the mixture heated to boiling under a nitrogen atmosphere. After 70 min boiling under reflux, the sol was allowed to cool. A small volume (< 1 mL) was removed for electron microscopy. An aliquot (5 mL) of ca. 0.2 M sodium hydroxide solution was then added and the sol concentrated down to ca. 5 mL while purging with nitrogen. There was no change in color during the last two processes and redilution revealed no change in optical spectrum. This sample was then retained for EXAFS.

Optical spectroscopy of the sol was performed using a PYE-Unicam SP-8800 spectrophotometer. Spectra were recorded in the range 400–800 nm with the

samples contained in quartz cells of 1-mm path length. Although the sols were prepared under nitrogen, exposure to air caused no noticeable change in the optical appearance of the sol, and no effort was made to protect the samples for EXAFS and HREM from air.

Specimens for electron microscopy were prepared by allowing a drop of the sol to contact briefly an amorphous carbon film supported on a copper grid. Initial TEM examination was carried out using a standard JEOL JEM-200CX fitted with a standard side-entry double-tilt goniometer and operated at 200 kV, subsequent high-resolution studies employing either our modified JEOL JEM-200CX [21] (C_s = 0.52 mm, C_c = 1.05 mm at 200 kV) or a JEOL JEM-4000EX (C_s = 1.0 mm, C_c = 1.7 mm at 400 kV) for structural characterization at interpretable point resolutions of 1.95 Å and 1.7 Å, respectively. For these studies suitably oriented particles were located on the grid on a trial-and-error basis. Care was taken to ensure the correct alignment of the illumination system [22], and residual objective-lens astigmatism was corrected by observations of the granularity of the amorphous carbon film. All high-resolution micrographs were recorded at electron-optical magnifications in the range 300000 to 700000.

EXAFS spectra were obtained from the highly concentrated (ca. 0.1 M) sol in transmittance mode on Beam Line 9 of the Synchrotron Radiation Source at the SERC Daresbury Laboratory, and the spectrum of platinum metal powder (Johnson Matthey Chemicals) also obtained for comparison. Background subtraction was achieved using smooth polynomial curves for both pre- and post-edge in the program PAXAS [23]. Window limits for Fourier filtration of the spectra around the first shell were 1.98 to 3.42 Å and 1.97 to 3.47 Å for the metal and the colloid, respectively, in the non-phase-shifted spectra. Fourier filtration has two functions; it ensures that any contributions from more distant shells are removed and produces a spectrum with 200 evenly distributed points in k space.

All calculations employed the spherical wave theory of *Lee* and *Pendry* [24], utilizing algorithms suitable for polycrystalline or amorphous samples [25]. Twenty-five phase shifts were used in calculating the backscattering terms. The excited atom wave function was calculated for an atom in which the outer electrons are fully relaxed in the presence of a 2p core hole. A constant imaginary potential of -7 eV was used to model inelastic processes. This low value is an adequate model for the short core hole lifetimes of metals.

Analysis involved least-squares minimization of the fit index

$$S_i(k^3(X_i^T - X_i^E))^2$$

where X_i^T and X_i^E are the theoretical and experimental EXAFS, respectively. However, this is dependent on the absolute amplitude of the spectrum. A discrepancy index, R, is therefore reported as a measure of the precision of the fit.

$$R = \frac{\int |(X^T(k) - X^E(k))| k^3 \, dk \times 100}{\int |X^E(k)| k^3 \, dk}$$

The parameters refined were: the interatomic distance from the absorber to the nearest-neighbor backscattering shell, R1; the Debye–Waller factor for the first shell of nearest neighbors, A1, described by $A1 = 2\,s^2$; the energy of the emitted photoelectron at $k = 0$, E0.

Received: October 25, 1988 [Z 3025 IE]
German version: *Angew. Chem. 101* (1989) 610

[1] M. J. Yacaman, K. Heinemann, C. Y. Yang, H. Poppa, *J. Cryst. Growth 47* (1979) 187.
[2] H. Hofmeister, H. Haefke, M.Krohn, *J. Cryst. Growth 58* (1982) 507.
[3] D. G. Duff, A. C. Curtis, P. P. Edwards, D. A. Jefferson, B. F. G. Johnson, A. I. Kirkland, D. E. Logan, *Angew. Chem. 99* (1987) 688; *Angew. Chem. Int. Ed. Engl. 26* (1987) 676.
[4] D. J. Smith, L. D. Marks, *J. Cryst. Growth 54* (1981) 433.
[5] G. Schmid, *Struct. Bonding (Berlin) 62* (1985) 51.
[6] J. M. Thomas, G. R. Millward, A. Harriman, *New J. Chem. 11* (1988) 757.
[7] H. Hirai, *J. Macromol. Sci.—Chem. Part A 13* (1979) 633.
[8] H. Hirai, Y. Nakao, N. Toshima, *J. Macromol. Sci.—Chem. Part A 13* (1979) 727.
[9] D. N. Furlong, A. Launikonis, W. H. F. Sasse, J. V. Sanders, *J. Chem. Soc. Faraday Trans. 80* (1984) 571.
[10] C. G. Granqvist, R. A. Buhrman, *J. Appl. Phys. 47* (1976) 2200.
[11] L. R. Wallenberg, J-O. Bovin, A. K. Petford-Long, D. J. Smith, *Ultramicroscopy 20* (1986) 71.
[12] G. Schmid, N. Klein, *Angew. Chem. 98* (1986) 910; *Angew. Chem. Int. Ed. Engl. 25* (1986) 922.
[13] M. L. Sattler, P. N. Ross, *Ultramicroscopy 20* (1986) 21.
[14] D. A. Jefferson, A. I. Kirkland, *Institute of Physics Short Meetings Series* (Institute of Physics, Bristol, U.K.) *11* (1988) 71.
[15] D. G. Duff, P. P. Edwards, D. A. Jefferson, B. F. G. Johnson, A. I. Kirkland, unpublished.
[16] J. H. Sinfelt, G. H. Via, F. W. Lytle, *J. Chem. Phys. 68* (1978) 2009.
[17] B. Moraweck, G. Clugnet, A. J. Renouprez, *Surf. Sci. 81* (1979) L361.
[18] C. Solliard, M. Flueli, *Surf. Sci. 156* (1985) 487.
[19] S. N. Khanna, J. P. Bucher, J. Buttet, F. Cyrot-Lackmann, *Surf. Sci. 127* (1983) 165.
[20] P. R. van Rheenen, M. J. McKelvy, W. S. Glaunsinger, *J. Solid State Chem. 67* (1987) 151.
[21] D. A. Jefferson, G. R. Millward, J. M. Thomas, R. Brydson, A. Harriman, K. Tsuno, *Nature 323* (1986) 428.
[22] D. J. Smith, L. A. Bursill, G. J. Wood, *Ultramicroscopy 16* (1985) 19.
[23] N. Binsted, *Program for the Analysis of X-ray Absorption Spectra (PAXAS)*, University of Southampton (U.K.) 1988.
[24] P. A. Lee, J. B. Pendry, *Phys. Rev. B 11* (1975) 2795.
[25] S. J. Gurman, N. Binsted, I. Ross, *J. Phys. C 17* (1984) 143.

Efficient Photoinduced Intramolecular Energy Transfer in an Oblique Bis-Porphyrin System

By *Sylvie Chardon-Noblat, Jean-Pierre Sauvage,** and *Paul Mathis*

Multifunctional molecular systems able to perform intramolecular electron or energy transport are of particular relevance both for handling and carrying signals at the molecular level[1] and for understanding the function of the chromophores involved in natural photosynthetic systems.[2] In order to mimic the initial charge-separation step of photosynthesis, numerous bipartite compounds consisting of a porphyrin linked to an electron acceptor[3] have been synthesized and studied, a promising extension being provided by tripartite systems consisting of an electron donor, a porphyrin, and an electron acceptor.[4] Energy transfer and migration is also of great importance in natural photosynthesis.

Intramolecular singlet energy transfer has been observed in covalently linked but highly flexible bis-porphyrin systems.[5] We have recently described a rigid oblique bis-porphyrin[6] built on a 1,10-phenanthroline spacer insuring geometrical features close to those found in the reaction center of photosynthetic bacteria.[7] We now report a method for rapid synthesis of the bis-porphyrin system **5** as well as its intramolecular energy-transfer properties.

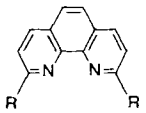
Compound **1** was obtained as previously described[6] from 4-lithiotoluene and 1,10-phenanthroline in 65% yield. Treatment of **1** with *N*-bromosuccinimide (3 equivalents) in refluxing benzene under light irradiation ($\lambda > 320$ nm; 30 min) gave **2**. After filtration, washing (H_2O), and solvent evaporation, the crude product was directly treated with NaOH in refluxing propionic acid. Workup and chromatographic purification (silica; CH_2Cl_2/AcOEt) afforded **3** as a yellow, glassy solid in 20% yield from **1**.

Compound **3** was allowed to react with pyrrole and 3,5-di-*tert*-butylbenzaldehyde (1:16:15) in refluxing propionic acid for 16 h. After workup, repeated chromatographic separation on silica (hexane/toluene), and recrystallization in benzene/ethanol, a 2.6% yield of **4** was obtained as a purple solid. Compound **7** was isolated from the same reaction mixture in 16% yield.

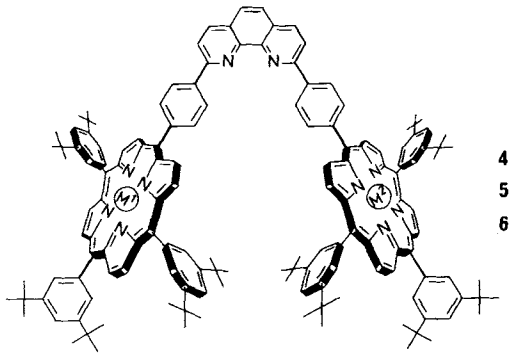
Compound **4** was treated with 1.1 equivalents of zinc acetate in CH_3OH/CH_2Cl_2 (1:3) under reflux for 1.5 h. After chromatography (alumina; CH_2Cl_2/hexane), the three com-

[*] Dr. J.-P. Sauvage, S. Chardon-Noblat
Laboratoire de Chimie Organo-Minérale, Institut de Chimie
1, rue Blaise Pascal, F-67008 Strasbourg (France)
Dr. P. Mathis
Service Biophysique, C.E.N. de Saclay
F-91198 Gif-sur-Yvette (France)

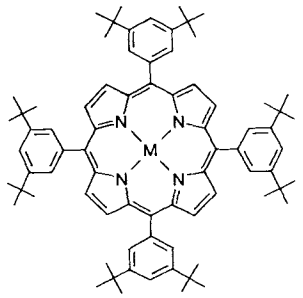
[**] We thank the C.N.R.S. for financial support.



1: R = *p*-C_6H_4-CH_3
2: R = *p*-C_6H_4-$CHBr_2$
3: R = *p*-C_6H_4-CHO



4: $M^1 = M^2 = 2H$
5: $M^1 = Zn$, $M^2 = 2H$
6: $M^1 = M^2 = Zn$



7: M = 2 H
8: M = Zn

pounds **4**, **5**, and **6** were isolated in 20, 35, and 20% yield, respectively.

In order to determine whether **5** can undergo a photoinduced intramolecular electron-transfer reaction, the electrochemical properties of this compound and of **4**, **6**, and the monoporphyrins **7** and **8**, similar to the constitutive subunits of **5**, have been studied (Table 1).

Table 1. Electrochemical properties of the porphyrin compounds **4**–**8** [a].

Compound	E° (oxidation)			E° (reduction)	
	−1e	−2e	−3e	+1e	+2e
4	1.04	1.38		−1.20	
5	0.80	1.01	1.14	−1.20	< −1.5
6	0.82	1.17		< −1.5	
7	1.01			−1.24	
8	0.62	0.91		< −1.5	

[a] Cyclic voltammetry measurements on 2.5×10^{-4} M solutions (**4**–**6**) or 5×10^{-4} M solutions (**7**, **8**) in degassed CH_2Cl_2 on Pt wire; successive redox potentials of reversible couples in *V* vs. SCE with 0.1 M $nBu_4N^{\oplus}BF_4^{\ominus}$ in CH_3CN junction; 0.1 M $nBu_4N^{\oplus}BF_4^{\ominus}$ as supporting electrolyte; scan rate, 80 mV s^{-1}.

The absorption spectra of **4**, **5**, and **6** in CH_2Cl_2 display a single, relatively sharp Soret band (at $\lambda = 421.5$ nm with $\varepsilon = 1.1 \times 10^6$ cm^{-1} mol^{-1} L for **5**). The spectra correspond rather precisely to those of **7** or **7** + **8** (data not shown). This indicates that the two chromophores are not or only very weakly coupled, in contrast to *Tabushi*'s gable porphyrin.[8] Interesting observations related to the influence of the geometry of the system on the inter-chromophore interaction have recently been reported for flat, twisted, and gable bis-porphyrins.[9, 10] Some dipole–dipole interaction seems to exist in the gable system, contrary to the presently described molecules. This different behavior may originate in larger edge-to-edge (ca. 9 Å) and center-to-center (ca. 13 Å) separation of the two porphyrin units in **5** compared with gable bis-porphyrins.[8, 9]

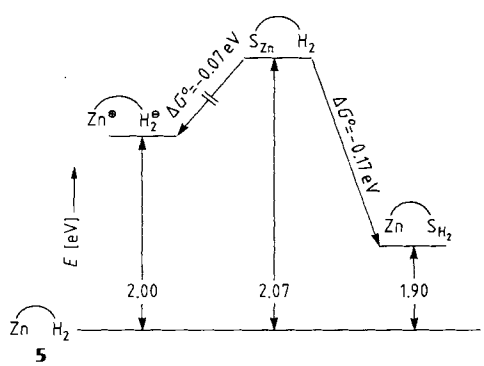
Table 2. Emission data of the porphyrin compounds **4**–**8** [a].

Compound	λ_{max} (emission, relative intensity in parentheses) [nm]		
4	–	654 (120)	720 (30)
5	–	654 (180)	718 (30)
6	603 (40)	653 (30)	–
7	–	654 (100)	718 (30)
8	600 (70)	651 (60)	–

[a] Emission spectra at room temperature in degassed CH_2Cl_2; 2×10^{-6} M porphyrin in each case; excitation wavelength, 550 nm.

In contrast to its absorption spectrum, the emission spectrum of the mixed dimer **5** is dramatically different from the superposition of the spectra of its constitutive parts (Table 2). Interestingly, the singlet state of the zinc-containing porphyrin in **5** is completely quenched (600 nm) whereas the emission spectrum corresponding to the non-metalated part (singlet state) is strongly enhanced: at 654 nm, the emission intensity of **5** is 1.8 times that of **7**. This shows that efficient energy transfer has occurred between the zinc porphyrin part (singlet energy donor) and the non-metalated subunit (singlet energy acceptor). It is the singlet state of this latter porphyrinic subunit that is generated regardless of which porphyrinic part is photoexcited in the initial photonic process. As a reference, the emission spectrum of a mixture of **7** and **8** is roughly the superposition of the emission spectra of the two components.

The efficient photoinduced intramolecular energy transfer observed in **5** is in agreement with the energy level of the singlet excited state of each component of the bis-porphyrin (Scheme 1). The ΔG° values and the energy levels were calculated using the electrochemical data (Table 1) and the emission spectra (Table 2). Clearly, the driving force for the electron-transfer reaction (0.07 eV) is much smaller than that for the intramolecular energy migration (0.17 eV).



5

Scheme 1. Energy transfer in electronically excited **5**. Zn = Zn-containing porphyrinic part; H_2 = non-metalated porphyrinic part; S = excited singlet state.

 © VCH Verlagsgesellschaft mbH, D-6940 Weinheim, 1989 0570-0833/89/0505-0594 $ 02.50/0

Excitation of **5**, **7**, and **8** (10^{-4} M in degassed CH_2Cl_2 at room temperature) by a 20-ps laser pulse at 530 nm was used for transient absorption measurements at 820 nm (triplet state absorption; see Ref. [11]) with an apparatus already described.[12] Simultaneously, time-resolved emission measurements were performed. In **5**, emission at 600 nm is completely quenched whereas emission at 660 nm is enhanced as compared to **7** under the same conditions. The formation rate of the triplet state localized on the non-metalated subunit (10^8 s^{-1} at room temperature in degassed CH_2Cl_2) is similar to the decay rate of the singlet state (non-metalated ring). Furthermore, the emission quantum yield at 660 nm and the quantum yield of triplet state generation (absorption at 820 nm) for **5** are roughly twice those for **7**, corroborating the data of Table 2 obtained by classical emission spectroscopy. No evidence was obtained for light-induced electron transfer. These observations are in full agreement with the postulated reaction of efficient intramolecular singlet energy transfer from the zinc porphyrin part to the non-metalated ring.

The present oblique bis-porphyrin may be related to the hypothetical mechanism of the photosynthetic bacterial reaction center. Energy migration from the special pair to the isolated bacteriochlorophyll followed by electron transfer or initial electron transfer from the special pair may be operative.[2]

Received: November 17, 1988 [Z 3055 IE]
German version: *Angew. Chem. 101* (1989) 631

CAS Registry numbers:
1, 116287-98-0; **2**, 120085-98-5; **3**, 120085-99-6; **4**, 120086-00-2; **5**, 120086-01-3; **6**, 120086-02-4; **7**, 89372-90-7; **8**, 116123-17-2; pyrrole, 109-97-7; 3,5-di-*tert*-butylbenzaldehyde, 17610-00-3.

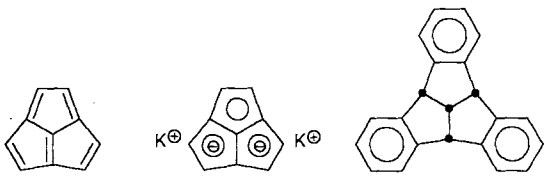
[1] F. Effenberger, H. Schlosser, P. Bäuerle, S. Maier, H. Port, H. C. Wolf, *Angew. Chem. 100* (1988) 274; *Angew. Chem. Int. Ed. Engl. 27* (1988) 281.
[2] S. F. Fischer, P. O. J. Scherer, *Chem. Phys. 115* (1987) 151; R. A. Marcus, *Chem. Phys. Lett. 133* (1987) 471; A. Ogrodnik, N. Remy-Richter, M. E. Michel-Beyerle, R. Feick, *ibid. 135* (1987) 576; M. Bixon, J. Jortner, M. E. Michel-Beyerle, A. Ogrodnik, W. Lersch, *ibid. 140* (1987) 626; P. O. J. Scherer, S. F. Fischer, *ibid. 141* (1987) 179; Y. Won, R. A. Friesner, *J. Phys. Chem. 92* (1988) 2208; A. Warshel, S. Creighton, W. W. Parson, *ibid. 92* (1988) 2696.
[3] J. L. Sessler, M. R. Johnson, *Angew. Chem. 99* (1987) 679; *Angew. Chem. Int. Ed. Engl. 26* (1987) 678; A. C. Chan, J. Dalton, L. R. Milgrom, *J. Chem. Soc. Perkin Trans. 2 1982*, 707; T. F. Ho, A. R. McIntosh, A. C. Weedon, *Can. J. Chem. 62* (1984) 967; M. R. Wasielewski, M. P. Niemczyk, *J. Am. Chem. Soc. 106* (1984) 5043 and the numerous references cited in these publications.
[4] M. R. Wasielewski, M. P. Niemczyk, W. A. Svec, E. B. Pewitt, *J. Am. Chem. Soc. 107* (1985) 5562; D. Gust, T. A. Moore, L. R. Makings, P. A. Liddell, G. A. Nemeth, A. L. Moore, *ibid. 108* (1986) 8028.
[5] F. P. Schwartz, M. Gouterman, Z. Muljiani, D. H. Dolphin, *Bioorg. Chem. 2* (1972) 1; J. A. Anton, P. A. Loach, R. Govindjee, *Photochem. Photobiol. 28* (1978) 235; R. Selensky, D. Holten, M. W. Windsor, J. B. Paine III, D. Dolphin, M. Gouterman, J. C. Thomas, *Chem. Phys. 60* (1981) 33; J. C. Mialocq, G. Giannotti, P. Maillard, M. Momenteau, *Chem. Phys. Lett. 112* (1984) 87; A. Regev, T. Galili, H. Levanon, A. Harriman, *ibid. 131* (1986) 140; O. Gonen, H. Levanon, *J. Chem. Phys. 84* (1986) 4132.
[6] S. Noblat, C. O. Dietrich-Buchecker, J.-P. Sauvage, *Tetrahedron Lett. 28* (1987) 5829.
[7] J. Deisenhofer, O. Epp, K. Miki, R. Huber, H. Michel, *J. Mol. Biol. 180* (1984) 385.
[8] I. Tabushi, T. Sasaki, *Tetrahedron Lett. 23* (1982) 1913.
[9] J. L. Sessler, M. R. Johnson, T. Y. Lin, S. E. Creager, *J. Am. Chem. Soc. 110* (1988) 3659.
[10] A. Osuka, K. Maruyama, *Chem. Lett. 1987*, 825; A. Osuka, K. Maruyama, I. Yamazaki, N. Tamai, *J. Chem. Soc. Chem. Commun. 1988*, 1243.
[11] R. L. Brookfield, H. Ellul, A. Harriman, *J. Chem. Soc. Faraday Trans. 2 81* (1985) 1837.
[12] Y. Takahashi, O. Hansson, P. Mathis, K. Satoh, *Biochim. Biophys. Acta 893* (1987) 49.

Towards Tribenzoacepentalene: Tribenzotriquinacene, Dihydrotribenzoacepentalenediide, and the Tribenzoacepentalene Radical Anion**

By *Dietmar Kuck,** *Andreas Schuster, Björk Ohlhorst, Volker Sinnwell,* and *Armin de Meijere**

Dedicated to Professor Kurt Heyns on the occasion of his 80th birthday

Benzoannelation can increase the stability of cyclically conjugated, nonaromatic hydrocarbons that, owing to unfavorable electron configuration and/or unfavorable HOMO energies, are unstable and therefore highly reactive. To explore this possibility for acepentalene **1**, only the dianion of which, $\mathbf{1}^{2\ominus}$, is so far known,[1] we synthesized tribenzotriquinacene (tetrahydrotribenzoacepentalene) **2** and investigated its deprotonation-dehydrogenation both in solution and in the gas phase.

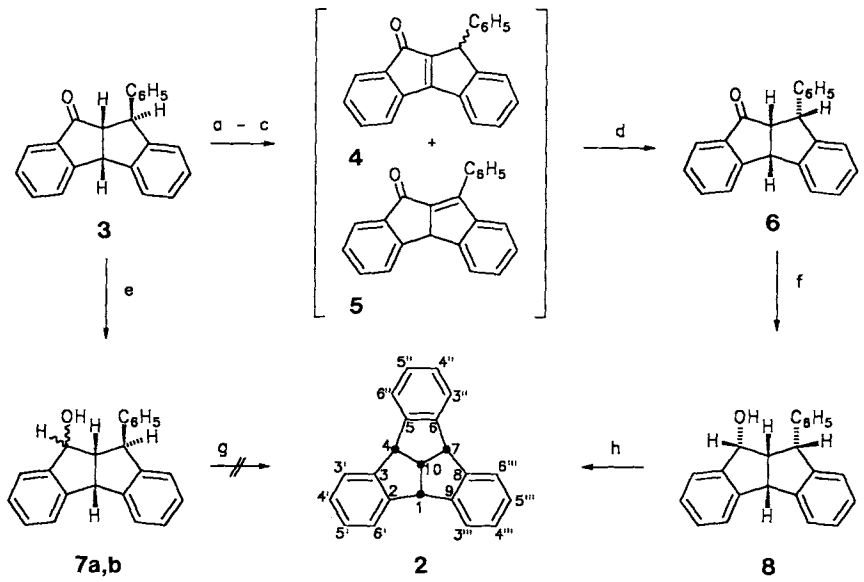


1 $\quad$ $\mathbf{1}^{2\ominus}/2K^{\oplus}$ $\quad$ **2**

Tribenzotriquinacenes with substituents on the central C atom are accessible by double cyclodehydration of the correspondingly substituted 2-benzhydryl-1,3-indandiols.[2] The unsubstituted hydrocarbon **2**, however, could be obtained only in low yields via this route. Starting from cinnamic acid, *Baker* et al.[3] synthesized the diquinane ketone **3** in three steps; bromination/dehydrobromination then gave the enone **4** in moderate yield. In our attempts to synthesize **2** and higher benzoannelated centropolyquinanes,[4] the ketone **3** and the alcohols **7a, b**[3] derived therefrom were identified as 8-*exo*-phenyl stereoisomers on the basis of their mass spectra;[5] thus, the cyclodehydration **7** → **2** attempted by *Baker* et al.[3] was doomed to failure for steric reasons. The enone **4**, together with the isomer **5**,[8] is accessible on a preparative scale (overall yield 25%, Scheme 1) by an alternative route involving phenylsulfenylation of **3**, oxidation, and thermal elimination of the phenylsulfinyl derivative.[6, 7] Subsequently, **4** and **5** can be rehydrogenated with palladium on charcoal in dioxane to afford the isomeric diquinane ketone **6** with high selectivity. After reduction to the alcohol **8**, bearing an *endo*-phenyl group, the cyclodehydration to the tricyclic compound **2** occurs readily, as expected. Compound **2** crystallizes from hot xylene as sparingly soluble, colorless, long, hard needles having an unusually high melting point (390 °C). The identity of **2** was established on the basis of its analytical[9] and spectroscopic data.[10]

[*] Dr. D. Kuck, Dipl.-Chem. A. Schuster
Fakultät für Chemie der Universität
Universitätsstrasse, D-4800 Bielefeld 1 (FRG)
Prof. Dr. A. de Meijere, Dipl.-Chem. B. Ohlhorst, Dr. V. Sinnwell
Institut für Organische Chemie der Universität
Martin-Luther-King-Platz 6, D-2000 Hamburg 13 (FRG)

[**] This work was supported by the Deutsche Forschungsgemeinschaft, the Stiftung Volkswagenwerk, the Fonds der Chemischen Industrie, Chemetall GmbH, Hoechst AG, BASF AG, and Hüls AG (donation of chemicals). *B. O.* thanks the Fonds der Chemischen Industrie for a doctoral fellowship.



Scheme 1. a) $LiNiPr_2$/THF, −40 °C → 0 °C, $(PhS)_2$/THF, room temperature (RT), 1 h (76%); b) *m*-chloroperoxybenzoic acid/CH_2Cl_2, −30 °C → RT, then 10 h (91%); c) Δ/toluene, 110 °C, 4 d (36%); d) H_2/Pd,C/dioxane, RT (71% [9]); e) $LiAlH_4/Et_2O$ [3] or $Al(OiPr)_3$/*i*PrOH/toluene [3]; f) $LiAlH_4/Et_2O$, 3 h, 36 °C (95%); g) $CuSO_4$/xylene [3]; h) H_3PO_4/xylene, 135 °C, 4 h (58%). The numbering in **2** is unsystematic; the numbers 1–10 refer to the triquinacene.

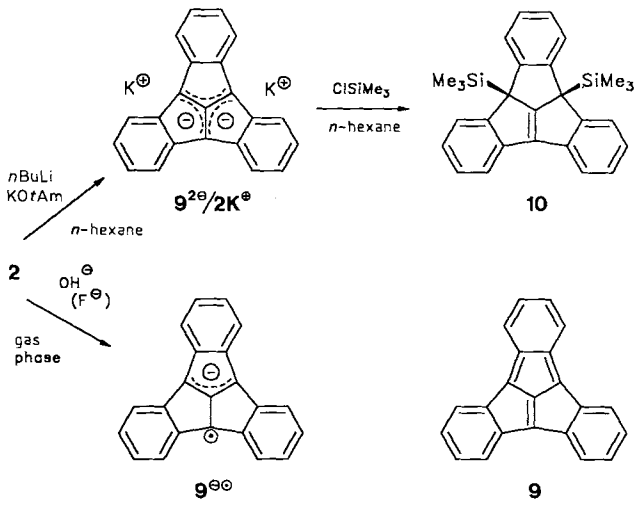
Upon treatment of a suspension of **2** in *n*-hexane with *n*-butyllithium and potassium *tert*-amyl alkoxide (molar ratio 1:4.7:2.5), the mixture turns carmine red within 30 min. After 24 h at room temperature and an additional 24 h at reflux temperature, the reaction mixture was filtered under argon. The red-brown solid was washed four times with *n*-hexane and once with diethyl ether and then dried at 40 °C/0.1 torr. In addition to dipotassium dihydrotribenzoacepentalenediide ($\mathbf{9}^{2\ominus}/2K^{\oplus}$),[11] the pyrophoric solid contained lithium and potassium as the hydrides and *tert*-amyl alkoxides, as well as, possibly, butyllithium. Despite the impurities, $\mathbf{9}^{2\ominus}$ could be unambiguously characterized by NMR spectroscopy in [D_{10}]dimethoxyethane (Table 1). Particularly surprising is the position of the signal of the central C atom (C-10) at extremely high field ($\delta = 173.17$); its assignment is confirmed by the unchanged half-width ($\nu_{1/2} = 5.5$ Hz) in the broadband- and "gated"-decoupled ^{13}C NMR spectrum. This ^{13}C chemical shift and those of the peripheral acepentalene C atoms (C-2,3,5,6,8,9) indicate that, for $\mathbf{9}^{2\ominus}$, another resonance structure besides that with Y-like delocalization[12] of the negative charges, shown here, contributes even less to the resonance hybrid than for $\mathbf{1}^{2\ominus}$.

Table 1. Characteristic NMR data for dipotassium dihydrotribenzoacepentalenediide $\mathbf{9}^{2\ominus}/2K^{\oplus}$ and its trapping product **10**. For numbering, see Scheme 1. The cross peaks of magnetically equivalent atoms are not listed separately.

$\mathbf{9}^{2\ominus}$: ^1H NMR (400 MHz, [D_{10}]DME, 293 K): $\delta = 6.69$ (AA'BB, $^3J = 5.57$ Hz, 6H, 4',5',4'',5'',4''',5'''-H), 7.74 (AA'BB', $^3J = 5.57$ Hz, 6H, 3',6',3'',6'',3''',6'''-H), ^{13}C NMR (100.62 MHz, [D_{10}]DME, 273 K, "gated"): $\delta = 99.86$ (s, $\nu_{1/2} = 9$ Hz, C-1,4,7), 113.95 (d, C-4',5',4'',5'',4''',5''', $^1J_{CH} = 146$ Hz), 119.59 (d, C-3',6',3'',6'',3''',6''', $^1J_{CH} = 146$ Hz), 137.77 (s, C-2,3,5,6,8,9), 173.17 (s, $\nu_{1/2} = 5.5$ Hz, C-10). In the H,C-COLOC spectrum[13] (SF(2) = 100.62 MHz, SF(1) = 400.14 MHz), the following cross peaks were found: C-1/3',6'-H, C-2/3',5',6'-H, C-3'/4',5'-H, C-4'/3',6'-H

10: ^1H NMR (400 MHz, [D_8]THF, 297 K): $\delta = 0.22$ (s, 18H, $Si(CH_3)_3$), 7.10 (AA'BB', $^3J = 5.8$ Hz, 2H, 4'',5''-H), 7.14 (dt, $^3J = 7.6$, $^4J = 1.1$ Hz, 2H, 3',6''-H); 7.27 (dt, $^3J = 7.6$, $^4J = 1.1$ Hz, 2H, 5',4'''-H); 7.42 (AA'BB', $^3J = 5.8$ Hz, 2H, 3'',6''-H), 7.69 (dd, $^3J = 7.4$ Hz, 2H, 6',3'''-H), 7.72 (dd, $^3J = 7.6$ Hz, 2H, 4',5'''-H). Assignment of the protons was made from the H,H COSY spectrum: ^{13}C NMR (100.62 MHz, [D_8]THF, 297 K): $\delta = 0.49$ (−, $Si(CH_3)_3$), 61.60 (0, C-4,7), 121.60 (−, C-3',6'''), 124.50 (−, C-4',5'''), 125.88 (−, C-6',3'''), 125.91 (−, C-3'',6''), 128.86 (−, C-4'',5''), 127.10 (−, C-5',4'''), 143.66 (0, C-2,9), 148.76 (0, C-5,6), 156.46 (0, C-1), 159.4 (0, C-3,8), 182.32 (0, C-10). The assignment was made from the DEPT spectrum with 135° pulse (+ = positive signal for CH_2; − = negative signal for CH, CH_3; 0 = no signal for quart. C) and a C-H correlation.—In the H,C-COLOC spectrum[13] (SF2 = 100.62 MHz, SF1 = 400.14 MHz), the following cross peaks were found: C-1/6'-H, C-2/3',5',6'-H, C-3/3',4',6'-H, C-4/CH_3,3',6''-H, C-5/5'',6''-H

The chemical proof for the constitution of $\mathbf{9}^{2\ominus}$ was accomplished, as for $\mathbf{1}^{2\ominus}$,[1] by trapping with chlorotrimethylsilane in *n*-hexane. The bis(trimethylsilyl)dihydrotribenzoacepentalene **10** (colorless crystals, m.p. 191 °C (dec.); for spectroscopic data, see Table 1), isolated in 97% yield (based on **2**), was much easier to purify than the corresponding parent compound; in addition, $\mathbf{9}^{2\ominus}/2K^{\oplus}$ is markedly more stable than $\mathbf{1}^{2\ominus}/2K^{\oplus}$. The special stabilization of $\mathbf{9}^{2\ominus}$ is also supported by the fact that it is formed from 10-methyltribenzotriquinacene[2] with formal expulsion of methane under the same conditions as it is formed from **2**.



In the gas phase, compound **2** also undergoes ready deprotonation to give the monoanion $[2-H]^{\ominus}$ under the conditions of negative chemical ionization (NCI).[14,15] Moreover, at low pressure of the reactant gas (i.e., for a higher average excitation of the $[2-H]^{\ominus}$ ions), predominant formation of $[2-2H]^{\ominus\odot}$ and $[2-4H]^{\ominus\odot}$ ions ($\triangleq \mathbf{9}^{\ominus\odot}$) is observed, indicating elimination or abstraction of up to three hydrogen atoms (see Fig. 1). Correspondingly, the NCI spectrum of 10-methyltribenzotriquinacene[2] is governed by the $[M-2H-CH_4]^{\ominus\odot}$ peak at low reactant gas pressures. Apparently, therefore, the (unsolvated!) radical anion $\mathbf{9}^{\ominus\odot}$ of

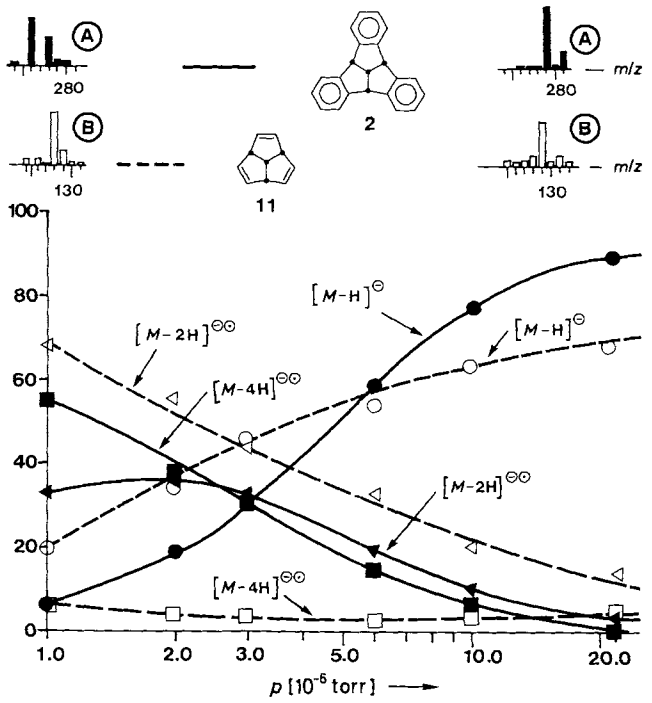


Fig. 1. Relative ion abundances in the NCI (N_2O/CH_4) mass spectra [15] of triquinacene **11** (– – –) and tribenzotriquinacene **2** (——) as a function of the (nominal) pressure of the reactant gas. (The values are ^{13}C-corrected and normalized with respect to $\Sigma[C_{22}H_x]^{\ominus}$ and $\Sigma[C_{10}H_y]^{\ominus}$, respectively.) (A) and (B): the [M – nH] region of the NCI-MS of **2** (M = 280) and **11** (M = 130), respectively.

tribenzoacepentalene **9** is very stable—in marked contrast to **1**. Under identical conditions, triquinacene **11** is deprotonated to the monoanion $[\mathbf{11}-H]^{\ominus}$, but, at lower pressure of the reactant gas, only $[\mathbf{11}-2H]^{\ominus\ominus}$ along with a small amount of $[\mathbf{11}-4H]^{\ominus\ominus}$ ($\triangleq \mathbf{1}^{\ominus\ominus}$, see Fig. 1) is formed. Accordingly, the neutral tribenzoacepentalene **9** must also be appreciably more stable than the parent system **1** and might even be detectable in pure form.

Received: November 24, 1988 [Z 3065 IE]
German version: *Angew. Chem. 101* (1989) 626

CAS Registry numbers:
2, 120022-86-8; **3**, 120057-05-8; **4**, 116665-59-9; **5**, 120022-87-9; **6**, 120057-06-9; **8**, 120057-07-0; $\mathbf{9}^{\ominus}$, 120022-88-0; $\mathbf{9}^{2\ominus}\cdot 2K^{\oplus}$, 120022-90-4; **10**, 120022-89-1.

[1] T. Lendvai, T. Friedl, H. Butenschön, T. Clark, A. de Meijere, *Angew. Chem. 98* (1986) 734; *Angew. Chem. Int. Ed. Engl. 25* (1986) 719.
[2] D. Kuck, *Angew. Chem. 96* (1984) 515; *Angew. Chem. Int. Ed. Engl. 23* (1984) 508.
[3] W. Baker, J. F. W. McOmie, S. D. Parfitt, D. A. M. Watkins, *J. Chem. Soc. 1957*, 4026.
[4] D. Kuck, A. Schuster, *Angew. Chem. 100* (1988) 1222; *Angew. Chem. Int. Ed. Engl. 27* (1988) 1192, and references cited therein.
[5] D. Kuck, *Adv. Mass Spectrom. 1986*, 773.
[6] a) B. M. Trost, T. N. Salzmann, K. Hiroi, *J. Am. Chem. Soc. 98* (1976) 4887; b) B. M. Trost, *Chem. Rev. 78* (1978) 363.
[7] a) H. J. Reich, J. M. Renga, I. L. Reich, *J. Am. Chem. Soc. 97* (1975) 5434; b) H. J. Reich, *Acc. Chem. Res. 12* (1979) 22.
[8] Compound **4** is also formed as a mixture with **5** by the route described by *Baker* et al. [3]: D. Kuck, E. Neumann, unpublished.
[9] All new compounds, except for **6** and $\mathbf{9}^{2\ominus}/2K^{\oplus}$, which were used as crude products, gave satisfactory elemental analyses.
[10] Spectroscopic data for **2**: ^1H NMR (300 MHz, $CDCl_3$): δ = 4.49 (q, ^3J = 9.7 Hz, 1H), 4.97 (d, ^3J = 9.7 Hz, 3H), 7.18, 7.46 (AA'BB', 12H). ^{13}C NMR (75.5 MHz, $CDCl_3$): δ = 51.2 (d), 56.0 (d), 124.3 (d), 127.4 (d), 145.9 (s). MS (EI, 70 eV): m/z 280 ($M^{\oplus\ominus}$, 100%), 279 (32), 278 (13), 277 (12), 276 (16), 203 (23), 202 (22). IR (KBr) [cm^{-1}]: $\tilde{\nu}$ = 3070 (w); 3020 (w), 2980 (w), 2900 (w), 1482 (m), 1476 (m), 1458 (m), 754 (s), 746 (s), 713 (m), 575 (s). UV (n-C_7H_{16}, $c = 8\times10^{-5}$ mol L^{-1}) [nm]: $\lambda_{max}(\varepsilon)$ = 276.5 (4850), 269 (3840), 263 (2350).
[11] All experimental findings indicate the presence of the dipotassium salt $\mathbf{9}^{2\ominus}/2K^{\oplus}$; cf. D. Wilhelm, T. Clark, P. von R. Schleyer, J. L. Courtneidge, A. G. Davies, *J. Organomet. Chem. 273* (1984) C1.
[12] Cf. H. Butenschön, A. de Meijere, *Helv. Chim. Acta 68* (1985) 1658.
[13] Cf. H. Kessler, C. Griesinger, J. Zarbock, H. R. Loosli, *J. Magn. Res. 57* (1984) 331.
[14] a) H. Budzikiewicz, *Angew. Chem. 93* (1981) 635; *Angew. Chem. Int. Ed. Engl. 20* (1981) 624; b) A. G. Harrison: *Chemical Ionization Mass Spectrometry*, CRC Press, Boca Raton 1983; c) H. Budzikiewicz, *Mass Spectrom. Rev. 5* (1986) 345.
[15] Measuring conditions: ZAB-2F mass spectrometer (Vacuum Generators); reactant gases CF_4 or CH_4/N_2O (1:1); reactant ions $F^{\ominus}$ and $OH^{\ominus}$, respectively; acceleration voltage 5.6 eV; electron energy 100 eV; emission 500 μA; source pressure, see Fig. 1; source temperature 190 °C. Comparative measurements (Fig. 1) were carried out with simultaneous admission of **2** and **11** (direct inlet system, 110 °C, and injection system, 150 °C, respectively).

Electron Densities, Deformation Densities, and Chemical Bonding**

By *W. H. Eugen Schwarz,* Klaus Ruedenberg, Lothar Mensching, Lance L. Miller, Petros Valtazanos,* and *Wolfgang von Niessen*

The frequently postulated relationship between electron density and chemical bonding has so far been investigated in two different, although fundamentally related, ways. According to the older method,[1,2] one uses the difference density $\Delta\varrho = \varrho_{molecule} - \Sigma\varrho_{atoms}$, where $\varrho_{molecule}$ is the electron density of the molecule and ϱ_{atom} the spherically averaged density of an unperturbed, correctly positioned atom. A chemical bond should be characterized by a positive $\Delta\varrho$ between the atoms. According to the more recent method,[3,4] instead of $\Delta\varrho$ one uses the second derivative of the molecular density $\nabla^2\varrho_{molecule}$. Large negative values of $\nabla^2\varrho_{molecule}$ between two atoms, especially in comparison with the spherically averaged atomic densities, are regarded as an indication of chemical bonding.

The ground states of most atoms with open valence shells, however, are degenerate (e.g., ^2P states for $C(1s^22s^22p^2)$ and $F(1s^22s^22p^5)$); that is, their electron density is anisotropic. The electron density of the free atoms can be oriented (e.g., F in the ^2P_z state, see Fig. 1c) without any increase in energy. Thus, molecules and crystals can be envisioned as consisting of suitably *positioned and oriented* atoms (whereby, owing to the Heisenberg uncertainty principle, even the positioning of noninteracting atoms requires the zero-point vibrational energy). The positions of the atomic cores along with their

[*] Prof. Dr. W. H. E. Schwarz, Dipl.-Chem. L. Mensching
Chemisches Institut der Universität
Postfach 101240, D-5900 Siegen (FRG)
Prof. Dr. K. Ruedenberg, Dr. P. Valtazanos, Dr. L. L. Miller
Ames Laboratory USDOE and Department of Chemistry of the Iowa State University
Ames, IA 50011 (USA)
Prof. Dr. W. von Niessen
Physikalisch-Chemisches Institut der Technischen Universität
Postfach 3329, D-3300 Braunschweig (FRG)

[**] This work was supported by the Deutsche Forschungsgemeinschaft, the U.S. Department of Energy (Office of Basic Energy Sciences, Contract No. 7405-Eng-82), NATO, and the Fonds der Chemischen Industrie. We thank Prof. Dr. *C. Krüger* for the experimental triazine data and Priv.-Doz. Dr. *B. Engelen* for helpful comments.

vibrational "smears", as well as the orientation and occupation of the open valence shells, is determined by the interactions between the atoms in the molecule or crystal. "Positional parameters" and "directional parameters" therefore provide information on these interactions. Particularly the directional parameters appear to be sensitive to the intermolecular interactions (see the discussion regarding Fig. 4b).

The interatomic interactions are often further revealed in a comparatively small deformation of the atomic electron densities. A shift of charge toward the center of the bond indicates normal covalent bonding. Constructive quantum-mechanical interference[5] of partially occupied, *strongly* overlapping, oriented AOs, as described well by the MO model, leads to an increase in density in the region of overlap and, at the same time, to a reduction in the functional describing the kinetic energy of the electrons ("electron sharing"). However, covalent bonds are also possible between partially occupied, *weakly* overlapping AOs if, owing to electron correlation, as described well in the VB model, the Coulombic repulsion between the electrons is reduced. This "correlation covalence" (e.g., in dichromium compounds[6]) is revealed to only a small extent in the charge density.

In the density analyses mentioned at the beginning, details are easily lost.[7, 8] Thus, the difference density $\Delta\varrho$ for F_2, derived from spherically averaged F-atom densities (electron configuration $1s^2 2s^2 2p_x^{5/3} 2p_y^{5/3} 2p_z^{5/3}$) shows an extreme density deficit along the bond axis and in the region of the lone pairs in σ orbitals (Fig. 1a). $\nabla^2 \varrho_{\text{molecule}}$ also fails to indicate the presence of a normal covalent bond.[8] Oriented, nonspherical F atoms ($1s^2 2s^2 2p_x^2 2p_y^2 2p_z^1$) can also be used as references, however (Fig. 1c); in this case the F–F σ bond arises quite naturally from the singly occupied F $2p_z$ AOs. The corresponding "chemical" deformation density in Figure 1b gives the characteristic charge shift for lone pairs in σ orbitals (A) as well as the small bond charge (B) characteristic of a weakly covalent σ bond.

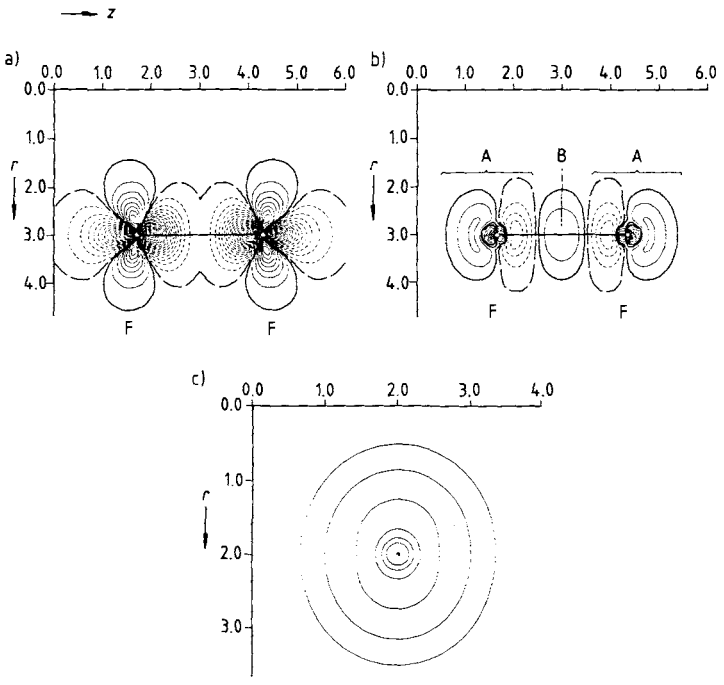


Fig. 1. Ab initio SCF electron difference densities of F_2. r in atomic units (1 a.u. = 0.529 Å). $\Delta\varrho$ values of the contour lines: —— $n \times 0.27$ eÅ^{-3} ($n = 1,2,3\ldots$), – – – – $n \times 0.27$ eÅ^{-3}, —— 0.07 Å^{-3}, – – – – 0.07 eÅ^{-3}. a) "Usual" difference densities derived from spherically averaged F-atom densities. b) "Chemical" deformation densities derived from oriented ground-state F atoms ($F\ 1s^2 2s^2 2p_x^2 2p_y^2 2p_z^1$). A = lone pair; B = bond charge. c) Total density of the oriented ground-state F atom (different scale!; $\Delta\varrho$ values of the contour lines: 0.67, 2, 6.7, 20, 67, 200 eÅ^{-3}).

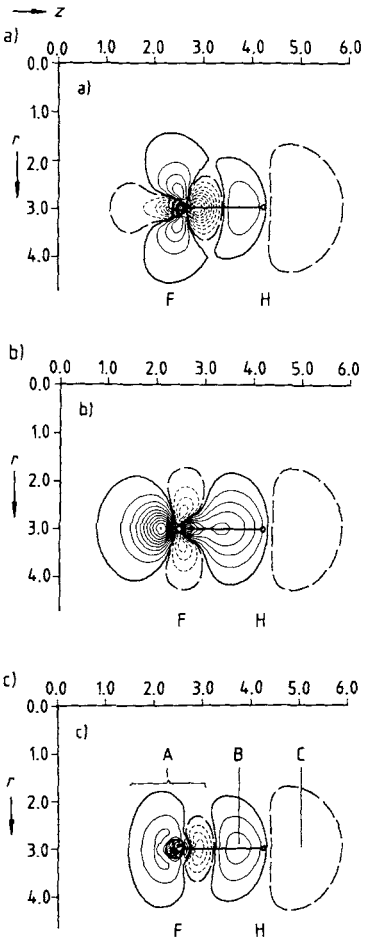


Fig. 2. Ab initio SCF electron difference densities of HF; cf. caption to Fig. 1. a) "Usual" difference densities derived from spherically averaged F-atom densities. b) "Naive" difference densities derived from maximally oriented F atom. c) "Chemical" deformation densities derived from empirically determined orientation of the F atom ($1s^2 2s^2 2p_x^{1.79} 2p_y^{1.79} 2p_z^{1.42}$). C = charge deficit of H ($H^{\delta\oplus}$).

Figure 2 shows difference densities of HF. Figure 2a was derived from spherically averaged F-atom densities and Figure 2b from completely oriented densities. Both difference densities are extremely large and hardly comparable to those in other molecules. Apparently, it is not wise to derive $\Delta\varrho$ from arbitrarily determined (spherically averaged or completely oriented) atom densities.

We have therefore developed a procedure to establish unambiguously both positions and orientations of the ground-state densities in molecules by means of an extremal principle, starting either from the calculated molecular electron density distribution[9] or from experimental X-ray diffraction data.[10] In the latter case, the coordinates and vibrational parameters of the atomic cores are fitted preferentially to the scattering data for large angles and the parameters for occupation and orientation of the valence shells to the data for small angles.

Analysis of the theoretical SCF densities of HF yields the occupation $2p_x^{1.79} 2p_y^{1.79} 2p_z^{1.42}$ for F, which represents a com-

promise between an oriented F atom in a nonpolar covalent bond and a spherical F anion in a purely ionic bond. The difference density in Figure 2c, derived for a uniquely defined, optimally oriented F atom, describes the true deformation of the atomic ground states of the HF molecule. This "chemical" deformation density displays three salient features: the charge shift characteristic of lone pairs in σ orbitals; the bond charge typical of a normally strong σ bond; and the decrease in charge density "behind" the hydrogen typical of acidic hydrogen (C).

Difference densities of singlet methylene are shown in Figure 3. For optimal fitting of the open 2p shell of the ground-state C atom to the molecular situation, which results in a 2p occupation $p_x^{0.94}p_y^{0.06}p_z^{1.00}$, the "chemical" deformation densities shown in Figures 3c and 3d are obtained. They show the charge shift typical of lone pairs in σ orbitals, the bond charge typical of a normal covalent σ bond, and the increase in density at the nuclear center typical of a neutrally bonded H atom. Figures 3a and 3b were derived for a spherically averaged C-atom density ($C\ 1s^2 2s^2 2p_x^{2/3} 2p_y^{2/3} 2p_z^{2/3}$). Again, all finer details of the molecular electron density are concealed by what is "in reality" the quadrupolar oriented electron density of the ground-state C atom in methylene.

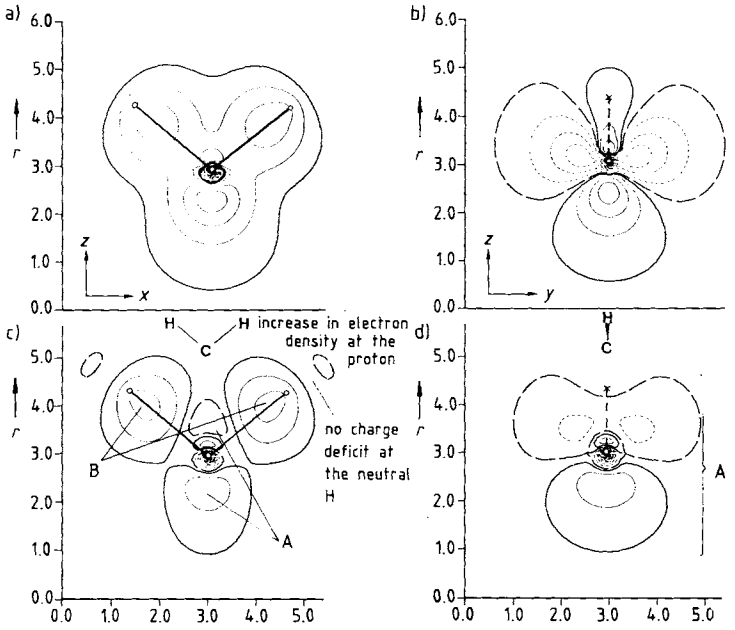


Fig. 3. Ab initio SCF electron difference densities of singlet methylene; cf. caption to Fig. 1. a) and b) "Usual" difference densities derived from spherically averaged C-atom densities ($C\ 1s^2 2s^2 2p_x^{2/3} 2p_y^{2/3} 2p_z^{2/3}$). c) and d) "Chemical" deformation densities derived from empirically optimized orientation of the ground-state C atom ($C\ 1s^2 2s^2 2p_x^{0.94} 2p_y^{0.06} 2p_z^{1.00}$).

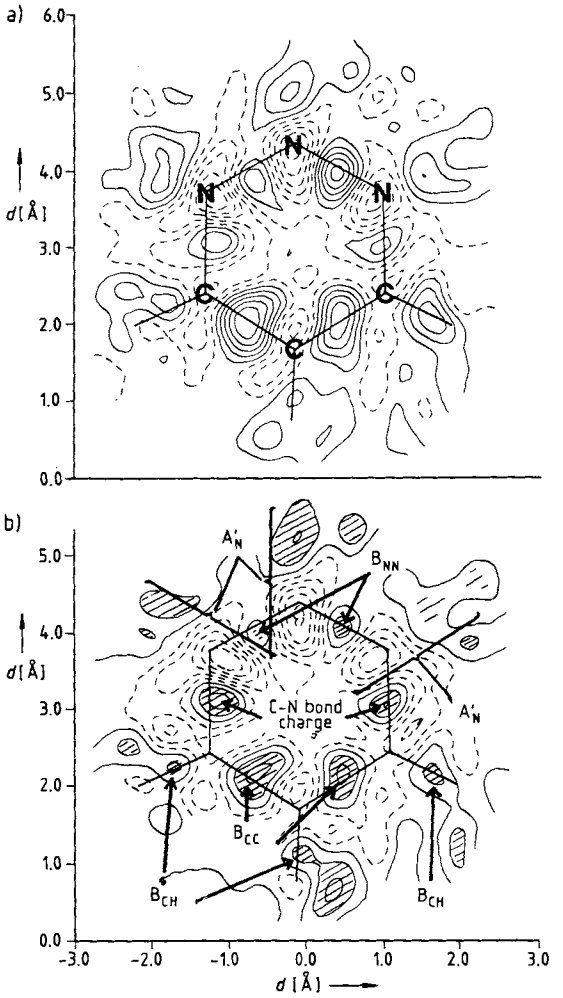


Fig. 4. Experimental static electron difference densities of 1,2,3-triazine [11]. $\Delta\varrho$ values of contour lines: —— $n \times 0.1\ e\text{Å}^{-3}$, ------ $-n \times 0.1\ e\text{Å}^{-3}$. a) "Usual" difference densities derived from spherically averaged C- and N-atom densities. b) "Chemical" deformation densities derived from oriented, optimally occupied p AOs. The curley brackets marked with A'_N indicate the dipolar charge shift corresponding to the lone pair on N. B_{CH}, B_{CC}, and B_{NN} denote the bond charges between the respective atoms.

Figure 4 shows the "experimental" difference density of 1,2,3-triazine in the standard form.[11] It is difficult to interpret in detail the pronounced qualitative asymmetry. Fitting of the p AO occupation to the molecular electron density affords $p_t^{1.08}p_r^{0.68}p_\pi^{0.24}$ for the C atoms and $p_t^{1.04}p_r^{1.42}p_\pi^{0.54}$ for the N atoms; the tangential and radial AOs, p_t and p_r, are strongly twisted, however (see Ref. [10]). The orbital occupations of the middle and terminal atoms of the E_3 units (E = C, N) do not differ significantly from each other. The high Np_r occupation is an indication of the lone pairs and also points to mixing of energetically higher-lying doublet states of the p^3 ground-state configuration of the N atom. The polarity of the molecule is reflected in the different Cp_π and Np_π occupations, whereas the p_t AOs forming the σ bonds in the ring are nearly identically occupied. The corresponding "chemical" deformation density in Figure 4b reflects the nearly ideal symmetry of the molecular framework in the crystal. The bond charges decrease on going from C-C to C-N to N-N. The strong interactions between the molecules in the crystal are manifested in the different twistings of the p AOs from the symmetry-adapted positions,[10] but influence the "chemical" deformation densities to only a small extent.

Electron densities allow the characterization of covalent bonds of "normal MO type" as well as of intermolecular interactions. The prerequisite for the reasonable construction and discussion of difference densities, however, is not to derive these arbitrarily from spherically averaged atomic ground-state densities. Combined refinement starting from the experimental or theoretical electron density data of a molecule allows the determination of not only the positional parameters of the atoms but also their respective directional parameters and quadrupole moments. Qualitative atomic

 © VCH Verlagsgesellschaft mbH, D-6940 Weinheim, 1989 0570-0833/89/0505-0599 $ 02.50/0

parameters as well as qualitative deformation density maps that are readily interpretable in chemical terms can then be obtained.

Received: August 8, 1988;
revised: January 11, 1989 [Z 2960 IE]
German version: *Angew. Chem. 101* (1989) 605

[1] R. F. W. Bader in B. M. Deb (ed.): *The Force Concept in Chemistry*, Van Nostrand-Reinhold, New York 1981, p. 39.
[2] P. Coppens, M. B. Hall: *Electron Distributions and the Chemical Bond*, Plenum, New York 1982.
[3] R. F. W. Bader, T. T. Nguyen-Dong, *Adv. Quantum Chem. 14* (1981) 63.
[4] D. Cremer, E. Kraka, *Croat. Chem. Acta 57* (1984) 1259.
[5] K. Ruedenberg, *Rev. Mod. Phys. 34* (1962) 326; W. Kutzelnigg, *Angew. Chem. 85* (1973) 551; *Angew. Chem. Int. Ed. Engl. 12* (1973) 546.
[6] R. A. Kok, *Dissertation*, A and M University, College Station, Texas, 1984; D. R. Salahub, *Adv. Chem. Phys. 69* (1987) 447.
[7] J. D. Dunitz, P. Seiler, *J. Am. Chem. Soc. 105* (1983) 7056; J. D. Dunitz, W. B. Schweizer, P. Seiler, *Helv. Chim. Acta 66* (1983) 123.
[8] D. Cremer, E. Kraka, *Angew. Chem. 96* (1984) 612; *Angew. Chem. Int. Ed. Engl. 23* (1984) 627; R. F. W. Bader, H. Essen, *J. Chem. Phys. 80* (1984) 1943.
[9] W. H. E. Schwarz, L. Mensching, P. Valtazanos, W. von Niessen, *Int. J. Quantum Chem. 30* (1986) 439; L. Mensching, W. von Niessen, P. Valtazanos, K. Ruedenberg, W. H. E. Schwarz, *J. Am. Chem. Soc.* (1989), in press.
[10] L. L. Miller, *Ph.D. Thesis*, Iowa State University, Ames, IA, USA 1988; K. Ruedenberg, W. H. E. Schwarz, unpublished; L. L. Miller, K. Ruedenberg, R. Jacobson, unpublished.
[11] K. Angermund, K. H. Claus, R. Goddard, C. Krüger, *Angew. Chem. 97* (1985) 241; *Angew. Chem. Int. Ed. Engl. 24* (1985) 237.

$P_6(C_5Me_5)_2$, a Tricyclic Polyphosphane

By *Peter Jutzi,* Rainer Kroos, Achim Müller,* and *Michael Penk*

Our detailed knowledge on cyclic polyphosphanes is due primarily to the extensive investigations of *M. Baudler* and her co-workers.[1] The structural diversity of this class of compounds is fascinating and is only exceeded by that of cyclic hydrocarbons. We describe here a preparatively simple route to a tricyclohexaphosphane with a previously unknown type of structure.

Upon heating tris(pentamethylcyclopentadienyl)cyclotriphosphane **1**[2] for several hours in refluxing benzene, 2,3,4,6-tetrakis(pentamethylcyclopentadienyl)bicyclo[3.1.0]-hexaphosphane **2** is formed in nearly quantitative yield [Eq. (a)]. Compound **2** crystallizes from *n*-hexane as yellow needles (mp. 98 °C (dec.), sealed tube), which are only slightly sensitive to air. The structure of **2** was determined by analysis of the two-dimensional ^{31}P–^{31}P shift-correlated NMR spectrum (COSY type) and from an X-ray structure analysis.[3] The structure is similar to that of P_6tBu_4,[4] the only compound so far known with this structure.

$$2\,(PC_5Me_5)_3 \xrightarrow[-(C_5Me_5)_2]{\Delta} P_6(C_5Me_5)_4 \xrightarrow[-(C_5Me_5)_2]{\Delta} P_6(C_5Me_5)_2 \quad (a)$$

1 **2** **3**

Thermolysis of **2** in refluxing xylene leads to the formation of 3,4-bis(pentamethylcyclopentadienyl)tricyclo[3.1.0.0^{2,6}]-hexaphosphane **3** in 46% yield [Eq. (a)]. Compound **3** is obtained from *n*-hexane as bright yellow rhombic crystals (m.p. 183 °C (dec.), sealed tube), which are only slightly sensitive to air.[5] Like **2**, compound **3** ist very soluble in aromatic hydrocarbons and in THF but less soluble in *n*-hexane. The structure was again elucidated by NMR spectroscopy and by X-ray structure analysis.

The 121-MHz ^{31}P NMR spectrum of **3** exhibits three groups of mirror-symmetric signals at $\delta = 105$, 70, and -237 (intensities 1:1:1). The high-field signal is a triplet, that at $\delta = 70$ corresponds to an AA'BB' system, and that at $\delta = 105$ is a complex multiplet.[6] The extreme high-field shift of one signal group and the high symmetry of the spectrum indicate that **3** has a tricyclo[3.1.0.0^{2,6}]hexaphosphane-type structure. The connectivity of the phosphorus atoms is revealed by analysis of the two-dimensional $^{31}P-^{31}P$ shift-correlated NMR spectrum (COSY type). Owing to the asymmetric environment of the two organosubstituted phosphorus atoms in **3**, both the sp^2 carbon atoms of the prochiral pentamethylcyclopentadienyl rings and their respective methyl groups are expected to be magnetically nonequivalent and diastereotopic. The ^{13}C NMR spectrum displays the four signals corresponding to the sp^2 carbon atoms. The mass spectrum of **3** shows, in addition to the molecular-ion ($M^{\oplus}$) peak, the peaks of the fragments $M^{\oplus} - C_5Me_5$ and $C_5Me_5^{\oplus}$.

The X-ray structure analysis[7] of **3** corroborates the structure determined from the spectroscopic data (Fig. 1). The P_2

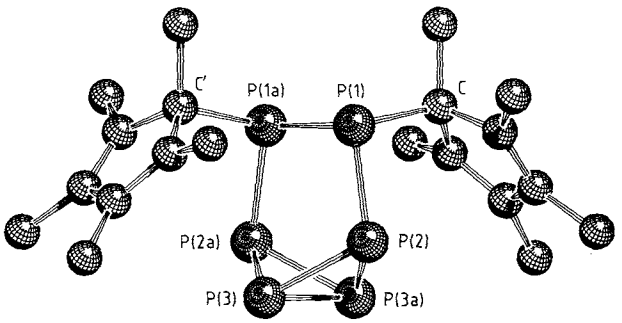


Fig. 1. The molecular structure of **3** [8]. Important bond lengths [Å], bond angles [°], and torsional angles [°]: P(1)–P(1a) 2.160 (2), P(1)–P(2) 2.184 (1), P(2)–P(3) 2.195 (1), P(2)–P(3a) 2.191(1), P(3)–P(3a) 2.192 (2); P(3)–P(3a)–P(2a) 59.9 (1), P(3)–P(2a)–P(3a) 60.0 (1), P(2a)–P(3)–P(3a) 60.1 (1), P(1)–P(2)–P(3) 107.3 (1), P(1)–P(2)–P(3a) 103.8(1), P(1a)–P(1)–P(2) 103.6 (1), P(2a)–P(3)–P(2) 94.2 (1), P(2)–P(1)–C 101.6 (1), P(1a)–P(1)–C 104.4 (1); P(2)–P(1)–P(1a)–P(2a) 10.7, C–P(1)–P(1a)–C' 158.6.

bridge results in an *endo–endo* substitution that is novel for phosphorus compounds with the bicyclo[1.1.0]tetraphosphane ("butterfly") structural element. This is markedly reflected in the ^{31}P NMR signals of the peripheral phosphorus atoms ($\delta = 105$), which are shifted strongly downfield compared with those of other phosphorus butterfly compounds.[2, 9]

The phosphorus–phosphorus bonds in **3** (average 2.187 Å) are significantly shorter than in **2** (average 2.225 Å) or P_4 (2.21 Å). Surprisingly, the bond between the two organosubstituted phosphorus atoms (2.160 Å) is quite short. The folding angle between the phosphorus triangles is 115.5° and is therefore 10° larger than in other structurally characterized phosphorus butterfly compounds.[9a, b, 10] The transannular phosphorus–phosphorus distance (P(2)-P(2a)) is 3.212 Å. Compound **3** can be viewed as a phospho-

[*] Prof. Dr. P. Jutzi, Dipl.-Chem. R. Kroos, Prof. Dr. A. Müller[+], Dipl.-Chem. M. Penk[+]
Fakultät für Chemie der Universität
Universitätsstrasse, D-4800 Bielefeld
[+] X-ray structure analysis

rus analogue of 3,4-dihydrobenzvalene or as a P_4 tetrahedron open at one edge and bridged by a P_2R_2 unit. The considerable stability of 3 toward air may be ascribed to the good steric shielding of the phosphorus framework by the pentamethylcyclopentadienyl ligands.

The syntheses of **2** and **3** from **1** are further examples of the preparative utility of the labile phosphorus–carbon bond in pentamethylcyclopentadienyl-substituted phosphorus compounds.[9c, 11] Clearly, the new cyclophosphanes **2** and **3** with their functionalized P_6R_x frameworks have promising synthetic potential.[11d]

Experimental Procedure

2: A solution of **1** (3.40 g, 6.82 mmol) in 35 mL of benzene was refluxed for 20 h. The solvent was then removed under vacuum from the clear, orange reaction solution until the viscous residue (ca. 3.5 g) began to form bubbles. Shortly after addition of 7 mL of *n*-hexane, the deep orange oil solidified to a yellow crystalline mass. After removal of the supernatant liquid, **2** was recrystallized from *n*-hexane. Yield: 2.05 g (66%) **2** · *n*-C_6H_{14}; correct elemental analysis. ^{1}H NMR (300 MHz, C_6D_6): δ = 0.9–2.2 (complex multiplet; C_5Me_5, *n*-C_6H_{14}). ^{13}C NMR (75 MHz, C_6D_6): δ = 11.0–23.0 (Me), 57.4–59.7 (P-C), 134.8, 135.5, 136.0, 136.4, 139.7, 141.0, 141.6, 141.7 (sp^2-C). ^{31}P NMR (121 MHz, C_6D_6): δ = 78 (2P), 60 (1P), –121 (2P), –129 (1P). MS (*m/z*; rel. int.): $P_6(C_5Me_5)_3^{\oplus}$ (591; 18), $P_6(C_5Me_5)_2^{\oplus}$ (456; 2), $P_3(C_5Me_5)_2^{\oplus}$ (363; 4), $P_6(C_5Me_5)^{\oplus}$ (321; 34), $C_5Me_5^{\oplus}$ (135; 100).

3: **2** · *n*-C_6H_{14} (5.50 g, 6.77 mmol) was refluxed in 70 mL of xylene for 45 min. After removal of the solvent, the orange residue was treated with 20 mL of *n*-hexane. The precipitated pale yellow powder (ca. 2.5 g) was filtered off and recrystallized several times from *n*-hexane. Yield: 1.42 g (46%) **3**; correct elemental analysis. ^{1}H NMR (300 MHz, C_6D_6): δ = 1.3–2.1, ^{13}C NMR (75 MHz, C_6D_6): δ = 10.9–21.7 (Me), 57.4 (P-C), 136.8, 137.7, 139.5, 140.2 (sp^2-C). ^{31}P NMR (121 MHz, C_6D_6): δ = 105, 70, –237 (intensities 1:1:1). MS (*m/z*; rel. int.): $M^{\oplus}$ (456; 9), $P_6(C_5Me_5)^{\oplus}$ (321; 44), $C_5Me_5^{\oplus}$ (135; 100).

Received: November 28, 1988 [Z 3070 IE]
German version: *Angew. Chem. 101* (1989) 628

CAS Registry numbers: **1**, 114029-17-3; **2**, 113924-88-2; **3**, 120295-56-9.

[1] Reviews: a) M. Baudler, *Angew. Chem.99* (1987) 429; *Angew. Chem. Int. Ed. Engl. 26* (1987) 419; b) *Z. Chem. 24* (1984) 352; c) *ACS Symp. Ser. 171* (1981) 261; d) *Angew. Chem. 94* (1982) 520; *Angew. Chem. Int. Ed. Engl. 21* (1982) 492; e) *Pure Appl. Chem. 52* (1980) 755.

[2] P. Jutzi, T. Wippermann, *J. Organomet. Chem. 287* (1985) C5.

[3] P. Jutzi, R. Kroos, A. Müller, H. Bögge, unpublished.

[4] a) M. Baudler, Y. Aktalay, K.-F. Tebbe, T. Heinlein, *Angew. Chem. 93* (1981) 1020; *Angew. Chem. Int. Ed. Engl. 20* (1981) 967; b) K.-F. Tebbe, T. Heinlein, *Z. Kristallogr. 160* (1982) 285.

[5] The thermolysis of **1** in xylene instead of benzene leads directly to **4**. The bis(pentamethylcyclopentadienyl) formed according to Equation (a) can be detected in the reaction solution in each case.

[6] The approximate contributions of the coupling constants were determined by analysis of the spectrum according to the rules for first-order spectra. Refinement of the parameters with the computer program PANIC (version 840419.0; Bruker) led to complete agreement of the calculated with the recorded NMR spectrum. AA'BB'X_2-type spectrum: contributions of the coupling constants in Hz (numbering of the centers as in Fig. 1): ^1J(P(1), P(2)) = ^1J(P(1a),P(2a)) = 387, ^1J(P(2),P(3, 3a)) = ^1J(P(2a),P(3, 3a)) = 217, ^1J(P(1), P(1a)) = 386, ^2J(P(1), P(2a)) = ^2J(P(1a), P(2)) = 8, ^2J(P(1), P(3, 3a)) = ^2J(P(1a), P(3, 3a)) = 0.5, ^2J(P(2), P(2a)) = 56.

[7] **3** forms monoclinic crystals: *C2/c*, a = 1104.4, b = 1308.2, c = 1684.2 pm, β = 106.4°, V = 2334.4 × 10^6 pm^3, Z = 4, ρ_{calcd} = 1.30 g cm^{-3}; solution of the structure by direct methods (SHELXTL), R = 0.052 for 1939 unique reflections with $F_o > 3.92\,\sigma(F_o)$, Syntex $P2_1$ four-circle diffractometer, $Mo_{K\alpha}$ radiation, graphite monochromator. Further details of the crystal structure investigation may be obtained from the Fachinformationszentrum Energie, Physik, Mathematik GmbH, D-7514 Eggenstein-Leopoldshafen 2 (FRG), on quoting the depository number CSD-53719, the names of the authors, and the journal citation.

[8] Drawn with the SCHAKAL 88 computer program.

[9] a) E. Niecke, R. Rüger, B. Krebs, *Angew. Chem. 94* (1982) 553; *Angew. Chem. Int. Ed. Engl. 21* (1982) 544; b) R. Riedel, H.-D. Hausen, E. Fluck, *ibid. 97* (1985) 1050, and *24* (1985) 1056; c) P. Jutzi, U. Meyer, *J. Organomet. Chem. 333* (1987) C18.

[10] E. Fluck, R. Riedel, H.-D. Hausen, G. Heckmann, *Z. Anorg. Allg. Chem. 551* (1987) 85.

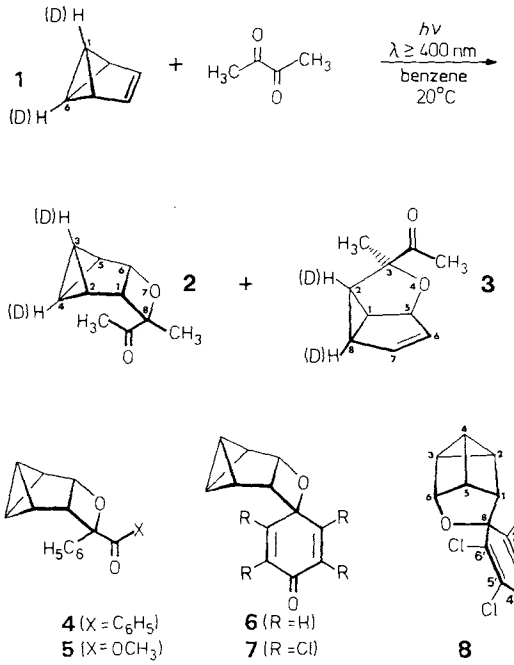
[11] a) P. Jutzi, U. Meyer, *Angew. Chem. 98* (1986) 894; *Angew. Chem. Int. Ed. Engl. 25* (1986) 919; b) P. Jutzi, H. Saleske, U. Meyer, *Phosphorus Sulfur 30* (1987) 161; c) P. Jutzi, U. Meyer, *Chem. Ber. 121* (1988) 559; d) P. Jutzi, R. Kroos, *ibid. 121* (1988) 1399.

Photocycloadditions of Benzvalene**

By *Manfred Christl** and *Max Braun*

In 1975, *Katz* and *Turro* et al.[1] reported that the sensitized photolysis of benzvalene **1** can lead to two rearrangements. Transformation to benzene occurs with sensitizers with a triplet energy $E_T > 65$ kcal mol^{-1}, whereas automerization (1,3-C migration) is induced by those with $E_T <$ 63 kcal mol^{-1}. Although the sensitizers used were mainly ketones, which are typical substrates for the Paterno–Büchi reaction,[2] the authors mentioned no products with oxetane structure. In view of the high reactivity of benzvalene toward a wide variety of electrophiles,[3] we wanted to know whether, besides the isomerizations noted above, photochemical cycloadditions of **1** take place.

Irradiation[4] of **1**[5] in the presence of acetone and benzophenone (E_T = 78 and 69 kcal mol^{-1}, respectively[2a]) resulted in the formation of benzene. However, with biacetyl (E_T = 56 kcal mol^{-1}[2a]), benzil (54 kcal mol^{-1}[2a]), methyl phenylglyoxylate (61.9 kcal mol^{-1},[6a] irradiation at –30 °C), 1,4-benzoquinone (50 kcal mol^{-1}[2a]), and chloranil (56.4 kcal mol^{-1},[6b] irradiation at –30 °C), the oxetanes **2** (19%), **4** (22%), **5** (38%), **6** (25%), and **7** (51%), respectively, were obtained.[7] In the experiment with biacetyl, we observed, in addition to **2**, the oxadihydrosemibullvalene **3** (**2**:**3** ≈ 30:1), which is also accessible, together with a small amount of its diastereomer, in 48% yield by treatment of **2** with $AgBF_4$ in $CDCl_3$ at 20 °C.[7] The experiment with chloranil afforded pure **7** only at –30 °C; at 20 °C, besides **7**, the rearrangement product **8**[7] (**7**:**8** = 4:1) was formed. For selected physical data for **2**–**8**, see Table 1.

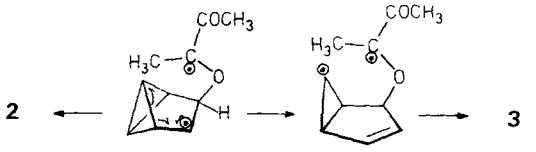


4 (X = C_6H_5)
5 (X = OCH_3)
6 (R = H)
7 (R = Cl)
8

[*] Prof. Dr. M. Christl, Dipl.-Chem. M. Braun
Institut für Organische Chemie der Universität
Am Hubland, D-8700 Würzburg (FRG)

[**] This work was supported by the Fonds der Chemischen Industrie and the Deutsche Forschungsgemeinschaft.

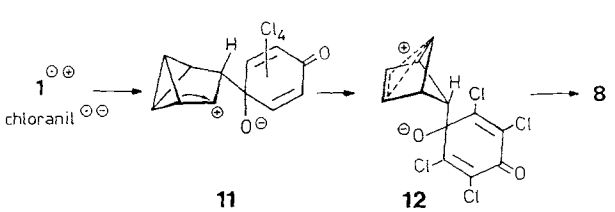
The formation of **3** confirms the multistep mechanism of the Paterno–Büchi reaction.[2] Compound **1** and biacetyl in its triplet state presumably give the diradical **9**, which can then either cyclize to **2** or undergo a cyclopropylmethyl–homoallyl rearrangement,[3a] to afford **10**, provided that, of the two C–C bonds in question in **9**, the bond *cis* to the biacetyl moiety breaks. Diradical **10** would then collapse to **3**. In agreement with this mechanism, [1,6-D_2]benzvalene yields the dideuterated products [3,4-D_2]-**2** and [2,8-D_2]-**3**.



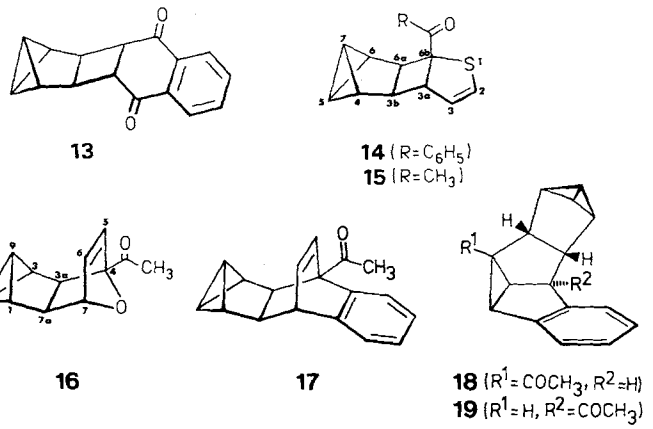
9 **10**

The finding that the labels in **2** are limited to positions 3 and 4[8] rules out the automerization of **1** by the excited sensitizer biacetyl. We arrived at the same conclusion by recovering unused [D_2]-**1** and allowing it to react with 2,4,6-trimethylbenzonitrile oxide. In the resulting dihydroisoxazole,[9] we found the deuterium atoms also restricted to the bicyclobutane bridgehead positions.[8] Interestingly, *Katz* and *Turro* et al.[1] included biacetyl in their table of sensitizers but did not enter a quantum yield for the automerization of **1**. The latter was given as ca. 0.2 for benzil as sensitizer. We have now confirmed that excited benzil effects the automerization of **1**. Adduct [D_2]-**4** was obtained from [1,6-D_2]-**1** with the ratio of the labels in positions 1 (6), 2 (5), and 3 (4) being 1:3:45.[8] Analysis of the 2,4,6-trimethylbenzonitrile oxide adduct revealed that the labels in unused [D_2]-**1** were more evenly distributed, namely in a ratio of 1:2:4 in the positions corresponding to those in **4**.[8] Irradiation of 1,4-benzoquinone and 2-benzoylthiophene (see below) in the presence of [1,6-D_2]-**1** did not lead to a 1,3-C migration in [1,6-D_2]-**1**. Whether benzvalene **1** undergoes automerization in the presence of ketones in the triplet state (E_T < 63 kcal mol^{-1}), therefore, is a question of relative reaction rates. With biacetyl, 1,4-benzoquinone, and 2-benzoylthiophene, the cycloaddition occurs appreciably faster than the energy transfer required for automerization of **1**; the two rates are similar in the case of benzil.

The structure of the product **8** indicates that it is not formed via a diradical analogous to **9**. A radical ion pair is known to be formed upon irradiation of chloranil in the presence of a donor;[10a] for **1** as donor, this was shown by CIDNP signals of **1** and benzene.[10b] Thus, **8** is presumably formed via the radical ion pair, which collapses to zwitterion



11 **12**



13 **14** (R=C_6H_5) **15** (R=CH_3) **16** **17** **18** (R^1=$COCH_3$, R^2=H) **19** (R^1=H, R^2=$COCH_3$)

Table 1. Selected physical data for **2**–**8** and **13**–**19**; the boiling point always refers to the temperature measured in the kugelrohr distillation apparatus; the assignment of the bands in the NMR spectra is based on NOE effects and ^{1}H–^{13}C correlations.

2: b.p. 30–50 °C/0.05 torr. IR (CCl_4): $\tilde{\nu}$ = 1713 cm^{-1} (C=O). ^{1}H NMR (200 MHz, $CDCl_3$): δ = 1.45 (s; 8-CH_3), 2.12 (dtt, J(3,4) = 8.8, J(2,4) = J(4,5) = 1.8, J(1,4) = J(4,6) = 1.0 Hz; 4-H), 2.17 (br.dt, J(2,3) = J(3,5) = 1.7 Hz, 3-H), 2.25 (s; CO–CH_3), 2.31 (br.dq, J(2,5) = 4.5, J(1,2) = 1.7 Hz; 2-H), 2.54 (dq, J(5,6) = 1.8 Hz; 5-H), 2.69 (ddd, J(1,6) = 6.0 Hz; 1-H), 4.71 (br.dd; 6-H). ^{13}C NMR (50 MHz, $CDCl_3$): δ = 1.2 (C-4), 8.8 (C-3), 24.8 and 25.2 (2 CH_3), 35.8 (C-2), 40.5 (C-5), 49.8 (C-1), 80.1 (C-6), 87.2 (C-8), 213.6 (C=O)

3: b.p. 30–50 °C/0.05 torr. IR (CCl_4): $\tilde{\nu}$ = 1710 cm^{-1} (C=O). ^{1}H NMR (200 MHz, $CDCl_3$): δ = 1.40 (s; 3-CH_3), 2.05 (dddd, J(2,8) = 6.6, J(1,8) = 6.0, J(7,8) = 2.4, J(6,8) = 0.6 Hz; 8-H), 2.17 (s; CO–CH_3), 2.27 (ddd, J(1,2) = 7.7, J(2,6) = 0.6 Hz; 2-H), 2.96 (dddd, J(1,5) = 4.9, J(1,6) = 0.5 Hz; 1-H), 5.19 (ddd, J(5,6) = 2.0, J(5,7) = 0.6 Hz; 5-H), 5.46 (ddq, J(6,7) = 5.4 Hz; 6-H), 5.84 (ddd; 7-H). ^{13}C NMR (50 MHz, $CDCl_3$): δ = 25.8 and 26.5 (2 CH_3), 31.7, 36.6 and 46.0 (C-1, C-2, C-8), 87.0 (C-5), 90.2 (C-3), 130.0 and 135.9 (C-6, C-7), 215.1 (C=O)

4: m.p. 85–86 °C. IR (KBr): $\tilde{\nu}$ = 1670 cm^{-1} (C=O)

5: m.p. 62–63 °C. IR (KBr): $\tilde{\nu}$ = 1735 cm^{-1} (C=O)

6: m.p. 72–73 °C. IR (KBr): $\tilde{\nu}$ = 1667, 1661 (C=O), 1627, 1602 cm^{-1} (C=C)

7: m.p. 140–142 °C. IR (KBr): $\tilde{\nu}$ = 1678 (C=O), 1600, 1568 cm^{-1} (C=C)

8: m.p. 163–165 °C. IR (KBr): $\tilde{\nu}$ = 1680 (C=O), 1607, 1574 cm^{-1} (C=C). ^{1}H NMR (400 MHz, C_6D_6): δ = 1.19 (dddd, J(2,5) = 4.7, J(2,3) = 4.5, J(2,4) = 3.2, J(1,2) = 2.6 Hz; 2-H), 1.70 (tdd, J(3,5) = 4.5, J(3,4) = 3.2, J(3,6) = 2.2 Hz; 3-H), 1.98 (td, J(4,5) = 1.0 Hz; 4-H), 2.14 (dd, J(1,5) = 4.5 Hz; 1-H), 2.60 (quint. d, J(5,6) = 4.7 Hz; 5-H), 4.58 (dd; 6-H). ^{13}C NMR (50 MHz, $CDCl_3$): δ = 15.5 and 17.3 (C-2, C-3), 22.3 (C-4), 48.6 (C-5), 59.7 (C-1), 82.4 (C-6), 87.3 (C-8), 128.8 and 131.1 (C-3′, C-5′),153.4 and 153.7 (C-2′, C-6′), 169.9 (C-4′)

13: m.p. 155–156 °C. IR (KBr): $\tilde{\nu}$ = 1665 (C=O), 1592, 1585 cm^{-1} (C=C)

14: m.p. 108–110 °C. IR (KBr): $\tilde{\nu}$ = 1679 (C=O), 1594, 1578 cm^{-1} (C=C). ^{1}H NMR (200 MHz, $CDCl_3$): δ = 1.86 (br.s, 5-H, 7-H), 1.94 (dq, J(4,6) = 4.3, J(6,6a) = J(5,6) = J(6,7) = 1.7 Hz; 6-H), 2.29 (dq, J(4,5) = J(3b, 4) = J(4,7) = 1.7 Hz; 4-H), 2.38 (ddd, J(3b,6a) = 7.3, J(3a,3b) = 3.8 Hz; 3b-H), 3.11 (br.d; 6a-H), 3.86 (≈ tt, J(3,3a) = 3.5, J(2,3a) ≈ J(3a,6a) ≈ 1.1 Hz; 3a-H), 5.63 (dd, J(2,3) = 5.9 Hz; 3-H), 6.09 (dd; 2-H), 7.47 (*m*-H), 7.54 (*p*-H), 7.91 (*o*-H). ^{13}C NMR (50 MHz, $CDCl_3$): δ = 0.9 (C-7), 6.6 (C-5), 37.3 (C-6), 38.3 (C-4), 45.9 (C-3b), 52.7 (C-3a), 55.8 (C-6a), 63.0 (C-6b), 123.7 (C-3), 124.9 (C-2), 128.6 (*m*-C), 128.9 (*o*-C), 133.0 (*p*-C), 135.1 (*ipso*-C), 195.5 (C=O)

15: b.p. 50–80 °C/0.01 torr. IR (neat): $\tilde{\nu}$ = 1705 cm^{-1} (C=O).

16: b.p. 80 °C/0.01 torr. IR (CCl_4): $\tilde{\nu}$ = 1711 cm^{-1} (C=O). ^{1}H NMR (440 MHz, C_6D_6): δ = 1.35 (dtd, J(1,3) = 4.5, J(1,2) = J(1,9) = 1.8, J(1,7a) = 1.0 Hz; 1-H), 1.63 (dtt, J(2,9) = 8.3, J(3,9) = 1.8, J(3a,9) = J(7a,9) = 1.2 Hz; 9-H), 1.68 (dt, J(2,3) = 1.8 Hz; 2-H), 1.84 (≈ dq, J(3,3a) = 1.1 Hz; 3-H), 2.07 (s; CH_3), 2.53 (dt, J(3a,7a) = 8.1 Hz; 3a-H), 2.58 (ddt, J(7,7a) = 4.6 Hz; 7a-H), 4.39 (dd, J(6,7) = 1.7 Hz; 7-H), 5.81 (dd, J(5,6) = 5.7 Hz; 6-H), 6.20 (d; 5-H). ^{13}C NMR (50 MHz, $CDCl_3$): δ = 5.6 and 9.3 (C-2, C-9), 25.9 (CH_3), 33.3 and 33.8 (C-1, C-3), 49.8 (C-7a), 51.9 (C-3a), 80.4 (C-7), 94.4 (C-4), 132.6 and 134.2 (C-5, C-6), 207.6 (C=O)

17: b.p. 140 °C/0.01 torr. IR (CCl_4): $\tilde{\nu}$ = 1711 cm^{-1} (C=O)

18: m.p. 128–130 °C. IR (KBr): $\tilde{\nu}$ = 1676 cm^{-1} (C=O)

19: oil. IR (CCl_4): $\tilde{\nu}$ = 1708 cm^{-1} (C=O)

11. A Wagner–Meerwein rearrangement in the cationic moiety of **11** involving migration of the bicyclobutane bridgehead carbon atom *trans* to the anionic moiety[3] would then have to occur to give **12**, which would subsequently yield **8**.

In contrast to the reaction with 1,4-benzoquinone, irradiation[4] of **1**[5] with 1,4-naphthoquinone (E_T = 57 kcal mol^{-1}[6c]) at −30 °C gave the cyclobutane **13**[7] (17%). Motivated by the work of *Cantrell*,[11] we also employed 2-benzoylthiophene (62.6 kcal mol^{-1}[11]) at room temperature as well as 2-acetylthiophene (64.5 kcal mol^{-1}[11]) and 2-acetylfuran (64.9 kcal mol^{-1}[11]) at −30 °C and obtained the [2 + 2] cycloadducts **14** (21%), and **15** (27%) as well as the [4 + 2] cycloadduct **16** (19%) together with its diastereomer (6%).[7] At −30 °C, excited 1-acetylnaphthalene (56.4 kcal mol^{-1}[6a]) and **1**[5] gave initially the [4 + 2] cycloadduct **17** (25%). Upon further irradiation, however, **17** was converted at a similar rate into **18** (41%) and **19** (9%)[7] (di-π-methane rearrangement). Selected physical data for **13**–**19** are given in Table 1.

We obtained no cycloadduct from **1** and cyclopent-2-en-1-one (E_T = 74 kcal mol^{-1}[2a]). In conclusion, **1**, too, can undergo photochemical cycloadditions, provided that the reaction partner has a triplet energy E_T < 65 kcal mol^{-1}.

Received: December 7, 1988 [Z 3078 IE]
German version: *Angew. Chem. 101* (1989) 636

CAS Registry numbers: **1**, 659-85-8; **2**, 120229-54-1; **3** isomer 1, 120229-55-2; **3** isomer 2, 120328-37-2; **4**, 120229-56-3; **5**, 120229-57-4; **6**, 120229-58-5; **7**, 120262-48-8; **8**, 120229-59-6; **13**, 120229-60-9; **14**, 120229-61-0; **15**, 120229-62-1; **16** isomer 1, 120229-63-2; **16** isomer 2, 120328-38-3; **17**, 120229-64-3; **18**, 120262-49-9; **19**, 120220-65-4; $(MeCO)_2$, 431-03-8; $(PhCO)_2$, 134-81-6; methylphenylglyoxylate, 15206-55-0; 1,4-benzoquinone, 106-51-4; chloranil, 118-75-2, 1,4-naphthoquinone, 130-15-4; 2-benzoylthiophene, 135-00-2; 2-acetylthiophene, 88-15-3; 2-acetylfuran, 1192-62-7; 1-acetylnaphthalene, 941-98-0.

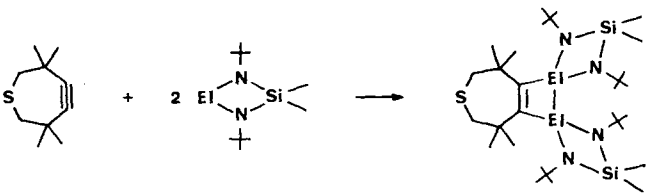
[1] C. A. Renner, T. J. Katz, J. Pouliquen, N. J. Turro, W. H. Waddell, *J. Am. Chem. Soc. 97* (1975) 2568.
[2] a) N. J. Turro: *Modern Molecular Photochemistry*, Benjamin/Cummings, Menlo Park, 1978; b) W. M. Horspool (Ed.): *Synthetic Organic Photochemistry*, Plenum Press, New York 1984.
[3] a) M. Christl, *Angew. Chem. 93* (1981) 515; *Angew. Chem. Int. Ed. Engl. 20* (1981) 529, and references cited therein; b) M. Christl, E. Brunn, F. Lanzendörfer, *J. Am. Chem. Soc. 106* (1984) 373.
[4] Light sources: medium-pressure Hg lamp (Hanovia, 450 W) in a Pyrex immersion well; radiation with λ < 400 nm was filtered out for colored substrates. 1,4-Naphthoquinone and 1-acetylnaphthalene were irradiated in a Rayonet® RPR 100 photoreactor with 350-nm and 300-nm light, respectively.
[5] We used **1** as a solution in hexane, which was diluted with the same or up to a fivefold quantity of benzene (experiments at room temperature) or toluene (experiments at −30 °C). The solutions, which were saturated with nitrogen before photolysis, were ca. 0.10 M in **1** and 0.05 M in the carbonyl compound.
[6] a) W. G. Herkstroeter, A. A. Lamola, G. S. Hammond, *J. Am. Chem. Soc. 86* (1964) 4537; b) P. Longin, A.-M. Lambert, M. A. Rousset, *C.R. Acad. Sci. Ser. B 273* (1971) 599; c) G. S. Hammond, J. Saltiel, A. A. Lamola, N. J. Turro, J. S. Bradshaw, D. O. Cowan, R. C. Counsell, V. Vogt, C. Dalton, *J. Am. Chem. Soc. 86* (1964) 3197.
[7] The isolation was carried out by flash chromatography with petroleum ether/ethyl acetate on SiO_2 (**4**–**8**, **13**–**15**) or on basic Al_2O_3, activity III (**17**–**19**), and by preparative gas chromatography with Carbowax 20M on Volaspher® A 2 (**2**, **3**) or silicon SE 30 on Chromosorb® W (**16** and diastereomer). Elemental analyses as well as mass, IR, and NMR spectra support the proposed structures. Except for **13**, the configurations were determined from the characteristic magnitudes of the coupling constants or from NOE effects.
[8] Analysis by ^2H NMR spectroscopy.
[9] M. Christl, B. Mattauch, H. Irngartinger, A. Goldmann, *Chem. Ber. 119* (1986) 950.
[10] a) J. Mattay, *Angew. Chem. 99* (1987) 849; *Angew. Chem. Int. Ed. Engl. 26* (1987) 825; b) C. J. Abelt, H. D. Roth, M. L.-M. Schilling, *J. Am. Chem. Soc. 107* (1985) 4148.
[11] T. S. Cantrell, *J. Org. Chem. 39* (1974) 2242.

Synthesis and Structure of Digerma- and Distannacyclobutenes **

By *Adolf Krebs*,* *Andrea Jacobsen-Bauer*, *Erhard Haupt*, *Michael Veith*,* and *Volker Huch*

The first germirenes (germacyclopropenes) were synthesized by reaction of 3,3,6,6-tetramethyl-1-thiacyclohept-4-yne **1** with suitable precursors of dialkylgermylenes (dialkylgermanediyls);[1] **1** combines high reactivity of the C–C triple bond with steric shielding of the resulting addition product, thereby often making possible the synthesis of systems otherwise accessible only with difficulty.[2] Since, until recently, no addition reactions of stannylenes to C–C triple bonds had been described,[3] we allowed **1** to react with the stabilized diaminogermylene **2**[4] as well as the diaminostannylene **3**[4] and obtained, in addition to the digermacyclobutene **4**, the first distannacyclobutene **5**. Compounds **4** and **5** are both dispiro compounds.

Addition of **1** to the red solution of **3** in various solvents (benzene, THF, *n*-hexane, diethyl ether) resulted in immediate precipitation of a yellow solid, whose ^1H and ^{13}C NMR spectroscopic data in concentrated solution indicate the formation of the 1:2 adduct **5**. In dilute solution, however, only the ^1H NMR signals of the starting materials were observed; in the ^{13}C NMR spectrum of **5**, the signal for the sp-hybridized C atom of **1** was absent. Proof for the presence of an Sn–Sn bond was provided by the ^{119}Sn NMR spectrum, which showed a signal at $\delta = +155$ (rel. to $Sn(CH_3)_4$; $J(^{119}Sn, ^{117}Sn) = 3723$ Hz). Compound **4** was synthesized in a similar way from **1** and **2**.



1 **2** El = Ge **4** El = Ge
3 El = Sn **5** El = Sn

The results of the X-ray structure analyses of **4** and **5** are given in Figure 1. They confirm the structure derived for **5** in solution. In both cases, there is a central four-membered ring containing two sp^2-hybridized carbon atoms and two four-fold coordinated germanium or tin atoms, respectively. Whereas in **5** the nearly planar peripheral diazasilastanna four-membered rings are perpendicular to the completely planar central distannacyclobutene (**5** has a C_2 axis in the crystal, the thiacycloheptene unit being disordered; only one of the two variants is shown in Fig. 1), the diazasilagerma four-membered rings in **4**, which are also planar, are twisted

[*] Prof. Dr. A. Krebs, Dipl.-Chem. A. Jacobsen-Bauer
Institut für Organische Chemie der Universität
Martin-Luther-King-Platz 6, D-2000 Hamburg 13 (FRG)
Dr. E. Haupt
Institut für Anorganische und Angewandte Chemie der Universität Hamburg
Prof. Dr. M. Veith, Dr. V. Huch
Institut für Anorganische Chemie der Universität
Im Stadtwald, D-6600 Saarbrücken 11 (FRG)

[**] Cyclic Diazastannylenes, Part 29. Part 28: M. Veith, V. Huch, R. Lisowsky, P. Hobein, *Z. Anorg. Allg. Chem.*, in press.

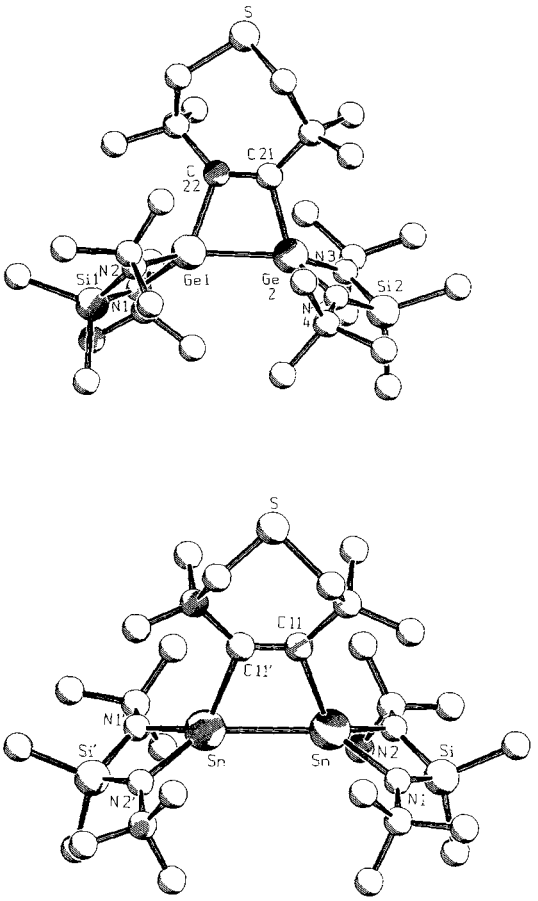
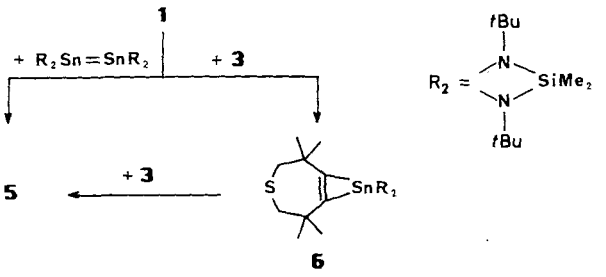


Fig. 1. Molecular structures of **4** (top) and **5** (bottom). Important bond lengths [Å] and angles [°] [5] in the dimetallacyclobutenes: **4**: Ge1-Ge2 2.459 (1), Ge1-C22 2.030 (7), Ge2-C21 2.028 (6), C21-C22 = 1.34 (1); C22-Ge1-Ge2 73.3 (1), Ge2-C21-C22 105.0 (1). **5**: Sn-Sn' 2.803 (1), Sn-C11 2.27 (1), C11-C11' 1.31 (2); C11-Sn-Sn' 70.7 (2), Sn-C11-C11' 109.3 (3) [5].

away from orthogonal positions with respect to the slightly puckered digermacyclobutene. This twisting is due to the sterically demanding *tert*-butyl groups on the nitrogen atoms of the two peripheral rings. Compound **5** is not twisted because the Sn–Sn distance is 0.344 Å longer, thereby reducing this steric interaction.

Whereas the bond lengths and angles of the central ring of **4** are in the expected range, the C=C bond in **5** is quite short (1.31 Å versus the expected value of 1.34 Å) and the Sn–C bonds are very long (2.27 Å versus the expected value of 2.17 Å). [6] For comparison, in the stannirene synthesized by *Sita* et al., [3] the bond lengths are d(C=C) = 1.34 Å and d(Sn-C) = 2.14 Å. The Sn–C bond is thus very weak, which would also explain the dissociation to the starting compounds observed in solution.

Compound **5** could have formed either via the stannirene **6** and subsequent insertion of **3** or by a [2 + 2] cycloaddition



of **1** and a dimer of **3** having an Sn–Sn double bond; since such dimers of **3** are not known [7] whereas a stannirene has already been isolated, [3] we believe that the pathway via **6** is more likely. Both pathways to the 1,2-digermacyclobutene are possible in the case of the dialkylgermylenes. [8] Phosphadistannacyclobutenes, however, are probably formed by [2 + 2] cycloaddition. [9]

Experimental Procedure

4, 5: Compound **1** (0.78 g, 4.68 mmol) was added dropwise under argon to **2** (1.28 g, 4.68 mmol) or **3** (1.5 g, 4.68 mmol) in 5 mL of dry benzene at + 10 °C over 5 min, resulting in the formation of yellow crystals. After purification (**4**, recrystallization from benzene; **5**, sublimation at 40–50 °C/10^{-3} torr), 1.43 g of **4** (86%) or 1.05 g of **5** (56%) was obtained.

Received: October 21, 1988 [Z 3020 IE]
German version: *Angew. Chem. 101* (1989) 640

CAS Registry numbers: **1**, 26825-18-3; **2**, 84806-15-5; **3**, 54724-62-8; **4**, 119787-85-8; **5**, 119793-90-7.

[1] A. Krebs, J. Berndt, *Tetrahedron Lett. 24* (1983) 4083; M. P. Egorov, S. P. Kolesnikov, Yu. T. Struchkov, M. Yu. Antipin, S. V. Sereda, O. M. Nefedov, *J. Organomet. Chem. 290* (1985) C 27.
[2] A. Krebs, J. Wilke, *Top. Curr. Chem. 109* (1983) 189.
[3] L. R. Sita, R. D. Bickerstaff, *J. Am. Chem. Soc. 110* (1988) 5208.
[4] M. Veith, M. Grosser, *Z. Naturforsch. B37* (1982) 1375; M. Veith, *Angew. Chem. 87* (1975) 287; *Angew. Chem. Int. Ed. Engl. 14* (1975) 263.
[5] **4**: $C_{30}H_{64}N_4SSi_2Ge_2$, space group $P2_1/n$, a = 10.761 (9), b = 31.85 (3), c = 12.54 (1) Å, β = 114.61 (7)°, V = 3908 Å^3, Z = 4, $\varrho_{calcd.}$ = 1.197 g cm^{-3}, $\mu(Mo_{K\alpha})$ = 16.25 cm^{-1}. 4634 unique reflections, 1047 classified as not observed ($F \leq 3\,\sigma(F)$). Reflection/parameter ratio = 15. R = 0.057.–**5**: $C_{30}H_{64}N_4SSi_2Sn_2$, space group $C2$, a = 17.135 (9), b = 10.223 (5), c = 14.233 (7) Å, β = 125.63 (4)°, V = 2026 Å^3, Z = 2, $\varrho_{calcd.}$ = 1.305 g cm^{-3}, $\mu(Mo_{K\alpha})$ = 12.52 cm^{-1}. 1410 unique reflections, 14 classified as not observed ($F \leq 3\,\sigma(F)$). Reflection/parameter ratio = 8.2. R = 0.044.–Further details of the crystal structure investigations may be obtained from the Fachinformationszentrum Energie, Physik, Mathematik GmbH, D-7514 Eggenstein-Leopoldshafen 2 (FRG), on quoting the depository number CSD-53 454, the names of the authors, and the journal citation.
[6] M. Veith, O. Recktenwald, *Top. Curr. Chem. 104* (1982) 1.
[7] M. Veith, *Angew. Chem. 99* (1987) 1; *Angew. Chem. Int. Ed. Engl. 26* (1987) 1.
[8] O. M. Nefedov, M. P. Egorov, A. M. Gal'minas, S. P. Kolesnikov, A. Krebs, J. Berndt, *J. Organomet. Chem. 301* (1986) C 21.
[9] A. H. Cowley, S. W. Hall, C. M. Nunn, J. M. Power, *Angew. Chem. 100* (1988) 874; *Angew. Chem. Int. Ed. Engl. 27* (1988) 838.

Highly Reduced Porphyrins**

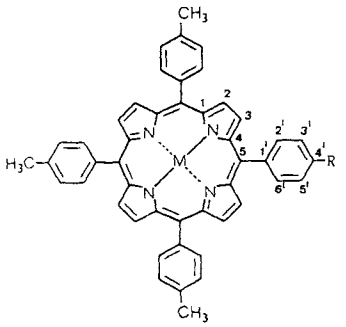
By *Robert Cosmo, Christian Kautz, Klaus Meerholz, Jürgen Heinze,** und *Klaus Müllen**

Can an organic π system be used to store charge by successive addition of electrons and is the storage capacity increased on going to higher analogues containing several redox centers? We have examined this question for the first time for porphyrins [1] and have found that the zinc complex **1** of *meso*-tetratolylporphyrin **2** can reversibly accept six electrons. The NMR spectra of the intermediate di- and tetra-

[*] Prof. Dr. K. Müllen, Dr. R. Cosmo, Dipl.-Chem. C. Kautz
Institut für Organische Chemie der Universität
J.-J.-Becher-Weg 18–22, D-6500 Mainz 1 (FRG)
Prof. Dr. J. Heinze, Dipl.-Chem. K. Meerholz
Institut für Physikalische Chemie der Universität
Albert-Strasse 21, D-7800 Freiburg (FRG)

[**] This work was supported by the Deutsche Forschungsgemeinschaft and the Fonds der Chemischen Industrie. *R.C.* thanks the Alexander von Humboldt Foundation for a fellowship.

anions demonstrate their annulene-like bonding. We "doubled" the zinc porphyrin complex **1** to form the stilbene-bridged diporphyrinyl system **3** and examined its redox properties in analogy to those of **1**. Complex **3** forms a dodecaanion!



1 : M=Zn, R=CH_3
2 : M=2H, R=CH_3
5 : M=2H, R=Br
6 : M=2H, R=CHO
7 : M=Zn, R=CHO

Reduction of **1**[2,3] in [D_8]THF at $-78\,^{\circ}C$ with active lithium or potassium results in several color changes; however, the characterization of a diamagnetic primary product (green-red) or a secondary product (black) by high-resolution NMR spectroscopy was only possible when the reaction was followed spectroscopically and the concentration of the intermediate radical anions was minimized. The number and the charge-induced shifts of the ^1H and ^{13}C NMR signals of the diamagnetic species (Table 1), as well as trapping experiments with dimethyl sulfate[4] and mass-spectrometric characterization of the adducts, show that a dianion and a tetraanion with intact porphyrin frameworks are formed.

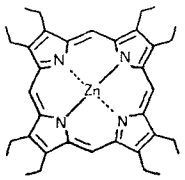
Table 1. ^1H and ^{13}C NMR chemical shifts ([D_8]THF]) of the porphyrins **1** and **4** and of the corresponding amines.

	δ_H				
	1	$\mathbf{1}^{2\ominus}$/2 $K^{\oplus}$	$\mathbf{1}^{4\ominus}$/4 $Li^{\oplus}$	**4**	$\mathbf{4}^{2\ominus}$/2 $Li^{\oplus}$
H-2,3	8.95	−0.9	6.70	–	–
H-2′,6′	8.10	4.95	7.85	–	–
H-3′,5′	7.55	6.05	6.59	–	–
CH_3	2.70	1.50	2.14	1.94	−0.60
H-5 (*meso*-H)	–	–	–	10.13	−3.9
CH_2	–	–	–	4.17	−1.53

	δ_c		
	1	$\mathbf{1}^{4\ominus}$/4 $Li^{\oplus}$	$\Delta\delta_c$
C-5 (*meso*-C)	121.1	92.8	+28.3
C-1,4	150.4	121.8	+28.6
C-2,3	131.9	110.0 [a]	+21.9
CH_3	21.5	23.4	−1.9
C-1′	140.0	148.8	−8.8
C-2′,6′	134.4	127.4 [a]	−7.0
C-3′,5′	127.2	130.2 [a]	−3.0
C-4′	137.0	142.4	−5.4

[a] Signal assignment by selective decoupling.

The salient features of the ^1H NMR spectra are the resonances of the β protons of the pyrrole units at high field ($\delta_H = -0.9$) in the dianion and at low field ($\delta_H = 6.70$)–despite charge-induced shielding–in the tetraanion. If the bonding in the neutral compound **1** is related to that in a diatropic diaza[18]annulene,[5,6] it follows necessarily that the corresponding dianion (tetraanion) has a paratropic (diatropic) 20 π (22 π) perimeter. We were able to carry out corresponding redox experiments involving dianion and tetraanion formation with an [18]annulene.[7] The paratropism of a doubly charged porphyrin perimeter is especially revealed in the resonance of the *meso* proton ($\delta_H = -3.9$) in the dianion (lithium salt) of the octaethyl zinc porphyrin **4**.[8]



4

The ^{13}C NMR spectrum of $\mathbf{1}^{4\ominus}$/4 $Li^{\oplus}$ provides information on the charge distribution. Whereas all carbon centers of the porphyrin ring experience an appreciable shielding upon tetraanion formation (see Table 1), the centers of the phenyl rings are deshielded. This finding indicates that, owing to twisting, the phenyl groups are not significantly involved in the charge delocalization.[9]

The cyclovoltammetric measurement of the reduction of **1** in absolutely dry dimethylamine[10] with tetrabutylammonium bromide as conducting electrolyte at temperatures below $-20\,^{\circ}C$ (Fig. 1 and Table 2) confirms that a stable tetraanion is formed. Furthermore, it shows that **1** can be reversibly reduced all the way to the hexaanion. The reduction of **1** to the dianion occurs in one-electron steps having separated potentials of $E^0(\mathbf{1}/\mathbf{1}^{\ominus}) = -1.44$ and $E^0(\mathbf{1}/\mathbf{1}^{2\ominus}) = -1.98$ V, whereas both the tetraanion and the hexaanion are formed in formal "two-electron" reactions at $E^0(\mathbf{1}^{2\ominus}/\mathbf{1}^{4\ominus}) = -2.78$ and $E^0(\mathbf{1}^{4\ominus}/\mathbf{1}^{6\ominus}) = -3.20$ V. Simulations revealed that the normal-potential separation between the $\mathbf{1}^{2\ominus}/\mathbf{1}^{3\ominus}$ ($\mathbf{1}^{4\ominus}/\mathbf{1}^{5\ominus}$) and the $\mathbf{1}^{3\ominus}/\mathbf{1}^{4\ominus}$ ($\mathbf{1}^{5\ominus}/\mathbf{1}^{6\ominus}$) redox pair is only 40 (50) mV.

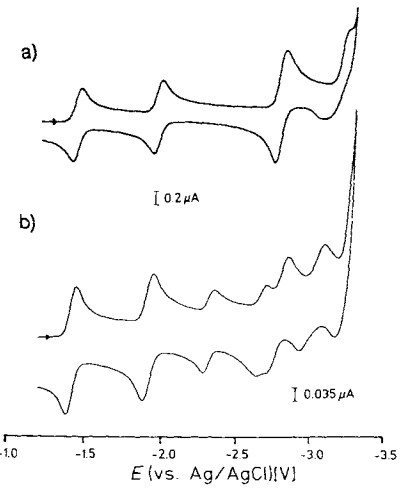


Fig. 1. Cyclic voltammogram of a) **1**, b) **3**; each 10^{-3} M in Me_2NH/0.1 M NBu_4Br.

Independent of the NMR data, cyclovoltammetric measurements on the Zn-free porphyrin system **2** showed that only the charge state of the porphyrin framework and not that of the $Zn^{2\oplus}$ ion is changed upon reduction of **1**. Here, too, six redox steps are observed (Table 2). However, the

Table 2. Redox potentials E^0 [V] of the compounds **1**–**4** [a].

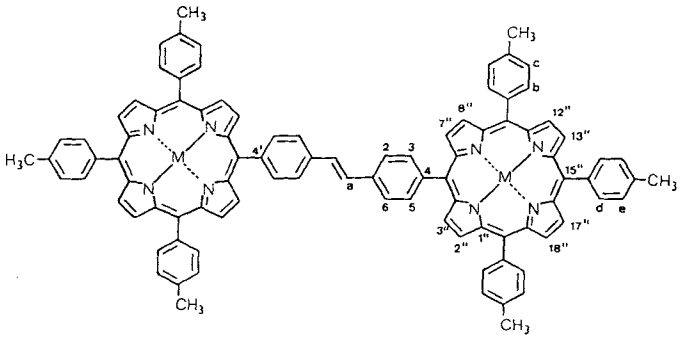
	1	**2**	**3**	**4**
$R/R^{\ominus}$	– 1.44	– 1.19	– 1.42 (10) [b]	– 1.68
$R^{\ominus}/R^{2\ominus}$	– 1.98	– 1.54		– 2.27
$R^{2\ominus}/R^{3\ominus}$	– 2.78 (44) [b]	– 2.60	– 1.92 (20) [b]	– 3.08
$R^{3\ominus}/R^{4\ominus}$		– 2.71		– 3.25 [c]
$R^{4\ominus}/R^{5\ominus}$	– 3.20 (50) [b]	– 3.00	– 2.32	–
$R^{5\ominus}/R^{6\ominus}$		– 3.09	– 2.67	–
$R^{6\ominus}/R^{8\ominus}$	–	–	– 2.73 (40) [b]	–
$R^{8\ominus}/R^{10\ominus}$	–	–	– 3.02 (70) [b]	–
$R^{10\ominus}/R^{12\ominus}$	–	–	– 3.27 [c]	–

[a] All potentials were determined by cyclic voltammetry with 10^{-3} M solutions of R in Me_2NH/0.1 M NBu_4Br with respect to the Ag/AgCl electrode (calibration with $Cp_2Co^{\oplus}/Cp_2Co$); $T = -65\,^{\circ}C$. [b] "Two-electron" redox steps (one-electron potential separation [mV] in parentheses). [c] $T = -85\,^{\circ}C$.

anions of **2** are appreciably less stable than those of **1**, so that, even for moderately fast scan rates, secondary reactions can occur, despite the low temperatures employed.

Previous cyclovoltammetric investigations on the formation of highly charged porphyrins had always shown[11,12] that protonated secondary products are formed beyond the trianion stage.[12] This is also true for the octaethyl zinc porphyrin **4**, which we were able, for the first time, to reduce reversibly to the tetraanion. The extreme potential values of – 3.08 and – 3.25 V, respectively, for the $\mathbf{4}^{2\ominus}/\mathbf{4}^{3\ominus}$ and $\mathbf{4}^{3\ominus}/\mathbf{4}^{4\ominus}$ redox pairs confirm, at the same time, that these stages are only accessible with difficulty by chemical reduction.

The connection of two porphyrin moieties through a stilbene group enticed us because stilbene is also a good electron acceptor ($E^0 = -2.26$ vs. Ag/AgCl) and because twisting around the formal single bond would allow a "decoupling" of the two moieties as well as a minimization of the Coulombic repulsion in the anions. The synthesis of the diporphyrinyl system 4,4'-bis[5-(10,15,20-tris(*p*-tolyl)porphyrinyl)]stilbene (as its zinc complex **3**) starts from the monobromo compound **5**,[2] which was metalated with butyllithium (9.2 equiv., 0 °C, diethyl ether, 2 h) and then formylated by reaction with dimethylformamide (6.8 equiv., 0 °C, 30 min) and hydrolysis with 2.5 M HCl to give the aldehyde **6**[13] (24% yield after chromatography on silica and recrystallization from $CHCl_3/CH_3OH$ 1/1). Compound **6** was converted into the zinc complex **7** (98% after recrystallization from $CHCl_3/CH_3OH$) by reaction with zinc acetate dihydrate[3] and then subjected to McMurry coupling[14] ($TiCl_4$/Zn, THF, 0 °C). Chromatography on silica and recrystallization ($CHCl_3/CH_3OH$) afforded the wine-red diporphyrinyl derivative **3** in 32% yield; **3** was sufficiently soluble in chloroform (1 mg in 0.14 mL $CHCl_3$).[15]



3: M=Zn

The cyclovoltammetric experiment in dimethylamine now shows (see Fig. 1 and Table 2) that **3** is reduced to the tetraanion in two formal "two-electron" redox steps. Two potentially separated, reversible one-electron transfers are observed for the next redox reactions; the first already occurs at – 2.32 V owing to the enlarged conjugation of the entire system—the stilbene bridge has to be coplanar with the two porphyrin frameworks in this charge state. The shift of the next electron transfer by 350 mV [$E^0(\mathbf{3}^{5\ominus}/\mathbf{3}^{6\ominus}) = -2.67$ V] is explained by the fact that the accumulation of charge to form the second trianionic electrophore is energetically disfavored by the Coulombic interaction through the coplanar stilbene bridge. After this critical charge state is attained, the sixfold charged dimer reversibly accepts another six (!) electrons to form the dodecaanion: however, the last stage already lies in the region of current rise due to electrolyte reduction. Since the electron transfers again occur in formal "two-electron" redox steps, the further accumulation of charge must take place locally in the two porphyrin units, without larger Coulombic effects acting through the stilbene bridge.

Thus, a tetraaryl porphyrin is a highly efficient electron acceptor. A doubling of the storage capacity per molecule can be achieved by suitable linking of the two porphyrin units. Current work is aimed at the development of analogous charge storage systems containing more than two porphyrin redox centers.

Received: August 4, 1988;
revised: January 12, 1989 [Z 2908 IE]
German version: *Angew. Chem. 101* (1989) 638

CAS Registry numbers:
1, 19414-67-6; $\mathbf{1}^{2\ominus}/2K^{\oplus}$, 119770-75-1; $\mathbf{1}^{4\ominus}/4Li^{\oplus}$, 119770-76-2; $\mathbf{1}^{6\ominus}$, 119787-46-1; **2**, 14527-51-6; **3**, 119787-45-0; **4**, 17632-18-7; $\mathbf{4}^{2\ominus}/2Li^{\oplus}$, 119770-77-3; $\mathbf{4}^{4\ominus}$, 119770-79-5; **5**, 119770-80-8; **6**, 119770-81-9; **7**, 119770-78-4.

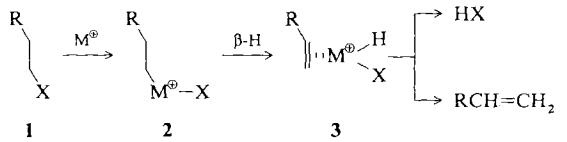
[1] For comparable investigations on phthalocyanine complexes, see R. Taube, *Z. Chem. 6* (1966) 8.
[2] A. D. Adler, F. R. Longo, J. D. Finarelli, J. Goldmacher, J. Assour, L. Korsakoff, *J. Org. Chem. 32* (1967) 476.
[3] A. D. Adler, F. R. Longo, F. Kampas, J. Kim, *J. Inorg. Nucl. Chem. 32* (1970) 2443.
[4] A. Botulinski, J. W. Buchler, N. E. Abbes, W. R. Scheidt, *Liebigs Ann. Chem. 1987*, 305; A. Botulinski, J. W. Buchler, K.-L. Lay, H. Stoppa, *ibid. 1984*, 1259.
[5] M. Gouterman in D. Dolphin (Ed.): *The Porphyrins, Vol. 3*, Academic Press, New York 1978, p. 1.
[6] E. Vogel, W. Haas, B. Knipp, J. Lex, H. Schmickler, *Angew. Chem. 100* (1988) 445; *Angew. Chem. Int. Ed. Engl. 27* (1988) 406, and references cited therein.
[7] K. Müllen, W. Huber, M. Nakagawa, M. Iyoda, *J. Am. Chem. Soc. 104* (1982) 5403.
[8] G. N. Sinyakov, A. M. Shul'ga, G. P. Gurinovich, *Zh. Prikl. Spektrosk. 28 (3)* (1978) 504; *Chem. Abstr. 89* (1978) 33752n.
[9] From the charge-induced shift of all ^{13}C NMR signals of the porphyrin ring (without tolyl substituents) in $\mathbf{1}^{4\ominus}/4\,Li^{\oplus}$ and the proportionality constant $K = 160$ ppm per unit charge, one obtains an estimate of $3.2\,e^{\ominus}$ for the excess charge in the porphyrin framework. If the same charge density is assumed for the four nitrogen centers as for the ring carbon atoms, one obtains an estimate of $3.9\,e^{\ominus}$ for the excess charge.
[10] K. Meerholz, J. Heinze, *J. Am. Chem. Soc. 111* (1989) 2325. The purification is accomplished by condensing gaseous dimethylamine (99% purity) on activated alumina. After heating at reflux for 1 h, the dimethylamine is condensed at reduced pressure into an electrochemical cell suitable for low-temperature measurement; see also R. P. VanDuyne, C. N. Reilley, *Anal. Chem. 44* (1972) 142.
[11] D. W. Clark, N. S. Hush, *J. Am. Chem. Soc. 87* (1965) 4238.
[12] G. Peychal-Heiling, G. S. Wilson, *Anal. Chem. 43* (1971) 545, 551.

[13] H. Ericsson, O. Wennerström, unpublished. We thank Prof. *O. Wennerström* for providing us with the results.
[14] J. E. McMurry, *Acc. Chem. Res. 16* (1983) 405.
[15] Spectroscopic data for **3**: m.p. > 300 °C; UV/VIS (CH_2Cl_2): λ_{max} = 228 nm (lg ε = 5.96), 304 (5.23), 402 sh (5.46), 424 (6.36), 550 (5.23), 591 (4.88); ^1H NMR (400 MHz, $CDCl_3$): δ = 9.06, 9.05 (AB_q, $J_{A,B}$ = 4.5 Hz, 8H, 2 × H-2'', 3'', 7'', 8''), 8.96 (s, 8H, 2 × H-12'', 13'', 17'', 18''), 8.29 (d, 4H, J = 7.9 Hz, 2 × H-3,5), 8.1 (m, 12H, 2 × (4 H-b, 2 H-d)), 8.05 (d, 4H, J = 7.9 Hz, 2 × H-2,6), 7.76 (s, 2H, 2 × H-a), 7.56 (m, 12H, 2 × (4 H-c, 2 × H-e)), 2.71 (s, 18H, 2 × (3 aryl-CH_3)); MS (zinc isotope pattern): *m/z* ($M^{\oplus}$) 1469.41 (20.9%), 1468.5 (45.2), 1467.44 (58.3), 1466.47 (75.7), 1465.5 (79.1), 1464.44 (100), 1463.41 (64.4), 1462.44 (83.5), 1461.44 (51.3), 1460.41 (33.0); *m/z* ($M^{2\oplus}$) 734.2 (65.8), 732.2 (100).

Revision and Modification of the Traditional Mechanism of C–H/C–C Activation by "Naked" Transition-Metal Ions**

By *Sigurd Karraß, Karsten Eller, Christian Schulze,* and *Helmut Schwarz**

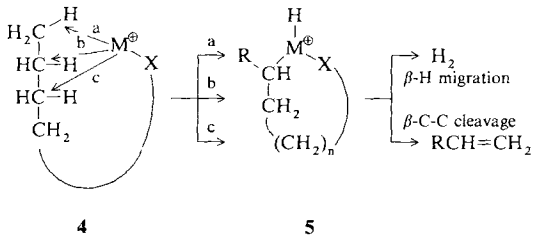
Many reactions of "naked" (i.e., ligand- and counterion-free) transition-metal ions $M^{\oplus}$ with substituted alkanes **1** in the gas phase can be satisfactorily explained in terms of a mechanism formulated for the first time by *Allison* and *Ridge*[1] (Scheme 1). Oxidative addition of the C–X bond to $M^{\oplus}$ (**1** → **2**) is followed by a β-hydrogen transfer; the resulting olefin complex **3** undergoes competitive loss of HX (reductive elimination) and $RCH{=}CH_2$.



1 **2** **3**

Scheme 1. X = OH, halogen, NH_2

For longer-chain CN-substituted *n*-alkanes (cf. **4**, X = CN), we recently found a new type of reaction.[2] In this case, the dominant process is due to an interaction of remote C–H bonds with the transition-metal ion $M^{\oplus}$ "anchored" to the functional group ("remote functionalization"[3]). Depending on $M^{\oplus}$ (e.g., $Fe^{\oplus}$, $Co^{\oplus}$, $Ni^{\oplus}$), *different* segments of the alkyl chain are activated in an oxidative addition (Scheme 2).



4 **5**

Scheme 2.

We report here on experiments that reveal a significant variant in the mechanism of the metal-ion-induced activation of C–H and C–C bonds and, further, provide insight into several fundamental aspects of elementary reactions of organometallic chemistry.

Electron-impact ionization (100 eV) of a mixture of $Fe(CO)_5$ and $C_3H_7NH_2$ (1:5) in a mass spectrometer affords a complex of composition $C_3H_9NFe^{\oplus}$, which, in a tandem mass spectrometry (MSMS) experiment,[4] gives the products shown in Equation (a). The identity of the neutral molecules, based on the mass differences (Δ*m*), is firmly established for energetic reasons.[5] Their origin can be determined by investigation of the $Fe^{\oplus}$ complexes of the deuterated propylamines **6a–d** (Table 1).

	Δm	Neutral molecule	[%]
$C_3H_7NH_2/Fe^{\oplus}$ **6**/$Fe^{\oplus}$	2	H_2	22
	17	NH_3	4
	28	C_2H_4	55
	42	C_3H_6	19

(a)

Table 1. Neutral isotopomers, generated from the $Fe^{\oplus}$ complexes of **6a–6d** [a].
$CH_3CH_2CH_2ND_2$ **6a** $CH_3CH_2CD_2NH_2$ **6b**
$CH_3CD_2CH_2NH_2$ **6c** $CD_3CH_2CH_2NH_2$ **6d**

Neutral isotopomers	**6a**/$Fe^{\oplus}$	**6b**/$Fe^{\oplus}$	**6c**/$Fe^{\oplus}$	**6d**/$Fe^{\oplus}$
H_2	100	100	–	–
HD	–	–	100	100
D_2	–	–	–	–
NH_3	–	50	50	100
NH_2D	–	50	50	–
NHD_2	100	–	–	–
C_2H_4	100	–	–	100
C_2H_3D	–	–	–	–
$C_2H_2D_2$	–	100	100	–
C_3H_6	100	–	–	–
C_3H_5D	–	50	50	–
$C_3H_4D_2$	–	50	50	–
$C_3H_3D_3$	–	–	–	100

[a] The product distribution is normalized with respect to the corresponding neutral compound ($\Sigma_{isotopomer}$ = 100%).

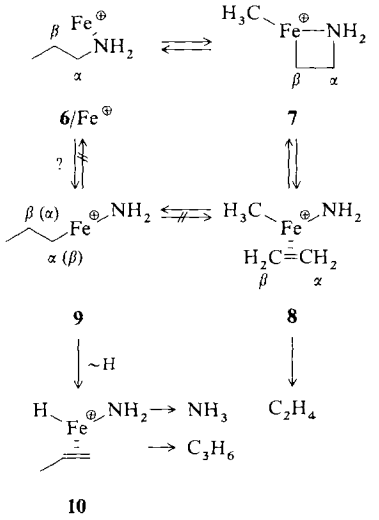
It was found that molecular hydrogen originates exclusively from the β and γ positions of the alkyl chain (1,2-elimination); hydrogen shifts do not occur. Scheme 2 (X = NH_2; pathway a) provides a satisfactory description of the reaction mechanism. Oxidative addition of an N–H bond, followed by β-H transfer and reductive elimination of H_2 to give an $Fe^{\oplus}$-complexed imine, plays *no* role.[6]

The elimination of ethylene from the complex $C_3H_7NH_2/Fe^{\oplus}$ is not explainable in terms of Scheme 1, since only propene should be formed from propylamine. The reaction mechanism shown in Scheme 2 is also wrong, since ethylene originates specifically from the α- and β-methylene groups of the amine (Table 1). The α- and β-methylene groups are also involved in the formation of NH_3 and C_3H_6—in fact, to the same extent (± 2%). According to Scheme 1, NH_3 should contain a hydrogen atom only from the β position of the alkyl chain, and this hydrogen atom should be absent in the propene formed (R = CH_3). The data in Table 1 show that, before the elimination of ammonia or propene, the α- and β-methylene groups are equilibrated. Hydrogen shifts (e.g., via dyotropic rearrangement[7]) are ruled out here (no loss of a hydrogen atom from the α-CH_2 group). Instead a (formal) interchange of the two *intact* methylene groups takes place, possibly via the olefin complex **8** (Scheme 3). Complex **8**

[*] Prof. Dr. H. Schwarz, Dipl.-Chem. S. Karraß, Dipl.-Chem. K. Eller, Dipl.-Chem. C. Schulze
Institut für Organische Chemie der Technischen Universität
Straße des 17. Juni 135, D-1000 Berlin 12

[**] This work was supported by the Fonds der Chemischen Industrie, the Stiftung Volkswagenwerk, and the Gesellschaft von Freunden der Technischen Universität Berlin.

could be formed by a combination of oxidative addition and cycloreversion (**6**/$Fe^{\oplus}$ → **7** → **8**) and fulfills two functions: (1) as immediate precursor for the elimination of $C^{\alpha}C^{\beta}H_4$; (2) as intermediate for the equilibration of the C(α)/C(β) methylene groups. Although the details of the equilibration are not known and thermodynamic data for the system $C_3H_7NH_2/Fe^{\oplus}$ are not yet available, it is not unreasonable to assume that a rotation around the $Fe^{\oplus}$-(C_2H_4) bond requires less energy than, for example, an alkene elimination.[8] Insertion of the olefin into the metal–carbon bond—a gas-phase analogue of the Ziegler–Natta reaction[9]—affords **9**, which can be formally regarded as the product of the direct insertion of $Fe^{\oplus}$ into the C–N bond of **6**/$Fe^{\oplus}$. Compound **9** undergoes fast, irreversible β-H transfer to give the propene complex **10**, which eliminates C_3H_6 and NH_3.



Scheme 3.

Whether **6**/$Fe^{\oplus}$–**9** are interconverted reversibly or whether these isomerizations are irreversible reactions is not known with certainty for all pairs, but can be determined for partial steps. At the very least, we consider the β-methyl transfer **9** → **8** unlikely as a necessary condition for the equilibration of C(α)/C(β) in an intermediate **9** generated directly from **6**, since this reaction could not be found in any system so far investigated by us.[2f, 10] We also rule out the reaction **9** → **6**/$Fe^{\oplus}$, since the β-H shift **9** → **10** should occur appreciably faster than the conceivable competing reactions. The direct reaction **6**/$Fe^{\oplus}$ → **9**, which, in view of the divergent thermodynamic data,[1b, 11] cannot be excluded on this basis, must be markedly slower than the rearrangement **6**/$Fe^{\oplus}$ ⇄ **7** ⇄ **8**. Sufficient precedence is known for the reversibility of the step **7** ⇄ **8** as well as for the reductive opening of metallacycles.[12, 13]

Other alternatives (e.g., an $Fe^{\oplus}$-induced isomerization $nC_3H_7NH_2 \rightarrow iC_3H_7NH_2$) were eliminated in favor of the reaction mechanism shown in Scheme 3. Both the distribution of label (Table 1) and the finding that exclusively H_2 (95%) and CH_4 (5%) are formed from independently generated $iC_3H_7NH_2/Fe^{\oplus}$ definitively rule out this variant.

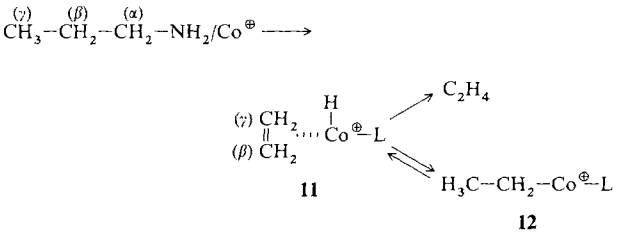
The gas-phase chemistry of the $C_3H_7NH_2/Co^{\oplus}$ complex ($Co^{\oplus}$ is generated by fast atom bombardment (FAB) of $CoCl_2$ with xenon (8 keV)[2f]) differs from that of the $C_3H_7NH_2/Fe^{\oplus}$ complex. In the MSMS experiment, the products shown in Equation (b) are formed unimolecularly; their origin was elucidated by investigations using the labeled amines.

	Δm	Neutral molecule	[%]	
$nC_3H_7NH_2/Co^{\oplus}$	2	H_2	12	(b)
	28	C_2H_4	81	
6/$Co^{\oplus}$	60	CoH	7	

Molecular hydrogen originates, as in the case of $nC_3H_7NH_2/Fe^{\oplus}$, exclusively from the β and γ positions (1,2-elimination); H scrambling was not observed.

Neutral CoH is formed by $Co^{\oplus}$-induced hydride abstraction[6, 11] from the α-methylene group of the amine (loss of CoD from **6b**/$Co^{\oplus}$ and of CoH from the $Co^{\oplus}$ complexes of the other isotopomers of **6**). The specificity of the reaction presumably is related to the facile formation of an iminium ion $CH_3CH_2CH{=}NH_2^{\oplus}$.

In contrast to $Fe^{\oplus}$, $Co^{\oplus}$ generates the olefin from the C(β)/C(γ) positions of the propylamine (loss of C_2H_4) instead of $C_2H_2D_2$ for **6b**/$Co^{\oplus}$). The investigation of the $Co^{\oplus}$ complexes of **6c** and **6d** reveals, however, that an incomplete hydrogen exchange within the β/γ positions must precede the ethylene elimination. Thus, $C_2H_2D_2$ and C_2H_3D are formed in a ratio of 2.8:1 from **6c** and $C_2H_2D_2$ and C_2HD_3 in a ratio of 2.7:1 from **6d**/$Co^{\oplus}$. For a complete exchange of an A_3B_2 system (A,B = H,D), the isotopomers $C_2A_2B_2$ and C_2A_3B, respectively, should be eliminated from **6c**/$Co^{\oplus}$ and **6d**/$Co^{\oplus}$ in the ratio 1.5:1. Presumably, the direct olefin elimination competes with the preceding exchange reaction of type **11** ⇄ **12** (Scheme 4).



Scheme 4. L = CH_2NH_2.

Collisional activation results in the formation of ca. 20% ethylene from the C(α)/C(β) positions of propylamine. The probable intermediate is a $Co^{\oplus}$ complex analogous to **8** (Scheme 3).

Received: December 15, 1988 [Z 3088 IE]
German version: *Angew. Chem. 101* (1989) 634

[1] a) J. Allison, D. P. Ridge, *J. Am. Chem. Soc. 101* (1979) 4998; b) see also S. J. Babinec, J. Allison, ibid. 106 (1984) 7718.

[2] a) C. B. Lebrilla, C. Schulze, H. Schwarz, *J. Am. Chem. Soc. 109* (1987) 98; b) T. Drewello, K. Eckart, C. B. Lebrilla, H. Schwarz, *Int. J. Mass Spectrom: Ion Processes 76* (1987) R1; c) C. B. Lebrilla, T. Drewello, H. Schwarz, *ibid. 79* (1987) 287; d) *J. Am. Chem. Soc. 109* (1987) 5639; e) G. Czekay, T. Drewello, H. Schwarz, *J. Am. Chem. Soc.*, in press; f) review: G. Czekay, T. Drewello, K. Eller, C. B. Lebrilla, T. Prüsse, C. Schulze, N. Steinrück, D. Sülzle, T. Weiske, H. Schwarz in H. Werner, G. Erker (Eds.): *Organometallics in Organic Synthesis*, Springer, Berlin, in press.

[3] a) R. Breslow, *Chem. Soc. Rev. 1* (1972) 553; b) *Acc. Chem. Res. 13* (1980) 170; c) R. Breslow, A. Adams, T. Guv, J. Hunger, *Lect. Heterocycl. Chem. 9* (1987) 43.

[4] ZAB-HF-3F mass spectrometer (Vacuum Generators), BEB configuration (B, magnetic sector; E, electrostatic sector). The ions generated in the ion source were accelerated to 8-keV kinetic energy; with a mass resolution of

ca. 3000 (10% valley definition), $C_3H_9NFe^{\oplus}$ was selected with BE; its unimolecular decay was recorded by "scanning" of B(2). 5–10 spectra were accumulated on-line with the VG data system 250/11. For a description of the apparatus, see T. Weiske, *Dissertation (D83)*, Technische Universität, Berlin 1985.

[5] a) Owing to insufficient sensitivity, it was not possible in this case to characterize the neutral fragments formed in the unimolecular decay of the complex by the otherwise very useful CIDI method (collisionally induced dissociative ionization), a variant of neutralization-reionization (NR) mass spectrometry: b) P. C. Burgers, J. L. Holmes, A. A. Mommers, J. K. Terlouw, *Chem. Phys. Lett. 102* (1983) 1; c) C. Wesdemiotis, F. W. McLafferty, *Chem. Rev. 87* (1987) 485; d) J. K. Terlouw, H. Schwarz, *Angew. Chem. 99* (1987) 829; *Angew. Chem. Int. Ed. Engl. 26* (1987) 805; e) J. K. Terlouw, *Adv. Mass Spectrom.* (1989) 984.

[6] The $Co^{\oplus}$-induced HD elimination from $CH_3CH_2ND_2$ and the absence of hydrogen elimination in the case of, for example, *tert*-butylamine and triethylamine, prompted *Radecki* and *Allison* to make the (unsupported) generalization that, for primary amines, the transition-metal ion mainly activates the NH bond: B. D. Radecki, J. Allison, *J. Am. Chem. Soc. 106* (1984) 946 (see also the results obtained for the system propylamine/$Co^{\oplus}$).

[7] Definition: M. T. Reetz, *Tetrahedron 29* (1973) 2189.

[8] The $M^{\oplus}$-olefin bond energies for many systems are ca. 40–60 kcal mol^{-1}; see z. B. M. A. Hanratty, J. L. Beauchamp, A. J. Illies, P. van Koppen, M. T. Bowers, *J. Am. Chem. Soc. 110* (1988) 1, and references cited therein. The barrier for ethylene rotation in complexes of the type $(CO)_4Fe$-olefin (ca. 10–15 kcal mol^{-1}) is significantly smaller; see, e.g., L. Kruczynski, L. K. K. Li Sing, Man J. Takats, *J. Am. Chem. Soc. 96* (1974) 4006; S. T. Wilson, N. J. Coville, J. R. Shapley, J. A. Osborn, *ibid. 96* (1974) 4038; J. A. Segal, B. F. G. Johnson, *J. Chem. Soc. Dalton Trans. 1975*, 677, 1990.

[9] P. L. Watson, *J. Am. Chem. Soc. 104* (1982) 337.

[10] a) T. Prüsse, C. B. Lebrilla, T. Drewello, H. Schwarz, *J. Am. Chem. Soc. 110* (1988) 5986; b) K. Eller, T. Drewello, W. Zummack, T. Allspach, U. Annen, M. Regitz, H. Schwarz, *ibid.*, in press; c) for a counterexample from the chemistry of alkanes with $M^{\oplus}$ see R. Houriet, L. F. Halle, J. L. Beauchamp, *Organometallics 2* (1983) 1818.

[11] S. W. Buckner, B. S. Freiser, *J. Am. Chem. Soc. 109* (1987) 4715.

[12] For bimolecular metathesis reactions of transition-metal ions in the gas phase, see a) A. E. Stevens, J. L. Beauchamp, *J. Am. Chem. Soc. 101* (1979) 6449; b) L. F. Halle, P. B. Armentrout, J. L. Beauchamp, *Organometallics 2* (1983) 1829; c) D. B. Jacobson, B. S. Freiser, *J. Am. Chem. Soc. 107* (1985) 2605; d) H. Kang, J. L. Beauchamp, *ibid. 108* (1986) 5663; e) S. W. Buckner, J. R. Gord, B. S. Freiser, *ibid. 110* (1988) 6606; f) S. W. Buckner, B. S. Freiser, *Polyhedron 7* (1988) 1583.

[13] a) J. L. Beauchamp, A. E. Stevens, R. R. Corderman, *Pure Appl. Chem. 51* (1979) 967; b) J. Allison, *Prog. Inorg. Chem. 34* (1986) 627.

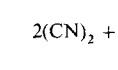
$S_4(CN)_8$, a Blue-Black High-Molecular Sulfur–Cyanogen Compound with 6π- and 8π-Electron Structural Elements**

By *Jörg Sundermeyer, Herbert W. Roesky,** and *Mathias Noltemeyer*

Paracyanogen films $(CN)_x$ are semiconductors at room temperature[1] and exhibit photoconductivity in the visible region.[2] Their structure has not yet been elucidated. To the best of our knowledge, in fact, no high-molecular compounds containing four or more cyanogen units covalently linked through heteroatoms have been structurally confirmed. The blue-black $S_4(CN)_8$, described here, is the first such compound having the general formula $S_x(CN)_y$.[3]

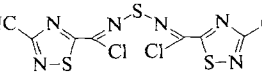
As we have already reported, reaction of cyanogen with elemental sulfur and copper as catalyst in dimethylformamide (DMF) gives 1,2,4-thiadiazole-3,5-dicarbonitrile **1**.[4]

$$2(CN)_2 + 1/8\ S_8 \xrightarrow[\text{[Cu]}]{\text{DMF}} S(CN)_4 \equiv \mathbf{1}$$



In the presence of catalytically active chloride ions, **1** reacts regioselectively with sulfur dichloride at the cyano function adjacent to sulfur to yield the reactive bis(imidoyl chloride) **2**.[5] Treatment of **2** with thiourea and pyridine results in

$$2\ \mathbf{1} + SCl_2 \xrightarrow[\text{[Cl}^{\ominus}\text{]}]{\text{THF}} S_3(CN)_8Cl_2 \equiv \mathbf{2}$$



spontaneous formation of a violet-blue reaction solution, from which blue-black crystalline needles of composition $S_4(CN)_8$ **3** (yield 55%) can be isolated.

$$\mathbf{2} \xrightarrow[(H_2N)_2CS]{\text{MeCN}} \xrightarrow[\text{pyridine}]{\text{MeCN}} S_4(CN)_8 \quad \mathbf{3}$$

The ^{13}C NMR spectrum of **3** shows four signals, indicating a structure with pairwise equivalent carbon atoms. No C≡N vibrational band is present in the IR spectrum. Raman-spectroscopic investigations failed owing to the strong fluorescence of **3**. The UV/VIS spectrum in MeCN shows four absorption maxima at λ = 543, 351, 286, and 218 nm.

Long black needles were obtained from toluene/pentane. Figure 1 shows the result of the single-crystal X-ray structure analysis of these crystals.[6]

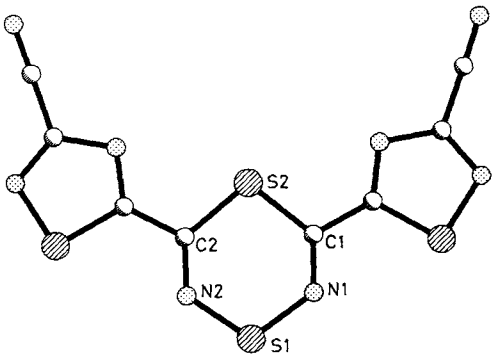


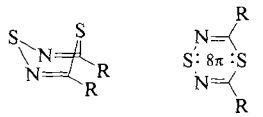
Fig. 1. Molecular structure of **3**. Selected bond lengths [pm] and angles [°]: S1-N1 165(8), N1-C1 126(4), C1-S2 178(9), S2-C2 179(1), C2-N2 128(1), N2-S1 165(2); N1-S1-N2 109.5(4), C1-S2-C2 99.5(5), S1-N1-C1 125.7(7), N1-C1-S2 129.7(7); torsional angle: N2-S1-N1-C1 6.9(0), S2-C2-N2-S1 0.1(1); Coplanarity of the symmetrical halves of the molecule: ± 1 pm.

In **3**, four cyanogen units are covalently linked through four sulfur atoms without cleavage of the respective C–C bonds, thereby forming a tricyclic system consisting of a central six-membered 1,4,2,6-dithiadiazine ring symmetrically substituted in the 3,5 positions with two 1,2,4-thiadiazole-3-carbonitrile ring systems. The three heterocycles are conjugated.

Recently, *C. W. Rees* et al.[7] characterized a phenyl-substituted 1,4,2,6-dithiadiazine of type **I**, which was formed in small yield upon reaction of diphenylacetylene with S_4N_4. The ring system **I** is not planar but rather adopts a boat conformation. Therefore, the orange compound **I**, R = Ph, is aromatic and not antiaromatic.

[*] Prof. Dr. H. W. Roesky, Dipl.-Chem. J. Sundermeyer, Dr. M. Noltemeyer
Institut für Anorganische Chemie der Universität
Tammannstrasse 4, D-3400 Göttingen (FRG)

[**] This work was supported by the Deutsche Forschungsgemeinschaft and the Fonds der Chemischen Industrie.



I

II

By contrast, the ring system of type **II** present in **3** deviates only slightly from planarity (max. deviation 6 (8) pm), and **3** is characterized by a blue-black color both in solution and in the crystal. In both compounds, the π bonds are localized. These three characteristics were also observed for six-membered CNS ring systems with 8π antiaromatic electron structure, first reported several years ago.[8]

We ascribe the structural differences between the two compounds to the different electronic properties of the substituents R. The thiadiazolyl moiety in **3** has a higher electron affinity than the phenyl moiety in *Rees'* compound. The electronic influence of the ligands on the planarity and electronic structure of unsaturated CNS heterocycles has also been observed for variously substituted 1,5-dithia-2,4,6,8-tetrazocines.[9]

Compound **3** opens up new perspectives in the search for high-molecular crystalline oligomers constructed mainly from condensed cyanogen molecules.

Experimental Procedure

5,5'-(1,4,2,6-Dithiadiazine-3,5-diyl)bis(1,2,4-thiadiazole-3-carbonitrile) **3**: **2** (7.50 g, 20 mmol) [5] and powdered thiourea (1.52 g, 20 mmol) were stirred in 150 mL of MeCN for 1 h at 40 °C. The suspension of greenish-yellow, microcrystalline solid thereby formed was filtered at 0 °C and the solid was washed with 50 mL of ether and then resuspended in 100 mL of MeCN. Pyridine (3.20 g, 40 mmol), diluted with 20 mL of MeCN, was added dropwise over 1 h at room temperature to this suspension; the resulting mixture immediately turned blue-black. After ca. 2 h, when almost all yellow solid had gone into solution, the volatiles were removed at 40 °C/0.01 mbar and the blue-black residue was extracted with 3 × 20 mL of toluene. Slow diffusion of pentane vapor into the concentrated toluene extracts resulted in the formation of long, blue-black needles, which lost toluene from the crystal lattice at 125 °C/0.01 mbar. Blue-black crystals (3.70 g, 55%; m.p. 169–170 °C) were thereby obtained. IR (Nujol): $\tilde{\nu}$ [cm^{-1}] = 1576, 1520, 1475, 1390, 1304, 1292, 988, 978, 857, 842, 812, 788, 710, 678, 665, 625, 555, 505, 432, 410. FI-MS: *m/z* 336 ($M^{\oplus}$, 100%). EI-MS: *m/z* 336 ($M^{\oplus}$, 55%), 252 ($M^{\oplus}-S(CN)_2$, 4), 200 ($M^{\oplus}-S(CN)_4$, 85%), 154 ($M^{\oplus}-S(CN)_4-SN$, 100%). ^{13}C NMR ($CDCl_3$): δ = 183.4, 147.1, 143.6, 111.2. UV-VIS (CH_3CN): λ_{max} [nm] = 218 (ε = 37200), 286 (20000), 351 (3680), 543 (3320).

Received: December 14, 1988 [Z 3087 IE]
German version: *Angew. Chem. 101* (1989) 609

CAS Registry numbers: **2**, 102247-21-2; **3**, 119877-45-1.

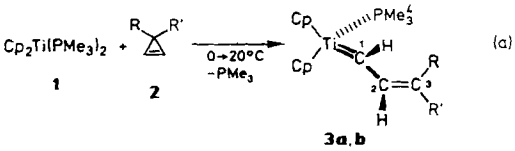
[1] M. E. Fabian, *J. Mater. Sci. 2* (1967) 424.
[2] L. S. Polak, A. F. Lunin, A. M. Nechushkin, *Izv. Vyssh. Uchebn. Zaved. Fiz. 10* (1967) 147; *Chem. Abstr. 67* (1967) 117 611.
[3] For coordination polymers of this class of substances, see H. W. Roesky, T. Gries, J. Schimkowiak, P. G. Jones, *Angew. Chem. 98* (1986) 93; *Angew. Chem. Int. Ed. Engl. 25* (1986) 84; H. W. Roesky, H. Hofmann, J. Schimkowiak, P. G. Jones, K. Meyer-Bäse, G. M. Sheldrick, *ibid. 97* (1985) 403 and *24* (1985) 417.
[4] H. W. Roesky, K. Keller, J. W. Bats, *Angew. Chem. 95* (1983) 904; *Angew. Chem. Int. Ed. Engl. 22* (1983) 881; *Angew. Chem. Suppl. 1983*, 1323; H. W. Roesky, K. Keller (Hoechst AG), DAS 3 309 515 (20 September 1984); *Chem. Abstr. 102* (1985) 45954e.
[5] H. W. Roesky, J. Sundermeyer, J. Schimkowiak, T. Gries, M. Noltemeyer, G. M. Sheldrick, *Z. Naturforsch. B41* (1986) 162.
[6] Crystal structure analysis of **3**: space group $P2_1/n$, a = 571.4 (8), b = 2278.4 (30), c = 1461.0 (20) pm, β = 99.4 (10)°, V = 1.877 nm^3, $C_8N_8S_4 \cdot PhCH_3$, Z = 4, ϱ_{calcd} = 1.516 Mg m^{-3}, $\mu(Mo_{K\alpha})$ = 0.5 mm^{-1}, 5055 measured reflections, 2443 symmetry-independent, 1408 with $F_o > 3\,\sigma(F_o)$ used in the refinement: R = 0.08, R_w = 0.064, $w^{-1} = \sigma^2(F) + 0.0004\,F^2$. Further details of the crystal structure investigation may be obtained from the Fachinformationszentrum Energie, Physik, Mathematik GmbH, D-7514 Eggenstein-Leopoldshafen 2 (FRG), on quoting the depository number CSD-53483, the names of the authors, and the journal citation.
[7] S. T. A. K. Daley, C. W. Rees, *J. Chem. Soc. Perkin Trans. 1 1987*, 207; S. T. A. K. Daley, C. W. Rees, D. J. Williams, *J. Chem. Soc. Chem. Commun. 1984*, 57.
[8] A. W. Cordes, M. Hojo, H. Koenig, M. C. Noble, R. T. Oakley, W. T. Pennington, *Inorg. Chem. 25* (1986) 1137; T. Chivers, F. Edelmann, J. F. Richardson, N. R. M. Smith, O. Treu, Jr., M. Trsic, *ibid. 25* (1986) 2119.
[9] I. Ernest, W. Holick, G. Rihs, D. Schomburg, G. Shoham, D. Wenkert, R. B. Woodward, *J. Am. Chem. Soc. 103* (1981) 1540; R. Gleiter, R. Bartetzko, D. Cremer *ibid. 106* (1984) 3437.

Vinylcarbene Complexes of Titanocene

By *Paul Binger,* Patrik Müller, Reinhard Benn,* and *Richard Mynott*

Titanocenecarbenes, usually obtained in situ from bis(cyclopentadienyl)titanacyclobutanes or the Tebbe reagent, are highly interesting, newly developed reagents in organic synthesis,[1] e.g., for the olefination of carbonyl compounds,[1] enolate formation,[2] olefin metathesis[3] and ring-opening polymerization.[4] Despite this broad spectrum of applications, surprisingly few titanocenecarbene complexes have thus far been isolated and characterized. Those described include alkylidene complexes detectable only in solution,[5, 6] some 1-allenylidene complexes[7] and a 2,2-dimethylbut-3-enylidene complex,[8] all stabilized by trialkylphosphane ligands.

We have now succeeded in preparing representatives of the previously unknown titanocene(vinylcarbene) complexes in a most simple way. Reaction of the readily accessible cyclopropenes[9] **2a** and **2b** with titanocenebis(trimethylphosphane) **1**[10] affords the titanocene(vinylcarbene) complexes **3a** and **3b** as microcrystalline, red powders in yields of 81% and 72%, respectively [Eq. (a)].

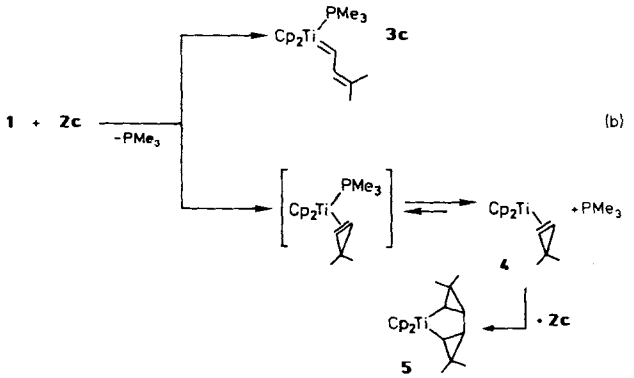


(a)

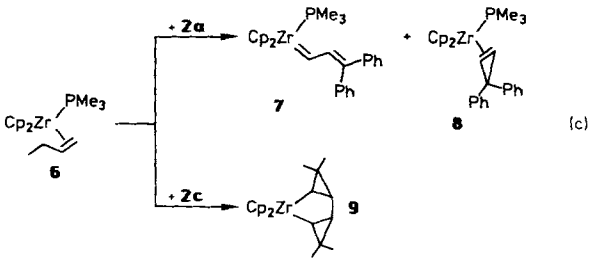
a, R=R'=Ph; **b**, R=Me, R'=Ph; **c**, R=R'=Me

The multifunctional behavior of the cyclopropenes towards transition metal compounds, long known in the case of Ni^0- and Pd^0-catalyzed cycloadditions,[11] is evident again in the reaction of 3,3-dimethylcyclopropene **2c** with **1** [Eq. (b)] or in the reaction of **2a** with (1-butene)(trimethylphosphane)zirconocene **6**[12] [Eq. (c)]. **1** reacts differently with **2c** depending on the molar ratio and the reaction conditions. With **2c** in excess (**1**:**2c** = 1:4; dropwise addition of an etheral solution of **1** to **2c** at 0 °C), the complex **5** is obtained. Equimolar amounts of **1** and **2c**, on the other hand, afford a mixture of the titanium complexes **3c** and **4** at 0 °C in a ratio of ca. 2:1. An NMR study showed that the complexes **3c** and **4** are formed in a ratio of ca. 2:1 at −30 °C; above 0 °C **4** reacts with further **2c** to give **5**.

[*] Prof. Dr. P. Binger, Dipl.-Chem. P. Müller, Priv.-Doz. Dr. R. Benn, Dr. R. Mynott
Max-Planck-Institut für Kohlenforschung
Kaiser-Wilhelm-Platz 1, D-4330 Mülheim a.d. Ruhr (FRG)



Reaction of **2a** and **6**[12] at 20 °C leads to the formation of equal amounts of the (diphenylvinyl)carbene complex **7** and the (η^2-diphenylcyclopropene) complex **8**, while the 3,3-dimethylcyclopropene **2c** reacts with **6** exclusively with oxidative coupling to give **9**. The complexes **7** and **8** do not equilibrate, nor can they be interconverted into each other by heating. These findings suggest that the vinylcarbene complexes **3a–3c** and **7** are formed by direct opening of the three-membered ring and not via an η^2-cyclopropene complex as intermediate.



The structures of the vinylcarbene complexes **3a–3c** and **7** can be unequivocally confirmed by NMR spectroscopy. The characteristic downfield shift to $\delta = 12.54–12.93$[13] is observed for the carbene proton 1-H [for numbering see Eq. (a)]. The downfield shift of the olefin proton 2-H ($\delta = 7.44–8.32$) is also significant. The presence of two Cp signals in the spectra of **3**[13] indicates that trimethylphosphane is bound perpendicular to the plane of the Ti=C double bond. Overall, the data indicate a tetrahedral structure for the complexes **3a–3c** and **7**. The ^{13}C NMR spectra are consistent with these structures, the chemical shift of the carbene C atoms ($\delta = 284–286$) being especially indicative.[6]

The synthesis of the titanium compounds **3a–3c** as outlined here opens up a novel entry to carbene complexes of titanium. At the same time, this finding demonstrates that, under certain conditions, transition metal compounds are able to convert cyclopropenes into vinylcarbenes. Hitherto, such a reaction has only been postulated, on the basis of reaction products formed catalytically from cyclopropenes.[11,14] With one exception,[15] attempts to synthesize vinylcarbene-transition metal complexes have led only to (vinylketene)metal complexes,[11] metallacyclohexadienes or (η^4-cyclopentadiene)metal complexes.[16]

Experimental

3a: A solution of **1** (3.18 g, 9.63 mmol) in pentane (200 mL) was treated dropwise at 0 °C with **2a** (1.85 g, 9.63 mmol). The cooling bath was removed and the solution stirred for 3 h at room temperature. The precipitated red, microcrystalline powder was then filtered. Yield 3.5 g (81%) of **3a** after washing twice with 10 mL of pentane and drying at 10^{-3} torr; decomp. at ca. 50 °C. 0.4 g (72%) of **3b** (decomp. at ca. 50 °C) was obtained analogously from **1** (0.48 g, 1.45 mmol) and **2b** (0.2 g, 1.5 mmol).

Received: November 6, 1988 [Z 3043 IE]
German version: *Angew. Chem. 101* (1989) 647

CAS Registry numbers:
1, 95936-00-8; **2a**, 22825-21-4; **2b**, 65051-83-4; **2c**, 3907-06-0; **3a**, 119747-43-2; **3b**, 119747-44-3; **3c**, 119747-46-5; **4**, 119747-47-6; **5**, 119747-45-4; **6**, 10753010; **7**, 119747-48-7; **8**, 119747-49-8; **9**, 119747-50-1.

[1] K. A. Brown-Wensley, S. L. Buchwald, L. F. Cannizzo, L. E. Clawson, S. Ho, J. D. Meinhart, D. Strauss, R. H. Grubbs, *Pure Appl. Chem. 55* (1983) 1733.
[2] J. R. Stille, R. H. Grubbs, *J. Am. Chem. Soc. 105* (1983) 1664.
[3] a) F. N. Tebbe, G. W. Parshall, D. W. Overall, *J. Am. Chem. Soc. 101* (1979) 5074; b) D. A. Strauss, R. H. Grubbs, *J. Mol. Catal. 28* (1975) 9.
[4] a) L. R. Gilliom, R. H. Grubbs, *J. Am. Chem. Soc. 108* (1986) 733; b) T. M. Swager, R. H. Grubbs, *ibid. 109* (1987) 894.
[5] F. W. Hartner, Jr., J. Schwartz, S. M. Clift, *J. Am. Chem. Soc. 105* (1983) 640
[6] B. J. J. van Heisteeg, G. Schat, O. S. Akkerman, F. Bickelhaupt, *J. Organomet. Chem. 310* (1986) C25.
[7] S. L. Buchwald, R. H. Grubbs, *J. Am. Chem. Soc. 105* (1983) 5490.
[8] L. R. Gilliom, R. H. Grubbs, *Organometallics 5* (1986) 721.
[9] P. Binger, *Synthesis 1974*, 190.
[10] L. B. Kool, M. D. Rausch, H. G. Alt, M. Herberhold, U. Thewalt, B. Wolf, *Angew. Chem. 97* (1985) 425; *Angew. Chem. Int. Ed. Engl. 24* (1985) 394.
[11] Review: P. Binger, H. M. Büch, *Top Curr. Chem. 135* (1987) 79.
[12] a) S. L. Buchwald, B. T. Watson, J. C. Huffman, *J. Am. Chem. Soc. 109* (1987) 2544; b) P. Binger, P. Müller, R. Benn, A. Rufińska, B. Gabor, C. Krüger, P. Betz, *Chem. Ber.*, in press.
[13] Spectroscopic data [numbering as in Eq. (a)]: **3a:** ^{31}P NMR (81 MHz, [D$_8$]THF, H_3PO_4 ext.): $\delta = 11.50$ (s).—^1H NMR (200 MHz, [D$_8$]THF): $\delta = 12.54$ (dd, $J_{1,2} = 14.5$, $J_{PH} = 7.0$ Hz, 1-H), 8.32 (dd, $J_{PH} = 3.5$ Hz, 2-H), 5.58 (d, $J_{PH} = 2.5$ Hz, Cp-H), 5.40 (d, $J_{PH} = 2.5$ Hz, Cp-H), 1.16 (d, $J_{PH} = 6.5$, 4-H), 7.19 (m), 6.91 (d) (R,R').—^{13}C NMR (75.5 MHz, [D$_8$]THF): $\delta = 285.6$ ($J_{CH} = 121$, $J_{CP} = 28.8$ Hz, C-1), 142.3 ($J_{CH} = 145$, $J_{CP} = 8.2$ Hz, C-2), 113.0 ($J_{CP} = 10.7$ Hz, C-3), 19.1 ($J_{CH} = 129$, $J_{CP} = 18.2$ Hz, C-4), 103.3 ($J_{CH} = 171$ Hz, Cp-C), 102.7 ($J_{CP} = 171$ Hz, Cp-C).—**3b:** ^{31}P NMR (81 MHz, [D$_8$]THF, H_3PO_4 ext.): $\delta = 12.46$ (s).—^1H NMR (200 MHz, [D$_8$]THF): $\delta = 12.93$ (dd, $J_{1,2} = 14.2$, $J_{PH} = 7.4$ Hz, 1-H), 8.26 (dd, $J_{PH} = 2.6$ Hz, 2-H), 1.79 (d, $J_{PH} = 4.1$ Hz, R), 1.17 (d, $J_{PH} = 6.7$ Hz, 4-H), 5.55 (d, $J_{PH} = 2.4$ Hz, Cp-H), 5.53 (d, $J_{PH} = 2.4$ Hz, Cp-H), 7.38 (m), 7.15 (m), 6.90 (d) (R').—^{13}C NMR (75.5 MHz, [D$_8$]THF): $\delta = 284.1$ ($J_{CH} = 120$, $J_{PC} = 29.7$ Hz, C-1), 142.6 ($J_{CH} = 143$, $J_{PC} = 8.2$ Hz, C-2), 104.8 ($J_{PC} = 10.1$ Hz, C-3), 15.3 ($J_{CH} = 126$, $J_{PC} = 3.0$ Hz, R), 19.4 ($J_{CH} = 129$, $-J_{PC} = 18.3$ Hz, C-4), 103.0 ($J_{CH} = 171$ Hz, Cp-C), 102.4 ($J_{CH} = 172$ Hz, Cp-C).
[14] a) P. Binger, J. McMeeking, H. Schäfer, *Chem. Ber. 117* (1984) 1551; b) P. Binger, B. Biedenbach, *ibid. 120* (1987) 601.
[15] a) J. Klimes, E. Weiss, *Angew. Chem. 94* (1982) 207; *Angew. Chem. Int. Ed. Engl. 21* (1982) 205; b) T. Valéri, F. Meier, E. Weiss, *Chem. Ber. 121* (1988) 1093.
[16] N. A. Grabowski, R. P. Hughes, B. S. Jaynes, A. L. Rheingold, *J. Chem. Soc. Chem. Commun. 1986*, 1694.

Pentamethylcyclopentadienylmercury Chloride: An Organomercury Compound with Novel Battlement-like Structure

By Jörg Lorberth, Theo F. Berlitz, and Werner Massa*

Dedicated to Professor Michael Fredrick Lappert on the occasion of his 50th birthday

The chemistry of the pentamethylcyclopentadienyl-complexes of main group metals is full of surprises:[1] for example, Cp* (Cp* = C_5Me_5) as η^1-bound ligand in the tin compounds [$Cp^*_2SnX_2$] is eliminated by an unknown mechanism

[*] Prof. Dr. J. Lorberth, Dr. T. F. Berlitz, Prof. Dr. W. Massa
Fachbereich Chemie der Universität
Hans-Meerwein-Strasse, D-3550 Marburg (FRG)

 © VCH Verlagsgesellschaft mbH, D-6940 Weinheim, 1989 0570-0833/89/0505-0611 $ 02.50/0

and forms, via C–C coupling, $C_{20}H_{30}$, decamethyldicyclopentadiene (dimeric Cp*),[2] the gas-phase and solid-state structures of which have already been reported.[3, 4] On attempting to synthesize $SbCp^*_3$ and $SbCp^*_5$ by reaction of $SbCl_3$ and $SbCl_5$, respectively, with KCp* we obtained $[\eta^1$-Cp*Sb$]_4$ and decamethyldicyclopentadiene.[5, 6] In another Cp*-main group metal compound, $[Cp^*_2BiCl]$, the ligand is η^5-bound: above $-30\,^\circ C$ it is eliminated with formation of $C_{20}H_{30}$[6, 7] and $[Cp^*BiCl_2]$.[8]

We have now investigated the reaction of potassium pentamethylcyclopentadienide with $HgCl_2$ at room temperature in ether; the title compound **1** was obtained in 74% yield.

$$HgCl_2 + KCp^* \longrightarrow 1/n\,[Cl\text{–}Hg\text{–}Cp^*]_n + KCl$$
$$\mathbf{1}$$

Decomposition, presumably of $HgCp^*_2$, which is formed in small amounts, still leads to elemental mercury and $C_{20}H_{30}$. Probably the reductive elimination of the hydrocarbon is a general reaction with such compounds and is difficult to suppress.

The crystal structure of $[Cp^*\text{–}Hg\text{–}Cl]_\infty$ **1** was determined by X-ray crystallography.[9] The basic units of this novel structural type consist of almost linear [Cl–Hg–Cp*] groups (Cl–Hg–C angles: 174 and 177°). These units are joined together via weak Hg···Cl contacts (310–324 pm) to give a double-chain structure (see Figs. 1 and 2).

Other than in the case of $[HgCl_2(PMe_3)]$, whose Cl–Hg–P dumbbells are all perpendicular to a planar ladder-like chain,[10] in **1** the covalent Hg–Cl bonds participate in the construction of the double chain: pairs of parallely oriented piece sections of a ladder. Because of the bulkiness of the Cp* terminals the dumbbells in such pairs—linked by symmetry centers—are oriented antiparallel. The incorporation of these dumbbell pairs as sidepiece sections is only possible with strong folding of the double chain; the folding angle at the "crosspieces" with short Hg–Cl bonds (Hg2–Cl2) is 129°, at those with long Hg1···Cl1 contacts 88°, thus resulting in a battlement-like structure of the double chain.

The pentamethylcyclopentadienyl rings do not deviate significantly from planarity (at Hg1 maximaly 1.3(15), at Hg2 maximally 3.5(11) pm). They are bent from the Hg–C bond axis at angles of about 113 and 108°, respectively, and form an organic protective covering round the "$[Hg_2Cl_2]_\infty$ battlement-like structure" (Fig. 3).

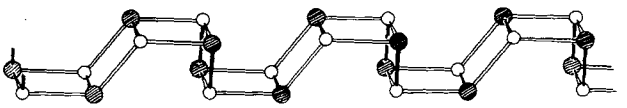


Fig. 1. Double chain or battlement-like structure of **1**. Hatched: Hg; white: Cl; C not shown. For details see text.

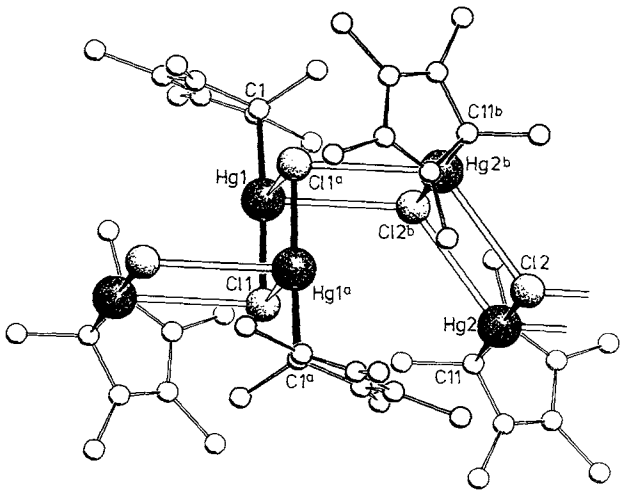


Fig. 2. Section of the polymer structure of **1** view approx. along the *c* axis. Chain orientation along the *a* axis (SCHAKAL drawing) [15]. Important bond lengths [pm] and angles [°]: Hg1-Cl1 236.1(5), Hg1-C1 208(2), Hg1-Cl1^a 309.8(5), Hg1-Cl2^b 323.8(7), Hg2-Cl2 235.0(6), Hg2-C11 210(2), Hg2^b-Cl1^a 323.2(6), Hg2-Cl2^b 317.7(6); Cl1–Hg1–C1 173.9(5), Cl1-Hg1-Cl1^a 87.2(2), Hg1-Cl1-Hg1^a 92.8(2), Cl1^a-Hg1-Cl2^b 75.2(2), Hg1-Cl1^a-Hg2^b 91.3(2), Cl1^a-Hg2^b-Cl2^b 86.1(2), Hg1-Cl2^b-Hg2^b 107.1(2), Cl2-Hg2-C11 176.8(7), Cl2-Hg2-Cl2^b 85.4(2), Hg2-Cl2-Hg2^b 94.6(2), Cl1-Hg1-Cl2^b 86.2(2), Hg1^a-Cl1^a-Hg2^b 90.4(2), Cl1^a-Hg2^b-Cl2 126.8(2), Hg1-Cl2^b-Hg2 128.2(2).

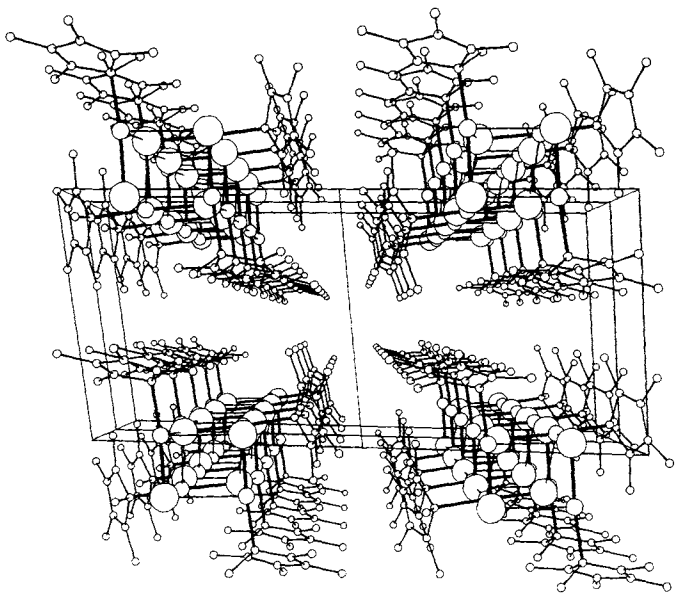


Fig. 3. Perspective ORTEP drawing [16] of the chain structure and packing of the double chains of **1** (projection along the *a* axis).

Double chain structures are also found, aside from in the already mentioned $[HgCl_2(PMe_3)]$, in, e.g., $[pyr\text{–}Cu\text{–}I]_\infty$ (pyr = C_5H_5N),[11] $[CH_3CN\text{–}Cu\text{–}Br]_\infty$[12] and $[F\text{–}Sn\text{–}NCS]_\infty$;[13] however, they are built of tetrahedral building blocks and exhibit simple zig-zag folding. $[Cp\text{–}Sn\text{–}Cl]_\infty$, with a formula type most comparable with the title compound, has a weakly folded ladder-like double chain structure in which all Cp–Sn–Cl dumbbells form "crosspieces".[14]

Experimental

1: A mixture of 3.83 g (14.1 mmol) of $HgCl_2$ and 2.46 g (14.1 mmol) of KCp* in 100 mL of absolute diethyl ether was heated under reflux for 12 h. The ether solution was filtered from the grey, fine-grained precipitate and concentrated by evaporation. On cooling the concentrated solution to $-37\,^\circ C$, yellow needle-like crystals separated out (m.p. 43 °C (decomp. at ca. 78 °C); yield 3.88 g (74%)).—^{1}H NMR ($CDCl_3$), 300 MHz, int. TMS): $\delta \approx 0.98$ (s, $^3J(^{199}Hg\text{–}C\text{–}C\text{–}^1H)$ 62.55 Hz), 1.59(s), 1.75(s).—^{13}C NMR ($CDCl_3$, 300 MHz, int. TMS): δ = 10.8, 12.42, 19.19 (all s, CH_3), 59.60, 132.98, 141.55 (all s, ring atoms).—EI-MS (70 eV), main fragments *m/z* rel. to base peak. 370 (3.95%, $M^\oplus$); 270(13.13%, $C_{20}H_{30}$); 200 (1.84%, Hg); 135 (100%, C_5Me_5); 105 (20.54%, C_5Me_3).

Received: December 8, 1988;
revised: February 17, 1989 [Z 3079 IE]
German version: *Angew. Chem. 104* (1989) 623

[1] P. Jutzi, *Comments Inorg. Chem. 6* (1987) 123.
[2] P. Jutzi, F. Kohl, *J. Organomet. Chem. 164* (1979) 141.
[3] R. Blohm, *Acta Chem. Scand. A 42* (1988) 445.
[4] J. Lorberth, S.-H. Shin, G. Braun, W. Massa, *Acta Crystallogr.*, in press.
[5] T. F. Berlitz, H. Sinning, J. Lorberth, U. Müller, *Z. Naturforsch. B 43* (1988) 744.

[6] J. Lorberth, T. F. Berlitz, S.-H. Shin, U. Müller, H. Sinning, *Abstr. XIIIth Int. Conf. Organomet. Chem.*, Torino 1988.
[7] J. Lorberth, S.-H. Shin, G. Baum, W. Massa, *Angew. Chem.* and *Angew. Chem. Int. Ed. Engl.*, in press.
[8] S.-H. Shin, *Dissertation*, Universität Marburg 1989.
[9] Crystallographic data of **1**: space group $P\bar{1}$, $Z = 4$, $a = 831.5(2)$, $b = 1185.9(2)$, $c = 1245.8(5)$ pm, $\alpha = 91.80(2)$, $\beta = 101.24(2)$, $\gamma = 109.34(2)^\circ$. 2015 observed reflections with $F_o > 4\,\sigma F_o$ were measured on a four-circle diffractometer (CAD4, Enraf-Nonius) with $Mo_{K\alpha}$ radiation at 190 K; empirical absorption correction (ψ scan, $\mu = 138\ cm^{-1}$). The structure was solved by Patterson methods. Refinement using anisotropic temperature factors for all atoms except hydrogen atoms, which were placed at calculated positions with common isotropic temperature factors (218 parameters) led to $R = 0.044$ and $wR = 0.038$ [$w = 1/\sigma^2(F_o)$] [17]. Further details of the crystal structure investigation are available on request from the Fachinformationszentrum Energie, Physik, Mathematik GmbH, D-7514 Eggenstein-Leopoldshafen 2 (FRG), on quoting the depository number CSD-53710, the names of the authors, and the journal citation.
[10] N. A. Bell, M. Goldstein, T. Jones, I. W. Nowell, *Inorg. Chim. Acta 48* (1981) 185.
[11] E. Eitel, D. Oelkrug, W. Hiller, J. Strähle, *Z. Naturforsch. B35* (1980) 1247.
[12] M. Massaux, M. J. Bernard, M.-T. Le Bihan, *Acta Crystallogr. Sect. B27* (1971) 2419.
[13] S. Vilminot, W. Granier, Z. Al Oraibi, L. Cot, *Acta Crystallogr. Sect. B34* (1978) 143.
[14] K. D. Bos, E. J. Bulten, J. G. Noltes, *J. Organomet. Chem. 99* (1975) 71.
[15] E. Keller: *SCHAKAL-86B, A FORTRAN Program for the Graphic Representation of Molecular and Crystallographic Models*, Freiburg 1986.
[16] C. K. Johnson: *ORTEP, Report ORNL-3794*, Oak Ridge National Laboratory, Oak Ridge, TN 1965.
[17] G. M. Sheldrick: *SHELX-76, Program for Crystal Structure Determination*, Cambridge 1976.

From 2,5-Dihydropyrazines to 2*H*-1,4-Diazepines and from Benzodihydroarenes to Benzocycloheptene Derivatives, Structural Variants of the Antidepressant Protriptyline

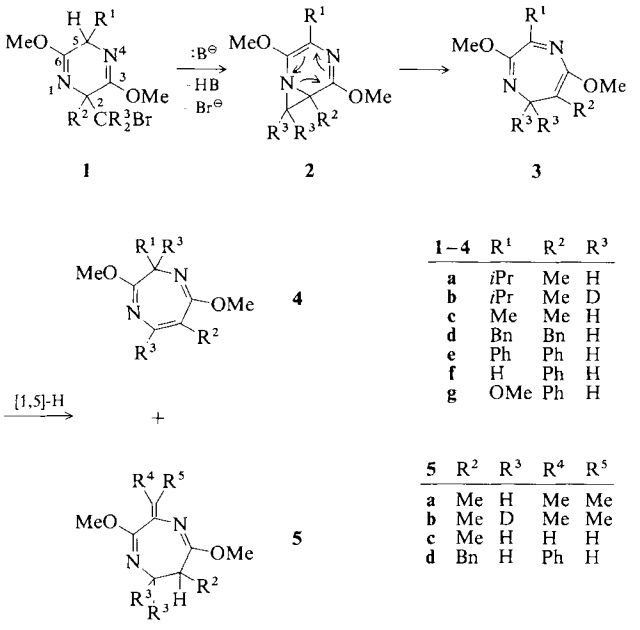
By *Ulrich Schöllkopf** and *Joachim Mittendorf*

Dedicated to Sir Derek Barton on the occasion of his 70th birthday

In our studies of the asymmetric synthesis of non-proteinogenic amino acids according to the bislactim method[1] we have observed that bislactim ethers **1** with a nucleofugal leaving group on C-1′ undergo a novel ring expansion of the six-membered ring to a seven-membered ring in the presence of bases such as potassium hydroxide or potassium *tert*-butoxide in dimethyl sulfoxide (DMSO) or dimethylformamide (DMF) at room temperature, whereby diazepines **4** are formed (Scheme 1). If R^1 is a CHR_2 group, relatively large amounts of dihydrodiazepines **5** are also formed, the ratio **4**:**5** depending upon the reaction conditions (Table 1).

As has been shown by a mechanistic study with deuterium-labeled compounds (e.g. **1b**),[3] the ring expansion begins with the deprotonation of **1** at C-5 and formation of the heteronorcaradiene **2**. This rearranges electrocyclically to 5*H*-1,4-diazepine **3**. So far we have only been able to isolate **3g**; the 1,4-diazepines **3a–f** undergo further rapid reaction involving a [1,5]-sigmatropic shift to give **4**. When $R^1 = CHR_2$ a deprotonation-reprotonation reaction is possible at the stage of **3** in the presence of a base, leading to the dihydrodiazepines **5**.

As already mentioned, when R^1 = OMe (**1g**) the "cycloheptatriene intermediate" **3g** is isolable, since the additional imino ether group strongly stabilizes the ground state. With



Scheme 1. Base-induced ring expansion of the bislactim ethers **1**.

1–4	R^1	R^2	R^3
a	*i*Pr	Me	H
b	*i*Pr	Me	D
c	Me	Me	H
d	Bn	Bn	H
e	Ph	Ph	H
f	H	Ph	H
g	OMe	Ph	H

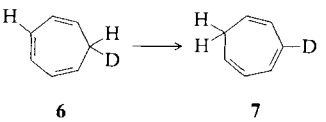
5	R^2	R^3	R^4	R^5
a	Me	H	Me	Me
b	Me	D	Me	Me
c	Me	H	H	H
d	Bn	H	Ph	H

Table 1. Reaction conditions of the ring expansion of **1** and yields of **4** and **5** [8].

1	Base/Solvent	T [°C]	t [h]	Yield [%] **4**	**5**
a	KO*t*Bu/DMSO	50	1	–	75
a	$DMSO^{\ominus}\ Li^{\oplus}$/DMSO	25	10	8	62
a	KOH/DMSO	25	24	73	6
a	KOH/DMSO	50	5	93	< 0.5
a	KOH/DMF	25	24	62	1
c	KOH/DMSO	25	96	14	44
c	KO*t*Bu/DMSO	50	1	–	71
d	KOH/DMSO	25	24	–	73
e	KOH/DMSO:DMF (1:1)	0	4	87	–
f	KOH/DMSO	25	2	59	–
g	KO*t*Bu/DMSO	25	0.2	7[a]	–

[a] Initially **3g** is obtained, which upon heating for 1 h at 90 °C completely rearranges to **4g**.

3g the (irreversible) transannular 1,5-hydrogen shift to give **4g** can be kinetically monitored. The rate constants are $k = (4.385 \pm 0.033) \times 10^{-4}\ s^{-1}$ at 70 °C and $(1.023 \pm 0.011) \times 10^{-4}\ s^{-1}$ at 55 °C.[4] In contrast, the rate constants for the isomerization **6** → **7**, the prototype of the transannular [1,5]-hydrogen shift are $k = 4.8 \times 10^{-8}\ s^{-1}$ at 98 °C, $6.6 \times 10^{-7}\ s^{-1}$ at 121 °C and $3.2 \times 10^{-6}\ s^{-1}$ at 140 °C.[5] Hence, the isomerization **3g** → **4g** at 70 °C is ca. 10^5 times faster than the reaction **6** → **7**. If one sets a lower limit of 96 kJmol^{-1} of the activation barrier of the [1,5]-hydrogen shifts **3** → **4**, in which **3** is not isolable, then it can be estimated that this rearrangement is at least 10^7 times faster than the rearrangement **6** → **7**.[7]

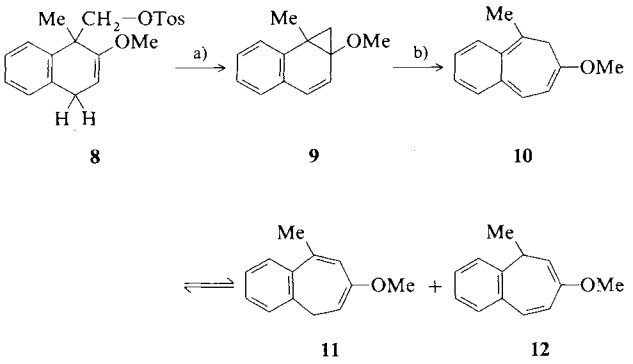


6 **7**

As expected, the ring expansion is not limited to the 2,5-dihydropyrazines, but can also be extended to analogous all-carbon compounds. Thus, reaction of the 1,4-dihydronaphthalene **8**[9] with potassium *tert*-butoxide affords the norcaradiene derivative **9**, which, on heating, is converted

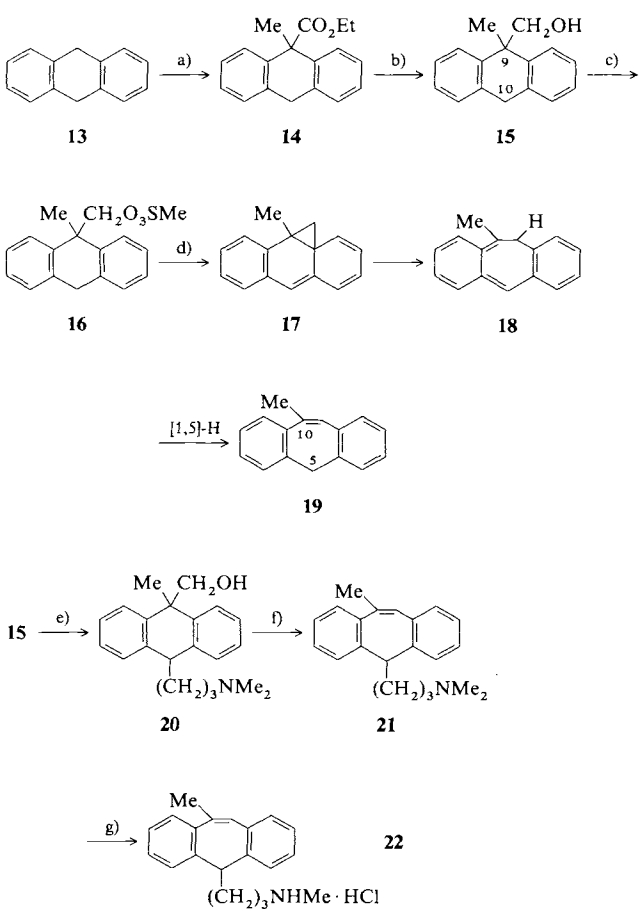
[*] Prof. Dr. U. Schöllkopf, Dipl.-Chem. J. Mittendorf
Institut für Organische Chemie der Universität
Tammannstrasse 2, D-3400 Göttingen (FRG)

via the "cycloheptatriene intermediate" **10** into a mixture of the benzocycloheptenes **11** and **12** (Scheme 2).



Scheme 2. Reaction conditions: a) KO*t*Bu, DMSO, 25 °C; 93%. b) 250 °C in *n*-icosane; 85% [8].

In an analogous way 9,10-dihydroanthracene **13** furnishes 10-methyl-5*H*-dibenzo[*a*,*d*]cycloheptene **19** via the intermediates **14** to **18** (Scheme 3). After introduction of a 3-dimethylaminopropyl group at position 10 of **15**, the compound **22** is formed analogously via the intermediates **20** and **21** (Scheme 3). Compound **22** warrants attention as 10-methyl analogue of the antidepressant protriptyline®. Since the substituent in position 10 of **22** is variable within wide limits, the ring expansion method described here opens up a simple and productive entry to structural variants of protriptyline.



Scheme 3. Reaction conditions: a) 1. *n*BuLi, THF, −78 °C; 2. Dropwise addition to $ClCO_2Et$ (fourfold excess) in THF, −78 °C; 3. KO*t*Bu, THF, 0 °C; 4. MeI, 0 °C; 85%. b) $LiAlH_4$, ther; 96%. c) $MeSO_2Cl$, NEt_3; 93%. d) KO*t*Bu, DMSO, 25 °C; 94%. e) 1. 2 equiv. *n*BuLi, THF, 0 °C; 2. $ClCH_2CH_2CH_2NMe_2$, 0 °C; 81%. f) 1. $MeSO_2Cl$, NEt_3; 2. KO*t*Bu, DMSO, 25 °C; 79%. g) 1. $ClCO_2Ph$, CH_2Cl_2, 25 °C; 2. NaOH, 50% aqueous ethanol, reflux; 3. HCl; 67% [8].

Received: October 31, 1988 [Z 3033 IE]
German version: *Angew. Chem. 101* (1989) 633

CAS Registry numbers:
1a, 119945-28-7; **1c**, 119909-37-4; **1d**, 119909-38-5; **1e**, 119909-39-6; **1f**, 119909-40-9; **1g**, 119909-41-0; **4a**, 119909-18-1; **4c**, 119909-19-2; **4e**, 119909-34-1; **4f**, 119909-35-2; **4g**, 119909-36-3; **5a**, 119909-17-0; **5c**, 119909-20-5; **5d**, 119909-21-6; **6**, 1541-12-4; 7, 65007-13-8; **8**, 119909-22-7; **9**, 119909-23-8; **10**, 119909-24-9; **11**, 119909-25-0; **12**, 119909-26-1; **13**, 613-31-0; **14**, 119909-27-2; **15**, 119909-28-3; **16**, 119909-29-4; **17**, 119909-30-7; **18**, 119909-31-8; **19**, 16204-28-7; **20**, 119909-32-9; **21**, 521-80-2; **22**, 119909-33-0.

[1] Reviews of the bislactim ether method for the asymmetric synthesis of amino acids: U. Schöllkopf in J. Streith, H. Prinzbach, G. Schill (Ed.): *Organic Synthesis: An Interdisciplinary Challenge*, Blackwell, Oxford 1985, p. 101; U. Schöllkopf, *Pure Appl. Chem. 55* (1983) 1799; *Chem. Scr. 25* (1985) 105.
[2] U. Groth, U. Schöllkopf, *Synthesis 1983*, 37.
[3] J. Mittendorf, *Diplomarbeit*, Universität Göttingen 1987, and unpublished results.
[4] The mole fraction of **3** was determined ^1H NMR spectroscopically as a function of time.
[5] A. P. ter Borg, H. Kloosterziel, N. van Meurs, *Recl. Trav. Chim. Pays-Jas 84* (1965) 717.
[6] *H. Kessler*, Angew. Chem. 82 (1970) 237; *Angew. Chem. Int. Ed. Engl. 9* (1970) 219.
[7] This easier [1,5]-hydrogen shift is said to be due to a change in the orbital energies and orbital coefficients (see also C. B. Argo, J. T. Sharp, *J. Chem. Soc. Perkin Trans. 1 1984*, 1581; N. Hoshi, H. Hagiwara, H. Uda, *Chem. Lett. 1979*, 1291, 1295, N. Hoshi, H. Uda, *J. Chem. Soc. Chem. Commun. 1981*, 1163). In the transition state of the rearrangement **3** → **4** the imino ether group has a relatively strong electron-withdrawing effect on both ends of the azapentadiene system. The energy of the HOMO of the azapentadienyl radical should be lowered thereby and the transition state should be stabilized compared to that in the cycloheptatriene system **6** (I. Fleming: *Frontier Orbitals and Organic Reactions*, Wiley, Chichester 1978, p. 27).
[8] Correct C,H analyses and ^1H and ^{13}C NMR and mass spectra were obtained for all the described compounds.

Total Enantiospecific Synthesis of (9*S*)- and (9*R*)-9-Hydroxyeicosatetraenoic Acid (9-HETE) Methyl Ester

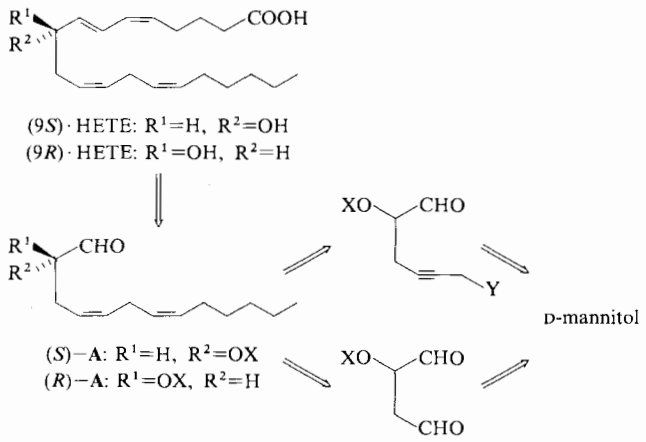
By *Michèle Saniere, Yves Le Merrer, Brigitte Barbe, Thierry Koscielniak, Jacques Dumas, Dominique Micas-Languin*, and *Jean-Claude Depezay**

It has recently been demonstrated that leukotrienes (LTC_4, LTD_4 and LTE_4) are formed in the central nervous system.[1] Furthermore, 9-hydroxyeicosatetraenoic acid (9-HETE) was isolated from incubations of sliced rat brain tissue,[2] thus pointing to a direct lipoxygenase activity in the brain. The formation of 9-HETE had previously never been observed in mammalian tissues.

Two syntheses of (±)9-HETE and (9*S*)-HETE have already been published.[3] In the interest of fully evaluating the biological properties of 9-HETE it was desirable to obtain adequate supplies of both enantiomers. We report here on the synthesis of the enantiomeric 9-HETE methyl esters from

[*] Prof. Dr. J.-C. Depezay, Dr. M. Saniere, Dr. Y. Le Merrer, B. Barbe, T. Koscielniak, J. Dumas, Dr. D. Micas-Languin
Université René Descartes,
Laboratoire de Chimie et Biochimie Pharmacologiques
et Toxicologiques (UA 400 CNRS)
45 rue des Saints Pères, F-75270 Paris Cedex 06 (France)

D-mannitol. The chiral protected α-hydroxyaldehydes (*R*)-**A** and (*S*)-**A** are the key intermediates for these syntheses. To obtain enantiomerically pure α-hydroxyaldehyde **A** with *R*- or *S*-configuration from D-mannitol we used two different methods, one providing selective access to the *R*-configurated aldehyde, the other to the *S*-configurated aldehyde (Scheme 1). Each method can be used for selective access to *R*- or to *S*- configurated aldehydes.



Scheme 1. Retrosynthetic analysis. X = protecting group (see Scheme 2).

Scheme 2 outlines the synthesis of (9*S*)-HETE from the enantiomerically pure diepoxide **1a**,[4] nucleophilic ring-opening of which by 2-lithio-2-propynyl tetrahydropyranyl ether, followed by benzoylation *in situ* afforded **2**. Direct conversion into the dibromide **3**,[5] and coupling with cuprate of 1-heptyne[3] in excess led to the tetrayne **4** (50% overall yield based on **1a**). Direct nucleophilic opening of diepoxide **1a** by various organometallics of decadiyne led to the tetrayne **4** in poor yield (ca. 15%). Selective hydrogenation of **4** to the tetraene **5a**, followed by removal of the ketal and oxidative cleavage of the resulting 3,4-diol gave the protected chiral α-hydroxyaldehyde (*S*)-**A** $[\alpha]_D^{20} = -11°$ (c = 1.2, CH_2Cl_2).

Reaction of (*S*)-**A** with formylmethylene(triphenyl)phosphorane afforded the unsaturated aldehyde (*S*)-**6** in 70% yield, $[\alpha]_D^{20} = +67°$ (c = 1.3, CH_2Cl_2), whose selective *cis* olefination with the ylide derived from the 4-carboxybutyl (triphenyl)phosphonium bromide furnished (*S*)-**7**[6] in 75% yield, $[\alpha]_D^{20} = +51°$ (c = 1.6, CH_2Cl_2). Esterification with diazomethane to give (*S*)-**8** followed by treatment with K_2CO_3 in methanol finally gave the HETE methyl ester (*S*)-**9**. ^{1}H NMR spectroscopic data for **A, 6, 7** and **9** are listed in Table 1.

Table 1. ^{1}H NMR data for compounds **A, 6, 7** and **9** (250 MHz, $CDCl_3$). Numbering sequence of carbons as for **9**.

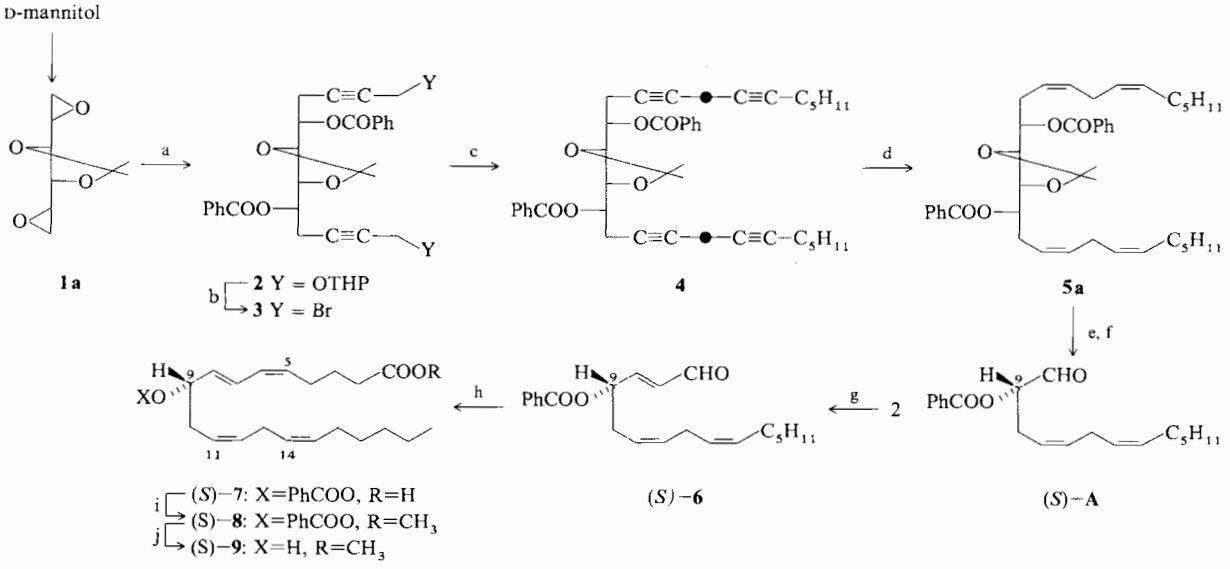
A: δ = 9.64 (s, 1H, CHO); 8.1, 7.50 (m, 5H, Ph); 5.6–5.2 (m, 5H, H-9,11,12,14,15); 2.81 (t, 2H, H-13, J = 7 Hz); 2.72 (t, 2H, H-9, J = 7 Hz); 2.01 (q, 2H, H-16, J = 7 Hz); 1.27 (m, 6H, H-17,18,19,); 0.86 (t, 3H, H-20, J = 7 Hz).

6: δ = 9.55 (d, 1H, CHO, J = 7.5 Hz); 7.90, 7.30 (m, 5H, Ph); 6.85 (dd, 1H, H-8, J = 4.5, 16 Hz); 6.30 (ddd, 1H, H-7, J = 1.5, 7.5, 16 Hz); 5.80 (m, 1H, H-9); 5.54–5.28 (m, 4H, H-11,12,14,15); 2.85 (m, 2H, H-13); 2.60 (m, 2H, H-10); 2.00 (m, 2H, H-16); 1.30 (m, 6H, H-17,18,19); 0.86 (t, 3H, H-20, J = 7 Hz).

7: δ = 8.1 7.5 (m, 5H, Ph); 6.58 (dd, 1H, H-7, J = 11, 16 Hz); 6.01 (t, 1H, H-6, J = 11 Hz); 5.66 (dd, 1H, H-8, J = 7.5, 16 Hz); 5.60–5.20 (m, 6H, H-5,9,11,12,14,15); 1.90–2.79 (m, 10H, H-2,4,10,13,16); 1.70 (m, 2H, H-3); 1.23 (m, 6H, H-17,18,19); 0.86 (t, J = 7 Hz, 3H, H-20).

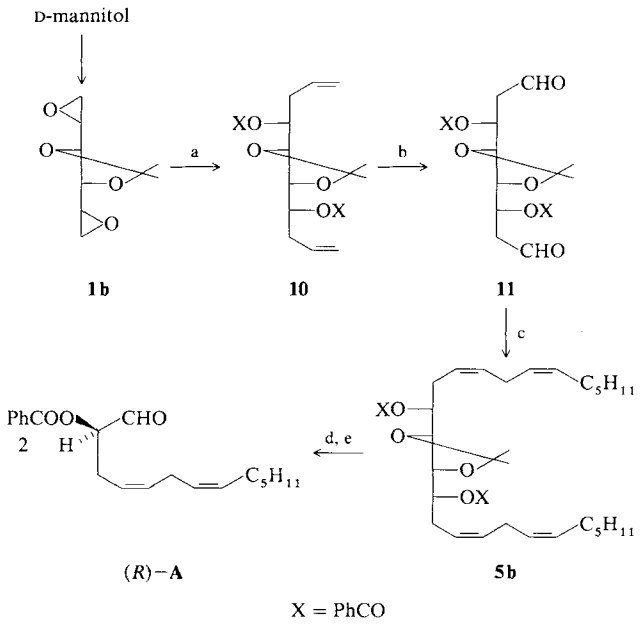
9: δ = 6.48 (ddd, 1H, H-7, J = 1.5, 11, 15.5 Hz); 6.0 (t, 1H, H-6, J = 11 Hz); 5.7 (dd, 1H, H-8, J = 6, 15.5 Hz); 5.4 (m, 5H, H-5,11,12,14,15); 4.2 (m, 1H, H-9); 3.68 (s, 3H, OCH_3); 2.8 (m, 2H, H-13); 1.9–2.5 (m, 8H, H-2,4,10,16); 1.70 (m, 2H, H-3); 1.25 (m, 6H, H-17,18,19); 0.9 (t, J = 7 Hz, 3H, H-20).

We also obtained the (9*R*)-HETE methyl ester from D-mannitol (Scheme 3): nucleophilic opening of the enantiomerically pure D-mannitol derivative **1b**[4] with lithium cyanodivinylcuprate,[7] followed by benzoylation *in situ* afforded **10** (90%), ozonolysis of which led to the crude di-



Scheme 2. [9] a) −5 °C, LiC≡C−CH_2OTHP (4 equiv.), THF/$(Me_2N)_3PO$ (HMPA) 10/1, reflux 20 h, then 0 °C, PhCOCl (5 equiv.), 80%; b) $Ph_2PC_2H_4PPh_2$-$2Br_2$ (4 equiv.), CH_2Cl_2, 1.5 h, 25 °C, 70%; c) C_5H_{11}−C≡CH (4 equiv.), CuBr · Me_2S (2 equiv.), THF, 30 min, −10 °C; then −78 °C, BuLi (2 equiv.), −78 °C → −40 °C, 20 min; then **3**, −78 °C → 0 °C; then HMPA, 0 °C − room temperature (RT), ca. 12 h, 90%; d) H_2, 5% Pd/$BaSO_4$, 1% quinoline, ethyl acetate, 60%; e) F_3C−COOH/H_2O 9/1, −5 °C, 30 min, 100%; f) $Pb(OAc)_4$ (1.2 equiv.), CH_2Cl_2, −10 °C, 1 h, 75%; g) $Ph_3P^{\oplus}$−CH_2−CHO $Br^{\ominus}$ (1.1 equiv.), NEt_3 (1.4 equiv.), C_6H_6, 25 °C, 24 h, 70%; h) $Ph_3P^{\oplus}$−$(CH_2)_4$−COOH $Br^{\ominus}$ (2.8 equiv.), $(CH_3)_3Si$−NLi−$Si(CH_3)_3$ (5.3 equiv.), THF/HMPA 4/1, 0 °C; then −78 °C, **6**, 75%; i) CH_2N_2, Et_2O; j) K_2CO_3, MeOH.

aldehyde **11**. This unstable dialdehyde (highly prone to elimination of benzoic acid) was not purfied but condensed immediately with the ylide derived from the (Z)-non-3-en-1-yl(triphenyl)phosphonium bromide[8] (overall yield based on **10** was 50%). Hydrolysis of the ketal function and oxidative cleavage of the resulting 3,4-diol afforded the protected α-hydroxyaldehyde (*R*)-**A**, $[\alpha]_D^{20} = +11°$ (c = 1.14, CH_2Cl_2).



Scheme 3. [9]. a) $(CH_2=CH)_2CuCNLi_2$ (3 equiv.), THF, −78 °C; −78 °C → RT, 2 h; then −40 °C, PhCOCl (6 equiv.), −40 °C → RT, 40 min, 90%; b) O_3, CH_2Cl_2, −78 °C, then Ph_3P (2 equiv.), −78 °C → RT, 24 h; c) (Z)-$Ph_3P^{\oplus}(CH_2)_2CH=CH-C_5H_{11}$ $Br^{\ominus}$ (4 equiv.), THF, BuLi (3.9 equiv.), −78 °C, 1 h, then **11**, −78 °C → RT, 2 h, yield (b + c) 50%; d) $F_3C-COOH/H_2O$ 9/1, −5 °C, 30 min, 100%; e) $Pb(OAc)_4$ (1.2 equiv.), CH_2Cl_2, −10 °C, 30 min, 76%.

Using the previously described reactions, the aldehyde (*R*)-**A** was transformed into the (9*R*)-HETE methyl ester. Analysis of the (9*S*)- and (9*R*)-HETE methyl esters using a chiral phase HPLC column revealed in each case the presence of a single enantiomer.

The method reported here can be used for the synthesis of various HETEs, metabolites of arachidonic acid.

Received: December 13, 1988 [Z 3086 IE]
German version: Angew. Chem. 101 (1989) 645

[1] a) J. A. Lindgren, T. Hökfelt, S. E. Dahlen, C. Patrono, B. Samuelsson, *Proc. Natl. Acad. Sci. USA 81* (1984) 6212; b) A. Dembinska-Kiec, T. Simmet, B. A. Peskar, *Eur. J. Pharmacol. 99* (1984) 57; c) M. A. Moskowitz, K. J. Kiwak, K. Hekimian, L. Levine, *Science (Washington D.C.) 224* (1984) 886.

[2] B. Samuelsson, S. E. Dahlen, J. A. Lindgren, C. A. Rouzer, C. N. Serhan, *Science (Washington D.C.) 237* (1987) 1171.

[3] a) J. Adams, J. Rokach, *Tetrahedron Lett. 25* (1984) 35; b) G. Just, Z. Yan Wang, *J. Org. Chem. 51* (1986) 4796.

[4] Y. Le Merrer, A. Duréault, C. Greck, D. Micas-Languin, C. Gravier, J. C. Depezay, *Heterocycles 25* (1987) 541.

[5] S. P. Schmidt, D. W. Brooks, *Tetrahedron Lett. 28* (1987) 767.

[6] Depending upon the procedure we obtained up to 10% of the *E*-isomer. In such cases, pure (*S*)-**7** was purified by HPLC.

[7] B. H. Lipshutz, R. S. Wilhelm, J. A. Kozlowski, *Tetrahedron 40* (1984) 5005.

[8] This phosphonium bromide salt was prepared according to the procedure described in: J. Rokach, Y. Girard, Y. Guindon, J. G. Atkinson, M. Larue, R. N. Young, P. Masson, G. Holme, *Tetrahedron Lett. 21* (1980) 1485.

[9] Satisfactory analytical and/or spectroscopic data were obtained for all the new compounds using chromatographically homogenous samples.

Pep5: Structure Elucidation of a Large Lantibiotic**

By *Roland Kellner, Günther Jung,* Michaela Josten, Cortina Kaletta, Karl-Dieter Entian,* and *Hans-Georg Sahl*

Dedicated to Professor Hans Zähner on the occasion of his 60th birthday

The thioether amino acids lanthionine (Lan) and 3-methyllanthionine (MeLan, cf. Fig. 1) have been identified in several biologically active polypeptides produced by Gram-positive bacteria. For these peptide antibiotics, we have proposed the collective name *lantibiotics*.[1] So far, the structures of eight lantibiotics have been elucidated. The most important lantibiotic is nisin,[2] produced by several *Streptococcus lactis* strains, which has found application as a food preservative;[3] others are subtilin,[4] cinnamycin and duramycin,[5] ancovenin,[6] epidermin,[7] Ro09-0198,[8], and gallidermin.[9] In addition to Lan and MeLan, most lantibiotics contain 2,3-unsaturated amino acids. The occurrence of the unusual amino acids causes considerable difficulties in determining the structure, as they are not detected unless specific modifications to sequenceable residues are made.

Recent isolation of the epidermin[7] structural gene from *Staphylococcus epidermidis* showed that lantibiotics are encoded by distinct genes.[1] This finding confirmed the hypothesis[10] that these peptide antibiotics originate from ribosomally synthesized precursor peptides as postulated, e.g., for epidermin.[7a] Recently, the structural genes were sequenced for subtilin,[11] nisin,[12,13] and gallidermin.[14]

All precursor sequences (prelantibiotics) consist of a leader sequence followed by a prosequence from which the lantibiotic is formed by modification.

Here, we report the structure elucidation of the large and strongly basic lantibiotic Pep5.[15] Pep5 is a membrane-modifying polypeptide. In lipid membranes it forms voltage-dependent ion channels by aggregation, and the conductance states depend on the number of monomers involved in the aggregate.[15c] The chemical sequencing enabled us to propose a prolantibiotic (cf. Fig. 4), to synthesize an appropriate DNA probe for isolating the Pep5 structural gene, and to determine the prelantibiotic including its leader sequence.[16]

Table 1. Some characteristic data of Pep5.

Amino acid composition: L-Ala (4), L-Arg (2), L-Asn (1), L-Gln (2), L-Gly (3), L-Ile (1), L-Leu (2), L-Lys (6), L-Phe (1), L-Pro (1), L-Val (2), *meso*-Lan (2), (2*S*,3*S*,6*R*)-3-MeLan (1), Dhb (2); N^{α}-2-oxobutyryl.

HPLC: Gradient: 12% B to 40% B in 15 min. Eluent A: 0.1% Tfa in water. Eluent B: 0.1% Tfa; 80% acetonitrile; 20% water.

Conditions: Nucleosil $5C_{18}$, 4.6 × 250 mm; flowrate 1 mL min^{-1}; UV detection 214 nm; retention time: 23 min.

Mass spectrum: (FAB-MS): *m/z* 3489 [Pep5 + H]$^{\oplus}$

[*] Prof. Dr. G. Jung, Dipl.-Chem. R. Kellner
Institut für Organische Chemie der Universität
Auf der Morgenstelle 18, D-7400 Tübingen (FRG)
Prof. Dr. K.-D. Entian, Dipl.-Biochem. C. Kaletta
Medizinisch-Naturwissenschaftliches Forschungszentrum der Universität
D-7400 Tübingen (FRG)
Prof. Dr. H.-G. Sahl, M. Josten
Institut für Medizinische Mikrobiologie der Universität
D-5300 Bonn (FRG)

[**] This work was supported by the Deutsche Forschungsgemeinschaft (SFB 323 and Sa 292/4-2) and the Fonds der Chemischen Industrie. We thank *G. J. Nicholson* for expert technical assistance. A doctorate stipend (*C. S.*) was given by Dechema, and *K.-D. E.* is the recipient of a Heisenberg grant from the Deutsche Forschungsgemeinschaft.

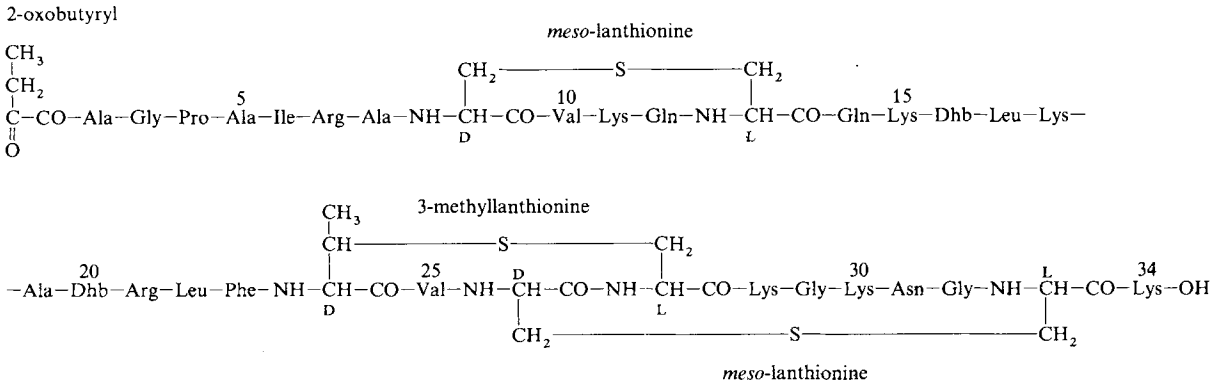


Fig. 1. Structure of the tricyclic lantibiotic Pep5. All amino acids have L-configuration with the exception of the *N*-terminal half of *meso*-lanthionine and (2*S*,3*S*,6*R*)-3-methyllanthionine. Dhb = dehydrobutyrine = 2-aminobut-2-enoic acid.

The polypeptide antibiotic Pep5 (Fig. 1) was isolated from culture supernatants of *Staphylococcus epidermidis* 5.[15] The acidic hydrolyzate of Pep5 contained twenty-five protein amino acids, two lanthionines and one 3-methyllanthionine (cf. Table 1). The configurational analysis by gas chromatography of trifluoroacetyl-amino acid *n*-propylesters on chiral stationary phases[17] revealed *meso*-lanthionine (Lan) and (2*S*,3*S*,6*R*)-3-methyllanthionine (MeLan); unsaturated amino acids were detected after chemical derivatization. The native antibiotic was *N*-terminally blocked, and therefore chemical and enzymic degradation failed. Having a content of eight cationic amino acids and an isoelectric point pI > 10.5, Pep5 is very hydrophilic and strongly basic and its chromatography therefore causes many problems. Moreover, a high number of enzymic cleavage sites and, particularly, the presence of two dehydrobutyrines (Dhb) caused further complications when elucidating the structure.

The key for sequencing the complex lantibiotic was the enzymic cleavage with chymotrypsin and endoproteinase Arg-C (Fig. 2). Other proteases, for example trypsin, gave a complex mixture of many fragments. The most important results were obtained by Edman degradation (Fig. 3),[18] even though the information was limited by the particular properties of the unusual components. Lanthionine and 3-

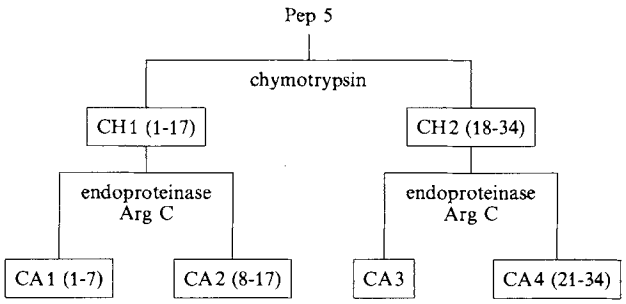


Fig. 2. Survey of enzymic cleavage used in sequencing the heterodet tricyclic 34-peptide antibiotic Pep5.

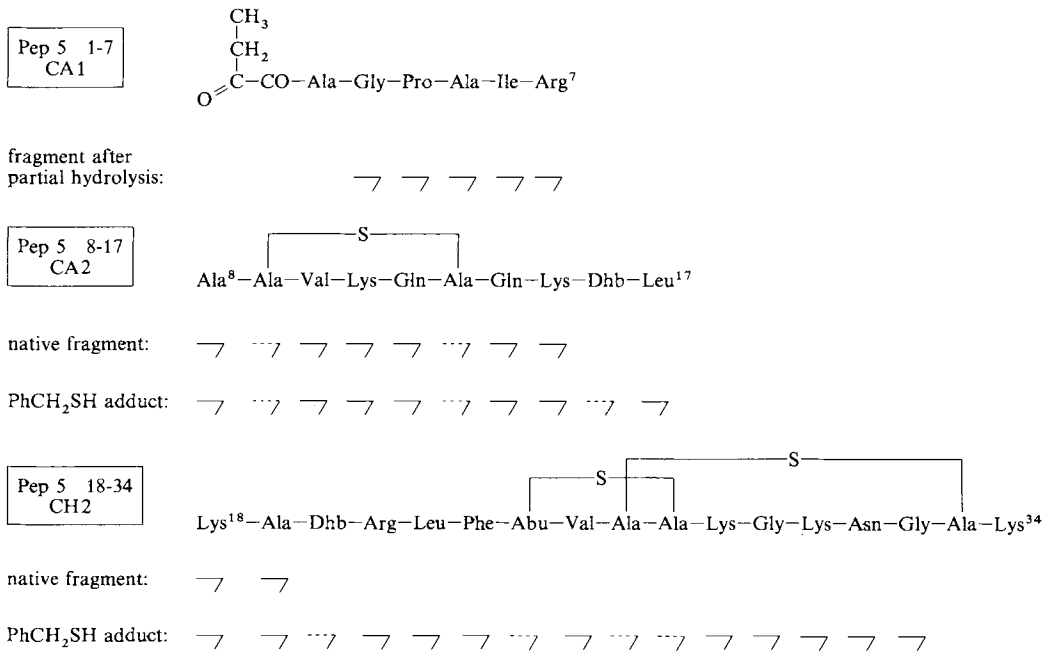


Fig. 3. Sequence information obtained by Edman degradation [18] of isolated fragments of Pep5 (cf. Fig. 2) and benzylthioalcohol adduct [19] (---), no PTH derivative was detected). Abu = α-aminobutyric acid.

methyllanthionine were not detectable during automated pulsed liquid-phase sequencing, because of the sulfide bridges and the peculiar chromatographic properties of their bis-PTH-derivatives. Fortunately, the Edman degradation proceeded further after the gap due to the Lan or MeLan residue. By contrast, the α,β-unsaturated amino acids blocked the Edman degradation by deamination with formation of an *N*-terminal 2-oxobutyryl residue, as found for position 14 in epidermin[7] and gallidermin.[9] The main products of chymotryptic cleavage of Pep5 were the two fragments, CH1 and CH2. The *N*-terminal part of Pep5, CH1, was further cleaved by endoproteinase Arg-C to give the fragments CA1 and CA2. Fragment CA1 was found to be *N*-terminally blocked as the native polypeptide, and the Edman degradation of CA2 stopped after eight residues. After adding benzylthioalcohol to the double bond,[19] the sequence 8–17 was obtained whereby positions 9 and 13 belonged to a Lan-residue and position 16 to an unsaturated amino acid.

In the same way the degradation of the C-terminal part of Pep5, CH2, stopped already after two amino acids, and again derivatization with benzylthioalcohol revealed the prolonged amino acid sequence 18–32. Hence, an additional unsaturated amino acid must have been located at position 20. The backbone positions for one Lan and one MeLan-residue were shown to be positions 24, 26, 27 and 33. After adding benzylthioalcohol, the acidic total hydrolyzates of Pep5 and its fragments were analyzed by GC-MS and *S*-benzyl-3-methylcysteine was detected as the addition product of Dhb. Lan and MeLan were detected again by GC-MS, but no further unusual residue was observed. The C-terminal residues of the fragments were obtained after cleavage with carboxypeptidase *A*/*B*.

26 to 33 for Lan. The fragment Leu^{22}-Phe^{23}-Abu^{24} was detected in the positive FAB mass spectrum of CA4 and, furthermore, different characteristic fragments resulted from the neighboring sulfur atoms containing sequence Ala^{26}(S)-Ala^{27}(S). The bridging positions were established in accordance to Pro-Pep5 with Thr/Cys as the precursor for MeLan and Ser/Cys for Lan (Fig. 4). The partial acid hydrolysis of Pep5 showed the turn segment Gly^3-Pro^4-Ala^5 to be preferably cleavable, and sequencing the isolated hydrolytic fragments established the amino acid sequence 3–15. From the amino acid composition, one Ala residue appeared to be missing and so must have been located at position 2.

Using ^{13}C NMR, Pep5 was found to contain a 2-oxobutyryl-residue probably located at the *N*-terminus. Therefore the tentative sequence of fragment CA1 consisting of 2-oxobutyryl-Ala^2-Gly-Pro-Ala-Ile-Arg^7 (Fig. 1), was synthesized and compared with the enzymatic fragment CA1 by HPLC and FAB-MS. This comparison showed the two fragments to be identical.

To sum up, Pep5 was shown to contain a 34-residue backbone (Fig. 1) and this was confirmed by FAB-MS and ^{13}C NMR. The 2-oxobutyryl residue at the *N*-terminus originating from threonine of the prelantibiotic is counted as position one. With the sequence of Pep5 obtained, the elucidation of the corresponding linear prepeptide sequence could be revealed by genetic methods.[1] This prepeptide sequence confirmed the chemically derived amino acid sequence and especially the positions of the unusual amino acids. The sequence of Pep5 shows no homology to any of the eight lantibiotics known so far. Thus, the versatility of the enzymes catalyzing the transformation of prelantibiotics to the various lantibiotics is remarkable, and one may expect a great potential for achieving useful biotransformations of

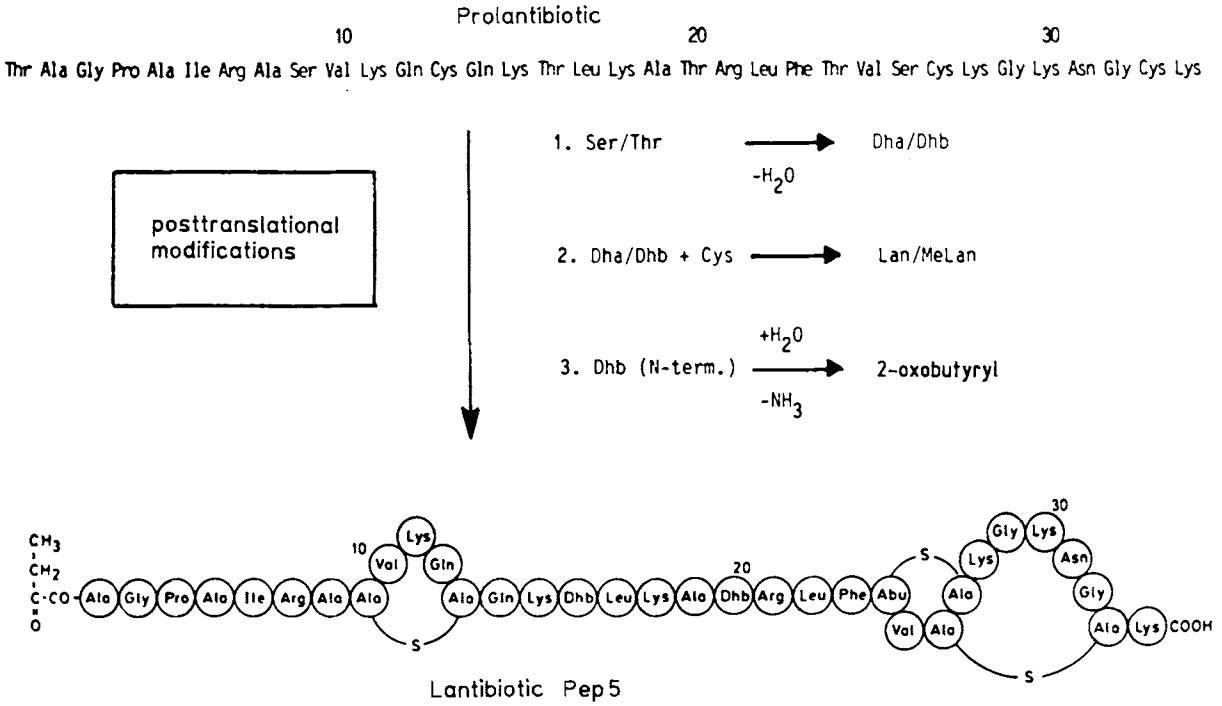


Fig. 4. Biosynthesis of lantibiotic Pep5. The ribosomally synthesized propeptide of Pep5 is posttranslationally modified by water elimination from L-serine and L-threonine residues and stereospecific addition of thiol groups of L-cysteines to the resulting possibly intermediate double bonds of dehydroalanine (Dha) and dehydrobutyrine (Dhb), thus forming *meso*-lanthionine and (2*S*,3*S*,6*R*)-3-methyllanthionine. Thereby the α-carbon atoms of the originally hydroxylated amino acids become D-configurated. The *N*-terminal dehydrobutyrine is unstable and after deamination a 2-oxobutyryl residue is formed.

Assignment of the thioether bridges in the C-terminal fragment CA4 was achieved by FAB-MS (*m*/*z* 1349 [M + $H^{\oplus}$]) and involved positions 24 to 27 for MeLan and suitably designed precursor peptides. However, none of the enzymes acting in lantibiotic biosynthesis has been isolated so far.

Received: January 2, 1989 [Z 3110 IE]
German version: *Angew. Chem. 101* (1989) 618

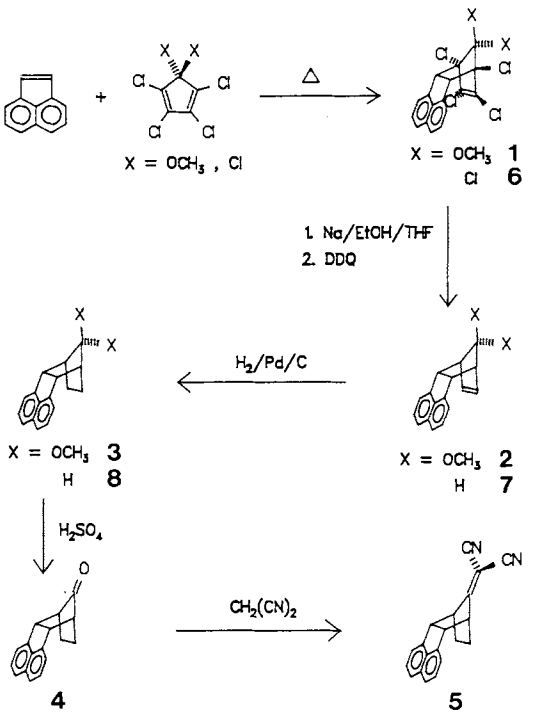
[1] N. Schnell, K.-D. Entian, U. Schneider, F. Götz, H. Zähner, R. Kellner, G. Jung, *Nature (London) 333* (1988) 276.
[2] E. Gross, J. L. Morell, *J. Am. Chem. Soc. 93* (1971) 4634.
[3] A. Hurst, *Adv. Appl. Microbiol. 27* (1981) 85.
[4] E. Gross, H. Kiltz, E. Nebelin, *Hoppe-Seyler's Z. Physiol. Chem. 354* (1973) 810.
[5] E. Gross, *Adv. Exp. Med. Biol. B86* (1977) 131.
[6] T. Wakamiya, Y. Ueki, T. Shiba, Y. Kido, Y. Motoki, *Tetrahedron Lett. 26* (1985) 665.
[7] a) H. Allgaier, G. Jung, R. G. Werner, U. Schneider, H. Zähner, *Angew. Chem. 97* (1985) 1052; *Angew. Chem. Int. Ed. Engl. 24* (1985) 1051; b) *Eur. J. Biochem. 160* (1986) 9.
[8] a) H. Kessler, S. Steuernagel, D. Gillessen, T. Kamiyama, *Helv. Chim. Acta 79* (1987) 726; b) H. Kessler, S. Steuernagel, M. Will, G. Jung, R. Kellner, D. Gillessen, T. Kamiyama, *ibid. 71* (1988) 1924.
[9] R. Kellner, G. Jung, T. Hörner, H. Zähner, N. Schnell, K. D. Entian, F. Götz, *Eur. J. Biochem. 177* (1988) 53.
[10] a) L. C. Ingram, *Biochim. Biophys. Acta 224* (1970) 263; b) C. Nishio, S. Komura, K. Kurahashi, *Biochem. Biophys. Res. Commun. 116* (1983) 751.
[11] S. Banerjee, J. N. Hansen, *J. Biol. Chem. 263* (1988) 9508.
[12] G. W. Buchman, S. Banerjee, J. N. Hansen, *J. Biol. Chem. 263* (1988) 16260.
[13] C. Kaletta, K.-D. Entian, *J. Bacteriol. 171* (1989) 1597.
[14] N. Schnell, K. D. Entian, F. Götz, T. Hörner, R. Kellner, G. Jung, *FEMS Microbiol. Lett. 58* (1989) 263.
[15] a) H.-G. Sahl, H. Brandis, *J. Gen. Microbiol. 127* (1981) 377; b) H.-G. Sahl, M. Grossgarten, W. R. Widger, W. A. Cramer, H. Brandis, *Antimicrob. Agents Chemother. 27* (1985) 836; c) M. Kordel, R. Benz, H.-G. Sahl, *J. Bacteriol. 170* (1988) 84.
[16] C. Kaletta, K.-D. Entian, R. Kellner, G. Jung, M. Reis, H.-G. Sahl, *Arch. Microbiol.*, in press.
[17] E. Küsters, H. Allgaier, G. Jung, E. Bayer, *Chromatographia 18* (1984) 287.
[18] For automated Edman degradation, a pulsed liquid-phase sequencer Model 477 A with an on-line Model 120 PTH-analyzer (Applied Biosystems) was used. Sequencing reagents and solvents were from Applied Biosystems. The acidic total hydrolysates were analyzed by gas chromatographic enantiomer analysis on the chiral phase Chirasil-Val [17], using a Sichromat Autoderivat 100 (Siemens). FAB-Mass spectra were recorded with a VG 70/250/SEQ and the samples were applied in a matrix of 3-nitrobenzylalcohol/methanol.
[19] a) E. Nebelin, E. Gross, *Hoppe-Seyler's Z. Physiol. Chem. 354* (1973) 807; b) E. Gross, J. L. Morell, *J. Am. Chem. Soc. 92* (1970) 2919.

Synthesis of a Rigid Electron-Donor/Acceptor Compound–Evidence for Intramolecular Charge Separation**

By *Hans Heitele,** *Peter Finckh,* and *Maria Elisabeth Michel-Beyerle*

Particularly suitable for investigating the factors which determine the rate of electron transfer reactions[1–12] are compounds in which an electron donor and an electron acceptor are rigidly bound together.[3–6] The mutual diffusion of the reaction partners and possible changes of conformation during the reaction are thereby excluded. Our investigations on electron transfer processes[10–12] have now led to the compound **5**, in which a (electronically excited) naphthylene residue acts as electron donor and a dicyanoethylidene residue as electron acceptor. Compound **8** served as reference standard for fluorescence measurements.

Essentially all the steps of the synthesis of **5** and **8** can be taken from Ref. [3]. (Scheme 1). Upon fusion, acenaphthalene reacts with polychlorocyclopentadienes at 110 °C in a Diels-Alder reaction to give the *endo* products **1** and **6** in 70–75% yield. By reduction with a large excess of sodium in boiling ethanol/THF and rearomatization by heating with 2,3-dichloro-5,6-dicyanobenzoquinone (DDQ) in benzene all the chlorine atoms can be replaced by hydrogen atoms (**2**, **7**; 63 and 32% yield respectively). The double bond is hydrogenated at normal pressure in ethyl acetate on 10% Pd/C (**3** and **8**). The ketal **3** is then cleaved in a mixture of THF and 40% H_2SO_4 (1:1) to give the ketone **4** (yield 78%), which upon Knoevenagel condensation with malonodinitrile in a Dean and Stark condenser (for removal of H_2O) affords the desired product **5** (yield 79%). All compounds form colorless crystals.



Scheme 1. Synthesis of the donor/acceptor compound **5** and the reference compound **8**.

The structures of the products are confirmed by ^{1}H NMR and mass spectra (Table 1). The large upfield shift ($\delta = 0.6$–0.9) of two of the four protons of the ethylene bridge in **3**, **4**, **5** and **8** in the *endo* isomers can be explained, in particular, by a ring current effect on the H atoms lying directly above the naphthalene system. The larger extinction coefficient in **5** at ca. 290 nm compared to that in **8** indicates a direct charge transfer absorption[3] in **5** below 300 nm.

A comparison of the fluorescence spectra[13] (not corrected) of the compounds **5** and **8** in methanol and *n*-hexane affords the first evidence for their electron transfer properties (Fig. 1). The shapes of the spectra of **5** and **8** in methanol are almost identical, the relative quantum yield ϕ in the case of **5** is, however, only 1% of the yield for **8**. The strong quenching is probably attributable to an intramolecular electron transfer from the excited naphthylene residue to the dicyanoethylidene residue, which competes with the fluorescence of the naphthylene residue. Intermolecular quenching processes can be ruled out because of the low concentration of the sample. From the ratio of the quantum yields $\phi_5/\phi_8 \leq 0.01$ and the fluorescence lifetime $\tau_8 \approx 40$ ns, a lower limit of ca. 2.5×10^9 s^{-1} can be given for the electron transfer rate in **5**.[14] The free enthalpy of this reaction in

[*] Dr. H. Heitele, Dr. P. Finckh, Prof. Dr. M. E. Michel-Beyerle
Institut für Physikalische und Theoretische Chemie der
Technischen Universität München
Lichtenbergstraße 4, D-8046 Garching (FRG)

[**] This work was supported by the Deutsche Forschungsgemeinschaft and the Volkswagenstiftung.

Table 1. Spectroscopic data of the compounds **1**–**8** [a].

1: m.p. 165.5–166 °C (from ethanol) ^{1}H NMR: δ = 3.6 (s, 3H; OCH_3), 3.75 (s, 3H; OCH_3), 4.5 (s, 2H; Aryl-CH), 7.2–7.7 (m, 6H; Aryl-H). MS: *m/z* 414 ($M^{\oplus}$, 19%), 381 (97), 379 (100), 343 (37), 152 (62)

2: m.p. 120.5–122.5 °C (from hexane). ^{1}H NMR: δ = 3.1–3.4 (m, 2H; C=C–CH); overlapping with 3.2 (s, 3H; OCH_3) and 3.37 (s, 3H; OCH_3), 4.2 (br., 2H; Aryl-CH), 5.45 (m, 2H; HC=CH), 7.0–7.6 (m, 6H; Aryl-H). MS: *m/z* 278 ($M^{\oplus}$, 100%), 263 (45), 250 (34), 203 (86), 152 (50)

3: m.p. 118–120 °C (from hexane). ^{1}H NMR: δ = 0.6–0.8 (m, 2H; *endo*-H of CH_2), 1.3–1.6 (m, 2H; *exo*-H of CH_2), 2.5 (br., 2H; CH), 3.3 (s, 3H; OCH_3), 3.4 (s, 3H; OCH_3), 4.1 (br., 2H; Aryl-CH), 6.9–7.6 (m, 6H; Aryl-H). MS: *m/z* 280 ($M^{\oplus}$, 97%), 265 (100), 205 (36)

4: m.p. 106.5–107.5 °C (sublimed at 10^{-3} mbar) ^{1}H NMR: δ = 0.8–1.7 (m, 4H; CH_2), 2.45 (br., 2H; CH), 4.1 (br., 2H; Aryl-CH), 7.0–7.6 (m, 6H; Aryl-H). MS: *m/z* 234 ($M^{\oplus}$, 67%), 179 (100)

5: m.p. 198–199 °C (from ethanol). ^{1}H NMR: δ = 0.9–1.6 (m, 4H; CH_2), 3.4 (br., 2H; CH), 4.1 (br., 2H; Aryl-CH), 7.1–7.7 (m, 6H; Aryl-H). MS: *m/z* 282 ($M^{\oplus}$, 29%), 153 (100), UV (MeOH): λ_{max}[nm](lg E) = 321 (3.06), 289 (3.96)

6: m.p. 189–190 °C from ethyl acetate). ^{1}H NMR: δ = 4.7 (s, 2H; Aryl-CH), 7.1–7.7 (m, 6H; Aryl-H). MS: *m/z* 422 ($M^{\oplus}$, 5%), 152 (100)

7: m.p. 54–55 °C (sublimed at 10^{-3} mbar). ^{1}H NMR: δ = 1.65 (m, 2H; CH_2), 3.23 (br., 2H; CH), 4.03 (br., 2H; Aryl-CH), 5.35 (m, 2H; HC = CH), 7.0–7.6 (m, 6H; Aryl-H). MS: *m/z* 218 ($M^{\oplus}$, 18%), 152 (100)

8: m.p. 84–85 °C (sublimed at 10^{-3} mbar). ^{1}H NMR: δ = 0.7–2.0 (m, 6H; CH_2), 2.6 (br., 2H; CH), 3.9 (br., 2H; Aryl-CH), 6.8–7.7 (m, 6H; Aryl-H). MS: *m/z* 220 ($M^{\oplus}$, 51), 179 (36), 153 (100). UV (MeOH): λ_{max}[nm](lg E) = 321 (3.12), 291 (3.84)

[a] The ^{1}H NMR spectra were recorded at 60 MHz in $CDCl_3$ and the mass spectra at 70 eV.

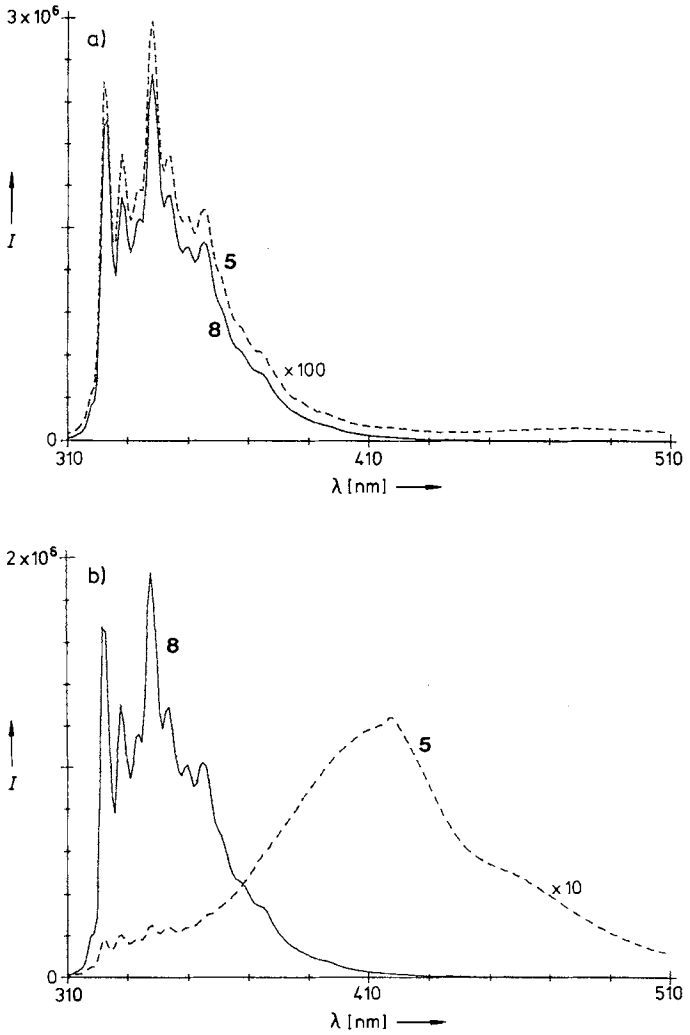


Fig. 1. Fluorescence spectra of the compounds **5** and **8** in methanol (a) and *n*-hexane (b). Spectra of **5**; 100 × and 10 ×, respectively.

methanol is estimated to be ca. −0.9 eV.[15] The emission spectrum of **5** in hexane shows, besides a small donor fluorescence with similar quantum yields as in methanol, a broad fluorescence band with a maximum at ca. 415 nm. The fluorescence excitation spectra in *n*-hexane (not shown) do not change upon variation of the wavelength of the observed fluorescence light between 330 and 470 nm and agree with the excitation spectrum of **8**, i.e. the initial state of the red-shifted emission is populated via the excitation of the napthylene residue. The strong quenching of the donor fluorescence shows that the intramolecular electron transfer in **5** is also thermodynamically possible in apolar solvents. The emission at 415 nm is presumably due to a recombination fluorescence (transition from the charge transfer state into the ground state of the molecule).[3] In polar solvents this emission is shifted into the infrared and its intensity decreases dramatically.[3] This explains the absence of a red shifted fluorescence band of **5** in methanol. A confirmation of this preliminary interpretation, however, requires further time resolved measurements.

The advantages of compound **5** are its simple synthesis, its completely rigid structure, the fact that electron transfer is possible in arbitrary solvents, and the long fluorescence lifetime of the unquenched donor, which makes changes in the rate—by decreasing the temperature—of three orders of magnitude measureable.

Received: December 27, 1988 [Z 3107 IE]
German version: *Angew. Chem. 101* (1989) 629

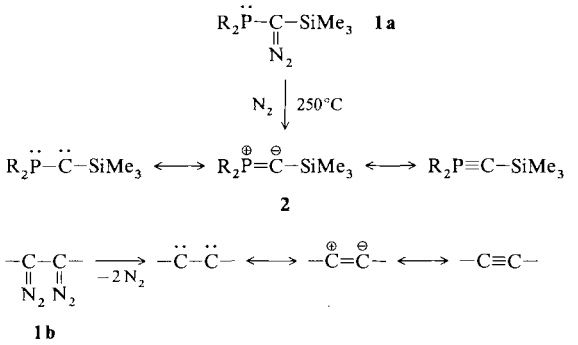
CAS Registry numbers:
1, 119945-29-8; **2**, 119909-42-1; **3**, 119909-43-2; **4**, 120010-45-6; **5**, 119924-07-1; **6**, 63784-80-5; **7**, 26159-42-2; **8**, 119945-30-1; $CH_2(CN)_2$, 109-77-3; acenaphthylene, 208-96-8; 5,5-dimethoxytentachlorocyclopentadiene, 2207-27-4; perchlorocyclopentadiene, 77-47-4.

[1] M. D. Newton, N. Sutin, *Annu. Rev. Phys. Chem. 35* (1984) 437, and references cited therein.
[2] R. A. Marcus, N. Sutin, *Biochim. Biophys. Acta 811* (1985) 265, and references cited therein.
[3] H. Oevering, M. N. Paddon-Row, M. Heppener, A. M. Oliver, E. Cotsaris, J. W. Verhoeven, N. S. Hush, *J. Am. Chem. Soc. 109* (1987) 3258.
[4] J. M. Warman, M. P. de Haas, M. N. Paddon-Row, E. Cotsaris, N. S. Hush, H. Oevering, J. W. Verhoeven, *Nature (London) 320* (1986) 615.
[5] M. R. Wasielewski, M. D. Niemczyk, W. A. Svec, E. B. Pewitt, *J. Am. Chem. Soc. 107* (1985) 1080.
[6] D. Heiler, G. McLendon, P. Rogalsky, *J. Am. Chem. Soc. 109* (1987) 604.
[7] G. L. Closs, L. T. Calcaterra, N. J. Green, K. W. Penfield, J. R. Miller, *J. Phys. Chem. 90* (1986) 3673.
[8] A. D. Joran, B. A. Leland, G. G. Geller, J. J. Hopfield, P. B. Dervan, *J. Am. Chem. Soc. 106* (1984) 6090.
[9] R. J. Harrison, B. Pearce, G. S. Beddard, J. A. Cowan, J. K. Sanders, *Chem. Phys. 116* (1987) 429.
[10] H. Heitele, M. E. Michel-Beyerle, *J. Am. Chem. Soc. 107* (1985) 8068.
[11] H. Heitele, M. E. Michel-Beyerle, P. Finckh, *Chem. Phys. Lett. 134* (1987) 273.
[12] P. Finckh, H. Heitele, M. Volk, M. E. Michel-Beyerle, *J. Phys. Chem. 92* (1988) 6584.
[13] Sample concentration 10^{-5} M, excitation wavelength 295 nm. The spectra are independent of the excitation wavelength between 290 and 320 nm. All samples were prepared shortly before the measurement and carefully freed of oxygen.
[14] Electron transfer rate $k = 1/\tau_8$ ($\phi_8/\phi_5 - 1$). Fluorescing impurities (e.g. residues of **4**) of ≤1% in **5** cannot, as yet, be excluded. The actual transfer rate could therefore be significantly greater than 2.5×10^9 s^{-1}.
[15] The free enthalpy of the electron transfer ΔG^0 is given by $\Delta G^0 = E_{ox} - E_{red} - e^2/\varepsilon d - \Delta E_{00}$, with the oxidation potential of the donor (acenaphthene) $E_{ox} \approx 1.35$ V [16], the reduction potential of the acceptor $E_{red} \approx -1.70$ V [3], the excitation energy of the acceptor $\Delta E_{00} = 3.85$ eV (from the absorption spectrum), and the coulomb energy of the ion pair with the ionic distance $d = 6$ Å and the dielectric constant of the solvent (methanol) $\varepsilon = 32$. This gives $\Delta G^0 \approx -0.9$ eV in methanol.
[16] A. J. Bard, L. Lund: *Encyclopedia of Electrochemistry of the Elements. Vol. XI*, Marcel Dekker, New York 1978.

[Bis(diisopropylamino)phosphino]trimethylsilylcarbene: A Stable Nucleophilic Carbene**

By *Alain Igau, Antoine Baceiredo, Georges Trinquier,* and *Guy Bertrand**

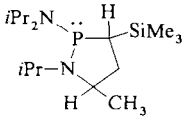
Recently, we were able to show that the thermolysis of [bis(diisopropylamino)phosphino](trimethylsilyl)diazomethane **1a**[1] leads, after loss of nitrogen, to a stable compound **2** ("1,1-Bis(diisopropylamino)-2-trimethylsilyl-1-phosphaacetylene")[2]. The NMR data and reactivity of **2** towards trimethylsilyl chloride, dimethyl sulfoxide and trimethylsilyl azide are characteristic for a phosphorus–carbon multiple bond (Scheme 1).



Scheme 1.

It is well-known[3] that α,α'-biscarbenes, generated from the corresponding bisdiazo derivatives **1b**, are stable compounds; however, from their reactivity they must be regarded as alkynes rather than as stable biscarbenes.

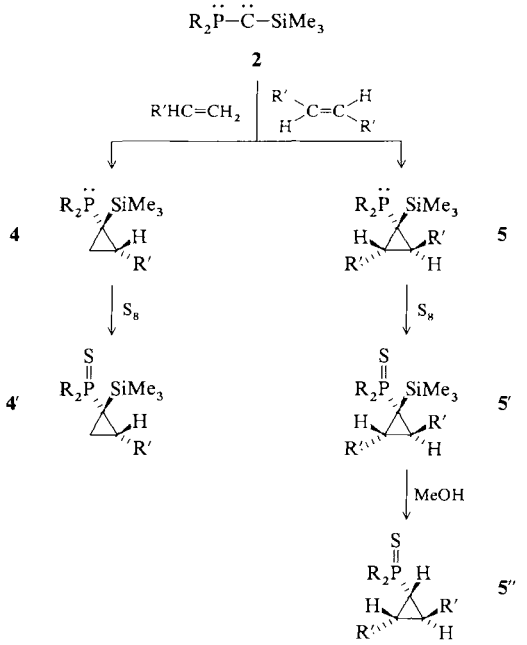
The only argument for the carbene character of **2** was based on the formation of the azaphospholidine **3** (carbene insertion into a carbon-hydrogen bond of an isopropyl substituent) upon thermolysis of **2** at 300 °C.[2] The experimental conditions used and the regioselectivity of the ring closure are consistent with this argument.



3

We now wish to report definitive evidence for the carbene character of **2**, based on cyclopropanation reactions, oxirane formation, and [1 + 1] addition to isocyanides.

Compound **2** does not react with alkyl-substituted alkenes or conjugated dienes,[4] but readily adds to electron-poor olefins such as methyl acrylate and dimethyl fumarate with formation of the cyclopropane derivatives **4** and **5**.[5] Reaction with sulfur affords the compounds **4'** and **5'** in 95 and 87% yield, respectively. In both cases only one diastereoisomer is obtained. The NMR spectroscopic data (see Table 1) of **4, 4', 5, 5'** and **5''** (obtained by methanolysis of **5'**), suggest a *syn* attack of the carbene **2**,[6] with retention of the stereochemistry about the double bond (Scheme 2). Compound **2** does not react with dimethyl maleate: the difference in reactivity between *cis* and *trans*-olefins towards carbenes has already been noted by *Moss* et al. with the methoxy(phenyl)carbene.[7] Note that products **4** and **5** are also obtained when the diazo derivative **1a** is irradiated, at 300 nm, in the presence of a stoichiometric amount of the corresponding alkene.



Scheme 2.

Electrophilic carbenes are known to react with carbonyl groups through the oxygen lone pair to give carbonyl ylides ($R_2C=\overset{\oplus}{O}-\overset{\ominus}{C}X_2$).[8] These 1,3 dipolar species are usually characterized by [3 + 2] cycloaddition or can even be isolated;[9] a small amount of the corresponding oxiranes is sometimes obtained.[8a, 10] Compound **2** does not react with dimethyl ketone but readily adds to benzaldehyde and cinnamaldehyde, affording oxiranes **6** and **7**. After treatment with elemental sulfur, **6'** and **7'** were isolated in 80 and 82% yield, respectively, as only one diastereoisomer. These results strongly suggest a concerted mechanism (route a): a zwitterionic intermediate such as **8** would have probably induced an oxygen attack at the phosphorus atom with subsequent formation of a phosphorylalkene (route b). Indeed, when a very electron-poor carbonyl group, such as ethyl cyanoformate, is used, a mixture of *Z*- and *E*-phosphorylalkenes **9** (Table 1) is obtained, and no trace of the corresponding oxiranes is detected (Scheme 3).[11]

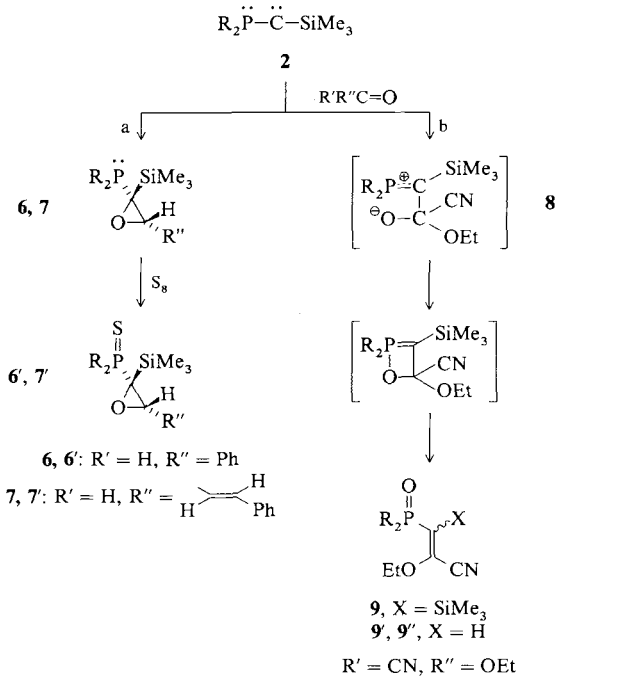
[*] Dr. G. Bertrand, Dr. A. Baceiredo, A. Igau
Laboratoire des Organométalliques, U.A. 477,
Université Paul Sabatier
118, Route de Narbonne, F-31062 Toulouse Cedex (France).
Dr. G. Trinquier
Laboratoire de Physique Quantique, U.A. 505,
Université Paul Sabatier
118, Route de Narbonne, F-31062 Toulouse Cedex (France)

[**] We thank Dr. *I. Tkatchenko*, Dr. *Y. Dartiguenave*, and Dr. *M. Dartiguenave* (Laboratoire de Chimie de Coordination du CNRS at Toulouse) for providing us laboratory facilities after the destruction, on March 25, 1987, of the chemistry building of Paul Sabatier University, and to the CNRS (GRECO basses coordinences) for financial support of this work.

Table 1. Some physical data of the new compounds. Abbreviations for solvents: I = acetonitrile/toluene, II = pentane, III = $CDCl_3$, IV = C_6D_6. ^{31}P NMR (32.438 MHz, standard H_3PO_4). IR (C=C=N).

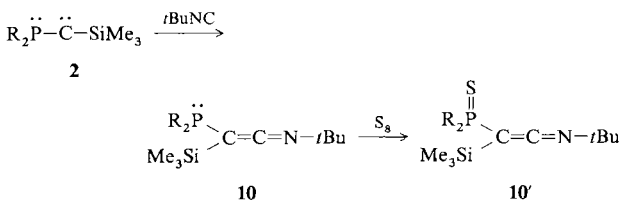
Cpd.	M.p. [°C] [a]	Solv.	Column chromatography hexane/ether	R_F	$\delta(^{31}P)$ Solv.		IR Solv.
4	168	I			78.4	III	
4′	153	II			90.73	III	
5	n.i.				86.3	III	
5′	oil		70/30	0.6	91.4	III	
5″	107	II			70.92	III	
6	n.i.				56.2	IV	
6′	149–151	II	95/5	0.8	83.1	III	
7	n.i.				56.2	IV	
7′	125	II	95/5	0.55	82.3	III	
9	n.i. [b]				23.69 and 23.76	IV	
9′	157 [c]	I			14.5	IV	
9″	n.i. [d]				13.0	IV	
10	n.i.				50.3	IV	2020 II
10′	95	II	97/3	0.8	72.5	III	2020 II

[a] n.i. = not isolated. [b] Z/E = 1.1. [c] Z or E. [d] Z or E, 35 % yield.



Scheme 3.

Lastly, carbene **2** reacts with *tert*-butyl isocyanide to give the corresponding ketene imine **10**, which was isolated, after sulfuration, as **10′** in 90% yield. The reaction of **2** to give **10** can be considered as a carbene–carbene coupling reaction.



These findings, as a whole, clearly establish that **2** is a nucleophilic carbene. Due to the phosphorus lone pair conjugation, the p_π LUMO is expected to lie significantly high in energy, preventing any electrophilic character. According to simple extended Hückel calculations, **2** should be located between dimethoxycarbene and dimethylamino(methoxy)-carbene on the "Moss carbene selectivity scale":[12] in the model $H_2P\ddot{C}H$ the p_π LUMO is calculated at −9.2 eV while it lies at −9.6 and −8.9 eV in $(MeO)_2\ddot{C}$ and $MeO\ddot{C}NMe_2$, respectively. On the other hand, the $n_\sigma > p_\pi$ separation is calculated at 2.7 eV for $H_2P\ddot{C}H$, 2.5 eV for $(MeO)_2\ddot{C}$, and 3.1 eV for $MeO\ddot{C}NMe_2$.

The stereospecificity of the cyclopropane formation as well as the coupling reaction with *tert*-butyl isocyanide suggest that **2** has a singlet ground state, although ab initio calculations[13] revealed a singlet-triplet energy separation of only 3 kcal mol^{-1} in favor of the singlet state.

Received: December 12, 1988 [Z 3085 IE]
German version: *Angew. Chem. 101* (1989) 617

CAS Registry numbers:
1a, 97135-48-3; **2**, 115797-19-8; **4**, 119946-27-9; **4′**, 119946-34-8; **5**, 119946-28-0; **5′**, 119946-35-9; **5″**, 119946-41-7; **6**, 119946-29-1; **6′**, 119946-36-0; **7**, 119946-30-4; **7′**, 119946-37-1; (*E*)-**9**, 119946-31-5; (*Z*)-**9**, 119946-32-6; (*E*)-**9′**, 119946-39-3; (*Z*)-**9′**, 119946-40-6; **10**, 119946-33-7; **10′**, 119946-38-2; *trans*-PhCH=CHCHO, 14371-10-9; *t*BuNC, 7188-38-7; *trans*-$MeO_2CCH=CHCO_2Me$, 624-49-7; $H_2C=CHCO_2Me$, 96-33-3; EtO(CN)C=O, 623-49-4; PhCHO, 100-52-7; dimethyl ketone 67-64-1.

[1] a) A. Baceiredo, G. Bertrand, G. Sicard, *J. Am. Chem. Soc. 107* (1985) 4781; b) A. Baceiredo, A. Igau, G. Bertrand, M. J. Menu, Y. Dartiguenave, J. J. Bonnet, *ibid. 108* (1986) 7868; c) J. M. Sotiropoulos, A. Baceiredo, G. Bertrand, *ibid. 109* (1987) 4711.
[2] A. Igau, H. Grützmacher, A. Baceiredo, G. Bertrand, *J. Am. Chem. Soc. 110* (1988) 6463.
[3] a) Th. Curtius, *Ber. Dtsch. Chem. Ges. 22* (1889) 2161; b) Th. Curtius, R. J. Kastner, *Prakt. Chem. 83* (1913) 215; c) W. Schlenk, E. Bergmann, *Justus Liebigs Ann. Chem. 463* (1928) 76; d) A. T. Blomquist, R. E. Burge, A. C. Sucsy, *J. Am. Chem. Soc. 74* (1952) 3636; e) A. T. Blomquist, L. H. Liu, J. C. Bohrer, *ibid. 74* (1952) 3643; f) D. J. Cram, M. Gordon, *ibid. 77* (1955) 4090.
[4] Dimethoxycarbene, the archetypical nucleophilic carbene, does not react with alkyl-substituted olefins. a) R. A. Moss, M. Wlostowski, S. Shen, K. Krogh-Jespersen, A. Matro, *J. Am. Chem. Soc. 110* (1988) 4443; b) R. W. Hoffmann, W. Lillienblum, B. Dittrich, *Chem. Ber. 107* (1974) 3395; c) R. W. Hoffmann, M. Reiffen, *ibid. 109* (1976) 2565.
[5] In a typical experiment: a solution (10 mL) of **2** (0.632 g, 2 mmol) in toluene was treated at room temperature with 0.172 g (2 mmol) of methyl acrylate. The reaction was followed by NMR spectroscopy. After stirring for 30 minutes, the solvent was removed and the residue recrystallized from toluene/acetonitrile. An excess of elemental sulfur was then added to a toluene solution of the cyclopropane **4**. After stirring for 5 hours, at room temperature, **4′** was isolated by column chromatography on silica gel. Products **5**, **6**, **7**, **9** and **10** were characterized in solution and only isolated as the corresponding thiphosphoryl derivatives **5′**, **6′**, **7′**, **9′**, **9″**, and **10′**.
[6] See for example: M. Brookhart, W. B. Studabaker, *Chem. Rev. 87* (1987) 411.
[7] R. A. Moss, S. Shen, L. M. Hadel, G. Kmiecik-Lawrynowicz, J. Wlostowska, K. Krogh-Jespersen, *J. Am. Chem. Soc. 109* (1987) 4341.
[8] a) P. De March, R. Huisgen, *J. Am. Chem. Soc. 104* (1982) 4952; b) *ibid. 104* (1982) 4953.
[9] D. S. Wulfman, B. Poling in R. A. Abramovitch (Ed.): *Reactive Intermediates Vol. 1*, Plenum, New York 1980, p. 321.
[10] M. Regitz, *Synthesis 1972*, 351.
[11] These results are in agreement with extended Hückel calculations which show that the gap $HOMO_{carb}$-$LUMO_{CO}$ is decreased by 1 eV, on going from aldehyde to cyanoaldehyde, favoring a charge control process rather than a fully concerted mechanism.
[12] For a detail study on the relative degree of electrophilicity or nucleophilicity of carbenes see: R. A. Moss, *Acc. Chem. Res. 13* (1980) 58; *ibid. 22* (1989) 15.
[13] M. T. Nguyen, M. A. McGinn, A. F. Hegarty, *Inorg. Chem. 25* (1986) 2185.

catena-Poly[bis-μ-(*o*-oxyphenyleneoxy)silicon]: Crystal Structure of the Orthosilicate of Catechol **

By *Wolfgang Hönle, Urszula Dettlaff-Weglikowska, Leonard Walz*, and *Hans Georg von Schnering**

The surprising conclusion drawn from the studies of *Meyer* and *Nagorsen*[1] on the structure of the title compound **1**, according to which a square-planar SiO_4 coordination is present, has led to recurrent discussion. With good reason, *Dunitz*[2] has pointed out that the argument used by *Meyer* and *Nagorsen* is not free of flaws and he suspects that the crystals investigated were not those of compound **1** but of the product of hydrolysis, namely catechol **2**. Neither the subsequent reply by *Nagorsen* and *Meyer*[3] nor theoretical studies[4] have as yet solved this problem. The true nature of this compound can not be elucidated from the structures of similar compounds, since the uncertainity relating to compound **1** always remains.

$[Si(o\text{-}O-C_6H_4-O)_2]_n$ **1** $o\text{-}HO-C_6H_4-OH$ **2**

The orthosilicate **1** is formed from $SiCl_4$ and catechol in solvents[5, 6] or from catechol and Si/Cu under H_2 in an autoclave.[7] Depending on the work-up, a transparent, amber colored resin,[5] or colorless glass[7] or colorless powder[6] is obtained. Apparently only *Meyer* and *Nargorsen* have succeeded in obtaining single crystals of **1**, but precisely these crystals, however, could have been catechol. Thus, the problem to be solved is clearly well-defined: 1) crystals of **1** must be prepared, and the structure must be determined; 2) it must be established whether these crystals are identical or not with those prepared by *Meyer* and *Nargorsen*.

The starting material for growing the crystals was prepared as previously described.[6, 8] The product thus obtained by us is a colorless X-ray amorphous powder. Single crystals of **1** are formed without complications and always reproducibly by sublimation in sealed, carefully baked-out ampules (length 15 cm, outer diameter 1.3 cm) under high vacuum ($p < 10^{-4}$ Pa) over the temperature range from 540 K to 523 K within four weeks. The sublimation can also be carried out at lower temperatures (540 K to 493 K). At $T < 423$ K, however, glassy, X-ray amorphous material separates out. The crystals are colorless, transparent, in part strongly intergrown robust rods, which upon subjection to the slightest mechanical stress separate into fibers like asbestos and become opaque. The structure determination was carried out on a 3-mm long fragment using only a selected glass-clear region for the intensity measurement.[9] Under such unfavorable conditions the structure determination (see below) is obviously not as accurate as usual.

According to differential thermal analysis in sealed quartz ampoules the crude product and selected crystals behave differently during the *first stage of heating*: the amorphous crude product shows a broad *exothermic* effect at 450 K (≈180 °C) and melts at 538 K (not sharply). The crystals melt without this effect at 543 K (sharply). During the *second* (and subsequent) *heating*, both samples exhibit the exothermic transformation before reaching the melting point. X-ray photographs at different temperatures show that the molten sample always forms X-ray amorphous phases during cooling, which then crystallize on heating to 450 K (exothermic effect). The crystalline phase is always identical with that obtained on sublimation. There are no indications of the formation of a second (e.g. monomeric) modification. The thermogravimetric analysis in a high vacuum ($p < 10^{-4}$ Pa) reveals the onset of sublimation already at 295 K and strong increase of this process at 430 K. As already described[6] the mass spectrum shows only the molecular peak (m/z 244) and the peaks of the fragments.

The crystal structure (Fig. 1) consists of one-dimensional infinite polymers $^1_\infty[Si(O-C_6H_4-O-)_{4/2}]$ with *tetrahedral*

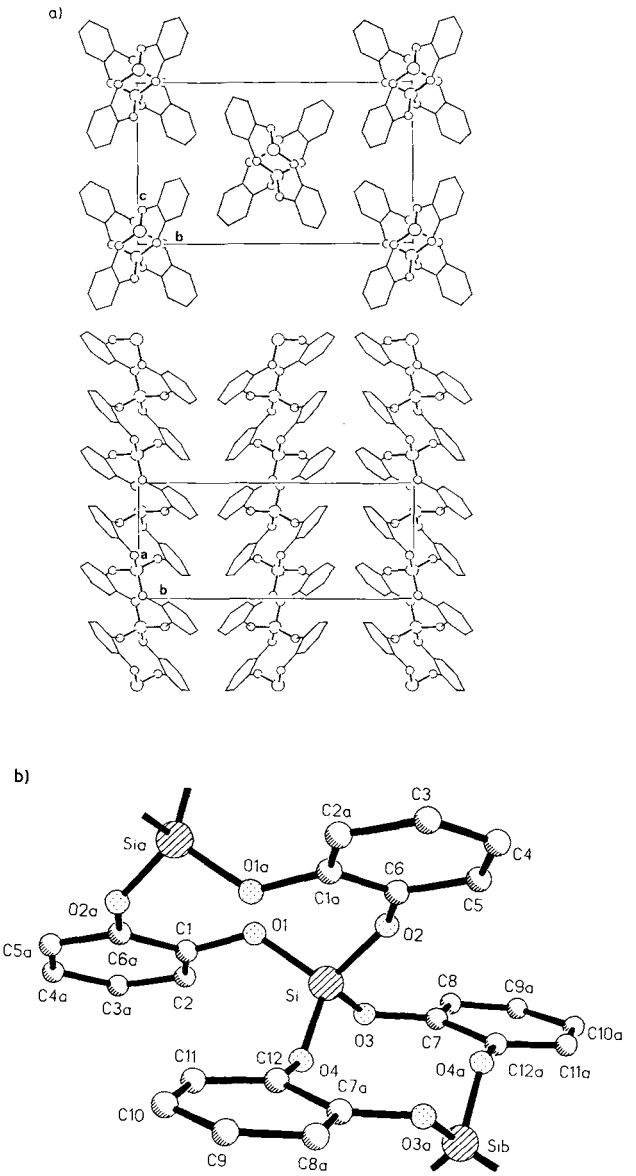


Fig. 1. a) Views of the unit cell of **1** along [100] and [001] showing the rodlike packing of the polymer strands. b) Section of the structure of **1** with crystallographic labeling of the atoms. Note the *trans,trans*-conformation of the heterocyclodecanes and the orientation of the Si atoms to the donor functions of the O atoms. Important bond lengths [pm] and angles [°]: Si–O2 160.2(7), Si–O4 160.2(8), Si–O3 160.7(8), Si–O1 160.8(8), O1–C1 138.3(14), O2–C6 138.6(13), O3–C7 137.2(15), O4–C12 135.6(12), C_1–C_1 138(3): O2–Si–O4 116.0(4), O2–Si–O3 108.8(4), O2–Si–O1 107.1(4), O4–Si–O3 104.7(4), O4–Si–O1 112.7(4), O3–S–O1 107.1(4), C1–O1–Si 134.4(8), C6–O2–Si 134.4(7), C7–O3–Si 131.4(7), C12–O4–Si 135.6(8).

[*] Prof. Dr. H. G. von Schnering, Dr. W. Hönle, Dr. M. Dettlaff-Weglikowska, Dr. L. Walz. Max-Planck-Institut für Festkörperforschung Heisenbergstrasse 1, D-7000 Stuttgart 80 (FRG)

[**] Our thanks are due to Herrn Ing. grad *C. Mensing* for carrying out the mass spectrometric measurements, Frau *S. Lacher* for performing the sublimation experiments, and Herrn Ing. grad *J. Curda* (all Max-Planck-Institut für Festkörperforschung, Stuttgart) for kindly recording the temperature-dependent powder diffraction measurements.

SiO_4 coordination. The bidentate *o*-phenylenedioxy groups are bound as bridge ligands and in all cases to two Si atoms. 1,3,6,8-Tetraoxa-2,7-disilacyclodeca-4,9-dienes (*trans,trans*-conformation) are coupled in a 2,7-spiro fashion along the polymer strands. The dihedral angle at the spiro atom is 90.2°. The strands are arranged in a hexagonal rodlike packing (a_{hex} = 938 pm, $\gamma = 118.15° \approx 120°$) and are held together only by van der Waals forces, which is consistent with the asbestos-like mechanical behavior of the crystals. The bond lengths $\bar{d}$(Si–O) = 160.5 pm are at the lower limits of the values previously determined in analogous compounds.[10] The bond angles O–Si–O vary over a broad range between 104.7 and 116.0°, whereby the smaller angles are endocyclic. The Si–O–C bond angles are relatively constant (131.4–135.6°), with the mean value 134° corresponding well to typical values observed for silicates.[10] An interesting feature is the position of the Si atoms relative to the ring planes of the ligands, which are characterized by the dihedral angle δ between the planes of the phenylene rings and the planes E_i(Si–O_i–C_j): $\delta(E_1) = 68.5°$, $\delta(E_2) = 35.5°$, $\delta(E_3) = 39.4°$, $\delta(E_4) = 87.2°$. Thus, the donor functions of the O atoms do not lie in the ring plane ($\delta = 0°$), as is usual in chelates. The inclination of the planes E_2 and E_3 to the ring plane is comparable with that in, e.g., "tris(catecholamide)iron" (an iron complex with three *N,N'*-dimethyl-2,3-dihydroxyterephthalamide units that, are bound via the methyl groups to two benzene rings),[12] while the planes E_1 and E_4 are almost oriented perpendicular to the ring plane.

Concerning the identity of the previously investigated crystals[1, 3] some questions still remain open, which actually can be answered only by the aforementioned authors. In our experiments, small amounts of the hydrolysis product catechol **2** were formed initially (m.p. 381 K), and since crystals of **1** rapidly become dull upon hydrolysis in air, there would be the tendency in this case to seek out accumulated crystals of **2** as the more interesting. Nevertheless, the lattice constants quoted by *Meyer* and *Nagorsen* deviate beyond the error limits of the correspondingly transformed values for catechol,[11] so that the question now is whether a further modification of **1** exists, e.g. with monomeric units. The cell volume would be suitable (165.53 $cm^3\,mol^{-1}$ according to Ref. [1], cf. 160.79 $cm^3\,mol^{-1}$ for compound **1**). However, with the observed values d(Si–O) = 162 pm, d(O–C) = 140 pm, one obtains an angle at the Si atom of 106° and for the angle at the O atom a value of 102°. The monomer would thus show considerable strain at the oxygen atom, which is removed by formation of the polymer. Such strain does not occur if the SiO_2 fragment is part of a six-membered ring, as in bis(1,8-naphthylenedioxy)silane,[13] or if aliphatic C atoms participate in the SiO_2–C_2 five-membered ring.[14] A further strong argument arises from the structure of the product of the first reaction step $(O_2C_6H_4)SiCl_2$, which crystallizes as dimer,[15] and can be regarded as a section of the polymeric structure of **1**.

Received. December 27, 1988 [Z 3105 IE]
German version: *Angew. Chem. 101* (1989) 615

CAS Registry number:
$(SiCl_4)$ (catechol) (polymeric), 119946-94-0.

[1] H. Meyer, G. Nagorsen, *Angew. Chem. 91* (1979) 587; *Angew. Chem. Int. Ed. Engl. 18* (1979) 551.
[2] J. D. Dunitz, *Angew. Chem. 92* (1980) 1070; *Angew. Chem. Int. Ed. Engl. 19* (1980) 1033.
[3] G. Nagorsen, H. Meyer, *Angew. Chem. 92* (1980) 1071; *Angew. Chem. Int. Ed. Engl. 19* (1980) 1034.
[4] E. U. Würthwein, P. von R. Schleyer, *Angew. Chem. 91* (1979) 588; *Angew. Chem. Int. Ed. Engl. 18* (1979) 553.
[5] R. Schwarz, W. Kuchen, *Z. Anorg. Allg. Chem. 266* (1951) 185.
[6] H. R. Allcock, T. A. Nugent, L. A. Smeltz, *Synth. Inorg. Met.-Org. Chem. 2* (1972) 97.
[7] J. J. Zuckerman, *J. Chem. Soc. 1962*, 873.
[8] Experimental procedure: **1**: All operations were carried out under strict exclusion of moisture and oxygen in an argon inert gas atmosphere. **2** was recrystallized from freshly distilled chloroform, dried under vacuum (oil pump), and stored under argon. Acetonitrile (Merck-Schuchardt p.a.) was heated under reflux for 12 h with P_2O_5 and distilled directly into the reaction flask (500 mL). Silicon that is commercially available tetrachloride (Aldrich) was used. All further steps of the synthesis were the same as in the procedure described by *Allcock* et al. [6]. Analysis of the crude product: Si and O were determined with ICP 35000 C (Applied Research Laboratories) and NOA 2003 (Leybold-Hereaus), respectively, % Si (found) 12.2 (calcd. 11.5); % O (found) 26.0 (calcd. 26.2). Amount of sample 20 mg and 10 mg, respectively. Single crystals were isolated in a glove box (MBraun GmbH; O_2 and $H_2O \leq 0.5$ ppm) with integrated microscope, fixation in capillary with baked-out silicon grease.
[9] X-ray structure analysis of **1**: space group $P2_1/c$ (No. 14), a = 689.0 (3), b = 1611.0 (8), c = 965.1 (5) pm, $\beta = 94.54(5)°$, Z = 4, Huber-Wiege 511 four-circle diffractometer, ($Mo_{K\alpha}$ graphite monochromator, scintillation counter), ω scan, $2\theta \leq 60°$, marked drop in intensity to $2\theta > 40°$, 1826 independent reflections *hkl*, 774 *hkl* with $F_o > 6\sigma(F_o)$. Structure solution by direct methods with SHELXS, refinements (179 parameters) with full matrix, least squares errors, protons located by AFIX in the SHELX, anisotropic (protons fixed, U = 0.08 $Å^2$) refinement to R (aniso) = 0.079, R(w, aniso) = 0.082, residual electron density in F synthesis 0.5 $eÅ^{-3}$. Further details of the crystal structure investigation are available on request from the Fachinformationszentrum Energie, Physik, Mathematik GmbH, D-7514 Eggenstein-Leopoldshafen 2 (FRG), on quoting the depository number CSD-53560, the names of the authors, and the journal citation.
[10] F. Liebau: *Structural Chemistry of Silicates*, Springer, Berlin 1985.
[11] H. Wunderlich, D. Mootz, *Acta Crystallogr. Sect. B 27* (1971) 1684.
[12] T. J. McMurry, M. Wais Hosseini, T. M. Garrett, F. E. Hahn, Z. E. Reyes, K. N. Raymond, *J. Am. Chem. Soc. 109* (1987) 7196.
[13] J. W. Bibber, C. L. Barnes, D. van der Helm, J. J. Zuckerman, *Angew. Chem. 95* (1983) 498; *Angew. Chem. Int. Ed. Engl. 22* (1983) 501.
[14] D. Schomburg, *Angew. Chem. 95* (1983) 52; *Angew. Chem. Int. Ed. Engl. 22* (1983) 65.
[15] W. Hönle, U. Dettlaff-Weglikowska, L. Walz, H. G. von Schnering, unpublished.

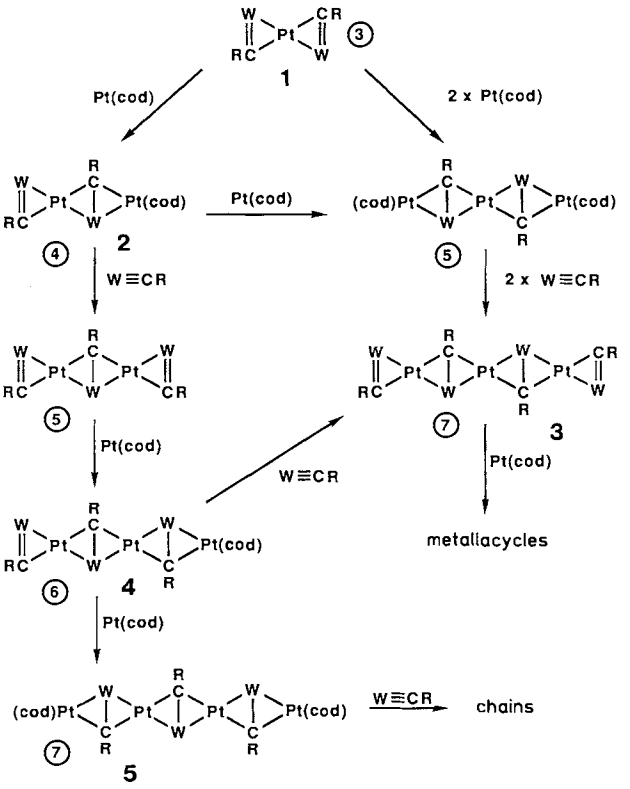
Chain Complexes with Eleven Metal Atoms**

By *Simon J. Davies, Judith A. K. Howard, Rupert J. Musgrove*, and *F. Gordon A. Stone**

The preparation of polynuclear metal complexes by rational procedures, rather than by serendipitous methods, represents a major challenge. For species with bonds between tungsten and platinum we have employed compounds of the Type **1** containing three metal atoms as precursors.[1] Chain-type complexes containing up to seven metal atoms may be obtained readily, and in a sequential manner, using the reagents $[Pt(cod)_2]$ or $[W(\equiv CR)(CO)_2Cp]$ as appropriate (Scheme 1). By using $[Ni(cod)_2]$ or $[Mo(\equiv CR)(CO)_2Cp]$[1, 2] the method has been successfully extended to incorporate Ni or Mo atoms in the chains. The various polynuclear metal compounds generally exist in solution as mixtures of diastereoisomers.[3] Attempts to extend the length of the chains via procedures which involve the intermediacy of heptanuclear metal clusters such as **3** with terminal C=M groups (M = Mo or W) have proved unsuccessful. This is because the stereochemistry of the previously available intermediates favored the formation of metallacycles ('star-clus-

[*] Prof. Dr. F. G. A. Stone, S. J. Davies, Dr. J. A. K. Howard and R. J. Musgrove
Department of Inorganic Chemistry, University of Bristol
Bristol BS8 1TS (UK)

[**] This work was supported by the U.S. Air Force of Scientific Research (Grant 86-0125).

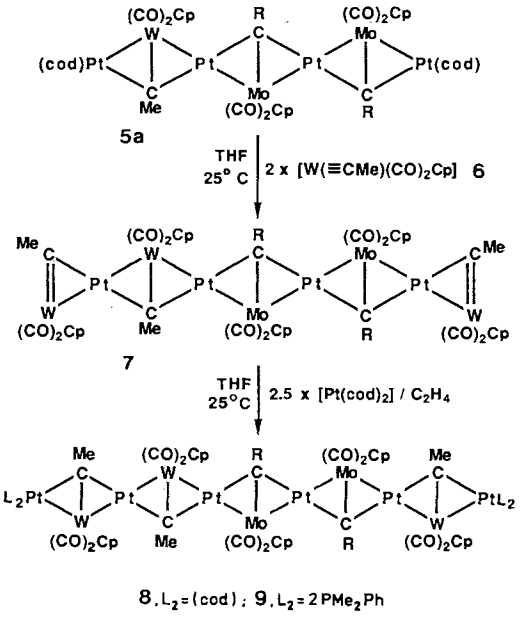


Scheme 1. Stepwise synthesis of polynuclear tungsten-platinum complexes. Numbers in circles refer to metal atoms in chains.
W≡CR = [W(≡CR)(CO)$_2$Cp]; R = alkyl; Cp = η^5-C_5H_5
Pt(cod) = [Pt(cod)$_2$]/C_2H_4; cod = 1,5-cyclooctadiene.

ters', Fig. 1a).[4] This problem has now been overcome by identifying heptanuclear metal compounds of type **5** having terminal Pt(cod) groups, which do not have chain conformations favoring metallacycle formation.

$[Mo_2WPt_3(\mu\text{-CMe})(\mu_3\text{-}CC_6H_4Me\text{-}4)_2(CO)_6(cod)Cp_3]$ **4a**

Treatment of th hexanuclear cluster **4a**[1b] with 1.5 equivalents of [Pt(cod)$_2$] in THF (tetrahydrofuran) afforded brown crystals of the heptanuclear species **5a**. It formed as a single isomer,[5] which then served (Scheme 2) as a starting compound for the synthesis of the nona- and undecanuclear compounds **7** and **8**, respectively. Only one isomer of each compound is formed, as revealed by the observation of signals corresponding to only one species in their NMR spectra.[5] It was not possible to grow crystals of **8** for an X-ray diffraction study. To overcome this difficulty treatment of **8** with PMe_2Ph in excess replaced the cod groups to yield quantitatively **9**, a product which did give suitable crystals.



Scheme 2. Stepwise synthesis of polynuclear metal clusters. R = C_6H_4Me-4.

The structure of **9** resulting from the X-ray analysis is shown in Figure 1b.[6] The molecule consists of five μ_3-$CMPt_2$ (M = Mo or W) groups linked together through four of the Pt atoms sharing vertices. Of the six Pt atoms present, all but Pt(1) and Pt(6) are approximately tetrahedrally coordinated by alkylidynemetal fragments. However, Pt(1) and Pt(6)

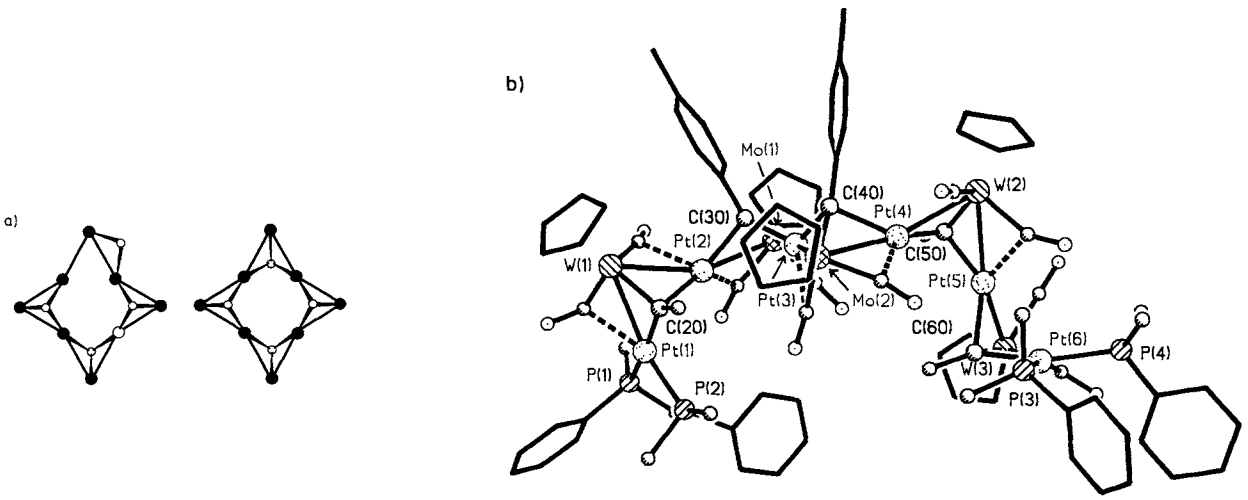


Fig. 1. a) The core structures of the 'asymmetric' and 'symmetric' isomers of the 'star-clusters' $[M_4M'_4(\mu\text{-CR})_4(CO)_8Cp_4]$ (M = Mo or W, M' = Ni or Pt) showing the metal atoms and the ligated carbon atoms of the alkylidyne groups. In solution, the asymmetric species, with one edge-bridging alkylidyne ligand, isomerize into the symmetrical isomers with four triply-bridging alkylidyne groups. These are sited alternately above and below the eight-metal atom rings. Experimental procedures may be adapted so as to produce metallacycles with different metal atom sequences, e.g. Mo · Pt · W · Ni · W · Pt · Mo · Ni or W · Pt · Mo · Ni · W · Pt · Mo · Ni. b) Structure of compound **9** in the crystal. Selected bond lengths [Å] (mean distances): Pt–W 2.751, Pt–Mo 2.745, Pt · · · Pt 3.040, μ_3-C–W 2.04, μ_3-C–Mo 1.98, P–Pt 2.30.

have essentially square planar coordination geometries, being ligated by one alkylidynetungsten fragment and two PMe_2Ph groups. All the CO ligands, except C(7)O(7) and C(9)O(9), semibridge W–Pt bonds.

Experimental

5a: A cold (0 °C) ethylene-saturated solution of $[Pt(cod)_2]$ (0.05 g, 0.12 mmol) in THF (20 mL) was treated with a solution of **4a** (0.15 g, 0.09 mmol) in the same solvent (25 mL). After 4 hours' stirring, the solvent was removed in vacuo and the residue was dissolved in CH_2Cl_2/light petroleum (15 mL, 4/1) and chromatographed on alumina. Elution with the same solvent mixture gave a brown eluate from which microcrystals of **5a** (0.11 g, 62%) were recovered after removal of solvent.

7: A solution of **5a** (0.15 g, 0.08 mmol) in THF (15 mL) was added to a solution of **6** (0.10 g, 0.30 mmol) in THF (10 mL). The mixture was stirred under C_2H_4 pressure (2 atm) for 3 h. The solvent was removed in vacuo, and the residue was dissolved in CH_2Cl_2 (10 mL) and chromatographed on alumina. Elution with the same solvent removed initially unreacted **6** followed by a brown fraction containing **7**. Removal of solvent in vacuo and crystallization from CH_2Cl_2/light petroleum gave **7** (0.17 g, 92%).

8, 9: A solution of **7** (0.15 g, 0.06 mmol) in THF (20 mL) was slowly added to a C_2H_4-saturated solution of $[Pt(cod)_2]$ (0.06 g, 0.17 mmol) in THF (20 mL, 0 °C). After warming to room temperature in vacuo and stirring for 3 h the residue was dissolved in CH_2Cl_2 (10 mL) and chromatographed. Elution with the same solvent removed a brown fraction, removal of solvent from which gave **8** (0.15 g, 80%), crystallized from CH_2Cl_2/light petroleum. Treatment of **8** (0.15 g, 0.05 mmol) in CH_2Cl_2 (15 mL) with PMe_2Ph (0.04 g, 0.30 mmol) for 30 min gave **9** (0.15 g, 90%).

Received: January 16, 1989 [Z 3126 IE]
German version: *Angew. Chem. 101* (1989) 613

CAS Registry numbers:
4a, 116994-81-1; **5a**, 120085-94-1; **6**, 72465-88-4; **7**, 120085-96-3; **8**, 120085-95-2; **9**, 120085-97-4; $Pt(cod)_2$, 12130-66-4; PMe_2Ph, 672-66-2.

[1] a) G. P. Elliott, J. A. K. Howard, T. Mise, I. Moore, C. M. Nunn, F. G. A. Stone, *J. Chem. Soc., Dalton Trans. 1986*, 2091; b) S. J. Davies, G. P. Elliot, J. A. K. Howard, C. M. Nunn, F. G. A. Stone, *ibid. 1987*, 2177.

[2] S. J. Davies, F. G. A. Stone, *J. Chem. Soc. Dalton Trans. 1989*, 785.

[3] The two C≡W bonds in the enantiomeric trimetal compounds **1** are at right angles to each other. Addition of a Pt(cod) fragment to one of these bonds occurs in such a manner as to produce the product **2** in two diastereomeric forms [1]. With increasing chain length, for each species the number of possible diastereoisomers increases. For the heptanuclear metal compounds there is a maximum of ten isomers, based on the different ways in which the metal triangles comprising the chain can be linked. However, not all the possible isomers (detected by NMR studies) are formed, presumably for steric reasons. Separation of the isomers by chromatography is generally possible, although re-equilibration occurs in solution [1, 2].

[4] (a) G. P. Elliott, J. A. K. Howard, T. Mise, C. M. Nunn, F. G. A. Stone, *Angew. Chem. 98* (1986) 183; *Angew. Chem. Int. Ed. Engl. 25* (1986) 190; b) *J. Chem. Soc. Dalton Trans. 1987*, 2189.

[5] Selected NMR data (270 and 400 MHz, CD_2Cl_2/CH_2Cl_2; J in Hz): **5a:** $^{13}C\{^1H\}$: δ = 267.1, 263.8, 259.8 (μ_3-C), 247.6, 244.2, 240.7, 236.9, 235.3, 277.1 (CO); $^{195}Pt\{^1H\}$ (to high frequency of Ξ (^{195}Pt), 21.4 MHz): δ = 1234, 946, 401, 311 (J(PtPt) 1211–78).—**7:** $^{13}C\{^1H\}$: δ = 329.4, 328.9 (μ_2-C), 275.9, 274.8, 273.7 (μ_3-C); $^{195}Pt\{^1H\}$; δ = 1284, 1181, 1073, 855.—**8:** $^{13}C\{^1H\}$: δ = 267.1, 266.2, 265.4, 262.6, 259.2 (μ_3-C), 245.7, 244.6, 242.2, 240.2, 236.5, 235.0, 233.7 (CO), 227.9 (2 × CO), 226.4 (CO); $^{195}Pt\{^1H\}$: δ = 1500, 1105, 959, 762, 339, 319 (J(PtPt) 1377–351).—**9:** $^{13}C\{^1H\}$: δ = 266.8 (d, μ_3-C, J(PC) 55), 266.1, 263.2 (μ_3-C), 261.3 (d, μ_3-C, J(PC) 52), 259.0 (μ_3-C), 247.8, 244.7 (CO), 241.8 (d, CO, J(PC) 9), 239.2 (d, CO, J(PC) 9), 238.0, 237.4, 234.5, 229.6, 223.4, 221.0 (CO); $^{31}P\{^1H\}$ (to high frequency of 85% H_3PO_4 (external)): δ = −4.75 (d, J(PP) 5, J(PtP) 3755), −5.12 (d, J(PP) 7, J(PtP) 3876), −7.45 (d, J(PP) 5, J(PtP) 3188), −8.25 (d, J(PP) 5, J(PtP) 3150 Hz).

[6] Monoclinic space group. $C2/c$ (No. 15), Z = 8, a = 42.37 (2), b = 12.262 (8), c = 40.71 (4) Å, β = 98.57 (7)°, V = 20920 (30) Å^3, $\varrho_{calc.}$ = 2.13 g cm^{-3}, F(000) = 12320, μ($Mo_{K\alpha}$) = 117.7 cm^{-1}; $2\theta < 50°$ ($Mo_{K\alpha}$ λ = 0.71073 Å, ω-2θ scans, 293 K); 18493 unique reflections but only 6160 with $F > 6\,\sigma(F)$ were used in the last stages of refinement (Nicolet P3/mv), R_1 = 0.091, R_2 = 0.092. Further details for the crystal structure analysis are available on request from the Cambridge Crystallographic Data Centre, University Chemical Laboratory, Lensfield Road, Cambridge CB2 1EW (U.K.). Any request should be accompanied by the full literature citation for this communication.

Chromatographic Separation of the Excess Enantiomer under Achiral Conditions**

By *Rudolf Matusch** and *Carsten Coors*

Enantioselective syntheses result in the formation of a non-racemic mixture of products in which one enantiomer predominates.[1] Whenever a pure enantiomer cannot be isolated in pure form by crystallization, some resolution method has to be employed. The search for an efficient method can be very time consuming, success being uncertain. But the advantage offered by the non-racemic mixture compared to the racemate still remains methodologically unexploited. We report here on the chromatographic separation of the excess enantiomer under achiral conditions.

Instead of trying to remove the undesired enantiomer, as in the resolution method we saw a general route in the separation of the excess enantiomer from the residual racemate.[2, 3] If the solvent chosen for a polar non-racemic mixture is so unpolar that self-asociation is possible in solution, homochiral and heterochiral associates can be formed.[4] These associates are diastereomeric and can thus be differentiated by achiral methods. Hence, in principle a chromatographic separation on an achiral stationary phase with an achiral mobile phase is possible.

In order to prevent decomposition of the associates on the stationary phase and/or to promote their formation, the phase must possess adequate donor properties and be spatially adaptable. We therefore chose, in contrast to other authors,[3] aminopropylsilica gel (LiChrosorb®-amine) as the stationary phase. The amino group is a good donor and can form hydrogen bonds. Furthermore, the propyl chain is long and flexible enough to enable the associates to bind (tentacle effect) without disadvantageously influencing the existing interactions.

As Figure 1a shows, the chromatography of 1,1′-bi-2-naphthol **1** with only 33% *ee* leads to a distinct separation into two signals with a difference in the retention times of 2.9 min. The synchronously recorded optical rotation increases sharply at first and after reaching a maximum decreases in accord with the UV curve. At the minimum of the UV curve, however, it drops steeply to zero. That is, the excess enantiomer is first eluted and then the non-rotating racemate and not vice versa. Accordingly, from a mechanistic point of view a temporary chiral imposition as a cause of the separation can be ruled out.

On loading a mixture with 86% *ee* (Fig. 1b) the difference in the retention times between excess enantiomer and racemate increases to 10.7 min. The separation factor α[5] is thus improved on increasing the enantiomeric excess.

The corresponding polarimeter curve is essentially of the same form as in Figure 1a, but the sharp drop on passage of the racemate is less clearly recognizable since the sensitivity limit of the flow polarimeter is reached. The detailed analysis of the eluate by analytical HPLC on a chiral stationary phase (ionic Pirkle phase[6]) shows that only the pure enantiomer is present down to the minimum of the UV curve, the racemate being first observed in the fraction following.

Since the formation of the diastereomeric associates is concentration dependent, the separation factor α is further enhanced upon increasing the loaded amount of material

[*] Prof. Dr. R. Matusch, Dr. C. Coors
Institut für Pharmazeutische Chemie der Universität
Marbacher Weg 6, D-3550 Marburg (FRG)

[**] Based on a lecture at the Jahrestagung der Deutschen Pharmazeutischen Gesellschaft, September 9, 1988, in Erlangen.

($\alpha = 1.24$ for 2.5 μg; $\alpha = 1.28$ for 10 μg; $\alpha = 1.39$ for 35 μg and $\alpha = 1.46$ for 100 μg throughput of a mixture with 86% *ee*). Thus α depends both on the enantiomeric composition and the amount of material loaded.

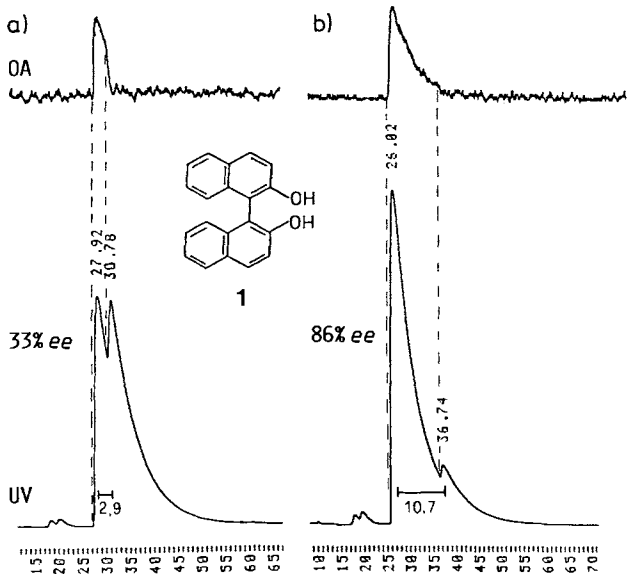


Fig. 1. Chromatography of 100 μg of 1,1'-bi-2-naphthol **1** with a) 33% *ee* and b) 86% *ee*. Bottom: UV detection, $\lambda = 228$ nm; top optical activity (OA, angle of rotation). Column: 250 × 4 mm ID, LiChrosorb®-amine, 5 μm; flowrate: 1 mL min^{-1}, hexane:2-propanol 6:4. Abscissa: t [min].

For further clarification, the retention times in the range of 100 μg to 0.025 μg were determined for the pure enantiomers and the racemate (Fig. 2). As expected the pure

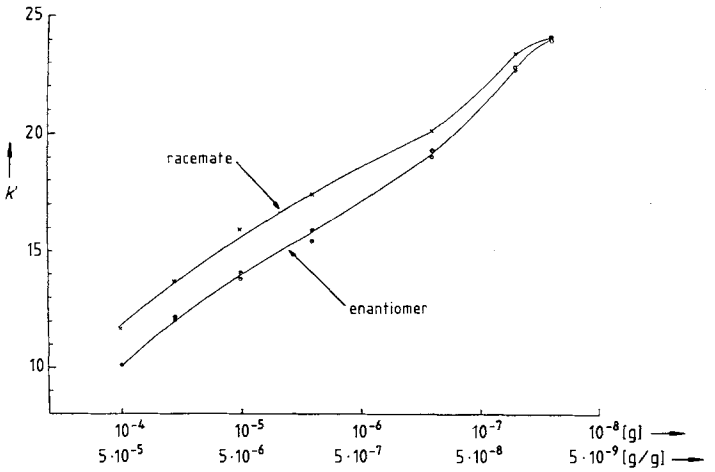
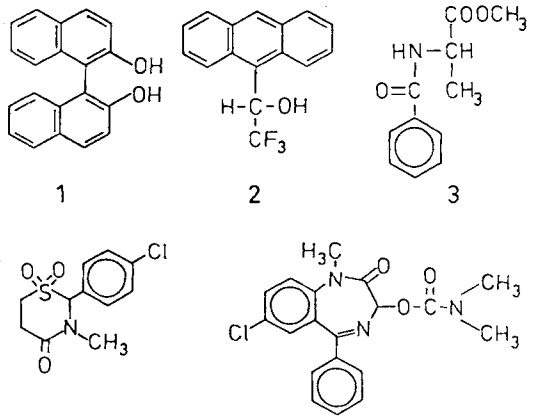


Fig. 2. Retention (given as capacity factor k' [5]) of (+/−)-, (+)-, and (−)-1,1'-bi-2-naphthol **1** versus amount of sample and amount of sample/amount of sorptive medium (semilog). Conditions as in Figure 1.

enantiomers behave similarly, whereas the racemate shows increased retention in each case. Only at loaded amounts which are four orders of magnitude less than in the case of "normal", i.e. non-complexing compounds, is the retention time noticeably constant.[7] The curve of the pure enantiomers also intercepts that of the racemate at this point. The explanation for this behavior is simple: below this concentration the medium gets diluted to such an extent that association is negligible and practically only monomers are still present. Their behavior on achiral phases is, however, logically the same.

In order to determine the scope of application of the method we arbitrarily chose, besides **1**, another four compounds: the chiral shift reagent 1-anthryl-2,2,2-trifluoroethanol **2**, *N*-benzoylalanine methyl ester **3**, and two drugs, the tranquilizer chloromezanone **4** and the benzodiazepine camazepam **5**.



Hexane/2-propanol mixtures were suitable for the separation of the excess enantiomer on Lichrosorb®-amine phases for all compounds except **2**, where hexane/dichloromethane was used. In all cases the excess enantiomer was eluted prior to the racemate. In no case did we observe splitting of the UV signal upon variation of the stationary phase (e.g. silica gel, Diol, RP18). Thus, the importance of the aminopropylsilica gel phase clearly manifests itself, and the postulated mechanism of separation is highly plausible.

In summary, it may be said that, in the separation of the excess enantiomer, a material property is effective whose practical application has hitherto been underestimated: the different interaction of homochiral and heterochiral associates with the stationary phase. Its exploitation, complementary to the progress made chemically by enantioselective synthesis, thus provides a chromatographic method for the isolation of the pure enantiomer, hitherto lacking, which ensures success even when the enantioselectivity is not quantitative.

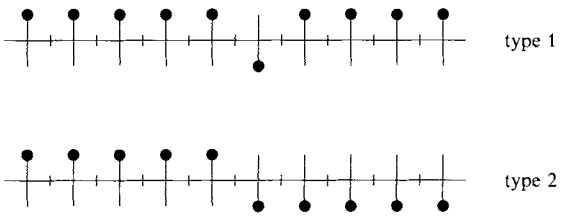
Received: December 5, 1988 [Z 3073 IE]
German version: *Angew. Chem. 101* (1989) 624

[1] Non-racemic is used here in the sense of "not 1/1 racemic".
[2] C. Coors, *Ph.D. thesis, Universität Marburg* 1988.
[3] a) K. C. Cundy, P. A. Crooks, *J. Chromatogr. 281* (1983) 17; b) R. Charles, E. Gil-Av, *ibid. 298* (1984) 516; c) A. Dobashi, Y. Motoyama, K. Kinoshita, S. Hara, N. Fukasaku, *Anal. Chem. 59* (1987) 2209; d) W. L. Tsai, K. Hermann, E. Hug, B. Rohde, A. S. Dreiding, *Helv. Chim. Acta 68* (1985) 2238.
[4] The associate formed from two enantiomeric molecules (+/−) is referred to as "heterochiral", that from two homomeric molecules (+/+ or −/−) as homochiral.
[5] α is a measure of the selectivity and is defined by the ratio k'_2/k'_1, where k'_1 is the capacity factor of the first eluted peak. For k', $(t_R - t_0)/t_0$; t_R = retention time, t_0 = dead time.
[6] W. H. Pirkle, J. M. Finn, *J. Org. Chem. 46* (1981) 2935.
[7] In the linear region of the adsorption isotherms the retention times are independent of the amount of sample. This region is also referred to as "linear capacity"; see S. R. Snyder: *Principles of Adsorption Chromatography*, M. Dekker, New York 1968, p. 75.

Double Stereodifferentiation in the Formation of Isotactic Polypropylene at Chiral $(C_5H_4CHMePh)_2ZrCl_2$/Methylalumoxane Catalysts**

By *Gerhard Erker,** *Rainer Nolte, Yi-Hung Tsay,* and *Carl Krüger*

The formation of two types of isotactic polypropylene at soluble $(RC_5H_4)_2MX_2$/alkylalumoxane catalysts (M = Ti, Zr, Hf) is well known. Isotactic block polymers (type 2, Scheme 1) can be prepared using achiral transition metal components (e.g. Cp_2TiPh_2);[1] the diastereoselectivity of the reaction is here effected by chirality centers at the end of the growing chain (chain end control). Isotactic polypropylene of type **1** (Scheme 1) is obtained using catalysts prepared from the chiral, Cp-bridged ansa-titanocene and -zirconocene complexes developed by *Brintzinger* et al.[2] In this case the chiral transition-metal center is controlling the stereoselectivity (enantiomorphic site control). Any "errors" occurring during polymer formation are corrected immediately and not propagated as in the case of type 2 polymer formation.



Scheme 1. Isotactic polypropylene type 1 (enantiomorphic site control) and type 2 (chain end control).

In fact, it is to be expected that these two different kinds of diastereoselective control of the C–C coupling of propene units are not independent, but mutally strengthen or weaken each other using a chiral catalyst. We have now been able to demonstrate experimentally for the first time the influence of double stereodifferentiation[3] in the formation of isotactic polypropylene using a *rac*-$(C_5H_4CHMePh)_2ZrCl_2$/$(AlMeO)_n$ catalyst.

We have prepared the known compound bis[(1-phenylethyl)cyclopentadienyl]zirconium dichloride **1**[4] via a novel synthetic variation: reaction of 6-methyl-6-phenylfulvene with isobutyllithium in ether afforded (1-phenylethyl)-cyclopentadienyllithium (60%), which, on treatment with zirconium tetrachloride in a 2:1 molar ratio in THF, furnished **1** as a diastereomeric mixture (73%). Repeated fractional crystallization gave *rac*-**1** containing < 1% *meso* diastereomer.[5a]

Complex *rac*-**1** was characterized by an X-ray structure analysis (Fig. 1).[5b] A remarkable feature is the chiral, approximately C_2 symmetric metallocene conformation in the crystal. The chiral substituents at the cyclopentadienyl units are oriented synclinally. The observed arrangement of the cyclopentadienyl units (methyl groups at C6 and C26 inwards, phenyl groups outwards) may be the sterically most favorable orientation. Presumably this conformation (**A**) is favored over that of the $R^*C_5H_4$–M rotational isomer (**B**), even in solution.

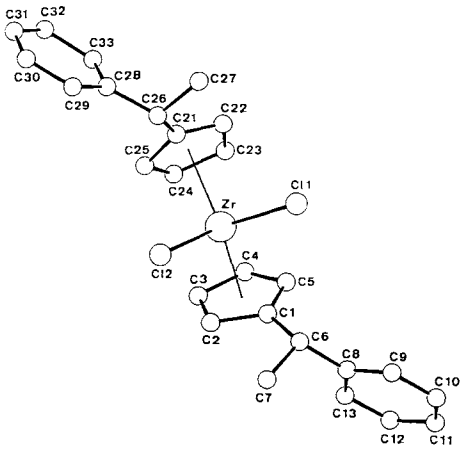
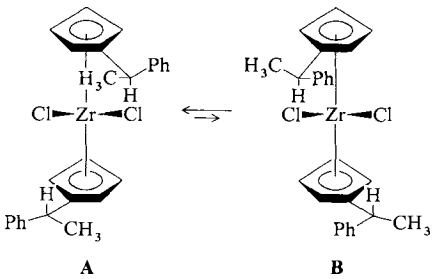


Fig. 1. Structure of *rac*-**1** in the crystal. Selected bond lengths [Å] and angles [°] Zr–Cl1 2.462 (2), Zr–Cl2 2.456 (2); Cl1-Zr-Cl2 96.6 (1), C1-C6-C7 113 (1), C1-C6-C8 111.8 (9), C7-C6-C8 111 (1).



We have used the *rac*-**1**/methylalumoxane system as a catalyst for the polymerization of propene. In a typical experiment with *rac*-**1**/$(AlMeO)_n$ (ratio Al/Zr = 3400) in toluene at − 79 °C we obtained isotactic polypropylene (catalyst activity: 143 g polymer/gZr · h). The configuration of the polymer ($\bar{M}_n$ = 10 000) was determined from the crude reaction product, without further work-up, by ^{13}C NMR spectroscopy.[1,6]

Under the conditions chosen for the ^{13}C NMR analysis (1,2,4-trichlorobenzene, 50 MHz, 92 °C) the signals of the methyl groups are satisfactorily resolved on the pentad level (Fig. 2, top). The polymer was quantitatively analyzed by applying the usual statistical treatment. The polymer obtained consists of ca. 35% of isotactic polypropylene of type 1 (enantiomorphic site control, $\alpha = 0.94$; average length of the sequences containing only m-diads $\langle m\rangle_{n,\alpha} = 16$) and ca. 65% of type 2 (chain end control, $\sigma = 0.85$, $\langle m\rangle_{n,\sigma} = 6.7$). The observed (calculated) relative intensities of the methyl ^{13}C NMR signals are: mmmm 0.60 (0.60), mmmr 0.16 (0.15), rmmr 0.02 (0.01), mmrr 0.06 (0.05), mmrm + rmrr 0.12 (0.13), mrmr 0.03 (0.02), rrrr 0.00 (0.00), rrrm 0.00 (0.00), mrrm 0.01 (0.01) (Fig. 2, top). The stereoselectivity of the propene C–C coupling at the *rac*-**1**/$(AlMeO)_n$

[*] Prof. Dr. G. Erker, Dipl.-Chem. R. Nolte
Institut für Organische Chemie der Universität
Am Hubland, D-8700 Würzburg (FRG)
Dr. Y.-H. Tsay, Prof. Dr. C. Krüger
Max-Planck-Institut für Kohlenforschung
Kaiser-Wilhelm-Platz 1, D-4330 Mülheim a.d. Ruhr (FRG)

[**] This work was supported by the Fonds der Chemischen Industrie, by the Bundesminister für Forschung und Technologie, and by the Alfred-Krupp-von Bohlen-und-Halbach-Stiftung.

catalyst changes only slightly with increasing temperature (-55 °C: 32% type 1, $\alpha = 0.95$, 68% type 2, $\sigma = 0.79$; -33 °C: 24% type 1, $\alpha = 0.96$, 76% type 2, $\sigma = 0.74$).

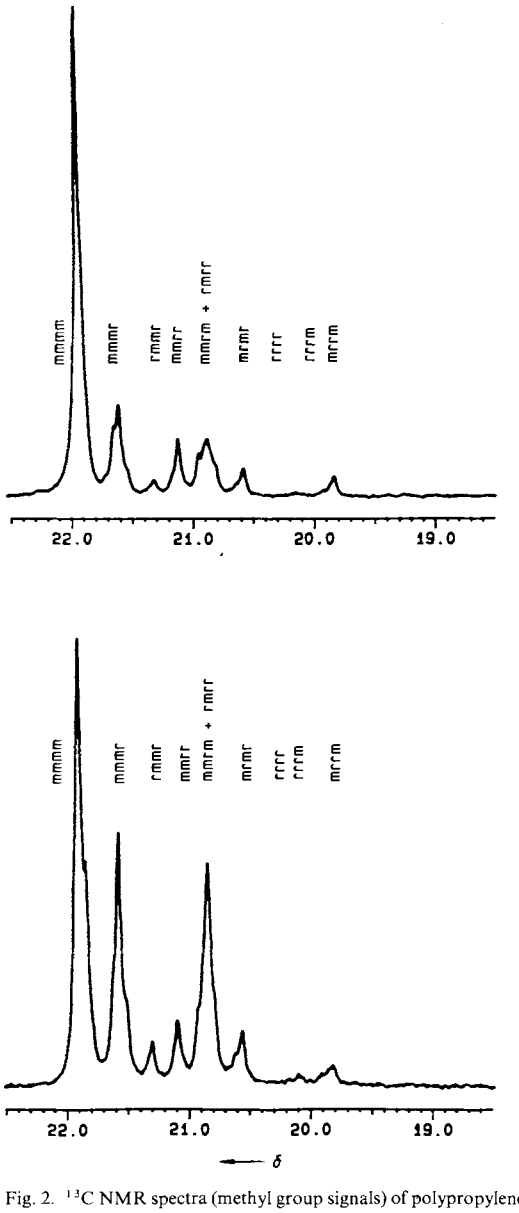


Fig. 2. ^{13}C NMR spectra (methyl group signals) of polypropylene, obtained at $(C_5H_4CHMePh)_2ZrCl_2$/methylalumoxane catalysts at -79 °C. Top: *rac*-**1**/*meso*-**1** > 99/1; bottom: 45/55.

According to the solubility behavior only a single type of polymer is obtained. Apparently a block polymer containing isotactic polypropylene of types 1 and 2 is formed at the *rac*-**1**/$(AlMeO)_n$ catalyst. Double stereodifferentiation (by the chiral metal center *and* the chiral chain end) leads thereby to an increase in $\langle m \rangle_{n,\alpha}$ (matched pair) and a decrease in $\langle m \rangle_{n,\sigma}$ (mismatched pair), assuming general isotactic stereocontrol by the chain end. According to this interpretation removal of the chirality information of the transition metal center under otherwise essentially unchanged steric conditions should result in the formation of a purely isotactic type-2 polymer. There is experimental evidence for this. The C–C coupling of propene at a soluble catalyst derived from methylalumoxane and a 55/45 mixture of *meso*-**1** and *rac*-**1** affords isotactic block polymers of type 2 at low temperatures (-50 °C; Al/Zr = 830; 132 g polypropylene/gZr · h, $\bar{M}_\eta = 28\,000$, $\sigma = 0.79$; -79 °C: Al/Zr = 860; 10 g polypropylene/gZr · h $\bar{M}_\eta = 35\,000$, $\sigma = 0.81$, $\langle m \rangle_{n,\sigma} \approx 5.3$; observed (calculated) relative intensities of the methyl-^{13}C NMR signals: mmmm 0.43 (0.43), mmmr 0.21 (0.20), rmmr 0.03 (0.02), mmrr 0.05 (0.05), mmrm + rmrr 0.22 (0.21), mrmr 0.04 (0.05), rrrr 0.00 (0.00), rrrm 0.01 (0.01), mrrm 0.02 (0.02); Fig. 2, bottom).[9]

In the development of asymmetric syntheses of low molecular weight organic compounds by olefin C–C coupling reactions at optically active homogeneous Ziegler catalysts,[10] stereochemically unproductive control by the chiral chain end must be excluded. In the case of conformationally flexible bent metallocene systems this can possibly be achieved by the use of bulky, chiral tertiary alkyl substituents attached to the cyclopentadienyl units, which, in contrast to the secondary alkyl substituents used in the case of **1**, favor a *trans* orientation in the lateral sectors of the bent metallocene unit.

Received: November 15, 1988 [Z 3050 IE]
German version: *Angew. Chem. 101* (1989) 642

CAS Registry numbers:
rac-**1**, 120203-01-2; *meso*-**1**, 120203-02-3; *i*-BuLi, 920-36-5; $ZrVl_4$, 10026-11-6; $(AlMeO)_n$, 120144-90-3; 6-methyl-6-phenylfulvene, 2320-32-3; (1-phenylethyl)cyclopentadienyllithium, 78759-82-7; propene, 115-07-1; polypropylene, isotactic, 25085-53-4.

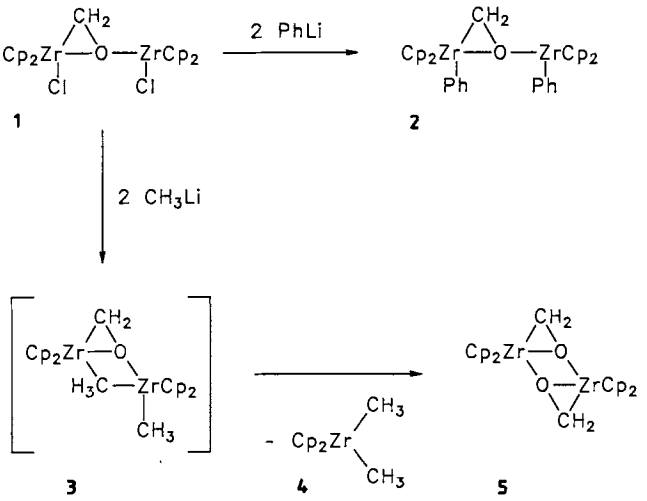
[1] J. A. Ewen, *J. Am. Chem. Soc. 106* (1984) 6355.
[2] W. Kaminsky, K. Külper, H. H. Brintzinger, F. R. W. P. Wild, *Angew. Chem.* 97 (1985) 507; *Angew. Chem. Int. Ed. Engl. 24* (1985) 507.
[3] S. Masamune, W. Choy, J. S. Petersen, L. R. Sita, *Angew. Chem. 97* (1985) 1; *Angew. Chem. Int. Ed. Engl. 24* (1985) 1.
[4] J. C. Leblanc, C. Moise, *J. Organomet. Chem. 120* (1976) 65; P. Renaut, G. Tainturier, B. Gautheron, *ibid. 148* (1978) 35; S. Couturier, B. Gautheron, *ibid. 157* (1979) C61; E. Cesarotti, R. Ugo, H. B. Kagan, *Angew. Chem. 91* (1979) 842; *Angew. Chem. Int. Ed. Engl. 18* (1979) 779.
[5] a) *rac*-**1**: m.p. 188 °C (CH_2Cl_2, -20 °C); correct element analysis (C, H); ^{13}C NMR ($CDCl_3$, 50 MHz): $\delta = 146.1$, 128.6, 127.7, 126.5 (Ph-*C*), 139.1, 116.9, 115.0, 112.5, 112.2 (Cp-*C*), 40.2 (CH), 22.0 (CH_3); ^{1}H NMR ($CDCl_3$, 200 MHz): $\delta = 7.33-7.14$ (m, 10H, Ph-H), 6.51, 6.18, 6.09, 5.86 (m, each 2H, Cp-H), 4.32 (q, 2H, CH), 1.57 (d, 6H, CH_3); *meso*-**1**: $\delta = 6.51$, 6.23, 6.13, 5.86 (m, each 2H, Cp-H), otherwise identical with *rac*-**1**; b) crystal structure analysis of *rac*-**1**: $C_{26}H_{26}Cl_2Zr$, $M = 500.6$, orthorhombic, $Pna2_1$, $a = 12.503$ (6), $b = 6.677$ (2), $c = 28.097$ (11) Å, $V = 2345.6$ Å^3, $Z = 4$, $\varrho_{calcd} = 1.42$ g cm^{-3}, $\mu = 7.0$ cm^{-1}, Enraf-Nonius diffractometer, 5672 measured reflections, 1506 observed ($I \geq \sigma(I)$), $R = 0.034$, $R_w = 0.034$ for 262 parameters. Further details of the crystal structure investigation are available on request from the Fachinformationszentrum Energie, Physik, Mathematik GmbH, D-7514 Eggenstein-Leopoldshafen 2 (FRG) on quoting the depository number CSD-53643, the names of the authors, and the journal citation.
[6] The statistical analysis was carried out using a model taking two controlling influences into account. Thereby, α and σ denote the probabilities of the formation of an m-diad, controlled by the chiral metal center and the chiral chain end, respectively (Bernoulli model): Y. Inoue, Y. Itabashi, R. Chujo, Y. Doi, *Polymer 25* (1984) 1640; see also M. Farina, *Top. Stereochem. 17* (1987) 1, and references cited therein.
[7] For examples of syndiospecific propene polymerization at catalysts of metallocene compounds of zirconium or hafnium see J. A. Ewen, R. L. Jones, A. Razavi, J. D. Ferrara, *J. Am. Chem. Soc. 110* (1988) 6255.
[8] According to the ^{13}C NMR analysis an almost identical isotactic type 1/2 block polypropylene is formed at a (neomenthyl-$C_5H_4)_2ZrCl_2$/methylalumoxane catalyst (G. Erker, S. Dehnicke, unpublished). An analogous experiment has been described, but was interpreted differently: W. Kaminsky, M. Buschermöhle, *NATO ASI Ser. Ser. C215* (1987) 503.
[9] The diastereomeric catalysts derived from *meso*-**1** and *rac*-**1** exhibit different reactivities. Under the reaction conditions applied ($T < -30$ °C) the amount of polypropylene originating from the less active *rac*-**1**/$(AlMeO)_n$ seems to be stereochemically of no importance.
[10] P. Pino, P. Cioni, J. Wei, *J. Am. Chem. Soc. 109* (1987) 6189.
[11] R. A. Howie, G. P. McQuillan, D. W. Thompson, *J. Organomet. Chem. 268* (1984) 149; G. Erker, T. Mühlenbernd, R. Benn, A. Rufińska, Y.-H. Tsay, C. Krüger, *Angew. Chem. 97* (1985) 336; *Angew. Chem. Int. Ed. Engl. 24* (1985) 321; G. Erker, R. Nolte, C. Krüger, R. Schlund, R. Benn, H. Grondey, R. Mynott, *J. Organomet. Chem.*, in press.

Dimeric $[Cp_2Zr(CH_2O)]$, a Novel (η^2-Formaldehyde)metal Complex from Carbon Monoxide **

By *Gerhard Erker,* Ursula Hoffmann, Roland Zwettler, Peter Betz,* and *Carl Krüger*

In the temperature range of interest for metal-catalyzed reactions in the condensed phase the formation of formaldehyde from H_2 and CO is endothermic,[1] whereas the formation of η^2-formaldehyde ligands in the coordination sphere of a metal is usually exothermic. Nevertheless, only a few examples of $(\eta^2\text{-}CH_2O)ML_n$ complexes are so far known in which the formaldehyde unit was synthesized by means of a carbonylation reaction.[2] We present here the very productive synthesis of a reactive (η^2-formaldehyde)zirconocene complex and describe some fundamental reactions of the metallaoxirane moiety.

According to *Floriani* et al.[3] carbon monoxide is hydrozirconated at room temperature and ambient pressure to give the dinuclear complex **1**. The stable substitution product **2** can be prepared by reaction of **1** with 2 molar equivalents of phenyllithium.[4] Not unexpectedly, the reaction with methyllithium proceeds somewhat differently. Presumably, in this case the methyl-bridged compound **3** is formed as an intermediate, which readily decomposes into its mononuclear organometallic components under the reaction conditions. We have isolated dimethylzirconocene **4** (quantitative yield) and dimeric (η^2-formaldehyde)zirconocene **5** (67%) as stable reaction products.



1 2 3 4 5

According to the results of an X-ray structure analysis,[5] in the complex **5** two (η^2-formaldehyde)zirconocene units are coupled to each other via their oxygen atoms, using the available lateral coordination sites at the bent metallocene. The Zr–O bonds in the three-membered ring are somewhat shorter than those connecting the monomeric $(\eta^2\text{-}CH_2O)ZrCp_2$ units. The C–O bonds are long; the Zr–C distance in the three-membered ring is typical for a ZrC_{sp^3} single bond. The $(\overline{CH_2\text{-}O})Zr$ units in **5** have metallaoxirane character.[6a, 7a]

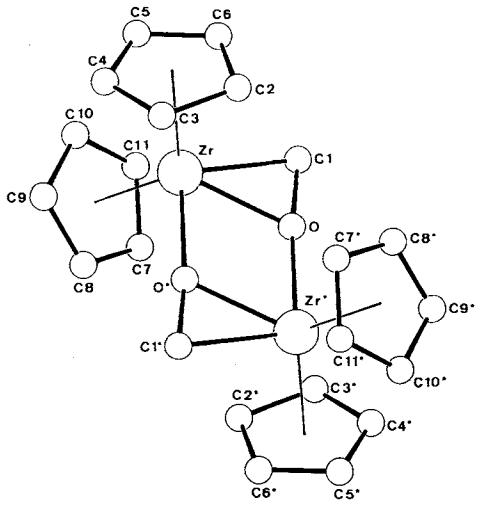


Fig. 1. Molecular structure of **5** in the crystal. Selected bond lengths [Å] and angles [°]: Zr-O 2.103 (2), Zr-C1 2.243 (3), C1-O 1.395 (4), Zr*-O 2.200 (2); O-C1-Zr 65.9 (2), C1-O-Zr 76.8 (2), C1-Zr-O 37.3 (1), Zr*-O-Zr 109.5 (1), Zr*-O-C1 173.5 (2), O*-Zr-O 70.5 (1).

Thermolysis (170 °C, 3 h) of the dimer **5** affords the known cyclotrimeric compound $[(\overline{CH_2\text{-}O})ZrCp_2]_3$.[8a] Complex **5** adds to many carbonylmetal complexes with opening of the reactive Zr–C bond of a metallaoxirane unit. At room temperature, **5** reacts with $CpCo(CO)_2$ selectively to give the adduct **6**.[7b, 8b] It also reacts with alkyl- and hydrido-aluminum complexes; upon reaction with diisobutylaluminum hydride at room temperature it forms the metallacyclic adduct **7**[7c] (Fig. 2). An X-ray structure analysis revealed that

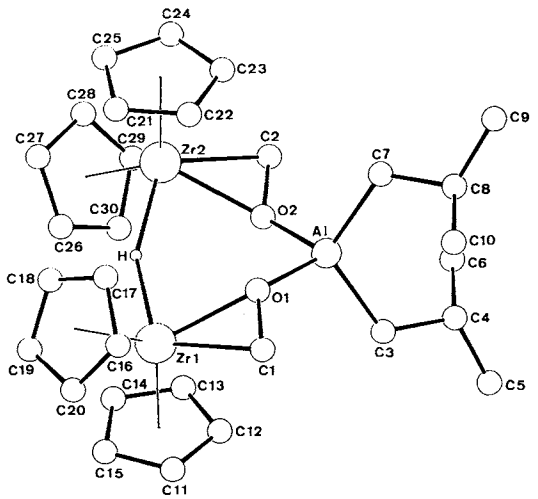
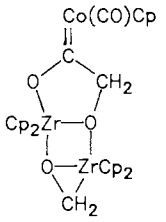


Fig. 2. Molecular structure of **7** in the crystal. Selected bond lengths [Å] and angles [°]: Zr1-O1, 2.153 (3), Zr1-C1 2.248 (5) C1-O1 1.430 (6), Zr2-O2 2.156 (3), Zr2-C2 2.230 (5), C2-O2 1.430 (6), Al-O1 1.815 (3), Al-O2 1.811 (3); Zr1-O1-Al 138.6 (2), Zr2-O2-Al 137.9 (2).

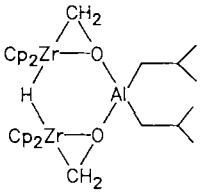
the (η^2-formaldehyde)zirconocene units in **7** also have pronounced metallaoxirane character.[9]

[*] Prof. Dr. G. Erker, Dipl.-Chem. U. Hoffmann, Dipl.-Chem. R. Zwettler
Institut für Organische Chemie der Universität
Am Hubland, D-8700 Würzburg (FRG)
Dr. P. Betz, Prof. Dr. C. Krüger
Max-Planck-Institut für Kohlenforschung
Kaiser-Wilhelm-Platz 1, D-4330 Mülheim a.d. Ruhr (FRG)

[**] This work was supported by the Fonds der Chemischen Industrie, the Deutsche Forschungsgemeinschaft, and by Alfred-Krupp-von-Bohlen-und-Halbach-Stiftung.



6



7

The reactions of **5** presented here confirm and extend the emerging consistent picture of the special behavior of metallaoxirane compounds of the early transition metals.[6, 9a, 10]

Received: October 12, 1988;
revised: December 27, 1988 [Z 3004 IE)
German version: *Angew. Chem. 101* (1989) 644

CAS Registry numbers:
1, 83385-36-8; **4**, 12636-72-5; **5**, 83385-20-0; **6**, 119747-76-1; **7**, 119747-77-2; $[(\overline{CH_2-O})ZrCp_2]_3$, 85442-82-6; $CpCo(CO)_2$,

[1] E. L. Muetterties, J. Stein, *Chem. Rev. 79* (1979) 479; C. K. Rofer-De Poorter, *ibid. 81* (1981) 447; see also J. F. Knifton, *J. Am. Chem. Soc. 103* (1981) 3959.

[2] G. Erker, *Acc. Chem. Res. 17* (1984) 103, and references cited therein; R. E. LaPointe, P. T. Wolczanski, *J. Am. Chem. Soc. 108* (1986) 3535; P. T. Wolczanski, R. S. Threlkel, J. E. Bercaw, *ibid. 101* (1979) 218; P. T. Barger, J. E. Bercaw, *Organometallics 3* (1984) 278; T. Beringhelli, G. D'Alfonso, G. Ciani, H. Molinari, *ibid. 6* (1987) 194.

[3] G. Fachinetti, C. Floriani, A. Roselli, S. Pucci, *J. Chem. Soc. Chem. Commun. 1978*, 269; S. Gambarotta, C. Floriani, A. Chiesi-Villa, C. Guastini, *J. Am. Chem. Soc. 105* (1983) 1690.

[4] G. Erker, K. Kropp, *Chem. Ber. 115* (1982) 2437.

[5] **5**: $C_{22}H_{24}O_2Zr_2$, $M = 502.9$, monoclinic, $P2_1/n$, $a = 8.9177$ (6), $b = 7.7670$ (6), $c = 13.917$ (1) Å, $\beta = 90.102$ (7)°, $V = 964.0$ Å^3, $Z = 2$, $\varrho_{calcd} = 1.73$ g cm^{-3}, $\mu(Mo)_{K\alpha} = 10.76$ cm^{-1}, Enraf-Nonius diffratometer, 4340 measured reflections, 3352 observed ($I > 2\,\sigma(I)$), heavy atom method, hydrogen positions calculated and not refined, $R = 0.047$, $R_w = 0.071$ for 118 paramters [9b].

[6] Cf. G. Erker, U. Dorf, P. Czisch, J. L. Petersen, *Organometallics 5* (1986) 668; G. Erker, P. Czisch, R. Schlund, K. Angermund, C. Krüger, *Angew. Chem. 98* (1986) 356; *Angew. Chem. Int. Ed. Engl. 25* (1986) 364; G. Erker, K. Kropp, C. Krüger, A.-P. Chian, *Chem. Ber. 115* (1982) 2447.

[7] **5**: m.p. = 220 °C (dec.); correct elemental analysis (C, H); MS (70 eV): *m/z* 500 ($M^{\oplus}$, 18%), 470 ($M^{\oplus} - CH_2O$, 100), 390 (33), 220 (60); ^{1}H NMR (200 MHz, $CDCl_3$): $\delta = 5.89$ (Cp), 2.42 (CH_2); ^{13}C NMR (50 MHz, $CDCl_3$): $\delta = 107.8$ (^1J(CH) = 171 Hz, Cp), 64.0 (^1J(CH) = 153 Hz, CH_2); b) **6**: yield 81%, m.p. 160 °C (dec.); correct elemental analysis (C, H); ^{1}H NMR (200 MHz, [D$_6$]benzene): $\delta = 5.81$, 5.45 (each s, each 10H, $ZrCp_2$), 5.08 (s, 5H, CoCp), 4.34 (s, 2H, CH_2), 2.58 (s, 2H, $ZrCH_2$); ^{13}C NMR (50 MHz, [D$_6$]benzene): $\delta = 290.0$ (carbene C), carbonyl C not observed, 113.0 ($ZrCp_2$), 107.8 ($ZrCp_2$), 95.4 (^1J(CH) = 143 Hz, CH_2), 84.5 (CoCp), 66.4 (^1J(CH) = 154 Hz, $ZrCH_2$); IR (KBr): $\tilde{\nu}$(CO) = 1905 cm^{-1}; c) **7**: yield 41%, m.p. 170 °C (dec.); MS (70 eV): *m/z* 642 ($M^{\oplus}$, 0.13%), 585 ($M^{\oplus} - CH_2CHMe_2$, 28%), 220 ($Cp_2Zr^{\oplus}$, 66%); ^{1}H NMR (200 MHz, [D$_6$]benzene): $\delta = 5.57$ (s, 20H, Cp), 2.39 (s, 4H, $ZrCH_2$), 2.21 (m, 2H, CH_2CH), 1.32 (d, 12H, $CH(CH_3)_2$), 0.15 (d, 4H, $AlCH_2CH$), −3.66 (s, 1H, ZrHZr); ^{13}C NMR (50 MHz, [D$_6$]benzene): $\delta = 105.8$ (Cp), 53.0 (^1J(CH) = 156 Hz, $ZrCH_2$), 29.0 (^1J(CH) = 123 Hz, $CHCH_3$), 26.8 (^1J(CH) = 118 Hz, $CHCH_3$), 22.1 (broad, $AlCH_2CH$).

[8] a) K. Kropp, V. Skibbe, G. Erker, C. Krüger, *J. Am. Chem. Soc. 105* (1983) 3353; b) cf. G. Erker, R. Lecht, J. L. Petersen, H. Bönnemann, *Organometallics 6* (1987) 1962.

[9] a) **7**: $C_{30}H_{43}AlO_2Zr_2$, $M = 645.1$, trichlinic, $P\bar{1}$, $a = 10.217$ (1), $b = 11.281$ (2), $c = 13.844$ (2) Å, $\alpha = 100.37$ (1), $\beta = 90.12$ (1), $\gamma = 106.36$ (1)°, $V = 1503.7$ Å^3, $Z = 2$, $\varrho_{ber} = 1.42$ g m^{-3}, $\mu(Mo_{K\alpha}) = 7.33$ cm^{-1}, Enraf-Nonius diffractometer, 7145 measured reflections, 4601 observed ($I \geq \sigma(I)$), $R = 0.042$, $R_w = 0.041$ for 445 parameters, b) further details of the crystal structure investigations are available on request from the Fachinformationszentrum Energie, Physik, Mathematik GmbH, D-7514 Eggenstein-Leopoldshafen 2 (FRG), on quoting the depository number CSD-53731, the names of the authors, and the journal citation.

[10] R. M. Waymouth, B. D. Santarsiero, R. J. Coots, M. J. Bronikowski, R. H. Grubbs, *J. Am. Chem. Soc. 108* (1986) 1427.

BOOK REVIEWS

Book reviews are written by invitation from the editor. Suggestions for books to be reviewed and for qualified book reviewers are welcome. Publishers should send brochures or (better) books to the following address: Redaktion Angewandte Chemie, Postfach 101161, D-6940 Weinheim, Bundesrepublik Deutschland. The editor reserves the right of selecting which books will be reviewed. Uninvited books not chosen for review will not be returned.

Preparative Acetylenic Chemistry (Series: Studies in Organic Chemistry, Vol. 34). 2nd Edition. By *L. Brandsma*. Elsevier, Amsterdam 1988. x, 322 pp., hard cover, HFl 220.00.—ISBN 0-444-42960-3

This book is a completely reviewed and updated version of the original 1971 publication, and has been enlarged by more than 100 pages. It is aimed at advanced students and preparative organic chemists.

As in other books by the same author (L. Brandsma, H. D. Verkruijsse: *Synthesis of Acetylenes, Allenes and Cumulenes*, Elsevier, Amsterdam 1981; L. Brandsma, H. D. Verkruijsse: *Preparative Polar Organometallic Chemistry*, Springer, Berlin 1987), all the preparative methods contained here have been carefully tested. The reader benefits from the author's many years of experience in acetylenic chemistry. The recommended reaction conditions take into account the reactivities of the starting compounds and intermediates. In practice a lack of knowledge of reactivities often leads to reactants being unnecessarily stirred under reflux for hours, despite the fact that the reaction is in fact completed within a few minutes. Much time and money can be saved when accurate information on reaction durations and reproducible laboratory recipes are available.

The topics covered in the book's twelve chapters are as follows. Chapter 1 gives practical advice of a general nature, and describes a number of extremely useful tricks from the author's wealth of experience. The rest of the chapters are: 2. Metallation of Acetylenes; 3. Functionalization of Metallated Acetylenes with Alkyl Halides, α-Haloethers, Epoxides and Alkyl Orthoformates; 4. Ethynylation and Alkynylation of Carbonyl Compounds; 5. Carboxylation, Alkylation and Related Reactions; 6. Silylation, Stannylation and Phosphorylation; 7. Sulfenylations and Related Reactions; 8. Halogenation and Cyanation; 9. Introduction of the Triple Bond by Elimination and Addition-elimination Reactions; 10. Couplings of Acetylenes Assisted by Copper and Palladium Compounds; 11. Base-promoted Interconversions of Acetylenes; 12. Miscellaneous Preparations of Acetylenic Derivatives. More than 500 acetylene derivatives, which can

be classified into 20 different groups on the basis of their functionality, are described in these chapters.

The concise factual style and the orderly arrangement of the material are pleasing features. Regrettably the pages do not have a headline identifying the chapter, and as a result cross-referencing often involves the reader in thumbing through the pages for a long time to find the required passage. The layout is attractive and the text contains hardly any printing errors. Although there are only 241 literature references this does not imply that the coverage is superficial; the smallness of the total is entirely a result of the author's rigorous criteria for choosing references.

To summarize, it can be said that this book, which is structured in the style of *Organic Syntheses*, gives an excellent and detailed overview of important synthetic building blocks containing C≡C bonds that are simple and obtainable in good yields. When the synthetic methods are read in conjunction with the "Introductions" which precede over half of them and the appended "Notes" on each one, the work is seen to be more than a mere "cook-book". It will certainly contribute to acetylenes assuming an even more important role in future in the planning of synthetic routes. The book will undoubtedly have a place in the standard reference collection of every chemistry library.

Rolf W. Saalfrank [NB 956 IE]
Institut für Organische Chemie
der Universität Erlangen-Nürnberg (FRG)

Organolithium Methods. (Series: Best Synthetic Methods.) By *B. J. Wakefield*. Academic Press, New York 1988. xvii, 189 pp., hard cover, $ 29.50.—ISBN 0-12-730940-3

The present reviewer has already remarked in this journal[*] that he regards the series title "Best Synthetic Methods" as a misleading description. Nevertheless, the volume on "Organolithium Methods" by *Wakefield* is very successful as an introduction to the topic with a strong emphasis on practical aspects. The author confines his treatment to organolithium compounds which are *not* stabilized by mesomeric effects (with the exceptions of allyl and benzyl derivatives of lithium). There are occasional passing references, perhaps unintentional, to the chemistry of compounds such as lithium enolates, but to cover these fully would have made the book too long.

The logical construction of the book together with its detailed contents list and the subject index allow one to quickly find the relevant chapter for each topic of interest (although the index is rather scanty). The introductory chapter is likely to be of particular value for newcomers to the field, such as students about to undertake their first work using organolithium compounds; it deals very briefly with constitution, reactivity and solvent effects, and, most importantly, gives much practical advice on matters such as the drying of solvents, use of inert atmosphere, handling of organolithium compounds, and quantitative analysis, illustrated in some cases by drawings of suitable apparatus.

The next chapter is devoted to the preparation of organolithium compounds, with a systematic and very instructive presentation of the principles, which are then translated into practical terms by giving laboratory recipes, most of which have been tested, and clear tables. The following chapters deal with the addition reactions of organolithium compounds to systems with multiple bonds, with the main emphasis, naturally, on carbonyl compounds as electrophiles. Next follow substitution reactions with the formation of C-C or C-heteroatom bonds, and related types of reactions. The following chapter describes some methods whereby organolithium compounds can be used to prepare organoboron, organosilicon and organophosphorus compounds, and—though only in outline—other organometallic species. Lastly, possibilities for using elimination reactions to form arynes, carbenes and ylides are briefly mentioned.

Every chapter includes detailed laboratory recipes and numerous examples in the form of tables. The relevant literature citations have been compiled with great thoroughness up to 1986; even a few references to work published in 1987 are included, making the coverage pleasingly up-to-date.

As each chapter includes a brief but succinct introduction summarizing the main features of current knowledge about mechanisms (or sometimes the lack of it), one can obtain from the book not only numerous practical hints and stimulating ideas, but also some basic science. Unfortunately, though, there is no reference to the principle of polar reversal of reactivity (umpolung), which has been and still is especially important for organolithium compounds.

The book is very attractively produced, and there are comparatively few printing errors (e.g., the formula scheme on page 37 has gone somewhat wrong). It is to be hoped that this book by *Wakefield* will achieve a wide circulation. It should at least be available in all libraries. However, although it would be especially useful to students, they will probably find it too expensive.

Hans-Ulrich Reissig [NB 952 IE]
Institut für Organische Chemie
der Technischen Hochschule Darmstadt (FRG)

The Bioinorganic Chemistry of Nickel. Edited by *J. R. Lancaster, Jr.* VCH Verlagsgesellschaft, Weinheim/VCH Publishers, New York 1988. xviii, 337 pp., hard cover, DM 175.00.—ISBN 3-527-26692-5/0-89573-338-2

Nickel was first discovered to play a physiological role in a biological system in 1965, and it was first found in a metalloenzyme a decade later. It is, in retrospect, surprising that the discovery of the importance of nickel in biology was made so late, but the fortunate result of this delay is that for nickel, unlike copper and iron, the tools of modern inorganic spectroscopy were used right from the beginning of the investigations of the biochemical properties of each newly discovered metal-containing biological system. The accounts of the elucidation of the properties of nickel-containing biological systems therefore read like a series of ongoing scientific detective stories. This is a well-written and well-organized volume that will be useful to a large number of readers. In addition, it is fortunate when a book such as this one describing a new field of research is written early enough that introductory material describing the methodology used, and the accounts of the background and current status of the field, all fit into one reasonably sized volume.

The volume consists of 14 chapters, each written by different experts in the field. The first four chapters provide the reader with an excellent introduction to the inorganic chemistry and spectroscopy of nickel. They are each written at an appropriate level that will enable the non-specialist to understand and to appreciate the significance of the spectroscopic results presented in the later chapters describing specific nickel-containing biological systems. These chapters are "The Coordination Chemistry of Nickel: An Introductory Survey" (*C. L. Coyle* and *E. I. Steifel*), "Nickel(III) Chemis-

[*] *Angew. Chem. Int. Ed. Engl.* 27 (1988) 1567

try and Properties of the Peptide Complexes of Ni(II) and Ni(III)" (*D. W. Margerum* and *S. L. Anliker*), "The EPR Spectra of Odd-Electron Nickel Ions in Biological Systems: Theory for d^7 and d^9 Ions" (*J. C. Salerno*), and "Electronic and Molecular Structure of Biological Nickel as Studied by X-ray Absorption Spectroscopy" (*M. K. Eidsness, R. J. Sullivan,* and *R. A. Scott*). The next two chapters provide an excellent overview of the role of nickel in biology: "Nickel in Biology: Nickel as an Essential Trace Element" (*D. Ankel-Fuchs* and *R. K. Thauer*) and "Biological Transport of Nickel" (*H. L. Drake*). The remaining eight chapters comprise more than half of the volume and describe in detail the results of the investigations of each of the types of nickel-containing metalloenzymes that have been found. They are "Urease—a Ni(II) Metalloenzyme" (*R. K. Andrews, R. L. Blakeley,* and *B. Zerner*), "Nickel in Hydrogenases from Sulfate-Reducing, Photosynthetic, and Hydrogen-Oxidizing Bacteria" (*R. Cammack, V. M. Fernandez,* and *K. Schneider*), "(Ni, Fe)Hydrogenases from Sulfate-Reducing Bacteria: Nickel Catalytic and Regulatory Roles" (*J. J. G. Moura, M. Teixeira, I. Moura* and *J. LeGall*), "Hydrogenases of *Methanobacterium thermoautotrophicum* strain ΔH" (*N. R. Bastian, D. A. Wink, L. P. Wackett, D. J. Livingston, L. M. Jordan, J. Fox, W. H. Orme-Johnston,* and *C. T. Walsh*), "Methyl-*S*-Coenzyme-M-Reductase: A Nickel-Dependent Enzyme Catalyzing the Terminal Redox Step in Methane Biogenesis" (*L. P. Wackett, J. F. Honek, T. P. Begley, S. L. Shames, E. C. Niederhoffer, R. P. Hausinger, W. H. Orme-Johnston,* and *C. T. Walsh*), "Structure and Properties of Coenzyme F_{430}" (*A. Pfaltz*), "Carbon Monoxide Dehydrogenase of Acetogens" (*G. Diekert*), and "Nickel in CO Dehydrogenase" (*S. W. Ragsdale, H. G. Wood, T. A. Morton, L. G. Ljungdahl,* and *D. V. DerVartanian*).

This book is a welcome addition to the literature of bioinorganic chemistry. It should be purchased by chemistry libraries and added to the personal libraries of bioinorganic chemists interested in nickel. It will also provide useful supplementary material for courses in bioinorganic chemistry. New workers in the field of nickel biochemistry will probably use this volume as a starting point in the future. (One warning: my copy has several pages where the print is very light. It might be a good idea to check your copy before you write your name in it.)

Joan Selverstone Valentine [NB 963 IE]
Department of Chemistry and Biochemistry
University of California
Los Angeles, CA 90024 (USA)

Math/Chem/Comp 1987. Edited by *R. C. Lacher*. Elsevier, Amsterdam 1988. 378 pp., $ 144.75.—ISBN 0-444-42930-1

This book, with its rather repulsive title, contains the proceedings of a conference on the interfaces between mathematics, chemistry and computer science which was held in Dubrovnik in June 1987. The conference is organized jointly by Florida State University and the Rugjer-Bošković Institute, Zagreb; according to the book's preface the meeting aims to encourage both interdisciplinary studies and those within a single discipline. The book contains 24 articles, which can be roughly grouped into the following topic areas: 1) Supercomputers and Chemistry, 2) Knot Theory, 3) Graph Theory and 4) Polymers. The main emphasis is not, as one might suppose from the abbreviation "Comp", on numerical quantum chemistry, but on topological methods of characterizing widely differing chemical structures.

The first two articles (by *D. Edelson* and *D. Edelson* et al., respectively) on supercomputers (vector computers) set out to review the current situation and likely future developments in the numerical treatment of scientific problems, a theme which has already been given a good deal of space in other publications during the past year. The second article reports specifically on the project at Florida State University to develop an expert system for chemistry.

The second section is more interesting. It includes an introduction to knot theory by *J. Simon* which is well worth reading; this is a special field of topology which has recently proved very useful for characterizing non-rigid cyclic polymers. Some advances have also occurred in the mathematics of knot theory; for example it has become possible to distinguish between the two chiral forms of the trefoil knot by means of the topological invariants (Jones polynomials) associated with them. However, for the reader interested in chemical aspects and applications it is regrettable that there are no contributions here on topics such as knotted strands of cyclic DNA molecules, the imaging of which has recently become possible through new experimental techniques.

A considerable proportion of the book is concerned with applications of graph theory in chemistry. The objective of graph theory is to translate structural characteristics of molecules into (mathematically defined) properties of graphs, and then to correlate these with physical-chemical properties, as described in the article by *N. Trinajstić*. The method is especially suitable for planar structures such as conjugated chains, which are dealt with in the article by *M. Randić* and *N. Trinajstić*. It emerges from the book that work is also in progress on a "three-dimensional graph theory" (*M. Randić*), for characterizing large molecules, i.e. synthetic and natural polymers. A reference to a 1985 paper indicates that graph theory can even contribute to cancer research, although this strikes the present reviewer as rather over-optimistic. Two articles by *R. Randell* deal with so-called conformation spaces, the object of which is to arrive at a description of flexible structures in chemistry. A typical problem posed here is: what is the minimum number of atoms in a cyclic structure for knotting to become possible?

The last of the main themes of the book and of the conference, polymers, brings into play the well known current catchphrases of this field: knot theory again, random walks, including those in restricted geometries (polymers in porous media), "lattice animals", scaling and critical exponents, Ising models. An exception to this is the review article by *L. Mandelkern* and *A. J. Peacock*, dealing from a purely phenomenological standpoint with the relationship between structure and mechanical properties of crystalline polymers. An analytical topological invariant for describing coiled polymer systems, the winding number, is introduced by *M. G. Brereton*. This quantity, defined as a path integral, does not distinguish as effectively between topologically different situations as do the polynomials of knot theory, but for dynamic processes its change or conservation provides an important indication of the type of reaction mechanism. Methods of analyzing polymers and branched polymers using the concepts of random walks or lattice animals have already been in common use for several years. Relationships to the description of disordered systems by fractals can be shown, and the renormalization theory which receives special mention in the article by *D. S. Gaunt* can also be used. Taken as a whole the section on polymers is the most interesting part of the book, as many physically relevant concepts are discussed here, and the articles give an insight into a large area of current research.

The value of having an index is not confined to textbooks; its presence would also be appreciated in this conference report. The price of the book is scarcely affordable for the private purchaser, and the same remains true for our libraries with their meagre budgets.

Werner Gans [NB 948 IE]
Institut für Physikalische Chemie
der Freien Universität Berlin

Houben-Weyl. Methoden der Organischen Chemie. Band E 20, Teil 1–3: Makromolekulare Stoffe. Edited by *H. Barte* and *J. Falbe*. Thieme, Stuttgart 1987. Part 1: lxxviii, pp. 1–688, bound, ISBN 3-13-219004-7; Part 2: xxx, pp. 689–1794, bound, ISBN 3-13-219004-7; Part 3: xxi, pp. 1795–2958, bound, ISBN 3-13-219004-7; price for Parts 1–3: DM 3400.00 (subscription and pre-ordered price: DM 3060.00).

There can hardly be a single chemistry library in the German-speaking world where "Houben-Weyl" is not to be found. It is a standard work of reference with which one is already familiar as a student, and which one reaches for whenever it becomes necessary to master a new topic.

It is certainly remarkable that a quarter of a century ago, under the series title "Methods of Organic Chemistry", the topic of "Macromolecular Substances" was already also included, in two volumes. The last twenty years have brought far-reaching changes in the polymer field, creating a pressing need for a revised version of this standard work. The breadth of the areas to be covered makes it impossible for the revision to be undertaken by only a small team of authors, let alone by one. There is no doubt that the editors have succeeded in engaging the services of many eminent experts to rewrite the different sections. There is a high degree of consistency in the style of treatment, and in view of the number of authors (86!) one may conclude from this that there has been a considerable amount of editing. Rules of nomenclature have been followed to a sensible extent, which contributes a good deal to easy readability.

The Part 1 volume is devoted entirely to preparative methods. A general introduction provides an easy entry into the field for the chemist who is less familiar with polymers. About 140 pages deal with the various methods for initiating the polymerization of monomers with multiple CC bonds. There is still much activity in this area, as shown by the fact that in some articles over 50% of the citations refer to work in the last ten years. Throughout the work as a whole the high proportion of recent citations provides a good overview of the main features of current research.

The largest amount of space is given to the description of free radical initiation. In describing the initiation of polymerization by CC cleavage, by azo initiators, peroxides, diacylperoxides and percarbonates, new results are included, and particular attention is given to systems with technological relevance. In addition to the conventional initiators, others such as the metal (O) compound/alkyl halide systems and electrochemical initiation are described. The term "living polymerization", which is wrongly applied in the literature to certain free radical polymerizations, is here rejected as being inaccurate, but to be consistent the section entitled "Living free radicals" should have been called "Long-lived free radicals". Polymerization initiation using energetic and high-intensity radiations is nowadays especially important in the manufacture of semiconductor chips and printed circuit boards, and it is pleasing to find that this "laser polymer chemistry" is described in detail.

Cationic polymerization and living polymerization have long seemed to be contradictory. This has changed. In the account of the current position in anionic polymerization, the main emphasis is on new results concerning ways of influencing the microstructure of polydienes, functionalization, and influencing copolymerization parameters. In the discussion of initiators for Ziegler-Natta coordination polymerization the current state of knowledge is summarized, with particular attention to the technologically important supported catalysts, to "linear low density" polyethylene, and to influences on the microstructure of polydienes. Group transfer polymerization is now just five years old, and the progress made on this topic is shown by a wealth of new results.

The theory of copolymerization is discussed from the standpoint of its practical applicability by the preparative chemist.

Over 200 pages are devoted to polymerization methods; particular emphasis is laid on technical polymerization procedures, as in bulk polymerization, and in solution, emulsion, suspension, precipitation and gas phase polymerization methods. Emulsion polymerization (approx. 100 pp.) is treated theoretically, and the colloidal properties of the products, such as the stability of the emulsions, coagulation and film formation, are reviewed. In the section on suspension polymerization the technologically important Pickering dispersing agents are discussed, as is also the synthesis of macroporous supports. Fluid bed processes for the polymerization of formaldehyde or ethylene are found under the heading "Gas phase polymerization". The equipment required for plasma polymerization and the capabilities of the method are also described. Solid phase polymerization and polymerization in thin films allow ordered systems to be produced. In addition to the classical case of diacetylene polymerization, polymerization in perovskites, inclusion compounds and ultrathin films are described.

The synthesis of carbon-heteroatom polymers is treated in the chapters that deal with the polymerization of monomers with CO or CN multiple bonds and with ring-opening polymerizations. The number of heterocyclic compounds that have been used in ring-opening polymerizations has grown enormously in the last 25 years; a short section is devoted to the free radical polymerization of heterocycles, but the main emphasis in this chapter is on the cationic and anionic ring-opening polymerization of heterocycles. The mechanistic aspects of the polymerization of oxacycles and lactones are clearly set out. Access to the literature on the copolymerization behavior of cyclic ethers is facilitated by the inclusion of more than 50 references.

In the chapter on "Polyadditions" the main emphasis is on polyurethane chemistry. The problems of synthesizing oligourethanes of uniform molecular structure are discussed in detail. The notion which *Otto Bayer* introduced of tailored synthesis in polyurethane chemistry is discussed, taking as an example the synthesis of segmented polyurethane elastomers. Other topics treated are the silane/olefin addition and the applications of the Diels-Alder reaction. Notwithstanding the enormous importance of the diisocyanate/diol reaction, the potential underlying the principle of polyaddition is still far from being exhausted.

The chapter on "Polycondensations" begins with a very comprehensive survey of the known structure-building reactions, but unfortunately no critical evaluation of yields and side-reactions is included. The prepolymer technique, which is especially suitable for synthesizing crosslinked polymers, is described in detail in accordance with its practical importance. Considerable space is also given to the description of

ordered structures in polycondensates in the form of segmented or block copolymers. The section on structure-property relationships is especially valuable for the preparative chemist. However, the generalizations that are made, e.g. concerning T_g and T_m, should only be regarded as approximate rules with many exceptions. The problems and the advantages and disadvantages of polycondensation in melts, in solutions and on surfaces are thoroughly discussed.

In considering reactions on macromolecules as a method of synthesis, the importance of the effects of neighboring groups on the structure of the polymer thus formed is usually underestimated. This chapter provides a good overview of this topic. Graft polymerization reactions offer a wide range of possibilities for modifying polymers, and are used in many different forms in industrial processes. In this article the choice of a suitable initiator for a given graft polymerization system is clearly explained.

The final chapter of the Part 1 volume describes modifications obtained by combining polymers. As well as interpenetrating networks, polymer blends offer ways of combining properties to achieve a desired result. The principles of producing modified polymers with high impact strength and thermoplastic elastomers are described.

In the Part 2 and Part 3 volumes the emphasis is on the different chemical classes of macromolecular substances. Over 100 pages are devoted to the polymerization of olefins, and the various methods are critically evaluated. Many laboratory recipes for both homo- and copolymerization are given. The densely packed information ranges from phase diagrams to safety aspects. Questions such as which comonomers should be used to stabilize an emulsion or to improve the adhesion strength of a film are answered, as well as those relating to ways of obtaining higher stereospecificity in the polymerization of propene. Under diene polymerization (over 100 pp.) the main emphasis is on microstructure, but in addition reaction regulators, and modifications through copolymerization and incorporating stabilizers are discussed. Metathesis reactions can nowadays be carried out as a form of living polymerization. However, many questions concerning the stereochemistry still remain unanswered. Here the current state of knowledge in this area is carefully set out. The section on "Styrene polymerization" concentrates on modifications, e.g. by copolymerization, grafting or ionic block copolymerization. It is remarkable that over 90% of the citations refer to the period since the publication of the previous edition. In addition fluoroolefins, chloroolefins, vinyl ethers, vinyl esters, unsaturated aldehydes and acrylic compounds as monomers are carefully and expertly discussed. Polymerization reactions of acetylenic monomers are not confined to acetylene itself—details of the polymerization of more than 40 acetylene derivatives are included. Diines too undergo polyaddition reactions to give many different polymers. Aliphatic and aromatic polyethers and aliphatic polyacetals are polymers that exhibit a very wide range of properties profiles. For these the importance of including alongside the polymerization processes the properties of the resulting polymers has been recognized, and representative data on technical products are also listed.

Polyesters in all their many variants are described in 50 pages. In addition to the familiar aryl-aliphatic polyesters there are detailed descriptions of unsaturated polyester resins, alkyd resins and polycarbonates. Sulfur-containing aliphatic and aromatic polymers are treated in the following chapter. These too include products of basically different types: on the one hand alternating copolymers of olefins and sulfur dioxide formed by free radical polymerization, which degrade easily as indicated by their low ceiling temperatures, and on the other hand high performance materials such as polyphenylenesulfide and polyphenylenesulfone.

In the area of polymers with main-chain nitrogen atoms the longest chapters are those on polyamides, polyurethanes and polyureas. The chapter on "Polyamides" deals with various polyheterocycles including polyimides, polyamidimides and polyether-imides, some of which also appear in Part 3 under the heading "Special polymers". Considerable advances have been made in the last 25 years in the field of ionomeric polyurethanes, and accordingly the preparative aspects of introducing ionic groups are discussed. In these 150 pages on polyurethanes an impressive account is given of the many possible variations of the molecular architecture. Other chapters in this volume are devoted to polymers with P, B, Si and metals as heteroatoms.

In the Part 3 volume phenolic and amino resins are described. In order to tailor the properties profile of formaldehyde resins to suit the many different applications a detailed knowledge of the basic reaction steps is essential. The short synopsis of areas of application given here is very useful. Epoxide resins are now more than 40 years old. In addition to their best known area of application in high performance composites, the wide range of variations that are possible in the underlying chemistry of starting materials and curing agents, as described here, opens up many different areas of use, e.g. in paints and other surface treatments.

The long third chapter of Part 3 (200 pp.) recognizes the enormous practical importance of the production of chemically modified polymers. The treatment is divided into synthetic polymers and polysaccharides. Under synthetic polymers a number of reactions have had to be omitted because of the need to be selective; those sacrificed include hydrolysis of esters and amides, imidization reactions and cyclization reactions in general. However, this still leaves a very wide range of topics. The conversion of polysaccharides is one of the oldest processes of polymer chemistry. Under the heading "Renewable raw materials" this has again become an important topic today. After a general discussion of structure-property relationships as influenced by the complex pattern of substitution, individual groups of cellulose ethers and cellulose esters are discussed. Special sections are devoted to starch and guarane derivatives.

In the next chapter we return to polymers produced by synthetic reactions. This chapter, on "Special polymers", is very varied in content. The topics covered are polymers formed by condensed heterocyclic rings, products from polymerization of ketene, polymers from carbon dioxide, liquid crystal polymers, chiral polymers and inorganic polymer chains. The section on "Condensed heterocyclic rings" is a good survey of the high temperature polymers known at present. That on "Liquid crystal polymers" suffers a little from the fact that aromatic polyesters and amides are treated elsewhere. The section on "Chiral polymers" consists of only one table. Under the heading "Inorganic polymers", polyphosphazenes, polyorganosilanes, silicones and polymers synthesized from metal phthalocyanines are described.

A considerable amount of space is given to characterization methods. Although the determination of chemical constitution by decomposition has nowadays become less important compared with spectroscopic methods, the analysis of end groups remains a problem, and this chapter offers some help in that respect. In the section on "Physical methods of polymer characterization", difficulties that may be encountered are briefly summarized and references are given for more detailed reading.

The final chapter of the work is concerned with toxicology and with environmental aspects of polymers. This is followed by a bibliography (approx. 100 pp.) listing further literature, mainly reviews, under the individual chapter headings. It is doubtful whether a reader who only makes occasional use of the work will find this additional material; perhaps it should have been put after the introduction or at the ends of the chapters.

As so often happens, there are problems with the subject index. One is used to looking for polystyrene (Polystyrol) under "Poly...". After realizing that one must look under "Styrol", further difficulties arise with "Polyethersulfon", as here one has to search under "Sulfon"; however, "Polyetherketon" does not appear under either "Etherketon" or "Keton".

The work contains hardly any printing errors, and the typography and presentation are attractive. There are a few errors which are likely to cause a smile: "Schmutzkolloide" on p. 188; in the contents list and in the index the Smith-Ebert theory appears instead of the emulsion theory, and on p. LIV under "General articles on large molecules" the "Encyclopedia of Polymer Science and Technology" is also cited.

The few shortcomings are small when weighed against the scientific value of the work. As an up-to-date work of reference for all scientists involved in polymer chemistry it is indispensable, and it will soon find its place in the libraries of polymer science departments and institutes. However, for those universities where macromolecular chemistry is not strongly represented the price may prove to be a serious obstacle.

Walter Heitz [NB 945 IE]
Fachbereich Physikalische Chemie
der Universität Marburg (FRG)

CORRESPONDENCE

One Pioneer or Several Pioneers? The Discovery of Noble-Gas Compounds

P. Laszlo and *G. J. Schrobilgen* have submitted the following **Addendum** to their article on noble-gas compounds (*Angew. Chem. 100* (1988) 495; *Angew. Chem. Int. Ed. Engl. 27* (1988) 479).

A letter from *Henry Selig* of August 29, 1988,[*] differs in the sequence of events, in respect to a key finding, from *John Malm*'s recollections, which we had no reason to doubt and have followed in our account. In Dr. *Selig*'s words: "... most members of the Argonne fluorine research group had gone to the Estes Park, Colorado, fluorine symposium leaving *Claassen, Malm* and myself behind. The actual experiment was planned by the three of us and carried out during that week. On the day of the very first experiment, Friday, August 2, 1962 *John Malm* was at home ill and *Claassen* and I conducted the experiment by heating Xe + F_2 in a nickel can at 400 °C. After pumping off the volatile materials and not finding any xenon we were still sceptical. We phoned *Malm* at home to apprise him of the results. The following week we identified the material in the weighing can as XeF_4, presenting our colleagues returning from Estes Park with a fait accompli."

We gratefully acknowledge Dr. *Selig*'s version of the first synthesis of XeF_4 at Argonne, an interesting variant with respect to the story we had reported. Our account, let us remind the readers, has as its main focus the prehistory of the discovery of noble-gas compounds.

Prof. P. Laszlo

Laboratoire de Chimie, École Polytechnique
F-91 128 Palaiseau Cédex (France)
Prof. G. J. Schrobilgen
Department of Chemistry, McMaster University
Hamilton, Ontario L8S 4M1 (Canada)

[*] To Prof. *Laszlo* (note added by the editorial staff).

Registered names, trademarks, etc. used in this journal, even when not marked as such, are not to be considered unprotected by law.

© VCH Verlagsgesellschaft mbH, D-6940 Weinheim, 1989. – Printed in the Federal Republic of Germany by Konrad Triltsch, Druck- und Verlagsanstalt Würzburg.

All rights reserved (including those of translation into foreign languages). No part of this issue may be reproduced in any form — by photoprint, microfilm, or any other means — nor transmitted or translated into a machine language without written permission from the publishers. Only single copies of contributions, or parts thereof, may be made for personal use. This journal was carefully produced in all its parts. Nevertheless, authors, editors and publisher do not warrant the information contained therein to be free of errors. Readers are advised to keep in mind that statements, data, illustrations, procedural details or other items may inadvertently be inaccurate.

Valid for users in the USA: The appearance of the code at the bottom of the first page of an article (serial) indicates the copyright owner's consent that copies of the article may be made for personal or internal use, or for the personal or internal use of specific clients. This consent is given on the condition, however, that the copier pay stated per-copy fee through the Copyright Clearance Center, Inc. (CCC), for copying beyond that permitted by Sections 107 or 108 of the U.S. Copyright Law. This consent does not extend to other kinds of copying, such as copying, for general distribution, for advertising or promotional purposes, for creating new collective works, or for resale. For copying from back volumes of this journal see 'Permissions to Photo-Copy: Publisher's Fee List' of the CCC.

Editorial office: Postfach 10 11 61, D-6490 Weinheim, Federal Republic of Germany, Telephone (06201) 60 22 55, Telex 465 516 vchwh d, Telefax (06201) 602 328.

Editor: *Peter Gölitz*

Associate editors: *D. I. Loewus, A. Stimson.* **Editorial assistant:** *E. Schweikart*

Publishers: VCH Verlagsgesellschaft mbH. (Managing Director: *Hans Dirk Köhler*), Pappelallee 3, D-6940 Weinheim, Federal Republic of Germany.

Advertising office (Advertising Manager *R. J. Roth*): Postfach 10 11 61, D-6940 Weinheim, Federal Republic of Germany, Telephone (0 62 01) 60 61 30, Telex 4 67 155, Telefax (0 62 01) 606 184.

ADVANCED MATERIALS

Materials Research—Current Issues and Future Directions

Editorial Essay

By John W. Collette* and Joel S. Miller*

"I am making the first announcement of a brand new chemical textile fiber. This textile fiber is the first man-made organic textile fiber prepared wholly from materials from the mineral kingdom...; Though wholly fabricated from such common materials as coal, water, and air, Nylon can be fashioned into filaments as strong as steel, as fine as a spider's web, yet more elastic than any of the common natural fibers."[1] This announcement by Du Pont's Vice-President, Dr. *Charles Stine*, on October 27, 1938, caught the public attention and can, perhaps more than any other single event, be viewed as the beginning of the *Age of Polymers*. Few if any futurists would have predicted how the subsequent avalanche of synthetic polymers would change the way man thinks about and uses materials. As part of the 50th anniversary celebrations of Nylon the "Advanced Materials Conference on Current Issues and Future Directions in Materials Research" was held in Wilmington, Delaware, USA, on October 23.–24., 1988. It provided an opportunity to focus on the theme of shaping the future in the evolving new world of materials and material systems.

Historically, the commercialization of Nylon culminated several decades of technological advances in Europe and the United States which had seen the growth of a polymer industry based largely on the chemical modification of cellulose. Major research efforts were also under way seeking a substitute for natural rubber. Then within one decade, a completely new series of synthetic materials—Neoprene rubber, styrene/butadiene rubber, polystyrene, polyvinylchloride, polyvinylbutyral, polymethylmethacrylate, Nylon and Teflon were developed which provided properties previously unattainable. Fifty years after its introduction, the worldwide market for nylon polyamides has grown to an annual size of 12 billion pounds. Sales are still expanding at a rate significantly faster than the gross national product. This, however, represents only a fraction of the global business in synthetic polymers.

There have been many technological developments during this period. New scientific advances in synthesis, in physical techniques, and in computational capabilities are increasing our ability to make, characterize, and understand the properties of specifically structured materials. The coalescence of macromolecular, metallurgical, and ceramic technologies around a common need to provide specific structural properties has catalyzed interdisciplinary work and synergized the translation of advances in one field to others. The increasing overlap of science with technology has seen scientific advances moving rapidly into technological development and advances in technology catalyzing scientific investigations into new materials.

Dr. *Ardent Bement*, Vice President for Technology at TRW Inc., in a keynote introduction to the conference, noted that never before have materials engineers been able to offer so many options to the design engineers in assisting them to reconcile conflicting ideals of efficiency, economy, functionality, durability, and aesthetics.[2] *Bement* provided a historical perspective of synthetic polymers in the evolution of materials science. He looked forward to even more exciting developments as microelectronic technology is combined with materials to provide a new generation of smart materials systems.

Prof. *Merton Flemings*, in his presentation entitled "National Perspectives on Materials Science and Engineering," observed that materials technologies are a key element in improved productivity and overall economic growth.[3] All leading nations and industries have targeted materials, and especially advanced polymers, as a theme for research emphasis. *Flemings* succinctly reviewed the preliminary findings from a forthcoming National Research Council Study on "Opportunities and Needs in Materials Science and Engineering" which he co-chaired. This study has identified important opportunities for improved materials in the aerospace, electronics, health care, automotive, chemical, and energy industries. Noteworthy conclusions include an urgent need for increased efforts on the synthesis and processing of materials and on education. Furthermore, improved interdisciplinary interaction between chemists involved in synthesis, physicists and physical chemists involved in structure and property determination, and engineers who process the material and fabricate the product are critical to future progress.

These themes were reiterated in the major technical talks (on which the following articles in this issue are based): Dr. *Michael Salkind* described the revolution taking place in aerospace materials to meet the challenges of lower weight with higher operating temperatures. The future will see increasing effort on so-called smart systems which can respond dynamically to external stresses (exemplified by the flying replica of the extinct reptile *Quetzalcoatl Northropi*). Dr. *David McCall* outlined the materials challenges in electronics applications as the drive towards miniaturization exacer-

[*] Dr. J. W. Collette, Dr. J. S. Miller
E. I. du Pont de Nemours & Co., Inc.
Central Research & Development, Experimental Station, Building 328
Wilmington, DE 19898 (USA)

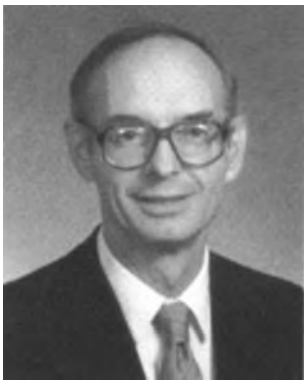
bates the complex interactions between the metals, ceramics, and polymers used in these systems. Prof. *David Williams* emphasized the embryonic character of materials technology in healthcare applications. Current materials used to replace bones or other body parts generally have only a single, simple function, usually a mechanical one. Truly functional replacements which combine mechanical properties with biological characteristics will require major advances in understanding how natural materials function and in the design of smart materials. Prof. *Walter Michaeli* used liquid crystal polymers to exemplify the importance of processing on materials properties. He also showed the value of computer modeling to guide part design based on knowledge of the behavior of the polymer during processing.

The importance of interdisciplinary work and of a systems approach to materials application was vividly apparent in the history of the development of Kevlar aramid fiber by Drs. *David Tanner, James Fitzgerald,* and *Brian Phillips.* With a highly engineered material such as Kevlar, market emphasis shifts from simply selling the product, to providing a system which meets a functional need. A complex composite, for example, may involve both organic and inorganic fiber reinforcement in a matrix of two or more different resins, all chosen to provide specific properties. The materials scientist has to be concerned not only that each individual material has the optimum properties needed but has also to understand the complex interactions between them in the final system.

The interdisciplinary nature inherent in materials research, the globalization of scientific effort and the intense international competition in advanced materials are combining to bring about many changes: partnerships between different companies to share technology, increased industrial/academic collaboration, and an effort by the government to facilitate technology transfer from government laboratories. This has affected the way research and development is carried out and placed new demands on the current science and engineering educational system. The particular issues of education and of collaboration between industry, academia, and government were addressed by the panel of industrial, academic, and government representatives. For a critical summary of this discussion see Prof. *Gerhard Wegner*'s contribution in this issue. The panel highlighted many of the changes already taking place. These include: 1) increased industrial support of academic research; 2) more collaborative programs between industry and individual university scientists; 3) visiting scientist programs to bring academic researchers to industry; 4) government policies aimed at encouraging effective liaisons between the different sectors; and 5) an increase in interdisciplinary training and research in academia. Some major gaps are the virtual absence of industrial scientists taking sabbaticals at universities and the limited number of Americans who study in Japan. A major issue discussed was how to increase interdisciplinary programs at universities without sacrificing the quality of the scientific training.

The materials field has never been so vibrant and full of expanding opportunities as it is today. Materials science is truly a dynamic global science of growing critical importance to mankind. The conceptual focus of materials research is changing from using available materials, to designing systems and materials in the context of a functional application. A major challenge for the future is to assure a climate which is conducive to effective R & D. We must optimize the fruitful partnership between industry, universities, and government. Educational programs at universities must be strengthened, and must recognize that advances will require experts who can communicate and cooperate in interdisciplinary programs. These goals must be met if we are to remain competitive in an increasingly technological world.

[1] D. Hounshell, J. K. Smith: *Science and Corporate Strategy*, Cambridge University Press, New York 1988, p. 270.
[2] A. L. Bement, *Metallurg. Trans. 18A* (1987) p. 363.
[3] J. P. Clark, M. C. Flemings, *Sci. Am. 255* (1986) No. 4, p. 50.



John W. Collette was chairman of the Organizing Committee for the Advanced Materials Conference held for the 50th anniversary of Nylon. A native of Calgary, Canada, he received his Ph.D. from the University of California (Berkeley) in 1958. He then joined Du Pont and has held a variety of managerial positions in polymer research and development. In 1987 he assumed his present position as Assistant to the Vice President of the Central R & D department. He holds 28 patents and has authored 22 publications in the fields of synthetic elastomers, high performance coatings, and polymerization catalysis.



Joel S. Miller received his Ph.D. from UCLA (1971). After a postdoctoral fellowship at Stanford University he joined the Xerox Webster Research Center in 1972 and in 1978 the Occidental Research Corporation. In 1983 he joined the Central R & D Department at Du Pont where he is currently a Research Supervisor for solid state science. His research interests focus on the solid state properties of molecular compounds and charge transfer complexes as well as the surface modification of solids. In addition to holding patents he has edited five monographs and published over 160 papers.

ADVANCED MATERIALS

Materials Issues in Electronic Systems

Chip Encapsulation
Semiconductors
Superconductors
Dielectrics
Multilayer Boards

By David W. McCall *

1. Introduction

The materials of electronic systems as illustrated in Figure 1 can be summarized in terms of relatively few basic elements and compounds. Integrated circuit (IC) chips are made of single crystal doped silicon with aluminum metallization and silicon dioxide or silicon nitride dielectrics. A glass (P-glass) or silicon nitride is used for passivation. For protection the chips are encapsulated in a plastic or ceramic package. Electrical connections are made via gold or aluminum wires from chip bonding pads, to leadframes constructed of copper or an alloy of iron and nickel. The leadframes are attached by solder to printed circuit boards that are composed of epoxy–glass (or sometimes polyimide) substrates which support copper interconnection patterns. In some cases alumina substrates are employed with refractory metals. Connections to other boards are made through connectors composed of molded plastic (poly(diallyl phthalate), poly(phenylene sulfide), etc.) with beryllium/copper contact fingers, and cables with copper conductors insulated with extruded plastic.

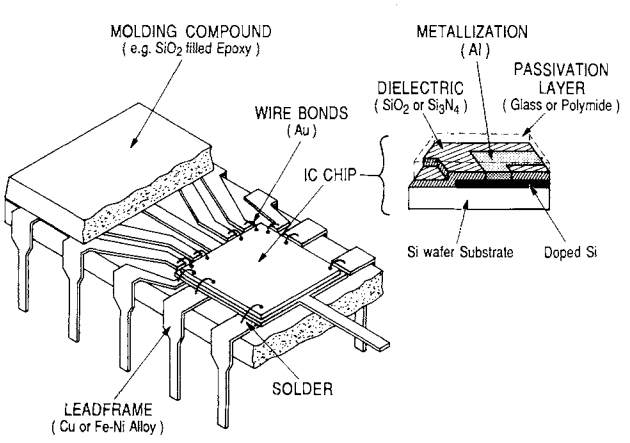


Fig. 1. Materials usage in integrated circuit chips.

This summary, while substantially accurate for the great majority of circuits, fails to reveal the enormous amount of materials engineering work that makes the manufacture and use of electronic systems possible. Each material has been carefully tailored for specific purposes, and issues of material compatibility are of critical importance. Process sequences, involving hundreds of steps, must be chosen such that conditions later in the sequence do not undermine structures formed earlier. The dimensions of all features of electronic circuits, from IC's to printed wiring boards have been decreasing logarithmically since the 1960's (Figure 2). As the

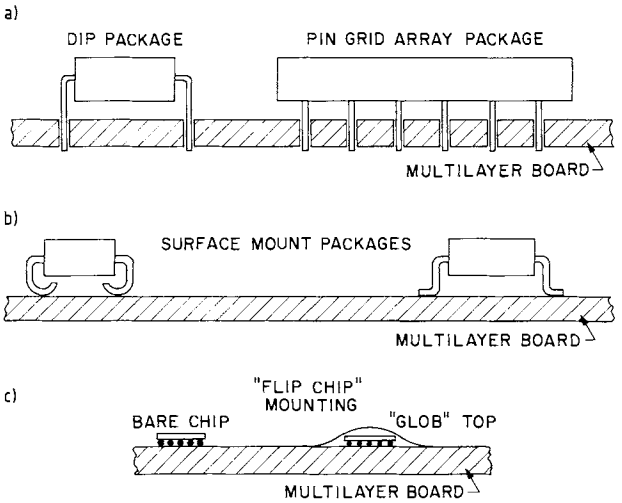


Fig. 2. Evolution of IC chip feature and interconnection dimensions for printed wiring boards (PWB), hybrids, and multichip modules (MCM).

circuit dimensions are reduced to two or three orders of magnitude above the sizes of the atoms themselves, compatibility of materials and processes becomes more important.

The foregoing capsule description includes only the materials that remain in the final product. In fact, many other materials are necessary to the processes that give rise to the structures, e.g. photoresists and electron beam resists, that define the lateral patterns on ever finer scales (a few thousand Ångstroms). Organometallic precursors are also employed to deposit metal films. Process control is increasingly critical, e.g., gate oxides of the order of 100 Å are necessary in advanced devices. Ion implantation places precisely known concentrations at controlled depths and molecular beam epitaxy lays down coherent layers atom-by-atom.

The packaging materials of the chip have different but extremely challenging demands. The package must provide

[*] Dr. D. W. McCall
AT & T Bell Laboratories
Murray Hill, NJ 07974 (USA)

timing information to all parts of all chips with manageable skew. Data must be delivered to and from chips with delays that are consistent with chip circuit switching times, and an increasing number of access points are required as chips evolve. Electrical power and ground must be supplied over leads of small impedance, which means extremely short paths. The heat generated by the chip circuitry must be transmitted to the environment effectively to prevent the chip temperature from rising disastrously. In material terms, the electrical signal paths require high conductivity metals such as copper, aluminum, gold, etc., and low dielectric constant insulation, e.g., polyimides and fluorinated polymers. The speed of light is a practical limiting factor in advanced circuits. For power delivery, high conductivity metals are again necessary, but high capacitance (i.e., low impedance) physically close to the chip requires high dielectric constant capacitor materials, usually ceramic. Thermal conductivity favors metal and other ceramic paths, as polymers are thermal insulators.

The thermal coefficient of expansion (TCE) is a critical factor in package design as mechanical stresses are created when temperature changes occur in manufacture, temperature cycle testing and use. Silicon has a low TCE compared with common metals and organic polymers. The problem, however, becomes more serious as the chip size decreases. Thinner sections of the molded body are more susceptible to thermal-mechanically induced failure by cracking. The TCE of polymeric materials can be controlled by addition of low TCE fillers, as is conventional for molding compounds and printed wiring board resins. Many packaging and interconnection materials are composites designed to improve the TCE match. The use of Kevlar fibers as reinforcement for polymer matrices is promising for TCE control. Also, there is a certain class of polyimides which has, by molecular design, been shown to exhibit very low TCE.

2. Materials Opportunities

Opportunities for material innovation continue to grow. After many years of promise GaAs is now finding real applications in advanced computers. Beryllium oxide, aluminum nitride and silicon carbide offer high thermal conductivity, and among the inorganic insulators, silica and cordierite have relatively low dielectric constants but suffer from poor thermal conductivity. Polymers offer low dielectric constants with opportunities for further substantial reduction in fluorinated materials. In all of these considerations material compatibility, adhesion, ionic impurities and many other factors are critical.

The physical properties of typically used organic, inorganic, and metallic materials are listed in Table 1. To give a more specific description of the use of organic materials in electronic systems, three areas will be discussed: chip packaging materials, printed circuit substrates, and interlayer dielectrics in hybrid circuits and other advanced structures.

2.1. Integrated Chip Packaging

Chip packaging is an area that requires careful attention to matters of material compatibility and process feasibility.

Table 1. Interconnection and Packaging Materials [a].

	T [°C]	ϱ [g cm^{-3}]	ε'	ε''	σ [Ω cm]	TCE [ppm K^{-1}]	K [W cm^{-1} K^{-1}]	Uses
Organics								
Epoxy (70% SiO_2)	170	1.8	3.8	0.03	4×10^{16}	20	0.002	Packaging
Epoxy Glass (FR-4)	120	1.9	4–5	0.05	10^{11}	15	0.02	Multilayer Board Substrate
Adv. Epoxy (Resin Only)	180	1.2	3.7	0.02	10^{14}	55	0.02	Multilayer Board Substrate
Triazine	250	1.26	3.1	0.001	$>10^{13}$	50	0.002	Hybrid Dielectric
BT Resin (Laminate)	290	1.28	4.0	0.01	10^{15}	15	0.005	Flexible Substrate
Polyimide	400	1.42	3.6	0.01	10^{16}	50	0.0007	Flexible Substrate
Polyimide	310	1.4	3.5–5	0.01	10^{16}	50	0.0007	Interlayer Dielectric
Inorganics								
Alumina (Ceramic)	1600	4.0	9.5	0.003	10^{14}	6.5	0.3	Hybrid Substrates/Chip Carriers
Silica (Fused)	1100	2.2	3.8	$<10^{-4}$	$>10^{17}$	0.6	0.02	Filter/Molding Epoxies
Silicon Nitride	2000	3	6	–	10^{16}	0.8	0.3	Candidate Substrates
Aluminum Nitride	1800	3.3	8.9	0.004	10^{13}	4.5	3.2	Candidate Substrates
Silicon Carbide	2100	3.2	40	0.2	10^{13}	3.7	2.7	Candidate Substrates
Silicon	1400	2.3	12	–	–	2.6	1.5	Candidate Substrates
Diamond	>3500	3.5	5.8	–	$>10^{20}$	0.9	20	Candidate Encapsulation
Glass-Ceramic	<1000	>4	7–10	–	–	>3	0.05	Candidate Substrates
Metals								
Aluminum	660	2.7	–	–	2.6×10^{-6}	23	2.1	Chip Conductor
Gold	1063	19.3	–	–	2.4×10^{-6}	14	3.4	Hybrid Conductor/Wire Bonds
Copper	1083	8.9	–	–	1.7×10^{-6}	17	3.8	Leadframe/Hybrid, PWB/Conductor
Lead	327	11	–	–	2.0×10^{-5}	29	0.3	Solder Attach
Molybdenum	2610	10	–	–	4.8×10^{-6}	4	1.3	Co-fired Ceramic Conductor
Tungsten	3380	19	–	–	5.5×10^{-6}	4	1.5	Co-fired Ceramic Conductor

[a] T: Melting, glass transition, softening or processing temperature, as appropriate; ϱ: Density; ε': Dielectric constant, permittivity; ε'': Dielectric loss, tan $\delta \equiv \varepsilon''/\varepsilon'$ = dissipation factor; σ: Resistivity; TCE: Thermal coefficient of expansion; K: Thermal conductivity.

As noted in Figure 2, the following steps are involved. The silicon chip is die bonded to a leadframe (usually copper or a nickel–iron alloy) employing either solder or a polymeric adhesive (gold alloy or silver-filled epoxy). The leadframe is then wire-bonded (gold or aluminum wire) to the bonding pads on the active side of the chip. The circuit may or may not be encapsulated with a conformal coating (silicone rubber or gel) and the assembly is transfer molded, usually silica-filled epoxy, leaving only the external leadframe visible. The component parts (silicon, copper, silica-filled epoxy, other) exhibit a considerable range of TCE's and considerable stresses develop as the package is cooled from the relatively high molding temperature. This stress may be reduced by increasing the concentration of silica filler (thus reducing the TCE) and addition of elastomeric materials to the epoxy. Good adhesion between the epoxy and the chip and leadframe surfaces is important as this reduces the effects of stress. For a large memory, the filler must be very pure, i.e., low in α-particle emitters, e.g., Th or U. The epoxy must be of low viscosity when it fills the mold cavity or it will distort the metal parts, particularly the gold or aluminum wires. The epoxy molding material preform should have minimal sensitivity to moisture and other extraneous factors which affect processing. At this time all of the foregoing processing and property factors have been accomodated by well-engineered epoxy molding compounds. Displacement of epoxies by other materials is unlikely in the foreseeable future.

An alternative to the transfer molding process is the use of chip carriers made of alumina or pre-molded plastic, usually epoxy or poly(phenylene sulfide). These options are easier to implement than direct epoxy encapsulation when the number of chip leads becomes large. Price, package area and lead impedance are high for chip carriers, and molded packages will probably continue to dominate where their use can be accomplished with reasonable yields. For finely spaced package leads (e.g., 0.635 mm) and large numbers of leads (> 100) the choice is not obvious. As lead counts approach 200, wire bonding and leadframe design become much more difficult and tape automated bonding (TAB) another packaging approach involving copper fanout patterns plated on a polyimide film, will grow in importance.

2.2. Chip or Package Attachment

The two major types of chip packaging, molded epoxy or hermetic ceramic, can exist in a variety of forms. Dual in line packages (DIP) and pin grid array packages have pins that are inserted through the printed circuit board and soldered into place, Figure 3a. A more recent development, called surface mount assembly (SMA) employs the same basic package types but the package leads are soldered to pads on the surface of the circuit board, Figure 3b. Components can be mounted on both sides with SMA and the absence of holes through the board leaves more room for circuit traces and interlayer vias. A still more efficient method is to directly attach the unpackaged chip to the circuit board by "flip chip" solder attachment, Figure 3c. This uses even less area of the printed circuit board and allows for more densely packed circuitry.

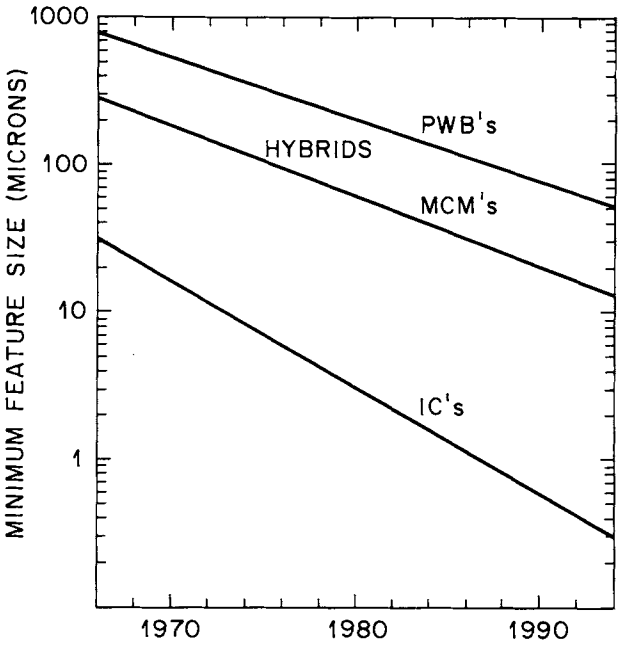


Fig. 3. Mounting options a) pins inserted in printed circuit boards; b) surface mount; c) "flip chip" mount.

2.3. Printed Circuit Boards

Packaged chips are interconnected by attachment to multilayer printed wiring boards (MLB's). These MLB structures are composed of copper circuit patterns on insulating substrates. Typically two to perhaps a dozen circuit layers are employed but advanced circuits may contain more than forty layers. The substrate dielectric is usually an epoxy polymer (based on the diglycidyl ether of bisphenol A) reinforced with glass fiber fabric. Multilayer structures are formed by printing copper circuits on partially cured (B-staged) epoxy and piling up the carefully registered sheets for final cure under pressure. Connections between layers (vias) are formed by drilling holes through the cured MLB and plating copper on the walls of the holes. Surface mount boards which have "buried" and "blind" vias are manufactured by similar but more complex processes.

As MLB circuits evolve to meet more difficult operating conditions and performance demands, the epoxy–glass–copper MLB materials will be challenged. Copper has no near-term competitors at this time. New epoxy compositions (highly functionalized novolacs) are being introduced for the most advanced circuits and their use will grow over the next few years. For circuits required to perform at high temperatures, polyimide and BT-resins (bis-maleimide/triazine) offer capabilities in the 300 °C region. When a low dielectric constant is needed, organic fibers (e.g., polyaramide) will be

ADVANCED MATERIALS

substituted for glass fiber reinforcement. Lower dielectric constant resins including hydrocarbons (e.g., bicyclobutadiene) and tetrafluoroethylene may also come into use. There will be many opportunities for special purpose compositions, but the epoxies are unlikely to be displaced in most conventional MLB applications.

2.4. Interlayer Dielectric

Organic dielectric layers are now being used in hybrid circuits which consist of metal patterns on alumina substrates. These patterns have dimensions between the range encountered in MLB's and those found on chips. Triazine formulations and polyimides are used in these applications. In recent years a great deal of activity has been devoted to the use of very fine interconnection circuits built up on silicon wafer substrates. Polyimides are generally the material of choice for this technology and many variations are being developed. Polyimides have been developed with very low and controllable TCE's. Dielectric constant, water absorption and other properties have been improved. Photopatternable materials are available but not widely used at this time. In some designs polyimides are being used as interlayer dielectrics on silicon chips. This is a very active area with polyimide formulation clearly dominant.

3. New Materials

The need for high conductivity interconnects has stimulated interest in the new oxide superconductors. This is an area that is developing rapidly and should be followed closely. Even if the formidable processing problems and current density limitations can be overcome, there will remain the question of high frequency performance. Present oxide superconductors are not very good at high frequencies and maximum current densities are rather low. If circuits are to be cooled to liquid nitrogen temperature, copper and aluminum will offer a substantial (a factor of eight) conductivity improvement. It should be kept in mind that the speed of signal transmission cannot be better than the speed of light which will be governed by the square root of the dielectric constant. Even so, superconductors continue to receive attention as candidates for interconnection structures and should be followed as a long-term option.

Finally, we mention diamond. Promising advances are being made with regard to the preparation of synthetic diamond films. If suitable films can be prepared in a manner compatible with other elements in electronic systems, diamond offers extremely attractive properties. The hardness, TCE and especially thermal conductivity are uniquely favorable. This is an active and promising line of research.

4. Conclusion

Electronic systems have evolved to the point at which opportunities for introducing new materials are highly favorable. As physical limits on circuit speed and power are approached, the advantages of special materials will increase.

Received: November 19, 1988.

Suggested further reading:

General Trends in Electronics: a) R. Hannemann, *IEEE Proc. 23* (1986) 48; b) J. D. Meindl, *Solid State Technol. 26* (1987) 85.

Organic Materials in Electronics: a) M. J. Bowden, S. R. Turner: *Polymers for High Technology—Electronics & Photonics, Am. Chem. Soc. Symp. Ser. 346* (1987); b) J. H. Lai, S. A. Jenekle, R. J. Jensen, M. Royer, *Solid State Technol. 27* (1984) November issue, p. 165; December issue, p. 149.

Inorganic Materials in Electronics: R. Tummala, *Am. Ceram. Soc. Bull. 67* (1988) 752.

Superconductors: J. G. Bednorz, K. A. Müller (Nobel lecture), *Angew. Chem. Int. Ed. Engl. Adv. Mater. 27* (1988) 735; *Angew. Chem. Adv. Mater. 100* (1988) 757; R. F. W. Pease, in P. Losleben (Ed.): *High Performance Packaging for VLSI Systems*, M.I.T. Press, Cambridge, MA, USA 1987.

Diamond: J. C. Augus, C. C. Hayman, *Science 241* (1988) 913; b) S. R. Kasi, Y. Lifshitz, J. W. Rabalais, G. Lempert, *Angew. Chem. Int. Ed. Engl. Adv. Mater. 27* (1988) 1203; *Angew. Chem. Adv. Mater. 100* (1988) 1245.

The following short communications will be published in future issues:

P. P. Edwards et al.:	High Resolution Electron Microscopy of the High Temperature Superconductor $Bi_{2+x}Sr_2Ca_{1-x}Cu_2O_{3+\delta}$
F. Dickert et al.:	Polymer Benzo[15]crown-5 Complexes as Sensor Materials for Solvent Vapors – Aromatic Halogenated Hydrocarbons and Polar Solvents
J. M. Thomas et al.:	Probing Changes in the Structure and Performance of a Lithium Nickel Oxide Catalyst During the High-Temperature Oxidative Coupling of Methane by in situ X-Ray Diffraction
A. Merz et al.:	Poly-[*N,N*-(1,4-divinylbenzene-β,β′-diyl)-4,4′-bipyridinium dibromide], a Novel Conducting Viologen Polymer
D. Schweitzer et al.:	Superconductivity at 7.5 K and Ambient Pressure in Polycrystalline Pressed Samples of β_p-(BEDT-TTF)$_2$I$_3$
R. Kniep et al.:	Structure of Anodic Oxide Coatings on Aluminum

ADVANCED MATERIALS

Materials Processing—a Key Factor

Injection and Extrusion Molding
Process Optimization
Computer Aided Design
Liquid Crystal Polymers

By Walter Michaeli *

1. Introduction

New polymers, computer-integrated manufacturing and quality requirements ask for a daily new, and never ending attempt to answer the question of how to optimize processing. The answer is very complex and requires fundamental knowledge of how, for a given polymer, the structure of a product correlates to its processing conditions since this influences crucially its final properties and performance.

Processing conditions are often dependent on the specific design of the processing equipment, the quality of the control systems, handling and pretreatment, for example, drying and compounding, and on environmental conditions. Moreover, the change of one parameter during processing can affect final product properties. Therefore, it is necessary to study the individual influences on a given material. However, before optimizing material processing it is first essential to optimize the plastics part design. It is the objective of many R & D departments in industry and academia to define rules, models, and software packages according to which a part is to be designed and processed. This has to be combined with the innovative potential of those who create new polymers.

In view of the increasingly more complex requirements put on part properties, computer-aided processes for part and tool design have become generally established in planning departments, and the necessary software packages are steadily improving. This will help to avoid a poor design and will lead to better processing and improved quality. Let me give some examples: As advanced composites with infinite fibers are formed during processing, the possibility of affecting product properties at this stage is increased. Voids and air entrapments have a tremendous influence on the mechanical properties of such a composite. This can be shown impressively by applying an interlaminar shear load, since the voids are mainly formed between the fiber and the matrix[1] and have a negative influence on the bonding. The strong influence of the void content on the interlaminar shear strength during dynamic loading is demonstrated in Figure 1.

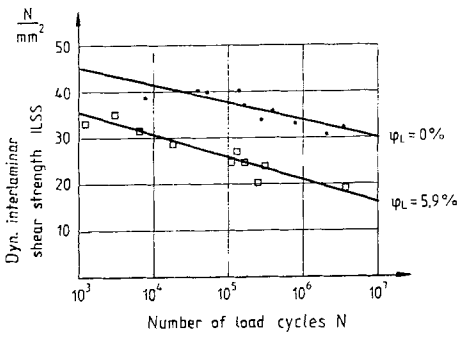


Fig. 1. The influence of void content φ_L on the mechanical properties of an FRP laminate, a composite material.

Another very important factor in part design and processing is the fiber orientation. Deviations from the given fiber orientation, e.g. of only 5°, may lead to a drop in strength of about 40 % for a fiber content of 60 vol-% (Figure 2).[2] This

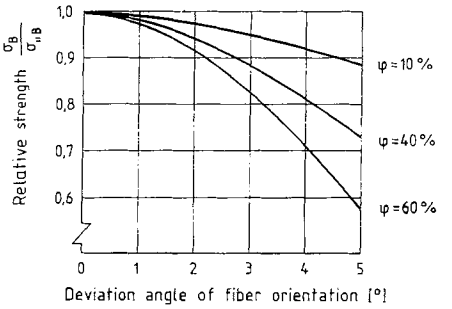


Fig. 2. The influence of fiber orientation on the mechanical properties of composite parts. φ = Filament volume ratio.

gives an idea of the importance of the reproducible laydown of fibers during material processing. There are many other key factors in material processing. To discuss them all is impossible but it is my intention to cover the most essential parameters used to set up process models, which give the key to separate and estimate the effect of single processing conditions on future products.

Manufacturing philosophy is that the final properties of a plastic part made from a well defined polymer should be independent of the production process used, in as much that it is the inner structure/morphology, crystallinity, fiber dispersion and distribution, orientation, and internal stress pattern, which determine the properties. However, if we analyze the processing of thermoplastic materials, we find that the structure formed is a function of thermal and mechanical

[*] Prof. Dr. Ing. W. Michaeli
Institut für Kunststoffverarbeitung
Technische Hochschule
D-5100 Aachen (FRG)

ADVANCED MATERIALS

influences. The absolute values of structural characteristics, like orientation or crystallinity, vary for different processes or products but can always be derived from the specific process conditions. Therefore, we have to analyze a process in terms of single steps for which the processing parameters are defined, and for which the internal properties (structure) and final properties are then determined.[3] This is depicted in Figure 3.

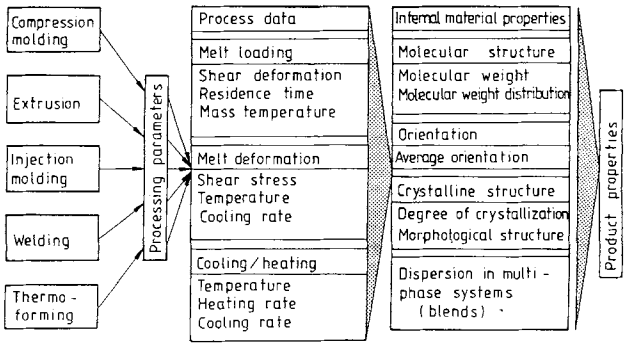


Fig. 3. Production process to part properties.

Process data are independent of molding- and processing equipment and are derived or calculated from the processing conditions and the specific geometrical boundary conditions of the equipment.

The material is more loaded (e.g. sheared, heated) during compression molding than during extrusion and therefore we expect alterations on the molecular level. A comparison of extrusion and injection molding gives a similar set of process data, but the pressure level and the shearing forces in injection molding are significantly higher than in extrusion.[3] The structural parameters (like orientation or boundary layers) are less distinct in extrusion. Similar cooling gradients exist, but due to the melt flow during the packing phase, high deformation rates at fairly low melt temperatures influence the internal structure. The morphology and internal stress patterns can be correlated for both processes to the cooling, pressure, and deformation conditions. A detailed analysis of these factors allows us to better understand materials processing.

2.1. Component (Part) Properties

To illustrate how properties, e.g. mechanical properties, are influenced by the internal morphology consider the following examples.[3] Figure 4 gives the thermal coefficient of expansion as a function of the degree of stretching λ (which correlates to orientation)[4] for different materials. Figure 5 shows for polypropylene (PP) how the Young's modulus E_0 and the tensile stress σ_s are influenced by crystallinity,[5] which is a function of the cooling and material deformation conditions during processing.

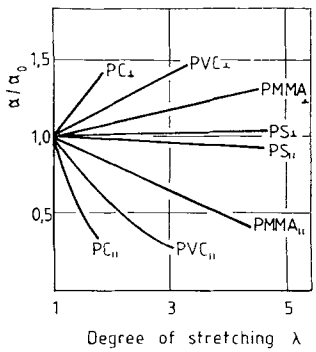


Fig. 4. Thermal expansion coefficient as a function of the degree of stretching.

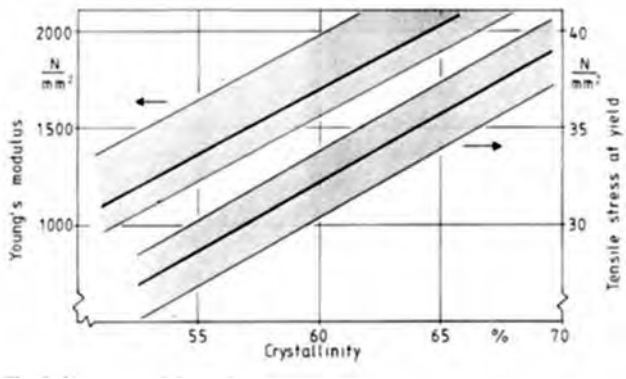


Fig. 5. Young's modulus and tensile stress (for polypropylene) as a function of crystallinity.

2.2. Influence of Melt Loading on Part Properties

The state of a thermoplastic material[3] while being processed and molded into a plastic part is defined by:

- melt loading (degradation)
- melt deformation (orientation) and
- cooling conditions

A certain molecular weight is necessary to achieve product properties like impact and corrosion resistance or dimensional stability under mechanical loading. Molecular weight and flow properties can be correlated, and also give a good correlation to degradation when the melt is loaded.[3] Figure 6[3] describes the effect of melt loading on the melt vis-

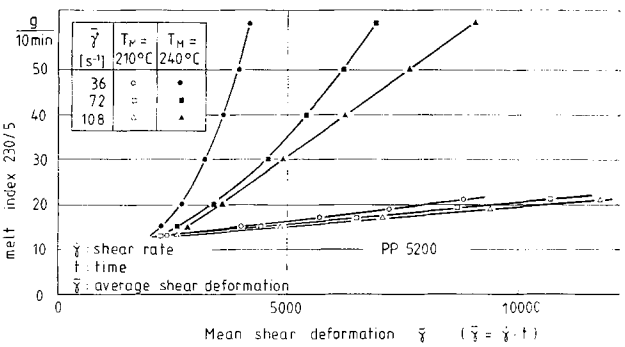


Fig. 6. Melt loading of polypropylene (PP).

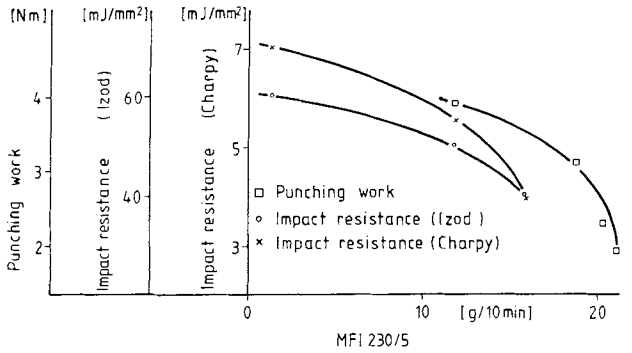


Fig. 7. Change in impact strength according to melt flow index (MFI).

cosity (melt index) as a function of mass temperature and shear deformation during extrusion. The significance of the mass temperature can clearly be seen. These experiments were made in extrusion but injection molding shows the same tendencies. Tensile tests often do not reveal the significance of the degradation, but impact resistance tests show how significantly chain scission influences performance (Fig. 7).[13]

3. Modeling of Part Design and Processing

If we wish to follow a straight line from the initial idea to the final product we have to structure our approach. The world-wide tendency to use software packages to guide us from the idea to the product is perhaps the strongest driving force bringing structure and unity to our approach. All steps from the idea to the final product have to be defined and have to be under control. This may sound simple to some or like utopia to others, but it is an essential objective.

The first step is to define the requirements the part has to fulfill (Fig. 8), and to select the right material.[6] Several software houses, and a large number of raw material manufacturers offer data banks for polymer materials, some even enabling the potential user to store his own proprietary knowledge and call it up as required.

The next step is the first layout of the geometry of the part. CAD-Macros defining and generating specific design elements of parts like snap-fit joints, gears, screw joints, rib reinforcements etc. are a most valuable tool and help to avoid poor designs. All design rules for the part will be automatically generated and observed. Fairly simple programs applying the basic rules of mechanics help to predimension a part. Here non-linear viscoelastic stress-strain relationships can be taken into consideration. The use of Finite Elements Methods (FEM) is commonplace in cases where the critical molding situation cannot be analyzed closely enough using empirical methods, or where complex or critical loads are involved. During mechanical analysis and structure optimization using FEM computer programs, the generally inhomogeneous, anisotropic and non-linear material behavior of plastics can be numerically approximated.

The next step is to check a design against accepted design rules (Figure 8). A software package for injection molded parts has been developed at our institute which examines the part geometry for material accumulations, draft angles and undercuts, checks the demoldability of a part and even defines the parting lines of a mold.[6]

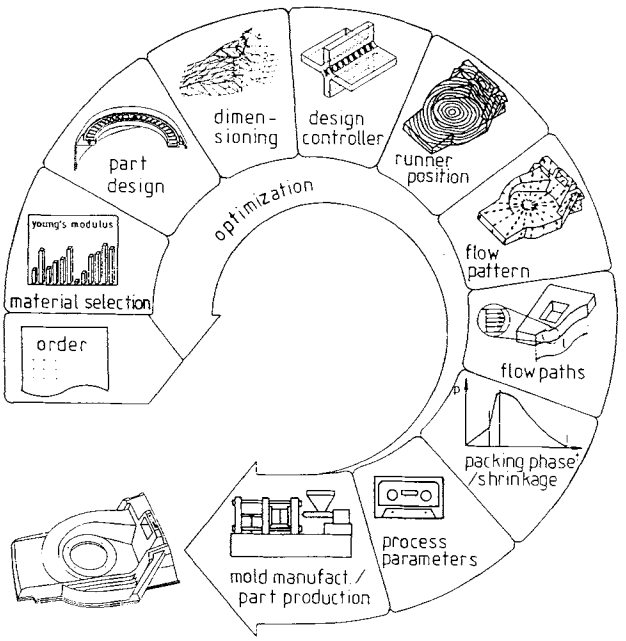


Fig. 8. Part and mold development.

At first sight, these rules and computer programs may appear to be trivial and obvious to the experienced designer. However, the automatic control of the geometry provides an additional check and helps to reduce costs by avoiding problems during materials processing. Such systems still have to be developed for advanced composites, where they will be especially important. The logical consequence of using a computer-guided approach in part design is also to use the computer to simulate processing and detect possible problems before going to the factory floor. The processing conditions can also be optimized in order to get the most out of the material with optimum economy.

Our institute has developed such a program system, called CADFORM-CADMOULD,[6] which incorporates programs

- for calculating the temporal melt front advance, which gives information about weld-lines, air entrapments, and the pressure distribution during the mold filling phase (Figure 9)
- for calculating the shear rates, shear stresses and melt temperatures along freely selected flow paths
- for analysis of the holding pressure phase and estimation of the shrinkage

- for determining the most favorable machine operating point and its dependence on operating parameters; say, to find better processing conditions
- for predicting the orientation pattern

This information is important to help design the mold and to minimize processing problems. In injection molding and extrusion, such programs for the rheological, thermal, and mechanical mold design are frequently and successfully used. Models for reactive materials processing are under development.

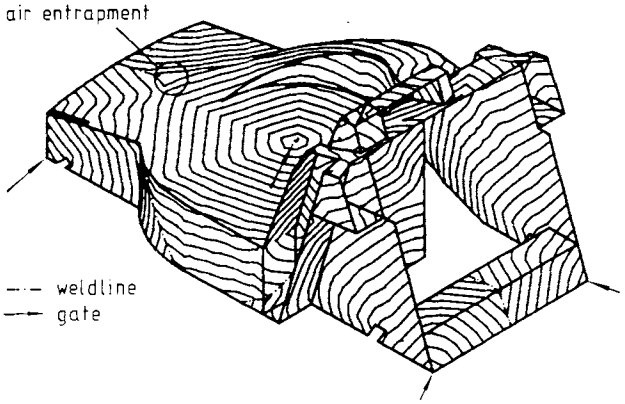


Fig. 9. Filling pattern of a complex part.

Modeling also provides the data to run the equipment, and it is no longer regarded as magic in advanced injection molding, to generate the best machine settings using a computer simulation, and to transfer these data directly to the control cabinet of the machine via the central and machine computers.[7, 8] It is very important to realize that next to reproducibility, proper transfer of information is a key factor in material processing, as is the choice of the most suitable equipment. If one knows, for example, the pressure drop in a cavity of an injection mold, one can predict the necessary clamping force and select the right machine. Such machine selection algorithms which are oriented towards optimum materials processing are to some extent already in existence.[9]

3.1. Processing and Properties of Short-Fiber Reinforced Polymers

If we want to make a part out of a short-fiber reinforced thermoplastic material we want to predict its mechanical properties and see how process variations will affect quality. Many independent investigations have found a symmetrical set-up of layers with different main fiber orientations in injection molded parts. The center layer is about 15% of the cross-section, the sheared layers about two-times 37.5% and the boundary layers about two-times 5%. This distribution

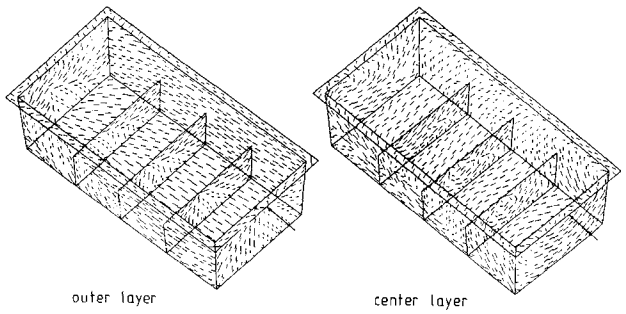


Fig. 10. Computed orientation of fibers.

varies little with injection rate, mass and mold wall temperature, or packing pressure for common wall thicknesses of the molding,[10] and holds true for almost all injection molded parts.

However, we have to keep in mind that there is always a distribution in fiber length and orientation angle, relative to the main orientation direction if we want to predict mechanical part performance. With the models described we can predict the fiber orientation according to the flow pattern during the filling of the cavity. The main orientation directions of the fibers are shown in Figure 10 for the center (core) and outer layers. We see the orientation in flow direction next to the wall and the perpendicular fiber arrangement in the central area.

The designer of a molding, and finally the customer, are in general interested in the overall mechanical properties of a part, and not only in the fiber orientation. Of special interest here, is the anisotropic elastic material behavior at each point of the molding. If this is known one can calculate the overall mechanical properties.[10]

3.2. Processing of Liquid Crystal Polymers

Modeling is a key factor in the processing of liquid crystal polymers (LCP). These new, self-reinforcing materials are very sensitive to their processing conditions. They show mechanical properties similar to steel and ceramics in the main orientation directions, but show little strength or stiffness transverse to the molecular chains. The orientation model shown in Figure 10 can also be found in these polymers (Fig. 11).[11] An attempt to predict their mechanical properties in the same way as for the short-fiber reinforced materials mentioned previously is presently being examined in our Institute.

There is still one problematic area in processing LCP's. The problem relates to those points where two flow fronts come into contact and form a weld-line. Figure 12 shows how two melt fronts will align parallel to each other.[12] This configuration results in poor mechanical performance, but it is possible to overcome this weakness to some extent by controlling the flow, through mold design and filling condi-

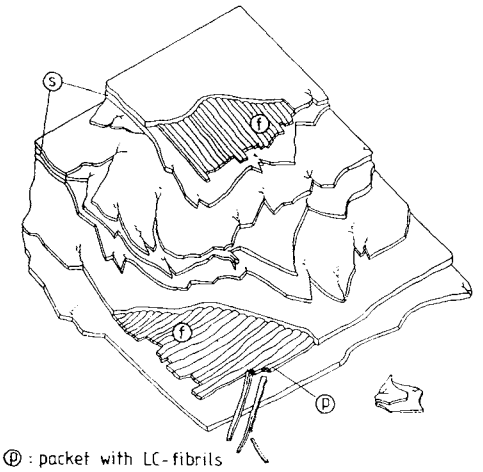


Fig. 11. Model of the "plywood-like structure" of liquid crystal polymers in moldings.

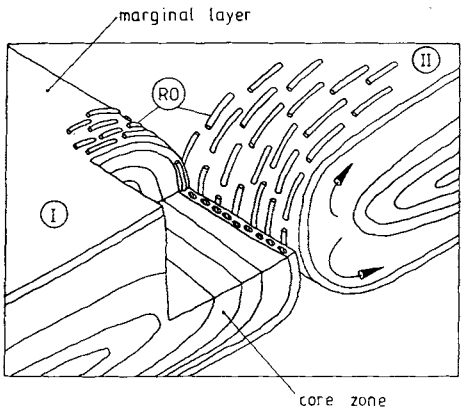


Fig. 12. Welding line in liquid crystal polymer molding. RO: Orientations in the marginal layers. I, II: Partial streams of the melt.

tions. Due to the anisotropic material properties, the analysis of the mold filling in conjunction with the calculation of the orientation pattern, is essential in order to exploit the high mechanical potential of this highly interesting group of polymers.

3.3. Processing of Composites

Advanced composites with endless fibers are relatively new materials with which many engineers and designers have little experience. Comprehensive rules, models, and design methods for composite parts have not been available to designers who are used to working with conventional materials. Today, however, composite parts are gaining importance in general mechanical engineering, especially in the design of rapidly moving parts which have to have a low weight. Designers now must deal with an added set of rules[13]:

- Anisotropic material properties. A part is stiff and strong in the fiber direction but weaker and more compliant in the perpendicular direction.
- Material properties are influenced by processing conditions. For example, the fiber content is influenced by the tension in the filament, the pressure in the parts, and by resin flow.
- Different material failure modes, e.g., if the interlaminar shear strength is exceeded, delamination occurs.

Therefore systematic sets of rules have emerged to aid the designer in laying out a composite part. The special rules that apply to fiber reinforced composites are now being incorporated into a computer aided design (CAD) and engineering (CAE) software program called CADFIBER. With this program, one can make predictions on part properties within reasonable time frames, reducing expensive and time consuming trial and error experiments to a minimum. When completely developed and implemented, CADFIBER will be able to design a part and simulate on minicomputers the processing of that part. The software program is composed of four main modules: materials data bank, construction and dimensioning, process simulation, and quality assurance.

4. Self-Optimization in Materials Processing

In materials processing, be it in product design, equipment design or in process adjustment and control, we are always striving for perfection. Optimization strategies which structure and direct our approach to our final goal are very helpful and of increasing importance. We are experimenting with the so called "evolution strategy" according to *Rechenberg*,[14] which is well suited for optimizing flow channels. We are also applying this strategy to optimize the parameters of electric controllers on-line during processing, and for adjusting injection molding machines. The initial results are very encouraging and will lead to new dimensions in answering questions concerning the optimization of materials processing.

In this paper the necessity to be assisted by the computer has been stressed. Although computerization is an essential factor in materials processing, we are aware that man, who analyzes and acts, is still *the* key factor. I have described an engineering point of view of materials processing. A chemist or a physicist might have another approach and may interpret things differently. That is good, since it is always best to look at things with different eyes. Let us put our expertise, knowledge and will together and face the challenge of future materials processing.

Received: December 19, 1988

[1] U. Seiler, *Doctoral Thesis*, ("Zur Auslegung statisch und dynamisch belasteter Bauteile aus Verbundwerkstoffen am Beispiel von GFK-Blattfedern"), Technische Hochschule Aachen, FRG, 1987.
[2] U.-P. Behrenbeck, *Doctoral Thesis*, ("Fertigungs- und werkstoffgerechte Konstruktion von Faserverbundbauteilen"), Technische Hochschule Aachen, FRG, 1987.
[3] U. Berghaus, N. El Barbari, H. Offergeld, G. Pötsch, H. Ries, "Material—Machine—End Product. Internal Structure as the Key to Component Properties", Preprint, 14. Kunststofftechnisches Kolloquium, Institut für Kunststoffverarbeitung Aachen, 9.-11. March 1988, Aachen, FRG.
[4] J. Hennig, *Kunststoffe 57* (1967) 385-390.
[5] G. Schönfeld, S. Wintergerst, *Kunststoffe 60* (1970) 177-184.
[6] E. Baur, P. Filz, H. Greif, S. Groth, V. Lessenich, S. Ott, G. Pötsch, K. Schleede, "Component and Mold Design in One Operation—the Modern Aid for the Designer", Preprint, 14. Kunststofftechnisches Kolloquium, Institut für Kunststoffverarbeitung Aachen, 9.-11. March 1988, Aachen, FRG.
[7] G. Menges, W. Benfer, E. Baur, "Rechnerintegrierte Prozeßgestaltung beim Spritzgießen", Innovations-Supplement "Fabrik der Zukunft" der Zeitschriften *Der Betriebsleiter* und *Der Konstrukteur*, Part 1: (1986) 12, p.8-16; Part 2: (1987) 1/2, p. 20-24.
[8] G. Menges, *Kunststoffe 76* (1986) 1019-1023.
[9] G. Weyer, M. Lauterbach, K. Bourdon, B. v. Eysmondt, "CIM in Plastics Processing—Applied in Injection Molding", Preprint, 14. Kunststofftechnisches Kolloquium, Institut für Kunststoffverarbeitung Aachen, 9.-11. March 1988, Aachen, FRG.
[10] U. Wölfel, *Doctoral Thesis* ("Verarbeitung faserverstärkter Formmassen im Spritzgießprozeß"), Technische Hochschule Aachen, FRG 1988.
[11] T. Schacht, *Doctoral Thesis* ("Spritzgießen von Liquid-Crystal-Polymeren"), Technische Hochschule Aachen, FRG 1986.
[12] G. Menges, T. Schacht, H. Becker, S. Ott, *Int. Polym. Processing 2* (1987) No. 2, p. 77.
[13] U.-P. Behrenbeck, M. Effing, K. Kirberg, W. Müller, U. Seiler, M. Wegener, "Designing with Fiber-Composite Materials—from Material Data to Machine Control Data", Preprint, 14. Kunststofftechnisches Kolloquium, Institut für Kunststoffverarbeitung Aachen, 9.-11. March 1988, Aachen, FRG.
[14] I. Rechenberg: *Evolutionsstrategie - Optimierung technischer Systeme nach den Prinzipien der biologischen Evolution*, Frommann-Holzborg, Stuttgart 1973.

The Kevlar Story—an Advanced Materials Case Study

Process Development
High Performance Fibers
High Impact Composites
Rigid-Rod Polymers

By David Tanner, James A. Fitzgerald, and Brian R. Phillips*

1. Introduction

The Kevlar story is an excellent example of the innovation process where a laboratory discovery is placed into commercial production. It started in the early 1960's with an identified need. In 1965, this led to an important scientific discovery. At this time the research and development phase was entered and in 1972 a 1 000 000 lb per year market development plant was built. By 1982 full commercialization was reached with a 45 000 000 lb/yr. plant. During this period several tough hurdles were encountered. To overcome these obstacles a multi-disciplinary approach was almost always required.

2. The Need for a Heat Resistant Stiff Fiber

The invention of Nylon and subsequent textile fibers provided powerful vision and direction for the research effort aimed at 'super' fibers. In the early 1960's Du Pont was driven by two goals, a fiber with the heat-resistance of asbestos and the stiffness of glass. A fiber of this type could be visualized to fill many market needs. Experimental work indicated that the route to such a material lay with stiff chain aromatic polyamides. These materials, however, had evaded the scientist by virtue of their extreme insolubility and intractability.

3. The Discovery of a Rigid Rod Spinnable Polymer

In 1965 *Stephanie Kwolek*, a research scientist at the Du Pont Experimental Station in Wilmington, made a major discovery. She found that *p*-aminobenzoic acid could be polymerized and solubilized under special conditions to yield a rigid-rod spinnable polymer. Initially, when these polymer solutions were first made, it was not believed that they would spin into fibers since the solution was opaque and could not be clarified by heating or filtration. This implied that there was inert matter dispersed in the spin dope which would plug the spinneret holes. However, the fibers spun well. We now know that this capacity was due to the formation of polymer

[*] Dr. D. Tanner, Dr. J. A. Fitzgerald, Dr. B. R. Phillips
Fibers Department, E. I. Du Pont de Nemours & Co., Inc.
Wilmington, DE 19898 (USA)

liquid crystals. The stress–strain curve of the first aramid fiber tested was startling, and the test was re-run several times for confirmation. A true step change in properties was achieved vs. existing synthetic textile fibers.[1]

The behavior of rigid-rod molecules in solution is quite different from flexible molecules (Fig. 1). Flexible polymers like Nylon, in dilute solution, have a low level of entanglement. However, at higher concentrations the random coils become highly entangled. Spinning and drawing lead to only partially extended chains due to the high level of entanglements. Hence, properties such as tenacity and modulus reach only a small fraction of the theoretical values.

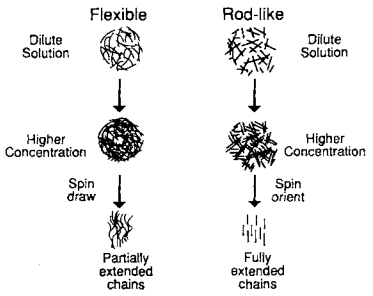


Fig. 1. Schematic illustration of the solution behavior of rigid and flexible polymers.

On the other hand, due to their rod-like conformation, more rigid polymers like the *p*-aramids, in going from dilute to higher concentration do not form random coils. At a critical concentration they can no longer populate the solution randomly. At this point, in order to pack more molecules into the solvent, they are forced to align parallel to each other in randomly oriented liquid crystalline domains.[2, 3] Under shear, as in a spinneret capillary, the liquid crystalline domains orient in the direction of the deformation. This leads to fully extended chains in fibers and the observed high strength and modulus.

4. Research and Development

Following *Kwolek*'s discovery, the first obstacle was encountered, i.e., the *p*-aminobenzoic acid raw material was too costly to justify scale-up. At this point a major research and development program was launched. The aim was to develop a deeper understanding of the formation of liquid crystalline solutions and to identify a lower cost rigid-rod polymer system. This effort led to a variety of rigid polymers with potential for formation of liquid crystalline spinning solutions and strong, stiff fibers.[4–6] The best candidate was the polymer from *p*-phenylenediamine and terephthalic acid (PPD-T). This polymer eventually became the basis for Kevlar. It had the lowest cost ingredients, the highest symmetry, and theoretically the highest stiffness. However, to produce the best properties the spinning solvent had to be 100% sulfuric acid, and the resulting spinning solutions were very viscous. Low spinning speeds were needed for good properties and therefore the process was uneconomical.

Thus, the second obstacle was encountered; the process was not practical. This became starkly apparent when the researchers first described the invention to the manufacturing and engineering groups who would have to design, build and operate the plant. They didn't want it! The sulfuric acid solvent was unconventional and highly corrosive, process yields and throughput were very low, and investment very high. These are the realities that research people do not pay much attention to when they are at the frontiers of discovery.

A major breakthrough came when another Du Pont research scientist, *Herbert Blades*, made two crucial discoveries.[7, 8] First, he found that PPD-T and sulfuric acid form a crystalline complex at a polymer concentration of 20% (vs. 10–12% by previous workers). He unexpectedly formed this complex by going against conventional wisdom and heating the polymer solution containing the 100% sulfuric acid. This complex melts around 70 °C and is composed of PPD-T:sulfuric acid in the ratio 1:10. This enabled spinning at much higher polymer concentrations than had been previously possible.

The second advance was in spinning where he used an air gap between the spinneret face and the quench bath (Fig. 2). When the PPD-T/sulfuric acid complex was melted and spun through the air gap into cold water, very high spinning speeds could be obtained through attenuation of the molten

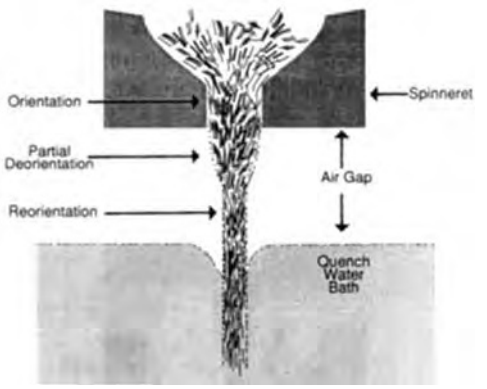


Fig. 2. Schematic of air gap spinning high concentration PPD-T solutions in sulfuric acid.

spinning solution in the air gap. Although partial deorientation occurs as the polymer solution emerges from the spinneret, the very high extensional shear in the air gap results in extraordinary orientation and tensile properties of the final as-spun fiber (Fig. 3). The air gap spinning technology gave birth to an improved product version which is today's Kevlar and ultimately led to Du Pont's heat strengthened high modulus Kevlar 49 product.

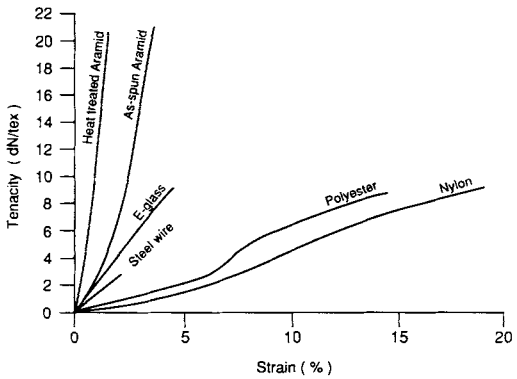
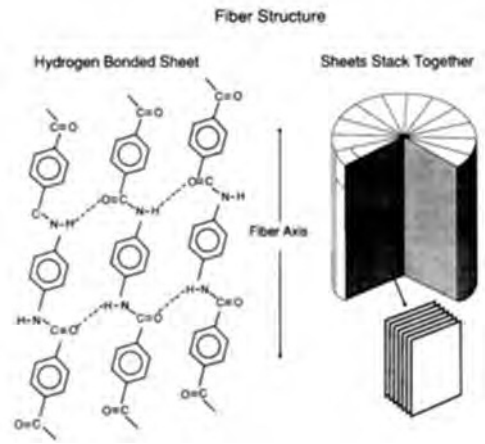


Fig. 3. Stress strain curves of reinforcing fibers.

The reason for these truly outstanding mechanical properties most likely lies in the microstructure of the fiber. Kevlar is a hydrogen bonded highly crystalline material.[9] Sheets of cells extend across the radius of the fiber resulting in almost perfect radial as well as longitudinal order. This level of three-dimensional order had never been observed in a fiber before. Kevlar has a molecular orientation parallel to the fiber axis, and a well defined radial crystalline orientation (Fig. 4).



5. Scale-Up to a Market Development Plant

The air-gap spinning discovery was an invention worthy of scale-up. The product was certainly unique, the process scalable and the economics satisfactory. The next step in the innovation process and the next obstacle was to scale-up to a market development plant. Translation of a laboratory discovery to a practical, scalable, commercializable process is one of the hardest tasks faced by any technology-driven industry. In the case of Kevlar, a task force of dozens of scientists and engineers of many disciplines was assembled. Some of the Wilmington researchers moved to the plant site in Richmond, VA, USA. The task was to develop the manufacturing basic data and tackle scale-up. In less than two years from *Blades'* laboratory discoveries, Kevlar was being shipped from a 1 000 000 lb per year market development plant. This timetable, considering the complexity of the process, was unprecedented in the Du Pont Fibers Department. Five years later the commercial product was being produced in a 15 million pound per year plant.

During the scale-up stage several difficult hurdles were encountered, some quite unusual and unexpected. A complex laboratory process had to be translated into a workable plant operation. The ingredients were corrosive, there were environmental concerns such as waste disposal, and the polymerization solvent had an unexpectedly high level of toxicity. Two of these hurdles are described below.

An unusual environmental problem arose involving waste disposal. The spinning solution is based on a complex containing five moles of sulfuric acid per PPD-T amide bond (or four pounds of sulfuric acid per pound of polymer). Disposal of the spent acid after spinning was a problem. The best option turned out to be conversion of the sulfuric acid into calcium sulfate (gypsum). For every pound of fiber seven pounds of gypsum is generated. This year the Kevlar plant is generating a lot of gypsum—quite a storage problem! As a matter of interest, the produced gypsum is attractive to both wallboard and cement manufacturers, and eventually the gypsum will be recycled.

The second hurdle deals with toxic materials. In the Kevlar process, two solvents are used. The spinning solvent is sulfuric acid, discussed above, and the polymerization solvent was hexamethylphosphoramide (HMPA). The Kevlar business was in the scale-up stage on a fast track heading toward full commercialization. Suddenly it came to a self-imposed barrier—the toxicity of the HMPA polymerization solvent. Du Pont pays much attention to the toxicity and handling of hazardous materials. Use of HMPA on a large scale was new, but the material was well known for many years and there were no highly unusual toxic effects reported. To be completely sure about HMPA toxicity, a lifetime exposure study with rats was initiated by Du Pont to determine any possible carcinogenicity potential.[10] This study was one of the first of its kind, and carried out purely as a precautionary measure. The results of that study showed that HMPA was an experimental animal carcinogen. Immediate steps were taken in the handling of HMPA to be certain that there was no hazard to the workers, the community, or the customers.

It is, however, preferable not to use a potentially hazardous material if a safer alternative can be found. Therefore, a crash technical program was mounted to find an HMPA replacement. The task was to find an acceptable polymerization solvent of low toxicity; one that would give polymer yielding fiber properties identical to those already introduced to the trade, as well as fitting into the process and the expensive equipment layout designed for polymerization in

HMPA. The chemistry turned out to be relatively straightforward.[11] The combination of *N*-methylpyrrolidone (NMP) and calcium chloride was selected as the solvent of choice. The engineering and product development were, however, formidable challenges.

Polymerization in NMP/$CaCl_2$ proceeded smoothly and a high inherent viscosity polymer was obtained with no difficulty. The polymer, however, could not be spun to the equivalent tenacity of the same inherent viscosity polymer prepared in HMPA. The problem turned out to be molecular weight distribution. The data showed that at equal inherent viscosity, the average molecular weight of polymer made in the NMP/$CaCl_2$ system was lower than in the HMPA system. Using a gel permeation chromatography technique, this difference was traced to the presence of a large low molecular weight fraction in the NMP/$CaCl_2$ system (Fig. 5). Further analysis showed that this resulted from precipitation of oligomers from the polymerization mixture. These were not

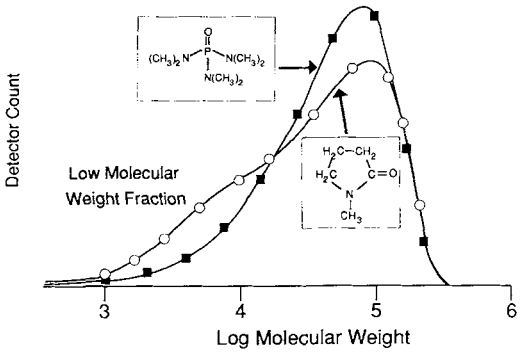


Fig. 5. Molecular weight distribution curve for PPD-T prepared in HMPA and in NMP/$CaCl_2$ by gel permeation chromatography (GPC).

present in the HMPA system because of it's superior solvating power. The problem was solved through the design of a reactor system to eliminate early nucleation and precipitation of low molecular weight polymer. This is another example where solving a problem required multidisciplinary chemical and engineering skills. Extensive internal and trade testing demonstrated that the Kevlar fibers made in the two polymerization systems were indistinguishable.

The program to find an alternative solvent took an estimated 40 man-years of technical effort. Throughout the scale-up phase there was an underlying confidence in the multidisciplinary team. There was no hurdle that could not be jumped, although at times it took considerable energy and support to do so.

6. Full Commercialization of Kevlar

Thus far, the need, the discovery phase, the obstacles in moving the R & D along, and the process development hurdles in scale-up to a market development plant have been described. Perhaps an even greater challenge was to demonstrate the market potential of Kevlar. This was necessary to justify the final step in the innovation process, a full scale commercial plant requiring a huge US $ 400,000,000 investment. Hence, throughout the development there was intensive parallel effort to find practical applications for this new fiber. For Kevlar to be a commercial success a sufficient value in use had to be found versus incumbent fibers like Nylon, steel, fiberglass and carbon to warrant a pricing structure that made economic sense.

7. Systems Approach to Applications for Kevlar

Early in the development, it was recognized that Kevlar was a unique fiber that would not automatically fit into existing applications. This became apparent from initial evaluation in tires, ballistics, composites, ropes, cables, etc. Each application had to be looked at as a "system" requiring a systems approach. Early partnerships with customers were vital to success. This part of the program can be as scientifically challenging and exciting as the *p*-aramid discovery itself.

As a framework for thinking about the total system a simple tetrahedral model can be visualized (Fig. 6). At the base, each corner represents a different knowledge center in the development. At the left corner is the chemical structure, e.g., the polymer composition. At the right corner is the physical structure, e.g., the degree of orientation or crystallinity. The back corner represents the fiber properties, e.g., tensile or surface characteristics. Ongoing iteration between these three base corners, which can be referred to as molecular and process engineering, is important. However, this model adds a third dimension at the apex of the tetrahedron. It involves the creative integration of the base technologies to give an advanced, composite structure. The selection of design criteria for parts, devices, and objects, i.e., "systems" engineering, has been vital to Kevlar product development. It requires the combined talents of professionals in many disciplines. A final advanced structure usually involves much interaction between each corner of the tetrahedron and

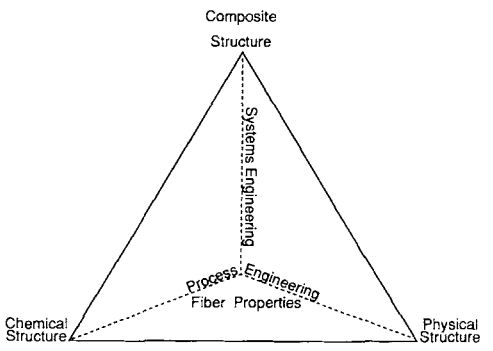


Fig. 6. Tetrahedral model of a systems approach to applications development.

sometimes multiple products organized into an integrated total system.

To illustrate the systems approach, two examples have been selected: Kevlar in ropes and cables and in composites. The main driving force for Kevlar in ropes and cables is the high strength per unit weight, inherent low elongation and low creep. In air, the specific strength is seven times, and in sea water more than twenty times that of steel. This means one can use smaller, lighter more easily handled lines. In long lengths where the self-weight of steel becomes critical, Kevlar can offer a greater payload.

The application to be described is that of a riser-tensioner line. The systems technology involved a specially engineered rope design to reduce internal stresses in order to increase wear life. Riser-tensioner lines are used on floating offshore oil drilling platforms, where their purpose is to keep the rise pipe or outer drill casing at a constant elevation and under uniform tension while the vessel surges with the waves. These are normally 44 mm diameter steel wire ropes which experience considerable cycling over pulleys as the platform moves. Laboratory studies had shown that small diameter Kevlar ropes could far surpass steel in cycling performance over pulleys. However, scale-up of the best small constructions to 44 mm diameter surprisingly gave rope lifetimes that were only 5–10% that of steel wire rope. Analysis showed that internal forces in the twisted rope rise rapidly with increasing diameter.[12, 13] These internal loads stem from radial squeezing forces which increase rapidly with increasing twist levels, bringing pressure against the pulleys and leading to high frictional heating, high internal abrasion, and shear fatigue failure of yarn as the rope elements move.

Cooperation with steel cable manufacturers lead to several design changes (i.e., Fig. 7) which improved the lifetime of

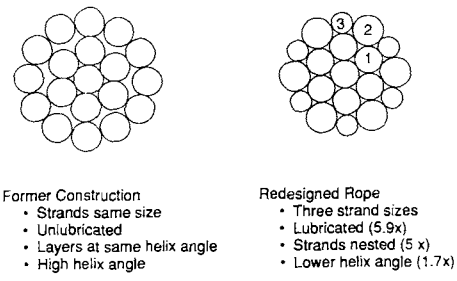


Fig. 7. Rope constructions.

Kevlar ropes over 50-fold. On the left is the former construction, and on the right the redesigned rope. One change was to increase the number of strand sizes from one to three. The purpose was to minimize cross-overs of inner and outer strand layers by nesting the outer strands in the inner layer. This compacted the structure and spread the lateral loads uniformly over a greater area giving a five-fold improvement in lifetime. A second change was to lubricate the strands by jacketing each strand with a braid impregnated with fluorocarbons. This reduced friction, heat buildup, abrasion and internal shear stresses resulting in a six-fold improvement. The third approach was to optimize the twist helix angle to minimize radial squeezing forces without seriously affecting other rope properties. This gave an additional two-fold improvement. The result was a rope having more than three times the life of steel in severe laboratory tests and more than five times in service. More than a dozen oil rigs have utilized Kevlar riser-tensioner lines, including those from major drilling contractors such as Santa Fe International, Western Oceanic, Zapata and Sedco.

A future application of Kevlar rope under development is that of deep water mooring lines for the same type of oil platforms that use riser-tensioner lines. Here the light weight of Kevlar gives less sag than heavy steel chain or steel wire rope. This allows operation at water depths several times that of steel. A one million pound break strength Kevlar rope has been deployed by Conoco in the Gulf of Mexico and by Petrobras off the coast of Brazil.

The next systems example involves the use of Kevlar in aircraft composites. The materials base is Kevlar, carbon fiber, and epoxy resin. The driving force is high tensile strength and modulus per unit of weight and toughness. The systems technology involves hybrids of Kevlar and carbon fibers reinforcing an epoxy resin to gain the best balance of mechanical properties and damage tolerance, i.e., the ability to tolerate abuse and to survive a catastrophic impact. Carbon fiber confers high stiffness and compressive strength but because of its rigid coplanar ring structure it is unyielding and fails by brittle fracture. Hence, it is unable to survive a catastrophic impact.

Kevlar has structural features that lead to good damage tolerance because of a ductile compressive failure mode. This can occur by a compressive buckling of PPD-T chains. At a compressive strain of about 0.5%, we believe that a buckling of *p*-aramid molecules occurs by molecular rotation of the amide C–N bonds to accomodate configurational changes. Figure 8 shows the shift that we believe is occurring from the *trans* configuration shown on the left to the *cis* shown on the right. This can result in a yielding to the imposed stress without bond cleavage. The result is an accordion-like collapse on impact. This continues to be a useful model for explaining the compressive properties of Kevlar composites.[14]

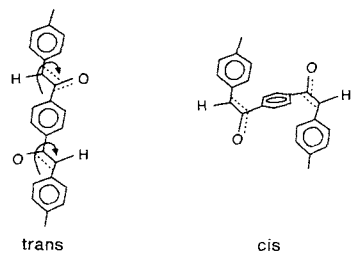


Fig. 8. PPD-T chain buckling under compression.

The response of Kevlar to compressive strain resembles that of aluminum. This metal-like ductility of Kevlar reinforced composites is illustrated by the flexural stress-strain behavior for epoxy matrix composites containing carbon, glass, Kevlar, and aluminum (Fig. 9). This is because in

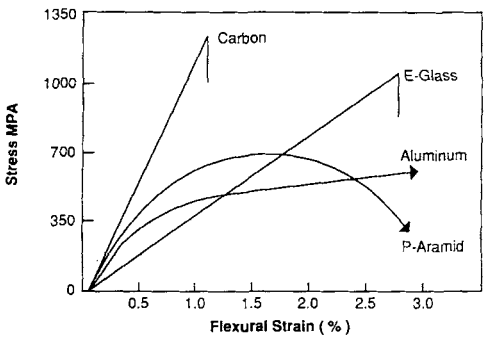


Fig. 9. Flexural stress strain curves of unidirectional epoxy matrix composites.

bending, one side of the composite is in compression and the accordion-like "yielding" contributes to the metal-like behavior. Crashworthy composite systems have been explored using a crushed tube test to compare materials. This test involves the crushing of filament wound tubes with a drop-weight impact tester. There is a marked difference between the failure modes of Kevlar aramid and carbon fiber-wound tubes. The tube reinforced with Kevlar fails by a progressive buckling mode, similar to that observed for an aluminum tube. The structure is damaged but still intact and able to sustain a load. The carbon fiber-wound tube shatters. However, it does reach and sustain a higher load just prior to failure, and absorbs more total energy in the crushing process than does the tube wound with Kevlar.

Hybrid technology that combines Kevlar and carbon fiber as a wound structure offers a better balance of properties. High energy absorption, within 7% of that of the all-carbon tubes, and good structural integrity after crushing, approaching that of the aramid-wound tube, is achieved. Hybrid composites of Kevlar and carbon fibers are used in commercial aircraft such as the Boeing 767, 757, and 737, as well as in helicopters and commuter aircraft. Other applications under development include filament wound structures, for example, those used in Trident missile cases and in pressure vessels. The Kevlar provides external damage protection, particularly during transport.

8. Summary

Limited space permits description of only two examples of Kevlar applications research. There are numerous others. In the early product development there were some indications that Kevlar would go mainly into tire reinforcement. This has turned out not to be true. In the mid-seventies Kevlar was participating in only ten market segments and less than fifty specific applications, but today, it is in more than twenty market segments, serving more than two hundred applications, and continued growth is anticipated. Kevlar is produced in a 45 million pound plant in Richmond, VA, USA. In 1988, a second plant was started up in Northern Ireland and plans for a third plant in Japan were announced. The Kevlar innovation story exemplifies the kind of obstacles, interdisciplinary skills and systems approach involved in bringing a laboratory discovery to commercial reality. The story is still unfolding and applications currently not envisioned will undoubtedly become important in the future.

Received: December 19, 1988.

[1] S. L. Kwolek, *U.S. Pat. Reissue* 30,352 (Du Pont) 1980.
[2] P. J. Flory, *Adv. Polym. Sci. 59* (1984) 1–36.
[3] S. P. Popkov, *Adv. Polym. Sci. 59* (1984) 76–99.
[4] P. W. Morgan, *Macromolecules 10* (1977) 1381.
[5] S. L. Kwolek, P. W. Morgan, J. R. Schaefgen, L. W. Gulrich, *Macromolecules 10* (1977) 1390.
[6] T. I. Bair, P. W. Morgan, F. L. Kilian, *Macromolecules 10* (1977) 1396.
[7] H. Blades, *U.S. Pat.* 3767756 (Du Pont) 1973.
[8] H. Blades, *U.S. Pat.* 3869429 (Du Pont) 1975.
[9] M. G. Northolt, *Eur. Polym. J. 10* (1974) 799.
[10] K. P. Lee, H. J. Trochimowicz, *Toxicol. Appl. Pharmacol. 62* (1982) 90–103.
[11] W. B. Black, J. Preston in H. Mark (Ed.): *Man-Made Fibers, Vol. 2*, Interscience, New York 1968, p. 297–301.
[12] P. T. Gibson: *Analytical and Experimental Investigation of Aircraft Arresting Gear Purchase Cable* (NTIS Report AD 904263) Battelle Memorial Institute, Columbus, OH, USA, July 3, 1967.
[13] P. T. Gibson: *Continuation of Analytical and Experimental Investigation of Aircraft Arresting Gear Purchase Cable* (NTIS Report AD 869092) Battelle Memorial Institute, Columbus, OH, USA, April 8, 1969.
[14] For an additional perspective on compressive failure see S. J. De Teresa, R. S. Porter, R. J. Farris, *J. Mater. Sci. 23* (1988) 1886–1894; *ibid. 20* (1985) 1645–1659.

The following reviews will be published in future issues:

T. Kodas: Generation of Complex Metal Oxides by Aerosol Processes: Superconducting Ceramic Particles and Films

H. Warlimont: Rapidly Quenched Materials

H.-W. Schmidt: Dichroic Dyes and Liquid Crystal Side Chain Polymers

R. Eidenschink: Liquid Crystals – New Compounds, New Applications

E. Hondros: Materials for the 21st Century

F. Stoddart: The Structure Directed Synthesis of New Organic Materials

ADVANCED MATERIALS

Aerospace Materials Research Opportunities**

Engineered Microstructures
Intermetallics
Advanced Composites
Materials Processing

By Michael Salkind*

As we approach the second century of aerospace, increased emphasis is being placed on endurance, reliability, ease of manufacture, and lower cost, in addition to weight saving. This change in emphasis will have a major effect on not only the selection of materials, but on how materials are integrated into the total system design process. Subsonic aircraft will continue to play a major role in our future with emphasis on increased durability and lower cost. Non-metals that do not corrode are attractive; however, the issues of reliable fracture resistance to ensure safety and durability as well as ease of manufacture and inspection will be key. Higher performance engines and hypersonic aircraft will require higher temperature materials (including a substantial amount of non-metals) along with reliable toughness and ease of manufacture. In space, weight will continue to be a major driving force along with the need for long term vacuum and radiation stability. Ease of assembly and multifunctional use (e.g. electrically or thermally conducting structure) will be additional needs for spacecraft materials. We have reached a point in the evolution of structural materials where we are moving away from processing naturally occurring materials toward synthesizing designed microstructures to perform specific functions. The mathematical modeling of microstructure–property relationships and new chemical and biotechnical synthesis techniques appear to be critical technologies for the future. In addition, the future materials developer will need a broader understanding of the total structural life cycle so that the impact of utilization, maintenance, and training requirements in the design of new materials can be considered.

1. Introduction

For more than 40 years, mankind has not had a major war nor used a nuclear weapon in anger. The USA and USSR are experiencing a decided recent warming in relations and western economic hegemony seems to be yielding to the Pacific miracle. We are seeing more and more transnational companies which challenge some of our assumptions about national economic competitiveness and indeed the definition of a company or a nation. In 1964, General *Schriever* said "The traditional geographical barriers are really meaningless in today's world ... (which) emphasizes ... the inseparability of political, military, economic, and psychological factors."[1] We are coming to grips with the facts that our environment is delicate and that our natural resources are finite. Against this background, we can conclude that the 21st century, the second century for aerospace, will surely bring great change.

The first century of aerospace was clearly dominated by performance considerations. In the future we will still be pushing back the weight and temperature barriers but within the context of limited mineral, financial, and human resources. We will need to provide improved performance for more capable military vehicles, more economical transport vehicles, and new hypersonic vehicles and spacecraft. However, these new capabilities must be more affordable, more reliable, easier to maintain, and less demanding of our environment, including our mineral and energy resources. An historical summary of tactical aircraft costs showing the inexorable climb in unit cost, Figure 1, led *Norman Augustine* to postulate that:

> "In the year 2054, the entire defense budget will purchase just one tactical aircraft. This aircraft will have to be shared by the Air Force and Navy three and a half days each per week, except for leap year, when it will be made available to the Marines for the extra day."
>
> *Augustine's First Law*[2]

Augustine's "first law" may be amusing hyperbole, but the underlying data are real and, taken together with the global economic realities, indicate that cost must be a far more significant consideration in future aerospace systems.

Maintenance costs of tactical aircraft also indicate the inexorable upward trend.[2] *Augustine* concluded:

> "Aircraft flight in the 21st century will always be in a westerly direction, preferably supersonic, to provide the additional hours needed each day to maintain all the broken parts ..."
>
> *Augustine's Second Law*[2]

[*] Dr. M. Salkind
Air Force Office of Scientific Research Washington, DC, 20332-6448 (USA)

[**] The author would like to thank his colleagues at AFOSR, *J. Dimmock, G. Haritos, A. Rosenstein, L. Schioler*, and *D. Ulrich*, for their assistance in preparing and reviewing the manuscript.

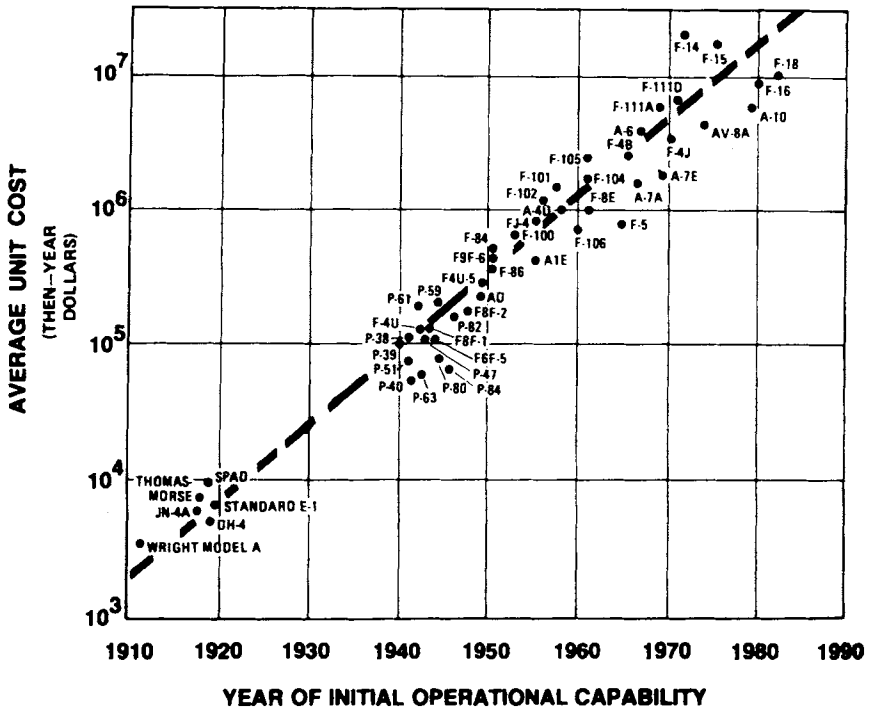


Fig. 1. The unit cost of tactical aircraft has increased consistently by a factor of four every ten years since the beginning of the aviation age. After *Augustine* [2].

Human resource support requirements are rising logarithmically while the capabilities are not. Thus we must conclude that in the 21st century, we will need to produce aerospace systems with more performance, but which, at the same time, are more affordable and supportable.

2. A New Age

"What Age is next?" asks an Alcoa advertisement.[3] *Forney* points out that we have, in rapid succession, entered the Atomic Age, the Space Age, the Information Age, and now the Age of Composites.[4] General *Schriever* called the advent of composites a new age in materials, comparable to the advent of the Iron Age.[1] *Inomori* has said we are entering Shin Sekki Jiddai (the New Stone Age).[5] The Alcoa advertisement goes on to say that we are entering the Engineered Materials Age. Clearly, composites, advanced ceramics, and metal alloys are all subsets of engineered materials or what *Drucker* describes as "... design of the microstructure to give any combination of macroscopic properties."[6] A recent study by the U.S. Congressional Office of Technology Assessment entitled "Advanced Materials By Design" captures this perspective.[7]

We are therefore experiencing a rapid change in materials technology simultaneously with rapid changes in the performance and economic demands on new materials. It is imperative that we see our role as *designers* of materials within the broader context of a systems design. The contrast between design with composites and design with metals is presented in Figure 2. Although the figure relates to fiber composites,

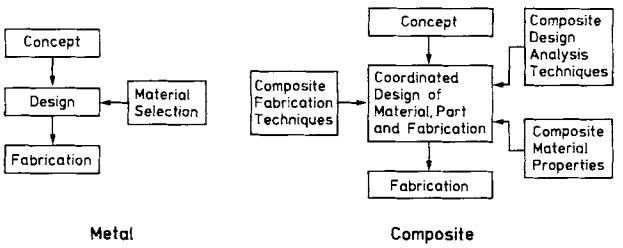


Fig. 2. The advent of materials with engineered microstructures, such as composites, is changing the way materials design is integrated into the total systems design. After *Salkind* [8].

it is a microcosm of the newer approach of designing the microstructure (whether metal, ceramic and/or polymer) for the requirement, compared with the former approach of separate materials development. The materials designer must be part of a design team that considers not only the function, but also the manufacture and life-cycle support of the system. This changing perspective implies changes in how we define ourselves, our organizational roles, our educational goals, and the context of future materials research. Materials research and development is no longer just the purview of the Materials Department.

3. Aerospace Needs

Types of aerospace systems and their range of operating temperatures, together with the capabilities of structural materials are summarized in Figure 3.[9] Materials are the limit-

ADVANCED MATERIALS

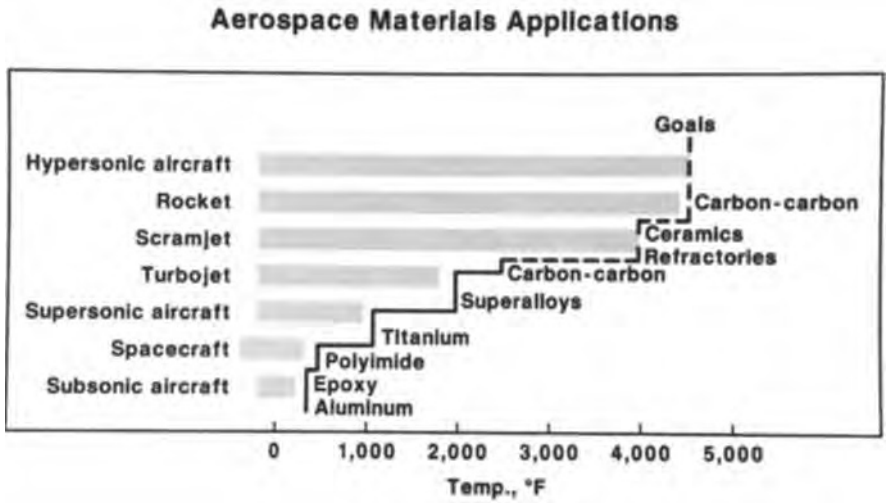
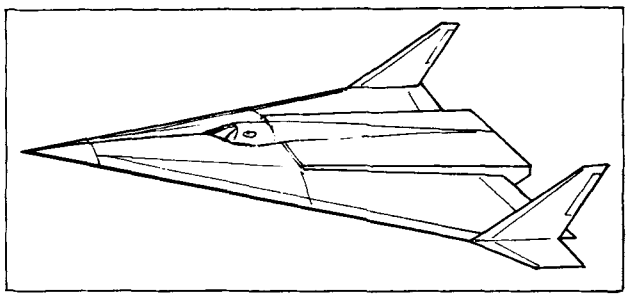


Fig. 3. Summary of Aerospace Materials Requirements and Materials Capabilities. After [9]. $x\,°F = \frac{5}{9}(x-32)\,°C$.

ing technology at the higher temperatures. Over the entire range of temperatures, both materials performance and cost are critical to the mission or commercial success of the system.

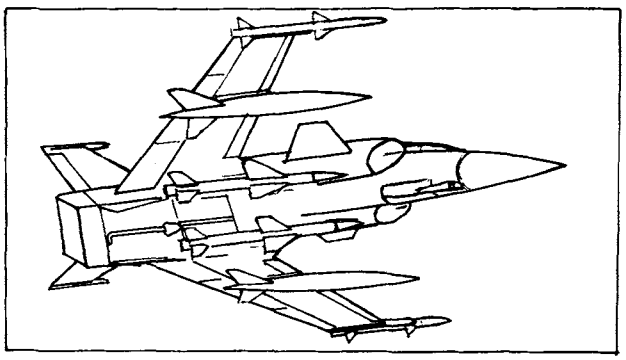
The National Aero-Space Plane (NASP) embodies both significant weight and temperature challenges. Such a hypersonic (Mach 5+) aircraft would take off and land on conventional runways and have both military and commercial applicability. A technology demonstrator, designated the X-30,[10] is planned to be flown in the 1990's to explore the complex aerodynamic, propulsion, structures and materials challenges for the next generation of operational aircraft. *Hadcock*[11] has projected the probable airframe materials and design criteria for such aircraft, as shown in Figure 4. The likely propulsion system, a supersonic ramjet or SCRAMJET, is basically an integral part of the airframe. Multi-phase materials with engineered microstructures will be dominant in such aircraft.

The Advanced Tactical Fighter (ATF) will be the Air Force's major tactical weapons system in the early 21st century.[12] It will combine high maneuverability with supersonic cruise, and employ low-observable technologies. In addition to superior performance, it must have double the maintenance interval of current fighters, be more readily supportable, and meet stringent cost requirements. *Hadcock* has summarized the probable material usage and design drivers for future fighters, Figure 5.[11] As with the NASP,



	Airframe Materials	Airframe Design Criteria
Wing/Fins	Oxidation-Stable Carbon/Carbon	Fail Safe
Fuselage	Superplastic Formed/Diffusion Bonded Refractory Alloys	Damage Tolerant
Internal Structure	Organic Matrix Composites	Extended Life
Inlets/Ducts	Ceramic Matrix Composites Rador Absorbing Structure	Maintainability
Nozzles	Ceramic Matrix Composites	High Reliability
Fittings	Titanium	Chemical, Biological, Nuclear and Laser Resistent
Landing Gear	Metal Matrix Composites.	

Fig. 4. Materials applications for 21st century hypersonic aircraft. After *Hadcock* [11].



	Airframe Materials	Airframe Design Criteria
Wing/Fins	Intermediate Modulus Graphite/ Bismaleimide	Low Vulnerability
Fuselage	Superplastic Formed/Diffusion Bonded Ti & Al	Damage Tolerant
Inlets/Ducts	Organic Matrix Composites Radar Absorbing Structure	Crashworthy Extended Life
Nozzles	Carbon/Carbon	High Reliability
Fairings	Self-Reinforcing Polymers	Maintainability
Fittings	Al Powder Metallurgy	Chemical, Biological, Nuclear Resistent
Landing Gear	Metal Matrix Composites	

Fig. 5. Materials applications for 21st century tactical aircraft. After *Hadcock* [11].

Table 1. Integrated High Performance Turbine Engine Technology (IHPTET) Goals Require Revolutionary Materials [14].

Engine Component	State-Of-The-Art Materials [a]	IHPTET Material Requirements [a]	Candidate Materials [a]
Cold Section (Fan/Compressor)	Titanium (to 800 °F) Nickel (to 1200 °F)	2–3 × Specific Strength 1200 °F–1800 °F	Ti Aluminide Composites Ti Composites Glass Composites High Temperature Al
Hot Section (Combustor/Turbine Augmentor/Nozzle)	Nickel (to 1900 °F) Cobalt	3–5 × Specific Strength 2800 °F with Cooling 3–4000 °F Uncooled	Ceramic/C–C Composites Adv. Aluminide Composites Refractory Metals
Nonstructural (Bearing/Lubes)	Liquid Lube (to 350 °F) Metal Bearings	up to 1500 °F	Solid Lubes to 1500 °F Liquid Lubes to 800 °F Ceramic Bearings

[a] $x\,°F = \frac{5}{9}(x-32)\,°C$.

the requirements are primarily multi-phase materials requiring engineered microstructures. The requirement for low-observable technology, including radar and infrared signatures, strongly drives the choice of the structural configuration as well as the material selection, particularly for stealth technology aircraft such as the B-2.[13] The materials for such aircraft must be designed to meet not only structural but also electromagnetic requirements. Such multiple purpose designs require the materials engineer (and ultimately the materials researcher) to define his or her role within the broader systems design concept as described earlier.

The joint Department of Defense/NASA/Industry Integrated High Performance Turbine Engine Technology (IHPTET) program[14] has the goal of doubling the performance (thrust-to-weight-ratio) of turbine engines by the beginning of the next century. The materials challenge, Table 1, involves major usage of non-metallic materials which have traditionally been avoided because of their low toughness.[14]

Although first cost, and total cost of ownership, are becoming far more important for military aircraft, such considerations have always been dominant for commercial aircraft. There currently exists an economic dilemma in terms of new materials usage in commercial planes.[15] Whereas the soaring fuel prices of the 1970's accelerated the need for fuel efficient technologies, including composites and aluminum–lithium alloys for weight reduction, the oil glut of the 1980's slowed down the introduction of new aircraft and consequently new technologies. According to *Swihart* the price premium that the market would bear for a 10% fuel saving dropped from 16% in the 1970's to 2.5% in 1985.[15] The cost of ownership has replaced the fuel cost as the largest part of the commercial transport direct operating cost.[16] The next generation of transport aircraft will likely consist of derivatives of current models. As a result, the opportunities for introduction of new materials will be very much dependent upon economic considerations. For composites, which could be as much as 65% of the structural weight of new transports,[16] the cost of fabrication is a major factor. The emphasis on cost further reinforces the theme that the materials design must be more fully integrated into the systems design.

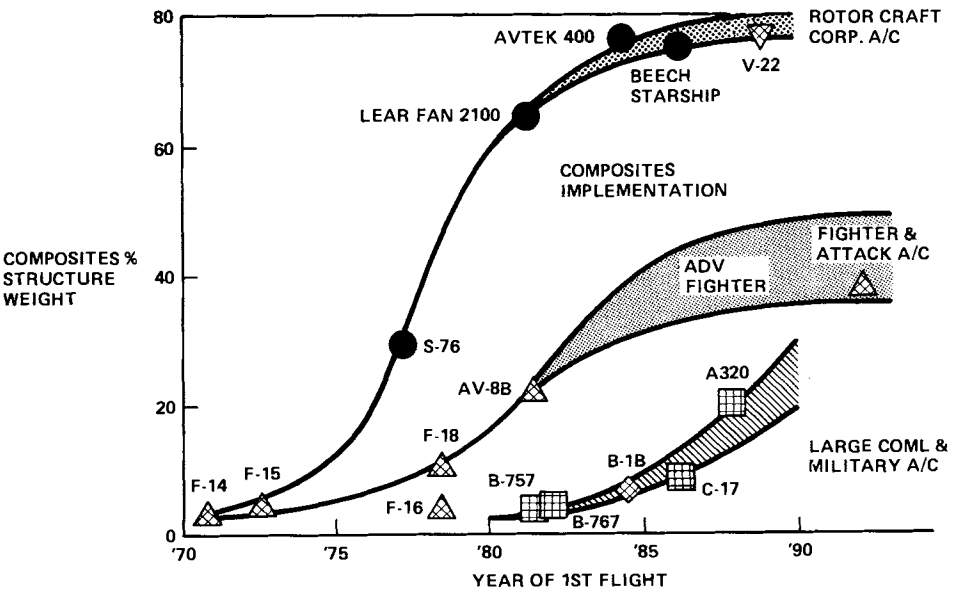


Fig. 6. Increased Usage of Composites in Aircraft. After *Hadcock* [11].

The introduction of new materials, such as composites, has been more rapid in helicopters and light aircraft than in tactical or transport aircraft, Figure 6.[11] Prototype all-composite helicopters have been built[17-19] and have demonstrated the potential for significant (30%) cost reduction. The cost reduction accrues primarily from an order of magnitude reduction in the number of parts and the attendant assembly labor reduction, which more than overshadows the higher materials costs.

There is significant future potential for both military and civilian usage of space. Whether or not the current world situation slows the development of space weapons, there will be a need for both military and civilian communication, surveillance, and navigational satellites. In addition, there is the potential for exploiting the space environment for materials (including biological materials) processing. The NASA Space Station represents a major thrust in space in the 21st Century. Because of the high launch costs, weight remains a more dominant factor in spacecraft than aircraft; however, long term durability continues to be an increasingly important consideration. The combined effects of vacuum, radiation, and thermal cycling are particularly challenging, especially for non-metals. The use of metal matrix composites for microwave packaging is typical of the emerging need to integrate the materials design with the total system requirement.[20] In this case the material functions simultaneously as a structure and a heat rejection mechanism, and meets stringent electromagnetic and thermal stability requirements. So-called "smart materials", that have embedded sensors and can change characteristics as required, are the obvious extension of the integration of materials design with systems design.

4. Research Opportunities

In examining research opportunities it is clear that we must posture ourselves to design microstructures to meet a broadened range of requirements. The relationship between microstructure and properties is the traditional domain of the materials scientist. The classic work of *Hall*[21] and *Petch*[22] in the 1950's, relating grain size in steel to mechanical properties, established the significance of quantitative microstructure–property relationships. There is a need to establish these relationships in a more precise quantitative form than has been done in the past. Traditional continuum mechanics, based on the assumption of homogeneous continua, cannot handle multi-phase materials nor discontinuities such as damage. Although micromechanics has been developed to handle some simple aspects of fiber composites, a new level of materials mechanics is needed to provide the mathematical basis to truly design a general microstructure.[23] Such an approach requires extensive collaboration between materials and mechanics researchers. There is also a need for a more precise and universal mathematical description of microstructure as the common language of this collaboration. Some metallurgical approaches[24,25] coupled with the use of fractals[26-28] appear promising. Fractal dimension can be a powerful mathematical description of microstructure. We need a standardized language to describe the shape and size distribution of each phase (including interfaces) and its spatial arrangement. Such a scheme must be able to characterize such complex structural materials as soils (solid particles plus liquid and gas phases), chemically bonded ceramics (including concrete and cement), and deliberately porous materials.

5. Tough Materials

It is clear that in developing a new quantitative mechanics of microstructures, the property we call toughness is probably least understood. Our emergence from the Stone Age, more than five thousand years ago, was prompted by the lack of toughness of ceramics. Because metals exhibit extensive plastic deformation, we have come to equate ductility with toughness and have assumed, erroneously, that uses of materials exhibiting little or no plastic deformation are limited by their brittleness or low toughness. In recent years, experience with multi-phase materials, especially fiber composites, has taught us that there are microstructural alternatives to plastic deformation which can handle stress concentrations and exhibit significant toughness.

Toughness tests normally involve notched or pre-cracked specimens and measure resistance to damage propagation. For inhomogeneous anisotropic materials, it is not always clear how such measured properties relate to actual performance in structures. The following discussion treats such measured resistance to damage propagation as an indicator of toughness. Ceramic and carbon fiber reinforced glass-ceramics have exhibited macroscopic toughness values over 20 MPa $m^{1/2}$ which is comparable to metal alloys.[29-30] *Cook* and *Gordon* described how the fiber matrix interface can open to blunt a crack, which is analogous to plastic deformation blunting the crack tip in metals.[31] The role of the fiber interface in imparting toughness has been the subject of extensive discussion. Fiber surface treatment has been shown to dramatically change the toughness of fiber reinforced polymers,[35] hydrated cement,[36] and ceramic/ceramic composites.[37-39] The research challenge of understanding the microstructure–toughness relationship is also dependent upon the complex state of stress determined by the other microstructural characteristics, such as the relative properties of the phases and their shape, size, and spatial arrangement.[37,40-44] The exact mechanism of toughening will be dependent upon the interaction of the relative and absolute properties of the phases and the interface. In addition to the composite approach to providing toughness to otherwise brittle materials, there have also been extensive efforts to control[48,49] and characterize microstructural defects and to provide phase transformation toughening.[50]

The groundwork for the required mathematical mechanics treatment of microstructure–property relationships has begun. *Kunin* has extended the description of elastic media to include microstructure.[51] Major efforts have been made to account for damage,[52, 53] and inelastic behavior.[54] A concerted effort is needed by materials and mechanics researchers to develop a more precise mathematical basis for the design of microstructure.

6. Biological Models for Designed Microstructures

In a fascinating new book, *Gordon* points out that living organisms provide manifold examples of structural materials, engineered within a total system design including cost (defined as metabolic cost).[55] Bone is a marvelous example of an engineered microstructure. It is a fiber composite containing stiff hydroxyapatite fibers in a collagen matrix. The fibers are oriented to resist the principal loads and, because living bone is constantly dissolving and regenerating its structure, can reorient the microstructure to respond to changes in loading (e.g. a fracture). In addition, bone microstructure simultaneously performs non-structural functions such as conveying blood via built-in tubular cells. Bone is not as structurally efficient as wood (another living engineered fiber composite), because it is optimized to function along with tendons and muscles in a total structural system.

In a remarkable example of man imitating nature, *MacCready* et al. built a flying replica of the extinct reptile *Quetzalcoatl Northropi* (QN).[56] In the course of doing so, he studied the detailed design of engineered materials in birds within the context of complex system design (Fig. 7). A key design factor in the QN replica was an on-board control system (brain analog) to maintain structural and dynamic flight stability under changing loading conditions. The structural materials design could not carry the flight loads in the absence of the control system, which was inadvertently demonstrated when the QN was accidently launched with its control system off. Analogously, the human body cannot stand straight with its control system (brain) off. So-called smart materials, containing sensors and actuators to change structural characteristics, are future materials research opportunities which could mimic the integrated systems of biological materials.



Fig. 7. A man-made *Quetzalcoatl Northropi* incorporating nature's design concepts. The materials design was fully integrated with structural and control design. Photo courtesy of Aerovironment Corp [56].

7. Processing Opportunities

Perhaps one of the most challenging materials research opportunities is processing. Not only will we be challenged to economically produce geometrically precise microstructures, but we will also likely shift away from energy intensive thermal processing toward more low temperature chemical and even biological processing. This will require an additional shift in our perspective and a blurring of the traditional roles of materials supplier, processer, and user.

Sol–Gel processing of ceramics is an example of a new lower temperature chemical technique.[57, 58] It consists of polymerizing a porous ceramic gel from solution and subsequently drying and densifying it. The technique allows processing below 500 °C compared with traditional melt processing at three times that temperature. Recent research has focussed on chemical additives to control the kinetics and therefore the pore size, distribution, and residual stresses.[59] Perhaps more important than low temperature processing, is the opportunity to produce composites by sol–gel processing.[58] By dispersing two or more phases in the sol, precisely controlled multiphase microstructures can be produced at fine scale. The term nanostructure or nanocomposite has been used to describe such structures with nanometer scale phased dimensions. Because the size of each phase is only a few atomic layers, such materials tend to have properties significantly different from bulk properties.[60] This has significant potential for both structural and electronic applications.

Another approach is reaction processing, in which the components react chemically in the solid state with a gas or liquid phase to provide densification.[61] An extreme example of this is self-propagating high temperature synthesis involving a combustion reaction.[62] The LANXIDE process involves forming solid oxide structures by the controlled reaction of a molten metal with an oxidizing vapor. By conducting the reaction in the presence of a solid second phase, composites can be fabricated.[63]

A very intriguing materials research opportunity lies in mimicking the way living organisms process ceramic composite structures such as bone and shell. *Calvert* and *Broad* have used such bio-mimetic processing to produce metal oxide materials.[64] Coupled with our new insights into the

structure of DNA and the ability to bioengineer designer organisms, it seems a natural extension to design organisms to produce precisely defined microstructures.

There are also significant research opportunities in the area of processing metal alloys and metal matrix composites.[65, 66] Castings are attractive because of the low cost and their potential for production of net-shape or near net-shape parts. Processes such as directional solidification to control or eliminate grain boundaries and hot isostatic pressing to eliminate defects have moved castings from the low to the high performance arena. Whisker reinforced cast aluminum exhibits properties approaching polymer matrix composites with the inherent low cost and handling familiarity of metals.[67, 68] The key technological issue is processing to provide a controlled whisker dispersion. Intermetallics have significant potential for higher temperature application, but with significant processing challenges.[69, 70]

The technology of polymers has been traditionally process oriented. The engineering of polymer chains probably represents the most extensive use of engineered microstructures.[71–73] Some of the newer oriented polymer fibers compete with some of the best inorganic fiber reinforcements. An exciting outgrowth of this area is the possibility of simultaneously polymerizing rigid rod fiber polymers in a matrix of a more flexible polymer thus creating a molecular composite.[73] Thermoplastic polymers are attractive because of their lower processing cost and cycle time compared with thermosets.[74, 75] Research challenges include synthesizing new higher performance (including higher temperature) thermoplastics with improved environmental resistance along with improved processability in composites. Polymer blending offers the potential for providing ease of processing with improved performance.[76, 77]

8. Conclusion

There are exciting challenges facing the materials research community. Although the technical needs are well known, and many important new approaches are well defined, it is important for the materials scientist to see himself or herself in a broadly expanded context. The design of materials as a part of the overall systems design will become the norm. As a result, such factors as cost, durability, supportability, and specialized functions will take on added importance in materials science, engineering research and education. Important research opportunities include joint materials–mechanics efforts to provide precise mathematical microstructural design tools, and new chemical and biochemical processing techniques to synthesize the designed microstructures. In particular, the advent of bioengineering offers the possibility of genetically engineering new biological species to produce precisely designed microstructures.

Received: December 19, 1988

[1] B. Schriever: *The Significance of Aerospace*, NATO Defense College, Paris, 15 June 1964.
[2] N. Augustine: *Augustine's Laws*, Am. Inst. Aero. Astro. (AIAA), New York 1983.
[3] Alcoa, *J. Met. 38* (1986) No. 8, back cover.
[4] R. Forney, *J. Met. 38* (1986) No. 3, p. 18.
[5] K. Inomori, in a speech to Kyocera Management, 1984, quoted in *High Technology*, August 1985, p. 50.
[6] D. Drucker, *Adv. Aero. Struct. Mater. AD-01*, Am. Soc. Mech. Eng., New York 1981, p. 1.
[7] *Advanced Materials by Design*, OTA-E-351, Congressional Office of Technology Assessment, U.S. Government Printing Office, Washington, DC, 1988.
[8] M. Salkind, *Proc. ICCM*, Am. Inst. Met. Eng., New York 1976, Vol. 2, p. 5.
[9] *Net Shape Technology in Aerospace Structures*, National Academy of Sciences Press, Washington, DC, 1986.
[10] C. Covault, *Aviat. Week Space Technol., 1988*, March 7 issue, p. 36.
[11] R. Hadcock: *Status and Viability of Composite Materials in Structures of High Performance Aircraft*, National Research Council, Aeronautics and Space Engineering Board, Naval Postgraduate School, Monterey, CA, 10. February 1986.
[12] A. Brown, *Aerosp. Am. 25* (1987) No. 4, p. 16.
[13] C. Lewis, *Mater. Eng. 105* (1988) No. 6, p. 37.
[14] R. Henderson, J. Petty, *Adv. Technol. for Aero Gas Turbine Components*, AGARD Conf. Proc. No. 421 (September 1987) p. 1–1.
[15] J. Swihart: *Cost Effective High-Technology Civil Transports*, Jpn. Aerosp. Soc., Nagoya, October 1985.
[16] D. Lovell, Boeing: *Future Materials Outlook*, SACMA 3rd Int. Conf., 3–4 May 1988.
[17] K. Grina, *Vertiflite 34* (1988) No. 1, p. 29.
[18] J. Goldberg ("Crashworthiness of the ACAP") *Proc. Am. Helo. Soc. Forum*, St. Louis, May 1983.
[19] W. Sonneborn, G. Alsmiller: *Usage of Composites in Rotorcraft*, Am. Soc. Mech. Eng. Design Eng. Conf., Chicago 1982.
[20] C. Thaw, R. Minet, J. Zemany, C. Zweben, *SAMPE J., 1987*, November/December issue, p. 40.
[21] E. Hall, *Proc. Phys. Soc. (London) 64 B* (1951) 747.
[22] N. Petch, *J. Iron Steel Inst. (London) 174* (1953) 747.
[23] G. Haritos, J. Hager, A. Amos, M. Salkind, A. Wang, *Int. J. Solids Struct. 24* (1988) 1081.
[24] E. Underwood: *Quantitative Sterology*, Addison Wesley, Reading, MA, USA 1970.
[25] R. DeHoff, *Sci. Sintering 16* (1984) 97.
[26] B. Mandelbrot, D. Passoja, A. Paullay, *Nature (London) 308* (1984) 721.
[27] E. Underwood, K. Banerji, *Mater. Sci. Eng. 80* (1986) 1.
[28] R. Messier, J. Yehoda, *J. Appl. Phys. 58* (1985) 3739.
[29] J. Brennan, K. Prewo, *J. Mater. Sci. 17* (1982) 2371.
[30] K. Prewo, *Philos. Trans. R. Soc. London, A 294* (1980) 551.
[31] J. Cook, J. Gordon, *Proc. R. Soc. London A 282* (1964) 508.
[32] M. Salkind: *Surfaces and Interfaces II*, Syracuse Univ. Press (1968) 417.
[33] M. Salkind in K. Kawata, S. Umekawa, A. Kobayashi (Eds.): *Composites 86*, Jpn. Soc. for Compos. Mater., Tokyo 1986, p. 845.
[34] *Interfaces in Composites*, STP 452, Am. Soc. Test. Mater., Philadelphia 1969.
[35] L. Drzal, *Adv. Polym. Sci. 75* (1986) 1.
[36] V. Li, Y. Wang, S. Backer ("*Bonding in Cementitions Composites*"), *Mater. Res. Soc. Proc.* Vol. 114, Pittsburgh 1988, p. 167.
[37] A. Evans, *J. Am. Ceram. Soc. 65* (1982) 127.
[38] D. Marshall, W. Oliver, *J. Am. Ceram. Soc. 70* (1987) 542.
[39] R. Singh, M. Brun, *Adv. Ceram. Mater. 3* (1988) 235.
[40] A. Evans: *Fracture in Ceramic Materials*, Noyes, New York 1984.
[41] R. Cook, B. Lawn, C. Fairbanks, *J. Am. Ceram. Soc. 68* (1985) 604.
[42] B. Budiansky, J. Hutchinson, A. Evans, *J. Mech. Phys. Solids. 34* (1986) 167.
[43] R. Rice, *Ceram. Eng. Sci. Proc. 6*, Am. Ceram. Soc. 1985, p. 589.
[44] T. Oh, J. Rodel, R. Cannon, R. Ritchie, *Acta Metall. 36* (1988) 2083.
[45] P. Lagasse, *Rubber World 192* (1985) No. 2, 27.
[46] L. Schioler, J. Stiglich, *Am. Ceram. Soc. Bull. 65* (1986) 289.
[47] K. Prewo, J. Brennan, G. Layden, *Am. Ceram. Soc. Bull. 65* (1986) 305.
[48] R. Katz, *Mater. Sci. Eng. 71* (1985) 227.
[49] J. Skalny, *Annu. Rev. Mater. Sci. 17* (1987) 35.
[50] T. Masaki, *J. Am. Ceram. Soc. 69* (1986) 638.
[51] I. Kunin: *Elastic Media with Microstructure*, Vol. I 1982, Vol. II 1983, Springer, Berlin.
[52] J. Dumont, *Comput. Struct. 8* (1987) 119.

[53] S. Bodner, Z. Hashin (Eds.): *Mechanics of Damage and Fatigue*, Pergamon, Oxford 1986.
[54] C. Herakovitch (Ed.): *Inelastic Behavior of Composite Materials*, AMD Vol. 13, Am. Soc. Mech. Eng., New York 1975.
[55] J. Gordon: *The Science of Structures and Materials*, Scientific American Library, New York 1988.
[56] A. Brooks, W. Morgan, P. Lissaman, P. MacCready, *Development of a Wing Flapping Flying Replica of a Pterosaur*. AIAA paper 85-1446, 1985, AIAA, Washington, DC.
[57] D. Ulrich, *J. Non-Cryst. Solids 100* (1988) 174.
[58] R. Roy, *Science 238 (Washington)* (1987) 1664.
[59] L. Hench: *Science of Ceramic Chemical Processing*, Wiley, New York 1986, p. 52.
[60] H. Gleiter, P. Marquardt, *Z. Metallkd. 75* (1984) 263.
[61] M. Washburn, W. Coblenz, *Am. Ceram. Soc. Bull. 67* (1988) 350.
[62] Z. Munir, *Am. Ceram. Soc. Bull. 67* (1988) 342.
[63] M. Newkirk, H. Lesher, D. White, C. Kennedy, A. Urquhart, T. Cloar, *Ceram. Eng. Sci. Proc. 8* (1987) 879.
[64] P. Calvert, A. Broad, *Atom. Mol. Proc. Elect. Ceram. Mater.*, Materials Res. Soc., Pittsburgh 1987, p. 89.
[65] F. Froes, *Mater. Edge 1988*, May/June issue, p. 19.
[66] R. Sundaresan, F. Froes, *J. Met. 39* (1987) August issue, p. 22.
[67] F. Froes, *Space Age Metals Technology*, SAMPE Azusa, CA, USA 1988, p. 1–19.
[68] D. Schuster, *Report AFWAL-TR-87-3042*, October 1986, AF Wright Aeronautical Labs., Ohio.
[69] H. Lipsitt: ("High Temperature Ordered Intermetallic Alloys"), *Mater. Res. Soc. Proc. 39*, Pittsburgh 1985, p. 351.
[70] R. Rowe, A. Taub, F. Froes, ("Developments in Rapidly Solidified Ni and Ti Intermetallics"), *Proc. ASM Int. Conf.*, Paris, September 1987.
[71] R. Tucker, *J. Met. 38* (1986) No. 3, 21.
[72] W. Adams, R. Eby, *Mater. Res. Soc. Bull. 12* (1987) No. 8, p. 22.
[73] D. Ulrich, *Polymer 28* (1987) 533.
[74] S. Witzler, *Adv. Compos. 3* (1988) 55.
[75] L. English, *Mater. Eng. 1988*, May issue, p. 68.
[76] I. Sanchez: *Polymer Blends*, Academic Press, New York 1978, Chapter 3.
[77] L. Kleiner, F. Karasz, W. Macknight, *Polym. Eng. Sci. 19* (1979) 519.

Challenges in Materials for Health Care Applications

Implanted Devices
Tissue Replacements
Biocompatible Polymers

By David F. Williams*

Important issues face the use of advanced materials in medical applications. It is now possible to replace or augment many tissues and parts of the body by implanted devices, but there are still severe limitations to functions they are able to perform and problems associated with their compatibility with the tissues. Biomaterials of the future need to simulate more closely the tissues they are replacing and both the current position and future outlook are reviewed in this light.

1. Introduction

In the fifty years that have now passed since the invention of Nylon by *Wallace Carothers*, we have witnessed many changes in materials science and in the contribution of materials science to the welfare of mankind. This paper will discuss and review the current status of, and future challenges for, the uses of materials in one specific aspect of this contribution, that of implantation within the tissues of the human body.

There are many reasons why it is necessary or desirable to place some of today's advanced materials within the body,[1] but it is not the purpose of this paper to review them in detail. Some of the major reasons, and the current technical advances that have been made, are now well-known (Table 1). The twin diseases of rheumatoid and osteoarthritis are unfortunately very common, but the surgical technique of joint replacement, developed to overcome the pain and disability caused by these diseases is widely practiced, and has become a familiar landmark of late twentieth century surgery. Cataracts in the eye are now effectively treated in some half

Table 1. Some current applications of implanted devices.

Clinical area	Implant	Tissue replaced or augmented
Orthopedic surgery	Total joint replacement	Bone, cartilage
	Fracture fixation	Bone
	Ligament repair	Ligament
Cardiovascular surgery	Mechanical heart valve	Valve leaflet
	Bioprosthetic heart valve	Valve leaflet
	Vascular prosthesis	Blood vessel
	Pacemaker	Nerve
Ophthalmology	Intraocular lens	Lens
	Keratoprosthesis	Cornea
Ear, nose and throat	Ossicular replacement	Bone
	Cochlear stimulation	Cochlea/nerve
Maxillofacial	Dental implant	Teeth
	Fracture fixation	Bone
	Mandibular reconstruction	Bone
Plastic surgery	Breast reconstruction	Soft tissue

[*] Prof. D. F. Williams
Institute of Medical and Dental Bioengineering
University of Liverpool
P.O. Box 147, Liverpool L69 3BX (UK)

a million patients a year by the removal of the offending clouded lens and its replacement with a polymeric intraocular lens. Dental caries and, to a lesser extent, periodontal disease, affect most people at some stage, and the various procedures of restorative dentistry used to replace or treat these tissues utilize a great variety and volume of synthetic materials. Fewer people suffer from disease of the cardiovascular and peripheral vascular system, but the problems, when they arise, are of far greater consequence and significance. One method of treatment of such disease is the surgical replacement of the affected tissue.

Within this range of uses, the precise requirements of function will also be varied. It must be noted that, at the present time, the functions performed by the materials and devices of implant reconstructive surgery are quite simple in relation to the functions of the tissues they replace. Ideally, a replacement should possess all of the functional characteristics of the tissues, but this is rarely possible. In most cases it is a simple mechanical or physical function that is obtained, very frequently the implant merely acting as a space filler. It is very exceptional for more complex functions, especially involving biological activity, to be sought or achieved. The challenge for materials in these applications is to provide more sophisticated function, including biological and pharmacological function, while maintaining the appropriate mechanical or physical performance.

2. The Functional Replacement of Tissues

If it is intended to replace diseased, damaged or otherwise lost tissue by a functionally analogous structure, it is sensible to consider the nature and characteristics of these natural tissues. At the molecular level there are many different components involved. Water is the most abundant compound; this is not a trivial comment, since virtually all synthetic materials are unhydrated. Dissolved in this water are a variety of acids and bases as well as a vast array of both soluble and structural proteins, carbohydrates, lipids and nucleic acids. Complex as these organic molecules may be, the development of materials to simulate or mimic them is not the real problem. Figure 1 demonstrates the close similarity between the repeating molecular units in a synthetic polyamide, and two common, although non-human organic molecules, silk and wool. Many other examples can be found of the essential

Nylon $\cdots\cdots C(=O)-NH-(CH_2)_n-C(=O)-NH-(CH_2)_y-C(=O)\cdots\cdots$

Silk $\cdots\cdots C(=O)-NH-CH_2-C(=O)-NH-CH_2-C(=O)\cdots\cdots$

Wool $\cdots\cdots C(=O)-NH-\underset{R}{CH}-C(=O)-NH-\underset{R}{CH}-C(=O)\cdots\cdots$

Fig. 1. A comparison of the molecular structures of a synthetic polymer (Nylon) and two natural polymers (silk, wool). After *Richardson*.

equivalence of the repeat units in natural biopolymers and synthetic polymers.

The real problem lies with the fact that these molecules constitute just the basic level in the structural hierarchy of tissues and that the higher levels are far more difficult to rebuild. The tissue itself, apart from the water, contains both cellular and extracellular structures. Cells are not only varied in their structure and function, but are also extremely complex entities whose activity is as much dependent upon the ability to receive information, for example for highly specific receptors on their membranes, as on the ability to react to this information. Perhaps the simplest cell is the erythrocyte, or red blood cell, since this consists of a thin membrane which contains a solution of hemoglobin. It has been possible to prepare structures which simulate this cell and possess some of the functions of hemoglobin transport, but the development of more complex artificial cells using conventional materials is rather difficult to contemplate.

Cells possess varying degrees of mobility. Some, notably those of the musculo-skeletal system, are essentially fixed within an extracellular matrix. This matrix often consists largely of structural proteins such as collagen and elastin and is in some cases reinforced by deposits of minerals, specifically hydroxyapatite in the case of bone, dentine and enamel. In this type of system it is as much the spatial distribution of the various components and their interfacial relationships that control the performance of the tissue, as it is the molecular nature of the components themselves.

The structure of bone provides an excellent example of this, which is, of course, very relevant to implantable devices.[3] The structural protein of bone is collagen, which has a well recognized molecular and fibrillar structure. The collagen is itself arranged with a microstructure, described in terms of a Haversian system, in which there are cylindrical, concentric layers of collagen (Fig. 2). There are lengthwise

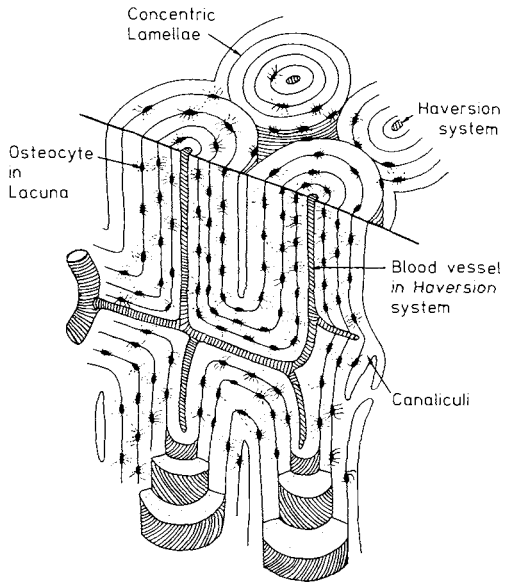


Fig. 2. The structure of bone.

canals containing blood vessels, small spaces containing the blood cells and a myriad of ultrafine canals, the canaliculi. The collagen contains a multitude of nanometer-sized crystallites of calcium hydroxyapatite.

At a macroscopic level, the bone may be arranged in a reasonably dense way (cortical bone) which comprises most of the major structural part of long bones such as the femur and tibia, or it may be arranged in a more open, porous form, known as cancellous bone, which is found in the ribs, the pelvis and elsewhere.

The mechanical and physical properties of a bone (as a structure) depend on all of the molecular, microstructural and macroscopic arrangements discussed above, making it a multicomponent composite structure, with considerable anisotropy. The functional characteristics of bone are complicated even more by its viable, dynamic nature. It does contain cells, which are in a state of constant turnover, and it does require a blood supply. Resistance to fatigue crack propagation is dependent on the vital ability of bone to blunt cracks. The relationship between the mineral phase and the collagen is controlled by mechanical stress via a number of mechanisms including piezoelectric and streaming potential effects. These and many other phenomena demonstrate the acute relationship between mechanical properties and biological characteristics which control functional performance.

Since bone, with this structure complexity, is one of the most straightforward of tissues to replace from a functional point of view, it is easy to appreciate the enormous difficulty of replacing some of the other tissues of the body. Two examples will serve to emphasize this point.

Skeletal muscle consists at the molecular level of proteins such as myosin and actin. They form long myofibrils combined to form muscle fiber which are arranged in bundles to form the muscular structure (Fig. 3). The molecular and fibrillar arrangement allows very high extensibility without excessive interatomic forces, a characteristic which is difficult to achieve in all but a few synthetic elastomers. The ability to elongate and contract, however, is not a simple passive function, but involves active movement of calcium ions, under the influence of electrical impulses, which initiates myosin and actin interactions and the sliding of myofibrils. The challenges to the functional replacement of muscle lie both within the extraordinary elastic performance and the ability to incorporate transducers in order to translate electrical impulses into elastic deformation.

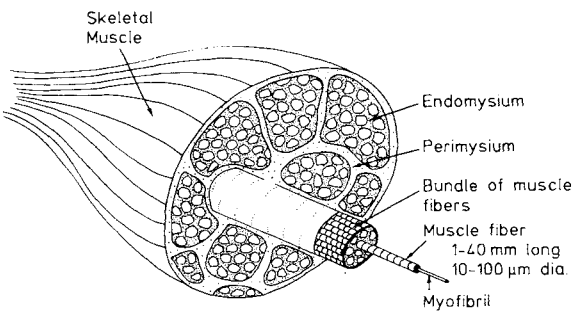


Fig. 3. The structure of skeletal muscle.

The vascular system, both in relation to the cardiac and peripheral circulation, appears to have a simple function, that of providing a series of conduits along which blood can flow, and gently assisting that flow. In reality, the mechanisms involved in producing the optimal hemodynamic conditions so that the organs and tissues receive their blood most efficiently are very complex. Considering the arterial system, an artery consists of a cylindrical connective tissue layer, a smooth-muscle layer within this, a cylindrical elastin membrane and finally, on the inner aspect, a layer of endothelial cells (Fig. 4). The functions of importance are two-

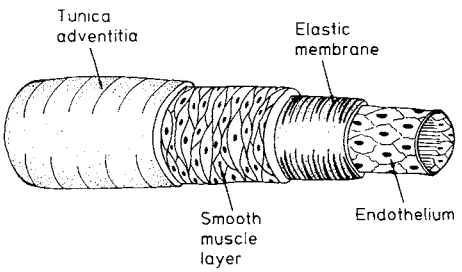


Fig. 4. The structure of an arterial wall.

fold, relating to the mechanical performance of the wall and also the interaction between the endothelial cells (or underlying connective tissue if damaged) and the blood. The mechanical performance is vital. Since it is necessary for blood to flow with laminar characteristics under pulsatile conditions, both the elasticity, compliance and geometry are important. Of equal, if not greater, importance is the need for this contact with flowing blood to take place without adverse effects on the blood. Blood is a medium that contains several defense mechanisms that can only operate under certain conditions, for example, blood has the ability to clot if the vessel is damaged. The clotting mechanism is very complex, but represents a sensitive balance between a variety of biochemical events. This balance can be easily upset and it is therefore a major functional requirement of these tissues that they do not themselves adversely interfere with these mechanisms.

3. The Characteristics of Current Biomaterials

At the present time, a wide selection of materials is used in implant surgery (Table 2) but in the majority of cases, because only a simple, single function is sought, these materials bear little resemblance to the tissues they replace. Examples include metals and alloys, such as an amalgam of mercury, silver and tin which replaces tooth structure,[4] and cobalt-based alloys, 316 stainless steel, titanium or Ti-Al-V alloys which replace or augment bone.[5] Clearly, these metallic materials have no molecular or structural similarities with

Table 2. Major currently used biomaterials.

Class	Material	Use
Metal	Amalgam	Restoration of teeth
	Titanium/Ti–Al–V	Bone replacement/repair Dental implant Maxillofacial implants Encapsulation of electronic devices
	Stainless steel	Bone replacement/repair
	Co-Cr alloy	Bone replacement/repair
Ceramic	Alumina	Bone, joint and tooth replacement
	Hydroxyapatite	Coating on bone/tooth replacement Bone augmentation
Polymer	Polyurethanes	Arteries and other blood contact devices
	Polymethylmethacrylate	Dental restorations Ophthalmology Fixation of bone/joint prostheses
	Polytetrafluoroethylene	Arteries, soft tissue
	Polyethylene	Joint replacement
	Polyesters	Arteries, sutures

the tissues. There are also some ceramics. High purity alumina and transformation-toughened alumina possess some attractive properties of wear resistance and inertness,[6] but otherwise are quite unlike natural tissues.

Polymer-based materials are widely used[7] and possess a greater claim for similarity with tissues than most materials. However, they still fall short, for although they are based, as indicated earlier, on an organic backbone, it is extremely difficult to organize their microstructure in an appropriately biological way. Current polymers in use include polyethylene and polypropylene, acrylics, polyamides, polyesters (both aromatic and aliphatic) polyurethanes and silicone polymers. Most of these are single phase structures, either thermoplastics, cross-linked polymers or elastomers, with little evidence of any structural hierarchy. In some cases multiphase structures with domains and segments are available and of course certain composites, both fiber and particulate, are emerging. Even here, however, there are still major structural differences from the anisotropic heterogeneous natural products.

4. Some Concepts in the Development of Biologically Analogous Materials

A few concepts and ideas that have emerged during the last few years are beginning to show real promise in the search for biologically analogous materials.[8] It should be said that the ultimate solution is the use of natural tissue itself. In many ways this is the most obvious and indeed oldest solution, for transplanted tissues have been used in selected cases for many years. Ranging from skin and bone grafts at one end of the range to heart transplants at the other, these materials and procedures are very variable in their success and applicability. The most successful procedures are those where simple tissues are transplanted from one part of a patient to another, but the occasions where a patient has an adequate supply of the required tissue, and when the loss from the donor site is repairable, are few and far between. The most difficult are those, such as major organ transplants, where donor and recipient are different, and although great strides have been made with immunosuppressive drugs to improve their acceptability, transplants of this type are always likely to have major problems facing their use.

Most of the technical as opposed to ethical and logistic problems associated with transplanted tissue relate to sterility and antigenicity issues. Foreign tissue generally elicits a response from the immune system and of course all tissue products transferred from one human to another have to be carefully screened for viruses such as those involved with hepatitis and AIDS. One potential solution to the dilemma of using natural tissues, but being concerned about sterility and antigenicity issues, is to take such tissues and treat them, rendering them non-viable but sterile and non-antigenic. The construction of prosthetic heart valves has employed this concept, with the use of bovine pericardium (the muscular tissue of the heart-wall of cows) or porcine valve tissue, in the fashioning of the leaflets of mitral and aortic valves, after fixation in glutaraldehyde.[9] While giving better biological performance than the alternative mechanical valves, these do suffer problems of long term calcification and degradation. It is not clear whether any treated soft tissue obtained in this way will ever be sufficiently stable for long term use in the body. Some success has been achieved with the use of bone harvested from donors and treated in some appropriate way, for example freeze-drying.

Tissue which is either transplanted in a viable state, or treated and rendered non-viable, usually retains its heterogeneity. An alternative approach to using these structurally complex tissues is to separate individual components from the tissue and use these for their specific properties. These components may be obtained by separation techniques using donor tissue or synthesized directly. Two examples are described here. First, there is considerable interest in the use of collagen preparations, especially for injection as soluble materials for cosmetic surgery.[10] Secondly, the mineral phase of bone, hydroxyapatite, may be used for bone reconstruction or bone bonding applications either in its own right as an alternative to bone graft or as a coating on a tough substrate. In the latter case there is strong evidence that synthetic apatite allows new tissue-derived hydroxyapatite to be deposited epitaxially on its surface, hence producing material–tissue bonding.[11]

As a ceramic, hydroxyapatite cannot offer all of the properties of bone itself and suffers from inferior mechanical properties. Some attempts have been made to produce composite materials that are structurally analogous to bone in the hope of finding equivalent properties. One example actually employs hydroxyapatite as the dispersed phase in a ma-

trix of polyethylene.[12] Others, including some carbon fiber reinforced thermoplastics, are less biological in composition, but possibly better mechanically. In situations where it is desirable to apply a biomaterial which can be shaped to a prepared bone cavity or to augment a deficient bone structure, for example the ridge of the mandible in patients without teeth, the same hydroxyapatite can be incorporated into some natural polymerizable substance. Of increasing interest here is the use of a fibrin glue as a matrix for the preparation of a composite with hydroxyapatite.

The assumption that natural tissue is the best replacement material, together with the problems of supply logistics, ethics, technique and acceptability, have resulted in several attempts to encourage regeneration of the patient's own tissues. Several years ago, for example, an "artificial" artery was prepared by the implantation of a mandril into tissues and utilizing the fibrous capsule that formed around it, although this was not particularly successful.[13] More recently, porous surfaces and totally porous materials have been employed, which, by manipulation of the pore characteristics can allow tissue ingrowth.[14] This may be used to secure anchorage of an implant to tissue via a porous surface or, when using a degradable porous material, complete tissue regeneration. Since it is usually only connective tissue that is able to regenerate in this way there are significant limitations to this approach and it cannot be used for highly specialized tissue.

The concept of using the biomaterial as a vehicle or matrix to support the growth of natural tissue has been taken in a different direction through the use of biomaterial-supported cells grown in culture. It is possible for certain cells, isolated from tissue and maintained under strictly controlled conditions in the laboratory, to carry out their usual function. If cells are taken from the tissue of a patient and grown in culture to an effective condition and concentration, they may be reimplanted, with an appropriate support, where they can provide an effective 'natural' replacement. This is being used, for example, for an artificial skin, in which epithelial cells from a patient with a major burns injury can be incorporated into a suitable degradable matrix and used in place of a skin graft. Also, endothelial cells may be cultured onto the surface of a vascular prosthesis, which will present a more natural surface to the flowing blood.[15]

A combination of cells and synthetic polymer has also been employed, at least experimentally, for an entirely different reason. The application mentioned above can only work if the cells are derived from the same patient in whom they are to be used because of the problem of the immune response to foreign proteins. If the cells of interest are not readily available in that patient, problems arise. Such a situation is seen in diabetic patients, for example. They do not have the cells that produce insulin, the Islets of Langerhans, and it is not possible to transplant such cells from a donor as they would be recognized as foreign and attacked by the immune defence system. However, it is possible to encapsulate donor cells in a polymeric membrane. If the structural characteristics of this membrane are selected carefully, it can allow the transport of glucose and insulin between the cells and the surrounding tissue, but prevent the passage of the much larger protein molecules of the immune system, inhibiting their immunological rejection.[16] This concept is leading to the development of so-called hybrid artificial organs such as, in this case, the pancreas.

A final approach to be mentioned here involves the surface modification of engineering materials to provide more biologically acceptable interfaces, especially those which attempt to mimic natural interfaces. Most examples are of blood-contacting surfaces.

Blood is a highly complex and sophisticated tissue which in the healthy patient flows through the cardiovascular and peripheral vascular systems without any interaction with the vessel walls. This lack of interaction represents a delicate balance between several events and many factors play a role. One of the more important factors is the relationship between the circulating platelets and the vessel wall.[17] Platelets do not normally interact with the endothelium, largely because the cells release a variety of substances, especially prostacyclin, which inhibit such interactions. If the vessel is damaged, or if a foreign material is placed within the vessel, then the platelets recognize a non-endothelial surface, adhere to it, and initiate a sequence leading to the formation of a clot. While this is a desirable reaction in the case of vessel injury, it is undesirable in the case of a biomaterial implanted within the vascular system for reconstructive purposes. There are many different approaches to controlling these blood interactions, but in one case a synthetic analogue of prostacyclin has been attached to the material surface. Such a surface imitates the natural endothelial surface and prevents platelet deposition.[18]

5. General Conclusions

This brief review has highlighted the major problems of implanting synthetic materials for advanced applications in the human body. If we are to succeed in using materials with greater reliability and more sophisticated performance, we need to face the challenges of developing advanced materials to meet the combined requirements of functional performance and biocompatibility. The more this approach leads to a merging of the concepts of synthetic materials and of natural materials, the better the prospects.

Received: December 19, 1988

[1] D. F. Williams, *Mater. Sci. Technol. 3* (1987) 787.
[2] R. J. Richardson in M. B. Bever (Ed.): *Encyclopedia of Materials Science and Engineering Vol. 5*, Pergamon, Oxford 1988, p. 3610.
[3] D. F. Williams: *Biocompatibility of Orthopedic Implants Vol. 1*, CRC Press, Boca Raton, FL, USA 1986, chapter 1.
[4] S. Espevik, *Annu. Rev. Mater. Sci. 7* (1977) 55.
[5] R. M. Pilliar, G. C. Weatherby, *CRC Crit. Rev. Biocompat. 1* (1985) 371.
[6] P. Griss, G. Heimke in D. F. Williams (Ed.): *Biocompatibility of Clinical Implant Materials Vol. 1*, CRC Press, Boca Raton, FL, USA 1981, chapter 6. See also: G. Heimke, *Adv. Mater. 1989*, 7; *Angew. Chem. Int. Ed.*

Engl. Adv. Mater. 28 (1989) 113; *Angew. Chem. Adv. Mater. 101* (1989) 113.
[7] G. G. Gebelein, F. F. Koblitz (Eds.): *Biomedical and Dental Applications of Polymers*, Plenum Press, New York 1981.
[8] D. F. Williams: Biocompatibility of Tissue Analogs Vols. I, II, CRC Press, Boca Raton, FL, USA 1985.
[9] F. J. Schoen, *J. Biomed. Mater. Res. 21* (1987) Part A, 91.
[10] R. Armstrong, L. S. Cooperman, T. M. Parkinson, K. A. Piez, in J. W. Boretos, M. Eden (Eds.): *Contemporary Biomaterials*, Noyes Publications, Park Ridge, NJ, USA 1984, chapter 25.
[11] M. Jarcho, *Clin. Orthop. 157* (1981) 259.
[12] W. Bonfield in D. F. Williams (Ed.): *Biocompatibility of Tissue Analogs Vol. II*, CRC Press, Boca Raton, FL, USA 1985, p. 89.
[13] C. H. Sparks, *Ann. Surg. 177* (1973) 293.
[14] R. M. Pilliar, *J. Biomed. Mater. Res. 21* (1987) A1.
[15] J. C. Stanley, W. E. Burkel, L. M. Traham, B. Lindblad, *Acta. Chir. Scand. Suppl. 29* (1985) 17.
[16] M. A. Goosen, *CRC Crit. Rev. Biocompat. 3* (1987) 1.
[17] J. M. Anderson, K. Kottke-Marchant, *CRC Crit. Rev. Biocompat. 1* (1985) 111.
[18] C. H. Bamford, I. P. Middleton, K. G. Al-Lamee, *Biochim. Biophys. Acta 924* (1987) 33.

Panel Discussion

Improving Effectiveness in Materials Research

By Gerhard Wegner*

High temperature materials, electronic materials, composites and superconductors are featured as regularly in the business press as in scientific journals. Materials science receives heavy management attention as well as public and political interest worldwide. The Materials Research Society (MRS), founded only a few years ago in the US, is rapidly growing into one of the largest professional societies, with offshoots on other continents. Despite the obvious successes of materials science as a field of industrial relevance and academic concern, the people involved do not seem to be very satisfied. One of the key issues is finding the proper balance between industrial or market driven research and development and the necessity to conduct in depth research of a basic nature to find and understand new materials. This issue is intimately related to the role of industry in defining and supporting research areas in academic institutions. Conversely, the transfer of basic knowledge, new insights and novel methods from the ivory tower of the university to the harsh and competitive ground of the industrial world does not seem to work well and finds many obstacles.

This, in a nutshell, was the content of a panel discussion organized and directed by Du Pont's *Rudolf Pariser*, Director for Advanced Materials Science in the Central Research and Development Center at Wilmington, Delaware, USA. The panel discussion was part of an Advanced Materials Conference celebrating the 50th anniversary of Nylon and the invention of Teflon, both products being cornerstones of the commercialization of polymeric materials.

[*] Prof. G. Wegner
Max-Planck-Institut für Polymerforschung
Jakob-Welder-Weg 11, D-6500 Mainz (FRG)

A Climate of Worldwide Competition and Collaboration

"The climate in Du Pont research is characterized by increasing worldwide competition and collaboration, the globalization of business and the need to respond quickly and specifically to market needs, energy and raw materials resources and environmental issues...", Dr. *Pariser* told the audience of more than 150 invited scientists from US and foreign universities, research institutes and agencies involved in materials science studies.

Du Pont's approach to research and development reflects the change of attitude towards materials science worldwide. As little as ten years ago, the laboratories were organized to emphasize specific polymeric materials, such as elastomers or textile fibers with relatively little interaction between them. Today, research has expanded beyond polymers and includes ceramics and metals as well. The emphasis is on materials systems and systems functionality. New fields are under development based on polymer composites and structural ceramics, inorganic fibers and molecular composites. Thus, an advanced materials laboratory has been created where many materials disciplines are combined into one organization with broad functional research themes. The trend is toward multidisciplinarity among the research staff as well. In addition, Du Pont has a rapidly increasing involvement with US universities. The more than US $ 25 million which were spent by Du Pont in 1988 alone to support university research programs was a substantial part of the total US $ 630 million by which US industry supported R & D at American universities.

Support of academic programs cannot be seen independently from the hiring policy. "We at Du Pont," Dr. *Pariser* said, "have always tried to hire the very best students. We are also emphasizing the ability to collaborate and interact with others, to communicate, and to show a high degree of initiative and self-management." As a policy, Du Pont tries to hire the best students from the classical disciplines, frequently from the top rated universities, despite the fact that these graduates need substantial reeducation and another two or more years further training to adapt to the R & D subjects of industry. Secondly, graduates are hired with specific expertise which is urgently required, for the exploration of polymer composites, thin film techniques or ceramic processing. The contribution of these graduates can be of immediate value but there exists the problem that they may be too specialized and lack the flexibility needed to respond to future challenges.

The rapid development of materials science and its impact on chemical industry obviously requires changes of emphasis in the education of scientists and engineers alike. An interdisciplinary education is absolutely necessary, otherwise the students and graduates will not learn to adapt to the unexpected developments which, for good reasons, are the basis for the further success of industry.

Graduate Education in Materials

What should an active and successful Department of Materials Science look like? How should it be organized? What about the balance between "core" subjects and specialized training programs?

These questions were raised by Dr. *Anthony Evans,* Chairman of the Department of Materials at the University of California, Santa Barbara. As a general philosophy he suggested a multidisciplinary curriculum with three fields of specialization. These, for example, could be:

- Structural materials
  (advanced composites, light weight alloys, tough ceramics)
- Electronic materials
  (compound semiconductors, optoelectronic devices, quantum wells)
- Macromolecular materials
  (high-strength fibers, interfaces, conducting polymers)

Furthermore, training and research projects should be favored, which have the integrated concept of devising a model, testing the properties and establishing the role of processing in the quality control of the materials and devices. This requires substantial investment in capital equipment and continuous support to maintain sophisticated equipment. Among others, the following facilities should be made available for training and research: machinery to process ceramics, metals, and polymer fibers and to prepare surface structures (molecular beam epitaxy); all methods for structure investigation, notably electron microscopy (SEM, TEM etc.) and, last but not least, sufficient computing hardware. Dr. *Evans* also emphasized the role of unconventional industry–university relationships which help to motivate the research students and faculty. Among other suggestions he mentioned "research condominiums," a term which describes a joint university–industry research program in which space, facilities, students and faculty are shared for a certain time to solve a specific but interdisciplinary problem which is of interest to one or more industrial partners. The active participation of researchers from industry in such "research condominiums" is the necessary ingredient which differentiates this from conventional industry supported programs.

The Impact of Government Policies

"The problem of revitalization of civilian R & D effort in the US is compounded by the heavy emphasis on military programs in our federal R & D budget. We spend almost twice as much on the military programs as on civilian efforts, with relatively little payoff in economic terms. This puts us at a significant disadvantage compared to our trading partners." This was one of a number of rather blunt statements by Dr. *John H. Moore,* Deputy Director of the National Science Foundation, describing current trends in the US-federal policy towards science and technology. He greatly deplored the fact that when only civilian R & D is considered, the US rate of investment, at 1.9% of the gross national product (GNP), is only about two-thirds the level of Japan and below that of West Germany and France. On the other hand, Dr. *Moore* reported, there was a major shift of the administration away from supporting applied research and development programs and toward basic research. As a result, basic research now gets about 40% of the non-defensive federal R & D dollar today as opposed to about 23% in 1977. Although the administration and its institutions recognize the importance of basic research as fundamental for further economic development, they also emphasize increased interaction between industry and academia. "We need explicit mechanisms," Dr. *Moore* said, "to make sure that results of our (academic) laboratories flow smoothly into industry." One such mechanism is the establishment of Engineering Research Centers (ERC's). Center topics include combustion processes, biotechnology, process engineering, robotics in microelectronics processing, composite materials and intelligent systems engineering. NSF presently supports 18 ERC's and plans to increase that number.

A Change of Culture is Needed

"University researchers will have to lose any lingering disdain for concern about marketability and profit of their discoveries. They will have to learn that directed research does

not automatically represent a threat to free academic inquiry" said Dr. *Alan Schriesheim,* Director of Argonne National Laboratory and Professor of Chemistry at the University of Chicago, to a somewhat startled audience. He reported on his attempts to increase the sensitivity of the research staff of the Argonne National Laboratory to the commercial potential of their work. One feature was to make patents and R & D awards a legitimate factor in promotion applications along with the traditional scientific publication list. Another feature was the creation of a Technology Transfer Center which became pro-active rather than re-active to commercial opportunity.

The Need of Goal Oriented Basic Research

Effective communication in the materials area is a challenge which requires the interdisciplinary approach illustrated in this issue of Advanced Materials. The Materials Research Society (MRS) has also taken on the challenge by sponsoring multidisciplinary meetings, *Kathleen C. Taylor,* past president of the MRS, told the audience. In addition, the MRS attempts to fill the gap between basic research and application by emphasizing goal oriented basic research. Improved effectiveness in research is reached by fast communication of recent results; however, it is not recommended to abandon peer review which would lead to a rapid decline in the quality of the published reports.

Dr. *Kathleen Taylor* is head of the Physical Chemistry Department at the General Motors Research Laboratory and is thus an expert at considering the needs in materials in the automobile industry. Summarizing the current trends and needs in that industry, she pointed to the increasing importance of plastics and composite materials. Plastics now comprise more than 200 lb of the weight of each vehicle, and when all polymer-based materials are considered including elastomers, paints, adhesives and sealants, this number is 400 lb. Reduction of the production costs in the manufacturing process and the decrease in number of individual parts by integral design is the advantage offered by polymers over conventional materials. The major deficiencies of ceramics as substitutes for metals are still the low reliability caused by brittle failure and the high cost of fabrication.

Another issue is the development of long life batteries, a prerequisite if the electric vehicle is to become a common feature. Fuel cell technology will require that efficient low cost membranes and electrocatalysts become available. Last but not least, it becomes more and more important to predict performance based upon a knowledge of chemical-physical characteristics and operating parameters—a wide open field for theoretical work.

Specialists or Generalists—the Role of Education

Coming back to the initial remarks of Dr. *Pariser* on the role of education and the impact of industry–university relationships in materials science, Harvard's Professor *George M. Whitesides* commented on the function of the universities. The key problem is that it takes a very long time to learn how to educate a good expert in a decent time and that professors are faced with the problem of teaching the right subject. Although being a chaired professor himself, he did not hesitate to remark that professors in general are not amenable to new ideas. He suggested therefore that industry should give preference to assistant professors who are eager to open up their own field of expertise. Professor *Whitesides* emphasized furthermore that if one wants to establish a meaningful interaction between industry and university the motivation must be clear. Finally, technology transfer will never work unless accompanied by the transfer of personnel. He thus called for an increased exchange of personnel over shorter or longer periods between university laboratories and industrial sites.

What is the Message?

Did the panel discussion convey a message to the audience, to the public, to the scientific community? This foreign observer, invited as a guest to participate in the celebration of the 50th anniversary of Nylon and Teflon, was left with mixed feelings. Du Pont deserves applause for the attempt to focus on the intellectual background of commercial enterprises in chemical industry and on the role of basic and academic research for past and present developments of product lines in materials. Many of the statements made by panelists from industry will be taken as encouragement by those who fight for better recognition of materials science as an academic subject in universities and academic circles. On the other hand, no solutions were given—and probably can never properly be given—how to bridge the gap between the needs of industry for more specific research on actual products and processing, and the aspiration of academia to work on very general aspects and laws controlling materials structure and dynamics.

Not too surprising to the foreign guest, the panel discussion was almost entirely centered on the US despite the initial remarks of Dr. *Pariser* on the global issues. Non-US developments were only mentioned in the context of how US industry and the US educational system could maintain leadership in technology and business or regain ground lost in the recent years to Japan or to Europe. The competition by Japan was seen as the major issue by many of the panelists although there are similar problems in this country when it comes to the central point of how materials science and materials science centers can be properly supported, and oriented toward goals worth the money invested.

Overall the panel discussion gave a snapshot of the current state of mind of US materials scientists in industry, universities and academic research centers, and that is certainly helpful for further orientation.

ADVANCED MATERIALS

Book Reviews

From Blood Substitutes to Semiconductors and beyond

Blood Substitutes. Preparation, Physiology and Medical Applications. Edited by *K. C. Lowe*, VCH Verlagsgesellschaft, Weinheim, 1988. 187 pp., bound, DM 168.—ISBN 3-527-26556-2.

The development of a blood substitute and, more generally, an effective injectable oxygen carrier, has become a pressing but considerable challenge. Extensive progress has been achieved in recent years. It is the objective of the multiauthor book edited by *K. C. Lowe* to provide a review of the state of the art in the field. It deals with both simple plasma substitutes for volume restoration and oxygen-delivering fluids, whether the latter are based on hemoglobin or on fluorocarbons as the gas carrier.

In an easy-to-read first chapter, *E. S. Parry* sets the search for O_2-carrying blood substitutes in a historical perspective. The chapter is mainly (ca. 85%) devoted to a detailed up-to-date account of the vicissitudes of the hemoglobin approach since the turn of the century, and of the progress achieved in recent years, but without attempting to minimize the numerous questions and concerns which remain to be answered before human trials can be safely envisaged. The more recent fluorocarbon and synthetic chelate approaches unfortunately receive a much shorter and scantier treatment, with literature coverage up to 1982 only; this leaves out the most recent developments, but the reader will fortunately find these in subsequent chapters.

Chapter 2 by *K. Messmer* is devoted to plasma substitutes for rapid volume restoration after hemorrhage. The author discusses and compares the role, advantages, limitations and adverse effects of isotonic electrolyte solutions, plasma substitutes based on natural colloids prepared from human plasma or placenta, and artificial colloids including dextran, gelatin and hydroxyethyl starch. While plasma substitutes have been used on a routine basis for several decades now, it is shown that there is still room for improvement and that they constitute an active field of research with, for example, the successful development of hapten inhibition of dextran-induced anaphylactic reactions, and exploration of the concept of small volume resuscitation by hypertonic/hyperosmotic solutions.

In Chapter 3 *G. W. Odling-Smee* and *B. G. Wilson* discuss hemoglobin as a blood substitute, and show how successive modifications—pyridoxylation then polymerization—can improve its oxygen-delivering capacity and intravascular persistence, which are both strongly reduced when hemoglobin is extracted from its natural environment. The authors give a brief summary of contradictory reports on the effectiveness and safety of such preparations, and end by stressing the outstanding problems, namely cardiovascular effects and effectiveness in the presence of red cells, which in the authors' opinion need to be addressed before they would recommend them for use in humans.

There follows a too-short chapter by *T. M. S. Chang* which concentrates on microencapsulation of hemoglobin as a way of preserving its oxygen-unloading characteristics, and (again) on cross-linked hemoglobins. A section on toxicity and safety expresses the author's concern about the immunogenicity of the modified crosslinked hemoglobins.

Polymerized pyridoxylated hemoglobins consist, indeed, of complex mixtures of chemically modified materials, difficult to reproduce, and each one of these more or less randomly occurring modifications can be the source of immunogenic problems. The chemist will remain unsatisfied, as none of the three chapters devoted to the modified hemoglobin approach to blood substitutes broaches the central and difficult question of the chemistry involved in these reactions. This is all the more regrettable as the lack of insight into what is really happening to the hemoglobin molecule, as well as the diversity, poor definition and poor reproducibility of the resulting preparations are probable reasons for many contradictory reports.

Turning to the fluorocarbon approach, *J. G. Riess* and *M. Le Blanc* give an authoritative and thoroughly documented account of the state of the art, including the criteria of selection, preparation procedures and properties of fluorocarbons and surfactants, formulation, preparation, characteristics and control of the emulsions. A stringent analysis of the shortcomings of the Fluosol-DA-type first generation of preparations enables them to delineate what research should be done with the aim of improving on this early emulsion. Emphasis is then laid on the advances that have already been achieved with respect to Fluosol-DA. Among these, the discovery of fluorocarbons with much shorter organ dwell time, and the preparation of five times more concentrated and room temperature stable fluid emulsions, are certainly the most remarkable breakthroughs. This strongly consolidates the potential of the fluorocarbon approach to blood substitutes, including use in case of hemorrhagic shock, where the early emulsions had only limited efficacy. Further improvement is shown to depend in large part on the synthesis and

selection of new biocompatible surfactants, more specifically designed for emulsifying fluorocarbons.

A solid chapter by *N. S. Faithfull* discusses the potential of fluorocarbon emulsions in medicine and research. The author's reminder that it is the carrier's oxygen delivering capacity rather than its oxygen dissolving capacity which is important, is welcome. He then emphasizes that the potential of fluorocarbon emulsions goes considerably beyond that of a substitute for blood. Microcirculatory support of the myocardium and central nervous system, use in radiology or for radiosensitization of hypoxic tumors, for organ preservation or during cardiopulmonary bypass, or percutaneous transluminal coronary angioplasty, treatment of respiratory failure, and stimulation of killer macrophages are among the most promising avenues that are being explored. The reader may regret that some of these applications are not discussed in greater depth.

K. C. Lowe left for himself the difficult task of summarizing the biological assessment of fluorocarbon emulsions, which is treated in a meticulous, detailed manner. Particular consideration is given to the uptake of emulsion components into lymphoid tissues and the reticuloendothelial system, and to the consequences these may have on immune defence in the recipients. Unfortunately the greater part of the available data still concern the early fluorocarbon-poor and Pluronic F-68 containing emulsions, Fluosol-DA and Fluosol-43. It will nevertheless be of great use by providing the reader with extensive information and numerous protocols which should prove helpful for evaluating the newer emulsions. The need for improved biocompatibility with respect to Fluosol-DA is indeed high-lighted.

Chapter 8, by *G. M. Vercellotti* and *D. E. Hammerschmidt*, reviews the clinical studies that have so far involved fluorocarbon emulsions. Again these studies concern *solely Fluosol-DA*; the data analyzed highlight the side effects and limitations of this particular preparation. These are by no means representative and cannot be extrapolated to other fluorocarbon emulsions. The authors then discuss the possible mechanisms for the adverse reactions noted with Fluosol-DA, and show that they can be assigned primarily to complement activation by Pluronic F-68, the main surfactant used in this preparation. As a result they call for the development of emulsions with a lower ability to activate plasma complement.

On the whole, *Lowe*'s book, in spite of some omissions (the chemistry of modified hemoglobin, for example) and repetitions (the compositions of Fluosol-DA is given no less than three times), inevitable in such a multi-author enterprise, reaches its objective. It is timely and useful—useful as it summarizes a considerable amount of recent information in a relatively small, compact volume—timely in view of the increasing demand for substitutes for blood, triggered by increased difficulties of transfusion, and also because the decisive breakthroughs that have recently been achieved, especially in the fluorocarbon approach, should lead to new preparations now becoming available for research.

There are few typographical errors in the text; the same is unfortunately not true of the chemical formulas and equations, which sadly appears to be a common fault in medically-oriented books.

Pierre Vierling
Department of Chemistry
University of Nice-Sophia Antipolis (France)

Electrons in Solids: An Introductory Survey. By *R. H. Bube*. Academic Press Inc., San Diego 1988. xiv, 315 pp., bound, $ 39.50.—ISBN 0-12-138552-3

The book is intended as an introductory survey for students with a background in materials science or other engineering disciplines. This is explicitly stated by the author in the preface to the first edition. The second edition has been updated in some chapters by including recent developments, and an additional chapter on "sample problems" has been included in the appendix.

The presentation is clear and supported by very good illustrations. Since the reader is not expected to have a knowledge of electrodynamics, quantum mechanics or basic solid state physics, the author has to cover a lot of ground before he can present the facts on various properties of solid state materials. In the first chapters he therefore has to give a short description of the above mentioned basic physics. After having discussed the general properties of waves in Chapters 1 and 2, he continues by describing lattice waves and light waves in Chapters 3 and 4. The usual examples of quantum mechanics are described in Chapter 5, and in the next two chapters the simplest models of solids are presented, namely the free electron model and the tight binding description. In the second half of the book we find the main topic, with chapters on optical, electrical and magnetic properties, and an additional chapter on junctions between different materials.

The treatment contains a good mixture of phenomenological descriptions, formal presentations of basic formulas, and comparison with experimental results. Nevertheless, I have the feeling that a student reading Chapter 4, for example, where on 14 pages the Maxwell equations are presented, may have difficulties in really understanding these basic equations. A good list of further references including textbooks on this subject should at least have been provided. The same problem for the reader might also arise with the topics in the other six introductory chapters.

The second half of the book discusses a quite extensive list of properties of the solid state, and again the clarity of the presentation is to be admired. The chapter on optical properties presents an overview of the various absorption processes. Unfortunately, there is no discussion on new developments, e.g. on various aspects of laser physics. The next chapter on electrical properties discusses the basic relaxation

mechanism in semiconductors, and a few pages are devoted to effects in superconductors. A topic of special interest for students in engineering science is presented in the chapter on junctions between various materials. The new and interesting properties of quantum wells and superlattices are only briefly touched on, and there is no discussion of the quantum Hall effect, for example. A final chapter on magnetic materials presents some basic facts on diamagnetism and ferromagnetism, and also includes a discussion of new magnetic materials. Looking through these chapters the question again arises whether a student in the engineering disciplines will really obtain a basic understanding of the various phenomena. I therefore suggest that further references to textbooks and original literature should be included at the end of each chapter.

The appendix includes useful formulas, as well as the above mentioned discussion of problems, which I think are very helpful for students. The list of problems at the end of the book is also attractive.

The book can be recommended for undergraduates with an engineering background, as a suitable introductory text on solid state physics. However, in teaching such a course one should give the students further material for background reading in the various topics.

Helmut Büttner
Physikalisches Institut
der Universität Bayreuth (FRG)

Optical Nonlinearities and Instabilities in Semiconductors. Edited by *H. Haug*. Academic Press, San Diego 1988. xi, 440 pp., bound, $ 65.—ISBN 0-12-332915-9

The investigation of optical nonlinearities in semiconductor materials and devices has recently become a field of rapidly increasing interest, mainly due to possible applications in optical data processing. Most important for these applications are the so called "resonance enhanced" nonlinear optical processes, which occur when the photon energy of the optical field is close to an electronic resonance of the semiconductor material, e.g. the fundamental band edge. According to the editor's statement in the introduction, the present book attempts to bring together all the investigations of the resonance enhanced nonlinear optical properties of semiconductors and their manifestation in optical instabilities. In the reviewer's opinion, this attempt has been highly successful.

The book contains 16 independent review articles on different, partly related topics, written by different authors, together with an introduction by the editor which contains some historical comments and a brief summary of the definitions and concepts employed to describe the nonlinear effects. The list of authors includes many leading scientists representing some of the most active laboratories in the field.

Most of the articles are devoted to optical nonlinearities due to electronic processes in semiconductors, including free carrier effects such as band filling, band gap shrinkage and inter-band absorption, as well as excitonic nonlinearities; however, thermally induced optical nonlinearities are also discussed (e.g. the contribution by *Wherret, Walker* and *Tooley*). Special attention is also paid to nonlinear phenomena in electronic systems with reduced dimensionality, as in semiconductor quantum well structures, and to optical nonlinearities in semiconductor devices, in particular semiconductor lasers.

The combination of theoretical and experimental work is one of the special features of this book. Fortunately, experiment and theory are not treated separately; instead, a close connection is maintained throughout the book, by means of jointly written reports, and careful arrangement of the respective papers.

The theoretical contributions cover fundamental topics such as the microscopic theory of optical band edge nonlinearities (*Haug*), the theory of dense nonequilibrium exciton systems (*Schäfer*), the nonlinear optical properties of semiconductor quantum wells (*Chemla, Miller* and *Schmitt-Rink*), including electric field effects as well as more device orientated problems such as the theoretical description of optical instabilities in semiconductors (*Koch*).

The experimental data collected in the present book cover bulk phenomena in different II–VI compounds, including semiconductor doped glasses (*Klingshirn, Peyghambarian* and *Gibbs*), exciton and biexciton processes in III–V (*Ulbrich*) and II–VI semiconductors (*Levy, Hönerlage* and *Grun*), optical phase conjugation (*Claude, Chase, Hulin* and *Mysyrowicz*), electronic transport (*Mahler, Kuhn, Forschel* and *Hillmer*), and some of the most recent results on optical nonlinearities in quantum well structures (*Chemla* et al.; *Miller* et al.; *Peyghambarian* et al.).

Device applications are described in several reports; in particular, self-electro-optic effect devices (SEED) based on electric field induced nonlinearities in quantum wells (*Miller* et al.), as well as bulk semiconductors (*Jäger* and *Forsmann*) are discussed. Finally, semiconductor lasers—which are essentially nonlinear optical devices—are considered in detail, including optical bistability in laser amplifiers (*Adams, Westlake* and *O'Mahony*), semiconductor lasers (*Harder* and *Yariv*), and higher order instabilities in semiconductor lasers, including chaotic emission (*Shore* and *Rozzi*).

The book provides a comprehensive overview of the basic physics and device applications of resonance enhanced nonlinear optical phenomena in semiconductors at a high scientific level. It is mainly addressed to research students and active research workers in this area, and for them this book will be indispensable.

Ernst O. Göbel
Fachbereich Physik
der Universität Marburg (FRG)

Rubberlike Elasticity—A Molecular Primer. By *J. E. Mark* and *B. Erman*. Wiley, Chichester 1988. viii, 196 pp., bound, £ 23.70.—ISBN 0-471-61499-8

This book is written by two former coworkers of the late *P. J. Flory*, and both of them are very active and highly esteemed scientists in the field of polymer networks. One of them (*J. E. Mark*) has developed new synthetic concepts for 20 years to obtain cross-linked materials with new and unconventional properties, the other (*B. Erman*) has specialized in problems concerning the theoretical description of rubber-like elasticity. However this book is not designed for experts in the area. Its approach is more that of an introductory course for chemists or engineers who wish to be confronted with the fundamental aspects of rubber-like elasticity and its molecular origin.

The first part of the book can be understood if the reader is familiar with some basic concepts of physical chemistry. Here, some rubber-like materials are presented and typical problems concerning network structure and routes of preparation are discussed. The basic theoretical concepts are presented without claiming completeness. Most of the logical steps are accompanied by references which simplify a reworking for readers with deeper interests. At the end of the first part, the dependence of the elastic force on deformation, temperature and structure is presented by means of typical examples of the authors' work. By reading through these chapters one becomes familiar with strain experiments and their physical meaning.

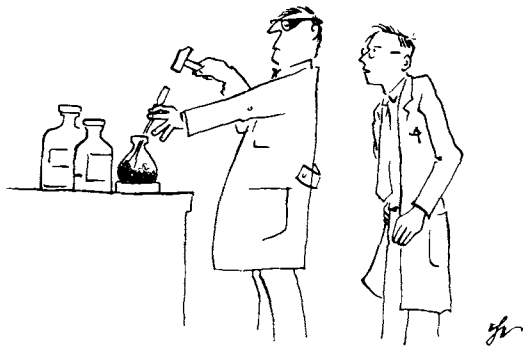
The purpose of part B of the book is completely different. Here, the authors wish to confront modern topics of network research, both new synthetic concepts and new methods for the characterization of network properties. This is very hard to realize, especially in a compressed and popular form, and consequently some of the chapters presented are fragmentary, (e.g. the treatment of neutron scattering experiments on networks) and a couple of modern developments are missing completely. However, the presentation of the authors' recent work in this area, for instance the treatise of bimodal networks and filled elastomers is convincing. Hence it should be regarded as a very personal point of view of the future of cross-linked materials.

However, in my opinion a good opportunity to give more detailed information to a readership with deeper interests has been missed. The later chapters are unbalanced in proportion, and their title "additional topics" may be misunderstood as an unstructured enumeration of sometimes very impressive, but sometimes not worked out, concepts. The textbook character of the first part should not be transfered to the second part. The very personal view-point of "modern topics" must be underlined, and with this understanding one can even enjoy some of the exceptionally elegant ideas which are presented. It is up to the readers with broader interests to complete their information with other publications.

In my opinion the book is not the missing textbook on polymer networks but it is a brief and stimulating introduction to this area of polymer materials. It can be recommended to all scientists who wish to learn something about networks without the necessity of a detailed discourse on special problems in research.

Markus Antonietti
Institut für Physikalische Chemie
der Universität Mainz (FRG)

Call for Short Communications · Call for Short Communications · Call for Short Communications



... doesn't melt, won't dissolve, just can't be broken down – let's send it to ADVANCED MATERIALS!

ADVANCED MATERIALS publishes short communications starting in June. Peer review, a wide circulation and short publication times are guaranteed. Please submit manuscripts or write for instructions for authors to:
ADVANCED MATERIALS · Editorial Office · P.O. Box 101161 · D-6940 Weinheim · Federal Republic of Germany

Call for Short Communications · Call for Short Communications · Call for Short Communications

Conference Calendar

June 1989

12–15 **Narrow-Gap Semiconductors and Related Materials**
Int. Conf.
Ogunquit (USA)
Contact: D. G. Seiler, Phys. Dept., Univ. of North Texas, P.O. Box 5368, Denton, TX 76203, USA

12–16 **Advanced Materials Chemistry Conf.**
St. Augustine (FL, USA)
Contact: Prof. R. S. Drago, Dept. of Chem., Univ. of Florida, Gainesville, FL 32611, USA

13–14 **Nonlinear Optical Polymers for Soldier Survivability**
Science Symp.
Natick (USA)
Contact: Th. Sklarsky, US Army Natick RD + E Center, Attn: STRNC-EMP, Natick, MA 01760-5014, USA, Tel. 508-651-4687

18–21 **Colloid & Surface Science**
63rd ACS Div. of Colloid & Surface Chem. Symp.
Seattle (USA)
Contact: J. Berg, Dept. of Chemical Eng. BF-10, Univ. of Washington, Seattle, WA 98105, USA

18–23 **Ceramic Materials and Production Methods**
1st Conf. of the Eur. Ceramic Soc. and Fair
Maastricht (Netherlands)
Contact: Mrs. L. M. J. Bos, P.O. Box 1630, 6201 BP Maastricht, Netherlands

19–21 **Composites**
Asia-Pacific 89
Adelaide (Australia)
Contact: The Secretariat, Techsearch, Composites Asia-Pacific '89, P.O. Box 2471, Adelaide S.A. 5001, Australia

20–21 **Modern Magnetic Materials**
Conf. and Exhibit. London (UK) Contact: S. Taylor, ERA Technology Ltd., Cleeve Rd., Leatherhead, Surrey KT22 7SA, UK



20–22 **SAMPE**
3rd Int. Electronics Conf.
Los Angeles (USA)
Contact: M. Smith, Business Director, SAMPE, P.O. Box 2459, Covina, CA 91722, USA, Tel. 818-331-0616

21–23 **Chemically Modified Surfaces**
Midland (USA)
Contact: W. T. Collins, Dow Corning Corp., Mail Stop C41C00, Midland, MI 48686, USA

21–23 **Electronic Materials**
Cambridge (USA)
Contact: The Metallurgical Soc., 420 Commonwealth Dr., Warrendale, PA 15086, USA

22–25 **Optics Asia '89**
Singapore (Singapore)
Contact: Asia '89, 994 Bendemeer Rd., N° 04-03, Singapore 1233, Singapore

25–29 **Composite Materials for High Temperature, Fundamental Principles and Performance**
Jerusalem (Israel)
Contact: Mrs. S. Cahana, Ministry of Sci. and Developm., P.O. Box 18195, 91181 Jerusalem, Israel

25–30 **Solid State Sensors and Actuators (Transducers-5)/ Eurosensors III**
Montreux (Switzerland)
Contact: COMST S.A., P.O. Box 415, CH-1001 Lausanne 1, Switzerland

26–28 **Molecular Design of Functional Polymers**
IUPAC Int. Symp.
Seoul (Korea)
Contact: IUPAC Int. Symp., c/o Polymer Soc. of Korea, Rm. 601, Hyecheon Bldg., 831 Yeoksam-dong, Kangnam-ku, Seoul 135-792, Korea

26–28 **Coherence and Quantum Optics**
Conf.
Rochester (USA)
Contact: L. Mandel, Univ. of Rochester, Dept. of Physics, Rochester, NY 14627, USA, Tel. 716-275-4361

26–30 **Solid State Chemistry**
2nd Int. Symp.
Pardubice (Czechoslovakia)
Contact: Dr. L. Koudelka, Inst. of Chem. Technol., Leninovo nam., 565, CS-53210 Pardubice, Czechoslovakia

26–30 **Supermembranes**
Trieste (Italy)
Contact: Int. Ctr. for Theoretical Physics, P.O. Box 586, I-34100 Trieste, Italy

26–30 **Ion Beam Analysis (IBA-9)**
Int. Conf.
Kingston (Canada)
Contact: J. F. Ziegler, IBM Research, POB 66, Hannover St., Yorktown Heights, NY 10598, USA

27–28 **Polymer Latex III**
London (UK)
Contact: Miss M. Peacock, Plastics and Rubber Inst., 11 Hobart Place, London SW1W 0HL, UK

28–30 **Chemically Modified Oxide Surfaces**
Midland (USA)
Contact: W. T. Collins, Mail Stop C41C00, Dow Corning Corp., Midland, MI 48686-0994, USA

July 1989

2–7 **Solid State Organic Materials**
9th Int. Conf.
Como (Italy)
Contact: Centro di Cultura Scientifica, "A. Volta", Villa Olmo, Via Cantoni 1, I-22100 Como, Italy

3–6 **Conduction and Breakdown in Solid Dielectrics**
3rd Int. Conf. (ICSD '89)
Trondheim (Norway)
Contact: Prof. Sletbak, ICSD '89, The Norwegian Inst. of Technol., Sem Sælands V 13, N-7034 Trondheim, Norway

3–7 **Martensitic Transformations**
Int. Conf. ICOMAT-89
Sydney (Australia)
Contact: N. Kennon, Dept. of Metallurgy and Materials Eng., Univ. of Wollongong, Wollongong, NSW 2500, Australia

3–8 **Light-Sensitive and Conducting Polymers**
Leipzig (German Dem. Rep.)
Contact: Prof. H. K. Roth, TH Leipzig, Sekt. Naturwissenschaften, P.O. Box 66, DDR-7030 Leipzig, GDR

3–28 **Liquids, Freezing and the Glass Transition**
NATO Adv. Study Inst.
Les Houches (France)
Contact: École d'Été de Physique Théorique, F-74310 Les Houches, France

4–7 **Nonlinear and Electro-Optics**
Int. Conf.
Cambridge (UK)
Contact: The Meetings Officer, The Inst. of Physics, 47 Belgrave Square, London SW1X 8QX, UK

9–14 **Scanning Tunneling Microscopy/Spectroscopy**
4th Int. Conf.
Oarai (Japan)
Contact: O. Nishikawa, The Graduate School of Nagatsuta, Tokyo Inst. of Technol., 4259 Nagatsuta, Midori-ku, Yokohama 227, Japan

9–14 **Zeolites**
8th Int. Conf.
Amsterdam (Netherlands)
Contact: M. Laboushere, 792 Keizersgracht, 1017 EC, Amsterdam, The Netherlands

Materials Related Gordon Research Conferences

General Information

Contact: Dr. A. M. Cruickshank, Director, Gordon Research Conf., Gordon Res. Ctr., Univ. of Rhode Island, Kingston, RI 02881-0801, USA
Locations: Colby-Sawyer College (N), (S): New London, NH;
New Hampton School: New Hampton, NH;
Kimball Union Academy: Meriden, NH;
Tilton School: Tilton, NH

June 1989

19–23 **Catalysis**
Colby-Sawyer College (N)
Chairman: L. D. Schmidt

26–30 **Polymers**
Colby-Sawyer College (N)
Chairman: J. P. Kennedy

July 1989

3–7 **Fiber Science**
Colby-Sawyer College (N)
Chairman: B. C. Goswami

3–7 **Thermosetting Polymers**
Colby-Sawyer College (S)
Chairman: N. J. Johnston

10–14 **Elastomers**
Colby-Sawyer College (N)
Chairman: G. Ver Strate

10–14 **Metal Hydrides**
Tilton School
Chairman: F. D. Manchester

17–21 **Corrosion**
Colby-Sawyer College (N)
Chairman: H. J. Grabke

17–21 **Chemistry at Interfaces**
Kimball Union Academy
Chairman: R. Johnson

17–21 **Superconducting Films**
Tilton School
Chairman: D. Gubser

31–4 **Ion-Containing Polymers**
Colby-Sawyer College (S)
Chairman: G. Wilkes

August 1989

7–11 **Physical Metallurgy**
Tilton School
Chairman: J. C. Williams

14–18 **Studies in Solid-State Ceramics**
Colby-Sawyer College
Chairman: U. Chowdhry

14–18 **Science of Adhesion**
New Hampton School
Chairman: R. A. Pike

10 **Bonding and Repair of Composite Materials**
Birmingham (UK)
Contact: John Herriot, Butterworth, P.O. Box 63, Westbury House, Bury St., Guildford GU2 5BH, UK

10–12 **Appl. Organomet. Chem.: an Entry to the New Technology**
The Pines Resort (Australia)
Contact: Dr. A. F. Masters, School of Chemistry, Univ. of Sydney, Sydney, N.S.W. 2006, Australia

10–13 **Magnetic Resonance in Polymers**
9th Spec. Colloq. Ámpere
Prague (Czechoslovakia)
Contact: P. M. M. Secretariat, c/o. Inst. of Macromol. Chem., Czech. Acad. of Sci., 16206 Prague, Czechoslovakia

10–14 **Ion Sources**
Int. Conf.
Berkeley (USA)
Contact: W. O'Connor, Lawrence Berkeley Lab., 50B-2270, Berkeley, CA 94720, USA, Tel. 415-486-6386, Fax 415-486-7000

10–14 **Electron Spectroscopy**
4th Int. Conf.
Honolulu (USA)
Contact: G. E. McGuire, Microelectronics Ctr. of North Carolina, P.O. Box 12889, Research Triangle Park, NC 27709, USA

10–14 **Organic Coatings Science and Technology**
15th Int. Conf.
Athens (Greece)
Contact: Dr. A. V. Patsis, Inst. in Materials Sci., State Univ. of New York, New Paltz, NY 12561, USA

11–14 **Numerical Analysis of Semiconductor Devices and Integrated Circuits**
6th Int. Conf.
Dublin (Ireland)
Contact: J. J. H. Miller, Nase-Code Conf., INCA, P.O. Box 2, Dún Laoghaire, Ireland

12–14 **Solid-State Laser/Optical Fiber Science and Electromagnetic Theory '89**
Top. Mtg./Sino-Japanese Joint Mtg.
Beijing (P.R. China)
Contact: Optical Soc. of America (OSA), 1816 Jefferson Pl. NW, Washington, DC 20036, USA

16–21 **Catalysis**
Eur. Conf.
Berlin (West)
Contact: Prof. G. Ertl, Fritz-Haber-Inst. der Max-Planck-Gesellsch., Faradayweg 4–6, D-1000 Berlin

17–20 **Polymer Blends**
Prague (Czechoslovakia)
Contact: P. M. M. Secretariat, c/o. Inst. of Macromol. Chem., Czech. Acad. of Sci., 16206 Prague, Czechoslovakia

18–20 **Polymer Chemistry: Aspects of Radical Polymerization**
Lancaster (UK)
Contact: Dr. J. R. Ebdon, Dept. of Chemistry, Univ. of Lancaster, Lancaster LA1 4YA, UK

18–21 **Integrated Optics and Optical Fiber Communications**
7th Int. Conf. (IOOC-7)
Kobe (Japan)
Contact: P. W. Shumate, Jr., Bell Communications Research, 435 S St., Morristown, NJ 07960, USA

23–24 **Computer-Aided Materials Characterization**
Int. Symp.
Charlotte (USA)
Contact: R. Biederman, Worcester Polytechn. Inst., Worcester, MA 01609, USA, Tel. 508-831-5453/5346

23–28 **Materials and Mechanisms of Superconductivity: High-T_c Superconductors**
Int. Conf. (HTSC-M^{2}S)
Stanford (USA)
Contact: Dr. T. H. Geballe, Dept. of Applied Phys., Stanford Univ., Stanford, CA 94305, USA

24–26 **Micro-Optics/Gradient-Index Optical Imaging Systems**
2nd Conf./8th Top. Mtg.
Tokyo (Japan)
Contact: K. Iga, Tokyo Inst. of Technol., Research Lab. of Precision Machinery and Electronics, 4259 Nagasuta, Midori-ku, Yokohama 227, Japan

Registered names, trademarks, etc. used in this journal, even when not marked as such, are not to be considered unprotected by law.

© VCH Verlagsgesellschaft mbH, D-6940 Weinheim, 1989. – Printed in the Federal Republic of Germany by Konrad Triltsch Druck- und Verlagsanstalt Würzburg.

All rights reserved (including those of translation into foreign languages). No part of this issue may be reproduced in any form — by photoprint, microfilm, or any other means — nor transmitted or translated into a machine language without written permission from the publishers. Only single copies of contributions, or parts thereof, may be made for personal use. This journal was carefully produced in all its parts. Nevertheless, authors, editors and publisher do not warrant the information contained therein to be free of errors. Readers are advised to keep in mind that statements, data, illustrations, procedural details or other items may inadvertently be inaccurate.

Valid for users in the USA: The appearance of the code at the bottom of the first page of an article (serial) indicates the copyright owner's consent that copies of the article may be made for personal or internal use, or for the personal or internal use of specific clients. This consent is given on the condition, however, that the copier pay stated per-copy fee through the Copyright Clearance Center, Inc. (CCC), for copying beyond that permitted by Sections 107 or 108 of the U.S. Copyright Law. This consent does not extend to other kinds of copying, such as copying, for general distribution, for advertising or promotional purposes, for creating new collective works, or for resale. For copying from back volumes of this journal see 'Permissions to Photo-Copy: Publisher's Fee List' of the CCC.

Editorial office: Postfach 10 11 61, D-6490 Weinheim, Federal Republic of Germany, Telephone (06201) 60 22 55, Telex 465 516 vchwh d, Telefax (06201) 602 328.

Editor: *Peter Gölitz*

Associate Editor: *Peter Gregory*

Publishers: VCH Verlagsgesellschaft mbH. (Managing Director: *Hans Dirk Köhler*), Pappelallee 3, D-6940 Weinheim, Federal Republic of Germany.

Advertising office (Advertising Manager *R. J. Roth*): Postfach 10 11 61, D-6940 Weinheim, Federal Republic of Germany, Telephone (0 62 01) 60 61 30, Telex 467 155 vchwh d, Telefax (0 62 01) 606 184.

ANGEWANDTE CHEMIE

International Edition in English

Volume 28 · Number 6
June 1989
Pages 677–828

The Search for Highly Colored Organic Compounds

By Jürgen Fabian* and Rudolf Zahradník*

Until now the study of organic compounds in which the π-electron system is excited by absorbed light has been mainly concentrated on the ultraviolet and visible regions of the electromagnetic spectrum. Various new applications, such as the use of conjugated organic compounds as dye lasers or as materials for storing information with the help of diode lasers, led to the synthesis of new compounds which absorb light in the near infrared (NIR). It is possible to use structure–color relationships to predict the properties of such new compounds when they belong to dyestuff classes which have already been studied in detail; in this case the approach involves decreasing the energy difference between the ground state and the first excited state. A less conventional starting point is provided by molecular structures in which from the outset there is only a very small energy difference between the lowest-energy electronic states; such diradicaloid molecules occupy a special position among the various types of organic compounds. It is possible by means of suitable structural modification to stabilize such molecules in a singlet form which absorbs light at very long wavelengths (i.e. at small wave numbers).

1. Introduction

During its history of more than a century color chemistry has produced thousands of colored molecules; today these are used in many fields other than as textile colorings. Over the last twenty years research has been concentrated mainly on dyes with specific and optimized properties ("tailormade dyes"). Theoretical methods have been used increasingly in pursuing this goal: complex syntheses are attempted only when the required spectral properties are to be expected on the basis of either empirical experience or theoretical considerations.[1] While the need for compounds which absorb at long wavelengths ("deeply colored" compounds) initially involved blue and green textile dyes, much more attention has been paid recently to non-textile dyes which absorb at wavelengths even longer (more "bathochromic") than those typical for known substances. These compounds have an absorption band at the boundary of the visible region (ca. 750 nm) and in the neighboring area of the near infrared (above 750 nm). If the wavelengths usually used by organic chemists and color chemists[2] are converted into the physically more appropriate wave numbers (these are proportional to the energy), then the spectral region of interest lies at wave numbers below ca. $\tilde{\nu} \approx 1.33\ \mu m^{-1}$ (see Fig. 1). Such compounds can serve as receptors for infrared light or as NIR dye lasers.[3] The former are used in the manufacture of optical storage disks which react to light emitted in the near infrared at ca. 800 nm either by cryptoion lasers[4a] or by the particularly economical semiconductor (GaAs or GaAlAs) lasers.[4b, 4c] The application of organic NIR dyes in the following areas is also being studied: in liquid crystal displays,[1a, 5a] in the photosemiconductor layer of laser printers,[5b] as absorbers in laser filters[1a] or in plasts in plant

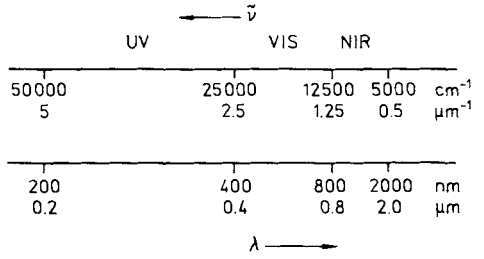


Fig. 1. The ultraviolet (UV), visible (VIS) and near infrared (NIR) spectral regions in wave number ($\tilde{\nu}$) and wavelength (λ) units.

[*] Dr. J. Fabian
Sektion Chemie der Technischen Universität Dresden
Mommsenstrasse 13, DDR-8027 Dresden (GDR)

[**] Dr. R. Zahradnik
J. Heyrovský-Institut für Physikalische und Elektrochemie
der Tschechoslovakischen Akademie der Wissenschaften
Dolejškova 3, CS 182 23 Prag 8 (Czechoslovakia)

 © VCH Verlagsgesellschaft mbH, D-6940 Weinheim, 1989 0570-0833/89/0606-0677 $ 02.50/0

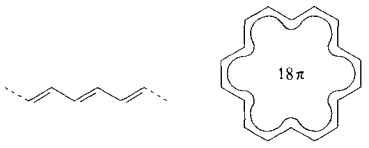
chemistry,[5c] as photochemotherapeutic agents[6] and as fluorescence dyes in HPLC laser fluorimetry.[7] The number of compounds available for such applications is at present very limited.

Known dyes have shown themselves to be suitable starting points in the search for compounds which absorb at extremely long wavelengths; they can be dealt with on the basis of either empirical experience or theoretical knowledge.[1] However, as we shall show in this article, it is also possible to begin from a completely different conceptual starting point: in this approach we shall consider diradicaloid compounds and vary their molecular structure in order to obtain compounds which absorb at long wavelengths.

Some examples will show that the conventional approach can also lead to the same compounds with absorption bands at long wavelengths. We should therefore commence by stating that the change in the reference point and in the point of view is intended less as a new type of classification of the deeply colored compounds than as a method for stimulating chemical intuition in the search for deeply colored systems.

2. On the Long-Wavelength Absorption of Some Conjugated Organic Compounds

In the course of studies on linear and cyclic conjugated hydrocarbons it has been observed that the absorption wavelength cannot be increased beyond a certain limit simply by increasing the size of the π-electron system: thus, the absorption maximum in carotenoid polyenes is shifted only up to ca. 600 nm.[8] The color of a film of pure *trans*-polyacetylene **1**, which is a unidimensional solid, varies between copper-red and blue;[9a] while the absorption coefficient increases rapidly below ca. 900 nm, even here the absorption maximum lies at only ca. 650 nm.[9b] In the case of the aromatic [18]annulenes **2** the long-wavelength absorption shoulder just reaches into the near infrared:[10] however, no absorption band at longer wavelengths is observed when the ring size is increased.[11]

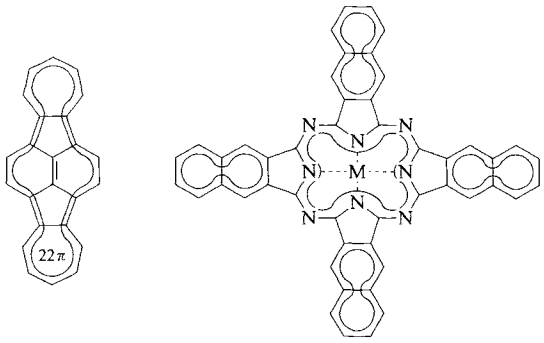


1 **2**

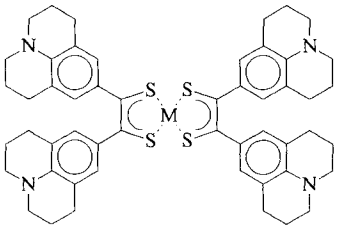
1: $\lambda \approx 650$ nm/$\tilde{\nu} \approx 1.53$ μm^{-1}, as a film [9b]
2: 768 nm/1.30 μm^{-1} (lg $\varepsilon = 2.15$), in chloroform [10].

The failure of the absorption wavelength to increase further in long-chain polyenes and large-ring annulenes is considered to be due to a localization (fixation) of the conjugated bonding system in bonds with preponderantly single or double bond character. This bond fixation is interpreted as an electron-vibration interaction of the molecule (Jahn-Teller distortion) or as an electron-photon interaction of the solid (Peierls distortion).[12a] Theoretical studies have shown that the properties of long-chain polyenes are determined by electron correlation effects.[12b, 12c] In the case of ring systems the bond fixation corresponds to the loss of the delocalization of the conjugated bonding system present in benzene ([6]annulene) and still present to a large extent in [18]annulene. In addition, various configurations are possible for larger rings, non-planar arrangements often being preferred.[11b] However, even when the molecule is forced into a nearly planar configuration by a transannular bond or by substituents,[13, 14] NMR spectroscopy has shown that the higher annulenes become increasingly polyenic. This has again been demonstrated recently in a comparison between a structurally partially fixed [38]annulene[14] and smaller rings in the same series. The loss of the benzenoid ("aromatic") character with increasing ring size is in agreement with theoretical considerations.[12b, 15]

However, cyclic hydrocarbons with a fixed geometry which favors electron delocalization do indeed exhibit absorption bands which lie in the infrared region (e.g. **3**[16]): in this connection we should mention the tetraazaporphyrins, which are related to [18]annulene,[5b, 17a] thus in compound **4** a central metal atom is incorporated into a rigid structure. Long-wave absorptions are also observed for other metal chelates. Dithiolenes such as **5** absorb in the visible or near infrared,[17b-d] and in suitable solvents even up to 1400 nm.[17c] In these planar complexes the transition metal forms part of the π-system; the absorption band of longest wavelength is due to a $\pi \rightarrow \pi^*$ transition.[18]



3 **4**

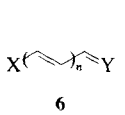


5

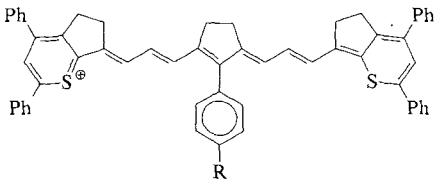
3: $\lambda = 900-1500$ nm/$\tilde{\nu} = 1.11-0.71$ μm^{-1} [16];
4: M = AlOH: 1204 nm/0.83 μm^{-1}, in acetyl chloride/$AlBr_3$ [17a];
5: M = Ni: 1298 nm/0.77 μm^{-1} (lg $\varepsilon = 4.68$), in dichloroethane [17c].

The polymethines **6** provide a general entry to extremely deeply-colored systems; polymethines differ from the polyenes **1** in that one of the terminal carbon atoms carries a donor group and the other an acceptor group. In this case we are dealing with meropolymethine dyes, merocyanines **6a** or, when the end groups are equivalent, with cyanine dyes (**6b**)

or oxonol dyes (**6c**).[8] The parent compounds for these three series are the streptopolymethines **6** and **7**.



6

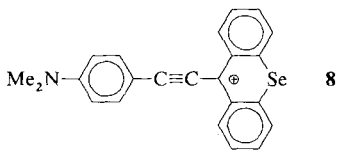


7

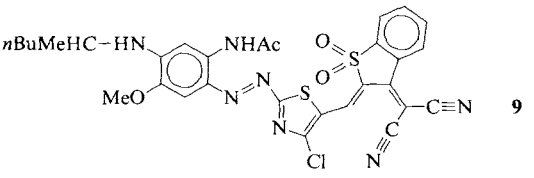
6a: X = NR_2; Y = O; **6b**: X = Y = $NR_2^{1/2\oplus}$; **6c**: X = Y = $O^{1/2\ominus}$;
7a: R = H: λ = 1500 nm/$\tilde{\nu}$ = 0.66 μm^{-1}, in dichlorobenzene [20b];
7b: R = $NHMe_2^{\oplus}$: 1500 nm/0.66 μm^{-1} (lg ε = 4.75) in dichloromethane [20c].

A large number of relatively stable NIR dyes has been made available by incorporating suitable cyclic end groups and by using methylene groups to stiffen the polymethine chains;[20] in the case of the polymethines **7** the absorption band lies at 1500 nm.[20b, c] While at present no upper limit for the absorption wavelength of the polymethine dyes is apparent, a limiting wavelength is expected for the unidimensional solid; this will depend on the end groups present.[21]

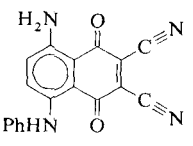
NIR dyes can also be found in other types of compounds which, though formally related to the polymethine dyes, traditionally form separate classes of dyes. These include the xanthenylium, thioxanthenylium and selenoxanthenylium dyes (e.g. **8**),[22] azo dyes (e.g. **9**),[23] naphtho- and anthraquinones (e.g. **10**),[5c, 24] indophenols and analogues (e.g. **11**)[25a] and other merocyanine-like dyes.[25b, c]



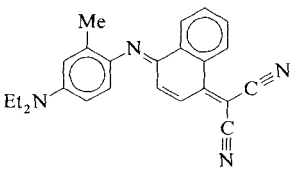
8



9



10



11

8: λ = 802 nm/$\tilde{\nu}$ = 1.25 μm^{-1} (lg ε = 4.93), in chloroform [22];
9: 778 nm/1.29 μm^{-1} (4.92), in dichloromethane [23];
10: 760 nm/1.32 μm^{-1}, in cyclohexane [24a];
11: 761 nm/1.31 μm^{-1} (4.49), in chloroform [25a].

The preparation of these and other dyes[26] was made easier by the application of quantum-chemical models and computation methods, in which a known chromophore structure was modified either in totality or as a linked donor-acceptor system. The theoretical estimation of the color-determining $\pi \rightarrow \pi^*$ transitions involved the use of a topological approach on the basis of the Hückel MO method, and also in some cases graph theory;[27] however, the main tool was the Pariser-Parr-Pople [PPP] method.[1a, 8b]

Since the color-determining electron transition in polymethines is very well described as a transition between the highest occupied MO (HOMO) and the lowest unoccupied MO (LUMO), qualitative approaches for decreasing the spectral excitation energy often involve diminishing the energy difference between the frontier orbitals (Fig. 2, left-hand

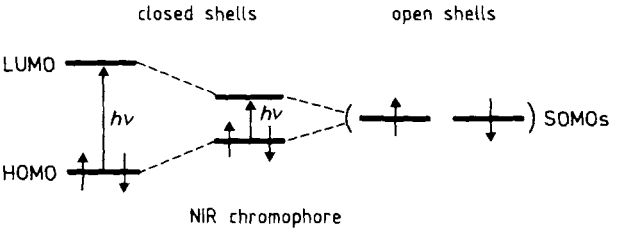


Fig. 2. HOMO-LUMO energy separation and spectral excitation energy of singlet configurations. SOMO = singly occupied molecular orbital.

side); even the simplest perturbation theory considerations can be very useful for this purpose.[8a] As the HOMO-LUMO energy difference decreases, so also does the spectral excitation energy; thus the absorption band will be shifted to longer wavelengths. Such arguments are generally used for structures which are of a more or less classical type.

One can however envisage that a small HOMO-LUMO difference can also be due to other factors. There are a number of structures with degenerate or nearly degenerate MOs which are occupied by only two electrons: these are diradical or diradicaloid compounds. When the MOs are degenerate the spectral excitation energy in fact appears to be zero when the electron interaction is not taken into account. The diradicals of interest here are acyclic or cyclic π,π-diradicals (π,π-diyls). The highly symmetrical compounds trimethylenemethane (C_{3v} symmetry) and cyclobutadiene (D_{2h} symmetry) are examples of hydrocarbon diradicals (compare Fig. 3); their degenerate MOs are non-bonding (NBMOs). *Zhixing* and *Sigun*[28] have shown how the occurrence of degenerate

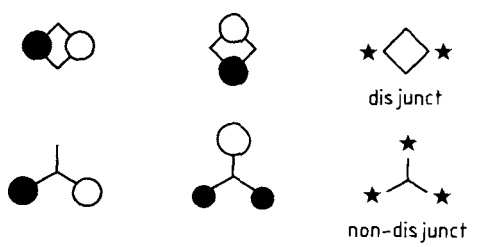


Fig. 3. The characteristics of the degenerate non-bonding π-MOs of two diradicals; the MOs can be either fully localized on different atoms (cyclobutadiene as a disjunct alternant diradical) or can have atoms in common (trimethylenemethane as a non-disjunct alternant diradical). A classification is possible using the "starring" procedure (see text).

NBMOs can be recognized from the topological matrix of the hydrocarbons.

A more detailed analysis of the degenerate MOs has shown that the linear combinations of the delocalized wave functions can either be localized on different atoms of the π-system (as for example in the case of cyclobutadiene, Fig. 3) or can have contributions common to like atoms (e.g. trimethylenemethane). According to the nomenclature used by *Borden* and *Davidson*, molecules of the first type are known as disjunct, alternant diradicals.[29a, b] These include alternant hydrocarbons in which the numbers of starred and unstarred atoms in the π-system are equal.[29c] This classification is of interest when the question posed is whether the diradical exists as a singlet or a triplet molecule.

The probability of obtaining a singlet configuration will always increase when the orbital degeneracy is removed. If the energy difference between the HOMO and the LUMO is small, we can expect an absorption at relatively long wavelengths.[30]

3. Chromophores Derived from Diradicaloid Compounds

3.1. Some General Remarks Concerning the Electronic Structure of Diradicals

The picture shown in Figure 2 of an electronic state in which two degenerate π-MOs are each occupied by one electron requires refinement. As was shown in detail by *Salem* and *Rowland*[31a, b] and by *Michl*,[31c] the diradicals defined in the two-electron-two-orbital model can take up one of six different electron configurations (compare Fig. 4): these correspond to a triplet state (T_1) and three singlet states (S_0, S_1, S_2).

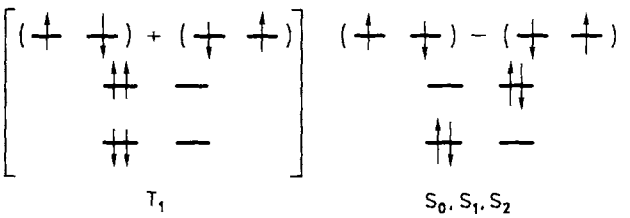


Fig. 4. The four electronic states of a diradical which result from different occupancy of two degenerate MOs by two electrons, taking the electron spin into account.

If the interactions between the electrons are taken into account, the energies of these configurations are in general no longer equal. *Bonačić-Koutecký*, *Koutecký* and *Michl* have dealt in detail with the relative energies of diradicals in the two-electron-two-orbital model in connection with the interpretation of the photophysical and photochemical properties of unsaturated organic molecules.[31d] In the case of the "homosymmetric" ("perfect") diradicals the degeneracy between S_0 and T_1 states is retained only for the so-called "pair" biradicals: these include the square cyclobutadiene shown in Figure 3. Of more interest for our discussions in this article are those diradicals in which the degeneracy between S_0 and S_1 is not lifted. According to *Bonačić-Koutecký* et al.[31d] these are always the "axial diradicals", which include trimethylenemethane (see Fig. 3). Although the energy difference between the singlet state S_0 and the triplet state T_1 is not an optimum criterium for a diradical, an S_0-T_1 splitting of the order of *RT* (ca. 10 kJ/mol) can be regarded as a characteristic feature of diradicals.[31e] The two-electron-two-orbital model also implies that an excitation from the lowest energy singlet state lies at lower energy than that of a triplet-triplet excitation, since the model includes only one single triplet state.[31e]

A configuration interaction is included in quantum-chemical calculations for diradicals. In the simplest calculations based on the two-electron-two-orbital method this interaction is limited to three singlet configurations (3 × 3 CI). In semiempirical calculations using the MNDO method the SCF wave functions are obtained in an approximation in which the valence electron system forms an open shell (half-electron method).[32] For limitation to a 2 × 2 CI a closed shell is assumed, and the configuration of the ground state is mixed with that of the doubly excited state. In principle the approach known as the two-configuration SCF method (TCSCF) is better: it has also been used in a semiempirical all-valence-electron approximation.[33] In MNDOC calculations electron correlations are treated in terms of perturbation theory.[34]

Reliable predictions regarding the energy spectrum of diradical structures only become possible when complex ab initio calculations are carried out. In the case of π,π-diyls these include all configurations of the π-space; MRD-CI and MCSCF-CI calculations include a suitable selection of configurations.[29a, 31d] However, because of the extreme complexity of the calculations the term schemes of larger conjugated organic molecules have not so far become available using these methods. Detailed calculations carried out for small molecules have shown that Hund's rule, which was derived for atoms and which requires that the triplet state of the diradicals should be of lower energy than the singlet state, should not strictly apply.[29a, 35, 36] The disjunct, alternant diradicals already mentioned are potential candidates for molecules with a singlet ground state. The relative stability with respect to the triplet state is said to be due to dynamic spin polarization.[36]

The degree to which the degeneracy of the MOs is lifted, and the energy difference between the HOMO and the LUMO increased, parallels the stabilization of the singlet state with respect to the triplet state. The "perfect" diradical undergoes a transition via a "non-perfect" diradicaloid[31d] to a normal molecule. The lifting of the degeneracy can have different origins; for instance, heteroatoms or groups containing heteroatoms may have replaced the CH or CH_2 groups of the diradical hydrocarbons. The reason may however also lie in a dynamic instability of the hydrocarbon which leads to a molecule of lower symmetry:[37] this phenomenon is known as the Jahn-Teller effect. Depending on the type of substitution, one or another Jahn-Teller distorted structure may occur in the derivatives of these diradicals.[38]

The diradical character of a diradicaloid structure can be judged on the basis of various criteria.[39] The occupation numbers of the natural orbitals, which are obtained from the density matrix, have proved particularly suitable.[39c] A fur-

ther criterion relates to the relative energies of the singlet and triplet states of lowest energy: according to *Wirz*[31e] a compound is a diradicaloid when the energy of the singlet-triplet splitting (S_0/T_1) lies between ca. 10 and 100 kJ/mol (800–8000 cm^{-1}); thus the energy difference can be greater than the thermal energy at room temperature.

According to the two-electron-two-orbital model we expect a term scheme for the diradicaloid singlet state which, apart from the triplet state, contains at least one excited singlet state which lies lower in energy than the ground state (Fig. 5). The $S_0 \rightarrow S_1$ excitation is then responsible for the long-wavelength light absorption.

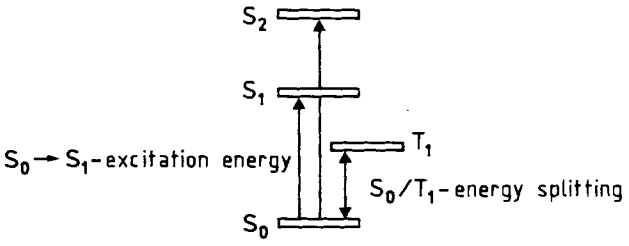


Fig. 5. Relative energies for the states of a diradical using the two-electron-two-orbital model for a diradicaloid with singlet ground state.

When the spectral excitation energy is described by a transition from the HOMO (a) to the LUMO (b), the singlet-singlet excitation energy ΔE_{ab} is, to a close approximation, given by Equation (1):

$$\Delta E_{ab} = \varepsilon_b - \varepsilon_a - J_{ab} + 2K_{ab} \quad (1)$$

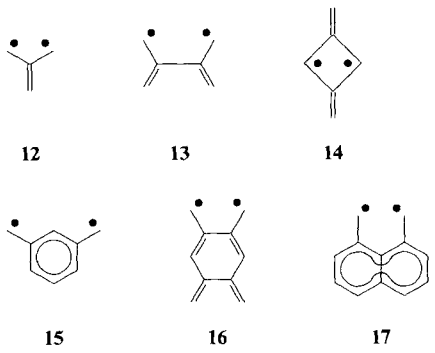
According to Equation (1) ΔE_{ab} is equal to the energy difference between the HOMO and the LUMO (ε_a, ε_b) minus the molecular Coulomb repulsion integral J_{ab} plus double the exchange integral K_{ab}. If the frontier orbitals formed from the degenerate MO describe spaces occupied by the electrons which are almost separate, K_{ab} will be relatively small; small K_{ab} values lead to a long-wavelength light absorption.[40] However, this same electron distribution character is also connected with a low transition probability for the electronic excitation, since then the transition dipole D_{ab} is relatively small. Since the oscillator strength f, which is proportional to the integral of the area under the absorption band, is given by Equation (2):

$$f = 1.085 \times 10^{-5}\, \Delta E_{ab}\, D_{ab}^2 \quad (2)$$

D_{ab} must be sufficiently large to compensate for the decrease in the oscillator strength which necessarily results from a small value of ΔE_{ab}.

3.2. Diradicaloid Non-Kekulé Structures

One group of diradicaloid compounds has "non-Kekulé" structures, i.e. the compounds cannot be described by conventional (Kekulé) structural formulas without the use of a long formal bond. They are derivatives of the hydrocarbons **12**–**17**, the diradical character of which is made clear by the following valence bond formulas.



These diradicals have been investigated in detail in the last few years,[29a] and they are now more readily available.[41] The compounds **12**–**17**[42–47] and some of their simple derivatives have shown themselves to be triplet diradicals.

Theoretical predictions according to which the singlet states of **13** and **16** should be of lower energy than the triplet states[35] have not so far been confirmed experimentally.[43,46]

According to PPP calculations carried out by *Gisin* and *Wirz*[48a] the triplet-triplet absorptions for a number of π,π-diradicals lie in the visible spectral range. Experimental details are available for **14**,[44] **15**[45] and the methylene-bridged **17**.[47] The discussion above suggests that singlet-singlet excitations should lie at lower energies than triplet-triplet absorptions. The absorption band of the singlet-singlet absorption was calculated to lie at 1000 nm for **17**[31e] and well above 1000 nm for **14**.[48b]

In order to stabilize the singlet state of a non-Kekulé hydrocarbon in comparison with the triplet state it is necessary to carry out a suitable structural modification of the hydrocarbon diradical. As shown in Figure 6 for the trimethylene **18a** (X = CH_2),[49] the replacement of the central CH_2 group by an atom X (with a doubly occupied p orbital) leads to a splitting of the NBMOs. Since only the symmetrical combination of the p_π-orbitals of the terminal carbon atoms[50] overlaps with the p_π-orbital of the heteroatom, the degeneracy is lifted and the lowest energy electronic transition is described by a one-electron transition from the symmetrical HOMO to the antisymmetrical LUMO. In Figure 6

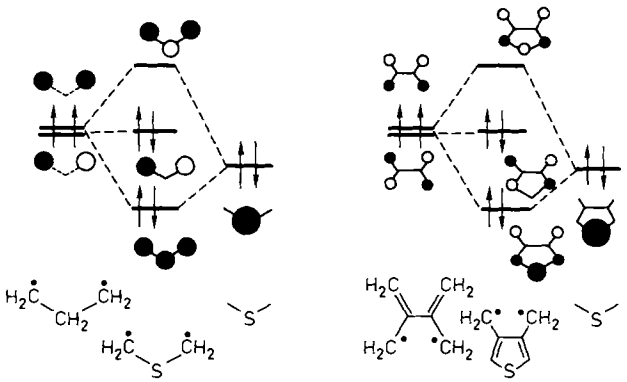
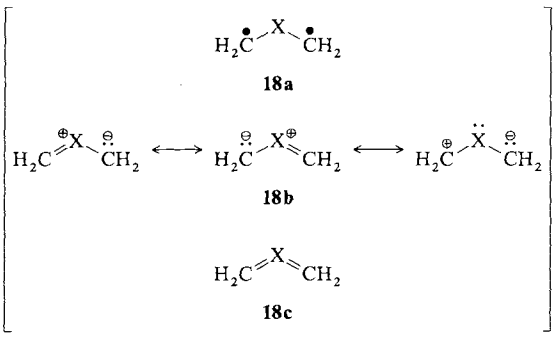


Fig. 6. Lifting of the degeneracy of the NBMOs of trimethylene (**18a**, X = CH_2) [50] when CH_2 is replaced by S (left) and on cyclization of trimethyleneethane **13** by means of S (right) via overlap of the symmetrical MOs of the diradicals with the p_π-orbital of the heteroatom.

this splitting is shown for the substitution of CH_2 by σ-bivalent sulfur to give **18a**, X = S.

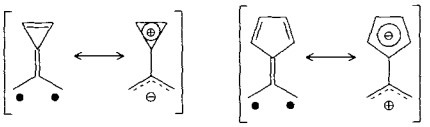
According to perturbation theory considerations in the MO picture, the HOMO-LUMO difference will, however, only be small when the heteroatom X is more electronegative than carbon and/or when the p_π-orbitals of carbon and the heteroatom overlap only slightly. When this prerequisite is not fulfilled, as for example in the case considered where X is sulfur, the π-system is more strongly delocalized and the degree of diradicaloid character is either slight or negligible. In this case the electronic structure is better represented by valence bond formulations such as **18b** in which X is a donor atom. One of the mesomeric structures of **18b** indicates the presence of 1,3-dipolar properties, which are often used in the interpretation of cycloaddition reactions of trimethylene and its derivatives.[51] In formula **18c** the heteroatom is bonded to the carbon atoms via an extension of its electron octet.[52]



18a **18b** **18c**

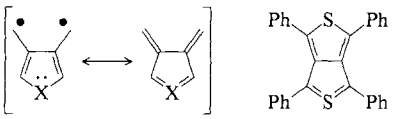
Before we discuss some derivatives of the biradical hydrocarbons **12–19**, it should be noted that here, just as for **18a–c**, the representation of the compound by a single valence bond structure is not possible. However, for the sake of simplicity and in spite of their deficiencies we have below used valence bond formulas of the type found in the literature.

Problems of this type exist not only for compounds containing heteroatoms but for the hydrocarbons themselves: a betaine structure is also indicated in the case of the non-Kekulé hydrocarbons **19** and **20**, which belong to the group of the non-alternant hydrocarbons. In contrast to **12–18, 19** and **20** do not have degenerate MOs but are still to be classified as diradicaloid hydrocarbons.[39c, 53]



19 **20**

The heterocycles 3,4-dimethylenefuran and 3,4-dimethylenethiophene (**21**, X = O, S) can be considered to be derivatives of trimethyleneethane **13**. These heterocycles have been synthesized;[54] their purple-red color is due to a singlet-singlet transition. The intensity of the color absorption band in **21** (X = S) is relatively high. The introduction of a heteroatom into **13** leads to the lifting of the degeneracy of the NBMOs (see Fig. 6), and the triplet hydrocarbon is converted into a heterocycle with singlet character. It has been shown by ab initio calculations[56] that the S_0/T_1 splitting increases with increasing donor ability of the heteroatom.

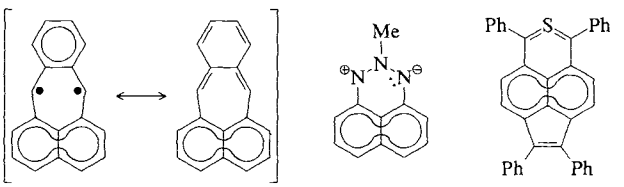


21 **22**

21: X = O: λ = 560 nm/$\tilde{\nu}$ = 1.79 μm^{-1} (lg ε > 3);
21: X = S: 572 nm/1.75 μm^{-1} (>4), in toluene [54];
22: 550 nm/1.82 μm^{-1} (4.01), in cyclohexane [55].

The synthetically available thieno[3,4-*c*]thiophene, which has been described according to formula **22** as a heterocycle with "tetravalent sulfur", is related to **21** (X = S) and also absorbs at relatively long wavelengths.[55] **22** differs in color from the isomeric thienothiophenes, which are classical thiophene derivatives with σ-bivalent sulfur.

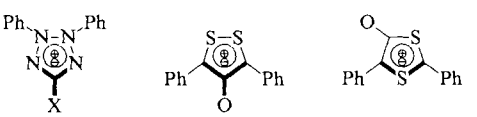
Derivatives of **17** include the blue pleiadene **23** and the (also blue) heterocycles **24** and **25**, which exhibit only relatively weak long-wavelength absorptions.



23 **24** **25**

23: $\lambda \approx$ 690 nm/$\tilde{\nu} \approx$ 1.45 μm^{-1}, in 3-methylpentane [57];
24: 607 nm/1.65 μm^{-1} (lg ε = 2.98), film [58];
25: 665 nm/1.50 μm^{-1} (3.37), in dichloromethane [59].

At this point we should also mention mesoionic compounds[60] which absorb at relatively long wavelengths when they contain sulfur as the heteroatom. Again their absorption bands lie at wavelengths considerably greater than those for isomeric non-mesoionic heterocycles; examples are compounds **26–28**. In the formulas shown below the diradical substructure, which is derived either from **12** (an example of a mesoion of the first kind) or from **18** (an example of a mesoion of the second kind), is denoted by bolder bonds.

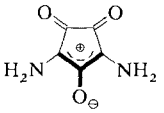


26 **27** **28**

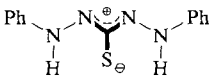
26: X = O: λ = 350 nm/$\tilde{\nu}$ = 2.86 μm^{-1} (lg ε = 3.68), in chloroform [61];
26: X = S: 468 nm/2.14 μm^{-1} (3.07), in chloroform [61];
26: X = $C(CH_2)_2$: 468 nm/2.14 μm^{-1} (2.97), in acetonitrile [62];
27: 575 nm/1.74 μm^{-1} (4.23), in benzene [63];
28: 553 nm/1.81 μm^{-1} (4.11), in dioxane [64].

Exactly as has been shown for **23**,[57] doubly excited configurations are also of importance in the description of mesoionic compounds, as for example in the case of the 1,2-dithiolylium-4-olates (e.g. **27**), which also absorb at relatively long wavelengths.[65, 66]

The diradicaloid oxyallyl substructure is also present in croconic acid derivatives such as **29**; however, it is so distorted that the singlet-singlet excitation energy is relatively large, and the compound is only yellow in color.[67] A substitution product of the diazathioxyallyl, however, absorbs at much longer wavelengths. The dithizone **30**, which has a chain structure with respect to **26** (X = S), dissolves in organic solvents to give a green solution.[68, 69]



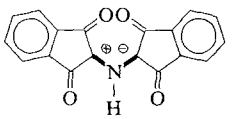
29



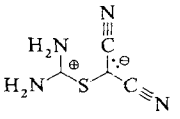
30

29: λ = 440 nm/$\tilde{\nu}$ = 2.27 μm^{-1} (lg ε = 4.11), in dichloromethane [67a];
30: 617 nm/1.62 μm^{-1} (4.44), in hexane [68].

31, which is derived from the diradicaloid **18**, has been described[70] as a stable dipolar azomethine ylide; its structure has been determined by X-ray crystallography. As in the case of capto-datively stabilized thiocarbonyl ylides such as **32**, the spectral excitation energy is relatively high,[71] and deeply-colored compounds of this type are so far unknown.



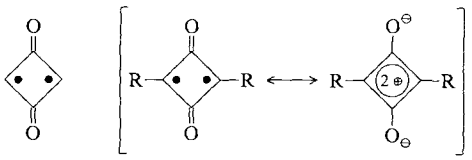
31



32

31: λ = 485 nm/$\tilde{\nu}$ = 2.06 μm^{-1} (lg ε = 4.20), in chloroform [70].

Finally, we should mention compounds in which several carbon atoms of a non-Kekulé hydrocarbon have been replaced by heteroatoms; although such a substitution removes the degeneracy in diradicals such as **15** and **17**, some derivatives do in fact exist as triplet molecules.[35c, 72] The dicarbonyl compound **33** formed by substitution of the exocyclic CH_2 group in **14** by oxygen is, according to *Gleiter* and *Hoffmann*, a singlet molecule ($\lambda_{calc.}$ = 610 nm).[73] **33**, which is so far unknown, forms a building block for the squaraines of general structure **34**; these absorb at long wavelengths and are of interest because of their possible application as materials for electrophotographic reproduction, in solar cells and in optical storage disks.[4a, 74] These compounds are generally described as betaine-type cyclobutenediylium diolates; however, according to the results of ab initio calculations for **34a** (NR_2 = NH_2) they do not in fact have such an electronic structure.[75]

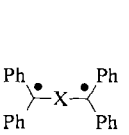


33

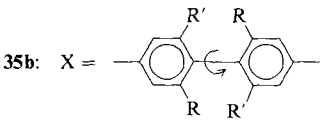
34a: R = NR_2
34b: R = NHC_6H_5
34c: R = *p*-$C_6H_4NH_2$

The diradical character of the parent hydrocarbon **14** is apparently destroyed by substitution; the color variation from **34a** (NR_2 = piperidine, yellow) via **34b** (red) to **34c** (blue)[8b, 76] apparently reflects the increasing π-delocalization rather than a stepwise perturbation of a diradicaloid electronic structure.

Compounds in which two radical fragments are only weakly coupled are closely related to diradicaloid non-Kekulé structures. While the bridging of two diphenylmethyl radicals via *p*-diphenylene to give the orange-red Thiel hydrocarbon **35a** results in a quinoid structure,[77] bridging via a twisted π-electron system should result in retention of the diradicaloid structure; examples are Tschitschibabin's hydrocarbon and its derivatives[77, 78] and Müller's hydrocarbon.[78e]



35a: X =



35b: X =

35a, R = R′ = H: λ = 574 nm/$\tilde{\nu}$ = 1.74 μm^{-1} (lg ε = 5.02), in benzene [77];
35b, R = H, R′ = Me: 600 nm/1.67 μm^{-1}, 690 nm/1.4 μm^{-1}, in benzene [78a].

35b, R = R′ = H, which has been obtained in the form of green crystals with a metallic sheen or as a violet powder[77] exists at room temperature to the extent of 98% in a singlet state.[78b] The methyl-substituted compound **35b**, like various chlorine-substituted products[78c, d] is certainly twisted about the central C–C bond.[79] The spectra of the unsubstituted hydrocarbon and the derivatives mentioned above exhibit an intense absorption at λ > 600 nm; only in the case of **35b** has the UV/VIS spectrum also been measured above 600 nm, and it has been found to have an additional weak absorption at almost 700 nm.[78a, 80]

Tschitschibabin's hydrocarbon and compounds of this type form a transition to another class of diradicaloid compounds which can be classified in terms of an intra- or intermolecular charge transfer model.

3.3. Diradicaloid Structures with Charge Transfer

A diradicaloid electronic system will form when an unsaturated compound is twisted about the double bond.[29a, 31b, 82] In the extreme case the two molecular frag-

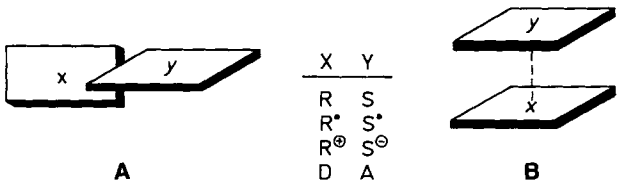


Fig. 7. Schematic representation of the geometry of a twisted molecule **A** and a sandwich complex **B** with partial structures X and Y. The fragments or single molecules X, Y represent radicals ($R^•$, $S^•$), ions ($R^⊕$, $S^⊖$) or donor and acceptor systems (D, A) of organic compounds with conjugated bonds.

ments will, as shown in Figure 7 by **A**, be approximately orthogonal.

The formation of a singlet ground state in diradicaloid structures of this type can be explained on the basis of the molecule-in-a-molecule model.[82] The no-bond (NB) ground state defined by the radical fragments is superimposed by a conformation which describes charge transfer (CT) in opposite directions; the mixing of the two configurations describes bonding between the two fragments (if these do in fact interact). If charge transfer plays a much more important role for the excited state than for the ground state, the transition from ground to excited state caused by light absorption will be accompanied by charge transfer; in such a case we are dealing with a charge transfer (CT) transition. However, the present case is that of a symmetrical molecule, so that the opposing charge transfer processes do not here lead to an effective charge shift: instead we have a charge redistribution (charge resonance, CR). In order to avoid any misunderstanding it is thus desirable in such cases to refer to a CR rather than a CT transition; this transition can lead to a long-wave CR band in the absorption spectrum.

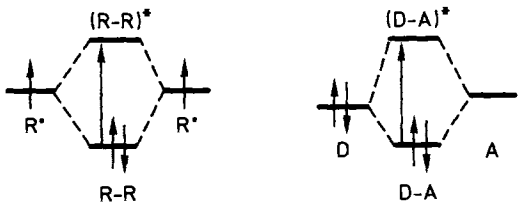


Fig. 8. Orbital splitting via overlap of the SOMOs of two radicals in a dimer structure (left) and of the HOMOs of a donor molecule with the LUMO of an acceptor molecule in a donor-acceptor complex with electronic excitation of CR or CT type respectively (right).

In Figure 8 the CR and CT absorptions are indicated in an MO picture for diradicaloid electron systems; the interacting MOs are of equal or approximately equal energy. For radical fragments R they are singly occupied (SOMOs), while the MO of a donor fragment (the HOMO) formally supplies two electrons to the bond and the lowest unoccupied MO of the acceptor fragment (the LUMO) none.

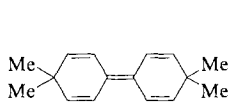
Our knowledge of compounds which are twisted about the double bond is limited. A torsion of this type must be forced by steric constraints, as for example in the case of the bridgehead olefin **36**.



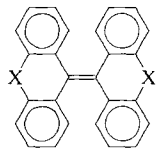
36

While the expected large effect on the electronic excitation is clearly present, it will hardly be possible to obtain highly colored compounds routinely on such a basis.[83]

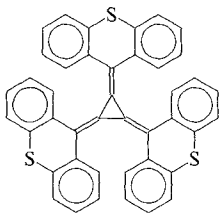
In sterically strained cross-conjugated compounds such as the dendralene hydrocarbon **37**,[84] dianthrone **38a**[85a, b] or dixanthylene **38b**,[85c, d] torsion about the double bond is replaced by folding. The green thermochromic form of the dianthrone **38a** is however due to a structure in which there is torsion about the double bond:[86] according to quantum-chemical calculations the torsional angle θ is ca. 57°.[33a, 87] The thermochromic form of the dixanthylene **38b** is probably also twisted.[88a, b] The recently synthesized highly colored [3]radialenes[88c, d] (e.g. **39**) are also definitely non-planar molecules.



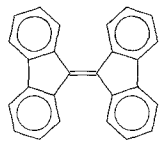
37



38a: X = CO
38b: X = O



39

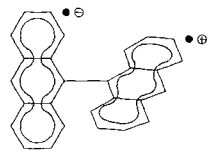


40

38a: λ = 675 nm/$\tilde{\nu}$ = 1.48 μm^{-1} (lg ε = 4.19), in dimethyl phthalate at 349 K [86b];
39: 600 nm/1.67 μm^{-1} (4.48), in dichloromethane [88c];
40: 460 nm/2.17 μm^{-1} (4.34), in benzene [89a].

Only in the case of 9,9'-bifluorenylidene **40** has the torsion of the molecule about the double bond been demonstrated by X-ray crystallography.[89a, b] Here the dihedral angle is relatively small (θ = 39°); the hydrocarbon is red. According to quantum-chemical calculations carried out using a semi-empirical two-configuration SCF method[33a, b] the twisted form of the difluorenylidene represents a global minimum while that of the dianthrone corresponds only to a local minimum on the potential energy hypersurface.

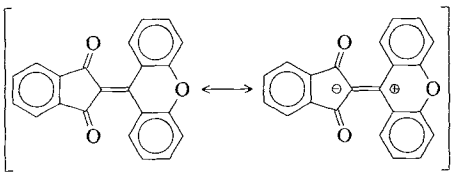
The situation can be expected to be similar for compounds with two dissimilar molecular "halves"; in this connection the TICT (Twisted Intramolecular Charge Transfer) molecules, which are at present the subject of intensive investigation,[90] should be considered; these include the twisted betainic 9,9'-dianthryl **41**.[90b, 91]



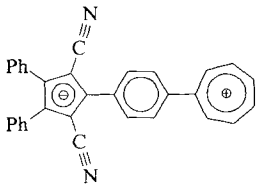
41

However, **41** and similar molecules are in fact relaxed molecules in an excited state; this can be recognized by the existence of an anomalous fluorescence or a rapid radiationless deactivation.[90b] The light absorption of interest here can be detected only by rapid spectroscopic methods; such studies[91a] have confirmed the twisted structure **41**, since characteristic absorptions of the fragment molecules could be detected. However, no information has yet been provided on the expected light absorption by **41** at extremely long wavelengths.

A betaine structure appears preferable when a diradicaloid structure is allowed to form from an unsymmetrical compound via torsion about a double bond. Although a few sterically hindered compounds of this type are known, little information is available on their molecular structure and spectral absorption. An example is compound **42** which was described by *Schönberg* et al. as being almost black in the solid state, deep blue when melted and violet in solution; in this compound the dihedral angle θ is 42.7°.[92] *Sandström* et al. showed that non-symmetrical sterically hindered double bond systems ("push-pull ethylenes") can also undergo a folding of the molecule rather than a torsion.[93]



42



43

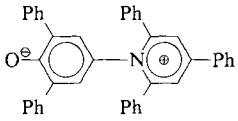
43: $\lambda = 934\,\text{nm}/\tilde{\nu} = 1.01\ \mu\text{m}^{-1}$, in bromobenzene; 672 nm/1.59 μm^{-1} ($\lg \varepsilon = 4.23$), in dimethyl sulfoxide [94].

Another type of compound with a basically similar structure, whose absorption in non-polar solvents lies well into the NIR, is derived from **43**.[94] The betaine character of **43** can be recognized from the hypsochromic shift of the color band which occurs when the non-polar solvent is replaced by a polar solvent (negative solvatochromic effect).

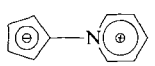
An interesting type of compound, whose long-wavelength spectral transition is characterized by a CT band, is provided by the extremely strongly solvatochromic pyridinium phenoxides (e.g. **44a**); these have been studied by *Reichardt* et al.[95] X-ray crystallography has shown that **44a** is also non-planar ($\theta = 65°$).

However, pyridinium betaines or colored pyridinium salts such as **44** (which are typical of many other conjugated organic compounds with similar structures) will only exhibit an absorption at long wavelengths when certain preconditions are fulfilled.

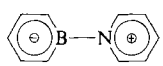
On the one hand, one half of the molecule (or a residue in the molecule) must be a strong electron donor (low ionization energy for the molecule derived from it), while the second half (or another residue) must be a strong electron acceptor (high electron affinity of the corresponding molecule). In this case the HOMO of the donor and the LUMO of the acceptor are almost degenerate, the CT excitation energy is small (long-wavelength CT band), and the compounds have structures of a diradicaloid type. The CT excitation energy will increase parallel to the extent that the donor and acceptor abilities diminish (left-hand side of Fig. 9a).



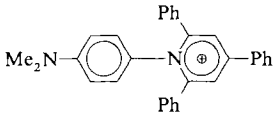
44a



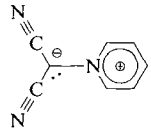
44b



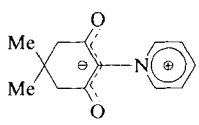
44c



44d



44e



44f

44a: $\lambda = 795\,\text{nm}/\tilde{\nu} = 1.26\ \mu\text{m}^{-1}$ ($\lg \varepsilon \approx 4.1$), in dioxane [95];
44b: 495 nm/2.02 μm^{-1} (4.28), in acetonitrile [96];
44c: 472 nm/2.12 μm^{-1} (3.45), in tetrahydrofuran [97];
44d: 468 nm/2.14 μm^{-1} (3.76), in dichloromethane [98];
44e: 393 nm/2.54 μm^{-1} (4.33), in acetonitrile [99];
44f: 358 nm/2.79 μm^{-1} (3.24), in 85% ethanol [100].

However, the absorption wavelength also depends on the overlap between the donor and acceptor fragments. Even when an absorption at a very long wavelength is expected from the nature of the fragments, it can fail to occur because there is a good overlap of the fragment MOs. A poor overlap is often caused by torsion within a donor-acceptor molecule X-Y (X = D, Y = A), as indicated by **A** in Figure 7. We can thus understand that the color band in a number of pyridinium compounds of type **44** occurs at long wavelengths, while in other compounds it occurs at relatively short wavelengths.

It must also be remembered in the interpretation of light absorption that the character of the chromophore changes with increasing overlap of the donor and acceptor fragments. Two extreme cases are shown on the left- and right-hand sides in Figure 9b: a molecule which is electrically neutral is on the left-hand side a betaine in the ground state, and is characterized by the formula $D^{\ominus}\,A^{\oplus}$. The electronic excitation, which is accompanied by an electron shift, then leads to DA. The decrease in the dipole moment caused by the excitation is generally accompanied by a negative solvatochromic effect. In the second case, on the right-hand side of the figure, the ground state is represented by DA, and $D^{\oplus}A^{\ominus}$ characterizes the excited state.[101] The excitation causes an increase in the dipole moment, and a positive solvatochromic effect will result. However, whether in fact such a charge transfer occurs and leads to a long-wave absorption depends entirely on the conditions discussed above.

If as the result of a good overlap between the fragments a considerable charge shift occurs even in the ground state, then the latter is not satisfactorily characterized either by $D^{\ominus}A^{\oplus}$ or by DA. Instead we must write $D^{\delta\oplus}A^{\delta\ominus}$ or $D^{\delta\ominus}A^{\delta\oplus}$

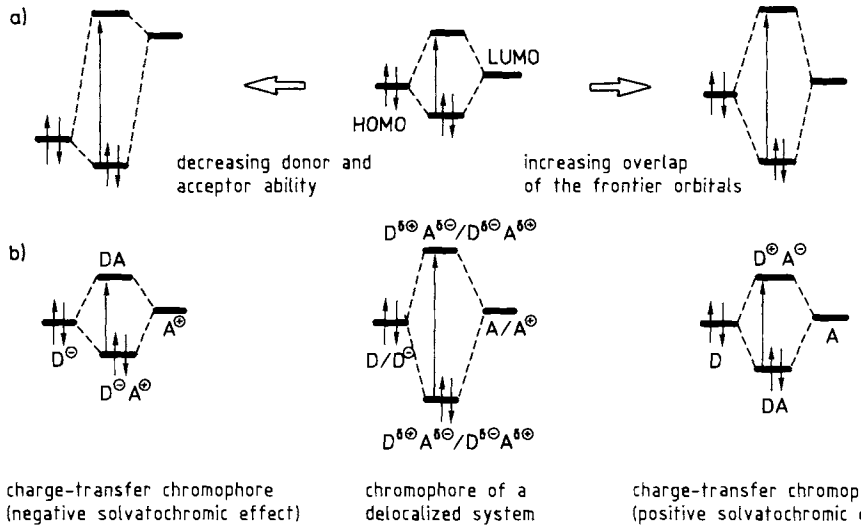


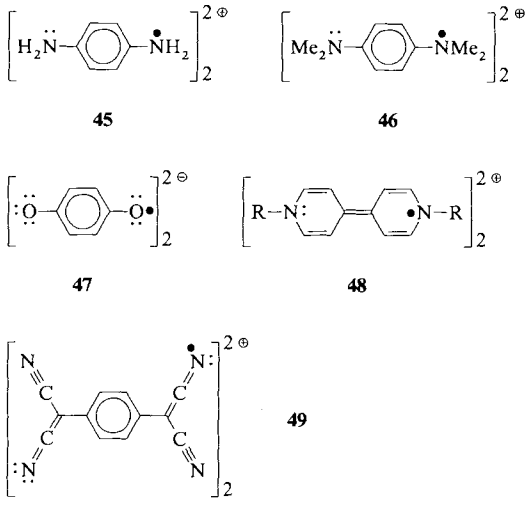
Fig. 9. a) Increase of the excitation energy (hypsochromic shift of the color band) as the result of an increasing HOMO-LUMO interaction and b) different characteristics of the change in charge distribution on excitation (vertical transitions).

and in this case the same type of electron distribution is also present in the excited state. This is shown in the center of Figure 9b. Since the electron excitation is no longer accompanied by a charge shift between the fragments but by a redistribution of the charge within the molecule as a whole, we are no longer dealing with a CT chromophore; the chromophore of a new delocalized π-system has been formed.[102]

The above discussion can also be applied to compounds which are not joined by a σ-bond (or several σ-bonds) as in case **A** in Figure 7, but in which intermolecular interactions lead to the formation of an aggregate (case **B**). Such an aggregate of organic π-systems, which can be a dimer (X = Y) or a donor-acceptor complex (X ≠ Y) exists preferentially in a stacked arrangement. In the Figure this arrangement in space is only indicated in principle. The overlap in sandwich complexes is naturally only small, and an absorption at relatively long wavelengths is thus observed.

A large number of π-radicals exhibit a long-wavelength absorption at higher radical concentrations or at lower temperatures which is not observed for the monomer. The tendency to dimerization is particularly pronounced in the case of radical anions of Wurster and Weitz types. The dimers (also called "pimers"[103]), which in contrast to the monomers exist in a singlet state, absorb at longer wavelengths than the radicals themselves:[106] examples are the dimers **45** to **49**.

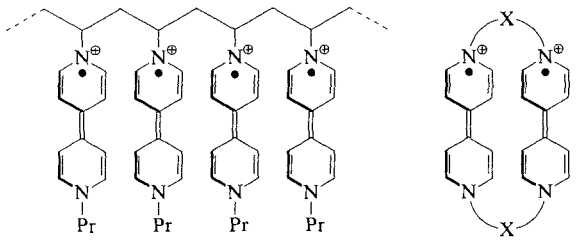
Since dimeric radicals can be described in terms of a symmetrical combination of CT-configurations, we are again dealing with an electronic excitation of the CR type.[107] The formation of dimeric structures can also be detected in the absorption spectra of polymers,[108] for example in **50**. The sandwich structure of the dimers is indicated by the spectra of compounds in which radicals are terminally bridged, e.g. **51**.[109] For the reasons stated above, the position of the dimer absorption should, for any one monomer, depend on the degree of overlap present: the absorption wavelength for compounds of type **51** does indeed increase with increasing distance between the radical fragments.[109]



45: λ = 605 nm/$\tilde{\nu}$ = 1.65 μm^{-1}, in ethanol [104a];
46: 780 nm/1.28 μm^{-1}, in ethanol [104a];
47: 585 nm/1.71 μm^{-1}, in ethanol [104a];
48: 870 nm/1.15 μm^{-1}, in water [103];
49: 1282 nm/0.78 μm^{-1}, in the crystal [105c].

The same long-wavelength band which is observed in solution for crystalline halides and perchlorates of radical cations[104b-d, 110] and for alkali metal salts of radical anions[105] is also observed (with small variations in the absorption wavelength) in their absorption and reflection spectra. The singlet-triplet energy splitting of the dimer band in salts of Wurster's blue is only ca. 250 cm^{-1}.[110] Crystallographic studies have shown that these radicals also dimerize in a stacked form.[111] The formation of the dimeric structures is accompanied by a decrease in the paramagnetic susceptibility.

When dissimilar partners are involved in aggregation (X ≠ Y) as in **B** (Fig. 7), charge-transfer complexes are formed; these have been studied in detail.[112] In the two-



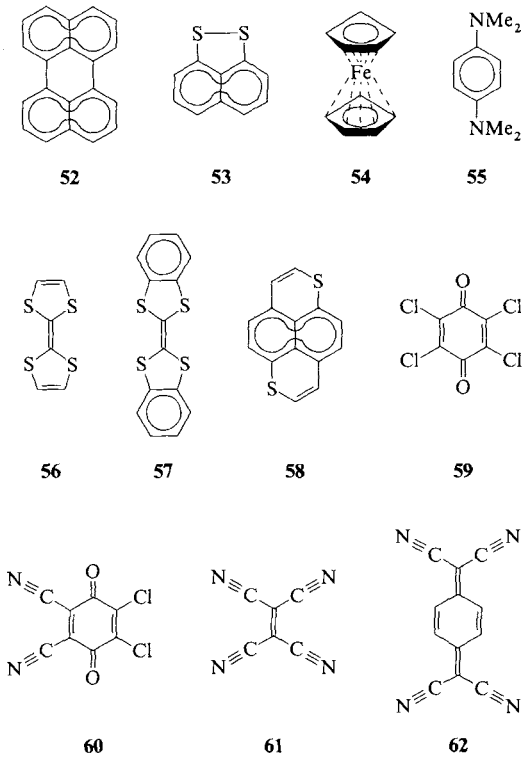
50 51

50: λ = 860 nm/$\tilde{\nu}$ = 1.19 μm^{-1}, in water [108b];
51, X = *o*-phenylene: 840 nm/1.19 μm^{-1}, in methanol [109];
51, X = *m*-phenylene: 920 nm/1.09 μm^{-1}, in methanol [109].

electron-two-orbital picture of the diradicaloid structure, both electrons are provided by the donor molecule. When the prerequisites referred to for compound **A** (X ≠ Y) are met, intermolecular CT bands are observed in the NIR. Examples are provided by the following complexes: the fused hydrocarbon perylene **52** and tetracyanoethylene (TCNE) **61** (**52/61:** λ = 870, 900 nm in dichloromethane[113]), the heterocycle naphthalene disulfide **53** and tetracyanoquinodimethane (TCNQ) **62** (**53/62:** λ = 925 nm in dichloromethane[114]) and the organometallic compound ferrocene and TCNE **61** (**54/61:** λ = 900 and 1075 nm in cyclohexane[115]). These absorption bands are of low intensity (lg $\varepsilon \approx 2$). As has been shown for **52/61** and many other cases, the same CT band can be detected in the spectrum of the solid. The band at the longest wavelength undergoes a bathochromic shift with respect to that in solution of almost 1000 cm^{-1}.[113]

A linking together of the donor-acceptor molecule via σ-bonds makes it possible to predetermine the spatial positions of the partial structures and to study steric influences on the spectral absorption. The overlap of the frontier orbitals is often increased by the bridging, so that the color band is shifted to shorter wavelengths. When for steric reasons overlap is either poor or impossible, an absorption at relatively long wavelengths is observed. *Murata*[116] has demonstrated this for triptycenes in which donor-substituted benzenes were linked to TCNQ. In a theoretical study, *Vogler*[117] has predicted the conditions under which an electron transition from the donor to the acceptor fragment will occur in a CT compound of the cyclophane type, thus leading to a diradical-ion ground state.

Radical ions can also be detected when CT complexes are studied in polar rather than non-polar solvents,[118] for example the system **55/59** in acetonitrile.[118a] In the case of **55/62** the equilibrium constant and the thermodynamic parameters have been determined for the equilibrium between the neutral compounds and the radical ions in acetonitrile. The tendency for electron transitions to occur is even larger in the crystalline state.[119] If the donor and (or) acceptor molecules form separate stacks in the crystal, then (as already stated) the long-wavelength absorption of a dimer structure (a CR band) is observed.[104b-d] The antiferromagnetic interaction of the radicals can also be inferred from the magnetic susceptibility value.[104c, 120] As for the CR bands of the dimeric radicals in solution, an absorption at ca. 1.0 μm (10000 cm^{-1}) is observed in saltlike CT complexes such as the crystalline complex **55/59**.[104c]



52 53 54 55

56 57 58 59

60 61 62

CT complexes are also known which absorb at considerably longer wavelengths; their absorption bands can lie even above 3 μm (at ca. 3000 cm^{-1}).[121-123] In such cases the electronic excitation spectrum overlaps the vibrational spectrum.[124] This unusual absorption behavior was observed by *Iida*[121] and later studied in detail by *Torrance* et al.[122] These extremely long-wavelength absorptions occur when the CT complex shows conducting properties. An important prerequisite is the formation of separate stacks for the complex partners in the crystal and a partial electron transfer between the molecules within the stacks; such complexes are thus also referred to as mixed valence CT complexes.[122b]

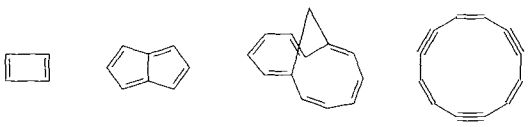
The absorption bands of these complexes are due to factors different from those responsible for the CT and CR bands of diradicaloid systems. They have their origin in the occurrence of free charge carriers[125] and have been interpreted in terms of band models.[122a] *Torrance* et al.[122c] and *Saito* et al.[123] have shown clearly from the reflection spectra of CT complexes (in KBr) that variation of the complex partner can cause a transition from the neutral complex (ionicity ca. zero) via the mixed-valence complex (ionicity ca. 0.5) to the complex of the radical salt (ionicity ca. 1); this transition is accompanied by characteristic changes in the spectra. While the neutral complex **57/62** shows a typical CT band, the organic conductors **56/62** and **57/60,** which are mixed-valence complexes, absorb at ca. 3.3 μm (3000 cm^{-1}).[122c] The complex **56/60,** however, is a radical salt, and the typical dimer band of the radicals caused by a CR transition is observed. A theoretical interpretation of the spectra of the various complexes has been given by *J. Tanaka* et al.[123c] A recent report has appeared on the IR spectra of mixed-valence complexes derived from Weitz-type donors, which also exhibit electrical conductivity and a spectral behavior analogous to, e.g., **58/62**.[123d]

3.4. Diradicaloid Cyclopolymethine-Type Structures

Electronic structures with a diradicaloid character can also be derived from cyclic conjugated systems. It can readily be seen from Frost's circle, a mnemonic method for deriving the MO energies of monocyclic hydrocarbons,[126] that occupancy of the MOs of such hydrocarbons by a total of $4n$ π-electrons leads to the presence of degenerate MOs which contain a total of two electrons; these MOs can be bonding, non-bonding or antibonding. Such molecules form anti-Hückel systems, for which *Breslow*[127a] and *Dewar*[127b] have coined the term antiaromatic. In the past few years a great deal of information has become available on such compounds.[128]

These molecules are distorted because of a second-order Jahn-Teller effect; annulenes with $4n$ π-electrons thus exist in a singlet ground state. When bond alternance is introduced via the choice of the resonance integrals $\beta_{C=C}$ and β_{C-C} in the Hückel approximation, a HOMO-LUMO energy difference of $2(\beta_{C=C} - \beta_{C-C})$ is obtained, independent of the ring size;[129] the $\pi \rightarrow \pi^*$ transition of lowest energy is forbidden. Even when the electronic interactions are taken into account there is no clear dependence of the absorption wavelength on ring size; according to PPP calculations the color of such compounds should vary between red and blue. This agrees with experimental results: thus [16]annulene is described as being purple.[11a] However, according to X-ray crystallography [16]annulene is non-planar, and D NMR studies show that in solution there is an equilibrium between conformers.[11b]

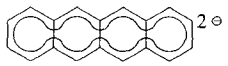
Cyclobutadiene **63** occupies a special position within the series of $4n$ π-annulenes. Studies on a peralkylated cyclobutadiene have indicated the (adiabatic) S_0/T_1 energy splitting to be only 50 kJ/mole,[130] so that this compound can also be described as a diradicaloid; however, an extremely large bond alternance, which has been confirmed experimentally for several derivatives,[131, 132] leads to an absorption at relatively short wavelengths.[130] According to ab initio calculations the absorption band observed for **63**[130b] corresponds to the $S_0 \rightarrow S_1$ transition of lowest energy.[130c]



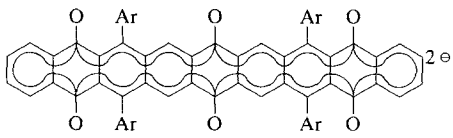
63 **64** **65** **66**

63: $\lambda \approx 300$ nm/$\tilde{\nu} \approx 3.33$ μm^{-1}, in a matrix [130b];
64: 594 nm/1.68 μm^{-1} ($\lg \varepsilon = 1.87$), in hexane [133];
65: 425 nm/2.35 μm^{-1} (2.38), in cyclohexane [134];
66: ca. 480 nm/$\approx$ 2.08 μm^{-1} ($\approx$ 2.2), in isooctane [135].

Planarity can be induced in cyclic compounds by the introduction of a transannular bond or a bridge (e.g. CH_2) or by "stiffening" the ring by replacement of a double bond by a triple bond (e.g. in **64–66**): however, π-bond equalization cannot be forced.[133, 136] The latter is realized better in acene dianions (e.g. **67**)[137] and their heteroanalogues[138] as far as the perimeter bonds are concerned; these ions are red, blue or green in solution, depending on the degree of annelation.[139] A clear relationship exists between the energy difference and the paramagnetic ring current determined from the NMR chemical shifts.[137]



67

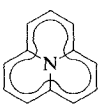


68

67: $\lambda = 673$ nm/$\tilde{\nu} = 1.49$ μm^{-1} ($\lg \varepsilon = 4.76$), in 1,2-dimethoxyethane [139b];
68: Ar = *p*-$(CH_3)_3C-C_6H_4$: 1900 nm/0.53 μm^{-1} (4.88) [140].

Dianions should be stabilized by acceptor substituents and dications by donor substituents; the long-wavelength light absorption of these ions does not necessarily have to be related to the presence of a diradicaloid "antiaromatic" chromophore. The electron configuration of prime importance in a description of the excited state of lowest energy is one which can in principle be derived from the two lowest unoccupied MOs of the corresponding neutral compound in the case of the anion and from the two highest occupied MOs in the case of the cation. From this point of view we are dealing with "unnatural" electronic transitions of the $\pi^* \rightarrow \pi^*$ or $\pi \rightarrow \pi$ type, in contrast to the "natural" $\pi \rightarrow \pi^*$ transitions. The differences in the energies of these MOs suggest that the former will lead to a light absorption at longer wavelengths than will the latter; such a picture had already proved extremely useful in the interpretation of the extremely long-wavelength absorption of many organic radicals.[26, 140] It also allows us to understand the extremely long wavelength (1–2 μm) of the absorption of the dianion of the triquinone **68**, which *Miller* et al. had observed in the study of the absorption spectra of polyacenequinone radicals.[140]

A simple derivative of the "antiaromatic" [12]annulene is [3.3.3]cyclazine **69**. This compound is probably characterized by a fairly complete equalization of the CC bond lengths; the color band of **69** lies in the near infrared.[141] Stepwise replacement of CH in the perimeter by nitrogen shifts the band from the infrared into the visible and finally into the UV region.[141a, 142]

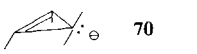


69

$\lambda = 1290$ nm/$\tilde{\nu} = 0.78$ μm^{-1}, in hexane [141a].

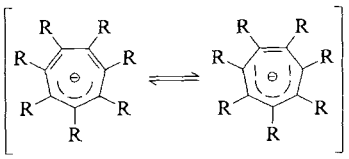
In contrast to the situation for rings with an even number of atoms, a long-wave absorption is expected for ionic rings

with $4n$ π-electrons even when a Jahn-Teller distortion leads to the formation of polyenic or carbopolymethine substructures. An exception is formed by the cyclopropenide, which ab initio calculations[143] indicate to be non-planar (see formula **70**).



70

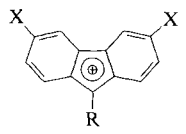
71



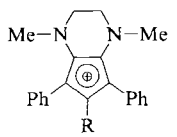
72

72: R = H: $\lambda \approx 750$ nm/$\tilde{\nu} \approx 1.33$ μm^{-1}, in tetrahydrofuran [153a];
72: R = Ph: 563 nm/1.78 μm^{-1}, in propylamine [153b].

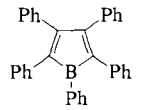
An absorption in the near infrared has been calculated[144] to occur for a planar structure of the Jahn-Teller distorted cyclopentadienyl cation **71**.[145] Pentaphenyl-**71**, which in solution has singlet and triplet molecules in equilibrium, is blue.[146] The products of benzo-condensation **73**[147,148] and amino-substitution **74**[149] are also long-wavelength absorbers (deeply colored); they have been characterized by their UV-VIS spectra and in some cases isolated.



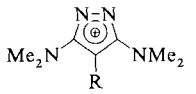
73



74



75

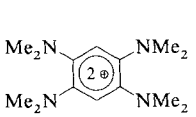


76

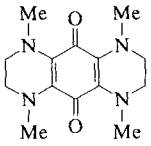
73: X = R = H: $\lambda = 670$ nm/$\tilde{\nu} = 1.49$ μm^{-1} (lg $\varepsilon \approx 3.1$), in conc. sulfuric acid [147];
73: X = NMe_2, R = Ph: 955 nm/1.05 μm^{-1} (≈ 4.3), in acetic acid [148];
74: R = NMe_2: 624 nm/1.60 μm^{-1} (2.71), in dichloromethane [149a];
74: R = OEt: 735 nm/1.36 μm^{-1}, in acetic anhydride [149a];
75: 567 nm/1.76 μm^{-1}, in toluene [151];
76: 583 nm/1.72 μm^{-1} (3.71), in acetonitrile [152].

Apart from the cyclopentadienylium salts, heterocycles such as **75** and **76**, the parent molecules of which are π-isoelectronic with **71**, are worthy of mention. The synthesis of these carbocyclic and heterocyclic cation salts and other diradicaloid structures was stimulated by studies on ferromagnetic organic compounds.[150]

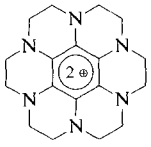
The stabilization of the cycloheptatrienyl anion **72**, which has been suggested to exist in a blue solution,[153] should be favored by acceptor substituents.[154] X-ray crystallography[155] showed that the recently prepared deep violet tetraiodide of the dication **77** is, as expected for a substituted antiaromatic dication, distorted; it contains two separate trimethinecyanine substructures.[156] In this connection we should also mention highly colored stellaquinones[157] such as the recently prepared **78**.[158]



77



78

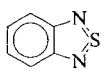


79

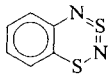
77: $\lambda = 573$ nm/$\tilde{\nu} = 1.74$ μm^{-1} (lg $\varepsilon = 3.38$), in acetonitrile [155];
78: 627 nm/1.59 μm^{-1} (2.28), in dichloromethane [158];
79: 523 nm/1.91 μm^{-1} (4.16), in acetonitrile [159b].

If the benzene dication bears six substituents, as in **79**, symmetry considerations indicate that it will again have a doubly degenerate MO containing two electrons. **79** has been shown by ESR spectroscopy to be a triplet molecule;[159a] however, the singlet molecule has been predicted to be 0.9 kcal/mol lower in energy in acetonitrile solution than the triplet molecule.[159b]

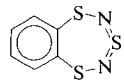
Heterocyclic compounds with $4n$ π-electrons can also exhibit a longer-wavelength absorption than the $(4n + 2)$ π-systems if their π-electron systems are planar: for example the heterocycle **81**, which is iso-π-electronic with a 12 π-hydrocarbon, absorbs at noticeably longer wavelengths than do **80** and **82** which have 10 and 14 π-electrons respectively.[160]



80



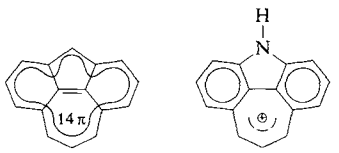
81



82

80: $\lambda = 304$ nm/$\tilde{\nu} = 3.29$ μm^{-1} (lg $\varepsilon = 4.15$), in cyclohexane;
81: 617 nm/1.62 μm^{-1} [160];
82: 384 nm/2.60 μm^{-1} [160].

In the above discussion we have dealt only with hydrocarbons in which the diradicaloid character is linked with the presence of $4n$ π-electrons in the perimeter ring; we shall now deal with the question as to whether under certain structural conditions a perimeter with $(4n + 2)$ π-electrons can also exhibit diradicaloid character. Examples of such behavior can perhaps be found for non-alternant hydrocarbons, which are often characterized by an absorption at relatively long wavelengths.[161] *Heilbronner* et al.[162] carried out a theoretical study on the cyclohepta[*def*]fluorene **83** and came to the conclusion that this (still unknown) hydrocarbon, which has 14 π-electrons in the outer ring and a central double bond, should exist as a triplet diradical.[163]



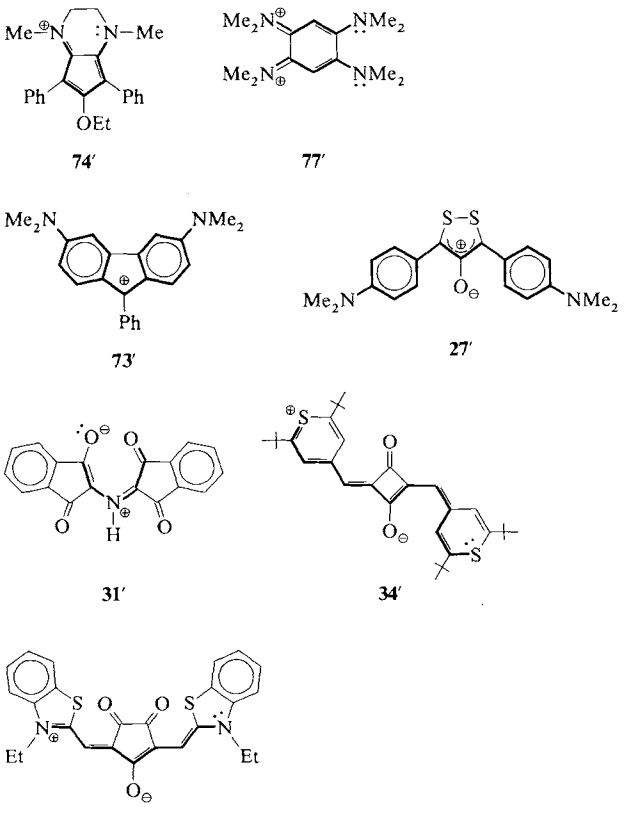
83 **84**

84: $\lambda \approx 690$ nm/$\tilde{\nu} \approx 1.45$ μm^{-1} ($\lg \varepsilon = 3.3$), in 60% $HClO_4$ [164].

Wirz et al. have suggested[164] that replacement of one of the methine groups in **83** by a heteroatom-containing group, as in **84**, will lead to a singlet molecule which will absorb at relatively long wavelengths; the heterocycle **84** is blue.

4. Classical *versus* Diradicaloid Chromophores

The compounds discussed above were investigated more or less from the point of view of diradicaloid structures; in this sense we can speak of colored substances with diradicaloid chromophores. However, this by no means excludes another reference for the color-determining π-electron system. This conclusion becomes particularly clear when the polymethine concept[8, 102] is used for the derivation of color-structure relationships. Many of the compounds listed above can indeed be considered as strongly structurally modified polymethine dyes, the absorption wavelengths of which can be qualitatively estimated with the help of empirical color rules. To make this clear we have again represented a number of the dyes dealt with above in terms of valence bond formulations which contain a polymethine substructure; the latter is emphasized by the use of bold bonding dashes.



Thus **74**, in the form of **74′**, can be derived from a streptopolymethinecyanine which has undergone cyclization via an additional bond.[156, 165] The long-wavelength absorption of the dye **77**, written as **77′**, consists of two weakly coupled trimethinecyanine units. Like **73′** and **27′** the compounds **73** and **27** are derivatives of a diphenylmethane and a vinylogous diphenylmethane dye respectively, while **31** in the form of **31′** is a protonated oxonol dye. Compounds with structures **34** and **29** have also been referred to above: in the case of the squarylium dye **34′** ($\lambda = 799$ nm[4a]) and the croconylium dye **29′** ($\lambda = 830$ nm[67b]) their relationship with polymethine dyes is made clear by the introduction of terminal heterocyclic groups; the carbonyl groups form bridges and the oxide residues substituents in *meso*-positions in heterocyclic polymethine dyes.[8b]

Whether or not these or other alternative formulations and chromophore reference structures have any justification can be decided on the basis of an objective analysis of the wave functions. It is possible using the configuration analysis method (CA) introduced by *Baba, Suzuki* and *Takemura*[166a] to relate the ground and excited states of the dyes to those structures which contain the same number of π-electrons and either a corresponding molecular skeleton or a composite molecule. The relationships between the ground states and the lowest-energy singly excited states of the chromophoric system or of a chromophoric system containing the subchromophore of the composite molecule can be evaluated on the basis of a number of suitable indices.[166] For example, it can be demonstrated by CA for **73** that in spite of the NIR absorption of this compound its relationship to the π-electron states of the diphenylmethane dyes is much closer than that to a structure constructed from a (Jahn-Teller distorted) diradicaloid cyclopentadienylium and two butadiene fragments. In Figure 10 the more or less completely hatched areas indicate graphically that the wave functions of the ground and first ππ* excited states of **74** are only very

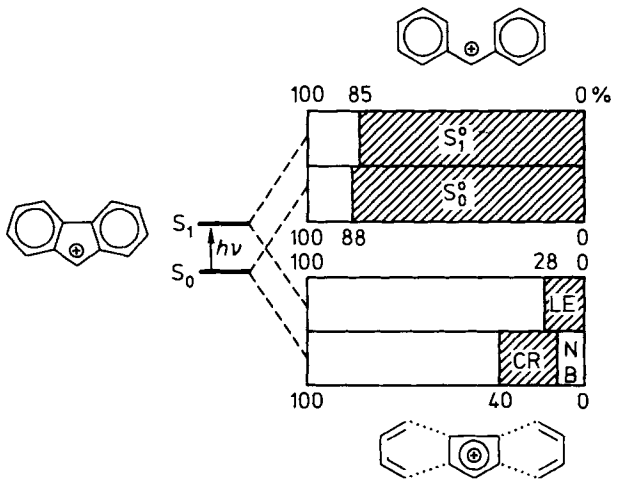


Fig. 10. Characterization of the ground and lowest excited states of the fluorenyl cation with respect to the ground and lowest excited state of the diphenylmethyl cation (top) and a composite molecule (bottom) consisting of a Jahn-Teller distorted cyclopentadienyl cation and two butadiene fragments. The degree of completeness of the representation in % is evaluated by projection of the wave function (configuration analysis). The contributions of the configurations in the composite molecule consist in the main of the no-bond (NB) ground state, the configuration of the lowest-energy local excitation (LE) in the five-membered ring and the configuration of the lowest-energy charge resonance (CR) from the butadiene fragments to the five-membered ring.

poorly described by the wave function of the fragmented molecule, while a comparison with the diphenylmethane dye resulting from the removal of only one bond gives a much better picture.[167] Because of the close relationships of the wave functions in the latter case, which are due to a good correlation of the MOs, *Dewar* et al. were able to successfully explain with MOs the spectral effects of the diphenylmethane dyes upon cyclization.[168] Configuration analyses have shown that relationships between chromophoric systems cannot reliably be described by the similarity of their spectral excitation energies but rather by correlation of the wave functions of those states which are responsible for the light absorption.[169]

Whether an NIR chromophore is regarded as the result of a diradicaloid structure or rather as a perturbed classical chromophore, the problem remains basically the same. If the spectral excitation energy falls to ca. 0.85 μm (1.2 μm^{-1}), the energy difference between S_0 and T_1 automatically becomes so small that we must refer to the compound as a diradicaloid: all the problems which occur in the description of such an electronic state will then be present.

5. Conclusion

At the beginning of the century it seemed likely on the basis of the studies then carried out on radical salts that the color band of dyes could be shifted from the visible into the near infrared, so that "higher-order colors" would occur;[170] today, in contrast, reliable information exists on NIR absorptions of many organic compounds resulting from an excitation of their electronic systems. In the case of light absorption by molecules from a singlet ground state these extend to almost 2 μm (0.5 μm^{-1}). Many dyes have been isolated which are suitable for information recording using commercial diode lasers at ca. 0.8 μm (1.25 μm^{-1}). A number of deeply colored compounds were obtained as "by-products" in the course of searches for organic conductors and ferromagnetics.

Although the specific modification of known chromophores has already made possible an approach to many chromophores which absorb at long wavelengths in the visible and NIR, the diradicaloid approach may provide pointers for the existence of further NIR chromophores which differ more radically from the conventional chromophores. However, the diradicaloid nature of compounds which absorb at very long wavelengths also indicates the difficulties which exist in the theoretical treatment of these chromophores. A limitation of the configuration interaction to singly excited configurations, which in the case of chromophores active in the UV/VIS region is justified by experience, becomes questionable for NIR chromophores. Proven semiempirical methods for the description of the $\pi \rightarrow \pi^*$ transitions of conjugated organic systems, such as the PPP method, are not suited to numerical predictions unless careful reparametrization is carried out when multiply-excited configurations are to be taken into account or when a complete CI is required.[171] A treatment of the vibronic interaction of NIR chromophores of the dimensions of organic dyes is also still outstanding.

We thank Prof. Dr. S. Hünig (Würzburg) and Prof. Dr. H. Bock (Frankfurt/Main) for their critical reading of the manuscript and for many useful comments.

Received: September 14, 1988 [A 719 IE]
German version: *Angew. Chem. 101* (1989) 693
Translated by Professor J. K. Mitchell, Dortmund (FRG)

[1] a) J. Griffiths, *Chem. Br. 22* (1986) 997; b) *Crit. Rep. Appl. Chem. 7* (1985) 1; c) H. Frühbeis, unpublished; cf. the report of the 9th Farbensymposium, Engelberg (Switzerland) 1985; *Chimia 39* (1985) 334.

[2] See for example J. P. Phillips, D. Bates, H. Feuer, B. S. Thyagarajan (Eds.): *Organic Spectral Data, Vol. 23*, Wiley, New York 1987.

[3] K. H. Drexhage in F. P. Schäfer (Ed.): *Dye Lasers*, 2nd edit., Springer, Berlin 1977, p. 144 ff; M. Maeda: *Laser Dyes, Properties of Organic Compounds for Dye Lasers*, Academic Press, New York 1984, and references cited therein.

[4] a) D. J. Gravesteijn, C. Steenbergen, J. Van der Veen, *Proc. SPIE Int. Soc. Opt. Eng. 420* (1983) 327; *Chem. Abstr. 100* (1983) 129783; b) M. Umehara, M. Abe, H. Oba, *J. Synth. Org. Chem. Jpn. 43* (1985) 334; c) J. E. Kuder, *J. Imaging Technol. 12* (1986) 140.

[5] a) M. Matsuoka, K. Takagi, K. Hamano, T. Kitao, *J. Jpn. Soc. Colour Mater. 57* (1984) 2; cited in [24b]; b) R. O. Loutfy, A.-M. Hor, C.-K. Hsiao, G. DiPaola-Baranyi, P. M. Kazmaier, *Pure Appl. Chem. 60* (1988) 1047; G. DiPaola-Baranyi, C.-K. Hsiao, P. M. Kazmaier, R. Burt, R. O. Loutfy, T. I. Martin, *J. Imaging Sci. 32* (1988) 60; c) N. Ito, H. Aiga, *Jpn. Kokai Tokkyo Koko*, JP 62132963; *Chem. Abstr. 107* (1987) 238195v.

[6] M. R. Detty, P. B. Merkel, S. K. Powers, *J. Am. Chem. Soc. 110* (1988) 5920.

[7] T. Imasaka, A. Yoshitake, N. Ishibashi, *Anal. Chem. 56* (1984) 1077; b) K. Sauda, T. Imasaka, N. Ishibashi, *ibid. 58* (1986) 2649.

[8] Reviews: a) J. Griffiths: *Colour and Constitution of Organic Molecules*, Academic Press, London 1976; b) J. Fabian, H. Hartmann: *Light Absorption of Organic Colorants*, Springer, Berlin 1980; c) P. F. Gordon, P. Gregory: *Organic Chemistry in Color*, Springer, Berlin 1983; H. Zollinger: *Color Chemistry*, VCH Verlagsgesellschaft, Weinheim 1987; d) S. Hünig, H. Quast in W. Foerst (Ed.): *Optische Anregung organischer Systeme*, Verlag Chemie, Weinheim 1966, p. 184 ff.

[9] a) H. Fujimoto, M. Tanaka, J. Tanaka, *Bull. Chem. Soc. Jpn. 56* (1983) 671; b) C. R. Fincher, Jr., M. Ozaki, M. Tanaka, D. Peebles, L. Lauchlan, A. J. Heeger, A. G. MacDiarmid, *Phys. Rev. B20* (1979) 1589; c) A. O. Patil, A. J. Heeger, F. Wudl, *Chem. Rev. 88* (1988) 183.

[10] H.-R. Blattmann, E. Heilbronner, G. Wagnière, *J. Am. Chem. Soc. 90* (1968) 4786.

[11] a) F. Sondheimer, *Chimia 28* (1974) 163, and references cited therein; *Acc. Chem. Res. 5* (1972) 81; b) J. F. M. Oth, *Pure Appl. Chem. 25* (1971) 573.

[12] a) J.-L. Calais, *Int. J. Quantum Chem. Quantum Chem. Symp. 11* (1977) 547; b) M. Takahashi, J. Paldus, *Int. J. Quantum Chem. 28* (1985) 459; c) P. Tavan, K. Schulten, *Phys. Rev. B36* (1988) 4337.

[13] a) E. Vogel, *Chimia 33* (1979) 57; *Pure Appl. Chem. 54* (1982) 1015; b) K. Yamamoto, S. Kuroda, M. Shibutani, Y. Yoneyama, J. Ojima, S. Fujita, E. Ejiri, K. Yonagihara, *J. Chem. Soc. Perkin Trans. 1 1988*, 395.

[14] J. Ojima, S. Fujita, M. Masumoto, E. Ejiri, T. Kato, S. Kuroda, Y. Nozawa, S. Hirooka, Y. Yoneyama, H. Tatemitsu, *J. Chem. Soc. Perkin Trans. 1 1988*, 385.

[15] R. C. Haddon, K. Raghavachari, *J. Am. Chem. Soc. 107* (1985) 289, and references cited therein.

[16] S. Itô, *Pure Appl. Chem. 54* (1982) 957.

[17] a) W. Freyer, *Z. Chem. 26* (1986) 263; b) G. N. Schrauzer, *Acc. Chem. Res. 2* (1969) 72; c) W. Freyer, *J. Prakt. Chem. 328* (1986) 253; *Z. Chem. 25* (1985) 104; d) I. Tabushi, K. Yamamura, H. Nonoguchi, *Chem. Lett. 1987*, 1373.

[18] In this report we have not discussed metal complexes with organic ligands, since the metal is responsible for their long-wavelength absorption; these are complexes whose spectral absorption is due to $d \rightarrow d^*$ transitions of transition metals [19a]. We have also not dealt with complexes which contain two metal atoms in different oxidation states and which exhibit relatively intense absorptions up to ca. 1600 nm (0.6 μm^{-1}) (mixed valence complexes) [19b]. These include the Ru^{II}/Ru^{III}-pyrazine complexes [19d] known as *Creutz-Taube* compounds and the ferrocene-type Fe^{II}/Fe^{III} complexes.

[19] a) A. B. P. Lever: *Inorganic Electronic Spectroscopy*, Elsevier, Amsterdam, 1984; b) C. Creutz, H. Taube, *J. Am. Chem. Soc. 91* (1969) 3988; c) C. LeVanda, K. Bechgaard, D. O. Cowan, U. T. Mueller-Westerhoff, P. Eilbracht, G. A. Candela, R. L. Collins, *ibid. 98* (1976) 3181; d) L.-T. Zhang, J. Ko, M. J. Ondrechen, *ibid. 109* (1987) 1666.

[20] a) G. A. Reynolds, K. H. Drexhage, *J. Org. Chem. 42* (1977) 885; b) B. Sens, *Dissertation*, Universität-Gesamthochschule Siegen 1984; c) M. A. Kudinova, Y. L. Slominskii, I. V. Shokod'ko, A. I. Tolmachev, *Ukr. Khim. Zh., Russ. Ed. 51* (1985) 95.

[21] N. Tyutyulkov, O. E. Polansky, F. Dietz, J. Fabian, A. Mehlhorn, *Theor. Chim. Acta 69* (1986) 247.
[22] S. Akiyama, S. Nakatsuji, K. Nakashima, M. Watanabe, *J. Chem. Soc. Chem. Commun. 1987*, 710.
[23] K. A. Bello, J. Griffiths, *J. Chem. Soc. Chem. Commun. 1986*, 1639.
[24] a) K.-Y. Chu, J. Griffiths, *J. Chem. Res. (S) 1978*, 180; *J. Chem. Res. (M) 1978*, 2319; b) K. Takagi, M. Kawabe, M. Matsuoka, T. Kitao, *Dyes Pigm. 6* (1985) 177; c) S. H. Kim, M. Matsuoka, Y. Kubo, T. Yoshida, T. Kitao, *ibid. 7* (1986) 93; S. H. Kim, S. Minami, M. Matsuoka, T. Kitao, *Chem. Express 2* (1987) 73; *Chem. Abstr. 106* (1987) 86211m.
[25] a) Y. Kubo, F. Mori, K. Yoshida, *Chem. Lett. 1987*, 1761; Y. Kubo, F. Mori, K. Komatsu, K. Yoshida, *J. Chem. Soc. Perkin Trans. 1 1988*, 2439; b) K. A. Bello, L. Cheng, J. Griffiths, *J. Chem. Soc. Perkin Trans. 2 1987*, 815; c) H. Junek, G. Uray, G. Zuschnig, *Dyes Pigm. 9* (1988) 137.
[26] Chromophoric organic radicals have also been excluded. Free radicals often absorb in the near infrared: P. Čársky, R. Zahradník, *Top. Curr. Chem. 43* (1973) 1, and references cited therein.
[27] a) G. G. Dyadyusha, A. D. Kachkovskii, *Teor. Eksp. Khim. 17* (1981) 393; b) M. Yu. Kornilov, G. G. Dyadyusha, V. I. Zamkovoi, M. L. Dekhtar', A. D. Kachkovskii, *Khim. Geterotsikl. Soedin. 1984*, 217; c) A. I. Tolmachev, *Teubner Texte zur Physik 13* (1987) 115.
[28] Ch. Zhixing, H. Siqun, *Theor. Chim. Acta 67* (1985) 409.
[29] a) W. T. Borden (Ed.): *Diradicals*, Wiley, New York 1982, and references cited therein; b) W. T. Borden, E. R. Davidson, *J. Am. Chem. Soc. 99* (1977) 4587; c) A. A. Ovchinnikov, *Theor. Chim. Acta 47* (1978) 297.
[30] J. Fabian, *Z. Chem. 27* (1987) 28; *Teubner Texte zur Physik 13* (1987) 151.
[31] a) L. Salem, C. Rowland, *Angew. Chem. 84* (1972) 86; *Angew. Chem. Int. Ed. Engl. 11* (1972) 92; b) L. Salem: *Electrons in Chemical Reactions: First Principles*, Wiley, New York 1982, and references cited therein; c) J. Michl, *Mol. Photochem. 4* (1972) 257; d) V. Bonačić-Koutecký, J. Koutecký, J. Michl, *Angew. Chem. 99* (1987) 216; *Angew. Chem. Int. Ed. Engl. 26* (1987) 170; e) J. Wirz, *Pure Appl. Chem. 56* (1984) 1289.
[32] a) R. C. Bingham, M. J. S. Dewar, *J. Am. Chem. Soc. 94* (1972) 9107; b) M. J. S. Dewar, C. Doubleday, *ibid. 100* (1978) 4935; c) M. J. S. Dewar, K. M. Merz, *J. Phys. Chem. 89* (1985) 4739.
[33] a) O. Kikuchi, K. Matsushita, K. Morihashi, M. Nakayama, *Bull. Chem. Soc. Jpn. 59* (1986) 3043; b) O. Kikuchi, Y. Kawakami, *J. Mol. Struct. 137* (1986) 365; c) J. M. Bofill, J. Gomez, S. Olivella, *ibid. 163* (1988) 285.
[34] a) W. Thiel, *J. Am. Chem. Soc. 103* (1981) 1420; b) A. Schweig, W. Thiel, *ibid. 103* (1981) 1425.
[35] a) P. Du, W. T. Borden, *J. Am. Chem. Soc. 109* (1987) 930; b) P. Du, D. A. Hrovat, W. T. Borden, P. M. Lahti, A. R. Rossi, J. A. Berson, *ibid. 108* (1986) 5072; c) J. A. Berson, *Pure Appl. Chem. 59* (1987) 1571, and references cited therein.
[36] H. Kollmar, V. Staemmler, *J. Am. Chem. Soc. 99* (1977) 3583; *Theor. Chim. Acta 48* (1978) 223.
[37] a) E. R. Davidson, W. T. Borden, *J. Phys. Chem. 87* (1983) 4783; b) I. B. Bersuker: *The Jahn-Teller-Effect and Vibronic Interaction in Modern Chemistry*, Plenum Press, New York 1984; I. B. Bersuker, N. N. Gorinchoi, V. Z. Polinger, *Theor. Chim. Acta 66* (1984) 161.
[38] J. Fabian, A. Mehlhorn, N. Tyutyulkov, *J. Mol. Struct. 151* (1987) 355.
[39] a) K. Fukui, K. Tanaka, *Bull. Chem. Soc. Jpn. 50* (1977) 1391; b) E. F. Hayes, A. K. Q. Siu, *J. Am. Chem. Soc. 93* (1971) 2090; c) D. Döhnert, J. Koutecký, *ibid. 102* (1980) 1789; d) K. Jug, *Tetrahedron Lett. 26* (1985) 1437; e) K. Yamaguchi, Y. Takahara, T. Fueno, K. N. Houk, *Theor. Chim. Acta 73* (1988) 337.
[40] *J. Michl* and *E. W. Thulstrup* have referred to the importance of the molecular exchange integral K_{ab} for the electronic excitation energy when they offered a simple explanation for the fact that azulene is blue and anthracene colorless, although the orbital energies of both structures are very similar: *Tetrahedron 32* (1976) 205.
[41] K. Haider, M. S. Platz, A. Despres, V. Lejeune, E. Migirdicyan, T. Bally, E. Haselbach, *J. Am. Chem. Soc. 110* (1988) 2318.
[42] R. Jain, L. McElwee-White, D. A. Dougherty, *J. Am. Chem. Soc. 110* (1988) 552, and references cited therein.
[43] P. Dowd, W. Chang, Y. H. Paik, *J. Am. Chem. Soc. 108* (1986) 7416; *ibid. 109* (1987) 5284.
[44] a) G. J. Snyder, D. A. Dougherty, *J. Am. Chem. Soc. 108* (1986) 299; b) P. Dowd, Y. H. Paik, *ibid. 108* (1986) 2788.
[45] V. Lejeune, A. Despres, E. Migirdicyan, J. Baudet, G. Berthier, *J. Am. Chem. Soc. 108* (1986) 1853.
[46] W. R. Roth, R. Langer, M. Bartmann, B. Stevermann, G. Maier, H. P. Reisenauer, R. Sustmann, W. Müller, *Angew. Chem. 99* (1987) 271; *Angew. Chem. Int. Ed. Engl. 26* (1987) 256.
[47] M. N. Burnett, R. Boothe, E. Clark, M. Gisin, H. M. Hassaneen, R. M. Pagni, G. Persy, R. J. Smith, J. Wirz, *J. Am. Chem. Soc. 110* (1988) 2527.
[48] a) M. Gisin, J. Wirz, *Helv. Chim. Acta 66* (1983) 1556; b) J. Pranata, D. A. Dougherty, *J. Am. Chem. Soc. 109* (1987) 1621.
[49] C. Doubleday, Jr., J. W. McIver, Jr., M. Page, *J. Phys. Chem. 92* (1988) 4367, and references cited therein.
[50] For the sake of clarity we shall neglect overlap with the central CH_2 group in the diradical trimethylene **18a** ($X = CH_2$) in our treatment using the π-approximation.
[51] Thiocarbonyl ylides such as thioformylium methylide (**18b**, X = S) are, like other ylides (1,3-dipoles), building blocks in cycloaddition reactions. See: A. Hosomi, S. Hayashi, K. Hoashi, S. Kohra, Y. Tominaga, *J. Chem. Soc. Chem. Commun. 1987*, 1442; R. Huisgen, C. Fulka, I. Kalwinsch, L. Xingya, G. Mloston, J. R. Moran, A. Pröbstl, *Bull. Soc. Chim. Belg. 93* (1984) 511; S. Araki, Y. Butsugan, *Chem. Letters 1985*, 1639. The blue-black conducting polymer polyisothionaphthene (band gap ca. 1 eV [9c]) contains thiocarbonyl ylide substructures, and dimers and clusters of the heteroanalogous azomethine ylides are of interest because their electronic structures are similar to that of the ferromagnetic CuO. See: K. Yamaguchi, Y. Takahara, T. Fueno, K. Nakasuji, I. Murata, *J. Appl. Phys. 27* (1988) L766.
[52] A formulation such as **18c** is often used when X is sulfur or an atom of another element of a higher group in the periodic table. Although in this case ab initio calculations indicate a higher contribution of d-type polarization functions at sulfur than in sulfur atoms in conventional sulfides, such a formula does not describe the actual situation satisfactorily. A larger contribution of polarization functions for heteroatoms in ylides is surprisingly also found when only second-row elements are present in the molecule. See: S. D. Kahn, W. J. Hehre, J. A. Pople, *J. Am. Chem. Soc. 109* (1987) 1871. For earlier discussions on hypervalency in valence bond formulas of betaine-type compounds see G. Berthier, B. Levy, L. Paoloni, *Theor. Chim. Acta 16* (1970) 316.
[53] a) W. C. Herndon, M. L. Ellzey, *Tetrahedron Lett. 1974*, 1399; b) M. Mestechkin, Yu. Vysotski, *ibid. 1975*, 109.
[54] a) K. J. Stone, M. M. Greenberg, J. L. Goodman, K. S. Peters, J. A. Berson, *J. Am. Chem. Soc. 108* (1986) 8088; b) K. W. Zilm, R. A. Merrill, M. M. Greenberg, J. A. Berson, *ibid. 109* (1987) 1567.
[55] a) M. P. Cava, M. V. Lakshmikantham, *Acc. Chem. Res. 8* (1975) 139; b) R. Gleiter, R. Bartetzko, G. Brähler, H. Bock, *J. Org. Chem. 43* (1978) 3893.
[56] P. Du, D. A. Hrovat, W. T. Borden, *J. Am. Chem. Soc. 108* (1986) 8086.
[57] J. Kolc, J. Michl, *J. Am. Chem. Soc. 95* (1973) 7391.
[58] R. Bartetzko, R. Gleiter, *Angew. Chem. 90* (1978) 481; *Angew. Chem. Int. Ed. Engl. 17* (1978) 468.
[59] J. M. Hoffman, Jr., R. H. Schlessinger, *J. Am. Chem. Soc. 91* (1969) 3953.
[60] For a detailed description see: W. D. Ollis, S. P. Standforth, C. A. Ramsden, *Tetrahedron 41* (1985) 2239, and references cited therein.
[61] P. B. Talukdar, S. K. Sengupta, A. K. Datta, *Indian J. Chem. 9* (1971) 1018.
[62] S. Araki, J. Mizuya, Y. Butsugan, *J. Chem. Soc. Perkin Trans. 1 1985*, 2439.
[63] a) D. Barillier, *Phosphorus Sulfur 8* (1980) 79; b) A. Schönberg, E. Frese, *Chem. Ber. 103* (1970) 3885.
[64] H. Gotthardt, M. C. Weisshuhn, B. Christl, *Chem. Ber. 109* (1976) 740.
[65] R. Mayer, J. Fabian, H. Viola, L. Jakisch, *Phosphorus Sulfur 31* (1987) 109.
[66] Estimates of spectral absorption of diradicaloid π-systems made using the PPP method, which normally does not take higher excited configurations into account, are not reliable. While the calculated wavelengths of the absorption bands for compounds such as **21** (X = S) with parameters used earlier for sulfur in sulfur heterocycles (J. Fabian, A. Mehlhorn, R. Zahradník, *J. Phys. Chem. 72* (1968) 3975) with a variable β_{CC} method for CC (J. Fabian, G. Tröger, *Teor. Eksp. Khim. 7* (1971) 170) and MNDO/2 × 2-CI geometries (J. Fabian, P. Birner, *Wiss. Z. Techn. Univ. Dresden 37* (1988) 119) lie relatively close to the experimental data, (**21**: λ_{calc} = 519 nm, λ_{exp} = 572 nm [54a]), the absorption wavelengths calculated for betaine-type olate and thiolate structures are much too high (see for example calculations for dithizone [68]).
[67] a) G. Seitz, J. Auch, W. Klein, *Chem.-Ztg. 87* (1987) 343; b) Y. Nishimura, T. Kimura, H. Matsuda, T. Eguchi, T. Nakagiri, K. Sakai, Jpn. Kokai Tokkyo Koho, JP 62149482, *Chem. Abstr. 108* (1988) 214047t.
[68] J. Fabian, G. Röbisch, R. Nöske, *Dyes Pigm. 8* (1987) 165.
[69] Only recently has it been shown by X-ray crystallography and spectral studies in solution that dithizone has the structure represented by **30**. It was previously assumed that in solution dithizone is a mixture of the tautomers *C*-mercaptoformazan and *N,N'*-diphenylthiocarbazone (see [68] and references cited therein) or a mixture of the latter compound and its deprotonated form: M. R. Mahmoud, A. A. Abd El Gaber, A. M. El Roudi, E. M. Soliman, *Spectrochim. Acta 43A* (1987) 1281.
[70] R. Grigg, J. F. Malone, T. Mongkolaussavaratana, S. Thianpatanagul, *J. Chem. Soc., Chem. Commun. 1986*, 421. Tautomeric structures were previously suggested for **31**, the protonated from of "Ruhemann's purple". It is however unclear why, in contrast to the normal situation, the protonation of the anionic dyes at nitrogen leads to a hypsochromic shift of the color band.
[71] a) W. J. Middleton, *J. Org. Chem. 31* (1966) 3731; b) P. Gronski, K. Hartke, *Chem. Ber. 111* (1978) 272; impurities which cannot be removed are probably responsible for the color of the thiocarbonyl ylides synthesized.
[72] D. E. Seeger, P. M. Lahti, A. R. Rossi, J. A. Berson, *J. Am. Chem. Soc. 108* (1986) 1251.
[73] R. Gleiter, R. Hoffmann, *Angew. Chem. 81* (1969) 225; *Angew. Chem. Int.*

Ed. Engl. 8 (1969; according to ab inition) 214 calculations the diketone **34**, R = H, has a folded geometry: P. von R. Schleyer, P. H. M. Budzelaar, D. Cremer, E. Kraka, *Angew. Chem. 96* (1984) 374; *Angew. Chem. Int. Ed. Engl. 23* (1984) 374.

[74] a) R. W. Bigelow, R.-J. Freund, *Chem. Phys. 107* (1986) 159, and references cited therein; b) K.-Y. Law, S. Kaplan, R. K. Crandall, *Dyes Pigm. 9* (1988) 187, and references cited therein.

[75] P. H. M. Budzelaar, H. Dietrich, J. Macheleid, R. Weiss, P. von R. Schleyer, *Chem. Ber. 118* (1985) 2118.

[76] J. Gauger, G. Manecke, *Chem. Ber. 103* (1970) 3553.

[77] L. K., Montgomery, J. C. Huffman, E. A. Jurczak, M. P. Grendze, *J. Am. Chem. Soc. 108* (1986) 6004.

[78] a) W. Theilacker, W. Ozegowski, *Ber. Dtsch. Chem. Ges. 73* (1940) 898; b) H.-D. Brauer, H. Stieger, H. Hartmann, *Z. Phys. Chem. (Frankfurt/Main) NF 63* (1969) 50; c) R. Sartorius, H.-D. Brauer, *Angew. Chem. 84* (1972) 546; *Angew. Chem. Int. Ed. Engl. 11* (1972) 531; d) M. Ballester, J. Riera, J. Castañer, C. Badía, J. M. Monsó, *J. Am. Chem. Soc. 93* (1971) 2215; cf. M. Ballester, J. Castañer, R. Riera, A. Ibáñez, *Tetrahedron Lett. 21* (1980) 2435; e) R. Schmidt, H.-D. Brauer, *Angew. Chem. 83* (1971) 498; *Angew. Chem. Int. Ed. Engl. 10* (1971) 506.

[79] X-ray crystallographic studies on Tschitschibabin's hydrocarbon showed unexpectedly that in the crystal the hydrocarbon has an almost planar biphenylylene bridge. In contrast to Thiel's hydrocarbon a quinoid bonding system is not formed.

[80] As was shown in [78 d] for the perchlorinated Tschitschibabin hydrocarbon, the intense absorption corresponds in wavelength to that of the perchlorinated diphenylmethyl radical. Just as for **35a**, the triplet structure of this derivative was demonstrated by its spectrum.

[81] Twisted ethene (dimethylene) and its heteroanalogues are transition structures in an *E/Z* isomerization. According to *Bonačić-Koutecký* et al. [31 d] an orthogonal arrangement of two planar CH_2 fragments gives a homosymmetric diradical, while at smaller dihedral angles a homosymmetric diradicaloid is present. Rotation about a double bond is of importance in the phenomenon of vision.

[82] For the method see: J. N. Murrell: *The Theory of the Electronic Spectra of Organic Molecules*, Wiley, New York 1963; H. Suzuki: *Electronic Absorption Spectra and Geometry of Organic Molecules*, Academic Press, New York 1967; J. Fabian, *J. Signalaufzeichnungsmater. 6* (1978) 307; *ibid. 7* (1979) 67, and references cited therein.

[83] J. Michl, J. G. Radziszewski, J. W. Downing, J. Kopecký, P. Kaszynski, R. D. Miller, *Pure Appl. Chem. 59* (1987) 1613. For further investigations on sterically hindered alkenes see A. Krebs, B. Kaletta, W. U. Nickel, W. Rüger, L. Tikwe, *Tetrahedron 42* (1986) 1693.

[84] M. Traetteberg, P. Bakken, A. Almenningen, W. Lüttke, J. Jannsen, *J. Mol. Struct. 81* (1982) 87.

[85] a) E. Harnik, G. M. J. Schmidt, *J. Chem. Soc. 1954*, 3295; b) J. F. D. Mills, S. D. Nyburg, ibid. 1963, 308; c) I. Agranat, Y. Tapuhi, *J. Am. Chem. Soc. 100* (1978) 5604; d) I. R. Gault, W. D. Ollis, I. O. Sutherland, *Chem. Commun. 1970*, 269.

[86] a) G. Kortüm, *Ber. Bunsenges. Phys. Chem. 78* (1974) 391; b) Y. Tapuhi, O. Kalisky, I. Agranat, *J. Org. Chem. 44* (1979) 1949.

[87] R. Korenstein, K. A. Muszkat, S. Sharafy-Ozeri, *J. Am. Chem. Soc. 95* (1973) 6177.

[88] a) J. F. D. Mills, S. C. Nyburg, *J. Chem. Soc. 1963*, 927; b) R. Korenstein, K. A. Muszkat, M. A. Slifkin, E. Fischer, *J. Chem. Soc. Perkin Trans. 2 1976*, 438; c) T. Sugimoto, Y. Misaki, T. Kajita, T. Nagatomi, Z. Yoshida, J. Yamauchi, *Angew. Chem. 100* (1988) 1129; *Angew. Chem. Int. Ed. Engl. 27* (1988) 1078; d) M. Iyoda, H. Otani, M. Oda, *ibid. 100* (1988) 1131 and *27* (1988) 1080.

[89] a) C. P. Fenimore, *Acta Crystallogr. 1* (1948) 195; b) N. A. Bailey, S. E. Hull, *ibid. B 34* (1978) 3289; c) J.-S. Lee, S. C. Nyburg, *ibid. C 41* (1985) 560.

[90] a) Z. R. Grabowski, K. Rotkiewicz, A. Siemiarczuk, D. J. Cowley, W. Baumann, *Nouv. J. Chim. 3* (1979) 443; b) W. Rettig, *Angew. Chem. 98* (1986) 696; *Angew. Chem. Int. Ed. Engl. 25* (1986) 971; c) E. Lippert, W. Rettig, V. Bonačić-Koutecký, F. Heisel, J. A. Miehe, *Adv. Chem. Phys. 68* (1987) 1, and references cited therein.

[91] a) T. Okada, N. Mataga, W. Baumann, A. Siemiarczuk, *J. Phys. Chem. 91* (1987) 4490; b) K. Yamasaki, K. Arita, O. Kajimoto, K. Hara, *Chem. Phys. Lett. 123* (1986) 277; O. Kajimoto, K. Yamasaki, K. Arita, K. Hara, *ibid. 125* (1986) 184.

[92] a) A. Schönberg, A. Mustafa, M. E. El-Din Sobhy, *J. Am. Chem. Soc. 75* (1953) 3377; b) A. Schönberg, E. Singer, W. Stephan, W. S. Sheldrick, *Tetrahedron 39* (1983) 2429.

[93] A. Z. Khan, J. Sandström, *J. Am. Chem. Soc. 110* (1988) 4843.

[94] K. Takahashi, F. Ishikawa, K. Takase, *Tetrahedron Lett. 1976*, 4655; K. Takahashi, K. Takase, *ibid. 1975*, 245.

[95] C. Reichardt, E. Harbusch, R. Müller in I. Bertini, L. Lunazzi, A. Dei (Eds.): *Advances of Solution Chemistry*, Plenum, New York 1981, p. 275 ff.

[96] E. M. Kosower, B. G. Ramsey, *J. Am. Chem. Soc. 81* (1959) 856.

[97] R. Boese, N. Finke, J. Henkelmann, G. Maier, P. Paetzold, H. P. Reisenauer, G. Schmid, *Chem. Ber. 118* (1985) 1644.

[98] A. T. Balaban, M. Paraschiv, *Rev. Roum. Chim. 27* (1982) 513.

[99] W. J. Linn, O. W. Webster, R. E. Benson, *J. Am. Chem. Soc. 87* (1965) 3651.

[100] S. V. Kalniń, O. Ya. Neiland, *Zh. Org. Khim. 7* (1971) 1606.

[101] A cursory examination indicates that the diradicaloid TICT state mentioned above corresponds to an excitation state of type $D^{\oplus}A^{\ominus}$. However, this state does not result from vertical excitation of the molecule, but only after a "horizontal" relaxation process.

[102] The change in the nature of the bond in the delocalized dye chromophore was already described by *Th. Förster* in the language of resonance theory: *Z. Phys. Chem. B 47* (1940) 245; *ibid. B 48* (1941) 12. However, it was *Dähne's* contribution to have recognized the characteristic electronic structure of the polymethines and the importance of the polymethine state for the dyes. It is a characteristic of the polymethines that the π-charges which alternate along the chain undergo redistribution on excitation: see S. Dähne, *Z. Chem. 5* (1965) 441; S. Dähne, D. Leupold, *Ber. Bunsenges. Phys. Chem. 70* (1966) 618; S. Dähne, F. Moldenhauer in R. W. Taft (Ed.): *Progress in Physical Organic Chemistry, Vol. 15*, Wiley, New York 1985, p. 1 ff., and references cited therein.

[103] The term "pimer" (or π-mer), which is due to *Kosower* (E. M. Kosower, J. L. Cotter, *J. Am. Chem. Soc. 86* (1964) 5524; E. M. Kosower, J. Hajdu, *ibid. 93* (1971) 2534) has the advantage of being clearly distinct from the dimerization with concomitant formation of a σ-bond which is typical for many radicals.

[104] a) K. Kimura, H. Yamada, H. Tsubomura, *J. Chem. Phys. 48* (1968) 440; b) J. Tanaka, M. Mizuno, *Bull. Chem. Soc. Jpn. 42* (1969) 1841; c) Y. Sato, M. Kinoshita, M. Sano, H. Akamatu, *ibid. 43* (1970) 2370; d) Y. Oohashi, T. Sakata, *ibid. 46* (1973) 765.

[105] a) R. Foster, T. J. Thomson, *Trans. Faraday Soc. 59* (1963) 296; b) Y. Iida, *Bull. Chem. Soc. Jpn. 42* (1969) 71; c) S. Hiroma, H. Kuroda, H. Akamatu, *ibid. 44* (1971) 9; d) M. Morinaga, T. Nogami, H. Hikawa, *ibid. 52* (1979) 3739.

[106] The pimerization leads to a change in color. The color of monomeric **48**, caused by an absorption at ca. 600 nm, changes to violet on dimerization because of the hypsochromic shift of this band [103]. The term "viologen" for the oxidized form of the radical (and "violenes" for polymethine radicals in general cf. S. Hünig, *Pure Appl. Chem. 15* (1967) 109) results from the incorrect assumption that the violet color of **48** is due to the radical. See Ref. [109].

[107] The term "CT band" is widely used in the literature because of the theoretical interpretation of this absorption of the dimerized radical in terms of a molecule which is described as a symmetrical combination of two (opposing) CT configurations (K. H. Hausser, J. N. Murrell, *J. Chem. Phys. 27* (1957) 500); for the theory see also K. Kimura, T. Yamazaki, S. Katsumata, *J. Phys. Chem. 75* (1971) 1768 and [123 d].

[108] a) S. Imabayashi, N. Kitamura, K. Tokuda, S. Tazuke, *Chem. Lett. 1987*, 915; b) Y. Nambu, K. Yamamoto, T. Endo, *J. Chem. Soc., Chem. Commun. 1986*, 574.

[109] W. Geuder, S. Hünig, A. Suchy, *Tetrahedron 42* (1986) 1665.

[110] T. Sakata, S. Nagakura, *Bull. Chem. Soc. Jpn. 43* (1970) 2414.

[111] J. L. de Boer, A. Vos, *Acta Crystallogr. B 28* (1972) 835, 839.

[112] The species known as charge-transfer (electron-donor-acceptor) complexes was described in detail by Mulliken et al.: R. S. Mulliken, W. B. Person: *Molecular Complexes: A Lecture and Reprint Volume*, Wiley, New York 1969. For a description of the theoretical model see also C. J. Bender, *Chem. Soc. Rev. 15* (1986) 475. Numerous spectral data are tabulated in: C. N. R. Rao, S. N. Bhat, P. C. Dwivedi, *Appl. Spectrosc. Rev. 5* (1971)) 1 ff. For dyes of the intermolecular CT-complex type, which are of interest for optical reproduction in the NIR, see M. Matsuoka, T. Yodoshi, L. Han, T. Kitao, *Dyes Pigm. 9* (1988) 343.

[113] H. Kuroda, M. Kobayashi, M. Kinoshita, S. Takemoto, *J. Chem. Phys. 36* (1962) 457.

[114] D. J. Sandman, G. P. Ceasar, P. Nielsen, A. J. Epstein, T. J. Holmes, *J. Am. Chem. Soc. 100* (1978) 202.

[115] M. Rosenblum, R. W. Fish, C. Bennett, *J. Am. Chem. Soc. 86* (1964) 5166.

[116] I. Murata, *Pure Appl. Chem. 55* (1983) 323.

[117] H. Vogler, *Croat. Chim. Acta 56* (1983) 297.

[118] a) R. Foster, T. J. Thomson, *Trans. Faraday Soc. 58* (1962) 860; b) J. Ferraris, D. O. Cowan, V. Walatka, Jr., J. H. Perlstein, *J. Am. Chem. Soc. 95* (1973) 948; c) A. Yamagishi, F. Watanabe, T. Masui, *J. Chem. Soc., Chem. Commun. 1977*, 273.

[119] a) B. G. Anex, E. B. Hill, Jr., *J. Am. Chem. Soc. 88* (1966) 3648; b) D. B. Chesnut, W. D. Phillips, *J. Chem. Phys. 35* (1961) 1002.

[120] J. S. Miller, A. J. Epstein, W. M. Reiff, *Chem. Rev. 88* (1988) 201.

[121] Y. Iida, *Bull. Chem. Soc. Jpn. 42* (1969) 637.

[122] a) J. B. Torrance, B. A. Scott, F. B. Kaufman, *Solid State Commun. 17* (1975) 1369; b) J. B. Torrance, *Acc. Chem. Res. 12* (1979) 79; c) J. J. Mayerle, J. B. Torrance, *Bull. Chem. Soc. Jpn. 54* (1981) 3170.

[123] a) G. Saito, H. Kumagai, J. Tanaka, T. Enoki, H. Inokuchi, *Mol. Cryst. Liqu. Cryst. 120* (1985) 337; b) K. Nakasuji, H. Kubota, T. Kotani, I. Murata, G. Saito, T. Enoki, K. Imaeda, H. Inokuchi, M. Honda, C. Katayama, J. Tanaka, *J. Am. Chem. Soc. 108* (1986) 3460; c) J. Tanaka, M. Tanaka, T. Kawai, T. Takabe, O. Maki, *Bull. Chem. Soc. Jpn. 49*

(1976) 2558; d) K. Yakushi, H. Kanbara, H. Tajima, H. Kuroda, G. Saito, T. Mori, *ibid. 60* (1987) 4251.

[124] An example was recently reported: A. Aumüller, P. Erk, S. Hünig, H. Meixner, J.-U. von Schütz, H.-P. Werner, *Liebigs Ann. Chem. 1987*, 977.

[125] The spectral behavior of the mixed-valence complexes is reminiscent of dimers which exist as free radicals. They absorb at wavelengths considerably longer than do the radicals of the monomers; cf. B. Badger, B. Brocklehurst, *Trans. Faraday Soc. 65* (1969) 2588; A. Kira, S. Arai, M. Imamura, *J. Chem. Phys. 54* (1971) 4890. The color-determining transitions of these dimers are of doublet-doublet character [26]. Thus we are not dealing here with singlet-singlet transitions as in the CR bands of dimers as they are formed on dimerization.

[126] The regular polygon of the monocyclic ring of interest is placed in a circle of radius 2β in such a way that an apex is pointing downwards. The points where the polygon touches the circle give the energy of the Hückel-MOs. For example, when a three-, four- or five-membered ring is populated by four π-electrons then two of these electrons must occupy two MOs of equal energy. For a detailed treatment see: W. Kutzelnigg: *Einführung in die Theoretische Chemie, Band 2*, Verlag Chemie, Weinheim 1978, p. 280 ff.

[127] a) R. Breslow, *Acc. Chem. Res. 6* (1973) 393; b) M. J. S. Dewar, *Angew. Chem. 83* (1971) 859; *Angew. Chem. Int. Ed. Engl. 10* (1971) 761.

[128] M. N. Gluchovtsev, B. Ya. Simkin, V. I. Minkin, *Usp. Khim. 54* (1985) 86; see also D. Lloyd: *Non-Benzenoid Conjugated Carbocyclic Compounds*, Elsevier, Amsterdam 1984; A. T. Balaban, M. Bancin, V. Ciorba: *Annulenes, Benzo-, Hetero-, Homo-Derivatives, and their Valence Isomers, Vol. 1–3*, CRC Press, Boca Raton, FL, USA 1987.

[129] P. G. Farrell, R. Grinter, S. F. Mason in W. Foerst (Ed.): *Optische Anregung organischer Systeme*, Verlag Chemie, Weinheim 1966; p. 88 ff., and references cited therein.

[130] a) J. Wirz, A. Krebs, H. Schmalstieg, H. Angliker, *Angew. Chem. 93* (1981) 192; *Angew. Chem. Int. Ed. Engl. 20* (1981) 192; b) G. Maier, B. Hoppe, *Tetrahedron Lett. 1973*, 861; S. Masamune, M. Suda, H. Ona, M. L. Leichter, *J. Chem. Soc., Chem. Commun. 1972*, 1268; c) G. Maier, *Angew. Chem. 100* (1988) 317; *Angew. Chem. Int. Ed. Engl. 27* (1988) 309.

[131] a) O. Ermer, E. Heilbronner, *Angew. Chem. 95* (1983) 414; *Angew. Chem. Int. Ed. Engl. 22* (1983) 402; b) M. Irngartinger, M. Nixdorf, N. H. Riegler, A. Krebs, H. Kimling, J. Pocklington, G. Maier, K.-D. Malsch, K. A. Schneider, *Chem. Ber. 121* (1988) 673.

[132] The CC bond lengths of cyclobutadienes were found to be ca. 1.34 and 1.60 Å [131], while the bond lengths in polyenes and cyclopolyenes are ca. 1.45 and 1.35 Å respectively. The extreme distortion of **63** is an expression of a destabilization of the square arrangement. The destabilization of the $4n$ π-annulenes decreases rapidly with increasing ring size. According to ab initio calculations **63** is the only annulene with a π-destabilization; see R. C. Haddon, *Pure Appl. Chem. 58* (1986) 129. Higher $4n$ π- and $(4n + 2)$ π-annulenes then differ only in their paramagnetic ring current.

[133] P. Bischof, R. Gleiter, K. Hafner, K. H. Knauer, J. Spanget-Larsen, H. U. Süss, *Chem. Ber. 111* (1978) 932.

[134] E. Vogel, H. Königshofen, K. Müllen, J. F. M. Oth, *Angew. Chem. 86* (1974) 229; *Angew. Chem. Int. Ed. Engl. 13* (1974) 283.

[135] a) F. Sondheimer, R. Wolovsky, P. J. Garatt, I. C. Calder, *J. Am. Chem. Soc. 88* (1966) 2610; b) *DMS-UV-Atlas organischer Verbindungen*, Verlag Chemie, Weinheim 1967; c) [135b], p. A14/2.

[136] A. Mugnoli, M. Simonetta, *J. Chem. Soc. Perkin Trans. 2 1976*, 822.

[137] a) A. Minsky, A. Y. Meyer, R. Poupko, M. Rabinovitz, *J. Am. Chem. Soc. 105* (1983) 2164; b) A. Minsky, A. Y. Meyer, M. Rabinovitz, *Tetrahedron 41* (1985) 785; c) M. Rabinovitz, *Top. Curr. Chem. 146* (1988) 99.

[138] a) Y. Cohen, J. Klein, M. Rabinovitz, *J. Chem. Soc., Chem. Commun. 1985*, 1033; b) Y. Cohen, A. Y. Meyer, M. Rabinovitz, *J. Am. Chem. Soc. 108* (1986) 7039.

[139] a) G. Levin, B. E. Holloway, M. Szwarc, *J. Am. Chem. Soc. 98* (1976) 5706; b) [135b], p. E4/5.

[140] T. H. Jozefiak, L. L. Miller, *J. Am. Chem. Soc. 109* (1987) 6560.

[141] a) W. Leupin, J. Wirz, *J. Am. Chem. Soc. 102* (1980) 6068; b) W. Leupin, S. J. Berens, D. Magde, J. Wirz, *J. Phys. Chem. 88* (1984) 1376.

[142] M. A. Rossman, N. J. Leonhard, S. Urano, P. R. LeBreton, *J. Am. Chem. Soc. 107* (1985) 3884.

[143] a) B. A. Hess, Jr., L. J. Schaad, P. Čársky, *Tetrahedron Lett. 25* (1984) 4721; b) G. Winkelhofer, R. Janoschek, F. Fratev, G. W. Spitznagel, J. Chandrasekhar, P. von R. Schleyer, *J. Am. Chem. Soc. 107* (1985) 332.

[144] A "non-classical" pyramidal structure has also been discussed for **71**, cf. V. I. Minkin, R. M. Minyaev, Yu. A. Zhdanov: *Nonclassical Structures of Organic Chemistry*, ST Chemical Series, MIR Publ., Moscow 1987, p. 100 ff. Among the doubly charged ions with $4n$ π-electrons and an even number of atoms in the ring, recent ab initio calculations have indicated that the benzene dianion should also be nonplanar; this molecular structure has been taken as a criterion for "antiaromaticity": B. L. Podlogar, W. A. Glauser, W. R. Rodriguez, D. J. Raber, *J. Org. Chem. 53* (1988) 2127.

[145] A. Mehlhorn, J. Fabian, N. Tyutyulkov, G. Olbrich, F. Dietz, *J. Prakt. Chem. 328* (1986) 603, and references cited therein.

[146] a) R. Breslow, H. W. Chang, W. A. Yager, *J. Am. Chem. Soc. 85* (1963) 2033; b) R. Breslow, R. Hill, E. Wasserman, *ibid. 86* (1964) 5349, see footnote [2].

[147] R. Zahradník, J. Pancíř, A. Kröhn, *Collect. Czech. Chem. Commun. 34* (1969) 2831.

[148] A. Barker, C. C. Barker, *J. Chem. Soc. 1954*, 1307.

[149] a) R. Gompper, H. Glöckner, *Angew. Chem. 96* (1984) 48; *Angew. Chem. Int. Ed. Engl. 23* (1984) 53; b) R. Gompper, T. Gessner, *ibid. 97* (1985) 996 and *24* (1985) 982.

[150] a) R. Breslow, *Pure Appl. Chem. 54* (1982) 927; b) H. Iwamura, *ibid. 58* (1986) 187; c) T. J. LePage, R. Breslow, *J. Am. Chem. Soc. 109* (1987) 6412.

[151] J. J. Eisch, J. E. Galle, S. Kozima, *J. Am. Chem. Soc. 108* (1986) 379.

[152] R. Gompper, R. Guggenberger, R. Zentgraf, *Angew. Chem. 97* (1985) 998; *Angew. Chem. Int. Ed. Engl. 24* (1985) 984.

[153] a) H. J. Dauben, Jr., M. R. Rifi, *J. Am. Chem. Soc. 85* (1963) 3041; b) R. Breslow, H. W. Chang, *ibid. 87* (1965) 2200.

[154] J. Petkov, J. Fabian, unpublished.

[155] K. Elbl, C. Krieger, H. A. Staab, *Angew. Chem. 98* (1986) 1024; *Angew. Chem. Int. Ed. Engl. 25* (1986) 1023.

[156] A. Mehlhorn, J. Fabian, *J. Mol. Struct. 109* (1984) 27.

[157] K. Wallenfels, W. Draber, *Angew. Chem. 70* (1958) 313; *Justus Liebigs Ann. Chem. 667* (1963) 55.

[158] R. Gompper, R. Binder, H.-U. Wagner, *Tetrahedron Lett. 27* (1986) 691.

[159] a) R. Breslow, P. Maslak, J. S. Thomaides, *J. Am. Chem. Soc. 106* (1984) 6453; b) J. S. Thomaides, P. Maslak, R. Breslow, *ibid. 110* (1988) 3970.

[160] A. W. Cordes, M. Hojo, H. Koenig, M. C. Noble, R. T. Oakley, W. T. Pennington, *Inorg. Chem. 25* (1986) 1137.

[161] R. Zahradnik, *Angew. Chem. 77* (1965) 1097; *Angew. Chem. Int. Ed. Engl. 4* (1965) 1039.

[162] P. Baumgartner, E. Weltin, G. Wagnière, E. Heilbronner, *Helv. Chim. Acta 48* (1965) 751.

[163] The hydrocarbon **3** belongs to the family of non-alternant hydrocarbons. Just like **83** it has a $(4n + 2)$ π-electron system along its perimeter ($n = 3$ for **83**, $n = 5$ for **3**), which is fixed by a double bond.

[164] B. Freiermuth, J. Wirz, *Angew. Chem. 100* (1988) 589; *Angew. Chem. Int. Ed. Engl. 27* (1988) 585.

[165] J. Fabian, *J. Prakt. Chem. 320* (1978) 361; *ibid. 323* (1981) 551.

[166] a) M. Baba, S. Suzuki, T. Takemura, *J. Chem. Phys. 50* (1969) 2078; b) J. Fabian, *Z. Chem. 20* (1980) 197; c) J. Fabian, A. Mehlhorn, F. Fratev, *Int. J. Quantum Chem. 17* (1980) 235.

[167] The configuration analysis of **73** (X = H) is based on PPP calculations carried out using a variable β-technique (see Ref. [67]). The inclusion of multiply excited configurations of the base structures would improve the quality of the projection but not the clarity of the interpretation.

[168] D. A. Brown, M. J. S. Dewar, *J. Chem. Soc. 1954*, 2134.

[169] J. Fabian, A. Mehlhorn, F. Dietz, N. Tyutyulkov, *Monatsh. Chem. 115* (1984) 21.

[170] J. Piccard, *Ber. Dtsch. Chem. Ges. 46* (1913) 1843. Proof that radical salts of Wurster type would actually absorb in the NIR was first provided decades later: M. Ertaman, Dissertation, Universität Basel 1952; U. Zenhäusern, Dissertation, Universität Basel 1965; cf. R. Wizinger, *Palette (Basel) 24* (1966) 24.

[171] Cf. P. Tavan, K. Schulten, *J. Chem. Phys. 70* (1979) 5407; *85* (1986) 6602.

General Aspects and Optimization of Enantioselective Biocatalysis in Organic Solvents: The Use of Lipases

New Synthetic Methods (76)

By Ching-Shih Chen* and Charles J. Sih*

Enantioselective biocatalysis in nonaqueous media is becoming increasingly important in preparative synthetic chemistry. This article discusses (1) the general catalytic properties of enzymes in nonaqueous environments, (2) the basic principles that govern lipase-catalyzed enantioselective esterification and transesterification reactions in organic media for the preparation of optically active acids and alcohols, (3) the determination of kinetic and thermodynamic parameters, and (4) the quantitative analysis of published data.

1. Introduction

Enzymatic reactions are generally conducted in aqueous media because of the general notion that an aqueous environment is optimal for maintaining the catalytically active conformations of the enzyme protein for binding and catalysis. In an aqueous medium, the folding of a soluble enzyme protein is driven by the tendency of hydrophobic amino acid residues to be excluded from water, so that they are buried in the interior of the molecule, whereas the charged and hydrophilic residues are on the surface in contact with the aqueous solvent. When water is replaced with an apolar solvent, the interior hydrophobic residues tend to disperse, resulting in a reorganization of the enzyme tertiary structure. This conjecture implies that the conformation of the enzyme protein is drastically altered and, in the extreme case, the enzyme pocket may be viewed as "turned inside out"[1] in organic media. Consequently, the catalytic behavior of the enzyme is expected to be less optimal than in water. This perception has perhaps impeded the investigation of the stereoselective properties of enzymes in nonaqueous media in the past. In more recent years, however, it has become increasingly apparent that many biocatalytic reactions in nonaqueous media can proceed with high degrees of enantioselectivity.

It has been known for some time that a variety of enzymes are catalytically active in apolar media (Table 1), and some of these enzymes have been used for the transformation of water-insoluble substrates[2] (such as the transesterification of fats) and for peptide synthesis[26] via reversal of the hydrolytic process. However, the enantioselective properties of the lipases[2-20] (triglycerol acylhydrolases EC 3.1.1.3), in particular, have attracted the attention of synthetic organic chemists because of their synthetic utility. Lipases are uniquely stable in nonpolar organic solvents and have the remarkable ability of assuming a variety of conformations to accomodate substrates of varying sizes and stereochemical complexities. Moreover, compounds that are unstable in water (anhydrides, halogenated compounds, etc.) could be used as substrates in nonaqueous media. But more importantly, lipase-catalyzed esterification reactions in organic solvents are often more enantioselective than the corresponding hydrolytic reactions in water. For these reasons, nonaqueous biocatalytic technology is becoming increasingly important as a method for the preparation of homochiral (optically active) compounds. This article is intended to bring this methodology to the attention of synthetic chemists by discussing the basic principles and the more recent studies, but limiting the treatment to the enantioselective properties of lipases in nonaqueous media. The recent development of enzyme catalysis in reverse micelles[31] and supercritical fluids[32] is not covered, and the enzymology and kinetics of lipases have been discussed elsewhere.[33]

Table 1. Representative enzyme catalysis in organic media.

Biocatalyst	Solvent	Catalyzed reaction	Ref.
Lipases (crude powder)	apolar solvents	ester synthesis/ interchange, peptide synthesis, macrocyclic lactone formation	[2-20] [21, 22] [23-25]
Proteases (thermolysin, subtilisin, *chymotrypsin*)	ethyl acetate, amyl alcohol, etc.	peptide synthesis	[26]
Immobilized carboxyesterase	methyl propionate	enantioselective acylation of racemic alcohols	[2, 9]
Immobilized alcohol dehydrogenase	isopropyl alcohol	asymmetric reduction of ketonic substrates	[27]
Immobilized polyphenol oxidase	*chloroform*	oxidative conversion of phenols to *o*-quinones	[28]
Immobilized mandelonitrile lyase	ethyl acetate	synthesis of optically active *R*-cyanohydrins	[29]
Cholesterol oxidase	heptane, CCl_4, butyl acetate	oxidation of 3β-hydroxy-steroids	[30]

2. Enzyme Catalysis in Organic Solvents – General Considerations

Three types of solvent systems are used in biocatalytic conversions: water-miscible organic cosolvent systems, anhydrous organic solvents (< 1% water), and biphasic systems consisting of water and a water-immiscible organic solvent. The potential advantages of conducting biocatalytic reactions in these solvent media have been summarized by many workers:[34-38] (1) efficient catalysis may be achieved with substrates poorly soluble in water; (2) reactions catalyzed by hydrolytic enzymes may be shifted towards the synthetic direction; (3) undesirable side reactions in organic media as well as substrate and product inhibition may be

[*] Prof. C. S. Chen
College of Pharmacy, University of Rhode Island
Kingston, RI 02881-0809 (USA)
Prof. C. J. Sih
School of Pharmacy, University of Wisconsin
Madison, WI 53706 (USA)

 © VCH Verlagsgesellschaft mbH, D-6940 Weinheim, 1989 0570-0833/89/0606-0695 $ 02.50/0

reduced; (4) recovery of product and biocatalyst from systems may be easier; (5) enzymes may be more stable in anhydrous organic media.

Water-miscible organic cosolvents such as acetone, methanol, ethanol, dimethylformamide (DMF), and dimethyl sulfoxide (DMSO) are often added to the aqueous reaction media to increase the solubility of substrates that are poorly soluble in water.[38] Moreover, they have been frequently used in peptide synthesis to shift the ionic equilibrium. By lowering the dielectric constant of the medium, the organic cosolvent diminishes the hydration of ionic groups, thereby reducing the acidity of the carboxyl group and the basicity of the α-amino group.[39] However, while lower concentrations of these polar solvents may not have serious adverse effects (concentrations of DMSO as high as 20% have been used in lipase-catalyzed enantioselective hydrolyses of ester[40]), higher solvent concentrations do progressively lead to protein denaturation and the attendant loss of stereochemical specificity. The use of suitable quantities of polar cosolvents may enhance the reaction rate and, in some cases, may also improve the stereoselectivity of biocatalytic systems.[41-43] However, this article will concentrate only on biocatalysis in anhydrous organic solvents or in biphasic solvent systems consisting of water and a water-immiscible organic solvent. Of special interest is the lipase-catalyzed esterification and transesterification reactions in organic solvents, because the observed enantioselectivity of condensation reactions in organic media is often higher than that of the corresponding hydrolytic reactions in water.[10, 18]

It is now well known that lipases can accept a broad range of artificial substrates of varying sizes in both aqueous and apolar media, which suggests that the protein backbone of lipases is flexible and can adopt a variety of conformations to accommodate substrate molecules. Thus, lipases must possess low energetic barriers for conformational transitions, a behavior reminiscent of "induced-fit"[44] enzymes. These features make it rather difficult for one to predict the stereochemical interaction of the enzyme with substrates. That is, in some cases the enantioselectivity of hydrolysis of esters in water is higher than the corresponding esterification reaction or vice versa. However, when hydrolytic reactions in aqueous media proceed with poor enantioselectivity, the corresponding esterification mode in organic solvent should be examined. In contrast, for "non-induced fit" enzymes, which possess more rigid conformations (high energetic barriers for the disruption of noncovalent forces), one envisages that they need not undergo major conformational changes to assume the catalytically active conformation in nonaqueous environments. Thus, this class of enzymes is expected to lose only a modicum of catalytic activity and enantioselectivity when water is replaced with apolar media, because the catalytic cavity is retained in nonaqueous media. However, these enzymes tend to have a more rigid substrate specificity and enhancement of enantioselectivity in apolar media is not expected.

The thermodynamic changes during formation of an enzyme–substrate (EnzSu) complex in water and in organic media have been considered by *Kieboom*.[45] In aqueous solutions, the polar groups in the catalytic site of the enzyme and the substrate molecules form hydrogen bonds with water. In the process of enzyme–substrate complexation, some

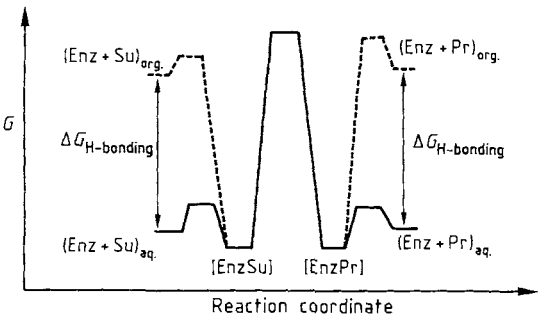


Fig. 1. Comparison of free energy profiles in aqueous solutions and organic solvents for an enzyme reaction in which substrate and product form hydrogen bonds with solvent water. Enz = enzyme, Su = substrate, Pr = product, H-bond = hydrogen bond.

of the hydrogen bonds are disrupted and the energy required for this disruption also contributes to the free energy change of complex formation (ΔG_{aq}) (Fig. 1). On the other hand, in a non-hydrogen-bonding solvent, the EnzSu-forming process does not involve the disruption of hydrogen bonds and the free energy of EnzSu complex formation[45] ($\Delta G_{org.}$) is given by Equation (1),

$$\Delta G_{org.} = \Delta G_{aq} - (n_{Enz} + n_{Su})\,\Delta G_{H\text{-bonding}} \quad (1)$$

where n_{Enz} and n_{Su} denote the number of hydrogen bonds disrupted between water and, respectively, the enzyme active site and the substrate. Thus, the relationship of the apparent association constants of the EnzSu complex in water ($K_{a\,(aq.)}$) and organic solvent ($K_{a\,(org.)}$) can be expressed by Equation (2).

$$K_{a\,(aq.)} = \exp[-(n_{Su} + n_{Enz})\,\Delta G_{H\text{-bonding}}\,RT] \cdot K_{a\,(org.)} \quad (2)$$

$$K_a = [EnzSu]/[Enz][Su]$$

It is noteworthy that although the energy of hydrogen bonding is relatively weak (4.5 kcal mol^{-1}), a transition from an aqueous to an apolar environment may result in an extremely large apparent association constant for either enzyme–substrate or enzyme–product complex for highly polar substrate molecules (e.g., polyhydroxy compounds or their phosphate derivatives) (Table 2). As a consequence, severe substrate and/or product inhibition will occur.

Table 2. Effect of hydrogen bonding energy on enzyme–substrate complexation in apolar solvents. Calculated for non-hydrogen-bonding solvents such as isooctane and hexane.

Number of hydrogen bonds ($n_{Enz} + n_{Su}$)	$K_{a(org.)}/K_{a(aq.)}$
1	2000
2	3.9×10^6
3	7.7×10^9
4	1.5×10^{13}

3. Lipases and Interfacial Catalysis

There are now about 20 different commercially available lipases from microbial, plant, and animal sources (Table 3). Many of these lipases have been purified to homogeneity and obtained in crystalline form. However, only the crystals of

Table 3. Source of commercial lipase preparations.

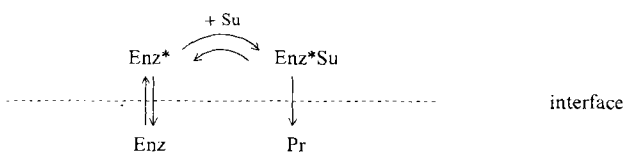
Source	Suppliers
Alcaligenes sp.	Amano
Achromobacter sp.	Meito Sangyo
Aspergillus niger	Amano
Bacillus subtilis	Towa Koso
Candida cylindracea	Sigma, Amano, Meito Sangyo, Boehringer-Mannheim
Candida lipolytica	Amano
Chromobacterium viscosum	Sigma, Toyo Jozo
Geotrichum candidum	Sigma, Amano
Humicola lanuginosa	Amano
Mucor miehei	Amano, NOVO
Penicillium camemberti	Rhône-Poulenc
Phycomyces nitens	Takeda Yakuhin
Porcine pancreas	Sigma, Amano, Boehringer-Mannheim
Pseudomonas aeruginosa	Amano
Pseudomonas fluorescens	Amano
Pseudomonas sp.	Sigma, Boehringer-Mannheim
Rhizopus arrhizus	Sigma, Boehringer-Mannheim
Rhizopus delemar	Sigma, Amano, Tanabe seiyaku
Rhizopus japonicus	Amano, Nagase Sangyo, Osaka Saiken Lab.
Rhizopus oryzae	Amano
Rhizopus sp.	Amano, Serva
Wheat germ	Sigma

the lipase of *Geotrichum candidum* have been investigated by X-ray analysis, which, at 6-Å[46] and 2.8-Å[47] resolution, revealed the presence of nine α-helices and four β-strands. The helical content was calculated to be about 20%. The molecule is ellipsoidal with dimensions of $50 \times 50 \times 70$ Å. Near the molecular center, there exists a large cleft, which is assumed to be the active site of the enzyme.

Very few studies have been made on the structure and function of lipases. For pancreatic lipase, serine and histidine residues and a carboxylate group were found to be essential for activity,[48] but in the case of *G. candidum*, there seems to be no involvement of a reactive serine residue. On the other hand, the lipase of *Humicola lanuginosa* requires histidine and tyrosine residues and a carboxylate group for activity.[49]

Lipases are characterized by a common catalytic feature – the involvement of a lipid–water interface in their catalytic process.[33] This unique feature of interfacial catalysis provides the lipases with an inherent affinity for hydrophobic environments and distinguishes them from other hydrolytic enzymes.

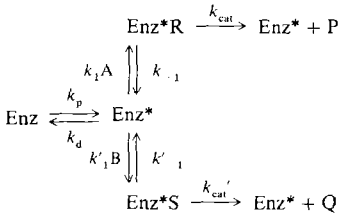
The general principles of interfacial enzyme catalysis were put forward by *Verger* et al.[50] and may be envisaged by Scheme 1, where Enz is enzyme in solution, Enz* is enzyme "penetrated" in the interface. Su represents lipid substrate molecules at the interface, and Pr represents reaction products.



Scheme 1.

Inherent in this model is the presence of two successive equilibria. The first step describes the reversible binding of the enzyme to the interface, which is designated as the penetration step and is assumed to confer on the biocatalyst a new conformation, Enz*. The second step is the reversible binding of the "penetrated" enzyme, Enz*, with the substrate, Su, to form Enz*Su, which undergoes catalysis to regenerate Enz* with liberation of products, Pr.

Using this concept, the action of lipolysis of two insoluble competing enantiomers,[51] A and B, may be envisioned as shown in Scheme 2.



Scheme 2.

This model makes the assumption that the catalytic step is irreversible, as is the case during initial stages of the reaction. It differs from the conventional enzyme model[52] for two competing substrates only by the presence of the additional Enz ⇄ Enz* interconversion step and is similar to the "C induced-fit" model described by *Fersht*.[53] Since the surface-active properties of the enantiomers are identical, the ratio k_d/k_p is a constant and independent of the relative concentration of the enantiomers in the interface. As a consequence, the penetration step does not participate in the discrimination process[44] and the enantioselectivity of *irreversible* lipase-catalyzed reactions in water-immiscible organic solvents or in anhydrous organic media also obeys the classical homocompetitive equation [Eq. (3)]. k_{cat}/K_m is the apparent second-order rate constant for the reaction of the enzyme and the substrate at infinitely low substrate concentrations to give product(s). k_{cat} and K_m denote catalytic and Michaelis constants, respectively, and E is the enantiomeric ratio.[52]

$$\frac{\ln([A]/[A_0])}{\ln([B]/[B_0])} = E = \frac{(k_{cat}/K_m)_A}{(k_{cat}/K_m)_B} \quad (3)$$

This relationship has indeed been independently confirmed by steady-state kinetics derivation. Moreover, kinetic data of phospholipase[50] and lipase[51] appear to obey this model reasonably well.

4. Stereochemical Specificity of Lipase Catalysis in Solvents

In organic solvents, lipases catalyze the transfer of acyl groups from suitable donors to a wide array of acceptors other than water. Depending on the type of acyl donors and acceptors, lipase-catalyzed reactions include esterification, transesterification, amidation, peptide synthesis, and macrocyclic lactone formation. Of these, enantioselective ester synthesis/interchange is of interest because it provides synthetic chemists with a facile method for the preparation of optically active acids and alcohols. Mechanistically, enzymatic ester synthesis/interchange has some features in common with the corresponding hydrolytic reaction, but the underlying principles governing the stereochemical specificity are somewhat different and thus warrant consideration.

4.1. Resolution of Racemic Acids via Enantioselective Ester Synthesis

The kinetics of lipase-catalyzed acyl transfer in organic media may be represented by a ping-pong reaction mechanism,[54] as depicted in Scheme 3. This synthetic mechanism is analogous to that of a hydrolytic reaction when $R^2 = H$. However, ester synthesis/interchange is further complicated by the reversibility of enzyme catalysis with the participation of an acyl acceptor (R^2OH), whose concentration and species may alter the thermodynamic and/or kinetic functions of the catalytic system.[10] Nevertheless, this synthetic mode of catalysis in organic media may often yield a higher degree of enantioselectivity than the corresponding hydrolytic reaction in water. The rationale may be envisaged as follows:

$$\text{Enz} \underset{-RCO_2R^1k_2}{\overset{+RCO_2R^1k_1}{\rightleftharpoons}} \text{Enz} \cdot RCO_2R^1 \underset{k_4}{\overset{k_3}{\rightleftharpoons}} \text{RCO-Enz} \cdot R^1OH$$

$$\underset{+R^1OHk_6}{\overset{-R^1OHk_5}{\rightleftharpoons}} \text{RCO-Enz} \underset{-R^2OHk_8}{\overset{+R^2OHk_7}{\rightleftharpoons}} \text{RCO-Enz} \cdot R^2OH$$

$$\underset{k_{10}}{\overset{k_9}{\rightleftharpoons}} \text{ENZ} \cdot RCO_2R^2 \underset{+RCO_2R^2k_{12}}{\overset{-RCO_2R^2k_{11}}{\rightleftharpoons}} \text{Enz}$$

$$\text{Enz} \underset{-R'CO_2R^1k_2'}{\overset{+R'CO_2R^1k_1'}{\rightleftharpoons}} \text{Enz} \cdot R'CO_2R^1 \underset{k_4'}{\overset{k_3'}{\rightleftharpoons}} \text{R'CO-Enz} \cdot R^1OH$$

$$\underset{+R^1OHk_6'}{\overset{-R^1OHk_5'}{\rightleftharpoons}} \text{R'CO-Enz} \underset{-R^2OHk_8'}{\overset{+R^2OHk_7'}{\rightleftharpoons}} \text{R'CO-Enz} \cdot R^2OH$$

$$\underset{k_{10}'}{\overset{k_9'}{\rightleftharpoons}} \text{Enz} \cdot R'CO_2R^2 \underset{+R'CO_2R^2k_{12}'}{\overset{-R'CO_2R^2k_{11}'}{\rightleftharpoons}} \text{Enz}$$

Scheme 3.

During the initial stages of the reaction, the complex catalytic sequence shown in Scheme 1 may be reduced to a minimal reaction mechanism consisting of the presence of two bond-breaking and two bond-forming steps (Scheme 4),

$$\underset{\mathbf{A}}{\text{Enz} + RCO_2R^1} \xrightarrow{-R^1OHk_a} \text{RCO-Enz} \xrightarrow{+R^2OHk_b} \text{Enz} + \underset{\mathbf{P}}{RCO_2R^2}$$

$$\underset{\mathbf{B}}{\text{Enz} + R'CO_2R^1} \xrightarrow{-R^1OHk_a'} \text{R'CO-Enz} \xrightarrow{+R^2OHk_b'} \text{Enz} + \underset{\mathbf{Q}}{R'CO_2R^2}$$

Scheme 4.

where k_a, k_b, k_a', and k_b' are net rate constants.[55] Kinetically, k_a and k_a' are equivalent to k_{cat}/K_m for A and B, respectively; k_b and k_b' represent the gross binding and catalytic performance of each diastereomeric acyl-enzyme complex toward the achiral nucleophile (R^2OH). The implication of these net rate constants can be further illustrated by the free energy diagram in Figure 2, where k_a and k_b are given by Equations 4 and 5, respectively. T_1 and T_2 refer to transition states.

$$k_a = \exp(-\Delta G_{T1}/RT) \tag{4}$$

$$k_b = \exp(-\Delta G_{T2}/RT) \tag{5}$$

If the reaction rate of substrate A is v_A and that of the competing substrate B is v_B, then application of the net rate constant method of *Cleland*[55] yields Equations (6) and (7), respectively.

$$[\text{Enz}]_0/v_A = 1/k_a[A] + (1/k_b + k_a'[B]/k_a k_b'[A]) \cdot 1/[\text{ROH}] \tag{6}$$

$$[\text{Enz}]_0/v_B = 1/k_a'[B] + (1/k_b' + k_A[A]/k_a' k_b[B]) \cdot 1/[\text{ROH}] \tag{7}$$

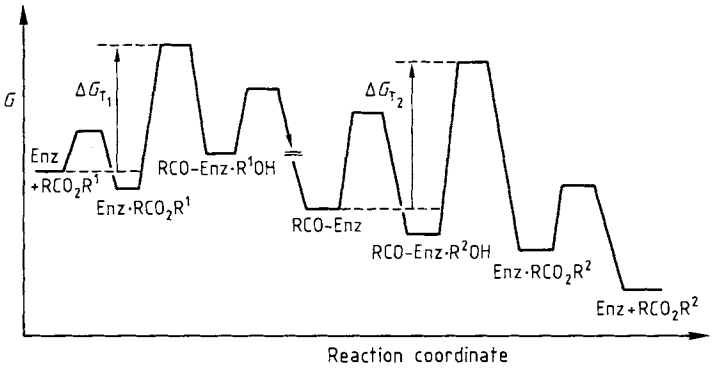


Fig. 2. Reaction-coordinate diagram illustrating a lipase-catalyzed esterification reaction.

These equations clearly indicate that the discrimination between two competing substrates depends on the entire reaction sequence.

For hydrolytic reactions, there will be a partial loss of specificity due to the high concentration of water solvent (55.5 M). As a consequence, the second terms in Equations (6) and (7), contributed mainly by the steps following the first irreversible step, can be neglected. Thus, Equations (8) and (9) are obtained.

$$[\text{Enz}]_0/v_A = 1/k_a[A] \tag{8}$$

$$[\text{Enz}]_0/v_B = 1/k_a'[B] \tag{9}$$

Combining Equations (8) and (9) affords the familiar Equation (10),[52] which indicates that in hydrolytic reac-

$$v_A/v_B = (k_a/k_a') \cdot ([A]/[B]) \tag{10}$$

tions, the enantioselectivity is solely contributed by the catalytic sequence leading to and including the first irreversible step. This difference explains why, in some instances, the enantiomeric purity can often be enhanced by conducting biocatalytic ester synthesis/interchange in organic solvents in lieu of the corresponding hydrolytic reaction in water.[10, 18, 57]

One should keep in mind that in enzyme-catalyzed condensation reactions, the gradual accumulation of products (R^1OH and RCO_2R^2) during the reaction will give rise to reverse catalysis. Thus, the equilibrium constant (K) plays a pivotal role not only in the expression of enzymatic enantioselectivity, but also in the maximal obtainable chemical conversion [$c = 1/(1 + K)$]. To envisage the progressive changes of the stereochemical behavior of enzymes, the reaction scheme is further simplified to Equations (11) and (12),

$$\text{Enz} + \text{A} \underset{k_2}{\overset{k_1}{\rightleftharpoons}} \text{Enz} + \text{P} \tag{11}$$

$$\text{Enz} + \text{B} \underset{k_4}{\overset{k_3}{\rightleftharpoons}} \text{Enz} + \text{Q} \tag{12}$$

where k_1, k_2, k_3, and k_4 are the rate constants for the forward and backward reactions. In an achiral environment, the equilibrium constants for the pair of enantiomers should be equal [Eq. (13)].

$$K = k_2/k_1 = k_4/k_3 \tag{13}$$

This relationship reveals that the sense of preferred chirality for the forward and reverse reactions is retained; i.e., if $k_2 > k_4$, then $k_1 > k_3$.

For reversible biocatalytic systems, assuming that the acyl acceptor is kept at saturating levels, a new expression, which incorporates the thermodynamic parameter K, is required for the calculation of the enantiomeric ratio, E [Eq. (14)], where $E = k_1/k_3$.

$$\frac{\ln[1-(1+K)(1-[A]/[A]_0)]}{\ln[1-(1+K)(1-[B]/[B]_0)]} = E \tag{14}$$

When k_2 and $k_4 = 0$, Equation (14) is reduced to the homocompetitive Equation (3) for the irreversible case.[52] Alternatively, Equation (14) may be transformed into Equations (15) and (16) to relate the extent of conversion (c) and the enantiomeric excess of substrate (ee_S) and product (ee_P).

$$\frac{\ln[1-(1+K)(c+ee_S\{1-c\})]}{\ln[1-(1+K)(c-ee_S\{1-c\})]} = E \tag{15}$$

$$\frac{\ln[1-(1+K)c(1+ee_P)]}{\ln[1-(1+K)c(1-ee_P)]} = E \tag{16}$$

These equations show that the enantioselectivity of enzyme-catalyzed synthesis depends on the complex interaction of both kinetic (E) and thermodynamic (K) functions. The computer-generated graphs[10] of Equations (15) and (16) (Fig. 3) show that the optical yield of both fractions is

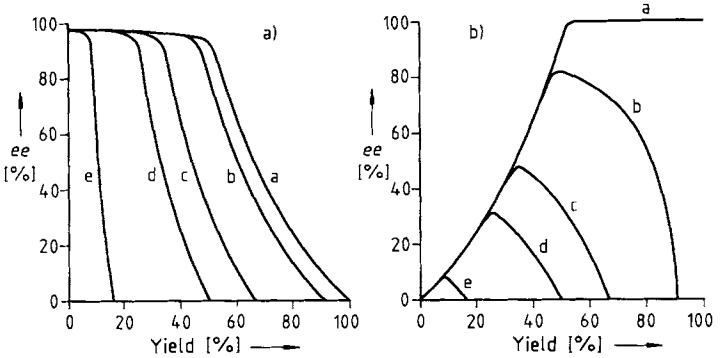


Fig. 3. Expression of the percentage enantiomeric excess of product (A) and remaining substrate fractions (B) as a function of the percentage conversion for $E = 100$ and $K = 0$ (a), 0.1 (b), 0.5 (c), 1.0 (d), and 5.0 (e) [10]. These curves were computer generated from Equations (13) and (14). [Reprinted with permission from *J. Am. Chem. Soc., 109* (1987) 2812. Copyright 1987 American Chemical Society.]

inversely related to the magnitude of K. In addition, high optical purity of the remaining substrate ($ee_S \geq 99\%$) cannot be attained by extending the conversion much beyond 50% even with a very small K value. These graphic representations allow one to predict precisely when to stop the kinetic resolution to maximize chemical and optical yields after the values of E and K have been defined.

4.2. Resolution of Racemic Alcohols via Enantioselective Ester Synthesis

In Scheme 5, ROH (A) and R'OH (B) represent two competing enantiomers. The nucleophilic group of each enantiomer may interact differently with the acyl-enzyme (R^1CO-Enz) to give different transition states (Fig. 4), and the size of this activation energy difference ($\Delta\Delta G_T$) will dictate the enantioselectivity of biocatalysis. Of the factors that influence the stereochemical properties of the biocatalytic system, the acyl donor is of special importance, and its role can be summarized as follows: (1) Because the kinetic differentiation between two enantiomers is independent of the transfer of the acyl group to the enzyme, the type of acyl donor, either acid or ester, does not affect discrimination or the E value. (2) Since the acyl group of the acyl-enzyme exerts steric and/or stereoelectronic effects on the deacylation process, it is possible, in principle, to achieve high enantioselective esterification by the selection of a suitable acyl donor. (3) Since the reaction is reversible, the concentration and the type of acyl donor may alter the equilibrium constant, which in turn influences the biocatalytic stereochemical behavior.

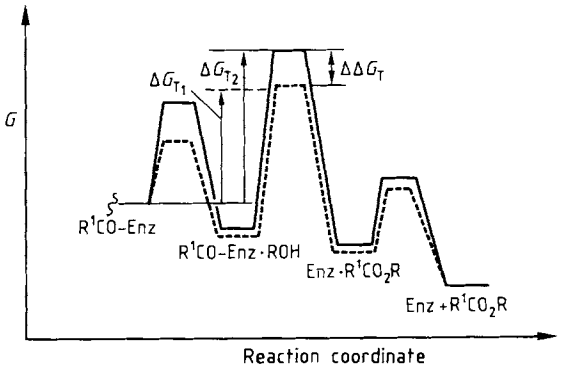
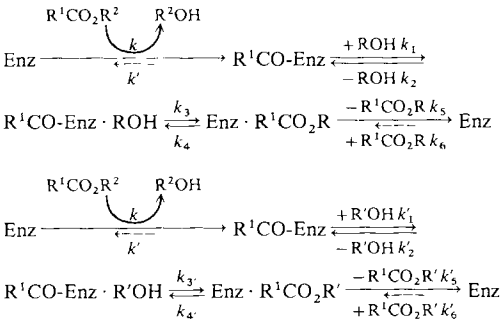
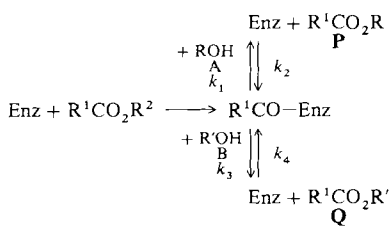


Fig. 4. Reaction-coordinate diagram illustrating an enzymatic resolution of a racemic alcohol via enantiospecific esterification. ----, enantiomer 1; ——, enantiomer 2.



Scheme 5.

To facilitate the kinetic treatment, the mechanism outlined in Scheme 5 may be simplified to Scheme 6.



Scheme 6.

The rate of disappearance of two enantiomers A and B can be described by Equations (17) and (18).

$$v_A = k_1[A][RCO\text{-}Enz] - k_2[P][Enz] \quad (17)$$

$$v_B = k_3[B][RCO\text{-}Enz] - k_4[Q][Enz] \quad (18)$$

These equations show that the relative concentration of acyl-enzyme and free enzyme affects both reaction rates. At saturating levels of acyl donor, the ratio of the acyl-enzyme to free enzyme remains constant. The combination of Equations (17) and (18) and the integration of the resulting equation lead to the same format as Equations (15) and (16). However, at low concentrations of the acyl donor, the amounts of acyl-enzyme and free enzyme vary as the reaction proceeds.[56] As a result, the stereochemical behavior of the system becomes more complicated and cannot be predicted by Equations (15) and (16). Practically speaking, it would be desirable to keep all the free enzyme in the acylated form so that the reverse reaction is negligible.

5. Experimental Considerations

5.1. Selection of Organic Solvent

The type of organic solvent will have profound effects on the reaction kinetics and stability of the biocatalyst. In general, the catalytic efficiency of enzymes diminishes as the polarity of the solvent increases.[57] Hydrophilic solvents may denature enzymes by penetrating into the hydrophobic core of proteins, thus disrupting their delicate functional structures,[58] or by stripping off the essential water from the enzyme.[59] Recently, some general empirical rules have been formulated for the optimization of biocatalytic activity in different organic solvents. The parameter P, the partition coefficient of the solvent between octanol and water,[60] was introduced as a quantitative measure of solvent polarity[61, 62] (Table 4). Generally, the catalytic activity is low in polar solvents having a log $P < 2$, is moderate in solvents having a log P between 2 and 4, and is high in apolar solvents having a log $P > 4$. However, the instability of biocatalysts in polar solvents can often be partially overcome by immobilizing the enzymes on hydrophilic supports.[61] (A detailed account of this "medium-engineering" of biocatalytic systems is given in Ref. [61].)

Another consideration is the solubility of substrate and product in the media.[63] Enzymes are catalysts and only serve to accelerate the attainment of chemical equilibrium. Therefore, the physical properties of the apolar environments may affect the position of equilibrium and thus the chemical yield of the enzyme reaction. It is conceivable that for lipase catalysis, owing to the unique interfacial catalytic property, one would choose a solvent system in which the substrate can form micelles or emulsions whereas the product is fully dispersed in solution. As a rule, apolar solvents such as hexane, isooctane, toluene, and cyclohexane are commonly used for lipase-mediated reactions. Also, halogenated hydrocarbons,[64] such as trichlorotrifluoroethane, and *tert*-butyl and diisopropyl ethers[65] have been successfully employed. However, when the substrates are highly hydrophilic, polar solvents such as DMF, pyridine, and butanol may be used at the expense of enzyme stability or immobilized enzymes may be employed.[61]

Table 4. The log P values of some commonly used solvents [a].

Solvent	log P	Comments
dodecane	6.6	Apolar solvents, suitable for reactions in which dry enzyme powders are used
octane	4.5	
heptane	4.0	
hexane	3.5	
cyclohexane	3.2	
toluene	2.5	
benzene	2.0	Moderately to highly polar solvents; may reduce enzyme's catalytic efficiency; enzyme immobilization is recommended for optimal activity.
chloroform	2.0	
butyl acetate	1.7	
diethyl ether	0.85	
butanol	0.80	
pyridine	0.71	
ethyl acetate	0.68	
tetrahydrofuran	0.49	
acetone	−0.23	
ethanol	−0.24	
acetonitrile	−0.33	
methanol	−0.76	
diemethylformamide	−1.0	
dioxane	−1.1	
dimethyl sulfoxide	−1.3	

[a] See [61] for a complete list of log P values of solvents. P is the partition coefficient in a standard octanol–water two-phase system.

5.2. Water Content of Organic Media

Esterification and transesterification reactions may be carried out in either monophasic, nearly anhydrous organic media (water content < 1 %) or in aqueous-organic biphasic systems. In the latter, the enzyme resides in the aqueous phase, surrounded by an organic phase. Since enzymes are insoluble in hydrophobic organic solvents, they form suspensions. Hence, unless the reaction mixture is stirred or shaken, the enzyme settles. Although published experimental procedures give no clear indication as to the optimal amount of exogenous water to be added to the organic solvent, there is a consensus that some water is absolutely needed for the catalytic function of the enzyme.[66] This is because water is involved in various types of noncovalent bonding interactions for the maintenance of catalytically active conformations of enzymes. For some esterification reactions, the immiscible organic solvent is saturated with water, because the rate of reaction appears to increase as the water content increases.[23] On the other hand, anhydrous organic media (no addition of exogenous water) are preferred for lactonization[25] (intramolecular esterification). In this case, the reaction rate is relatively slow and higher temperature (e.g., 65 °C) is used.

5.3. Choice of Acyl Donors and Acyl Acceptors

Another consideration is the choice of substrates; i.e., either chiral racemic acids or the corresponding chiral racemic esters could be used as substrates. Mechanistically, these two types of reactions proceed via different transition states for all steps leading to and including the formation of the acyl-enzyme intermediate (Scheme 1). Hence, despite the apparent similarity, the E and K values for esterification and ester interchange may be different. Also, the physical state of the substrate has a pronounced effect on the enzymatic rate. For

instance, in an organic medium, the ester substrate is fully dispersed and is less susceptible to enzymatic lipolysis due to a lack of lipid–water interface. On the other hand, the acid substrate forms micelles or emulsions, which are readily attacked by the lipase. However, if the acid is insoluble in the organic medium, the reaction rate is markedly reduced due to the sluggish enzymatic action on a solid substrate, but the physical separation of the substrate from the product is often much easier for the acid substrate than for the ester substrate.

To achieve high enantioselective esterification, it is imperative to minimize the extent of the reverse reaction. Several strategies may be used to circumvent the thermodynamic restraint imposed by equilibrium. These include: the use of enolesters[19] (R^1OH = aldehyde or acetone) or anhydride[18] as acyl donors so that no alcohol or water molecules are formed; the selection of a suitable acyl acceptor (R^2OH = secondary alcohol) to prevent the backward reaction;[10] the removal of R^1OH to shift the equilibrium position (e.g., by adding molecular sieve to remove water in esterification reactions); and the addition of a large excess of acyl acceptor to the medium to reduce the relative concentration of the competing nucleophile, R^1OH[10] (Scheme 3).

5.4. Determination of E and K Values

The enantioselectivity of biocatalytic reactions is normally expressed as the E value,[52] a biochemical constant that is independent of substrate concentration and the extent of conversion. Lipase-catalyzed esterification or transesterification reactions in aqueous-organic biphasic or anhydrous organic media also obey the conventional homocompetitive equation provided that the reaction is irreversible (saturating amounts of achiral acyl donor and acceptors are present). At the initial stages of the reaction, little product has accumulated. Normally, reversibility of the reaction becomes a significant problem only at conversions around 40% or greater (Fig. 3). Consequently, if the enantiomeric excess of the substrate (ee_S) and the product (ee_P) is determined at low conversions (< 20%), one can calculate the extent of conversion (c) using Equation (19).

$$c = \frac{ee_S}{ee_S + ee_P} \tag{19}$$

The E value can then be readily calculated using either Equation (20) or (21).[52]

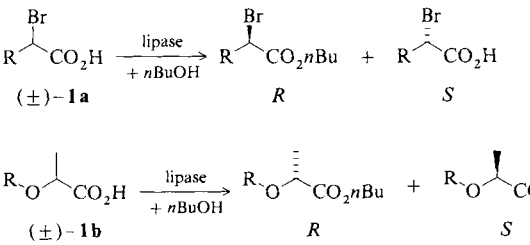
$$E = \frac{\ln[(1-c)(1-ee_S)]}{\ln[(1-c)(1+ee_S)]} \tag{20}$$

$$E = \frac{\ln[1-c(1+ee_P)]}{\ln[1-c(1-ee_P)]} \tag{21}$$

Moreover, by inserting the values of E, c, ee_S, and ee_P determined at a conversion greater than 40% into Equations (15) and (16), the value of K can also be determined.

The need for a quantitative treatment of biocatalytic resolution data in organic media may be best illustrated by an analysis of some published results (Tables 5 and 6). In the lipase-catalyzed enantioselective esterification of (±)-2-bromohexanoic acid **1a** and (±)-2-*p*-chlorophenoxy)propionic acid **1b**,[17] 1-butanol was used as the acyl acceptor. It is noteworthy that even though the reaction was conducted in hexane with only a very small amount of exogenous water (0.1%), the reactions are clearly reversible. Using Equations (20) and (21), the E values were calculated from the data of Table 5. As can be seen, the E value decreased from 300 (30% conversion) to 3 (67% conversion) for **1a** and from 17 (45% conversion) to 4 (65% conversion) for **1b**. If the reactions were irreversible, the E values should remain constant throughout the reaction. A similar observation was noted during the enantioselective esterification of (±)-menthol **1** using dodecanoic acid as the acyl donor.[6] Again, the E value decreased from a value of 92 (45% conversion) to 17 (57% conversion). Therefore, when the reactions are reversible, Equations (15) and (16) should be used instead of Equations (20) and (21) for the calculation of the E value to take into account the contribution of the equilibrium constant, K.

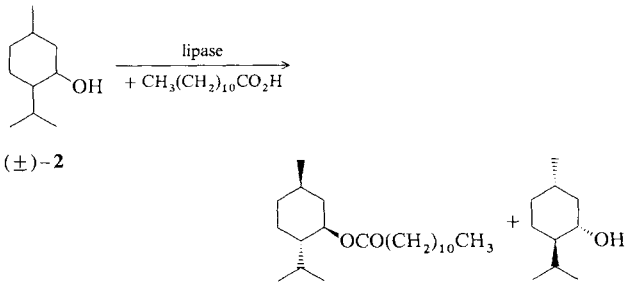
Table 5. Reversible enantioselective esterification of chiral racemic acids **1** catalyzed by *C. cylindracea* lipase with 1-butanol as acyl acceptor in hexane (containing 0.1% H_2O) [7]. *ee* = enantiomeric excess, E = enantioselectivity.



Substrate R	t [h]	Conversion [%]	*ee* [%] Product (*R* ester)	*ee* [%] Substrate (*S* acid)	E [a]
1a n-C_4H_9	19	30	99	–	300
	48	67	–	62	3
1b p-ClC_6H_4	40	45	79	–	17
	168	65	–	65	4

[a] Calculated using either Equation (20) or (21).

Table 6. Reversible enantioselective esterification of chiral racemic alcohol **2** catalyzed by *C. cylindracea* lipase with dodecanoic acid as acyl donor in hexane or heptane [6][a].



T [°C]	t [h]	Conversion [%]	*ee* [%] Product (ester)	*ee* [%] Substrate (alcohol)	E
45	8	45	95	–	92
40	88	57	69	88	17

[a] Ref. [6] does not indicate which solvent was used.

5.5. Determination of the Kinetic Parameters V_{max} and K_m

Frequently, it is of interest to know which of the kinetic parameters, the Michaelis constant, K_m, or the catalytic constant, V_{max}, is altered when a substituent is introduced onto the substrate molecule. As mentioned earlier, lipase-catalyzed reactions occur at the oil–water or micelle–water interface.[33] Since the lipase is reversibly adsorbed at the interface, the experimentally determined "apparent K_m" may represent the dissociation constant of the interfacial enzyme–substrate complex, termed interfacial K_m^*. Also, the "apparent V_{max}" measured at saturating amounts of lipid substrate is also an apparent quantity, namely, the real V_{max} multiplied by the factor $Su/(K_m^* + Su)$. This factor tells us what fraction of the enzyme molecules are in the Enz*Su form.

To overcome the complexity of this interfacial surface problem, *Hirohara* et al.[67] selected experimental conditions under which all enzyme molecules are adsorbed to the interface by increasing the area of interface with vigorous stirring (1000 rpm) and increasing the amount of substrate under these conditions. They assumed that the concentration of the enzyme in solution is that at the interface. Lineweaver–Burk plots with substrate concentration expressed in mole L^{-1} instead of $m^2\ L^{-1}$ gave straight lines to allow the calculation of K_m and V_{max}. In any event, accurate noncompetitive measurement of K_m and V_{max} is a difficult problem, especially the K_m for the more slowly reacting enantiomer.

In theory, the kinetic parameters, K_m and V_{max}, for both enantiomers, A and B, can also be calculated directly from competitive measurements using Equations (22) and (23),[68]

$$t(V_{max}/K_m)_A + ([A] - [A]_0)[1/(K_m)_A] + ([A]^{1/E} - [A]_0^{1/E}) \cdot x \cdot E \cdot [1/(K_m)_B] = \ln [A]_0/[A] \quad (22)$$

$$t(V_{max}/K_m)_B + ([B] - [B]_0)[1/(K_m)_B] + ([B]^E - [B]_0^E)(y/E) \cdot [1/(K_m)_A] = \ln [B]_0/[B] \quad (23)$$

where $[A]_0$ and $[B]_0$ denote initial concentrations, E is the enantiomeric ratio, $x = ([B]_0/[A]_0^{1/E})$, $y = ([A]_0/[B]_0^E)$, t = time, and $(K_m)_A$, $(K_m)_B$, $(V_{max})_A$, and $(V_{max})_B$ are the Michaelis constants and maximal velocities for A and B, respectively. By inserting the E value and at least three sets of experimental data $[(t_1, [A]_1), (t_2, [A]_2), (t_3, [A]_3)$ and $(t_1, [B]_1), (t_2, [B]_2), (t_3, [B]_3)]$ into Equations (22) and (23), respectively, the values of V_{max}/K_m, K_m, and V_{max} for each enantiomer A and B may be readily calculated.

6. Asymmetric Catalysis in Organic Solvents

Because lipase-catalyzed reactions are generally conducted in the hydrolytic mode in water,[69] it is not too surprising to find that there are relatively few published examples of enantioselective and enantiotopically selective esterification reactions in nonaqueous media. Nevertheless, the data presented in Tables 7–11 should provide chemists with a glimpse of the usefulness of this unconventional methodology. Although Equations (15) and (16) should be employed for the calculation of the E values, the equilibrium constants for these systems were unfortunately not determined. Therefore, the E values listed in Tables 7, 9, and 11 were calculated using Equations (20) and (21), and they represent apparent minimal values rather than intrinsic E values.

6.1. Optically Active Carboxylic Acids and Esters

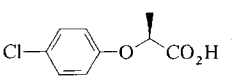
Most of the biocatalytic kinetic resolutions of chiral racemic acids were conducted in the hydrolytic mode in water,[69] because the hydrolytic rate in water is generally faster than the corresponding rate of esterification in organic media. That is, if the hydrolytic rate in water is slow, the corresponding rate of esterification in organic media in most cases is expected to proceed at an even slower rate. Hence, more enzyme is required for esterification in nonaqueous media.

The catalytic activity of enzymes is strongly influenced by both electronic and steric effects. For example, acids that possess electron-donating or bulky substituents (e.g., isopropyl or larger) adjacent to the carboxyl function are attacked slowly or not at all by lipases and the rate-determining segment of the reaction is the formation of the acyl-enzyme complex. In these cases, transesterification may be used as a means of improving the catalytic rate; the chiral racemic acid is first converted nonenzymatically into an activated ester (e.g., chloroethyl ester), which is more susceptible to nucleophilic attack by the biocatalyst. Using the lipase of *Candida cylindracea*, *Klibanov* et al.[7] observed good catalytic activity and enantioselectivity with substrates that possess an electron-withdrawing group adjacent to the carboxyl function, such as **1a** and **1b**, whereas low catalytic activity was noted with other substrates devoid of an electron-withdrawing substituent.

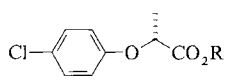
Table 7 compares the enantioselectivity of esterification versus hydrolysis of 2-(*p*-chlorophenoxy)propionates. In both sets of experiments, the observed enantioselectivity (E value) of esterification in organic media is four- to fivefold higher than the corresponding hydrolytic reaction in water. Similarly, the data in Table 8 show that the enantiomeric excess (*ee*) of the product, (*S*)-3-methylglutarate monomethyl ester, is higher when the product is prepared by enzymatic acylation by the corresponding anhydride in organic solvent[18a] than by enzymatic hydrolysis of the diester in water.

As far as the influence of the acyl acceptor on enantioselectivity is concerned, no prediction may be made with any degree of confidence at this stage. Although one might surmise that the enantioselectivity may perhaps be improved by the use of a chiral alcohol, in many cases the observed enantioselectivity using achiral alcohols as acyl acceptors is superior to that of chiral alcohols.[77] However, the matching of appropriate racemic acids with racemic alcohols in a double kinetic resolution experiment is an exciting area that warrants systematic exploration in the future.

The existence of reverse hydrolysis during the lipase-mediated enantioselective formation of 2-(*p*-chlorophenoxy)-propionic esters[10] **1c, d** is illustrated in Figure 5a. The *Candida* lipase preferentially attacked the (*R*) enantiomer in the

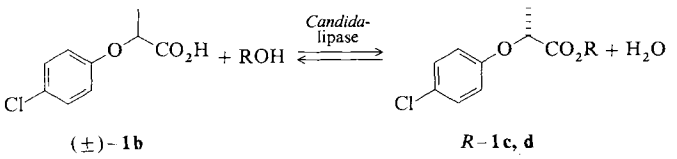


(*S*)-**1b**



(*R*)-**1c**, R = *n*Bu
(*R*)-**1d**, R = cyclohexyl

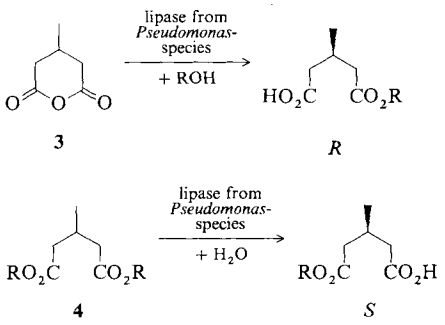
Table 7. Lipase-catalyzed enantioselective esterification of the acid (±)-**1b** in organic solvent versus enantioselective hydrolysis in water. Conditions: 24 h for butanol and 105 h for cyclohexanol, 25 °C, isooctane as solvent.



Synthesis	Stereo-preference R		ee_S [%]	ee_P [%]	Conversion [%]	E [a]
1c	*n*Bu	*R*	0.12	0.81	13	0
1d	cyclohexyl	*R*	0.25	0.97	20	84
Hydrolysis	Stereo-preference R		ee_S [%]	ee_P [%]	Conversion [%]	E [a]
1c	*n*Bu	*R*	0.24	0.20	55	2
1d	cyclohexyl	*R*	0.94	0.73	56	22

[a] Calculated using Equations (20) and (21).

Table 8. Lipase-catalyzed enantiotopically selective acylation by the anhydride **3** in organic solvent versus hydrolysis of the diester **4** in water. Conditions: 6 h, 25 °C, diisopropyl ether as solvent [18a].



Acylation R	Stereo-preference	*ee* [%]	Conversion [%]	Hydrolysis Stereo-preference	*ee* [%]	Conversion [%]
CH_3	pro-*R*	87	92	pro-*R*	74	50
*n*Bu	pro-*R*	91	74	–	–	–

presence of an excess amount of 1-butanol as the acyl acceptor. The E value for this system was moderate ($E = 12$) and the K value was found to be 0.15. As shown in Figure 5a, the characteristic feature of such a reversible system is that the optical purity of the remaining substrate (ee_S) decreases as the conversion is extended beyond 50%. This is in marked contrast to the irreversible case where ee_S increases as the conversion is extended. Figure 5b illustrates the advantage of using cyclohexanol as the acyl acceptor, because esters of secondary alcohols are more resistant to enzymatic hydrolysis than those of primary alcohols. The K value for this system is reduced to 0.02.

6.2. Optically Active Alcohols

With the exception of certain sterically hindered alcohols, lipases catalyze the asymmetric acylation of a wide range

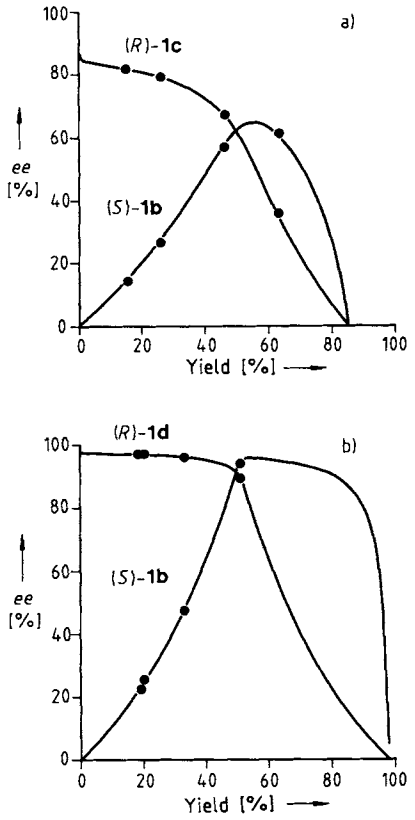


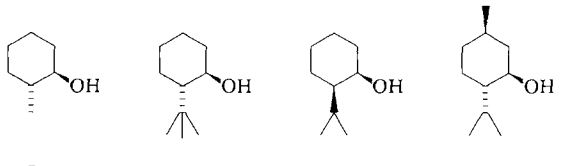
Fig. 5. Enantiospecific synthesis of the 2-(*p*-chlorophenoxy)propionic esters **1c** and **1d** from the acids (±)-**1b** in isooctane catalyzed by *Candida* lipase [10]. + = experimentally derived values. The curves depicting the relationship between enantiomeric excess and conversion were computer generated from Equations (15) and (16) with use of the apparent constants E and K. a) Formation of the butyl ester **1c**, E = 12, $K = 0.15$; b) formation of the cyclohexyl ester **1d**, $E = 84$, $K = 0.02$. [Reprinted with permission from *J. Am. Chem. Soc. 109* (1987) 2812. Copyright 1987 American Chemical Society.]

of cyclic and acyclic substrates with moderate to high enantioselectivity (Tables 9 and 10). To achieve highly enantioselective acylation, the selection of a suitable biocatalyst and the optimization of reaction conditions are important.

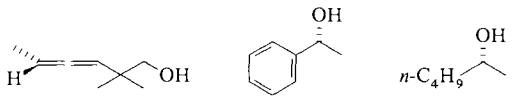
The acyl donor can have a marked effect on the stereochemical behavior of the enzyme system. This is illustrated by the examples of enantioselective acylation of racemic 1-phenethanol (±)-**9** mediated by *Candida cylindracea* lipase[70] (Table 11).

While the physical states of the acyl donor, either as an ester in a fully dispersed form or as an acid in a micelle form, had no effect on the enantioselectivity, different catalytic rates were observed. For example, the rate of the reaction using tributyrin (tributyrylglycerin) as the acyl donor was only about one-fifth of that of butyric acid. On the other hand, increasing the chain length of the acyl group from C_4 to C_{12} led to higher values of enantiomeric ratio E, but no significant difference in enantioselectivity was noted for acyl donors with chain lengths between C_{12} and C_{16}. Similar observations were reported for the *Mucor miehei* lipase, which was used for the resolution of (±)-2-octanol via enantioselective acylation.[16] In this case, the E value increased to > 50 with chain lengths of alkanoic acid up to C_8; it declined beyond C_8 but only to rise again to > 50 for the C_{16} acid. Therefore, it is noteworthy that the optimal chain

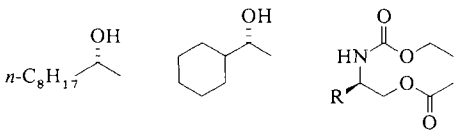
Table 9. Lipase-catalyzed enantioselective acylation of alcohols **5**–**17** and **2**.



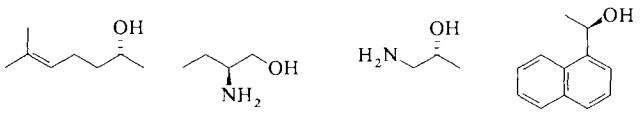
5 **6** **7** **2**



8 **9** **10**



11 **12** **13a**, R = C_2H_5; **13b**, R = CH_3



14 **15** **16** **17**

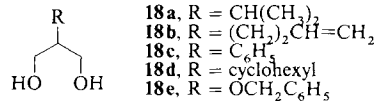
Substrate [a]	Stereo-preference	Acyl donor	Conversion [%]	ee_S [%]	ee_P [%]	E [b]	Ref.
Candida cylindracea lipase							
(±)-**5**	1*R*,2*R*	dodecanoic acid	44	80	98	>100	[6]
(±)-**6**	1*R*,2*S*	dodecanoic acid	34	–	≈100	>100	[6]
(±)-**7**	1*R*,2*R*	dodecanoic acid	30	–	88	23	[6]
(±)-**2**	1*R*,2*S*,5*R*	dodecanoic acid	45	–	95	92	[6]
(±)-**8**	*R*	dodecanoic acid	31	32	72	8	[12]
(±)-**9**	*R*	dodecanoic acid	35	50	93	45	[67]
Mucor miehei lipase							
(±)-**10**	*R*	octanoic acid	51	87	83	30	[16]
(±)-**11**	*R*	octanoic acid	49	83	87	38	[16]
(±)-**12**	*R*	octanoic acid	44	67	86	27	[16]
(±)-**9**	*R*	octanoic acid	45	71	87	31	[16]
Crude porcine pancreatic lipase (PPL)							
(±)-**13a**	*R*	ethyl acetate	41	65	≥95	78	[17]
(±)-**13b**	*R*	ethyl acetate	51	≥95	90	>100	[17]
(±)-**14**	*R*	trichloroethyl butyrate	30	66	88	22	[15]
(±)-**14**	*R*	trifluoroethyl dodecanoate	52	>97	91	>100	[13]
(±)-**15**	*S*	ethyl acetate	–	>95	>95	>100	[78]
(±)-**16**	*R*	ethyl acetate	–	–	>95	–	[78]
(±)-**17**	*R*	trichloroethyl butyrate	49	≈93	≈100	>100	[79]

[a] The enantiomers shown react preferentially. [b] Calculated using Equations (20) and (21).

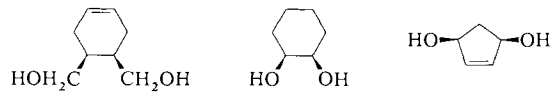
length of the acyl donor required for maximal enantioselection varies with the enzyme and the substrate.

The presence of competing enzymes in the crude lipase preparations should also be considered. In general, lipases from microbial sources are produced extracellularly and are virtually homogeneous in terms of lipolytic activity.[33] In contrast, crude mammalian and plant lipase preparations contain several other interfering enzymes, including proteases and esterases, which may possess opposite or poor stereo-

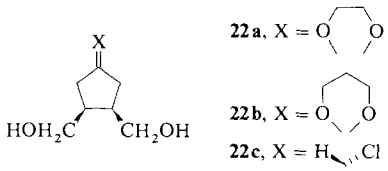
Table 10. Lipase-catalyzed enantiotopically selective acylation of alcohols **18**–**22**.



18a, R = $CH(CH_3)_2$
18b, R = $(CH_2)_2CH{=}CH_2$
18c, R = C_6H_5
18d, R = cyclohexyl
18e, R = $OCH_2C_6H_5$



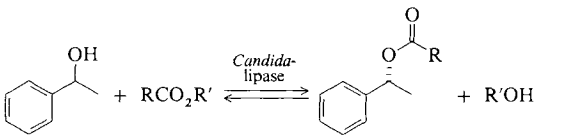
19 **20** **21**



22a, X = O
22b, X = O
22c, X = H, Cl

Substrate	Stereo-preference	Acyl donor	Conversion [%]	ee [%]	Ref.
P1 fraction from porcine pancreatic lipase					
18a	pro-*R*	methyl acetate	91	65	[9]
18b	pro-*R*	methyl acetate	70	90	[9]
18c	pro-*R*	methyl acetate	98	92	[9]
18d	pro-*R*	methyl acetate	90	58	[9]
19	pro-*R*	methyl acetate	–	96	[9]
Pseudomonas sp. lipase					
18e	pro-*S*	isopropenyl acetate	53	96	[19]
Crude porcine pancreatic lipase					
20	pro-*S*	methyl acetate	–	84	[14]
21	pro-*S*	trichloroethyl acetate	48	95	[20]
22a	pro-*S*	methyl acetate	57	26	[14]
22b	pro-*S*	methyl acetate	74	68	[14]
22c	–	methyl acetate	79	84	[14]

Table 11. Enantioselective acylation of (±)-1-phenethanol (±)-**9** catalyzed by *C. cylindracea* lipase.



(±)-**9**

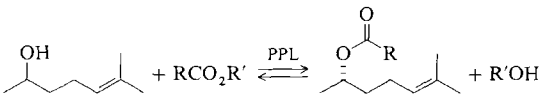
Acyl donor	t [h]	Conversion [%]	ee_S [%]	ee_P [%]	E [a]
butyric acid	66	39	54	84	20
tributyrin (tributyrylglycerin)	100	10	10	89	19
octanoic acid	66	20	24	94	41
tricapyrin (trioctanoylglycerin)	100	< 5	–	–	–
dodecanoic acid	66	19	22	95	46
hexadecanoic acid	66	14	15	95	45
5-phenylvaleric acid	100	< 5	–	–	–

[a] Calculated using Equations (20) and (21).

selectivity as compared with the lipase. As a consequence, low optical yields or unreproducible results are often encountered in using these crude lipases, depending on the state of the enzyme preparations. Therefore, to enhance the optical yield, a number of measures can be taken. These include:

treatment of the crude enzyme preparation with chemical reagents[71] (e.g., serine protease inhibitors) to inactivate interfering enzymes; treatment of the crude enzyme preparation by physical means (e.g., partial protein purification; lyophilization) to remove or selectively inactivate competing enzymes; and selection of a suitable acyl donor which serves as a poorer substrate for interfering enzymes and/or as a more efficient substrate for the target enzyme. These strategies of optical purity enhancement are illustrated by a number of recent examples where crude porcine pancreatic lipase (PPL) was used.

PPL exhibited a moderate enantioselectivity in the esterification of (±)-sulcatol (±)-**14**.[13] When the commercial Sigma crude PPL preparation was dehydrated to constant weight under vacuum, a threefold increase in the E value was noted. Although a general increase in the chain length of the acyl moiety had little effect on the enzyme specificity, the use of an activated ester, trifluoroethyl dodecanoate resulted in a fourfold increase in the E value. A combination of enzyme dehydration and ester selection gave rise to a nearly tenfold increase in E value.



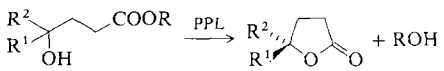
(±)-**14**

Some of the asymmetric esterification reactions in organic solvents were actually mediated by the competing enzymes in the crude lipase preparation. A recent study by *Ramos Tombo* et al.[72] has shown that an esterase fraction from crude PPL catalyzed highly enantioselective acylation of 2-substituted 1,3-propanediol, whereas pure PPL was virtually inactive. In addition, several hydrolytic enzymes, including cholesterol esterase and chymotrypsin, are present in crude PPL preparations. For example, the claim[22] that crude porcine pancreatic lipase (PPL) catalyzes the formation of peptide bonds may well be due to the contaminating chymotrypsin present in the preparation. Therefore, partial purification of enzyme preparations may result in more enantioselective biocatalysts. Finally, it is interesting to note the existence of pancreatic colipase whose main function appears to be to restore the activity of the bile-salt-inhibited lipase. However, it is unclear as to whether colipase can alter the V_{max} and K_m of the pancreatic lipase.[80]

6.3. Macrocyclic Lactones

Lipases have been used for the preparative syntheses of macrocyclic lactones via the lactonization of hydroxy acids and esters in organic solvents.[23, 24] However, more recent studies[73] show that the product profile varies with the length of the hydroxy acid and the lipase and is considerably more complex than those reported previously.[23, 24] For example, when 10-hydroxydecanoic acid was exposed to a variety of lipases in anhydrous isooctane, no decanolide was detected; instead, a complex mixture of di-, tri-, tetra-, and pentalactones was formed in different ratios depending on the lipase used. A similar product profile was obtained using methyl 10-hydroxydecanoate as substrate. On the other hand, hexadecanolide was found to be the dominant product after exposure of 16-hydroxyhexadecanoic acid to the lipases, except the lipase of *Mucor miehei* which formed hexadecanodiolide predominantly. Chiral (ω-1)-hydroxy acids (C_8 and C_{13}) were also lactonized by the lipases to yield a mixture mainly of di- and trilactones, but no monolactones were detected (Table 12). The enantioselectivity of the intramolecular esterification was examined using a series of acyclic diastereomeric dimers, prepared from (*R*)- and (*S*)-7-hydroxyoctanoic acids.[74] The relative rates of diolide formation were found to follow the order $R,R > R,S > S,S$, and no cyclization was noted with the (*S*,*R*) diastereomer. These results indicate that the stereochemistry of the hydroxyl at both chiral centers appears to influence the lactonization reaction.[73]

Porcine pancreatic lipase (PPL) in anhydrous organic solvents such as dry ether catalyzed the lactonization of a number of esters of γ-hydroxy acids **25** in nearly quantitative yields.[75] This highly enantioselective process was used for the synthesis of (*S*)-(−)-γ-methylbutyrolactone **26** ($R^1 = CH_3$; $R^2 = H$; $E = > 100$), (*R*)-(+)-methylbutyrolactone **26** ($R^1 = H$, $R^2 = CH_3$), and optically active γ-phenylbutyrolactone (the presence of the (*R*) or (*S*) form was not established).



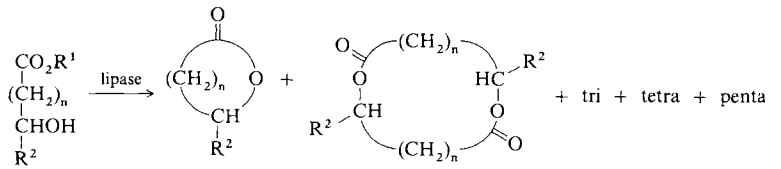
25 **26**

It was found that α-substituted γ-hydroxy esters were very poor substrates for the enzyme. The initial rates of lactonization of α-bromo-γ-hydroxybutyrate and of α-methyl-γ-hydroxybutyrate were, respectively, 200 and 50 times lower than that of γ-hydroxybutyrate. It is interesting to note that the PPL-catalyzed hydrolyses of γ-, δ-, and ε-chiral racemic lactones in water[76] proceeded with only modest enantioselectivity; E values ranged from 3 to 20.

Lipases also catalyzed the formation of macrocyclic lactones via the condensation of diacids and diols in anhydrous nonpolar organic solvents such as isooctane.[25] The major products of this reaction were mono- and dilactones accompanied by linear oligomeric esters and a small quantity of trilactones in some systems. The yield of the lactone products varied not only with different substrates, but also with reaction conditions. Optimal temperature for lactonization was between 55 and 75 °C; at lower temperatures (≤ 45 °C), oligomeric esters were the dominant products. Lipases accommodated acyclic diacids **27** (m = 2–12) and diols **28** (n = 5–16) of various sizes. However, the optimum yield of lactones was achieved when the size of the ring is in the range of 24–28.

Cyclic diacids and diols as well as acyclic diacids and diols bearing heteroatoms[77] also served as lactonization substrates for the lipases. However, the enantioselectivity of this unique biocatalytic reaction has yet to be systematically studied.

Table 12. Lipase-catalyzed lactonization of ω-hydroxy carboxylic acids and their esters.

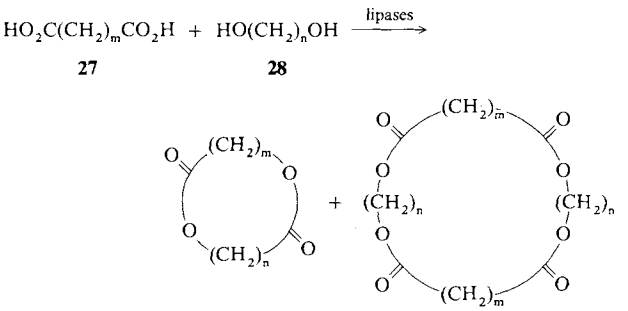


23, mono **24**, di

R^1	R^2	n	Origin of the lipase	Conditions [a]	**23** mono	Yield [%] [b] **24** di	tri	tetra	penta
H	H	8	*Pseudomonas* sp.	A	0	53	16	4	*
			Pseudomonas sp.	A	0	33	14	15	7
			porcine pancreas	A	0	57	20	6	2
			Candida cylindracea	B	0	2	24	13	*
			Mucor miehei	B	0	2	22	18	*
H	H	14	*Pseudomonas* sp.	A	66	26	*		
			Pseudomonas sp.	A	62	30	*		
			porcine pancreas	A	46	21	12		
			Candida cylindracea	A	19	15	9		
			Mucor miehei	A	3	43	15		
CH_3	H	8	porcine pancreas	A	0	55	24	9	4
			Candida cylindracea	B	0	0	27	13	6
			Mucor miehei	A	0	15	46	20	15
CH_3	H	14	porcine pancreas	A	54	5	6	*	
			Candida cylindracea	B	0	24	19	*	
			Mucor miehei	A	0	26	15	*	

R^1	R^2	n	Origin of the lipase	Conditions [a]	**23**, mono	Yield [%] [b] **24**, di *R,S*	*S,S* + *R,R*	tri-1	tri-2	tetra
H	CH_3	5	*Pseudomonas* sp.	C	0	5	12	4	3	2
H	CH_3	10	*Pseudomonas* sp.	D	0	13	30	11	9	*
			Pseudomonas sp.	D	0	4	20	17	20	*
			Candida cylindracea	A	0	7	21	13	12	*

[a] Reaction conditions: A 65 °C, 48 h; B 65 °C, 96 h; C 25 °C, 144 h; D 50 °C, 96 h. [b] An asterisk indicates that a trace quantity was detected by thin layer chromatography.



27 **28**

7. Epilogue

Enantioselective biocatalysis in organic media is a rapidly developing field but it is still at an early stage, because there is still much to learn about enzyme protein conformations in water and in organic media. Nevertheless, the usefulness of this nonaqueous methodology is clearly indicated by a number of published reports. Thus far, only the enantioselective properties of lipase-catalyzed esterification and transesterification reactions have been exploited to a large extent. By choosing a biocatalyst and an acceptor or donor in a suitable organic solvent, the biocatalytic reaction may often be more enantioselective than the corresponding hydrolytic reaction in water. As such, it provides the synthetic chemist with an additional methodology for the preparation of optically active compounds.

It is important to recognize the potential broad range of biocatalysts that may be used for biocatalytic resolution in organic media. We are therefore in the midst of an exciting stage in the development of this field. We hope this article will stimulate interest and greater activity in this relatively new area.

C.S.C. is grateful to the Petroleum Research Fund of the American Chemical Society for financial support.

Received: November 8, 1988;
supplemented: January 23, 1989 [A 721 IE]
German version: *Angew. Chem. 101* (1989) 711

[1] A. A. Klyosov, N. Van Viet, I. V. Berezin, *Eur. J. Biochem. 59* (1975) 3.
[2] A. R. Macrae, *J. Am. Oil Chem. Soc. 60* (1983) 291.
[3] B. Cambou, K. Klibanov, *J. Am. Chem. Soc. 106* (1984) 2687.
[4] B. Cambou, K. Klibanov, *Biotechnol. Bioeng. 26* (1984) 1449.
[5] S. Koshiro, K. Sonomoto, A. Tanaka, S. Fukui, *J. Biotechnol. 2* (1985) 47.
[6] G. Langrand, M. Secchi, G. Buono, J. Baratti, C. Triantaphylides, *Tetrahedron Lett. 26* (1985) 1857.
[7] G. Kirchner, M. P. Scollar, A. M. Klibanov, *J. Am. Chem. Soc. 107* (1985) 7072.

[8] G. Langrand, J. Baratti, G. Buono, C. Triantaphylides, *Tetrahedron Lett. 27* (1986) 29.
[9] G. M. Ramos Tombo, H.-P. Schaer, X. Fernandez I Busquets, O. Ghisalba, *Tetrahedron Lett. 27* (1986) 5707.
[10] C.-S. Chen, S.-H. Wu, G. Girdaukas, C. J. Sih, *J. Am. Chem. Soc. 109* (1987) 2812.
[11] A. L. Margolin, J.-Y. Crenne, A. M. Klibanov, *Tetrahedron Lett. 28* (1987) 1607.
[12] G. Gil, E. Ferre, A. Meou, J. Le Petit, C. Triantaphylides, *Tetrahedron Lett. 28* (1987) 1647.
[13] T. M. Stokes, A. C. Oehlschlager, *Tetrahedron Lett. 28* (1987) 2091.
[14] H. Hemmerle, H.-J. Gais, *Tetrahedron Lett. 28* (1987) 3471.
[15] A. Belan, J. Bolte, A. Fauve, J. G. Gourcy, H. Veschambre, *J. Org. Chem. 52* (1987) 256.
[16] P. E. Sonnet, *J. Org. Chem. 52* (1987) 3477.
[17] F. Francalanci, P. Cesti, W. Cabri, D. Bianchi, T. Martinengo, M. Foa, *J. Org. Chem. 52* (1987) 5079.
[18] a) K. Yamamoto, T. Nishioka, J. Oda, Y. Yamamoto, *Tetrahedron Lett. 29* (1988) 1717; b) D. Bianchi, P. Cesti, E. Battistel, *J. Org. Chem. 53* (1988) 5531.
[19] a) Y.-F. Wang, C.-H. Wong, *J. Org. Chem. 53* (1988) 3127; b) Y. F. Wang, J. J. Lalonde, M. Momongan, D. E. Bergbreiter, C. H. Wong, *J. Am. Chem. Soc. 110* (1988) 7200; c) Y. Terao, M. Murata, K. Achiwa, T. Nishio, M. Akamtsu, M. Kamimura, *Tetrahedron Lett. 29* (1988) 5173.
[20] F. Theil, S. Ballschuh, H. Schick, M. Haupt, B. Hafner, S. Schwarz, *Synthesis 1988*, 540.
[21] J. B. West, C.-H. Wong, *Tetrahedron Lett. 28* (1987) 1629.
[22] A. L. Margolin, A. M. Klibanov, *J. Am. Chem. Soc. 109* (1987) 3802.
[23] I. L. Gatfield, *Ann. N.Y. Acad. Sci. 434* (1984) 569.
[24] A. Makita, T. Nihira, Y. Yamada, *Tetrahedron Lett. 28* (1987) 805.
[25] Z.-W. Guo, C. J. Sih, *J. Am. Chem. Soc. 110* (1988) 1999.
[26] W. Kullman: *Enzymatic Peptide Synthesis*, CRC Press, Boca Raton, FL 1987.
[27] J. Grundwald, B. Wirtz, M. P. Scollar, A. M. Klibanov, *J. Am. Chem. Soc. 108* (1986) 6732.
[28] R. Z. Kazandjian, A. M. Klibanov, *J. Am. Chem. Soc. 107* (1985) 5448.
[29] F. Effenberger, T. Ziegler, S. Förster, *Angew. Chem. 99* (1987) 491; *Angew. Chem. Int. Ed. Engl. 26* (1987) 458.
[30] A. M. Snijder-Lambers, H. J. Doddema, H. J. Grande, P. H. van Lelyveld, *Biocatal. Org. Media, Proc. Int. Symp. 1986*, 87, see *Stud. Org. Chem. (Amsterdam) 29* (1987).
[31] P. L. Luisi, *Angew. Chem. 97* (1985) 449; *Angew. Chem. Int. Ed. Engl. 24* (1985) 439.
[32] T. W. Randolph, H. W. Blanch, J. M. Praunitz, C. R. Wilke, *Biotechnol. Lett. 7* (1985) 325.
[33] H. L. Bruckman in B. Borgström, H. L. Brockman (Eds): *Lipases*. Elsevier, Amsterdam 1984, p. 3.
[34] L. E. S. Brink, J. Tramper, *Biotechnol. Bioeng. 27* (1985) 1258.
[35] C. Laane, S. Boeren, K. Vos, C. Veeger, *Biotechnol. Bioeng. 30* (1987) 81.
[36] G. Carrea, *Trends Biotechnol. 2* (1984) 102.
[37] L. G. Butler, *Enzyme Microb. Technol. 1* (1979) 253.
[38] M. W. Empie, A. Gross, *Annu. Rep. Med. Chem. 23* (1988) 305.
[39] G. A. Homandberg, J. A. Mattis, M. Laskovski, Jr., *Biochemistry 17* (1978) 5220.
[40] R. Dernoncour, R. Azerad, *Tetrahedron Lett. 28* (1987) 4661.
[41] F. Bjorkling, J. Boutelje, J. Gatenbeck, S. Hult, T. Norin, *Tetrahedron Lett. 26* (1985) 4957.
[42] L. K. P. Lam, R. A. H. F. Hui, J. B. Jones, *J. Org. Chem. 51* (1986) 2047.
[43] F. Bjorkling, J. Boutelje, M. Hjalmarsson, K. Hult, T. Norin, *J. Chem. Soc. Chem. Commun. 1987*, 1041.
[44] D. Herschlag, *Bioorg. Chem. 10* (1987) 62.
[45] A. P. G. Kieboom, *Recl. Trav. Chim. Pays-Bas 107* (1988) 347.
[46] Y. Hata, Y. Matsuura, N. Tanaka, M. Kakudo, A. Sugihara, M. Iwai, Y. Tsujisaka, *J. Biochem. 86* (1979) 1821.
[47] Y. Hata, N. Tanaka, N. Kakudo, A. Sugihara, M. Iwai, Y. Tsujisaka, *Acta Crystallogr. Sect. A 37* (1981) C 38.
[48] M. Sémériva, P. Desnuelle, *Adv. Enzymol. Relat. Areas Mol. Biol. 48* (1979) 360.
[49] W. H. Liu, T. Beppa, K. Arima, *Agric. Biol. Chem. 41* (1977) 131.
[50] R. Verger, M. C. F. Mieras, G. H. DeHaas, *J. Biol. Chem. 248* (1973) 4023.
[51] J. Lavayre, J. Verrier, J. Baratti, *Biotechnol. Bioeng. 24* (1982) 2175.
[52] C. S. Chen, Y. Fujimoto, G. Girdaukas, C. J. Sih, *J. Am. Chem. Soc. 104* (1982) 7294.
[53] A. R. Fersht: *Enzyme Structure and Mechanism*, 2nd ed., Freeman, New York 1985, Chapter 12.
[54] A. Zaks, A. M. Klibanov, *Proc. Natl. Acad. Sci. USA 82* (1985) 3192.
[55] W. W. Cleland, *Biochemistry 14* (1975) 3220.
[56] G. Langrand, J. Baratti, G. Buono, C. Triantaphylides, *Biocatalysis 1* (1988) 231.
[57] P. Aldercreutz, B. Mattiasson, *Biocatalysis 1* (1987) 99.
[58] M. V. Rodionova, A. B. Belova, V. V. Mozhaev, K. Martinek, I. V. Berezin, *Dokl. Akad. Nauk USSR 292* (1987) 913; *Chem. Abstr. 106* (1987) 171823.
[59] A. Zaks, A. M. Klibanov, *J. Biol. Chem. 263* (1988) 3194.
[60] A. Leo, C. Hansch, D. Elkins, *Chem. Rev. 71* (1971) 525.
[61] C. Laane, S. Boeren, R. Hilhorst, C. Veeger, *Biocatal. Org. Media, Proc. Int. Symp. 1986*, 65, see *Stud. Org. Chem. (Amsterdam) 29* (1987).
[62] C. Laane, *Biocatalysis 1* (1987) 17.
[63] K. Martinek, A. N. Semenov, I. V. Berezin, *Biochim. Biophys. Acta 658* (1981) 76.
[64] C. Gancet, C. Gaignard, P. Fourmentreaux, Eur. Pat. Appl. 239470.A1 (1987); *Chem. Abstr. 108* (1988) 73744d.
[65] M. Reslow, P. Adlercreutz, M. Mattiasson, *Biocatal. Org. Media, Proc. Int. Symp., 1986*, 349, see *Stud, Org. Chem. (Amsterdam) 29* (1987).
[66] A. M. Klibanov, *CHEMTECH 1986*, 354.
[67] H. Hirohara, S. Mitsuda, E. Ando, R. Komaki, *Biocatal. Org. Synth., Proc. Int. Symp. 1985*, 119, see *Stud. Org. Chem. (Amsterdam) 22* (1985).
[68] C. S. Chen, C. J. Sih, unpublished data.
[69] C. J. Sih, S. H. Wu, *Top. Stereochem. 19* (1989), in press.
[70] C.-S. Chen, unpublished data.
[71] D. V. Patel, F. VanMiddlesworth, J. Donaubauer, P. Gannett, C. J. Sih, *J. Am. Chem. Soc. 108* (1986) 4603.
[72] G. M. Ramos Tombo, H.-P. Schaer, X. Fernandez I Busquets, O. Ghisalba: *Biocatal. Org. Media, 1986*, 43, see *Stud, Org. Chem. (Amsterdam) 29* (1987).
[73] Z. W. Guo, T. K. Ngooi, A. Scilimati, G. Fülling, C. J. Sih, *Tetrahedron Lett. 29* (1988) 4927.
[74] A. Scilimati, T. K. Ngooi, C. J. Sih, *Tetrahedron Lett. 29* (1988) 5583.
[75] A. L. Gutman, K. Zuobi, A. Boltansky, *Tetrahedron Lett. 28* (1987) 3861.
[76] L. Bianco, E. Buigé-Jampel, G. Rousseau, *Tetrahedron Lett. 29* (1988) 1915.
[77] Z. W. Guo, C. J. Sih, unpublished data.
[78] V. Gotor, R. Brieva, F. Rebolledo, *J. Chem. Soc. Chem. Commun. 1988*, 957.
[79] P. D. Theisen, C. H. Heathcock, *J. Org. Chem. 53* (1988) 2374.
[80] B. Borgström, C. E. Albertsson in B. Borgström, H. L. Brockman (Hrsg.): *Lipases*, Elsevier, Amsterdam 1984, p. 151.

Solid Ion Conductors in Heterogeneous Catalysis

By Hans-Günther Lintz* and Costas Georgios Vayenas*

The electrochemical measurement of oxygen activity using ion-conducting solid electrolytes (λ-sensors) has become widely known, at least since the application of three-way catalysts in the postcombustion of exhaust gases from spark-ignition engines. However, the use of solid ion conductors is not limited to control devices. There are various other potential applications and numerous problems which can be studied: the formation of oxides in the course of catalytic reactions on metal surfaces, the improvement of selectivity and yield of catalytic reactions, such as the epoxidation of ethylene on silver catalysts and, finally, the cogeneration of electrical energy during oxidation reactions, such as the partial oxidation of methanol to formaldehyde.

1. Introduction

Solid ion conductors have found numerous applications in research and in technology. Electrochemical measurements in the domain of thermodynamics (free enthalpies, partial pressures, activities) and of kinetics (oxygen diffusion on metals, formation of coating layers) are widely known.[1, 2] Ion conducting solids are used in fuel cells, batteries, sensors and as chemotronic components.[3] Examples of special applications are: in research, the measurement of inertial forces,[4] and in industry the measurement of pH in aqueous systems at high temperatures and pressures.[5] So far only oxygen ion conductors have been used in the field of heterogeneous catalysis. Among the rare earth oxides ZrO_2, ThO_2 and CeO_2 (see Table 1 in Ref. [3]), zirconium dioxide is the most frequently used. It is usually doped with Y_2O_3 instead of CaO in order to maintain high conductivity in the low temperature range.

The electrochemical measurement of oxygen activity using oxygen ion conductors has become widely known since the introduction of catalytic converters for the post-treatment of automobile exhausts. Hydrocarbons, carbon monoxide and nitrogen oxides are simultaneously eliminated on three-way catalysts when the exhaust gas composition is within certain specified limits. The oxygen content in the exhaust is measured by the so-called λ-sensor and the air-to-fuel ratio of the engine feed is controlled accordingly. The oxygen content in the exhaust gas is determined electrochemically by measuring the potential difference between the electrodes of the solid electrolyte cell.

exhaust | electrode || solid electrolyte || electrode | air
(measuring side) (reference side)

However, the application of solid ion conductors in heterogeneous catalysis is not restricted to regulation and control. *Wagner*[6] had originally proposed the use of solid electrolyte potentiometry (SEP) for the measurement of oxygen activity simultaneously with the reaction rate during oxidation reactions. In this case an open system is investigated in (measuring side) constitutes simultaneously the catalytically active surface. The measurement of the oxygen activity thus leads to a quantity which is characteristic of the catalyst surface under reaction conditions. *Vayenas* and *Saltsburg*[7] were the first to perform such measurements during the investigation of SO_2 oxidation on platinum. In addition there had been early attempts to influence the reaction kinetics by electrochemical transport of oxygen from or to the catalyst surface using the same device and applying an external potential.[8] Finally, the possibility has been investigated[9] of using the potential difference generated by an electrochemical reaction between the electrodes in order to simultaneously generate electrical power and useful chemical products.

In the following we first describe the principles of the electrochemical measurements and the methods of preparation of the galvanic cell and of the electrodes. We then discuss some examples of the three different applications of solid ion conductors in the field of heterogeneous catalysis.

2. Principles of Measurement and Electrode Preparation

The potentiometric determination of pH is the most well known electrochemical method for measuring an activity. When the normal hydrogen electrode is used, the potential determining reaction takes place at the three-phase boundary line between the gas, the metal and the electrolyte. The pH of a solution relative to the known hydrogen ion activity in a second solution is determined by measuring the potential difference between the two electrodes of a galvanic cell when the same hydrogen partial pressure is imposed on both electrodes.

When an oxygen partial pressure is measured electrochemically using a solid electrolyte cell, again the potential determining reaction (1)

$$O_2 + 4\,e^- \rightleftarrows 2\,O^{2-} \qquad (1)$$

takes place at the three-phase boundary line gas–electrode–electrolyte. In contrast to the pH measurement, the oxygen ion activity is now the same at both electrodes but the oxygen partial pressure is different. The potentiometric measurement thus indicates the value of the oxygen partial pressure $p^{M}_{O_2}$ at the working electrode relative to the known value $p^{R}_{O_2}$

[*] Prof. Dr. H.-G. Lintz
Institut für Chemische Verfahrenstechnik der Universität
Postfach 6380
Kaiserstrasse 12, D-7500 Karlsruhe (FRG)
Prof. Dr. C. G. Vayenas
Institute of Chemical Engineering and
High Temperature Chemical Processes
P.O. Box 1239, GR-26110 Patras (Greece)

at the reference side (e.g., air), according to the Nernst equation.

$$E = \frac{RT}{4F} \ln \frac{p^{M}_{O_2}}{p^{R}_{O_2}} \qquad (2)$$

The experimental setup is depicted schematically in Figure 1.

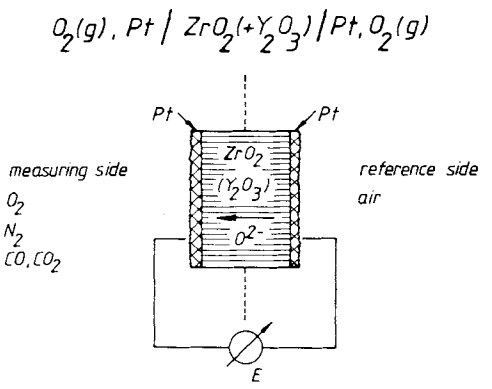


Fig. 1. The electrochemical cell: schematic diagram of the measuring arrangement.

The validity of the Nernst equation is based on the following assumptions:

- there is only one potential determining reaction, namely reaction (1);
- the conductivity of the solid electrolyte is exclusively due to oxygen ions;
- the elementary steps of reaction (1) at both electrodes are in equilibrium.

The first requirement is always fulfilled in mixtures of oxygen and inert gases. Also it has been proven that in the case of the electrolyte normally used, i.e. Y_2O_3-doped zirconium dioxide, the numbers of electrons and cations transferred are negligibly small.[10-12]

The third assumption is in principle fulfilled only under open-circuit conditions, but can be closely approximated in practice. Considering as an example the case of platinum electrodes one can distinguish the following elementary steps:

- dissociative chemisorption of oxygen
- concentration equilibrium within the chemisorbed layer
- electrochemical reaction at the gas–metal–electrolyte three-phase boundary line

Figure 2 shows a schematic diagram of a porous electrode. The above assumptions require the absence of concentration gradients both in the gas phase and in the chemisorbed layer. Moreover, there must be no concentration polarization within the electrolyte.

In the measurement proposed by *Wagner*[6] the electrode on the working side is simultaneously the catalyst. If, for example, carbon monoxide and oxygen are present in the gas phase, the reaction (3)

$$CO + 1/2\ O_2 \rightarrow CO_2 \qquad (3)$$

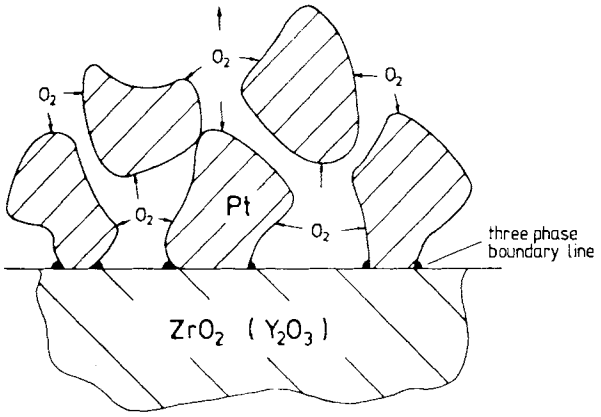


Fig. 2. Schematic diagram of the porous platinum electrode.

will take place at the electrode surface. Consequently, not only oxygen and carbon monoxide, but also carbon dioxide are in contact with the working electrode. This is shown schematically in Figure 3. The oxygen activity at the electrode will, in general, no longer be in equilibrium with the oxygen activity (partial pressure) in the gas phase. One now potentiometrically measures a quantity which is characteristic of the catalyst surface under reaction conditions. The value $p^{V}_{O_2}$ of the oxygen partial pressure, calculated from the measured potential difference by means of the Nernst equation, is now, in general, smaller than the partial pressure value in the gas phase $p^{M}_{O_2}$. The value of $p^{V}_{O_2}$ corresponds to a virtual oxygen pressure which would be in equilibrium with the oxygen activity at the electrode catalyst surface in the absence of reaction.

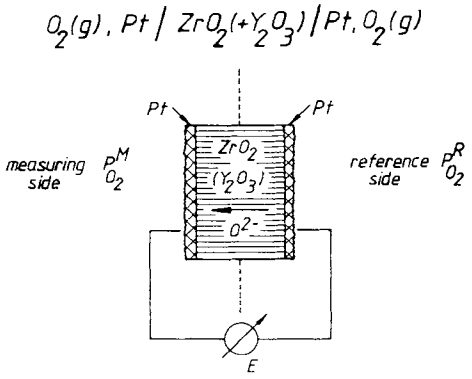


Fig. 3. The electrochemical cell (open system): schematic diagram of the setup for potentiometric measurements in a reacting system.

Naturally, the formal application of Equation (2) in the case of a reaction system is meaningful only if the potential determining reaction is still unambiguously described by Equation (1) despite the presence of additional species.

The oxygen activity value obtained potentiometrically is not an equilibrium value but is determined primarily by the oxygen coverage of the electrode under stationary conditions. This stationary value of the activity may be altered by oxygen ion transport to or from the catalyst surface by the application of an external voltage. The aim of this approach is to change the rate or selectivity of the catalytic reaction. One may consider as an example the partial oxidation of

methanol on Ag where the goal is to promote the formation of formaldehyde [Eq. (4a)]

$$CH_3OH + 1/2\,O_2 \rightarrow CH_2O + H_2O \qquad (4a)$$

which competes with the complete oxidation [Eq. (4b)]

$$CH_3OH + 3/2\,O_2 \rightarrow CO_2 + 2\,H_2O \qquad (4b)$$

A typical experimental setup is shown in Figure 4 where the oxygen ion current between the catalyst and the counter electrode is controlled galvanostatically. A third (reference) electrode can also be used as shown in Figure 4 to monitor the catalyst potential.

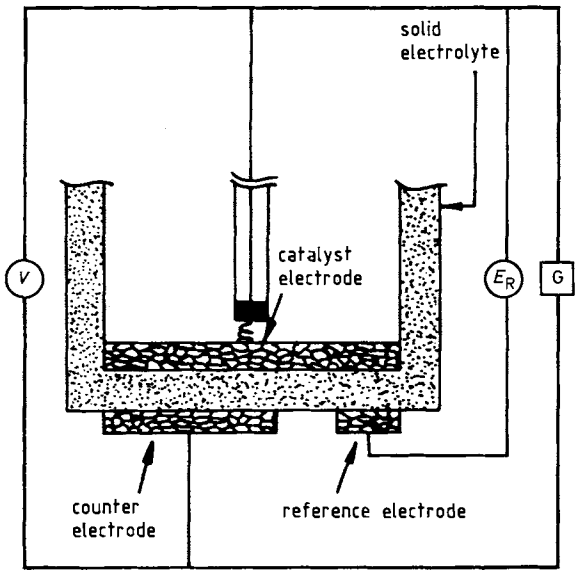


Fig. 4. Three-electrode system for controlling the oxygen ion current. V: applied potential: E_R: catalyst potential with respect to reference electrode; G: galvanostat.

A conceptually similar device can be used to study the possibility of simultaneously producing chemicals and electrical energy in a fuel cell. In this mode of operation no gas phase oxygen is fed to the anode and oxygen is supplied entirely by O^{2-} transport through the solid electrolyte. In the case of the partial oxidation of methanol to formaldehyde [Eq. (4a)] the anodic reaction is [(Eq. (5)]:

$$CH_3OH + O^{2-} \rightarrow CH_2O + H_2O + 2\,e^- \qquad (5)$$

The corresponding oxygen reduction to O^{2-} at the cathode is again described by Equation (1).

Oxygen activity measurements are useful only when they can be performed within the temperature range of interest for catalytic processes. The lower temperature limit for potentiometric measurements is determined by the fact that at low temperatures (e.g. $< 300\,^{\circ}C$) the Nernst equation is no longer satisfied due to polarization phenomena.

In order to avoid concentration polarization in the electrolyte it is important for the solid electrolyte to have the highest possible conductivity. Consequently, Y_3O_3-doped zirconium dioxide is generally used instead of CaO-doped zirconium dioxide. Furthermore, the three-phase boundary line must be extended as far as possible to avoid activation polarization effects, which have been observed during potentiometric measurements in the case of Pt/O_2 electrodes in the low-temperature range.[13] The length of the three-phase boundary line is determined by the mode of electrode preparation. The quality of electrodes can be assessed by measuring the exchange current density.

Porous electrodes can be prepared by vacuum evaporation,[14] electron beam evaporation,[15] or sputtering.[8] However, metal pastes or paints are used in most studies. The pastes are applied to form a thin layer on the solid electrolyte and are then subjected to an appropriate temperature treatment, usually in air. The organic material is evaporated or oxidized during the thermal treatment. Such pastes are commercially available and have been used in the preparation of platinum,[7,16-20] silver,[16,21] gold,[16,22] and nickel[23] electrodes. Because the pastes frequently contain fluxing agents, the possibility of catalyst contamination has to be checked[20] in the study of heterogeneous kinetics. A modified preparation technique uses powdered metal oxides suspended in an organic matrix. The porous oxide layer is reduced after drying.[24]

If one aims to determine the oxygen activity at the surface of an oxide catalyst, there are two main possibilities for preparing the solid electrolyte cell. If the oxide conductivity is sufficiently high then the potential determining reaction (1) can proceed at the three-phase boundary line gas–oxide–electrolyte. In other cases the oxide is directly deposited on a porous metal electrode[25,26] and the electrochemical reaction takes place at the three-phase boundary line oxide–metal–electrode. However, in this case the oxide layer must be impervious, since any reaction of the gas phase at the metal electrode would falsify both the kinetic and the potentiometric measurements.

3. Applications of Solid Ion Conductors in Heterogeneous Catalysis

3.1. Potentiometric Measurement of the Oxygen Activity on Catalyst Surfaces under Operating Conditions

During these measurements the temperature T and the reactant concentrations c_i are control variables and are kept constant. The measured quantities are the reaction rate $r\,(T, c_i)$ and the potential difference E between the catalyst and the reference electrode. It is convenient in the presentation of results to use the corresponding oxygen activity a_0 rather than the virtual oxygen partial pressure $p^{v}_{O_2}$ derived by using the Nernst equation (2), particularly when oxidants other than oxygen are involved [Eq. (6)].

$$a_0^2 \equiv p^{v}_{O_2} \qquad (6)$$

After the initial study of SO_2 oxidation on platinum mentioned in Section 1,[7] the potentiometric method has been used in a series of investigations involving the oxidation of ethylene on silver[21] and platinum,[27] the oxidation of propene on silver,[28] the sorption of oxygen on platinum,[29] the oxidation of platinum[30] and the interaction of carbon monoxide and oxygen on platinum.[19,31,32]

In the latter case the question has also been addressed as to whether the reaction (1)

$$O_2 + 4\,e^- \rightleftarrows 2\,O^{2-} \qquad (1)$$

is the only potential determining electrode reaction. If the competing reaction (7)

$$CO + 2\,O^{2-} \rightleftarrows CO_2 + 4\,e^- \qquad (7)$$

takes place simultaneously then a mixed potential will be measured.[32] This question has been discussed in detail.[33, 34, 38]

The benefits and limitations of the potentiometric method (SEP) had already become apparent after the first investigation:[7]

- The assumption of equilibrium between gaseous oxygen and chemisorbed oxygen, frequently used to interpret kinetic results, is generally not valid. The oxygen activity measured at the catalyst surface can be orders of magnitude lower than the gas phase oxygen activity.
- The domains of gas phase composition in which a distinct rate law is obeyed correspond to definite ranges of surface oxygen activity as a function of gas composition. The technique is not restricted to high vacuum conditions and allows the study of catalysis under pressure and temperature conditions relevant to industrial practice.

On the other hand, the measured oxygen activity is a thermodynamic property which does not permit any direct calculation of the oxygen concentration at the surface, i.e., of the oxygen surface coverage. This would be possible only with the additional knowledge of the oxygen adsorption isotherm. Therefore, such thermodynamic observations alone do not, in general, lead to more certain conclusions regarding the surface elementary reactions than does the experimentally determined dependence of reaction rate on gas composition.

An example of the above mentioned relationship between kinetically distinguishable domains and ranges of surface oxygen activity is shown in Figure 5 for the case of carbon monoxide oxidation by nitrogen monoxide on platinum.[35] As shown in this figure (Fig. 5b) high values of surface oxygen activity are measured in the range where the reaction rate is first order in carbon monoxide. When the reaction order with respect to carbon monoxide changes from first order to negative order there is an abrupt concomitant decrease in oxygen activity to extremely low values. However, the values corresponding to equilibrium with the gas phase are never attained. The observation that the rate is apparently inhibited by nitrogen monoxide (Fig. 5a) at high NO gas concentrations ($X_{NO} = 0.08$) can be easily explained by the fact that an increasing amount of undissociated NO is adsorbed on the surface. This explanation is not inconsistent with the experimentally measured surface oxygen activity values.[35, 63]

The potentiometric measurements give essential information under conditions where the phase composition of the catalyst may change during the course of the reaction and where this phase change is kinetically controlled. In these cases the experimental value of the surface oxygen activity

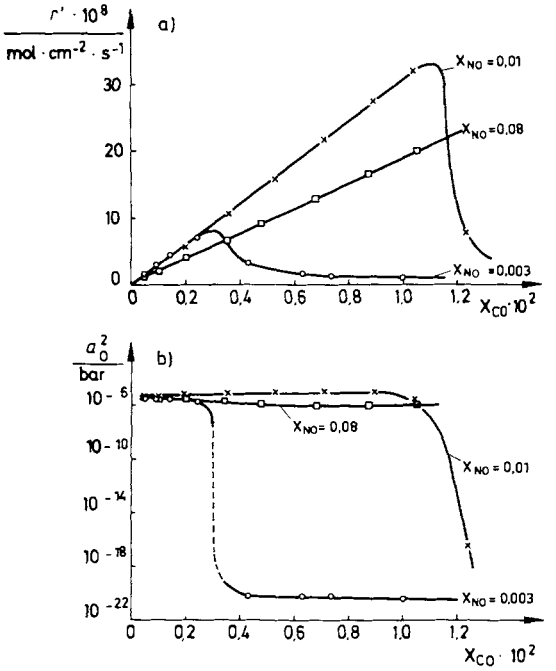


Fig. 5. Oxidation of carbon monoxide by nitrogen monoxide on platinum. a) Specific reaction rate r' and b) oxygen activity a_O^2 for different NO mole fractions at constant $T = 773$ K; $p = 1$ bar.

indicates the phase which is thermodynamically stable, and the variation in reaction rate shows the extent to which a phase change has indeed taken place. This has been demonstrated, for example, in the case of platinum oxide formation during carbon monoxide oxidation on platinum.[36]

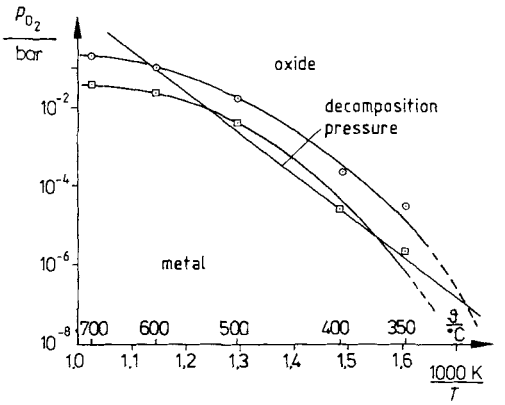


Fig. 6. Oxidation of carbon monoxide by oxygen on platinum. Temperature dependence of the oxygen activity at the platinum surface under reaction conditions; $X_{CO} = 3 \times 10^{-3}$; O: $X_{O_2} = 0.2$; □: $X_{O_2} = 0.04$ (after Ref. [36]).

Figure 6 shows the temperature dependence of the dissociation pressure of surface platinum oxide[30] and of the potentiometrically determined surface oxygen activity values under constant reactant partial pressures at 1 bar total pressure. It can be seen that over a certain temperature range the oxygen activity at the catalyst surface is greater than the dissociation pressure. Within this domain platinum oxide is the thermodynamically stable phase. At high temperatures the dissociation pressure is higher than the surface oxygen activity and, consequently, the metal is stable. In the low temperature range the surface is covered by chemisorbed CO and therefore the oxygen activity is again too low to permit

oxide formation. The thermodynamically allowed oxide formation in the intermediate temperature range has been observed under operational conditions and has been confirmed by photoelectron spectroscopy.[36]

The phase transformation of solids is considered to be one of the causes of non-linear phenomena in heterogeneous catalysis and of the occurrence of reaction rate oscillations.[37] The usefulness of the potentiometric method is not restricted to oxygen activity measurements under stable steady state conditions. It can also be used to monitor variations in oxygen activity. An example is given in Figure 7, again for the case of CO oxidation on Pt.[38] This figure shows the variation with time of both the effluent CO_2 mole fraction in the system (as a measure of the reaction rate r', Fig. 7a, c) and the potential difference E (Fig. 7b, d). Both temporal variations show clearly the same pattern. The differences in the two sets of data shown, which were obtained under identical conditions, arise from different catalyst pretreatment. The Pt catalyst is either preoxidized (Fig. 7a, b) or prereduced (Fig. 7c, d).

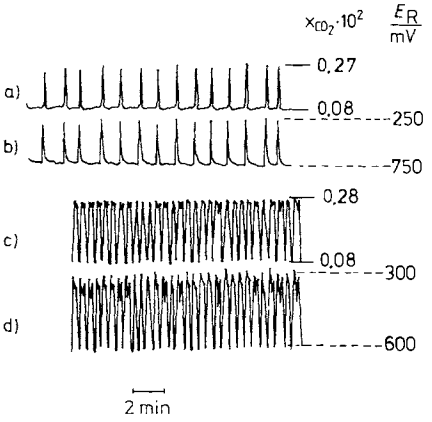


Fig. 7. Oxidation of carbon monoxide by oxygen on platinum. Oscillations of reaction rate and oxygen activity at the catalyst surface during the reaction at 610 K. a)–d), see text. Reactor inlet gas mixture composition: $X_{O_2} = 4.26 \times 10^{-2}$; $X_{CO} = 3.85 \times 10^{-3}$; balance N_2. Reaction rate: $1.3 < r' \times 10^9 < 4.5$ mol cm^{-2} s^{-1}.

Such measurements have been performed during the study of ethylene oxidation on platinum,[27] carbon monoxide oxidation on platinum[19, 32, 38] and hydrogen oxidation on nickel.[39] The results unequivocally confirm the hypothesis that periodic oxidation and reduction of the solid is the main cause of rate oscillations.

Kinetically induced transitions in the phase composition of solid catalysts are particularly important in technical applications when, as in the case of the partial oxidation of hydrocarbons, the selectivity of the reaction is altered substantially.[40] In such cases the surface oxygen activity must be maintained and controlled between specific limits to promote the desired reaction, even when the gas phase composition changes during the course of the reaction. The relationship between selectivity and oxygen activity can be studied in principle by the potentiometric method if one succeeds in working with oxide or oxide-covered electrodes. Increased efforts have been undertaken recently in this direction.[25, 41, 42]

3.2. Modification of the Course of Catalytic Reactions by Electrochemical Transport of Oxygen from or to the Catalyst Surface

Oxygen can be transferred from or to the catalytically active electrode by application of an external voltage to a stabilized zirconium dioxide cell. In the following we refer to this procedure as electrochemical oxygen transport. The surface oxygen activity can be altered by electrochemical oxygen transport even at constant gaseous composition. The aim of the procedure is to influence the course of the catalytic reaction by the additional source or sink of oxygen.

The catalytic reaction rate can now be measured as a function of temperature, gas composition and galvanostatically controlled current i: $r = r(T, c_i, i)$. The change in reaction rate [Eq. (8)] can be compared with the rate of electro-

$$\Delta r = r(i) - r(i = 0) \tag{8}$$

chemical oxygen transport $i/2F$. One can define an enhancement factor Λ[59] from:

$$\Lambda = \frac{\Delta r}{|i/2F|} \tag{9}$$

The case $|\Lambda| > 1$ is called non-Faradaic behavior,[59] sincethe variation in catalytic rate is larger than the rate of oxygen transport. The effect has been confirmed unambiguously.[59–62]

In the following we first summarize the results of previous studies.

The decomposition of nitrogen monoxide on platinum is inhibited by chemisorbed oxygen. *Amirnazmi* et al.[43] give the following kinetic expression (10) for the decomposition rate:

$$r = \frac{k\,[NO]}{1 + K[O_2]} \tag{10}$$

When the surface oxygen is eliminated electrochemically then the reaction rate increases.[8] A rather unexpected increase in the rate of NO decomposition was observed when the applied external voltage exceeded a certain critical value.[22] This effect was attributed to zirconium dioxide reduction at the cathode and formation of metallic zirconium. The observed critical potential value of 2.2 V is in good agreement with the thermodynamically computed decomposition voltage of ZrO_2, i.e., 2.28 V at 900 °C. It has been reported[44] that practically the same decomposition voltage value applies to the solid electrolyte used, i.e. 10 mol-% Y_2O_3 in ZrO_2.

The effect of the decrease in oxygen activity caused by cathodic currents has been studied for the case of carbon monoxide methanation on Pt, Fe, Ni and Co.[17] It was found that the rate of methanation could be increased by a factor of up to five. Cathodic currents promote the rate of CO disproportionation but the effect may again be related to partial reduction of the electrolyte.[17]

The rate of metal-catalyzed oxidations is usually increased by electrochemical oxygen transport to the catalyst. In a first attempt to influence the selectivity of a partial oxidation reaction, the oxidative dehydrogenation of ethylbenzene to styrene on platinum was investigated in a solid electrolyte

cell operating as a fuel cell with ethylbenzene as the fuel.[45] It was found that the rate of CO_2 production increases linearly with the current density, while the rate of styrene production is enhanced to a lesser extent. Consequently, the selectivity of the partial oxidation is not influenced positively on increasing the current in this reaction system.

Hayakawa et al.[14] have studied the oxidation of propene on gold, which was found to be inactive under open-circuit conditions. Electrochemical oxygen transport to the gold catalyst led to the formation of acrolein and other partial and complete oxidation products. The rate of acrolein production was found to increase in proportion to the rate of electrochemical oxygen transport. Only preliminary results have been reported so far regarding attempts to influence the oxidative coupling of methane to C_2-hydrocarbons by electrochemical oxygen transport.[24, 26, 46]

The effect of electrochemical oxygen transport on the epoxidation of ethene and propene on silver catalysts has been investigated in more detail.[47, 48] It was found that the selectivity and yield of ethene oxide can be strongly influenced by electrochemical oxygen transport to the catalytically active surface. It was also observed that the increase in oxidation rate can be more than two orders of magnitude higher than the rate of electrochemical oxygen transport to the catalyst. This shows that the state of the catalyst changes considerably. The catalyst modification was found to be reversible. The catalytic rate relaxation time constants during galvanostatic transients are of the order of several minutes. This marked effect was originally explained by assuming that electrochemical oxygen transport to or from the catalyst changes the surface concentration of a catalytically active silver-oxygen species.

The results obtained during ethene and propene epoxidation on silver illustrated for the first time the possibility of a non-Faradaic electrochemical modification of catalytic activity (NEMCA). It has recently been found[59–62] that the effect is not limited to epoxidation reactions on Ag. The various reactions which have been found so far to exhibit the NEMCA effect, i.e., non-Faradaic behavior, are listed in Table 1. For most of the reactions studied[59–62] it has been

Table 1. List of reactions showing non-Faradaic behavior (taken from [59]).

Reactants	Products	Catalyst	ϑ/°C	Λ	Ref.
$CH_2{=}CH_2$, O_2	ethene oxide, CO_2	Ag	320–420	300	[47]
propene, O_2	propene oxide, CO_2	Ag	320–420	300	[48]
$CH_2{=}CH_2$, O_2	CO_2	Pt	260–420	15000	[59]
CO, O_2	CO_2	Pt	300–550	500	[59]
CH_3OH	H_2CO, CO, H_2	Ag	550–700	−10	[59]
CH_3OH, O_2	CO_2, H_2CO	Pt	400–500	12000	[59]

found that over wide ranges of temperature, gas composition and applied current, catalytic rates depend exponentially on the catalyst potential [Eq. (11)]:

$$\ln\frac{k(i)}{k(i=0)} = \frac{aF}{RT}(E_R - E_R^*) \qquad (11)$$

where E_R is the catalyst potential with respect to the reference electrode and a and E_R^* are catalyst- and reaction-specific constants.[60–62]

The electrochemically induced modification of catalytic activity and the formation of certain phases could be of interest as a method of controlling the catalytic behavior of solids. As an example one can consider the case of carbon monoxide oxidation on platinum. As already discussed in Section 3.1, one can explain the observed reaction rate oscillations by assuming that the surface is subject to periodic oxidation and reduction. It is now possible to resort to electrochemical oxygen transport in order to exceed the necessary oxygen activity values for triggering the rate oscillations.

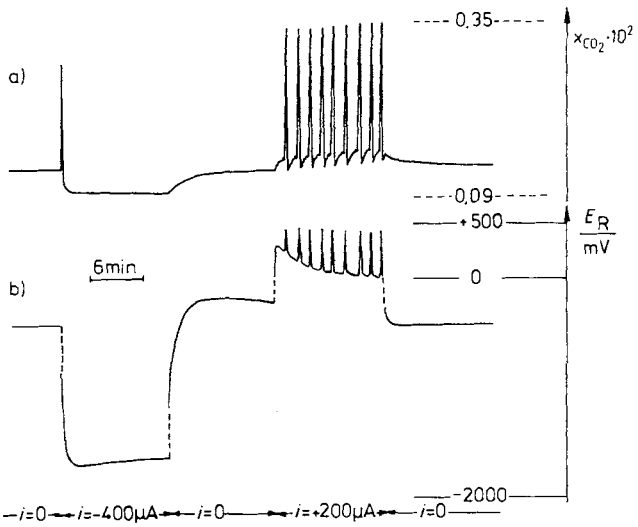


Fig. 8. Oxidation of carbon monoxide by oxygen on platinum. Modification of reaction rate by electrochemical oxygen transport, $T = 570$ K. Reactor inlet gas mixture composition: $X_{O_2} = 0.16$; $X_{CO} = 4.7\times10^{-3}$; balance N_2.

Figure 8 shows some results that have been obtained in this way. The mole fraction of the reaction product CO_2 is shown in the upper part (a) and the resulting potential of the catalyst with respect to the reference (air, Pt) electrode in the lower part (b) of the figure. At the beginning, without electrochemical oxygen transfer, the resulting oxygen activity is low and the value of the equivalent virtual oxygen pressure, 1.7×10^{-14} bar, is considerably lower than the decomposition pressure of PtO_2 at the reaction temperature, i.e., 4.8×10^{-8} bar.[30] Consequently oxygen removal from the catalyst created by a cathodic current ($i = -400$ μA) leads only to a decrease in reaction rate. If, however, an anodic current is applied ($i = +200$ μA) sufficient oxygen is supplied to the surface to exceed the corresponding oxygen activity value for oxide formation and reaction rate oscillations are induced. The final measurement under open-circuit conditions shows that the behavior of the system is reversible, as the initial values of reaction rate and potential are obtained again. The interactions between oscillations and electrochemical oxygen transfer are discussed in detail elsewhere.[49]

3.3. Cogeneration of Chemicals and Electrical Energy in Catalytic Processes

The application of oxygen ion conductors in fuel cells has been studied in detail. Results obtained with hydrogen and carbon monoxide as fuels have been reviewed recently.[50]

In addition, it has recently been proposed to combine the concepts of a fuel cell and of a chemical reactor. This aims at the cogeneration of chemicals and electrical power. The concept was first demonstrated in 1980 when electrical energy was produced during the anodic oxidation of ammonia to nitric oxide at the platinum electrode of a fuel cell.[9, 51] Subsequent studies have shown that several other exothermic reactions of technological interest can be carried out in solid electrolyte fuel cells with appropriate electrocatalytic anodes. The reactions which have been investigated so far are the oxidation of methanol to formaldehyde,[52] the synthesis of HCN in the Andrussow process,[53] the oxidative dehydrogenation of ethylbenzene to styrene[45, 54] and of 1-butene to butadiene[55] as well as the oxidation of H_2S to SO_2.[56] The results and possibilities have recently been discussed in detail.[57]

We therefore limit ourselves to the example of methanol partial oxidation to formaldehyde on a silver anode.[57] The cell is operated between 800 K and 900 K. The oxygen necessary for the oxidation reaction is supplied to the anode by spontaneous O^{2-} transport through the solid electrolyte. Oxygen anions O^{2-} are produced at the cathode, which is exposed to air. Typical results, presented in Figure 9, show

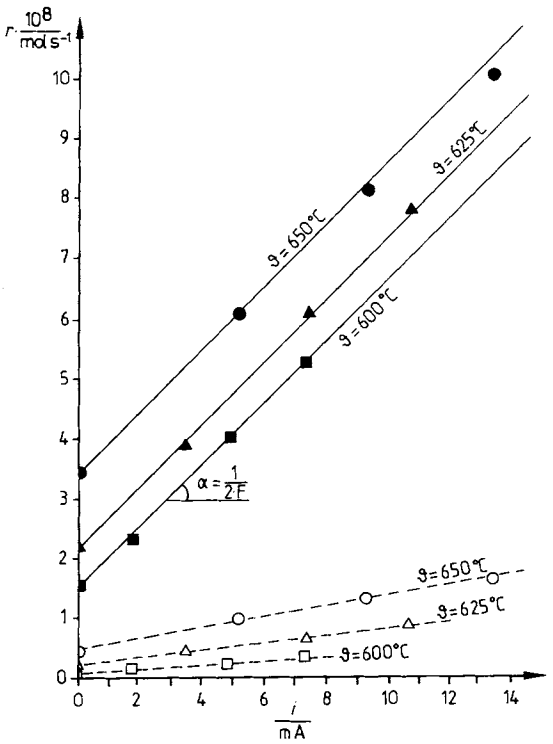


Fig. 9. Partial oxidation of methanol by oxygen on silver with simultaneous generation of electrical current. Reactor inlet gas mixture composition: $X_{CH_3OH} = 5.1 \times 10^{-2}$; balance N_2. ●, ■, ▲ = H_2CO; ○, □, △ = CO, CO_2. (Current is controlled by the resistance of the external circuit.)

that up to 95% of the methanol is oxidized to formaldehyde in the lower temperature range. The results prove that good product selectivity, which is essential even if one aims at cogeneration, can be attained under conditions where the production of electrical energy is possible. The rate measured without oxygen transfer ($i = 0$) is due to the catalytic dehydrogenation of methanol to formaldehyde and CO and to other secondary catalytic reactions.[57]

Conventional state-of-the-art solid electrolyte fuel cells exhibit power densities of the order of 400 mW cm^{-2} for thousands of hours.[58] In the above cited investigation the power density was of the order of a few mW cm^{-2}. No information is yet available on the long term cell performance. Clearly, the state of development is still in its infancy.

Outlook

There are various applications of solid oxygen ion conductors in the domain of heterogeneous catalysis. Different investigations reviewed in this article have different motivations. They range from the search for fundamental information regarding elementary catalytic steps to the, currently distant, industrial scale applications.

Presently, the applications of the different electrochemical methods are focused on the study and interpretation of elementary reaction kinetics and on explaining the efficiency of catalytically active solids. The potentiometric method (SEP) is particularly useful in this context. Future investigations will be concerned with extending the measurements to lower temperatures and also to oxide catalysts. In the latter case, particularly, SEP should give indications as to why and how product selectivity and the existence of certain solid phases can be controlled and maintained by various promotors and additives in many commercial catalysts of special composition.

The galvanostatic investigations have revealed the effect of non-Faradaic electrochemical modification of catalytic activity (NEMCA)[59–62] where both the rate and selectivity of catalytic reactions can be altered dramatically. However, potential industrial applications cannot yet be evaluated.

Investigations on the cogeneration of electrical energy and chemicals are still in a preliminary stage. Future applications will depend crucially on the commercialization of hydrogen fueled solid electrolyte fuel cells. If the latter become commercially available they could be used for chemical cogeneration purposes after minor modifications.

The present article resulted from the collaboration of our two Institutes in Karlsruhe and Patras which is sponsored by the Volkswagen foundation. We are very grateful for this support. Helpful discussions with Professor Lothar Riekert are gratefully acknowledged.

Received: July 21, 1988; revised: October 20, 1988 [A 718 IE]
German version: *Angew. Chem. 101* (1989) [A 725]

[1] H. Rickert: *Einführung in die Elektrochemie fester Stoffe*, Springer, Berlin 1973.
[2] H. Rickert: *Electrochemistry of Solids. An Introduction*, Springer, Berlin 1982.
[3] H. Rickert, *Angew. Chem. 90* (1978) 38; *Angew. Chem. Int. Ed. Engl. 17* (1978) 37.
[4] M. Betsch, H. Rickert, R. Wagner, *Ber. Bunsen-Ges. Phys. Chem. 89* (1985) 113.
[5] L. W. Niedrach, *Angew. Chem. 99* (1987) 183; *Angew. Chem. Int. Ed. Engl. 26* (1987) 161.
[6] C. Wagner, *Adv. Catal. 21* (1970) 323.
[7] C. G. Vayenas, H. Saltsburg, *J. Catal. 57* (1979) 296.
[8] S. Pancharatnam, R. A. Huggins, D. M. Mason, *J. Electrochem. Soc. 122* (1975) 869.
[9] C. G. Vayenas, R. D. Farr, *Science (Washington D.C.) 208* (1980) 593.
[10] H. Schmalzried, *Ber. Bunsen-Ges. Phys. Chem. 66* (1962) 572.
[11] D. T. Bray, *J. Electrochem. Soc. 111* (1964) 447.

[12] L. Burke, H. Rickert, R. Steiner, *Z. Phys. Chem. NF 74* (1971) 146.
[13] E. Häfele, H.-G. Lintz, *Solid State Ionics 23* (1987) 235.
[14] T. Hayakawa, T. Tsunoda, H. Orita, T. Kameyama, H. Takahashi, K. Takehira, K. Fukuda, *J. Chem. Soc. Chem. Commun. 1986*, 961.
[15] H. Okamoto, H. Obayashi, T. Kudo, *Solid State Ionics 1* (1980) 319.
[16] D. Y. Wang, A. S. Nowick, *J. Electrochem. Soc. 128* (1981) 55.
[17] T. M. Gür, R. A. Huggins, *J. Catal. 102* (1986) 443.
[18] H. S. Isaacs, L. J. Olmer, *J. Electrochem. Soc. 129* (1982) 366.
[19] R. E. Hetrick, E. M. Logothetis, *Appl. Phys. Lett. 34* (1979) 117.
[20] J. J. Ehrhardt, E. Häfele, H.-G. Lintz, A. F. Martins, *Ber. Bunsen-Ges. Phys. Chem. 89* (1985) 894.
[21] M. Stoukides, C. G. Vayenas, *J. Catal. 64* (1980) 18.
[22] T. M. Gür, R. A. Huggins, *J. Electrochem. Soc. 126* (1979) 1067.
[23] C. Sarranteas, M. Stoukides, *J. Catal. 93* (1985) 417.
[24] K. Otsuka, S. Yokohama, A. Morikawa, *Chem. Lett. 1985*, 319.
[25] E. M. Breckner, S. Sundaresan, J. B. Benziger, *Appl. Catal. 30* (1987) 277.
[26] S. Seimanides, M. Stoukides, *J. Electrochem. Soc. 133* (1986) 1536.
[27] C. G. Vayenas, B. Lee, J. N. Michaels, *J. Catal. 66* (1980) 36; C. G. Vayenas, C. Georgakis, J. N. Michaels, J. Tormo, *ibid. 67* (1981) 348.
[28] C. G. Vayenas, M. Stoukides, *J. Catal. 74* (1982) 266.
[29] H. Okamoto, G. Kawamura, T. Kudo, *Electrochim. Acta 28* (1983) 379.
[30] C. G. Vayenas, J. N. Michaels, *Surf. Sci. 120* (1982) L405.
[31] H. Okamoto, H. Obayashi, T. Kudo, *Solid State Ionics 3* (1981) 453.
[32] H. Okamoto, G. Kawamura, T. Kudo, *J. Catal. 82* (1983) 332.
[33] C. G. Vayenas, *J. Catal. 90* (1984) 371.
[34] H. Okamoto, G. Kawamura, T. Kudo, *J. Catal. 90* (1984) 374.
[35] E. Häfele, *Dissertation*, Universität Karlsruhe 1987.
[36] E. Häfele, H.-G. Lintz, *Ber. Bunsen-Ges. Phys. Chem. 90* (1986) 298.
[37] L. Riekert, *Ber. Bunsen-Ges. Phys. Chem. 85* (1981) 29.
[38] I. V. Yentekakis, S. Neophytides, C. G. Vayenas, *J. Catal. 111* (1988) 152.
[39] D. Eng, M. Stoukides, T. McNally, *J. Catal. 106* (1987) 342.
[40] M. Greger, B. Ihme, M. Kotter, L. Riekert, *Ber. Bunsen-Ges. Phys. Chem. 88* (1984) 427; M. Greger, L. Riekert, *ibid. 91* (1987) 1007.
[41] P. P. Zhuk, A. A. Vecher, R. Hartung, V. V. Samokhval, H. H. Moebius, *Vestsi Akad. Navuk BSSR, Ser. Khim. Navuk 1986*, (6), 44.
[42] B. Harrison, Johnson Matthey Ltd., private communication.
[43] A. Amirnazmi, J. E. Benson, M. Boudart, *J. Catal. 30* (1973) 55.
[44] S. Weppner, *Electrochim. Acta 22* (1977) 721.
[45] J. N. Michaels, C. G. Vayenas, *J. Catal. 85* (1984) 477.
[46] B. C. H. Steele, I. Kelly, H. Middleton, R. Rudkin, *6th Int. Meet. Solid State Ionics*, Garmisch-Partenkirchen 1987.
[47] M. Stoukides, C. G. Vayenas, *J. Catal. 70* (1981) 137.
[48] M. Stoukides, C. G. Vayenas, *J. Electrochem. Soc. 131* (1984) 839.
[49] I. V. Yentekakis, C. G. Vayenas, *J. Catal. 111* (1988) 170.
[50] E. C. Subbarao: *Solid Electrolytes and their Applications*, Plenum Press, New York 1980.
[51] R. D. Farr, C. G. Vayenas, *J. Electrochem. Soc. 127* (1980) 1478; C. Sigal, C. G. Vayenas, *Solid State Ionics 5* (1981) 567.
[52] S. Neophytides, C. G. Vayenas, J. Electrochem. Soc., in press.
[53] N. Kiratzis, M. Stoukides, *J. Electrochem. Soc. 134* (1987) 1925.
[54] J. N. Michaels, C. G. Vayenas, *J. Electrochem. Soc. 131* (1984) 2544.
[55] M. Manton, *Sc. D. Thesis*, M.I.T. 1986.
[56] I. V. Yentekakis, C. G. Vayenas, *J. Electrochem. Soc., 136* (1989) 996.
[57] C. G. Vayenas, *Solid State Ionics 28–30* (1988) 1521.
[58] A. O. Isenberg, *Solid State Ionics 3/4* (1981) 431.
[59] C. G. Vayenas, S. Bebelis, S. Neophytides, *J. Phys. Chem. 92* (1988) 5083.
[60] S. Bebelis, C. G. Vayenas, *J. Catal.* (1989), in press.
[61] S. Neophytides, C. G. Vayenas, *J. Catal.* (1989), in press.
[62] C. G. Vayenas, S. Bebelis, S. Neophytides, I. V. Yentekakis, *Appl. Phys. A* (1989), in press.
[63] E. Häfele, H.-G. Lintz, *Ber. Bunsen-Ges. Phys. Chem. 92* (1988) 188.

Gene Synthesis

By Joachim W. Engels* and Eugen Uhlmann*

Dedicated to Professor Hansgeorg Gareis on the occasion of his 60th birthday

New Synthetic Methods (77)

Oligonucleotide synthesis, until a few years ago the rather exotic preserve of a few experts, has become an integral part of the arsenal of molecular-biological techniques. The last decade, in particular, has seen unbelievably rapid development in this area. DNA synthesis has been automated and can now produce genes greater than 1000 base pairs in length. Tailor-made synthetic genes also permit the synthesis of altered or even novel proteins (de novo protein design) by gene-technological methods. Together with modern methods of gene isolation, sequencing, and expression, gene synthesis has played a major part in the enormous advances achieved in gene technology.

1. Introduction

The basic structure and chemical nature of DNA have been known since *Watson* and *Crick*'s fundamental paper of 1953.[1] Starting from nucleotide chains built up of sugar, phosphate, and heterocycles (Fig. 1), the primary structure of the double helix can be deduced as two single strands running antiparallel to each other. Because of complementarity between the individual heterocycles and the hydrogen bonds that are therefore possible between them, an ordered structure results. To describe such complex molecules in a short but comprehensible manner, the following nomenclature has been adopted. The heterocycles in the DNA, called nucleobases, are given the abbreviations A (adenine), C (cytosine, G (guanine), and T (thymine), while the fundamental sugar, 2′-deoxyribose, is indicated with d and has the numbering 1′ to 5′. Figure 1 shows a section of a dodecamer whose X-ray structure[2] forms the basis of our current understanding of B-DNA, one of the three-dimensional forms of DNA. In chemical DNA synthesis, the two complementary strands are constructed separately; i.e., only single-stranded DNA (oligonucleotides) can be synthesized. These are then hybridized (formation of hydrogen bonds) and linked to larger DNA units by enzymatic coupling in order to construct genes or their regulatory units. Although there are several definitions of a gene, our working definition[3] here is that genes are the DNA sequences responsible for the production of polypeptides. With DNA recombination techniques, it is now possible to construct any given DNA, whether synthetic or natural, to reproduce it, and to convert it into polypeptides using whole cell systems.

Starting with the chemical basis of oligonucleotide synthesis and its automation, we will describe actual chemoenzymatic gene synthesis[4–7] and its applications, which open the door to completely new peptides and proteins. The fundamentals for applying the methods outlined here have already been described in detail in this journal.[7,8]

[*] Prof. Dr. J. W. Engels
Institut für Organische Chemie der Universität
D-6000 Frankfurt am Main 50 (FRG)
Dr. E. Uhlmann
Hoechst AG
D-6230 Frankfurt am Main 80 (FRG)

2. Synthesis and Application of Oligonucleotides

2.1. Strategies in Oligonucleotide Synthesis

Oligonucleotides are polymers built up by the polycondensation of nucleoside phosphates. In this process, synthesis is possible in two directions, by 3′–5′ and 5′–3′ phosphate coupling. Because of the higher reactivity of the primary hydroxyl group, the 3′–5′ direction is the one used almost exclusively in synthesis, while nature uses the reverse direction, based on 5′-triphosphates.

Synthesis of a long oligomer or of a polymer can be carried out either by stepwise addition of single monomers or by coupling of oligomeric building blocks. Since DNA consists of only four different nucleotides, 16 dimeric oligonucleotide blocks[9–11] or 64 (4^3) trimeric ones can be prepared,[12,13] and these can be used as building blocks in the synthesis of any desired DNA sequence. Both concepts have been realized. In choosing between them, two factors must be considered: the difficulty of synthesizing the oligonucleotide blocks and the yields obtainable by monomer addition. The diagram in Figure 2 correlates the coupling yield with the length of the DNA and convincingly shows that for a yield of 99% per addition – which, astonishingly, can be achieved for all four nucleotides – pieces long enough to be used in gene synthesis can be synthesized in acceptable yields. In practical solid-phase synthesis, the stepwise addition of monomeric building blocks has become standard.

2.2. Methods for Oligonucleotide Synthesis

Methods for synthesizing defined oligonucleotides are differentiated primarily by the way in which the phosphate ester bond is formed. Thus, according to the nature of the phosphorus component, one distinguishes the so-called triester (Fig. 3a), phosphite (Fig. 3b, X = Cl), phosphoramidite (Fig. 3b, X = N*i*Pr$_2$), and H-phosphonate (Fig. 3c) methods. The corresponding protected nucleoside derivative functions as the starting compound. Although an enormous number of protecting groups are known[14] and have also been tested in oligonucleotide synthesis,[15–18] only a few are routinely used, owing to automation (and commercialization) of DNA synthesis. These are primarily those introduced by *Khorana* et al.:[19] acyl groups on the exocyclic amino functions of adenine, guanine, and cytosine and a

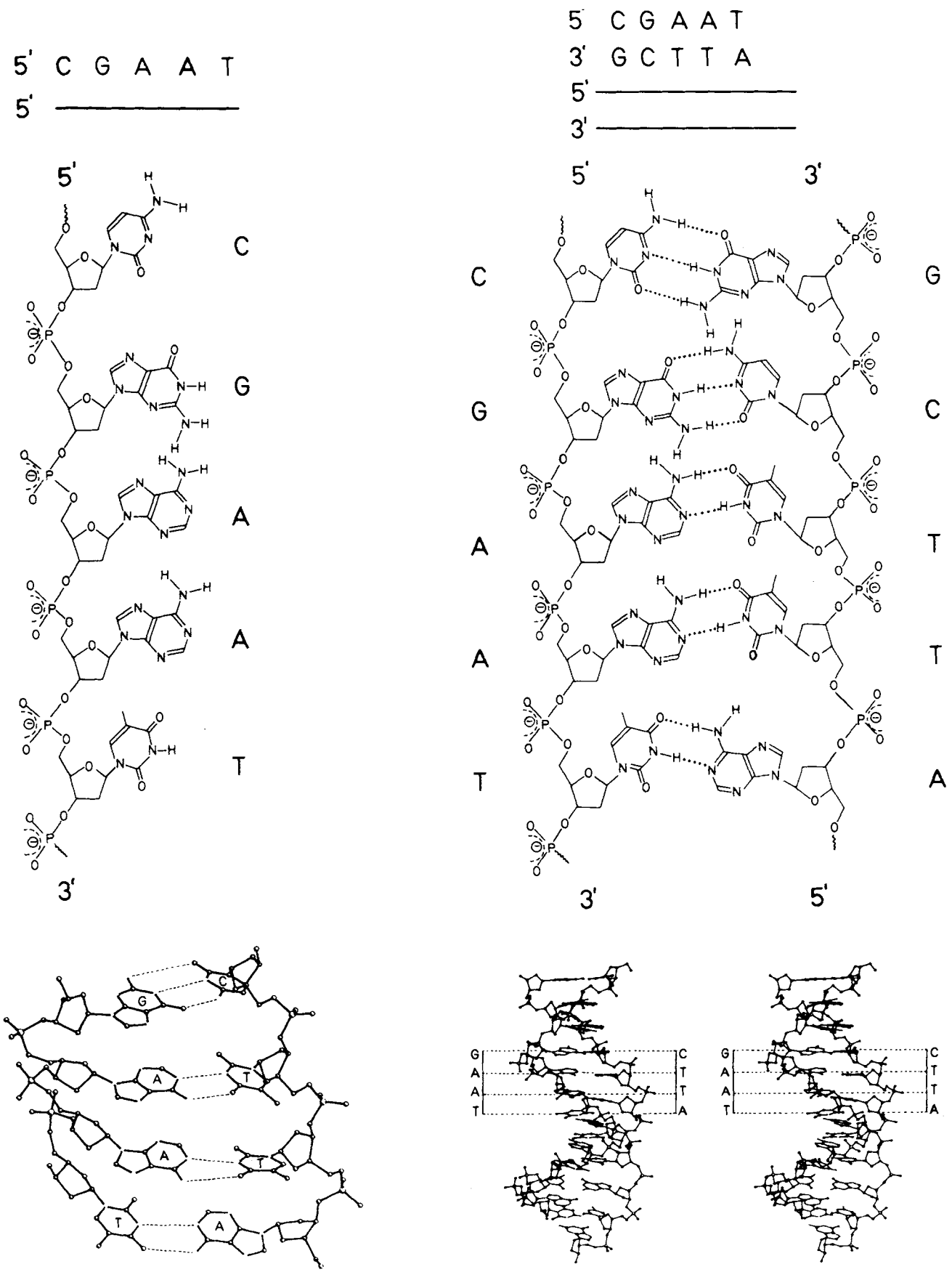


Fig. 1. Single-stranded and double-stranded B-DNA (dodecamer) CGCGAATTCGCG. Top left: 5'-CGAAT single strand. Top right: Idealized Watson–Crick base pairing. Bottom left: Section GAAT, retaining the base pairing. Bottom right: Stereopair of dodecamer.

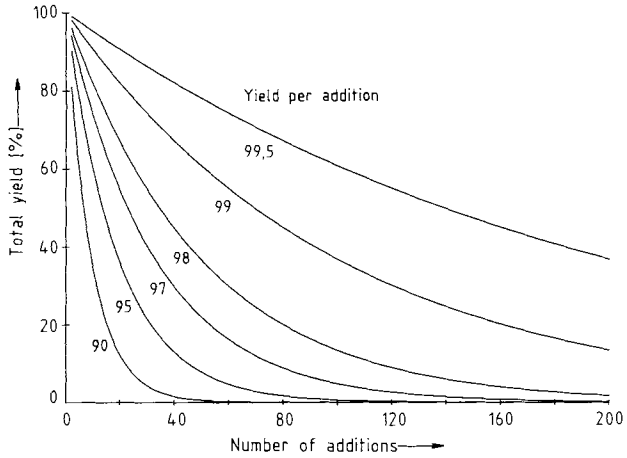


Fig. 2. Correlation of total yield per addition with the number of reaction cycles (i.e., the length of the DNA).

dimethoxytrityl group on the 5'-hydroxyl group of the deoxyribose. Today, they can be introduced easily and in good yield by the "transient protection" method of *Ti* et al.[20] Intermediate protection of the sugar OH groups as their trimethylsilyl ethers allows the amino groups to be specifically protected by acylation reagents. More labile acyl[21] and amidine[22, 23] protecting groups are finding increasing use;

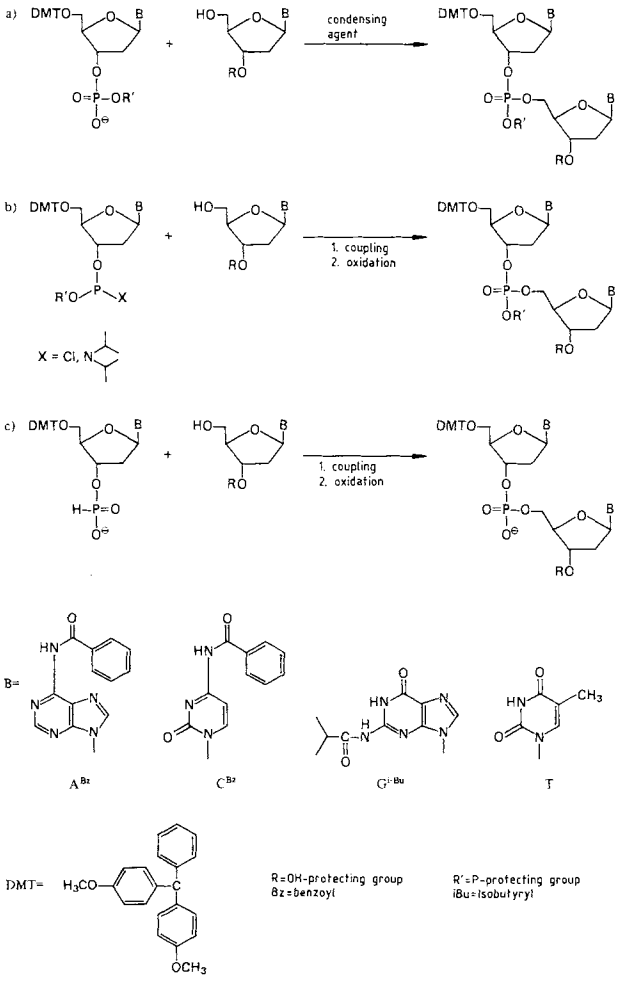


Fig. 3. Methods of oligonucleotide synthesis: a) triester, b) amidite, and c) H-phosphonate.

they are of particular advantage in the synthesis of modified DNA with more labile functionality. A comprehensive list of all the protecting groups used in oligonucleotide synthesis up to 1986 can be found in *Sonveaux*.[18] Especially when synthetic methods using very reactive phosphorus derivatives are employed, it is important to consider undesired derivatization of the amide functions of guanine and thymine.[24–26] Here, too, several protecting groups have been used to convert the amide into the iminoether.[27–30] For the phosphoramidite method, we have been able to show that optimization of the synthesis is preferable to excessive use of protecting groups.[31]

The corresponding protected nucleosides are then phosphorylated with suitable reagents. These can be either mono- or bifunctional. For synthesis on a solid support by the Merrifield strategy, however, it has proved advantageous to synthesize stable monomeric nucleotide building blocks which can be stored ready to be used as needed in synthesis. A multitude of different functions have been used as protecting groups on phosphorus.[18] Here, too, as with the nucleobases, automation has brought about simplification. A point worth mentioning is the chemical mechanism by which the phosphorus protecting group is removed. Reactions at phosphate phosphorus have been shown by *Westheimer* et al.[32] to proceed by addition-elimination mechanisms, with the possibility of pseudorotations. To avoid potential problems, such as undesired hydrolysis, protecting groups are preferred in which attack of the reagent takes place directly at the protecting groups without affecting the phosphate center.[33] Alkyl groups such as methyl and benzyl have been used here, as have β-cyanoethyl, arylsulfonylethyl, arylethyl, and haloethyl groups, all of which can be removed by β-elimination. Isomerization of the phosphate bond is largely prevented and strand breaks avoided by this strategy.

2.2.1. *Triester Method*

This synthetic method (Fig. 3a) was introduced by *Todd* et al.[34] and is based on suitable activation of a protected nucleoside phosphate diester with acid derivatives of the arylsulfonic acid azolide type. The activated phosphate diester then reacts with the unprotected 5'-OH of the nucleoside, giving the corresponding dinucleoside phosphate triester. A large number of such reagents have been used[35–38] as their phosphoric and sulfonic acid derivatives. Of the azolides, tetrazole and 3-nitrotriazole have proved particularly useful. The low initial reactivity of P^V compounds can thus be increased to a sufficient level. Decisive advantages of this method include the good stability of the starting diesters and their potential recovery (e.g., as barium salts).[39] A disadvantage lies in the side reactions brought about by the condensing agent (e.g., sulfonation at the 5'-OH position).

2.2.2. *Phosphoramidite Method*

Here, a suitably protected nucleoside phosphoramidite (Fig. 3b) is converted into a phosphite triester by reaction with a 5'-OH nucleoside in the presence of tetrazole. Subsequent oxidation leads to the corresponding triester (see Fig. 3a). The higher reactivity of P^{III} compounds has always made them attractive starting materials,[40] but for routine oligonucleotide synthesis their poor handleability and

availability and especially the difficulty of storing the monomeric building blocks have hampered their use. With the introduction by *Caruthers* et al.[41,42] of phosphoramidites, which can be activated by acid, the breakthrough was made. Although the initial choice fell on the dimethylamino group as the amidite component and on the methoxy protecting group,[43] today, after further optimization of reaction conditions, the diisopropylamino compound,[44] in combination with a β-cyanoethyl protecting group,[45] is regarded as the best compromise. The most important advantage of this method is the activation by the mild reagent tetrazole, which is practically free of side reactions.

2.2.3. H-Phosphonate Method

Todd et al.[46] were quick to recognize and use the synthetic potential of H-phosphonates. Here, a protected nucleoside H-phosphonate (Fig. 3c) is converted into a dinucleoside phosphonate diester by reaction with a 5'-OH nucleoside in the presence of a condensing agent, usually an acid chloride.[47,48] Subsequent oxidation leads to the corresponding triester. No intermediate protecting group is required on the phosphorus, and the oxidation of the H-phosphonate is carried out only at the end of the synthesis, not after each addition, as in the amidite method. On the other hand, side reactions (acylations) of the condensing agent (e.g., pivaloyl chloride) do occur, as in the triester method. Moreover, the yields in the H-phosphonate method do not match those of the phosphoramidite method, despite optimization (e.g., use of adamantoyl chloride as the condensing agent).[49]

2.3. Oligonucleotide Syntheses on Solid Supports

Because oligonucleotide synthesis is a repetitive technique, synthesis on a solid support has come to be preferred to synthesis in solution or polycondensation.[50] Since the introduction of solid-phase synthesis by *Merrifield*[51] and *Letsinger*,[52,53] the following fundamental requirements have been worked out: (1) The polymeric matrix must be insoluble and as inert as possible in the solvent used. (2) Functional groups on the polymeric support must allow covalent binding of the product to be synthesized. (3) The structure of the polymer must not interfere with the chemical reaction too much (e.g., by hindering diffusion of the reacting molecules).

A large number of materials have been tested, from polystyrene[54] to polyacrylamide,[55] cellulose,[56] polytetrafluoroethylene,[57] and silica gel.[9,58,59] The most widely used today are silica gel and specially defined glass beads, so-called controlled pore glass (CPG) material.[44,60,61] The solid support is connected to the initial nucleoside through a spacer (most simply an alkylamine; Fig. 4). Since synthesis proceeds in the 3'–5' direction, the initial nucleoside is linked to the spacer through its 3'-hydroxyl function and a dicarboxylic acid (e.g., succinic acid).[59] At present, supports carrying the four nucleosides A, G, C, and T or a universal anchor[62] are in use.

Of the requirements listed above, the first two are easy to satisfy. However, the requirement that the solid support have as little effect as possible on the growing chain is not so

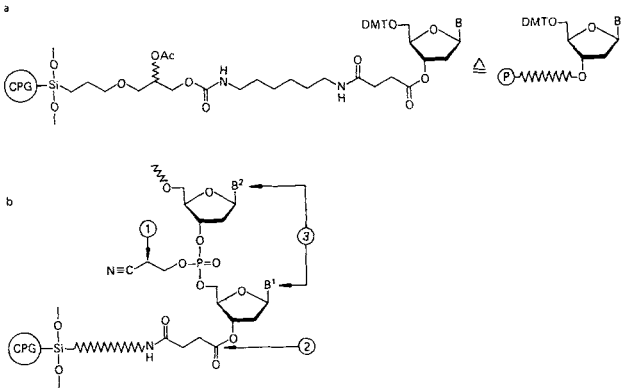


Fig. 4. a) Attachment of the starting nucleoside to the solid support. b) Cleavage (1) of the protecting group on phosphorus, (2) of the oligonucleotide from the support, and (3) of the base protecting groups.

easily met. A very good compromise has been found in the CPG materials now being successfully used. It is interesting to note that when 500-Å CPG material is used, the coupling yield of each addition decreases when a length of 80 bases is exceeded. Changing to 1000-Å material, however, permits synthesis of chain lengths of up to 200 bases.[63] The support material appears to be a decisive limiting factor of the method.

The strategy for carrying out simultaneous syntheses is also worth mentioning here. For solid-phase synthesis, automatic synthesizers have been in use since 1980. With these, one or several (three or four) oligonucleotides can be synthesized simultaneously. However, since in principle only four different reactants (A,G,C,T) are possible in the synthesis of natural DNA, the filter-disc method[64–66] (20 to 100 oligonucleotides) has proved itself as an alternative. The handicaps of this method are slightly reduced yields and difficulties in automation.

Automation was the decisive step in making oligonucleotide synthesis broadly applicable. Thus, the synthetic protocols that had been worked out were put together into the reaction cycle shown schematically in Figure 5. The important steps in such a cycle are:

1. deprotection of the 5'-OH position by treatment with acid;
2. activation of the nucleotide component with tetrazole;
3. addition of the nucleotide;
4. capping of unreacted 5'-OH groups;
5. oxidation (in the case of P^{III} compounds).

Several washes were placed between these crucial chemical steps to rinse away excess reagents and equilibrate the reactions concerned. While steps (1)–(3) are routine for all methods, the necessity of step (4), the capping of unreacted 5'-OH groups, is disputed. Although the individual additions are practically quantitative, this step has proved invaluable in avoiding failure sequences. After completion of the synthesis on the solid support, the oligonucleotides are freed from their protecting groups while still in the automatic synthesizer (step (6), Fig. 5). As a result, cleavage conditions are also simplified. In the phosphoramidite method – which we favor – this reaction is carried out with concentrated aqueous ammonia. The nucleotide mixture obtained is then purified by efficient methods like preparative gel electrophoresis or high-performance liquid chromatography (HPLC).[67]

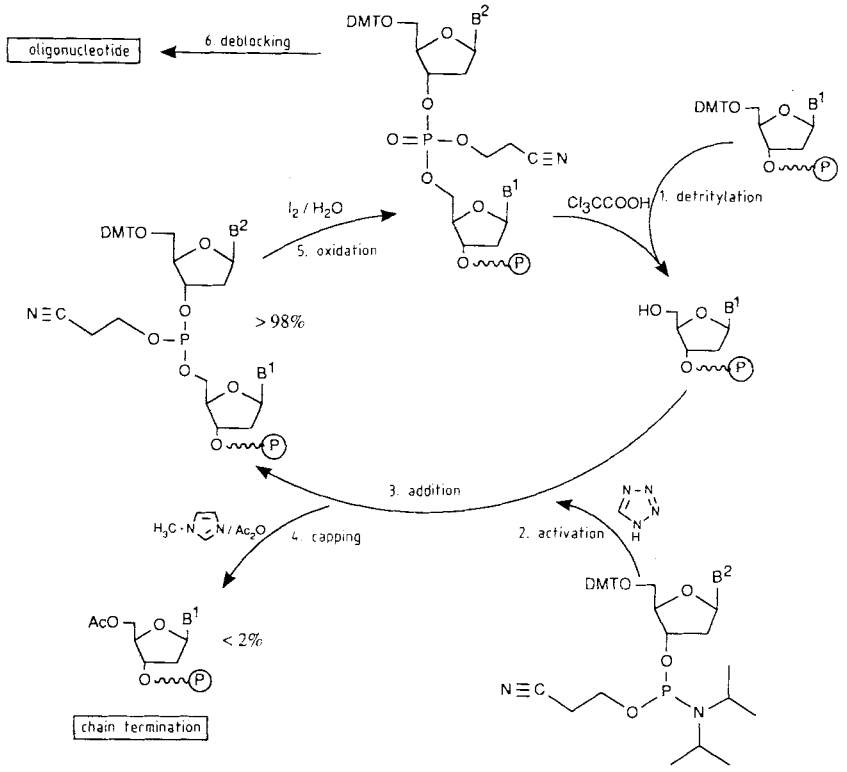


Fig. 5. Synthetic cycle for the phosphoramidite method.

2.4. Application of Synthetic Oligonucleotides

On the basis of the complementarity principle formulated by *Watson* and *Crick*, oligodeoxynucleotides can hybridize with both DNA and RNA. Experiments have shown that the duplex with exact base-pair complementarity is the highest melting. By gradual annealing, therefore, extremely specific analyses can be performed. This principle appears to give especially promising results in genome analysis (i.e., the diagnosis of gene defects).[68] This aspect will not be dealt with further here; rather, the application of the synthesized oligonucleotide building blocks to gene synthesis will be discussed in detail.

3. Construction of Synthetic Genes

3.1. Historical Development of Gene Synthesis

Before methods for the design and synthesis of genes are discussed in detail, the enormous developments in DNA synthesis during the last two decades will be illustrated with a few instructive examples (Table 1). In the sixties and early seventies, crucial pioneering work was carried out by *Khorana* et al., who synthesized the genes for yeast alanine-specific transfer RNA (tRNA)[69] and *E. coli* tyrosine-suppressor tRNA.[70–82] The fundamental methods and strategies developed there are still being used for the synthesis of numerous genes.

Table 1. Historical developments in gene synthesis.

Gene for	Length of the gene [bp]	Number of oligo-nucleotides	Method for oligonucleotide synthesis [a]	Length of synthesized oligonucleotide	Length of overlap	Year of appearance	Ref.
Alanine-specific tRNA from yeast	77	15	diester	5–20	4–7	1970	[69]
Angiotensin II	33	7	diester	6–11	5–6	1975	[83]
Tyrosine-suppressor tRNA from *E. coli*	126	26	diester	6–13	4–7	1976	[70–82]
Somatostatin	56	8	triester	11–16	5–8	1977	[84]
Insulin							
B chain	104	18	blocks of triester	10–12	4–6	1978	[85]
A chain	77	12	blocks of triesters	10–15	5–8		
Interferon-α	514	67	triester/sp	14–21	7–10	1981	[87]
Epidermal growth factor	170	10	amidite/sp	11–59	7–24	1983	[97]
Interferon-γ	453	66	chloridite/sp	9–14	5–8	1984	[116]
Interferon-γ	452	34	amidite/sp	18–33	6 [b]	1984	[115]
Growth hormone	584	78	triester/sp	7–26	4–10	1984	[89]
Interleukin-2 receptor protein	753	38	amidite/sp/A	27–51	6–12 [b]	1986	[90]
Bovine rhodopsin	1057	72	amidite/sp/A	15–40	4–5 [b]	1986	[168]
Bovine prochymosin [d]	1108	28	amidite/sp/A	59–102	4 [b]		
	1126	26		72–102	7–8 [b]	1987	[92]
HMG CoA reductase	1400	19	amidite/sp/A	86–147	[c]	1988	[93]
t-Plasminogen activator	1610	101	amidite/sp/A	17–37	4–20	1988	[91]

[a] sp = solid phase; A = automated DNA synthesis. [b] Preformed duplex DNA. [c] Not by ligation of the oligonucleotides. [d] Two syntheses performed.

Despite *Khorana*'s sensational work and exceptional successes, the time was not yet ripe for application of synthetic genes, since many of the important molecular-biological tools and techniques (e.g., restriction enzymes, DNA sequencing) were not discovered or developed until later. The real breakthrough did not occur until a decade later, with the synthesis and expression of structural genes (i.e., genes that code for valuable peptides or proteins). "Expression" of a gene is understood as its transcription into a messenger RNA (mRNA) and subsequent translation of the mRNA into the corresponding polypeptide. Although by 1975, *Köster* et al.[83] had reported the first successful synthesis of a structural gene, that coding for the octapeptide angiotensin II, the breakthrough in synthetic genes took a few more years, since this gene could not be successfully expressed at that time. The route to expression of synthetic genes had thus been foreshadowed, but the expression of the first synthetic gene in bacteria, achieved by *Itakura* et al. in 1977,[84] was without doubt one of the highlights of genetic engineering. The tetradecapeptide obtained, somatostatin, was, in addition, the first peptide hormone to be detected in *E. coli* produced by recombinant DNA methods. In another remarkable paper the following year, the same research group reported the successful synthesis of the insulin A and B chains,[85] which were later expressed in *E. coli*.[86]

A further milestone in the history of gene synthesis was the total synthesis of the gene for leukocyte interferon (IFN-α) in 1981.[87] The length of the gene, 514 base pairs (bp), coding for 166 amino acids, was impressive, as was the fact that for the first time the synthetic gene was derived not from the peptide sequence but from the published nucleotide sequence (cDNA).[88] Previously, genes had been produced manually and in solution, a process which would have been impracticable for a gene of this size. Only since the introduction of solid-phase techniques has the synthesis of larger genes of the length of the interferon gene, for example, become a reality. With the introduction of the technique of sequential cloning, the construction of larger genes became possible. Sequential cloning means division of a gene into fragments which are cloned separately and, only after verification of the partial sequences, combined to form the total gene. For example, the syntheses of a gene for human growth hormone (192 amino acids), put together in two fragments from 78 oligonucleotides, was accomplished in 1984.[89] The gene syntheses published after 1984 have been largely carried out using DNA synthesizers.

The first example of a synthetic gene for a receptor protein was presented in 1986.[90] It consisted of 753 base pairs and was synthesized from only 38 synthetic oligonucleotides via three subclones. The longest synthetic gene to date contains 1610 base pairs and codes for human t-plasminogen activator (h-tPA).[91] This gene required the synthesis of 101 oligonucleotides with an average length of 32 nucleotide units. With a cycle time of 12.5 min per nucleotide addition, one can thus calculate a total synthesis time of about 30 days for the entire tPA gene. The main task was linking together the 101 oligonucleotides to make the complete gene.[91]

Indirectly, Table 1 reflects the extremely rapid progress in oligonucleotide synthesis in recent years, as seen in the growing chain length of the oligonucleotides used. If one ignores the tPA gene for the moment, the trend is clearly towards the use of longer oligonucleotides,[92,93] simplifying construction of the gene and also admitting the development of new strategies for gene synthesis. It is not difficult to predict that in the future great but easily justifiable efforts will go into making even longer synthetic genes.

To date, over 150 genes have been synthesized, coding for hormones,[83-85,89,94-113] interferons and lymphokines,[90,127-130] growth factors,[131-140] enzymes,[92,93,141-152] neuropeptides,[153-157] calcium-binding proteins,[158,159] gastrointestinal peptides,[106,160] proteinase inhibitors,[161-167] and other products.[69,82,91,168-188]

3.2. Routes to Double-Stranded DNA

3.2.1. Fundamental Enzymatic Reactions: The DNA Ligase and DNA Polymerase Reactions

Genetic information is stored in the form of the nucleotide triplet in the coding strand of DNA and indirectly in the noncoding strand. The double helix structure of DNA (Fig. 1) serves to stabilize the DNA and is also a requirement for its replication. The natural ability of single-stranded oligo- or polynucleotides to bind to one another in a defined manner through base pairing can be exploited for the construction of double-stranded DNA from suitable chemically synthesized oligonucleotides.

In principle, two types of enzymatic reactions can be applied in the construction of double-stranded DNA, those catalyzed by DNA ligase and DNA polymerase. The enzyme T4-DNA ligase catalyzes the formation of phosphodiester bonds between neighboring 5'-phosphate and 3'-hydroxyl ends in a DNA duplex in the presence of ATP (Fig. 6). Sin-

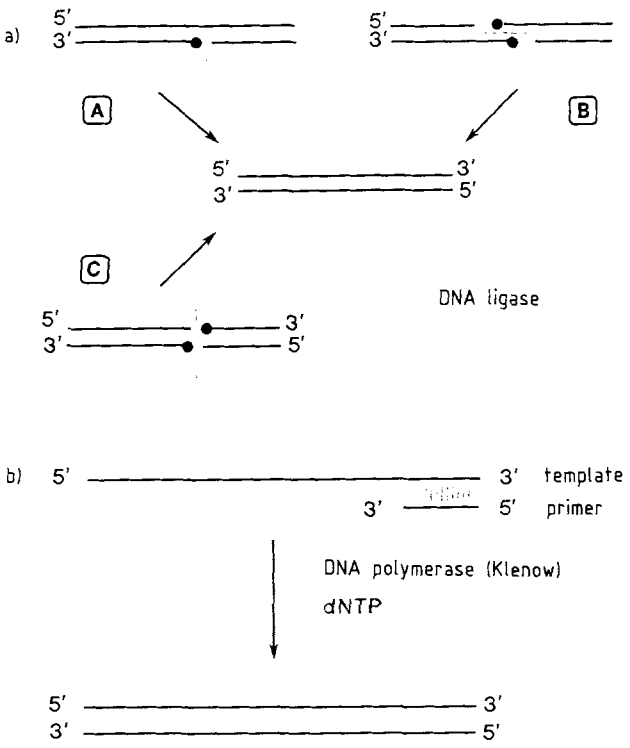


Fig. 6. Fundamental enzymatic reactions in the construction of double-stranded DNA from oligonucleotides: a) DNA ligase reaction; b) DNA polymerase reaction.

gle-stranded oligonucleotides, by contrast, are not substrates of DNA ligases. In reaction-type A, the oligonucleotides to be coupled are held together by an intact region on the complementary oligonucleotide. In contrast, in reaction-type B the overlapping ends of the two strands are joined. Like the DNA fragments that arise from cutting with restriction enzymes, the ends can be ligated in a 5′-overhanging or a 3′-overhanging manner. Reaction-type C, in which "blunt ends" are ligated, is rarely used in gene synthesis, since the lack of base pairing leads to low selectivity in this reaction. In addition, these blunt-end ligations are much less efficient than so-called sticky-end ligations. If the oligonucleotides to be joined have not already been synthesized as 5′-phosphates,[189, 190] phosphorylation of the 5′-hydroxyl nucleotides with polynucleotide kinase and ATP is necessary. In this enzymatic step, the oligonucleotides can be radioactively labeled using [γ-^{32}P]ATP, a process which can be useful in the ligation of subnanomolar quantities. The enzyme DNA polymerase I (Klenow fragment), which lacks the 5′–3′ exonuclease activity of the complete enzyme, can, in the presence of the deoxynucleoside 5′-triphosphates, synthesize a complementary copy of a single-stranded polynucleotide, starting at the 3′-hydroxyl end of a short, hybridized oligonucleotide primer (Fig. 6b). In principle, this "fill-in" reaction can be performed by any of the DNA polymerases from other organisms that have been used for DNA sequencing according to the *Sanger* procedure.[202]

3.2.2. *Strategies for Gene Synthesis*

Retrosynthetically, the gene to be synthesized can be dissected into single-stranded oligonucleotides along any of the paths A–E in Figure 7. The number of required oligonucleotides will depend on their length.

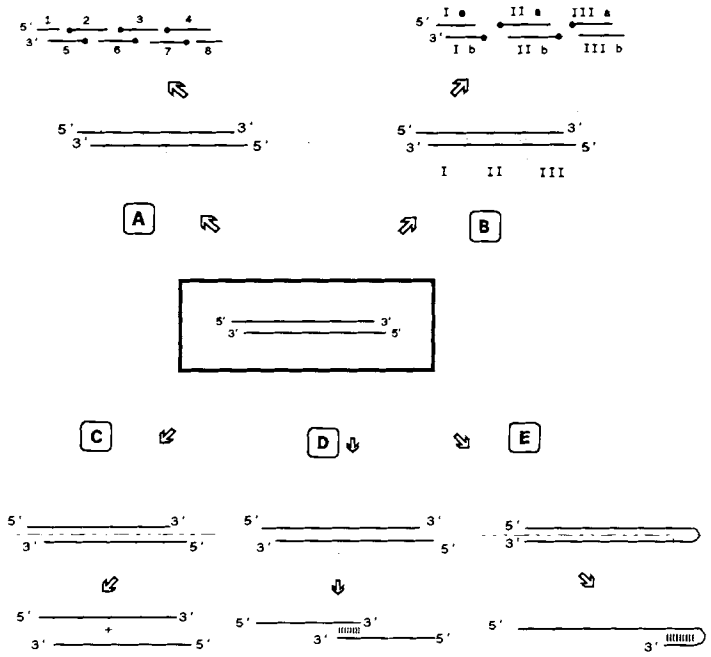


Fig. 7. Strategies for gene synthesis: A) ligation procedure according to *Khorana*; B) sequential ligation of preformed DNA duplexes; C) direct hybridization and cloning of longer oligonucleotides; D) fill-in method for overlapping oligonucleotides; E) fill-in method for autoprimer oligonucleotides.

Path A: Ligation of Overlapping Oligonucleotides by the Khorana Procedure

The classical procedure of *Khorana*[69, 191] is outlined in path A. It is based on ligation-type A of Figure 6a, whereby the gaps to be closed are situated alternately in the upper and lower strands. This strategy requires the synthesis of a set of overlapping oligonucleotides (here, for example, eight of them) and their ligation to form a complete gene or gene fragment. Only the internal oligonucleotides (2–7) must be present as their 5′-phosphates. Because of base complementarity, heating a solution of all the oligonucleotides and cooling it slowly results in correct annealing and formation of a hybrid molecule that is not yet covalently bonded. In the presence of ATP, DNA ligase then generates the desired phosphodiester bonds. In this way, for example, 20 oligonucleotides could be coupled in a single ligase reaction to give a 280-bp structural gene.[131] In our hands, however, six to ten oligonucleotides proved optimal with regard to yield and size of the gene. The general rule is that the yield of the completely ligated product falls as the number of oligonucleotides to be coupled in a reaction increases.[176] Using longer oligonucleotides of 40 to 60 bases leads to an increase in the efficiency of the enzymatic ligation reactions.[192]

Ligation according to path A is exemplified by the synthesis of a gene for tyrosine-suppressor tRNA from *E. coli*, reported by *Khorana* et al. in twelve consecutive publications in 1976.[70–81] The 126-bp gene was first divided into four fragments, and these were then further divided into a total of 26 oligonucleotides. This was done in such a way that at least four to six base pairs could overlap between the individual oligonucleotides. Another aspect was the economy of the synthesis, for example the repeated use of synthetic blocks. The total synthesis of the gene thus required the chemical synthesis of 26 oligonucleotides by the phosphodiester method, which at that time was the most labor-intensive part of the synthesis. These oligonucleotides were then ligated in groups into four fragments, which were subsequently coupled to give the complete gene. Coupling of the fragments proved to be quicker and more efficient than the previous ligation of single-stranded oligonucleotides, a fact that was taken into account in later developments (cf. strategy B). Today, *Khorana*'s ligation procedure is still the most popular strategy, especially for oligonucleotide chain lengths between 15 and 50 units. Since the filter-disc method[64–66] works mainly in this length region and can also be used to synthesize a large number of oligonucleotides simultaneously, ligation strategy A is the method of choice in this case. These days, longer genes are divided into several subclones (subfragments)[115] and are not constructed in a ligation cascade without intermediate cloning, as was the case for the leukocyte interferon gene.[87] Among others, the 1610-bp gene for tPA[91] was constructed from 101 oligonucleotides by this strategy, via three subclones.

Path B: Sequential Ligation of Preformed DNA Duplexes

Just as DNA can be cut with restriction enzymes, genes can also be retrosynthetically divided into smaller DNA fragments. This approach presumes a certain chain length for the synthesized oligonucleotides, however, in order that stable DNA duplexes are formed. Strategy B has the advan-

tage over strategy A that the oligonucleotides are hybridized pairwise into small DNA double strands, which can then be ligated, either sequentially or in one pot, to form the complete gene in good yield. In this way undesired hybridizations are prevented (for example, Ia with IIb in Fig. 7). DNA double strands can also be easily purified on agarose gels (2–4%). The overlapping ends can be planned to overlap either 3′ or 5′, as desired. Usually overlaps of four to eight bases are chosen, but overlaps of up to twelve base pairs have been used with success.[90] Although longer overlaps lead to more stable hybrids, with large overlaps one is potentially struggling against problems of secondary structure (cf. Section 4.1) and incorrect intermolecular interactions, so that a compromise must be sought between the opposing effects.

Path C: Direct Hybridization and Cloning of Longer Oligonucleotides

Division of a gene into a coding and a noncoding strand is the simplest possible route to the total synthesis of a gene, but was not practicable in the past because chemical synthesis could not produce oligonucleotides of sufficient length. Today, however, the synthesis of oligonucleotides up to 200 units in length is possible. This means that genes or gene fragments coding for up to 65 amino acids are accessible by the synthesis of only two oligonucleotides and their hybridization. Recently, the synthesis and cloning of a calcitonin gene by this procedure was reported for the first time.[109] This strategy has the following advantages: the manual work to be performed is greatly reduced, since no enzymatic ligation is required; the chemical synthesis is performed by a synthesizer; purification of only two oligonucleotides is needed. On application of sequential cloning (subcloning) of gene fragments, this strategy also becomes an attractive method for the synthesis of larger genes. In principle it is a logical further development of the preformation of DNA duplexes (strategy B). Depending on the chain length of the oligonucleotides used and on the choice of retrosynthetic cleavages, there is a smooth transition from strategy A through B to C. In this light, subcloning is nothing more than moving the sequential ligation of preformed duplexes into a plasmid, though with the great advantages that the sequence of the synthetic fragments can be verified at an intermediate stage and that an inexhaustible source of the particular gene fragment is obtained. A combination of strategies B and C is found in the synthesis of the ca. 1100-bp-long gene for bovine prochymosin.[92]

Path D: Fill-in Method of Overlapping Oligonucloeotides

The so-called fill-in procedure, making use of DNA polymerase, was farsightedly suggested by *Khorana*[191] in 1968, but was not realized until 1982 by *Rossi* et al.[193] It relies on the synthesis of two long oligonucleotides with perfect base-pairing sequences at their 3′ ends. After correct hybridization of these oligonucleotides, the DNA polymerase (Klenow) reaction shown schematically in Figure 6b can be applied, with the 3′ end of each strand acting as a primer for template-dependent synthesis of a copy of the other strand. In this manner some 40% of the chemical synthesis work can be spared. Nonetheless, this strategy has not really become established and only a few examples are known.[161, 162, 178, 194–196] The size of the gene fragments used has been about 60 to 100 base pairs. In our own work on the synthesis of a gene fragment for interferon-γ[3] we encountered the following problems: (1) Difficulties sometimes arise in "filling-in" the last nucleotide at the 5′ end. It is therefore advisable to synthesize two or three extra nucleotides, which can later be cleaved off with an appropriate restriction enzyme. Restriction enzymes that, on cutting, leave overhanging ends, are advantageous, since these ends are easier to ligate than blunt ones. (2) Product quality was seldom as good as the DNA obtained from ligase reactions. We therefore think that the main problem in this strategy is the formation of unwanted secondary structures, especially when, for reasons of economy, very long oligonucleotides are used.

Path E: Fill-in Method using Autoprimer Oligonucleotides

One immediate consequence of these disadvantages was the introduction of a new method, which also uses the intrinsically economic DNA polymerase reaction.[197, 198] This strategy is based on the use of long oligonucleotides carrying a short, repeated sequence at the 3′ end. The resulting hairpin structure is unusually stable[198–201] and serves as a primer in the DNA polymerase-catalyzed formation of the complementary strand. This type of oligonucleotide is accordingly designated an "autoprimer". Following the fill-in reaction with the deoxynucleotide triphosphates, easily ligated, overhanging ends are generated by cleavage with appropriate restriction enzymes, which simultaneously dissolve the hairpin structure. Use of autoprimer oligonucleotides (strategy E) has numerous advantages over overlapping oligonucleotides (strategy D): (1) No special hybridization is necessary, since the autoprimer oligonucleotides are obtained in their entropically favored hairpin configuration. (2) The strand-separation activity of the DNA polymerase is circumvented, since the primer is covalently bound to the template. (3) One has the option of synthesizing either the coding or the noncoding strand, and constructing the complementary strand with the aid of the problem-free, enzymatic polymerase reaction. In this way the chemical synthesis of long purine-rich sequences, which often affords problems, can be avoided.

Thus, a 117-bp gene for calcitonin-Gly(33) could be produced[197] from a single 140-base oligonucleotide. With the aid of subcloning techniques, however, genes of any size can be synthesized. For example, from only three autoprimer oligonucleotides it was possible, by enzymatic processing, to synthesize a 310-bp fragment.[198] Just as in *Sanger*'s DNA-sequencing procedure,[202] which is also based on the DNA-polymerase reaction, four to eight reactions can be carried out simultaneously without difficulty.

3.2.3. Selection Criteria: Gene Size, Oligonucleotide Length, Mutation Frequency

In planning the synthesis of a gene, the following questions must first be considered. How long is the gene? Can it be synthesized as one block, or must it be divided into gene fragments? What chemical methods are available for synthesis of the oligonucleotides, and what oligonucleotide lengths can be achieved?

In principle, one attempts to synthesize a gene in one cloning step from the longest possible oligonucleotides, since there is then a minimum number of oligonucleotides to purify and of ligation points to couple. Set against this, however, is the mutation frequency, which rises with the chain length of the oligonucleotides and becomes a limiting factor as the gene grows longer. Recently reported mutation frequencies lie between 0.05% and 0.32% per oligonucleotide.[92, 173, 198, 203, 204] Taking an average value of 0.15%, in every 1000 nucleotides about one or two errors are to be expected. The chance, then, of finding a correct clone in direct cloning of a 500-bp gene is at best 50%. In practice, therefore, one has to sequence at least two clones in order to identify a correct one. All kinds of mutations are found: transitions, transversions, insertions, and deletions. The most frequent, however, appears to be the mutation of a GC base pair into an AT base pair.[139, 204] A possible explanation for this is a chemical modification of the carboxamide function (O^6) of deoxyguanosine during oligonucleotide synthesis. On treatment with ammonia, the base 2,6-diaminopurine may be formed at the corresponding position and can base-pair with both cytosine and thymine.

The longest subcloned gene fragment to date, with 710 base pairs, codes for the serine protease domain of tPA.[91] Following the cloning of this fragment, three clones were sequenced, of which one was correct and the other two showed a total of three mutations. At the present time it is advisable to subdivide large genes into fragments of about 250 to 300 base pairs, so that the labor saved in the gene construction is not overcompensated for by subsequent DNA sequencing. Table 2 compares the mutation frequencies per oligonucleotide pair given in recent articles. While for short oligonucleotides (33-bp average)[173] only every twelfth clone shows an error, for longer oligonucleotides (85 to 132 bp) this is the case for about every fourth clone.[92, 203] A significantly lower error frequency is observed when autoprimer oligonucleotides are used in a fill-in reaction. This is reasonable, since only one strand of the DNA is chemically synthesized, while the opposite strand is formed by a virtually error-free enzymatic reaction. All in all, the mutation frequency very clearly reflects the purity of the oligonucleotides used, so optimal retrosynthetic analysis of a gene may only be possible after some experience has been gained. Selection criteria other than those named are also of practical significance and will be discussed later. Subdivision of a gene into various small subclones, for example, can be worthwhile despite the greater initial effort involved, if many variants of the gene are to be synthesized subsequently.

Table 2. Mutation frequency in cloning synthetic oligonucleotides.

Number of oligonucleotide pairs	Strategy used in gene synthesis (cf. Fig. 7)	Mutation frequency per oligonucleotide pair x/y [b]	[%]	Ref.
33	A	1/12	8	[173]
105	E	2/18	11	[198]
85	B, C [a]	34/139	24	[92]
132	C	10/36	28	[203]
80	C	8/20	40	[204]
100	B	6/9	67	[139]

[a] Combination of various strategies, including the "shot-gun" method.
[b] x = number of incorrect clones; y = total number of clones sequenced.

3.3. Rapid Methods of Gene Synthesis

In this section, several special variations on the principal methods outlined above will be described. These allow rapid synthesis of genes, but no longer conform to the ideal of the original *Khorana* papers, namely, the characterization of the intermediate products. These rapid methods were made possible by the enormous progress made both in nucleotide synthesis and DNA sequencing and in the utilization of more efficient selection procedures in the cloning step.

3.3.1. The "Shotgun" Method

In this procedure, the gene is put together from a number of overlapping oligonucleotides without intermediate control or purification, by immediately ligating it into an appropriate M13 vector and cloning it in *E. coli* (Fig. 8a). *Grundström* et al.[205] have reported the synthesis of a number of SV40 DNA segments which were constructed from a set of 15 oligonucleotides. Since the synthetic DNA fragment contains the overhanging sequences for incorporation into a suitable vector, only completely ligated products possessing the correct ends are finally integrated into the vector. Incompletely ligated products do not lead to recircularization of the vector and therefore remain mute. It was found that about half of the clones analyzed contained the desired sequence.[205] Starting with five sets of oligonucleotides, containing eleven, three times seven, and two oligonucleotides, *Brodin* et al.[158] produced a gene for a bovine Ca-binding protein. Since then, numerous other gene syntheses of this type have been published.

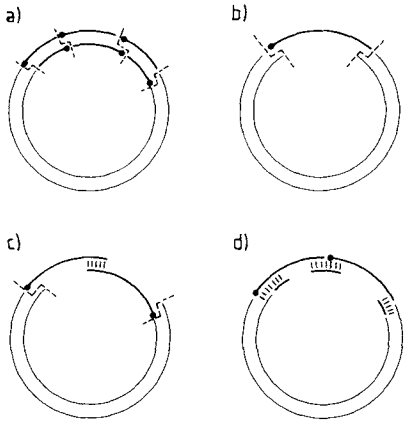


Fig. 8. Rapid procedures for gene synthesis: a) shotgun procedure; b) single-stranded cloning of an oligonucleotide; c) single-stranded cloning of 3'-overlapping oligonucleotides; d) single-stranded cloning using an auxiliary oligonucleotide.

"In vivtro" cloning[206] is a further development of the shotgun method, where the enzymatic machinery of the cell is utilized to phosphorylate and to ligate the synthetic oligonucleotides. Since the procedure combines the characteristics of in vitro and in vivo reactions, the term "in vivtro" appears justified. Basically, one proceeds as in the shotgun technique, but hybridizes the oligonucleotides directly with a

suitable open vector and further transforms them in competent cells without in vitro phosphorylation and ligation.

3.3.2. *Single-Strand Cloning by Repair of DNA Gaps*

In principle, the genetic information in a gene is defined by one DNA strand, while the second strand serves to maintain the double-helical structure, thus allowing replication and proofreading. Almost half the chemical synthesis work can therefore be spared if single-stranded DNA is ligated into vectors suitable for this task. On subsequent transformation of bacteria with these incomplete vectors, the repair machinery of the host cells completes the vector ("in vivo" gap repair). This procedure was realized[207] in the synthesis of a gene fragment coding for amino acids 198–231 of bacteriorhodopsin. Here, an oligonucleotide was ligated, patchlike, into a vector having a 3'-overhanging, single-stranded DNA sequence on one side and a 5'-overhanging sequence on the other, complementary to the 5' and 3' ends, respectively, of the oligonucleotide (see Fig. 8b). Up to now this method has only been applied to relatively short oligonucleotides and the efficiency observed has been low.[208] By using an "in vitro fill-in" reaction (or a tricky sequential ligation procedure) and a large excess of oligonucleotide, the desired clones were obtained in significantly increased yields.[209] Finding pairs of restriction enzymes that always open the vector with 5' and 3' overhangs is not a limiting factor if one uses two single-stranded oligonucleotides hybridized through their complementary 3' ends (Fig. 8c). In this case a vector possessing 5'-overhanging ends on both sides can also be used for ligation.[207] To raise the ligation yield, auxiliary oligonucleotides can also be employed, in order to lengthen the double-stranded region at the ligation points. Thus, the cloning of a 290-bp gene was recently reported;[185] it was made from two long oligonucleotides (144 and 139 bases) which were coupled together through three smaller oligonucleotides (11–16 bases) and ligated into a vector (Fig. 8d). As far as the efficiency of this variant is concerned, it was reported that of 48 clones analyzed, seven contained the desired gene, and of three completely sequenced clones only one possessed the correct sequence.

Although the ideas behind Figures 8c and 8d could theoretically be expanded as far as desired by using a still larger number of oligonucleotides, there are practical limits, since yields fall with an increasing number of oligonucleotides. Under certain circumstances, single-stranded ligation of oligonucleotides bearing a ribonucleotide at their 3' end, catalyzed by T4 RNA ligase, could be of benefit here.[210–212]

The M13-insertion technique is a special form of in vitro mutagenesis.[213] The principle of oligonucleotide-directed site-specific M13 mutagenesis (cf. Section 4.2) is based on designing an oligonucleotide that is complementary to a single-stranded M13 template, but has a single base mismatch which generates the desired mutation (see Fig. 11). After annealing the oligonucleotide onto the template, the second strand is formed with the aid of DNA polymerase. Finally, the vector is circularized with DNA ligase. In order to insert a long DNA sequence into a defined site in the vector (gene synthesis)[214] this must replace the mismatch. After replication of the partially mismatched vector, appropriate methods are used to select the clones with the desired insert from the wild-type clones which are generated at the same time. An interesting further application of single-stranded cloning to gene synthesis is based on oligonucleotide-directed repair of a DNA double-stranded break.[215]

3.3.3. *Solid-Phase Gene Synthesis*

In Section 2.2, it was stated that in a ligase reaction the yield of fully ligated products decreases as the number of oligonucleotides to be coupled increases. From this, it seems that sequential coupling of small gene fragments is an advantage and that an excess of the fragment to be ligated may greatly increase the yield. Just as an oligonucleotide may be synthesized on a solid support, entire genes may be built up by repetitive ligation of gene fragments. The advantages of solid-phase gene synthesis were first described by *Hostomský* et al.,[164] using the example of a bovine colostrum trypsin inhibitor gene. In the initial step, a starter oligonucleotide was anchored covalently by its 3' end to Sephacryl S-500, using cyanogen bromide activation. In the subsequent stepwise addition, DNA duplexes, prepared from three to four oligonucleotides by hybridization, were annealed to complementary oligonucleotides through relatively long overhanging ends of 15 nucleotides. At this stage the growing chain is therefore held together merely by the hydrogen bonds of the bases. In the last elongation step, the entire gene is covalently linked together with DNA ligase. The linearized cloning vector is best added while the gene is still on the support and before the whole construct is cleaved from it and circularized. This procedure has the advantage that only complete DNA chains with the appropriate ends can be integrated into the vector. The time-consuming derivatization of the solid support with the anchor oligonucleotide is a disadvantage, as are the unprotected, long overhangs on the oligonucleotides, which can potentially interact with themselves and thereby lead to inefficient or even incorrect ligation.

Problems of this nature can easily be avoided, however, by fixing partially double-stranded anchor oligonucleotides onto the support via appropriately modified unpaired nucleotides.[216] In addition, the autoprimer oligonucleotides described in the previous section are of great benefit in the chain extension, if one generates overhanging ends on only one side by restriction enzyme digestion after the fill-in reaction and retains the loop structure on the other. By using an excess of these fragments, they can be ligated very efficiently onto the growing chain.[198] The hairpin structure, which prevents multiple addition, can be removed by scission with a suitable restriction enzyme, allowing a further chain extension.

3.4. Construction Planning for Synthetic Genes

The quality of the planning for a synthetic gene is crucial both in the success of the gene synthesis and in successful expression of the gene. Systematic planning, drawing on computer programs, is therefore to be recommended, following the flow diagram shown in Figure 9, for example. The bigger the gene to be synthesized, the more detailed and polished the synthetic planning will have to be. Plans for expression will be discussed in Section 3.4.2. Obviously,

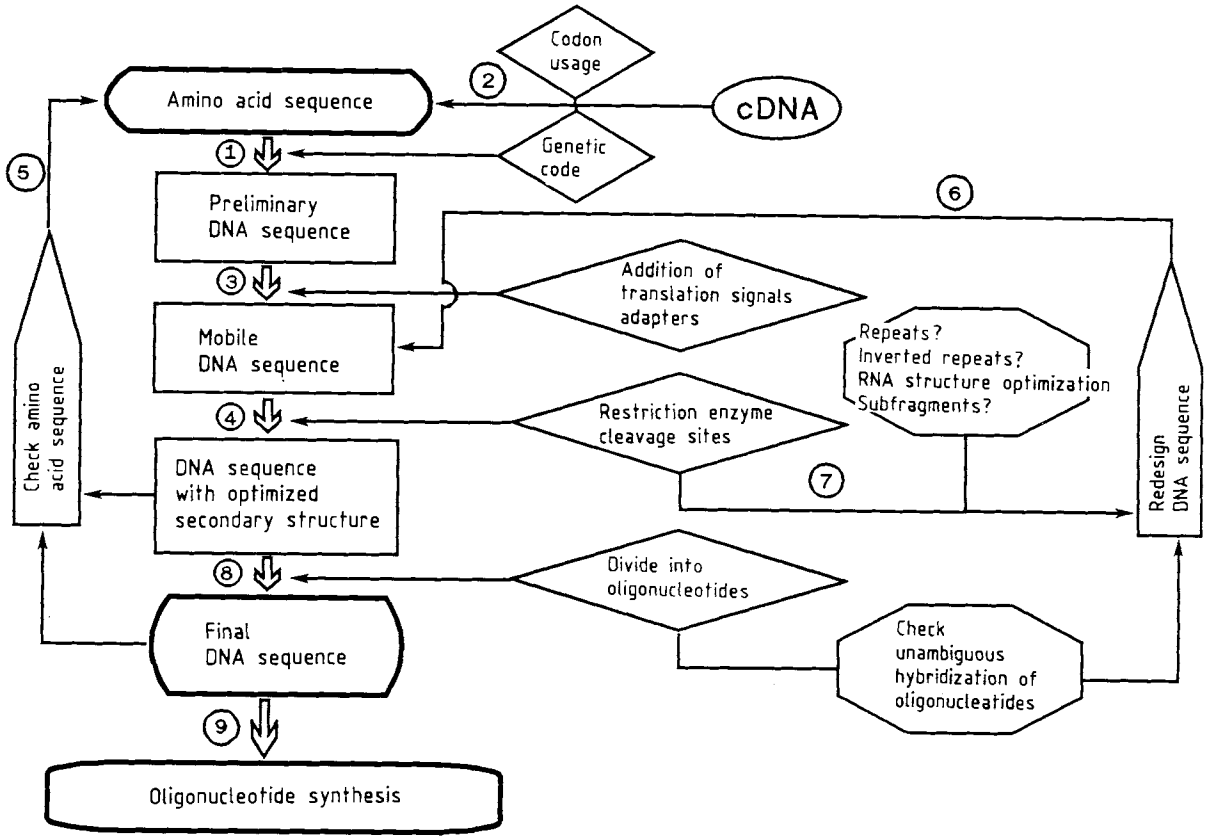


Fig. 9. Planning and design of a synthetic gene.

however, these considerations must play a part in the final design of a gene.

3.4.1. Design of a Synthetic Gene

Genetic Code and Host Specificity of the DNA

Total synthesis of a gene is especially useful when the amino acid sequence of a protein has been determined but the DNA sequence of the corresponding gene is not yet known. If one knows the genetic code (Table 3), the amino acid sequence can be translated into a DNA sequence (step 1, Fig. 9). The genetic code is degenerate, however; this means that for most amino acids several nucleotide triplets can be chosen. Because synonymous codons are not used with the same frequency in natural DNA and also because the nonstatistical use of these codons is related to the level of gene expression, there seems to be a set of "optimal" codons for synthetic genes. According to the species of host organism, one follows the codon usage of genes that are highly expressed in *E. coli*,[217-219] for example, or in other hosts.[220,221] The value of this codon usage should not be overrated, though, at least in the case of *E. coli*, because so far no conclusive experimental data on this problem are available. Nonetheless, preferred codon usage has been taken into consideration for most synthetic genes.

Table 3. Codon usage in strongly and weakly expressed genes in *E. coli* (from *Grosjean* and *Fiers* [217]). Codon pairs that are read by only one tRNA are framed. Amber, ochre, and opal correspond to stop codons.

	U			C			A			G			
		strong	weak		strong	weak		strong	weak		strong	weak	
U	Phe	39	151	Ser	93	36	Tyr	34	96	Cys	13	34	U
		113	102		87	49		98	65		23	39	C
	Leu	12	71		6	37	ochre			opal			A
		16	64		12	62	amber			Trp	25	66	G
C	Leu	26	73	Pro	21	29	His	19	95	Arg	223	99	U
		33	69		2	46		75	59		101	133	C
		→ 3	22		26	45	Gln	38	90		→ 3	27	A
		345	294		162	101		169	166		→ 1	42	G
A	Ile	67	156	Thr	103	46	Asn	13	101	Ser	10	56	U
		262	118		137	119		159	98		49	61	C
		→ 2	27		15	32	Lys	259	163	Arg	→ 3	28	A
	Met	140	130		28	76		106	44		→ 1	17	G
G	Val	192	108	Ala	173	87	Asp	116	183	Gly	226	124	U
		41	66		48	178		204	106		174	140	C
		119	48		119	107	Glu	333	210		→ 4	42	A
		83	123		129	149		106	98		→ 14	66	G

Chemical gene synthesis is also useful, though, when the amino acid sequence has been derived by back-translation of the cDNA sequence. Apart from the adjustment to optimal codons (step 2), this also has the advantage of the speed with which tailor-made genes are accessible. Since proteins are often synthesized as precursors in nature, the cDNA is frequently missing the corresponding translation signals. A start codon (ATG) for methionine, plus one or two translation stop codons and additional adaptor sequences for the integration of the synthetic gene into a plasmid, can easily be added to a coding sequence for synthetic genes and leads to a mobile DNA sequence (step 3). Reconstruction of isolated cDNA often requires considerable effort in order to arrive at a mobile DNA sequence.

Restriction Enzyme Cleavage Sites

The introduceability of unique restriction enzyme scission sites into a synthetic gene (step 4) is one of the greatest ad-

vantages of synthetic genes over natural, isolated genes. Such restriction sites, which generally are evenly distributed over the gene sequence, are not only helpful in subcloning during the construction of a gene, but also permit easy variation (mutagenesis) of the original DNA sequence (cf. Section 4.2). Restriction sites that lead to the formation of cohesive ends on cleavage are preferred (Table 4). Such sites are

Table 4. Recognition sequences for some selected restriction enzymes.

Recognition sequence [a]	Restriction enzyme
5'-G↓AATTC- 3'-CTTAA↑GA	EcoR I
5'-CTGCA↓G- 3'-G↑ACGTC-	Pst I
5'-GG↓CC- 3'-CC↑GG-	Hae III
5'-GAAGA(N)$_7$N↓N- 3'-CTTCT(N)$_7$N'↑N'-	Mbo II
5'-GAAN N↓NN TTC- 3'-CTTN'↑N' N'N'AAG-	Xmn I
5'-GTPy↓Pu AC- 3'-CAPu↑PyTG-	Hind II

[a] Cut position marked with an arrow. N = G, A, T, or C; N' = the respective complementary base; Py = C or T, Pu = G or A.

made use of in the cloning of genes or in the subcloning of gene fragments. They are also present in commercially available plasmids, for example the pUC plasmids[222] or the M13mp plasmids,[223] which contain polylinkers (multiple cloning sites).

However, if the restriction sites required are not available in the commercial plasmids, temporary restriction sites can be used. One possibility is to increase the length of the gene or gene fragment by a few nucleotides, in order to incorporate a clonable (temporary) recognition sequence. After integration of the gene into a suitable plasmid and replication, the desired gene sequence can be isolated by cutting with the originally planned restriction enzymes.

Another possibility for the generation of temporary restriction sites is to build a short string of nucleotides into the DNA sequence to give a clonable restriction enzyme recognition sequence. The additional nucleotides can be removed later by successive cleavage with the relevant restriction enzyme, and single-strand-specific nuclease S1.[195]

The planning of unique restriction sites is relatively complex and can only be performed with appropriate computer programs.[224, 225] At present about 600 different restriction enzymes are known.[226–228]

Secondary Structure Considerations

After optimization of a DNA sequence with respect to codon usage and restriction sites, the secondary structure of the corresponding mRNA must be examined (step 7). Direct repetitions of nucleotide sequences ("repeats") can interfere with the construction of the gene, while inverted repeats can lead additionally to undesired secondary structures in the mRNA, making efficient expression of the gene impossible. Hairpin structures, which inhibit the initiation of translation, can drastically diminish expression.[229, 230] In dividing a gene up into oligonucleotides (step 8), each of the oligonucleotides must be checked for adverse intra- and intermolecular interactions. A large number of programs are available for calculating desired and undesired secondary structures and interactions.[224, 231–233] The necessity of reasonably comprehensive calculations depends very much on the strategy used for gene construction (Fig. 7). If a relatively large number of short oligonucleotides are used in a single hybridization step, clearly many more undesired interactions are to be expected than in the hybridization and subsequent cloning of long oligonucleotides.[203]

In designing a synthetic gene all the points discussed so far must be taken into consideration. If one does this stepwise, as shown in Figure 9, repeated alterations of the DNA sequence can be necessary (step 6: redesign), for example, after steps 4, 7, and 8. Since errors can creep in here, it is a good idea to check the amino acid sequence from time to time by back-translation of the DNA sequence (step 5). The actual experiment begins with the chemical synthesis of the oligonucleotides (step 9).

3.4.2. Strategies for Expression of Synthetic Genes

There are three fundamental procedures for the expression of synthetic or natural genes: (1) direct expression, (2) expression as a fusion protein, (3) transport expression (Fig. 10).

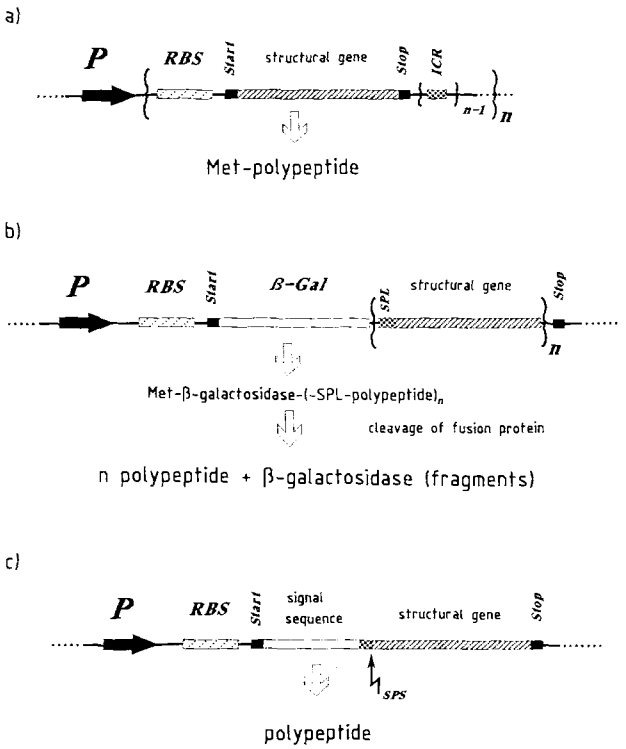


Fig. 10. Strategies for expression of synthetic genes: a) direct expression; b) expression as a fusion protein; c) transport expression. ICR = intercistronic region, P = promoter, RBS = ribosome binding site, SPL = cleavage linker, SPS = signal peptidase.

Direct Expression

Direct expression of a gene under the control of a constitutive or inducible[115] regulatory unit is the simplest mode of

expression in prokaryotes, provided the product being formed is stable and nontoxic to the host organism (Fig. 10a, $n = 1$). Since the structural gene must be preceded by a translation start codon, coding for methionine, a methionyl protein is formed. In most cases the additional methionine does not interfere with the activity of the protein, but it can be removed by cleavage with cyanogen bromide or with specific aminopeptidases.[140] In order to increase the expression yield, direct expression can also be carried out on a polycistronic tandem gene system. This variation, in which n copies of the same structural gene (Fig. 10a, $n = 2, 3 \ldots$), one behind the other, are separated by intercistronic regions (ICR), makes use of the gene-dosage effect. In a similar manner to polycistronic bacterial lactose or tryptophan operons, the common transcription unit consists of a promoter and a ribosome binding site (RBS) and forms a single mRNA. This methodology has been applied successfully in the expression of leukocyte interferon;[234] the amount of interferon expressed was directly proportional to the number of interferon genes in the plasmid ($n = 1$ to 4).

Expression as a Fusion Protein

The direct expression of polypeptides 50–80 amino acids in length often fails because these relatively small proteins are rapidly proteolytically degraded in the host organism. Thus, the tetradecapeptide somatostatin could only be successfully expressed by stabilization as a fusion protein with β-galactosidase (Fig. 10b). The somatostatin was isolated by cyanogen bromide cleavage from the fusion protein, which consisted of about 1000 amino-terminal amino acids of the β-galactosidase, followed by methionine and the tetradecapeptide somatostatin moiety. If the desired protein contains an internal methionine, alternative cleavage sequences must be planned at the gene level: e.g., Asp-Pro (acid-labile),[235] Asn-Gly (hydroxylamine),[236] Arg-Arg (trypsin, carboxypeptidase B),[237] or Ile-Glu-Gly-Arg (blood coagulation factor X_a).[238] Often just a small fused moiety yields sufficient stabilization; examples include portions of Trp E,[99] interferon-γ,[100] or growth hormone[144] or short homooligopeptide tails.[239] One variant is the inclusion of several genes, which are not, however, separated by intercistronic regions as described above, but are linked instead by cleavage sequences. In the case of proinsulin, which because of its short half-life in *E. coli* ($t_{1/2} = 2$ min) cannot be directly expressed in good yields, stable fusion proteins could be synthesized by coupling three or four genes to each other (Fig. 10b, $n = 3$ or 4) through a cleavage linker (SPL) coding for Arg-Arg-Asn-Ser-Met.[240] By cleavage of the fusion protein with cyanogen bromide and subsequent treatment with trypsin/carboxypeptidase B, proinsulin was obtained. This multigene-copy procedure has been described for substance P,[153] growth hormone releasing factor,[102] and Met-enkephalin,[154] among others, and has the clear advantage over β-galactosidase fusions that the host cells have to produce less ballast, which can interfere in the cleavage and workup of the fusion protein.

Transport Expression

A serious disadvantage of expression as a fusion protein is that the proteins are generally obtained in a biologically inactive form. Occasionally the folding of the proteins into biologically active structures can be difficult. With transport expression (Fig. 10c) a procedure is now available which largely allows one to avoid the problems discussed above (additional methionine, protein folding, disulfide bridge formation, protease lability). Its advantage is based on the fact that the growing polypeptide chain is channeled out through the cytoplasmic membrane with the aid of a signal sequence and hence out of the reducing cytoplasmic environment. According to the hypothesis of *Blobel* and *Dobberstein*,[241] the signal sequence is cleaved off by a signal peptidase (SPS) as the polypeptide passes through the membrane. For example, epidermal growth factor (EGF),[101] hirudine,[242] and growth hormone[243] have all been transported into the periplasm of *E. coli* using the signal sequence of alkaline phosphatase. We have previously reported a synthetic DNA fragment for the signal peptide of alkaline phosphatase, which allows proinsulin secretion.[244] For transport expression purposes, however, *E. coli* is not necessarily the host organism of choice. Better product yields are often obtained in other organisms like staphylococci,[245] *B. subtilis*,[246] or yeast, because the product is then secreted into the medium. *Saccharomyces cerevisiae* is of special interest in connection with the α-factor signal sequence,[247, 248] with which the synthetic genes for atrial natriuretic peptide[98] and for connective tissue activating peptide were successfully expressed, for example. However, one problem in transport expression into the medium, which should not be underestimated, is that of host-cell extracellular proteases, if these are able to degrade the expressed product. In yeast, glycosylatable proteins may also be converted into glycoproteins whose glycosyl moiety is not identical with that of the natural product.

4. Applications and Advantages of Synthetic Genes

4.1. Tailor-made Genes

Especially for small proteins of up to about 200 amino acids whose primary structures have been clarified by peptide sequencing, chemical enzymatic synthesis offers an alternative to the isolation of the natural gene. Synthetic genes for proteins of this size can now be synthesized and cloned in a few weeks or months. In contrast to natural genes, which, after isolation, have to be reconstructed to allow expression (in bacteria, for example), synthetic genes can be planned right from the start so that they can be expressed immediately after cloning. As demonstrated in the previous section, host specificity can be taken into consideration here by using preferred codons. In addition, unique restriction-enzyme recognition sites can be built into synthetic genes at reasonable intervals (about every 50 to 100 bp), greatly simplifying subsequent alteration of the genes and gene products. Finally, gene synthesis can also include regulatory DNA sequences which achieve transcription and translation of the structural gene. Specific alteration of structural genes or of regulatory DNA sequences is a valuable method in the study of structure–activity and structure–function relationships.

4.2. Specific Alteration and Optimization of Protein Properties

Although today DNA from any given source can be specifically altered using so-called oligonucleotide-directed site-specific M13 mutagenesis (cf. Section 3.3.2),[249] synthetic DNA is predestined for such use. While the various methods for implementation of M13 mutagenesis[213,249-255] always yield the wild-type gene along with the desired mutant, modular or cassette mutagenesis, when correctly performed, leads exclusively to the specifically altered gene (Fig. 11). After correct planning of a synthetic gene, suitably positioned restriction sites permit rapid alteration of the protein product: a DNA segment flanked by two unique restriction sites is replaced by a corresponding fragment containing the mutation (modular mutagenesis[255]). Thus, particular genes[96,141,159,169] have been specifically planned with regard to subsequent alterations. In the case of growth hormone releasing hormone (GHRH), we replaced the codon for methionine 27 with a codon for leucine, in order to allow the GHRH derivative to be liberated from a fusion protein with β-galactosidase by cyanogen bromide cleavage.[96] Using so-called cassette mutagenesis, the DNA fragment to be changed is replaced by a cassette of oligonucleotides that have not been synthesized in an unambiguous manner.[256,257] This generates numerous mutants in one cloning step. Particular forms of cassette mutagenesis permit the cloning of single-stranded oligonucleotides.[208,209,258]

Alterations in enzymes can, for example, make them resistant to oxidation,[259] shift their pH dependence,[260] or even achieve a reversal of an allosteric inhibition into an activation.[261] Pharmacologically interesting proteins like γ-interferon[262] or interleukin-2[263,264] have been successfully subjected to structure–activity studies. In the most favorable case, mutations led to an increase in biological activity, as in two particular muteins of interleukin-1[265] and interleukin-2.[266]

Genes can also be altered in such a way that selective post-translational modification of the expressed precursor protein is possible. Thus, in nature many smaller proteins (<50 amino acids) occur as their C-terminal carboxylic amides, which in prokaryotes are not directly accessible by expression. Recently, we were able to show[96,267] that, by planning at the DNA level, a precursor of GHRH can be synthesized which contains an additional glycine at the C-terminus. This serves as a signal for an amino-acid-amidating enzyme[268] to convert the precursor protein into the desired GHRH carboxamide.

One particular variation of gene synthesis, also called the "hybrid" or "mispairing" procedure, permits simultaneous

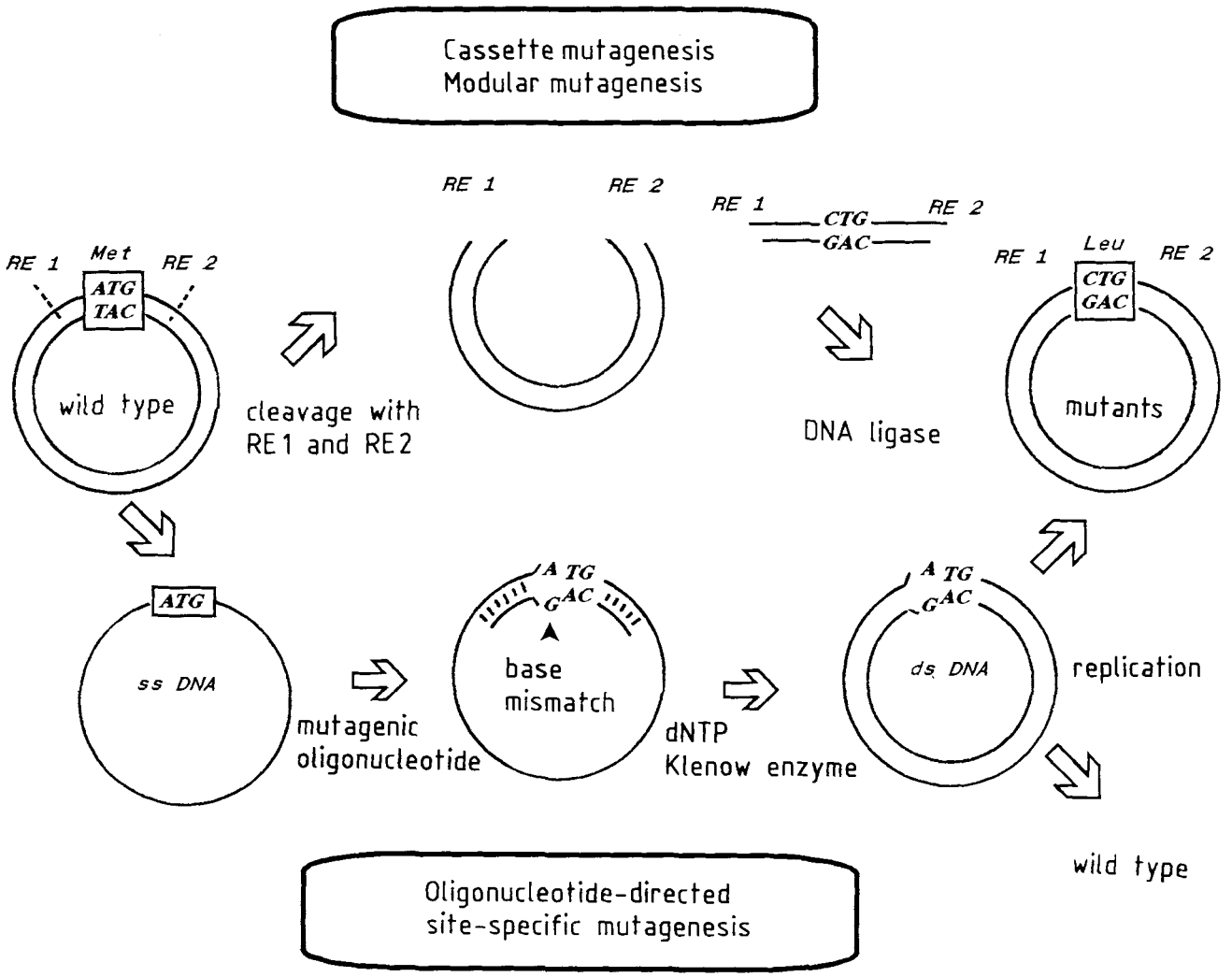


Fig. 11. Alternative methods for specific alteration of a gene.

production of closely related genes. A partially base-mismatched gene is synthesized whose two strands code for different proteins.[95] Thus, a gene was synthesized where one strand coded for human epidermal growth factor (hEGF), while the other coded indirectly for mouse EGF.[132]

4.3. Control of Gene Expression by Synthetic DNA

A further tremendous advantage of synthetic genes is that, in addition to the structural gene, the transcription or translation control regions that direct the expression of the synthetic gene can also be included in the synthesis planning. Using the building-block system, individual control elements can be put together in a modular way to form a complete regulatory unit. In the expression of interferon-γ, for example, we used a synthetic regulatory unit[3] consisting of an idealized promoter, an operator, and a ribosome binding site. One should not, however, gain the impression that a combination of individually very efficient modules always leads to optimal gene expression; in practice, the reverse can also occur. Rather, the great value of the building block system is that a very great number of different module combinations can be synthesized quickly and efficiently in order to find the optimal combination for gene expression.

Transcription can be controlled by synthetic promoters, operators, and terminators. By using synthetic ribosome binding sites and by planning a favorable mRNA secondary structure, translation can also be positively influenced. A promoter is a special DNA sequence which interacts with the RNA polymerase to allow synthesis of the mRNA. The efficiency of this control region, which is generally found in the nontranslated 5′ region, is crucial for the amount of mRNA formed. Numerous promoters have already been synthesized.[3, 196, 269–274]

Promoters may be always switched on (constitutive) or of an inducible type. Those that can be regulated also contain, in addition to the RNA polymerase interaction region described above, a so-called operator. Probably the best-investigated system is the lac operon,[275] which is subject to negative regulation; the start of transcription is inhibited by binding of the lac-repressor protein to the lac-operator sequence. By adding isopropyl-β-D-thiogalactopyranoside (IPTG), which forces the repressor into a form which cannot bind the operator, the lac promoter can be induced. Interestingly, idealized synthetic lac operators have been synthesized[276, 277] which bind to the lac repressor up to eight times more strongly than the natural operator. By coupling of a constitutive promoter to a lac-operator sequence, an inducible system can be synthesized.[278]

Particularly when strong promoters are used to initiate transcription, an efficient transcription terminator is an advantage. Thus, the expression yield for interferon-α was increased by a factor of two[279] and that for EGF by one of five to ten[280] when strong terminators were added downstream of the structural gene. Sensibly, synthetic terminators were cosynthesized with the corresponding gene.[158]

The efficiency of translation of the mRNA is controlled by the ribosome binding site (RBS) and the mRNA structure. The RBS in prokaryotes is most usually the sequence AAGGA, also called the Shine–Dalgarno (SD) sequence.[281] It is responsible for initiation of protein biosynthesis, by binding to the 3′ end of the 16S RNA. The SD sequence is generally four to nine nucleotides long and is found some three to twelve nucleotides upstream of the translation start codon. Genes from eukaryotic sources have no RBS that is recognized by prokaryotic ribosomes. Synthetic RBSs have therefore been used for some time for the expression of eukaryotic genes in bacteria.[3, 279, 280, 282–284] Apparently, the RBS should be easily accessible to the 16S RNA. One assumes that the RBS also includes that portion of the structural gene coding for the amino-terminal region of the protein, and it therefore seems reasonable to track down adverse secondary structures with suitable computer programs.[231–233] In the expression of interferon-α, fluctuations of a factor of fifty were observed when nucleotides in particular positions close to the translation initiation region were exchanged. These results could be explained on the basis of mRNA secondary-structure calculations.[230] From our own studies on the expression of interferon-γ we have learned, however, that predictions of the level of expression using mRNA structural calculations alone are barely possible. Expression must, after all, be experimentally optimized.

5. Future Prospects

Recombination techniques, especially those based on synthetic genes and oligonucleotides, have led to a wealth of biologically active proteins. It has become clearer, however, that our understanding of the structure and function of more complex polypeptides is very limited. In searching for an answer to the question "Which protein sequence gives which properties?", polypeptide synthesis from synthetic genes ideally complements chemical peptide synthesis.[285, 286] Because of the general validity of the genetic code, it is possible to synthesize a corresponding DNA for any polypeptide, or, more generally, for any defined sequence of linked amino acids, and to express it by recombination in a suitable vector for the host organism concerned. The synthesis of new and unknown polypeptides,[143, 180] so-called de novo protein design,[287–291] should be especially stressed here, since it now allows us to build novel proteins and to test the underlying hypotheses concerning their construction and properties (Fig. 12). In the scheme shown in Figure 12, the relation-

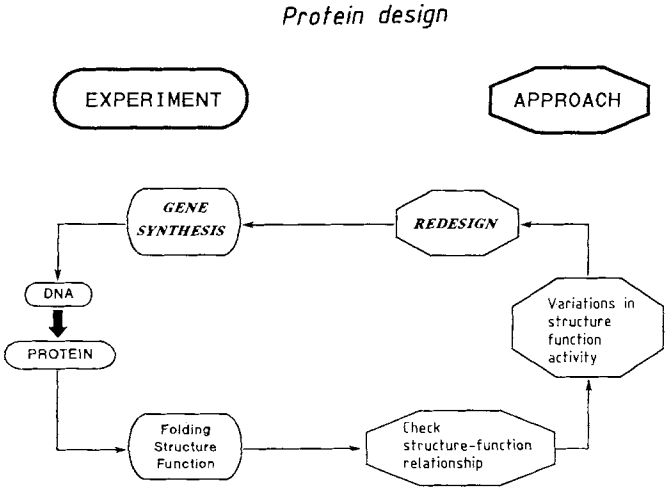


Fig. 12. De novo protein design using synthetic genes.

ship between protein sequence, structure and function, and the underlying DNA sequence is portrayed as a cyclic type of process.

As yet the prediction of protein tertiary structure is a largely unsolved problem.[292] The synthesis of certain secondary structures like α-helices and β-pleated sheets is of special interest.[293] These structures are more predictable[294] and form supersecondary structures or so-called motifs. An experiment of this sort, with a helix bundle composed of four α-helices, is currently being addressed by both peptide chemistry and recombinant techniques. A gene coding for the product has been synthesized, and the artificial product can indeed be produced by expression in *E. coli*.[295] For future research in this field it is encouraging to note that this work constitutes an experimental starting point for one of the greatest challenges in molecular biology, the determination of the relationship between peptide sequence, polypeptide structure, and function.

We are grateful to the Deutsche Forschungsgemeinschaft, the Fonds der Chemischen Industrie, the Bundesministerium für Forschung und Technologie, and Hoechst AG for their financial support. Special thanks are due to E. Groeneveld for preparation of the text and to H. Zimmermann for the diagrams.

Received: September 26, 1988 [A 720 IE]
German version: *Angew. Chem. 101* (1989) 733
Translated by *Dr. Michael Kertesz*, Melbourne, Australia

[1] J. D. Watson, F. H. C. Crick, *Nature (London) 171* (1953) 737.
[2] R. E. Dickerson, H. R. Drew, *J. Mol. Biol. 149* (1981) 761.
[3] J. Engels, M. Leineweber, E. Uhlmann in J. Streith, H. Prinzbach, G. Schill (Eds.): *Organic Synthesis: an Interdisciplinary Challenge*, Blackwell, Oxford 1985, p. 205.
[4] J. Engels, E. Uhlmann in A. Fiechter (Ed.): *Advances in Biochemical Engineering/Biotechnology*, Springer, Berlin 1988, p. 75.
[5] R. Frank, H. Blöcker in B. Wittmann-Liebold (Ed.): *Advanced Methods in Protein Microsequence Analysis*, Springer, Berlin 1986, p. 387.
[6] M. Edwards, *Int. Biotechnol. Lab. 5* (1987) 19.
[7] J. E. Davies, H. G. Gassen, *Angew. Chem. 95* (1982) 26; *Angew. Chem. Int. Ed. Engl. 22* (1983) 26.
[8] F. Wengenmayer, *Angew. Chem. 95* (1983) 874; *Angew. Chem. Int. Ed. Engl. 22* (1983) 842.
[9] F. Chow, T. Kempe, G. Palm, *Nucleic Acids Res. 9* (1981) 2807.
[10] G. Kumar, M. S. Poonian, *J. Org. Chem. 49* (1984) 4905.
[11] R. Letsinger, E. P. Groody, N. Lander, N. Tanaka, *Tetrahedron 40* (1984) 137.
[12] T. Hirose, R. Crea, K. Itakura, *Tetrahedron Lett. 20* (1979) 2449.
[13] K. Miyoshi, T. Miyake, T. Hozumi, K. Itakura, *Nucleic Acids Res. 8* (1980) 5473.
[14] T. W. Greene: *Protective Groups in Organic Synthesis*. Wiley, New York 1981.
[15] H. Kössel, H. Seliger, *Fortschr. Chem. Org. Naturst. 32* (1975) 297.
[16] V. Amarnath, A. D. Broom, *Chem. Rev. 77* (1977) 183.
[17] S. A. Narang, *Tetrahedron 39* (1983) 3.
[18] E. Sonveaux, *Bioorg. Chem. 14* (1986) 274.
[19] H. G. Khorana, *Bioorg. Chem. 1* (1978) 351.
[20] G. S. Ti, B. L. Gaffney, R. A. Jones, *J. Am. Chem. Soc. 104* (1982) 1316.
[21] J. C. Schulhof, D. Molko, R. Teoule, *Nucleic Acids Res. 15* (1986) 397.
[22] L. J. McBride, M. H. Caruthers, *Tetrahedron Lett. 24* (1983) 2953.
[23] B. C. Froehler, M. D. Matteuci, *Nucleic Acids Res. 22* (1983) 8031.
[24] C. B. Reese, A. Ubasawa, *Tetrahedron Lett. 21* (1980) 2265.
[25] B. L. Gaffney, L. A. Marky, R. A. Jones, *Tetrahedron 40* (1984) 3.
[26] A. D. Barone, J. Y. Tang, M. H. Caruthers, *Nucleic Acids Res. 12* (1984) 4051.
[27] C. B. Reese, P. A. Skone, *J. Chem. Soc. Perk. Trans. 1 1984*, 1263.
[28] F. Himmelsbach, B. S. Schulz, T. Trichtinger, R. Charubala, W. Pfleiderer, *Tetrahedron Lett. 40* (1984) 59.
[29] S. S. Jones, C. B. Reese, S. Sibande, A. Ubasawa, *Tetrahedron Lett. 22* (1981) 4755.
[30] T. Kaminura, M. Tsuchiya, K. Koura, M. Sekine, T. Hata, *Tetrahedron Lett. 24* (1983) 2775.
[31] M. Mag, J. W. Engels, *Nucleic Acids Res. 16* (1988) 3525.
[32] F. H. Westheimer, *Acc. Chem. Res. 1* (1968) 70.
[33] a) J. Engels, *Habilitationsschrift*, Universität Konstanz 1978; b) E. Uhlmann, W. Pfleiderer, *Nucleic Acids Res. Symp. Ser. 4* (1978) 25; c) E. Uhlmann, W. Pfleiderer, *Helv. Chim. Acta 64* (1981) 1688.
[34] A. M. Michelson, A. R. Todd, *J. Chem. Soc. 1955*, 2632.
[35] S. Stawinski, T. Hozumi, S. A. Narang, *Can. J. Chem. 54* (1976) 670.
[36] J. H. van Boom, P. M. J. Burgers, G. van der Marel, C. H. M. Verdegaal, G. Wille, *Nucleic Acids Res. 4* (1977) 1047.
[37] J. B. Chattopadhyaya, C. B. Reese, *Tetrahedron Lett. 20* (1979) 5059.
[38] J. Engels, U. Krahmer, L. Zsolnai, G. Huttner, *Liebigs Ann. Chem. 1982*, 745.
[39] G. R. Gough, M. J. Brunden, P. T. Gilham, *Tetrahedron Lett. 22* (1981) 4177.
[40] R. L. Letsinger, *J. Am. Chem. Soc. 97* (1978) 3278.
[41] S. L. Beaucage, M. H. Caruthers, *Tetrahedron Lett. 22* (1981) 1859.
[42] M. H. Caruthers, A. D. Barone, S. L. Beaucage, D. R. Dodds, E. F. Fisher, L. J. McBride, M. D. Matteucci, Z. Stabinsky, J.-Y. Tang, *Methods Enzymol. 154* (1987) 287.
[43] G. W. Daub, E. E. van Tamelen, *J. Am. Chem. Soc. 99* (1977) 3526.
[44] S. P. Adams, *J. Am. Chem. Soc. 105* (1983) 661.
[45] N. D. Sinha, J. Biernat, H. Köster, *Tetrahedron Lett. 24* (1983) 5843.
[46] R. H. Hall, A. Todd, R. F. Webb, *J. Chem. Soc. 1957*, 3291.
[47] B. C. Froehler, P. G. Ng, M. D. Matteucci, *Nucleic Acids Res. 14* (1986) 5399.
[48] P. J. Garegg, I. Lindh, T. Regberg, J. Stawinski, R. Stromberg, C. Henrichson, *Tetrahedron Lett. 27* (1986) 4051.
[49] Applied Biosystems, *User Bull. 44* (1987) 1.
[50] W. S. Zielinski, L. E. Orgel, *Nature (London) 327* (1987) 346.
[51] R. B. Merrifield, *J. Am. Chem. Soc. 85* (1963) 2149.
[52] R. L. Letsinger, M. J. Kornet, *J. Am. Chem. Soc. 85* (1963) 3045.
[53] R. L. Letsinger, V. Mahadevan, *J. Am. Chem. Soc. 87* (1965) 3526.
[54] H. Ito, Y. Ike, S. Ikuta, K. Itakura, *Nucleic Acids Res. 10* (1982) 1755.
[55] K. Miyoshi, R. Arentzen, T. Huang, K. Itakura, *Nucleic Acids Res. 8* (1980) 5507.
[56] R. Crea, T. Horn, *Nucleic Acids Res. 8* (1980) 2331.
[57] V. K. Potapov, V. P. Veiko, O. N. Koroleva, Z. A. Shabarova, *Nucleic Acids Res. 6* (1979) 2041.
[58] H. Köster, *Tetrahedron Lett. 1972*, 1527.
[59] M. D. Matteucci, M. H. Caruthers, *J. Am. Chem. Soc. 103* (1981) 3185.
[60] G. R. Gough, M. J. Brunden, P. T. Gilham, *Tetrahedron Lett. 22* (1981) 4177.
[61] G. R. Gough, M. J. Brunden, P. T. Gilham, *Tetrahedron Lett. 24* (1983) 5321.
[62] J. S. deBaer, J. A. Hayes, M. P. Koleck, G. R. Gough, *Nucleosides & Nucleotides 6* (1987) 821.
[63] J. W. Efcavitch, L. J. McBride, S. C. Eadie in K. S. Bruzik, W. J. Stec (Eds.): *Biophosphates and Their Analogues – Synthesis, Structure, Metabolism and Activity*, Elsevier, Amsterdam 1987, p. 65.
[64] a) R. Frank, W. Heikens, G. Heisterberg-Moutsis, H. Blöcker, *Nucleic Acids Res. 11* (1983) 4365; b) R. Frank, A. Meyerhans, K. Schwellnus, H. Blöcker, *Methods Enzymol. 154* (1987) 221.
[65] a) H. W. D. Matthes, W. M. Zeneke, T. Grundstroem, *EMBO J. 3* (1984) 801; b) H. W. D. Matthes, A. Staub, P. Chambon, *Methods Enzymol. 154* (1987) 250.
[66] W. Bannwarth, P. Iaiza, *DNA 5* (1986) 413.
[67] a) M. J. Gait: *Oligonucleotide Synthesis, a Practical Approach*, IRL Press, Oxford 1984; b) Applied Biosystems, *User Bull. 13* (1987) 1.
[68] K. Itakura, J. J. Rossi, R. B. Wallace, *Annu. Rev. Biochem. 53* (1984) 323.
[69] K. L. Agarwal, H. Büchi, M. H. Caruthers, N. Gupta, H. G. Khorana, K. Kleppe, A. Kumar, E. Ohtsuka, U. L. Rajbhandary, J. H. van de Sande, V. Sgaramella, H. Weber, T. Yamada, *Nature (London) 227* (1970) 27.
[70] H. G. Khorana, K. L. Agarwal, P. Besmer, H. Büchi, M. H. Caruthers, P. Cashion, M. Fridkin, E. Jay, K. Kleppe, R. Kleppe, A. Kumar, P. Loewen, R. C. Miller, K. Minamoto, A. Panet, U. Rajbhandary, B. Ramamoorthy, T. Sekyia, T. Takeya, J. H. van de Sande, *J. Biol. Chem. 251* (1976) 565.
[71] J. H. van de Sande, M. H. Caruthers, A. Kumar, H. G. Khorana, *J. Biol. Chem. 251* (1976) 571.
[72] K. Minamoto, M. H. Caruthers, B. Ramamoorthy, J. H. van de Sande, N. Sidorova, H. G. Khorana, *J. Biol. Chem. 251* (1976) 587.
[73] K. L. Agarwal, M. H. Caruthers, M. Fridkin, A. Kumar, J. H. van de Sande, H. G. Khorana, *J. Biol. Chem. 251* (1976) 599.
[74] E. Jay, P. J. Cashion, M. Fridkin, B. Ramamoorthy, K. L. Agarwal, M. H. Caruthers, H. G. Khorana, *J. Biol. Chem. 251* (1976) 609.
[75] K. L. Agarwal, M. H. Caruthers, H. Büchi, J. H. van de Sande, H. G. Khorana, *J. Biol. Chem. 251* (1976) 624.
[76] T. Sekiya, P. Besmer, T. Takeya, H. G. Khorana, *J. Biol. Chem. 251* (1976) 634.
[77] P. C. Loewen, R. C. Miller, A. Panet, T. Sekiya, H. G. Khorana, *J. Biol. Chem. 251* (1976) 642.
[78] A. Panet, R. Kleppe, K. Kleppe, H. G. Khorana, *J. Biol. Chem. 251* (1976) 651.

[79] M. H. Caruthers, R. Kleppe, K. Kleppe, H. G. Khorana, *J. Biol. Chem. 251* (1976) 658.
[80] R. Kleppe, T. Sekiya, P. C. Loewen, K. Kleppe, K. L. Agarwal, H. Büchi, P. Besmer, M. H. Caruthers, P. J. Cashion, M. Fridkin, E. Jay, A. Kumar, R. C. Miller, K. Minamoto, A. Panet, U. L. Rajbhandary, B. Ramamoorthy, N. Sidorova, T. Takeya, J. H. van de Sande, H. G. Khorana, *J. Biol. Chem. 251* (1976) 667.
[81] B. Ramamoorthy, R. G. Lees, D. G. Kleid, H. G. Khorana, *J. Biol. Chem. 251* (1976) 676.
[82] E. L. Brown, B. Ramamoorthy, M. Ryan, H. G. Khorana, *Methods Enzymol. 68* (1979) 109.
[83] H. Köster, H. Blöcker, R. Frank, S. Geussenhainer, W. Kaiser, *Hoppe-Seylers Z. Physiol. Chem. 356* (1975) 1585.
[84] K. Itakura, T. Hirose, R. Crea, A. D. Riggs, H. Heyneker, F. Bolivar, H. Boyer, *Science (Washington) 198* (1977) 1056.
[85] R. Crea, A. Kraszewski, T. Hirose, K. Itakura, *Proc. Natl. Acad. Sci. USA 75* (1978) 5765.
[86] D. Goeddel, D. G. Kleid, F. Bolivar, H. Heyneker, D. Y. Yansura, R. Crea, T. Hirose, A. Kraszewski, K. Itakura, A. D. Riggs, *Proc. Natl. Acad. Sci. USA 76* (1979) 106.
[87] M. Edge, A. R. Greene, G. R. Heathcliffe, P. A. Meacock, W. Schuch, D. B. Scanlon, T. C. Atkinson, C. R. Newton, A. Markham, *Nature (London) 292* (1981) 756.
[88] N. Mantei, M. Schwarzenstein, M. Streuli, S. Panem, S. Nagata, C. Weissmann, *Gene 10* (1980) 1.
[89] M. Ikehara, E. Ohtsuka, T. Tokunaga, S. Iwai, K. Kitano, S. Miyamoto, T. Ohgi, Y. Sakuragawa, K. Fujiyama, T. Ikari, M. Kobayashi, T. Miyake, S. Shibahara, A. Ono, T. Ueda, T. Tanaka, H. Baba, A. Sakurai, T. Oishi, O. Chisaka, K. Matsubara, *Proc. Natl. Acad. Sci. USA 81* (1984) 5956.
[90] J. Engels, W. Becker, T. Beckers, D. Hüsken, W. Wetekam, *Pure Appl. Chem. 59* (1987) 437.
[91] L. D. Bell, J. C. Smith, R. Derbyshire, M. Finlay, I. Johnson, R. Gilbert, P. Slocombe, E. Cook, H. Richards, P. Clissold, D. Meredith, C. H. Powell-Jones, K. M. Dawson, B. L. Carter, K. G. McCullagh, *Gene 63* (1988) 155.
[92] M. A. Wosnick, R. W. Barnett, A. M. Vicentini, H. Erfle, R. Elliott, M. Sumner-Smith, N. Mantei, R. W. Davies, *Gene 60* (1987) 115.
[93] E. Uhlmann, F. Hein, S. Hein, L. Hornung, R. Schardt, unpublished.
[94] R. Wetzel, D. G. Kleid, R. Crea, H. L. Heyneker, D. G. Yansura, T. Hirose, A. Kraszewski, A. D. Riggs, D. V. Goeddel, *Gene 63* (1981) 63.
[95] W. L. Sung, D. M. Zahab, F.-L. Yao, C. S. Tam, *Biochem. Cell. Biol. 64* (1986) 133.
[96] J. W. Engels, J. Glauder, H. Müllner, E. Uhlmann, W. Wetekam, T. Hashimotoh Gotoh, B. Scheikl-Lenz, *Nucleosides & Nucleotides 6* (1987) 185.
[97] M. S. Urdea, J. P. Merryweather, G. T. Mullenbach, D. Coit, U. Heberlein, P. Valenzuela, P. J. Barr, *Proc. Natl. Acad. Sci. USA 80* (1983) 7461.
[98] G. P. Vlasuk, G. H. Bencen, R. S. Scarborough, P.-K. Tsai, J. L. Whang, T. Maack, M. J. F. Camargo, S. W. Kirsher, J. A. Abraham, *J. Biol. Chem. 261* (1986) 4789.
[99] J. Smith, E. Cook, I. Fortheringham, S. Pheby, R. Derbyshire, M. A. E. Eaton, M. Doel, D. M. J. Lilley, J. F. Pardon, T. Patel, H. Lewis, L. D. Bell, *Nucleic Acids Res. 10* (1982) 4467.
[100] I. Ivanov, L. Gigova, E. Jay, *FEBS Lett. 210* (1987) 56.
[101] T. Oka, S. Sakamoto, K.-I. Miyoshi, T. Fuwa, K. Yoda, M. Yamasaki, G. Tamura, T. Miyake, *Proc. Natl. Acad. Sci. USA 82* (1985) 7212.
[102] T. Kempe, F. Chow, S. M. Peterson, P. Baker, W. Hays, G. Opperman, J. J. L'Italien, G. Long, P. Paulson, *Bio/Technology 4* (1986) 565.
[103] F. Kishimoto, H. Gomi, M. Kanaoka, T. Nakatani, A. Ito, T. Katoh, H. Agui, S. Sumida, S. Ogino, *Gene 45* (1986) 311.
[104] Y. Ovchinnikov, V. A. Efimov, I. N. Ivanova, S. V. Reverdatto, N. P. Skiba, O. G. Chakhmakhcheva, *Gene 31* (1984) 65.
[105] R. Brousseau, R. Scarpulla, W. Sung, H. M. Hsiung, S. A. Narang, R. Wu, *Gene 17* (1982) 279.
[106] K.-I. Miyoshi, A. Hasegawa, M. Tomiyama, T. Miyake, *Nucleic Acids Res. Symp. Ser. 10* (1981) 197.
[107] A. Cravador, P. Jacobs, A. van Elsen, C. Lacroix, B. Colau, P. van Alphen, A. Herzog, A. Bollen, *Biochimie 67* (1985) 829.
[108] H. Seliger, A. Herold, U. Kotschi, J. Lyons, G. Schmidt, F. Eisenbeiß, *Nucleosides & Nucleotides 6* (1987) 137.
[109] F. Hein, H. W. Jansen, E. Uhlmann, *Nucleosides & Nucleotides 6* (1987) 489.
[110] I. Ivanov, J. Tam, P. Wishart, E. Jay, *Gene 59* (1987) 223.
[111] M. Lennick, J. R. Haynes, S.-H. Shen, *Gene 61* (1987) 103.
[112] S. A. Rabbani, T. Yasuda, H. P. J. Bennett, W. L. Sung, D. M. Zahab, C. S. Tam, D. Goltzman, G. Hendy, *J. Biol. Chem. 263* (1988) 1307.
[113] S. Villa, G. De Fazio, S. Donini, G. Tarchi, U. Canosi, *Eur. J. Biochem. 171* (1988) 137.
[114] K. Alton, Y. Stabinski, R. Richards, B. Ferguson, L. Goldstein, B. Altrock, L. Miller, N. Stebbing in E. DeMaeyer, E. Schellekens (Eds.): *The Biology of the Interferon System*, Elsevier, Amsterdam 1983, p. 119.
[115] J. Engels, M. Leineweber, E. Uhlmann, *Angew. Chem. 96* (1984) 969; *Angew. Chem. Int. Ed. Engl. 23* (1984) 961.
[116] E. Jay, D. MacKnight, C. Lutze-Wallace, D. Harrison, P. Wishart, W.-Y. Liu, V. Asundi, L. Pommeroy-Cloney, J. Rommens, L. Eglington, J. Pawlak, F. Jay, *J. Biol. Chem. 259* (1984) 6311.
[117] S. Tanaka, T. Oshima, K. Ohsuye, T. Ono, A. Mizono, A. Ueno, H. Nakazato, M. Tsujimoto, N. Higashi, T. Noguchi, *Nucleic Acids Res. 11* (1983) 1707.
[118] P. W. Gray, B. B. Aggarwal, C. V. Benton, T. S. Bringman, W. J. Henzel, J. A. Jerrett, D. W. Leung, B. Moffat, P. Ng, L. P. Svedersky, M. A. Palladino, G. E. Nedwin, *Nature (London) 312* (1984) 721.
[119] M. D. Edge, A. R. Greene, G. R. Heathcliffe, V. E. Moore, N. J. Faulkner, R. Camble, N. N. Petter, P. Trueman, W. Schuch, J. Hennam, T. C. Atkinson, C. R. Newton, A. F. Markham, *Nucleic Acids Res. 11* (1983) 6419.
[120] S. M. Zurawski, K. Pope, H. Cherwinski, G. Zurawski, *Gene 49* (1986) 61.
[121] A. G. Porter, L. D. Bell, J. Adair, G. H. Catlin, J. Clarke, J. A. Davies, K. Dawson, R. Derbyshire, S. M. Doel, *DNA 5* (1986) 137.
[122] R. Camble, N. N. Petter, P. Trueman, C. R. Newton, F. J. Carr, R. C. Hockney, V. E. Moore, A. R. Greene, D. Holland, M. D. Edge, *Biochem. Biophys. Res. Commun. 134* (1986) 1404.
[123] W. C. Leung, A. P. Liu, X. Wu, S. E. Hasnain, G. Ritzel, G. Jing, in H. Kirchner (Eds.): *Biol. Interferon Syst. Proc. TNO-ISIR Meet.*, Elsevier, Amsterdam 1985, p. 419.
[124] Y. Nagase, N. Nakamura, J. Tohyama, S. Watanabe, H. Ogino, K. Horikoshi, A. Nii, M. Soma, M. Nobuhara, *Nucleic Acids Res. Symp. Ser. 12* (1983) 83.
[125] D. C. Humber, M. Allsopp, B. A. Coomber, L. G. D'Urso, C. W. Dykes, A. N. Hobden, M. Mitchell, S. A. Noble, *Nucleosides & Nucleotides 6* (1987) 413.
[126] D. P. Williams, K. Parker, P. Bacha, W. Bishai, M. Borowski, F. Genbauffe, T. B. Strom, J. R. Murphy, *Protein Eng. 1* (1987) 493.
[127] R. Wetzel, H. L. Heyneker, D. V. Goeddel, P. Jhurani, J. Shapiro, R. Crea, T. L. K. Low, J. E. McClure, G. B. Thurman, A. L. Goldstein, *Biochemistry 19* (1980) 6096.
[128] W. Mandecki, K. W. Mollison, T. J. Bolling, B. S. Powell, G. W. Carter, J. L. Fox, *Proc. Natl. Acad. Sci. USA 82* (1985) 3543.
[129] G. E. Armah, S. Nishikawa, C. Kondo, K.-I. Tomita, *Nucleic Acids Res. Symp. Ser. 19* (1988) 165.
[130] A. Calenda, A. Cordonnier, F. Lederer, D. K. H. Le, J. M. Pleau, *Biotechnol. Lett. 10* (1988) 155.
[131] G. T. Mullenbach, A. Tabrizi, R. W. Blacher, K. S. Steimer, *J. Biol. Chem. 261* (1986) 719.
[132] W. L. Sung, D. M. Zahab, F.-L. Yao, S. A. Narang, *Nucleic Acids Res. 14* (1986) 6159.
[133] B. S. Sproat, M. J. Gait, *Nucleic Acids Res. 13* (1985) 2959.
[134] A. Elmblad, L. Fryklund, L.-O. Heden, E. Holmgren, S. Josephson, M. Lake, B. Löwenadler, G. Palm, A. Skottner-Lundin in *3rd Eur. Congr. Biotechnol. Vol. III*, Verlag Chemie, Weinheim 1984, p. 287.
[135] G. Buell, M.-F. Schulz, G. Selzer, A. Chollet, N. R. Movva, D. Semon, S. Escanez, E. Kawashima, *Nucleic Acids Res. 13* (1985) 1923.
[136] G. Allen, C. A. Payneter, M. D. Winther, *J. Cell. Sci. Suppl. 3* (1985) 29.
[137] M. A. Peters, E. P. Lau, D. L. Snitman, J. J. van Wyk, L. E. Underwood, W. E. Russel, M. E. Svoboda, *Gene 35* (1985) 83.
[138] M. L. Bayne, M. C. Cascieri, B. Kelder, J. Applebaum, G. Chicchi, J. A. Shapiro, F. Pasleau, J. J. Kopchick, *Proc. Natl. Acad. Sci. USA 84* (1987) 2638.
[139] P. Denefle, S. Kovarik, J.-D. Guitton, T. Cartwright, J.-F. Mayaux, *Gene 56* (1987) 61.
[140] R. Shapiro, J. W. Harper, E. A. Fox, H.-W. Jansen, F. Hein, E. Uhlmann, *Anal. Biochem. 175* (1988) 450.
[141] K. N. Nambiar, J. Stackhouse, D. M. Stauffer, W. Poindexter Kennedy, J. K. Eldredge, S. A. Benner, *Science (Washington) 223* (1984) 1299.
[142] Y. Jigami, M. Muraki, N. Harada, H. Tanaka, *Gene 43* (1986) 273.
[143] L. Bülow, K. Mosbach, *FEBS Lett. 210* (1987) 147.
[144] M. Ikehara, E. Ohtsuka, T. Tokunaga, S. Nishikawa, S. Uesugi, T. Tanaka, Y. Aoyama, S. Kikyodani, K. Fujimoto, K. Yanase, K. Fuchimura, H. Morioka, *Proc. Natl. Acad. Sci. USA 83* (1986) 4695.
[145] D. P. Gearing, G. McMullen, P. Nagley, *Biochem. Int. 10* (1985) 907.
[146] T. Horn, J. S. Allen, M. S. Urdea, *Nucleosides & Nucleotides 6* (1987) 335.
[147] J. Phipps, J. J. Michniewicz, F.-L. Lao, S. A. Narang, *Biochem. Biophys. Res. Commun. 145* (1987) 190.
[148] S. A. Narang, F.-L. Yao, J. J. Michniewicz, G. Dubuc, J. Phipps, R. L. Samorjai, *Protein Eng. 1* (1987) 481.
[149] K. P. Nambiar, J. Stackhouse, S. R. Presnell, S. A. Benner, *Eur. J. Biochem. 163* (1987) 67.
[150] S. Nishikawa, H. Morioka, T. Kimura, Y. Ueda, T. Tanaka, S. Uesugi, T. Hakoshima, K.-I. Tomita, E. Ohtsuka, M. Ikehara, *Eur. J. Biochem. 173* (1988) 389.
[151] T. Tanaka, S. Kimura, Y. Ota, *Gene 64* (1988) 257.
[152] P. S. Vermersch, G. N. Bennett, *DNA 7* (1988) 243.
[153] T. Kempe, S. B. H. Kent, F. Chow, S. M. Petersom, W. I. Sundquist, J. J. L'Italien, D. Harbrecht, D. Plunkett, W. J. DeLorbe, *Gene 39* (1985) 239.
[154] Z. Hostomsky, J. Smrt, V. Paces, *Gene 39* (1985) 269.

[155] J. Tank, Z. X. Zhou, Z. Liang, B. Zon, X. Gao, X. Yang, C. Chen, D. Wang, *Sci. Sin. Ser. B (Engl. Ed.) 27* (1984) 466.
[156] S. Tanaka, T. Oshima, K. Ohsue, T. Ono, S. Oikawa, I. Takano, T. Noguchi, K. Kanagawa, N. Minamino, H. Matsuo, *Nucleic Acids Res. 10* (1982) 1741.
[157] V. N. Dobrynin, V. G. Korobko, I. V. Severtsova, V. P. Vlasov, N. S. Bystrov, M. N. Kolosov, *Biorg. Khim. 7* (1981) 1745.
[158] P. Brodin, T. Grundström, T. Hofmann, T. Drakenberg, E. Thulin, S. Forsen, *Biochemistry 25* (1986) 5371.
[159] D. M. Roberts, R. Crea, M. Malecha, G. Alvarado-Urbina, R. H. Chiarello, D. M. Watterson, *Biochemistry 24* (1985) 5090.
[160] N. Y. Theriault, C.-S. Tomich, W. Wierenga, *Nucleosides & Nucleotides 5* (1986) 15.
[161] C. Bergmann, J. Dodt, S. Köhler, E. Fink, H. G. Gassen, *Biol. Chem. Hoppe-Seyler 367* (1986) 731.
[162] H. Rink, M. Liersch, P. Sieber, F. Meyer, *Nucleic Acids Res. 12* (1984) 6369.
[163] E. Fortkamp, M. Rieger, G. Heisterberg-Moutses, S. Schweitzer, R. Sommer, *DNA 5* (1986) 511.
[164] a) Z. Hostomsky, J. Smrt, L. Arnold, Z. Tocik, V. Paces, *Nucleic Acids Res. 12* (1987) 4849; b) Z. Hostomsky, J. Smrt, *Nucleic Acids Res. Symp. Ser. 18* (1987) 241.
[165] E. Auerswald, W. Schröder, M. Kotick, *Biol. Chem. Hoppe-Seyler 367* (1987) 1413.
[166] P. Flecker, *Eur. J. Biochem. 166* (1987) 151.
[167] M. Strauss, F. O. Bartsch, J. Stollwerk, M. Trstenjak, A. Böhning, H. G. Gassen, W. Machleidt, V. Turk, *Biol. Chem. Hoppe-Seyler 369 Suppl.* (1988) 209.
[168] L. Ferretti, S. S. Karnik, H. G. Khorana, M. Nassal, D. D. Oprian, *Proc. Natl. Acad. Sci. USA 83* (1986) 599.
[169] M. T. Doel, M. T. Eaton, E. A. Cook, H. Lewis, T. Patel, N. H. Carey, *Nucleic Acids Res. 8* (1980) 4575.
[170] V. P. Kumarev, M. I. Rivkin, V. S. Bogachev, L. V. Baranova, V. M. Merkulov, V. N. Rybakov, *FEBS Lett. 114* (1980) 273.
[171] J. B. Ohlrogge, P. D. Beremand, D. N. Kuhn, P. E. Parker, *Biochem. Soc. Trans. 14* (1986) 579.
[172] K. Miura, Y. Inoue, H. Nakamori, S. Iwai, E. Ohtsuka, M. Ikehara, S. Noguchi, S. Nishimura, *Jpn. J. Cancer Res. 77* (1986) 45.
[173] S. Heaphy, M. Singh, M. J. Gait, *Protein Eng. 1* (1987) 425.
[174] A. Rosenthal, R. Ulrich, H. Billwitz, R. Frank, H. Blöcker, *Nucleic Acids Res. Symp. Ser. 18* (1987) 233.
[175] D. D. Oprian, R. S. Molday, R. J. Kaufman, H. G. Khorana, *Proc. Natl. Acad. Sci. USA 84* (1987) 8874.
[176] M. Nassal, T. Mogi, S. S. Karnik, H. G. Khorana, *J. Biol. Chem. 262* (1987) 9264.
[177] K. D. Preuss, H. Sachse, H. S. Sharma, G. Hagendorff, K. H. Scheit, *Biol. Chem. Hoppe-Seyler 368* (1987) 501.
[178] J. Biernat, H. Hasselmann, B. Hofer, N. Kennedy, H. Köster, *Protein Eng. 1* (1987) 345.
[179] J. Biernat, H. Köster, *Protein Eng. 1* (1987) 353.
[180] R. Moser, S. Frey, K. Münger, T. Hehlgans, S. Klauser, H. Langen, E.-L. Winnacker, R. Mertz, B. Gutte, *Protein Eng. 1* (1987) 339.
[181] D. J. Ecker, T. R. Butt, J. Marsh, E. J. Sternberg, N. Margolis, B. P. Monia, S. Jonnalagadda, M. I. Khan, P. L. Weber, L. Mueller, S. T. Crooke, *J. Biol. Chem. 262* (1987) 14213.
[182] V. M. Reyes, J. Abelson, *Anal. Biochem. 166* (1987) 90.
[183] J.-M. Masson, P. Meuris, M. Grunstein, J. Abelson, J. H. Miller, *Proc. Natl. Acad. Sci. USA 84* (1987) 6815.
[184] D. J. Ecker, M. I. Khan, J. Marsh, T. R. Butt, S. T. Crooke, *J. Biol. Chem. 262* (1987) 3524.
[185] S. E. Adams, I. D. Johnson, M. Braddock, A. J. Kingsman, R. M. Edwards, *Nucleic Acids Res. 16* (1988) 4287.
[186] J.-H. Lee, J. L. Weickmann, R. K. Koduri, P. Ghosh-Dastidar, K. Saito, L. C. Blair, T. Date, J. S. Lai, S. M. Hollenberg, R. L. Kendall, *Biochemistry 27* (1988) 5101.
[187] T. P. Sakmar, H. G. Khorana, *Nucleic Acids Res. 16* (1988) 6361.
[188] A. G. Stewart, H. Richards, S. Roberts, J. Warwick, K. Edwards, L. Bell, J. Smith, R. Derbyshire, *Nucleic Acids Res. 11* (1983) 6597.
[189] E. Uhlmann, J. Engels, *Tetrahedron Lett. 27* (1986) 1023.
[190] E. Uhlmann, J. Engels, *Chem. Scr. 26* (1986) 217.
[191] H. G. Khorana, *Pure Appl. Chem. 17* (1968) 349.
[192] N. Y. Theriault, J. B. Carter, S. P. Pulaski, *BioTechniques 6* (1988) 470.
[193] J. J. Rossi, R. Kierzek, T. Huang, P. A. Walker, K. Itakura, *J. Biol. Chem. 257* (1982) 9226.
[194] R. C. Scarpulla, S. Narang, R. Wu, *Anal. Biochem. 121* (1982) 356.
[195] O. G. Chakhmakhcheva, V. A. Efimov, O. V. Mirskikh, R. V. Reverdatto, A. A. Buryakova, Y. A. Ovchinnikov, *Chem. Scr. 26* (1986) 31.
[196] J. J. Rossi, X. Soberon, Y. Marumoto, J. McMahon, K. Itakura, *Proc. Natl. Acad. Sci. USA 80* (1983) 3203.
[197] E. Uhlmann, F. Hein, *Nucleic Acids Res. Symp. Ser. 18* (1987) 237.
[198] E. Uhlmann, *Gene 71* (1988) 29.
[199] D. H. Hare, B. R. Reid, *Biochemistry 25* (1986) 5341.
[200] S. Ikuta, R. Chattopadhyaya, *Biochemistry 25* (1986) 4840.
[201] R. Chattopadhyaya, S. Ikuta, K. Grzeskowiak, R. E. Dickerson, *Nature (London) 334* (1988) 175.
[202] a) F. Sanger, S. Nicklen, A. R. Coulson, *Proc. Natl. Acad. Sci. USA 74* (1977) 5462; b) Nobel-Aufsatz: F. Sanger, *Angew. Chem. 93* (1981) 937.
[203] F. Hein, H. W. Jansen, E. Uhlmann, *Nucleosides & Nucleotides 7* (1988) 497.
[204] W. H. McClain, K. Foss, K. L. Mittelstadt, J. Schneider, *Nucleic Acids Res. 14* (1986) 6770.
[205] T. Grundström, W. M. Zenke, M. Wintzerith, H. W. D. Matthes, A. Staub, P. Chambon, *Nucleic Acids Res. 13* (1985) 3305.
[206] S. A. Narang, G. Dubuc, F. L. Yao, J. J. Michniewicz, *Biochem. Biophys. Res. Commun. 134* (1986) 407.
[207] O. G. Chakhmakhcheva, V. A. Efimov, Y. A. Ovchinnikov, *Nucleosides & Nucleotides 6* (1987) 321.
[208] A. R. Oliphant, A. L. Nussbaum, K. Struhl, *Gene 44* (1986) 177.
[209] K. M. Derbyshire, J. J. Salvo, N. D. F. Gringley, *Gene 46* (1986) 145.
[210] C. A. Brennan, R. I. Gumport, *Nucleic Acids Res. 13* (1985) 8665.
[211] R. Cosstick, L. W. McLaughlin, F. Eckstein, *Nucleic Acids Res. 12* (1984) 1791.
[212] D. Zeh, H. Seliger, *Nucleosides & Nucleotides 6* (1987) 485.
[213] M. J. Zoller, M. Smith, *Nucleic Acids Res. 10* (1982) 6487.
[214] H. J. Fritz, *Biol. Chem. Hoppe-Seyler 367 Suppl.* (1986) 86.
[215] a) W. Mandecki, *Proc. Natl. Acad. Sci. USA 83* (1986) 7177; b) W. Mandecki, T. J. Bolling, *Gene 68* (1988) 101; c) M. A. Hayden, W. Mandecki, *DNA 7* (1988) 571.
[216] S. Pochet, B. Arcangioli, T. Huynh-Dinh, *Nucleic Acids Res. 16* (1988) 1619.
[217] H. Grosjean, W. Fiers, *Gene 18* (1982) 199.
[218] T. Ikemura, *J. Mol. Biol. 158* (1982) 573.
[219] T. Togunaga, S. Iwai, H. Gomi, K. Kodama, E. Ohtsuka, M. Ikehara, O. Chisaka, K. Matsubara, *Gene 39* (1985) 117.
[220] a) T. Maruyama, T. Gojobori, S.-I. Aota, T. Ikemura, *Nucleic Acids Res. 14* (1986) Suppl. r151; b) S.-I. Aota, T. Gojobori, T. Maruyama, T. Ikemura, *ibid. 16* (1988) Suppl. r315.
[221] G. O'Neill, S. H. Goh, R. A. J. Warren, D. G. Kilburn, R. C. Miller Jr., *Gene 44* (1986) 325.
[222] J. Vieira, J. Messing, *Gene 19* (1982) 259.
[223] J. Messing, B. Gronenborn, B. Müller-Hill, P. H. Hofschneider, *Proc. Natl. Acad. Sci. USA 74* (1977) 3642.
[224] a) *Nucleic Acids Res. 10* (1982) 1–456; b) *ibid. 12* (1984) 1–853; c) *ibid. 14* (1986) 1–621; d) *ibid. 16* (1988) 1655–1877.
[225] S. R. Presnell, S. A. Benner, *Nucleic Acids Res. 16* (1988) 1693.
[226] a) R. J. Roberts, *Nucleic Acids Res. 13* (1985) Suppl. r165; b) *ibid. 15* (1987) Suppl. r189.
[227] C. Kessler, H. J. Höltke, *Gene 47* (1986) 1.
[228] R. J. Roberts, *Nucleic Acids Res. 16* (1988) Suppl. r271.
[229] A. C. Looman, J. Bodlaender, M. de Gruyter, A. Vogelaar, P. H. van Knippenberg, *Nucleic Acids Res. 14* (1986) 5481.
[230] L.-H. Tessier, P. Sondermeyer, T. Faure, D. Dreyer, A. Benavente, D. Villeval, M. Courtney, J.-P. Lecocq, *Nucleic Acids Res. 12* (1984) 7663.
[231] M. Zucker, P. Stiegler, *Nucleic Acids Res. 9* (1981) 133.
[232] R. Nussinov, G. Pieczenik, J. R. Riggs, D. J. Kleitman, *SIAM J. Appl. Math. 35* (1978) 68.
[233] C. Papanicolaou, M. Gouy, J. Ninio, *Nucleic Acids Res. 12* (1984) 31.
[234] N. Lee, J. Cozzitorto, N. Wainwright, D. Testa, *Nucleic Acids Res. 12* (1984) 6797.
[235] a) P. R. Szoka, A. B. Schreiber, H. Chan, J. Murthy, *DNA 5* (1986) 11; b) M. Landon, *Methods Enzymol. 47* (1977) 145.
[236] J. K. Blodgett, G. M. Loudon, K. D. Collins, *J. Am. Chem. Soc. 107* (1985) 4305.
[237] C. Lazure, N. G. Seidah, D. Pelaprat, M. Chretien, *Can. J. Biochem. Cell. Biol. 61* (1983) 501.
[238] K. Nagai, H. C. Thoegersen, *Nature (London) 309* (1984) 810.
[239] W. L. Sung, F.-L. Yao, D. M. Zahab, S. A. Narang, *Proc. Natl. Acad. Sci. USA 83* (1986) 561.
[240] S.-H. Shen, *Proc. Natl. Acad. Sci. USA 81* (1984) 4627.
[241] B. Blobel, B. Dobberstein, *J. Cell. Biol. 67* (1975) 835.
[242] J. Dodt, T. Schmitz, T. Schäfer, C. Bergmann, *FEBS Lett. 202* (1986) 373.
[243] G. L. Grey, J. S. Baldridge, K. S. McKeown, H. L. Heyneker, C. Nan Chang, *Gene 39* (1985) 247.
[244] E. Uhlmann, J. Engels, W. Wetekam, *Nucleosides & Nucleotides 4* (1985) 259.
[245] B. Nilsson, E. Holmgren, S. Josephson, S. Gatenbeck, L. Philipson, M. Uhlen, *Nucleic Acids Res. 13* (1985) 1151.
[246] K. Ohmura, K. Nakamura, H. Yamazaki, T. Shiroza, K. Yamane, Y. Jigami, H. Tanaka, K. Yoda, M. Yamasaki, G. Tamura, *Nucleic Acids Res. 13* (1984) 5307.
[247] K. M. Zsebo, H.-S. Lu, J. C. Fieschko, L. Goldstein, J. Davis, K. Duker, S. V. Suggs, P. H. Lai, G. A. Bitter, *J. Biol. Chem. 261* (1986) 5858.
[248] S. D. Emr, R. Schekman, M. C. Flessel, J. Thorner, *Proc. Natl. Acad. Sci. USA 80* (1983) 7080.
[249] M. Smith, *Annu. Rev. Genet. 19* (1985) 423.

[250] W. Kramer, V. Drutsa, H. W. Jansen, B. Kramer, M. Pflugfelder, H. J. Fritz, *Nucleic Acids Res. 12* (1984) 9441.
[251] M. J. Zoller, M. Smith, *DNA 3* (1984) 479.
[252] W. Kramer, K. Schughart, H. J. Fritz, *Nucleic Acids Res. 10* (1982) 6475.
[253] P. Carter, H. Bedouelle, G. Winter, *Nucleic Acids Res. 13* (1985) 4431.
[254] T. A. Kunkel, *Proc. Natl. Acad. Sci. USA 82* (1985) 488.
[255] J. W. Taylor, J. Ott, F. Eckstein, *Nucleic Acids Res. 13* (1985) 8764.
[256] M. D. Matteucci, H. L. Heyneker, *Nucleic Acids Res. 11* (1983) 3113.
[257] J. A. Wells, M. Vasser, D. B. Powers, *Gene 34* (1985) 315.
[258] S. W. Cline, M. Yarus, P. Wier, *DNA 5* (1986) 37.
[259] D. A. Estell, T. P. Graycar, J. A. Wells, *J. Biol. Chem. 260* (1985) 6518.
[260] P. G. Thomas, A. J. Russel, A. R. Fersht, *Nature (London) 318* (1985) 375.
[261] K. T.-K. Lau, A. R. Fersht, *Nature (London) 326* (1987) 811.
[262] Y.-R. Hsu, B. Ferguson, M. Narachi, R. M. Richards, Y. Stabinsky, N. K. Alton, N. Stebbing, T. Arakawa, *J. Interferon Res. 6* (1986) 663.
[263] F. E. Cohen, P. A. Kosen, I. D. Kuntz, L. B. Epstein, T. L. Ciardelli, K. A. Smith, *Science (Washington) 234* (1986) 349.
[264] A. Wang, S.-D. Lu, D. F. Mark, *Science (Washington) 224* (1984) 1431.
[265] J. J. Huang, R. C. Newton, R. Horuk, J. B. Matthew, M. Covington, K. Pezzella, Y. Lin, *FEBS Lett. 223* (1987) 294.
[266] T. Arakawa, T. Boone, J. M. Davis, W. C. Kenney, *Biochemistry 25* (1986) 8274.
[267] J. W. Engels, J. Glauder, H. Müllner, D. Tripier, E. Uhlmann, W. Wetekam, *Protein Eng. 1* (1987) 195.
[268] A. Bradbury, M. D. F. Finnie, D. G. Smyth, *Nature (London) 298* (1982) 686.
[269] H. J. Fritz, *Nucleic Acids Res. Spec. Publ. 4* (1978) s243.
[270] V. N. Dobrynin, V. G. Korobko, I. V. Severtsova, N. S. Bystrov, S. A. Chuvpilo, M. N. Kolosov, *Nucleic Acids Res. Symp. Ser. 7* (1980) 365.
[271] P. L. DeHaseth, R. A. Goldman, C. L. Cech, M. H. Caruthers, *Nucleic Acids Res. 11* (1983) 773.
[272] J. Rommens, D. MacKnight, L. Pomeroy-Cloney, E. Jay, *Nucleic Acids Res. 11* (1983) 5921.
[273] E. Jay, J. Rommens, L. Pomeroy-Cloney, D. MacKnight, C. Lutze-Wallace, P. Wishart, D. Harrison, W. Y. Lui, V. Asundi, M. Dawood, F. Jay, *Proc. Natl. Acad. Sci. USA 81* (1984) 2290.
[274] J. D. Windass, C. R. Newton, J. De Maeyer-Guignard, V. E. Moore, A. F. Markham, M. D. Edge, *Nucleic Acids Res. 10* (1982) 6639.
[275] F. Jacob, J. Monod, *J. Mol. Biol. 3* (1961) 318.
[276] J. R. Sadler, H. Sasmor, J. L. Betz, *Proc. Natl. Acad. Sci. USA 80* (1983) 6785.
[277] A. Simons, D. Tils, B. von Wilcken-Bergmann, B. Müller-Hill, *Proc. Natl. Acad. Sci. USA 81* (1984) 1624.
[278] J. Brosius, A. Holy, *Proc. Natl. Acad. Sci. USA 81* (1984) 6929.
[279] G. Simons, E. Remaut, B. Allet, R. Devos, W. Fiers, *Gene 28* (1984) 55.
[280] J.-I. Flock, I. Fotheringham, J. Light, L. Bell, R. Derbyshire, *MGG Mol. Gen. Genet. 195* (1984) 246.
[281] J. Shine, L. Dalgarno, *Nature (London) 254* (1975) 34.
[282] E. Dworkin-Rastl, P. Swetly, M. B. Dworkin, *Gene 21* (1983) 237.
[283] P. Stanssens, E. Remaut, W. Fiers, *Gene 36* (1985) 211.
[284] D. M. Marquis, J. M. Smolec, D. H. Katz, *Gene 42* (1986) 175.
[285] R. E. Offord, *Protein Eng. 1* (1987) 151.
[286] M. Mutter, *Angew. Chem. 97* (1985) 639; *Angew. Chem. Int. Ed. Engl. 24* (1985) 639; S. Vuilleumier, M. Mutter, *ibid. 101* (1989) 551 and *28* (1989) 535.
[287] R. Moser, S. Klauser, T. Leist, H. Langen, T. Epprecht, B. Gutte, *Angew. Chem. 97* (1985) 737; *Angew. Chem. Int. Ed. Engl. 24* (1985) 719.
[288] V. L. Rath, R. J. Fletterick, *Cell 49* (1987) 583.
[289] T. L. Blundell, B. L. Sibanda, M. J. E. Sternberg, J. Thornton, *Nature (London) 326* (1987) 347.
[290] W. V. Shaw, *Biochem. J. 246* (1987) 1.
[291] T. Blundell, D. Carney, S. Gardner, F. Hayes, B. Howlin, T. Hubbard, J. Overington, D. A. Singh, B. L. Sibanda, M. Sutcliffe, *Eur. J. Biochem. 172* (1988) 513.
[292] R. Jaenicke, *Prog. Biophys. molec. Biol. 49* (1987) 117; *Angew. Chem. 96* (1984) 385; *Angew. Chem. Int. Ed. Engl. 23* (1984) 395.
[293] J. van Brunt, *Bio/Technology 6* (1988) 655.
[294] J. F. Gibrat, J. Garnier, B. Robson, *J. Mol. Biol. 198* (1987) 425.
[295] L. Regan, W. F. Degrado, *Science (Washington) 241* (1988) 976.

Communications may be submitted in English *or* in German. Further details regarding the submission of communications can be found in the "Notice to Authors" reproduced in the January issue of the journal. Copies thereof may be obtained from the editorial office upon request.

Pentabenzylcyclopentadienylpotassium · 3 THF, an Organopotassium Compound with "Piano Stool" Geometry

By *Jörg Lorberth,* Sung-Hee Shin, Sigrid Wocadlo,* and *Werner Massa*

The anions of pentamethylcyclopentadiene[1] and pentabenzylcyclopentadiene are good ligands for stabilizing complexes of both transition metals and main-group metals in low oxidation states. Recent examples include Sb^{I} compounds[2] for pentamethylcyclopentadienide and Ge^{II}, Sn^{II}, Pb^{II},[3] and Tl^{I} compounds for pentabenzylcyclopentadienide.[4,5]

We have now obtained the potassium salt **1** of the "bulky" pentabenzylcyclopentadiene, $C_5H(CH_2C_6H_5)_5$, in a smooth reaction as described by Equation (a).

$$K + C_5H(CH_2C_6H_5)_5 \xrightarrow{THF} \underset{\mathbf{1}}{K[C_5(CH_2C_6H_5)_5] \cdot 3\,THF} + \tfrac{1}{2}H_2 \qquad (a)$$

In contrast to organolithium and -sodium compounds, only a few crystal structures of the corresponding potassium compounds have been reported;[6] for example, the molecular and crystal structures of KCD_3[7] and $K[C_5H_4(SiMe_3)]$[8] were described only recently. We have obtained single crystals of **1** and have subjected these to X-ray structure analysis.[9] The potassium ion is bonded in an η^5 fashion to a planar cyclopentadienyl ring, the "ring slippage" being only 17.4 pm. The three oxygen atoms of the THF molecules complete the coordination polyhedron around the central atom to give a coordination number of 8 (Fig. 1).

Three of the benzyl substituents and the three THF molecules are oriented in an eclipsed fashion with respect to one another, so that the geometry around the potassium ion may also be described as a trigonal prism, two faces of which are capped by benzyl substituents; in KCH_3, the $CH_3^{\ominus}$ ions are coordinated by the $K^{\oplus}$ ions in a trigonal-prismatic fashion and the $K^{\oplus}$ ions, in turn, are surrounded pseudooctahedrally by $CH_3^{\ominus}$ ions.[10]

One THF molecule is bent away for steric reasons, thus clearly demonstrating the large spatial demands of the benzyl groups. In the dimer $[Tl^{I}\{C_5(CH_2C_6H_5)_5\}]_2$, three benzyl substituents of each Cp ring are oriented towards the heavy atom[3] and largely shield the two thallium ions. The first X-ray structure analysis of a transition-metal

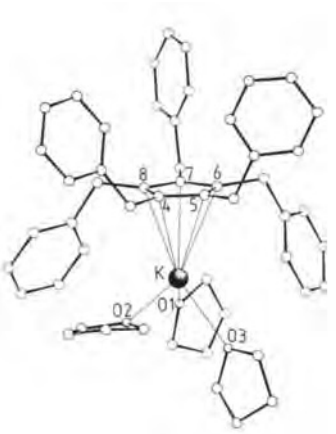


Fig. 1. SCHAKAL drawing [15] of the structure of **1** in the crystal. Important distances [pm] and angles [°]: K-O1 269.0(4), K-O2 273.7(4), K-O3 277.9(5) (average 273.5), K-C4 296.8(5), K-C5 305.1(5), K-C6 309.5(5), K-C7 307.0(5), K-C8 298.9(5) (average 303.5), K-Cp ring center 278.8(3), "ring slippage" = distance between the perpendicular projection of the metal on the ring plane and the ring center 17.4, C4-C5 143.3(7), C5-C6 140.5(7), C6-C7 139.6(7), C7-C8 141.0(7), C4-C8 139.7(7) (average 140.8); O1-K-O2 118.2(1), O1-K-O3 92.3(1), O2-K-O3 75.4(1).

complex containing a pentabenzylcyclopentadienyl ligand, $[\{C_5(CH_2C_6H_5)_5\}Co(CO)_2]$, shows that four of the five benzyl groups are oriented away from cobalt.[10]

The K–Cp(ring center) distance is 278.8(3) pm, the average K–C distance 303.5 pm. For comparison, the K–C distance in KCH_3 (center of gravity of the CH_3 group) is 322[11] and the average value of the K–C distances in $K[C_5H_4(SiMe_3)]$ is 300 pm.[8] The average K–O distance is 273.5 pm; the distance to the O1–O2–O3 plane, which forms an angle of 19.4° with the nearly planar cyclopentadienyl ring (maximal deviation of the C atoms from the "best plane" 4.9 pm), is 133(1) pm. For comparison, the average K–O distance in $K[C_5(NO_2)_2Cl_3]$, in which the potassium ion is surrounded by an irregular octahedron of oxygen atoms,[12] is ca. 258–294 pm and in $K[C_5(CO_2Me)_5] \cdot MeOH$ ca. 264–288 pm.[13]

The C–C bond lengths in the Cp ring vary only from 139.6(7) to 143.3(7) pm, averaging 140.8 pm, and are therefore similar to those in cyclopentadiene, C_5H_6 (141 pm).[14]

Experimental Procedure

Potassium (2.27 g, 58.09 mmol), the surface of which was cleaned with 1-butanol prior to use, was dissolved in 100 mL of liquid NH_3 in a 250-mL Schlenk flask. NH_3 was evaporated and the powdery residue was dried under high vacuum and then suspended in 80 mL of dry THF. Pentabenzylcyclopentadiene (30 g, 58.09 mmol), dissolved in 50 mL of dry THF, was added dropwise to this suspension at room temperature. After the potassium metal had gone into solution, the reaction solution was kept at ca. −37 °C; colorless, transparent crystals with a melting range of 35–45 °C (uncorrected) were obtained: the yield was 31.33 g (ca. 70%).

Received: February 2, *1989 [Z 3152 IE]*
German version: *Angew. Chem. 101* (1989) 793

CAS Registry numbers:
1, 120686-85-3; $C_5H(CH_2C_6H_5)_5$, 67209-29-4.

[*] Prof. Dr. J. Lorberth, MSc S.-H. Shin, S. Wocadlo, Prof. Dr. W. Massa
Fachbereich Chemie der Universität
Hans-Meerwein-Strasse, D-3550 Marburg (FRG)

[1] P. Jutzi, *Comments Inorg. Chem. 6* (1987) 123.
[2] T. F. Berlitz, H. Sinning, J. Lorberth, U. Müller, *Z. Naturforsch. B43* (1988) 744.
[3] H. Schumann, C. Janiak, E. Hahn, J. Loebel, J. J. Zuckermann, *Angew. Chem. 97* (1985) 765; *Angew. Chem. Int. Ed. Engl. 24* (1985) 773; H. Schumann, C. Janiak, E. Hahn, C. Kolax, J. Loebel, M. D. Rausch, J. J. Zuckermann, *Chem. Ber. 119* (1986) 2656.

[4] H. Schumann, C. Janiak, J. Pickardt, U. Börner, *Angew. Chem. 99* (1987) 788; *Angew. Chem. Int. Ed. Engl. 26* (1987) 789.
[5] H. Schumann, C. Janiak, M. A. Khan, J. J. Zuckermann, *J. Organomet. Chem. 354* (1988) 7.
[6] C. Schade, P. von R. Schleyer, *Adv. Organomet. Chem. 27* (1987) 169.
[7] E. Weiss, T. Lambertsen, B. Schubert, J. K. Cockcraft, *J. Organomet. Chem. 358* (1988) 1.
[8] P. Jutzi, W. Leffers, B. Hampel, S. Pohl, W. Saak, *Angew. Chem. 99* (1987) 563; *Angew. Chem. Int. Ed. Engl. 26* (1987) 583.
[9] **1** crystallizes in the space group $P2_1/n$; $Z = 4$; $a = 1198.2(7)$, $b = 1530.6(2)$, $c = 2458.7(13)$ pm, $\beta = 102.07(3)°$. 3875 observed reflections with $F_o > 3\sigma(F_o)$ were measured on a four-circle diffractometer (CAD4, Enraf-Nonius) with $Cu_{K\alpha}$ radiation at 193 K; no absorption correction ($\mu = 12\ cm^{-1}$). The structure was solved by direct methods. All heavy atoms were refined with anisotropic temperature factors; the H atoms were included at calculated positions with groupwise common isotropic temperature factors (509 parameters). The use of weighting factors $w = 1/\sigma^2(F_o)$ and inclusion of an extinction correction [F_c(corr.) $= F_c(1 - \varepsilon F_c^2/\sin\theta)$ with $\varepsilon = 1.8 \times 10^{-7}$] resulted in residual indices of $R = 0.070$ and $R_w = 0.055$ [16]. Further details of the crystal structure investigation may be obtained from the Fachinformationszentrum Karlsruhe, Gesellschaft für wissenschaftlich-technische Information mbH, D-7514 Eggenstein-Leopoldshafen 2 (FRG), on quoting the depository number CSD-53777, the names of the authors, and the journal citation.
[10] J. W. Chambers, A. J. Baskar, S. G. Bott, J. L. Atwood, M. D. Rausch, *Organometallics 5* (1986) 1635.
[11] E. Weiss, G. Sauermann, *Chem. Ber. 103* (1970) 265; *Angew. Chem. 80* (1968) 123; *Angew. Chem. Int. Ed. Engl. 7* (1968) 133.
[12] Y. Otaka, F. Marumo, Y. Saito, *Acta Crystallogr. Sect. B28* (1972) 1590.
[13] M. I. Bruce, J. K. Walton, M. L. Williams, S. R. Hall, B. W. Skelton, A. H. White, *J. Chem. Soc. Dalton Trans. 1982*, 2209.
[14] G. Liebling, R. E. Marsh, *Acta Crystallogr. 19* (1965) 202.
[15] E. Keller, *SCHAKAL-86 B* (A FORTRAN Program for the Graphic Representation of Molecular and Crystallographic Models), Freiburg 1986.
[16] G. M. Sheldrick, *SHELX-76* (Program for Crystal Structure Determination), Cambridge 1976; *SHELXS-86* (Program for Crystal Structure Solution), Göttingen 1986.

Gas-Chromatographic Enantiomer Separation of Unfunctionalized Cycloalkanes on Permethylated β-Cyclodextrin**

By *Volker Schurig,* Hans-Peter Nowotny,* and *Dieter Schmalzing*

The enantiomer separation of simple, unfunctionalized, saturated hydrocarbons is a challenge,[1] since no procedure based on the formation of diastereomers or on chemical, diastereomeric interaction with chiral auxiliaries (NMR, GC)[2] can be used. Even the determination of optical purity is often difficult owing to unknown maximum specific rotations. In 1981, we began experiments on the gas-chromatographic separation of the enantiomers of tetraalkylmethanes, $R^1R^2R^3R^4C$ (R = alkyl), on glass capillary columns coated with permethylated β-cyclodextrins in polysiloxane solution.[3] Although these experiments have been unsuccessful so far, it has recently been shown that peralkylated cyclodextrins are suitable for the enantiomer separation of unfunctionalized olefins.[4, 5] Packed columns coated with α-cyclodextrin in formamide were also successfully used, despite their poor efficiency, to separate the enantiomers of *trans*-pinane (semiquantitatively) and *cis*-pinane[6] as well as the diastereomers of *cis*/*trans*-dimethylcycloalkanes. In the latter case, the chiral isomers were not resolved into enantiomers.[7]

The quantitative separation of a series of alkylcyclohexanes by gas chromatography has now been achieved on permethylated β-cyclodextrin in OV-1701 on glass capillaries between 23 and 60 °C (cf. Fig. 1 and Table 1).

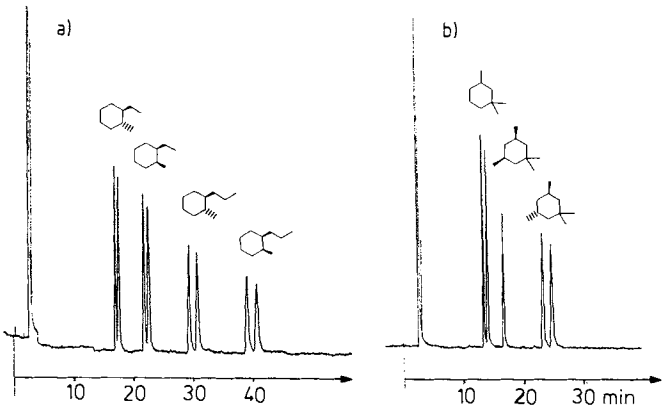


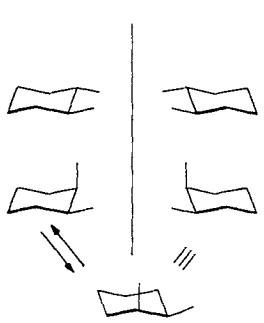
Fig. 1. a) Separation of the enantiomers of *trans*- and *cis*-1-ethyl-2-methylcyclohexane and *trans*- and *cis*-1-methyl-2-propylcyclohexane on a glass capillary column (25-m × 0.25-mm inner diameter) coated with 10% heptakis(2,3,6-tri-*O*-methyl)-β-cyclodextrin in OV-1701 (0.08 m). Oven temperature 50 °C; carrier gas pressure 0.7 bar helium. b) Separation of the enantiomers and diastereomers of 1,1,3-trimethylcyclohexane and *cis*- and *trans*-1,1,3,5-tetramethylcyclohexane; conditions same as in a) except for the oven temperature (45 °C).

Table 1. Gas-chromatographic data for enantiomer separation on permethyl-β-cyclodextrin in OV-1701.

Compound	T [°C]	p [bar]	Separation factor α	Resolution R_s
trans-1,2-dimethylcyclohexane	23	1.0	1.06	0.85
trans-1,3-dimethylcyclohexane	23	1.0	1.07	1.28
cis-1-ethyl-2-methylcyclohexane	60	0.7	1.04	1.40
trans-1-ethyl-2-methylcyclohexane	60	0.7	1.03	1.00
cis-1-methyl-2-propylcyclohexane	60	1.0	1.03	1.60
trans-1-methyl-2-propylcyclohexane	60	1.0	1.04	1.69
1,1,3-trimethylcyclohexane	60	0.7	1.05	1.47
trans-1,1,3,5-tetramethylcyclohexane	60	0.7	1.05	2.00
cis-pinane	40	1.0	1.10	2.28
trans-pinane	40	1.0	1.03	0.89

Since the enantiomers of both *cis*-1-ethyl-2-methylcyclohexane and *cis*-1-methyl-2-propylcyclohexane are separated, the cyclodextrin phase should, in principle, discriminate between the enantiomers of the homologous *cis*-1,2-dimethylcyclohexane, the chair conformation of which is chiral. Rapid inversion of the chair conformation, however, leads (without change in configuration at the chiral centers) to formation of the enantiomeric conformer.[8] The appearance of only one peak is therefore interpreted as an interesting example of an extremely rapid enantiomerization ("peak coalescence of the first kind"[9]).

Hitherto, the investigation of the separation of enantiomers on cyclodextrin phases has not allowed a clear distinction to be made between the contributions from the nonpolar interactions in the interior of the cavity (inclusion) and



[*] Prof. Dr. V. Schurig, Dipl.-Chem. H.-P. Nowotny, Dipl.-Chem. D. Schmalzing
Institut für Organische Chemie der Universität
Auf der Morgenstelle 18, D-7400 Tübingen (FRG)

[**] This work was supported by the Deutsche Forschungsgemeinschaft and the Fonds der Chemischen Industrie.

the polar interactions with the alkoxy groups on the outside of the torus. Our results on unfunctionalized, saturated hydrocarbons, for which polar interactions can be excluded, indicate that inclusion represents the decisive contribution, whereby the methoxy groups shield the cavity only slightly and, moreover, increase the flexibility of the cyclodextrin ring ("induced fit").[10] Heptakis(2,6-di-*O*-methyl-3-*O*-trifluoroacetyl)-β-cyclodextrin does not separate the enantiomers of the cycloalkanes discussed here.

The direct separation of the enantiomers of unfunctionalized cycloalkanes described here allows a simple investigation of enantioselective synthesis (e.g., asymmetric hydrogenation of aromatic or olefinic compounds) or of enzymatic or chemical transformations (kinetic resolution of enantiomers). The method is also suitable for extrapolation and quantification of chiroptic data.

Received: January 23, 1989 [Z 3137 IE]
German version: *Angew. Chem. 101* (1989) 785

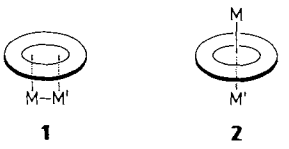
CAS Registry numbers:
trans-1,2-dimethylcyclohexane, 6876-23-9; *trans*-1,3-dimethylcyclohexane, 2207-03-6; *cis*-1-ethyl-2-methylcyclohexane, 4923-77-7; *trans*-1-ethyl-2-methylcyclohexane, 4923-78-8; *cis*-1-methyl-2-propylcyclohexane, 4926-71-0; *trans*-1-methyl-2-propylcyclohexane, 42806-77-9; 1,1,3-trimethylcyclohexane, 3073-66-3; *trans*-1,1,3,5-tetramethylcyclohexane, 50876-31-8; *cis*-pinane, 6876-13-7; *trans*-pinane, 33626-25-4; permethyl-26-cyclodextrin, 55216-11-0.

[1] V. Schurig, *Angew. Chem. 96* (1984) 733; *Angew. Chem. Int. Ed. Engl. 23* (1984) 747.
[2] V. Schurig, *Kontakte (Darmstadt), 1985*(1), 54; *1985*(2), 22; *1986*(1), 3.
[3] Ref. 16 in [4].
[4] V. Schurig, H.-P. Nowotny, *J. Chromatogr. 441* (1988) 155.
[5] J. Ehlers, W. A. König, S. Lutz, G. Wenz, H. tom Dieck, *Angew. Chem. 100* (1988) 1614; *Angew. Chem. Int. Ed. Engl. 27* (1988) 1556.
[6] T. Koscielski, D. Sybilska, S. Belniak, J. Jurczak, *Chromatographia 19* (1984) 292.
[7] T. Koscielski, D. Sybilska, *J. Chromatogr. 349* (1985) 3.
[8] E. L. Eliel; *Stereochemistry of Carbon Compounds*, McGraw-Hill, New York 1962, p. 212.
[9] V. Schurig, W. Bürkle, *J. Am. Chem. Soc. 104* (1982) 7573.
[10] K. Harata, K. Uekama, M. Otagiri, F. Hirayama, *J. Inclusion Phenom. 2* (1984) 583.

Triple-Decker Complexes as Intermediates in Ring-Ligand Transfers**

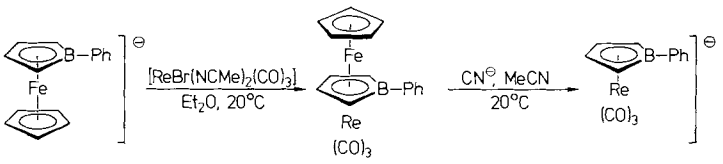
By *Gerhard E. Herberich,** *Barry J. Dunne*, and *Bernd Heßner*

The principle and the preparative value of ring-ligand transfer[2] was first shown by *Maitlis* et al. for (cyclobutadiene)metal complexes.[3] They found, for example, that $[(\eta^4\text{-}C_4Ph_4)PdBr_2]_2$ reacts with $Fe(CO)_5$ to give $[(\eta^4\text{-}C_4Ph_4)Fe(CO)_3]$, Pd metal, CO, and $FeBr_2$.[3b] They suggested a mechanism in which the transferred ligand is never free but, instead, changes its metallic center via intermediates of type **1** with a monofacially bridging ligand.[3b] This hypothesis is supported by the identification of compounds with monofacially bridging ligands.[4] However, the Maitlis mechanism has not yet been proved and several mechanistic alternatives are conceivable. We show here that, for 1*H*-borole complexes, ring-ligand transfer can also occur via triple-decker intermediates **2** with bifacially bridging ring ligands.



1 **2**

The sodium borataferrocene Na-**3**[5] reacts with $[ReBr(NCMe)_2(CO)_3]$[6] as electrophile in ether to give the stable, wine-red triple-decker complex **4**. The triple-decker structure of **4** is confirmed by the typical small coupling constant $N = {}^3J_{23} + {}^4J_{24}$ of 4.1 Hz for the bridging borole ligands.[7] Nucleophilic degradation with KCN transforms **4** into the rhenate **5**,[8] which can be isolated as $NMe_4^{\oplus}$ salt **6** ($N = 5.9$ Hz) or, after protonation, as hydride **7** ($N = 6.2$ Hz). The overall result of the electrophilic stacking reaction and nucleophilic degradation is the transfer of the 1*H*-borole ligand from iron to rhenium.



3 **4** **5**

$[(\eta^5\text{-}C_4H_4BPh)ReH(CO)_3]$ **7**

The neutral cobalt complex **8**[7] undergoes a similar electrophilic stacking reaction with **9a**[9] in acetone to afford the reddish-brown triple-decker salt **10a**, which is isolable in pure form and undergoes degradation with NaI in acetone[8] to give the known (borole)ruthenium complex **11a**.[10] The labile triple-decker salt **10b** was observed in the analogous reaction with the iridium complex **9b**[11] in an NMR tube; in this case, however, the degradation product **11b** appears in the reaction mixture before the cobalt complex **8** is completely consumed. Again, the preparative degradation is carried out with NaI.

$$[CpCo(\eta^5\text{-}C_4H_4BPh)] + [LM(OCMe_2)_3](BF_4)_2 \rightarrow$$
8
9a; LM = $Ru(\eta^6\text{-}C_6Me_6)$
9b; LM = $Ir(\eta^5\text{-}C_5Me_5)$

$$[(\mu\text{-}\eta^5\text{-}C_4H_4BPh)(CoCp)(ML)](BF_4)_2 \xrightarrow{NaI} [LM(\eta^5\text{-}C_4H_4BPh)]$$
10a, b **11a, b**

The transfer of the borole ligands affords the first borole complexes of rhenium (**4**–**7**) and iridium (**10b, 11b**) and, at the same time, the first triple-decker complexes of these metals. The direct observation of triple-decker intermediates was made possible by the way in which the reaction was performed.

Even when no intermediates are observed in ring-ligand transfers, it is possible, in principle, to distinguish between the different mechanisms. According to the Maitlis mechanism, the transferred ligand is coordinated to the *same* side in the starting material and the product. By contrast, the transferred ligand is bound to *different* sides in the starting material and product when the reaction proceeds via triple-decker intermediates. If the reaction involves a free ligand, on the other hand, the stereochemical information is lost. Chiral complexes should allow one to distinguish between these cases.

[*] Prof. Dr. G. E. Herberich, B. J. Dunne, B. Sc., Dr. B. Heßner
Institut für Anorganische Chemie der Technischen Hochschule
Professor-Pirlet-Strasse 1, D-5100 Aachen (FRG)

[**] Triple-Decker Complexes, Part 7. This work was supported by the Deutsche Forschungsgemeinschaft and the Fonds der Chemischen Industrie. Part 6: [1].

Experimental Procedure

4: $[Re(NCMe)_2(CO)_3]$ (825 mg, 1.91 mmol) was added to Na · **3** (625 mg, 2.22 mmol) in 50 mL of Et_2O and the reaction mixture was stirred for ca. 12 h. Filtration, concentration, and crystallization from Et_2O/hexane at −30 °C afforded 701 mg (69%) of **4** as wine-red crystals, m.p. 146 °C, dec. at 289 °C [12]. MS: *m/z* 532 (90%, $M^{\oplus}$), 448 (100, $M^{\oplus}$ − 3 CO). IR (hexane): $\tilde{\nu}$(CO) = 2032, 1945, 1935 cm^{-1}. ^1H NMR (80 MHz, CD_2Cl_2, int. TMS): δ = 7.70 (m, $2H_o$), 7.38 (m, $2H_m + H_p$), 4.27 (s, CpH), 4.94 (m, borole H−3,4), 3.32 (m, borole H−2,5, N = 4.1 Hz). ^{11}B NMR (32.08 MHz, CD_2Cl_2, ext. $BF_3 \cdot OEt_2$): δ = 11.2.

Degradation of **4** to give **6** and **7**: Compound **4** (264 mg, 0.497 mmol) in 40 mL of acetonitrile and KCN (0.35 g, 5.4 mmol) were stirred in the dark for 3 d at room temperature. The solvent was removed, the residue was dissolved in water, and the resulting solution was filtered. **6**: Addition of NMe_4Br (102 mg, 0.66 mmol) to the aqueous filtrate resulted in precipitation of a colorless crude product. Recrystallization from CH_2Cl_2/OEt_2 afforded 164 mg (68%) of **6** as thin, colorless plates m.p. 141–142 °C, dec. at 265 °C [12]. IR (CH_2Cl_2): $\tilde{\nu}$(CO) = 1970, 1867, 1855 sh cm^{-1}. ^1H NMR (80 MHz, CD_2Cl_2, int. TMS): δ = 7.45 (m, $2H_o$), 7.08 (m, $2H_m + H_p$), 5.01 (m, borole H−3,4), 3.56 (m, borole H−2,5, N = 5.9 Hz), 2.82 (s, NMe_4). ^{11}B NMR (32.08 MHz, CD_2Cl_2, ext. $BF_3 \cdot OEt_2$): δ = 16.3.

7: The aqueous filtrate obtained from the degradation of **4** was layered with pentane, acidified with 85% phosphoric acid (0.40 mL, 5.9 mmol), and extracted with pentane. Concentration of the pale yellow extract solution, drying with Na_2SO_4, and crystallization at −30 °C afforded 128 mg (63%) of **7** as orange-yellow needles, m.p. 77 °C, dec. at 243 °C [12]. IR (hexane): $\tilde{\nu}$(CO) = 2054, 1987, 1982 cm^{-1}. ^1H NMR (80 MHz, [D$_6$]acetone, int. TMS): δ = 7.57 (m, $2H_o$), 7.15 (m, $2H_m + H_p$), 4.61 (m, borole H−3,4), 3.39 (m, borole H−2,5, N = 6.2 Hz), −7.59 (s, ReH). ^{11}B NMR (32.08 MHz, CD_2Cl_2, ext. $BF_3 \cdot OEt_2$): δ = 6.3.

10a: $AgBF_4$ (195 mg, 1.00 mmol) in 15 mL of acetone was added to $[(\eta^6\text{-}C_6Me_6)RuCl_2]_2$ [9b] in 10 mL of acetone, the precipitated AgCl was filtered off after 30 min, **8** (132 mg, 0.50 mmol) [7] was added to the filtrate, and the resulting solution was kept at room temperature for 16 h. Concentration to 10 mL and addition of 50 mL of OEt_2 afforded 198 mg (57%) of reddish-brown needles of **10a**, m.p. 190 °C (dec.) [12]. ^1H NMR (80 MHz, [D$_6$]acetone, int. TMS): δ = 7.90 (m, $2H_o$), 7.50 (m, $2H_m + H_p$), 6.05 (s, Cp), 6.42 (m, borole H−3,4), 5.17 (m, borole H−2,5), 2.20 (s, C_6Me_6). ^{11}B NMR (32.08 MHz, [D$_6$]acetone, ext. $BF_3 \cdot OEt_2$): δ = 13.0, −0.8.

11a: Compound **10a** (443 mg, 632 µmol) and NaI (0.75 g, 5.0 mmol) were stirred in 20 mL of acetone for 2 h at room temperature. Removal of the acetone, extraction of the residue into OEt_2, filtration through Al_2O_3, and crystallization from CH_2Cl_2 afforded 84 mg (33%) of **11a**.

10b, 11b: $[(\eta^5\text{-}C_5Me_5)IrCl_2]_2$ [11b] in 20 mL of acetone, $AgBF_4$ (390 mg, 2.00 mmol) in 30 mL of acetone, and **8** (264 mg, 1.00 mmol) were treated as described for **10a, 11a**. NaI (1.5 g, 10 mmol) was then added and the resulting solution was stirred for an additional 20 h at room temperature. Workup as described for **11a** gave 156 mg (33%) of **11b** as colorless plates m.p. 158–160 °C [12]. **10b**: ^1H NMR (80 MHz, [D$_6$]acetone, int. TMS): δ = 7.9 (m, $2H_o$), 7.5 (m, $2H_m + H_p$), 6.17 (s, Cp), 6.46 (m, borole H−3,4), 5.35 (m, borole H−2,5, N = 3.2 Hz), 1.88 (s, C_5Me_5). ^{11}B NMR (32.08 MHz, [D$_6$]acetone, ext. $BF_3 \cdot OEt_2$): δ = 13, −0.5. **11b**: ^1H NMR (80 MHz, [D$_6$]acetone, int. TMS): δ = 7.42 (m, $2H_o$), 7.16 (m, $2H_m + H_p$), 4.77 (m, borole H−3,4), 3.89 (m, borole H−2,5, N = 5.0 MHz), 1.88 (s, C_5Me_5). ^{11}B NMR (32.08 MHz, [D$_6$]acetone, ext. $BF_3 \cdot OEt_2$): δ = 11.9.

Received: February 10, 1989 [Z 3168 IE]
German version: *Angew. Chem. 101* (1989) 798

CAS Registry numbers:
3, 118657-25-3; **4**, 20686-87-5; **5**, 120686-88-6; **6**, 120711-19-5; **7**, 120686-89-7; **8**, 111800-73-8; **9a**, 101810-21-3; **9b**, 96097-01-7; **10a**, 120686-91-1; **10b**, 120711-21-9; **11a**, 112198-52-4; **11b**, 120741-62-0; $ReBr(NCMe)_2(CO)_3$, 28862-30-8; $[(\eta^6\text{-}C_6Me_6)RuCl_2]_2$, 67421-02-7; $[(\eta^5\text{-}C_5Me_5)IrCl_2]_2$, 12354-84-6.

[1] G. E. Herberich, I. Hausmann, N. Klaff, *Angew. Chem. 101* (1989) 328; *Angew. Chem. Int. Ed. Engl. 28* (1989) 319.
[2] P. E. Garrou, *Adv. Organomet. Chem. 23* (1984) 95; A. Efraty, *J. Organomet. Chem. 57* (1973) 1; H. Werner, *Fortschr. Chem. Forsch. 28* (1972) 141; A. Z. Rubezhov, S. P. Gubin, *Adv. Organomet. Chem. 10* (1972) 347.
[3] a) P. M. Maitlis, M. L. Games, *J. Am. Chem. Soc. 85* (1963) 1887; b) P. M. Maitlis, *Adv. Organomet. Chem. 4* (1966) 95.
[4] H. Werner, *Angew. Chem. 89* (1977) 1; *Angew. Chem. Int. Ed. Engl. 16* (1977) 1; $[(\mu\text{-}\eta^3\text{-}2\text{-}MeC_3H_4)(\mu\text{-}Cp)\{Pd(PPh_3)\}](Pd\text{-}Pd)$: H. Werner, D. Tune, G. Parker, C. Krüger, D. J. Brauer, *ibid. 87* (1975) 205 and *14* (1975) 185; $[(\mu\text{-}C_6H_6)_2 \cdot \{Pd(Al_2Cl_7)\}_2]$ (*Pd-Pd*): G. Allegra, A. Immirzi, L. Porri, *J. Am. Chem. Soc. 87* (1965) 1394.
[5] G. E. Herberich, B. Heßner, D. P. J. Köffer, *J. Organomet. Chem. 362* (1989) 243.
[6] M. F. Farona, K. F. Kraus, *Inorg. Chem. 9* (1970) 1700.
[7] G. E. Herberich, B. Heßner, R. Saive, *J. Organomet. Chem. 319* (1987) 9.
[8] The fate of the cleaved fragment is not known.
[9] a) M. A. Bennett, T. W. Matheson, G. B. Robertson, W. L. Steffen, T. W. Turney, *J. Chem. Soc. Chem. Commun. 1979*, 32; b) M. A. Bennett, T. W. Matheson, G. B. Robertson, A. K. Smith, P. A. Tucker, *Inorg. Chem. 19* (1980) 1014.
[10] G. E. Herberich, W. Boveleth, B. Heßner, M. Hostalek, D. P. J. Köffer, M. Negele, *J. Organomet. Chem. 319* (1987) 311.
[11] a) C. White, S. J. Thompson, P. M. Maitlis, *J. Chem. Soc. Dalton Trans. 1977*, 1654; b) J. W. Kang, K. Moseley, P. M. Maitlis, *J. Am. Chem. Soc. 91* (1969) 5970.
[12] Suitable C, H analyses were obtained.

Complete Identification of C–C Connectivities by Two-Dimensional INADEQUATE NMR Spectroscopy with Composite Pulses

By *Jörg Lambert, Hans Jochen Kuhn, and Joachim Buddrus* *

Two-dimensional INADEQUATE NMR spectra (*I*ncredible *N*atural *A*bundance *D*ouble *Qua*ntum *T*ransfer *E*xperiment)[1, 2] allow a direct and unambiguous elucidation of C–C connectivities and have become an important tool for determining constitutions of organic molecules.[3] The wide use of this technique, however, has been opposed not only by its low sensitivity but also by the fact that satellite signals belonging to large double-quantum frequencies are often of very weak intensity ("off-resonance" effects). We report here a modified 2D INADEQUATE experiment that avoids these intensity drawbacks.

Off-resonance effects are due to a high-frequency field strength B_1 that, compared with the width of the ^{13}C frequency range f, is too small ($\gamma B_1/2\pi < f$, cf. Ref. [4]); they

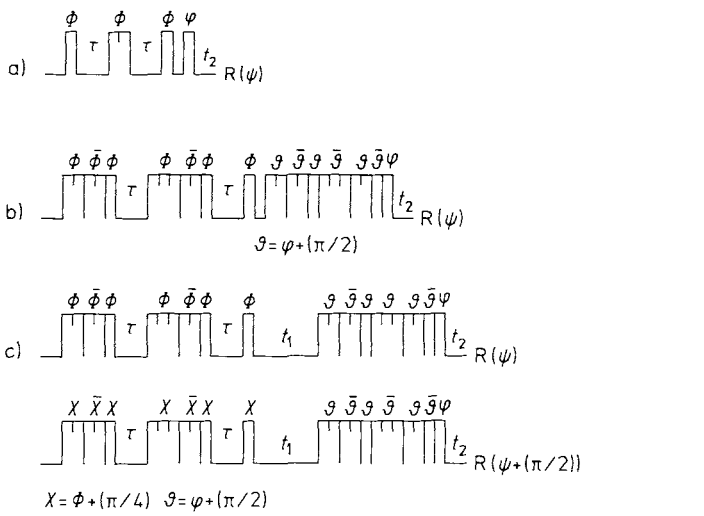


Fig. 1. INADEQUATE pulse sequences. Rectangles with zero, one, and two "cuts" symbolize 90°, 180°, and 270° pulses, respectively. Φ, φ, ϑ, χ, and ψ give the phases of the transmitter and receiver R; bars over the phase symbols (e.g., $\bar{\Phi}$) indicate inverted phases. The phases have fixed relationships to one another. $\tau = 1/(4J(c, c))$; t_2 = acquisition time. a) One-dimensional experiment, simple pulses; for phase relationship see [3]. b) One-dimensional experiment, composite pulses. c) Two-dimensional experiment, composite pulses. The FIDs of the two pulse sequences are added.

[*] Prof. Dr. J. Buddrus, Dr. J. Lambert
Institut für Spektrochemie und angewandte Spektroskopie
Bunsen-Kirchhoff-Strasse 11, D-4600 Dortmund 1 (FRG)
Dr. H. J. Kuhn
Max-Planck-Institut für Strahlenchemie
Stiftstrasse 34–36, D-4330 Mühlheim an der Ruhr (FRG)

are especially noticeable in an INADEQUATE experiment, since, in this case, pulses are applied to two ^{13}C nuclei.[5, 6] To eliminate the off-resonance effects, composite pulses have been suggested and were used in a *one-dimensional* version of the INADEQUATE experiment.[5, 7] These sequences also compensate for inhomogeneities in the B_1 field, which especially appear when concentrated solutions of ionic compounds are employed.[8]

Two-dimensional INADEQUATE NMR spectra, which are of incomparably greater value in determining constitutions, may be obtained with quadrature detection in the f_1 dimension either by the method of *Bax* et al.[1] or by that of *Mareci* and *Freeman*.[2] The former approach involves inserting a 45_z° pulse into the delay time t_1; the latter uses a read pulse $\alpha \neq 90^\circ$ (e.g., 135°). The second method is ca. 20% more sensitive, but its application with composite pulses is difficult owing to the required 135° pulse.[9] We therefore chose the first method for establishing a pulse sequence made up of composite pulses—although the likewise off-resonance-sensitive 45_z° pulse was replaced with a 45° phase shift of the first three pulses in the experiment (Fig. 1).

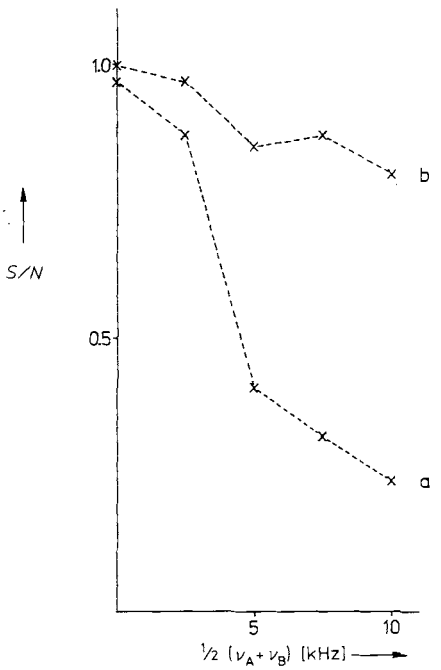
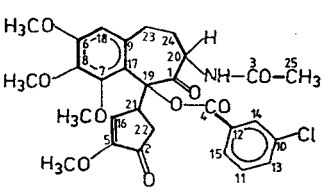


Fig. 2. Signal/noise ratio (S/N) of the satellite signals generated by the 2D INADEQUATE experiment performed on 2-butanol as a function of the offset parameter $(\nu_A + \nu_B)/2$ [12]. Length of the 90° pulse, 25 μs (10-mm probe head). Curve a obtained by the pulse sequence described in [1] with simple pulses, curve b by the pulse sequence shown in Figure 1c with composite pulses.

Figure 2 compares the experimental offset dependence of the signal intensities of the model compound 2-butanol over a range of 10 000 Hz for the 2D INADEQUATE experiment with and without composite pulses. The intensity increases by a factor of up to three when the sequence with composite pulses is used.



The sequence with composite pulses allowed elucidation of the structure of the product obtained upon oxidation of **1** with *m*-chloroperbenzoic acid followed by workup under basic conditions (Fig. 3). This product could not be identified unambiguously either by standard NMR techniques[10] or by X-ray structure analysis (unsuitable crystals).

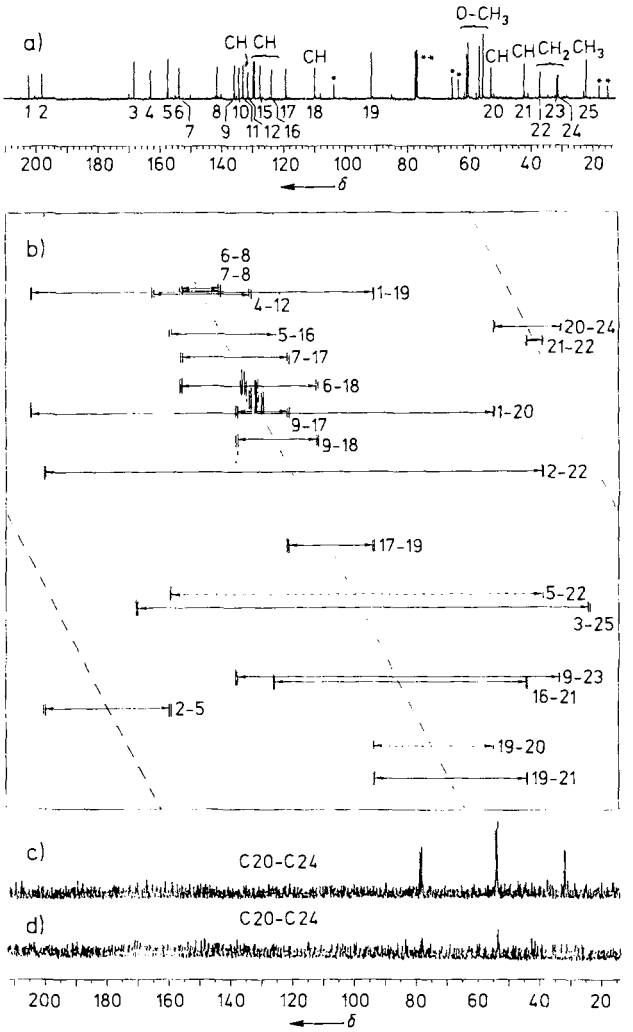


Fig. 3. 100-MHz ^{13}C NMR spectra of **2** (1.4 g) and [Cr(acac)$_3$] (15 mg) in 3.5 mL of $CDCl_3$. a) Proton-decoupled spectrum with signal assignment according to the numbering in the above formula. Signals not assigned to CH_n are due to quaternary C atoms. * = signals due to impurities; ** = signals of $CDCl_3$. b) 2D INADEQUATE NMR spectrum [13]: for pulse sequence see Figure 1c: t_1 noise of the $CDCl_3$ signal removed for clarity. c) Spectral trace of the connectivity C20–C24 from b). d) Spectral trace of the same connectivity recorded with the simple pulse sequence described in [2].

The 2D INADEQUATE NMR spectrum with composite pulses (Fig. 3b) directly shows the presence of a carbon framework corresponding to that of **2**.[11] By contrast, the 2D INADEQUATE NMR spectrum recorded with simple pulses does not reveal some C–C connectivities. The spectral traces in Figures 3c and 3d show just how large these differences can be.

Composite pulses overcome the problem of unequal signal intensities in 2D INADEQUATE NMR spectra in a striking way, even for broad frequency regions. Moreover, they result in a significant increase in sensitivity for this unsensitive technique.

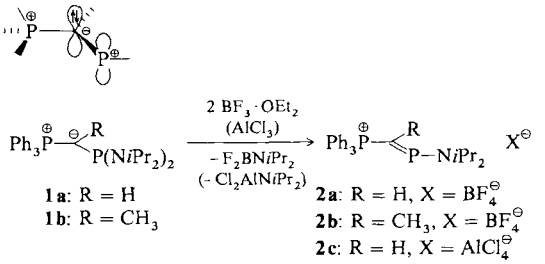
Received: December 23, 1988;
supplemented: March 9, 1989 [Z 3102]
German version: *Angew. Chem. 101* (1989) 797

[1] A. Bax, R. Freeman, T. A. Frenkiel, M. H. Levitt, *J. Magn. Reson. 43* (1981) 478.
[2] T. H. Mareci, R. Freeman, *J. Magn. Reson. 48* (1982) 158.
[3] Review: J. Buddrus, H. Bauer, *Angew. Chem. 99* (1987) 642; *Angew. Chem. Int. Ed. Engl. 26* (1987) 625.
[4] R. R. Ernst, G. Bodenhausen, A. Wokaun: *Principles of Nuclear Magnetic Resonance in One and Two Dimensions*, Oxford University Press, Oxford 1987, p. 119.
[5] M. H. Levitt, R. R. Ernst, *Mol. Phys. 50* (1983) 1109.
[6] K. V. Schenker, W. von Philipsborn, *J. Magn. Reson. 66* (1986) 219.
[7] M. H. Levitt, *Prog. Nucl. Magn. Reson. Spectrosc. 18* (1986) 61.
[8] W. E. Hull, Heidelberg, personal communication.
[9] If the suggestion of *W. E. Hull* (*Methods Stereochem. Anal. 9* (1987) 198) is taken and the last 90° pulse of the read-pulse cluster in Figure 1b is replaced by a 135° pulse, one obtains a sequence compensating for the off-resonance effects, but all satellite signals with negative frequencies appear reflected on the line $f_1 = 0$. This reflection obscures the spectrum, thus obviating much of the advantage of the two-dimensional version.
[10] J. Buddrus, A. Defoin, C. Krüger, Y.-H. Tsay, H. J. Kuhn, unpublished.
[11] The configuration could not be determined, not even from the large NOE effect (H NMR spectrum) between the methoxy group on C-5 and the methyl group on C-3.
[12] The offset parameter is equal here to half of the double-quantum frequency.
[13] $\tau = 1/(4J)$, ($J = 45$ Hz). $f_2 = 19920$ Hz (8K data points), $f_1 = 19920$ Hz (64 data points). 64 rows with 1536 accumulations each were recorded. Repeat interval 4 s (total time 4.5 days). The FID in f_2 was multiplied by an exponential function, that in f_1 by a Gauss function after zero filling to 128. The connectivity 23–24 cannot be identified, since a strongly coupled AB spin system is present; connectivities obtained from long-range couplings are shown by broken lines; the signals of the chlorophenyl moiety were assigned in part by comparison with literature values.

A New Route to Phosphaalkenes**

By *Hansjörg Grützmacher** and *Hans Pritzkow*

2-Phosphonio-substituted 1-phospha-1-alkenes[1, 2] are interesting because, formally, a phosphonium and a phosphenium ion compete in them for the electron density on the bridging carbon atom (Scheme 1).[3] We report here a new synthesis of these compounds.



Scheme 1.

The phosphonio-substituted phosphaalkenes **2a–c** are obtainable in yields of > 90% by reaction of the readily accessible phosphinomethylenetriphenylphosphoranes **1a, 1b**[4] with two equivalents of $BF_3 \cdot OEt_2$ or $AlCl_3$ in CH_2Cl_2. The ^{31}P NMR signals of the low-coordinated phosphorus atoms in **2a** and **2b**, $\delta = 303.5$ and 302.5, respectively, are characteristic of both phosphenium ions and phosphaalkenes.[5] As in the 1-(2-phosphaethenyl)-1-phosphoniaindans described by *Karsch* et al.,[11] the ^{13}C NMR signals of the bridging carbon atoms are shifted markedly to high field (**2a**, $\delta = 88.40$; **2b**, $\delta = 104.29$) – which is untypical of phosphaalkenes.

An X-ray structure investigation of **2a**[6] (Fig. 1) revealed that the length of the P1–C1 bond (1.79 Å) lies in the range

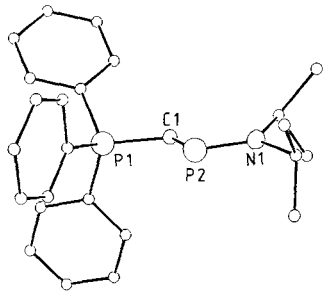
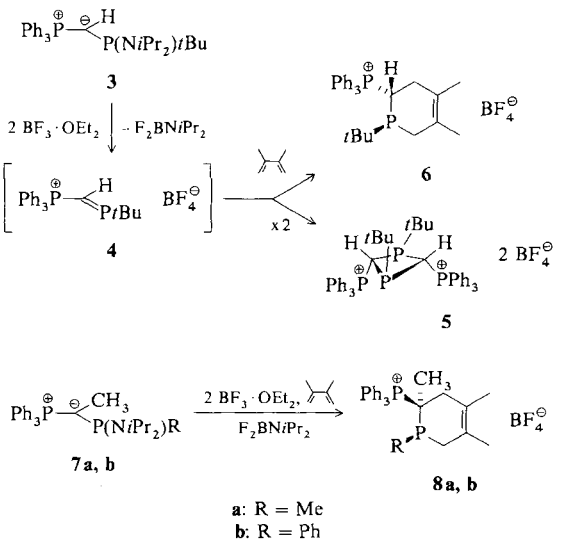


Fig. 1. Molecular structure of **2a**. Important bond lengths [Å] and angles [°]: P1-C1 1.788(14), C1-P2 1.684(14), P2-N1 1.617(13); P1-C1-P2 115.5(8), C1-P2-N1 105.3(7).

observed for P^v–$C(sp^2)$ single bonds, whereas the P2–C1 bond (1.68 Å) is much shorter and typical of phosphaalkenes.[7] The slight increase in length compared with the bonds in *P*-aryl-substituted phosphaalkenes[8] is presumably due to the conjugation of the lone pair on N1 with the P=C bond. The relatively short P2–N1 bond (1.61 Å) further supports this conjecture. In addition to the bands of the phenyl groups, the UV/VIS spectra (in CH_3CN) of **2a** and **2b** show bands for the C=P π–π^* transition at $\lambda = 307$ nm ($\varepsilon = 0.61 \times 10^3$ L mol^{-1} cm^{-1}) and 316 nm (2.4×10^3 L mol^{-1} cm^{-1}), respectively. The phosphaalkenes with coplanar amino substituents on phosphorus that *Gudat* and *Niecke* synthesized and investigated by UV/VIS spectroscopy are excited in the same wavelength region (e.g., $(Me_3Si)_2C{=}P{-}NiPr_2$, 307 nm; $(Me_3Si)_2C{=}P{-}NMe_2$, 317 nm).[9]

An attempt to synthesize the *P*-alkyl-substituted derivative **4** was unsuccessful – instead, the head-to-tail dimer **5** was obtained and characterized by NMR spectroscopy and X-ray structure analysis.[10] 1,3-Diphosphetanes are well



Scheme 2.

[*] Dr. H. Grützmacher, Dr. H. Pritzkow
Anorganisch-chemisches Institut der Universität
Im Neuenheimer Feld 270, D-6900 Heidelberg (FRG)

[**] This work was supported by the Deutsche Forschungsgemeinschaft and the Fonds der Chemischen Industrie. *H.G.* thanks Prof. Dr. *W. Sundermeyer* for financial support.

known as dimerization products of phosphaalkenes.[11] The intermediacy of **4** was confirmed by trapping experiments with 2,3-dimethylbutadiene; the product **6**, formed by [2 + 4] cycloaddition to the P=C bond, was obtained in nearly quantitative yield.[12] Similarly, the reaction of **7a, b** with $BF_3 \cdot OEt_2$ in the presence of 2,3-dimethylbutadiene in excess leads to the heterocycles **8a** and **8b**. However, the reaction of **7b** is not uniform. Loss of F_2BPh, instead of F_2BNiPr_2, results in the formation of **2b** as a side product. Compounds **6, 8a**, and **8b**[13] are formed as racemates with no observed formation of diastereomers. This finding supports a concerted [2 + 4] cycloaddition. Compounds **2a** and **2b** do not react with 2,3-dimethylbutadiene under the conditions described here. Moreover, products of a [1 + 4] cycloaddition were not observed.[14]

The bonding parameters obtained from a structure investigation and the data derived from the UV/VIS spectra of **2a** and **2b**, as well as the reactivity of compounds **4, 7a**, and **7b**, are similar to those of previously reported phosphaalkenes. The syntheses described here offer attractive variants for the synthesis of phosphaalkenes, since the phosphinomethylenetriphenylphosphoranes required as starting materials are readily accessible and widely variable.

Received: January 24, 1989 [Z 3139 IE]
German version: *Angew. Chem. 101* (1989) 768

[1] H. H. Karsch, H.-U. Reisacher, G. Müller, *Angew. Chem. 98* (1986) 467; *Angew. Chem. Int. Ed. Engl. 25* (1986) 454.
[2] G. Becker, W. Becker, R. Knebl, H. Schmidt, U. Hildenbrandt, M. Westerhausen, *Phosphorus Sulfur 30* (1987) 349.
[3] Theoretical analysis of the bonding in phosphorus ylides and phosphaalkenes: M. M. Francl, R. C. Pellow, L. C. Allen. *J. Am. Chem. Soc. 110* (1988) 3723.
[4] K. Issleib, R. Lindner, *Justus Liebigs Ann. Chem. 699* (1966) 40; H. Schmidbauer, *Adv. Organomet. Chem. 9* (1970) 259.
[5] J. G. Verkade, L. D. Quin (Eds.): *Methods in Stereochemical Analysis, Vol. 8*, VCH Verlagsgesellschaft, Weinheim 1987.
[6] **2a**: $Pbn2_1$; $a = 9.225(5)$, $b = 15.097(9)$, $c = 19.419(12)$ Å, $V = 2704$ Å^3, $Z = 4$. 1035 observed reflections with $I > 2\sigma(I)$ (four-circle diffractometer, $Mo_{K\alpha}$ radiation, ω scan). $R = 0.089$, $R_w = 0.048$ (P refined anisotropically, F, N, C, B isotropically; the disordered anion refined with two rigid BF_4 tetrahedrons, the methyl groups and phenyl rings as rigid groups with a common temperature factor for the H atoms). Further details of the crystal structure investigation may be obtained from the Fachinformationszentrum Karlsruhe, Gesellschaft für wissenschaftlich-technische Information, D-7514 Eggenstein-Leopoldshafen 2 (FRG), on quoting the depository number CSD-53721, the names of the authors, and the journal citation.
[7] R. Appel, F. Knoll, I. Ruppert, *Angew. Chem. 93* (1981) 771; *Angew. Chem. Int. Ed. Engl. 20* (1981) 771.
[8] A. H. Cowley, R. A. Jones, J. G. Lasch, N. C. Norman, C. A. Stewart, A. L. Stuart, J. L. Atwood, W. E. Hunter, H.-M. Zhang, *J. Am. Chem. Soc. 106* (1984) 7015.
[9] D. Gudat, *Dissertation*, Universität Bielefeld 1987; D. Gudat, E. Niecke, *Phosphorus Sulfur 30* (1987) 796.
[10] L. Zsolnai, G. Huttner, unpublished.
[11] G. Becker, W. Uhl, *Z. Anorg. Allg. Chem. 475* (1981) 35; R. Appel, V. Winkhaus, F. Knoch, *Chem. Ber. 119* (1986) 2466, and references cited therein.
[12] R. Appel, F. Knoch, R. Zimmermann, *Chem. Ber. 118* (1985) 814; R. Appel, J. Menzel, F. Knoch, *ibid 118* (1985) 4068.
[13] General experimental procedure: The respective phosphinomethylenetriphenylphosphorane (**1a,b, 3, 7a,b**; 5 mmol), was dissolved in 30 mL of dry CH_2Cl_2 and treated at -78 °C with 1.13 mL of freshly distilled $BF_3 \cdot OEt_2$ (10 mmol) in ether. In the cycloaddition reactions, 2,3-dimethylbutadiene (2.1 g, 25 mmol) was then added. The reaction solution was warmed to room temperature, the volatiles were removed at 0.01 torr, and the residue was washed with ether and recrystallized from CH_2Cl_2/ether. **2a**: m.p. 146 °C. $^{31}P\{^1H\}$ NMR (36.19 MHz, $CDCl_3$, 27 °C): $\delta = 19.5$ (d, PPh_3); 303.5 (d, PN, $^2J = 124.6$ Hz). ^1H NMR (89.99 MHz, $CDCl_3$, 27 °C): $\delta = 1.25$ (d, 12H, CH_3, $^3J = 6.6$ Hz); 3.75–4.46 (m, 2H, CH); 6.41 (dd, 1H, CH, $^2J(P^{III}H) = 10.7$, $^2J(P^VH) = 1.7$ Hz); 7.49–7.60 (m, 15H, arene-CH). $^{13}C\{^1H\}$ NMR (22.49 MHz, $CDCl_3$, 25 °C): $\delta = 20.96$ (s, CH_3); 25.87 (s, CH_3); 51.25 (s, CH); 52.76 (s, CH); 88.40 (dd, CH, $^1J(P^{III}C) = 92.5$, $^1J(P^VC) = 34.3$ Hz); 121.58 (d, *ipso*-C, $^1J(P^VC) = 89.4$ Hz); 129.72 (d, *m*-C, $^3J(P^VC) = 12.5$ Hz); 133.2 (d, *o*-C, $^2J(P^VC) = 10.1$ Hz), 134.2 (s, *p*-C). **2b**: m.p. 143 °C. $^{31}P\{^1H\}$ NMR (36.19 MHz, $CDCl_3$, 27 °C): $\delta = 28.5$ (d, PPh_3), 302.5 (d, PN, $^2J = 168.6$ Hz). ^1H NMR (89.99 MHz, $CDCl_3$, 27 °C): $\delta = 1.11$ (d, 12H, CH_3, $^3J = 6.9$ Hz); 2.15 (dd, 3H, CH_3, $^3J(P^VH) = 17$, $^3J(P^{III}H) = 7.2$ Hz); 4.03 (sept., 2H, CH, $^3J = 6.9$ Hz); 7.46–7.55 (m, 15H, arene-CH). $^{13}C\{^1H\}$ NMR (22.49 MHz, $CDCl_3$, 27 °C: $\delta = 19.02$ (dd, CH_3, $^2J(P^VC) = 8.8$, $^2J(P^{III}C) = 3.0$ Hz); 24.16 (d, CH, $^3J(P^{III}C) = 7.4$ Hz); 51.37 (d, CH, $^2J(P^{III}C) = 6.1$ Hz); 104.29 (dd, CCH_3, $^1J(P^{III}C) = 76.2$, $^1J(P^VC) = 68.9$ Hz) 119.79 (dd, *ipso*-C, $^1J(P^VC) = 89.4$, $^3J(P^{III}C) = 7.3$ Hz); 129.45 (d, *m*-C, $^3J(P^VC) = 13.2$ Hz); 133.64 (d, *o*-C, $^2J(P^VC) = 13.2$ Hz); 133.83 (s, *p*-C). **5**: m.p. 249 °C. $^{31}P\{^1H\}$ NMR (36.19 MHz, CD_3CN 27 °C): $\delta = 21.42$ (m, AA'XX' system). ^1H NMR (89.99 MHz, CD_3CN, 27 °C): $\delta = 0.43-0.57$ (m, 18H, CH_3); 3.5 (m, 2H, CH); 7.34–7.75 (m, 30H, arene CH). **6**: m.p. 166–167 °C. $^{31}P\{^1H\}$ NMR (36.19 MHz, $CDCl_3$, 27 °C): $\delta = -25.2$ (d, P*t*Bu); 24.76 (d, PPh_3, $^2J = 80.6$ Hz). **8a**: m.p. 193 °C. $^{31}P\{^1H\}$ NMR (36.19 MHz, CD_3CN, 27 °C): $\delta = -24.8$ (d, PCH_3); 36.3 (d, PPh_3, $J = 95.1$ Hz). **8b**: $^{31}P\{^1H\}$ NMR (36.19 MHz, $CDCl_3$, 0 °C): $\delta = -20.97$ (d, PPh); 31.2 (d, PPh_3, $^2J = 85.3$ Hz).
[14] E. Niecke, D. Gudat, W. W. Schoeller, P. Rademacher, *J. Chem. Soc. Chem. Commun. 1985*, 1050; V. D. Romanenko, A. B. Drapailo, A. V. Ruban, L. N. Markovskii, *Zh. Obshch. Khim. 57* (1987) 1402; *J. Gen. Chem. USSR (Engl. Transl.) 57* (1987) 1253.

On the Structure of Eumelanins: Identification of Constitutional Patterns by Solid-State NMR Spectroscopy**

By *Martin G. Peter** and *Hans Förster*

Melanins are complex polyphenolic polymers. They are usually formed in nature by enzyme-catalyzed oxidative polymerization of *o*-diphenols (for reviews, see Refs. [1–3]). The deep black eumelanins, derived from Dopa **1** or dopamine **3**, are distinguished from the yellow to brown phaeomelanins obtained from Dopa in the presence of cysteine. Characteristic of eumelanins are the indole units, which are formed from catecholamines by intramolecular addition of the amino groups to the oxidatively generated *o*-quinones (Fig. 1). During polymerization of these indoles, C–C and C–O bonds are formed by nucleophilic additions and by oxidative radical phenol couplings. Allomelanins are polyarenes obtained from nitrogen-free catechols.

In contrast to Dopa-melanin, dopamine-melanin is basic in character and is capable of being benzoylated to a greater extent than Dopa-melanin.[1] According to *Swan*,[2] Dopamelanin has the following statistical composition (Fig. 1): ca. 10% **1** and **2**, ca. 10% **7** and **9**, ca. 65% **11** and **12**, and ca. 15% pyrrolecarboxylic acids. Dopamine-melanin contains ca. 35% **3** and **4**, ca. 55% **11, 12, 8,** and **10**, and ca. 10% pyrrolecarboxylic acid units. The latter are not shown in Figure 1 (cf. Refs. [1, 2, 5]). The relative amounts of noncyclic units in Dopa- and dopamine-melanin correspond roughly to the ratio of the rate constants k_c of the cyclization (Dopa, $k_c = 72$ s^{-1};[6] dopamine, $k_c = 25.6$ s^{-1}[7]). The rates of rearrangement of dopachrome **9** and dopaminochrome **10** to 5,6-dihydroxyindole **11** have not yet

[*] Prof. Dr. M. G. Peter
Institut für Organische Chemie und Biochemie
der Universität
Gerhard-Domagk-Strasse 1, D-5300 Bonn 1 (FRG)
Dr. H. Förster
Bruker Analytische Meßtechnik GmbH
Silberstreifen, D-7512 Rheinstetten 4 (FRG)

[**] This work was supported by the Deutsche Forschungsgemeinschaft and the Fonds der Chemischen Industrie.

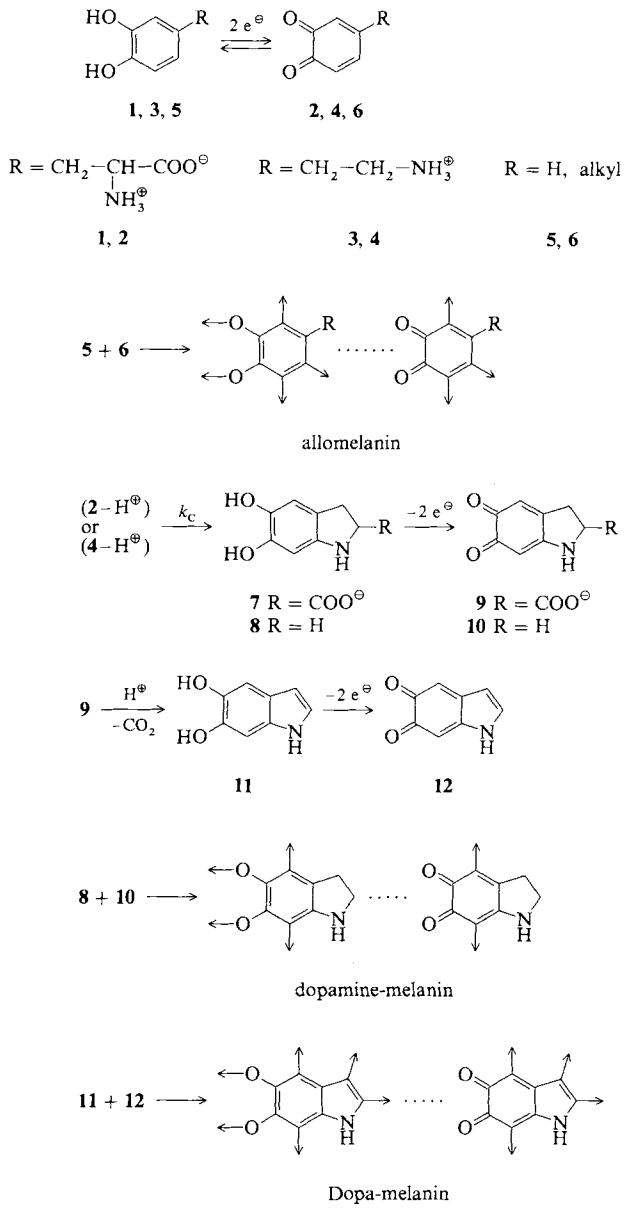


Fig. 1. Schematic drawing of the formation of melanins from catechols.

been determined to the best of our knowledge. In basic to neutral media, however, the decarboxylation of the dihydroindole should proceed faster than the deprotonation. The dopamine-melanin generated at pH 7 should therefore consist to a larger extent of dopamine and dihydroindole units than of indole units.

These conclusions are confirmed by solid-state ^{13}C NMR spectra. We prepared Dopa- and dopamine-melanin by oxidation of Dopa and dopamine, respectively, with excess $K_3[Fe(CN)_6]$ in water. The elemental analysis (double determination) gave the following results for Dopa-melanin: $49.02 \pm 0.03\%$ C, $3.71 \pm 0.01\%$ H, and $8.29 \pm 0.03\%$ N ($C_9H_{8.15}N_{1.30}$). For dopamine-melanin, the values were $50.83 \pm 0.11\%$ C, $4.20 \pm 0.03\%$ H, and $9.52 \pm 0.01\%$ N ($C_8H_{7.92}N_{1.28}$).

The CP/MAS ^{13}C NMR spectrum of Dopa-melanin is shown in Figure 2b. The signal assignment given in Table 1 was made by comparison with the solid-state ^{13}C NMR spectrum of Dopa (Fig. 2a).

In the aliphatic region, the side-chain C atoms of the Dopa units and C2 of the dihydroindole units can also be identified upon improvement of the resolution by Gauss modification.

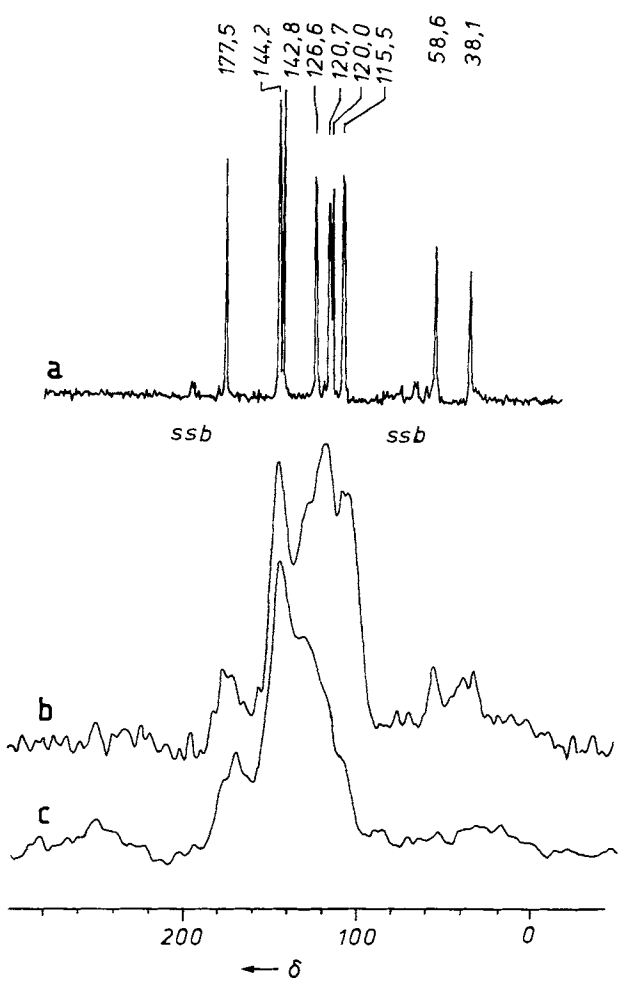


Fig. 2. CP/MAS ^{13}C NMR spectra of a) Dopa, b) Dopa-melanin, and c) Dopa-melanin recorded with an NQS sequence using 60-μs delay times; $^1H-^{13}C$ cross-polarization with sample rotation around the magic angle; spin frequency 5.19 kHz; decoupling field strength 20 G; contact time 500 μs; 1606 accumulations at 297 K; rotation side bands (SSB) were largely suppressed.

Table 1. Assignment of the signal groups in the CP/MAS ^{13}C NMR spectrum of Dopa-melanin (Fig. 2b).

δ	Assignment
175	Carboxyl and quinoid carbonyl C atoms
144	Diphenolic phenoxy C atoms
127–116	Arene *C*-H and *C*-C; C2, C3a, C4, and C6a of indole units
107–104	C3 of indole and pyrrole units
54, 36, and 31	Side-chain C atoms of noncyclized Dopa and C2 of dihyroindole units

If the resonances of non-quaternary C atoms are suppressed with an NQS sequence, the signals in the aliphatic region as well as those of the respective indole and pyrrole C atoms at $\delta = 107-104$ disappear (Fig. 2c). In the region of the arene C atoms, a decrease in intensity is observed owing to the suppression of the resonances of the unsubstituted phenyl and indole C atoms. Thus, the partial structures contained in the constitutional scheme of Dopa-melanin are unambiguously confirmed by the solid-state ^{13}C NMR spectrum.

The CP/MAS ^{13}C NMR spectrum of dopamine-melanin, shown in Figure 3b, differs markedly from that of Dopa-melanin (cf. Fig. 2b). Owing to the absence of carboxyl groups in the starting material, the carbonyl resonances ($\delta \approx 170$) are weaker than in Dopa-melanin. The C-3 signals of the unsubstituted indole and pyrrole units can hardly be

identified for dopamine-melanin. The intense aliphatic signals correlate unambiguously with the side-chain C atoms of dopamine (Fig. 3a); the signal of dihydroindole C2, expected at $\delta \approx 46$, is not resolved. Suppression of non-quaternary C atoms affords a spectrum very similar to that of the NQS spectrum of dopa-melanin (Fig. 3c).

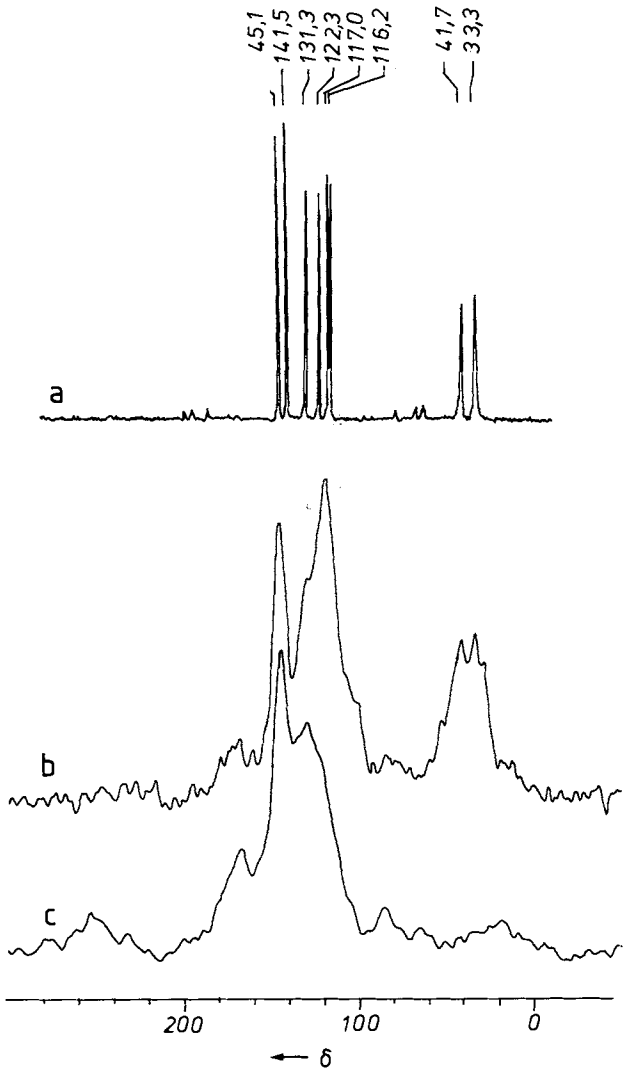


Fig. 3. CP/MAS ^{13}C NMR spectra of a) dopamine (hydrochloride), b) dopamine-melanin, and c) dopamine-melanin recorded with an NQS sequence using 60-μs delay times. For measuring parameters, see Figure 2.

Comparison of the relative intensities of individual groups of signals in the spectra of the monomeric precursor and the polymer reveal that dopamine-melanin contains a much larger proportion of unmodified side chains compared with Dopa-melanin. Accordingly, dopamine-melanin is formed to a correspondingly greater extent by polymerization of the open-chain precursors **3** and **4** (Fig. 1) and contains substructures of the allomelanin type (cf. the polymerization of **5** and **6** in Fig. 1). In addition, constitutional patterns resulting from copolymerization of **3** and **4** with **8, 10, 11,** and **12** are present to a lesser extent. In Dopa-melanin, on the other hand, the polymerization of **11** with **12** predominates.

The solid-state ^{13}C NMR spectra also allow an estimate of the oxidation state of the polymer. Comparison of the intensities of the carbonyl and the diphenolic phenoxy C signals reveals a high proportion of catechol units; this indicates that the polymerization occurs by oxidative phenol couplings.

Duff et al.[8] recently described CP/MAS ^{13}C and ^{15}N NMR spectra of autooxidatively generated Dopa-melanin as well as of melanoma- and sepia-melanin, isolated from biological material. The signal assignments largely agree with those in Figure 2b discussed here. However, the indole, pyrrole, and dihydroindole units in the spectrum published in Ref. [8] are not unambiguously identifiable owing to the comparatively low resolution. In the CP/MAS ^{15}N NMR spectrum, on the other hand, signals for aliphatic amino groups are present.

The CP/MAS ^{13}C NMR spectrum of melanin generated enzymatically from tyrosine with tyrosinase (monophenol monooxygenase, EC 1.14.18.1) agrees qualitatively with Figure 2b, although the carboxyl/carbonyl signals in tyrosine-melanin are more intense. The signals of the phenoxy C atoms at $\delta \approx 145$ are less intense than those of the other arene C atoms. However, indole C3 atoms and pyrrole C atoms can be unambiguously identified. The CP/MAS ^{13}C NMR spectrum of a phaeomelanin, prepared by oxidation of a mixture of Dopa and cysteine with $K_3[Fe(CN)_6]$, is characterized above all by the prominent carboxyl signal and the signals of the aliphatic amino-acid C atoms.

The results show that solid-state NMR spectroscopy is very suitable for nondestructive investigation of complex biopolymers. The analysis of the constitutional pattern not only leads to new insights into structural relationships, but also is essential for the assignment of unknown polyphenolic natural products to specific melanin classes.

Experimental Procedure

Preparation of Dopa-melanin: A solution of L-Dopa (1.0 g, 5.07 mmol) and $K_3[Fe(CN)_6]$ (8 g, 23.4 mmol) in 1 L of H_2O was adjusted to pH 8 with ca. 2 N KOH and then stirred vigorously in an open Erlenmeyer flask at 22 °C. After 7 h, the reaction mixture was acidified with 10 mL of conc. HCl. The black melanin that settled out was centrifuged off and washed thoroughly with 10 × 50 mL of H_2O. It was then suspended in H_2O and lyophilized. Yield: 897 mg Dopa-melanin. Dopamine-melanin was synthesized similarly.

Received: January 5, 1989 [Z 3113 IE]
German version: *Angew. Chem. 101* (1989) 753

[1] R. A. Nicolaus: *Melanins*, Hermann, Paris 1968.
[2] a) G. A. Swan, *Fortschr. Chem. Org. Naturst. 31* (1974) 521; b) R. H. Thomson, *Angew. Chem. 86* (1974) 355; *Angew. Chem. Int. Ed. Engl. 13* (1974) 305.
[3] M. G. Peter, *Angew. Chem. 101* (1989) 572; *Angew. Chem. Int. Ed. Engl. 28* (1989) 555.
[4] P. Palumbo, M. d'Ischia, O. Crescenzi, G. Prota, *Tetrahedron Lett. 28* (1987) 467.
[5] R. M. B. Deibel, M. R. Chedekel, *J. Am. Chem. Soc. 106* (1984) 5884.
[6] T. E. Young, J. R. Griswold, M. H. Hulbert, *J. Org. Chem. 39* (1974) 1980.
[7] T. E. Young, B. W. Babbitt, *J. Org. Chem. 48* (1983) 562.
[8] G. A. Duff, J. E. Roberts, N. Foster, *Biochemistry 27* (1988) 7112.

$[Et_4N]_6[Na_{14}Mo_{24}P_{17}O_{97}(OH)_{31}] \cdot xH_2O$: A Hollow Cluster Filled with 12 $Na^{\oplus}$ Ions and a H_3PO_4 Molecule

By *Robert C. Haushalter** and *Frank W. Lai*

Dedicated to Professor Hans Bock on the occasion of his 60th birthday

Compared to the solid-state layer and tunnel structures composed of either all octahedral or all tetrahedral building blocks, relatively little attention has been given to solids built up from octahedral-tetrahedral frameworks.[1] During our

[*] Dr. R. C. Haushalter, F. W. Lai
Exxon Research and Engineering Co.
Annandale, NJ 08801 (USA)

recent investigations of the factors affecting framework formation and stability in the mixed octahedral-tetrahedral system M-Mo-P-O (M = metal cation) in the solid-state compounds built up from MoO_6 octahedra and PO_4 tetrahedra, we and others discovered a large number of new tunnel or layer structures. These compounds include $Cs_2Mo_4P_6O_{26}$,[2] $Cs_4Mo_8P_{12}O_{52}$,[2] $AgMo_5P_8O_{33}$,[3] $CsMoP_2O_7$,[4] $Cs_4Mo_{10}P_{18}O_{66}$,[5] $Cs_4Mo_6P_{10}O_{38}$,[6] and $Mo_3P_5SiO_{19}$[7] as well as metal–metal-bonded $[Mo_4O_4]^{6\oplus}$ cubes in $Cs_3Mo_5P_6O_{25}$[8] and $Cs_3Mo_4P_3O_{16}$,[9] all of which contain Mo in an oxidation state less than + 6. Since these reduced molybdenum phosphates formed so readily in the solid state, we were interested to see if similar species could exist in solution.

The chemistry of molybdenum in phosphoric acid solution is dominated by the familiar heteropolymolybdates, Keggin-type anions, and other species with Mo in an oxidation state

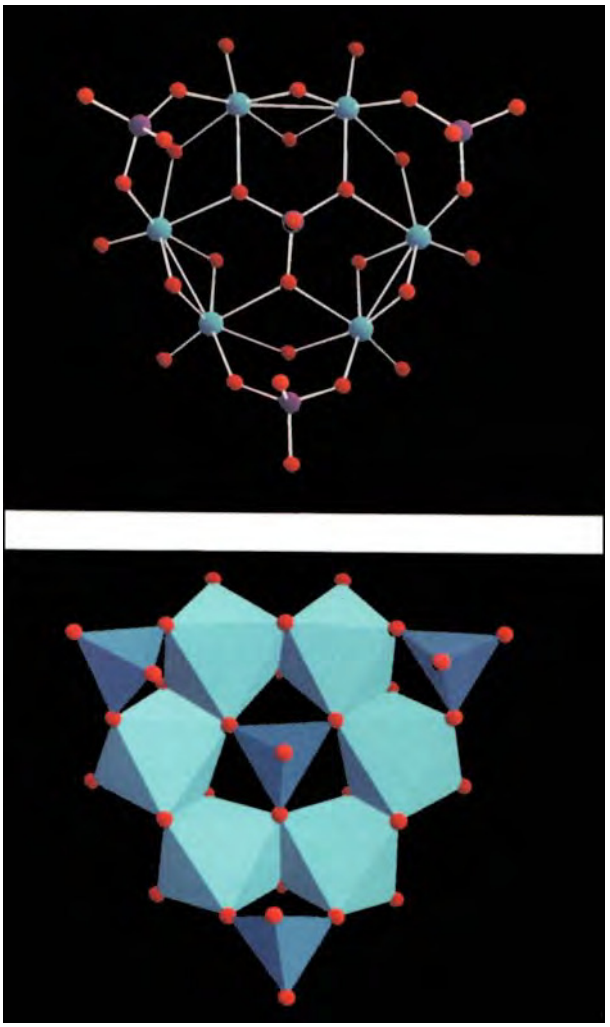


Fig. 1. Chem-X representation [16] of the $[Mo_6P_4O_{24}(OH)_7]^{5\ominus}$ ion perpendicular to the plane defined by the six Mo atoms. Top: Ball-and-stick model. O, red; P, violet; Mo, light blue. Bottom: Polyhedral representation, emphasizing the edge-sharing octahedra. MoO_6 octahedra, light blue; PO_4 tetrahedra, dark blue; O, red.

near + 6,[10] but at least one low-valent molybdenum phosphate with a Mo–Mo bond[11] is known. We have found that if the oxidation state of Mo is maintained at + 5 or below, several novel reduced molybdenum phosphates can be isolated from phosphoric acid solution. The synthesis and structure of one such phosphate, **1**,[12] a hollow cluster enclosing twelve $Na^{\oplus}$ ions and a phosphoric acid molecule, is described here.

$[Et_4N]_6[Na_{14}Mo_{24}P_{17}O_{97}(OH)_{31}] \cdot xH_2O$ **1**

Hydrothermal treatment of a mixture of Na_2MoO_4, Mo, Et_4NOH, H_3PO_4, and H_2O in a mole ratio of 2:1:2:6:100 (200 °C, 3 d) gives, in addition to some unreacted Mo metal, a >90% yield (based on sodium molybdate) of dark red crystals of **1**. Compound **1** was identified by a single-crystal

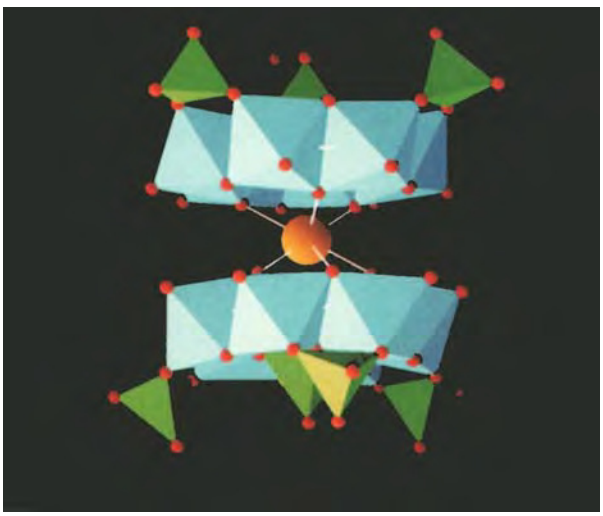


Fig. 2. Structure of the $Na^{\oplus}$-bridged dimer of $[Mo_6P_4O_{24}(OH)_7]^{5\ominus}$. MoO_6 octahedra, light blue; PO_4 tetrahedra, green; $Na^{\oplus}$, yellow.

X-ray diffraction study combined with subsequent comparison of the powder X-ray diffraction pattern of the bulk sample with the simulated pattern generated from the coordinates of the single-crystal data. Without the presence of the Mo metal, the familiar heteropolymolybdates are the major Mo-containing species obtained.

The solid-state structure of **1** is interesting because of the unique $[Na_{12}Mo_{24}P_{17}O_{97}(OH)_{31}]^{8\ominus}$ clusters present as well as an unusual motif of intersecting, $Et_4N^{\oplus}$-filled tunnels. The basic structural building block in **1** is the novel anion **2**,

$[Mo_6P_4O_{24}(OH)_7]^{5\ominus}$ **2**

which is shown in Figure 1 and consists of six MoO_6 octahedra, each containing an Mo=O group and sharing two edges with neighboring octahedra (Fig. 1). This $[\mu^2\text{-O–Mo=O}]_2$ unit is commonly found with $Mo^{5\oplus}$ coordinated to oxo ligands.[13] Mo–Mo single bonds (2.59 Å) alternate with nonbonding Mo···Mo contacts (3.55 Å). The unique central phosphate group has one terminal OH and provides three μ^3 oxygens that bridge the bonding Mo···Mo contacts, while the remaining three PO_4 groups each have two terminal OH groups and span the nonbonding Mo–Mo contacts.

In **1**, and other molybdenum phosphates,[6] the anion **2** is bonded to another identical anion via an octahedrally coordinated $Na^{\oplus}$ ion to give a dimer of Mo_6 subunits (Fig. 2) with the $Na^{\oplus}$ ion enclosed by an octahedron of oxygen atoms and shielded from the external environment by the twelve intermeshing Mo=O groups. Note that all of the PO_4 groups lie on one side of the plane defined by the six Mo atoms (Fig. 2).

The three-dimensional structure[14] of **1** is built up in the cubic space group $Pn\bar{3}$ from the dimers as follows: four different dimers are bound to each other through one end into a complicated hydrogen-bonded pattern and are centered about the Wyckoff *a* site (site symmetry 23) at 1/4, 1/4, 1/4. This yields a large, hollow $[Mo_{24}P_{16}O_{96}(OH)_{28}]$ aggregate

(Fig. 3), which also displays overall 23 symmetry (i.e., the four $[Mo_6P_4O_{24}(OH)_7]$ clusters lie at the vertices of a tetrahedron with the Mo_6 plane perpendicular to the threefold axis of the tetrahedron.). This mode of aggregation leaves a large void, which is filled with a H_3PO_4 group, whose P atom is on the special position at 1/4, 1/4, 1/4, and twelve $Na^{\oplus}$ ions that are coordinated to oxygens on the interior surface of the $[Mo_6P_4O_{24}(OH)_7]_4$ cluster (Fig. 3). The unique central

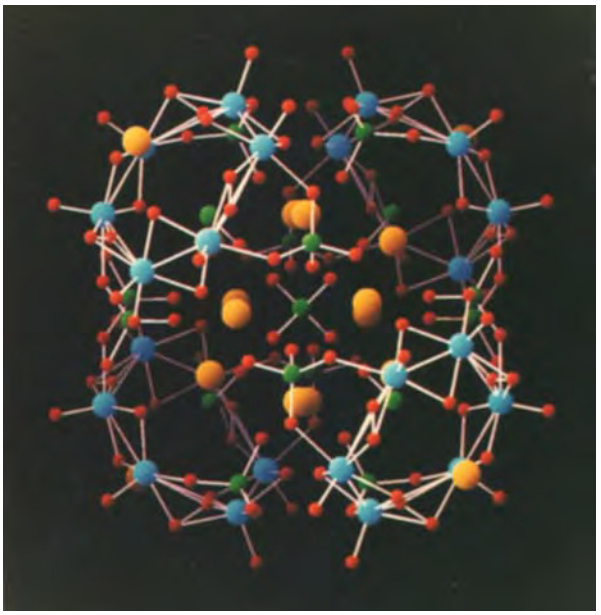


Fig. 3. Ball-and-stick representation of the $[Na_{12}MO_{24}P_{17}O_{97}(OH)_{31}]^{8\ominus}$ cluster in **1**. Mo, light blue; P, green; O, red; Na, yellow.

H_3PO_4 molecule is hydrogen bonded to the other phosphates that are part of the dimer[12] and is enclosed in a distorted icosahedron of $Na^{\oplus}$ ions with each O atom of the phosphate bonded to three $Na^{\oplus}$ ions (Fig. 3). The other ends of the four dimers forming this large unit take part in the formation of four different $[Mo_{24}P_{17}O_{97}(OH)_{31}]$ clusters.

An alternative description of the anionic framework in this compound is that of $[Na_{12}Mo_{24}P_{17}O_{97}(OH)_{31}]^{8\ominus}$ clusters connected into a tetrahedral array by $Na^{\oplus}$ ions. The voids left by packing the anions together form an unusual array of one-dimensional tunnels, which are filled with $Et_4N^{\oplus}$ ions and run parallel to the six $\langle 100 \rangle$ directions in the unit cell as shown in Figure 4. If one considers the cubic unit cell to be divided into octants, then the P atoms of the central H_3PO_4 molecules of the $[Mo_{24}P_{17}O_{97}(OH)_{31}]$ clusters are at 1/4, 1/4, 1/4 and 3/4, 3/4, 3/4, while the one-dimensional tunnels intersect at the centers of the other six octants. There are also six water molecules per Mo_{24} unit. These water molecules, which were difficult to model satisfactorily, sit on threefold rotation and threefold inversion axes (two on the Wyckoff *c* site and four on the *e* site).

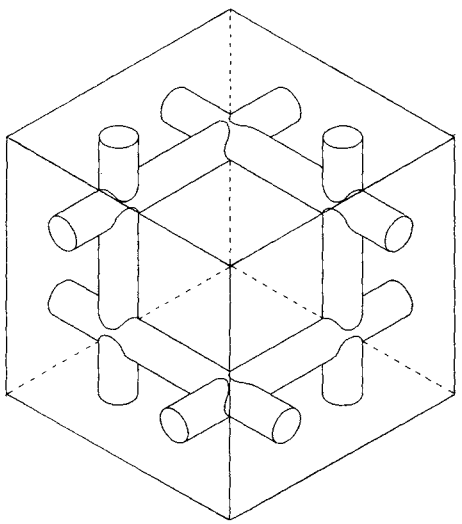


Fig. 4. A schematic view of the $Et_4N^{\oplus}$-filled tunnels in **1**.

These results show that it is possible to prepare molybdenum phosphates in acidic aqueous solution that differ greatly from the well-known heteropolymolybdates. The assembly of such a complex structure as **1** in very high yield from simple starting materials is somewhat surprising. As will be discussed elsewhere,[6] one possible rationalization for the gross structure of this and other molybdenum phosphates prepared by us may be in terms of hydrophilic-hydrophobic interactions, since the MoO_6 groups appear to be relatively less polar than the phosphate portion of the structure. For example, in **1**, the sixteen PO_4 groups are oriented toward the $Na^{\oplus}$ ions and the unique H_3PO_4 molecule in the interior of the aggregate, while the twenty-four Mo=O groups are all on the exterior facing the relatively nonpolar tetraalkylammonium ions. In other words, the tunnels containing the relatively nonpolar $Et_4N^{\oplus}$ ions are "lined" with Mo=O groups as shown in the projection of the unit cell contents in Figure 5. The overall structure is reminiscent of a small amount of a polar species and a detergent in a nonpolar liquid. This material may be an interesting candidate for a description in terms of periodic minimal surfaces.[15]

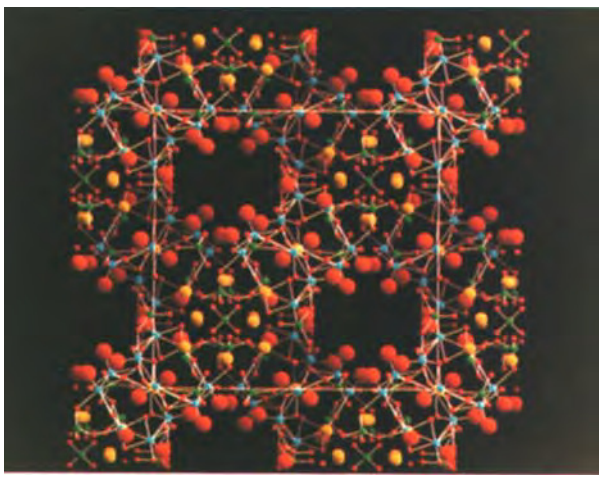


Fig. 5. The unit cell of **1** with the Mo=O oxygen atoms (red) represented with exaggerated size to emphasize their segregation onto the "lining" of the tunnels where the $Et_4N^{\oplus}$ ions reside (not shown). Mo, light blue; P, green; Na, yellow.

Received: February 3, 1989;
revised: April 14, 1989 [Z 3156IE]
German version: *Angew. Chem. 101* (1989) 802

[1] B. Raveau, *Proc. Ind. Acad. Sci. 88* (1986) 419.
[2] K.-H. Lii, R. C. Haushalter, *J. Solid State Chem. 69* (1987) 320.
[3] K.-H. Lii, D. C. Johnston, D. P. Goshorn, R. C. Haushalter, *J. Solid State Chem. 71* (1987) 131.
[4] K.-H. Lii, R. C. Haushalter, *Acta Crystallogr. C43* (1987) 2036.
[5] R. C. Haushalter, F. W. Lai, *J. Solid State Chem. 76* (1988) 218.
[6] R. C. Haushalter, F. W. Lai, unpublished results.
[7] S. L. Wang, C. C. Wang, K.-H. Lii, *J. Solid State Chem. 74* (1988) 409.
[8] R. C. Haushalter, K.-H. Lii, C. M. O'Connor, *Angew. Chem. 99* (1987) 576; *Angew. Chem. Int. Ed. Engl. 26* (1987) 549.

[9] R. C. Haushalter, *J. Chem. Soc. Chem. Commun. 1987*, 374.
[10] M. T. Pope: *Heteropoly and Isopoly Oxometalates*, Springer, New York 1983; D. L. Kepert ("Isopolyanions and Heteropolyanions") in J. C. Bailar (Ed.): *Comprehensive Inorganic Chemistry, Vol. 4*, Pergamon, Oxford 1973, pp. 607–672.
[11] A. Bino, F. A. Cotton, *Angew. Chem. 91* (1979) 496; *Angew. Chem. Int. Ed. Engl. 18* (1979) 462.
[12] This formulation for this material assumes, based on the observed geometry and the P–O bond lengths, that all of the terminal OH groups on the PO_4 groups, including the unique central PO_4, are protonated. Bond strength–bond length calculations, based on the observed Mo–O bond lengths and the geometry about the Mo atoms, clearly show the Mo to be in the + 5 oxidation state. If one assumes that all Mo atoms are $Mo^{5\oplus}$ and the solvate water molecules are not protonated, then the central phosphate is required to be H_3PO_4, consistent with the observed hydrogen-bonding pattern.
[13] a) E. I. Stiefel, *Prog. Inorg. Chem. 22* (1976) 1; b) F. A. Cotton, G. Wilkinson: *Advanced Inorganic Chemistry*, Wiley, New York 1980, p. 867.
[14] Crystal data for **1**: Cubic, space group $Pn\bar{3}$ (# 201) with $a = 20.404(1)$ Å, $V = 8494$ Å^3 at -115 °C; $Mo_{K\alpha}$ radiation, $\mu = 19.7$ cm^{-1}, empirical absorption correction. For 1170 unique reflections with $I > 3\sigma(I)$, $R(R_w) = 0.049$ (0.051) with maximum and minimum values of 1.27 and -0.78 eÅ^{-3} in the final difference map. Further details of the crystal structure investigation may be obtained from the Fachinformationszentrum Karlsruhe, Gesellschaft für wissenschaftlich-technische Information mbH, D-7514 Eggenstein-Leopoldshafen 2 (FRG), on quoting the depository number CSD-53847, the names of the authors, and the journal citation.
[15] H. G. von Schnering, R. Nesper, *Angew. Chem. 99* (1987) 1097; *Angew. Chem. Int. Ed. Engl. 26* (1987) 1059.
[16] Chem-X, designed and distributed by Chemical Design, Ltd., Mahwah, NJ, USA.

The Organization of Two "Soft" ($Cu^{2\oplus}$, $Ni^{2\oplus}$) Metal Centers in Heterotrinuclear Complexes of a Macrocyclic Ligand by Cocomplexation with $Ba^{2\oplus}$ **

By *Frank C. J. M. van Veggel, Martinus Bos, Sybolt Harkema, Willem Verboom*, and *David N. Reinhoudt* *

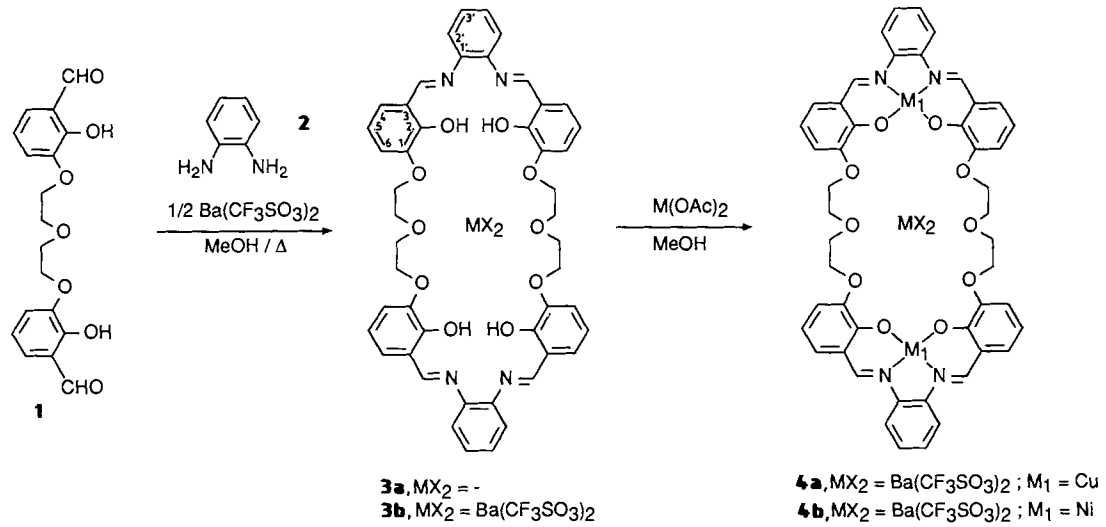
Almost all the reported model compounds for the active site in dicopper metalloproteins like hemocyanin, tyrosinase, and dopamine β-hydroxylase[1] contain dinucleating ligands in which a hydroxide, a phenolate, or an alkoxide group acts as a bridge between the two copper sites. As part of our work on the complexation of neutral molecules by macrocyclic receptor molecules,[2] we have recently reported the complexation of urea and its derivatives by macrocycles in which "soft" cations are immobilized as electrophilic centers.[3] In addition, we have shown that hard cations, like alkali and alkaline-earth cations, can be cocomplexed in such metallomacrocycles to give heterodinuclear complexes.[4, 5]

We describe here the synthesis of a barium complex containing a novel type of macrocyclic ligand and its subsequent reaction with copper or nickel acetate to yield heterotrinuclear complexes in which the arrangement of the two soft metal centers is completely different from that in known dicopper complexes.

The synthesis of the complexes **3b** and **4**, containing the macrocyclic ligand **3a**, is outlined in Scheme 1. Complex **3b** was prepared by simultaneous slow addition of a solution of *o*-phenylenediamine (**2**) and a solution of the dialdehyde **1**[6] to a refluxing solution of $Ba(CF_3SO_3)_2$ in MeOH and obtained as a red crystalline material in 63% yield.[7] The FAB mass spectrum of **3b** shows the parent peak at *m/z* 1123, which corresponds to $[M-CF_3SO_3]^{\oplus}$.

Ruby red crystals of **3b** were obtained by slow diffusion of petroleum ether into a solution of **3b** in MeOH. The structure of one of the two independent molecules in the asymmetric unit is shown in Figure 1.

The macrocycle is folded around the barium, thereby allowing coordination by all ten oxygen atoms of the macrocycle ($Ba^{2\oplus}\cdots O$ 2.69–3.14 Å). The eleventh position around the barium ion is occupied by an oxygen of a triflate ion ($Ba^{2\oplus}\cdots O$ 2.82 Å). The two conjugated *N,N'-o*-phenylenebis(salicylidenaminato) (salophen) units are not planar, the angles between the two opposite aromatic rings being 17.3 and 29.5°. The mean planes through the four heteroatoms of the salophen units are approximately parallel, with an angle of 12.6°.



Scheme 1.

The conversion of the barium complex **3b** into the trinuclear complexes **4** was carried out by reaction with 2 equivalents of copper or nickel acetate.[8, 9] The parent peaks in the FAB mass spectra of **4a** (*m/z* 1245) and

[*] Prof. Dr. Ir. D. N. Reinhoudt, Ir. F. C. J. M. van Veggel, Dr. M. Bos, Dr. S. Harkema, Dr. W. Verboom
Department of Chemical Technology, University of Twente
P.O. Box 217, NL-7500 AE Enschede (The Netherlands)

[**] We thank Akzo International Research BV for financial support and Prof. *N. Nibbering* and *R. R. Fokkens*, Amsterdam, for recording the FAB mass spectra.

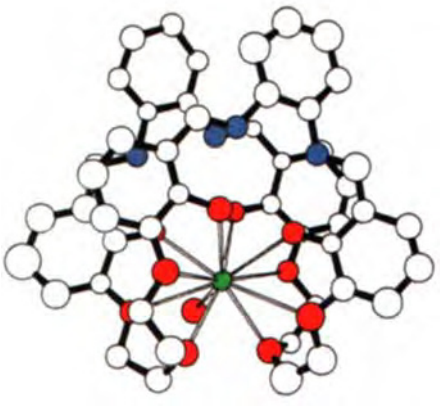


Fig. 1. Crystal structure of **3b**. The asymmetric unit contains two independent molecules, of which one is shown. The noncoordinating triflate ion and hydrogen atoms are omitted for clarity. Green = Ba, red = O, blue = N. Crystal data [16]: triclinic, $a = 21.950(2)$, $b = 16.993(2)$, $c = 14.502(2)$ Å, $\alpha = 84.15(5)$, $\beta = 79.04(5)$, $\gamma = 88.79(5)°$, $V = 5283(8)$ Å^3, space group $P\bar{1}$, $Z = 4$, $\varrho_{calcd} = 1.60$ g cm^{-3}, $\mu(Mo_{K\alpha}) = 9.18$ cm^{-1}. Final R factor for 4388 significant [$I > 5\,\sigma(I)$, $\theta = 3-25°$] reflections is 0.060.

4b (m/z 1234) correspond to $[M-CF_3SO_3]^{\oplus}$ and $[M-CF_3SO_3+H]^{\oplus}$, respectively.

Suitable crystals for an X-ray analysis of the dicopper/barium complex **4a** were obtained by slow diffusion of Et_2O into a solution of **4a** in a mixture of MeOH and CH_3CN (1:1). The structure of the folded macrocycle is shown in Figure 2. It is similar to that of **3b**.

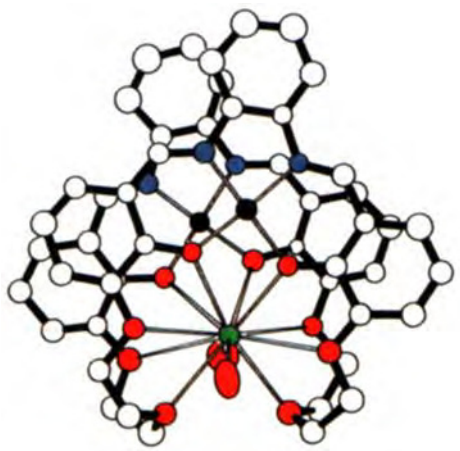


Fig. 2. Crystal structure of **4a** · 2 H_2O. Only the coordinating oxygen atom of the triflate anion (ellipse) is drawn for clarity. The noncoordinating triflate ion, water molecule, and hydrogen atoms are omitted for clarity. Green = Ba, black = Cu, red = O, blue = N. Crystal data [16]: orthorhombic, $a = 28.589(9)$, $b = 27.786(4)$, $c = 13.383(3)$ Å, $V = 10631(6)$ Å^3, space group $Pbca$, $Z = 8$, $\varrho_{calcd} = 1.74$ g cm^{-3}, $\mu(Mo_{K\alpha}) = 16.9$ cm^{-1}. Final R factor for 2589 significant [$I > 3\,\sigma(I)$, $\theta = 3-22.5°$] reflections is 0.078.

The two copper ions in **4a** are complexed in an almost square-planar fashion in the "soft" salophen cavities and the barium ion is complexed in the large polyether cavity. The two conjugated salophen parts of the macrocycle are not completely planar, the angles between the opposite aromatic rings being 8.2 and 8.7°. The mean planes through the coordinating atoms of the copper ions are approximately parallel, with an angle of 5.8°. A view perpendicular to one salophen unit shows that the other unit is not exactly under it but displaced by about 1.4 Å. The barium ion is coordinated by all ten oxygens of the macrocycle ($Ba^{2\oplus}\cdots O$ 2.76–3.63 Å), one water molecule ($Ba^{2\oplus}\cdots O$ 3.01 Å), and one triflate ion ($Ba^{2\oplus}\cdots O$ 2.89 Å). The metal–metal distances in the cation cluster **4a** are: $Ba^{2\oplus}\cdots Cu^{2\oplus}$ 3.70 and 3.85; $Cu^{2\oplus}\cdots Cu^{2\oplus}$ 3.50 Å. The angle $Cu^{2\oplus}$-$Ba^{2\oplus}$-$Cu^{2\oplus}$ is 55.1°.

Dark red single crystals of the dinickel/barium complex **4b** were similarly obtained by slow diffusion of Et_2O into a solution of **4b** in a mixture of CH_3CN and dimethyl sulfoxide (DMSO). The structure of **4b** resembles that of **4a**. The two nickel ions are complexed in the "soft" salophen cavities in an almost square-planar fashion. The mean planes through the coordinating atoms of the nickel ions are approximately parallel to each other, with an angle of 7.4°. A view perpendicular to one salophen unit shows that the other unit is not exactly under it but displaced by about 0.95 Å. The barium ion is complexed in the "hard" cavity by all crown ether oxygens ($Ba^{2\oplus}\cdots O$ 2.72–3.09 Å) and one water molecule ($Ba^{2\oplus}\cdots O$ 2.87 Å). The metal–metal distances in the cation cluster **4b** are: $Ba^{2\oplus}\cdots Ni^{2\oplus}$ 3.66 and 3.73; $Ni^{2\oplus}\cdots Ni^{2\oplus}$ 3.42 Å. The angle $Ni^{2\oplus}$-$Ba^{2\oplus}$-$Ni^{2\oplus}$ is 55.1°.

The electrochemical properties of the trinuclear complexes **4a** and **4b** were investigated by polarography and cyclic voltammetry at a mercury drop electrode in DMSO with 0.1 M $Et_4N^{\oplus}ClO_4^{\ominus}$ as supporting electrolyte.[10]

The polarogram of the dicopper/barium complex **4a** shows two waves between −0.2 and −1.4 V [$E_{1/2} = -1.065$ and −1.110 V (slope 52 and 50 mV, respectively)].[11] The ratio of the limiting currents is 1, which indicates two one-electron reductions.[12] Cyclic voltammograms of **4a** were recorded at scan rates of 0.5 to 6 V s^{-1}. At these scan rates the two-step process is reflected as a shoulder on a peak in the reductive as well as in the oxidative sweep. This two-electron reduction/oxidation is *chemically* reversible, because, when five scans at scan rates of 0.5 and 6 V s^{-1} were applied, five identical cyclic voltammograms were recorded. This reduction can be regarded as taking place by a simple EE mechanism, that is, two one-electron transfers via a (formally) M_1^{II}/M_1^{I} oxidation state to a (formally) M_1^{I}/M_1^{I} oxidation state.

The polarogram of **4b** shows two waves between −0.2 and −1.4 V [$E_{1/2} = -1.036$ and −1.137 V (slope 50 and 46 mV, respectively)].[11] The ratio of the limiting currents is about 1. The cyclic voltammograms of **4b** at scan rates

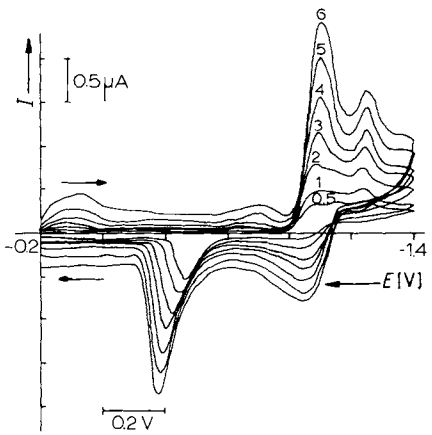


Fig. 3. Cyclic voltammograms of **4b** in DMSO, with 0.1 M $Et_4N^{\oplus}ClO_4^{\ominus}$ as supporting electrolyte, at scan rates of 0.5 to 6 V s^{-1} (shown on the curves); vs. Ag/AgCl.

of 0.5 to 6 V s^{-1} between −0.2 and −1.4 V are shown in Figure 3.

Cyclic voltammetry showed that the reduction/oxidation of **4b** is also *chemically* reversible, because, when 30 scans were applied at scan rates of 2 and 6 V s^{-1} between −0.2 and −1.4 V, 30 identical voltammograms were recorded. However, this reduction/oxidation cannot be regarded as two simple one-electron transfers[13] but is complicated by reversible intra- and intermolecular C–C coupling of two (reduced) C=N bonds. This reductive C–C coupling of two C=N bonds in Ni(salophen) units has also been observed in the solid state by *Floriani* et al. upon reduction of Ni(salophen) with one equivalent of lithium and sodium metal.[14] They showed that the C–C coupling product could be oxidized to give the original Ni(salophen), which demonstrates the reversibility of this reductive C–C coupling. The reduced Ni(salophen) can be regarded as a complex of Ni^{II} with a radical anion ligand, as was demonstrated by *Gosden* et al.[15] by ESR measurements of reduced Ni(salophen) at 77 K.

Currently we are studying the interaction of the trinuclear complexes **4** with small anions and neutral molecules.

Received: January 26, 1989 [Z 3142 IE]
German version: *Angew. Chem. 101* (1989) 800

CAS Registry numbers:
1, 121073-78-7; **2**, 95-54-5; **3b**, 121073-80-1; **4g**, 121073-84-5; **4a**·$2H_2O$, 121073-85-6; **4b**, 121073-82-3.

[1] For recent reviews on mimics of dicopper metalloproteins, see J.-M. Latour, *Bull. Soc. Chim. Fr. 1988*, 508; T. N. Sorrell, *Tetrahedron 45* (1989) 3.

[2] P. D. J. Grootenhuis, J. W. H. M. Uiterwijk, D. N. Reinhoudt, C. J. van Staveren, E. J. R. Sudhölter, M. Bos, J. van Eerden, W. T. Klooster, L. Kruise, S. Harkema, *J. Am. Chem. Soc. 108* (1986) 780; J. W. H. M. Uiterwijk, C. J. van Staveren, D. N. Reinhoudt, H. J. den Hertog, Jr., L. Kruise, S. Harkema, *J. Org. Chem. 51* (1986) 1575; V. M. L. J. Aarts, C. J. van Staveren, P. D. J. Grootenhuis, J. van Eerden, L. Kruise, S. Harkema, D. N. Reinhoudt, *J. Am. Chem. Soc. 108* (1986) 5035; C. J. van Staveren, V. M. L. J. Aarts, P. D. J. Grootenhuis, J. van Eerden, S. Harkema, D. N. Reinhoudt, *ibid. 108* (1986) 5271; J. van Eerden, P. D. J. Grootenhuis, P. J. Dijkstra, C. J. van Staveren, S. Harkema, D. N. Reinhoudt, *J. Org. Chem. 51* (1986) 3918; C. J. van Staveren, V. M. L. J. Aarts, P. D. J. Grootenhuis, W. J. H. Droppers, J. van Eerden, S. Harkema, D. N. Reinhoudt, *J. Am. Chem. Soc. 110* (1988) 8134.

[3] C. J. van Staveren, J. van Eerden, F. C. J. M. van Veggel, S. Harkema, D. N. Reinhoudt, *J. Am. Chem. Soc. 110* (1988) 4994.

[4] F. C. J. M. van Veggel, S. Harkema, M. Bos, W. Verboom, C. J. van Staveren, G. J. Gerritsma, D. N. Reinhoudt, *Inorg. Chem., 28* (1989) 1133.

[5] F. C. J. M. van Veggel, S. Harkema, M. Bos, W. Verboom, G. Klein Woolthuis, D. N. Reinhoudt, *J. Org. Chem.*, in press.

[6] Compound **2** was prepared by reaction of 2,3-dihydroxybenzaldehyde and diethylene glycol ditosylate (2:1) in DMSO under basic conditions (NaH); see [3] for the synthesis of analogous dialdehydes.

[7] **3b**: 63% yield; m.p. 270–280 °C (MeOH/petroleum ether 40–60, dec.). ^1H NMR ([D_6]DMSO): δ = 13.37 (s, 4H, OH), 8.92 (s, 4H, N=CH), 7.45 (s, 8H, aryl H), 7.3–7.1 (m, 8H, aryl H), 6.9–6.7 (m, 4H, aryl H), 4.1–4.0 (m, 8H, aryl OCH_2), 4.0–3.9 (m, 8H, OCH_2). ^{13}C NMR ([D_6]DMSO): δ = 163.5 (d, N=C), 151.4 (s, C-3), 146.4 (s, C-2), 140.7 (s, C-1'), 127.3, 124.2, 118.7, 117.6, 117.3 (d, C-4–C-6, C-2',C-3'), 118.6 (s, C-1), 68.5, 67.8 (t, OCH_2). IR (KBr): $\tilde{\nu}$ = 1620 cm^{-1} (N=C). FAB-MS: *m/z* 1123 $[M-CF_3SO_3]^{\oplus}$. Satisfactory C, H, N analysis for $C_{48}H_{44}BaF_6N_4O_{16}S_2$.

[8] Complex **4a** was obtained as a green solid in 74% yield: m.p. >300 °C [MeOH/CH_3CN (1:1), Et_2O as precipitant]. IR (KBr): $\tilde{\nu}$ = 1608 cm^{-1} (N=C). FAB-MS: *m/z* 1245 $[(M-CF_3SO_3)]^{\oplus}$. Satisfactory C, H, N analysis for $C_{50}H_{40}BaCu_2F_6N_4O_{16}S_2 \cdot 2H_2O$. Complex **4b** was obtained as a dark red solid in 64% yield: m.p. >300 °C [MeOH/CH_3CN (1:1), Et_2O as precipitant]. ^1H NMR ([D_6]DMSO): δ = 8.39 (s, 4H, N=CH), 7.7–7.5 (m, 4H, aryl H), 7.2–7.0 (m, 4H, aryl H), 7.0–6.6 (m, 4H, aryl H), 6.5–6.3 (m, 8H, aryl H), 4.9–3.6 (m, 16H, OCH_2). ^{13}C NMR ([D_6]DMSO): δ = 156.9 (d, N=C), 151.6 (s, C-3), 147.3 (s, C-2), 140.7 (s, C-1), 127.7, 125.1, 115.6, 115.3, 113.7 (d, C-4–C-6, C-2', C-3'), 119.4 (s, C-1), 67.3, 66.2 (t, OCH_2). IR (KBr): $\tilde{\nu}$ = 1610 cm^{-1} (N=C). FAB-MS: *m/z* 1234 $[M-CF_3SO_3+H]^{\oplus}$. Satisfactory C, H, N analysis for $C_{50}H_{40}BaF_6N_4Ni_2O_{16}S_2 \cdot 2H_2O$.

[9] The barium-free dicopper and dinickel complexes could be made by reaction of **3a** with two equivalents of copper and nickel acetate, respectively, but these complexes are insoluble in all normal organic solvents.

[10] Measurements were performed in 0.1 M $Et_4N^{\oplus}ClO_4^{\ominus}$ solution in DMSO at 20 °C. The apparatus was operated in a three-electrode mode with a mercury drop as cathode, a platinum wire as auxiliary electrode, and an Ag/AgCl electrode as reference. The reference electrode (Ag/AgCl) was filled with 1 M Et_4NCl in MeOH and brought into contact via a salt bridge, filled with 0.1 M $Et_4N^{\oplus}ClO_4^{\ominus}$ in DMSO, with the sample solution. See [4,5] for a more detailed description of the apparatus and procedures.

[11] Determination of the half-wave potentials ($E_{1/2}$) was done manually. The slopes were estimated with $E_{3/4}-E_{1/4}$. The peak at about −0.3 V, which occurs at higher scan rates, is due to capacitance effects. This peak is also found in the blank.

[12] The one-electron reduction of the Cu(salophen) unit is well known; see, e.g., D. F. Rohrbach, W. R. Heineman, E. Deutsch, *Inorg. Chem. 18* (1979) 2536.

[13] The one-electron reduction of the Ni(salophen) unit is well known; see, e.g. [15].

[14] S. Gambarotta, F. Urso, C. Floriani, A. Chiesi-Villa, *Inorg. Chem. 22* (1983) 3966.

[15] C. Gosden, J. B. Kerr, D. Pletcher, R. Rosas, *J. Electroanal. Chem. 117* (1981) 101.

[16] All calculations were done with the Structure Determination Package program [17]. Further details of the crystal structure investigation are available from the Director of the Cambridge Crystallographic Data Center, University Chemical Laboratory, Lensfield Road, Cambridge CB2 1EW (England) by quoting the full literature citation.

[17] B. A. Frenz and Associates Inc., College Station, TX, USA, and Enraf-Nonius, Delft 1983.

A Novel Type of Anionic Cluster Containing a Pt_4Ag_2 Core**

By *Rafael Usón, Juan Forniés, Milagros Tomás,* and *José M. Casas*

The electron-rich metal centers in mono- and binuclear platinum(II) complexes containing perhalophenyl ligands are able to donate electron density to suitable Lewis acids, such as $Ag^{\oplus}$ and $(AgL)^{\oplus}$, to afford unusual polynuclear complexes containing Pt→Ag bonds.[1–6] Specifically, the anionic binuclear complexes **1** react with $AgClO_4$ without elimination of AgX to give the trinuclear complexes **2**.

$(NBu_4)_2[Pt_2(\mu\text{-}X)_2(C_6F_5)_4]$ **1**

$(NBu_4)[Pt_2Ag(\mu\text{-}X)_2(C_6F_5)_4OEt_2]$ **2**

a, X = Cl; **b**, X = Br; **c**, $X = C_6F_5$

The structures of **2a** and **2c** have been established by single-crystal X-ray studies. In both cases[4, 5] the bent binuclear $[Pt_2(\mu\text{-}X)_2(C_6F_5)_4]$ fragment acts as a bidentate chelating ligand with both platinum donor atoms bonded to the silver atom through otherwise unsupported Pt→Ag bonds. The diethyl ether molecule is coordinated to the silver atom (Fig. 1).

However, the analogous binuclear pentachlorophenyl derivatives **3**[7] behave differently. Upon reaction with $AgClO_4$ (under similar conditions as those used in the syn-

[*] Prof. R. Usón, Prof. J. Forniés, Dr. M. Tomás, Dr. J. M. Casas
Departamento de Química Inorgánica. Instituto de Ciencia de Materiales de Aragón
Universidad de Zaragoza
E-50009 Zaragoza (Spain)

[**] This work was supported by the Spanish Comisión Asesora de Investigación Científica y Técnica (CAICYT) (project PB85-0128).

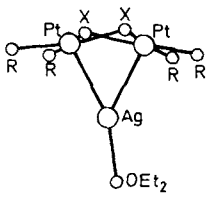


Fig. 1. Schematic drawing of the structure of **2**. R = C_6H_5.

thesis of **2**), they afford complexes **4**[8] with the same stoichiometry as **2** but lacking the OEt_2 molecule.

$(NBu_4)_2[Pt_2(\mu\text{-}X)_2(C_6Cl_5)_4]$ **3**

$\{(NBu_4)[Pt_2Ag(\mu\text{-}X)_2(C_6Cl_5)_4]\}_2$ **4**

a, X = Cl; **b**, X = Br

This difference, along with previous observations revealing dramatic structural differences between pentafluoro-[1] and pentachlorophenyl[2] platinum(II) derivatives of *identical* stoichiometry, **5** and **6**, respectively, made it worthwhile

$\{(NBu_4)[PtAgCl_2(C_6X_5)_2]\}_n$

5, X = F, n = 2; **6**, X = Cl, n = ∞

to solve[9] the structure of complex **4a**, which happens to be unprecedented and very different from that of **2** (see Fig. 1).

Complex **4a** consists of a hexanuclear anion $[Pt_4Ag_2(\mu\text{-}Cl)_4(C_6Cl_5)_8]^{2\ominus}$ and two $NBu_4^{\oplus}$ cations. The cluster (Fig. 2)

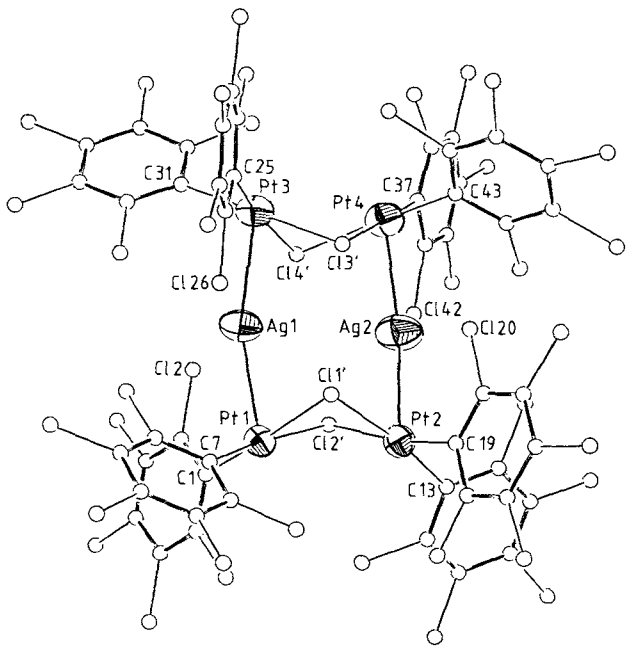


Fig. 2. Molecular structure of the anion $[Pt_4Ag_2Cl_4(C_6Cl_5)_8]^{2\ominus}$ **4a**. Selected bond lengths [Å] and bond angles [°]. Ag1-Pt1 2.766(4), Ag1-Pt3 2.755(4), Ag2-Pt2 2.781(4), Ag2-Pt4 2.748(4), Pt1-C1 2.003(23), Pt1-C7 2.069(24), Pt1-Cl1′ 2.429(12), Pt1-Cl2′ 2.429(4), Pt2-C13 2.009(26), Pt2-C19 1.965(23), Pt2-Cl1′ 2.390(11), Pt2-Cl2′ 2.424(11), Pt3-C25 1.973(25), Pt3-C31 2.085(26), Pt3-Cl3′ 2.403(11), Pt3-Cl4′ 2.440(12), Pt4-C37 2.017(30), Pt4-C43 1.976(32), Pt4-Cl3′ 2.407(12), Pt4-Cl4′ 2.424(12); Pt1-Ag1-Pt3 163.2(8), Pt2-Ag2-Pt4 163.3(2), Pt1-Cl′-Pt2 85.5(4), Pt1-Cl2′-Pt2 84.8(3), Pt3-Cl3′-Pt4 85.5(4), Pt3-Cl4′-Pt4 84.3(4).

comprises two $[Pt_2(\mu\text{-}Cl)_2(C_6Cl_5)_4]$ units doubly bridging two Ag atoms. The best least-square plane through the six metal atoms almost contains Ag1 (0.007 Å), but the other metal atoms lie distinctly above (Pt2 0.344; Pt3 0.268 Å) or below (Pt1 0.283; Ag2 0.263; Pt4 0.224 Å) this plane.[10] The Pt–Ag bond distances are given in the caption to Figure 1. The long Ag–Ag distance (3.87 Å) excludes any bonding interaction. The environment around each platinum atom is a distorted square pyramid, but the Ag–Pt bond is not perpendicular to the basal plane (formed by the platinum atom, two chlorine atoms, and two carbon atoms). The deviations are in the range 18.83–26.25°.[10] The dihedral angles, formed by the planes Pt1-Cl1′-Cl2′ and Pt2-Cl1′-Cl2′ and by the planes Pt3-Cl3′-Cl4′ and Pt4-Cl3′-Cl4 are 129.25 and 127.70°.[10] The long distance between Pt1 and Pt2 (3.272(3) Å) and between Pt3 and Pt4 (3.265(3) Å) excludes any significant Pt–Pt bond.

The environment of the silver atom is not linear; the Pt–Ag–Pt angles are 163.2(3) and 163.3(3)°. Furthermore, short contacts with *o*-Cl atoms of the C_6Cl_5 groups are observed, as in other perhalophenyl platinum–silver complexes. In fact, Ag1 shows contacts to Cl2 (2.783(14) Å) and Cl26 (2.788(13) Å) and Ag2 shows contacts to Cl20 (2.821(13)) and Cl42 (2.867(14) Å). These contacts of each Ag atom with two *o*-Cl atoms are shorter than any previously observed ones in pentachlorophenyl platinum–silver complexes.[2, 11] We think they imply donation of electron density (*o*-Cl → Ag), thereby enhancing the stability of the cluster. Moreover, the bridging chloride ligands are also close to the silver atoms, although some of these contacts are here longer and more irregular: Ag1-Cl1′ 3.033(11); Ag1-Cl3′ 3.145(12), Ag1-Cl4′ 3.159(11); Ag2-Cl1′ 3.285(11), Ag2-Cl2′ 2.826(12), Ag2-Cl3′ 3.024(13) Å. If these bridging chloride ligands are also donating electron density to the silver atoms, this situation would be another unprecedented feature in this very unusual structure.

Received: January 30, 1989 [Z 3149 IE]
German version: *Angew. Chem. 101* (1989) 782

CAS Registry numbers:
3a, 86392-08-7; **3b**, 86392-10-1; **4a**, 120610-97-1; **4b**, 120610-99-3; $AgClO_4$, 7783-93-9.

[1] R. Usón, J. Forniés, B. Menjón, F. A. Cotton, L. R. Falvello, M. Tomás, *Inorg. Chem. 24* (1985) 4651.
[2] R. Usón, J. Forniés, M. Tomás, J. M. Casas, F. A. Cotton, L. R. Falvello, *Inorg. Chem. 25* (1986) 4519.
[3] F. A. Cotton, L. R. Falvello, R. Usón, J. Forniés, M. Tomás, J. M. Casas, I. Ara, *Inorg. Chem. 26* (1987) 1366.
[4] R. Usón, J. Forniés, M. Tomás, J. M. Casas, F. A. Cotton, L. R. Falvello, *Inorg. Chem. 26* (1987) 3482.
[5] R. Usón, J. Forniés, M. Tomás, J. M. Casas, F. A. Cotton, L. R. Falvello, R. Llusar, *Organometallics 7* (1988) 2279.
[6] $PtMe_2$(bpy) shows a similar behavior; G. J. Arsenault, C. M. Anderson, R. J. Puddephatt, *Organometallics 7* (1988) 2094.
[7] R. Usón, J. Forniés, F. Martinez, M. Tomás, I. Reoyo, *Organometallics 2* (1983) 1386.
[8] **4a**: To CH_2Cl_2 solution (30 mL) of **3a** (0.2 g, 0.1039 mmol), $AgClO_4$ (0.0213 g, 0.1029 mmol) was added and the mixture, under exclusion of light, was stirred at room temperature for 4 h. No AgX precipitation was observed. The solution was evaporated to dryness and the resulting oily residue was treated with diethyl ether (20 mL). The resulting solid (a mixture of NBu_4ClO_4 and **4a**) was washed with 3 × 5 mL of 2-propanol to remove the soluble NBu_4ClO_4. Yield 83%; dec. 188 °C; molar conductivity (acetone $c \approx 5 \times 10^{-4}$ M) 92 $ohm^{-1}\,cm^2\,mol^{-1}$. IR (nujol): C_6Cl_5 groups [12]: 845w, 832w, ν(Pt-C) 625vs; others 1332vs, 1317vs, 1295vs, 1216s, 675vs; ν(Pt-Cl) 252m. **4b** was prepared similarly from **3b** (0.2 g, 0.0984 mmol), CH_2Cl_2 (35 mL), and $AgClO_4$ (0.0204 g, 0.0984 mmol). Yield 72%; dec. 180 °C. **4b** is unstable in acetone solution. Very similar IR bands due to the C_6Cl_5 groups are observed. Satisfactory microanalytical data were obtained for **4a** and **4b**.
[9] Crystals of **4a** suitable for crystal structure investigation were obtained by slow diffusion (ca. 2 weeks at −30 °C) of *n*-hexane into a solution of the complex in dichloromethane. X-ray structure analysis: $Pt_4Ag_2Cl_{44}N_2C_{80}H_{72}$; space group $P2_{1/n}$, $a = 14.528(9)$, $b = 42.615(12)$, $c = 19.942(10)$ Å, $\beta = 96.08(5)°$, $V = 12.276$ Å^3 Size 0.5 × 0.25 × 0.04 mm. $\mu(Mo_{K\alpha}) = 56\ cm^{-1}$, 20% decay during the data collection time.

Interpolative decay and empirical absorption correction [13] were applied (minimum and maximum transmission factors 0.248 and 0.583, respectively). Four-circle diffractometer, Siemens/Stoe AED2. Profile-fitted intensities [14] $3 \leq 2\theta \leq 40°$. Total number of reflections 12376. 4300 unique reflections with $F_o \geq 6\,\sigma(F_o)$. The structure was solved by Direct Methods [15] and refined to $R = 0.071$, $R_w = 0.0677$ [16]. Pt and Ag atoms and 15 Cl atoms were anisotropic. The carbon frames of the C_6Cl_5 groups were refined as idealized rigid groups with C-C 1.395 Å. The weighting scheme was $w^{-1} = \sigma^2(F) + 0.0007\,F^2$; 558 variables. Δ/esd (max) 0.11. Highest peaks: 5 peaks between 1.31 and 1.0 e/Å^3 close to heavy atoms. Further details of the crystal structure investigation are available from the Cambridge Crystallographic Data Centre, University Chemical Laboratory, Lensfield Road, Cambridge CB2 1EW (England), on quoting the full journal citation.

[10] M. Nardelly, *Comput. Chem. 7* (1983) 95.

[11] R. Usón, J. Forniés, M. Tomás, *J. Organomet. Chem. 358* (1988) 525, and references cited therein.

[12] E. Maslowsky, Jr.: *Vibrational Spectra of Organometallic Compounds*; Wiley, New York 1977, p. 437, and references cited therein.

[13] N. Walker, D. Stuart, *Acta Crystallogr. Sect. A39* (1983) 158.

[14] W. Clegg, *Acta Crystallogr. Sect. A37* (1981) 22.

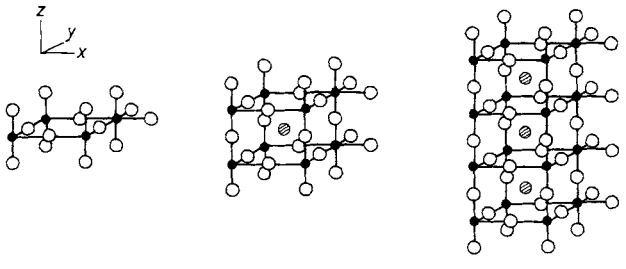
[15] G. M. Sheldrick, SHELX-86, Universität Göttingen 1986.

[16] G. M. Sheldrick, SHELX-76 "Program of Crystal Structure Determination", University of Cambridge, Cambridge (England) 1976.

Aurivillius Phases: A Possible New Class of Metal Oxide Superconductors**

By *Kyeong Ae Yee, Thomas A. Albright, Dongwoon Jung,* and *Myung-Hwan Whangbo**

A number of $AB_{n-1}M_nO_{3n+1}$ phases contain layered M_nO_{3n+1} perovskite structures, where M is typically an early transition metal (e.g., Ti, Nb, Ta, Cr, W, Fe), B is an electropositive atom (e.g., Na, K, Ca, Sr, Ba, Gd, La, Y, Pr, Sn, Pb, Bi), and n is the number of MO_2 layers within the perovskite slab.[1-3] The prototype perovskite slabs for n = 1, 2, and 4 are shown in **1**, **2**, and **3**, respectively. Most Aurivillius phases, for which A represents Bi_2O_2 layers separating the perovskite slabs and $n \leq 5$, are ferroelectric materials. In a similar class of $AB_{n-1}M_nO_{3n+1}$ compounds with A = Li, Na, K, Rb, Cs, Tl, Sr, Ba, or NR_4 (R = alkyl), perovskite slabs with n as large as 7 have been reported.[4] The crystal structures of Aurivillius phases are strikingly similar to those of the new high-temperature Bi–Ca–Sr–Cu–O and Tl–Ca–Ba–Cu–O superconductors,[5] as has been pointed out by *von Schnering* et al.[5b] However, the electron count at the metal is d^0 in known Aurivillius phases, while it is close to d^9 in the copper–oxide superconductors. On the basis of tight-binding band structure calculations[6-8] on **1–3**, we shall show that layered perovskite structures of the Aurivillius type with metal electron counting close to d^3 have electronic structures strikingly similar to those of the Cu–O superconductors and thus might form a new class of superconductors.



1 2 3

● M, ⊘ B, ○ oxygen

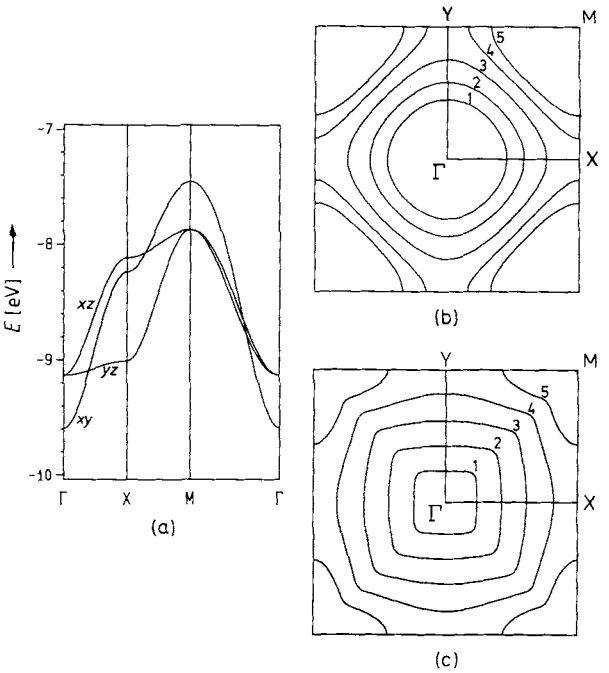


Fig. 1. a) Dispersion relations of the t_{2g}-block bands calculated for a TiO_4 layer in **1**, where $\Gamma = (0,0)$, $X = (a^*/2,0)$, and $M = (a^*/2, b^*/2)$. Fermi surfaces of the xy band in (b) and the xz band in (c), calculated for a d^x (x = 1–5) electron count, where the numbers 1–5 refer to the d-electron count d^1–d^5, respectively.

Figure 1a shows the dispersion relations of the t_{2g}-block bonds calculated for a TiO_4 layer (**1**, M = Ti). The dispersion characteristics and density-of-states profile of the xy band are very similar to the x^2-y^2 bands of the CuO_2 layers in Cu–O superconductors.[9,10] Here, xy is antibonding to oxygen p orbitals in a π fashion, whereas, in the Cu–O layers x^2-y^2 is antibonding to oxygen in a σ sense. The Fermi surfaces calculated for d^x (x = 1–5) are shown in Figure 1b and 1c for the xy and xz bands, respectively. The yz band has Fermi surfaces identical with those of the xz band but centered at the M point. Since all the Fermi surfaces are closed, the three bands are two-dimensional metallic. In particular, the Fermi surfaces for a d^3 count are very close in shape to those found for the nearly half-filled x^2-y^2 bands of the copper–oxide superconductors.[9,10] Thus, layered perovskite structures of the Aurivillius type with electron counting close to d^3 might give rise to a new class of superconductors. Valence or charge fluctuations, presumed to be essential for the Cu–O superconductors,[9b,11] would be present in such perovskite slabs. Hole states (at M or O), introduced via chemical doping or having the s bands associated with B (for $n \geq 2$), cut across the Fermi surface. The linear electron-hole

[*] Prof. T. A. Albright, K. A. Yee
Department of Chemistry, University of Houston
Houston, Texas 77204-5641 (USA)
Prof. M.-H. Whangbo, D. Jung
Department of Chemistry, North Carolina State University
Raleigh, North Carolina 27695-8204 (USA)

[**] *T. A. A.* thanks the Robert A. Welch Foundation, the Petroleum Research Fund (administered by the American Chemical Society), and the Texas Center for Superconductivity at the University of Houston (prime grant MDA 972-88-G-0002 from the Defense Advanced Research Projects Agency and the State of Texas) for support and the NSF for a generous allocation of computer time at the Pittsburgh Supercomputer Center. *M. H. W.* thanks DOE, Office of Basic Sciences, Division of Materials Sciences, for support of this research under grant DE-FG05-86ER45259.

electron-pair model[12] will operate in a way analogous to that suggested for the Cu–O superconductors: concerted in-plane M–O breathing motions can be established via local Jahn–Teller instabilities. Our band calculations on **1** with two Bi_2O_2 layers sandwiching it show no significant contribution of the Bi_2O_2 layers to the t_{2g}-block bands. Our calculations on **2** and **3** without the embedded atoms, B, show that the essential features of the t_{2g}-block bands remain unaltered. Small coupling exists between the xz and yz bands via the out-of-plane oxygen atoms that bridge the MO_2 layers, while the xy bands are not coupled via the out-of-plane oxygen atoms. The x^2-y^2 bands of the Cu–O superconductors behave identically.[9, 10]

So far, all synthetic work on the $AB_{n-1}M_nO_{3n+1}$ phases has been directed towards d^0 systems. The wide tolerance for atomic substitution of A, B, and M suggests that higher d-electron variants are possible. The t_{2g}-block bands of **2** and **3** are strongly perturbed by embedded Bi atoms (although this may well be an artifact of parameterization); thus, more electropositive atoms are suggested for B. With n = 4 as a working example, species **4**–**7** are possible.

$(Bi_2O_2)Pb_3W_4O_{13}$ (d^3 electron count at each W) **4**

$(Bi_2O_2)LaPb_2W_4O_{13}$ ($d^{2.75}$) **5**

$La_4W_4O_{13}$ ($d^{2.5}$) **6**

$YLa_3W_4O_{13}$ ($d^{2.5}$) **7**

Another viable series of candidates for superconductivity, phases with an electron count close to d^1 at M, should not be discounted. If the out-of-plane M–O distances become shorter than the in-plane ones, as expected for higher electron counts,[13] the xz and yz bands will be raised and the xy band can become nearly half-filled, even with d^1 metals. For the n = 4 model, **8** and **9** are possibilities, which lead to d^1 for

$(Bi_2O_2)Ba_{1+x}La_{2-x}Nb_4O_{13}$ (x = 0) **8**

$Sr_{2+x}La_{2-x}Nb_4O_{13}$ (x = 0) **9**

x = 0. The latter composition is particularly interesting in view of the recent report of high-temperature superconductivity in Sr–La–Nb–O films.[14] Substitution of the out-of-plane oxygens with stronger π-donor nitrogen atoms may also serve to push the xz and yz bands above the xy band. For n values other than 4, a large number of stoichiometries can also be proposed. We are well aware of fluorite or pyrochlore structural alternatives and also of the electronic instabilities such as charge and spin density waves that may frustrate superconductivity. We have not pinpointed a global mechanism for superconductivity nor calculated a T_c for any of these materials. Nevertheless, the persistent electronic analogy between these layered structures and the Cu–O superconductors strongly merits experimental investigation.

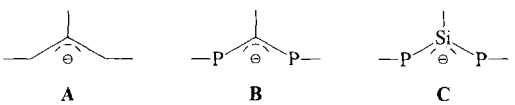
Received: January 25, 1989 [Z 3140 IE]
German version: *Angew. Chem. 101* (1989) 789

[1] B. Aurivillius, *Ark. Kemi 1* (1949) 463, 499; *2* (1950) 519; *5* (1952) 39.
[2] R. E. Newnham, R. W. Wolfe, J. F. Dorrian, *Mater. Res. Bull. 6* (1971) 1029.
[3] L. E. Cross, R. C. Pohanka, *Mater. Res. Bull. 6* (1971) 939.
[4] a) A. J. Jacobson, J. W. Johnson, J. T. Lewandowski, *Inorg. Chem. 24* (1985) 3727; b) J. Gopalakrishnan, V. Bhat, B. Raveau, *Mater. Res. Bull. 22* (1987) 413; M. A. Subramanian, J. Gopalakrishnan, A. W. Sleight, *ibid. 23* (1988) 837.
[5] See, e.g., a) M. A. Subramanian, C. C. Torardi, J. C. Calabrese, J. Gopalakrishnan, K. J. Morrissey, T. R. Askew, R. B. Flippen, U. Chowdhry, A. W. Sleight, *Science (Washington D.C.) 239* (1988) 1015; C. C. Torardi, M. A. Subramanian, J. C. Calabrese, J. Gopalakrishnan, K. J. Morrissey, T. R. Askew, R. B. Flippen, U. Chowdhry, A. W. Sleight, *ibid. 240* (1988) 631; M. A. Subramanian, J. C. Calabrese, C. C. Torardi, J. Gopalakrishnan, T. R. Askew, R. B. Flippen, K. J. Morrissey, U. Chowdhry, A. W. Sleight, *Nature (London) 332* (1988) 420; b) H. G. von Schnering, L. Walz, M. Schwarz, W. Becker, M. Hartweg, T. Popp, B. Hettich, P. Müller, G. Kämpf, *Angew. Chem. 100* (1988) 604; *Angew. Chem. Int. Ed. Engl. 27* (1988) 574; c) Z. Z. Sheng, A. M. Hermann, *Nature (London) 332* (1988) 55; d) C. W. Chu, J. Bechtold, L. Gao, P. H. Hor, Z. J. Huang, R. L. Meng, Y. Y. Sun, Y. Q. Wang, Y. Y. Xue, *Phys. Rev. Lett. 60* (1988) 941.
[6] The atomic parameters employed in our calculations on **1** (TiO_4; NbO_4), its sandwich analogue $(Bi_2O_2)_2NbO_4$, **2** ($BiNb_2O_7$; Nb_2O_7), and **3** ($Bi_3Nb_4O_{13}$; Nb_4O_{13}) are as follows: The valence shell ionization potentials and orbital exponents are −32.3 eV and 2.275 for O 2s, −14.8 eV and 2.275 for O 2p, −21.2 eV and 2.76 for Bi 6s, −13.0 eV and 2.29 for Bi 6p, −10.10 eV and 1.89 for Nb 5s, −6.86 eV and 1.85 for Nb 5p, −8.97 eV and 1.50 for Ti 4s, and −5.44 eV and 1.50 for Ti 4p. The 3d orbitals of Ti and the 4d orbitals of Nb are represented by two Slater functions with mixing coefficients in parentheses: −10.81 eV with 4.55 (0.5206) and 1.40 (0.7839) for Ti 3d, −12.49 eV with 4.08 (0.6401) and 1.64 (0.5516) for Nb 4d.
[7] M.-H. Whangbo, R. Hoffmann, *J. Am. Chem. Soc. 100* (1978) 6093.
[8] R. Hoffmann, *J. Chem. Phys. 13* (1963) 1397; H. H. Ammeter, H.-B. Bürgi, J. C. Thibeault, R. Hoffmann, *J. Am. Chem. Soc. 100* (1978) 3686.
[9] See, e.g., a) M.-H. Whangbo, M. Evain, M. A. Beno, J. M. Williams, *Inorg. Chem. 26* (1987) 1829, 1831, 1832; b) J. K. Burdett, G. V. Kulkarni, K. Levin, *ibid. 26* (1987) 3652; c) L. F. Mattheiss, *Phys. Rev. Lett. 58* (1987) 1028; L. F. Mattheiss, D. R. Hamann, *Solid State Commun. 63* (1987) 395.
[10] F. Herman, R. V. Kasowski, W. Y. Hsu, *Phys. Rev. B38* (1988) 204.
[11] a) A. Simon, *Angew. Chem. 99* (1987) 602; *Angew. Chem. Int. Ed. Engl. 26* (1987) 579; b) M. J. S. Dewar, *ibid. 99* (1987) 1313 and *26* (1987) 1273.
[12] M.-H. Whangbo, E. Canadell, M. Evain, J. M. Williams, *Inorg. Chem. 27* (1988) 2394.
[13] R. A. Wheeler, M.-H. Whangbo, T. Hughbanks, R. Hoffmann, J. K. Burdett, T. A. Albright, *J. Am. Chem. Soc. 108* (1986) 2222.
[14] T. Ogushi, Y. Hakuraku, H. Honjo, G. N. Suresha, S. Higo, Y. Ozono, I. Kawano, T. Numota, *J. Low Temp. Phys. 70* (1988) 485.

Synthesis, Structure, and Reactivity of a 1,3-Diphospha-2-silaallyl Anion**

By *Edgar Niecke,* Elke Klein,* and *Martin Nieger*

The formal replacement of the two terminal positions in allyl anion **A**[1] by phosphorus centers of coordination number 2 leads to the 1,3-diphosphaallyl system **B**,[2] which is becoming increasingly important as a complex ligand.[3] We report here the synthesis of the 1,3-diphospha-2-silaallyl anion **C**, which is analogous to **B** and is the first example of a stable, delocalized 3p(π) bonding system.



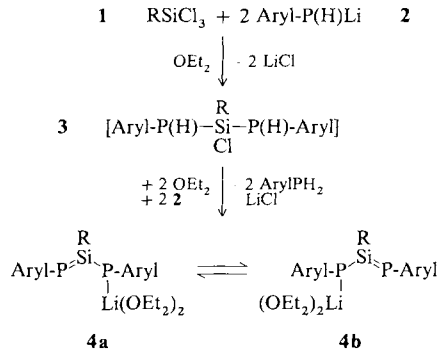
A **B** **C**

The surprisingly simple preparation of **C** was achieved in a one-pot reaction by treatment of *tert*-butyltrichlorosilane **1** with four equivalents of lithiophosphane **2** in diethyl ether.[4] The lithium salt of the allyl anion is obtained as the diether adduct **4** in the form of deep red, extremely moisture-sensitive, thermally stable crystals (m.p. 150–152 °C). These are

[*] Prof. Dr. E. Niecke, Dipl.-Chem. E. Klein, M. Nieger
Institut für Anorganische Chemie der Universität
Gerhard-Domagk-Strasse 1, D-5300 Bonn 1 (FRG)

[**] This work was supported by the Deutsche Forschungsgemeinschaft and the Fonds der Chemischen Industrie.

stable for several weeks under inert atmosphere at room temperature. The constitution of **4** was established by elemental analysis, NMR spectroscopy,[5] and X-ray structure analysis.[6]



R = *t*Bu; Aryl = 2,4,6-*t*Bu$_3$C$_6$H$_2$

The ^{31}P NMR spectrum of **4** (25 °C, C_6D_6) displays four equally spaced lines in the high-field region ($\delta = -45.1$), thus showing an interaction with the lithium nucleus ($J_{PLi} = 46.5$ Hz).[5] This finding can be interpreted in terms of a rapid exchange process, **4a** $\rightleftharpoons$ **4b**.

The X-ray structure analysis[6] (Fig. 1) corroborates the spectroscopic results. In the solid state, **4** is present as an

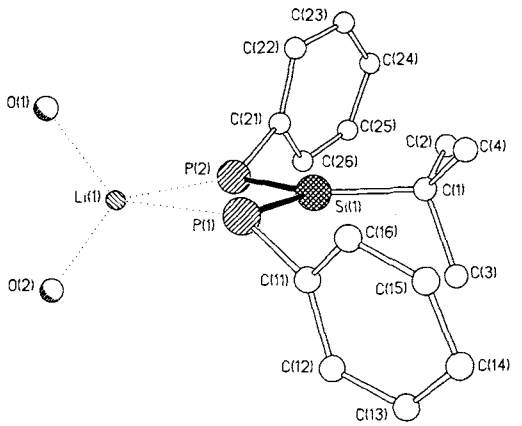
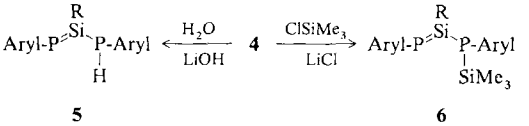


Fig. 1. Molecular structure of **4** (peripheral groups omitted). Important bond lengths [pm] and angles [°]: Si1-P1 211.4(3), Si1-P2 211.3(3), Si1-C1 191.5(7) Li1-P1 263.9(14), Li1-P2 267.0(13), Li1-O1 193.9(13), Li1-O2 193.8(12); P1-Si1-P2 104.9(1), Si1-P1-Li1 88.8(3), P1-Li1-P2 78.3(3), Si1-P2-Li1 88.0(3), O1-Li1-O2 110.1(6). The atoms P1-Si1-P2-Li1 lie in a plane ($\sigma = 0.20$ pm).

η^2-lithio-1,3-diphospha-2-silaallyl system ("frozen transition state" of **4a** $\rightleftharpoons$ **4b**); the position of the lithium with respect to the P1–Si1–P2 plane of **4** is indicative of a σ complex. Owing to the coordination of the lithium to two phosphorus centers, the Li–P bonds (264–267 pm) are, as expected, longer than those in the lithiophosphanes investigated so far.[7] The bonding in the anion fragment with the observed planar arrangement of the framework C11-P1-Si1 [-C1]-P2-C21, as well as the very short P–Si distances (211 pm; sum of the covalent radii for a single bond, 224 pm[8]), is in agreement with a description of **4** as a four-electron, three-center 3 p(π) bonding system. The relatively small P1–Si1–P2 angle (105°) may be ascribed to the chelating effect of the lithium atom. Both aryl ligands are orthogonal to the p(π) system owing primarily to steric effects ("steric bulk" of the *tert*-butyl groups). The coordination vacancies at lithium are filled by two solvent molecules (Et_2O), which create a distorted tetrahedral geometry for the "cation".



In the presence of traces of moisture, **4** is immediately converted into the phosphino derivative **5**. Reaction of **4** with trimethylchlorosilane affords the silylphosphino compound **6**. Both **5** and **6** contain a P–Si double bond, as revealed by the ^{31}P NMR spectra (**5**, $\delta = 142$, -125 ($J_{PP} = 6$ Hz); **6**, $\delta = 83.3$, -110.1 ($J_{PP} = 63$ Hz)). Such compounds are well known through the work of *Bickelhaupt* et al.[9]

Experimental Procedure

4: 2,4,6-*t*Bu$_3$-C$_6$H$_2$PH$_2$ (4.18 g, 15 mmol) [10] in 20 mL of anhydrous ether was treated at room temperature with an equimolar amount of *n*-butyllithium (15% in *n*-hexane). The reaction mixture was then stirred for 1 h. The solution of the lithiophosphane **2** obtained in this way was added slowly dropwise to **1** (0.72 g, 3.75 mmol) in 15 mL of anhydrous ether at -65 °C. The resulting gold-yellow solution turned deep red on warming to 25 °C. The ^{31}P NMR spectrum of the reaction mixture shows, in addition to the signals of **4**, only those of the primary phosphane [9] ($\delta = -132$ (t, $J_{PH} = 207$ Hz)). After evaporation of the solvent, the residue was dissolved in dry *n*-hexane, the LiCl was filtered off, and the filtrate was concentrated in vacuo. Deep red crystals of **4** were obtained from an ether/hexane mixture (1:3): yield 2.25 g (77%).

Received: January 13, 1989 [Z 3118 IE]
German version: *Angew. Chem. 101* (1989) 792

CAS Registry numbers:
1, 18171-74-9; **4**, 120496-38-0; **5**, 120477-62-5; **6**, 120477-63-6; 2,4,6-*t*Bu$_3$-C$_6$H$_2$PH$_2$, 83115-12-2.

[1] D. J. Cram: *Fundamentals of Carbanion Chemistry*, Academic Press, New York 1965.

[2] a) H. H. Karsch, *Phosphorus Sulfur 30* (1987) 419; b) W. Schuhn, *Dissertation*, Universität Bonn 1988; R. Appel, W. Schuhn, unpublished.

[3] a) R. Appel, W. Schuhn, F. Knoch, *Angew. Chem. 97* (1985) 421; *Angew. Chem. Int. Ed. Engl. 24* (1985) 420; b) *J. Organomet. Chem. 319* (1987) 345; c) R. Appel, W. Schuhn, *ibid. 329* (1987) 179; d) R. Appel, W. Schuhn, M. Nieger, *Angew. Chem. 100* (1988) 437; *Angew. Chem. Int. Ed. Engl. 27* (1988) 416.

[4] The intermediacy of a bisphosphinosilane **3** has been structurally confirmed for R = Cl: E. Niecke, E. Klein, M. Nieger, H. Ranaivonjatovo, unpublished.

[5] ^{7}Li NMR (C_6D_6, 25 °C): $\delta = 2.66$ (t, $J_{LiP} = 49$ Hz).

[6] Crystal structure analysis of **4** ($C_{48}H_{87}O_2P_2SiLi$): Red crystals from ether/hexane; crystal dimensions $0.5 \times 0.5 \times 0.8$ mm^3, $M_r = 793.2$; space group $P2_1/n$, $a = 18.107(8)$, $b = 16.193(13)$, $c = 19.492(14)$ Å, $\beta = 112.22(5)°$, $V = 5.291$ nm^3, $Z = 4$, $\varrho_{calcd} = 0.99$ g cm^{-3}, $\mu(Mo_{K\alpha}) = 0.13$ mm^{-1}; 6922 symmetry-independent reflections ($2\theta_{max} = 45°$), 3483 with $|F| > 4\sigma(F)$ used in the structure solution (Direct Methods) and refinement (485 parameters); non-hydrogen atoms refined anisotropically (disordered *tert*-butyl groups on Si isotropic; site occupancy factor (C2, C3, C4 = 0.67(1)); H atoms refined using a "riding" model; $R = 0.083$ ($R_w = 0.080$, $w^{-1} = \sigma^2(F) + 0.0012\,F^2$). Further details of the crystal structure investigation may be obtained from the Fachinformationszentrum Karlsruhe, Gesellschaft für wissenschaftlich-technische Information mbH, D-7514 Eggenstein-Leopoldshafen 2 (FRG), on quoting the depository number CSD-53667, the names of the authors, and the journal citation.

[7] The sum of the covalent radii of Li and P is 244 pm.

[8] No structural data are available for the P–Si p(π) bonding system. For the parent compound HP=SiH$_2$, theoretical calculations give a value of 204 pm: K. J. Dykema, T. N. Truong, M. S. Gordon, *J. Am. Chem. Soc. 107* (1985) 4535.

[9] F. Bickelhaupt, C. N. Smit, *Organometallics 6* (1987) 1156.

[10] M. Yoshifuji, L. Shima, N. Inamoto, *J. Am. Chem. Soc. 105* (1983) 2495.

Additivities of Electrostatic and Hydrophobic Interactions in Host–Guest Complexes**

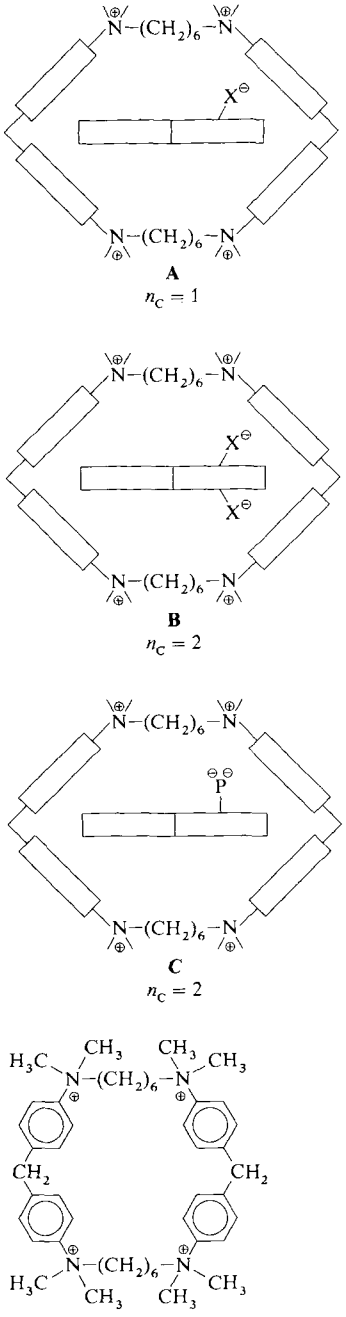
By *Hans-Jörg Schneider** and *Isolde Theis*

Noncovalent interactions play a major role in biological systems as well as in synthetic host–guest complexes. The importance of quantification of electrostatic contributions[1] has been recognized, for example, in the study of enzyme–substrate binding mechanisms by site-directed mutagenesis[2] and of polyamine binding to nucleic acids.[3] Synthetic analogues of receptor–substrate complexes[4] offer the advantage of planned variations of the nature and the geometries of interacting groups within relatively well defined conformations. We demonstrate here that the analysis of salt bridges in a large number of very different synthetic receptor models in water gives a surprisingly uniform value of 5 ± 1 kJ mol^{-1} per ion pair as long as electrostatic interactions dominate.

Many substrates and coenzymes are bound by electrostatic as well as by hydrophobic forces. The complexes **A**–**C** (Scheme 1), formed between azoniacyclophanes **1** and naphthalene derivatives bearing negative charges,[5,6] are examples in which the predominant lipophilic or hydrophobic binding contributions can be quantified by the dependence of the association constants on solvent hydrophobicity.[7] Since many electroneutral naphthalene derivatives show quite similar complexation free energies of $\Delta G = 19 \pm 1$ kJ mol^{-1} (Table 1, row a), one can subtract these values from the higher ΔG values observed for corresponding compounds of similar shape bearing anionic substituents X in order to obtain typical Coulomb interaction increments. Measurements with four naphthalene derivatives with anionic substituents at C-2 indeed show a rather uniform increase of $\Delta G \approx 3$ kJ mol^{-1} (Table 1, row b). With anionic substituents at C-1 (row c) a similar value is observed, particularly if the substituent is attached to an intervening CH_2 or O group which allows a better contact of $X^{\ominus}$ to the $^{\oplus}N$ counterion of the macrocycle; otherwise, the predominating pseudoequatorial inclusion of the naphthalene unit,[8] necessary for an optimal hydrophobic interaction, would be distorted. Similar reasons may explain the small ΔG increase observed for substrates with $X^{\ominus}$ at C-1 and C-8 (Table 1, row d; cf. **B** in Scheme 1); only if the position of the charges allows the simultaneous contact of both charged substituents with the host counterion is a concomitant ΔG increase observed; this is remarkably the case when both charges reside in *one* phosphate unit (**C** in Scheme 1).

The complex **D** (Scheme 2) formed from a macrocyclic tetraphenolate **2** with four delocalized negative charges and a host compound, represents a case in which Coulomb interactions dominate almost entirely. This is shown, for instance, by the decrease in the complexation free energy ΔG for the substrates Y from 25 kJ mol^{-1} for Y = $^{\oplus}NMe_4$ to 4 kJ mol^{-1} for Y = $HOCMe_3$.[9] If one considers the interactions in all of these complexes[9] to be additive, the resulting Coulomb interaction between singly charged ions ($n_c = 1$) is $\Delta G = 21/4 = 5.2$ kJ mol^{-1}.

Association constants in water for complexes held together *exclusively* by electrostatic forces have been reported. Those determined by *Williams* et al.[10] for complexes of type



Scheme 1.

E (Scheme 2) all fall into the same range within the limits of error, yielding 5 ± 1 kJ mol^{-1} per salt bridge ($n_c = 1$) for 25 different salts. The same values are obtained for the complexes of type **F** and **G** (Scheme 2) described by *Lehn* et al.[4a,11] if those systems are disregarded in which the counterions for geometric reasons cannot contact each other closely and if the interactions between one ion and several counterions at similar distances are counted separately.

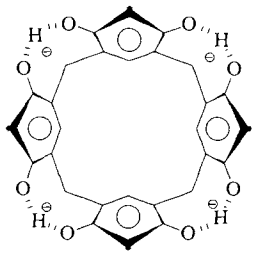
Thus, the complexation free energies of more than 35 complexes can be described by a simple Coulomb correlation (Fig. 1). The underlying cation–anion combinations comprise groups of quite different sizes, polarizabilities, and charge densities: $^{\oplus}NH_2R_2$, $^{\oplus}NR_4$ (R = alkyl), aromatic positively charged nitrogen heterocycles, $CO_2^{\ominus}$, $HPO_4^{\ominus}$, $PO_4^{2\ominus}$, and charge-delocalized phenolates. As a first approximation it is obviously sufficient to consider only the electrostatic interactions between nearest neighbors.

[*] Prof. Dr. H.-J. Schneider, Dipl.-Chem. I. Theis
Fachrichtung Organische Chemie der Universität
D-6600 Saarbrücken 11 (FRG)

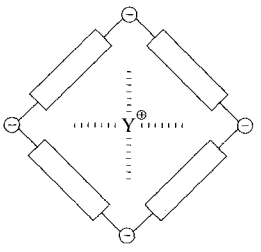
[**] Host–Guest Chemistry, Part 21. This work was supported by the Deutsche Forschungsgemeinschaft and the Fonds der Chemischen Industrie. Part 20: H.-J. Schneider, T. Blatter, S. Simova, I. Theis, *J. Chem. Soc. Chem. Commun.*, in press.

Table 1. Complexation free energies ΔG [kJ mol^{-1}] of the complexes formed from the azoniacyclophane **1** and naphthalene derivatives with substituents X [a]

	X	ΔG	X	ΔG	X	ΔG	X	ΔG	X	ΔG
a	H	19	1-OH	21	2-OH	19	2-COOH	18	1-NH_2	19
b	2-$COO^{\ominus}$	22	2-$CH_2COO^{\ominus}$	22	2-$SO_3^{\ominus}$	23	2-O-$PO_3H^{\ominus}$	22		
c	1-$COO^{\ominus}$	20	1-$CH_2COO^{\ominus}$	21	1-O-$PO_3H^{\ominus}$	22				
d	1,8-$(COO^{\ominus})_2$	23	2,3-$(COO^{\ominus})_2$	26	1-O-$PO_3^{2\ominus}$	22	2-O-$PO_3^{2\ominus}$	24.5		



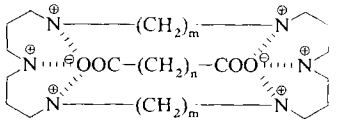
2



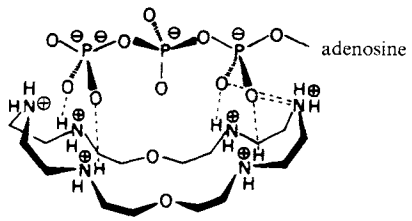
D
$n_C = 4$



E
$n_C = 2$



F
$n_C = 2 \times 3$



G
$n_C = 2 \times 3 + 2 \times 3$

Scheme 2.

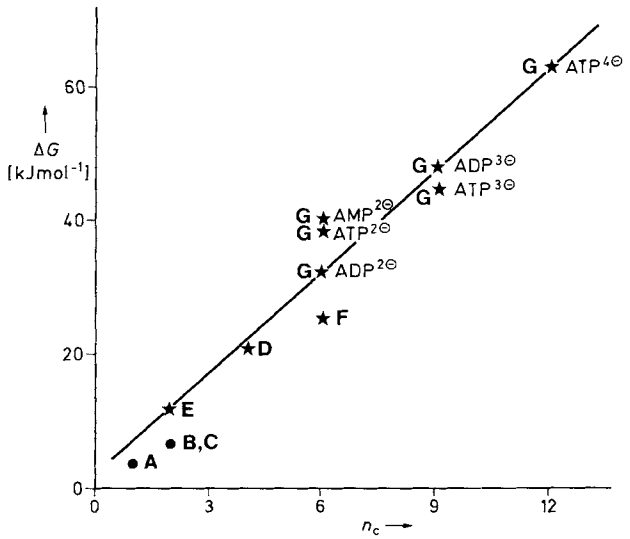


Fig. 1. Complexation free energies ΔG in water plotted versus the number of ion pairs (n_c). Correlation coefficient $r = 0.967$; reliability measure $\Psi = 8\%$; weight = 1.0 for **D** (5 values)[8], **E** (25 values)[10], **F**[11], **G**[11]; weight = 0.0 for **A**–**C**.

Apparently, the differences in complexation free energies between the charged systems **A** to **C** (Table 1, rows b–d) and their electroneutral counterparts (row a) are uniformly smaller ($\Delta G \approx 3$ kJ mol^{-1}) than the general Coulomb increment (ca. 5 kJ mol^{-1}). The reason for this can be seen in the decrease in the hydrophobic van der Waals interactions – which dominate in all these complexes[6, 7] – upon introduction of the charged groups in the naphthalene guest molecules, so that the Coulomb attraction gained is partially compensated.

Received: January 9, 1989 [Z 3116 IE]
German version: *Angew. Chem. 101* (1989) 757

[1] A. Warshel, S. T. Russel, *Q. Rev. Biophys. 17* (1984) 283; S.-C. Tam, R. J. P. Williams, *Struct. Bonding (Berlin) 63* (1985) 103.
[2] M. J. E. Sternberg, F. R. F. Hayes, A. J. Russell, P. G. Thomas, A. R. Fersht, *Nature (London) 330* (1987) 86.
[3] G. S. Manning, *Q. Rev. Biophys. 11* (1978) 179; K. D. Stewart, *Biochem. Biophys. Res. Commun. 152* (1988) 1441, and references cited therein.
[4] Recent reviews: a) J.-M. Lehn, *Angew. Chem. 100* (1988) 91; *Angew. Chem. Int. Ed. Engl. 27* (1988) 89; b) F. Diederich, *ibid. 100* (1988) 372 and *27* (1988) 362.
[5] K. Odashima, K. Koga in P. M. Kuhn, S. M. Rosenfeld (Eds): *Cyclophanes, Vol. 2*, Academic Press, New York 1983, pp. 629–677.
[6] a) H.-J. Schneider, K. Philippi, J. Pöhlmann, *Angew. Chem. 96* (1984) 907; *Angew. Chem. Int. Ed. Engl. 23* (1984) 908; b) H.-J. Schneider, T. Blatter, *ibid. 100* (1988) 1211 and *27* (1988) 1163.
[7] H.-J. Schneider, R. Kramer, S. Simova, U. Schneider, *J. Am. Chem. Soc. 110* (1988) 6442.
[8] H.-J. Schneider, J. Pöhlmann, *Bioorg. Chem. 15* (1987) 183.
[9] H.-J. Schneider, D. Güttes, U. Schneider, *J. Am. Chem. Soc. 110* (1988) 6449.
[10] S.-C. Tam, R. J. P. Williams, *J. Chem. Soc., Faraday Trans. 1 80* (1984) 2255.
[11] a) M. W. Hosseini, J.-M. Lehn, *J. Am. Chem. Soc. 104* (1982) 3525; b) M. W. Hosseini, J.-M. Lehn, M. P. Mertes, *Helv. Chim. Acta 66* (1983) 2454.

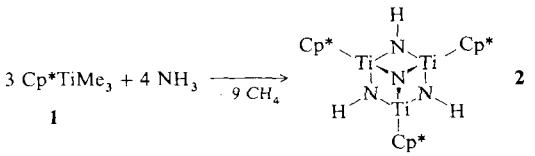
Synthesis and Structure of $[\{(\eta^5\text{-}C_5Me_5)Ti(NH)\}_3N]$, a Titanium Imide Nitride **

By *Herbert W. Roesky,** *Yüniu Bai,* and *Mathias Noltemeyer*

In our investigations of metal–nitrogen heterocycles, we recently succeeded in synthesizing $[Cp^*TaN(Cl)]_3$, which can be regarded as a trimer of a metal nitride, by reaction of Cp^*TaCl_4 ($Cp^* = C_5Me_5$) with $N(SnMe_3)_3$.[1] Whereas metal nitrides are known to have a wide variety of structures,[2] transition-metal complexes with NH ligands (imides) have been little investigated. Imides might occur as intermediates in the formation of TiN from $TiCl_4$ and ammonia.[3] We now report an imide nitride of titanium, prepared by reaction of Cp^*TiMe_3 **1**[4] with excess ammonia at room temperature. Loss of methane leads to the formation of $[\{Cp^*Ti(NH)\}_3N]$ **2** in good yield.

[*] Prof. Dr. H. W. Roesky, Yüniu Bai, Dr. M. Noltemeyer
Institut für Anorganische Chemie der Universität
Tammannstrasse 4, D-3400 Göttingen (FRG)

[**] This work was supported by the Deutsche Forschungsgemeinschaft, the VW-Stiftung, and the Fonds der Chemischen Industrie.



Evidence for the composition and structure of **2** is already provided by the ^{1}H NMR spectrum and the mass spectrum. Equivalent pentamethylcyclopentadienyl ($\delta = 2.01$) and NH ($\delta = 13.4$) groups are found. The molecular ion (m/z 608) is observed with 100% relative intensity in the mass spectrum. In the field-ionization mass spectrum, only the signal of $[M + 1]^{\oplus}$ (m/z 609) appears. The IR spectrum shows two of the three (2 A', 1 A'') absorptions (3357 and 3345 cm^{-1}) expected for C_s symmetry. We assign these to the N–H valence vibrations.

Single crystals suitable for an X-ray structure analysis (Fig. 1)[5] were obtained by recrystallization from *n*-hexane.

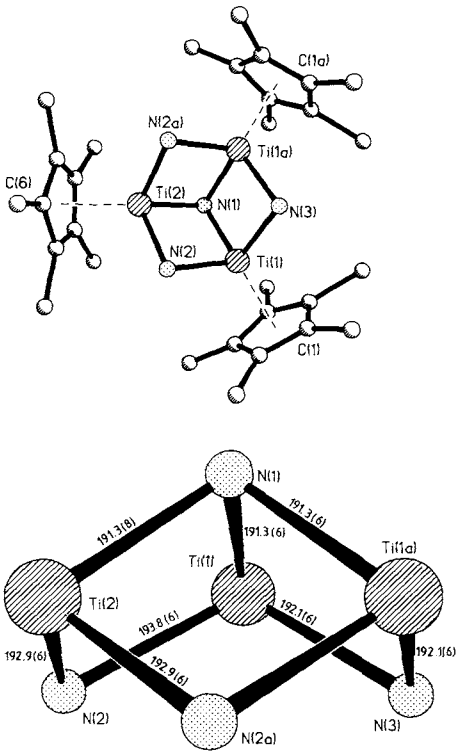


Fig. 1. Molecular structure of **2**. Top: View from above. Below: Side view of the Ti_3N_4 core. Selected bond lengths [pm] and angles [°]: Ti(1)-Ti(2) 280.3(3); Ti(2)-Ti(1)-N(1) 42.9(2), N(1)-Ti(1)-N(2) 85.9(3), N(1)-Ti(1)-N(3) 85.8(3). Further bond lengths are given in the lower part of the figure.

The six-membered $(TiNH)_3$ ring with tetrahedrally coordinated titanium atoms exists in chair conformation. The three titanium atoms are bridged by a further nitrogen atom, N(1). The molecule exhibits C_s symmetry (mirror plane through Ti(2), N(1), N(3)). The Ti–N bond lengths (average 192.4 pm) lie between those in $[CpTiCl_2NPPh_2]$ (177.5 (13) pm)[6] and $[CpTiCl_2NPPh_2NS(O)Me_2]$ (176.4(2) pm)[7] on the one hand and those in $[\{PhC(NSiMe_3)_2\}_2TiCl_2]$ (206.6 and 210.1 pm)[8] on the other.

Oxygen-containing titanium compounds with similar structures have been described by *Garcia Blanco* et al.[9] and *Bottomley* et al.[10] Methyl-substituted organometallic compounds are well known,[11] so that their reaction with ammonia should afford further imides and nitrides.

Experimental Procedure

Excess ammonia was admitted over 3 h to a solution of **1** (1.14 g, 5 mmol) in 30 mL of *n*-hexane at room temperature. The initially yellow solution turned red and a yellow solid formed. The reaction was over when no more solid precipitated. Excess ammonia and the solvent were then removed in vacuo and the residue was washed with a small amount of *n*-hexane. Yield: 0.67 g (67%) of **2**. The compound slowly decomposes above 200 °C. Only a doublet is present in the ^{15}N NMR spectrum ($CDCl_3$, ext. $MeNO_2$): $\delta = 90.7$ ($^1J_{NH} = 63.5$ Hz).

Received: February 3, 1989 [Z 3153 IE]
German version: *Angew. Chem. 101* (1989) 788

CAS Registry numbers:
1, 107333-47-1; **2**, 120686-86-4.

[1] H. Plenio, H. W. Roesky, M. Noltemeyer, G. M. Sheldrick, *Angew. Chem. 100* (1988) 1377; *Angew. Chem. Int. Ed. Engl. 27* (1988) 1330.
[2] K. Dehnicke, J. Strähle, *Angew. Chem. 93* (1981) 451; *Angew. Chem. Int. Ed. Engl. 20* (1981) 413; N. N. Greenwood, A. Earnshaw: *Chemistry of the Elements*, Pergamon, Oxford 1984, p. 480ff.
[3] L. Maya, *Inorg. Chem. 25* (1986) 4213; F. A. Cotton, G. Wilkinson: *Advanced Inorganic Chemistry*, Wiley, New York 1988, p. 658; P. Ehrlich, *Z. Anorg. Allg. Chem. 259* (1949) 1; A. Brager, *Acta Physicochim. USSR 11* (1939) 617; H. Harnisch, G. Heymer, E. Schallas, *Chem. Ing. Tech. 35* (1963) 7; H. Winterhager, K. Hanusch, *Ber. Dtsch. Keram. Ges. 46* (1969) 181; F. H. Pollard, G. W. A. Fowles, *J. Chem. Soc. 1952*, 2444.
[4] M. Mena, M. A. Pellinghelli, P. Royo, R. Serrano, A. Tiripicchio, *J. Chem. Soc. Chem. Commun. 1986*, 1118.
[5] $C_{30}H_{48}N_4Ti_3$, $M_r = 608.4$, orthorhombic *Pnma*, $a = 1184.8(6)$, $b = 1930.7(10)$, $c = 1402.4(9)$ pm, $V = 3.20798$ nm^3, $Z = 4$, $\varrho = 1.26$ Mg m^{-3}, $\mu_{MoK\alpha} = 0.74$ mm^{-1}, crystal dimensions $0.1 \times 0.3 \times 0.3$ mm^3, STOE four-circle diffractometer, 6093 reflections to $2\Theta = 45°$, 2167 symmetry-independent reflections and 1546 with $F_0 > 4\delta(F_0)$ used in the refinement (SHELX): $R = 0.089$, $R_w = 0.095$, $w^{-1} = \delta^2(F_0) + 0.0008\,F_0^2$. The relatively poor R value is explained by the high thermal motion of the Cp* rings. For this reason, a total of 48 hydrogen atoms were not included. The standard deviation for the Ti–N bond lengths is ca. 0.6 pm and for the C–C bond lengths (in Cp*) between 1 and 2 pm. Residual electron density ± 0.6 e Å^{-3}. Further details of the crystal structure investigation may be obtained from the Fachinformationszentrum Karlsruhe, Gesellschaft für wissenschaftlich-technische Information mbH, D-7514 Eggenstein-Leopoldshafen 2 (FRG), on quoting the depository number CSD-53121, the names of the authors, and the journal citation.
[6] I. A. Latham, G. J. Leigh, G. Huttner, I. Jbril, *J. Chem. Soc. Dalton Trans. 1986*, 377.
[7] H. W. Roesky, F. Schrumpf, M. Noltemeyer, *Z. Naturforsch. B44* (1989) 35.
[8] H. W. Roesky, B. Meller, M. Noltemeyer, H. G. Schmidt, U. Scholz, G. M. Sheldrick, *Chem. Ber. 121* (1988) 1403.
[9] S. Garcia Blanco, M. P. Gómez Sal, S. Martinez Carreras, M. Mena, P. Royo, R. Serrano, *J. Chem. Soc. Chem. Commun. 1986*, 1572.
[10] F. Bottomley, G. O. Egharevba, P. S. White, *J. Am. Chem. Soc. 107* (1985) 4353.
[11] G. Wilkinson, F. G. A. Stone, E. W. Abel (Eds.): *Comprehensive Organometallic Chemistry*, Pergamon, Oxford 1982.

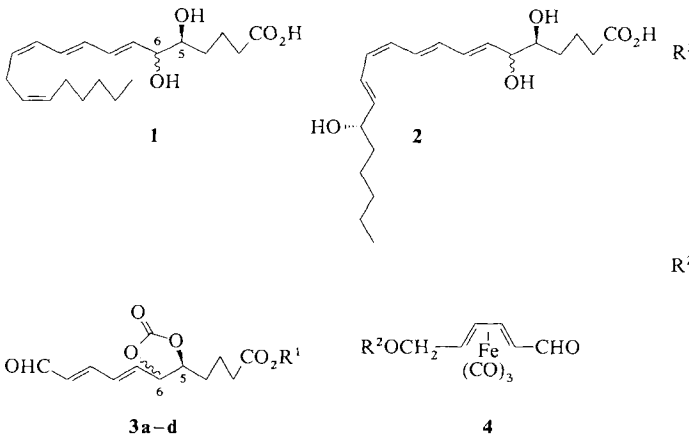
A New Synthesis of Key Intermediates for the Preparation of 5,6-DiHETE and Lipoxin A_4

By *Agnès Gigou, Jean-Paul Lellouche, Jean-Pierre Beaucourt,* Loïc Toupet,* and *René Grée**

Polyhydroxylated metabolites of the arachidonic acid cascade are attractive target molecules not only because of their

[*] Dr. J.-P. Beaucourt, A. Gigou, Dr. J.-P. Lellouche
Service des Molécules Marquées, Bât. 547
CEN Saclay
F-91191 Gif-Sur-Yvette (France)
L. Toupet
Départment de Physique Cristalline, UA CNRS 804
Université de Rennes I
F-35042 Rennes Cedex (France)
Dr. R. Grée
Laboratoire de Chimie Organique Biologique, CNRS UA 704
ENSCR
Avenue du Gal Leclerc, F-35700 Rennes-Beaulieu (France)

interesting stereochemistry but also because of their potent biological properties. 5,6-DiHETE **1**[1] and lipoxin A_4 **2**[2] (Scheme 1) are representative examples of a group of metabolites characterized by a glycol structure vicinal to a polyenic system. The carbonates **3a** and **3b**, which are key intermediates for the total synthesis of **1** and **2** have already been prepared by multistep sequences starting from 2-deoxy-D-ribose (for the *erythro* isomer) and from xylose (for the *threo* isomer).[3]



1 **2** **3a–d** **4**

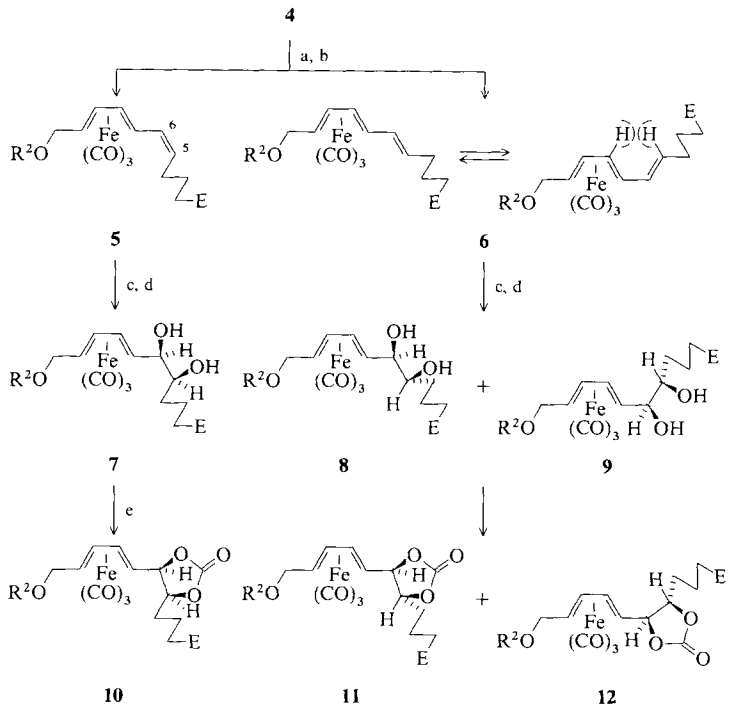
Scheme 1. **3a, b**, $R^1 = C_2H_5$; **3c, d**, $R^1 = CH_3$; **4**, $R^2 = SiPh_2tBu$. The *erythro* isomers **3a,c** have the (5*S*,6*R*) configuration, the *threo*-isomers **3b,d** the (5*S*,6*S*) configuration.

Here we describe a new, stereoselective synthesis of racemic **3c** and **3d** starting from the butadiene–tricarbonyl–iron complex **4**.[4] The key step of this novel approach is the diastereoselective osmylation of double bonds vicinal to the organometallic complex fragment.[5]

The Wittig reaction of **4** with 5-(triphenylphosphoranediyl)pentenoic acid, followed by in situ esterification, gives a 4:1 mixture of the complexed trienes **5** and **6** (Scheme 2), which are easily separated by chromatography.[6] Their osmylation occurs readily and without decomplexation to give, in almost quantitative yield, only one complexed diol **7** starting from **5** and two diastereoisomeric diols **8** and **9** starting from **6** (HPLC and 300-MHz ^{1}H NMR controls). Compound **7** is converted into the carbonate **10** (63% overall yield from **5**; see Table 1 for spectral data); in the same way, the diols **8** and **9** give a 9:1 mixture of the two complexed *threo* carbonates **11** and **12** (77–81% overall yield from **6**), which can be separated by chromatography.

The configurations of the carbonates **10–12** have been unambiguously established by X-ray crystallography.[7] Interestingly, in each case, the addition of OsO_4 to the free double bond occurs *anti* to the $Fe(CO)_3$ moiety; for the *E* alkene, it is possible to consider an equilibrium between the *s-trans* conformer (leading to **8**) and the *s-cis* conformer (giving the minor derivative **9**). This result is in good agreement with the addition of diazo compounds to structurally related trienes.[8]

Correlation of these derivatives with carbonates **3c** and **3d** is done by a three-step sequence: decomplexation ($Ce^{4\oplus}$, MeOH, −15 °C, 80–95%), desilylation ($nBu_4N^{\oplus}F^{\ominus}$, 3 H_2O, THF, 0 °C, *erythro* 80%, *threo* 77%), and oxidation (pyridinium dichromate, CH_2Cl_2, 20 °C, *erythro* 80%, *threo* ≥95%) leads to racemic **3c** starting from **10**, while its isomer **3d** is exclusively obtained starting from **11**.[10]



5 **6** **7** **8** **9** **10** **11** **12**

Scheme 2. E = CO_2Me; $R^2 = SiPh_2tBu$. 0.5 mmol **4** was employed. a) $Br^{\ominus}Ph_3P^{\oplus}(CH_2)_4CO_2H$ (0.92 mmol, 1.83 equiv.), $(Me_3Si)_2NLi$ (1.83 mmol, 1.83 equiv.), THF (4.5 mL), HMPA (0.6 mL), 1.5 h −20 °C → 0 °C; **4** (0.5 mmol), THF (2.5 mL), 1.5 h −78 °C, then 1.5 h −20 °C. b) Me_2SO_4 (4.2 mmol, 8.4 equiv.), 18 h, −10 °C (80–90% from **4**). c) **5** or **6** (0.4 mmol), OsO_4 (0.6 mmol, 1.5 equiv.), Py (8 mL), 2 h 20 °C. d) $Na_2S_2O_5$ (10.5 mmol), H_2O (20 mL), 16 h, 20 °C (95% from **5** or **6**). e) **7** (0.43 mmol), Im_2CO (0.47 mmol, 1.09 equiv.), benzene (13 mL), 2 h 40 °C, then Im_2CO (0.47 mmol, 1.09 equv.), 1 h 64 °C (66%). f) **8** + **9** (0.21 mmol), Im_2CO (1.05 mmol, 5.0 equiv.), benzene (11 mL), 1 h 20 °C (81–85%).

Table 1. Spectral data of **10**.

IR (KBr pellet): $\tilde{\nu}$ = 2045 (s), 1985 (s), 1950 (s), 1790 (s), 1735 (m) cm^{-1}. MS(EI): *m/z* 504.1 (8.6%), 448.0 (5.7%), 28.0 (100.0%). ^{1}H NMR (300 MHz, C_6D_6): δ = 0.32 (dd, 1H, *J* = 8.5, 7.3 Hz), 1.07–1.21 (m, 1H), 1.16 (s, 9H), 1.22–1.30 (m, 2H), 1.32–1.70 (m, 2H), 1.94 (t, 2H, *J* = 6.8 Hz), 3.34 (s, 3H), 3.50 (dd, 1H, *J* = 6.2, 12.3 Hz), 3.64 (dd, 1H, *J* = 7.6, 8.1 Hz), 3.72 (dd, 1H, *J* = 5.2, 12.4 Hz), 3.75 (dt, 1H, *J* = 7.2, 6.6 Hz), 4.46 (dd, 1H, *J* = 5.1, 7.7 Hz), 4.57 (dd, 1H, *J* = 5.1, 8.8 Hz), 7.20–7.30 (m, 6H), 7.70–7.80 (m, 4H).

These results confirm the potential of the butadiene–tricarbonyl–iron complexes in synthesis and some aspects of this approach are noteworthy:

1. Although this preliminary study has been done only in racemic form, extension to asymmetric synthesis appears possible since **4** has recently been resolved.[9]
2. It should be possible to take advantage of the presence of the $Fe(CO)_3$ moiety to differentiate between the two hydroxyl groups in **7** and **8**[12] and then to obtain new modified analogues of fatty acid metabolites.
3. This methodology could be extended to other derivatives such as 11,12- or 14,15-DiHETE. This is currently under investigation in our laboratories.

Experimental Procedure

7: To a solution of the alkene **5** (240.0 mg, 0.41 mmol) in anhydrous pyridine (5 mL) was added dropwise 3 mL (1.45 equiv.) of a 0.2 M osmium tetroxide solution in pyridine under nitrogen at 20 °C. The mixture was stirred for 2 h at 20 °C. The osmate ester, added with an excess of an aqueous solution of $Na_2S_2O_5$ (10.5 mmol, 18.0 equiv.), was decomposed by stirring the mixture for 16 h. The dark red solution was transferred to a separatory funnel containing

25 mL of 3% hydrochloric acid and extracted with two 25-mL portions of ethyl acetate. The combined organic phases were washed with a saturated ammonium chloride solution (2 × 10 mL), dried over anhydrous $MgSO_4$, and concentrated under reduced pressure. The resulting yellow oil was then filtered in methanol on a KC 18 reverse-phase cartridge (SEP PAK) to yield 96% of the diol **7**, which was used in the next step without further purification.

10: To a solution of the *erythro* diol **7** (266.9 mg, 0.43 mmol) in anhydrous benzene (1 mL) was added dropwise a suspension of *N,N'*-carbonyldiimidazole (76 mg, 0.47 mmol; 1.09 equiv.) in anhydrous benzene (10 mL). The mixture was stirred for 1 h at 45 °C, then a second portion of *N,N'*-carbonyldiimidazole (76 mg, 0.43 mmole; 1.09 equiv.) was added at 64 °C. Stirring was continued for 1.5 h at this temperature and the mixture was then transferred to a separatory funnel containing water (25 mL) and extracted with ethyl acetate (3 × 25 mL). The combined organic layers were washed with water (3 × 25 mL), dried over anhydrous $MgSO_4$, and concentrated under reduced pressure. The resulting cake was purified by flash chromatography on silica gel (eluant: cyclohexane:ethyl acetate 80:20), yielding 209 mg (75%) of pure yellow crystalline carbonate **10**.

11/12: The carbonation of the mixture of *threo* diols **8** and **9** was simpler, since it occurred within 1.5 h at 20 °C following one addition of *N,N'*-carbonyldiimidazole (170 mg, 5.0 equiv.). Extraction and chromatographic separation of the two yellow crystalline *threo* carbonates **11** and **12** were performed as described above for **10** (**11** + **12**: 115.9 mg, 85% overall yield, **11**:**12** = 90:10).

Received: January 23, 1989 [Z 3136 IE]
German version: *Angew. Chem. 101* (1989) 794

CAS Registry numbers:
1 (isomer 1), 82948-87-6; **1** (isomer 2), 82948-88-7; **2** (isomer 1), 94292-80-5; **2** (isomer 2), 89663-86-5; (±)-cis-**3c**, 120665-90-9; (±)-trans-**3d**, 120710-11-4; **4**, 120665-91-0; **5**, 120665-92-1; **6**, 120786-12-1; **7**, 120665-93-2; **8**, 120710-12-5; **9**, 120710-13-6; **10**, 120665-94-3; **11**, 120710-14-7; **12**, 120710-15-8; $Br^{\ominus}Ph_3P^{\oplus}(CH_2)_4CO_2H$, 17814-85-6.

[1] 5,6-DiHETE (biosynthesis and biological properties): E. J. Goeltz, W. C. Pickett, *J. Exp. Med. 153* (1981) 482; P. Sirois, S. Roy, G. Beraldin, P. Valleraud, P. Borgeat, *Prostaglandins 24* (1982) 405; J. Haeggström, J. Meijer, O. Radmark, *J. Biol. Chem. 261* (1986) 6332; J. F. Medina, J. Haeggström, A. Wetterholm, A. Wallin, O. Radmark, *Biochem. Biophys. Res. Commun. 143* (1987) 697; J. Haeggström, A. Wetterholm, M. Hamberg, J. Meijer, R. Zipkin, O. Radmark, *Biochem. Biophys. Acta 958* (1988) 469; N. Ueda, S. Yamamoto, *J. Biol. Chem. 263* (1988) 1937.

[2] Lipoxin A_4 (biosynthesis and biological properties): C. N. Serhan, M. Hamberg, B. Samuelsson, *Proc. Natl. Acad. Sci. USA 81* (1984) 5335; J. Palmblad, H. Gyllen-Hammar, B. Ringertz, C. N. Serhan, B. Samuelsson, K. C. Nicolaou, *Biochem. Biophys. Res. Commun. 145* (1987) 168; K. F. Badr, C. N. Serhan, K. C. Nicolaou, B. Samuelsson, *ibid. 145* (1987) 408; B. Samuelsson, S. E. Dahlén, J. A. Lindgren, C. A. Rouzer, C. N. Serhan, *Science (Washington) 237* (1987) 1171; G. Feuerstein, A. L. Siren, *FEBS Lett. 232* (1988) 51.

[3] J. Adams, B. J. Fitzsimmons, Y. Girard, Y. Leblanc, J. F. Evans, J. Rokach, *J. Am. Chem. Soc. 107* (1985) 464.

[4] The synthesis of **4**, starting from another complex [*Tetrahedron Lett. 22* (1981) 1961] will be described in a full paper.

[5] For an earlier example see: B. F. G. Johnson, J. Lewis, D. G. Parker, S. R. Postle, *J. Chem. Soc., Dalton Trans. 1977*, 794. An example of the osmylation of a double bond far from the dienyl-$Fe(CO)_3$ moiety has also been described: A. J. Pearson, *Metallo-Organic Chemistry*, Wiley, New York 1985, p. 269.

[6] **5** and **6** have been separated by medium pressure liquid chromatography on silica gel (Merck Kieselgel 60, hexane:ether 9:1). The geometry of the uncomplexed double bond is secured by the $^3J(H_5, H_6)$ coupling value (300 MHz, C_6D_6); **5**, 10.5 Hz; **6**, 15.1 Hz).

[7] L. Toupet, A. Gigou, T-P. Lellouche, J.-P. Beaucourt, R. Grée, *Acta Crystallogr. Sect. C*, in press.

[8] M. Franck-Neumann, D. Martina, M. P. Heitz, *J. Organomet. Chem. 301*(1986) 61.

[9] P. Mangeney, A. Alexakis, J. F. Normant, *Tetrahedron Lett. 29* (1988) 2677.

[10] The racemic carbonates **3c** and **3d** have spectral properties that agree well with the proposed structures. The stereochemistry (*erythro* vs. *threo*) has been established by comparison of their spectral (300-MHz; ^1H NMR, MS) and physicochemical properties (TLC, HPLC) with those of (5*S*,6*R*)-**3c** and (5*R*,6*R*)-**3d** obtained by another route [11].

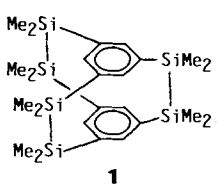
[11] C. Kugel, T-P. Lellouche, T-P. Beaucourt, G. Niel, T-P. Girard, T-C. Rossi, unpublished.

[12] Preliminary results indicate, for instance, that selective monotosylation of **7** and **8** is possible in position 5.

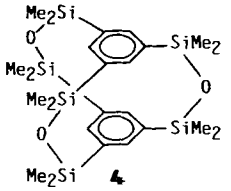
1,2,9,10,17,18-Hexasila[2.2.2](1,3,5)cyclophane, a Cage-like Phane Containing Three Si–Si Units**

By *Akira Sekiguchi, Tetsuo Yatabe, Chizuko Kabuto,* and *Hideki Sakurai**

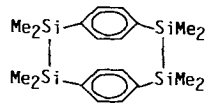
In connection with our studies on cyclophanes containing Si–Si units,[1] we herein report the physical and chemical properties and X-ray structure analysis of the cyclophane **1**, which contains three Si_2Me_4 units. In 1986 we reported the preparation of 1,1,2,2,9,9,10,10-octamethyl-1,2,9,10-tetrasila[2.2]paracyclophane **2** by reaction of a Grignard reagent derived from bis(*p*-bromophenyl)tetramethyldisilane with 1,2-dichlorotetramethyldisilane.[1b] The unique properties of **2** resulting from the through-bond interaction of σ – π mixing between Si–Si bonds and aromatic π-systems are demonstrated.[1c]



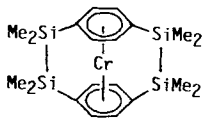
1



4



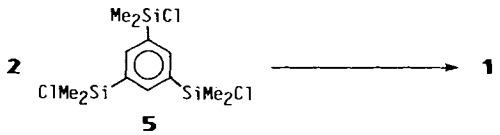
2



3

Shortly after our report,[1b] *Elschenbroich* et al. described the synthesis of (octamethyltetrasila-η^{12}-[2.2]paracyclophane)chromium **3** in 3.5% yield by a coupling reaction of bis[η^6-1,4-di(chlorodimethylsilyl)benzene]chromium with naphthalenelithium.[2] A template effect was indicated. This prompted us to attempt a direct coupling of 1,4-di(chlorodimethylsilyl)benzene under various conditions. The compound **2** was indeed obtained in 2.2% yield upon reaction with sodium in the presence of [18]crown-6. Furthermore, we have extended this reaction to a one-step synthesis of **1** via a reductive coupling reaction of 1,3,5-tris(chlorodimethylsilyl)benzene. The properties of **1** are of special interest because of the extremely rigid structure and the strong σ – π conjugation to be expected in such a system.

Reductive coupling of 1,3,5-tris(chlorodimethylsilyl)benzene **5** with sodium in toluene in the presence of [18]crown-6 afforded the cyclophane **1**.[3] This provides the most direct route to **1**, but the yields are minimal (0.22%). The presence of [18]crown-6 is essential, for without the crown ether only polymeric substances were obtained, and no **1**.



5

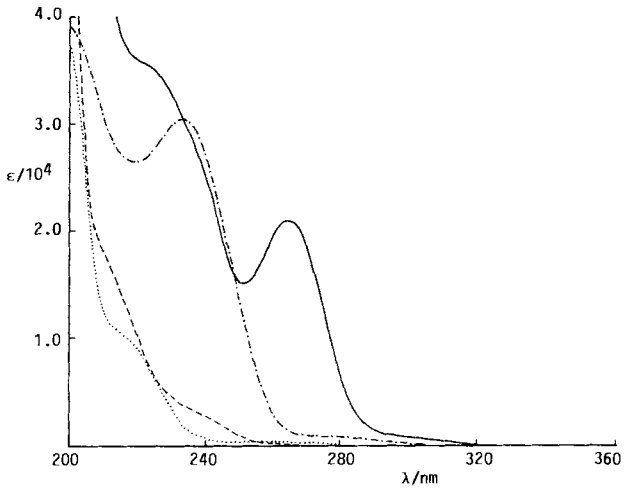
The cyclophane **1** is stable and remains unchanged upon heating to 300 °C. **1** is, however, readily oxidized at the

[*] Prof. Dr. H. Sakurai, Dr. A. Sekigurchi, Dipl.-Chem. T. Yatabe, Dr. C. Kabuto
Department of Chemistry, Faculty of Science, Tohoku University
Sendai, 980 (Japan)

[**] Chemistry of Organosilicon Compounds, Part 258.–Part 257: K. Sakamoto, K. Obata, H. Hirata, M. Nakajima, H. Sakurai, *J. Am. Chem. Soc.*, in press

Si–Si units by trimethylamine oxide in refluxing benzene, giving the cyclophane **4** containing Si–O–Si bonds.[4]

In the ^{1}H NMR spectrum, the aromatic protons of **1** appear at $\delta = 6.69$ and are shifted appreciably upfield compared to those of **2** ($\delta = 6.79$); this points to shortening of the inter-ring distance. The UV spectrum of **1** shows an absorption maximum at 264 nm ($\varepsilon = 20\,900$), whereas **4** exhibits no marked absorption band (see Fig. 1). The UV spectra of the related compounds, 1,3,5-tris(pentamethyldisiloxanyl)benzene **6** and 1,3,5-tris(pentamethyldisiloxanyl)-benzene **7** are also shown in Figure 1. The large bathochromic shift in the spectrum of **1** relative to that that in the spectrum of **6** ($\lambda = 233$ nm, $\varepsilon = 30\,500$) is the result of a strong interaction of the Si–Si σ bonds with the π-systems in the ground state.[5] Such an orbital interaction causes considerable destablization of the HOMO level.



1,3,5-$(Me_3Si-SiMe_2)_3C_6H_3$ **6** 1,3,5-$(Me_3Si-O-SiMe_2)_3C_6H_3$ **7**

Fig. 1. Electronic absorption spectra of **1** (–), **4** (-------), **6** (–·–·–·–), and **7** (·····) in hexane.

The crystal structure of **1** is shown in Figure 2.[6] The molecule has no crystallographic symmetry; the three Si–Si bonds have different lengths, and, on average are slightly longer (2.378 Å) than a normal Si–Si bond (2.34 Å), while those in **2** (2.376 Å) are almost the same as each other. The aromatic carbon atoms (C1, C3, C5, C7, C9, C11) attached to the silicon atoms lie only slightly outside (0.003–0.029 Å) the mean planes of the aromatic rings. However, the Si–C(ring) bonds deviate considerably from the planes of the benzene rings (av. 14.1°), similarly as in the case of **2** (15.0°).

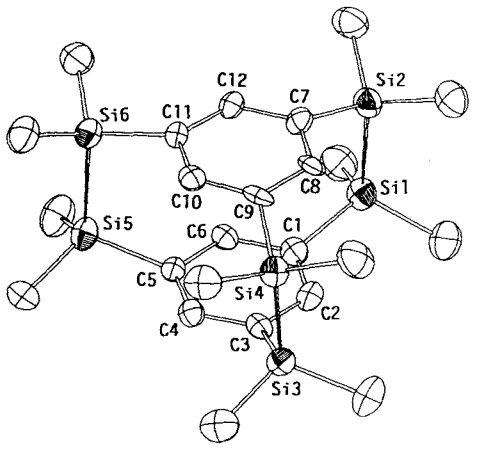


Fig. 2. ORTEP drawing of **1**: All hydrogen atoms omitted for clarity. Selected bond lengths and [Å] angles [°]: Si(1)–Si(2) 2.378(6), Si(3)–Si(4) 2.373(6), Si(5)–Si(6) 2.384(5); Selected bond C(1)–Si(1)–Si(2) 102.6(4), C(3)–Si(3)–Si(4) 104.3(4), C(5)–Si(5)–Si(6) 104.7(4), C(7)–Si(2)–Si(1) 105.7(4), C(9)–Si(4)–Si(3) 105.4(4), C(11)–Si(6)–Si(5) 104.1(4); Interplanar angles (°): C(2)–C(1)–C(6)/Si(1)–C(1) 11.0, C(2)–C(3)–C(4)/Si(3)–C(3) 13.5, C(4)–C(5)–C(6)/Si(5)–C(5) 12.6, C(8)–C(7)–C12)/Si(2)–C(7) 14.8, C(8)–C(9)–C(10)/Si(4) C(9) 16.6, C(10)–C(11)–C(12)/Si(6)–C(11) 16.2.

The two aromatic rings are arranged in the eclipsed position. The average distance between the two aromatic rings is 3.32 Å, much greater than that in [2.2.2](1,3,5)cyclophane (2.79 Å),[7] but somewhat shorter than that in **2** (3.40 Å).

Experimental

A suspension of molten sodium (0.71 g, 30.9 mmol) in boiling toluene was treated dropwise in the presence of [18]crown-6 (1.31 g, 4.96 mmol) with a toluene solution of 1,3,5-tris(chlorodimethylsilyl)benzene (1.74 g, 4.89 mmol). Chromatography on silica gel with hexane and subsequent separation by GLC furnished 2.7 mg (0.22%) of pure **1** as a white solid.

Received: February 13, 1989 [Z 3174 IE]
German version: *Angew. Chem. 101* (1989) 778

CAS Registry numbers:
1, 120666-37-7; **2**, 109828-61-7; **4**, 120666-39-9; **5**, 120666-38-8; 1,4-bis(chlorodimethylsilyl)benzene, 1078-97-3.

[1] a) H. Sakurai, Y. Nakadaira, A. Hosomi, Y. Eriyama, *Chem. Lett. 1982*, 1971; b) H. Sakurai, S. Hoshi, A. Kamiya, A. Hosomi, C. Kabuto, *ibid. 1986*, 1781; c) R. Gleiter, W. Schäfer, G. Krennrich, H. Sakurai, *J. Am. Chem. Soc. 110* (1988) 4117.

[2] C. Elschenbroich, J. Hurley, W. Massa, G. Baum, *Angew. Chem. 100* (1988) 727; *Angew. Chem. Int. Ed. Engl. 27* (1988) 684.

[3] **1**: m.p. > 300 °C; ^{1}H NMR (300 MHz, $CDCl_3$): $\delta = 0.39$ (s, 36H), 6.69 (s, 6H); ^{13}C NMR (75.5 MHz, $CDCl_3$): $\delta = -5.30$, 137.94, 138.02; ^{29}Si NMR (59.6 MHz, $CDCl_3$): $\delta = -15.08$; UV (hexane): λ_{max}/nm (ε) = 224 (35200, sh), 264 (20900); MS (70 eV, rel. int.) *m/z* 498 ($M^{\oplus}$, 67) 483 (39), 439 (13), 425 (14), 409 (15), 365 (11), 351 (14), 249 (19), 73 (100), 59 (13); high-resolution mass: calcd for $C_{24}H_{42}Si_6$: 498.1902; found: 498.1901.

[4] **4**: m.p. 236–237 °C; ^{1}H NMR ($CDCl_3$): $\delta = 0.40$ (s, 36H), 7.35 (s, 6H); ^{13}C NMR ($CDCl_3$): $\delta = -0.71$, 136.18, 139.42; ^{29}Si NMR ($CDCl_3$): $\delta = -0.69$; IR(KBr): 1053 cm^{-1} (Si–O–Si); MS (70 eV) *m/z* 546 ($M^{\oplus}$); high-resolution mass: calcd for $C_{24}H_{42}Si_6O_3$: 546.1750; found: 546.1751.

[5] H. Sakurai, *J. Organomet. Chem. 200* (1980) 261. The interaction between Si–Si (σ) and π orbitals with b_{3u} and b_{2u} symmetry should be considered for the electronic structure of **1**.

[6] A 0.2 × 0.2 × 0.2 mm crystal was used for the data collection on a Rigaku-Denki AFC 5R four-circle diffractometer with graphite monochromatized $Mo_{K\alpha}$ radiation ($\lambda = 0.71069$ Å). A total of 2692 reflections within $2\theta = 40°$ were collected by the $2\theta - \omega$ scan method with a scan rate of 4°/min. **1**: $C_{24}H_{42}Si_6$, $M_r = 499.1$, $a = 19.346(7)$, $b = 11.758(3)$, $c = 14.050(6)$ Å, $\beta = 95.08(3)°$, $V = 3183.4(19)$ Å^3, space group $P2_1/n$, $Z = 4$, $\varrho_{calc} = 1.04$ g/cm^3. The final R factor was 0.072 for 1758 reflections of $F_0 > 3\sigma(F_0)$. Further details of the crystal structure investigation can be obtained from the Fachinformationszentrum Energie, Physik, Mathematik, D-7514 Eggenstein-Leopoldshafen 2, by quoting the depository number CSD-53906, the names of the authors and the journal citation.

[7] a) V. Boekelheide, R. A. Hollins, *J. Am. Chem. Soc. 95* (1973) 3201; b) A. W. Hanson, *Cryst. Struct. Commun. 9* (1980) 1243.

$PbMo_5O_8$ and $Tl_{0.8}Sn_{0.6}Mo_7O_{11}$, Novel Clusters of Molybdenum and Thallium

By *R. Dronskowski* and *A. Simon**

The structures of numerous reduced oxomolybdate phases can be described with the concept of condensed metal clusters.[1] The structure of $NaMo_4O_6$[2] contains *infinite* chains of *trans*-edge-sharing Mo_6 octahedra; but examples of *oligomeric* chain-like building blocks are also known: according to single crystal investigations, $In_3Mo_{11}O_{17}$ and

[*] Prof. Dr. A. Simon, Dipl.-Chem. R. Dronskowski
Max-Planck-Institut für Festkörperforschung
Heisenbergstr. 1, D-7000 Stuttgart 80 (FRG)

$In_{11}Mo_{40}O_{62}$ contain chain fragments of n = 5, or n = 4 and 5 *trans*-edge-sharing Mo_6 octahedra, respectively.[3,4] The limiting case of the isolated Mo_6 octahedron is realized in the structure of $BaMo_6O_{10}$.[5] X-ray powder investigations on $LaMo_5O_8$ indicate the existence of chain fragments consisting of n = 2 condensed metal octahedra.[6]

With $PbMo_5O_8$ **1** a further compound isotypic with $LaMo_5O_8$ was obtained, which with a slightly different electron balance, contains clusters of n = 2 condensed octahedra.[7,8] $Tl_{0.8}Sn_{0.6}Mo_7O_{11}$ **2** is structurally closely related with **1** and contains the hitherto missing cluster of the series consisting of n = 3 condensed octahedra.[7,9]

Figure 1 shows [010] projections of the metal-atom substructures for both compounds, from which the layered stacking of octahedral twins (and octahedral triplets) is clearly recognizable.

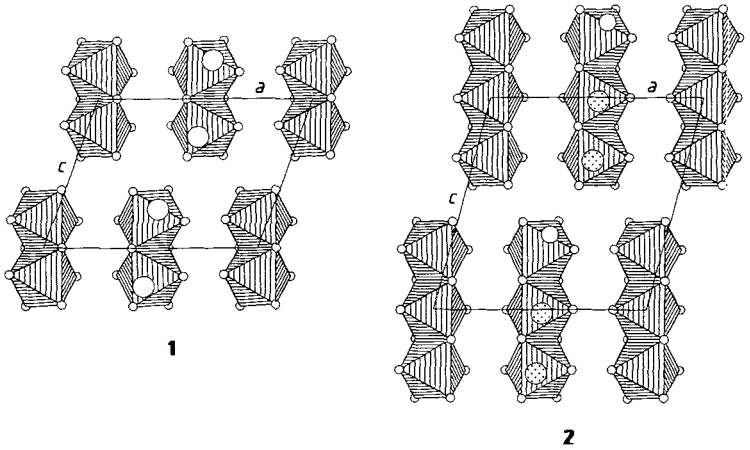


Fig. 1. Polyhedral projection [19] of the condensed Mo_6 octahedra in **1** and **2** along [010]; Mo atoms as small circles. (Cluster centers in $0\frac{1}{2}0$ and $\frac{1}{2}00$; Pb,Tl, Sn in $y \approx \frac{1}{2}$.) In **1** Pb atoms as large circles; in **2** Tl atoms as large dotted circles, Sn atoms as medium sized open circles (only one of the two possible positions of the Sn-Tl-Tl sequence is shown, cf. Ref. [9]).

The Mo_6 octahedra are surrounded at all free edges (in the manner of the M_6X_{12} cluster) by O atoms. In the crystal, O atoms occupy further positions at the apices of octahedra of neighboring clusters (Fig. 2).

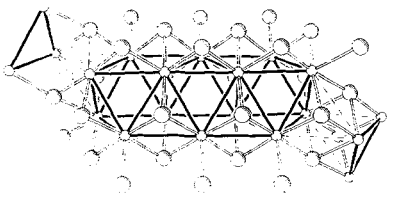


Fig. 2. Perspective diagram [16] of the molybdenum cluster in **2**; Mo atoms as small circles, O atoms as large circles. The shortest inter-cluster bonds are shown as unbroken thin lines, the longer as broken lines. (To give a better view of the inter-cluster bonds one O atom on the right has been omitted.)

All the compounds thus far reported in which fragments of the Mo_4O_6 chain (n = 1 to 5 condensed Mo_6 octahedra) have been identified as building blocks show an identical coupling of the clusters which can be described by the general formula $Mo_{4n+2}O_{6n+2}O_{4/2}$.

The Mo-O distances in **1** range from 195 to 215 pm (average 206 pm); in **2** they lie between 191 and 218 pm (average 206 pm). They do not differ significantly from those in $In_{11}Mo_{40}O_{62}$ (average 207 pm).

The Mo-Mo distances in the cluster of **1** lie between 261 and 284 pm (average 275 pm). The shortest distances between neighboring cluster units (278, 303(2×) and 308 pm(2×)) are surprisingly short. In the octahedral triplet of **2** the Mo-Mo distances are 270 to 286 pm (average 278 pm). The shortest inter-cluster distances here are 299, 304(2×) and 312 pm(2×). A comparison with the average Mo-Mo distances in $In_{11}Mo_{40}O_{62}$ (intra-cluster: 279 pm; inter-cluster: ≥ 320 pm) shows that the intra-cluster distances are scarcely affected by the degree of condensation, whereas the inter-cluster distances with shorter chain lengths (and increasing charge on the counterion) markedly decrease.

This finding is qualitatively easy to explain: the optimal valence electron concentration per Mo atom for Mo-Mo bonds in such oligomeric clusters has been estimated by way of appropriate fragmentation.[10] Accordingly, the values (in each case ± 0.2) 2.9 (n = 2), 3.1 (n = 3) and 3.2 (n = 4) are expected. Excess electrons must be accomodated in bonds between the clusters. The short inter-cluster distances quoted (see Fig. 2) correspond, according to *Pauling*,[11] to a bond order of 1.3 for the cluster in **1** and of 0.9 for the cluster in **2**. As expected, for $LaMo_5O_8$[6] this value (1.6) is higher than for $PbMo_5O_8$ **1**.

For a quantitative electron balance the valence of the cations (Pb, Tl, Sn) must be analyzed: according to bond length-bond strength calculations[12,13] the Pb atoms in **1** are present as isolated $Pb^{2\oplus}$; the next nearest Pb atoms are at a (nonbonding) distance of 372 pm.

Interestingly, in **2** one finds pairs of Tl atoms which are shifted towards each other from the centroid of their respective coordination polyhedron (cube). This leads to a distance d(Tl-Tl) = 284.0(3) pm, which corresponds to a single bond.[14] The analysis of the Tl-O distances gives $Tl^{2\oplus}$ for these two Tl atoms. Hence, (by stabilization with oligomeric transition metal clusters[3]) the formation of a Tl-Tl bond is achieved. M-M bonded Tl_2 units have, to our knowledge, never been described structurally. The Tl-Sn distance in **2** (374 pm) is non-bonding; the Sn atoms, as expected according to the Sn-O distances, are present as $Sn^{2\oplus}$.

With inclusion of the valence of the Pb (and Tl/Sn) atoms and the number of the electrons in inter-cluster bonds (see above), the Mo valence electron concentrations for intra-cluster bonds in **1** are calculated to be 2.94 and in **2** to be 3.12, in very good agreement with the above predictions for the optimal values.

Received: January 23, 1989 [Z 3138 IE]
German version: *Angew. Chem. 101* (1989) 775

[1] A. Simon, *Angew. Chem. 93* (1981) 23; *Angew. Chem. Int. Ed. Engl. 20* (1981) 1.
[2] C. C. Torardi, R. E. McCarley, *J. Am. Chem. Soc. 101* (1979) 3963.
[3] A. Simon, W. Mertin, Hj. Mattausch, R. Gruehn, *Angew. Chem. 98* (1986) 831; *Angew. Chem. Int. Ed. Engl. 25* (1986) 845.
[4] Hj. Mattausch, A. Simon, E.-M. Peters, *Inorg. Chem. 25* (1986) 3428.
[5] K. H. Lii, C. C. Wang, S. L. Wang, *J. Solid State Chem. 77* (1988) 407.
[6] S. J. Hibble, A. K. Chectham, A. R. L. Bogle, H. R. Wakerley, D. E. Cox, *J. Am. Chem. Soc. 110* (1988) 3295.
[7] Stoichiometric amounts of powdered Mo (LAB, Merck), MoO_2 (Ventron) and elemental Pb (p.a. Merck) (or Tl/Sn (LAB/p.a. Merck)) were well mixed and pelletized. The synthesis was carried out in evacuated quartz glass ampules heated to 1200-1300 °C for 7 d. Black, metallic shiny crystals were formed in almost quantitative yields.
[8] $PbMo_5O_8$ crystallizes in smooth platelets with hexagonal (!) habit; the unit cell, however, has monoclinic symmetry, as can be shown by electron diffraction analyses of powdered material [18]. Precession layer photographs confirm that the monoclinic cell tripletizes about the b axis (60°). The monoclinic b axis and the face normal of the platelet coincide thereby. By pulverizing the triplets, fragments were obtained with ca. 0.04 mm-edges, each of which showed only reflections of an individual monoclinic crystal. The investigation showed: space group $P2_1/a$ (No. 14),

$a = 999.3(2)$, $b = 924.7(1)$, $c = 753.6(2)$ pm, $\beta = 109.39(2)°$, $Z = 4$, Enraf-Nonius CAD4 four-circle diffractometer, $Mo_{K\alpha}$; 2099 reflections, 1235 with $|F_0| \geq 3\sigma|F_0|$; solution of structure by direct methods [15], refinement by least squares method [16]; $R_{aniso} = 0.057$, $R_w = 0.047$ [9b].

[9] a) The irregular shapes of the crystals of $Tl_{0.8}Sn_{0.6}Mo_7O_{11}$ resemble the star-shaped crystals of $In_{11}Mo_{40}O_{62}$. The investigation of an undistorted crystal obtained as described in Ref. [8] gave: space group $P2_1/a$ (No. 14), $a = 997.2(1)$, $b = 936.2(1)$, $c = 1036.2(1)$ pm, $\beta = 104.14(1)°$, $Z = 4$; Syntex $P\bar{1}$ four-circle diffractometer, $Mo_{K\alpha}$; 1822 reflections, 1438 with $|F_0| \geq 3\sigma|F_0|$; solution of structure by direct methods [15], refinement by least squares method [16], $R_{aniso} = 0.051$, $R_w = 0.046$. In the refined structure the Sn–Tl–Tl unit shows a positional disorder about the inversion center. X-ray crystallographically, each unit gives the composition $Sn_{0.6}Tl_{0.4}Tl_{0.4}$. This composition corresponds within the limits of experimental error to that determined analytically. In Figure 1, only one of the two possible orientations is shown. Refinements in the acentric space groups Pc or $P2_1$ assuming an inversion twin (Program SFLS [17]) led only to R values of about 0.19; b) Further details of the crystal structure investigations are available on request from the Fachinformationszentrum Energie, Physik, Mathematik GmbH, D-7514 Eggenstein-Leopoldshafen 2 (FRG), on quoting the depository number CSD-53673, the names of the authors, and the journal citation.

[10] A. Simon, *Angew. Chem. 100* (1988) 163; *Angew. Chem. Int. Ed. Engl. 27* (1988) 159.

[11] $\lg s = (261.4 \text{ pm} - d)/60$.

[12] I. D. Brown in M. O'Keeffe, A. Navrotsky (Eds.): *Structure and Bonding in Crystals, Vol. II*, Academic Press, New York 1981.

[13] I. D. Brown, D. Altermatt, *Acta Crystallogr. Sect. B41* (1985) 244.

[14] L. Pauling: *The Nature of the Chemical Bond*, Cornell University Press, Ithaca, NY, USA 1960.

[15] G. M. Sheldrick, *SHELXS-86*, Universität Göttingen 1986.

[16] *SHELXTL-PLUS, Rel. 3.4*, Nicolet Instrument Corporation 1988.

[17] M. Eitel, H. Bärnighausen, *SFLS, Version zur Verfeinerung von Datensätzen verzwillingter oder verdrillingter Kristalle nach der Methode der kleinsten Quadrate*, Universität Karlsruhe 1986.

[18] W. Mertin, R. Dronskowski, A. Simon, R. Gruehn, unpublished.

[19] R. X. Fischer, *J. Appl. Crystallogr. 18* (1985) 258.

Laser Desorption/Ionization Mass Spectrometry of Proteins of Mass 100 000 to 250 000 Dalton**

By *Michael Karas,* Ute Bahr, Arndt Ingendoh,* and *Franz Hillenkamp*

In the last few years several new ionization techniques have been developed for the mass spectrometric analysis of thermally labile biomolecules. With these so-called "soft" ionization methods the accessible mass range has been continuously extended. While fast atom bombardment (FAB) or liquid secondary ion mass spectrometry (SIMS) find their main applications in the mass range below 5000 Dalton, plasma desorption mass spectrometry (PD-MS) made it possible for the first to ionize proteins of up to 35 000 Dalton;[1] however, it is routinely used below 15 000 Dalton only.[2,3]

Recently, it was reported that ultraviolet-laser desorption/ionization (UVLDI) mass spectrometry, up to now mainly used for analysis of small molecules up to 1000 Dalton, is able to desorb and ionize proteins in the 100 000 Dalton range.[4–6] This technique requires embedding the proteins in a matrix which resonantly absorbs the incident laser light.

We report here new results with the matrix-assisted UV-laser desorption showing that this method promises to become a fast, sensitive and precise method for detemining the molecular weights of proteins in the mass range up to at least 250 000 Dalton.

[*] Dr. M. Karas, Dr. U. Bahr, A. Ingendoh, Prof. Dr. F. Hillenkamp
Institut für Medizinische Physik, Universität Münster
Hüfferstrasse 68, 4400 Münster (FRG)

[**] This work was supported by the Deutsche Forschungsgemeinschaft and the Bundesministerium für Forschung und Technologie. Technical support by Finnigan MAT, Bremen, is thankfully acknowledged.

The mass spectrometer used is a time-of-flight instrument with 3 keV acceleration energy. For desorption and ionization of the sample a frequency-quadrupled Nd-YAG l at 266 nm wavelength and a pulse width of 10 ns is used pical laser parameters are focus diameters between 10–50 μm and irradiances of $1-5 \times 10^7$ W/cm^2. For detection the ions are post-accelerated to 20 keV. The ion signals for each laser pulse were recorded and stored with a transient recorder (LeCroy 9400) at a time resolution of 40 or 80 ns/chanal. Each spectrum covers the whole mass range. The spectra shown are sum spectra of 30–50 single laser shots.

The proteins β-D-galactosidase (*e. coli*; Sigma G 8511) and catalase (bovine liver; Serva 26902) were used as obtained, glucose isomerase was provided by Prof. *Witzel*, Münster. 10^{-6} M solutions of proteins in highly purified water were mixed with nicotinic acid as matrix in a molar ratio of 1:50 000. 1 μL of this solution (corresponding to 500 fmol of protein) was dripped onto a silver target and dried. Total time for sample preparation and measurement is typically 10 minutes.

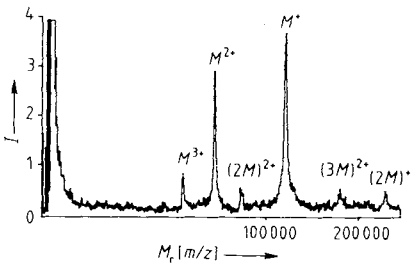


Fig. 1. LDI mass spectrum of β-D-galactosidase. Measured molecular weight: 117 130. Sum of 30 single spectra. I = relative intensity in arbitrary units.

Figure 1 shows the LDI mass spectrum of β-D-galactosidase. The molecular weight as determined by the peak centroids is 117 130. The base peak represents the singly charged molecular ion. The multiply charged molecular ions like $M^{2\oplus}$ and $M^{3\oplus}$, as well as cluster ions like $(2M)^{\oplus}$, $(3M)^{2\oplus}$ and $(2M)^{3\oplus}$ are typical for LDI spectra of high molecular weight proteins. Their appearance and relative intensity distribution depend on the laser irradiance used for desorption. Generally, the singly charged molecular ion forms the base peak of the protein ions.

Although the ion peaks in these spectra are rather wide, corresponding to a mass resolution of about $m/\Delta m = 50$, the peak centroids can be determined with a much better precision. For several proteins independent mass calibration of successive spectra, based on one or more matrix ions in the low mass range and the integer mass relation of multiply charged and oligomer ions of the protein yielded a standard deviation of 0.1 % or less. In cases in which the exact absolute mass of the proteins used for the analysis was known to that accuracy with certainty, the known and measured masses agreed within this uncertainty. In a few other cases deviations up to 1 % occurred, which however, could also derive from an inaccurate mass determination from the supplier.

Figure 2 shows the spectrum of glucose isomerase, summed over 30 single shot spectra. Again, the singly charged molecular ion with a measured mass of 172 400 shows up in surprisingly high intensity. The velocity of these ions at the conversion dynode is only 0.48×10^4 m/s^{-1}. The detection efficiency should therefore be very low.[7] Again multiply charged molecular ions $M^{n\oplus}$ (n = 2 – 4) are found

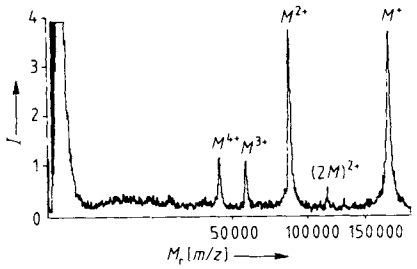


Fig. 2. LDI mass spectrum of glucose isomerase. Measured molecular weight: 172420. Sum of 30 single spectra.

as well as a cluster ion $(2M)^{3\oplus}$ with lower intensity. All signals can be used to improve mass determination precision. The fact that glucose isomerase, which consists of four noncovalently bound subunits, is desorbed at least predominantly, if not only as the intact protein is a further proof for the extreme softness of the matrix-UVLDI technique.

The total sample amount deposited on the target was 500 fmol, spread over an area of several mm^2. At least several thousand single spectra can be obtained from such a preparation. An estimate of the sample consumption per single spectrum gives ca. 10^{-17} mol[6] leaving much room for a further reduction of sample amount necessary.

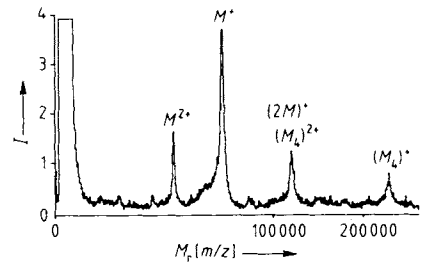


Fig. 3. LDI mass spectrum of catalase. Measured molecular weight: 236230. Sum of 50 single spectra.

Figure 3 shows the spectrum of catalase with a measured molecular weight of 236230, summed over 50 single laser shots. Again, the molecular ion, $(M_4)^{\oplus}$, consisting of 4 equal subunits with a molecular weight of 59060 each, is clearly detected, as well as the doubly charged species $(M_4)^{2\oplus}$. Because of the absence of a triply charged molecular ion it can be concluded that the peak at m/z 59060 originates from the singly charged subunit $(M_1)^{\oplus}$ and not the quadruply charged molecular ion $(M_4)^{4\oplus}$. Correspondingly the signal at m/z 29500 represents the doubly charged subunit $(M_1)^{2\oplus}$. Whether or not the protein mostly decayed into its subunits upon preparation (and evaporation of the solvent) already, or the decomposition was predominantly induced by or during the desorption process still needs further investigation.

As in all desorption techniques sample preparation plays the key role in LDI of high mass molecules. Highly purified samples and the use of ultrapure water for protein and matrix solutions is a prerequisite for a successful mass analysis, indicating that the salt contamination commonly present can disturb the homogeneity of the protein-matrix-association necessary for high mass ion desorption. Under such conditions, all spectra show a very good signal-to-noise ratio. The mass spectra shown are typical for matrix-UVLDI: so far no fragmentation of covalent bonds has been observed. The intense signals in the mass range below ca. 1000 Dalton are caused exclusively by the matrix. Whether a successive fragmentation, which would most suitably be done by a second laser, enables sequencing of peptides and proteins comparably to Collision-Induced-Dissociation has yet to be investigated.

Received: February 13, 1989 [Z 3172 IE]
German version: *Angew. Chem. 101* (1989) 805

[1] A. G. Craig, A. Engström, H. Bennich, I. Kamensky, 35th ASMS Conf. Mass Spectrom. Allied Top., Denver, CO, USA 1987, p. 528.
[2] P. Roepstorff, P. F. Nielsen, K. Klarskov, P. Hojrup, *Biomed. Environm. Mass Spectrom. 16* (1988) 9.
[3] R. J. Cotter, *Anal. Chem. 60* (1988) 781A.
[4] K. Tanaka, H. Waki, Y. Ido, S. Akita, Y. Yoshida, T. Yoshida, *Rapid Commun. Mass Spectrom. 8* (1988) 151.
[5] M. Karas, F. Hillenkamp, *Anal. Chem. 60* (1988) 2299.
[6] M. Karas, U. Bahr, F. Hillenkamp, *Int. J. Mass Spectrom. Ion Processes*, in press.
[7] R. J. Beuhler, *J. Appl. Phys. 54* (1983) 4118.

Diisocyanogen or Isocyanogen?**

By Lorenz S. Cederbaum, Francesco Tarantelli, Hans-Georg Weikert, Markus Scheller,* and *Horst Köppel*

While the stable cyanogen molecule (NCCN) has long been known, the synthesis of its isomers diisocyanogen (CN-NC) and isocyanogen (CNCN) has posed considerable difficulties. Only recently has the experimental formation of CN-NC been reported for the first time.[1] The precursor norbornadienone azine was flash-pyrolyzed and the ^{13}C and ^{14}N NMR spectra of the pyrolysis products were consistent with the presence of CNNC.[1] More recently the He(I) photoelectron (PE) spectrum of CNNC was reported.[2] This clean spectrum was interpreted on the basis of experimental considerations augmented by the results of Hartree-Fock-Slater calculations. The calculations indicated the presence of strong correlation effects and made it quite clear that more sophisticated theoretical methods are necessary to correctly understand the experimental findings.[2]

The PE spectrum of cyanogen has been successfully calculated in the past using Green's functions theory.[3] We have now computed the PE spectrum of CNNC using both Green's functions and configuration interaction (CI) methods. The CI result is shown in Figure 1c. It is seen that the calculated spectrum does not compare with the experimental spectrum, which is schematically depicted in Figure 1a. In particular, the energy difference between the two σ-ionization potentials is much smaller than the experimental one. This difference is very constant with respect to the various calculations performed. In addition, the calculated π_u-ionization potential is, over and beyond the uncertainties of the theory, too large compared to the experimental value. We should mention that correlation effects are indeed substantial and an interpretation of the calculated spectrum via orbital energies is rather meaningless.

The geometry of CNNC used for the calculation of the PE spectrum was optimized at the CI level and was found, due to the presence of correlation effects, to be somewhat different from the SCF geometry reported in the literature[4]

[*] Prof. Dr. L. S. Cederbaum, Dr. F. Tarantelli,[+] H.-G. Weikert, M. Scheller, Dr. H. Köppel
Physikalisch-Chemisches Institut der Universität
D-6900 Heidelberg (FRG)
[+] Alexander von Humboldt fellow; Permanent adress:
Dipartimento di Chimica Università di Perugia 06100 Perugia (Italy)

[**] We thank *C. A. deLange* for making the PE spectrum available prior to publication and for many interesting discussions.

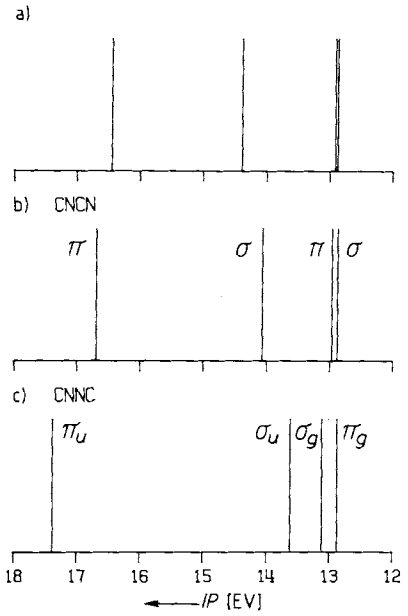
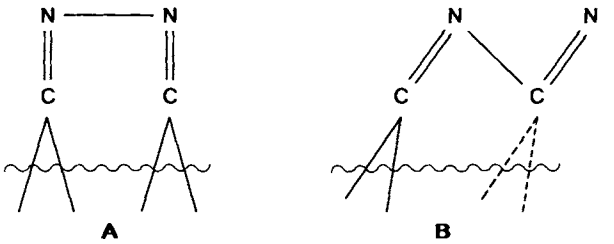


Fig. 1. a) The experimental [2] (schematic drawing) and b), c) calculated PE spectra.

(R_{CN} = 1.181 Å, R_{NN} = 1.291 Å). This difference in geometry is, however, by far too small to lead to substantial changes of the ionization potentials. In particular, the $\sigma_g - \sigma_u$ separation remains unchanged. To remedy the situation we searched for a linear but non-symmetric CNNC (a non-linear CNNC would exhibit six ionization potentials instead of the four found in the PE spectrum). Although we have invested considerably in this search and the potential energy surface has been found to be very flat along the asymmetric distortion, no additional minima could be detected and we conclude that CNNC is indeed symmetric. Moreover, we must conclude that the molecule whose PE spectrum has been measured is *not* diisocyanogen.

Since the molecule that has been synthesized contains two C atoms and two N atoms, we must assume that either a different isomer has been obtained, or that CNNC has isomerized to the more stable CNCN before the PE spectrum was recorded. The spectrum, however, does not exhibit signs of an additional isomer and, therefore, we tend to assume that it is not CNNC which has been synthesized. **B** is *one* possible explanation for the formation of CNCN from norbornadienone azine, whereas **A** would correspond to the formation of CNNC as suggested in Ref. [1].



Since the NMR measurements are carried out in the condensed phase we cannot rule out the formation of ordered CN-chains.

The ionization potentials of CNCN have been calculated before[5] and agree well with the experimental values.[2] To be consistent with the calculation on CNNC, we have repeated the calculation of the PE spectrum of CNCN using the same procedures and basis sets as for the newly computed CI geometry (CNC'N': R_{CN} = 1.180 Å, $R_{NC'}$ = 1.320 Å, $R_{C'N'}$ = 1.157 Å). The technical details of the Green's function and CI calculations of both CNCN and CNNC will be given elsewhere.[6] The resulting PE spectrum of CNCN is shown in Figure 1 b. It compares very convincingly with the experimental spectrum (Fig. 1 a). It is now obvious that the measurements in Ref. [2] were performed on CNCN.[7]

Received: February 17, 1989 [Z 3178 IE]
German version: *Angew. Chem. 101* (1989) 770

CAS Registry numbers:
diisocyanogen, 78800-21-2; cyanoisocyanogen, 83951-85-3.

[1] T. van der Does, F. Bickelhaupt, *Angew. Chem. 100* (1988) 998; *Angew. Chem. Int. Ed. Engl. 27* (1988) 936.
[2] O. Grabant, C. A. deLange, R. Mooyman, T. van der Does, F. Bickelhaupt, *Chem. Phys. Lett. 155* (1989) 221.
[3] L. S. Cederbaum, W. Domcke, W. von Niessen, *Chem. Phys. 10* (1975) 459.
[4] M. Sana, G. Leroy, *J. Mol. Struct. 76* (1981) 259.
[5] W. von Niessen, L. S. Cederbaum, J. Schirmer, G. H. F. Diercksen, W. P. Kraemer, *J. Electr. Spectr. 28* (1982) 45.
[6] F. Tarantelli, L. S. Cederbaum et al., unpublished.
[7] Authors' note: After submission of our manuscript a relevant paper has appeared (F. Stroh and W. Winnewisser, *Chem. Phys. Lett. 155* (1989) 21) in which the experimental infrared and microwave spectra of the molecule of [1] are presented and analyzed and likewise attributed to CNCN.

Surprising Reactions of Decamethylsilicocene with π-Systems of the Type X=C=Y

By *Peter Jutzi** and *Andreas Möhrke*

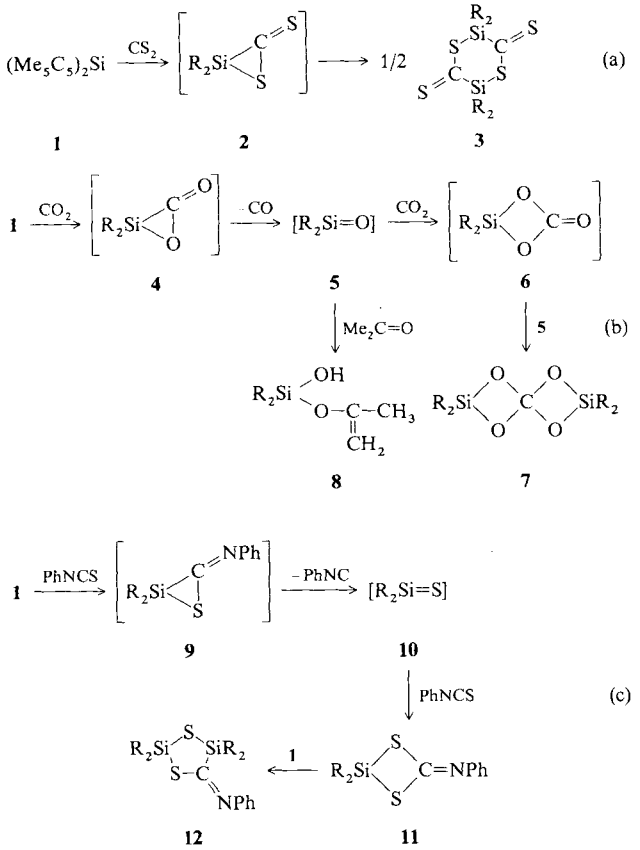
We recently reported the synthesis of decamethylsilicocene **1**.[1] This metallocene-like π-complex is so far the only divalent silicon compound that is stable under normal conditions. In the framework of our investigations of the chemistry of **1** we have, inter alia,[2] carried out reactions with simple organic compounds of the type X=C=Y. In the following we describe some, in part, surprising observations we made in the reaction of **1** with carbon disulfide, carbon dioxide, and phenyl isothiocyanate.

Already at room temperature **1** reacts with carbon disulfide in benzene solution to give the cyclic thioester **3** in almost quantitative yield. This suggests that the reaction involves an initial [2+1]-cycloaddition leading to the unstable thiasilirane **2**, which immediately dimerizes to give **3** [Eq. (a)].

The reaction of **1** with carbon dioxide proceeds quite differently: passage of CO_2 into a solution of **1** in toluene at room temperature surprisingly leads to almost quantitative formation of the spiro compound **7**. The reaction probably proceeds as follows: the initial [2+1]-cycloaddition product **4** formed analogously to Equation (a) loses carbon monoxide to give the silanone **5**, which reacts with carbon dioxide in a [2+2]-cycloaddition to give the cyclic silanediyl carboxylate **6**; this then reacts with further silanone **5** to give the final product **7** [Eq. (b)]. The carbon monoxide formed in this reaction sequence was detected in the form of a carbonyl complex.[3] If the reaction according to Equation (b) is carried out in the presence of acetone the hydroxysilylenol ether

[*] Prof. Dr. P. Jutzi, Dipl.-Chem. A. Möhrke
Fakultät für Chemie der Universität
Postfach 8640, D-4800 Bielefeld (FRG)

8 is formed quantitatively in an ene reaction via the postulated intermediate silanone **5**.



Scheme 1. R = C_5Me_5.

1 reacts somewhat differently with phenyl isothiocyanate: In toluene at about 60 °C, the dithiasiletane **11** is formed in high yields. In accord with the reaction postulated in Equation (c) an initial [2+2]-cycloaddition leads to the silirane **9** analogous to **2** and **4**; the three-membered ring system **9** then reacts with further phenyl isothiocyanate to give **11**. In contrast to **6**, the heterocycle **11** is stable under the reaction conditions. The phenyl isocyanide required as byproduct can be detected NMR spectroscopically.[5] So far it has not been possible to trap the postulated intermediate silathione **10**.

Reaction of **1** and **11** in toluene at about 100 °C leads via insertion of **1** between one of the two sulfur–carbon bonds of **11** to formation of the dithiodisilolane **12**. If the reaction of **1** with phenyl isocyanate is carried out from the beginning at higher temperature **12** is formed directly, irrespective of the molar ratio of the reactants.

The composition and constitution of **3, 7, 8, 11** and **12** are confirmed by NMR and MS spectra and by elemental analyses. In contrast to **1**, the pentamethylcyclopentadienyl ligand in these compounds is in each case bound monohapto to the silicon atom. The slight change in hapticity is presumably the reason for **1**, which is extremely electron-rich in the ground state due to π-bonding, being able to react as an electron deficient dialkylsilanediyl.[6] To our knowledge the heterocycles forming the basis of the compounds **3, 7, 11** and **12** were hitherto unknown. The pentamethylcyclopentadienyl ligand lends an additional functionality to this system.

As shown by the reactions (a)–(c) the reaction of decamethylsilicocene **1** with substrates of the type X=C=Y provides access to novel silacycles. Moreover, the possibility of generating pπ–pπ double-bonded systems $R_2Si{=}X$ from reactive three-membered ring precursors of the type $R_2\overline{Si-X-C}=Y$ deserves special mention.

Experimental

3: A solution of **1** (0.60 g, 2.0 mmol) in benzene (10 mL) was treated with 1.26 mL (20.0 mmol) of carbon disulfide and the mixture allowed to stand for 20 h at room temperature. Upon subsequent addition of *n*-pentane a fine, colorless precipitate separated out which, after filtration and crystallization from toluene, precipitated in the form of colorless cubes. Yield: 85%; m.p. 237 °C; ^{29}Si NMR ($CDCl_3$): $\delta = +21.6$; MS (70 eV): *m/z* 748 ($M^{\oplus}$, 12%).

7: Carbon dioxide was passed through a solution of **1** (1.46 g, 4.9 mmol) in toluene (25 mL) at room temperature for 3 h. Thereafter, the solution was stirred for a further 16 h in a CO_2 atmosphere. The solvent was removed under vacuum and the residue washed with *n*-pentane and crystallized from toluene. Yield 83%; m.p. 175 °C (decomp.); ^{29}Si NMR($CDCl_3$): $\delta = +10.3$; MS (70 eV): *m/z* 672 ($M^{\oplus}$, 29%).

8: CO_2 was passed through a solution of **1** (1.59 g, 5.36 mmol) in acetone (70 mL) at room temperature for 1 h and the solution stirred for a further 18 h in a CO_2 atmosphere. After removal of the solvent the residue was purified by sublimation (0.01 bar, 90 °C). Yield 92%; m.p. 42 °C; ^{29}Si NMR ($CDCl_3$): $\delta = -24.0$; MS (70 eV): *m/z* 372 ($M^{\oplus}$, 21%).

11/12: A solution of **1** (1.50 g, 5.03 mmol) in toluene was treated with 1.5 mL (12.5 mmol) of phenyl isothiocyanate and the mixture stored at 65 °C for 5 h (**11**) and 100 °C for 20 h (**12**) respectively. After removal of volatile components by distillation there remained an orange-red residue, which was recrystallized from *n*-pentane (**11**) and toluene (**12**), respectively. **11**: pale yellow rhombs, yield 55%; m.p. 118 °C (decomp); ^{29}Si NMR ($CDCl_3$): $\delta = +12.0$, MS (70 eV): *m/z* 465 ($M^{\oplus}$, 4%). **12**: bright yellow powder, yield 67%; m.p. 264 °C; ^{29}Si NMR ($CDCl_3$): $\delta = +21.4, -0.4$; MS (70 eV): 763 ($M^{\oplus}$, 60%).

Received: February 10, 1989 [Z 3167 IE]
German version: *Angew. Chem. 101* (1989) 769

CAS Registry numbers:
1, 100189-23-9; **3**, 120577-98-2; **7**, 120577-99-3; **8**, 120578-00-9; **11**, 120578-01-0; **12**, 120578-02-1; CS_2, 75-15-0; CO_2, 124-38-9; $Me_2C{=}O$, 67-64-1; PhNCS, 103-72-0.

[1] P. Jutzi, D. Kanne, C. Krüger, *Angew. Chem. 98* (1986) 163; *Angew. Chem. Int. Ed. Engl. 25* (1986) 164.
[2] P. Jutzi, U. Holtmann, H. Bögge, A. Müller, *J. Chem. Soc. Chem. Commun. 1988*, 305.
[3] Reaction with $[(C_5H_5)Fe(Me_2S)_3]BF_4$ to give the carbonyl complex; $\tilde{\nu}$(CO) = 1980, 1730 cm^{-1}.
[4] A comparable ene reaction with acetone in Si=C chemistry has been described: N. Wiberg, G. Preiner, G. Wagner, H. Köpf, *Z. Naturforsch. B42* (1987) 1062.
[5] ^{13}C-NMR of PhNC: $\delta = 165.5$ (in H. D. Kalinowski, S. Berger, S. Braun: *^{13}C-NMR-Spektroskopie*; Thieme, Stuttgart 1984: $\delta = 165.7$).
[6] Despite extensive investigations with reactive silylenes, reactions with substrates of the type X=C=Y have thus far not been reported in the literature: see also P. P. Gaspar, *React. Intermed. (Wiley) 3* (1985) 335.

The Novel Complex $[LRu^{IV}(\mu\text{-}O)_3Ru^{IV}L][PF_6]_2 \cdot H_2O$ – a Molecular Section of the Structures of $BaRu^{IV}O_3$ (High-Pressure Phase) and $Ba_{5/6}Sr_{1/6}Ru^{IV}O_3$**

By *Peter Neubold, Beatriz S.P.C. Della Vedova, Karl Wieghardt,* Bernd Nuber,* and *Johannes Weiss*

The ternary oxides $BaRuO_3$ (H4 high-pressure phase) and $Ba_{5/6}Sr_{1/6}RuO_3$ contain face-sharing, binuclear

[*] Prof. Dr. K. Wieghardt, Dipl.-Chem. P. Neubold, Dr. B. S.P.C. Della Vedova
Lehrstuhl für Anorganische Chemie I der Universität
Postfach 102148, D-4630 Bochum (FRG)
Dr. B. Nuber, Prof. Dr. J. Weiss
Anorganisch-Chemisches Institut der Universität
Im Neuenheimer Feld 270, D-6900 Heidelberg (FRG)

[**] This work was supported by the Fonds der Chemischen Industrie. – L = *N,N'N''*-trimethyl-1,4,7-triazacyclononane.

$[O_3Ru^{IV}(\mu\text{-}O)_3Ru^{IV}O_3]$ units with a very short Ru···Ru distance (2.473 Å).[1, 2] These units are then coupled edge-to-edge via oxo bridges in the crystalline state. The magnetic properties of these oxides (weak antiferromagnetism?) are not yet fully understood. This motivated our interest to synthesize a binuclear complex with two face-sharing, octahedrally coordinated L'_3Ru^{IV}-units and three μ_2-oxo bridges and to study its magnetic properties. Such complexes were hitherto unknown.

Oxidation of the blue, mixed-valence complex **1**, described here for the first time, with $S_2O_8^{2\ominus}$ at pH = 7 furnishes the Ru_2^{III}-complex **2**; subsequent atmospheric oxidation of this species in alkaline solution (pH > 10) leads to **3**, a tri(μ-oxo)diruthenium(IV) complex. **1**, **2** and **3** were isolated in crystalline form as hexafluorophosphate salts; the structures of **1a** and **3a** were determined X-ray crystallographically.[3]

$[LRu^{II}(\mu\text{-}OH)_3Ru^{III}L][PF_6]_2 \cdot 0.5\,H_2O$	blue	**1a**
$[LRu^{III}(\mu\text{-}OH)_3Ru^{III}L][PF_6]_3$	yellow	**2a**
$[LRu^{IV}(\mu\text{-}O)_3Ru^{IV}L][PF_6]_2 \cdot H_2O$	green	**3a**

L = *N*,*N*′,*N*″-trimethyl-1,4,7-triazacyclononane, $C_9H_{21}N_3$

Figure 1 shows the structure of the cation **1**; that of the cation **3** in crystals of **3a** is very similar. In both cases we

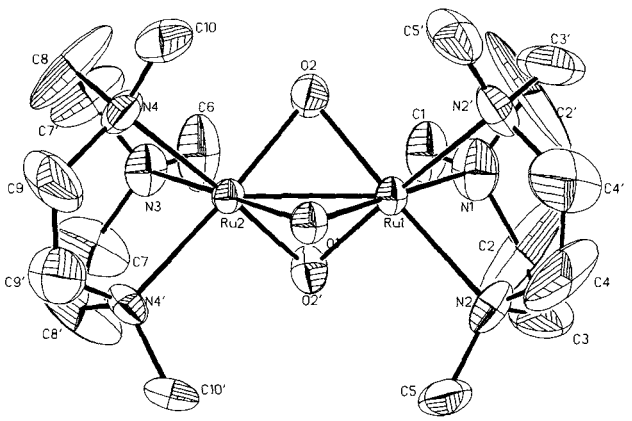


Fig. 1. Structure of the cation **1** of **1a**. The structures of the cation **3** of **3a** is similar and is not shown here. Important bond lengths [Å] and angles [°] in **1**: Ru1–Ru2 2.401 (2), Ru1–O1 1.96(1), Ru1–O2 1.967(7), Ru1–N1 2.22(2), Ru1–N2 2.20(1), Ru2–O1 1.943(9), Ru2–O2 1.950(7), Ru2–N3 2.17(1), Ru2–N4 2.18(1); Ru1–O1–Ru2 76.0(3), Ru1–O2–Ru2 75.5(3), N–Ru–N (mean) 82.4(5), O–Ru–O (mean) 86.7(5), N–Ru–O (mean) 95.6(5).—Important bond lengths [Å] and angles [°] in **3**: Ru1–Ru2 2.363(2), Ru1–O1 1.937(9), Ru1–O2 1.918(7), Ru1–N1 2.15(1), Ru1–N2 2.136(9), Ru2–O1 1.899(9), Ru2–O2 1.919(7), Ru2–N3 2.14(1), Ru2–N4 2.14(1), Ru1–O1–Ru2 76.1(3), Ru1–O2–Ru2 76.0(3), N–Ru–N (mean) 82.2(4), O–Ru–O (mean) 86.5, N–Ru–O (mean) 95.7.

have a binuclear complex consisting of two face-sharing octahedra (three hydroxo- and three-oxo bridges, respectively); the $[N_3RuO_3RuN_3]$ frameworks each have idealized D_{3h} symmetry.

2 has an analogous structure with three (μ-OH)-bridges.[4] A comparison of the Ru···Ru distances in **1** and **3** with those in the cation **4** of **4a**[5] shows that direct Ru–Ru bonds are present in **1** and **3** whereas *no* such bond exists in the

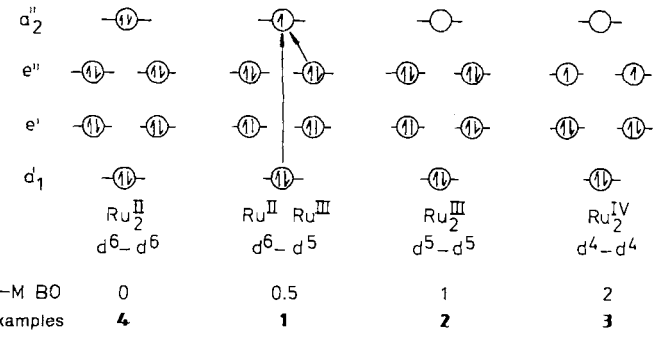


Fig. 2. MO scheme of the metal–metal bond in face-sharing complexes of the type $[L'RuX_3RuL']^{n\oplus}$ (X = OH, O). The two allowed electronic transitions for **1** are indicated by arrows.

diamagnetic $[Ru^{II}(\mu\text{-}OH)_3Ru^{II}]^{\oplus}$ complexes (such as **4**) (Ru···Ru ≈ 2.98 Å).[5, 6]

$[(\eta^6\text{-}C_6H_6)Ru^{II}(\mu\text{-}OH)_3Ru^{II}(\eta^6\text{-}C_6H_6)]Cl \cdot 3H_2O$ **4a**

Figure 2 shows the MO scheme for face-sharing octahedra with D_{3h} symmetry.[7] One bonding σ orbital (a'_1) and two degenerate, bonding π orbitals (e′) and the corresponding antibonding orbitals (a''_2, e″) can be constructed from the t_{2g} atomic orbitals of the Ru centers. In Ru_2^{II} complexes these orbitals are occupied, and the resulting Ru···Ru bond order (BO) is therefore zero; in **1** the formal BO is 0.5, then in **2** 1.0, and in **3** it is 2.0. The Ru–Ru distance in **1** and **3** decreases with increasing oxidation state of the Ru centers.

The magnetic behavior of these complexes is consistent with the MO scheme (Fig. 2): the Ru_2^{II} species such as **4a** are diamagnetic (d^6 low-spin configuration at each Ru^{II} center); **1a** has a temperature-independent magnetic moment between 9 K and 293 K (μ = 1.73 μ_B), corresponding to one unpaired electron per binuclear unit. **2a** is diamagnetic, and **3a** has a temperature-dependent magnetic moment. At 293 K it corresponds to almost two unpaired electrons per binuclear unit (μ_{eff}(9 K) = 1.77 μ_B; μ_{eff} (293 K) = 2.26 μ_B per binuclear unit).[10]

The electron spectra of **1**, **2** and **3** are shown in Figure 3. The spectrum of **1** is typical for mixed-valence complexes of

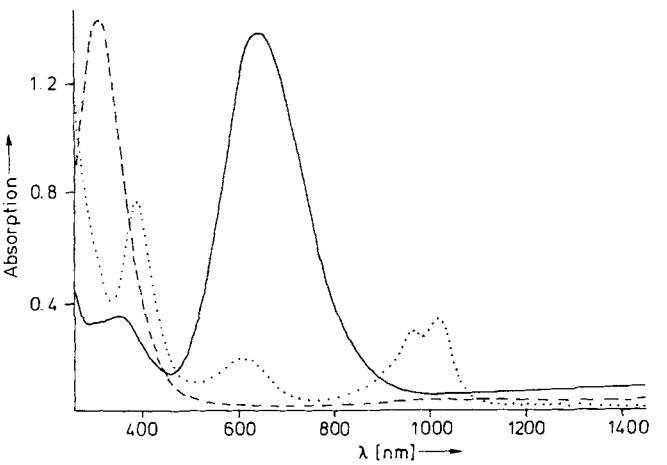


Fig. 3. Electron spectra of **1** (—), **2** (-----) and **3** (·····) in CH_3CN at 20 °C. ([**1**] = 3.8×10^{-4} M; [**2**] = 1.95×10^{-4} M; [**3**] 3.7×10^{-4} M; 1-cm cell). Absorption maxima in the NIR region (> 1400 nm) are not shown.

the type $[Ru(\mu\text{-}X)_3Ru]^{2\oplus}$ (X = Cl,Br).[8] **1** is the first tri(μ-hydroxo)diruthenium complex of this type. The intense band at 648 nm is, as usual, assigned to the $\sigma \rightarrow \sigma^*$ transition ($a_1' \rightarrow a_2''$; Fig. 2) and the weaker band in the NIR region at 1470 nm to the $e'' \rightarrow a_2''$ transition. The unpaired electron in **1** is completely delocalized; both Ru ions are equivalent. The degree of oxidation is 2.5 on the time scale for electronic transitions and vibrations, since the observed half-width of the band at 648 nm of $\approx 4400\ cm^{-1}$ is smaller than it is when calculated according to the Hush relationship ($[\Delta\tilde{\nu}_{1/2} = 2310\ \tilde{\nu}_{max}]^{1/2}$) for complexes of class II according to *Robin* and *Day* ($5970\ cm^{-1}$); and it is independent of the solvent.

The cyclovoltammogram (CV) of **1a** in CH_3CN (Pt electrode; 0.1 M nBu_4NPF_6) shows a reversible one electron transition at −0.11 V versus the normal hydrogen electrode (NHE);[9] the same transition was observed when **2a** was used as starting material [Eq. (1)].

$$\underset{\mathbf{2}}{[LRu(\mu\text{-}OH)_3RuL]^{3\oplus}} + e^{\ominus} \rightleftharpoons \underset{\mathbf{1}}{[LRu(\mu\text{-}OH)_3RuL]^{2\oplus}} \quad (1)$$

Under the same conditions, the CV of **3a** in CH_3CN shows two reversible one-electron transitions at $E^1_{1/2} = +1.12$ V and $E^2_{1/2} = -0.46$ V versus NHE, which correspond to an oxidation of **3** to the mixed valence $Ru^{IV}Ru^{V}$ complex **5** and a reduction to the mixed valence $Ru^{III}Ru^{IV}$ complex **6** [Eqs. (2, 3)]. The assignment of oxidation steps to individual metal centers is only to be understood formally here; delocalized valences are not to be ruled out.

$$\underset{\mathbf{5}}{[LRu^{IV}(\mu\text{-}O)_3Ru^{V}L]^{3\oplus}} + e^{\ominus} \rightleftharpoons \underset{\mathbf{3}}{[LRu^{IV}(\mu\text{-}O)_3Ru^{IV}L]^{2\oplus}} \quad (2)$$

$$\mathbf{3} + e^{\ominus} \rightleftharpoons \underset{\mathbf{6}}{[LRu^{III}(\mu\text{-}O)_3Ru^{IV}L]^{\oplus}} \quad (3)$$

Coulometric measurements on **3a** in CH_3NO_2 at +1.05 V versus ferrocenium/ferrocene revealed that 0.99 ± 0.1 electrons are removed per cation **3**. The color of the solution changes thereby from dark green to bright green; a subsequently measured CV agreed with that of **3a**. A similar electrochemical behavior was recently described by *Anson* et al.[12a] and *Meyer* et al. for two μ-oxo-bridged diruthenium complexes in solution. $Ru^{IV}Ru^{V}$ complexes exhibit catalytic activity in the oxidation of H_2O and alcohols.[12b] This aspect is currently being investigated for the case of **3**.

3 is the first tri(μ-oxo)diruthenium(IV) complex with an extremely short Ru–Ru bond of 2.363(2) Å. Its magnetic properties closely resemble those of the ternary oxides $BaRuO_3$ (H4 high-pressure phase) and $Ba_{5/6}Sr_{1/6}RuO_3$.[10] The $[Ru(O_3)Ru]$ unit in **3** is thus to be regarded as a section from the structure of these oxides.

Experimental

1a: To a suspension of 0.25 g (0.25 mmol) $[L_2Ru^{III}_2(\mu\text{-}O)(\mu\text{-}CH_3CO_2)_2] \cdot [PF_6]_2$ [11] in 15 mL H_2O was added 25 g of Zn amalgam (Zn content 2–3%) and the mixture adjusted to pH 2 with a small amount of 0.05 M H_2SO_4. After 2 hours' heating at 50 °C in the absence of air the clear yellow solution was separated from the Zn amalgam and treated with NaOH (pH = 12) and 0.30 g of $NaPF_6$. Upon gently heating in the presence of air the color of the solution turned deep blue and crystallization of blue **1a** was observed. Stirring of the solution was continued for a further hour at 20 °C in the absence of air and, after cooling to 0 °C, the blue crystals were filtered off and recrystallized from alkaline, aqueous solution. Yield 0.08 g (35%). UV/VIS (CH_3CN): λ_{max} (ε, L $mol^{-1}\ cm^{-1}$ per binuclear complex) = 1470(240), 648 (3.3×10^3), 354(925).

2a: A solution of **1a** (0.10 g, 0.11 mmol) in warm H_2O (15 mL) was treated with a solution of $Na_2S_2O_8$ (0.04 g, 0.16 mmol) in H_2O (3 mL). The color of the solution changed from blue to yellow. After briefly heating to 90 °C the solution was treated with 0.25 g of $NaPF_6$ and cooled to 0 °C for 12 h. Yellow-green crystals of **2a** separated out. Yield 0.11 g (95%). UV/VIS (CH_3CN): λ_{max} (ε, L $mol^{-1}\ cm^{-1}$ per binuclear complex) = 1634(323), 1450(sh), 1150(200), 314(7.4×10^3).

3a: A solution of **2a** (0.10 g, 1.1 mmol) in H_2O (10 mL) was treated with 0.02 g of NaOH and the stirred mixture heated at 80 °C for 10 min in the presence of air. The yellow solution turned dark green. The warm solution was then treated with 0.05 g of $NaPF_6$ dissolved in 1 mL of H_2O. After 12 h at 0 °C green crystals of **3a** could be filtered off. Yield 0.05 g (60%). UV/VIS (CH_3CN): λ_{max}(ε, L $mol^{-1}\ cm^{-1}$ per binuclear complex) = 1010(897), 964(754), 612(461), 391 (1.94×10^3).

All the complexes gave correct elemental analyses.

Received: February 6, 1989;
supplemented: March 22, 1989 [Z 3160 IE]
German version: *Angew. Chem. 101* (1989) 780

[1] a) J. M. Longo, J. A. Kafalas, *Mater. Res. Bull. 3* (1968) 687; b) P. C. Donohue, L. Katz, R. Ward, *Inorg. Chem. 5* (1966) 335; c) A. Calaghan, C. W. Moeller, R. Ward, *ibid. 5* (1966) 1572.

[2] E. A. Seddon, K. R. Seddon in R. J. H. Clark (Ed.): *The Chemistry of Ruthenium, Topics in Inorganic and General Chemistry, Monograph 19*, Elsevier, Amsterdam 1984.

[3] **1a**: orthorhombic, space group *Pnma* (D^{16}_{2h}; No. 62), $a = 10.089(2)$, $b = 16.234(3)$, $c = 19.585(4)$ Å, $V = 3187.95$ Å, $Z = 4$, $\delta_{calc} = 1.88\ g\ cm^{-3}$, AED II (Siemens) diffractometer, 2θ-ω scan, graphite monochromator, $Mo_{K\alpha}$ radiation. The structure was solved by Patterson and difference Fourier syntheses and refined anisotropically: $R = 0.067$, $R_w = 0.056$ for 2410 unique reflections with $I > 2.5\sigma(I)$ ($\theta < 30°$). – **3a**: orthorhombic, space group *Pnma* (D^{16}_{2h}; No.62), $a = 10.057(5)$, $b = 16.12(1)$, $c = 19.237(9)$ Å, $V = 3118.7$ Å, $Z = 4$, $\varrho_{calcd} = 1.91\ g\ cm^{-3}$; Syntex R3 diffractometer, ω scan, graphite monochromator, $Mo_{K\alpha}$ radiation. The structure was solved as for **1a** and refined anisotropically: $R = 0.054$, $R_w = 0.049$ for 1374 independent reflections with $I > 2.5\sigma(I)$ ($\theta < 25°$). – In **1a** and **3a** the ligand conformations are disordered; attempts to describe this disorder by a split-atom model failed. Further details of the crystal structure investigations are available on request from the Fachinformationszentrum Energie, Physik, Mathematik GmbH, D-7514 Eggenstein-Leopoldshafen 2 (FRG), on quoting the depository number CSD-53761, the names of the authors, and the journal citation.

[4] This follows from a crystal structure analysis on a qualitatively poor single crystal of $[L_2Ru_2(\mu\text{-}OH)_3][ClO_4]_3$ **2b** (*R* value: 0.086). The Ru–Ru distance is 2.505(6) Å.

[5] T. D. Kim, T. J. McNeese, A. L. Rheingold, *Inorg. Chem. 27* (1988) 2554.

[6] Further crystal structures of complexes with a $[Ru^{II}(\mu\text{-}OH)_3Ru^{II}]^{\oplus}$-framework: a) T. V. Ashworth, M. J. Nolte, R. H. Reimann, E. Singleton, *J. Chem. Soc. Chem. Commun. 1977*, 937; b) R. O. Gould, C. L. Jones, T. A. Stephenson, D. A. Tocher, *J. Organomet. Chem. 264* (1984) 365.

[7] a) R. H. Summerville, R. Hoffmann, *J. Am. Chem. Soc. 101* (1979) 3821; b) W. S. Togler, *Inorg. Chem. 19* (1980) 697.

[8] a) N. S. Hush, J. K. Beattie, V. M. Ellis, *Inorg. Chem. 23* (1984) 3339; b) L. Dubicki, E. Krausz, *ibid. 24* (1985) 4461.

[9] Experimentally, the redox potentials were measured against the internal standard ferrocenium/ferrocene, for which a redox potential in CH_3CN of 0.40 V versus NHE was assumed: H. M. Koep, H. Wendt, H. Strehlow, *Z. Elektrochem. 64* (1960) 483.

[10] The magnetic moment per Ru^{IV} center in $Ba_{5/6}Sr_{1/6}RuO_3$ [1c] varies from 0.69 μ_B (77 K) to 2.10 μ_B (971 K); in the case of **3a** somewhat higher values were measured: 1.25 μ_B/Ru (93 K) and 1.60 μ_B/Ru (293 K). It is conceivable that the unpaired electrons of one binuclear complex in the oxide are coupled weakly antiferromagnetically with those of a second and a third complex and thus the effective magnetic moments in the oxide are somewhat lower than in **3a**. The similarity of the magnetic properties in the oxide and in **3a** is, however, remarkable; it is determined, above all, by the binuclear $[Ru^{IV}(\mu\text{-}O)_3Ru^{IV}]$ unit.

[11] P. Neubold, K. Wieghardt, B. Nuber, J. Weiss, *Angew. Chem. 100* (1988) 990; *Angew. Chem. Int. Ed. Engl. 27* (1988) 933; *Inorg. Chem. 28* (1989) 459.

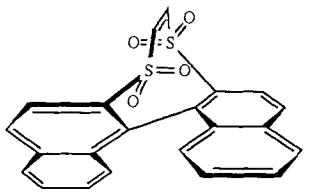
[12] a) R. B. Baar, F. C. Anson, *J. Electronal. Chem. 187* (1985) 265; b) S. J. Raven, T. J. Meyer, *Inorg. Chem. 27* (1988) 4478.

 © VCH Verlagsgesellschaft mbH, D-6940 Weinheim, 1989 0570-0833/89/0606-0765 $ 02.50/0

Ethylenebis(sulfonyl)-bridged 1,1′-Binaphthalene, an Atropisomeric Dienophile for Highly Diastereoselective Diels-Alder Reactions

By *Sergio Cossu, Giovanna Delogu, Ottorino De Lucchi,* Davide Fabbri,* and *Giulia Licini*

The recent development of (*Z*)- and (*E*)-1,2-bis(phenylsulfonyl)ethylenes as reactive equivalents of ethylene[1] and acetylene[2] in cycloaddition reactions[3] has led to a noticeable improvement in the synthesis of otherwise difficulty accessible molecules[1,2] and to the preparation of new ones.[4] We now wish to report on the cycloaddition behavior of the title compound **1**,[5] a chiral variant of the above mentioned dienophiles, which, owing to its peculiar structure, exhibits enhanced reactivity.[6] Dienophile **1** reacts with virtually complete diastereoselection (a single adduct as determined by 200-MHz ^{1}H NMR spectra) with a number of non-symmetric dienes and represents the first specifically designed equivalent of acetylene in asymmetric Diels-Alder reactions. Furthermore, **1** is the first example of an atropisomeric sulfur dienophile and of an asymmetric dienophile possessing a rigid C_2 symmetry intrinsic in the shape of the molecule and not arising from chiral carbon or sulfur atoms.[7]



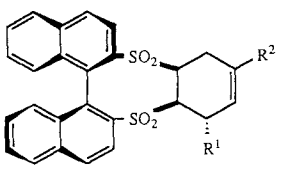
1

For the synthesis of **1**, racemic[8] or optically active[9] disodium [1,1′-binaphthalene]-2,2′-dithiolate was allowed to react with (*Z*)-1,2-dichloroethylene to give the disulfide **1**, S instead of SO_2 (m.p. 210 °C),[2] which was oxidized to the disulfone **1** (m.p. 320 °C). Optically active [1,1′-binaphthalene]-2,2′-dithioethers, which are accessible by kinetically controlled enantioselective oxidations with modified Sharpless reagents,[10] can also be transformed into **1**.

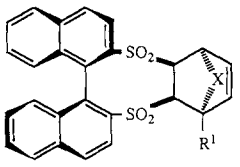
Addition at room temperature of 1-methoxy-3-(trimethylsilyloxy)-1,3-butadiene directly into an NMR tube containing a deuterochloroform solution of dienophile **1** leads to disappearence of the signals of the starting reagents and formation of a new set of signals which is attributable to a single diastereoisomer. Upon addition of ether, crystalline **2a** precipitated in almost quantitative yield. The orientation of the substituents relative to the binaphthyl group was determined on the basis of NMR data, NOE experiments and correlation of the spectral data with those of **2d** (see below) whose stereochemistry has been ascertained by X-ray analysis. Surprisingly, the methoxy group is *trans* to the two sulfonyl groups, thereby suggesting an *exo* transition state.[11]

The rigid conformational array of the dienophile **1**, which has two of the four oxygens in the plane containing the double bond and the other two parallel to each other but pointing in opposite directions (see structural formula of **1**). This geometry is probably decisive for the diastereoselectivity of the cycloaddition.

In order to determine the effect of the position of the substituents in the diene, reactions with various 1- and 2-substituted dienes have been carried out.[12] In reactions with 1-substituted dienes (both open chain and cyclic), exclusively one diastereoisomer was formed (cf. **2b–d**), even with (*E*)-1,3-piperylene in which the stereochemical bias is controlled only by a methyl group.[13] Of the 2-substituted dienes examined, only 2-trimethylsilyloxy-1,3-butadiene produced a single stereoisomer (**2e**), while isoprene gave a ca. 8:2 mixture of adducts (cf. **2f** as predominating isomer). The position of the substituents in these adducts was established, as before, on the basis of ^{1}H NMR spectral data. Cyclic dienes gave *endo* products, as was deduced from the ^{1}H-NMR coupling constants (cf. **2g, h**). The adduct **2h** was reduced with sodium amalgam in buffered methanol (NaH_2PO_4) to give the corresponding bicyclic diene, thus confirming the applicability of **1** as acetylene equivalent in cycloaddition reactions.



2a: R^1 = OMe, R^2 = $OSiMe_3$ (m.p. 185–186 °C)
2b: R^1 = OMe, R^2 = H (m.p. 250 °C)
2c: R^1 = $OSiMe_3$, R^2 = H (m.p. 266–268 °C)
2d: R^1 = Me, R^2 = H (m.p. 311–313 °C)
2e: R^1 = H, R^2 = $OSiMe_3$ (m.p. 230 °C)
2f: R^1 = H, R^2 = Me



2g: R^1 = OMe, X = O (m.p. 180 °C)
2h: R^1 = OMe, X = $-(CH_2)_2-$ (m.p. 307 °C)

The dienophile described herein is only one example of the several chiral synthons which may be accessible from [1,1′-binaphthalene]-2,2′-dithiol and whose diastereoselectivity is effected by atropisomerism.

Received: December 20, 1988 [Z 3092 IE]
German version: *Angew. Chem. 101* (1989) 767

CAS Registry numbers:
1, 120546-24-9; **2a**, 120546-17-0; **2b**, 120546-18-1; **2c**, 120546-19-2; **2d**, 120546-20-5; **2e**, 120546-21-6; **2f**, 120546-22-7; **2g**, 120546-23-8; **2h**, 120577-40-4; CH_2=C(OTMS)CH=CHOMe, 59414-23-2; CH_2=CHCH=CHOMe, 3036-66-6; CH_2=CHCH=CHOTMS, 6651-43-0; CH_2=CHCH=$CHCH_3$, 2004-70-8; CH_2=C(OTMS)CH=CH_2, 38053-91-7; CH_2=$C(CH_3)$CH=CH_2, 78-79-5; 2-methoxyfuran, 25414-22-6; 1-methoxy-1,3-cyclohexadiene, 2161-90-2.

[*] Prof. Dr. O. De Lucchi, Dipl.-Chem. S. Cossu, Dr. D. Fabbri
Dipartimento di Chimica dell'Università
via Vienna 2, I-07100 Sassari (Italy)
Dr. G. Delogu
Istituto C.N.R. per l'Applicazione delle Tecniche Chimiche Avanzate ai Problemi Agrobiologici
via Vienna 2, I-07100 Sassari (Italy)
Dr. G. Licini
Dipartimento di Chimica Organica dell'Università
via Marzolo 1, I-35131 Padova (Italy)

[1] O. De Lucchi, L. Pasquato, *Gazz. Chim. Ital. 114* (1984) 349.
[2] O. De Lucchi, V. Lucchini, L. Pasquato, G. Modena, *J. Org. Chem. 49* (1984) 596; O. De Lucchi, V. Lucchini, M. Zamai, G. Modena, *Can. J. Chem. 62* (1984) 2487; U. Azzena, S. Cossu, O. De Lucchi, G. Melloni, *Synth. Commun. 18* (1988) 351; S. Mirsadeghi, B. Rickborn, *J. Org. Chem. 50* (1985) 4340; A. Padwa, J. R. Gasdaska, *J. Am. Chem. Soc. 108* (1986) 1104; A. C. Brown, L. A. Carpino, *J. Org. Chem. 50* (1985) 1749; I. V. Kazimirchik, K. A. Lukin, I. L. Taranyuk, G. F. Bebikh, N. S. Zefirov, *Zh. Org. Khim. 21* (1985) 313 [*Chem. Abstr. 103* (1985) 536735v].
[3] O. De Lucchi, G. Modena, *Tetrahedron 40* (1984) 2585; O. De Lucchi, L. Pasquato, *ibid. 44* (1988) 6755.

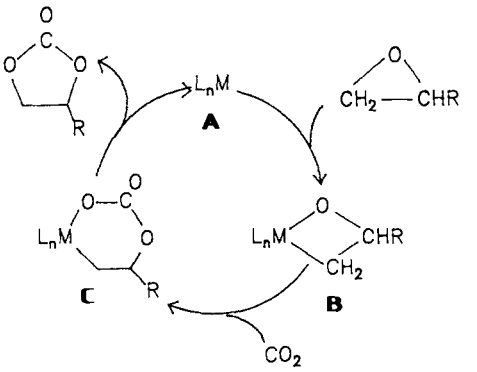
[4] L. A. Paquette, H. Künzer, K. E. Green, O. De Lucchi, G. Licini, L. Pasquato, G. Valle, *J. Am. Chem. Soc. 108* (1986) 3453; L. A. Paquette, T. M. Kravetz, P. Charumilind, *Tetrahedron 42* (1986) 1789; T. M. Kravetz, L. A. Paquette, *J. Am. Chem. Soc. 107* (1985) 6400; L. A. Paquette, U. S. Racherla, *J. Org. Chem. 52* (1987) 3250; L. A. Paquette, M. Kugelchuk, M. L. McLaughlin, *ibid. 52* (1987) 4732.
[5] IUPAC name: Dinaphtho[2,1-*e*:1′,2′-*g*][1,4]dithiocin *S,S,S,S*-tetraoxide.
[6] Control experiments confirm the higher reactivity of **1** compared to the bis(phenylsulfonyl)ethylenes. The reason may be attributed to the relief of strain at the dienophilic carbons upon change of hybridization from sp^2 to sp^3. 1,4-Benzodithiin *S,S,S,S*-tetraoxide, which is structurally related to **1**, has also been reported to be more reactive: E. Wenkert, C. A. Broka, *Finn. Chem. Lett. 1984*, 126; J. Nakayama, Y. Nakamura, M. Hoshino, *Heterocycles 23* (1985) 1119.
[7] G. Helmchen, R. Karge, J. Weetman in R. Scheffold (Ed.): *Modern Synthetic Methods*, Vol. 4, Springer, Berlin 1986, p. 261; L. A. Paquette in J. D. Morrison (Ed.): *Asymmetric Synthesis*, Vol. 3, Academic Press, New York 1984, p. 455; W. Oppolzer, *Angew. Chem. 96* (1984) 840; *Angew. Chem. Int. Ed. Engl. 23* (1984) 876; *Tetrahedron 43* (1987) 1969; H. Würziger, *Kontakte 1984 (Darmstadt) (2)*, 3.
[8] D. J. Cram, R. C. Helgeson, K. Koga, E. P. Kyba, K. Madan, L. R. Sousa, M. G. Siegel, P. Moreau, G. W. Gokel, J. M. Timko, G. D. Y. Sogah, *J. Org. Chem. 43* (1978) 2758.
[9] W. L. F. Armarego, E. E. Turner, *J. Chem. Soc. 1957*, 13.
[10] F. Di Furia, G. Licini, G. Modena, O. De Lucchi, *Tetrahedron Lett. 30* (1989) 2575.
[11] S. Danishefsky, T. Kitahara, C.-F. Yan, J. Morris, *J. Am. Chem. Soc. 101* (1979) 6996.
[12] All reactions for checking the diastereoselectivity were carried out directly in the NMR tube in deuterochloroform mixtures and for the preparative runs in dichloromethane. All reactions were complete within 24–48 h at room temperature, except for isoprene whose reaction was run in refluxing chloroform. Isolated yields are in all cases > 90%. All the new compounds have been fully characterized. The simplicity of the reaction is remarkable as in many instances simple mixing of the reagents at room temperature leads to precipitation of a single crystalline adduct.
[13] An X-ray structure determination confirms the stereochemical assignment. The diffractometric analysis was performed by Dr. *G. Valle* (Centro Studi Biopolimeri del C.N.R., via Marzolo 1, I-35131 Padova, Italy).

Coupling of Epoxides to Pt^{II}-Complexes with Carbon Dioxide and the Structure of a Cyclic Metallacarbonate**

By *Khin-Than Aye, George Ferguson,* Alan J. Lough* and *Richard J. Puddephatt**

The use of both epoxides and carbon dioxide as reagents in organic synthesis has been increasing rapidly, and transition metal catalysts are often necessary.[1–6] One important example is the coupling of epoxides with CO_2 to give cyclic carbonates;[3–6] and for electron rich catalysts such as $[M(PR_3)_4]$, M = Ni or Pd, the general mechanism of Scheme 1 has been proposed.[5]

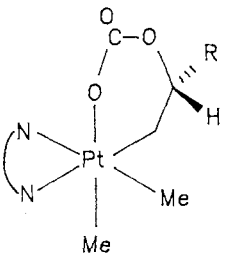
The formation of oxametallacyclobutanes, **B**, by oxidative addition of epoxides has been observed only with activated epoxides such as tetracyanoethylene oxide[7] or in a cryogenic matrix.[8] This is especially unfortunate since oxametallacyclobutanes are also thought to be key intermediates in the oxidation of alkenes to epoxides by cytochrome P-450, and the catalytic step in which the epoxide is formed by reductive elimination is obviously related to the reverse of the first step in Scheme 1 (**A** → **B**).[9] We are therefore prompted to report the oxidative addition of some



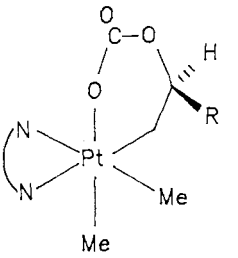
Scheme 1.

simple epoxides to the complexes $[PtMe_2(\widehat{NN})]$ (**1a**: $\widehat{NN}$ = 2,2′-bipyridine; **1b**: $\widehat{NN}$ = 1,10-phenanthroline), in which the unstable complexes **B** are trapped by reaction with carbon dioxide to give the stable metallacarbonate complexes **C**. Similar metallacarbonates have recently been reported to be formed upon reaction of carbon dioxide with $[Ir(CH_2CMe_2O)(\eta\text{-}C_5Me_5)(PMe_3)]$ and with $[RhClH(CH_2COMe)(PMe_3)_3]$.[10]

Reaction of **1a** or **1b**, which are highly reactive towards oxidative addition,[11,12] with ethylene oxide under inert atmosphere gave a mixture of products, but under one atmosphere of CO_2 the products **2a** and **2b** were formed cleanly. The reactions are complete within 1–2 days at 0 °C, and even ambient CO_2 pressure is sufficient to give **2a** and **2b** as major products.



Cpd	$\widehat{NN}$	R
2a,	bpy	H
2b,	phen	H
3a,	bpy	Ph
3b,	phen	Ph
4a,	bpy	CH_2OPh
4b,	phen	CH_2OPh



Cpd	$\widehat{NN}$	R
3a′,	bpy	Ph
3b′,	phen	Ph
4a′,	bpy	CH_2OPh
4b′,	phen	CH_2OPh

Figure 1 shows the crystal structure of **2b**.[13] The six-membered platinum-containing heterocycle adopts a boat conformation and there is a marked bowing of the 1,10-phenanthroline ring.

The analogous compounds **3a,b** and **4a,b** are formed upon reaction of styrene oxide and 2-(phenoxymethyl)oxirane, respectively, with **1a, b**, and each was shown by NMR to exist as a mixture of isomeric forms (for example, **3a/3a′**) which could not be separated. The NMR data, especially the ^{13}C NMR data, showed clearly that the substituent R was in the β-position to the platinium in all cases studied. Thus, the α-carbon atom could easily be identified by the large value of

[*] Dr. R. J. Puddephatt, K.-T. Aye
Department of Chemistry, University of Western Ontario
London N6A 5B7 (Canada)
Dr. G. Ferguson, Dr. A. J. Lough
Department of Chemistry, University of Guelph
Guelph N1G 2W1 (Canada)
[**] This work was supported by N.S.E.R.C. (Canada)

Table 1. Selected spectroscopic properties of complexes **2**–**4** [a].

Complex	^{1}H NMR						IR	^{13}C NMR								
	$\delta(Me^a)$	$^2J(PtH)$	$\delta(Me^b)$	$^2J(PtH)$	$\delta(CH_2^\alpha)$	$\delta(CH^\beta)$	$\tilde{\nu}(C=O)$ [cm^{-1}]	$\delta(Me^a)$	$^1J(PtC)$	$\delta(Me^b)$	$^1J(PtC)$	$\delta(C^\alpha)$	$\delta(C^\beta)$	$^1J(PtC^\alpha)$	$^2J(PtC^\beta)$	$\delta(C=O)$
2a	0.43	78	1.28	70	2.20	3.9	1669	− 3.02	698	− 2.88	698	19.2	64.6	663	45	187.6
2b	0.37	78	1.39	70	2.24	4.0	1630, 1670	− 15.48	734	− 2.00	721	17.5	67.9	693	56	[c]
3a	0.39	76	1.43	68	2.2	5.0	1655	− 2.67	719	− 2.43	719	26.3	74.9	701	38	187.2
3a′	0.32	74	1.41	68				− 3.19	719	[c]	[c]	24.6	[c]	666	[c]	[c]
3b	0.35	77	1.54	68	2.3	5.1	1649	− 15.59	720	− 1.11	720	25.9	79.4	696	48	[c]
3b′	0.44	76	1.59	68				− 15.6	720	− 1.59	[c]	[c]	[c]	[c]	[c]	[c]
4a	0.48	77	1.46	68	2.3	4.3	1636, 1651	− 15.39	719	− 1.13	719	18.4	75.8	701	50	187.3
4a′	0.58	76	1.34	68				− 15.57	719	− 3.08	683	16.3	[c]	647	[c]	[c]
4b	0.39	77	1.46	68	2.3	4.2	1647, 1666 [b]	− 15.53	722	− 1.75	718	18.1	72.1	707	54	158.5 [d]
4b′	0.48	76	1.35	68				− 19.25	720	− 3.51	720	16.1	[c]	687	[c]	157.7 [d]

[a] For pairs of isomers such as **3a/3a′**, the major isomer is arbitrarily assigned the structure **3a**. The opposite assignment is possible also. [b] In **4b***, prepared from $^{13}CO_2$, $\tilde{\nu}(C=O)$ = 1599, 1624 cm^{-1}. [c] Not resolved. [d] Measured for **4b***.

Table 2. Kinetic data for the reactions in acetone solution [a].

Complex	Epoxide	k_2[L mol^{-1} s^{-1}]	ΔH^*[kJ mol^{-1}]	ΔS^*[J K^{-1} mol^{-1}]
1a	$PhOCH_2CHCH_2O$	9.2×10^{-5}	48 ± 2	−160 ± 15

[a] k_2, at 25 °C, is measured for disappearance of **1a** but, when measured in the presence of CO_2, also applies to formation of **3a/a′** or **4a/a′** (see text).

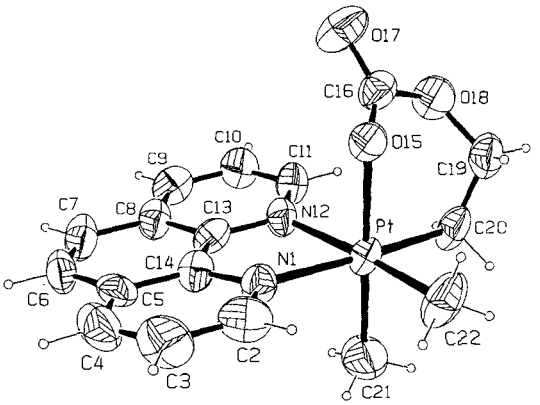


Fig. 1. Crystal structure of **2b**. Important bond lengths [Å] and angles [°]: Pt–O15 21.144(9); O15–C16 1.235(16); C16–O17 1.236(16); C16–O18 1.388(15); O18–C19 1.428(17); C19–C20 1.480(22); C20–Pt 2.034(14); O15–Pt–C20 89.3(5).

$^1J_{PtC}$ = 663–707 Hz and was shown to be a CH_2 group in every case by APT measurements (Table 1).

The kinetics of the reaction could be followed by monitoring the decay of the band due to **1** at 475 nm in the UV/VIS spectrum. Using a large excess of epoxide, the reactions followed first order kinetics and the first order rate constants were linearly dependent on the concentration of epoxide but were independent of the concentration of CO_2. Thus, overall second order kinetics, first order in both platinum(II) and epoxide reagent, were established. This indicates that the rate determining step involves oxidative addition of the epoxide (formation of **B** in Scheme 1) and that the subsequent CO_2 insertion is fast. The activation parameters given in Table 2 are typical of those expected for an S_N2 oxidative addition mechanism, and suggest that a dipolar intermediate $[Me_2(\widehat{NN})Pt^{\oplus}-CH_2CHRO^{\ominus}]$ is formed by nucleophilic attack by platinum(II) on the least substituted carbon atom of the epoxide steric effects are then responsible for the observed selectivity on formation of complexes **3** and **4**. This finding gives strong support for the mechanism of catalysis in Scheme 1,[5, 10] and also suggests that the formation of epoxides in transition metal catalysis[9] may involve dipolar intermediates.

Received: January 30, 1989 [Z 3147 IE]
German version: *Angew. Chem. 101* (1989) 765

CAS Registry numbers:
1a, 52594-52-2; **1b**, 52594-55-5; **2a**, 120610-86-8; **2b**, 120610-87-9; **2b**·0.5 C_5H_2, 120610-88-0; **3a**, 120610-82-4; **3a′**, 120709-21-9; **3b**, 120610-83-5; **3b′**, 120707-80-4; **4a**, 120610-84-6; **4a′**, 120707-81-5; **4b**, 120610-85-7; **4b′**, 120707-82-6; $PhOCH_2CHCH_2O$, 96-09-3; $PhOCH_2CHCH_2O$, 122-60-1; CO_2, 124-38-9; ethylene oxide, 75-21-8.

[1] D. Walther, *Coord. Chem. Rev. 79* (1987) 135.
[2] A. Behr, U. Kanne, *J. Organomet. Chem. 309* (1986) 215; review: A. Behr, *Angew. Chem. 100* (1988) 681; *Angew. Chem. Int. Ed. Engl. 27* (1988) 661.
[3] B. M. Trost, S. R. Angle, *J. Am. Chem. Soc. 107* (1985) 6123.
[4] H. Kisch, R. Millini, I.-J. Wang, *Chem. Ber. 119* (1986) 1090.
[5] R. J. De Pasquale, *J. Chem. Soc. Chem. Commun. 1973*, 157.
[6] T. Fujinanii, T. Suzuki, M. Kamiya, S. Fukuzawa, S. Sakai, *Chem. Lett. 1985*, 199.
[7] R. Schlodder, J. A. Ibers, M. Lenarda, M. Graziani, J. *Am. Chem. Soc. 96* (1974) 6893.
[8] Z. H. Kafafi, R. H. Hauge, W. E. Billups, J. L. Margrave, *J. Am. Chem. Soc. 109* (1987) 4775.
[9] J. T. Groves, Y. Watanabe, *J. Am. Chem. Soc. 108* (1986) 507.
[10] D. P. Klein, J. C. Hayes, R. G. Bergman, *J. Am. Chem. Soc. 110* (1988) 3704. M. Farmer, M. A. Khan, K. M. Nicholas, *J. Chem. Soc. Chem. Commun. 1988* 1384.
[11] G. Ferguson, P. K. Monaghan, M. Parvez, R. J. Puddephatt, *Organometallics 4* (1985) 1669.
[12] K.-T. Aye, D. Colpitts, G. Ferguson, R. J. Puddephatt, *Organometallics 7* (1988) 1454.
[13] Crystallstructure data of **2b**: $C_{17}H_{18}N_2O_3Pt\cdot0.5C_5H_{12}$, M_r = 1059.02, monoclinic, space group $C2/c$ (No. 15), a = 28.793(7) Å, b = 11.823(3) Å, c = 12.473(2) Å, β = 93.30(2)°, V = 4239.0 Å^3, Z = 8, ρ_{calcd} = 1.66 g cm^{-3}, $F(000)$ = 2056, $Mo_{K\alpha}$ radiation (λ = 0.71073 Å), $\mu(Mo_{K\alpha})$ = 67.1 cm^{-1}. Intensity data were measured at 23 °C using an Enraf-Nonius CAD4 diffractometer; Lorentz, polarization, and absorption corrections were applied to the data. The structure was solved by the heavy atom method. A loosely held *n*-pentane molecule of solvation with 0.5 occupancy was also found. Full matrix least-squares refinement, with hydrogens allowed for as riding atoms, gave R_1 = 0.045 and R_2 = 0.063 for 2451 reflections with $I \geq 3\sigma(I)$. A final difference map was devoid of chemically significant features. – The atomic coordinates for this work are available on request from the Director of the Cambridge Crystallographic Data Centre, University Chemical Laboratory, Lensfield Road, Cambridge CB2 1EW (UK). Any request should be accompanied by the full literature citation for this communication.

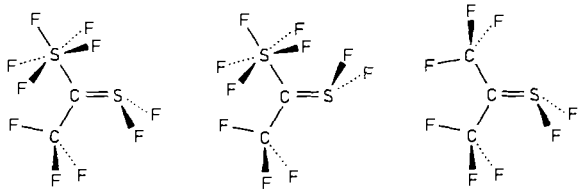
Alkylidene Sulfur Difluorides: $F_5S(F_3C)C=SF_2$ and $(F_3C)_2C=SF_2$. Synthesis, Structure, and Structure Predictions**

By *Reinhard Damerius, Konrad Seppelt,** and *Joseph S. Thrasher*

In the isomerization reaction between $F_5S-HC=CF_2$ **1** and $F_4S=CH-CF_3$ in the presence of highly active CsF,[1] we have obtained a compound of formula **3** in very small yield. A detailed investigation of this reaction has led to a smooth synthesis of this compound, the first alkylidene sulfur difluoride.

$$F_5S-HC=CF_2 \xrightarrow[CsF]{SF_4} [(F_5S)(F_3C)HC-SF_3] \xrightarrow[-HF]{} F_5S(F_3C)C=SF_2$$
1 **2** **3**

The alkylidene sulfur difluoride **3** is a colorless, stable liquid at room temperature and can be characterized by the usual physical methods. The ^{19}F NMR spectrum is particularly revealing; the F_5S, F_3C, and $\rangle C=SF_2$ resonances are clearly separated from one another and fully coupled (see *Experimental Procedure*). Moreover, compound **3** is present as two isomers in a ratio of ca. 8:1. Accordingly, the plane formed by the substituents on carbon bisects the SF_2 angle (see Fig. 1).



3a **3b** **6**

Fig. 1. Structural model of alkylidene sulfur difluoride **3** (isomers **3a** and **3b**) as well as of **6**.

Interconversion of the isomers is not observed up to 100 °C: thus, the torsional barrier for the C=S double bond (or the inversion barrier of the $\rangle C=SF_2$ group) can be estimated to be at least 100 kJ mol^{-1}.

The corresponding reaction of $F_3C-HC=CF_2$ affords $(F_3C)_2C=SF_2$ **6** in poor yields; owing to its characteristic rearrangement to $(F_3C)_2FC-SF$ **7**, compound **6** cannot be synthesized in pure form. The ^{19}F NMR spectra of **6** show nonequivalence of the F_3C groups. This is expected from the structural principles derived for **3** (see Fig. 1). It has not been possible so far to extend this simple synthesis reaction to other olefins.

The observed structural rigidity of compounds **3** and **6**, which is a characteristic feature of double bonds, contrasts sharply with the free rotation around the C–S bond in the sulfur ylides **4**.[2] Of all phosphorus ylides reported, only one example is known in which rotation around the P–C bond is hindered below -10 °C and this is presumably due to steric factors.[3] For the recently discovered compound $OFC-HC=SF_2=O$, C=S torsion is frozen out below -30 °C.[4]

The reactivity of the alkylidene sulfur difluorides **3** and **6** also differs from that of the sulfur ylides **4**, which are mainly employed as carbene sources. By contrast, **3** and **6** are transformed into the sulfenyl fluorides **5** and **7**, respectively, upon irradiation or slow heating.

$$\underset{\mathbf{4}}{R_2\overset{\ominus}{C}-\overset{\oplus}{S}R'_2} \longrightarrow R_2C: + SR'_2$$

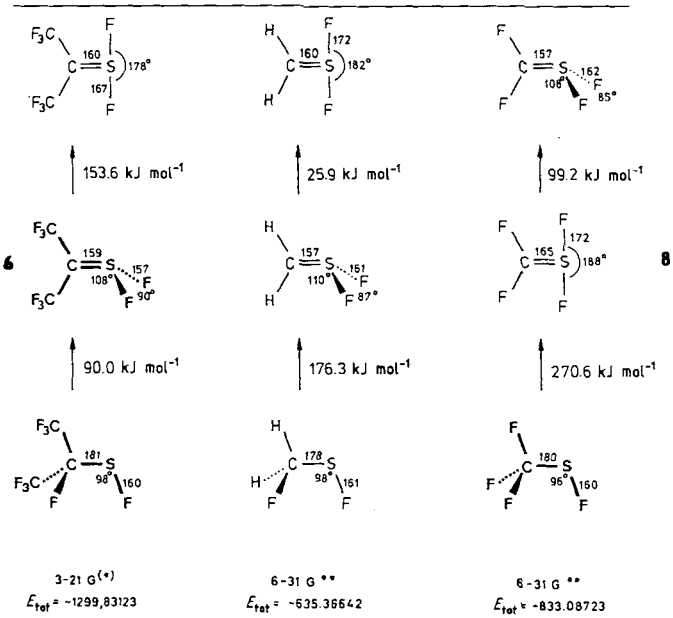
$$\underset{\mathbf{3}}{F_5S(F_3C)C=SF_2} \xrightarrow[\Delta,\,100\,^\circ C]{h\nu,\,20\,^\circ C} \underset{\mathbf{5}}{F_5S(F_3C)FC-SF}$$

$$\underset{\mathbf{6}}{(F_3C)_2C=SF_2} \xrightarrow{\Delta\,40\,^\circ C} \underset{\mathbf{7}}{(F_3C)_2FC-SF}$$

Only a few sulfenyl fluorides have been reported so far;[5–7] these are moderately stable derivatives of the very unstable SF_2.[8] The 1,2-fluorine shift is reminiscent of the transformation of FS–SF to $S=SF_2$.[9] From a thermodynamic point of view, a reversal of the stability in favor of the single bond is plausible. In this rearrangement, the CF bond is formed at the expense of a weaker SF bond.

If the structural isomers **3** and **6** are simplified to $H_2C=SF_2$ and those of **5** and **7** to H_2FC-SF, one obtains molecular structures whose sizes and relative energies are accessible to ab initio methods of calculation [(3–21G(*))-6–31G**]. The ground state is H_2FC-SF in the *gauche* conformation; the other rotamers are higher in energy by 5–30 kJ mol^{-1}. $H_2C=SF_2$, corresponding to the structures shown in Figure 1, is higher in energy by 176.3 kJ mol^{-1}. It has a short C=S bond length of 157 pm (see Table 1; cf. 155 pm in $H_2C=SF_4$[10]).

Table 1. Ab initio results for alkylidene sulfur difluorides $R_2C=SF_2$ compared with those for fluoroalkyl sulfenyl difluorides R_2FC-SF. Bond lengths in pm, E_{tot} in Hartree; known compounds drawn with thick lines.



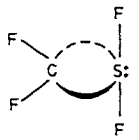
The energies of the isomer pair **6/7** could only be calculated with the 3–21 G(*) basis set; the energy difference in this case is 90.0 kJ mol^{-1}. The energy value obtained upon rota-

[*] Prof. Dr. K. Seppelt, Dipl.-Chem. R. Damerius
Institut für Anorganische und Analytische Chemie
der Freien Universität
Fabeckstrasse 34–36, D-1000 Berlin 33
Prof. Dr. J. S. Thrasher
Department of Chemistry, University of Alabama
Tuscaloosa, Alabama 35487 (USA)

[**] This work was supported by the Deutsche Forschungsgemeinschaft and the Fonds der Chemischen Industrie as well as by a generous allotment of computer time by the Alabama Supercomputer Network.

tion of the $=SF_2$ group by 90° relative to the $=C(CF_3)_2$ group is 91 kJ mol^{-1} higher; this provides a qualitative idea of the amount of C–S double bonding, which was calculated to be approximately 122 kJ mol^{-1} for alkylidene sulfur tetrafluorides.[1]

The calculation could also be performed for the isomer pair $F_2C=SF_2/F_3C-SF$ using once again the larger basis set. Surprisingly, a new structure **8** was predicted to be more stable. This molecule is fully planar and the SF_2 group is nearly linear. The C–S π bond lies outside of the molecular plane to the extent of 98%. This atomic arrangement corresponds to a minimum since all eigenvalues of the second-derivative matrix are positive. This molecule, which cannot be easily described according to conventional models, presents a challenge for the experimentalist. A possible model is of-



8

fered by **8**. It has thus been shown once again that SF_5 substitution stabilizes unusual bonding patterns.

Experimental Procedure

3: **1** (3.8 g, 20 mmol), SF_4 (2.16 g, 20 mmol), and CsF (9 g, 59 mmol) were stirred in a stainless-steel autoclave at 70 °C for 3 d. The product was isolated in a −78 °C trap by fractional condensation under dynamic vacuum. Colorless liquid (b.p. 64 °C, extrapolated from the vapor pressure curve), overall yield of the isomeric mixture 84%, isomer ratio 8:1 (according to ^{19}F NMR). Raman (liq.): strong bands at $\tilde{\nu}$ = 989.0 (s,p), 734.5 (s,p), 717.0 (vs,p), 678.0 (vs,p), 466.5 (s,p), 453.5 (vs,p), 406.0 (s,p), 324.0 (s,dp), 314.0 (s,dp), 288.0 (vs,p), 231.0 (s,dp) cm^{-1}. IR (gas): strong bands at $\tilde{\nu}$ = 1274 (vs), 1228 (vs), 1180 (vs), 901 (vs), 887 (vs), 854 (vs), 834 (s) cm^{-1}. ^{19}F NMR (84.25 MHz, CCl_3F), $AB_4C_2D_3$ type (values for the minor isomer in parentheses): δ_A = 73.2 (77.1), δ_B = 80.0 (86.5), δ_C = −3.6 (−7.5), δ_D = −54.6 (−55.2), J_{AB} = 147.3 (144.0), J_{AC} = 2.0 (1.5), J_{AD} = 1.4 (1.1), J_{BC} = 20.5 (23.0), J_{BD} = 10.1 (11.1), J_{CD} = 18.8 (17.2) Hz. MS: m/z 278 ($M^{\oplus}$, 45% based on $SF_5^{\oplus}$ = 100%) as well as numerous lighter fragments.

5: Irradiation of **3** in a pyrex glass apparatus for 1 h at 20 °C with a high-pressure Hg lamp gave pure **5**. Colorless liquid (b.p. 55 °C, extrapolated from the vapor pressure curve), quantitative yield. Raman (liq.): strong bands at $\tilde{\nu}$ = 1147.5 (s,p), 733.0 (s,p), 702.5 (vs,p), 682.0 (vs,p), 402.0 (vs,p), 278.0 (s,p), 244.0 (s,p) cm^{-1}. IR (gas): strong bands at $\tilde{\nu}$ = 1256 (s), 1240 (s), 1232 (vs), 1216 (vs), 1033 (s), 1028 (s), 905 (vs), 888 (vs), 834 (s), 795 (s) cm^{-1}. ^{19}F NMR (84.25 MHz, CCl_3F), AB_4C_3DE type: δ_A = 66.4, δ_B = 55.0, δ_C = −73.8, δ_D = −125.0 (CF), δ_E = −329.5 (SF), J_{AB} = 146.3, J_{BC} = 22.5, J_{BD} = 5.4, J_{BE} = 3.6, J_{CD} = 26.0, J_{CE} = 3.6, J_{DE} = 11.0 Hz. MS: m/z 278 ($M^{\oplus}$, 5% based on $S_2^{\oplus}$ = 100%) as well as numerous lighter fragments.

6: $F_3C-HC=CF_2$ (2.64 g, 20 mmol) [11], SF_4 (2.16 g, 20 mmol), and CsF (9 g, 59 mmol) were agitated in an autoclave at 20 °C for 5 d. Thermally unstable **6**, together with **7**, was formed. Yield 2%. ^{19}F NMR (84.25 MHz, CCl_3F), $A_2B_3C_3$ type: δ_A = −5.5, δ_B = −55.9, δ_C = −56.4, J_{AB} = 16.2, J_{AC} = 18.6, J_{BC} = 6.3 Hz. Warming to 40 °C resulted in complete rearrangement to **7** (for physical data see [5]).

Ab initio calculations: GAUSSIAN 86 program, geometry optimization with 3-21 G(*) (*: d orbitals on sulfur) and, if possible, energy optimization of this geometry with 6-31 G** basis set (**: d orbitals on S, C, F, p orbitals on H).

Received: January 26, 1989 [Z 3143 IE]
German version: *Angew. Chem. 101* (1989) 783

[1] T. Grelbig, B. Pötter, K. Seppelt, *Chem. Ber. 120* (1987) 815.
[2] E. F. Perozzi, I. C. Paul in C. J. Sterling (Ed.): *The Chemistry of the Sulfonium Group*, Wiley, Chichester 1981; *B. M. Trost, L. S. Melvin, Jr.: Organic Chemistry, Vol. 31; "Sulfur Ylides,"* Academic Press, New York 1975.
[3] B. Neumüller, E. Fluck, *Phosphorus Sulfur 29* (1986) 23.
[4] T. Krügerke, K. Seppelt, *Chem. Ber. 121* (1988) 1977.
[5] R. M. Rosenberg, E. L. Muetterties, *Inorg. Chem. 1* (1962) 756.
[6] F. Seel, W. Gombler, R. Budenz, *Angew. Chem. 79* (1967) 686; *Angew. Chem. Int. Ed. Engl. 6* (1967) 706.
[7] L. M. Zaborowski, J. M. Shreeve, *Inorg. Chim. Acta 5* (1971) 311.
[8] F. Seel, *Adv. Inorg. Chem. Radiochem. 16* (1974) 297.
[9] B. Solouki, H. Bock, *Inorg. Chem. 16* (1977) 665.
[10] A. Simon, E. M. Peters, D. Lentz, K. Seppelt, *Z. Anorg. Allg. Chem. 468* (1980) 7; H. Bock, J. E. Boggs, G. Kleemann, D. Lentz, H. Oberhammer, E. M. Peters, K. Seppelt, A. Simon, B. Solouki, *Angew. Chem. 91* (1979) 1008; *Angew. Chem. Int. Ed. Engl. 18* (1979) 944.
[11] Synthesis of $F_3C-CH=CF_2$ similar to that of $C_3F_7-CH=CF_2$: J. D. LaZerte, K. J. Koshar, *J. Am. Chem. Soc. 77* (1955) 910.

Location of *para*-Xylene in Yb-Faujasite (Zeolite Y) by Neutron Diffraction**

By *Mirjam Czjzek, Thomas Vogt,* and *Hartmut Fuess**

Synthetic Y-zeolite is employed as catalyst in the petrochemical industry, e.g. in isomerizations and alkylation.[1] The activity and selectivity of the Y-zeolites (mineral name faujasite) increases when the alkali metal ions are replaced by ions of the rare-earth metals.[2, 3]

In the isomerization of xylenes, disproportionation occurs as competing reaction. Both reactions proceed via a carbocation, and toluene and trimethylbenzenes as well as the isomeric xylenes are as products.[4, 5] On using an H-Y-zeolite as catalyst, mainly the products of disproportionation are obtained, whereas when Y-zeolites with rare-earth cations are employed the amount of isomerization products increases with increasing content of rare-earth cations.

To gain an insight into the catalytic process at the molecular level, a knowledge of the structural arrangement of the chemisorbed molecules in the zeolite is required. A knowledge of the structure and the thermodynamic, kinetic and spectroscopic data are prerequisite for a discussion of theoretical models.[6] Since single crystals of catalytically synthetic zeolites are seldom available for a structure analysis, the analysis of powder data has to be resorted to. For this purpose the Rietveld method for the profile analyses[7] of highly resolved neutron powder pattern has proven advantageous. The first results obtained for the location of chemisorbed molecules in zeolites have only recently been reported.[8, 9] We have now investigated the isomerization of *para*-xylene in Yb-zeolite Y (Yb-Y) and report here on the location of the xylene molecules in the zeolite framework.

The sample of Yb-Y was prepared from synthetic Y-zeolite (Union Carbide) by cation exchange with a 0.04 molar aqueous $Yb(NO_3)_3$ solution. The sample was dehydrated by slowly heating to 400 °C in a stream of oxygen and thereafter under vacuum for 12 h. Chemisorption of 0.25 ml of deuterated *p*-xylene in 3.22 g of Yb-Y was achieved within 2.5 h at room temperature in a vacuum. The sample was characterized by the composition $Yb_{13}Na_{17}Al_{56}Si_{136}O_{384}$ 9.4 C_8H_{10}. Neutron powder spectra were recorded on the D1A diffractometer[10] at the Institut Laue-Langevin (Grenoble).[11] The positions of the cations in the zeolite loaded with *p*-xylene differ only slightly from those in the pure Yb-Y.[12] Figure 1 shows the neutron powder pattern.

[*] Prof. Dr. H. Fuess, Dipl.-Chem. M. Czjzek
Institut für Kristallographie der Universität
Senckenberganlage 30, D-6000 Frankfurt am Main (FRG)
Dr. T. Vogt
Institut Laue-Langevin
Avenue des Martyrs, F-38042 Grenoble (France)

[**] This work was supported by the Bundesminister für Forschung und Technologie. The samples were prepared at the Institut des Recherches sur la Catalyse, CNRS, Villeurbanne, Lyon (France).

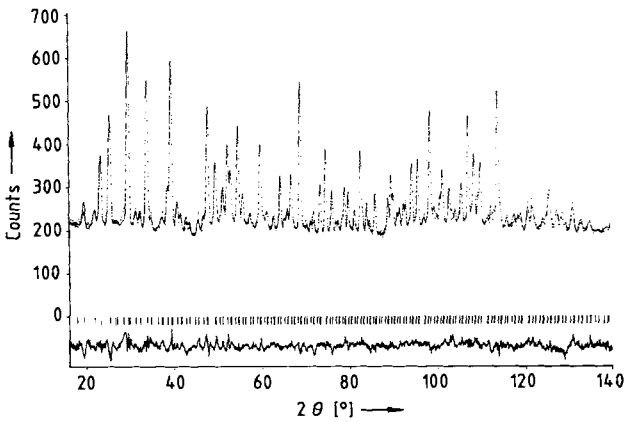


Fig. 1. Neutron diffraction pattern of Yb-faujasite with *p*-xylene. Dots: experiment. Upper curve: calculated diagram. Line series: positions of reflections. Lower curve: difference between observed and calculated intensities.

The $Yb^{3\oplus}$ ions are located at the position SI′ in the sodalite cage. Ce[14] and La[15] have already been found in this position too. The 17 $Na^{\oplus}$ ions are located in the six-membered ring windows between sodalite- and supercage. A comparison of the lattice constants of Na-Y (2485.36(3) pm[8]), Yb-Y (2458.50(6) pm[12]) and Yb-Y · 9.4 C_8D_{10} (2454.92(6) pm) reveals that the lattice contracts. $Yb^{3\oplus}$ is surrounded octahedrally by three oxygen atoms of the lattice at a distance of 239.2 pm and three water molecules at a distance of 236.3(14) pm. This interaction of the Yb ion with the framework gives rise to a lengthening of the Si–O(3) bond in the framework from 166.6(4) pm in Na-Y to 168.0(7) pm in Yb-Y. This bond is further lengthened to 171.31(8) pm by chemisorption of C_8D_{10}. The Si–O(4) bond, whose oxygen is not bound to the cations, on the other hand, is shortened from 164.8(4) pm in Na-Y through 157.5(7) pm to 156.6(8) pm in Yb-Y-C_8H_{10}. The position of the *p*-xylene molecules was determined by difference Fourier syntheses and refined with incorporation of structural boundary conditions (chemical constraints) for the geometry of the adsorbed molecule according to *Waser*.[16] For each supercage there are two crystallographically different positions, each of which is present four times (Fig. 2). The molecules are arranged perpendicular to the threefold axis. With eight super cages per cell, complete occupation leads to 32 molecules per position in the unit cell. Such a complete occupation of this type, however, is not possible for steric reasons. In position A there are on average 2 molecules, in position B 7.4. This corresponds to an average occupancy of 1.175 molecules of *p*-xylene per supercage, distributed over the eight crystallographic positions. If more than one molecule resides at an equivalent position in the cage then the molecular planes form an angle of 59.4°. The shortest C–C distance between the methyl groups of two molecules is 360(10) pm. The ring planes in the two positions A and B are rotated through 30° with respect to each other. The deuterium atom D(3) of the methyl group in position A is at a distance of 273(6) pm from O(1) and 273(6) pm from O(4). The deuterium atom D(6) of the methyl group in the *p*-xylene of position B is at a short distance of 270(6) pm from O(1)′ and in the *para* position thereto at a large distance of 301(6) pm from O(1)′. These distances are indicative of an interaction of the methyl group of the *p*-xylene with the skeletal framework.

The centroid of the aromatic ring in position A is at a distance of 255(5) pm from $Na^{\oplus}$ whereas in position B the distance is much shorter (241(5) pm). Similar short distances have been observed by *Fitch* et al.[8] in Na-Y · C_6D_6. They found a distance of 270(1) pm at lower occupancy and of 264(1) pm at higher occupancy. They interpret their results in terms of a cluster formation of neighboring arene molecules; a homogeneous distribution of the molecules on the supercage does not occur. This is also demonstrated by small angle measurements,[7] which show that, with occupancies of more than one molecule per supercage, the cluster formation will be given preference over the homogeneous distribution. Also ^2H NMR investigations by *Zibrowius* et al.[18] on chemisorbed benzene in Y-zeolites afford evidence of strong intermolecular interactions of the chemisorbed molecules and of a possible interaction of the π-electrons of the benzene rings with the Na ions.

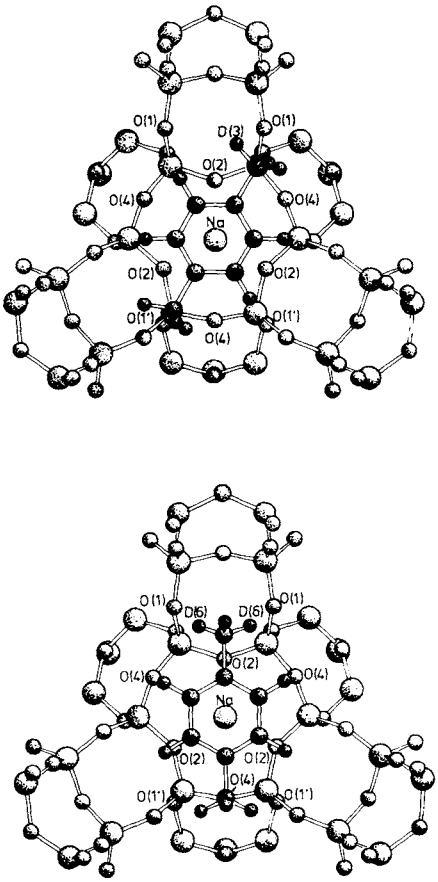


Fig. 2. Position of the *p*-xylene molecule in the supercage of Yb-faujasite. By rotating the molecule through 60° and 120° one obtains further symmetry-equivalent positions. The molecule appears (statistically distributed) in all three positions. Above: position A. Below: position B.

Received: October 31, 1988;
revised: February 24, 1989 [Z 3032 IE]
German version: *Angew. Chem. 101* (1989) 786

CAS Registry numbers:
Yb, 7440-64-4; C_8D_{10}, 41051-88-1; *p*-xylene, 106-42-3.

[1] J. A. Rabo, M. L. Poutsma, *ACS Monogr. (Molecular Sieve Zeolites I) 101* (1970) 209.
[2] P. E. Eberly, L. N. Kimberlin, *ACS Monogr. (Molecular Sieve Zeolites I) 101* (1970) 283.
[3] J. W. Ward, *J. Catal. 13* (1969) 321.
[4] F. Gajewski, B. Sulikowski, *React. Kinet. Catal. Lett. 9* (1978) 395.
[5] B. Sulikowski, *React. Kinet. Catal. Lett. 31* (1986) 215.
[6] S. Yashonath, J. M. Thomas, A. K. Nowak, A. K. Cheetham, *Nature (London) 331* (1988) 601; M. Mabilia, R. A. Pearlstein, A. J. Hopfinger, *J. Am. Chem. Soc. 109* (1987) 7960; S. Ramdas, J. M. Thomas, P. W. Betteridge, A. K. Cheetham, E. K. Davies, *Angew. Chem. 96* (1984) 629; *Angew.*

Chem. Int. Ed. Engl. 23 (1984) 671; J. M. Thomas, *ibid. 100* (1988) 1735 and *27* (1988) 1673.
[7] H. M. Rietveld, *J. Appl. Crystallogr. 2* (1969) 65.
[8] A. N. Fitch, H. Jobic, A. Renouprez, *J. Phys. Chem. 90* (1986) 1311.
[9] P. A. Wright, J. M. Thomas, A. K. Cheetham, A. K. Nowak, *Nature (London) 318* (1985) 611.
[10] A. W. Hewat, I. Bailey, *Nucl. Instrum. Methods 137* (1976) 463.
[11] The samples were transferred under He into cylinder-shaped vanadium containers (16 mm diameter) sealed with an indium wire. The spectrum was measured at 5K with a wavelength of 190.51 pm in the 2θ range of 6–156° in steps of 0.05°. Rietveld refinements [13] in the space group $Fd\bar{3}m$ led to the following figures of merit: $R(wp) = \sqrt{\sigma[w(y_{obs} - y_{calc})^2]/\sigma[wy_{obs}]^2} = 0.115$ with $R(\exp) = \sqrt{[N - P + c]/\sigma[wy_{obs}]^2} = 0.068$ and $R(I) = (\sigma[\mathrm{Mod}(I_{obs} - I_{calc})/\sigma y_{obs}) = 0.073$. The positions of the carbon atoms of the *p*-xylene were taken from difference Fourier maps. Deuterium positions were first calculated and subsequently refined with chemical constraints [16]. The range up to 16° in 2θ was excluded from the refinement since the first four Bragg reflections show an asymmetry due to the finite detector opening that cannot be fitted with the fundamental Gauss profile.
[12] M. Czjzek, H. Fuess, T. Vogt, unpublished results.
[13] J. K. Cockroft, unpublished Rietveld Program.
[14] P. Gallezot, B. Imelik, *J. Chem. Phys. Physicochim. Biol. 68* (1971) 34.
[15] J. M. Bennet, J. V. Smith, *Mater. Res. Bull., 3* (1968) 865.
[16] J. Waser, *Acta Crystallogr. 16* (1963) 1091.
[17] A. J. Renouprez, H. Jobic, R. C. Oberthür, *Zeolites 5* (1985) 222.
[18] B. Zibrowius, J. Caro, H. Pfeiffer, *J. Chem. Soc. Faraday Trans. 1 84* (1988) 2347.

Amine-Bis(ethene)nickel(0) Complexes; Structure of 1-Azabicyclo[2.2.2]octanebis(ethene)nickel(0)**

By *Wilfried Kaschube, Klaus R. Pörschke,** *Werner Bonrath, Carl Krüger,* and *Günther Wilke*

Behrens and *Hieber* et al. reported that in liquid NH_3 or in pyridine above −25 °C $Ni(CO)_4$ forms readily disproportionating substitution complexes $[(NH_3)Ni(CO)_3]$ and $[(NH_3)_2Ni(CO)_2]$ (isolated as mixture)[3a] or $[(C_5H_5N)Ni(CO)_3]$ (IR detection).[3b] According to the HSAB concept of *Pearson*,[4] in the former compounds the "soft" Lewis acid nickel(0) is coordinated by a "hard" base. Our investigations show a decrease in acceptor strength of nickel(0) for the σ-donors $R^{\ominus}$ [5] and $H^{\ominus}$ [6] in the series

$$Ni(cdt) < Ni(C_2H_4)_2 < Ni(CO)_3$$

(cdt = *trans,trans,trans*-1,5,9-cyclododecatriene). Thus the amine–nickel(0) bond of the alkene-stabilized complexes should be even more labile than that of the carbonyl derivatives. It was therefore surprising that isolable, crystalline complexes of the type $[(amine)Ni(C_2H_4)_2]$ could be obtained,[7] whose syntheses and properties we describe herein.

Equimolar amounts of tris(ethene)nickel(0)[8] and 1-azabicyclo[2.2.2]octane in pentane afford a clear yellow reaction solution below 0 °C, from which small yellow cuboids of the title compound **1** separate in 70% yield on cooling to −78 °C. The crystals of **1** slowly decompose above 0 °C. Upon reaction of solid **1** with cyclooctatetraene ethene is liberated quantitatively and can thus be determined; in THF solution, **1** reacts smoothly with cyclooctadiene (cod) at −30 °C with displacement of all ligands to give $Ni(cod)_2$.

Analogously to the preparation of **1**, the complex **2** (long yellow needles, 56%) is obtained with the secondary amine Et_2NH, whereas no reaction is observed with NEt_3. Passage of ammonia into a solution of $Ni(C_2H_4)_3$ in pentane at −78 °C leads to immediate separation of **3** as a yellow precipitate (decomp. −50 °C). With pyridine a red solution was obtained, from which **4** crystallized as yellow cubes (86%), while with the diamine 1,4-diazabicyclo[2.2.2]octane the binuclear complex **5** (fine yellow cubes, 21%, decomp. at 20 °C) was isolated. Tetramethylethylenediamine (tmeda) possibly reacts with $Ni(C_2H_4)_3$ to form a binuclear complex analogous to **5**, which however could not be isolated.[9] The reactions according to Equations (a) and (b) are obviously equilibrium reactions.

$$Ni(C_2H_4)_3 \xrightarrow[-C_2H_4]{+\text{ amine}} \begin{cases} [(C_7H_{13}N)Ni(C_2H_4)_2] & \mathbf{1} \\ [(Et_2NH)Ni(C_2H_4)_2] & \mathbf{2} \\ [(H_3N)Ni(C_2H_4)_2] & \mathbf{3} \\ [(C_5H_5N)Ni(C_2H_4)_2] & \mathbf{4} \end{cases} \quad (a)$$

$$2\ Ni(C_2H_4)_3 \xrightarrow[-2\ C_2H_4]{+\text{ diamine}} [(\mu\text{-}C_6H_{12}N_2)\{Ni(C_2H_4)_2\}_2] \quad \mathbf{5} \quad (b)$$

amine = 1-azabicyclo[2.2.2]octane, diethylamine, ammonia;
diamine = 1,4-diazabicyclo[2.2.2]octane

The compounds **1**–**5** are very soluble in cold ether and THF. The 200-MHz ^1H NMR ([D_8]toluene) and 75.5-MHz ^{13}C NMR spectra ([D_8]THF) of **1** showed signals for the ethene ligands at $\delta(H) = 2.95$ and $\delta(C) = 55.7$, no broadening or splitting of which is observable down to −80 °C (^1H) and −100 °C (^{13}C), respectively; the ethene ligands obviously rotate about the bond axes to the nickel atom with a relatively low energy barrier. The shielding of the ethene protons and C atoms is less than in the corresponding phosphane complexes, in which the ethene rotation can, in addition, be frozen-in (cf. $(Me_3P)Ni(C_2H_4)_2$ in [D_8]THF, −80 °C: $\delta(H) = 2.44, 2.31$; $\delta(C) = 49.4, 48.7$; $\Delta G^{\neq} = 43.4$ kJ mol^{-1}).[5b]

The crystal structure analysis (173 K) of **1**[10] (Fig. 1) showed a trigonal planar coordination of the nickel, with an

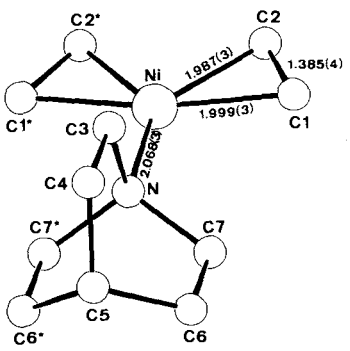


Fig. 1. Crystal structure of **1** [10]. Bond lengths in [Å].

[*] Priv.-Doz. Dr. K. R. Pörschke, Dr. W. Kaschube, Dr. W. Bonrath [+], Prof. Dr. C. Krüger [+], Prof. Dr. G. Wilke
Max-Planck-Institut für Kohlenforschung
Postfach 10 13 53, D-4330 Mülheim a. d. Ruhr 1 (FRG)

[+] Single crystal X-ray analysis.

[**] Amine–Nickel Complexes, Part 5 and On the Lewis Acidity of Nickel(0), Part 11 – Parts 4 and 10: [1] and [2], respectively.

ethene ligand and the amine nitrogen atom each occupying a coordination site. Ni, N, C3, C4 and C5 lie in a mirror plane determined by the space-group. The two equivalent ethene ligands are attached coplanar to the nickel with NiC distances which, within the limits of experimental error, are equal. The angle subtended at the nickel to the mid-points of the ethene ligands in **1** is 126.2°; the corresponding angle at the N atom is 116.9°. The other structurally investigated ligand-Ni(C_2H_4)$_2$ complexes[2, 5a, 11] have lower symmetries than **1**. The Ni–N distance in **1** (2.068(3) Å) lies between the values found for (tmeda)nickel(0) complexes with trigonal-planar (1.97–2.02 Å; with strong π-acceptors)[12] and tetrahedral coordination geometry of the nickel (2.14–2.17 Å).[1, 13] As in the free amine,[14] the C–N–C angles in the 1-azabicyclo[2.2.2]octane ligands are 107.4° (mean value).

1 reacts with CO in THF at 0 °C to give the carbonyl complex **6**, which can be isolated at −78 °C in the form of yellow cubic shaped crystals (37%, recrystallizable from pentane); if the reaction is carried out below 0 °C more byproducts are formed. The IR spectrum of **6** shows C≡O valence vibrations ($\tilde{\nu}$ = 2030 (A_1) and 1970 cm^{-1}(E)) as are characteristic for L–Ni(CO)$_3$ complexes.[15] We could not isolate a pyridine derivative formed by reaction of **4** with CO either (cf. Ref. [3b]).

$$\underset{\mathbf{1}}{(C_7H_{13}N)Ni(C_2H_4)_2} + 3\,CO \xrightarrow[THF]{0\,^\circ C} \underset{\mathbf{6}}{(C_7H_{13}N)Ni(CO)_3} + 2\,C_2H_4$$

Formation of an adduct of Ni(cdt) with amines was not observed. The decrease in acceptor strength of nickel(0) as outlined at the beginning (in extension of Ref. [6b], Eq. (1) and Ref. [5c], Eq. (2)) we now have the following sequence of reduced σ-donor strength of the ligands:

$$R^{\ominus} > R_3Al-H^{\ominus} \geq R_3P^{\oplus}-CH_2^{\ominus} > Me_2S(O)^{\oplus}-CH_2^{\ominus} \approx R_3N$$

Experimental

1: A reaction solution of 10 mmol of Ni(C_2H_4)$_3$ [8] and 1.11 g (10 mmol) of 1-azabicyclo[2.2.2]octane in 20 mL of pentane was freed of excess ethene at −30 °C by stirring under vacuum (oil pump); sparingly soluble impurities were then removed by filtration. On cooling the filtrate below −50 °C yellow cuboid crystals separated out; these were, after withdrawing the mother liquor with a capillary pipette, washed twice with cold pentane, and dried in a high vacuum at −60 °C. Yield 1.55 g (70%); correct elemental analysis. 400-MHz ^{1}H NMR ([D$_8$]toluene, −80 °C): δ = 2.95 (8H, C_2H_4), 2.77 (6H, NCH_2), 1.28 (1H, CH), 1.00 (6H, CH_2); 75.5-MHz ^{13}C NMR ([D$_8$]THF, −80 °C): δ = 55.7 (4C, C_2H_4), 53.6 (3C, NCH_2), 27.35 (3C, CH_2), 21.2 (1C, CH).

2: Procedure as for **1**, but with 731 mg (10.0 mmol) of Et_2NH. At −78 °C long needles, yield 1.05 g (56%). 200-MHz ^{1}H NMR ([D$_8$]THF, −80 °C): δ = 4.74 (m, 1H, ^3J(HH) = 11.4 and 3.4 Hz, NH), 2.82 (m, 2H, ^2J(HH) = −10.9 Hz, $^3J(HH)_{CH_3}$ = 7.1 Hz, NC*H*H), 2.65 (m, 2H, $^3J(HH)_{CH_3}$ = 7.3 Hz, NCH*H*), 2.30 (8H, C_2H_4), 1.11 (t, 6H, CH_3); 75.5-MHz ^{13}C NMR ([D$_8$]THF, −80 °C): δ = 51.45 (4C, C_2H_4), 49.8 (2C, NCH_2), 15.7 (2C, CH_3).

3: Procedure as for **1**, but with 250 mL (ca. 10 mmol) of gaseous NH_3 at −78 °C. A bright yellow precipitate immediately separated out; this was recovered by filtration, washed twice with cold pentane and dried at −78 °C in a high vacuum. Yield 990 mg (75%); decomp. −50 °C, an elemental analysis could not be carried out. 200-MHz ^{1}H NMR ([D$_8$]THF, −80 °C): δ = 2.74 (3H, NH_3), 2.25 (8H, C_2H_4).

4: Procedure as for **1**, but with 791 mg (10.0 mmol) of pyridine. Fine yellow crystals separated out from the bright-red filtrate at −78 °C. Yield 1.66 g (86%). 200-MHz ^{1}H NMR ([D$_8$]THF, −80 °C): δ = 8.79 (2H, NCH), 7.80 (1H, CH), 7.41 (2H, CH, C_5H_5N), 2.51 (8H, C_2H_4); 75.5-MHz ^{13}C NMR ([D$_8$]THF, −80 °C): δ = 152.7 (2C, NCH), 136.2 (1C, CH), 125.5 (2C, CH, C_5H_5N), 55.4 (4C, C_2H_4).

5: Procedure as for **1**, but with 560 mg (5.0 mmol) of 1,4-diazabicyclo-[2.2.2]octane in 20 mL of ether. At −50 °C fine yellow crystals, yield 360 mg (21%). 400-MHz ^{1}H NMR ([D$_8$]THF, −80 °C): δ = 3.17 (12H, NCH_2), 2.41 (16H, C_2H_4); 75.5-MHz ^{13}C NMR ([D$_8$]toluene, −105 °C): δ = 55.8 (8C, C_2H_4), 52.6 (6C, NCH_2).

6: 330 mL (13.5 mmol) of CO were taken up at 0 °C in a stirred solution of **1** (2.21 g, 10.0 mmol) in ether (60 mL). The dark-brown precipitate that separated out was removed by filtration and the filtrate evaporated to dryness under vacuum (oil pump) at −30 °C. the yellow crude product (756 mg, 37%) was recrystallized from pentane. Yellow cubic crystals; yield 395 mg (20%); correct elemental analysis. IR (THF solution): $\tilde{\nu}$[cm^{-1}] = 2030 (A_1), 1970 (E, C≡O).

Received: January 13, 1989 [Z 3119 IE]
German version: *Angew. Chem. 101* (1989) 790

CAS Registry numbers:
1, 120611-06-5; **2**, 120611-07-6; **3**, 120611-08-7; **4**, 120611-09-8; **5**, 120611-10-1; **6**, 120636-95-5; $C_7H_{13}N$, 100-76-5; $C_6H_{12}N_2$, 280-57-9; Ni(C_2H_4)$_3$, 50696-82-7; Ni(cod)$_2$, 1295-35-8; cod, 111-78-4.

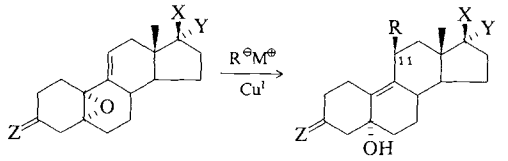
[1] W. Kaschube, K. R. Pörschke, K. Seevogel, C. Krüger, *J. Organomet. Chem. 367* (1989) 233.
[2] W. Kaschube, K. R. Pörschke, K. Angermund, C. Krüger, G. Wilke, *Chem. Ber. 121* (1988) 1921.
[3] a) H. Behrens, H. Zizlsperger, *J. Prakt. Chem. 4. Reihe, 14* (1961) 249; b) W. Hieber, J. Ellermann, E. Zahn, *Z. Naturforsch. B 18* (1963) 589.
[4] R. G. Pearson, *J. Am. Chem. Soc. 85* (1963) 3533; *J. Chem. Educ. 45* (1968) 581, 643.
[5] a) K. R. Pörschke, K. Jonas, G. Wilke, R. Benn, R. Mynott, R. Goddard, C. Krüger, G. Wilke, *Chem. Ber. 118* (1985) 275; b) K. R. Pörschke, G. Wilke, R. Mynott, *ibid. 118* (1985) 298; c) K. R. Pörschke, *ibid. 120* (1987) 425.
[6] a) K. R. Pörschke, G. Wilke, *Chem. Ber. 118* (1985) 313; b) W. Kleimann, K. R. Pörschke, G. Wilke, *ibid. 118* (1985) 323.
[7] W. Kaschube, *Dissertation*, Universität Bochum 1987.
[8] K. Fischer, K. Jonas, G. Wilke, *Angew. Chem. 85* (1973) 620; *Angew. Chem. Int. Ed. Engl. 12* (1973) 565.
[9] W. Schröder, K. R. Pörschke, *J. Organomet. Chem. 322* (1987) 385.
[10] a) Crystal structure analysis of **1**: space group *Pnma*, a = 13.310(1), b = 11.565(1), c = 7.303(1) Å, V = 1124.1 Å^3, Z = 4, T = −100 °C, ϱ_{calcd} = 1.34 g cm^{-3}, $\mu(Mo_{K\alpha})$ = 16.92 cm^{-1}, CAD4 Enraf-Nonius diffractometer, 5031 measured reflections, 1700 unique reflections, 1310 observed ($I \geq 2\sigma(I)$), 67 refined parameters, R = 0.042, R_w = 0.049. b) Further details of the crystal structure investigation are available on request from the Fachinformationszentrum Energie, Physik, Mathematik GmbH, D-7514 Eggenstein-Leopoldshafen 2 (FRG), on quoting the depository number CSD-53485, the names of the authors, and the journal citation.
[11] a) C. Krüger, Y.-H. Tsay, *J. Organomet. Chem. 34* (1972) 387; b) K. Jonas, K. R. Pörschke, C. Krüger, Y.-H. Tsay, *Angew. Chem. 88* (1976) 682; *Angew. Chem. Int. Ed. Engl. 15* (1976) 621; c) C. Krüger, J. C. Sekutowski, Y.-H. Tsay, *Z. Kristallogr. 149* (1979) 109; d) K. R. Pörschke, W. Kleimann, G. Wilke, K. H. Claus, C. Krüger, *Angew. Chem. 95* (1983) 1032; *Angew. Chem. Int. Ed. Engl. 22* (1983) 991; *Angew. Chem. Suppl. 1983*, 1527; e) K. R. Pörschke, G. Wilke, C. Krüger, *ibid. 95* (1983) 564 and *22* (1983) 547 and *1983*, 726.
[12] a) [(tmeda)Ni(Ph_2C=O)]: K. Jonas, C. Krüger, unpublished; K. Blum, *Dissertation*, Universität Bochum 1978; b) [(tmeda)Ni(C_2F_4)]: W. Kaschube, K. R. Pörschke, K. Angermund, C. Krüger, unpublished and Ref. [7].
[13] W. Schröder, K. R. Pörschke, Y.-H. Tsay, C. Krüger, *Angew. Chem. 99* (1987) 953; *Angew. Chem. Int. Ed. Engl. 26* (1987) 919.
[14] R. Fourme, *J. Phys. (Orsay, Fr.) 40* (1979) 557.
[15] C. A. Tolman, *J. Am. Chem. Soc. 92* (1970) 2953.

Stereo- and Regiospecific 6-*endo-trig*-Cyclization of Aryl Radicals, an Entry to Novel Progesterone-Antagonists of the Androstane Series

By *Eckhard Ottow,* Günter Neef,* and *Rudolf Wiechert*

An elegant, preparatively simple route[1] to 11 β-substituted steroids **2** of the estrane series, namely the regio- and stereospecific S_N2'-opening of the α,β-unsaturated epoxides **1** has been known since the end of the seventies.

[*] Dr. E. Ottow, Dr. G. Neef, Prof. Dr. R. Wiechert
Schering AG, Institut für Arzneimittelchemie
Müllerstrasse 170–178, D-1000 Berlin 65



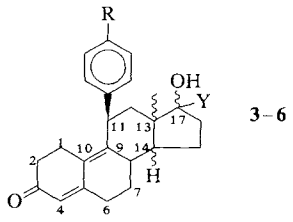
(a)

1 **2**

a, Z = OCH_2CH_2O, X = C≡N, Y = $OSiMe_3$
b, Z = $OCH_2C(CH_3)_2CH_2O$, X = OH, Y = H
R = alkyl, aryl; M = Li, MgCl, MgBr

At the beginning of the eighties this key reaction enabled the synthesis of the first competitive progesterone antagonists.[2] The exploration of the pharmacological profile and potential of these antihormones on the one hand, and the search for new antigestagens on the other, have since then been the subject of intensive studies.[3]

The competitive antiprogesterones **3–6** (Table 1)[4] that have so far been reported contain, aside from the antigestagen pharmacophore – the 11 β-aryl-substituent – also a 4,9-diene-3-oxo system.



3–6

Table 1. Characterization of the antiprogesterones **3–6**.

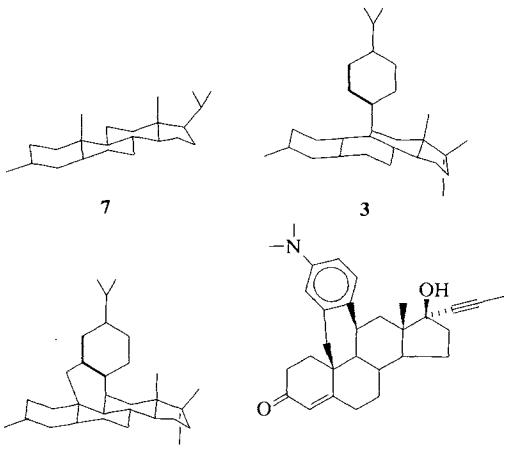
Cp.	Designation	Configuration at C-13	C-14	Position of 17-OH	R	Y
3	RU 38 486	β	α	β	$N(CH_3)_2$	$C\equiv C-CH_3$
4	ZK 112 993	β	α	β	$COCH_3$	$C\equiv C-CH_3$
5	ZK 98 299	α	α	α	$N(CH_3)_2$	$CH_2CH_2CH_2OH$
6	ZK 131 589	β	β	α	$N(CH_3)_2$	$CH_2CH_2CH_2OH$

This clearly demonstrates in which way the synthetic entry according to (a) on the one hand and the established sterically demanding 11 β-substituent on the other restrict conceivable variations at the carbon atoms 9 and 10 of these steroids. The approximate coplanarity of the 9,11 bond with the plane of the phenyl ring, as is revealed by X-ray structure analyses of the antigestagens **3–6**,[5] makes it plausible why even attempts to incorporate the least sterically demanding of all residues, a hydrogen atom, in the 10 β-position have failed.[6]

The coplanarity leads to a strong steric hindrance between the *ortho* proton of the 11-aryl moiety, which is turned towards the carbon atom 10, and a potential 10 β-substituent. This hindrance and a comparison of the structure with that of the natural gestagen, progesterone **7**, make a methylene bridging, as in the enone **8**, appear extremely attractive as synthetic goal (Scheme 1).

The establishment of this structural element was accomplished surprisingly easy by radical initiated cyclization of 19-(2-haloaryl)-9(11)-androstene derivatives **10**. These are accessible in good yields by 1,2-opening of the epoxide **1b** with (2-haloaryl)methylmagnesium halides **9**[7] (Table 2).

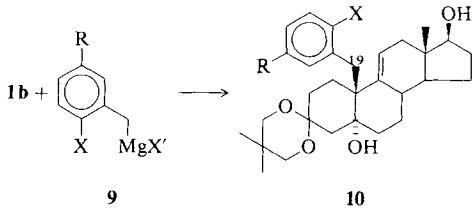
Of the conceivable methods[8] for the generation of the necessary intermediary phenyl radicals **11** (see Scheme 2) two



Antigestagens of the androstane series

7 **3** **8**

Scheme 1. Structure of an antigestagen of the androstane series derived from the structures of progesterone **7** and the antigestagen of the estrane series (only the atomic couplings between non-H atoms are shown), and **8** as possible realization of this structure.



(b)

1b + **9** → **10**

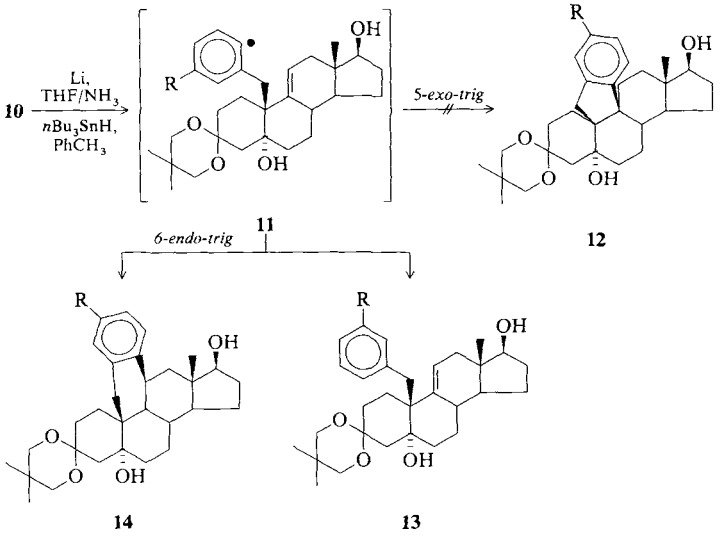
Table 2. Definition of the residues R, X′ and X in Equation (b) and yields of **10a–f**.

	R	X′	X	Yield of **10** [%]
a	H	F	Cl	83
b	H	Cl	Cl	86
c	H	Br	Br	81
d	OCH_3	Cl	Cl	79
e	OCH_3	Br	Br	86
f	$N(CH_3)_2$	Cl	Cl	78

in particular were used: the reaction with lithium and that with tributylstannane. On treating the aryl halides **10a–g** (the starting material **10g** (X = Br) was obtained by bromination of the dehalogenation product **13f** with *N*-bromosuccinimide in dichloromethane in the presence of triethylamine) with lithium in a mixture of tetrahydrofuran and liquid ammonia at − 65 °C the cyclization proceeds in good to very good yields independently of the nature of the halogen[9] (Table 3). The ratio of cyclization product **14** to noncyclized dehalogenation product **13** (Scheme 2) is thereby influenced by the halide ion as already described by *Bunnett* et al.[10]

The more reactive bromobenzenes **10e** and **10g** can also be cyclized with tributylstannane in toluene with the same success[11] (Table 3).

Particularly noteworthy is the regioselectivity of this ring closure. The perfect 6-*endo-trig*-regiospecificity[12] is in complete contrast to the reaction course in more simple systems.[13] As various studies have shown, especially the excellent preparative and mechanistic investigations of *Beckwith* et al.,[15] analogous alkenylphenyl radicals cyclize preferen-

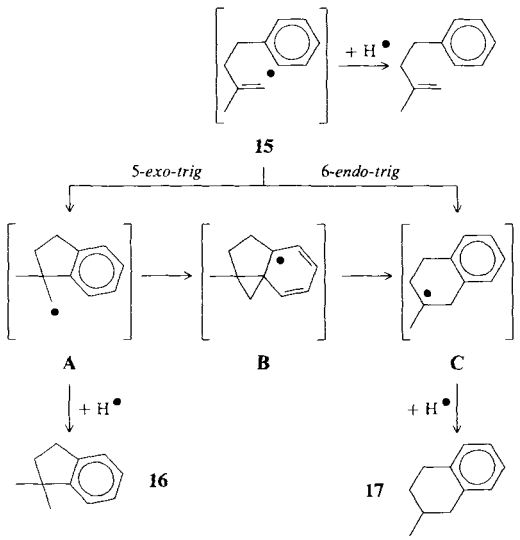


Scheme 2. Radical initiated cyclization of **10** to **14**. In all cases the dehalogenation product **13** is formed as byproduct.

Table 3. Radical cyclization of **10** according to Scheme 2. Concentration of **10**: 0.02 M.

Starting material	Method	Ratio **14**:**13**	Yield of **14** [%]
10a	Li	> 10 : 1	82
10b	Li	> 10 : 1	81
10c	Li	> 10 : 1	85
10d	Li	9 : 1	73
10e	nBu$_3$SnH	14 : 1	92
10e	Li	13 : 1	89
10f	Li	6 : 1	79
10g	nBu$_3$SnH	12 : 1	89
10g	Li	9 : 1	85

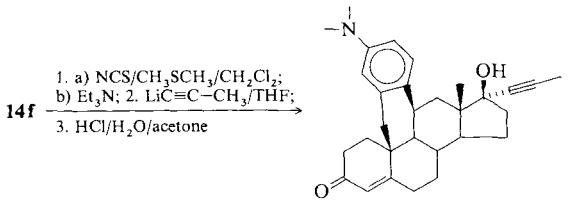
tially or exclusively in a 5-*exo-trig* fashion. Thus, for example, predominantly the five-membered ring compound **16** is formed from the phenyl radical **15**.



A neophyl rearrangement[16] in analogy to **15** → **A** → **B** → **C** → **17**, evidently[16] explaining larger amounts of six-membered ring products in certain cases, is unlikely in the case of **11** for energetic reasons. Semiquantitative estimations[18] of the relative energies of the transition states of direct 5-*exo-trig*- and 6-*endo-trig*-cyclizations that have to be taken into consideration in analogy to the force field calculations carried out by *Beckwith* et al.[19] are in good agreement with the experimental results.

In the simplest cases, conversion of the intermediates **14** into the finally desired active substances merely requires attachment of a side chain to carbon atom 17 and the removal of the protective groups. As example, in the case of **14f** the introduction of a 17α-propynyl group to give **8** is demonstrated [Eq. (c); NCS = *N*-chlorosuccimimide].

The described regiospecific 6-*endo-trig*- cyclization of the 19-(2-haloaryl)-9(11)-androstene derivative **10** is thus a general route to the synthesis of antigestagens of the androstane series. Structural modifications of the A/B part of these



(c)

steroid antihormones, as are known from potent synthetic gestagens,[20] are thus accessible for the first time or at least in simpler ways. Moreover, the double fixation of the 11 β-substituents opens up the possibility of specifically characterizing the gestagen/antigestagen binding site of the progesterone receptor with respect to the spatial environment of the arene.

Experimental

13a–f/14a–f [21]: 80 mL of anhydrous ammonia was condensed at −78 °C in the absence of moisture into a round flask. After addition of 2 mmol of lithium and appearance of the characteristic blue color the mixture was treated with a solution of 5 mmol of the aryl halide **10** in 160 mL of tetrahydrofuran. The resulting mixture was then stirred for 20 min (DC control) and the excess lithium removed by dropwise addition of ethanol (decoloration). The major part of the ammonia was then removed by evaporation, the reaction mixture poured into water, and the aqueous phase extracted several times with ethyl acetate. The combined organic phases were washed with sodium chloride solution, dried over sodium sulfate and evaporated to dryness under vacuum. The residue was either chromatographed on aluminum oxide (neutral, grade III) with ethyl acetate/hexane or taken up in a suitable solvent and the mother liquor remaining after crystallization of **13** chromatographed as described above (see Table 3).

Received: December 5, 1988 [Z 3074 IE]
German version: *Angew. Chem. 101* (1989) 776

CAS Registry numbers:
1b, 104068-77-1; **8**, 119056-06-3; **9a**, 120608-58-4; **9b**, 29874-00-8; **9c**, 56812-60-3; **9d**, 120577-91-5; **9e**, 120577-92-6; **9f**, 120577-93-7; **10a**, 120608-59-5; **10b**, 119053-87-1; **10c**, 119055-79-7; **10d**, 119055-88-8; **10e**, 120608-60-8; **10f**, 119056-02-9; **13a,b,c**, 120577-94-8; **13d,e**, 120577-95-9; **13f,g**, 120577-96-0; **14a,b,c**, 119070-69-8; **14d,e**, 119055-89-9; **14f,g**, 119056-03-0; **10g**, 120577-97-1.

[1] a) J. G. Teutsch, A. Belanger, *Tetrahedron Lett. 1979*, 2051; b) A. Belanger, D. Philibert, J. G. Teutsch, *Steroids 37* (1981) 361.
[2] D. Philibert, R. Deraedt, C. Tournemine, I. Mary, J. G. Teutsch: *RU 38486—A Potent Antiprogesterone* (*6th Int. Congr. of Hormonal Steroids*, Jerusalem, Israel 1982), Abstract f204.

[3] a) M. K. Agarwal (Ed.): *Adrenal Steroid Antagonism*, de Gruyter, New York 1984, p. 43; b) W. Elger, S. Beier, K. Chwaliz, M. Fähnrich, S. H. Hasan, D. Henderson, G. Neef, R. Rhode, *J. Steroid Biochem. 25* (1986) 835.
[4] a) J. G. Teutsch, G. Costerousse, D. Philibert, R. Deraedt, Eur. Pat.-Anm. 0 110 434 (1982), Roussel-Uclaf; b) G. Neef, G. Cleve, E. Ottow, A. Seeger, R. Wiechert, *J. Org. Chem. 52* (1987) 4143; c) R. Wiechert, G. Neef, *J. Steroid Biochem. 27* (1987) 851; d) H. J. J. Loozen, Eur. Pat.-Anm. 0 277 676 (1988), Akzo N. V.
[5] a) V. J. van Geerestein, J. A. Kanters, J. Kroon, *Acta Crystallogr. Sect. C 42* (1986) 469; b) C. Herrmann, G.-A. Hoyer, G. Neef, D. Schomburg, R. Wiechert, *Liebigs Ann. Chem. 1986*, 1317.
[6] G. Neef, G. Sauer, R. Wiechert, *Tetrahedron Lett. 24* (1983) 5205.
[7] E. Ottow, R. Wiechert, G. Neef, S. Beier, W. Elger, D. Henderson, Int. Pat.-Anm. WO 88/07051 (1987), Schering AG.
[8] a) C. Galli, *Chem. Rev. 88* (1988) 765; b) B. Giese (Ed.): *Radicals in Organic Synthesis: Formation of Carbon-Carbon Bonds*, Pergamon Press, Oxford 1986.
[9] These studies were carried out concomitantly with and independently of the studies cited in Ref. [10].
[10] G. F. Meijs, J. F. Bunnett, A. L. J. Beckwith, *J. Am. Chem. Soc. 108* (1986) 4899.
[11] G. Stork, N. H. Baine, *J. Am. Chem. Soc. 104* (1982) 2321.
[12] For the definition of the term *endo/exo-trig* see J. E. Baldwin, *J. Chem. Soc. Chem. Commun. 1976*, 734.
[13] A. L. J. Beckwith, C. H. Schiesser, *Tetrahedron 41* (1982) 3925.
[14] a) Y. Ueno, K. Chino, M. Okawara, *Tetrahedron Lett. 23* (1982) 2575; b) K. Shankaran, C. P. Sloan, A. Snieckus, *ibid. 26* (1985) 6001; c) L. J. Johnson, J. Lusztyk, D. D. M. Wayner, A. N. Abeywickrema, A. L. J. Beckwith, J. C. Scaiano, K. U. Ingold, *J. Am. Chem. Soc. 107* (1985) 4594.
[15] A. N. Abeywickrema, A. L. J. Beckwith, *J. Chem. Soc. Chem. Commun. 1986*, 464.
[16] K. A. Parker, D. M. Spero, K. C. Inman, *Tetrahedron Lett. 27* (1986) 2833.
[17] A. N. Abeywickrema, A. L. J. Beckwith, S. Gerba, *J. Org. Chem. 52* (1987) 4072.
[18] R. Wiechert et al. unpublished.
[19] A. L. J. Beckwith, C. H. Schiesser, *Tetrahedron Lett. 26* (1985) 373.
[20] R. Wiechert, F. Neumann, *Arzneim. Forsch. 15* (1965) 244.
[21] All the new compounds were characterized completely.

$FeI_3SC(NMe_2)_2$, a Neutral Thiourea Complex of Iron(III) Iodide**

By *Siegfried Pohl,** *Ulrich Bierbach,* and *Wolfgang Saak*

According to the textbooks, iron(III) iodide compounds are either unstable or nonexistent.[1] Recently, the synthesis of FeI_3 from $FeI_2(CO)_4$ and iodine was reported.[2] In solution the compound decomposes to FeI_2 and iodine, but in the solid state it can be stored for several months. So far, however, a characterization of the solid has not been possible, since it could only be isolated in small amounts.

By reaction of iron(II) iodide, iodine and tetramethylthiourea in dichloromethane we have now been able to prepare triiodo(1,1,3,3-tetramethylthiourea-*S*)iron(III) **1** in almost quantitative yield according to Equation (a).[3] The

$$FeI_2 + \tfrac{1}{2} I_2 + SC(NMe_2)_2 \rightarrow \underset{\mathbf{1}}{FeI_3SC(NMe_2)_2} \qquad (a)$$

compound was characterized by IR and UV/VIS spectra, elemental analysis, and an X-ray structure analysis.[4]

The iron(III) center in **1** is coordinated tetrahedrally by three iodine atoms and one sulfur atom (Fig. 1). The Fe–I distances compare with the values that have also been found in tetraiodoferrate(III) ions.[5,6] The Fe–S distance

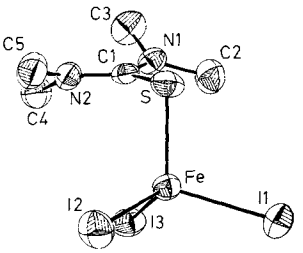


Fig. 1. Structure of **1** in the crystal (ORTEP, vibration ellipsoids at the 50% probability level). Important bond lengths [Å] and angles [°]: [pm] Fe–I1 255.3(1), Fe–I2 253.0(1), Fe–I3 253.7(1), Fe–S 231.1(2), C1–S 174.6(7), C1–N1 133.8(9), C1–N2 133.2(9); I1–Fe–I2 111.6(1), I1–Fe–I3 110.3(1), I2–Fe–I3 108.6(1), S–Fe–I1 106.2(1), S–Fe–I2 110.7(1), S–Fe–I3 109.3(1), C1–S–Fe 101.4(2). The planes through N1–C2–C3 and N2–C4–C5 are rotated through 27.4° and −24.9°, respectively, with respect to the plane through S–C1–N1–N2.

found in tetraiodoferrate(III) ions.[5,6] The Fe–S distance (231.1 pm) is only slightly greater than the Fe–S bond lengths in $Et_4N[Fe^{III}(SPh)_4]$ (mean value 229.6 pm).[7]

The synthesis of **1** parallels that of tetraiodoferrate(III) [Eq. (b)].[8,9]

$$FeI_2 + \tfrac{1}{2} I_2 + I^{\ominus} \xrightarrow{CH_2Cl_2} FeI_4^{\ominus} \qquad (b)$$

Like $FeI_4^{\ominus}$ (e.g., as Et_4NFeI_4), **1** is thermodynamically stable towards self-decomposition under normal conditions. Even with additional ligands, **1** and $FeI_4^{\ominus}$ react analogously—in each case iron is reduced [Eqs. (c) and (d), resp.].[8]

$$2\ \underset{\mathbf{1}}{FeI_3SC(NMe_2)_2} + 2\ SC(NMe_2)_2 \xrightarrow{CH_2Cl_2} \underset{\mathbf{2}}{Fe_2I_4[SC(NMe_2)_2]_3} + I_2 \cdot SC(NMe_2)_2 \qquad (c)$$

$$2\ FeI_4^{\ominus} + 3\ I^{\ominus} \xrightarrow{CH_2Cl_2} 2\ FeI_4^{2\ominus} + I_3^{\ominus} \qquad (d)$$

This reduction of iron with excess ligand is probably the reason for iron(III) iodide compounds being regarded as unstable.

In contrast to $FeI_4^{\ominus}$,[6] however, **1** reacts with iodine—with oxidation of tetramethylthiourea [Eq. (e)]. (The compounds **2** and **3** were also characterized by X-ray structure analysis.[10])

$$2\ \underset{\mathbf{1}}{FeI_3SC(NMe_2)_2} + I_2 \xrightarrow{CH_2Cl_2} \underset{\mathbf{3}}{[(Me_2N)_2CS-SC(NMe_2)_2]^{2\oplus}(FeI_4^{\ominus})_2} \qquad (e)$$

A reaction comparable with (e) with an oxidizing agent which, unlike iodide, does not coordinate in reduced form to iron, is possibly the most favorable route to FeI_3.

Received: January 30, 1989 [Z 3146 IE]
German version: *Angew. Chem. 101* (1989) 796

[*] Prof. Dr. S. Pohl, U. Bierbach, Dipl.-Chem. W. Saak
Fachbereich Chemie der Universität
Postfach 2503, D-2900 Oldenburg (FRG)

[**] This work was supported by the Deutsche Forschungsgemeinschaft and the Fonds der Chemischen Industrie.

[1] See, for example, N. N. Greenwood, A. Earnshaw: *Chemistry of the Elements*, Pergamon, Oxford 1985, p. 1266. *Chemie der Elemente*, VCH Verlagsgesellschaft, Weinheim 1988, p. 1388.
[2] K. B. Yoon, J. K. Kochi, *Z. Anorg. Allg. Chem. 561* (1988) 174.
[3] Procedure: A mixture of 1.55 g (5 mmol) of freshly sublimed FeI_2, 0.66 g (5 mmol) of tetramethylthiourea and 0.64 g (2.5 mmol) of iodine in 50 mL of dichloromethane was stirred until complete dissolution of the FeI_2 (ca. 6 h). After evaporation of the solution to 20 mL and addition of 50 mL of toluene, crystallization was observed to set in. The first crystal fraction furnished 1.81 g (64%) of **1**. After work-up of the mother liquor, the yield was almost quantitative; satisfactory C,H,N analyses. **1** forms black, platelet-like, hygroscopic crystals.
[4] X-ray structure analysis: monoclinic, $P2_1/c$, $a = 794.6(1)$ $b = 1356.5(1)$, $c = 1335.2(1)$ pm, $\beta = 95.00(1)°$, $V = 1433.74 \times 10^6$ pm^3, $Z = 4$, $\varrho_{calcd} = 2.635$ g cm^{-3}, 2419 unique reflections, 2113 observed ($I > 2\sigma(I)$), number

of variables 109, empirical absorption correction, $R = 0.039$, $R_w = 0.038$. – Program: G. M. Sheldrick, *SHELX-76* (Program for Crystal Structure Determination), Cambridge England 1976; *SHELXS-86*, Göttingen (FRG) 1986; drawing: C. K. Johnson, *ORTEP-II, Report ORNL-5138*, Oak Ridge National Laboratory, Oak Ridge, USA 1976. – Further details of the crystal structure investigation are available on request from the Fachinformationszentrum Energie, Physik, Mathematik GmbH, D-7514 Eggenstein-Leopoldshafen 2 (FRG), on quoting the depository number CSD-53831, the names of the authors, and the journal citation. – IR spectra: $\tilde{\nu}$ of the asymmetric CN valence vibration [cm^{-1}]: tetramethylthiourea(L): 1508; **1**: 1558; FeI_2L_2 [10]: 1548. – Electron excitation spectrum λ [nm]: 261, 340, 390(sh), 425(sh), 524, 645, 720(sh). The band at 261 nm corresponds to an electron transfer within the thiourea ligand.

[5] S. Pohl, W. Saak, *Z. Anorg. Allg. Chem. 523* (1985) 25.

[6] W. Saak, S. Pohl, *Z. Anorg. Allg. Chem. 552* (1987) 186.

[7] S. A. Koch, L. E. Maelia, *J. Am. Chem. Soc. 105* (1983) 5944.

[8] S. Pohl, W. Saak, *Z. Naturforsch. B39* (1984) 1236.

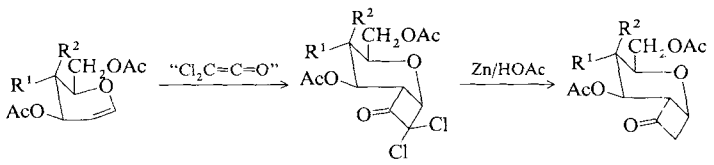
[9] For the synthesis of $FeI_4^{\ominus}$ from $FeCl_4^{\ominus}$ see J. L. Ryan, *Inorg. Chem. 8* (1969) 2058. The observed rapid decomposition of $FeI_4^{\ominus}$ at normal temperature motivated attempted syntheses at low temperatures. According to our results, however, this decomposition is not due to a thermodynamic instability towards self-decomposition, but exclusively to the behavior of $FeI_4^{\ominus}$ towards excess ligand (see text).

[10] U. Bierbach, W. Saak, S. Pohl, unpublished.

Chiral Cyclobutanones by [2+2]-Cycloaddition of Dichloroketene to Carbohydrate Enol Ethers**

By *Hartmut Redlich,* Jan B. Lenfers,* and *Jürgen Kopf*

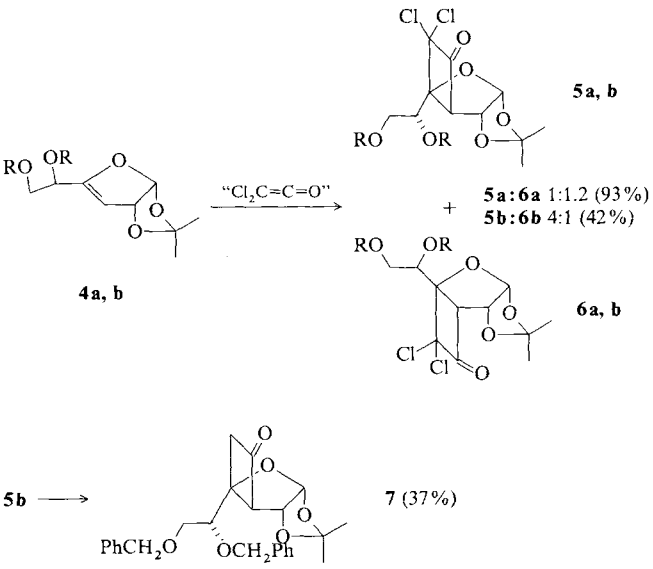
Reaction of dichloroketene[1] (generated in situ) with carbohydrate derivatives containing an enol ether unit (**1a,b, 4a,b,** and **8a,b**)[2] furnishes the [2+2]-cycloaddition products (**2a,b, 5a,b, 6a,b** and **9a,b**),[3] in some cases in excellent yields. Reduction of these compounds with zinc/glacial acetic acid leads to dehalogenated chiral cyclobutanones (**3a,b, 7** and **10a,b**).[4] Optically active cyclobutanones, which are preparatively valuable building blocks, can be obtained very easily in this way. Thus, e.g., with compound **10a** a Baeyer-Villiger oxidation can be carried out to give the corresponding lactone.



1a, b — **2a** (89%), **2b** (95%) — **3a** (55%), **3b** (58%)

a: R^1 = OAc, R^2 = H; **b**: R^1 = H, R^2 = OAc

In the case of **1a,b** and **8a,b,** the stereochemical course of the addition of dichloroketene to the carbohydrate enol ether is uniform; as a result of the regiochemistry established by the enol ether, in each case only one of the possible diastereomers is formed. Should the reaction of the two glycals **1a,b** to give the "α-oriented" products **2a,b** seem plausible, then an interpretation of the findings for the reactions of **4a,b, 8a,b** and **11** is more difficult. Extensive data for comparison from carbohydrate chemistry demonstrate that sp^3- and sp^2-hybridized carbon atoms at positions 3 and 4 of derivatives of 1,2;5,6-di-*O*-isopropylidene-α-D-glucofuranose are almost always attacked from above the sugar ring plane (the β side), irrespective of the reagent used. In contrast, in the case of **4a** (R,R = isopropylidene) attack from the α-side is slightly favored (**5a:6a** 1:1.2). If the protecting



4a, b — **5a, b** — **5a:6a** 1:1.2 (93%) + **5b:6b** 4:1 (42%) — **6a, b**

5b → **7** (37%)

a: R, R = $>CMe_2$; **b**: CH_2Ph

groups on C5 and C6 are replaced by $PhCH_2O$ groups (**4b**), then the expected product **5b** is formed in excess (**5b:6b** 4:1). The (*E*)/(*Z*) isomers **8a,b** are attacked exclusively from the α-side. The structures of the resulting compounds **9a,b** and of the dehalogenated secondary products **10a,b** could not be elucidated NMR spectroscopically. Upon irradiation at the frequency of H3 of compound **10a**, NOE experiments reveal an interaction with both H5 as well as H72 (for numbering cf. Fig. 1). Hence, only the (*Z*)-geometry is verified in

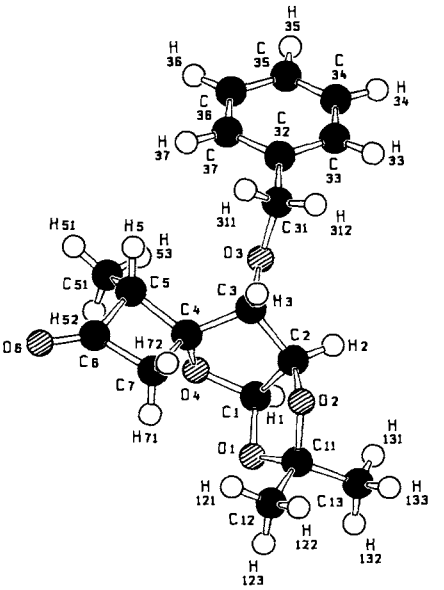


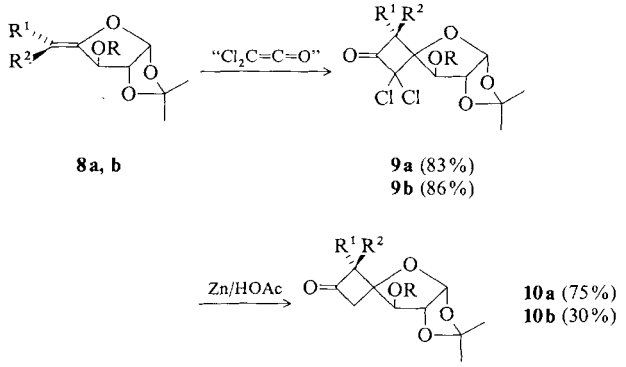
Fig. 1. Crystal structure of **10a**.

[*] Prof. Dr. H. Redlich, Dr. J. B. Lenfers
Institut für Organische Chemie der Universität
Martin-Luther-King-Platz 6, D-2000 Hamburg 13 (FRG)
Priv.-Doz. Dr. Jürgen Kopf [+]
Institut für Anorganische Chemie der Universität Hamburg (FRG)

[+] X-ray structure analysis

[**] This work was supported by the Deutsche Forschungsgemeinschaft and the Fonds der Chemischen Industrie.

the starting olefin **8a**. An X-ray structure analysis of **10a**[6] (cf. SCHAKAL diagram[7] in Fig. 1) was necessary, however, before conclusions could be drawn about the unusual stereochemical course of the reaction, according to which the dichloroketene adds to the double bond from the α-side. This would seem to be possible only when the dichloroketene generated "in situ" is fixed in the sphere of the carbohydrate derivative **8a** such that the orientation of the addition is not controlled by normal steric effects. In particular the two halogen atoms of the dichloroketene must penetrate far into

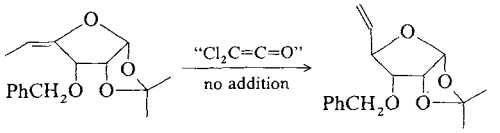


8a, b → **9a** (83%), **9b** (86%)

→ **10a** (75%), **10b** (30%)

a: R^1 = Me, R^2 = H, **b**: R^1 = H, R^2 = Me
R = CH_2Ph

the concave region of the sugar molecule during the addition – an orientation which normally cannot be expected.



11 → **12** (50%)

The compound **11** 3-epimeric to the olefin **8b** does not add dichloroketene. Instead, the double bond migrates, and predominantly the olefin **12** is formed. It is thus clear that merely a slight shielding of the α-side by the 3-*O*-benzyl group in **11** changes the course of the reaction.

Experimental

Reaction with dichloroketene: A well-stirred suspension of the respective sugar (1 mmol) and zinc powder activated with copper [1] (330 mg, 5 mmol) in absolute diethyl ether (10 mL) was treated dropwise under nitrogen with a solution of trichloroacetyl chloride (0.36 g, 2 mmol) in absolute diethyl ether (5 mL) such that the reaction temperature did not exceed 30 °C (2 h). After a further two hours at room temperature the mixture was treated with 15 mL of pentane and the reaction solution decanted off from precipitated zinc salts. The residue was washed once with 10 mL of pentane/diethyl ether (1:1), and the organic phase was washed with 10 mL of saturated $NaHCO_3$, dried over $MgSO_4$ and filtered. The combined organic phases were evaporated down and the concentrate co-distilled several times with toluene under vacuum. The resulting syrup can, as a rule, be characterized NMR spectroscopically without resort to further purification.

Reduction with zinc: A solution of the dichlorocyclobutanone derivative (1 mmol) in glacial acetic acid (5 mL) was stirred at 50 °C and treated portionwise with a total of 10 mmol of zinc powder. On completion of reaction (up to 7 h) the mixture was cooled to room temperature, filtered, and the filtrate concentrated by evaporation under vacuum. In order to remove the last traces of glacial acetic acid the concentrate was co-distilled several times with toluene. The residue was taken up in diethyl ether, washed with water, and the organic phase dried over Na_2SO_4, filtered, and evaporated down under vacuum. The product was finally purified by column chromatography.

Received: January 27, 1989 [Z 3145 IE]
German version: *Angew. Chem. 101* (1989) 764

CAS Registry numbers:
1a, 2873-29-2; **1b**, 4098-06-0; **2a**, 120497-59-8; **2b**, 120575-47-5; **3a**, 120497-60-1; **3b**, 120575-48-6; **4a**, 2774-28-9; **4b**, 120497-61-2; **5a**, 120523-82-2; **5b**, 120497-62-3; **6a**, 120576-15-0; **6b**, 120575-49-7; **7**, 120497-63-4; **8a**, 120575-50-0; **8b**, 99096-64-7; **9a**, 120497-64-5; **9b**, 120575-51-1; **10a**, 120497-65-6; **10b**, 120575-52-2; **11**, 120575-53-3; **12**, 23537-43-1; dichloroketene, 4591-28-0; trichloroacetyl chloride, 76-02-8.

[1] Dichloroketene was prepared from trichloroacetyl chloride and Zn/Cu pair: L.-F. Tietze, T. Eicher, *Reaktionen und Synthesen im organisch-chemischen Praktikum*, Thieme, Stuttgart 1981, p. 229.
[2] **1a, b**: W. Roth, W. Pigman, *Methods Carbohydr. Chem. 2* (1963) 405; **4a**: T. W. Flechtner, *Carbohydr. Res. 77* (1979) 262; **4b, 8a, b**: J. B. Lenfers, *Dissertation*, Universität Hamburg 1988.
[3] Isocyanates with strong electron attracting substituents also add in the sense of a [2+2]-cycloaddition – e.g. to glycals; cf. also M. Chmielewski, Z. Kaluza, C. Belzecki, P. Salanski, J. Jurcazk, H. Adamowicz, *Tetrahedron 41* (1985) 2441; M. Chmielewski, Z. Kaluza, *Carbohydr. Res. 167* (1987) 143.
[4] The chloro cycloaddition products were characterized exclusively by ^1H and ^{13}C NMR spectroscopy. The dehalogenated cyclobutanone derivatives were characterized, in addition, by elemental analyses and optical rotation.
[5] D. Belluš, B. Ernst, *Angew. Chem. 100* (1988) 820; *Angew. Chem. Int. Ed. Engl. 27* (1988) 797.
[6] To our knowledge this is the first X-ray structure analysis of a carbohydrate derivative containing a carbocyclic four-membered ring. – Enraf-Nonius CAD4 diffractometer, $Cu_{K\alpha}$ radiation, λ = 154.05 pm, graphite monochromator. Space group $P2_12_12_1$ (No. 19), orthorhombic, a = 551.8(2), b = 1010.6(2), c = 2968.6(7) pm, ϱ_{calcd} = 1.28 g cm^{-3}, Z = 4, μ = 9.14 cm^{-1}. 1948 reflections, 1738 observed; $F_o > 3\sigma(F_o)$, R = 0.056, R_w = 0.042. Further details of the crystal structure investigation are available on request from the Fachinformationszentrum Energie, Physik, Mathematik GmbH, D-7514 Eggenstein-Leopoldshafen 2 (FRG), on quoting the depository number CSD-53471, the names of the authors, and the journal citation.
[7] E. Keller, *Chem. Unserer Zeit 14* (1980) 56.

$Pt_{309}Phen^*_{36}O_{30\pm10}$, a Four-Shell Platinum Cluster **

By *Günter Schmid*,* *Bernd Morun*, and *Jan-Olle Malm*

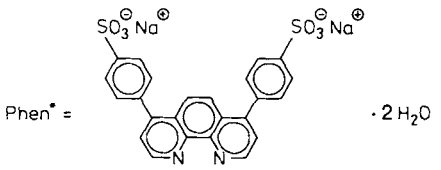
In medium to large transition-metal clusters, the arrangement of the metal atoms increasingly resembles that of the metal itself as the size of the clusters increases. Therefore, most clusters may be described as cutouts of metal lattices, the outer atoms being protected by suitable ligands in order to prevent intermolecular interactions and coagulation processes like those observed for naked clusters.[1] The systematic construction of higher-nuclear clusters according to the principle of cubic (ccp) or hexagonal (hcp) close packing results in the attainment of "magic numbers" when a complete outer form is reached, namely, a cubeoctahedron (for ccp) or an anticubeoctahedron (for hcp). This process can

[*] Prof. Dr. G. Schmid, Dipl.-Chem. B. Morun
Institut für Anorganische Chemie der Universität
Universitätsstrasse 5–7, D-4300 Essen 1 (FRG)
M. Sc. J.-O. Malm,
National Center for High Resolution Electron Microscopy
Inorganic Chemistry 2, Chemical Center
P.O. Box 124, S-22100 Lund (Sweden)

[**] Large Transition-Metal Clusters, Part 7. This work was supported by the Commission of the European Community, Brüssel, the Fonds der Chemischen Industrie, and the Swedish National Science Research Council. We would like to thank Prof. Dr. *F. Bandermann* and *D. Jacobi*, Institut für Technische Chemie der Universität Essen for ultracentrifuge determinations of the molecular weights. Part 6: G. Schmid, N. Klein, L. Korste, U. Kreibig, D. Schönauer, *Polyhedron 7* (1988) 605.

best be understood in terms of the shell model, according to which the first shell consists of 12 atoms, the second shell 42 atoms, and, in general, the n-th shell $(10n^2 + 2)$ atoms. So far, ligand-stabilized clusters containing 13 (one shell),[2] 55 (two shells),[3,4] and roughly 561 atoms (five shells)[5,6] have been prepared.

We have now succeeded in synthesizing a four-shell platinum cluster. It is impossible, of course, to give the exact number of metal atoms in such large clusters. However, electron microscopy clearly and reliably reveals the number of [110] and [100] atomic planes (shells) and allows a justifiable estimate of the ideal number of atoms. The exact determination of the ligands is not straightforward either. The number of oxygen atoms in the present case is especially difficult to determine.



The platinum cluster is synthesized by stirring an acetic acid solution of platinum(II) acetate and Phen* · H_2O (molar ratio 7–8:1) under hydrogen until gas absorption has ceased (2.5–3 h). The brown-black reaction solution is then exposed to an oxygen atmosphere to oxidize the free surface atoms. Workup yields a water-soluble, air-stable cluster of idealized composition $Pt_{309}Phen^*_{36}O_{30\pm10}$ in ca. 30% yield. This composition is derived from (1) multiple elemental analyses of all elements present, (2) molecular-weight determinations using an ultracentrifuge,[7] and (3) transmission-electron-microscopy investigations. The above formula corresponds to a molecular weight of 81.368 g mol^{-1}. Repeated molecular-weight determinations on aqueous solutions of the cluster give an average value of 79.500 with an error range of ca. ± 10% owing to the method used.

To perform the electron-microscopy investigations, the platinum cluster was dissolved in an acetone–water mixture. A carbon-coated copper grid was dipped into the solution and then transferred to the JEM 4000 EX transmission electron microscope, operating at 400 kV. The ca. 0.16-nm resolution of the microscope is sufficient for atomic resolution of the [110] and [100] directions in platinum. High-resolution electron microscopy and image simulation have repeatedly demonstrated the ability to distinguish between various types of structures and particle forms of metal fragments.[8,9] The platinum clusters investigated here have nearly exclusively cubeoctahedral structure with cubic close-packed atoms. Figure 1 shows a typical sample of the Pt_{309} cluster. Such large-area images are important for establishing the uniformity of the samples. The largest number of clusters by far have a diameter of 1.7–1.8 nm, as calculated for a four-shell platinum cluster.

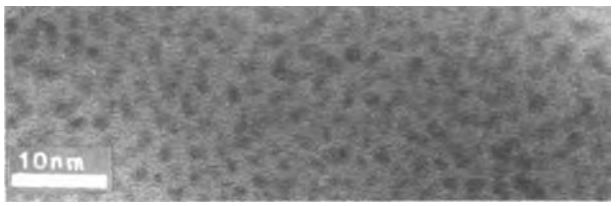


Fig. 1. Typical micrograph of a Pt_{309} cluster on amorphous carbon. The cluster particles that have not undergone any aggregation processes have diameters of 1.7–1.8 nm (very good agreement with the size of a four-shell Pt cluster).

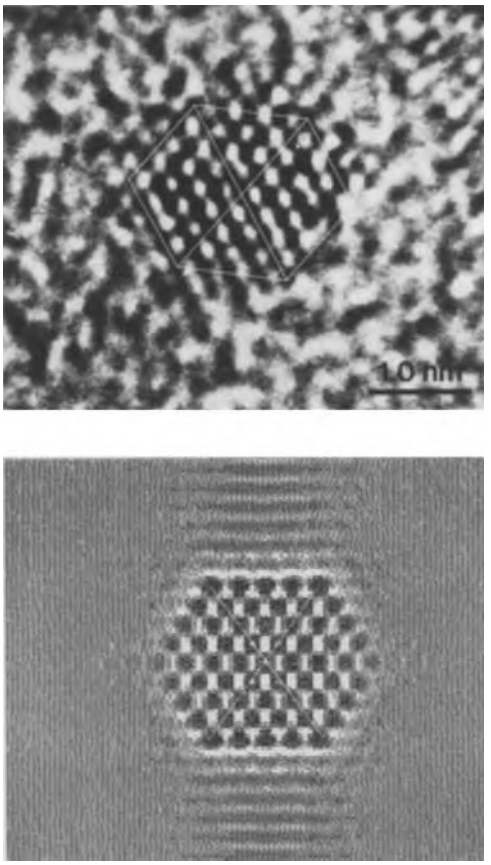


Fig. 2. Top: High-resolution transmission-electron micrograph of a four-shell Pt cluster in the [110] direction. Because of the contrast of the amorphous carbon support, it is difficult to distinguish completely the surface atoms. Nonetheless, the cubeoctahedral shape is clearly revealed. The diameter (111 separations) is 1.8 nm (calcd 1.81 nm). Bottom: Computer-simulated image of an M_{309} cluster in the [110] direction.

The structure of a single cluster is shown in Figure 2. Readily apparent is the ccp arrangement of the 309 Pt atoms in the [110] direction. For comparison, Figure 2 also shows a computer simulation of a four-shell cluster viewed from the same direction.

X-ray powder diffraction diagrams of several samples show very broad reflections, the maxima of which agree with the values obtained for metallic platinum. Reflections were observed for $d_{111} = 2.26$ Å ($Pt_{met.}$: 2.265), $d_{220} = 1.38$ Å ($Pt_{met.}$: 1.387), and $d_{113} = 1.18$ Å ($Pt_{met.}$: 1.1826). From the half-width of the [111] reflections[10] the particle sizes were calculated to be 17.5 ± 1 Å. Owing to the large half-widths and the relatively low reflection intensities, this value is subject to a relatively large error, but it lies in the correct range.

The presence of 33 Phen* ligands in the four-shell cluster is readily explained by the model and leads to an optimal "envelope" of the Pt_{309} core of the cluster. More difficult to understand is the oxygen content determined by elemental analysis. Crystalline Phen* · H_2O contains three molecules of water per molecule, one on each of the SO_3Na groups and one between the N atoms. The latter should be absent in the complexed state, whereas the former should still be bound to the sulfone groups in the cluster, as deduced from a comparison of the IR spectra of hydrated and nonhydrated SO_3Na groups.[11] Thus, 288 oxygen atoms should be present in the 36 Phen* ligands. The value of 6.22 ± 0.24% O determined by elemental analysis leaves 30 ± 10 atoms to occupy the platinum atoms at the surface. The error of ±0.24% results from five oxygen determinations on different samples. For a

constant number of Phen* ligands, the small variation in the analytical value has a marked effect on the surface oxygen atoms. It is not yet possible to determine whether these are bound as O_2 units or as $O^{2\ominus}$. We suspect the presence of O_2 groups.

Experimental Procedure

Platinum(II) acetate (380 mg, 1.2 mmol) was placed under N_2 atomosphere in a 100-mL flask, which was connected through a stopcock with a 100-mL gas burette, and then dissolved in 40 mL of conc. acetic acid with stirring. Phen* · H_2O (95 mg, 0.16 mmol) was dissolved in 1 mL of H_2O and treated with 20 mL of conc. acetic acid. The resulting solution was then added to the solution of the platinum salt. The apparatus was subsequently flushed with H_2. After 15–20 min, the solution began to absorb gas, the uptake ending after 2.5–3 h [H_2 consumption 38–39 mL (ca. 1.7 mmol)]. During hydrogen uptake, the solution turned brown-black. The hydrogen was flushed out with nitrogen and the apparatus was then filled with oxygen. Upon stirring, the solution absorbed O_2, the uptake ending after consumption of 17–18 mL (ca. 0.8 mmol). A black solid was separated using a laboratory centrifuge and then treated several times with conc. acetic acid followed each time by centrifugation, until the solution was colorless. The product was treated with ethanol in the same way. After drying under vacuum, the solid was treated with completely desalted water. The remaining undissolved solid was washed several times with water. Removal of water from the combined centrifuge fractions under vacuum yielded 60–70 mg of a black product, which was stored under N_2 (prolonged exposure of the product to air results in changes which are reflected in an increasing oxygen content). Elemental analysis (average value of five determinations performed on different samples): found, C 12.62 ± 1.0, H 0.81 ± 0.07, N 1.13 ± 0.12, Na 1.95 ± 0.20, O 6.22 ± 0.24, Pt 74.5 ± 0.5, S 2.49 ± 0.26%; calcd for $C_{864}H_{648}N_{72}Na_{72}O_{318}Pt_{309}S_{72}$, C 12.75, H 0.80, N 1.24, Na 2.03, O 6.25, Pt 74.09, S 2.84.

Received: January 20, 1989 [Z 3132 IE]
German version: *Angew. Chem. 101* (1989) 772

CAS Registry numbers:
Pt, 7440-06-4; $C_{24}H_{16}N_2O_6S_2 \cdot 2Na$, 53744-42-6; O_2, 7782-44-7.

[1] G. Schmid, N. Klein, *Angew. Chem. 98* (1986) 910; *Angew. Chem. Int. Ed. Engl. 25* (1986) 922.
[2] V. G. Albano, A. Ceriotti, P. Chini, G. Ciani, S. Martinengo, W. M. Anker, *J. Chem. Soc. Chem. Comm. 1975*, 859.
[3] G. Schmid, R. Boese, R. Pfeil, F. Bandermann, S. Meyer, G. H. M. Calis, J. W. A. van der Velden, *Chem. Ber. 114* (1981) 3634.
[4] G. Schmid, W. Huster, *Z. Naturforsch. B41* (1986) 1028.
[5] M. N. Vorgaftik, V. P. Zagorodnikov, I. P. Stolyarov, I. I. Moiseev, V. I. Likholobov, D. I. Kochubey, A. L. Chuvilin, V. I. Zaikowsky, K. I. Zamaraev, G. I. Timofeeva, *J. Chem. Soc. Chem. Comm. 1985*, 937.
[6] G. Schmid, *Nachr. Chem. Tech. Lab. 34* (1987) 249.
[7] The method is described in detail in [3].
[8] J.-O. Malm, J.-O. Bovin, A. K. Petford-Long, D. J. Smith, G. Schmid, N. Klein, *Angew. Chem. 100* (1988) 80; *Angew. Chem. Int. Ed. Engl. 27* (1988) 555.
[9] M. Flueli, R. Spycher, P. A. Stadelmann, P. A. Buffat, J. P. Borel, *Europhys. Lett. 6* (1988) 349.
[10] Determination of the particle sizes by means of the Scherrer formula: *Göttinger Nachrichten 2* (1918) 98; H. P. Klug, L. E. Alexander: *X-Ray Diffraction Procedures*, 2nd ed., Wiley, New York 1973.
[11] A. F. Borowski, J. Cole-Hamilton, G. Wilkinson, *Nouv. J. Chim. 2* (1978) 137.

The Complexation of Gold Colloids**

By *Günter Schmid** and *Andreas Lehnert*

The formation of metallic states is still one of the largely unexplained phenomena of chemistry and physics. However, the development of cluster chemistry in recent years has led to considerable advances in our understanding, insofar as we can now use a long series of increasingly larger clusters to follow, in atomic steps, the formation of very small cutouts of metal lattices.[1] Clusters with specific ("magic") numbers of metal atoms appear to be characterized by particular stability; they are frequently formed if metal atoms are allowed to aggregate with minimal disturbance, M_{13},[2] M_{55},[3,4] M_{309},[5] and M_{561}[6,7] clusters are striking examples. Although metallic properties have not been observed for any of these clusters, behavior untypical of low-molecular clusters has been found.[8] The concept of a meta-metal has been developed to account for these properties.[8]

The transition from a cluster to a colloid can be assumed to occur in a continuous fashion, although examples of intermediate species are lacking. There is a huge gap between the largest ligand-stabilized cluster of ca. 2.5-nm diameter[6,7] and a small colloid of 10–20-nm diameter. Nonetheless, the same chemical principles should hold for colloids as for clusters. Two important differences should be noted, however. Colloids display a size distribution, which, in some cases, can be down to ±10%, and they are generally polycrystalline. Still, colloids can serve as models for very large clusters, as shown by the results presented here.

Colloids have already been stabilized by protecting colloids, which prevent the coagulation of the colloids in solution. Examples include gelatins, albumin and other peptides,[9] and macromolecules like polyethyleneimine, polyvinylimidazole,[10] and polyvinyl alcohol.[11] To the best of our knowledge, however, colloids have never been treated in terms of clusters and stabilized by the low-molecular-weight ligands known from complex chemistry.

We employed an aqueous solution of gold colloids prepared according to the sodium citrate method,[12] since their size distribution should be relatively narrow (ca. 20 nm ± 10%). We treated this solution with the water-soluble phosphane $(C_6H_5)_2PC_6H_4SO_3Na$, which has proved useful in the chemistry of large clusters.[13] Since it was difficult to specify the molar ratio exactly, we used a large excess of the ligand (Au: ligand ca. 1:1). The ligand-stabilized colloids are accessible in a largely pure form as follows: After addition of phosphane, the solution, which is still red, is concentrated under water-pump vacuum at room temperature until most of the colloid has separated out as a black precipitate and the solution is practically colorless. The precipitate, collected by centrifugation, dissolves instantly in water, the solution turning dark red. A second purification is accomplished by precipitating the stabilized colloid with ethanol from the aqueous solution, centrifuging off the precipitate, and drying it under vacuum. From 50 mg of gold, 60 mg of phosphane-stabilized colloid is obtained as golden leaves, which redissolve in water to give almost any desired concentration. These golden leaves contain on the average 90% gold and 5% carbon, which corresponds to an Au:ligand ratio of approximately 20:1. The adsorption of other species (e.g., $Cl^{\ominus}$ ions) on the colloids surface in amounts below the limits of analytical detection cannot be ruled out. An overall negative surface charge of the colloids is revealed by electrophoresis experiments, which show a migration of the colloids toward the anode. The particle sizes of the gold colloids remain practically unchanged upon coordination of phosphane molecules, as shown by comparison of the UV/VIS spectra. Both the original colloid solution and an aqueous solution prepared from isolated, phosphane-stabilized colloid show an absorption maximum at $\lambda = 520$ nm.

Molecular-weight determinations with an analytical ultracentrifuge[14] gave a value of $(38 \pm 8) \times 10^6$ g mol^{-1}, which, in turn, allowed calculation of the volume of the gold colloids, not including the ligand shell. From the volume, a diameter of 18 ± 1 nm was determined.[15]

[*] Prof. Dr. G. Schmid, Dipl.-Chem. A. Lehnert
Institut für Anorganische Chemie der Universität
Universitätsstrasse 5–7, D-4300 Essen 1 (FRG)

[**] This work was supported by the Commission of the European Community, Brüssel, and by the Fonds der Chemischen Industrie. We would like to thank Prof. Dr. *F. Bandermann* and *D. Jacobi*, Institut für Technische Chemie der Universität Essen, for their ultracentrifuge measurements.

The average particle diameter can also be determined from X-ray diffraction experiments. X-ray powder diffraction diagrams of the isolated colloid show all reflections of metallic gold, which proves that the gold atoms in this case are arranged primarily in a cubic face-centered lattice, as in the bulk metal. The presence of significant amounts of icosahedral or polytetrahedral[16] structures, which were postulated earlier, can therefore be ruled out. The average particle size of the metal nuclei (17 nm) was determined from the half-width of the intense [111] reflection by use of the Scherrer formula.[17]

Evaluation of the electron-microscopic image (Fig. 1) of a sample of the phosphane-stabilized colloid gave nearly a

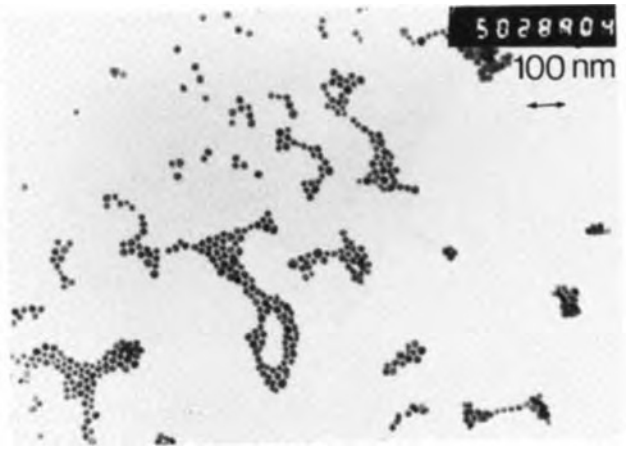


Fig. 1. Electron-microscopic images of phosphane-stabilized gold colloids obtained from aqueous solution (100 kV). Distribution maximum, 18.6 ± 0.1 nm.

Gauss distribution with a maximum at 18.6 ± 0.1 nm and a standard deviation of 2.8 nm.[18]

In summary, gold colloids can be regarded as extremely large clusters and isolated as their solid "phosphane complexes". These complexes are readily soluble in water, so that colloid solutions of any desired concentration can be prepared and stored. Further, colloids prepared in this way can also be investigated in the solid state. Of particular interest are conductivity measurements, especially in comparison with measurements performed on clusters with identical or similar ligands. Preliminary attempts to stabilize Cu, Ag, Pd, and Pt colloids in a similar way are in progress.

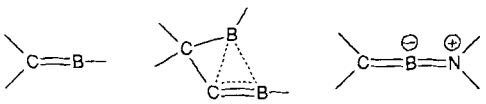
Received: January 20, 1989 [Z 3133 IE]
German version: *Angew. Chem. 101* (1989) 773

[1] Cf., for example, G. Schmid, *Chem. Unserer Zeit 22* (1988) 85.
[2] V. G. Albano, A. Ceriotti, P. Chini, G. Ciani, S. Martinengo, W. M. Anker, *J. Chem. Soc. Chem. Commun. 1975*, 859.
[3] G. Schmid, R. Boese, R. Pfeil, F. Bandermann, S. Meyer, G. H. M. Calis, J. W. A. van der Velden, *Chem. Ber. 114* (1981) 3634.
[4] G. Schmid, W. Huster, *Z. Naturforsch. B41* (1986) 1028.
[5] G. Schmid, B. Morun, J.-O. Malm, *Angew. Chem. 101* (1989) 772 *Angew. Chem. Int. Ed. Engl. 28* (1989) 778.
[6] M. N. Vargaftik, V. P. Zagorodnikov, I. P. Stolyarov, I. I. Moiseev, V. A. Likholobov, D. I. Kochubey, A. L. Chuvilin, V. I. Zaikovsky, K. I. Zamaraev, G. I. Timofeeva, *J. Chem. Soc. Chem. Commun. 1985*, 937.
[7] G. Schmid, *Nachr. Chem. Tech. Lab. 34* (1987) 249.
[8] L. J. De Jongh, H. B. Brom, G. Longoni, P. R. Nuysteren, B. J. Pronk, G. Schmid, M. P. J. van Staveren, R. C. Thiel, *Physics and Chemistry of Small Clusters, Series B: Physics 158* (1987) 807.
[9] B. Matuszewska, W. Wojciak, *Colloid Polym. Sci. 255* (1977) 492.
[10] H. Thiele, J. Kowallik, *Kolloid Z. Z. Polym. 234* (1969) 1017.
[11] P. C. Lee, D. Meisel, *Chem. Phys. Lett. 99* (1983) 262.
[12] J. Turkevich, P. C. Stevenson, J. Hillier, *Discuss. Faraday Soc. 11* (1951) 55.
[13] G. Schmid, N. Klein, L. Korste, U. Kreibig, D. Schönauer, *Polyhedron 7* (1988) 605.
[14] The procedure is described in [3].
[15] $V = M/\varrho N_L$ (M = molecular weight, $\varrho_{Au} = 19.32\ g\ cm^{-3}$, N_L = Loschmidt constant. $d = 2\sqrt[3]{3M/4\pi\varrho N_L}$.
[16] M. R. Harrison, P. P. Edwards in P. P. Edwards, C. N. R. Raz (Eds.): *The Metallic and Nonmetallic States of Matter*, Taylor and Franus, London 1985.
[17] P. Scherrer, *Göttinger Nachrichten 2* (1918) 98; H. P. Klug, L. E. Alexander, *X-Ray Diffraction Procedures*, 2nd ed., Wiley, New York 1973.
[18] The electron-microscopic images were provided by Prof. Dr. *A. Kreibig*, Fachbereich Physik der Universität des Saarlandes.

Stable Methyleneboranes of High Lewis Acidity**

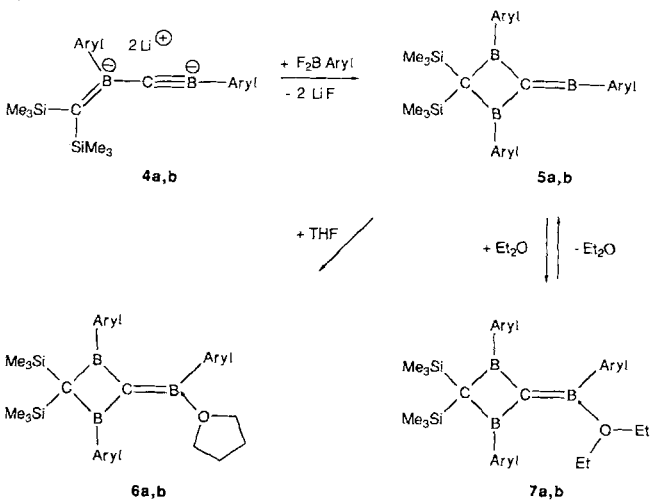
By *Ralf Hunold, Monika Pilz, Jürgen Allwohn, Matthias Stadler, Werner Massa, Paul von Ragué Schleyer*, and *Armin Berndt**

Methyleneboranes **1** with empty p-orbitals on boron should be strong Lewis acids.[1] The previously described stable methyleneboranes of type **2**[2] and **3**[3] are at best only weak[4, 5] Lewis acids since their empty p-orbital on the boron is filled up intramolecularly by neighboring electron pairs.



1 **2** **3**

The existence of methyleneboranes of high Lewis acidity could hitherto only be demonstrated by trapping reactions.[4, 6] We now present the 2-boranediyl-1,3-diboretanes **5a,b** as stable methyleneboranes which form adducts with weak Lewis bases such as THF and diethyl ether. Moreover, they add 4-*tert*-butylpyridine. **5a,b** are formed by reaction of the dilithium compounds **4a**[7] and **4b** with mesityl and duryldifluoroborane, respectively, in pentane at room temperature.



a: Aryl = 2,4,6-$Me_3C_6H_2$; **b**: Aryl = 2,3,5,6-Me_4C_6H

[*] Prof. Dr. A. Berndt, Dr. R. Hunold, M. Pilz, J. Allwohn, M. Stadler, Prof. Dr. W. Massa
Fachbereich Chemie der Universität
Hans-Meerwein-Strasse, D-3550 Marburg (FRG)
Prof. Dr. P. von R. Schleyer
Institut für Organische Chemie der Universität Erlangen-Nürnberg
Henkestrasse 42, D-8520 Erlangen (FRG)

[**] This work was supported by the Deutsche Forschungsgemeinschaft and the Fonds der Chemischen Industrie.

With THF, **5a,b** form the stable tetrahydrofuran adducts **6a,b**. The diethyl ether adducts **7a,b** which are obtained upon crystallization of **5a,b** from diethyl ether, are in strongly temperature-dependent equilibrium with **5a,b** and diethyl ether in solution ($CDCl_3$, CD_2Cl_2). At room temperature, the ^{13}C NMR spectra of **7a,b** are almost identical to those of **5a,b** and diethyl ether; at $-80\,^{\circ}C$ on the other hand they resemble those of the THF adducts **6a,b**. That is, the electron deficiency of the dicoordinated boron atom in **5** is not satisfied intramolecularly to the extent found in **2** and **3**. Hence of all the isolable methyleneboranes, **5a** and **5b** are so far the closest to the prototype **1** with a formally empty p-orbital on the dicoordinated boron atom.

An insight into the electronic structure of the B-C double bond in **5** is provided by the crystal structure[8] of **5b** (Fig. 1a) and its comparison with that of **7b** (Fig. 1b) as well as by the ^{11}B and ^{13}C NMR shifts (Table 1).

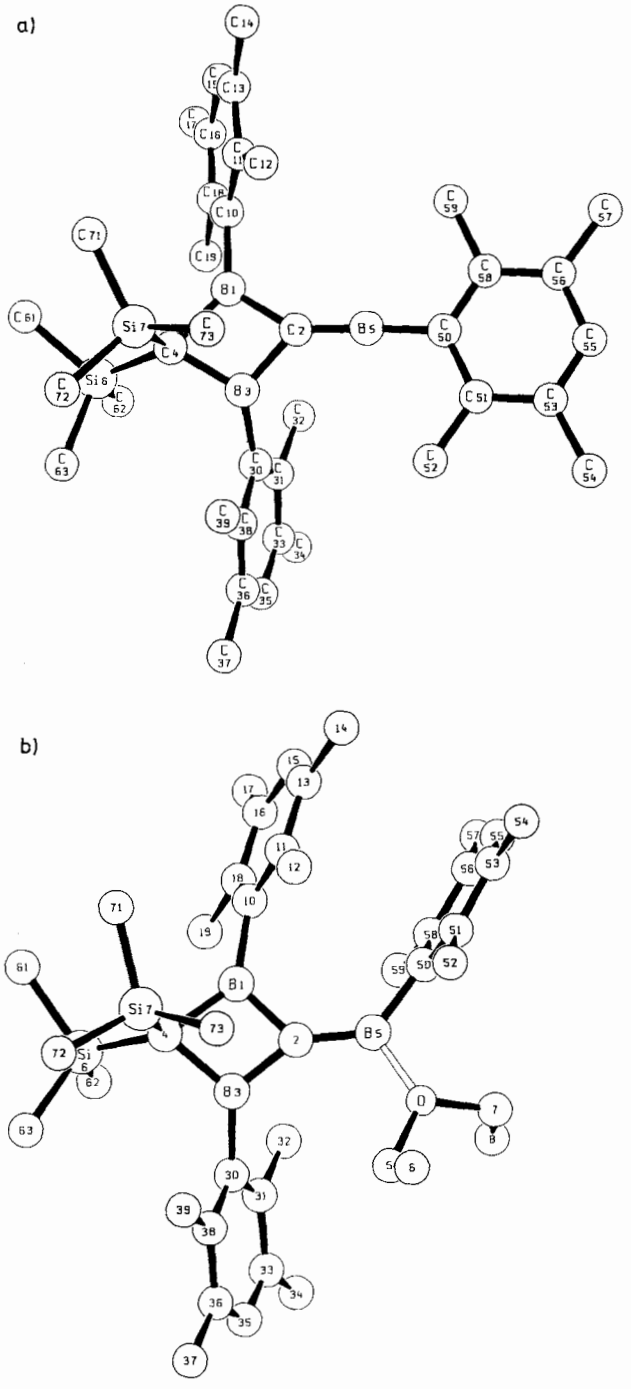


Fig. 1. Schakal diagrams of the molecular structures of a) **5b** and b) **7b** in the crystal. Projection onto the best plane through the atoms of the C_2B_2 four-membered ring. Important bond lengths [pm] and angles [°]: **5b**: C2–B1 155.7(8), C2–B3 156.6(8), C2–B5 137.4(8), C4–B1 160.3(8), C4–B3 159.8(8), B5–C50 150.5(8), B1–C10 158.5(8), B3–C30 157.6(8); B1–C2–B3 78.3(4), B1–C4–B3 76.1(4), B1–C2–B5 148.2(5), B3–C2–B5 133.3(5), C2–B5–C50 176.7(6). – **7b**: C2–B1 152.2(7), C2–B3 150.7(8), C2–B5 143.1(8), C4–B1 164.4(7), C4–B3 162.8(7), B5–C50 158.4(8), B1–C10 163.6(8), B3–C30 162.2(7), O–B5 158.2(7), O–C5 149.2(6); B1–C2–B3 81.3(4), B1–C4–B3 74.2(4), B1–C2–B5 130.1(5), B3–C2–B5 146.1(5), C2–B5–C50 132.1(5), O–B5–C50 109.2(4), C2–B5–O 118.4(5); B1–C2–B5–C50 –3.5(9); B1–C2–B5–O –177.3(5), B3–C2–B5–C50 –157.6(7), B3–C2–B5–O 29(1).

Table 1. Some physical data of the compounds **5**–**7** and **9**. All form colorless crystals. Spectra in $CDCl_3$ (**5a, b, 7a, 9**) [D_8]THF (**6a, b**), CD_2Cl_2 (**7b**).

5a: m.p. 60 °C, yield 92%; ^1H-NMR: $\delta = 0.18$ (s, 18H, $Si(CH_3)_3$), 2.19 (s, 6H, CH_3), 2.25 (s, 9H, CH_3), 2.46 (s, 12H, CH_3), 6.75 (s, 6H, *m*-H); ^{13}C-NMR (–40 °C): $\delta = 4.5$ (6C, $Si(CH_3)_3$), 21.1 (2C, CH_3), 21.9 (1C, p-CH_3), 22.5 (2C, CH_3), 24.8 (4C, *o*-CH_3), 56.6 (br., 1C, Si_2C), 116.1 (br., 1C, CB_3), 122.0 (br., 1C, *i*-C), 127.4 (2C, *m*-C), 127.7 (4C, *m*-C), 136.6 (2C, *p*-C), 138.3 (4C, *o*-C), 141.7 (br., 2C, *i*-C), 144.6 (1C, *p*-C), 146.8 (2C, *o*-C); ^{11}B-NMR: $\delta = 61$ ($\nu_{1/2} = 2200$ Hz), signal of B5 masked by broad signal of B1, B3; IR (Hostaflon): $\tilde{\nu} = 1685$ with shoulder at 1715 cm^{-1} (m, C=B)

5b: m.p.147 °C, yield 81%; ^1H-NMR: $\delta = 0.20$ (s, 18H, $Si(CH_3)_3$), 2.14, 2.21, 2.41 (each s, each 12H, CH_3), 6.92 (s, 2H, *p*-H), 7.06 (s, 1H, *p*-H); ^{13}C-NMR: $\delta = 4.7$ (q, 6C, $Si(CH_3)_3$), 18.9, 20.0 (each q, each 2C, CH_3), 19.9, 21.9 (each q, each 4C, CH_3), 56.8 (br. s, 1C, Si_2C), 115.5 (br. s, 1C, CB_3), 126.6 (br. s, 1C, *i*-C), 130.6 (d, 2C, *p*-C), 133.0 (s, 4C, *o*-C), 133.9 (s, 2C, *m*-C), 134.1 (s, 4C, *m*-C), 136.9 (d, 1C, *p*-C), 142.3 (s, 2C, *o*-C), 146.0 (br. s, 2C, *i*-C); ^{11}B-NMR (toluene, 95 °C): $\delta = 62$ (2B, B1, B3, $\nu_{1/2} = 426$ Hz), 71 (1B, B5, $\nu_{1/2} = 1021$ Hz); IR (CH_2Cl_2): $\tilde{\nu} = 1686$ cm^{-1} (m, C=B)

6a: m.p. 128 °C (decomp.), yield: NMR-spectroscopically quantitative; ^1H-NMR: $\delta = 0.00$ (s, 18H, $Si(CH_3)_3$), 1.74 (m, 4H, CH_2 of THF), 2.02 (s, 6H, CH_3), 2.12 (s, 9H, CH_3), 2.23 (s, 12H, CH_3), 3.58 (m, 4H, OCH_2 of THF), 6.48 (s, 2H, *m*-H), 6.50 (s, 4H, *m*-H); ^{13}C-NMR (–60 °C): $\delta = 5.8$ (6C, $Si(CH_3)_3$), 21.2, 22.6 (each 2C, CH_3), 21.3 (1C, *p*-CH_3), 25.3 (4C, *o*-CH_3), 26.3 (2C, CH_2 of THF), 50.7 (1C, Si_2C), 79.4 (br., 2C, OCH_2 of THF), 127.4 (2C, *m*-C), 127.7 (4C, *m*-C), 134.7 (2C, *p*-C), 136.4 (1C, *i*-C), 137.6 (1C, *p*-C), 138.8 (4C, *o*-C), 139.9 (2C, *o*-C), 140.4 (br., 1C, CB_3), 144.8 (2C, *i*-C); ^{11}B-NMR: 56 ($\nu_{1/2} = 2200$ Hz)

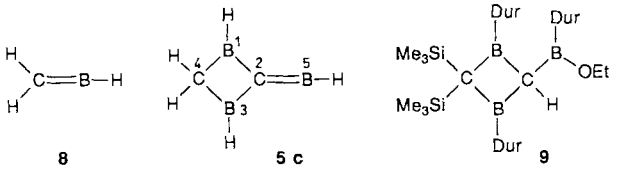
6b: m.p. 116 °C, yield: NMR-spectroscopically quantitative; ^1H-NMR: $\delta = 0.01$ (s, 18H, $Si(CH_3)_3$), 1.85 (m, 4H, CH_2 of THF), 1.87, 1.96 (each s, each 6H, CH_3), 2.04, 2.12 (each s, each 12H, CH_3), 4.13 (m, 4H, OCH_2 of THF), 6.68 (s, 2H, *p*-H), 6.72 (s, 1H, *p*-H); ^{13}C-NMR (–40 °C) $\delta = 5.3$ (6C, $Si(CH_3)_3$), 19.5 19.8 (each 2C, CH_3), 20.1, 21.9 (each 4C, CH_3), 24.9 (br., 2C, CH_2 of THF), 51.4 (1C, Si_2C), 78.3 (br., 2C, OCH_2 of THF), 128.4 (2C, *p*-C), 130.6 (1C, *p*-C), 131.7 (4C, *o*-C), 132.5 (2C, *o*-C), 134.1 (4C, *m*-C), 134.7 (2C, *m*-C), 137.7 (br., 1C, CB_3), 138.5 (br., 1C, *i*-C), 147.0 (br., 2C, *i*-C); ^{11}B-NMR (toluene): $\delta = 58$ ($\nu_{1/2} = 2380$ Hz)

7a: loses Et_2O at 40 °C, yield 70%; ^1H-NMR: $\delta = 0.24$ (s, 18H, $Si(CH_3)_3$), 1.23 (t, 6H, CH_3 of Et_2O), 2.23 (s, 6H, CH_3), 2.28 (s, 3H, *p*-CH_3), 2.29 (s, 6H, CH_3), 2.51 (s, 12H, *o*-CH_3), 3.56 (q, 4H, CH_2 of Et_2O), 6.78 (s, 2H, *m*-H), 6.79 (s, 4H, *m*-H); ^{13}C-NMR (CD_2Cl_2, –80 °C): $\delta = 4.6$ (6C, $Si(CH_3)_3$), 13.3 (br., 2C, CH_3 of Et_2O), 20.6, 22.3 (each 2C, CH_3), 20.8 (1C, *p*-CH_3), 24.4 (4C, *o*-CH_3), 50.0 (1C, Si_2C), 74.0 (br., 2C, CH_2 of Et_2O), 126.6 (6C, *m*-C), 133.5 (1C, *i*-C), 134.1 (2C, *p*-C), 136.6 (br., 1C, CB_3), 137.0 (1C, *p*-C), 138.1 (4C, *o*-C), 139.5 (2C, *o*-C), 143.4 (2C, *i*-C)

7b: loses Et_2O at 40 °C, yield 70%; ^1H-NMR: $\delta = 0.17$ (s, 18H, $Si(CH_3)_3$), 1.25 (t, 6H, CH_3 of Et_2O), 1.96, 1.98 (each s, each 6H, CH_3), 2.19, 2.37 (each s, each 12H, CH_3), 3.60 (q, 4H, CH_2 of Et_2O), 6.90 (s, 2H, *p*-H), 7.03 (s, 1H, *p*-H); ^{13}C-NMR (–55 °C): $\delta = 4.8$ (br., q, 6C, $Si(CH_3)_3$), 13.2 (q, 2C, CH_3 of Et_2O), 19.3, 19.93 (each q, each 2C, CH_3), 19,85, 21.9 (each q, each 4C, CH_3), 50.9 (br. s, 1C, Si_2C), 74.6 (br., t, 2C, CH_2 of Et_2O), 128.6 (d, 2C, *p*-C), 130.5 (d, 1C, *p*-C), 132.0 (s, 4C, *o*-C), 132.6 (s, 2C, *o*-C), 134.3 (s, 4C, *m*-C), 135.2 (s, 2C, *m*-C), 136.9 (br. s, 1C, CB_3), 137.3 (br. s, 1C, *i*-C), 147.3 (br. s, 2C, *i*-C)

9 (from **5b** and EtOH): m.p. 149 °C, yield: NMR-spectroscopically quantitative; ^1H-NMR: $\delta = 0.04$, 0.36 (each s, each 9H, $Si(CH_3)_3$), 0.96 (t, $^3J = 7.0$ Hz, 3H, OCH_2CH_3), 1.53, 2.04 (each s each 6H, CH_3), 2.13, 2.18 (each s, each 12H, CH_3), 2.71 (s, 1H, B_3CH), 3.51 (q, $^3J = 7.0$ Hz, 2H, OCH_2CH_3), 6.79 (s, 1H, *p*-H), 6.91 (s, 2H, *p*-H); ^{13}C-NMR: $\delta = 4.5$, 5.9 (each q, each 3C, $Si(CH_3)_3$), 16.3 (q, 1C, $BOCH_2CH_3$), 17.9, 19.3 (each q, each 2C, CH_3), 19.7, 22.0 (2q, each 4C, CH_3), 62.1 (t, 1C, $BOCH_2CH_3$), 69.4 (s, 1C, Si_2C), 71.3 (d, $^1J_{C,H} = 100.4$ Hz, 1C, B_3C), 130.2 (d, 1C, *p*-C), 130.5 (d, 2C, *p*-C), 132.8, 133.2 (each s, each 4C, *o*- and *p*-C), 132.6, 133.4 (each s, each 2C, *o*- and *p*-C), 143.6 (br. s, 1C, *i*-C), 144.2 (br. s, 2C, *i*-C); ^{11}B-NMR: $\delta = 51$ (1B, CBO, $\nu_{1/2} = 1700$ Hz), 77 (2B, BC_2, $\nu_{1/2} = 2213$ Hz)

The B-C double bond in **5b** (137 pm[9]) is shorter than in amino(methylene)boranes **3** (139[3c]–142[3b] pm) and of similar length to that calculated for the unsubstituted methyleneborane **8** (138 pm, 6-31 G*).[10] The B-C distances calculated (6-31 G*) for the unsubstituted boranediyl-1,3-diboretane **5c** agree excellently with those in **5b** (Table 2).



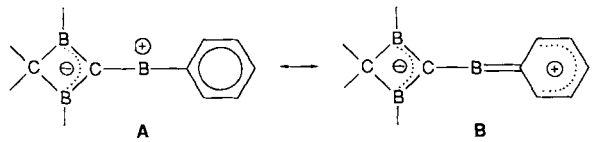
8 **5c** **9**

Dur = 2,3,5,6-Me_4C_6H

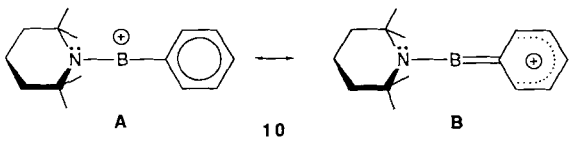
Table 2. Experimental (**5b**, cf. Fig. 1a) and calculated (6-31 G*) (**5c**) C–B distances [pm] in boranediyl-1,3-diboretanes.

	5b (exp.)	**5c** (calcd)
C2–B5	137.4(8)	137.3
C2–B1	155.7(8)	155.9
C2–B3	156.6(8)	155.9
C4–B1	160.3(8)	159.9
C4–B3	159.8(8)	159.9

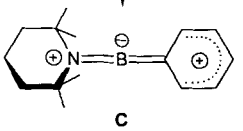
From the similarity in the lengths of the B-C double bonds in **5b,c** and **8** it may not be concluded however that the boron atoms of the four-membered ring have no significant influence on the electronic structure of the B-C double bond. In **5a,b** these boron atoms are shielded by $\Delta\delta \approx 15$ compared to the corresponding ones in **9** (cf. Table 1), i.e. they carry negative π-charge corresponding to the resonance formula **5a,b A**. In the case of **5c** a Mulliken population analysis gives π-charges of −0.173 each on the ring boron atoms B1 and B3, −0.159 on C2 and +0.504 on the exocyclic boron atom B5.[11]



A **5 a,b** **B**



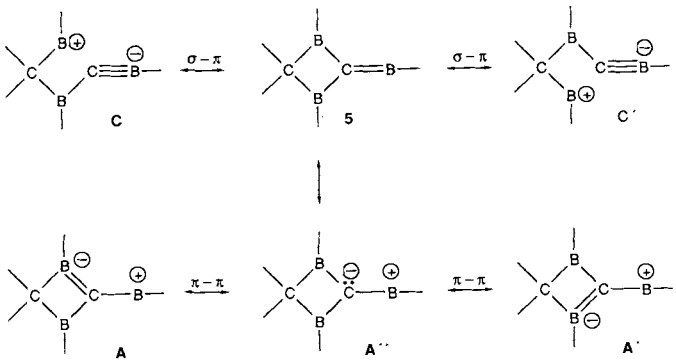
A **10** **B**



C

The positive charge on B5 leads to delocalization of the π electrons of the aryl ring on B5 corresponding to the resonance formula **5a,b B**; this manifests itself in deshielding of the *ortho* and *para* C atoms of $\Delta\delta = 6-9$ compared to the corresponding atoms in aryl rings on B1 and B3. In the amido(phenyl)boron cation **10**[13] the corresponding delocalization (**B**) leads to deshielding of the *ortho* and *para* C atoms of $\Delta\delta = 9-14$.

The boron p-orbital in the plane of the aryl ring is, in the case of **10**, filled up by delocalization of the electron pair on the nitrogen, resulting in a normal allene geometry with *orthogonal* π systems and substituent planes. In contrast **5b** has a *planar*[14] heteroallene framework (anti-van't-Hoff geometry[15]). In **5** the electron deficiency on B5 in the plane of the aryl ring is stabilized by hyperconjugation[16] with the C2–B σ bonds of the four-membered ring corresponding to the resonance formulas **5C,C'**.



C **5** **C'**

A **A''** **A'**

Mulliken population analysis of **5c** indicates a π charge of −0.194 in the p-orbital on B5 in the B_2CB plane. A comparison of the resonance formulas **5C,C'** (σ-π delocalization) and **5A,A'** (π–π delocalization) shows that the two effects compensate themselves regarding bond strengthening and weakening if they are comparatively strong. In addition, the formal charges arising from opposing delocalizations, are then removed.

The significantly longer C2–B1 and C2–B3 bonds in **5b** (155.7, 156.6 pm) compared to those in **7b** (152.2, 150.7 pm) inspite of similar π–π delocalization in **5** and **7**,[17] indicate C–B hyperconjugation corresponding to **5C,C'**.

Received: January 16, 1989;
revised: March 9, 1989 [Z 3122/3123 IE]
German version: *Angew. Chem. 101* (1989) 759

CAS Registry numbers:
4a, 114958-96-2; **4b**, 120637-66-3; **5a**, 120637-67-4; **5b**, 120637-68-5; **5c**, 120637-71-0; **6a**, 120637-72-1; **6b**, 120637-73-2; **7a**, 120637-74-3; **7b**, 120637-75-4; **9**, 120637-70-9; 2,4,6-$Me_3C_6H_2BF_2$, 119615-26-8; 2,3,5,6-$Me_4C_6HBF_2$, 120637-69-6.

[1] P. Jutzi, *Angew. Chem. 87* (1975) 269; *Angew. Chem. Int. Ed. Engl. 14* (1975) 232.
[2] a) H. Klusik, A. Berndt, *Angew. Chem. 95* (1983) 895; *Angew. Chem. Int. Ed. Engl. 22* (1983) 877; b) P. H. M. Budzelar, P. von R. Schleyer, K. Krogh-Jespersen, *ibid. 96* (1984) 809 bzw. *23* (1984) 825; c) G. Frenking, H. F. Schaefer III, *Chem. Phys. Lett. 109* (1984) 521.
[3] a) B. Glaser, H. Nöth, *Angew. Chem. 97* (1985) 424; *Angew. Chem. Int. Ed. Engl. 24* (1985) 416; b) B. Glaser, E. Hanecker, H. Nöth, H. Wagner, *Chem. Ber. 120* (1987) 659; c) R. Boese, P. Paetzold, A. Tapper, *ibid. 120* (1987) 1069.
[4] H. Lukasch, G. Schmidt-Lukasch, U. Lippold, A. Berndt, *Angew. Chem. 100* (1988) 959; *Angew. Chem. Int. Ed. Engl. 27* (1988) 960.
[5] A methyleneborane of type **3** synthesized by us does not form an adduct with 4-*tert*-butylpyridine: G. Schmidt-Lukasch, A. Berndt, unpublished.
[6] C. Pues, G. Baum, W. Massa, A. Berndt, *Z. Naturforsch. B43* (1988) 275.
[7] R. Hunold, J. Allwohn, G. Baum, W. Massa, A. Berndt, *Angew. Chem. 100* (1988) 961; *Angew. Chem. Int. Ed. Engl. 27* (1988) 961.
[8] X-ray structure analysis of **5b**: $C_{38}H_{57}B_3Si_2$, space group *Pbca*, $Z = 8$, $a = 930.3(2)$, $b = 3925.0(3)$, $c = 2038.4(4)$. 3278 unique reflections with $F_0 > 3\sigma$ measured on a four-circle diffractometer (CAD4, Enraf Nonius) with $Cu_{K\alpha}$ radiation at −90 °C; no absorption correction ($\mu = 9.5\ cm^{-1}$),

methyl groups refined as rigid groups using isotropic temperature factors groupwise for the H atoms. Anisotropic temperature factors were used for all other atoms. 460 parameters, $R = 0.0704$, $wR = 0.0558$ (weighting $w = 1/\sigma^2(F_o)$). **7b**: $C_{42}H_{67}B_3Si_2O$, space group $P2_1/c$, $Z = 4$, $a = 2226.8(11)$, $b = 913.7(2)$, $c = 2040.4(8)$ pm, $\beta = 92.59(3)°$. 4131 unique reflections with $F_o > 3\sigma$ measured corresponding to **5b**, no absorption correction ($\mu = 9.1\ cm^{-1}$), methyl groups refined as rigid groups using isotropic temperature factors groupwise for the H atoms. Anisotropic temperature factors used for all other atoms. Refinement in a block diagonal matrix method with threefold blocking. 519 parameters, $R = 0.0699$, $wR = 0.0644$ (weighting $w = 1/\sigma^2(F_o)$). – The moderate reliability factors for **5b** and **7b** may be due to numerous strongly vibrating methyl groups. Further details of the crystal structure investigation are available on request from the Fachinformationszentrum Energy, Physik, Mathematik, GmbH, D-7514 Eggenstein-Leopoldshafen 2 (FRG) on quoting the depository number CSD-53790, the names of the authors, and the journal citation.

[9] The length of the B-C double bond in **7b** (143 pm) is comparable with that in $(mesityl)_2B^{\ominus}=CH_2$ (144 pm; M. M. Olmstead, P. P. Power, K. J. Weese, *J. Am. Chem. Soc. 109* (1987) 2541) which also has a tricoordinated boron atom.

[10] P. von R. Schleyer, D. Kost, *J. Am. Chem. Soc. 110* (1988) 2105, and references cited therein.

[11] π-Charges of −0.18 and −0.22 on the C atom and of +0.18 and +0.22 on the B atom respectively have been calculated for **8** [12, 2c]; that is, the different electronegativities of boron (2.0) and carbon (2.5) alone lead to far less polarity of the π-bond part of the B-C double bond. 3-21 G calculations show that **5c** is a stronger Lewis acid than **8**: the bonding energy of H_2O to **5c** is about 3 kcal mol^{-1} greater than that of H_2O to **8**, and the B–O distance in the H_2O-adduct of **5c** (158.7 pm) is distinctly shorter than in the H_2O adduct of **8** (162.6 pm).

[12] B. T. Luke, J. A. Pople, M.-B. Krogh-Jespersen, Y. Apeloig, M. Karni, J. Chandrasekhar, P. von R. Schleyer, *J. Am. Chem. Soc. 108* (1986) 270.

[13] H. Nöth, R. Staudigl, H. U. Wagner, *Inorg. Chem. 21* (1982) 706.

[14] In the crystal of **5b** the duryl group on the dicoordinated boron atom B5 lies almost in the B1, C2, B3 plane (interplanar angle 12.7(4)°); the 1,3-diboretane rings are folded at the B···B axis through 23.2(6)° (**5b**) and 21.8(5)° (**7b**), respectively.

[15] K. Krogh-Jespersen, D. Cremer, D. Poppinger, J. A. Pople, P. von R. Schleyer, J. Chandrasekhar, *J. Am. Chem. Soc. 101* (1979) 4843.

[16] *Nöth* et al. [13] have already drawn attention to the importance of C-C and C-H hyperconjugation in diphenylboron cation and in amido(organo)boron cations. C-B hyperconjugation is considerably more effective owing to the lower electronegativity of boron, particularly of boron with negative π charge: cf. A. Höfner, B. Ziegler, W. Massa, A. Berndt, *Angew. Chem. 101* (1989) 188; *Angew. Chem. Int. Ed. Engl. 28* (1989) 186 and references cited therein.

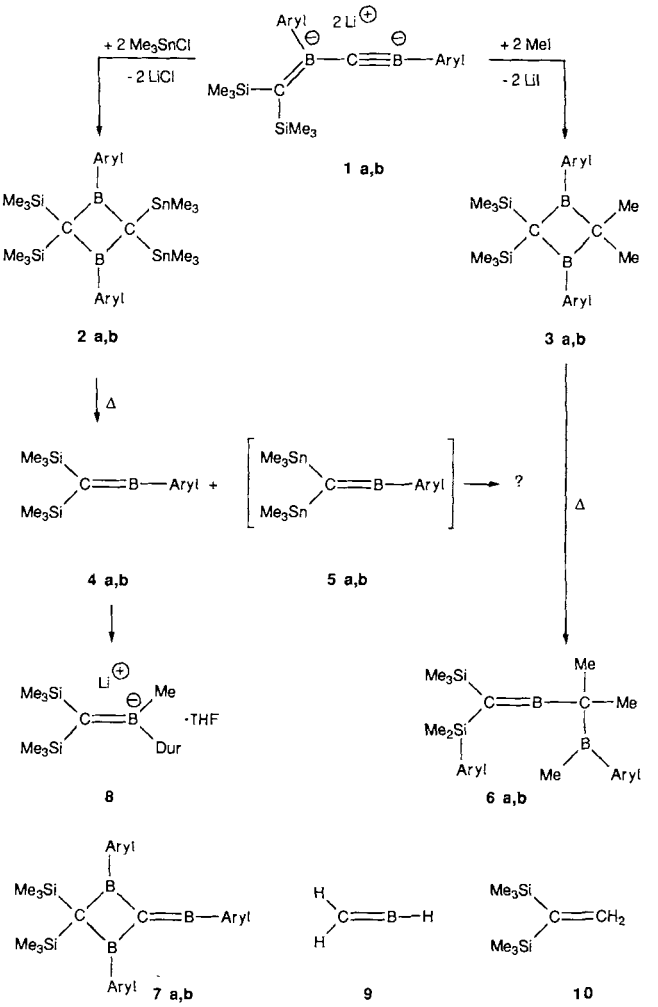
[17] Similar π–π delocalization in **5** and **7** follows from the similarity of the ^{11}B shifts of B1 and B3 in **5b** (61) and **6b** (58) and the almost identical ^{13}C NMR data of **6b** and **7b**, which justify assumption of a similar electronic structure for **7b** as for **6b**. In the case of **7b**, $\delta(^{11}B)$ is not experimentally accessible. Attempts to determine the crystal structure of **6b** have so far been unsuccessful.

Thermal Cleavage and Isomerization of 1,3-Diboretanes to Stable Methyleneboranes**

By *Monika Pilz, Matthias Stadler, Ralf Hunold, Jürgen Allwohn, Werner Massa,* and *Armin Berndt**

The dilithium compounds **1a, b**[1] react with two equivalents of trimethyltin chloride and with methyl iodide to give the 1,3-diboretanes **2a, b** and **3a, b** respectively. Upon melting (148 and 177 °C, respectively) **2a, b** furnish the readily volatile methyleneboranes **4a, b**, which can be separated by condensation (yield ca. 35%) from mixtures of predominantly higher boiling products of still unknown structure. We presume that the diboretanes **2a, b** are converted via a cycloreversion[2] into **4a, b** and **5a, b** and that the latter react further to secondary products. Upon melting (157 and 152 °C, resp.) the 1,3-diboretanes **3a, b** are cleanly transformed into the methyleneboranes **6a, b**; the four-membered ring is opened at a bond to the silyl-substituted C atom, a methyl group migrates from silicon to boron, and an aryl group migrates from the other boron atom to the silicon atom.

In contrast to **7a, b**,[11] **4a, b** add neither diethyl ether nor THF, but, like **7a, b**, form deep-red adducts with 4-*tert*-butylpyridine.[3] Reaction of **4b** with methyllithium leads to formation of the duryl(methyl)methyleneborate **8**.



a: Aryl = 2,4,6-$Me_3C_6H_2$ (= Mes); **b**: Aryl = 2,3,5,6-Me_4C_6H (= Dur)

The structures of **2–4, 6** and **8** are consistent with the ^1H-, ^{13}C- and ^{11}B-NMR spectra (Table 1); the structure of **6b** is confirmed by an X-ray structure analysis[4] (Fig. 1).

The C1–B1–C2 angle is 177°, the sum of the bond angles at C1 360°; that is, B1 is practically linear coordinated, and C1 trigonal-planar coordinated. The boron-carbon double bond in **6b** (136 pm) is slightly shorter than that found in the boranediyl-1,3-diboretane **7b** (137 pm),[11] and that calculated for the unsubstituted methyleneborane **9** (138 pm, 6-31 G*).[5]

[*] Prof. Dr. A. Berndt, M. Pilz, M. Stadler, Dr. R. Hunold, J. Allwohn, Prof. Dr. W. Massa
Fachbereich Chemie der Universität
Hans-Meerwein-Strasse, D-3550 Marburg (FRG)

[**] This work was supported by the Deutsche Forschungsgemeinschaft and the Fonds der Chemischen Industrie.

Table 1. Some physical data of the compounds **2**–**4** and **6** and **8**. Spectra in $CDCl_3$, **8** in [D_8]THF.

2a: pale yellow crystals, m.p. 148 °C (decomp.), yield 93%; ^{1}H-NMR: $\delta = 0.04, 0.06$ (each s, each 18 H, $Si(CH_3)_3$ and $Sn(CH_3)_3$), 2.26 (s, 6 H, *p*-CH_3), 2.46 (s, 12 H, *o*-CH_3), 6.76 (s, 4 H, *m*-H); ^{13}C-NMR: $\delta = -0.4$ (6 C, $Sn(CH_3)_3$), 6.7 (6 C, $Si(CH_3)_3$), 21.2 (2 C, *p*-CH_3), 25.6 (4 C, *o*-CH_3), 46.6, 49.0 (each br., each 1 C, CB_2), 129.0 (4 C, *m*-C), 138.3 (2 C, *p*-C), 138.9 (4 C, *o*-C), 142.2 (br., 2 C, *i*-C); ^{11}B-NMR: $\delta = 82$ ($\nu_{1/2} = 1400$ Hz)

2b: colorless crystals, m.p. 177 °C (decomp.), yield 98%; ^{1}H-NMR: $\delta = 0.00$, 0.55 (each s, each 18 H, $Si(CH_3)_3$ and $Sn(CH_3)_3$), 2.18, 2.37 (each s, each 12 H, *o*- and *m*-CH_3), 6.92 (s, 2 H, *p*-H); ^{13}C-NMR: $\delta = -0.5$ (q, 6 C, $Sn(CH_3)_3$), 6.3 (q, 6 C, $Si(CH_3)_3$), 20.0, 23.3 (each q, each 4 C, *o*- and *m*-CH_3), 47.5, 49.9 (each br. s, each 1 C, CB_2), 131.7 (d, 2 C, *p*-C), 133.6, 134.4 (each s, each 4 C, *o*- and *m*-C), 145.5 (br. s, 2 C, *i*-C); ^{11}B-NMR: $\delta = 81$ ($\nu_{1/2} = 1445$ Hz)

3a: bright-yellow crystals, m.p. 157 °C (decomp.), yield 89%; ^{1}H-NMR: $\delta = 0.19$ (s, 18 H, $Si(CH_3)_3$), 1.33 (s, 6 H, $C(CH_3)_2$), 2.28 (s, 6 H, *p*-CH_3), 2.37 (s, 12 H, *o*-CH_3), 6.80 (s, 4 H, *m*-H); ^{13}C-NMR: $\delta = 6.5$ (6 C, $Si(CH_3)_3$), 21.0 (2 C, *p*-CH_3), 24.5 (4 C, *o*-CH_3), 25.9 (2 C, $C(CH_3)_2$), 53.4, 64.1 (each br., each 1 C, CB_2), 128.0 (4 C, *m*-C), 137.9 (2 C, *p*-C), 138.7 (br., 2 C, *i*-C), 139.7 (4 C, *o*-C); ^{11}B-NMR: $\delta = 76$ ($\nu_{1/2} = 1000$ Hz)

3b: colorless crystals, m.p. 152 °C (decomp.), yield: NMR-spectroscopically quantitative; ^{1}H-NMR: $\delta = 0.31$ (s, 18 H, $Si(CH_3)_3$), 1.47 (s, 6 H, $C(CH_3)_2$), 2.33, 2.38 (each s, each 12 H, *o*- and *m*-CH_3), 7.09 (s, 2 H, *p*-H); ^{13}C-NMR: $\delta = 6.6$ (q, 6 C, $Si(CH_3)_3$), 19.8, 21.9 (each q, each 4 C, *o*- and *m*-CH_3), 25.8 (q, 2 C, $C(CH_3)_2$), 52.1, 64.4 (each br. s, each 1 C, CB_2), 131.7 (d, 2 C, *p*-C), 133.3, 135.0 (each s, each 4 C, *o*- and *m*-C), 142.7 (br. s, 2 C, *i*-C); ^{11}B-NMR: $\delta = 77$ ($\nu_{1/2} = 1360$ Hz)

4a: bright-yellow liquid, b.p. 60 °C/5×10^{-3} torr, yield 35%; ^{1}H-NMR: $\delta = 0.40$ (s, 18 H, $Si(CH_3)_3$), 2.61 (s, 3 H, *p*-CH_3), 2.83 (s, 6 H, *o*-CH_3), 7.11 (s, 2 H, *m*-H); ^{13}C-NMR: $\delta = 4.0$ (q, 6 C, $Si(CH_3)_3$), 21.8 (q, 1 C, *p*-CH_3), 23.3 (q, 2 C, *o*-CH_3), 61.5 (br. s, 1 C, Si_2CB), 123.7 (br. s, 1 C, *i*-C), 127.6 (d, 2 C, *m*-C), 144.3 (s, 1 C, *p*-C), 148.8 (s, 2 C, *o*-C); ^{11}B-NMR: $\delta = 63$ ($\nu_{1/2} = 1020$ Hz); IR (film): $\tilde{\nu}$ (C=^{11}B, C=^{10}B) = 1639, 1681 cm^{-1}

4b: bright-yellow liquid, b.p. 76 °C/5×10^{-4} torr, yield 42%; ^{1}H-NMR: $\delta = 0.33$ (s, 18 H, $Si(CH_3)_3$), 2.35, 2.75 (each s, each 6 H, *o*- and *m*-CH_3), 7.26 (s, 1 H, *p*-H); ^{13}C-NMR: $\delta = 4.0$ (q, 6 C, $Si(CH_3)_3$), 19.6, 20.8 (each q, each 2 C, *o*- and *m*-CH_3), 60.9 (br. s, 1 C, Si_2CB), 127.5 (br. s, 1 C, *i*-C), 133.7, 144.2 (each s, each 2 C, *o*- and *m*-C), 137.0 (d, 1 C, *p*-C); ^{11}B-NMR: $\delta = 63$ ($\nu_{1/2} = 1274$ Hz); IR (film): $\tilde{\nu}$ (C=^{11}B, C=^{10}B) = 1638, 1680 cm^{-1}

6a: pale yellow oil, yield: NMR-spectroscopically ca. 95%; ^{1}H-NMR: $\delta = 0.23$ (s, 9 H, $Si(CH_3)_3$), 0.69 (s, 6 H, $Si(CH_3)_2$), 1.17 (s, 3 H, B-CH_3), 1.22 (s, 6 H, $C(CH_3)_2$), 2.39, 2.41 (each s, each 3 H, *p*-CH_3), 2.27, 2.72 (each s, each 6 H, *o*-CH_3), 6.92, 6.93 (each s, each 2 H, *m*-H); ^{13}C-NMR: $\delta = 4.1$ (q, 3 C, $Si(CH_3)_3$), 8.6 (q, 2 C, $Si(CH_3)_2$), 14.4 (br. q, 1 C, B-CH_3), 20.9 (q, 1 C, *p*-CH_3), 21.0 (q, 3 C, 2 CH_3 and *p*-CH_3), 22.5, 25.1 (each q, each 2 C, CH_3), 29.1 (br. s, 1 C, $C(CH_3)_2$), 55.4 (br. s, 1 C, Si_2CB), 127.3, 129.3 (each d, each 2 C, *m*-C), 134.3 (s, 2 C, *o*-C), 135.4 (s, 1 C, *i*-C of Si-Mes), 136.5, 138.2 (each s, each 1 C, *p*-C), 143.8 (br. s, 1 C, *i*-C of B-Mes), 144.1 (s, 2 C, *o*-C); ^{11}B-NMR (toluene, 90 °C): $\delta = 87, 69$ ($\nu_{1/2} = 500$ and 550 Hz)

6b: colorless crystals, m.p. 69 °C, yield: NMR-spectroscopically quantitative; ^{1}H-NMR: $\delta = 0.15$ (s, 9 H, $Si(CH_3)_3$), 0.58 (s, 6 H, $Si(CH_3)_2$), 0.99 (s, 3 H, B-CH_3), 1.05 (s, 6 H, $C(CH_3)_2$), 2.02, 2.21, 2.23, 2.49 (each s, each 6 H, *o*- and *m*-CH_3), 6.89, 6.98 (each s, each 1 H, *p*-H); ^{13}C-NMR: $\delta = 4.2$ (q, 3 C, $Si(CH_3)_3$), 9.1 (q, 2 C, $Si(CH_3)_2$), 14.2 (br. q, 1 C, B-CH_3), 19.1, 20.1, 20.6, 21.5 (each q, each 2 C, *o*- and *m*-CH_3), 21.1 (q, 2 C, $C(CH_3)_2$), 28.9 (br. s, 1 C, $C(CH_3)_2$), 55.4 (br. s, 1 C, Si_2CB), 130.3, 132.6 (each d, each 1 C, *p*-C), 129.9, 133.4, 136.7, 140.1 (each s, each 2 C, *o*- and *m*-C), 140.2 (s, 1 C, *i*-C of Si-Dur), 147.2 (br. s, 1 C, *i*-C of B-Dur); ^{11}B-NMR (toluene, 90 °C): $\delta = 86, 69$ ($\nu_{1/2} = 600$ and 700 Hz)

8: ^{1}H-NMR: $\delta = -0.52, 0.00$ (each s, each 9 H, $Si(CH_3)_3$), 0.31 (s, 3 H, B-CH_3), 1.74 (t, 4 H, CH_2 of THF), 2.00, 2.14 (each s, each 6 H, *o*- and *m*-CH_3), 3.59 (t, 4 H, OCH_2 of THF), 6.32 (s, 1 H, *p*-H); ^{13}C-NMR (−40 °C): $\delta = 6.5$, 7.6 (each q, each 3 C, $Si(CH_3)_3$), 13.7 (br. q, 1 C, B-CH_3), 20.1, 20.8 (each q, each 2 C, *o*- and *m*-CH_3), 26.3 (t, 2 C, CH_2 of THF), 65.3 (br. s, 1 C, Si_2CB), 68.3 (t, 2 C, OCH_2 of THF), 126.3 (d, 1 C, *p*-C), 130.3, 132.8 (each s, each 2 C, *o*- and *m*-C), 163.3 (br. s, 1 C, *i*-C); ^{11}B-NMR: $\delta = 49$ ($\nu_{1/2} = 510$ Hz)

The similarity of **4a, b** and **6a, b**[6] is immediately apparent in the chemical shifts of the atoms of the B–C double bonds (see also Table 1):

	4a	**4b**	**6a**	**6b**
$\delta(^{13}C)$	61.5	60.9	55.4	55.4
$\delta(^{11}B)$	63	63	69	69

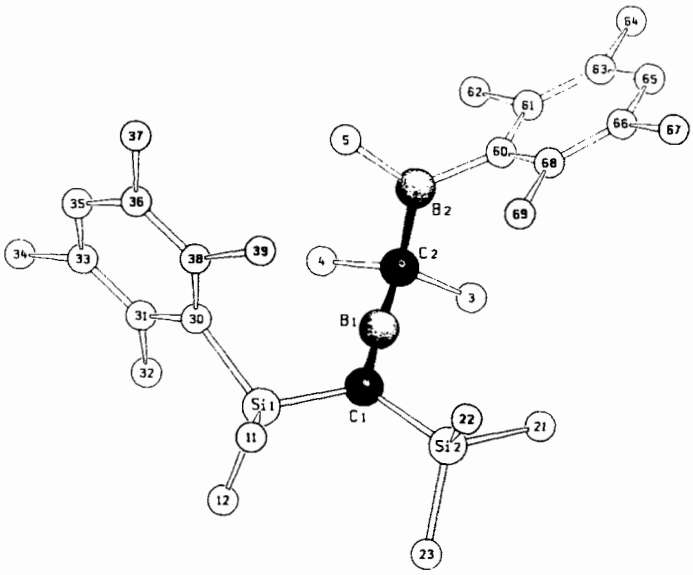
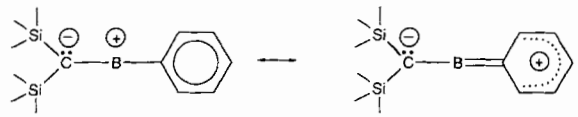


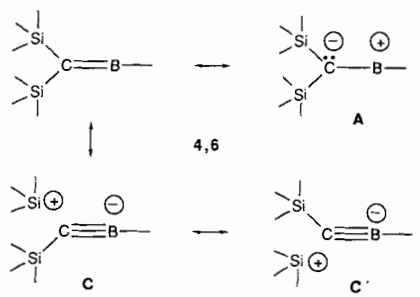
Fig. 1. Schakal drawing of the molecular structure of **6b** in the crystal. Important bond lengths [pm] and angles [°]: C1–B1 136.3(9), C2–B1 156(1), C2–B2 158.7(8), Si1–C1 182.8(6), Si2–C1 187.6(6), Si1–C30 189.6(6), B2–C60 157.7(9), B2–C5 155(1); C1–B1–C2 176.6(7), B1–C2–B2 106.8(5), Si1–C1–Si2 122.0(3), Si1–C1–B1 120.1(5), Si2–C1–B1 117.9(5), C2–B2–C60 121.6(6); B1–C2–B2–C60 110.2(7), C31–C30–Si1–C1 106.3(5), C61–C60–B2–C2 84.6(7), B1–C1–Si1–C30 −22.5(5).

The C atoms of the B–C double bonds are, for tricoordinated C-atoms, very strongly shielded (by $\Delta\delta = 93-98$) compared to the C atom bound to two trimethylsilyl groups in **10** ($\delta(^{13}C) = 153.5$).[7] From their chemical shifts, π charges of ca. −0.5 can be estimated for these C-atoms using the modified Spieseke-Schneider relationship.[8] The corresponding positive π charge (resonance formula **A**), on boron leads in **4a, b** to significant delocalization of the π-electrons of the aryl rings (resonance formula **B**). This is shown by the similar deshielding of their *ortho*- and *para*-C atoms as in **7a, b**.[1]



4 a,b

The polarity of the B–C π bond, which is due to different electronegativity of boron (2.0) and carbon (2.5), is considerably smaller: For **9**, π charges of ca. −0.2 at the C atom and ca. +0.2 at the B atom were calculated.[9, 10] The substantially stronger polarity of the B–C π bond in **4** and **6** can easily be explained by the silyl substituents. They can stabilize negative charge in the α-position[11] and empty orbitals in the β-position (β-Si-effect)[12] – usually of carbenium



ions, here on a partly positive boron atom – by C–Si hyperconjugation (resonance formulas **C, C'**).[13]

We consider the C–Si hyperconjugation to be the main reason for the B–C double bond in **6b** being very short in spite of weaker π-bonding (resonance formula A).[15] The electronic stabilization of the B–C double bond by the silyl groups might also contribute to the easy formation of **4** and **6**. In addition, the steric requirements of the silyl substituents contribute decisively to the kinetic stability of these methyleneboranes.

Received: January 27, 1989;
revised: March 16, 1989 [Z 3144 IE]
German version: *Angew. Chem. 101* (1989) 761

CAS Registry numbers:
1a, 114958-96-2; **1b**, 120637-66-3; **2a**, 120638-15-5; **2b**, 120638-19-9; **3a**, 120638-16-6; **3b**, 120638-20-2; **4a**, 120638-17-7; **4b**, 120638-21-3; **6a**, 120638-18-8; **6b**, 120638-22-4; **8**, 120638-23-5; Me_3SnCl,1066-45-1.

[1] R. Hunold, M. Pilz, J. Allwohn, M. Stadler, W. Massa, A. Berndt, *Angew. Chem. 101* (1989) 759; *Angew. Chem. Int. Ed. Engl. 28* (1989) 781.
[2] Previously there were indications of the reverse reaction path, i.e. the [2+2]-cycloaddition of methyleneboranes to give 1,3-diboretanes: B. Glaser, E. Hanecker, H. Nöth, *Chem. Ber. 120* (1987) 659.
[3] Color test for methyleneboranes, cf. H. Lukasch, G. Schmidt-Lukasch, U. Lippold, A. Berndt, *Angew. Chem. 100* (1988) 959; *Angew. Chem. Int. Ed. Engl. 27* (1988) 960. The color test fails in the case of **6a, b**, apparently for steric reasons.
[4] **3b**: X-ray structure analysis: $C_{30}H_{50}B_2Si_2$, space group $P\bar{1}$, $Z = 2$, $a = 981.3(9)$, $b = 1313.8(9)$, $c = 1357.4(10)$ pm; $\alpha = 64.17(8)$, $\beta = 85.53(5)$, $\gamma = 81.16(6)°$; 2994 unique reflections with $F_0 > 3\sigma(F_0)$ measured on a four-circle diffractometer (CAD4, Enraf-Nonius) with $Cu_{K\alpha}$ radiation at −80 °C; no absorption correction ($\mu = 10.5\ cm^{-1}$). H atoms were refined groupwise with common isotropic temperature factors. The methyl groups on Si were assumed to be rigid groups. Anisotropic temperature factors were used for all other atoms. 446 parameters, $R = 0.067$, $wR = 0.058$ ($w = 1/\sigma^2(F_0)$). Further details of the crystal structure investigation are available on request from the Fachinformationszentrum Energie, Physik, Mathematik GmbH, D-7514 Eggenstein-Leopoldshafen 2 (FRG), on quoting the depository number CSD-53 833, the names of the authors, and the journal citation.
[5] P. von R. Schleyer, D. Kost, *J. Am. Chem. Soc. 110* (1988) 2105, and references cited therein.
[6] In the methyleneboranes **4, 6** and **7** the C atoms that are bound to the dicoordinated B atoms are shielded by ca. $\Delta\delta = 20$ compared to comparable C atoms bound to tricoordinated B atoms. Similar shieldings are observed for C atoms on dicoordinated C atoms of alkynes. *Nöth* has drawn attention to the corresponding shielding in an amido(methyl)boron cation and in benzoyl and thiobenzoyl cations: H. Nöth, R. Staudigl, H. W. Wagner, *Inorg. Chem. 21* (1982) 706.
[7] G. Fritz, W. Himmel, *Z. Anorg. Allg. Chem. 448* (1979) 55.
[8] G. Boche, H. Etzrodt, M. Marsch, W. Thiel, *Angew. Chem. 94* (1982) 141; *Angew. Chem. Int. Ed. Engl. 21* (1982) 132; *Angew. Chem. Suppl. 1982*, 345, and references cited therein.
[9] B. T. Luke, J. A. Pople, M. B. Krogh-Jespersen, Y. Apeloig, M. Karni, J. Chandrasekhar, P. von R. Schleyer, *J. Am. Chem. Soc. 108* (1986) 270.
[10] G. Frenking, H. F. Schaefer III, *Chem. Phys. Lett. 109* (1984) 521.
[11] Concerning the extent of stabilization of carbanions by α-silyl substituents see: D. M. Wetzel, J. I. Braumen, *J. Am. Chem. Soc. 110* (1988) 8333; for interpretation: P. von R. Schleyer, T. Clark, A. J. Kos, G. W. Spitznagel, C. Rohde, D. Arad, K. N. Houk, N. G. Rondan, *ibid. 106* (1984) 6467.
[12] For the stabilization of vinyl cations isoelectronic with methyleneboranes by β-silyl substituents see: S. G. Wierschke, J. Chandrasekhar, W. L. Jorgensen, *J. Am. Chem. Soc. 107* (1985) 1496.
[13] The geometric requirements for C–Si hyperconjugation [14] are optimal in bis(silyl)methyleneboranes such as **4** and **6** since an empty p-orbital on the boron lies in the plane of the C–Si σ-bonds. Furthermore, greater overlap is facilitated by the short B=C distance. The σ-π interaction is energetically favored by the positivization of the boron atom, i.e. the increase in its electronegativity (lowering of the LUMOs).
[14] Cf., e.g.: I. Fleming: *Grenzorbitale und Reaktionen organischer Verbindungen*, Verlag Chemie, Weinheim 1979, pp. 96–97.
[15] For bond shortening by hyperconjugation see also A. Höfner, B. Ziegler, W. Massa, A. Berndt, *Angew. Chem. 101* (1989) 188; *Angew. Chem. Int. Ed. Engl. 28* (1989) 186, and references cited therein.

BOOK REVIEWS

Book Reviews are written by invitation from the editor. Suggestions for books to be reviewed and for book reviewers are welcome. Publishers should send brochures or (better) books to the following address: Redaktion Angewandte Chemie, Postfach 101161, D-6940 Weinheim, Federal Republic of Germany. The editor reserves the right of selecting which books will be reviewed. Uninvited books not chosen for review will not be returned.

Coordination Compounds en gros and en détail

Comprehensive Coordination Chemistry. The Synthesis, Reactions, Properties and Applications of Coordination Compounds. (In 7 volumes). Edited by *G. Wilkinson, R. Gillard* and *J. A. McCleverty*. Pergamon Press, Oxford 1987. Approx. 7000 pp. in total, hard cover, $ 2450.00.– ISBN 0-08-026232-5

Volume 1: Theory and Background

A total of 18 authors have here set themselves the task of compiling the introductory volume of this new work of reference. Its 17 chapters aim to provide the intending user of "Comprehensive Coordination Chemistry" with a summary of those general aspects of chemistry that are relevant to coordination compounds. The volume concludes with a subject index and a formula index.

The chapters that have been chosen for inclusion in this introductory volume can be divided into several subject groups. Chapters 1.1 and 1.2 are historical reviews of the development of coordination chemistry. The period up to 1930 is dealt with by *G. B. Kauffman*, who is well known for his reviews and essays on this subject, while the period from 1930 on is covered by an outstanding coordination chemist, *J. C. Bailar, Jr.*, who has himself made important contributions to the development of the field. These two introductory chapters undoubtedly provide useful background knowledge on this segment of inorganic chemistry, though Chapter 1.2 can highlight only the most important trends and insights. The custom of starting a major collected work with the historical development of the field of study, describing not only

its chronology but also the scientists involved and their individual contributions, is one that is worth preserving. Other chapters too in this volume are very impressive. *D. L. Kepert*'s treatment of coordination numbers and geometries (Chapter 2), in which complexes with coordination numbers from 5 to 12 are discussed on the basis of the VSEPR principle, is detailed, sound and well illustrated with figures, its only omission being the absence of alternative descriptions of coordination polyhedra and their polytopic rearrangements (e.g. those based on quantum mechanics). Chapter 3 is a lesson by *T. B. Sloan* on the nomenclature of coordination compounds; the necessity for this and the content of the article are beyond question. In Chapter 4 *I. G. Dance* provides a very useful classification of metal cluster compounds and clathrates in list form (with clear structural formulas which are a welcome aid to the reader). As is always the case with undertakings of this sort, the question arises here (as also in other chapters) of how up-to-date the information can be made. Published work up to 1983 is taken into account, but quite a lot has happened in the field of clusters in the intervening years. A few of the sections in this chapter, such as those on bonding (where only clusters of the cubane type are covered), or on synthetic methods (one and a half pages of text), are too rudimentary. In Chapter 5, on isomerism in coordination complexes, the ground covered by *J. M. Harrowfield* and *S. B. Wild* is essentially the same as is usually treated in inorganic chemistry textbooks or elementary lecture courses on complex chemistry, apart from unnecessarily introducing the newly coined words "allogonism" and "allogone" in connection with geometrical isomers, failing to mention the "bond-stretch" isomerism whose existence was recently established, and the inclusion of some material which overlaps with that in Chapter 2. Ligand field theory and its modifications, and the "angular overlap" model, which are treated in Chapter 6 (*B. N. Figgis*), are undoubtedly an important part of the theoretical background of coordination chemistry, but after looking through this chapter one is left with doubts about its usefulness. These topics are treated in several excellent and considerably more detailed monographs and textbooks (not least those by the same author). Many of the points are merely touched on briefly (e.g. "Excited States and Photochemistry" is given only one and a half lines of text with four literature references), and the omission of other electronic structural theories of coordination compounds from this chapter, the only one devoted to bonding theory, gives a somewhat unbalanced picture of the quantum chemistry of inorganic complexes.

A further five chapters deal with the general theme "Reaction Mechanisms". Chapters 7.1 on substitutions (*M. L. Tobe*), 7.2 on electron transfer reactions (*T. J. Meyer* and *H. Taube*), and 7.3 on photochemical processes (*C. Kutal* and *A. W. Adamson*), are all written by authors whose names are inseparable from the respective chapter titles. They are impressive, especially that which has the doyen of this subject, *Taube*, as one of its authors. The treatment of photochemical processes includes more than 200 literature references; newcomers to the research topic will note this with considerable satisfaction, as there is scarcely one useful monograph on this topic, and even less in the way of textbooks. Chapter 4, in which *D. St. C. Black* fills the greater part of the 44 pages with formula schemes, mainly describing the reactions of metal-bonded chelate ligands, is followed by a short chapter by *H. E. LeMay, Jr.* on solid state reactions of coordination compounds, which reveals how little knowledge exists about this area. Next follow three very brief reviews of electrochemical aspects of coordination chemistry. Although it is true that brevity can often be the soul of wit, it seems odd that the first of these three chapters (with its very general sounding title "Electrochemistry and Coordination Chemistry") by *C. J. Pickett* contains only material which could easily have been integrated into the two following chapters (by *D. H. Vaughan* and *C. J. Pickett* respectively). These latter two are likewise not very informative, and could have been combined together. Following Chapter 9 by *D. H. Vaughan*, from which one learns something about solvent effects on the rates of reactions, redox potentials and equilibrium constants of coordination compounds, the final chapter by *H. M. N. H. Irving* reviews the important applications of coordination compounds in analytical chemistry. This article again is mainly useful for its collection of relevant literature references, which gives the non-specialist easy access to appropriate background reading.

The overall impression from this first volume of "Comprehensive Coordination Chemistry" is one of rather wide variations in the quality, quantity, usefulness and importance of the individual chapters. Excellent surveys appear alongside other chapters that could with equal benefit be replaced by lists of relevant review articles. It would perhaps be not such an outrageous idea if multi-volume works of this sort were to have, instead of a whole volume devoted to "Theory and Background", just one chapter covering as many as possible of the most up-to-date relevant reviews and monographs, even though the saving of one volume would probably not lead to a significant reduction in the price of the whole set.

Peter Hofmann
Anorganisch-chemisches Institut
der Technischen Universität München, Garching (FRG)

Volume 2: Ligands

In multi-volume works it is a truism that a systematic and well-organized treatment of the subject makes the collection attractive, and reduces the gaps left for other authors and publishers to fill; in practice, however, a successful recipe is not found in every case. Comparing the present work with "Comprehensive Organometallic Chemistry"[*] it emerges that significant progress has been made in this respect. Volume 2 (together with Vol. 6) gives probably one of the most obvious indications of this.

In the past the attitudes of metal complex chemists and organometallic chemists have been strongly metal-orientated. In contrast, there is now a trend towards thinking more in terms of ligands. Which ligand should one choose in order to make a complex more stable or more labile? Which ligand offers the best possibilities as an analytical probe? How can molecules in the coordination sphere be switched around? This volume directly or indirectly answers many of these and similar questions. For this reason the collection will become an important standard work, not only for organometallic chemists but also for organic chemists, biochemists and biologists. There are, of course, too many instances of overlapping in content between this and the other volumes, and this must ultimately have an effect on the total price of the work. However, the volume on "Ligands" is so useful that such a consideration will not prevent it being bought.

The ligands are grouped according to the obvious classification based on donor atoms. Thus there are eight chapters on nitrogen-containing ligands, one on ligands containing elements of Main Group 5, with the greatest emphasis on phosphorus, nine on oxygen-containing ligands, six on sulfur-containing ligands, and one each on ligands in which the

[*] Cf. *Angew. Chem. 95* (1983) 819; *Angew. Chem. Int. Ed. Engl. 22* (1983) 797.

donor atom is selenium, tellurium, a halogen or hydrogen. A further eight chapters deal with ligands having two or more different donor atoms. Especially noteworthy is the extensive treatment of macrocycles with nitrogen and oxygen donor centers (sulfur analogs of these are listed only briefly under thioethers). Next a separate chapter is devoted to ligands of natural origin (covered only very briefly, however, omitting alkaloids for example). Further chapters treat cyanides and fulminates, then ligands containing silicon, germanium, tin and lead, and lastly mercury as a ligand; however, the analogous copper ligands and the gold ligands which have been particularly thoroughly studied are unaccountably omitted.

In more than a thousand pages many well-known experts have here applied their best efforts to bringing order to this many-faceted subject. The result stands up to scrutiny; it is a mine of information for all chemists, from the student to the committed researcher or the industrial chemist. An "exhaustive" treatment is, of course, something aimed for but never fully attained. Some readers will find that "their" ligands are not covered or are not given due attention. Those that may be missed include the nitrido ligand, the intentionally (but unjustifiably) omitted dinitrogen, thiazyl fluoride and thioformaldehyde ligands, and the trialkylamines, especially with regard to their interaction with alkali metal ions. Many of the chapters contain useful directions concerning nomenclature. Regrettably, though, hardly any of the chapters give an indication of the date up to which the literature has been scanned.

Unfortunately the editors have missed an important opportunity by failing to impose uniformity in the manner whereby the properties and bonding capabilities of the ligands are presented and discussed; this would have made comparisons easier, an important matter from the reader's standpoint. The only chapter sub-sections in which this has been done are 13.2 to 13.4 (N-donor ligands), 15.2 (on the ligands O_2, $O_2^{\ominus}$ and $O_2^{2\ominus}$), 16.1 to 16.3 (S-donor ligands) and 19 (hydrogen and hydrides); the discussion on the bonding of ligands containing phosphorus and its homologs is especially worth mentioning. In many of the articles the authors have been content to include sub-sections with titles such as "Properties", "Structure", "Spectroscopic Data" or "Types of Coordination". However, to describe the ligands the authors use many different concepts or terms: the coordination number, "soft" or "hard", a good or poor donor or acceptor, the position in the spectroscopic series; information on isoelectronic ligands is occasionally given. The energies of the HOMOs or LUMOs are missing, as are their relative sizes.

At the end of the volume there is a subject index (37 pages) and a formula index (75 pages). Unfortunately the latter is only arranged according to the metal atoms, with the result that a ligand can be located from its empirical formula only with difficulty.

Frank H. Köhler
Anorganisch-chemisches Institut
der Technischen Universität München, Garching (FRG)

Volume 3: Main Group and Early Transition Elements

Volume 3, with 25 chapters consisting of 1400 pages, describes the coordination chemistry of the Main Group elements and the "early transition elements". The article on the coordination chemistry of phosphorus could not be completed in time, and will appear later in the journal *Polyhedron* (note also "Technetium" in Volume 4). All the chapters (except that on molybdenum) have a similar construction, being arranged according to the various ligands for a given central atom. This results in a consistency within the volume which is by no means always found in multi-author reference works of this type. Organometallic/metalloid compounds have deliberately been excluded, with very few exceptions, a fact which is not immediately apparent from the title of the reference work, but is explained in the preface. Readers are there referred to the sister series "Comprehensive Organometallic Chemistry" for this class of compounds.

The first 300 pages are devoted to the coordination chemistry of the Main Group elements. The contribution by *D. E. Fenton* on the coordination behavior of the alkali and alkaline earth metals (70 pp., with 598 references extending up to 1985) has turned out very successfully, with the main emphasis, as expected, on the complexation of these metals with polydentate and macrocyclic ligands (crown ethers, cryptates, porphyrins etc.). The resulting structures are shown very clearly, either schematically or as pictorial molecular diagrams. This feature proves especially useful in the final section of the chapter (10 pp.), which deals with naturally occurring ionophores as ligands. The currently topical question of what factors influence the selectivity and the stability of the complexes is discussed in detail.

The chapter on the coordination chemistry of boron by *J. Emri* and *B. Györi* (20 pp., 172 references extending up to 1984) treats the complexes, classified according to ligands, in text linked to tables, each with a separate bibliography; thus the reader has no difficulty in quickly finding the required reference. This useful arrangement is also found in the other chapters.

The following chapters by *M. J. Taylor* on the coordination chemistry of aluminum and gallium (37 pp., 690 references up to 1985) and by *D. G. Tuck* dealing with indium and thallium (22 pp., 438 references up to 1983) are packed with much information; however, as might be guessed from the small numbers of pages, the form of presentation is less user-friendly in this case. Complicated structures are merely described rather than drawn, and the reader is hurried from one heading to the next.

The chapter by *P. G. Harrison* on the coordination chemistry of silicon, germanium, tin and lead (40 pp., 663 references up to 1985) reviews a considerable amount of well-established knowledge, but also includes a more topical section on "Multiple Bonding Involving Silicon, Germanium and Tin". Thus the chapter does not completely exclude the occurrence of carbon itself as a "ligand". Several pages are also devoted to the cyclopentadiene ligand and to the related carbaboranes. The presentation as a whole lacks clarity, and cannot be said to be satisfactory. Moreover, many aspects of the chemistry of these elements cannot be regarded as "coordination chemistry" without straining the definition.

The chapter by *C. A. McAuliffe* on the coordination chemistry of arsenic, antimony and bismuth consists of 56 pages, and reviews 272 publications (extending up to 1985) in a clear comprehensible style. The three elements are treated separately. Although this procedure facilitates searching for specific compounds, comparisons within the triad of elements, which can often be very useful, are thereby made more difficult; in a "parallel" method of treatment such comparisons emerge naturally. However, the easy style makes refreshing reading, and valuable glimpses of matters of current controversy are included.

The appropriately brief chapters on the coordination chemistry of sulfur, selenium, tellurium and polonium (*F. J. Berry*, 8 pp., 85 references up to 1983), and of the halogens and inert gases (*A. J. Edwards*, 10 pp., 102 references up to

 © VCH Verlagsgesellschaft mbH, D-6940 Weinheim, 1989 0570-0833/89/0606-0788 $ 02.50/0

1984), are followed by chapters on the "Early Transition Metals" (i.e. titanium to chromium, the lanthanides and the actinides). A separate chapter is devoted to the iso- and heteropolyanions (*M. T. Pope*, 25 pp., 140 references up to 1985). The coordination chemistry of molybdenum is covered in six chapters, written respectively by *A. G. Sykes, G. L. Leigh, R. L. Richards, C. D. Garner, J. M. Charnock* and *E. I. Stiefel*. These molybdenum chapters have been placed at the end for reasons of timing, and are preceded by the chapters on titanium (*C. A. McAuliffe* and *D. S. Baratt*), zirconium and hafnium (*R. C. Fay*), vanadium (*L. F. Vilas Boas* and *J. Costa Pessoa*), niobium and tantalum (*L. G. Hubert-Pfalzgraf, M. Postel* and *J. G. Riess*), chromium (*L. F. Larkworthy, K. B. Nolan* and *P. O'Brien*), tungsten (*Z. Dori*), the lanthanides (*F. A. Hart*) and the actinides (*K. W. Bagnall*). All the chapters are competently written, and they will be useful to a wide readership. In contrast the preceding 300 pages on the coordination chemistry of the Main Group elements are out of place in this volume.

Hubert Schmidbaur
Anorganisch-chemisches Institut
der Technischen Universität München, Garching (FRG)

Volume 4: Middle Transition Elements

Having already introduced the semantically questionable terms "early" and "late" to classify the transition elements, this bad practice is now continued in Volume 4 of the work with the so-called "middle transition elements". These comprise the elements of the manganese, iron and cobalt groups of the Periodic Table. The coordination chemistry of these elements—with the exception of the article on technetium, which was not ready in time and will appear later in the journal *Polyhedron*—is described in 1400 pages, the contributions being of a consistently high quality. The chapter on manganese (by *B. Chiswell, E. D. McKenzie* and *L. F. Lindoy*) is quite extensive, well organized and reasonably comprehensive; the only area dealt with too briefly is that of manganese compounds with coordination numbers of five to seven. Another pleasing contribution to this volume is the carefully prepared account of the inorganic chemistry of rhenium, which is skilfully organized according to ligands and structural units. However, the treatment in this chapter of the higher valency hydrides especially seems unsatisfactory with regard to completeness and presentation; the applications of this class of compounds in the chemistry of "CH activation" ought to have been included (e.g. the work of *Felkin*). The chapter on rhenium (*K. A. Conner* and *R. A. Walton*) is a valuable mine of information for all whose work involves this element, or who would like to make a start in rhenium chemistry. The two chapters on iron also are clearly structured, under the heading of Fe(II) complexes and lower oxidation states (*P. N. Hawker* and *M. V. Twigg*) and that of Fe(III) compounds and higher oxidation states (*S. M. Nelson*). However, these chapters lack detailed descriptions of biologically relevant systems with an adequate coverage of the literature, and also references to modern developments in organo-iron chemistry. For the contribution on osmium the editors have found in *W. P. Griffith* an especially competent and expert author. This chapter, clearly set out according to ligands, with sub-divisions for the different oxidation states of osmium, is a really excellent resource for researchers engaged in osmium chemistry. The expert selection and presentation of the structural chemistry details here deserves a special mention. The author also gives a correct and historically aware account of the development of the osmium tetraoxide catalyzed olefin oxidation process (*cis*-hydroxylation, p. 590 ff.). The elements cobalt (*D. A. Buckingham* and *C. R. Clark*) and rhodium (*V. H. Jardine* and *P. S. Sheridan*) receive the most extensive and detailed treatment (altogether 460 pages and 2500 references). The Wilkinson complexes of the $ClRh(PR_3)_3$ type are deservedly given the most detailed treatment including tables. In the chapter on iridium (*N. Serpone* and *M. A. Jamieson*), with its sometimes badly proportioned pictorial formulas (e.g. on pages 1102, 1105, 1112, 1115 and 1151), a pleasing feature is the account of the catalytic activity of this element (see the tables on page 1159); although short, it includes a very useful compilation of key references.

Wolfgang A. Herrmann
Anorganisch-chemisches Institut
der Technischen Universität München, Garching (FRG)

Volume 5: Late Transition Elements

This volume contains chapters on the coordination chemistry of the nickel, copper and zinc triads of the Periodic Table. It begins with an excellent survey of the coordination chemistry of nickel by *L. Sacconi, F. Mani* and *A. Bencini*. In this, the longest of the chapters with about 350 pages, more than 3200 publications are competently reviewed. In a few instances literature published up to 1985 is included, but in general the coverage extends up to 1984. The material is arranged primarily according to increasing nickel oxidation states, then further divided according to ligands. An especially commendable and useful feature is the clear way in which the different ligand systems are presented, as also are the many tabulations of physical-chemical data and the enumeration of related ligand systems. It is only by these means that an adequate coverage of the large variety of ligands can be given. In this and the following chapters important molecular structures are reproduced directly from the original papers, in contrast to the practices usually followed in tertiary publications of this sort. In addition stereochemical diagrams are used in important cases to make intermolecular interactions clearer to the reader. This form of representation is a welcome aid, as it helps one to understand three-dimensional molecular relationships.

D. M. Roundhill, in his chapter on the coordination chemistry of platinum, with 182 pages of text and about 2000 literature references, adopts a quite different arrangement of the material. Here the system is based on the ligands, ordered according to the position of the donor atom in the Periodic Table—a method of classification which does not always make for clarity of presentation.

In the account of the coordination chemistry of copper by *B. J. Hathaway*, which is quite a lengthy one with 250 pages, the spatial relationships of the many cluster compounds included are in some cases not shown very effectively. The coordination chemistry of silver (*R. J. Lancashire*) is treated in a less comprehensive fashion, with only 500 literature references.

R. J. Puddephatt's contribution on the coordination chemistry of gold illustrates that much advantage can be gained by having articles on related topics written by the same author, even though the aims may be different. Although some overlapping is almost inevitable in works of this scale, such an arrangement would have considerably reduced the duplication between articles in this series and others in the sister series "Comprehensive Organometallic Chemistry".

The article on zinc and cadmium (122 pp., 1470 references) by *R. H. Prince* includes detailed sections devoted to

industrial applications and to biological aspects of these elements, which are very useful. Although these important facets are also touched on in the chapter on copper, they are absent or less clearly stated in the rest of the chapters. The account by *K. Brodersen* and *H. U. Hummel* of the coordination chemistry of mercury (124 pp., 600 references) follows very conventional lines in the choice of material, indicating an outlook which has now almost disappeared from the German literature. Even the introduction strikes one as awkward and constrained.

To conclude these comments, the articles on the coordination chemistry of palladium by *C. F. J. Barnard* and *M. J. H. Russell,* and by *A. T. Hutton* and *C. P. Morley,* both much too brief, with altogether only 660 literature references (only a few of which are more recent than 1980), give a rather inadequate account of the current state of knowledge in this field. Applications, such as those to catalysis, are not discussed at all. These chapters are definite weaknesses of the volume, and the reader would be well advised to refer also to the complementary volume of "Comprehensive Organometallic Chemistry" (see footnote on p. 787) for additional information.

Carl Krüger
Max-Planck-Institut für Kohlenforschung
Mülheim a. d. Ruhr (FRG)

Volume 6: Applications

In the 16 chapters of this volume, experts from universities and industry describe the applications and importance of coordination chemistry in a wide variety of currently topical fields. It is no surprise to find that the publications cited show a bias towards those in the English language. On the other hand it is regrettable in a work published in 1987 that, whereas the important and lengthy chapter by *M. N. Hughes* cites papers as recent as 1986, in others, such as those on "Dyes and Pigments" (Chapter 58) and on "Applications in Photography" (Chapter 59), the most recent citations are to 1983 papers (and even these are only patents or patent applications). As a result the usefulness of these parts of Volume 6 as reports on the "current" situation in applied research is considerably reduced. This turns out to be the case for all the areas that are undergoing rapid development, e.g. in "Electrochemical Applications" (Chapter 57), and in "Compounds with Novel Electrical Properties" (Chapter 60), although it is true that there are as yet few actual applications in the form of fully developed systems.

Chapter 61 consists of five sections: "Stoichiometric Reactions of Coordinated Ligands", "Catalytic Activation of Small Molecules" (which in particular describes hydrogenations, hydroformylations and carbonylations, classified according to the metals involved), "Metal Complexes in Oxidation Reactions", "Lewis Acid Catalysis in Reactions of Coordinated Ligands", and "Decomposition of Water into its Elements".

The treatment of biological and medical aspects in Chapter 62.1 (the longest) is detailed and pleasingly up-to-date, as are those on the applications of coordination compounds in chemotherapy (Chapter 62.2) and in radiopharmacology (Chapter 65).

Geochemical aspects and prebiotic systems are discussed in Chapter 64. The articles on "Metal Extraction" (hydrometallurgy) (Chapter 63) and on "Nuclear Fuel Cycles" (Chapter 65) describe well-established technological applications. Finally Chapter 66 summarizes miscellaneous applications, ranging from hydrogen storage to uses in agricultural chemistry and in reducing toxic smoke emission from burning of PVC.

Despite the fact that the literature coverage is not always ideal, this is on the whole a well-written and very clearly presented volume, and reading through it or merely browsing will reveal plenty of new ideas, and perhaps surprises, whether the reader's interests lie in basic research or in applications. This useful volume should find a place in every library, as an aid both to those starting in a new field and to others wishing to round off their knowledge.

Heinz P. Fritz
Anorganisch-chemisches Institut
der Technischen Universität München, Garching (FRG)

Volume 7: Indexes

The formula and subject indexes for Volumes 1 to 6 are collected together in this volume. It also includes a list of review articles relevant to this subject area.

[NB 920 IE]

Metal-Ligand Multiple Bonds. By *W. A. Nugent* and *J. M. Mayer.* Wiley, Chichester/New York 1988. xi, 334 pp., hardcover, £ 35.15/$ 55.00. – ISBN 0-471-85440-9

This superb book by *W. A. Nugent* and *J. A. Mayer* on metal–ligand multiple bonds provides a thorough review on the chemistry of transition-metal complexes with M–O, M–N, and M–C multiple bonds. This is the first time that these related types of complexes have been treated together comprehensively and compared with one another.

The seven chapters describe the electronic and geometric structures, the synthesis and spectroscopic properties, and the reactivity and catalytic activity of these complexes. The first chapter introduces the different types of complexes: oxo complexes, nitrido, imido, and hydrazido complexes, and different compounds with M–C multiple bonds, including Fischer- and Schrock-type carbene complexes as well as carbyne complexes. Unfortunately, complexes in which the metal exhibits multiple bonds to main-group elements other than O, N, and C are not discussed, although these complexes are equally interesting and a focus of current attention. Inclusion of these complexes would have allowed more extensive comparisons. Presumably, however, this would also have led to an unwieldy text. In the second chapter, the bonding and electronic structure of these complexes are discussed. The following two chapters provide a detailed description of the currently available routes to compounds with metal–ligand multiple bonds and a summary of their vibrational and NMR spectra. The O, N, and C NMR resonances are discussed extensively. Chapter five offers a comprehensive review of the crystal structures and, in particular, the M–O, M–N, and M–C bond lengths. Chapters six and seven thoroughly treat the reactivity of metal–ligand multiple bonds and their role in catalysis.

This book is a gold mine for all chemists interested in the area of metal–ligand multiple bonds or requiring specific information on such complexes. Especially valuable is the exhaustive literature survey, including publications appearing in 1987, which may be rapidly scanned and helps the reader in finding answers to specific questions. The book is excellent as a basic text for advanced study in courses and seminars. Despite the cutbacks in library budgets, which have placed severe limitations on the purchase of new mono-

 © VCH Verlagsgesellschaft mbH, D-6940 Weinheim, 1989 0570-0833/89/0606-0790 $ 02.50/0

graphs, this book is an essential acquisition for every chemistry library. Only in this way will it be readily available to students. The numerous, clearly drawn figures, tables, and formulas are didactically well placed in the text, which has been carefully proofread and is practically free of errors. An exception, however, is found in Table 4.7, where the columns for ν_s and ν_{as} of the M=N=M bridge vibrations are interchanged. Moreover, it would have been better to refer to antisymmetric vibrations instead of asymmetric vibrations.

All in all, this book is a must for every chemistry library and for every scientist interested in this area, as well as for advanced students. I recommend it without reservation.

Joachim Strähle [NB 978 IE]
Institut für Anorganische Chemie
der Universität Tübingen (FRG)

Biomedical Magnetic Resonance Imaging. Principles, Methodology and Applications. Edited by *F. W. Wehrli, D. Shaw,* and *J. B. Kneeland.* VCH Verlagsgesellschaft, Weinheim/VCH Publishers, New York 1988. xviii, 601 pp., hardcover, DM 195.00.—ISBN 3-527-26701-8/0-89573-349-8

This book of 600 pages describes the physical basis, clinical applications, and recent developments (up to 1986) in the field of NMR imaging and *in vivo* NMR spectroscopy. It consists of 13 chapters written by a total of 18 physicists and medical scientists with relevant experience.

The method-oriented part of the book gives an account of the fundamentals of NMR spectroscopy and of the techniques used to produce spatially resolved NMR signals. These chapters are particularly successful, since they are not merely a repetition of conventional introductions to NMR spectroscopy, but constantly keep in mind the special conditions of *in vivo* experiments. Some of the topics treated are the spatial resolution, image contrast, relaxation phenomena, the use of paramagnetic agents for enhancing contrast, (rapid) imaging techniques and gradient switching, techniques for suppressing water signals, effects of the chemical shift, detection of flow processes, problems caused by motion, and the use of surface coils. Other sections are concerned with special topics such as NMR imaging using nuclei other than hydrogen (fluorine, phosphorus, sodium), problems of spatial localization in *in vivo* NMR spectroscopy, and spectroscopic imaging. One chapter is devoted to safety aspects.

Since this area of research, especially *in vivo* NMR spectroscopy, is developing very rapidly, some of the evaluations and predictions given here are already out of date as a consequence of the date of completion of the manuscript. For example, the limitation of spectroscopic applications to studies of energy metabolism by ^{31}P NMR measurements is no longer valid. Major advances in image-controlled localized ^{1}H NMR spectroscopy, with scientific and medical applications in studies of the metabolism of amino acids and neurotransmitters in the human brain, were reported only during last year.

Clinical applications discussed are those relating to the central nervous system, the cardiovascular system, the abdominal and pelvic regions, and the skeletal muscular system. Unfortunately, some of the examples are based on old image material. Not enough space is given to the important brain and spine studies, and for cardiac applications the greatly increased capabilities offered by ECG-synchronized ciné NMR imaging studies are not mentioned. Nevertheless, the clinical chapters provide non-medical readers with valuable insights into the importance of the techniques in medicine; for those who are only interested in using the methods for clinical applications, other more extensive collections of imaging data are available.

Taken as a whole the book commendably follows the main stream of developments and applications. This is undoubtedly due to the editors' and authors' close connections with industry and clinical practice. In this continually changing area of research *realistic* developments in *in vivo* NMR are always characterized by their human applicability. This feature seems to be a prerequisite for a successful adaptation of "classical" NMR techniques to the field. The individual articles are detailed for an introduction, but not long-winded, and they are competently written. The book is very clearly structured, and the method-oriented sections especially are very well prepared from a learning point of view. An extensive bibliography at the end of each chapter provides easy access to the original literature. In contrast to some other "rapidly produced" works on NMR imaging, this book is a valuable addition to the literature. It is suitable for chemists, physicists, biologists and medical scientists who wish to begin work in this field, or would like to gain a deeper understanding of it, or who simply need a work of reference to direct them to further reading in their daily work.

Jens Frahm [NB 942 IE]
Max-Planck-Institut für Biophysikalische Chemie
Göttingen (FRG)

Introduction to Synchrotron Radiation. By *G. Margaritondo.* Oxford University Press, Oxford 1988, xi, 280 pp., hard cover, £ 32.00.—ISBN 0-19-504524-6

Amongst the growing number of publications on synchrotron radiation this book by *G. Margaritondo* occupies a special position: here the wealth of applications of synchrotron radiation in chemistry, physics, biology, medicine and engineering is treated as a consistent whole by a single author. The numerous cross-references link together topics that appear widely disparate: to give an example, the concept of phase space runs like a scarlet thread through subjects ranging from the production of synchrotron radiation in electron storage rings, and the design of synchrotron radiation guides, mirrors and monochromators, to the interaction of the radiation with the samples being studied.

One third of the book is concerned with the description of sources of synchrotron radiation and with instruments for using such radiation. Optical components and detectors are discussed, as well as wigglers and undulators that are incorporated into the latest storage rings for the production of synchrotron radiation tailored for specific applications. Also not neglected, of course, is the outlook for third generation storage rings, of which the chief representative is the European ESRF synchrotron radiation facility in Grenoble. The information given about working conditions in the vicinity of synchrotron radiation sources is also very useful.

The following third of the book deals with the applications of synchrotron radiation in optical spectroscopy, X-ray absorption spectroscopy and photoemission spectroscopy, also including spin-polarized photoemission. The importance of these techniques in surface studies is discussed in detail.

Of the various elastic X-ray scattering techniques, one which has profited at a relatively early stage from the laser-like collimation of synchrotron radiation is low angle X-ray scattering. This is also the case in X-ray topography. By taking advantage of anomalous dispersion one can introduce some features of spectroscopy into X-ray structural analysis. Techniques for determining the phase of the scattered X-rad-

iation are described in detail in view of the growing importance of this method. Lastly the importance of the polarization of synchrotron radiation for measuring magnetic X-ray scattering is discussed.

X-ray lithography is associated with some important industrial applications, and the investigation of coronary arteries (angiography) by differential absorption measurements on iodine offers definite prospects for becoming a routine application of synchrotron radiation in medical diagnosis. Other promising possibilities for synchrotron radiation include X-ray microscopy, time-resolved fluorescence measurements, X-ray stationary waves and inelastic X-ray scattering. However, mention should also have been made here of Mössbauer scattering.

The book is not a substitute for further reading of more comprehensive handbooks on synchrotron radiation, but is intended rather as an elementary introduction. The author has achieved this aim to the full by means of clear descriptions avoiding complicated formulas, illustrated by attractive diagrams. The book is highly recommended, especially for readers from all fields of science, engineering and medicine who are beginners in the use of synchrotron radiation.

Heinrich Stuhrmann [NB 964 IE]
GKSS Forschungszentrum
Geesthacht GmbH, Geesthacht (FRG)

Electron Nuclear Double Resonance Spectroscopy of Radicals in Solution. By *H. Kurreck, B. Kirste* and *W. Lubitz*. VCH Verlagsgesellschaft, Weinheim/VCH Publishers, New York 1988. xii, 374 pp., hardcover, DM 148.00.—ISBN 3-527-26791-3/0-89573-324-2

This monograph on applications of ENDOR (Electron Nuclear Double Resonance) spectroscopy to studies of free radicals in solution, in both organic chemistry and biology, has been written by acknowledged experts in this field, and fills a gap in the existing range of books.

ESR spectrometers have been commercially available for about 25 years, and provide the organic chemist with a routine method for studying free radicals in solution. ENDOR spectroscopy was developed more than 30 years ago as a technique for simplifying complex ESR spectra; however, it was then a laborious procedure, and was only used in special cases. A few years ago ENDOR instruments were introduced commercially, making this method also accessible to the organic chemist who uses routine equipment. It is therefore likely that it will be used increasingly in the future, especially in studying radicals with very large numbers of coupling nuclei, where the interpretation of the ESR spectra would otherwise be impossible, or at best ambiguous.

The book is aimed at two groups of readers. Firstly it takes into account the needs of the reader who wishes to learn about the ways in which the ENDOR technique can be used in organic and biological chemistry. Secondly it offers the specialist a review of results obtained up to now. The arrangement of the contents reflects these two aims.

The introduction explains the basic fundamentals for the non-specialist in a concise and easily understandable form. This is followed by two more detailed chapters dealing with the principles and theory of the method; the first of these is aimed mainly at the organic chemist, while the second—written in collaboration with a physicist (Dr. *Plato* of the Free University of Berlin)—is addressed mainly to the spectroscopist. The fourth chapter, which is devoted to the basic principles of ENDOR spectroscopy applied to hetero nuclei, completes the general part of the book.

The fifth chapter deals systematically with ENDOR spectroscopic observations on various types of free radicals in solution, grouped according to the identity of the central atom. This is a clearly presented and critical summary of the results, with many literature references to enable the interested reader to delve further. The last third of the book consists of four chapters describing some special applications of ENDOR spectroscopy: studies of intramolecular dynamic processes, free radicals in liquid crystals, organic multi-spin systems, and biological systems.

The book will undoubtedly become an indispensable item in every library that aims to give a complete picture of the applications of spectroscopic methods in organic chemistry. It is not intended as an alternative to other monographs on the ESR spectroscopy of free radicals in solution, but as an extension of these. The appearance of a new complete work on ESR spectroscopy would therefore be very welcome—for example a revised and updated edition of the standard work published in 1970 by *Scheffler* and *Stegmann*. At present the reader needing more complete data on the ESR spectroscopy of free radicals in solution must rely on the comprehensive tabulated work provided in Landolt-Börnstein.

Manfred Lehnig [NB 932 IE]
Institut für Organische Chemie
der Universität Dortmund (FRG)

Registered names, trademarks, etc. used in this journal, even when not marked as such, are not to be considered unprotected by law.

© VCH Verlagsgesellschaft mbH, D-6940 Weinheim, 1989. – Printed in the Federal Republic of Germany by Konrad Triltsch, Druck- und Verlagsanstalt Würzburg.

All rights reserved (including those of translation into foreign languages). No part of this issue may be reproduced in any form — by photoprint, microfilm, or any other means — nor transmitted or translated into a machine language without written permission from the publishers. Only single copies of contributions, or parts thereof, may be made for personal use. This journal was carefully produced in all its parts. Nevertheless, authors, editors and publisher do not warrant the information contained therein to be free of errors. Readers are advised to keep in mind that statements, data, illustrations, procedural details or other items may inadvertently be inaccurate.

Valid for users in the USA: The appearance of the code at the bottom of the first page of an article (serial) indicates the copyright owner's consent that copies of the article may be made for personal or internal use, or for the personal or internal use of specific clients. This consent is given on the condition, however, that the copier pay stated per-copy fee through the Copyright Clearance Center, Inc. (CCC), for copying beyond that permitted by Sections 107 or 108 of the U.S. Copyright Law. This consent does not extend to other kinds of copying, such as copying, for general distribution, for advertising or promotional purposes, for creating new collective works, or for resale. For copying from back volumes of this journal see 'Permissions to Photo-Copy: Publisher's Fee List' of the CCC.

Editorial office: Postfach 10 11 61, D-6490 Weinheim, Federal Republic of Germany, Telephone (06201) 60 22 55, Telex 465 516 vchwh d, Telefax (06201) 602 328.

Editor: *Peter Gölitz*

Associate editors: *D. J. Loewus, A. Stimson.* **Editorial assistant:** *E. Schweikart*

Publishers: VCH Verlagsgesellschaft mbH. (Managing Director: *Hans Dirk Köhler*), Pappelallee 3, D-6940 Weinheim, Federal Republic of Germany.

Advertising office (Advertising Manager *R. J. Roth*): Postfach 10 11 61, D-6940 Weinheim, Federal Republic of Germany. Telephone (0 62 01) 60 61 30, Telex 4 67 155, Telefax (0 62 01) 606 184.

ADVANCED MATERIALS

Generation of Complex Metal Oxides by Aerosol Processes: Superconducting Ceramic Particles and Films

Aerosol Decomposition
Superconducting Films
Oxygen Diffusion
Ferroelectric Ceramics
Ferrimagnetic Ceramics
Powder Generation

By Toivo T. Kodas*

Complex metal oxides, including ferroelectric, ferrimagnetic and superconducting ceramics, have a variety of technologically useful properties that can be exploited for a number of applications. Fabrication of complex metal oxide ceramics with specific properties requires high-purity powders with controlled chemical compositions, size distributions, and morphologies. Powders with these characteristics can be produced by aerosol processes in which fine particles are generated in gaseous flow systems. The particles can also be deposited from the gas phase onto surfaces to form films. This paper will discuss the use of aerosol processes for the generation of complex metal oxide powders. A review of aerosol processes will be presented first, followed by a discussion of the methods used for the generation of superconducting ceramic powders. Examples include the production of $YBa_2Cu_3O_7$, $La_{1.85}Sr_{0.15}CuO_4$, and Tl-Ca-Ba-Cu-O powders and films. Emphasis will be placed on defining the conditions required for the generation of chemically homogeneous particles with controlled morphologies.

1. Introduction

The fabrication of complex metal oxides with specific electrical, magnetic, optical and superconductor properties begins with molecular precursors which must be transformed into the product film or part. A versatile class of methods for accomplishing this transformation is aerosol processes. The term aerosol process is used here to describe systems in which particles are formed in the gas phase as the result of chemical or physical processes and systems in which particles or droplets are deposited from the gas phase onto surfaces to form films. For this discussion, the terms particle and droplet will include clusters, collections of a small number of atoms or molecules in which an appreciable fraction of the atoms or molecules are at the surface.[1, 2] Table 1 lists the major types of aerosol processes that have been used for the generation of metal oxide particles and films. Systems such as laser-heated reactors[3] which have been used primarily for non-oxide ceramics are not included.

The processes in Table 1 can be grouped into gas to particle conversion, intraparticle reaction, and hybrid processes. In gas to particle conversion processes (Fig. 1) a supersaturated vapor of a condensable gaseous species is formed either as the result of chemical reactions which create new molecules[4, 5] or physical processes such as cooling which reduce the vapor pressure of the condensable species.[6] At a sufficiently high supersaturation, new particle formation occurs by homogeneous nucleation. Nucleation is followed by particle growth, and for sufficiently high particle concentrations, by coagulation and agglomeration. Gas to particle conversion processes can be coupled with particle deposition from the gas phase to provide methods for film fabrication.[7] Particle deposition from the gas phase onto surfaces can take place by mechanisms including impaction, thermophoresis, and diffusion.[8–10]

In intraparticle reaction processes, often called spray pyrolysis, evaporative decomposition, spray roasting or aero-

Table 1. Aerosol processes for the generation of metal oxide powders and films.

Films	Powders
1. Gas to particle conversion	
1.1 Physically induced processes	
Ionized cluster beam [75–82]	Supercritical fluid expansion [83, 84]
Supercritical fluid expansion [83, 84]	Condensation processes [85–87]
1.2 Chemical Reaction Processes	
Laser evaporation/deposition [88–91]	Flame reactors [92–96]
Heated-wall reactors [12]	Heated-wall reactors [97–102]
Plasma spraying [103–105]	Plasma reactors [106–108]
2. Intraparticle Reaction	
Spray pyrolysis or pyrosol process [55, 56, 109–130]	Spray pyrolysis, evaporative decomposition, spray roasting or aerosol decomposition [43–48, 51–54, 61, 62, 131–139]
3. Hybrid processes	
	Condensation/intraparticle reaction [50, 140–145]

[*] Prof. T. T. Kodas
Center for Micro-Engineered Ceramics and
Chemical and Nuclear Engineering Department
University of New Mexico
Albuquerque, NM 87131 (USA)

ADVANCED MATERIALS

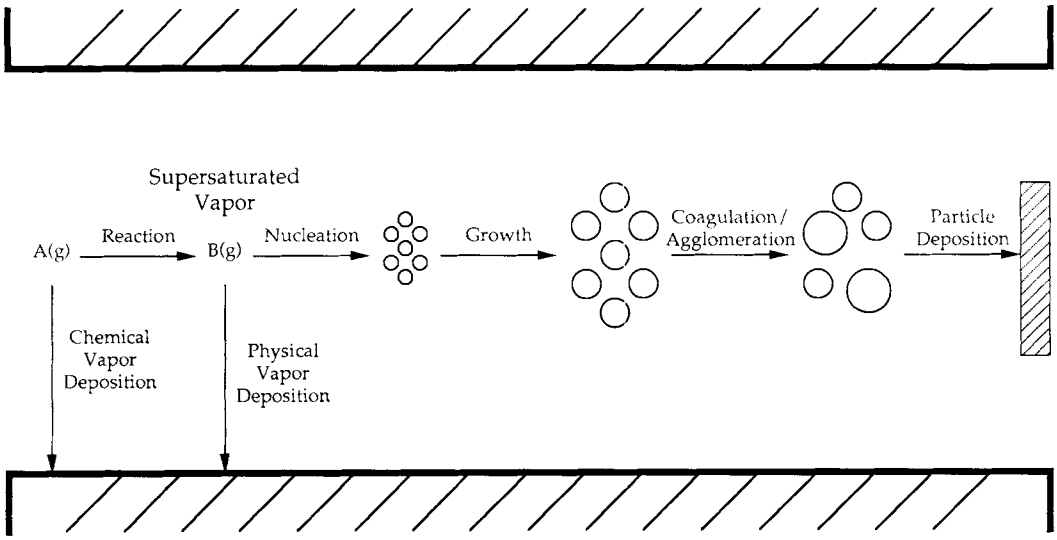


Fig. 1. Particle generation by gas to particle conversion.

sol decomposition, particles containing precursors are formed mechanically using a droplet or particle generator (Fig. 2a). The precursors in each particle are then reacted with a gaseous species or are pyrolyzed in the particulate phase to form the product. A modification of the aerosol decomposition process, spray pyrolysis (the same name as for the powder generation process), or the pyrosol process, can be used for film generation. The liquid droplets are deposited onto a heated substrate where the precursors decompose, and further heating results in the formation of the product film. One variation of this process is to first form solid particles in the gas phase, deposit them onto a substrate, and sinter them to form the solid ceramic film.[11] Another variation (Fig. 2b) is to use volatile reactants which evaporate into the gas phase and deposit materials by chemical vapor deposition. Although gas to particle conversion processes and intraparticle reaction processes provide convenient groups for classifying aerosol processes, some methods incorporate elements of both processes. For example, in the hybrid process cited in Table 1, droplets of an organometallic species can be formed by nucleation and condensational growth and then be converted to a ceramic species by intraparticle chemical reaction.

Aerosol methods have been used to produce a wide variety of metal oxide ceramics as shown in Table 2. These studies have shown that aerosol processes allow the generation of particles with a unique combination of properties that in many cases cannot be obtained by other processes. Typical properties include:

- high purity
- single-crystal or polycrystalline
- multicomponent materials
- coated/multilayer or chemically homogeneous
- porous or non-porous
- size from clusters to 5 μm
- unagglomerated, soft or hard agglomerates

An example of a process which can produce complex metal oxide powders with these characteristics, aerosol decomposition, will be discussed later.

The advantages of aerosol deposition for film fabrication include:

- high purity
- multicomponent materials
- high deposition rates

One of the best examples of a process which exploits these advantages for film formation is optical fiber production in which high-purity SiO_2 is deposited at high rates onto the inside surface of a tube which is eventually filled in and drawn into an optical waveguide.[12]

Aerosol processes for the generation of metal oxide ceramics have been used primarily for simple metal oxides and to a lesser extent for complex metal oxides containing two metallic or semiconducting species (Table 2). A smaller number of studies have examined the generation of powders containing three or more of these species. However, rapidly advancing technologies in areas such as superconductivity, electronics, solar cells, optics, and high-tech ceramics for structural applications are requiring increasingly complex materials which often contain three or more metallic or semiconducting species in addition to oxygen, nitrogen and other nonmetallic species. Examples of such materials are given in Table 3. Both powders and films with controlled chemical compositions and microstructures are required.

This paper will discuss the use of aerosol processing for the fabrication of complex metal oxide ceramic powders and films. Emphasis will be placed on the aerosol decomposition process for powder and film generation (see Tables 1 and 2) since it is the only aerosol technique that has demonstrated the ability to produce complex metal oxides. The present status of research in this area will be discussed first. Superconducting ceramic powder generation by intraparticle reac-

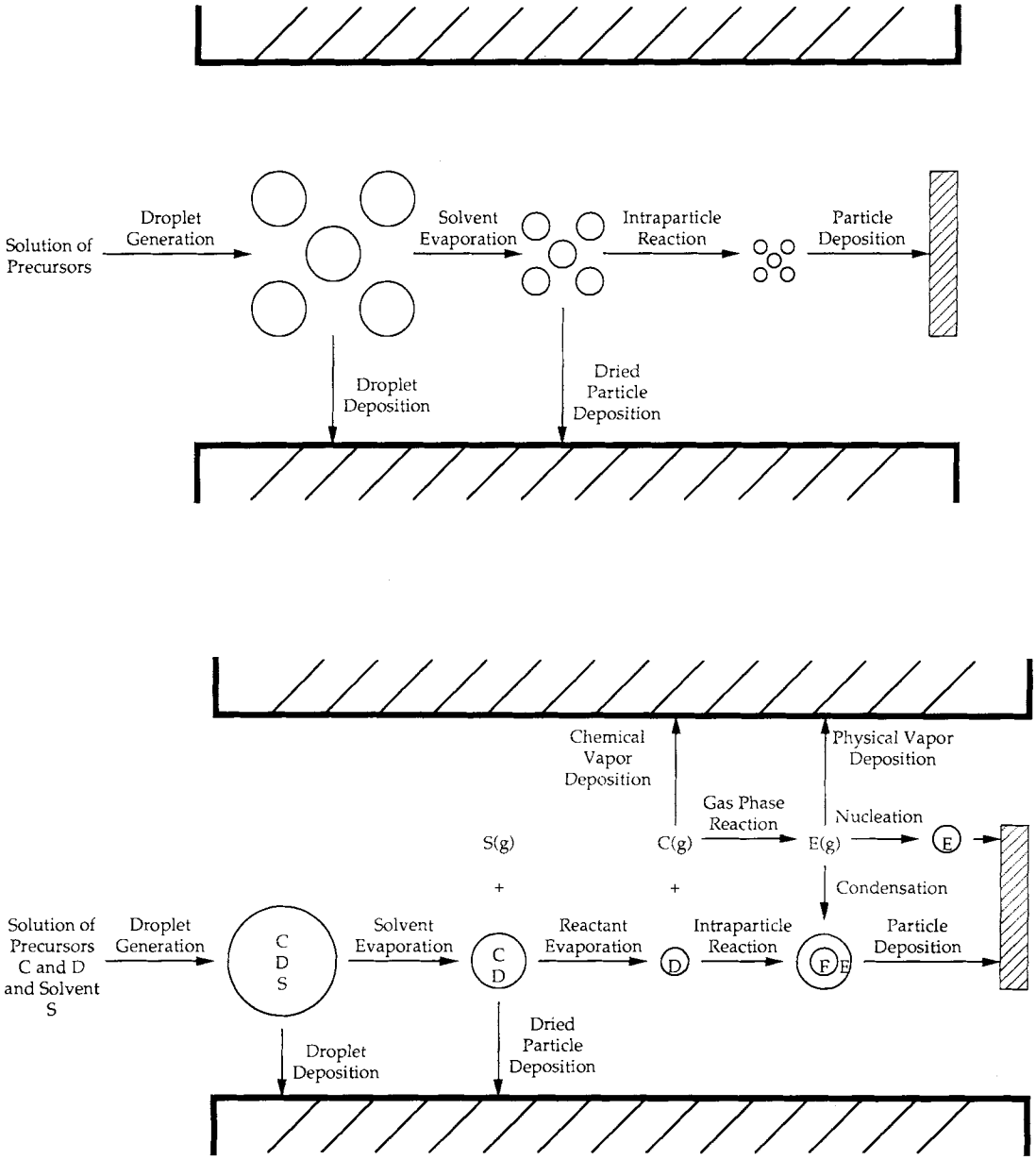


Fig. 2. Particle generation by aerosol decomposition. a) Pure intraparticle reaction and b) combined intraparticle reaction and gas to particle conversion.

tion and a combination of gas to particle conversion and intraparticle reaction will be discussed along with deposition of the particles onto surfaces to form films. New results will be presented with a review of previous work. Emphasis will be placed on describing the physical and chemical processes which control the chemical composition and morphology of complex metal oxide particles and films produced by aerosol decomposition. A goal of the paper is to identify the problems which must be solved in order to increase the range and number of applications of aerosol processes for the generation of powders and films.

2. Present Status of Research on Aerosol Processing of Complex Metal Oxides

2.1. Theory

Gas to particle conversion and intraparticle reaction methods for powder generation can involve a variety of physicochemical processes (see Figs. 1, 2a and b). These processes include:

- gas-phase chemical reactions
- single-particle chemical processes such as surface and intraparticle chemical reactions

ADVANCED MATERIALS

Table 2. Examples of metal oxides synthesized by aerosol processes.

Complex metal oxides	
Superconductors	
$YBa_2Cu_3O_7$	films [11, 74, 88–91, 116–118, 146–148] powders [11, 37–41]
Bi-Sr-Ca-Cu-O	films [57, 119, 120] powders [11]
Tl-Ca-Ba-Cu-O	powders [11]
La-Sr-Cu-O	powders [11]
Magnetic materials	
$M_xM_yFe_{3-(x+y)}O_4$	where M = Bi, Zn, Mg, Ni, Mn, films [77, 78, 109] powders [43, 52, 136]
Assorted	
$NiMn_2O_4$	powders [52]
$NiMgO_2$	powders [43]
$MgCr_2O_4$	powders [43]
$CoCr_2O_4$	powders [43]
$CaAl_2O_4$	powders [138]
$MgAl_2O_4$	powders [54]
$Gd_3Fe_5O_{12}$	films [121]
Simple metal oxides	
Al_2O_3	films [81, 111, 126, 149–151] powders [45, 53, 86, 93,96, 107, 108, 131, 138, 141, 142, 144, 145]
BeO	films [75]
CaO	powders [86]
CeO_2	powders [86]
Cr_2O_3	films [111, 115] powders [43]
Fe_2O_3	films [110, 113, 115, 122, 125, 127, 129, 130] powders [52, 96, 98, 134, 135]
Ga_2O_3	films [152]
GeO_2	films [84] powders [84, 96]
In_2O_3	films [111, 115, 123]
La_2O_3	powders [48]
MgO	powders [46, 51, 85, 86, 97, 107]
NiO	powders [52]
SiO_2	films [12, 76, 83, 84] powders [84, 86, 92, 107, 140, 145]
SnO_2	films [111, 115, 123, 128]
TiO_2	films [80, 111] powders [92, 94, 96, 101, 143, 145]
VO_x	films [96, 111, 115]
Y_2O_3	films [111]
Yb_2O_3	films [105]
ZnO	films [79, 112, 114] powders [47, 52, 62, 85]
ZrO_2	films [105, 111] powders [48, 86, 96, 100, 107, 133]

Table 3. Examples of complex metal oxides of technological importance.

Superconducting ceramics [66, 153,154]	
$M_wM_xM_yM_zO_u$ where M = Cu, Tl, Bi, Ca, Sr, Ba, Pb, Sb, Y, etc.	
Examples	
$YBa_2Cu_3O_7$	power transmission, magnets
Bi-Pb-Sr-Ca-Cu-O	electronic devices
Tl-Pb-Ca-Ba-Cu-O	
Ferroelectric ceramics [155, 156]	
$(M_wM_xM_yM_z)O_3$ where M_i = K, Zn, Nb, Fe, W, Pb, Ba, Ni, Zr, Ti, Li, Ca, Sr, Sn, Ta, etc.	
Examples	
$(Sr_{1-x}Ca_x)[(Li_{1/4}Nb_{3/4})]_{1-y}Ti_yO_3$	electric resonators
$K(Ta_xNb_{1-x})O_3$	optical oscillators
Ferrimagnetic ceramics [157]	
$M_xM_yFe_{3-x-y}O_4$ where M = Mg, Zn, Mn, Ni, etc.	
Examples	
$Mg_{1-x}Zn_xFe_2O_4$	circuit elements
Sialon ceramics [158]	
$M_x(Si, Al)_{12}(O, N)_{16}$ where M = Li, Mg, Ca, Y or rare earths	

- single-particle physical processes such as nucleation, evaporation and condensation
- multi-particle physical processes such as coagulation and agglomeration
- mass transport including diffusion and deposition of gases and particles
- heat and momentum transport leading to nonuniform velocity and temperature fields
- effects associated with plasmas, photons, electric fields, supercritical fluids, and other complicating features

The processes which occur depend on the mode of aerosol reactor operation. One of the simplest cases, aerosol decomposition, can involve only intraparticle chemical reactions for particles in nonuniform temperature and velocity fields (Fig. 2a). Gas to particle conversion processes can, however, involve many of the processes mentioned above (Fig. 1). Similarly, aerosol decomposition processes with one or more volatile species (Fig. 2b) can involve many of these processes. Because of this variety of processes that can occur, a complete understanding of aerosol methods for film and particle generation will only be obtained by an interdisciplinary approach.

A large number of studies have theoretically examined the behavior of aerosol processes for film and particle generation. However, few have studied the behavior of multicomponent systems. Fortunately, many of the results from single-component systems can be used to understand qualitatively the behavior of the more complicated multicomponent systems. Models for single-component systems incorporating gas phase reaction, particle formation and growth, nonuniform velocity profiles and diffusion of gaseous reactants and products in flow systems have been developed.[13–23] The added complexities of coagulation and transport of particles have also been added to these models.[24–25] The aerosol dynamics in well-mixed systems (continuously stirred tank reactor) with exponential residence time distributions have been examined,[26,27] and the roles of particle nucleation, growth and coagulation in determining particle characteristics have been studied in detail.[28–35,99] These and other studies have provided a basis for the understanding of the aerosol dynamics in a variety of systems for powder and film generation.

2.2. Experimental Results

The only aerosol method that has demonstrated the ability to produce chemically homogeneous complex metal oxides, including superconducting ceramics,[11,36–41] is aerosol decomposition. The powder generation process begins by pass-

ing a solution of precursors through an aerosol generator to form fine droplets.[42] The droplets are then passed through a furnace where chemical reactions convert the precursors to the product powder which is then collected on a filter.

This process has several advantages over gas to particle conversion processes for the generation of multicomponent materials. Particles with a uniform chemical composition can be produced in many cases since the precursors are present in the correct stoichiometry in each droplet produced by the aerosol generator. Volatile precursors are not required; thus, a wide variety of reactants can be used while avoiding the need for carbon-containing precursors. Gas to particle conversion or nucleation processes have not been successful in producing multicomponent materials due primarily to difficulties in controlling the nucleation process when several species are involved (see section 3.2.2). In contrast, aerosol decomposition processes can produce multicomponent materials. The generation of multicomponent ceramic powders can be carried out on an industrial scale using only a few unit operations; the ability to scale up these systems for production of ton-quantities of conventional ceramic oxide powders has already been demonstrated.[43, 44]

The morphology of particles produced by aerosol decomposition strongly influences the properties of ceramics produced by sintering the particles. The primary difficulty with the intraparticle reaction route for powder generation has been that in most cases porous polycrystalline particles have been formed.[43–48] This morphology can lead to difficulties in sintering to near-theoretical density, a crucial problem for superconducting ceramics where porosity can lead to degraded superconductor and mechanical properties.

The morphology of the particles depends on a variety of physicochemical processes including reactant crystallization in the particle during solvent evaporation, chemical reaction in the particles, and transport of gaseous reactants and products into and out of the particles. Few studies have examined how solvent evaporation influences the final particle morphology. Conditions leading to solid particles during evaporation are believed to be a nuclei-free system, high solute solubility, low drying rates and low relative humidities.[49] The rate of intraparticle reaction of water vapor with metal alkoxide droplets has been measured optically, but little information about particle morphology was reported.[50]

A variety of precursors have been used for the generation of ceramic powders by aerosol decomposition. They include chlorides, oxalates, lactates, citrates, nitrates, acetates, alkoxides, sulfates and acetylacetonates (Table 2). However, only a few studies have examined the role of the precursors in determining the morphology of particles produced by spray pyrolysis. The difference between using nitrate, chloride and acetate salts of Mg as precursors for MgO generation has been examined.[46, 51] The acetate gave dispersed particles while the nitrate and chloride gave large aggregates. A similar study was carried out for ZnO, NiO, $NiMn_2O_4$, $ZnFe_2O_3$, and Fe_2O_3 generation from the nitrate and acetate salts. The acetates gave powders ranging from hard aggregates to fine unagglomerated particles while the nitrates gave hard agglomerates under all conditions.[52] However, unagglomerated $YBa_2Cu_3O_7$ particles have been obtained by aerosol decomposition using the nitrates.[36–41] Little information is available for other precursors.

The processing of powders produced by aerosol decomposition has been investigated only in a few studies. Examples include processing of Al_2O_3 to form 96% dense ceramic[45, 53] and $MgAl_2O_4$ to form 93% dense material.[54] The processing of most other powders produced by aerosol techniques (see Table 2) has not been investigated. Further work is required to characterize the powders and to study the fabrication of ceramics using these powders.

Films of many materials have been deposited by spray pyrolysis (see reviews[55, 56] and Table 2). The gas phase processes occurring during film generation are similar to those occurring during powder generation by spray pyrolysis (Figs. 2a and b). As for powder generation, few studies have used modern aerosol techniques to determine how the properties of the films can be improved by controlling the droplet size distribution, reactor design and operating conditions. Instead, the large majority of these studies have concentrated on characterizing the electrical, optical, and magnetic properties of simple metal oxide films.

Deposition of particles from the gas phase onto surfaces followed by sintering has been used for many years for the fabrication of optical waveguides.[12] However, this process has only recently been exploited for the generation of films of materials other than SiO_2. An example is the formation of thick films of superconducting ceramics by the deposition of superconducting ceramic particles formed by aerosol decomposition[11] (see section 3.5). Advantages of the process include in situ formation of films while minimizing exposure to contaminants, adaptability to different chemical systems, and the integration of materials synthesis and processing steps. A modification of this process has been used to produce Bi-Sr-Ca-Cu-O films.[57] Amorphous particles generated by a non-aerosol process were entrained in a carrier gas to form an aerosol and then deposited from the gas phase onto heated surfaces to form crystalline films. Films have also been generated by simultaneous deposition of particles and vapor from the gas phase. Deposition rates were orders of magnitude higher than those achieved by conventional chemical vapor deposition processes.[7]

3. Generation of Superconducting Ceramics by Aerosol Decomposition

Typical superconducting ceramics contain three or more metallic species and oxygen. Examples include Bi-Pb-Sr-Ca-Cu-O, Tl-Pb-Ca-Ba-Cu-O and Y-Ba-Cu-O. The motivation behind using aerosol processes for superconducting powder generation is the need for high-purity multi-component powder composed of unagglomerated particles with a uni-

form chemical composition and controlled size distribution,[58-60] characteristics which can only be obtained by aerosol decomposition. No other aerosol methods have demonstrated the ability to produce complex metal oxide powders with these characteristics. A further motivation for studies of these materials is that, because of the large number and variety of species involved, they are excellent model systems for studies of the generation of other ceramic powders by aerosol processes (Table 3).

3.1. Experimental

Powders were generated by the following method. Metal-containing species were dissolved in a solvent and passed through an aerosol droplet generator to form micron-sized solution droplets. Aqueous solutions of the nitrate salts of the metals are used to minimize carbon contamination from either the solvent or precursors. The droplets were then passed through a furnace where chemical reaction took place to convert the reactants to the product powder. Average residence times were typically 1 to 25 seconds with temperatures of 800–1200 °C. The powders were collected on silver-membrane filters to minimize contamination. Powders based on the $YBa_2Cu_3O_7$, $La_{2-x}Sr_xCuO_4$, Bi-Sr-Ca-Cu-O, and Tl-Ca-Ba-Cu-O systems have been generated by this technique.[11, 36-41]

3.2. Mechanism of Particle Formation

The process of forming ceramic particles by aerosol decomposition can be viewed in the simplest case as the drying of droplets followed by solid and liquid phase chemical reactions in a microreactor (the particle) suspended in a gas to form the product. However, the actual behavior of the system is in many cases more complicated. The microreactor can exhibit two types of behavior which are determined by the nature of the species transported into the gas phase. If only nonmetallic species (O_2, CO, CO_2, NO, NO_2) are transported across the particle/gas interface, only intraparticle and surface reactions occur, and the product stoichiometry can be precisely controlled during mixing of the precursor solution (Fig. 2a). As will be shown, samples of $YBa_2Cu_3O_7$ and $La_{1.85}Sr_{0.15}CuO_4$ formed from the metal nitrates exhibit this type of behavior. If metal-containing species are exchanged across the interface, gas phase, surface and intraparticle chemical reactions can occur. In this case, control of the stoichiometry and phase purity becomes far more difficult than for the case of a purely intraparticle reaction. An example of a system exhibiting this type of behavior is the formation of Tl-Ca-Ba-Cu-O from the metal nitrates where volatile Tl-containing species are transported across the particle/gas interface.

3.2.1. Intraparticle Reaction: $YBa_2Cu_3O_7$ and $La_{1.85}Sr_{0.15}CuO_4$

In the purely intraparticle reaction mode where only gaseous species are transported across the particle/gas interface (Fig. 2a) the solvent evaporates from the droplets formed by the aerosol generator followed by nucleation of the metal salts in the particle to form one or more solid phases. This is followed at higher temperatures by decomposition of the metal salts in the particles to form reaction intermediates. As the reaction proceeds, these intermediates diffuse together and react to form the final product. Since no metal-containing species leave the particles, the spread of the particle size distribution is limited by the spread of the size distribution of the droplets formed by the aerosol generator. Thus, nearly monodispersed particles can be produced by using ultrasonic droplet generators.[38, 40, 41]

The intraparticle reaction mode occurs during formation of $YBa_2Cu_3O_7$ by decomposition of metal nitrates. The melting points of the oxides of Cu, Y, and Ba (1326–2410 °C) are far above the typical reactor operating temperature (900–1000 °C); thus, evaporation of the oxides does not occur. Similarly, no evidence of evaporation of any of the nitrate species or reaction intermediates was found by examination of the powders by transmission electron microscopy (TEM) electron diffraction, X-ray diffraction, and wet chemical analysis of the composition of the powders. Since the Y, Ba, and Cu are confined to the particles, it is possible to form $YBa_2Cu_3O_7$ particles (Fig. 3) with the following characteristics:[36, 37]

- Completely reacted (thermogravimetric analysis (TGA))
- Single phase (X-ray diffraction (XRD))
- Superconducting with $T_c > 90$ K (magnetic susceptibility)

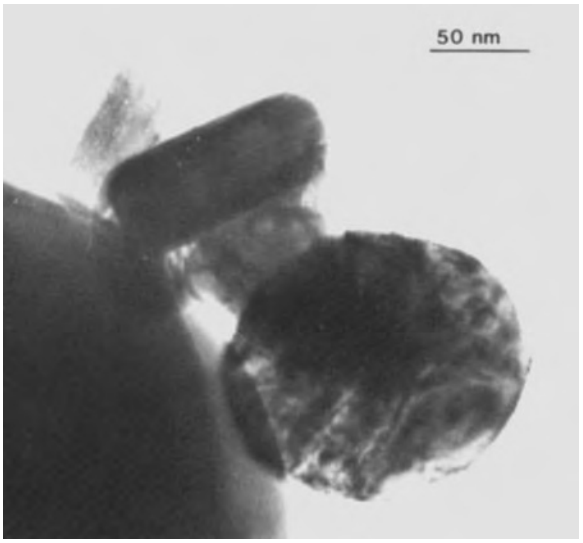


Fig. 3. Single-crystal $YBa_2Cu_3O_7$ particles generated by aerosol decomposition at 1000 °C.

- Single-crystal particles (electron diffraction)
- Uniform composition from particle to particle (energy dispersive spectroscopy (EDS))
- Solid particles (TEM and Brunauer, Emmett, Teller (BET) surface area measurements)
- Fully oxygenated (iodometric titration)
- 1:2:3 ratio of Y:Ba:Cu (wet chemical analysis)
- Equiaxed and spherical shapes

Similar results were obtained for the $La_{1.85}Sr_{0.15}CuO_4$ system. The X-ray diffraction pattern for the powder generated by aerosol decomposition of the nitrates at 1100 °C is shown in Figure 4. TGA showed that the material was fully reacted. Sintered and annealed material had a T_c at approximately 35 K.

Although $YBa_2Cu_3O_7$ and $La_{1.85}Sr_{0.15}CuO_4$ particles with a uniform chemical composition can be formed, cases exist where intraparticle reaction leads to chemically nonuniform particles. One example is the formation of $YFeO_3$ and Fe_2O_3 instead of yttrium-iron garnet ($Y_3Fe_5O_{12}$) during intraparticle reaction of the sulfates of yttrium and iron at 1000 °C. The preferential formation of the $YFeO_3$ and Fe_2O_3 was attributed to fast nucleation of the $YFeO_3$ phase.[61] Another example of the formation of multiphase materials by aerosol decomposition is the generation of Bi-Sr-Ca-Cu-O powders by reaction of the nitrates. Experiments under conditions which produced single phase $YBa_2Cu_3O_7$ and $La_{1.85}Sr_{0.15}CuO_4$ produced only multiphase Bi-Sr-Ca-Cu-O particles. In this case, both thermodynamic and kinetic limitations may have been responsible for the multiphase material.

3.2.2. Combined Intraparticle Reaction and Gas to Particle Conversion: Tl-Ca-Ba-Cu-O

Spray pyrolysis systems for powder generation can also be operated under conditions where both intraparticle reaction and gas-to-particle conversion occur (Fig. 2b). Gas to particle conversion can occur if one or more of the precursors (C and D), reaction intermediates, or reaction products (E and F) are transported across the particle/gas interface. The precursors or reaction intermediates in the gas phase (C) can react to form products which may be the same as or different from the products of intraparticle reaction (E). Any of the gaseous species, either after being formed by chemical reaction in the gas phase or during cooling while exiting the reactor, may condense on the walls of the system, condense on the particles from which they evaporated, or nucleate homogeneously to form new particles. These types of behavior have been observed during the operation of single and multicomponent systems. Zinc acetate evaporation, gas phase chemical reaction and nucleation to form ZnO has been observed during ZnO particle formation,[47, 62] and Na_2O loss has been observed during generation of powders containing Na, Mg and Al by spray pyrolysis.[53]

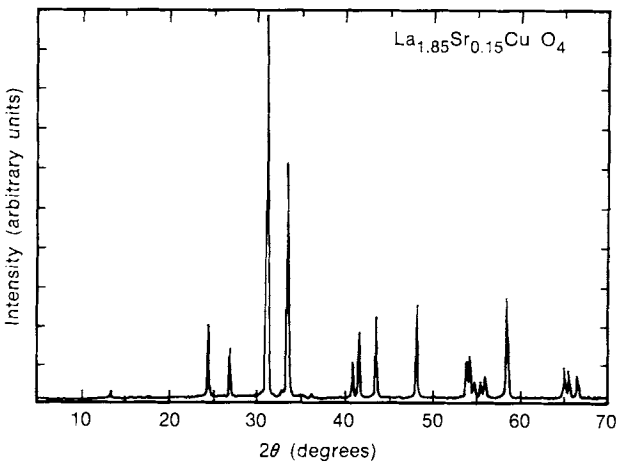


Fig. 4. X-Ray diffraction pattern for $La_{1.85}Sr_{0.15}CuO_4$ generated by aerosol decomposition at 1100 °C showing single-phase material.

The physicochemical processes shown in Figure 2b influence the properties of the product powders and hence the properties of ceramics produced from the powders. Total condensation onto the existing particles (particles of F coated with E) restores the initial stoichiometry, but only in a volume average sense; the particles are no longer chemically homogeneous and consist of a multicomponent core covered by a single-component layer of the condensed material. Homogeneous nucleation to form new particles (E) without condensation on the walls again conserves the composition of the powders averaged over the total particle volume. However, the powder consists of fine particles of one material (E) mixed with larger particles of E and F which are now depleted in the volatile species (E). Condensation on the walls results in a change in the volume average composition of the powder. Since the fraction of the volatile species remaining in the particles is difficult to control, this situation is usually the least desirable of the possibilities. Fortunately, wall losses can be eliminated by appropriate design and operation of the reactor. Studies of gas to particle conversion in tubular flow reactors suggest that rapid cooling rates which lead to high saturation ratios will result in new particle formation.[13–21] Slow cooling rates allow condensation on the particles and walls since the saturation ratio can be kept below the critical value for particle formation. The relative amounts of condensation on the walls and particles are controlled mainly by the surface area of the preexisting particles and the reactor radius. Larger aerosol surface areas and larger reactors favor condensation onto existing particles.

Experiments at a variety of temperatures and reactor residence times showed that aerosol decomposition of the Tl, Ca, Ba, and Cu nitrates resulted in particle generation by a combination of intraparticle reaction and evaporation/condensation. X-ray diffraction of collected powders showed only peaks corresponding to Tl_2O_3 (Fig. 5). TEM, EDS and electron diffraction analysis of the powders, however, showed that the Ca, Ba and Cu were present mainly in an

ADVANCED MATERIALS

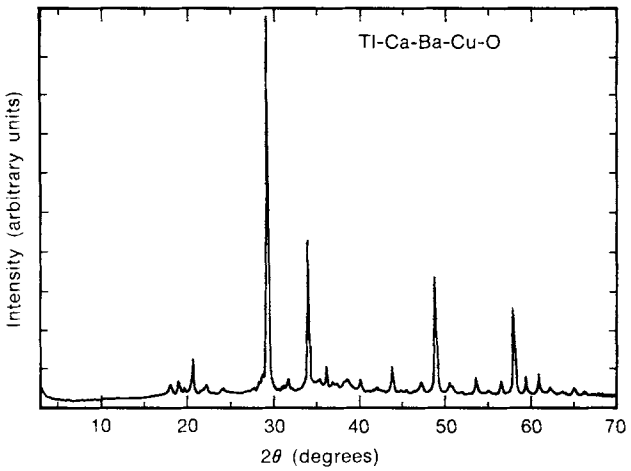


Fig. 5. X-Ray diffraction pattern corresponding to Tl_2O_3 for powder generated by aerosol decomposition of Tl, Ca, Ba, and Cu nitrates. Ba, Ca and Cu are present mainly as amorphous material.

amorphous form with the Tl present in a crystalline oxide form on the surfaces of the particles (Fig. 6). Wet chemical analysis of collected powders showed that all the species were present in the appropriate ratios, except for Tl whose concentration was reduced by up to 50%. The observed Tl loss from the particles was consistent with the observation of a coating on the walls of the system. The coated particles (depleted of Tl by 50%) could be sintered to produce Tl-Ca-Ba-Cu-O ceramics showing zero resistance at 110 K (onset at 125 K) (Fig. 7).

These results can be explained by the high volatility of the Tl-containing species. Under typical conditions, Tl nitrates, Tl_2O_3 and Tl_2O evaporate into the gas phase resulting in loss of Tl from the particles. Because of the high vapor pressure of the Tl_2O (roughly 500 Torr at 1000 °C),[63] the Tl exists mainly in the gas phase until cooling while exiting the reactor where the Tl-containing species condense and coat the existing particles. The particles are not superconducting as produced since the Tl was not in contact with the Ba, Ca and Cu at the temperature required for formation of any of the superconducting phases. However, EDS analysis suggested that the Ca, Ba and Cu in each particle were well-mixed. Since the mobilities of Tl species are high at typical processing temperatures, Tl-coated Bi-Sr-Ca-O particles may provide a beneficial route for formation of this particular class of superconducting ceramics.

In the case where two or more species enter the gas phase, a multicomponent nucleation/condensation problem can occur. This may take place for superconductors containing Tl and Pb[64] in which two components have significant vapor pressures under typical operating conditions (approximately 1 Torr for PbO and 500 Torr for Tl_2O at 1000 °C)[63] or for systems in which two or more precursors have significant vapor pressures under the operating conditions. This type of system has not been studied extensively, but useful information can be obtained from studies of the behavior of single-component aerosol flow reactors relying on gas-to-particle conversion.[13-35] This work and that by other investigators has shown that the aerosol dynamics depend strongly on the rate of formation, surface energy, and vapor pressure of the condensing species. These parameters are usually different

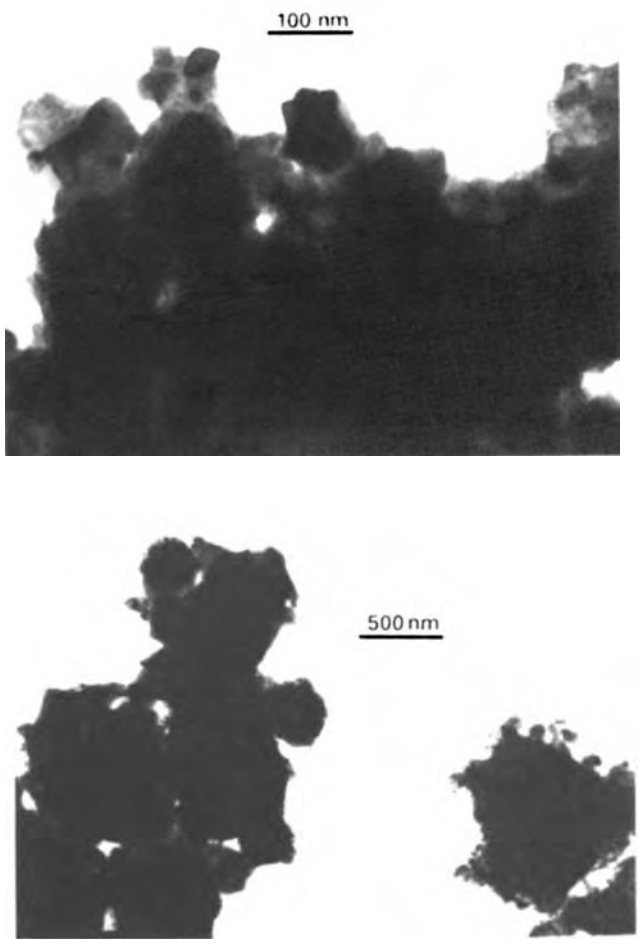


Fig. 6. Powder generated by aerosol decomposition of Tl, Ca, Ba, and Cu in 2:2:2:3 ratio. Energy dispersive spectroscopy showed the presence of Tl-containing crystallites on the surface of the particles.

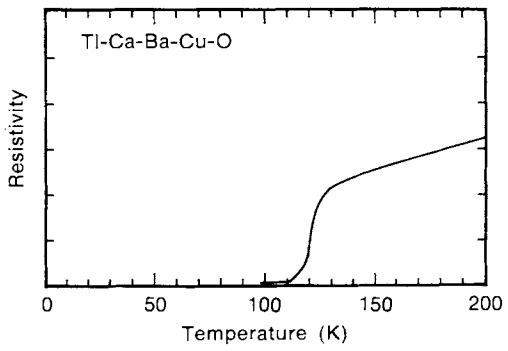


Fig. 7. Resistivity as function of temperature for sample generated by sintering aerosol powder with Tl:Ca:Ba:Cu ratio of 1:2:2:3.

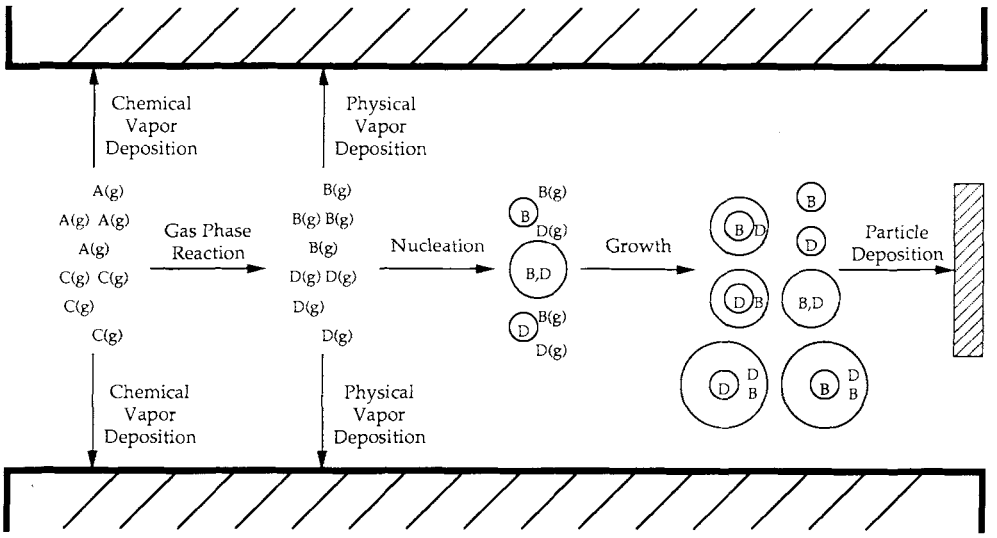


Fig. 8. Physicochemical processes occurring during a two component reaction/nucleation/condensation process.

for each species resulting in unequal nucleation rates and unequal condensation rates on existing particles and walls. Thus, simultaneous condensation to form chemically homogeneous particles is difficult to achieve. Instead, nucleation of separate particles of each species can occur.

Figure 8 shows some of the processes that can occur for two reactant species in the gas phase in the absence of existing particles. The situation in the presence of existing particles, as would be the case for aerosol decomposition, is even more complicated. Particles of one product (B), the other product (D) and a mixture of both products (B and D) may be formed by homogeneous nucleation. These species may grow by addition of B and D from the vapor phase. Many particle compositions and morphologies are possible: uniform mixtures of B and D, pure B, pure D, B coated with D, D coated with B, and other combinations.

The result of the processes outlined above is particles with a broad size distribution, a nonuniform distribution of chemical species with respect to particle size, and a nonuniform chemical composition within each particle. The spread of the size distribution and the distribution of the various chemical species with respect to particle size strongly influence the properties of superconducting ceramics obtained by processing the powders. Broad particle size distributions can lead to difficulties in obtaining high density material. Nonuniform chemical composition within a particle and from particle to particle leads to inhomogeneous material resulting in degraded superconductor properties. Thus, research is required to determine if the nucleation process can be controlled to provide particles with predetermined compositions: for example, a uniform mixture of B and D or particles of one species coated with the other species.

3.2.3. Implications For Other Systems

Although the previous sections discussed superconducting ceramic powder generation by intraparticle chemical reaction and a combination of intraparticle chemical reaction and gas to particle conversion, the results have implications for other systems where particles containing superconducting ceramics or their precursors are formed or suspended in a gas at high temperatures. Examples (Table 1) of such processes include plasma spraying, flame spraying and spray pyrolysis systems for film generation and plasma reactors, flame reactors, and electrohydrodynamic atomization[65] for powder production.

Because of the small particle dimensions involved, transport processes for individual particles in the gas phase can occur extremely rapidly. In general, transport of a reactant, intermediate or product to or from the interior of an aerosol particle consists of three steps, gas phase transport, interfacial processes including adsorption and chemical reaction and transport in the particle.[8-10] The time needed for the gas phase concentration profile around an aerosol particle to achieve a steady state for typical conditions is in the order of microseconds or less for a 1 μm particle. The time to reach interfacial equilibrium is a function of the operating conditions, but can be rapid compared to the characteristic time for solid state diffusion.[8] Thus, the time required for a volatile species to evaporate from a particle or for a species such as oxygen to diffuse into a particle can be controlled by the rate of diffusion in the solid or liquid particle. Further generalizations are difficult, however, because diffusion coefficients in liquids and solids vary tremendously with changes in temperature and composition.

An estimate of the time required for complete evaporation of a species from a particle can be made for the Tl-containing ceramics. If gase phase transport and interfacial processes are rapid, the time depends on the diffusion coefficient of the Tl-containing species in the particle. A diffusion coefficient of 10^{-8} cm^2/sec will allow complete evaporation in roughly 1 second for a 1 μm particle. Thus, if the particle's residence time at the elevated temperatures is greater than 1 second, complete evaporation can occur. In the case of plasma spray or flame spray processes, the heating of Tl-containing particles may result in the loss of Tl from the particles and subsequent segregation of Tl from the other species. A similar situation may occur during spray pyrolysis for film generation. As a droplet is transported to the substrate it is heated, and Tl-containing species may evaporate into the gas phase. Since deposition rates for particles and gaseous species can differ greatly,[22] this mechanism can lead to the incorrect stoichiometry in the deposited films.

3.3. Control of Particle Morphology and Phase Purity

Although most previous studies of particle formation from the nitrates have produced porous particles,[45–48] single-crystal $YBa_2Cu_3O_7$ particles (Fig. 3) can be formed from the nitrates by aerosol decomposition at temperatures near 1000 °C.[39] Single-crystal particle formation is favored by operating at reactor temperatures near the melting point of the material being formed. Thus, operation at lower temperatures can result in porous polycrystalline particles.[39] Other conditions that favor single-crystal particle formation include long residence times and small particle diameters which allow diffusion and reaction in each particle to form solid particles.

Particle formation proceeds as follows. Water droplets containing the nitrate salts of the metals enter the heated reactor where the water evaporates to form porous particles. As the temperature increases, the metal salts decompose to yield porous particles composed of the metal oxides. As the particles are heated further, the metal oxides react and nucleate to form a crystallite of the superconducting phase at a temperature near its metling point. Because of the high temperature relative to the melting point and the short diffusion distances involved, diffusion of the species in the particle to the crystallite results in a collapse of the porous particle to form a solid particle and complete mixing of the various species to form the product. Alternatively, the particle may start as a polycrystalline entity and the preferential growth of one crystallite at the expense of the other crystallites may lead to single-crystal particles.

Materials generation by chemical reaction in a microreactor (each particle) has one major advantage over bulk solid state chemical reaction. In bulk solid state reaction processes, liquid phases that form can percolate through the material resulting in macroscopic segregation. Further heating results only in further aggregation. In contrast, any liquid phases formed during reaction in a particle suspended in a gas are confined to the particle. Since the liquid phase cannot leave the micron-sized particle, macroscopic aggregation of species cannot occur. Thus, the thermodynamically favored product can eventually be formed even when prior melting of the reactants, intermediates or products has occurred.

3.4. Oxygen Diffusion in Single-Crystal $YBa_2Cu_3O_7$ Aerosol Particles

Intraparticle mass transport processes play a critical role in determining the properties of superconducting ceramics. As discussed earlier for the Tl-Ca-Ba-Cu-O system, these processes determine whether or not chemically homogeneous material is obtained. These transport processes can also control the oxygen content of superconducting ceramics. $YBa_2Cu_3O_{7-x}$ formed at temperatures of 900–1000 °C is not a superconductor and must be annealed in oxygen at temperatures of the order of 500 °C to allow the oxygen to diffuse into the material and convert it to the superconductor.[66] Previous methods for the measurement of oxygen diffusion coefficients in $YBa_2Cu_3O_{7-x}$ have examined sintered and annealed material.[67–70] In general, diffusion in sintered ceramics can proceed by several mechanisms including bulk, surface and grain boundary diffusion. Thus, the apparent diffusion coefficient depends in a complicated way on the concentration and distribution of impurities, the structure of grain boundaries and the density of the sintered ceramic part. The relative importance of these different diffusion mechanisms could be sorted out if bulk diffusion coefficients were available.

Bulk diffusion coefficients for oxygen in $YBa_2Cu_3O_{7-x}$ can be obtained by measuring the time required to oxygenate equiaxed single-crystal aerosol particles of known size suspended in oxygen. A temperature-averaged diffusion coefficient was obtained from experiments in which the size of the particles, their oxygen content after being cooled to roughly 100 °C, and the temperature/time history of the particles were measured.[71] Titration measurements[72] gave an oxygen content of $7.04 \pm .03$ for the $YBa_2Cu_3O_{7-x}$ powder indicating that the particles were fully oxygenated. XRD and TGA also showed that the powder was fully oxygenated. Oxygenation of the powder is limited by the time needed for oxygen to diffuse into the largest particles. This time is of the order of r_p^2/D where r_p is the radius of the largest particles and D is the diffusion coefficient of oxygen in $YBa_2Cu_3O_{7-x}$ averaged over the temperature range where diffusion took place.[73] The largest particle radius observed was roughly 1 μm. The time the particles spent cooling from 1000 °C to 100 °C was less than 10 seconds. Thus, the temperature averaged diffusion coefficient was roughly 10^{-9} cm^2/sec. The primary advantage of this method is the ability to measure diffusion coefficients for

single crystals in the absence of grain boundary effects and impurities. Further work is necessary to obtain diffusion coefficients as a function of temperature.

3.5. Thick Film Formation by Aerosol Deposition

Aerosol deposition has been used extensively for the generation of optical waveguides.[112] The formation of thick films of other materials has been investigated only in a few cases. This section will discuss recent results for the formation of thick $YBa_2Cu_3O_7$ films by aerosol deposition.

The fabrication of superconductor/metal wires and tapes with high critical current densities is complicated by difficulties in eliminating impurities such as carbon and obtaining the correct oxygen content in the superconductor. These problems can be minimized by producing high-purity $YBa_2Cu_3O_7$ particles in a gaseous flow system as described earlier, depositing the particles directly from the gas phase onto surfaces by thermophoresis, and then sintering and annealing the deposited particulate films in an oxygen flow to form thick superconducting coatings.[111] Copper tubes with uniform, adherent coatings on their inside surfaces were produced. The coatings showed sharp superconducting transitions above 91 K and critical current densities (J_c) of roughly 100 A cm^{-2}. Advantages of the process include the ease of obtaining the correct oxygen content in the superconductor (since oxygen can be passed through the center of the tube) and the ability to fabricate wires and tapes with arbitrary shapes. A similar process has been used to produce thick Bi-Sr-Ca-Cu-O films with J_c of 8000 A cm^{-2}.[74] Further work is necessary to improve the J_c values and to investigate the formation of thick films on other types of substrates.

4. Summary and Conclusions

The most successful aerosol process for generation of complex metal oxides is aerosol decomposition without transport of metal-containing species across the particle/gas interface. This process has demonstrated the ability to produce $YBa_2Cu_3O_7$ and $La_{1.85}Sr_{0.15}CuO_4$ particles with the following properties:

- Single-crystal
- Fully oxygenated
- Single phase
- Superconducting as produced with $T_c > 90$ K
- Equiaxed and spherical shape
- Uniform chemical composition

An advantage of carrying out materials synthesis in a micron-sized reactor (an aerosol particle) is that segregation is minimized since any liquid phases formed cannot leave the particle. This can be contrasted with bulk processes where macroscopic segregation of species can occur when liquid phases are formed.

Aerosol decomposition can also be carried out under conditions for which metal-containing species can be transported across the particle/gas interface. This can result in the formation of new particles, vapor wall losses, and condensation on existing particles. An example of this mode of reactor operation for superconducting ceramics is generation of Tl-containing powders. In this case, Tl-Ca-Ba-Cu-O particles with a nonuniform chemical composition and a nonuniform distribution of Tl with respect to particle size are obtained. In addition, the particles are not superconducting as produced. However, the particles which consist of a core containing Ca, Ba, and Cu coated with Tl oxides can be processed to produce bulk superconducting ceramics. Thus, the Tl-coated particles provide a useful starting point for the fabrication of bulk ceramics.

Superconducting ceramic aerosol particles can also be exploited for measurements of properties as a function of particle size and for film formation. Oxygen diffusion coefficients can be measured in single-crystal aerosol particles to provide values of bulk diffusion coefficients in the absence of the effects of grain boundary diffusion. Thick superconducting ceramic films can be formed by depositing particles directly from the gas phase onto surfaces.

5. Future Trends

With respect to the general problem of forming complex metal oxides, including superconductors and ferroelectric and ferrimagnetic materials, some of the open questions are as follows:

- For aerosol scientists: How do evaporation, reaction, condensation and nucleation of volatile precursors, reaction intermediates and reaction products influence the chemical composition and morphology of the particles and films?
- For chemists: How can the chemical composition and morphology of particles of existing materials be improved by developing novel precursors? What new materials can be generated using novel precursors?
- For chemical engineers: How do transport processes on a micron-scale such as solvent evaporation, intraparticle transport and intraparticle chemical reaction and heat and mass transport on a reactor-scale influence the morphology and chemical composition of the particles?
- For materials scientists and physicists: What changes in the properties of the powders must be made to

ADVANCED MATERIALS

improve the properties of ceramics formed by processing the powders?

The possibility of producing high quality $YBa_2Cu_3O_7$ has been demonstrated. Powders of other materials with similar characteristics are required for a number of processing schemes for the generation of superconducting ceramic parts and films. Several areas need to be explored in order to increase the number and variety of applications of powders produced by aerosol processes:

- Tl-Pb-Ca-Ba-Cu-O, Bi-Pb-Sr-Ca-Cu-O, and Sb-containing powders produced by aerosol processes may have characteristics that cannot be obtained by other processes. For example, coated and non-equiaxed particles may be useful for the fabrication of bulk ceramics.
- Deposition of superconducting ceramic aerosol particles to form films at higher rates and purities than is currently possible may be feasible.
- The fabrication of bulk superconducting ceramics needs to be studied in conjunction with powder generation by aerosol processes in order to determine the optimum powder generation and processing conditions.

Received: March 29, 1989

[1] A. Castleman, R. Keese, *Acc. Chem. Res. 19* (1986) 413.
[2] P. Marquardt, D. Stauffer, W. Weiss, *Science 242* (1988) 1671.
[3] W. R. Cannon, S. C. Danforth, J. H. Flint, J. S. Haggerty, R. A. Marra, *J. Am. Ceram. Soc. 65* (1982) 324.
[4] S. K. Friedlander, *Aerosol Sci. Technol. 1* (1982) 3.
[5] S. K. Friedlander, *Ann. N.Y. Acad. Sci. 404* (1983) 354.
[6] P. Wegener, P. Mirabel, *Naturwissenschaften 74* (1987) 111.
[7] H. Komujama, T. Osawa, H. Kazi, T. Konno, in B. Vincenzini (Ed.): *High Tech Ceramics*, Elsevier, Amsterdam 1987, p. 667.
[8] J. H. Seinfeld: *Atmospheric Chemistry and Physics of Air Pollution*, Wiley, New York 1986.
[9] S. K. Friedlander: *Smoke, Dust and Haze*, Wiley, New York 1977.
[10] G. Hidy, J. Brock: *The Dynamics of Aerocolloidal Systems*. Pergamon, New York 1970.
[11] T. T. Kodas, V. Y. Lee, E. M. Engler, *Appl. Phys. Lett. 54* (1989) 1923.
[12] J. MacChesney, P. O'Connor, H. Presby, *Proc. IEEE 62* (1974) 1278.
[13] T. T. Kodas, S. E. Pratsinis, S. K. Friedlander, *Ind. Eng. Chem. Res.* 26 (1987) 1999.
[14] A. Pesthy, R. Flagan, J. Seinfeld, *J. Colloid Interface Sci. 91* (1983) 525.
[15] T. T. Kodas, S. Pratsinis, S. Friedlander, *J. Colloid Interface Sci. 111* (1986) 102.
[16] S. Pratsinis, T. T. Kodas, A. Sood, *Ind. Eng. Chem. Res. 27* (1988) 105.
[17] S. Pratsinis, T. T. Kodas, S. Friedlander, *Chem. Eng. Sci. 41* (1986) 693.
[18] S. Pratsinis, T. T. Kodas, M. Dudukovic, S. Friedlander, *Powder Technol. 47* (1986) 17.
[19] T. T. Kodas, S. Friedlander, *AIChE J. 34* (1988) 551.
[20] J. Turner, T. T. Kodas, S. Friedlander, *J. Chem. Phys. 88* (1988) 457.
[21] E. Davis, S. Liao, *J. Colloid Interface Sci. 50* (1975) 488.
[22] J. Castillo, D. Rosner, *Int. J. Multiphase Flow 14* (1988) 99.
[23] S. E. Pratsinis, T. T. Kodas, M. P. Dudukovic, S. K. Friedlander, *Ind. Eng. Chem. Prod. Res. Dev. 25* (1986) 634.
[24] S. Pratsinis, *J. Colloid Interface Sci. 124* (1988) 416.
[25] K. Kim, S. Pratsinis, *AIChE J. 34* (1988) 912.
[26] J. Crump, J. Seinfeld, *AIChE J. 26* (1980) 610.
[27] S. Pratsinis, S. K. Friedlander, A. Pearlstein, *AIChE J. 32* (1986) 177.
[28] D. R. Warren, J. H. Seinfeld, *Aerosol Sci. Technol. 3* (1984) 135.
[29] D. Warren, J. Seinfeld, *J. Colloid Interface Sci. 105* (1985) 136.
[30] G. Ulrich, N. Subramanian, *Combust. Sci. Technol. 17* (1977) 119.
[31] G. Ulrich, *Combust. Sci. Technol. 4* (1971) 47.
[32] C. Seigneur, A. Hudischewskyj, J. Seinfeld, K. Whitby, E. Whitby, J. Brock, H. Barnes, *Aerosol Sci. Technol. 5* (1986) 205.
[33] K. Alam, R. Flagan, *Aerosol Sci. Technol. 5* (1986) 237.
[34] D. Warren, J. Seinfeld, *J. Colloid Interface Sci. 105* (1985) 136.
[35] J. Stern, J. Wu, R. Flagan, J. Seinfeld, *J. Colloid Interface Sci. 110* (1986) 533.
[36] T. T. Kodas, E. M. Engler, V. Y. Lee, R. Jacowitz, T. H. Baum, K. Roche, S. P. Parkin, W. Young, S. Hughes, J. Kleder, W. Auser, *Appl. Phys. Lett. 52* (1988) 1622;
[37] T. T. Kodas, E. M. Engler, V. Y. Lee, R. Jacowitz, T. Baum, K. Roche, S. P. Parkin in C. Burnham, R. Kane (Eds.): *Proc. 1st World Congr. Superconductivity*, World Scientific, USA 1988, p. 177.
[38] A. Pebler, R. Charles, *Mater. Res. Bull. 23* (1988) 1337.
[39] T. T. Kodas, A. Datye, E. Engler, V. Y. Lee, *J. Appl. Phys. 65* (1989) 2149.
[40] S. Shimazu, T. Uematsu, S. Matsuda, Y. Kuwasana, *Mod. Phys. Lett. B2* (1988) 501.
[41] N. Tohge, M. Tatsumisago, T. Minami, K. Okuyama, M. Adachi, Y. Kousaka, *Jpn. J. Appl. Phys. 7* (1988) L292.
[42] M. Kerker, *Adv. Colloid Interface Sci. 5* (1975) 105.
[43] M. I. Ruthner, in P. Vincenzini (Ed.): *Ceramic Powders*, Elsevier, Amsterdam 1983, p. 515.
[44] R. Roettenbacher, R. Schmidberger, in P. Vincenzini (Ed.): *High Tech Ceramics*, Elsevier, Amsterdam 1987, p. 539.
[45] A. Kato, Y. Hirata, Y. Tokunaga, T. Maeda, H. Nishi, in P. Vincenzini (Ed.): *Ceramic Powders*, Elsevier, Amsterdam 1983, p. 835.
[46] T. Gardner, J. Messing, *Thermochim. Acta 78* (1984) 17.
[47] K. Seitz, E. Ivers-Tiffee, H. Thomann, A. Weiss in P. Vincenzini (Ed.): *High Tech Ceramics*, Elsevier, Amsterdam 1987, p. 1753.
[48] G. Kanapilly, O. Raabe, G. Newton, *Aerosol Sci. 1* (1970) 313.
[49] K. Leong, *J. Aerosol Sci. 12* (1981) 417.
[50] B. Ingebrethsen, E. Matijevic, *J. Colloid Interface Sci. 100* (1984) 1.
[51] T. Gardner, G. Messing, *Am. Ceram. Soc. Bull 63* (1984) 1498.
[52] D. Sproson, G. Messing, T. Gardner, *Ceram. Int. 12* (1986) 3.
[53] A. Kato, Y. Hirata, *Mem. Fac. Eng. Kyushu Univ. 45* (1985) 251.
[54] Y. Suyama, A. Kato, *Ceram. Int. 8* (1982) 17.
[55] M. Tomar, F. Garcia, *Prog. Cryst. Growth Charact. 4* (1981) 221.
[56] J. Mooney, S. Rodding, *Ann. Rev. Mater. Sci. 12* (1982) 81.
[57] R. Baker, W. Hurng, H. Steinfink, *Appl. Phys. Lett. 54* (1989) 371.
[58] N. J. Jubb, H. K. Bowen, *J. Mater. Sci. 22* (1987) 1963.
[59] H. K. Bowen, *Mater. Sci. Eng. 44* (1980) 1.
[60] E. Barringer, H. K. Bowen, *Appl. Phys. A45* (1988) 271.
[61] M. Multani, N. Nanadikar, N. Verkataramani, V. Ragupathy, A. Pansare, A. Gurjar, *Mater. Res. Bull. 14* (1979) 1251.
[62] T. Liu, O. Sakurai, N. Mizutani, M. Kato, *J. Mater. Sci. 21* (1986) 3698.
[63] R. H., Lamoreaux, D. L. Hildenbrand, L. Brewer, *J. Phys. Chem. Ref. Data 16* (1987) 419.
[64] Y. Yamada, S. Murase, *Jpn. J. Appl. Phys. Lett. 27* (1988) L996.
[65] G. G. Levi, V. Jayaram, J. Valencia, R. Mehrabian, *J. Mater. Res. 3* (1988) 969.
[66] G. F. Holland, A. M. Stacy, *Acc. Chem. Res. 21* (1988) 8.
[67] K. Tu, S. Park, C. Tsuei, *Appl. Phys. Lett. 51* (1987) 2158.
[68] E. O'Sullivan, B. Chang, *Appl. Phys. Lett. 52* (1988) 1441.
[69] A. Yoshida, H. Tamura, S. Morohashi, S. Hasuo, *Appl. Phys. Lett. 53* (1988) 811.
[70] J. H. Park, P. Kostic, *Mater. Sci. Lett. 6* (1988) 393.
[71] V. Lee, E. Engler, T. T. Kodas, unpublished results.
[72] A. Nazzal, V. Lee, E. Engler, R. Jacowitz, Y. Tokura, J. Torrance, *Physica C 153* (1988) 1367.
[73] J. Crank: *The Mathematics of Diffusion*, Clarendon, Oxford 1975, p. 104.
[74] S. Matsuno, K. Egawa, K. Yoshizaki, H. Watari, *MRS Int. Meet. Adv. Mater.*, May 30–June 3, 1988, Tokyo, Japan.
[75] T. Takagi, K. Matsubara, H. Takaoka, *J. Appl. Phys. 51* (1980) 5419.
[76] Y. Minowa, K. Yamanishi, K. Tsukamoto, *J. Vac. Sci. Technol. B1* (1983) 1148.
[77] A. Matsumoto, H. Sadamura, A. Inubishi, M. Okubo, S. Masuda, K. Suzuki, *Mater. Sci. Monogr. 38C* (1987) 2119.
[78] A. Matsumoto, H. Sadamura, A. Inubishi, M. Okubo, S. Masuda, K. Suzuki, *Mater. Sci. Monogr. 38C* (1987) 1421.
[79] K. Matsubara, I. Yamada, N. Nagoe, K. Tominaga, T. Takagi, *Surf. Sci., 86* (1979) 290.
[80] K. Fukushima, I. Yamada, T. Takagi, *J. Appl. Phys. 58* (1985) 4140.
[81] H. Takaoka, J. Ishikawa, T. Takagi, *Thin Solid Films 157* (1988) 143.
[82] K. Yamanishi, S. Yasunaga, K. Imada, K. Sato, Y. Hashimoto, *Mater. Res. Soc. Symp. Proc. 99* (1988) 343.
[83] R. Petersen, D. Matson, R. Smith, *J. Am. Chem. Soc. 108* (1986) 2100.
[84] D. W. Matson, R. Peterson, R. Smith, *J. Mater. Sci. 22* (1987) 1919.

[85] L. Pokrovski, N. Samolyuk, V. Gribkov, L. Borovinskii, E. Umantsev, V. Osipov, *Inorg. Chem. 13* (1977) 697.
[86] D. Ramsay, R. Avery, *J. Mater. Sci. 9* (1974) 1681.
[87] R. Siegel, S. Ramasamy, H. Hahn, L. Zongquan, L. Ting, R. Gronsky, *J. Mater. Res. 3* (1988) 1367.
[88] C. Becker, J. Pallix, *J. Appl. Phys. 44* (1988) 5152.
[89] D. Geohegan, D. Machburn, R. Culbertson, S. Pennycock, J. Budai, R. Valiga, B. Sales, D. Lowndes, L. Boatner, E. Sonder, D. Eres, D. Christen, W. Christie, *J. Mater. Res. 3* (1988) 1169.
[90] L. Lynds, B. Weinberger, G. Peterson, H. Krasinski, *Appl. Phys. Lett. 52* (1988) 320.
[91] T. Venkatesan, X. Wu, A. Inam, J. Wachtman, *Appl. Phys. Lett. 52* (1988) 1193.
[92] G. D. Ulrich, *Chem. Eng. News 1984*, August 6, p. 22.
[93] M. Sokolowski, A. Sokolowska, A. Michalski, B. Gokieli, *J. Aerosol Sci. 8* (1977) 219.
[94] A. George, R. Murley, E. Place, *Faraday Symp. Chem. Soc. 7* (1973) 143.
[95] A. Hurd, W. Flower, *J. Colloid Interface Sci. 122* (1988) 178.
[96] M. Formenti, F. Juillet, P. Mereaudeau, S. Techner, P. Vergnon in G. Hidy (Ed.): *Aerosols and Atmospheric Chemistry*, Academic, New York 1972, p. 45.
[97] A. Kato, in P. Vincenzini (Ed.): *High Tech Ceramics*, Elsevier, Amsterdam 1987, p. 459.
[98] K. Okuyama, Y. Kousaka, N. Tohge, M. Adachi, *J. Mater. Sci. Lett. 6* (1987) 1466.
[99] J. J. Wu, R. C. Flagan, O. J. Gregory, *Appl. Phys. Lett. 49* (1986) 82.
[100] K. Masdiyasni, C. Lynch, J. Smith, *J. Am. Ceram. Soc. 48* (1965) 372.
[101] Y. Suyama, A. Kato, *J. Am. Ceram. Soc. 59* (1976) 146.
[102] K. Mazdiyasni, C. Lynch, J. Smith, *J. Am. Ceram. Soc. 48* (1965) 372.
[103] K. Tachikawa, I. Watanabe, S. Kosuge, M. Kabasawa, Y. Suzuki, Y. Matsuda, Y. Shinbo, *Appl. Phys. Lett. 52* (1988) 1011.
[104] R. Neiser, J. Kirkland, H. Herman, W. Elam, E. Skelton, *Mater. Sci. Eng. 91* (1987) L 13.
[105] S. Stecura, *Thin Solid Films 150* (1987) 15.
[106] C. M. Hollabaugh, D. E. Hull, L. R. Newkirk, J. Petrovic, *J. Mater. Sci. 18* (1983) 3190.
[107] C. Pickles, A. McLean, *Am. Ceram. Soc. Bull. 62* (1983) 1004.
[108] M. Gani, R. McPherson, *J. Mater. Sci. 15* (1980) 1915.
[109] S. Talisa, K. Yoo, M. Abe, T. Itoh, *J. Appl. Phys. 64* (1988) 5819.
[110] M. Langlet, M. Labeau, B. Bochu, J. Joubert, *IEEE Trans. Magn. 22* (1986) 151.
[111] G. Blandenet, M. Court, Y. Lagarde, *Thin Solid Films 77* (1981) 115.
[112] A. Ortiz, C. Falcony, M. Garcia, A. Sanchez, *J. Phys. D 20* (1987) 670.
[113] M. Sharon, B. Prasod, *Sol. Energy Mater. 8* (1983) 457.
[114] J. Aranovich, A. Ortiz, R. Bube, *J. Vac. Sci. Tech. 16* (1979) 994.
[115] J. Vigue, J. Spitz, *J. Electrochem. Soc. 122* (1975) 585.
[116] M. Kawai, T. Kawai, H. Masuhira, M. Takahasi, *Jpn. J. Appl. Phys. 26* (1987) L 1740.
[117] J. Chu, R. Liu, J. Kung, P. Wu, L. Chen, *J. Appl. Phys. 64* (1988) 2523.
[118] R. Henry, H. Lessoff, E. Swiggard, S. Qudri, *J. Cryst. Growth 85* (1987) 615.
[119] E. Cooper, E. Geiss, A. Gupta, *Mater. Lett. 7* (1988) 5.
[120] D. Vaslow, G. Dieckmann, D. Elli, A. Ellis, D. Holmes, A. Lefkow, M. MacGregor, J. Nordman, M. Peters, Y. Yang, *Appl. Phys. Lett. 53* (1988) 324.
[121] D. Bahadur, D. Roy, S. Ram, *Adv. Ceram. 16* (1984) 651.
[122] S. K. Pawar, S. H. Pawar, *Mater. Res. Bull. 18* (1983) 211.
[123] W. Siefert, *Thin Solid Films 121* (1984) 275.
[124] A. Murthy, K. Reddy, *Mater. Res. Bull. 19* (1984) 241.
[125] K. Nomura, Y. Ujihira, K. Itoh, K. Honda, *Thin Solid Films 128* (1985) 225.
[126] D. Nguyen, M. Von Roode, S. Johar, *Thin Solid Films 135* (1986) L 19.
[127] K. Nomura, Y. Ujihira, *Hyperfine Interact. 29* (1986) 1471.
[128] S. Arya, *Cryst. Res. Technol. 21* (1986) K 38.
[129] A. Murthy, K. Reddy, *Mater. Res. Bull. 19* (1984) 241.
[130] C. Uma, L. Malhotra, K. Chopra, *Bull. Mater. Sci. 8* (1986) 385.
[131] D. W. Sproson, G. L. Messing, *Commun. Am. Ceram. Soc.* May (1984) C-92.
[132] S. Kanzaki, H. Tabata, N. Otsuka, Z. Nakagawa, K. Hamano, *Yogyo-Kyokai shi 81* (1983) 344.
[133] H. Ishizawa, O. Sakurai, N. Mizutani, M. Kato, *Am. Ceram. Soc. Bull. 65* (1986) 1399.
[134] T. O'Holleran, R. Neurgonkar, D. Roy, R. Roy, *Am. Ceram. Soc. Bull 57* (1978) 459.
[135] S. Nafis, Z. Tang, B. Dale, C. Sorensen, G. Hadjipanayis, K. Klabunde, *J. Appl. Phys. 64* (1988) 5835.
[136] K. Kumar, A. Petrovich, C. Williams, J. Van der Sande, *J. Appl. Phys. 64* (1988) 5665.
[137] R. LaBauve, G. Kanapilly, N. Stalnaker, J. McWhinney, *J. Aerosol. Sci. 10* (1979) 251.
[138] D. Roy, R. Neurgonkar, T. O'Holleran, R. Roy, *Am. Ceram. Soc. Bull. 56* (1977) 1023.
[139] S. Kanzaki, H. Tabata, T. Kumazawa, S. Ohta, *J. Am. Ceram. Soc. 68* (1985) C 6.
[140] E. Matijevic, *Langmuir 2* (1986) 12.
[141] B. Ingebrethsen, E. Matijevic, R. Partch, *J. Colloid. Interface Sci. 95* (1983) 228.
[142] T. T. Kodas, S. Pratsinis, A. Sood, *Powder Technol. 50* (1987) 47.
[143] M. Visca, E. Matijevic, *J. Colloid. Interface Sci. 68* (1979) 308.
[144] B. Ingebrethsen, E. Matijevic, *J. Aerosol. Sci. 11* (1980) 271.
[145] E. Matijevic in P. Vincenzini (Ed.): *High Tech Ceramics*. Elsevier, Amsterdam (1987) p. 441.
[146] K. Tachikawa, I. Watanabe, S. Kosuge, M. Kabasawa, T. Suzuki, Y. Matsuda, Y. Shinbo, *Appl. Phys. Lett. 52* (1988) 1011.
[147] Cuomo, C. Guarnieri, S. Shivashankar, R. Roy, D. Yee, R. Rosenberg, *Adv. Ceram. Mater. 2* (1987) 422.
[148] W. Elam, J. Kirkland, R. Neiser, E. Skelton, S. Sampath, H. Herman, *Adv. Ceram. Mater. 2* (1987) 411.
[149] M. Baraton, P. Chagnon, P. Quintard, *J. Mol. Struct. 115* (1984) 87.
[150] P. Boch, C. Gault, F. Platon, in P. Vincenzini (Ed.): *Ceramic Powders*, Elsevier, Amsterdam 1983, p. 825.
[151] D. Chuanxian, R. Zatorski, H. Herman, P. Ott, *Thin Solid Films 118* (1984) 467.
[152] H. Kim, W. Kim, *J. Appl. Phys. 62* (1987) 2000.
[153] E. M. Engler, *CHEMTECH 17* (1987) 542.
[154] A. P. Malozemoff, N. J. Gallagher, R. E. Schwall in *High Temperature Superconductivity (ACS Symp. Ser. 351* (1987) 280), Am. Chem. Soc., Washington, D.C.
[155] F. Galasso: *Structure, Properties and Preparation of Perovskite-Type Compounds*, Pergamon, New York 1968.
[156] K. Okazaki, *Ceram. Bull 67* (1988) 1946.
[157] Y. Bando, T. Akashi, in S. Saito (Ed.): *Fine Ceramics*, Elsevier, New York 1985, p. 122.
[158] K. Wakino in S. Saito (Ed.): *Fine Ceramics*. Elsevier, New York 1985, p. 251.

The following reviews will be published in future issues:

B. Joyce: Tailoring Semiconductor Crystals to Atomic Dimensions

H. Warlimont: Rapidly Quenched Materials

H.-W. Schmidt: Dichroic Dyes and Liquid Crystal Side Chain Polymers

R. Eidenschink: Liquid Crystals – New Compounds, New Applications

E. Hondros, E. Bullock: Materials for the 21st Century

J. F. Stoddart: The Structure Directed Synthesis of New Organic Materials

Communications

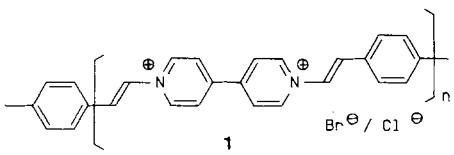
Manuscripts intended for publication as communications should be sent to ADVANCED MATERIALS PO Box 101161, D-6940 Weinheim, FRG. Authors are requested to consult the "Instructions to Authors" which are reproduced in the January issue of the journal or are available from the editorial office on request.

Poly-[*N*,*N*-(1,4-divinylbenzene-β,β′-diyl)-4,4′-bipyridinium dibromide], a Novel Conducting Viologen Polymer**

By *Andreas Merz** and *Stefan Reitmeier*

Dedicated to Professor Gottfried Märkl on the occasion of his 60th birthday

The title compound **1** is a new, easily accessible π-conjugated viologen polymer. Properties of particular interest are its conductivity of 1×10^{-3} S cm^{-1} and electroactivity in the potential region from −0.1 to −0.6 V vs. Ag/AgCl.

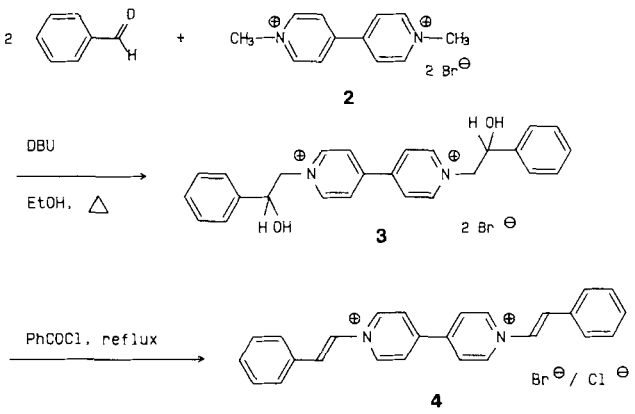


1

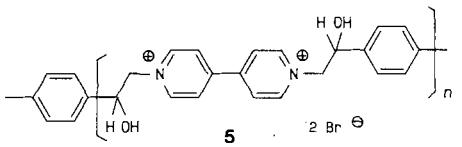
The electrical conductivity of π-conjugated electron rich organic polymers like polypyrrole, polythiophene, and polyaniline is increased by chemical or electrochemical oxidation (p-doping with positive charge carriers).[1] The doping process occurs simultaneously with polymer film formation at the electrode surface during anodic oxidation. On discharging at negative potentials in an electrochemical cell the polymer films become insulating. Polyphenylene and polyacetylene are also electroactive at very negative potentials.[2] The reduction process corresponds to n-doping with negative charge carriers. It was assumed that suitable π-conjugated polymeric viologen structures should be reducible at moderately negative potentials and possibly show conductivity in this potential region.

Methyl viologen **2** displays two reversible redox transitions at −0.57 and −0.92 V.[3] Compound **2** and its homologues have frequently been used as redox catalysts[4] and as electron relays in photocatalyzed water cleavage.[5] Polymeric viologens are also known, with the viologen moiety either as a pendant group on the polymer chain,[6] or as an interconnecting member of the chain.[7]

The orange styryl viologen **4** was prepared as a model monomer in a two step synthesis, following a procedure of *Kröhnke* for the preparation of *N*-alkenyl pyridinium salts,[8] starting from methyl viologen and benzaldehyde and proceeding via the bis-hydrated salt **3** (Scheme 1).[9] The 250 MHz ^{1}H NMR shows that the *E*/*Z* ratio of the styryl units of **4** is 3.6:1. The extended π-system of **4** as compared with **2** is demonstrated by a positive shift of the viologen redox signals and the presence of a third reversible couple which is not likely to be due to the *E*/*Z* isomers.[10]



The same synthetic method is readily applied to the preparation of **1**.[11] Reaction of methyl viologen with 1,4-benzenedialdehyde (1:1) in 90% aqueous ethanol, in the presence of 1,8-diazabicyclo[5.4.0]undec-7-ene (DBU) for 3–4 d at 70 °C gives the polyhydroxy salt **5** as a tan solid in 60% yield. After drying, this is converted to **1** by dehydration in neat benzoylchloride for 10 h at 100 °C.



5

Polymer **1** is obtained as an amorphous black powder. It is paramagnetic, giving a single unresolved ESR signal with $g = 2.009$, a peak to peak width of 5.9 G and a spin density of 5×10^{-17} spins per gram. Elemental analysis shows that the bromide anion has been partially exchanged for chloride which stems from the dehydrating agent. The halogen content is 30% less than calculated for **1** although the C:H:N ratio is correct. The same effect is observed for the hydroxy-polymer salt **5**. The reason for the deviation from the stoichiometric values is not clear at this time, although it may result from the terminal groups or from the irreversible side reaction of some viologen groups. The IR spectrum suggests the presence of water (see[8]) and possibly the benzoate anion. The presence of conjugated viologen structural elements has been confirmed by cyclic voltammetry of 5% of **1** in a

[*] Prof. Dr. A. Merz, Dipl.-Chem. S. Reitmeier
Institut für Organische Chemie der Universität
Universitätsstraße 31, D-8400 Regensburg (FRG)

[**] This work was supported by the Deutsche Forschungsgemeinschaft and the Fonds der Chemischen Industrie.

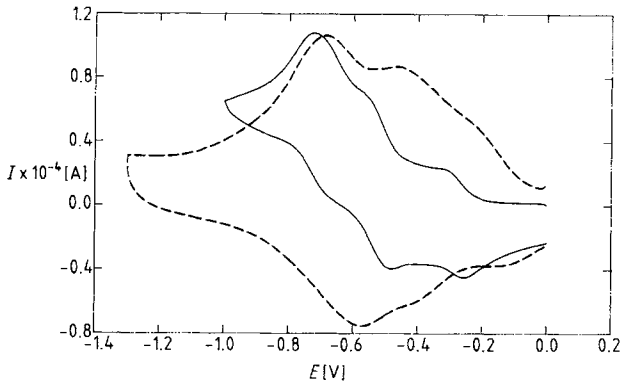


Fig. 1. Cyclovoltammograms of **1** and **4**. (– – –): Voltammogram of **1** embedded in a carbon paste electrode [12] in DMSO/0.1 M Bu_4NClO_4, scan rate 1 mV s^{-1}, E_p(red) = −0.20, −0.46, −0.69 V; E_p(ox) = −0.15, −0.41, −0.58 V. (——): Solution cyclic voltammogram of **4** in DMSO/0.1 M Bu_4NClO_4 on a 0.07 cm^2 Pt disk; scan rate 0.1 V s^{-1}, current scale in this case should be changed to 10^{-5}. Potentials are recorded vs. Ag/AgCl [3]. E_p(red) = −0.31, −0.55, −0.71 V; E_p(ox) = −0.26, −0.48, −0.68 V.

carbon paste electrode[12] (Fig. 1). The voltammogram is very similar to that of **4**. The further positive shift indicates more extended conjugation. The area under the slow sweep voltammogram in Figure 1 corresponds to 1.4 F mol^{-1} for both reduction and oxidation.

Polymer **1** is easily pressed into pellets which have an electrical conductivity[13] of $(1.3 \pm 0.2) \times 10^{-3}$ S cm^{-1}. Neither the ESR spectrum nor the conductivity change on storage in air for two months. Likewise, **1** is stable in water and in many organic solvents. Exposure of the polymer to iodine vapors increases its conductivity by a factor of 2–3. Gaseous SO_2 has no effect. Doping experiments in solvent suspensions with I_2 and $FeCl_3$ for the oxidative process, or with $Na_2S_2O_4$ for the reductive process resulted in almost complete loss of conductivity. Thus, it appears that the necessary conditions for conductivity are produced during the dehydration process without the need for additional doping.

Received: January 27, 1989

[1] A. Diaz, J. Bargon in T. A. Skotheim (Ed.): *Handbook of Conducting Polymers*, Marcel Dekker, New York 1986, Vol. 1, p. 81.

[2] J. F. Fauvarque, M. A. Petit, A. Digue, G. Froyer, *Makromol. Chem. 188* (1987) 1833; R. B. Kaner, S. J. Porter, A. G. McDiarmid, *J. Chem. Soc., Faraday Trans. 82* (1986) 2323.

[3] The potentials reported were measured vs an AgCl coated silver wire in dimethyl sulfoxide (DMSO); the zero potential on this scale is 339 mV negative of the ferrocene signal.

[4] H. Simon, J. Bader, H. Günther, S. Neumann, J. Thanos, *Angew. Chem. Int. Ed. Engl. 24* (1985) 539; *Angew. Chem. 97* (1985) 541; L. Coche, J.-C. Moutet, *J. Electroanal. Chem. 224* (1987) 111.

[5] I. Tabushi, S. Kugimiya, *J. Am. Chem. Soc. 107* (1985) 1859.

[6] K. Ageishi, T. Endo, M. Okawara, *J. Polym. Sci. Chem. 21* (1983) 175.

[7] A. Factor, G. E. Heinsohn, *J. Polym. Sci. Part B9* (1971) 289.

[8] F. Kröhnke, J. Wolff, G. Jeutsch, *Chem. Ber. 84* (1951) 399.

[9] ^{1}H NMR spectrum of **3** (in CD_3OD): δ = 4.54 (2H; OH), 4.82 (2H; CH_2), 5.05 (2H; CH_2), 5.27 (1H). ABX system with J_{AB} = 15.8 Hz, J_{ax} = 8.0, J_{BX} = 3.1; C*H*OH), 7.32–7.51 (10H, m; C_6H_5), 8.67 (4H), 9.18 (4H, AA'BB' system with J_{AB} = 6.2 Hz). Voltammetric data of **3**: E_p(red) = −0.57, −0.94 V; E_p(ox) = −0.49, −0.87 V.—^{1}H NMR spectrum of **4** in [D_6]DMSO: δ = 7.53–7.66 (6H, m; *m*-, *p*-C_6H_5), 7.72–7.78 (4H, m; *o*-C_6H_5), 7.94 (0.44H), 8.43 (0.44H, AB system with J_{AB} = 14.2 Hz), 8.79 (0.88H), 9.53 (0.88H, AA'BB' system with J_{AB} = 6.6 Hz), 8.05 (1.56H), 8.51 (1.56H, AB system with J_{AB} = 14.5 Hz), 9.02 (3.12H), 9.70 (3.12H, AA'BB' system with J_{AB} = 6.6 Hz). UV spectrum of **4**: λ_{max} = 362 nm ($\varepsilon = 2.21 \times 10^4$).

[10] S. I. Imabashi, N. Kitamura, S. Tazuka, K. Tokuda, *J. Electroanal. Chem. 239* (1988) 397; T. W. Ebbesen, R. Akaba, K. Tokumaru, M. Washio, S. Tagawa, Y. Tabata, *J. Am. Chem. Soc. 110* (1988) 2147.

[11] C, H, N, Hal. analysis found (calculated): **1** $(C_{20}H_{16}Br_{1.66}Cl_{0.33}N_2)_n$, (428.7) × n: C 56.1(56.0), H 4.2(3.7), Br 20.5(30.9), Cl 1.8(2.7), N 5.5(6.5). **5** $(C_{20}H_{20}Br_2N_2O_2)_n$, (464.7) × n: C 50.2(50.0), H 5.0(4.2), Br 23.5(33.5), N 5.7(5.8).

[12] The carbon paste was prepared with DMSO solvent in an experimental arrangement as given in: P. Audebert, G. Bidan, *Synth. Metals 14* (1986) 71. We thank Dr. *P. Audebert* and Dr. *C. Andrieux*, University of Paris 7, for kind assistance in these experiments.

[13] L. J. van der Pauw, *Philips Techn. Rundsch. 20* (1958/1959) 220.

Probing Changes in the Structure and Performance of a Lithium Nickel Oxide Catalyst by in situ X-Ray Diffraction During the High-Temperature Oxidative Coupling of Methane**

By *Ingrid J. Pickering, Peter J. Maddox* and *John M. Thomas**

Heterogeneous catalysts and their precursors are customarily characterized under conditions profoundly different from those that prevail in the actual catalytic reaction. The active solid may possess structural features quite unlike those deduced from measurements conducted at ambient temperatures and pressures. This calls for the increased use of in situ methods for the characterization of heterogeneous

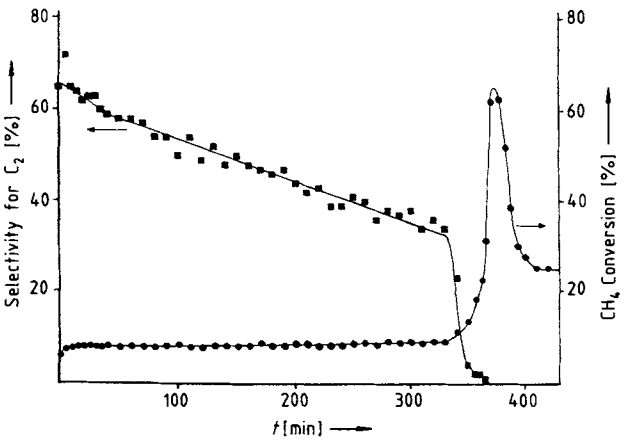


Fig. 1. The changes with time of conversion of methane and selectivity for C_2 hydrocarbons are shown for the duration of the experiment. Percentage conversion of methane is derived as $(100 \times \Sigma n V_{C_n})/V_{CH_4} + \Sigma n V_{C_n}$ and percentage selectivity for ethane and ethene as $(100 \times (2 V_{C_2H_6} + 2 V_{C_2H_4}))/\Sigma n V_{C_n}$ where V_{C_n} is the percentage volume of C_n hydrocarbon product (CO, CO_2, C_2H_4, C_2H_6) in the gas chromatographic analysis. (These values do not take into account any carbon which forms carbonate or other solid phases).

[*] Prof. Dr. J. M. Thomas, I. J. Pickering, Dr. P. J. Maddox
Davy Faraday Research Laboratory
The Royal Institution of Great Britain
21, Albemarle Street, London W1X 4BS (UK)

[**] We thank the Science and Engineering Research Council for a studentship (to *IJP*), a fellowship (to *PJM*) and an equipment grant (to *JMT*).

ADVANCED MATERIALS

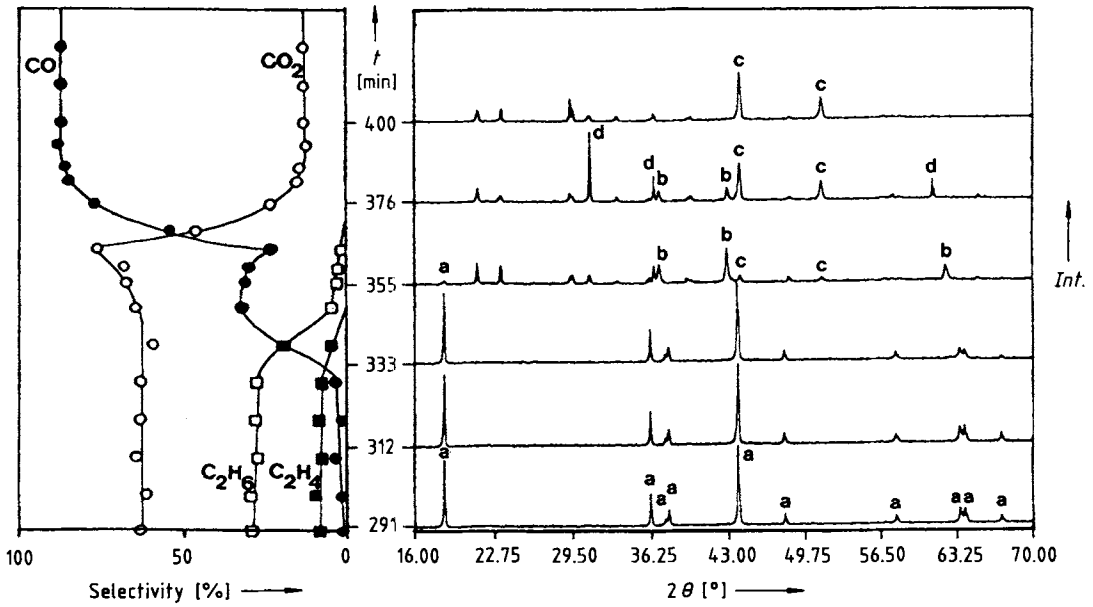


Fig. 2. Variation in selectivities and diffraction patterns as a function of time for the final stages of the reaction. Left: individual percentage selectivities for the various products. Right: corresponding in situ diffraction patterns of the catalyst. The vertical position of the diffraction pattern represents the time at which the scan was commenced, at 16° (2 θ). Diffraction peaks labelled as follows: a: $Li_{0.45\pm0.02}Ni_{0.55\pm0.02}O$, b: NiO, c: Ni metal and d: unknown transient.

catalysts. Here we illustrate the advantages of in situ X-ray diffraction in clarifying the onset and nature of distinct kinds of catalytic action exhibited by a lithium nickel oxide for the oxidation of methane at elevated temperatures.[1, 2]

A sample of 1.01 g of the powdered solid of composition $Li_{0.45\pm0.02}Ni_{0.55\pm0.02}O$ was placed in a porous quartz sample holder in a specially-constructed, resistively-heated, quartz reaction cell fitted with mica windows.[3] The cell was attached to a slightly modified Siemens D500 diffractometer equipped with a rotating anode source (CuK_α radiation), which allowed rapid structural characterization. Under the flow of the reaction gas mixture (composition: CH_4 19.68%, O_2 3.00%, balance N_2; flowrate: 50 mL min^{-1}), the catalyst was rapidly heated to and maintained at 700 °C. A series of diffraction patterns was recorded (2 θ range 16 to 70°), each pattern requiring some 19 min, and concurrently the outlet product gases were analyzed by gas chromatography.

The conversion of methane, and the selectivity for C_2 hydrocarbons during the 7 h catalytic run are shown in Figure 1. After about 330 min the nature of the catalysis changes dramatically (see also expanded version with the appropriate diffraction patterns in Fig. 2). It should be noted that there are three distinct regimes of catalysis associated with correspondingly distinct structural features.

During the initial regime (up to 330 min) the fractional conversion of methane remains essentially constant at ca. 8%; concomitantly the selectivity of C_2 products starts at 65% and gradually drops, for reasons that are at present obscure, to a value of 33% at t = 330 min. The diffraction patterns reveal that a single phase, lithium nickel oxide, functions as the oxidative coupling catalyst. The structure,[4] schematized in Figure 3a, is of the rocksalt type with different cation distributions on alternate close-packed layers.

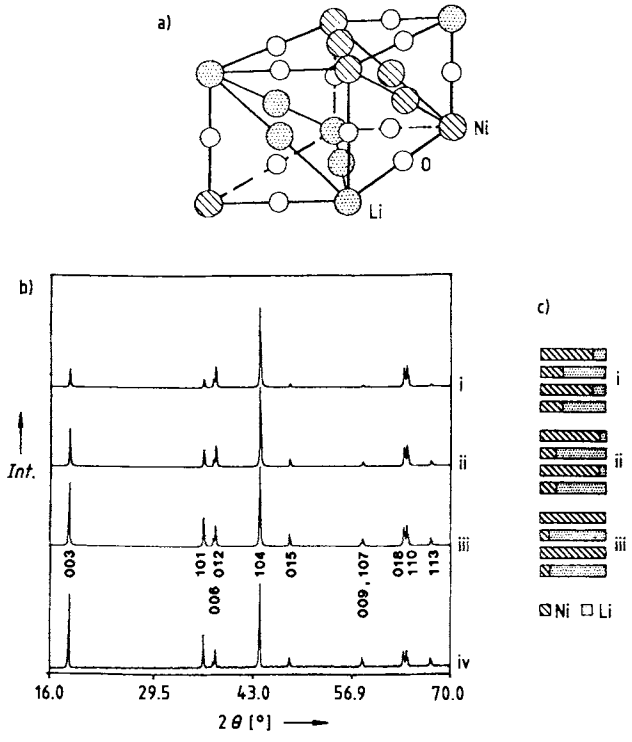


Fig. 3. a) The idealized structure of $Li_xNi_{1-x}O$ for x = 0.5. Its relationship to the rocksalt structure is shown, lithium and nickel ions occupy alternate close-packed layers between the oxygens. b) Diffraction patterns of $Li_xNi_{1-x}O$ for x = 0.43. i, ii and iii are simulated diffraction patterns for increasing order between the layers. Lattice parameters for the simulations are taken from the experimental data (a = 2.905, c = 14.361 Å). iv is the first experimental diffraction pattern collected at reaction temperature (700 °C). c) Representation of the ordering of Li and Ni between the layers. i, ii and iii are the models for i, ii and iii in part b, respectively. i has 20% Li in the predominantly Ni layer, 66% in the other layer; likewise ii 10 and 76%; iii 0 and 86%, i.e. totally ordered.

Diffraction patterns have been simulated (Fig. 3 b, i to iii) for different degrees of ordering[5] of lithium and nickel ions between the layers (represented in Fig. 3c, i to iii). Comparison with the initial diffraction pattern at 700 °C (Fig. 3 b, iv) shows that the lithium ions are essentially fully ordered between the layers. The unit cell is hexagonal, $R\bar{3}m$ with computed cell dimensions of $a = 2.904$ and $c = 14.36$ Å with a slight axial distortion away from the true cubic close packing ($c/a = 4.945$; ideal cubic = 4.899). This distortion is greater than at room temperature ($a = 2.885$, $c = 14.21$ Å, $c/a = 4.925$). The Figures 2 and 3 show that, during the initial period of catalytic activity the lithium nickel oxide structure remains invariant within the limits of our technique. The oxide appears to function as a uniform heterogeneous catalyst in the sense previously elaborated.[6]

In the second regime, 330–360 min, there is dramatic change; at least two crystallographic phases are present as the parent $Li_{0.46}Ni_{0.54}O$ is reduced to its daughter phase NiO (labelled b in Fig. 2). Accompanying the appearance of NiO there is a sharp rise in the degree of conversion of CH_4, and the principal product is CO_2. Production of C_2 hydrocarbons decreases to zero as the Li-Ni-O phase disappears.

In the third and final regime, 360 min and longer, metallic nickel (c in Fig. 2) along with some Li_2CO_3, is the predominant crystallographic phase. It is also noted that new, sharp peaks appear (labelled d); these are as yet unidentified and rapidly disappear (see top diffraction pattern of Fig. 2) before the catalyst is finally converted to metallic nickel and lithium carbonate. In this regime CO is the dominant gaseous product of catalytic reaction, and there is now no longer a uniform heterogeneous catalyst.

In summary, it has been shown that in situ X-ray diffractometry coupled with parallel gas chromatography throws fresh light on the structure of reactive solid catalysts. In the case of the Li-Ni-O system studied here, three distinct regimes could be readily identified each with different gaseous products. Furthermore, although the experimental conditions were not optimized, it was possible to detect the presence of an as yet unidentified transitory solid product as well as those expected on the basis of the known chemistry of the parent, monophasic mixed oxide catalyst. Greater time resolution may be attained with our set-up by using a higher flux of X-rays and a more sensitive detector.

Received: January 30, 1989

[1] M. Hatano, K. Otsuka, *Inorg. Chim. Acta 146* (1988) 243–247.
[2] R. K. Ungar, X. Zhang, R. M. Lambert, *Appl. Catal. 42* (1988) L1–L4.
[3] P. J. Maddox, J. Stachurski, J. M. Thomas, *Catal. Lett. 1* (1988) 191.
[4] L. D. Dyer, B. S. Borie, Jr., G. P. Smith, *J. Am. Chem. Soc. 76* (1954) 1499.
[5] J. B. Goodenough, D. G. Wickham, W. J. Croft, *J. Phys. Chem. Solids 5* (1958) 107.
[6] J. M. Thomas, *Angew. Chem. Int. Ed. Engl. 27* (1988) 1673; *Angew. Chem. 100* (1988) 1735.

The following short communications will be published in future issues: *D. Schweitzer et al:* Superconductivity at 7.5 K and Ambient Pressure in Polycrystalline Pressed Samples of β_p-(BEDT-TTF)$_2$I$_3$ – *R. Kniep et al:* Structure of Anodic Oxide Coatings on Aluminum – *G. Gray et al:* Siloxane Copolymers with Laterally and Terminally Attached Mesogenic Side Chains

High Resolution Electron Microscopy of the High-T_c Superconductor $Bi_{2+x}Sr_2Ca_{1-x}Cu_2O_{8+\delta}$

By *W. Zhou, A. I. Kirkland, K. D. Mackay, A. R. Armstrong, M. R. Harrison, D. A. Jefferson, W. Y. Liang* and *P. P. Edwards**

The structure of the 85 K Bi-Sr-Ca-Cu-O superconductor has been investigated by means of high resolution electron microscopy combined with image simulation. An ordered one-in-five substitution of calcium by bismuth ions is proposed as the explanation for the observed superlattice formation. This model is consistent with the reports of the recent analytical studies carried out on the same system.

The discovery of high temperature superconductivity in the Bi-Sr-Ca-Cu-O system has demonstrated conclusively that this phenomenon is not confined to compounds containing yttrium and rare-earth elements.[1–4] Several groups have isolated a high-T_c phase in this system and single crystal X-ray[4–6] and neutron diffraction[7] studies have shown both similarities and differences between these new cuprate superconductors and the previously known 40 K and 90 K materials.[4–6] A superstructure has also been observed in these diffraction studies and various structural models for its formation have been proposed.[8–10] Equally important was the indication of additional electron density at the Ca site suggesting a variable Bi:Sr:Ca occupancy.[5, 6] Here the results of high resolution electron microscopy (HREM) and model image simulation of the title compound are presented from which an ordered compositional variation in atomic arrangement, which leads naturally to the superlattice for-

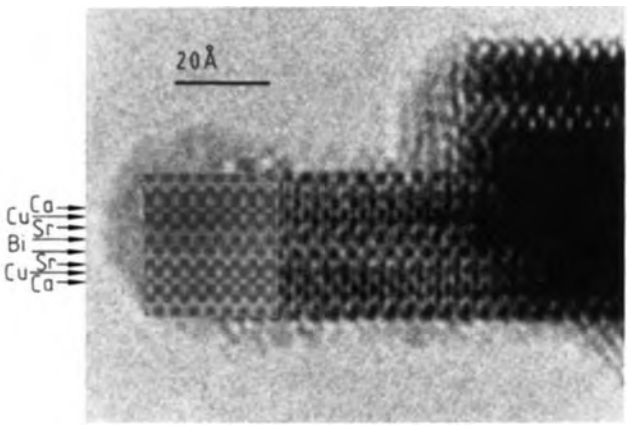


Fig. 1. HREM image of the tip of one crystal a single c lattice vector wide viewed down [110] of the published unit cell together with a calculated image inset (defocus = 950 Å, crystal thickness = 20 Å). The image clearly shows in cross section the metal layers in the order (Bi-Sr-Cu-Ca-Cu-Sr-Bi).

[*] Dr. P. P. Edwards, Dr. W. Zhou, Dr. A. I. Kirkland, Dr. K. D. Mackay, Dr. A. R. Armstrong, Dr. D. A. Jefferson, Dr. W. Y. Liang
Interdisciplinary Research Centre in Superconductivity
University of Cambridge
Madingley Road, Cambridge CB3 0HE (UK)
Dr. M. R. Harrison
General Electric Company
Hirst Research Centre
East Lane, Wembley, Middlesex HA9 7PP (UK)

[**] We thank the SERC, P.A. Technology (*W. Z.*), Alcan Chemical Ltd. (*A. I. K.*), and B.P. Research (*A. R. A.*) for financial support.

ADVANCED MATERIALS

mation, is proposed. The substitution of Bi on the Ca site also leads to oxygen incorporation and concomitant oxidation.

The crystallites invariably possessed a plate-like morphology and images were readily obtained down the [001] zone axis. These images and electron diffraction patterns confirmed the essentially square 5.4 Å basic unit cell in this projection, and also indicated the pronounced superlattice. Some crystallites were also found to fracture perpendicular to their main cleavage plane or alternatively to curl up at the edges. It was then possible to obtain images in [110] or [100] projections. Figure 1 shows an image of a crystal in its [110] projection and the crystal is only one *c* lattice vector or unit cell wide. No evidence of the superlattice is visible in this projection. It appears that the projected charge density approximation[11] can be used to interpret the image and that the dark dots in the image can thus be correlated with the cation positions, although the oxygen atoms cannot be observed directly. The one-dimensional superlattice can be seen when the crystals are viewed in the [100] orientation, as shown in Figure 2. In this case the image is from the edge of a curled-

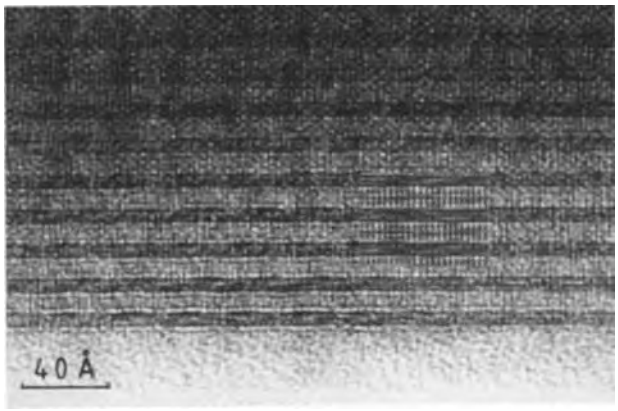


Fig. 2. HREM image of a crystal viewed down the [100] direction, with the one-dimensional superlattice being visible. The model simulation (insert) was calculated for a crystal thickness of 30 Å and an objective lens defocus of −1600 Å.

up platelet crystal some 200–300 Å thick, and clearly shows both the layer-like nature of the material, and a subtle variation of fringe contrast in a direction along the plane of the layers indicating the existence of the superlattice. No drastic variations in the basic arrangement of lattice fringes were observed, implying that a relatively minor effect, such as cation substitution or displacement may be responsible for the superlattice. In general, the superlattice was observed in one dimension as shown in Figure 3a, but a two-dimensional variant was also observed in certain cases (Fig. 3b). The periodicity of the superlattice, whether one- or two-dimensional is predominantly five basic cell repeats, though periods of four and six unit cells were also recorded. In addition, these superlattice vectors have occasionally been observed to be slightly inclined to the basic cell axes. No platelets were obtained which did not exhibit the superlattice.

Two structural models have been proposed[4–6] for this new high temperature superconductor based on single crystal X-ray studies. These models have virtually identical cation distributions, but differ in the arrangement of oxygen ions in the Bi_2O_2 bilayer. In the first,[4] oxygen ions are placed between the sheets of bismuth ions, in an arrangement similar to that found in Aurivillius layered oxides,[12] whereas the second[5–7] has a coplanar arrangement of bismuth and oxygen. The [110] projection is most suitable for comparing the two models, and accordingly images from both were simulated and compared with experimental results. At a focus slightly beyond the optimum both simulations gave a broad overall agreement with the features of the experimental image, although with the oxygens in the same plane as the bismuth the scattered intensity from this plane appeared to be slightly enhanced, and this manifested itself as a more pronounced white fringe between the bismuth-oxygen components and the rest of the structure. The differences between the simulations from the two models were, however, minimal and it was concluded that the scattering from the oxygen ions was insufficient at this value of specimen thickness to distinguish between them. However, with the onset of increased multiple scattering at greater specimen thicknesses differences were expected to occur,[13] but interpretation of images of thick crystals of such strong scatterers is difficult, particularly for those involving inelastic electrons.[14] In addition, there exists the possibility of crystal bending. Consequently no further attempts at image matching were made, although studies of this problem are continuing.

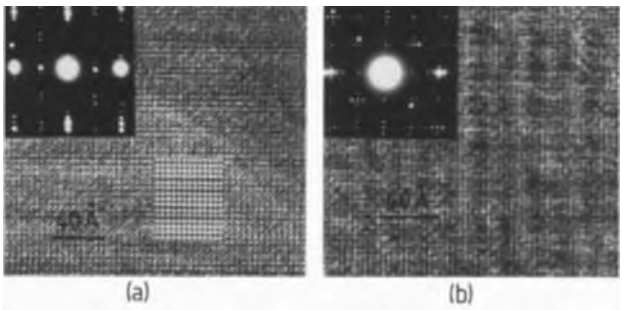


Fig. 3. HREM image of a crystal viewed in the [001] orientation, with insert selected area electron diffraction patterns, a) with one-dimensional superlattice, b) with an apparent two-dimensional superlattice. The inset image simulation in a) was calculated for a crystal thickness of 60 Å and an objective lens defocus of −2200 Å.

This same model was used to simulate images in the [100] projection and again it gave good agreement with the basic image contrast. However, in this projection a superlattice was also visible, which can be seen as a periodic darkening of the overall contrast in a direction perpendicular to the *b* axis (Fig. 2). Image simulations from the basic structure reveal that the darker component represents the Bi_2O_2 layer and the lighter parts the Sr-Ca-Cu-O. This darkening might therefore arise from the inclusion of heavier cations within the Sr-Ca-Cu-O component. Bearing in mind the established tendency of bismuth to replace calcium, it is proposed that this is the origin of the modulating image contrast. Accordingly a model was constructed for such a superlattice and this is shown schematically in Figure 4. Here rows of calcium ions parallel to the [100] axis were replaced by bismuth in

every fifth unit cell. The proposed substitution of the Ca by Bi ions will necessitate a conversion of the square pyramids of oxygen around copper atoms into linked octahedra which effectively constitute a small section of perovskite structure and will also require a local expansion of the structure in the [001] direction. Between the regions of additional bismuth, the layers in the model of Figure 4 suffer a contraction, and, as the regions of excess bismuth are staggered in adjacent layers, the average layer spacing is that of the published structure. Interestingly in this construction, each Bi substituent is accompanied by two oxygen atoms which over-compensate for the increased charge on the bismuth. Thus the resultant stoichiometry is $Bi_{2.2}Ca_{0.8}Sr_2Cu_2O_{8.4}$, giving a nominal average copper valency of +2.33, reminiscent of the copper valency in $YBa_2Cu_3O_7$ superconductors. Images simulated from this model are in good agreement with those obtained experimentally in the [001] projection (Fig. 3). The same model was also used to simulate images in the [100] projection with some displacement/relaxation of the anion lattice at the positions of the inserted oxygen ions as indicated in Figure 4, and the basic superlattice contrast was again obtained. It is therefore concluded that this substitution scheme provides a plausible explanation for both the non-stoichiometry of this material and the observed superlattice. Furthermore, it is assumed that the occasional departure of the superlattice period from five to either four or six unit cell repeats is a means by which the lattice can reduce the strain energy built up by this distortion.

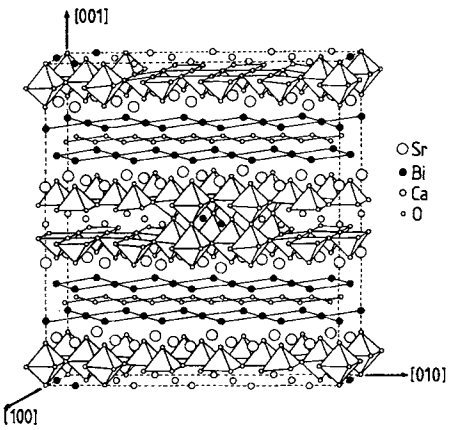


Fig. 4. One superlattice unit cell of the structure model used for the image simulations of Figures 1, 2 and 3. The copper atoms are located at the centers of the square pyramids or octahedra. Unit cell dimensions are $a = 5.4$ Å, $b = 5.4$ Å, $c = 30.7$ Å.

In compositional terms, our model is consistant with the analytical data of *Chippindale* et al.,[15] and would correspond to their predominant phase. Detail differences in cation ratio could well arise from the presence of the superlattice and its variable periodicity, and our structure model can be regarded as an intermediate between two possibly hypothetical end-member phases, namely $Bi_2CaSr_2Cu_2O_8$ and $Bi_3Sr_2Cu_2O_9$. With the general formula $Bi_{2+x}Ca_{1-x}Sr_2Cu_2O_{8+2x}$, the main phase described by *Chippindale* et al.[15] would correspond to $x = 0.143$. On the other hand, their second phase cannot fit easily into this scheme due to the much reduced copper content. This phase, which has a reduced c parameter, may be constructed, however, if a complete Cu-O layer together with a Sr-O layer, were removed, giving the stoichiometry $Bi_{2+x}Ca_{1-x}SrCuO_6$, with $x = 0.286$.

Experimental

Samples with nominal stoichiometry $Bi_{2+x}Sr_2Ca_{1-x}Cu_2O_{8+\delta}$, where $x \approx 0.2$ and $\delta \approx 0.4$, were prepared by reacting Bi_2O_3, $CaCO_3$, $SrO_2/Sr(NO_3)_2$ and CuO in appropriate proportions at 800 °C in air for 20 hours. Samples were tested for superconductivity in the temperature range 10–300 K using both four-probe electrical resistance and field exclusion measurements, and the results in Figure 5 show that a zero resistance state is obtained at 83 K. The samples showed a Meissner effect comparable to those obtained for $YBa_2Cu_3O_{6.9}$ in the same apparatus.

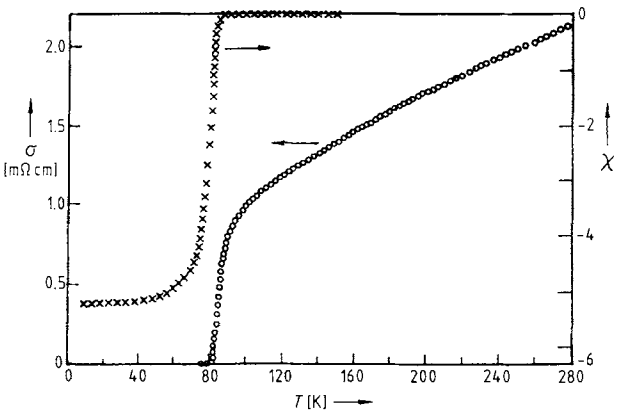


Fig. 5. Variation with temperature of resistivity and AC susceptibility of a pressed pellet of $Bi_{2+x}Ca_{1-x}Sr_2O_{8+\delta}$, where nominally $x \approx 0.2$ and $\delta = 0.4$. The resistivity vanishes at 83 K coinciding with the sharp turn in the susceptibility.

Specimens were prepared for HREM examination by grinding the synthesized material in an agate mortar and pestle in either acetone or liquid nitrogen; the latter being used to embrittle the sample and encourage non-standard cleavage. A drop of the suspension was then placed onto a copper grid coated with a holey carbon film. HREM investigations were carried out with a modified JEOL JEM-200CX instrument [16] operated at 200 kV, with objective lens characteristics $C_s = 0.52$ mm, $C_c = 1.05$ mm and an interpretable point resolution of 1.95 Å at the optimum defocus. Crystals were chosen by examination in the selected-area diffraction mode, and they were oriented such that the beam was parallel to each of the main high symmetry zone axes. After careful correction of residual astigmatism and illumination system misalignments [17], images were recorded at a magnification of ca. 450.000 X. For comparison with experimental images, model-simulated images were computed using the multislice method [18] for [100], [110] and [001] projections of the previously identified basic unit cell over a systematic range of crystal thicknesses and objective lens defocus values.

Received: November 8, 1988;
supplemented version: March 20, 1989

[1] C. Michel, M. Hervieu, M. M. Borel, A. Grandin, F. Deslandes, B. Raveau, *Z. Phys. B68* (1987) 421.
[2] H. Maeda, Y. Tanaka, M. Fukutomi, T. Asano, *Jpn. J. Appl. Phys. Lett. 27* (1988) L 209.
[3] C. W. Chu, L. Gao, P. H. Hor, Z. J. Huang, R. L. Meny, Y. Y. Sun, Y. Q. Wang, Y. Y. Xue, *Phys. Rev. Lett. 60* (1988) 941.
[4] M. A. Subramanian, C. C. Torardi, J. C. Calabrese, J. Gopalkrishnan, K. J. Morrisey, T. R. Askew, R. B. Flippeu, U. Chowdhry, A. W. Sleight, *Science 239* (1988) 1015.

ADVANCED MATERIALS

[5] S. A. Sunshine, T. Siegrist, L. F. Schneemeyer, D. W. Murphy, R. J. Cava, B. Batlogg, R. B. van Dover, R. M. Fleming, S. H. Glarum, S. Nakahara, R. Farrow, J. J. Krajewski, S. M. Zahurak, J. V. Waszczak, J. H. Marshall, P. Marsh, L. W. Rupp, Jr., W. F. Peck, *Phys. Rev. B38* (1988) 893.
[6] J. M. Tarascon, Y. Le Page, P. Barboux, B. G. Bagley, L. H. Greene, W. R. McKinnon, G. W. Hull, M. Giroud, D. M. Whang, *Phys. Rev. B37* (1988) 9382.
[7] H. G. von Schnering, L. Walz, M. Schwarz, W. Becker, M. Hartweg, T. Popp, B. Mettich, P. Müller, G. Kämpf, *Angew. Chem. Int. Ed. Engl. 27* (1988) 574; *Angew. Chem. 100* (1988) 604.
[8] Y. Matsui, H. Maeda, Y. Tanaka, S. Horiuchi, K. Ibe, *Inst. Phys. Soc. Conf. Ser. 93* (1988) 231.
[9] L. R. Wallenberg, J. S. Anderson, J. G. Thompson, R. L. Withers, J. D. Fitzgerald, *Inst. Phys. Soc. Conf. Ser. 93* (1988) 237.
[10] M. D. Kirk, J. Nogami, A. A. Baski, D. B. Mitzi, A. Kapitulnik, T. H. Geballe, C. F. Quate, *Science 243* (1988) 1673.
[11] D. F. Lynch, M. A. O'Keefe, *Acta Crystallogr. A28* (1972) 536.
[12] B. Aurivilius, *Arh. Kemi. 2* (1950) 519.
[13] N. P. Huxford, D. J. Englesham, C. J. Humphreys, *Nature London 329* (1987) 812.
[14] W. O. Saxton, W. M. Stobbs, *J. Microsc. 151* (1988) 171.
[15] A. M. Chippindale, S. J. Hibble, J. A. Hriljac, L. Cowey, D. M. S. Baggley, P. Day, A. K. Cheetham, *Physica C152* (1988) 198.
[16] D. A. Jefferson, J. M. Thomas, G. R. Millward, K. Tsuno, A. Harriman, R. D. Brydson, *Nature London 323* (1986) 428.
[17] D. M. Smith, W. O. Saxton, M. A. O'Keefe, G. J. Wood, W. M. Stobbs, *Ultramicroscopy 11* (1983) 263.
[18] J. M. Cowley, A. F. Moodie, *Acta Crystallogr. 10* (1957) 609.

Polymer Benzo[15]crown-5 Complexes as Sensor Materials for Solvent Vapors—Aromatic Halogenated Hydrocarbons and Polar Solvents**

By *Franz L. Dickert** and *Doris Zeltner*

Dedicated to Professor Gerd Wedler on the occasion of his 60th birthday

For the first time thin layers of polymer-metal complexes with crown ether ligands have been applied as sensor materials for the detection of solvent vapors. The hydrophobic properties of these films enable the detection of even halogenated and aromatic hydrocarbons through conductivity measurements.

The crown ether[1] [15]crown-5 (15C5) forms 1:1 complexes with Mg^{II}, Zn^{II}, Co^{II} and Ni^{II} ions (because they fit well into the cavity of this macrocyclic ligand) and can act as a tetra- or pentadentate ligand.[2, 3] Complexes with the composition $[M^{II}(15C5)\ (S)_2]^{2\oplus}$ have been identified in donor solvents (S). In inert solvents, however, even the usually non-coordinating $ClO_4^{\ominus}$ ion yields inner sphere complexes.[3] The reversible substitution reaction of coordinated anions $X^{\ominus}$ (e.g. $ClO_4^{\ominus}$) by donor molecules [Eq. (a)] has been applied to develop sensor materials for solvent vapors:

$$[M^{II}(15C5)(X)_2] + 2\,S \rightleftharpoons [M^{II}(15C5)(S)_2]^{2\oplus} + 2\,X^{\ominus} \qquad (a)$$

[*] Prof. Dr. F. L. Dickert, Dr. D. Zeltner
Institut für Physikalische und Theoretische Chemie
der Universität Erlangen-Nürnberg
Egerlandstraße 3, D-8520 Erlangen (FRG)

[**] This work was supported by Siemens AG, Central Research and Development (ZFE F1 AMF 32, Dr. *G. Mages*), and the Fonds der Chemischen Industrie.

The formation of a charged complex and anions through the interaction of the initial complex with solvent molecules can easily be detected by conductivity measurements. For practical use formaldehyde resins[4] synthesized from benzo[15]crown-5 (B15C5) are more convenient (§B15C5). These polymer materials form complexes with $Mg^{2\oplus}$ such as **1** in $CH_3OH/CHCl_3$ solution.

Solutions of these polymer complexes are dropped onto interdigital structures to perform conductivity measurements. Stable amorphous films with a thickness of approximately 0.2 μm to 1 μm are obtained after evaporation of the solvent.

The sensor effect consists of two steps. First, an absorption of solvent vapors by the solid macrocyclic layers occurs followed by a chemical reaction according to equation (a). Macrocyclic complexes are very favorable materials for the absorption of different kinds of solvent since these ions have pronounced hydrophobic properties. Strong absorption occurs in the case of protic and aprotic polar solvents such as alcohols, ketones, esters etc. and also for aromatic and halogenated hydrocarbons.

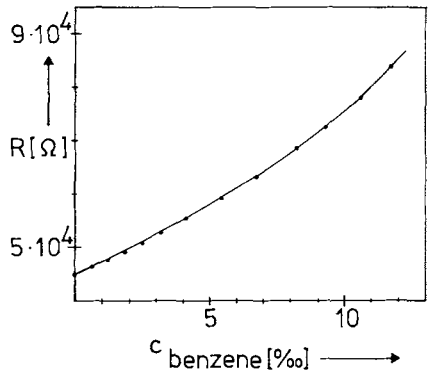


Fig. 1. Dependence of the resistance of the 1:1 complexes of $Mg(ClO_4)_2$ with §B15C5 on an interdigital structure (5 μm electrode distances) on the amount of benzene in the air at 20 °C and 50% humidity.

A typical measurement, e.g. the detection of benzene in the air, is depicted in Figure 1. The resistance of the sensor layers increases parallel with the amount of solvent vapor in the air produced by a gas mixing apparatus.[5] Solvents with no donor properties also result in this sensor effect, since water stemming from the humidity of the air is removed from the sensor layers by the incorporated benzene. Since ionic conductivity is responsible for the described effect, as the ion concentration is diminished according to equation (a) the resistance of the sensor layers increases. The sensitivity of the proposed sensor materials to water vapors can be reduced by increasing the hydrophobic properties of the layers. This can be achieved by the inclusion of cross linking agents such as anisole which enlarge the aromatic ring content in the resins. The addition of ingredients with solvating power such as polyethyleneglycols enables sensors to be designed with characteristic properties. As shown in Figure 2 this procedure can yield a zero slope for certain solvent vapors (e.g. dichloromethane) whereas other solvents (e.g. ethanol) give

a sensor response. Ions other than **1** can also be used. The B15C5 ligand acts in the case of the $K^{\oplus}$ ion as a cap since the ion diameter is larger than the cavity dimension of this crown ether. The application of arrays of these sensors with different characteristic lines makes it possible, in combination

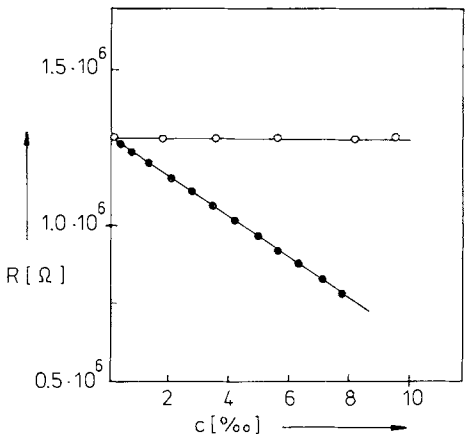


Fig. 2. Dependence of the resistance of the 1:1 complexes of KCl with § B15C5 after the addition of polyethyleneglycol (100 wt.-%, M_r 1000) on an interdigital structure (5 µm electrode distances) on the amount of dichloromethane (○) and ethanol (●) in the air at 20 °C and 30% humidity.

with the methods of pattern recognition,[6–8] to detect organic vapors in the air independent of the humidity. More generally, the selectivity of these sensors can be improved by sophisticated signal processing.

These gas phase measurements can also be applied to detect traces of organic solvents in water. For this purpose a Teflon membrane was applied to separate the sensor element in the gas phase from the water. The solvent vapor is able to penetrate the membrane and a constant vapor pressure of water is obtained in this way. Results for ethanol and dichloromethane are presented in Figure 3. The absorption of the coordinating ethanol [eq. (a)] leads to a decrease in the resistance whereas the opposite effect is observed for dichloromethane as already described for benzene (Fig. 1).

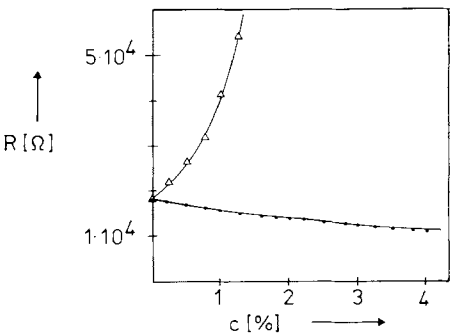
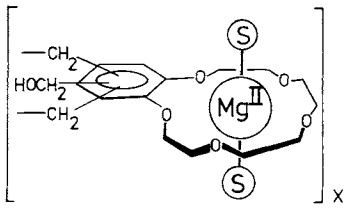


Fig. 3. Dependence of the resistance of the 1:1 complexes of $Mg(ClO_4)_2$ with §B15C5 on interdigital structures (5 µm electrode distances) on the amount of ethanol (●) and dichloromethane (△) in water at 20 °C for a dipping sensor. The sensor element and the water are separated by a permeable Teflon membrane.

The detection limits can easily be determined from the characteristic lines. According to Figure 1, 17 ppm benzene in air or 40 ppm ethanol and 6 ppm dichloromethane in water (Fig. 3) are detectable if a resolution of 10^{-3} for the relative changes in the resistance are assumed.

It is possible to construct low cost equipment for the detection of solvent vapors based on the proposed polymer macrocyclic complexes **1**. The conductivity measurements



1

are easily performed with oscillator circuits incorporating a free running multivibrator. Another possibility is the application of a chemical field-effect transistor (ChemFET).[9] In this method the sensor material is applied to the gate of a ChemFET and electrical contact is realized throuh the use of a perforated electrode[10] which is permeable to gas. In this way compatibility to integrated circuits can be achieved.

Received: February 7, 1989

[1] E. Weber, F. Vögtle, *Top. Curr. Chem. 98* (1981) 1.
[2] F. L. Dickert, M. Waidhas, *Angew. Chem. Int. Ed. Engl. 24* (1985) 575; *Angew. Chem. 97* (1985) 569.
[3] F. L. Dickert, W. Gumbrecht, S. W. Hellmann, M. Waidhas, *Ber. Bunsenges. Phys. Chem. 89* (1985) 875.
[4] E. Blasius, K.-P. Janzen, W. Klein, H. Klotz, V. B. Nguyen, T. Nguyen Tien, R. Pfeiffer, G. Scholten, H. Simon, H. Stockemer, A. Toussaint, *J. Chromatogr. 201* (1980) 147.
[5] F. L. Dickert, E. Lehmann, S. Schreiner, G. Mages, H. Kimmel, *Anal. Chem. 60* (1988) 1377.
[6] P. Geladi, B. R. Kowalski, *Anal. Chim. Acta 185* (1986) 1.
[7] R. Müller, E. Lange, *Sens. Actuators 9* (1986) 39.
[8] G. Bertlein, F. L. Dickert, unpublished.
[9] P. Bergveld, *IEEE Trans. Biomed. Eng. BME 19* (1972) 342.
[10] P. Tischer in W. Heywang, R. Müller (Eds): *Sensorik*, Springer Verlag, New York, 1986, p. 166.

Manuscripts intended for publication as communications should be sent to ADVANCED MATERIALS PO Box 101161, D-6940 Weinheim, FRG. Authors are requested to consult the "Instructions to Authors" which are reproduced in the January issue of the journal or are available from the editorial office on request.

Conference Reports

Martensitic Transformations in Bochum

By Norbert Jost *

The European Conference on The Martensitic Transformation in Science and Technology held on March 8.–10. 1989 in Bochum, was a sequence of more or less informal meetings of researchers from western European countries interested in martensitic transformation.** It was organized by *E. Hornbogen* and *N. Jost* from the Institute of Materials at the Ruhr University, Bochum, and *V. Schumacher* from the German Society of Materials (DGM), Oberursel.

The martensitic transformation is a particular type of first order structural phase transformation in crystalline solids. Among its characteristics are its diffusionless nature and the rather large amount of shear displacement associated with the change in crystal structure. Consequently, its onset and course is not only determined by thermodynamic equilibria and nucleation, but also by internal and external shear stresses. It has been found in all types of crystalline materials: ceramics (ZrO_2), polymers (PTFE), and metals (steels, shape memory alloys). The differences in the characteristics of the martensitic transformation from similar transformations in crystalline solids are shown in Table 1.

Table 1. Definition of the martensitic transformation in comparison with some similar solid state reactions.

characteristics / transformation	no diffusion $D \approx 0$	no change in chemical composition $\Delta C \approx 0$	first order transformation 1. Order	large lattice variant shear $\gamma_{\beta\alpha} \gg 0$
martensitic	+	+	+	+
pre-martensitic (and similar)	+	+	○	○
bainitic	○	○	+	+
massive	○	+	+	○

Due to the strong response to the conference announcement two parallel oral sessions in addition to posters were necessary. The topics of the conference were subdivided into four large groups: 1) Fundamentals; 2) Iron Based Alloys, Steels; 3) Shape-Memory Alloys; and 4) Mn-, Ti-, Zr-Alloys and Ceramics.

[*] N. Jost
Institut für Werkstoffe
Ruhr-Universität Bochum
D-4630 Bochum 1 (FRG)

[**] Conference proceedings will be published by the "DGM-Informationsgesellschaft", Deutsche Gesellschaft für Metallkunde e.V., D-6370 Oberursel, FRG. Editors: E. Hornbogen, N. Jost.

Five invited lecturers summarized recent research interests and 75 contributed papers covered a wide range of more specialized subjects. Additionally, two workshop discussions dealing with "Residual Austenite and Measurement Techniques" and "Future of Shape Memory" were held.

The aim of the conference was to bring together the various interested groups in western European research institutes and industry in order to review the present situation, to assess the prospects, and to define tasks for the future.

For about 3000 years mankind was baffled by the phenomenon of the hardening of steel. About 100 years ago the first successful scientific efforts were made for the scientific clarification of this problem by *Sorby* (1865) in Sheffield. *Adolf Martens* (1850–1914), the ex-president of the Royal Institute for the Testing of Materials, Berlin, gave his name to the main theme of the conference, and an introductory lecture ("*Adolf Martens* and Early Research on Martensite") commemorated the 75th anniversary of his death. This was given by *H. Czichos*, the vice-president of the present Federal Institution for the Testing of Materials (BAM) in Berlin. He recalled some of the highlights of the fundamental work of this great researcher and presented some very interesting original drawings made by *A. Martens* in the 19th century using a specially developed microscope.

The sessions on shape memory alloys (SMA) were led off by three keynote lectures. In the first one, *L. Delaey* (Katholieke Universiteit Leuven, Belgium) gave a review of the potential shape memory alloys. Because SM-effects are not shown in all martensitic alloy systems, all SME "candidate" systems were pointed out, and three groups of technologically important SMA were highlighted. Besides the characteristics of copper- and nitinol based alloys, two recently developed iron based alloys (Fe-Mn-Si and Fe-Ni-Co-Ti) were discussed. The subjects of the second keynote presentation by *R. Gotthardt* (Ecole Polytechnique Federale de Lausanne, Switzerland) were the TEM mobility of austenite-martensite interfaces as well as hysteresis and internal friction. *G. Guenin* (Institut National des Sciences Appliquees, Villeurbanne, France) discussed the two way memory effect in relation to the nucleation and growth of martensite.

The session on the fundamentals of the martensitic transformation was started by a paper by *W. Krauss, S. K. Papi* and *H. Gleiter* (Universität des Saarlandes, Saarbrücken, FRG) in which the mechanism of martensite nucleation was

reviewed. *I. Müller* (Technische Universität Berlin, West) discussed a model for the simulation of shape memory behavior after which the session was concluded by *J. Ortin* and *A. Planes* (University of Barcelona, Spain). They pointed out the thermodynamics of the thermoelastic martensitic transformations in relation to calorimetric measurements.

The second session on shape memory alloys was concerned with thermal and thermomechanical aspects. It was led off by *M. Sade* (a von Humboldt fellow on leave from Centro Atomico Bariloche, Argentina) who gave a report on the thermal and mechanical fatigue of shape memory alloys. The other papers in this session discussed the effect of aging and the thermal and thermomechanical stability of Cu-based SMA.

Many contributions were presented on alloy development and applications, most of them concerned with Ni-Ti alloys. The report of *P. M. Kleinherenbrink* and *J. Beyer* (Univerisity of Twente, Enschede, Netherlands) dealt with the control of the transformation temperatures of Ni-Ti alloys by ternary additions and *T. Duerig* and *K. Melton* (Raychem Corp., Menlo Park, USA) presented details of a very effective way to obtain wide hysteresis in Ni-Ti alloys by the addition of niobium. *J. Beyer, E. J. M. Hiensch* and *P. A. Besselink* from the university of Twente, Enschede, Netherlands reported work on the possibility of the resistance welding of Ni-Ti SMA. The results of this work may be very interesting for the future, especially for new industrial applications of SMA. In the same way this could be said for the "CADSMA", the computer aided design of SMA. A large group of authors from the university of Leuven and *N. V. Proteus* (Kortijk, Belgium) outlined the special problems concerned with construction using SMA. In the next three lectures *P. Tautzenberger* (G. Rau GmbH, Pforzheim, FRG) and *D. Stöckel* (Raychem Corp., Menlo Park, USA) gave an overview of the industrial application of SMA and drew a comparison to the properties of thermobimetals. *J. M. Welter* and *P. Naudot* (Trefimetaux, Serifontaine, France) reported about the development in industrial scale fabrication of Cu-based SMA.

A whole session was concerned with new iron based SMA. It was led off by *M. Sade* who gave a review of the SME in Fe-Mn-Si alloys. *Y. Vanderveken* and his coauthors (Katholieke Universiteit Leuven, Belgium) continued the session with a report on the influence of thermomechanical treatment on the one way effect in Fe-Mn-Si alloys. *P. Donner* and *E. Hornbogen* (Ruhr-Universität Bochum, FRG) described the production of Fe-Mn based SMA by melt spinning and discussed the results in relation to the influence of rapid solidification on the SM behavior. The session was concluded by two papers from *N. Jost* and *K. Escher* (Ruhr-Universität Bochum, FRG) in which the effect of the austenite microstructure on the martensitic transformation and the mechanical properties of Fe-Ni-Co-Ti SMA were analyzed.

The last session on SMA was concerned with special transformation characteristics and hysteresis. It began with a paper by *L. Lu, E. Aernoudt* and *L. Delaey* on the modeling of hysteresis in martensitic transformations after which *J. Stoiber, J. van Humbeeck* and *R. Gotthardt* described the hysteresis effects during martensitic transformation in Cu-Zn-Al SMA. The report of *G. Airoldi* and *G. Riva* (Universita di Milano, Italy) dealt with the stepwise, stress free, martensitic transformation in the Ni-Ti system. The last paper of this session was presented by *L. Manosa* (University of Barcelona, Spain) who had studied the origin of acoustic emission during thermoelastic martensitic transformation.

In addition to these oral sessions 21 posters concerned with SM and a workshop on the future of shape memory held by *E. Hornbogen* gave the participants of the conference the opportunity to discuss more of the fundamental as well as specialized subjects. A systematic survey of shape memory effects and applications in the different fields of engineering was given by *E. Hornbogen* as a basis for the workshop discussion. It can be seen from Table 2 that a large field of applications exist.

Table 2. Systematic survey of shape memory effects and applications in engineering.

technology \ SM effect	one-way	two-way	pseudo-elasticity
connecting, fastening	couplings, pipe connections expanding rivets		seals, spectacle frames
control		valve control, temperature protection greenhouse opener	
motor vehicle		opening of fog lights gear adjustments	high noise absorption
data processing	plug connections for circuits	head/disc system magnetic data memory color changes for optical storage	
engines/ power		rotating machines, solar battery control	
automation	manipulators	robot hands	
medicine	implants (osteosynthesis)	endoscope control	dental braces
clothing	fabric reinforcement		rubber substitute

Besides the sessions on SM, the second large group of contributions was concerned with new developments in steels. It was begun by the keynote paper from *I. Schmidt* (Zahnradfabrik Friedrichshafen AG, FRG) who gave an overview of metastable ferrous austenites and the consequences on fracture and tribology.

The session was continued by *B. Skrotzki* and *E. Hornbogen* (Ruhr-Universität Bochum, FRG) who described a volume fraction vs. temperature function of the martensitic transformation in iron based alloys. *H. Weiland, L. M.*

Matthews and *H. J. Bunge* (Technische Universität Clausthal, FRG) reported work on the texture and microstructure of lath martensite and *H. Berns* (Ruhr-Universität Bochum, FRG) traced the development of new martensitic nitrogen steels, discussing his results with special reference to the technological applications of this steel. *D. Löhe, R. Bartels* and *E. Macherauch* (Universität Karlsruhe, FRG) then dealt with the interaction of dynamic strain aging and the transformation of retained austenite to martensite, after which *K. Ullako* and *J. Pietikäinen* (Helsinki University of Technology, Espoo, Finland) reported their results on the carbon redistribution in low temperature deformed and aged martensite. Fe-Ni-C alloys were the subject of a paper by *X. M. Zhang* (Institute of Metal Research, Shenyang, China) who had studied the effect of plastic deformation on the lenticular martensitic transformation. *T. Abe* and *C. M. Sellars* gave an overview on the effect of thermo-mechanical treatment on the reverse transformation behavior and micro-duplex formation in Fe-Ni alloys. The last lecture of this session was given by *H. Vetters* (Institut für Werkstofftechnik, Bremen, FRG) who discussed the influence of unidirectional and cyclic loading on the martensite formation in austempered ductile iron.

The second session on steels was concerned with the mechanical properties. It began with a paper by *E. Gautier* and coauthors (Laboratoire de Science et Genie des Materiaux Metalliques, Nancy, France) on the transformation plasticity and resulting microstructures for strain induced martensitic transformation in Fe-Ni-C alloys. *Y. Zhang* (on leave from Shangai Iron and Steel Institute, China) reported on reverse austenite and its effect on mechanical properties. The microstructure-strength relationship of low carbon bainite and martensite was discussed by *W. Österle* (BAM, Berlin, FRG), and then *A. Schulz-Beenken* and *H. P. Hougaray* (Max-Planck-Institut für Eisenforschung, Düsseldorf, FRG) reported on a development of high strength martensite. They have shown that the age hardening of coherent intermetallic precipitates is a very effective way to obtain such martensites. In the last paper of the session *J. B. Vogt* and his coauthors (Universite de Lille, France) discussed the influence of nitrogen on the low temperature stress induced martensitic transformation of stainless steel.

In the workshop "Residual Austenite and Measurement Techniques" held by *I. Schmidt* and in five additional posters, interesting aspects on the development of steels were discussed in detail.

The session on transformations in Mn-, Ti-, Zr-alloys and ceramics was led off by *H. Warlimont* and coworkers (Vacuumschmelze Hanau, FRG). They gave an overview of displacive transformation phenomena in high-T_c-superconductors. The lecture by *G. Vogl* and coauthors (Universität Wien, Austria) dealt with the martensitic phase transition and soft phonons in the pure metals Ti and Zr. *M. Humbert* and coworkers (University of Metz, France) explained a simulation model for the texture transformation which occurs during the martensitic $\alpha-\beta$ transformation of Zr sheets. The fractal aspects of the martensitic transformation in Zirconia were discussed by *W. Wunderlich* (MPI-Düsseldorf, FRG) who made special reference to the study of fractal geometry as a new method for the characterization of microstructures. *S. Schmauder* (MPI Stuttgart, FRG) discussed the nucleation of the martensitic transformation of ZrO_2 in the system Al_2O_3-ZrO_2 before *M. Ellner* (MPI Stuttgart, FRG) closed the session by describing the structure of the high temperature phase $Mn_{0.8}Al$ (h) and the martensitic transformation of this phase to Mn_5Al_8.

The last contribution of the conference was the presentation of an educational film by *S. Keller* (Gewerbeschule Hamburg, FRG) and *J. F. Edgar* (Stockport College of Technology, England) in which the crystallographic characteristics of the martensitic transformation in steels were shown with hard sphere models.

The conference was an exciting and important meeting and provided an excellent opportunity for researchers from academic institutions and industry to meet and discuss problems and aspects of martensitic transformation.

Composites and Particle Technology in Las Vegas

By Wolfgang A. Kaysser *

The 118th TMS Annual Meeting and Joint TMS/SME (The Minerals, Metals and Materials Society/Society of Metallurgical Engineering) Exhibition from February 27 to March 2, 1989 in Las Vegas, Nevada, USA confirmed the growing importance of particulate technology as the major production route to new high performance materials. It is increasingly accepted that the required property combinations such as high temperature strength, creep resistance and toughness at low temperatures are not achievable in mono-

[*] Dr. W. A. Kaysser
Max-Planck-Institut für Metallforschung
Institut für Werkstoffwissenschaften
Pulvermetallurgisches Laboratorium
Heisenbergstraße 5, D-7000 Stuttgart 80 (FRG)

lithic materials and tailored composite microstructures are needed.

Many advanced materials such as intermetallics, ceramic matrix composites and to a lesser extent metal matrix composites suffer from low fracture toughness. New micromechanics models of composite toughening, presented at the conference, require microstructures which permit toughening through the removal of weakly bonded fibers and the bridging of strongly bonded ductile particles. Titanium aluminides are a nice example of attempts to improve the properties of a monolithic base, e.g. Ti_3Al, by introducing stiffening particulates (SiC) which also enhance creep properties, and second phase ductile inclusion (Nb) which results in an increased toughness at lower temperatures. Other intermetallics such as advanced nickel-aluminide alloys have been recognized as potential composite matrix materials for elevated temperature structural applications. The usefulness of monolithic nickel-aluminide single phase material itself, however, is becoming increasingly doubtful due to a combination of limitations in room temperature formability, and creep, oxidation and pest resistance. Reinforced nickel-aluminide alloys should, instead, form a composite with low density, high tensile strength and acceptable creep resistance.

Typical examples of new materials tailored by particulate technology were presented in sessions such as "Light Weight Alloys for Aerospace Applications". Almost all presentations dealt with materials produced from rapidly solidified or mechanically alloyed powders. Major interest focussed in intermetallics on Ti_3Al, TiAl and NiAl compounds or highly modified multiphase Ni-Al composites. In addition, P/M magnesium alloys were shown to be of growing interest because of their low density. Insufficient mechanical performance and corrosion resistance of coarse grained materials has restricted their application up to now. Rapid solidification leads to a substantial refinement of the microstructure, yielding a considerable increase in strength.

Forming methods for materials with rapidly solidified microstructures or composite nature include powder processing, such as particulate liquid infiltration, melt oxidation or mushy state mixing, hot isostatic pressing, forging, rolling and extrusion as well as spray forming or reactive liquid phase sintering. Developments in these processing techniques were emphasized strongly.

Multiphase composites are far from equilibrium, hence, detrimental chemical reactions between the different phases, in particular between the reinforcement and the matrix, can rapidly degrade the strength of the composite. Attempts to solve these problems include variation of the processing parameters to suppress additional intermetallic phases forming at the interfaces, for example in TiB_2/NiAl composites. In most cases coating of the reinforcing phases is necessary to prevent or slow the interface reactions. Coating of SiC fibers or particulates with TiB_2, TiC and Al_2O_3 is used in nickel aluminides and titanium aluminides. Systems such as Ti_3Al and TiB_2 containing coated SiC create a large number of non-equilibrium heterophase boundaries. The prediction of phase stabilities at these interfaces from thermodynamic data and the definition of rules on the time interval of heterophase compatibility from kinetic evaluations (with respect to the mechanical properties) will be of future importance.

Since many of the advanced composites are intended to be used at elevated temperatures, creep becomes a major issue of composite materials characterization. Materials in which the reinforcements are small enough to act as dispersoids, affecting the creep properties, can be treated by the classical microstructural hardening theory. Materials in which reinforcements are large and interact with the matrix elements must be understood in terms of continuum mechanics. Complimentary approaches are needed to understand the creep properties of these materials, for example a mechanics approach that focusses on the load transfer between the matrix and the fiber, and a mechanisms approach that focusses on the interaction of moving dislocations and gliding grain boundaries with larger particles such as fibers. For very high volume fractions of reinforcements the material can almost be locked against creep due to the high constraint levels generated. Lengthy periods of transient response can occur and tertiary behavior can develop due to the failure of the reinforcements. Especially serious consideration was given to superplastic flow in tensile stress loaded metal matrix composites annealed under thermal cycling. The inequality of the thermal expansion coefficients of metal matrix and reinforcement results in very high tensile elongation at low strain rates and low stresses.

It is understood that the expensive powder technology processing of these advanced composites pays off only for elaborate materials designed for the highest performance. This raises the question of the economical viability, i.e. to what extent these materials will be used in applications other than special tasks such as the NASP (National Aero Space Plane) or the former SDI program. It should be noted, however, that the spin-off result of high level targets in materials science for broader applications has been much greater than in other research areas. The use of SiC reinforced aluminum alloys in the pistons of diesel engines in Japan may be nothing other than a first glimpse of the abundant possible applications of these advanced multiphase composites.

The session on the injection molding of powdered metals and ceramics showed the increasingly detailed understanding of this novel powder forming process. Major concerns were the influence of particle size distributions on viscosity, formability and debindering time. Feedstock consisting of spherical 316L stainless steel powder and a polymer binder showed a trend of increasing viscosity with decreasing particle spacing and with a decreasing ratio of particle spacing to particle size. For a number of alloys it is now obvious, however, that second phases forming a liquid during sintering need to be present to achieve full density products after the sintering of the debindered greens. A typical example are injection molded nickel aluminides.

Book Reviews

Corrosion, Thin Films, Glasses, Sensors ...

DECHEMA Corrosion Handbook, Vol. 3. Edited by *D. Behrens*. VCH Verlagsgesellschaft, Weinheim 1988. ix, 282 pp., bound, DM 775.—ISBN 3-527-26654-2

The DECHEMA Corrosion Handbook is a completely new English edition of the DECHEMA Werkstoff-Tabelle and describes the corrosion properties of metallic, inorganic non-metallic, organic and composite materials in different corrosive media. The third volume summarizes the corrosion in acid halides, amine salts, bromides, bromine, carbonic acids and lithium hydroxide, the literature being cited approximately up to 1985.

The general layout of the third volume is identical to the previous ones. Again, the contents are clearly arranged and it is therefore easy for the user to find the desired information quickly. A criticism of the earlier volumes was the rather frequent statement of electrode potentials without any reference system. In the third volume, most of the potentials mentioned in the text, figures or tables refer explicitly to different reference systems (standard hydrogen electrode, standard calomel electrode) although in the chapters concerning bromide (p. 115, 116, Table 12), carbonic acids (Figs. 17, 44, 45) and lithium hydroxide (Fig. 1) the reference system is missing. A list of all reference electrodes used in the Corrosion Handbook, should be included into the introduction, citing their potentials versus the Standard Hydrogen Electrode.

Chapter 1 discusses corrosion properties in acid halides. The introduction to this chapter is very extensive and makes up half of the chapter. Different acid halides are described in detail, including their chemical properties, technical importance and corrosivity with respect to different materials. Then, a detailed description of the corrosion properties of the individual materials with respect to the different acid halides is given. The discussion of the properties of the corrosion system, the medium (introduction), as well as the material is clearly arranged for the reader, despite the overlap in the information provided in the introductory and the later part of the chapter. At the end of this chapter, informative tables summarize the usability of the individual materials in varying concentrations of the different acid halides.

Chapter 2 summarizes the corrosion properties of materials in amines. The short introduction touches only slightly the major importance of amines as inhibitors, and a detailed discussion of the adsorption properties of inhibitors, their technological use and the dangers accompanied with their use (e.g. localized corrosion, if the inhibitor concentration is too low, H-embrittlement in certain solvents) is missing. In the second part of this chapter a detailed description of the corrosion properties of the different materials in solvents containing amines is given. The inhibiting properties of the individual amines are discussed in detail, with special emphasis on their use as vapor-phase-inhibitors in order to inhibit the atmospheric corrosion of Cu and Fe.

Chapters 3 and 4 summarize the corrosion induced by bromides and bromine. In this context, especially the localized corrosion induced by bromides is of importance. The first part of chapter 3 gives a short introduction to the topic, but the determination of pitting potentials by potentiostatic and potentiodynamic experiments is described insufficiently as is the determination of repassivation potentials (although repassivation potentials are mentioned on p. 115). In addition, there is no discussion of the importance of corrosion potentials with respect to pitting potentials nor one on cathodic currents, which have to balance the anodic dissolution of the metal in pits in order to allow pitting corrosion to occur.

Chapter 5 is concerned with corrosion in carbonic acid with special emphasis on the corrosion of Cu and steel in CO_2 containing tap-water. The well written introduction provides the reader with a lot of information concerning the physical properties of CO_2 containing water, water hardness and the electrochemical principles of the corrosion in this system. The general background which is provided in this introduction, is complementary to the detailed description of the individual corrosion properties which are presented in the following part of the chapter. The latter parts are well written, providing lots of information on the corrosion of materials in CO_2 containing media. Techniques mentioned (CERT-test, Fig. 32), should have been explained in more detail for the non-specialist users of the handbook. Figures 44 & 45 discuss pitting corrosion and repassivation, using techniques and terms which have been introduced in chapter 3. It would have been much better to summarize such important techniques and corrosion mechanisms in an individual chapter than to distribute this type of information widely throughout the book. The last chapter is devoted to lithium hydroxide, and is in general well written.

Overall, as a reference book, the third volume of the DECHEMA Corrosion Handbook is highly recommended to anyone working as an engineer or scientist in the corrosion area.

Martin Stratmann
Max-Planck-Institut für Eisenforschung
Düsseldorf (FRG)

Ionized-Cluster Beam Deposition and Epitaxy. Edited by *T. Takagi*. Noyes Publications, Park Ridge, NJ, USA 1988. viii, 231 pp., bound, US $ 48.—ISBN 0-8155-1168-X

The various techniques for ion-assisted deposition of thin films composed of metals, semiconductors, insulators, magnetic materials, composites etc. are of great importance for application in industrial production as well as for fundamental studies in research laboratories. This volume, of the series Materials Science and Process Technology, deals with the deposition of thin films by means of beams composed of

ionized aggregates of a few hundred to a few thousand atoms rather than individual atoms or molecules. These clusters are formed by the condensation of evaporated atoms during adiabatic expansion through a narrow aperture into a high vacuum region. They are then ionized by electron impact and uniformly accelerated in an electric field between source and substrate surface. A single charge on the cluster is thus used to accelerate many hundreds of atoms. A cluster consisting of 500 atoms has a diameter of the order of 30 Å. The size, charge, and acceleration voltage of the clusters are intimately related with the film formation process.

The author of this book is considered to be the pioneer of the ionized-cluster beam technique. He started the research in this field at Kyoto University (Japan) in 1972. The various activities of the author to promote the spreading of this method throughout the world largely determine also the character of this book. In 60 of the 100 references *T. Takagi* is one of the authors. This unbalanced selection of the material implies that a critical comparison of the ionized-cluster beam deposition with both conventional evaporation and sputter deposition as well as low-energy ion deposition is unfortunately not given. Throughout the entire text the author emphasizes the advantages of "his" technique. In the case of crystalline semiconducting materials, like e.g. Si or GaAs, this point of view is totally misleading, because the quality of thin films prepared by ionized-cluster deposition is far inferior to that of films prepared by either chemical vapor deposition or by molecular beam epitaxy. Unfortunately, most aspects of ionized-cluster beam deposition discussed in this book are treated only qualitatively. A number of misprints and errors should be eliminated in a following edition.

Due to the partiality and the lack of an in-depth treatment of the subject this book is of limited use only. It can, however, serve as an introduction to the field.

Klaus Ploog
Max-Planck-Institut für
Festkörperforschung, Stuttgart (FRG)

Mathematical Approach to Glass. By *M. B. Volf.* Elsevier Science Publishers, Amsterdam 1988. 420 pp., bound, DFL 275.—ISBN 0-444-98951-X

There are different approaches to glass science and technology. One approach is based on chemistry and attempts to answer the question of how the properties of a glass change after the substitution of one component by another. A second approach investigates the structure of the glasses and tries to set up structural models. Of course, structure and properties are related to each other. Glass formation, on the other hand, may also be related to thermodynamic and kinetic arguments, both being of equal importance.

In this book the chemical approach to glass is stressed. The text is essentially based on the finding that the properties of glass are roughly determined by the properties of the constituent atoms or ions and by their bonds. Projected into calculations, this in most cases makes it possible to predict in what way an element will behave when bound to oxygen in an oxide glass. Optimization of properties may then also be possible in a given type of glass. Thanks to the rapid introduction of computer technology ranging from pocket calculators to large computers, the field of applied mathematics in glass is expanding.

The book contains four main chapters. In the first, general ideas and models are described, e.g. models on the chemistry and technology of glass, the chemical model as a theoretical base for the calculations in the chemistry of glass, questions of composition and composition factors, characteristics of mass and volume, activation energy for describing temperature dependencies, and questions of acidobasicity.

The second chapter deals with the affinity of properties, that means, how one property is related to another property. This interdependence of properties is, of course, essential for the approach described in this book.

The third main chapter, on the dependence of properties on composition, contains the known and developed methods, e.g. additivity principles, the methods of *Winkelmann* and *Schott, Gehlhoff* and *Thomas, Huggins* and *Sun, Appen, Gan Fu-Xi, Demkina, Mackenzie* et al., and some regressive and statistical schedules.

The fourth main chapter is the most comprehensive one and discusses the physical dependence of properties. The properties investigated are density, optical properties, permittivity, thermal properties, elasticity, strength, hardness, photoelasticity constant, thermal expansion coefficient, resistance to thermal shock, surface tension, viscosity, electrical properties, and chemical durability. Some supplements and a list of references conclude the book.

This book is of importance to people working in the glass industry and who want to know how a property changes with the change of a component. In most cases the absolute value is not necessary. However, the tendency of the change is more important. This book, of course, has also some value to people who are not so familiar with glasses and their properties and who want to get a feeling of how chemistry influences glass properties. However, there are many anomalously behaving glasses, e.g. borate-containing or mixed alkali glasses. In those cases possible differences between prediction and measurements have to be checked.

Günther H. Frischat
Institut für Nichtmetallische Werkstoffe
der Technischen Universität
Clausthal-Zellerfeld (FRG)

Encyclopedia of Materials Science and Engineering, Supplementary Volume 1. Edited by *R. W. Cahn,* Senior advisory Ed. *M. B. Bever.* Pergamon Press, Oxford 1988. xiii, 653 pp., hardcover, US $ 295.—ISBN 0-08-032551-1.

The Encyclopedia of Materials Science and Engineering, published in the spring of 1986, is a comprehensive reference work and source of information for a wide readership, including but not restricted to practitioners in the broad domain of materials. It consists of eight volumes containing 1580 articles, the production of which involved almost 1500 experts all over the world. The Encyclopedia has been well received by reviewers and has been acquired by institutions worldwide.

It is clear that change in some areas is so rapid that publication must be a continuing activity if the Encyclopedia is to

retain its position as an authoritative and up to date systematic compilation of our knowledge and understanding of materials. This is the prime objective of the Supplementary Volumes of the Encyclopedia of Materials Science and Engineering, of which this is the first. The Supplementary Volumes are designed to be used in conjunction with the Main Encyclopedia.

Supplementary Volume 1 contains 113 articles which fall into three categories; articles covering new materials, processing and characterization techniques, models and interpretations, all discovered or developed after the spring of 1985 when the main encyclopedia went to press; articles covering mature topics which for a variety of reasons were not treated in the main encyclopedia; and articles designed to bring the treatment of topics already covered in the main encyclopedia up to date. The later articles are divided into two subsidiary categories.

a) Supplementary articles which are intended to be read in conjunction with the original article of the same, or similar, title in the main encyclopedia; generally a subsidiary phrase such as "recent developments" has been added to the title.

b) Replacement articles which are intended to substitute entirely for the original article and therefore have the title of that article. These articles generally refer to topics in which there have been rapid recent developments: their inclusion does not imply a critical judgement on the original articles.

All articles in Supplementary Volume 1, are furnished with cross-references to relevant articles in the main encyclopedia as well as to other articles in this supplementary volume itself, where appropriate.

As with the Encyclopedia of Materials Science and Engineering itself the careful selection of experts by the two editors has resulted in comprehensive articles. If this standard is maintained in further supplementary volumes the encyclopedia will receive continuously increasing well justified attention and become a must for all libraries covering topics in materials science.

Wolfgang A. Kaysser
Max-Planck-Institut für Metallforschung
Stuttgart (FRG)

Solid State Electrochemistry and its Applications to Sensors and Electronic Devices. By *K. S. Goto*. Elsevier Science Publishers, Amsterdam 1988. x, 454 pp., bound, US $ 119.50.—ISBN 0-444-42912-3.

The title of the book is somewhat misleading, implying that the coverage is much broader than it is in reality. It is in fact restricted to the electrochemistry of solid and liquid (melts, slags) oxides at temperatures in the range 200–2000 °C. The monograph is based on lecture notes of a course given by the author on this specific theme at the Tokyo Institute of Technology since 1971. About 100 "Problems" for discussion and calculations found in the appendix of the book are indicative of this origin.

The book can be divided roughly in two parts, chapters 1–9 "Fundamentals" and chapters 10–13 "Applications". In the course of the first part, which makes up about 60% of the book, a thorough treatment of the following fundamental properties of oxides is given from an electrochemical point of view:

a) Transport properties, diffusion, electronic and ionic conduction in binary oxides and multicomponent systems (chapters 2–5).

b) Thermodynamics of solid state galvanic cells, including the electrochemical Knudsen effusion cell. This is the only location, where the work of *H. Rickert* (erronneously cited throughout as "H. Richert") has been mentioned. His monographs on solid ionic electrochemistry are ignored, as is also the case (with one exception) for the pioneering work of *C. Wagner* (chapters 6–7).

c) Electrochemical kinetics. The chapters 8 and 9 are very useful and overpotential phenomena at the phase boundaries metal/solid oxide as well as metal/liquid-oxide melts are treated thoroughly. The author also introduces the use of the Pt-rotating disc electrode in PbO–SiO_2 melts at 1000 °C.

The final four chapters are devoted to various applications of solid state (sss) devices, with a strong emphasis on oxygen sensors for metallurgy and on MOS-sensors (another name for ISFETS; however, this term is not used in the book). In cooperation with the Japanese steel industry, the author has developed various sensor designs to measure the oxygen activity in molten iron as well as in molten slag. Typical values are 10^{-9} atm and 10^{-8} atm, respectively. Interesting correlations to the carbon content in the iron, the duration of oxygen blasting or the ratio of Fe^{III}/Fe^{II} in the slag have been found. This section is most authoritative, and the predominance of Japanese references is more justified here than in other parts of the book. The work of *Janke* et al. is also adequately discussed. Some parts, however, lie outside the scope "high temperature application" such as those in section 13.3 which include electrochromic displays, coulometric timers or pacemaker batteries. A brief account that electrochemical reactions are relevant to impurity effects and long term behavior (corrosion) of electronic devices, is given in chapter 1, but it is not followed up later in the book.

The typed manuscript has been directly reproduced, unfortunately without line balance, but typing errors are minimal. The price is high, as with many other specialized monographs, but although the variety of the possible subject matter in this area is extremely large, for example, stoichiometry, texture, phases and the result of various combinations, the book is clearly written and a guide in this broad field. It is also clear, that "in the future, many more electronic devices will surely be developed to utilize the physical and chemical properties of solid oxides".

Fritz Beck
Fachgebiet Elektrochemie der Universität
Gesamthochschule Duisburg (FRG)

Handbook of Thin-Film Deposition Processes and Techniques. Edited by *K. K. Schuegraf*. Noyes Publications, Park Ridge, N.J., USA 1988. xvii, 413 pp., bound, US $ 72.—ISBN 0-8155-1153-1

The book gives a thorough account of a large number of thin film deposition processes. Emphasis lies on the techniques which are either already in extensive use in high technology areas, especially in the microelectronics industry, or may be expected to become competitive in the future. Apart from the introduction, which gives a somewhat broader overview, the treatise has been confined to processes in which the films are deposited from the gas phase at pressures ranging from atmospheric to ultra-high vacuum. The techniques treated in this volume can be classified into the following three categories:

1) Chemical methods: They entail chemical vapor deposition (CVD) and its variants, like low pressure chemical vapor deposition (LPCVD) or metal-organic CVD (MOCVD). In these techniques one or several gaseous species react in the vicinity of, or on, the substrate and condense to form a solid film. Apart from the supply of purely thermal energy for reaction initiation a number of additional means are used, leading to higher reaction rates at lower temperatures, such as photochemical vapor deposition (PHCVD) and laser assisted CVD (LCVD). In the former, UV-photons are used to dissociate or excite molecules in the gas phase or on the substrate surface to form a thin film. The latter method either uses a laser beam for the same purpose or for highly localized substrate heating. In electron beam assisted CVD (EBCVD) a high energy electron beam is used instead to dissociate the gas molecules by impact ionization.

2) Physical methods: These include plasma techniques, such as RF and DC sputtering and ion beam deposition, the latter being applied in either of two modes: a) Sputtering mode allowing for a better control over the sputter parameters and a lower operating pressure in the deposition chamber than conventional techniques and b) ion assisted deposition (IAD) in which a beam of ions is directed towards the substrate during the deposition from another source. Conventional vacuum evaporation and electron beam evaporation are not treated in this text, apart from their most advanced application, i.e. in molecular beam epitaxy (MBE). This method offers probably the best control of single crystal growth on a monolayer scale of all deposition techniques in current use. As a result, a number of devices relying on superlattices or quantum well structures have been fabricated, some of which are described in the text. Equally promising is one of the latest developments, namely ionized cluster beam deposition (ICB), in which ionized particles containing typically 100–2000 atoms impinge on a substrate where they spread and eventually condense into a thin film.

3) Physico-chemical methods. They are in essence a combination of the physical and chemical methods mentioned above, the chemical reactions taking place in a plasma generated in a number of ways. Plasma-enhanced or plasma-assisted chemical vapor deposition (PECVD, PACVD) use a plasma generated in a glow discharge. Ions and free radicals produced in the discharge greatly accelerate reaction rates, allowing film deposition at lower substrate temperatures than in purely thermal CVD. Much higher ionizing efficiencies, yielding high deposition rates at still lower substrate temperatures, are offered by electron cyclotron resonance deposition (ECR), in which electrons orbiting in a magnetic field absorb microwave radiation under resonance conditions.

Reactive sputtering, in which a reactive gas is mixed with the inert sputter gas, also belongs to this category.

A special chapter is devoted to plasma and high pressure oxidation of silicon for very large and ultra large scale integration.

Apart from the deposition processes, the book covers a number of other equipment-related topics, such as etching techniques (sputter etching, reactive ion etching, ion beam etching, etc.), resist patterning, including self-development and beam-induced thermal processes.

The book gives a short overview of the physical principles, underlying the various deposition techniques. The basic design and the performance of the deposition equipment are thoroughly outlined. Numerous tables and figures describing the properties and the uniformity of the deposited films are given, enabling the reader to compare the advantages and the limitations of each method. A considerable part of the applications in many chapters has been devoted to silicon technology, in particular to silicon epitaxy, polysilicon, silicides and dielectrics, like silicon oxide, silicon nitride and -oxynitride. The increasing importance of low temperature processing, especially in future ULSI is becoming apparent in view of the many techniques capable of low temperature deposition. III/V-epitaxy and its applications are the leading topics in the chapters on MOCVD and MBE. Other applications include metal films and especially metal-insulator-semiconductor heterostructures, where important advances have been made, particularly by ICB.

The extensive bibliography will be valuable help, especially for newcomers in any of the fields, the references covering the period up to 1986.

In general the book can be recommended to all engineers and scientists wishing to become acquainted with current trends and future outlooks in thin film technology. Since prime importance has been laid on the practical aspects, the production capabilities of the various techniques and their limitations with respect to large scale applications can easily be assessed by the practically minded reader.

Hans von Känel
Laboratorium für Festkörperphysik
der ETH Zürich (Switzerland)

Publishers: Please send books intended for review to ADVANCED MATERIALS, PO BOX 101161, D-6940 Weinheim, Federal Republic of Germany. Book reviews are written at the invitation of the editors but suggestions concerning both suitable books to review and reviewers are welcome. The editors reserve the right to select the books to be reviewed. Books not selected for review will not be returned.

Conference Calendar

July 1989

9–14 **Scanning Tunneling Microscopy/Spectroscopy**
4th Int. Conf.
Oarai (Japan)
Contact: O. Nishikawa, The Graduate School of Nagatsuta, Tokyo Inst. of Technol., 4259 Nagatsuta, Midori-ku, Yokohama 227, Japan

9–14 **Zeolites**
8th Int. Conf.
Amsterdam (Netherlands)
Contact: M. Laboushere, 792 Keizersgracht, 1017 EC, Amsterdam, The Netherlands

10 **Bonding and Repair of Composite Materials**
Birmingham (UK)
Contact: John Herriot, Butterworth, P.O. Box 63, Westbury House, Bury St., Guildford GU2 5BH, UK

10–12 **Appl. Organomet. Chem.: an Entry to the New Technology**
The Pines Resort (Australia)
Contact: Dr. A. F. Masters, School of Chemistry, Univ. of Sydney, Sydney, N.S.W. 2006, Australia

10–13 **Magnetic Resonance in Polymers**
9th Spec. Colloq. Ámpere
Prague (Czechoslovakia)
Contact: P. M. M. Secretariat, c/o. Inst. of Macromol. Chem., Czech. Acad. of Sci., 16206 Prague, Czechoslovakia

10–14 **Ion Sources**
Int. Conf.
Berkeley (USA)
Contact: W. O'Connor, Lawrence Berkeley Lab., 50B-2270, Berkeley, CA 94720, USA, Tel. 415-486-6386, Fax 415-486-7000

10–14 **Electron Spectroscopy**
4th Int. Conf.
Honolulu (USA)
Contact: G. E. McGuire, Microelectronics Ctr. of North Carolina, P.O. Box 12889, Research Triangle Park, NC 27709, USA

10–14 **Organic Coatings**
15th Int. Conf.
Athens (Greece)
Contact: Dr. A. V. Patsis, Inst. in Materials Sci., State Univ. of New York, New Paltz, NY 12561, USA



11–14 **Numerical Analysis of Semiconductor Devices and Integrated Circuits**
6th Int. Conf.
Dublin (Ireland)
Contact: J. J. H. Miller, Nase-Code Conf., INCA, P.O. Box 2, Dún Laoghaire, Ireland

12–14 **Solid-State Laser/Optical Fiber Science and Electromagnetic Theory '89**
Top. Mtg./Sino-Japanese Joint Mtg.
Beijing (P.R. China)
Contact: Optical Soc. of America (OSA), 1816 Jefferson Pl. NW, Washington, DC 20036, USA

16–21 **Catalysis**
Eur. Conf.
Berlin (West)
Contact: Prof. G. Ertl, Fritz-Haber-Inst. der Max-Planck-Gesellsch., Faradayweg 4–6, D-1000 Berlin

17–20 **Polymer Blends**
Prague (Czechoslovakia)
Contact: P. M. M. Secretariat, c/o. Inst. of Macromol. Chem., Czech. Acad. of Sci., 16206 Prague, Czechoslovakia

18–20 **Polymer Chemistry: Aspects of Radical Polymerization**
Lancaster (UK)
Contact: Dr. J. R. Ebdon, Dept. of Chemistry, Univ. of Lancaster, Lancaster LA1 4YA, UK

18–21 **Integrated Optics and Optical Fiber Communications**
7th Int. Conf. (IOOC-7)
Kobe (Japan)
Contact: P. W. Shumate, Jr., Bell Communications Research, 435 S St., Morristown, NJ 07960, USA

23–24 **Computer-Aided Materials Characterization**
Int. Symp.
Charlotte (USA)
Contact: R. Biederman, Worcester Polytechn. Inst., Worcester, MA 01609, USA, Tel. 508-831-5453/5346

23–28 **Materials and Mechanisms of Superconductivity: High-T_c Superconductors**
Int. Conf. (HTSC-M^{2}S)
Stanford (USA)
Contact: Dr. T. H. Geballe, Dept. of Applied Phys., Stanford Univ., Stanford, CA 94305, USA

24–26 **Micro-Optics/Gradient-Index Optical Imaging Systems**
2nd Conf./8th Top. Mtg.
Tokyo (Japan)
Contact: K. Iga, Tokyo Inst. of Technol., Research Lab. of Precision Machinery and Electronics, 4259 Nagasuta, Midori-ku, Yokohama 227, Japan

24–26 **Composite Structures**
5th Int. Conf.
Paisley (UK)
Contact: Dr. I. H. Marshall, Dept. of Mechanical and Production Eng., Paisley College of Technol., High St., Paisley PA 12BE, UK

25–26 **Computer-Aided Microscopy and Quality Control**
Int. Conf.
Charlotte (USA)
Contact: J. Braun, EG + G Mound Appl. Technologies, Miamisburg, OH 45343-0987, USA, Tel. 513-865-3829

31–2 **Biologically-Engineered Polymers**
Cambridge (UK)
Contact: Royal Soc. of Chemistry, Burlington House, London W1V 0BN, UK

31–3 **Photoacoustic and Photothermal Phenomena**
6th Int. Mtg.
Baltimore (USA)
Contact: J. Murphy, Johns Hopkins Appl. Physics Lab., Johns Hopkins Rd., Laurel, MD 20707, USA, Tel. 301-953-6214

August 1989

2–7 **Pure and Applied Chemistry**
32nd IUPAC Congr.
Stockholm (Sweden)
Contact: Stockholm Convention Bureau, P.O. Box 6911, S-10239 Stockholm, Sweden

13–26 **High-T_c Superconductors**
NATO Adv. Study Inst.
Bad Windsheim (Fed. Rep. Germany)
Contact: R. Kossowsky, Applied Res. Lab., Pennsylvania State Univ., P.O. Box 30, State College, PA 16804, USA

14–17 **Shock Compression of Condensed Matter**
APS Top. Conf.
Albuquerque (USA)
Contact: A. Roach, MS-P 915, Los Alamos Nat. Lab., Los Alamos, NM 87545, USA

14–18 **Hopping Transport**
8th Conf.
Chapel Hill (USA)
Contact: M. Pollak, Dept. of Phys., Univ. of California, Riverside, CA 92521, USA

16–18 **Properties Through Processing**
Amherst (USA)
Contact: H. H. Winter, Dept. Chem. Eng., Univ. of Massachusetts, Amherst, MA 01003, USA

20–24 **Imaging Systems—150 Years of Photography**
Int. Symp. (ISIS '89)
Dresden (German Dem. Rep.)
Contact: Conf. Secretary, ISIS '89, Technische Univ. Dresden, Sektion Physik, Wissenschaftsbereich Photophysik, Mommsenstr. 13, DDR-8027 Dresden, GDR

20–25 **Crystal Growth: Progress in Science and Technology**
9th Int. Conf.
Sendai (Japan)
Contact: Prof. T. Nishinaga, Inter Group Corp., Akasaka Yamakatsu Bldg., 8-5-32, Akasaka Minato-ku, Tokyo 107, Japan

21–24 **Amorphous and Liquid Semiconductors**
13th Int. Conf.
Asheville (USA)
Contact: D. E. Sayers, P.O. Box 8202, North Carolina State Univ., Raleigh, NC 27695-8202, USA

21–25 **Phonons 89**
Heidelberg (Fed. Rep. Germany)
Contact: Inst. f. Angew. Physik II, Univ. of Heidelberg, Albert-Überle-Str. 3–5, D-6900 Heidelberg, FRG

21–26 **Photochemistry**
Int. Conf.
Beijing (P.R. China)
Contact: Prof. S. Wu, Inst. of Photographic Chem., Academia Sinica, Beijing, P.R. China

22–26 **Particles in Gases and Liquids: Detection, Characterization and Control**
2nd Symp. and 20th Annu. Mtg. of Fine Particle Soc.
Boston (USA)
Contact: Dr. K. L. Mittal, IBM U.S. Techn. Education, 500 Columbus Ave., Thornwood, NY 10594, USA, Tel. 914/742-5745

22–26 **Particles in Gases and Liquids: Detection, Characterization and Control**
2nd Symp. and 20th Annu. Mtg. of Fine Particle Soc.
Boston (USA)
Contact: Dr. K. L. Mittal, IBM U.S. Techn. Education, 500 Columbus Ave., Thornwood, NY 10594, USA, Tel. 914/742-5745

27–1 **Supramolecular Organic Chemistry and Photochemistry**
Workshop
Saarbrücken (Fed. Rep. Germany)
Contact: Prof. Dr. H.-J. Schneider, FR Organ. Chem., Univ. des Saarlandes, D-6600 Saarbrücken, FRG

28–31 **Dynamical Processes in Excited States of Solids**
7th Int. Conf. (DPC '89)
Athens (USA)
Contact: DPC '89, Prof. J. E. Rives, Dept. of Physics and Astronomy, Univ. of Georgia, Athens, GA 30602, USA

28–1 **Surface Modification Technologies**
3rd Int. Conf.
Neuchatel (Switzerland)
Contact: The Metallurgical Soc., 420 Commonwealth Dr., Warrendale, PA 15086, USA, Tel. 412-776-9050

28–1 **Magnet Technology**
Int. Conf.
Tsukuba (Japan)
Contact: S. Shimamoto, Japan Atomic Energy Res. Inst., Naka-gun, Ibaraki-ken 311-01, Japan

28–1 **Ferroelectricity**
7th Int. Mtg., (IMF-7)
Saarbrücken (Fed. Rep. Germany)
Contact: Dr. J. Albers, Univ. des Saarlandes, Fachbereich Physik, D-6600 Saarbrücken, FRG

28–1 **Sintering**
7th World Round Table Conf.
Herceg-Novi (Yugoslavia)
Contact: Dr. D. P. Uskoković, Serbian Academy of Sci. and Arts, Knez-Mihailova 35, 11000 Beograd, Yugoslavia

28–1 **X-Ray Optics and Microanalysis**
12th Int. Congr.
Cracow (Poland)
Contact: S. Jasienska, Academy of Mining and Metallurgy, Inst. of Metallurgy, 30-059 Cracow, Poland

28–2 **Photochemistry for High Technology**
Int. Summer School
Leuna-Merseburg (German Dem. Rep.)
Contact: Prof. H.-J. Timpe, Section Chemie, Technische Hochschule für Chemie, Leuna-Merseburg, Gensaerstr., DDR-42 Merseburg, GDR

29–2 **Innovation and Perspectives in Solid Phase Synthesis**
Int. Symp.
Oxford (UK)
Contact: R. Epton, School of Appl. Sci., Wolverhampton Polytech., Wolverhampton WV1 1SB, UK

September 1989

3–5 **Advanced Ceramics and PM Materials, Development and Applications**
Int. New Business and High Tech. Conf.
Jyväskylä (Finland)
Contact: EAMI, Ms. R. Häninen, Reumantie 4, 18100 Heinola, Finland, Tel. 358-10-57062, Fax 358-10-57161

4–6 **Magnetic Recording Media**
Int. Conf.
Rimini (Italy)
Contact: Dr. L. Pareti, MASPEC, Via Chiavari 18, I-43100 Parma, Italy

4–8 **Liquid and Amorphous Metals**
Kyoto (Japan)
Contact: Prof. A. Ueda, Dept. of Appl. Mathematics and Physics, Kyoto Univ., Kyoto 606, Japan

4–8 **Electronic Properties of Two-Dimensional Systems**
Int. Conf.
Grenoble (France)
Contact: J. C. Maan, SNCI-HML, 166x, F-38042 Grenoble Cedex, France

4–8 **High-T_c Superconductivity**
Beijing (P.R. China)
Contact: Prof. Z. X. Zhao, Chin. Acad, of Sci., Inst. of Physics, POB 603, Beijing 100080, P.R. China

4–8 **Electrically and Optically Active Polymers**
21st Europhysics Conf.
Lodz (Poland)
Contact: Dr. J. Ulanski, Polymer Inst., Techn. Univ. of Lodz, Zwirki 36, 90-924 Lodz, Poland

4–8 **Macromolecules 89**
Eur.-Am. Conf. on Functional Polymers and Biopolymers
Oxford (UK)
Contact: Prof. R. Epton, School of Appl. Sci., The Polytechnic, Wolverhampton WV1 1SB, UK

4–8 **Olefin Metathesis and Polymerization**
8th Int. Symp.
Bayreuth (Fed. Rep. Germany)
Contact: Office ISOM 8, Lab. für Anorg. Chem., Univ. Bayreuth, Postfach 101251, D-8580 Bayreuth, FRG

5–7 **Interfacial Phenomena in Composite Materials**
Int. Conf.
Sheffield (UK)
Contact: J. Herriot, Butterworth, P.O. Box 63, Westbury House, Bury St., Guildford GU2 5BH, UK

5–8 **Optical, Electrical and Acoustic Properties**
Kent (UK)
Contact: M. D. Shuttleworth, Plastics and Rubber Inst., 11 Hobart Pl., London SW1W 0HL, UK

5–8 **Polymers, Laminations and Coatings**
TAPPI Conf.
Orlando (FL, USA)
Contact: Mtg. Dept., TAPPI Technology Park, P.O. Box 105113, Atlanta, GA 30348-5113, USA

5–9 **Accelerators in Appl. Res. Technology**
1st Eur. Conf.
Frankfurt (Fed. Rep. Germany)
Contact: K. Bethge, Inst. f. Kernphysik, August-Euler-Str. 6, D-6000 Frankfurt 90, FRG

6–8 **New Materials and Processes for Tooling**
2nd Int. Tooling Conf.
Bochum (Fed. Rep. Germany)
Contact: Ruhr-Univ. Bochum, Unikontakt-Tooling, POB 102148, D-4630 Bochum, FRG

6–9 **Magnetic Materials and Applications (EMMA '89)**
Rimini (Italy)
Contact: L. Pareti, EMMA '89, Istituto Maspec, Via Chiavari 18/A, I-43100 Parma, Italy, Phone 521-95811, Fax 521-96315

7–9 **Biomaterials**
8th Eur. Congr.
Heidelberg (Fed. Rep. Germany)
Contact: Dr. U. Soltesz, Fraunhofer-Institut für Werkstoffmechanik, Wöhlerstr. 11, D-7800 Freiburg, FRG

10–11 **Ceramics in Medicine**
2nd Int. Symp.
Heidelberg (Fed. Rep. Germany)
Contact: Dtsch. Keram. Gesellsch., Frankfurter Str. 196, D-5000 Köln 90, FRG

10–12 **Colloidal Dispersions**
Faraday Discussion 90
Bristol (UK)
Contact: Prof. R. H. Ottewill, School of Chemistry, Univ. of Bristol, Bristol BS8 1TS, UK

10–14 **Optical Communications**
15th Eur. Conf.
Gothenburg (Sweden)
Contact: P. A. Andrekson, Dept. of Optoelectronics, Chalmers Univ. of Technol., S-41296 Gothenburg, Sweden

10–15 **Materials and Fluid Sciences in Microgravity**
Eur. Conf.
Oxford (UK)
Contact: Dr. H. U. Walter, Eur. Space Agency, Microgravity Office, 8–10 rue Mario-Nikis, F-75738 Paris Cedex 15, France

10–23 **Molecular Dynamics of Liquid Crystals**
NATO Adv. Study Inst.
Il Ciocco, Lucca (Italy)
Contact: Prof. C. A. Veracini, Dipartimento di Chimica, Universita di Pisa, Viale Risorgimento 35, I-56100 Pisa, Italy

11–13 **Charge Transfer in Polymeric Systems**
RSC, Faraday Div.
Contact: Dr. J. F. Gibson, Royal Soc. of Chemistry, Burlington House, Piccadilly, London W1V 0BN, UK

11–13 **Holographic Systems, Components and Applications**
2nd Int. Conf.
Bath (UK)
Contact: Inst. of Electronic and Radio Eng., Conf. Dept., Savoy Hill House, London WC2R 0JD, UK

11–13 **Surface Analysis Techniques and Applications**
Manchester (UK)
Contact: E. Wellingham, Conf. Secretariat, Field End House, Bude Close, Nailsea, Bristol BS19 2FQ, UK

13–15 **Microscopy**
150th Anniversary Commemorative Mtg.
London (UK)
Contact: Microscopical Soc., 37–38 St. Clements, Oxford OX4 1AJ, UK

17–22 **Defect Recognition and Image Processing in Semiconductors**
3rd Mtg. (DRIP-3)
Yokohama (Japan)
Contact: Prof. T. Ogawa, Gakushuin Univ., Dept. of Physics, 1-5-1 Mejiro, Toshima-ku, Tokyo 171, Japan

17–22 **Optics and Optical Engineering**
Cambridge Symp.
Cambridge (USA)
Contact: Soc. of Photo-Optical Instrumentation Eng. (SPIE), P.O. Box 10, Bellingham WA 98227, USA

18–22 **Quantum Electronics**
9th Natl. Conf.
Oxford (UK)
Contact: Mrs. M. Sherwen, Rutherford Appleton Lab., Chilton, Didcot, Oxon OX11 0QX, UK

19–21 **High-T_c Superconductors**
Birmingham (UK)
Contact: Dr. C. Greaves, School of Chemistry, Univ. of Birmingham, POB 363, Birmingham B15 2TT, UK, Tel. 021/414-4397

19–21 **Superconductivity and Applications**
3rd Annu. Conf.
Buffalo (USA)
Contact: NYSIS, 330 Bonner Hall, State Univ. of New York, Buffalo, NY 14260, Tel. 716/636-3463

19–22 **Structure and Dynamics of Colloidal Systems**
3rd Eur. Coll. and Interface Soc. Conf. and ILL Workshop
Basel (Switzerland)
Contact: Dr. M. Zulauf, c/o F. Hoffmann-La Roche + Co., ZFE 65–509, CH-4002 Basel, Switzerland, Tel. 0041/616885746, Fax 0041/616919391

20–22 **Structural Adhesives in Engineering**
SAE II '89
Bristol (UK)
Contact: J. Herriot, SAE II '89, Butterworth Scientific Ltd., P.O. Box 63, Westbury House, Bury St., Guildford, Surrey GU2 5BH, UK

20–22 **Manmade Fibers**
Int. Congr.
Dornbirn (Austria)
Contact: Austrian Manmade Fibers Inst., Plossigasse 8, A-1041 Vienna, Austria

21–22 **Fire Retardant Polymers**
Torino (Italy)
Contact: Prof. L. Costa, Dipl. di Chim. dell'Università di Torino, Via P. Giuria, 7, 10125 Torino, Italy

24–28 **Metallization of Polymers**
Int. Colloquium
Montreal (Canada)
Contact: Ed. Sacher, Ecole Polytechnique, Université de Montreal, Quebec H3C 3A7, Canada

25–26 **Additive Approaches to Improved Polymer Performance**
Toronto (Canada)
Contact: Jeff Hood, Stochem. Inc., 106 Summerlea Rd., Brampton, Ontario L6T 4X3, Canada

25–27 **Structure Formation in Polymer Solutions**
22nd Europhysics Conf.
Leuven (Belgium)
Contact: Prof. H. Berghmans, Lab. for Polymer Res., Katholieke Univ. Leuven, Celestijnenlaan 200F, B-3030 Leuven, Belgium, Tel. 16/200656, Fax 16/201215

25–27 **Surface Engineering with High Energy Beams**
2nd Int. Seminar
Lisbon (Portugal)
Contact: Secretariat of ISHT '89 Seminar, Ctr. of Mech. and Mater. of the Tech. Univ. Lisbon (CEMUL), 1096 Lisboa Codex, Portugal

25–29 **Ceramics' 89 "C89"**
4. Int. Conf. Limoges (France)
Contact: Comité Régional D'Expansion Economique du Limousin (CREEL), 27, Boulevard de la Corderi, F-87000 Limoges, France, Tel. 0033/55451830, Fax 0033/55797789

25–29 **Vacuum Solid Surfaces**
IVC-11/CSS-7
11th Int. Conf./7th Int. Conf.
Cologne (Fed. Rep. Germany)
Contact: D. A. Benninghoven, Physikalisches Inst. der Univ. Münster, Wilhelm-Klemm-Str. 10, D-4000 Münster, FRG

25–30 **Epitaxial Crystal Growth**
Int. Conf.
Budapest (Hungary)
Contact: Dr. E. Lendfay, Hung. Acad. of Sci., Inst. for Techn. Physics, Ujpest 1, POB 76, H-1325 Budapest, Hungary

26–28 **Optical Memory**
Int. Symp. (ISOM '89)
Kobe (Japan)
Contact: ISOM '89 Secretariat, Business Ctr. for Academic Soc. Japan, 3-23-1 Hongo, Bunkyo-ku, Tokyo 113, Japan

26–28 **SAMPE**
21st Int. Techn. Conf.
Atlantic City (USA)
Contact: SAMPE, 843 W. Glentana, P.O. Box 2459, Covina, CA 91722, USA, Tel. 818-331-0616

26–29 **Structure and Dynamics of Colloidal Systems**
3rd Eur. Colloid and Interface Conf.
Basle (Switzerland)
Contact: Dr. M. Zulauf, F. Hoffmann-La Roche & Co, ZFE 65-509, CH-4002 Basel, Switzerland

27–29 **Polymer Reaction Engineering**
3rd Berlin Int. Workshop
Berlin (West)
Contact: Prof. Dr. K.-H. Reichert, Inst. f. Techn. Chemie, TU Berlin, Straße des 17. Juni 135, D-1000 Berlin 10

27–29 **New Polymers**
1st Materials Symp.
Regensburg (Fed. Rep. Germany)
Contact: OTTI-Fortbildung, Martin-Luther-Straße 10, D-8400 Regensburg, FRG

30–4 **High-T_c Thin Films and Single Crystals**
Int. Conf.
Ustron (Poland)
Contact: M. W. Gutowski, Inst. of Physics, ON-3 Polish Acad. of Sci., Al. Lotnikow 32/46, PL-02668 Warszawa, Poland

October 1989

1–4 **Interfaces in Condensed Systems Equilibria and Dynamic Phenomena**
Annu. Mtg. Dtsch. Kolloid-Gesellsch. Bochum (Fed. Rep. Germany)
Contact: Prof. Dr. G. H. Findenegg, Physikal. Chem. II, Ruhr-Univ., P.O. Box 102148, D-4630 Bochum 1, FRG, Tel. 0234/700429

1–5 **The Metallurgical Society**
Fall Mtg.
Indianapolis (USA)
Contact: Mtgs. Dept., TMS, 420 Commonwealth Dr., Warrendale, PA 15086, USA

1–5 **Halide Glasses**
6th Int. Symp.
Clausthal (Fed. Rep. Germany)
Contact: Prof. G. Frischat, Techn. Univ. Clausthal, Fak. für Bergbau, Hütten- und Maschinenwesen, Adolf-Römer-Str. 2A, D-3392 Clausthal-Zellerfeld, FRG

2–3 **Makromoleculares Symposium**
Hamburg (Fed. Rep. Germany)
Contact: Prof. Dr. W. Kaminsky, Inst. f. Techn. u. Makromol. Chemie, Univ. Hamburg, Bundesstr. 45, D-2000 Hamburg 13, FRG

2–4 **Electron and Optical Beam Testing of Integrated Circuits**
2nd Eur. Conf.
Duisburg (Fed. Rep. Germany)
Contact: E. Kubalek, Werkstoffe der Elektronik, Univ. Duisburg, Kommandanten-Str. 60, D-4100 Duisburg 1, FRG

2–4 **High Temperature Polymers**
Cleveland (USA)
Contact: Vivian E. Malpass, Ferro Corp., Technical Ctr., 7500 East Pleasant Valley Rd., Independence, OH 44131, USA

2–5 **Materials Week**
Technical Conf.
Indianapolis (IN, USA)
Contact: Technicol Dept. Marketing, ASM Int., Metals Park, OH 44073, USA

4–6 **Fabrication and Characterization of Semiconductor Optoelectronic Devices and Integr. Circuits**
1st Int. Mtg.
Tokyo (Japan)
Contact: Univ. of Tokyo, Dept. of Electronic Eng., Hongo, Bunkyo-ku, Tokyo 113, Japan

8–11 **Organometallic Vapor Phase Epitaxy**
4th Biennial Workshop
Monterey (USA)
Contact: B. Kamperman, TMS, 420 Commonwealth Dr., Warrendale, PA 15086, USA, Tel. 412/776-9050, Fax 412/776-3770

9–10 **Quasicrystals**
DFG-workshop
Bad Honnef (Fed. Rep. Germany)
Contact: Dr. J. Tobolski, Dtsch. Forschungsgem., Bad Godesberg, Kennedyallee 40, D-5300 Bonn 2, FRG

9–11 **Dtsch. Keramische Gesellsch. Jahrestagung 1989**
Coblenz (Fed. Rep. Germany)
Contact: Dtsch. Keramische Gesellsch., Frankfurter Str. 196, D-5000 Köln 90, FRG, Tel. 02203-69069, Fax 2203-69301

10–13 **Ion Beams in Materials Research and Technology**
4th Europhysics Ind. Workshop Bad Honnef (Fed. Rep. Germany) Contact: G. Thomas, Eur. Physical Soc., POB 69, CH-1213 Petit-Lancy 2, Switzerland

11–13 **Materials for Electrochemistry**
Stuttgart (Fed. Rep. Germany)
Contact: Prof. F. von Sturm, Jahnstr. 26, D-8901 Biberbach, FRG

11–13 **Surface Technology Forum**
SURTEC '89
Berlin (West)
Contact: AMK Berlin, M 3/Surtec, Messedamm 22, D-1000 Berlin 19

15–18 **Unconventional Photoactive Solids**
4th Int. Conf.
San Jose (USA)
Contact: Dr. C. G. Willson, IBM Almaden Research Ctr., 650 Harry Road, San Jose, CA 95120, USA

16–19 **High-Tech-Coating**
Congr. and Exhibition
Wiesbaden (Fed. Rep. Germany)
Contact: Demat Exposition Managing, P.O. Box 110611, D-6000 Frankfurt, FRG

17–18 **Optics in Computing**
Int. Symp.
Toulouse (France)
Contact: Secretariat Des Conferences, OPTO-Informatique, ONERA-CERT, BP 4025, F-31055 Toulouse Cedex, France

17–18 **Superconductivity: the Manufacturing Challenge**
Oak Brook (USA)
Contact: K. L. Kammerer, SME, Techn. Committee, Projects Dept., 1 SME Drive, POB 930, Dearborn, MI 48121-0930, USA, Tel. 313/271-1500/542

17–19 **Optical Storage for Large Systems**
4th Annu. Conf.
New York, (USA)
Contact: Rothchild Consult., 256 Laguna Honda Blvd., San Francisco, CA 94116-1496, USA

22–28 **Solid-State and Integrated Circuit Technology**
2nd Int. Conf.
Beijing (P.R. China)
Contact: Continuing Education in Eng., Univ. Extension, Univ. of California, 2223 Fulton St., Berkeley CA 94720, USA

23–24 **Modern Aspects of Superconductivity**
Int. Conf.
Paris (France)
Contact: Dr. R. Suryanarayanan, Lab. de Physique des Solides, 1, Place Aristide Briand, 92195 Meudon, France, Fax 1/45344696

23–24 **High-T_c Superconductors and Crystal Chemistry III**
Bad Honnef (Fed. Rep. Germany)
Contact: Dr. J. Debrus, Physikzentrum, Hauptstr. 5, D-5340 Bad Honnef 1, FRG

Registered names, trademarks, etc. used in this journal, even when not marked as such, are not to be considered unprotected by law.

© VCH Verlagsgesellschaft mbH, D-6940 Weinheim, 1989. – Printed in the Federal Republic of Germany by Konrad Triltsch Druck- und Verlagsanstalt Würzburg.

All rights reserved (including those of translation into foreign languages). No part of this issue may be reproduced in any form — by photoprint, microfilm, or any other means — nor transmitted or translated into a machine language without written permission from the publishers. Only single copies of contributions, or parts thereof, may be made for personal use. This journal was carefully produced in all its parts. Nevertheless, authors, editors and publisher do not warrant the information contained therein to be free of errors. Readers are advised to keep in mind that statements, data, illustrations, procedural details or other items may inadvertently be inaccurate.

Valid for users in the USA: The appearance of the code at the bottom of the first page of an article (serial) indicates the copyright owner's consent that copies of the article may be made for personal or internal use, or for the personal or internal use of specific clients. This consent is given on the condition, however, that the copier pay stated per-copy fee through the Copyright Clearance Center, Inc. (CCC), for copying beyond that permitted by Sections 107 or 108 of the U.S. Copyright Law. This consent does not extend to other kinds of copying, such as copying, for general distribution, for advertising or promotional purposes, for creating new collective works, or for resale. For copying from back volumes of this journal see 'Permissions to Photo-Copy: Publisher's Fee List' of the CCC.

Editorial office: Postfach 10 11 61, D-6490 Weinheim, Federal Republic of Germany, Telephone (06201) 60 22 55, Telex 465 516 vchwh d, Telefax (06201) 602 328.

Editor: *Peter Gölitz*

Associate Editor: *Peter Gregory*

Publishers: VCH Verlagsgesellschaft mbH. (Managing Director: *Hans Dirk Köhler*), Pappelallee 3, D-6940 Weinheim, Federal Republic of Germany.

Advertising office (Advertising Manager *R. J. Roth*): Postfach 10 11 61, D-6940 Weinheim, Federal Republic of Germany, Telephone (0 62 01) 60 61 30, Telex 467 155 vchwh d, Telefax (0 62 01) 606 184.

ANGEWANDTE CHEMIE
International Edition in English
Volume 28 · Number 7
July 1989
Pages 829–968

The Photosynthetic Reaction Center from the Purple Bacterium *Rhodopseudomonas viridis* (Nobel Lecture)**

By Johann Deisenhofer* and Hartmut Michel*

In our lecture we first describe the history and methods of membrane protein crystallization, before we show how the structure of the photosynthetic reaction center from the purple bacterium *Rhodopseudomonas viridis* was solved. The structure of this membrane protein complex is then correlated with its function as a light-driven electron pump across the photosynthetic membrane. Finally, we draw conclusions on the structure of the photosystem II reaction center of plants and discuss the aspects of membrane protein structure. Sections 1 (crystallization), 4 (conclusions on the structure of photosystem II reaction center and evolutionary aspects) and 5 (aspects of *membrane* protein structure) were presented and written by *H. M.*, sections 2 (determination of the structure) and 3 (structure and function) by *J. D.* We have arranged the manuscript in this way in order to facilitate continuous reading.

1. The Crystallization

1.1. The Background

As in many instances of new scientific developments and technical inventions a chance observation initiated a series of experiments, which ultimately resulted in the elucidation of the three-dimensional structure of a photosynthetic reaction center. In August 1978 I accidently observed the formation of solid, most likely glass-like aggregates, when lipid-free bacteriorhodopsin prepared according to the method of *Happe* and *Overath*[1] (1976) was stored in the freezer. These aggregates are shown in Figure 1 A. From that time on I was convinced that it should be possible not only to produce these solid bodies but also to prepare three-dimensional crystals. The availability of well-ordered three-dimensional crystals is a prerequisite for a high resolution X-ray crystallographic analysis, which – despite the progress made by *Henderson* and *Unwin*[2] (1975) with electron microscopy and electron diffraction on bacteriorhodopsin – was, and still is the only way to obtain a detailed structural knowledge of large biological macromolecules.

At the time I was working at the University of Würzburg as a post-doc in *Dieter Oesterhelt*'s lab, who, in collaboration with *Walter Stoeckenius*, had discovered bacteriorhodopsin[5] and was the first to propose its function.[6] My intention to try to produce well-ordered three-dimensional crystals of bacteriorhodopsin received his immediate support. It turned out that he had already tried to crystallize a modified form of bacteriorhodopsin from organic solvents.

Bacteriorhodopsin, the protein component of the so-called purple membrane, resembles the visual pigment rhodopsin and acts as a light energy converting system. It is part of a simple "photosynthetic" system in halobacteria, and is an integral membrane protein, which forms two-dimensional crystals in the purple membrane. At that time the general belief was that it was impossible to crystallize membrane proteins in three dimensions. With the exception of bacteriorhodopsin there was no information about the three-dimensional structure of membrane proteins, which might

[*] Prof. Dr. J. Deisenhofer
Howard Hughes Medical Institute and Department of Biochemistry
University of Texas Southwestern Medical Center
5323 Harry Hines Boulevard, Dallas, Tx 75235 (USA)
Prof. Dr. H. Michel
Max-Planck-Institut für Biophysik
Heinrich-Hoffmann-Strasse 7,
D-6000 Frankfurt am Main 71 (FRG)

[**] Copyright © The Nobel Foundation 1989. – We thank the Nobel Foundation, Stockholm, for permission to print this lecture.

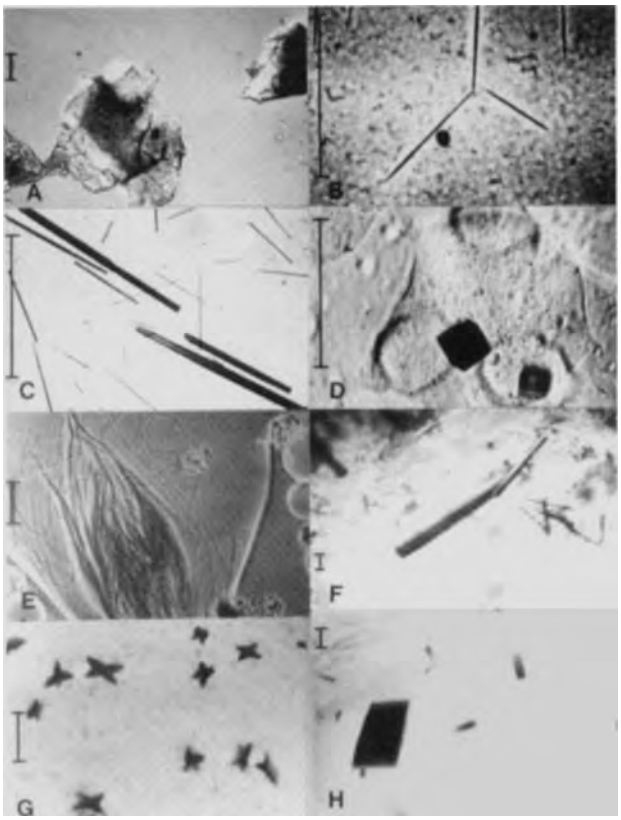


Fig. 1. Optical micrographs showing crystals and aggregates of bacteriorhodopsin and the photosynthetic reaction center from *Rhodopseudomonas viridis*: A) "glass-like" aggregates of bacteriorhodopsin obtained after freezing of lipid-free bacteriorhodopsin; B) rolled up sheets of the two-dimensionally crystalline orthorhombic form of purple membrane (after *Michel* and *Oesterhelt* [3]); C) needle-like crystals of bacteriorhodopsin obtained with sodium phosphate as precipitant; D) cube-like crystals of bacteriorhodopsin obtained with ammonium sulfate as precipitant; E) filamentous aggregates of bacteriorhodopsin and a few cubes (arrows) obtained with ammonium sulfate as precipitant (after *Michel* [4a]); F) hexagonal columns of bacteriorhodopsin obtained in the presence of 3% heptane-1,2,3-triol with ammonium sulfate as precipitant; G) star-like crystals of the reaction center obtained within 2 days (starting conditions: 1 mg protein/ml, 3% heptane-1,2,3-triol, 1.5 M ammonium sulfate) by vapor diffusion against 3 M ammonium sulfate (after *Michel* [4b]); H) tetragonal crystals of the reaction center obtained within 3 weeks (starting conditions as under G) by vapor diffusion against 2.4 M ammonium sulfate (after *Michel* [4b]). In all photographs the bar indicates 0.1 mm.

have provided insights into their various functions, e.g. as carriers, energy converters, receptors or channels.

In our first experiments we tried to decrease the negative surface charge of purple membrane by the addition of long chain amines, and, by subsequent treatment with Triton X100, a detergent, to facilitate rearrangement of the bacteriorhodopsin molecules, which were partly solubilized by the detergent. This procedure may be a way (see Fig. 3) to obtain the type I crystals described below. Within four weeks we obtained the "needles" illustrated in Figure 1 B. Electronmicroscopic studies carried out in collaboration with *Richard Henderson* in Cambridge showed that the "needles" were a new two-dimensionally crystalline membrane form of bacteriorhodopsin. In this new form the membranes are rolled up like tobacco leaves in a cigar.[7]

1.2. A More Systematic Approach

Based on the properties of membrane proteins outlined below, a new strategy was developed.[8] Membrane proteins are embedded into the electrically insulating lipid bilayers. Difficulties are encountered in the handling of membrane proteins because of the amphipathic nature of their surface. It is hydrophobic where the membrane proteins have contact with the alkane chains of the lipids, and it is hydrophilic where the membrane proteins have contact with the aqueous phase (on both sides of the membrane) or with the polar head-groups of the lipids (see Fig. 2). As a result membrane

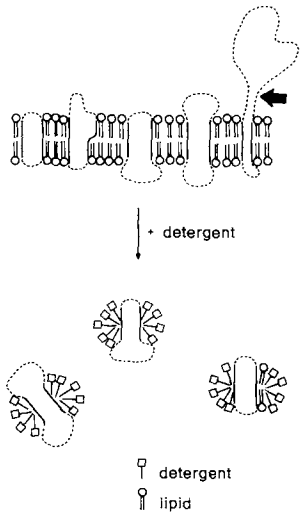


Fig. 2. Schematic drawing of a biological membrane consisting of a lipid bilayer in which membrane proteins are embedded (top), and its solubilization by detergents (bottom). The hydrophilic part of the membrane protein surface is indicated by broken lines (modified after *Michel* [8]).

proteins are not soluble in aqueous buffers or in organic solvents with low dielectric constants. In order to solubilize membrane proteins one has to add detergents. Detergents are amphiphilic molecules which form micelles above a certain concentration, the so-called critical micellar concentration. The detergent micelles take up the membrane proteins and shield the hydrophobic parts of the surface of the membrane protein from contact with water. A schematic drawing of a biological membrane and its solubilization with detergents is presented in Figure 2. The membrane protein in the detergent micelle then has to be purified by chromatographic methods.

Once the protein has been isolated and is available in large quantities, one can try to crystallize it. For membrane proteins, which are merely anchored in the membrane, the most promising approach is to remove the membrane anchor by proteases or to use genetically modified material where the part of the gene coding for the membrane anchor has been deleted. Four examples of highly resolved structures of the hydrophilic domains have already been reported: cytochrome b_5,[9] hemagglutinin[10] and neuraminidase[11] from influenza virus and the human class I histocompatibility antigen, HLA-A2.[12]

There are two possibilities for generating true three-dimensional crystals of really integral membrane proteins:

1) One could think of forming stacks of two-dimensional crystals of membrane proteins. Perpendicular to the membrane the two-dimensional crystals must be ordered with respect to translation, rotation and orientation during or after their formation. In most cases the lipids might still be

present in the form of bilayers and compensate the hydrophobicity of the intramembranous protein surface. Hydrophobic and polar interactions would stabilize the crystals in the membrane planes, whereas polar interactions would dominate in the third dimension (Fig. 3, left). In a reasonable

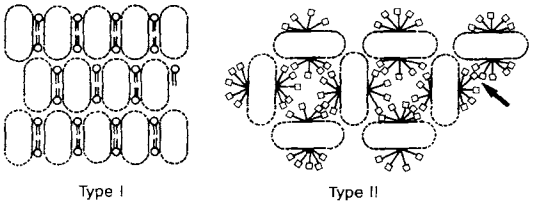


Fig. 3. The two basic types of membrane protein crystals. Type I: stacks of membranes containing two-dimensionally crystalline membrane proteins, which are then ordered in the third dimension. Type II: A membrane protein crystallized with detergents bound to its hydrophobic surface. The hydrophilic surface part of the membrane proteins is indicated by broken lines. The symbols for lipids and detergents are the same as in Figure 2 (after *Michel* [8]).

crystallization procedure one would have to increase both types of interaction at the same time. This seems to be difficult to achieve.

2) The alternative is to crystallize the membrane proteins within their detergent micelles. The crystal lattice will be formed by the membrane proteins via polar interactions between the polar parts of the surface. Figure 3 (right) shows one example of such a crystal. It is immediately clear that membrane proteins with large extramembranous domains should form this type of crystal much easier than those with small polar domains. The size of the detergent micelle plays a crucial role. A large detergent micelle might prevent the required close contact between the polar surface domains of the membrane proteins. One way to achieve a small detergent micelle is to use small linear detergents like octyl glucopyranoside. However, for membrane biochemists, a general experience is that membrane proteins in micelles formed by a detergent with a short alkyl chain are not very stable. An increase in length of the alkyl chain by one methylene group frequently leads to an increase in stability by a factor of two to three. One therefore has to find a compromise.

The advantage of the type II crystals is that basically the same procedures to induce supersaturation of the membrane protein solution can be used as for soluble proteins, namely vapor diffusion or dialysis with salts or polymers like polyethylene glycol as precipitating agents. Frequently a viscous detergent phase is formed, which seems to consist of precipitated detergent micelles (see, e.g., Ref. [13]). This phase separation is a serious problem. Membrane proteins are enriched in the detergent phase, and frequently undergo denaturation. In several examples crystals which were already formed are redissolved.

Bacteriorhodopsin, solubilized in octyl glucopyranoside, forms needle-like crystals (Fig. 1 C) when phosphate is used as precipitant (Fig. 1 C) and cubic crystals when ammonium sulfate[3] (Fig. 1 D) is used. The cubic crystals are not very stable, and transform into hairy, thread-like material (Fig. 1 E) after several weeks.[4] In this hairy material bacteriorhodopsin probably forms membranes again.

OmpF-porin, an outer membrane protein from *Escherichia coli*, was also crystallized – after solubilization in octyl glucopyranoside – by *Garavito* and *Rosenbusch*.[14] We received knowledge of this parallel development when *D. Oesterhelt* and *J. P. Rosenbusch* met in China at the end of 1979.

1.3. The Improvement

My opinion regarding the lack of final success with bacteriorhodopsin was always that the detergent micelles were still too large. The use of even smaller detergents was impossible due to insufficient stability of the bacteriorhodopsin in detergents with a shorter alkyl chain or a smaller polar head group. For several reasons, one way out was to add small amphiphilic molecules:[4a, 8] (i) these molecules might displace detergent molecules which are too large to fit perfectly into the protein's crystal lattice in certain positions. (ii) The small amphiphilic molecules are too small to form micelles themselves, but they are incorporated into the detergent micelles. These mixed micelles are smaller than the pure detergent micelles and the curvature of their surface is different. As a result the protein's could come closer together. (iii) Their polar head group is smaller than that of the detergent and less of the protein's polar surface would be covered by the polar part of the mixed small amphiphile/detergent micelle.

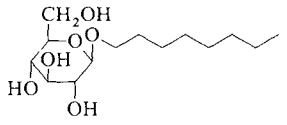
I had a look through the major chemical companies' catalogues and ordered nearly everything which was polar at one end and hydrophobic at the other. In addition I synthesized about 20 amphiphilic compounds, mainly alkylpolyols and alkyl *N*-oxides. These compounds were added during our attempts to crystallize bacteriorhodopsin. Several of the compounds had the effect that hexagonal columns were obtained (see Fig. 1 F), whereas cubes (Fig. 1 D) had been obtained without the additives. The most effective compound was heptane-1,2,3-triol, but it had a slightly denaturing effect on bacteriorhodopsin. The diffraction quality of the bacteriorhodopsin crystals was improved: Using synchroton radiation *H. Bartunik, D. Oesterhelt* and I were occasionally able to achieve a resolution of 3 Å, but only in one direction.

1.4. The Turn to Classical Photosynthesis

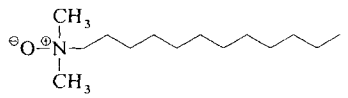
Frustrated from the failure to make a final breakthrough with bacteriorhodopsin, which was partly due to the absence of large extramembranous domains in this protein, I looked for more promising membrane proteins for crystallization. I chose the photosynthetic reaction centers from the purple bacteria *Rhodospirillum rubrum* and *Rhodopseudomonas viridis* and the light-harvesting chlorophyll a/b protein from spinach. I was influenced by the fact that these proteins (or protein-complexes) were said to be already part of a two-dimensional crystalline array in their native environment. As additional benefits they were available in large quantities, could easily be isolated, were colored and denaturation of the proteins was indicated by color changes.

I learnt about the *Rhodopseudomonas viridis* system when *Ernst Wehrli* from the ETH Zürich presented the results of electron microscopic studies during a workshop at Burg Gemen, Germany, in June 1979 (see Ref. [15]). Initially, I received some isolated photosynthetic membranes from him in December 1980. At that time I had moved with *D.*

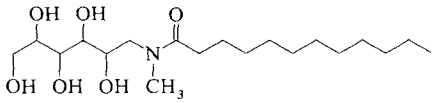
Oesterhelt to the Max-Planck-Institut für Biochemie at Martinsried near Munich and I was just back from a stay at the MRC in Cambridge where we had carried out X-ray diffraction experiments on the bacteriorhodopsin crystals. We isolated the reaction center using hydroxyapatite chromatography according to a procedure published by Clayton and Clayton in 1978.[16] We tried to crystallize the isolated reaction centers, but without success. I developed a new procedure of isolation using only molecular sieve chromatography and tried again, and met with immediate success. The conditions were nearly identical to those found to be optimal for bacteriorhodopsin. The exception was that I could use *N,N*-dimethyldodecylamine *N*-oxide as detergent instead of octyl glucopyranoside (see Fig. 4). In the presence of 3%



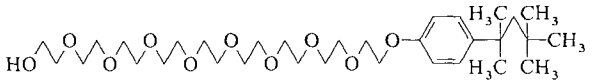
octyl-β-D-glucopyranoside (OG)



N, *N*-dimethyldodecylamine-*N*-oxide (LDAO)



decanoyl-*N*-methylglucamide (DMG)



Triton X 100

Fig. 4. Structural formulas of commonly used detergents: octyl β-D-glucopyranoside, *N,N*-dimethyldodecylamine *N*-oxide, decanoyl *N*-methylglucamide are promising for membrane protein crystallization, whereas Triton X100 is not.

heptane-1,2,3-triol (high melting point isomer) and 1.5 to 1.8 M ammonium sulfate, star-like crystals were obtained upon vapor diffusion against 2.5 to 3 M ammonium sulfate in two days; more regular tetragonal columns with a length of up to 2 mm were formed upon vapor diffusion against 2.2 to 2.4 M ammonium sulfate in two to three weeks (see Figs. 1 G, 1 H). The much smaller polar head group of *N,N*-dimethyldodecylamine *N*-oxide is certainly of importance. Unfortunately, this detergent denatures bacteriorhodopsin. *D. Oesterhelt* generously considered the reaction center as my project.

The crystals turned out to be of excellent quality from the beginning. After a scaling-up of the isolation procedure, a continuous supply of crystals was guaranteed. Initially with the help of *Wolfram Bode* and *Robert Huber*, I could now start collecting the X-ray data. Figure 5 shows a rotation photograph similar to that used for the data collection.

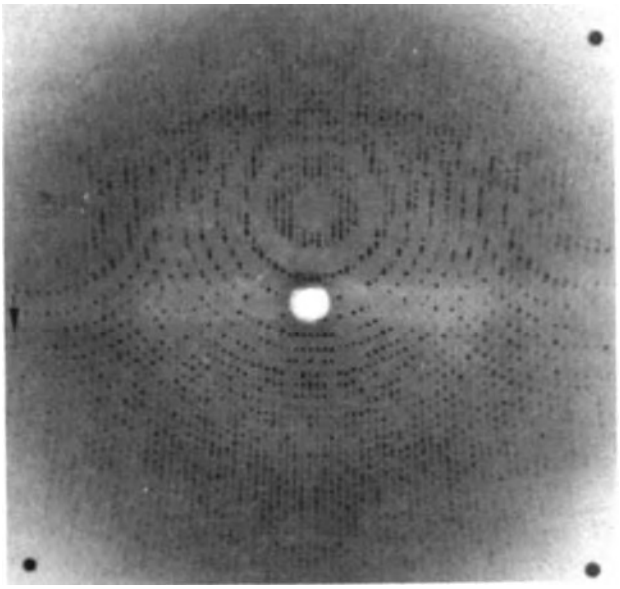


Fig. 5. X-ray diffraction pattern of a single crystal of the reaction center (1° rotation). Exposure time: 20 h, $Cu_{K\alpha}$ radiation, crystal to film distance: 100 mm. The arrow indicates 3.0 Å resolution (after *Michel* [4b]).

2. Determination of the Structure

In spring 1982 I (*J. D.*) joined *H. M.* in order to determine the three-dimensional structure of the reaction center. The tetragonal crystals have unit cell dimensions of $a = b = 223.5$ Å, $c = 113.6$ Å, and the symmetry of space group $P4_32_12$.[4, 17] As it turned out, there is one reaction center with a molecular weight of 145000 Daltons in the asymmetric unit.

2.1. Collection of X-ray Reflection Intensity Data

For data collection we used the rotation method with a rotating anode X-ray generator as the source, and photographic film as the detector.[17] The large unit cell of the reaction center crystals, in combination with the resolution limit of the diffraction pattern at 2.9 Å, limited the rotation interval per film exposure to 0.5°, so that more than two thirds of the reflections on any given film were only partially recorded. However, the long lifetime of the crystals in the X-ray beam at about 0 °C, and their positional stability allowed to add up partially recorded reflections from successive exposures, so that their treatment did not present a serious problem. Nevertheless, it took about three to four months to collect a complete data set. Data collection for the heavy atom derivatives was speeded up by choosing a rotation interval of 0.6° per exposure. A later re-collection of the native data set at the HASYLAB facilities of DESY in Hamburg was carried out at 2.3 Å resolution in rotation intervals of 0.4° by *Irmgard Sinning*, *Gerhard Schertler*, and *H. M.* The most tedious and time consuming task in this type of data collection was the processing of films. *Kunio Miki* and later *Otto Epp* provided invaluable help during that period of the work. We used the computer programs FILME[18, 19] and OSC[20, 21] for film evaluation, and PROTEIN (principal author: *W. Steigemann*) for scaling and merging data.

2.2. Solution of the Phase Problem

To solve the phase problem for the crystal structure of the reaction center we used the method of isomorphous replacement with heavy atom compounds. The experimental part was performed by *H. M.*, the film evaluation and data analysis by myself with support from *Kunio Miki* and *Otto Epp*.

In order to find the heavy atom derivatives, crystals were soaked for three days in 1 mM solutions of the respective heavy atom compounds in a soak buffer similar to the mother liquor. A number of compounds like K_2PtBr_4, $K_2Pt(CN)_4$, $KHg(CN)_2$, K_2HgI_4 and $EuCl_3$ could not be used since they induced the separation of the soak buffer phase into a viscous detergent phase and an aqueous phase. It was established from the beginning that X-ray diffraction no longer occurred on using large heavy atom compounds like $(C_6H_5)_3PbNO_3$ or C_6H_5HgCl, whereas the smaller homologues $(CH_3)_3PbCl$ or C_2H_5HgCl reduced the diffraction to about 6 Å resolution. However, after additional purification of the reaction centers prior to the crystallization the diffraction quality of the crystals was unchanged by the small heavy atom compounds. One compound ($KAuCl_4$) caused a shrinkage of the *c*-axis. Rotation photographs (1°) showing a large part of the 1,*k*,*l* lattice plane were taken and inspected visually for changes in the diffraction pattern. For promising candidates, ca. 50% complete data sets were collected and evaluated.

On average, each heavy atom derivative had nine heavy atom binding sites.[17] The major binding sites were found with the automatic search procedure in the PROTEIN program package. Using five different heavy atom derivatives, we could calculate phases to 3.0 Å resolution, and an electron density map.[17] Phases and map were further improved by solvent flattening.[22]

2.3. Model Building

Map interpretation and model building was done in three stages: First the prosthetic groups in the reaction center were identified. We found the four heme groups, the four bacteriochlorophyll-b molecules, the two bacteriopheophytin-b molecules, and one quinone molecule.[17] Next, the polypeptide chains were built with polyalanine sequence —except in the amino terminal regions of the subunits L, M, and cytochrome where partial amino acid sequences were known[23] and could be used to distinguish between the subunits. At that stage, some use was made of the local symmetry of the subunits L and M. Finally, as the gene sequences of the reaction center subunits were determined[24–26] the model of the protein subunits was completed. The sequence information not only led to an overall verification but also to a number of minor corrections of the polypeptide backbone model, since in the previous model building stage the electron density was not always clear enough to allow determination of the correct number of amino acids.

Our tools for model building were interactive graphics display systems: a Vector General 3400 system (black and white), and later an Evans & Sutherland PS 300 system (color). For both systems we used *Alwyn Jones*' program package FRODO.[27] The model library of this package was extended to include bacteriochlorophyll-b, bacteriopheophytin-b, menaquinone-7, and ubiquinone-1. Frequent use was made of the real-space refinement facility in FRODO which allowed correct incorporation of long stretches of helical structure into the electron density.

2.4. Model Refinement

The reaction center model, with about half of the side chains of the cytochrome subunit still missing, already had the rather low crystallographic *R*-value of 0.359 at 2.9 Å resolution ($R = \Sigma(||F_{obs}| - |F_{calc}||)/\Sigma|F_{obs}|$; F_{obs} and F_{calc} are observed and calculated structure factors, respectively). Crystallographic refinement of the model was started at 2.9 Å resolution, and continued at 2.3 Å resolution. The program packages used for refinement were PROTEIN, EREF,[28, 29] TNT,[30] and again FRODO.

As a result of the refinement the *R*-value was brought down to 0.193 for 95762 unique reflections at 2.3 Å resolution, the refined model consists of 10288 non-hydrogen atoms. Errors in the initial model, e.g. peptide groups and side chains with wrong orientations, were removed. New features were added to the model: a partially ordered carotenoid molecule, a ubiquinone in the partially occupied Q_B binding pocket, a complete detergent molecule (LDAO, see Fig. 4), a candidate for a partially ordered LDAO or similar molecule, seven candidates for negative ions; and 201 ordered water molecules. The upper limit of the mean coordinate error was estimated to be 0.26 Å.[31] A detailed description of refinement and refined model of the photosynthetic reaction center from *Rhodopseudomonas viridis* will be given elsewhere (*J. Deisenhofer, O. Epp, I. Sinning, H. Michel*, to be published).

3. Structure and Function

3.1. Structure Overview

An overall view of the structure of the photosynthetic reaction center from *Rhodopseudomonas viridis* is shown in Figure 6. It is a complex of four protein subunits, and of 14 cofactors. The protein subunits are called H (heavy), M (medium), L (light), and cytochrome; the names H, M, and L were chosen according to the apparent molecular weights of the subunits, as determined by electrophoresis. The core of the complex is formed by the subunits L and M, and their associated cofactors: four bacteriochlorophyll-b (BChl-b) molecules, two bacteriopheophytin-b (BPh-b) molecules, one non-heme iron ion, two quinone molecules, one carotenoid molecule. Structural properties, e.g. the hydrophobic nature of the protein surface, and functional considerations strongly indicate that the subunits L and M span the bacterial membrane. This aspect of the structure will be discussed in Section 5. Each of the subunits L and M contains five membrane spanning polypeptide segments, folded into long helices. The polypeptide segments connecting the transmembrane helices form flat surfaces parallel to the membrane surfaces.



Fig. 6. Stereoview of the overall reaction center of *Rhodopseudomonas viridis*. Protein chains are drawn in smoothed form; green, cytochrome; blue, M-subunit; brown, L-subunit; purple, H-subunit. The atoms of the cofactors are drawn in bright colors: yellow, carbon; blue, nitrogen; red, oxygen; green, magnesium. Smoothed backbone representations of polypeptide chains were produced following an idea of *Richard J. Feldman*, with help from *Marius G. Clore*.

The H subunit contributes another membrane spanning helix with its *N*-terminus near the periplasmic membrane surface. The *C*-terminal half of the H subunit forms a globular domain that is bound to the L–M complex near the cytoplasmic membrane surface. On the opposite side of the membrane the cytochrome subunit with its four covalently bound heme groups is attached to the L–M complex. Both the cytochrome subunit and the globular domain of the H-subunit have surface properties typical for water soluble proteins.

The total length of the reaction center, from the tip of the cytochrome to the H subunit is about 130 Å. The core has an elliptical cross section with axes of 70 Å and 30 Å.

The photosynthetic reaction centers from purple bacteria are the best characterized among all photosynthetic organisms (reviews: Refs. [32, 33]). All of them contain the three subunits H, M, and L; some bacteria lack the tightly bound cytochrome subunit. An example of a reaction center without a bound cytochrome subunit is that from *Rhodobacter sphaeroides*, which was also crystallized;[34, 35] its structure has been shown to be very similar to the reaction center of *Rhodopseudomonas viridis*.[36, 37]

3.2. Subunit Structure

The folding of the polypeptide chains of the four reaction center subunits is shown schematically in Figure 7. As mentioned above, major elements of secondary structure in the subunits L and M are the five membrane spanning helices. A comparison of the polypeptide chain folding in both subunits reveals a high degree of similarity. Structurally similar segments include the transmembrane helices and a large fraction of their connections. In total, 216 α-carbons from the M-subunit can be superimposed onto corresponding α-carbons of the L-subunit with an r.m.s. deviation of only 1.22 Å. The superposition of the subunits is achieved by a rotation of ca. 180° about an axis running perpendicular to the membrane surface; we call this axis the central local symmetry axis. Table 1 lists the helices in both subunits, and Table 2 lists the structurally similar regions in both subunits. Besides the transmembrane helices, called LA, LB, LC, LD, LE, and MA, MB, MC, MD, ME, with lengths between 21 and 28 residues, there are shorter helices in the connecting segments, notably helix de (between transmembrane helices D and E), and helix cd. Subunit M (323 residues) is 50 residues longer than L (273 residues). The insertions in M,

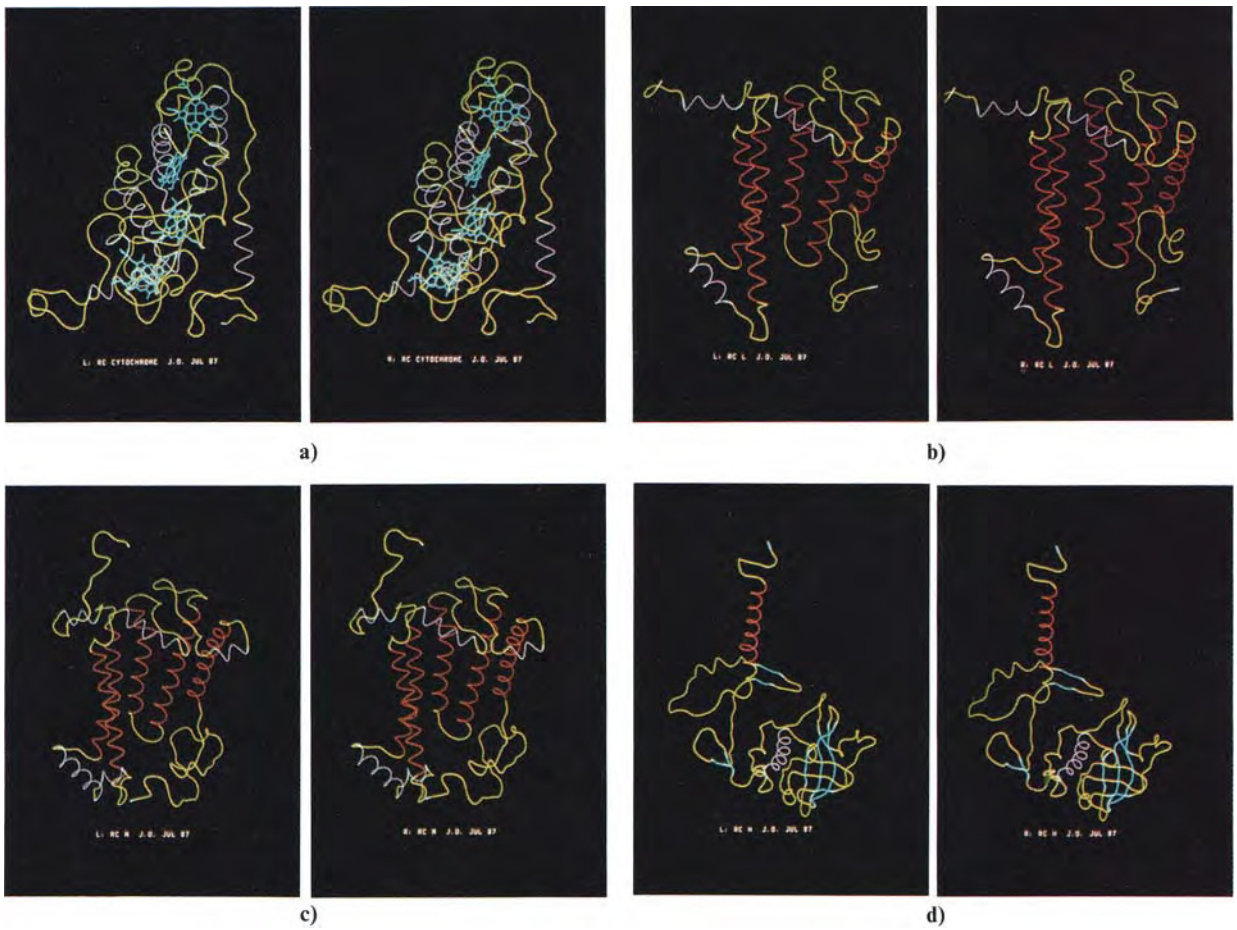


Fig. 7. Stereoview of the smoothed backbone representations of the protein subunits. The secondary structure is indicated in color: yellow, no apparent secondary structure; red, transmembrane helices; purple, other helices; blue, antiparallel β-sheets. a) Cytochrome (with the four heme groups); b) L-subunit; c) M-subunit; d) H-subunit. *N*-termini are marked blue, *C*-termini are marked red.

Table 1. Helical segments in subunits L and M.

Helix	Segment (length)	
	subunit L	subunit M
transmembrane		
A	L33–L53 (21)	M52–M76 (25)
B	L84–L111 (28)	M111–M137 (27)
C	L116–L139 (24)	M143–M166 (24)
D	L171–L198 (28)	M198–M223 (26)
E	L226–L249 (24)	M260–M284 (25)
periplasmic		
	– –	M81–M87 (7)
cd	L152–L162 (11)	M179–M190 (12)
ect	L259–L267 (9)	M292–M298 (7)
cytoplasmic		
	– –	M232–M237 (6)
de	L209–L220 (12)	M241–M254 (14)

with respect to L, are located near the *N*-terminus (20 residues), in the connection between the helices MA and MB (7 residues), in the connection between MD and ME (7 residues), and at the *C*-terminus (16 residues). The insertions at the *N*- and *C*-termini make the M-subunit dominate the contacts with the peripheral subunits. The insertion between MD and ME, containing another small helix (see Table 1) is of importance for the different conformations of the quinone binding sites in L and M, and for binding of the non-heme iron (see below).

Table 2. Regions with similar polypeptide chain folding in subunits L and M.

Subunit M		Subunit L	Length
M49–76	→	L29–56	28
M88–96	→	L61–69	9
M100–224	→	L73–197	125
M243–290	→	L209–256	48
M291–296	→	L258–263	6

The H-subunit with 258 residues can be divided into 3 structural regions with different characteristics (see Fig. 7). The *N*-terminal segment, beginning with formylmethionine,[24] contains the only transmembrane helix of subunit H; it consists of 24 residues (H12 to H35). Near the end of the transmembrane helix the sequence shows seven consecutive charged residues (H33 to H39). Residues H47 to H53 are disordered in the crystal, so that no significant electron density can be found for them.

Following the disordered region the H chain forms an extended structure along the surface of the L–M complex, apparently deriving structural stability from that contact. The surface region contains a short helix and two two-stranded antiparallel β-sheets.

The third structural segment of the H-subunit, starting at

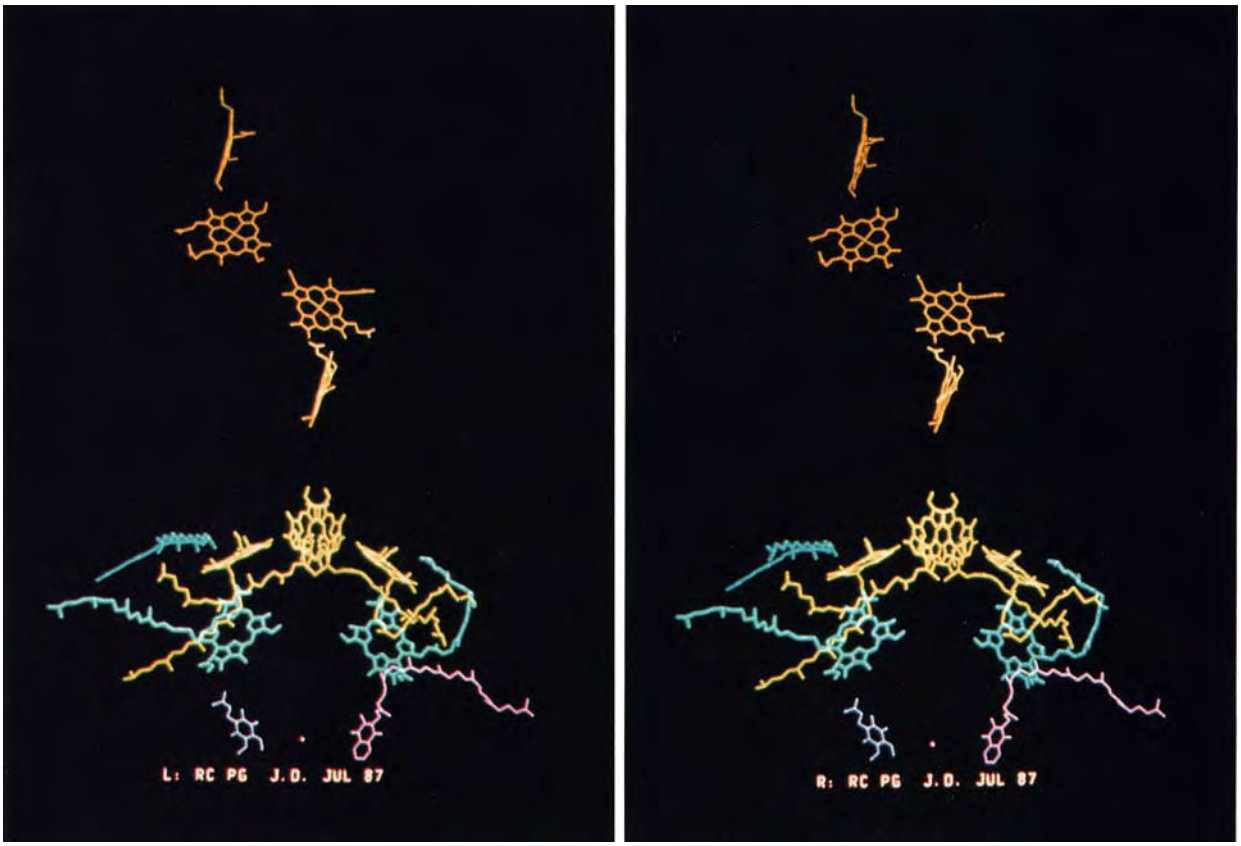


Fig. 8. Stereoview of the cofactors: brown, heme groups; yellow, bacteriochlorophyll-b; light blue, bacteriopheophytin-b; blue, carotenoid (dihydroneurosporene; *I. Sinning, H. Michel*, unpublished results); purple, quinones (right: Q_A, left: Q_B); red dot, non-heme iron.

about H105 forms a globular domain. This domain contains an extended system of antiparallel and parallel β-sheets between residues H134 and H203, and an α-helix (residues H232 to H248). The β-sheet region, the only larger one in the whole reaction center, forms a pocket with highly hydrophobic interior walls. This structural property reminds one of transport proteins like the retinol binding protein[38] and the biline binding protein;[39] however, the strand topology is different. So far, no evidence for a ligand has been found.

With 336 residues[26] the cytochrome is the largest subunit in the reaction center complex. Its last four residues, C333 to C336, are disordered. Also disordered is the lipid molecule-bound to the *N*-terminal cysteine residue.[40] The complicated structure of the cytochrome can be summarized as follows: The structure consists of an *N*-terminal segment, two pairs of heme binding segments, and a segment connecting the two pairs. Each heme binding segment consists of a helix with an average length of 17 residues, followed by a turn and the Cys-X-Y-Cys-His sequence typical for c-type cytochromes. The hemes are connected to the cysteine residues via thioether linkages. This arrangement leads to the heme planes being parallel to the helix axes. The sixth ligand to the heme iron is in three of the four cases a methionine residue within the helix. The iron of heme 4 has histidine C124, located in a different part of the structure, as a sixth ligand. The two pairs of heme binding segments, containing hemes 1 and 2, and 3 and 4, respectively, are related by a local twofold symmetry. From each pair 65 residues obey this local symmetry with an r.m.s. deviation between corresponding α-carbon atoms of 0.93 Å. The local symmetry of the cytochrome is not related to the central local symmetry.

3.3. Arrangement of Cofactors

Figure 8 shows the arrangement of the 14 cofactors associated with the reaction center protein subunits. The four heme groups of the cytochrome, numbered according to the order of attachment to the protein, form a linear chain that points to a closely associated pair of bacteriochlorophyll (BChl-b) molecules. This pair, the so-called "special pair" is the origin of the two branches of cofactors, each consisting of another BChl-b (the "accessory" BChl-b), a bacteriopheophytin-b (BPh-b), and a quinone. The non-heme iron sits between the quinones. The tetrapyrrole rings of BChl-b, BPh-b and quinone molecules approximately follow the same local symmetry that is displayed by the L- and M-chains. The branches of cofactors from the special pair to the BPh-b molecules can be clearly associated with subunits L or M, so that we speak of an L-branch and an M-branch. This is the basis for our nomenclature: BChl-b and BPh-b are called BC_{XY} and BP_X, respectively, where X denotes the branch (L or M), and Y is P for "special pair" or A for "accessory". At

the level of the quinones the situation is more complicated because the subunits interpenetrate here, and the quinone at the end of the L-branch is actually bound in a pocket of the M-subunit and vice versa. Therefore, we prefer the nomenclature Q_A and Q_B with Q_A at the end of the L-branch; Q_A is menaquinone-9, and Q_B is ubiquinone-9.[41] The local symmetry is violated by the phytyl chains of BChl-b and BPh-b, by the different chemical nature and different occupancy of the quinones, and by the presence of a carotenoid molecule near the accessory BChl-b molecule of the M-branch.

3.4. Functional Overview

Our current understanding of the function of the reaction center was developed by combining structural information with information from other experimental techniques, notably spectroscopy, as described in recent reviews.[42-44] Figure 9 shows a schematic view of the reaction center with its

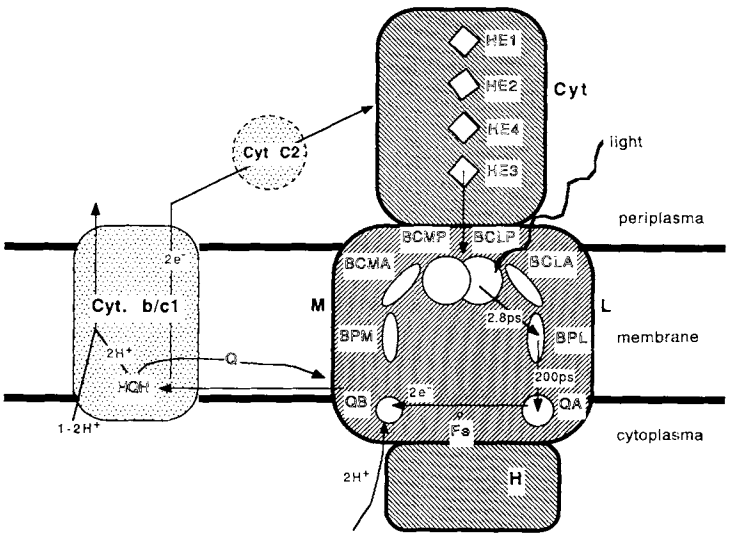


Fig. 9. Schematic view of the reaction center, showing the light-driven cyclic electron flow.

cofactors in the bacterial membrane. The special pair, P, is the starting point for a light-driven electron transfer reaction across the membrane. Absorption of a photon, or energy transfer from light harvesting complexes in the membrane puts P into an excited state, P*. From P* an electron is transferred to the bacteriopheophytin on the L-branch (here: BP_L) with a time constant of 2.8 ps.[45,46] The distinction between the two bacteriopheophytin molecules was possible because they absorb at slightly different wavelengths, and, with a knowledge of the crystal structure, linear dichroism absorption experiments could distinguish between the two chromophores.[47-49]

From BP_L the electron is transferred to Q_A with a time constant of ca. 200 ps. At this point the electron has crossed most of the membrane. Both these electron transfer steps function at very low temperatures (ca. 1 K) with time constants even shorter than at room temperature.[50,51]

From Q_A the electron moves on to Q_B in about 100 μs. The non-heme iron does not seem to play an essential role in this step.[52]

Q_B can pick up two electrons and, subsequently, two protons.[53] In the Q_BH_2 state it dissociates from the reaction center, and the Q_B site is re-filled from a pool of quinones dissolved in the membrane. Electrons and protons on Q_BH_2 (here: HQH) are transferred back through the membrane by the cytochrome b/c_1 complex. The electrons are shuttled via a soluble cytochrome c_2 to the reaction center's cytochrome from which the photo-oxidized special pair is reduced with a time constant of ca. 270 μs. This time constant increases with decreasing temperature down to ca. 100 K, and remains constant for lower temperatures. The whole process can be described as a light-driven cyclic electron flow, the net effect of which is the generation of a proton gradient across the membrane that is used to synthesize adenosine triphosphate, as described by *P. Mitchell*'s chemiosmotic theory. A number of still unsolved problems preclude a complete understanding of the reaction center's function. The nature of the electron transfer steps described above, and their speed and temperature dependence have not yet been explained theoretically. The first step, imposing the question of the role of the bridging BC_{LA}, is a subject of fascinating debate.

One of the greatest surprises in the structure analysis was the symmetry of the core structure, raising the question of the factors leading to the use of only the L-branch of cofactors and of the significance of the apparently unused branch. Further open questions relate to electron transfer between Q_A and Q_B, the role of the non-heme iron, and the function of Q_B as two-electron gate and proton acceptor. Finally, the purpose of the cytochrome, as well as details of the electron transfer from the soluble cytochrome to the cytochrome in the reaction center, and within the four hemes, are yet not fully understood.

3.5. Structural Details in Relation to Function

Here I describe the arrangement of the cofactors and their environment in some detail. Observations relating to open functional questions are emphasized.

Figure 10 shows the BChl-b ring system of the special pair, the primary electron donor of the photosynthetic light reaction. On the basis of spin resonance experiments the existence of a special pair had been postulated some time ago.[54] The two molecules overlap with their pyrrole rings I in such a way that, when viewed in a direction perpendicular to the ring planes, the atoms of these rings eclipse each other. The orientation of the rings leads to a close proximity between the ring I acetyl groups and the Mg^{2+} ions; however, the acetyl groups do not act as ligands to the Mg^{2+} ions. The pyrrole rings I of both BChl-b molecules are nearly parallel, and ca. 3.2 Å apart. Both tetrapyrrole rings, however, are non-planar; planes through the pyrrole nitrogens of each BChl-b form an angle of 11.3°.

The BChl-b molecules of the special pair are arranged with a nearly perfect twofold symmetry. This is illustrated in Figure 11 which shows a view along the twofold axis.[55] The BChl-b rings of the special pair are nearly parallel to this symmetry axis. Further structural elements shown in Fig-

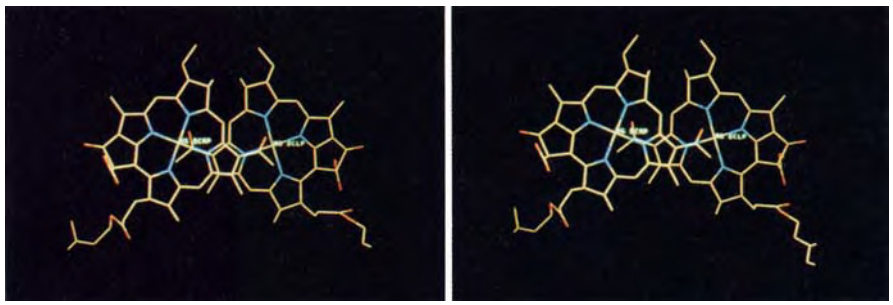


Fig. 10. Stereoview of the special pair with atoms and bonds in color: yellow, carbon; blue, nitrogen; red, oxygen; green, magnesium.

ure 11 that obey the central local twofold symmetry are the histidine residues (L173, M200) acting as ligands to the special pair Mg^{2+} ions, the rings of the accessory BChl-b molecules, the water molecules H-bonded between histidine nitrogen atoms and ring-V carbonyl groups of the accessory

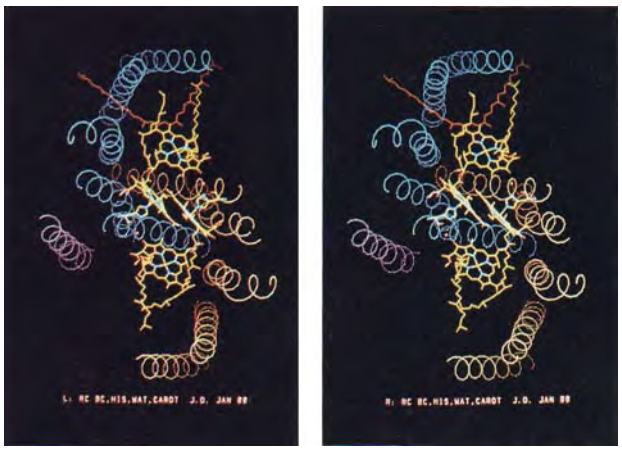


Fig. 11. Stereodiagram of a part of the reaction center (view along the central local twofold axis): special pair with histidine ligands, accessory bacteriochlorophyll-b molecules (BC_{LA} bottom, BC_{MA} top), two water molecules; the transmembrane helices of subunits L (brown), M (blue), and H (purple) are shown in smoothed backbone form.

BChl-b molecules, and the transmembrane helices of subunits L and M. The carotenoid molecule in contact with the accessory BChl-b (BC_{MA}), the side chains of the accessory BChl-b molecules, and the transmembrane helix of the H-subunit are examples of structural elements that break the twofold symmetry. A more subtle deviation from symmetry is the different degree of non-planarity of the two BChl-b ring systems of the special pair. The tetrapyrrole ring of BC_{MP} is considerably more deformed than that of BC_{LP}. This can cause an unequal charge distribution between the two BChl-b systems of the special pair, which in turn can be part of the reason for unidirectional electron transfer.[56]

Even though the tetrapyrrole rings of the BChl-b and BPh-b molecules of the L- and M-branches can be rotated on top of each other using a single transformation with the reasonably low r.m.s. deviation of 0.38 Å between the positions of equivalent atoms, a closer inspection shows considerable differences between the local symmetry operations of the special pair, the accessory BChl-b molecules, and the BPh-b molecules. Optimum superposition of the tetrapyrrole rings of the special pair alone is achieved by a rotation of 179.7°, for the accessory BChl-b molecules by a rotation of $-175.8°$, and for the BPh-b molecules by a rotation of

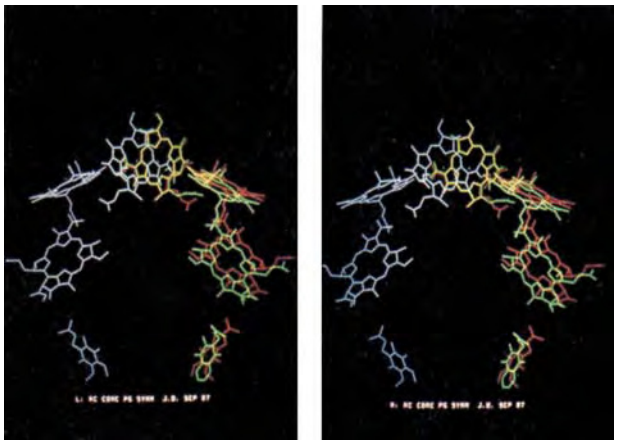


Fig. 12. Stereoview of the cofactors of the M-branch (purple), and of the L-branch (green); the phytyl chains are omitted for clarity. Red: cofactors of M-branch, rotated using a transformation that optimally superimposes the tetrapyrrole ring of BC_{MP} onto that of BC_{LP}.

$-173.2°$. This deviation from twofold symmetry is illustrated in Figure 12, where the cofactors of the M-branch were rotated using the transformation that optimally superimposes the special pair tetrapyrrole rings. It is clear that, due to the imperfect symmetry, interatomic distances and interplanar angles are different in both branches. For example, the closest distance between the atoms involved in double bonds in the special pair, and in BP_L is shorter by 0.7 Å than the corresponding distance between special pair and BP_M. Another example is provided by the angles between the tetrapyrrole rings of the special pair, and those of the accessory BChl-b molecules: the angles for BP_L are about 6° smaller than for BP_M. These structural differences lead to differences in overlap of the orbitals, and are expected to lead to different electron transfer properties in the two branches. This may be another contribution to the unidirectional charge separation in the reaction center.

Yet another observation that may relate to the different electronic properties of the L- and M-branches is the different degree of structural order. The amount of disordered structure, measured by the number of atoms without significant electron density, is larger in constituents of the M-branch than in those of the L-branch. Both phytyl side chains of BC_{MA} and BP_M are partially disordered at their ends; the phytyl chains of BC_{LA} and BP_L have a different conformation and are well ordered. The carotenoid near BC_{MA} may contribute to this difference in phytyl chain structure since its presence prevents an identical arrangement of phytyl chains on both sides.

A measure of the rigidity of the structure are the atomic *B*-values obtained during crystallographic refinement. These

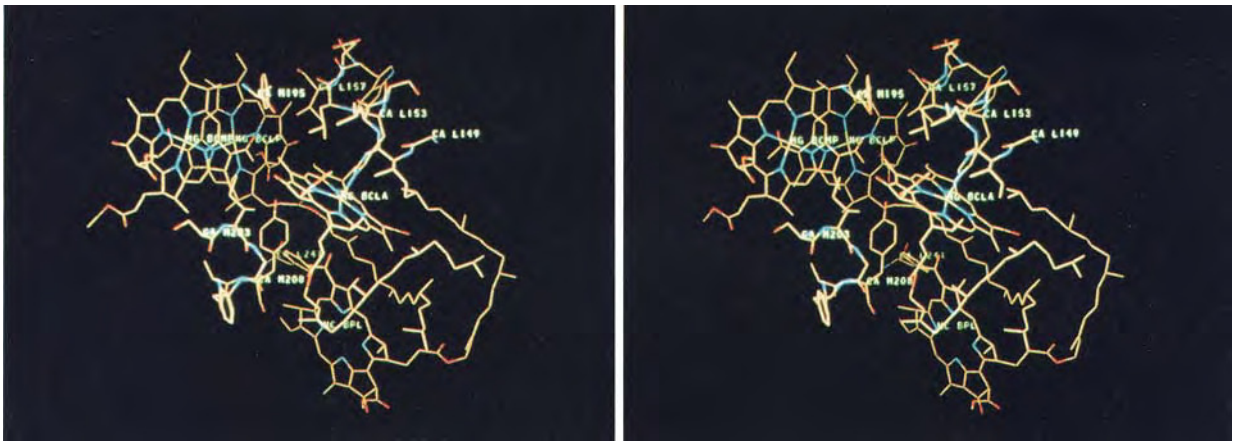


Fig. 13. Stereoview of the special pair, BC_{LA}, BP_L, and selected residues with colored atoms and bonds. Colors as in Fig. 10.

values are higher in the M-branch than in the L-branch. An example is the tetrapyrrole ring of BP_M with an average B value of 21.1 Å^2; in BP_L, B is only 10.3 Å^2.

A major source of asymmetry are the protein subunits L and M surrounding the core pigments. Their overall sequence homology is only 25%.[25] Although key residues like the histidines that are ligands to the Mg^{2+} ions of the BChl-b molecules and to the non-heme iron are strictly conserved, most of the residues in contact with the core pigments are different in the two branches.

I will now describe details of the protein environment of the pigments along the pathway of the electron, and mention additional differences between the branches that may be functionally important. Figure 13 shows a close-up view of the structures that are directly involved in the first step of the light-driven electron transfer reaction: the special pair (P), the accessory BChl-b BC_{LA}, and the first electron acceptor (BP_L). In addition, a few amino acid residues in close contact with these pigments are shown. BC_{LA} is in van der Waals contact with both the special pair and BP_L. The closest approach between the tetrapyrrole rings of the special pair and BP_L is 10 Å (atoms in double bonds). The phytyl chain of BC_{LP} follows a cleft formed by BC_{LA} and BP_L; it is in van der Waals contact with both tetrapyrrole rings.

At first glance this arrangement suggests that the electron should follow the path P → BC_{LA} → BP_L. However, attempts to observe bleaching of the absorption bands of BC_{LA} due to transient reduction failed. Spectroscopic experiments with ultrafast laser systems indicated direct reduction of BP_L from P* without intermediate steps.[45, 46, 50] This result triggered off heated discussions of the mechanism of electron transfer from P to BP_L, and of the role of BC_{LA} in this process. As indicated in Figure 13 with the example of tyrosine M208, it seems plausible that the protein plays an important role, not only as a scaffold to keep pigments in place, but also in influencing functional properties.

Numerous protein-pigment interactions are apparent also for the special pair itself,[57] as shown in Figure 14. These interactions include bonds from N_ε atoms of histidines L173 and M200 to the Mg^{2+} ions of BC_{LP} and BC_{MP}, respectively. Both acetyl groups of the special pair are hydrogen bonded: BC_{LP} to histidine L168, and BC_{MP} to tyrosine M195. A further hydrogen bond is found between the carbonyl oxygen of ring V and the OH group of threonine L248; there is no equivalent hydrogen bond for BC_{MP}.

The special pair environment is rich in aromatic residues: five phenylalanines, three tyrosines, and three tryptophans are in direct contact with the tetrapyrrole rings of the special

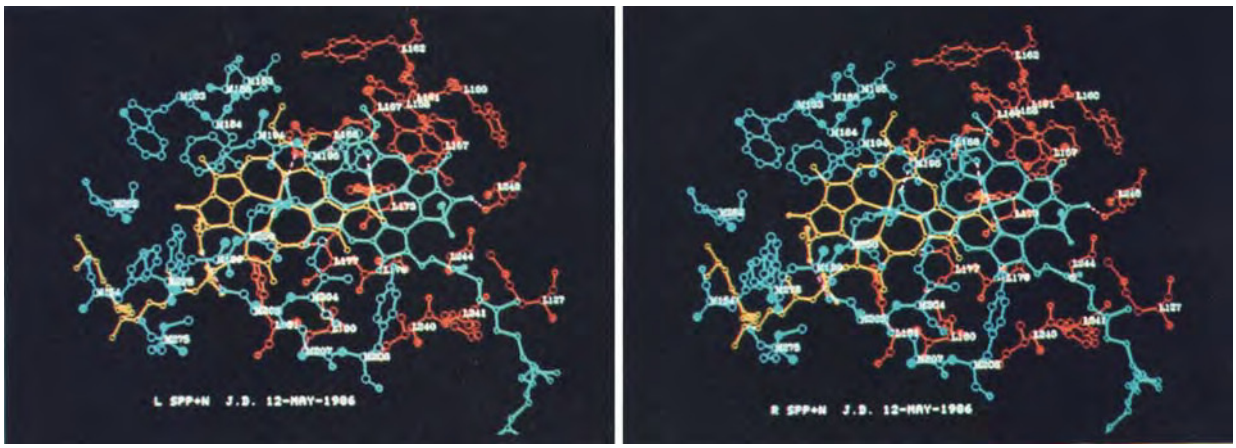


Fig. 14. Stereoview of the special pair and of its protein environment (after *Michel* et al. [57]): brown-red, residues from the L-subunit; blue, residues from the M-subunit; green, BC_{LP}; yellow, BC_{MP}; hydrogen bonds are indicated in purple. The hydrogen bond between serine M203 and BC_{MP} is no longer present in the refined model.

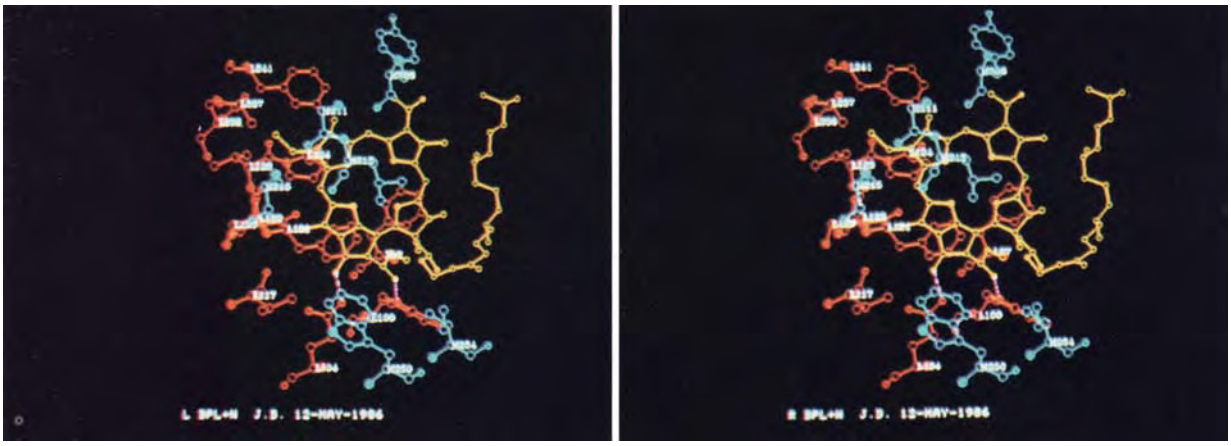


Fig. 15. Stereoview of BP_L (yellow) and its protein environment; colors as in Fig. 14.

pair. Tyrosine L162 is located between the special pair and the closest heme group (HE3) of the cytochrome, and may play a role during reduction of the photooxidized special pair (P^+) by cytochrome.[57]

Figure 15 shows BP_L, the first electron acceptor, with its protein environment.[57] The BPh-b molecules are held in their places by non-covalent interactions only. In the positions where histidine ligands of BChl-b molecules would be expected, we find leucine M212 in the case of BP_L (see Fig. 15), and methionine L184 in the case of BP_M. BP_L forms two hydrogen bonds to the protein. The one between the ester carbonyl group of ring V and tryptophan L100 has an equivalent in a hydrogen bond between BP_M and tryptophan M127. The other hydrogen bond, between the keto-carbonyl oxygen of ring V and glutamic acid L104 is unique for the L-branch; the residue on the M-side corresponding to glutamic acid L104 is valine M131. Glutamic acid L104 is conserved in all currently known sequences of reaction center L-subunits from purple bacteria. Its position in the electron transfer pathway strongly suggests that it is protonated; otherwise, the negative charge of the ionized glutamic acid side chain would make electron transfer to BP_L energetically highly unfavorable.

As for the special pair, aromatic residues are found in the neighborhood of the BPh-b; the neighborhood of BP_L is richer in aromatic residues than that of BP_M. An especially noteworthy aromatic residue is tryptophan M250 whose side chain forms a bridge between BP_L and the next electron acceptor, Q_A. The M-branch residue equivalent to tryptophan M250 is phenylalanine L216 which, due to the smaller side chain, cannot perform a similar bridging function between BP_M and Q_B.

The environment of the quinone molecules and of the non-heme iron[57] is shown in Figure 16. Instead of the quinone, however, the figure shows the herbicide terbutryne in the Q_B binding pocket. The non-heme iron appears in the center of the drawing, between the binding sites of Q_A and Q_B, very near the central local twofold symmetry axis. It is bound by five protein side chains, four histidines (L190, L230, M217, M264), and glutamic acid M232, whose carboxylate group acts as a bidentate ligand. The iron sits in a distorted octahedral environment with the axial ligands histidine L230 and histidine M264, and equatorial ligands histidine L190, histidine M217, and glutamic acid M232. Histidine L190 and histidine M217 also contribute significantly to the binding of Q_B and Q_A, respectively. The location of the iron and its binding to residues from subunits L and M immediately suggests that a part of the iron's role is to increase the structural stability of the reaction center. It is surprising that its role in electron transfer between the quinones seem to be relatively minor.[58]

The head group of Q_A is bound in a highly hydrophobic pocket; its carbonyl oxygens are hydrogen bonded to the peptide NH groups of alanine M258, and to the N_δ atoms of the histidine M217 bound to iron. As mentioned above, tryptophan M250 forms part of the Q_A's binding pocket; its indole ring is nearly parallel to the head group of Q_A at a distance of 3.1 Å. The isoprenoid side chain of Q_A is folded along the surface of the L-M complex; the last three isoprenoid units are disordered in the crystal. The Q_A binding pocket is well shielded from the cytoplasm by the globular domain of the H-subunit.

The Q_B binding site in the crystals of the reaction center is only partially occupied; the Q_B model is therefore less reliable than the other parts of the structural model discussed above. Nevertheless, the crystallographic data suggest a highly plausible arrangement of the Q_B head group in its pocket; the Q_B side chain remains undefined. Apparently Q_B, similarly to Q_A, forms hydrogen bonds to the protein with its two carbonyl oxygens: one to the N_δ atom of the histidine L190 bound to iron, and a bifurcated hydrogen bond to the OH group of serine L223, and to the NH group of glycine L225. Like tryptophan M250 in the case of Q_A, phenylalanine L216 forms a significant part of the Q_B binding pocket. Major differences between the binding sites of Q_A and Q_B are the more polar nature of the Q_B site, and the presence of pathways through the protein, through which protons may enter the Q_B site. The bottom of the Q_B site is formed to a large part by the side chain of glutamic acid L212. Protons can move from the cytoplasm along a path marked by charged or polar residues to glutamic acid L212 and from there, by an as yet unknown mechanism, to the doubly reduced Q_B^{2-}.

Some herbicides are competitive inhibitors of Q_B binding to reaction centers of purple bacteria. Crystallographic binding studies with the herbicide terbutryne (see Fig. 16), and with *o*-phenanthroline[57, 59] demonstrated binding of these molecules in the Q_B binding pocket, and provided a structur-

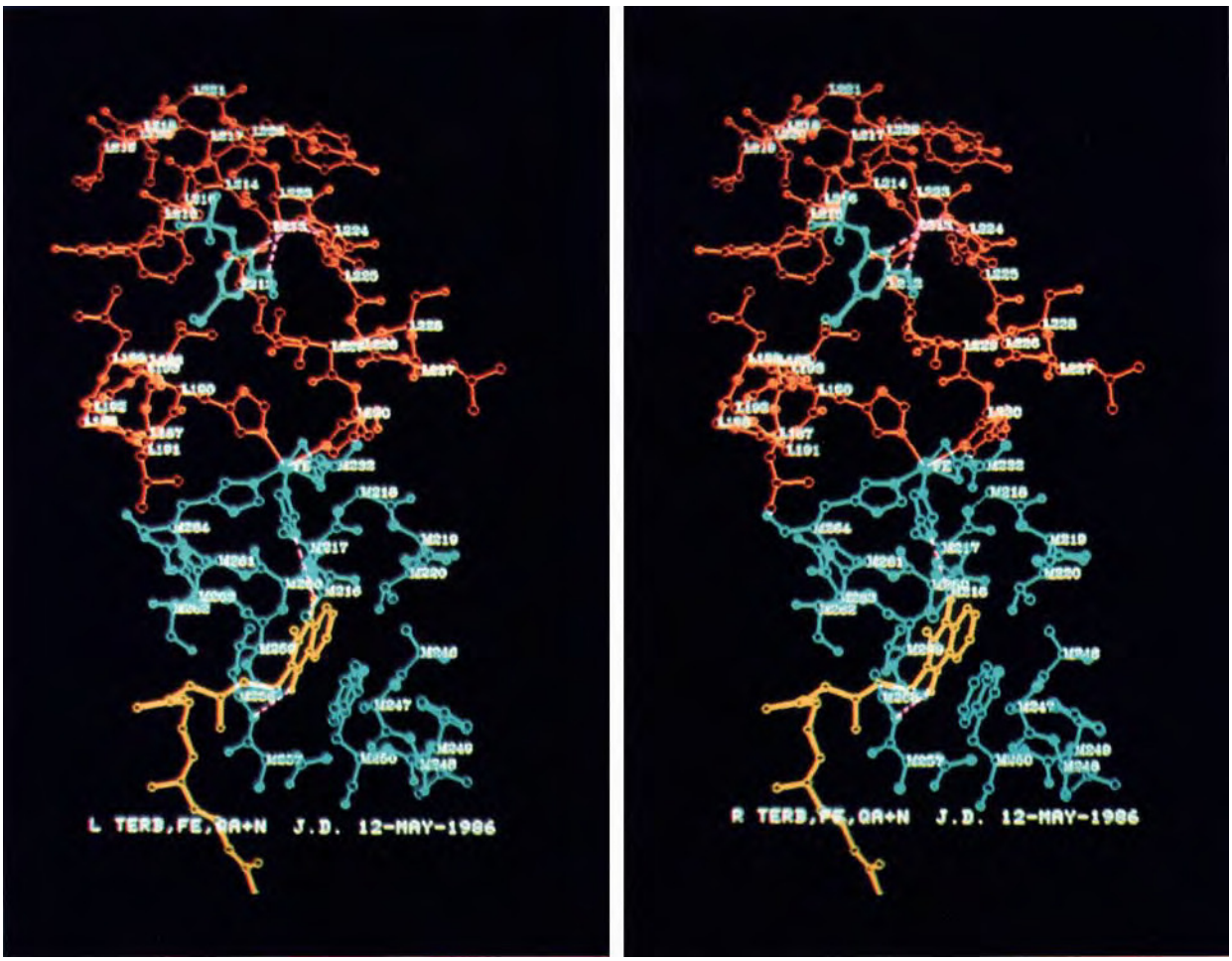


Fig. 16. Stereoview of the primary quinone (Q_A) of the non-heme iron, of the herbicide terbutryne (blue-green) in the Q_B binding pocket, and of the protein environment of these cofactors; colors as in Fig. 14 (after *Michel* et al. [57]).

al basis for understanding mutations that lead to herbicide-resistant *Rps.-viridis*.[60,61] The fact that herbicides which were developed to inhibit photosystem II reaction centers of green plants can also inhibit reaction centers of purple bacteria is one of the many indications of a close structural similarity between these kinds of photosynthetic reaction centers (see also Section 4 and Ref. [62]).

4. The Relation to Photosystem II and Evolutionary Aspects

4.1. Conclusions on the Structure of Photosystem II Reaction Center

The most surprising result of the X-ray structure analysis was the discovery of the nearly symmetric arrangement of the reaction center core formed by the homologous L- and M-subunits together with the pigments. The primary electron donor as well as the ferrous non-heme iron (II) are found at the interface between both subunits. Both subunits are needed to establish the reaction center.

Parallel to our X-ray structure analysis the following results suggesting a close relation between the reaction centers from purple bacteria and photosystem II were or became available: i) Photosystem II reaction center and the reaction center from purple bacteria both possess two pheophytin molecules.[32,63] Upon removal of the quinones or prereduction of them it is possible to trap one electron on one of them.[64,65] ii) Both reaction centers possess a magnetically coupled Q_A–Fe–Q_B complex. iii) The L-subunit of the reaction center of purple bacteria and the D1 protein (which is the product of the psbA-gene and also called Q_B protein, 32 kD-protein or herbicide binding protein) bind the herbicide azidoatrazine upon photoaffinity labeling.[66,67] iv) Weak but significant sequence homologies between the L- and M-subunits of the purple bacteria,[25,57,68–70] and the D1 proteins,[71] and later on also D2 proteins[72–75] of the photosystem II were discovered.

The conclusion to be drawn from the results was obvious: The reaction center of photosystem II from plants and algae had to be expected to be formed by the D1 and D2 proteins with D1 corresponding to the L-subunit and D2 corresponding to the M-subunit. This, however, was at variance with the accepted view[76] that the so-called CP47, a chlorophyll-binding protein with apparent molecular weight of 47000, is the apoprotein of the photosystem II reaction center. Figure 17 compares the amino acid sequences of the L- and M-subunits from two purple bacteria with the D1 and D2 proteins from spinach chloroplasts. Significant sequence homology starts with the glycine-glycine pair (L83, 84, M110,

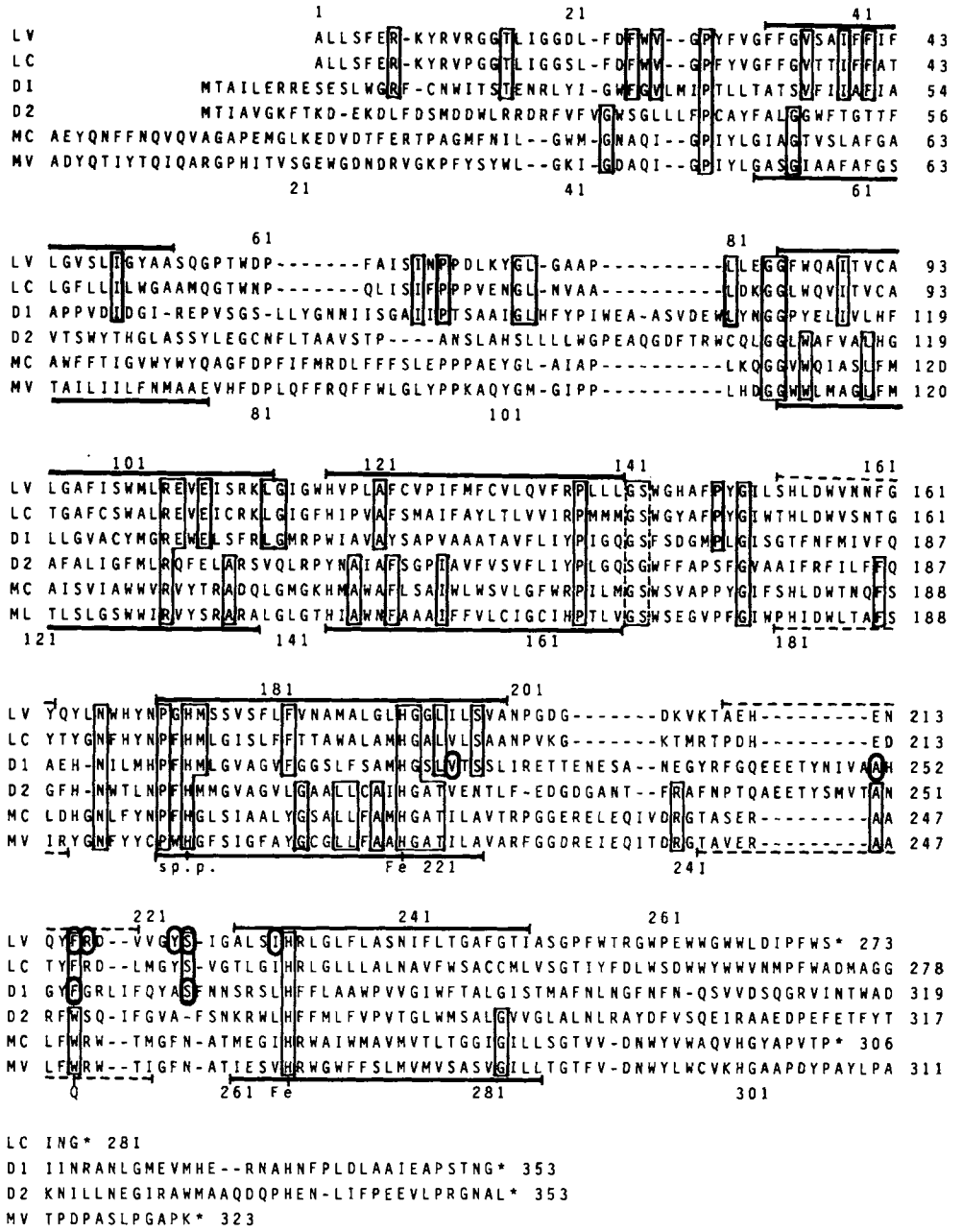


Fig. 17. The amino acid sequences of the L and M subunits of the purple bacteria *Rps. viridis* (LV, MV) [25] and *Rb. capsulatus* (LC, MC) [70] and of the D1 and D2 proteins. Amino acids common to all six subunits, the L subunits and D1, or the M subunits and D2 are boxed. The position of the transmembrane α-helices in the *Rps. viridis* reaction center is indicated by bars above the sequences of the L subunits and below the sequences of the M subunits. The positions of the short α-helices in the connections of transmembrane α-helices C and D, as well as D and E, are indicated by dashed lines. The histidine ligands of the special pair bacteriochlorophyll molecules and of the non-heme iron atom are labeled sp.p. and Fe, respectively. Circles show amino acids known to be mutated in herbicide-resistant reaction centers of purple bacteria or photosystem II (after *Michel* and *Deisenhofer* [62]).

111) at the beginning of the second transmembrane helix. Mainly amino acids of structural importance such as glycines, prolines and arginines are conserved. Part of the amino acids involved in the binding of the pigments and cofactors are also conserved: The histidine-ligands to the magnesium atoms of the special-pair chlorophyll molecules (L173, M200) and to the non-heme iron atom. In the L-subunit and in the D1 protein, a phenylalanine residue (L216, D1-255) and a serine residue (L223, D1-264) are found in the corresponding sequence positions. These residues are involved in the binding of the *s*-triazine herbicides like atrazine and terbutryne, which presumably compete with the secondary quinone Q_B for its binding site. Mutations of these amino acids cause herbicide resistance in the purple bacteria, in plants and in algae. The phenylalanines L216 and D1-255 correspond to tryptophans M250 and D2-254, which form the major part of the binding site of the primary quinone Q_A (see Section 3.5).

Several important differences exist between the reaction centers of photosystem II and those of the purple bacteria: the amino acids involved in the binding of the accessory bacteriochlorophylls in the purple bacteria, and a glutamic acid (M232) which is a bidentate ligand to the ferrous non-heme iron are not conserved. There is no indication of the existence of an analogue to the H-subunit in the reaction center of the photosystem II. The overall structure of the photosystem II reaction center core, however, must be very similar to the reaction center from purple bacteria formed by the L- and M-subunits. Figure 18 shows those helices which are presumably conserved between the reaction center cores of the purple bacteria and photosystem II and the position of the amino conserved between the L- and M-subunits and the D1 and D2 proteins. The identities of amino acids which are found specifically in the L-subunits and the corresponding positions of the D1 proteins, or specifically in the M-subunits and the corresponding positions of the D2 proteins,

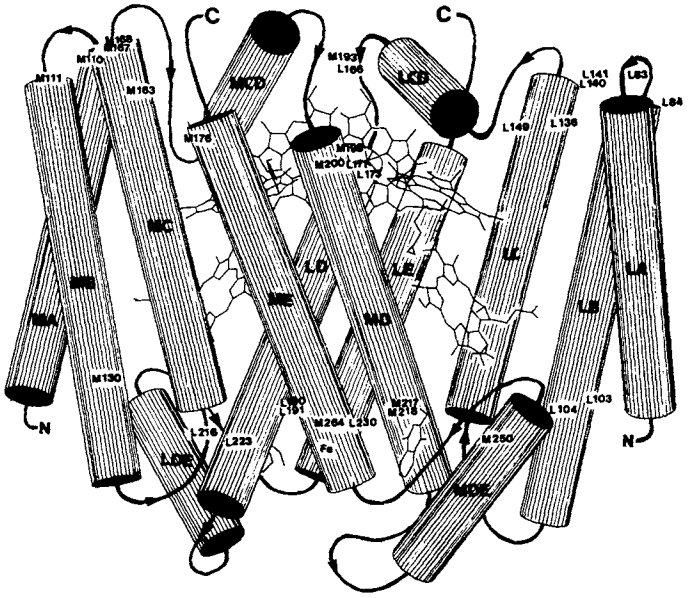


Fig. 18. Column model of the core of the reaction center of *Rps. viridis*. Only helices which are presumably conserved in photosystem II reaction center are shown. The connections of the helices are only indicated schematically. The transmembrane helices of the L (M) subunit are labeled LA-LE (MA-ME) and the major helices in the connections are labeled LCD (MCD) and LDE (MDE). Bacteriochlorophyll molecules of the special pair are at the interface of the L and M subunits between the D and E helices, while the bacteriopheophytin molecules are near the L helices. The binding site for Q_B is between the LDE and LD helices. The location of the amino acids conserved between all L and M subunits and the D1 and D2 proteins, as well as those forming the quinone binding sites, is indicated by their sequence numbers (after *Michel* and *Deisenhofer* [62]).

and are involved in the quinone binding, might be the result of convergent evolution. Their location is also shown.

The photooxidized primary electron donor (P^+) in the reaction center of *Rhodopseudomonas viridis* is reduced by the cytochrome subunit. In the position equivalent to this subunit in the photosystem II reaction center we have to expect the water soluble proteins forming part of the manganese-containing complex which evolves oxygen.

Experimental proof of the existence of a similar reaction center core in photosystem II was the recent isolation of a complex consisting of the proteins D1, D2 and cytochrome b559 from spinach chloroplasts which contains four to five chlorophyll molecules and two pheophytin molecules.[77] It has been shown to be active in electron transport to one of the pheophytins. Recently, evidence has been presented by two groups that a tyrosine residue located on the D1 subunit in the third transmembrane helix is an intermediate electron carrier between the primary electron donor of photosystem II and the oxygen-evolving manganese cluster.[78–80] A topic of speculation at the moment is whether or not the manganese cluster is also bound to the D1 and D2 proteins.

As a result of the work on the bacterial photosynthetic reaction center our entire view on the photosystem II reaction centers from plants and algae has changed.

4.2. Evolutionary Aspects

The sequence similarities discussed above suggest that the reaction centers from purple bacteria and photosystem II are evolutionarily related. A common ancestor possessed an entirely symmetric reaction center with two parallel electron transporting pigment branches across the membrane. This symmetric reaction center was formed by two copies of the same protein subunit encoded by one gene, i.e. was a homodimer. After a gene duplication and subsequent mutations the formation of the asymmetric dimer ("heterodimer") and the use of only one pigment branch for electron transfer became possible. It is an open question whether in evolution this gene duplication occurred only once (before the lineages leading to the purple bacteria and the organisms containing photosystem II split) or twice, after the splitting into these two lineages. In the latter case the specific sequence similarities between L and D1, as well as those between M and D2, would be the result of convergent evolution, whereas the identities of the structurally important amino acids would date back to the original symmetric dimer. Sequence comparisons are in favor of the latter possibility (see Ref. [81]): The similarity of the sequences in the D1 and D2 proteins is much greater than that in the L- and M-subunits. This observation possibly indicates that the gene duplication giving rise to separate D1 and D2 proteins occurred later during evolution than the gene duplication leading to the L- and M-subunits. On the other hand, due to more and stronger interactions with neighboring proteins, the D1 and D2 proteins had less freedom to mutate than the L- and the M-subunits. As a result, sequence comparisons might be misleading.

These evolutionary relationships also indicate that there must be an advantage for reaction centers possessing only one active electron transport chain with two quinones acting in series. There might be rather trivial explanations for the use of only one branch, e.g. an asymmetry in the protein environment can cause an asymmetry in the distribution of electrons in the excited state and subsequently lead to a preferred release of an electron only in one direction. This existing polarity might lead to a faster rate of the first electron transfer step, a minimization of competing reactions, and thus a higher quantum yield for the electron transfer.

A clear advantage of the present day's reaction centers is that the two quinones act in series, and only the released secondary quinone, Q_B, is a two-electron carrier. Consider the situation of the ancient symmetric reaction center: After the first excitation the electron is transferred to the quinone at the end of one pigment branch. The resulting semiquinone is not stable and its electron is lost within a period of seconds. Only if it receives a second electron can it be protonated and energy stored in the form of the quinol. With two identical parallel electron transfer chains the probability for the second electron to be funneled into the same chain to the same quinone as the first electron is only 50%. A possible electrostatic repulsion by the negatively charged semiquinone might even decrease this probability. In a frequent situation the absorption of two photons leads to the formation of two semiquinones in the same reaction center and energy is not stored in a stable way. Clearly, the way out of this dilemma is to switch the two quinones in series and to allow protonation and release only to the final quinone, which is then Q_B in the electron transfer chain, as is observed in the reaction centers of purple bacteria and photosystem II. A considerable increase in the efficiency of light energy conversion must result, especially under poor light conditions.

5. Aspects of Membrane Protein Structure

5.1. The Membrane Anchor of the Cytochrome Subunit

X-ray structure analyses established that the L and M subunits are firmly integrated into the membrane, both possessing five transmembrane helices, whereas the H subunit is anchored to the membrane by one transmembrane helix. The X-ray work showed no indication of any intramembraneous part of the cytochrome subunit. Nevertheless, in the hands of the biochemists it behaved like a membrane protein and aggregated easily. A strange observation during the protein sequencing was that upon Edman-degradation of the isolated cytochrome subunit no *N*-terminal amino acid could be identified after the first degradation, but a normal sequence could be obtained starting with the second amino acid from the *N*-terminus. With the help of *F. Lottspeich, K. A. Weyer* was then able to isolate a modified amino-terminal amino acid, and, in collaboration with *W. Schäfer* to elucidate its structure using mass spectrometry.[40, 82] The result is shown in Figure 19. The *N*-terminal amino acid is a cysteine linked to a glycerol residue via a thioether bridge. Two fatty acids are then esterified to the two OH-groups of the glycerol. The fatty acids are a statistical mixture of singly unsaturated C_{18} fatty acids and singly hydroxylated C_{18} fatty acids. These experiments firmly established that the cytochrome subunit also possesses a membrane anchor, but this is now of a lipid type and not of a peptide type. The membrane anchor is very similar to that of the bacterial lipoproteins (see, e.g., Refs. [83, 84]). The cytochrome subunit of the reaction center is the first cytochrome molecule known to contain such a membrane anchor.

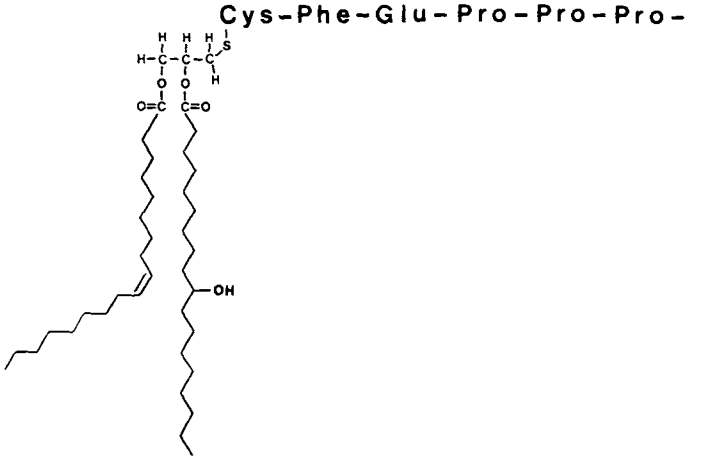


Fig. 19. The *N*-terminus of the cytochrome subunit. Two fatty acids are esterified with the *N*-terminal *S*-glycerocysteine. The fatty acids are a mixture of 18:OH (two isomers) and 18:1 (three isomers) acids roughly in a 1:1 ratio, which are represented by oleic acid and 10-hydroxystearic acid in the figure (after *Weyer* et al. [40]).

5.2. Protein Lipid Contacts

The interaction between lipids and protein occurs at the surface of the proteins. Therefore a closer examination of the surface of the protein complex might be very informative. For this purpose a space filling model of the reaction center is shown in Figure 20a. Carbon atoms approaching the surface of the reaction center are shown as white spheres. A central section perpendicular to the approximate twofold rotation axis can be seen where carbon atoms form the surface of the protein almost exclusively. They are mainly side chain atoms of the amino acids leucine, isoleucine and phenylalanine. This central zone must correspond to the hydrophobic part of the protein surface, which in the membrane is in contact with the alkane chains of the lipids. Approaching the cytoplasmic rim of that central zone a row of nitrogen atoms is seen at the protein surface. These nitrogen atoms are side chain atoms of the basic amino acids arginine and histidine. The role of these basic residues might be to determine the position of the reaction center perpendicular to the membrane via specific interaction between negatively charged phosphate groups of the lipids and the positively charged amino acid side chains of the reaction center protein subunits.

Figure 21 shows the percentage of the "accessible surface area" occupied by carbon atoms, as layers perpendicular to the central twofold rotation axis. The twofold rotation axis runs through the non-heme iron atom near the cytoplasmic side and relates the special-pair bacteriochlorophyll molecules near the periplasmic side of the membrane. Two important conclusions can be drawn from Figure 21: (i) The primary electron donor (special pair), is located in the hydrophobic non-polar part of the membrane, whereas the non-heme iron atom is already in that zone where the protein surface is polar and most likely interacts with the polar head groups of the lipids. (ii) The thickness of the hydrophobic zone perpendicular to the membrane is 30 to 31 Å only. This value is smaller than expected for a lipid bilayer composed of lipids with C_{18} fatty acids.

5.3. Distribution of Amino Acids and Bound Water Molecules

Figure 20b shows the distribution of the strongly basic amino acids arginine and lysine, and of the strongly acidic amino acids glutamic acid and aspartic acid, which at neutral pH possess electric charges at the ends of their side chains. A central zone, where none of these amino acids is found, has a thickness of about 25 Å and is thus slightly thinner than the hydrophobic surface zone shown in Figures 20 and 21. This slight discrepancy is due to two arginine residues and one glutamic acid residue, which are apparently in a hydrophobic environment without counter charges. The role of the positive charges of the arginine side chains seems to be structural. They possibly cancel the partial negative charge at the carboxy-terminal ends of the short helices in the connections of the long D and E transmembrane helices. These short de helices partly intrude into the hydrophobic zone of the membrane and a positive charge seems to be necessary so that the peptide chain can change its direction. The glutamic acid (L104) seems to be protonated and thus neutral, and forms a hydrogen bond with one of the bacteriopheophytin molecules (BP_L)[57] (see also Section 3.5).

Within the L and M subunits the glutamate and aspartate, as well as lysine and arginine residues show an interesting asymmetric distribution with respect to cytoplasmic and periplasmic sides. If one calculates "net charges" for the

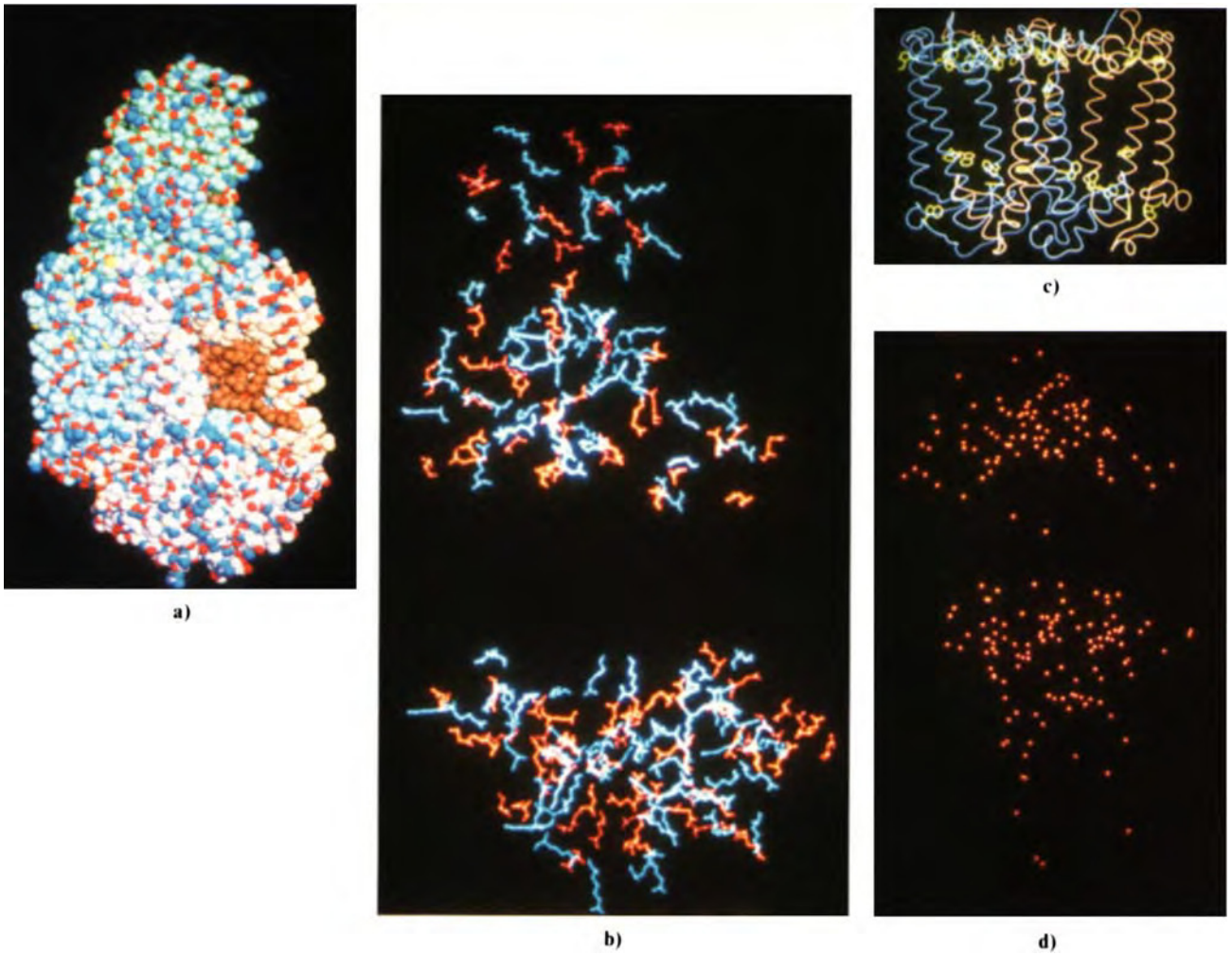


Fig. 20. a) Space-filling model of the photosynthetic reaction center of *Rps. viridis*. Carbon atoms are shown in white, nitrogen atoms in blue, oxygen atoms in red, and sulfur atoms in yellow. The atoms of a bacteriopheophytin molecule visible on the surface are represented in brown. b) Distribution of the "charged" amino acids in the photosynthetic reaction center of *Rps. viridis*. The negatively charged amino acids (aspartic, glutamic) are shown in red, the positively charged amino acids (arginine, lysine) in blue. c) Distribution of tryptophan residues (green) in the L- (brownish) and M-subunits (blue). d) Distribution of bound water molecules in the reaction center. The reaction centers and the L- and M-subunits are always viewed parallel to the membrane.

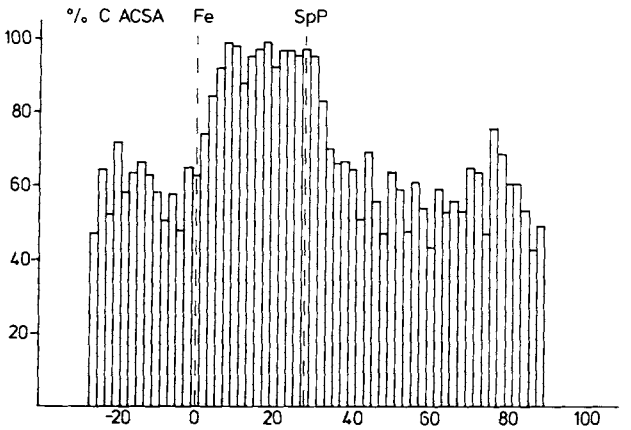


Fig. 21. Percentage of the accessible surface area (ACSA) occupied by carbon atoms; shown for 3 Å-thick layers perpendicular to the noncrystallographic twofold rotation axis, which runs through the ferrous non-heme iron atom (Fe) and the special pair (SpP).

peptide chains on the periplasmic side of the membrane and compares them with the net charges of the cytoplasmic side (assuming that all glutamic acid residues, aspartic acid residues and the carboxy-termini are negatively charged, whereas all the arginine and lysine residues and the amino-termini are positively charged) one finds that the cytoplasmic ends of the transmembrane helices and their respective connections are nearly always less negatively charged than their counterparts on the periplasmic side. This phenomenon is illustrated schematically in Figure 22: As a result the cytoplasmic part of the M-subunit carries four positive net charges and the periplasmic part four negative charges, the cytoplasmic part of the L-subunit two positive charges and the periplasmic part four negative charges. The charge asymmetry becomes even more pronounced if one considers the existence of the firmly bound non-heme iron atom on the cytoplasmic side and the presumed protonation of glutamic acid L104. Thus, these membrane proteins are strong electric dipoles. This result can be correlated with the fact that the interior of bacteria is negatively charged, due to the action of electrogenic ion pumps. This means that the L- and M-subunits are oriented in the membrane in the energetically more favorable manner. Conversely, the combination of the electric field across the membrane, established by the ion pumps, and the anisotropic distribution of negatively and positively charged amino acids in the protein may be one of the factors which determine the orientation of membrane proteins with respect to the inside and outside of the cell.

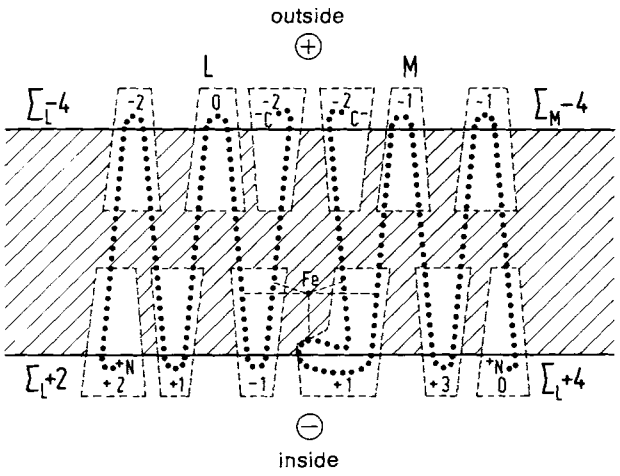


Fig. 22. Schematic drawing of the transmembrane helices and the helix connections of the L and M subunits of the *Rps. viridis* reaction center in the membrane to show the net charges at the ends of the helices and the helix connections. The negatively charged interior of the cell is indicated by the minus sign at the bottom, the positively charged extracellular medium by the plus sign at the top (after *Michel* and *Deisenhofer* [85]).

In the L- and M-subunits the remarkably uneven distribution of the amino acid tryptophan as shown in Figure 20c was quite unexpected. About two thirds of the tryptophans are found at the ends of transmembrane helices or in the helix connections on the periplasmic side. Only a few tryptophan residues are seen in the hydrophobic zone, where they interact with pigments. The residual tryptophans are located in the transition zone between hydrophobic and polar surface or in the polar part of the L- and M-subunits near the cytoplasmic surface. The indole rings of the tryptophans are oriented preferentially towards the hydrophobic zone of the membrane.

Figure 20d shows the distribution of the bound water molecules which have been tentatively identified by X-ray crystallographic analysis. Only five of them are found in the hydrophobic zone of the membrane. A closer inspection shows that they may perform an important structural role. Figure 23 shows one of these water molecules and its probable hydrogen-bonding pattern. It apparently cross-links two transmembrane helices, one from the L-subunit, the other from the M-subunit by donating hydrogen bonds to two peptide oxygen atoms. Another hydrogen bond with an asparagine side chain is possible. Just how much these water molecules contribute to the stability of the structure of the reaction center has still to be clarified.

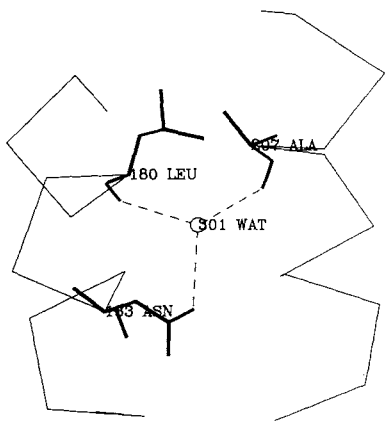


Fig. 23. A firmly bound water-molecule (301 WAT) in the hydrophobic part of the membrane cross-linking two transmembrane helices by forming hydrogen bonds with the peptide oxygen atoms of leucine L180 and alanine M207. Another hydrogen bond with the side chain of asparagine L183 is possible.

5.4. Crystal Packing and Detergent Binding

As outlined in Section 1, the most promising strategy was to crystallize the reaction center within a detergent micelle. According to this concept the crystal lattice should be formed by polar interactions between polar surface domains of the reaction center. This expectation was confirmed by the results of the structural analysis. Mainly the polar surfaces of the cytochrome subunit and the H-subunit are involved in the crystal packing, and only to a minor extent the polar surface part of the M-subunit.

As expected for detergents in a micelle most of the detergent is crystallographically not ordered and, with one exception, cannot be seen in the electron density map: The single transmembrane helix of the H-subunit, two transmembrane helices of the M-subunit, and part of the pigments seem to form a pocket in which one detergent molecule is bound. Its polar head-group apparently undergoes specific interactions with the protein near the cytoplasmic end of the hydrophobic surface zone. Specific binding of this particular detergent molecule might explain why crystals of the photosynthetic reaction center from *Rhodopseudomonas viridis* could be grown only with *N,N*-dimethyldodecylamine *N*-oxide as detergent, but not when octyl glucopyranoside or similar detergents were used.

In collaboration with *M. Roth* and *A. Bentley-Lewit* from the Institut Laue-Langevin in Grenoble the detergent micelle could be made visible by neutron crystallography and H_2O/D_2O contrast variation. A rather flat, monolayer-like ring of detergent molecules surrounding the hydrophobic surface zone of the reaction center became visible. Regions where the detergent micelles are in contact can also be seen. Therefore, attractive interactions between detergent micelles may also contribute to the stability of the protein's crystal lattice. In general, the strategy to crystallize membrane proteins within their detergent micelles[8, 86] now seems to be successful; however, the progress made in crystallizing other membrane proteins has been unexpectedly slow. Well diffracting crystals have only been obtained in the case of bacterial photosynthetic reaction centers and bacterial porins. The necessary fine tuning with respect to the size of the detergent micelle and the size of the polar head group of the detergent is still a formidable task which has to be solved empirically for each individual membrane protein.

We wish to express our sincere gratitude to persons and organizations who helped to make our work possible and successful: Our colleagues Otto Epp, Heidi Grünberg, Friedrich Lottspeich, Kunio Miki, Wolfram Schäfer, Irmgard Sinning, Karl-Alois Weyer and Wolfgang Zinth made important direct contributions as mentioned in the text. Dieter Oesterhelt and Robert Huber, their departments and the whole Max-Planck-Institut für Biochemie provided facilities and a stimulating and supportive atmosphere. Dieter Oesterhelt's backing especially during the intitial, frustrating phases, and the stable environment in the Max-Planck-Gesellschaft allowed us to start a project of unknown duration and outcome. Financially

the project was supported by the Deutsche Forschungsgemeinschaft through Sonderforschungsbereich 143 (Teilprojekt A3 to H.M., Teilprojekt A6 to J.D. and H.M.) and the Max-Planck-Gesellschaft.

Received: February 27, 1989 [A 726 IE]
German version: *Angew. Chem. 101* (1989) 872

[1] M. Happe, P. Overath, *Biochem. Biophys. Res. Commun. 72* (1976) 1504–1511.
[2] R. Henderson, P. N. T. Unwin, *Nature (London) 257* (1975) 28–32.
[3] H. Michel, D. Oesterhelt, *Proc. Natl. Acad. Sci. USA 77* (1980) 1283–1285.
[4] a) H. Michel, *EMBO J. 1* (1982) 1267–1271; b) *J. Mol. Biol. 158* (1982) 567–572.
[5] D. Oesterhelt, W. Stoeckenius, *Nature New Biol. 233* (1971) 149–152.
[6] D. Oesterhelt, *Hoppe-Seyler's Z. Physiol. Chem. 353* (1972) 1554–1555.
[7] H. Michel, D. Oesterhelt, R. Henderson, *Proc. Natl. Acad. Sci. USA 77* (1980) 338–342.
[8] H. Michel, *Trends Biochem. Sci. 8* (1983) 56–59.
[9] F. S. Mathews, P. Argos, M. Levine, *Cold Spring Harbor Symp. Quant. Biol. 36* (1972) 387–397.
[10] I. A. Wilson, J. J. Skehel, D. C. Wiley, *Nature (London) 289* (1981) 366–373.
[11] J. N. Varghese, W. G. Laver, P. M. Colman, *Nature (London) 303* (1983) 35–40.
[12] P. J. Björkman, M. A. Saper, B. Samraoui, W. S. Bennett, J. L. Strominger, D. C. Wiley, *Nature (London) 329* (1987) 506–512.
[13] M. Zulauf, K. Weckstrom, J. B. Hayter, V. Degeorgio, M. Corti, *J. Phys. Chem. 89* (1985) 3411–3417.
[14] R. M. Garavito, J. P. Rosenbusch, *J. Cell Biol. 86* (1980) 327–329.
[15] W. Baumeister, W. Vogell (Eds.): *Electron Microscopy at Molecular Dimensions*, Springer, Berlin 1980.
[16] R. K. Clayton, B. J. Clayton, *Biochim. Biophys. Acta 501* (1978) 478–487.
[17] J. Deisenhofer, O. Epp, K. Miki, R. Huber, H. Michel, *J. Mol. Biol. 180* (1984) 385–398.
[18] P. Schwager, K. Bartels, A. Jones, *J. Appl. Crystallogr. 8* (1975) 275–280.
[19] T. A. Jones, K. Bartels, P. Schwager in U. W. Arndt, A. J. Wonacott (Eds.): *The Rotation Method in Crystallography*, North Holland, Amsterdam 1977, pp. 105–117.
[20] M. G. Rossmann, *J. Appl. Crystallogr. 12* (1979) 225–238.
[21] M. F. Schmid, L. H. Weaver, M. A. Holmes, M. G. Gruetter, D. H. Ohlendorf, R. A. Reynolds, S. J. Remington, B. W. Matthews, *Acta Crystallogr. Sect. A 37* (1981) 701–710.
[22] B. C. Wang, *Meth. Enzymol. 115* (1985) 90–112.
[23] H. Michel, J. Deisenhofer, K. Miki, K. A. Weyer, F. Lottspeich in E. Quagliariello, F. Palmieri (Eds.): *Structure and Function of Membrane Proteins*, Elsevier, Amsterdam 1983, pp. 191–197.
[24] H. Michel, K. A. Weyer, H. Gruenberg, F. Lottspeich, *EMBO J. 4* (1985) 1667–1672.
[25] H. Michel, K. A. Weyer, H. Gruenberg, I. Dunger, D. Oesterhelt, F. Lottspeich, *EMBO J. 5* (1986) 1144–1158.
[26] K. A. Weyer, F. Lottspeich, H. Gruenberg, F. Lang, D. Oesterhelt, H. Michel, *EMBO J. 6* (1987) 2197–2202.
[27] T. A. Jones, *J. Appl. Crystallogr. 11* (1978) 268–272.
[28] A. Jack, M. Levitt, *Acta Crystallogr. Sect. A 34* (1978) 931–935.
[29] J. Deisenhofer, O. Epp, K. Miki, R. Huber, H. Michel, *Nature (London) 318* (1985) 618–624.
[30] D. E. Tronrud, L. F. Ten Eyck, B. W. Matthews, *Acta Crystallogr. Sect. A 43* (1987) 489–501.
[31] P. V. Luzzati, *Acta Crystallogr. 5* (1952) 802–810.
[32] G. Feher, M. Y. Okamura, in R. K. Clayton, W. R. Sistrom (Eds.): *The Photosynthetic Bacteria*, Plenum Press, New York 1978, pp. 349–386.
[33] M. Y. Okamura, G. Feher, W. Nelson in Govindjee (Ed.): *Photosynthesis: Energy Conversion by Plants and Bacteria, Vol. 1*, Academic Press, New York 1982, pp. 195–272.
[34] J. P. Allen, G. Feher, *Proc. Natl. Acad. Sci. USA 81* (1984) 4795–4799.
[35] C. H. Chang, M. Schiffer, D. Tiede, U. Smith, J. Norris, *J. Mol. Biol. 186* (1985) 201–203.
[36] J. P. Allen, G. Feher, T. O. Yeates, D. C. Rees, J. Deisenhofer, H. Michel, R. Huber, *Proc. Natl. Acad. Sci. USA 83* (1986) 8589–8593.
[37] C. H. Chang, D. Tiede, J. Tang, U. Smith, J. Norris, M. Schiffer, *FEBS Lett. 205* (1986) 82–86.
[38] M. E. Newcomer, T. A. Jones, J. Aqvist, J. Sundelin, U. Eriksson, I. Rask, P. A. Peterson, *EMBO J. 3* (1984) 1451–1454.
[39] R. Huber, M. Schneider, O. Epp, I. Mayr, A. Messerschmidt, J. Pflugrath, H. Kayser, *J. Mol. Biol. 195* (1987) 423–434.
[40] K. A. Weyer, W. Schäfer, F. Lottspeich, H. Michel in S. Papa, B. Chance, L. Ernster (Eds.): *Cytochrome Systems*, Plenum, New York 1987, pp. 325–331.
[41] P. Gast, T. J. Michalski, J. E. Hunt, J. R. Norris, *FEBS Lett. 179* (1985) 325–328.
[42] W. W. Parson, B. Ke in Govindjee (Ed.): *Photosynthesis: Energy Conversion by Plants and Bacteria, Vol. 1*, Academic Press, New York 1982, pp. 331–384.
[43] W. W. Parson, in J. Amesz (Ed.): *New Comprehensive Biochemistry: Photosynthesis*, Elsevier, Amsterdam 1987, pp. 43–61.
[44] C. Kirmaier, D. Holten, *Photosynth. Res. 13* (1987) 225–260.
[45] J. Breton, J. L. Martin, A. Migus, A. Antonetti, A. Orszag, *Proc. Natl. Acad. Sci. USA 83* (1986) 5121–5125.
[46] G. R. Fleming, J. L. Martin, J. Breton, *Nature (London) 333* (1988) 190–192.
[47] W. Zinth, W. Kaiser, H. Michel, *Biochim. Biophys. Acta 723* (1983) 128–131.
[48] W. Zinth, E. W. Knapp, S. F. Fischer, W. Kaiser, J. Deisenhofer, H. Michel, *Chem. Phys. Lett. 119* (1985) 1–4.
[49] E. W. Knapp, S. F. Fischer, W. Zinth, M. Sander, W. Kaiser, J. Deisenhofer, H. Michel, *Proc. Natl. Acad. Sci. USA 82* (1985) 8463–8467.
[50] C. Kirmaier, D. Holten, W. W. Parson, *Biochim. Biophys. Acta 810* (1985) 49–61.
[51] C. Kirmaier, D. Holten, W. W. Parson, *Biochim. Biophys. Acta 810* (1985) 33–48.
[52] R. J. Debus, G. Feher, M. Y. Okamura, *Biochemistry 25* (1986) 2276–2287.
[53] S. M. Dracheva, L. A. Drachev, A. A. Konstantinov, A. Y. Semenov, V. P. Skulachev, A. M. Arutjunjan, V. A. Shuvalov, S. M. Zaberezhnaya, *Eur. J. Biochem. 171* (1988) 253–264.
[54] J. R. Norris, R. A. Uphaus, H. L. Crespi, J. J. Katz, *Proc. Natl. Acad. Sci. USA 68* (1971) 625–628.
[55] J. Deisenhofer, H. Michel in J. Breton, A. Vermeglio (Eds.): *The Photosynthetic Bacterial Reaction Center Structure and Dynamics*, Plenum Press, New York 1988, pp. 1–3.
[56] M. E. Michel-Beyerle, M. Plato, J. Deisenhofer, H. Michel, M. Bixon, J. Jortner, *Biochim. Biophys. Acta 932* (1988) 52–70.
[57] H. Michel, O. Epp, J. Deisenhofer, *EMBO J. 5* (1986) 2445–2451.
[58] C. Kirmaier, D. Holten, R. J. Debus, G. Feher, M. Y. Okamura, *Proc. Natl. Acad. Sci. USA 83* (1986) 6407–6411.
[59] J. Deisenhofer, S. J. Remington, W. Steigemann, *Meth. Enzymol. 115* (1985) 303–323.
[60] I. Sinning, H. Michel, *Z. Naturforsch. C 42* (1987) 751–754.
[61] I. Sinning, H. Michel in J. Biggins (Ed.): *Progress in Photosynthesis Research, Vol. 3*, Martinus Nijhoff, Dordrecht 1987, pp. III.11.771–III.11.773.
[62] H. Michel, J. Deisenhofer, *Biochemistry 27* (1988) 1–7.
[63] T. Ornata, M. Murata, K. Satoh, *Biochim. Biophys. Acta 765* (1984) 403–405.
[64] D. M. Tiede, R. C. Prince, G. H. Reed, P. L. Dutton, *FEBS Lett. 65* (1976) 301–304.
[65] V. H. Shuvalov, U. V. Klimov, *Biochim. Biophys. Acta 440* (1976) 587–599.
[66] C. de Vitry, B. Diner, *FEBS Lett. 167* (1984) 327–331.
[67] K. Pfister, K. E. Steinback, G. Gardner, C. J. Arntzen, *Proc. Natl. Acad. Sci. USA 78* (1981) 981–985.
[68] J. C. Williams, L. A. Steiner, R. C. Ogden, M. I. Simon, G. Feher, *Proc. Natl. Acad. Sci. USA 80* (1983) 6505–6509.
[69] J. C. Williams, L. A. Steiner, G. Feher, M. I. Simon, *Proc. Natl. Acad. Sci. USA 81* (1984) 7303–7307.
[70] D. C. Youvan, E. J. Bylina, M. Alberti, H. Requsch, J. E. Hearst, *Cell (Cambridge, Mass.) 37* (1984) 949–957.
[71] G. Zurawski, H. J. Bohnert, P. R. Whitfeld, W. Bottomley, *Proc. Natl. Acad. Sci. USA 79* (1982) 7699–7703.
[72] J. Alt, J. Morris, I. Westhoff, R. G. Hermann, *Curr. Genet. 8* (1984) 597–606.
[73] K. Holschuh, W. Bottomley, P. R. Whitfield, *Nucleic Acids Res. 12* (1984) 8819–8834.
[74] O. F. Rasmussen, G. Bookjans, B. M. Stummann, K. W. Henningen, *Plant Mol. Biol. 3* (1984) 191–199.
[75] J. D. Rochaix, M. Dron, M. Rahire, P. Maloe, *Plant Mol. Biol. 3* (1984) 363–370.
[76] H. Y. Nakatani, B. Ke, E. Dolan, C. J. Arntzen, *Biochim. Biophys. Acta 765* (1984) 347–352.
[77] O. Nanba, K. Satoh, *Proc. Natl. Acad. Sci. USA 84* (1987) 109–112.
[78] R. J. Debus, B. A. Barry, G. T. Babcock, L. McIntosh, *Proc. Natl. Acad. Sci. USA 85* (1988) 427–430.
[79] W. F. Vermaas, A. W. Rutherford, Ö. Hansson, *Proc. Natl. Acad. Sci. USA 85* (1988) 8477–8481.
[80] C. W. Hoganson, G. T. Babcock, *Biochemistry 27* (1988) 5848–5855.
[81] J. C. Williams, L. A. Steiner, G. Feher, *Proteins: Struct. Funct. Genet. 1* (1986) 312–325.
[82] K. A. Weyer, W. Schäfer, F. Lottspeich, H. Michel, *Biochemistry 26* (1987) 2909–2914.
[83] A. P. Pugsley, C. Chapon, M. Schwartz, *J. Biol. Chem. 256* (1986) 2194–2198.
[84] F. Yu, S. Inouye, M. Inouye, *J. Biol. Chem. 261* (1986) 2284–2288.
[85] H. Michel, J. Deisenhofer, *Chem. Scr. 27B* (1987) 173–180.
[86] R. M. Garavito, Z. Markovic-Housley, J. A. Jenkins, *J. Crystal. Growth 76* (1986) 701–709.
[87] B. Lee, F. M. Richards, *J. Mol. Biol. 55* (1971) 379–400.

A Structural Basis of Light Energy and Electron Transfer in Biology (Nobel Lecture)**

By Robert Huber*

Dedicated to Christa

Aspects of intramolecular light energy and electron transfer are discussed for three protein cofactor complexes whose three-dimensional structures have been elucidated by X-ray crystallography: the light harvesting phycobilisomes of cyanobacteria, the reaction center of purple bacteria, and the blue multi-copper oxidases. A wealth of functional data is available for these systems which allows specific correlations to be made between structure and function and general conclusions to be drawn about light energy and electron transfer in biological materials.

Introduction***

All life on earth depends ultimately on the sun, whose radiant energy is captured by plants and other organisms capable of growing by photosynthesis. They use sunlight to synthesize organic substances which serve as building materials or stores of energy. This was clearly formulated by *L. Boltzmann*, who stated that "there exists between the sun and the earth a colossal difference in temperature ... The equalization of temperature between these two bodies, a process which must occur because it is based on the law of probability will, because of the enormous distance and magnitude involved, last millions of years. The energy of the sun may, before reaching the temperature of the earth, assume improbable transition forms. It thus becomes possible to utilize the temperature drop between the sun and the earth to perform work as is the case with the temperature drop between steam and water ... To make the most use of this transition, green plants spread the enormous surface of their leaves, and, in a still unknown way, force the energy of the sun to carry out chemical syntheses before it cools down to the temperature level of the earth's surface. These chemical syntheses are to us in our laboratories complete mysteries..."[1]

Today many of these 'mysteries' have been resolved by biochemical research and the protein components and their basic catalytic functions have been defined.[2]

I will focus in my lecture on *Boltzmann*'s 'improbable transition forms', namely excited electronic states and charge transfer states in modern terminology, the structures of biological materials involved and the interplay of cofactors (pigments and metals) and proteins. I will discuss some aspects of the photosynthetic reaction center of *Rhodopseudomonas viridis* (see the original publications cited later and short reviews[3-5]) and of functionally related systems, whose structures have been studied in my laboratory: light harvesting phycobilisomes of cyanobacteria and blue oxidases. A wealth of structural and functional data is available for these three systems, which makes them uniquely appropriate examples to derive general principles of light energy and electron transfer in biological materials. Indeed, there are very few systems known in sufficient detail for such purposes.*

We strive to understand the underlying physical principles of light and electron conduction in biological materials with considerable hope for success as these processes appear to be more tractable than other biological reactions, which involve diffusive motions of substrates and products and intramolecular motions. Large-scale motions have been identified in many proteins and shown to be essential for many functions.[12,13] Theoretical treatments of these reactions have to

[*] Prof. Dr. Robert Huber
Max-Planck-Institut für Biochemie
Am Klopferspitz, D-8033 Martinsried (FRG)

[**] Copyright © The Nobel Foundation 1989. – We thank the Nobel Foundation, Stockholm for permission to print this lecture.

[***] Abbreviations:
PBS phycobilisomes, light harvesting organelles peripheral to the thylakoid membrane in cyanobacteria, which carry out oxygenic photosynthesis and have photosystems I and II.
PE, PEC, PC, APC phycoerythrin, phycoerythrocyanin, phycocyanin, allophycocyanin, biliprotein components in PBS with covalently attached tetrapyrrole (bilin) pigments.
PS I, II photosynthetic reaction centers in chloroplasts and cyanobacteria.
RBP retinol binding protein.
BBP bilin (biliverdin IXγ) binding protein in *Pieris brassicae*.
Rps. viridis Rhodopseudomonas viridis, bacteriochlorophyll-b containing purple bacterium carrying out anoxygenic photosynthesis.
RC reaction center.
C, H, L, M the four subunits of the reaction center from *Rps. viridis*: the cytochrome c subunit (C), with four hemes displaying two redox potentials (c_{553}, c_{558}) is located on the periplasmic side of the membrane; the L- and M-subunits are integrated in the membrane and their polypeptide chains span the membrane with 5 α-helices each, labeled A, B, C, D, E; they bind the bacteriochlorophyll-b (BChl-b or BC), bacteriopheophytin-b (BPh-b or BP), menaquinone-9 (Q_A), ubiquinone-9 (UQ, Q_B) and Fe^{2+} cofactors; the subscripts P, A, M, L indicate pair, accessory, M-, L-subunit association, respectively; the H-subunit is located on the cytoplasmic side and its *N*-terminal α-helical segment (H) spans the membrane.
P_{680}, P_{960} primary electron donors in PS II and the RC of *Rps. viridis*, respectively, indicating the long wavelength absorption maxima.
P*, D* electronically excited states of P, D (donor), A (acceptor)
LHC light harvesting complexes.
$LH_{a,b}$ light harvesting protein pigment complexes in BChl-a, b containing bacteria.
Car carotenoids.
Sor Soret bands of chlorophyll and bacteriochlorophyll.
PCY plastocyanin, electron carrier in the photosynthetic apparatus of plants.
LAC laccase, oxidase in plants and fungi.
AO ascorbate oxidase, oxidase in plants.
CP ceruloplasmin, oxidase in mammalian plasma.

[*] The structure of the *Rb. sphaeroides* RC is closely related to the *Rps. viridis* RC [6, 7, 151]. A green bacterial bacteriochlorophyll-a containing light harvesting protein is well defined in structure [9] but not in function. In the multiheme cytochromes [10, 11] the existence/or significance of intramolecular electron transfer is unclear.

take flexibility and solvent into account and become theoretically tractable only by applying the rather severe approximations of molecular dynamics[14, 15] or by limiting the system to a few active site residues, which can then be treated by quantum mechanical methods.

Light and electron transfer processes seem to be amenable to a more quantitative theoretical treatment. The substrates are immaterial or very small and the transfer processes on which I focus are intramolecular and far removed from solvent. Molecular motions seem to be unimportant, as shown by generally small temperature dependences. The components active in energy and electron transport are cofactors, which, in a first approximation, suffice for a theoretical analysis, simplifying calculations considerably.

1. Models for Energy and Electron Transfer

To test theories developed for energy and electron transfer appropriate model compounds are essential. Although it would be desirable, these models need not be mimics of the biological structures.

Förster's theory of inductive resonance[16] treats the cases of strong and very weak coupling in energy transfer. Strong interactions lead to optical spectra which are very different from the component spectra. Examples include concentrated solutions of some dyes, crystalline arrays, and the bacteriochlorophyll pair (BC_P) discussed in Section 3.1. The electronic excitation is in this case delocalized over a molecular assembly. A very weak coupling produces little or no alteration of the absorption spectra, but the luminescence properties may be quite different. Structurally defined models for this case are scarce. The controlled deposited dye layers of *Kuhn* and *Frommherz* et al.[17, 18] may serve this purpose and have demonstrated the general validity of *Förster*'s theory, but with deviations.

Synthetic models with electron transfer are abundant and have recently been supplemented by appropriately chemically modified proteins.[19–21] They are well covered in reviews (see, e.g., Refs. [22–29]). Figure 1 shows the essential elements of such models: Donor D (of electrons) and acceptor A may be connected by a bridging ligand (B) with a pendant group (P) embedded in a matrix M.

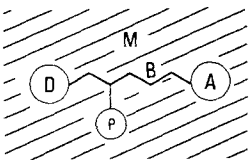


Fig. 1. Determinants of electron transfer models. D: Donor, A: Acceptor, B: Bridge, P: Pendant group, M: Matrix

Models with porphyrins as donors and quinones as acceptors are mimics of the reaction center (RC).[30, 31] Models with peptide bridging ligands[32] merit interest especially in relation to the blue oxidases. The effect of pendant groups (P), which are not in the direct line of electron transfer[22] is noteworthy in relation to the unused electron transfer branches in the RC and the blue oxidases. It is clear, however, that the biological systems are substantially more complex than synthetic models. The protein matrix is inhomogeneous and unique in each case. Despite these shortcomings, theory and models provide the framework within which the factors controlling the transfer of excitation energy and electrons and competing processes are to be evaluated.

1.1. Determinants of Energy and Electron Transfer

The important factors are summarized in Table 1. They may be derived from *Förster*'s theory and variants of *Marcus*' theory[26] for excitation and electron transfer, respectively. These theoretical treatments may in turn be derived from classical considerations or from *Fermi*'s Golden Rule with suitable approximations (see, e.g., Ref. [33]). Excitation and electron transfer depend on the geometric relation between donors and acceptors. Excitation energy transfer may occur over wide distances when the transition dipole moments are favorably aligned. Fast electron transfer requires sufficient electronic orbital overlap. Fast electron transfer over wide distances must therefore involve a series of closely spaced intermediate carriers with low lying unoccupied molecular orbitals or suitable ligands bridging donor and acceptor. Bridging ligands may actively participate in the transfer process and form ligand radical intermediates (chemical mechanism) or the electron may at no time be in a bound state of the ligands (resonance mechanism).[34] The spectral overlap and the 'driving force', for energy and electron transfer, respectively, have obvious effects on the transfer rates and are largely determined by the chemical nature and geometry of donors and acceptors. Nuclear reorganization of donor, acceptor, and the surrounding medium accompanying electron transfer is an important factor but difficult to evaluate, even qualitatively, in a complex protein system; we observe that the protein typically binds donors and acceptors firmly and rigidly, keeping reactant reorganization effects small. Surrounding polar groups may, as a result of their reorientation, slow down rapid electron transfer. However, a polar environment also contributes to the energetics by stabilizing ion pairs ($D^+ A^-$) or lowering activation and tunneling barriers and may thus increase 'driving force' and rate. The energy transfer also depends on the medium and is disfavored in media with high refractive index.

Table 1. Factors controlling the rate of transfer of excitation energy and electrons.

Excitation energy transfer $D^* + A \rightarrow D + A^*$ (very weak coupling)	Distance and orientation (coupling of excited states); Spectral overlap of emission and absorption of D and A; Refractive index of medium
Electron transfer from excited state $D^* + A \rightarrow D^+ + A^-$	Distance and orientation (electronic coupling, orbital overlap);
and from ground state $D^- + A \rightarrow D + A^-$	Free energy change ('driving force'); Reorganization in D and A; Orientation polarization of medium

Processes competing with productive energy and electron transfer from excited states 'lurk' everywhere (Table 2). Quite generally they are minimized by high transfer rates and a conformational rigidity of the cofactors in the protein ensemble.

I will discuss these factors in relation to the biological structures later on.

Table 2. Processes competing with the transfer of excitation energy and electrons.

Excitation energy transfer $D^* + A \rightarrow D + A^*$ (very weak coupling)	Non-radiative relaxation of D^* by photoisomerization and other conformational changes; Excited state proton transfer; Intersystem crossing; Chemical reactions of D^*, A^*, D^+, A^- with the matrix; Fluorescence radiation of D^*
Electron transfer from excited state $D^* + A \rightarrow D^+ + A^-$	Energy transfer; as above; Back reaction to ground state D,A
from ground state $D^- + A \rightarrow D + A^-$	–

2. The Role of Cofactors

The naturally occurring amino acids are transparent to visible light and seem also, with the exception of tyrosine, to be unsuitable as single electron carriers. Tyrosyl radicals have been identified in PS II as excited intermediates Z* and donors D*, which are involved in electron transfer from the water-splitting manganese protein complex to the photooxidized P^+_{680} (for reviews, see Refs. [35, 36]). Their identification has been assisted by the observation that Tyr L162 lies in the electron transfer path from the cytochrome to the bacteriochlorophyll pair (BC_{LP}) in the bacterial RC[37] (see Section 3.2.2.2 and Fig. 10c). A tyrosyl radical is not generated in the bacterial system, because the redox potential of P^+_{960} does not suffice.

Therefore cofactors, i.e. pigments and metal ions, generally serve as light energy acceptors and redox active elements in biological materials.

Figure 2 is a gallery of the pigments and metal clusters which will be discussed further on, namely the bile pigments phycocyanobilin and biliverdin IXγ in the light harvesting

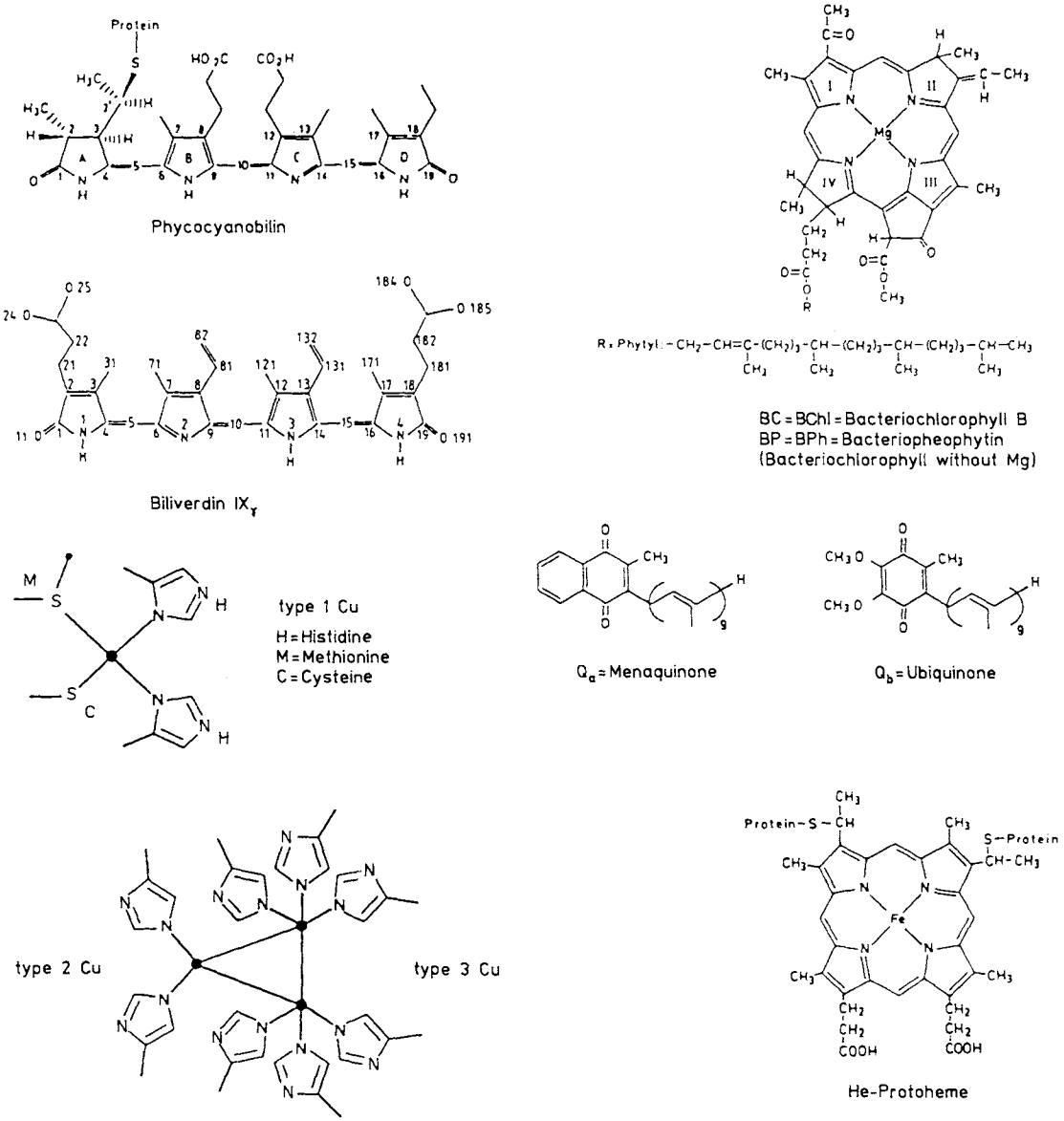


Fig. 2. Cofactors in phycocyanin (PC), bilin binding protein (BBP), ascorbate oxidase (AO) and the reaction center (RC) of the purple bacteria. Phycocyanobilins are covalently bound by thioether linkages to the protein. Biliverdin IXγ is non-covalently bound to the protein BBP. Type-1, type-2, type-3 copper ions are linked to the enzyme AO by coordination to the amino acid residues indicated. Four BChl-b molecules and two 2 BPh-b molecules are bound to the reaction center (RC) of the purple bacteria. A pair of BChl-b serves as the primary electron donor, a menaquinone-9 (Q_A) is the primary electron acceptor and an ubiquinone-9 (Q_B) the secondary acceptor. The four heme groups are bound by thioether linkages to the cytochrome c.

complexes, the BChl-b, BPh-b and quinones in the purple bacterial RC, and the copper centers in the blue oxidases.

The physicochemical properties of these cofactors determine the general features of the protein pigment complexes, whereas the protein part has a decisive influence on the spectral and redox properties.

3. The Role of the Protein

The role of the protein follows a hierarchy in determining the properties of the functional protein cofactor complexes shown in Table 3. The interactions listed in the table are different for the various systems and shall be described separately, except point 1, as there are common features in the action of proteins as polydentate ligands which can be ascribed to a 'rack mechanism'.

Table 3. Hierarchy of protein cofactor interactions.

1. Influence on configuration and conformation of the cofactors by the nature and geometry of ligands (the protein as a *polydentate ligand*)
2. Determination of the spatial arrangements of arrays of cofactors (the protein as a *scaffold*)
3. The protein as the *medium*
4. Mediation of the interaction with other components in the supramolecular biological system

3.1. The Protein as Polydentate Ligand

The 'rack mechanism' was introduced by *Lumry* and *Eyring*[38] and *Gray* and *Malmström*[39] to explain unusual reactivities and spectral and redox properties of amino acids and cofactors by the distortion enforced by the protein.

A comparison of isolated and protein bound bile pigments clearly demonstrates this effect. Isolated bile pigments in solution and in the crystalline state prefer a macrocyclic helical geometry with configuration *ZZZ* and conformation *syn,syn,syn* and show a weak absorption in the visible range and a low fluorescence quantum yield.[40-42] When bound as cofactors to light harvesting phycocyanins, however, they absorb and fluoresce very strongly in the visible range (Fig. 3). The auxochromic shift, essential for the light harvesting functions, is due to a strained conformation of the chromophore, which has configuration *ZZZ* and conformation *anti,syn,anti* stabilized by tight polar interactions with the protein[44-46] (Fig. 4). Particularly noteworthy is an aspartate residue (A87 here) bound to the central pyrrole nitrogen atoms, and conserved in all pigment binding sites. It influences the protonation, charge, and spectral properties of the tetrapyrrole systems. Tight binding is also effective against deexcitation by conformational changes. The structure shown in Figure 3 as representative for the free pigment is in fact observed in a bilin binding protein from insects.[41,42] This protein serves a different function and prefers the low energy conformer. The open chain tetrapyrrole bilins are conformationally adaptable, a property which makes them appropriate cofactors for different purposes.

The cyclic bacteriochlorophyll in the reaction center of purple bacteria is conformationally restrained but responds

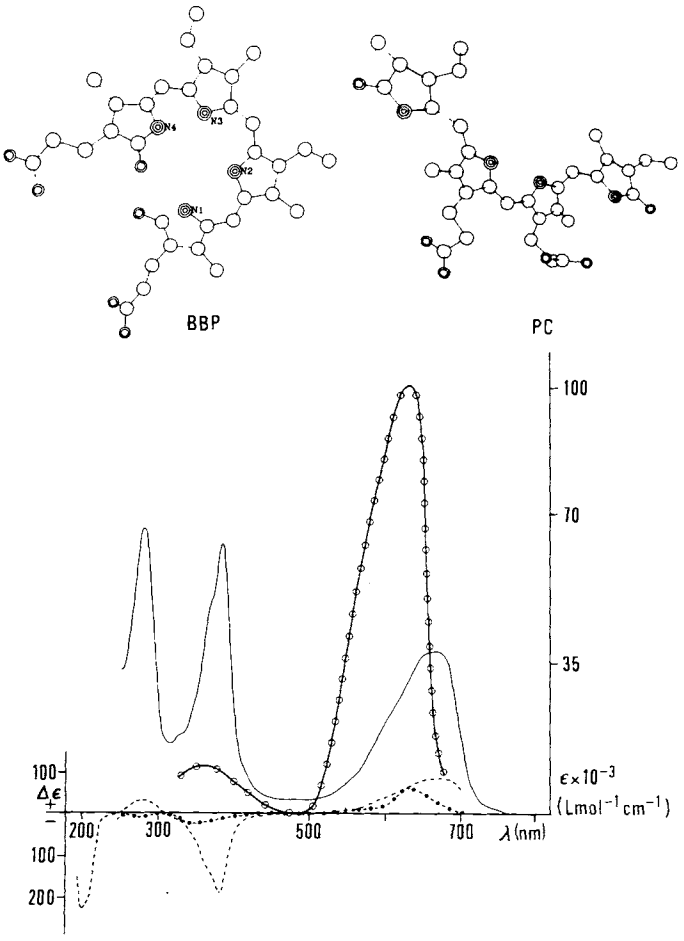


Fig. 3. Tetrapyrrole structures in PC and BBP and the associated optical and circular dichroism spectra [42, 44]. Absorption (———) and CD spectrum (– – –) of BBP; absorption (⊖) and CD spectrum (– · –) of PC.

to the environment by twisting and bending of the macrocycle. This may be one of the reasons for the different electron transfer properties of the two pigment branches in the RC (cf. Section 3.2.2.2). A more profound influence of the protein on the RC pigment system is seen in the absorption spectra, which differ from the composite spectra of the individual components (Fig. 5). The protein binds a pair of BChl-b (BC_P) in such a way that the two BChl-b molecules interact strongly via the pyrrole rings I, the acetyl substituents, and the central magnesium ions.[47] Alignment of the transition dipole moments and proximity of the BChl-b molecules lead to excitonic coupling, which partly explains the long wavelength absorption band P_{960}.[49]

The change in the optical spectra of blue copper proteins compared with those of cupric ions in normal tetragonal coordination is even greater (Fig. 6). The redox potential is also raised, to about 300–500 mV vs. 150 mV for Cu^{2+} (aq).[51] These effects are caused by the distorted tetrahedral coordination of the type-1 copper (a strained conformation stabilizing the cuprous state) and a charge transfer transition from a ligand cysteine $S^- \rightarrow Cu^{2+}$.[39,52]

The examples presented demonstrate the influence of the protein on the cofactors by various mechanisms: the stabilization of unstable conformers and strained ligand geometries and the generation of contacts between pigments leading to strong electronic interaction.

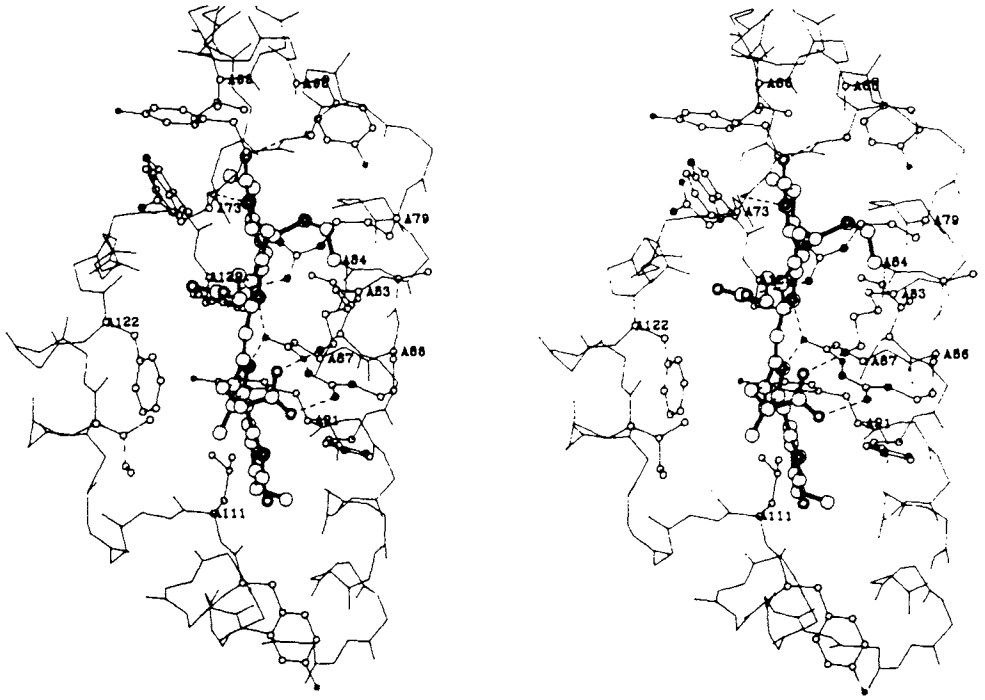


Fig. 4. Stereodrawing of phycocyanobilin A84 (thick bonds) and its protein environment (thin bonds). All polar groups of the bilin except those of the terminal D pyrrole ring are bound by hydrogen bonds and salt links to protein groups [44].

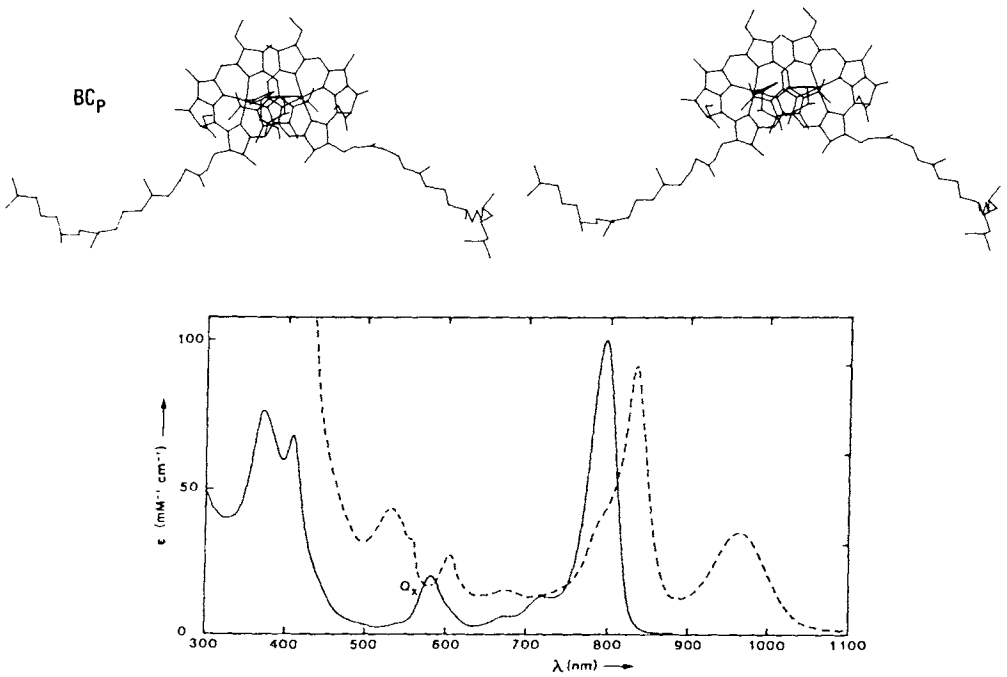


Fig. 5. Stereodrawing of the special pair BC_P in the reaction center (RC) [47] mainly responsible for the spectral alterations and the long wavelength absorption of the RC of *Rps. viridis* (– – –) compared with the spectra of BChl-*b* in ether solution (———) (spectra from Ref. [48]).

The fixation of the relative arrangements of systems of cofactors forms the basis of the energy and charge transfer properties in each system.

3.2. Protein as a Scaffold

3.2.1. Light Harvesting by Phycobilisomes

The limited number of pigment molecules associated with the RC would absorb only a small portion of incident sunlight. The RCs are therefore associated with LHC, which may be located within the photosynthetic membrane or form layers or antenna-like organelles in association with the photosynthetic membrane. Cyanobacteria contain particularly intricate light harvesting systems, the phycobilisomes (PBS), as organelles peripheral to the thylakoid membrane. Compared to PS I and PS II they absorb light of shorter wavelengths and thus use a wider spectral range of sunlight (Fig. 7). The PBS are assembled from components with fine-

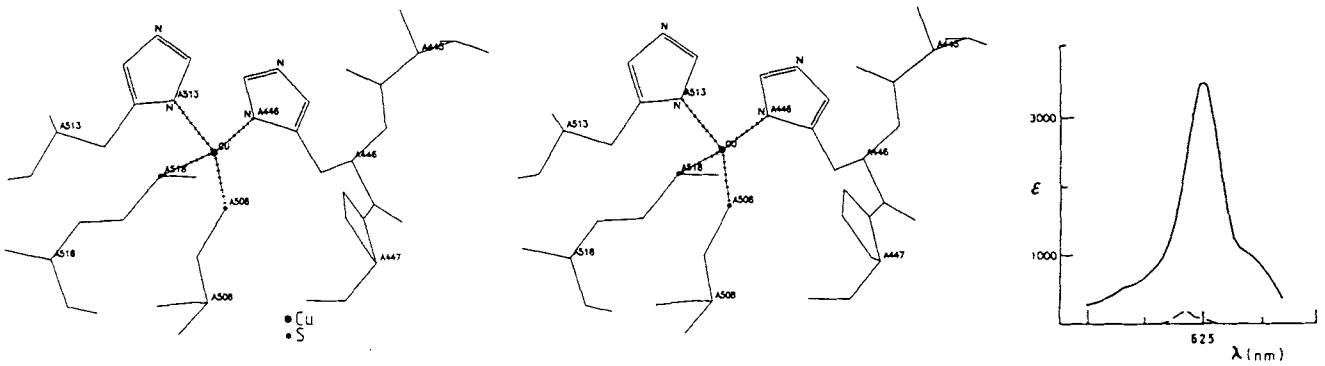


Fig. 6. Stereodiagram of the type-1 copper and its ligands in the ascorbate oxidase (AO). The coordination of the copper is to His A446, His A513, Met A518, Cys A508 [50]. The optical absorption spectra of 'blue' copper in copper proteins (———) are compared with the spectrum of normal tetragonal copper (– – –) (spectra from Ref. [51]).

ly tuned spectral properties such that the light energy is channeled along an energy gradient to PS II.

3.2.1.1. Morphology of the Phycobilisomes

The phycobilisomes consist of biliproteins and linker polypeptides. Biochemical and electron microscopy studies[54–57] led to the model representative of a hemidiscoidal phycobilisome (PBS) in Figure 7. Accordingly, PBS rods are assembled in a polar way from phycoerythrin (PE) or phycoerythrocyanin (PEC) and phycocyanin (PC), which is attached to a central core of allophycocyanine (APC). APC is next to the photosynthetic membrane and close to PS II (for a review, see Ref. [53]). The PC component consists of α- and β-protein subunits, which are arranged as $(\alpha\beta)_6$ disc-like aggregates with the dimensions 120 Å × 60 Å (for reviews, see Refs. 58–63]).

From crystallographic analyses, a detailed picture of the PC and PEC components has emerged.[44–46, 64, 65] The homology in the amino acid sequences suggests that all components have similar structures.

3.2.1.2. Structure of Phycocyanin

The α- and β-subunits of the phycocyanin (PC) (in *Mastigocladus laminosus*) have 162 and 172 amino acid residues, respectively. The phycocyanobilin chromophores (cf. Fig. 2) are linked via thioether bonds to cysteine residues at position 84 of both chains (A84, B84) and at position 155 of the β-subunit (B155).[66] Both subunits have similar structures and are folded into eight α-helices (X, Y, A, B, E, F, G, H: see Fig. 13). A84 and B84 are attached to helix E, B155 to the G-H loop. α-helices X and Y form a protruding antiparallel pair essential for formation of the (αβ) unit.

The isolated protein forms $(\alpha\beta)_3$-trimers with C_3 symmetry and hexamers $(\alpha\beta)_6$ as head-to-head associated trimers with D_3 symmetry (Fig. 8). The inter-trimer contact is exclusively mediated by the α-subunits, which are linked by an intricate network of polar bonds. The inter-hexamer contacts within the crystal (and in the native PBS rods) are made by the β-subunits.[44]

3.2.1.3. Oligomeric Aggregates: Spectral Properties and Energy Transfer

The spectral properties, absorption strength and fluorescence quantum yield of biliproteins depend on the state of aggregation. The absorption spectrum of the (αβ) unit resembles the sum of the spectra of the constituent subunits, but the fluorescence quantum yield is somewhat higher than

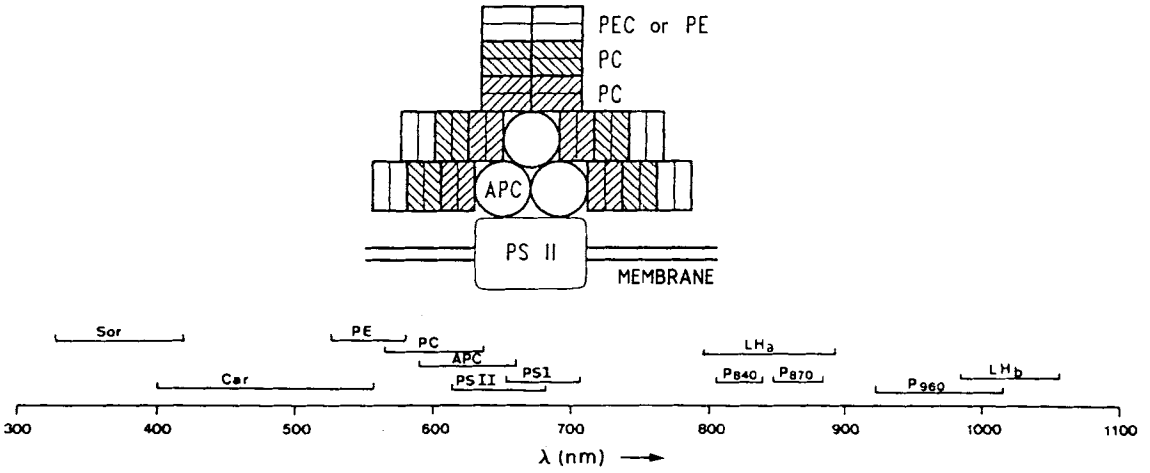


Fig. 7. Scheme of a typical phycobilisome (PBS) with the arrangements of the components and the putative spatial relationship to the thylakoid and photosystem II (PS II; for reviews see Refs. [53, 54]). The component labeled PS II is thought to represent PS II and the phycobilisome attachment sites. The main absorption bands of photosynthetic protein cofactor complexes in photosynthetic organisms are also shown. The PBS components absorb differently to cover a wide spectral range and permit energy flow from phycoerythrocyanin (PEC)/phycoerythrin (PE) via phycocyanin (PC) and allophycocyanin (APC) to PS II (for abbreviations see footnote [***] to the Introduction).

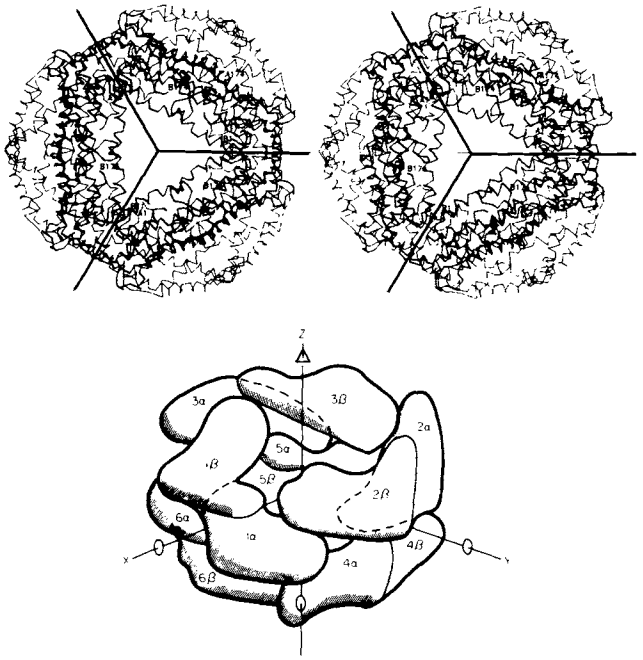


Fig. 8. Stereodrawing of the polypeptide chain fold of an $(\alpha\beta)_6$ hexamer of phycocyanin (PC) seen along the disk axis (top). The scheme (bottom) indicates the packing of subunits in the packing of subunits in the hexamer seen from the side.

the sum of the fluorescence yields of the constituent subunits. Upon trimer formation, the absorption is red-shifted and its strength and the quantum yield of fluorescence are increased[67, 68] (for a review, see Ref. [60]). In the $(\alpha\beta)_6$-linker complexes, the fluorescence is further increased and the absorption spectrum further altered.[69]

These observations can be rationalized by the structure of the aggregates. Formation of $(\alpha\beta)$ units causes little change in the environment of the chromophores. They remain quite widely separated at distances of > 36 Å (Fig. 9a). Upon trimer formation, the environment of chromophore A84 changes profoundly due to approach of chromophore B84 of the related symmetrically bound unit (Fig. 9a, top). In the hexamer (Fig. 9a, middle) the A84 and B155 chromophores strongly interact pairwise across the trimer interface. Furthermore, the molecular structures become more rigid with increasing size of the aggregates, as seen in the crystals of the trimeric and hexameric aggregates.[44, 46] Rigidity hinders excitation relaxation by isomerization and thus increases the fluorescence quantum yield.

The chromophores can be divided into subsets of s (sensitizing) and f (fluorescing) chromophores.[70, 71] The s-chromophores absorb at the blue edge of the absorption band and rapidly transfer excitation energy to the f-chromophores. This transfer is accompanied by depolarization.[72] Excitation at the red absorption edge (f-chromophores), however, results in little depolarization, suggesting that the energy is transferred along stacks of similarly oriented f-chromophores (Fig. 9a, bottom).[73] The assignment of the chromophores to s and f was accomplished by steady-state spectroscopy on various aggregates,[68] by chemical modification guided by the spatial structure,[74] and conclusively by measurement of the linear dichroism and polarized fluorescence on single crystals.[75] Accordingly, B155 is the s-, B84 the f-, and A84 the intermediate chromophore.

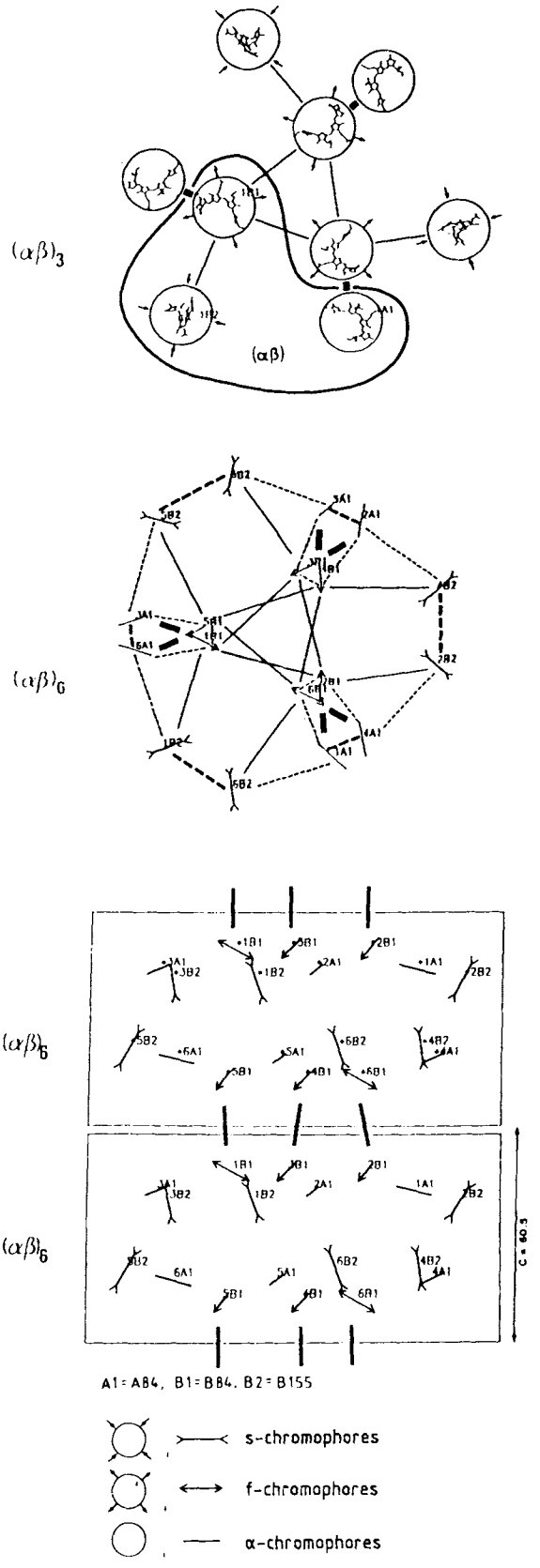


Fig. 9a. Arrangement of chromophores and preferred energy transfer pathways in $(\alpha\beta)_3$ trimers, $(\alpha\beta)_6$ hexamers and stacked hexamers (based on Table 10 from Ref. [44]). For the trimer the detailed structures of the chromophores are drawn, otherwise their approximate transition dipole directions are indicated. For the trimer and hexamer the view is along the disk axis; for the stacked hexamers it is perpendicular. In the stacked hexamers only the inter-hexamer transfers are indicated. The strength of coupling is indicated by the thickness of the connecting lines. Transfer paths within and between the trimers are represented by full and broken lines, respectively.

Light energy is transferred rapidly within 50 to 100 ps from the tips to the core of the PBS (for reviews, see Refs. [60, 73, 76–80]). The transfer times from the periphery to the base are several orders of magnitude faster than the intrinsic fluorescence life-times of the isolated components.[72, 76] The distances between the chromophores within and between the hexamers are too large for strong (excitonic) coupling, but efficient energy transfer by inductive resonance occurs. A Förster radius of about 50 Å has been suggested by *Grabowski* and *Gantt*.[81] The relative orientations and distances of the chromophores as obtained by *Schirmer* et al.[44] were used as basis for the calculation of the energy transfer rates in Figure 9a, which shows the preferred energy transfer pathways in $(\alpha\beta)$ units, $(\alpha\beta)_3$ trimers, $(\alpha\beta)_6$ hexamers and stacked disks as models for native antenna rods. There is very weak coupling of the chromophores in the $(\alpha\beta)$ units. However, some energy transfer takes place, probably between B155 and B84, as indicated by steady-state polarization measurements.[68, 82] Trimer formation leads to strong coupling between A84 and B84, but B155 is integrated only weakly. In the hexamer many additional transfer pathways are opened and B155 is efficiently coupled. Hexamers are obviously the functional units, as the energy can be distributed and concentrated on the central f-chromophores, which couple the stacks of hexamers. Kinetic studies[60, 68, 73, 83] have confirmed the picture of energy transfer along the rods as a random walk (trap or diffusion limited) along a one-dimensional array of f-chromophores. *Sauer* et al.[84] have successfully simulated the observed energy transfer kinetics in PC aggregates on the basis of the structures using *Förster*'s mechanism. The PEC component at the tips of PBS rods is extremely similar to PC.[64, 65] Its short wavelength absorbing chromophore A84 is located at the periphery (cf. Fig. 10a), as are the additional chromophores in PE, which is also a tip component (Fig. 9b).

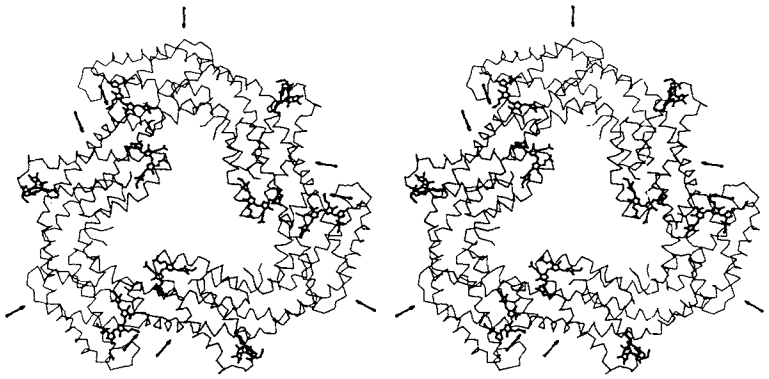


Fig. 9b. Model of the PE $(\alpha\beta)_3$ trimer of phycoerythrin (PE) on the basis of the structure of phycocyanin (PC). The locations of the additional phycoerythrobilins are indicated by arrows.

The phycobilisome rods act as light collectors and energy concentrators from the peripheral to the central chromophores, that is, as excitation energy funnels from the periphery to the center and from the tip to the bottom.

The linker polypeptides determine the functional properties of the aggregates. Some of them are believed to be located in the central channel of the hexamers, where they may interact with B84.

3.2.2. *Electron Transfer in the Reaction Center*[*]

3.2.2.1. *The Composition of the Reaction Center*[**]

The reaction center of *Rps. viridis* is a complex of the four protein subunits C, L, M, H and cofactors arranged as in Figure 10a. The proteins consist of 336, 273, 323, and 258 amino acid residues, respectively.[43, 87, 89] The c-type cytochrome contains four heme groups covalently bound via thioether linkages. The cofactors are four BChl-b (BC_{MP}, BC_{LP}, BC_{LA}, BC_{MA}), two BPh-b (BP_M, BP_L), one menaquinone-9 (Q_A), and a ferrous ion involved in electron transfer. A second quinone (ubiquinone-9 UQ, Q_B), which is a component of the functional complex, is partially lost during preparation and crystallization of the reaction center.

3.2.2.2. *Chromophore Arrangement and Electron Transfer*

The chromophores are arranged in L- and M-branches, which meet at BC_P and are related by an axis of approximate two-fold symmetry.[47] This axis is normal to the plane of the membrane.

While many of the optical properties of the pigment system are rather well understood on the basis of the spatial structure,[49] electron transfer is less well understood. The excited BC_P is quenched by electron transfer to BP_L in 3 ps and then further to the primary acceptor Q_A in about 200 ps, driven by the redox potential gradient between P^*/P^+ (about -760 mV) and Q_A/Q_A^- (about -110 mV). The redox potential of BP/BP^- is intermediate with a value of about -400 mV.[90–99] These functional data are summarized in Figure 10a. General factors controlling the transfer rates have been summarized in Table 1 and are detailed here specifically for the reaction center:

Fast electron transfer requires effective overlap of the molecular orbitals. The orbital interaction decreases exponentially with the edge-to-edge distance of donor and acceptor and is insignificant at distances larger than about 10 Å.[29, 100] In the reaction center the distance between BC_P

[*] A historical background of the development of concepts and key features of the purple bacterial reaction center is given by *Parson* [85].

[**] The arrangement of the reaction center in the thylakoid membranes of *Rps. viridis* as obtained by electron microscopy is described by *Stark* et al. [86].

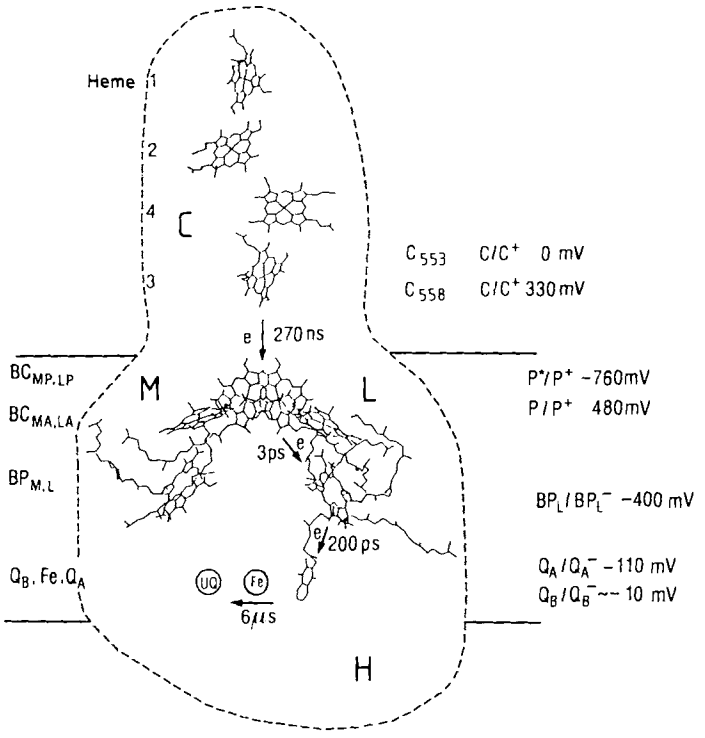


Fig. 10a. Scheme of the structure of the reaction center of *Rps. viridis* showing the cofactor system, the outline of the protein subunits (C, M, L, H), the electron transfer half-times, and the redox potentials of defined intermediates (for references see Section 3.2.2.2; for abbreviations see footnote [***] to the Introduction).

and Q_A is far too large to allow fast direct electron transfer; instead the electron migrates via BP_L. BP_L^- is a spectroscopically and kinetically well defined intermediate. Although located between BC_P and BP_L, BC_{LA}^- is not an intermediate but probably involved in electron transfer by a 'superexchange' mechanism mediating a strong quantum mechanical coupling[101] (for a review, see Ref. [102]). The distance between BP_L and Q_A seems large for a fast transfer. Indeed, in the L branch of the pigment system, this gap is bridged by the aromatic side chain of Trp M250 (Fig. 10b),[37, 88] which might mediate coupling via appropriate orbitals. In addition, the isoprenoid side chain of Q_A is close to BP_L. Electron transfer via long connecting chains by through-bond coupling of donor and acceptor orbitals has been observed[100, 103, 104] but, in the reaction center, there are only Van der Waals contacts.

A second important factor for electron transfer is the free energy change (ΔG), which is governed by the chemical nature of the components, by geometrical factors, and by the environment (solvent polarity). It depends on the ionization potential of the donor in its excited state, on the electron affinity of the acceptor, and on the coulombic interaction of the radical ion pair, which is probably small, as donor and acceptor (BC_P and Q_A in the RC) are far apart. The influence of the environment may be substantial in the stabilization of the radical ion pair by ionic interactions and hydrogen bonds. ΔG is *one* important factor of the activation energy of electron transfer. Also important is the nuclear rearrangement of the reactants and the environment. As the charge on donor and acceptor develops, the nuclear configurations change. These changes are likely to be small in the RC, as the BChl-b macrocycles are relatively rigid and are tightly packed in the protein, and the charge is distributed over the extended aromatic electron system. Reorientable dipolar groups (peptide groups and side chains) may contribute considerably to the energy barrier of the electron transfer. On the other hand, a matrix with high electronic polarizability stabilizes the developing charge in the transition state of the reaction and reduces the activation energy. An alternative picture is that the potential energy barrier to electron tunneling is decreased. Aromatic compounds which are concentrated in the vicinity of the electron carriers in the RC have these characteristics (see Trp M250).

The electron transfer from P* to Q_A occurs with very low activation energy[91, 94, 96, 105–108] and proceeds readily, even at 1 K. Thermally activated processes, nuclear motions, and collisions are therefore not important for the first very fast charge separation steps. There is even a slight increase in rate with decrease in temperature, due either to a closer approach of the pigments at low temperature or to changes of the vibrational levels, which may lead to a more favorable Franck-Condon factor.

The electron transfer between primary and secondary quinone acceptors, Q_A and Q_B, is rather different from the previous processes, because it is much slower (about 6 μs at pH 7 according to *Carithers* and *Parson*[91]) and has a sub-

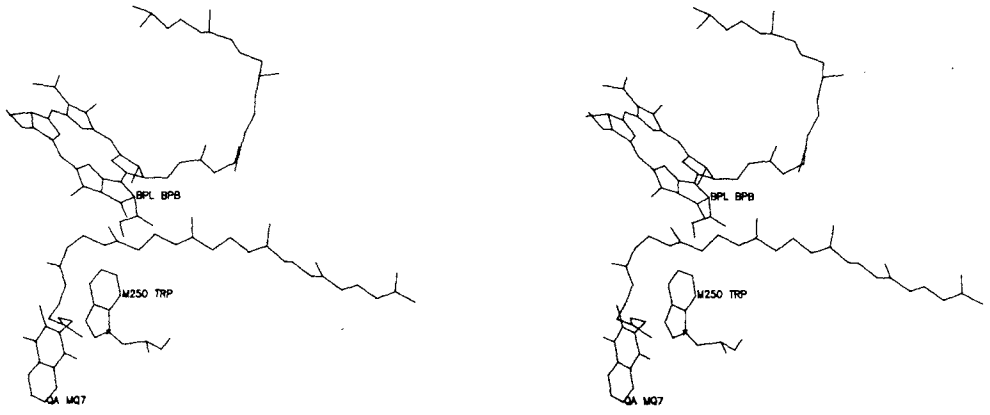


Fig. 10b. Stereodrawing of the arrangement of BP_L, Trp M250 and Q_A in the L-branch of the pigment system of the reaction center.

stantial activation energy of about 8 kcal mol^{-1}. In *Rps. viridis*, Q_A is a menaquinone-9 and Q_B a ubiquinone-9, which differ in their redox potentials in solution by about 100 mV. In other purple bacteria, both Q_A and Q_B are ubiquinones. The redox potential difference required for efficient electron transfer in these cases is generated by the asymmetric protein matrix. The protein matrix is also responsible for the quite different functional properties of Q_A and Q_B. Q_A accepts only one electron (leading to a semiquinone anion), which is transferred to Q_B before the next electron transfer can occur. Q_B, however, accepts two electrons and is protonated to form a hydroquinone, which diffuses from the reaction center (two-electron gate[109]). Q_B is close to Glu L212, which opens a path to the H-subunit and may protonate Q_B. The electron transfer between Q_A and Q_B takes place in an environment which differs considerably from the environment of the primary electron transfer components. The line connecting Q_A and Q_B (the Q_B binding site has been inferred from the binding mode of competitive inhibitors and ubiquinone-1 in *Rps. viridis* crystals[37]) is occupied by the iron and its five coordinating ligands—four histidine residues (M217, M264, L190, L230) and a glutamic acid (M232) residue. His M217 forms a hydrogen bond to Q_A. His L190 is close to Q_B. Q_A and Q_B are separated by an edge-to-edge distance of about 15 Å, which might explain the slow transfer. If electron transfer and protonation are coupled, the observed pH dependence of the electron transfer rate from Q_A to Q_B[110] could be explained, and conformational changes required for proton transfer may generate the observed activation energy barrier. The role of the charged Fe-His_4-Glu complex in the Q_A to Q_B electron transfer is poorly understood at present, as it occurs also in the absence of the iron;[111] its role seems to be predominantly structural.

The cycle of electron transfer is closed by the rereduction of BC_P^* by cytochrome c (subunit C of the reaction center), whereby a distance of about 11 Å between the pyrrole ring I of heme 3 and the pyrrole ring III of BC_{LP} has to be bridged. The transfer time is 270 ns[95] (cf. Ref. [147]); the transfer is considerably slower than the first electron transfer steps. Tyr L162, which is located midway (Fig. 10c), may facilitate electron transfer by mediating electronic coupling between the widely spaced donor and acceptor. The biphasic temperature dependence indicates a complex mechanism in which nuclear motions play a role at high temperatures (for reviews, see Refs. [112, 113]).

The favorable rate controlling factors that have been discussed are a necessary but not sufficient condition for the electron transfer, which competes with other quenching processes summarized in Table 2 and now described in detail for the reaction center:

The transfer of energy from P* back to the light harvesting complex or to other pigments may be favored by orientation and proximity but is disfavored energetically. The special pair BC_P usually absorbs (but not in *Rps. viridis* where the absorption maxima of the RC and the LHC are at 960 and 1020 nm respectively, see Fig. 7) at longer wavelengths than other pigments of the photosynthetic apparatus and thus represents the light energy sink. The natural radiative lifetime of the excited singlet state P* is around 20 ns[107, 114] and may serve as an estimate of the times involved in the other wasteful quenching processes. Clearly, electron transfer is much faster. Non-radiative relaxation of BC_P^* by isomerizations and conformational changes is unlikely, since the cyclic pigment systems are tightly packed in the protein matrix.

The back reaction $P^+Q_A^-$ to PQ_A has a favorable driving force (Fig. 10a) and is temperature independent, but is slow and insignificant under physiological conditions (for a review, see Ref. [94]). The physical basis for this has yet to be explained. It may be related to a gating function of BP_L by its negative redox potential compared to Q_A, to electronic properties of P^+ disfavoring charge transfer, and to conformational changes induced by electron transfer.

The profound influence of the protein matrix on electron transfer in the reaction center manifests itself in the observed asymmetry of electron transfer in the bacteriochlorophyll-b (BC) and bacteriopheophytin (BP) pigments, depending upon whether they belong to the L or the M branch. Only the

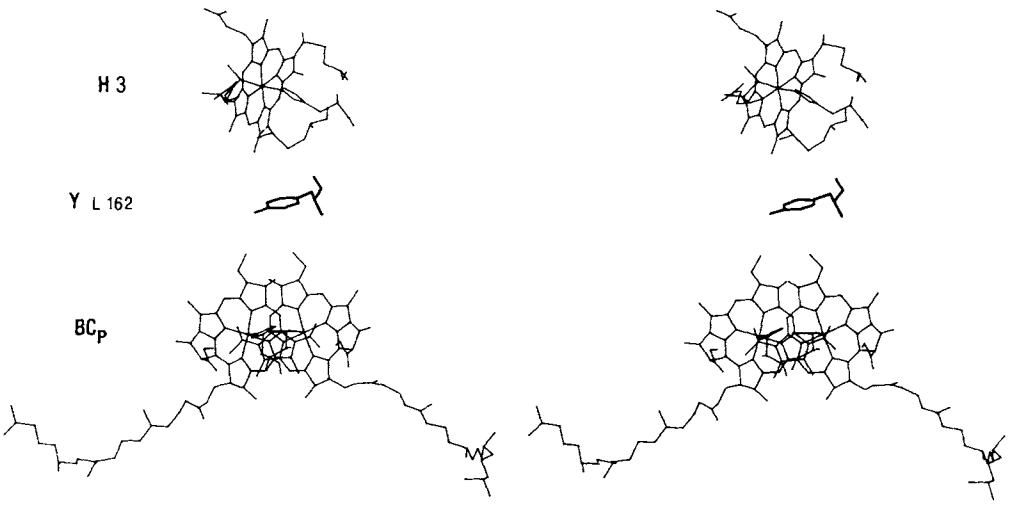


Fig. 10c. Stereodrawing of heme 3 (H3) of the cytochrome c, the special pair BC_P and the intercalating Tyr L162 (Y L162) of the L-subunit [37]. The His and Met ligands to the iron of H3 and the His ligands to the magnesium ions of the BC_P are also shown.

branch more closely associated with the L-subunit is active. An explanation is offered perhaps by the finding that the protein environment of the two branches, although formed by homologous proteins (L and M), is quite different, in particular by virtue of the Trp M250 located between BP_L and Q_A and the numerous differences in the Q_A and Q_B binding sites.[37, 88] Asymmetry is observed in the BC_P due to different distortions and hydrogen bonding of the macrocycles and in the slightly different spatial arrangements of the BC_A and BP. It has been suggested that electron release into the L-branch is thereby facilitated.[115] The M-branch may, however, have influence as a pendant group.

The protein matrix also serves to dissipate the excess energy of about 650 mV[92] of the excited special pair ($P^* Q_A$) compared to the radical ion pair $P^+ Q_A^-$. These processes are probably very fast.

In summary, the very fast electron transfer from BC_P^* to Q_A occurs between closely spaced aromatic macrocycles with matched redox potentials. The protein matrix in which the pigments are tightly held is lined predominantly with apolar amino acid side chains with a high proportion of aromatic residues. The path taken by the electrons is far removed from the water phase.

3.2.3. *The Blue Oxidases*

Oxidases catalyze the reduction of dioxygen by single electron transfers from substrates. Dioxygen requires four electrons and four protons to be reduced to two water molecules. Oxidases must provide recognition sites for the two substrates, a storage site for electrons and/or the means to stabilize reactive partially reduced oxygen intermediates.[116–118]

The 'blue' oxidases are classified according to the distinct spectroscopic properties of the three types of copper which they contain: Type-1 Cu^{2+} is responsible for the deep blue color of these proteins; type-2 or normal Cu^{2+} has no recognizable optical absorption; type-1 and type-2 cupric ions are paramagnetic; type-3 copper has a strong absorption around 330 nm and is antiferromagnetic, indicating coupling of the spin of a pair of cupric ions. The characteristic optical and electron paramagnetic resonance spectra disappear upon reduction.

Studies of the catalytic and redox properties of the 'blue' oxidases have been well documented in several recent reviews (e.g. for laccase,[119] for ascorbate oxidase,[120] for ceruloplasmin[121]). Basically, type-1 Cu^{2+} is reduced by electron transfer from the substrate. The electron is transferred further to the type-3 and type-2 copper ions. The second substrate, dioxygen, is associated with the type-3 and/or type-2 copper ions.

3.2.3.1. *Ascorbate Oxidase, Composition and Copper Arrangement*

Ascorbate oxidase is a polypeptide of 553 amino acid residues folded into three tightly associated domains.[50] It is a dimer in solution; the functional unit, however, is the monomer. Ascorbate oxidase belongs, together with laccase and ceruloplasmin, to the group of 'blue' oxidases.[122]

Structures of copper proteins containing only one of the different types of copper are known: Plastocyanin has a 'blue' type-1 copper, which is coordinated to two histidine residues and the sulfur atoms of cysteine and methionine in a distorted tetrahedral geometry.[123] Cu–Zn-superoxide dismutase contains a type-2 copper, which has four histidine ligands with slightly distorted square coordination.[124] Hemocyanin of *Panulirus interruptus* contains as type-3 copper, a pair of copper ions 3.4 Å apart with six histidine ligands.[125]

In domain 3 of ascorbate oxidase (see Section 4.4) a copper ion is found in a strongly distorted tetrahedral (approaching trigonal pyramidal geometry) coordination with the ligands His, Cys, His, Met as has already been shown in Figure 6. It resembles the blue type-1 copper in plastocyanin. A trinuclear copper site is enclosed between domains 1 and 3 of ascorbate oxidase (Fig. 11a). Four (–His–X–His–) amino acid sequences provide the eight histidine ligands. The trinuclear copper site contains a pair of coppers (Cu 31, Cu 32), each with three histidyl (A108, A451, A507; A64, A106, A509) ligands, forming a trigonal prism. It is the type-3 copper pair; a comparable arrangement is observed in

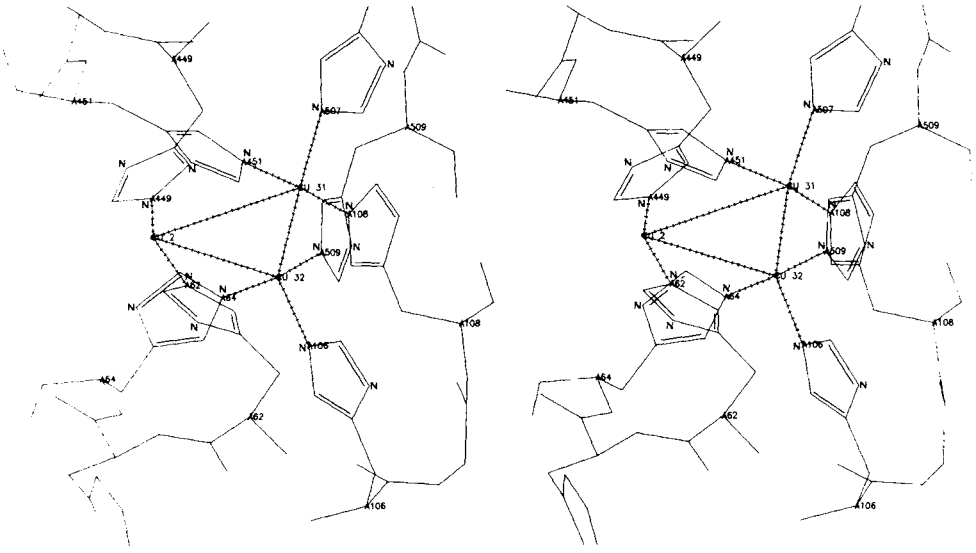


Fig. 11a. Stereodrawing of the trinuclear copper site in ascorbate oxidase. Coordination bonds between the copper ions and the protein residues are marked (dotted lines) [50].

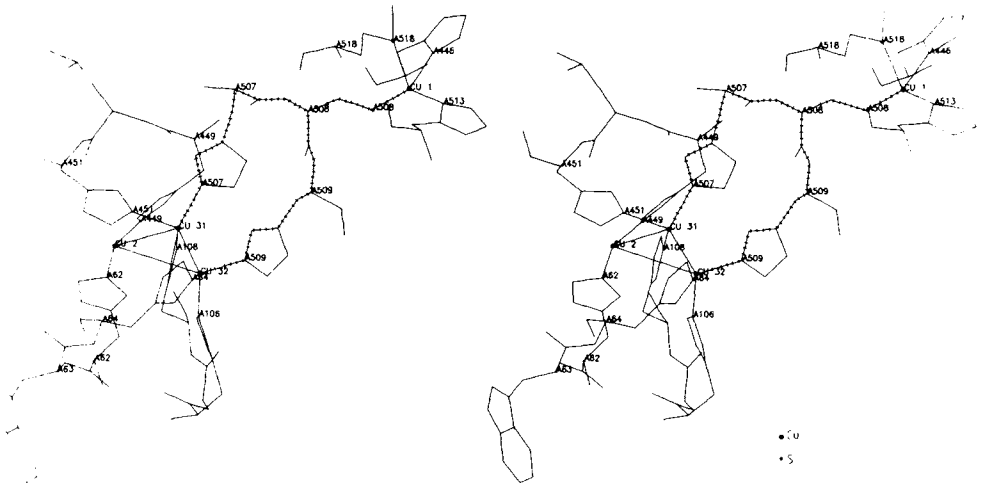


Fig. 11 b. Stereodrawing of the tridentate peptide ligand (–His 507–Cys 508–His 509–) in ascorbate oxidase bridging type-1 copper (Cu 1) and the trinuclear cluster (Cu 31, Cu 32, Cu 2) [50].

hemocyanin. The remaining copper (Cu 2) has two histidyl ligands (A62, A449) and is type-2 copper. The trinuclear copper cluster is the site where dioxygen binds; details of the structure including the presence of exogenic ligands still require clarification. The close spatial association of the three copper ions in the cluster suggests facile electron exchange. The cluster serves as electron storage site and may function as cooperative three-electron donor for the oxygen molecule, to irreversibly cleave the O–O bond.

3.2.3.2. Intramolecular Electron Transfer in Ascorbate Oxidase

Electrons are transferred from the type-1 copper to the trinuclear site. The shortest pathway is via Cys-A508 and His-A507 or His-A509. The (His–X–His–) segment links electron donor and acceptor and thus bridges a distance of 12 Å (Fig. 11 b). The cysteine sulfur and the imidazole components of the bridging ligand have low lying unoccupied molecular orbitals and may favor a chemical mechanism of electron transfer, but the intervening aliphatic and peptide chains are unlikely to form transient radicals and may well participate by resonance. The optical absorption of the 'blue' copper assigned to a cysteine $S^- \rightarrow Cu^{2+}$ charge transfer transition supports the suggested electron pathway.

The putative electron path branches at the C^α atom of Cys A508. Model compounds have shown inequivalence and faster transfer in the N–C direction of amide linking groups.[131] This may apply also to the blue oxidases and cause preferred transfer to A507.

The difference in redox potential between the type-1 copper and the type-3 copper is –40 mV in ascorbate oxidase. Unfortunately, there are no direct measurements of the intramolecular electron transfer rates available. The turnover number serves as a lower limit and is $7.5 \times 10^3\ s^{-1}$ in ascorbate oxidase,[126, 127] indicating a fairly rapid transfer despite the long distance and small driving force. The electron pathway is intramolecular and far removed from bulk water.

The characteristic distribution of the redox centers as mono- and trinuclear sites in the blue oxidases may also be found in the most complex oxidase, cytochrome oxidase (see the hypothetical model of *Holm* et al.[128]) and in the water-splitting manganese protein complex of the photosystem II, which carries out the reverse reaction of the oxidases. For its $(Mn)_4$ cofactor, either two binuclear or a tetranuclear metal center is favored,[129] but mono- and trinuclear arrangements cannot be excluded.

3.3. The Protein as Medium

The boundary between protein as ligand and as medium is fluid. The extreme microscopic complexity of structure, polarity and polarizability of protein media may influence the energy and electron transfer. There are no obvious common structural features in the protein systems discussed except a high proportion of aromatic residues (particularly tryptophans) bordering the electron transfer paths in the reaction center of purple bacteria and in ascorbate oxidase and their wide separation from bulk water by internal location within the protein and the hydrocarbon bilayer (in the reaction center). These effects have been mentioned in Sections 1.3 and 3.2.2.2.

4. Structural Relationships and Internal Repeats

All four protein systems mentioned in the following show internal repetition of structural motifs or similarities to other proteins of known folding patterns. This is a quite common phenomenon and not confined to energy and electron transfer proteins. It is also not uncommon that these relationships often remained undetected on account of the amino acid sequences; in effect this reflects our ignorance of the sequence structure relationships. An analysis of the structural relationships will shed light on the evolution and function of protein systems and is thus appropriate here.

4.1. Retinol and Bilin Binding Proteins

The simplest case is shown in Figure 12, where bilin-binding protein (BBP)[142] is compared with retinol-binding

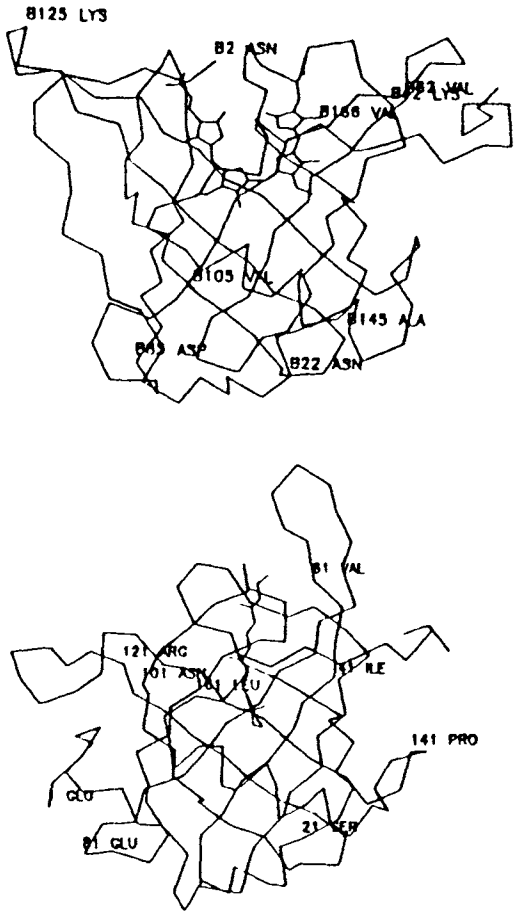


Fig. 12. Comparison of the polypeptide chain folds of bilin-binding protein (BBP) and retinol-binding protein (RBP) with bound cofactors.

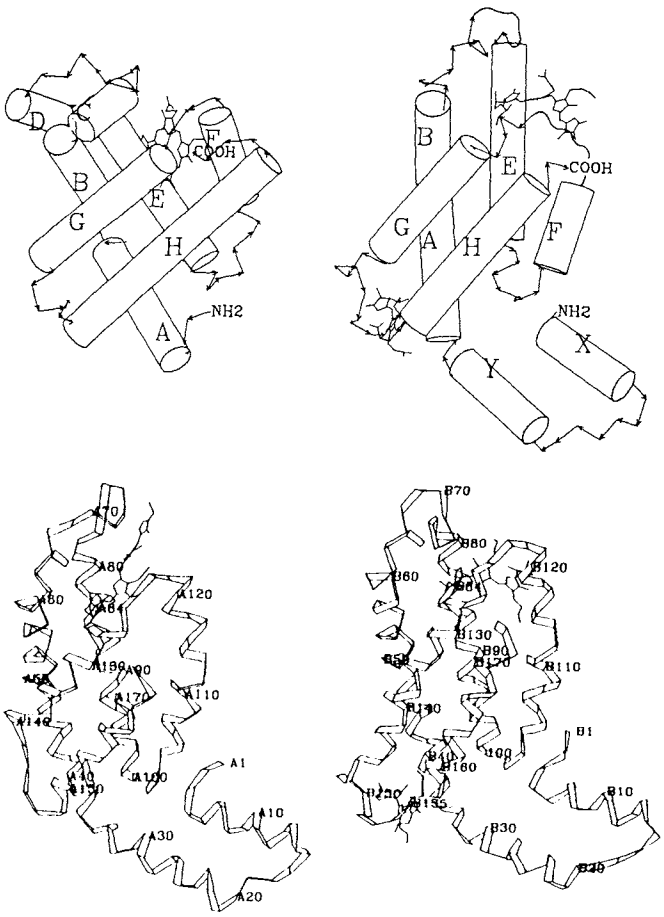


Fig. 13. Polypeptide chain folds of the α- and β-subunits of phycocyanin [44] (lower part, left and right) and comparison of the arrangements of α-helices in myoglobin and phycocyanin (upper part, left and right).

protein (RBP).[130] For the bottom of the β-barrel structure, the structural similarity is obvious, while the upper part, which is involved in the binding of the pigments biliverdin and retinol, differs considerably. The molecule is apparently subdivided into framework and hypervariable segments which determine binding specificity in analogy to the immunoglobulins.[131] This relationship suggests carrier functions for BBP as for RBP, although RBP also serves for pigmentation in butterflies.

4.2. Phycocyanin

In the protein part, phycocyanin (PC) consists of two polypeptide chains α and β which are clearly related in structure (Fig. 13, bottom), and probably originate from a common precursor.

The α-subunit is shorter in the G–H turn and lacks the s-chromophore B155 (see Section 3.2.1.3.). The loss or acquisition of chromophores during evolution may be less important than differentiation of the α and β subunits, which occupy non-equivalent positions in the $(\alpha\beta)_3$ trimer, so that the homologous chromophores A84 and B84 are non-equivalent with B84 lying on the inner wall of the disk. In addition the α and β subunits play very different roles in the formation of the $(\alpha\beta)_6$ hexamer, as has already been shown in Figure 8. Symmetrical precursor hexamers might have existed and could have formed stacks, but would lack the differentiation of the chromophores, in particular the inequivalence and close interaction of A84 and B84 in the trimer. Functional improvement has probably promoted divergent evolution of the α- and β-subunits.

A most surprising similarity was discovered between the PC subunits and the globins shown in Figure 13 (top). The globular helical assemblies A to H show similar topology. The U-shaped extension of phycocyanin formed from the *N*-terminal X,Y α-helices is essential for the formation of the αβ substructure. Comparison of the amino acid sequence after structural superposition reveals some homologies, suggesting divergent evolution of phycobiliproteins and globins;[44] however, what function a precursor of light harvesting and oxygen binding proteins might have had remains a mystery.

4.3. Reaction Center

The reaction center of *Rps. viridis* lacks symmetry across the membrane plane. This is not surprising for a complex which catalyzes a vectorial process across the membrane. However, there is quasi-symmetry relating the L- and M subunits and the pigment system. The structural similarity and the homology of the amino acid sequences of the L- and M-subunits suggest a common evolutionary origin. This relationship is extended to the photosystem II components D1 and D2 on the basis of sequence homology and conservation of residues involved in cofactor binding (for reviews, see

Refs. [132, 133]). The putative precursor was a symmetrical dimer with identical electron transfer pathways. The interaction with the H subunit introduces asymmetry, particularly noteworthy at the *N*-terminal transmembrane α-helix of the H-subunit (H), which is close to the E transmembrane α-helix of the M-subunit, the L-branch of the pigment system, and Q_A (Fig. 14). The improvement of the interaction with the H-subunit, which appears to play a role in the electron transfer from Q_A to Q_B and in protonation of Q_B might have advanced divergent evolution of the L- and M subunits at the expense of the inactivation of the M pigment branch. However, the electron transfer from BC_P to Q_A is extremely fast and not rate-limiting for the overall reaction. The evolutionary conservation of the M branch of pigments may be of functional significance as a pendant group in light harvesting and electron transfer. There are also structural reasons, for its deletion would leave a void.

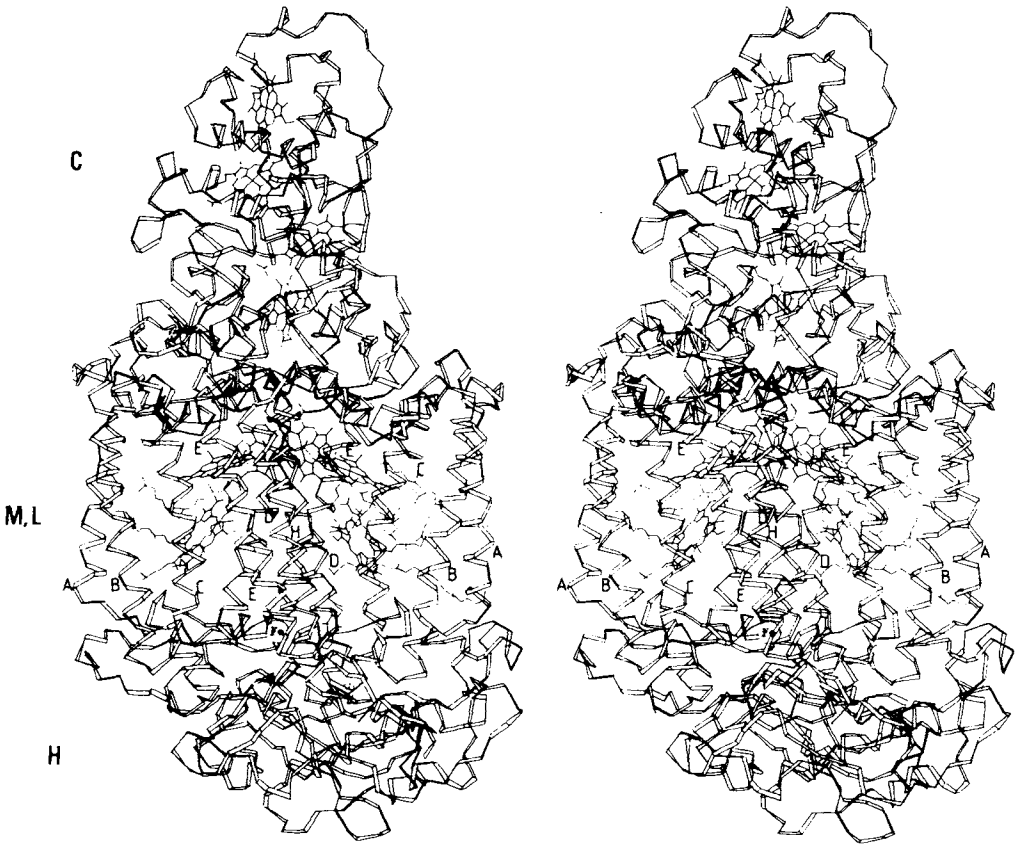


Fig. 14. Stereodrawing of the reaction center of *Rps. viridis* (complete complex of subunits and cofactors). The membrane-spanning α-helices of the L- and M-subunits (A, B, C, D, E in sequential and A, B. C, E, D in spatial order) and the H-subunit (H) are labeled [37] (cf. Fig. 10 a).

The cytochrome subunit (C) contributes to the asymmetry of the L–M complex and shows, in itself, an internal duplication.[37] All four heme groups are associated with a helix-turn-helix motif, but the turns are short for heme groups 1 and 3 and long for heme groups 2 and 4.

4.4. Blue Oxidases

Gene multiplication and divergent evolution is most evident in the blue oxidase, ascorbate oxidase. Figure 15 shows the polypeptide chain of 553 amino acid residues folded into three closely associated domains of similar topology.[50] Although nearly twice as large, they resemble the simple, small copper protein plastocyanin (Fig. 16).[123] In the blue oxidase the domains I and III enclose the trinuclear copper cluster in a quasi-symmetrical fashion, but only domain III contains the type 1 copper, the electron donor to the trinuclear site. A potential electron transfer pathway in domain I is not realized, reminiscent of the M-branch of pigments in the reaction center (cf. Section 3.2.2.2). Similarly to the H subunit in the reaction center, the linking domain II introduces asymmetry in the ascorbate oxidase, which might have promoted evolutionary divergence of domains I and III.

The proteins plastocyanin, ascorbate oxidase, laccase, and ceruloplasmin are members of a family of copper proteins, as indicated by structural relations and sequence homology.[50, 135–137] They provide a record from which an evolutionary tree may be mapped out (Fig. 17). The simplest molecule is plastocyanin containing only a type-1 copper. A dimer of plastocyanin-like molecules could provide the two times four histidyl ligands for the trinuclear copper cluster, representing a symmetrical oxidase. From this hypothetical precursor the modern blue oxidases and ceruloplasmin might have evolved following different paths of gene (domain) insertion and loss or acquisition of copper. In both, the arrangement of the *N*- and *C*-terminal domains, which



Fig. 15. Stereodrawing of the polypeptide chain folds of ascorbate oxidase and exploded view of its three domains from top to bottom [50]. β-strands are indicated as arrows and α-helices as cylinders (produced by the plot program of *Lesk* and *Hardman* [134]).

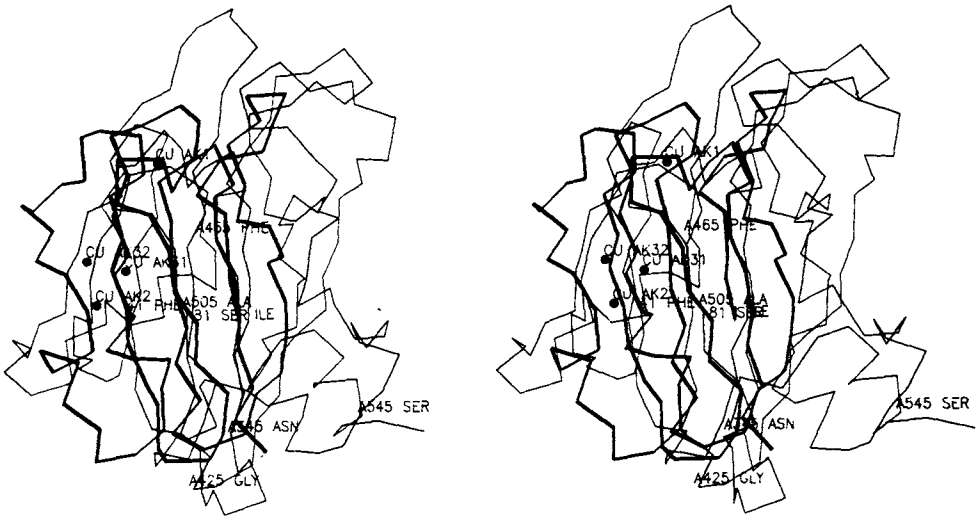


Fig. 16. Stereodrawing and superposition of domain III of ascorbate oxidase (thin lines) and plastocyanin (thick lines). The trinuclear copper site in ascorbate oxidase is buried between domain I (not shown) and domain III.

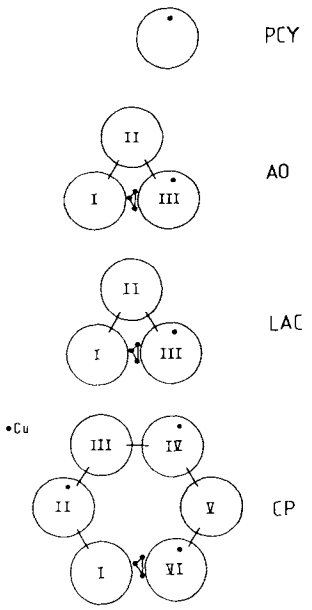


Fig. 17. Homologous domains in plastocyanin (PCY), ascorbate oxidase (AO), laccase (LAC) and ceruloplasmin (CP). The mono- and trinuclear copper sites are indicated.

contain the functional copper cluster, has been preserved. Recombinant DNA technology provides the possibility of reconstructing the hypothetical precursor oxidase. This is under investigation.

5. Implications from the Structure of the Reaction Center for Membrane Proteins in General

The structures of water soluble proteins show a seemingly unlimited diversity, despite their being built from only a few well defined secondary structural elements such as helices, β-sheets and turns and despite their construction from domains and recurring structural motifs. The proteins under discussion provide ample evidence of this. That there seems to be a limited set of basic folds may be related to the evolution of proteins from a basis set of structures and/or to constraints by protein stability and rates of folding. These basic folding motifs do not represent rigid building blocks, however, but adapt to sequence changes and respond to the environment and to association with other structural elements. Adaptability and plasticity (which is not to be confused with flexibility) is related to the fact that the entire protein and solvent system, and not its individual components, must attain the global energy minimum. Water is a good hydrogen bond donor and acceptor and is thus able to saturate polar peptide groups exposed on the surface almost as well as intraprotein hydrogen bonds do (entropic effects excluded).

Membrane proteins face the inert hydrocarbon part of the phospholipid bilayer and must saturate their hydrogen bonds intramolecularly. Only two secondary structures fulfill this condition for the polypeptide main chains, namely the α-helix and the β-barrel. For the assembly of α-helices packing rules have been derived which predict certain preferred angles between the helix axes albeit with a broad scatter. Similarly, the arrangement of strands in β-sheets and β-barrels follows defined rules.[138]

5.1. Structure of the Membrane Associated Parts of the Reaction Center

The reaction center was the first membrane protein whose structure could be determined at atomic resolution. Only the low resolution structure of bacteriorhodopsin was known previously. Both structures have some common features.[139] The structure of the reaction center may permit some conclusions to be drawn about membrane proteins in general. The reaction center contains 11 transmembrane α-helices, which, with 26 residues (H-subunit) or 24–30 residues (L- and M-subunits), have appropriate lengths to span the membrane. The amino acid sequences of these segments are devoid of charged residues (Fig. 18). Few charged residues occur close to the ends of the α-helices. Glycine residues initiate and terminate almost all α-helical segments, both the transmembrane and the connecting α-helices. It is well known from soluble proteins that glycine residues are abundant in turns and often associated with flexible regions of proteins.[12] They may be important for the insertion into the membrane by enabling structural rearrangements. The angles between the axes of the contacting α-helices of the L- and M-complex are 20° to 30°, a packing angle range also preferred by α-he-

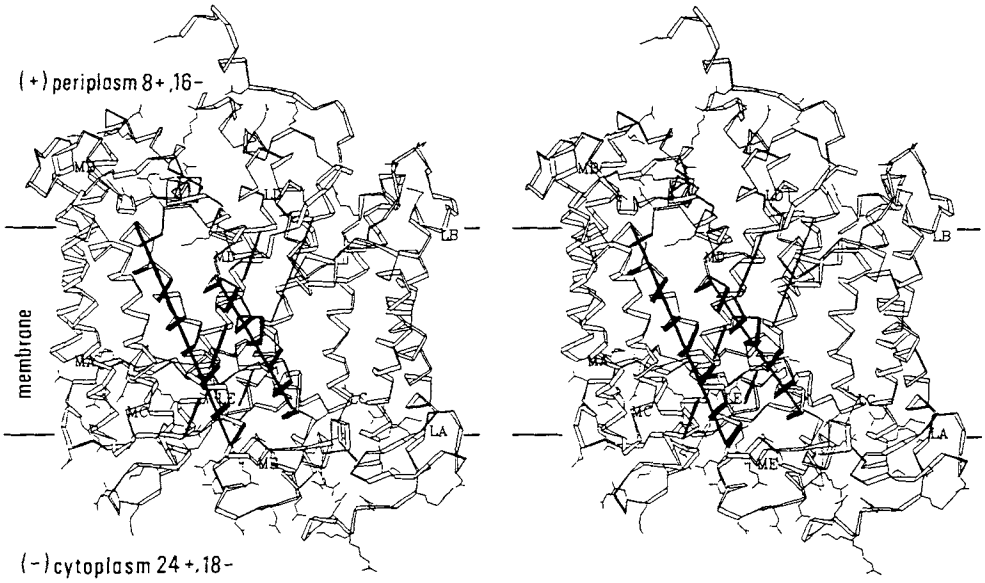


Fig. 18. Stereodrawing of the polypeptide chains of the L- and M-subunits of the reaction center in ribbon representation. The *N*-terminal residues of the membrane-spanning α-helices are labeled (including the prefix M and L) and the tetrahelical motif of the D and E α-helices is marked by shading and lines. The side chains of charged residues are drawn. Asp, Glu, and carboxy-termini are counted as negatively charged, and Lys, Arg and amino-termini are counted as positively charged and added for the cytoplasmic and periplasmic sides [5, 37].

lices in soluble proteins. They have features in common with buried α-helices in large globular proteins, which are also characterized by the absence of charged residues and the preferred location of glycines and prolines at the termini.[140, 141] Furthermore, the D- and E-α-helices of the L- and M-subunits (Fig. 18) find counterparts in soluble proteins. They are associated around the local diad axis and form the center of the L–M module, which binds the iron and the bacteriochlorophyll pair BC_P.

The four D- and E-α-helices of the L- and M-subunits are arranged as a bundle, held together by the iron ion and splayed out towards the cytoplasmic side to accommodate the large special pair. This motif is quite common in water-soluble electron transfer proteins.[142] I will resume this discussion later and suggest appropriate substructures of soluble proteins as models for pore forming membrane proteins.

5.2. Membrane Insertion

The structure of the reaction center is also important regarding our views of the mechanism of integration of membrane proteins into the phospholipid bilayer. The reaction center is composed of components which are quite differently arranged with respect to the membrane: The C-subunit is located on the periplasmic side. The H-subunit is folded into two parts: a globular part located on the cytoplasmic side and a transmembrane α-helix. The L- and M-subunits are incorporated into the phospholipid bilayer. Consequently, cytochrome (the C-subunit) has to be completely translocated across the membrane from its intracellular site of synthesis. In the H-, L-, and M-subunits the transmembrane α-helices are embedded in the bilayer. Only the *N*-terminal segment of H and the *C*-termini and connecting segments of the α-helices located at the periplasmic side of L and M (A–B, C–D) require transfer.

It is interesting to note that only the cytochrome gene possesses a prokaryotic signal sequence, as indicated by the sequence of the gene.[89] Transfer of the large hydrophilic C-subunit may require a complex translocation system and a signal sequence, while H, L, and M may spontaneously insert into the bilayer due to the affinity of the contiguous hydrophobic segments for the phospholipids (for a review of this and related problems see Ref. [143]). A "simple" dissolution still requires transfer across the membrane of those charged residues which are located at the periplasmic side.[37, 88] The increasingly favorable protein lipid interaction which develops with insertion may assist in this process. M and L have considerably more charged residues at the cytoplasmic side (41) than at the periplasmic side (24), providing a lower activation energy barrier for correct insertion. The net charge distribution of the L–M complex is asymmetric, with six positive charges at the cytoplasmic side and eight negative charges at the periplasmic side. As the intracellular membrane potential is negative, the observed orientation of the LM complex is energetically favored (Fig. 18).

The H-subunit has a very polar amino acid sequence at the *C*-terminus of the transmembrane α-helix with a stretch of seven consecutive charged residues (H33–H39)[37, 87] which may efficiently stop membrane insertion. Similarly, there are three to eleven charged residues in each of the connecting segments of the α-helices at the cytoplasmic side of the L- and M-subunits which might stop the transfer of α-helices or α-helical pairs.[144] As an alternative to sequential insertion the L- and M-subunits may be inserted into the membrane as assembled protein pigment complexes, because they cohere tightly by protein–protein and protein–cofactor interactions.

5.3. Models of Pore Forming Proteins

It is not absolutely clear whether the structural principles observed in the reaction center apply also to 'pore' or 'channel' forming α-helical proteins. These could, in principle, elaborate quite complex structures within the aqueous chan-

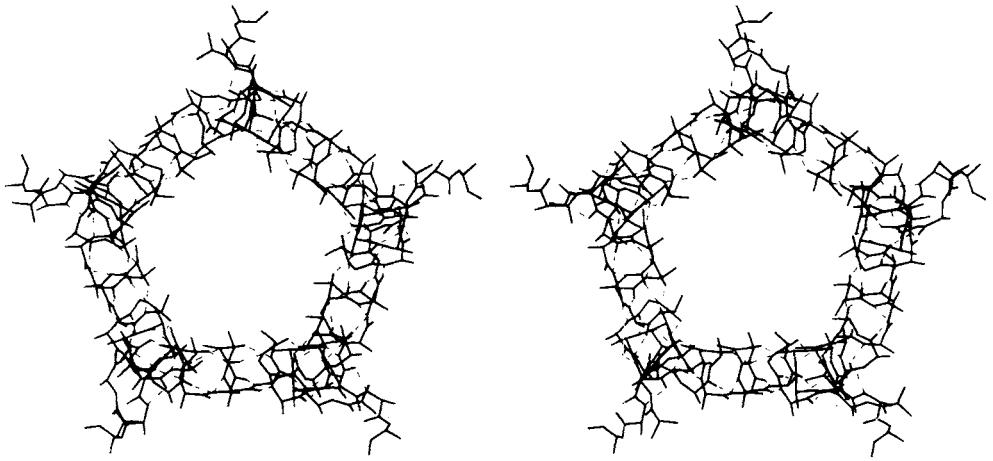


Fig. 19. Stereodrawing of the pentahelical pore in heavy riboflavin synthase [148].

nel,[145] but available evidence at low resolution for gap junction proteins[146] indicates in this specific case a simple hexameric arrangement of membrane-spanning amphiphilic α-helices, whose polar sides face the aqueous channel.

Guided by the observation that rules for structure and packing of α-helices derived for soluble proteins apply also to the reaction center, we may derive models for membrane pore forming proteins from appropriate soluble protein substructures. The penta-helical pore seen at high resolution in the icosahedral multi-enzyme complex riboflavin synthase seems to be a suitable model[148] (Fig. 19). Five amphiphilic α-helices of 23 residues each are nearly perpendicular to the capsid surface. The coiled coil of α-helices has a right-handed twist and forms a pore for the putative import of substrates and export of products. They pack with their apolar sides against the central four-stranded β-sheet of the protein, which mimics the hydrocarbon part of a phospholipid bilayer, and project charged residues into the aqueous channel.

Similar modeling of membrane protein structures may be extended to another class of membrane proteins which have β-structures spanning the outer membrane, the bacterial porins.[149] The β-barrels observed in soluble proteins have four to eight or more strands. The lower limit is determined by the distortion of the regular hydrogen bonds. An upper limit may be given by the possible sizes of stable protein domains. A four-stranded β-barrel with 4 parallel strands duplicated head-to-head with symmetry D_4 is observed in the ovomucoid octamer.[150] The β-strands lean against the hydrophobic core of the molecule and project their (short) polar residues into the channel (which is extremely narrow here).

6. Some Thoughts on the Future of Protein Crystallography

Thirty years after the elucidation of the first protein crystal structures by *Perutz* and *Kendrew* and after steady development, protein crystallography is undergoing a revolution. Recent technical and methodical developments enable us to analyze large functional protein complexes like the reaction center,[37,151] large virus structures (to mention only Refs. [152–154]), protein DNA complexes (to mention only Ref. [155]), and multienzyme complexes like riboflavin synthase.[148]

The significance of these studies for understanding biological functions is obvious and has excited the interest of the scientific community in general.

In addition, it was recognized that detailed structural information is a prerequisite for the rational design of drugs and proteins. As an illustration I chose human leucocyte elastase, which is an important pathogenic agent. On the basis of its three-dimensional structure (Fig. 20)[156] and the criteria of optimal stereochemical fit, potent inhibitors are

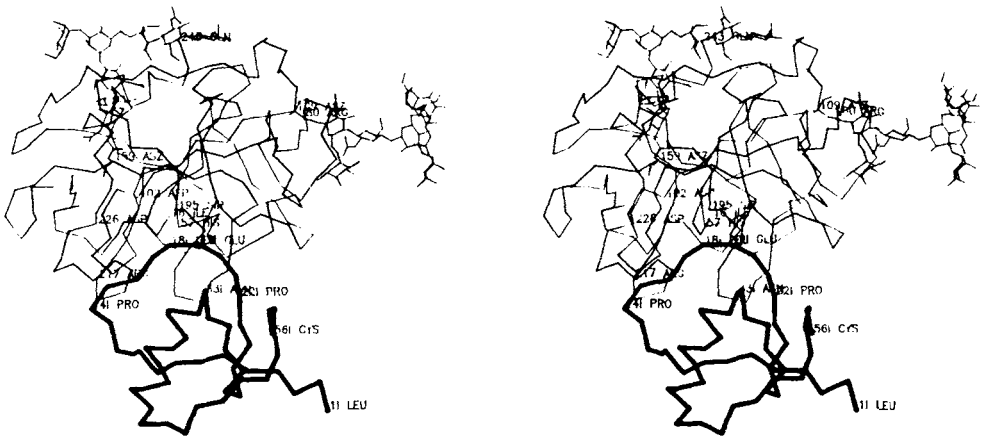


Fig. 20. Stereodrawing of the complex between human leucocyte elastase (thin lines) and turkey ovomucoid inhibitor (thick lines) [156].

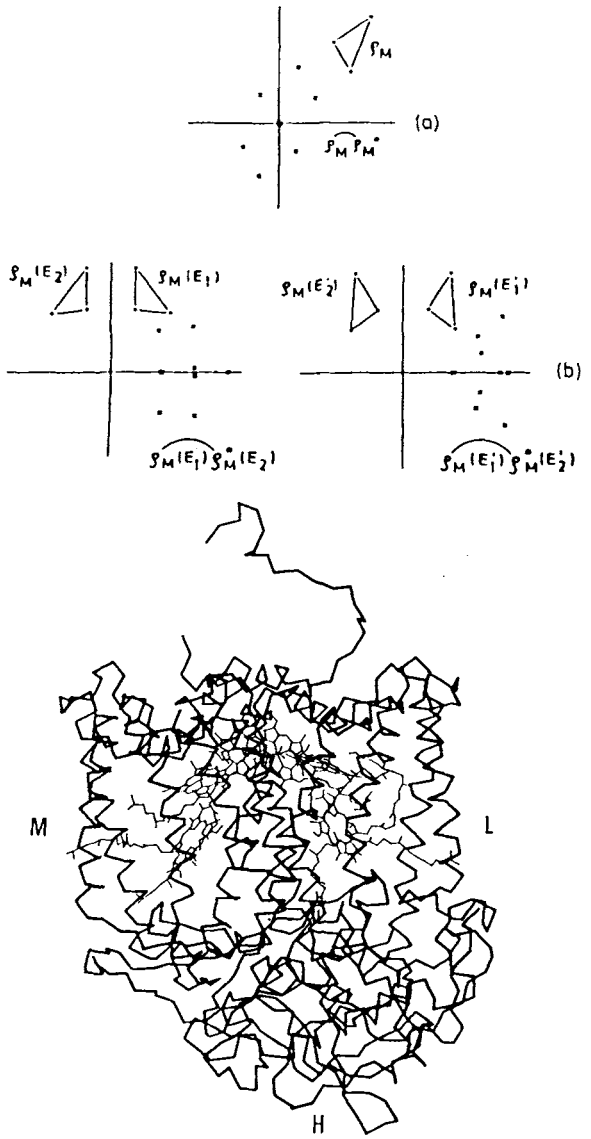


Fig. 21. Faltmolekül construction. Upper part: $\varrho_M\varrho_M^*$ (a) and $\varrho_M(E1)\varrho_M^*(E2)$ (b) are the intra- and intermolecular vector sets of a triangular structure ϱ_M, respectively. Their sum represents the Patterson function. The intramolecular vector set can be constructed from the molecular structure, is located at the origin, and permits the determination of the orientation. From the intermolecular vector set the translation component relative to the mirror plane can be derived. In (b) the intermolecular vector sets corresponding to two different orientations of ϱ_M are shown [164]. Lower part: Drawing of the main chain of the M-, L-, H-subunits and the cofactors which served as search model to solve the phase problem for the crystal structure of the reaction center of *Rb. sphaeroides*. For the calculation all homologous main chain and side chain atoms were included [6].

now being synthesized or natural inhibitors modified by use of recombinant DNA technology in many scientific and commercial institutions. Other, equally important proteins are also being studied. This field especially benefits from the readily available molecular modeling software (e.g. FRODO[157]) and a standard depository of structural data, the Protein Data Bank.[158]

Success *and* the new technical and methodical developments spur protein crystallography's progress. These new developments are indeed remarkable: Area detectors for automatic recording of diffraction intensities have been designed. Brilliant X-ray sources (synchrotrons) are available for very fast measurements and now permit use of very small crystals or radiation-sensitive materials. Their polychromatic radiation is used to obtain diffraction data sets within milliseconds by Laue techniques,[159] and their tunability allows the optimal use of anomalous dispersion effects.[160, 161]

Refinement methods including crystallographic and conformational energy terms provide improved protein models. Methods which allow the analysis of large protein complexes with internal symmetry averaging procedures have been developed[162] leading from blurred to remarkably clear pictures. A priori information of a relationship to known proteins can be used to great advantage as it is possible to solve an unknown crystal structure using a known model of a variant structure by a method discovered and named the 'Faltmolekül' method by my teacher, *W. Hoppe*. It has become a very powerful tool in protein crystallography.

With this last paragraph I wish to pay tribute to *W. Hoppe* who in 1957 laid the foundation to Patterson search methods by discovering that the Patterson function (the Fourier transform of the diffraction intensities) of molecular crystals can be split into sums of intra- and intermolecular vector sets[163] from which orientation and translation of the molecules can be derived when their approximate structure is known (Fig. 21). *Hoppe*'s method has been elaborated, computerized, and reformulated.[8, 165, 166] It provided a shortcut to the crystal structure of the reaction center of *Rb. sphaeroides* which was solved on the basis of the molecular structure of the reaction center of *Rps. viridis* and subsequently refined.[6, 151] The molecular architectures are very similar, although the *Rb. sphaeroides* reaction center lacks the permanently bound cytochrome. The structure solution was independently confirmed using similar methods.[7] With the Faltmolekül method the orientation and location of a molecule in a crystal cell can be determined. The detailed molecular structure and its deviations from the parent model have to be worked out by crystallographic refinement, to which *W. Steigemann* and *J. Deisenhofer* (in his thesis work) laid a foundation in my laboratory.[167, 168]

Recently, NMR techniques have demonstrated their efficiency in the determination of three-dimensional structures of small proteins in solution. In one case a detailed comparison of crystal and solution structures has shown very good correspondence,[169, 170] but further development is called for to extend the power of the method to larger protein structures.

Protein crystallography is the only tool available to unravel in detail the architecture of the large protein complexes described here, and it will continue in the foreseeable future to be the only experimental method that provides atomic resolution data on atom–atom and molecule–molecule interactions. It is such a method which *Emil Fischer* had in mind in 1907 in his 9th Faraday Lecture when pointing out that an understanding of "the precise nature of the assimilation process ... will only be accomplished when biological research, aided by improved analytical methods, has succeeded in following the changes which take place in the actual chlorophyll granules."[171] Yet an ultimate goal for which we all struggle is the solution of the folding problem. The growing number of known protein structures and the design of single residue variants by recombinant DNA technology and their analysis by protein crystallography has brought us nearer to this goal. We are able to study contributions of

individual residues to rates of folding, structure, stability, and function. Also theoretical analysis of protein structures has progressed (to mention only *Levitt* and *Sharon*[172]), but a clue to the code relating sequence and structure is not in sight.[173] Like *Carl von Linné* who 250 years ago created a system of plant classification on the basis of morphology (Genera plantarum, Leiden 1737), we classify proteins according to their shapes and structures. Whether this may lead to a solution of the folding problem is unclear, but it is certain that the end of protein crystallography will only come through it itself.

Acknowledgement

J. Deisenhofer's and my interest in structural studies on the photosynthetic reaction center of *Rps. viridis* was awakened by the establishment of *D. Oesterhelt*'s department in Martinsried in 1980; he brought with him *H. Michel*, with whom a fruitful collaboration on the analysis of the crystal structure of this large protein complex began. Later, other members of my group, *O. Epp* and *K. Miki*, became involved. We had been studying enzymes, proteases and their natural inhibitors, immunoglobulins, and had developed methods to improve data collection, electron density map interpretation, and crystallographic refinement. The tools were available to solve the structure of the reaction center, which was and still is the largest asymmetric protein whose structure has been determined with atomic resolution.

The "eureka" moment of protein crystallography is at the very end when one sees for the first time a new macromolecule with the eyes of a discoverer of unknown territories. To reach this moment much, sometimes tedious work has to be done with the ever present possibility of failure. I am deeply grateful to my collaborators, present and past, for their dedicated and patient work over many years. I mention by name those involved in the studies of the light harvesting cyanobacterial proteins and the blue oxidases: W. Bode, M. Duerring, R. Ladenstein, A. Messerschmidt, T. Schirmer. These projects were collaborative undertakings with biochemists in Switzerland (H. Zuber, W. Sidler), USA (M. L. Hackert) and Italy (M. Bolognesi, A. Marchesini, A. Finazzi-Agro).

Scientific work needs a stimulating environment which was provided at the Max-Planck-Institut für Biochemie and it needs steady financial support, which has been provided by the Max-Planck-Gesellschaft and the Deutsche Forschungsgemeinschaft.

I thank R. Engh, S. Knof, R. Ladenstein, M. Duerring, E. Meyer for their helpful comments on this manuscript.

Received: January 13, 1989 [A 724 IE]
German version: *Angew. Chem. 101* (1989) 849

[1] L. Boltzmann, Lecture delivered at the jubilee meeting of the Kaiserlichen Akademie der Wissenschaften, May 29, 1886, in *L. Boltzmann-Gesamtausgabe, Bd. 7*, Akademische Druck- und Verlagsanstalt Vieweg, Wiesbaden 1919, pp. 26–46. English translation from D. L. Arnon (1961) in W. D. McElroy, B. Glass (Eds.): *Light and Life*, The Johns Hopkins Press, Baltimore, pp. 489–569.

[2] M. Calvin, J. A. Bassham: *The Photosynthesis of Carbon Compounds*, Benjamin, New York 1962, pp. 1–127.

[3] J. Deisenhofer, H. Michel, R. Huber, *Trends Biochem. Sci. Pers. Ed. 10* (1985) 243–248.

[4] J. Deisenhofer, R. Huber, H. Michel, *Nachr. Chem. Tech. Lab. 34* (1986) 416–422.

[5] J. Deisenhofer, R. Huber, H. Michel in G. D. Fasman (Ed.): *Prediction of Protein Structure and the Principles of Protein Conformation*, Plenum, New York 1989, in press.

[6] J. P. Allen, G. Feher, T. O. Yeates, D. C. Rees, J. Deisenhofer, H. Michel, R. Huber, *Proc. Natl Acad. Sci. USA 83* (1986) 8589–8593.

[7] C.-H. Chang, D. Tiede, J. Tang, U. Smith, J. Norris, M. Schiffer, *FEBS Lett. 205* (1986) 82–86.

[8] R. A. Crowther, D. M. Blow, *Acta Crystallogr. 23* (1967) 544–548.

[9] D. E. Tronrud, M. F. Schmid, B. W. Matthews, *J. Mol. Biol. 188* (1986) 443–454.

[10] M. Pierrot, R. Haser, M. Frey, F. Payan, J.-P. Astier, *J. Biol. Chem. 257* (1982) 14341–14348.

[11] Y. Higuchi, M. Kusunoki, Y. Matsuura, N. Yasuoka, M. Kakudo, *J. Mol. Biol. 172* (1984) 109–139.

[12] W. S. Bennet, R. Huber, *CRC Crit. Rev. Biochem. 15* (1984) 291–384.

[13] R. Huber, *Angew. Chem. 100* (1988) 79; *Angew. Chem. Int. Ed. Engl. 27* (1988) 79–88.

[14] M. Karplus, J. A. McCammon, *CRC Crit. Rev. Biochem. 9* (1981) 293–349.

[15] U. Burkert, N. L. Allinger: *Molecular Mechanics*, American Chemical Society Monograph, Washington 1982.

[16] a) T. Förster, *Ann. Phys. (Leipzig) 2* (1948) 55–75; b) T. Förster in M. Florkin, E. H. Stotz (Eds.): *Comprehensive Biochemistry, Vol. 22*, Elsevier, Amsterdam 1967, pp. 61–80.

[17] H. Kuhn, *J. Chem. Phys. 53* (1970) 101–108.

[18] P. Frommherz, G. Reinbold, *Thin Solid Films 160* (1988) 347–353.

[19] S. L. Mayo, W. R. Ellis, R. J. Crutchley, H. B. Gray, *Science (Washington, D. C.) 233* (1986) 948–952.

[20] H. B. Gray, *Chem. Soc. Rev. 15* (1986) 17–30.

[21] J. L. McGoutry, S. E. Peterson-Kennedy, W. Y. Ruo, B. M. Hoffman, *Biochemistry 26* (1987) 8302–8312.

[22] H. Taube, E. S. Gould, *Acc. Chem. Res. 2* (1969) 321–329.

[23] J. J. Hopfield, *Proc. Natl. Acad. Sci. USA 71* (1974) 3640–3644.

[24] W. A. Cramer, A. R. Crofts: *Electron and Proton Transport in Photosynthesis: Energy Conversion by Plants and Bacteria, Vol. 1*, Academic Press, New York 1982, p. 387.

[25] L. Eberson, *Adv. Phys. Org. Chem. 18* (1982) 79–185.

[26] R. A. Marcus, N. Sutin, *Biochim. Biophys. Acta 811* (1985) 265–322.

[27] K. V. Mikkelsen, M. A. Ratner, *Chem. Rev. 87* (1987) 113–153.

[28] P. Kebarle, S. Chowdhury, *Chem. Rev. 87* (1987) 513–534.

[29] G. McLendon, *Acc. Chem. Res. 21* (1988) 160–167.

[30] D. Gust, T. A. Moore, P. A. Lidell, G. A. Nemeth, L. R. Makings, A. L. Moore, D. Barrett, P. J. Pessiki, R. V. Bensasson, M. Rougée, C. Chachaty, F. C. De Schryver, M. Van der Anweraer, A. R. Holzwarth, J. S. Connolly, *J. Am. Chem. Soc. 109* (1987) 846–856.

[31] J. A. Schmidt, A. R. McIntosh, A. C. Weedon, J. R. Bolton, J. S. Connolly, J. K. Hurley, M. R. Wasielewski, *J. Am. Chem. Soc. 110* (1988) 1733–1740.

[32] S. Isied, A. Vassilian, R. Magnuson, H. Schwarz, *J. Am. Chem. Soc. 107* (1985) 7432–7438.

[33] J. A. Barltrop, J. D. Coyle: *Principles of Photochemistry*, Wiley, Chichester 1978.

[34] A. Hains, *Acc. Chem. Res. 8* (1975) 264–272.

[35] J. Barber, *Trends Biochem. Sci. Pers. Ed. 12* (1987) 321–326.

[36] R. C. Prince, *Trends Biochem. Sci. Pers. Ed. 13* (1988) 286–288.

[37] J. Deisenhofer, O. Epp, K. Miki, R. Huber, H. Michel, *Nature (London) 318* (1985) 618–624.

[38] R. Lumry, H. Eyring, *J. Phys. Chem. 58* (1954) 110–112.

[39] H. B. Gray, B. G. Malmström, *Comments Inorg. Chem. 2* (1983) 203–209.

[40] C. Scharnagl, E. Köst-Reyes, S. Schneider, H.-P. Köst, H. Scheer, *Z. Naturforsch. C 38* (1983) 951–959.

[41] R. Huber, M. Schneider, O. Epp, I. Mayr, A. Messerschmidt, J. Pflugrath, H. Kayser, *J. Mol. Biol. 195* (1987) 423–434.

[42] R. Huber, M. Schneider, I. Mayr, R. Müller, R. Deutzmann, F. Suter, H. Zuber, H. Falk, H. Kayser, *J. Mol. Biol. 198* (1987) 499–513.

[43] H. Michel, K. A. Weyer, H. Gruenberg, I. Dunger, D. Oesterhelt, F. Lottspeich, *EMBO J. 5* (1986) 1149–1158.

[44] T. Schirmer, W. Bode, R. Huber, *J. Mol. Biol. 196* (1987) 677–695.

[45] T. Schirmer, W. Bode, R. Huber, W. Sidler, H. Zuber, *J. Mol. Biol. 184* (1985) 257–277.

[46] T. Schirmer, R. Huber, M. Schneider, W. Bode, M. Miller, M. L. Hackert, *J. Mol. Biol. 188* (1986) 651–676.

[47] J. Deisenhofer, O. Epp, K. Miki, R. Huber, H. Michel, *J. Mol. Biol. 180* (1984) 385–398.

[48] W. W. Parson, A. Scherz, A. Warshel in M. E. Michel-Beyerle (Ed.): *Antennas and Reaction Centers of Photosynthetic Bacteria*, Springer, Berlin 1985, pp. 122–130.

[49] E. W. Knapp, S. F. Fischer, W. Zinth, M. Sander, W. Kaiser, J. Deisenhofer, H. Michel, *Proc. Natl. Acad. Sci. USA 82* (1985) 8463–8467.

[50] A. Messerschmidt, A. Rossi, R. Ladenstein, R. Huber, M. Bolognesi, G. Gatti, A. Marchesini, T. Petruzzelli, A. Finazzi-Agro, *J. Mol. Biol. 206* (1989) 513–530.
[51] H. B. Gray, E. I. Solomon in T. G. Spiro (Ed.): *Copper Proteins*, Wiley, New York 1981, pp. 1–39.
[52] D. F. Blair, G. W. Campbell, J. R. Schoonover, S. I. Chan, H. B. Gray, B. G. Malmström, I. Pecht, B. F. Swanson, W. H. Woodneff, W. K. Cho, A. R. English, A. H. Fry, V. Lum, K. A. Norton, *J. Am. Chem. Soc. 10* (1985) 5755–5766.
[53] R. MacColl, D. Guard-Friar: *Phycobiliproteins*, CRC Press, Boca Raton, FL 1987, pp. 157–173.
[54] M. Nies, W. Wehrmeyer, *Arch. Microbiol. 129* (1981) 374–379.
[55] E. Mörschel, K.-P. Koller, W. Wehrmeyer, H. Schneider, *Cytobiologie 16* (1977) 118–129.
[56] D. A. Bryant, G. Guglielmi, N. Tandeau de Marsac, A.-M. Castets, G. Cohen-Bazire, *Arch. Microbiol. 123* (1979) 113–127.
[57] E. Gantt, C. A. Lipschultz, B. Zilinskas, *Biochim. Biophys. Acta 430* (1976) 375–388.
[58] H. Scheer in F. K. Fong (Ed.): *Light Reaction Path of Photosynthesis*, Springer, Berlin 1982, pp. 7–45.
[59] G. Cohen-Bazire, D. A. Bryant in N. G. Carr, B. Whitton (Eds.): *The Biology of Cyanobacteria*, Blackwell, London 1982, pp. 143–189.
[60] A. N. Glazer, *Annu. Rev. Biophys. Biophys. Chem. 14* (1985) 47–77.
[61] B. A. Zilinskas, L. S. Greenwald, *Photosynth. Res. 10* (1986) 7–35.
[62] H. Zuber, *Photochem. Photobiol. 42* (1985) 821–844.
[63] H. Zuber, *Trends Biochem. Sci. Pers. Ed. 11* (1986) 414–419.
[64] a) M. Duerring, W. Bode, R. Huber, *FEBS Lett. 236* (1988) 167–170; b) M. Duerring, *Dissertation*, Technische Universität München 1989.
[65] M. Duerring, W. Bode, R. Huber, R. Rümbeli, H. Zuber, in preparation.
[66] G. Frank, W. Sidler, H. Widmer, H. Zuber, *Hoppe-Seyler's Z. Physiol. Chem. 359* (1978) 1491–1507.
[67] A. N. Glazer, S. Fang, D. M. Brown, *J. Biol. Chem.* 248 (1973) 5679–5685.
[68] M. Mimuro, P. Flüglistaller, R. Rümbeli, H. Zuber, *Biochim. Biophys. Acta 848* (1986) 155–166.
[69] D. J. Lundell, R. C. Williams, A. N. Glazer, *J. Biol. Chem. 256* (1981) 3580–3592.
[70] F. W. J. Teale, R. E. Dale, *Biochem. J. 116* (1970) 161–169.
[71] B. Zickendraht-Wendelstadt, J. Friedrich, W. Rüdiger, *Photochem. Photobiol. 31* (1980) 367–376.
[72] P. Hefferle, M. Nies, W. Wehrmeyer, S. Schneider, *Photobiochem. Photobiophys. 5* (1983) 41–51.
[73] T. Gillbro, Å. Sandström, V. Sundström, J. Wendler, A. R. Holzwarth, *Biochim. Biophys. Acta 808* (1985) 52–65.
[74] S. Siebzehnrübl, R. Fischer, H. Scheer, *Z. Naturforsch. C42* (1987) 258–262.
[75] T. Schirmer, M. G. Vincent, *Biochim. Biophys. Acta 893* (1987) 379–385.
[76] G. Porter, C. J. Tredwell, G. F. W. Searle, J. Barber, *Biochim. Biophys. Acta 501* (1978) 232–245.
[77] G. F. W. Searle, J. Barber, G. Porter, C. J. Tredwell, *Biochim. Biophys. Acta 501* (1978) 246–256.
[78] J. Wendler, A. R. Holzwarth, W. Wehrmeyer, *Biochim. Biophys. Acta 765* (1984) 58–67.
[79] I. Yamazaki, M. Mimuro, T. Murao, T. Yamazaki, K. Yoshihara, Y. Fujita, *Photochem. Photobiol. 39* (1984) 233–240.
[80] A. R. Holzwarth, *Photochem. Photobiol. 43* (1986) 707–725.
[81] J. Grabowski, E. Gantt, *Photochem. Photobiol. 28* (1978) 39–45.
[82] S. C. Switalski, J. Sauer, *Photochem. Photobiol. 40* (1984) 423–427.
[83] A. R. Holzwarth in M. E. Michel-Beyerle (Ed.): *Antennas and Reaction Centers of Photosynthetic Bacteria*, Springer, Berlin 1985, pp. 45–52.
[84] K. Sauer, H. Scheer, P. Sauer, *Photochem. Photobiol. 46* (1987) 427–440.
[85] W. W. Parson in R. K. Clayton, W. R. Sistrom (Eds.): *The Photosynthetic Bacteria*, Plenum, New York 1978, pp. 317–322.
[86] N. Stark, W. Kuhlbrandt, I. Wildhaber, E. Wehrli, K. Mühlethaler, *EMBO J. 3* (1984) 777–783.
[87] H. Michel, K. A. Weyer, H. Gruenberg, F. Lottspeich, *EMBO J. 4* (1985) 1667–1672.
[88] H. Michel, O. Epp, J. Deisenhofer, *EMBO J. 5* (1986) 2445–2451.
[89] K. A. Weyer, F. Lottspeich, H. Gruenberg, F. Lang, D. Oesterhelt, H. Michel, *EMBO J. 6* (1987) 2197–2202.
[90] R. J. Cogdell, A. R. Crofts, *FEBS Lett. 27* (1972) 176–178.
[91] R. P. Carithers, W. W. Parson, *Biochim. Biophys. Acta 387* (1975) 194–211.
[92] R. C. Prince, J. S. Leigh, P. L. Dutton, *Biochim. Biophys. Acta 440* (1976) 622–636.
[93] T. L. Netzel, P. M. Rentzepis, D. M. Tiede, R. C. Prince, P. L. Dutton, *Biochim. Biophys. Acta 460* (1977) 467–479.
[94] J. R. Bolton in R. K. Clayton, W. R. Sistrom (Eds.): *The Photosynthetic Bacteria*, Plenum, New York 1978, pp. 419–442.
[95] D. Holten, M. W. Windsor, W. W. Parson, J. P. Thornber, *Biochim. Biophys. Acta 501* (1978) 112–126.
[96] N. W. Woodbury, M. Becker, D. Middendorf, W. W. Parson, *Biochemistry 24* (1985) 7516–7521.
[97] J. Breton, *Biochim. Biophys. Acta 810* (1985) 235–245.
[98] J. Breton, D. L. Farkas, W. W. Parson, *Biochim. Biophys. Acta 808* (1985) 421–427.
[99] J. Breton, J.-L. Martin, A. Migus, A. Antonetti, A. Orszag, *Proc. Natl. Acad. Sci. USA 83* (1986) 5121–5125.
[100] G. J. Kavarnos, N. J Turro, *Chem. Rev. 86* (1986) 401–449.
[101] G. R. Fleming, J. L. Marti, J. Breton, *Nature (London) 333* (1988) 190–192.
[102] J. Barber, *Nature (London) 333* (1988) 114.
[103] P. Pasman, F. Rob, J. W. Verhoeven, *J. Am. Chem. Soc. 104* (1982) 5127–5133.
[104] T. A. Moore, D. Gust, P. Mathis, J.-C. Bialocq, C. Chachaty, R. V. Bensasson, E. J. Land, D. Doizi, P. A. Liddell, W. R. Lehman, G. A. Nemeth, A. L. Moore, *Nature (London) 307* (1984) 630–632.
[105] W. Arnold, R. D. Clayton, *Proc. Natl. Acad. Sci. USA 46* (1960) 769–776.
[106] W. W. Parson, *Annu. Rev. Microbiol. 28* (1974) 41–59.
[107] W. W. Parson, R. J. Cogdell, *Biochim. Biophys. Acta 416* (1975) 105–149.
[108] a) C. Kirmaier, D. Holten, W. W. Parson, *Biochim. Biophys. Acta 810* (1985) 33–48; b) *ibid. 810* (1985) 49–61.
[109] C. A. Wraight in B. L. Trumpower (Ed.): *Function of Quinones in Energy Conserving Systems*, Academic Press, London 1982, pp. 181–197.
[110] D. Kleinfeld, M. Y. Okamura, G. Feher, *Biochim. Biophys. Acta 809* (1985) 291–310.
[111] R. J. Debus, G. Feher, M. Y. Okamura, *Biochemistry 25* (1986) 2276–2287.
[112] P. L. Dutton, R. C. Prince in R. K. Clayton, W. R. Sistrom (Eds.): *The Photosynthetic Bacteria*, Plenum, New York 1978, pp. 525–565.
[113] D. DeVault, B. Chance, *Biophys. J. 6* (1966) 825–847.
[114] L. Slooten, *Biochim. Biophys. Acta 256* (1972) 452–466.
[115] M. E. Michel-Beyerle, M. Plato, J. Deisenhofer, H. Michel, M. Bixon, J. Jortner, *Biochim. Biophys. Acta 932* (1988) 52–70.
[116] B. G. Malmström: *New Trends in Bio-inorganic Chemistry*, Academic Press, New York 1978, pp. 59–77.
[117] B. G. Malmström, *Annu. Rev. Biochem. 51* (1982) 21–59.
[118] O. Färver, I. Pecht in R. Lontie (Ed,): *Copper Proteins and Copper Enzymes, Vol. 1*, CRC Press, Boca Raton, FL 1984, pp. 183–214.
[119] B. Reinhammar in R. Lontie (Ed.): *Copper Proteins and Copper Enzymes, Vol. 3*, CRC Press, Boca Raton, FL 1984, pp. 1–35.
[120] B. Mondovi, L. Avigliano in R. Lontie (Ed.): *Copper Proteins and Copper Enzymes, Vol. 3*, CRC Press, Boca Raton, FL 1984, pp. 101–118.
[121] L. Rydén in R. Lontie (Ed.): *Copper Proteins and Copper Enzymes, Vol. 3*, CRC Press, Boca Raton, FL 1984, pp. 34–100.
[122] R. Malkin, B. G. Malmström, *Adv. Enzymol. 33* (1970) 177–243.
[123] J. M. Guss, H. C. Freeman, *J. Mol. Biol. 169* (1983) 521–563.
[124] J. S. Richardson, K. A. Thomas, B. H. Rubin, D. C. Richardson, *Proc. Natl. Acad. Sci. USA 72* (1975) 1349–1353.
[125] W. P. J. Gaykema, W. G. J. Hol, J. M. Verijken, N. M. Soeter, H. J. Bak, J. J. Beintema, *Nature (London) 309* (1984) 23–29.
[126] C. R. Dawson in J. Peisach, P. Aison, W. E. Blumberg (Eds.): *The Biochemistry of Copper*, Academic Press, New York 1966, pp. 305–337.
[127] B. Gerwin, S. R. Burstein, J. Westley, *J. Biol. Chem. 249* (1974) 2005–2008.
[128] L. Holm, M. Sarastre, M. Wikström, *EMBO J. 6* (1987) 2819–2823.
[129] G. T. Babcock in J. Amesz (Ed.): *Oxygen-evolving Process in Photosynthesis*, Elsevier, Amsterdam 1987.
[130] E. M. Newcomer, T. A. Jones, J. Åqvist, J. Sundelin, U. Eriksson, I. Rask, P. A. Peterson, *EMBO J. 3* (1984) 1451–1454.
[131] R. Huber in P. Gronski, F. R. Seiler (Eds.): *Behring-Institut Mitteilungen, Vol. 76*, Medizinische Verlagsgesellschaft, Marburg 1984, pp. 1–14.
[132] A. Trebst, *Z. Naturforsch. C41* (1986) 240–245.
[133] H. Michel, J. Deisenhofer, *Biochemistry 27* (1988) 1–7.
[134] A. M. Lesk, K. D. Hardman, *Science (Washington, D.C.) 216* (1982) 539–540.
[135] J. Ohkawa, N. Okada, A. Shinmyo, M. Takano, *Proc. Natl. Acad. Sci. USA 86* (1989) 1239–1243.
[136] U. A. Germann, G. Müller, P. E. Hunziker, K. Lerch, *J. Biol. Chem. 263* (1988) 885–896.
[137] N. Takahashi, T. L. Ortel, F. W. Putnam, *Proc. Natl. Acad. Sci. USA 81* (1984) 390–394.
[138] C. Chothia, *Annu. Rev. Biochem. 53* (1984) 537–572.
[139] R. Henderson, P. N. T. Unwin, *Nature (London) 257* (1975) 28–32.
[140] H. Loebermann, R. Tokuoka, J. Deisenhofer, R. Huber, *J. Mol. Biol. 177* (1984) 531–556.
[141] S. Remington, G. Wiegand, R. Huber, *J. Mol. Biol. 158* (1982) 111–152.
[142] P. C. Weber, F. R. Salemme, *Nature (London) 287* (1980) 82–84.
[143] T. A. Rapoport, *CRC Crit. Rev. Biochem. 20* (1986) 73–137.
[144] D. M. Engelman, T. A. Steitz, A. Goldman, *Annu. Rev. Biophys. Chem. 15* (1986) 321–353.
[145] H. F. Lodish, *Trends Biochem. Sci. Pers. Ed. 13* (1988) 332–334.
[146] L. C. Milks, N. M. Kumar, R. Houghten, N. Unwin, N. B. Gilula, *EMBO J. 7* (1988) 2967–2975.
[147] G. D. Case, W. W. Parson, J. P. Thornber, *Biochim. Biophys. Acta 223* (1970) 122–128.

[148] R. Ladenstein, M. Schneider, R. Huber, H.-D. Bartunik, K. Wilson, K. Schott, A. Bacher, *J. Mol. Biol. 203* (1988) 1045–1070.
[149] B. Kleffel, R. M. Garavito, N. Baumeister, J. P. Rosenbusch, *EMBO J. 4* (1985) 1589–1592.
[150] E. Weber, E. Papamokos, W. Bode, R. Huber, F. Kato, M. Laskowski, *J. Mol. Biol. 149* (1981) 109–123.
[151] J. P. Allen, G. Feher, T. O. Yeates, H. Kemiya, D. C. Rees, *Proc. Natl. Acad. Sci. USA 84* (1987) 6162–6166.
[152] S. C. Harrison, A. J. Olson, C. E. Schutt, F. K. Winkler, G. Bricogne, *Nature (London) 276* (1978) 368–373.
[153] M. G. Rossmann, E. Arnold, J. W. Erickson, E. A. Frankenberger, J. P. Griffith, H.-J. Hecht, J. E. Johnson, G. Kamer, M. Luo, A. G. Mosser, R. R. Rueckert, B. Sherry, G. Vriend, *Nature (London) 317* (1985) 145–153.
[154] J. M. Hogle, M. Chow, D. J. Filman, *Science (Washington, D.C.) 229* (1985) 1358–1365.
[155] D. Ollis, P. Brick, R. Hamlin, N. G. Xuong, T. A. Steitz, *Nature (London) 313* (1985) 762–766.
[156] W. Bode, A. Wei, R. Huber, E. Meyer, P. Travis, S. Neumann, *EMBO J. 5* (1986) 2453–2458.
[157] A. T. Jones, *J. Appl. Crystallogr. 11* (1978) 268–272.
[158] F. C. Bernstein, T. F. Koetzle, G. J. B. Williams, E. F. Meyer, Jr., M. D. Brice, J. R. Rodgers, O. Kennard, T. Shimonouchi, M. Tasumi, *J. Mol. Biol. 112* (1977) 535–542.
[159] J. Hajdu, K. R. Acharya, D. A. Stuart, D. Barford, L. Johnson, *Trends Biochem. Sci. Pers. Ed. 13* (1988) 104–109.
[160] W. A. Hendrickson, J. L. Smith, R. P. Phizackerly, E. A. Merritt, *Proteins 4* (1988) 77–88.
[161] J. M. Guss, E. A. Merritt, R. P. Phizackerly, B. Hedman, M. Murata, K. O. Hodgson, H. C. Freeman, *Science (Washington, D.C.) 241* (1988) 806–811.
[162] G. Bricogne, *Acta Crystallogr. Sect. A 32* (1976) 832–847.
[163] W. Hoppe, *Acta Crystallogr. 10* (1957) 750–751.
[164] R. Huber in P. Machin (Ed.): *Molecular Replacement*, Proceedings of the Daresbury Study Weekend, Daresbury Laboratory 1985, pp. 58–61.
[165] M. G. Rossmann, D. M. Blow, *Acta Crystallogr. 15* (1962) 24–31.
[166] R. Huber, *Acta Crystallogr. 19* (1965) 353–356.
[167] R. Huber, D. Kukla, W. Bode, P. Schwager, K. Bartels, J. Deisenhofer, W. Steigemann, *J. Mol. Biol. 89* (1974) 70–101.
[168] J. Deisenhofer, W. Steigemann, *Acta Crystallogr. Sect. B31* (1975) 238–280.
[169] A. D. Kline, W. Braun, K. Wüthrich, *J. Mol. Biol. 189* (1986) 377–382.
[170] J. W. Pflugrath, G. Wiegand, R. Huber, L. Vertesy, *J. Mol. Biol. 189* (1986) 383–386.
[171] E. Fischer, *J. Chem. Soc. 91* (1907) 1749–1765.
[172] M. Levitt, R. Sharon, *Proc. Natl. Acad. Sci. USA 85* (1988) 7557–7561.
[173] R. Jaenicke in E.-L. Winnacker, R. Huber (Eds.): *39. Mosbacher Kolloquium*, Springer, Berlin 1988, pp. 16–36.

The Purine Path to Chemotherapy (Nobel Lecture)**

By Gertrude B. Elion*

Introduction

When I joined the Wellcome Research Laboratories in 1944, World War II was in progress. Since the work I am about to discuss covers a period of some 40 years, it may be pertinent to consider the "state of the art" at that time. Our ultraviolet absorption spectra were measured with a Bausch and Lomb spectrograph which had a carbon arc as the light source and photographic plates for recording the amount of light absorbed at each wavelength. There was no paper or ion-exchange chromatography, and purines were isolated and separated as copper and silver salts, or picrates, by fractional crystallization. Tritium and ^{32}P were available, but no ^{14}C or ^{35}S. Geiger counters were used for counting radioactivity; scintillation counters came much later. Some heavy isotopes (e.g., ^{15}N and ^{13}C) were obtainable but required the use of a mass spectrometer, which few laboratories had. The state of knowledge of nucleic acids was rather rudimentary. We knew they contained purines and pyrimidines, but the sequences were not known. The prevailing theory was that there were two purines and two pyrimidines in each tetranucleotide and that these tetranucleotides were strung together in some fashion. However, the nature of the internucleotide linkage had not been established and the helical structure of DNA had not yet been proposed.

In 1940 *Woods*[1] and *Fildes*[2] had put forth the antimetabolite theory to explain the action of sulfonamides on bacteria, suggesting that the sulfonamides interfered with the utilization of a necessary nutrient, *para*-aminobenzoic acid. *Hitchings* theorized that, since all cells required nucleic acids, it might be possible to stop the growth of rapidly dividing cells (e.g., bacteria, tumors, protozoa) with antagonists of the nucleic acid bases. One might hope to take advantage of the faster rate of multiplication of these cells compared with normal mammalian cells and eventually sort out the biochemical differences between various types of cells by the way they responded to these antimetabolites.[3,4] It was my assignment to work on purines, pteridines, and some other condensed pyrimidine systems.

It was, of course, necessary to have some biological systems to determine the potential activities of the new compounds. Essentially nothing was known at that time about the anabolic pathways leading to the utilization of purines for nucleic acid synthesis. A number of catabolic enzymes were known: nucleases, nucleotidases, nucleosidases, deaminases (for guanine, adenine, adenosine, and adenylic acid), xanthine oxidase, and uricase. In 1947 *Kalckar* described the reversibility of nucleoside phosphorylase.[5] The enzymes guanase and xanthine oxidase were useful in our laboratory to examine the purines as substrates or inhibitors of these enzymes.[6,7] However, it was the microorganism *Lactobacillus casei* upon which we mainly relied. It could grow on adenine, guanine, hypoxanthine, or xanthine, provided the pyrimidine thymine was added. It could also synthesize purines and thymine, if given a source of folic acid in the form of liver powder. (The structure of folic acid was not elucidated until 1946 by the *Lederle* group.[8]) *Hitchings* and *Falco* had devised a screening test in which it was possible to determine whether a compound could substitute for thymine[9] or a natural purine[4,10] or inhibit its utilization, and they could also determine whether a compound was a folic acid antagonist.[11,12]

Few chemists were interested in the synthesis of purines in those days and I relied mainly on methods in the old German literature. The transformation reactions were carried out mainly by the methods of *Emil Fischer* and the syntheses from pyrimidine intermediates by the methods of *Traube*. The direct replacement of oxygen by sulfur by the method of *Carrington*[13] also proved to be exceedingly useful for synthesizing the mercaptopurines.[14,15]

In 1950 we reported that 2,6-diaminopurine (DAP) inhibited the growth of *L. casei* very strongly and that the inhibition was reversed specifically by adenine, but not by the other natural purines.[4,16] However, the effects of low concentrations of DAP could also be reversed by folic acid, an attribute which DAP had in common with other diaminopyrimidines and diaminopyrimidine condensed systems.[10] Studies on a DAP-resistant strain of *L. casei* revealed that it grew poorly on adenine as a source of purine. We deduced that adenine and DAP must be anabolized by the same enzyme and that the product of DAP anabolism interfered with purine interconversion.[17] That enzyme was reported by *Kornberg* et al. in 1955 to be adenylate pyrophosphorylase (adenine phosphoribosyltransferase).[18] When tested on mouse tumors and the Ak4 mouse leukemia[19] or tumor cells in tissue culture,[20] DAP proved to be strongly inhibitory. It produced two good clinical remissions in chronic granulocytic leukemia in adults but produced severe nausea and vomiting, as well as severe bone marrow depression, in two other patients.[21] Interestingly, DAP showed activity against vaccinia virus, a DNA virus, in vitro,[22] but its toxicity in animals led us to abandon that possible utility.

Antileukemic Drugs

By 1951 we had made and tested over 100 purines in the *L. casei* screen[23] and discovered that the substitution of oxygen by sulfur at the 6-position of guanine and hypoxanthine produced inhibitors of purine utilization. 6-Mercaptopurine (6-MP) and 6-thioguanine (TG) were tested at the Sloan-Kettering Institute, with whom we had established a

[*] Prof. G. B. Elion
Wellcome Research Laboratories
Burroughs Wellcome Co.
3030 Cornwallis Road
Research Triangle Park, NC 27709 (USA)

[**] Copyright © The Nobel Foundation 1989. We thank the Nobel Foundation, Stockholm, for permission to print this lecture.

collaboration, and were found to be active against a wide spectrum of rodent tumors and leukemias. Of special interest was the finding by *Clarke* et al.[24] that 6-MP–treated tumors, although they had not regressed completely in the host mouse, were not transplantable into other mice. After some animal toxicology studies by *Philips* et al.,[25] *Burchenal* et al. proceeded rapidly to clinical trial with 6-MP in children with acute leukemia.[26] At that time the only drugs available for the treatment of these terminally ill children were methotrexate (MTX) and steroids and the median life expectancy was between three and four months; only 30% lived for as long as one year. The findings that 6-MP could produce complete remissions of acute leukemia in these children, although most of them relapsed at various intervals thereafter, led the Food and Drug Administration to approve the drug for this use in 1953, a little more than two years after its synthesis and microbiological investigation. A symposium on 6-MP was held at the New York Academy of Sciences in 1954.[27] The addition of 6-MP to the antileukemia armamentarium increased the median survival time to 12 months in these children, and a few remained in remission for years with 6-MP and steroids. This convinced us, as well as many other investigators in the cancer field, that antimetabolites of nucleic acid bases were fruitful leads to follow. Today 6-MP remains one of the dozen or more drugs found useful in the treatment of acute leukemia. With the use of combination chemotherapy with three or four drugs to produce and consolidate remission, plus several years of maintenance therapy with 6-MP and methotrexate, almost 80% of children with acute leukemia can now be cured.

Although we felt we were on the right track in 1952, there were still many unanswered questions. How did 6-MP work? What was the reason for its differential effect on neoplastic cells? How could one improve this differential effect? Reversal studies with 6-MP in *L. casei* did not pinpoint antagonism for any single purine. The inhibition was reversed by hypoxanthine, adenine, guanine, and xanthine.[28] However, studies with a 6-MP–resistant strain of *L. casei* revealed that the strain was unable to utilize hypoxanthine for growth.[29] Again, as with the earlier studies with 2,6-diaminopurine, we concluded that 6-MP and hypoxanthine were anabolized by the same enzyme and that interference with purine interconversions at the nucleotide level was involved.[30] In 1955 (two years after the introduction of 6-MP into clinical use), the enzyme that converts hypoxanthine and 6-MP into their respective nucleotides was identified as hypoxanthine phosphoribosyltransferase (HGPRT).[18] Also in the mid-fifties, the pioneering work of *Greenberg*[31] and of *Buchanan*[32, 33] and their co-workers revealed the pathways of the biosynthesis of purines and the importance of hypoxanthine ribonucleotide (inosinic acid, IMP) as the first purine nucleotide formed in this biosynthetic pathway. It took a number of investigators and a period of years to unravel all of the pathways in which the nucleotide of 6-MP, thioinosinic acid (TIMP), and nucleotides derived from TIMP participated as substrates or inhibitors (Fig. 1).[34]

Our current knowledge of enzyme inhibition constants and the concentrations of the various nucleotides achieved with the therapeutic regimens indicates that the principal modes of action are feedback inhibition of de novo purine synthesis (particularly by methylthioinosinic acid), inhibition of inosinate dehydrogenase, and incorporation into DNA in the form of TG.[35] Selectivity for neoplastic cells probably depends on the levels of the individual anabolic and catabolic enzymes. Catabolic enzyme levels are generally much lower in tumor cells than in normal cells. In addition, mitotic rate, drug transport, and metabolite pool sizes can be responsible for selective toxicity.

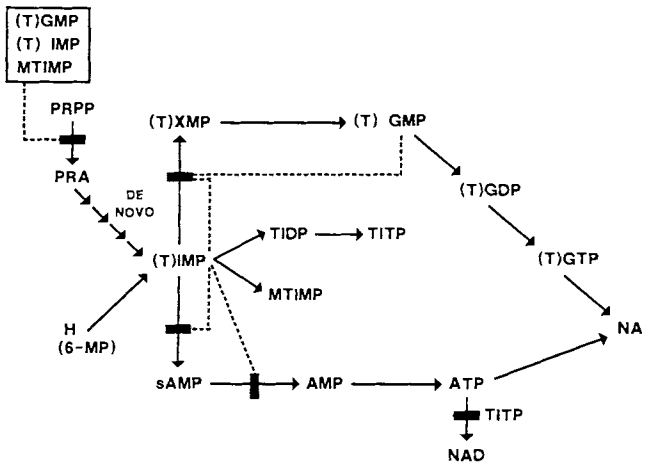


Fig. 1. Pathways in the anabolism of 6-MP and loci of action of the nucleotides derived from 6-MP. In addition, TGDP is converted into dTGDP and dTGTP for incorporation into DNA. MP, DP, and TP are mono-, di-, and triphosphate, respectively. T = thio, M = methyl, G = guanosine, X = xanthosine, PRPP = 5-phosphoribosyl-1-pyrophosphate, PRA = phosphoribosylamine, sAMP = adenylosuccinate.

While these biochemical studies were going on, we studied the metabolic fate of 6-MP, first in mice[36] and then in humans.[37] Pharmacokinetic and metabolic studies were then in their infancy, perhaps because the methodology for separation of metabolites and the counting of radioactive samples as thin films in a flow Geiger counter were so tedious and time-consuming. Nevertheless, using Dowex-1 and Dowex-50 ion-exchange columns and paper chromatography, we investigated the fate of 6-MP in vivo and attempted to discover whether it was possible to modify this metabolism and thus improve the efficacy of 6-MP. We continued to synthesize derivatives of 6-MP and TG and to investigate structure–activity relationships.[38–40] Thioguanine, which we had synthesized earlier than 6-MP, was more active but also more toxic.[25] It was also more difficult to synthesize and, since its mechanism of action appeared to be similar to that of 6-MP, its metabolic fate and clinical activity were explored somewhat later.[41–43] Thioguanine later found its main utility, in combination with cytosine arabinoside, in the treatment of acute myelocytic leukemia in adults.

Studies of the urinary metabolites of 6-MP revealed that extensive metabolic transformations occurred in vivo.[36, 37, 44–46] The single product present in highest amount was 6-thiouric acid, formed by the action of xanthine oxidase on 6-MP. In addition, there were various substances in which the sulfur had been methylated and the methylthio derivative had been oxidized on the sulfur or on the purine ring. A considerable amount of the sulfur had been removed and converted by oxidation into inorganic sulfate, which also appeared as sulfate esters. Very little 6-MP was excreted unchanged.

In an attempt to modify the metabolism of 6-MP, we introduced substituents at the 2- and/or 8-positions of the purine ring and on the ring nitrogens. This led to the loss of antitumor activity, with the exception of the 2-amino-6-mercapto derivative, thioguanine, which we had previously found to have strong antimetabolic activity. Attempts were then made to protect the sulfur from oxidation and hydrolysis by blocking groups which might be removed intracellularly to release 6-MP, hopefully by some tumor-specific enzyme. The most successful compound to emerge from this approach was the *S*-(1-methyl-4-nitroimidazol-5-yl) derivative. This compound, now known as azathioprine (Imuran®), acts as a pro-drug for 6-MP. Because of the proximity of the *ortho*-nitro group, azathioprine is subject to attack by sulfhydryl groups and other nucleophiles[45-49] (Fig. 2). In

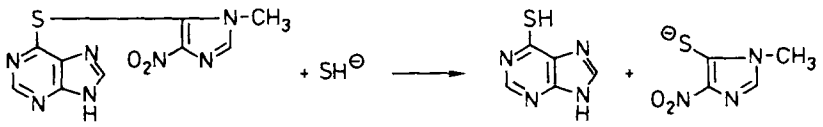


Fig. 2. Reaction of hydrogen sulfide with azathioprine to release 6-MP. Reproduced from [46] with permission.

particular, the glutathione present in red blood cells reacts with azathioprine, releasing 6-MP back into the plasma.[47] This compound had a better therapeutic index in mice bearing adenocarcinoma 755, being as active as 6-MP but less toxic.[50] In patients with leukemia, however, the chemotherapeutic index of 6-MP was similar to that of azathioprine.[51]

Imunosuppression and Transplantation

In 1958 a new horizon appeared. *Robert Schwartz*, working with *William Dameshek* in Boston, investigated the effect of 6-MP on the immune response, based on the rationale that the immunoblastic lymphocyte formed during an immune response closely resembled leukemic lymphocytes. *Schwartz* et al. showed that when 6-MP was administered to rabbits for several days, beginning with the time of injection of a foreign antigen (e.g., bovine serum albumin) the rabbits were unable to mount an antibody response to that antigen.[52] Schwartz and his co-workers worked out the importance of drug dose and timing and showed that 6-MP was most effective when treatment was started at the time of antigen administration.[52, 53] They also demonstrated that animals could be made tolerant to a particular antigen while still retaining immunological reactivity to other antigens.[54] At *Schwartz*'s instigation, we set up an immunological screening test that consisted of measuring the antibody response of mice to sheep red blood cells.[55, 56] It enabled us to identify new active agents and synergistic combinations of drugs and to show that immunosuppression was greater at higher doses of antigen and of drug.

Roy Calne, a young British surgeon, stimulated by the papers of *Schwartz* and his co-workers, decided to examine the effect of 6-MP on kidney transplant rejection in dogs. He obtained a 44-day survival of a kidney from an unrelated donor in a dog given daily doses of 6-MP.[57] This was considerably longer than the expected 9- to 10-day graft survival in control animals. When *Calne* asked us for compounds related to 6-MP which he might investigate, we suggested that azathioprine might have some advantages. The following studies showed azathioprine to be superior to 6-MP for preventing rejection of canine kidney homografts.[58, 59] Successful transplantation of kidneys to unrelated recipients became a reality in man in 1962, with regimens of immunosuppression consisting of azathioprine and prednisone.[60] By 1977, the Kidney Registry had records of 25000 kidney transplants done between 1965 and 1972[61] and the number of transplants done each year has continued to increase.[62, 63] Today the procedure is considered therapeutic rather than experimental, and the importance of histocompatibility matching is recognized.[63] Other organ transplants (e.g., liver, heart, and lung) have likewise become possible. Other immunosuppressive drugs (e.g., cyclosporin) have come into use in recent years, but azathioprine remains a mainstay in kidney transplantation.

The immunosuppressive effects of azathioprine have been studied in a wide variety of immunological systems. The earlier work is reviewed in Ref. [64] and more recent studies in Ref. [65]. Immunosuppressive drugs have also shown utility in the treatment of autoimmune disease. Remissions with 6-MP, thioguanine, and azathioprine have been reported in autoimmune hemolytic anemia, systemic lupus, and chronic active hepatitis.[65] Azathioprine is now an approved drug for the treatment of severe rheumatoid arthritis.[66]

Gout and Hyperuricemia

It was time now to try a new approach to the potentiation of 6-MP activity. Since we knew from metabolic studies that 6-thiouric acid was one of the principal products of 6-MP catabolism, it seemed possible that we could interfere with this oxidation by inhibiting the enzyme responsible for it, xanthine oxidase. In the early days of seeking antimetabolites for the natural purines in our laboratory, xanthine oxidase had been one of the test enzymes. *Doris Lorz* had identified many substrates as well as inhibitors of this enzyme.[7] These compounds had also been tested on *L. casei* and on animal tumors. To test for xanthine oxidase inhibition in vivo, we chose a compound that had no inhibitory effects on bacteria or tumors and was nontoxic, but which was a potent inhibitor of xanthine oxidase. This compound was the hypoxanthine analogue 4-hydroxypyrazolo[3,4-*d*]pyrimidine (allopurinol). When allopurinol was given to mice together with 6-MP, it did indeed inhibit the oxidation of 6-MP and potentiated the antitumor and immunosuppressive properties of 6-MP three- to fourfold.[45, 67, 68] Moreover, the toxicity of 6-MP to mice appeared to be potentiated only twofold, so that the chemotherapeutic index of 6-MP had been in-

creased. Was it possible that the same phenomenon would occur in man? With the collaboration of *Wayne Rundles*, we explored this possibility in patients with chronic granulocytic leukemia, in whom the efficacy and metabolism of 6-MP could be investigated. As had happened in mice, the oxidation of 6-MP to thiouric acid (TU) was inhibited in a dose-related manner and the antileukemic activity of 6-MP was potentiated proportionally.[45, 69–71] Figure 3 illustrates the

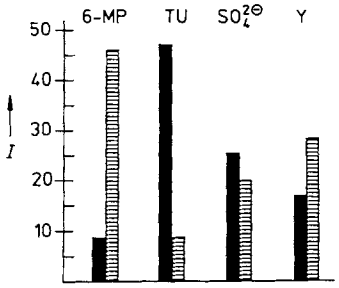


Fig. 3. Radioactive metabolites in the urine following administration of 110 mg of [35S]6-MP to a patient with (▤) and without (■) 300 mg of allopurinol. Reproduced from [71] with permission. Y = other metabolites, I = percent of radioactivity in urine.

fourfold reduction in TU and increase in 6-MP when 300 mg of allopurinol was given together with 110 mg of 6-MP. Later investigations[72] showed that the increased activity of 6-MP was accompanied by a proportional increase in toxicity. Thus, although less 6-MP was required to produce an antileukemic effect, the therapeutic index of 6-MP for leukemia remained unchanged.

Xanthine oxidase is responsible not only for the oxidation of 6-MP, but also for the formation of uric acid from hypoxanthine and xanthine (Fig. 4). Consequently, treatment

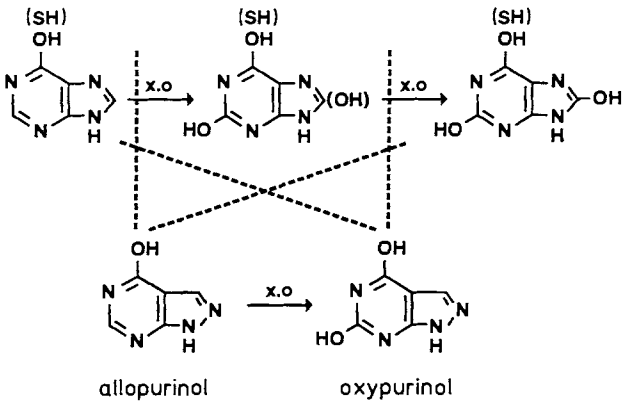


Fig. 4. Pathways in the oxidation of hypoxanthine and 6-MP by xanthine oxidase (x.o.) inhibited by allopurinol and oxypurinol. For 6-MP, the intermediate is 8-hydroxy-6-MP; for hypoxanthine, the intermediate is 2,6-dihydroxypurine (xanthine).

with allopurinol produces a marked decrease in both serum and urinary uric acid.[69, 71, 73, 74] This presented the possibility of a unique approach to the treatment of gout and other forms of hyperuricemia.

It was recognized at the outset that the inhibition of an enzyme like xanthine oxidase in vivo might present some difficulties. First, there was the question as to whether the inhibitor had a sufficiently long half-life in the body to produce a persistent reduction in uric acid production. There was also the possibility that the inhibition would result in an unacceptable accumulation of the intermediates hypoxanthine and xanthine, the latter compound being about as insoluble as uric acid. Moreover, it was possible that more enzyme would be induced by the presence of excess amounts of the intermediates, leading to the need for ever-increasing amounts of inhibitor. Finally, one had to consider carefully the long-term effects of this inhibitor, since gout patients would probably continue to take the drug for life. All of these possibilities were thoroughly examined, first in animals and then in man.

Allopurinol is not only a potent competitive inhibitor of xanthine oxidase but also a substrate,[75] its oxidation resulting in the corresponding xanthine analogue, oxypurinol (called alloxantine, oxoallopurinol, or oxipurinol in early papers), which is also a xanthine oxidase inhibitor (Fig. 4). Oxypurinol also has the unusual property of binding very tightly to the reduced form of the enzyme, thereby inactivating it.[75, 76]. The enzyme activity can be restored by oxidation, which takes place slowly in the presence of air.[76, 77] Allopurinol itself has a short half-life in plasma (about 90 to 120 minutes). However, oxypurinol has a very long half-life of 18 to 30 hours,[75, 78, 79] because it is reabsorbed in the proximal tubule of the kidney.[80] Consequently, steady-state levels of oxypurinol are achieved in a few days and uric acid concentrations can be maintained at the desired level by proper dose adjustment.[80] Because allopurinol is completely absorbed orally, whereas oxypurinol is not, allopurinol remains the ideal pro-drug for oxypurinol.

The fate of the intermediate oxypurines, hypoxanthine and xanthine, turned out to be a fascinating one. These oxypurines do not accumulate in the serum. In fact, their serum levels rise very little during allopurinol treatment[79, 81] for two reasons. First, hypoxanthine and xanthine can be reutilized for nucleic acid synthesis via the enzyme hypoxanthine-guanine phosphoribosyltransferase (HGPRT).[82, 83] The nucleotides formed, IMP and XMP, are the normal intermediates for adenine and guanine nucleotides (AMP, GMP). Second, through a process of feedback inhibition, IMP, AMP, and GMP can reduce the de novo synthesis of purines by inhibiting PRPP-amidotransferase.[84] Thus, the salvage of hypoxanthine and xanthine serves to regulate purine biosynthesis, reducing it when it is excessive. When the oxypurines are not reutilized, they are excreted by the kidney by glomerular filtration, since they are not reabsorbed by the kidney tubule to any significant degree.[85, 86]

Long-term studies with allopurinol in animals and in man have shown that new enzyme is not induced and that allopurinol is a safe and effective drug for long-term treatment.[87] A few percent of patients develop a rash when taking allopurinol. Patients with poor kidney function require lower doses of drug because of the pharmacological properties of oxypurinol and its long half-life.[88]

Allopurinol helps to alleviate several of the clinical problems associated with gout. The hyperuricemia of gout produces deposits of small crystals of uric acid in joints, which result in extreme pain, or large deposits, tophi, which result in gouty arthritis and restricted joint movement. In patients who excrete excessive amounts of uric acid in the urine, urate stones often form in the kidney. With allopurinol it has been possible to prevent and reduce the tophaceous deposits and

to prevent urate stone formation.[74, 81, 87, 89, 90] Likewise, the secondary hyperuricemia associated with the therapy of malignancy can be reduced with allopurinol treatment.[91]

Antiprotozoal Effects of Allopurinol

I would like to digress at this point, to describe another use for allopurinol which materialized about 10 years later, because it typifies the kind of chemotherapeutic selectivity which can be achieved with purine analogues as the result of differences in the specificities of parasitic and mammalian enzymes. The finding by *Joseph Marr* et al.[92] that allopurinol inhibits the replication of *Leishmania donovani* led us into an extended collaboration with *Marr* to discover the biochemical basis for this unexpected activity.[93–101] Leishmaniae and trypanosomes, like many other unicellular parasites, lack the ability to synthesize purines de novo. They do, however, have ample quantities of salvage enzymes which enable them to utilize preformed purines and nucleosides present in the mammalian blood stream. Leishmaniae and trypanosomes have large amounts of the enzyme HGPRT capable of utilizing allopurinol as a substrate to a much greater extent than does the human enzyme.[97] Moreover, the enzyme adenylosuccinate synthetase, which has as its function the conversion of IMP to sAMP, the intermediate for AMP, has a broader substrate specificity than does the mammalian enzyme.[96, 101] The protozoal enzymes consequently convert allopurinol ribonucleotide into the adenylate analogue, 4-aminopyrazolo[3,4-*d*]pyrimidine ribonucleotide, which is then converted into a di- and triphosphate and incorporated into RNA.[93, 94, 98, 100] In the mammalian host this amination does not occur and allopurinol is not incorporated into nucleic acids.[102] The differences in the metabolism of allopurinol by the mammalian host and the trypanosomes are illustrated in Figure 5. Allopurinol has shown activity in the treatment of Leshmaniasis[103] and of Chagas' disease (caused by *Trypanosoma cruzi*).[104]

Allopurinol riboside, a minor urinary metabolite of allopurinol in man, can likewise be converted by leishmaniae in this way,[94] whereas allopurinol riboside is not further metabolized in man.

Antiviral Drugs

In 1968 we decided to return to a path that had intrigued us as early as 1948, the path to antivirals. The antiviral activity of 2,6-diaminopurine (DAP) had been provocative,[22] although its toxicity had been discouraging. Meanwhile, the pursuit of 6-MP, thioguanine (TG), azathioprine, and allopurinol had occupied 20 years. When it was discovered that adenine arabinoside (ara-A) inhibited the growth of both DNA and RNA viruses,[105] the information started a train of thought. Would the arabinoside of DAP (ara-DAP) be equally active? After all, DAP had mimicked adenine in many reactions and could be converted into a nucleoside and nucleotide by adenine-metabolizing enzymes. Moreover, diaminopurine riboside was a poorer substrate for adenosine deaminase than was adenosine. It therefore seemed possible that ara-DAP might persist longer than ara-A, a compound which is rapidly deaminated in vivo.

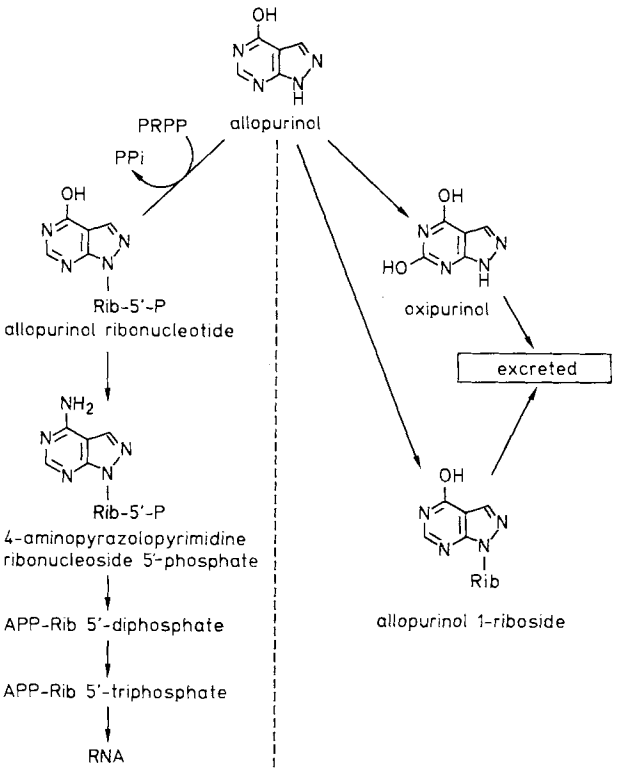


Fig. 5. Metabolic pathways of allopurinol in trypanosoma (left) and man (right).

Diaminopurine arabinoside was synthesized by *Janet Rideout*, and, since we did not have a virus laboratory on site at the time, we sent the compound to our colleague, *John Bauer*, in the Wellcome Research Laboratories in the U.K. for antiviral screening. In a few weeks he informed us that this compound was highly active against both herpes simplex virus and vaccinia virus. Moreover, the compound was less cytotoxic to mammalian cells than ara-A. Thus began our antiviral odyssey. For several years my group pursued studies on the purine arabinosides, exploring structure–activity relationships, seeking better synthetic methods, and doing metabolic studies in mice.[106] *Bauer* and *Collins* studied the activity of these compounds in rabbits and mice.[106] We found that ara-DAP was deaminated to guanine arabinoside in mice and that the guanine derivative (ara-G) was as active an antiviral as ara-DAP. In this respect, ara-G had an advantage over the deamination product of ara-A, hypoxanthine arabinoside, which had very poor antiviral activity. We were not certain whether this advantage was sufficient to warrant the full-scale development of ara-DAP.

In 1970 our laboratories moved to North Carolina and *Howard Schaeffer* joined us as head of the Organic Chemistry Department. He had been studying analogues of adenosine as substrates and inhibitors of the enzyme adenosine deaminase, and he had examined a variety of acyclic side chains on the 9-position of adenine to determine what changes the enzyme would tolerate in a substrate.[107] He found that 9-{(2-hydroxyethoxy)methyl}adenine could still serve as a substrate for adenosine deaminase. This suggested that other enzymes might also recognize such a side chain as a pentose and that nucleoside analogues of this kind might have antimetabolite properties.

When the acyclic adenosine analogue was tested in the antiviral screen, it showed antiherpetic activity in vitro at about twice the concentration of ara-A. The antiviral program now concentrated on the acyclic nucleoside analogues, with the syntheses conducted by *Schaeffer* and *Beauchamp*, the antiviral testing by *Bauer* and *Collins*, and the mechanisms of action, enzymology, and in vivo metabolism by my group.[108, 109] As was the case with the purine arabinosides, the DAP analogue proved highly active on herpes simplex virus in vivo as well as in vitro. However, unexpectedly, the guanine analogue, acyclovir (ACV, acycloguanosine), was over 100 times as active as the diamino compound.[109] Acyclovir is a metabolic product of the DAP derivative, formed by the action of adenosine deaminase and is undoubtedly responsible for the antiviral activity of the diamino compound observed in vivo.[110–112]

Acyclovir

One of the most intriguing aspects of the antiviral activity of ACV is not only its high potency but its unusual degree of selectivity (Fig. 6).[108, 109, 113–115] It is highly active against

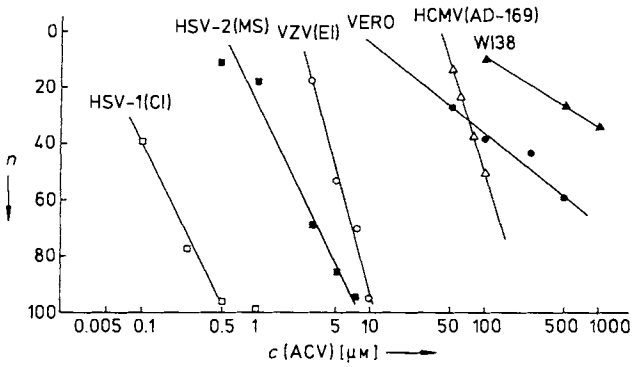


Fig. 6. Dose–response curves of various viruses and cells to ACV. Reproduced from [108] with permission. n = percent inhibition, c = concentration.

herpes simplex virus, types 1 and 2 (HSV-1 and HSV-2), and varicella-zoster (chicken pox) virus. It has activity against several other herpes-type viruses, for example, Epstein-Barr virus (EBV) and pseudorabies virus, but only slight activity against the human cytomegalovirus (HCMV). It is not cytotoxic to the mammalian cells in which these viruses are grown at concentrations hundreds of times greater than those required for antiviral activity. Moreover, the compound is inactive against other DNA viruses (e.g., vaccinia virus) as well as RNA viruses.[109]

We decided that it was highly important to determine the reason for this unusual selectivity, since this would undoubtedly offer exploitable information about the herpes viruses. In order to do these biochemical studies effectively, we set up a virus laboratory in-house with *Phillip Furman* as its head. Radioactive ACV labeled in the 8-position of the guanine with ^{14}C or with ^{3}H in the side chain was synthesized. Vero cells, uninfected or infected with HSV-1, were incubated with both types of radioactive ACV for seven hours. Extracts of these cells were then examined by high-pressure liquid chromatography. The extracts of the uninfected cells showed only the presence of unchanged ACV. In the HSV-infected cells three new radioactive compounds were formed.[108] These products were identified by enzymatic methods as the mono-, di-, and triphosphates of ACV (ACV-MP, ACV-DP, ACV-TP), and this was later confirmed by comparison with authentic synthetic samples.

The enzyme responsible for the conversion of ACV to its monophosphate was laboriously isolated, purified, and identified by *James Fyfe* as a herpesvirus-specified thymidine kinase.[108, 116] While this enzyme had been reported to be formed in herpesvirus-infected cells, it was unexpected that an acyclic nucleoside of guanine could serve as its substrate. A similar enzyme is specified by the varicella-zoster virus. Once the first phosphate has been added, the second phosphate is added by cellular guanylate kinase,[117] while several other cellular kinases can add the third phosphate.[118] Since the cellular thymidine kinase cannot use ACV as a substrate, very little ACV-TP is formed in uninfected cells.[108, 119] The small amount of phosphorylation that occurs in normal cells is due to a 5′-nucleotidase.[120] The pathways for the formation of ACV-TP are shown in Figure 7.

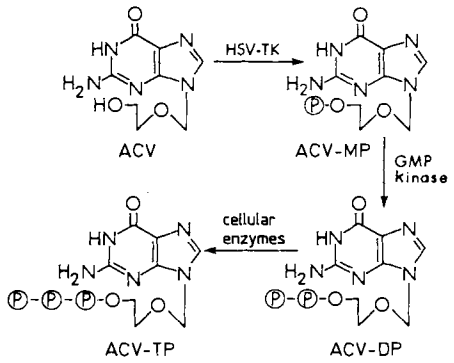


Fig. 7. Pathways for the formation of ACV mono-, di-, and triphosphate. Reproduced from [108] with permission.

When it was apparent that the active antiviral compound was ACV-TP, the interaction of this compound with viral and cellular DNA polymerases was investigated. ACV-TP proved to be a more potent inhibitor of the herpes virus DNA polymerase than of cellular DNA polymerase-α.[121, 122] The quantitative aspects of these differences in the amounts of ACV-TP formation and DNA polymerse inhibition (K_i value) by ACV-TP in virus-infected cells and uninfected cells are illustrated in Figure 8.[123] Moreover, ACV-TP serves as a substrate for the herpes virus DNA polymerase, but chain termination occurs when it is incorporated, because of the absence of the 3′-hydroxyl group needed for chain elongation.[113] Thus, only very small fragments of viral DNA are formed.[124] In addition, ACV-TP not only inhibits but also inactivates the viral DNA polymerase following the formation of the enzyme–template–ACV-MP complex.[125] This inactivation does not occur with cellular DNA polymerase.

The high selectivity of ACV for those herpes viruses that induce a herpes-specified thymidine kinase can thus be explained. This enzyme has proved to be a very useful tool for determining the structural requirements for other potential substrates of this enzyme.[126] Its absence or alteration also explains the resistance of some herpes virus isolates to ACV.[127–129] On the other hand, transfection of cells with

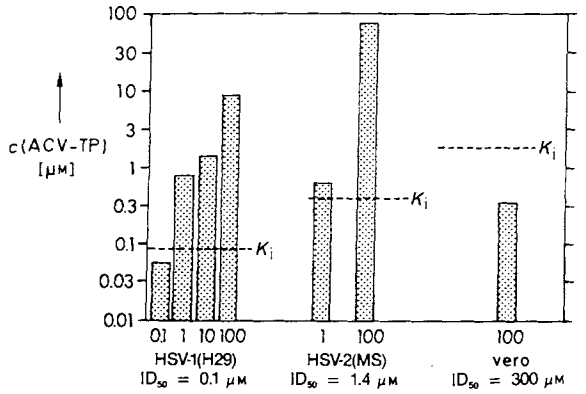


Fig. 8. Amounts of ACV-TP formed in uninfected Vero cells and in HSV-1- and HSV-2-infected Vero cells in the presence of varying concentrations of ACV. Dotted lines represent the K_i values for the individual DNA polymerases. ID_{50} values are concentrations for 50% inhibition of plaque formation. Reproduced from [123] with permission.

a portion of the herpesvirus genome containing the HSV thymidine kinase gene transforms normally resistant cells into ACV-sensitive cells.[130] Resistance to ACV may also result from mutations in the viral DNA polymerase.[127-129]

Epstein-Barr virus and HCMV infection do not induce a specific kinase capable of phosphorylating ACV. However, the DNA polymerase of Epstein-Barr virus is exquisitely sensitive to the small amount of ACV-TP formed in EBV-infected cells.[131] Interestingly, although HCMV-infected cells do not phosphorylate ACV to any extent, they do phosphorylate the closely related ACV derivative, ganciclovir (formerly called BW B759U, DHPG, or 2'NDG), which has an extra hydroxymethyl group on the side chain. Consequently, ganciclovir has proven to be a much better inhibitor of HCMV replication than ACV.[132-134]

Investigation of the pharmacokinetics and metabolism of ACV first in several animal species and then in man revealed that it was a remarkably stable compound. Only two metabolites were found, 9-{(2-carboxymethoxy)methyl}guanine (CMMG) and 8-hydroxyacyclovir.[135] In man, the carboxy derivative CMMG accounted for 9-14% of an intravenous dose of ACV, while essentially none of the 8-hydroxy metabolite appeared in the urine.[136,137] In other species there were somewhat increased amounts of both metabolites.[135,137,138] Acyclovir has a plasma half-life of approximately three hours,[139] so that an intravenous infusion is generally given every eight hours. Because ACV is excreted at about twice glomerular filtration rate and has a limited solubility in water (2.5 mg mL^{-1} at 37 °C), it is administered as a one-hour intravenous infusion rather than as a bolus injection. The compound is also active topically and orally. Although the oral bioavailability is limited, the blood levels attained by oral administration of ACV are adequate for therapeutic efficacy against herpes simplex and varicella-zoster viruses.[140]

The compound is distributed in all body tissues and crosses the blood-brain barrier.[109,135,141] Toxicology studies in mice, rats, and dogs showed the drug to be nontoxic at doses well above those required for therapeutic efficacy.[142]

Acyclovir has now been in clinical use for about eight years and it seems appropriate to mention some of the areas in which it has decreased suffering and saved lives. First episodes of genital herpes infections are characterized by pain, prolonged viral excretion, and slow healing of lesions. Acyclovir, given by either the intravenous or oral routes, produces a significant alleviation of symptoms and decreases the time of viral shedding and time to healing (Table 1).[143]

Table 1. Effect of ACV on first episodes of genital herpes.

Route of application	Median duration in days (ACV/placebo) Virus shedding	Pain	Healing	Ref.
i.v.	2/13	3/7	9/21	[144]
p.o.	1/13	4/8	6/11	[145]
p.o. [a]	3.9/13.4	2.8/3.4	9.5/13.7	[146]

[a] Women only; mean duration.

Recurrent episodes of genital herpes are generally much shorter and less severe than the initial one. Therefore, the benefits of ACV treatment appear to be less dramatic. However, in a study in which patients initiated oral therapy, there was a significant difference in new lesion formation, 23% on placebo, 6.5% on ACV.[147] For patients with frequently recurring genital herpes (e.g., once a month) of several years duration, it has been possible to decrease the frequency of recurrence to a mean of 1.8 episodes during the first year and 1.4 episodes during the second year by oral prophylaxis with ACV.[148] The percentage of patients having no recurrences in a year of oral prophylactic therapy was 45-50%.[149]

Herpes zoster, commonly known as shingles, is caused by a reactivation of latent varicella-zoster virus. It produces severe pain during the acute two-to-three-week episode, as well as a post-herpetic neuralgia months later in about 10 percent of patients. Acyclovir causes a significant decrease in the duration of acute pain but has little effect on the post-herpetic neuralgia.[150] In immunocompromised individuals, herpes zoster can produce serious sequelae in the form of progressive skin dissemination and visceral disease. The latter can be fatal in a small percentage of patients. Intravenous treatment with ACV has effectively prevented this dissemination.[151]

Herpes simplex infections in immunosuppressed individuals is a serious medical problem. Virus continues to be shed for a long time and healing is slow. In two studies that involved 97 immunocompromised patients[152] with a variety of diseases and 34 bone marrow transplant recipients,[153] the effects of intravenous ACV treatment on viral shedding, pain, and time to healing were highly significant (Table 2). In

Table 2. Effect of intravenous ACV on HSV infections in immunocompromised patients.

Patients	Median duration in days (ACV/placebo) Virus shedding	Pain	Healing
All (97)	2.8/16.8	8.9/13.1	13.7/20.1
Bone marrow transplants (34)	3/17	10/16	14/28

bone marrow transplant patients and in leukemic patients, prophylaxis with ACV has made it possible to prevent the reactivation of latent virus during therapy, so that the patients can remain free of herpetic episodes during the period of maximum immunosuppression.[154,155] The treatment of herpes encephalitis, a frequently fatal disease, with intra-

venous ACV has been successful in a large percentage of patients if begun before the patient is comatose.[156, 157]

In addition to the clinical utility of ACV, the lessons learned from its development have proven to be extremely valuable for subsequent antiviral research. In-depth studies of mechanisms of action have led to a better understanding of the enzymatic differences between normal and virus-infected cells and have given impetus to the search for other viral-specific enzymes which are capable of therapeutic application.

Outlook

In my attempt to cover 40 years of research on purines and purine analogues, I have been able to give you only a bird's eye view. However, I hope that I have successfully conveyed our philosophy that chemotherapeutic agents are not only ends in themselves but also serve as tools for unlocking doors and probing Nature's mysteries. This approach has served us well and has led into many new areas of medical research. Selectivity remains our aim and understanding its basis our guide to the future.

Received: January 27, 1989 [A 722 IE]
German version: *Angew. Chem. 101* (1989) 893

[1] D. D. Woods, *Br. J. Exp. Pathol. 21* (1940) 74.
[2] P. Fildes, *Lancet 1940 I*, 955.
[3] G. H. Hitchings, G. B. Elion, E. A. Falco, P. B. Russell, M. B. Sherwood, H. VanderWerff, *J. Biol. Chem. 183* (1950) 1.
[4] G. H. Hitchings, G. B. Elion, E. A. Falco, P. B. Russell, H. VanderWerff, *Ann. N. Y. Acad. Sci. 52* (1950) 1318.
[5] H. M. Kalckar, *J. Biol. Chem. 167* (1947) 461.
[6] G. H. Hitchings, E. A. Falco, *Proc. Natl. Acad. Sci. USA 30* (1944) 294.
[7] D. C. Lorz, G. H. Hitchings, *Fed. Proc. Fed. Am. Soc. Exp. Biol. 9* (1950) 197.
[8] R. B. Angier, J. H. Boothe, B. L. Hutchings, J. H. Mowat, J. Semb, E. L. R. Stokstad, Y. Subbarow, C. W. Waller, D. B. Cosulich, M. J. Fahrenbach, M. E. Hultquist, E. Kuh, E. H. Northey, D. R. Seeger, J. P. Stickels, J. M. Smith, *Science (Washington) 103* (1946) 667.
[9] G. H. Hitchings, E. A. Falco, M. B. Sherwood, *Science (Washington) 102* (1945) 251.
[10] G. B. Elion, G. H. Hitchings, *J. Biol. Chem. 185* (1950) 651.
[11] G. H. Hitchings, G. B. Elion,, H. VanderWerff, E. A. Falco, *J. Biol. Chem. 174* (1948) 765.
[12] G. H. Hitchings, G. B. Elion, H. VanderWerff, *J. Biol. Chem. 174* (1948) 1037.
[13] H. C. Carrington, *J. Chem. Soc. 1944*, 124.
[14] G. B. Elion, E. Burgi, G. H. Hitchings, *J. Am. Chem. Soc. 74* (1952) 411.
[15] G. B. Elion, G. H. Hitchings, *J. Am. Chem. Soc. 77* (1955) 1676.
[16] G. B. Elion, G. H. Hitchings, *J. Biol. Chem. 187* (1950) 511.
[17] G. B. Elion, H. VanderWerff, G. H. Hitchings, M. E. Balis, D. H. Levin, J. B. Brown, *J. Biol. Chem. 200* (1953) 7.
[18] A. Kornberg, I. Lieberman, E. S. Simms, *J. Biol. Chem. 215* (1955) 417.
[19] J. H. Burchenal, A. Bendich, J. B. Brown, G. B. Elion, G. H. Hitchings, C. P. Rhoads, C. C. Stock, *Cancer (Philadelphia) 2* (1949) 119.
[20] J. J Biesele, R. E. Berger, A. Y. Wilson, G. H. Hitchings, G. B. Elion, *Cancer (Philadelphia) 4* (1951) 186.
[21] J. H. Burchenal, D. A. Karnofsky, E. M. Kingsley-Pillers, C. M. Southam, W. P. L. Myers, G. C. Escher, L. F. Craver, W. Dargeon, C. P. Rhoads, *Cancer (Philadelphia) 4* (1951) 549.
[22] R. L. Thompson, M. L. Wilkin, G. H. Hitchings, G. B. Elion, E. A. Falco, P. B. Russell, *Science (Washington) 110* (1949) 454; R. L. Thompson, M. L. Price, S. A. Menton, Jr., G. B. Elion, G. H. Hitchings, *J. Immunol. 65* (1950) 529.
[23] G. B. Elion, G. H. Hitchings, H. VanderWerff, *J. Biol. Chem. 192* (1951) 505.
[24] D. A. Clarke, F. S. Phillips, S. S. Sternberg, C. C. Stock, G. B. Elion, G. H. Hitchings, *Cancer Res. 13* (1953) 593.
[25] F. S. Philips, S. S. Sternberg, L. Hamilton, D. A. Clarke, *Ann. N. Y. Acad. Sci. 60* (1954) 283.
[26] J. H. Burchenal, M. L. Murphy, R. R. Ellison, M. P. Sykes, C. T. C. Tan, L. A. Leone, D. A. Karnofsky, L. F. Craver, H. W. Dargeon, C. P. Rhoads, *Blood 8* (1953) 965.
[27] C. P. Rhoads (Ed.): *6-Mercaptopurine* (*Ann. N. Y. Acad. Sci. 60* (1954) 183).
[28] G. B. Elion, S. Singer, G. H. Hitchings, *Ann. N. Y. Acad. Sci. 60* (1954) 200.
[29] G. B. Elion, S. Singer, G. H. Hitchings, *J. Biol. Chem. 204* (1953) 35.
[30] M. E. Balis, D. H. Levin, G. B. Brown, G. B. Elion, H. C. Nathan, G. H. Hitchings, *Arch. Biochem. Biophys. 71* (1957) 358.
[31] a) G. E. W. Wolstenholme, C. M. O'Connor (Eds.): *The Chemistry and Biology of Purines*, Churchill, London 1957; b) G. R. Greenberg, L. Jaenicke in [31a] pp. 204–232.
[32] J. M. Buchanan, J. G. Flaks, S. C. Hartman, B. Levenberg, L. N. Lukens, L. Warren in [31a], pp. 233–252.
[33] J. M. Buchanan, S. C. Hartman, *Adv. Enzymol. Relat. Subj. Biochem. 21* (1959) 199.
[34] G. H. Hitchings, G. B. Elion in I. Brodsky, S. B. Kahn, J. H. Moyer (Eds.): *Cancer Chemotherapy II, Twenty-Second Hahnemann Symposium*, Grune & Stratton, New York 1972, pp. 23–32.
[35] G. B. Elion: *Pharmacological Basis of Cancer Chemotherapy*, Williams & Wilkins, Baltimore 1975, pp. 547–564.
[36] G. B. Elion, S. Bieber, G. H. Hitchings, *Ann. N. Y. Acad. Sci. 60* (1954) 297.
[37] L. Hamilton, G. B. Elion, *Ann. N. Y. Acad. Sci. 60* (1954) 304.
[38] G. B. Elion, *Proc. R. Soc. Med. 50* (1957) 7.
[39] D. A. Clarke, G. B. Elion, G. H. Hitchings, C. C. Stock, *Cancer Res. 18* (1958) 445.
[40] G. B. Elion, I. Goodman, W. Lange, G. H. Hitchings, *J. Am. Chem. Soc. 81* (1959) 1898.
[41] G. B. Elion, S. Bieber, G. H. Hitchings, *Cancer Chemother. Rep. 8* (1960) 36.
[42] G. B. Elion, S. W. Callahan, G. H. Hitchings, R. W. Rundles, *Cancer Chemother. Rep. 8* (1960) 47.
[43] G. B. Elion, S. W. Callahan, G. H. Hitchings, R. W. Rundles, *Proc. Int. Congr. Hematol. 8th 1960* (1962) 642–645.
[44] G. B. Elion, S. Mueller, G. H. Hitchings, *J. Am. Chem. Soc. 81* (1959) 3042.
[45] G. B. Elion, S. Callahan, R. W. Rundles, G. H. Hitchings, *Cancer Res. 23* (1963) 1207.
[46] G. B. Elion, *Fed. Proc. Fed. Am. Soc. Exp. Biol. 26* (1967) 898.
[47] P. deMiranda, L. M. Beacham III, T. H. Creagh, G. B. Elion, *J. Pharmacol. Exp. Ther. 187* (1973) 588.
[48] G. B. Elion, G. H. Hitchings, *Handb. Exp. Pharmacol. 38* (1975) 404–425.
[49] P. deMiranda, L. M. Beacham III, T. H. Creagh, G. B. Elion, *J. Pharmacol. Exp. Ther. 195* (1975) 50.
[50] G. B. Elion, S. Callahan, S. Bieber, R. W. Rundles, *Cancer Chemother. Rep. 14* (1961) 93.
[51] R. W. Rundles, J. Laszlo, T. Itoga, G. B. Hobson, F. E. Garrison, Jr., *Cancer Chemother. Rep. 14* (1961) 99.
[52] R. Schwartz, J. Stack, W. Dameshek, *Proc. Soc. Exp. Biol. Med. 99* (1958) 164.
[53] D. Chanmougan, R. S. Schwartz, *J. Exp. Med. 124* (1966) 363.
[54] R. Schwartz, W. Dameshek, *Nature (London) 183* (1959) 1682.
[55] H. C. Nathan, S. Bieber, G. B. Elion, G. H. Hitchings, *Proc. Soc. Exp. Biol. Med. 107* (1961) 796.
[56] S. Bieber, G. B. Elion, G. H. Hitchings, D. C. Hooper, H. C. Nathan, *Proc. Soc. Exp. Biol. Med. 111* (1962) 334.
[57] R. Y. Calne, *Lancet 1960 I*, 417.
[58] R. Y. Calne, *Transplant. Bull. 28* (1961) 65.
[59] R. Y. Calne, G. P. J. Alexandre, J. E. Murray, *Ann. N. Y. Acad. Sci. 99* (1962) 743.
[60] J. E. Murray, J. P. Merrill, J. H. Harrison, R. E. Wilson, G. J. Dammin, *N. Engl. J. Med. 268* (1963) 1315.
[61] Advisory Committee to the Renal Transplant Registry: *The Twelfth Report of the Human Renal Transplant Registry (JAMA J. Am. Med. Assoc. 233* (1975) 787).
[62] S. T. Perdue, P. I. Terasaki, S. Cats, M. R. Mickey, *Transplantation 36* (1983) 658.
[63] H. Takiff, D. J. Cook, N. S. Himaya, M. R. Mickey, P. I. Terasaki, *Transplantation 45* (1988) 410.
[64] G. H. Hitchings, G. B. Elion, *Pharmacol. Rev. 15* (1963) 365.
[65] G. Wolberg, *Handb. Exp. Pharmacol. 85* (1988) 517–533.
[66] T. Hunter, M. B. Urowitz, D. A. Gordon, H. A. Smythe, M. A. Ogryzlo, *Arthritis Rheum. 18* (1975) 15.
[67] G. B. Elion, S. W. Callahan, G. H. Hitchings, R. W. Rundles, J. Laszlo, *Cancer Chemother. Rep. 16* (1962) 197.
[68] G. B. Elion, S. Callahan, H. Nathan, S. Bieber, R. W. Rundles, G. H. Hitchings, *Biochem. Pharmacol. 12* (1963) 85.
[69] R. W. Rundles, J. B. Wyngaarden, G. H. Hitchings, G. B. Elion, H. R. Silberman, *Trans. Assoc. Am. Physicians 76* (1963) 126.
[70] R. W. Rundles, *Ann. Rheum. Dis. 25* (1966) 615.

[71] G. H. Hitchings, G. B. Elion, *Cancer Res. 45* (1985) 2415.
[72] W. R. Vogler, J. A. Bain, C. M. Huguley, Jr., H. G. Palmer, Jr., M. E. Lowrey, *Am. J. Med. 40* (1966) 548.
[73] G. H. Hitchings, *Ann. Rheum. Dis. 25* (1966) 601.
[74] J. T. Scott (Ed.): *Symposium on Allopurinol (Ann. Rheum. Dis. 25* (1966) 599).
[75] G. B. Elion, *Ann. Rheum. Dis. 25* (1966) 608.
[76] V. Massey, H. Komai, G. Palmer, G. B. Elion, *J. Biol. Chem. 245* (1970) 2837.
[77] V. Massey, H. Komai, G. Palmer, G. B. Elion, *Vitam. Horm. (N.Y.) 28* (1970) 505.
[78] G. B. Elion, A. Kovensky, G. H. Hitchings, E. Metz, R. W. Rundles, *Biochem. Pharmacol. 15* (1966) 863.
[79] G. B. Elion, *Handb. Exp. Pharmacol. 51* (1978) 485–514.
[80] G. B. Elion, T.-F. Yü, A. B. Gutman, G. H. Hitchings, *Am. J. Med. 45* (1968) 69.
[81] T.-F. Yü, A. B. Gutman, *Am. J. Med. 37* (1964) 885.
[82] R. Pomales, S. Bieber, R. Friedman, G. H. Hitchings, *Biochim. Biophys. Acta 72* (1963) 119.
[83] R. Pomales, G. B. Elion, G. H. Hitchings, *Biochim. Biophys. Acta 95* (1965) 505.
[84] J. B. Wyngaarden, D. M. Ashton, *J. Biol. Chem. 234* (1959) 1492.
[85] S. Goldfinger, J. R. Klinenberg, J. E. Seegmiller, *J. Clin. Invest. 44* (1965) 623.
[86] J. R. Klinenberg, S. E. Goldfinger, J. E. Seegmiller, *Ann. Intern. Med. 62* (1965) 639.
[87] R. W. Rundles, *Arch Intern. Med. 145* (1985) 1492.
[88] a) A. Rapado, R. W. E. Watts, C. H. M. M. DeBruyn (Eds.): Purine Metabolism in Man III, Plenum, New York 1980; b) G. B. Elion, F. M. Benezra, T. D. Beardmore, W. N. Kelley in [88a] Part A, pp. 263–267.
[89] R. W. Rundles, E. Metz, H. R. Silberman, *Ann. Intern. Med. 64* (1966) 229.
[90] A. deVries, M. Frank, U. A. Liberman, O. Sperling, *Ann. Rheum. Dis. 25* (1966) 691.
[91] I. H. Krakoff, *Arthritis Rheum. 8* (1965) 896.
[92] M. A. Pfaller, J. J. Marr, *Antimicrob. Agents Chemother. 5* (1974) 469.
[93] D. J. Nelson, C. J. I. Bugge, G. B. Elion, R. L. Berens, J. J. Marr, *J. Biol. Chem. 254* (1979) 3959.
[94] D. J. Nelson, S. W. LaFon, J. V. Tuttle, W. H. Miller, R. L. Miller, T. A. Krenitsky, G. B. Elion, R. L. Berens, J. J. Marr, *J. Biol. Chem. 254* (1979) 11 544.
[95] J. Marr, R. Berens, D. Nelson, *Science (Washington) 201* (1978) 1018.
[96] T. Spector, T. E. Jones, G. B. Elion, *J. Biol. Chem. 254* (1979) 8422.
[97] T. A. Krenitsky, G. W. Koszalka, J. V. Tuttle, D. L. Adamczyk, G. B. Elion, J. J. Marr in [88a] Part B, pp. 271–276.
[98] R. L. Berens, J. J. Marr, D. J. Nelson, S. W. LaFon, *Biochem. Pharmacol. 29* (1980) 2397.
[99] S. W. LaFon, D. J. Nelson, R. L. Berens, J. J. Marr, *Biochem. Pharmacol. 31* (1982) 231.
[100] R. L. Berens, J. J. Marr, F. Steele De Cruz, D. J. Nelson, *Antimicrob. Agents Chemother. 22* (1982) 657.
[101] T. Spector, R. L. Berens, J. J. Marr, *Biochem. Pharmacol. 31* (1982) 225.
[102] D. J. Nelson, G. B. Elion, *Biochem. Pharmacol. 24* (1975) 1235.
[103] P. A. Kager, P. H. Rees, B. T. Wellde, W. T. Hockmeyer, W. H. Lyerly, *Trans. R. Soc. Trop. Med. Hyg. 75* (1981) 556.
[104] C. I. Meirovich, H. L. Montrull, R. H. Gallerano, R. R. Sosa, *Arq. Bras. Cardiol. 45* (1985) 217.
[105] F. M. Schabel, Jr., *Chemotherapy (Basel) 13* (1968) 321.
[106] G. B. Elion, J. L. Rideout, P. deMiranda, P. Collins, D. J. Bauer, *Ann. N. Y. Acad. Sci. 255* (1975) 468.
[107] H. J. Schaeffer, S. Gurwara, R. Vince, S. Bittner, *J. Med. Chem. 14* (1971) 367.
[108] G. B. Elion, P. A. Furman, J. A. Fyfe, P. deMiranda, L. Beauchamp, H. J. Schaeffer, *Proc. Natl. Acad. Sci. USA 74* (1977) 5716.
[109] H. J. Schaeffer, L. Beauchamp, P. deMiranda, G. B. Elion, D. J. Bauer, P. Collins, *Nature (London) 272* (1978) 583.
[110] S. S. Good, P. deMiranda, *Fed. Proc. Fed. Am. Soc. Exp. Biol. 41* (1982) 1733.
[111] H. C. Krasny, S. H. T. Liao, S. S. Good, B. Petty, P. S. Lietman, *Clin. Pharmacol. Ther. (St. Louis) 33* (1983) 256.
[112] T. Spector, T. E. Jones, L. M. Beacham III, *Biochem. Pharmacol. 32* (1983) 2505.
[113] G. B. Elion, *Am. J. Med. 73* (1982) 7.
[114] P. Collins, *J. Antimicrob. Chemother. 12 Suppl. B* (1983) 19.
[115] G. B. Elion, *J. Antimicrob. Chemother. 12 Suppl. B* (1983) 9.
[116] J. A. Fyfe, P. M. Keller, P. A. Furman, R. L. Miller, G. B. Elion, *J. Biol. Chem. 253* (1978) 8721.
[117] W. H. Miller, R. L. Miller, *J. Biol. Chem. 255* (1980) 7204.
[118] W. H. Miller, R. L. Miller, *Biochem. Pharmacol. 31* (1982) 3879.
[119] P. A. Furman, P. deMiranda, M. H. St. Clair, G. B. Elion, *Antimicrob. Agents Chemother. 20* (1981) 518.
[120] P. M. Keller, S. A. McKee, J. A. Fyfe, *J. Biol. Chem. 260* (1985) 8664.
[121] P. A. Furman, M. H. St. Clair, J. A. Fyfe, J. L. Rideout, P. M. Keller, G. B. Elion, *J. Virol. 32* (1979) 72.
[122] M. H. St. Clair, P. A. Furman, C. M. Lubbers, G. B. Elion, *Antimicrob. Agents Chemother. 18* (1980) 741.
[123] G. B. Elion in J. Mills, L. Corey (Eds.): *Antiviral Chemotherapy: New Directions for Clinical Application and Research*, Elsevier, New York 1986, pp. 118–137.
[124] P. V. McGuirt, J. E. Shaw, G. B. Elion, P. A. Furman, *Antimicrob. Agents Chemother. 25* (1984) 507.
[125] P. A. Furman, M. H. St. Clair, T. Spector, *J. Biol. Chem. 259* (1984) 9575.
[126] P. M. Keller, J. A. Fyfe, L. Beauchamp, C. M. Lubbers, P. A. Furman, H. J. Schaeffer, G. B. Elion, *Biochem. Pharmacol. 30* (1981) 3071.
[127] L. E. Schnipper, C. S. Crumpacker, *Proc. Natl. Acad. Sci. USA 77* (1980) 2270.
[128] P. A. Furman, D. M. Coen, M. H. St. Clair, P. A. Schaffer, *J. Virol. 40* (1981) 936.
[129] K. K. Biron, J. A. Fyfe, J. E. Noblin, G. B. Elion, *Am. J. Med. 73* (1982) 383.
[130] P. A. Furman, P. V. McGuirt, P. M. Keller, J. A. Fyfe, G. B. Elion, *Virology 102* (1980) 420.
[131] J. S. Pagano, J. W. Sixbey, J.-C. Lin, *J. Antimicrob. Chemother. 12 Suppl. B* (1983) 113.
[132] W. T. Ashton, J. D. Karkas, A. K. Field, R. L. Tolman, *Biochem. Biophys. Res. Commun. 108* (1982) 1716.
[133] Y. C. Cheng, S. P. Grill, G. E. Dutschman, K. Narayama, K. F. Bastow, *J. Biol. Chem. 258* (1983) 12 460.
[134] K. K. Biron, S. C. Stanat, J. B. Sorrell, J. A. Fyfe, P. M. Keller, C. U. Lambe, D. J. Nelson, *Proc. Natl. Acad. Sci. USA 82* (1985) 2473.
[135] P. deMiranda, H. C. Krasny, D. A. Page, G. B. Elion, *J. Pharmacol. Exp. Ther. 219* (1981) 309.
[136] P. deMiranda, S. S. Good, O. L. Laskin, H. C. Krasny, J. D. Connor, P. S. Lietman, *Clin. Pharmacol Ther. (St. Louis) 30* (1981) 662.
[137] P. deMiranda, S. S. Good, H. C. Krasny, J. D. Connor, O. L. Laskin, P. S. Lietman, *Am. J. Med. 73* (1982) 215.
[138] S. S. Good, P. deMiranda, *Am. J. Med. 73* (1982) 91.
[139] P. deMiranda, R. J. Whitley, M. R. Blum, R. E. Keeney, N. Barton, D. M. Cocchetto, S. Good, G. P. Hemstreet, L. E. Kirk, D. A. Page, G. B. Elion, *Clin. Pharmacol. Ther. (St. Louis) 26* (1979) 718.
[140] P. deMiranda, M. R. Blum, *J. Antimicrob. Chemother. 12 Suppl. B* (1983) 29.
[141] M. R. Blum, S. H. T. Liao, P. deMiranda, *Am. J. Med. 73* (1982) 186.
[142] W. E. Tucker, *Am. J. Med. 73* (1982) 27.
[143] G. B. Elion, *Cancer Res. 45* (1985) 2943.
[144] L. Corey, J. Benedetti, C. Critchlow, G. Mertz, J. Douglas, K. Fife, A. Fahnlander, M. L. Remington, C. Winter, J. Dragavon, *J. Antimicrob. Chemother. 12 Suppl B* (1983) 79.
[145] A. E. Nilsen, T. Aasen, A. M. Halsos, B. R. Kinge, E. A. L. Tjotta, K. Wikstrom, A. P. Fiddian, *Lancet 1982 II*, 571.
[146] Y. J. Bryson, M. Dillon, M. Lovett, G. Acuna, S. Taylor, J. D. Cherry, B. L. Johnson, E. Wiesmeier, T. Creagh-Kirk, R. Keeney, *N. Engl. J. Med. 308* (1983) 916.
[147] R. C. Reichman, G. J. Badger, G. J. Mertz, L. Corey, D. D. Richman, J. D. Connor, D. Redfield, M. C. Savoia, M. N. Oxman, Y. Bryson, D. Tyrrell, J. Portnoy, T. Creagh-Kirk, R. E. Keeney, T. Ashikaga, R. Dolin, *JAMA J. Am. Med. Assoc. 251* (1984) 2103.
[148] G. J. Mertz, L. Eron, R. Kaufman, L. Goldberg, B. Raab, M. Conant, J. Mills, T. Kurtz, L. G. Davis, *Am. J. Med. 85* (1988) 14.
[149] H. R. Mattison, R. C. Reichman, J. Benedetti, D. Bolgiano, L. G. Davis, A. Bailey-Farchione, M. Remington, C. Winter, L. Corey, *Am. J. Med. 85* (1988) 20.
[150] B. Bean, C. Braun, *Lancet 1982 II*, 118.
[151] H. H. Balfour, K. A. McMonigal, B. Bean, *J. Antimicrob. Chemother. 12 Suppl. B* (1983) 169.
[152] J. D. Meyers, J. C. Wade, C. D. Mitchell, R. Saral, P. S. Lietman, D. T. Durack, M. J. Levin, A. C. Segreti, H. H. Balfour, *Am. J. Med. 73* (1982) 229.
[153] J. C. Wade, B. Newton, C. McLaren, N. Fluornoy, R. E. Keeney, J. D. Meyers, *Ann. Intern. Med. 96* (1982) 265.
[154] R. Saral, W. H. Burns, O. L. Laskin, G. W. Santos, P. S. Lietman, *N. Engl. J. Med. 305* (1981) 63.
[155] R. Saral, R. F. Ambinder, W. H. Burns, C. M. Angelopulos, D. E. Griffin, P. J. Burke, P. S. Lietman, *Ann. Intern. Med. 99* (1983) 773.
[156] B. Sköldenberg, M. Forsgren, K. Alestig, T. Bergstrom. L. Burman, E. Dahlqvist, A. Forkman, A. Fryden, K. Lovgren, K. Norlin, R. Norrby, E. Olding-Stenkvist, J. Stiernstedt, I. Uhnoo, K. DeVahl, *Lancet 1984 II*, 707.
[157] R. J. Whitley, C. A. Alford, M. S. Hirsch, R. T. Schooley, J. P. Luby, F. Y. Aoki, D. Hanley, A. J. Nahmias, S. J. Soong, *N. Engl. J. Med. 314* (1986) 144.

Selective Inhibitors of Dihydrofolate Reductase (Nobel Lecture)**

By George H. Hitchings, Jr.*

Introduction

My interest in nucleic acids, their constituents, and their metabolism can be traced to the discovery of adenosine triphosphate in muscle by *Fiske* and *Subbarow*.[1] I had entered Harvard University as a candidate for a Ph.D. degree in 1928 and transferred to Harvard Medical School in 1929. *Otto Folin*, then head of the Department of Biological Chemistry, designated my first predoctoral year to be spent with *Cyrus J. Fiske*, then involved in the momentous discoveries of phosphocreatine and the labile phosphorus compounds of muscle and other tissues. I was soon immersed in the discovery of analytical tools with which to follow the metabolism of adenosine triphosphate.[2]

Other lines of thought coalesced with this interest when I joined Burroughs Wellcome Co. in 1942 as the sole member of the Biochemistry Department. In the meantime, the antimetabolite principle had been expressed by *Woods*[3] and *Fildes*.[4] I saw the opportunity to explore nucleic acid biosynthesis in a new and revealing way by employing synthetic analogues of the purine and pyrimidine bases in a system utilizing these heterocyclic compounds for biosynthesis.

I was able to interest *Elvira Falco*, who was then an assistant in the company's Bacteriology Department. Together we worked out a system using *Lactobacillus casei*, which would grow either with a then unknown "L. casei" growth factor or with a mixture of thymine and a purine (Fig. 1).[5]

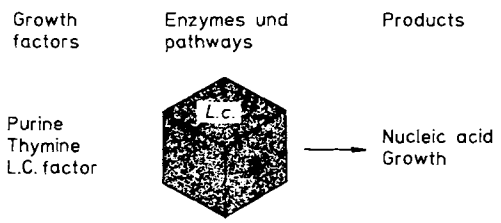


Fig. 1. The use of *Lactobacillus casei* as a black box of enzymes and metabolic pathways concerned with nucleic acid metabolism [9].

This system quickly gave us encouraging results. In a simple screening test for antibacterial activity, analogues were found to inhibit strongly not only the *L. casei* system but pathogenic bacteria as well. We had added toxicity testing in growing rats and other biological screening procedures and were becoming more and more excited by the results.

By 1947 six or seven of us were pursuing this work, and the feeling in the group was, "Now we have the chemotherapeutic agents; we need only to find the diseases in which they will be active." At that point I made two arrangements for collaborative studies, one with Sloan Kettering Institute for antitumor testing using sarcoma 180 (S-180) in mice, and another with outside laboratories for expansion of antibacterial and antimalarial testing. The antimalarial testing was included through the insight of *Peter B. Russell*, also a member of our research group. *Russell* noted the resemblance of a 2,4-diamino-5-phenylpyrimidine to a hypothetical conformation of the antimalarial proguanil. It turned out later that this theory was prescient; the dihydrotriazine is the active metabolite of proguanil.[6]

The next year two leads developed almost simultaneously. *Falco* began a series of selective inhibitors of dihydrofolate reductase (DHFR) with the synthesis of 2,4-diamino-5-phenoxypyrimidine, and *Gertrude Elion* synthesized 2,6-diaminopurine.[7] The latter was among the first four compounds we submitted to Sloan Kettering Institute. It was found to be active in the S-180 test, was taken into clinical trial by *Joseph H. Burchenal*, and gave at least one spectacular remission.[8] This was sufficient to establish cancer chemotherapy as a continuing primary goal of our group. The purine analogue story, which has been a major theme in *Gertrude Elion*'s career, is the topic of her Nobel lecture.[*]

The Discovery of DHFR Inhibitors

The main theme of this essay is the continuing topic of selective inhibitors of dihydrofolate reductase. Biochemical knowledge of the role of folates was developing concomitantly. Figure 2 shows that dihydrofolate is synthesized de novo in prokaryotes (microorganisms), while the higher species of eukaryotes (host) must have the vitamin preformed. I will pick up the story of selective inhibitors of DHFR *in medias res* and carry it forward to current exciting developments.

A short review of our line of research was presented in a symposium honoring *Sir Henry Wellcome*.[9] Several papers[10-12] tell the story of selectivity among 2,4-diaminopyrimidines from its first recognition before 1950 to its confirmation. Proof was developed through inhibitor analysis, sequencing, conformations, induced mitogenesis, computer-assisted conformation studies, and new syntheses based on this type of information.

The earliest proof of the mechanism of action of these compounds is illustrated in Figure 3.[13] The growth of *Streptococcus faecium* was easily inhibited by a diaminopyrimidine when the growth was induced by folate, but it took 500 to 1000 times as much inhibitor when tetrahydrofolate (H_4FA) was supplied. This was correctly interpreted as

[*] Prof. G. H. Hitchings
Wellcome Research Laboratories
Burroughs Wellcome Co.
3030 Cornwallis Road
Research Triangle Park, NC 27709 (USA)

[**] Copyright © The Nobel Foundation 1989. We thank the Nobel Foundation, Stockholm, for permission to print this lecture.

[*] See preceding article.

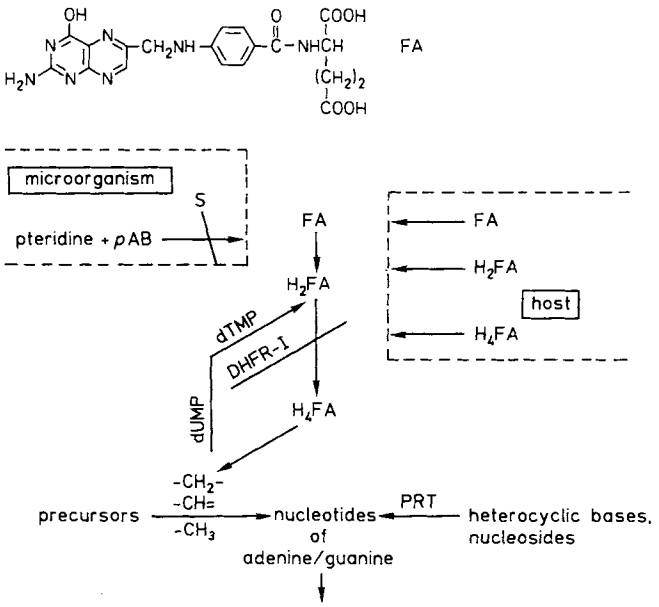


Fig. 2. Folate metabolism. Upper left shows biosynthesis in prokaryotes; upper right shows the uptake of preformed vitamin in mammals. The subsequent utilization for the biosynthesis of nucleic acid components is shown below. The importance of DHFR and the selectivity of its inhibitors takes a central place. FA = folate; H_2FA = dihydrofolate; H_4FA = tetrahydrofolate; dTMP = thymidylate; dUMP = deoxyuridylate; pAB = *p*-aminobenzoic acid; PRT = phosphoribosyl transferase [10].

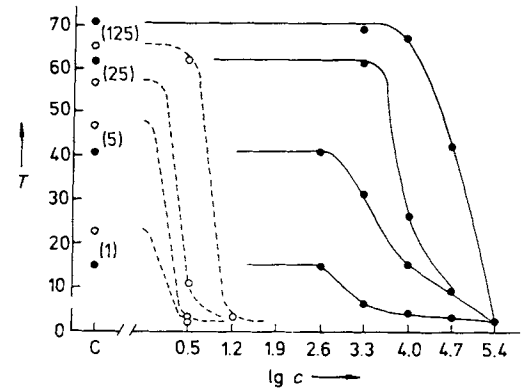


Fig. 3. The concentration (c in 10^{-9} g per 10 mL) of pyrimethamine (Pyr) required to inhibit growth of *Streptococcus faecium* depends on whether FA (○ – – – ○) or a form of H_4FA (●——●) is used in the medium [13]. T = turbidity.

inhibition of the yet unknown enzyme responsible for the reduction of folate to tetrahydrofolate.

By 1950 we had concluded that we were dealing with selective inhibitors of dihydrofolate reductase. From this work it appeared probable that details of fine structure in DHFR vary from species to species and that a given inhibitor may exhibit considerable selectivity as a result of looser or tighter binding to the corresponding enzyme of host or parasite.[14] The full structural analogue methotrexate (MTX) shows little selectivity, while pyrimethamine (Pyr) is highly active against the malarial enzyme and trimethoprim (Tmp) against a bacterial enzyme. Neither has notable toxicity against the rat liver enzyme.

Isolation and characterization of DHFR from various organisms led first to inhibitor analysis (Table 1). This documented unequivocally the different structures of representative dihydrofolate reductases from different sources. This

Table 1. The concentration ($IC_{50} \times 10^8$) of MTX, Pyr, or Tmp required to inhibit the DHFR derived from *E. coli*, rat liver, and *P. berghei* [9].

Inhibitor	Enzyme from		
	E. coli	Rat liver	*P. berghei*
MTX	0.1	0.2	0.07
Pyr	250	70	0.05
Tmp	0.5	3×10^3	7.0

was soon followed by amino acid analyses and sequence determinations.

Concomitantly developing knowledge of the roles of folate derivatives in biosyntheses and metabolism gave a fuller appreciation of the significance of inhibition of DHFR (Figs. 4, 5). The activity of the enzyme is necessary to pro-

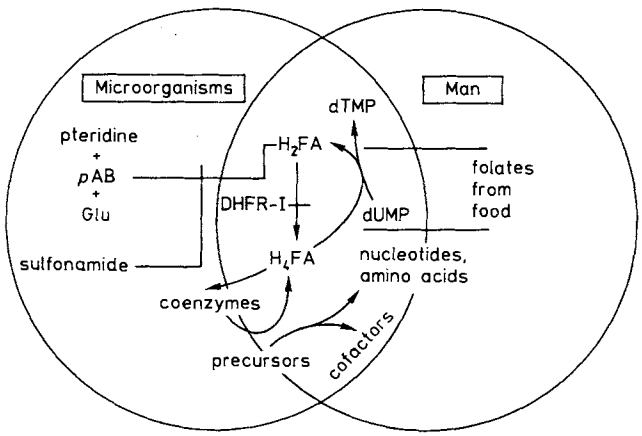


Fig. 4. The metabolic reactions catalyzed by derivatives of H_4FA. GLU = glutamate [12].

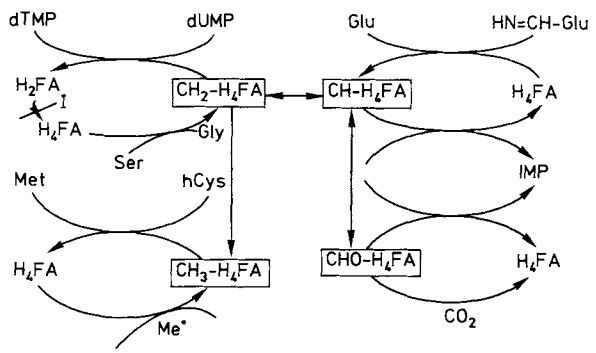


Fig. 5. Details of reactions of specific folate-containing cofactors. Counterclockwise: N^{10}-formyl, N^5,N^{10}-methenyl, methylene, and N^5-methyl tetrahydrofolates. Ser = serine; Met = methionine; IMP = inosinic acid [12].

duce H_4FA initially and to recycle it after its reoxidation in the formation of thymidylate from deoxyuridylate.

Amino acid sequence determinations brought out a full appreciation of the high variability of the basic constituents of this enzyme in a range of species.[15] Between the enzymes of two bacterial species there is only 30 percent homology, and between prokaryotes and eukaryotes only 30 percent. It is only the higher species that exhibit as much as 90 percent homology. *Hitchings* and *Roth* found 16 identities between the enzymes from *Escherichia coli* and those from the mouse tumor L1210.[12] They predicted correctly that study of a wider range of enzymes would reduce the number of identi-

ties. If one takes into account enzymes not in the mainstream, for example, those from protozoa plasmids, the number is even smaller.

The mainstream enzymes (from bacterial and mammalian sources) have similar conformations. That published by *Richardson*[16] may be regarded as the representative type (Fig. 6). Although mammalian enzymes are larger than this

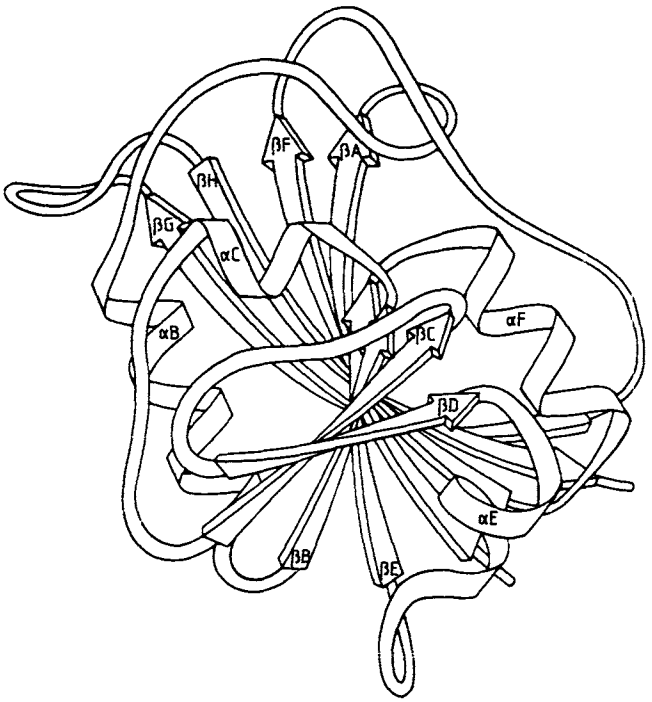


Fig. 6. A graphic illustration of the configuration of DHFR [16].

bacterial enzyme by some 3000 daltons, the extra residues exist as loops that do not greatly alter the main conformation. On the other hand, the enzymes from other types of organism can be so different as to raise doubts about whether they are intrinsically dihydrofolate reductases, or whether their DHFR activity is secondary to some other unknown function (cf. *Matthews* et al.[17]). Figure 7[18] shows some possible origins of Type II DHFR.

If its normal function is:

To reduce H_2FA	To reduce/oxidize other compounds
1. Other intestinal coliforms	1. Pteridine/flavin
2. T4 phage	2. Nonspecific dehydrogenases
3. Anaerobes	
4. Fungi (yeasts)	
5. Protozoa	

Fig. 7. Possible origins of untypical dehydrofolate reductases (DHFR II) [18].

Uses of DHFR Inhibitors

Synergistic Combinations

It is pertinent at this point to refer to some of the applications of selective inhibitors of DHFR. An important application is, of course, the use of co-trimoxazole as an antibacterial. Its creation derived from the knowledge that in combining trimethoprim with sulfamethoxazole, one was creating a sequential blockade of a major biosynthetic pathway in a bacterium or in other prokaryotes (Table 2). The minimal

Table 2. Effect on minimal inhibitory concentration (MIC) of combining one part Tmp with 20 parts sulfamethoxazole [19].

Organism	MIC [μg mL^{-1}] of			
	Sulfamethoxazole		Tmp	
	Alone	Mixture	Alone	Mixture
Streptococcus pyogenes	> 100	1	1	0.05
Streptococcus pneumoniae	30	2	2	0.1
Staphylococcus aureus	3	0.3	1	0.015
Haemophilus influenzae	10	0.3	1	0.015
Bordetella pertussis	50	4	3	0.2
Klebsiella pneumoniae	> 100	4	1	0.2
Klebsiella aerogenes	> 100	4	1	0.2
Escherichia coli	3	1	0.3	0.05
Salmonella typhimurium	10	1	0.3	0.05
Shigella sonnei	10	1	0.3	0.05
Proteus vulgaris	30	3	3	0.15

effects on the host reflect the absence in eukaryotes of the reactions leading to the biosynthesis of dihydrofolate such as occurs in prokaryotic cells.

The strong potentiation that occurs is indicated by the data of Table 2,[19] which show that minimum inhibitory concentrations of one component may be reduced as much as 10- or 20-fold when the second component is also present. Moreover, the combination may be effective against organisms that would not be inhibited by the individual drugs (e.g., *Klebsiella sp.* and *Streptococcus* Group C), where the individual inhibitory concentrations would be borderline or unattainable.

One further illustration of the possible utility of biochemically related inhibitors is given in Figure 8,[20] where the

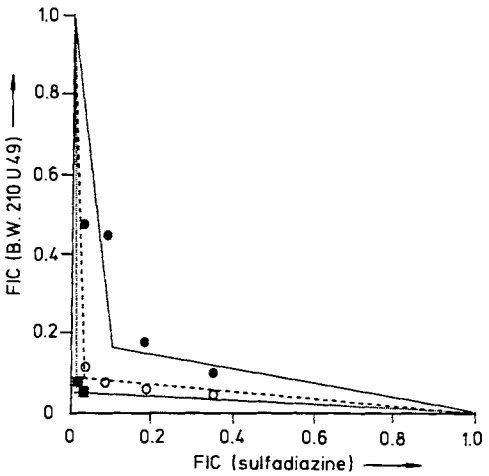


Fig. 8. Fractional inhibitory concentrations (FIC) of B.W. 210U49 and sulfadiazine required for 50 percent inhibition of *P. vulgaris* in the presence and absence of 8-azaguanine: ●—●, no 8-azaguanine; o - - - o, 1 μg mL^{-1}; ■—■, 10 μg mL^{-1} [20].

addition of 8-azaguanine to an already potentiative combination of diaveridine (B.W. 210U49) with sulfadiazine enhances the potency. Such biochemically oriented triple combinations have not been used in a major way, but their potential remains exploitable.

I should like to focus now on the uses of individual DHFR inhibitors.

Trimethoprim and Its Derivatives

Chronologically first, and perhaps still first in importance in cancer chemotherapy, is methotrexate (MTX) from the Lederle Laboratories. Methotrexate had assumed a role in the therapy of acute leukemia as early as 1948[21] and is still of major interest today. As shown in Figure 2, however, it is relatively unselective. Its therapeutic utility depends mainly on differences in uptake, glutamylation, cellular excretion, cellular metabolic balance, and other factors.

Whereas MTX is a close structural analogue of folate, our own "antifols" were significantly different and highly selective. These facts will be brought out by examination of details of the structures and active centers of several enzymes.

For example, the fine structure of the complex of MTX and cofactor in *L. casei* DHFR (Fig. 9)[22] may be contrast-

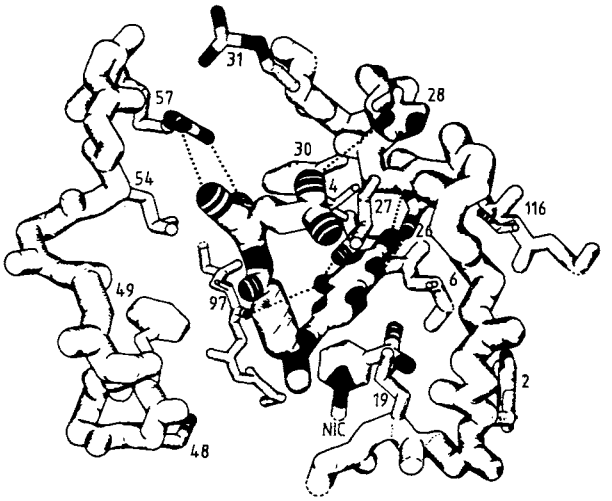


Fig. 9. Schematic illustration of the active site of *L. casei* DHFR showing the binding of MTX and nicotinamide adenine dinucleotide phosphonate [22].

ed with that of Tmp and cofactor in the chicken liver enzyme (Fig. 10).[23] It is obvious that the MTX molecule is much more space-filling than Tmp. Such contrasts are observable in all situations where the small-molecule inhibitors are observed, and the contrasts in the active centers of the enzymes are consistent with the selectivities of the small-molecule inhibitors.

There have been a number of studies of the functions of specific amino acid residues. One of the most cogent was reported by *Kraut* et al.[24] in a paper that combined several experiments. In this study of the *E. coli* enzyme, the replacement of aspartate by asparagine reduced activity to 0.1 % of that of the unaltered enzyme, showing the importance of the ionizable carboxyl group (Fig. 11). The substitution of alanyl for glycyl completely inactivated the enzyme, probably by distorting its conformation. However, substitution of SH for OH (cysteine for serine) had little effect. This type of experiment may provide the background for the synthesis of new and useful inhibitors.

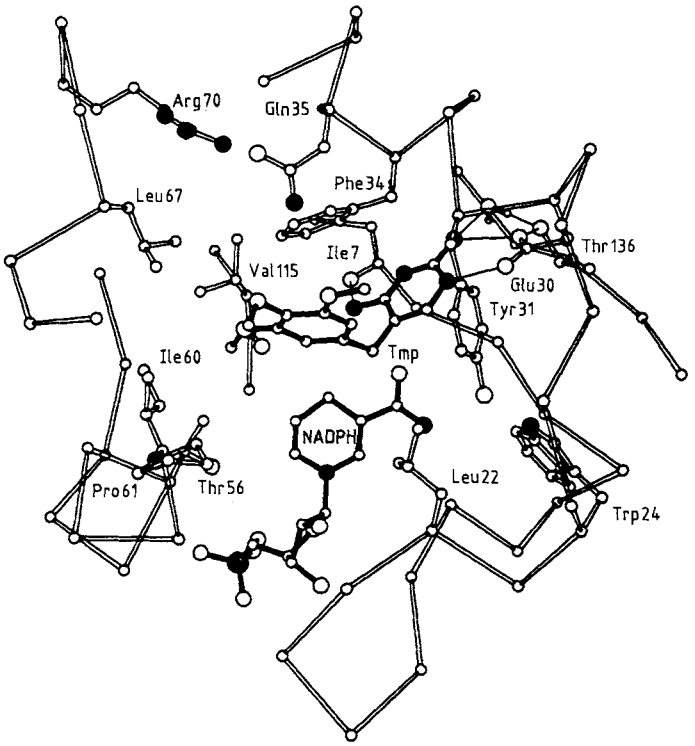


Fig. 10. Schematic illustration of the cofactor in chicken liver DHFR showing the binding of Tmp and nicotinamide adenine dinucleotide phosphonate [23].

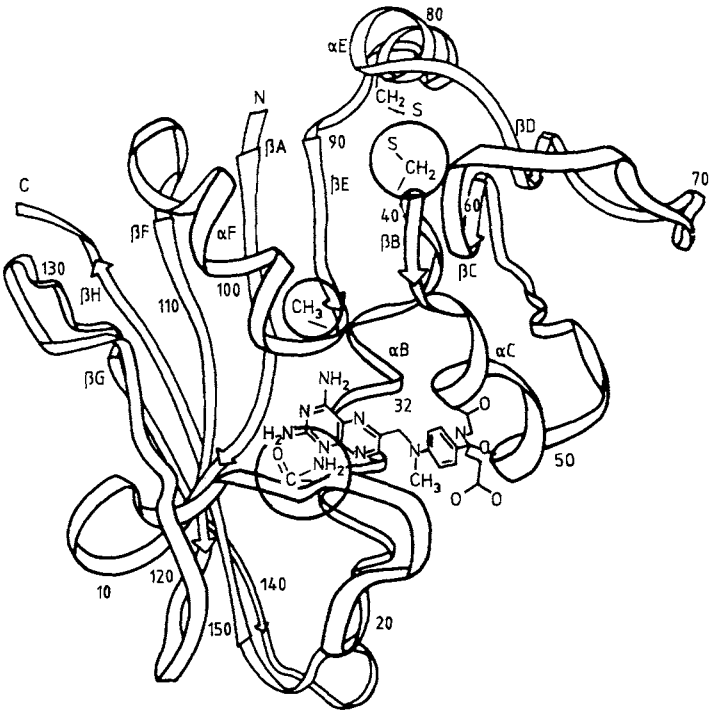


Fig. 11. *E. coli* DHFR with induced specific mutations [24].

An aspect of folate metabolism that appeared relatively late is the identification of the high-molecular-weight derivatives of folic acid as polyglutamates. Since the chain length of most of these exceeds that of the longest form that can be transported into the cell efficiently, most cells contain a pteroylpolyglutamate synthetase. The number of glutamyl residues varies with time and with cell type. The immense

complexities of this situation are only beginning to appear. Nevertheless, it is interesting and instructive to compare the binding constants and kinetic values of polyglutamates in some of the enzymatic reactions involved in folate metabolism (Table 3).[25]

Table 3. Comparison of binding constants (K_m) and kinetic values of polyglutamates in enzymatic reactions in folate metabolism. TS = thymidylate synthase; AICAR TF = AICAR transformylase; GAR TF = GAR transformylase [25].

Enzyme	n	$n/1$	
		K_m	v_{max}
DHFR	5	1	–
Serin-$HOCH_2$-transferase	5	0.0025	–
N^5,N^{10}-CH_2-H_4FA-dehydrogenase	3	< 1	1.7
N^{10}-CHO-H_4FA-synthetase	3	0.01	0.5
N^{10}-CHO-H_4FA-synthetase	5	0.001	0.25
N^5,N^{10}-CH-H_4FA-cyclohydrolase	5	0.5	1.5
T_aS_α	3	0.2	–
T_aS_α	5	0.014	3
AICAR-TF	3	0.01	1
GAR-TF	3	0.8	5

The inhibitor MTX, as well as the tetrahydrofolate, is subject to polyglutamylation. In many cases the ratio of folate polyglutamate to inhibitor polyglutamate is not markedly changed, but it is predictable that among the vast number of possibilities some of the anomalies and some of the therapeutic indices will find solid explanations. A few of the effects of glutamylation on specific biosynthetic enzymes are shown in Table 4.[26]

Table 4. The effect of pentaglutamylation on the binding of MTX to specific tetrahydrofolate-utilizing synthetic enzymes [26].

Enzyme	Folate cofactor	K_i [μM]		K_i(MTX) / K_i(MTX-Glu_5)
		MTX	MTX-Glu_5	
TS	N^5,N^{10}-CH_2-H_4PteGlu$_1$	13.0	0.047	277
	N^5,N^{10}-CH_2-H_4PteGlu$_5$	14.3	0.056	254
AICAR-TF	N^{10}-CHO-H_4PteGlu$_1$	143.9	0.057	2508
	N^{10}-CHO-H_4PteGlu$_5$	40.0	5.89	6.8
GAR-TF	N^{10}-CHO-H_4PteGlu$_1$	80	2.5	32
	N^{10}-CHO-H_4PteGlu$_5$	84	22.0	4

I wish to turn now to the intimate details of the structure of specific enzymes and their exploitation in the synthesis of more active inhibitors. Figure 12[27] shows the fit of Tmp in the DHFR of *E. coli*. In the upper left (residue 57), one can see the guanidino group of arginine. This was exploited by *Lee Kuyper* who replaced the *m*-methoxyl group of Tmp with a series of carboxyalkoxy radicals. The optimum length proved to be five carbon atoms, and the product, the carboxyl amyloxy derivative, bound the enzyme some 50 times more tightly than did Tmp.[28] In the same vein, *Barbara Roth* synthesized a bromoacetoxyphenoxy analogue of Tmp and found that the derivative bound to the histidine-22 residue of the enzyme with a covalent linkage.[29] These examples may be regarded as probes of a vast and exciting future.

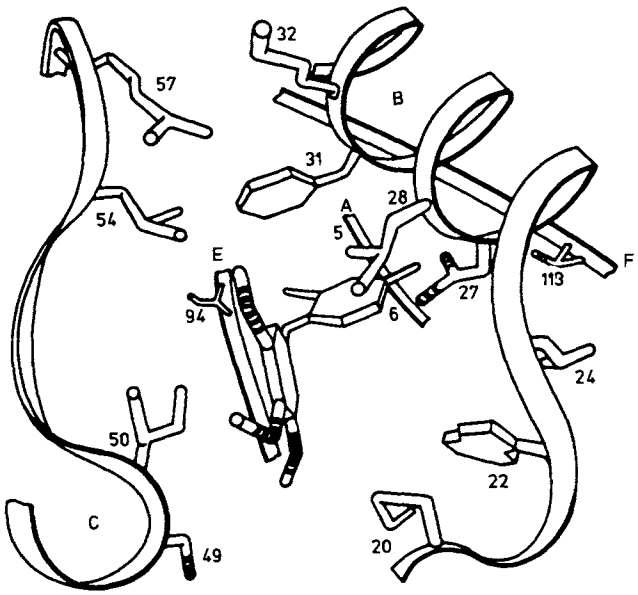


Fig. 12. Fit of trimethoprim (center) in the DHFR of *E. coli* [27].

Lipophilic DHFR Inhibitors

Multiple forms of resistance to antifols appeared soon after work on these inhibitors began. Among these various expressions of resistance (Fig. 13) was a loss of the cellular

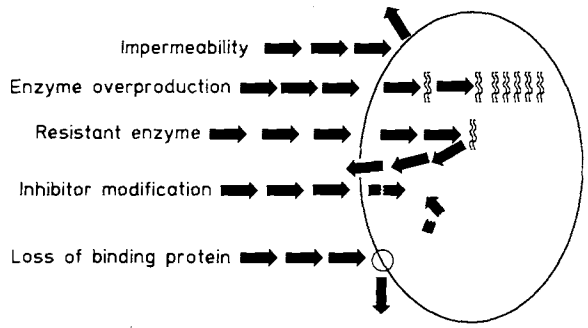


Fig. 13. Mechanisms of resistance to inhibitors of DHFR [18].

transport mechanism, which has stimulated the investigation of lipophilic inhibitors that do not depend on this mechanism for transport into the cell. At present the two potentially useful drugs are trimetrexate and piritrexim (Fig. 14). Exploitation of these inhibitors is in its infancy, but each has exhibited interesting properties of its own. The effects of trimetrexate and MTX are compared in Table 5.[30] Both trimetrexate and piritrexim have shown interesting activities

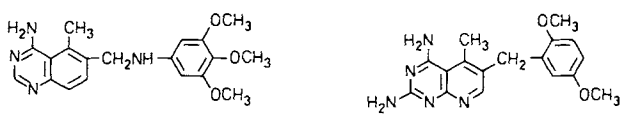


Fig. 14. Chemical structures of trimetrexate (left) and piritrexim (right), two potentially useful DHFR inhibitors.

Table 5. Efficacy of trimetrexate and MTX against transplantable rodent tumors and in xenografts [30].

	Tumor system	Trimetrexate	MTX
Murine	L1210 leukemia	++	++
	P388 leukemia	++	++
	B16 melanoma	++	−−
	Lewis lung carcinoma	−−	−−
	colon 26	++	−−
	colon 38	+	−−
	CD8F1 mammary	++	+
Human xenograft	mammary MX-1	−−	−−
	lung LX-1	−−	−−
	colon CX-1	−−	−−

against infectious prokaryotic organisms. The combination of trimetrexate and leucovorin has been used successfully to treat pneumocystic pneumonia in AIDS patients.[31] Table 6 shows the effect of combining piritrexim and sulfadiazine to treat murine toxoplasmosis.[32]

Table 6. Effect of the piritrexim(P)–sulfadiazine(S) combination in treatment of murine toxoplasmosis. Sulfadiazine was administered orally by gavage at concentrations of 4, 40, and 500 mg kg^{-1} per day, and piritrexim was administered i.p. at a concentration of 20 mg kg^{-1} per day [32].

Treatment [a]	Percent cumulative mortality after n days. [%]						
	$n = 3$	6	9	12	15	18	20
None	0	0	100	–	–	–	–
S(4)	0	20	60	100	–	–	–
P + S(4)	0	20	40	60	80	80	80
S(40)	0	20	40	100	–	–	–
P + S(40)	20	20	20	40	80	80	80
S(400)	0	0	80	100	–	–	–
P + S(400)	0	0	0	0	0	0	0

[a] Sulfazidine concentration given in parentheses.

Inhibitors of other Enzymes

Finally to be mentioned is a selective inhibitor of thymidylate synthase (TS) (Fig. 15). The first of these is 5,8-dideazaisopteroylglutamate (IAHQ) (Fig. 16). IAHQ and specific inhibitors of other biosynthetic reactions involving tetrahydrofolate represent the beginning of a biochemically oriented, improved cancer chemotherapy.[33]

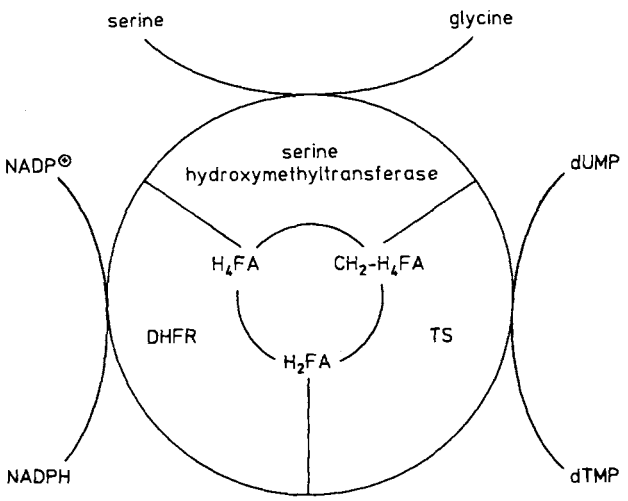


Fig. 15. The thymidylate synthetic cycle.

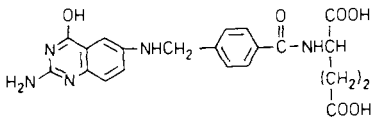


Fig. 16. Chemical structure of IAHQ, a selective inhibitor of TS.

Outlook

I am incredibly blessed to have been involved for well over four decades in a field that continues to become more exciting with every passing year. Figure 17[34] charts the history

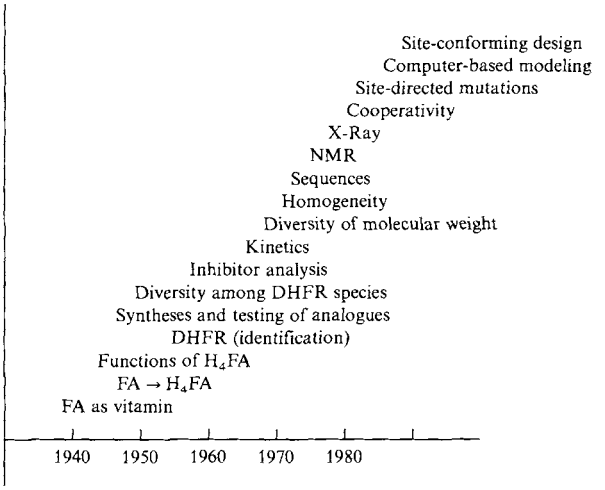


Fig. 17. Accrual of information about DHFR, beginning with untargeted studies in the 1940s and continuing in the 1980s with discovery of new useful compounds and methods of drugs design [34]. The ordinate is a measure of utility in synthetic design.

of increasing knowledge concerning dihydrofolate reductase, beginning with our work in the 1940s. Those early, untargeted studies led to the development of useful drugs for a wide variety of diseases (Fig. 18) and has justified our belief

Base Analogues	
Antileukemic	*Immunosuppressant*
2,6-Diaminopurine	→
6-Thioguanine	→
6-Mercaptopurine →	Azathioprine
Hypouric	*Antiprotozoal*
Allopurinol →	Allopurinol riboside
DHFR Inhibitors	
Pyrimethamine	*Antimalarial*
Trimethoprim	*Antibacterial*
Piritrexim	*Antitumor*
Sugar Analogues	
Acyclovir (acyclic guanosine)	*Antiherpetic*
3-Azidothymidine (zidovudine)	*Anti-AIDS*

Fig. 18. Drug therapies that have emerged from DHFR inhibitors.

that this approach to drug discovery is more fruitful than narrow targeting. In 1988 this line of research continues to generate useful new compounds.

I should like to close with a quotation from one of my own papers:[35]

To the biochemical chemotherapist, it is not only a matter of faith, but an obvious fact, that every cell type must have a characteristic biochemical pattern, and therefore be susceptible to attack at some *locus* or *loci* critical for its survival and replication.

I am greatly indebted to Mara Gabriel and Coyla Barry for skillful and energetic work that made completion of this paper possible.

Received: January 27, 1989 [A 723 IE]
German version: *Angew. Chem. 101* (1989) 903

[1] C. J. Fiske, Y. Subbarow, *Science (Washington) 70* (1929) 381.
[2] G. H. Hitchings, *Dissertation*, Harvard University 1933.
[3] D. D. Woods, *Br. J. Exp. Pathol. 21* (1940) 74.
[4] P. Fildes, *Lancet 1940 I*, 955.
[5] G. H. Hitchings, E. A. Falco, M. B. Sherwood, *Science (Washington) 102* (1945) 251.
[6] E. A. Falco, G. H. Hitchings, P. B. Russell, H. VanderWerff, *Nature (London) 164* (1949) 107.
[7] G. H. Hitchings, G. B. Elion, H. VanderWerff, E. A. Falco, *J. Biol. Chem. 174* (1948) 765.
[8] J. H. Burchenal, D. A. Karnofsky, E. M. Kingsley-Pillers, C. M. Southam, W. P. Laird Meyers, G. C. Escher, L. F. Craver, H. W. Dargeon, C. P. Rhoads, *Cancer (Philadelphia) 4* (1951) 549.
[9] G. H. Hitchings, *Drug Intell. Clin. Pharm. 16* (1982) 843.
[10] G. H. Hitchings, J. J. Burchall, *Adv. Enzymol. Relat. Subj. Biochem. 27* (1965) 417.
[11] G. H. Hitchings, S. L. Smith, *Adv. Enzyme Regul. 18* (1980) 349.
[12] G. H. Hitchings, B. Roth in M. Sandler (Ed.): *Enzyme Inhibitors as Drugs*, University Park Press, Baltimore 1980, pp. 263–280.
[13] G. H. Hitchings, E. A. Falco, G. B. Elion, S. Singer, G. B. Waring, D. J. Hutchison, J. H. Burchenal, *Arch. Biochem. Biophys. 40* (1952) 479.
[14] G. H. Hitchings in L. G. Goodwin, R. H. Nimmo-Smith (Eds.): *Drugs, Parasites and Hosts*, Little-Brown, Boston 1962, pp. 196–210.
[15] A. C. Y. Chang, J. H. Nunberg, R. J. Kaufman, H. A. Erlich, R. T. Schimke, S. N. Cohen, *Nature (London) 275* (1978) 617.
[16] S. Richardson, *Adv. Protein Chem. 34* (1981) 167.
[17] D. A. Matthews, S. L. Smith, D. P. Baccanari, J. J. Burchall, S. J. Oatley, J. Kraut, *Biochemistry 25* (1986) 4194.
[18] J. Burchall, *Wellcome Scientist Lecture 1983*.
[19] S. R. M. Bushby in M. Finland, E. H. Kass (Eds.): *Trimethoprim-sulfamethoxazole, Microbiological, Pharmacological and Clinical Considerations*, University of Chicago Press, Chicago, USA, 1973, pp. 10–30.
[20] G. B. Elion, S. Singer, G. H. Hitchings, *Antibiot. Chemother (Washington) 10* (1960) 556.
[21] S. Farber, L. K. Diamond, R. F. Mercer, R. F. Sylvester, J. A. Wolff, *N. Engl. J. Med. 238* (1948) 787.
[22] B. Roth, E. Bliss, C. R. Beddell in S. Neidle, M. J. Waring (Eds.): *Molecular Aspects of Anti-Cancer Drug Action*, Macmillan, London 1983, pp. 363–393.
[23] D. A. Matthews, J. T. Bolin, J. M. Burridge, D. J. Filman, K. W. Volz, B. T. Kaufman, C. R. Beddell, J. N. Champness, D. K. Stammers, J. Kraut, *J. Biol. Chem. 260* (1985) 381.
[24] J. E. Villafranca, E. H. Howell, D. H. Voet, M. S. Strobel, R. C. Ogden, J. N. Abelson, J. Kraut, *Science (Washington) 222* (1983) 782.
[25] J. J. McGuire, J. K. Coward in R. L. Blakley, S. J. Benkovic (Eds.): *Folates and Pterins, Vol. 1*, Wiley, New York 1984, pp. 135–190.
[26] C. J. Allegra, J. C. Drake, J. Jolivet, B. A. Chabner in I. D. Goldman (Ed.): *Proceedings of the Second Workshop on Folyl and Antifolyl Polyglutamates*, Praeger, New York 1985, pp. 348–359.
[27] C. R. Beddell in A. S. Horn, C. J. DeRanter (Eds.): *X-ray Crystallography and Drug Action*, Oxford University Press, Oxford 1984, pp. 169–193.
[28] L. F. Kuyper, B. Roth, D. P. Baccanari, R. Ferone, C. R. Beddell, J. N. Champness, D. K. Stammers, J. G. Dann, F. E. Norrington, D. J. Baker, *J. Med. Chem. 28* (1985) 303.
[29] J. H. Chan, L. F. Kuyper, B. Roth, *Abstr. Pap. Am. Chem. Soc. 189* (1985) 87.
[30] J. T. Lin, J. R. Bertino, *J. Clin. Oncol. 5* (1987) 2032.
[31] C. J. Allegra, B. A. Chabner, C. U. Tuazon, D. Ogata-Arakaki, B. Baird, J. C. Drake, J. T. Simmons, E. E. Lack, J. H. Shelhamer, F. Balis, R. Walker, J. A. Kovacs, H. C. Lane, H. Masur, *N. Engl. J. Med. 317* (1987) 978.
[32] F. Aruajo, D. R. Guptill, J. S. Remington, *J. Infect. Dis. 156* (1987) 828.
[33] D. J. Fernandes, J. R. Bertino, J. B. Hynes, *Cancer Res. 43* (1983) 1117.
[34] G. H. Hitchings in A. Burgen (Ed.): *Discoveries*, Cambridge University Press, Cambridge, in press.
[35] G. H. Hitchings, *Cancer Res. 29* (1969) 1895.

Drugs from Emasculated Hormones: The Principle of Syntopic Antagonism (Nobel Lecture)**

By Sir James W. Black*

In this lecture I want to give an outline of the early stages in the discovery of adrenaline β-receptor antagonists and of the histamine H_2-receptor antagonists. I will end with a brief personal view about future research.

Adrenaline β-Receptor Antagonists

The work that is the theme of this lecture began in the early summer of 1958 when I joined Imperial Chemical Industries' Pharmaceuticals Division. I had gone there to pursue a very clear project that had been developing in my mind for several years. The idea had clinical, therapeutic, physiological, and pharmacological elements.

Clinically, angina pectoris was known to be precipitated by anxiety and emotion just as well as by exercise. Indeed, the initiation of pain by an injection of adrenaline had been used as a diagnostic test. Partial thyroidectomy had been found to relieve severe angina pectoris whether or not associated with hyperthyroidism. At that time, tachycardia seemed to me to be the connecting link in these disorders.

Therapeutically, nitroglycerine could quickly relieve and attack of angina. Nitroglycerine also produced facial flush and headache. The relief of angina was attributed to similar vasodilatation in the coronary arteries. However, the newer, synthetic, selective coronary vasodilators, such as dipyridamole, were clinically ineffective despite the enhanced coronary artery dilatation that they provided. Here was a question mark against the widely practiced industrial strategy of seeking better drugs to increase coronary blood flow for angina.

Physiologically, Smith and *Lawson*[1] had found that hyperbaric oxygen, at two atmospheres pressure, reduced the incidence of ventricular fibrillation associated with occlusion of a coronary artery, even though the oxygen-carrying capacity of the blood had increased by a maximum of only 25%. Might not an equivalently small *decrease* in the myocardial demand for oxygen be just as effective? That was my question.

Myocardial oxygen consumption is determined by the work of the heart and is a function of arterial blood pressure and heart rate. Lowering blood pressure by systemic vasodilatation might dangerously reduce the perfusion pressure and blood flow through disease-narrowed coronary arteries. Indeed, hypotension was known to be able to induce a heart attack. Heart rate, on the other hand, is largely determined by the cardiac autonomic nervous system. Heart rate would thus be reduced by cardiac sympathetic blockade. In addition, there was much discussion in those days about a postulated "anoxiating" action of adrenaline, proposing that the price of rapidly increasing cardiac power was a decrease in cardiac metabolic efficiency.

These clinical, therapeutic, and physiological features of hearts coping with coronary artery disease all seemed to point to the potential advantage of annulling the actions of the sympathetic hormones, noradrenaline and adrenaline, on the heart.

Pharmacologically, the antiadrenaline drugs were a well-recognized class in 1958. All of them showed a pattern of actions similar to those seen by *Dale*[2] with the ergot alkaloids. Characteristically, they reversed the blood pressure rise produced by adrenaline to a fall in pressure, but they did not suppress the associated tachycardia. *Konzett*[3] had shown that isoprenaline, the purely synthetic isopropyl derivative of noradrenaline, produced only the actions such as tachycardia, vasodilatation, and bronchodilatation which the antiadrenaline drugs were not able to suppress. These were the actions of isoprenaline that *Ahlquist*[4] could not explain on the basis of *Cannon* and *Rosenbleuth*'s prevailing hypothesis involving sympathins E and I.[5] *Ahlquist* went on to propose that the wide-spread physiological effects of adrenaline were mediated by two classes of receptors, α and β. In this new classification, the antiadrenaline drugs of the day were α-receptor antagonists and isoprenaline was a selective stimulant of β-receptors.

So I started at I.C.I. with a clear goal – I wanted to find a β-receptor antagonist. I expected this to reduce pulse rates at rest and during exercise and hoped that it would decrease the susceptibility of patients to angina pectoris. The unknown factor for me at that time was the significance of adrenaline's "anoxiating" activity.

John Stephenson was the medicinal chemist assigned to work with me. As no compounds were known to annul the actions of adrenaline on the heart, the program had to be cold-started. The structure of isoprenaline (Fig. 1), the selective β-receptor stimulant, was our only clue. We thought that if N-substitution of adrenaline with an isopropyl group produced a selective *agonist*, then perhaps substitution with a different, larger group might produce a selective *antagonist.* We thought that symmetrical, "doubled-up" analogues of isoprenaline, dibenzylethylamines, might be interesting targets.

We were making compounds and testing them, admittedly without success, when, early in 1959, we read *Powell* and *Slater*'s report[6] about the properties of dichloroisoprenaline (DCI), an analogue of isoprenaline in which the ring hydroxyl groups were replaced by chlorine atoms (Fig. 1). In trying to exploit the bronchodilator properties of isoprenaline by making a long-acting variant, the Lilly group had discovered a compound that intrigued them by displaying – instead of isoprenaline's bronchodilator activity – the

[*] Prof. James Black
James Black Foundation
King's College School of Medicine and Dentistry
68 Half Moon Lane, Dulwich, GB-London SE24 9 JE (UK)

[**] Copyright © The Nobel Foundation 1989. We thank the Nobel Foundation, Stockholm, for permission to print this lecture.

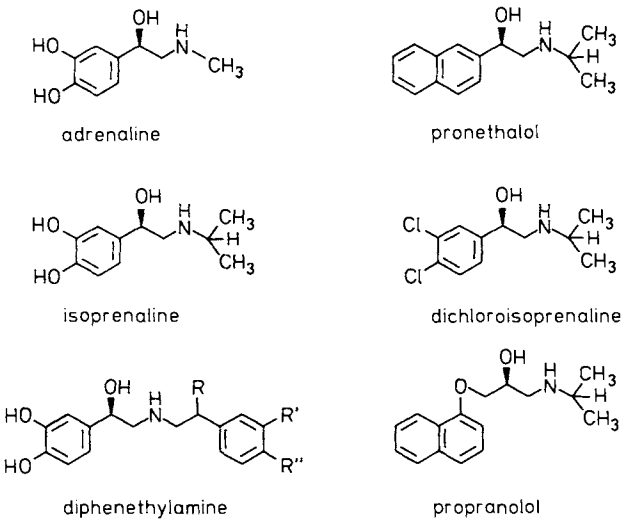


Fig. 1. Chemical structures of adrenaline-related compounds.

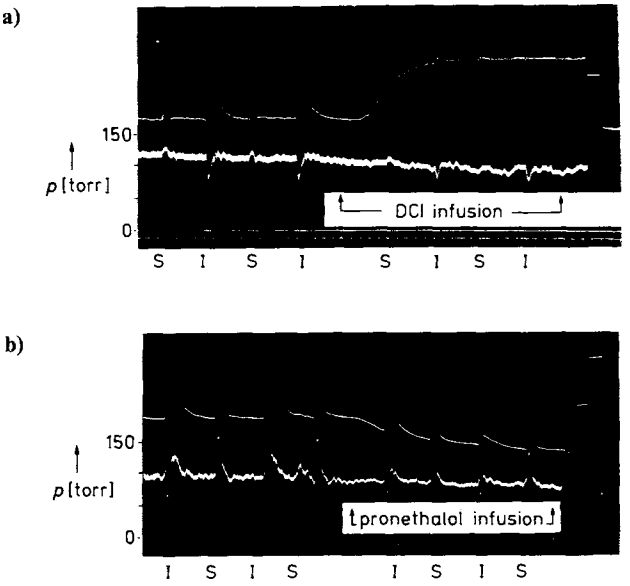


Fig. 2. Effects of a) DCI (100 μg kg^{-1} min^{-1}) and b) pronethalol (100 μg kg^{-1} min^{-1}) infusion upon heart rate and blood pressure responses to injections of isoprenaline (I) (0.4 μg kg^{-1} i.v.) and to sympathetic stimulation (S) (square wave pulses, 10-ms duration, 2.5 V, 15 pulses per second for 30 s) in anesthetized cats. Lower axis shows time markers in one-minute intervals.

opposite property, namely antagonism. Soon afterwards, *Moran* and *Perkins*[7] reported that DCI could annul the inotropic effects of adrenaline on the heart and classified DCI as a β-receptor antagonist. *Stephenson* immediately made some DCI for us to test.

We had started our bioassays using the classical Langendorff preparation, the isolated, spontaneously beating, guinea-pig heart. Isoprenaline is a powerful stimulant of both the rate and force of beating in this preparation, but we measured the amplitude of contractions, which compounded both changes. In this system DCI turned out to be as powerful a stimulant as isoprenaline and so was not at all what we were looking for. We had also developed a technique for simultaneously recording blood pressure and heart rate, in analogue form, in anesthetized animals. Potential antagonists could now be given economically by slow intravenous infusion, and this allowed the effect on a wide range of systems to be monitored. Here, too, the powerful stimulant effects of DCI on heart rate were clearly seen, although there was less hypotension due to vasodilatation than we had expected (Fig. 2). On the basis of these experiments, we decided that DCI was not the lead we needed.

As analytical pharmacologists, what we are allowed to see of a new molecule's properties is totally dependent on the techniques of bioassay we use. The prismatic qualities of an assay distort our view in obscure ways and degrees. Our only defense lies in restless improvement in technique and experimental design, in the hope that collimation of several techniques will improve the reliability of our vision. We would make the change self-consciously today, but then it was intuitive.

We developed a new in vitro assay based on guinea-pig cardiac papillary muscles as a way of measuring the contractile effects of isoprenaline independently of rate changes. Then, we reassessed many early compounds, including DCI. On the new preparation, DCI had no stimulant activities itself but simply antagonized the effects of adrenaline and isoprenaline, although the stimulant activity on pacemaker tissue could be clearly seen in the atrial preparation. We were astonished. Today, we classify DCI as a partial agonist. *Ariens*[8] and *R. P. Stephenson*[9] had introduced the concept of partial agonists a few years earlier but nothing in their writing, as far as I recall, alerted us to expect that the agonist activity of these compounds could be so tissue dependent.

I shall never forget *John Stephenson*'s reaction to this discovery: "We'll make the naphthyl analogue of isoprenaline" (Fig. 1).[35] He had realized immediately that while a fused benzene ring would have similar steric and electronic properties to the two chlorine atoms, there was also the possible advantage of extended π bonding. Compound ICI 38174—nicknamed nethalide for a time, but finally christened pronethalol (Fig. 1)—was conceived in excitement and thrilled us at its birth. Pronethalol was an antagonist without any sign of agonist activity in both atrial and ventricular tissues. In anesthetized animals, pronethalol reduced the resting heart rate and depressed the increments from isoprenaline or stimulation of cardiac sympathetic nerves (Fig. 2b).

Having got over the first hurdle much more easily than I had dared to imagine, I was impatient to tackle the next one. How would someone, restricted by β-receptor blockade, cope with a surge of adrenaline or a burst of exercise? I had always imagined that the combination of *Starling*'s "Law of the Heart" and the buffering capacity of the arterio-venous oxygen difference ought to be able to take up the slack of a reduction in cardiac output. We had developed the noninvasive technique of acceleration ballistocardiography to estimate the force of cardiac contractions in anesthetized dogs (Fig. 3). Adrenaline increased heart rate, aortic blood pressure, and force of contractions. After pronethalol, heart rate and force were reduced and the effects of adrenaline were abolished. However, the vasodilator effects of adrenaline were also blocked, thus exposing the heart to a vasoconstrictor load mediated by the unblocked α-receptors. The heart was able to maintain its output and produced an enhanced rise in blood pressure. This was the experiment that convinced me that the new compound might be more than a laboratory curiosity. In fact, I did notice in these early exper-

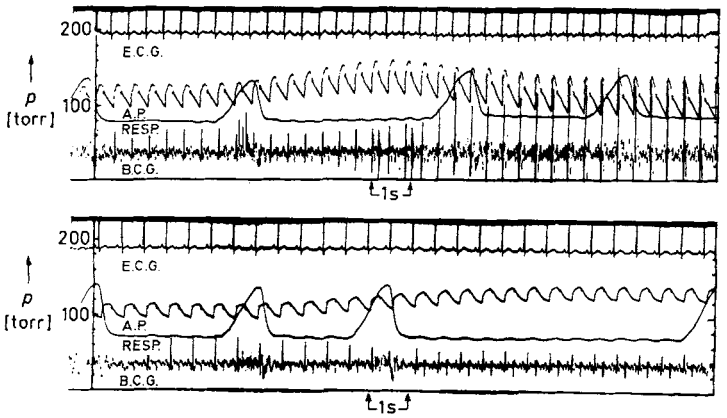


Fig. 3. Cardiac and respiratory responses to adrenaline (1 μg kg^{-1} i.v.) in anesthetized dogs. Top: Before addition of pronethalol. Bottom: 15 minutes after addition of pronethalol. The arrow indicates when adrenaline was administered. E.C.G., electrocardiogram; A.P., aortic blood pressure; RESP, respiration; B.C.G., ballistocardiogram.

iments that the cardiac ballistic action was reduced under load. I noticed also that the time taken from ventricular excitation to the opening of the aortic valves – that is, from the R-wave to the upstroke of aortic pressure – was increased under load. These were tell-tale signs that the cardiac reserve was reduced, but I persuaded myself at the time that this was a reasonable price to pay for the possibility of increasing the work capacity of a heart with restricted coronary flow.

The early clinical studies seemed to confirm that judgment. *Dornhorst* and *Robinson*[10] studied the interaction between pronethalol and isoprenaline in healthy volunteers. Isoprenaline, infused into the brachial artery, produced a large increase in forearm blood flow. However, when repeated after an intraarterial infusion of pronethalol, the first route of administration into man, the vasodilator effect was abolished. Isoprenaline given by slow intravenous infusion increased heart rate, respiratory amplitude, arterial pulse pressures, and forearm blood flow. The subjects in these studies often seemed to get a fear of impending doom and became visibly restless. After pronethalol, all of these effects of isoprenaline were suppressed (Fig. 4). By chance, an athlete and a loafer were the first pair to do maximal exercise after pronethalol. Compared to the control run, the athlete's heart rate at rest and exercise were little changed and his capacity to work was reduced. The loafer's heart rate was substantially reduced by pronethalol at rest and during exercise. He was less distressed by his lower heart rate. The potential benefits of β-adrenoceptor blockade for people with embarrassed hearts was also seen in the first patient with angina of effort. After administration of pronethalol, he was able to do more work before the onset of pain forced him to stop when his heart rate had eventually reached the same level as in the control run (Fig. 5).

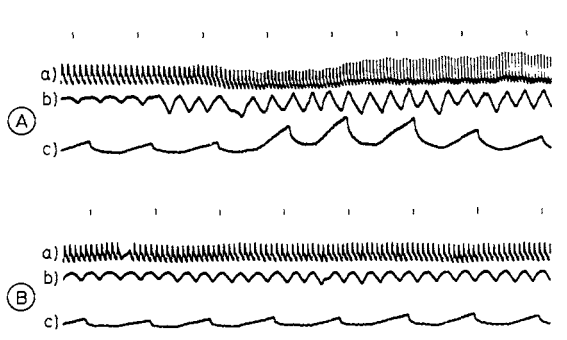


Fig. 4. Effects of intravenous infusion of isoprenaline (10 μg min^{-1}), before Ⓐ and after Ⓑ intravenous infusion of pronethalol (110 mg) on arterial blood pressure (a), respiration (b), and forearm blood flow (c) in a healthy volunteer (reproduced by kind permission from [10]). Time intervals: 10 sec.

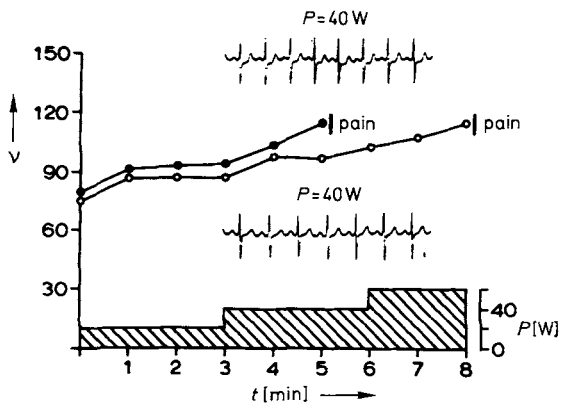


Fig. 5. Effect of pronethalol (250 mg p.o.) on time taken and work exerted before the onset of chest pain in a patient with angina pectoris performing graded exercise on a bicycle. Inserts show the ECG before (top) and after (bottom) administration of pronethalol (reproduced by kind permission from [10]). •, without pronethalol; o, with pronethalol. v = pulse rate.

Pronethalol always seemed to us to be a prototype drug, good enough to answer questions of principle but not good enough to be marketable. So a large chemical group, directed by *Crowther*,[11] was assembled to try to find a more active, safer replacement for pronethalol. The discovery of ICI 45520, propranolol, a naphthyloxy propanolamine derivative, was the result (Fig. 1).

Our bioassays, which had been developed as qualitative screens, had now to be adapted for comparative quantitative bioassay. The isolated, spontaneously beating, guinea-pig right atrial preparation proved to be excellent for these assays. The nature of the surmountable antagonism by propranolol was analyzed by relating the rightward displacement of cumulatively derived dose–response curves to the concentration of antagonist.[34] The linearity and slope of the Schild plot relating these variables indicated the likelihood that adrenaline and propranolol were competing for the same sites. This is the evidence that propranolol can be classified as a *syntopic* antagonist to the native hormones which activate β-adrenoceptors. Note here that I follow *A. J. Clark*[12] in using the term "hormone" very broadly: when one cell secretes a chemical to which another responds physiologically, I define that chemical as a hormone.

Histamine H_2-Receptor Antagonists

In 1964, I went to Smith, Kline & French Laboratories Ltd. to pursue another project that I had been thinking about for some time. Again, the idea had clinical, therapeutic, physiological, and pharmacological implications.

The *clinical* problem was gastric and duodenal ulcers. I had thought a lot about the problem when I worked with

Adam Smith on the effects of 5-hydroxytryptamine on gastric secretion.[13] The immediate cause of ulceration was recognized to be hypersecretion of acid but the nature of the driving stimulus was unknown. The one clear fact was that patients with duodenal ulcers gave an exaggerated secretory response to histamine, the basis of a diagnostic test.

The *therapeutic* problem was that only surgical intervention, partial gastrectomy in those days, was recognized to be effective. The potential value of anticholinergic drugs, like atropine, was obscured by unacceptable side effects. Antacids could be shown to promote ulcer healing but only with clinically unacceptable regimens.

The *physiological* problem was the relationship between gastrin and histamine, both of them powerful stimulants of acid secretion and both synthesized in the mucous membrane of the stomach. *MacIntosh*[14] had proposed that histamine was the final stimulant of secretion when the vagus was stimulated and *Code*,[15] as well as *Kahlson* and *Rosengren*,[16] had extended that idea to gastrin as well, making histamine the *final* common chemostimulant. Mainstream thinking in gastroenterology, however, regarded gastrin as the *direct* hormone of secretion in its own right; thus, the question of the function of histamine in the stomach was unsettled.[17]

The *pharmacological* problem was the selective blocking properties of the antihistamines.[18] The available antihistamines were a diverse group, chemically unrelated to histamine and reminiscent in this respect of the class of adrenaline α-receptor antagonists. They were powerful inhibitors of histamine-induced visceral muscle contractions but had no effect at all against histamine-induced acid secretion, uterine relaxation, or cardiac stimulation. Other effects of histamine, such as vasodilatation, were well known to be insensitive to the antihistamines. The parallels with the spectrum of activity of the antiadrenalines seemed obvious.

In 1964, I had no doubts that histamine had its "β-receptors" and that a new type of selective histamine antagonist could be found. Ambiguity about the physiological role of histamine in acid secretion left me unsure about the clinical value of such drugs. At the very least, however, I expected to answer the physiological question of the gastrin–histamine connection.

The bioassay systems were easily selected. For in vitro assays, guinea-pig ileal muscle was the classical system for studying antihistamines such as mepyramine. Guinea-pig atrial tissue looked like a good assay for mepyramine-refractory histamine responses. The assay for acid secretion was harder to choose. No in vitro assays were available at that time. We chose the Ghosh and Schild method[19] of lumen perfusion of the stomach of anesthetized rats, but the method worked reliably only after it had been substantially modified by *Parsons*, my new colleague.[20]

The chemical program, from the start, concentrated on making analogues and derivatives of histamine. As the whole project was conceived by analogy with the adrenaline β-receptor story, I was particularly anxious to concentrate on varying the imidazole-ring end of histamine. Some of the early ring-substituted compounds turned out to be very important (Fig. 6).[21] Methyl substitution on either of the ring nitrogens produced inactive compounds. Methyl substitution on the 2-position gave compounds that were less active

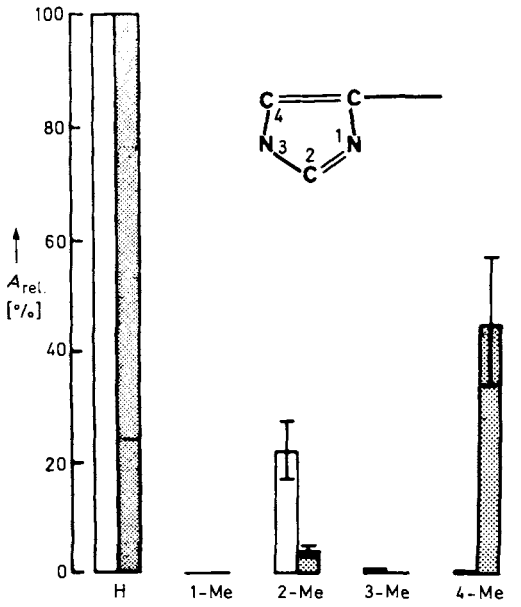


Fig. 6. Selectivity of histamine (H) and several methyl-substituted analogues in the guinea-pig ileum (histamine H_1-receptor assay, □) and right atrium (histamine H_2-receptor assay, ⊠). Activity values, relative to histamine (A_{rel}), were calculated from parallel line assays. Error bars show 95% confidence limits.

than histamine itself but nevertheless showed a clear preference for the ileal assay. However, 4-methylhistamine was exciting for me. Nearly half as active as histamine on the atrial assay, 4-methylhistamine was practically inactive on the ileal assay. We were able to confirm this selectivity in vivo (Fig. 7). In the anesthetized rat preparation, an injection of

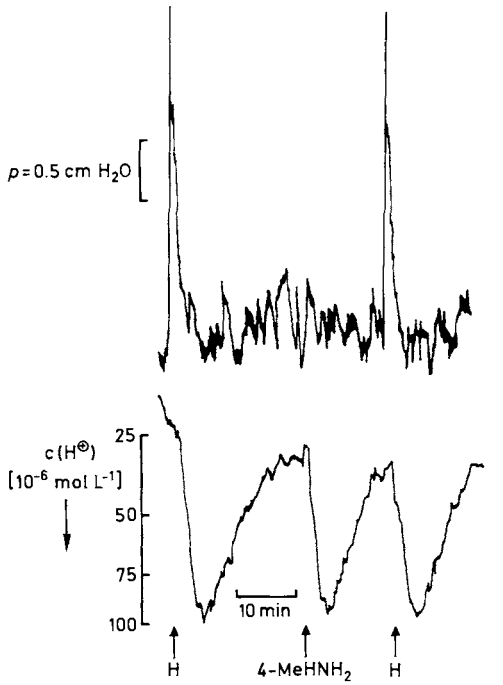


Fig. 7. Effects of intravenous bolus injections of histamine (H, 2 μg kg^{-1}) and 4-methylhistamine (4-$MeHNH_2$, 5 μg kg^{-1}) on secretion of gastric acid (bottom) and stomach wall contraction (top) in an anesthetized rat. c = concentration, p = pressure.

histamine produced a fast, spasmodic contraction of the stomach wall followed by a phasic burst of acid secretion; 4-methylhistamine produced an equivalent output of acid without any muscle contractions. Thus, 4-methylhistamine

was a selective agonist analogous to isoprenaline at adrenergic receptors. This result was the compelling clue which kept us going through several lean years of negative screening.

This observation assumed even greater importance when we compared 4-methylhistamine and 2-methylhistamine with the 1,2,4-triazole analogue of histamine. Using a number of additional assays, both in vitro and in vivo, we found that the triazole analogue was clearly nonselective, whereas 2-methylhistamine was selective for the mepryamine-sensitive responses and 4-methylhistamine was selective for the refractory responses (Fig. 8). When *Ash* and *Schild* proposed

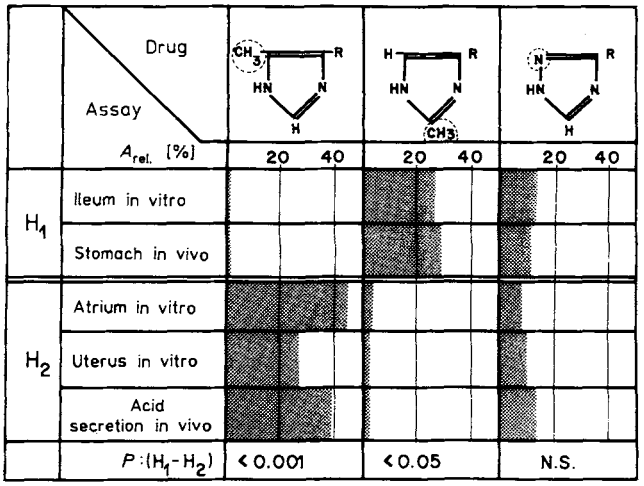


Fig. 8. Selectivity of 2-methylhistamine, 4-methylhistamine, and 1,2,4-triazole analogue of histamine in several in vitro and in vivo, histamine H_1- and H_2-receptor assays. The activity relative to histamine (A_{rel} was calculated from parallel line assays. p (H_1-H_2) = probability value for the difference between H_1 and H_2 results.

in 1966 that the mepyramine-sensitive histamine receptors should be classified as H_1,[22] we used this pattern of bioassay results to argue for the homogeneity of a non-H_1 class of histamine receptor.

A very large number of compounds were made, predominantly ring substitutions and fused-ring heterocycles, all of them inactive. I vividly remember wondering suddenly if the strategy was all wrong. Perhaps we should have spent more time exploring the role of the side-chain amino group. On this suggestion, *Parsons* quickly scanned through the earlier compounds looking for examples of side-chain variations. He came up with N^{α}-guanylhistamine (Fig. 9). This compound was one of the earliest we had tested and had proved to be quite a potent agonist when injected, like histamine, intravenously. However, over the years we had changed the design of the screening assay. A continuous intravenous infusion of histamine was used to produce a stable background of near-maximal acid secretion. A new compound could now be quickly screened by giving a succession of increasing doses intravenously. Even antagonism of very short duration would be detectable. In the new experimental design, the guanidino analogue of histamine now exhibited a small degree of inhibition, about 5% reduction. There it was – a partial agonist! Guanylhistamine on histamine receptors was the analogue of DCI on β-adrenoceptors. However, unlike DCI, the efficacy of histamine had been reduced by modifying the side-chain rather than the ring system.

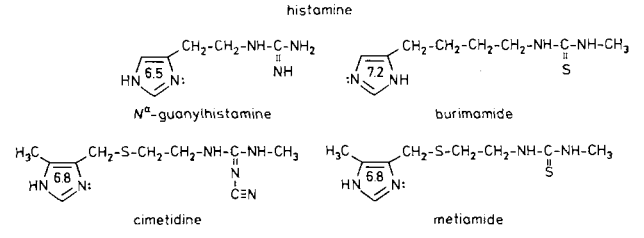


Fig. 9. Chemical structures of histamine-related imidazoles. The numbers inside the rings are pK_a values.

This was the lead that *Ganellin* and his colleagues in chemistry had been waiting for. In one of the early analogues, IPG, the length of the side chain was simply increased from ethyl to propyl. In the rat stomach assay this compound showed good antagonism of histamine without much agonist activity of its own. However, in other species, particularly cat and dog, the compound was nearly a full agonist. Similarly, in the isolated guinea-pig atrial preparation, although much less potent than histamine, the compound achieved a maximum response of about 80% of the histamine maximum. The true nature of this partial agonism could be seen by repeating the dose–response curve in the presence of a nearly maximal concentration of histamine. Only *antagonism* was now seen with the maximum inhibition, about 20%, being equal to the agonist maximum (Fig. 10).

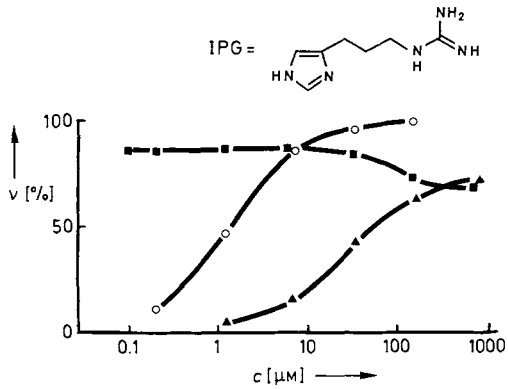


Fig. 10. Effects of cumulative additions of histamine (○), imidazolylpropylguanidine (IPG, ▲), and IPG in the presence of 10 μM histamine (■) on the pacemaker frequency (ν) of the isolated guinea-pig right atrium. Error bars have been removed for clarity (n = 7). ν given in % of the maximum of histamine.

Lengthening the side chain to four carbon atoms and replacing the strongly basic guanidino group by the neutral methyl thiourea group produced burimamide (Fig. 9), the first antagonist of moderate activity which had low enough efficacy to avoid being an agonist in any of our assays. Burimamide, having relatively low potency and poor oral bioavailability, was clearly only a prototype. *Ganellin* saw the way forward. The nonbasic, electron-releasing side chain in burimamide, compared to the basic, electron-withdrawing side chain in histamine, raised the pK_a of the ring and favored the 3*H* tautomer. Inserting the electronegative thioether linkage in place of a methylene and introducing the

4-methyl group to favor H_2-receptor selectivity produced metiamide (Fig. 9), which was much more potent and better absorbed than burimamide. Toxicity associated with thiourea was then eliminated by replacing the thiourea sulfur with a C=N–CN group to produce cimetidine (Fig. 9).

On the atrial assay in vitro, burimamide produced surmountable antagonism, shown by rightward parallel displacement of the histamine dose–response curves. When analyzed by the Schild method, burimamide behaved like a syntopic antagonist to histamine. The estimated dissociation constants (K_B) were found to be independent of the potency of the titrating agonist and also independent of the tissue (atrium or uterus) used for the assay, substantially confirming the syntopic classification (Fig. 11). The high value on the ileum, an H_1 system, disclosed the compound's selectivity. As *Ash* and *Schild*[22] had proposed the notation H_1, we proposed that burimamide should be classed as an H_2-receptor antagonist.

	Atrium	Uterus	Ileum
Histamine	7.8	6.6	288
4-Methylhistamine	7.2		
2-Methylhistamine	6.9		

Fig. 11. Equilibrium dissociation constants (K_B [μM]) for burimamide in guinea-pig right atrium and rat uterus (histamine H_2-receptor assays) and in guinea-pig ileum (histamine H_1-receptor assay) against histamine and its analogues.

The analytical capability to distinguish an antagonist that acts at the same site as the native hormone from one that does not act syntopically – which is a functional antagonist – seems to me to be important in drug research for two reasons. For a defined homogeneous population of receptors, widely disseminated across tissues, the properties of the syntopic antagonist can be generalized. As the mechanism of action of the functional antagonist is unknown, however, its properties have to be identified on a tissue-by-tissue basis. Again, the analytical power of a syntopic antagonist – that is, its ability to prove hormonal involvement in physiological processes – is likely to be greater than for a functional antagonist. Of course, a compound that is a syntopic antagonist at one receptor system can also be a functional antagonist at a different receptor system. However, a possible combination of syntopic and functional properties would be expected to vary between different molecules, and the confusion can be eliminated by building up a class of syntopic antagonists that are chemically distinct but pharmacologically homogeneous. Syntopic antagonists are the best tools that analytical pharmacologists possess.

This problem of the resolving power of a receptor antagonist was seen from the beginning with metiamide. The histamine-induced acid secretion in the rat assay, having reached a plateau, was promptly inhibited when metiamide was given intravenously. Metiamide was found to be equally effective at inhibiting pentagastrin-induced secretion but much less effective against carbachol-induced secretion. Failure to inhibit cholinergically stimulated secretion showed that metiamide was not a nonspecific inhibitor of acid secretion. The ability of metiamide to inhibit the effects of gastrin pointed to potential clinical utility, but it was not at all clear that this result might contribute to a resolution of the gastrin–histamine controversy.

The problem became clear when the interactions between metiamide and the various stimulants were studied quantitatively in dogs with Heidenhain pouches.[23] Metiamide displaced the histamine dose–response curves in parallel to the right, as would be expected for a surmountable, syntopic antagonist (Fig. 12). Carbachol's steep dose–response curves were relatively refractory to inhibition. However, the flatter dose–response curves to pentagastrin were depressed downwards as well as being displaced to the right (Fig. 12).

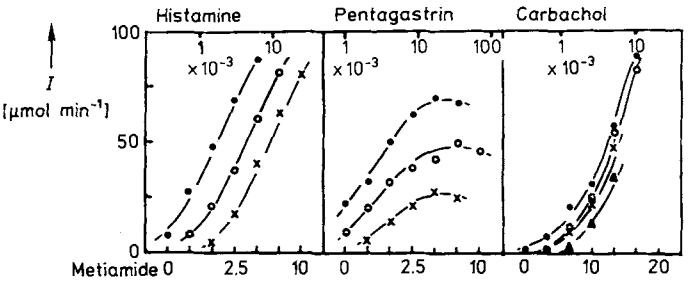


Fig. 12. Effects of intravenous infusion of metiamide against histamine-, pentagastrin-, and carbachol-induced gastric acid secretion in anesthetized dogs with Heidenhain pouches. Doses shown are μmol kg^{-1} min^{-1} for the agonists (upper abscissae); μmol kg^{-1} h^{-1} for metiamide (● = 0, ○ = 2.5, × = 10, ▲ = 20 μmol kg^{-1} h^{-1}). I = acid secretion. Reproduced by kind permission from [23]).

At that time I did not know what to expect if H_2-receptor blockade inhibited gastrin only because histamine was the final common chemostimulant. I could not rule out the possibility that these drugs were functional antagonists of gastrin. Subsequently, when other workers had confirmed the different patterns of inhibition in other species, and with different compounds, an unspecific inhibitory action seemed unlikely. The pattern also became understandable when I was able to model indirect competitive antagonism and applied the model to tyramine, a well-characterized indirectly acting agonist, to show that it was inhibited insurmountably by propranolol, just like the gastrin–metiamide interaction.[24]

When we took the H_2-receptor antagonists into human volunteers, there were no surprises in the patterns of secretory inhibition. However, we did get a surprise, right at the start, with burimamide. We followed the standard clinical practice of giving the volunteers mepyramine before giving them histamine intravenously. Even so, the subjects showed marked skin and conjunctival vasodilatation. The surprise was that treatment with burimamide completely blocked this vasodilatation. In the laboratory, burimamide alone had had no effect on histamine-induced vasodilatation. As both H_1- and H_2-receptors were involved, both antagonists were needed. This finding thus explained the results of *Folkow* et al.[25] of 30 years earlier.

Hormone-Receptor Antagonists in the Future

The histamine project was started by analogy with my experience of the adrenaline project. In retrospect, I think they have some features in common which helped them to

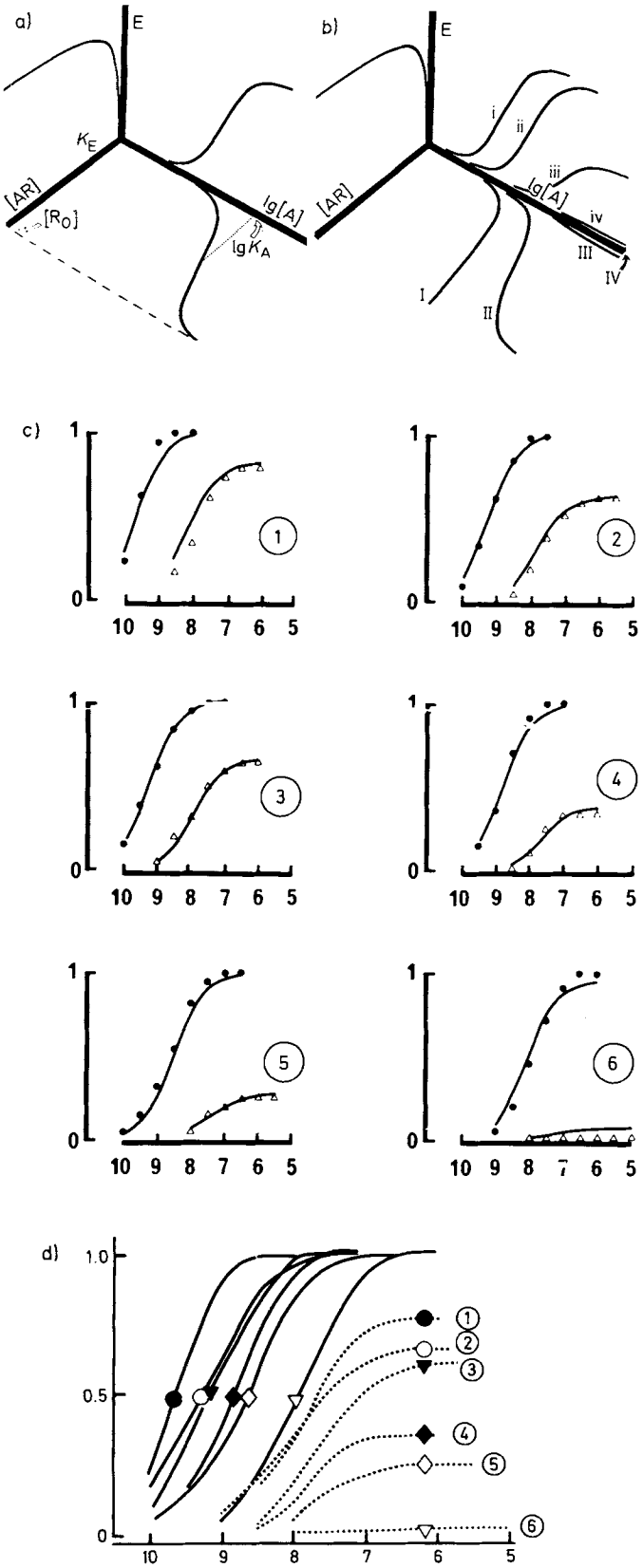


Fig. 13. a) Three-dimensional display of the operational model of agonism [26]. E, pharmacological effect; lg [A], logarithmic concentration of agonist A; lg K_A, log equilibrium agonist dissociation constant; [R_0], operational receptor concentration; [AR], concentration of receptors occupied by A; K_E, concentration of AR required for half-maximal tissue response. The three planes of the figure represent pharmacological effect (right panel), binding or affinity (base panel), and efficacy or transduction (left panel). b) Predictions of the influence of changes in [R_0] on pharmacological effect using the operational model of agonism. Curves I to IV show [R_0] values decreasing successively by tenfold giving rise to effect curves i to iv, respectively. c) Behavior of isoprenaline (●) and prenalterol (△) in guinea-pig tracheal muscle ①, cat left atria ②, rat left atria ③, cat papillary ④, guinea-pig left atria ⑤, and guinea-pig extensor digitorum longus muscle ⑥ [27]. The data has been regressed to the operational model of agonism allowing only [R_0] to vary between tissues. Abscissa: negative log molar agonist concentration [M]. Ordinate: Fractional response to isoprenaline. d) Representation of the model-simulated curves from Figure 13c superimposed on a single pair of axes. ——, isoprenaline; ···, prenalterol. ①–⑥ and axes: see Figure 13c.

succeed. Both started from well-recognized clinical problems at a time when they could be illuminated by specific hypothetical modeling at the laboratory level. The laboratory modeling defined the chemical starting points and the types of bioassay. The clinical problem defined how the newly classified drug should be tested in volunteers and patients. If the intimate coupling of clinical experience and pharmacological modeling has the effect of helping to eliminate wishful thinking in drug research, then the limiting step in the future will be the development and improvement of these models.

Models in analytical pharmacology are not meant to be descriptions, pathetic descriptions, of nature; they are designed to be accurate descriptions of our pathetic thinking about nature. They are meant to expose assumptions, define expectations, and help us to devise new tests.

Traditionally, pharmacological modeling of hormone-receptor systems has been based on the application of the Law of Mass Action to reversible interactions. Therefore, they are all chemical, molar models characterized by thermodynamic parameters. The discovery, often in a homologous series of compounds, that not all agonists could produce the same maximum response (now defined as partial agonists) led to models which had both binding, or affinity, parameters and efficacy, or response-generating, parameters. In both of the studies that I have sketched for you today, chemical modification of a native hormone produced, first of all, selective agonists, then quite separate chemical changes produced partial agonists and finally pure antagonists. The assumption is that partial agonists and antagonists are associated with a relative loss of efficacy – emasculated hormones.

The discovery of partial agonists was, in both studies, crucial to the development of syntopic antagonists. Yet I very nearly, and could quite easily, have failed to discover them. The choice of tissue for the assay was vital. So, why is the expression of efficacy so tissue dependent? How can we try to choose tissues which are most likely to allow us to detect partial agonists?

To illuminate these questions, *Leff* and I developed an operational model of agonism which defined three mutually connected surfaces such that knowing the shape of the function on any two allowed us, syllogistically, to deduce the necessary shape of the function on the third space (Fig. 13a).[26] On the right-hand side of the graphical display of the model is the measured function that relates agonist concentration, on a logarithmic scale (lg [A]), to the tissue effect which it produces. The pharmacological assumption is that the agonist initiates an effect by binding to a receptor (R); then the bound receptor (AR) activates a messenger system that produces the effect. Therefore, the base of the display shows the assumed relationship between agonist concentration and the concentration of bound receptors – the *affinity* relation.

Then, the left-hand panel shows the deduced relation between bound receptor concentration and effect – the *efficacy* relation. The behavior of this model is critically determined by the ratio of $[R_0]$, the total receptor concentration, to K_E, the concentration of bound receptor needed to produce a half-maximal effect. For example, when $[R_0]$ is equal to K_E the agonist can only produce a half-maximal response, thus defining a 50% partial agonist (Fig. 13b).

One of the first uses of the model was to fit simultaneously all of the data which *Kenakin* and *Beek*[27] had got from comparing isoprenaline and prenalterol, a partial agonist at β-receptors, on six different tissues (Fig. 13c). The model of agonism allowed all of the data to be fitted by the theoretical curves shown when only one parameter, total receptor density, was allowed to vary. The concentration of receptors is now known to vary between tissues, so that this seems to me to be an attractive way of accounting for the tissue dependence of a partial agonist's efficacy. Superimposing all the dose–response curves clearly demonstrates that the tissues most sensitive to isoprenaline support the greatest maximum responses to prenalterol and vice versa (Fig. 13d). Practically, therefore, the best way to avoid missing a partial agonist is to measure the potency of the native hormone or full agonist on as many tissues as possible and select assays expressing both high and low efficacy. This seems to be a robust test, relatively insensitive to the mechanisms underlying the differences in sensitivity.

Partial agonists, as empirical facts, have been recognized for many years. Pharmacological modeling of partial agonism and the related concept of efficacy has, however, developed more slowly. Fundamental problems about the nature of efficacy, either as a molar, thermodynamic concept or as a molecular problem in wave mechanics have still to be tackled. However, there seems no doubt about the pragmatic utility in drug research of distinguishing potency changes from efficacy changes in the bioassay of hormone analogues. The discovery of a partial agonist is the vital clue in developing useful syntopic antagonists.

We have gone on to use the model to study the effects of the slope of dose–response curves,[28] functional antagonism,[29] indirect competitive antagonism,[30] dual receptor systems, and receptor distribution when there is a relatively high concentration of transducer molecules.

The dose–response relation can, of course, be broken down into any two necessarily connected steps. Thus, the gastrin dose–response curve of acid secretion can be broken down into the gastrin/histamine-released relation followed by the histamine-released/acid secretion response relation. Two of the relations are known from measurement and the third, the gastrin/histamine-released relation, can be deduced. Using this model, *Shankley* and I were able to make a correct estimate of the K_B of an H_2-receptor antagonist from the family of unsurmountable curves produced by its interaction with pentagastrin, an important piece of evidence linking local histamine release to the physiological action of gastrin.

The approach I have outlined so far has regarded hormones and their conjugate receptors as simple, linear, "command-control" systems. The approach has undoubtedly had some success. Nevertheless, I think if we want to continue to try to develop new drugs by mimicking and manipulating physiological chemical control systems, our ideas will have to become more sophisticated. There is plenty of evidence now that hormone receptors and their dependent messengers are not insulated from each other. Mutually enhancing interactions between any two receptor–messenger systems can occur at many different points, leading to different kinds of physiological advantage.

When one hormone can interact with two allosterically linked receptors on the same cell, the continuous gearing can change the relatively flat concentration–response curve characteristic of the Mass-Action-Law behavior of a one-receptor system into steep curves. This greatly reduces the change in concentration needed to sweep the cellular response through its full range. This could be an advantage for fast-responding cells. When there are two hormones and two receptors, mutual potentiation can lead to threshold changes and pulsing signals and, more importantly, by making the activity of one hormone depend on the other, the convergence changes the type of behavior from obligatory responses to conditional responses, like those of nerve cells, based on summation (Fig. 15).

The rich possibilities of hormonal convergence plus inter-receptor amplification are now being discovered in the area of neuroendocrine secretion. While coexistence of multiple hormones in a single nerve ending does not necessitate co-transmission, there seems as yet no need to doubt it. *Hokfelt* et al., in a recent review,[31] pointed out that the distribution of these hormones was not random. For example, neurones classified as 5-HT-, noradrenaline-, or dopaminetransmitting each had different groups of peptides coexisting in their terminals. Neurobiologists have plenty of ideas about the significance of the very large and rapidly growing number of pharmacologically active substances which have been identified in nervous tissue. However, as an outsider looking in on all their excitement, I sense that my colleagues have problems with the Principle of Parsimony. Neurotransmission involving discrete, microscopic events is unlikely to generate problems with chemical cross talk in the brain at large. So, is there not now an embarrassing number of potential neurotransmitters?

On the other hand, biologists concerned with brain development probably do need an abundance of specific cell markers. *Sperry*'s chemoaffinity hypothesis,[32] one of the earliest attempts to account for the details of pattern development in the embryonic brain, required that cells have individual chemical identification markers almost down to the level of single cells. *Edelman*'s modulation hypothesis[33] – how the composition and density of nerve cell adhesion molecules can be locally regulated by the cells themselves – is chemically much more economical. These molecules subserving cell-to-cell interactions can provide a framework for guiding neurite growth cones. Diffusible growth factors, such as the specific nerve growth factor, can provide a general engine for neural growth into a supporting network. The question that intrigues me, however, is whether the framework and the engine are enough to account for the exquisite fine-tuning of synaptic connections which occurs during brain maturation and for the control of synaptic plasticity now known to be a feature of the mature brain.

I like the idea that these synaptic connections are determined chemotactically. An effective chemotactic address

might then involve the cooperative signaling of two or more chemicals. The possibilities for chemotactic signatures are factorial. If an effective signal involved just three chemicals, then 100 hormones could provide over a hundred thousand different signatures in any one compartment.

As our ideas about hormone–receptor systems become progressively more complicated in terms of multiplex pathways, hierarchy due to cellular conjunctions and biochemical cascades, the reductionist methods of molecular biology would seem to offer modern drug research a way out: simplify the systems by receptor isolation and expression. Molecular biology undoubtedly holds out the promise of the most direct and productive route ever to screening chemicals as hormone receptor reagents. However, once classified at the molecular level, a new reagent will have to be evaluated at the level of tissue complexity to confirm its classification and define its selectivity. These tissue bioassays, such as I have discussed today, may seem old-fashioned but, properly designed, they are arguably the best methods we have for making reliable predictions about clinical outcomes. They have served us well but they need to be continually improved, both technically and in their related operational models, to match our changing ideas. Molecular biology will continue to provide drug research with extraordinary analytical methods and lend a richer texture to our imagination.

These reflections suggest that there will be both great opportunities, and potential dangers, for the development of specific hormone receptor reagents in the future. The limiting factors, however, are likely to be the verisimilitude of our models and the complexity of our bioassays.

Received: January 27, 1989 [A 725 IE]
German version: *Angew. Chem. 101* (1989) 910

[1] G. Smith, D. D. Lawson, *Scott. Med. J. 3* (1958) 346.
[2] H. H. Dale, *J. Physiol. (London) 34* (1906) 163.
[3] H. Konzett, *Naunyn-Schmiedebergs Arch. Exp. Pathol. Pharmakol. 197* (1940) 27.
[4] R. P. Ahlquist, *Am. J. Physiol. 153* (1948) 586.
[5] W. B. Cannon, A. Rosenbleuth: *Autonomic Neuroeffector Mechanisms*, Macmillan, New York 1939.
[6] C. E. Powell, I. H. Slater, *J. Pharmacol. Exp. Ther. 122* (1958) 480.
[7] N. C. Moran, M. E. Perkins, *J. Pharmacol. Exp. Ther. 124* (1958) 223.
[8] E. J. Ariens, *Arch. Int. Pharmacodyn. Ther. 99* (1954) 32.
[9] R. P. Stephenson, *Br. J. Pharmacol. Chemother. 11* (1956) 379.
[10] A. C. Dornhorst, B. F. Robinson, *Lancet 1962 II*, 314.
[11] J. W. Black, A. F. Crowther, R. G. Shanks, L. H. Smith, A. C. Dornhorst, *Lancet 1964 I*, 1080.
[12] A. J. Clark: *The Mode of Action of Drugs in Cells*, Edward Arnold, London 1933.
[13] J. W. Black, E. W. Fisher, A. N. Smith, *J. Physiol. (London) 141* (1958) 27.
[14] F. C. MacIntosh, *Q. J. Exp. Physiol. Cogn. Med. Sci. 28* (1938) 87.
[15] C. F. Code, *Fed. Proc. Fed. Am. Soc. Exp. Biol. 24* (1965) 1311.
[16] G. Kahlson, E. Rosengren, *Experientia 28* (1972) 993.
[17] S. P. Grossman, *Handb. Physiol. Sect. 6 Aliment. Canal Vol. 1* (1967) 287.
[18] E. R. Loew, *Physiol. Rev. 27* (1947) 542.
[19] M. N. Ghosh, H. O. Schild, *Br. J. Pharmacol. Chemother. 13* (1958) 54.
[20] M. E. Parsons, *Ph.D. Thesis*, University of London 1969.
[21] J. W. Black, W. A. M. Duncan, G. J. Durant, C. R. Ganellin, M. E. Parsons, *Nature (London) 236* (1972) 385.
[22] A. S. F. Ash, H. O. Schild, *Br. J. Pharmacol. Chemother. 27* (1966) 427.
[23] J. W. Black in C. J. Wood, M. A. Simkins (Eds.): *Int. Symp. on Histamine H_2-Receptor Antagonists*, SK & F, Welwyn Garden City, Großbritannien 1973, p. 219.
[24] J. W. Black, D. H. Jenkinson, T. P. Kenakin, *Eur. J. Pharmacol. 65* (1980) 1.
[25] B. Folkow, K. Maeger, G. Kahlson, *Acta Physiol. Scand. 15* (1948) 264.
[26] J. W. Black, P. Leff, *Proc. R. Soc. London B 220* (1983) 141.
[27] T. P. Kenakin, D. Beek, *J. Pharmacol. Exp. Ther. 213* (1980) 406.
[28] J. W. Black, P. Leff, N. P. Shankley, J. Wood, *Br. J. Pharmacol. 84* (1985) 561.
[29] P. Leff, G. R. Martin, J. M. Morse, *Br. J. Pharmacol. 85* (1985) 655.
[30] J. W. Black, P. Leff, N. P. Shankley, *Br. J. Pharmacol. 86* (1985) 589.
[31] T. Hokfelt, D. Millhorn, K. Seroogy, Y. Tsuruo, S. Ceccatelli, B. Lindh, D. Meister, T. Melander, M. Schalling, T. Bartfai, L. Terenius, *Experientia 43* (1987) 768.
[32] R. W. Sperry, *Proc. Natl. Acad. Sci. USA 50* (1963) 703.
[33] G. M. Edelman, *Annu. Rev. Neurosci. 7* (1984) 339.
[34] J. W. Black, W. A. M. Duncan, R. G. Shanks, *Br. J. Pharmacol. Chemother. 25* (1965) 577.
[35] J. W. Black, J. S. Stephenson, *Lancet 1962 II*, 311.

Communications may be submitted in English *or* in German. Further details regarding the submission of communications can be found in the "Notice to Authors" reproduced in the January issue of the journal. Copies thereof may be obtained from the editorial office upon request.

The First PE-Spectroscopic Investigations of Lithium, Sodium, and Potassium *tert*-Butoxide **

By *Manfred Braun,** *Delia Waldmüller,* and *Bernhard Mayer*

Lithium, sodium, and potassium *tert*-butoxide, reagents widely used by several generations of chemists, are monomeric neither in the crystal nor in nonpolar solvents, although this is suggested by the usual formulas $LiOC(CH_3)_3$ **1**, $NaOC(CH_3)_3$ **2**, and $KO(CH_3)_3$ **3**. For example, potassium *tert*-butoxide was found by X-ray structure analysis to exist as a tetramer,[1] whereas, in the case of the corresponding sodium alkoxide, both hexamers and nonamers are present in the crystal.[2, 3] An incomplete X-ray structure investigation of lithium *tert*-butoxide also revealed the possible presence of hexameric aggregates.[4] In THF, the alkoxides **1**–**3** all form tetramers, whereas the lithium alkoxide **1** forms hexameric[5–7] aggregates in benzene, toluene, and cyclohexane.[8] Even in the gas phase (up to ca. 200 °C), the readily sublimable alkoxides do not dissociate to monomers. Thus, mass-spectrometric investigations indicate that, in the gas phase, lithium *tert*-butoxide is present exclusively as the hexamer.[9] Besides hexamers, heptamers of sodium *tert*-butoxide were also found in the gas phase.[2] On the other hand, potassium *tert*-butoxide is tetrameric in the gas phase according to mass spectrometry.[1]

With the goal of studying the "inherent" properties of the aggregated alkoxides **1**–**3**, uninfluenced by a solvent, we have recorded the photoelectron (PE) spectra of these compounds in the gas phase at temperatures between 150 and 180 °C.[10, 11] Figure 1 shows the PE spectrum of lithium *tert*-butoxide and, below it, the orbital energies calculated for aggregates of various size by the MNDO procedure.[12] The characteristic broad double band ① in the region of 8.0 to 9.8 eV presumably arises from molecular orbitals with predominant contributions from the oxygen atoms. This is suggested by a comparison of this PE spectrum with that of *tert*-butyl alcohol, the lowest ionization potential of which lies at 10.23 eV,[13] and confirmed by a comparison of the alkoxide spectrum with the calculated orbital energies (Fig. 1).

The orbital energies of 9.08 eV of the degenerate HOMOs in the monomer (line a), assignable to the nonbonding electron pairs of the oxygen atom, contrast markedly with the spectroscopically observed broad splitting of band ①. This broadening can be explained by the presence of aggregates in the gas phase.[14] For dimeric lithium *tert*-butoxide (line b), the calculations thus predict the existence of four HOMOs that are clearly separated at lower energy from the remaining orbitals. Structure **4**, with a planar four-membered ring, was assumed in these calculations.[15] Since mass-spectrometric investigations have shown that lithium *tert*-butoxide is a hexamer in the gas phase,[9] it was of particular interest to calculate its electronic structure. Structure **5**, in which each oxygen atom is coordinated by three lithium atoms,[16] was used in these calculations. As expected, further splitting was observed in region ① (line c) in comparison with the dimer.[17]

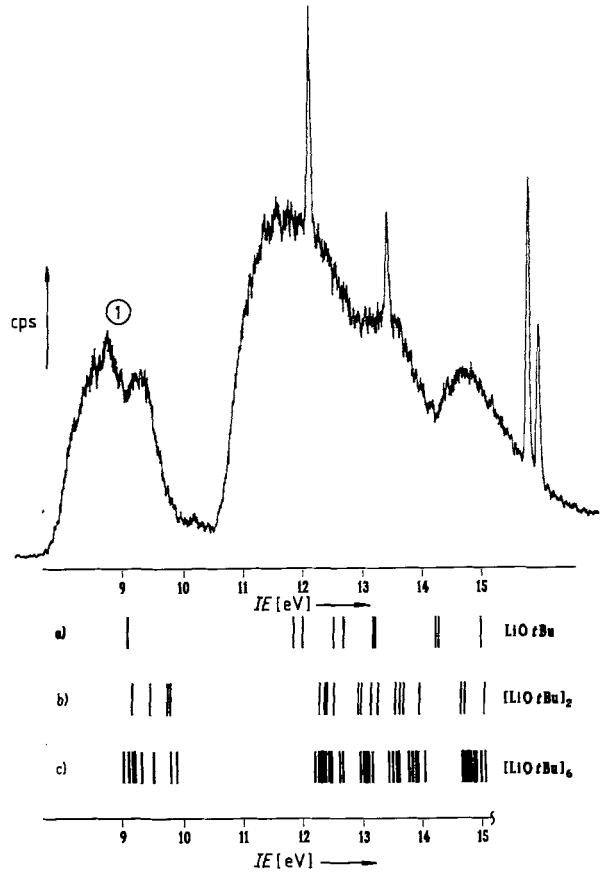
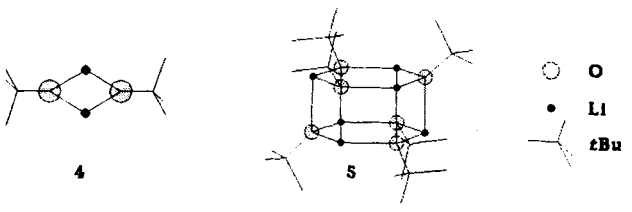


Fig. 1. PE spectrum of lithium *tert*-butoxide in the gas phase and calculated orbital energies [eV] for monomeric, dimeric, and hexameric lithium *tert*-butoxide.



Comparison of the PE spectrum of lithium *tert*-butoxide in the gas phase with those of sodium and potassium *tert*-butoxide (Fig. 2) reveals a clear shift of the lowest ionization potential to lower energies on going from lithium to sodium to potassium (cf. ①, ②, ③).

[*] Prof. Dr. M. Braun, Dipl.-Chem. D. Waldmüller, Dr. B. Mayer
Institut für Organische und Makromolekulare Chemie der Universität
Universitätsstrasse 1, D-4000 Düsseldorf 1 (FRG)

[**] This work was supported by the Fonds der Chemischen Industrie.

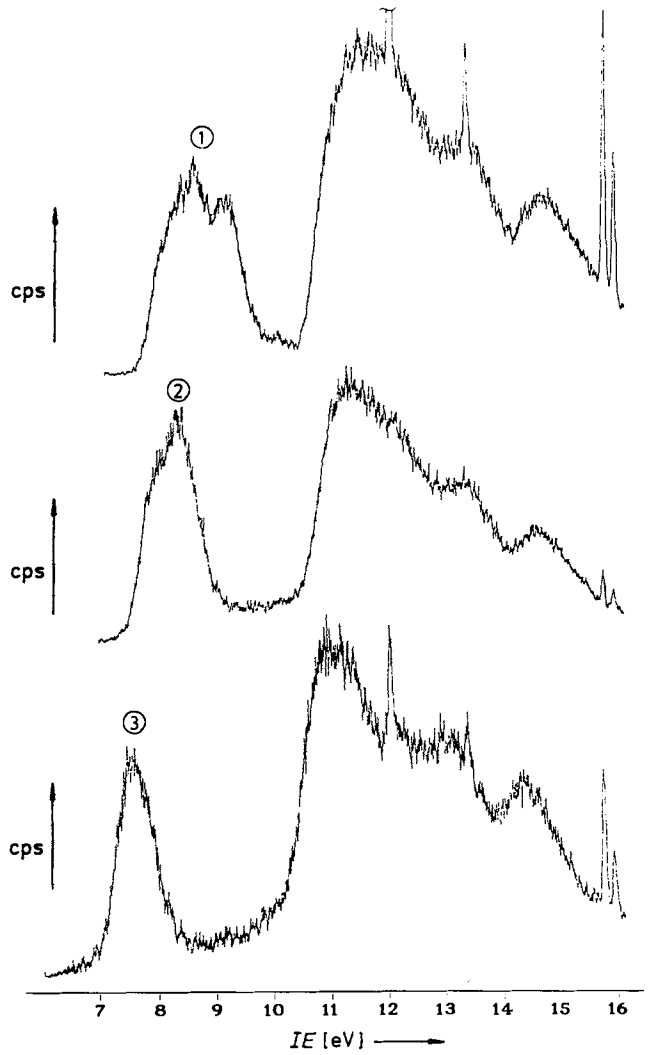


Fig. 2. PE spectra of lithium (top), sodium (middle), and potassium *tert*-butoxide (bottom) in the gas phase.

Assuming that the ionic character of the metal–oxygen bond increases in the order "LiO*t*Bu" < "NaO*t*Bu" < "KO*t*Bu", these spectra appear to support the conclusion that the ionization of alkoxides to their corresponding radical cations becomes easier as the electron density at the oxygen atom is increased. For the hexameric lithium *tert*-butoxide, MNDO calculations give a charge of −0.45 at the oxygen atom; for the monomer, on the other hand, a charge of −0.60 was calculated. Accordingly, a more highly aggregated species should be more difficult to ionize, as has already been shown for hydroxides of lithium, sodium, and potassium by PE spectroscopy.[18] It remains to be determined, however, whether ionization potentials can generally be correlated with a charge separation in alkali metal–heteroatom bonds.

Received: February 20, 1989 [Z 3180 IE]
German version: *Angew. Chem. 101* (1989) 953

[1] E. Weiss, H. Alsdorf, H. Kühr, H.-F. Grützmacher, *Chem. Ber. 101* (1968) 3777–3786.
[2] T. Greiser, E. Weiss, *Chem. Ber. 110* (1977) 3388–3396.
[3] J. E. Davies, J. Kopf, E. Weiss, *Acta Crystallogr. Sect. B 38* (1982) 2251–2253.
[4] H. Huml, *Czech. J. Phys. B 15* (1965) 699–700. More recent investigations have not resulted in an unambiguous structure either, owing to the poor quality of the crystals. However, the available data support the existence of hexameric aggregates (E. Weiss, personal communication 1989).
[5] Thermoelectric, cryoscopic, and ebullioscopic molecular-weight determinations: V. Halaska, L. Lochmann, D. Lim, *Collect. Czech. Chem. Commun. 33* (1968) 3245–3253.
[6] Comparison of the IR spectra of pure and dissolved species.: P. Schmidt, L. Lochmann, B. Schneider, *J. Mol. Struct. 9* (1971) 403–411.
[7] ^{7}Li relaxation: G. E. Hartwell, A. Allerhand, *J. Am. Chem. Soc. 93* (1971) 4415–4418.
[8] Dissociation to monomers and free ions has only been observed so far in DMSO: J. H. Exner, E. C. Steiner, *J. Am. Chem. Soc. 96* (1974) 1782–1787.
[9] G. E. Hartwell, T. L. Brown, *Inorg. Chem. 5* (1966) 1257–1259. Mass spectra recorded by the retarding potential difference (RPD) technique show an $Li_6R_5^{\oplus}$ peak of high intensity for an appearance potential of 9.6 eV. Smaller fragments, such as $Li_4R_3^{\oplus}$, only appear at appreciably higher potentials.
[10] Leybold-Heraeus UPG 200, Köln; He I line; calibration peaks Xe (12.14, 13.44 eV) and Ar (15.76, 15.94 eV).
[11] To the best of our knowledge, no PE-spectroscopic investigations of alkali metal alkoxides in the gas phase were carried out previously. A PE measurement of lithium surfaces exposed to methanol vapor has been reported: J. A. Schultz, S. M. Gates, L. G. Pedersen, R. C. Jarnagin, *Chem. Phys. Lett. 72* (1980) 156–161; *Surf. Sci. 118* (1982) 634–648.
[12] M. J. S. Dewar, W. Thiel, *J. Am. Chem. Soc. 99* (1977) 4899, 4907; *QCPE 438, QCPE Bull. 2* (1982) 63. We thank Prof. *H.-D. Martin* (Universität Düsseldorf) for stimulating discussions in connection with carrying out the calculations.
[13] A. D. Baker, D. Betteridge, N. R. Kemp, R. E. Kirby, *Anal. Chem. 43* (1971) 375–381; M. B. Robin, N. A. Kuebler, *J. Electron Spectrosc. Relat. Phenom. 1* (1972/1973) 13–28; H. Ogata, H. Onizuka, Y. Nihei, H. Kamada, *Bull. Chem. Soc. Jpn. 46* (1973) 3036–3040.
[14] In this connection, both mass-spectrometric and PE-spectroscopic investigations at higher temperatures would be interesting, since, under these conditions, a dissociation to monomers is conceivable (cf. [18]). Corresponding investigations are in progress.
[15] This structure is obtained from ab initio calculations, for example of $(LiOH)_2$: K. Raghavachari, *J. Chem. Phys. 76* (1982) 5421–5426; cf. also E. Kaufmann, T. Clark, P. von R. Schleyer, *J. Am. Chem. Soc. 106* (1984) 1856–1858, and references cited therein.
[16] Optimized geometry: Li-O 2.10, O-C 1.38, C-C 1.58 Å. For simplification, the calculations were carried out for D_{3d} symmetry. Analogous structures have been found experimentally for ketone enolates as well as for lithiated secondary amides. P. G. Williard, G. B. Carpenter, *J. Am. Chem. Soc. 108* (1986) 462–468; D. Seebach, unpublished.
[17] MO energies [eV] of **5** (symmetries of the highest occupied orbitals) calculated by MNDO: 9.004 (E_g), 9.110 (E_u), 9.196 (A_{2u}), 9.198 (A_{2u}), 9.319 (E_u), 9.509 (E_g), 9.794 (A_{1g}), 9.900 (A_{1u}).
[18] J. M. Dyke, M. Feher, A. Morris, *J. Electron Spectrosc. Relat. Phenom. 41* (1986) 343–355.

Non-Chelate-Controlled Addition of 1-Bromo-1-lithio-1-alkenes to *O*-Protected Lactaldehydes**

By *Manfred Braun** and *Hellmut Mahler*

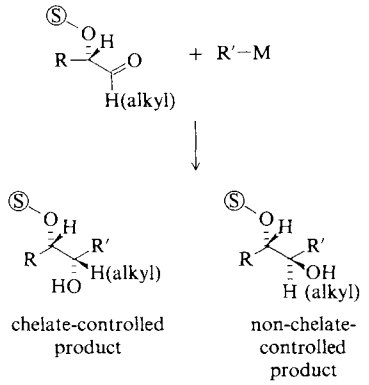
In memoriam Hans Musso

Acyclic chiral α-alkoxyaldehydes and α-alkoxyketones react with Grignard reagents[1] as well as with a variety of other organometallic compounds[2] according to *Cram*'s cyclic model[3] to yield preferentially the "chelate-controlled"[4] product (Scheme 1, left). On the other hand, "non-chelate control" (Scheme 1, right), sometimes called "Felkin–Anh selectivity",[5] is generally difficult to accomplish.[4] Recently, additions involving mainly non-chelate control have been realized, for example with weakly Lewis-acidic alkyltitanium reagents[4] and with allylsilanes in the presence of boron trifluoride,[4] as well as by the Cr^{II}-induced

[*] Prof. Dr. M. Braun, Dipl.-Chem. H. Mahler
Institut für Organische und Makromolekulare Chemie der Universität
Universitätsstrasse 1, D-4000 Düsseldorf 1 (FRG)

[**] This work was supported by the Deutsche Forschungsgemeinschaft, the Fonds der Chemischen Industrie, and BASF AG (donation of chemicals).

reaction of vinyl and allyl halides.[6] Organolithium compounds add to the above-mentioned carbonyl compounds sometimes with chelate control,[1a, 7] sometimes without any significant selectivity.[8]



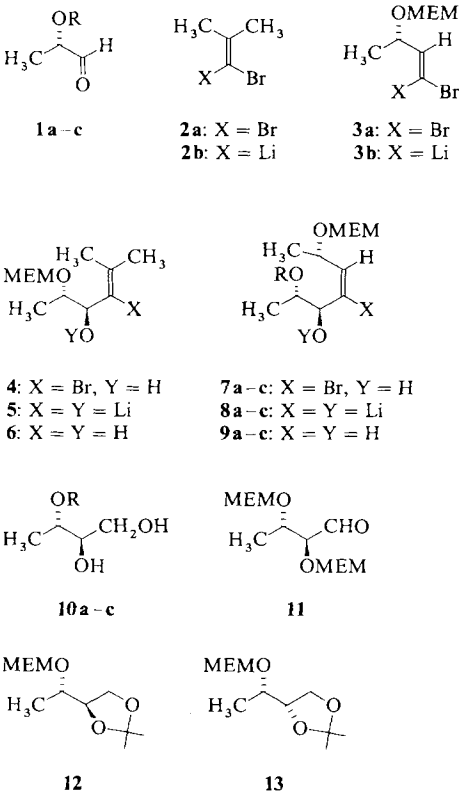
Scheme 1. Ⓢ: protecting group. M: e. g., Li, MgX, ZnX, TiX_3.

We have now observed, for the first time, a largely non-chelate-controlled addition of organolithium compounds to *O*-protected lactaldehyde **1a**. Although, owing to its crown-ether-like structure, the (2-methoxyethoxy)methyl (MEM) protecting group of the aldehyde would seem predestined[1b] to direct the addition in the way predicted by *Cram*'s cyclic model, reaction with the lithium reagent **2b**, generated in situ from the dibromoalkene **2a**, results in preferential attack on the *Re* side, yielding the non-chelate-controlled product **4** (yield 86.3%, *de* = 85%). The chiral vinyllithium reagent (*S*)-**3b**, generated analogously from the dibromoalkene (*S*)-**3a**,[9] adds to achiral aldehydes preferentially with *ul* (unlike) topicity[10] (i.e., also from the *Re* side). As expected, in the addition of **3b** to the *O*-protected lactaldehydes **1a–c**, the selectivity can therefore be considerably increased in favor of the non-chelate-controlled products **7a–c** (**7a**, yield 78%, *de* = 91%; **7b**, 79.5/92; **7c**, 83.5/95).

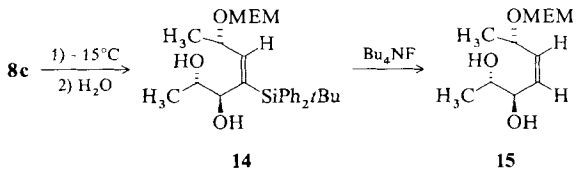
The C–C double bond in the nucleophiles **2b** and **3b** can be cleaved oxidatively to give a hydroxymethylene or a formyl unit; the stereoselective introduction of a $^{\ominus}CH_2OH$ or $^{\ominus}CHO$ synthon with d^1 reactivity[11] is thus possible. To demonstrate this, we transformed the adducts **4** and **7a–c** into the olefins **6** and **9a–c**, respectively, in yields of 89–95% by bromine/lithium exchange at −78 °C (cf. **5** and **8a–c**) followed by protonation. The configuration of the double bond[12] was completely retained in the products. Ozonolysis afforded, after workup with $LiAlH_4$, the diols **10a** (from **6** or **9a**) and **10b,c** (from **9b,c**) in yields of between 78 and 88%. Introduction of a further MEM protecting group into the alkene **9a**, followed by ozonolysis, yields the aldehyde **11** (81%).[13]

Cleavage of the double bond also serves to establish the configuration of the adducts **4** and **7a**. The (2*R*,3*S*)-diol **10a**, prepared from these adducts, was converted into the acetal **12**. To differentiate between the isomers **12** and **13**, reference samples were prepared by addition of methylmagnesium iodide to D-1,2-di-*O*-isopropylideneglyceraldehyde,[14] which occurs with only moderate diastereoselectivity (non-chelate-control), followed by ether formation with MEM-Cl (**12**:*ent*-**13** 69:31). Since these two compounds differ significantly in their ^1H and ^{13}C NMR data,[13] an unambiguous structural assignment of the adducts **4** and **7** was possible.[15]

If the vinyl anion **8c**, generated by bromine/lithium exchange, is not protonated at −78 °C, but instead at −15 °C, O → C migration of the silyl moiety occurs to give quantitatively the vinylsilane **14**, which undergoes fluoride-induced desilylation to yield the olefin **15** with (*Z*) configuration.



1, 7–10: **a**, R = MEM; **b**, R = $SiMe_2tBu$; **c**, R = $SiPh_2tBu$



Since (*S*)-lactaldehyde was used as the starting material, all the products described here are obtained in enantiomerically pure form. Diastereomeric excesses—of the alkenes **9a, b**, for example—can be increased by distillation or column chromatography to *de* > 98%. The (*R*)-lactic esters, also available, afford access to the corresponding enantiomers. The non-chelate control in the reaction of 1-bromo-1-lithio-1-alkenes **2b** and **3b** with *O*-protected lactaldehydes serves to reemphasize that such carbenoids are not only intermediates with unusual structural and spectroscopic properties,[16] but also species with surprising reactivity. The lacking tendency of "ligands" like **1a** to form chelates demonstrates that 1-bromo-1-lithio-1-alkenes do not at all display the typical character of electron-deficient compounds expected for organolithium compounds.

Received: March 6, 1989 [Z 3215 IE]
German version: *Angew. Chem. 101* (1989) 948

CAS Registry numbers:
1a, 88722-70-7; **1b**, 87727-28-4; **1c**, 87696-33-1; **2b**, 2799-45-3; **3b**, 120854-23-1; **4**, 120854-13-9; **7a**, 120854-14-0; **7b**, 120854-15-1; **7c**, 120854-16-2; **10a**, 120854-17-3; **11**, 120854-18-4; **12**, 120854-19-5; **13**, 120854-20-8; **14**, 120854-21-9; **15**, 120854-22-0.

[1] a) D. J. Cram, D. R. Wilson, *J. Am. Chem. Soc. 85* (1963) 1245–1249; b) W. C. Still, J. H. McDonald III, *Tetrahedron Lett. 21* (1980) 1031–1034; c) K. C. Nicolaou, D. A. Claremon, W. E. Barnette, *J. Am. Chem. Soc. 102* (1980) 6611–6612.

[2] a) With Lewis-acidic organotitanium reagents as well as under the conditions of the Mukaiyama reaction: M. T. Reetz, K. Keßler, S. Schmidtberger, B. Wenderoth, R. Steinbach, *Angew. Chem. 95* (1983) 1007–1008; *Angew. Chem. Int. Ed. Engl. 22* (1983) 989–990; C. Gennari, P. G. Cozzi, *Tetrahedron 44* (1988) 5965–5974; b) with cuprates: K. Mead, T. L. Macdonald, *J. Org. Chem. 50* (1985) 422–424; c) with zinc alkyls K. T. Mead, *Tetrahedron Lett. 28* (1987) 1019–1022.

[3] a) D. J. Cram, F. A. Abd Elhafez, *J. Am. Chem. Soc. 74* (1952) 5828–5835; J. Kallmerten, M. Balestra, *J. Org. Chem. 51* (1986) 2855–2857; b) review: E. L. Eliel in J. D. Morrison (Ed.): *Asymmetric Synthesis, Vol. 2. Part A*, Academic Press, New York 1983, pp. 125–155; J. Mulzer, *Nachr. Chem. Tech. Lab. 32* (1984) 16–18.

[4] Review: M. T. Reetz, *Angew. Chem. 96* (1984) 542–555; *Angew. Chem. Int. Ed. Engl. 23* (1984) 556–569.

[5] M. Cherest, H. Felkin, N. Prudent, *Tetrahedron Lett. 1968*, 2199–2204; N. T. Anh, *Top. Curr. Chem. 88* (1980) 145–162.

[6] H. Jin, J. Uenishi, W. J. Christ, Y. Kishi, *J. Am. Chem. Soc. 108* (1986) 5644–5646; J. Mulzer, T. Schulze, A. Strecker, W. Denzer, *J. Org. Chem. 53* (1988) 4098–4103.

[7] D. J. Cram, K. R. Kopecky, *J. Am. Chem. Soc. 81* (1959) 2748–2755.

[8] Cf. [2c] and [3b] as well as U. Mahler, R. M. Devant, M. Braun, *Chem. Ber. 121* (1988) 2035–2044. Unusually high selectivity was recently observed for the chelate-controlled addition of a lithium enolate to *N*-(2-siloxyalkylidene)silylamine: G. Cainelli, M. Panunzio, D. Giacomini, G. Martelli, G. Spunta, *J. Am. Chem. Soc. 110* (1988) 6879–6880.

[9] H. Mahler, M. Braun, *Tetrahedron Lett. 28* (1987) 5145–5149.

[10] D. Seebach, V. Prelog, *Angew. Chem. 94* (1982) 696–702; *Angew. Chem. Int. Ed. Engl. 21* (1982) 654–660.

[11] D. Seebach, *Angew. Chem. 91* (1979) 259–278; *Angew. Chem. Int. Ed. Engl. 18* (1979) 239–258.

[12] Formal inversion of configuration for **4** → **6** and **7** → **9** owing to a change in substituent priority.

[13] The new compounds gave correct C,H analyses. Characteristic physical and spectroscopic data: **4**: b.p. 91–93 °C/0.005 torr; $de = 85\%$; α_D^{20} ($c = 0.8$, 95% aq. ethanol) = 9.7°. ^{1}H NMR (300 MHz, $CDCl_3$, TMS int.): $\delta = 1.29$ (d, $J = 6$ Hz, 3H), 1.88 (s, 3H), 1.92 (s, 3H), 2.42 (d, $J = 7$ Hz, 1H), 3.38 (s, 3H), 3.48–3.69 (m, 4H), 3.74–3.88 (m, 1H), 4.32 (dd, $J = 8.5$, 6 Hz, 1H), 4.67–4.73 (m, 2H). **7a**: $de = 91\%$; α_D^{20} ($c = 2.4$, 95% aq. ethanol) = −91.2°, ^{1}H NMR (300 MHz, $CDCl_3$, TMS int.): $\delta = 1.27$ (d, $J = 6$ Hz, 6H), 3.3 (s, 1H), 3.39 (s, 3H), 3.40 (s, 3H), 3.54–3.80 (m, 8H), 3.90–3.99 (m, 1H), 4.42 (d, $J = 6$ Hz, 1H), 4.69–4.89 (3m, 5H), 6.01 (d, $J = 9.5$ Hz, 1H).**7b**: b.p. 132 °C/0.005 torr; $de = 95\%$; α_D^{20} ($c = 1.3$, 95% aq. ethanol) = 86.6°. ^{1}H NMR (300 MHz, $CDCl_3$, TMS int.): $\delta = 0.1$ (s, 6H), 0.89 (s, 9H), 1.21 (d, $J = 6$ Hz, 3H), 1.27 (d, $J = 6$ Hz, 3H), 2.95 (d$J = 5.5$ Hz, 1H), 3.39 (s, 3H), 3.54–3.57 (m, 2H), 3.62–3.79 (m, 2H), 3.98–4.08 (m, 1H), 4.27 (dd, $J = 6.5$, 5.5 Hz 1H), 4.66–4.88 (2m, 3H), 6.00 (d, $J = 9$ Hz, 1H).**7c**: $de = 96\%$; α_D^{20} ($c = 2.5$, 95% aq. ethanol) = −39.2°. ^{1}H NMR (300 MHz, $CDCl_3$, TMS int.): $\delta = 1.07$ (s, 9H), 1.09 (d, $J = 6$ Hz, 3H), 1.22 (d, $J = 6$ Hz, 3H), 3.04 (d, $J = 5$ Hz), 3.37 (s, 3H), 3.51–3.56 (m, 2H), 3.62–3.72 (m, 2H), 4.02–4.11 (m, 1H), 4.36 (dd, $J = 6$, 5 Hz, 1H), 4.63–4.79 (m, 2H), 4.80–4.89 (m, 1H), 5.97 (d, $J = 9.5$ Hz, 1H), 7.34–7.46 (m, 3H), 7.67–7.74 (m, 2H). **10a**: 79.6%; $de = 90\%$; α_D^{20} ($c = 1$, 95% aq. ethanol) = 12.1° ^{13}C NMR (75 MHz, $CDCl_3$, TMS int.): $\delta = 16.05$, 58.99, 62.82, 67.18, 71.71, 74.37, 75.02, 94.17. **11**: 81%; $de = 90\%$; α_D^{20} ($c = 2.6$, 95% aq. ethanol) = −30.8° ^{1}H NMR (300 MHz (300 MHz, $CDCl_3$, TMS int.): $\delta = -1.26$ (d, $J = 6.5$ Hz, 3H), 3.38 (s, 3H), 3.39 (s, 3H), 3.51–3.58 (m, 4H), 3.68–3.87 (m, 4H), 4.04 (dd, $J = 1.5$, 4 Hz, 1H), 4.10–4.17 (m, 1H), 4.77 (s, 2H), 4.85 (s, 2H), 9.69 (d, $J = 1.5$ Hz, 1H). **12**: 86.2%; $de = 83\%$; α_D^{20} ($c = 1.2$, 95% aq. ethanol) = 11.5°. ^{13}C NMR (75 MHz, $CDCl_3$, TMS int.): $\delta = 16.49$, 25.30, 26.45, 59.04, 66.46, 67.00, 71.74, 73.53, 78.75, 94.17, 109.25. *ent*-**13** (from D-1,2-di-*O*-isopropylideneglyceraldehyde): ^{13}C NMR (75 MHz, $CDCl_3$, TMS int.): $\delta = 15.90$, 25.36, 26.51, 58.99, 65.81, 66.84, 71.74, 73.71, 78.87, 94.28, 109.44. For the reaction of **3a** with aldehydes see [9]. For **2a**, 1.05 equiv. of *n*BuLi in THF was used in the lithiation; otherwise, the procedure was the same as that for **3a**.

[14] J. Mulzer, A. Angermann, *Tetrahedron Lett. 24* (1983) 2843–2846; A. Angermann, *Dissertation*, Freie Universität Berlin 1986.

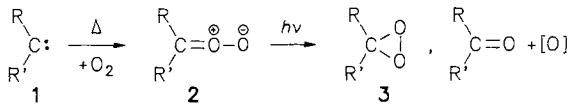
[15] Correlation of **7b, c** with **7a** was carried out in each case, after dehalogenation, by cleavage of the silyl and introduction of MEM protecting groups to give **11** upon ozonolysis.

[16] D. Seebach, H. Siegel, J. Gabriel, R. Hässig, *Helv. Chim. Acta 63* (1980) 2046–2053; D. Seebach, R. Hässig, J. Gabriel, *ibid. 66* (1983) 308–337.

Dimethyldioxasilirane**

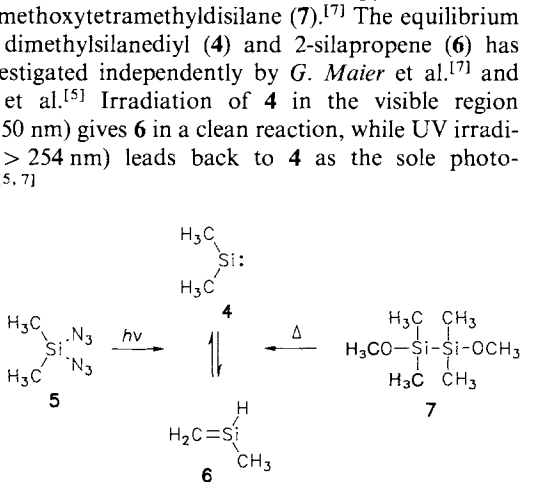
By *Andreas Patyk, Wolfram Sander,* Jürgen Gauss,* and *Dieter Cremer**

The reaction of carbenes (**1**) with molecular oxygen yields carbonyl *O*-oxides (**2**), dioxiranes (**3**), or carbonyl compounds and oxygen atoms. These species are powerful oxygen-atom transfer reagents; especially dioxiranes have proved to be useful in preparative organic chemistry.[1] The relative amount of **2, 3,** or oxygen atoms formed depends greatly on the constitution of the carbene and on the reaction conditions.[2]



Whereas the mechanism of carbene oxidation is quite well understood, not much is known about silanediyl oxidation. Recently, *Ando* et al.[3] reported the formation of a silanone *O*-oxide in the oxidation of dimesitylsilanediyl in oxygen matrices at 10 K. The assignment of this species was based on the observation of one IR absorption at 1084 cm^{-1}, which showed an ^{18}O-isotopic shift of 40 cm^{-1}. We have now investigated the reaction of dimethylsilanediyl (**4**) and O_2. In contrast to the observations of *Ando* et al., a dioxasilirane rather than a silanone *O*-oxide is formed as the primary thermal adduct at low temperature.

Silanediyl **4** was generated in argon matrices either by short-wavelength photolysis ($\lambda > 254$ nm, 10 K)[4] of diazidodimethylsilane (**5**)[5, 6] or by flash vacuum pyrolysis (FVP) of 1,2-dimethoxytetramethyldisilane (**7**).[7] The equilibrium between dimethylsilanediyl (**4**) and 2-silapropene (**6**) has been investigated independently by *G. Maier* et al.[7] and *J. Michl* et al.[5] Irradiation of **4** in the visible region ($\lambda_{max} = 450$ nm) gives **6** in a clean reaction, while UV irradiation ($\lambda > 254$ nm) leads back to **4** as the sole photoproduct.[5, 7]



When **5** is irradiated ($\lambda > 254$ nm, 10 K) in argon matrices doped with low O_2 concentrations (0.1–0.5%), the formation of **4** (and traces of **6**) along with a photooxidation product **A** can be monitored by IR spectroscopy.[8] At higher O_2 content (> 2%), **4** is completely oxidized to **A** upon irradiation.

[*] Dr. W. Sander, Dipl.-Chem. A. Patyk
Organisch-Chemisches Institut der Universität
Im Neuenheimer Feld 270, D-6900 Heidelberg (FRG)
Prof. Dr. D. Cremer, Dipl.-Chem. J. Gauss
Lehrstuhl für Theoretische Chemie der Universität
Greinstrasse 4, D-5000 Köln 41 (FRG)

[**] This work was supported by the Deutsche Forschungsgemeinschaft, the Fonds der Chemischen Industrie, and the Stiftung Volkswagenwerk. We thank Prof. Dr. *R. Gleiter* for supporting this work and Prof. Dr. *G. Maier* for the communication of unpublished results.

The thermal reaction between unreacted **4** and O_2 (in 0.1–0.5% O_2-doped Ar matrices) is induced by annealing the matrix at 35–42 K. After several hours at this temperature, most of **4** has reacted to give a new product, **B**. The formally spin-forbidden reaction of (singlet) **4** and $^3O_2$ *is—as expected—much slower than the analogous reaction* of triplet carbenes.[2] Compound **A** is not formed in the thermal reaction and **6** does not react with O_2 under these conditions.

Interestingly, thermal adduct **B** is also formed in the gas-phase reaction of **4** and O_2 at high temperature. FVP of disilane **7** (700 °C, 10^{-4} mbar) and trapping of the products in Ar at 10 K produces a mixture of **4** and **6**.[9] If small amounts of O_2 are added in the reaction zone, **4** is almost completely trapped to give a mixture of **A** and **B**. Again, **6** is much less reactive towards O_2 and is not trapped in the gas phase. **B** proves to be photolabile towards visible light irradiation (λ = 436 nm). Photolysis produces **A** as the sole product within several minutes; compound **A** is stable even towards UV irradiation (λ > 220 nm).

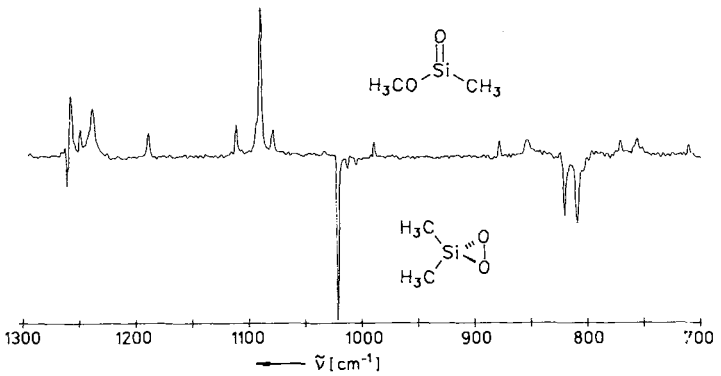


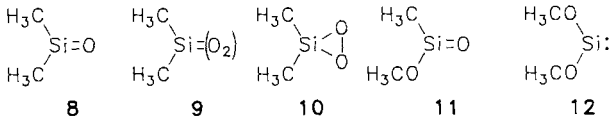
Fig. 1. IR difference spectra showing the photochemistry of **B**, matrix-isolated in a 0.2% $^{16}O_2$-doped Ar matrix at 10 K. Bottom: Bands assigned to **B**, disappearing on irradiation (λ = 436 nm). Top: Bands assigned to **A**, appearing on irradiation.

Table 1. IR-spectroscopic data of **B**, matrix-isolated in Ar at 10 K ($\tilde{\nu}$ [cm^{-1}], Δ, isotopic shift).

[$^{16}O_2$]-**B**	[$^{16}O^{18}O$]-**B** [a]	Δ	[$^{18}O_2$]-**B**	Δ	Assignment [b]
1431.4 (w)	1430.9 (w)	− 0.5	1430.4 (w)	− 1.0	δ_{as} (CH_3)
1260.3 (m)	1260.3 (m)	0.0	1258.8 (m)	− 1.5	δ_s (CH_3)
1021.1 (s)	1009.6 (s)	−11.5	997.0 (s)	−24.1	ν_s(Si−O)
1012.9 (w)	1005.2 (m)	− 7.7	988.8 (w)	−24.1	[c]
1005.7 (w)	993.2 (w)	−12.5	981.1 (w)	−24.6	ν_{as}(Si−O) [c]
820.1 (m)	814.8 (m)	− 5.3	810.4 (m)	− 9.7	δ(CH_3) [d]
			809.5 (m)	−10.6	
809.5 (m)			800.8 (w)	− 8.7	δ(CH_3) [d]
554.4 (w)			530.8 (w)	−23.6	ν(O−O)

[a] Owing to the presence of three isotopomers in the spectra, not all bands could be assigned. [b] Approximate description on the basis of observed isotopic shifts and by comparison with ab initio calculations. [c] The assignment of the weak bands at 1012.9 and 1005.7 is not definite. [d] Rocking mode.

The IR spectra of **A** and **B** show strong absorptions in the region between 1000 and 1100 cm^{-1}, characteristic of Si–O stretching modes (Fig. 1, Table 1). When the experiments were repeated using $^{18}O_2$, strong isotopic shifts towards lower wave numbers were observed for these bands, which shows that both compounds contain oxygen. Structures for **A** and **B** that have to be considered are dimethylsilanone (**8**), dimethylsilanone *O*-oxide (**9**), dimethyldioxasilirane (**10**), methoxymethylsilanone (**11**), and dimethoxysilanediyl (**12**). Compounds **8**[10] and **12**[11] can be readily excluded by comparison with published matrix IR spectra.



To exclude structures with more than one O_2 molecule added to silanediyl **4**, experiments with mixtures of $^{16}O_2$ and $^{18}O_2$ were performed. If a 1:1 mixture is used, the spectra obtained are exact superpositions of the spectra of the pure $^{16}O_2$ and $^{18}O_2$ isotopomers. Thus, **A** and **B** can only contain one or two O atoms from one O_2 molecule.

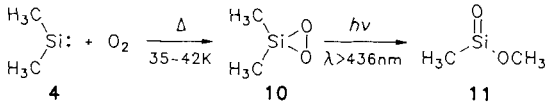
The symmetry of **A** and **B** was examined by using a 1:2:1 mixture of $^{16}O_2$, $^{16}O^{18}O$, and $^{18}O_2$. If **A** or **B** contain only one O atom, no additional $^{16}O^{18}O$ isotopomer should be observed. A compound with two equivalent O atoms should give one "mixed" $^{16}O^{18}O$ isotopomer, whereas two different O atoms should lead to two $^{16}O^{18}O$ isotopomers.

Compound **B** gives one mixed $^{16}O^{18}O$ isotopomer together with the "pure" $^{16}O_2$ and $^{18}O_2$ isotopomers in a ratio of 2:1:1. The bands assigned to the $^{16}O^{18}O$ isotopomer are located halfway between the IR bands of the $^{16}O_2$ and $^{18}O_2$ isotopomers (Table 1). This demonstrates that the two O atoms are equivalent; thus, **B** has structure **10**.[12] In contrast, **A** forms two $^{16}O^{18}O$ isotopomers and therefore contains two nonequivalent O atoms. The two new isotopomers can be recognized best in the region between 1090 and 1050 cm^{-1}. Other bands are broadened owing to the presence of the additional two isotopomers. The most reasonable structure for **A**, compatible with both the IR data and the observed absence of photochemistry,[13] is methoxymethylsilanone (**11**).

On the basis of the ^{18}O isotopic shifts, several bands of **10** were assigned (Table 1). These assignments were confirmed by ab initio calculations,[14] which show that the symmetrical Si–O stretching mode (calculated at 1006 cm^{-1}) is—in agreement with the experiment—the strongest band in the IR spectrum of **10**, with calculated isotopic shifts of 21 and 33 cm^{-1} upon incorporation of one and two ^{18}O atoms, respectively. There are only two other vibrational modes in the calculated IR spectrum with similarly strong isotopic shifts: the asymmetric Si–O stretching mode, which is very weak, but should exhibit the strongest isotopic shifts, and the O–O stretching mode, which should lead to a weak but somewhat more intense band than that for the asymmetric Si–O stretching mode. From the ab initio calculations it follows that the observed weak band at 1005.7 cm^{-1} corresponds to the asymmetric Si–O stretching mode. All other assignments given in Table 1 have been made on the basis of the calculated normal modes.

The strong band of silanone **11** at 1090.1 cm^{-1} shows an isotopic shift of −30.9 cm^{-1} in $^{18}O_2$-**11** and is assigned to a Si–O stretching mode.[15] The mixed $^{16}O^{18}O$ isotopomers absorb at 1087 and 1062 cm^{-1}, which are close to the vibrations of the "pure" isotopomers. This demonstrates that the second O atom is not much involved in this Si–O stretching mode. Other bands in **11** that exhibit strong ^{18}O-isotopic shifts are found at 1249.7 (−29.9) and 1238.1 cm^{-1} (−29.4 cm^{-1}).[15] These absorptions are found at higher

wavenumbers than Si–O stretching modes and assigned to the Si=O stretching mode. The splitting of the band can be rationalized by matrix site effects or by the formation of different rotamers in the matrix. The corresponding band in silanone **8** is observed at 1210 cm^{-1} [10] and in dichlorosilanone at 1240 cm^{-1} (^{18}O isotopic shift: -37 cm^{-1}).[16]



4 10 11

The thermal reaction of silanediyl **4** and O_2 at low temperature leads exclusively to dioxasilirane **10**. In contrast, carbenes only give carbonyl *O*-oxides. The difference in the behavior of silanediyls and carbenes becomes clear on the basis of the ab initio calculations. The calculated isomerization barrier of silanone *O*-oxide is just 6.5 kcal mol^{-1},[17] whereas that of carbonyl oxide is 22.8 kcal mol^{-1}.[18] If silanone *O*-oxide is formed in the thermal reaction of **4** and O_2, then it will immediately isomerize to **10** in an exothermic process releasing 63.8 kcal mol^{-1}.[17]

Received: February 6, 1989 [Z 3159 IE]
German version: *Angew. Chem. 101* (1989) 920

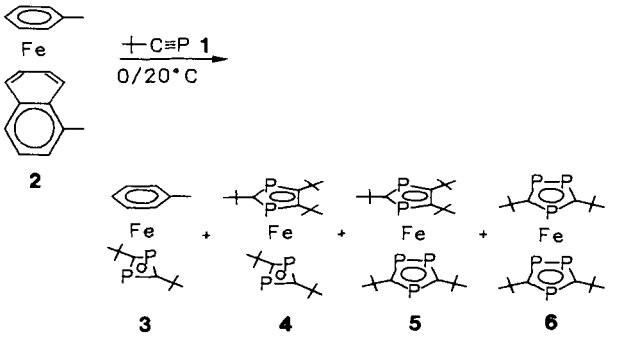
CAS Registry numbers:
4, 6376-86-9; **5**, 4774-73-6; **7**, 10124-62-6; **10**, 120854-11-7; **11**, 120854-12-8.

[1] a) R. W. Murray, R. Jeyaraman, M. K. Pillay, *J. Org. Chem. 52* (1987) 746; b) D. Cremer, M. Schindler, *Chem. Phys. Lett. 133* (1987) 293; c) L. Cassidei, M. Fiorentino, R. Mello, O. Sciacovelli, R. Curci, *J. Org. Chem. 52* (1987) 699; d) W. Adam, Y.-Y. Chan, D. Cremer, J. Gauss, D. Scheutzow, M. Schindler, *ibid. 52* (1987) 2800; e) R. W. Murray, M. K. Pillay, R. Jeyaraman, *ibid. 53* (1988) 3007; f) A. L. Baumstark, P. C. Vasquez, *ibid. 53* (1988) 3437.
[2] a) W. Sander, *Angew. Chem. 98* (1986) 255; *Angew. Chem. Int. Ed. Engl. 25* (1986) 254; b) *Spectrochim. Acta A43* (1987) 637; c) *J. Org. Chem. 53* (1988) 121; d) *ibid. 53* (1988) 2091; e) *ibid. 54* (1989) 333.
[3] T. Akasaka, S. Nagase, A. Yabe, W. Ando, *J. Am. Chem. Soc. 110* (1988) 6270.
[4] Irradiations were carried out by using high-pressure mercury arc lamps in combination with cutoff filters (50% transmission at the wavelength specified) or interference filters (band maximum at the wavelength specified).
[5] G. Raabe, H. Vancik, R. West, J. Michl, *J. Am. Chem. Soc. 108* (1986) 671.
[6] For a recent discussion of the photochemistry of silanediyl precursors, see: P. P. Gaspar, D. Holten, S. Konieczny, Y. Corey, *Acc. Chem. Res. 20* (1987) 329.
[7] G. Maier, G. Mihm, H. P. Reisenauer, D. Littmann, *Chem. Ber. 117* (1984) 2369.
[8] A Bruker IFS66 FT-IR spectrometer was used to record the spectra. The resolution was generally 1 cm^{-1}. For experimental details see [2b,c].
[9] The relative amounts of **4** and **6** depend on the pyrolysis temperature: see [7].
[10] A. K. Maltsev, V. N. Khabashesku, O. N. Nefedov, N. D. Zelinski in E. R. Corey, J. Y. Corey, P. P. Gaspar (Eds.): *Silicon Chemistry*, Ellis Horwood, Chichester 1988, Chap. 21.
[11] G. Maier, H. P. Reisenauer, K. Schöttler, U. Wessolek-Kraus, in press.
[12] The same method has been used to establish the structure of a dioxirane: I. R. Dunkin, C. J. Shields, *J. Chem. Soc. Chem. Commun. 1986*, 154.
[13] Carbonyl *O*-oxides are extremely labile towards long-wavelength irradiation ($\lambda > 600$ nm) [2], whereas **A** is stable even towards UV irradiation.
[14] HF/6-31G(d) and MP2/6-31G(d) calculations have been carried out for dioxasilirane and the dimethyl derivative **10**. For the latter molecule, the IR spectrum was only calculated at the HF/6-31G(d) level owing to calculational limitations.
[15] **11**: IR (Ar, 10 K): 1469.0 (w), 1406.3 (vw), 1258.3 (m), 1249.7 (w), 1238.1 [m, ν(Si=O)], 1189.4 (m), 1111.8 (m), 1090.1 [s, ν(Si–O)], 1079.0 (w), 770.9 (w), 769.0 (w), 759.8 (w), 710.2 (w) cm^{-1}. [$^{18}O_2$]-**11**: IR (Ar, 10 K): 1469.5 (w), 1255.0 (m), 1219.8 (m), 1208.7 [s, ν(Si=O)], 1177.8 (w), 1079.0 (w), 1059.2 [s, ν(Si–O)], 1050.5 (s), 764.2 (w), 756.9 (w), 710.2 (w), 708.7 (w) cm^{-1}.
[16] H. Schnöckel, *Z. Anorg. Allg. Chem. 460* (1980) 37.
[17] MP2/6-31G(d) energies for silanone *O*-oxide, the transition state leading to dioxasilirane, and dioxasilirane are -440.07176, -440.06145, and -440.17340 hartree, respectively.
[18] D. Cremer, T. Schmidt, J. Gauss, T. P. Radhakrishnan, *Angew. Chem. 100* (1988) 431; *Angew. Chem. Int. Ed. Engl. 27* (1988) 427.

Polycyclic Polyphosphorus Hydrocarbons**

By *Dongqi Hu, Hartmut Schäufele, Hans Pritzkow,* and *Ulrich Zenneck**

The highly efficient synthesis of *tert*-butylphosphaacetylene **1** published by *G. Becker* et al. in 1981[1] provided the foundation for the use of phosphaalkynes in a wide variety of organic and organometallic[2, 3] cycloadditions. With one exception, a maximum of three units of **1** are coupled in the metal-promoted cycloadditions. The exception is the reaction of $TaCl_5$ with **1**, which leads to a complexed tricyclic trimer of **1** as the main product and the $TaCl_6^{\ominus}$ salt of the polycyclic cation $[P_7(CCMe_3)_6]^{\oplus}$ as side product.[4]



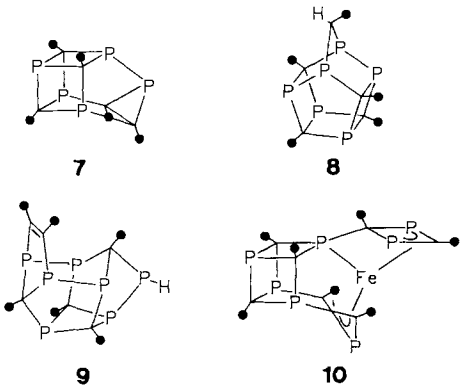
The reaction of (η^4-1-methylnaphthalene)(η^6-toluene)-iron **2**[5] with **1** at 0 to 20 °C affords, in addition to **3**, which contains a cyclodimer as ligand, the substances **4** to **6**,[6, 7] the formation of which requires the breaking of PC triple bonds. This finding suggested that more complex products might also be obtained from these systems. Systematic workup of the reaction allowed optimization of the conditions for synthesis of **5**, obtained eventually in 30% yield when **1** and **2** were used in the stoichiometrically required amounts (mole ratio 5:1). Use of a very large excess of **1**, accessible by a new synthetic route,[8] results in reaction of approximately nine moles of **1** per mole of **2** within one day at room temperature. Unreacted **1** can be separated under vacuum from the products.

Besides **3** to **6**, the amounts of which are less than those obtained when a smaller amount of **1** is used, the product mixture yields at least ten other fractions upon medium pressure chromatography (MPLC). When this mixture is heated under vacuum to approximately 100 °C, one obtains, in ad-

[*] Dr. U. Zenneck, Dipl.-Chem. D. Hu,
Dipl.-Chem. H. Schäufele, Dr. H. Pritzkow
Anorganisch-chemisches Institut der Universität
Im Neuenheimer Feld 270, D-6900 Heidelberg (FRG)

[**] Reactive π Complexes of Electron-Rich Transition Metals (SFB 247), Part 9. This work was supported by the Land Baden-Württemberg and the Deutsche Forschungsgemeinschaft (SFB 247). Part 8: D. Hu, H. Pritzkow, H. Schäufele, C. Tolxdorff, U. Zenneck in H. Werner, G. Erker (Eds.), *Organometallics in Organic Synthesis*, Springer, Heidelberg 1989, in press.

dition to the known compounds, the new substances **7** to **10**, which can be isolated in small yields and characterized by X-ray crystal structure analysis.



The pale yellow $(PCCMe_3)_5$ **7** (Fig. 1a) is a polycyclic pentamer of **1**. Its structure may be derived from that of the so far unknown tetraphosphacubane[19a] by replacing a corner with a three-membered ring. A structurally analogous hydrocarbon is known,[9] but neither an organophosphorus compound nor a polyphosphide. The bond lengths and angles[10] of **7**, except for those of the three-membered ring, lie in the range expected for a completely saturated compound. The strikingly small angle C3-P4-C3′ (49.7°) in the three-membered ring is reminiscent of that in the corresponding 1-phosphirane.[11]

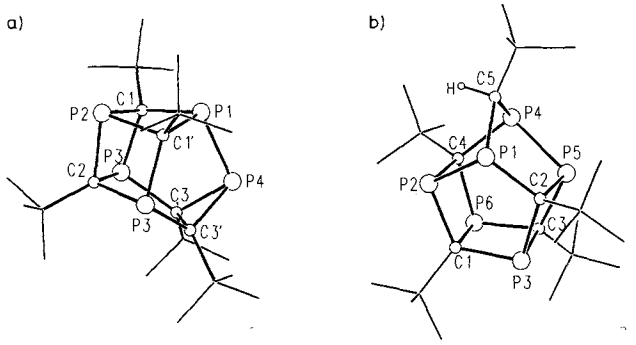


Fig. 1. a) Molecular structure of $(PCCMe_3)_5$ **7**. Selected distances [Å] and angles [°]: P1-P4 2.175(2), C3-C3′ 1.588(7), P-C 1.849–1.902(5); C3-P4-C3′ 49.7(1), P4-C3-C3′ 65.2(4), P1-C1-P2 92.4(1), C1-P1-C1′ 86.1(1), C1-P2-C1′ 84.7(1). b) Molecular structure of $P_6(CCMe_3)_5H$ **8**. Selected distances [Å] and angles [°]: P1-P2 2.196(1), P4-P5 2.203(1), P-C 1.864–1.914(4). The P–C distances in the two five-membered rings of the bases are shorter on average than those between the rings: 1.878 and 1.911 Å. Angles at P: 87.1–88.0 (in C_2P_2), 95.5–103.0 (in C_2P_3); at C: 90.7–92.5 (in C_2P_2), 107.9–117.0 (in C_2P_3).

The almost colorless $P_6(CCMe_3)_5H$ **8** is a heteroanalogue of homopentaprismane[12] (Fig. 1b). Compound **8** is not an oligomer of **1** but instead, as in the case of **4**, **6**, and **9**, a product formed by cleavage and intermolecular exchange of the components of **1**; the number of phosphorus atoms and the number of $CCMe_3$ fragments are therefore different. An additional hydrogen atom is bonded to C5.[13]

$P_7(CCMe_3)_6H$ **9**, which is again pale yellow, may be derived formally from **8** by addition of one more unit of **1** (Fig. 2a). Apart from the charge of the ion $[P_7(CCMe_3)_6]^{\oplus}$ and the additional hydrogen H1 of **9**, these two cage compounds are isomers with markedly different structures.[4, 14]

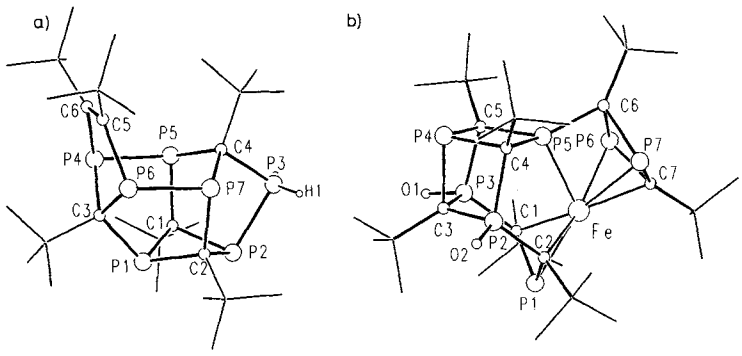


Fig. 2. a) Molecular structure of $P_7(CCMe_3)H$ **9**. Selected distances [Å] and angles [°]: P2-P3 2.154(2), P4-P5 = P6-P7 2.240(1), C5-C6 1.338(6), P-C 1.848–1.904(5); C1-P1-C2 = C1-P2-C2 85.2(5), P1-C1-P2 = P1-C2-P2 87.0(2). b) Molecular structure of (partially oxidized) $(PCCMe_3)_7Fe$ **10** (projection as in Fig. 1a). Selected distances [Å] (some averaged): Fe-P1 2.265(2), Fe-P5 2.281(2), Fe-P6(7) 2.396(2), Fe-C1 2.112(5), Fe-C2 2.131(6), Fe-C7 2.121(5), P6-C6 = P7-C6 1.921(7), P6-C7 = P7-C7 1.780(8), P1-C1 = P1-C2 1.780(7), P2-C2 = P3-C1 1.826(7); the remaining P–C distances are between 1.844 and 1.915 Å.

In **9**, H1 is bonded to a phosphorus atom, in **8** to a carbon atom. Compound **9**, which has a double bond between C5 and C6, displays a near plane of symmetry through C3, C4, P1, P2, and P3. The H atom on P3 can be either above or below this plane; the two positions are occupied roughly to the same extent.

To the best of our knowledge, **9** represents a new type of structure. Consideration of only part of the framework, for example the section C1-C2-C4-P2-P3-P5-P7, reveals some similarities with organopolyphosphanes of the type P_7R_3.[15]

The ligand in the olive-brown iron complex $(PCCMe_3)_7Fe$ **10** (Fig. 2b) is a polycyclic heptamer of **1**. X-ray structure analysis revealed that the substance is partially oxidized at P2 and P3 after workup.[16, 19b] The metal-complex fragment of this paramagnetic cage compound contains 16 valence electrons on iron; P6, C7, and P7 of the four-membered ring, joined to the cage through only a σ bond, form a 1,3-diphosphaallyl ligand, whereas C1, P1, and C2 coordinate as a 2-phosphaallyl ligand. An additional coordination site is occupied by the lone pair of P5. In comparison to other 16-VE complexes of iron, **10** is very stable[17]—presumably because of the chelate effect and the steric shielding of the metal by the *tert*-butyl groups.

The cage portion of **10**, composed of five units of **1**, is remarkably similar to the pentamer **7**. The essential difference is that the atoms of the three-membered ring in **7** serve there as a phosphaallyl ligand and the contact between the phosphorus atoms, which are directly bonded to one another in **7**, is established through the iron atom in **10**. Otherwise, all phosphorus atoms and CR fragments occupy corresponding positions and the bond angles and lengths are very similar.

In view of the large number of possible isomers, it seems reasonable to interpret such structural commonalities in **7** and **10** as a hint of a chemical relationship. Further experimental investigations are necessary to determine whether the analogous eclipsed arrangement of the triphospholyl ligands of **6**,[7] as well as the base five-membered rings of **8**, is a mere coincidence.

Experimental Procedure

1 (11.24 g, 112.4 mmol) and **2** (1.45 g, 5 mmol) were combined in 40 mL of toluene under N_2 at −18 °C and the stirred mixture was allowed to react for 24 h, the temperature rising slowly to room temperature. The toluene and

68.3 mmol of unreacted **1** were removed under vacuum. The residue was extracted into petroleum ether 40/60 and chromatographed several times (column and MPLC: silica gel 60 Merck/5% water; petroleum ether, toluene, THF, and binary mixtures of these solvents). Fourteen colored fractions were isolated. Five have been identified so far, namely, **3, 4, 5, 6,** and **10** (oxygen free [19b], dec. 220 °C).

Heating of the residue under 1 Pa to 100 °C results in complete distillation of **3** and 1-methylnaphthalene. The remaining residue was subjected several times to MPLC, resulting in the isolation of several new fractions. Compound 7 (m.p. 255 °C) crystallized from a brown petroleum ether fraction. Compounds **8** and **9** precipitated as crystalline masses (no sharp melting point) within 14 d from a red-violet petroleum ether solution, the intensity of the color thereby decreasing. The crystals could be separated manually.

When Al_2O_3/5% water was used as the stationary phase in the chromatography and the main components of the mixture were eluted, a brown residue was removed with THF from the top of the column. Concentration of this solution resulted in crystallization of partially oxidized **10**.

The yields of the isolated crystalline compounds **7**–**10** were all about 1%. The NMR spectra of the diamagnetic speices **7**–**9** are very complicated and have not yet been completely analyzed. Compound **10** gives strongly broadened and paramagnetically shifted ^{1}H NMR signals; ^{13}C and ^{31}P NMR signals are not observable.

Received: February 16, 1989 [Z 3177 IE]
German version: *Angew. Chem. 101* (1989) 929

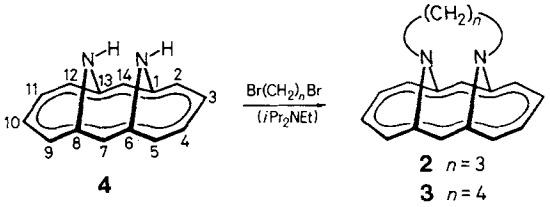
CAS Registry numbers:
1, 78129-68-7; **2**, 116018-76-9; **3**, 116018-77-0; **4**, 116018-78-1; **5**, 114993-20-3; **6**, 115426-03-4; **7**, 120883-33-2; **8**, 120905-04-6; **9**, 120883-34-3; **10**, 120883-35-4; 1-methylnaphthalene, 90-12-0.

[1] G. Becker, G. Gresser, W. Uhl, *Z. Naturforsch. B36* (1981) 16.
[2] M. Regitz, P. Binger, *Angew. Chem. 100* (1988) 1541; *Angew. Chem. Int. Ed. Engl. 27* (1988) 1484, and references cited therein.
[3] J. F. Nixon, *Chem. Rev. 88* (1988) 1327, and references cited therein.
[4] G. Becker, W. Becker, R. Knebl, H. Schmidt, U. Weeber, M. Westerhausen. *Nova Acta Leopold. 59* (1985) 55.
[5] H. Schaufele, D. Hu, H. Pritzkow, U. Zenneck, *Organometallics 8* (1989) 396.
[6] M. Drieß, D. Hu, H. Pritzkow, H. Schaufele, U. Zenneck, M. Regitz, W. Rösch, *J. Organomet. Chem. 334* (1987) C35.
[7] Compounds **5** and **6** are accessible via another route, too: R. Bartsch, P. B. Hitchcock, J. F. Nixon, *J. Chem. Soc. Chem. Commun. 1987*, 1146.
[8] W. Rösch, U. Hees, M. Regitz, *Chem. Ber. 120* (1987) 1645.
[9] E. L. Allred, B. R. Beck, *J. Am. Chem. Soc. 95* (1973) 2393.
[10] **7**: *Pnma*, $a = 9.918(3)$, $b = 16.472(6)$, $c = 17.155(5)$ Å, $V = 2803$ Å^3 $Z = 4$. 1488 observed reflections ($I > 2\sigma_{II}$), four-circle diffractometer ($Mo_{K\alpha}$ radiation, ω scan, $\theta_{max} = 25°$). The refinement (167 parameters, P and C anisotropic, methyl groups as rigid groups with a common isotropic temperature factor) gave $R = 0.043$, $R_w = 0.028$ ($w = 1/\sigma_F^2$) [18].
[11] R. Appel, T. Gaitzsch, F. Knoch, G. Lenz, *Chem. Ber. 119* (1986) 1977.
[12] E. C. Smith, J. C. Barborak, *J. Org. Chem. 41* (1976) 1433; A. P. Marchand, T.-C. Chou, J. D. Ekstrand, D. van der Helm, *ibid. 41* (1976) 1438; P. E. Eaton, L. Cassar, R. A. Hudson, R. H. Deng, *ibid. 41* (1976) 1445.
[13] **8**: *P*1, $a = 10.149(5)$, $b = 12.188(6)$, $c = 12.356(6)$ Å, $\alpha = 98.76(4)$, $\beta = 96.57(4)$, $\gamma = 101.79(4)°$, $V = 1462$ Å^3, $Z = 2$. 3694 observed reflections ($I > 2\sigma_{II}$), four-circle diffractometer ($Mo_{K\alpha}$ radiation, ω scan, $\theta_{max} = 25°$). The refinement (456 parameters, P and C anisotropic, one methyl group as rigid group with a common isotropic temperature factor for the H atoms, the remaining H atoms refined isotropically) gave $R = 0.054$, $R_w = 0.042$ [18].
[14] **9**: $P2_1$, $a = 10.562(2)$, $b = 10.106(1)$, $c = 17.061(4)$ Å, $\beta = 74.02(2)°$, $V = 1751$ Å^3, $Z = 2$. 4091 observed reflections ($I > \sigma_I$), two-circle diffractometer ($Mo_{K\alpha}$ radiation, ω scan, $\theta_{max} = 28°$). The refinement (505 parameters, P and C anisotropic, methyl groups partly refined as rigid groups with a common isotropic temperature factor and partly refined isotropically) gave $R = 0.051$, $R_w = 0.046$ [18].
[15] M. Baudler, *Angew. Chem. 99* (1987) 429; *Angew. Chem. Int. Ed. Engl. 26* (1987) 419; H. G. von Schnering, W. Hönle, *Chem. Rev. 88* (1988) 243, and references cited therein.
[16] **10** (with oxygen on P2 and P3; cf. Fig. 2b): $P2_1/c$, $a = 10.068(5)$, $b = 34.36(4)$, $c = 12.202(10)$ Å, $\beta = 110.34(6)°$, $V = 3957$ Å^3, $Z = 4$. 4763 observed reflections ($I > 2\sigma_{II}$), two-circle diffractometer ($Mo_{K\alpha}$ radiation, ω scan, $\theta_{max} = 25°$). The refinement (478 parameters, Fe, P, O, and C refined anisotropically, methyl groups refined as rigid groups) gave $R = 0.066$, $R_w = 0.066$. The occupation densities of the two oxygen atoms were ca. 0.5 and 0.3 [18, 19b].
[17] H. Hoberg, K. Jenni, K. Angermund, C. Krüger, *Angew. Chem. 99* (1987) 141; *Angew. Chem. Int. Ed. Engl. 28* (1987) 153.
[18] Further details of the crystal structure investigations may be obtained from the Fachinformationszentrum Karlsruhe, Gesellschaft für wissenschaftlich-technische Information mbH, D-7514 Eggenstein-Leopoldshafen 2 (FRG), on quoting the depository number CSD-53825, the names of the authors, and the journal citation.
[19] Notes added in proof (April 17, 1989): a) This gap has been closed in the meantime: T. Wettling, J. Schneider, O. Wagner, C. Kreiter, M. Regitz, *Angew. Chem. 101* (1989); *Angew. Chem. Int. Ed. Engl. 28* (1989), in press; b) Oxygen-free **10** was also confirmed by an X-ray structure analysis. Apart from the two oxygen atoms, the two molecular structures are not significantly different.

The Radical Cation of *N,N'*-Tetramethylene-*syn*-1,6:8,13-diimino[14]annulene. An Experimental Study of the N–N Three-Electron σ Bond**

By *Fabian Gerson,* Georg Gescheidt, Urs Buser, Emanuel Vogel, Johann Lex, Margareta Zehnder,* and *Andreas Riesen*

The N–N three-electron σ bond in radical cations has been the subject of numerous experimental[1–4] and theoretical[5] studies. When such a bond is formed intramolecularly, the N–N distance in the radical cation should be considerably shorter than in the neutral counterpart. This expectation has so far been experimentally borne out solely for 1,6-diazabicyclo[4.4.4]tetradecane (**1**)[1e] and *N,N'*-trimethylene-*syn*-1,6:8,13-diimino[14]annulene (**2**),[2b] because only in the case of these two compounds could the structures of the corresponding radical cations $\mathbf{1}^{\cdot\oplus}$ and $\mathbf{2}^{\cdot\oplus}$ be determined by X-ray crystallography. Here we report an X-ray crystallographic structure analysis performed on the radical cation of *N,N'*-tetramethylene-*syn*-1,6:8,13-diimino[14]annulene (**3**). As will be demonstrated below, $\mathbf{3}^{\cdot\oplus}$ also exhibits a N–N three-electron σ bond. The lengthening of the polymethylene chain on going from $\mathbf{2}^{\cdot\oplus}$ to $\mathbf{3}^{\cdot\oplus}$ leads to an essential change in the "structure" of the two N atoms.



4

2 $n = 3$
3 $n = 4$

The tetramethylene derivative **3**[6] was synthesized from the parent compound **4**[7] by the same procedure as its trimethylene homologue **2**.[2b] In the cyclic voltammogram of **3**,[8] a reversible oxidation wave appears at $E_{1/2} = +0.29$ V (vs. SCE). Accordingly, **3** can be as readily oxidized as **2** ($E_{1/2} = +0.24$ V)[2b] to its radical cation with a variety of reagents ($Tl(OAc)_3$, $AgClO_4$, $(p\text{-}BrC_6H_4)_3NSbCl_6$). The ESR spectrum of $\mathbf{3}^{\cdot\oplus}$ ($g = 2.0035 \pm 0.0001$) at several temperatures is shown in Figure 1. The temperature dependence is due to an interconversion between two equivalent conformations of the tetramethylene chain and a concomitant modulation of the β-proton coupling constants:

[*] Prof. Dr. F. Gerson, Dr. G. Gescheidt, U. Buser
Institut für Physikalische Chemie der Universität
Klingelbergstrasse 80, CH-4056 Basel (Switzerland)
Prof. Dr. E. Vogel, Dr. J. Lex
Institut für Organische Chemie der Universität
Greinstrasse 4, D-5000 Köln 41 (FRG)
Priv.-Doz. Dr. M. Zehnder, Dr. A. Riesen
Institut für Anorganische Chemie der Universität
Spitalstrasse 51, CH-4056 Basel (Switzerland)

[**] This work was supported by the Schweizerischer Nationalfonds zur Förderung der wissenschaftlichen Forschung.

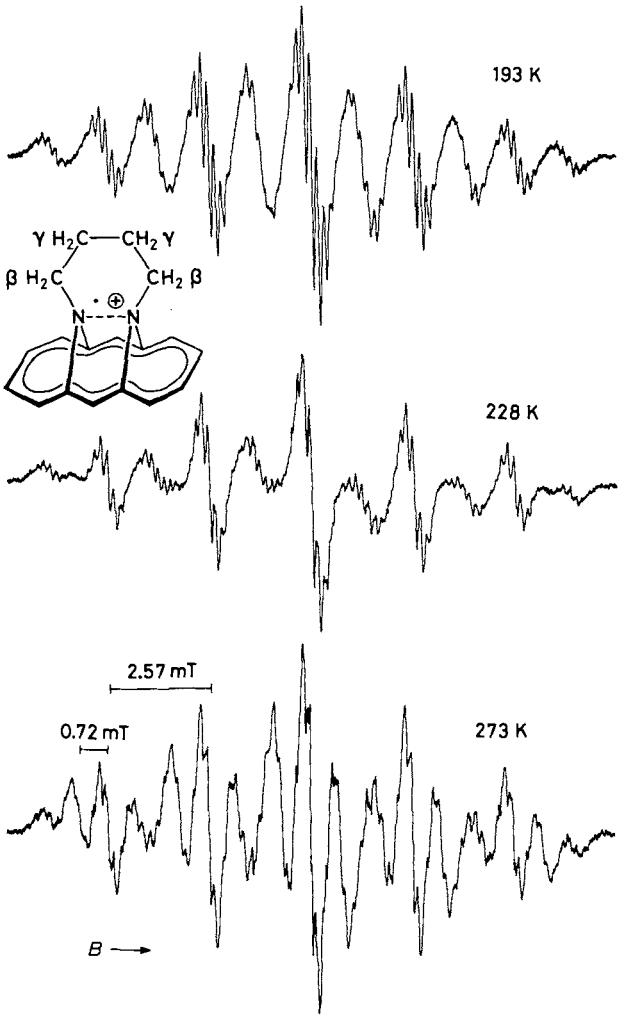
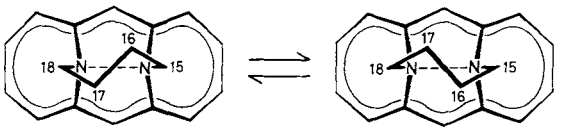


Fig. 1. ESR spectrum of $3^{\cdot\oplus}$ at several temperatures. Solvent, CH_2Cl_2; counterion, $SbCl_6^{\ominus}$.



Although only an average value of 0.72 ± 0.01 mT (fast interconversion) could be exactly measured for these coupling constants, an Arrhenius activation energy E_A was readily calculated for the chain inversion according to a previously described method;[9] simulations of the ESR spectra[10] yielded an E_A value of 22 ± 2 kJ mol^{-1}. A conspicuous spectral feature is the very large coupling constant (a_N = 2.57 ± 0.01 mT) of the two ^{14}N nuclei. It greatly exceeds the corresponding value for $2^{\cdot\oplus}$ (1.685 mT[2]), but it is substantially lower than that for $1^{\cdot\oplus}$ (3.59 mT[1d]). As confirmed by the ENDOR spectra of $3^{\cdot\oplus}$, the protons at the 14-membered π perimeter and the γ protons of the tetramethylene chain give rise to relatively small coupling constants (6H, 0.175 ± 0.005; 4H, 0.150 ± 0.005 mT).

The crystalline perchlorate salt of $3^{\cdot\oplus}$ was prepared by oxidation of **3** with $AgClO_4$ in CH_3CN. Figure 2 gives the mean values of the bond lengths and two selected bond angles in $3^{\cdot\oplus}$ and **3**, as determined by X-ray crystallographic structure analyses.[11] The N–N distance in $3^{\cdot\oplus}$ (218.9 pm) is shortened by 37.1 pm relative to that in **3** (256.0 pm). It compares favorably with the experimentally found N–N bond lengths in $1^{\cdot\oplus}$ (229.5 pm[1e]) and $2^{\cdot\oplus}$ (216.0 pm[2b]), as well as with the analogous value calculated for

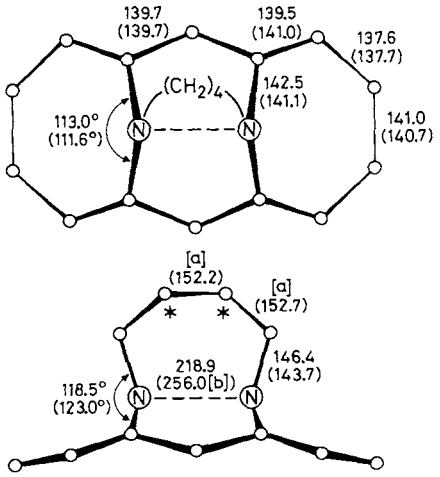


Fig. 2. Mean values for the bond lengths [pm] and two selected bond angles in $3^{\cdot\oplus}$ (**3**). Standard deviations of the bond lengths and bond angles: 0.7 (0.2) pm and 0.4 (0.1)°, respectively. [a] The C atoms, marked here by asterisks, are disordered, because the two conformations of the tetramethylene chain in the asymmetric unit cell are superimposed. [b] No bonding.

$[H_3N\cdots NH_3]^{\cdot\oplus}$ (216.4[5a] and 215.1 pm[5b]). The X-ray crystallographic data thus clearly point to the formation of a N–N three-electron σ bond in $3^{\cdot\oplus}$, a conclusion that could already be drawn from the thermodynamic and kinetic stability of this radical cation and from its large ^{14}N and β-proton coupling constants.

Since the N AOs participating in the N–N three-electron σ bond accommodate almost the entire spin population in $1^{\cdot\oplus}$–$3^{\cdot\oplus}$, the steep rise of the a_N values in the order $2^{\cdot\oplus}$ (1.685 mT) < $3^{\cdot\oplus}$ (2.57 mT) < $1^{\cdot\oplus}$ (3.59 mT) cannot be due to an enhancement of this population, but must be caused by a change in the "character" of the pertinent N AOs. A plot of a_N versus the average C–N–C angles χ[12] in $1^{\cdot\oplus}$ (114.0°[1e]), $2^{\cdot\oplus}$ (119.1°[2b]), and $3^{\cdot\oplus}$ (116.7°) results in an almost perfect straight line with the regression equation (a) (Fig. 3).

$$a_N = (46.18 \pm 0.30) - (0.3736 \pm 0.0026)\,\chi \qquad \text{(a)}$$

The a_N value of 1.35 ± 0.01 mT, obtained by extrapolating χ to 120°, corresponds to two sp^2-hybridized N atoms, each lying in the plane of the three neighboring C atoms. In this

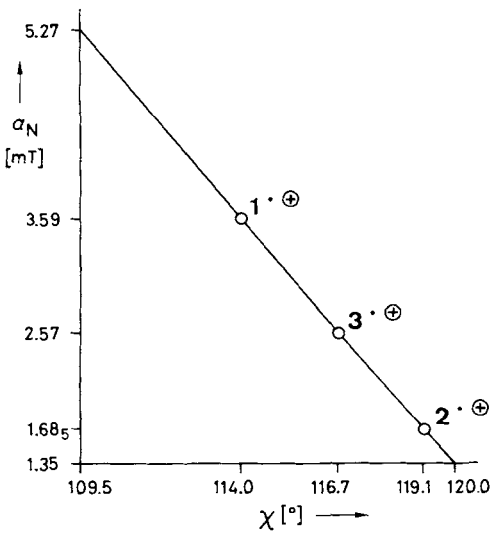


Fig. 3. ^{14}N coupling constants (a_N) versus the average C–N–C angle χ in $1^{\cdot\oplus}$–$3^{\cdot\oplus}$.

 © VCH Verlagsgesellschaft mbH, D-6940 Weinheim, 1989 0570-0833/89/0707-0903 $ 02.50/0

case, a three-electron σ bond, formed by N AOs of a pure p character, is perpendicular to the planes of the two "flat" N atoms. The N–N bond in $\mathbf{2}^{\cdot\oplus}$ ($\chi = 119.1°$) approaches such a structure. On decreasing the angle χ, the hybridization of the N atoms changes from sp^2 in the direction of sp^3, and each of them increasingly deviates from the coplanar arrangement with the three neighboring C atoms. The "pyramidalization" of the N atoms enhances the s contribution to the AOs responsible for the N–N bond and thus readily rationalizes the observed rise of the ^{14}N coupling constants with decreasing angle χ: $\mathbf{2}^{\cdot\oplus}$ (119.1°) < $\mathbf{3}^{\cdot\oplus}$ (116.7°) < $\mathbf{1}^{\cdot\oplus}$ (114.0°). In the borderline case, where the two N atoms are sp^3-hybridized ($\chi = 109.5°$), extrapolation yields an a_N value of 5.27 ± 0.02 mT (Fig. 3).

Experimental Procedure

3: Ethyldiisopropylamine (0.52 mL, 3.0 mmol) and 1,4-dibromobutane (0.18 mL, 1.5 mmol) were added to a solution of **4** (312 mg, 1.5 mmol) in 30 mL of toluene in a glass ampoule. After flushing with argon, the sealed ampoule was left standing for 48 h at 150 °C. The reaction mixture was dissolved in diethyl ether, washed three times with water, and dried with magnesium sulfate. Chromatography in pentane on aluminum oxide (particle size 0.063–0.200 mm; column 10 × 2 cm) and recrystallization from diethyl ether afforded 106 mg (27%) of **3** as deep-violet needles (m.p. 130–131 °C).

$\mathbf{3}^{\cdot\oplus}$ $ClO_4^{\ominus}$: anhydrous $AgClO_4$ (16.5 mg, 0.08 mmol) in 2 mL of dry, degassed acetonitrile was added to a solution of **3** (21 mg, 0.08 mmol) in 2 mL of likewise purified acetonitrile. The ampoule was sealed under high vacuum and left standing for several hours at room temperature. Opening of the ampoule and working up the mixture were carried out under argon. Distilling off the solvent, extraction of the residue with dichloromethane, and recrystallization first from dichloromethane and then from nitrobenzene/THF (10:1) gave ca. 4 mg (10%) of red-brown needles of $\mathbf{3}^{\cdot\oplus}$ $ClO_4^{\ominus}$ (m.p. ca. 180 °C), which were stable under argon. Correct elemental analysis [13].

Received: February 21, 1989 [Z 3186 IE]
German version: *Angew. Chem. 101* (1989) 938

CAS Registry numbers:
1, 75863-17-1; **3**, 120789-29-9; $\mathbf{3}^{\cdot\oplus}\cdot ClO_4^{\ominus}$, 120789-30-2; $Br(CH_2)_4Br$, 110-52-1.

[1] a) R. W. Alder, R. Gill, N. C. Goode, *J. Chem. Soc. Chem. Commun. 1976*, 973; b) R. W. Alder, R. B. Sessions, *J. Am. Chem. Soc. 101* (1979) 3651; c) R. W. Alder, *Acc. Chem. Res. 16* (1983) 321; d) B. Kirste, R. W. Alder, R. B. Sessions, M. Bock, H. Kurreck, S. F. Nelsen, *J. Am. Chem. Soc. 107* (1985) 2635; e) R. W. Alder, A. G. Orpen, J. M. White, *J. Chem. Soc. Chem. Commun. 1985*, 949.

[2] a) F. Gerson, *J. Mol. Struct. 141* (1986) 27; b) F. Gerson, J. Knöbel, U. Buser, E. Vogel, M. Zehnder, *J. Am. Chem. Soc. 108* (1986) 3781.

[3] J. P. Dinnocenzo, T. E. Banach, *J. Am. Chem. Soc. 110* (1988) 971.

[4] G. W. Eastland, M. C. R. Symons, *Chem. Phys. Lett. 45* (1977) 422; N. Ganghi, J. L. Wyatt, M. C. R. Symons, *J. Chem. Soc. Chem. Commun. 1986*, 1424.

[5] a) W. J. Bouma, L. Radom, *J. Am. Chem. Soc. 107* (1985) 345; b) P. M. W. Gill, L. Radom, *ibid. 110* (1988) 4931.

[6] Physical data of **3**: MS: *m/z* 262 (100%, $M^{\oplus}$), 233 (14, $M^{\oplus}$-C_2H_5), 219 (15, $M^{\oplus}$-C_3H_7), 206 (14, $M^{\oplus}$-C_4H_8), 103 (33, $[M\text{-}C_4H_8]^{2\oplus}$; identified by the ^{13}C satellite at *m/z* 103.5). IR (CsI): $\tilde{\nu}$ = 3035 (=C–H), 1557, 1518 cm^{-1} (–C≡C–). UV (MeOH): λ_{max} = 295 (ε = 130100), 367 (7800), 487 (320), 565 nm (sh 240). ^1H NMR (300 MHz, CD_2Cl_2, 193 K): δ = 8.44 (s, H-7,14), 8.05–7.85 (AA′ part of AA′BB′, 4H, H-2,5,9,12), 7.55–7.35 (BB′ part of AA′BB′, 4H, H-3,4,10,11), 0.59 (s, 4H, H-15,18), 0.17 (s, 4H, H-16,17). ^{13}C NMR (75.5 MHz, CD_2Cl_2, 193 K): δ = 134.37 (C-7,14), 134.02 (C-2,5,9,12), 127.66 (C-3,4,10,11), 120.13 (C-1,6,8,13), 51.13 (C-15,18), 28.34 (C-16,17).

[7] E. Vogel, F. Kuebart, J. A. Marco, R. Andree, H. Günther, R. Aydin, *J. Am. Chem. Soc. 105* (1983) 6982.

[8] Working electrode, platinum disc; counterelectrode, glassy carbon; solvent, acetonitrile; supporting salt, Et_4NBF_4; T = 298 K; voltage scan, 200 mV s^{-1}.

[9] F. Gerson, H. Ohya-Nishiguchi, G. Plattner, *Helv. Chim. Acta 65* (1982) 551.

[10] J. Heinzer, *J. Magn. Reson. 13* (1974) 124.

[11] Both structures were solved and refined by direct methods and a difference-Fourier procedure. Crystallographic data for $\mathbf{3}^{\cdot\oplus}$ ($C_{18}H_{18}N_2ClO_4$) [and **3** ($C_{18}H_{18}N_2$)]; M = 361.807 [262.358]; space group $P2_1$ (No. 4) [$P2_1/c$ (No. 14)]; a = 855.2(1) [1192.9(1)], b = 1263.4(5) [662.4(1)], c = 854.9(1) [1911.7(2)] pm; β = 113.82(14) [108.86(1)]°; V = 0.8450 [1.42958] nm^3; Z = 2 [4]: ϱ_{calcd} = 1.422 [1.219] g cm^{-3}, T = 293 [293] K; θ_{max} = 26 [27]°; $\mu(Mo_{K\alpha})$ = 2.06 [0.672] cm^{-1}; independent reflections 1749 [3122]; observed reflections 1219 [2121]; variables 243 [253]; R = 0.064 [0.033]; R_w = 0.069 [0.044]; $w^{-1} = 1.008\,\sigma^2(F_o) + 0.0032\,F_o^2$; [$\sigma^2(F)$]. Further details of the crystal structure investigation are available from the Director of the Cambridge Crystallographic Data Centre, University Chemical Laboratories, Lensfield Road, Cambridge CB2 1EW, England, by quoting the full literature citation.

[12] E.g., for $\mathbf{3}^{\cdot\oplus}$: $\chi = (1/3)(113.0° + 2 \times 118.5°) = 116.7°$.

[13] We thank Dr. *L. Strauch*, Institut für Organische Chemie der Universität Basel, for this elemental analysis.

Bis-Stilbene Systems: Reduction to the Tetraanions**

By *Rainer Schenk, Joachim Hucker, Henning Hopf, Hans-Joachim Räder*, and *Klaus Müllen**

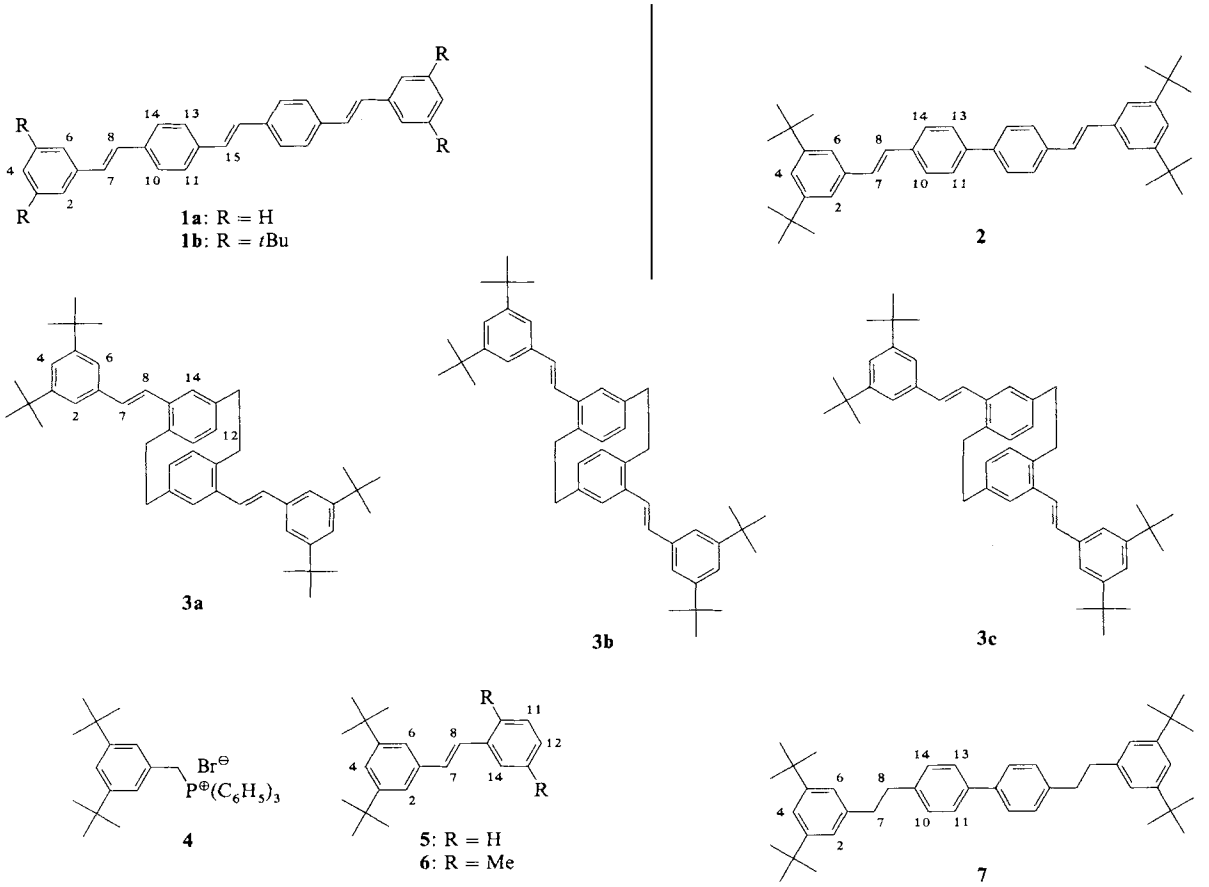
Recently, we synthesized a homologous series of soluble oligo-*p*-phenylenevinylenes and studied the dependence of their reduction potentials on chain length.[1] Extrapolation of the results to the analogous polymer compelled us to revise the theoretical concepts[2, 3] used to describe the addition of electrons to linear π systems. However, two questions remain unanswered: What is the maximum number of electrons that can be added to these systems upon reduction? What charge distribution results in a minimization of Coulombic interactions? Using compounds **1**–**3**, in which two stilbene moieties are linked through a vinylene group (**1**) or a single bond (**2**) or interact through space (**3**), we have studied the addition of electrons to polyene chains.

The stilbene systems **1b**, **2**, and **3**[4] were prepared by Wittig reaction of the phosphonium salt **4**[1] (2 equiv.) and, respectively, 4,4′-stilbenedicarbaldehyde, 4,4′-biphenyldicarbaldehyde, and 4,12-[2.2]paracyclophanedicarbaldehyde.[5] The positions of the *tert*-butyl substituents, necessary to increase the solubility of the compounds, were chosen so as to avoid steric perturbation of the π conjugation. For comparison, compounds **5** and **6**[4] were also prepared from **4**. Comparison of the cyclophanes **3** with the stilbene **6** by UV spectroscopy revealed that the longest-wavelength band (**3**, λ = 309, 323 (sh) nm, ε = 46000, 41000; **6**, λ = 297, 317 (sh), 333 (sh) nm, ε = 22200, 17600, 7500) of **3** is shifted bathochromically and has lost fine structure. This finding is in agreement with the observations made for the pair 1,2-bis(*p*-tolyl)ethane and [2.2]paracyclophane and is ascribed to a transannular π, π interaction in the cyclophane system.[6]

Compounds **1b**, **2**, and **3** were reduced with alkali metals in [D_8]THF at −78 °C. The blue to violet products were characterized by ^1H and ^{13}C NMR spectroscopy (see Table 1 and Ref. [7, 8]) as well as by quenching reactions. In each case, trapping with dimethyl sulfate afforded tetramethyl adducts. In agreement with this result, the reduction product of **2** was protonated to give the tetrahydro derivative **7**.[4] Independent of the way in which these structurally related π systems are linked, therefore, reduction yields the alkali-metal salt of the respective tetraanion. This is remarkable, since reduction of **1b**, for example, results in transfer of only

[*] Prof. Dr. K. Müllen, Dipl.-Chem. R. Schenk, Dipl.-Chem. H.-J. Räder
Institut für Organische Chemie der Universität
Johann-Joachim-Becher-Weg 18–22, D-6500 Mainz 1 (FRG)
Dipl.-Chem. J. Hucker, Prof. Dr. H. Hopf
Institut für Organische Chemie der Universität
Hagenring 30, D-3300 Braunschweig (FRG)

[**] This work was supported by the Deutsche Forschungsgemeinschaft and the Fonds der Chemischen Industrie.



Scheme 1. The numbering of the centers is arbitrary.

Table 1. ^{1}H NMR chemical shifts (coupling constants [Hz]) of the lithium salts of $\mathbf{1b}^{4\ominus}$, $\mathbf{2}^{4\ominus}$, $\mathbf{5}^{2\ominus}$, $\mathbf{3}^{4\ominus}$, and $\mathbf{6}^{2\ominus}$.

	4	2,6	7,8	10,14	11,13	15[12]	*t*Bu
$\mathbf{1b}^{4\ominus}$	4.92s	5.05s, 5.68s	3.30d (10.8), 3.17d (10.8)	5.03d, 5.70d	6.00d, 6.11d	5.38s	1.07s, 1.12s
$\mathbf{2}^{4\ominus}$	4.70s	5.54s, 4.78s	3.13d (10.3), 2.79d (10.3)	5.74d, 5.16d	6.35d, 6.14d		1.10s, 1.05s
$\mathbf{5}^{2\ominus}$	4.82s	5.58s, 4.94s	3.04d (10.4), 2.98d (10.4)	5.56d, 4.96d	6.09t, 5.76t	[4.55t]	1.10s, 1.05s

	2,4,6,14	7,8	11	12	Me [methylene]	*t*Bu
$\mathbf{3}^{4\ominus}$	6.13s, 5.99s, 5.72s, 5.36s, 5.31s, 5.15s, 5.12 (2H,s)	3.80d (9.3), 2.70d (9.3), 3.43d (8.8), 3.10d (8.8)	6.17d, 6.04d	5.04d, 4.42d	[2.1–2.8m]	1.21 (9H,s), 1.18 (9H,s), 1.12 (18H,s)
$\mathbf{6}^{2\ominus}$	5.71s, 5.27s, 5.08s, 4.96s	3.18d (10.1), 2.80d (10.1)	5.88d	4.76d	1.80s, 1.61s	1.13s, 1.08s

three electrons according to cyclic voltammetry.[11] These tetraanions are all stable at room temperature in the absence of air. For comparison with **1b**,[7] **2**, **3**, and their tetraanions, the stilbenes **5** and **6** were converted into their dianions (see Table 1 and Ref. [7, 8]). Protonation of the latter afforded the corresponding ethane derivatives.

Although the reductions of **1b**, **2**, and **3** were followed by NMR spectroscopy, it was not possible to obtain high-resolution NMR spectra of the intermediate dianions. This was achieved, however, for the more poorly soluble parent compound **1a**.[7]

Structural elucidation of the anions by NMR spectroscopy is hampered by the presence of conformational isomers for $\mathbf{1a}^{2\ominus}/2M^{\oplus}$, $\mathbf{1b}^{4\ominus}/4K^{\oplus}$, and $\mathbf{3}^{4\ominus}/4M^{\oplus}$ (M = Li,K in each case). Conformational isomers were not observed, however, for $\mathbf{1b}^{4\ominus}/4Li^{\oplus}$ and $\mathbf{2}^{4\ominus}/4Li^{\oplus}$. The conformational isomerism is presumably due to slower rotation around the formal single bonds on the NMR time scale because of the higher π-bond order.[9] In each case, rotation of the terminal phenyl units is no longer observed at −20 °C. The number of ^{1}H NMR signals for $\mathbf{1b}^{4\ominus}/4M^{\oplus}$ indicates that the Li salt is only present as a symmetric conformer. The K salt, on the other hand, forms all three possible conformers owing to slow rotation around the formal single bonds C8-C9 and C12-C15.[10] In the case of $\mathbf{3}^{4\ominus}/4M^{\oplus}$, hindered rotation around the formal single bonds C8-C9 (C8′-C9′) can lead to three non-isodynamic conformers **3a–c**, only two of which are centrosymmetric (**3a,b**). The equal intensities of all NMR signals may best be explained by the existence of only *one* non-centrosymmetric structure **3c** with different twisting angles (ca. 0, 180°) with respect to C8-C9 (C8′-C9′).

The two stilbene moieties of $\mathbf{3}^{4\ominus}/4M^{\oplus}$ differ markedly in their ^{1}H and ^{13}C NMR chemical shifts as well as in the coupling constants of their vicinal (olefinic) protons (see Table 1). These effects are due primarily to the conformational isomerism.[10] Even comparison with $\mathbf{6}^{2\ominus}/2M^{\oplus}$ revealed no anisotropic ring-current effects. A shift of charge to the outer styryl units due to electrostatic repulsion within the cyclophane element was not observed.

The calculated π-charge densities q_π in the dianion of **1a** and **1b** decrease in the series $q_\pi(C15) > q_\pi(C7) > q_\pi(C8)$. The additional charge in the tetraanion is localized above all in the terminal double bond, resulting in the series $q_\pi(C7) > q_\pi(C8) > q_\pi(C15)$. As expected based on the correlation of

^{13}C and ^{1}H NMR chemical shifts with π charge densities,[11] H15 in $\mathbf{1a}^{2\ominus}/2M^{\oplus}$ absorbs at highest field, whereas the difference in shifts of H15, H8, and H7 in $\mathbf{1b}^{4\ominus}/4M^{\oplus}$ is significantly smaller. The δ values of $\mathbf{2}^{4\ominus}$ reveal no evidence of "uncoupling" of the stilbene units by twisting around the biphenyl single bond, since the calculated relative charge densities of C7 and C8 are not affected by the twisting. The characterization of all these tetraanions by NMR spectroscopy reveals (also in comparison with $\mathbf{5}^{2\ominus}$ and $\mathbf{6}^{2\ominus}$) the existence of two separate, only slightly perturbed stilbene subunits.

The first two reduction potentials E_1 and E_2 of **1b**, **2**, and **3** were found to be $-1.96/-2.14$, $-2.11/-2.28$, and $-2.30/-2.52$ V, respectively, by cyclic voltammetry (dimethylformamide; NBu_4PF_6 as supporting electrolyte; $T = 288$ K; scan rate 100 mVs^{-1}; potentials vs. SCE, measured using Ag wire as a quasi reference, ferrocene calibration; reversible one-electron transfers in each case). The E_1 and E_{pc} values[12] of **5** and **6**, for comparison, are $-2.39/-2.95$ and $-2.40/-2.95$ V, respectively. The radical anion of **3**—in which the stilbene units interact "more weakly"—thus appears to be less stable than the radical anions of **1b** and **2**, but more stable than those of the reference compounds **5** and **6**. The potential differences $E_1 - E_2$, a measure of the interaction energies of the excess electrons, are 0.18 (**1b**), 0.17 (**2**), and 0.22 V (**3**), and reveal that the interaction of the two charged stilbene units in the dianions of **2** and **3** is small.

Received: February 20, 1989 [Z 3183 IE]
German version: *Angew. Chem. 101* (1989) 942

CAS Registry numbers:
1a, 64496-23-7; $\mathbf{1a}^{2\ominus}/2Li^{\oplus}$, 120926-83-2; **1b**, 120926-88-7; $\mathbf{1b}^{4\ominus}/4K^{\oplus}$, 120942-29-2; **2**, 120926-78-5; $\mathbf{2}^{4\ominus}/4Li^{\oplus}$, 120926-84-3; **3**, 120926-79-6; $\mathbf{3}^{4\ominus}/4Li^{\oplus}$, 120926-85-4; **4**, 36393-44-9; **5**, 120926-80-9; $\mathbf{5}^{2\ominus}/2Li^{\oplus}$, 120926-86-5; **6**, 120926-81-0; $\mathbf{6}^{2\ominus}/2Li^{\oplus}$, 120926-87-6; **7**, 120926-82-1; 4,4'-biphenyldicarbaldehyde, 66-98-8; 4,12-[2.2]paracyclophanedicarbaldehyde, 120964-23-0; benzaldehyde, 100-52-7; 2,5-dimethylbenzaldehyde, 5779-94-2.

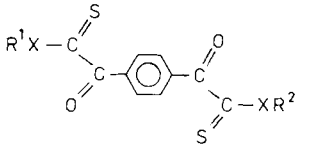
[1] J. Heinze, J. Mortensen, K. Müllen, R. Schenk, *J. Chem. Soc. Chem. Commun. 1987*, 701.
[2] J. L. Bredas, J. C. Scott, K. Yakushi, G. B. Street, *Phys. Rev. B30* (1984) 1023; J. L. Bredas, *Mol. Cryst. Liq. Cryst. 118* (1985) 49.
[3] S. A. Brazowskii, N. N. Kirava, *JEPT Lett. (Engl. Transl.) 33* (1981) 4.
[4] **2**: m.p. 203 °C, ^{1}H NMR ($CDCl_3$, 200 MHz): $\delta = 7.62$ (br.s, 8H; H10, 11, 13, 14), 7.35–7.40 (m, 6H; H2, 4, 6), 7.22, 7.11 (2d, $^{3}J = 16.2$ Hz, 4H; H7, 8), 1.38 (s, 36H; *t*Bu), ^{13}C NMR ($CDCl_3$, 50 MHz): $\delta = 151.1$ (C3, 5), 139.6, 136.8, 136.6 (C1, 9, 12), 130.0, 127.5 (C7, 8) 127.0, 126.9 (C10, 11, 13, 14), 122.2 (C4), 120.9 (C2, 6), 34.9, 31.5 (*t*Bu). **3**: m.p. 273 °C, ^{1}H NMR ($CDCl_3$, 200 MHz): $\delta = 7.38-7.45$ (m, 6H; H2, 4, 6), 7.21, 6.94 (2d, $J = 16$ Hz, 4H; H7, 8), 6.71 (s, 2H; H14), 6.69, 6.43 (2d, $J = 10$ Hz, 4H; H11, 12), 2.8–3.7 (m, 8H; CH_2), 1.40 (s, 36H; *t*Bu), ^{13}C NMR ($CDCl_3$, 50 MHz): $\delta = 151.2$ (C3, 5), 139.5, 138.1, 137.7, 137.2 (C1, 9, 10, 13), 133.6, 130.5, 130.1, 129.4, 126.6 (C7, 8, 11, 12, 14), 122.1 (C4), 120.9 (C2, 6), 35.0, 31.6 (*t*Bu), 34.6, 33.5 (CH_2). **5**: m.p. 57 °C. ^{1}H NMR ($CDCl_3$, 200 MHz): $\delta = 7.2-7.55$ (m, 8H; arene protons), 7.17, 7.07 (2d, $J = 16.3$ Hz, 2H; H7, 8), 1.36 (s, 18H; *t*Bu), ^{13}C NMR ($CDCl_3$, 50 MHz): $\delta = 151.2$ (C3, 5), 137.9, 136.8 (C1, 9), 130.1, 128.2, 127.5 (C7, 8, 12), 128.8, 126.6 (C10, 11, 13, 14), 122.2 (C4), 121.0 (C2, 6), 35.0, 31.7 (*t*Bu). **6**: m.p. 78 °C, ^{1}H NMR ([D$_8$]THF, 200 MHz): $\delta = 7.44$ (br.s, 1H; H14), 7.40 (d, $^{4}J = 1.8$ Hz, 2H; H2, 6), 7.36 (t, $^{4}J = 1.8$ Hz, 1H; H4), 7.34, 7.06 (2d, $J = 16$ Hz, 2H; H7, 8), 7.03, 6.93 (2d, $J = 7.8$ Hz; H11, 12), 2.37, 2.31 (2s, 6H; 2Me), 1.36 (s, 18H; *t*Bu), ^{13}C NMR ($CDCl_3$, 50 MHz): $\delta = 151.1$ (C3, 5), 137.2, 136.6, 135.5, 132.7 (C1, 9, 10, 13), 131.1, 130.3, 128.2, 126.3, 126.2 (C7, 8, 11, 12, 14), 122.1 (C4), 121.0 (C2, 6), 34.9, 31.6 (*t*Bu), 21.1, 19.5 (Me). **7**: ^{1}H NMR ($CDCl_3$, 200 MHz): $\delta = 7.5$ (d, $J = 8.1$ Hz, 4H; H11, 13), 7.28 – 7.23 (m, 6H; H4, 10, 14), 7.03 (d, $J = 1.7$ Hz, 4H; H2, 6), 2.95 (s, 8H; H7, 8), 1.31 (s, 36H; *t*Bu), ^{13}C NMR ($CDCl_3$, 50 MHz): $\delta = 150.6$ (C3, 5), 140.9, 140.7, 138.8 (C1, 9, 12), 128.9, 126.9 (C10, 11,13,14), 122.7 (C2, 6), 119.8 (C4), 38.4, 37.8 (C7, 8), 34.8, 31.5 (*t*Bu).
[5] H. Hopf, F.-W. Raulfs, *Isr. J. Chem. 25* (1985) 210.
[6] S. Misumi in P. M. Keehn, S. M. Rosenfeld (Ed.): *Cyclophanes, Vol. II*, Academic Press, New York 1983, p. 579 ff.
[7] $\mathbf{1b}^{4\ominus}/4K^{\oplus}$: ^{1}H NMR ([D$_8$]THF, 400 MHz, −20 °C): $\delta = 3.3-3.5$ (m, 2H), 3.9–4.0 (m, 2H), 4.5–4.7 (m, 4H), 4.9–5.2 (m, 4H), 5.5–5.9 (m, 8H) 0.9–1.2 (m, 36H, tBu). $\mathbf{1a}^{2\ominus}/2Li^{\oplus}$: ^{1}H NMR ([D$_8$]-THF, 400 MHz, −50 °C): $\delta = 4.9-5.0$ (m, 2H; H15), 5.3–5.4 (m, 2H; H7), 5.5–6.3 (m, 20H).
[8] $\mathbf{2}^{4\ominus}/4Li^{\oplus}$: ^{13}C NMR ([D$_8$]THF, 100 MHz, 25 °C): $\delta = 152.5$, 147.0 (C3, 5), 140.0, 137.9 (C1, 9), 124.8, 123.1 (C11, 13), 118.3, 112.0, 103.6, 96.2 (C2, 6, 10, 14), 116.4 (C12), 93.2 (C4), 61.0, 56.0 (C7, 8), 34.9, 34.4, 32.1, 31.8 (*t*Bu). $\mathbf{3}^{4\ominus}/4Li^{\oplus}$: ^{13}C NMR ([D$_8$]THF, 100 MHz, 25 °C): $\delta = 160.8$, 151.9, 151.3, 148.4, 148.0, 145.3, 144.7, 144.4, 134.5, 133.4, 130.8, 124.8, 112.1 (2C), 112.0 (2C), 99.6, 99.0, 98.1 (2C), 96.9, 96.6, 87.9, 86.4 (arene C), 65.4, 61.9, 58.5, 58.1 (C7, 8), 35.1 (2C), 34.8, 34.7, 32.32, 32.23, 32.21, 32.16 (*t*Bu), 34.0, 33.1, 27.9, 25.8 (bridge C). $\mathbf{3}^{4\ominus}$ is the first example of a [2.2] cyclophane tetraanion. $\mathbf{5}^{2\ominus}/2Li^{\oplus}$: ^{13}C NMR ([D$_8$]THF, 100 MHz, 25 °C): $\delta = 152.4$, 147.5 (C3, 5), 141.6, 140.6 (C1, 9), 131.5, 127.4 (C11, 13), 117.6, 111.8, 102.8, 96.9 (C2, 6, 10, 14), 97.5 (C12), 94.3 (C4), 59.8, 59.1 (C7, 8), 34.9, 34.2, 32.1, 31.8 (*t*Bu). $\mathbf{6}^{2\ominus}/2Li^{\oplus}$: ^{13}C NMR ([D$_8$]THF, 100 MHz, 25 °C): $\delta = 151.8$, 147.5 (C3, 5), 143.2, 137.5, 136.6 (C1, 9, 13), 127.9 (C11), 117.3 (C10), 112.0, 102.0, 98.6 (C2, 6, 14), 98.6 (C12), 95.3 (C4), 58.1, 57.9 (C7, 8), 35.0, 34.5, 32.1, 31.9 (*t*Bu), 22.5, 21.2 (Me).
[9] W. Huber, K. Müllen, *Acc. Chem. Res. 19* (1986) 300.
[10] R. Schenk, W. Huber, P. Schade, K. Müllen, *Chem. Ber. 121* (1988) 2201.
[11] K. Müllen, *Chem. Rev. 84* (1984) 603; B. Eliasson, U. Edlund, K. Müllen, *J. Chem. Soc. Perkin Trans. 2 1986*, 937.
[12] The dianion potentials of **5** and **6** are not half-wave potentials but rather cathodic peak potentials (E_{pc} values), since, under the measuring conditions, the dianion stage is irreversible.

Radical Tri- and Pentaanions of Benzenedi- and Benzenetriglyoxylate Thioesters**

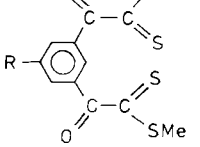
By *Andrzej Sawluk* and *Jürgen Voß**

Although radical monoanions of numerous compounds with π-electron systems have been known for decades,[1] molecular radicals with more than two negative charges have only been described recently: for example, radical trianions of aromatic hydrocarbons having a network of conjugated double bonds, more highly charged ionic hydrocarbons such as the decacyclene hexaanion,[2] or oligoanions of tetramers and pentamers of the phenylene-vinylene type,[3] in which Coulombic repulsion of the electrons is reduced by delocalization.[4] Stabilization may also be achieved, however, by incorporation of functional groups containing atoms with higher polarizability such as sulfur.

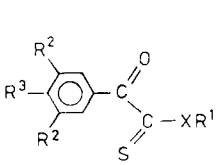
We have now found that compounds **1**–**4**,[5–7] which are thiono- and dithioesters of benzenedi- and benzenetrigly-



1 [5]: $XR^1 = XR^2 = OEt$
2a [6]: $XR^1 = XR^2 = SMe$
2b [6, 7]: $XR^1 = XR^2 = SiPr$
2c [5, 6]: $XR^1 = SMe$, $XR^2 = SiPr$



3a [6]: R = H
3b [6]: R = *t*Bu
4 [7]: R = CO-CS-SMe



5a [5, 8]: $XR^1 = OEt$, $R^2 = H$, $R^3 = tBu$
5b [9]: $XR^1 = SMe$, $R^2 = H$, $R^3 = tBu$
6 [8]: $XR^1 = SMe$, $R^2 = tBu$, $R^3 = H$

[*] Prof. Dr. J. Voß, Dr. A. Sawluk
Institut für Organische Chemie der Universität
Martin-Luther-King-Platz 6, D-2000 Hamburg 13 (FRG)

[**] ESR Investigations on Carboxylic Esters, Part 11. This work was supported by the Deutsche Forschungsgemeinschaft and the Fonds der Chemischen Industrie. *A.S.* thanks the Konrad-Adenauer-Stiftung for a Promotionsstipendium. Part 10: R. Edler, J. Voß, *Chem. Ber. 122* (1989) 187.

oxylic acid, readily accept several electrons, even though they contain only one benzene ring. This is shown not only by the electroanalytic measurements but also by the ESR spectra.[5] Five maxima ($E_{1/2} = -0.13$, -0.35, -0.59, -1.31, and -1.62 V; cf. Fig. 1) are observed in the differential pulse polarogram of the tris(dithioester) **4**, measured in dimethylformamide (DMF).[10]

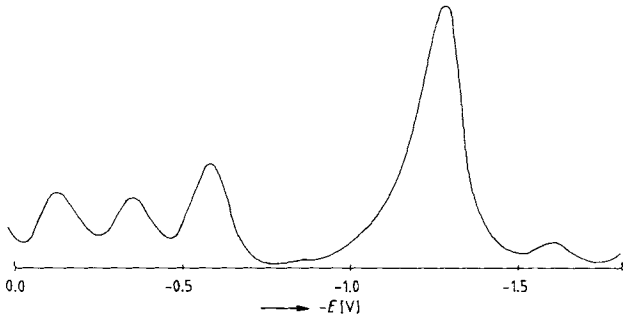


Fig. 1. Differential pulse polarogram of **4**, recorded in DMF/nPr$_4$Br versus Ag/Ag$^{\oplus}$.

The two striking examples in Figure 2 show the completely different ESR spectra of the radical monoanions and the corresponding radical oligoanions obtained by in situ electroreduction at different potentials.[11] We assign the spectrum shown in Figure 2, bottom, to the pentaanion of **4**, because it appears when a cathode potential of -1.0 V, the value at which the corresponding polarographic step begins, is applied to the ESR measuring cell – but, above all, because this assignment provides the only clear explanation of the proton hyperfine structure of the ESR spectrum.

The different spin density distributions arising in the molecule after it accepts one or more electrons result in different coupling constants (Table 1), which can be used to simulate reliably the ESR spectra. In the triply charged radical ions of **1**–**3**, one of the functional groups is capable of bearing two negative charges; in $\mathbf{4}^{\cdot 5\ominus}$, two of the functional groups can each bear two negative charges. These substituents thereby become "diamagnetic", while the benzene ring, with one functional group, contains the unpaired electron. The ESR spectra thus obtained strongly resemble those of the radical anions of *tert*-butyl-substituted thionoesters (e.g., **5a**)[5, 8] and dithioesters (e.g., **5b**, **6**)[9] of phenylglyoxylic acid (compare the ESR spectrum of $\mathbf{5a}^{\cdot\ominus}$, Fig. 3, with that of $\mathbf{1}^{\cdot 3\ominus}$, Fig. 2); on the other hand, the radical monoanions $\mathbf{1}^{\cdot\ominus}$–$\mathbf{4}^{\cdot\ominus}$ exhibit a spin density distribution corresponding to the molecular symmetry. The higher spin density in one thioester group is reflected in the g factors of the radical oligoanions, which are increased by the heavy atom effect of the sulfur atom (Table 1).

Owing to the different alkyl moieties, unsymmetrical radical trianions $\mathbf{2c}^{\cdot 3\ominus}$ exist as two characteristic species, whose overlapping ESR spectra display different coupling constants and g factors (Table 1).

We assume that, in the multiply charged species, each spin label group – defined in terms of the ESR time scale – is coplanar with the ring, so that spin delocalization is possible. By contrast, the other, doubly negatively charged functional groups are twisted out of the ring plane (Fig. 4). For the radical monoanions, such a conformation is also apparently adopted at low temperatures to a certain extent. For instance, on cooling to -49 °C, $\mathbf{2a}^{\cdot\ominus}$ and $\mathbf{3a}^{\cdot\ominus}$ show new ESR spectra, which do not arise by line broadening of the spectra recorded at room temperature. Instead, they resemble much

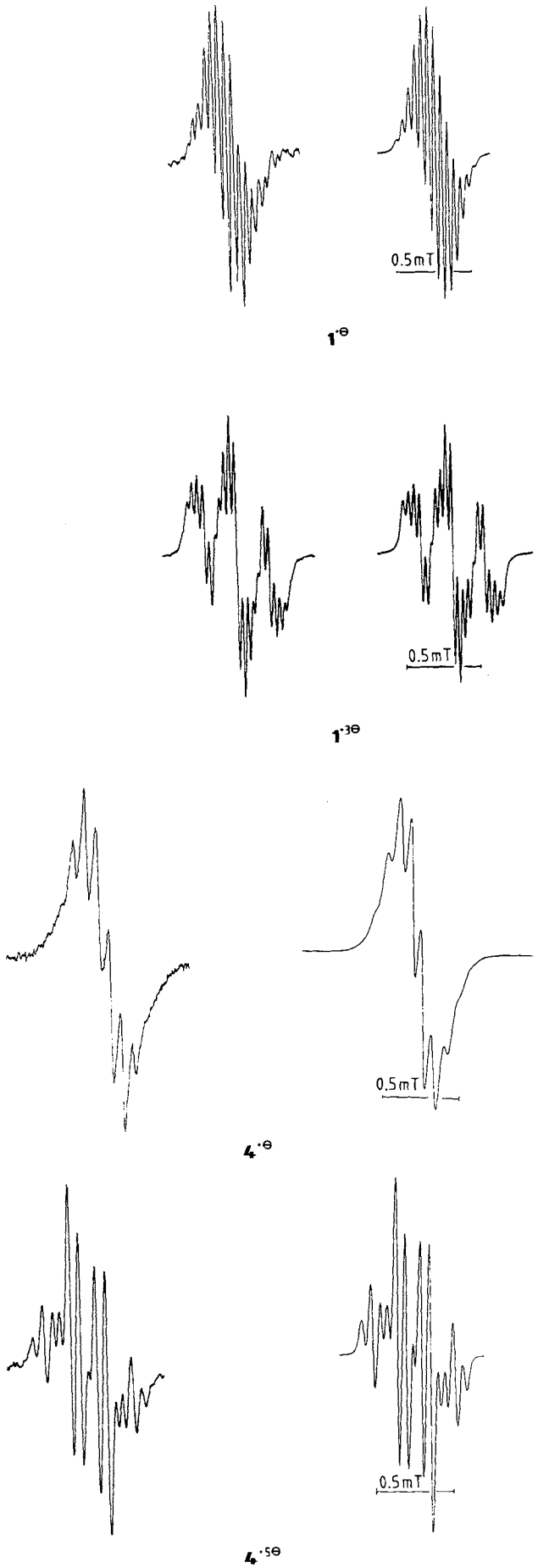
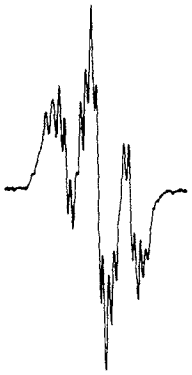


Fig. 2. Measured and simulated ESR spectra of $\mathbf{1}^{\cdot\ominus}$, $\mathbf{1}^{\cdot 3\ominus}$, $\mathbf{4}^{\cdot\ominus}$, and $\mathbf{4}^{\cdot 5\ominus}$.



$5a^{\cdot\ominus}$

Fig. 3. Measured ESR spectrum of $5a^{\cdot\ominus}$.

Table 1. Proton coupling constants a(H) [a] [mT] and g factors of the radical anions of **1–6**.

Compd	E_{red} [b]	$a(H_{2,6})$	$a(H_{3,5})$ ($a(H_4)$)	$a(H_{XCH})$ [c]	n [d]	g factor
$\mathbf{1}^{\cdot\ominus}$	−0.3	0.042	0.042	0.083	4	2.00736
$\mathbf{1}^{\cdot 3\ominus}$	−0.9	0.070	0.035	0.21	2	2.00792
$\mathbf{2a}^{\cdot\ominus}$	−0.2	0.025	0.025	0.075	6	2.01094
$\mathbf{2a}^{\cdot 3\ominus}$	−1.3	0.052	0.030	0.158	3	2.01143
$\mathbf{2b}^{\cdot 3\ominus}$	−1.0	0.052	0.030	0.050	1	2.01112
$\mathbf{2c}^{\cdot 3\ominus}$	−1.3	0.055 0.063	0.027 0.032	0.131 0.072	3 1	2.01140 2.01130
$\mathbf{3a}^{\cdot\ominus}$	−0.2	0.036 [e]	[f] ([f])	0.063	6	2.01101
$\mathbf{3a}^{\cdot 3\ominus}$	−0.7	0.050 [e]	0.026 (0.057) [e]	0.150	3	2.01118
$\mathbf{3b}^{\cdot 3\ominus}$	−1.2	0.050 [e]	(0.062) [e]	0.149	3	2.01111
$\mathbf{4}^{\cdot\ominus}$	−0.2	0.022	(0.022)	0.067	9	2.01103
$\mathbf{4}^{\cdot 5\ominus}$	−1.0	0.053	(0.066)	0.158	3	2.01123
$\mathbf{5a}^{\cdot\ominus}$	−0.6	0.060	0.030	0.18	2	2.00809
$\mathbf{5b}^{\cdot\ominus}$	−0.4	0.047	0.028	0.152	3	2.01105
$\mathbf{6}^{\cdot\ominus}$	−1.1	0.045	(0.049)	0.149	3	2.01108

[a] In cases of doubt, position 1 is the ring position with the spin-bearing functional group. [b] Potential [V] of the in situ electroreduction, with respect to an internal $Ag/Ag^{\oplus}/AgBr$ reference electrode, whose potential is shifted by −0.61 relative to that of the SCE. [c] Alkyl proton coupling, X = O (**1**, **5a**) or X = S (**2–4**, **5b**, **6**). [d] Number of coupled alkyl protons. [e] These values could not be assigned unambiguously. [f] Unresolved couplings.

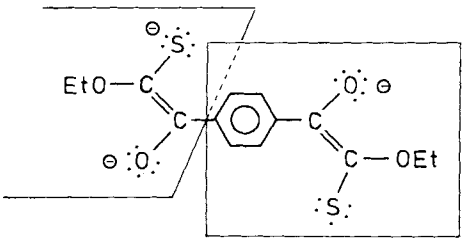


Fig. 4. Twisted conformation of the radical anion $\mathbf{1}^{\cdot 3\ominus}$

more strikingly the spectra of the trianions $\mathbf{2a}^{\cdot 3\ominus}$ and $\mathbf{3a}^{\cdot 3\ominus}$ and are due to a different, less symmetric spin density distribution.[5]

Different ESR spectra are also obtained when dithioesters of 4-nitrophenylglyoxylic acid are reduced at different potentials, so that they accept one or more electrons.[5] By contrast, no multiply charged radical anions are detectable for the sulfur-free esters of benzenediglyoxylic esters.[5]

Received: November 17, 1988;
revised: April 5, 1989 [Z 3056 IE]
German version: *Angew. Chem. 101* (1989) 927

CAS Registry numbers:
$\mathbf{1}^{\ominus}$, 120637-51-6; $\mathbf{1}^{3\ominus}$, 120637-52-7; $\mathbf{2a}^{\ominus}$, 120637-54-9; $\mathbf{2a}^{3\ominus}$, 120637-55-0; $\mathbf{2b}^{3\ominus}$, 120637-57-2; $\mathbf{2c}^{3\ominus}$, 120637-58-3; $\mathbf{3a}^{\ominus}$, 120665-61-4; $\mathbf{3a}^{3\ominus}$, 120637-59-4; $\mathbf{3b}^{3\ominus}$, 120637-60-7; $\mathbf{4}^{\ominus}$, 120665-62-5; $\mathbf{4}^{5\ominus}$, 120637-61-8; $\mathbf{5a}^{\ominus}$, 120637-53-8; $\mathbf{5b}^{\ominus}$, 120637-56-1; $\mathbf{6}^{\ominus}$, 120637-62-9.

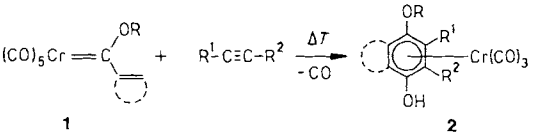
[1] F. Gerson: *Hochauflösende ESR-Spektroskopie*, Verlag Chemie, Weinheim 1967.
[2] J. Mortensen, J. Heinze, *J. Electroanal. Chem. Interfacial Electrochem. 175* (1984) 333; J. Heinze, *Angew. Chem. 96 (1984) 823; Angew. Chem. Int. Ed. Engl. 23* (1984) 831.
[3] J. Heinze, J. Mortensen, K. Müllen, R. Schenk, *J. Chem. Soc. Chem. Commun. 1987*, 701.
[4] F. Gerson, W. Huber, *Acc. Chem. Res. 20* (1987) 85; K.-U. Klabunde, W. Huber, J. Lex, K. Müllen, *Chem. Ber. 120* (1987) 1491; H. Kurreck, B. Kirste, W. Lubitz, *Angew. Chem. 96* (1984) 171; *Angew. Chem. Int. Ed. Engl. 23* (1984) 173.
[5] A. Sawluk, *Dissertation*, Universität Hamburg 1987.
[6] A. Sawluk, J. Voß, *Synthesis 1987*, 968.
[7] A. Sawluk, *Diplomarbeit*, Universität Hamburg 1982.
[8] G. Adiwidjaja, H. Günther, J. Voß, *Angew. Chem. 92* (1980) 559; *Angew. Chem. Int. Ed. Engl. 19* (1980) 563.
[9] H. Günther, *Dissertation*, Universität Hamburg 1980.
[10] DMF was purified by azeotropic distillation with benzene, dried, and stored over molecular sieves at 4 °C. The potentials are given relative to an internal silver electrode (Ag wire in a 0.1 M solution of tetrapropylammonium bromide in DMF); cf. footnote [b] in Table 1.
[11] The radical ions were generated, as described in [12], by internal electrolysis of 3×10^{-3} M solutions of thioesters in dry DMF (0.1 M in tetrapropylammonium bromide as electrolyte) at a Pt cathode. The ESR spectra were recorded with a Bruker 420 s spectrometer [12].
[12] J. Voß, F.-R. Bruhn, *Liebigs. Ann. Chem. 1979*, 1931; C.-P. Klages, S. Köhler, E. Schaumann, W. Schmüser, J. Voß, *J. Phys. Chem. 83* (1979) 738; D. Helling, C.-P. Klages, J. Voß, *ibid. 84* (1980) 3638.

The Mechanism of the Dötz Reaction: Chromacyclobutenes by Alkyne–Carbene Coupling?**

By *Peter Hofmann** and *Martin Hämmerle*

Dedicated to Professor Hans Hofmann on the occasion of his 60th birthday

The reaction of Fischer carbene complexes **1** with alkynes, first described by *Dötz* (Dötz reaction),[1] has proved to be of exceptionally broad preparative value.[2–5] The complexity of this template reaction is revealed by the fact that – depending on reaction conditions and starting materials – roughly ten other types of products have so far been isolated in addition to phenol derivatives **2**.



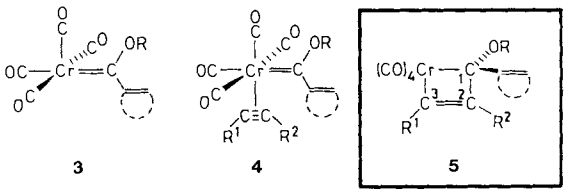
1 **2**

Although the mechanism of the Dötz reaction and its variants is still largely unknown, all mechanistic proposals start from a *cis* CO dissociation in **1** followed by alkyne coordination to intermediates **3** giving species **4**. Kinetic investigations[6] and studies on tungsten analogues of **1**[7] seem to support this assumption. In a subsequent step, chromacyclobutenes **5** are postulated to be the key intermediates formed[8] by (regioselective) alkyne–carbene coupling at the

[*] Prof. Dr. P. Hofmann, Dipl.-Chem. M. Hämmerle
Anorganisch-chemisches Institut der Technischen Universität München
Lichtenbergstrasse 4, D-8046 Garching (FRG)

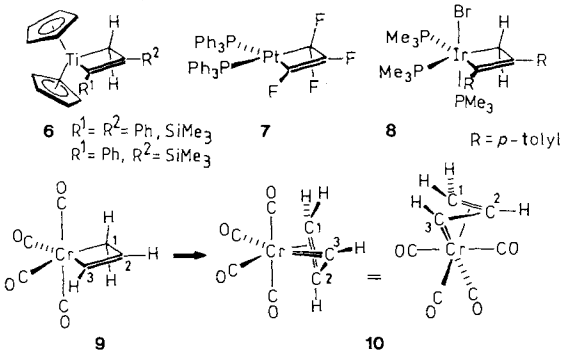
[**] This work was supported by the Stiftung Volkswagenwerk and by the Fonds der Chemischen Industrie.

metal. It is the stereochemistry of their electrocyclic ring-opening ("mode of rotation" at C1) and of the vinylcarbene complexes thereby formed which was recently suggested to govern the course of further transformations and therefore the chemoselectivity of the overall reaction.[9]



3 4 5

Here we report MO model calculations[10] which demand some modification of these concepts and which are relevant to the stereo- and chemoselectivity of the Dötz reaction. Although planar metallacyclobutenes similar to **5** are known and their structures have been established (**6**,[11] **7**,[12] **8**[13]), analogous ground-state geometries for $Cr(CO)_4$ (d^6-ML_4, isolobal to $CH_2^{2\oplus}$, $CH^{\oplus}$) as metal fragment are unrealistic.



6 $R^1 = R^2 = Ph, SiMe_3$; $R^1 = Ph$, $R^2 = SiMe_3$ 7 8 $R = p$-tolyl

9 10

This is clearly revealed in Figure 1, which shows the computed interaction diagram between a $Cr(CO)_4$ fragment[14] and a C_3H_4 ligand[15] for the unsubstituted, planar model system **9**.

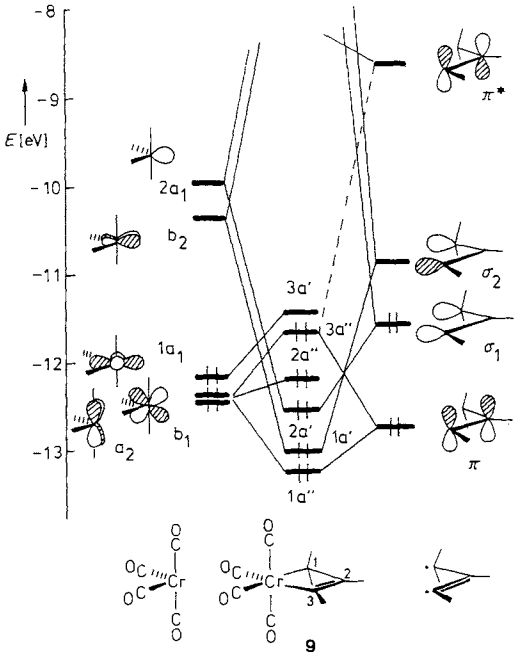


Fig. 1. Interaction diagram between $Cr(CO)_4$ (C_{2v}, "octahedral" fragment) and the C_3H_4 ligand (C_s) for structure **9**. Only the relevant contributions to the molecular orbitals are shown schematically.

Interaction of the fragment MOs σ_1 and σ_2 with $2a_1$ and b_2 of $Cr(CO)_4$[14] results in the MOs 1a' and 2a' of the two Cr–C σ bonds. The π MO of the C_3H_4 system cannot satisfy the electronic requirements of the chromium center in **9**. Thus, as typical of such cases, an "open-shell" 16-electron system with only a small separation between HOMO and LUMO emerges. The character of the two frontier orbitals of **9**–3a' largely corresponds to the empty x^2-y^2 AO on chromium and 3a'' is mainly localized on C3 of the π MO of the C2–C3 double bond – implies an out-of-plane distortion of the metallacyclobutene ring, that is, a 2nd-order Jahn–Teller stabilization.[14] Figure 2 shows a calculated Walsh diagram and the corresponding total energy for a "ring folding" of **9** (H atoms relaxed). The resulting structure **10**, which is 26 kcal mol^{-1} more stable than **9**, has a large frontier orbital energy separation and an 18-electron configuration. Analogous structure characteristics have been found

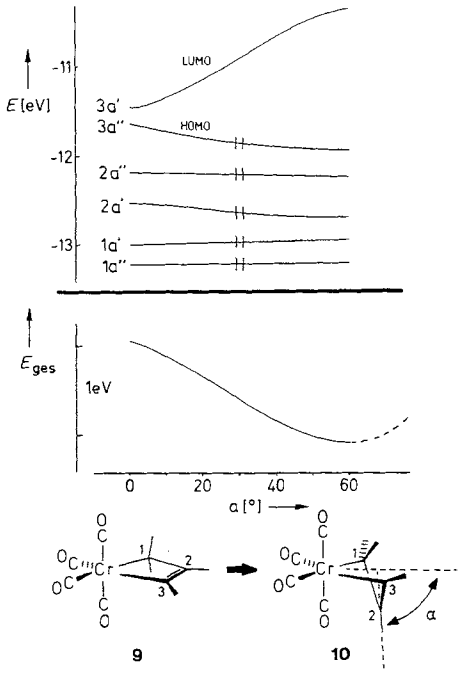
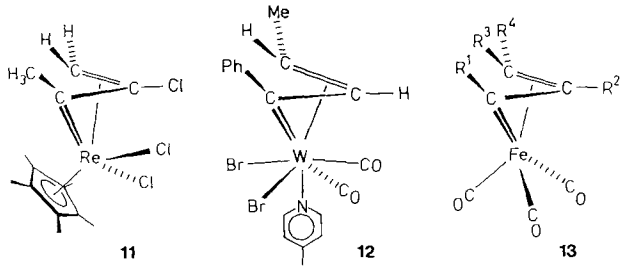


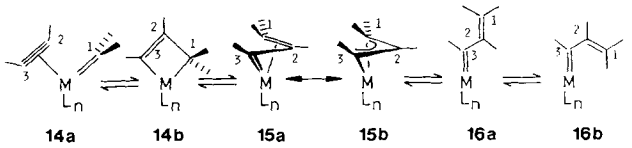
Fig. 2. Walsh diagram and total energy curve for a "folding" of the metallacyclobutene ring of **9** around the C1–C3 axis; H atoms simultaneously relaxed, interatomic distances constant.

experimentally for **11**[16] and **12**[17] and for representatives of **13**.[18] Thus, within the structural continuum **14**–**16**, $[(CO)_4Cr(C_3H_4)]$, in accord with **15a/15b**, has to be regarded as an η^3-vinylcarbene complex in which the double bond saturates the electron deficiency of chromium intramolecularly. The calculations indicate that the vinyl π system is coordinated relatively loosely to the metal (weak back-bonding). For $ML_n = Cr(CO)_4$, therefore, the isomeric structures **15** (= **10**) and **16a/16b** have similar total energies and, even without complete geometry optimization, are ca. 25–30 kcal mol^{-1} more stable than the most energetically favored structure of **9**! In **10**, unlike **9**, the double bond is no longer localized between C2 and C3; instead, the calculated overlap populations indicate that it resides more between C1 and C2 or is delocalized in the C_3 system. True η^1-vinylcarbene ligands such as those in **16** are known at, for example, $Cr(CO)_5$[19] and $Cp_2Ti(PMe_3)$.[20]

Analogous calculations for Cp_2Ti, $(PH_3)_2Pt$, and $Fe(CO)_3$ as metal fragments correctly reproduce the ground-state geometries found experimentally for **6**, **7**, and **13**: planar metallacyclobutene structures for $Cp_2Ti(C_3H_4)$ and

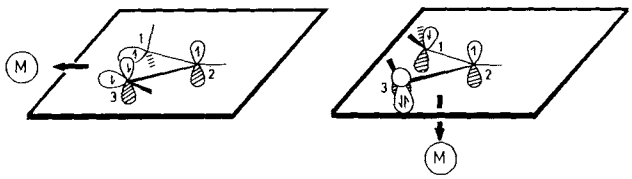


11 12 13



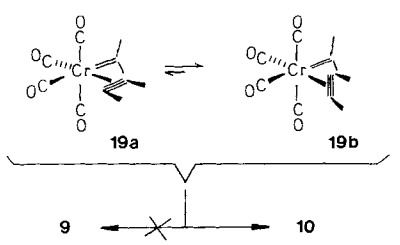
14a 14b 15a 15b 16a 16b

$(PH_3)_2Pt(C_3H_4)$, η^3-vinylcarbene type for $(CO)_3Fe(C_3H_4)$. In the series d^2-ML_6 (Cp_2Ti in **6**), d^4-ML_5 ([Cp*$ReCl_2$] in **11** and $[W(CO)_2Br_2$(4-picoline)] in **12**), d^6-ML_4 ($Cr(CO)_4$ in **10**), d^8-ML_4 ($Ir(PMe_3)_3Br$ in **8**), and d^{10}-ML_2 ($(PPh_3)_2Pt$ in **7**), the coordination mode of the organic ligand therefore adjusts to the symmetry and occupation of the valence orbitals (the isolobal character) of the respective metal unit and serves as a two-electron donor **17** ("in plane") or a four-electron donor **18** ("out of plane").



17 18

The details of the real structures **11**–**13** (C–C and M–C bond lengths, weight of **15a** versus **15b**, degree of backbonding, etc.) depend on the specific fragment ML_n and on the substitution of the C_3 system. The appreciably lower total energy of **10** compared with **9** means that, in the Dötz reaction, alkyne carbene complexes **4** do not react via chromacyclobutenes **5**. Model calculations on **19**, the η^2-C_2H_2 ligand of which, like ethene,[21] prefers conformation **19b** by ca. 5 kcal mol^{-1}, indeed lead to an energy maximum approximately 23 kcal mol^{-1} above **19a** for the "in plane" alkyne–carbene coupling **19a** → **9** (C_s symmetry), in marked contrast to the exothermic reaction course calculated for Cp_2Ti as metal fragment.[11b] In neither case is the reaction symmetry forbidden.



19a 19b

9 10

Preliminary calculations, even without full optimization of the reaction pathway, reveal, however, that the activation barrier disappears nearly completely for a direct rearrangement of **19b** to **10** (C_1 symmetry). This suggests that alkyne carbene complexes **4**, formed via **3**,[22] should they exist as discrete intermediates at all,[23] may rearrange directly to η^3-vinylcarbene complexes. This mechanism would establish both the regioselectivity of alkyne incorporation and the chemoselectivity of the overall reaction (via *exo*/*endo* or *cis*/*trans* position of the substituents at C1 of intermediates of type **10** and **16**) without a need to invoke chromacyclobutenes **5** and their electrocyclic ring opening.[9] The consequences of the results described here with respect to a mechanistic understanding of the Dötz reaction or of alkyne polymerization with Fischer carbene complexes of tungsten,[24] where intermediates like **5** have also been assumed, are self-evident.

Received: March 13, 1989 [Z 3227 IE]
German version: *Angew. Chem. 101* (1989) 940

CAS Registry numbers:
9, 121126-05-4; **10**, 121126-06-5; Cr, 7440-47-3.

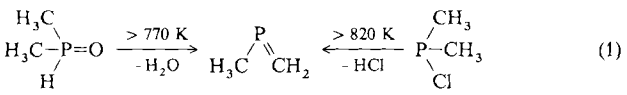
[1] a) K. H. Dötz, *Angew. Chem. 87* (1975) 672; *Angew. Chem. Int. Ed. Engl. 14* (1975) 644; b) *ibid. 96* (1984) 573 and *23* (1984) 587.
[2] a) W. D. Wulff, P. C. Tang, K. S. Chan, J. S. McCallum, D. C. Yang, S. R. Gilbertson, *Tetrahedron 41* (1985) 5813; b) W. D. Wulff in L. S. Liebeskind (Ed.): *Advances in Metal-Organic Chemistry, Vol. 1*, JAI press Inc., Greenwich 1987.
[3] H. U. Reissig, *Nachr. Chem. Tech. Lab. 34* (1986) 22.
[4] M. F. Semmelhack, J. J. Bozell, L. Keller, T. Sato, E. J. Spiess, W. D. Wulff, A. Zask, *Tetrahedron 41* (1985) 5803.
[5] C. P. Casey, *React. Interned. 2* (1981) 155.
[6] H. Fischer, J. Mühlemeier, R. Märkl, K. H. Dötz, *Chem. Ber. 115* (1982) 1355.
[7] a) H. C. Foley, L. M. Strubinger, T. S. Targos, G. L. Geoffroy, *J. Am. Chem. Soc. 105 (1983) 3064*; b) *S. E. J. Bell, K. C. Gordon, J. J. McGarvey, ibid. 110* (1988) 3107.
[8] K. H. Dötz in H. tom Dieck, A. de Meijere (Eds.): *Organometallics in Organic Synthesis: Aspects of a Modern Interdisciplinary Field*, Springer, Berlin 1988.
[9] J. S. McCallum, F.-A. Kunng, S. R. Gilbertson, W. D. Wulff, *Organometallics 7* (1988) 2346.
[10] Extended Hückel-type calculations were employed: R. Hoffmann, *J. Chem. Phys. 39* (1963) 1397. H_{ij} matrix elements: J. H. Ammeter, H.-B. Bürgi, J. C. Thibeault, R. Hoffmann, *J. Am. Chem. Soc. 100* (1978) 3686. Atom parameters for Cr, Fe, Pt: T. A. Albright, R. Hoffmann, J. C. Thibeault, R. D. L: Thorn, *ibid. 101* (1979) 3801; for Ti: J. W. Lauher, R. Hoffmann, *ibid. 98* (1976) 1729; for C, H, O, P: EH standard parameters. Model geometries idealized from X-ray structure data of relevant complexes with standard bond lengths.
[11] a) F. N. Tebbe, R. L. Harlow, *J. Am. Chem. Soc. 102* (1980) 6149; b) R. J. McKinney, T. H. Tulip, D. L. Thorn, T. S. Coolbaugh, F. N. Tebbe, *ibid. 103* (1981) 5584.
[12] R. C. Hemond, R. P. Hughes, D. J. Robinson, A. L. Rheingold, *Organometallics 7* (1988) 2239.
[13] J. C. Calabrese, D. C. Roe, D. L. Thorn, T. H. Tulip, *Organometallics 3* (1984) 1223.
[14] T. A. Albright, J. K. Burdett, M.-H. Whangbo: *Orbital Interactions in Chemistry*, Wiley, New York 1985.
[15] For reasons of consistency with C_3H_4 as vinylcarbene, uncharged fragments were chosen. For recent ab initio work on various C_3H_4 isomers and states see: M. Yoshimine, J. Pacansky, N. Honjou, *J. Am. Chem. Soc. 111* (1989) 2785.
[16] W. A. Herrmann, R. A. Fischer, E. Herdtweck, *Angew. Chem. 99* (1987) 1286; *Angew. Chem. Int. Ed. Engl. 26* (1987) 1263.
[17] A. Mayr, M. F. Asaro, T. J. Glines, *J. Am. Chem. Soc. 109* (1987) 2215.
[18] a) T. Mitsudo, H. Watanabe, T. Sasaki, Y. Takegami, Y. Watanabe, *Organometallics 8* (1989) 368; b) J. Klimes, E. Weiss, *Angew. Chem. 94* (1982) 207; *Angew. Chem. Int. Ed. Engl. 21* (1982) 205; *Angew. Chem. Suppl. 1989*, 477; c) T. Valéri, F. Meier, E. Weiss, *Chem. Ber. 121* (1988) 1093.
[19] R. Aumann, H. Heinen, *Chem. Ber. 120* (1987) 537, zit. Lit.
[20] P. Binger, P. Müller, R. Benn, R. Mynott, *Angew. Chem. 101* (1989) 647; *Angew. Chem. Int. Ed. Engl. 28* (1989) 648.
[21] F. Volatron, O. Eisenstein, *J. Am. Chem. Soc. 108* (1986) 2173.
[22] A coordination of the double bond (or of the aryl group), which is then displaced by the alkyne, presumably occurs for **3** as it does for **10**.
[23] The only stable *cis*-alkyne carbene complexes known are those containing the fragments $W(PMe_3)_2Cl_2$ and $CpW(CO)^{\oplus}$ (both d^4-ML_4 with two fewer valence electrons than **4**): A. Mayr, K. S. Lee, M. A. Kjelsberg, D. Van Engen, *J. Am. Chem. Soc. 108* (1986) 6097; H. G. Alt, *J. Organomet. Chem. 256* (1983) C12. In the case of d^8-ML_3 [13] and d^2-ML_6 [11], for which the coupling products have been isolated, such intermediates are not detectable.

Water Elimination from Phosphorus–Oxygen Compounds: The Formation of 2-Phosphapropene by Thermolysis of Dimethylphosphane Oxide**

By *Hans Bock** and *Martin Bankmann*

Dedicated to Professor Gottfried Märkl on the occasion of his 60th birthday

Unsaturated organophosphorus compounds containing the structural units $-C\equiv P$, $\diagdown C=P-$, $-P=C=P-$, $-C\equiv P\diagup\diagdown$, or $\diagup C-P\diagup\diagdown$ with a wide variety of substituents have recently been synthesized by numerous routes.[1, 2] However, their preparation by thermal dehydration, for example of dialkylphosphane oxides, $R_2HP=O$, which are now being produced on a large scale,[3] has not been reported.[4] The P=O bond, which exhibits a bond dissociation enthalpy of 520 to 720 kJ mol^{-1},[5, 6] is generally regarded as being highly favored energetically; its preferential formation is exploited in the Wittig and Arbusov reactions.[5] Here we report on the gas-phase thermolysis of dimethylphosphane oxide[2, 3] to give 2-phosphapropene [Eq.(1)], which has already been generated by HCl elimination from dimethylchlorophosphane.[1, 2]



(1)

When the decomposition of $(H_3C)_2HP=O$ on quartz wool is followed by PE-spectroscopic real-time analysis,[7] a method that has proved especially valuable for studying reactive molecules in the gas phase, the ionization pattern recorded at room temperature provides no evidence of a hydroxy isomer[8] (Fig. 1, top). The decomposition starts above 770 K, as revealed by the appearance of the characteristic sharp peak at 12.6 eV corresponding to H_2O ionization. Undecomposed dimethylphosphane oxide can be removed by inserting a 230 K cold trap, so that the bands of H_2O and the dehydration product (cf. Ref. [1]: 9.7, 10.0, 12.4, and 14.3 eV) dominate the spectrum. Above 970 K, methane is eliminated ($H_3C-P=CH_2 \rightarrow HC\equiv P+CH_4$), as observed earlier.[1]

The thermal decomposition of dimethylphosphane oxide thus results in water elimination! By carrying out this novel preparation of 2-phosphapropene on finely granulated silica, for example, the reaction can be optimized[2] and even made superior to the HCl elimination from dimethylchlorophosphane, which needs finely tuned reaction conditions and affords only moderate yields.[1] Condensation of the highly reactive 2-phosphapropene in a 77 K cold trap and careful fractional reevaporation allows, for example, the head-to-tail dimer, *trans*-1,3-dimethyl-1,3-diphosphetane, to be characterized by mass and PE spectroscopy,[2, 8] while a viscous, glassy polymeric residue is obtained as the main product.

This surprising dehydration of dimethylphosphane oxide represents an unprecedented type of reaction in organophosphorus chemistry.[5] To rationalize the unexpected observation, a section of the MNDO energy hypersurface has been calculated, which, by appropriate choice of the coordinates

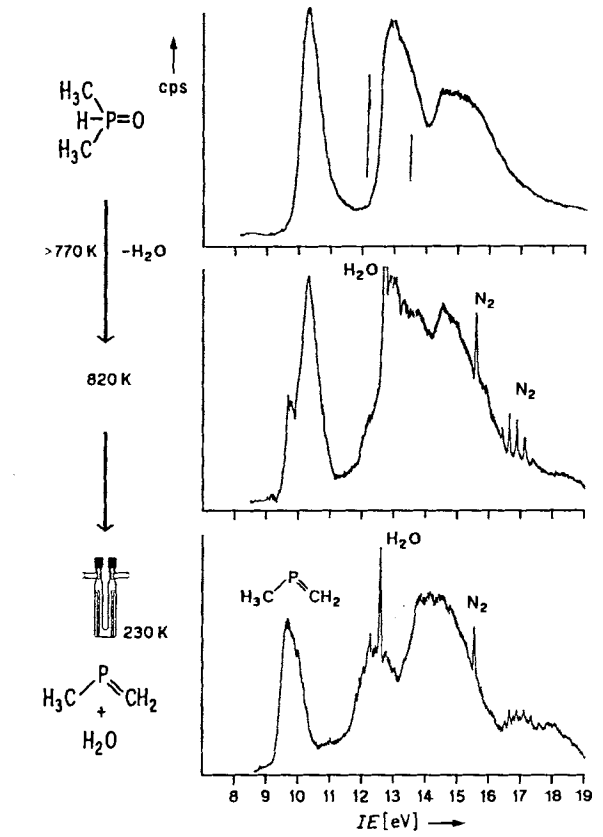


Fig. 1. He(I) PE spectra of dimethylphosphane oxide (top) and its thermolysis products on quartz wool at 820 K, H_2O and $H_3C-P=CH_2$ (middle), as well as the spectrum after removing undecomposed $(H_3C)_2HP=O$ in a 230 K cold trap (below).

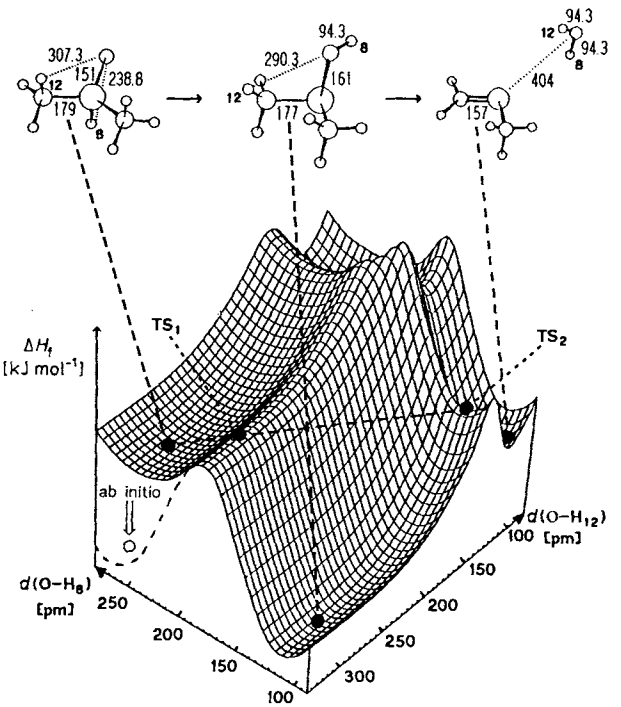
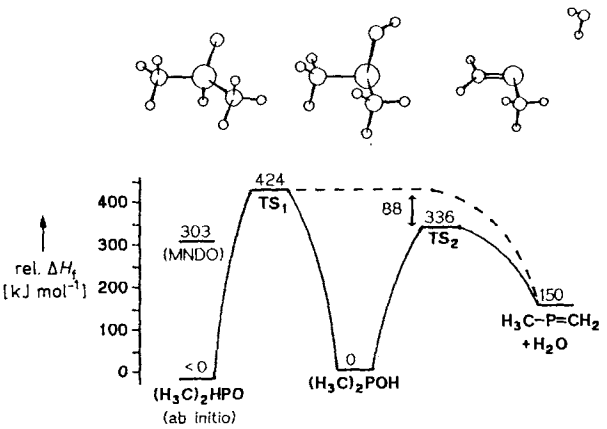


Fig. 2. Section of the two-parameter MNDO hypersurface for the isomerization of dimethylphosphane oxide to dimethylhydroxyphosphane and the H_2O elimination to $H_3C-P=CH_2$, as well as MNDO-optimized structures of these compounds (○: value extrapolated from ab initio calculations, cf. text).

[*] Prof. Dr. H. Bock, Dipl.-Chem. M. Bankmann
Institut für Anorganische Chemie der Universität
Niederurseler Hang, D-6000 Frankfurt am Main 50 (FRG)

[**] Gas-Phase Reactions, Part 75. This work was supported by the Deutsche Forschungsgemeinschaft, the Fonds der Chemischen Industrie, Hoechst AG, and the Land Hessen. We thank Prof. *K. Kühlein* (Hoechst AG) for donation of chemicals. Part 74: H. Bock, B. Solouki S. Patai; Z. Rappoport (Eds.): *The Chemistry of Organic Silicon Compounds*, Wiley, Chichester 1989, pp. 555–653.

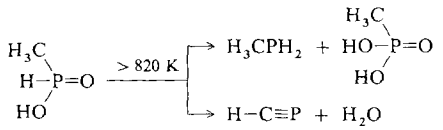
$d(O\cdots H_8)$ and $d(O\cdots H_{12})$ from the total of $(3\times 11-6)=27$ degrees of freedom, contains the two isomers of the starting material, $(H_3C)_2HP=O$ and $(H_3C)_2P-OH$, as well as the two products, $H_3C-P=CH_2$ and H_2O (Fig. 2).[9] With respect to the assumptions introduced, these calculations afford the following speculative insights into the thermolysis pathway: The MNDO enthalpies of formation suggest a relatively shallow potential well for dimethylphosphane oxide, which is considerably deepened by including d-polarization functions in an ab initio basis set (Fig. 2: ○). The barrier for the isomerization $(H_3C)_2P-OH \rightarrow (H_3C)_2HP=O$, calculated by MNDO to amount to approximately 420 kJ mol^{-1}, agrees with reported values.[10] The minimum-energy reaction path crosses the first and highest energy transition state, TS_1, and then follows the slope of the hypersurface to the saddle point TS_2 for the 1,2-HOH elimination at 88-kJ mol^{-1} lower energy (Scheme 1).



Scheme 1. Enthalpy differences ΔH_f from MNDO calculations.

The overall endothermic H_2O elimination is apparently preferred over the energetically more favorable isomerization because of the entropy increase. Considering the numerous approximations and, in particular, the selection among the many degrees of freedom, the reaction profile (Scheme 1) is also in agreement with the experimental result that not even traces of the possible isomerization product $(H_3C)_2P-OH$ are revealed by PE spectroscopy. Under the nearly unimolecular thermolysis conditions (pressure 10 Pa), only the simultaneous elimination of water allows an effective dissipation of the activation energy stored in the "chemically activated" $(H_3C)_2P-OH$.[11]

This type of reaction, in which unsaturated phosphorus(III) compounds are prepared by thermal elimination of water from phosphane oxides, can be extended to other derivatives.[2] For example, methylphosphinic acid, on gas-phase thermolysis at 820 K, only partially disproportionates to methylphosphane and methylphosphonic acid, while phosphaacetylene is formed in approximately the same yield by water elimination.[2]



Received: March 20, 1989 [Z 3236 IE]
German version: *Angew. Chem. 101* (1989) 950

CAS Registry numbers: $(H_3C)_2HP=O$, 7211-39-4; $H_3CP=CH_2$, 89149-01-9.

[1] H. Bock, M. Bankmann, *Angew. Chem. 98* (1986) 287; *Angew. Chem. Int. Ed. Engl. 25* (1986) 265, and references cited therein. In the meantime, also 1-phosphapropene has been characterized by PE spectroscopy: S. Lacombe, D. Gonbeau, J.-L. Cabioch, B. Pellerin, J.-M. Denis, G. Pfister-Guillozo, *J. Am. Chem. Soc. 110* (1988) 6984.

[2] Cf. M. Bankmann *Dissertation*, Universität Frankfurt 1989, and the comprehensive references therein. Recent review articles: M. Regitz, P. Binger, *Angew. Chem. 100* (1988) 1541; *Angew. Chem. Int. Ed. Engl. 27* (1988) 1484; J. I. G. Cadogan, P. K. G. Hodgson, *Phosphorus Sulfur 30* (1987) 3; K. Karaghiosoff, A. Schmidtpeter, *ibid. 36* (1988) 217.

[3] Cf., e.g., the scientific symposium "125 Jahre Hoechst", Festschrift Hoechst AG 1989, p. 72.

[4] A careful literature search revealed that, upon heating at 60 °C/1 Torr, cyclohexyl- and (3-pentyl)phosphane oxides afford mixtures of products, from which tetraalkyltetraphosphetanes, $(RP)_4$, can be isolated in small yields: W. M. A. Henderson, Jr., M. Epstein, F. S. Seichter, *J. Am. Chem. Soc. 85* (1963) 2462.

[5] Cf. J. E. Huheey: *Inorganic Chemistry: Principles of Structure and Reactivity*, Harper and Row, New York 1978, p. 839f.

[6] Calculations for substituted phosphane oxides XYHP=O with X,Y=H,CH_3,NH_2,OR,F [M. S. Gordon, J. A. Boatz, M. W. Schmidt, *J. Phys. Chem. 88* (1984) 2998; *ibid. 91* (1987) 1743] revealed that the oxo forms are usually more stable than the hydroxy isomers XYP-OH and that the activation barrier for the isomerization $H_3P=O \rightarrow H_2POH$ should be approximately 300 kJ mol^{-1}. Elimination of HX or XY has been proposed as a possible thermolysis pathway. Experimentally, the hydroxy form has been observed only for acceptor-substituted derivatives like $(F_3C)_2P-OH$ [J. E. Griffith, A. B. Burg, *J. Am. Chem. Soc. 84* (1962) 3442] or on complex stabilization, e.g., in $[(OC)_4HalMn\cdots PR_2OH]$ [E. Lindner, B. Schilling, *Chem. Ber. 110* (1977) 3266].

[7] H. Bock, B. Solouki, S. Aygen, M. Bankmann, O. Breuer, R. Dammel, J. Dörr, M. Haun, T. Hirabayashi, D. Jaculi, J. Mintzer, S. Mohmand, H. Müller, P. Rosmus, B. Roth, J. Wittmann, H.-P. Wolf, *J. Mol. Struct. 173* (1988) 31, and references cited therein.

[8] Vertical ionization energies of $(CH_3)_2HP=O$ with assignment: 10.32 (n_O,$\pi_{P=O}$), 12.9 (σ_{PC}, σ_{PH},σ_{PO}), and >14.5 eV (σ_{CH}). *trans*-1,3-Dimethyl-1,3-diphosphetane: *m/z* 120 ($M^{\oplus}$), 105 ($M^{\oplus}$-CH_3), 92, 77, 75, 57, 45; IE^V = 8.0 ($4b_g$), 9.3 ($6a_g$), 11.3 ($3b_g$, $3a_u$, $5b_u$), 12.9–15.5 eV; ΔH(MNDO) = −274.1 kJ mol^{-1}.

[9] According to the literature, bond enthalpies of four-coordinate phosphorus(v) compounds obtained from MNDO calculations are usually too high, because d-polarization functions are not included in the MNDO parameter set. [cf. M. J. S. Dewar, M. L. McKee, H. S. Rzepa, *J. Am. Chem. Soc. 100* (1978) 3607]. On the other hand, ab initio studies [6], in agreement with the experimental data, indicate that nearly all derivatives HXYPO are 10–60 kJ mol^{-1} more stable than the corresponding tautomers XYPOH. According to the Hammond principle [*J. Am. Chem. Soc. 77* (1955) 334], the transition states of endothermic reactions should be productlike. Therefore, the MNDO results for both the isomerization and the H_2O elimination of the phosphorus(III) derivatives are assumed to satisfactorily approximate this part of the energy hypersurface (Fig. 2). For the phosphorus(v) compound $(H_3C)_2HP=O$, the ab initio total energy [6] also given (Fig. 2: ○) demonstrates that the potential well calculated by MNDO is too shallow.

[10] Cf., e.g., M. W. Schmidt, S. Yabushita, M. S. Gordon, *J. Phys. Chem. 88* (1984) 32 as well as [6]. C. J. Cramer, C. E. Dykstra, S. E. Denmark, *Chem. Phys. Lett. 136* (1987) 17, calculated isomerization barriers $R_2POH \rightarrow R_2HP=O$ between 290 and 365 kJ mol^{-1}.

[11] Cf. H. Bock, R. Dammel, *Angew. Chem. 99* (1987) 518; *Angew. Chem. Int. Ed. Engl. 26* (1987) 504, and references cited therein. The "chemically activated" $H_2C=NH$, generated by methyl azide pyrolysis, eliminates H_2 in the subsequent reaction channel and forms HCN at a temperature 500 K lower than after prior isolation in a 180 K cold trap.

Amides Nonplanar Solely by C–N Bond Rotation**

By *Terrence J. Collins** and *José M. Workman*

Because of its central significance, the structural properties of the amide functional group have been studied extensively.[1] As a result of the distinctive bonding features, the C, N, and O atoms and their substituent atoms lie in a planar array for almost all amides, a structural generality having

[*] Prof. T. J. Collins, J. M. Workman
Department of Chemistry, Carnegie Mellon University
4400 Fifth Avenue, Pittsburgh, PA 15213 (USA)

[**] Support by the National Science Foundation (Grant No. CHE-8714720) is gratefully acknowledged.

many notable consequences. Nonplanar amides are rare and arise in organic chemistry primarily when amide groups are constrained by rings.[2] Three separate classes of distinctly nonplanar amide groups bonded to metals have been identified in the last several years.[2, 3] Parameterization of nonplanar deformations was exquisitely defined in the early seventies, allowing amide nonplanarity to be assessed meaningfully in terms of the C–N twist angle and planar-to-pyramidal distortions at carbon and nitrogen.[4]

Deformation by twisting of the C–N bond or by pyramidalization at C are extremely rare. Pyramidalization at nitrogen is the lowest-energy deformation and the dominating occurrence. Here we describe a unique molecule, **2**, with a ligand containing two nonplanar amide groups in which twisting of the C–N bonds is appreciable, but pyramidalization at the N and C atoms is nonexistent.

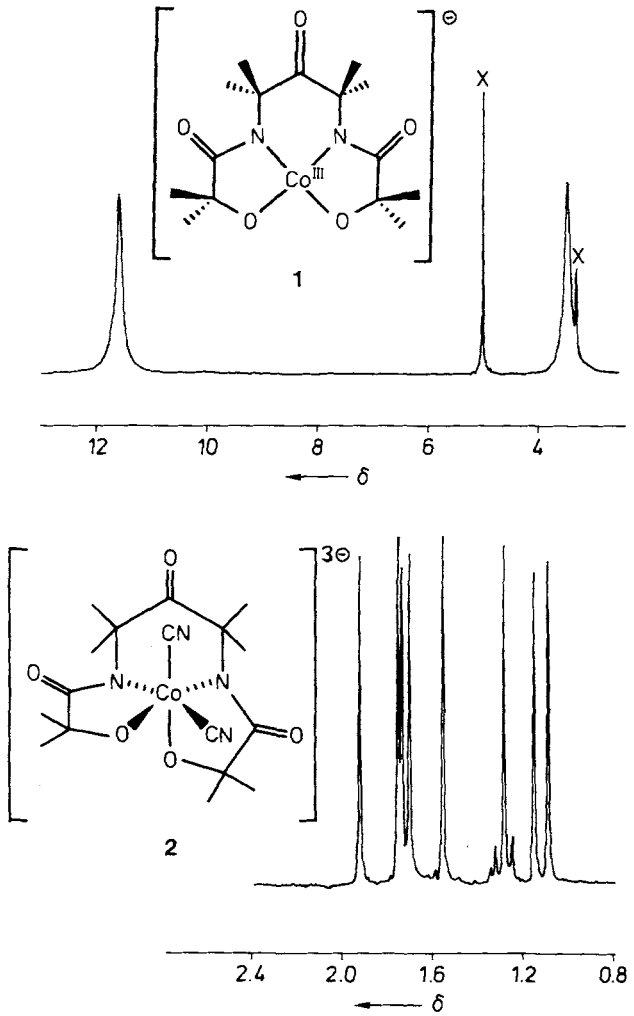


Fig. 1. ^{1}H NMR spectra of **1** (top) and **2** (bottom) (300 MHz, in CD_3OD. ×: solvent peak.

When a CD_3OD solution of the paramagnetic square-planar cobalt(III) complex **1** (Fig. 1), as a sodium salt,[5] is treated with two equivalents of potassium cyanide, the ^{1}H NMR spectrum indicates the formation of a low-symmetry diamagnetic complex, **2**, in which the tetradentate ligand cannot be planar (the two equivalent sets of four methyl groups of **1** are split to eight singlets in **2**; see Fig. 1). The appearance of two ν_{CN} bands in the IR spectrum at 2121 and 2111 cm^{-1} (Nujol mull) is consistent with an octahedral complex containing *cis* CN ligands. Previous experience[2, 3] suggested that the tetradentate ligand can be compatible with a nonplanar octahedral stereoisomer only if the amide groups are distorted. An increase in the IR stretching frequency of the highest amide band (1610 cm^{-1} in **1** to 1654, 1648, 1632 cm^{-1} in **2**) indicates significant amide nonplanarity. The results of an X-ray crystal structure determination[6] for **2** and the Dunitz amide nonplanarity parameters[4, 7] are shown in Figure 2.

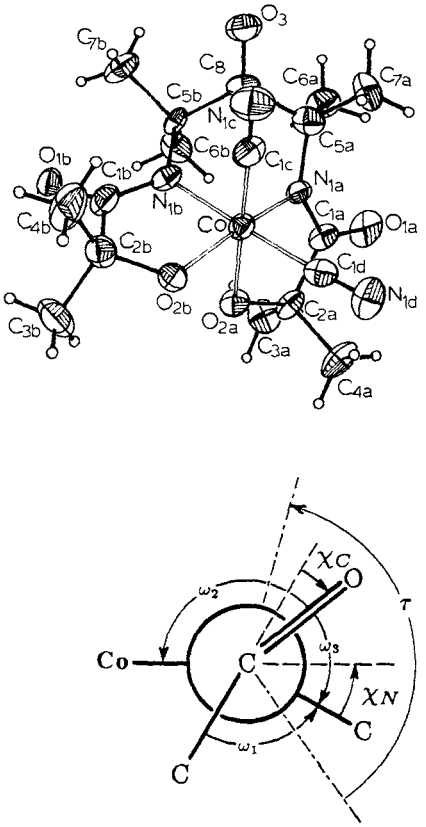


Fig. 2. Top: Molecular structure of **2** [6]. Bottom: Dunitz amide nonplanarity parameters [4]. See also [7].

As expected, both amide groups in **2** are significantly distorted. However, the N atoms remain rigorously trigonal planar ($\chi_{N1b} = -1°$, $\chi_{N1a} = 1°$) with all distortions being accommodated by twisting of the C–N bond ($\bar{\tau}_{N1b-C1b} = 15°$, $\bar{\tau}_{N1a-C1a} = 17°$). As expected,[3a] the amide C atoms remain planar ($\chi_{C1b} = \chi_{C1a} = 1°$). The results suggest that there is $p \rightarrow d\pi$ bonding between the amide N atoms and the Co atom as an additional force holding the amide N atoms planar. This bonding term should be encouraged by the presence of the strong π-back-bonding CN ligands.

Received: January 9, 1989 [Z 3114 IE]
German version: *Angew. Chem. 101* (1989) 924

[1] W. E. Stewart, T. H. Sidall, III, *Chem. Rev. 70* (1970) 517.
[2] T. J. Collins, R. J. Coots, T. T. Furutani, J. T. Keech, G. T. Peake, B. D. Santarsiero, *J. Am. Chem. Soc. 108* (1986) 5333, and references cited therein.
[3] a) F. C. Anson, T. J. Collins, S. L. Gipson, J. T. Keech, T. E. Krafft, G. T. Peake, *J. Am. Chem. Soc. 108* (1986) 6593; b) T. J. Collins, T. Lai, G. T. Peake, *Inorg. Chem. 26* (1987) 1674.
[4] a) J. D. Dunitz, F. K. Winkler, *J. Mol. Biol. 59* (1971) 169; b) *Acta Crystallogr., Sect. B31* (1975) 251; c) A. Walshal, M. Leviyy, S. Lifson, *J. Mol. Spectrosc. 33* (1970) 84.

[5] J. C. Brewer, T. J. Collins, M. R. Smith, B. D. Santarsiero, *J. Am. Chem. Soc. 110* (1988) 423.

[6] Crystal data for NaK_2-**2**·$CH_3OH \cdot 3\,H_2O$: space group $P2_1/c$, $a = 9.869(1)$, $b = 17.323(2)$, $c = 16.083(3)$ Å, $\beta = 94.85(1)°$, $V = 2739.7(7)$ Å^3, $Z = 4$; 1606 independent reflections with $I > 3\sigma(I)$; four-circle diffractometer, $Cu_{K\alpha}$, $3° \leq 2\theta \leq 115°$. Lorentz, polarization, and adsorption corrections and corrections for linear decay were applied to the 3766 independent reflections collected. Anomalous dispersion corrections were applied for Co, K, and Na. The 35 non-hydrogen atoms were located using the SHELXTL Direct Methods programs and the hydrogen atom positions were located. Final cycles of least-squares refinement, which employed anisotropic thermal parameters for non-hydrogen atoms and isotropic parameters for hydrogen atoms, gave $R_1 = 0.053$, $R_w = 0.058$. Further details of the crystal structure investigation may be obtained from the Director of the Cambridge Crystallographic Data Centre, University Chemical Laboratory, Lensfield Road, Cambridge CB2 1EW (England), by quoting the full literature citation.

[7] The twist angle τ and the pyramidalization terms χ_C and χ_N were obtained from the primary torsion angles ω_1, ω_2, and ω_3 as follows: $\tau = (\omega_1 + \omega_2)/2$; $\chi_N = (\omega_2 - \omega_3 + \pi) \bmod 2\pi$; $\chi_C = (\omega_1 - \omega_3 + \pi) \bmod 2\pi$. Here we use the modified twist angle, $\bar{\tau}$: $\bar{\tau} = (\tau) \bmod \pi$ [3a]. $\bar{\tau}$ maximizes at $\pm 90°$ and can be interpreted as the angle between the idealized positions of the $p\pi$ orbitals on C and N. The pyramidalization terms maximize at $\pm 60°$.

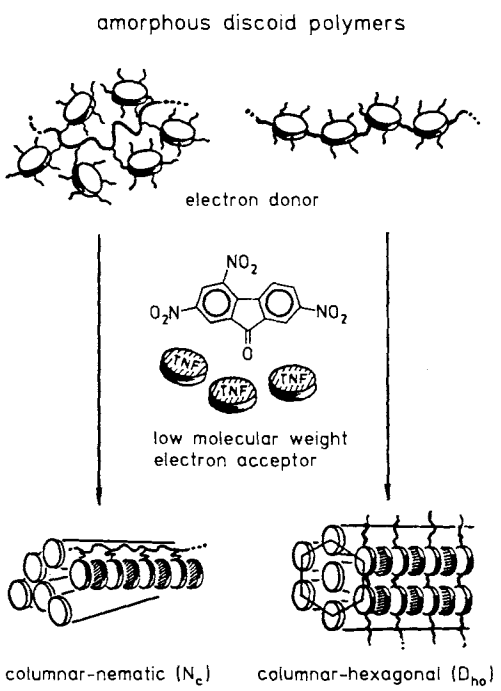


Fig. 1. Schematic presentation of the induction of discotic mesophases in amorphous discoid polymers via charge-transfer interactions with low molecular weight electron acceptors. Left: Side-group polymers. Right: Main-chain polymers. TNF = 2,4,7-trinitrofluorenone as acceptor. D_{ho} = discotic hexagonal ordered (hexagonal long-range order of columns, whose discs are stacked with regular spacings). N_C = nematic columnar (nematic order, i.e., exclusively one long-range orientational order of the columns, whose discs are also stacked with regular spacings). In contrast to the N_C phase, the known discotic-nematic N_D phases [3] do not consist of columns but rather of individual discs ordered in nematic fashion.

Induction of Liquid Crystalline Phases: Formation of Discotic Systems by Doping Amorphous Polymers with Electron Acceptors

By *Helmut Ringsdorf,* Renate Wüstefeld, Elfriede Zerta, Martina Ebert,* and *Joachim H. Wendorff*

Doping of liquid crystals: Structure–property relationships of low molecular weight and polymeric liquid crystals[1] are of current interest, in particular those between molecular structure and properties such as color,[2a] ferroelectricity,[2b] photoreactivity,[2c] and nonlinear optical activity.[2d] These functionalities may be introduced into liquid crystals and also varied not only by chemical synthesis but also by doping.[2a, b, d] It has been found that doping electron-rich discoid polymers with electron acceptors introduces new functional behavior and, moreover, even allows the induction of mesophases in previously non-liquid-crystalline polymers.

Because of charge-transfer (CT) interactions, disc-shaped parts of side-group or main-chain polymers can be arranged in columns, which leads to discotic-columnar mesophases (Fig. 1). Although the functionalization of liquid crystals by doping has been extensively studied,[2a, b, d] induction of mesophases by mixing of non-liquid-crystalline substances has only been established for a few examples of rod-shaped, low molecular weight compounds.[4] Induction of mesophases in amorphous discoid polymers is of special importance since, although numerous amorphous discoid polymers are known,[5] only a few liquid crystalline discotic polymers have been reported.[6, 7]

Polyacrylates[8] and polyesters[9] containing disc-shaped, electron-rich triphenylene units were employed in these induction experiments. The induction agents were fluorenone derivatives[10] with different acceptor strengths: 2,4,7-trinitrofluorenone (TNF) and 2,4,7-trinitrofluoren-9-ylidenemalonodinitrile (TNF-CN). Doping of the polymers was achieved by mixing in solution.[11] The functionalized polymers were characterized by polarization microscopy, differential calorimetry, and X-ray diffraction.[12]

Induction of columnar mesophases in amorphous side-group polymers: The polymethacrylate **1** ($T_g = 30$ °C) and the polyacrylate **2** ($T_g = -6$ °C) were used as amorphous polymers containing electron-rich triphenylene side groups.[5a, 8] When combined with the electron acceptor TNF,[11] these polymers form discotic phases due to CT interactions. Mesophases are obtained after addition of only 25 mol% TNF; they become isotropic at 170 °C (**1**/TNF) and 88 °C (**2**/TNF) (Fig. 2).

Samples containing different amounts of TNF were prepared from **2** (Table 1). Only those with between 20 and 25 mol% TNF exhibit liquid crystalline phases. A mixture containing 10 mol% TNF is amorphous, as is the neat polymer **2**. Mixtures containing high amounts of TNF (molar ratio 2/1 and 1/1) phase-separate during preparation.[11] The enthalpies of clearing are very small (< 0.4 J g^{-1}) for the induced liquid crystalline phases.

The structures of these mesophases were established by X-ray diffraction studies (Fig. 3 and Table 1). The flat plate photograph in Figure 3a shows three reflections. A regular spacing of 3.4 Å between the molecules (triphenylene units, TNF) within the columns can be derived from the sharp, oriented reflection in the wide-angle region.[13] The same value was also found for the intracolumnar spacing in noninduced discotic phases of polysiloxanes containing tripheny-

[*] Prof. Dr. H. Ringsdorf, Dipl.-Chem. R. Wüstefeld, Dipl.-Chem. E. Zerta
Institut für Organische Chemie der Universität
J.-J.-Becher-Weg 18–20, D-6500 Mainz (FRG)
Dipl.-Phys. M. Ebert, Prof. Dr. J. H. Wendorff
Deutsches Kunststoff-Institut
Schlossgartenstrasse 6 R, D-6100 Darmstadt (FRG)

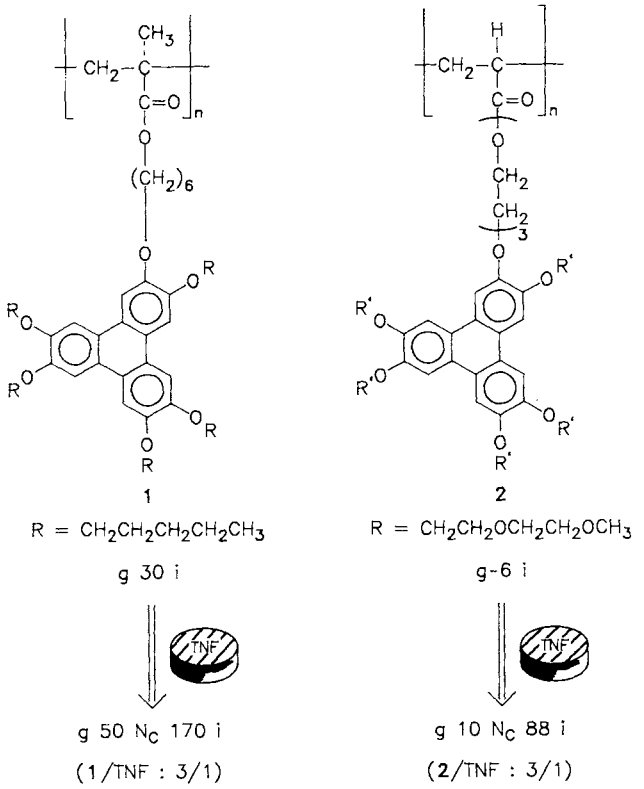


Fig. 2. Induction of nematic-columnar mesophases (N_C) in the amorphous discoid side-group polymers **1** and **2** via CT interactions with the low molecular weight electron acceptor TNF.

lene side groups.[6e] The weak-intensity halo at 4.2 Å is ascribed to the liquidlike short-range order of the alkyl chains.[14] The strong-intensity small-angle reflection at 16.7 Å is related to ordering of the columns. It is diffuse and higher order reflections are absent. This is evidence against a positional long-range order of the columns as present in, for example, D_{ho} phases. Orientational long-range order of the columns, however, is present because the samples can be macroscopically oriented. These results indicate the existence of nematic-columnar phases (N_C, Fig. 1), which have until now been found for lyotropic[15] but not for thermotropic liquid crystals. Nematic N_C phases align in such a way that the column axes are parallel to the direction of strain (Fig. 3c). The columns and the polymer chain of higher-ordered columnar phases of undoped discotic side-group polymers have also been found to be oriented in the same direction.[6e]

Table 1. Induction of discotic phases in amorphous side-group polymers via CT interactions. Structure and temperature range of mixtures of TNF and the amorphous polyacrylates **1** and **2**.

Polymer	Polymer/TNF [a]	Temperature range [°C]	Phase	Structure: Spacings within the columns [b]	Structure: Spacings between the columns [c]	Halo [d]
2	9/1	g −6 i	amorphous	[e]	[e]	[e]
2	4/1	g 10 N_C 47 i	nematic-columnar	3.40	19.3	4.1
2	3/1	g 10 N_C 88 i	nematic-columnar	3.40	19.0	4.2
2	2/1	(g −7 i)	amorphous	–	–	–
2	1/1	(g −5 i)	two-phase	–	–	–
1	3/1	g 50 N_C 170 i	nematic-columnar	3.42	19.3	4.6

[a] Mole ratio. [b] ±0.03 Å. [c] ±0.3 Å. [d] ±0.1 Å. [e] Nonoriented, diffuse reflections.

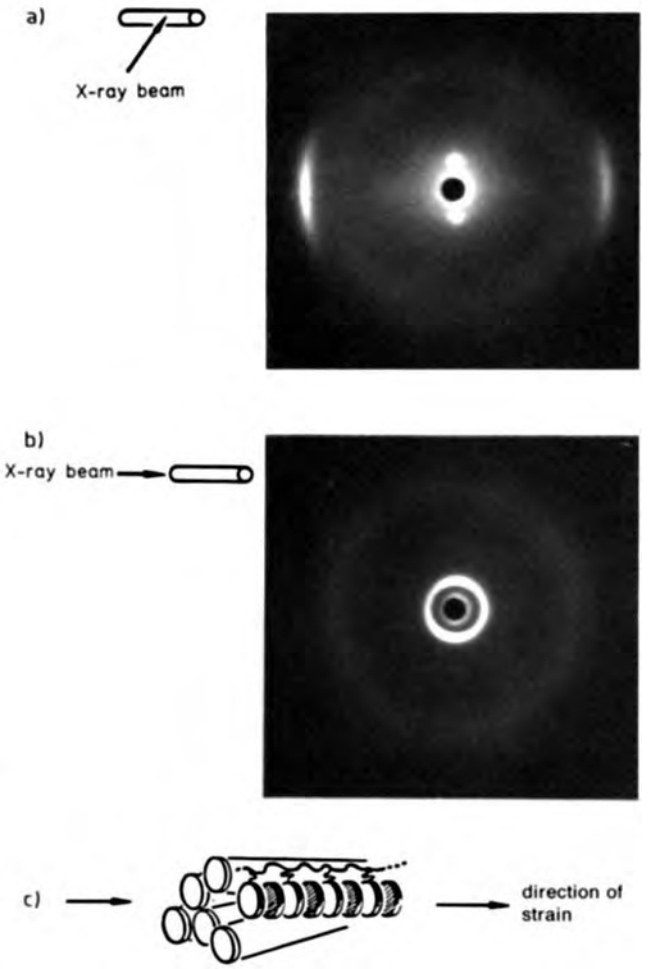
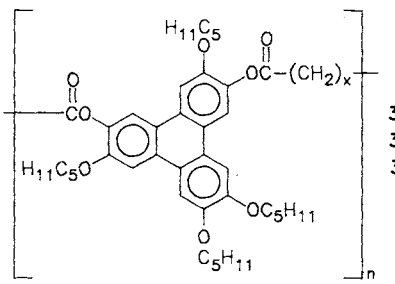


Fig. 3. Flat plate photograph of the nematic-columnar mesophase (N_C) induced in the amorphous side-group polymer **2** for a 4/1 mol ratio of **2**/TNF. X-ray beam impinges perpendicular (a) and parallel (b) to the direction of strain. c) The columns are oriented with the column axes in the direction of strain.

Induction of columnar mesophases in amorphous main-chain polymers: The induction of columnar mesophases in discoid main-chain polymers was studied for the polyester **3c**, which contains triphenylene units in the main chain. The three polymers **3a**,[5] **3b**,[5,6c] and **3c**[5] differ only in the length of the spacer: **3a** and **3b**, with shorter spacers, form D_{ho} phases; the polymer **3c** is amorphous (T_g = 35 °C).



3a, x = 10 : g 50 D_{ho} 220 i
3b, x = 14 : g 60 D_{ho} 150 i
3c, x = 20 : g 35 i

When **3c** is doped with TNF, however, CT complexation increases the interaction between the discs in the main chain, leading to the induction of discotic phases. The phase diagram (Fig. 4) reveals that mesophase induction starts at even

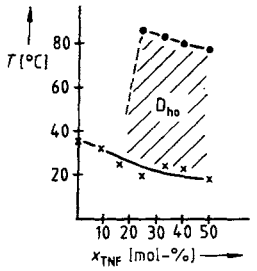


Fig. 4. Phase behavior of mixtures of the amorphous discoid main-chain polymer **3c** and TNF. For amounts of TNF ≥ 25 mol%, higher-ordered discotic phases are induced. For 1/1 and 2/1 mixtures of **3c**/TNF, D_{ho} phases are present. For 1.5/1 (40 mol% TNF) and 3/1 (25 mol% TNF) ratios, the mesophase type could not be determined.

25 mol% TNF. Clearing temperatures decrease slightly (from 83 to 76 °C) with increasing amounts of TNF. Simultaneously, glass transition temperatures decrease from 35 °C for the undoped polymer **3c** to 17 °C, so that the phase width remains constant over the entire doping range (to 50 mol%). Enthalpies of clearing (0.6–1.3 J g^{-1}) are roughly a factor of 10 smaller than for undoped discotic polymers. If a stronger electron acceptor, like TNF-CN, is used instead of TNF, the clearing temperatures increase, for example, for a 2/1 ratio of **3c** to electron acceptor, from 83 °C for TNF to 165 °C for TNF-CN. This shows that the electron acceptor, in addition to inducing mesophases, also strongly influences the mesomorphic temperature range.

X-ray diffraction studies reveal that higher-ordered columnar phases (D_{ho}) are present for the TNF-containing discotic main-chain polymers (Figs. 1 and 5). Such phases are already known for undoped discotic main-chain polymers such as **3a, b.**[6, 7] Thus, the structural features – for example, the values for inter- and intracolumnar spacings of doped and undoped discotic polymers may be compared (Table 2). Figure 5 shows X-ray flat plate photographs of the

Table 2. Induction of discotic phases in amorphous main-chain polymers via CT interactions. Structure and temperature range of mixtures of TNF and the amorphous polyester **3c** as well as comparison with the liquid crystalline polyesters **3a** and **3b**.

Polymer	Polymer/TNF [a]	Temperature range [°C]	Phase	Structure Spacings within the columns [b]	Structure Spacings between the columns [c]	Halo [d]
3c	–	g 35 i	amorphous	[d]	[d]	[d]
3c	9/1	g 32 i	amorphous	[d]	[d]	[d]
3c	5/1	g 25 i	amorphous	[d]	[d]	[d]
3c	3/1	g 20 $D_?$ 85 i	$D_?$	[e]	[e]	[e]
3c	2/1	g 22 D_{ho} 83 i	D_{ho}	3.40	26.9	4.4
3c	1/1	g 17 D_{ho} 76 i	D_{ho}	3.41	26.6	4.4
3a [5a]	–	g 50 D_{ho} 220 i	D_{ho}	3.50	20.4	4.2
3b [6b, f]	–	g 60 D_{ho} 150 i	D_{ho}	3.50	21.3	4.2

[a] Mole ratio. [b] ±0.03 Å. [c] ±0.1 Å. [d] Nonoriented, diffuse reflections. [e] Only the Bragg spacings are known so far: 3.40, 21.6/15.5, 4.4 Å; the column spacings cannot be given, since the phase type ($D_?$) is still unknown.

induced mesophases of the polyester **3c** containing 50 and 33 mol% TNF. The sharp wide-angle reflection is assigned to the intracolumnar disc spacings; the sharpness of the reflection indicates a regular arrangement with spacings of between 3.38 and 3.40 Å.

The hexagonal order in the induced D_{ho} phase becomes most evident in the hexagonal pattern of the X-ray photograph in Figure 5b. Values of approximately 27 Å are

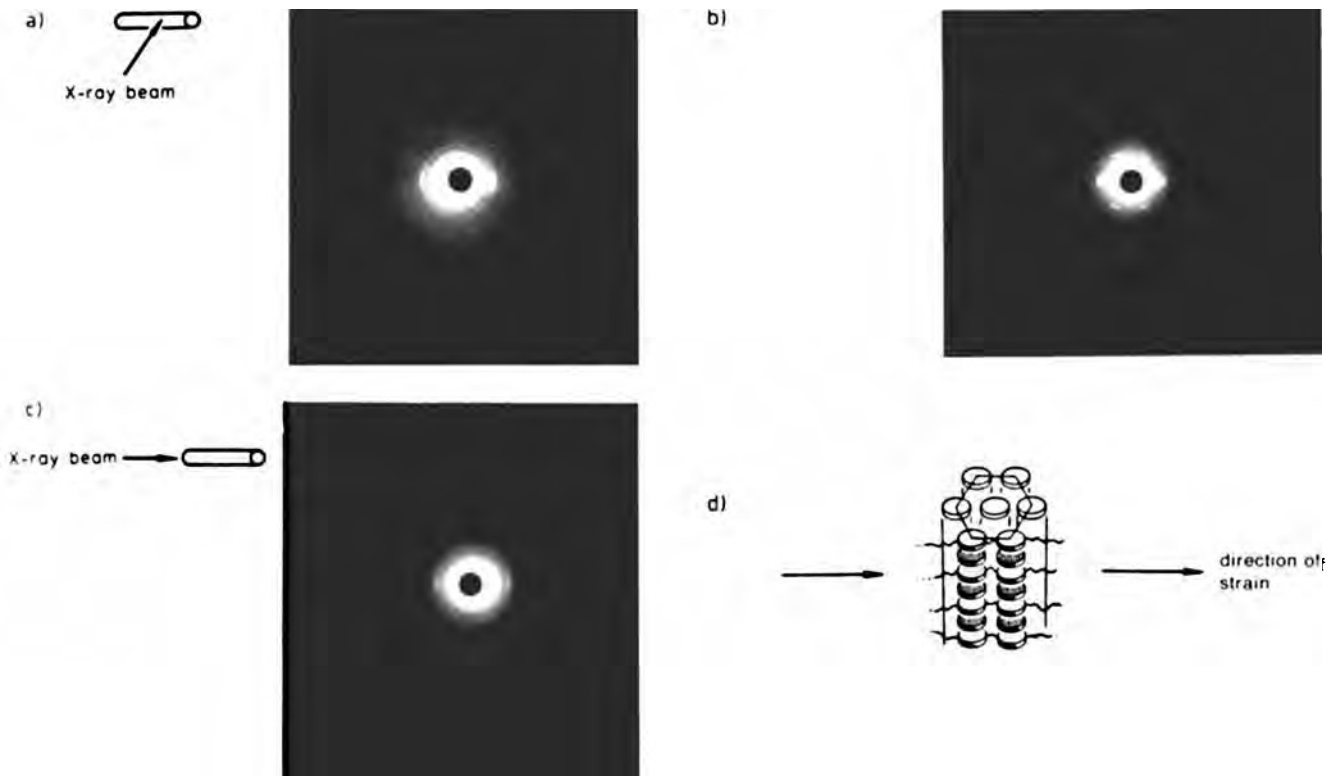


Fig. 5. Flat plate photographs of the hexagonal-columnar mesophase (D_{ho}) induced in the amorphous main-chain polymer **3c** for a 1/1 (a and c) and a 2/1 (b) mole ratio of **3c**/TNF. Impingement of the X-ray beam perpendicular (a, b) and parallel (c) to the direction of strain. d) In contrast to the side-group polymers **1** and **2**, but in analogy to the undoped discotic main-chain polymers [6b, f], the columns are oriented perpendicular to the direction of strain. This means that the polymer chains and not the columns undergo extension upon stretching the polymer.

calculated for the spacing between the columns (= hexagonal lattice constant). These intercolumnar spacings are about 6–7 Å larger than those in noninduced discotic phases of **3a**[5a] (20.4 Å) and **3b**[6] (21.6 Å). Strikingly, they are even larger than the diameter of the hexasubstituted triphenylene discs with extended pentyloxy chains (23–24 Å). Using density measurements to explain this result,[16] a structural model seems likely in which the TNF molecules are not arranged exclusively within the columns but also exist in the side-chain region between the columns.

Induction of columnar mesophases in polymer blends: CT interactions may help to increase the miscibility of polymers, resulting in the formation of one-phase polymer blends.[17] This observation suggested the idea to combine the improved miscibility of polymers due to CT interactions with the induction of discotic mesophases. In the first experiment, TNF and two non-liquid-crystalline discoid polymers containing triphenylene side groups (polyacrylate **2**[8] and polymalonate **4**[18]) were employed (Fig. 6). Polymers **2** and **4** are immiscible. Addition of TNF results not only in miscibility of the two incompatible polymers but also in the formation of columnar mesophases. For a molar ratio of 1/1/1.2 for **2**/**4**/TNF, the polymer blend **5**, in analogy to the polyacrylate **2**/TNF system, exhibits a nematic-columnar N_C phase (temperature range -13 to 89 °C).

Induction and functionalization of liquid crystalline phases: Induction of mesophases by CT interactions opens a wide range of possibilities for polymeric discotic liquid crystals. The synthesis of polymeric as well as low molecular weight[19] discotic liquid crystals is no longer restricted to the classical disc-shaped mesogens. The TNF derivatives used here are nonmesogenic electron acceptors. Furthermore, a greater variety of structures is possible for disc-shaped electron-donor molecules; one possibility is the introduction of normally sterically perturbing functional groups. The type of phase and the phase width may be varied over a wide range by an appropriate choice of polymer system and mixing ratio. Mesophase induction due to CT interactions also opens up a route to liquid crystalline polymer blends. In addition to blends consisting of polymeric discoid donors and low molecular weight acceptors, other combinations are conceivable, such as mixtures of main- and side-chain polymers or of discoid acceptor and donor polymers. Noteworthy is the simultaneous induction of liquid crystalline phases and the introduction of functional behaviors such as color, polarity, and photoreactivity. This approach to functional discotic liquid crystals makes the induction of columnar phases via CT interactions of interest for technical applications in such areas as electrical and photoconductive systems.

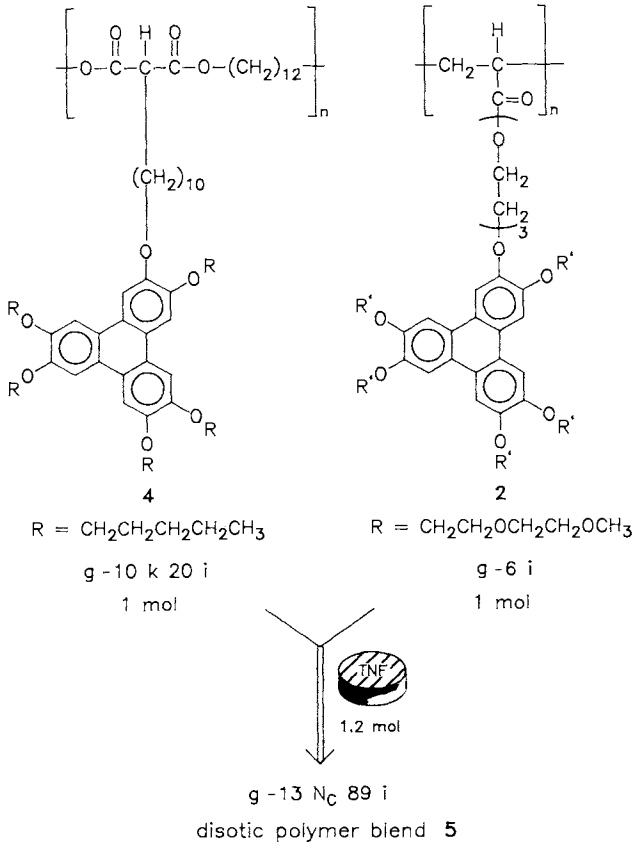


Fig. 6. Induction of discotic mesophases and miscibility in polymer blends via CT interactions with the electron acceptor TNF.

Received: February 2, 1989 [Z 3185 IE]
German version: *Angew. Chem. 101* (1989) 934

[1] a) H. Kelker, R. Hatz: *Handbook of Liquid Crystals*, Verlag Chemie, Weinheim 1980; b) H. Finkelmann, *Angew. Chem. 99* (1987) 840; *Angew. Chem. Int. Ed. Engl. 26* (1987) 816.

[2] a) A. V. Ivashchenko, V. G. Rumyantsev, *Mol. Cryst. Liq. Cryst. 150* (1987) 1; b) L. A. Beresnev, L. M. Blinov, M. A. Osipov, S. A. Pikin *ibid. 158* (1988) 979; c) I. Cabrera, V. Krongauz, H. Ringsdorf, *Angew. Chem. 99* (1987) 1204; *Angew. Chem. Int. Ed. Engl. 26* (1987) 1178; d) D. J. Williams, *ibid. 96* (1984) 637 and *23* (1984) 690.

[3] Nguyen Huu Tinh, C. Destrade, H. Gasparoux, *Phys. Lett. A 72* (1979) 251.

[4] a) K. Araya, Y. Matsunaga, *Bull. Chem. Soc. Jpn. 53* (1980) 3079; b) Y. Matsunaga, N. Kamiyama, Y. Nakayasu, *Mol. Cryst. Liq. Cryst. 147* (1987) 85.

[5] a) W. Kreuder, *Dissertation*, Universität Mainz 1986; b) O. Karthaus, *Diplomarbeit*, Universität Mainz 1988.

[6] Discotic polymers containing triphenylene mesogens: a) W. Kreuder, H. Ringsdorf, *Makromol. Chem. Rapid. Commun. 4* (1983) 807; b) O. Herrmann-Schönherr, J. H. Wendorff, W. Kreuder, H. Ringsdorf, *ibid. 7* (1985) 97; c) W. Kreuder, H. Ringsdorf, P. Tschirner, *ibid. 6* (1985) 97; d) G. Wenz, *ibid. 6* (1985) 577; e) B. Hüser, H. Spiess, *ibid. 9* (1988) 337; f) O. Herrmann-Schönherr, *Dissertation*, Technische Hochschule Darmstadt 1987.

[7] Discotic polymers containing benzene and phthalocyanine mesogens: a) C. Sirlin, L. Bosio, J. Simon, *J. Chem. Soc. Chem. Commun. 1987*, 379; b) A. Beck, H. Hanack, H. Lehmann, *Synthesis 1987*, 703; c) [6c].

[8] The discoid side-group polymers were obtained by radical polymerization of acrylates and methacrylates in solution. Relative molecular weights of the discoid polymethacrylate **1** from GPC measurements: M_{GPC1} = 3800000 g mol^{-1} (polystyrene (PS) standard, THF, measurement of the refractive index (RI detection)), M_{GPC2} = 4300000 g mol^{-1} (polymethylmethacrylate standard, THF, RI detection): this corresponds to degrees of polymerization P of 3900 and 5500, respectively. Relative molecular weight of discoid polyacrylate **2**: M_{GPC} = 380000 g mol^{-1} (PS standard, $CHCl_3$, UV detection) corresponds to P = 370.

[9] The main-chain polyesters **3a–3c** were each obtained by melt condensation of an isomeric mixture [6a, c] of two triphenylenediacetates and the corresponding 1,ω-dicarboxylic acids (catalyst: *p*-toluenesulfonic acid). **3c**: M_{GPC} = 13000 g mol^{-1} (PS standard, $CHCl_3$, UV detection); corresponds to P = 14.

[10] J. E. Kuder, J. M. Pchan, S. R. Turner, D. L. F. Hinman, *J. Electrochem. Soc. 11* (1978) 1750.

[11] Upon combination of the colorless and yellow solutions, respectively, of the polymer and electron acceptor (in dichloromethane or THF), the color turned red (**3**/TNF) or violet (**1,2**/TNF). The mixtures were stirred for several hours at room temperature. Evaporation of the solvent resulted in separation of a black film, which was dried under oil-pump vacuum for one to two days.

[12] Ortholux II POL-BK (Leitz), microscope used for polarization microscopy investigations; DSC-4 (Perkin-Elmer) calorimeter used for differential calorimetry investigations, heating and cooling rate = 20 K min^{-1} (the melting and clearing temperatures were taken from the peak maxima, the glass transition temperatures were taken from the inflection point of the

curve); X-ray diffraction measurements with nickel-filtered Cu_{K_α} radiation ($\lambda = 0.154$ nm) (oriented samples were obtained by stretching or by applying pressure at a given direction of flow [6b]).

[13] The interplanar separations of many low molecular weight CT complexes containing TNF and polycyclic arenes lie between 3.1 and 3.5 Å; see, for example, L. J. E. Hofer, W. C. Peebles, *Analyt. Chem. 24* (1952) 822.

[14] A M. Levelut, *J. Phys. Lett. 40* (1979) 81.

[15] N. Boden, R. J. Bushby, L. Ferris, C. Hardy, F. Sixl, *Liq. Cryst. 1* (1986) 109.

[16] Taking the hexagonal lattice parameter and the intracolumnar distance (see Table 2), it is possible to calculate the densities ϱ_1 and ϱ_2 for different arrangements of the TNF molecules in the liquid crystalline phase (see Table 3). $\varrho_1 \triangleq$ all TNF molecules are arranged within the columns; $\varrho_2 \triangleq$ no TNF molecule is arranged within a column, that is, all TNF molecules are located in the region between the columns. For the 1/1 mixture, the measured ϱ_3 value agrees with the ϱ_2 value. For the 2/1 mixture, the measured density ϱ_3 is higher than the ϱ_2 value; in this case, the structural arrangement appears to be more complex.

Table 3. Calculated and experimentally found densities of liquid crystalline phases of polymer **3c** with TNF.

3c/TNF	ϱ_1 [gcm^{-3}]	ϱ_2 [g cm^{-3}]	ϱ_3 [g cm^{-3}]
1/1 0.50	1.00	1.04	
2/1 0.57	0.86	1.04	

[17] a) T. Sulzberg, R. J. Cotter, *J. Polym. Sci. Part A-1 8* (1970) 2747; b) J. M. Rodriguez-Parada, V. Percec, *Macromolecules 19* (1984) 55; c) C. Pugh, V. Percec, *ibid. 19* (1984) 65.

[18] The polymalonate **4** was obtained by Ti^{IV}-catalyzed transesterification of a triphenylene malonate with dodecanediol [5b].

[19] Discotic-columnar phases can also be induced in low molecular weight discoid systems through CT interactions, for example by addition of TNF to non-liquid-crystalline triphenylene derivatives or to discotic-nematic hexaphenylethynylene benzenes: M. Ebert, B. Kohne, K. Praefcke, H. Ringsdorf, J. H. Wendorff, R. Wüstefeld, E. Zerta, unpublished results.

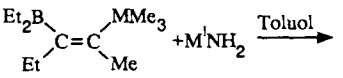
Pentacoordinated Elements of the 4th Main Group with Four Organic Residues

By *Roland Köster, Günter Seidel, Bernd Wrackmeyer,* Klaus Horchler* and *Dieter Schlosser*

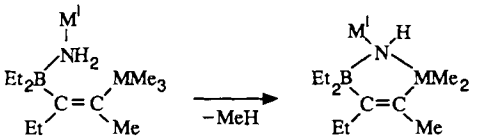
Hypervalent species of heavy elements of the fourth main group of the periodic system, especially silicon,[1] are of particular interest because of their importance as starting materials and reactive intermediates (e.g. silicon hydride[2]) in synthesis and because of their biological activity (e.g. silatranes[3]). A coordination number > 4 in the case of silicon, however, has only been documented for compounds with at least two electro-negative substituents on the silicon atom.[1, 4, 5] We report here on the first NMR spectroscopic detection of a long-lived species with a pentacoordinated silicon atom, which has a coordinative Si–N bond besides four organic residues. In addition, the results of NMR investigations on analogous tin and lead derivatives are reported. Whereas an intramolecular Sn–N bond, analogous to that in stannatrane, has been postulated for certain tetraorganostannanes,[6] and pentaorganostannates $[R_5Sn]^{\ominus}$ have already been detected NMR spectroscopically,[7] an increase in the coordination number of lead in tetraorganoplumbanes was hitherto unknown.

[*] Prof. Dr. B. Wrackmeyer, Dipl.-Chem. K. Horchler
Laboratorium für Anorganische Chemie der Universität
Postfach 101251, D-8580 Bayreuth (FRG)
Prof. Dr. R. Köster, G. Seidel
Max-Planck-Institut für Kohlenforschung
Kaiser-Wilhelm-Platz 1, D-4330 Mülheim a. d. Ruhr (FRG)
Dr. D. Schlosser
Chemische Fabrik Pfersee
Postfach 101409, D-8900 Augsburg (FRG)

The sodium and potassium aminoborates **2**,[9, 10] which are readily accessible from (*E*)-alkenylboranes **1**[8] by reaction with $NaNH_2$ and KNH_2, respectively, are intermediates in the synthesis of the cyclic compounds **3** and are thus ideal species for investigating intramolecular M–N interactions. **2a** splits off methane already at room temperature, forming an Si–N bond.[11]



1 (1)

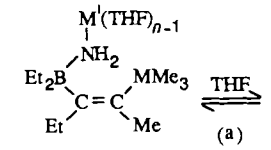


2 **3**

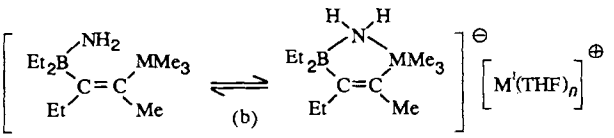
a: M=Si, **b**: M=Sn, **c**: M=Pb; M': Na, K

2b reacts similarly,[12a] whereas **2c** does not undergo any simple secondary reaction. Although the cleavage of methane permits assumption of M–N interactions at least for N = Si, Sn, proof of the existence of the anions derived from **2** [(b) in Eq. (2)] with a coordination number of 5 for M is first furnished by the NMR spectra in THF at several temperatures (Table 1).

In coordinating solvents such as THF or upon addition of suitable crown ethers in THF or nonpolar solvents, the equilibrium (a) in Equation (2) can be shifted in such a way that the alkali metal ion $M^{\oplus}$ prefers a coordination other than in **2**. The position of the equilibria (a) and (b) in dilute solutions depends on M' and M and on the temperature, as shown by the δ(M) values measured under various conditions (cf. Table 1). The difference of the $\delta(^{29}Si)$ values in THF (25 °C) for **2a**, M' = Na ($\delta = -18.6$), and **2a**, M' = K ($\delta = -61.0$), typically demonstrates the dependence on the alkali metal. The influence of M is e.g. immediately clear from the fact that the $\delta(^{119}Sn)$ value for **2b**, M' = Na or for **2b**, M' = K, in THF at 25 °C ($\delta = -166.0$) changes only slightly compared to the value at −50 °C ($\delta = -175.6$). Thus, in THF, the Sn–N interaction successfully competes with the M'–N interaction at room temperature, i.e. the coordinative Sn–N bond is stronger than the coordinative Si–N



2 · $(THF)_{n-1}$ (2)



2 · $(THF)_n$

Table 1. ^{11}B-, ^{13}C-, ^{29}Si-, ^{119}Sn- and ^{207}Pb-NMR-data of **2a–c** and **4a–c** [a]

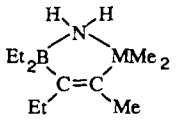
	a, M′ = Na	**a**, M′ = K	**b**, M′ = Na	**c**, M′ = Na
$\delta(^{13}C)$ **2** [b]:				
M–CH_3	12.9 [n.d.]	13.2 [n.d.]	1.0 [c], 1.2 [c] [450.0], [n.d.]	5.6 [d] [131.4]
M–C=	131.1 [n.d.]	131.5 [81.0]	131.4 [861.9]	139.0 [1144.4] [e]
=C–CH_3	19.0	19.0	20.5 [136.2]	23.9 [254.0]
B–C=	179.7 br	179.1 br	175.1 br	172.3 br
=C–CH_2CH_3	25.6, 14.6	25.5, 14.6	25.4, 14.8 [127.0], [16.8]	26.4, 15.1 [268.2], [31.6]
B–CH_2CH_3	18.5 br, 12.0	18.6 br, 12.0	19.1 br, 11.9	20.8 br, 12.3
$\delta(^{11}B)$ (**2**, −30 °C):	−6.8	−7.0	−7.2	−7.3
δ(M) (**2**):	−74.0 [f]	−81.0 [g]	−175.6 [h]	−146.5 [i]
δ(M) (**4**) [j]:	+21.3	+21.3	+116.0	+427.5
$\Delta\delta$(M) [k]:	−95.3	−102.3	−291.6	−574.0

[a] In [D$_8$]THF (ca. 10%); δ-values versus ext. Et_2O-BF_3 (δ^{11}B), Me_4Si (δ^{13}C), Me_4Si (δ^{29}Si), Me_4Sn (δ^{119}Sn), Me_4Pb (δ^{207}Pb); [coupling constants J(M^{13}C)/Hz], [n.d.] = not detected. [b] **2a**, M′ = Na, K at −60 °C, **2b**, M′ = Na at −80°, **2c**, M′ = Na at −75 °C. [c] Signals in the ratio 2:1; at −20 °C an averaged signal with $^1J(^{119}Sn^{13}C)$ = 308.7 Hz is found. [d] At −90 °C despite satisfactory signal-to-noise ratios no ^{207}Pb-satellite signals are observed; upon further cooling solid **2c** separates, M′ = Na, even from very dilute THF-solutions. [e] At 25 °C: $^1J(^{207}Pb^{13}C)$ = 836.6 Hz. [f] At −50 °C; further measurements in [D$_8$]THF: δ (^{29}Si) (−30 °C) −52.1, (25 °C) −18.6, (25 °C, addition of one equiv. [18]crown-6) −78.8; in toluene δ (^{29}Si) (25 °C) −15.0, (−50 °C) −15.1. [g] At −60 °C; further measurements in [D$_8$]THF: δ (^{29}Si) (−90 °C) −82.4, (25 °C) −61.0. [h] At −50 °C; further measurements in [D$_8$]THF: δ (^{119}Sn) (−30 °C) −175.2, (25 °C) −166.0. [i] At −74 °C; further measurements in [D$_8$]THF: δ (^{207}Pb) (−100 °C) −150.5, (−90 °C) −147.8, (−53 °C) −137.0, (−30 °C) −94.0, (−10 °C) −68.0, (25 °C) ca. −50 (extremely broad), (25 °C, addition of [18]crown-6) no ^{207}Pb-signal; in toluene: δ (^{207}Pb) (25 °C) −56.0. [j] In toluene at 27 °C. [k] $\Delta\delta$M = δM (**2**) − δ(M) (**4**).

bond. **2c**, M′ = Na, in THF at 25 °C, shows only one very broad ^{207}Pb-NMR signals at δ = −50, the position of which is similar to that of the signal in toluene (δ = −56.0). After addition of [18]crown-6 the ^{207}Pb-NMR signal disappears as a consequence of the dynamics of the equilibrium (b). In contrast, the ^{29}Si-NMR signal of **2a**, M′ = Na, in THF (25 °C) is shifted from δ = −18.6 to −78.7 upon addition of the crown ether. It follows from these observations that the strength of the coordinative M–N bond decreases along the series Sn > Si > Pb at room temperature.

The δ(M) values of **2** are clearly influenced by the increase in coordination number of M. The neutral five-membered ring compounds **4** provide the best reference system:[12] one of the anionic equilibrium components of $\mathbf{2}\cdot(THF)_{n-1}$ [Eq. (2)] differs from these merely by an additional methyl group on M and the negative overall charge. $\Delta\delta(^{29}Si)$ [= $\delta(Si_{2a}) - \delta(Si_{4a})$, Table 1] with a value of ca. −100 lies in the same region as $\Delta\delta(^{29}Si)$ for spirocyclic pentacoordinated and tetracoordinated cyanosilicates.[4c] Likewise, $\Delta\delta(^{119}Sn)$ = −291.6 compares very well with the $\Delta\delta(^{119}Sn)$ value of −227 for $[Me_5Sn]^{\ominus}$ and Me_4Sn.[7]

A distorted trigonal-pyramidal environment is expected for pentacoordinated M in **2**, whereby the NH_2 group prefers axial orientation[13] and the olefinic C atom should always be equatorial. The second axial position must accordingly be occupied by a methyl group. Owing to the low activation energy for pseudorotation when the coordination number of M is 5, the signals for the MMe_3 group in the ^{1}H or ^{13}C NMR spectrum do not split down to −95 °C, neither in the case of **2a** nor in the case of **2c**. In the case of **2c** the dynamic behavior is apparent, since ^{207}Pb satellite signals [$^1J(^{207}Pb)^{13}C$)] are no longer observable at −90 °C (other than at −80 °C). In the case of **2b**, the ^{13}C NMR spectrum shows two signals in the ratio 1:2 for the Me_3Sn group at ca. −80 °C. The activation energy for the interchange of the methylene groups is $\Delta G^{\ddagger}_{-75\,°C} = 42 \pm 2$ kJ mol^{-1}. The $^{117/119}$Sn satellite signals of the signal of lower intensity ($SnMe_{ax}$unit) cannot be assigned, whereas for the other signal ($SnMe_{2(eq)}$unit) $^1J(^{119}Sn^{13}C)$ = 450 Hz. Since the mean value for $^1J(^{119}Sn^{13}C_{Me})$ at −20 °C (308.7 Hz) is known it follows that $^1J(^{119}Sn^{13}C)$ = 26 Hz for the axial methyl group. This is in agreement with the expected low s character of the Sn–C_{ax}-hybrid orbital (cf. also with the extrapolated values $^1J(^{119}Sn^{13}C)$ of 441 Hz and 17 Hz for the equatorial and axial methyl groups, respectively in $[Me_5Sn]^{\ominus}$[7]).



4a–c

Received: February 21, 1989 [Z 3188 IE]
German version: *Angew. Chem. 101* (1989) 945

CAS Registry numbers:
1a, 79483-02-6; **1b**, 66088-90-2; **1c**, 86108-50-1; **2a** (M′ = K), 79483-26-4; **2a** (M′ = Na), 79483-25-3; **2b** (M′ = Na), 121192-71-0; **2c** (M′ = Na), 121192-72-1; **4a** [B(III)], 121192-69-6; **4a** [chelat], 121192-74-3; **4b** [B(III)], 100585-22-6; **4b** [chelat], 100581-15-5; **4c** [B(III)], 121192-70-9; **4c** [chelat], 121192-73-2; (*E*)-$[Me_3PbC(Me)=C(Et)BEt_2Me]^{\ominus}Na^{\oplus}$, 121192-75-4; ^{29}Si, 14304-87-1; ^{119}Sn, 14314-35-3; ^{207}Pb, 14119-29-0.

[1] a) R. Damrauer, S. E. Danahey, *Organometallics 5* (1986) 1490; b) S. N. Tandura, M. G. Voronkov, N. N. Alexeev, *Top. Curr. Chem. 131* (1986) 191; c) V. E. Shklover, Y. T. Struchkov, M. G. Voronkov, *Main Group Met. Chem. 11* (1988) 109; d) D. Schinzer, *Nachr. Chem. Tech. Lab. 37* (1989) 28.

[2] a) R. J. P. Corriu, R. Perz, C. Reye, *Tetrahedron 39* (1983) 999; b) R. J. P. Corriu, G. F. Lanneau, M. Perrot, *Tetrahedron Lett. 29* (1988) 1271; c) B. Becker, R. J. P. Corriu, C. Guerin, B. Hemer, *J. Organomet. Chem. 359* (1989) C33; d) J. J. Eisch, C. S. Chiu, *ibid. 358* (1988) C1.

[3] M. G. Voronkov, *Top. Curr. Chem. 84* (1979) 77.

[4] a) H. Bürger, *Angew. Chem. 85* (1973) 519; *Angew. Chem. Int. Ed. Engl. 12* (1973) 474; b) R. J. P. Corriu, C. Guerin, J. J. E. Moreau, *Top. Stereochem. 15* (1984) 158; c) D. A. Dixon, W. R. Hertler, D. B. Chase, W. B. Farnham, F. Davidson, *Inorg. Chem. 27* (1988) 4012.

[5] a) Exceptions: gas-phase studies indicate short-lived anionic pentacoordinated species with four or even five Si–C bonds [5b], and 1,1,5,5,9,9-hexamethyl-1,5,9-trisilacyclododecane ("[12]silacrown-3") has transport properties for $Cl^{\ominus}$ and $Br^{\ominus}$ which are attributable to the increase in coordination number of the silicon [5c]; b) R. Damrauer, L. W. Burggraf, L. P. Davis, M. S. Gordon, *J. Am. Chem. Soc. 110* (1988) 6601; c) M. E. Jung, H. Xia, *Tetrahedron Lett. 29* (1988) 297.

[6] K. Jurkschat, A. Tzschach, *J. Organomet. Chem. 272* (1984) C13.

[7] H. J. Reich, N. H. Phillips, *J. Am. Chem. Soc. 108* (1986) 2102.

[8] a) **1a**: P. Binger, R. Köster, *Synthesis 1973*, 309; b) **1b**: G. Menz, B. Wrackmeyer, *Z. Naturforsch. B32* (1977) 1400; c) **1c**: B. Wrackmeyer, *Int. J. Spectrosc. 1* (1982) 201.

[9] A suspension of sodium amide (0.40 g, 10 mmol) or potassium amide (0.5 g, 10 mmol) in toluene (15 mL) was treated at −78 °C with equimolar amounts of the compounds **1a–c**, and the mixtures warmed to 0 °C and stirred for 2 h. After removal of the toluene by distillation, **2a–c** were obtained in quantitative yield as colorless air- and moisture-sensitive solids which are only moderately soluble in toluene and benzene but very soluble in THF.—^{1}H NMR (300 MHz) of the Na compounds in [D$_8$]THF, −70 °C: **2a**: δ = −0.17 (s, 9H; Me_3Si), 0.0 (m, 4H), 0.53 (t, 6H; Et_2B), 1.52 (s, 3H; =CMe), 1.95 (q, 2H), 0.73 (t, 3H; =CEt).—**2b**: $\delta[J(^{119}Sn^1H)/Hz]$ = −0.67 (br. s, 2H; NH_2), −0.32 (br. s, 9H; Me_3Sn), −0.18 (m, 2H), 0.05 (m, 2H), 0.52 (t, 6H; Et_2B); 1.71 [71.7] (s, 3H; =CMe), 2.03 (q, 2H), 0.79 (t, 3H; =CEt).—**2c**: $\delta[J(^{207}Pb^1H)/Hz]$ = −1.04 [ca. 40] (br. s, 2H; NH_2), 0.21 [41.5] (s, 9H; Me_3Pb), −0.47

(m, 2H), 0.28 (m, 2H), 0.54 (t, 6H; Et_2B), 2.00 [149.8] (s, 3H; =CMe), 2.03 (q, 2H), 0.80 (t, 3H; =CEt).

[10] **2a, b** can be obtained according to Equation (1) in toluene and in THF. **2c** rapidly underwent further reaction with **1c** in THF, leading, inter alia, to a detectable novel tetraorganoborate ion (*E*)-[$Me_3PbC(Me)$=$C(Et)BEt_2Me$]$^{\ominus}$; characteristic NMR data: $\delta(^{13}C)$ [$^1J(^{13}C^{11}B)$/Hz] 21.9 (BCH_2) [41.4], 10.3 (BCH_3) [42.5]; $\delta(^{11}B) = -13.9$, $\delta(^{207}Pb)$ [$^3J(^{207}Pb^{11}B)$/Hz] −66.7 [54.8]. If **2c** is prepared in toluene its solutions in THF are stable.

[11] a) R. Köster, G. Seidel, *Angew. Chem. 93* (1981) 1009; *Angew. Chem. Int. Ed. Engl. 20* (1981) 972; b) R. Köster, G. Seidel, R. Boese, B. Wrackmeyer, *Chem. Ber. 120* (1987) 669.

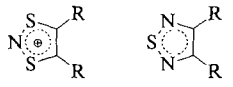
[12] a) **4a**: R. Köster, G. Seidel, B. Wrackmeyer, unpublished; b) **4b**: S. Kerschl, B. Wrackmeyer, *Z. Naturforsch. B40* (1985) 845; c) **4c**: K. Horchler, B. Wrackmeyer, unpublished.

[13] a) R. R. Holmes, *Acc. Chem. Res. 12* (1979) 257; b) R. R. Holmes, *J. Am. Chem. Soc. 100* (1978) 433; c) R. Willem, M. Gielen, J. Meunier-Piret, K. Jurkschat, A. Tzschach, *J. Organomet. Chem. 277* (1984) 335; d) D. Schomburg, R. Krebs, *Inorg. Chem. 23* (1984) 1378.

1,3,5-Trithia-2,4,6-triazapentalenyl — a Stable Sulfur-Nitrogen Radical**

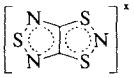
By *Gotthelf Wolmershäuser** und *Rudolf Johann*

1,3,2-Dithiazolylium ions **1**[1,2] may be regarded as aromatic 6π-heterocycles. The same holds true for the neutral 1,2,5-thiadiazoles **2**.[3] Upon one-electron reduction the respective radical species are formed.[1,2,4] Owing to their favorable redox potential, their planarity, and the stability of their reduced radical state, benzoannelated derivatives of **1** are suitable building blocks for conductive CT complexes.[2,5]



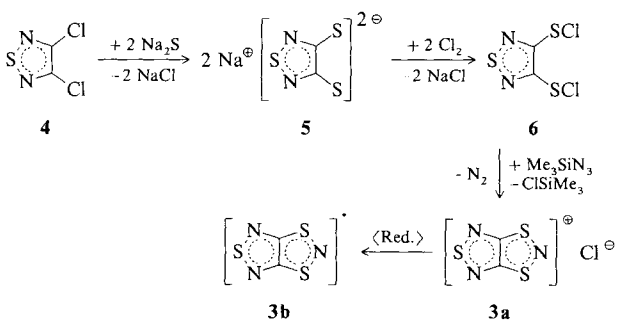
1 **2**

We were now interested in whether the novel pentalene analogue **3**, in which the two ring systems **1** and **2** are coupled, are also suitable for the synthesis of conductive systems.



3a: x = ⊕
3b: x = ·

Reaction of the thiadiazole **4** with Na_2S leads to formation of the dianion **5**, which *Rees* et al.[6] had already obtained via another route. By reaction with elemental chlorine, **5** can be converted into the corresponding sulfenyl chloride **6**. As we have already shown, 1,2-disulfenyl chlorides react with trimethylsilyl azide yielding dithiazolylium chlorides.[2] This reaction also takes place in high yields with **6**; **3a**$Cl^{\ominus}$ is obtained as a bright-orange colored solid that is moderately soluble in polar solvents and melts at 195–196 °C with decomposition.



4 **5** **6**

3b **3a**

Treatment of a suspension of **3a**$Cl^{\ominus}$ with sodium dithionite, triphenylantimony or TCNQ-lithium leads rapidly to a deep-blue solution of **3b**. From petroleum ether solutions, which are stable for days even in the presence of air, **3b** crystallizes in the form of black needles. Well-shaped, deep-violet crystals suitable for an X-ray structure analysis are formed upon slow sublimation in a high vaccum.

Information on the structure of **3b** was provided by ESR spectroscopic investigations and an X-ray structure analysis.[7] Of the cell parameters, most striking is the short *b* axis (3.697 Å), from which it follows that the molecules are stacked along this axis. The face normal is inclined about 35.1° to the stacking axis. In the crystal, **3b** has, within the limits of error, C_{2v} symmetry, i.e. the molecules are planar (max. deviation of an atom from the mean plane 0.003 Å; Fig. 1). This result is consistent with findings on the reso-

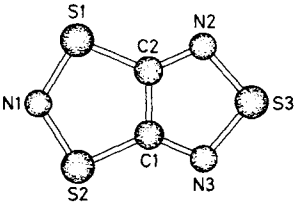
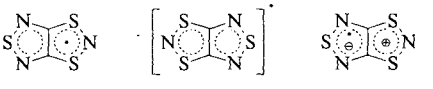


Fig. 1. Structure of **3b** in the crystal. Bond distances [Å] and angles [°]: -C2-C1 1.426(4), N3-C1 1.312(4), S2-C1 1.730(3), N2-C2 1.316(4), S1-C2 1.725(3), S1-N1 1.653(3), S2-N1 1.648(3), S3-N2 1.642(3), S3-N3 1.642(3); N3-C1-C2 114.4(3), S2-C1-C2 113.3(2), S2-C1-N3 132.3(2), N2-C2-C1 114.0(3), S1-C2-C1 114.0(2), S1-C2-N2 132.1(2), S2-N1-S1 116.8(2), S3-N2-C2 106.2(2), S3-N3-C1 106.1(2), N1-S1-C2 97.8(1), N1-S2-C1 98.1(1), N3-S3-N2 99.3(1).

nance-stabilized benzobisdithiazole radical cation (BBDTA$^{\cdot\oplus}$).[8] In the case of benzothiazole (BDTA),[1] on the other hand, the dithiazole ring is slightly bent. In **3b**, the S–N distances in both parts of the molecule are about equal (1.65 and 1.64 Å, resp.), thus indicating single bonds with double bond character (BDTA:[1] 1.65 Å, BBDTA$^{\cdot\oplus}$:[8] 1.62 Å). d(S–N) = 1.62 Å has also been found in the **3b** analogue 1,4-dithia-2,3,5,6-tetraazapentalene.[9] Also the C–C bond(1.426(4) Å) as well as the C–N and the C–S bonds (1.32 Å and 1.73 Å) are best described as single bonds with partial double bond character. Comparison of the bond lengths in **3b** with those in dithiazolylium salts, dithiazolyls and thiadiazoles indicates that the resonance formula **3b′** predominates over that of the formulation **3b‴**. However,



3b′ **3b″** **3b‴**

[*] Dr. G. Wolmershäuser, Dipl.-Chem. R. Johann
Fachbereich Chemie der Universität
Erwin-Schrödinger-Strasse, D-6750 Kaiserslautern (FRG)

[**] This work was supported by the Deutsche Forschungsgemeinschaft.

the formulation **3b**″ gives an adequate description, particularly if the planarity of the molecule is taken into account.

Whereas relatively short intermolecular S···S contacts are found in other dithiazole radicals (e.g. in BDTA[1] 3.17 Å), in **3b** the shortest intermolecular S···S distance is 3.38 Å; the distance between the molecular planes (3.7 Å) even corresponds to the van-der-Waals distance. Apparently the spin delocalization over the whole molecule makes closer intermolecular contacts unneccessary.

The ESR spectrum of **3b** is consistent with the X-ray structure analysis. In dichloromethane (20 °C) a triplet [a(N) = 11.21 G for N1] of quintets [a(N) = 0.85 G for the equivalent atoms N2 and N3] is observed. The g value is 2.0061. The nitrogen coupling constants of the 1,3,2-dithiazole-2-yls known so far lie between 10.4 and 11.4 G.[10] In contrast, 1,2,5-thiadiazole radical anions with two equivalent N atoms have a(N) values of ca. 5.3 G.[11]

As expected the mass spectrum of **3b** obtained at lower ionization energies shows an intense molecular peak. The IR spectra of **3a** and **3b** are very simple and closely resemble each other. The UV-VIS spectrum of **3b** in dichloromethane shows, besides a broad band at 595.5 nm (blue color), bands at 373.2, 346.3 and 267.7 nm; the longest wavelength band shows vibrational fine structure in nonpolar solvents.

Experimental

5: A solution of Na_2S (906 mg, 11.61 mmol) in 70% ethanol (50 mL) was treated with a solution of **4** (900 mg, 5.81 mmol) in ethanol (5 mL). After 45 min the (now bright orange) solution was evaporated to dryness. The residue was extracted with 2 × 15 mL of ethanol and the combined extracts evaporated to dryness. The dark-orange, glassy solid was dried in a vacuum. Yield: 575 mg (51%). IR (KBr): $\tilde{\nu}$ = 1415(w), 1375(w), 1290(s), 1220(m), 1190(m), 1015(s), 795(m), 605(w) cm^{-1}.

3a: A suspension of finely powdered **5** (700 mg, 3.61 mmol) in carbon tetrachloride (40 mL) was cooled to − 20 °C. Chlorine was passed into the suspension for 10 min. After a further 10 min the reaction mixture was allowed to warm to − 5 °C and, after removal of excess chlorine, centrifuged. The yellow solution was evaporated to dryness and the oily residue taken up in 30 mL of dichloromethane and treated at 20 °C with 0.42 g (3.65 mmol) of trimethylsilyl azide. After completion of evolution of nitrogen (ca. 1 h) the yellow-orange solid was separated off and dried in a vacuum. Yield: 270 mg (38% based on initial amount of **5**). IR(KBr): $\tilde{\nu}$ = 1163(vw), 1005(vw), 895(vw) 827(s), 773(w), 733(s), 549(w), 521(m), 509(s), 421(m), 401(vw) cm^{-1}. M.p 195–196 °C (decomp.).

3b: A vigorously stirred suspension of finely powdered sodium dithionite (1.5 g, 8.6 mmol) in acetonitrile (15 mL) was treated with 100 mg (0.51 mmol) of **3a**. The reaction mixture was covered with a layer of petroleum ether (20 mL). After a few minutes the petroleum ether phase (which was now blue) was replaced by fresh petroleum ether; this procedure was continued until the petroleum ether phase remained colorless. The combined petroleum ether phases were then evaporated to dryness; purification was possible by sublimation in a vacuum. Yield 55.9 mg (68%) black needles. IR(KBr): $\tilde{\nu}$ = 1347(vw), 1214(m), 833(vw), 779(m), 775(s), 680(s), 671(w), 505(m), 485(m) cm^{-1}. Decomposition above ca. 100 °C.

Received: March 30, 1989 [Z 3265 IE]
German version: *Angew. Chem. 101* (1989) 952

CAS Registry numbers:
3a, 121143-49-5; **3b**, 121143-50-8; **4**, 5728-20-1; **5**, 121143-48-4.

[1] a) G. K. MacLean, J. Passmore, M. J. Schriver, P. S. White, C. D. Bethell, R. S. Pilkington, L. H. Sutcliffe, *J. Chem. Soc. Chem. Commun. 1983*, 807–808; G. K. MacLean, J. Passmore, M. N. S. Rao, M. J. Schriver, P. S. White, D. Bethell, R. S. Pilkington, L. H. Sutcliffe, *J. Chem. Soc. Dalton Trans. 1985*, 1405–1416; b) E. G. Awere, N. Burford, C. Mailer, J. Passmore, J. Schriver, P. S. White, A. J. Banister, H. Oberhammer, L. H. Sutcliffe, *J. Chem. Soc. Chem. Commun. 1987*, 66–69.

[2] G. Wolmershäuser, M. Schnauber, T. Wilhelm, *J. Chem. Soc. Chem. Commun. 1984*, 573–574; *Mol. Cryst. Liq. Cryst. 120* (1985) 323–326.

[3] L. M. Weinstock, I. Shinkai in A. R. Katritzky, C. W. Rees (Hrsg.): *Comprehensive Heterocyclic Chemistry, Vol. 6/4 B*, Pergamon Press, Oxford 1984, S. 513–543.

[4] N. M. Atherton, J. N. Ockwell, R. Dietz, *J. Chem. Soc. A 1967*, 771–777; H. Bock, P. Hänel, R. Neidlein, *Phosphorus Sulfur 39* (1988) 235–252.

[5] G. Wolmershäuser, M. Schnauber, T. Wilhelm, L. H. Sutcliffe, *Synth. Met. 14* (1986) 239–244; E. Dormann, M. J. Nowak, K. A. Williams, R. O. Angus, Jr., F. Wudl, *J. Am. Chem. Soc. 109* (1987) 2594–2599.

[6] J. L. Morris, C. W. Rees, *J. Chem. Soc. Perkin Trans. 1 1987*, 217–223.

[7] **3b**: monoclinic, $P2_1/c$, a = 9.4071(8), b = 3.6967(4), c = 15.0071(11) Å, β = 104.56(1)°, Z = 4; 896 unique reflections ($Mo_{K\alpha}$, 1.5° ≤ θ ≤ 26°), 782 observed with $F_0^2 \geq 2\sigma(F_0^2)$, 74 parameters. R = 0.032, R_w = 0.035. – Further details of the crystal structure investigation are available on request from the Fachinformationszentrum Energie, Physik, Mathematik GmbH, D-7514 Eggenstein-Leopoldshafen 2 (FRG) on quoting the depository number CSD-53887, the names of the authors, and the journal citation.

[8] G. Wolmershäuser, G. Wortmann, M. Schnauber, *J. Chem. Res. (S) 1988*, 358–359.

[9] J. Kane, R. Schaeffer, *Cryst. Struct. Commun. 10* (1981) 1403–1404.

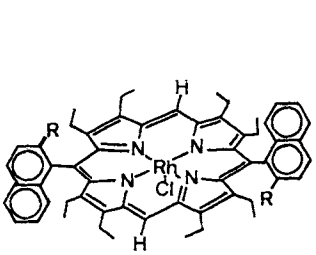
[10] K. F. Preston, J. P. B. Sandall, L. H. Sutcliffe, *Magn. Reson. Chem. 26* (1988) 755–759.

[11] C. L. Kwan, M. Carmack, J. K. Kochi, *J. Phys. Chem. 80* (1976) 1786–1792.

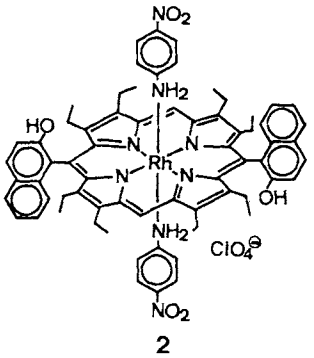
Amide Bond Scission via Bifunctional Activation with Bimetallic Porphyrin Systems with Two Different Metal Centers**

By *Yasuhiro Aoyama**, *Tadahiro Motomura*, and *Hisanobu Ogoshi**

Multicenter interaction is very important for biomimetic catalysts and receptors.[1] It has recently been shown that the metalloporphyrin **1a**, which contains two OH groups enables a bifunctional activation of ketones[2] and a two-point fixation of amino acids.[3] The object of the present study was to develop bimetallic porphyrin systems as a new type of bifunctional catalysts and receptors.[4] We report here that a Rh–Ag system resulting from interaction of $AgClO_4$ with **1a**



1a : R = OH
1b : R = OCH_3
1c : R = H



2

activates amides and esters toward alcoholysis reactions under mild and neutral conditions, as a consequence of intramolecular cooperation of the two metal ions.[5]

[*] Prof. Dr. Y. Aoyama, T. Motomura
Department of Chemistry, Nagaoka University of Technology
Kamitomioka, Nagaoka, Niigata 940-21 (Japan)
Prof. Dr. H. Ogoshi
Department of Synthetic Chemistry, Kyoto University
Sakyo-Ku, Kyoto 606 (Japan)

[**] Catalytic Reactions of Metalloporphyrins, Part 5. This work was supported by a Grant-in-Aid for Scientific Research from the Ministry of Education, Science, and Culture of Japan. – Part 4: Y. Aoyama, K. Midorikawa, H. Toi, H. Ogoshi, *Chem. Lett. 1987*, 1651.

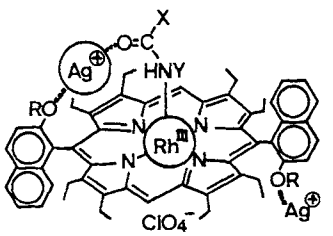
In the presence of $AgClO_4$, the chlororhodium(III) complex of *trans*-5,15-bis(2-hydroxy-1-naphthyl)octaethylporphyrin **1a**[2] promoted the methanolysis of *p*-nitroacetanilide in benzene at 50 °C according to reaction (a) under the following conditions: $[\mathbf{1a}] = 4.0 \times 10^{-6}$ M, $[AgClO_4] = 4.4 \times 10^{-5}$ M, [amide] $= 2.0 \times 10^{-5}$ M, and $[CH_3OH] = 1.3 \times 10^{-3}$ M. The reaction is rather slow (approximate halftime 30 h) and is stoichiometric, since the bis(*p*-nitroaniline) complex **2** formed is no longer active.[6] Under similar conditions, ethyl acetate as substrate underwent ester exchange [reaction (b)]. This reaction is much faster than reaction (a) and is catalytic, since the products do not deactivate the porphyrin catalyst; the yield after 100 h is 2500% based on **1a** under the following conditions:

$$2\,p\text{-}CH_3CONHC_6H_4NO_2 + \mathbf{1a} + 2\,CH_3OH \xrightarrow[AgClO_4]{} \mathbf{2} + 2\,CH_3CO_2CH_3 \quad (a)$$

$$CH_3CO_2CH_2CH_3 + CH_3OH \xrightarrow[AgClO_4]{\mathbf{1a}} CH_3CO_2CH_3 + CH_3CH_2OH \quad (b)$$

$[\mathbf{1a}] = 2.0 \times 10^{-6}$ M, $[AgClO_4] = 4.4 \times 10^{-5}$ M, and [ester] $= [CH_3OH] = 2.5 \times 10^{-3}$ M in benzene at 50 °C. In the absence of $AgClO_4$, reactions (a) and (b) were found to be unmeasurably slow. These reactions are also accelerated by the dimethoxynaphthyl derivative **1b**,[7] although somewhat less effectively than by **1a**. In marked contrast, no reaction takes place with the dinaphthyl derivative **1c** or with the free base of the porphyrin **1a** under otherwise identical conditions, indicating that the central Rh^{III} ion and an OR group (R = H or CH_3) in the same molecule in addition to $AgClO_4$ are essential for the present reactions.

Treatment of **1a**, **1b**, or **1c** with $AgClO_4$ (excess) resulted in a facile anion exchange to give a perchlorate salt of cationic Rh^{III}-porphyrin with concomitant precipitation of AgCl, as in the case of the octaethylporphyrin complex.[8] ^1H NMR spectroscopy of the complexes in C_6D_6 showed that upon interaction with $AgClO_4$ the OCH_3 protons of **1b** and the naphthalene ring protons of **1a** and **1b**, but not of **1c**, undergo characteristic downfield shifts, while the protons of the ethyl groups and *meso* positions remain unaffected; *e.g.*, $\delta(OCH_3) = 3.39$ and 3.24 (two s, each 3H) for **1b** and 3.44 (s, 6H) for **1b**-$AgClO_4$. IR spectroscopy of $CHCl_3$ solutions of **1a** showed a significant shift of ν_{OH} to lower wave numbers upon reaction with $AgClO_4$ ($\nu_{OH} = 3520\ cm^{-1}$ for **1a** and $3440\ cm^{-1}$ for **1a**-$AgClO_4$). These observations can be taken as evidence that excess $Ag^{\oplus}$ ions coordinate with OR groups (R = H or CH_3) of **1a** and **1b**.



3 (R = H, CH_3)

The resulting Rh-Ag-porphyrin forms 1:1 adducts (**3**) with amides (in excess), as evidenced by sharp ^1H NMR signals for bound substrates which are high-field shifted due to the porphyrin ring-current effect:[9] for the *N*-methylacetamide adduct (**3**, X = Y = CH_3) $\delta = -2.70$ (s, 3H, $NHCH_3$) and -0.19 (s, 3H, CH_3CO);[10] for the *p*-nitroacetanilide adduct (**3**, X = CH_3 and Y = *p*-$C_6H_4NO_2$) $\delta = -2.25$ (s, 3H, CH_3CO) and 4.29 (AB q, 2H, $C_6H_4NO_2$ *ortho* to the acetamino group).[11] Considerable high-field shifts for the *N*-methyl and *ortho* *N*-aryl protons ($\Delta\delta \approx 5.5$ and 3.4 ppm, respectively), in the light of the "shielding map" of rhodium porphyrins,[9] suggest that the adducts have a coordinative Rh^{III}-N bond as shown in **3**. An indication of the stability of the adduct **3** comes from the observation of sharp ^1H NMR signals for bound amide without undergoing averaging with those for free amide which is present in excess in the bulk solution; this can be taken as evidence that the exchange between bound and free amide molecules is rather slow at room temperature. Such an adduct with sharp NMR signals could be detected neither in the absence of $AgClO_4$ nor in its presence but with **1c** in place of **1a** or **1b**, indicating that an electrophilic Rh^{III} center and an $Ag^{\oplus}$ ion coordinated with OR groups are essential for the formation of **3**. The prechlorate salt of Rh^{III} porphyrin has been shown to be such a powerful electrophile that it is capable of metalating arenes.

Adduct **3** (X = CH_3, Y = *p*-$C_6H_4NO_2$) is presumably an intermediate of the methanolysis of *p*-nitroacetanilide, since addition of methanol to a solution of **3** leads to facile generation of **2** with concomitant formation of methyl acetate. Nucleophilic attack of methanol on the substrate may be facilitated by an electrophilic *double* activation of the amide bond, both in the leaving group (NHY) and in the carbonyl moiety, by the Rh^{III} and $Ag^{\oplus}$ centers.

Received: February 6, 1989 [Z 3157 IE]
German version: *Angew. Chem. 101* (1989) 922

CAS Registry numbers:
1a, 109362-30-3; **1b**, 121157-58-2; **2**, 121141-73-9; **3** (X = Y = Me), 121141-76-2; **3** (X = Me Y = *p*-$C_6H_4NO_2$), 121141-71-7; **3** (X = H Y = Me), 121141-68-2; **3** (X = Me Y = H), 121157-57-1; AcOEt, 141-78-6; *p*-$AcNHC_6H_4NO_2$, 104-04-1.

[1] Reviews: a) R. Breslow, *Acc. Chem. Res. 13* (1980) 170; b) I. Tabushi, *ibid. 15* (1982) 66; c) Y. Murakami, *Top. Curr. Chem. 115* (1983) 107; d) S. Shinkai, O. Manabe, *ibid. 121* (1984) 67; e) F. Vögtle, H.-G. Löhr, J. Franke, D. Worsch, *Angew. Chem. 97* (1985) 721; *Angew. Chem. Int. Ed. Engl. 24* (1985) 727; f) F. P. Schmidtchen, *Top. Curr. Chem. 132* (1986) 101; g) J. Rebek, Jr., *Science (Washington) 235* (1987) 1478; h) J.-M. Lehn, *Angew. Chem. 100* (1988) 91; *Angew. Chem. Int. Ed. Engl. 27* (1988) 89; i) F. Diederich, *ibid. 100* (1988) 372 and *27* (1988) 362; j) D. J. Cram, *ibid. 100* (1988) 1041 and *27* (1988) 1009.

[2] Y. Aoyama, A. Yamagishi, Y. Tanaka, H. Toi, H. Ogoshi, *J. Am. Chem. Soc. 109* (1987) 4735.

[3] Y. Aoyama, Y. Yamagishi, M. Asagawa, H. Toi, H. Ogoshi, *J. Am. Chem. Soc. 110* (1988) 4076.

[4] For metal complexes of cofacial diporphyrins, see for example: a) J. P. Collman, P. Denisevich, Y. Konai, M. Marrocco, C. Koval, F. C. Anson, *J. Am. Chem. Soc. 102* (1980) 6027; b) H. Y. Liu, M. Weaver, C. B. Wang, C. K. Chang, *J. Electrochem. 145* (1983) 439; c) C. K. Chang, I. Abdalmuhdi, *Angew. Chem. 96* (1984) 154; *Angew. Chem. Int. Ed. Engl. 23* (1984) 164.

[5] The catalysis by an intramolecular hydroxy phenol group in the hydrolysis of a Co^{III}-coordinated amide substrate has recently been reported: A. Schepartz, B. Breslow, *J. Am. Chem. Soc. 109* (1987) 1814.

[6] **2**: ^1H NMR ($CDCl_3$): $\delta = 6.65$ and ca. 2.53 (AB q, each 2H, $C_6H_4NO_2$); IR (KBr): $\tilde{\nu}_{max} = 1148$, 1125, 1093 cm^{-1} (ν_{ClO}); UV-VIS (CH_2Cl_2): $\lambda_{max} = 415$, 528, 560 nm. An authentic specimen of **2** was readily obtained by reaction of **1a** with *p*-nitroaniline in the presence of $AgClO_4$.

[7] Prepared and characterized in a similar manner as **1a** and **1c** [2].

[8] Y. Aoyama, T. Yoshida, K. Sakurai, H. Ogoshi, *Organometallics 5* (1986) 168.

[9] H. Ogoshi, J. Setsune, T. Omura, Z. Yoshida, *J. Am. Chem. Soc. 97* (1975) 6461.

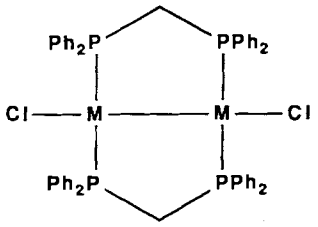
[10] The *N*-Methylformamide adduct (**3**, X = H and Y = CH_3) and acetamide adduct (**3**, X = CH_3 and Y = H) show the corresponding methyl signals at $\delta = -2.79$ (s, 3H, $NHCH_3$) and -0.36 (s, 3H, $COCH_3$), respectively.

[11] The signals of the *meta* protons could not be identified because of overlap with those of the naphthalene ring protons.

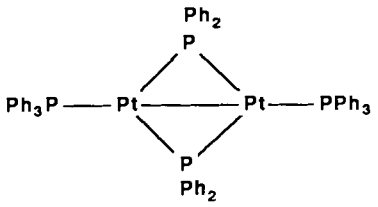
Agostic-type Gold Ligand and Incipient μ_3-PPh_2 Coordination in the $Au_2Pt_2P_6$ "Hammock" Skeleton of the Cluster $[Au_2Pt_2(\mu\text{-}PPh_2)_2(PPh_3)_4][PF_6]_2$

By *Robert Bender, Pierre Braunstein,*[*] *Alain Dedieu,* and *Yves Dusausoy*

The addition of electrophilic metal reagents to electron-rich (neutral or anionic) complexes is a method of choice for the stepwise construction of heterometallic clusters.[1] Thus, for example, the behavior of the metal–metal bond in dipalladium(I)- and diplatinum(I)-complexes such as **1** towards $HgCl_2$ and group 11 electrophiles has recently been the subject of detailed investigations.[2] These 30-electron complex-

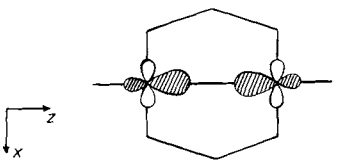


1a, M = Pd
1b, M = Pt



2

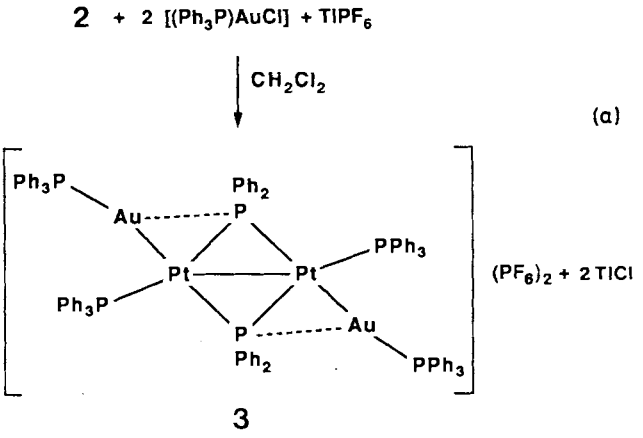
es were found to lead either to "A-frame" clusters through direct involvement of the d^9–d^9 metal–metal bond[2a, b]—more specifically of the HOMO (Scheme 1) formed from the bonding combination of the two d_{z^2} orbitals—or to clusters of higher nuclearity resulting from molecular rearrangements induced by the reactivity of the



Scheme 1. HOMO of complexes of type 1.

M–Cl bond of **1** towards the electrophilic reagent.[2c, d] We have now found that the 30-electron complex **2**,[3] which also contains a d^9–d^9 Pt–Pt bond but no M–Cl bond, reacts with $[Au(PPh_3)]^{\oplus}$ in yet a different manner, leading to an unprecedented raft structure which displays an agostic-type $Au(PPh_3)$ ligand and an incipient triply bridging diphenylphosphido ligand.

Reaction of **2** in CH_2Cl_2 with two equivalents of $[(Ph_3P)AuCl]$ in the presence of $TlPF_6$ resulted in a red solution of **3**[4] and the precipitation of TlCl [Eq. (a)].



3

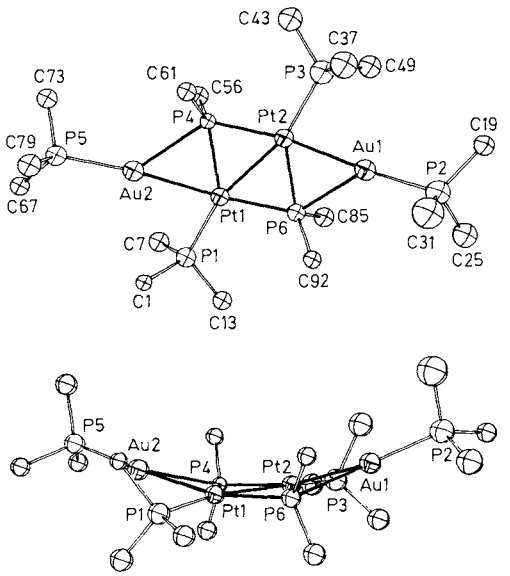
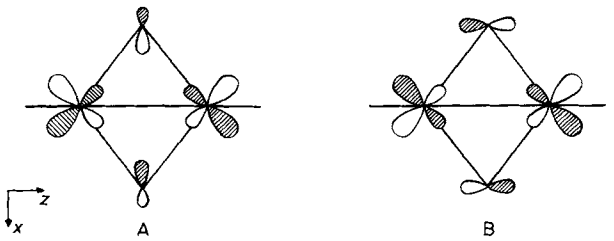


Fig. 1. Views of the molecular structure of the cation of **3**. Only the *ipso* C atoms of the Ph groups are shown. Important bond distances [Å] and angles [°]; Pt1–Pt2 2.660(2), Pt1–Au2 2.667(1), Pt2–Au1 2.634(1), Pt1–P1 2.294(8), Pt1–P4 2.341(7), Pt1–P6 2.301(7), Pt2–P3 2.263(8), Pt2–P4 2.308(7), Pt2–P6 2.315(7), Au1–P2 2.306(8), Au1–P6 2.682(7), Au2–P4 2.629(7), Au2–P5 2.288(8); Au2–Pt1–Pt2 115.5(1), Au1–Pt2–Pt1 117.3(1), Au2–Pt1–P4 62.9(2), Au1–Pt2–P6 65.3(2), Au2–Pt1–P6 165.0(2), Au1–Pt2–P4 164.4(2), Au2–Pt1–P1 82.3(2), Au1–Pt2–P3 80.4(2), P4–Pt1–Pt2 54.5(2), P6–Pt2–Pt1 54.6(2), P4–Pt1–P6 109.5(2), P6–Pt2–P4 110.2(2), P4–Pt1–P1 141.8(3), P6–Pt2–P3 142.4(3), Pt2–Pt1–P1 162.2, Pt1–Pt2–P3 162.3(2), Pt2–Pt1–P6 55.0(2), Pt1–Pt2–P4 55.7(2), P6–Pt1–P1 107.8(3), P4–Pt2–P3 106.9(3), Pt2–Au1–P2 169.6(2), Pt1–Au2–P5 173.3(2), Pt2–Au1–P6 51.6(2), Pt1–Au2–P4 52.5(2), P6–Au1–P2 135.0(3), P4–Au2–P5 132.2(3), Pt1–P6–Pt2 70.4(2), Pt1–P4–Pt2 69.8(2), Pt1–P6–Au1 130.1(3), Pt2–P4–Au2 131.6(3), Pt2–P6–Au1 63.1(2), Pt1–P4–Au2 64.6(2).

Figure 1 shows the molecular structure of the cation of **3** established by an X-ray diffraction study.[5] The $Pt_2Au_2P_6$ skeleton is pseudo-C_2 symmetric with the twofold axis perpendicular to the Pt1, Pt2, P4, P6 mean plane and intersecting the middle of the Pt1–Pt2 bond. The hammock conformation resulting from the slight folding of the $Pt_2Au_2P_6$ raft along Pt1–P4 and Pt2–P6 edges is noteworthy. Thus, the Pt1–Au2–P4, and Pt2–Au1–P6 planes form with the Pt1, Pt2, P4, P6 mean-plane an angle of 15.6 and 17.9°, respectively. The Pt1–Pt2 distance of 2.660(2) Å is longer than that in **2** (2.604(1) Å) and the Pt1–Au2 (2.667(1) Å) and Pt2–Au1 (2.634(1) Å) distances compare with the other known Pt–Au distances.[9]

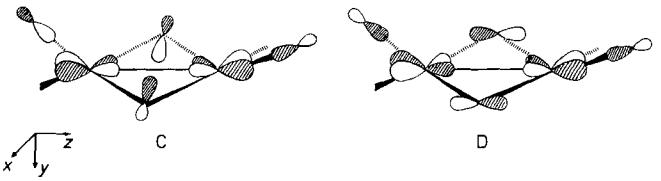
[*] Dr. P. Braunstein, Dr. R. Bender
Laboratoire de Chimie de Coordination
UA 416 CNRS, Université Louis Pasteur
4 rue Blaise Pascal, F-67070 Strasbourg Cédex (France)
Dr. A. Dedieu
Laboratoire de Chimie Quantique
ER 139 CNRS, Université Louis Pasteur
4 rue Blaise Pascal, F-67070 Strasbourg Cédex (France)
Prof. Y. Dusausoy
Laboratoire de Minéralogie et Cristallographie
UA 809 CNRS, Université de Nancy I
B.P. 239, F-54506 Vandoeuvre-les-Nancy (France)

The most remarkable features of **3** are that: (i) addition of $[Au(PPh_3)]^{\oplus}$ to **2** occurs *"externally"* to the $Pt_2(\mu\text{-}P)_2$ core without formation of a $Pt_2[\mu\text{-}Au(PPh_3)]$ unit, in contrast to **1** ; (ii) the relatively short Au1–P6 and Au2–P4 distances of 2.682(7) and 2.629(7) Å, respectively, suggest a bonding interaction between the corresponding atoms and an incipient μ_3-bonding mode for the μ-PPh_2 ligands. The Au1 and Au2 atoms are slightly out of the Pt1–Pt2–P4–P6 mean plane by 0.737(1) and 0.646(1) Å, respectively. The μ_3-bridging of a phosphido group has previously been reported only for Li[10a] or Cu[10b,c] complexes. Note that by virtue of the isolobal analogy between $Au(PPh_3)$ and H, the present structure also suggests that polynuclear systems containing a *bridging phosphane ligand* might exist.



Scheme 2. The two highest occupied orbitals of type 2 complexes.

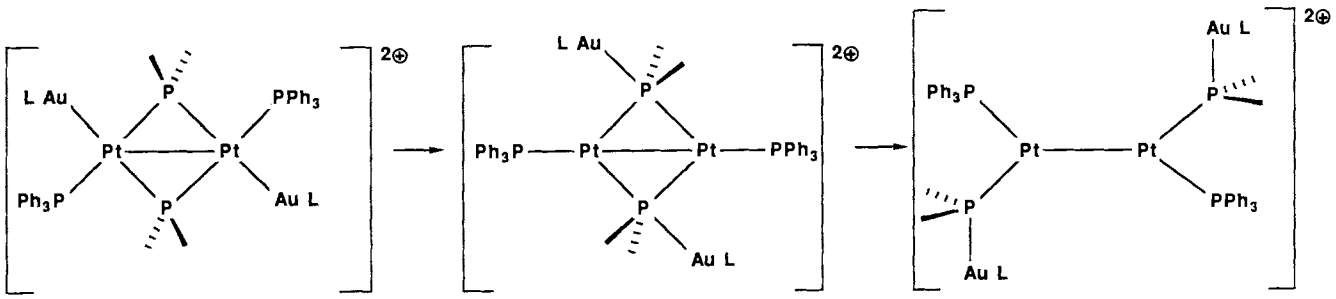
The unusual bonding in **3** can be easily rationalized through a fragment molecular orbital analysis[11] based on extended Hückel calculations.[12, 13] In this system, the two highest occupied orbitals (A and B, Scheme 2) are now essentially made of the bonding and antibonding combinations of the two d_{xz} orbitals. The bonding combination of the two d_{z^2} orbitals which accounts for the metal–metal bond is at a much lower energy. Hence the orbitals A and B interact primarily with the unoccupied acceptor orbital of the incoming electrophile. Since these two orbitals are polarized outward, away from the metal–metal bond,[17] one expects the attack to occur "externally" to the $Pt_2(\mu\text{-}P)_2$ core. A slight deviation of the Ph_3P–Pt–Pt angle from 180°, as in **3**, does not appreciably modify A and B. It opens on the other hand a reactive channel for the incoming $[Au(PPh_3)]^{\oplus}$ by allowing the two bonding interactions C and D (Scheme 3) to take place. The slight out-of-plane disposition of $Au(PPh_3)$ seems to be governed by electronic rather than by steric interactions: the electrophilic attack in the Pt_2P_4 plane requires a greater deviation of the Ph_3P–Pt–Pt angle from 180°. This in turn destabilizes the d_{xz} orbitals and polarizes them toward the metal–metal bond region,[18] the net result being an overall destabilization of the system and a weakening of its metal–metal bond.



Scheme 3. Bonding interactions between $(Ph_3P)Au$ acceptor orbitals and the orbitals A and B of Scheme 2.

Is the short Au–P distance between the $Au(PPh_3)$ and μ-PPh_2 moieties the result of some bonding interaction? The fragment molecular orbital analysis indeed points to a favorable overlap factor.[19] But the interaction remains rather weak, at least weaker than the interaction of the $Au(PPh_3)$ moiety with the d_{xz} orbitals, owing to an unfavorable energy difference factor (the orbitals of the bridging PPh_2 fragments are at a much lower energy than the d orbitals of the metal framework). That the Au–PPh_3 axis points toward the Pt metal center (P–Au–Pt 171°) rather than halfway between the Pt atom and the phosphido bridge is certainly the best illustration of the domination of the $(Ph_3P)Au$–Pt interaction over the $(Ph_3P)Au$–PPh_2 interaction.

The structure of the cluster **3** is therefore the result of a subtle balance between various possible bonding interactions. It might also be viewed as the result of an agostic-type three-center, two-electron interaction in the $Au(\mu\text{-}PPh_2)Pt$ ring system, somewhat equivalent to the classical M ← H–C agostic interaction. In fact, related M ← Au–C agostic interactions where $Au(PPh_3)$ replaces H have been described.[20] But in **3** the agostic interaction of $Au(PPh_3)$ is with the μ-PPh_2 ligand rather than with the Pt atom. One may conceptually link the two situations by considering them as frozen-in intermediates of the interconversion of the two extremes **4** and **5**.



Calculations, to be detailed elsewhere, indicate that the conversion of **4** into **5** is orbital symmetry allowed. There might however be some spin conservation problems arising from a possible triplet ground state for **5**. On the other hand, the further conversion of **5** into **6** is symmetry forbidden (with retention of the C_{2h} symmetry). The same behavior is displayed by the system which one obtains through the isolobal replacement of $Au(PPh_3)$ by H (or by an alkyl group), an interesting additional feature being that the first step of the migration process corresponds to a reductive elimination at the metal.[21]

Received: February 6, 1989 [Z 3158 IE]
German version: *Angew. Chem. 101* (1989) 931

[1] a) See many contributions in P. Braunstein (Ed.): *Recent Advances in Di- and Polynuclear Chemistry (New J. Chem. 12* (1988) 307–720), and references cited therein; b) R. Bender, P. Braunstein, C. de Méric de Bellefon, *Polyhedron Symp. in-Print No 8* (1988) 2271.

[2] a) P. R. Sharp, *Inorg. Chem. 25* (1986) 4185; b) G. J. Arsenault, L. Manojlovic-Muir, K. W. Muir, R. J. Puddephat, I. Treurnicht, *Angew. Chem. 99* (1987) 79; *Angew. Chem. Int. Ed. Engl. 26* (1987) 86; c) P. Braunstein, M. A. Luke, A. Tiripicchio, M. Tiripicchio Camellini, *ibid. 99* (1987) 802 and *26* (1987) 768; d) in Ref. [1a], p. 429.

[3] N. J. Taylor, P. C. Chieh, A. J. Carty, *J. Chem. Soc. Chem. Commun. 1975*, 448.

[4] A mixture of $[(Ph_3P)AuCl]$ (100 mg, 0.2 mmol) and $TlPF_6$ (70 mg, 0.2 mmol) in CH_2Cl_2 was stirred under nitrogen for 15 min. Complex **2** (128 mg, 0.1 mmol) was added and the resulting red solution was stirred for 2 h. After removal of TlCl by filtration, layering of the solution with hexane (40 ml) and cooling to $-20\,^{\circ}C$ afforded red crystals of **3** in ca. 80% yield. When only one equivalent of $[(Ph_3P)AuCl]$ was used, only **3** and ca. 50% of **2** were recovered.—**3**: $^{31}P\{^1H\}$ NMR (CH_2Cl_2/CD_2Cl_2, H_3PO_4 ext.) $\delta = 228$ (m, $^1J(PPt) = 2190$, $^1J(PPt) = 1550$, $^2J(PP) = 225$, $J(PP) = 68$ Hz, μ-PPh_2), 50.8 (complex m, Ph_3PAu), 26.5 (d with ^{195}Pt satellites, $^1J(PPt) = 4600$, $^2J(PP) = 225$ Hz, Ph_3PPt), -143.4 (hept, $PF_6^{\ominus}$).

[5] Crystal data for **3**: orthorhombic, space group *Pbca*, $a = 31.770(5)$, $b = 24.724(3)$, $c = 23.720(2)$ Å, $V = 18632$ Å^3, $Z = 8$, $\varrho_{calcd} = 1.765$ g cm^{-3}, $F(000) = 9583$, $\lambda = 0.70930$ Å, $\mu(Mo_{K\alpha_1}) = 115.6$ cm^{-1}, intensities of 15140 reflections with $1 < 2\theta < 25^{\circ}$ were measured on a Enraf-Nonius CAD 4 4F diffractometer, $\omega/2\theta$ scan mode with ω scan width $= 0.8 + 0.35 \tan\theta$, $\sin\theta/\lambda_{max} = 0.596$ Å^{-1}, dimensions of crystal selected $0.1 \times 0.1 \times 0.12$ mm. Data reduction was made using the SDP program package with decay correction [6]. Empirical absorption corrections were applied using Difabs [7]. The metal atoms were found by direct methods and the remaining non-hydrogen atoms from subsequent difference Fourier syntheses [8]. All hydrogen atoms were placed in calculated positions and included in the refinement with fixed isotropic thermal parameters ($B = 5$ Å). The structure was refined by full matrix least-squares using 4494 data with $I/\sigma(I) \geq 6$ to $R = 0.057$ and $R_w = 0.062$ with the error in an observation of unit weight of 0.25. Further details of the crystal structure investigation can be obtained from the Fachinformationszentrum Energie, Physik, Mathematik GmbH, D-7514 Eggenstein-Leopoldshafen 2 (FRG), by quoting the depository number CSD-53789, the names of the authors, and the journal citation.

[6] *SDP Structure Determination Package*; Enraf-Nonius, Delft 1977.

[7] N. Walker, D. Stuart, *Acta Crystallogr. Sect. A 39* (1983) 159.

[8] G. M. Sheldrick: *Programs for Crystal Structure Determination*, Göttingen 1976.

[9] T. Blum, P. Braunstein, A. Tiripicchio, M. Tiripicchio Camellini, in Ref. [1a], p. 539 and references cited therein.

[10] a) R. A. Jones, A. L. Stuart, T. C. Wright, *J. Am. Chem. Soc. 105* (1983) 7459; b) D. J. Brauer, P. C. Knüppel, O. Stelzer, *J. Chem. Soc. Chem. Commun. 1988*, 551; c) F. Gol, P. C. Knüppel, O. Stelzer, W. S. Sheldrick, *Angew. Chem. 100* (1988) 1008; *Angew. Chem. Int. Ed. Engl. 27* (1988) 956.

[11] R. Hoffmann, *Science (Washington) 211* (1981) 995.

[12] a) R. Hoffmann, *J. Chem. Phys. 39* (1963) 1397; b) R. Hoffmann, W. N. Lipscomb, *ibid. 36* (1962) 3179; *ibid. 37* (1962) 2872.

[13] Computational details. The parameters used in the extended Hückel calculations for Pt and Au were taken from Refs. [14] and [15]. The modified Wolfsberg-Helmolz formula [16] was used throughout this work. The geometries used for the cluster calculations were somewhat idealized from the experimental ones using for instance C_2 geometries for **3**–**6**.

[14] R. H. Summerville, R. Hoffmann, *J. Am. Chem. Soc. 98* (1976) 7240.

[15] S. Komiya, T. A. Albright, R. Hoffmann, J. K. Kochi, *J. Am. Chem. Soc. 98* (1976) 7255.

[16] J. H. Ammeter, H. B. Bürgi, J. C. Thibeault, R. Hoffmann, *J. Am. Chem. Soc. 100* (1978) 3686.

[17] The two d_{xz} orbitals are hybridized out, away from the metal–metal region in order to minimize the out of phase (and hence repulsive) mixing with the σ and π orbitals of the two PPh_2 bridging ligands.

[18] The reversal in the hybridization is induced by the need to minimize the repulsive interactions with the lone pair of the terminal phosphane ligands, which become greater than the repulsive interactions with the orbitals of the bridging ligands.

[19] The overlap between the sp hybrid orbital of $Au(PPh_3)$ with the π orbitals of the PPh_2 fragment amounts to 0.31 (compared with a value of 0.26 and 0.28 for the overlap with the d_{xz} components of A and B respectively (Scheme 2)).

[20] a) V. G. Andrianov, Yu. T. Struchkov, E. R. Rossinskaja, *J. Chem. Soc. Chem. Commun. 1973*, 338; b) G. A. Carriedo, J. A. K. Howard, F. G. A. Stone, M. J. Went, *J. Chem. Soc. Dalton Trans. 1984*, 2545; c) A. D. Horton, M. J. Mays, M. McPartlin, *J. Chem. Soc. Chem. Commun. 1987*, 424.

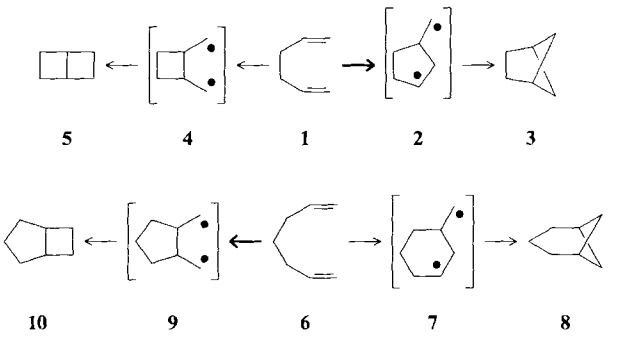
[21] A similar alkyl shift in a mononuclear Pd system has been analyzed recently and shown to be also symmetry allowed: J. V. Ortiz, Z. Havlas, R. Hoffmann, *Helv. Chim. Acta 67* (1984) 1.

Regiochemistry of the Intramolecular [2+2]-Photocycloaddition of Cyclohexenone to Vinyl Ethers**

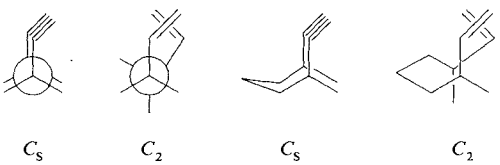
By *Evelyn Fischer* and *Rolf Gleiter**

Dedicated to Professor Margot Becke-Goehring on the occasion of her 75th birthday

The "rule of five" is an empirical rule frequently employed for predicting the regiochemistry of intramolecular [2+2]-photocycloadditions of open-chain, non-conjugated dienes.[1–3] It states that that regioisomer is preferentially formed in which a five-membered ring diradical can be formulated as intermediate. This is illustrated in Scheme 1 for the cyclization of 1,5-hexadiene **1** und 1,6-heptadiene **6**. This rule also applies when one or two double bonds are incorporated in complex systems.[4, 5] Since the rule of five does not satisfactorily explain the stability of the possible intermediates, we proposed a concurrence of electronic and steric effects in the transition state.[6] In the case of **1** the natural sequence of the frontier orbitals should be interchanged by the strong through-bond effect of the ethano bridge with a



Scheme 1.



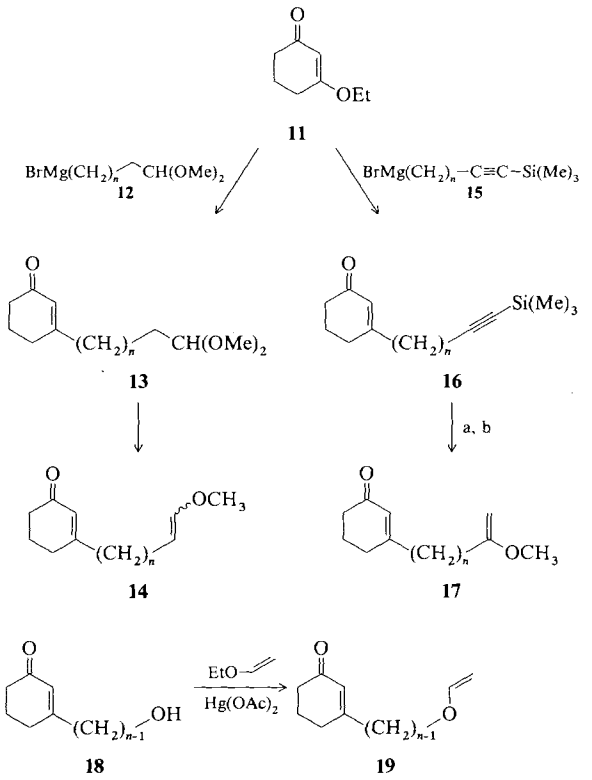
Scheme 2.

C_2- or C_s-transition state;[6] therefore, the activation energy should be dependent upon electronic factors both in the case of a C_s- as well as a C_2-transition state. The more favorable steric circumstances in the C_2-conformation (Scheme 2, left) should then be decisive for this transition state. In the case of **6** and dienes with longer chains we expect the natural sequence of the π-MOs (π_+, π_-; π_+^*, π_-^*), and, in contrast to the C_2 conformation no electronic contribution to the activation energy for the C_s conformation (Scheme 2, right). Steric effects should be less than in the case of **1** when **6** and dienes with longer bridges are considered. To explore the influence of electronic effects on the intramolecular [2+2]-photocycloaddition we investigated the compounds **14**

[*] Prof. Dr. R. Gleiter, Dr. E. Fischer
Organisch-Chemisches Institut der Universität
Im Neuenheimer Feld 270
D-6900 Heidelberg (FRG)

[**] This work was supported by the Deutsche Forschungsgemeinschaft, the Fonds der Chemischen Industrie and BASF AG. *E. F.* thanks the Land Baden Württemberg for a postgraduate grant.

($n = 2$–4), **17** ($n = 2,3$) and **19** ($n = 2,4$) (Scheme 3). Each of these compounds consists of a cyclohexenone moiety whose photochemistry[3b, 7] and photophysics[8] are well documented, and a vinyl ether fragment in which the polarity of the double bond is controlled by the alkoxy group. We assume that an exciplex is formed between the cyclohexenone moiety and the electron-rich vinyl ether moiety in the excited state.



Scheme 3. a) KF. b) $Hg(OAc)_2$, MeOH, $NaBH_4$, NaOH. See text.

The synthesis of the model compounds **14, 17** and **19** according to conventional methods is outlined in Scheme 3. Irradiation was carried out on 10^{-3} M solutions of the compounds in cyclohexane using a 366-nm interference filter. The product compositions[9] proved to be independent of the presence of a sensitizer (acetophenone, benzophenone); they are listed together with the quantum yields in Table 1. The lifetimes of the respective triplet states τ_{RT} for **14** ($n = 2$–4) and **19** ($n = 4$) quoted in the same table were obtained from the slope of the Stern-Volmer plot ($k_{qT}\tau_{RT}$).[10]

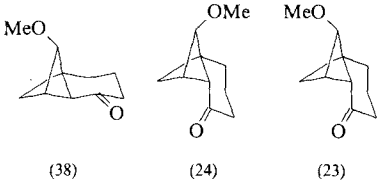
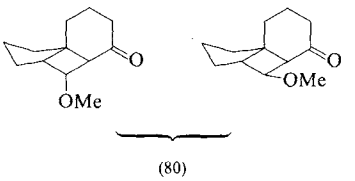
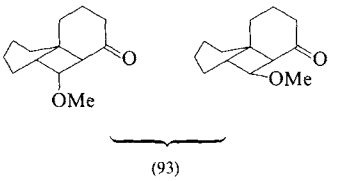
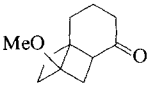
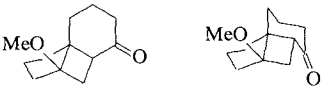
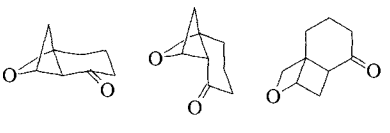
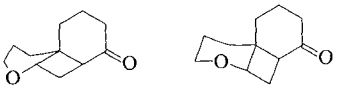
We interpret the results in Table 1 in terms of the polarization of the triplet cyclohexenone and of the vinyl ether moiety shown in Scheme 4.[11, 12] A comparison of the data in Table 1 shows that:

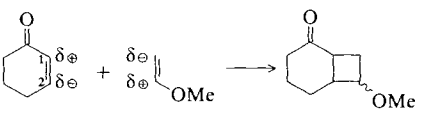
1) Compounds with $n = 3$ furnish only 1,2-bridged head-to-head adducts. The polarization of the enol ether double bond by methoxy groups has no influence on the regioselectivity, but does influence the quantum yield. With compound **17**, $n = 3$, where the polarization favors the head-to-head cycloaddition, the quantum yield is higher (0.71) than in the case of **14**, $n = 3$ (0.46).

2) Dienes with four-membered chains show the same regioselectivity as dienes with $n = 3$. The quantum yields are generally lower than for $n = 3$ and also reflect the polarization of the double bonds [Φ(**14**, $n = 4$) < Φ(**19**, $n = 4$)].

3) When $n = 2$, the regioselectivity is strongly dependent on the polarization of the enol ether double bond. In the case of **14** with $n = 2$, this favors the head-to-tail [2+2]-cycloaddition, and only tricyclo[5.2.1.$0^{1,6}$]decane is formed. However, the quantum yield (0.30) is lower than in the case of **14**, $n = 3$ (0.46), where chain length and enol-ether polarization are opposing each other. If the polarization is reversed (**17**, $n = 2$; **19**, $n = 2$), the quantum yield for the head-to-tail [2+2]-cycloaddition drops to zero.

Table 1. Ratio of head-to-head (□) and head-to-tail [2+2]-cycloaddition (X), quantum yield Φ, lifetime of the triplet state τ_{RT}, and products of the [2+2]-photocycloaddition of **14** ($n = 2,4$), **17** ($n = 2,3$) and **19** ($n = 2,4$).

Starting cpd.	Ratio □ : ×	Φ (τ_{RT}[ns])	Photoproducts (yield in % according to GC)
14, $n = 2$	0:100	0.30 (0.24)	 (38) (24) (23)
14, $n = 3$	100:0	0.46 (0.09)	 (80)
14, $n = 4$	100:0	0.31 (1.1)	 (93)
17, $n = 2$	100:0	0.13	 (75)
17, $n = 3$	100:0	0.71	 (36) (40)
19, $n = 2$	70:30	0.06	 (5) (6) (25)
19, $n = 4$	100:0	0.50 (1.8)	 (81) (11)



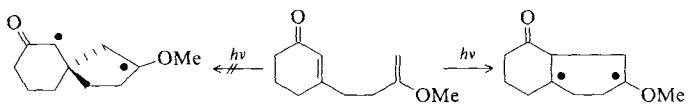
Scheme 4.

 © VCH Verlagsgesellschaft mbH, D-6940 Weinheim, 1989 0570-0833/89/0707-0926 $ 02.50/0

These results confirm the hypothesis that one of the main reasons for the "rule of five" is to be sought in the through-bond interaction. The absence of an electronic contribution to the activation energy for the C_S transition state with chains where $n = 3,4$ determines the regioselectivity of the cycloaddition;[6] all polarization effects of the substituents are overruled. On the other hand, in the case of compounds with $n = 2$, whose C_S and C_2 transition states experience an electronic activation energy,[6] the polarization of the vinyl ether double bond is decisive for the regiochemistry.

The increased activation energy for $n = 2$ compared to $n = 3,4$ can also be anticipated from the τ_{RT} values: whereas τ_{RT} for **19**, $n = 4$, and **14**, $n = 4,3$ becomes smaller with decreasing chain length, as one would expect for a diffusion controlled process, in the case of **14**, $n = 2$, an increased activation energy seems to outplay the advantage of the short chain and to increase the triplet lifetime.

Deviations from the rule of five can easily be explained in terms of the polarization of the two double bond systems; however, questions remain open, if one does not assume an exciplex,[13] but refers to the stability of possible diradicals.[1-5,14] It can be concluded from the stereochemistry of the products that such diradicals are preferred in which one of the radical centers is located at the carbon atom substituted by the alkoxy group. There would appear to be no preference for C-1 or C-2 (cf. Scheme 4) as second radical carbon atom. On the basis of these considerations one of the questions that arise is why exclusively the secondary product of the six-membered ring radical **20** is formed from **17**, $n = 2$, even though the five-membered ring radical **21** should be more stable. Polarization, however clearly favors **20** over **21**.



21 **17**, $n = 2$ **20**

Received: February 13, 1989 [Z 3170 IE]
German version: *Angew. Chem. 101* (1989) 925

CAS Registry numbers:
(*Z*)-**14**(n = 2), 121056-69-7; (*E*)-**14**(n = 2), 121056-70-0; **14**(n = 3), 93136-22-2; **14**(n = 4), 121056-71-1; **17**(n = 2), 121056-72-2; **17** (n = 3), 121056-73-3; **19**(n = 2), 121056-74-4; **19**(n = 4), 121056-75-5; 10-Methoxytetracyclo[4.3.1^{1,7}.0^{1,6}]decan-2-one (isomer 1), 121056-76-6; (isomer 2), 121123-99-7; (isomer 3), 121124-00-3; 6-Methoxytricyclo[5.4.0^{1,5}]undecan-8-one (isomer 1), 121056-77-7; (isomer 2), 121124-01-4; 7-Methoxytricyclo[6.4.0^{1,6}]dodecan-9-one (isomer 1), 121056-78-8; (isomer 2), 121124-02-5; 8-Methoxytricyclo[4.4.0^{1,6}]decan-5-one, 121056-19-9; 5-Methoxytricyclo[5.4.0^{1,5}]undecan-8-me (isomer 1), 121056-80-2; (isomer 2), 121124-03-6; 8-oxatetracyclo[4.3.1^{1,7}.0^{1,6}]decan-5-one (isomer 1), 121056-81-3; 8-oxatetracyclo[4.3.1^{1,7}.0^{1,6}]decan-5-one (isomer 2), 121056-82-4; 3-oxatricyclo[4.4.0^{1,4}]decan-7-one; 121056-83-5; 5-oxatricyclo[6.4.0^{1,6}]dodecan-9-one (isomer 1), 121056-84-6; (isomer 2), 121124-04-7.

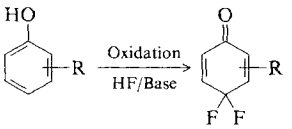
[1] R. Srinivasan, K. H. Carlough, *J. Am. Chem. Soc. 89* (1967) 4932.
[2] R. S. H. Liu, G. S. Hammond, *J. Am. Chem. Soc. 89* (1967) 4936.
[3] a) W. L. Dilling, *Chem. Rev. 66* (1966) 373; b) N. J. Turro: *Modern Molecular Photochemistry*, Benjamin/Cummings, Menlo Park, CA 1978.
[4] J. D. White, D. N. Gupta, *Tetrahedron 25* (1969) 3331; F. T. Bond, H. C. Jones, L. Scerbo, *Tetrahedron Lett. 1965*, 4685; T. N. Gibson, W. F. Erman, *J. Org. Chem. 37* (1972) 1148; J. R. Scheffer, R. A. Wostradowski, *ibid. 37* (1972) 4317.
[5] a) S. Wolff, W. C. Agosta, *J. Am. Chem. Soc. 105* (1983) 1292; b) A. R. Matlin, C. F. George, S. Wolff, W. C. Agosta, *ibid. 108* (1986) 3385; c) C. Schröder, S. Wolff, W. C. Agosta, *ibid. 109* (1987) 5491; d) M. T. Crimmins, *Chem. Rev. 88* (1988) 1453, and references cited therein.
[6] R. Gleiter, W. Sander, *Angew. Chem. 97* (1985) 575; *Angew. Chem. Int. Ed. Engl. 24* (1985) 566.
[7] D. O. Cowan, J. D. Drisko: *Elements of Organic Chemistry*, Plenum Press, New York 1976; W. Oppolzer, *Acc. Chem. Res. 15* (1982) 135; A. C. Weedon in W. M. Horspool (Ed): *Synthetic Organic Photochemistry*, Plenum Press, New York 1984; P. A. Wender in J. D. Coyle (Ed): *Photochemistry in Organic Synthesis*, The Royal Society of Chemistry, London 1986; see also [5d].
[8] G. Marsh, D. R. Kearns, K. Schaffner, *Helv. Chim. Acta 51* (1968) 1890; *J. Am. Chem. Soc. 93* (1971) 3129; R. Bonneau, *ibid. 102* (1980) 3816.
[9] The products were identified on the basis of the ^{1}H NMR data of the ketones; the dinitrophenylhydrazones were used for elemental analyses.
[10] The quench experiments were carried out with piperylene. The lifetime τ_{RT} was calculated from the diffusion constants in cyclohexane [3b]: $k_{diff} = 7 \times 10^9$ L mol^{-1} s^{-1}.
[11] E. J. Corey, J. D. Bass, R. Le Mahieu, R. B. Mitra, *J. Am. Chem. Soc. 86* (1964) 5570; P. de Mayo, *Acc. Chem. Res. 4* (1971) 41.
[12] The indicated polarization is also reflected in the HOMO of the enol ether and in the LUMO of the cyclohexenone.
[13] D. I. Schuster, G. E. Heibel, P. B. Brown, N. J. Turro, C. V. Kumar, *J. Am. Chem. Soc. 110* (1988) 8261.
[14] M. Ohsaku, *J. Chem. Soc. Perkin Trans. 2 1987*, 1027.

Oxidative Fluorination of Arenes**

By *Jan H. H. Meurs**, *David W. Sopher*, and *Wolf Eilenberg*

Selectively fluorinated arenes are often biologically active and thus interesting compounds which find many uses as pharmacologically active substances, agrochemicals, or as building blocks for their synthesis.[1] Methods for the selective fluorination of arenes, however, often involve several synthetic steps or are based on the use of highly reactive reagents such as elemental fluorine. We now report the selective oxidative fluorination of some selected phenol and benzene derivatives in an HF/base mixture, in which hydrogen fluoride is present in complexed form.

Hydrogen fluoride/base complexes are well known as reagents for direct fluorination or as sources of fluorine in oxidative fluorination.[2] In the latter case aryl cations or aryl radical cations are formed oxidatively; these react with fluoride ions in situ with formation of the new fluorine–carbon bonds.[3,4] In this way we were able to convert the phenols **1a–e** into the dienones **2a–d** and **2'** in an HF/base mixture in the presence of stoichiometric amounts of lead(IV) compounds or at the anode (Table 1). Without addition of bases no dienones are formed, but only polymers.[5]



1 **2**

The dienones **2a–d** and **2'** are useful intermediates in the synthesis of substituted fluorophenols. For example, hydrogenation of **2a** leads almost quantitatively to *p*-fluorophenol **3**. Numerous nucleophiles undergo a Michael addition with **2a**, whereupon a rearomatization takes place in situ with cleavage of HF. In this way 4-fluoro-3-hydroxybenzonitrile **4**, for example, is accessible in 90% yield. The addition of

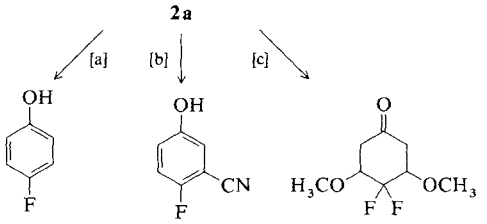
[*] J. H. H. Meurs, D. W. Sopher, W. Eilenberg
Koninklijke/Shell-Laboratorium, Amsterdam (Shell Research B.V.)
Postbus 3003, 1003 AA Amsterdam (The Netherlands)

Table 1. Conversion of the phenols **1a–e** into dienones in an HF/base mixture.

Phenol	R	Oxidation	HF/		
Base	Yield	Dienone			
				[wt.-%]	[a]
1a	H	PbO_2	HF/H_2O 37/63 (w/w)	12	**2a** [b]
		PbO_2	HF/pyridine 70/30 (w/w)	30(50)	
		PbF_4	9 HF/KF	60(65)	
		Pb_3O_4	9 HF/KF	37(41)	
		$Pb(OAc)_4$	9 HF/KF	42(48)	
		Anode	3 HF/Et_3N	25	
1b	2 Cl	PbO_2	HF/pyridine 70/30 (w/w)	25	**2b**
1c	2 CH_3	$Pb(OAc)_4$	9 HF/KF	10	**2c**
1d	3 CH_3	PbO_2	HF/pyridine 70/30 (w/w)	17	**2d**
1e	4 CH_3	PbO_2	HF/pyridine 70/30 (w/w)	36	**2'** [c]

[a] Determined by GC analysis of the isolated product. [b] Byproduct: benzoquinone. [c] **2'**: 4-fluoro-4-methylcyclohexadienone.

methoxy groups to **2a** leads to **5** in 80% yield; cleavage of HF, however, could not be achieved (Scheme 1).



3 (90%) **4** (90%) **5** (80%)

Scheme 1. [a] Pt 10% on carbon, MeOH, 1 bar H_2. [b] KCN, DMF, 30 min, 20°C; ^{13}C NMR (200 MHz, $CDCl_3$): 157.2, 155.8, 123.4, 119.2, 117.6, 114.8(CN) 100.7. [c] K_2CO_3, MeOH, 4 h, 60°C; ^{19}F NMR (200 MHz, $CFCl_3$): 122.75(2 F, J_{HF} = 8.8 Hz).

Owing to its high oxidation potential, benzene **6** reacts only slowly with PbO_2, and in HF/pyridine 70/30 (w/w) it is converted into **2a** (13%) in 5 d. **6** and other non-activated aromatics such as **7–9** can, however, be readily oxidized in an Et_3N/HF mixture (Scheme 2). In some cases secondary alkylamines (e.g., dipropylamine) or tetraethylammonium fluoride are equally suitable as bases; primary amines lead to electrode passivation.

The system Et_3N/3 HF as electrolyte and source of fluorine, has a series of advantages: it is stable towards oxidation up to over + 2 V/SCE, good electrical conductivity (no addition of supporting electrolytes), and satisfactory dissolution of the substrates that are mentioned here (additional solvent unnecessary). Moreover, it is distillable as azetrope (ratio Et_3N/HF 1/3) and can thus, in principle, be recovered.[6]

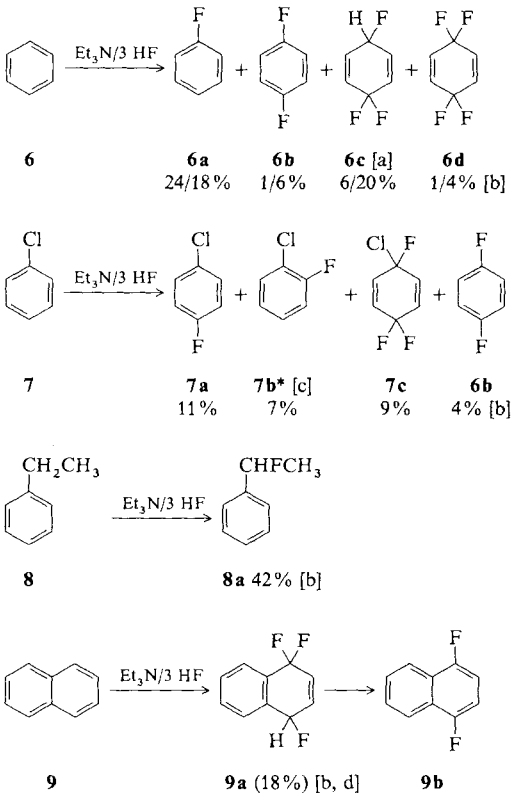
The applicability of HF/base complexes in electrochemical fluorination to various classes of substances is presently the subject of further investigation.

Experimental

Oxidation with Pb^{IV} reagents. **2a**: 0.94 g (10 mmol) of **1a** and 4.78 g (20 mmol) of PbO_2 were added with stirring in 20 min at 35°C to 10 mL of HF/pyridine (7/3 w/w) in 50 mL of CH_2Cl_2 (two phases). After 30 min the organic phase was decanted off, washed with 50 mL each of aqueous Na_2CO_3 solution and H_2O, and dried over $MgSO_4$. Subsequent chromatographic purification (silica gel, $CH_2Cl\,CH_2Cl_2$/pentane 1/1 v/v) furnished 0.39 g (30%) of **2a** as a pale yellow solid (highly lachrymatory). ^{13}C NMR (250 Hz; $CDCl_3$): 183.5, 137.0, 131,2, 109.9; ^{19}F NMR (250 MHz, $CFCl_3$): − 98.94.

1b–1e were oxidized analogously using the reagents quoted in Scheme 1. All products afforded correct ^1H NMR/^{13}C NMR data; e.g. ^{19}F NMR ($CFCl_3$, 250 MHz): **2d** − 103.16; **2'**, − 92.03.

Electrochemical oxidation: the electrolyses were carried out in unpartitioned plate cells (3 × 17 cm, electrode separation 1.5–2 mm) of platinum anodes (cathode: Monel) current controlled (5 mA/cm^2) with cell voltages of 3–5 V.



Scheme 2. Anodic oxidation of **6–9**. [a] **6c** can be converted quantitatively into **6b** by base- or acid-catalysis. [b] Conversion: **6**: 60/86%; **7**, 76%; **8**, 63%; **9**, 96%. [c] Experiments with deuterium-labeled compounds confirm attack of the radical cations of **7** in the *o*-position by $F^{\ominus}$. [d] Product unstable: cleavage of HF leads to **9b**.

The electrolyte was pumped through a degassing vessel (evolution of H_2) with the aid of an HF-resistant hose pump (30–50 mL/min).

2a: A solution of **1a** (0.47 g, 5 mmol) in Et_3N/3 HF (14 mL) was electrolyzed up to a charge consumption of 4.5 F mol^{-1} (conversion 90%). The electrode compartments were partitioned by a microporous polyethylene membrane. The reaction mixture was diluted with 50 mL of H_2O, extracted with CH_2Cl_2, and worked up as described above; yield of **2a**: 0.13 g (20%).

6–9 were oxidized analogously; ^{19}F NMR (250 MHz, $CFCl_3$): **7c**, − 92.7, − 103.6. **8a**: − 167.4; **9a**: − 77.3, − 86.6, − 171.5.

The ^{19}F NMR data of all the other compounds are consistent with those quoted in Ref. [7].

Received: February 20, 1989 [Z 3181 IE]
German version: *Angew. Chem. 101* (1989) 955

CAS Registry numbers:
1a, 108-95-2; **1b**, 95-57-8; **1c**, 95-48-7; **1d**, 108-39-4; **1e**, 106-44-5; **2a**, 42539-98-0; **2b**, 105277-17-6; **2c**, 105277-18-7; **2d**, 105277-19-8; **2'**, 77249-33-3; **3**, 371-41-5; **4**, 104798-53-0; **5**, 120788-52-5; **6**, 71-43-2; **6a**, 462-06-6; **6b**, 540-36-3; **6c**, 74298-20-7; **6d**, 22060-77-1; **7**, 108-90-7; **7a**, 352-33-0; **7b**, 348-51-6; **7c**, 114589-03-6; **8**, 100-41-4; **8a**, 7100-97-2; **9**, 91-20-3; **9a**, 120788-51-4; benzoquinone, 106-51-4.

[1] a) R. Filler, *J. Fluorine Chem. 33* (1986) 361; b) R. Filler, Y. Kobayashi: *Biomedical Aspects of Fluorine Chemistry*, Elsevier, Amsterdam 1982; c) J. T. Welch, *Tetrahedron 43* (1987) 3123.
[2] a) J. R. Ballinger, F. W. Teare, *Electrochim. Acta 30* (1985) 1075; b) E. Laurent, B. Marquet, E. Tardivel, H. Thiebault, *Bull. Soc. Chim. Fr. 1986*, 955; c) G. A. Olah, J. T. Welch, Y. D. Vankar, M. Nojima, I. Kerekes, J. A. Olah, *J. Org. Chem. 44* (1979) 3872.
[3] I. N. Rozhkov, *Russ. Chem. Rev. (Engl. Transl.) 1976*, 615.
[4] I. Ya. Aliev, I. N. Rozhkov, I. L. Knunyants, *Izv. Akad. Nauk, SSSR Ser. Khim. 6* (1973) 1430.
[5] A. E. Feiring, *J. Org. Chem. 44* (1979) 1252.
[6] R. Franz, *J. Fluorine Chem. 15* (1980) 423.
[7] A. Zweig, R. G. Fischer, J. E. Lancaster, *J. Org. Chem. 45* (1980) 3597.

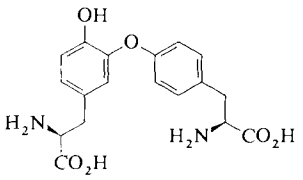
Synthesis of (*S*,*S*)-Diisotyrosine and Its Incorporation in an Ansa Tripeptide**

By *Ulrich Schmidt,* Regina Meyer, Volker Leitenberger,* and *Albrecht Lieberknecht*

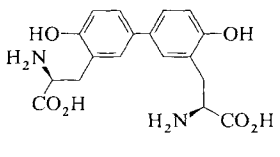
In numerous biologically highly active metabolic products of fungi and bacteria, diaminodicarboxylic acids have been found as characteristic building blocks, which – as in plant metabolism – are formed by dimerizing radical oxidation of hydroxylated phenylalanines.

Diphenyl ether structures have been found in the cyclopeptides piperazinomycin,[1] OF-4949 I–IV[2] K-13,[3] bouvardin and deoxybouvardin,[4] RA I–VII[5] and the very complex glycopeptide antibiotics vancomycin, teicoplanin and ristocetin.[6] Isodityrosine **1** was prepared during the synthesis of piperazinomycin,[7] deoxybouvardin,[8] OF-4949,[9–11] and K-13.[11]

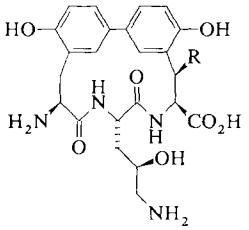
Biphenyl structures have been detected in some glycopeptide antibiotics.[6] WS-43708 A (**3a**) and B(**3b**),[12] highly active antibacterial metabolites from *Streptomyces griseorubiginosus* No-43708, contain diisotyrosine **2** (3,3'-(*p*,*p*'-dihydroxybiphenyl-*m*,*m*'-diyl)dialanine) and its β-hydroxy derivative as characteristic building blocks.



1



2

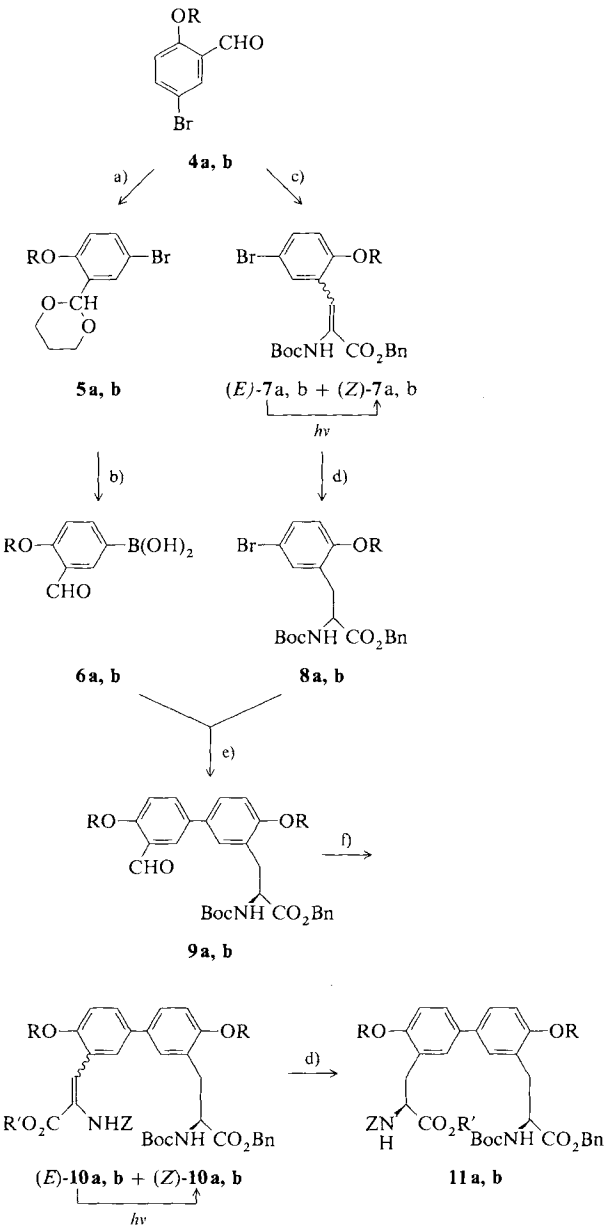


3a: R = OH
3b: R = H

We synthesized diisotyrosine as ether-masked species with four different protecting groups on amino and carboxyl groups (Scheme 1, **11a,b**; for physical data see Table 1).

The biphenyl skeleton was formed from **6** and **8** by Pd^0-catalyzed arylboronic acid-aryl bromide coupling.[13] Key reactions in the synthesis of the amino acid units were condensation reactions of the aldehydes **4** and **9** with (dialkoxyphosphoryl)glycine esters to give didehydroamino acid compounds and their enantioselective and diastereoselective hydrogenation. Since the homogeneous catalyst $[Rh(dipamp)]^{\oplus}$[15] hydrogenates *E*-didehydroamino acid derivatives only very slowly and without high stereoselectivity, we hydrogenated only *Z*-**7a, b** and *Z*-**10a, b** and converted the *Z*-compounds into the *E* compounds by photochemical isomerization. The enantioselectivity or diastereoselectivity of the hydrogenations was greater than 99%. The amino and carboxy protecting groups required on the diisotyrosine for subsequent cyclopeptide synthesis were already introduced during synthesis of the didehydroamino acids with appropriately protected (dialkoxyphosphoryl)glycine.[14]

The ansa-tripeptide **16** was synthesized from the monomethoxy compound **11c** – prepared analogously to **11a, b** – and (*S*)-alanine (Scheme 2). The site of coupling is often crucial for the successful ring closure via ω-aminopentafluo-

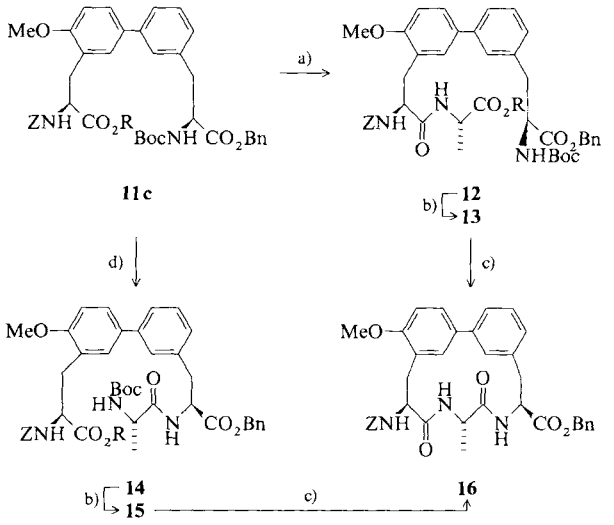


a: R = Me, **b**: R = $C_6H_5CH_2$; Boc = *t*BuOCO, Bn = $C_6H_5CH_2$, Z = $C_6H_5CH_2OCO$, R' = $Me_3SiCH_2CH_2$

Scheme 1. a) 1,3-propanediol/$BF_3 \cdot Et_2O$/toluene/reflux/4 h, **5a**: 87%, **5b**: 81%. b) 1. Mg/THF/20 °C/2 h, 2. $B(OCH_3)_3$/–60 to 20 °C/6 h, 3. $H^{\oplus}/H_2O$, **6a**: 64%, **6b**: 50%. c) *N*-*tert*-Butoxycarbonyl-2-(dimethoxyphosphoryl) glycinebenzyl ester/KO*t*Bu/CH_2Cl_2/–60 to 20 °C/14 h, **7a**: 84% (*E*:*Z* 30:70), **7b**: 80% (*E*:*Z* 37:63). d) $[Rh(dipamp)]^{\oplus}/H_2/CH_3OH$/20 °C/72 h, quant. e) $Pd(PPh_3)_4$/THF/2 M Na_2CO_3/Rückfluß/14 h, **9a**: 86%, **9b**: 62%. f) *N*-benzyloxycarbonyl-2-(dimethoxyphosphoryl) glycine-(2-trimethylsilylethyl) ester/KO*t*Bu/CH_2Cl_2/-60 to 20 °C/14 h, **10a**: 89% (*E*:*Z* 41:59), **10b**: 91% (*E*:*Z* 37:64).

[*] Prof. Dr. U. Schmidt, Dipl.-Chem. R. Meyer, Dipl.-Chem. V. Leitenberger, Dr. A. Lieberknecht
Institut für Organische Chemie, Biochemie und Isotopenforschung der Universität Pfaffenwaldring 55, D-7000 Stuttgart 80 (FRG)

[**] Amino Acids and Peptides, Part 72; Cyclopeptides, Part 17. This work was supported by the Fonds der Chemischen Industrie, the Deutsche Forschungsgemeinschaft, and BASF AG. – Part 71: U. Schmidt, M. Kroner, H. Griesser, *Synthesis*, in press; Part 16: U. Schmidt, U. Beutler, A. Lieberknecht, *Angew. Chem. 101* (1989) 344; *Angew. Chem. Int. Ed. Engl. 28* (1989) 333.



11c, 12, 14: R = $Me_3SiCH_2CH_2$; **13, 15**: R = C_6F_5

Scheme 2. a) 1. Bu_4NF/DMF/1 h, 2. (*S*)-Alanine-(2-trimethylsilylethyl)ester/EDCl/hydroxybenzotriazole/CH_2Cl_2/ −15 to 20 °C/14 h, 82%. b) 1. Bu_4NF/DMF/1 h, 2. C_6F_5OH/EDCl/CH_2Cl_2/ −15 to 20 °C/14 h. c) 1. $Me_3SiOSO_2CF_3$/CH_2Cl_2/ −40 to 20 °C/2 h, 2. $CHCl_3$/sat. $NaHCO_3$/20 °C/3 h, 80%. d) 1. $Me_3SiOSO_2CF_3$/CH_2Cl_2/ − 40 to 20 °C/2 h, 2. Boc-(*S*)-Ala-OH/EDCl/CH_2Cl_2/ − 15 to 20 °C/14 h, 85%.

rophenylester[16] to the ansa-peptide; we therefore investigated the cyclization at the carboxy group and at the amino group. For this purpose we synthesized the peptides **12** and **14** by conventional methods, cleaved the trimethylsilylethyl esters with fluoride ions, and converted the carboxylic acids into the pentafluorophenyl esters **13** and **15** with EDCl[17]

Table 1. Some physical data of the compounds **11a, b** and **16**.

11a: ^{1}H-NMR (300 MHz, $CDCl_3$): δ = 0.01 (s; 9H), 0.93 (dd, J = 7.8, 9.3 Hz; 2H), 1.36 (s; 9H), 3.05–3.15 (m; 4H), 3.83 (s; 3H), 3.84 (s; 3H), 4.14–4.22 (m; 2H), 4.57–4.62 (m; 2H), 5.04 (d, J = 0.9 Hz; 2H), 5.12 (s; 2H), 5.27 (d, J = 0.9 Hz; 2H), 5.52 (d, J = 7.5 Hz; 1H), 6.83–6.89 (m; 2H), 7.24–7.38 (m; 14H); correct elemental analysis; $[\alpha]_D^{20}$ = +3.95 (c = 1.60; $CHCl_3$)

11b: ^{1}H-NMR (300 MHz, $CDCl_3$): δ = − 0.03 (s; 9H), 0.88 (t, J = 8.3 Hz; 2H), 1.35 (s; 9H), 3.06–3.25 (m; 4H), 4.07–4.17 (m; 2H), 4.58–4.65 (m; 2H), 5.00–5.12 (m; 8H), 5.37 (d, J = 7.8 Hz; 1H), 5.60 (d, J = 7.8 Hz; 1H), 6.92 (t, J = 8.0 Hz; 2H), 7.23–7.47 (m; 24H); correct elemental analysis; $[\alpha]_D^{20}$ = +11.23 (c = 1.44; $CHCl_3$)

16: ^{1}H-NMR (300 MHz, [D_6]DMSO): δ = 1.19 (d, J = 7.0 Hz; 3H), 2.79 (dd, J = 2.0, 12.6 Hz; 1H), 3.01–3.27 (m; 3H), 3.57 (s; 3H), 4.68–4.87 (m; 3H), 5.06 (d, J = 2.6 Hz; 2H), 5.20 (s; 2H), 6.30 (d, J = 7.5 Hz; 1H), 6.97 (d, J = 8.6 Hz; 1H), 7.10 (s; 1H), 7.26–7.52 (m; 15H), 8.74 (d, J = 8.9 Hz; 1H), 9.07 (d, J = 9.0 Hz; 1H); MS (20 eV): m/z 635.5 ($M^{\oplus}$, 22%), 527.3 ($M^{\oplus}$-108, 100)

pentafluorophenol. After deblocking of the *N*-protecting groups with trimethylsilyl triflate in dichloromethane, the solution of the open-chain pentafluorophenyl ester was added dropwise into a vigorously stirred mixture of $CHCl_3$/saturated $NaHCO_3$ and the ring compound **16** (Table 1) isolated in 80% yield from the two precursors **13** as well as **15**.

Received: February 28, 1989 [Z 3209 IE]
German version: *Angew. Chem. 101* (1989) 946

[1] Isolation and Structure: S. Tamai, M. Kaneda, S. Nakamura, *J. Antibiot. 35* (1982) 1130; M. Kaneda, S. Tamai, S. Nakamura, T. Hirata, Y. Kushi, T. Suga, *ibid. 35* (1982) 1137.
[2] Isolation and Structure: S. Sano, K. Ikai, H. Kuroda, T. Nakamura, A. Obayashi, Y. Ezure, H. Enomoto, *J. Antibiot. 39* (1986) 1674; S. Sano, K. Ikai, K. Katayama, K. Takesako, T. Nakamura, A. Obayashi, Y. Ezure, H. Enomoto, *ibid. 39* (1986) 1685.
[3] Isolation and structure: H. Kase, M. Kaneko, K. Yamada, *J. Antibiot. 40* (1987) 450; T. Yasuzawa, K. Shirahata, H. J. Sano, *ibid. 40* (1987) 455.
[4] Isolation and structure: S. D. Jolad, J. J. Hoffman, S. J. Torrance, R. M. Weidhopf, J. R. Cole, S. K. Arora, R. B. Bates, R. L. Gargiulo, G. R. Kriek, *J. Am. Chem. Soc. 99* (1977) 8040.
[5] Isolierung und Struktur: H. Itokawa, K. Takeya, N. Mori, T.Hamanaka, T. Sonobe, K. Mihara, *Chem. Pharm. Bull. 32* (1984) 284; H. Itokawa, K. Takeya, K. Mihara, N. Mori, T. Hamanaka, T. Sonobe, Y. Iitaka, *ibid. 31* (1983) 1424.
[6] Review: D. H. Williams, *Acc. Chem. Res. 17* (1984) 364.
[7] S. Nishiyama, K. Nakamura, S. Suzuki, S. Yamamura, *Tetrahedron Lett. 27* (1986) 4481.
[8] T. Inaba, I. Umezawa, M. Yuasa, T. Inoue, S. Mihashi, H. Itokawa, K. Ogura, *J. Org. Chem. 52* (1987) 2958.
[9] S. Nishiyama, Y. Suzuki, S. Yamamura, *Tetrahedron Lett. 29* (1988) 559.
[10] U. Schmidt, D. Weller, A. Holder, A. Lieberknecht, *Tetrahedron Lett. 29* (1988) 3227.
[11] D. A. Evans, J. A. Ellman, *J. Am. Chem. Soc. 111* (1989) 1063; S. Nishiyama, Y. Suzuki, S. Yamamura, *Tetrahedron Lett. 30* (1989) 379.
[12] Isolation and structure: M. Ezaki, M. Iwami, M. Yamashita, S. Hashimoto, T. Komori, K. Umehara, Y. Mine, M. Kohsaka, H. Aoki, H. Imanaka, *J. Antibiot. 38* (1985) 1453; I. Uchida, N. Shigematsu, M. Ezaki, M. Hashimoto, H. Aoki, H. Imanaka, *ibid. 38* (1985) 1462; I. Uchida, M. Ezaki, N. Shigematsu, M. Hashimoto, *J. Org. Chem. 50* (1985) 1342; R. Kannan, D. H. Williams, *ibid. 52* (1987) 5435.
[13] M. J. Sharp, W. Cheng, V. Snieckus, *Tetrahedron Lett. 28* (1987) 5093.
[14] U. Schmidt, A. Lieberknecht, J. Wild, *Synthesis 1984*, 53.
[15] B. D. Vineyard, W. S. Knowles, M. J. Sabacky, G. L. Bachman, D. J. Weinkauff, *J. Am. Chem. Soc. 99* (1977) 5946; dipamp = *p,p'*-ethylenbis[*o*-methoxyphenyl(phenyl)phosphane].
[16] U. Schmidt, A. Lieberknecht, H. Griesser, J. Talbiersky, *J. Org. Chem. 47* (1982) 3261; im zweiphasigen System: U. Schmidt, R. Utz, A. Lieberknecht, H. Griesser, B. Potzolli, J. Bahr, K. Wagner, P. Fischer, *Synthesis 1987*, 236; U. Schmidt, M. Kroner, H. Griesser, *Tetrahedron Lett. 29* (1988) 4407.
[17] EDCl = 1-[3-(dimethylamino)propyl]-3-ethylcarbodiimide hydrochloride.

Direct Observation of Ground State Splitting in the Chromium(III) Acetate Trimer by Inelastic Neutron Scattering**

By *Upali A. Jayasooriya,* Roderick D. Cannon,* Ross P. White*, and *Gordon J. Kearley*

The electronic states of triangular clusters of paramagnetic ions have been studied extensively.[1] For homonuclear clusters of first-row transition metals bridged by anions, antiferromagnetic coupling predominate **1**, and the Heisenberg model of spin–spin interaction, assuming all three metal ions to be equivalent, leads in every case to an energy level scheme with a multiply degenerate ground state. For example, the Cr_3^{III} triangle in **1** (Fig. 1), is predicted to have a

$[Cr_3O(O_2CCH_3)_6(OH_2)_3]Cl \cdot 5H_2O$ **1**

multiplicity of four.[2] Physical measurements however, imply that in general the degeneracy is lifted by a lowering of symmetry of the metal ion triangle. Temperature-dependent magnetic susceptibility and specific heat data require at least two different coupling constants J(Cr–Cr).[1] Moreover, the low-temperature crystal structure of the chloride salt contains two sets of crystallographically non-equivalent trimer complex molecules.[3] From specific heat data, *Sorai* et al. deduced that both sets are distorted from equilateral geometry, to different extents[4] and more recently *Ferguson* and

[*] Dr. U. A. Jayasooriya, Dr. R. D. Cannon
School of Chemical Sciences, University of East Anglia
Norwich NR4 7TJ (England)
Dr. R. P. White, Dr. G. J. Kearley
Institut Laue-Langevin, BP 156X
38042 Grenoble Cédex (France)

[**] This work was supported by the UK Science and Engineering Research Council.

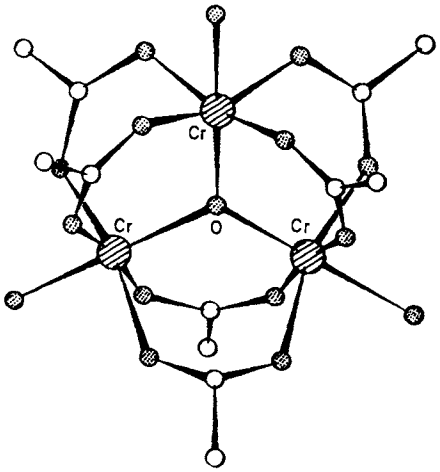


Fig. 1. Structure of the complex cation $[Cr_3O(O_2CCD_3)_6(OD_2)_3]^{\oplus}$.

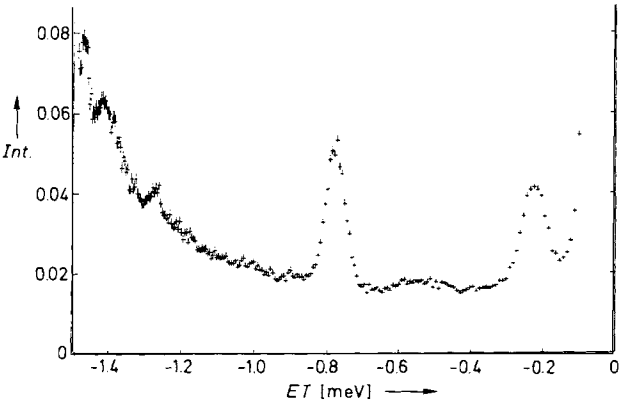


Fig. 2. INS spectrum of $[Cr_3O(O_2CCD_3)_6(OD_2)_3]Cl \cdot 5D_2O$, $T = 1.4$ K, wavelength of incident beam 5.5 Å. Measured on IN5 at the Institut Laue-Langevin, Grenoble. ET = energy transfer, Int. = intensity (in arbitrary units).

Güdel reached the same conclusion from luminescence measurements.[5]

We now report, for the first time, *direct* observation of spectroscopic transitions between the split components of the ground states of these molecules, using inelastic neutron scattering spectroscopy (INS).

The spectrum of the (deuterated) chloride salt is shown in Figure 2. Two well-resolved peaks are seen. The variation in intensity with momentum transfer confirms their magnetic character, and the similarity in intensity is consistent with their originating from two chromophores, present in equal numbers and having equal transition probabilities. Assuming local C_{2v} symmetry, the Heisenberg model interprets each energy as $4|\Delta J| = 4|J_{ca} - J_{ab}|$, where subscript c labels the unique Cr atom and a, b label the two equivalent atoms. We find $\Delta J = 0.778$ and 0.222 meV (6.3 and 1.8 cm^{-1}) for the two sets of complexes in the crystal, in good agreement with previous estimates.[4, 5]

Received: March 3, 1989 [Z 3211 IE]
German version: *Angew. Chem. 101* (1989) 923

[1] R. D. Cannon, R. P. White, *Prog. Inorg. Chem.* 36 (1988) 195.
[2] R. L. Martin, in: E. A. V. Ebsworth, A. G. Maddock, A. G. Sharpe (Eds.): *New Pathways in Inorganic Chemistry*, Cambridge University Press, Cambridge, 1968, pp. 175–231.
[3] S. C. Chang, G. A. Jeffrey, *Acta Crystallogr. B 26* (1970) 673.
[4] M. Sorai, M. Tachiki, H. Suga, S. Seki, *J. Phys. Soc. Jpn. 30* (1971) 750.
[5] J. Ferguson, H. U. Gudel, *Chem. Phys. Lett. 17* (1972) 547.

BOOK REVIEWS

Book Reviews are written by invitation from the editor. Suggestions for books to be reviewed and for book reviewers are welcome. Publishers should send brochures or (better) books to the following address: Redaktion Angewandte Chemie, Postfach 101161, D-6940 Weinheim, Federal Republic of Germany. The editor reserves the right of selecting which books will be reviewed. Uninvited books not chosen for review will not be returned.

Combination Effects in Chemical Carcinogenesis. By *D. Schmähl*. VCH Verlagsgesellschaft, Weinheim/VCH Publishers, New York 1988. 279 pp., hard cover, DM 128.00.—ISBN 3-527-267-26742-5/0-89573-670-5

This slender and well produced volume summarizes 20 years of work at the Deutsche Forschungsgemeinschaft on the effects of combinations of chemicals on carcinogenesis. While some readers will, understandably, wish that Professor *Schmähl* had attempted to cover all the available information in this area, it must be realized that the large literature, the considerable amount of information of a dubious or unhelpful nature, and the need to present a clear focus on the nature of the interactions, would make this a Herculean task. This volume is a good beginning insofar as it reviews in detail a substantial collection of data of consistently high quality.

Much information on how cancer arises has been accumulated over the past 20 years and is highly relevant to the understanding of chemical interactions in carcinogenesis. The importance of metabolic activation and of the usefulness of genotoxicity tests are considered in some detail in separate chapters. There are no such summaries of the relevance of other factors such as cellular proliferation induced by hormonal mimetic effects or by cytotoxicity followed by regeneration, or by immunotoxicological effects, or by physiological pharmacokinetics, or by cell to cell cooperation. This means that most of the topics are considered from the point of view of what happens when two or more chemicals act together to form tumors, rather than on why it happens.

A further result of focussing the text on the work of a single institute is that some salient features in the development of the subject have been omitted. Thus, in a consideration of the development of tumors in the mouse skin, no mention is made of the classical work of *Berenblum* and *Shubik* which established the importance of multi-agent interactions in the two-stage process. Also no mention is made

of the recent work of *Slaga* and of *Kinsel* that has indicated there may be three stages in the induction of these tumors, each mediated by a separate chemical. Such deficiencies in information limit the value of the book mainly to those who already have a working knowledge of the chemical induction of cancer. It greatly reduces the value of the book all not so well versed in the background of carcinogenesis.

The individual topics in this volume are very well presented, with an abundance of charts and figures to convey the basic data. The interactions described are of major importance in the practical sense, and impinge on many areas of importance to the general human environment. For example, experimental studies on combination effects in inhalation carcinogenesis, the effects of ethanol, interactions between low levels of potent carcinogens that affect the same tissue, combinations of carcinogens and non-carcinogens, interactions between the various components of cancer chemotherapeutic agents used to treat human cancer, interactions between the different components of cigarette smoke, and the all-important subject of the influence of diet, stressing the possibly greater importance of total calories consumed than of fat, are each carefully considered.

Overall, this volume will prove to be of value to those experienced in carcinogenesis, especially in relation to its bearing on the human environment. It will achieve its full potential if it persuades a dedicated group of scientists to attempt to organize the entire literature of interactions in a rational and comprehensive manner.

David B. Clayson [NB 940 IE]
Toxicology Research Division, Bureau of Chemical Safety
Food Directorate, Health Protection Branch
Health and Welfare Canada
Ottawa (Canada)

Chemical Carcinogens. Activation Mechanisms, Structural and Electronic Factors, and Reactivity. Bioactive Molecules Series, Vol. 5. Edited by *P. Politzer* and *F. J. Martin, Jr.*, Elsevier, Amsterdam 1988. xiv, 366 pp., hard cover, HFl 280.00. – ISBN 0-444-43008-3

Since 1978 an "Interdisciplinary Cancer Research Workshop" has been held annually at the University of New Orleans. Following the tenth meeting it was decided to publish a detailed report to mark the first decade of this conference. This book is the result. It consists of 15 chapters dealing with the most important aspects of research on chemical carcinogenesis: 1. Metabolic and chemical activation of carcinogens: an overview; 2. Reactive metabolites of carcinogens and their interactions with DNA; 3. DNA adducts in vitro and in vivo; 4. Carcinogenic halogenated aliphatic compounds; 5. Chemistry, reactivity and carcinogenicity of chloroethers; 6. Carcinogenicity of ethylene and its derivatives: structural considerations; 7. Reactions of vinyl chloride and its metabolites with bases in nucleic acids and the potential biological consequences; 8. Computational studies of olefin and epoxide carcinogenicity; 9. Irregularities of DNA structure and their effects on DNA replication; 10. Nucleic acid alkylation by *N*-nitroso compounds related to organ-specific carcinogenesis; 11. Nitro-polycyclic aromatic hydrocarbons: structural features, genotoxicity, and risk evaluation; 12. Methyl bay region diol epoxides: key intermediates in the metabolic activation of carcinogenic methylated polynuclear aromatic hydrocarbons; 13. Estrogen carcinogenicity: hormonal, morphologic and chemical interactions; 14. Theoretical implications of the k_e carcinogen-screening test; 15. A microspectrofluorimetric study of the cell's multiorganelle detoxification complex and intracellular carcinogen interactions.

The book reports the latest state of knowledge, since all the chapters have been prepared by acknowledged experts in their respective fields. Direct reproduction of the original typescripts has ensured rapid publication. This technique is known to reduce the likelihood of having a good key-word index, a fact which is also confirmed here: the index is less than four pages in length. Thus, "Aflatoxin" is missing, as is "2-Aminofluorene", to give only two examples. Careful scanning of the detailed contents list is therefore needed in order to find a given subject of interest, and it should have been possible to do better than this! Despite this failing the editors have put together a collection of articles which every chemist who is interested in chemical carcinogenesis should have – and their number should increase. The price of the book, however, is rather high.

Gernot Boche [NB 977 IE]
Fachbereich Chemie
der Universität Marburg (FRG)

Angular Momentum: Understanding Spatial Aspects in Chemistry and Physics. By *R. N. Zare*. Wiley, New York 1988. xi, 349 pp., hard cover, $ 39.95. – ISBN 0-471-85892-7

This book by *Richard Zare* is based on the Baker Lectures which he gave in 1980 at Cornell University, and on lectures given to post-graduate students at Stanford University in the following years. It is a gem amongst the excellent books that have emerged over a period of many years from the celebrated Baker Lectures; many chemists will be familiar with *C. K. Ingold*'s "Structure and Mechanism in Organic Chemistry" (1953), and with *Linus Pauling*'s "The Nature of the Chemical Bond", which were products of the early years of this lecture series.

The aim of the book is to give the reader a sound and detailed understanding of angular momentum in atomic and molecular physics. It begins by introducing angular momentum operators and wave functions. Chapter 2 treats the case of coupling between two angular momentum vectors, and Clebsch-Gordan coefficients. Chapter 3 contains a very detailed treatment of rotational transformations. Chapter 4 deals briefly with couplings involving more than two angular momentum vectors (with 6 and 9 *j* symbols), and Chapter 5 describes tensor operators. Finally Chapter 6 treats the energy levels and wave functions of a rigid rotor. The appendix gives some short Fortran programs for numerically evaluating 3, 6 and 9 *j* symbols.

The book is a masterpiece of didactic clarity. By means of numerous carefully set out exercises and examples from atomic and molecular physics, it enables the reader to work systematically through the material, and to gain an effective "practical" understanding of the subject. In this respect the book differs markedly from the many which adopt a more rigidly formal approach to angular momentum theory. *Richard Zare*'s approach is aimed not at theoretical physicists but at experimentalists, spectroscopists and chemists. Nevertheless, theoreticians too would benefit from the many examples of applications. *Zare* develops all the important basic theory needed, and the book is therefore eminently suitable for individual study or for reading in conjunction with a course of lectures. However, nuclear spin is treated very scantily from a chemist's point of view.

 © VCH Verlagsgesellschaft mbH, D-6940 Weinheim, 1989 0570-0833/89/0707-0932 $ 02.50/0

To sum up it is appropriate to quote from the preface of "Angular Momentum": "This is not the first book on angular momentum theory, but it differs from others in the emphasis placed on making it a learning text for those with a minimum background in quantum mechanics. It also differs in the choice of examples that are drawn almost entirely from atomic and molecular phenomena. I believe that it is not possible to present this material too simply to anyone learning angular momentum theory for the first time. Consequently, many intermediate steps are left in the text, which, to the initiated, may appear inelegant, if not annoying. At the same time this text serves a secondary purpose of being a reference work; the vast majority of formulas needed to solve any problem in angular momentum theory are contained in this book". It only remains for me to add that the book is strongly recommended as a textbook for students and prospective researchers (and is very sensibly priced!). I hope that it will run into many printings.

Martin Quack [NB 972 IE]
Laboratorium für Physikalische Chemie
der Eidgenössischen Technischen Hochschule
Zürich (Switzerland)

Chemiluminescence. By *A. K. Campbell*. Ellis Horwood, Chichester/VCH Verlagsgesellschaft, Weinheim/VCH Publishers, New York 1988. 608 pp., hard cover, DM 280.00.— ISBN 3-527-26342-X/0-89573-501-6; ISSN 0930-3367.

In separate chapters, the author covers the history of chemiluminescence, detection and quantification, bioluminescence, the need for chemiluminescence analysis, measurement of enzymes and metabolites, ultraweak chemiluminescence, indicators for inorganic ions, an alternative to radioactive labels, energy transfer, and "hills and horizons." Five appendices follow: a glossary, names of luminescent organisms, instructions for finding luminescent organisms, chemiluminescence demonstrations, and commercial sources of equipment.

The book contains a very large amount of information, but concentrated on the biological aspects. The subtitle on the cover "Principles and Applications in Biology and Medicine" is a better description. The historical aspects of the subject are developed in considerable depth, and the tabulation of the numerous units for light in Chapter 2 is particularly helpful. The text and figures are free from typographical errors.

The book unfortunately has a number of faults. In spite of the fact that chemiluminescence is my own specialty, I found the book rather tedious to read. On page 233 we are told that Mexican women use bioluminescent adornments in headwear. The same fact appears in a table on page 240, and again in the text on page 241. Lucigenin appears in a table on page 247 as an indicator of "reactive oxygen metabolites", again on page 302 in a table on limits of detection of oxygen metabolite measurement, with no data entry, and in a third table (page 364) as an indicator of reactive oxygen metabolites O_2^- and $^1O_2$. In most of the tables there is only one bit of information per entry. Aside from redundancies, *Campbell* seems unwilling to allow the reader to use his intelligence and imagination to figure out anything for himself. Half of page 242 is a photographed control experiment that shows absolutely nothing. In the appendix on collecting specimens at night, he gives a useful tip that a squirt of KCl solution will stimulate organisms to emit light, but then spoils it by dutifully itemizing a shovel, a bucket, and a flashlight as necessary equipment for any nocturnal expedition.

The author's enthusiasm for the subject is quite evident, and one is inclined to blame the editors for not showing a more businesslike hand in dealing with numerous artistic literary digressions into topics ranging from children's nursery rhymes to Welsh nationalism. Since footnotes do not appear in the text, it is at times difficult to separate fact from entertaining speculation. The encyclopedic scope of the book is probably best suited for biochemists and medical people with limited background who are interested in entering the field.

David Mendenhall [NB 953 IE]
Department of Chemistry and Chemical Engineering
Michigan Technological University
Houghton, MI (USA)

The Chemistry of the Quinonoid Compounds. Vol. 2. Parts 1 and 2. Edited by *S. Patai* and *Z. Rappoport*. Wiley, Chichester 1987. Part 1: xiv, pp. 1–878, hardcover, £ 175.00.—ISBN 0-471-91285-9; Part 2: xiv, pp. 879–1711, hardcover, £ 175.00.—ISBN 0-471-91914-4 (2-volume set £ 325.00.—ISBN 0-471-91916-0)

The first "Patai" on quinones appeared in 1974. Since then the preparative chemistry of quinones has been described in "Houben-Weyl" in 1977 and in 1979, whereas a recent account of naturally occurring quinones is available in Volume 3 of Thomson's series. Thus, after nearly 15 years, the new "Patai" presents a much needed survey that covers the broad spectrum of quinone chemistry. These books are timely and most useful for everyone who is concerned with quinonoids in research and teaching.

Chapter 1 is a general introduction into the theoretical chemistry, such as orbital calculations, spectroscopy and reactivity of simple quinones, quinonemethides, quinoneimines and thioquinones. Three chapters on analytical aspects follow: the first one contains numerous references on NMR, IR, and UV/VIS spectroscopy, as well as on chromatographic and electrochemical methods. Unfortunately actual results are mentioned in only a few instances, and the reader will find it necessary to consult the library in order to uncover the essential information hidden in Chapter 2. Some fundamental publications by *Sealy* et al. on ESR/ENDOR spectroscopy appear to have been ignored. Chapter 3 contains numerous data on electron impact ionization mass spectroscopy of anthraquinones, and Chapter 4 deals with the chiro-optical properties (ORD and CD) of chiral quinones that are of interest primarily to the natural products chemist.

The physical chemistry of quinones is described in five chapters. The impressive development in the field of photoelectron spectroscopy is reflected in Chapter 5, which contains a thorough discussion of quantum chemical calculations and many results in tabular form. This chapter also includes three-, four-, and five-membered ring systems as well as heteroquinonoids. Chapter 6 is a more specialized account of the photo-, thermo-, and piezochromism of bianthrones and bianthrylidenes. Chemiluminescence follows in Chapter 7. A comprehensive account of the electrochemistry is given in Chapter 12. An informative review on the reactions and spectroscopic properties of free radicals is found in Chapter 14, which also contains some examples of biochemically important quinonoids.

The remarkable progress in the synthesis of quinonoid compounds is summarized in Chapter 8. More than 500

original articles are covered in 162 pages, and the subjects are properly ordered under methodological subheadings, such as oxidations, annulations, cyclizations and condensations. Organometallic chemistry is covered as well as protective group chemistry with silylated quinones. One third of the chapter deals with the synthesis of naturally occurring quinones, and some of the reactions discussed earlier are repeated here. Nevertheless, this section illustrates the preparative aspects in a very informative way.

The second large chapter on preparative chemistry (Chapter 11, 182 pages, nearly 800 references) summarizes the use of quinones in organic synthesis. Vinylogous additions, reactions at the carbonyl group, cycloadditions, alkylations and substitutions are discussed comprehensively. Numerous examples are given concerning the use of quinones in heterocyclic synthesis. The biochemist will find many hints to analogies of quinone reactions in biological systems. Preparative and mechanistic photochemistry is reviewed in Chapter 13, which contains an orderly arranged survey of the reactions and results, including many tables. A more specialized account of dehydrogenation reactions of quinones in Chapter 23 deals mostly with DDQ. Many interesting examples of allylic and benzylic oxidations are cited.

Chapter 19 illustrates the importance of isotopically labeled quinones in mechanistic and biosynthetic investigations. The detailed, handbook-style listing of various compounds and their synthesis is most appreciated by those concerned with the preparation and use of labeled quinones. However, some of the examples seem to be unnecessary, such as the synthesis of [7-^{14}C]-geraniol and [7α-^{14}C]-methoxycephalosporin. Also the rather extensive description of general tracer methodology is superfluous. Some overlap exists in the contents of Chapters 19 and 22. The latter, entitled "The Biochemistry of Quinones", actually contains a very thorough and informative review of the biosynthesis of quinones, divided into sections on polyketides, shikimate metabolites and isoprenoids. Further sections deal with the metabolization of quinones into other natural products, e.g. aflatoxins, and with the role of vitamin K in blood clotting.

Several classes of quinonoid compounds are discussed under preparative, mechanistic or theoretical aspects in eleven chapters. The chemistry of *o*-quinonoids is presented in a rather lengthy way in Chapter 9. A discussion on *m*-quinones and related non-Kekulé structures follows in Chapter 10. The preparation and reactions of quinone bis- and monoketals is described in a clear style and with many tables in Chapter 15. Chapter 16 deals with quinhydrones and semiquinones, including their metal complexes, and there is a partial overlap with Chapter 14. Again, redox potentials, pK_a values and UV spectroscopic data are listed in tabular form. Some biologically important semiquinones are mentioned.

The synthesis and reactions of heterocyclic quinones are described in Chapter 17, which contains many references to organometallic reagents. Some overlap exists with the contents of Chapter 8, e.g. the synthesis of the mitomycins. The following Chapter 18 on polymerization reactions deals almost exclusively with substituted *p*-quinodimethanes. It includes an extensive compilation of data on the reaction kinetics. The solid state photochemistry of tetrahydronaphthoquinones is described in the rather specialized Chapter 20. *p*-Quinoneimines, which are particularly useful in industrial applications as coloring materials, are discussed in Chapter 21. Azulene quinones and polycyclic quinones, including annulenes and non-benzenoid systems, are found in Chapters 24 to 26, where some overlap exists in the description of the theoretical aspects in Chapters 24 and 26.

In summary, the new "Patai" presents an impressive collection of articles on nearly all aspects of quinone chemistry. More than 4500 references covering the period between 1974 and 1986 have been evaluated. In accordance with the intention of the editors, the literature prior to 1974 is cited very sparingly. Some subjects were not included in the collection: there is no separate chapter on quinone methides. They are mentioned, however, on several occasions throughout the books. One would have liked to see a separate chapter on quinonoid biopolymers and on chemical modifications of various biopolymers by quinones, though some biochemically important reactions are mentioned occasionally.

The text is quite heterogenous with respect to style and density of information. Some very specialized topics are distributed among some broad and general overviews. Eventually, an attempt to achieve more consistency in some chapters might lead to a smaller degree of overlapping. A further suggestion to the editors is that each volume should include a list of abbreviations. As it is now, searching for the meaning of abbreviations used in some chapters can become a time-consuming task. The subject index is not extensive enough, e.g. the key-word "daunorubicin" does not lead to the important data in Chapter 14 (p. 893). The sequence of chapters should be arranged more consistently with respect to the general topics.

Technically, the books are thoroughly prepared. Only a few errors or sloppy formulations were noted (e.g., on p. 495 *c,c*- and *t,t*-2,4-hexadienes... should read: *ZZ*- and *EE*...; p. 1301: 25-iso-caproyl... should read 2*S*-isocaproyl). Very few corrections are necessary in the reaction diagrams and formula schemes (e.g., p. 590, eq. 168: it is not evident from the formulas that the oxidative deamination leads to a 2-keto sugar which is then reduced to the 2-deoxy sugar shown; p. 652, eq. 359: the formula of the butadiene derivative is incorrect in the original paper; p. 681, eq. 452: the formula of homophthalimide is wrong). According to the latest published work, the mechanism of the cytotoxic action of mitomycin on p. 1058 should be revised. Nevertheless, these are minor mishaps which do not at all diminish the value of this important volume. The "Quinone Patai" will find its place in the libraries of most research and teaching institutions. Unfortunately, the high price is prohibitive for purchase by individuals. The list of those who will greatly appreciate these books includes scientists from the fields of physical and synthetic organic chemistry, natural products and pharmaceutical chemistry, and, last but not least, organometallic and biological chemistry.

Martin G. Peter [NB 944 IE]
Institut für Organische Chemie und Biochemie
der Universität Bonn (FRG)

Principles of Organometallic Chemistry. 2nd Edition. By *P. Powell*. Chapman and Hall, London/New York 1988. xv, 415 pp., paperback, £ 13.95. – ISBN 0-412-27590-2. – hard cover, £ 13.95. – ISBN 0-412-27580-5

Anyone who, like this reviewer, was a chemistry student in the early 1970s and was fascinated by the then still young and rapidly developing subject of organometallic chemistry, will clearly remember the first edition of this book, published in 1968 with four authors (*G. E. Coates, M. L. H. Green. P. Powell* and *K. Wade*). That, together with its German translation published in 1972, was almost the only textbook on organometallic chemistry tailored to the needs of students, unless one was prepared to use the two-volume "Coates".

In contrast to that time, there now exists a pleasingly large choice of rival books of varying size and aims, with which this new edition must compete. Of course, the book no longer has a lot in common with the first edition of twenty years ago – apart from its title, little more remains than the subdivision of the contents. Regrettably, however, Chapter 1 ("General Survey") has scarcely been revised. A historical summary of 26 lines, a mini-paragraph (11 lines) on physical properties, an outdated survey of types of bonding, and some very general remarks concerning the stability of organometallic compounds, fail to meet the level of treatment that is nowadays expected of a textbook. Fortunately this chapter is not typical of the rest of the book, and the topics on which it touches are treated in much greater deal and more accurately in later chapters.

The following three chapters (130 pp.) deal with the organometallic chemistry of the elements in Main Groups 1 to 5 and Sub-Groups 1 and 2. After a general discussion of the most important methods of synthesis, arranged according to the groups in the Periodic Table, these chapters deal, at a level and with an amount of detail appropriate for an introductory textbook, with the preparation, structures, reactions and uses of the various classes of compounds. Even such topical matters as the MOCVD (metal organic chemical vapor deposition) technique, arene complexes of Main Group elements, organo-polysilanes, and compounds with low coordination numbers, are briefly covered. The section on "$p_\pi - p_\pi$ Bonding in Compounds of Groups 4 and 5" is outdated, and too short even for an introductory textbook (despite the title, no Group 5 compounds with $p_\pi - p_\pi$ bonds are included).

Next comes a chapter of very heterogeneous content, which is concerned mainly with the chemistry of metal carbonyls and phosphine complexes, while also including the mechanisms of substitution and addition reactions of metal complexes. This is followed by a chapter on the classification of ligands and the treatment of the bonding of π-ligands by MO theory, and a short introduction to complexing by fragment orbitals (although regrettably the isolobal concept is not mentioned). These chapters lead into the organometallic chemistry of the transition metals, classified according to ligand types. The treatment of alkyl and aryl metal complexes is very comprehensive and up-to-date, even including C-H activation. In contrast, the discussion of carbene and carbyne complexes only gives the situation up to about 1975, apart from a mention of the synthesis of vitamin E by *Dötz*; for example, the only mention of a Schrock carbene complex is one structural formula with no related text. An appropriate amount of space (about 100 pp.) is devoted to metal π-complexes, covering the most important aspects, though largely ignoring heteroalkene and heteroarene complexes. A good feature of this section is the discussion of dynamic processes, the understanding of which is greatly helped by the inclusion of figures showing typical NMR spectra.

The book ends with three comparatively short chapters on cluster compounds, on mechanisms of industrial processes which use homogeneous catalysts, and on organoactinides and -lanthanides. The first of these three chapters seems out of place in an introductory book on organometallic chemistry, and the last chapter, with only five pages, does not do justice to the growing importance of this class of compounds. However, the chapter on catalysis is appropriate to the importance of the topic and is up-to-date.

The book declares itself to be aimed at undergraduates. With these readers in mind the author lists selected review articles at the end of each chapter, but no references to original papers. Also at the end of each chapter are a few problems of varying degrees of difficulty, mostly examination questions from British universities. The preface states that a book of answers is available from the publishers.

The right selection of material for an introductory textbook and its proper weighting is no easy task at the present stage of development in organometallic chemistry, and different authors have different approaches. In my view the level of treatment in this book is much more uneven than in other comparable books, and the discrepancies in the extent to which the different chapters are up-to-date have already been mentioned. To the question as to whether the book fills a gap, the answer must be a definite no. If confronted with the choice I would prefer, even for beginners, "Organometallchemie" by *C. Elschenbroich* and *A. Salzer* (also now available in an English translation), which despite its somewhat wider subject coverage gives a clearer, more up-to-date, and better balanced treatment.

Ulrich Schubert [NB 969 IE]
Institut für Anorganische Chemie
der Universität Würzburg (FRG)

Kinetics of Electrochemical Metal Dissolution. (Series: Studies in Physical and Theoretical Chemistry, Vol. 47). By *L. Kiss*, Elsevier, Amsterdam 1988. 260 pp., bound, HFl 200.00.—ISBN 0-444-98964-1

The dissolution and precipitation of metals is the subject of numerous research projects in industry and universities. Thermodynamics gives information as to whether or not a particular reaction can occur. However, it is much more important to know the rate at which a metal is dissolved, e.g. so as to be able to predict the lifetimes of industrial components. Kinetics provides answers to these questions. The appearance of a book dealing specifically with this subject is therefore to be welcomed.

The book is concerned essentially with the uniform dissolution of pure homogeneous metals in solutions of electrolytes. Other types of metal dissolution such as stress crack corrosion (season cracking) or the selective corrosion of alloys are not treated. The book has a logical structure, and at the beginning of each chapter the relevant fundamentals are explained so that the kinetics even of complex electrode reactions can be understood. Much of the cited literature consists of papers from Eastern Europe, some of which are published in Russian. Consequently the English translation of this Hungarian work is of particular interest to readers in the West, enabling them to get an overview of research in those countries on the theme of the book. Published work up to 1983 is covered.

The first chapter deals with equilibria in chemical and electrochemical reactions. The calculation of electrode potentials and potential-pH diagrams is clearly described in textbook style. The author has taken care throughout to ensure that the reader can follow his reasoning, and the book can therefore be recommended as a student text. The second chapter is concerned with the kinetics of electrode processes. The fundamentals of the kinetics are presented clearly and thoroughly. In addition to the penetration and diffusion overpotentials treated here there are, however, other types of overpotentials which, although unimportant for metal dissolution, are certainly important for metal precipitation (e.g. the crystallization overpotential). These could at least have been mentioned briefly. The high level of generality in the formulas and equations means that there are a large number of qualifying statements which require much vigilance on the

part of the reader, especially for complicated reaction equations. These general formulations (e.g. where diffusion and penetration overpotentials are present simultaneously in a reaction with several steps) are made specific to particular situations depending on which is the rate-determining step in the reaction. It would have been desirable to illustrate the relevance of these distinctions for practical situations by giving more examples.

Whereas the fundamentals of metal dissolution are treated in great detail, the dependence of the kinetics of dissolution on the microstructure of the metal surface is unfortunately not discussed. This fails to take account of recent findings that the inhomogeneous nature of real surfaces (points where dislocations meet the surface, grain boundaries, semicrystalline regions, etc.) has crucial effects on the kinetics of metal dissolution. The experimental techniques using rotating disk or disk-and-ring electrodes which are important in electrochemical investigations are thoroughly described. In contrast, however, the various mechanisms of iron dissolution are treated only briefly in relation to their importance, despite the fact that a great deal of detailed work on this topic has been published.

The chapters on the passivity of metals and their transpassive dissolution are well and clearly written. It would also have been of interest to include a more detailed discussion of the effects which the build-up of the passive layer has on the kinetics of dissolution. Treating the transpassivity of metals together with the occurrence of pitting corrosion (p. 173) is of doubtful value, as the two mechanisms are fundamentally unrelated. It would have been better to have included a separate chapter on the kinetics of pitting corrosion.

The final chapter describes the application of kinetics to corrosion calculations, well illustrated by figures. Here again it becomes necessary to distinguish between a number of different cases, showing, for example, the influence of the oxidizing medium or of diffusion processes on calculations of the corrosion current or of the free corrosion potential. The author illustrates very well the usefulness of the polarization resistance for determining corrosion rates, and also details the sort of errors that can arise when the anodic or cathodic partial reactions are no longer controlled purely by ion penetration. The discussion of the different possible types of corrosion protection turns out to be rather brief; however, the book does not set out to cover this topic.

To summarize, this book discusses all aspects of electrode kinetics that are important in the dissolution of pure undeformed metals. Readers who already have some previous knowledge of corrosion will find here a very useful introduction to the kinetics of metal dissolution, a topic which is not covered in such detail in mainstream books in the field.

Ralf Feser [NB 949 IE]
Max-Planck-Institut für Eisenforschung
Düsseldorf (FRG)

Surfactant Science and Technology. By *D. Myers*. VCH Verlagsgesellschaft, Weinheim/VCH Publishers, New York 1988. xiv, 351 pp., hard cover, DM 88.00.– ISBN 3-527-26695-X/0-89573-339-0

The physical chemistry of surfactant solutions is a topic which continues to attract increasing attention. For this reason the appearance of new textbooks aimed at enabling the reader to enter this field is not unexpected.

In the book reviewed here the author has succeeded well in that aim. The easily readable English text is concisely written, and helps towards a sound understanding of the phenomena described. Although it is not clear why the word "technology" appears in the title, this is, in fact, a good textbook which contains 466 literature references and a bibliography listing 35 books.

The contents are arranged in eight chapters on the following subjects: Overview; The Organic Chemistry of Surfactants; Micellization; Solubilization, Microemulsions and Micellar Catalysis; Surface Activity and the Liquid/Vapor Interface; Emulsions; Foams; Surfactants at the Solid/Liquid Interface.

An exhaustive coverage is not to be expected of a textbook. Thus, for example, rheology is not included at all, and consequently viscoelastic solutions and gels are not treated. Also the phase behavior at the inversion point is not explained in accordance with the most recent findings.

The quality of the book stands out above that of many rapidly produced publications, and it should achieve a wide readership.

Gerhard Platz [NB 958 IE]
Institut für Physikalische Chemie
der Universität Bayreuth (FRG)

Registered names, trademarks, etc. used in this journal, even when not marked as such, are not to be considered unprotected by law.

© VCH Verlagsgesellschaft mbH, D-6940 Weinheim, 1989. - Printed in the Federal Republic of Germany by Konrad Triltsch Druck- und Verlagsanstalt Würzburg.

All rights reserved (including those of translation into foreign languages). No part of this issue may be reproduced in any form — by photoprint, microfilm, or any other means — nor transmitted or translated into a machine language without written permission from the publishers. Only single copies of contributions, or parts thereof, may be made for personal use. This journal was carefully produced in all its parts. Nevertheless, authors, editors and publisher do not warrant the information contained therein to be free of errors. Readers are advised to keep in mind that statements, data, illustrations, procedural details or other items may inadvertently be inaccurate.

Valid for users in the USA: The appearance of the code at the bottom of the first page of an article (serial) indicates the copyright owner's consent that copies of the article may be made for personal or internal use, or for the personal or internal use of specific clients. This consent is given on the condition, however, that the copier pay stated per-copy fee through the Copyright Clearance Center, Inc. (CCC), for copying beyond that permitted by Sections 107 or 108 of the U.S. Copyright Law. This consent does not extend to other kinds of copying, such as copying, for general distribution, for advertising or promotional purposes, for creating new collective works, or for resale. For copying from back volumes of this journal see 'Permissions to Photo-Copy: Publisher's Fee List' of the CCC.

Editorial office: Postfach 101161, D-6490 Weinheim, Federal Republic of Germany, Telephone (06201) 602255, Telex 465516 vchwh d, Telefax (06201) 602328.

Editor: *Peter Gölitz*

Associate editors: *D. I. Loewus, A. Stimson.* **Editorial assistant:** *E. Schweikart*

Publishers: VCH Verlagsgesellschaft mbH. (Managing Director: *Hans Dirk Köhler*), Pappelallee 3, D-6940 Weinheim, Federal Republic of Germany.

Advertising office (Advertising Manager *R. J. Roth*): Postfach 101161, D-6940 Weinheim, Federal Republic of Germany, Telephone (06201) 606130, Telex 467155, Telefax (06201) 606184.

ADVANCED MATERIALS

The European Materials Research Society (E-MRS)

Editorial Essay

By Eberhard F. Krimmel*

It was on February 17, 1986, when the European Materials Research Society (E-MRS) was registered at court as a non-profit making learned society with its seat at the "Centre de Recherches Nucléaires" in Strasbourg, France. The history of the Society, however, started many years before when a group of French scientists used to discuss once a year new results and problems of ion implantation, laser and electron beam annealing, etc.

The number of persons participating in the symposia organized by this group of very active scientists continuously increased, the symposia found international recognition and were greatly in demand. Seeing this encouraging development a small circle of scientists from different countries within Europe who were attending one of the symposia in 1982/83 realized that it was time to become organized at the European level. The society to be founded should have an interdisciplinary character and be open to all scientists such as chemists, engineers, physicists, etc., interested and working in research and development within materials science. This nucleus of scientists became the basic unit of the European Materials Research Society. The enthusiasm of the involved scientists, most of them very young scientists, is such that the Society runs on a honorary basis, and although perfectionism is not requested vitality is. The philosophy is that it doesn't matter if a young scientist makes a mistake as not even experienced ones are perfect and in any case mistakes can be corrected!

The categories of membership of the Society are as follows:

First of all there are the ordinary members. These are physical persons active in the domain of materials science and technology or people who contribute to the development of these fields of science. Another catagory concerns sustaining members which are corporate persons such as associations, societies, groups, laboratories, and industrial companies. They must show evidence of supporting activity.

In the United States a society, the Materials Research Society (MRS), was already active with a similar program to that proposed by the European scientists. It was obvious that the American colleagues should be contacted in order to establish international links for the benefit of everybody. Thus, the idea emerged to establish an international federation of autonomous societies having similar structures and aims, all being devoted to materials research and development. These activities concern societies in the USA, Europe, Australia, China, Japan, South America, India, etc.

The E-MRS was founded with the knowledge that over the turn of the century the social future of Europe will depend on the progress that is made in new technologies especially in the development of the materials sciences. These new technologies must also be ecologically beneficial. The aim of the E-MRS is to contribute to this progress by promoting relevant efforts. Chemists, engineers and physicists are scientists who work in different fields and at different levels of a very complex whole. They have to cooperate and intercommunicate to obtain the results which benefit a growing society and which guide the development of our civilization and culture. Thus the E-MRS provides a forum to these scientists for efficient and rapid intercommunication. To this end, the E-MRS organizes conferences, workshops, summer schools, etc. which cover all disciplines of materials science such as ceramics, metals, semiconductors, composites, polymers, and biomaterials. Symposia arranged at short notice on present-day topics, e.g. high-T_c superconductors demonstrate the vitality and quick response of the Society.

In order to emphasize the idea of an unified Europe the main conferences of the E-MRS take place at the seat of the Council of Europe in Strasbourg. Workshops or co-sponsored meetings may be held in other places. The plenary sessions of the main conferences in Strasbourg host the best scientists as speakers on topics which reflect key areas of research on an interdisciplinary level. This years meeting, the largest yet, was attended by 850 people from many nations. Professors Friedel (University of Paris, France) and von Klitzing (Max Planck Institute for Solid State Research, Stuttgart, FRG) led off the extremely strong program of more than 450 lectures, posters and discussion sessions which lasted for four days. The educational potential of the program is always high and therefore special attention has been directed to make it feasible for students to attend the conferences, and publication of conference proceedings and reports serves to disseminate the latest scientific findings to a broad audience.

The interdisciplinary nature of the cooperation and scientific exchange between university and industry R & D efforts is the basis of the E-MRS. Thus the E-MRS coordinates "European Networks" in the field of materials research. At present, 16 Networks covering various fields in electronic and non-electronic materials research and development are in action and more than 200 industrial and university laboratories are involved. Brief details are given in the box.

[*] Prof. Dr. E. F. Krimmel
Mendelssohnstraße 7
D-8023 Pullach (FRG)

ADVANCED MATERIALS

European Networks of the E-MRS

Non-electronic Materials:

Network 2: Coordinator: Balkanski; Title: Solid state ionics.
Network 3: Coordinator: Fredriksson; Title: Crystal growth and solidification of metals.
Network 4: Coordinator: Bøttiger; Title: New methods in metastable alloy production.
Network 8: Coordinator: Muster; Title: Biomaterials.
Network 10: Coordinator: Chadwick; Title: Pressure casting and metal matrix composites.
Network 12A: Coordinator: Rizzuto; Title: High-T_c massive superconductors.
Network 13: Coordinator: Legros; Title: Materials research in microgravity.
Network 15: Coordinator: Waysand; Title: Materials for low temperature detectors.

Electronic Materials:

Network 1: Coordinators: Boyd, Krimmel; Title: Laser chemistry, beam and photon processing.
Network 5: Coordinators: Sirtl, Wagner; Title: High-resolution, high-sensitivity analysis of semiconductors.
Network 6: Coordinator: Bentini; Title: Ion beam processing of electronic materials.
Network 7: Coordinator: Triboulet; Title: II–VI Telluride-based semiconductors.
Network 9: Coordinators: Wettling; Title: Gallium arsenide.
Network 11: Coordinator: Zerbi; Title: Polyconjugated polymers.
Network 12B: Coordinators: Bongers, Habermeier; Title: High-T_c thin film superconductors.
Network 14: Coordinator: Quillec; Title: Indium phosphide-based semiconductors.

Further details are available from the author.

Also along these lines the E-MRS attaches importance to a fruitful cooperation with other more specialized societies. Such cooperation is already successfully taking place bringing bilateral benefits.

A further topic of activity concerns the critical analysis of the educational situation in the different parts of Europe. The necessity has been recognized of offering, for example, short intensive courses in the various fields of materials science, to individuals not normally having such training possibilities and to other interested parties, including students, to improve their professional skill and to broaden their area of expertise. Up to now more than 10 European intensive courses have already been implemented at the initiative of the E-MRS, exemplified by the Biomaterials course which was part of the Strasbourg meeting.

The E-MRS has been rapidly growing over the last three years and it doesn't take a clairvoyant to see that this will continue. 1992 is coming soon and the importance of materials science is just beginning to be realized.



Eberhard Krimmel studied physics at the University of Tübingen, FRG being awarded a diploma in 1958 in molecular spectroscopy and a Ph.D. in electron interferometry (1961). After a stay of two years at the University of Illinois, Urbana, USA as an Assistant Professor studying radiation damage in metals he started a career with Siemens in Munich, FRG as manager of a research department concentrating on semiconductor and laser technology (1970–1987). From 1982–1985 he was a part-time Professor at the Rand Afrikaans University, South Africa and since 1986 has been an honorary Professor at the University of Frankfurt/Main continuing his interest in semiconductors and ceramics. He was a founding member of the E-MRS (1983) and from 1985–1989 was its Secretary.

An extra large ADVANCED MATERIALS "Materials Science in Britain" is planned for the double issue August/September to coincide with the British Association for the Advancement of Science (BAAS) meeting to be held in Sheffield (UK) September 10.–14. The issue will contain five review articles from top British materials scientists including *B. A. Joyce* "Tailoring Semiconductor Materials to Atomic Dimensions" and *J. M. Thomas* "Catalysts". *R. W. Cahn, G. W. Gray* and *C. J. Humphreys* (amongst others) contribute to the other sections of the journal.

ADVANCED MATERIALS

Dichroic Dyes and Liquid Crystalline Side Chain Polymers**

Anisotropic Glasses
Optical Storage
LC-Displays

By Hans-Werner Schmidt*

1. Introduction

Thermotropic liquid crystalline (LC) side-chain polymers have attracted much attention in the last few years. In LC-side-chain polymers, rod-like mesogenic units are attached as side groups to the polymer backbone. The potential of LC-side-chain polymers is based on the unique combination of specific polymer properties with the anisotropic physical properties of conventional low molar mass liquid crystals. The developments in the area demonstrate the practical interest in this new class of materials, especially for optical and opto-electronic applications. Several review articles and books have been published describing the synthesis, characterization, properties and potential applications of LC side-chain polymers.[1]

The reason for the interest in liquid crystalline systems which contain dissolved or incorporated dichroic dyes is that the anisotropic order of liquid crystalline phases causes the molecular orientation of the guest molecules and the anisotropic properties of these guest molecules can be detected. The interplay of the molecular alignment with the different possibilities for macroscopic orientation is the basis for several spectroscopic methods as well as for commercial display applications. For instance, dichroic dye molecules or fluorescent dyes have been used as probes to study order phenomena in different thermotropic and lyotropic systems.

Mixtures of dichroic dyes, dissolved as guest molecules in low-molar-mass liquid crystals, are used in displays operating on the principle of dichroism. The electro-optical effect, a color intensity change, is based on the cooperative alignment of the dye in the host phase and the dependence of absorption on the macroscopic orientation. This effect is schematically demonstrated in Figure 1 for a nematic guest-host system with positive dielectric anisotropy in a typical Heilmeier cell.[2]

In the off-state (left) the nematic phase and the dye molecules are oriented parallel (homogeneously planar) to the glass plates and parallel to the polarization plane of a polarizer. If the transition moment of the absorption of visible light is in the same direction, maximum absorption occurs. In the on-state (right) the molecules are aligned perpendicular to the glass plates by an electric field. As a result, absorption is low. The areas of the display in the on-state appear colorless, while the ones in the off-state are colored. Suitable dichroic dyes for application should have high order parameters, high solubilities, high absorption coefficients and good photochemical stability. A large number of guest-host mixtures have been investigated and correlations between dye structure and properties have been discussed.[3]

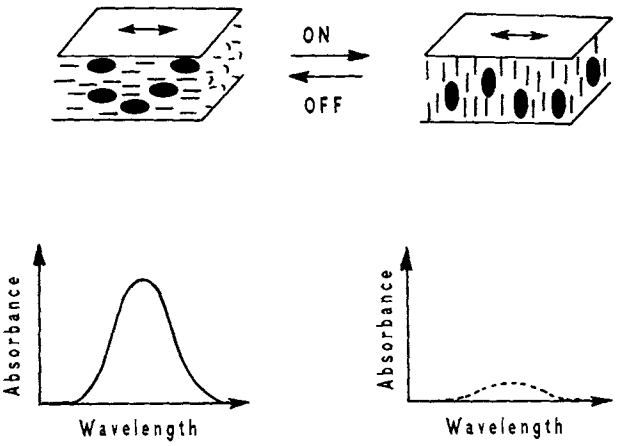


Fig. 1. Schematic representation of the on- and off-states for a guest-host system ($\Delta\varepsilon$ positive) in a Heilmeier cell, and the corresponding absorption spectra. ●: Dichroic dye moiety; ——: mesogenic unit; ↔: polarization plane.

This article focuses on the combination of LC side-chain polymers with dissolved or incorporated dichroic dyes but the results and conclusions are transferable to other types of guest molecules. The structure and properties of different dye containing liquid crystalline systems will be discussed and particular attention is given to copolymers with dichroic dyes and mesogens as side groups. Principal differences to low molar mass guest-host mixtures will be demonstrated and some potential applications of these materials such as dichroic polymer films, media for optical information storage or use as guest components in low molar mass liquid crystals for displays will be discussed.

[*] Dr. H.-W. Schmidt
FB Physikalische Chemie – Polymere, Philipps-Universität
Hans-Meerwein-Strasse, D-3550 Marburg (FRG)

[**] The author is grateful to Dr. *H. Eilingsfeld*, Dr. *K.-H. Etzbach*, Dr. *G. Wagenblast* (BASF AG, Ludwigshafen) and to Dr. *G. Baur*, and Dr. *R. Kiefer* (Fraunhofer-Institut für Angewandte Festkörperphysik, Freiburg) for fruitful collaboration and to Prof. *H. Ringsdorf* (University of Mainz) for his continuous support.

ADVANCED MATERIALS

2. Dichroic Dyes in Combination with LC-Side-Chain Polymers

Guest-host systems based on LC-side-chain polymers can be classified into three different types. The schematic structures of these types are shown in Figure 2.

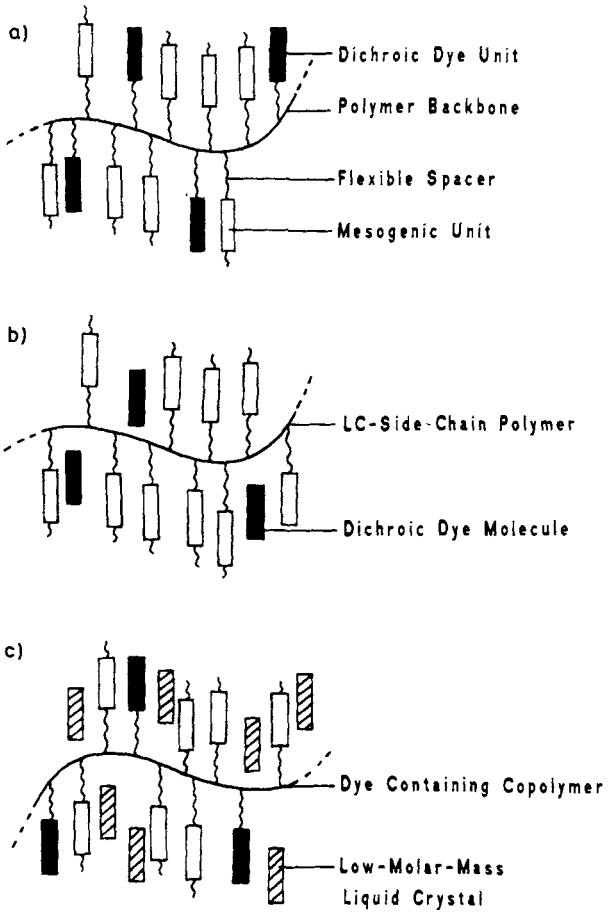


Fig. 2. Schematic structures of host-guest systems in combination with LC-side-chain polymers. a) LC copolymers with dichroic dyes and mesogens as side groups. b) Dichroic dyes dissolved as guests in LC-side-chain polymers. c) Dye containing copolymers as guests in low molar mass LC hosts.

A polymeric guest-host system is a copolymer with dichroic dyes and mesogens as side groups (Fig. 2a). The mesogenic groups as well as the dichroic dyes are covalently attached via flexible spacers to the polymer backbone.[4] This covalent bonding of the mesogenic units and dyes causes significant differences to low-molar mass mixtures. In the case of copolymers, liquid crystalline materials can be prepared with high dye concentrations, but the solubility of dichroic dyes is limited in low molar mass mixtures. In addition, the dye content to the copolymers is independent of the temperature and the type of mesophase. Another important difference is the fact that the order of the liquid crystalline melt does not change for LC-side-chain polymers when they are frozen in the solid state. As a result, the material becomes an anisotropic glass.[5] In contrast to this behavior, the liquid-crystalline order of low molar mass guest-host mixtures is generally destroyed upon cooling by crystallization.

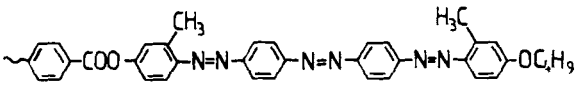
Another approach is the dissolution of dye molecules as guests in LC-side-chain polymers (Fig. 2b).[4d, 5, 6] This approach is limited by the solubility of the dye in the polymer matrix, but is suitable for the use of low dye concentrations. However, it can happen that the dye molecules phase separate and recrystallize above the glass transition temperature.

LC-copolymers with dichroic dyes and mesogens as side groups can be dissolved as guest components in low molar mass liquid crystals (Fig. 2c).[4c] The use of dye containing copolymers in mixtures is a general concept which achieves sufficiently high concentrations of dyes which have otherwise very poor solubility in low molar mass liquid crystals. The mesogenic side groups can be regarded as solubility enhancers for the dye moieties. The properties of such guest-host mixtures with respect to possible display applications are discussed in section 6.

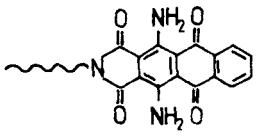
3. Synthesis and LC-Behavior of Dye Containing Copolymers

LC-copolymers with dichroic dyes as side groups can be obtained using the same synthetic procedures as for LC-side-chain polymers. The majority of published copolymers are polyacrylates, synthesized by a free radical copolymerization of mesogenic monomers and monomeric dyes. Another method is the reaction of mesogenic monomers and dyes containing terminal alkene groups with poly(methyl hydrogen siloxane) resulting in a dye containing copolymers with a siloxane backbone. Some functional groups of the dye moiety cause these procedures to fail and other polymerization techniques such as group transfer polymerization, or polycondensation procedures are necessary.

Azo- (mono, bis and tris)-, stilbene-, anthraquinone-, violanthrone-, and spiropyrane-dyes have been investigated in dye-containing LC side chain copolymers.[4] Of particular interest was the preparation of 'black' copolymers which absorb over the entire spectrum of visible light. Such copolymers can be prepared by the attachment of several dyes to one polymer backbone. Examples of dichroic dyes which are covalently attached in LC-side-chain copolymers are the yellow tris azo dye **1**,[4b] the blue anthraquinone dye **2**[4b] and

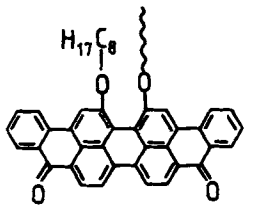


1

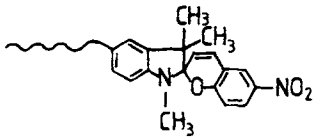


2

the violanthrone dye **3**.[7] All three dyes are known to have good photochemical stability and high absorption coefficients. *Cabrera* et al. investigated LC-side-chain copolymers with the photochromic spiropyrane dye **4**.[4e,f]

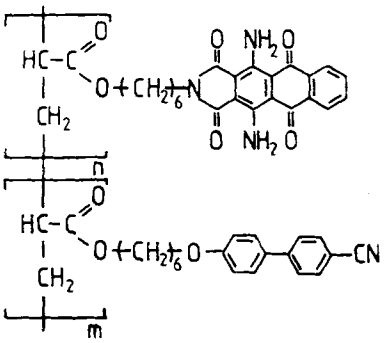


3



4

The liquid crystalline behavior of the copolymers depends on the dye content and on the molecular structure of the dyes. It was observed that anthraquinone- and spiropyrane-dyes generally destroy the mesophase. In contrast, the tris azo dye **1** increases the clearing temperatures and strongly broadens the mesophase range as the dye content increases. This behavior was found to be independent of the investigated mesogenic side groups in the copolymer. The liquid crystalline behavior of a polyacrylate copolymer **5** with the blue



5

anthraquinone dye **2** and a cyanobiphenyl mesogenic unit as side group will be discussed in more detail. The differential scanning calorimetry (DSC) curve of a copolymer with a dye-content of 2 wt.-% is shown in Figure 3.

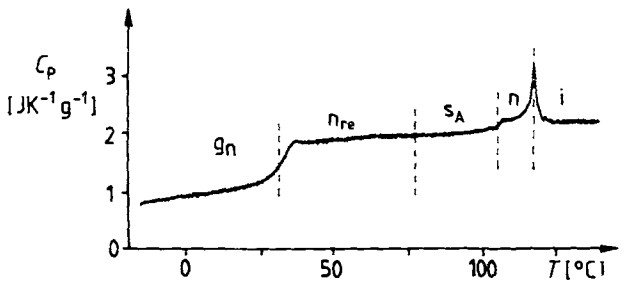


Fig. 3. DSC-heating curve of the anthraquinone-containing LC copolymer **5** (dye content 2 wt.-%). i: isotropic, n: nematic, s_A: smectic-A, n_{re}: reentrant nematic. g_n: nematic glass.

The copolymer has a glass transition at 36 °C and shows several additional endothermic transitions. The following LC behavior was observed using a polarizing microscope. On cooling from the isotropic melt, a nematic phase is formed at 120 °C and at 107 °C a transition to a smectic-A phase is observable. On further cooling a reentrant nematic phase is formed at about 75 °C and becomes a nematic glass below the glass transition temperature. The LC homopolymer without dye has the same phase sequence.[8] With increasing dye content the formation of the smectic-A phase is suppressed and copolymers with more than 10 wt.-% anthraquinone dye are only nematic. The phase diagram for copolymers with a dye content of up to 36 wt.-% is shown in Figure 4. The nematic to isotropic transition is lowered and

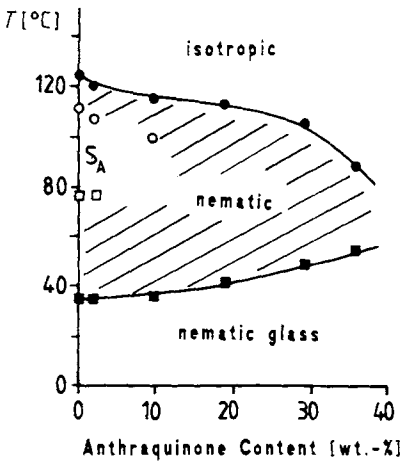


Fig. 4. Influence of the anthraquinone content on the LC behavior of copolymer series **5**. Transition temperatures plotted versus copolymer composition (wt.-% of the dye monomeric unit). ■: glass transition. □: transition reentrant nematic to smectic-A. ○: transition smectic-A to nematic. ●: transition nematic to isotropic.

the glass transition is increased with increasing anthraquinone content. Remarkably the copolymer with 36 wt.-% anthraquinone dye is still nematic. It should be mentioned that similar anthraquinone dyes in low molar mass nematic hosts in general have poor solubilities (below 0.5 wt.-%).

These results demonstrate that it is possible to synthesize liquid crystalline copolymers containing anthraquinone dyes, or other types of dichroic dyes, with very high dye concentrations. These high dye concentrations allow the preparation of thin LC polymer films (down to 1 μm thickness) with adjustable optical densities and absorption properties.

4. Orientational Order in Anisotropic Glasses

The microscopic LC order of side chain polymers can be macroscopically oriented by surface effects, or by magnetic or electric fields in a similar manner to low molar mass liquid crystals. Important is that the macroscopic orientation can

ADVANCED MATERIALS

be transferred to the solid state upon cooling below the glass transition temperature. An optically uniform, transparent, anisotropic glass is obtained. This was demonstrated for nematic as well as smectic glasses. If dye containing LC side-chain copolymers are used, dichroic polymer films are obtained. The oriented films can be prepared between glass plates in a display type cell configuration with a thickness of 0.5 mm to 1 μm (typically 10–20 μm). Uniform films on a substrate are also obtainable by spin coating.

The orientational order of dyes in the anisotropic glasses can be determined from the optical absorbance spectra parallel $A_{\parallel}$ and perpendicular $A_{\perp}$ to the direction of the homogeneous planar orientation (see Fig. 1, on-state). The dichroic ratio R and the order parameter of the dye S_D, characterizing the orientational order of the transition moment of the dyes, are calculated using the following expressions.[3] The order parameters vary from zero for an isotropic system to one for a perfectly aligned system.

$$R = \frac{A_{\perp}}{A_{\parallel}} \qquad S_D = \frac{A_{\parallel} - A_{\perp}}{A_{\parallel} + 2A_{\perp}}$$

As in low molar mass host-guest mixtures the dye structure and type of the liquid crystalline phase have an influence on the order parameter. In Figure 5a the absorption spectra

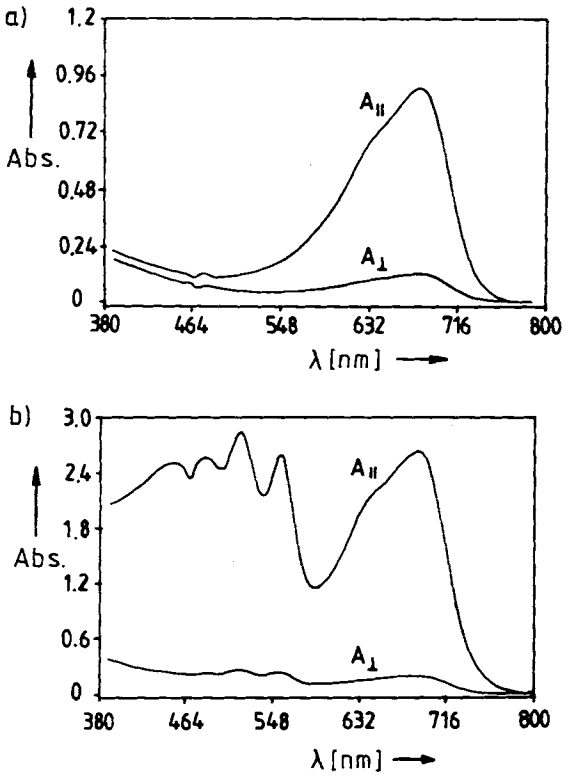


Fig. 5. a) Absorption spectra taken parallel ($A_{\parallel}$) and perpendicular ($A_{\perp}$) to the alignment direction of the anthraquinone containing copolymer **5** in an oriented nematic glass. b) Absorption spectra for a 'black' copolymer with three dyes (yellow tris azo dye, red and blue anthraquinone dyes) in an oriented smectic-A glass.

$A_{\parallel}$ and $A_{\perp}$ for copolymer **5** with the blue anthraquinone dye in the nematic glass are shown. The dichroic ratio is 7.6 and the corresponding order parameter 0.69. The order parameter of the mesogenic side group (0.71) was determined by IR-dichroism measurements, using the vibration of the cyano group attached to the biphenyl unit. The observed S_D values are comparable with those for similar anthraquinone dyes dissolved in low molar mass nematics. Higher dye order parameters are obtainable in smectic glasses, where the host phase has a more ordered structure. The same anthraquinone dye has an order parameter of 0.78 in a smectic-A glass of a polyacrylate with methoxyphenylbenzoate side groups (g 23 s_A 86 n 106 i).

The shape of the dyes and their fixation has also an important influence on the order parameter. The covalently attached rod-like tris azo dye **1** has an order parameter of 0.72 in the nematic glass and 0.84 in the smectic-A glass. For the more plate-like violanthrone dye **3**, which is attached perpendicular to its main molecular axis, lower order parameters were observed as expected. The S_D value in the nematic glass of a polyacrylate with cyanophenylbenzoate side groups (g 32 n 120 i) is only 0.42. In the smectic-A glass (g 30 s_A 93 n 119 i) the order parameter is 0.60.

Figure 5b shows the absorption spectra for a 'black' LC-side-chain copolymer in an oriented smectic-A glass. In this copolymer three dyes are covalently attached to the same polymer backbone: a yellow tris azo dye, and a red and a blue anthraquinone dye. The overall dichroic ratio R for the dyes from 400 to 750 nm is about 10.8.

These examples demonstrate that optically uniform dichroic polymer films, with high dichroic ratios, can be prepared from dyes containing LC-side-chain copolymers. Higher order parameters and dichroic ratios should be obtainable by optimizing the dye structure and the mesogenic side groups.

5. Optical Information Storage with Dye Containing Copolymers

LC-side-chain polymers are considered as one possible organic medium for non-erasable and erasable optical information storage.[9] The interest in this class of materials is based on the various states of order and orientation which they exhibit combined with the possibility of storing defined structures below the glass transition temperature or in highly viscous smectic phases. Storage in low molar mass liquid crystals requires a nematic phase and an additional viscous smectic phase. LC-side-chain polymers allow storage of information in nematic and smectic glasses. Optical storage effects, based on thermal (heat mode)[10] and photochemical (photon mode)[4e,f,11] mechanisms, have been reported for LC-side-chain polymers. Photochemical reactions in cholesteric polysiloxanes doped with benzophenone or carbon black were used for optical write-once storage.[12]

Optical storage based on thermal effects is generally related to a texture change in the LC film. This texture change can be a formation of scattering regions or a defined deformation of the LC-structure with or without the effects of additional external fields. The thermal energy required for a texture change can be generated on the surface or within the active LC film by dye molecules. The latter process has the advantage of higher sensitivity and better resolution. Dye molecules which are either dissolved[10b, 10d] or, like in our work, chemically incorporated into LC-side-chain polymers, can be used for thermal addressing. The covalent fixation of the dye moieties and the possibility of high dye content have additional advantages with respect to the matching of the sensitivity and thermal absorption with the characteristics of the applied laser. This can be done for variable film thicknesses.

As an example, the generation of optical scattering regions in optically clear macroscopically oriented films will be discussed. One possible write-store-erase cycle is schematically shown in Figure 6 for a dye-containing copolymer with a

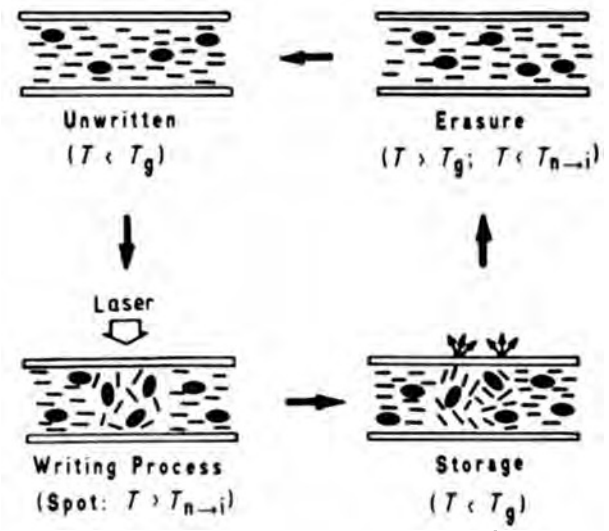


Fig. 6. Schematic representation of a write-store-erase cycle starting from a homogeneous planar oriented nematic glass of a dye-containing copolymer.

nematic phase. The unwritten state is an optically clear, nematic glass with homogeneous planar orientation. The writing process is based on local heating with a focused laser beam above the clearing temperature. On cooling, unoriented light scattering regions can be formed and stored below the glass transition temperature. Erasure is accomplished by heating the material into the nematic phase. The same write-store-erase cycle is possible with copolymers exhibiting a nematic and a smectic-A phase although in this case the information is stored in a smectic glass.

Figure 7 shows laser written scattering lines (width 2–3 mm) written with a He-Ne-laser (4 mW, 633 nm) between crossed polarizers within the macroscopically oriented glass of an anthraquinone dye-containing LC-copolymer.

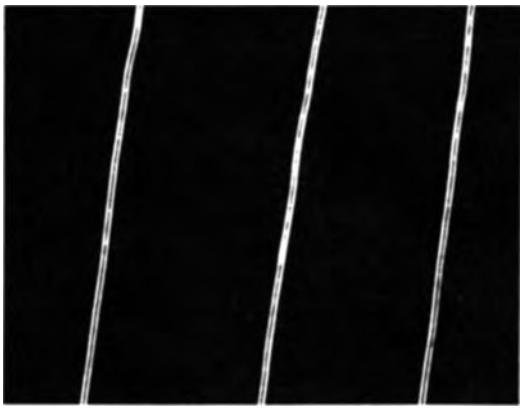


Fig. 7. Scattering lines (width: 2–3 μm) within a homogeneous planar oriented nematic glass (thickness 5 μm) of copolymer **5** (dye content: 10 wt.-%), written with a He-Ne laser (4 mW) at 633 nm. Photomicrograph between crossed polarizers and parallel to the director orientation (IAF, Freiburg).

The series of photographs in Figure 8 demonstrates the storage and erasure process. Figure 8a shows optically isotropic spots with a diameter of 60 μm written with a He-Ne laser in the homogeneous planar orientation of an anthraquinone dye containing copolymer. The information is stored below the glass transition temperature. If the sample is heated for one hour at 50 °C, slightly above the glass transition temperature, reorientation begins and the spot become smaller (Fig. 8b). After heating for an additional hour at 80 °C the spots are completely erased and the original homogeneous planar orientation is again obtained (Fig. 8c).

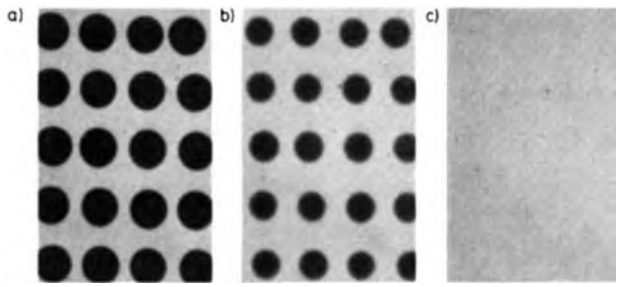


Fig. 8. Photomicrographs between crossed polarizers (45° relative to the director of the macroscopic orientation) of laser written spots on an anthraquinone dye-containing LC-side-chain copolymer (BASF, Ludwigshafen). a) information stored at room temperature. b) sample heated for one hour at 50 °C. c) sample heated for an additional hour at 80 °C.

As mentioned earlier, the writing process is also possible by laser addressing via a conducting IR-absorbing surface. Figure 9 shows a photograph of a cell drawn with a scanning Ne-YAG-laser at room temperature on a homogeneous planar aligned sample of LC-homopolymer with cyanobiphenylene side groups (**5** without the anthraquinone dye). Today, after more than three years, the information is still stable.

Photochemical storage effects in dyes contaning LC-polymers based on the cis-trans isomerization of the azobenzene side groups have been demonstrated by *Eich* et al.[11] and used for reversible digital and holographic optical storage.

ADVANCED MATERIALS

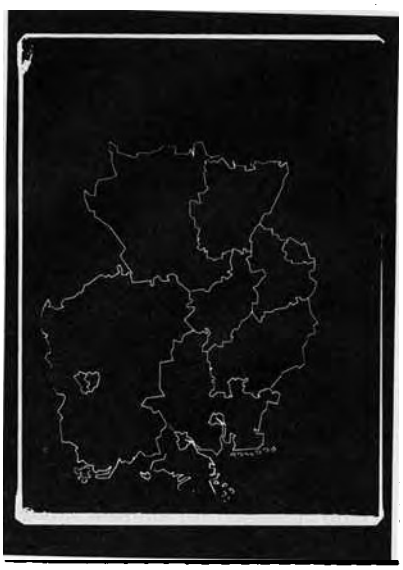


Fig. 9. Outlines of the Federal Republic of Germany and the German Democratic Republic drawn by a Ne-YAG-laser onto a homogeneous aligned nematic LC-homopolymer. Photomicrograph between crossed polarizers and parallel to the orientation of the director. (Cell: 4 cm × 3 cm; thickness: 10 μm; line width: 20–30 μm, IAF, Freiburg).

The photochromic and thermochromic behavior of spiropyrane dyes **4** in liquid crystalline polyacrylates and polysiloxanes have been recently described by *Cabrera* et al.[4e,f] The yellow spiropyrane dye was converted by UV-irradiation into its blue merocyanine form. Heating above the glass transition temperature caused the merocyanine side groups to form red dimers. The reverse photoconversion from the merocyanine structures occurred on irradiation with visible light.

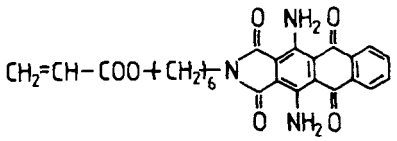
The examples discussed above demonstrate that dye-containing LC side chain copolymers can be used in principle as a medium for different modes of reversible optical storage. Studies have to be done on the different systems to further investigate application criteria such as speed, sensitivity, resolution, image density, storage stability, read-out stability, erasability and rewritability.

6. Copolymers as Guests in Low Molar Mass LC-Hosts

Nematic dye-containing copolymers in displays show the same orientation behavior and electrooptical effects as low molar mass host-guest mixtures.[4a] Due to the higher bulk viscosity of the polymers, the response times are longer under comparable conditions. The switching times can be shortened by raising the temperature, applying higher voltages and reducing the cell thickness. Recently, *Kiefer*[13] demonstrated that it is possible to achieve rise times in the order of 25 msec for dye-containing copolymers in thin cells (typically 2 μm) with an applied voltage of 16 V.

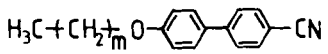
A different approach to shortening the switching times is the reduction of the bulk viscosity by adding low molar mass liquid crystals. LC-side-chain polymers are in general miscible with low molar mass liquid crystals if a) the chemical structure of the liquid crystal is similar to the mesogenic side groups and b) if both components have the same mesophase.[14] In the same manner, dye-containing copolymers can be dissolved in low molar mass liquid crystals. The mesogenic side group in the copolymer can be regarded as a solubility enhancer for the dye molecules. The use of dye-containing copolymers as guests is a general concept and is an alternative to the chemical modification of low molar mass dichroic dyes. Several types of dye-containing copolymers were investigated in different nematic low molar mass hosts with respect to the dye solubility, the order parameter S_D and the switching behavior in displays.[4c, 15]

As an example, a mixture of anthraquinone copolymer **5** in a binary nematic host consisting of cyanobiphenyls **7** and **8** (40 mol-% **7**; 60 mol-% **8**) will be discussed. Mixtures with



6

a dye concentration of 1.5wt.-% were prepared. The total polymer concentration in the mixtures can be adjusted by using copolymers with different dye contents. It should be noted that 1.5 wt.-% is not a maximum value, but is already three times higher than the achievable dye concentration of the corresponding dye monomer **6** in the binary host. Dye-containing copolymers can also be dissolved in multicomponent commercial mixtures, which are currently used in LC displays.



7: m = 4 **8**: m = 6

The mixtures have relatively low viscosities. Therefore commercial displays can be easily filled by capillary action and the LC mixture macroscopically aligned into a homogeneous planar orientation by surface effects. The order parameter of the dichroic dye moieties can be determined in the same manner as described in section 4. Figure 10 compares the order parameters S_D of a mixture of copolymer **5** (anthraquinone content 19 wt.-%) dissolved in the binary cyanobiphenyl host, with a mixture of the monomeric dye **6** in the same host. The order parameters S_D are plotted versus the reduced temperature (T_{red}). The reduced temperature is defined by the ratio of actual temperature (K) to the clearing

temperature (K). The value of S_D and the temperature dependence are almost identical for both systems and are not influenced by the polymer fixation of the dye.

Displays filled with copolymer containing host-guest mixtures can be switched by an electric field as shown in Figure 1. As an example, switching conditions and switching times for a mixture of 14.1 wt.-% of an anthraquinone copolymer (dye content 13 wt.-%) in the commercial nematic phase ZLI 1840 (Merck, Darmstadt) are given. The rise time is about 60 msec and the decay time 350 msec in a display (thickness 8.0 μm) at 20 °C and an applied voltage of 7 V. The response times are longer by a factor of 3.8 (rise) and 5.5 (decay) than those measured for host phase ZLI 1840 under the same conditions. It should be noted that a dissolved low molar mass dichroic dye also increases the response times. Additional switching experiments have to be carried out in order to study the influence of the polymer content and of the molecular weight of the copolymers. The results have to be compared with low molar mass host-guest mixtures.

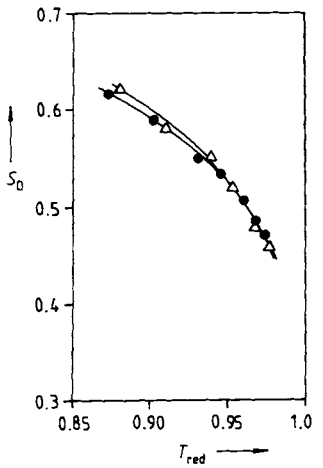


Fig. 10. Order parameter S_D versus T_{red} for the anthraquinone monomer **6** (△) and copolymer **5** (●) in the binary nematic biphenyl host of **7** and **8** (Compositions see [16]).

7. Summary and Outlook

Functional guest molecules incorporated into LC-side-chain polymers lead to polymeric materials which combine the physical and optical anisotropic properties of liquid crystals with the special functions of the guest components. This contribution focused on dichroic dyes, but the results are transferable to other guest moieties. The covalent fixation of the dye to the polymer backbone affords several advantages. Liquid crystalline materials with high dye concentrations were obtained opening the way to the preparation of highly ordered, optical uniaxial films with adjustable thickness and optical density. Thin well aligned LC-polymer films can in principle be used as an active medium for reversible optical information storage and mixtures of dye-containing copolymers in low molar mass liquid crystals can be used in displays. Current developments in the area of ferroelectric chiral smectic-C side-chain polymers will further enhance interest in this area.

Only a small part of the rapidly growing field of LC-polymer materials with specific optical and electrooptical properties has been discussed in this contribution. Combinations of novel polymeric LC-structures with or without special functional guest moieties will certainly lead to a variety of advanced polymeric materials with enormous potential in the areas of integrated optics, non-linear optics, optoelectronics, display and information storage technology.

Received February 20, 1989

[1] See e.g.: a) N. A. Plate, V. P. Shibaev: *Comb-shaped Polymers and Liquid Crystals*, Plenum Press, New York 1987; b) H. Finkelmann in A. Ciferri, W. R. Krigbaum, R. B. Meyer (Eds.): *Polymer Liquid Crystals*, Academic Press, New York 1982; c) C. Noel, *Makromol. Chem., Macromol. Symp. 22* (1988) 95; d) H. Finkelmann, *Angew. Chem. Int. Ed. Engl. 26* (1987) 816; *Angew. Chem. 99* (1987) 840.

[2] G. H. Heilmeier, J. A. Castellano, L. A. Zanoni, *Mol. Cryst. Liq. Cryst. 8* (1969) 293.

[3] See e.g.: G. W. Gray, *Dyes Pigm. 3* (1982) 203; b) R. Eidenschink, *Kontakte (Darmstadt) 2* (1984) 25; c) F. Jones, T. J. Reeve, *J. Soc. Dyers Colour. 95* (1979) 352.

[4] a) H. Ringsdorf, H.-W. Schmidt, *Makromol. Chem. 185* (1984) 1327; b) H. Ringsdorf, H.-W. Schmidt, H. Eilingsfeld, K.-H. Etzbach, *ibid. 188* (1987) 1355; c) H. Ringsdorf, H.-W. Schmidt, G. Baur, R. Kiefer in L. L. Chapoy (Ed.): *Recent Advances in Liquid Crystalline Polymers*, Elsevier Appl. Sci. Publ., Barking 1985, p. 253; d) H. Finkelmann, H. Benthack, G. Rehage, *J. Chem. Phys. 80* (1983) 163; e) I. Cabrera, V. Krongauz, H. Ringsdorf, *Angew. Chem. Int. Ed. Engl. 26* (1987) 1178; *Angew. Chem. 100* (1987) 1204; f) I. Cabrera, V. Krongauz, H. Ringsdorf, *Mol. Cryst. Liq. Cryst. 155* (1988) 221.

[5] H. Ringsdorf, H.-W. Schmidt, G. Baur, R. Kiefer, F. Windscheid, *Liq. Cryst. 1* (1986) 319.

[6] See e.g.: a) R. V. Talroze, V. P. Shibaev, V. V. Sinitzyn, N. A. Plate, *Polym. Prepr., (Am. Chem. Soc. Div. Polym. Chem.) 24* (1983) 309; b) G. R. Meredith, J. G. Van Dusen, D. J. Williams, *Macromol. 15* (1982) 1385; c) H. J. Coles, *Faraday Discuss. Chem. Soc. 79* (1985) 201; d) U. Quotschalla, W. Haase, *Mol. Cryst. Liq. Cryst. 153* (1987) 83.

[7] H.-W. Schmidt, K.-H. Etzbach, unpublished results.

[8] P. Le Barny, J.-C. Dubois, C. Friedrich, C. Noel, *Polym. Bull. 15* (1986) 341.

[9] See e.g.: a) G. Kämpf, *Polym. J. (Tokyo) 19* (1987) 257; b) M. G. Clark, *Chem. & Ind. London* (1985) 258.

[10] a) V. P. Shibaev, S. G. Kostromin, N. A. Plate, S. A. Ivanov, V. Y. Vetrov, I. A. Yakovlev, *Polym. Commun. 24* (1983) 364; b) H. J. Coles, R. Simon, *Polymer 26* (1985) 1801; c) R. Simon, H. J. Coles, *Liq. Cryst. 1* (1986) 281; d) C. B. McArdle, M. G. Clark, C. M. Haws, M. C. K. Wiltshire, A. Parker, G. Nestor, G. W. Gray, D. Lacey, K. J. Toyne, *ibid 2* (1987) 573.

[11] M. Eich, J.-H. Wendorff, B. Reck, H. Ringsdorf, *Makromol. Chem. Rapid Commun. 8* (1987) 59.

[12] J. Pinsl, C. Bräuchle, F. H. Kreuzer, *J. Mol. Electron. 3* (1987) 9.

[13] R. Kiefer, G. Baur, *Liq. Cryst. 4* (1989).

[14] See e.g.: a) G. Sigaud, M. F. Achard, F. Hardouin, H. Gasparoux, *Mol. Cryst. Liq. Cryst. 155* (1988) 443; b) H. Benthack-Thomas, H. Finkelmann, *Makromol. Chem. 186* (1985) 1895; c) H. Ringsdorf, H.-W. Schmidt, A. Schneller, *Makromol. Chem. Rapid Commun. 3* (1982) 745.

[15] H.-W. Schmidt, R. Kiefer, unpublished results.

[16] Binary host: 40 mol-% **7** and 60 mol-% **8**; dye monomer **6**: 0.5 wt.-% dissolved in binary host; copolymer **5** (19 wt.-% dye) 7.8 wt.-% dissolved in binary host, resulting dye content 1.5 wt.-%.

Production and Application of Rapidly Quenched Materials

Soft Magnetic Materials
Intermetallics
Brazing Alloys

By Hans Warlimont *

1. Introduction

The development of metallic glasses, i.e. amorphous metals produced by rapid quenching from the melt, has an impact on four areas of materials technology:
- substitution of existing materials
- innovation in applications
- instigation of competing material developments
- opening more widely the field of rapid solidification technology

In this overview both ribbon shaped soft magnetic materials and flake shaped hard magnetic materials are included, with emphasis on the former. It should be noted that other rapid solidification processes and products such as rapidly solidified powders, e.g. of aluminum alloys, and the formation of bulk materials by melt-spraying are also being developed and introduced commercially.

Table 1. Commercial applications of cooling wheel based RST.

	Single Roll		Double Roll	Centrifugal Water Cooling Wheel
Form of Product	strip	powder	strip	wire
Materials	amorphous magnetic alloys brazing alloys crystalline brazing alloys	$Fe_{14}Nd_2B$ Al alloys high speed steels hard facing alloys various steels (fibers)	Fe–Si	amorphous
Producers	Allied Signal Metglas Products Hitachi Metals Toshiba TDK VAC SISR I Shanghai CISRI, BMRI Beijing	Delco Remy Allied Signal Metglas Products Marko Materials Fibretech/Ribtec	Kawasaki Steel	Unitika

Table 1 shows a (possibly incomplete) compilation of the major materials, producers and forms of product of rapid solidification technology (RST). Table 2 shows an assessment of the products and applications of RST for 1988 indicating the uncertainty in quantitative data but giving some probable ranges. It should be noted that there are many more pilot productions in operation other than by those companies named in Table 1 and that thin strip casting is being developed on a much larger scale and for a much wider range of products than those comprised in Table 2. In most cases, however, product thickness is larger and cooling rates are lower, and therefore productivity rather than rapid solidification effects are sought.

Table 2. Rapid solidification technology – products and applications 1988.

Products	Applications	Quantities [tons]
amorphous ribbons Fe based	distribution transformers and large chokes	$10^2 \ldots < 10^3$
amorphous ribbons Fe and Co based	inductive components, sensors	$< 10^2$
microcrystalline $Fe_{14}Nd_2B$ powders	bonded permanent magnets	$> 10^2$
amorphous brazing alloys	aerospace	?
microcrystalline Al based powders	aerospace	?
microcrystalline steels	tools, reinforcement	?

2. Power Applications of Amorphous Metals

For this and the following section on the magnetic applications of metallic glasses, recent reviews[1, 2] and publications of conference proceedings[3, 4] should be consulted for details.

Figure 1 shows a comparison of different materials and operating conditions (peak induction $\hat{B}$) with regard to the

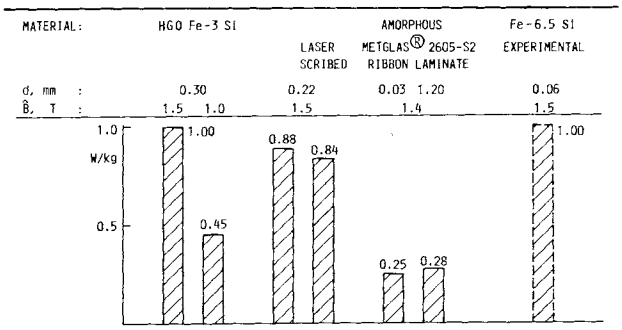


Fig. 1. 60 Hz power loss for typical Fe–Si and amorphous transformer materials.

Prof. Dr. H. Warlimont
Vacuumschmelze GmbH
D-6450 Hanau (FRG)

power loss p_{Fe} in transformers operating at a power grid frequency of $f = 60$ Hz. It is obvious that amorphous metals are substantially superior to the other materials but that progress has been made in the case of silicon steels and operating conditions are also yielding drastic differences. This indicates that economic aspects, such as investment and life cycle costs, will be decisive in the final use of transformer materials. The largest producer of amorphous core transformers in the USA, the General Electric Company, reports that their sales (over the last several years) total just 10000 amorphous core transformers (typically in the 30 kVA power range) but that they expect sales to double in each of the next few years. This should be compared with the total number of 1.2 million transformers sold in the USA annually. Jacksonville Electric Authority in Florida has so far bought 1600 amorphous-metal transformers which have cut power losses by 60%. The transformers are priced about 25% higher than conventional ones.[5]

3. Speciality Magnetic Applications of Amorphous Metals

The drastic reduction of iron loss in amorphous vs. crystalline soft magnetic materials is a major reason for their applications in power transformers. Their low coercivity H_c reduces their hysteresis losses, but their low ribbon thickness $d \lesssim 0.030$ mm and their high electrical resistivity $\rho \gtrsim 130$ μΩcm are still more effective in reducing the eddy current losses, which are proportional to d^2/ρ. This leads to the competitive situation between amorphous metal ribbons and ferrites shown in Figure 2. The ferrites have been improved in the sequence N27, N67, H_{7c4} (commercial designations) but the Co based amorphous ribbons are superior at all frequencies if their ribbon thickness is reduced to $d \simeq 15$ μm which is technically and economically feasible. Apart from lower losses another favorable property of amorphous metal cores with a Z type loop is their high squareness.

Table 3 is a compilation of speciality applications of soft magnetic amorphous metals. They have reached different degrees of importance. The use of amorphous cores in current compensated chokes may be pointed out as a special case. The effectiveness of these chokes in suppressing common mode interference is expressed by the insertion loss as a function of the frequency of the noise spectrum. Figure 3 shows the superiority of amorphous core chokes compared to permalloy and ferrite core chokes which exhibit lower insertion losses and pronounced minima at certain frequencies due to resonance effects.

Table 3. Magnetic speciality applications of amorphous metals.

Field of Application	Specific Application
power supplies	switched mode power supplies: - inverter transformers - chokes for magnetic amplifiers - storage chokes - RF current compensated chokes high repetition rate pulse compressors: - step-up transformers - saturable reactors
other HF circuits	- transformers - chokes
magnetic heads	- audio - data storage
magnetic shielding	- flexible shields
sensors	- magnetic field - position, displacement - force, torque - identification and anti-theft markers

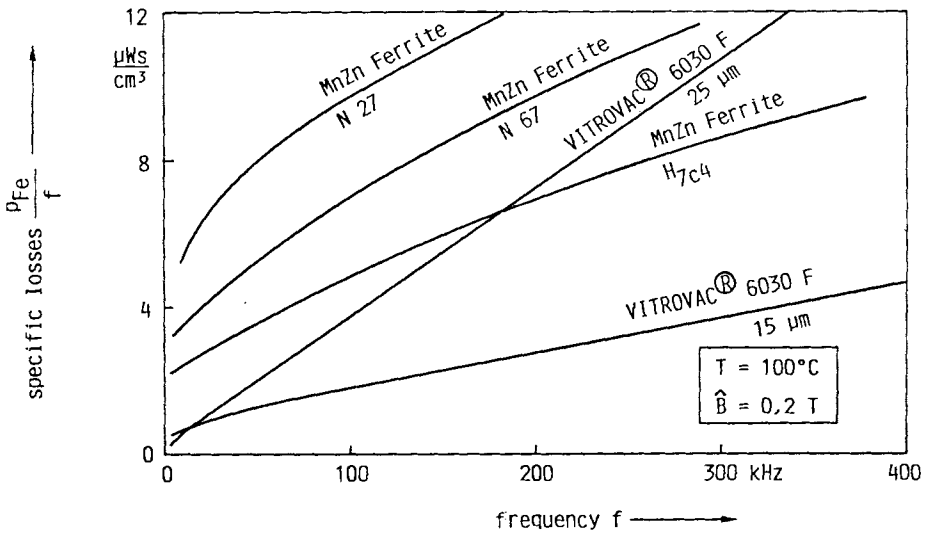


Fig. 2. Power losses per cycle for medium frequency materials.

ADVANCED MATERIALS

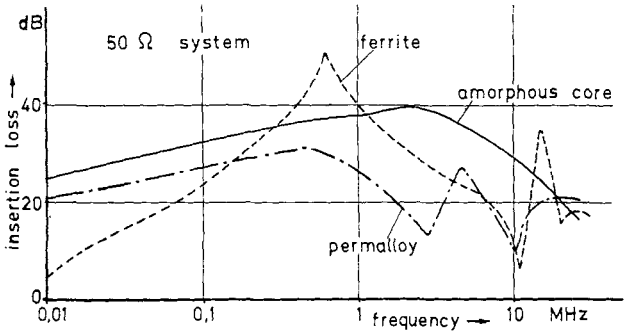


Fig. 3. Insertion loss of common mode interference in current compensated chokes.

4. Rapidly Quenched $Fe_{14}Nd_2B$

The hard magnetic compound $Fe_{14}Nd_2B$ is becoming important among the rare earth bearing permanent magnetic materials because of its high ratio of performance vs. cost. It is produced both by conventional powder metallurgical processing and by RST. To utilize the magnetic material to the full, anisotropic magnets are produced using powder metallurgy. Rapid solidification yields a higher coercivity and a somewhat lower temperature coefficient of the remanence B_r which is useful in some applications, and it allows the production of bonded magnets which are formed more easily yielding in certain cases an economic advantage. Since the material is produced by ribbon formation in the amorphous state, followed by disintegration into flakes and crystallization of the intermetallic compound, the magnetic easy axis is oriented randomly yielding isotropic properties. However, it has been found that uniaxial hot pressing of the flakes induces oriented selective grain growth such that anisotropic properties result. Table 4 gives properties of powders which

Table 4. Properties of rapidly quenched $Fe_{14}Nd_2B$ powders [a].

Type	Remanence B_r [T]	Coercivity ${}_iH_c$ [kA/cm]	$(dB_r/dT)/B_r$ [%/K (25...100 °C]
A. isotropic	0.75	12	− 0.13
B. isotropic	0.80	7	− 0.11
C. anisotropic	0.95	9	− 0.12
E. anisotropic	0.86	10	− 0.17

[a] Magnequench by Delco Remy.

are commercially available. In the present state of evaluation it is to be expected that sintered and rapidly quenched $Fe_{14}Nd_2B$ hard magnetic materials will be supplementing rather than competing with each other.

5. Further Materials Developments and Perspectives

Apart from the soft magnetic amorphous materials and the microcrystalline hard magnetic $Fe_{14}Nd_2B$ compound, other RST materials are beginning to assume commercial importance such as brazing alloys, nanocrystalline soft magnetic alloys and others (Table 2).

Rapid solidification of brazing alloys has yielded two advantageous aspects: a) amorphous and microcrystalline structures impart favorable mechanical properties to brazing alloys; b) supersaturation effects and favorable brazing behavior permit the design of active brazing alloys with technical and economic advantages. Active brazing involves an alloy containing an oxygen getter which eliminates the use of flux media for metal brazing and the need to metallize ceramic parts to be brazed. The resulting simplification of the brazing process is indicated in Figure 4. A typical alloy which was developed for this application is Ag–Cu–Ti.[6]

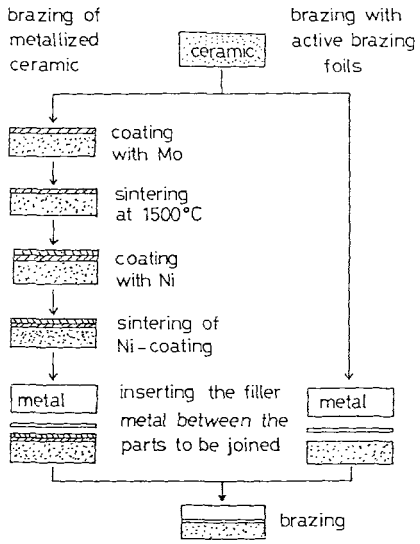


Fig. 4. Comparison of brazing processes for metal-ceramic joints.

A recent development by Hitachi Metals Ltd.[7] has yielded a rapidly solidified soft magnetic material with an extremely low grain size in the nm range. A typical composition

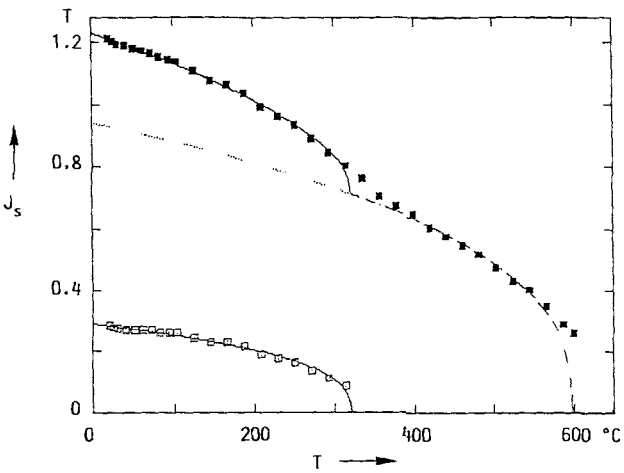


Fig. 5. Magnetization vs. Temperature of rapidly quenched $Fe_{73.5}Cu_1Nb_3Si_{13.5}B_9$ annealed 1 h at 520 °C.

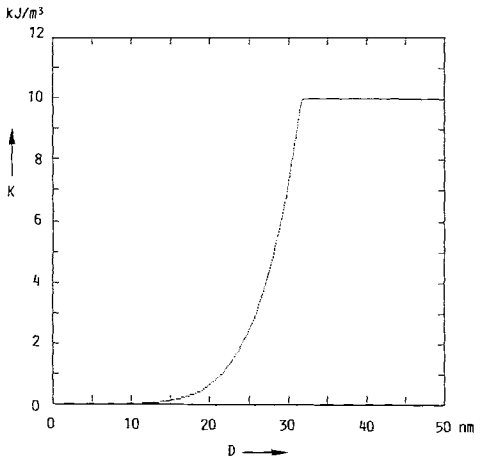


Fig. 6. Computed magnetocrystalline anisotropy K vs. grain diameter D.

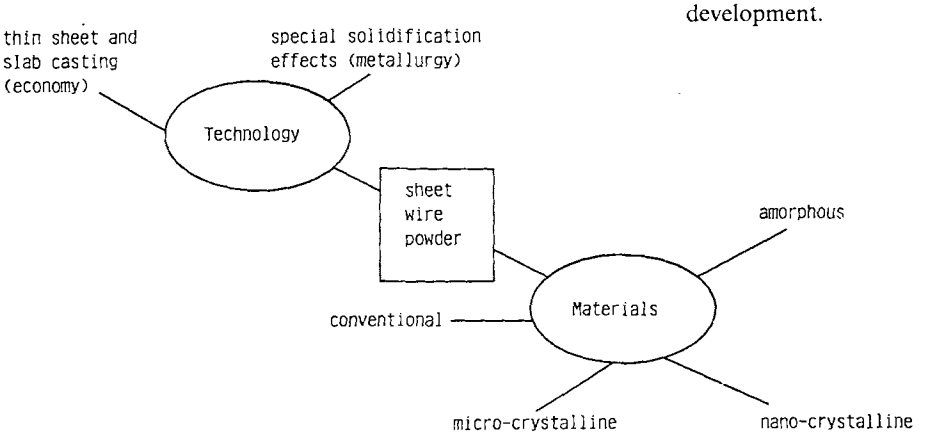


Fig. 7. Perspectives of rapid Solidification technology.

is $Fe_{73.4}Cu_1Nb_{3.1}Si_{13.4}B_{9.1}$. At variance to normal behavior where the coercivity H_c is expected to vary as the inverse of the grain diameter D, this material has a very low coercivity in the same range as that of the best amorphous materials. The explanation was found[8] by first determining the temperature dependence of the saturation polarization shown in Figure 5. It indicates clearly the presence of two ferromagnetic phases with different Curie temperatures which are due to a crystalline Fe–Si rich phase (high-T_c) and probably an amorphous phase (lower-T_c) forming a grain boundary layer. In a second step the magnetocrystalline anisotropy of such a microstructure was computed as a function of grain diameter D, Figure 6. It can be seen that magnetic isotropy prevails up to $D \lesssim 15$ nm. This is one of the essential prerequisites of a low magnitude of H_c. Combined with further favorable magnetic properties such as high B_r and low magnetostriction λ_S and losses p_{Fe} this material is quite promising for a number of applications.

Brazing alloys and nm-range crystalline soft magnetic alloys are just two examples of the versatility and the range of potential developments of rapid solidification technology. In Figure 7 a schematic view of the field is given. One important feature is the technology which allows on one hand for the design of special structural and microstructural effects and on the other, the economy of a one-step process from the melt to the final (or a near-final) product. The second aspect of the application of this technology is the different materials which can be produced possessing a variety of properties. It is obvious that this field has a great potential for further development.

Received March 14, 1989

[1] H. Warlimont, in H. Steeb, H. Warlimont (Eds.): *Rapidly Quenched Metals*, Elsevier Science Publishers, Amsterdam 1985.
[2] T. H. O'Dell, *Mater. Sci. Technol. 4* (1988) 493.
[3] S. Steeb, H. Warlimont (Eds.): *Rapidly Quenched Metals*, Elsevier Science Publishers, Amsterdam 1985.
[4] R. W. Cochrane, J. O. Ström-Olsen (Eds.): *Rapidly Quenched Metals 6*, Elsevier Applied Science, New York 1988.
[5] B. Paul, *The Wall Street Journal*, October 26., 1988.
[6] K. Emmerich, in: P. W. Lee, R. S. Carbonara (Eds.): *Rapidly Solidified Materials*, American Society for Metals, Metals Park, USA 1985.
[7] K. Yoshizawa, S. Oguma, K. Yamauchi, presented at Intermag 1988.
[8] G. Herzer, presented at Intermag 1989.

The following review articles will be published in future issues:

J. F. Stoddart: Structure Directed Synthesis of New Organic Materials
B. A. Joyce: Tailoring Semiconductor Crystals to Atomic Dimensions
E. D. Hondros et al: Materials for the Next Millenium
J. O. Williams: Metal-Organic Chemical Vapor Deposition (MOCVD)
J. M. Thomas: Advanced Catalysts: Interfaces in the Physical and Biological Sciences
R. Zentel: Liquid Crystal Elastomers
R. Eidenschink: Liquid Crystals, New Compounds, New Applications

Communications

Structure of Anodic Oxide Coatings on Aluminum **

By *Rüdiger Kniep,** *Peter Lamparter* and *Siegfried Steeb*

Porous surface coatings on aluminum are produced by anodic oxidation in acid electrolytes.[1] Pore sizes (10–250 nm) as well as pore densities (10^{12}–10^{15} m^{-2}) are mainly controlled by the anodizing voltage; the thickness of the layers may reach more than 100 μm and is determined by the amount of charge transferred. The remarkably uniform array of the pores in the centers of the almost hexagonally shaped cells makes the films of interest for application in the field of synthetic membranes and as supports for active materials.[2, 3] Furthermore, the coatings are widely used as protective layers which can also be colored by impregnation of the pores with organic dyes or by precipitation of inorganic pigments in the pores.[4, 5] After coloring, the pores are closed by treatment with water or steam. This "sealing" process causes the formation of gelatinous boehmite and amorphous oxide hydroxide by reaction of the pore wall material with water.[6]

The structure of the (amorphous) porous coatings is not clear at present. It is assumed that they are structurally related to the non-porous "barrier-layer" (in direct contact with the metal; thickness 0.1–0.2 μm) which consists of almost pure Al_2O_3 and contains the η- and γ-phases of alumina (spinel-type structures). This assumption is supported by the primary products of crystallization which are formed by thermal treatment of the porous coatings and which were identified as the γ- and γ'-phases of alumina.[7] A recent IR-investigation of dried porous layers[8] is consistent with coordination numbers of four and six (tetrahedral and octahedral) for the aluminum atoms.

In the present work freshly prepared porous coatings were investigated with X-ray and neutron diffraction methods. The aluminum atoms were found mostly to be surrounded tetrahedrally by four oxygen atoms. The close similarities of the radial distribution function (RDF) of the porous layers to that of vitreous silica suggest that the same structural model should be applied for both materials.

Samples for the diffraction experiments were prepared by anodic oxidation of aluminum foils applying the following parameters: bath temperature 12 °C; natural bath convection; current 1.5 A/dm²; voltage 15 V; $Al^{3\oplus}$ content in the bath 5.2 g/l; $H_2SO_{4(total)}$ 200 g/l; $H_2SO_{4(free)}$ 172 g/l. The layers were removed from the metal by treatment with Br_2/MeOH mixtures. The chemical composition of a large number of samples was determined using XFA (Al and S), IC ($SO_4^{2\ominus}$), EDX (Al and S) and TG (H_2O) and yielded a mean brutto-formula of $(5\,Al_2O_3 \cdot SO_3 \cdot 0.66\,H_2O) \cdot 1.33\,H_2O$ with deviations less than one wt-% for the distinct components. The amount of water given inside the brackets of the formula is regarded as the water of constitution (OH-groups) which is released only at temperatures above 470 °C; the amount of water given outside the brackets is regarded as H_2O-molecules (structural water and/or adsorbed water at the pore walls) which is already released between 80 °C and 250 °C.

Figure 1 (a) shows the X-ray structure factors $S^x(Q)$ from angular dispersive X-ray diffraction (ADXD) and from energy dispersive X-ray diffraction (EDXD). Both curves have the same overall shape without sharp reflexes, giving evidence that the anodic oxide coating material is amorphous. In the region of the first peak near $Q = 2$ Å^{-1} the EDXD reflects lower resolution, whereas the high Q-tail of the ADXD curve near $Q = 12$ Å^{-1} we judge to be less reliable. The observation of extended oscillations up to $Q = 23.5$ Å^{-1} demonstrates the power of the EDXD method. The same high-Q oscillations are observed with the neutron structure factor $S^N(Q)$ in Figure 1 (b). At smaller Q, however, S^N is different from S^X where the most drastic difference is the appearance of a large sharp peak in S^N at $Q = 2.8$ Å^{-1} which in S^X shows up only as a small hump. The reduced pair correlation functions $G(R)$, calculated from the structure factors by Fourier-transformation are shown in Figure 2. The restriction of the range, up to only $R = 6$ Å, is justified by the abrupt loss of any correlations in the X-ray curves $G^X(R)$ beyond $R = 4.6$ Å. This signifies that the structural units built up by the aluminum and oxygen atoms in the amorphous phase have a very small extension of maximum of about 5 Å. On the other hand, the neutron curve $G^N(R)$

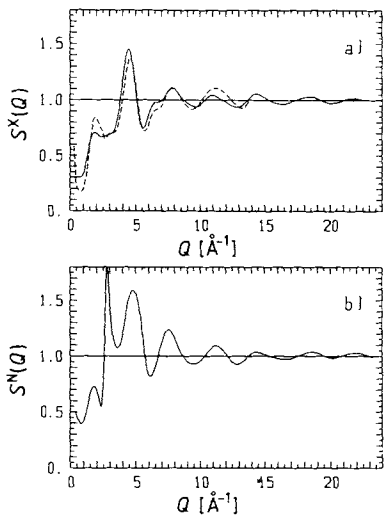


Fig. 1. Amorphous anodic oxide coatings on aluminum. Structure factors $S(Q)$, calculated from a) ADXD (– – –), EDXD (——) and b) Neutron diffraction. $S(Q) = (I(Q) - [\langle b^2\rangle - \langle b\rangle^2])/\langle b\rangle^2$ where $I(Q)$ = coherently scattered intensity per atom; $\langle b^2\rangle$ = mean squared scattering length per atom; $\langle b\rangle$ = mean scattering length (with X-rays depending on Q).

[*] Prof. Dr. R. Kniep
Eduard-Zintl-Institut
Technische Hochschule Darmstadt
Hochschulstraße 10
D-6100 Darmstadt (FRG)
Dr. P. Lamparter, Prof. Dr. S. Steeb
Max-Planck-Institut für Metallforschung
Institut für Werkstoffwissenschaft
Seestraße 92
D-7000 Stuttgart 1 (FRG)

[**] This work was supported by the Fonds der Chemischen Industrie and by the Henkel KGaA

exhibits very extended oscillations up to $R = 20$ Å. Obviously, these extended correlations involve hydrogen atoms which are practically invisible to X-rays. Details of the hydrogen scattering will not be under consideration in this study.

For the identification of the peaks in the $G(R)$ functions in Figure 2 the weighting factors of the ten partial correlation

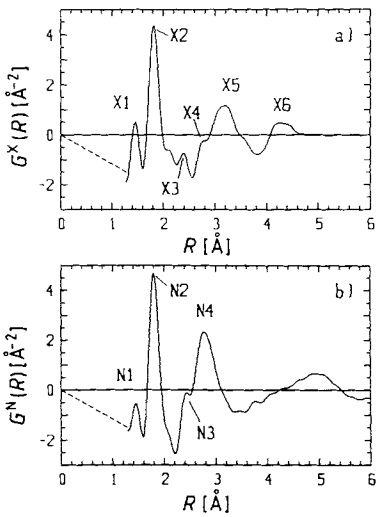


Fig. 2. Amorphous anodic oxide coatings on aluminum. Correlation functions $G(R)$, calculated by Fourier transformation from the structure factors $S(Q)$ in Fig. 1 (a): EDXD; (b): Neutron diffraction; $G(R) = \frac{2}{\pi} \cdot \int Q[S(Q) - 1] \sin QR \, dQ$ where $G(R) = 4\pi R[\varrho(R) - \varrho_0]$; $\varrho(R)$ = pair density distribution function; ϱ_0 = mean number density; R = distance in real space.

functions $G_{i,j}(R)$, (i, j = Al,O,S,H), which contribute to $G(R)$ are listed in Table 1.

The most important information on the short range order in the amorphous coatings is extracted from the main peak of $G(R)$ at $R = 1.80-1.82$ Å (X2 and N2 in Fig. 2) which represents the Al-O nearest neighbors. The almost equal W_{A10} for X-rays and neutrons (Tab. 1) are in accordance

Tab. 1. Weighting factors W_{ij} of the partial correlation functions $G_{ij}(R)$ (i,j = Al,O,S,H). Upper numbers for X-rays; lower numbers for neutrons. $G(R) = \sum_{ij} W_{ij} G_{ij}(R)$, where $W_{ij} = \delta c_i c_j b_i b_j / \langle b \rangle^2$; c_i = atomic concentration; $\delta = 1$ when i = j, $\delta = 2$ when i ≠ j.

	Al	O	S	H
Al	0.176	–	–	–
	0.062	–	–	–
O	0.433	0.266	–	–
	0.418	0.703	–	–
S	0.043	0.053	0.003	–
	0.010	0.035	0.000	–
H	0.011	0.013	0.001	0.000
	– 0.054	– 0.181	– 0.005	0.012

with the equal amplitudes of the corresponding peaks. From the area under the peaks in the radial distribution functions ($RDF^{X,N}(R) = 4\pi R^2 \varrho^{X,N}(R) = RG^{X,N}(R) + 4\pi R^2 \varrho_0$) the coordination number of oxygen atoms around Al is obtained as $4 \leqq Z_{A10} \leqq 5$ depending on the choice of ϱ_0, i.e., the macroscopic density D. According to this method the aluminum atoms are mostly surrounded tetrahedrally by four oxygen atoms. $Z_{A10} = 4$ is obtained using the macroscopic density $D = 2.75$ g cm^{-3} as determined by the Archemedean method. This experimental D-value might be somewhat too small, due to amounts of adsorbed air in the pores of the films. An estimated extrapolation of the densities of amorphous $SiO_2 \cdot Al_2O_3$ materials ($Z = 4.3-4.6$)[9] yields $D = 3.3$ g cm^{-3} for pure amorphous Al_2O_3. The Al-O distance at 1.81 Å in the amorphous porous coatings (Fig. 2) is smaller than the octahedral Al(6)-O distances observed in α-Al_2O_3 (1.86–1.97 Å[10]) and in boehmite (1.88–1.94 Å[11]) and is somewhat larger than the tetrahedral bond lengths Al(4)-O/OH (1.73–1.78 Å) in the isolated dimeric anion $[Al_2O(OH)_6]^{\ominus}$.[12]

According to the significant amount of sulfate in the porous anodic oxide coatings, the peaks X1 (N1) and X3 (N3) in Figure 2 can be attributed to SO_4-tetrahedra. The peaks X1 (N1) at $R = 1.45$ Å correspond to S–O bonds (1.47–1.50 Å) in $SO_4^{2\ominus}$ groups. Its height scales well with the respective W_{SO} in Table 1. The O-O distance along an edge of a SO_4-tetrahedron is expected at $R_{O-O} = \sqrt{8/3}\, R_{S-O} = 2.38$ Å, and shows up at X3 (N3) in the correlation functions. In accordance with W_{O-O} the peak appears higher with neutrons.

In the following we discuss the $G(R)$ curves in Figure 2 on the basis of the structural model for the short range order in the amorphous anodic coatings as presented in Figure 3:

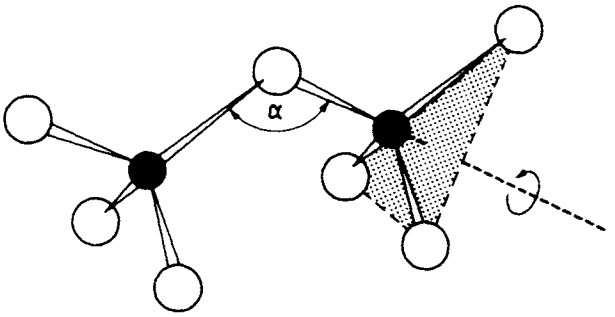


Fig. 3. Short range order in amorphous anodic oxide coatings on aluminum.

Two AlO_4 tetrahedra share a common oxygen corner; the irregular three dimensional structure is then controlled by the possible variations of the angle α, (Al-O-Al), as well as by the conformational statistics resulting from "free" rotation of the tetrahedra around their O-Al-axes. Preferred tetrahedral coordination of aluminum (Al-O 1.81 Å) has already been deduced from the peaks X2 (N2) in Figure 2. The distance between two O-atoms along an edge of a tetrahedron is expected for the case of perfect tetrahedra at $R_{O-O} = \sqrt{8/3}\, R_{Al-O} = 2.95$ Å. We attribute the peaks X4 (N4) at 2.80 Å to this O-O distance which, according to Table 1, appears stronger with neutrons. The average O-O distance along an edge of a tetrahedron in the structure of $K_2[Al_2O(OH)_6]$ is 2.86 Å.[12] With X-rays, a peak X5 appears at larger $R = 3.20$ Å which reflects Al···Al distances resulting from

ADVANCED MATERIALS

corner-sharing AlO_4 tetrahedra; according to Table 1 its contribution is much weaker with neutrons. The angle Al(4)-O(2)-Al(4) of 132° in the isolated dimeric tetrahedral anion $[Al_2O(OH)_6]^{\ominus}$ [12] corresponds with a respective distance Al···Al of 3.18 Å. Larger Al-O as well as O-O distances give rise to the peak X6 around 4.3 Å. Whether the fine structure in $G^N(R)$ in this region is real or is caused by Fourier-ripples cannot be decided presently. It is expected that the broad peaks X5 and X6 are also contributed by non-bonding interactions which reflect the partial substitution of aluminum by sulfur in the amorphous structure.

It should be noted that the short range order in amorphous anodic oxide coatings on aluminum shows close similarities to the short range order reported for vitreous silica.[13-17]

Standardization of the chemical composition $(5\ Al_2O_3 \cdot SO_3 \cdot 0.66\ H_2O) \cdot 1.33\ H_2O$ of the porous anodic oxide coatings to a structural formula $(A)^n[X_{n/2}]$, which in the case of $n = 4$ represents the idealized structure of vitreous silica, leads to $(Al_{0.91}\ S_{0.09})^{[3.39]}\ [O_{3.15/2}\ (OH)_{0.24/2}]$ with the water outside the brackets of the oxide formula not taken into consideration. The coordination number of oxygen atoms around aluminum ($4 \leq Z_{A10} \leq 5$) which is derived from the $RDF^{X,N}$ shows that the oxygen and hydroxyl-groups are not exclusively bound to only two adjacent cations, an observation which is also valid for the structure of vitreous silica.[17]

A final remark should be made concerning the morphology of the almost hexagonally shaped cells (each containing a pore) which has been discussed as an indication of crystallinity of the anodic oxide layers. The isotropic (circular) growth of cells starts at nuclei which are homogeneously distributed over the surface of the aluminum metal. In the course of growth the cells come into contact and develop a homogeneous nearly hexagonal array of cell boundaries which covers the complete coating surface. A pore size near 150 Å and a distance between the pores of about 370 Å was determined from small angle neutron scattering (SANS)[18] studies on a deuterated sample which was prepared under the same anodizing conditions as applied for the materials for the structural investigations.

Experimental

The X-ray diffraction experiments were performed in transmission mode using two different techniques: Angular dispersive X-ray diffraction (ADXD) with a conventional D500-Siemens diffractometer and energy dispersive X-ray diffraction (EDXD) with a laboratory-built set up.[19] The sample material was powdered and filled into a flat container with Kapton-foil windows mounted in a vacuum chamber. With ADXD (EDXD) the scattering could be recorded up to the scattering vectors $Q = 13.5\ Å^{-1}$ ($23.5\ Å^{-1}$), where $Q = 4\pi\sin\theta/\lambda$. Correction methods and normalization to absolute units were applied as described elsewhere.[20, 21] The structure factors $S(Q)$ were calculated according to the Faber-Ziman definition.[22]

The neutron diffraction experiments were performed at the Institute-Laue-Langevin using the instrument D4B up to $Q = 23.3\ Å^{-1}$. The evaluation of the structure factor $S(Q)$ was done essentially as reported elsewhere.[23] However, in the present case the incoherent scattering contribution of the hydrogen in the sample had to be corrected for. This was achieved by fitting a smooth function through the absorption corrected intensity curve in such a way that after the subtraction of the smooth H-contribution the resulting structure factor oscillated properly around one. This smooth function agreed very well with a previously reported[24] hydrogen scattering function. Furthermore, from its intensity an H-content of 10.6 at-% was calculated which corresponds well to the analytical value of 11.4 at-%.

Received April 13, 1989

[1] V. F. Henley: *Anodic Oxidation of Aluminum and Its Alloys*, Pergamon Press, New York 1982.
[2] R. C. Furneaux, W. R. Rigby, A. P. Davidson, *Nature London 337* (1989) 147.
[3] D. L. Cocke, D. E. Johnson, R. P. Merrill, *Catal. Rev. Sci. Eng. 26* (1984) 163.
[4] S. Tajima, *Adv. Corr. Sci. Technol. 1* (1970) 227.
[5] K. Wefers, P. F. Wallace, *Aluminium (Düsseldorf) 52* (1976) 485.
[6] K. Wefers, *Aluminium (Düsseldorf) 49* (1973) 622.
[7] A. Roth, *Z. Anorg. Allg. Chem. 244* (1940) 48.
[8] A. B. Kiss, E. Szontagh, G. Kresztury, *Aluminium (Düsseldorf) 61*(1985) 821.
[9] H. Morikawa, S. Miwa, M. Miyake, F. Marumo, T. Sata, *J. Am. Ceram. Soc. 65* (1982) 78.
[10] R. E. Newnham, Y. M. de Haan, *Z. Krist. 117* (1962) 235.
[11] R. J. Hill, *Clays Clay Miner. 29* (1981) 435. C. E. Corbato, R. T. Tettenhorst, G. C. Christoph, *ibid 33* (1985) 71.
[12] G. Johansson, *Acta Chem. Scand. 20* (1966) 505.
[13] R. J. Bell, P. Dean, *Philos. Mag. 25* (1972) 1381.
[14] K. Zickert, H. Steil, C. Geik, G. Herms, G. Becherer, *Krist. Tech 14* (1979) 1147.
[15] R. L. Mozzi, B. E. Warren, *J. Appl. Cryst. 2* (1969) 164.
[16] B. E. Warren, H. Krutter, O. Morningstar, *J. Am. Ceram. Soc. 19* (1936) 202.
[17] A. Felz: *Amorphe und glasartige anorganische Festkörper*, Akademie-Verlag, Berlin 1983.
[18] R. Kniep, P. Lamparter, S. Steeb, unpublished.
[19] R. Utz: *Diploma Thesis*, University Stuttgart, 1987.
[20] P. Lamparter, A. Habenschuss, A. H. Narten, *J. Non-Cryst. Solids 86* (1986) 109.
[21] T. Egami, *J. Appl. Phys. 50* (1979) 1564.
[22] T. E. Faber, J. M. Ziman, *Philos Mag. 11* (1965) 153.
[23] P. Lamparter, W. Sperl, S. Steeb, J. Blétry, *Z. Naturforsch. 37a* (1982) 1223.
[24] P. Chieux, R. de Kouchkovski, B. Boucher, *J. Phys. F14* (1984) 2239.

Superconductivity at 7.5 K and Ambient Pressure in Polycrystalline Pressed Samples of β_p-(BEDT-TTF)$_2$I$_3$**

By *Dieter Schweitzer**, *Emil Gogu*, *Hans Grimm*, *Siegfried Kahlich* and *Heimo J. Keller*

Recently, bulk superconductivity at ambient pressure in polycrystalline pressed samples of an organic metal—α_t-(BEDT-TTF)$_2$I$_3$—was observed.[1] This is a remarkable fact because this finding shows that organic superconductors can in principle be used for the production of electronic devices, such as squids, and might even be suitable for the preparation of superconducting cables similar to the high temperature superconductors of the copper oxides.

The polycrystalline pressed samples of α_t-(BEDT-TTF)$_2$I$_3$ were prepared from pulverized single crystals of α-(BEDT-TTF)$_2$I$_3$ and the pressed samples had to be anealed at 75 °C

[*] Prof. Dr. D. Schweitzer
Physikalisches Institut der Universität Stuttgart
Pfaffenwaldring 57, D-7000 Stuttgart 80 (FRG)
Dipl. Phys. E. Gogu, Dr. H. Grimm, Dipl. Phys. S. Kahlich
Max Planck Institut für Medizinische Forschung, AG Molekülkristalle
Heidelberg (FRG)
Prof. Dr. H. J. Keller
Anorganisch Chemisches Institut der Universität Heidelberg
Heidelberg (FRG)

[**] We gratefully acknowledge financial support of this work by the Deutsche Forschungsgemeinschaft.

for one or two days in order to obtain the α_t-phase and to observe bulk superconductivity with an onset temperature of about 9 K.[1] Nevertheless, the superconducting transition was rather broad with respect to single crystals of α_t-(BEDT-TTF)$_2$I$_3$ and zero resistivity was found at 2.2 K. On the other hand, single crystals of (BEDT-TTF)$_2$Cu(NCS)$_2$ show the highest transition temperature known so far among the organic superconductors of 10.4 K,[2] although no bulk superconductivity could be found.[1] The reason for the loss of the bulk superconductivity in the polycrystalline pressed sample compared to the single crystals of (BEDT-TTF)$_2$Cu(NCS)$_2$ is not quite clear, but is probably due to a phase transition of the material during the preparation of the sample under pressure.

Here we report the surprising fact that polycrystalline pressed samples of β-(BEDT-TTF)$_2$I$_3$ show bulk superconductivity with an onset temperature to superconductivity of 9 K, zero resistivity at 3.2 K and the middle of the resistive transition at 7.5 K. In contrast to the polycrystalline samples, single crystals of β-(BEDT-TTF)$_2$I$_3$ show a rather sharp superconducting transition but only at 1.4 K (onset temperature 1.6 K).[3] Under an isotropic pressure of about 1 kbar the single crystals of β-(BEDT-TTF)$_2$I$_3$ show a superconducting transition at 7.5 K.[4, 5] After a pressure-temperature cycling procedure, pressurizing the crystal up to 1 kbar at room temperature and then releasing the helium gas pressure at temperatures below 125 K, superconductivity at 8 K and ambient pressure in β-(BEDT-TTF)$_2$I$_3$ was found.[6, 7] However, this specially prepared superconducting state at 8 K and ambient pressure is metastable because superconductivity at 8 K can only be obtained as long as the temperature of the single crystals does not exceed 125 K. It is therefore very surprising that in the polycrystalline pressed samples of β-(BEDT-TTF)$_2$I$_3$ a stable superconducting state with an onset temperature of 9 K at ambient pressure exists. For this reason we term the polycrystalline pressed samples of the β-phase β_p-(BEDT-TTF)$_2$I$_3$, where the index p indicates the polycrystalline *pressed* material.

Samples of the size $4 \times 1 \times 0.5$ mm^3 were prepared from pulverized single crystals of β-(BEDT-TTF)$_2$I$_3$ (the resulting crystallites from the graining process had typical diameters of 0.1–10 μm) by applying a pressure of about $1.5 \cdot 10^4$ kg/cm^2 to the powder. The β_p-(BEDT-TTF)$_2$I$_3$ samples prepared in this way are mechanically very stable and were not tempered as in the case of the previously reported pressed samples of α_t-(BEDT-TTF)$_2$I$_3$. The conductivity was measured with the usual four point method. Typical room temperature conductivities σ_{300} lie between 5 and 10 $(\Omega\,\mathrm{cm})^{-1}$ and are about a factor of 2 lower than in the polycrystalline pressed samples of α_t-(BEDT-TTF)$_2$I$_3$. Figure 1 shows the typical temperature dependence of the resistivity of polycrystalline pressed samples of β_p-(BEDT-TTF)$_2$I$_3$ as well as of α_t-(BEDT-TTF)$_2$I$_3$. It can clearly be seen that the resistivity characteristics of the samples of β_p-(BEDT-TTF)$_2$I$_3$ differ remarkably from those of α_t-(BEDT-TTF)$_2$I$_3$ samples (and in fact also from the resistivity characteristics of single crystals of β-(BEDT-TTF)$_2$I$_3$).[8] While in the α_t-samples the resistivity decreases as it does in a metal as the sample is cooled from room temperature, in the case of the β_p-(BEDT-TTF)$_2$I$_3$ samples the resistivity first increases slowly on lowering the temperature. At around 220 K, the temperature at which an incommensurate structural modulation in single crystals of β-(BEDT-TTF)$_2$I$_3$ occurs,[9] a maximum in resistivity is observed, and below 220 K again as in a metal the resistivity decreases.

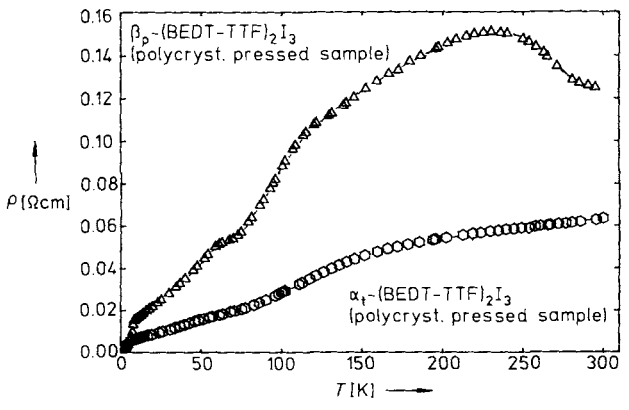


Fig. 1. Temperature dependence of the resistivity of polycrystalline pressed samples of β_p-(BEDT-TTF)$_2$I$_3$ and α_t-(BEDT-TTF)$_2$I$_3$.

Figure 2 shows the resistivity of β_p-(BEDT-TTF)$_2$I$_3$ samples in the temperature range below 16 K. As can be seen the onset of superconductivity lies at around 9 K and zero resistivity is found below 3.2 K indicating a rather broad transition. Nevertheless, the middle of the resistive transition is at around 7.5 K. The onset temperature for superconductivity here in β_p-(BEDT-TTF)$_2$I$_3$ is much higher than that in the single crystals of β-(BEDT-TTF)$_2$I$_3$. The reason for this is not yet clear, but the material probably undergoes a phase transition during the preparation of the polycrystalline samples under pressure. On the other hand, it is clear that the new β_p-phase is not identical with the known α_t-phase indicated by their different resistivity characteristics. In addition, first measurements of the upper critical fields H_{c2} have shown that the polycrystalline pressed samples of the β_p- and α_t-phases have different upper critical fields H_{c2},[10] but these are in both cases much higher than the upper critical field H_{c2} in crystals of α_t-(BEDT-TTF)$_2$I$_3$.[11]

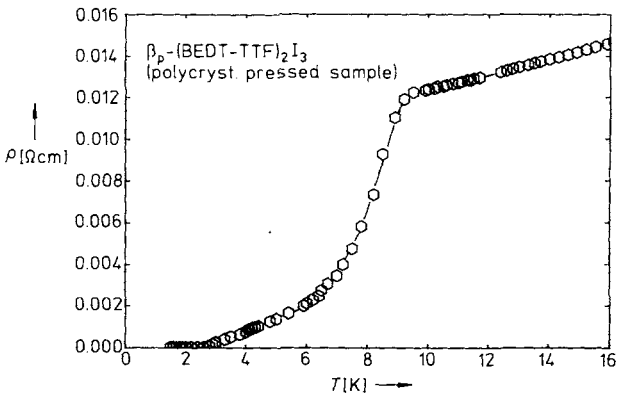


Fig. 2. Temperature dependence of the resistivity of polycrystalline pressed samples of β_p-(BEDT-TTF)$_2$I$_3$ in the temperature range below 16 K.

In order to obtain information on whether the observed superconductivity is a bulk effect of the sample or not, the

ADVANCED MATERIALS

AC susceptibility was measured at a frequency of 3 MHz with a field of about 0.2 Gauss. Figure 3 shows the increase in the resonance frequency of the LC-circuit due to exclusion of the RF-field by diamagnetic shielding currents in the polycrystalline pressed sample of β_p-(BEDT-TTF)$_2$I$_3$. There is clear evidence of an onset of diamagnetic shielding below 6 K (in samples of α_t-(BEDT-TTF)$_2$I$_3$ below 7 K). Here in the polycrystalline sample the onset for the diamagnetic shielding is far above the temperature where the resistivity becomes zero as is usually observed in single crystals of organic superconductors. The signal in Figure 3 which still

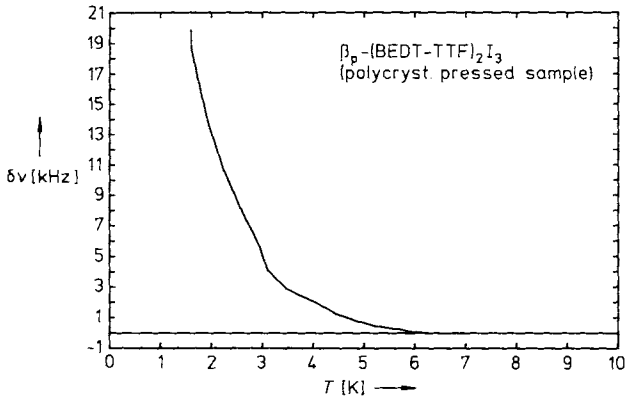


Fig. 3. Increase of the resonance frequency of an LC-circuit (3 MHz) due to exclusion of the RF-field by diamagnetic shielding currents (AC susceptibility) in a polycrystalline pressed sample of β_p-(BEDT-TTF)$_2$I$_3$ caused by cooling the sample from 10 K down to 2 K.

increases on cooling down to 2 K, corresponds to about 50% that expected for a perfect superconductor, indicating a clear bulk effect on the superconductivity in the polycrystalline pressed β_p-(BEDT-TTF)$_2$I$_3$ samples. Nevertheless, the large temperature range in which the frequency shift of the resonance frequency is observed shows that an inhomogeneous distribution of superconducting transitions exists in the sample. A similar broad distribution was already observed in the case of the polycrystalline pressed samples of α_t-(BEDT-TTF)$_2$I$_3$.

It should be mentioned that tempering of the polycrystalline pressed samples of β_p-(BEDT-TTF)$_2$I$_3$ for one or two days at 75 to 90 °C (as in the case of the samples of α_t-(BEDT-TTF)$_2$I$_3$) does not change the physical properties of the samples.

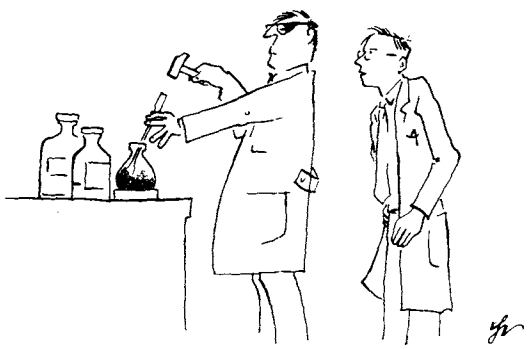
In conclusion, superconductivity at ambient pressure and 7.5 K exists in samples of β_p-(BEDT-TTF)$_2$I$_3$. The superconducting state is stable and the superconductivity is a bulk effect of the sample. Similar to the polycrystalline samples of α_t-(BEDT-TTF)$_2$I$_3$ here again structural phase transitions during the preparation of the samples under pressure seem to play an important role.

As a consequence of the structural phase transition, here in β_p-(BEDT-TTF)$_2$I$_3$, the transition temperature into the superconducting state is increased. This behavior reemphasizes that organic superconductors might also be of interest for industrial applications, as in the preparation of electronic devices polycrystalline materials are easier to use than single crystals. In addition, the discovery of bulk superconductivity in large pressed samples of crystallites of an organic metal of the typical diameter of 1 μm indicates that the observation of superconductivity in conducting polymers should also be possible.

Received: March 13, 1989

[1] D. Schweitzer, S. Gärtner, H. Grimm, E. Gogu, H. J. Keller, *Solid State Commun. 69* (1989) 843.
[2] H. Urayama, H. Yamochi, G. Saito, K. Nozawa, T. Sugano, M. Kinoshita, S. Saito, K. Oshima, A. Kawamoto, J. Tanaka; *Chem. Lett. 1988* 617.
[3] E. B. Yagupskii, I. F. Shegolev, V. N. Laukhin, P. A. Kononovich, M. V. Kartsovnik, A. V. Zwarykina, L. I. Buravov; *Sov. Phys. JETP Lett. 39* (1984) 12.
[4] K. Murata, M. Tokumoto, H. Anzai, H. Bando, G. Saito, K. Jajimura, T. Ishiguro; *J. Phys. Soc. Jpn. 54* (1985) 1236.
[5] V. N. Laukhin, E. E. Kostyuchenko, Yu. V. Sushko, I. F. Shegolev E. B. Yagupskii, *Sov. Phys. JETP Lett. 41* (1985) 81.
[6] F. Creuzet, G. Creuzet, D. Jérome, D. Schweitzer, H. J. Keller, *J. Phys. (Paris) Lett. 46* (1985) L-1079.
[7] F. Creuzet, D. Jérome, D. Schweitzer, H. J. Keller, *Europhys. Lett. 1* (1986) 461.
[8] M. Weger, K. Bender, T. Klutz, D. Schweitzer, F. Gross, C. P. Heidmann, C. Probst, K. Andres, *Synth. Metals 25* (1988) 49.
[9] P. C. W. Leung, T. J. Emge, M. A. Beno, H. H. Wang, J. M. Williams, *J. Am. Chem. Soc. 106* (1984) 7644.
[10] E. Gogu, D. Schweitzer, H. J. Keller, unpublished.
[11] E. Gogu, D. Schweitzer, H. J. Keller; *Physica C153-155* (1988) 491.

Call for Short Communications · Call for Short Communications · Call for Short Communications



... doesn't melt, won't dissolve, just can't be broken down – let's send it to ADVANCED MATERIALS!

ADVANCED MATERIALS

Biomaterials Highlights II

Materials for Biomedical Applications – High Long-Term Success Rates Might Pose New Problems**

By Günther Heimke*

The main influences on the survival rate of implants for a given purpose are:

- the implantation technique and the skill of the surgeon
- the implant material or materials
- the shape of the implant

At a first approximation, the second and third influences are typical engineering aspects. However, as the size, the shape, and the stiffness of an implant can influence the operational procedure, the implantation technique might also be influenced by engineers.

All three major groups of solids have been considered or are used as implant materials: organic solids (like plastics, textiles, even wood, but also ivory and other animal hard tissue) metals, and ceramics.

Plastics are widely used in soft tissue replacements and have stood the test of several decades of service in such different applications as resorbable and non-resorbable sutures, vascular grafts, intraocular lenses, and in many areas of corrective surgery. Their most common applications in orthopedic surgery are the polyethylene sockets in total hip replacements, inlays on the tibial components of total knee protheses and the polymethylmethacrylate (PMMA) bone cement.

The main metallic implant materials are the stainless steels, the Co–Cr–Mo alloys, and some titanium alloys. Today, the application of the stainless steels is essentially confined to temporary implants like bone plates and screws, intramedullary rods, and pins and wires because of their relatively high corrosion rate[1] (more than 75% of all retrieved stainless steel components show evidence of pitting and crevice corrosion). The Co–Cr–Mo alloys have increasingly replaced the stainless steels in all long term (if possible life long) applications like joint replacements and dental implants. In the latter field, these Co based alloys have been substituted almost completely by titanium and some of its alloys. In joint replacements, titanium alloys are also gaining ground.

In spite of being the oldest man made material, the ceramics have been the last group of materials to be considered and tested for implant purposes.[2] Some essentially bioinert oxide ceramics, in particular the highly pure and dense version of alumina ceramic, have found widespread applications for the articulating components in total joint replacements[3] and as dental implants.[4] The fascinating ability of some Ca-phosphate based ceramics, glasses and glass-ceramics (socalled bioactive ceramics) to form a strong bond to bony tissue has not yet be exploited for the fixation of load bearing implants because of the relatively poor mechanical strength and the instability of these materials in the body environment. Trials to overcome these problems by combining them with high strength metals are presently under way.

All of the well established implant materials have stood the test of short and, with the exception of the stainless steels, medium term clinical applications. They have contributed to the considerable increase of survival times and allowed for the use of such devices in younger and younger patients. This, in turn, necessitates the extension of the time of reliable service of all components of such implant systems to much more than ten years. However, all of these implant materials release some matter into their environment.

The presently used plastics and in particular their wear debris have been kept under careful observation without resulting in any alarming finding beyond their influence on the formation and widening of the radiolucencies along adjacent PMMA to bone interfaces. The destruction of the polyethylene sockets of total hip replacements by wear and cold working can be partially counteracted by the use of alumina ceramic for the heads instead of metal.[5] The contribution of the aging of the PMMA bone cement to the increases of the failure rates of total joint replacements has been the main motivation for the attempts to find other modes of implant fixation.

A carcinogenicity test on alumina ceramic was commenced together with the early compatibility studies of this material and proved negative.[6] No reports are yet available which would allow any judgment on medium or long term systemic effects of the bioactive ceramics to be made.

[*] Prof. G. Heimke
Department of Bioengineering
College of Engineering
Clemson University
Clemson, SC 29634-0905 (USA)

[**] For Part I see *Adv. Mater. 1989* 122; *Angew. Chem. Int. Ed. Engl. 28* (1989) 518; *Angew. Chem. 101* (1989) 534.

ADVANCED MATERIALS

There is, however, some concern about the long term systemic effects of the corrosion products from metals. Their corrosion rates are estimated to be 0.15 to 0.3 microgram/cm^2/day[7, 8] or about 11 to 22 mg/year for a typical total hip prosthesis. This was confirmed in a paper[9] presented at the recent US Biomaterials Conference. In 24 patients with an average implantation time of 9.8 years, total metal concentrations ranging from 2.6 to 248 microgram/g of dry tissue with an average of 35 microgram/g were found. (For comparison, the total body burden of an average person is less than 10 mg with concentrations in the order of 0.1 nanogram/g.[10])

Of course, the biological effects of the metals used in these alloys differ considerably. Traces of some of them are even needed in normal metabolism, like cobalt in vitamin (B_{12}) synthesis. The concentrations mentioned above, however, are far beyond such limits. Allergies to some of the metals, in particular nickel, cobalt, and chromium, are known and can be avoided by using titanium based materials. Titanium actually is the only metal with a record of several decades of clinical application during which no adverse effects have been reported in spite of the fact that sometimes considerable accumulations of fine Ti particles are seen in the vicinity of such implants.

Until now, there have been not more than ten reports of the occurance of tumors in direct relation to orthopedic implants, but three were published in 1986 and 1987 alone. With the extension of the survival times to the 15 and even 20 years region, information from the epidemiology of human workplace exposure to metal-bearing chemicals and other possible carcinogens with latencies in this order of magnitude must be considered.[10] In the same issue, a group from New Zealand reported on a statistical evaluation of the records of 1358 patients who had received total hip replacements between 21 and 15 years earlier.[11] Using the data of the New Zealand Cancer Registry, they could identify which of these 1358 individuals had developed malignant tumors and compare these numbers with the average rate of tumor occurance in this population. For 298 individuals no data could be made available. They were assumed in the main analysis to be healthy survivers. Table 1 shows the results of this evaluation which is based on a total of 14 286 person-years.

Table 1. The incidence of different kinds of cancer in patients with total hip replacements in comparison to the average population (summarized from [11]), expressed as the ratio of (cases observed in this study)/(cases expected in the average population).

follow-up in years	person years	Type of Cancers (ICD) all	breast (174)	colon & rectum (153 & 154)	bronchus & lung (162)	lymphatic & haemopoietic systems (200 to 208)
Less than 1	1328	1.31	–	0.31	0.71	5.26 $^+$
1 to 2	1293	0.46 *	–	–	0.93	–
2 to 5	3687	0.61 $^+$	0.24	0.38 *	1.16	1.62
5 to 10	5330	0.77 *	0.30 *	0.52 *	0.54	1.38
Over 10	2648	1.60 $^+$	1.01	1.48	1.51	1.66
Total	14286	0.91	0.36 $^+$	0.62 *	0.92	1.68 *
0 to 10		0.74 $^+$	0.22 $^+$	0.41 $^+$		

* p 0.05, $^+$ p 0.01

Generally, a significant decrease in overall cancer incidence up to ten years after operation and a significant increase in those followed for longer than 10 years can be seen. This initial decrease was no longer significant if the 298 individuals of uncertain status at the end of the study were removed from the evaluation.

There is, however, a significant increase overall in the incidence of tumors of the lymphatic and haemopietic systems. The cumulative effect remained significant through the entire study. If the tumors observed in the first two years were excluded, the increase in incidence in the remainder of the study period persisted, but decreased in significance (16/10.57 = 1.51, p = 0.07). The diagnosis for the total hip replacements in these 21 patients was 17 cases of osteoarthritis, two rheumatoid arthritis, and one each with idiopatic aseptic necrosis and Paget's desease.

After discussing many factors which might have influenced their results, the authors point to the fact that the risk of developing a lymphoreticular neoplasm remains small, increasing from 2 per 1000 in the normal population to 6 per 1000 in the study group over 10 years. Nevertheless, the long term biological effects of implants definitly require more detailed attention as their survival times increase.

Along the lines of this warning an Editorial in the January 1989 issue of the British Journal of Bone and Joint Surgery asked its readers to report all cases of malignant tumors along with the necessary details in order to find out if the ten cases reported until now may just be the tip of an iceberg. In addition, animal experiments are presently underway attempting to quantify serveral parameters in order to allow for a more reliable judgement on the risks and to provide possible recommendations to cope with these problems.

[1] S. D. Cook, *Clin. Orthop. 194* (1985) 236.
[2] G. Heimke, *Adv. Mater. 1989* 7; *Angew. Chem. Int. Ed. Engl. 28* (1989) 111; *Angew. Chem. 101* (1989) 113.
[3] P. Griss, G. Heimke in D. F. Williams (Ed.): *Biocompatibility of Clinical Implant Materials*, Vol. 1, CRC-Press, Boca Raton, FL 1981, p. 155.
[4] W. Schulte, *Zahnärztl. Mitt. 71* (1981) Issues 19 and 20.
[5] M. Semlitsch, M. Lehmann, H. Weber, E. Dörre, H.-G. Willert, *J. Biomed. Mater. Res. 11* (1977) 537.
[6] P. Griss, E. Werner, R. Buchinger, C. M. Büsing, G. Heimke, *Arch. Orthop. Unfall-Chir. 90* (1977) 29.
[7] S. G. Steinemann in G. D. Winter, J. L. Leray, K. de Groot (Eds.): *Evaluation of Biomaterials*, Wiley, Chichester 1980, p. 1.
[8] S. G. Steinemann, in A. Luterjering, U. Zwicker, W. Bunk (Eds.): *Titanium, Science and Technology*, Vol. 2, Deutsche Gesellschaft für Metallkunde, Berlin 1985, 1373.
[9] F. Betts, K. K. Hansraj, M. Bansal, T. W. Wright, Transactions of the 15th Annual Meeting of the Society for Biomaterials, April 28–May 2, 1989, 145.
[10] J. Black, *J. Bone Jt. Surg. Br. 70-B* (1988) 517.
[11] W. J. Gillespie, C. M. A. Frampton, R. J. Henderson, P. M. Ryan, *ibid*, 539.

Conference Reports

Magnetism in Washington

By Frans Greidanus *

The 1989 INTERMAG (International Magnetics Conference, Washington, USA, March 28.–31.) provided a forum for engineers and scientists to discuss the field of magnetics, from basic research to applications. The sessions included invited and contributed papers, poster sessions, workshops and tutorials. The total number of participants was approximately 800. The diversity of the field was indicated by presentations covering all branches of magnetics and related technologies. Topics discussed included recording heads, superconductivity, microwave components, numerical techniques and field calculations, hard magnets, amorphous magnets, magnetic measurements, recording systems, coercivity mechanisms, domains and domain walls, magneto-optics, magnetic separation and biomagnetism, thin film media, soft magnetic materials, perpendicular recording, and bubble and bloch line memories. Most of the conference took place in six parallel sessions. In the plenary session on March 29. Professor *Iwasaki* from Tohoku University was awarded the 1989 Cledo Brunetti Award for his contributions to the miniaturization of magnetic recording systems.

Also on March 29. a workshop on scanning electron microscopy with polarization analysis (SEMPA) was organized by *J. Unguris* from the National Institute of Standards and Technology (formerly called NBS). SEMPA is a relatively new technology which enables high resolution imaging of magnetic domains by the analysis of the polarization state of electrons reflected from a magnetic surface. In general there was much interest in magnetic domain imaging and related new techniques. Another new tool in this field is the magnetic force microscope. Its possibilities were reviewed in an excellent paper by *Rugar, Mamin, Stern, Fontana, Kasiraj, Mc-Fadyen* and *Lambert* from IBM and optical imaging techniques were reviewed in a paper by *Argyle*, also from IBM.

Materials played an important role at the 1989 INTERMAG conference. Examples are Ba-ferrite as a promising new magnetic recording material, the use of magnetic Co/Pt multilayers for magneto-optical recording, and the application of NdFeB permanent magnets in magnetic imaging devices for clinical applications using NMR.

A substantial number of papers dealt with magnetic recording. Of these about 100 were devoted to magnetic recording, and about 40 to magneto-optical recording. On March 28. a symposium on the status and future of magnetic and magneto-optical disk-drive technologies was organized by Professor *M. Kryder* from Carnegie Mellon University. In this symposium *G. Hughes* (Seagate), *F. Greidanus* (Philips), *D. Rugar* (IBM) and *T. Toshima* (NTT) presented their views. Magneto-optical recording will find its place in the market, but the question whether it will (partially) replace Winchester technology remains to be answered.

An important issue in magneto-optical recording is "direct overwrite." Papers by *Nakao, Sukeda, Ojima, Taka* and *Nishiyama* (Hitachi) and *Greidanus, Jacobs, Spruit* and *Klahn* (Philips) discussed the field-modulation technique. *Kryder, Shieh, Schultz* (Carnegie Mellon), *Meiklejohn* and *Skoda* (MOVID Information Technology) showed real time movies of the writing and erasing of domains with a single laser, operating under different conditions. *Van den Berg* and *Röckelein* (Siemens) proposed two new "direct overwrite" schemes, employing two magnetic layers separated by a thermal insulating layer. It is clear that this subject will attract more attention in the coming years.

Kano, Shono, Kuroda, Koshino and *Ogawa* (Fujitsu) reviewed the possibilities of sputtered garnets for future applications in magneto-optical disks. With garnet layers deposited on Gandolinium Gallium Garnet (GGG) single crystals

[*] Dr. F. J. A. M. Greidanus
Philips Research Laboratories
Eindhoven (Netherlands)

ADVANCED MATERIALS

they have been able to achieve a carrier to noise ratio (CNR) of 60 dB ($v = 0.5$ MHz, $bw = 30$ kHz, $v = 10$ m/s). By depositing the same layers on glass substrates the CNR dropped to 50 dB. Most papers in the session on magneto-optical recording materials were devoted to multilayers (or layered structures) consisting of alternating Co and a non-magnetic metal e.g. Pt or Pd, each individual layer having a thickness of only a few atomic layers. *Ochiai, Hashimoto* and *Aso* (Sony) reported on the magnetic and magneto-optical properties of Co/Pt and Co/Pd ultrathin multilayered films. *Tsunashima, Nagase, Nakamura* and *Uchiyama* (Nagoya Univ.) discussed the possible role of magnetostriction in Pd/PdCo multilayers. *Zeper, Greidanus* and *Carcia* (Philips-Du Pont) were the first to report on thermally written domains and recording experiments in Co/Pt multilayers. In thin (20 nm) films they obtained a CNR of 53 dB ($v = 1.0$ MHz, $bw = 30$ kHz, $v = 5$ m/s). This value approaches the CNR-values obtained in GdTbFe thin films. Multilayers of Co and Pt offer the advantage of increased magneto-optical efficiency in the blue, an important feature for future higher density recording. Furthermore, they are very resistant against corrosion and oxidation and there is no need to apply protective layers. The application of multilayers for magneto-optical recording is an exciting possibility, and increased activitity in this area is anticipated.

In this short report it is impossible to review all subjects discussed at the 1989 INTERMAG. Those who are interested in further information I refer to the contributed and invited papers which will be published in the IEEE Transactions on Magnetics.

Liquid Crystals in Schladming

By Peter Laggner*

One hundred years after the discovery of liquid crystals by the Austrian botanist *Friedrich Reinitzer* was a good time for the VI. European Liquid Crystal Winter Conference (5.–10. March 1989) to be held in Schladming, Austria. This triennial series of 'European' conferences tends to be different from the bigger 'International' conferences as the program is topically confined in order to promote coherent discussion, to reflect the interests of the groups in the organizer's country, and to leave plenty of time and opportunity for less formal interaction.

A specific attraction of this series of conferences is the choice of venue. Previous conferences were held at Les Arcs (France), Madonna di Campiglio (Italy), Garmisch-Partenkirchen (FRG), Bovec (Yugoslavia) and Borovets (Bulgaria) all being winter sports centers. A sport hotel at Schladming this year served this purpose admirably.

The aim of this conference was to bring into fusional contact the two traditionally separate nuclei of liquid crystal research, biology and technology, in order to cross-fertilize the separately developed but related physical and chemical concepts. Thus, under the title "Liquid Crystals in Biology and Technology: Supramolecular Structure, Dynamics and Function" about 130 scientists from 21 nations (not only European) gave 17 lectures (35 min.) and 20 oral contributions (15 min.) and presented 69 posters, representing fields of interest ranging from medical biophysics, chemistry and physics to polymer and display science and technology.

[*] Prof. P. Laggner
Institut für Röntgenfeinstrukturforschung
Österreichische Akademie der Wissenschaften
Steyrergasse 17, 8010 Graz (Austria)

The topics covered in biology included the following: Biomembrane structure and dynamics, polymorphism and dynamics of lipids, Langmuir-Blodgett films, and carbohydrate liquid crystals. Technological topics included amphotropic polymer liquid crystals, chiral main-chain liquid crystals, thermal imaging systems and plastic materials.

An overlap region was presented in the fields of molecular engineering, membrane mimetic chemistry, and drug delivery systems. The first day was devoted to these overlapping topics where concepts from the study of biological membranes combined with synthetic chemistry are used to design devices in the true sense of molecular engineering. *A. Ruaudel-Teixier* (CEN, Saclay, France) and *J. Fendler* (Syracuse University, USA) presented two technically distinct approaches, the LB-film technique on solid interfaces and the BLM (bilayer lipid membrane) technique, where a single membrane of a few nanometers thickness separates two macroscopic aqueous compartments. Both approaches were originally analytical tools in membrane biophysics but are now developing rapidly in the direction of molecular electronics, photonics and sensing devices of ultimate miniaturization. Still in its infancy, as far as marketable products are concerned, this line of research was shown to hold great promise.

Ambitious molecular engineering projects require intelligent chemistry combined with structural information. *L. Feigin* (USSR Academy of Sciences, Moscow) emphasized this point and showed how X-ray small-angle diffraction techniques can provide useful data on the supramolecular architecture of oligo- and multilayer systems of high complexity. Particularly instructive, also in this context, was the

presentation of new X-ray and neutron reflectivity techniques on monolayers at a liquid surface (*J. Als-Nielsen*, Risø National Lab., Denmark). The spectacular achievement of performing the X-ray structure analysis of a single monolayer, can only be realized with high-flux photon sources such as synchrotrons.

The second day's program moved further into the more classical field of lyotropic liquid crystal phase structures and dynamics. An analytical approach to the interpretation of periodic, two-dimensional domain patterns in monolayers under conditions of 'solid-fluid' phase coexistence was presented and discussed in terms of electrostatic and interfacial forces by *R. M. Weis* (Univ. of Massachusetts, Amherst, USA). *P. Fromherz* (Univ. Ulm, FRG) discussed conservative and dissipative instabilities in lipid bilayers which are involved in the formation of different supramolecular structures, such as micelles or closed bilayer vesicles, and in the appearance of oscillatory or solitary waves in a 'fluid-mosaic' membrane containing ion-channel proteins.

A long standing problem of general physico-chemical interest concerns the kinetics and mechanism of phase transitions. This problem was addressed by *B. Tenchov* (Bulg. Acad. of Sci., Sofia, Bulgaria) and *P. Laggner* (Institute for X-ray Fine Structure Research, Graz, Austria) with time-resolved X-ray diffraction studies, using synchrotron X-ray sources, on the specific question of the thermal transitions of lipid bilayers. A wealth of hitherto unavailable information on short-lived intermediate states promises to fill the gap between largely unknown structural mechnisms and the thermodynamic and spectroscopic data which have already reached a high standard but which contain less structural information. Fluorescence spectroscopy on liposomes and LB-films, was reported by *P. Kinnunen* (Univ. Helsinki, Finland) to show indications of regular distribution patterns which might be related to the minimization of steric elastic strain in an assembly of host-guest molecules of different sizes. This phenomenon may be functionally important in biomembranes but also has implications for technological lipid film design.

Deuterium NMR spectroscopy, as a tool to probe molecular interactions at membrane surfaces, was covered by *A. Watts* (Univ. Oxford, U.K.). Being practically nonperturbing and amenable to site-specific labeling, this technique continues to provide new and important information, particularly with regard to lipid-protein interactions. Still with a strong analytical accent in membrane biophysics, but already pointing towards a potential in biosensor development, *L. Tamm* (Biocenter, Univ. Basel, Switzerland) presented studies on monoclonal anti-lipid antibodies and their interaction with fluorescence labeled lipid membranes supported on silicon wafers. Lateral diffusion and domain segregation depending on the thermotropic state of the lipids were analyzed. Similar investigations were extended to other interesting membrane proteins, such as signal peptides which are important components in cellular protein biosynthesis and processing.

Both biologically and technologically important systems were discussed on the third day. *D. Small* (Boston Univ., USA) presented a comprehensive overview on the lyotropic and thermotropic phase behavior of soaps and acid-soap complexes. A profound combination of thermodynamic and X-ray diffraction data linked to the scholarly use of Gibbs phase rule demonstrated the value but also the complexity of physical chemistry in this field. The potential of lipid/bile salt systems, analyzed with respect to their mesomorphic structure and dynamics by NMR and light-scattering techniques as suitable media for controlled drug delivery systems was discussed by *B. Lindman* (Lund Univ., Sweden). Cubic phases formed by monoolein-water were described as particularly promising candidates for systems that can encapsulate both hydrophilic and lipophilic drugs as they are stable under the wide range of conditions required for pharmaceutical purposes.

The chemical and structural aspects of a hitherto rather neglected class of mesogenic substances based upon inositol-derived compounds were reviewed by *K. Praefcke* (Techn. Univ. Berlin, FRG). These discotic carbohydrates form strongly hydrogen-bonded superlattices with thermotropic liquid crystalline behavior and frequently contain hexagonal columnar phases.

Structure-property relationships of liquid crystalline polymers were discussed by *E. Chiellini* (Univ. Pisa, Italy). His presentation focussed on chiral main-chain polyesters produced by the poly-condensation or polyaddition of chiral and non-chiral components. These polymers offer opportunities for the design of materials with specific properties and a wide variety of thermotropic states. The concept of amphotropic liquid crystal polymers was presented by *F. Kuschel* (Univ. Halle, GDR). Here, lyotropic properties are confered to linear polymers by the attachment of alcohol side-chains resulting in comb-like polymeric structures. These structures, which are in principle rather similar to smectic lipid multilayer systems, show stable mesomorphic behavior which can be influenced discretely by variations in main chain flexibility, length and nature of the side chains, and by swelling in water. Apart from being interesting models for the investigation of the intermolecular forces that govern mesomorphism, these systems also show promise as matrix components in pharmaceutical applications.

The last day of the conference was devoted to liquid crystal materials in fields where industrial applications already exist or are imminent. *B. Holcroft* (Thorn-EMI Res. Labs, Hayes, UK) discussed recent advances in the fabrication of thermal imaging films based upon the Langmuir-Blodgett technique. LB films optimized for pyroelectric properties and low thermal conductance of the substrate have been shown to be promising as practical devices for low-light thermal imaging.

Finally *D. Fleischer* (Hoechst AG, Frankfurt, FRG) gave an overview on high performance polymers based upon thermotropic liquid crystals. This presentation highlighted the manifold merits of such materials for extreme applications,

ADVANCED MATERIALS

e.g. in microelectronic devices, in chemical industry, aerospace technology and medicine. He also gave an impression of the many criteria that have to be optimized in industrial high-tech product development.

The framework of lectures complemented well the short contributions and poster presentations. A best-poster award was presented to *G. Hertel, H. Hoffmann* and *J. Kalus* (Univ. Bayreuth, FRG) for their neutron small-angle scattering study on the magnetic field alignment of the nematic phases of surfactants.

On the whole, the attempt to combine biological and technological aspects of liquid crystal research in one conference was well received and stimulated much discussion.

A book of abstracts is available from the author of this report.

Ferromagnetic and High Spin Molecular Based Materials in Dallas

By Joel S. Miller * and Dennis A. Dougherty *

The first symposium focusing on several aspects directly related to high spin and molecular/polymeric ferromagnets convened April 9–12, 1989 as part of the 197th National American Chemical Society meeting in Dallas, Texas, USA. This multidisciplinary meeting brought together inorganic, organic, organometallic, polymer, and physical chemists as well as theoretical and experimental condensed matter physicists from Japan, the USSR, the UK, France, Germany, Italy, Spain, Bulgaria, and the USA. The symposium was comprised of a tutorial and sessions devoted to the preparation and characterization of a 'designer magnet' from organic, organometallic, inorganic, and polymeric materials. This broad interdisciplinary symposium was unusual as it was co-sponsored by the Divisions of Inorganic, Organic, Polymer, and Physical Chemistry of the ACS and additionally supported by the Petroleum Research Fund and Gordon & Breach (Science Publisher). A total of 39 verbal and 25 poster papers were presented and the proceedings will be published as a forthcoming volume of *Molecular Crystals, Liquid Crystals*.

The tutorial session enabled attendees to appreciate the conceptual framework on which the current understanding of cooperative magnetic phenomena in molecular/organic/polymeric systems is based. *D. A. Dougherty* (Caltech) concisely reviewed the key criteria for stabilizing a triplet ground state, the building block of a high spin molecule or polymer. *J. S. Miller* (Du Pont) described the existing paradigms, while the fundamental physics of magnetism were reviewed by *A. J. Epstein* (Ohio State). Models for magnetic order and neutron diffraction aspects were presented by *P. Day* (Institut Laue-Langevin) and insight into the realities of opportunities for molecular based magnets was provided by *R. M. White* (Control Data Corp.). Due to their low density, high molecular weight, and low spin-orbit coupling, competition with existing magnets seems unlikely; however, opportunities might exist in fine particle and magnetooptic recording.

The strategies for designing molecular/polymeric materials with ferromagnetic coupling include: a) unpaired electrons in orthogonal orbitals sharing the same spatial region, b) Heitler-London spin exchange, c) antiferromagnetic coupling of sites with differing S values (ferrimagnet), d) conjugated odd-alternate hydrocarbons, e) polaronic, conjugated block copolymers, and f) configurational admixture of triplet charge transfer excited states. High spin systems demonstrating the feasibility of several of the strategies were discussed and a few high moment materials were described. It was emphasized universally that the rational design of solid state structures remains an art that limits our ability to prepare the secondary and tertiary structures needed to test many concepts in solid state science. Frequently, complex, solvated compositions with undesired or new structure types form instead of the desired phase. Additionally, several polymorphs may form in lieu of the desired structure type. This is particularly crucial for the formation of a bulk ferromagnet as ferromagnetism is a 3-D (bulk) not a 1-D property.

[*] Dr. J. S. Miller
Central R & D Department
E. I. du Pont de Nemours & Co., Inc
Wilmington, DE 19880-0328 (USA)
Prof. D. A. Dougherty
Department of Chemistry
California Institute of Technology
Pasadena, CA 91125 (USA)

The challenge of rationally controlled spin preferences of small organic molecules was addressed by *J. A. Berson* (Yale), *W. T. Borden* (Univ. Washington), *P. Dowd* (Pittsburgh) and *D. J. Klein* (Univ. Texas at Galveston). While there have been considerable successes, it is clear that for finely balanced systems, present computational methods cannot yet predict the singlet-triplet energy gap to better than a few kcal/mol for modest-sized molecules. A means to experimentally determine the singlet/triplet gap particularly for ground state triplet substances is unavailable, but would be of great value. *H. Iwamura* (Univ. Tokyo) and *K. Itoh* (Osaka City University) have prepared variously substituted extended carbene systems, reaching spin states as high as $S = 5$ in a pentacarbene. The spin coupling capacities of various π topologies were discussed, and the first ferrimagnetically coupled organic molecule was reported by *Itoh*. *Dougherty* described a high spin state ($S = 2$) in a partially localized system, involving ferromagnetic coupling through a cyclobutane ring.

The most extensively characterized organic, organometallic, and inorganic high spin compounds exhibiting magnetic or incipient magnetic order were galvinoxyl [*M. Kinoshita* (Univ. Tokyo)], decamethylferrocenium tetracyanoethenide [DMeFc][TCNE] (*Epstein* and *Miller*) and $Mn^{II}Cu^{II}$[oxamido-*N,N'*-bis(2-benzoato)] · H_2O, [*O. Kahn* (Univ. Paris, South)] and Mn(hexafluoroacetylacetonate)$_2$tetramethyl-*n*-propylnitronylnitroxide [*D. Gatteschi* (Florence)]. Galvinoxyl exhibits strong ferromagnetic coupling (Curie-Weiss $\theta = +19$ K), however, a still to be understood phase transition, which can be suppressed by doping with hydroxygalvinoxyl, occurs at ~ 85 K. The Mn^{II} containing coordination polymers exhibit spontaneous magnetization in accord with ferrimagnetic ordering at 14 and 8.6 K, respectively. The most extensively characterized molecular magnet, [DMeFc][TCNE] [i.e., $\theta = +30$ K, 1 kOe coercive field, α–δ critical constants, and ferromagnetic ordering at 4.8 K confirmed by neutron diffraction], comprises isolated radical cations and radical anions without the benefit of an extended network solid state structure. Substitution of chemically important features of [DMeFc][TCNE] lead to the characterization of several ferromagnetically coupled systems. An additional bulk ferromagnet, however, remains elusive. The extended McConnell model of the configurational admixture of triplet charge transfer excited states appears at present to provide the best understanding of the mechanism of ferromagnetic coupling for this system and enables the prediction of magnetic coupling for related systems.

Based upon this McConnell model several groups have targeted the preparation of radicals to test the model and its special cases. Three-fold or higher symmetry donors containing nitrogen were discussed by *R. Breslow* (Columbia) and *D. A. Dixon* (Du Pont), whereas *L. Y. Chiang* (Exxon) reported on an oxygen containing donor and *F. Wudl* (UCSB), *J. Yamaguchi* (Kyoto), and *J. P. Morand* (Bordeaux) described their successes in preparing sulfur containing donors. *Wudl* also elaborated upon the preparation of 1,3,5,-tris(tricyanovinyl)benzene. In the best characterized system, the six-fold symmetric hexaazaoctadecahydrocoronene system, *Breslow* and *Dixon* noted that distortions to the diamagnetic dication readily occurred and conjectured that this distortion may be circumvented by going to a three-fold symmetric system. Ferromagnetically coupled systems, however, have yet to be prepared with such donors.

Two unusual ferromagnetically coupled high spin polynuclear clusters were reported. *D. C. Johnston* (Iowa) and *D. N. Hendrickson* (UCSD) reported $S = 6$ $[Cr_4^{III}S(O_2CMe)_8(H_2O)_4]^{2\oplus}$ and $S = 14$ $[Mn_8^{III}Mn_4^{IV}O_{12}(O_2CPh)_{16}(H_2O)_4]$, respectively. A microscopic understanding of the mechanism of spin exchange is unknown; however, the 'orbital ordering' mechanism described by *Day* in for example Rb_2CrCl_4 may be applicable. Additionally, a ferromagnetically coupled $S = 9/2$ $Cr^{III}Ni_3^{II}$ cluster was described by *Kahn* and a $S = 12$ $[Mn^{II}$(nitronylnitroxide)$]_6$ ferrimagnetic ring was presented by *Gatteschi* and *Rey*. Novel liquid crystals (*W. Haase*, Darmstadt) exhibiting antiferromagnetic and ferromagnetic order and monomolecular films (*H. M. McConnell*, Stanford) exhibiting long range order captured the imagination of the audience.

The preparation of organic polymers exhibiting high spin if not ferromagnetic order is attracting significant attention. *Iwamura* described materials based on polyacetylenes with radical pendant groups. *A. L. Buchachenko* (Institute of Chemical Physics, USSR), *M. Ota* (Gumna U.), *A. A. Ovchinnikov* (Institute of Chemical Physics, USSR), and *J. B. Torrance* (IBM) described their respective approaches, i.e., silicone based polymers, photooxidation of triarylmethane based polymers, pyrolysis of polyacrylonitrile, polymerization of nitroxyl containing diacetylenes, and iodine oxidation of 1,3,5-triaminobenzene. A reproducibly prepared, well characterized system has been elusive. In post deadline poster contributions *D. W. Wiley* (Du Pont) and *C. J. O'Connor* (Univ. New Orleans) independently reported that prototype dinitroxyl diacetylenes monomers (each crystallizing into two polymorphs) to test the concept of preparing high spin polymer, could not be topochemically polymerized and did not exhibit high spin, ferromagnetically coupled behavior. Theoretical guidance for designing new polymers was additionally described by *N. N. Tyutyukov* (Bulgaria Academy of Science) and *T. Hughbanks* (Texas A & M at College Station).

Clearly the embryonic quest for molecular/polymer based magnetic materials is a thriving area of research. The synthetic challenges are formidable as ferromagnetism, being a bulk and not a molecular property, requires that materials with specific primary, secondary, and tertiary structures be made. The rational design of solids remains an art that limits our ability to prepare such structures.

Nonetheless, several examples of deliberately designed high moment, magnetically ordered materials have been prepared and we look toward a future where ferromagnetic phenomena can be added to the repertoire of physical properties enjoyed by molecular/polymeric materials.

Book Reviews

Microbeams, Surfaces and Sieves

Spectroscopy of Surfaces. Edited by *R. J. H. Clark* and *R. E. Hester*. Wiley, Chichester 1988. xxi, 488 pp., bound US $ 190. – ISBN 0-471-91895-4

This book gives a comprehensive review on the state of the art in selected surface spectroscopies. Except for the chapters by *J. C. Vickermann* on Static Secondary Ion Mass Spectroscopy and by *F. P. Netzer, J. A. D. Matthew* and *E. Bertel* on Electron Excited Surface Spectroscopies, vibrational spectroscopies are discussed. The articles describing the principles and theoretical background of Raman-, IR-reflection absorption-, Inelastic Tunneling- and High Resolution Electron Energy Loss Spectroscopy are comprehensive and clearly written. The book is a good introductory text for advanced graduate students and a useful reference text for researchers in surface and interface science.

The first chapter "Structure and Orientation in Thin Films: Raman Studies with Integrated Optical Techniques" is written by *J. F. Rabolt* and *J. D. Swalen* who pioneered the use of optical spectroscopies to probe organic thin films prepared by Langmuir-Blodgett techniques or by self-assembly through adsorption on a solid surface. They describe the theory of Waveguide Raman Spectroscopy (WRS) starting from basic principles and discuss layered structures to which the technique can be applied. Examples are given to show how different modes of the light beam can be used to emphasize the signal from different layers of the thin films and how polarization dependent measurements are used to determine the molecular structure in thin films. The application to adhesion studies and molecular interactions between thin films is demonstrated for a poly(vinylalcohol)/poly(methylmethacrylate) (PVA/PMMA) composite wave guide.

In chapter two "The Selection Rules for Surface-Enhanced Raman Spectroscopy (SRS)" by *J. A. Creighton* the different physical mechanisms leading to the SERS effect are explained. Their relative contributions to the resulting enhancements are discussed with reference to the spectra of molecular adsorbates at metal-electrolyte and metal-gas interfaces. In a clear and concise way the criteria to distinguish between electromagnetic, resonance and modulated charge transfer enhancement are described and suggestions for further experiments are given. Utilizing the SERS effect to determine the orientation in adsorbed organic films is clearly one of the future applications of the technique.

T. M. Cotton reviews the application of SERS to biological systems in her chapter "The Application of Surface Enhanced Raman Scattering in Biochemical Systems". As an introduction to the subject, she summarizes the theories of electromagnetic and charge transfer enhancement and the experimental aspects of SERS. The biological application of SERS are demonstrated with data obtained for DNA, proteins, lipids and studies of the interaction of dissolved enzymes with coenzymes and substrates. Absolute detection limits in the picogram range have been achieved for aromatic compounds and dyes which make SERS a powerful analytical technique in materials science.

In chapter four *J. C. Vickerman* reviews Secondary Ion Mass Spectrometry (SIMS) and discusses new applications in surface science and materials analysis. Static SIMS applied to the study of thermodynamic quantities in adsorbed layers, and imaging SIMS are two examples in this comprehensive review.

The technique of Inelastic Electron Tunneling Spectroscopy (IETS) for the study of vibrational modes of surface species is free from the normal selection rules other vibrational surface spectroscopies are subject to. In chapter five *N. M. D. Brown* discusses this technique where the adsorbates to be measured are introduced as dopants in the insulator component of a metal-insulator-metal tunnel junction.

Chapter six, written by *F. P. Netzer, J. A. D. Matthew* and *E. Bertel*, is devoted to exited electron spectroscopies in surface science. Whereas Auger-Electron Spectroscopy is routinely used to determine the chemical composition of surfaces, detailed information about the chemical state of the adsorbate and its adsorption site can also be determined from the Auger transitions involving valence electrons and from angular effects. Electron Energy Loss Spectroscopy (EELS) on clean and adsorbate covered surfaces, involving electronic transitions, is discussed in detail. Excellent summaries including illustrative examples are given for Electron Stimulated Ion Desorption (ESD) and Inverse Photoemission Spectroscopy (IPES).

The last two chapters of the book are devoted to vibrational surface spectroscopies, i.e. "High Resolution Electron Energy Loss Spectroscopy" (HREELS) applied to clean and adsorbate covered surfaces is reviewed by *M. A. Chesters* and *N. Sheppard*, and "Infrared Reflection-Absorption Spectroscopy (IRAS) of Adsorbed Molecules" is discussed by *A. M. Bradshaw* and *E. Schweizer*. *Chesters* and *Sheppard* make detailed comparisons of HREELS with IRAS and Raman spectroscopy and emphasize the relative merits of the techniques. This article on HREELS is an excellent introduction to this important technique. *Bradshaw* and *Schweizer* review the use of IRAS on metal and semiconductor surfaces, discuss those factors which are important in the optimization of the IRAS experiment, and compare dispersive and interferometric instruments. The examples given to demonstrate the state of the art in IRAS include hydrogen adsorption on tungsten and silicon surfaces, CO adsorption on Pt(111), K/Pt(111) and stepped platinum surfaces, and the detailed spectroscopic study of surface formate and surface methoxy species.

Like the last article, the book as a whole is not only an excellent introduction to modern techniques in surface science. The many practical hints and comments make it a valuable hand-book in materials science and surface science laboratories.

Michael Grunze
Angewandte Physikalische Chemie
Universität Heidelberg (FRG)

Zeolite Molecular Sieves. By *A. Dyer*. Wiley, Chichester 1988. xi, 149 pp., bound, £ 25.70.—ISBN 0-471-91981-0

Crystalline microporous solids replete with cavities and channels of molecular dimension (3 to 10 Å diameter) are all the rage these days. Not only are they important, as they have been for several decades past, as adsorbents, ion-exchangers and catalysts, they are also promising materials for applications such as second harmonic generation (in laser technology), as the basis of novel microdevices for electro- and photo-catalysis, and potentially as novel membranes in a range of new laboratory-scale and commercially viable fuel cells.

Good books on the fundamentals of zeolite structure and properties exist already, the ones by *Breck* (Wiley, 1974) and *Barrer* (Academic, 1978) and Special Publication No. 23 "The Properties and Applications of Zeolites" (edited by *R. P. Townsend*, the Chemical Society, London, 1980) as well as ACS Symposium Series 218 on "Intrazeolite Chemistry" (Ed. *G. D. Stucky* and *F. G. S. Dwyer*), being particularly noteworthy. There is also a relatively large collection of admirable review articles devoted to various aspects of the science and technology of zeolites which have appeared in the last five years.

This book adds very little to the information already collated in the open literature. It consists of ten brief chapters, the contents of which provide hardly any new items of information and precious few chemical or other surprises. For that reason alone it cannot be recommended as a favored introductory text, which is what it purports to be. In parts the text reads like advertisers copy. Thus, on p. 84, we are told in arid terms that horticultural applications (of clinoptilolite and mordenite) generally use 5 to 10% incorporation of the zeolite into growing media. "The value of this has been shown in the production of tomatoes, bell peppers, house plants and strawberries", and that "obviously ion exchange has a role in these phenomena".

There are a number of misprints. On p. 81 there is talk of "large part mordenite" (not large port) and Figure 80 is labelled 'Tonic' rather than 'Ionic' radius.

More serious, however, is the improper use of figures and micrographs published elsewhere. Figures 42 and 43, for example, appeared in ACS Symposium Series 218 (p. 183, (1983)) and the Springer Series in Surface Science 5 (p. 124, 1986). Had the senior author of these original publications been consulted, and his permission to re-publish sought (a common courtesy), this text would not, as now, be in breach of copyright law.

John M. Thomas
Royal Institution of Great Britain
London (UK)

Problem-Solving with Microbeam Analysis. By *K. Kiss*. Elsevier, Amsterdam 1988. 410 pp., hard cover, Dfl 245.00.—ISBN 0-444-98949-8

Microbeam techniques have matured into appropriate methods for the characterization of materials on the micron- and even submicron scale. During the last two decades, instruments such as the electron microprobe and the scanning electron microscope went on the production line and are now in third generation development. Other instruments, e.g. the electron- and ion probes have been constructed and have become commercially available, and, although numerous further instruments have been designed and significant applications have been announced, their ultimate breakthrough has not yet been achieved.

On the other hand, the characterization of microstructures is of high-ranking value in quality assurance and materials research. More and more applications become known, and more commercially available instruments become useful in the guidance of research, especially in high-tech industries. Obviously, each one of these techniques has special capabilities, but none of them are suited to uniquely cope with all the complex problems. Besides, instrument prices in the range of 100 000 to 600 000 US $, and operation costs are very high.

Each technique has its own specific literature, but apart from reviews and proceedings, there exists as yet no survey on the various techniques and their respective fields of application. This book fills this gap and will help engineers, analysts and scientists facing various microanalytical problems to work with those techniques or to select the above mentioned expensive intruments.

Part 1 deals with optical and electron microscopy, X-ray and electron spectroscopy, with ion beam methods as well as Raman and laser techniques. One chapter summarizes those methods especially used for the control of microelectronic devices, another is devoted to the combination of complementary techniques and the last chapter is involved with the strategy of selecting the most suitable technique for solving the problem.

Part 2 includes a great variety of case histories and selected applications of the various techniques. Two entire chapters are devoted to synthetic polymers and microelectronics, a third to miscellaneous problems in metallurgy and corrosion as well as glasses and ceramics, catalysts, fibers, food products, cosmetics and the environment. The numerous examples of failure analysis and trouble shooting reflect the author's wide experience. The book concludes with a bibliography of 829 references, a glossary of acronyms and a subject index with about 1200 keywords.

The advantages and limitations of the individual techniques are evaluated adequately and critically and listed concisely. It is intentional that the finer details of the various methods have been omitted or abridged. However, this reviewer would have wished for some more fundamental information on particular techniques: (i) Optical microscopy is insufficiently described. The principle is mentioned, and some variants such as phase or interference contrast microscopy are discussed briefly, but knowledge of the fundamental figures of merit like spatial resolution, magnification and depth of field are assumed. (ii) X-ray spectroscopy is, in general, based on the Moseley law, and focusing spectrometers fulfill the Rowland condition: no mention is made of either of these two rules. On the other hand, an entire page (p. 54) is spent on artifact peaks called escape-peaks, although the formula $E = E_c - 1.74$ keV would have been self explanatory. (iii) The chapter describing electron spectroscopy in only eleven pages is meagre throughout and in this case a comparison of advantages and limitations is missing. (iv)

The basic modes of operation within microbeam analysis; the recording of line scans, area maps and depth profiles, are certainly not common knowledge and should have been described.

The main emphasis is placed on the methods and applications in the semiconductor and microelectronic industries. Recent innovations like the small-spot ESCA and the LMIS (liquid metal ion source) have been considered and modern analytical electron microscopy is treated in greater detail. On the other hand, there is no mention of the recent development of the STM (scanning tunneling microscope) and the two methods, PIXE (proton-induced X-ray emission) and SXRF (synchrotron X-ray fluorescence), have not even been briefly referred to. Both methods, like RBS (Rutherford backscattering) are dependent on accelerators or storage rings which are scarcely available to the general public, but are very effective.

The literature coverage in both parts of the book is somewhat dated, the mean value lying in the middle of the 70's (only 14% of the citations are dated after 1983) and about 25% of the references are second-rate (sales brochures, internal reports, technical notes, etc.). Some representations are also poor (e.g. Figure 1-74).

Overall, the book is generously illustrated with figures and relatively free of printing errors (Rushka instead of *Ruska*, p. 20; $K_{1,2}$ instead of $K\alpha_{1,2}$, p. 123). However, a great disadvantage is imposed by the great number of figures of poor quality. Of the 306 figures contained in the book, more than half are photographs, mainly included in Part 2, and the majority of these are reproduced badly. This is partly due to bad models, partly to poor quality of the paper – and this at a price which cannot be considered as low. Only the photographic reproduction of Figures 2-35 to 2-38 and the five color photographs is acceptable.

It is for these reasons that the book cannot be recommended without reservations. But since the demand for such a survey is certainly great, the author as well as the publishers should be encouraged to commence with preparations for a revised edition.

Reinhold Klockenkämper
Institut für Spektrochemie
und angewandte Spektroskopie,
Dortmund (FRG)

Conference Calendar

August 1989

13–26 **High-T_c Superconductors**
NATO Adv. Study Inst.
Bad Windsheim (Fed. Rep. Germany)
Contact: R. Kossowsky, Applied Res. Lab., Pennsylvania State Univ., P.O. Box 30, State College, PA 16804, USA

14–17 **Shock Compression of Condensed Matter**
APS Top. Conf.
Albuquerque (USA)
Contact: A. Roach, MS-P 915, Los Alamos Nat. Lab., Los Alamos, NM 87545, USA

14–18 **Hopping Transport**
8th Conf.
Chapel Hill (USA)
Contact: M. Pollak, Dept. of Phys., Univ. of California, Riverside, CA 92521, USA



16–18 **Properties Through Processing**
Amherst (USA)
Contact: H. H. Winter, Dept. Chem. Eng., Univ. of Massachusetts, Amherst, MA 01003, USA

20–24 **Imaging Systems—150 Years of Photography**
Int. Symp. (ISIS '89)
Dresden (German Dem. Rep.)
Contact: Conf. Secretary, ISIS '89, Technische Univ. Dresden, Sektion Physik, Wissenschaftsbereich Photophysik, Mommsenstr. 13, DDR-8027 Dresden, GDR

20–25 **Crystal Growth: Progress in Science and Technology**
9th Int. Conf.
Sendai (Japan)
Contact: Prof. T. Nishinaga, Inter Group Corp., Akasaka Yamakatsu Bldg., 8-5-32, Akasaka Minato-ku, Tokyo 107, Japan

21–24 **Amorphous and Liquid Semiconductors**
13th Int. Conf.
Asheville (USA)
Contact: D. E. Sayers, P.O. Box 8202, North Carolina State Univ., Raleigh, NC 27695-8202, USA

21–25 **Phonons 89**
Heidelberg (Fed. Rep. Germany)
Contact: Inst. f. Angew. Physik II, Univ. of Heidelberg, Albert-Überle-Str. 3–5, D-6900 Heidelberg, FRG

21–26 **Photochemistry**
Int. Conf.
Beijing (P.R. China)
Contact: Prof. S. Wu, Inst. of Photographic Chem., Academia Sinica, Beijing, P.R. China

22–26 **Particles in Gases and Liquids: Detection, Characterization and Control**
2nd Symp. and 20th Annu. Mtg. of Fine Particle Soc. Boston (USA)
Contact: Dr. K. L. Mittal, IBM U.S. Techn. Education, 500 Columbus Ave., Thornwood, NY 10594, USA, Tel. 914/742-5745

22–26 **Particles in Gases and Liquids: Detection, Characterization and Control**
2nd Symp. and 20th Annu. Mtg. of Fine Particle Soc.
Boston (USA)
Contact: Dr. K. L. Mittal, IBM U.S. Techn. Education, 500 Columbus Ave., Thornwood, NY 10594, USA, Tel. 914/742-5745

27–1 **Supramolecular Organic Chemistry and Photochemistry**
Workshop
Saarbrücken (Fed. Rep. Germany)
Contact: Prof. Dr. H.-J. Schneider, FR Organ. Chem., Univ. des Saarlandes, D-6600 Saarbrücken, FRG

28–31 **Dynamical Processes in Excited States of Solids**
7th Int. Conf. (DPC '89)
Athens (USA)
Contact: DPC '89, Prof. J. E. Rives, Dept. of Physics and Astronomy, Univ. of Georgia, Athens, GA 30602, USA

28–1 **Surface Modification Technologies**
3rd Int. Conf.
Neuchatel (Switzerland)
Contact: The Metallurgical Soc., 420 Commonwealth Dr., Warrendale, PA 15086, USA, Tel. 412-776-9050

28–1 **Magnet Technology**
Int. Conf.
Tsukuba (Japan)
Contact: S. Shimamoto, Japan Atomic Energy Res. Inst., Naka-gun, Ibaraki-ken 311-01, Japan

28–1 **Ferroelectricity**
7th Int. Mtg., (IMF-7)
Saarbrücken (Fed. Rep. Germany)
Contact: Dr. J. Albers, Univ. des Saarlandes, Fachbereich Physik, D-6600 Saarbrücken, FRG

28–1 **Sintering**
7th World Round Table Conf.
Herceg-Novi (Yugoslavia)
Contact: Dr. D. P. Uskoković, Serbian Academy of Sci. and Arts, Knez-Mihailova 35, 11000 Beograd, Yugoslavia

28–1 **X-Ray Optics and Microanalysis**
12th Int. Congr.
Cracow (Poland)
Contact: S. Jasienska, Academy of Mining and Metallurgy, Inst. of Metallurgy, 30-059 Cracow, Poland

28–2 **Photochemistry for High Technology**
Int. Summer School
Leuna-Merseburg (German Dem. Rep.)
Contact: Prof. H.-J. Timpe, Section Chemie, Technische Hochschule für Chemie, Leuna-Merseburg, Gensaerstr., DDR-42 Merseburg, GDR

29–2 **Innovation and Perspectives in Solid Phase Synthesis**
Int. Symp.
Oxford (UK)
Contact: R. Epton, School of Appl. Sci., Wolverhampton Polytech., Wolverhampton WV1 1SB, UK

September 1989

3–5 **Advanced Ceramics and PM Materials, Development and Applications**
Int. New Business and High Tech. Conf.
Jyväskylä (Finland)
Contact: EAMI, Ms. R. Häninen, Reumantie 4, 18100 Heinola, Finland, Tel. 358-10-57062, Fax 358-10-57161

4–6 **Magnetic Recording Media**
Int. Conf.
Rimini (Italy)
Contact: Dr. L. Pareti, MASPEC, Via Chiavari 18, I-43100 Parma, Italy

4–8 **Liquid and Amorphous Metals**
Kyoto (Japan)
Contact: Prof. A. Ueda, Dept. of Appl. Mathematics and Physics, Kyoto Univ., Kyoto 606, Japan

4–8 **Electronic Properties of Two-Dimensional Systems**
Int. Conf.
Grenoble (France)
Contact: J. C. Maan, SNCI-HML, 166x, F-38042 Grenoble Cedex, France

4–8 **High-T_c Superconductivity**
Beijing (P.R. China)
Contact: Prof. Z. X. Zhao, Chin. Acad. of Sci., Inst. of Physics, POB 603, Beijing 100080, P.R. China

4–8 **Electrically and Optically Active Polymers**
21st Europhysics Conf.
Lodz (Poland)
Contact: Dr. J. Ulanski, Polymer Inst., Techn. Univ. of Lodz, Zwirki 36, 90-924 Lodz, Poland

4–8 **Macromolecules 89**
Eur.-Am. Conf. on Functional Polymers and Biopolymers
Oxford (UK)
Contact: Prof. R. Epton, School of Appl. Sci., The Polytechnic, Wolverhampton WV1 1SB, UK

4–8 **Olefin Metathesis and Polymerization**
8th Int. Symp.
Bayreuth (Fed. Rep. Germany)
Contact: Office ISOM 8, Lab. für Anorg. Chem., Univ. Bayreuth, Postfach 101251, D-8580 Bayreuth, FRG

5–7 **Interfacial Phenomena in Composite Materials**
Int. Conf.
Sheffield (UK)
Contact: J. Herriot, Butterworth, P.O. Box 63, Westbury House, Bury St., Guildford GU2 5BH, UK

5–8 **Optical, Electrical and Acoustic Properties**
Kent (UK)
Contact: M. D. Shuttleworth, Plastics and Rubber Inst., 11 Hobart Pl., London SW1W 0HL, UK

5–8 **Polymers, Laminations and Coatings**
TAPPI Conf.
Orlando (FL, USA)
Contact: Mtg. Dept., TAPPI Technology Park, P.O. Box 105113, Atlanta, GA 30348-5113, USA

5–9 **Accelerators in Appl. Res. Technology**
1st Eur. Conf.
Frankfurt (Fed. Rep. Germany)
Contact: K. Bethge, Inst. f. Kernphysik, August-Euler-Str. 6, D-6000 Frankfurt 90, FRG

6–8 **New Materials and Processes for Tooling**
2nd Int. Tooling Conf.
Bochum (Fed. Rep. Germany)
Contact: Ruhr-Univ. Bochum, Unikontakt-Tooling, POB 102148, D-4630 Bochum

6–9 **Magnetic Materials and Applications (EMMA '89)**
Rimini (Italy)
Contact: L. Pareti, EMMA '89, Istituto Maspec, Via Chiavari 18/A, I-43100 Parma, Italy, Phone 521-95811, Fax 521-96315

7–9 **Biomaterials**
8th Eur. Congr.
Heidelberg (Fed. Rep. Germany)
Contact: Dr. U. Soltesz, Fraunhofer-Institut für Werkstoffmechanik, Wöhlerstr. 11, D-7800 Freiburg, FRG

10–11 **Ceramics in Medicine**
2nd Int. Symp.
Heidelberg (Fed. Rep. Germany)
Contact: Dtsch. Keram. Gesellsch., Frankfurter Str. 196, D-5000 Köln 90, FRG

10–12 **Colloidal Dispersions**
Faraday Discussion 90
Bristol (UK)
Contact: Prof. R. H. Ottewill, School of Chemistry, Univ. of Bristol, Bristol BS8 1TS, UK

10–14 **Optical Communications**
15th Eur. Conf.
Gothenburg (Sweden)
Contact: P. A. Andrekson, Dept. of Optoelectronics, Chalmers Univ. of Technol., S-41296 Gothenburg, Sweden

10–15 **Materials and Fluid Sciences in Microgravity**
Eur. Conf.
Oxford (UK)
Contact: Dr. H. U. Walter, Eur. Space Agency, Microgravity Office, 8–10 rue Mario-Nikis, F-75738 Paris Cedex 15, France

10–23 **Molecular Dynamics of Liquid Crystals**
NATO Adv. Study Inst.
Il Ciocco, Lucca (Italy)
Contact: Prof. C. A. Veracini, Dipartimento di Chimica, Universita di Pisa, Viale Risorgimento 35, I-56100 Pisa, Italy

11–13 **Charge Transfer in Polymeric Systems**
RSC, Faraday Div.
Contact: Dr. J. F. Gibson, Royal Soc. of Chemistry, Burlington House, Piccadilly, London W1V 0BN, UK

11–13 **Holographic Systems, Components and Applications**
2nd Int. Conf.
Bath (UK)
Contact: Inst. of Electronic and Radio Eng., Conf. Dept., Savoy Hill House, London WC2R 0JD, UK

11–13 **Surface Analysis Techniques and Applications**
Manchester (UK)
Contact: E. Wellingham, Conf. Secretariat, Field End House, Bude Close, Nailsea, Bristol BS19 2FQ, UK

13–15 **Microscopy**
150th Anniversary Commemorative Mtg.
London (UK)
Contact: Microscopical Soc., 37–38 St. Clements, Oxford OX4 1AJ, UK

17–22 **Defect Recognition and Image Processing in Semiconductors**
3rd Mtg. (DRIP-3)
Yokohama (Japan)
Contact: Prof. T. Ogawa, Gakushuin Univ., Dept. of Physics, 1-5-1 Mejiro, Toshima-ku, Tokyo 171, Japan

17–22 **Optics and Optical Engineering**
Cambridge Symp.
Cambridge (USA)
Contact: Soc. of Photo-Optical Instrumentation Eng. (SPIE), P.O. Box 10, Bellingham WA 98227, USA

18–22 **Quantum Electronics**
9th Natl. Conf.
Oxford (UK)
Contact: Mrs. M. Sherwen, Rutherford Appleton Lab., Chilton, Didcot, Oxon OX11 0QX, UK

19–21 **High-T_c Superconductors**
Birmingham (UK)
Contact: Dr. C. Greaves, School of Chemistry, Univ. of Birmingham, POB 363, Birmingham B15 2TT, UK, Tel. 021/414-4397

19–21 **Superconductivity and Applications**
3rd Annu. Conf.
Buffalo (USA)
Contact: NYSIS, 330 Bonner Hall, State Univ. of New York, Buffalo, NY 14260, Tel. 716/636-3463

19–22 **Structure and Dynamics of Colloidal Systems**
3rd Eur. Coll. and Interface Soc. Conf. and ILL Workshop
Basel (Switzerland)
Contact: Dr. M. Zulauf, c/o F. Hoffmann-La Roche + Co., ZFE 65–509, CH-4002 Basel, Switzerland, Tel. 0041/616885746, Fax 0041/616919391

20–22 **Structural Adhesives in Engineering**
SAE II '89
Bristol (UK)
Contact: J. Herriot, SAE II '89, Butterworth Scientific Ltd., P.O. Box 63, Westbury House, Bury St., Guildford, Surrey GU2 5BH, UK

20–22 **Manmade Fibers**
Int. Congr.
Dornbirn (Austria)
Contact: Austrian Manmade Fibers Inst., Plossigasse 8, A-1041 Vienna, Austria

21–22 **Fire Retardant Polymers**
Torino (Italy)
Contact: Prof. L. Costa, Dipl. di Chim. dell'Università di Torino, Via P. Giuria, 7, 10125 Torino, Italy

24–28 **Metallization of Polymers**
Int. Colloquium
Montreal (Canada)
Contact: Ed. Sacher, Ecole Polytechnique, Université de Montreal, Quebec H3C 3A7, Canada

25–26 **Additive Approaches to Improved Polymer Performance**
Toronto (Canada)
Contact: Jeff Hood, Stochem. Inc., 106 Summerlea Rd., Brampton, Ontario L6T 4X3, Canada

25–27 **Structure Formation in Polymer Solutions**
22nd Europhysics Conf.
Leuven (Belgium)
Contact: Prof. H. Berghmans, Lab. for Polymer Res., Katholieke Univ. Leuven, Celestijnenlaan 200F, B-3030 Leuven, Belgium, Tel. 16/200656, Fax 16/201215

25–27 **Surface Engineering with High Energy Beams**
2nd Int. Seminar
Lisbon (Portugal)
Contact: Secretariat of ISHT '89 Seminar, Ctr. of Mech. and Mater. of the Tech. Univ. Lisbon (CEMUL), 1096 Lisboa Codex, Portugal

25–29 **Ceramics' 89 "C89"**
4. Int. Conf. Limoges (France)
Contact: Comité Régional D'Expansion Economique du Limousin (CREEL), 27, Boulevard de la Corderi, F-87000 Limoges, France, Tel. 0033/55451830, Fax 0033/55797789

25–29 **Vacuum Solid Surfaces**
IVC-11/CSS-7
11th Int. Conf./7th Int. Conf.
Cologne (Fed. Rep. Germany)
Contact: D. A. Benninghoven, Physikalisches Inst. der Univ. Münster, Wilhelm-Klemm-Str. 10, D-4000 Münster, FRG

25–30 **Epitaxial Crystal Growth**
Int. Conf.
Budapest (Hungary)
Contact: Dr. E. Lendfay, Hung. Acad. of Sci., Inst. for Techn. Physics, Ujpest 1, POB 76, H-1325 Budapest, Hungary

26–28 **Optical Memory**
Int. Symp. (ISOM '89)
Kobe (Japan)
Contact: ISOM '89 Secretariat, Business Ctr. for Academic Soc. Japan, 3-23-1 Hongo, Bunkyo-ku, Tokyo 113, Japan

26–28 **SAMPE**
21st Int. Techn. Conf.
Atlantic City (USA)
Contact: SAMPE, 843 W. Glentana, P.O. Box 2459, Covina, CA 91722, USA, Tel. 818-331-0616

Registered names, trademarks etc. used in this journal, even when not marked as such, are not to be considered unprotected by law.

© VCH Verlagsgesellschaft mbH, D-6940 Weinheim, 1989. – Printed in the Federal Republic of Germany by Konrad Triltsch Druck- und Verlagsanstalt Würzburg.

All rights reserved (including those of translation into foreign languages). No part of this issue may be reproduced in any form — by photoprint, microfilm, or any other means — nor transmitted or translated into a machine language without written permission from the publishers. Only single copies of contributions, or parts thereof, may be made for personal use. This journal was carefully produced in all its parts. Nevertheless, authors, editors and publisher do not warrant the information contained therein to be free of errors. Readers are advised to keep in mind that statements, data, illustrations, procedural details or other items may inadvertently be inaccurate.

Valid for users in the USA: The appearance of the code at the bottom of the first page of an article (serial) indicates the copyright owner's consent that copies of the article may be made for personal or internal use, or for the personal or internal use of specific clients. This consent is given on the condition, however, that the copier pay stated per-copy fee through the Copyright Clearance Center, Inc. (CCC), for copying beyond that permitted by Sections 107 or 108 of the U.S. Copyright Law. This consent does not extend to other kinds of copying, such as copying, for general distribution, for advertising or promotional purposes, for creating new collective works, or for resale. For copying from back volumes of this journal see 'Permissions to Photo-Copy: Publisher's Fee List' of the CCC.

Editorial office: Postfach 101161, D-6490 Weinheim, Federal Republic of Germany, Telephone (06201) 602255, Telex 465516 vchwh d, Telefax (06201) 602328.

Editor: *Peter Gölitz*

Associate Editor: *Peter Gregory*

Publishers: VCH Verlagsgesellschaft mbH. (Managing Director: *Hans Dirk Köhler*), Pappelallee 3, D-6940 Weinheim, Federal Republic of Germany.

Advertising office (Advertising Manager *R. J. Roth*): Postfach 101161, D-6940 Weinheim, Federal Republic of Germany, Telephone (06201) 606130, Telex 467155 vchwh d, Telefax (06201) 606184.

ANGEWANDTE CHEMIE
International Edition in English
Volume 28 · Number 8
August 1989
Pages 969–1146

The Stereoselectivity of Intermolecular Free Radical Reactions

New Synthetic Methods (78)

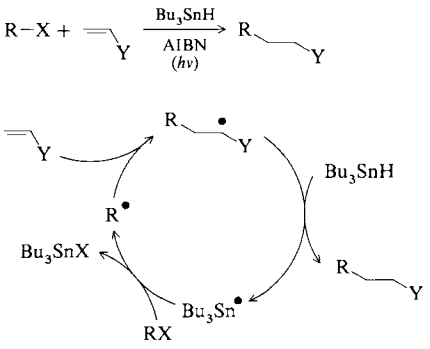
By Bernd Giese*

Dedicated to Professor Christoph Rüchardt on the occasion of his 60th birthday

The regio- and chemoselectivities of free radical reactions are often high and largely predictable; systematic studies have now shown that the stereoselectivity of free radical reactions can also be directed. Examples involving five- and six-membered cyclic radicals will be used to show how steric and stereoelectronic effects influence the diastereoselectivity of reactions of cyclic radicals with olefins. The temperature, the solvent, and the nature of the radical scavenger used also play a role, so that, if the correct reaction conditions are used, the stereoselectivity of reactions for cyclic reactants can be very high. Lower stereoselectivities are often observed for reactions between acyclic radicals and acyclic alkenes. However, preliminary experiments have indicated that under certain conditions such systems can also react in a stereoselective manner.

1. Introduction

Since the beginning of the present decade, organic synthesis has been enriched by advances in free radical chemistry as chemists have learned how to generate and to trap short-lived radicals in a selective manner.[1] Of particular preparative importance are chain reactions in which the decisive synthetic steps are those involving reactions between radicals and nonradicals. In the case of C–C bond formation via the "tin-method" (Scheme 1) we have shown in detail that the various radicals produced within the chain must have differing selectivities (selectivity condition), but must not lose their high reactivity (reactivity condition).[1, 2]



Scheme 1. AIBN = azobisisobutyronitrile.

It only became possible to use free radical reactions for selective syntheses after mechanistic studies had revealed the effects which influence the reactivity and selectivity of free radicals. *C. Rüchardt* and his co-workers demonstrated the influence of steric effects in free radical chemistry at an early stage.[3] In addition, polar effects (which can today be ex-

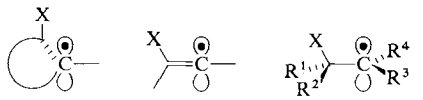
[*] Prof. Dr. B. Giese
Institut für Organische Chemie
der Technischen Hochschule
Petersenstrasse 22, D-6100 Darmstadt (FRG)
New address:
Institut für Organische Chemie
der Universität Basel
St. Johanns-Ring 19, CH-4056 Basel (Switzerland)

 © VCH Verlagsgesellschaft mbH, D-6940 Weinheim, 1989 0570-0833/89/0808-0969 $ 02.50/0

plained in terms of frontier orbital theory[4]) and radical-stabilizing effects play important parts.[5] Regio- and chemoselectivities of radical reactions can be predicted and understood on the basis of these effects.

Less is known about the stereoselectivity of radical reactions. Although the steric course of *intra*molecular reactions, and in particular of cyclization and rearrangement reactions, is known to a large extent,[1, 6] the control of *inter*molecular reactions is still a great problem. Only when this problem is solved will it become possible to use free radicals widely in organic synthesis. This review article will describe the present research situation and indicate some perspectives for the future.

In most carbon-centered free radicals the unpaired electron occupies an orbital which has mainly p-character (i.e., they are π radicals), allowing attack from two sides. Thus, high stereoselectivity requires that the radicals (1) react from preferred conformations and (2) be attacked predominantly from one side. The influence of substituents X on the stereoselectivity in reactions of cyclic radicals **1** and of vinyl radicals **2** has been studied in detail; however, little is presently known about the possibilities for influencing the stereoselectivity of acyclic radicals **3**.



1 **2** **3**

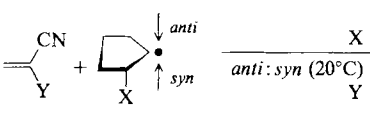
Reactions of five-membered cyclic radicals can demonstrate how *anti*:*syn* stereoselectivity is determined by shielding substituents, since on a time average the highly flexible five-membered ring can be considered to be almost planar. Six-membered cyclic radicals can be used to study the equatorial:axial stereoselectivity. At the end of this article we shall indicate the conditions under which acyclic radicals react in a stereoselective manner.

2. Five-Membered Cyclic Radicals

2.1. Addition Reactions

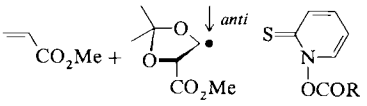
In reactions involving addition to β-substituted radicals, the *anti*:*syn* ratio depends on the substituents of both the radical and the radical trap. In a few cases the solvent can also exert a small influence on the stereoselectivity of the addition. The influence of the substituent X in the cyclopentyl radical **4** on *anti* versus *syn* attack by alkenes has been studied in detail.[7]

An alkoxy substituent shields the *syn* side of the radical **4** only slightly against attack of acrylonitrile (Y = H; 20 °C, CH_2Cl_2; X = OEt, *syn*:*anti* 77:23; O*t*Bu, 80:20): however, the presence of a methyl group leads to a stereoselectivity of 92:8, and an acetamido group directs the attack of α-chloroacrylonitrile nearly completely to the *anti*-side (> 98:2). The ester group in the radical **5** is also sufficient to ensure predominant *anti* addition of methyl acrylate.[8] The sulfur atom of the thiocarbonyl group in **6** also attacks the radical **5** *anti* to the ester group.



X	OEt	O*t*Bu	Me	NHAc
anti:*syn* (20°C)	77:23	80:20	92:8	> 98:2
Y	H	H	H	Cl

4



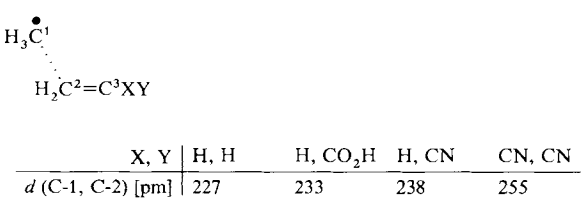
5 **6**

Substituents on the alkene have a great influence on the stereoselectivity of the C–C bond formation, both the reactivity and the shielding of the alkene playing a role thereby. Thus, the *anti*:*syn* selectivity in addition reactions to the β-ethoxycyclopentyl radical **4**, X = OEt, increases from 72:28 to 90:10 when α-chloroacrylonitrile is replaced by styrene, which reacts 200 times more slowly (Table 1).[7a, 9]

Table 1. Stereoselectivity (*anti*:*syn* attack) of the β-ethoxycyclopentyl radical **4**, X = OEt, in reactions with alkenes (20 °C, CH_2Cl_2) and relative reactivity (k_{rel}) of the alkenes with respect to cyclohexyl radicals (20 °C).

Alkene	*anti*:*syn* Attack	k_{rel}
$H_2C=CClCN$	72:28	31
$H_2C=CHCN$	77:23	3.6
$H_2C=CHCOMe$	86:14	2.0
$H_2C=CHCO_2Me$	88:12	≡ 1.0
$H_2C=CHPh$	90:10	0.15
trans-$NCCH=CHCN$	60:40	41
trans-$MeO_2CCH=CHCO_2Me$	88:12	4.0
$(MeO_2C)_2C=C(CO_2Me)_2$	> 98:2	1.1

When terminal alkenes attack the radical **4**, X = OEt, there is a direct relationship between decreasing reactivity and increasing stereoselectivity. This conforms with the reactivity-selectivity principle[10a] and the Hammond postulate,[10b] according to which the steric shielding of the radical substituent has more effect in the later transition state of the slower reaction. Ab initio calculations[11a] for the addition of methyl radicals to terminal alkenes have demonstrated that the distance between the radical and the olefinic carbon atoms in the transition state increases[11b] as the reactivity of the alkene is increased by electron-withdrawing substituents (Scheme 2).[4] The shielding effect of a substituent on the stereoselectivity should decrease as the distance between the radical and the olefinic C atoms in the transition state increases.



X, Y	H, H	H, CO_2H	H, CN	CN, CN
d (C-1, C-2) [pm]	227	233	238	255

Scheme 2.

This relationship also applies when, as in the case of fumarodinitrile, the alkene carbon atom undergoing attack bears

a small cyano group. On going to the more bulky ester groups, the reactivity effects are compensated by steric effects: the shielding substituents increase the stereoselectivity, so that even in the case of diethyl fumarate the *anti*:*syn* ratio is 88:12. Only the *anti* product can be detected in the reaction with tetraethyl ethenetetracarboxylate, although the reactivity of the latter would lead us to expect the same selectivity as that shown by acrylate esters.[7a, 9]

It is also noteworthy that in the case of the β-ethoxycyclopentyl radical **4**, X = OEt, the stereoselectivity is influenced by the solvent: thus, the *anti*:*syn* ratio for the addition of acrylonitrile at 20 °C increases from 68:32 (cyclohexane) to 76:24 (THF), 77:23 (CH_2Cl_2), and 81:19 (CH_3CN).[7a, 9] This increase in stereoselectivity could be due to better solvation of ethoxy substituent. The introduction of an oxygen atom into the five-membered ring also influences the stereoselectivity of attack, the tetrahydrofuranyl radical **7** reacting somewhat more selectively than the cyclopentyl radical **4**, X = OEt[7a] (Table 2).

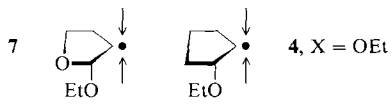
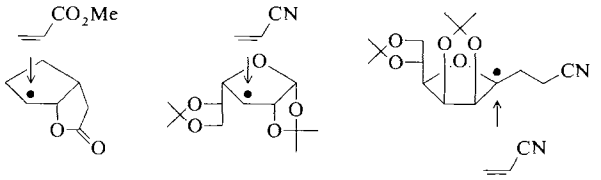


Table 2. Stereoselectivity (*anti*:*syn* attack) in the addition of unsubstituted alkenes to **4**, X = OEt, and **7**.

Radical	*trans*-NCCH=CHCN	H_2C=CHCN	H_2C=CHCOMe	H_2C=$CHCO_2Me$
7	64:36	86:14	88:12	93:7
4, X = OEt	60:40	77:23	86:14	88:12

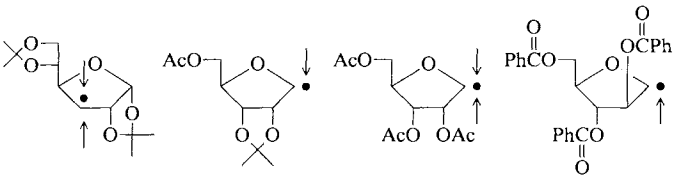
The greater selectivity of the tetrahydrofuranyl radical **7** is probably due to the spatial arrangement of the ethoxy substituent; according to the anomeric effect the ethoxy group in **7** should occupy an axial position and thus be able to shield the *syn* side of the radical more effectively than in **4**, X = OEt. This effect makes it clear that an exact prediction of the stereoselectivity can only be made when the conformations of the radicals are known. How substituents influence conformations will be discussed in the case of six-membered cyclic radicals, for which detailed ESR studies have been carried out.

When more than one substituent is present, the spatial arrangement of the substituents can increase or decrease the stereoselectivity. The presence of a second or third *cis* substituent, as in the radicals **8**–**10**, leads to exclusive *anti* attack even with acrylates or acrylonitrile.[12]



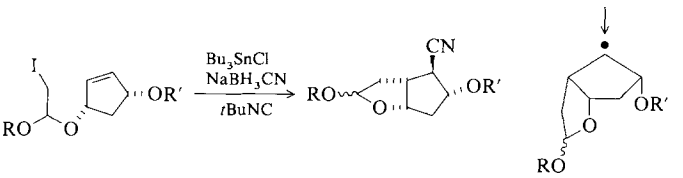
8 **9** **10**

In the glucofuranosyl radical **11**, however, the substituent at C-4 is *trans* to the substituents at C-1 and C-2; this leads to a drastic decrease in the stereoselectivity,[12b] whereby the dioxolane ring annelated at C-1/C-2 shields one side of the radical more strongly than does the alkyl substituent at C-4 (β:α attack of acrylonitrile 73:27).



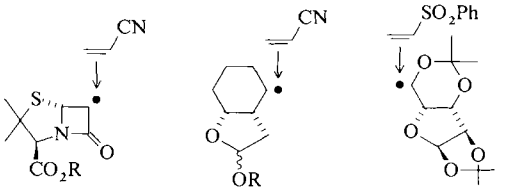
11 **12** **13** **14**

The *cis*-fused dioxolane ring gives the molecule a bent shape. Comparison of the high stereoselectivity observed with radical **12** with the unselective behavior of **13** (β:α attack 50:50) indicates the magnitude of the influence of the annelated ring.[13] However, inversion of the configuration at C-2 suffices to induce a high stereoselectivity (radical **14**; attack from the α side).[14] *Stork* et al. have made use of the high "shape selectivity" in prostaglandin synthesis:[15] in the reaction **15** → **17**, radical **17** is trapped stereoselectively by *tert*-butyl isocyanide.



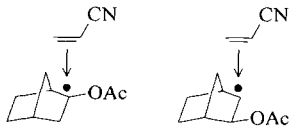
15 **17** **16**

The shape selectivity resulting from the annelation of a five-membered ring also occurs in four- and six-membered cyclic radicals (e.g., **18**–**20**).[13c, 16]



18 **19** **20**

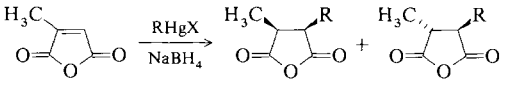
Radicals of the norbornyl type also react in a clearly shape-selective manner. Thus, acrylonitrile attacks not only the norbornyl radical **21**, which is substituted at the radical center, but also the β-substituted norbornyl radical **22** from the *exo* side.[7a, 17]



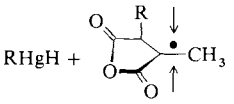
21 22

2.2. Abstractions

Systematic studies on the influence of substituents on the stereoselectivity of hydrogen abstraction reactions have been carried out. As in addition reactions, a β substituent directs attack to the *anti* side of the radical. Hydrogen abstraction involves the transfer of only a small hydrogen atom, so that, in contrast to the C–C bond-forming reaction, hydrogen abstraction leads to the formation of the thermodynamically less stable products. Thus, in the reaction of methylmaleic anhydride (**23**) with an alkylmercury salt in the presence of $NaBH_4$, the *cis*-product **25** is formed preferably.[18] The five-membered cyclic radical **24**, formed as an intermediate, is subsequently attacked by the alkylmercury hydride.



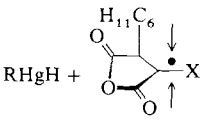
23 25 26



24

R	*n*-C_6H_{13}	*c*-C_6H_{11}	*t*Bu
25:**26**	62:38	89:11	94:6

The degree to which *anti* attack is favored, leading to an increasing amount of the thermodynamically less stable *cis*-product **25**, increases as the shielding substituent R in the radical **24** becomes larger. Not only β but also α substituents influence the stereoselectivity: thus, the *anti*:*syn* stereoselectivity increases in the case of the radical **27** from 70:30 for X = F to 95:5 for X = *t*Bu.[19] The reason for this increase in the stereoselectivity is not yet known.



27

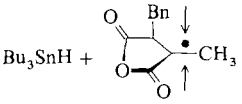
X	F	Ph	*c*-C_6H_{11}	Me	OMe	OAc	*t*Bu
anti:*syn*	70:30	73:27	80:20	89:11	91:9	94:6	95:5

The differences in the shielding of the *syn* and *anti* sides by substituents of varying size are also reflected in the enthalpy of activation and therefore in the temperature dependence of the stereoselectivity. Thus, the difference in the enthalpy of activation for *syn* versus *anti* attack increases from 5 to 9 and 12 kJ mol^{-1} when the β substituent in the radical **24** increases in size from the primary 1-hexyl group to the secondary cyclohexyl and the *tert*-butyl groups, respectively.[20] Variation of the hydrogen donor (alkylmercury hydride, tributyltin hydride, cyclohexane) surprisingly has very little effect on the stereoselectivity. However, variation of the H donor permits the temperature influence on the stereoselectivity to be measured over the range 0–260 °C.[20, 21] As expected, the stereoselectivity decreases with increasing reaction temperature (Table 3).

Table 3. Influence of temperature on the stereoselectivity (*anti*:*syn* attack) of the H transfer by cyclohexylmercury hydride, tributylstannane, and cyclohexane to radical **24** (R = *c*C_6H_{11}).

T [°C]	*anti*:*syn* Attack by $C_6H_{11}HgH$	Bu_3SnH	C_6H_{12}
0	90:10		
20	84:16	85:15	
40	80:20	80:20	
60	76:24	76:24	
80		75:25	
110		70:30	
200			66:34
220			64:36
240			61:39
260			59:41

The influence of the solvent on the stereoselectivity of hydrogen transfer reactions has not yet been studied in detail; however, reactions of the radical **28** with tributyltin hydride in benzene [*anti*:*syn* attack 76:24 (0 °C), 63:37 (80 °C)] and tetrahydrofuran [80:20 (0 °C), 69:31 (80 °C)] indicate that small solvent effects can occur.[20] These are possibly due to variations in the solvation of the tin hydride.



28 Bn = $PhCH_2$

T	0°C	80°C
anti:*syn* in benzene	76:24	63:37
anti:*syn* in THF	80:20	69:31

The stereoselectivity of hydrogen transfer and alkene addition can be compared directly using the radicals **4**, X = OEt, **9**–**11**, and **21**.[17, 22] It is found that for five-membered cyclic radicals the shielding effects for hydrogen transfer and for addition to reactive terminal alkenes are similar (Table 4).

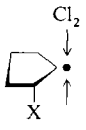
Table 4. Comparison of the stereoselectivities (*anti*:*syn* attack) of free radical addition and D or H abstraction of the radicals **4**, X = OEt, **9**–**11** and **21**.

Radical	Addition of $H_2C{=}CHCN$	Abstraction
4, X = OEt	77:23	90:10 [a]
9	> 98:2	> 98:2 [a]
10	> 98:2	> 98:2 [a]
11	73:27	85:15 [a]
21	> 95:5	80:20 [b]

[a] Bu_3SnD. [b] RHgH.

The stereoselectivity of halogen transfer to five-membered cyclic radicals is influenced by the same effects that are involved in addition and hydrogen transfer reactions: (1) β substituents favor *anti* attack; (2) attack on annelated systems occurs from the convex side; (3) *exo* attack is preferred in norbornyl systems. β-Chloro and, in particular, β-bromo substituents cause a pronounced *anti* selectivity; thus, the *anti*:*syn* ratio in the chlorination of the β-chlorocyclopentyl radical **29** [98:2 (40 °C), 93:7 (108 °C)] and the β-bromocyclopentyl radical **30** [> 99:1 (40 °C)][23] is much larger than that found for the β-methylcyclopentyl radical **31** [57:43 (104 °C)].[24]

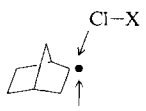
29: X = Cl
30: X = Br
31: X = CH_3



	29	30	31
T [°C]	40 (108)	40	104
anti:*syn*	98:2 (93:7)	> 99:1	57:43

A coplanar arrangement of the semi-occupied orbital and the carbon-halogen bond would explain this finding. Such a conformational effect is of particular importance in the stereoselectivity of addition in acyclic systems (see Section 4.1). It was possible using the norbornyl radical **32** as an example to show that the stereoselectivity can also depend on the nature of the halogen donor.[25]

32



X	Cl	*t*BuO	SO_2Cl	CCl_3
T [°C]	80	40	40	80
exo:*endo*	71:29	87:13	95:5	98:2

3. Six-Membered Cyclic Radicals

The difference between the axial and equatorial positions is greater in six-membered than in five-membered rings. Thus, the stereoselectivity of six-membered cyclic radicals will be analyzed below with particular reference to the equatorial:axial selectivity.

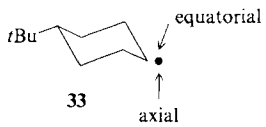
3.1. Torsional Effects

The stereoselectivity of the 4-*tert*-butylcyclohexyl radical **33** has been studied in detail.[26] "Axial" attack at the radical center of **33** is faster for OH-, D-, Cl-, and Br-transfer reagents than is "equatorial" attack (Table 5).[26, 34] This is reminiscent of the stereoselectivity of nucleophilic attack at the carbonyl carbon in cyclohexanone, which is also sp^2-hybridized. Calculations by *K. N. Houk* et al. have shown that in the transition state for axial attack on cyclohexanone the steric strain caused by the torsional effect is smaller than that for equatorial attack.[27a] Analogous torsional effects may perhaps influence the stereoselectivity of the cyclohexyl radicals.

Table 5. Stereoselectivity (equatorial:axial attack) of the 4-*tert*-butylcyclohexyl radical (**33**) in abstraction and addition reactions.

Reagent	Reaction type	eq:ax
RCO_2-OH	HO abstraction	20:80
Cl_3C-Cl	Cl abstraction	23:77
Bu_3Sn-D	D abstraction	30:70
Cl_3C-Br	Br abstraction	31:69
$H_2C=C(CO_2Et)_2$	alkene addition	44:56
$H_2C=CHCN$	alkene addition	55:45
NCCH=CHCN [a]	alkene addition	60:40
$CH_3CH=CHCN$ [b]	alkene addition	74:26
$CH_3CH=C(CO_2Et)_2$	alkene addition	73:27
$iC_3H_7CH=C(CO_2Et)_2$	alkene addition	88:12

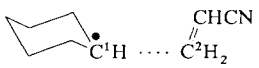
[a] *trans* isomer. [b] *cis*:*trans* mixture 1:1.



33

This torsional effect is counteracted by the 1,3-diaxial interactions which occur in axial attack. The larger the reagent is, the larger will be the influence of these 1,3-diaxial interactions. Thus, the proportion of equatorial attack in the addition of the cyclohexyl radical **33** to alkenes increases from 44 to 88% when an isopropyl group replaces hydrogen at the olefinic carbon atom which is attacked (Table 5).[28]

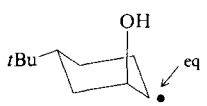
The equatorial:axial ratio also depends on the distance between the reacting molecules in the transition state. This has been demonstrated by force-field calculations,[27b] in which the distance between the radical C atom of the cyclohexyl radical and the methylene group of acrylonitrile is varied continuously. At a hypothetical distance of 207 pm in the transition state, the equatorial:axial ratio is 70:30, whereas at a distance of 247 pm the equatorial:axial ratio is shifted to 43:57.



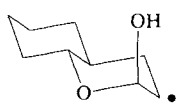
d (C-1, C-2) [pm]	207	217	227	233	238	247
äqu:ax	70:30	64:36	57:43	52:48	48:52	43:57

3.2. Steric Substituent Effects

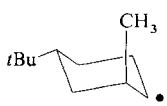
As in five-membered rings, substituents in six-membered rings in a β position with respect to the radical center lead to an increase in *anti* attack. Axial substituents cause a shift in the direction of axial attack (radicals **34**–**36**)[29] and equatorial substituents direct the reaction towards equatorial attack (radical **37**).[30] Whereas the shielding of the *syn* side of



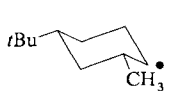
34
$H_2C=CHCN$
eq:ax 27:73



35
$H_2C=CHCN$
eq:ax 28:72



36
RCO_2-OH
eq:ax 10:90

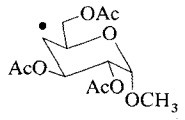


37

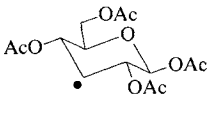
$H_2C=C(CO_2Et)_2$	eq:ax 73:27
$H_2C=CHCN$	eq:ax 79:21
trans-NCCH=CHCN	eq:ax > 97:3
$H_3CCH=C(CO_2Et)_2$	eq:ax > 97:3

the radical by an axial substituent is not surprising, the magnitude of the influence of equatorial substituents on the stereoselectivity is remarkable. The equatorial selectivity increases with increasing size of the substituent at the olefinic carbon atom undergoing attack; thus, even the reaction of fumarodinitrile with the radical **37** leads exclusively to the product of equatorial addition.[30]

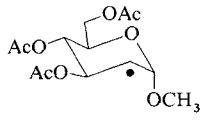
A second axial or equatorial β substituent increases the proportion of axial or equatorial attack even further.[12a, 31] A comparison of the stereoselectivity of the carbohydrate radicals **38–41** shows that equatorial substituents are almost as effective as axial substituents when acrylonitrile is the alkene undergoing attack.



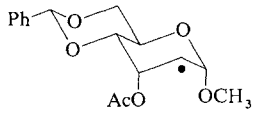
38



39



40



41

Table 6. Stereoselectivity (equatorial:axial attack) in the addition of alkenes to the doubly β-substituted radicals.

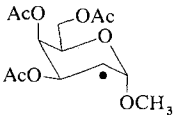
Alkene	equatorial:axial **38**	**39**	**40**	**41**
$H_2C=CHCN$	82:18	76:24	55:45	17:83
$H_2C=CHCH_2SnBu_3$	–	85:15	60:40	–
trans-NCCH=CHCN	> 98:2	> 95:5	84:16	52:48

However, fumarodinitrile attacks preferentially in an equatorial manner. This is due to a drastic retardation of axial attack on going from acrylonitrile to fumarodinitrile. While the cyclohexyl radical **33** reacts about ten times faster with fumarodinitrile than with acrylonitrile in both an axial and an equatorial manner, β substituents in the radical reverse this sequence.[31b, 32] Thus, acrylonitrile is three to six times more reactive than fumarodinitrile with respect to equatorial attack on the radicals **38–41.** However, this reactivity difference is even more pronounced for axial attack. The ratio of reactivities of acrylonitrile and fumarodinitrile (k_{AN}/k_{FN}) with respect to axial attack changes by a factor of 200 to 500 on going from the cyclohexyl radical **33** to the carbohydrate radicals **38–41** (see Table 7).[32] This is caused

Table 7. Ratio of the reactivities of acrylonitrile and fumaronitrile ($k_{AN}:k_{FN}$) in equatorial and axial attack on six-membered cyclic radicals.

	33	**38**	**39**	**40**	**41**
$(k_{AN}:k_{FN})_{eq}$	0.1	4.2	3.1	3.9	19
$(k_{AN}:k_{FN})_{ax}$	0.09	> 45	> 40	19	28

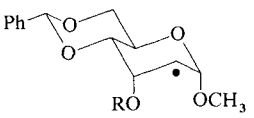
by steric effects which increase with the degree of shielding of the olefinic carbon atom undergoing attack. The galactosyl radical **42**[31c] provides a clear example.



42

$H_2C=CHCN$	eq:ax 65:35
trans-NCCH=CHCN	eq:ax 90:10
$MeO_2CCH=CHCO_2Me$	eq:ax > 95:5
$H_3CCH=C(CN)_2$	eq:ax > 98:2

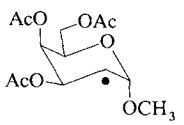
The type of substituents at the radical can also influence the stereoselectivity of the reaction: in the reaction of radical **43** with acrylonitrile, the axial versus equatorial selectivity increases from 64:36 via 74:26 and 83:17 to 94:6 on going from the alcohol (R = H) via the ether (R = CH_3) and ester (R = OAc) to the lithium salt (R = Li).[31b, c] The large effect of the lithium salt is due to chelation of the lithium ion by the two axial oxygen atoms of the β substituent of **43**.



43

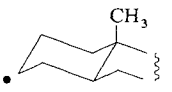
R = H	ax:eq 64:36
R = CH_3	ax:eq 74:26
R = OAc	ax:eq 83:17
R = Li	ax:eq 94:6

Axial γ and δ substituents also affect the stereoselectivity, as is shown by the reactions of the galactosyl radical **42** and the steroid radical **44**. For steric reasons the axial γ substituent in **42** favors equatorial attack,[31] whereas the axial δ substituent in **44** favors axial attack[33] (compare the data for **40** and **33**, respectively).



42

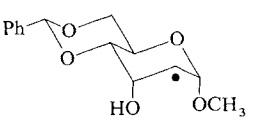
Alkene	eq:ax **42**	**40**
$H_2C=CHCN$	65:35	55:45
NCCH=CHCN	90:10	84:16



44

Alkene	eq:ax **44**	**33**
$H_2C=CHCN$	40:60	55:45
$H_3CCH=CHCN$	68:32	74:26

As in the case of the five-membered cyclic radical **4**, X = OEt, the stereoselectivity of reaction with the six-membered cyclic radical **45** also increases slightly with increasing polarity of the solvent. The equatorial:axial ratio for attack of acrylonitrile changes from 64:36 in toluene to 76:24 in methanol. This small effect is again probably due to an increase in the solvation of the β substituents.[31c]



45

toluene	eq:ax 64:36
THF	eq:ax 65:35
acetonitrile	eq:ax 70:30
methanol	eq:ax 76:24

Substituents on the six-membered cyclic radical have similar effects on the stereoselectivity of abstraction reactions as on that of addition reactions. However, the torsional effect

can cause the proportion of axial product to be considerably larger in abstraction reactions. The stereoselectivities of deuterium trapping and addition to acrylonitrile are compared in Table 8.[30, 31, 34, 35]

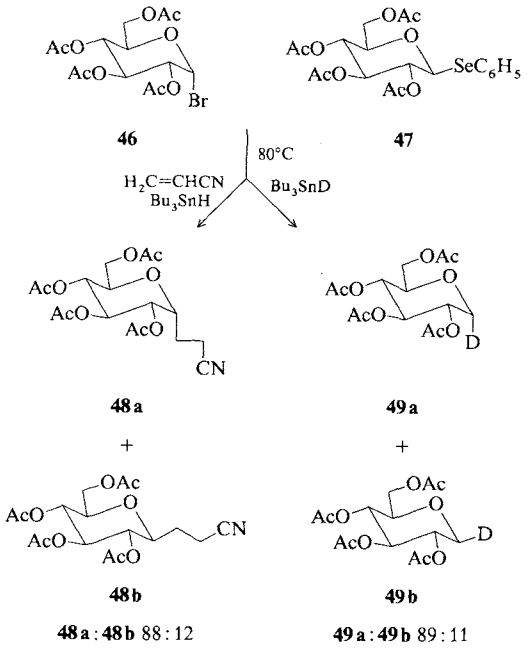
Table 8. Stereoselectivity (equatorial:axial attack) of free radical D abstraction and addition to acrylonitrile of **33** and **37–41**.

	equatorial:axial					
	33	**37**	**38**	**39**	**40**	**41**
D abstr.	30:70 [a]	56:44 [a]	58:42 [a]	53:47 [a]	34:66 [b]	< 4:96 [b]
addition	55:45	79:21	82:18	76:24	55:45	17:83

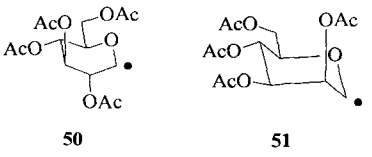
[a] Bu_3SnD, 80 °C. [b] RHgD, 25 °C.

3.3. Stereoelectronic Effects

Glucosyl radicals, in which the radical center is the anomeric carbon atom, yield predominantly α-substituted products. For example, the main products obtained from the α-glucosyl bromide **46** and the β-glucosyl selenide **47** are **48a** in radical addition to acrylonitrile and **49a** in deuterium abstraction from tributyltin deuteride;[31a, 36] the selectivity of the glucosyl radical is independent of whether the radical precursor is an α or β anomer.

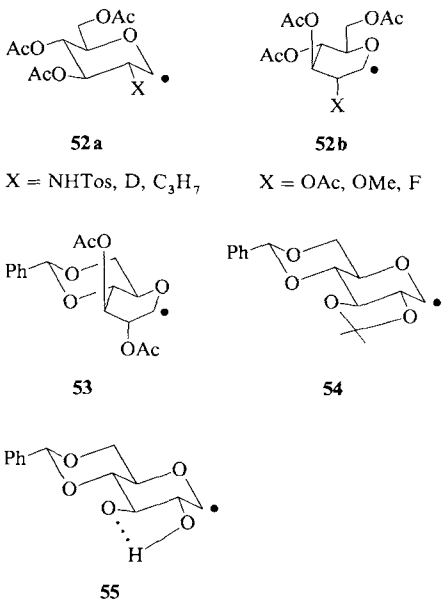


This stereoselectivity is caused by stereoelectronic effects which influence both the radical conformations and the direction of attack on the radicals. ESR studies indicate that the glucosyl radical **50** exists in a slightly distorted $B_{2,5}$ boat conformation, while the mannosyl radical **51** remains in the $^4C_1$ chair conformation of its precursor.[37]



Common to both radicals is the axial arrangement of the neighboring acetoxy group; stabilizing interactions may well exist between the unpaired electron and the neighboring carbon–oxygen bond. This stereoelectronic effect overcompensates the steric repulsion which occurs during the chair–boat interconversion in the glucosyl radical. Analogous conformational changes are not observed in the case of pyranosyl radicals, which have their radical center at C-2 to C-4; thus the radicals **38–40** exist in an only slightly flattened $^4C_1$ chair conformation.[38] The ring oxygen atom adjacent to the radical center of **50** is therefore apparently of critical importance.

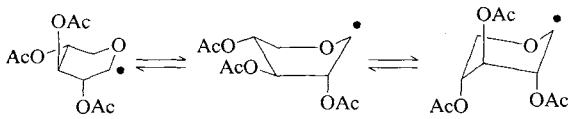
According to the frontier orbital theory, this stabilizing effect is due to interaction of the SOMO with the LUMO of the neighboring carbon-oxygen bond. Interaction of the semioccupied orbital with the oxygen lone pair results in a higher SOMO energy, making the SOMO–LUMO stabilization significant.[37] This rationalization is supported by the influence exerted on the conformation of the radicals **52** by the substituent X: only for X = OR or F is the boat form **52b** energetically more favored than the chair form **52a**.[39] Electron-attracting substituents X lower the LUMO energy of the C–X bond and thus increase the stabilizing effect of the SOMO–LUMO interaction. When X = NHTos, D, or C_3H_7, however, only the chair conformer **52a** is observed in the ESR spectrum. In the case of these substituents, the stereoelectronic effect does not suffice to compensate for the increase of the steric strain in the course of the chair–boat interconversion.[39]



The equilibrium between the chair and the boat conformations can also be influenced by ring annelation or by hydrogen bonding. Thus, while the bicyclic radical **53** still exists in a boat form, the annelated five-membered ring in **54** causes the latter to take up a chair conformation. Even the energy of the hydrogen bonds in **55** suffices to suppress the chair-boat interconversion to a large extent.[37]

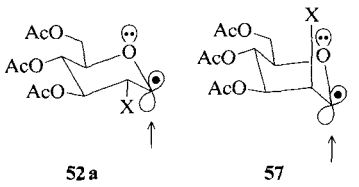
In the pentopyranosyl radicals the substituent at C-5 is absent; these systems are thus more flexible, and the three radicals **56a–c** can be detected in the ESR spectrum of the

triacetylxylosyl system; in all conformers the carbon–oxygen bond next to the radical center is axial.[40]



56a **56b** **56c**

Not only the conformation but also the direction of attack on substituted oxyalkyl radicals is influenced by stereoelectronic effects. Thus, the glycopyranosyl radicals **52a** and **57**,



52a **57**

which exist in the $^4C_1$ conformation, are attacked axially in both addition and abstraction reactions.

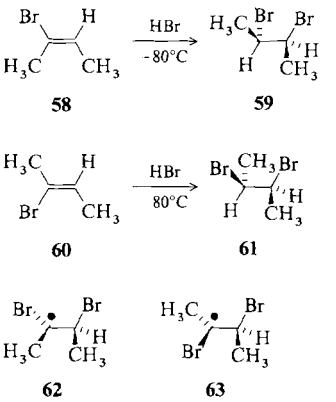
Only in the case of axial attack on the radicals **52a** or **57** is the overlap between the nonbonding electron pair of the ring oxygen atom and the unpaired electron of the radical center (or the newly formed bond) maintained en route to the transition state; only α products are formed.[39] In the case of radicals in the boat conformation **52b**, the stereoselectivity is somewhat smaller. The decrease in stereoselectivity is probably due to the fact that boat conformers are more flexible than chair conformers.[36, 37] There is only a small energy difference between a $B_{2,5}$ boat (e.g., **56a**) and a $^{1,4}B$ boat (e.g., **56b**). According to the stereoelectronic effect, $B_{2,5}$ conformers afford α-products, whereas β products are formed from $^{1,4}B$ conformers. In the xylosyl radicals the selectivity is in fact reversed in favor of the β products, since here, apart from the $B_{2,5}$ boat form **56a**, not only the $^{1,4}B$ boat form **56a** but also the $^1C_4$ chair form **56c** is present.[31b, 41]

4. Acyclic Radicals

High stereoselectivities are only possible when the radicals (1) react from preferred conformations and (2) are attacked preferentially from one side. Until now only a few experiments have been carried out using acyclic radicals for which both these conditions are fulfilled. However, there are indications as to how the stereoselectivity can be increased.

4.1. Alkyl Radicals

Saturated alkyl radicals can adopt a preferred conformation if, for example, there are stabilizing interactions between the radical center and a neighboring substituent. One example is the free radical addition of HBr to the alkenes **58** and **60**.[42] At −80 °C the products **59** and **61** of *anti* addition are obtained, because the interaction between the radical center and the neighboring carbon–bromine bond locks the intermediate radicals into the conformations **62** and **63**, respectively; these radicals are then attacked *anti* to the shielding bromine atom.

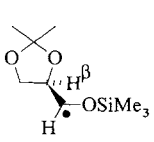


58 **59**

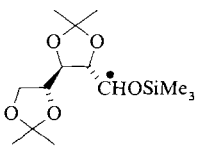
60 **61**

62 **63**

This stereoselectivity decreases when the reaction temperature increases, and disappears at 20 °C.[42] This is perhaps due to the fact that rotation around the central C–C bond can compete with hydrogen abstraction at higher temperatures. The influence of temperature on the rotation of acyclic radicals that exist in a preferred conformation for stereoelectronic reasons is shown by the β coupling constant a(β-H) in the ESR spectrum of the radical **64**.[43] The interaction between the β carbon–oxygen bond and the unpaired electron of the siloxyalkyl radical leads to the preferred conformation **64**. However, the temperature dependence of the β coupling constant shows that rotation around the C–C bond increases as the temperature rises.



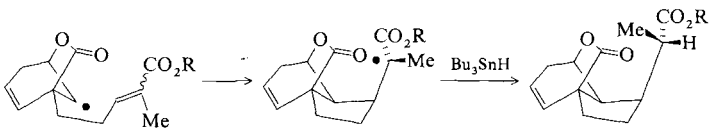
a (β-H)	T [°C]
6.33	−22
6.93	15
7.72	45
8.17	75



64 **65**

Addition reactions of the radical **64** and the arabinosyl radical **65** at 80 °C afford products in which the diastereomeric excess (*de*) is only just above 30%;[44] higher diastereoselectivity may result at lower temperatures.

Preferred conformations can also be induced by dipole–dipole interactions; thus, the radical **67**, formed from **66**, is trapped with high stereoselectivity by Bu_3SnH to give the product **68** (*de* = 90–94%).[45]

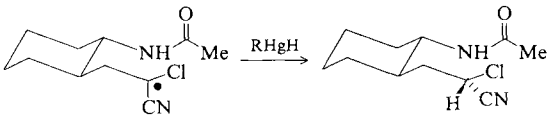


66 **67** **68**

de = 90–94% (80 °C)

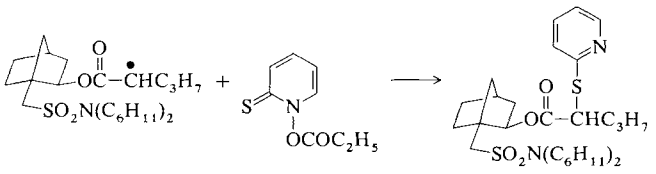
The stereoselectivity does not depend on the configuration of the alkene **66**; the radical center presumably adopts the preferred conformation shown in **67** because of dipole–dipole interactions. The radical will then be attacked from the less shielded side. The radical **69** also affords products

with high selectivity, probably via the conformation shown;[7b] the hydrogen transfer agent in this reaction is an alkylmercury hydride.



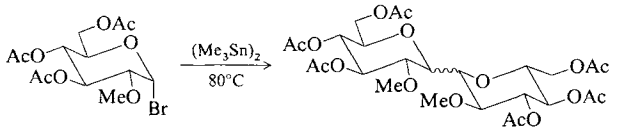
69 **70**
de = 90% (25°C)

The bent shape of the unsymmetrically substituted norbornyl group directs the addition of the radical **71** to the sulfur atom of the thiocarbonyl compound **72**; at −35 °C the product **73** is obtained with a diastereomeric excess of 66%.[46]



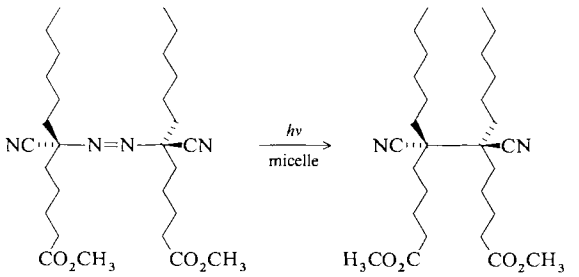
71 **72** **73**
de = 66% (−35°C)

Chiral products can be formed in recombination reactions of radicals that are formed from chiral precursors. However, the stereoselectivity is low in solution: thus, the glucosyl bromide **74** gives the dimers **75** in statistical proportions, although the trapping reactions of corresponding glucosyl radicals with nonradicals can be highly selective.[47]



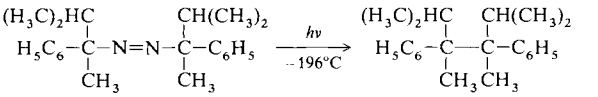
74 **75**

Selective radical–radical recombination reactions do however occur in micelles. This is shown by the photolytic cleavage of nitrogen from the azo compound **76** when the latter is embedded in phospholipid micelles; the reaction occurs with a high degree of retention.[48] The majority of the radicals in the micelle recombine before rotation occurs. These experiments make it clear why the stereoselectivity of radical reactions in enzymes can be different from that in solution.[49]

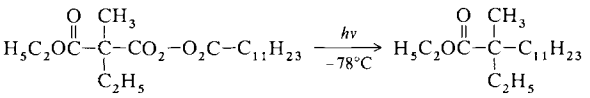


76 **77**
de = 72% (30°C)

Recombination reactions of radicals in the solid state are often stereoselective: thus, the photolytic cleavage of nitrogen from the azo compound **78** at −196 °C in a matrix affords the dimer **79** with a very high degree of retention,[50] and the photochemical decarboxylation of the diacyl peroxide **80** in the solid state at −78 °C gives the recombination product **81** with 80% retention.[51]



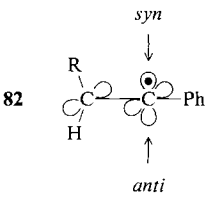
78 **79**



80 **81**

4.2. Vinyl Radicals

In vinyl radicals, rotation around the C=C bond does not occur and substituents can shield the two sides of the π radical to different extents. The hydrogen transfer to the vinyl radical **82** therefore occurs preferably *anti* to the alkyl substituent R with formation of the thermodynamically less stable *cis* alkene.[51]



82

R	*T*[°C]	*anti*:*syn*	H donor
c-C_6H_{11}	0	72:28	RHgH
	80	67:33	
*t*Bu	0	96:4	RHgH
	80	88:12	
Ad	80	> 98:2	Bu_3SnH

The stereoselectivity increases with increasing size of the shielding substituents, so that only formation of the *cis* alkene is observed in the case of the adamantane substituent. The stereoselectivity also depends on the nature of the hydrogen donor: the difference in activation enthalpy between *syn* and *anti* attack increases with decreasing reactivity of the hydrogen donor (see Table 9). However, the influence of the

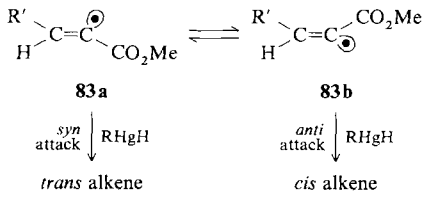
Table 9. Difference in activation enthalpies ($\Delta\Delta H^{\neq} = \Delta H^{\neq}_{anti} - \Delta H^{\neq}_{syn}$) and activation entropies ($\Delta\Delta S^{\neq} = \Delta S^{\neq}_{anti} - \Delta S^{\neq}_{syn}$) in reactions of the vinyl radical **82** (R = *c*C_6H_{11}) with H donors of differing reactivity (k_H).

H donor	$\Delta\Delta H^{\neq}$ [kJ mol^{-1}]	$\Delta\Delta S^{\neq}$ [J mol^{-1} K^{-1}]	k_H [L mol^{-1} s^{-1}]
cC_6H_{11}HgH	2.5	1	10^7
Bu_3SnH	4.5	7	10^6
cC_6H_{12}	12	28	1

activation entropies acts in an opposite direction, so that, in the case of the hydrogen donors in Table 9, the isoselective temperature lies at ca. 100 °C.[52b]

Lower selectivities are observed in reactions of σ radicals, since in this case the stability of the two interconverting

σ radicals, the rate at which equilibrium is attained, and the rate of the trapping reaction become important. The influence of the olefinic substituent on the equilibrium position and on the rate of the subsequent reactions acts in opposite directions; in the case of the hydrogen transfer reactions of the radicals **83a** and **83b**, this leads to an actual reversal of the selectivity on going from a *tert*-butyl to an *n*-hexyl substituent.[52a, 53]



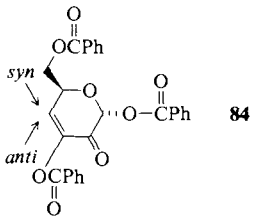
R'	*n*-C_6H_{13}	*c*-C_6H_{11}	*t*-C_4H_9
anti:*syn* (0°C)	34:66	46:54	70:30

5. Additions of Radicals to Alkenes with Stereogenic Centers

Alkyl radicals without chiral centers can also react in a stereoselective manner when radical traps with stereogenic centers are used. High stereoselectivities have been observed for trapping with chiral alkenes. However, only very little is known about stereoselective abstraction reactions involving radicals in nonenzymatic systems.

5.1. Cyclic Alkenes

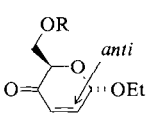
The stereoselectivity of cyclic alkenes and the reactions of cyclic radicals are influenced by steric effects in a similar manner; thus, alkyl radicals add to C-4 of the enolone **84** preferably *anti* to the substituent at C-5.[54] The *anti* selectivity increases with increasing size of the radical.



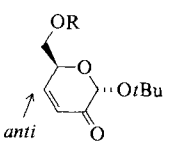
84

Radikal	*n*-$C_6H_{13}^{\bullet}$	*c*-$C_6H_{11}^{\bullet}$	*t*-$C_4H_9^{\bullet}$
anti:*syn* (80°C)	75:25	95:5	> 98:2

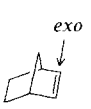
The cyclic alkenes **85** and **86** are also attacked preferably in an *anti* manner,[55] and norbornene **87** is attacked almost solely from the *exo* side.[56]



85



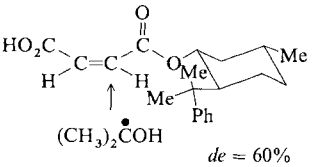
86



87

5.2. Acyclic Alkenes

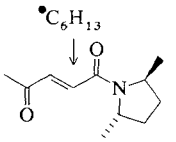
There are so far only a few examples of intermolecular radical reactions with acyclic alkenes in which attack is more selective than 3:1. With terminal alkenes no cases of high stereoselectivity are known. It thus appears to be very important that the olefinic carbon atom undergoing attack should bear the chiral substituent. For example, the photochemically produced 1-hydroxy-1-methylethyl radical adds to the chiral maleic ester **88** with a diastereoselectivity of 60%.[57]



88

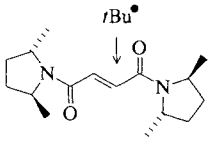
de = 60%

The decisive breakthrough occurred with α,β-unsaturated amides.[58] Alkyl radicals add to the alkenes **89** and **90** with diastereoselectivities which increase with decreasing temperature and increasing size of the radicals; even at 20 °C *tert*-butyl radicals add to the fumaric acid diamide **90** with a diastereoselectivity of 96%.[59a]



89

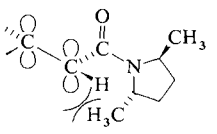
de = 78% (80°C)
87% (20°C)



90

de = 88% (110°C)
96% (20°C)

This high selectivity observed in the amide cases is due to the two stereogenic centers of the amine component. Because of the C_2 symmetry of the amines, the conformation does not change when rotation around the carbon–nitrogen bond occurs. The two methyl groups of the amine component shield the two sides of the alkene to different degrees. This is made clear by formula **91**; the methyl group below the plane of the



91

paper is closer to the alkene than the methyl group directed upwards. The attack on the olefinic C atom that is substituted by the amide group is thus hindered to different degrees by the two methyl groups, and the radical addition is stereoselective.[59b]

These initial experiments with α,β-unsaturated amides make it clear that radical reactions of acyclic systems can indeed be highly stereoselective.

6. Future Prospects

The results obtained in the last few years have shown that cyclic radicals and cyclic radical traps react with predictable and in part high stereoselectivity. Preliminary experiments have shown that the reactions of acyclic radicals with acyclic alkenes can also be stereoselective. However, it must be left to future work to show how preferred conformations of acyclic radicals or acyclic radical traps can be stabilized; both stereoelectronic effects and complexation with metal salts could be of use here. Since stereoselectivities are reflected in differences in activation enthalpies, a reduction of the reaction temperature will also increase the radical selectivity. It is important that the radicals be reactive enough to react at low temperatures. This presupposes, however, that it will be possible to generate radicals at low temperatures under the synthetic conditions required; photochemical techniques, in particular, will be of importance. It would also be desirable to develop alternatives to photochemical generation of radicals. Whether it will be possible to use free radical chemistry for enantioselective syntheses – for example, via chiral metal complexes – remains to be seen. Until now it has not been possible to influence the stereoselectivity of radical reactions with, for example, the chiral ligands of vitamin B_{12}.[60]

The importance of free radical chemistry for organic synthesis will depend on the degree to which stereoselectivity can be controlled. However, the wide use of radicals (for example, in industrial processes) will require the development of methods in which organotin compounds are no longer necessary. It appears to me that this problem can be solved: for example, the method developed by *Barton* et al.[61] using thiopyridine compounds or the use of organocobalt compounds[33,62] make it possible to work without tin. Very recent studies have shown that stannanes can also be replaced by silanes.[63] The use of silanes, in particular, should make possible a wide practical use of free radicals in organic synthesis.

Our own work in this area has been made possible by the generous support of the Deutsche Forschungsgemeinschaft, the VW-Stiftung and the Fonds der Chemischen Industrie. I thank my co-workers, whose names can be found in the list of references, for their hard work and dedication. I am grateful to Prof. Sustmann and Dr. Korth for the ESR studies, Prof. K. N. Houk for help and advice concerning calculations, Prof. H. J. Lindner for X-ray analyses, and Prof. N. A. Porter for extensive and helpful discussions.

Received: February 1, 1989 [A 728 IE]
German version: *Angew. Chem. 101* (1989) 993
Translated by Prof. Dr. *T. N. Mitchell*, Dortmund

[1] For a comprehensive review, see B. Giese: *Radicals in Organic Synthesis: Formation of Carbon-Carbon Bonds*, Pergamon, Oxford 1986. For further reviews: D. J. Hart, *Science (Washington D.C.) 223* (1984) 883; M. Ramaiah, *Tetrahedron 43* (1987) 3541; W. P. Neumann, *Synthesis 1987*, 665; D. P. Curran, *ibid. 1988*, 417, 489.

[2] B. Giese, *Angew. Chem. 97* (1985) 555; *Angew. Chem. Int. Ed. Engl. 24* (1985) 553.

[3] C. Rüchardt, *Angew. Chem. 82* (1970) 845; *Angew. Chem. Int. Ed. Engl. 9* (1970) 830; *Top. Curr. Chem. 88* (1980) 1.

[4] See, e.g., J. Sorba, J. Fossey, D. Lefort, *Bull. Soc. Chim. Fr. 1977*, 967; A. Citterio, F. Minisci, O. Porta, G. Sesane, *J. Am. Chem. Soc. 99* (1977) 7960; B. Giese, J. Meixner, *Angew. Chem. 91* (1979) 167; *Angew. Chem. Int. Ed. Engl. 17* (1979) 154; B. Giese, *ibid. 95* (1983) 771 and *22* (1983) 753.

[5] For good reviews, see H. G. Viehe, Z. Janousek, R. Merenyi (Eds.): *Substituent Effects in Radical Chemistry*, Reidel, Dordrecht 1986.

[6] See, e.g., A. L. J. Beckwith, C. H. Schiesser, *Tetrahedron 41* (1985) 3925.

[7] a) B. Giese, K. Heuck, H. Lenhardt, U. Lüning, *Chem. Ber. 117* (1984) 2132; b) R. Henning, H. Urbach, *Tetrahedron Lett. 24* (1983) 5343.

[8] D. H. R. Barton, A. Gateau-Olesker, S. D. Gero, B. Lacher, C. Tachdjian, S. Z. Zard, *J. Chem. Soc. Chem. Commun. 1987*, 1790.

[9] U. Lüning, *Dissertation*, Technische Hochschule Darmstadt 1984.

[10] a) B. Giese, *Angew. Chem. 89* (1977) 162; *Angew. Chem. Int. Ed. Engl. 16* (1977) 125; b) G. S. Hammond, *J. Am. Chem. Soc. 77* (1955) 334.

[11] a) Ab initio calculations (3-21G//3-21G/UHF) for the addition of methyl radicals to ethylene, see: K. N. Houk, M. N. Paddon-Row, D. C. Spellmeyer, N. G. Rondan, S. Nagase, *J. Org. Chem. 51* (1986) 2874; b) K. N. Houk, B. Giese, Y. Li, D. C. Spellmeyer, H. Zipse, unpublished results.

[12] a) S. D. Burke, W. F. Fobare, D. H. Armistead, *J. Org. Chem. 47* (1982) 3348; b) B. Giese, J. A. González-Gómez, T. Witzel, *Angew. Chem. 96* (1984) 51; *Angew. Chem. Int. Ed. Engl. 23* (1984) 69; c) J. Dupuis, B. Giese, J. Hartung, M. Leising, H.-G. Korth, R. Sustmann, *J. Am. Chem. Soc. 107* (1985) 4332.

[13] a) J. Dupuis, *Dissertation*, Technische Hochschule Darmstadt 1985; b) Y. Araki, T. Endo, M. Tanji, J. Nagasawa, Y. Ishido, *Tetrahedron Lett. 29* (1988) 351; c) D. H. R. Barton, *Pure Appl. Chem. 60* (1988) 1549.

[14] T. Linker, *Diplomarbeit*, Technische Hochschule Darmstadt 1988.

[15] G. Stork, P. M. Sher, H. L. Chen, *J. Am. Chem. Soc. 108* (1986) 6384.

[16] a) G. Stork, P. M. Sher, *J. Am. Chem. Soc. 108* (1986) 302; b) G. Sacripante, G. Just, *J. Org. Chem. 52* (1987) 3659.

[17] B. Giese, U. Erfort, *Chem. Ber. 116* (1983) 1240.

[18] B. Giese, J. Meixner, *Tetrahedron Lett. 1977*, 2783.

[19] B. Giese, G. Kretzschmar, *Chem. Ber. 117* (1984) 3175.

[20] B. Giese, H. Farshchi, unpublished results.

[21] J. Metzger, personal communication.

[22] a) J. J. Patroni, R. V. Stick, *J. Chem. Soc. Chem. Commun. 1978*, 449; b) W. Kitching, A. R. Atkins, G. Wickham, V. Alberts, *J. Org. Chem. 46* (1981) 563; c) F. Baumberger, A. Vasella, *Helv. Chim. Acta 66* (1983) 2210.

[23] G. A. Russell, A. Ito, *J. Am. Chem. Soc. 85* (1963) 2983.

[24] D. S. Ashton, J. M. Tedder, *J. Chem. Soc. B 1971*, 1719.

[25] P. D. Bartlett, G. N. Fickes, F. C. Haupt, R. Helgeson, *Acc. Chem. Res. 3* (1970) 177.

[26] a) F. D. Greene, C. C. Chu, J. Walia, *J. Org. Chem. 29* (1964) 728; b) D. Lefort, J. Fossey, M. Gruselle, J.-Y. Nedelec, *Tetrahedron 41* (1985) 4237.

[27] a) Y.-D. Wu, K. N. Houk, *J. Am. Chem. Soc. 109* (1987) 908; b) Force-field calculations were carried out with the program MM2 of *Allinger* (1980) and the parameters of the radical cyclization [D. C. Spellmeyer, K. N. Houk, *J. Org. Chem. 52* (1987) 959]: K. N. Houk, B. Giese, H. Zipse, unpublished results.

[28] B. Giese, J. Hartung, J. He, O. Hüter, A. Koch, *Angew. Chem. 101* (1989) 334; *Angew. Chem. Int. Ed. Engl. 28* (1989) 325.

[29] T. Haßkerl, *Dissertation*, Technische Hochschule Darmstadt 1987.

[30] O. Hüter, *Diplomarbeit*, Technische Hochschule Darmstadt 1988.

[31] a) B. Giese, K. S. Gröninger, *Tetrahedron Lett. 25* (1984) 2743; b) B. Giese, J. Dupuis, K. S. Gröninger, T. Haßkerl, M. Nix, T. Witzel in [5], p. 28; c) K. S. Gröninger, *Dissertation*, Technische Hochschule Darmstadt 1987.

[32] M. Nix, *Dissertation*, Technische Hochschule Darmstadt 1986.

[33] K. Kroder, *Diplomarbeit*, Technische Hochschule Darmstadt 1988; c.f. also R. Scheffold, *Chimia 39* (1985) 203.

[34] B. Giese, J. Hartung, unpublished results.

[35] J. R. Rasmussen, C. J. Slinger, R. J. Kordish, D. D. Newman-Evans, *J. Org. Chem. 46* (1981) 4843.

[36] a) J. P. Praly, *Tetrahedron Lett. 24* (1983) 3075; b) B. Giese, J. Dupuis, *ibid. 25* (1984) 1349; c) B. Giese, J. Dupuis, M. Nix, *Org. Synth. 65* (1987) 236.

[37] a) J. Dupuis, B. Giese, D. Rüegge, H. Fischer, H.-G. Korth, R. Sustmann, *Angew. Chem. 96* (1984) 887; *Angew. Chem. Int. Ed. Engl. 23* (1984) 896; b) H.-G. Korth, R. Sustmann, J. Dupuis, B. Giese, *J. Chem. Soc. Perkin Trans. 2 1986*, 1453.

[38] H.-G. Korth, R. Sustmann, K. S. Gröninger, T. Witzel, B. Giese, *J. Chem. Soc. Perkin Trans. 2 1986*, 1461.

[39] B. Giese, *Pure Appl. Chem. 60* (1988) 1655.

[40] H.-G. Korth, R. Sustmann, B. Giese, unpublished results.

[41] B. Giese, J. Dupuis, M. Leising, M. Nix, H. J. Lindner, *Carbohydr. Res. 171* (1987) 329.

[42] P. S. Skell, K. J. Shea in J. K. Kochi (Ed.): *Free Radicals, Vol. 2*, Wiley, New York 1973, p. 809.

[43] H.-G. Korth, R. Sustmann, R. Rupaner, B. Giese, unpublished results.

[44] R. Rupaner, *Dissertation*, Technische Hochschule Darmstadt 1989.

[45] C. P. Chuang, D. J. Hart, *J. Org. Chem. 48* (1983) 1782; D. J. Hart, H. C. Huang, *Tetrahedron Lett. 26* (1985) 3749.

[46] D. Crich, J. W. Davies, *Tetrahedron Lett. 28* (1987) 4205.

[47] B. Giese, B. Rückert, K. S. Gröninger, R. Muhn, H. J. Lindner, *Liebigs Ann. Chem. 1988*, 997.

[48] W. J. Brittain, N. A. Porter, P. J. Krebs, *J. Am. Chem. Soc. 106* (1984) 7652.
[49] J. Rétey in F. Minisci (Ed.): *Free Radicals in Synthesis and Biology*, Kluwer, Dordrecht 1989, p. 373.
[50] P. D. Bartlett, J. M. McBride, *Pure Appl. Chem. 15* (1967) 89.
[51] M. Feldhues, H. J. Schäfer, *Tetrahedron 41* (1985) 4213.
[52] a) B. Giese, S. Lachhein, *Angew. Chem. 94* (1982) 780; *Angew. Chem. Int. Ed. Engl. 21* (1982) 768; b) B. Giese, J. A. González-Gómez, S. Lachhein, J. O. Metzger, *ibid. 99* (1987) 475 and *26* (1987) 479; c) M. Ohno, K. Ishizaki, S. Eguchi, *J. Org. Chem. 53* (1988) 1285.
[53] S. Lachhein, *Dissertation*, Technische Hochschule Darmstadt 1982.
[54] B. Giese, T. Witzel, *Tetrahedron Lett. 28* (1987) 2571.
[55] a) B. Fraser-Reid, N. L. Holder, D. R. Hicks, D. L. Walker, *Can. J. Chem. 55* (1977) 3978; b) U. E. Udodong, B. Fraser-Reid, *J. Org. Chem. 53* (1988) 2131.
[56] a) D. I. Davies, L. T. Parfitt, C. K. Alden, J. A. Claisse, *J. Chem. Soc. C 1969*, 1585; b) J. G. Traynham, A. Laue, N. S. Bhacca, *J. Org. Chem. 34* (1969) 1302; c) A. G. Ludwick, J. C. Martin, *ibid. 34* (1969) 4108.
[57] R. Vaßen, J. Runsink, H.-D. Scharf, *Chem. Ber. 119* (1986) 3492.
[58] High diastereoselectivities with α,β-unsaturated amides were first observed in macrocyclizations: N. A. Porter, B. Lacher, V. H. T. Chang, D. R. Magnin, unpublished results.
[59] a) N. A. Porter, D. M. Scott, B. Lacher, H. G. Zeitz, B. Giese, unpublished results; b) This interpretation is supported by the X-ray structure analysis of the addition product of **91** carried out by *H. J. Lindner*.
[60] R. Scheffold, personal communication.
[61] D. H. R. Barton, S. Z. Zard, *Pure Appl. Chem. 58* (1986) 675.
[62] a) M. Tada, M. Okabe, *Chem. Lett. 1980*, 201; b) V. F. Patel, G. Pattenden, *J. Chem. Soc. Chem. Commun. 1987*, 871; c) A. Ghosez, T. Göbel, B. Giese, *Chem. Ber. 121* (1988) 1807.
[63] B. Giese, B. Kopping, C. Chatgilialoglu, *Tetrahedron Lett. 30* (1989) 681.

Calorimetric Studies of Biopolymers and Aggregates of Phospholipids

By Theodor Ackermann*

Dedicated to Professor Christoph Rüchardt on the occasion of his 60th birthday

The structural transformations that biopolymers undergo in aqueous solution are complex processes, whose mechanisms can only be explained by the coupling of various partial processes. A spectroscopic analysis of the states of the system often requires considerable effort. In many cases, calorimetric studies have proven to be sufficient for a general characterization of the behavior of the system. These measurements provide information on the stability of the initial state and on the cooperativity of the total process. From the thermodynamic parameters of the system, knowledge on the structure-determining influence of the various types of inter- and intramolecular interactions is obtained. This not only applies to solutions of biopolymers and analogous model substances, but also to solutions of biopolymer complexes with low-molecular-weight ligands and to aqueous suspensions of self-aggregating phospholipids. Possibilities and limitations of the calorimetric methods of measurement are demonstrated for typical examples from the numerous polypeptide and polynucleotide systems and the phospholipid bilayer systems that have been studied. In addition, the special problems involved in carrying out measurements on dilute solutions are pointed out. Here, the latest advances made in measuring techniques are readily apparent.

1. Introduction

The structure of proteins and nucleic acids is characterized by a high degree of molecular order, which is not limited to the covalently bonded atomic building blocks (primary structure). The helix sequences of the secondary structure, stabilized by hydrogen bonds, are a characteristic feature of these biopolymers. The functional diversity of these substances reflects the diversity of the three-dimensional folding pattern (tertiary structure). Hydrophobic interactions, together with other intermolecular interactions, stabilize the aggregation of molecules having defined tertiary structures (quaternary-structure formation). These molecular aggregates, often embedded in the matrix system of the lipid bilayer of biomembranes, are the building elements of biological functional units.

Phospholipids are the most important structural components of biological membranes. Their fatty acid chains are more or less closely packed in the hydrophobic region of the lipid matrix. In the hydrocarbon chains of phospholipid molecules, rotation about the bond between neighboring CH_2 groups is limited. The ideal conformation of this chain is *all trans*. However, this ordered state seldom occurs in membranes. Normally, the CH_2 groups of lipid molecules are in a state characterized by several *gauche-trans-gauche* kinks. In regard to the molecular dynamics of the lipid system, this means that the mobility of the molecular chains in biomembranes is much higher than in the ideal quasi-crystalline lipid bilayer. In an exact description of the state of order of phospholipids, the relative orientation of the neighboring polar head groups must also be considered.

The biological functions of proteins and nucleic acids are optimal only in a narrow temperature range and for an almost constant composition of the surrounding aqueous medium. Any temperature change, as well as any pH shift or change in the solvent composition, leads to a conformational change of biopolymers associated with a reduction in function (denaturation). Examples of this kind of process include the helix–random coil transition of polypeptides and the denaturation of the DNA double helix. The transformation of a polypeptide chain from the ordered helix state to the disordered randomly coiled state is schematically shown in Figure 1. During this conformational change, a variety of different intermediate states can occur in a group of dissolved macromolecules. These intermediate states must be

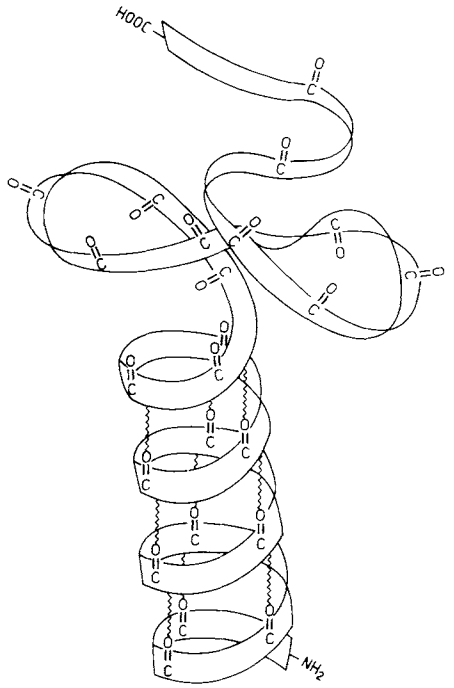


Fig. 1. Helix–random coil transition of a polypeptide chain (schematic).

[*] Prof. Dr. T. Ackermann
Institut für Physikalische Chemie der Universität
Albertstrasse 23a, D-7800 Freiburg (FRG)

 © VCH Verlagsgesellschaft mbH, D-6940 Weinheim, 1989 0570-0833/89/0808-0981 $ 02.50/0

considered in any statistical thermodynamic theory of helix–random coil transitions.[1-3] Molecular states characterized by a relatively small number of randomly coiled regions between continuous helix sequences are preferred. In the helix–random coil transformation, concerted transitions of connected helix regions to the randomly coiled state take place. The overall process is cooperative and is similar to a phase transition. Therefore, the thermally induced helix denaturation is often compared with a melting process, although it is not a first-order phase transition.

The transition from the ordered helix state to the disordered state is reflected in numerous physical changes when solutions are studied. For example, the optical rotatory power of polypeptide solutions is influenced by the helix–random coil transition. A simple procedure for recording transition curves, in which the degree of helix transformation is represented as a function of temperature, is based on this effect.[4] In measurements on polynucleotide solutions, the helix denaturation curves can be recorded in a similarly easy manner, because base unstacking, which progresses with denaturation, causes a reduction of the hypochromic effect (i.e., increased UV absorption).[5]

Information on the stability of secondary structures with different units can be obtained from denaturation curves. An exact analysis of the combined effects of the various types of weak interactions is only possible if the thermodynamic parameters of the system are known. The most important thermodynamic parameters are the enthalpy of transition and the entropy of transition as well as additional parameters describing the degree of cooperativity of the conformational change. If the observed transformation is coupled with the release of low-molecular-weight ligands, the relevant values for the binding enthalpy and binding entropy must be determined.

Phospholipid bilayer vesicles[6] in aqueous suspension may be considered as lipid-matrix model systems for biological membranes. These lipid systems also change from a quasi-crystalline gel state to a less ordered liquid-crystalline state above a characteristic transition temperature. This transformation, characterized by a reduction in the packing density and increased chain mobility, also takes place within a narrow temperature interval. This cooperative process is called a lipid phase transition.[7] The characteristic transition temperature not only depends on the state of the polar phospholipid head groups, but also on the number of double bonds in the hydrocarbon chains of the lipid and the chain length. The phase transition of lipid bilayers is also influenced by the addition of other components (e.g., cholesterol). In lipid systems with low water content, in addition to the simply structured bilayer vesicles, other more complicated lipid aggregates can also occur. The areas where these "phases" exist can be assigned by a lipid phase diagram. Knowledge of the thermodynamic equilibrium parameters of lipid systems is required for a molecular theoretical interpretation of the phenomena observed in these systems.

There are several methods for determining the thermodynamic parameters of biopolymer solutions and phospholipid systems. Based on studies of simple model systems, several research groups have prepared extensive experimental data which have recently been critically studied and summarized in review articles[8, 9] and data collections.[10] It is not possible to discuss all these data within the framework of this article. Instead, its aim is to present the calorimetric methods described in Sections 4 and 5 as an important procedure for studying biopolymers and phospholipid systems and to exemplify the results obtained with these methods.

2. Degree of Conversion and Enthalpy of Transition

The simplest model system for a biopolymer solution with a temperature-dependent helix–random coil equilibrium is a group of homopolypeptide molecules with the same chain lengths. The peptide units of these molecules are called "segments". If the cooperative interactions are neglected, the state of this system can be described by a two-state equilibrium (segment in α-helix state (B) $\rightleftarrows$ segment in randomly coiled state (A)). The fraction of the segments bound in the helix state is called the degree of helix formation θ.[1-3] The helix formation constant s is the equilibrium constant for process (1).

$$\cdots \text{ABBAA} \cdot \rightleftarrows \cdot \text{ABBBA} \cdots \tag{1}$$

The temperature dependence of the quantity $1-\theta$ is shown in the upper part of Figure 2. The temperature T_m (or

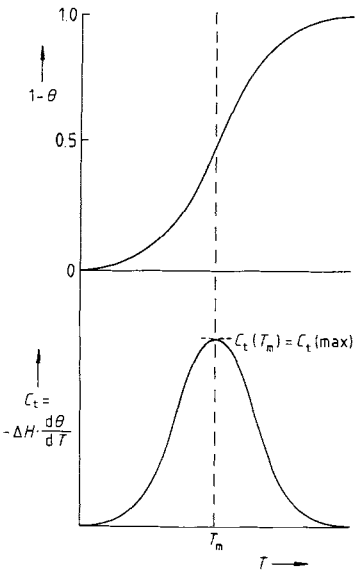


Fig. 2. The temperature dependence of the degree of transformation $1-\theta$ (top) and the conformational excess heat capacity C_t (bottom) of a thermally induced helix–random coil transition according to Equations (3) and (7).

the corresponding ϑ_m of the celsius scale) that is assigned to $\theta = 0.5$ is called the transition temperature. If no cooperative interactions need to be considered, the typical shape of the curve obtained by plotting $1-\theta$ versus T is derived from the temperature dependence of the equlibrium constant s, which, according to the laws of thermodynamics, is expressed by Equation (2).

$$\frac{d\ln s}{dT} = \frac{\Delta H_{v.H.}}{RT^2} \tag{2}$$

In Equation (2), $\Delta H_{v.H.}$ represents the van't Hoff's enthalpy of helix formation or the enthalpy of transition per mole of segmental unit or per mole of lipid. At the transition

point, $s = 1$ and $\theta(1-\theta) = 1/4$. From this and the simplifying assumptions already mentioned,[3] Equation (3) is derived.

$$\left(\frac{d(1-\theta)}{dT}\right)_{T_m} = -\frac{\Delta H_{v.H.}}{4RT_m^2} \tag{3}$$

Based on Equation (3), $\Delta H_{v.H.}$ can be obtained from the slopes of the transition curves recorded by optical methods.

The helix–random coil transition facilitates the addition of solvent molecules to the dissolved polypeptide molecules (solvation). Solvation is an exothermic process. The state of association of the solvent also changes with the state of solvation of dissolved substances. Thus, the overall helix–random coil transition is a process in which endothermic and exothermic partial processes overlap and, except for a relatively insignificant amount, are compensated in the energy balance. Therefore, the molar enthalpy of transition calculated for a peptide segment with an average hydrogen bond dissociation energy[11] of 30 kJ mol^{-1} cannot be significantly greater than 5 kJ mol^{-1}. For a comprehensively studied peptide system (poly(γ-benzyl-L-glutamate)[12,13] dissolved in a mixture of dichloroacetic acid and 1,2-dichloroethane; see Section 7.1), however, a much higher $\Delta H_{v.H.}$ value of approximately 400 kJ mol^{-1} was obtained from the evaluation of transition curves. Apparently, the stabilizing effects of neighboring segments of a peptide chain cannot be neglected, because the formation of a helix sequence is strongly favored by the immediately neighboring segments already in the helix state. This facilitation means that the neighboring segments of a helix sequence in peptide chains change from the helix state to the random state in a concerted process. The influence of this cooperativity is exhibited in the pronounced sharpness of the transition curves.

3. Cooperativity Parameters and Average Cooperative Lengths

Theoretical formulations[1-3,13] allow the derivation of a quantitative relationship for the temperature dependence of the frequencies and neighboring distribution of the segments in the helix and randomly coiled states. This provides information on the average number of united segments still in a helix sequence at temperature T_m. The number N_0 of segments that cooperatively transform to the randomly coiled state at the transition point is called the average cooperative length.[1] When the cooperativitiy is considered, the true molar enthalpy of transition ΔH_t is not used for $\Delta H_{v.H.}$ in Equation (3), but rather the product $N_0 \cdot \Delta H_t$. Equation (4)

$$H_{v.H.} = N_0 \cdot \Delta H_t \tag{4}$$

applies, since, instead of the individual peptide segment, the number of segments (N_0) is used as a molar stoichiometric unit for the conformational change. Evaluation of transition curves that are, for example, determined by measurements of the temperature dependence of optical rotatory power always provides only the product $N_0 \cdot \Delta H_t$. Normally, the average cooperative length N_0 is not known. Often, it cannot be theoretically calculated if there is no exact data on the chain lengths of the polypeptide molecules studied and their influence on the sharpness of the transition curves. In the theory of the helix–random coil transformation, the cooperativity parameter σ should be given central importance. If s is the equilibrium constant for the growth step defined by Equation (1), the product $\sigma \cdot s$ is the equilibrium constant for the nucleation step (5) ($\sigma < 1$). *Applequist*[3] showed that there is a simple relationship [Eq. (6)]

$$\cdots AAAAA \cdot \rightleftarrows \cdot ABAAA \cdots \tag{5}$$

$$N_0 = \sigma^{-1/2} \tag{6}$$

between the cooperativity parameter and the average cooperative length N_0. For example, for $\sigma = 10^{-4}$, $N_0 = 100$. If the value for N_0 is not known, no information on the true molar enthalpy of transition per segment (ΔH_t) can be obtained with the described procedure. However, knowledge of the ΔH_t values is especially important for an understanding of the enthalpy balance that contributes to the stability of secondary structures. Therefore, direct calorimetric procedures should be used to determine ΔH_t values.

The influence of the cooperative interactions discussed here for the helix–random coil transition of a polypeptide system is similarly reflected in the thermally induced denaturation of nucleic acid double-helix sequences. Thus, if chain-length effects are considered, the true enthalpies of denaturation per mole of base pairs (bp) for poly- or oligonucleotides can only be obtained from the different slopes of the so-called melting curves determined by recording UV absorbance of substances with different chain lengths.

The cooperative effect has a particularly dramatic effect on the transition of a lipid bilayer system from the gel state to the liquid-crystalline state. The strong similarities of this change of state with a first-order phase transition lead to the conclusion that this process is highly cooperative. In the physico-chemical characterization of these systems, the exact determination of the true enthalpy of transition can often only be achieved by means of direct calorimetric measurements. Suitable methods for these measurements are explained below.

4. True Enthalpies of Transition and the Conformational Excess Heat Capacity

If the temperature is limited to the relative narrow range of a cooperative conformational transformation, the molar enthalpy of transition ΔH_t can be considered a constant system parameter. Since the total mole number n_g for all segments is given, with the differential mole number change $dn = -n_g d\theta$ and the increase in enthalpy $dH = \Delta H dn$, Equation (7) is obtained, where C_t is the conformational ex-

$$C_t = \frac{1}{n_g}\frac{dh}{dT} = -\Delta H_t \frac{d\theta}{dT} \tag{7}$$

cess heat capacity per mole of segment. The temperature dependence of C_t is schematically represented in Figure 2 (bottom). The symmetric curve shows the proportionality between the value of C_t and the differential quotient $d\theta/dT$.

Since the total enthalpy of transition of the system does not depend on the type of intermediate state, the true molar enthalpy of transition ΔH can be determined by measuring the area under the curve shown in Figure 2 (bottom). Since the transition curve reaches its maximum sharpness at temperature T_m, $C_t(T)$ also has a maximum at this point. Consideration of Equations (4) and (6) gives Equation (8) for T_m.

$$C_t(T_m) = \frac{1}{4\sigma^{1/2}} \frac{(\Delta H_t)^2}{RT_m^2} \tag{8}$$

If the temperature dependence of the heat capacity of a solution of biopolymers is exactly recorded, the parameters ΔH_t and $C_t(T_m)$ can be determined. If these two parameters are inserted into Equation (8), σ and thus N_0 can be calculated based on Equation (6). The prerequisite for an exact determination of the cooperativity parameters is, however, a distortion-free reproduction of the function $C_t(T)$, which can only be achieved if the rate of heating is low and the measuring arrangement is relatively inert to thermal lag effects.

In cases of model substances with uniform primary structures (homopolypeptides and homopolynucleotides) and some transfer ribonucleic acids, the conformational transformation can be reversed by cooling via the same path achieved by heating. In enzyme proteins, deviations from the renaturation equilibrium curve[14] are also rarely observed. In contrast to polypeptides partial renaturation of native DNA samples following thermal denaturation can only be achieved by very slow cooling.[15] Between these two extremes, complete renaturation and nonreversible denaturation, there are numerous hysteresis-like phenomena. The importance of these phenomena in regard to possible information storage effects are discussed in detail by *E. Neumann*.[16] Hysteresis effects are observed during variations of pH values and during thermally induced conformational transformations of several polynucleotide solutions and lipid suspensions. An example of a polynucleotide system with thermally induced hysteresis is the mixed system of poly(deoxyriboadenylic acid)(poly(dA)) and poly(ribothymidylic acid)-(poly (T)).[17] Phosphatide acid systems are lipid systems exhibiting thermal hysteresis.[18] The hysteresis effect is also reflected in the course of the $C_t(T)$ curves. When the equilibrium of hysteresis-free systems is quickly reached, the $C_t(T)$ curves recorded upon heating and cooling must agree. Since the primary objective of thermodynamic measurements is the characterization of changes of state occurring between equilibrium states, it should always be checked whether the system studied goes through a series of equilibrium states during the conformational transformation or whether significant deviations from equilibrium take place. Thus, the development of heating–cooling calorimeters,[19] which make it possible to record $C_t(T)$ curves during heating and cooling, should receive special attention. If the enthalpy area under the $C_t(T)$ curve is constant, the problems related to distortion-free recording of these curves are insignificant if only the ΔH_t values are to be determined.

5. Experimental

The first measurements on solutions of polypeptides[20] and polynucleotides[21] were made with adiabatic recording calorimeters. For special measurements of some samples dissolved in nonaqueous corrosive solvents, glass calorimeter vessels had to be used.[22, 23] In most cases, measurements on aqueous solutions can be done with suitable metal calorimeter vessels (e.g., gold-plated silver vessels[24]). The most suitable method for recording C_t curves is the DSC method (differential scanning calorimetry).[25] The principle of this twin calorimeter method (recording the additional electrical heating power needed for the compensation of the conformational excess heat capacity when heat exchanges with the surroundings are largely excluded) is well-known and described in detail in the latest specialized literature on measuring procedures in calorimetry.[26] However, only some of the specialized types of commercial DSC apparatuses are suitable for measurements on solutions of biopolymers and analogous model substances. Special demands on sensitivity inevitably result from the fact that the major contribution to the enthalpy increase observed in thermally induced conformational transformations is not caused by the structural change of the solute but by the high heat capacity of the solvent. While the increase in enthalpy caused by structural changes strongly contributes to the total heat capacity in the study of homogeneous solid samples (e.g., solid polymer materials), the conformational excess heat capacity for biopolymer solutions is normally no more than one or two percent of the calorimetrically measurable total effect. Thus, the sensitivity for the difference effect to be determined must also be particularly high when the major contribution to the heat capacity caused by the solvent is eliminated by compensation based on the principle of the twin calorimeter. In addition, only instruments with hermetically sealable sample chambers can be used for calorimetric measurements on solutions of biopolymers owing to the volatility of the solvent.

The requirements mentioned are met by the DASM-1M calorimeter (Mashpriborintorg, Moscow, USSR) equipped with gold vessels, which was developed by *P. L. Privalov* et al.[27] An improved version (DASM-4M) is now available. With this type of apparatus, measurements on biopolymer solutions with relatively small concentrations (1–2 mg mL^{-1}) can be made without particular difficulty. The Microcal MC1 (Microcal Inc., Amherst, MA, USA) developed by *J. F. Brandts* et al.[28] is also suitable to make measurements on biopolymer solutions. The Perkin-Elmer DSC apparatus (Perkin-Elmer Corporation, Norwalk, CT, USA) can also be used to study concentrated lipid suspensions (5–10 wt%). However, with this apparatus, the small sample volumes (20 to 25 μL) have a negative influence on the calorimetrically measurable effect. In view of the relatively small number of suitable calorimeters offered, the further development of DSC instruments for the above mentioned purpose would be useful.

Figure 3 shows the construction scheme and the twin vessel unit of a DPSC apparatus (differential power scanning calorimeter) developed in our institute by *M. Grubert*.[29] In Figure 4, as example, a $C_t(T)$ curve of a polynucleotide solution recorded with this type of apparatus is shown.[30] Since the ΔH_t value obtained from the area under the $C_t(T)$ curve corresponds to a small difference effect of two endothermic effects eliminated by compensation, this ΔH_t value cannot be assigned a particularly high degree of relative accuracy. Normally, the ΔH_t values determined with the DSC method are

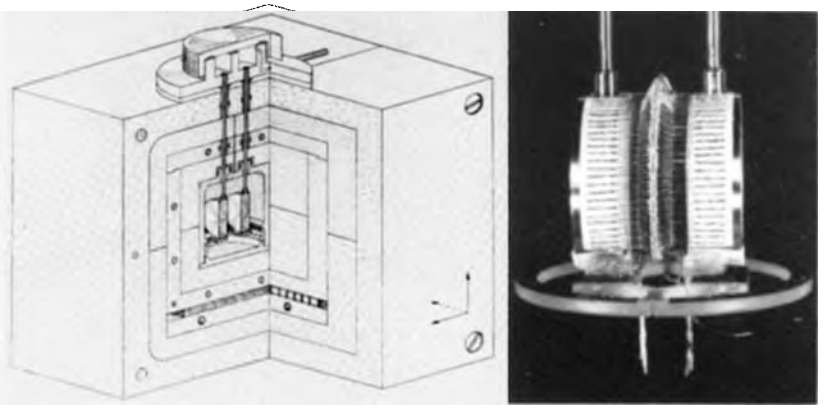


Fig. 3. A construction scheme (left) and twin-vessel unit (right) of a DPSC apparatus (according to *M. Grubert*[29]). The twin-vessel unit fixed to the inlet tubes is surrounded by an adiabatic shield regulated by means of multijunction thermocouples. A constant temperature of the surroundings is maintained by means of a thermostated outer shield with a Peltier battery, which surrounds the adiabatic shield (outer protective end: aluminum block with a pressure-resistant lid; lining of the space between the outer shields: polyurethane-foam fillers).

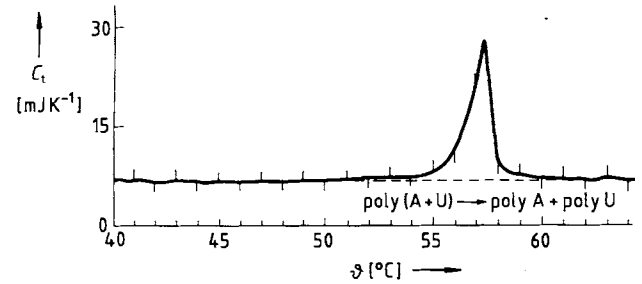


Fig. 4. A $C_t(T)$ curve of a polynucleotide system (equimolar mixture of polyribouridylate and polyriboadenylate in aqueous buffer solution; see Section 6) recorded with DPSC apparatus.

reproducible with an accuracy of $\pm$ 2%. In most cases where thermodynamic data are needed for numerical calculations, this accuracy has proved to be sufficient.

For the thermodynamic characterization of biopolymer systems with ligand binding,[31] direct calorimetric determination of the enthalpy of binding should also be carried out if possible. The LKB mixture calorimeter[32] (model 10700-2; LKB, Broma, Sweden) is suitable for these kinds of experiments. Such measurements have also been made by several research groups.[33]

6. Results from Measurements on Polynucleotide Solutions

Calorimetric measurements on nucleic acids and synthetically prepared poly- and oligonucleotides have been made. The results are summarized in the data collection mentioned previously.[10] Here, several typical examples will be briefly described and explained.

6.1. Deoxyribonucleic Acids

The magnitude of the ΔH_t values per mole of base pairs (mol bp) for the thermally induced denaturation of dissolved deoxyribonucleic acids is approximately 35 kJ/mol bp.[34-37] For a number of different DNA samples, the dependence of ΔH_t values on guanine/cytosine (GC) content has been studied.[38, 39] From the ΔH_t values determined for different T_m values, the entropy of denaturation (ΔS_t values) and the ΔG_t values can be calculated and summarized in a state diagram.[10] With increasing GC content, the ΔH_t values increase (see Fig. 5): that is, they show a T_m dependence that corresponds to the dependence of T_m values on GC content in DNA samples determined by *Marmur* and *Doty*.[5]

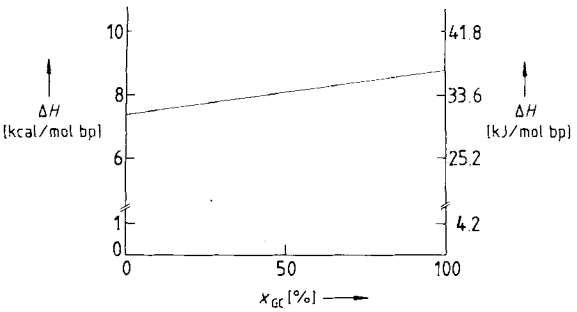


Fig. 5. Dependence of the DNA enthalpy of denaturation ΔH_t on the guanine–cytosine content x of the samples [34, 39].

Exact measured values of the enthalpy of denaturation can therefore be used as an additional analytical criterion for the relative base composition of DNA samples. However, the dependence of ΔH_t values on the GC content is not as pronounced as might be expected in a double helix stabilized solely by hydrogen bonds. From all the ΔH_t values measured on DNA samples, it can be concluded that the hydrogen-bond-enthalpy effect does not contribute significantly to the stabilization of secondary structures and that the double-helix structure is primarily stabilized by means of base stacking. This is understandable if it is considered that solvated single strands are formed during denaturation. The ΔH values for the partial processes of base unstacking listed in Table 2 (Section 9) are approximately 25 kJ/mol bp. The comparison with the value for the enthalpy of DNA denaturation (35 kJ/mol bp) implies that approximately 70% of the total enthalpy effect of the double helix denaturation can be attributed to base unstacking. Thus, the hydrogen-bond systems are of primary importance in regard to the specificity of base pairing, but only of secondary significance for the stability of secondary structures.

In the discussion of ΔH_t values, it is to be noted that the thermodynamic data of dissolved electrolytes are normally related to the standard state of ideal dilution.[40] Calorimetric measurements on polynucleotide solutions of different polynucleotide concentrations have shown that the ΔH_t values of these substances exhibit only a small degree of concen-

tration dependence.[41] The deviations of the ΔH_t^0 values extrapolated to the state of ideal dilution and the measured ΔH_t values from moderately concentrated solutions are within the stated limit of error of $\pm 2\%$. Therefore, the experimentally determined ΔH_t values can be referred to as standard values of first approximation. Up to now, however, this simplified assumption has proven valid only for aqueous polynucleotide solutions.

By means of measurements on selected DNA samples, it was possible to show that the DSC method could also be used in the characterization of highly repetitive sequences in eukaryotic DNA. The repetitive sequences occurring in certain satellite DNAs can be assigned to different discrete peaks in the $C_t(T)$ diagram of the samples studied. From the T_m values determined with this method, the average base composition of the repetitive sequences can be obtained.[42]

6.2. Ribonucleic Acids

The specific transfer ribonucleic acids (tRNAs), which are indispensable for protein biosynthesis, exhibit a characteristic base-pairing pattern (cloverleaf model) and a distinctive tertiary structure (see Fig. 6). Their molecular weights differ

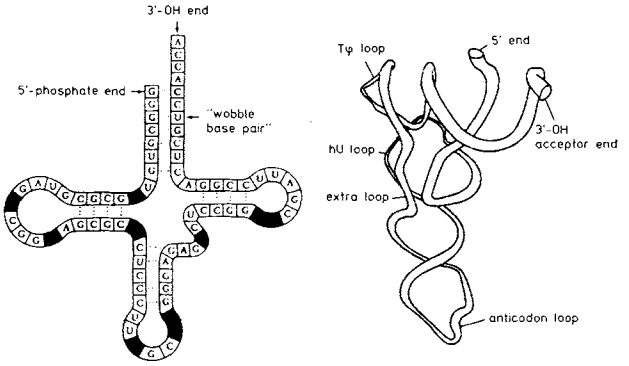


Fig. 6. Simplified drawing of the secondary structure ($tRNA^{Ala}$, left) and the tertiary structure ($tRNA^{Phe}$, right) of transfer ribonucleic acids.

only slightly. However, characteristic differences in the secondary structures of different specific transfer ribonucleic acids can be recognized in the number of base pairs determined by various physicochemical methods.[43] In the largely reversible thermally induced denaturation of dissolved tRNA samples, the endothermic degradation processes of the tertiary and secondary structures overlap.[44, 45] Despite this overlapping of two effects, a significant, nearly linear dependence of the enthalpies of denaturation on the number of hydrogen bonds given by the secondary structure was determined by means of calorimetric measurements on solutions of different specific tRNAs.[46] The ΔH_t value for the denaturation of tRNA samples is approximately 1500 kJ mol^{-1} per mole of tRNA. This value corresponds to an average of approximately 20 base pairs[43] and is thus significantly higher than the calculated values, which were determined using the base-pair denaturation increments listed in Table 2 (Section 9).[46] Based on this, a substantial proportion (approximately 30%) of the total enthalpy of transition of the tRNA sample must be used for the denaturation of the tertiary structures.

Viroids are circular, single-stranded ribonucleic acids (molecular weight of approximately 120000), which as infectious particles lead to a number of plant diseases.[47] Detailed information on the secondary structure of these ribonucleic acids was derived from precise measurements of the temperature dependence of UV absorption of dissolved viroid samples.[48] The model of the secondary structure adapted to the denaturation behavior of the viroid samples[49] is the basis for an estimate of the enthalpy of denaturation, which can be calorimetrically determined using the methods described in this paper. For the CPFV (cucumber pale fruit viroid), enthalpies of denaturation of 3930 ± 150 kJ mol^{-1} were measured with the DPSC method.[50] This value agrees relatively well with the value of 4080 kJ mol^{-1} derived from the model secondary structure. Thus, the model of secondary structure of CPFV suggested by *Riesner* et al.[49] is essentially correct.

6.3. Model Substances (Poly- and Oligonucleotides)

The double helix–random coil transition of equimolar mixtures of complementary homopolyribonucleotides is characterized by a high degree of cooperativity and is easily accessible to studies using the calorimetric methods of measurement described. This is exemplified by the results of measurements on aqueous solutions of polyriboadenylate (poly A) and polyribouridylate (poly U), a system that has been comprehensively studied.[21, 30, 51, 52] The formation and thermally induced degradation of triple helices can be followed relatively well by means of measurements on this system. In Figure 7 $C_t(T)$ curves, recorded at pH 6.8 and a

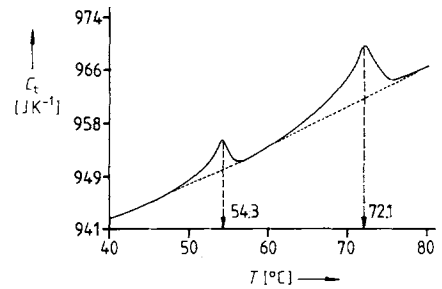


Fig. 7. $C_t(T)$ curve of an equimolar mixture (0.0078 M) of polyriboadenylate (poly A) and polyribouridylate (poly U). The experimental conditions are stated in the text.

$Na^{\oplus}$ concentration of 0.5 mol L^{-1}, are presented. The transition peak at 54.3 °C corresponds to the "disproportionation" (9).

$$2\,\text{poly}(A + U) \rightleftarrows \text{poly}(A + 2U) + \text{poly}\,A \qquad (9)$$

During transformation, a triple helix composed of poly (A + 2U) is formed, accompanied by the release of a molar equivalent of poly A. The pronounced maximum of the heat capacity at 72.1 °C corresponds to a transformation in which the components poly A and poly U are released from the triple-helical complex [Eq. 10]. The model system

$$\text{poly}(A + 2U) \rightleftarrows \text{poly}\,A + 2\,\text{poly}\,U \qquad (10)$$

poly(I + C), that is, an equimolar aqueous mixture of polyriboinosylate (poly I) and polyribocytidylate (poly C) has also been largely characterized with calorimetric methods.[53]

From the ΔH_t values of polynucleotide systems, which are related to a double helix denaturation, information on the relative stability of different complementary base combinations can be obtained, because the corresponding entropies of transition differ only slightly.[10] For example, the ΔH_t value[54] of 30 kJ/mol bp determined for alternating poly-d(A-T) fits well into the explanations in regard to the system described in Figure 5. In this context, the experiments on the thermodynamic characterization of the "wobble base pairs" GU postulated by *Crick*[55] (e.g., see Fig. 6, left) should be noted.[56] Using spectroscopic and calorimetric measurements on equimolar aqueous mixtures of poly(A, G) with poly U (also poly(C,U) with poly G), it was possible to show that the ΔH_t value of 28 kJ/mol bp determined for the guanine–uracil base combination differs only slightly from the value for the AU base pair (33 kJ/mol bp). In these cases, the different stabilities of the base combinations are reflected in the different values of the entropies of transition.[56] At the standard temperature of 25 °C, the ribonucleotide secondary structures are also stabilized by the guanine–uracil base combination, although this base combination is characterized by a particularly high dynamic flexibility.[57] The poly A released during transformation based on Equation (9) is not in the randomly coiled form but rather in a partially ordered secondary structure. The enthalpies of transition assigned to the thermally induced degradation of this secondary structure can also be determined with calorimetric measurements.[10] In the determination of enthalpies of transition, the enthalpy changes caused by changes in the secondary structure of single-stranded polynucleotides must in any case be taken into account.

The thermodynamic characterization of oligonucleotide systems[58] is important because these systems provide an especially good basis for the study of the effects of certain base sequences on the relative stability of various secondary-structure elements (e.g., hairpin loops, see Fig. 6). Sequence-specific effects can be better determined by studying short oligonucleotide sequences than by determining the characteristics of polynucleotides. With a suitable set of thermodynamic parameters of oligonucleotides, the stability of certain models of secondary structures (e.g., of viroids) can be approximated. By means of measurements on oligonucleotide systems, it was shown that there is no significant difference between the enthalpies of base unstacking of ribonucleotides and deoxyribonucleotides with identical base pairs.[58] The stabilizing or destabilizing effects of dangling ends on the stability of helix structures can be quantitatively determined by denaturation experiments on solutions of double-helical oligonucleotide complexes.[59] It should be noted that a relatively small slope of the transformation curves is expected even for extremely high degrees of cooperativity, because the average cooperative lengths [see Eq. (4)] cannot be greater than the sequence length of the molecule. For the same reason, only broad and flat $C_t(T)$ curves are obtained from calorimetric measurements on oligonucleotide systems. Thus, the amount of substance used for calorimetric determination in such systems is much greater than the quantity used for measurements on polynucleotide systems. Despite this disadvantage, calorimetric measurements should always be carried out when oligonucleotide systems are studied, provided that there is a sufficient quantity of sample substance. The calorimetrically measured ΔH_t values do not depend on the type of model (two-state model or multistep model) that must be assumed when transition curves are evaluated. A process that corresponds to the simple two-state model exists if the calorimetrically measured total molar enthalpy of transition agrees with the van't Hoff enthalpy of transition $\Delta H_{v.H.}$ derived from the transition curves. This applies, for example, to the deoxyribonucleotide system $d(GC)_3$ ($\Delta H_{v.H.} = 240\ kJ\ mol^{-1}$) studied by *Breslauer* et al.[60] If, on the other hand, $\Delta H_{v.H.}$ is less than the calorimetrically measured total enthalpy of transition, the system goes through a series of intermediate states (for example, rA_7U_7)[61] during the thermally induced helix–random coil transition. Further measured data and experimental details have already been summarized.[58]

6.4. Ligand Binding (Intercalation)

A typical example of an interaction of dissolved biopolymers with low-molecular-weight ligands is the binding of ethidium and acridine dyes to deoxyribonucleic acids. Here, the noncompetitively bound ligands (dye cations) are largely shielded from their surroundings by intercalation.[62,63] In contrast, the competitively (externally) bound ligands can be displaced by competitor salt ions. These types of binding differ in the values of the binding constants; the standard entropy of binding is greater for external binding. In regard to the van't Hoff enthalpies of binding ($-30\ kJ\ mol^{-1}$) derived from the temperature dependence of the binding constants, both types of binding are similar. For the thermodynamic characterization of the binding of dyes to deoxyribonucleic acids, systematic studies with physicochemical methods have been carried out by *H. Zimmermann* and his coworkers.[64] The enthalpies of ligand binding can be calorimetrically determined with a suitable mixing calorimeter and the resulting ΔH values agree relatively well with values derived from binding studies under comparable conditions. This agreement is remarkable, because often difficulties can occur in the calculation of formal standard enthalpies of binding[64] from the temperature dependence of the binding constant owing to the complexity of the binding. Calorimetrically determined formal standard enthalpies of binding are temperature-dependent.[31] This ("apparent") temperature dependence can be primarily attributed to the overlapping of the two binding processes mentioned above and to the effects on the electrolyte equilibria and buffer dissociation equilibria associated with these processes. Detailed discussions of these temperature-dependent binding equilibria have been presented elsewhere.[31,64]

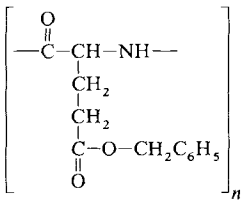
7. Results from Measurements on Solutions of Polypeptides and Proteins

The results from measurements of enthalpies of protein denaturation have been described and summarized in ta-

bles.[65] Some of the most important aspects of these studies are explained here using several examples.

7.1. Polypeptide Systems

Several authors[22, 66] have reported exact calorimetric measurements on solutions of the polypeptide poly(γ-benzyl-L-glutamate) **1** in a mixture of dichloroacetic acid and



1

1,2-dichloroethane. The nonaqueous solvent mixture containing the strongly solvating component dichloroacetic acid was chosen for this model system, because relatively simple assumptions could be made for the polypeptide-solvent interactions (quasi-stoichiometric solvation). This system has already been comprehensively studied by *Zimm, Doty,* and *Iso*[4] and is characterized by the enhanced formation of a polypeptide α-helix (see Fig. 1) when samples are warmed. At low temperatures, solvated polypeptide molecules are largely in the randomly coiled state. Thus, a necessary precondition for helix formation is the release of solvent molecules (dichloroacetic acid) from the polypeptide, thereby making available hydrogen-bond-acceptor and -donator sites. Therefore, the overall process of α-helix formation in this solvent mixture is endothermic. For the thermodynamic characterization of this polypeptide system, all preconditions for the use of the equations developed by *Zimm* and *Bragg*[2] for quantitative determination of the transition curves are satisfied. The optical rotatory power and the heat capacities (measured with a suitable adiabatic calorimeter[23]) of a solution of poly(γ-benzyl-L-glutamate) **1** (0.257 mole per kilogram of solvent) in a mixture of dichloroacetic acid and 1,2-dichloroethane (81:19) result in a temperature curve corresponding to the scheme presented in Figure 2. The enthalpy of transition determined from this data is dependent on the concentration of the dissolved poylpeptide.[22] The ΔH_t value of 3.99 kJ per mole of segment extrapolated to standard ideal dilution agrees well with the ΔH_t value determined from the temperature dependence of the optical rotatory power, where the length of the polymer chain was taken into consideration. From the maximum value of the conformational excess heat capacity, it was possible to calculate the cooperativity parameter σ for this system from Equation (8). A value of $\sigma = 10^{-4}$ was determined for the standard state of ideal dilution. This value agrees well with the value approximated by *Zimm, Doty* and *Iso*.[4] The effects of solvent composition on the magnitude of the ΔH_t values has also been studied.[67] It should be noted that not all polypeptide systems are suitable for a physico-chemical characterization using calorimetric methods. For example, the helix–helix transformation of poly(L-proline) comprehensively studied by *Engel* et al.[68] cannot be induced by a change in temperature ($\Delta H \approx 0$).

7.2. Proteins

The free energy of denaturation of proteins (Gibbs free energy change associated with protein unfolding) is an important parameter for the evaluation of the ability of organisms to live under extreme conditions (thermophilic, psychrophilic behavior).[69] In this context, the determination of enthalpies of denaturation of dissolved proteins is of fundamental importance.[65, 70] The values of the calorimetrically determined enthalpies of denaturation range from 1134 kJ mol^{-1} (pepsinogen, M_r = 38000 g mol^{-1}) to 97 kJ mol^{-1} (tryptophane synthase, α subunit, mutant (Ser 49), M_r = 29000 g mol^{-1}). The numerous interactions between various molecular regions are reflected in the size of the ΔH values. This applies especially to the systems with protein–protein association[71] that have also been thermodynamically characterized (example: tobacco mosaic virus protein TMVP[72]). In the study of association or polymerization of polymer subunits, both positive and negative values for the standard entropies of transition have been found.[72]

Another important aspect of protein thermodynamics is the protein–ligand interaction.[73] Of the numerous ligand binding systems that have been studied, but which cannot be discussed in detail here, five kinds of interactions are particularly noteworthy, namely, the binding of inorganic ions including $H^{\oplus}$ ions, the binding of denaturing agents (e.g., urea),[74] the hapten–antibody interaction,[75, 76] the interaction of proteins (e.g., muscle proteins) with ADP and ATP,[77, 78] and the binding of $NAD^{\oplus}$ and analogous ligands to enzymes (e.g., lactate dehydrogenase from porcine heart muscle).[79]

The interaction between protein subunits[80] and the protein nucleic acid interactions[81] are considered to be especially important. A typical example of the interaction of protein subunits is that between S-peptide and S-protein of ribonuclease S'.[80]

The results from these studies are the basis for the investigation of model concepts on the structure–function relationship of protein systems.

8. Aqueous Lipid Systems

The discussion of thermodynamic parameters of lipid suspensions is limited to the explanation of a few typical examples. For measurements on lipid systems with low water contents, the reader is referred to a recent summary[9] and to the original literature.[82]

8.1. Transition Temperatures, Enthalpies of Transition, and Apparent Molar Heat Capacities

In Table 1 the thermodynamic parameters for 16 different phospholipids, each containing two identical hydrocarbon chains, are summarized. The abbreviations almost always used in the relevant literature[6, 8] (e.g., DSPC for distearoyl phosphatidylcholine) are derived from the trivial names of the fatty acids and of the head-group components linked to the phosphate groups (see footnote to Table 1). The T_m val-

Table 1. Transition temperatures (T_{m1}) and transition enthalpies (ΔH_t) of pretransition as well as transition temperatures, enthalpies of transition, and entropies of transition (T_{m2}, ΔH_2, ΔS_2) of the main transformation of phospholipids with two identical hydrocarbon chains in dilute aqueous suspension (taken from *A. Blume* [9, 83, 84]).

Lipid [a]	T_{m1} [°C]	T_{m2} [°C]	ΔH_t [kJ mol^{-1}]	ΔH_2 [kJ mol^{-1}]	ΔS_2 [J mol^{-1} K^{-1}]
DMPC	15.3	24.0	5.4	27.2	91.5
DPPC	35.5	41.5	6.7	41.9	115.9
DSPC	51.0	54.3	7.5	45.6	139.4
DAPC	62.1	64.1	7.1	51.5	157.4
DBPC		72.5		62.4	180.4
DLPE		30.5		18.0	59.4
DMPE		49.9		27.6	85.4
DPPE		63.9		36.0	106.7
DSPE		72.5		43.9	127.2
DAPE		81.1		51.1	144.4
DLPA (pH 6)		33.5		14.2	46.5
DMPA (pH 6)		52.2		23.8	73.2
DPPA (pH 6)		65.0		33.1	97.9
DMPA (pH 12)		22.4		17.2	58.2
DPPA (pH 12)		43.1		23.9	74.5
DHPC	33.0	43.5	5.9	35.6	111.8
DHPE		68.5		31.8	93.3
DHPA (pH 6)		73.3		29.7	85.8
DHPA (pH 12)		53.8		24.3	74.5

[a] DMPC, dimyristoylphosphatidylcholine; DHPC, 1,2-dihexadecyl-*sn*-glycero-3-phosphocholine; DHPE, 1,2-dihexadecyl-*sn*-glycero-3-phosphoethanolamine; DHPA, 1,2-dihexadecyl-*sn*-glycero-3-phosphoric acid.

ues and the enthalpies of transition (ΔH_2) increase with increasing hydrocarbon chain lengths.

Figure 8 shows, as example, the DSC curves of aqueous suspensions of different phosphatidylethanolamines record-

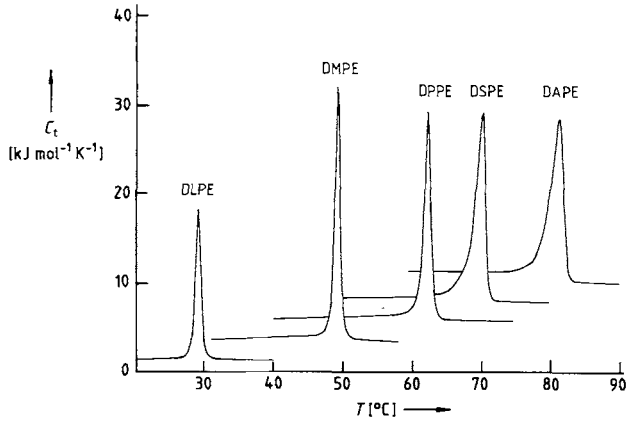


Fig. 8. $C_t(T)$ curve of aqueous suspensions of five phosphatidylethanolamines with different hydrocarbon chain lengths (c = 1 mg mL^{-1}).

ed under identical conditions and at a concentration of 1 mg mL^{-1}. The entropies of transition (ΔS_2) shown in Table 1 vary systematically in an analogous way. The magnitudes of these ΔS values are much lower than the entropies of melting of corresponding long-chain fatty acids or corresponding pure hydrocarbons. This finding clearly shows that the degree of order of the lipid bilayers of liposomes[7] in the liquid-crystalline phase is significantly greater than it is in an isotropic liquid phase. In some lipid systems (e.g., DPPC) a so-called pretransition[6, 85] is observed. Where it was possible to determine enthalpies of transition for this transformation, these values (ΔH_1) are also listed in Table 1. The magnitude of the ΔH_2 values depends not only on the length and degree of saturation of the hydrocarbon chains, but also on the type of phospholipid head groups. As a comparison of the values for distearoyl phosphatidylethanolamine (DSPE) and distearoyl phosphatidylcholine (DSPC) listed in Table 1 shows, the T_m values of phosphatidylethanolamines (PEs) are greater and the ΔH_2 values are smaller than the corresponding values for phosphatidylcholines (PCs) having identical hydrocarbon chain lengths. This finding, which is reflected in the different values of methyl-group increments[84] of ΔH_2 values, indicates that the PE molecules are more closely packed than corresponding PC molecules in the liquid-crystalline phase because of a possible hydrogen-bond linkage of $NH_3^{\oplus}$ head-group components. For quantitative determination of the influence of the size of head groups, *Hinz* et al.[86] made calorimetric measurements on suspensions of different synthetically prepared glycolipids. It is remarkable that for the phospholipids with two different fatty acid chains largely present in biomembranes, a significant dependence of the ΔH_t values on the binding position of these fatty acid chains at the glycerol backbone is observed.[87] Since, for steric reasons, a line joining the three glycerol carbon atoms cannot run parallel to the surface of the bilayer, the effective number of methylene groups in the lipophilic zone is reduced by approximately two units (effective chain shortening effect). Based on this, a lipophilic zone with a largely regular arrangement of hydrocarbon chains with identical effective chain lengths results for MPPC. In contrast, the PMPC bilayer is characterized by a packing of hydrocarbon chains with different effective lengths, resulting in a lower ΔH_2 value. Finally, it should be noted that with the DSC method, the apparent molar heat capacities[88, 89, 95, 96] defined by Equation (11)

$$^{\Phi}C_p = \frac{C_{p,\text{mixture}} - n_{H_2O} \cdot C_{p,H_2O}}{n_{\text{lipid}}} \qquad (11)$$

can be determined and that information on the state of order of lipid molecules can also be derived from these apparent molar heat capacities.[90, 91, 95, 96] Contributions to the apparent molar heat capacities come not only from the excitation of internal degrees of freedom of the molecules, but also from interactions with the surrounding aqueous medium. The negative contributions come from the hydration of the polar groups and the change in the association structure of water[92] caused by hydration. Normally, additional positive $^{\Phi}C_p$ contributions can be attributed to the hydrophobic interaction of nonpolar groups with the bordering regions of the water structure.[93, 94]

8.2. Multicomponent Systems, Lipid–Protein Interaction, and Mixing and Titration Calorimetry

In the formal description of the mixing behavior of multicomponent lipid systems, the methods of classical phase thermodynamics can be used in largely unchanged form.[97] The phase diagrams can be obtained from DSC curves recorded for different mixing ratios.[9] In connection with lipid–protein interactions, the question concerning the state of order of lipid molecules in the immediate surrounding (annulus zone) of integrated membrane proteins is of particular interest.[98] Figure 9 shows, as an example, a set of DSC

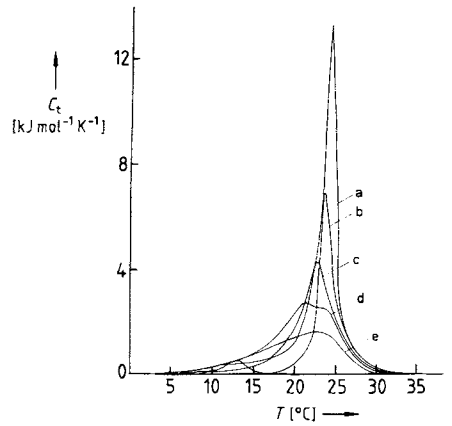


Fig. 9. DSC curve of DMPC–bacteriorhodopsin mixed-vesicle suspensions with the mixture proportions a) ∞, b) 552, c) 316, d) 188, e) 91 (taken from [99]).

curves of aqueous suspensions of vesicles[99, 100] formed from dimyristoyl phosphatidylcholine (DMPC) and bacteriorhodopsin for different values of the mixing ratio. From a comparison of simulated transition curves, based on a simple model, with experimentally determined transition curves, it can be concluded that the state of order of approximately 60 DMPC molecules is influenced by an intercalated bacteriorhodopsin molecule accompanied by a reduction of the individual ΔH_t values of these molecules (approximately 30%). Accordingly, an effective "order effect" beyond the immediate bordering zone can be attributed to the intercalated protein. Similar conclusions are drawn from measurements made in reaction and mixing calorimeters for the characterization of the phospholipid–melittin system.[9]

The investigation of reaction (12) exemplifies measure-

$$DMPA^{\ominus} + OH^{\ominus} \rightleftarrows DMPA^{2\ominus} + H_2O \qquad (12)$$

ments made with a mixing calorimeter.[32, 9] The reaction enthalpy ΔH_{diss} for the $DMPA^{\ominus}$ deprotonation reaction is obtained by subtracting the enthalpy of neutralization from the measured total reaction enthalpy when the dilution enthalpy of NaOH is eliminated by compensation in a twin calorimeter arrangement. From the graphical presentation of the temperature dependence of the ΔH_{diss} values (Fig. 10),

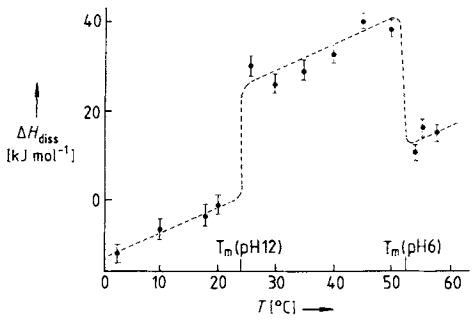


Fig. 10. Temperature dependence of the dissociation enthalpy for the second dissociation step of dimyristoyl phosphatidic acid [9].

three characteristic temperature areas can be recognized. For temperatures below 22 °C, in addition to deprotonation, a change in the angle of inclination of the fatty acid chains takes place (phase transition $L_\beta \rightarrow L_{\beta'}$) between 22 °C and 51 °C, the $L_\beta \rightarrow L_\alpha$ phase transition overlaps the deprotonation;[9] above 51 °C, the experimentally determined ΔH_{diss} values are nearly equal to the enthalpies of denaturation because, in this temperature range, the phase state of lipids does not change. These results are discussed in detail elsewhere.[9]

9. Summary

An opportunity to compare the magnitudes of the ΔH values of different important processes is provided by Table 2. The range of application of calorimetric methods for thermodynamic characterization of biopolymers and suspended lipids is also shown in this table.

Table 2. Magnitude of characteristic ΔH values for different types of structural transformations in biopolymer solutions and aqueous lipid suspensions.

Model substance	Process	Molecular subunit	ΔH [kJ mol^{-1}]	Ref.
Specific transfer ribonucleic acids	Denaturation of the secondary structure	tRNA molecule	1180	[44, 46]
Deoxyribonucleic acid	Double helix–random coil transformation	Base pair	35	[38, 39]
Polyriboadenylic acid	Base unstacking	Nucleotide residue	15	[10]
DNA and ethidium bromide (EB)	Reversal of the "intercalation"	EB molecule	20	[31]
Viroid	Denaturation of the secondary structure	CPFV molecule	3900	[50]
Poly(γ-benzyl-glutamate) in dichloroacidic acid/1,2-dichloroethane	α-Helix formation	Amino acid residue	4	[22]
$(Pro,Pro,Gly)_{15}$	Polyproline II helix-random coil transition	Amino acid residue	2	[10]
Poly(N^5-hydroxypropyl-L-glutamine)	α-Helix-random coil transition	Chain segment	0.5	[10]
Protein	Denaturation	α-Subunit of tryptophan synthase mutant (Ser 49) (M_r = 29000 g mol^{-1})	100	[10, 65, 70]
Phospholipid vesicle in aqueous suspension	Lipid phase transition: gel-liquid-crystalline	DPPC molecule	42	[83]
Phosphatidic acid	Deprotonation (second step)	DMPA molecule or ion	10	[9]

I wish to thank the Deutsche Forschungsgemeinschaft and the Fonds der Chemischen Industrie for their support of our scien-

tific work. In particular, I would like to thank my former and present co-workers mentioned in the references for their tireless efforts and numerous helpful discussions.

Received: June 16, 1987;
revised: November 15, 1988 [A 727 IE]
German version: *Angew. Chem. 101* (1989) 1005
Translated by Dipl.-Chem. *B. Jackson*, Brussels, Belgium

[1] J. Engel, G. Schwarz, *Angew. Chem. 82* (1970) 468; *Angew. Chem. Int. Ed. Engl. 9* (1970) 389.
[2] B. H. Zimm, J. K. Bragg, *J. Chem. Phys. 31* (1959) 526.
[3] J. Applequist, *J. Chem. Phys. 38* (1963) 934.
[4] B. H. Zimm, P. Doty, K. Iso, *Proc. Natl. Acad. Sci. USA 45* (1959) 1601.
[5] J. Marmur, P. Doty, *J. Mol. Biol. 5* (1962) 109.
[6] D. Chapman, R. M. Williams, B. D. Ladbrooke, *Chem. Phys. Lipids 1* (1967) 445.
[7] J. A. Lucy in D. Chapman (Ed.): *Biological Membranes*, Academic Press, London 1968, p. 261ff.
[8] D. Bach in D. Chapman (Ed.): *Biomembrane Structure and Function*, Verlag Chemie, Weinheim 1984, p. 1ff.
[9] A. Blume in C. Hidalgo (Ed.): *Physical Properties of Membranes, Functional Implications*, Plenum Press, New York 1988, p. 71.
[10] H.-J. Hinz (Ed.): *Thermodynamic Data for Biochemistry and Biotechnology*, Springer, Berlin 1986.
[11] G. C. Pimentel, A. L. McClellan: *The Hydrogen Bond*, Freeman, New York 1960.
[12] S. Lifson, A. Roig, *J. Chem. Phys. 34* (1961) 1963.
[13] N. Davidson: *Statistical Mechanics*, McGraw-Hill, New York 1962, p. 385ff.
[14] R. Jaenicke, *Angew. Chem. 96* (1984) 385; *Angew. Chem. Int. Ed. Engl. 23* (1984) 395.
[15] J. Marmur, D. Lane, *Proc. Natl. Acad. Sci. USA 46* (1960) 453.
[16] E. Neumann, *Angew. Chem. 85* (1973) 430; *Angew. Chem. Int. Ed. Engl. 12* (1973) 356.
[17] D. Barszcz, D. Shugar, *Eur. J. Biochem. 5* (1968) 91.
[18] H. Träuble, H. Eibl in F. O. Schmitt, D. M. Schneider, D. M. Crothers (Eds.): *Functional Linkage in Biomolecular Systems*, Raven Press, New York 1975, p. 59ff.
[19] G. Messner, M. Grubert, *J. Phys. E 16* (1983) 131.
[20] T. Ackermann, H. Rüterjans, *Z. Phys. Chem. (Frankfurt/Main) 41* (1964) 116.
[21] E. Neumann, T. Ackermann, *J. Phys. Chem. 73* (1969) 2170.
[22] T. Ackermann, H. Rüterjans, *Ber. Bunsen-Ges. Phys. Chem. 68* (1964) 850.
[23] T. Ackermann, *Ber. Bunsen-Ges. Phys. Chem. 62* (1958) 411.
[24] M. Grubert, T. Ackermann, *Z. Phys. Chem. (Frankfurt/Main) 93* (1974) 255.
[25] T. Ackermann in D. B. Davies, W. Saenger, S. S. Danyluk (Eds.): *Structural Molecular Biology*, Plenum, New York 1982, p. 305ff.
[26] W. Hemminger, G. Höhne: *Calorimetry*, Verlag Chemie, Weinheim 1984.
[27] P. L. Privalov, V. V. Plotnikov, V. V. Filimonov, *J. Chem. Thermodyn. 7* (1975) 41.
[28] K. S. Krishnan, J. F. Brandts, *Methods Enzymol. 49* (1978) 1.
[29] M. Grubert, *Z. Phys. Chem. (Frankfurt/Main) 93* (1974) 255.
[30] C. L. Stevens, G. Felsenfeld, *Biopolymers 2* (1964) 293.
[31] W. Burkart, H. Klump, *Ber. Bunsen-Ges. Phys. Chem. 85* (1981) 371.
[32] I. Wadsö, *Acta Chem. Scand. 22* (1968) 927.
[33] W. Burkart, H. Klump, *Ber. Bunsen-Ges. Phys. Chem. 85* (1981) 375.
[34] H. Klump, T. Ackermann, *Biopolymers 10* (1971) 513.
[35] P. L. Privalov, D. R. Monaselidze, *Zh. Eksp. Teor. Fiz. 47* (1964) 2073.
[36] L. G. Bunville, P. E. Geiduschek, M. A. Rawitscher, J. M. Sturtevant, *Biopolymers 3* (1965) 213.
[37] J. M. Sturtevant, S. Rice, P. E. Geiduschek, *Discuss. Faraday Soc. 25* (1958) 138.
[38] H. Klump, *Thermochim. Acta 85* (1985) 457.
[39] H. Klump, K. Herzog, *Ber. Bunsen-Ges. Phys. Chem. 88* (1984) 20.
[40] G. N. Lewis, M. Randall: *Thermodynamics*, 2nd ed. (revised by K. S. Pitzer, L. Brewer), McGraw-Hill, New York 1961, p. 246ff.
[41] T. Ackermann in H. D. Brown (Ed.): *Biochemical Microcalorimetry*, Academic Press, New York 1969, p. 128ff.
[42] H. Klump, *Ber. Bunsen-Ges. Phys. Chem. 91* (1987) 206.
[43] U. Schernau, T. Ackermann, *Biopolymers 16* (1977) 1735.
[44] D. Bode, U. Schernau, T. Ackermann, *Biophys. Chem. 1* (1974) 214.
[45] H.-J. Hinz, V. V. Filimonov, P. L. Privalov, *Eur. J. Biochem. 72* (1977) 79.
[46] F. J. Schott, M. Grubert, W. Wangler, T. Ackermann, *Biophysical Chemistry 14* (1981) 25.
[47] D. Riesner, H. J. Gross, *Annu. Rev. Biochem. 54* (1985) 531.
[48] D. Riesner, G. Steger, J. Schumacher, H. J. Gross, J. W. Randles, H. L. Sänger, *Biophys. Struct. Mech. 9* (1983) 143.
[49] J. Langowski, H. Henco, D. Riesner, H. L. Sänger, *Nucleic Acids Res. 5* (1978) 1589.
[50] H. Klump, D. Riesner, H. L. Sänger, *Nucleic Acids Res. 5* (1978) 1581.
[51] E. Neumann, T. Ackermann, *J. Phys. Chem. 71* (1967) 2377.
[52] H. Krakauer, J. M. Sturtevant, *Biopolymers 6* (1968) 491.
[53] H.-J. Hinz, W. Haar, T. Ackermann, *Biopolymers 9* (1970) 923.
[54] D. W. Gruenwedel, *Biochim. Biophys. Acta 395* (1975) 246.
[55] F. H. C. Crick, *J. Mol. Biol. 19* (1966) 548.
[56] J. Stulz, T. Ackermann, *Ber. Bunsen-Ges. Phys. Chem. 87* (1983) 447.
[57] D. Söll, *J. Mol. Biol. 29* (1967) 113.
[58] K. J. Breslauer in H.-J. Hinz (Ed.): *Thermodynamic Data for Biochemistry and Biotechnology*, Springer, Berlin 1986, p. 402.
[59] S. M. Freier, M. Petersheim, D. R. Hickey, D. H. Turner, *J. Biomol. Struct. Dynam. 1* (1983) 1229.
[60] D. Albergo, L. A. Marky, K. J. Breslauer, D. H. Turner, *Biochemistry 20* (1981) 1409.
[61] K. J. Breslauer, J. M. Sturtevant, I. Tinoco Jr., *J. Mol. Biol. 99* (1975) 549.
[62] A. R. Peacocke in R. M. Acheson (Ed.): *Acridines*, 2nd ed., Wiley, New York 1973, p. 723ff.
[63] M. J. Waring in E. F. Gale, E. Cundliffe, P. E. Reynolds, M. H. Richmond, M. J. Waring (Eds.): *The Molecular Basis of Antibiotic Action*, 2nd ed., Wiley, New York 1981, p. 273ff.
[64] H. W. Zimmermann, *Angew. Chem. 98* (1986) 115; *Angew. Chem. Int. Ed. Engl. 25* (1986) 115.
[65] W. Pfeil in H.-J. Hinz (Ed.): *Thermodynamic Data for Biochemistry and Biotechnology*, Springer, Berlin 1986, p. 349.
[66] F. E. Karasz, J. M. O'Reilly, H. E. Bair, *Nature (London) 202* (1964) 693.
[67] T. Ackermann, E. Neumann, *Biopolymers 5* (1967) 649.
[68] V. Ganser, J. Engel, D. Winklmair, G. Krause, *Biopolymers 9* (1970) 329.
[69] R. Jaenicke, *Annu. Rev. Biophys. Bioeng. 10* (1981) 1.
[70] W. Pfeil, P. L. Privalov in M. N. Jones (Ed.): *Biochemical Thermodynamics (Studies in Modern Thermodynamics, Vol. 1)*, Elsevier, Amsterdam 1979, p. 75ff.
[71] P. D. Ross in H.-J. Hinz (Ed.): *Thermodynamic Data for Biochemistry and Biotechnology*, Springer, Berlin 1986, p. 227.
[72] J. M. Sturtevant, G. Veliceleby, R. Jaenicke, M. A. Lauffer, *Biochemistry 20* (1981) 3792.
[73] H. Wiesinger, H.-J. Hinz in H.-J. Hinz (Ed.): *Thermodynamic Data for Biochemistry and Biotechnology*, Springer, Berlin 1986, p. 211.
[74] M. I. Paz Andrade, M. N. Jones, H. A. Skinner, *Eur. J. Biochem. 66* (1976) 127.
[75] J. F. Halsey, R. L. Biltonen, *Biochemistry 14* (1975) 6221.
[76] M. F. M. Johnston, B. G. Barisas, J. M. Sturtevant, *Biochemistry 13* (1974) 390.
[77] T. Kodama, I. D. Watson, R. C. Woledge, *J. Biol. Chem. 252* (1977) 8085.
[78] T. Kodama, R. C. Woledge, *J. Biol. Chem. 254* (1979) 6382.
[79] C. W. Niekamp, H.-J. Hinz, R. Jaenicke, C. Woenckhaus, R. Jeck, *Biochemistry 19* (1980) 3144.
[80] R. P. Hearn, F. M. Richards, J. M. Sturtevant, G. D. Watt, *Biochemistry 10* (1971) 806.
[81] H.-J. Hinz, S. Srinivasan, E. M. J. Jaspars, *Eur. J. Biochem. 95* (1979) 107.
[82] E. Jürgens, G. Höhne, E. Sackmann, *Ber. Bunsen-Ges. Phys. Chem. 87* (1983) 95.
[83] A. Blume, T. Ackermann, *FEBS Lett. 43* (1974) 71.
[84] A. Blume, *Biochemistry 22* (1983) 5436.
[85] R. J. Wittebort, C. F. Schmidt, R. G. Griffin, *Biochemistry 20* (1981) 4223.
[86] H.-J. Hinz, L. Six, K.-P. Ruess, M. Liefländer, *Biochemistry 24* (1985) 806.
[87] J. Stümpel, H. Eibl, A. Niksch, *Biochem. Biophys. Acta 727* (1983) 246.
[88] G. Wedler: *Lehrbuch der Physikalischen Chemie*, Verlag Chemie, Weinheim 1982, p. 237.
[89] G. Kortüm, H. Lachmann: *Einführung in die chemische Thermodynamik*, Verlag Chemie, Weinheim 1981, p. 124.
[90] See [40], p. 375ff.
[91] P. Privalov, N. N. Khechinashvili, *J. Mol. Biol. 86* (1974) 556.
[92] E. Wicke, *Angew. Chem. 78* (1966) 1; *Angew. Chem. Int. Ed. Engl. 5* (1966) 106.
[93] G. C. Kresheck in F. Franks (Ed.): *Water, A Comprehensive Treatise, Vol. 4*, Plenum Press, New York 1975, p. 95ff.
[94] F. M. Menger, *Acc. Chem. Res. 12* (1979) 111.
[95] N. Nichols, R. Sköld, C. Spink, J. Suurkuusk, I. Wadsö, *J. Chem. Thermodyn. 8* (1976) 1081.
[96] G. Roux, G. Perron, J. E. Desnoyers, *Can. J. Chem. 56* (1978) 2808.
[97] A. G. Lee, *Biochem. Biophys. Acta 472* (1977) 285.
[98] N. J. Singer, G. L. Nicholson, *Science (Washington, DC) 175* (1972) 720.
[99] M. P. Heyn, A. Blume, M. Rehorek, N. A. Dencher, *Biochemistry 20* (1981) 7109.
[100] M. P. Heyn, R. J. Cherry, N. A. Dencher, *Biochemistry 20* (1981) 840.

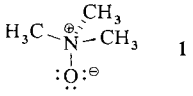
Covalent versus Dative Bonds to Main Group Metals, a Useful Distinction

By Arne Haaland*

Textbooks of inorganic chemistry describe the formation of adducts by coordination of an electron donor to an electron acceptor, often using the amine-boranes, $X_3N \rightarrow BY_3$, as examples. In the Lewis (electron dot) formulas of the compounds, the dative bond in $H_3N \rightarrow BH_3$ and the covalent bond in H_3C–CH_3 are both represented by a shared electron pair. In the simple molecular orbital or valence bond models the wave functions of both electron pairs would be constructed in the same manner from the appropriate sp^3 type atomic orbitals on the bonded atoms: the difference between the covalent and the dative bond becomes apparent only after the orbital coefficients have been analyzed. This may be the reason why many structural chemists seem reluctant to distinguish between the two types of bonds. The object of this article is to remind the reader that the physicochemical properties of covalent and dative bonds may be – and often are – quite different, and to show that a distinction between the two provides a basis for understanding the structures of a wide range of main group metal compounds.

1. Introduction

In his book *The Nature of the Chemical Bond*, probably the most influential book of this century on structural chemistry, *Linus Pauling* classifies chemical bonds as electrostatic, covalent or metallic. In the subsection on covalent bonds in the introductory chapter he represents the bonding in trimethylamine oxide in the following way



1

and adds[1] that the N–O bond "may be considered a sort of double bond consisting of one single covalent bond and one ionic bond of unit strength. A bond of this type has sometimes been called a semipolar double bond. The name coordinate link has also been used, together with a special symbol $\rightarrow$ to indicate the transfer of electric charge from one atom to the other". "We shall not find it convenient to make use of these names or these symbols".

Other chemists have written or edited whole books on electron donor-acceptor adducts, e.g. *E. N. Guryanova* et al.,[2] *R. G. Pearson*,[3] and *V. Gutmann*.[4]

In this article we first discuss the structure of simple molecules containing covalent or dative bonds between atoms of Groups 15, 16 or 17 and metal atoms of Groups 2 and 12–14. Our aim is to bring together information – some of it new, some of it quite old – which highlights the different properties of covalent and dative bonds between the same atom pair, for instance Al and N or Zn and O. In particular we shall be concerned about bond distances. Secondly, we wish to show how the bond distances of intermediate magnitude found in more complicated, polynuclear species may be rationalized in terms of the magnitude of covalent and dative bonding contributions determined by enumeration of canonical forms with localized covalent and dative bonds.

[*] Prof. A. Haaland
Department of Chemistry, University of Oslo,
P.O. Box 1033, Blindern, 0315 Oslo 3 (Norway)

In most of the adducts that we shall discuss, both donor and acceptor are neutral molecules, but we shall include a few species where the donor is a halide ion or the acceptor is a molecular ion with charge +1. Even though solvation of ions like $Mg^{2\oplus}$ or $Al^{3\oplus}$,[5] "secondary bonding" as encountered for instance in the solid trihalides of the heavy Group 15 elements,[6] and hydrogen bonding[7] all involve electron donor acceptor interactions, they are not within the scope of this article.

2. Prototype Covalent and Dative Bonds: Ethane and Amine-borane

H_3C–CH_3 and $H_3N \rightarrow BH_3$ provide convenient prototypes for covalent and dative bonds: The two molecules are isoelectronic, and, at least on paper, one species may be converted into the other by transfer of one proton between the nuclei of the bonded atoms.

It has sometimes been said that "the only difference between a covalent and a dative bond is where you think the electrons come from": When H_3NBH_3 is formed from H_3N and BH_3 the two BN bonding electrons are provided by N, but, since H_3CCH_3 may be formed by coordination of $H_3C^{\ominus}$ to $^{\oplus}CH_3$, it would seem that a distinction between covalent and dative bonds is artificial.

However, regardless of how H_3CCH_3 and H_3NBH_3 have been formed, the molecules differ in the nature of the fragments obtained when the central bonds are broken:

Rupture of the dative bond in $H_3N \rightarrow BH_3$ yields either two species without net charge or spin (H_3N: and BH_3) or two species with both net charge and net spin ($H_3N^{\bullet\oplus}$ and $BH_3^{\bullet\ominus}$). Rupture of the covalent bond in H_3C–CH_3, on the other hand, yields either species with net spin ($H_3C^{\bullet}$) or species with net charge ($H_3C:^{\ominus}$ and $CH_3^{\oplus}$).

Minimum-energy rupture of the central bond in either molecule yields neutral species; rupture of the dative bond in $H_3N \rightarrow BH_3$ proceeds heterolytically, rupture of the covalent bond in H_3C–CH_3 proceeds homolytically.

Since the electron affinities of the halogen atoms are smaller than the ionization energies of the alkali metal

 © VCH Verlagsgesellschaft mbH, D-6940 Weinheim, 1989 0570-0833/89/0992 $ 02.50/0

atoms, minimum energy rupture of the bonds in the gaseous monomeric alkali halides—like the covalent bond in ethane—proceeds homolytically to yield neutral, radical species (atoms).

In the following we shall denote a bond in a neutral diamagnetic molecule as *normal* if minimum-energy rupture in the gas phase or in an inert solvent proceeds homolytically to yield neutral, radical species. The term covers both covalent and ionic bonds as well as bonds of intermediate polarity. We shall use this term rather than the word covalent when discussing very polar bonds and when we wish to make general statements.

We shall define a bond in a neutral, diamagnetic molecule as *dative* if minimum-energy rupture in the gas phase or in an inert solvent proceeds heterolytically to yield neutral, diamagnetic species. The category to which a bond belongs may then be determined experimentally or deduced from measureable quantities like ionization energies and electron affinities.

The C–C bond rupture enthalpy of ethane at 298 K is $\Delta H^0_{dis} = 89.8 \pm 0.5$ kcal mol^{-1}.[8] The bond rupture enthalpy of $H_3N \rightarrow BH_3$ may be estimated to the nearest kcal mol^{-1} from the dissociation enthalpies of seven methylated amine boranes listed in Table 1; $\Delta H^0_{dis}(H_3N \rightarrow BH_3) = 31.1$ $\pm$ 1.0 kcal mol^{-1}.[*] The strength of the prototype dative bond is thus one third the strength of the prototype covalent bond. The difference in bond strength is reflected in the bond distances (Table 2); the covalent C–C bond distance in ethane is 1.533(2) Å by GED[10] (gas electron diffraction); the dative N → B bond distance in H_3NBH_3 is 1.658(2) Å by MW[11] (microwave spectroscopy).[**]

Table 1. Gas phase dissociation enthalpies, ΔH^0_{dis} (in kcal mol^{-1}), of the donor–acceptor complexes of BH_3 and BMe_3 with H_3N and the methylamines $Me_nH_{3-n}N$, n = 1–3.

Donor \ Acceptor	BH_3	BMe_3 [21]
H_3N	31.1 ± 1.0 [a]	13.8 ± 0.3
MeH_2N	35.0 ± 0.8 [b]	17.6 ± 0.2
Me_2HN	36.4 ± 1.0 [b]	19.3 ± 0.2
Me_3N	34.8 ± 0.5 [b]	17.6 ± 0.2

[a] Estimated by us from the other entries in the Table. [b] Calculated from the standard enthalpies of the reactions $2\,Me_nH_{3-n}N \rightarrow BH_3(g) \rightarrow B_2H_6(g) + 2\,Me_nH_{3-n}N(g)$ [19] and the dissociation enthalpy of diborane [20].

While the dipole moment of ethane is, by virtue of its symmetry, zero, the dipole moment of H_3NBH_3[11] is 5.22 D as compared with 1.47 D for free NH_3.[8] The negative pole is undoubtedly at the acceptor. If the electron pair was shared equally between donor and acceptor atoms, corresponding to the transfer of one full electron, $H_3N^{\oplus}$–$B^{\ominus}H_3$, the bond dipole calculated from point charges would be 8.0 D. The observed dipole moment indicates that the electron pair remains more closely associated with the donor than with the acceptor atom.

Table 2. Comparison of the physicochemical data of compounds with covalent and dative bonds.

	H_3C–CH_3	$H_3N \rightarrow BH_3$	Me_3Si–$SiMe_3$	$Me_3P \rightarrow AlMe_3$
ΔH^0_{dis} [kcal mol^{-1}]	90	31 [a]	74 [15]	21 [17]
R [Å]	1.53	1.66	2.34 [16]	2.53(4) [18]
μ [D]	0	5.2		
M.p. [°C]	−183	124		

[a] See footnote to Table 1.

The gross atomic populations obtained by analysis of MOs obtained with a split valence basis indicate that adduct formation is accompanied by transfer of 0.20 $e^{\ominus}$ from N to B.[12] Somewhat surprisingly, the electron density on B appears to be slightly less in the adduct than in free BH_3; the acceptor atom appears to compensate for the acquired electron density by passing a slightly larger negative charge on to its substituent H atoms. Similarly, the donor atom N appears to compensate for the charge transfer to B by extracting a slightly larger negative charge from *its* substituent H atoms: the charge transferred from donor to acceptor originates at the substituents of the donor atom and ends up at the substituents of the acceptor atom. The reader may wonder about the effect of replacing the substituent H atoms on N or B with more or less electron-withdrawing atoms or groups. We shall return to this point in the following section.

H_3NBH_3 is a solid at room temperature. The melting point[13] is about 124 °C and it sublimes at 60 °C/0.001 torr.[14] The melting point of ethane is − 183 °C and the normal boiling point is − 89 °C.[8] The difference is undoubtedly due to strong intermolecular dipole-dipole attractions in the adduct.

Another pair of covalently/datively bonded molecules that are isoelectronic and related through transfer of one proton between the bonded nuclei is provided by Me_3Si–$SiMe_3$ and $Me_3P \rightarrow AlMe_3$ (Table 2). In this case the strength of the dative bond is less than a third of the strength of the covalent bond, and the bond distance is about 10% greater.

3. Inductive Effects

Comparison of the gas phase dissociation enthalpies of complexes of BH_3 and BMe_3 with the methylamines $Me_nH_{3-n}N$, n = 1–3 (Table 1), shows that replacement of three H atoms on the acceptor atom by three Me groups reduces the dissociation enthalpy by about 17 kcal mol^{-1}, i.e. by a factor of 1/2.

If the destabilization were due to increased strain following the introduction of the more voluminous Me groups, introduction of one or more Me groups on N in $H_3N \rightarrow BMe_3$ should lead to still greater destabilization. Instead, it is found that introduction of the first Me group on N *stabilizes* the complex by about 4 kcal mol^{-1} and the second by about 2 kcal mol^{-1}, while the third Me group leads to a small destabilization.

It might be argued that the low dissociation enthalpy of the BMe_3 adducts is the result of high reorganization energy, i.e. that it would take more energy to pyramidalize BMe_3 than BH_3. In fact the molecular force fields indicate that the

[*] This estimate is in reasonable agreement with the dissociation energy D_e obtained by SCF MO calculations with triple zeta plus polarization basis with electron correlation Møller-Plesset calculations to the fourth order, $D_e = 34.7$ kcal mol^{-1}. Correction for zero-point vibrational energies yielded $D_0 = 28.7$ kcal mol^{-1} [9].

[**] As we shall see in Section 9 a *covalent* N–B single bond distance may be estimated to be 1.47 Å, i.e. 0.19 Å shorter than the dative bond in $H_3N \rightarrow BH_3$.

deformation energy of BH_3 is higher than that of BMe_3.[22] We therefore interpret the strong destabilization produced by Me groups on the acceptor atom and the weak stabilization produced by Me groups on the donor atom as an inductive effect due to the greater electron-releasing tendency of the Me group.

If introduction of electron-releasing Me groups on the acceptor atom destabilizes the complex, introduction of electron withdrawing Cl atoms would be expected to stabilize it. As far as we know, the dissociation enthalpy of Me_3NBCl_3 has not been determined. However, the gas phase dissociation enthalpies of $py \rightarrow BMe_3$ (py = pyridine) and $py \rightarrow BCl_3$ are available for comparison. The former, 17 kcal mol^{-1},[23] is similar to that of $Me_3N \rightarrow BMe_3$, while the latter, 38 kcal mol^{-1} [24] is similar to that of $Me_3N \rightarrow BH_3$. In borane complexes the replacement of H atoms on B by Cl atoms appears to have little effect on the dissociation enthalpy.

It is normally assumed that bond distances may serve as indicators of bond strength with the shorter distance associated with the stronger bond. Indeed, the N–B bond distance in $Me_3N \rightarrow BMe_3$, 1.70 ± 0.01 Å by MW,[25] is significantly longer than the bond distances in $Me_3N \rightarrow BH_3$, 1.64 ± 0.01 Å by MW[26] and 1.656(2) Å by GED,[27] and $Me_3N \rightarrow BCl_3$, 1.659(6) Å[28] and 1.652(9) Å[29] by two independent GED studies.

It is noteworthy that the bond distance in $Me_3N \rightarrow BCl_3$ decreases by about 0.06 Å on going from the gaseous to the solid state: two independent crystal structure determinations have yielded N—B = 1.609(6) Å[30] and 1.575(11) Å.[31] Since donor–acceptor bonds are relatively weak, they are relatively easy to compress or elongate. The dipole moment of $Me_3N \rightarrow BCl_3$ in benzene is 6.28 ± 0.02 D.[32] In the crystals, nearest neighbors are aligned with antiparallel N → B vectors. This arrangement stabilizes greater charge transfer, i.e. a stronger dative bond. An early X-ray crystallographic study of our prototype adduct H_3NBH_3 yielded an N–B bond distance of 1.56 ± 0.05 Å,[33] which – although very inaccurate – suggests a shortening of 0.05 Å or more relative to the gas phase.

Before proceeding to allane complexes we pause to take note of H_3BCO, which appears to be the only carbonyl complex of a main group element that is stable under the conditions of normal temperatures and pressures. Molecular orbital calculations indicate that there is considerable back donation of BH bonding electrons into the antibonding CO π-orbital (hyperconjugation).[12] The B–C bond distance is 1.534(10) Å,[34] about 0.04 Å shorter than the covalent $B-C_{sp^3}$ bond distance in BMe_3,[35] and hence only 0.04 Å longer than estimated for a covalent $B-C_{sp}$ bond distance. The gas phase dissociation enthalpy, however, is only 18.8 kcal mol^{-1},[36] or about one fifth of the mean disruption enthalpy of the covalent B–C bonds in BMe_3.[15]

Alane complexes appear to be as sensitive to inductive effects as borane complexes: thus the gas phase dissociation enthalpy of $Me_3N \rightarrow AlCl_3$ is $\Delta H^0 = 47.5 \pm 2.0$ kcal mol^{-1} as compared to $\Delta H^0_{dis} = 30.7 \pm 0.3$ kcal mol^{-1} for $Me_3N \rightarrow AlMe_3$.[37] The bond strength difference is clearly reflected in the N → Al bond distances, 1.96(1) Å by X-ray diffraction in the chloro compound[38] versus 2.10(1) Å by GED in the methyl compound.[37] The dissociation enthalpy of $Me_3N \rightarrow AlH_3$ is unknown, but the N → Al bond distance, 2.063(8) Å by GED,[39] indicates that the compound more closely resembles the $AlMe_3$- than the $AlCl_3$-complex.

In their book on the donor-acceptor bond,[2] *Guryanova* and her coauthors list the dissociation enthalpies of about 700 complexes where both donor and acceptor atoms are main group elements. The entries cover complexes where the acceptor atom is a Group 12 element (Zn), a Group 13 element (B, Al, Ga and In), a Group 14 element (Sn), a Group 15 element (As and Sb) and a halogen atom (Br and I). The donor atoms are Group 15 elements (mainly N and P) and Group 16 elements (mainly O and S). The bond dissociation enthalpies range from 0.2 kcal mol^{-1} to nearly 50 kcal mol^{-1}. The strongest bonds to a given acceptor appear to be formed by N donors. The strongest bonds to a given donor appear to be formed by Al acceptors, followed by B and Ga. Starting with Group 13 the strength of the donor-acceptor bond appears to decrease with increasing group number of the acceptor atom. If the free acceptor carries only hydrocarbon substituents the dissociation enthalpy is less than or equal to 30 kcal mol^{-1} (as in $Me_3N \rightarrow AlMe_3$). If the acceptor atom carries more electronegative substituents, the dissociation enthalpy is higher, and may approach 50 kcal mol^{-1} (as in $Me_3N \rightarrow AlCl_3$). The strength of a donor–acceptor bond between main group elements may be as high as about half the strength of a covalent bond, but often it is much weaker.

4. Dative Bonds and the VSEPR Model

In Figure 1 we compare the structure of the free donor Me_3P[40] and the structure of the free acceptor $AlMe_3$[41]

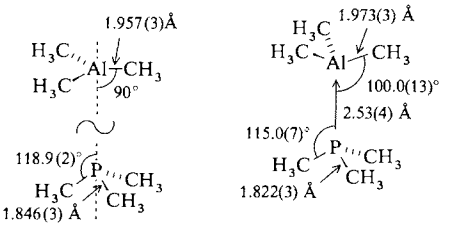


Fig. 1. Structural parameters of free Me_3P [40], free $AlMe_3$ [41] and the adduct $Me_3P \rightarrow AlMe_3$ [18].

with the structure of the adduct $Me_3P \rightarrow AlMe_3$.[18] In free $AlMe_3$ the metal atom is surrounded by three bond electron pairs and the coordination is trigonal planar in agreement with the VSEPR (*V*alence *S*hell *E*lectron *P*air *R*epulsion) model.

As the adduct is formed and a fourth electron pair is introduced (accepted), the Al–C bonds are bent back, and the C-Al-C angles are reduced from 120° to 113°. At the same time the bonds are slightly, but significantly, elongated from 1.957(3) Å to 1.973(3) Å. Both these changes are in the direction predicted from the VSEPR model. It should be noted, however, that after the adduct has been formed the C-Al-C angle remains greater than the tetrahedral angle 109.5°, suggesting that the spatial requirements of the covalent or normal bond pairs (NBP) are greater than the steric requirement of the accepted bond pair (ABP): NBP > ABP.

The P atom in Me_3P is surrounded by three covalent bond pairs (NBP) and one electron lone pair (LP). The structure is pyramidal, in agreement with the VSEPR model, and the C-P-C angle is less than tetrahedral, in agreement with the assumption that the spatial requirement of an LP is greater than that of a NBP.

As the adduct is formed and the lone pair is partially removed (donated), the C-P-C angles increase from 98.6(3)° to 103.4(8)°, and there is a slight but significant decrease in the P–C bond distances from 1.846(3) Å to 1.822(3) Å. Both these changes are in the direction predicted from the VSEPR model. After the adduct has been formed, however, the C-P-C angle remains less than tetrahedral, indicating that the spatial requirement of a donated electron bond pair (DBP) remains larger than that of a covalent bond pair: LP > DBP > NBP.

Similar changes in the structure of the donor have been observed in Me_3PBH_3[42] and Me_3PBCl_3.[43] When Me_3As forms a complex with BH_3 the As–C bond distance decreases from 1.968(3) Å[44] to 1.945 Å[45] and the C-As-C angle increases from 96.1(5)°[44] to 105°.[45]

The structures of the adducts of $AlMe_3$ and $AlCl_3$ with another donor, viz. Me_3N are shown in Figure 2. The structure of the acceptor ($AlMe_3$) in the adduct with Me_3N is very similar to the structure in the adduct with Me_3P and may be rationalized in the same manner. Monomeric $AlCl_3$ is trigonal planar in the gas phase with Al–Cl = 2.064(4) Å.[46] On formation of the adduct the Cl-Al-Cl angle is reduced from 120° to 114° and the Al-Cl bond distance increases to 2.121(4) Å; again the changes are those predicted from the VSEPR model.

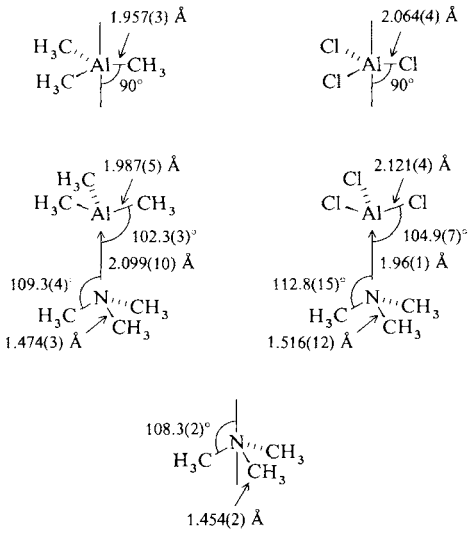


Fig. 2. Structural parameters of free $AlMe_3$ [41], free $AlCl_3$ [46], free Me_3N [47] and the adducts $Me_3N \rightarrow AlMe_3$ [37] and $Me_3N \rightarrow AlCl_3$ [48] (the Al–N bond length was determined X-ray crystallographically [38].

We now turn our attention to the structure of the donor: In free Me_3N the N atom is surrounded by three CBP and one LP. According to the VSEPR model the molecule should be pyramidal and the C-N-C angle less than tetrahedral. The C-N-C angle is, however, found to be slightly greater than tetrahedral, 110.6(6)° by GED[47] and 110.9(6)° by MW,[49] presumably because of steric repulsion between the Me groups. Formation of the adducts with $AlMe_3$ and $AlCl_3$ leaves the C-N-C angle unchanged or slightly decreased while the N–C bond distance *increases* from 1.454(2) Å in free NMe_3 to 1.473(3) Å in the complex with $AlMe_3$ and to 1.516(12) Å in the still stronger adduct with $AlCl_3$.

It appears that while the structural changes in Me_3P could be rationalized in terms of VSEPR, the structural changes in Me_3N on adduct formation are in the opposite direction and must be rationalized in terms of steric repulsion between the atoms and groups bonded to N.[*]

Consideration of steric repulsion between the ligands bonded to the acceptor atom (Al) leads to the prediction that Al–Y bonds should be elongated and Y-Al-Y angles reduced when the adduct is formed. On the acceptor atom VSEPR and steric interactions reinforce one another, on the donor atom they are opposed. When the donor atom is small (N or O), steric factors may prevail.

According to *Gutmann*'s rules on bond length variation,[4] adduct formation should always lead to elongation of bonds to both donor and acceptor atoms. This rule appears to be generally valid for bonds to the acceptor atoms, but is broken for bonds to the donor atom when Me_3P and Me_3As form adducts with boranes or allanes. We presume that it may be broken in other cases when the donor atom is large enough to make steric interaction between the substituents unimportant.

5. 2:1 Amine-Alane Complexes

Both $Me_3N \rightarrow AlH_3$ and $Me_2HN \rightarrow AlCl_3$ will add a second mole of the electron donor. The resulting coordination around Al is trigonal-bipyramidal with the donor atoms in axial positions as expected from the VSEPR model with the additional postulate that NBP > ABP.

The N → Al distances in the 2:1 adducts (Fig. 3) are considerably longer than in the 1:1 adducts, indicating saturation of the acceptor: in $(Me_2HN)_2AlCl_3$,[53] N → Al = 2.059(3) Å compared to 1.96(1) Å in Me_3NAlCl_3[38] (Fig. 2). In $(Me_3N)_2AlH_3$,[54, 55] N → Al = 2.18(1) Å compared to 2.063(8) Å in the 1:1 adduct. The N → Al bonds in

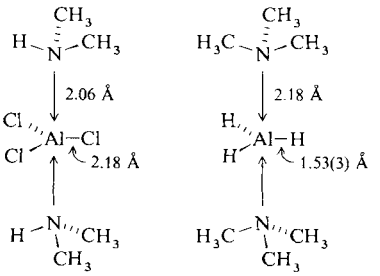


Fig. 3. The structural parameters of $(Me_2HN)_2AlCl_3$ [53] and $(Me_3N)_2AlH_3$ determined by X-ray diffraction [54] and gas-phase electron diffraction [55].

[*] This difference between N and P appears to be carried over to tetraalkylammonium and -phosphonium ions: The mean N–C bond distance in $[Me_4N]F \cdot 4\,H_2O$ is 1.499(2) Å [50], 0.04_5 Å *longer* than in free $(CH_3)_3N$, while the mean P–C bond distance in $[Me_4P][Cu_2Cl_3]$ is 1.779(3) Å [51], 0.06_7 Å *shorter* than in Me_3P. The average of 319 N–C* bond distances (C* = tetrahedral C atom carrying only C and H as additional substituents) in NC_4^+-type ammonium ions is 1.510 Å, 0.04_1 Å longer than the average of 1042 N–C bond distances in NC_3^+-type amines, while the average of 35 P–C* bond distances in C_3PC^*-type phosphonium ions is 1.800 Å, 0.04_5 Å shorter than the average of 23 bond distances in C_2PC^* phosphanes [52].

$(Me_2HN)_2AlCl_3$ are about 0.12 Å shorter than in $(Me_3N)_2AlH_3$, again indicating that $AlCl_3$ is a better acceptor than AlH_3. The N → Al bond distances in the 1:1 adducts indicate that $AlMe_3$ is a poorer acceptor than AlH_3; indeed Me_3NAlMe_3 will not add another mole of the base: it appears that 2:1 adducts are as sensitive to inductive effects as the 1:1 adducts.

Both VSEPR and steric considerations suggest that covalent Al–Y bonds should be further elongated on addition of the second donor. Indeed, in $(Me_2HN)_2AlCl_3$, Al–Cl = 2.180(1) Å[53] as compared to 2.121(4) Å in Me_3NAlCl_3.[48]

We are not aware of any observation indicating the existence of 2:1 amine-borane adducts.

6. Some Adducts of Beryllium, Magnesium, Zinc, and Mercury

Quinuclidine forms 2:1 adducts with both dimethylberyllium and dimethylmagnesium. The coordination geometries around the metal atoms as determined by X-ray crystallography[56, 57] are shown in Figure 4.[*] The main features are

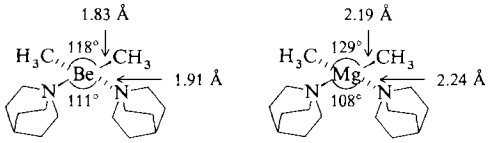


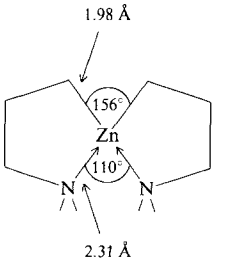
Fig. 4. Structural parameters of the 2:1 adducts of quinuclidine with $Be(CH_3)_2$ and $Mg(CH_3)_2$ [56, 57].

in agreement with the principles already outlined: $BeMe_2$ is linear in the gas phase with R(Be–C) = 1.70 Å;[58] coordination of two donor atoms decreases the C-Be-C angle to 118° and increases Be–C to 1.83 Å. In monomeric, base-free bisneopentylmagnesium the C-Mg-C angle is 180° and R(Mg–C) = 2.13 Å;[59] in the $MgMe_2$ adduct the values are 129° and 2.19 Å.

In each complex the metal atom is surrounded by two covalent electron bond pairs and two accepted bond pairs; the structure is distorted tetrahedral. Even though the datively bonded quinuclidine ligands are more bulky than the covalently bonded Me groups, the C-M-C angles are considerably larger than the N-M-N angles, in agreement with the postulate that NBP > ABP.

The interaction enthalpy between 2,2′-bipyridine and dimethylzinc in toluene is 17.6 kcal mol^{-1}.[60] Since 2,2′-bipyridine presumably acts as a bidentate ligand, this corresponds to a mean N → Zn dissociation enthalpy of 9 kcal mol^{-1}. The Zn–N bonds in the amides $Zn[N(SiMe_3)_2]_2$ are assumed to be single bonds with negligible π-components.[61] The bond energy term[62] is 49 kcal mol^{-1}, i.e. the strength of the covalent bond appears to be four or five times that of the dative bond.

We are not aware of the structure of any simple adduct between a dialkylzinc and an N-centered donor, but the structure of $Zn[(CH_2)_3N(CH_3)_2]_2$ **2** has been determined by



2

both X-ray and GED.[63] The Zn–C bonds are about 0.05 Å longer than in dipropylzinc,[64] the dative N → Zn bonds are 0.50 Å longer than the covalent Zn–N bonds in $Zn[(NSiMe_3)_2]_2$.[61] The weakness of the donor–acceptor interaction is indicated by the large C-Zn-C valence angle and the large N → Zn r.m.s. vibrational amplitude found in the GED study, l = 0.17(3) Å, two or three times greater than the amplitude of the Zn-C bond. The donor–acceptor bonds appear to be about 0.08 Å shorter in the solid phase than in the gas phase.

The structure of the 2:1 complex of pyridine with $ZnCl_2$[65] is shown in Figure 5. The N → Zn bond distance is about 0.25 Å *longer* than the covalent bond distance in $Zn[N(SiMe_3)_2]_2$ but 0.25 Å shorter than the N → Zn bond in **2**; the latter difference is presumably an inductive effect. The Zn–Cl bond is 0.15 Å longer than in gaseous monomeric $ZnCl_2$.[66]

In Figure 5 we also show the coordination sphere of the mercury atom in the related adduct of bis(2-pyridyl) disulfi-

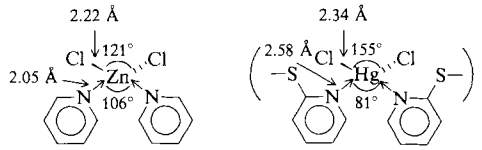
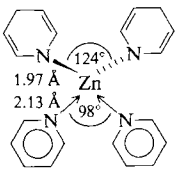


Fig. 5. Structural parameters of $ZnCl_2 \cdot 2$ pyridine [65] and $HgCl_2 \cdot$ bis(2-pyridyl) disulfide [67] in the crystal.

de with $HgCl_2$ in the solid phase.[67] Mercury compounds are known as poorer acceptors than their zinc analogues. The weakness of the interaction is indicated both by the large N → Hg bond distance, more than 0.50 Å longer than the covalent Hg–N bond in the amide $Hg[N(SiMe_3)_2]_2$,[68] and by the large Cl-Hg-Cl angle. The valence angles at the Hg atom are such that a description in terms of sp-hybridization with electron donation into pure p-orbitals may be more appropriate than a discussion in terms of sp^3-hybridization. The elongation of the Hg–Cl bond compared to that in gaseous monomeric $HgCl_2$ is 0.09 Å.[69]

The most interesting N → Zn adduct may be bis(1,4-dihydropyridin-1-yl)-bis(pyridine)zinc, **3**, which is formed from



3

ZnH_2 and four moles of pyridine.[70, 71] In this complex we see for the first time the difference between covalent and dative bonds between the same atom pair demonstrated in the same molecular unit.

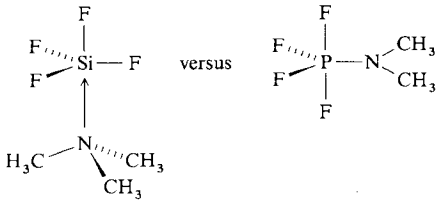
The covalent Zn–N bonds are about 0.15 Å longer than in $Zn[N(SiMe_3)_2]_2$: this elongation is similar to the elongation

[*] In the following we omit estimated standard deviations of less than 0.01 Å or 1°.

of the bonds in $ZnCl_2$ on coordination of two pyridine molecules. The covalent Zn–N bonds in **3** are, however, still 0.16 Å shorter than the dative bonds. The bulks of the four ligands are very nearly equal, and, as expected from VSEPR considerations, the angle subtended by the covalently bonded N atoms (124°) is considerably larger than that subtended by the datively bonded N atoms (98°).

7. Some Adducts of Silicon

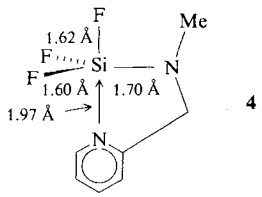
The 1:1 adducts of SiF_4 with the amines $Me_nH_{3-n}N$, n = 0,1,2,3, in argon matrices have been investigated by infrared spectroscopy.[72, 73] The coordination around Si was found to be trigonal bipyramidal with the amine occupying an axial position. A structural chemist has commented:[74] "This conclusion is remarkable. Of the huge range of five-coordinate derivatives known of P and S, all examples with only monodentate groups have the axial sites occupied by the most electronegative ligand...". In other words, why does the N atom in Me_3NSiF_4 occupy an axial position when the N atom in Me_2NPF_4[75] is equatorial (Scheme 1)?



Scheme 1. Structures of Me_3NSiF_4 and Me_2NPF_4.

We suggest that the contradiction is removed if a distinction is made between covalently bonded ligands (F and NMe_2) and datively bonded ligands (NMe_3). If the distinction is made, VSEPR considerations combined with the postulate NBP > ABP lead to the observed structures for both molecules.

The crystal structure of 2-{[methyl(trifluorosilyl)amino]-methyl}pyridine **4** shows that the coordination of Si is trigo-

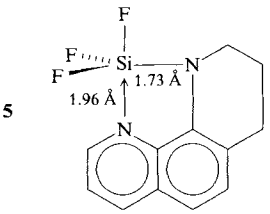


4

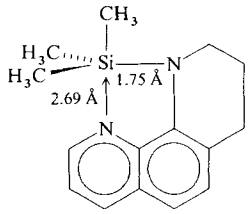
nal bipyramidal.[76] Two F atoms and the covalently bonded amide N atom occupy the equatorial sites, while the axial sites are occupied by the third F and the datively bonded pyridine N atom. The Si–F_{eq} and Si–F_{ax} distances are very similar, 1.603(4) Å and 1.621(5) Å, respectively. The equatorial Si–N distance is 1.70 Å, a normal value for a covalent Si–N bond, the dative, axial N → Si distance is 1.97 Å.

^{19}F-NMR spectra show that axial and equatorial F atoms undergo rapid exchange at room temperature.[76] There is evidence that the exchange proceeds via dissociation of the dative N → Si bond followed by rotation of the SiF_3 group and recoordination of the pyridine N atom. The activation energy (13.2(9) kcal mol^{-1}) determined by line shape analysis[76] is then the sum of the N → Si bond dissociation enthalpy and the barrier to rotation of the SiF_3 group in the uncoordinated intermediate.

Comparison of the axial N → Si bond distances found in the crystal structures of the related compounds **5**[77] and **6**[78] indicates that the dative N → Si bonds are even more



5



6

sensitive to inductive effects than N → Al or N → B bonds: replacement of three F atoms on Si by three Me groups increases the dative N → Si bond distance by 0.73 Å!

The covalent Si–N bond distance appears to increase by 0.02 Å on going from **5** to **6**, but the combined uncertainty is so large that it is doubtful whether the difference is real. A more accurate estimate of the effect on covalent bond distances when three F are replaced by three Me groups, is obtained by comparing the Si–F bonds in SiF_4[79] and Me_3SiF[80] and the Si–C bonds in $MeSiF_3$[80] and Me_4Si:[81] in both cases the bond distances increase by 0.05 Å. The difference between the N → Si bonds in **5** and **6** is thus more than an order of magnitude greater than the elongation expected for covalent bonds.

8. Influence of the Donor Atom and Net Charge

8.1. A Comparison of Donor Atoms

Trimethylaluminum forms stable complexes with a wide range of electron donors. Some D → Al bond distances and gas phase dissociation enthalpies [Eq. (a)] are listed in Table 3.

$$D \rightarrow AlMe_3(g) \rightarrow D(g) + AlMe_3(g) \qquad (a)$$

Table 3. Al–D bond lengths and gas phase dissociation enthalpies of some complexes of $AlMe_3$ and electron donors D.

Donor D	R [Å]	ΔH^0_{dis} [kcal mol^{-1}]
Me_3N [37]	2.10	31
Me_3P [17, 18]	2.53(4)	23
Me_2O [17, 82]	2.01(2)	22
Me_2S [83, 84]	2.55(2)	18
Me_2Se [85]	–	16

Complexes of trimethylaluminum with alkyl fluorides or chlorides have not been isolated; the donor–acceptor interaction is obviously not strong enough to compensate for the enthalpy required to produce one mole $AlMe_3$ by dissociation of the dimer, viz. 10 kcal mol^{-1}.[83] It should be noted, however, that Et_3SiF forms a stable complex with $AlEt_3$.[86] The enthalpy required to break the dative F → Al bond is

obviously greater than the enthalpy gained by dimerization of one mole of Et_3Al (9 kcal mol^{-1}[87]).

BH_3 will only form complexes with electron donors in those cases when the donor–acceptor interactions are strong enough to compensate the diborane dissociation enthalpy. No such limitations exist for BF_3 which is monomeric. Gas phase dissociation enthalpies are available for the complexes with Me_3N, Me_2O, Me_3P and Me_2S and the structures of the former two have been determined by GED (Table 4).

Table 4. B–D bond lengths and gas phase dissociation enthalpies of some complexes of BF_3 and electron donors.

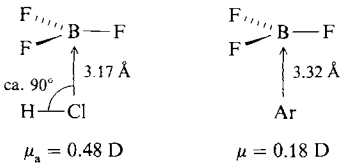
Donor D	R [Å]	ΔH^0_{dis} [kcal mol^{-1}]
Me_3N [88, 89]	1.67	27
Me_3P [92]	–	19
Me_2O [90, 91]	1.75(2)	13
Me_2S [93]	–	4

The enthalpy ΔH^0_r of reaction (b) is equal to the sum of

$$D \rightarrow BF_3(s) \rightarrow D(g) + BF_3(g) \qquad (b)$$

the sublimation and dissociation enthalpies. The experimental values are[94] 45 kcal mol^{-1} for $D = Me_3P$ and 20 kcal mol^{-1} for $D = Me_3As$. Subtraction of the dissociation enthalpy of Me_3PBF_3 from the value for Me_3P yields a sublimation enthalpy of 26 kcal mol^{-1} for the adduct. Since the sublimation enthalpy of Me_3AsBF_3 is expected to be greater than that of the P-analogue, it follows from the value $\Delta H^0_r = 20$ kcal mol^{-1} for Me_3As that the dissociation enthalpy of the As-adduct is *negative* (less than -6 kcal mol^{-1}). It seems that in this case intermolecular forces in the crystal are sufficient to stabilize an adduct where the donor–acceptor interaction is repulsive in the gas phase!

The structures of the adducts $HClBF_3$[95] and $ArBF_3$[96] have been determined by microwave spectroscopy (Scheme 2).



Scheme 2. Structural parameters of $HClBF_3$ and $ArBF_3$.

These species are commonly regarded as van der Waals complexes, but may also be described as weak donor–acceptor adducts. Comparison of the Ar → B and Cl → B bond distances, and comparison of the dipole moment of $ArBF_3$ with the dipole moment component μ_a along the Cl → B bond in $HClBF_3$, indicates that Ar is the weaker donor. HCl and Ar are isoelectronic; on paper, HCl may be formed from Ar by withdrawing one proton from the nucleus. The reader may wonder what effect it would have on the donor–acceptor interaction if the proton was completely removed to leave $[ClBF_3]^{\ominus}$. We shall return to such species in Section 8.3.

We have already pointed out that the strongest dative bonds to a given main group acceptor atom are formed by N donors. Beginning with Group 15 the strength of the donor–acceptor bond appears to decrease with increasing group number of the donor atom. With B and Al acceptors the strength of the interaction decreases monotonically with increasing principal quantum number of the valence electrons of the donor atom, but this does not appear to be true for all acceptors.

8.2. Cationic Complexes

Since the introduction of electron-withdrawing substituents on the acceptor atom often leads to a significant increase in the dissociation enthalpy of a donor–acceptor adduct, it is hardly surprising that cationic acceptors form stronger dative bonds than related neutral molecules.

The tetramethyl derivatives of Si, Ge or Sn do not appear to interact with electron donors. Introduction of a Cl atom on Sn leads to the formation of a stable 1:1 adduct with pyridine, the dissociation enthalpy in benzene being 11.0 ± 1.0 kcal mol^{-1}.[97] The interaction enthalpies of Me_3SiCl or Me_3GeCl with pyridine in the same solvent are, however, of the order of -2 kcal mol^{-1} or less.[97]

In striking contrast the dissociation enthalpies of the adducts of the cations $Me_3M^{\oplus}$ with the donor H_2O determined by high pressure mass spectrometry are 30.1 ± 1.9 kcal mol^{-1} for M = Si,[98] 28.6 ± 0.5 kcal mol^{-1} for M = Ge,[99] and 25.7 ± 1.0 kcal mol^{-1} for M = Sn.[100][*]

When $Me_3M^{\oplus}$ is formed from Me_4M by removal of $CH_3^{\ominus}$, a coordination site becomes vacant both in a steric sense since the coordination number has been reduced from four to three, and in an electronic sense since the number of electrons in the valence shell of M has been reduced from eight to six. At the same time the formal charge on the metal atom has increased from zero to +1.

Me_3Al, Me_3Ga and Me_3In are isoelectronic and isoleptic with $Me_3M^{\oplus}$, M = Si, Ge and Sn respectively. Comparison of the dissociation enthalpies of related adducts (Table 5) shows that the introduction of a unit positive charge on the acceptor atom doubles or triples the dissociation enthalpy. Comparison of the dissociation enthalpies of $Et_2O \rightarrow GaMe_3$, $Et_2O \rightarrow GaCl_3$ and $[H(Me)O \rightarrow GeMe_3]^{\oplus}$ indicates that in this series the stabilization accompanying the introduction of a net positive charge on the acceptor is twice as large as the stabilization accompanying the introduction of three electron-withdrawing Cl atoms.

The dissociation enthalpies in Table 5 also show that replacement of an H on the donor atom with a more electron-releasing methyl group invariably leads to stabilization of the adduct, and that the first methyl group introduced has the largest stabilizing effect.

Before we go any further, we note that while the acceptor ability of the cations $Me_3M^{\oplus}$ decreases in the order

[*] In the absence of evidence to the contrary we assume that low-energy rupture of M–O bonds in $[H_2OMMe_3]^{\oplus}$ would proceed heterolytically to yield H_2O and $Me_3M^{\oplus}$, i.e. that the O–M bond is dative according to the definition given above.

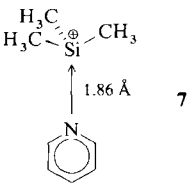
Table 5. Gas phase dissociation enthalpies, ΔH^0_{dis} of cationic and neutral donor–acceptor adducts.

Donor	Acceptor	ΔH^0_{dis} [kcal mol^{-1}]
H_2O	$Me_3Si^{\oplus}$ [98]	30.1 ± 1.9
MeOH	$Me_3Si^{\oplus}$ [98]	39.2
EtOH	$Me_3Si^{\oplus}$ [98]	42.0
Et_2O	$Me_3Si^{\oplus}$ [98]	44.2
Et_2O	Me_3Al [a]	20.2 ± 0.2
H_2O	$Me_3Ge^{\oplus}$ [99]	28.6 ± 0.5
MeOH	$Me_3Ge^{\oplus}$ [99]	35.0
Et_2O	Me_3Ga [101]	12.1 ± 0.2
Et_2O	Cl_3Ga [102]	26.6
H_2O	$Me_3Sn^{\oplus}$ [100]	25.7
MeOH	$Me_3Sn^{\oplus}$ [100]	32.6 ± 1.0
NH_3	$Me_3Sn^{\oplus}$ [100]	36.9
$MeNH_2$	$Me_3Sn^{\oplus}$ [100]	42.1
Me_2NH	$Me_3Sn^{\oplus}$ [100]	44.2
Me_3N	$Me_3Sn^{\oplus}$ [100]	45.6
Me_3N	Me_3In [103]	19.9 ± 0.5

[a] in hexane [17].

$Si^{\oplus} > Ge^{\oplus} > Sn^{\oplus}$, the normal order for neutral molecules is considered to be Sn > Ge > Si.[97]

Both $Me_3Si^{\oplus}$ and $Me_3Ge^{\oplus}$ may be prepared in solution.[104, 105] The structure of **7**, the adduct of $Me_3Si^{\oplus}$ with pyridine, has been determined by X-ray diffraction.[106] The



7

mean Si–C distance is not significantly different from the mean Si–C distance in the neutral five-coordinate complex **6**, but the dative N → Si distance is more than 3/4 Å shorter: again we find that the dative bond is more susceptible to inductive/charge effects than covalent bonds. It may be noted that even the very short dative bond in **7** is 0.11 Å longer than the covalent, equatorial Si–N bond in **6**.

8.3. Anionic Complexes

We now turn our attention to adducts where the donor is a negatively charged, monatomic ion. The structure of the anion of $[Me_4As][Me_3GaCl]$ is distorted tetrahedral with a mean Cl–Ga–C angle of 103° and a mean C-Ga-C angle of 115°.[107] The mean Ga–C bond distance (2.05(2) Å) is not accurately determined, but appears to be 0.08(2) Å longer than in free Me_3Ga[108] and 0.05(2) Å longer than in the adduct Me_3NGaMe_3.[109] The Ga–Cl distance (2.38 Å) is 0.28 Å longer than the terminal bond distance in Ga_2Cl_6 (2.10 Å),[110] which may serve as a reference value for a single normal Ga–Cl bond. If it is assumed that the electron affinity of Cl is greater than that of Me_3Ga, it follows that minimum-energy rupture of the Ga–Cl bond in $[Me_3GaCl]^{\ominus}$ would proceed heterolytically to yield Me_3Ga and $Cl^{\ominus}$, i.e. that the Ga–Cl bond is dative, Ga ← $Cl^{\ominus}$, according to our definition. In the following we adopt this description which is in good agreement with the observed bond distances and angles.

In Figure 6 we compare the average bond distances in the ions $[Me_{4-n}GaCl_n]$ (n = 1–4).[107, 111, 112] The two Ga–Cl bond distances in $[Me_2GaCl_2]^{\ominus}$ are indistinguishable, the

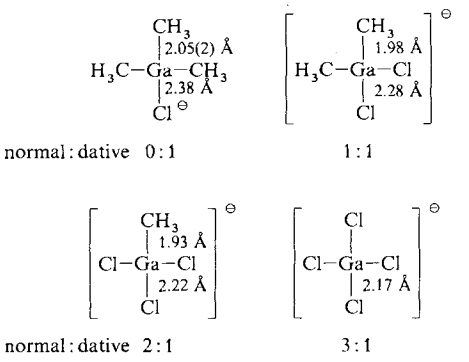
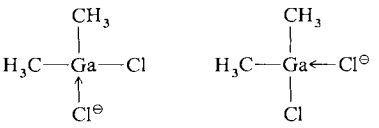


Fig. 6. Average Ga–C and Ga–Cl bond distances in the ions $[(CH_3)_{4-n}GaCl_n]^{\ominus}$ (n = 1, 2, 3 or 4) as determined by X-ray diffraction with $[Me_4As]^{\oplus}$ or $[Me_4Sb]^{\oplus}$ as counterion [107, 111, 112] and the ratio of covalent to dative contributions to the Ga–Cl bonds.

mean value (2.28 Å) is 0.10 Å shorter than the Ga ← $Cl^{\ominus}$ bond distance in $[Me_3GaCl]^{\ominus}$ and 0.18 Å longer than the terminal Ga–Cl distance in Ga_2Cl_6.[110] The bonding may be described in terms of the canonical forms **A** and **B**, where the



Ga atom forms three normal and one dative bond in each. Delocalization (resonance) would yield equal contributions of dative Ga ← $Cl^{\ominus}$ and normal Ga–Cl bonding to each of the two Ga–Cl bonds in the real ion. We note that the observed Ga–Cl distances are reasonably close to the mean of dative Ga ← $Cl^{\ominus}$ and normal Ga–Cl bond distances [(2.10 Å + 2.38 Å)/2 = 2.24 Å] and choose, therefore, to describe the Ga–Cl bonds as intermediate between pure normal and pure dative bonds. This description is consistent with the expected fragmentation behavior of the ion; one Ga–Cl bond (the first) is expected to yield Me_2GaCl and $Cl^{\ominus}$, the other (the second) to yield Me_2Ga and Cl.

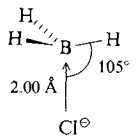
Similarly, the bonding in $[MeGaCl_3]^{\ominus}$ may be discussed in terms of three canonical forms, each with three normal Ga–C or Ga–Cl bonds and one dative bond (Ga ← $Cl^{\ominus}$). Delocalization yields normal to dative bonding contributions equal to 2:1, and the Ga–Cl bond distance in the real ion may be estimated from (2 × 2.10 Å + 3.28 Å)/3 = 2.19 Å, versus an observed value of 2.22 Å.

Finally, the Ga–Cl bonds in $[GaCl_4]^{\ominus}$ may be described in terms of 3:1 contributions of normal and dative bonding, and the bond distance estimated from (3 × 2.10 Å + 2.38 Å)/4 = 2.17 Å, equal to the observed value.

All things considered, we feel that the agreement between estimated and observed Ga–Cl bond distances is as good as can be expected for a linear, two-parameter model. If

the standard bond distances $R(Ga-Cl) = 2.12$ Å and $R(Ga \leftarrow Cl^{\ominus}) = 2.40$ Å had been chosen, the four bond distances in Figure 6 and the terminal bond distance in Ga_2Cl_6 would all have been predicted with a deviation of 0.02 Å or less.

The crystal structure of $[Ph_3PNPPh_3][ClBH_3]$ has recently been determined by both X-ray and neutron diffraction (Scheme 3).[113] The $[ClBH_3]^{\ominus}$ ion is pyramidal with a mean B–H bond distance of 1.20 Å and a Cl-B-H angle of 105°.



Scheme 3. Structural parameters of $[ClBH_3]^{\ominus}$.

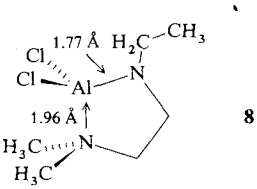
The authors remark: "The observed bonding parameters are quite normal, except that the B–Cl distance on the anion is anomalously long", and add that this "can be ascribed to incorporation of approximately 19% $(B_2H_7)^{\ominus}$ into the $(ClBH_3)^{\ominus}$ site".

We would suggest that the observed bond distance of 2.00 Å may be quite appropriate for a dative bond from $Cl^{\ominus}$ to B: the difference of 0.38 Å between the dative Ga–Cl bond in $[Me_3GaCl]^{\ominus}$ and the B–Cl bond in $[ClBH_3]^{\ominus}$ corresponds to the difference in the bonding radii of Ga and B. SCF MO calculations on $[ClBH_3]^{\ominus}$ with a 6-31G* basis set yields an optimum structure close to the experimental, and a binding energy relative to BH_3 and $Cl^{\ominus}$ of 19.9 kcal mol^{-1}.[114] In the complex $HCl \rightarrow BF_3$ (see Section 8.1) the B–Cl bond distance was 3.17 Å; as expected $Cl^{\ominus}$ is a better electron donor than HCl.

The covalent B–Cl bond distance in BCl_3 is 1.74 Å.[115] The $[BCl_4]^{\ominus}$ ion in $[NS_2Cl_2][BCl_4]$ is slightly distorted tetrahedral with all B–Cl bond distances close to the mean value of 1.84 Å.[116] Since B, like Ga, can form three covalent bonds to Cl and one dative bond to $Cl^{\ominus}$, delocalization yields covalent to dative bonding contributions equal to 3:1. The estimated bond distance $[(3 \times 1.74\ Å + 2.00\ Å)/4 = 1.83\ Å]$ is in good agreement with the observed value.

9. Covalent Al–N, Al–O and B–N Bond Distances

The two Al–N bond distances in **8** differ by 0.19 Å.[117] The longest bond, from Al to the four-coordinate N atom, has the same length as the Al–N bond in $Me_3N \rightarrow AlCl_3$ and



8

must be described as a dative bond. About the shorter bond, from Al to the three-coordinate N atom, the authors write: "It has previously been suggested that aluminum-nitrogen bonds that fall at about 1.78 Å are in effect double bonds, with dative nitrogen lone pair to aluminum 3d π-donation,...". We note that the Al–N bond distance calculated from the modified Schomaker-Stevenson (MSS) rule [Eq. (c)][118] is 1.77 Å, and suggest that the shorter Al–N bond should be described as a single covalent bond.

$$R(A-B) = r_A + r_B - 0.085|\chi_A - \chi_B|^{1.4} \qquad (c)$$

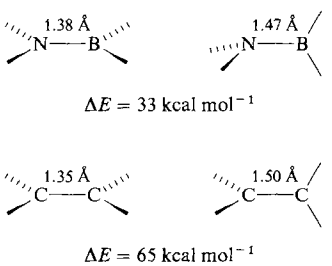
The trisamide $Al[N(SiMe_3)_2]_3$ is monomeric with trigonal planar configuration at Al and $R_{Al-N} = 1.78(2)$ Å.[119] In this species, where Al is tricoordinate, the Al–N bonds may be shortened by dative π-bonding. Comparison with the bond distance quoted above indicates that the effect is modest.

Aluminum trisisopropoxide $Al(OiPr)_3$ is tetrameric in the solid phase.[120] The central Al atom is connected to three terminal Al atoms through double alkoxide bridges. Each terminal Al atom is surrounded by two bridging and two terminal isopropoxide groups. The terminal Al–O distances (1.71 Å) are in good agreement with the covalent bond distance calculated according to the MSS rule[118] (1.72 Å). This covalent bond distance is 0.30 Å shorter than the dative $O \rightarrow Al$ bond distance in $Me_2O \rightarrow AlMe_3$ (2.01(2) Å).

The structure of the monomeric aminoborane, H_2NBH_2, generated by pyrolysis of diborane and ammonia at 500 °C, has been determined by MW spectroscopy.[121] The molecule has a planar ethene-like structure with a N–B bond distance of 1.391(2) Å. This bond may be described as having partial double bond character; a covalent σ-bond plus a dative π-bond. What is the effect of the π-bonding on the bond distance? The author of a recent review[122] surveyed the (dative) bond distances in amine–boranes and adopted N–B = 1.58 Å as reference value for a single (covalent) bond distance. This value would indicate that dative π-bonding in H_2NBH_2 shortens the BN distance by 0.19 Å, which is similar to the difference between single and double CC bond distances.

If the *dative* bond distance in an amine–borane is to serve as expectation value for a single *covalent* bond distance in H_2NBH_2, the logical choice would be the bond distance in H_3NBH_3, B–N = 1.66 Å.[11] Adoption of this value indicates that dative π-bonding in H_2NBH_2 shortens the BN bond by 0.27 Å, which is considerably more than the difference between single and double CC bond distances.

The bonding in H_2NBH_2 has been studied by *ab initio* molecular orbital calculations with a double zeta (DZ) basis (Scheme 4).[123] Complete structure optimization yielded an



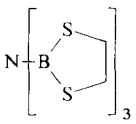
Scheme 4. Calculated structural parameters for planar and orthogonal H_2NBH_2 and C_2H_4.

equilibrium B–N bond distance of 1.378 Å, in good agreement with the experimental value. When the π-bond is broken by twisting the BH_2 fragment through 90° into an orthogonal form, the B–N bond distance increases to 1.469 Å and the configuration at N becomes pyramidal.

The energy of this relaxed orthogonal form is 33.3 kcal mol^{-1} above the energy of the planar equilibrium structure. This energy difference appears reasonable when compared to the barrier to internal rotation in $Me_2NBMePh$ obtained by line shape analysis of ^1H NMR spectra, 26.3 kcal mol^{-1}.[124]

MCSCF calculations on the planar and orthogonal forms of ethene[125] (Scheme 4) yield a π-bond energy of 65 kcal mol^{-1}, in good agreement with experimental estimates. It appears that the dative π-bond energy in H_2NBH_2 is about half the covalent π-bond energy in ethene. The C–C distance in the orthogonal form of ethene is that expected for a single bond between two sp^2 hybridized carbon atoms.

In the trisborylamine **9** one B_2N–BS_2 fragment adopts an orthogonal conformation, presumably for steric rea-



9

sons.[126] The corresponding B–N bond distance is 1.47 Å, in agreement with the theoretical value. In the following we shall adopt this as a standard value for a single covalent B–N bond distance. If this value is accepted, it follows that π-bonding shortens the B–N bond in H_2NBH_2 by about 0.07 Å, a third of the difference between single and double CC bond distances.

Coordination of an increasing number of π-donors (amido groups) to the same π-acceptor (B), would be expected to lead to saturation effects. Indeed, the BN bond distance in $B(NHMe)_3$ is 1.432(2) Å.[127, 128]

Hexagonal boron nitride (α-BN) has a graphite-like structure consisting of parallel, planar BN sheets.[129] Each B and N are trigonal planar, the B–N bond distance is 1.446 Å, and the perpendicular distance between the layers is 3.30 Å as compared to 3.35 Å in graphite. The B–N bond distance is slightly, but significantly, longer than in $B(NHMe)_3$, perhaps because each N atom is coordinated to three π-acceptors rather than one.

According to *Gmelins Handbook of Inorganic Chemistry*:[129] "Die Natur der B–N-Bindung ist umstritten. Einerseits ähnelt die BN-Struktur weitgehend der Graphitstruktur, die Bindungslängen C–C und B–N sind nur wenig voneinander verschieden, und die zwischenatomaren Kräfte beider Substanzen liegen in der gleichen Größenordnung." "Die BN-Bindungslänge in der Schichtebene beträgt 1.446 Å und ist damit sehr viel kürzer als die Summe der kovalenten Radien bei Einfachbindung (1.57 Å)". "Es liegt also nahe, für BN eine Resonanzstruktur wie in Graphit anzunehmen. Andererseits weichen gewisse Eigenschaften des BN stark von denen des Graphits ab. So hat BN eine geringe elektrische Leitfähigkeit, ist farblos, und seine diamagnetische Suszeptibilität ist gering, während die des Graphits abnorm groß ist. Diese Eigenschaften des BN lassen sich durch das Vorhandensein von Einfachbindungen erklären."[*]

We note that the B–N bond distance in α-BN is in fact close to our estimate of a covalent single bond distance, 1.45 Å vs 1.47 Å; the contradiction has been removed.

A rough estimate of the strength of a single covalent B–N bond may be obtained by calculating the energy of atomization of hexagonal boron nitride (at 25 °C) [Eq. (d)][130]

$$\Delta E^0_{at}(BN,hex) = \Delta H^0_f(B,g) + \Delta H^0_f(N,g) - \Delta H^0_f(BN,hex) - 2\,RT = 307.3 \text{ kcal mol}^{-1}, \quad (d)$$

and assuming the energy of atomization to be equal to the energy required to break three σ- and one π-bond [Eq. (e)].

$$\Delta E^0_{at}(BN,hex) = 3\,E(B\text{–}N) + E_\pi(B\text{–}N) \quad (e)$$

$E_\pi(B\text{–}N) = 33$ kcal mol^{-1} yields the mean B–N single bond energy of $E(B\text{–}N) = 91$ kcal mol^{-1}. An independent, though equally rough estimate based on the energy of atomization of cubic boron nitride (β-BN) yields $E(B\text{–}N) = 92$ kcal mol^{-1}.[**]

Both these values are overestimates; "delocalization energies" or "resonance energies" have been disregarded. We believe $E(B\text{–}N) = 88 \pm 2$ kcal mol^{-1} to be a more realistic estimate. In any case there is little doubt that covalent B–N bonds are as strong as or stronger than covalent C–C bonds: the mean C–C bond energy derived from the energy of atomization of diamond is 85 kcal mol^{-1}. The characteristics of covalent and dative B–N bonds are listed in Table 6.

Table 6. Comparison of covalent and dative B–N bonds.

	Covalent [a]	Dative [b]
E [kcal mol^{-1}]	88 ± 2	31
R [Å]	1.47 ± 1	1.66

[a] Derived from comparison data. [b] Determined on $H_3N \rightarrow BH_3$.

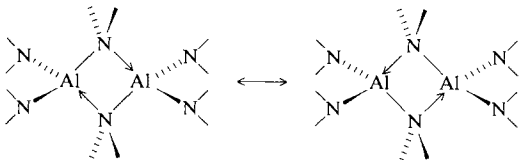
10. Some Polynuclear AlN Compounds

The trisamide $Al(NMe_2)_3$ is dimeric in the solid phase.[132] Each Al atom is surrounded by two bridging and two terminal NMe_2 groups. The terminal Al–N bonds have a length of 1.81 Å and may be described as single covalent bonds. The bridging Al–N bonds are 1.97 Å in length and

[*] "The nature of the B–N bond is controversial. On the one hand the BN and graphite structures are very similar, the difference between the C–C and B–N bond distances is very small, and the interatomic forces in the two substances are of the same order of magnitude". "The B–N bond distance in the sheets is 1.446 Å and thus much shorter than the sum of the covalent radii 1.57 Å". "It is therefore reasonable to assume a resonating (single and double bond) structure as in graphite. On the other hand, some properties of BN differ sharply from those of graphite. Thus, BN has a low electric conductivity, is colorless, and its diamagnetic susceptibility is small while that of graphite is abnormally large. These properties are in agreement with a single bond model".

[**] Cubic BN has a diamond-like structure, each B atom is bonded to four N atoms at a bond distance of 1.56 Å. The enthalpy of the transformation from hexagonal to cubic BN is 0.84 kcal mol^{-1} [131], and the energy of atomization is ΔE^0_{at} (BN, cub) = ΔE^0_{at}(BN, hex) − 0.8 kcal mol^{-1} = 306.5 kcal mol^{-1}. By assuming that the energy of atomization is equal to the energy required to break three single covalent bonds and one dative bond, $\Delta E^0_{at} = 3\,E(B\text{–}N) + E(N \rightarrow B)$, and that $E(N \rightarrow B) = \Delta H^0_{dis}$ $(H_3N \rightarrow BH_3) = 31.1$ kcal mol^{-1}, we obtain $E(B\text{–}N) = 92$ kcal mol^{-1}.

may be described as having equal covalent and dative bonding contributions:



Scheme 5. Canonical structures of $[Al(NMe_2)_3]_2$.

The results of molecular orbital bond index calculations on $[Al(NH_2)_3]_2$ and similar compounds have just been published.[133] The authors note that the bond index of the Al–N terminal bond ist nearly twice the bond index of the bridging Al–N bond and conclude: "This indicates a greater strength for the terminal bonds [...] than previously estimated, the difference arising because the capacity of terminal ligands with lone pair electrons to indulge in dative π-bonding has been underestimated in earlier work". As will be clear from the preceding discussion, we prefer to regard the terminal bonds as single covalent bonds, and the bridging bonds as less than that, viz. as half covalent and half dative. Using the terminal Al–N distance as a reference value for a covalent Al–N bond and the mean of the N→Al bond distances in Me_3NAlH_3 and Me_3NAlMe_3 (2.08 Å) as a reference value for a dative bond distance, we calculate a mean value of 1.95 Å, in reasonable agreement with the observed value of 1.97 Å. A description of each of the four bonds as half covalent and half dative is consistent with the expected fragmentation behavior: two Al–N bonds are expected to break heterolytically to yield the monomeric amides, the next two to break homolytically to yield $(Me_2N)_2Al^{\bullet}$ and $^{\bullet}NMe_2$.

In the following we shall briefly discuss the bond distances in some polynuclear AlN compounds (see Fig. 7). In order to minimize inductive effects we confine ourselves to species with hydrogen and alkyl substituents.

The Al–N bonds in $(H_2AlNMe_2)_3$[132] and $(Me_2AlNMe_2)_2$[134] may also be described as half covalent and half dative. The calculated mean (1.95 Å) is in good agreement with the observed values.

The Al–N bond distance in the cage compounds (HAlN*i*Pr)$_4$[135] and (HAlN*n*Pr)$_6$[136] may be described in terms of 2:1 covalent and dative bonding contributions. From the reference values we calculate a bond distance of 1.90 Å, again in good agreement with the observed values.

Finally, one may describe the bonds in crystalline AlN[137] as 3:1 resonances between covalent and dative bonds. The corresponding calculated bond distance is 1.88 Å. Again, a linear, two-parameter model has been able to reproduce the Al–N bond distances in Figure 7 with a deviation of 0.02 Å or less.

This model is not equally successful in all cases. Thus, the Al–N bridge bonds in $(Cl_2AlNMe_2)_2$ are 1.91 Å,[138] 0.04 Å shorter than calculated from the reference bond distances. The deviation may be interpreted as an inductive effect of the electron withdrawing Cl atoms. But adoption of the Al–N and N→Al distances in **8** as reference values does not lead to improvement, the calculated mean is 1.87 Å, 0.04 Å less than the observed value.

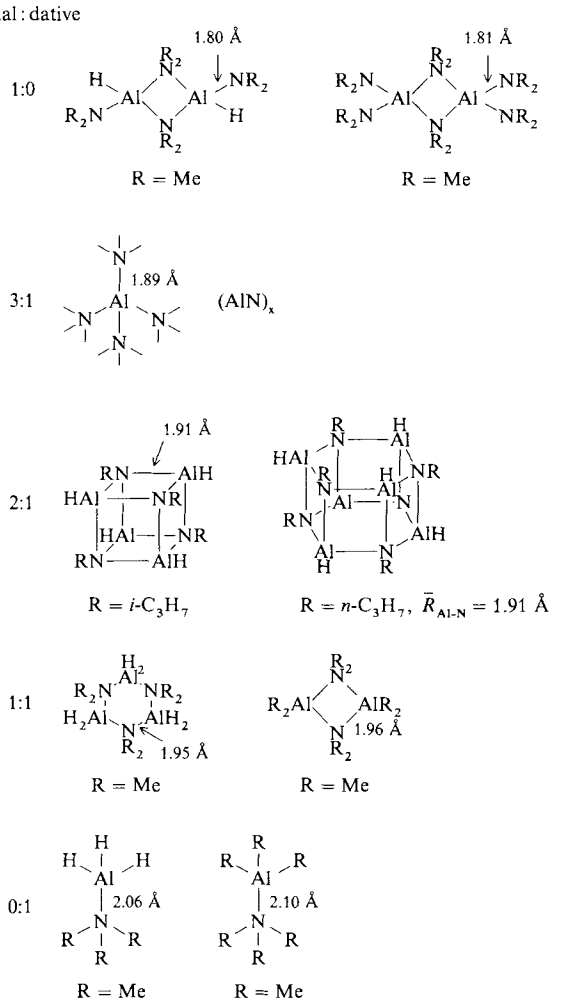


Fig. 7. The structure of some polynuclear AlN compounds and the ratio of normal to dative contributions to the Al–N bonds.

But even in those cases where the model fails in a quantitative way, it remains true that bond distances generally increase with increasing dative bonding contributions. The molecular structures of **10**–**14** have all been determined by

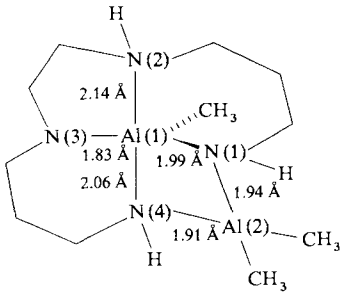
$(Me_2Al)_3(\mu\text{-}PMe_2)_3$ **10**[139] $(Me_2Al)_3(\mu\text{-}OMe)_3$ **11**[140]
$(Me_2Al)_2(\mu\text{-}SMe)_2$ **12**[141] $(Me_2Al)_4(\mu\text{-}F)_4$ **13**[142]
and $(Me_2Al)_2(\mu\text{-}Cl)_2$ **14**[143]

gas electron diffraction. In all these compounds we describe the endocyclic bonds as half dative and half covalent. The Al–P bond in **10** (2.43 Å) is 0.10 Å shorter than in adducts between $AlMe_3$ and phosphanes,[18, 144] and 0.06 Å longer than the bond distance in solid aluminum phosphide, which we would regard as 3/4 covalent and 1/4 dative; we are not aware of any molecule containing what might be described as a single covalent Al–P bond, but expect it to be about 2.32 Å.

The Al–O bond distance in **11** (1.85 Å) is close to the mean of the terminal covalent Al–O distance in tetrameric aluminum trisisopropoxide (1.72 Å)[120] and the dative O→Al distance in $Me_2O \rightarrow AlMe_3$ (2.01(2) Å). The Al–S bond distance in **12** (2.37 Å) is about 0.18 Å shorter than the dative S→Al distance in $Me_2S \rightarrow AlMe_3$,[84] while the Al–F distance in **13** (1.81 Å) is 0.18 Å greater than the normal Al–F distance in gaseous monomeric AlF_3.[145] Finally, the Al–Cl

bond distance in **14** (2.30 Å) is 0.24 Å longer than the normal bond distance in gaseous, monomeric $AlCl_3$.[46]

Before going on to other metals we pause to take note of the dinuclear complex **15**, containing a five-coordinate Al atom,[146] and the cationic complex **16**[147] prepared with $[AlCl_4]^{\ominus}$ as counterion.

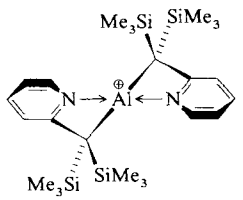


15

The five-coordinate Al(1) atom in **15** is trigonal bipyramidal, the four Al(1)–N bond distances range from 1.83 to 2.14 Å. The Al–C and Al(1)–N(3) bonds (1.83 Å) are clearly covalent, the Al(1)–N(2) bond (2.14 Å) clearly dative. As expected the covalently bonded C and N(3) occupy equatorial positions, the datively bonded N(2) an axial position.

Al(1) is bonded to the four-coordinate atom Al(2) through two amido nitrogen atoms, N(1) and N(4). We have seen that when two four-coordinate Al atoms are connected through two amido bridges as in $(Me_2AlNMe_2)_2$, covalent and dative bonding contributions are delocalized to yield four equal Al–N bonds at about 1.95 Å. In **15** the bond distances in the four-membered Al_2N_2 ring range from 1.91 to 2.06 Å.

There are probably several reasons for this variation. Firstly, as we have seen, bond distances to the acceptor atom are expected to increase with increasing coordination number, the mean of the bond distances from N((1) and N(4) to the five-coordinate Al is about 0.10 Å greater than the mean of the bond distances to the four-coordinate Al. Secondly, in compounds of the main group elements with trigonal bipyramidal coordination the bonds to axial ligands tend to be a few hundreths of an Å unit longer than those to equatorial ligands. Finally, we interpret the small but significant difference between the bond distances to the four-coordinate Al(2) (1.935(2) Å and 1.911(3) Å) as an indication that covalent and dative bonding contributions are not completely delocalized over the Al_2N_2 ring: the shortest bond, Al(2)–N(4), and consequently also the Al(1)–N(1) bond appear to be slightly more than half covalent, the longer bonds Al(2)–N(1) and Al(1)–N(4) appear to be slightly more than half dative. We further suggest that the reason for the incomplete delocalization is that it would require energy to increase the covalent contribution to the axial Al(1)–N(4) bond at the expense of the equatorial Al(1)–N(1) bond.



16

Al–C 1.96(2) Å
∢ CAlC 152°
Al–N 1.92(2) Å
∢ NAlN 115°

The mean Al–C distance in the cationic complex **16** is not significantly different from the Al–C bond distances in free $AlMe_3$ or Me_3NAlMe_3, but the dative N→Al distances, 1.92(2) Å, are 0.18 Å shorter than in the latter adduct. It should be noted, however, that even this very short N→Al bond distance is about 0.11 Å greater than the reference value for a covalent Al–N bond that we adopted above.

11. Three-coordinate Lithium Amides

The structure of the adduct of tetramethylethylenediamine and a monomeric Li-amide is shown in Figure 8.[148]

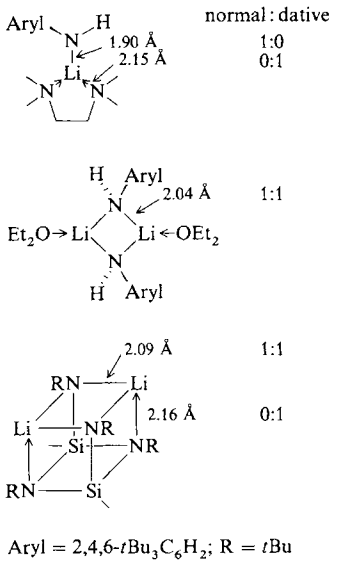


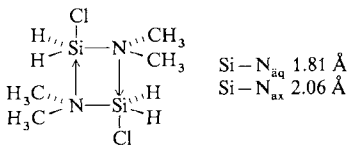
Fig. 8. Bond distances in some three-coordinate lithium amides and the ratio of normal to dative contributions to the Li–N bonds.

Here again we are able to compare dative and normal bond distances between the same atom pair in the same molecular species: Li–N = 1.90 Å and N → Li = 2.15 Å.

In $[Et_2OLi(\mu\text{-}NHAryl)_2]_2$ (Fig. 8, center) the Li atom is datively bonded to the O atom, while each of the four endocyclic bonds must be regarded as half dative and half normal.[149] The observed Li–N distance is in good agreement with the mean of the pure normal and dative bond distances in the adduct above shown at the top of Figure 8, 2.03 Å. Finally, we turn our attention to the cubic complex at the bottom of Figure 8.[150] The Si atoms are seen to be four-coordinate, and all Si—N distances are of the magnitude expected for covalent bonds. Since the Si–N bonds in the basal plane and the terminal N–C bonds are covalent, it follows that the perpendicular N–Li bonds are dative as indicated. If N is assumed to be capable of forming three covalent and one dative bond, and Li to be capable of forming one normal and two (or more) dative bonds, it follows that since the Li–N bonds in the upper face are all similar, each must be half normal and half dative. The observed mean value, 2.09 Å, is in moderate agreement with the estimated value of 2.03 Å.

12. Two Associated Si Amides

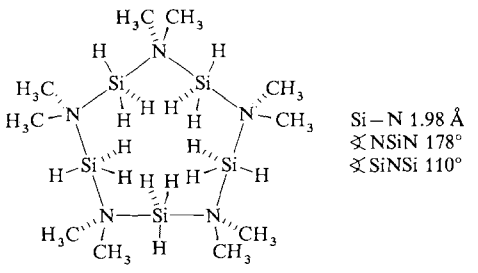
Me_2NSiH_2Cl is monomeric in the gas phase, but dimeric in the solid.[151] The monomeric units in the dimer **17** are held together by two dative N → Si bonds. The coordination around the two Si atoms is trigonal bipyramidal with the datively bonded N atom and the Cl atom in apical positions. The Si–N and N → Si bond distances are comparable to those in the mononuclear adducts **4** and **5** discussed in Section 7.



17

We have seen that when two NR_2 groups bridge two four-coordinate Al or two three-coordinate Li atoms, covalent and dative bonding is delocalized to give four equal bond distances. We suggest that this does not take place in the present compound because it requires energy to increase the covalent bonding contribution to the axial Si–N bond at the expense of the equatorial bond.

Replacement of the Cl atom by a hydrogen atom leads to a radical change of the solid state structure: Me_2NSiH_3 is pentameric in the solid phase as indicated in **18**.[152]



18

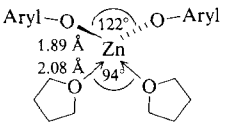
The covalently bonded N atom has moved into the apical position formerly occupied by the Cl atom: formation of dimers is prevented by the N-Si-N angle of 180°, the degree of association is now determined by the valence angle at N.

The Si–N bond distances in the ten-membered ring of **18** are indistinguishable. Each of them may be described in terms of equal covalent and dative bonding contributions, though the observed bond distance is somewhat larger than the average of the localized Si–N and N → Si distances in **17** (1.93 Å). We suggest that delocalization is stabilizing in the case of **18** because both N atoms occupy apical positions.

13. Some Zinc-Oxygen Compounds

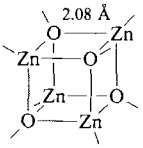
The Zn atom in the complex **19** formed from $Zn(OAryl)_2$ and two moles of tetrahydrofuran is covalently bonded to two O atoms and datively bonded to two others.[153] The difference between the two bond distances is 0.19 Å.

Solid ZnO has a wurzite structure, each Zn atom is surrounded by four O atoms at an average distance of 1.98 Å.[154] The bonding may be described in terms of equal covalent and dative bonding contributions; the mean of the Zn–O and O → Zn bond distances in **19** is 1.99 Å, in good agreement with the observed value.



19, Aryl = 2,4,6-tBu$_3$C$_6$H$_2$

Tetrameric MeZnOMe has the cubane structure **20**.[155] The external Zn–C bond distance corresponds to a covalent



20

bond. If it is assumed that Zn is capable of forming one more covalent bond and two (or more) dative bonds, it follows that each Zn–O bond in the cube is 1/3 covalent and 2/3 dative. The observed bond distance in **20** is indeed longer than the 1:1 bond in solid ZnO and shorter than the pure dative bond in **19**, but it is significantly longer than the appropriate mean of the bond distances in **19** (2.02 Å), perhaps as an effect of the presence of an electron-releasing methyl group.

14. "Tetrahedral Covalent Radii"

Working with the evidence available at the time when *The Nature of the Chemical Bond*[1] was written, *Pauling* clearly found no reason to distinguish between covalent and dative bonds. He described bonding in solid ZnO, AlN or cubic BN as "covalent bonds with some ionic character". N and O atoms were assigned tetrahedral covalent radii equal to the normal covalent radii determined from the observed bond distances in amines, ethers and related compounds. The "tetrahedral covalent radii" of Zn and the other Group 12 metals were then adjusted to reproduce the observed interatomic distances in oxides and other binary compounds with Group 16 elements. Similarly, the radii of Al and the other Group 13 elements were adjusted to reproduce the observed interatomic distance in nitrides and other binary compounds with group 15 elements.

The observed interatomic distances that we have adopted as reference values for pure, single covalent bonds to four-coordinate metal atoms are consistently shorter than the estimates obtained by adding the "tetrahedral covalent radii" for the two atoms: for Al–N 1.81 Å versus 1.91 Å, for Al–O 1.71 Å versus 1.92 Å, and for Zn–O 1.89 Å versus 1.97 Å. For B–N we have adopted 1.47 Å as a reference value for a single covalent bond to trigonal B; the sum of the "tetrahedral covalent radii" is 1.58 Å.

The reason for the discrepancy is clear. In our terminology the bonds in solid ZnO, AlN or cubic BN are not pure covalent bonds, but bonds of intermediate type with significant dative bonding contributions. The "tetrahedral covalent radii" are therefore incapable of reproducing either of the bond distances in species like **16**, which contain what according to our terminology are *pure* covalent and dative bonds.

We have quoted a few instances where this discrepancy has led investigators to the conclusion that the covalent bonds are shortened by additional π-bonding; there are more instances in the literature.

If the distinction between covalent and dative bonds is made, there arises the need for a new set of covalent radii based on observed pure, single covalent bond distances. In view of the great sensitivity of dative bond distances to inductive effects, it would hardly be profitable to attempt to establish a set of dative bond radii.

15. Conclusion

In this review we have defined a chemical bond as *normal* if minimum-energy rupture proceeds homolytically and as *dative* if minimum-energy rupture proceeds heterolytically. The term normal covers covalent and ionic bonds as well as bonds of intermediate polarity. We have compared the physicochemical properties of chemical bonds between the same atom pair DM where D is a donor element in groups 15, 16 or 17 and M is a main group metal: bonds to transition metals have not been considered. We find that:

1. The strength of a dative, or donor–acceptor, bond is very sensitive to inductive effects, particularly at the acceptor atom. Thus, while $SnMe_4$ does not appear to interact with electron donors such as amines or pyridine, the N → Sn bond rupture enthalpy of pyr → $SnMe_3Cl$ is 11 kcal mol^{-1} and of $Me_3N \rightarrow Sn^{\oplus}Me_3$ 46 kcal mol^{-1}. The variation in bond strength is clearly reflected in bond distances. Thus, while the N → Si bond distances in neutral (five-coordinate) Si^{IV} adducts range from 2.70 to 1.95 Å with increasing electronegativity of the substituents, the N → Si bond distance in pyr → $Si^{\oplus}Me_3$ is 1.86 Å.

2. The available evidence for metals in groups 12, 13 and 14 suggests that the strength of a dative bond rarely exceeds half the strength of an isoelectronic normal bond or a normal bond between the same atom pair.

Again the difference is reflected in bond distances: covalent Si–N distances to four- or five-coordinate Si^{IV} range from 1.70 to 1.80 Å, dative N → Si distances range from 1.95 to 2.70 Å. Normal and dative AlN bond distances in the same molecular unit **8** are 1.77 and 1.96 Å, respectively. Normal and dative LiN bond distances in the adduct at the top of Figure 8 are 1.90 and 2.15 Å, respectively, and the ZnO bond distances in **19** are 1.89 and 2.08 Å.

3. The coordination geometry of the acceptor atom may be predicted from the VSEPR model with the additional postulate that the spatial requirements of a (partially) "accepted" bond pair are less than the spacial requirements of a normal bond pair (NBP > ABP). This means that in five-coordinate trigonal pyramidal adducts the electron donors will occupy the axial positions.

The VSEPR model leads to the prediction that bonds to the acceptor atom will be elongated and the angles between them reduced on coordination of (another) electron donor. Both effects will be reinforced by steric repulsion between donor molecule and acceptor atom substituents.

4. In some molecular species bond distances are found to be equal, though no reasonable Lewis structure in which all are covalent or all dative can be found. Bonding in such species is conveniently described in terms of canonical forms containing localized covalent and dative bonds. Delocalization of bonding (resonance) yields bonds that are intermediate between pure covalent and dative bonds. The covalent or dative contributions to a particular bond in the real molecule may be determined by counting the number of canonical forms in which it is covalent or dative. The lengths of such bonds are generally found to be intermediate between the lengths of a pure covalent and a pure dative bond and to increase with increasing dative bonding contributions. In favorable cases bond distances may be predicted to within two or three hundreths of an Å unit by calculating the appropriate mean of reference values for pure normal and pure dative bond distances.

This approach is particularly useful for describing bonding in symmetric $M_2(\mu^2\text{-}NR_2)$, $M_2(\mu^2\text{-}OR)$ or $M_2(\mu^2\text{-}X)$ fragments; each M–N/O/X bond is half normal and half dative. Similarly, each M–N bond in a symmetric $M_3(\mu\text{-}NR)$ fragment is 2/3 normal and 1/3 dative, and each M–O/X bond in symmetric $M_3(\mu^3\text{-}OR)$ or $M_3(\mu^3\text{-}X)$ fragments are 1/3 normal and 2/3 dative.

We are grateful to the Norwegian Research Council for Science and the Humanities (NAVF) for financial support. We thank. Anne-Lise Ågren for typing – and retyping – the manuscript, and Snefrid Gundersen for preparing the figures. Finally I am grateful to Professors M. F. Lappert, P. Paetzold and P. von R. Schleyer and two anonymous referees for constructive criticism and helpful comments.

Received: January 26, 1989;
revised: February 20, 1989 [A 729 IE]
German version: *Angew. Chem. 101* (1989) 1017.

[1] L. Pauling: *The Nature of the Chemical Bond*, 3rd edit., Cornell University Press, Ithaca, NY, USA 1960.
[2] E. N. Guryanova, I. P. Goldstein, I. P. Romm: *The Donor-Acceptor Bond*, Wiley, New York 1975.
[3] R. G. Pearson (Ed.): *Hard and Soft Acids and Bases*, Dowden, Hutchinson and Ross, Stroudsburg, PA, USA 1973.
[4] V. Gutmann: *The Donor-Acceptor Approach to Molecular Interactions*, Plenum, New York 1978.
[5] Y. Marcus: *Ion Solvation*, Wiley, New York 1985.
[6] J. F. Sawyer, R. J. Gillespie: *The Stereochemistry of Sb^{III} Halides and Some Related Compounds* (*Prog. Inorg. Chem. 34* (1986)).
[7] P. Schuster, G. Zumbel, C. Sandorfy (Eds.): *The Hydrogen Bond, Vol. II, Structure and Spectroscopy*, North-Holland, Amsterdam 1976.
[8] R. C. Weast (Ed.): *CRC Handbook of Chemistry and Physics*, 67th edit., CRC Press, Boca Raton, FL, USA 1987.
[9] J. S. Binkley, L. R. Thorne, *J. Chem. Phys. 79* (1983) 2932.
[10] K. Kuchitsu, *J. Chem. Phys. 49* (1968) 4456.
[11] L. R. Thorne, R. D. Suenram, F. J. Lovas, *J. Chem. Phys. 78* (1983) 167.
[12] H. Umeyama, K. Morokuma, *J. Am. Chem. Soc. 98* (1976) 7208.
[13] J. Beres, A. Dodds, A. Morabito, R. M. Adams, *Inorg. Chem. 20* (1971) 2072.
[14] E. Mayer, *Inorg. Chem. 11* (1972) 866.
[15] G. Pilcher, H. A. Skinner in F. R. Hartley, S. Patai (Eds.): *The Chemistry of the Metal-Carbon Bond*, Wiley, New York 1982, p. 67.

[16] B. Beagley, J. J. Monaghan, T. G. Hewitt, *J. Mol. Struct. 8* (1971) 401.
[17] C. H. Henrickson, D. Duffy, D. P. Eyman, *Inorg. Chem. 7* (1968) 1047. The quoted ΔH^0_{dis} for Me_3PAlMe_3 has been obtained in hexane solution. In the gas phase ΔH^0_{dis} may be 1 or 2 kcal mol^{-1} higher.
[18] A. Almenningen, L. Fernholt, A. Haaland, J. Weidlein, *J. Organomet. Chem. 145* (1978) 109.
[19] R. E. McCoy, S. H. Bauer, *J. Am. Chem. Soc. 78* (1956) 2061.
[20] A. B. Burg, Y.-C. Fu, *J. Am. Chem. Soc. 88* (1966) 1147.
[21] H. C. Brown, H. Bartholomay, Jr., M. D. Taylor, *J. Am. Chem. Soc. 66* (1944) 435. The authors give ΔH^0_{dis} to the nearest 0.01 kcal mol^{-1}, but no error limits.
[22] a) For BH_3: M. Gelus, W. Kutzelnigg, *Theor. Chim. Acta 28* (1973) 103; b) for BMe_3: H. Siebert, *Z. Anorg. Allg. Chem. 268* (1952) 13; W. J. Lehmann, C. O. Wilson, I. Shapiro, *J. Chem. Phys. 31* (1959) 1071.
[23] H. C. Brown, G. K. Barbaras, *J. Am. Chem. Soc. 69* (1947) 1137.
[24] N. N. Greenwood, P. G. Perkins, *J. Chem. Soc. 1960,* 1144.
[25] P. M. Kuznesof, R. L. Kuczkowski, *Inorg. Chem. 17* (1978) 2308.
[26] P. Cassoux, R. L. Kuczkowski, P. S. Bryan, R. C. Taylor, *Inorg. Chem. 14* (1975) 126.
[27] K. Iijima, N. Adachi, S. Shibata, *Bull. Chem. Soc. Jpn. 57* (1984) 3269.
[28] M. Hargittai, I. Hargittai, *J. Mol. Struct. 39* (1977) 79.
[29] K. Iijima, S. Shibata, *Bull. Chem. Soc. Jpn. 53* (1980) 1908.
[30] P. H. Clippard, J. C. Hanson, R. C. Taylor, *J. Cryst. Mol. Struct. 1* (1971) 363.
[31] H. Hess, *Acta Crystallogr. Sect. B 25* (1969) 2338.
[32] G. M. Phillips, J. S. Hunter, L. E. Sutton, *J. Chem. Soc. 1945,* 146.
[33] E. W. Hughes, *J. Am. Chem. Soc. 78* (1956) 502.
[34] A. C. Venkatachar, R. C. Taylor, R. L. Kuczkowski, *J. Mol. Struct. 38* (1977) 17.
[35] L. S. Bartell, B. L. Carrol, *J. Chem. Phys. 42* (1965) 3076.
[36] See [19].
[37] G. A. Andersen, F. R. Forgaard, A. Haaland, *Acta Chem. Scand. 26* (1972) 1947.
[38] D. F. Grant, R. C. G. Killean, J. L. Lawrence, *Acta Crystallogr. Sect. B 25* (1969) 377.
[39] A. Almenningen, G. Gundersen, T. Haugen, A. Haaland, *Acta Chem. Scand. 26* (1972) 3928.
[40] L. S. Bartell, L. O. Brockway, *J. Chem. Phys. 32* (1960) 512.
[41] A. Almenningen, S. Halvorsen, A. Haaland, *Acta Chem. Scand. 25* (1971) 1937.
[42] P. S. Bryan, R. L. Kuczkowski, *Inorg. Chem. 11* (1972) 553.
[43] K. Iijima, S. Shibata, *Bull. Chem. Soc. Jpn. 52* (1979) 3204.
[44] R. Blom, A. Haaland, R. Seip, *Acta Chem. Scand. Ser. A 37* (1983) 595.
[45] J. R. Durig, B. A. Hudgens, J. D. Odom, *Inorg. Chem. 13* (1974) 2306.
[46] V. P. Spiridonov, A. G. Gershikov, E. Z. Zasorin, N. I. Popenko, A. A. Ivanov, L. I. Ermolayeva, *High Temp. Sci. 14* (1981) 285.
[47] B. Beagley, T. G. Hewitt, *Trans. Faraday Soc. 64* (1968) 2561.
[48] A. Almenningen, A. Haaland, T. Haugen, D. P. Novak, *Acta Chem. Scand. 27* (1973) 1821.
[49] J. E. Wollrab, V. W. Laurie, *J. Chem. Phys. 51* (1969) 1580.
[50] W. C. McLean, G. A. Jeffrey, *J. Chem. Phys. 47* (1967) 414.
[51] W. G. Haije, J. A. L. Dobbelaar, W. J. A. Maaskant, *Acta Crystallogr. Sect. C 42* (1986) 1485.
[52] F. H. Allen, O. Kennard, D. G. Watson, L. Brammer, A. G. Orpen, R. Taylor, *J. Chem. Soc. Perkin Trans. 2 1987,* S1.
[53] A. Ahmed, W. Schwarz, J. Weidlein, H. Hess, *Z. Anorg. Allg. Chem. 434* (1977) 207.
[54] C. W. Heitsch, C. E. Nordman, R. W. Parry, *Inorg. Chem. 2* (1963) 508.
[55] V. S. Mastryukov, C. V. Golubinskii, L. V. Vilkov, *J. Struct. Chem. (Engl. Transl.) 20* (1979) 921.
[56] J. L. Atwood, C. D. Whitt, *J. Organomet. Chem. 32* (1971) 17.
[57] J. Toney, G. D. Stucky, *J. Organomet. Chem. 22* (1970) 241.
[58] A. Almenningen, A. Haaland, G. L. Morgan, *Acta Chem. Scand. 23* (1969) 2921.
[59] E. C. Ashby, L. Fernholt, A. Haaland, R. Seip, R. S. Smith, *Acta Chem. Scand. Ser. A 34* (1980) 213.
[60] H. Rau, K. H. Thiele, *Z. Anorg. Allg. Chem. 355* (1967) 253.
[61] A. Haaland, K. Hedberg, P. P. Power, *Inorg. Chem. 23* (1984) 1972.
[62] I. E. Gümrükcüoglü, J. Jeffrey, M. F. Lappert, J. B. Pedley, A. K. Rai, *J. Organomet. Chem. 341* (1988) 53.
[63] J. Dekker, J. Boersma, L. Fernholt, A. Haaland, A. L. Spek, *Organometallics 6* (1987) 1202.
[64] A. Almenningen, T. U. Helgaker, A. Haaland, S. Samdal, *Acta Chem. Scand. Ser. A 36* (1982) 159.
[65] W. L. Steffen, G. Palenik, *Acta Crystallogr. Sect B 32* (1976) 298.
[66] M. Hargittai, J. Tremmel, I. Hargittai, *Inorg. Chem. 25* (1986) 3163.
[67] M. M. Kadooka, E. Hilti, L. G. Warner, K. Seff, *Inorg. Chem. 15* (1976) 1186.
[68] E. C. Alyea, K. J. Fisher, T. Fjeldberg, *J. Mol. Struct. 130* (1985) 263.
[69] K. Kashiwabara, S. Konaka, M. Kimura, *Bull. Chem. Soc. Jpn. 46* (1973) 410.
[70] A. J. de Koning, J. Boersma, G. J. M. van der Kerk, *J. Organomet. Chem. 186* (1980) 159.
[71] A. L. Spek, *Cryst. Struct. Commun. 11* (1982) 1621.
[72] B. S. Ault, *Inorg. Chem. 20* (1981) 2817.
[73] T. J. Lorenz, B. S. Ault, *Inorg. Chem. 21* (1982) 1758.
[74] C. J. Marsden, *Inorg. Chem. 22* (1983) 3177.
[75] L. S. Khaikin, L. G. Andrutskaya, L. V. Vilkov, *IX Hung. Diffr. Conf. (Pécs) 1978,* Abstr. p. 23.
[76] G. Klebe, M. Nix, K. Hensen, *Chem. Ber. 117* (1984) 797.
[77] G. Klebe, K. Hensen, H. Fuess, *Chem. Ber. 116* (1983) 3125.
[78] G. Klebe, *J. Organomet. Chem. 293* (1985) 147.
[79] K. Hagen, K. Hedberg, *J. Chem. Phys. 59* (1973) 1549.
[80] B. Rempfer, H. Oberhammer, N. Auner, *J. Am. Chem. Soc. 108* (1986) 3893.
[81] B. Beagley, J. J. Monaghan, T. G. Hewitt, *J. Mol. Struct. 8* (1971) 401.
[82] A. Haaland, S. Samdal, O. Stokkeland, J. Weidlein, *J. Organomet. Chem. 134* (1977) 165.
[83] C. H. Henrickson, D. P. Eyman, *Inorg. Chem. 6* (1967) 1461.
[84] L. Fernholt, A. Haaland, M. Hargittai, R. Seip, J. Weidlein, *Acta Chem. Scand. Ser. A 35* (1981) 529.
[85] G. E. Coates, *J. Chem. Soc. 1951,* 2003.
[86] H. Schmidbaur, H. F. Klein, *Angew. Chem. 78* (1966) 750; *Angew. Chem. Int. Ed. Engl. 5* (1966) 726.
[87] M. B. Smith, *J. Organomet. Chem. 46* (1972) 31.
[88] S. H. Bauer, R. E. McCoy, *J. Phys. Chem. 60* (1956) 1529.
[89] K. Iijima, S. Shibata, *Bull. Chem. Soc. Jpn. 52* (1979) 711.
[90] H. C. Brown, R. M. Adams, *J. Am. Chem. Soc. 64* (1942) 2557.
[91] K. Iijima, T. Yamada, S. Shibata, *J. Mol. Struct. 77* (1981) 271.
[92] E. A. Fletcher, *Ph. D. Thesis,* Purdue University, Lafayette, IN, USA 1952; R. S. Drago, G. C. Vogel, T. E. Needham, *J. Am. Chem. Soc. 93* (1973) 6014.
[93] H. L. Morris, N. I. Kulevsky, M. Tamres, S. Searles, Jr., *Inorg. Chem. 5* (1966) 124.
[94] D. C. Mente, J. L. Mills, R. E. Mitchell, *Inorg. Chem. 14* (1975) 123.
[95] J. M. LoBue, J. K. Rice, T. A. Blake, S. E. Novick, *J. Chem. Phys. 85* (1986) 4261.
[96] K. C. Janda, L. S. Bernstein, J. M. Steed, S. E. Novick, W. Klemperer, *J. Am. Chem. Soc. 100* (1978) 8074.
[97] J. N. Spencer, S. W. Barton, B. M. Cader, C. D. Corsico, L. E. Harrison, M. E. Mankuta, C. H. Yoder, *Organometallics 4* (1985) 394.
[98] A. C. M. Wojtyniak, J. A. Stone, *Int. J. Mass Spectrom. Ion Processes 74* (1986) 59.
[99] J. A. Stone, W. J. Wytenburg, *Can. J. Chem. 65* (1987) 2146.
[100] J. A. Stone, D. E. Splinter, *Int. J. Mass Spectrom. Ion Processes 59* (1984) 169.
[101] A. K. Baev, I. L. Gaidyn, *J. Gen. Chem. USSR (Engl. Transl.) 46* (1976) 823.
[102] N. N. Greenwood, T. S. Srivastava, *J. Chem. Soc. A 1966,* 270.
[103] G. E. Coates, R. A. Whitcombe, *J. Chem. Soc. 1956,* 3351.
[104] J. B. Lambert, W. J. Schultz, Jr., J.-A. A. McConnel, W. Schilf, *J. Am. Chem. Soc. 110* (1988) 2201.
[105] J. B. Lambert, W. Schilf, *Organometallics 7* (1988) 1659.
[106] K. Hensen, T. Zengerly, P. Pickel, G. Klebe, *Angew. Chem. 95* (1983) 739; *Angew. Chem. Int. Ed. Engl. 22* (1983) 725; *Angew. Chem. Suppl. 1983,* 973.
[107] H. D. Hausen, H. J. Guder, W. Schwarz, *J. Organomet. Chem. 132* (1977) 37.
[108] B. Beagley, D. C. Schmidling, I. A. Steer, *J. Mol. Struct. 21* (1974) 437.
[109] L. M. Golubinskaya, A. V. Golubinskii, V. S. Mastryukov, L. V. Vilkov, V. I. Bregadze, *J. Organomet. Chem. 117* (1976) C4.
[110] Q. Shen, *Thesis,* Oregon State University, Corvallis, OR, USA 1973.
[111] H. J. Widler, W. Schwarz, H. D. Hausen, J. Weidlein, *Z. Anorg. Allg. Chem. 435* (1977) 179.
[112] H. D. Hausen, H. Binder, W. Schwarz, *Z. Naturforsch. B 33* (1978) 567.
[113] S. H. Lawrence, S. G. Shore, T. F. Koetzle, J. C. Huffman, C.-Y. Wei, R. Bau, *Inorg. Chem. 24* (1985) 3171.
[114] A. E. Reed and T. Clark (Erlangen-Nürnberg), private communication.
[115] S. Konaka, Y. Murata, K. Kuchitsu, Y. Morino, *Bull. Chem. Soc. Jpn. 39* (1966) 1134.
[116] O. Glemser, B. Krebs, J. Wegener, E. Kindler, *Angew. Chem. 81* (1969) 568; *Angew. Chem. Int. Ed. Engl. 8* (1969) 598.
[117] M. J. Zaworotko, J. L. Atwood, *Inorg. Chem. 19* (1980) 268.
[118] R. Blom, A. Haaland, *J. Mol. Struct. 128* (1985) 21.
[119] G. M. Sheldrick, W. S. Sheldrick, *J. Chem. Soc. A 1969,* 2279.
[120] N. Ya. Turova, V. A. Kozunov, *J. Inorg. Nucl. Chem. 41* (1979) 5.
[121] M. Sugie, H. Takeo, C. Matsumura, *J. Mol. Spectrosc. 123* (1987) 286.
[122] P. Paetzold, *Adv. Inorg. Chem. Radiochem. 31* (1987) 123.
[123] O. Gropen, H. M. Seip, *Chem. Phys. Lett. 25* (1974) 206.
[124] T. Totani, K. Tori, J. Murakami, H. Watanabe, *Org. Magn. Reson. 3* (1971) 627.
[125] M. W. Schmidt, P. N. Truong, M. S. Gordon, *J. Am. Chem. Soc. 109* (1987) 5217.
[126] H. Nöth, R. Staudigl, W. Storch, *Chem. Ber. 114* (1981) 3024.
[127] A. Almenningen, G. Gundersen, M. Mangerud, R. Seip, *Acta Chem. Scand. Ser. A 35* (1981) 341.
[128] G. Gundersen, *Acta Chem. Scand. Ser. A 35* (1981) 729.

[129] *Gmelin Handbuch der Anorganischen Chemie, Band 13, Borverbindungen, Teil 1*, Springer, Berlin 1974, p. 18ff.
[130] Standard enthalpies of formation ΔH_f^0 from *J. Phys. Chem. Ref. Data Suppl. 11* (1982).
[131] N. N. Sirota, N. A. Kofman, *Dokl. Akad. Nauk SSSR 249* (1979) 1346; *Chem. Abstr. 92* (1980) 102465x.
[132] K. Ouzounis, H. Riffel, H. Hess, U. Kohler, J. Weidlein, *Z. Anorg. Allg. Chem. 504* (1983) 67.
[133] S. J. Bryan, W. Clegg, R. Snaith, K. Wade, E. H. Wong, *J. Chem. Soc. Chem. Commun. 1987*, 1223.
[134] H. Hess, H. Hinderer, S. Steinhauser, *Z. Anorg. Allg. Chem. 377* (1970) 1.
[135] G. del Piero, M. Cesari, G. Dozzi, A. Mazzei, *J. Organomet. Chem. 129* (1977) 281.
[136] M. Cesari, G. Perego, G. del Piero, S. Cucinella, E. Cernia, *J. Organomet. Chem. 78* (1974) 203.
[137] G. A. Jeffrey, Q. S. Parry, R. L. Mozzi, *J. Chem. Phys. 25* (1956) 1024.
[138] A. Ahmed, W. Schwarz, H. Hess, *Acta Crystallogr. Sect. B33* (1977) 3574.
[139] A. Haaland, J. Hougen, H. V. Volden, G. Hanika, H. H. Karsch, *J. Organomet. Chem. 322* (1987) C24.
[140] D. A. Drew, A. Haaland, J. Weidlein, *Z. Anorg. Allg. Chem. 398* (1973) 241.
[141] A. Haaland, O. Stokkeland, J. Weidlein, *J. Organomet. Chem. 94* (1975) 353.
[142] G. Gundersen, T. Haugen, A. Haaland, *J. Organomet. Chem. 54* (1973) 77.
[143] K. Brendhaugen, A. Haaland, D. P. Novak, *Acta Chem. Scand. Ser. A 28* (1974) 45.
[144] D. C. Bradley, H. Chudzynska, M. M. Faktor, D. M. Frigo, M. B. Hursthouse, B. Hussain, L. M. Smith, *Polyhedron 7* (1988) 1289.
[145] A. N. Utkin, G. V. Girichev, N. I. Giricheva, S. V. Khaustov, *J. Struct. Chem. (Engl. Transl.) 27* (1986) 212.
[146] G. H. Robinson, S. A. Sangokoya, F. Moise, W. T. Pennington, *Organometallics 7* (1988) 1887.
[147] L. M. Engelhardt, U. Kynast, C. L. Raston, A. W. White, *Angew. Chem. 99* (1987) 702; *Angew. Chem. Int. Ed. Engl. 26* (1987) 681.
[148] T. Fjeldberg, P. B. Hitchcock, M. F. Lappert, A. J. Thorne, *J. Chem. Soc. Chem. Commun. 1984*, 822.
[149] B. Çetinkaya, P. B. Hitchcock, M. F. Lappert, M. C. Misra, A. J. Thorne, *J. Chem. Soc. Chem. Commun. 1984*, 148.
[150] M. Veith, F. Goffing, V. Huch, *Chem. Ber. 121* (1988) 943.
[151] D. G. Anderson, A. J. Blake, S. Cradock, E. A. V. Ebsworth, D. W. H. Rankin, H. E. Robertson, A. J. Welch, *J. Chem. Soc. Dalton Trans. 1987*, 3035.
[152] A. J. Blake, E. A. V. Ebsworth, A. J. Welch, *Acta Crystallogr. Sect. C40* (1984) 895; see also E. A. V. Ebsworth, *Acc. Chem. Res. 20* (1987) 295.
[153] R. L. Geerts, J. C. Huffman, K. G. Caulton, *Inorg. Chem. 25* (1986) 1803.
[154] S. C. Abrahams, J. L. Bernstein, *Acta Crystallogr. Sect. B25* (1969) 1233.
[155] H. M. M. Shearer, C. B. Spencer, *Acta Crystallogr. Sect. B36* (1980) 2046.

Communications may be submitted in English *or* in German. Further details regarding the submission of communications can be found in the "Notice to Authors" reproduced in the January issue of the journal. Copies thereof may be obtained from the editorial office upon request.

The First Heterodinuclear Complexes with Bis(cyclopentadienyl)methane Bridges**

By *Peter Härter,* Günther Boguth, Eberhardt Herdtweck,* and *Jürgen Riede*

Dinuclear complexes have become increasingly interesting because of the possibility that the properties of the two fragments might complement each other, thereby leading to novel reactions.[1] Recent attention has focused on complexes with $(C_5H_4)_2X$ bridges (X = $SiMe_2$ and $(CH_2)_n$, n = 0, 1, 2), for example, since they are particularly stable. However, little is known about the especially interesting heterodinuclear derivatives of this class of compounds owing to the lack of suitable synthetic routes. Only the multistep syntheses of heterodinuclear fulvalene complexes[2] and 1,2-bis(cyclopentadienyl)ethane-bridged complexes[3] have been described. No examples of heterodinuclear complexes of the bis(cyclopentadienyl)methane series have been presented so far. Here we report a simple route to this class of substances.

We have found that the reaction of dilithioferrocene with 6-dimethylaminofulvene to give bis(6-fulvenyl)ferrocene, described by *Mueller-Westerhoff* et al.,[4] can be extended to other complexes containing a lithiated cyclopentadienyl ring. Reaction of tricarbonyl(lithiocyclopentadienyl)manganese **1**[5] with 6-dimethylaminofulvene **2a** or 1-(dimethylaminoethylene)-1 *H*-indene **2b**[6] in THF solution affords, after hydrolysis and chromatographic workup, the new fulvenyl complexes **3a** and **3b**, respectively.

The spectroscopic data for these compounds are consistent with the structures shown. An X-ray structure determination of **3a** confirms this formulation: the bond lengths and angles are typical of $C_5H_5Mn(CO)_3$ derivatives[7] (Fig. 1). The fulvenyl moiety displays the clear alternation of double bonds characteristic of fulvenes. The distance C6–C7 (146.6 pm), as well as the dihedral angle of 16.4° between the two rings, indicates the absence of significant π interaction between the manganese moiety and the fulvenyl moiety.

Reaction of **3a** with "superhydride" ($Li[HB(C_2H_5)_3]$) in THF solution results in quantitative formation of the anionic complex **4**, which precipitates as a pale yellow powder upon addition of hexane to the reaction solution. Further treatment of **4** with freshly prepared tetracarbonyl(iodo)cobalt[8] at −78 °C affords, after warming the reaction mixture to room temperature and extraction with hexane, complex **5** as a reddish-brown oil in 63% yield.

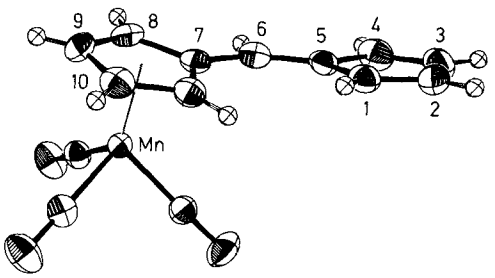
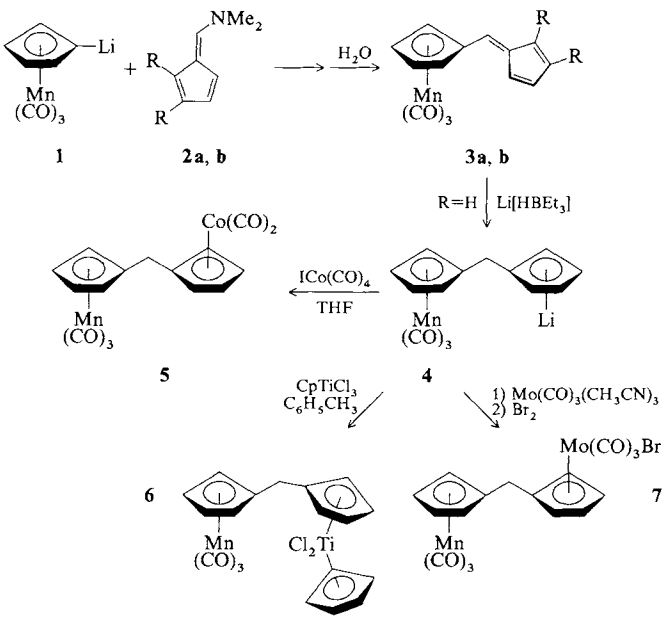


Fig. 1. Molecular structure of the 6-fulvenyl complex **3a** (ORTEP). The complex crystallizes from *n*-hexane in the orthorhombic space group *Pbca*. Selected distances [pm] and angles [°]: Mn–Cp 177.1 (center of the C_5H_4 ring), Mn–CO (average) 179.4(2), C1–C2 132.5(3), C1–C5 147.4(3), C2–C3 145.8(3), C3–C4 133.3(3), C4–C5 145.8(3), C5–C6 135.2(3), C6–C7 146.6(3), C7–C8 142.8(3), C8–C9 140.3(3), C9–C10 140.5(3); C5–C6–C7 128.4(2), dihedral angle Cp–Fulv 16.4. Further details of the crystal structure investigation may be obtained from the Fachinformationszentrum Karlsruhe, Gesellschaft für wissenschaftlich-technische Information mbH, D-7514 Eggenstein-Leopoldshafen 2 (FRG), on quoting the depository number CSD-53895, the names of the authors, and the journal citation.

The IR spectrum of **5** shows CO absorptions at 1944 (E, vs) and 2025 cm^{-1} (A, s), typical of $C_5H_5Mn(CO)_3$ derivatives. The CO vibrational bands of the cobalt moiety are found at 1970 and 2033 cm^{-1} (s). The ^1H NMR spectrum, displaying three groups of lines, corroborates the proposed structure. In a second reaction, **4** was treated with a molar equivalent of trichloro(η^5-cyclopentadienyl)titanium in toluene solution. Extraction of the reaction solution with CH_2Cl_2 afforded complex **6** as a peach-colored, microcrystalline powder. The IR spectrum displays the band pattern typical of $C_5H_5Mn(CO)_3$ derivatives. The proposed structure is supported by the ^1H NMR spectrum. Finally, reaction of complex **4** with tris(acetonitrile)tricarbonylmolybdenum, followed by oxidation with bromine, gives compound **7**.



a, R = H; **b**, R-R = CH=CH–CH=CH

[*] Dr. P. Härter, G. Boguth, Dr. E. Herdtweck, J. Riede
Anorganisch-chemisches Institut der Technischen Universität München
Lichtenbergstr. 4, D-8046 Garching (FRG)

[**] This work was supported by the Stiftung Volkswagenwerk and the Leonhardt-Lorenz-Stiftung.

The ready availability of **3a** opens up a route to other interesting manganese-containing dinuclear complexes. Furthermore, the synthetic strategy described here may be extended to other half-sandwich complexes, since numerous complexes of type **1** are now known.[9]

Experimental Procedure

3a: **1** (2.04 g, 10 mmol) was allowed to react with 4 mL of *n*BuLi (2.5 M *in* hexane) and 1.5 mL of TMEDA in a stirred solution of THF (30 mL) for 1 h at −78 °C. Compound **2a** (1.21 g, 10 mmol) was then added and the reaction mixture was allowed to warm to room temperature. After 5 h of additional stirring, 50 mL of water was added to the mixture. Extraction with diethyl ether and removal of the solvent left a residue, which was chromatographed on kieselgel 60 (activity 2–3) with hexane as eluent. The product (orange band) was obtained with hexane/ether (10:1) in 57% yield (1.50 g). IR (CH_2Cl_2 ν(CO) [cm^{-1}]): 1942 (E, vs), 2024 (A_1, s). ^1H NMR (270 MHz, $CDCl_3$): δ = 4.83, 5.18 (C_5H_4Mn); 6.2 (1H, m), 6.55 (1H, m), 6.60 (1H, m), 6.63 (2H, m). ^{13}C NMR (270 MHz, $CDCl_3$): δ = 83.15, 85.85, 95.73 (C_5H_4Mn), 119.07, 126.72, 130.01, 131.24, 135.52, 145.02 fulvenyl), 224 (CO).

Compound **3b** was obtained in a similar way in 42% yield (1.40 g). IR (CH_2Cl_2, ν(CO) [cm^{-1}]) 1941 (E, vs), 2024 (A_1, s), ^1H NMR (400 MHz, C_6D_6): δ = 7.28 (1H), 7.11 (2H), 7.10 (1H), 6.69 (1H), 6.54 (2H), 4.39 ("t", 2H), 3.93 ("t", 2H).

5: **3a** (280 g, 1 mmol) was treated with 1 mL of "superhydride", $Li[HB(C_2H_5)_3]$ (1 M in THF). The solution turned initially red. After the color had changed to yellow, 10 mL of *n*-hexane was added, the precipitate was filtered off, and the solid (**4**) was washed twice with *n*-hexane and then dissolved in 20 mL of THF. This solution was added to 10 mL of a THF solution of freshly prepared $Co(CO)_4I$ (330 mg, 1.1 mmol) at −78 °C. After the reaction mixture had warmed to room temperature, it was stirred for an additional 1 h. The solvent was then removed in vacuo and the residue extracted with *n*-hexane. Filtration and extraction of the *n*-hexane solution afforded **5** as a reddish-brown oil in 63% yield (250 mg). IR (ν(CO) [cm^{-1}]): 1944 (vs), 1970 (s), 2025 (s), 2033 (s), ^1H NMR (270 MHz, $CDCl_3$): δ = 2.51 (s, CH_2), 3.92, 3.84 (A_2B_2, C_5H_4Mn), 4.35, 4.30 (A_2B_2, C_5H_4Co).

6: $(C_5H_5)TiCl_3$ (220 mg, 1 mmol) was added to a solution of **4** in toluene (20 mL), prepared as described for the synthesis of **5**. The reaction solution was stirred for 2 h at room temperature and then evaporated to dryness. The residue was extracted with 3 × 10 mL of CH_2Cl_2 and the extracts filtered. The filtrate was concentrated until onset of crystallization and then cooled to − 34 °C. The microcrystalline, peach-colored product was collected on a frit and dried under vacuum for ca. 12 h. Yield 270 mg (69%). IR (CH_2Cl_2, ν(CO) [cm^{-1}]): 1933 (E, vs), 2020 (A_1, s). ^1H NMR (400 MHz, [D_6]acetone): δ = 3.71 (s, CH_2), 6.65 (s, Cp), 4.85, 4.97 ("t", C_5H_4Mn), 6.44, 6.72 ("t", C_5H_4Ti). ^{13}C NMR (400 MHz, [D_6]acetone): δ = 30.6, 83.2, 84.6, 105.6, 116.6, 121.0, 124.4, 123.8, 226.

7: $(CH_3CN)_3Mo(CO)_3$ (300 mg, 1 mmol) was added to a solution of **4** in THF (20 mL), prepared as described for the synthesis of **5**, and the reaction mixture was stirred for 2 h at room temperature. It was then cooled to 0 °C and a solution of bromine (50 µL) in 10 mL of THF was added dropwise. The red solution was stirred for 1 h at room temperature and the solvent removed in vacuo. The residue was transferred to silica and eluted with ether. Removal of the ether gave **7** as a microcrystalline red powder (235 mg, 60%). IR (CH_2Cl_2, ν(CO) [cm^{-1}]): 1936 (vs), 1966 (vs), 2022 (s), 2042 (s). ^1H NMR (400 MHz, C_6D_6): δ = 2.80 (s, CH_2); 4.61 ("t", C_5H_4Mo), 4.35 ("t", C_5H_4Mo), 3.95 ("t", C_5H_4Mn), 3.87 ("t", C_5H_4Mn), ^{13}C NMR (400 MHz, $CDCl_3$): δ = 28.02, 82.03, 83.44, 91.39, 95.05, 102.62, 115.95, 224.2, 227.0, 241.2.

Received: December 27, 1988;
supplemented: May 3, 1989 [Z 3106 IE]
German version: *Angew. Chem. 101* (1989) 1058

CAS Registry numbers:
1 (H instead of Li), 12079-65-1; **2a**, 696-68-4; **2b**, 2750-90-5; **3a**, 121575-50-6; **3b**, 121575-55-1; **4**, 121575-51-7; **5**, 121575-52-8; **6**, 121575-53-9; **7**, 121575-54-0; $CpTiCl_3$, 1270-98-0; $Mo(CO)_3(CH_3CN)_3$, 15038-48-9.

[1] a) T. E. Bitterwolf, *J. Organomet. Chem. 312* (1986) 197; b) H. E. Bryndzay, R. G. Bergman, *J. Am. Chem. Soc. 101* (1979) 4766; c) H. Werner, H. J. Scholz, R. Zolk, *Chem. Ber. 118* (1985) 4531; d) K. P. C. Vollhardt, T. W. Weidman, *J. Am. Chem. Soc. 105* (1983) 1676; e) *Organometallics 3* (1984) 82; f) J. S. Drage, K. P. C. Vollhardt, *ibid. 4* (1985) 191.

[2] M. A. Huffman, D. A. Newman, M. Tilset, W. B. Tolman, K. P. C. Vollhardt, *Organometallics 5* (1986) 1926.

[3] J. F. Buzinkai, R. R. Schrock, *Organometallics 6* (1987) 1447.

[4] A. Cassens, P. Eilbracht, A. Nazzal, W. Prössdorf, U. T. Mueller-Westerhoff, *J. Am. Chem. Soc. 103* (1981) 6367.

[5] A. N. Nesmeyanov, N. N. Sedova, Y. V. Volgin, V. A. Sazonova, *Izv. Akad. Nauk SSSR Ser. Khim. 10* (1977) 2352.

[6] K. Hafner, K. H. Vöpel, G. Ploss, C. König, *Org. Synth. 47* (1967) 52.

[7] a) R. E. Schmidt, M. Birkhahn, W. Massa, P. Kiprof, E. Herdtweck, STRUX-II, program for analyzing X-ray data, Universität Marburg (1980) and Technische Universität München (1985/87). **3a** crystallizes as orange-red prisms from hexane. The observed extinctions (0*kl*: $k = 2n + 1$, *h*0*l*: $l = 2n + 1$, 0*kl*: $l = 2n + 1$) are consistent with the orthorhombic space group *Pbca* (Nr. 61); a = 1465.0(1), b = 1604.1(1), c = 1036.7(1) pm; $V = 2436 \times 10^6$ pm^3; $C_{14}H_9MnO_3$; $Z = 8$; ϱ_{calcd} = 1.528 g cm^{-3}; Syntex $P2_1$, $Mo_{K\alpha}$ radiation (λ = 71.073 pm), graphite monochromator; $T = -50 \pm 1$ °C; $1.0° \leq \theta \leq 26.0°$; ω scan; variable scan width and measuring time t_{max} = 70 s. 2983 measured reflections, 2039 (NO) unique reflections with $I > 1.0\,\sigma(I)$ and 192 (NV) parameters, full-matrix least-squares refinement. $R = \Sigma(|F_o| - |F_c|)/\Sigma F_o = 0.037$; $R_w = [\Sigma w(|F_o| - |F_c|)^2/\Sigma w F_o^2]^{1/2} = 0.033$; GOF = $[\Sigma w(|F_o| - |F_c|)^2/(NO - NV)]^{1/2} = 2.047$ with $w = 1/\sigma^2(F_o)$. The structure was solved by Patterson methods and the difference Fourier technique; empirical absorption correction, μ = 10.4 cm^{-1}. The positions of the hydrogen atoms were obtained from difference Fourier syntheses and refined with a collective isotropic temperature factor. Anomalous dispersion was taken into consideration. After the final cycle of refinement, the residual electron density was + 0.32 $e^-_0/Å^3$ and − 0.38 $e^-_0/Å^3$ for shift/err < 0.00. b) M. Tasi, T. Ranga, G. Palyi in R. B. King, J. J. Eisch, (Eds): *Organometallic Syntheses, Vol. 4*, Elsevier, Amsterdam 1988, p. 262.

[8] A. F. Berndt, R. E. Marsh, *Acta Crystallogr. 16* (1963) 118.

[9] G. L. Croco, J. A. Gladysz, *Chem. Ber. 121* (1988) 375, and references cited therein.

Hydrooligomerization of Alkynes, a New Catalytic Reaction Promoted by $[Co(py)_6]^{\oplus}$ in the Presence of H_2**

By *Paolo Biagini, Anna M. Caporusso, Tiziana Funaioli,* and *Giuseppe Fachinetti**

Neutral half-sandwich Co^I complexes of the type $[YCoL_2]$ (Y = η^5-cyclopentadienyl or other 6-electron donor ligand, L = neutral ligand) are among the most effective and widely studied compounds in promoting alkyne cyclotrimerization to give benzenes[1] or co-cyclotrimerization with nitriles[2] or alkenes[3] to give pyridines or cyclohexadienes. Throughout these catalytic cycles the group Y is suggested to remain attached to the cobalt, and neutral organocobalt(III)cyclopentadienes are believed to be the common intermediate species.[4]

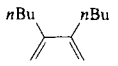
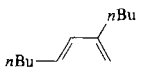
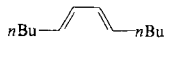
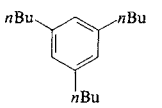
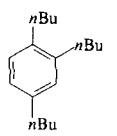
The Co^I cationic coordination compound $[Co(py)_6]^{\oplus}$ **1** (py = pyridine) is one of the most reactive known complexes in promoting alkyne cyclotrimerization to yield arenes.[5] It appears, therefore, that the reaction between $[Co(py)_6][BPh_4]$[6] and alkynes in pyridine as solvent results in the formation of new cationic cobaltacyclopentadiene intermediates. We report now that these intermediates react with H_2: conjugated dienes, trienes, or tetraenes are formed in an unprecedented reductive oligomerization of alkynes.

As stated earlier,[5] the reaction of C_2Ph_2 with **1** in pyridine as solvent represents a particular case with respect to other alkynes in that the stoichiometric formation of $[(\eta^6\text{-}C_6Ph_6)Co(C_2Ph_2)]$ and $[Co(py)_6]^{2\oplus}$ was observed. However, when an equimolar amount of C_2Ph_2 (0.6 M in pyridine) was added to a stirred pyridine solution of **1** (0.05 M) under H_2 at atmospheric pressure, the color of the solution changed initially from deep blue to dark brown and gas absorption took place (0.5 moles of H_2 per mole of C_2Ph_2 in 4 minutes at 20 °C). At the end of the gas absorption, the blue color of the solution was restored. This cycle

[*] Prof. Dr. G. Fachinetti, Dr. P. Biagini, Prof. Dr. A. M. Caporusso, Dr. T. Funaioli
Dipartimento di Chimica e Chimica Industriale
Università di Pisa
Via Risorgimento, 35, I-56100 Pisa (Italy)

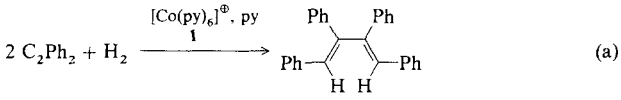
[**] This work was supported by Ministero della Pubblica Istruzione, Rome. We thank Prof. *F. Calderazzo* for helpful discussions.

Table 1. The effect of H_2 pressure on the reductive dimerization of 1-hexyne promoted by **1** [a].

P_{H_2} [atm]					
1	2	6	1	20	71
90	26	39	4	4	27

[a] For reaction conditions see text. Numbers refer to percentage product distribution. Conversion of 1-hexyne was > 95% in both cases. Organic products were identified by comparison of their GLC/MS data with those of authentic samples.

was repeated ten times with similar results. Evaporation of the resulting solution to dryness and extraction with Et_2O gave colorless crystals of (*E,E*)-1,2,3,4-tetraphenyl-1,3-butadiene[7] in quantitative yield [Eq. (a)].

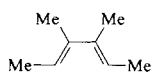
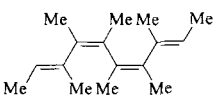


$$2\ C_2Ph_2 + H_2 \xrightarrow[\mathbf{1}]{[Co(py)_6]^{\oplus},\ py} \text{(Ph, Ph, Ph, Ph, H, H)} \qquad \text{(a)}$$

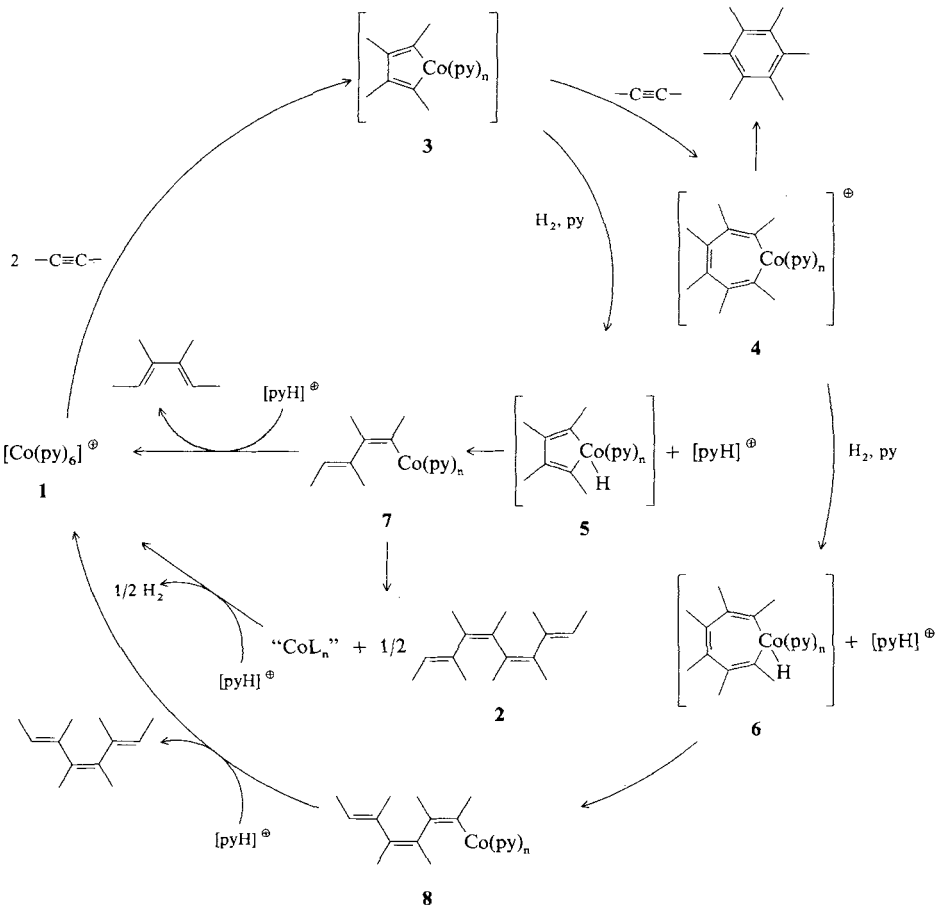
Conjugated dienes were also obtained in similar experiments carried out with 1-hexyne (Table 1) or 2-butyne (Table 2); in addition, considerable amounts of aromatic hydrocarbons were formed. Moreover, in the case of 2-butyne, GLC/MS indicated the formation of a linear conjugated triene[8] and of a linear conjugated tetraene. The latter, isolated by fractional distillation, was characterized by ^1H and ^{13}C NMR spectra[9] as **2** (Table 2).

These findings indicate that alkyne cyclotrimerization and hydrogenation to give conjugated polyenes are competing reactions promoted by **1**. Owing to the possible synthetic utility of the formation of conjugated polyenes by reductive oligomerization, we carried out experiments under elevated hydrogen pressure in order to minimize arene formation. By

Table 2. Reductive oligomerization of 2-butyne promoted by **1** [a].

P_{H_2} [atm]		$C_{12}H_{20}$ (conj. Triene)	 **2**	C_6Me_6
1 [b]	26	9	31	34
90 [b]	41	12	47	–
50 [c]	1	16	81	2

[a] For reaction conditions see text. Numbers refer to percentage product distribution. Conversions of 2-butyne were > 95% in all cases. Diene and hexamethylbenzene were identified by comparison of their GLC/MS data with those of authentic samples. For the identification of triene and tetraene **2** see text. [b] Addition of alkyne to **1**. [c] Addition of **1** to alkyne.



Scheme 1. Proposed mechanism of alkyne oligomerization promoted by **1**.

means of a high-pressure pump, 1-hexyne or 2-butyne, both 0.6 M in pyridine, was injected into a rocking steel autoclave pressurized with 90 atm of H_2 and containing a 0.1 M solution of **1** in pyridine; 30 moles of alkyne per mole of **1** was added over 3 hours at room temperature. GLC analyses of the resulting solutions (Tables 1 and 2) showed that for both alkynes, high hydrogen pressure reduces the formation of aromatic hydrocarbons: high yields of three conjugated dienes were obtained in the case of 1-hexyne, while 2-butyne was converted into a nearly equimolar mixture of diene and tetraene **2**, together with a linear conjugated triene in small amounts.

Although a systematic study of all the reaction parameters has not been made yet, we found a selective hydrotetramerization to occur when catalyst **1** (0.05 M in pyridine) and 2-butyne (1.3 M in pyridine) were added in the reverse order at room temperature under 50 atm hydrogen pressure (Table 2).

As anticipated before, diene and triene formation can be rationalized in terms of the interception by H_2 of cobaltacyclopentadiene or cobaltacycloheptatriene complexes **3** and **4**, respectively (Scheme 1). Presumably, H_2 activation occurs through pyridine-assisted heterolytic cleavage,[10] a step for which the positive charge of cobaltacycle intermediates appears to be an essential requirement. In fact, hydrooligomerization of alkynes is not observed when the neutral Co^I complex $[CoCp(CH_2CH_2)_2]$ is employed in place of **1** under high H_2 pressure. Although the neutral organometallic fragment $CoCp$[1] still promotes cyclotrimerization of alkynes to arenes, variable amounts of olefins and alkanes, depending on experimental conditions, are formed as a consequence of alkyne hydrogenation.

The selective formation of the linear tetraene **2** from 2-butyne is presumably not due to H_2 interception by a cationic cobaltaoctamethylcyclononatetraene. In the absence of H_2, such an intermediate would be expected to reductively eliminate octamethylcyclooctatetraene, which was not found among the products of the cyclooligomerization of 2-butyne promoted by **1**.[5] The selective hydrotetramerization reported here presumably arises from a dimerization of alkadienyl **7** (formed from **3** via **5**) to give **2** and labile Co^0 complexes, which are oxidized back to **1** by the pyridinium cation (Scheme 1). Possible pathways to the diene (via **7**) and the triene (via **4**, **6**, and **8**) are also shown in Scheme 1.

Received: February 13, 1989 [Z 3169 IE]
German version: *Angew. Chem. 101* (1989) 1079

CAS Registry numbers:
1-(BPh_4), 117236-96-1; **2**, 121440-64-0; $CH_2=C(Bu)C(Bu)=CH_2$, 5731-93-1; $BuCH=CH-C(Bu)=CH_2$; 61063-95-4; $BuCH=CH-CH=CHBu$, 30651-68-4; $1,3,5\text{-}(Bu)_3C_6H_3$, 841-07-6; $1,2,4\text{-}(Bu)_3C_6H_3$, 14800-16-9; MeCH=C(Me)C(ME)=CHMe, 18265-39-9; MeCH=C(Me)C(Me)=C(Me)C(Me)=CHMe, 121496-74-0; C_6Me_6, 87-85-4; 1-hexyne, 693-02-7; 2-butyne, 503-17-3.

[1] K. Jonas, *Angew. Chem. 97* (1985) 292; *Angew. Chem. Int. Ed. Engl. 24* (1985) 295.
[2] H. Bönnemann, *Angew. Chem. 97* (1985) 264; *Angew. Chem. Int. Ed. Engl. 24* (1985) 248.
[3] a) Y. Wakatsuki, H. Yamazaki, *J. Organomet. Chem. 139* (1977) 169; b) E. Duñach, R. L. Halterman, K. P. C. Vollhardt, *J. Am. Chem. Soc. 107* (1985) 1664.
[4] J. P. Collman, L. S. Hegedus, J. R. Norton, R. G. Finke: *Principles and Applications of Organotransition Metal Chemistry*, University Science Books, Mill Valley, CA, USA 1987, section 9.5 b.
[5] P. Biagini, T. Funaioli, G. Fachinetti, F. Laschi, P. F. Zanazzi, *J. Chem. Soc. Chem. Commun. 1989*, 405.
[6] G. Fachinetti, T. Funaioli, P. F. Zanazzi, *J. Chem. Soc. Chem. Commun. 1988*, 1100.
[7] H. H. Freedman, G. A. Doorakian, V. R. Sandel, *J. Am. Chem. Soc. 87* (1965) 3019.
[8] $C_{12}H_{20}$ (conjugated triene): MS (70 eV): *m/z* 164 (30%, $M^{\oplus}$), 149(100), 133(28), 119(16), 105(11), 91(13), 77(8), 41(11).
[9] **2**: ^1H NMR ($CDCl_3$): $\delta = 1.53$ (d, $J = 6.8$ Hz, 6H), 1.57 (d, $J = 1.2$ Hz, 6H), 1.64 (s, 6H), 1.66 (s, 6H), 5.18 (dq, $J = 6.8$, 1.2 Hz, 2H). ^3C NMR ($CDCl_3$): $\delta = 13.34$, 15.29, 18.17, 19.52, 119.83, 132.85, 132.95, 139.08. MS (70 eV): *m/z* 218 (68%, $M^{\oplus}$), 203(69), 189(16), 163(50), 149(70), 136(91), 121(63), 105(43), 83(85), 69(29), 55(100), 41 (86).
[10] G. J. Kubas, *Acc. Chem. Res. 21* (1988) 120, and references cited therein.

$[\{Ph_2PCH_2C(CF_3)_2O\}NiH(PCy_3)]$: Support for a Nickel Hydride Mechanism in Ethene Oligomerization**

By *Ulrich Müller, Wilhelm Keim,* Carl Krüger,* and *Peter Betz*

Dedicated to Dr. Günther Ohloff on the occasion of his 65th birthday

The selective oligomerization of ethene to give linear α-olefins is carried out industrially in the Shell SHOP process. A capacity of nearly one million tons in 1990 makes this procedure one of the largest applications of transition metals in homogeneous catalysis.[1]

The metallacycloalkane and the metal hydride mechanisms have usually been discussed as C–C bond-forming pathways in oligomerizations.[2–4] In the latter mechanism, metal hydride complexes have been proposed as the catalytically active species. However, attempts to trap and isolate nickel hydride compounds in oligomerizations have met with little success so far. Here we describe the isolation and in situ NMR measurements of nickel hydride complexes which support the hydride mechanism.

The reaction of 3-diphenylphosphino-1,1,1-trifluoro-2-trifluoromethyl-2-propanol **1** with $Ni(cod)_2$ (cod = 1,5-cyclooctadiene) in toluene gives a system that catalyzes the

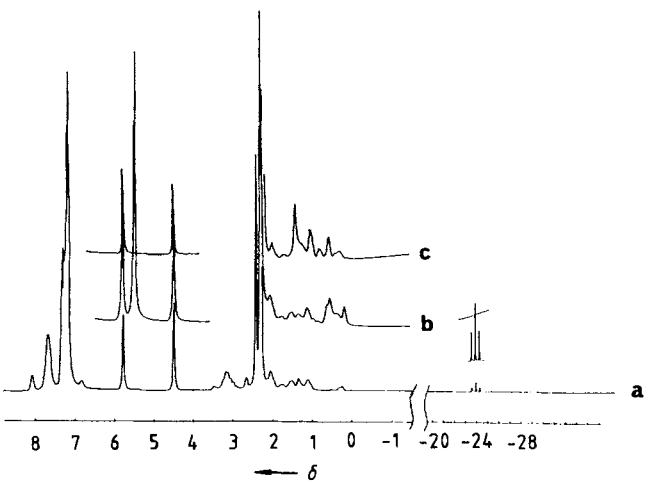


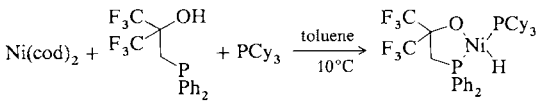
Fig. 1. ^1H NMR spectra of in situ experiments. Spectra: a) $Ni(cod)_2$ plus $Ph_2PCH_2(CF_3)_2OH$ **1**; b) plus ethene after 5 min; c) after 15 min (solvent $[D_8]$toluene at 10 °C).

[*] Prof. Dr. W. Keim, Dr. U. Müller
Institut für Technische Chemie und Petrolchemie
der Technischen Hochschule
Worringer Weg 1, D-5100 Aachen (FRG)
Prof. Dr. C. Krüger[+], Dr. P. Betz[+]
Max-Planck-Institut für Kohlenforschung
Kaiser-Wilhelm-Platz 1, D-4330 Mülheim a. d. Ruhr (FRG)
[+] Crystal structure analysis.

formation of higher olefins from ethene (50 bar) at 50 °C. The C_4–C_{30} oligomers were shown by gas chromatography to be present in a geometric distribution. Linear olefins, 98% of which are α-olefins, predominate to the extent of 99%. Activities of more than 5000 moles of ethene per mole of $Ni(cod)_2$ are attained. When the reaction of **1** with $Ni(cod)_2$ is followed in situ at −10 °C by ^{1}H NMR spectroscopy (Fig. 1, spectrum a), a nickel hydride signal ($\delta = -23.8$) is observed as a triplet.[5]

When ethene is introduced, the hydride signal vanishes immediately and a new signal appears at $\delta = 0.6$, which can be assigned to a nickel alkyl complex (Ni–CH_2; spectrum b). The reaction with ethene was complete after 15 min (spectrum c). Signals at $\delta = 1.12$ and 1.51 indicate the presence of higher nickel alkyl compounds. The presence of the expected α-olefins in the reaction solution could be demonstrated by gas chromatography.

Attempts to isolate the catalytically active nickel hydride complex were unsuccessful. When $Ni(cod)_2$ and **1** were allowed to react in the presence of tricyclohexylphosphane, however, it was possible to isolate complex **2** (Scheme 1).



1 **2**

Scheme 1. Formation of the nickel hydride complex **2**. Cy = cyclohexyl.

An X-ray structure analysis (Fig. 2) confirmed the structure of complex **2**, which has a square-planar configuration

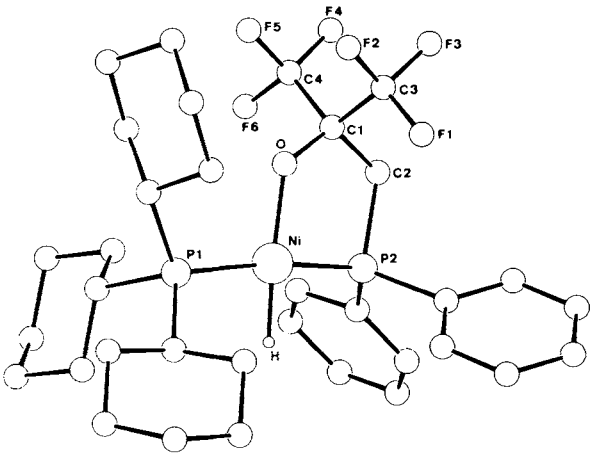


Fig. 2. Molecular structure of complex **2**. Selected bond lengths [Å] and angles [°]: Ni–P1 2.181(1), Ni–P2 2.140(1), Ni–O 1.873(2), Ni–H 1.37(3); P1–Ni–O 99.1(1), O–Ni–P2 87.8(1), P2–Ni–H 89.(1), H–Ni–P1 84(1). Crystal data for **2**: $P\bar{1}$, $a = 10.6169(5)$, $b = 12.0185(6)$, $c = 14.1276(7)$ Å, $\alpha = 102.63(1)$, $\beta = 90.45(1)$, $\gamma = 101.02(1)°$, $V = 1724.3$ Å^3, $Z = 2$, $\varrho_{calcd} = 1.36$ g cm^{-3}, $\lambda = 1.54179$ Å, $\mu = 21.93$ cm^{-1}, $R = 0.044$, $R_w = 0.053$; 7096 unique reflections, 5989 observed with $I > 2\sigma(I)$, 535 refined parameters, residual electron density 0.40 eÅ^{-3}. The positions of the hydrogen atoms, obtained by difference Fourier synthesis, were included in the refinement with fixed isotropic temperature factors ($U(H) = 0.08$ Å^2); all other atoms were refined anisotropically. Further detail of the crystal structure investigation may be obtained from the Fachinformationszentrum Karlsruhe, Gesellschaft für wissenschaftlich-technische Information mbH, D-7514 Eggenstein-Leopoldshafen 2 (FRG), on quoting the depository number CSD-53678, the names of the authors, and the journal citation.

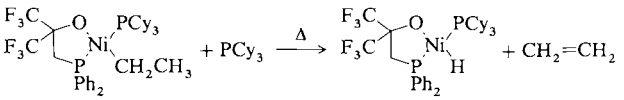
around nickel. The complex is characterized by a large P1–Ni–O angle (99.1(1)°); the chelate ring is folded by 13.5° along the Ni–C2 axis.

Complex **2** does not catalyze the oligomerization of ethene; the PCy_3 ligand presumably blocks the necessary free coordination site. Complex **3** was also isolated. A triplet at $\delta = -24.98$ in the ^{1}H NMR spectrum indicates the coordination of only two phosphorus atoms.

$[\{Ph_2PCH_2C(CF_3)_2O\}NiH(PCy_3)_2]$ **3**

The nickel hydride mechanism would be supported by the trapping and isolation of nickel alkyl complexes in analogy to the reaction shown in Scheme 1. To this end, a solution of $Ni(cod)_2$/**1** in [D_8]toluene was allowed to react with ethene at −20 °C. Addition of PCy_3 led to the formation of a yellow-orange complex, **4**, which could be isolated.

A pseudo triplet in the ^{13}C NMR spectrum of **4** ($\delta = -10.32$) exhibits two C–P couplings with coupling constants of 22.63 and 21.12 Hz, which are in agreement with the presence of two phosphorus atoms coordinated in different fashions to alkyl-substituted nickel. As expected, the methyl C atom gives rise to a singlet at $\delta = 15.29$. In the ^{1}H NMR spectrum, the signals of the Ni–CH_2 group are found at $\delta = 0.2$–0.7. The ^{1}H NMR shift assignments were confirmed on the basis of reference data.[6, 7] When **4** is warmed to room temperature, ethene is lost in a β-hydride elimination step (Scheme 2), resulting in the formation of **2**.



4 **2**

Scheme 2. β-Elimination of ethene from **4**.

Compounds **2** and **4** can serve as models for intermediates in the catalytic cycle and provide important support for the hydride mechanism. The nickel hydrides present in the catalysis solution are rapidly trapped by ethene. The resulting nickel ethyl complex can react further with ethene to give the nickel butyl complex, the nickel hexyl complex, etc. The β-hydride elimination of the nickel alkyl species affords the α-olefins, present in a geometric distribution.

Experimental Procedure

2: $Ni(cod)_2$ (620 mg, 2.25 mmol) was dissolved under argon in 10 mL of toluene in a Schlenk tube equipped with a stirring bar and the resulting solution was cooled to −30 °C. Compound **1** (825 mg, 2.25 mmol) [8] was dissolved likewise in 10 mL of toluene and then slowly added dropwise to the stirred solution of $Ni(cod)_2$. After an additional hour at −10 °C, PCy_3 (659 mg, 2.3 mmol) in toluene was added. The filtered toluene solution contains a nearly quantitative amount of liberated 1,5-cyclooctadiene. The crude yellow-brown product was recrystallized from toluene/petroleum ether (1/10). Yield 1.3 g (62%). ^{1}H NMR ([D_8] toluene): $\delta = 7.7$–6.99 (m, 10H, Ph_2P), 2.97 (d, 2H, CH_2), 2.1–1.2 (m, 33H, PCy_3), −24.85 (dd, 1H, Ni–H).

Complex **3** was prepared in a similar fashion. However, the reaction was performed at 20 °C and twice as much PCy_3 was used. Yield 81%. ^{1}H NMR ([D_8] toluene): $\delta = 7.0$–7.6 (m, 10H, PPh_2), 2.88 (d, 2H, CH_2), 1.2–2.1 (m, 66H, PCy_3), −24.98 (t, 1H, Ni–H).

All new compounds gave correct elemental analyses. The NMR spectra, with detailed coupling constants, are contained in the dissertation of *U. Müller* [9].

Received: February 21, 1989;
revised: May 8, 1989 [Z 3187 IE]
German version: *Angew. Chem. 101* (1989) 1066

CAS Registry numbers:
1, 98331-76-1; **2**, 121288-88-8; **3**, 121288-89-9; **4**, 121288-90-2; $Ni(cod)_2$, 1295-35-8; PCy_3, 2622-14-2; ethene, 74-85-1.

[1] M. Peuckert, W. Keim, *Organometallics 2* (1983) 594.
[2] J. P. Collman, L. S. Hegedus, J. R. Norton, R. G. Finke, *Principles and Applications of Organotransition Metal Chemistry*, University Science Books, Mill Valley, CA 1987, pp. 578–584.

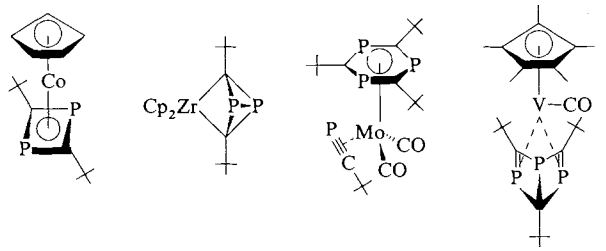
[3] W. Keim, A. Behr, M. Röper, in G. Wilkinson, F. Gordon, A. Stone, (Ed.): *Comprehensive Organometallic Chemistry, Vol. 8*, Pergamon, Oxford 1982, p. 373.
[4] G. Wilke, *Angew. Chem. 100* (1988) 203; *Angew. Chem. Int. Ed. Engl. 27* (1988) 185.
[5] C. A. Tolman, *Chem. Rev. 77* (1977) 313.
[6] A. Yamamoto, T. Yamamoto, T. Saruyama, Y. Nakamura, *J. Am. Chem. Soc. 95* (1973) 4073.
[7] P. W. Jolly, K. Jonas, C. Krüger, Y. H. Tsay, *J. Organomet. Chem. 33*(1971) 109.
[8] R. T. Boere, C. D. Montgomery, N. C. Payne, C. J. Willies, *Inorg. Chem. 24* (1986) 3680.
[9] U. Müller, *Dissertation*, Technische Hochschule Aachen, 1988.

Tetra-*tert*-butyltetraphosphacubane: The First Thermal Cyclooligomerization of a Phosphaalkyne**

By *Thomas Wettling, Jürgen Schneider, Oliver Wagner, Cornelius G. Kreiter,* and *Manfred Regitz**

Dedicated to Professor Gottfried Märkl on the occasion of his 60th birthday

The extremely rapid development of phosphaalkyne chemistry has focused above all on cycloaddition reactions and ligand properties.[1] Of particular interest have been the cyclodimerization and cyclotrimerization reactions in the coordination sphere of metals. Thus, *tert*-butylphosphaacetylene **5** can be dimerized, for example, to give cobalt complexes containing diphosphacyclobutadiene (**1**[2, 3]) and diphosphabicyclo[1.1.0]butane ligands (**2**[4]). Complexes with cyclotrimer ligands derived from 1,3,5-triphosphabenzene **3**[5] and its Dewar derivatives **4**[6] are also known.



1 **2** **3** **4**

The use of metal complexes in cyclooligomerization reactions is not always necessary, as shown by the thermal cyclotetramerization of **5**. Although most phosphaalkynes are not particularly thermally stable,[1] the behavior of these species upon heating has not been studied.

When neat phosphaalkyne **5** is heated for a long period of time at 130 °C and the product distilled, pale yellow crystals are obtained which exhibit a high melting point and are stable toward air. Elemental analysis and mass spectrometry revealed that the product is a tetramer of **5**, compound **7**. The stepwise decomposition of the tetramer to the monomer occurs upon electron-collision-induced fragmentation.[7]

The NMR spectra of **7** support a tetraphosphacubane structure with alternating C and P atoms. The $^{13}C\{^1H\}$ NMR spectrum (100.62 MHz, C_6D_6) shows three multiplets at $\delta = -29.07$, 21.57, and 30.64 (Fig. 1). These represent the

[*] Prof. Dr. M. Regitz, Dipl.-Chem. T. Wettling, Dipl.-Chem. J. Schneider, Dipl.-Chem. O. Wagner, Prof. Dr. C. G. Kreiter
Fachbereich Chemie der Universität
Erwin-Schrödinger-Strasse, D-6750 Kaiserslautern (FRG)

[**] Unusual Coordinated Phosphorus Compounds, Part 37. This work was supported by the Deutsche Forschungsgemeinschaft and the Fonds der Chemischen Industrie. Part 36: W. Schnurr, M. Regitz, *Synthesis 1989*, im Druck.

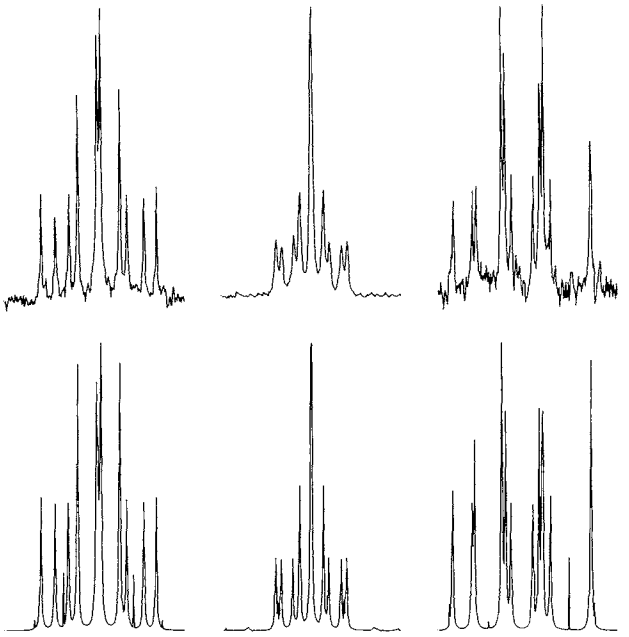


Fig. 1. Measured (top) and simulated (bottom) ^{13}C NMR spectrum of **7** (sequence of the signals from left to right: $C(CH_3)_3$, $C(CH_3)_3$, cage C; see text).

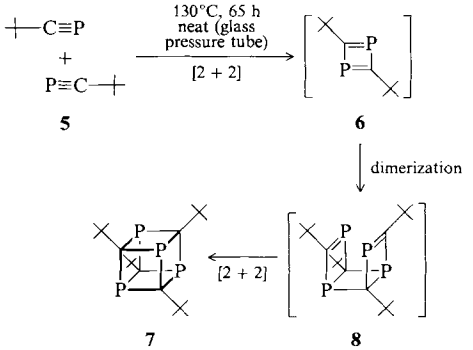
A portions of AX_3Y spin systems, each composed of one ^{13}C and four ^{31}P atoms. Different ^{13}C-induced shifts of the two kinds of phosphorus atoms have to be taken into consideration in calculating the signals.[8] Especially noteworthy is the isotope-induced shift for the spin system containing the cage ^{13}C atom, as revealed by the unsymmetrical appearance of the signal. The separation of the signals due to the two kinds of P atoms is less for the spin system containing the quaternary ^{13}C atom of a *tert*-butyl group or the ^{13}C atom of a methyl group. The $^2J(^{31}P\text{-}^{31}P)$ and the $^nJ(^{31}P\text{-}^{13}C)$ coupling constants (n = 1–5) lie in a narrow range (Table 1).

Table 1. Calculated ^{31}P NMR chemical shifts of the AX_3Y spin systems as well as $^2J(^{31}P\text{-}^{31}P)$ and $^nJ(^{31}P\text{-}^{13}C)$ coupling constants of the $^{13}C\{^1H\}$ NMR signals of **7**.

$\delta(X)-\delta(Y)$	$^2J(^{31}P\text{-}^{31}P)$	$^nJ(^{31}P\text{-}^{13}C)$	$^{n+2}J(^{31}P\text{-}^{13}C)$	n [a]
7.8	8.52	13.43	− 2.05	1
1.3	8.52	10.10	1.49	2
0.3	8.52	6.58	− 0.17	3

[a] n = 1, cage C; n = 2, $C(CH_3)_3$; n = 3, $C(CH_3)_3$.

Unusual is both the strong low-field shift of the phosphorus signals of **7** ($\delta = 257.4$, $CDCl_3$) and the high-field shift of the cage ^{13}C signal ($\delta = -29.07$). Presumably, this reflects a shift of electron density from phosphorus to carbon.



5 **6** **7** **8**

The formation of the pentacyclic system presumably begins with a head-to-tail dimerization of the phosphaalkyne (**5** → **6**), followed by either dimerization to give the tricyclic compound **8** or sterically controlled cycloaddition of two molecules of **5** to **6**,[9] which leads to the same result. The final step, **8** → **7**, is not surprising, since analogous intermolecular phosphaalkene dimerizations are known.[10]

Unequivocal confirmation of the phosphaalkyne tetramer as being tetraphosphacubane **7** was achieved by crystal structure analysis, which revealed a distorted cubelike structure (Fig. 2).

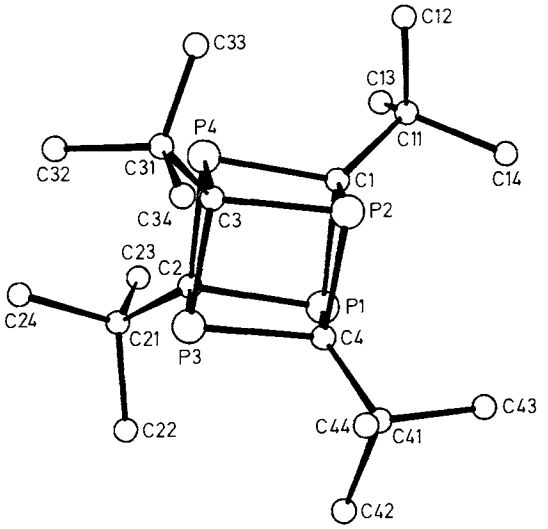


Fig. 2. Molecular structure of **7**: $C_{20}H_{36}P_4$; $P2_1/c$, $a = 9.678(3)$, $b = 14.365(4)$, $c = 17.019(5)$ Å, $\beta = 92.24(2)°$, $T = 20$ °C, $Z = 4$, $\varrho_{calcd} = 1.12$ g cm^{-3}. Enraf-Nonius CAD 4 diffractometer, monochromatic $Mo_{K\alpha}$ radiation, 3089 unique reflections with $2.0 \leq \theta \leq 22.5°$, absorption correction ($\mu = 3.14$ cm^{-1}), full matrix refinement with 2654 reflections [$I > 2\sigma(I)$] and 217 variables. $R = 0.042$, $R_w = 0.037$ [11]. Selected bond lengths [Å] and bond angles [°]: P1-C1 1.880(3), P1-C2 1.886(3), P1-C4 1.877(3), P2-C1 1.883(3), P2-C3 1.891(3), P2-C4 1.882(4), P3-C2 1.881(3), P3-C3 1.875(4), P3-C4 1.886(3), P4-C1 1.885(3), P4-C2 1.876(3), P4-C3 1.875(4); C1-P1-C2 85.4(1), C1-P1-C4 85.7(1), C2-P1-C4 85.6(1), C1-P2-C3 85.5(2), C1-P2-C4 85.5(1), C3-P2-C4 85.7(2), C2-P3-C3 85.0(2), C2-P3-C4 85.5(1), C3-P3-C4 86.1(2), C1-P4-C2 85.6(1), C1-P4-C3 85.9(1), C2-P4-C3 85.2(2), P1-C1-P2 94.2(2), P1-C1-P4 94.3(2), P2-C1-P4 94.1(1), P1-C2-P3 94.2(2), P1-C2-P4 94.3(2), P3-C2-P4 94.7(1), P2-C3-P3 93.9(2), P2-C3-P4 94.2(2), P3-C3-P4 94.9(2), P1-C4-P2 94.3(2), P1-C4-P3 94.4(2), P2-C4-P3 93.9(2).

Comparison of the internal bonding angles of the rings with those of unsubstituted cubanes, which are about 90°,[12] reveals that the C–P–C angles of **7** are on average 4.4° smaller (85.6°), which requires an increase in the P–C–P angles to 94.4°; the exocyclic P–C–C bond angles are 122.2°. The average P–C bond length in the cube is 1.881 Å, the same magnitude as in 1,3-diphosphacyclobutanes.[10]

Experimental Procedure

7: **5** (3.50 g, 35.0 mmol) [13] was stirred with a magnetic stirring bar for 65 h at 130 °C under argon atmosphere in a preheated Schlenk pressure tube. The red, viscous reaction mixture was dissolved in 10 mL of pentane, transferred by pipette to a round-bottomed flask, and evaporated at 25 °C/10^{-2} torr. Kugelrohr distillation of the residue (10 h at 155 °C (oven temperature)/10^{-2} torr) afforded crystalline **7**, which was separated from an oily side product [14] by recrystallization from *n*-pentane. Yield: 280 mg (8%) pale yellow, cube-shaped crystals, m.p. 241 °C [15].

Received: March 14, 1989;
supplemented: May 5, 1989 [Z 3232 IE]
German version: *Angew. Chem. 101* (1989) 1035

CAS Registry numbers:
5, 78129-68-7; **7**, 121097-72-1.

[1] Review: R. Regitz, P. Binger, *Angew. Chem. 100* (1988) 1541; *Angew. Chem. Int. Ed. Engl. 27* (1988) 1485.
[2] P. B. Hitchcock, M. J. Maah, J. F. Nixon, *J. Chem. Soc. Chem. Commun. 1986*, 737.
[3] P. Binger, R. Milczarek, R. Mynott, M. Regitz, W. Rösch, *Angew. Chem. 98* (1986) 645; *Angew. Chem. Int. Ed. Engl. 25* (1986) 644; P. Binger, R. Milczarek, R. Mynott, Y-H. Tsai, E. Raabe, C. Krüger, M. Regitz, *Chem. Ber. 121* (1988) 637.
[4] P. Binger, B. Biedenbach, C. Krüger, M. Regitz, *Angew. Chem. 99* (1987) 798; *Angew. Chem. Int. Ed. Engl. 26* (1987) 764.
[5] A. R. Barron, A. H. Cowley, *Angew. Chem. 99* (1987) 956; *Angew. Chem. Int. Ed. Engl. 26* (1987) 907.
[6] R. Milczarek, W. Rüsseler, P. Binger, K. Jonas, K. Angermund, C. Krüger, M. Regitz, *Angew. Chem. 99* (1987) 957; *Angew. Chem. Int. Ed. Engl. 26* (1987) 907.
[7] **7**: MS (70 eV): *m/z* [%] 400 [$M^{\oplus}$, 71], 331 [$M^{\oplus}-(H_3C)_3CC$, 5], 300 [$M^{\oplus}-(H_3C)_3CCP$, 7], 262 [$M^{\oplus}-2(H_3C)_3CC$, 76], 231 [$M^{\oplus}-(H_3C)_3CCP$, $-(H_3C)_3CC$, 10], 200 [$M^{\oplus}-2(H_3C)_3CCP$, 11], 169 [$M^{\oplus}-2(H_3C)_3CCP$, $-$ P, 100], 162 [$M^{\oplus}-(H_3C)_3CCP$, $-2(H_3C)_3CC$, 12], 131 [$M^{\oplus}-2(H_3C)_3CCP$, $-(H_3C)_3CC$, 24], 100 [$M^{\oplus}-3(H_3C)_3CCP$, 25]. We thank Dr. *R. Graf*, Fachrichtung Organische Chemie der Universität Saarbrücken, for recording the spectra.
[8] PANIC simulations program, Bruker, Karlsruhe.
[9] The cycloaddition of **5** to cyclobutadienes and azetes is known: J. Fink, W. Rösch, U.-J. Vogelbacher, M. Regitz, *Angew. Chem. 98* (1986) 265; *Angew. Chem. Int. Ed. Engl. 25* (1986) 280; U.-J. Vogelbacher, M. Ledermann, T. Schach, G. Michels, U. Hees, M. Regitz, *ibid. 100* (1988) 304 and *27* (1988) 272.
[10] G. Becker, W. Massa, O. Mundt, R. Schmidt, *Z. Anorg. Allg. Chem. 485* (1982) 23, and references therein; R. Appel, C. Casser, F. Knoch, *Chem. Ber. 117* (1984) 2693.
[11] Further details of the crystal structure investigation may be obtained from the Fachinformationszentrum Karlsruhe, Gesellschaft für wissenschaftlich-technische Information mbH, D-7514 Eggenstein-Leopoldshafen 2 (FRG), on quoting the depository number CSD-53729, the names of the authors, and the journal citation.
[12] E. B. Fleischer, *J. Am. Chem. Soc. 86* (1964) 3889; Synthese: P. Eaton, T. Cole, *ibid. 86* (1964) 3157.
[13] G. Becker, G. Gresser, W. Uhl, *Z. Naturforsch. B.36* (1981) 16; the improved procedure of W. Rösch, U. Hees, M. Regitz, *Chem. Ber. 120* (1987) 1645 is better suited for the preparation of larger amounts.
[14] This product is also presumably a tetramer of **5** (correct elemental analysis), as shown by the number of NMR resonances. ^{1}H NMR (90 MHz, $CDCl_3$): $\delta = 0.83, 1.14, 1.41, 1.45$ (*t*Bu); ^{13}C-NMR (125.8 MHz, $CDCl_3$): $\delta = 32.9, 55.4, 173.3, 177.8$ (ring C). ^{31}P NMR (80.8 MHz, $CDCl_3$): $\delta = -242.5, -155.7, 82.4, 87.7$.
[15] Note added in proof (May 5, 1989): For the cyclooligomerization of **5** with (η^4-1-methylnaphthalene)(η^6-toluene)iron, see the recent communication by D. Hu, H. Schäufele, H. Pritzkow, U. Zenneck, *Angew. Chem. 101* (1989) 929; *Angew. Chem. Int. Ed. Engl. 28* (1989) 900. A tetraphosphatetrasilacubane has also been reported in the meantime: M. Baudler, G. Scholz, K.-F. Tebbe, M. Fehér, *ibid. 101* (1989) 352 and *28* (1989) 339.

A Phosphane–Dithioformate Adduct as a Five-Electron Bridging Ligand $[Mn_2(CO)_6\{S_2C(H)P(cyclo\text{-}C_6H_{11})_3\}_2]$**

By *Daniel Miguel, Jesús A. Miguel, Victor Riera,** and *Xavier Soláns*

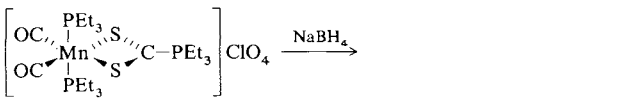
Coordinated trialkylphosphoniodithiocarboxylato ligands S_2CPR_3 undergo nucleophilic attack on the carbon atom, thus giving a variety of coordinated 1,1-dithiolato ligands such as xanthates and dithio- and trithiocarbonates.[1]

[*] Prof. Dr. V. Riera, Dr. D. Miguel
Departamento de Química Organometálica, Universidad de Oviedo
E-33071 Oviedo (Spain)
Dr. J. A. Miguel
Laboratorio de Química Inorgánica, Universidad de Valladolid
E-47005 Valladolid (Spain)
Prof. Dr. X. Soláns
Departamento de Cristalografía, Mineralogía y Depósitos Minerales, Universidad de Barcelona
Martí y Franqués s/n, E-08028 Barcelona (Spain)

[**] We thank C.A.I.C.Y.T. for financial support.

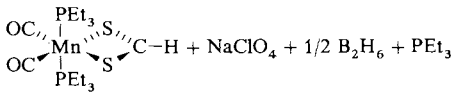
When the nucleophile used in these reactions is the hydride ion, two types of products can be obtained: either the hydride ion displaces the phosphane producing a coordinated dithioformate $^{\ominus}S_2CH$, or the PR_3 group remains attached to the carbon atom and an $^{\ominus}S_2C(H)PR_3$ ligand is formed. The final result seems to depend on both structural and electronic factors.[2, 3] Here we report a preliminary study of hydride additions to coordinated S_2CPR_3 ligands (R = cyclohexyl (Cy, Et)) in octahedral manganese(I) complexes, in which a spontaneous dimerization leads to the formation of a dinuclear Mn^I compound containing two five-electron unsymmetrically bridging $^{\ominus}S_2C(H)PCy_3$ ligands coordinated in an $^2\eta,^1\eta$ fashion.

The reaction of complex **1** [Eq. (a)] with $NaBH_4$ gives a bright red solution of the dithioformate complex **2**, which can be isolated as red crystals. Analytical and spectroscopic data are in good agreement with the structure depicted for **2**



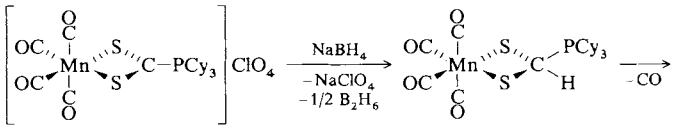
1

(a)



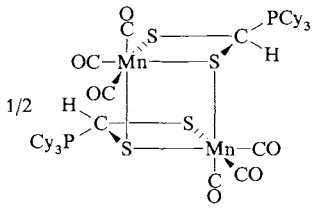
2

in Equation (a). On the other hand, treatment of complex **3**[5] with $NaBH_4$ [Eq. (b)] yields a yellow solution from which the dinuclear complex **4** can be isolated as a crystalline solid.



3

(b)



4

The IR spectrum of **4** shows five $\tilde{\nu}_{CO}$ maxima, in a pattern consistent with an $Mn_2(CO)_6$ grouping, but the available spectroscopic data[4] did not give enough information about the structure of this compound. An X-ray structure analysis was therefore carried out on a crystal of **4**[6] (Fig. 1).

Compound **4** is a dimer in which each $^{\ominus}S_2C(H)PCy_3$ ligand is coordinated to one manganese in an η^2-*S,S'* chelate fashion and one sulfur atom of each ligand serves as a bridge to bind the other manganese atom, thus forming a distorted Mn_2S_2 square with Mn–S distances ranging from 2.379(2) to 2.445(2) Å, values not very different from those found in $[Mn_2(CO)_6(\mu\text{-}SC(SMe)NMe)_2]$.[7] Both manganese atoms are surrounded by a six-coordinate octahedral environment, and the distance Mn1-Mn2 is large enough to prevent any significant interaction between them. The molecule consists of two tricarbonylmanganese units held together by two $^{\ominus}S_2C(H)PCy_3$ bridging ligands and, since no Mn–Mn bond

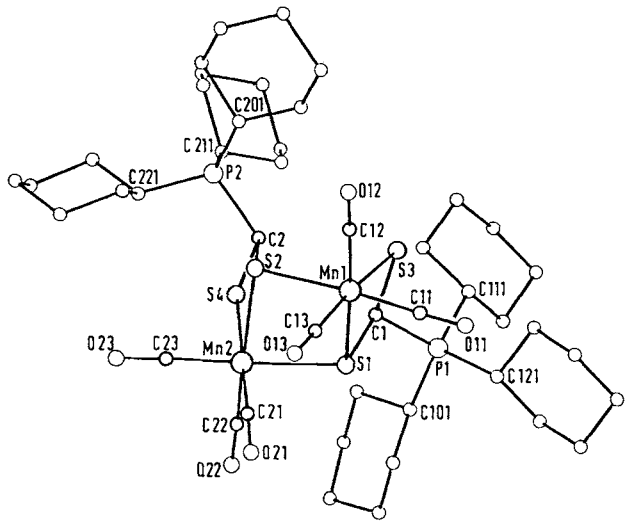


Fig. 1. Molecular structure of the cation of **4**. Selected bond lengths [Å] and angles [°]: Mn1-S1 2.379(2), Mn1-S2 2.426(2), Mn1-S3 2.388(2), Mn2-S1 2.445(2), Mn2-S2 2.410(2), Mn2-S4 2.375(2), C1-S1 1.827(7), C1-S3 1.816(7), C2-S2 1.826(7), C2-S4 1.828(7); S1-Mn1-S2 83.3(1), S1-Mn1-S3 75.1(1), S2-Mn1-S3 95.0(1), S1-Mn2-S2 82.3(1), S1-Mn2-S4 96.0(1), S2-Mn2-S4 75.0(1), Mn1-S1-Mn2 94.2(1), Mn2-S1-C1 110.8(2), Mn1-S2-Mn2 93.9(1), Mn1-S2-C2 108.9(2), S1-C1-S3 105.8(3), S2-C2-S4 105.7(3).

exists, each bridge must donate five electrons to satisfy the 18-electron rule. The carbonyls on each $Mn(CO)_3$ grouping adopt a *facial* arrangement with C–Mn–C angles very close to 90° and the six $Mn–C_{carbonyl}$ distances are normal. On the other hand, the positions of the sulfur atoms deviate considerably from ideal octahedral coordination, the main deviations being induced by the small bite of the chelate ligands (angles S3-Mn1-S1 = 75.1(1)°, S4-Mn2-S2 = 75.0(1)°).

The hydrogens on the central carbons of the ligands, H1 and H2, are close to one manganese and three sulfur atoms, the distances (Table 1) being shorter than the sum of the van

Table 1. Important distances [Å] between the central H atoms of **4** and other atoms. H1 is the H atom on C1, H2 that on C2.

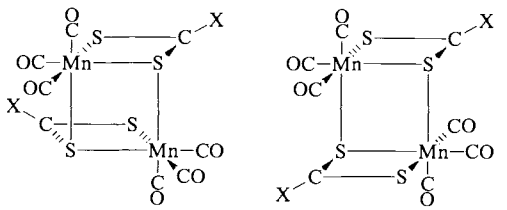
H1-C1 1.06(6), H1-S1 2.36(2), H1-S3 2.39(2), H1-S4 2.55(2), H1-Mn2 3.29(1), H2-C2 1.13(6), H2-S2 2.34(2), H2-S3 2.37(2), H2-S4 2.35(2), H2-Mn1 3.09(1)

der Waals radii of the atoms involved. This implies some degree of interaction between these hydrogens and the manganese and sulfur atoms, which could explain some unusual spectroscopic features, such as the position of the signal of these hydrogens in the ^1H NMR spectrum at lower fields ($\delta = 9.29$) than the range reported for other complexes containing $^{\ominus}S_2C(H)PR_3$ ligands ($\delta = 5.20-6.25$)[3, 8-10] and also the broadening of this signal, which precludes the observation of P–H coupling.

The formation of **4** can be rationalized by a two-step mechanism as shown in Equation (b). First, hydride addition to the carbon atom of the S_2PCy_3 ligand produces the neutral complex $[Mn(CO)_4(S_2C(H)PCy_3)]$, which cannot be isolated. Second, a dimerization, in which a carbonyl ligand on each manganese is displaced by a sulfur atom of the chelate ring of the opposite manganese, yields the final dinuclear product.

As far as we know, **4** is the first complex in which a phosphane–dithioformate adduct acts as a five-electron bridging ligand. However, this kind of dimerization (either spontaneous or thermally induced) has been observed before in other manganese complexes containing 1,1-dithiolato lig-

ands such as S_2CSMe and $^{\ominus}S_2CNR_2$.[7, 11, 12] In the final products of these dimerizations, the two chelate ligands can adopt, in principle, either a *cisoid* (**5**) or a *transoid* (**6**) disposition. However, the factors leading to one or the other geometry are not yet well understood. In the special case of **4**, the intramolecular interactions of the hydrogens with the manganese and sulfur atoms could play a significant role in the adoption of the *cisoid*[13] configuration, since these interactions would not be possible in the *transoid* geometry. However, this kind of hydrogen interaction has been absent in the other dimeric structures (either *cisoid* or *transoid*) reported so far.



5 cisoid

6 transoid

Received: February 20, 1989 [Z 3184 IE]
German version: *Angew. Chem. 101* (1989) 1078

CAS Registry numbers:
1, 121846-70-6; **2**, 121846-72-8; **3**, 112364-33-7; **4**, 121846-71-7; $NaBH_4$, 16940-66-2; HS_2CHPEt_3, 110375-43-4; HS_2CHPCy_3, 121846-68-2.

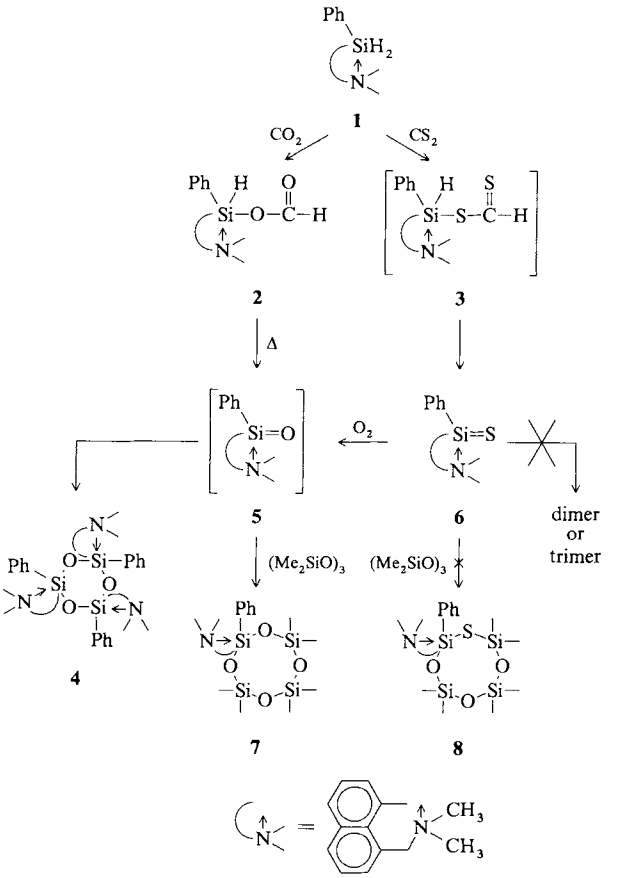
[1] C. Bianchini, A. Meli, A. Orlandini, *Inorg. Chem. 21* (1982) 4166.
[2] C. Bianchini, P. Innocenti, A. Meli, A. Orlandini, G. Scapacci, *J. Organomet. Chem. 233* (1982) 233.
[3] C. Bianchini, A. Meli, P. Daporto, A. Tofanari, P. Zanello, *Inorg. Chem. 26* (1987) 3677.
[4] Selected analytical and spectroscopic data. **2**: 90% yield; correct C, H analysis for $C_{15}H_{31}MnO_2P_2S_2$. IR (hexane): $\tilde{\nu}_{max}$(CO) [cm^{-1}]: 1919s, 1853s. ^1H NMR 300.1 MHz, $CDCl_3$): $\delta = 10.64$ (t, 1H, S_2CH; J(P–H) = 7.3 Hz), 1.86 (m, 12H, CH_2), 1.13 (m, 18H, CH_3). $^{31}P\{^1H\}$ NMR (121.5 MHz, $CDCl_3$): $\delta = 49.3$. The structure of **2** has been recently confirmed by an X-ray diffraction study. **4**: 89% yield; correct C, H analysis for $C_{44}H_{68}Mn_2O_6P_2S_4$. IR (THF): $\tilde{\nu}_{max}$(CO) [cm^{-1}] = 2006s, 1984vs, 1912s, 1895vs, 1887sh. ^1H NMR (300.1 MHz, $CDCl_3$): $\delta = 9.26$ (br s, 2H, S_2CH), 3.1–1.3 (m, 66H, cyclohexyl H). $^{31}P\{^1H\}$ NMR (121.5 MHz, $CDCl_3$): $\delta = 28.0$(s).
[5] D. Miguel, V. Riera, J. A. Miguel, C. Bois, M. Philoche-Levisalles, Y. Jeannin, *J. Chem. Soc. Dalton Trans. 1987*, 2875.
[6] Crystal structure data for **4** ($M = 993.09$); monoclinic, $a = 22.670(4)$, $b = 12.694(2)$, $c = 16.426(3)$ Å, $\beta = 91.46(2)°$, $V = 4725(1)$ Å^3, space group $P2_1/a$, $\varrho_{calcd} = 1.396$ g cm^{-3}, $Z = 4$, $F(000) = 2096$, $\lambda(Mo_{K\alpha}) = 0.7169$ Å, $\mu(Mo_{K\alpha}) = 8.49$ cm^{-1}, $T = 288$ K. 3435 reflections in the range $2 \leq \theta \leq 25°$. 3272 observed ($I \geq 2.5\,\sigma(I)$). $R = 0.045$ ($R_w = 0.046$). Further details of the crystal structure investigation can be obtained from the Fachinformationszentrum Karlsruhe, Gesellschaft für wissenschaftlich-technische Information mbH, D-7514 Eggenstein-Leopoldshafen 2 (FRG), by quoting the depository number CSD-53775, the names of the authors, and the journal citation.
[7] S. R. Finnimore, R. Goddard, S. D. Killops, S. A. R. Knox, P. Woodward, *J. Chem. Soc. Dalton Trans. 1978*, 1247.
[8] H. Werner, W. Bertleff, *Chem. Ber. 113* (1980) 267.
[9] C. Bianchini, A. Meli, A. Orlandini, *Inorg. Chem. 21* (1982) 4161.
[10] T. Ashworth, E. Singleton, M. Laing, *J. Chem. Soc. Chem. Commun. 1976*, 875.
[11] K. Tanaka, Y. Miya-Uchi, T. Tanaka, *Inorg. Chem. 14* (1975) 1545.
[12] E. W. Abel, M. O. Dunster, *J. Chem. Soc. Dalton Trans. 1973*, 98.
[13] The formation of any significant amount of the *transoid* isomer can be ruled out from spectroscopic data. The carbonyl stretching region of the IR spectra is highly informative: only three active bands (3 A_u) are expected [12] for the centrosymmetric *transoid* structure (point group C_i), whereas six (3 A + 3 B) bands are predicted for the noncentrosymmetric *cisoid* structure (point group C_2). For compound **4**, five bands are observed, probably owing to accidental degeneracy. Since IR and ^1H NMR solution spectra do not change upon crystallization of **4** from the reaction mixture, or upon recrystallization from CH_2Cl_2/hexane, it can be concluded that only very minor quantities of the *transoid* isomer, if any, are produced in the dimerization process.

Formation and Reactivity of Silicon–Sulfur and Silicon–Selenium Double Bonds. The First X-Ray Structure of a Silanethione

By *Prabhat Arya, Jacqueline Boyer, Francis Carré, Robert Corriu,* Gérard Lanneau, Jacques Lapasset, Myriam Perrot,* and *Christian Priou*

Experimental evidence for the existence of multiply bonded silicon compounds has accumulated in the last few years.[1] Compounds containing Si=C,[2] Si=Si,[3] and Si=N[4] double bonds have been isolated. A method of stabilizing them with respect to dimerization is to form adducts with donor molecules or anions.[5, 6]

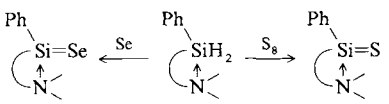
In 1986, we described the enhanced chemical reactivity of the pentacoordinated functional silane **1** towards carbonyl groups,[7] acyl chlorides,[8] and carboxylic acids.[9] CO_2 reacts with insertion[10] into the Si–H bond of **1** to give silyl formate **2**. Warming **2** at 85 °C decomposes the ester into formaldehyde and the transient silanone **5**, which trimerizes immediately to yield **4**. The silanone **5** has also been trapped[11] with $(Me_2SiO)_3$ to give the eight-membered ring compound **7**.



[*] Prof. Dr. R. Corriu, Dr. P. Arya [+], Dr. J. Boyer, Dr. F. Carré, Dr. G. Lanneau, M. Perrot, C. Priou
Institut de Chimie Fine
Université des Sciences et Techniques du Languedoc
Unité Associée C.N.R.S. U.A. 1097
Place E. Bataillon, F-34060 Montpellier Cedex (France)
Prof. Dr. J. Lapasset
Groupe de Dynamique des Phases Condensées LA 233
Université des Sciences et Techniques du Languedoc
Place E. Bataillon, F-34060 Montpellier Cedex (France)
[+] Present address:
Chemistry Department, McGill University
Montreal H3A 2K6 (Canada)

Here we describe the analogous reaction of **1** with CS_2. The unexpectedly easy decomposition of the silyl ester **3** of dithioformic acid at room temperature leads to the formation of the first isolable silanethione, **6**.[1a, 12]

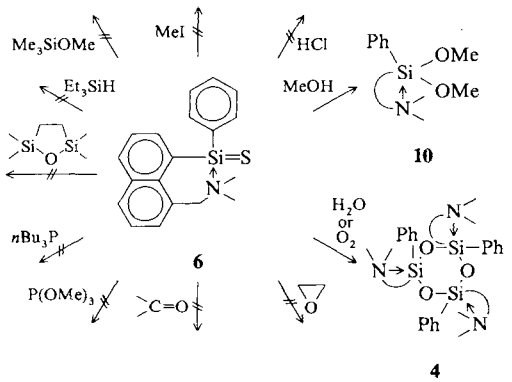
The ^1H NMR spectrum provides the strongest evidence for this structure. Two diastereotopic signals are observed for the methyl groups of the dimethylamino naphthyl substituent and they are clearly deshielded relative to the signals of the parent silane **1**. The IR spectrum exhibits a new band at 645 cm^{-1}.[13] Although **6** is relatively long-lived in solution ($t_{1/2}$: 3 d in $CDCl_3$ at 25 °C), extreme precautions must be taken to avoid exposure to minute amounts of air. The fast oxidation of **6** gives the same trimeric siloxane **4** obtained in the reaction of **1** with CO_2.[10] If the reaction of **1** with CS_2 is performed in the presence of $(Me_2SiO)_3$ no product **8** corresponding to the insertion[1a, 12] of the silanethione **6** into $(Me_2SiO)_3$ is obtained (even after 48 h). However, we observed the formation of the eight-membered ring derivative **7** when the oxidation of **6** was performed in the presence of $(Me_2SiO)_3$; this suggests that the oxidation probably involves the transient formation of silanone **5**. Addition of sulfur to **1** also gives **6**. A small excess of S_8 is necessary to complete the reaction at room temperature, but **6** is the only silicon-containing product. The insertion of sulfur into the Si–H bond normally requires more drastic conditions.[14]



9 **1** **6**

There has been only one report of the transient formation of an $R_2Si=Se$ compound.[15] The addition of Se to **1** gives, similarly to S_8, the monomeric Si=Se species **9**. The reaction is slightly slower than with S_8. Like **6**, compound **9** is extremely sensitive to air. Compound **9** is characterized by a downfield ^{29}Si chemical shift ($\delta = +29.4$) and a high coupling constant with ^{77}Se ($J_{SeSi} = 257$ Hz).

The reactivity of the coordinated Si=S compound **6** with electrophiles and nucleophiles is unexpectedly low. Phosphanes, phosphites, ketones, epoxides, MeI, and HCl are unreactive, as are alkoxysilanes and siloxanes. Methanolysis gives the dimethoxysilane **10**[16] but only if methanol is introduced in a large excess. Hydrolysis leads to the trimer **4**.[10]



The structure of the more bulky silanethione **11**, containing *two* α-naphthyl substituents, has been obtained by X-ray analysis[17] (Fig. 1). The Si–S bond (2.013 Å) is shorter than a Si–S single[18] bond (2.16 Å); an 8% reduction in bond

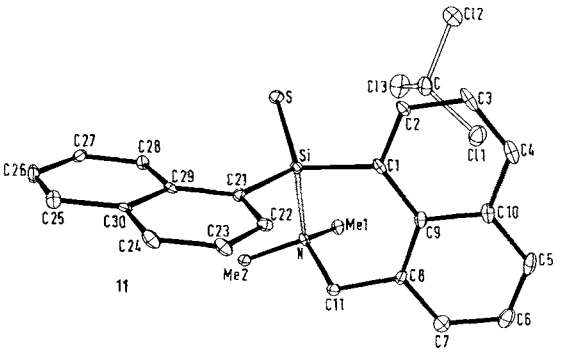
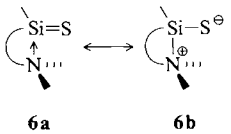


Fig. 1. ORTEP drawing of the molecular structure of **11**·$CHCl_3$. Thermal ellipsoids at the 10% probability level. Important distances [Å] and angles [°]: Si-S 2.013(3), Si-N 1.964(8), Si-C1 1.885(7), Si-C21 1.876(8); S-Si-C1 114.5(3),

length is typical of π-bonded species at silicon. The Si–N distance (1.96 Å), slightly longer than[19] a Si–N σ bond (1.79 Å), supports a very strong association of the aminoaryl substituent with silicon. Generally, the coordinate bond length determined with the same coordinating group lies in the range 2.3–2.6 Å.[20] The silicon center displays a distorted tetrahedral environment with the C1–Si–C21 angle (110°) nearly equal to the Si–Si–N angle (110.9°). The N–Si–C1 angle (96°) and the S–Si–C21 angle (120°) differ considerably, but the sum of the bond angles S-Si-C1, C1-Si-C21, S-Si-C21 is 344.9°, which is intermediate between $sp^2 + p$ (360°) and sp^3 (328.5°). Important to note is the position of the sulfur atom, which is situated outside the plane of the naphthyl–silicon unit, which means that the extra stabilization is not due to aromatic delocalization.

Also noteworthy is the solubility of the internally coordinated silicon compounds **6**, **9**, and **11**. They are insoluble in common organic solvents (CCl_4, Et_2O, THF, benzene, hexane) and only moderately soluble in $CHCl_3$ and CH_2Cl_2, but highly soluble in nucleophilic solvents (DMF, acetone, tetramethylurea, HMPT, $(MeO)_3PO$); the latter solvents are known to have a strong affinity for coordination at silicon.[21]

It is reasonable to expect that the resonance betaine structure **6b** strongly participates in the electronic distribution of **6** and **11**.



6a **6b**

Such a structure would partly explain the unexpectedly low reactivity of the silanethione towards nucleophiles and electrophiles, as well as its low solubility in organic solvents.

Experimental Procedure

Preparation of **6** from **1** and CS_2: The reaction was performed under argon using vacuum line techniques. CS_2 was purified by distillation and repeated freeze/thaw cycles just prior to use. In a typical experiment, 10 mL of CS_2 (12.6 g, 0.16 mol) was added dropwise at room temperature to **1** (2.91 g, 0.01 mol) with stirring. After a 5-min induction period, an exothermic reaction ensued with evolution of gas. After 1 h, the two phases were separated with a cannula. The lower phase was dried in vacuo, giving a yellow-white precipitate, which was dissolved in $CDCl_3$ (freshly distilled). Yield 67%; m.p. 170–171 °C. ^{29}Si NMR (49.69 MHz, $CDCl_3$, TMS int.): $\delta = +22.3$. ^{13}C NMR (62.9 MHz, $CDCl_3$, TMS int.): $\delta = 45.6$, 46.4 ($N(CH_3)_2$), 63.7 (NCH_2), ^1H NMR (62.9 MHz, $CDCl_3$, TMS int.): $\delta = 2.5$, 2.7 (2s, 6H, $N(CH_3)_2$), 4.3 (bd, 2H, NCH_2), 6.9–8.1 (m, 11H, aryl-H). MS (70 eV): *m/z* (rel. int. %): 321(33), 306(100), 245(15), 228(40), 215(20), 167(13), 141(18), 91(11), 84(8), 58(12). MS

(15 eV): *m/z* (rel. int. %): 321(15), 306(100), 245(6), 228(13), 91(2), 84(6), 58(3). FAB-MS (pos.): *m/z* (rel. int. %): 321(10), 306(100), 245(8), 228(30), 215(15), 167(10), 141(12), 91(8), 76(15), 58(8); M_r (calcd) for $C_{19}H_{19}SiSN$ = 321.008. Relative distribution: theoretical 321.008(100), 322.1030(27.838), 323.0999(11.442), 324.1009(2.263); experimental 321(100), 322(27.85), 323(11.74).

Preparation of **6** from **1** and S_8: **1** (0.589 g, 2 mmol) and S_8 (0.088 g, 2.76 mmol) were mixed in degassed $CDCl_3$ (2.5 mL). After 1 h, the NMR spectrum of the yellow solution was recorded. All the starting **1** had been consumed. The spectral data were identical to those of compound **6** isolated from the CS_2 reaction.

Preparation of **9** from **1** and Se: A mixture of **1** (0.5 g, 1.7 mmol) and selenium (0.225 g, 2.8 mmol) in $CDCl_3$ (5 mL) was kept for 30 min at 25 °C and then analyzed spectroscopically. Yield 84%; m.p. >80 °C (dec.). ^{29}Si NMR (49.69 MHz, $CDCl_3$, TMS int.): $\delta = +29.4$ ($J_{SeSi} = 257$ Hz). ^{13}C NMR (62.9 MHz, $CDCl_3$, TMS int.): $\delta = 45.72$, 47.32 (2s, $N(CH_3)_2$), 64.23 (s, NCH_2); ^{1}H NMR (60 MHz, $CDCl_3$, TMS int.): $\delta = 2.6$, 2.8 (2s, 6H), 5.4 (br., 2H), 6.8–8.2 (m, 11H). MS (70 eV): *m/z* (rel. int. %): 369(30), 354 (100), 276(45), 237(30).

Received: February 27, 1989;
revised: May 16, 1989 [Z 3196/3197 IE]
German version: *Angew. Chem. 101* (1989) 1069

[1] Reviews: a) L. E. Gusel'nikov, N. S. Nametkin, *Chem. Rev. 79* (1979) 529; b) G. Raabe, J. Michl, *ibid. 85* (1985) 419; T. J. Barton, *Pure Appl. Chem. 52* (1980) 615; G. Bertrand, G. Trinquier, P. Mazerolles, *J. Organomet. Chem. Libr. 12* (1981) 1; N. J. Wiberg, *J. Organomet. Chem. 273* (1984) 141; R. West, *Science (Washington, D.C.) 225* (1984) 1109.

[2] A. G. Brooks, F. Abdesaken, B. Gutekunst, G. Gutekunst, R. K. Kalbury, *J. Chem. Soc. Chem. Commun. 1981*, 191.

[3] R. West, M. J. Fink, J. Michl, *Science (Washington, D.C.) 214* (1981) 1343.

[4] N. Wiberg, K. Schurz, G. Fischer, *Angew. Chem. 97* (1985) 1058; *Angew. Chem. Int. Ed. Engl. 24* (1985) 1053; M. Hesse, U. Klingebiel, *ibid. 98* (1986) 638 and *25* (1986) 649; S. S. Zigler, L. M. Johnson, R. West, *J. Organomet. Chem. 341* (1988) 187.

[5] N. Wiberg, G. Wagner, G. Müller, *Angew. Chem. 97* (1985) 220; *Angew. Chem. Int. Ed. Engl. 24* (1985) 229; N. Wiberg, G. Wagner, G. Müller, J. Riede, *J. Organomet. Chem. 271* (1984) 381; N. Wiberg, H. Kopf, *ibid. 315* (1986) 9.

[6] N. Wiberg, K. Schurz, G. Reber, G. Müller, *J. Chem. Soc. Chem. Commun. 1986*, 591; N. Wiberg, K. Schurz, *Chem. Ber. 121* (1988) 581; N. Wiberg, K. Schurz, G. Müller, J. Riede, *Angew. Chem. 100* (1988) 979; *Angew. Chem. Int. Ed. Engl. 27* (1988) 935.

[7] J. Boyer, C. Breliere, R. Corriu, A. Kpoton, M. Poirier, G. Royo, *J. Organomet. Chem. 311* (1986) C39.

[8] R. J. P. Corriu, G. F. Lanneau, M. Perrot, *Tetrahedron Lett. 29* (1988) 1271.

[9] R. Corriu, G. Lanneau, M. Perrot, *Tetrahedron Lett. 28* (1987) 3941.

[10] P. Arya, J. Boyer, R. J. P. Corriu, G. Lanneau, M. Perrot, *J. Organomet. Chem. 346* (1988) C11.

[11] For typical Me_2SiO trapping experiments, see: C. M. Golino, R. D. Bush, L. H. Sommer, *J. Am. Chem. Soc. 97* (1975) 7371; H. S. Soysa, H. Okinoshima, W. P. Weber, *J. Organomet. Chem. 133* (1977) C17; D. Seyferth, T. F. O. Lim, D. P. Duncan, *J. Am. Chem. Soc. 100* (1978) 1626; see also T. J. Barton, S. Bain, *Organometallics 7* (1988) 528; H. Okinoshima, W. P. Weber, *J. Organomet. Chem. 149* (1978) 279.

[12] L. H. Sommer, J. McLick, *J. Organomet. Chem. 101* (1975) 171; H. S. Dilanjan Soysa, I. Nam Yung, w. P. Weber, *ibid. 171* (1979) 177; H. Sakurai, K. Sakamoto, M. Kira, *Chem. Lett. 1987*, 1075; T. J. Barton, G. C. Paul, *J. Am. Chem. Soc. 109* (1987) 5292; C. Guimon, G. Pfister-Guillouzo, H. Lavayssiere, G. Dousse, J. Barrau, J. Satgé, *J. Organomet. Chem. 249* (1983) C17.

[13] L. E. Gusel'nikov, V. V. Volkova, V. G. Avakyan, N. S. Nametkin, M. G. Voronkov, S. V. Kirpichenko, E. N. Suslova, *J. Organomet. Chem. 254* (1983) 173.

[14] R. Calas, N. Duffaut, B. Martel, C. Paris, *Bull. Soc. Chim. Fr. 1961*, 886; B. Becker, W. Wojnowski, *Synth. React. Inorg. Met.-Org. Chem. 12* (1982) 565, and references cited therein; B. Becker, R. Corriu, B. Henner, W. Wojnowski, K. Peters, H. G. von Schnering, *J. Organomet. Chem. 312* (1986) 305.

[15] D. P. Thomson, P. Boudjouk, *J. Chem. Soc. Chem. Commun. 1987*, 1466.

[16] Spectroscopic data for **10**: ^{1}H NMR (60 MHz, $CDCl_3$, TMS int.): $\delta = 1.92$ (s, 6H, $N(CH_3)_2$), 3.54 (s, 6H, OCH_3), 4.07 (s, 2H, $N-CH_2$), 7–8.5 (m, 11H, aryl-H). ^{29}Si NMR (49.69 MHz, $CDCl_3$, TMS int.): $\delta = 32.03$; ^{13}C NMR (62.9 MHz, $CDCl_3$, TMS int.): $\delta = 45.46$, 51.25 ($N(CH_3)_2$), 63.35 (NCH_2), 124.48–139.40 (m, aryl).

[17] Crystallographic data: Enraf-Nonius CAD-3 diffractometer, $Cu_{K\alpha}$ radiation, $\lambda = 1.5404$ Å, graphite monochromator, orthorhombic, space group $Pna2_1$, $a = 15.283(5)$, $b = 21.776(7)$, $c = 7.121(3)$ Å, $\varrho_{calcd} = 1.376$ g cm^{-3}, $Z = 4$, $\mu(Cu_{K\alpha}) = 49.7$ cm^{-1}. 1762 unique reflections, 1604 observed [$F > 3.5\,\sigma(F)$]. Anisotropic temperature factors for all atoms; the hydrogen atoms were taken into account in the refinement with isotropic temperature factors. $R = 0.0640$, $R_w = 0.0635$ for 129 parameters in the last refinement cycle. Further details of the crystal structure investigation are available on request from the Cambridge Crystallographic Data Center, University Chemical Laboratory, Lensfield Road, Cambridge CB2 1EW (UK), on quoting the full journal citation.

[18] W. E. Schklower, Yu. T. Strutchkow, L. E. Gusel'nikov, W. W. Wolkowa, W. G. Awakyan, *Z. Anorg. Allg. Chem. 501* (1983) 153; R. West, D. J. De Young, K. J. Haller, *J. Am. Chem. Soc. 107* (1985) 4942.

[19] See, for example: W. Fink, *Angew. Chem. 78* (1966) 803; *Angew. Chem. Int. Ed. Engl. 5* (1966) 760; A. J. Blake, E. A. V. Ebsworth, A. J. Welch, *Acta Crystallogr. Sect. C*, 40 (1984) 895; G. Klebe, J. W. Bats, K. Hensen, *Z. Naturforsch. B38* (1983) 825; *J. Chem. Soc. Dalton Trans. 1985*, 1.

[20] C. Breliere, F. Carré, R. J. P. Corriu, M. Poirier, G. Royo, *Organometallics 5* (1986) 388; J. Boyer, C. Breliere, F. Carré, R. Corriu, A. Kpoton, M. Poirier, G. Royo, J. C. Young, *J. Chem. Soc. Dalton Trans.* (1989) 43.

[21] R. J. P. Corriu, M. Henner, *J. Organomet. Chem. 74* (1974) 1; S. N. Tandura, M. G. Voronkov, N. V. Alekseev, *Top. Curr. Chem. 131* (1986) 99, and references cited therein; A. R. Bassindale, J. C. Y. Lau, P. G. Taylor, *J. Organomet. Chem. 341* (1988) 213; for a recent summary, see: R. J. P. Corriu, J. C. Young: *"Hypervalent Silicon Compounds", in S. Patai, Z. Rappoport (Eds.): The Chemistry of Organic Silicon Compounds*, Wiley, Chichester 1989, chap. 20, pp. 1241–1288.

$[Mes_2SbCu(PMe_3)_2]_2$: The First Cu^I Antimonide **

By *Alan H. Cowley,* Richard A. Jones,* Christine M. Nunn,* and *Donald L. Westmoreland*

Copper(I) amides and phosphides display an interesting variety of structures which range from dinuclear to octanuclear in character. The Cu^I amides are tetrameric,[1] while all the Cu^I phosphides except $[tBu_2PCu]_4$[2] are coordinated with Lewis bases.[3] Interestingly, the heavier congeners of Cu^I amides and phosphides are unknown. We report here the preparation and X-ray crystal structure of $[Mes_2SbCu(PMe_3)_2]_2$, the first example of an antimonide of a late transition metal (Mes = mesityl).

Dimesitylstibane (Mes_2SbH) was prepared by the reduction of trimesitylstibane[4] with excess lithium, followed by protonation with $[Me_3NH]Cl$. This method avoids the intermediacy of a halostibane. Mes_2SbH is surprisingly stable and does not show any signs of oxidation over a period of weeks. The X-ray crystal structure of Mes_2SbH (Fig. 1),[5] which, to our knowledge, constitutes the first such information for a secondary stibane, revealed that the molecules possess a C_2 axis which bisects the C1–Sb–C1′ angle. Each of the aryl rings is twisted out of the C1–Sb–C1′ plane by an angle of 68.06°. The presence of the Sb-H moiety could not be discerned in the electron density map; however, its identity was confirmed by the detection of a singlet at $\delta = 4.90$ in

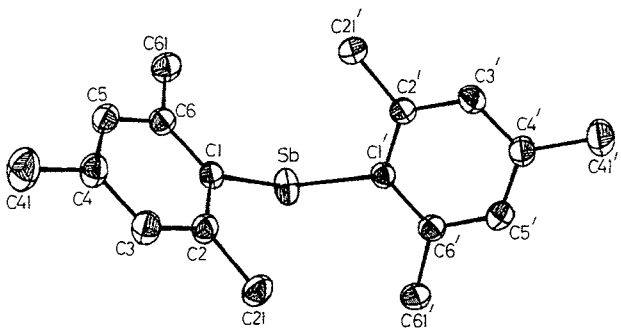


Fig. 1. The structure of Mes_2SbH in the crystal. Selected bond lengths and angles: Sb–C1 2.168(2) Å; C1–Sb–C1′ 101.70(8)°.

[*] Prof. R. A. Jones, Prof. A. H. Cowley, Dr. C. M. Nunn, D. L. Westmoreland
Department of Chemistry
The University of Texas at Austin
Austin, TX 78712 (USA)

[**] Acknowledgement is made to the National Science Foundation and the Robert A. Welch Foundation for support of this research.

the ^{1}H NMR spectrum and a stretching vibration at $\tilde{\nu}_{Sb-H}$ 1887.3 cm^{-1} in the IR spectrum.

Lithiation of Mes_2SbH with *n*BuLi produced Mes_2SbLi, which, upon addition to a THF solution of CuCl and Me_3P, afforded yellow crystalline $[Mes_2SbCu(PMe_3)_2]_2$. Its solid-state structure (Fig. 2)[5] comprises two crystallographically

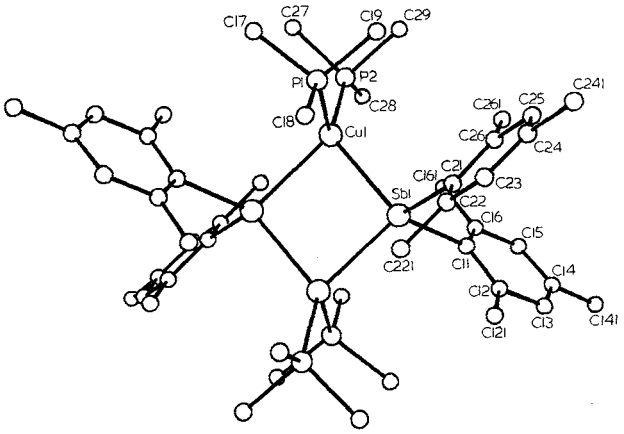


Fig. 2. The structure of $[Mes_2SbCu(PMe_3)_2]_2$ in the crystal [5]. There are two crystallographically independent molecules. Selected bond lengths [Å] and bond angles [°] shown in parentheses (for the second molecule): Sb1–Cu1 2.676(2) (2.661(2)), Sb1–Cu1 2.657(1) (2.681(1)), Cu1–P1 2.288(3) (2.272(3)), Cu1–P2 2.281(3) (2.285(4)), Cu1–Sb1–Cu1' 95.34(5) (94.88(5)), Sb1–Cu1–Sb1' 84.66(4) (85.12(5)), P1–Cu1–P2 105.3(1) (105.4(1)), C11–Sb1–C21 95.2(4) (93.7(4)).

independent molecules with similar dimensions. Both molecules are centrosymmetric and feature a planar Cu_2Sb_2 core of alternating Cu and Sb atoms. The average Sb–Cu–Sb' and Cu–Sb–Cu' angles are 95.11(5) and 84.89(5)°, respectively. Four-coordination of each Cu is achieved by the attachment of two Me_3P ligands. The geometry at both Cu and Sb is distorted tetrahedral. The average Cu–Sb distance is 2.669(2) Å, which is close to the sum of covalent radii for these elements (2.68 Å),[6] but somewhat longer than the only previously measured bond length of 2.554(2) Å in the stibane complex $[(Ph_3Sb)_3CuCl]$.[7] The Cu–Cu separation in the title compound (3.95 Å) precludes any type of bonding interaction between these atoms. The antimonide is moderately stable in the crystalline form in the absence of air. However, surface decomposition occurs in the presence of light. Solutions of the compound decompose in a few hours at 25 °C.

The reaction of Mes_2SbLi with CuCl in the absence of Me_3P resulted in reduction of Cu^I to Cu^0 and formation of the distibane Mes_4Sb_2.[8] Similar observations have been made previously with metal phosphides.[9]

Experimental Procedure

Mes_2SbH: A solution of Mes_2Sb (33 g, 68.8 mmol) and Li powder (2 g, 288.2 mmol) in THF (750 mL) was stirred at 25 °C for 12 h. After filtration of the deep orange solution, solid $[Me_3NH]Cl$ (9.2 g, 172 mmol) was added in one portion. After stirring the reaction mixture for 2 h, the volume was reduced to ca. 200 mL and 500 mL of toluene was added. Filtration through Celite, followed by solvent evaporation, left crude Mes_2SbH as an oily solid. Recrystallization from 3:1 toluene/hexane (−15 °C) afforded a 68% (16.9 g) yield of off-white crystals of Mes_2SbH, m.p. 112–15 °C. X-ray quality crystals were grown from hexane. ^{1}H NMR (300 MHz, C_6D_6, TMS ext.): δ = 2.08 (s, 3H, *p*-Me), 2.31 (s, 6H, *o*-Me), 4.90 (s, 1H, SbH), 6.72 (s, 2H, *m*-H). $[Mes_2SbCu(PMe_3)_2]_2$: Mes_2SbLi was prepared by addition of *n*BuLi (1.5 mL of a 1.6 M solution in hexane) to a solution of Mes_2SbH (0.86 g, 2.38 mmol) in 60 mL of THF at −78 °C. The resulting solution was stirred for 3 h at 25 °C, then added dropwise to a solution of CuCl (0.235 g, 2.37 mmol) and Me_3P (1 mL) in 75 mL of THF at −78 °C. After stirring the reaction mixture at −10 °C for 2 h, the solvent was removed in vacuo. The resulting dark solid was extracted with two 40-mL portions of hexane and filtered through Celite. Concentration and cooling of the solution (−15 °C) afforded a 41% yield (0.51 g) of yellow crystalline $[Mes_2SbCu(PMe_3)_2]_2$, m.p. 160 °C (dec.). X-ray quality crystals were grown from hexane. ^{1}H NMR (300 MHz, C_6D_6, TMS ext.): δ = 0.90 (br, PMe), 2.06 (s, 3H, *p*-Me), 2.47 (s, 6H, *o*-Me), 6.65 (s, 2H, *m*-H). $^{31}P\{^1H\}$ NMR (121.5 MHz, C_6D_6, 85% H_3PO_4 ext.): δ = −34.43(s).

Received: March 2, 1989 [Z 3210 IE]
German version: *Angew. Chem. 101* (1989) 1089

CAS Registry numbers:
$[Mes_2SbCu(PMe_3)_2]_2$, 121844-94-8; Mes_2SbH, 121810-02-4; $[Me_3NH]Cl$, 593-81-7; Li, 7439-93-2; Mes_3Sb, 23822-17-5.

[1] H. Hope, P. P. Power, *Inorg. Chem. 23* (1984) 936; S. Gamarotti, M. Bracci, C. Floriani, A. Chiesi-Villa, C. Guasanti, *J. Chem. Soc. Dalton Trans. 1987*, 1883.

[2] A. H. Cowley, D. M. Giolando, R. A. Jones, C. M. Nunn, J. M. Power, *J. Chem. Soc. Chem. Commun. 1988*, 208.

[3] T. Greiser, E. Weiss, *Chem. Ber. 111* (1978) 516; G. van Koten, J. G. Noltes, A. L. Spek, *J. Organomet. Chem. 159* (1978) 441; F. Gol, P. C. Knüppel, O. Stelzer, W. S. Sheldrick, *Angew. Chem. 100* (1988) 1008; *Angew. Chem. Int. Ed. Engl. 27* (1988) 956; T. A. Annan, R. Kumar, D. G. Tuck, *J. Chem. Soc. Chem. Commun. 1988*, 446; D. J. Brauer, P. C. Knüppel, O. Stelzer, *ibid. 1988*, 551.

[4] D. Henning, G. Kempter, K. D. Worlitzer, *Z. Chem. 9* (1969) 306; M. Benmalek, H. Chermette, C. Martelet, D. Sandino, J. Tousset, *J. Organomet. Chem. 67* (1974) 53.

[5] Crystal structure data for Mes_2SbH: monoclinic, space group $C2/c$ (No. 15), $Z = 4$, $a = 13.162(3)$, $b = 9.358(3)$, $c = 13.699(2)$ Å, $\beta = 103.01(2)°$. $V = 1644(1)$ Å^3, $\varrho_{calcd} = 1.459$ g/cm^3, ($Mo_{K\alpha}$, $\lambda = 0.71069$ Å, $\mu = 16.7$ cm^{-1}), 2175 unique data collected (ω-2θ scans, $3.0 \le 2\theta \le 50.0°$), of which 1780 had $I > 3.0\,\sigma(I)$ and were used for structure solution and refinement. $[Mes_2SbCu(PMe_3)_2]_2$: triclinic, space group $P\bar{1}$ (No. 2), $Z = 2$; $a = 12.466(7)$, $b = 12.496(6)$, $c = 20.026(15)$ Å, $\alpha = 75.22(5)$, $\beta = 80.07(5)$, $\gamma = 78.57(4)$, $V = 2932(1)$ Å^3; $\varrho_{calcd} = 1.305$ g/cm^3, ($Mo_{K\alpha}$, $\lambda = 0.71069$ Å, $\mu = 17.8$ cm), 8121 unique data collected (ω-2θ scans, $3.0 \le 2\theta \le 46.0°$), of which 5228 had $I > 3.0\,\sigma(I)$ and were used for structure solution and refinement. Both data sets were collected on an Enraf-Nonius CAD4 diffractometer at 293 K and were corrected for Lorentz, polarization, crystal decay, and X-ray absorption (empirical ψ-scan method). The structures were solved by Patterson syntheses, which located the heavy-atom positions. Refinement (full-matrix least-squares) gave $R = 0.027$ and $R_w = 0.035$ for Mes_2SbH and $R = 0.060$ and $R_w = 0.084$ for $[Mes_2SbCu(PMe_3)_2]_2$. Atoms C(33), C(34), and C(341) of the second molecule of $[Mes_2SbCu(PMe_3)_2]_2$ were refined isotropically; all other non-hydrogen atoms were refined anisotropically. Further details of the crystal structure investigations can be obtained from the Fachinformationszentrum Karlsruhe, Gesellschaft für wissenschaftlich-technische Information mbH, D-7514 Eggenstein-Leopoldshafen 2 (FRG), by quoting the depository number CSD-53858, the names of the authors, and the journal citation.

[6] L. Pauling, *The Nature of the Chemical Bond*, Cornell University Press, Ithaca, NY, USA 1960, p. 246.

[7] A. L. Rheingold, M. E. Fountain, *J. Crystallogr. Spectrosc. Res. 14* (1984) 549.

[8] M. Ates, H. J. Breunig, A. Soltani-Neshan, M. Tegeler, *Z. Naturforsch. B41* (1986) 321.

[9] K. Issleib, H. O. Fröhlich, *Chem. Ber. 95* (1962) 375; K. Issleib, E. Wenschuh, *Z. Naturforsch. B19* (1964) 199.

One-Dimensional Metal Chains in a Chiral Environment – The Crystal Structure of Helical Bis(dicarbonylrhodium(I))-3,3'-hexafluoroglutarylbis-(1*R*)-camphorate **

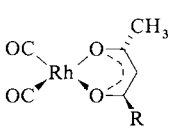
By *Volker Schurig,* Hans Gaus, Peter Scheer, Leonhard Walz,* and *Hans Georg von Schnering*

The propensity of four-coordinate square-planar d^8-transition-metal compounds, for example, dicarbonylrhodium(I)-

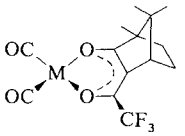
[*] Prof. Dr. V. Schurig, H. Gaus, Dipl.-Chem. P. Scheer
Institut für Organische Chemie der Universität
Auf der Morgenstelle 18, D-7400 Tübingen (FRG)
Dr. L. Walz, Prof. Dr. H. G. von Schnering
Max-Planck-Institut für Festkörperforschung
D-7000 Stuttgart (FRG)

[**] This work was supported by the Fonds der Chemischen Industrie and the Stiftung Volkswagenwerk.

2,4-pentanedionate **1**[1] or $K_2[Pt(CN)_4]Cl_{0.32}(H_2O)_{2.6}$,[2] to form one-dimensional metal chains in the solid state is well established.[2] It has previously been demonstrated that the presence of *chiral* β-diketonate ligands in the inner coordination sphere of the d^8-metal ions Rh^I or Ir^I may efficiently control the degree and mode of molecular stacking. Thus, enantiomerically pure dicarbonylrhodium(I)-3-(trifluoroacetyl)-(1*R*)-camphorate (1*R*)-**2a** crystallizes as a yellow solid devoid of molecular stacking, while the racemate (1*R*/1*S*)-**2a** forms dark dichroic crystals in which the rhodium atoms are linked along a one-dimensional metal chain in a pairwise alternating mode to ligands with -[(1*R*-1*R*-1*S*-1*S*)]$_\infty$- configuration.[3, 4]



1, R = CH_3
3, R = CF_3

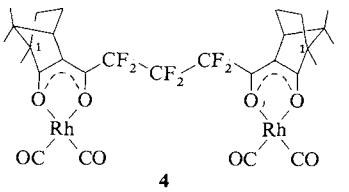


(1*R*)-**2a**, M = Rh
(1*R*)-**2b**, M = Ir

The concept of structure control by chiral ligands has subsequently been employed for the engineering of a totally ordered columnar structure consisting of a one-dimensional -[Rh-Rh-Ir-Ir]$_\infty$- metal chain in the solid state simply by mixing the quasi-enantiomers of yellow (1*S*)-**2a** and yellow (1*R*)-**2b** to yield a black quasi-racemate.[5, 6]

We have now synthesized dinuclear bis(dicarbonylrhodium(I)-3,3'-hexafluoroglutarylbis-(1*R*)-camphorate **4** in which two square-planar rhodium(I) entities are linked via a short perfluoroalkyl bridge.

In contrast to the yellow enantiomers of **2a** and **2b**, homochiral **4** forms dark crystals, indicating the formation of a columnar structure. An X-ray structure analysis of **4**[7]



4

showed unexpected features (Fig. 1). Dinuclear **4** does not participate in the bridging of segregated stacks, as might have been expected; instead, both rhodium atoms are incorporated into a single one-dimensional metal chain. This requires the formation of a twisted, helical conformation of **4** in the solid state. In the unit cell *two* independent dinuclear complexes of **4** are observed which differ by *opposite* screw senses of their helical conformations (Rh1-Rh2 (+)-(*P*) and Rh1'-Rh2' (−)-(*M*)) and which are arranged pairwise along the one-dimensional metal chain with the following repetitive sequence (Fig. 1b):

$$\cdots Rh1\text{-}Rh2(P)\cdots Rh1'\text{-}Rh2'(M)\cdots Rh2'\text{-}Rh1'(M)\cdots Rh2\text{-}Rh1(P)\cdots]\cdots_\infty$$

Since all rhodium atoms reside in the homochiral environment of (1*R*)-configurated camphor moieties, the energetically different diastereoisomers (1*R*)-(*P*)-(1*R*) and (1*R*)-(*M*)-(1*R*) (Fig. 2) occur as a result of stereoisomerism in the solid state.[8] Therefore, the one-dimensional metal chains are characterized by two different *intra*molecular metal–metal distances (Rh1-Rh2 (*P*), 3.419 Å; Rh1'-Rh2' (*M*), 3.313 Å) and by three different *inter*molecular metal–metal distances (Rh2$\cdots$Rh1' (*P*/*M*), 4.191 Å; Rh2'$\cdots$Rh2' (*M*/*M*), 3.373 Å, and Rh1$\cdots$Rh1 (*P*/*P*) 3.693 Å). Obviously, there is much stronger interaction between two adjacent (*M*) complexes than between the two (*P*) complexes, and a very weak metal–metal interaction between a (*P*) complex and an (*M*) complex. Despite the high steric constraint imposed by the

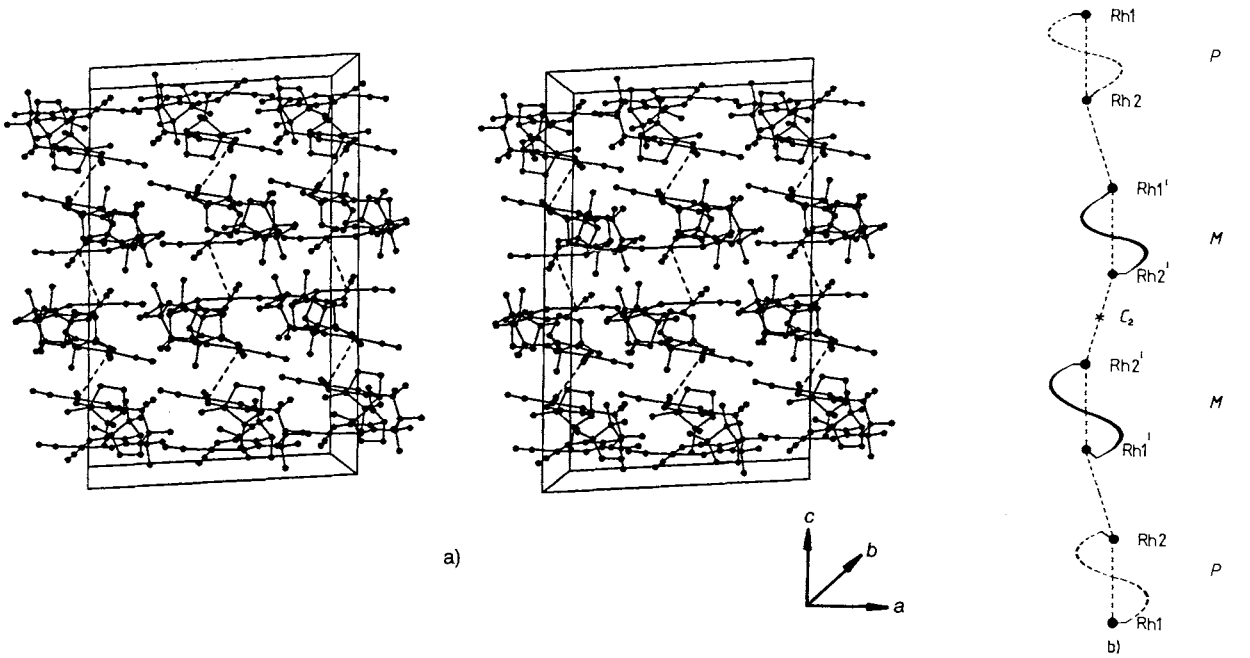


Fig. 1. a) Stereoview of the crystal structure of **4**; b) idealized arrangement of **4** in the one-dimensional metal chain.

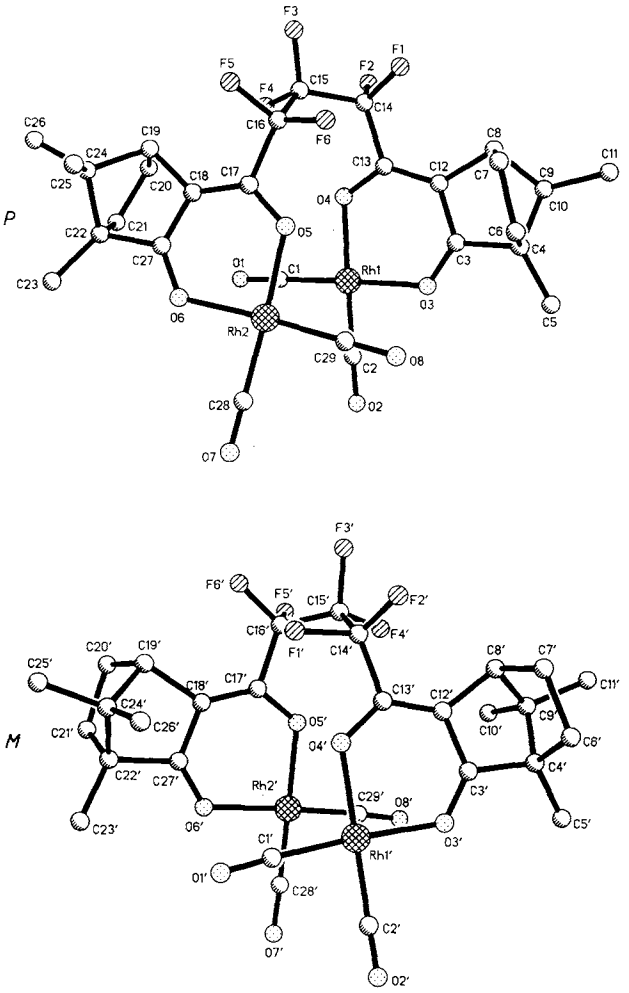
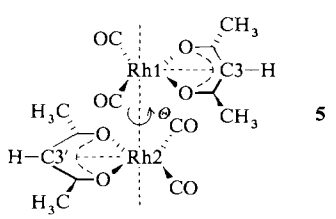


Fig. 2. Molecular structure of (*P*)-**4** (top) and (*M*)-**4** (bottom).

bicyclic camphor moiety, the Rh–Rh distances are comparable to that of planar dicarbonylrhodium(I)-1,1,1-trifluoro-2,4-pentanedionate **3** (Rh-Rh, 3.34 Å),[9] but nevertheless the distances are large with respect to a single Rh–Rh bond (2.50 Å).

In solid **1** the molecules are stacked in an *anti* position (i.e., $\theta = 180°$, interplanar angle C3-Rh1-Rh2-C3′; cf. **5**).[10]

Such nearly *anti* arrangement is observed in the unit cell of **4** between entities with the longest intermolecular metal–metal contact (Rh2 $\cdots$ Rh1′, $\theta = -175.5°$). The other entities exhibit lower interplanar angles (Rh2′ $\cdots$ Rh2′, $\theta = -120.9°$, and Rh1 $\cdots$ Rh1, $\theta = +119.2°$). Because of structural requirements, the intramolecular interplanar angles are much smaller, and different, for the diastereoisomers (1*R*)-(*P*)-(1*R*) (Rh1-Rh2, $\theta = +81.1°$) and (1*R*)-(*M*)-(1*R*) (Rh1′-Rh2′, $\theta = -78.3°$). Since the one-dimensional metal chain is not linear, the planes of the dicarbonylrhodium(I)-β-diketonate entities are not coplanar, but are tilted.[11]



5

In conclusion, the occurrence of opposite helical conformations of **4** (*P* and *M*) in a homochiral environment causes *stereoisomerism in the solid state* and thus deviations from an idealized molecular stacking.[12]

Experimental Procedure

3,3′-Hexafluoroglutarylbis-(1*R*)-camphorate (cf. V. Schurig, *Inorg. Chem. 11* (1972) 736): 3-Bromo-(1*R*)-camphor (6.9 g, 0.03 mol) (recrystallized from ethanol and dried over P_4O_{10}), magnesium powder (0.73 g, 0.03 mol), and diethyl hexafluoroglutarate (4.44 g, 0.015 mol) were refluxed in diethyl ether until most of the metal was consumed. The brown reaction mixture was hydrolyzed with 10% hydrochloric acid, the organic phase separated, and the product freed from volatiles by distillation and sublimation (camphor, ethyl 3-hexafluoroglutarylmono-(1*R*)-camphorate). The residue was chromatographed (dichloromethane/*n*-heptane (5:1, v/v)) on silica. Yield: 2 g (4 mmol, 27%). $[\alpha]_D^{23} + 150$ ($c = 4{,}5$, toluene). MS: *m/z* 509 ($M + 1$) (28%), 508 ($M^{\oplus}$) (100). ^{13}C NMR (25 MHz, $CDCl_3$): $\delta = 213.9, 120.0, 58.0, 49.0, 47.6, 30.2, 26.7, 20.4, 18.7, 8.5$.

4: Equimolar amounts of the ligand and $[(CO)_4Rh_2Cl_2]$ were refluxed in toluene in the presence of an excess of barium carbonate for 24 h. After flash chromatography on inactive neutral alumina, the complex was recrystallized from *n*-hexane at -20 °C. Yield 35%. M.p. 139 °C, red crystals. $[\alpha]_D^{23} + 75$ ($c = 0.4$, dichloromethane). MS: *m/z*: 824 ($M^{\oplus}$) (14%), 796 (48), 768 (100), 740 (30), 712 (26), 682 (13), 610 (12). IR (KBr) [cm^{-1}]: $\tilde{\nu} = 2960, 2935, 2875, 2080, 2015, 1975, 1620, 1490, 1175$. **4** may also be obtained by ligand exchange reaction of 3,3′-hexafluoroglutarylbis-(1*R*)-camphorate and **1** in *n*-hexane.

Received: February 27, 1989;
supplemented: April 25, 1989 [Z 3201 IE]
German version: *Angew. Chem. 101* (1989) 1037

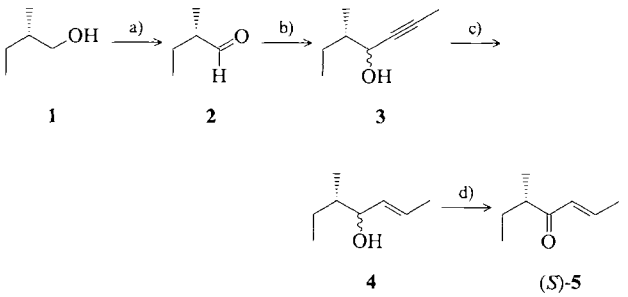
[1] F. Bonati, G. Wilkinson, *J. Chem. Soc. 1964*, 3156; J. P. Collman, L. M. Slifkin, L. M. Ballard, L. K. Monteith, C. G. Pitt, *Decomp. Organomet. Comp. Refract. Ceram., Met., Met. Alloys, Proc. Int. Symp., 1967*, S. 268.
[2] K. Krogmann, *Angew. Chem. 81* (1969) 10; *Angew. Chem. Int. Ed. Engl. 8* (1969) 35.
[3] V. Schurig, *Angew. Chem. 93* (1981) 806; *Angew. Chem. Int. Ed. Engl. 20* (1981) 807.
[4] V. Schurig, *Mol. Cryst. Liq. Cryst. 96* (1983) 271.
[5] V. Schurig, W. Pille, W. Winter, *Angew. Chem. 95* (1983) 327; *Angew. Chem. Int. Ed. Engl. 22* (1981) 327.
[6] V. Schurig, W. Pille, K. Peters, H. G. von Schnering, *Mol. Cryst. Liq. Cryst. 120* (1985) 385.
[7] Crystals of **4** (from *n*-hexane) are monoclinic, space group *C*2, $a = 16.249(5)$, $b = 15.365(5)$, $c = 25.652(8)$ Å, $\beta = 93.57°$, $Z = 8$, $R = 0.0421$, $V = 6392$ Å^3, $\varrho_{calcd} = 1.713$ g cm^{-3}, $\mu(Mo_{K\alpha}) = 9.96$ cm^{-1}. Further details of the crystal structure investigation may be obtained from the Fachinformationszentrum Karlsruhe, Gesellschaft für wissenschaftlich-technische Information mbH, D-7514 Eggenstein-Leopoldshafen 2 (FRG), by quoting the depository number CSD-53841, the names of the authors, and journal citation.
[8] (*P*)-**4** and (*M*)-**4** differ, for example, by the juxtaposition of the neopentyl bridge of camphor (*exo* (*P*) or *endo* (*M*)) towards the intramolecular metal–metal contact. The isomer (1*R*)-(*M*)-(1*R*) (Fig. 2, bottom) is obviously more stable then the diastereoisomer (1*R*)-(*P*)-(1*R*) (Fig. 2, top), because only the former and its enantiomer (1*S*)-(*P*)-(1*S*) are found in the solid state structure (unpublished) of *racemic* **4**; cf. [12].
[9] N. A. Bailey, E. Coates, G. B. Robertson, F. Bonati, R. Ugo, *Chem. Commun. 1967*, 1041.
[10] F. Huq, A. C. Skapski, *J. Cryst. Mol. Struct. 4* (1974) 411.
[11] The angles between the normals of the dicarbonylrhodium(I)-β-diketonate planes are 18.4° for *P* and 11.9° for *M*.
[12] The structure of **4** allows for intentional changes such as *heterochiral* variations ((1*R*,1*S*)-**4** (meso) or (1*R*,1*R*)-**4** + (1*S*,1*S*)-**4** (racemate)) and *heterometallic* combinations (Rh,Ir). If the structural motif of solid (1*R*,1*R*)-**4** is retained, the construction of highly ordered columnar structures with one-dimensional metal chains -[Rh,Ir,Rh,Ir]$_\infty$-, -[Rh,Rh,Ir,Ir]$_\infty$-, or -[Rh,Rh,Rh,Rh,Ir,Ir,Ir,Ir]$_\infty$- can be envisaged, when, for example, iridium is attached to the (1*R*)-configurated ligand and rhodium is attached to the (1*S*)-configurated ligand of **4**. These investigations are currently being pursued.

Isolation, Synthesis, and Absolute Configuration of Filbertone – the Principal Flavor Component of the Hazelnut**

By *Johann Jauch, Dieter Schmalzing, Volker Schurig,* Roland Emberger, Rudolf Hopp, Manfred Köpsel, Wilhelm Silberzahn,* and *Peter Werkhoff*

Chiral, acyclic, aliphatic (conjugated) enones occur in nature as pheromones and flavors. For example, (*E*,6*S*)-4,6-dimethyloct-4-en-3-one, manicone, has been identified in the mandibular gland of the ant *Manica mutica*[1] and (*E*)-5-methylhept-2-en-4-one, filbertone **5**, has been isolated[2] from hazelnut extracts and identified as the principal flavor component of filberts[3] (name synonymous with hazelnut; derived from *St. Philibert*).

The determination of the enantiomeric composition, the assignment of the absolute configuration, and the establishment of a relationship between chirality and olfaction necessitated both the enantioselective synthesis and the quantitative enantiomer separation of **5**. (*E*,5*S*)-Methylhept-2-en-4-one (*S*)-**5** was prepared according to Scheme 1 utilizing the (*S*)-*sec*-butyl chirality pool.



Scheme 1. a) $K_2Cr_2O_7/H_2SO_4/H_2O$; 70 °C/140 torr. b) $LiC{\equiv}CCH_3$/THF; −80 °C, 2 h; allowed to warm in ca. 12 h to +25 °C. c) $LiAlH_4$/THF, 4 h reflux. d) MnO_2/*n*-pentane, 40 h.

Commercially available (*S*)-(−)-2-methylbutan-1-ol **1** was oxidized to (*S*)-(+)-2-methylbutanal **2**,[4,5] which was then coupled with propynyllithium[6] to give (4*R*/4*S*,5*S*)-5-methylhept-2-yn-4-ol **3**. Stereoselective $LiAlH_4$ reduction[7] afforded exclusively (*E*,4*R*/4*S*,5*S*)-5-methylhept-2-en-4-ol **4**, which was oxidized with MnO_2 to (*E*,5*S*)-5-methylhept-2-en-4-one (*S*)-**5** (purity (by GLC) > 98%; overall yield, 20%, with steps a and d not yet optimized).[8]

Whereas racemic and natural **5** had previously been separated by GLC[9] after conversion to the oxime on a diamide phase,[10] the *underivatized* enone can be resolved directly by chiral complexation gas chromatography on nickel(II) bis[3-(heptafluorobutanoyl)-(1*R*)-10-methylcamphorate][11] in 8 min at 50 °C [phase 1] (Fig. 1) and by chiral inclusion gas chromatography on heptakis(2,6-di-*O*-methyl-3-*O*-trifluoroacetyl)-β-cyclodextrin[12] in 12 min at 110 °C [phase 2] (Fig. 2), thus permitting the simple complementary enantiomer analysis of synthetic (*S*)-**5** and *trace amounts* of natural **5**.

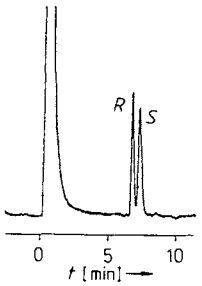


Fig. 1. Enantiomer separation of racemic (*E*)-5-methylhept-2-en-4-one **5** (filbertone) by chiral complexation gas chromatography on nickel(II)bis[3-(heptafluorobutanoyl)-(1*R*)-10-methylcamphorate] in OV-1 (ca. 0.1 m) at 50 °C [phase 1] [11]. Column: 10 m × 0.25 mm (I.D.) fused silica capillary. Carrier: 0.5 bar N_2.

The enantiomeric excess of synthetic (*S*)-**5** was determined on phase 1 and 2 to be *ee* = 92 ± 1% (Fig. 2c). On both phases 1 and 2, the (*S*) enantiomer is eluted as the second peak. Surprisingly, natural **5** exhibits only a rather low enantiomeric excess, varying with the origin of the hazelnuts: *ee* = 54.4% [phase 1], *ee* = 56.2% [phase 2] (Fig. 2a) (filberts from Turkey) and *ee* = 62.5% [phase 1], *ee* = 62.6% [phase 2] (filberts from Italy). Comparison of the elution order of synthetic (*S*)-**5** and natural filbertone established (*S*) configuration for the enantiomer in excess (Fig. 2a and 2c). Thus, it has been shown that **5** isolated from filberts is enriched with the (*S*) enantiomer of varying degree of enantiomeric purity.[9] The observation of differing enantiomeric compositions of natural compounds has a precedent in chiral pheromones (e.g., for *endo*-brevicomin[13]).

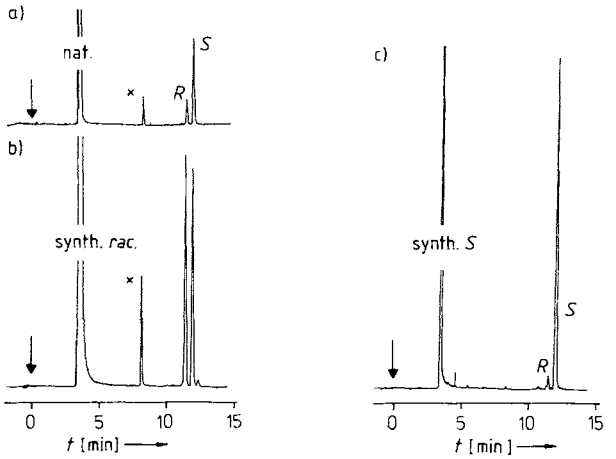


Fig. 2. Enantiomer separation of (*E*)-5-methylhept-2-en-4-one **5** by chiral inclusion gas chromatography on heptakis(2,6-di-*O*-methyl-3-*O*-trifluoroacetyl)-β-cyclodextrin in OV-1701 (0.05 m) at 110 °C [phase 2] [12]. Column: 40 m × 0.25 mm (I.D.) glass capillary. Carrier: 1 bar N_2. a) Natural **5** (filbertone), isolated from filberts [2]; b) racemic **5**, synthesized according to Scheme 1; c) (*S*)-**5**, synthesized according to Scheme 1.

[*] Prof. Dr. V. Schurig, Dipl.-Chem. J. Jauch, Dipl.-Chem. D. Schmalzing
Institut für Organische Chemie der Universität
Auf der Morgenstelle 18, D-7400 Tübingen (FRG)
Dr. R. Emberger, Dr. R. Hopp, Dr. M. Köpsel, Dr. W. Silberzahn, Dr. P. Werkhoff
Haarmann & Reimer GmbH, Research Department
D-3450 Holzminden (FRG)

[**] This work was supported by the Fonds der Chemischen Industrie. The identification and isolation of filbertone was performed in Holzminden, its enantiomer separation and the synthesis of the (*S*) enantiomer was carried out in Tübingen. The supply of filberts by *H. Teckenburg*, Schwartau GmbH, Bad Schwartau (FRG), is gratefully acknowledged.

Aided by the efficient analytical enantiomer separation (cf. Fig. 2c), racemization studies on (*S*)-**5** were also performed. No racemization, albeit appreciable thermal decomposition of **5** was observed in the gas phase at 120 °C over 21 days. In the presence of silica no racemization occurred at 22 °C over 21 h, but the *ee* dropped from 92% to 74% in the presence of *basic* alumina at 22 °C over 21 h. These results imply that the low enantiomeric purity of natural filbertone is an inherent property of the natural compound and is unlikely to have been caused by racemization during isolation.[2]

The sensory evaluation of *R*- and *S*-filbertone, separated on phase 2 (Fig. 2b), established a marked olfactory difference between the enantiomers in respect to odor intensity and quality. Also the sensory evaluation of synthetic racemic **5** and enantiomeric (*S*)-**5**, prepared according to Scheme 1, revealed striking olfactory differences. Thus, filbertone represents a new example of the importance of chirality in olfaction, thereby stressing the need to develop efficient chromatographic procedures for stereochemical analyses.[14]

Received: April 3, 1989 [Z 3269 IE]
German version: *Angew. Chem. 101* (1989) 1039

[1] H. J. Bestmann, A. B. Attygalle, J. Glasbrenner, R. Riemer, O. Vostrowsky, *Angew. Chem. 99* (1987) 784; *Angew. Chem. Int. Ed. Engl. 26* (1987) 784.

[2] Good quality raw hazelnuts (filberts) (600 g) of a Turkish variety (1988 crop) were ground to a fine slurry in an Ultra-Turrax blender with 1.5 L of distilled water and subsequently transferred into a 10-L round-bottom flask. 4.5 L of distilled water was added and the finely chopped nuts were subjected to a simultaneous steam distillation/extraction procedure with 150 mL of *n*-pentane/diethyl ether (2:1, v/v) for 2.5 h at atmospheric pressure as described by *Likens-Nickerson* (S. T. Likens, G. B. Nickerson, *Proc. Am. Soc. Brew. Chem. 1964*, 5.). The extract was dried over anhydrous sodium sulfate and the organic solvent was removed on a 25-cm × 1-cm Vigreux distillation column. The process was repeated several times, and about 50 mL of an aroma concentrate was obtained from a total of about 5 kg of raw filberts. The aroma concentrates had the characteristic and intense odor of raw filberts. A separation according to the polarity of the volatile components was carried out by adsorption chromatography. The total flavor extract was preseparated on silica gel 60 (70–230 mesh, Merck, Darmstadt) by using a stepwise gradient of increasing amounts of diethyl ether in *n*-pentane. Filbertone was isolated from a medium-polar silica fraction by means of preparative capillary gas chromatography employing a wide-bore fused silica open-tubular column (30-m × 0.53-mm I.D., DB-1/film thickness 1 μm).

[3] R. Emberger, M. Köpsel, J. Brüning, R. Hopp, T. Sand, DOS 3525604 A1 (22. Jan. 1987), *Chem. Abstr. 106* (1987) 155899f; DOS 3345784 (27 June 1985), *Chem. Abstr. 103* (1985) 140657q; R. Emberger, *43. Diskussionstagung des Forschungskreises der Ernährungsindustrie*, 25/26 March 1985, Bremen.

[4] D. Seebach, V. Ehrig, M. Teschner, *Justus Liebigs Ann. Chem. 1976*, 1357.

[5] W. Kirmse, H. Arold, *Chem. Ber. 104* (1971) 1800.

[6] Very expensive propyne has been replaced by the cheap welding gas mixture MAPP (*M*ethyl-*A*cetylene, *P*ropadiene, *P*ropene) (Messer-Griesheim, 4000 Düsseldorf), which contains up to 13.5% propyne.

[7] M. L. Midland, A. Tramontano, A. Kazubski, R. S. Graham, D. J. S. Tsai, D. B. Cardin, *Tetrahedron 40* (1984) 1371.

[8] ^{13}C NMR (62.9 MHz, $CDCl_3$): δ = 18.1 (C1), 142.2 (C2), 130.4 (C3), 203.8 (C4), 45.1 (C5), 26.0 (C6), 11.5 (C7), 16.0 (C8). ^1H NMR (250 MHz, $CDCl_3$): δ = 1.81 (dd, H1), 6.82 (dquart. H2), 6.15 (dquart. H3), 2.66 (sext, H5), 1.70 (m, H6), 1.40 (m, H6), 0.80 (t, H7), 1.07 (d, H8).

[9] W. Silberzahn, *Dissertation*, Technische Universität Berlin, Berlin 1988.

[10] W. A. König, I. Benecke, K. Ernst, *J. Chromatogr. 253* (1982) 267.

[11] V. Schurig, R. Link in D. Stevenson, I. D. Wilson (Eds.): *Chiral Separations*, Plenum, London, **12** (1989) 383.

[12] H.-P. Nowotny, D. Schmalzing, D. Wistuba, V. Schurig, *HRC & CC, J. High Resolut. Chromatogr. Chromatogr. Commun., 12* (1989) 383.

[13] R. Weber, V. Schurig, *Naturwissenschaften 71* (1984) 408.

[14] V. Schurig in P. Schreier (Ed.): *Bioflavour '87*, de Gruyter, Berlin 1988, p. 35

The Active Site of Glutathione Reductase: An Example of Near Transition-State Structures**

By *Reiner Sustmann,** *Willi Sicking*, and *Georg E. Schulz**

Dedicated to Professor Christoph Rüchardt on the occasion of his 60th birthday

The ubiquitous flavoenzyme glutathione reductase serves an important function in intracellular redox processes by making available free thiols in the form of reduced glutathione.[1] The catalysis proceeds in two separable steps. In the first step investigated here, two electrons are transferred from NADPH to the enzyme, leading to the reduced enzyme as a stable intermediate.

$$H^{\oplus} + NADPH + E_{ox} \rightleftharpoons E_{red}H_2 + NADP^{\oplus}$$

In the second step, glutathione disulfide is reduced.

$$E_{red}H_2 + GSSG \rightleftharpoons E_{ox} + 2\,GSH$$

The active center consists of isoalloxazine (from FAD) and the adjacent disulfide bridge Cys58:Cys63, both of which are buried in the protein. The reducing NADPH binds to the isoalloxazine side of this arrangement and the glutathione being reduced binds to the disulfide side.[2] The geometries have been determined by X-ray structure analysis at resolutions between 2.0 Å and 1.54 Å.[3]

Since the active center is located in a very densely packed, internal region of the protein, which is far apart from all intermolecular contacts with the enzyme crystal lattice[3] and since the enzyme remains active in the crystal, it is safe to assume that the geometry established for the average positions of the non-hydrogen atoms agrees with the geometry of the cellular enzyme to within 0.1–0.2 Å. The mechanism of the reduction is still not known in detail: the important question of whether a hydride transfer or successive one-electron transfers are involved remains unanswered.

Using calculations at the MNDO level that incorporate the most recent PM3 parametrization,[4] we have begun to analyze the interactions in the active center of the enzyme. These calculations are supplemented using perturbation calculations with the PERVAL[5] program, also subjected to PM3 parametrization. The latter allows the direct determination of the interactions of two molecules and the interpretation of the results on the basis of covalent stabilization as well as of polar and noncovalent contributions (closed shell repulsion). The analysis is based on the coordinates of the non-hydrogen atoms obtained from the X-ray structure analysis, complemented with hydrogen atoms introduced with standard bond lengths and bond angles. Since even semiempirical calculations are too unwieldy for FAD and NADPH, only the partial structures important for the reaction, that is, the isoalloxazine ring with and without ribitol and dihydronicotinamide with ribose, were included in the calculations. Hydrogen atoms were placed at the sites of the omitted moieties. The disulfide bridge between Cys58 and Cys63 was treated similarly; the bonds to the remaining protein were replaced by hydrogen atoms. The calculations indeed show that the frontier orbitals of the reactants impor-

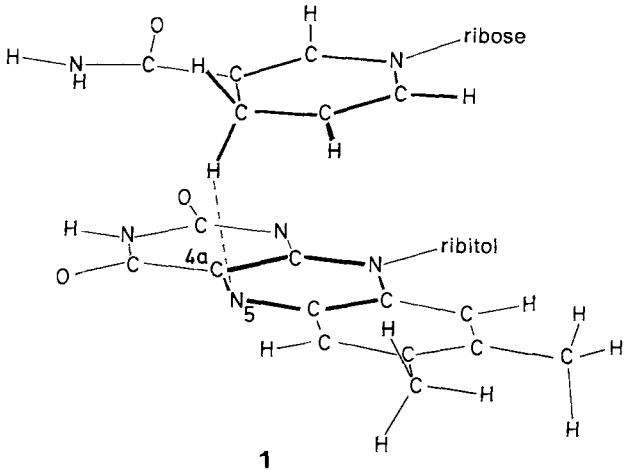
[*] Prof. Dr. R. Sustmann, Dipl.-Ing. W. Sicking
Institut für Organische Chemie der Universität
Postfach 103764, D-4300 Essen 1 (FRG)
Prof. Dr. G. E. Schulz
Institut für Organische Chemie und Biochemie der Universität
Albertstrasse 21, D-7800 Freiburg (FRG)

[**] This work was supported by the Deutsche Forschungsgemeinschaft.

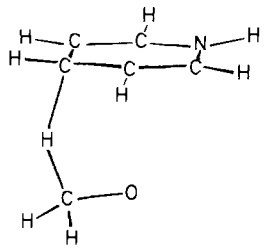
tant for the reaction are localized exclusively in the isoalloxazine and dihydronicotinamide moieties. In addition, the calculations show that the LUMO that is crucial for the reduction of the disulfide bridge is found in the SS bond. These findings are strong evidence that the primary function of the surrounding protein is to hold the reacting molecules in a fixed array.

Here we report on the following aspects of this reaction: (1) the interaction of the dihydronicotinamide of NADPH with the isoalloxazine ring of FAD (see **1**) and (2) the interaction of the reduced isoalloxazine ring with the protein disulfide bridge Cys58:Cys63 (see **5**, bottom). A comparison with the transition-state structures of hydride transfer from dihydropyridine to formaldehyde (see **2**)[6] and from methylamine to the methyleneiminium ion (see **3**),[7] obtained by ab initio calculations, proves useful.

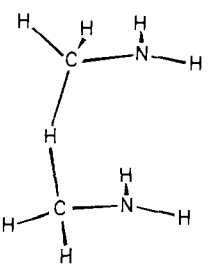
In **1–3**, the X-ray structure of the complex formed between dihydronicotinamide and the isoalloxazine ring of



1

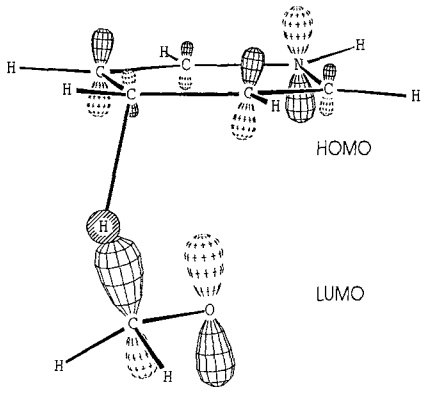


2



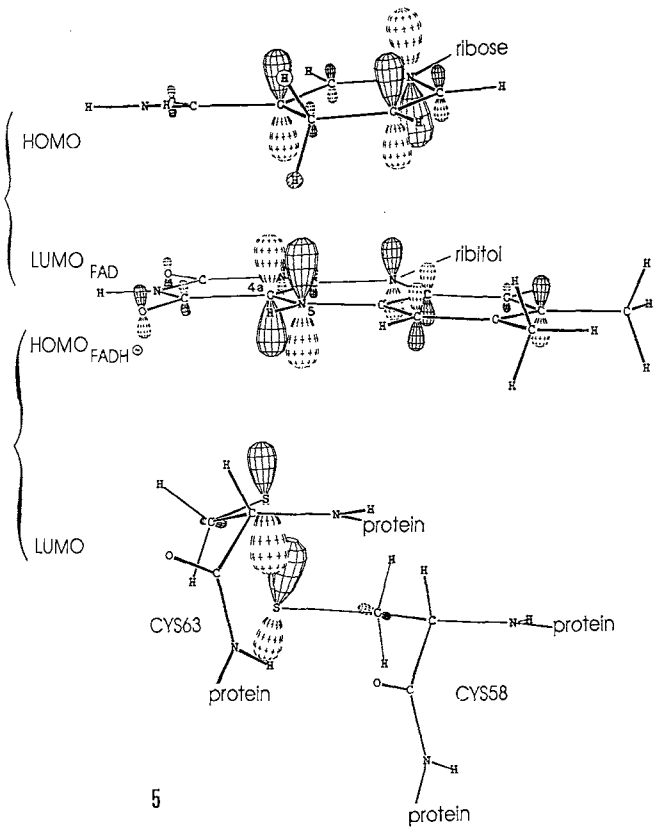
3

FAD is compared with the transition structures obtained from the two ab initio calculations. The agreement of **1–3** in the region of the atoms participating in the reaction is striking. It should be remembered, however, that **1** does not represent a transition structure. The calculated interaction of the molecules in complex **1** ($+6.5$ kcal mol^{-1}) is weakly repulsive. The separation of the atoms between which the hydrogen atom is exchanged is 3.2 Å in the enzyme and thus ca. 0.5–0.6 Å larger than in the transition structures **2** (2.70 Å) and **3** (2.55 Å). The question of whether the atoms participating in the reaction adopt a linear arrangement[8] is answered by the ab initio calculations (the atoms lie in a bent arrangement with an angle of ca. 140–150°). The enzyme structure forms a comparable angle of 134°, which is evidence for a similar mechanism. Such an arrangement results in optimal frontier orbital interactions, as is shown in **4** for the dominating $HOMO_{dihydropyridine}$–$LUMO_{formaldehyde}$ interaction (cf. **2**). The PERVAL calculations predict that this interaction accounts for 63% of the total covalent stabilization of the transition state for hydride transfer in **4**. The orientation of the orbitals in **4** serves to emphasize why a nonlinear arrangement is more favorable. In this arrangement, a maximal overlap of the participating orbitals is achieved in proceeding from the starting molecules to the reaction products.



4

The calculated HOMO of the dihydronicotinamide (with ribose) in the enzyme (see **5**, top) has nearly the same structure as that of dihydropyridine (cf. **4**). The LUMO of the isoalloxazine ring (with ribitol) exhibits the largest contribution at the nitrogen atom N-5, which would accept the H atom during hydride transfer. This LUMO nearly agrees with the HOMO of the reduced isoalloxazine moiety $FADH^{\ominus}$ given in **5** (middle). $HOMO_{FADH^{\ominus}}$ and $LUMO_{FAD}$ differ mainly in the contributions of the atoms N-5 and C-4a, the contribution of N-5 being somewhat larger than that of C-4a in $LUMO_{FAD}$. As in **4**, the $HOMO_{dihydronicotinamide}$–$LUMO_{isoalloxazine}$ interaction contributes the most to the



5

covalent stabilization, thus being the dominant interaction. The similarity of the structures **1**–**3** and of their interactions indicates that NADPH and FAD are arranged in a nearly ideal fashion for a hydride transfer to N-5 of the isoalloxazine ring in the enzyme.

In the second step, $FADH^{\ominus}$ transfers reduction equivalents to the disulfide bridge Cys58:Cys63 (cf. **5**, bottom). In this process, the direct nucleophilic attack of the reduced isoalloxazine ring offers an attractive possibility corresponding to the usual proposal of nucleophilic attack on FAD.[9] In such an attack, the nucleophile forms a covalent bond to C-4a of the isoalloxazine. Crystal structure analysis and calculation supports such a mechanism. Especially interesting is the observed unusual conformation of the disulfide bridge,[3] which, in the given fixed position relative to the isoalloxazine ring, leads to an exact orientation of the antibonding LUMO of the bridge toward C-4a, as is shown by the scaled reproduction of the crystal structure of **5**. C-4a of the isoalloxazine ring and the S atoms of the disulfide bridge lie next to each other in a linear fashion, and the energetically nearly degenerate frontier orbitals ($HOMO_{FADH^{\ominus}}$–$LUMO_{Cys58:Cys63}$) result in a strong covalent interaction between C-4a and the sulfur atom of Cys63. Structure **5** serves to emphasize the favorable orientation of the orbitals for back-side attack of C-4a on the disulfide bond. The mechanism can be described as a nucleophilic cleavage of the SS bridge with formation of a covalent bond between C-4a of the isoalloxazine and the S atom of Cys63. Transfer of the proton from N-5 to the S atom of $Cys58^{\ominus}$ and fragmentation by intramolecular nucleophilic substitution to give $Cys63^{\ominus}$ should follow. It is interesting to note that the MNDO PM3 calculation for the interaction of FAD with $Cys63^{\ominus}$, the relative position of which is known from X-ray data, gives a stabilization of -2.6 kcal mol^{-1} and shows no repulsion, although this is usually observed between molecules with closed valence shells. The calculation apparently confirms the spectroscopically established formation of a CT complex[1, 2] between FAD and $Cys63^{\ominus}$.

The MNDO PM3 calculations and the perturbation analysis of the structure of the active site of glutathione reductase show that, in the enzyme, the reaction partners NADPH and FAD, as well as $FADH^{\ominus}$ and Cys58:Cys63, are positioned in such a way that they are localized near the transition state along the reaction coordinates of the hydride transfer and the nucleophilic cleavage of the disulfide bridge, respectively. This positioning eliminates the decrease in entropy required for this reaction and is in agreement with proposals concerning enzyme-catalyzed reactions in general. Furthermore, other mechanisms, such as one-electron transfers, become improbable. Further investigations, which also consider the reduction of glutathione and include some important amino acids in the vicinity of the active center, are in progress.

Received: March 3, 1989;
supplemented: May 11, 1989 [Z 3213 IE]
German version: *Angew. Chem. 101* (1989) 1056

[1] C. H. Williams, Jr. in P. D. Boyer (Ed.): *The Enzymes, Vol. 13*, Academic Press, New York 1976, p. 89.
[2] E. F. Pai, G. E. Schulz, *J. Biol. Chem. 258* (1983) 1752; E. F. Pai, P. A. Karplus, G. E. Schulz, *Biochemistry 27* (1988) 4465; P. A. Karplus, E. F. Pai, G. E. Schulz, *Eur. J. Biochem. 178* (1989) 693.
[3] P. A. Karplus, G. E. Schulz, *J. Mol. Biol. 195* (1987) 701; P. A. Karplus, G. E. Schulz, *J. Mol. Biol.*, in press.
[4] J. J. P. Stewart, *J. Comput. Chem.*, in press. We thank Dr. *T. Clark*, Universität Erlangen-Nürnberg, for providing us with a program containing the MNDO PM3 parameters.
[5] R. Sustmann, W. Sicking, *Chem. Ber. 120* (1987) 1323; R. Sustmann, P. Daute, R. Sauer, W. Sicking, *Tetrahedron Lett. 29* (1988) 4699, and references cited therein.
[6] O. Tapia, R. Cardenas, J. Andres, P. Colonna-Cesari, *J. Am. Chem. Soc. 110* (1988) 4046.
[7] Y-D. Wu, K. N. Houk, *J. Am. Chem. Soc. 109* (1987) 906.
[8] J. W. Verhoeven, W. van Gerresheim, F. M. Martens, S. M. van der Kerk, *Tetrahedron 42* (1986) 975.
[9] C. Walsh, *Acc. Chem. Res. 13* (1980) 148.

Are Lithiosulfones Configurationally Stable?**

By *Hans-Joachim Gais,* Gunther Hellmann, Harald Günther, Fernando Lopez, Hans J. Lindner* and *Sigmar Braun*

Dedicated to Professor Christoph Rüchardt on the occasion of his 60th birthday

According to crystal structure analyses, lithiosulfones **1**[1] have chiral anions even when their α-C atom, bearing different groups, is coordinated in a planar rather than in a tetrahedral fashion.[2] In this respect they differ fundamentally from lithium enolates.[3] This is due to a favored C_α–S conformation in which the two Li-bound O atoms are arranged *gauche* to the lone pair on the α-C atom (cf. Fig. 1 and the formula shown). Earlier H/D-exchange experiments on optically active sulfones **2** have already provided compelling evidence for the chirality of counterion-free α-sulfonyl carbanions and shown that hindered C_α–S rotation, not C_α inversion, is responsible for their observability.[4] Ab initio calculations came to a similar conclusion.[5] According to these results negative hyperconjugation (n_c–$\sigma^*_{SR^3}$) and Coulombic interaction are the dominant mechanisms of stabilization. How stable, however, are the configurations of the lithiosulfones **1**? This important question has remained unanswered so far. In particular, no evidence has been provided for the chirality of **1** in solution.[6] We were also especially interested in whether optically stable lithiosulfones **1** can be generated enantioselectively from optically active sulfones **2**.

$[R^1R^2C-SO_2R^3]^{\ominus}\ Li^{\oplus}$ **1** $\quad R^1R^2C(H)-SO_2R^3$ **2**

1/2	R^1	R^2	R^3
a	Me	Ph	Ph
b	$PhCH_2$	Ph	Ph
c	$PhCH_2$	Me	Ph
d	$PhCH_2$	Me	CF_3
e	$PhCH_2$	Ph	CF_3

When the metalation of optically active phenyl sulfone **2a** with *n*BuLi in THF was followed by polarimetry, only rapid

[*] Prof. Dr. H.-J. Gais, Dipl.-Ing. G. Hellmann
Institut für Organische Chemie und Biochemie der Universität
Albertstrasse 21, D-7800 Freiburg (FRG)
Prof. Dr. H. Günther, Dr. F. Lopez
Fachbereich 8, Organische Chemie II der Universität
Postfach 101240, D-5900 Siegen (FRG)
Prof. Dr. H. J. Lindner, Dr. S. Braun
Institut für Organische Chemie der Technischen Hochschule
Petersenstrasse 22, D-6100 Darmstadt (FRG)

[**] This work was supported by the Deutsche Forschungsgemeinschaft, the Fonds der Chemischen Industrie, the Wissenschaftliche Gesellschaft in Freiburg, and the Alexander von Humboldt Foundation (*F. L.*). We thank Dr. *W. Bauer* for the cryoscopic measurements, Dr. *A. Powell* and Dr. *H. Paulus* for the crystallographic data sets, and Dr. *E. Keller* for a version of Schakal-88.

racemization with formation of *rac*-**1a** was observed, even at $-80\,^{\circ}C$. ^1H DNMR measurements on the benzyl-substituted lithio(*phenyl*)sulfones *rac*-**1b** and *rac*-**1c**, in which the exchange of nonequivalent methylene protons was observed in [D_8]THF, gave the following results: *rac*-**1b**, the α-C atom of which should be coordinated in a planar fashion,[2] has an enantiomerization barrier $\Delta G^{\neq}_{215}$ of 9.6 ± 0.2 kcal mol^{-1} ($c = 1.8 \times 10^{-1}$ mol L^{-1}); *rac*-**1c**, the α-C atom of which should be coordinated, by contrast, in a tetrahedral fashion,[2] likewise has a $\Delta G^{\neq}_{215}$ value of only 9.7 ± 0.2 kcal mol^{-1} ($c = 2.8 \times 10^{-1}$ mol L^{-1}).[7] Over a concentration range of 7×10^{-2} to 36×10^{-2} mol L^{-1}, the $\Delta G^{\neq}$ value for *rac*-**1b** does not change, but it increases to 10.1 ± 0.2 kcal mol^{-1} in the presence of four equivalents of hexamethylphosphoric triamide.[8]

Trifluoromethyl sulfones (*triflones*) are ca. 10 pK_a units more acidic than phenyl sulfones.[9] We found that lithiotriflones are also appreciably more configuratively stable than lithio(phenyl)sulfones. Metalation of the optically active triflone (+)-**2d**[10] with *n*BuLi in THF at $-95\,^{\circ}C$ resulted in formation of the optically active lithiotriflone (−)-**1d** with an extrapolated half-life of 30 d at $-78\,^{\circ}C$. The time dependence of the racemization of (−)-**1d** was followed polarimetrically at low temperatures for a concentration range of 5×10^{-3} to 120×10^{-3} mol L^{-1}. It obeys first-order kinetics with a racemization barrier $\Delta G^{\neq}_{239}$ of 17.2 ± 0.1 kcal mol^{-1} ($k_{rac} = 9.40 \times 10^{-4}$ s^{-1}, $t_{1/2} = 12.3$ min).[11] A $\Delta H^{\neq}$ value of 16.7 ± 0.3 kcal mol^{-1} and a $\Delta S^{\neq}$ value of -1.9 ± 1.1 cal K^{-1} mol^{-1} were derived from the temperature dependence (-44 to $-24\,^{\circ}C$) of k_{rac}. A linear relation between α and *t* was also obtained for the racemization of (−)-**1d** in THF in the presence of four equivalents of 1,3-dimethyltetrahydropyrimidine-2(1*H*)-one.[3] In this case, the lifetime of (−)-**1d** ($t_{1/2} = 42$ min at $-34\,^{\circ}C$) is longer. By ^1H DNMR measurements on *rac*-**1d**, the α-C atom of which should be tetrahedrally coordinated,[2] an enantiomerization barrier $\Delta G^{\neq}_{333}$ of 17.8 ± 0.2 kcal mol^{-1} ($c = 3.2 \times 10^{-1}$ mol L^{-1}) was found following the exchange of methylene protons in [D_{14}]diglyme.[8] For the enantiomerization of *rac*-**1e**, the α-C atom of which has been shown to be coordinated in a planar fashion (cf. Fig. 1), the NMR measurements in [D_8]THF gave a $\Delta G^{\neq}_{333}$ value of 16.0 ± 0.2 kcal mol^{-1} ($c = 1.9 \times 10^{-1}$ mol L^{-1}).[7] According to cryoscopic measurements,[12a] **1e** is *monomeric* in THF at $-103\,^{\circ}C$ and concentrations of 7.1×10^{-2} and 13.6×10^{-2} mol L^{-1},[12b, c] and, based on NMR analysis, associated with two molecules of THF. The results of NMR investigations on (−)-**1d** and *rac*-**1d** ([D_8]THF, $-80\,^{\circ}C$, $c = 3.1 \times 10^{-1}$ mol L^{-1}) are in agreement with these findings. Under these conditions, chiral and achiral dimers would have to be present in addition to chiral monomers. There are no differences in the positions of either the ^1H or the ^{13}C NMR signals, and only one species is observed. The appreciably higher acidity of **2d,e** and the greater configurative stability of **1d,e** are in accord with the stabilization of α-sulfonyl carbanions by negative hyperconjugation and Coulombic interaction.[5, 13] Hindered C_α–S rotation is the reason for the observability of chirality in **1e**. This should also be true for **1a–d**, whereby the α-C atoms in **1c–d** might be coordinated in a tetrahedral rather than a planar fashion.[2]

The metalation of (*R*)-**2d** and the protonation of (−)-**1d** occur enantioselectively and with retention of configuration! Reaction of (−)-**1d** ($c = 7.3 \times 10^{-2}$ mol L^{-1}), generated from (*R*)-**2d**[10] and one equivalent of *n*BuLi at $-90\,^{\circ}C$ in THF, with CF_3COOH in THF at $-105\,^{\circ}C$ afforded (*R*)-**2d** (93%) with $[\alpha]^{21}_{365} = +10.9$ ($c = 2.8$, THF).

Are the differences in the stability of deprotonated and lithiated triflones and phenyl sulfones reflexted in C_α–S bonds of different length? To answer this question, crystal structure analyses of (**1e** · TMEDA)$_2$[14a] and **2e**[14b] were carried out.[15] Single crystals of (**1e** · TMEDA)$_2$ were obtained in the usual way by metalation of **2e** with *n*BuLi in *N,N,N',N'*-tetramethylethylenediamine (TMEDA). (**1e** · TMEDA)$_2$ crystallizes as a typically achiral dimer[1] with (*M*) or (*P*) configuration[16] of the two anions, the α-C atoms of which are coordinated in a planar fashion (Fig. 1).

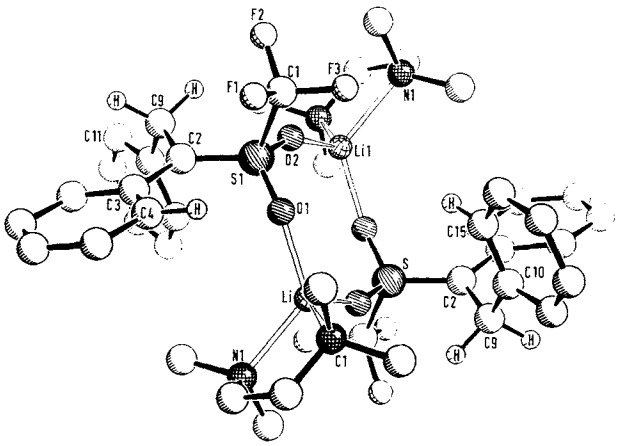


Fig. 1. Molecular structure of one of the two crystallographically independent dimers of (**1e** · TMEDA)$_2$ [17]. Selected bond lengths [Å] and angles [°] for both dimers: S1–O1 1.455(4), S1–O2 1.446(5), C1–S1 1.856(6), C2–S1 1.608(6), C2–C3 1.455(9), Li1–O1 1.920(9), Li1–O2 1.877(9), Li1–N1 2.131(9), Li1–N2 2.099(11); C3–C2–S1 124.1(4), C9–C2–S1 116.6(5), C9–C2–C3 119.2(5) C2–S1–C1 114.9(3); C1–S1–C2–C3 −80.1, C1–S1–C2–C9 96.7. S1–O1 1.445(4), S1–O2 1.459(4), C1–S1 1.823(8), C2–S1 1.611(6), C2–C3 1.480(9), Li2–O1 1.910(12), Li2–O2 1.907(9), Li2–N1 2.132(14), Li2–N2 2.130(11); C3–C2–S1 123.0(4), C9–C2–S1 116.5(5), C9–C2–C3 120.4(5), C2–S1–C1 112.3(3); C1–S1–C2–C3 83.8, C1–S1–C2–C9 −92.6.

Apart from the N atoms of the TMEDA molecules, only the O atoms of the sulfonyl groups are bound to the Li atoms.[18] Bonds do not exist between the Li and the α-C atoms. The anions have the characteristic C_α–S conformation;[1] however, their C_α–S bond is shortened by 11% to 1.609 Å (average value) compared with that in **2e**. It is thus shorter than that in (**1a** · diglyme)$_2$ (1.652 Å),[2b] the α-C atoms of which are also coordinated in a planar fashion, and of the same length as that in [$(CH_2SO_2Ph)Li$ · TMEDA]$_2$.[19] So far, shortenings of the C_α–S bond in metalated sulfones of only ca. 8% have been found.[1] The O–Li distances are of roughly the same length as those in all other lithiosulfones, while the S–O distances are slightly increased. Noteworthy is the fact that the S1–C1 bonds in (**1e** · TMEDA)$_2$ (average 1.839 Å) are no longer than the corresponding bond in **2e** (average 1.853 Å).

Finally, it was important to determine whether the Li atom of monomeric **1e** in solution occupies the same position (*O*-associated) as the Li atoms in (**1e** · TMEDA)$_2$ in the crystal. To this end, ^6Li,^1H heteronuclear NOE experiments[20] were performed on **1e** at 25 °C.[21] For these experiments, a solution of crystalline (**1e** · TMEDA)$_2$ prepared with 95% ^6Li in [D_8]THF ($c = 3 \times 10^{-1}$ mol L^{-1}) was used. On the one hand, 2D NMR experiments using the HOESY pulse sequence[20a, 22] allow one to observe intense correlation peaks for the CH_3 and CH_2 protons of TMEDA, which indicate that, even in [D_8]THF solution, the Li atom is chelated by TMEDA. On the other hand, correlation peaks

for 11-H/15-H ($\delta = 7.38$) as well as for 4-H/8-H and/or 12-H/14-H were observed; the signals of the latter ($\delta = 7.21$ and 7.14, respectively) lie very close to each other.[23] Against expectations, however, no interactions with the diastereotopic CH_2 protons could be obtained in this experiment, despite variation of the mixing time over a range of 2 to 5 s. Therefore, one-dimensional NOE difference experiments were also carried out and, upon irradiation of the resonance frequencies of the CH_2 protons, the expected intensity enhancements were observed. Moreover, the Li,H interactions already appearing in the HOESY spectrum were revealed in the corresponding 1D NOE difference measurements (Fig. 2). Furthermore, despite the small difference in shifts,

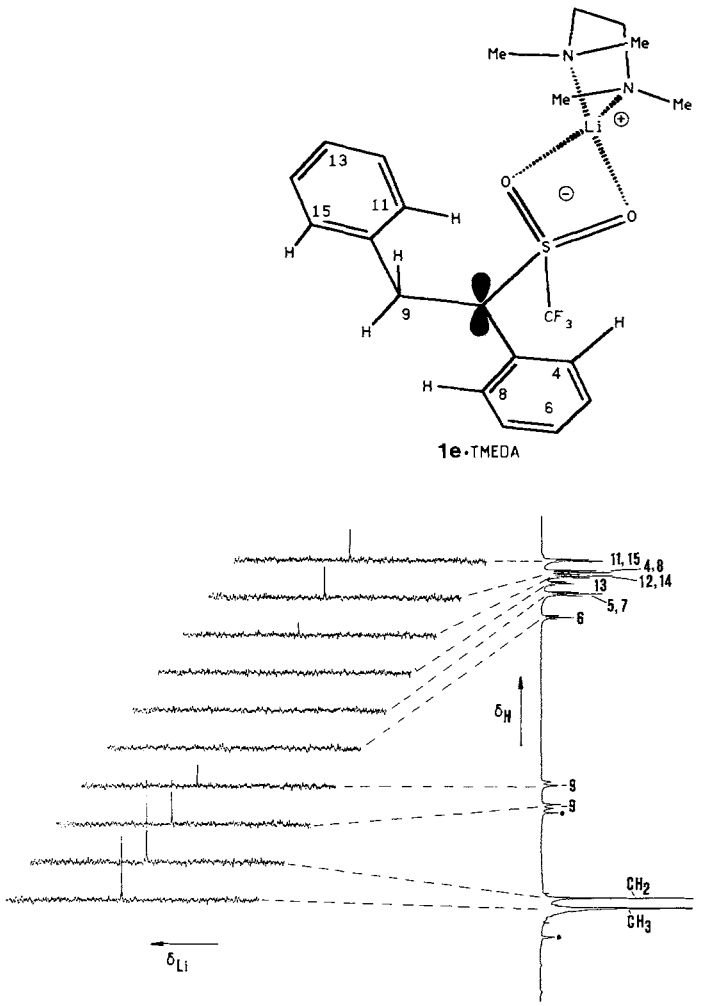


Fig. 2. $^6Li\{^1H\}$ NOE difference spectra of **1e** · TMEDA (see formula for numbering) in [D_8]THF at 298 K. The irradiation in the ^1H NMR spectrum and the resulting ^6Li NMR difference spectra are joined by broken lines. ● = solvent signal.

measurement with decreasing irradiation energy showed that only 4-H/8-H/11-H/15-H, and not 12-H/14-H, exert an NOE on the ^6Li atom. The short Li–H distances found[24] and the other results make a chiral structure of the type shown in the formula for **1e** · TMEDA in THF solution very probable. An (achiral) structure of this type has already been found in an X-ray structure analysis of $[(Me_3Si)_2C\text{-}SO_2Ph]K \cdot [18]$crown-6[25] and in theoretical investigations of $(CH_2SO_2Me)Li$.[5b]

Received: March 8, 1989;
Supplemented: April 27, 1989 [Z 3220 IE]
German version: *Angew. Chem. 101* (1989) 1061

[1] Review on crystal structures of lithiosulfones: G. Boche, *Angew. Chem. 101* (1989) 286; *Angew. Chem. Int. Ed. Engl. 28* (1989) 277.
[2] a) $[(Me_2CSO_2Ph)Li \cdot diglyme]_2$ [2b] and $[(CH_2{=}CHC(H)SO_2Ph)Li \cdot diglyme]_2$ [2c] have tetrahedrally coordinated α-C atoms and $[(PhC(H)SO_2Me)Li \cdot TMEDA]_2$ [1], $[(PhC(Me)SO_2Ph)Li \cdot diglyme]_2$, [2b] and $[(Me_3SiC(H)SO_2Ph)Li \cdot TMEDA]_2$ [1] have planar-coordinated α-C atoms; b) H.-J. Gais, J. Vollhardt, G. Hellmann, H. Paulus, H. J. Lindner, *Tetrahedron Lett. 29* (1988) 1259; c) H.-J. Gais, J. Vollhardt, H. J. Lindner, *Angew. Chem. 98* (1986) 916; *Angew. Chem. Int. Ed. Engl. 25* (1986) 939.
[3] Review on the crystal structures of lithium enolates: D. Seebach, *Angew. Chem. 100* (1988) 1685; *Angew. Chem. Int. Ed. Engl. 27* (1988) 1624.
[4] E. J. Corey, T. H. Lowry, *Tetrahedron Lett. 1965*, 803; J. N. Roitman, D. J. Cram, *J. Am. Chem. Soc. 93* (1971) 2225.
[5] a) S. Wolfe, *Stud. Org. Chem. (Amsterdam) 19* (1985) 133; b) D. A. Bors, A. Streitwieser, Jr., *J. Am. Chem. Soc. 108* (1986) 1397.
[6] *Cram* et al. (A. Ratajczak, F. A. L. Anet, D. J. Cram, *J. Am. Chem. Soc. 89* (1967) 2072) showed by ^1H NMR spectroscopy that lithio(2,2-dimethylcyclopropyl) phenyl sulfone is chiral and found an enantiomerization barrier $\Delta G^{\ddagger}_{328}$ of 18.0 kcal mol^{-1}.
[7] Estimated from the coalescence point as described by R. J. Kurland, M. B. Rubin, M. B. Wise, *J. Chem. Phys. 40* (1964) 2426.
[8] Result of a line-shape calculation as described by S. Alexander, *J. Chem. Phys. 37* (1962) 974.
[9] F. G. Bordwell, *Acc. Chem. Res. 21* (1988) 456.
[10] (*R*)-**2d** ($[\alpha]^{21}_{365}$ + 14.5 (*c* = 2.8, THF) was prepared from (*R*)-$PhCH_2CH(Me)SH$ ($[\alpha]^{23}_{D}$ − 13.5 (neat [10b]) by reaction with CF_3Br (NH_3/THF, − 80 °C, *hv*) according to *Ignat'ev* et al. [10c] to give (*R*)-$PhCH_2CH(Me)SCF_3$ ($[\alpha]^{21}_{365} = -3.2$ (*c* = 5.0, THF), 72%) followed by oxidation (H_2O_2, H_2WO_4, glacial acetic acid, 92%) according to *Hazeldine* et al. [10d]; b) C. L. Arcus, P. A. Hallgarten, *J. Am. Chem. Soc. 1956*, 1987; c) N. V. Ignat'ev, V. N. Boiko, L. M. Yagupol'skii, *J. Org. Chem. (USSR) 21* (1985) 592; d) R. Hazeldine, R. B. Rigby, A. E. Tipping, *J. Chem. Soc. Perkin Trans. 1 1973*, 676.
[11] A first order reaction was verified graphically over at least four half-lives. The calculation of k_{rac} ($K_{rac} = 2\,k_{enan}$) as well as of the activation parameters (Eyring procedure) was carried out with a kinetic program.
[12] a) W. Bauer, D. Seebach, *Helv. Chim. Acta 67* (1984) 1972; b) W. Bauer (Erlangen), private communication; c) $[PhC(H)SO_2Ph]Li$ is also monomeric in + 25 °C and a concentration range of $c = 1.35 \times 10^{-4}$ to 14.0×10^{-4} mol L^{-1}: M. J. Kaufmann, S. Gronert, D. A. Bors, A. Streitwieser, Jr., *J. Am. Chem. Soc. 109* (1987) 602.
[13] a) M. J. Janssen in C. J. M. Stirling (Ed.): *Organic Sulphur Chemistry*, Butterworths, London 1975, p. 19; b) Interestingly, the N–S rotation barrier in $R^1R^2NSO_2R^3$ for R^3 = Cl is appreciably higher than for R^3 = Me or Ph: W. B. Jennings, R. Spratt, *J. Chem. Soc. 1970*, 1418.
[14] a) (**1e** · TMEDA)$_2$: space group $P\bar{1}$, $a = 10.987(6)$, $b = 11.256(5)$, $c = 19.556(8)$ Å, $\alpha = 81.49(4)$, $\beta = 84.12(4)$, $\gamma = 76.99(4)°$, $V = 2324.5$ Å^3, $Z = 4$, $\varrho_{calcd} = 1.247$ g cm^{-3}, $\mu(Mo_{K\alpha}) = 1.42$ cm^{-1}. Intensity measurements at room temperature, CAD-4 diffractometer, $Mo_{K\alpha}$ radiation, graphite monochromator, 6592 measured reflections ($2° < 2\theta < 48°$), 3747 symmetry-independent reflections with $F > 3\,\sigma(F)$. SHELX86; direct methods yielded two crystallographically independent centrosymmetric dimers which do not differ significantly. Anisotropic refinement of the positioned H atoms, 562 variables, $R = 0.084$, $R_w = 0.087$. Maximal residual electron density 0.63 e/Å^3 near the S atoms. b) **2e**: $Pn2_1a$ ($Pna2_1$), $a = 18.693(5)$, $b = 10.527(3)$, $c = 15.234(4)$ Å, $V = 2997.8$ Å^3, $Z = 8$, $\varrho_{calcd} = 1.393$ g cm^{-3}. $R = 0.041$, $R_w = 0.056$. Selected bond-length [Å] and angles [°] (for numbering see Fig. 1): S1–O1 1.427(3), S1–O2 1.426(3), C1–S1 1.850(6), C2–S1 1.807(3), C2–C3 1.518(4); C2–S1–C1 102.6(2), S1A–O1A 1.425(3), S1A–O2A 1.421(3), C1A–S1A 1.857(5), C2A–S1A 1.803(3), C2A–C3A 1.506(5); C2A–S1A–C1A 102.9(2). Further details of the crystal structure investigations may be obtained from the Fachinformationszentrum Karlsruhe, Gesellschaft für wissenschaftlich-technische Information mbH, D-7514 Eggenstein-Leopoldshafen 2 (FRG), on quoting the depository number CSD-53850, the names of the authors, and the journal citation.
[15] Crystal structure of $Rb[CH(SO_2CF_3)_2]$: K. T. Davoy, T. Gramstad, S. Huseby, *Acta Chem. Scand. A33* (1979) 359.
[16] V. Prelog, G. Helmchen, *Angew. Chem. 94* (1982) 614; *Angew. Chem. Int. Ed. Engl. 21* (1982) 567.
[17] E. Keller, *Schakal-88, A FORTRAN Programm for the Graphic Representation of Molecular and Crystallographic Models*, Freiburg 1988.
[18] The crystal structure of (**1e** · 2 THF)$_2$ corresponds essentially to that of (**1e** · TMEDA)$_2$: H. J. Lindner, H.-J. Gais, G. Hellmann, unpublished.
[19] H.-J. Gais, H. J. Lindner, J. Vollhardt, *Angew. Chem. 97* (1985) 865; *Angew. Chem. Int. Ed. Engl. 24* (1985) 859.
[20] a) W. Bauer, M. Feigel, G. Müller, P. von R. Schleyer, *J. Am. Chem. Soc. 110* (1988) 6033; W. Bauer, P. von R. Schleyer, *Magn. Reson. Chem. 26* (1988) 827, and references cited therein; b) H. Günther, D. Moskau, P. Bast, D. Schmalz, *Angew. Chem. 99* (1987) 1242; *Angew. Chem. Int. Ed. Engl. 27* (1987) 1212.
[21] ^6Li, ^1H HOESY experiments: Bruker AC 300, program HOESY (Bruker Software): 128 increments in t_1 with 48 pulses each, mixing time 4 s, delay

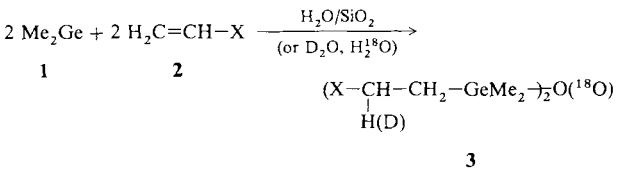
time 4 s, data matrix 256 (t_1) × 512 (t_2), Gauss filter. ^{6}Li{^{1}H} NOE difference spectra: program NOEDIFF: irradiation time 3 s, power 35 L, delay time 7 s, 160 pulses per experiment.
[22] C. Yu, G. C. Levy, *J. Am. Chem. Soc. 106* (1984) 6533.
[23] The assignment of the phenyl group signals in the ^{1}H NMR spectrum was achieved by ^{1}H,^{1}H-COSY and ^{13}C,^{1}H-shift correlation beginning with the ^{1}H and ^{13}C resonances of 6-H and C-6, respectively, which are shifted to high field owing to the benzyl resonance (S. Bradamante, G. A. Pagani, *J. Chem. Soc. Perkin Trans. 2 1986*, 1035).
[24] (**1e** · TMEDA)$_2$ also has such short Li–H distances in the crystal (Li–H4 3.838, Li–H9 3.361, Li–H11 3.437, Li–CH$_3$ 2.852, Li–CH$_2$ 3.240).
[25] H.-J. Gais, J. Vollhardt, C. Krüger, *Angew. Chem. 100* (1988) 1108; *Angew. Chem. Int. Ed. Engl. 27* (1988) 1092.

Addition of Free Me_2Ge: to Alkenes and Alkynes on Glass Surfaces in the Presence of Water**

By *Wilhelm P. Neumann,* Hideki Sakurai,* Gilbert Billeb, Hartmut Brauer, Jürgen Köcher,* and *Sabine Viebahn*

Dedicated to Professor Christoph Rüchardt on the occasion of his 60th birthday

Free Me_2Ge: (dimethylgermanediyl or "dimethylgermylene") **1** undergoes a surprising variety of additions to π systems of alkenes, 1,3-dienes, alkynes, and enones, most of them being regio- or stereospecific.[1] Now we have found that reaction of **1** with conjugated substituted alkenes **2** or with alkynes **4** gives products that contain two Ge atoms and are generated by water adsorbed at the surface of glass or silica gel.

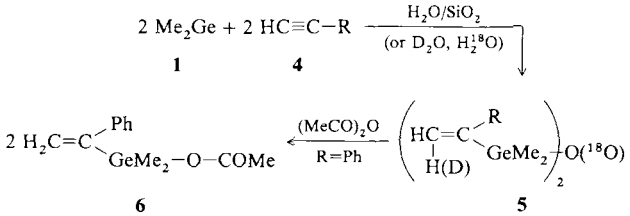


a, X = CN; **b**, X = COOMe; **c**, X = COMe

When we generated free **1** thermally in the presence of acrylonitrile **2a** or other conjugated substituted olefins (**2b, c**) in a glass flask with the usual careful exclusion of air and moisture, we obtained a moderate yield of compounds **3**, the hydrogen contents of which were higher than expected. The additional hydrogens are not contributed via free radical reactions between the partners or with the solvent, as suspected at first. This was established by the lack of influence of cumene and triphenylmethane, as well as of *t*BuBr, which is a powerful scavenger of Ge radicals. Finally, after several difficulties, oxygen was found to be present in the product and structure **3** was established. Compound **3**, a dimer of the adduct expected originally, contains an additional molecule of water. Saturation of the solvent benzene with water did not improve the yields of **3**, and D_2O gave no deuterated **3**. When we added finely powdered glass or silica gel saturated with water and dried at 10^{-3} Torr, however, we obtained nearly quantitatively **3a**; in the same way, reaction with D_2O and with $H_2{}^{18}O$ gave [D_2]**3a** and [^{18}O]**3a**, respectively.

Indeed, water adsorbed at or in the glass[2] is involved stoichiometrically in the reaction. This is evidenced additionally by cross checks: Using a quartz flask after heating it for 4 h at 150 °C/10^{-3} Torr, we found a yield of only 45% instead of 70%. Silylation of its inner surface by means of F_3C-CO-NMe-$SiMe_3$ (MSTFA)/Me_3SiCl over 4 h at 70 °C caused the yield of **3a** to decrease to 35%.

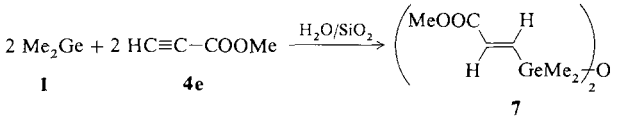
These surprising results required a reinvestigation of the reactions of **1** with alkynes. We had obtained earlier with phenylacetylene **4a** a mixture of unsaturated four-, five-, and six-membered germacycles.[1] Erratically, a minor byproduct with a 1-alkenyl group had been observed (^{1}H NMR), but could not be identified at first. When we now added wet silica gel before starting the reaction, high yields of the new digermoxane **5a** could be obtained instead of the expected products. Alkynes **4b–d** behaved analogously. The structures **5** have been clearly established, also by using $H_2^{18}O$. It should be noted that with **4c**, for example, no product could be detected earlier in the absence of H_2O/SiO_2.



a, R = Ph; **b**, R = Bu; **c**, R = *t*Bu; **d**, R = CH_2OAc

The germoxy group of **5** affords access to new organogermanium compounds, for example to the vinylgermyl acetate **6** starting from **5a** and acetic anhydride. This is additional evidence for the structure of compound **5**.

The structure of the product obtained from methyl acetylenecarboxylate **4e** and **1** was, at first, puzzling. The *E*-olefin **7** was found exclusively instead of the expected 1-alkenyl compound corresponding to **5a–d.**



Elucidation of the mechanism of the participation of adsorbed water thus became a priority task. Compound **1** could react with water in a first step giving the previously unknown hydride $Me_2Ge(H)OH$, which could yield, via hydrogermylation, compounds **3, 5,** and **7**. In the absence of alkene **2** or alkyne **4**, however, water/silica gel and **1** gave only the polygermane $(Me_2Ge)_n$, which we futilely tried to observe.[1] Thus, the intermediacy of a germoxy compound is excluded. An attempted in situ reaction of **1** with methanol led to new ^{1}H NMR absorptions of a hydride XMe_2GeH, but acrylonitrile **2a**, added consecutively, remained unchanged under the standard conditions. Further, no 1-alkenyl structure corresponding to **5** could be observed when phenylacetylene **4a** was hydrogermylated analogously by $Et_2Ge(H)OMe$; instead, the product of an inverse orientation was obtained.[3]

Therefore, the first step is presumably a reaction between **1** and the alkene or alkyne. The resulting intermediate, which

[*] Prof. Dr. W. P. Neumann, Dipl.-Chem. G. Billeb, Dipl.-Chem. H. Brauer, Dr. J. Köcher, Dipl.-Chem. S. Viebahn
Lehrstuhl für Organische Chemie I der Universität
D-4600 Dortmund 50 (FRG)
[**] Prof. Dr. H. Sakurai
Department of Chemistry, Faculty of Science
Tohoku University, Sendai 980 (Japan)

[**] This work was supported by the Fonds der Chemischen Industrie. We are grateful to Dr. *H. Hillgärtner* for very skilfull mass spectrometric investigations.

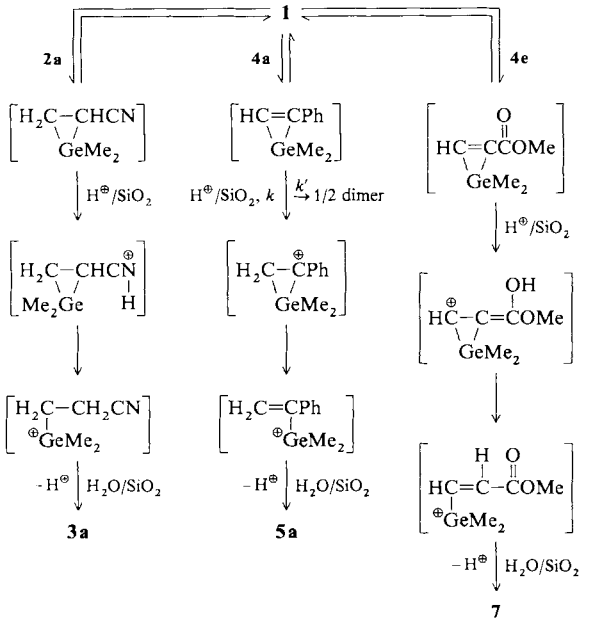
has not yet been detected directly, has a lifetime sufficient for diffusion to the wall of the flask, where it is stabilized by "reactive water". This term is used in the following way: at the surface of glass, not only (monomeric) H_2O has to be taken into account, but also the products of its reaction with the glass surface [Eq. (a)–(c)].[2]

$$(-\overset{\backslash}{\underset{/}{Si}})_2O + H_2O \rightleftharpoons 2\ -\overset{\backslash}{\underset{/}{Si}}-OH \qquad (a)$$

$$(-\overset{\backslash}{\underset{/}{Si}})_2O + H_2O \rightleftharpoons (-\overset{\backslash}{\underset{/}{Si}})_2O\cdot HOH \quad \text{or} \quad (-\overset{\backslash}{\underset{/}{Si}})_2O^{\oplus}\text{-}H + OH^{\ominus} \qquad (b)$$

$$(-\overset{\backslash}{\underset{/}{Si}})_2O^{\oplus}\text{-}H \rightleftharpoons (-\overset{\backslash}{\underset{/}{Si}})_2O + H^{\oplus} \qquad (c)$$

Protonations of the initially formed intermediates seem to best explain the experimental results. In all cases, the most stable cation is apparently formed and is decisive for the structure of the final product (Scheme 1). Thus, also the structural differences between products obtained with **4a–c** and **4e** can be understood now.



Scheme 1. Proposed mechanisms for the formation of **3a**, **5a** and **7**.

When "reactive water" is lacking, the intermediate decomposes reversibly (**4c**) or dimerizes (**4a**, **4b**[1]), or, in the case of other alkynes, butadienes, or styrene, undergoes rapid insertion forming the corresponding five-membered rings.[1]

We have thus been able to demonstrate that, in the reactions of alkenes and alkynes with **1** to give the new types of compounds **3**, **5**, and **7**, molecules of water, or their products present at and in the glass even after heating,[2] are capable of participating in the reaction in a surprising manner. This "reactive water" generates new products stoichiometrically and completely, when finely powdered glass or silica gel is used. This is probably done by proton donation to unstable intermediates. Our current efforts are directed at the definite identification of the intermediates and at broadening the scope of this new reaction principle.

Experimental Procedures[4]

3: SiO_2 (1.0 g, Celite 545, Nagel & Co.) was heated five times at 150 °C/0.001 Torr in a 50-mL two-necked Duran flask. At room temperature, H_2O (D_2O, $H_2{}^{18}O$) (0.300 mL), 7,7-dimethyl-1,4,5,6-tetraphenyl-7-germa-2,3-benzonorbornadiene [1] (2.0 g, 3.7 mmol), **2** (0.74 mL, 11.1 mmol), and benzene (25 mL) were added. The mixture was heated at 70 °C for 4 h under dry argon. After removal of the solvent at 14 Torr, the residue was stirred twice with 20 mL of pentane and filtered from 1,2,3,4-tetraphenylnaphthalene and SiO_2. The solution was evaporated at 14 Torr. Crude yields (^{1}H NMR) of **3**: 80–85%; rest, $(Me_2Ge)_n$. Equal yields were obtained with 1.5 g of powdered glass of a reaction flask. Without SiO_2, only 50% yields (**3a**) were found. The products were purified by kugelrohr distillation at 0.01–0.001 Torr.

5, **7**: Analogously to **3**, but with 1.0 g of the norbornadiene[1], 0.700 mL of H_2O (D_2O, $H_2{}^{18}O$), 10 mmol of **4**, and 10 mL of benzene, 3.5 h under reflux. Yields of crude products: 90–95%.

Received: March 8, 1989 [Z3224 IE]
German version: *Angew. Chem. 101* (1989) 1074

CAS Registry numbers:
1, 74963-95-4; **2a**, 107-13-1; **2b**, 96-33-3; **2c**, 78-94-4; **3a**, 121393-65-5; (D_2) **3a**, 121393-73-5; (^{18}O) **3a**, 121393-74-6; **3b**, 121393-66-6; **3c**, 121393-67-7; **4a**, 536-74-3; **4b**, 693-02-7; **4c**, 917-92-0; **4d**, 627-09-8; **4e**, 922-67-8; **5a**, 121393-68-8; (^{18}O) **5a**, 121393-75-9; **5b**, 121393-69-9; **5c**, 121393-70-2; **5d**, 121393-71-3; **6**, 121424-80-4; **7**, 121393-72-4; SiO_2, 7631-86-9; 7,7-dimethyl-1,4,5,6-tetraphenyl-7-germa-2,3-benzonorbornadiene, 76054-64-3.

[1] M. Schriewer, W. P. Neumann, *J. Am. Chem. Soc. 105* (1983) 897; J. Köcher, W. P. Neumann, *ibid. 106* (1984) 3861; *Organometallics 4* (1985) 400; E. Michels, W. P. Neumann, *Tetrahedron Lett. 27* (1986) 2455; G. Billeb, W. P. Neumann, G. Steinhoff, *ibid. 29* (1988) 5245.

[2] There have been controversial discussions about the amount, kind of bonding, mobility, and splitting of water in glasses. H. Scholze: *Glas*, 3rd ed., Springer, Berlin 1988. See also references therein.

[3] M. Massol, J. Satgé, P. Rivière, J. Barrau, *J. Organomet. Chem. 22* (1970) 599.

[4] The products give correct elemental analyses and have been identified unequivocally: ^{1}H, ^{13}C NMR: Bruker AM 300, TMS_{int}, $CDCl_3$; MS: Varian CH7, Finnigan-MAT 8230; [^{18}O]**3a**: $M^{\oplus}$ – Me by simulation and subtraction of the unlabeled **3a**; FT-IR: Bruker IFS 131v; Raman: Coderg T800, λ = 514.5 nm.

3a: MS (EI): *m/z* 315 ($M^{\oplus}$ – Me, 27%; high resolution: found 315.0352, calcd 315.0369). ^{1}H NMR: δ = 0.44 (s, 12H, GeMe), 1.18 (t, J = 7.8 Hz, 4H, CH_2), 2.51 (t, J = 7.8 Hz, 4H, CH_2); Raman: $\tilde{\nu}$ (GeO) = 460 cm^{-1}. [D_2]**3a**: MS (EI): *m/z* 317 ($M^{\oplus}$ – Me, 35%). ^{1}H NMR: δ = 0.34 (s, 12H, GeMe), 1.08 (d, ^3J(H,H) = 8.1 Hz, 4H, CH_2), 2.39 (tt, ^3J(H,H) = 8.1, ^2J(D,H) = 2.6 Hz, 2H, CDH). [^{18}O]**3a**: MS (EI): *m/z* 317 ($M^{\oplus}$ – Me, 36%). **3b**: MS (EI): *m/z* 381 ($M^{\oplus}$ – Me, 7%). ^{1}H NMR: δ = 0.38 (s, 12H, GeMe), 1.12 (t, J = 7.8 Hz, 4H, CH_2), 2.45 (t, J = 7.8 Hz, 4H, CH_2), 3.68 (s, 6H, CO_2Me). **3c**: MS (EI): *m/z* 349 ($M^{\oplus}$ – Me, 7%). ^{1}H NMR: δ = 0.27 (s, 12H, GeMe), 0.92 (t, J = 6.6 Hz, 4H, CH_2), 2.02 (s, 6H, COMe), 2.49 (t, J = 6.6 Hz, 4H, CH_2). **5a**: MS (EI): *m/z* 428 ($M^{\oplus}$, 4%), 413 ($M^{\oplus}$ – Me, 6%). ^{1}H NMR: δ = 0.38 (s, 12H, GeMe), 5.10, 5.47 (each d, ^2J(H,H) = 2.0 Hz, each 2H, =CH_2), 6.80 (m, 10H, Ph). IR (KBr): $\tilde{\nu}$ (GeO) = 855 cm^{-1}. [^{18}O]**5a**: MS (EI): *m/z* 430 ($M^{\oplus}$, 4%). **5b**: MS (EI): *m/z* 388 ($M^{\oplus}$, 3%), 373 ($M^{\oplus}$ – Me, 40%). ^{1}H NMR: δ = 0.34 (s, 12H, GeMe), 0.89–2.20 (18H, Bu), 5.22, 5.48 (each m, ^4J(H,H) = 1.3, ^2J(H,H) = 2.3 Hz, each 2H, =CH_2). **5c**: MS (EI): *m/z* 388 ($M^{\oplus}$, 2%), 373 ($M^{\oplus}$ – Me, 54%). ^{1}H NMR: δ = 0.47 (s, 12H, GeMe), 1.20 (s, 18H, *t*Bu), 5.30, 5.60 (each d, ^2J(H,H) = 1.6 Hz, each 2H, =CH_2). **5d**: MS (EI): *m/z* 405 ($M^{\oplus}$ – Me, 33%). ^{1}H NMR: δ = 0.40 (s, 12H, GeMe), 2.00 (s, 6H, CH_3), 4.70 (m, ^4J(H,H) = 1.4 Hz, ^4J(H,H) = 1.6 Hz, 4H, CH_2). **6**: ^{1}H NMR: δ = 0.66 (s, 6H, GeMe), 1.93 (s, 3H, COMe), 5.67, 5.93 (each d, ^2J(H,H) = 2.0 Hz, each 1H, =CH_2), 7.23 (s, 5H, Ph). **7**: MS (EI): *m/z* 377 ($M^{\oplus}$ – Me, 100%). ^{1}H NMR: δ = 0.52 (s, 12H, GeMe), 3.80 (s, 6H, CH_3), 6.25, 7.37 (each d, ^3J(H,H) = 19.0 Hz, each 2H, =CH).

Visualization of Chromatographic Separations by NMR Imaging

By *Ernst Bayer*,* *Winfried Müller*, *Martin Ilg*, and *Klaus Albert*

Nuclear magnetic resonance imaging[1, 2] has been very successful in medical diagnosis, since it allows noninvasive observation of liquid and gel-like states as well as of dynamic

[*] Prof. Dr. E. Bayer, Dr. W. Müller, M. Ilg, Dr. K. Albert
Institut für Organische Chemie der Universität
Auf der Morgenstelle 18, D-7400 Tübingen (FRG)

processes. This method has also proved useful in the investigation of exchange, flow, and diffusion processes in chemistry.[3, 4] Liquid chromatography is one of the most common such processes. Chromatographic interactions between eluent and stationary phase in the column cannot be observed in situ. It is therefore impossible to monitor exactly the elution profile and to determine the factors leading to band broadening and other irregularities. Even colored substances, the separation of which led *Tswett* to coin the term chromatography, only provide information on the zone boundaries; they afford no insight into the profile within the column.

^{1}H NMR imaging yields proton images of any desired volume element of a packed column. An unambiguous correlation between position and resonance frequency is achieved with three mutually orthogonal field gradients, which exactly define the positional dependence of the magnetic field. The NMR image is obtained from the signal intensities of the volume elements thus generated. These signal intensities depend on many parameters, such as relaxation times T_1 and T_2, spin density, flow and diffusion phenomena, and chemical shift. Differences in these parameters lead to a high-contrast image. Since these parameters are differently influenced by the interactions between stationary phase, mobile phase, and eluent, it is possible to obtain an image of a chromatogram or a column in either a stationary or a dynamic state. Thus, variations in the packing density along the diameter or length of the column, channel formation, and differences in the degree of wetting can be clearly recognized and subsequently used to develop an optimal method for packing the column. This is of particular importance for preparative columns.

The relaxation times T_1 and T_2 are key factors in imaging, since they provide information on the mobility of the solvent in the stationary phase. Stationary phases of low porosity and large absorption capacity absorb water more strongly than materials having large pores. This is reflected in smaller relaxation times T_1 and T_2 in fine-pored materials, as is shown by the values in Table 1. In the fine-pored gels Sephadex G10 and G15, the mobility of water is highly restricted. In the wide-pored material G100, on the other hand, T_1 and T_2 approach the normal relaxation times of water. Owing to the high polarity of silica gel 60, the mobility of water in this stationary phase is even more restricted than in Sephadex G10. Similar relationships are also observed for other solvents.

Table 1. Proton relaxation times T_1 and T_2 of water in swelled Sephadex gels.

Sephadex	T_2 [ms]	T_1 [ms]
G10	103	490
G15	164	585
G25	305	843
G100	494	2460

Interestingly, a decrease in the relaxation time T_1 is observed along the length of a column from top to bottom, as is shown in Figure 1 for silica columns in a stationary state with acetonitrile and with water as mobile phases. This is ascribed to a denser packing of the silica at the bottom of the column.

Rapid imaging sequences, such as FLASH (Fast Low Angle Shot Imaging),[5] allow the continuous monitoring of a chromatographic process. These sequences are based on the attainment of a dynamic equilibrium magnetization by the use of small flip angles ($\alpha < 90°$). A high transverse magnetization and an only slightly reduced longitudinal magnetization is thereby achieved, so that, even for very short repetition times, high contrast and good signal-to-noise ratios were obtained for measuring times of only a few seconds. This method allows one to monitor a running chromatogram by recording images every 30 s and combining them into a single film.

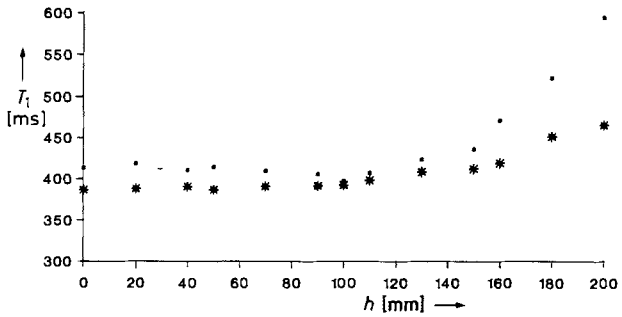


Fig. 1. Relaxation time T_1 in various regions of a silica column. 0 mm is the bottom of the column. Inversion-recovery sequence, Siemens Magneton 1.5 T whole-body system. ■, acetonitrile/SiO_2; *, H_2O/SiO_2.

The development of the profile of the chromatographic bands can be followed in each volume segment of the column rather than merely at the walls. The images thereby obtained allow one to view the elution profile through cross sections or along the length of the column or as a complete set of three-dimensional images (3D FLASH). The separation of both single-component and multicomponent systems has been followed in this way, as shown in Figure 2 (left) for the separation of amavadin, a naturally occurring vanadium(IV) complex,[6, 7] on Sephadex. In this case, the chromatographic bands were followed along a central longitudinal cut through the interior of the column by recording images of a 4-mm-thick slice (see Fig. 2, right). The band broadening and the variation in the elution profile with time are clearly revealed. The analysis of such flow profiles can be carried out even better by chromatographing the diethylenetriaminepentaacetic acid gadolinium complex (Gd-DPTA). This compound is used as a contrasting agent in magnetic resonance tomography at concentrations of 10^{-3} to 10^{-4} M[8] and affords high contrast in this concentration range. The development of the chromatogram was followed continuously and the images were combined into a single

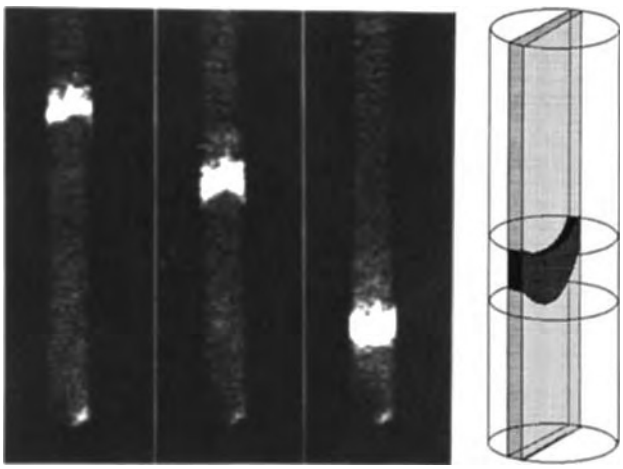


Fig. 2. Left: Fast images of the chromatography of amavadin/H_2O on Sephadex (FLASH sequence, TE = 20 ms, TR = 60 ms) after an elution time of 37 min, 63 min, and 110 min. Right: Schematic drawing of the slice selected in the chromatographic images.

 © VCH Verlagsgesellschaft mbH, D-6940 Weinheim, 1989 0570-0833/89/0808-1030 $ 02.50/0

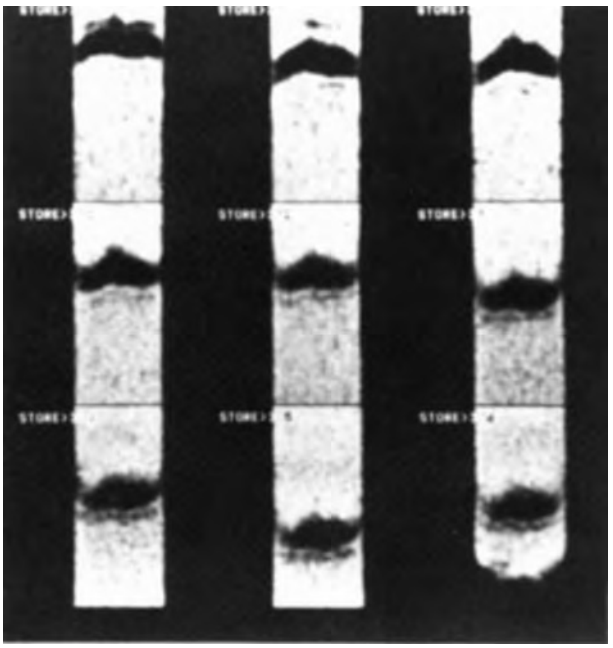


Fig. 3. Development of the elution front (proton image) during the chromatography of Gd-DPTA/H_2O on Sephadex (FLASH, TE = 20 ms, TR = 60 ms). Images from a film [9] at time intervals of 15 min. The images should be viewed along a line, not a column.

film,[9] nine individual images of which are shown in Figure 3.

At the beginning of the column, a parabolic flow profile is formed. This is due to the wall effect; the column packing is less dense at the walls and the interaction between eluent and stationary phase is therefore less strong, allowing a faster band migration. Although the wall effect has been theoretically predicted, in particular with respect to preparative columns, it has not been investigated in situ.[10, 11] This is the first time it has been made visible. Also clearly revealed at the beginning of the chromatogram is the effect of nonuniform sample application. As the elution proceeds, the wall effects become less important and the separation of the individual components is clearly seen. The eluent is observed to move most rapidly through the center of the column. This effect is ascribed to the higher temperature at the center of the column owing to the heat of absorption. The column material has a relatively poor thermal conductivity and cannot transfer the heat rapidly enough to the walls. Still later, band broadening occurs owing to diffusion effects. Also interesting are the contrasts in the column outside the respective elution regions. These differences remain constant with respect to their position during the entire chromatographic separation. We ascribe this to different degrees of wetting of the column material.

In addition to protons, other nuclei, such as ^{19}F, ^{23}Na, and ^{13}C, can also be used in NMR imaging. Because of the low NMR sensitivity of these nuclei, however, the imaging is restricted to larger volume elements with smaller spatial resolution. Nonetheless, mobile and bound sodium ions can be distinguished owing to the effects of their different T_2 relaxation times on the image contrast. A Dowex column loaded with $Na^{\oplus}$ exhibits only weak contrast. Various stages of the elution are shown in Figure 4. Because of the increase in T_2, the now mobile $Na^{\oplus}$ ions are clearly contrasted. In this case, nonuniformities in the column packing, which lead to channel formation, are visible.

These first attempts at following the chromatographic process by means of NMR imaging show that this method

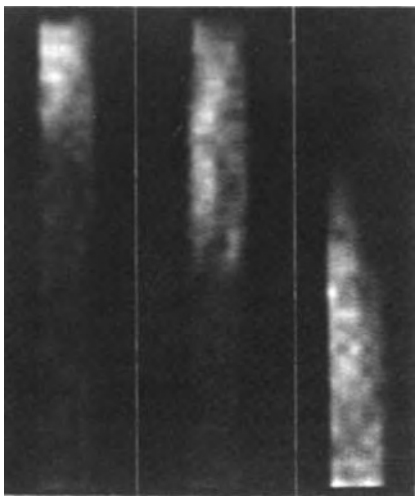


Fig. 4. Flash images (^{23}Na images) of ion exchange on an ion-exchange column during elution with 2 N HCl at time intervals of 40 min (column 30 cm × 3 cm, 3D FLASH, TE = 5 ms, TR = 20 ms).

offers new possibilities for basic investigations. Flow effects, which have so far only been investigated either theoretically or, when experimentally, with concomitant interference in the process, can be studied noninvasively. Optimization of the column packing should be of special value in opening up new applications to preparative chromatography.

The imaging of flow systems in packed and open columns is of interest for many other processes besides chromatography. Imaging allows the observation of chromatographic processes independent of the color of the substances being eluted. Thus, the term chromatography, as coined by *Tswett*, again takes on a general meaning.

So far the resolution of this method has not allowed the diffusion processes in individual particles to be viewed. Model studies on larger particles, however, can be carried out with micro-imaging instruments.[12, 13] Figure 5 shows polystyrene spheres of ca. 500-μm diameter with a planar resolution of 20 μm × 20 μm after swelling in benzene. The

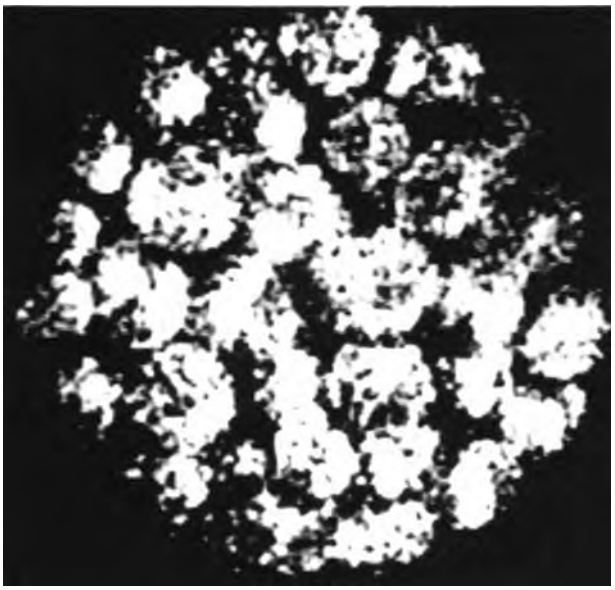


Fig. 5. Micro-image of polystyrene beads in benzene, pixel resolution 20 μm, slice thickness 200 μm (spin-echo sequence, Bruker AM 300 WB instrument). We thank *W. Kuhn*, Bruker Analytische Messtechnik, Karlsruhe-Forchheim, for this image.

distribution of the solvent inside the polymer spheres is revealed by the contrast in brightness. The further development of NMR imaging to include nearly microscopic resolution offers the possibility of numerous applications in polymer chemistry and cell biology.

Received: March 17, 1989 [Z 3235 IE]
German version: *Angew. Chem. 101* (1989) 1033

[1] P. C. Lauterbur, *Nature (London) 242*, (1973) 190.
[2] F. W. Wehrli, D. Shaw, J. B. Kneel (eds.): *Biochemical Resonance Imaging*, VCH Publishers, New York 1988.
[3] B. Blümich, *Angew. Chem. 100* (1988) 1460; *Angew. Chem. Int. Ed. Engl. 27* (1988) 1406.
[4] L. A. Weisenberger, J. L. König, *Polym. Prepr. Am. Chem. Soc. Div. Polym. Chem. 29* (1988) 98.
[5] A. Haase, J. Frahm, D. Matthaei, K. D. Merboldt, W. Hänicke, *J. Magn. Reson. 67* (1986) 217.
[6] E. Bayer, E. Koch, G. Anderegg, *Angew. Chem. 99* (1987) 570; *Angew. Chem. Int. Ed. Engl. 26* (1987) 545.
[7] H. Kneifel, E. Bayer, *J. Am. Chem. Soc. 108* (1986) 3075.
[8] W. Grodd, R. C. Brasch, *Roe Fo Fortschr. Geb. Roentgenstr. Nuklearmed. 145* (1986) 130.
[9] E. Bayer, lecture and film at the 12th Symposium on Column Liquid Chromatography, Washington, June 19–24, 1988.
[10] E. Bayer, *Chimia 17* (1963) 414.
[11] G. Guichon, S. Ghodbane, S. Golshan-Shirazi, L. Bingcheng, lecture at the 17th International Symposium on Chromatography, Vienna, Sept. 25–30, 1988.
[12] J. Aguayo, S. Blackband, J. Schoeniger, M. Mattingly, M. Hintermann, *Nature (London) 322* (1986) 190.
[13] W. Kuhn, *Bruker Rep. 1987 (1)* 40.

Insertion of $Cr(CO)_3$ into $As_7^{3\ominus}$ to Form $[As_7Cr(CO)_3]^{3\ominus}$: An Inorganic Nortricyclane-to-Norbornadiene Conversion

By *Bryan W. Eichhorn, Robert C. Haushalter,** and *John C. Huffman*

Dedicated to Professor Hans Bock on the occasion of his 60th birthday

The pioneering work of *von Schnering* and co-workers in the development of polyatomic pnictide anions revealed a remarkable family of clusters with unusual structures and properties.[1] Most notable among these compounds are the extensive series of phosphides that include $P_7^{3\ominus}$, $P_{11}^{3\ominus}$, $P_{16}^{2\ominus}$, and $P_{21}^{3\ominus}$.[2] Subsequent studies[3, 4] have shown that the later pnictide elements can adopt structures different from those of the phosphides, such as the square $M_4^{2\ominus}$ (M = Sb, Bi)[5] and the linked bis-trishomocubane $As_{22}^{4\ominus}$.[6] Reactions of these species with transition metals have been virtually unexplored aside from a few examples of transition-metal main-group clusters that include $P_7[FeCp(CO)_2]_3$[7] and the remarkable $^1_\infty[Rb \cdot NbAs_8^{2\ominus}]$.[8] We have been interested in inserting unsaturated transition-metal fragments into various polyatomic p-block cluster anions (Zintl ions) to effect topological rearrangements within the main-group fragment and probe the flexibilities of the cluster frameworks. Thus far, we have isolated and characterized *closo*-$[Sn_9Cr(CO)_3]^{4\ominus}$[9] along with a variety of telluride complexes that include $[Mo_4Te_{16}(en)_4]^{2\ominus}$ (en = ethylenediamine),[10] $[Cr(\eta^2\text{-}Te_2)_2(CO)_2]^{2\ominus}$,[11] and $[Pd(Te_4)_2]^{2\ominus}$.[12] Here we describe the synthesis and structure of $[As_7Cr(CO)_3]^{3\ominus}$, comprising a norbornadiene-related As_7 core derived from the nortricyclic $As_7^{3\ominus}$ ion.

[*] Dr. R. C. Haushalter, Dr. B. W. Eichhorn [+]
Exxon Research and Engineering Company
Route 22 East, Annandale, NJ 08801 (USA)
Dr. J. C. Huffman,
Molecular Structure Center
Indiana University
Bloomington, IN 47405 (USA)
[+] Current address:
Department of Chemistry
University of Maryland
College Park, MD 20742 (USA)

Toluene solutions of $[Cr(CO)_3(\eta^6\text{-mes})]$ (mes = 1,3,5-$Me_3C_6H_3$) react with ethylenediamine extracts of Rb_3As_7[1e] in the presence of three equivalents of 4,7,13,16,21,24-hexaoxa-1,10-diazabicyclo[8.8.8]hexacosane (crypt) to form the chromium-arsenide complex **1** [Eq. (a)]. Transparent red-orange crystals of complex **1** can be isolated in good yield from concentrated reaction mixtures at room temperature.

$$[Cr(CO)_3(\eta^6\text{-mes})] + Rb_3As_7 + 3\ \text{crypt} \xrightarrow{\text{en/toluene}} \underset{\mathbf{1}}{[As_7Cr(CO)_3][(Rb \cdot \text{crypt})_3] \cdot 0.5\ \text{toluene}} + \text{mes} \quad \text{(a)}$$

The crystalline solid must be stored at $-20\,^\circ C$ or below and is very air and moisture sensitive in solution and the solid state. Complex **1** has been characterized by energy-dispersive X-ray analysis (EDAX), bulk elemental analysis, solution and solid-state IR spectroscopy, and single-crystal X-ray diffraction.

Compound **1** crystallizes in the space group $P\bar{1}$ with two independent anions, six $(Rb \cdot crypt)^\oplus$ ions, and a toluene solvate molecule in the asymmetric unit (197 heavy atoms);[14] one anion is partially disordered. The structure of the $[As_7Cr(CO)_3]^{3\ominus}$ ion **2** (Fig. 1) contains an opened As_7 cage that is bound in an η^4 fashion to the $Cr(CO)_3$ fragment. The As_7 fragment in **2** bears a striking resemblance to the coordinated norbornadiene ligand in $PdCl_2$(norbornadiene)[15] and represents a new structure type for seven-atom p-block clusters; however, similar P_7 fragments can be identified in the interior of some larger polyphosphorus compounds[1, 2] and certain forms of elemental phosphorus.[16] The As_7 cage in **2** is closely related to the parent $As_7^{3\ominus}$ ion, differing only by the absence of one As–As bond (Fig. 2, left). The site of attachment of the $Cr(CO)_3$ fragment is shown in Figure 2, right. The Cr–As distances in **2** (average 2.67(6) Å) are long in comparison with metal–arsenic distances in related compounds such as $[Cr_2(CO)_6(AsMe)_9]$ (2.44(1) Å)[17] and $[(\mu_3\text{-}As)Cr_2Mn(CO)_{14}]$ (2.38(6) Å).[18] The anion possesses a virtual mirror plane (C_s symmetry). As a result, C13 and C11 are aligned *trans* to As4 and As5, thereby lengthen-

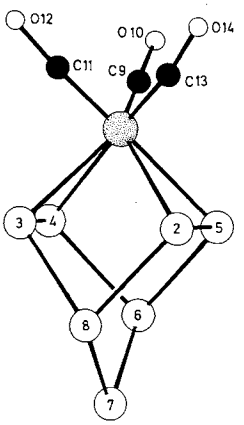


Fig. 1. Ball-and-stick Chem-X [20] representation of **2**. Pertinent distances [Å] and angles [°]: Cr1–As2 2.636(10), Cr1–As3 2.630(11), Cr1–As4 2.685(10), Cr1–As5 2.730(10), Cr1–C9 1.78(5), Cr1–C11 1.67(5), Cr1–C13 1.82(6), C11–O12 1.28(5), C9–O10 1.18(5), C13–O14 1.15(5); C13–Cr1–As4 177(2), C11–Cr1–As5 175(2), C9–Cr1–As2 132(1), C9–Cr1–As3 140(1), Cr1–As4–As6, Cr1–As5–As6 99.5(2) (average), Cr1–As2–As8, Cr1–As3–As8 103.9(1) (average).

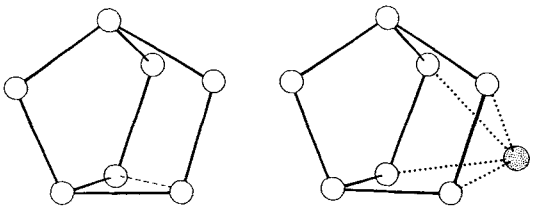


Fig. 2. Two views of the As_7 fragment of **2**. Left: Perspective showing the relationship to the parent $As_7^{3\ominus}$ ion. The separation denoted by the dashed line (3.2 Å) is 0.7 Å longer than in $As_7^{3\ominus}$ (2.49 Å) (see [1e]). Right: Perspective showing the site of attachment of the $Cr(CO)_3$ fragment relative to the parent $As_7^{3\ominus}$ framework.

ing these Cr–As bond distances (average 2.71(2) Å) relative to the Cr–As bond distances to As2 and As3 (average 2.64(2) Å) due to the high *trans* influence of CO. The As–As bond distances occur in two ranges: long contacts for As8–As2,3 and As6–As4,5 (average 2.46(2) Å) and short contacts for As2–As5, As3–As4, and As7–As8,6 (average 2.35(2) Å). The latter distances are typical for bonds to two-coordinate As atoms in polyarsenide cluster anions.[1, 2, 4, 6] The As2–As3 and As4–As5 separations of 3.09(1) and 3.29(1) Å, respectively, reflect a slight asymmetry in the As_7 core but can be considered nonbonding.

A significant amount of electron density has been transferred onto the Cr atom, as evidenced by low CO stretching frequencies in the IR spectrum of **2** [$\tilde{\nu}$(CO) = 1823, 1742, 1706 cm^{-1}] and short Cr–C bond distances (d(Cr,C) = 1.74(8) Å). These values are intermediate between those of $[M_9Cr(CO)_3]^{4\ominus}$ (M = Sn, Pb) and $[Cr(CO)_3(\eta^6\text{-}C_6H_6)]$, as is expected based on ligand donor properties and charge considerations (see Table 1). For electron bookkeeping purposes, it is convenient to consider **2** as a composite of a 14-electron $[Cr(CO)_3]^{2\ominus}$ fragment and a 4-electron-donor (norbornadiene-like) $As_7^{\ominus}$ fragment that satisfies the 18-valence-electron requirement at the Cr center.

Table 1. IR and structural data.

Complex	$\tilde{\nu}$(CO) [cm^{-1}]	d(Cr, C) [Å]	d(C,O) [Å]
$[Cr(CO)_3(\eta^6\text{-}C_6H_6]$ [13a]	1970, 1894	1.83	1.15
$[Sn_9Cr(CO)_3]^{4\ominus}$ [9]	1809, 1703	1.65(7)	1.29(4)
$[Pb_9Cr(CO)_3]^{4\ominus}$ [13b]	1791, 1688	1.76(5)	1.20(7)
$[As_7Cr(CO)_3]^{3\ominus}$	1823, 1724	1.76(9)	1.20(8)

The formation of **1** represents the conversion of a nortricyclic $As_7^{3\ominus}$ cluster into a norbornadiene-like As_7 fragment at a transition-metal center. This transformation closely resembles the organic chemistry occurring at a $(CO)_nCr$(norbornadiene) center (n = 3,4), where norbornadiene-to-nortricyclane conversions are facile.[19] Anion **2** represents the beginning of a growing class of transition-metal pnictide clusters with bare main-group fragments (cf. also Refs. [7, 8]).

Experimental Procedure

Under a He atmosphere a melt of nominal composition Rb_3As_7 (200 mg, ca. 0.26 mmol) was extracted into ethylenediamine (ca. 5 mL), producing a red-orange solution. In a separate reaction vessel, $[Cr(CO)_3(\eta^6\text{-mes})]$ (80 mg, 0.31 mmol) was dissolved in toluene (ca. 1 mL), producing a pale-yellow solution. The toluene solution was added dropwise to the ethylenediamine extract. Three equivalents of crypt (290 mg, 0.78 mmol) were added to the red-orange reaction mixture. No color changes occurred. The mixture was filtered twice and concentrated under vacuum to ca. 3 mL total volume. After 48 h, 320 mg (0.15 mmol) of pale orange red crystals were isolated, washed with toluene, and dried in vacuo (58% crystalline yield based on Rb_3As_7). Elemental analysis calculated for $Rb_6As_{14}Cr_2C_{121}H_{224}N_{12}O_{42}$: As, 24.52; Cr, 2.43; C, 35.95; H, 5.47; N, 3.93. Found: As, 25.06; Cr, 2.48; C, 34.73; H, 5.39; N, 4.02. A disordered en solvate molecule in the crystal lattice, which is typical for cryptated Zintl clusters [3, 9], would explain the high nitrogen content.

Received: February 7, 1989 [Z 3164 IE]
German version: *Angew. Chem. 101* (1989) 1081

CAS Registry numbers:
1, 121808-74-0; $[Cr(CO)_3(\eta^6\text{-mes})]$,12129-67-8.

[1] a) For review see H. G. von Schnering, *Angew. Chem. 93* (1981) 44; *Angew. Chem. Int. Ed. Engl. 20* (1981) 33; b) W. Hönle, H. G. von Schnering, *ibid. 98* (1986) 370 and *25* (1986) 352; c) W. Hönle, V. Manriquez, C. Mujica, D. Weber, H. G. von Schnering, *Chem. Future Proc. IUPAC Congr. 29th* (Köln 1983), *Abstr.* p. 36; d) H. G. von Schnering, T. Meyer, W. Hönle, W. Schmettow, U. Hinze, W. Bauhofer, G. Kliche, *Z. Anorg. Allg. Chem. 553* (1987) 261; e) H. G. von Schnering in A. Cowley (Ed.): *Rings, Clusters, and Polymers of the Main Group Elements, ACS Symposium Series 232* (1983) 69.

[2] For a review see M. Baudler, *Angew. Chem. 99* (1987) 429; *Angew. Chem. Int. Ed. Engl. 26* (1987) 419.

[3] a) D. G. Adolphson, J. D. Corbett, D. J. Merryman, *J. Am. Chem. Soc. 98* (1976) 522; b) R. C. Burns, J. D. Corbett, *Inorg. Chem. 24* (1985) 1489.

[4] a) J. Roziere, A. Seigneurin, C. Belin, A. Michalowicz, *Inorg. Chem. 24* (1985) 3710; b) C. H. E. Belin, *J. Am. Chem. Soc. 102* (1980) 6036.

[5] A. Cisar, J. D. Corbett, *Inorg. Chem. 16* (1977) 2482.

[6] R. C. Haushalter, B. W. Eichhorn, A. L. Rheingold, S. J. Geib, *J. Chem. Soc. Chem. Commun. 1988*, 1027.

[7] G. Fritz, K. D. Hoppe, W. Hönle, D. Weber, C. Mujica, V. Manriquez, H. G. von Schnering, *J. Organomet. Chem. 249* (1983) 63.

[8] H. G. von Schnering, J. Wolf, D. Weber, R. Ramirez, T. Meyer, *Angew. Chem. 98* (1986) 372; *Angew. Chem. Int. Ed. Engl. 25* (1986) 353.

[9] B. W. Eichhorn, R. C. Haushalter, W. T. Pennington, *J. Am. Chem. Soc. 110* (1988) 8704.

[10] B. W. Eichhorn, R. C. Haushalter, F. A. Cotton, B. Wilson, *Inorg. Chem. 27* (1988) 4084.

[11] B. W. Eichhorn, R. C. Haushalter, W. T. Pennington, results to be published.

[12] R. D. Adams, T. A. Wolfe, B. W. Eichhorn, R. C. Haushalter, *Polyhedron 8* (1989) 701.

[13] a) O. S. Mills, *Pure Appl. Chem. 20* (1969) 117; b) B. W. Eichhorn, R. C. Haushalter, results to be published.

[14] X-ray data: space group $P\bar{1}$(No.2); a = 23.32(4), b = 26.11(5), c = 14.96(3) Å, α = 102.58(8), β = 101,63(7), γ = 89.33(8)°, V = 8699(1) Å^3, Z = 4. $Mo_{K\alpha}$ radiation; 16344 unique reflections, 7823 with $F \geq 2.33\,\sigma(F)$. R = 0.110, R_w = 0.125. The structure was refined in blocked segments due to the large volume. One $[As_7Cr(CO)_3]^{3\ominus}$ anion was slightly disordered (ca. 25%). Further details of the crystal structure investigation may be obtained from the Fachinformationszentrum Karlsruhe, Gesellschaft für wissenschaftlich-technische Information mbH, D-7514 Eggenstein-Leopoldshafen 2 (FRG), on quoting the depository number CSD-53848, the names of the authors, and the journal citation.

[15] a) N. C. Baenziger, J. R. Doyle, C. L. Carpenter, *Acta Crystallogr. 14* (1961) 303; b) N. C. Baenziger, G. F. Richards, J. R. Doyle, *ibid. 18* (1965) 924.

[16] H. Thurn, H. Krebs, *Angew. Chem. 78* (1966) 1101; *Angew. Chem. Int. Ed. Engl. 5* (1966) 1047.

[17] P. S. Elmes, B. M. Gatehouse, D. J. Lloyd, B. O. West, *J. Chem. Soc. Chem. Commun. 1974*, 953.

[18] G. Huttner, U. Weber, B. Sigwarth, O. Scheidsteger, H. Lang, L. Zsolnai, *J. Organomet. Chem. 282* (1985) 331.

[19] a) D. J. Darensbourg, H. H. Nelson, M. A. Murphy, *J. Am. Chem. Soc. 99* (1977) 896; b) G. Platbrood, L. Wilputte-Steinert, *J. Organomet. Chem. 70* (1974) 393, 407.

[20] Chem-X, developed and distributed by Chemical Design Ltd., Oxford, England.

Trigonal-Bipyramidal Lanthanoid Complexes with Interstitial Oxygen Atoms**

By Herbert Schumann, Pil Ryul Lee,* and *Jörg Loebel*

Lanthanoid trichlorides react with $K[HB(pz)_3]$ to form the tris(pyrazolyl)borato complexes $[\{HB(pz)_3\}LnCl_2]$,[1]

[*] Prof. Dr. H. Schumann, Dr. P. R. Lee, Dipl.-Chem. J. Loebel
Institut für Anorganische und Analytische Chemie der
Technischen Universität
Strasse des 17. Juni 135, D-1000 Berlin 12

[**] Organometallic Compounds of the Lanthanoids, Part 49. This work was supported by the Fonds der Chemischen Industrie and the Deutsche Forschungsgemeinschaft. Part 48: H. Schumann, R. D. Köhn, F. W. Reier, A. Dietrich, J. Pickardt, *Organometallics 8* (1989) 1388.

$[\{HB(pz)_3\}_2LnCl]$,[1,2] $[\{HB(pz)_3\}_3Ln]$,[1,3] and $[\{HB(pz)_3\}_2Ln(CH_3COCHCOCH_3)]$,[4] in which the tris(pyrazolyl)borato ligands are coordinated to the lanthanoid atom through one nitrogen atom on each of the three pyrazole rings. The pyrazolyl ligand, $C_3H_3N_2^{\ominus}$(pz), and the 3,5-dimethylpyrazolyl ligand, $(CH_3)_2C_3HN_2^{\ominus}$ ($pzMe_2$), however, have two nitrogen atoms capable of coordination; thus, they can be employed as 1,2-μ-bridging ligands in the formation of (η^2-$pzMe_2$) complexes, for example, $[Ni(NO)(pzMe_2)]_2$,[5] and of (η^2-pz) complexes, for example, $[(C_5H_5)_2Ti(pz)_2Ti(C_5H_5)_2]$.[6] X-ray structure analyses of the first pyrazolyl complexes of the inner transition metals, $[(C_5H_5)_3U(pz)]$[7] and $[(C_5Me_5)_2U(pz)_2]$,[8] reveal an η^2 coordination.

We found that lanthanoid trichlorides, $LnCl_3$, react with Na(pz) and $Na(pzMe_2)$ in tetrahydrofuran under inert atmosphere to give organolanthanoid pyrazolates, some of which have complicated formulas. The products could be characterized by elemental analyses and NMR spectra.[9] Traces of water in the reaction mixture result in the incorporation of an $O^{2\ominus}$ ion between the strongly oxophilic lanthanoids. Reaction of YCl_3, $HoCl_3$, $YbCl_3$, and $LuCl_3$ with $Na(pzMe_2)$ thus yielded complexes **1a–4a** as colorless to pink crystals; a molecule of tetrahydrofuran is coordinated to each sodium atom.[10] Extraction of the reaction products with toluene results in replacement of the two tetrahydrofuran molecules coordinated to the two sodium atoms with two 3,5-dimethylpyrazoles (**1b–3b**).[10]

$$3\,LnCl_3 + 11\,Na(pzMe_2) + H_2O \xrightarrow{THF} [Ln_3(\mu\text{-}pzMe_2)_6(\eta^2\text{-}pzMe_2)_3(\mu_3\text{-}O)Na_2(thf)_2] + 9\,NaCl + 2\,H(pzMe_2)$$

Ln = Y (**1a**), Ho (**2a**), Yb (**3a**), Lu (**4a**)

$$3\,LnCl_3 + 11\,Na(pzMe_2) + H_2O \xrightarrow{toluene} [Ln_3(\mu\text{-}pzMe_2)_6(\eta^2\text{-}pzMe_2)_3(\mu_3\text{-}O)Na_2\{H(pzMe_2)\}_2] + 9\,NaCl$$

Ln = Y (**1b**), Ho (**2b**), Yb (**3b**)

The X-ray crystal structure analyses[11] of **2b** and **3a** revealed trigonal bipyramids containing an oxygen atom at the center, three lanthanoid atoms in the equatorial positions, and two sodium atoms at the apical vertices (Figs. 1 and 2). Holmium and ytterbium each are heptacoordinated by four nitrogen atoms of the bridging pyrazolyl ligands, two nitrogens of the terminal pyrazolyl ligands, and the central oxygen atom. In both clusters, the N–N bonds of the bridging pyrazolyl group are not parallel to the sides of the triangle formed by the lanthanoid atoms; thus, in each case, only one of the nitrogen atoms is coordinated to a sodium atom (average distance 248.5 pm in **2b**, 242.9 pm in **3a**). Therefore, together with the THF oxygen atom or a nitrogen atom of the neutral pyrazole ligand, respectively, the sodium atom has a tetrahedral coordination geometry.

Coordination of 3,5-dimethylpyrazole, which is sterically demanding relative to tetrahydrofuran to sodium, forces one of the terminal pyrazole rings in **2b** to lie nearly perpendicular (99.93°) to the plane of the holmium atoms, while the other terminal pyrazole ligands in **2b** and **3a** form angles of only 14.95–33.06° with respect to this plane. One of the bridging pyrazole ligands in **2b** is so strongly tilted that N15 is coordinated to two holmium atoms and N16 exhibits a relatively short distance (236.6(4) pm) to Na1. The nitrogen atoms of the terminal η^2-dimethylpyrazolyl ligands, which exhibit Ln–N distances of 227.5 and 234.8 pm in **3a** and of 230.7 and 239.1 pm in **2b**, are ca. 10 pm closer to the metal atom than those of the bridging ligands (240.2–247.6 pm in **3a** and 243.7–256.7 pm in **2b**). In **2b**, the Na–O distances (272.8(3) and 290.7(3) pm), as well as the Ho–O distances

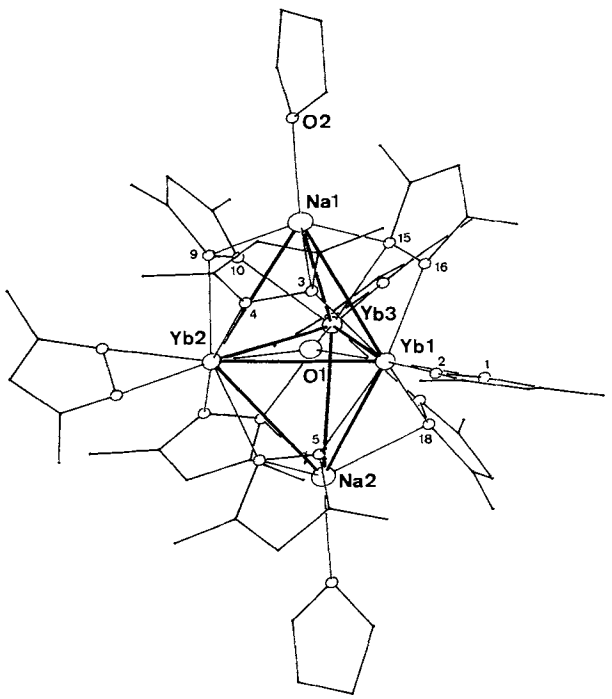


Fig. 1. Molecular structure of **3a**. The N atoms are numbered. For clarity, the C atoms are drawn in a simplified way (H atoms omitted). Selected distances [pm] and angles [°]: Yb1–N1 234.8(5), Yb1–N2 229.8(5), Yb1–N3 244.6(4), Yb1–N5 (243.9(5), Yb1–N16 244.5(4), Yb1–N18 244.8(4), Yb1–O1 213.8(4), Yb2–O1 213.0(4), Yb3–O1 213.2(3), Na1–O1 274.4(3), Na1–O2 227.0(4), Na1–N3 243.5(5), Na1–N4 270.3(5), Na1–N9 240.2(6), Na1–N10 297.6(5), Na1–N15 242.5(5), Na1–N16 274.8(5); Na1–O1–Na2 178.0(2), Yb1–O1–Yb2 120.3(1), Yb1–O1–Yb3 121.3(2), Yb2–O1–Yb3 118.4(2).

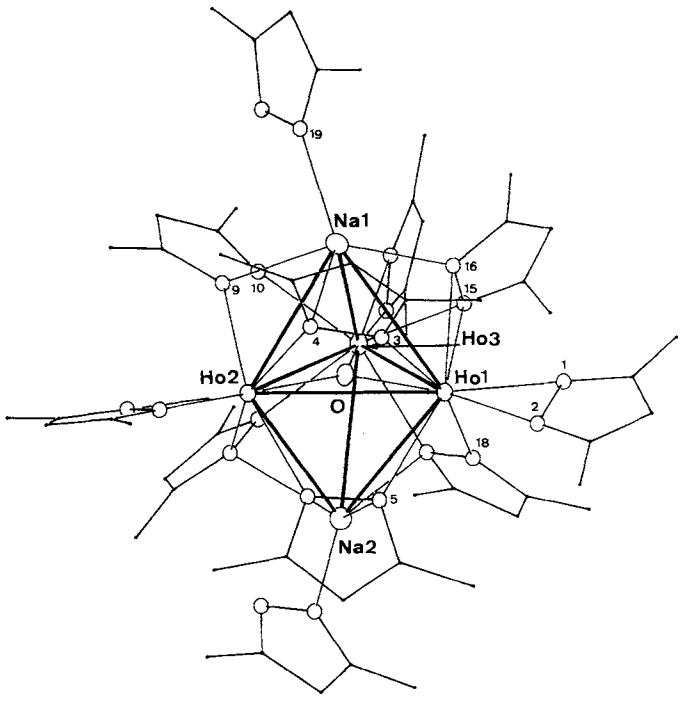


Fig. 2. Molecular structure of **2b**. The N atoms are numbered. For clarity, the C atoms are drawn in a simplified way (H atoms omitted). Selected distances [pm] and angles [°]: Ho1–N1 233.8(3), Ho1–N2 236.8(3), Ho1–N3 244.4(3), Ho1–N5 250.3(3), Ho1–N15 255.5(3), Ho1–N16 256.7(3), Ho1–N18 245.3(4), Ho1–O 217.8(3), Ho2–O 214.2(3), Ho3–O 214.2(3), Na1–O 272.8(3), Na1–N3 278.0(4), Na1–N4 247.6(4), Na1–N9 259.2(4), Na1–N10 283.2(4), Na1–N16 236.6(4), Na1–N19 236.3(5); Na1–O–Na2 174.5(1), Ho1–O–Ho2 123.1(1), Ho1–O–Ho3 111.2(1), Ho2–O–Ho3 125.7(1).

(214.2(3), 214.2(3), and 217.8(3) pm), are significantly different, whereas they are nearly identical in **3a** (274.4(3) and 276.7(3); 213.0(4), 213.2(3), and 213.8(4) pm). Furthermore, the Na–O–Na angle in **2b** (174.5(1)°) deviates more from linearity than in **3a** (178.0(2)°).

The tendency toward higher coordination numbers, together with the strong oxophilicity, leads to the preferential formation of organolanthanoid clusters with a central oxygen atom, as has already been demonstrated in the synthesis of cyclopentadienyllanthanoid alkoxides, whereby complexes **5**, Ln = Y[12] and Gd,[13] were isolated, and in the

$[(C_5H_5)_5Ln_5(\mu\text{-}OCH_3)_4(\mu_3\text{-}OCH_3)_4(\mu_5\text{-}O)]$ **5**

reaction of yttrium with refluxing 2-propanol, which resulted in the formation of **6**.[14] The same tendency to accept

$[Y_5(\mu_3\text{-}O\mathit{i}Pr)_4(\mu_2\text{-}O\mathit{i}Pr)_4(O\mathit{i}Pr)_5(\mu_5\text{-}O)]$ **6**

oxygen from "pure" organic solvents, leading to the formation of oxo-centered clusters, is shown by organouranium compounds like the likewise fortuitously obtained compounds **7**[15] and **8**.[16]

$[\{C_9H_7UBr(CH_3CN)_4\}_2O][UBr_6]$ **7**

$[\{C_5Me_5U[\mu\text{-}(CH_2)P(C_6H_5)_2(CH_2)]\}_2Mg\{CH_2P(CH_3)(C_6H_5)_2\}_2\text{-}(\mu_3\text{-}O)(\mu_2\text{-}O)(\mu_2\text{-}Cl)_2]$ **8**

Received: March 20, 1989 [Z 3239 IE]
German version: *Angew. Chem. 101* (1989) 1073

[1] K. W. Bagnall, A. C. Tempest, J. Takats, A. P. Masino, *Inorg. Nucl. Chem. Lett. 12* (1976) 555.
[2] D. L. Reger, J. A. Lindeman, L. Lebioda, *Inorg. Chem. 27* (1988) 3923.
[3] M. V. R. Stainer, J. Takats, *J. Am. Chem. Soc. 105* (1983) 410.
[4] M. A. J. Moss, C. J. Jones, A. J. Edwards, *Polyhedron 7* (1988) 79.
[5] K. S. Chong, S. J. Rettig, A. Storr, J. Trotter, *Can. J. Chem. 57* (1979) 3090.
[6] B. F. Fieselmann, D. G. Stucky, *Inorg. Chem. 17* (1978) 2074.
[7] C. W. Eigenbrot, K. N. Raymond, *Inorg. Chem. 20* (1981) 1553.
[8] C. W. Eigenbrot, K. N. Raymond, *Inorg. Chem. 21* (1982) 2653.
[9] P. R. Lee, *Dissertation*, Technische Universität, Berlin 1988.
[10] *Experimental Procedure*: All operations were performed under an argon atmosphere using carefully degassed solutions. **1a**: 3,5-dimethylpyrazolylsodium (1.87 g, 16 mmol) in 50 mL of THF was slowly added to a suspension of YCl_3: (0.97 g, 5 mmol) in 150 mL of THF. The reaction mixture was stirred for 48 h at room temperature and then refluxed for 5 d. After decantation of NaCl and concentration of the solution, colorless crystals of **1a** formed. Yield: 0.85 g (44%). Correct C,H,N analysis. M.p. 270–272 °C. ^{1}H NMR (80 MHz, C_6D_6): δ = 1.27 (m, THF), 2.21 (s, $CH_3(\mu\text{-}pzMe_2)$), 2.37 (s, $CH_3(\eta^2\text{-}pzMe_2)$), 3.20 (m, THF), 5.82 (s, $H(\mu\text{-}pzMe_2)$), 6.40 (s, $H(\eta^2\text{-}pzMe_2)$). ^{13}C NMR (20.1 MHz, C_6D_6): δ = 13.67 (CH_3), 25.45 (THF), 70.60 (THF), 105.23, 110.02, 145.53, 152.23. – **1b**: A reaction mixture containing YCl_3 (0.41 g, 2.1 mmol) and $Na(pzMe_2)$ (0.78 g, 6.6 mmol) in 70 mL of THF was refluxed for 6 d. The solvent was then completely removed in vacuo and replaced by 30 mL of toluene. After filtration of the precipitated NaCl, the solution was concentrated to half of its initial volume, resulting in the formation of colorless crystals of **1b** (0.43 g, 52%). Decomposition point: 230 °C. Correct C,H,N analysis. ^{1}H NMR (80 MHz, C_6D_6): δ = 1.92 (s, $CH_3(H(pzMe_2))$), 2.19 (s, $CH_3(\mu\text{-}pzMe_2)$), 2.36 (s, $CH_3(\eta^2\text{-}pzMe_2)$), 5.60 (s, $H(H(pzMe_2))$), 5.83 (s, $H(\mu\text{-}pzMe_2)$), 6.40 (s, $H(\eta^2\text{-}pzMe_2)$), 9.76 (s, $NH(H(pzMe_2))$). ^{13}C NMR (20.1 MHz, C_6D_6): δ = 11.53, 13.31, 13.45, 103.81, 104.75, 110.09, 144.31, 145.31, 152.24.
[11] *Crystal structure analyses*: Enraf-Nonius CAD-4 diffractometer, $Mo_{K\alpha}$ radiation, graphite monochromator, T = 138(5) K, empirical absorption corrections, SHELX 76 program, Patterson methods. **3a**: triclinic, space group $P\bar{1}$, a = 1298.1(3), b = 1423.3(4), c = 2213.3(3) pm, α = 92.01(2), β = 94.88(2), γ = 114.84(2)°, $V = 3686 \times 10^{-30}$ m^3, Z = 2, ϱ_{calcd} = 1.620 g cm^{-3}, $\mu(Mo_{K\alpha})$ = 36.64 cm^{-1}, crystal dimensions 0.432 × 0.360 × 0.288 mm^3, (ω-2θ) scan, $2\theta_{max}$ = 50°, 12358 unique reflections, $R(R_w)$ = 0.0321 (0.0341) for 11276 reflections with $F_0 \geq 6\sigma(F_0)$, all non-hydrogen atoms refined with anisotropic temperature factors, calculated H Positions. **2b**: monoclinic, space group $P2_1/n$, a = 1677.8(2), b = 1855.3(4), c = 2067.4(4) pm, β = 97.78(19)°, $V = 6376.1 \times 10^{-30}$ m^3, Z = 4, ϱ_{calcd} = 1.672 g cm^{-3}, $\mu(Mo_{K\alpha})$ = 35.74 cm^{-1}, crystal dimensions 0.756 × 0.403 × 0.396 mm^3, (ω-2θ) scan, $2\theta_{max}$ = 55°, 13726 unique reflections, $R(R_w)$ = 0.0274 (0.0313) for 12416 reflections with $F_0 \geq 6\sigma(F_0)$, all non-hydrogen atoms refined with anisotropic temperature factors, calculated H positions. Futher details of the crystal structure investigation may be obtained from the Fachinformationszentrum Karlsruhe, Gesellschaft für wissenschaftlich-technische Information mbH, D-7514 Eggenstein-Leopoldshafen 2 (FRG), on quoting the depository number CSD-53951, the names of the authors, and the journal citation.
[12] W. J. Evans, M. S. Sollberger, *J. Am. Chem. Soc. 108* (1986) 6095.
[13] H. Schumann, G. Kociok, J. Loebel, unpublished.
[14] O. Poncelet, W. J. Sartain, L. G. Hubert-Pfalzgraf, K. Folting, K. G. Caulton, *Inorg. Chem. 28* (1989) 263.
[15] W. Beeckman, J. Goffart, J. Rebizant, M. R. Spirlet, *J. Organomet. Chem. 307* (1986) 23.
[16] R. E. Cramer, M. A. Bruck, J. W. Gilje, *Organometallics 7* (1988) 1465.

Nickel(0)-Catalyzed Preparation of Isomeric Carboxamides – Ligand-Controlled β-H or β′-H Elimination

By *Heinz Hoberg** and *Dieter Guhl*

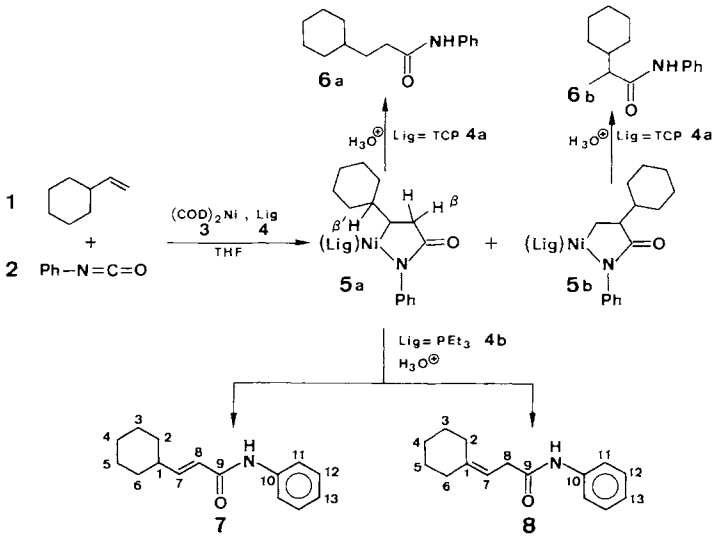
We have presented numerous examples of the diverse ways in which isocyanates can undergo C–C bond forming reactions with C–C multiple-bond systems at nickel(0) complexes, whereby, in addition to stoichiometric reactions, catalytic reactions have become increasingly important.[1] Azanickelacycles formed by oxidative coupling are the proposed intermediates. An important partial step in catalysis is often β-H elimination. It leads to H-Ni amide species which release the unsaturated compound in a reductive elimination step and regenerate the (Lig)Ni^0 starting complex. Until now, only CH groups whose C atoms are part of the azanickelacycle have been employed in the β-H elimination. In principle, however, it should also be possible to involve β-H atoms bound to an exocyclic C atom. Whereas in the first case α,β-unsaturated carboxamides are formed, in the second the β, γ isomers should be obtained.

To determine whether such alternative β-H abstractions are possible in these azanickelacycles, vinylcyclohexane **1** was selected. This alkene contains a tertiary CH bond, the H atom of which exhibits partial "hydride" character; it should therefore be especially well suited as a trial reagent. We have found that, by varying the reaction-controlling ligands **4** and by exploiting steric and/or electronic effects,[2] it is possible to activate selectively the different β-H positions in such a way that the products can be formed with high selectivity and even catalytically.

When a suspension of **1**, phenyl isocyanate **2**, bis(1,5-cyclooctadiene)nickel ($(cod)_2Ni$) **3**,[3] and tricyclohexylphosphane (TCP) **4a** in a molar ratio of 2:1:1:1 in THF at −78 °C is allowed to warm to room temperature (stoichiometric reaction[1]) and then hydrolyzed (2 N H_2SO_4), the saturated carboxamides **6a, b**, derived from the nickelacycles **5a, b**, are obtained in a molar ratio of ca. 95:5. (Scheme 1). The high regioselectivity of the reaction corresponds to that observed for other monosubstituted alkenes.[1] Since isomer **5b**, formed in small amounts, has only one β-H position, the products resulting from it were neglected in this investigation. If the sterically less demanding triethylphosphane **4b** is

[*] Prof. Dr. H. Hoberg, Dipl.-Chem. D. Guhl
Max-Planck-Institut für Kohlenforschung
Kaiser-Wilhelm-Platz 1, D-4330 Mülheim a.d. Ruhr (FRG)

used instead of **4a** in the reaction of **1** with **2** and **3** and the reaction mixture is heated to 50 °C, protonolysis yields, in addition to small amounts of **6a**, the β-H elimination products **7** and **8** in a molar ratio of ca. 1:1 (yield 19%); both products are derived from the coupling product **5a** (Scheme 1).

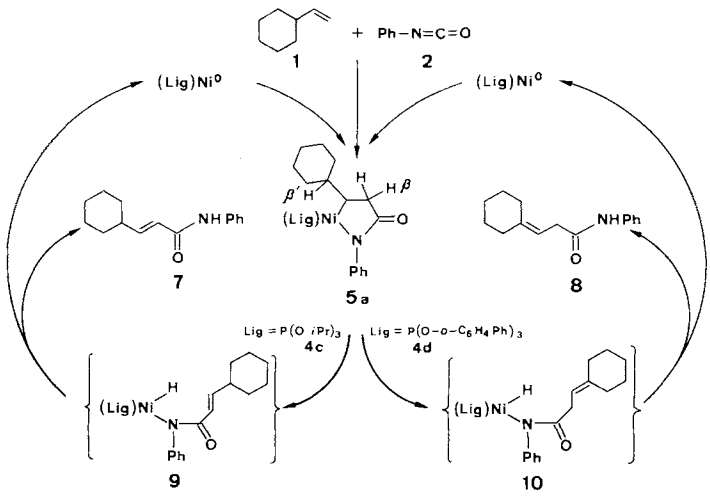


Scheme 1. Effect of the ligands on the reaction of **1** with **2** at nickel(0) complexes. **6a, b** are products of stoichiometric reaction; **7** and **8** are products of catalytic reaction. Arbitrary numbering in **7** and **8**.

This result clearly demonstrates that ligand **4b** activates the β-H and β′-H positions of **5a** to the same extent for elimination. Control experiments confirmed that the isomeric carboxamides **7** and **8** are formed as a result of different β-H abstraction steps rather than by subsequent isomerization. Neither **7** nor **8** is converted into the other product in the presence of (Lig)Ni^0 or 2 N H_2SO_4.

This stoichiometric reaction can be made catalytic under certain conditions.[1] After four catalytic cycles, the product ratio **7:8** remains constant (1:1) when ligand **4b** is used. Changing the ligand properties allows the product formation to be controlled. Thus, the sterically less demanding triisopropylphosphite **4c** induces β-H elimination at the metallacycle, resulting in an isomer distribution of **7:8** = 95:5. By contrast, the sterically demanding ligand tri-*ortho*-phenylphenylphosphite **4d** activates the β′ position. The product distribution is reversed (**7:8** = 14:86; Scheme 2).

Moreover, the use of ligands **4c, d** gave four of the theoretically expected maximum of ten cycles (based on the amount of **2** employed). We propose the mechanism formulated in Scheme 2 for the formation of carboxamide. The catalytic cycles begin with 1:1 C–C coupling of **1** with **2** at (Lig)Ni^0 to give the central nickelacycle **5a**; the subsequent reactions depend on the ligands used. Ligand **4c** leads to β-H elimination at the nickelacycle with formation of intermediate **9**. Subsequent reductive elimination results in release of **7** and regeneration of the (Lig)Ni^0 starting complex (left-hand cycle in Scheme 2). On the other hand, ligand **4d** activates the exocyclic β′-H position (formation of intermediate **10**); reductive elimination results in release of **8** and makes (Lig)Ni^0 available again for the catalytic cycle (right-hand cycle in Scheme 2).



Scheme 2. Catalytic cycles and product control by the ligands **4c** and **4d**.

The results presented here demonstrate for the first time, to the best of our knowledge, that different β-H positions of a metallacycle can be activated for H elimination with high selectivity by an appropriate choice of ligands. This reaction thus represents a novel variant of β-H elimination, which, in view of the possibility of using different alkenes, promises a wide range of applications in preparative chemistry.

Typical Experimental Procedure

Cyclohexylidenepropionanilide **8** (catalytic): A suspension of **3** (0.38 g, 1.38 mmol), **4d** (0.74 g, 1.38 mmol), and **1** (6.08 g, 55.27 mmol) in ca. 40 mL of THF was placed in a steel autoclave (200 mL) cooled to −30 °C. Compound **2** (1.64 g, 13.8 mmol), as a 1 M solution in THF, was added in a controlled fashion over ca. 8 h to the stirred reaction solution by means of a proportioning pump [4], whereby the mixture was heated simultaneously to +50 °C. After an additional 50 h, the cooled solution was hydrolyzed with ca. 10 mL of 2 N H_2SO_4 and then extracted several times with diethyl ether. The organic phase was dried over $MgSO_4$ and the solvent was then removed. The residue was separated by column chromatography (silica gel 60; eluant, toluene/ether, 1/1). Obtained: 0.17 g (0.72 mmol) **7** (5.2%) and 0.90 g (3.93 mmol) **8** (28.5%). Physical data for **8**: m.p. 101 °C; MS: *m/z* 229 ($M^{\oplus}$); correct elemental analysis IR (KBr): $\tilde{\nu}_{NH}$ = 3250 cm^{-1}, $\tilde{\nu}_{CO}$ = 1650 cm^{-1}. ^1H NMR ($CDCl_3$, 20 °C, 200.1 MHz): δ = 7.94 (s, 1H; NH), 7.51 (m, 1H; 13-H), 7.28 (m, 2H; 12-H), 7.07 (m, 2H; 11-H), 5.34 (t, 1H, $J_{7,8}$ = 7.5 Hz; 7-H), 3.13 (d, 2H; 8-H), 2.16 (m, 4H; 2-,6-H), 1.57 (m, 6H; 3-,4-,5-H). ^{13}C NMR ($CDCl_3$, 20 °C, 50.3 MHz): δ = 170.1 (s; C-9), 146.1 (s; C-1), 137.8 (s; C-10), 128.8 (d, $J_{C,H}$ = 160 ± 2 Hz; C-12), 124.1 (d, $J_{C,H}$ = 161 ± 2 Hz; C-13), 119.7 (d, $J_{C,H}$ = 161 ± 2 Hz; C-11), 113.0 (d, $J_{C,H}$ = 163 ± 2 Hz; C-7), 36.9 (t, $J_{C,H}$ = 128 ± 1 Hz; C-8), 36.0 (t, $J_{C,H}$ = 126 ± 1 Hz; C-6), 28.7, 28.4, 27.6, 26.4 (t, C-2,-3,-4,-5). Cyclohexylacrylanilide **7** (catalytic): amounts of reagents, 0.4 g (1.45 mmol) **3**, 0.30 g (1.45 mmol) **4c**, 6.38 g (58.0 mmol) **1**, 1.74 g (14.6 mmol) **2**; 1 M solution in toluene; solvent 40 mL toluene; reaction time, 17 h. Obtained: 0.076 g (0.33 mmol) **8** (2.2%) and 1.442 g (6.3 mmol) **7** (43.1%). Physical data for **7**: m.p. 125 °C; MS: *m/z* 229 ($M^{\oplus}$); correct elemental analysis. IR (KBr): $\tilde{\nu}_{NH}$ = 3250 cm^{-1}, $\tilde{\nu}_{CO}$ = 1670, 1640 cm^{-1}, $\tilde{\nu}_{C=C}$ = 980 cm^{-1}. ^1H NMR ($CDCl_3$, 20 °C, 200.1 MHz): δ = 8.6 (s, 1H; NH_2), 7.59 (m, 2H; 11-H), 7.24 (m, 2H; 12-H), 7.05 (m, 1H; 13-H), 6.89 (dd, 1H, $J_{7,8}$ = 16 Hz, $J_{7,1}$ = 6.9 Hz, 7-H), 5.98 (dd, 1H, $J_{8,1}$ = 1.2 Hz; 8-H), 2.10 (m, 1H; 1-H), 1.71–0.96 (m, 10H; 2-,3-,4-,5-,6-H). ^{13}C NMR ($CDCl_3$, 20 °C, 50.3 MHz): δ = 165.2 (s; C-9), 151.1 (d, $J_{C,H}$ = 151 ± 1 Hz; C-7), 138.4 (s; C-10), 128.8 (d; C-12), 124.1 (d; C-13), 121.8 (d, $J_{C,H}$ = 157 ± 1 Hz; C-8), 120.3 (d; C-11), 40.3 (d; C-1), 31.8 (t; C-2, C-6), 25.9 (t; C-4), 25.7 (t; C-3, C-5).

Received: March 14, 1989 [Z3231 IE]
German version: *Angew. Chem. 101* (1989) 1091

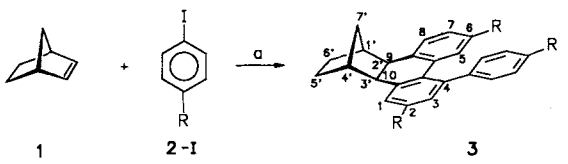
[1] H. Hoberg, *J. Organomet. Chem. 358* (1988) 507.
[2] C. A. Tolman, *Chem. Rev. 77* (1977) 313.
[3] B. Bogdanovic, M. Kröner, G. Wilke, *Justus Liebigs Ann. Chem. 699* (1966) 1.
[4] Reichelt Chemietechnik (Heidelberg) RCZ precision pump M16.

Selective 1:3 Coupling of Norbornene and Iodobenzene: A Facile Synthesis of Benzo[*e*]pyrenes with Annelated Cycloaliphatic Moieties**

By *Oliver Reiser, Martin Weber,* and *Armin de Meijere**

Dedicated to Professor Hans-Jörg Sinn on the occasion of his 60th birthday

Palladium(0)-catalyzed coupling of olefins with aryl halides, the so-called Heck reaction,[1] is becoming increasingly important in organic synthesis.[2] Frequent reports of new applications show that the potential of this reaction is far from being exhausted.[3] Under certain conditions, Pd^0-catalyzed coupling of norbornene with bromobenzene, investigated intensively by *Chiusoli* et al.,[4] leads to a 1:2 adduct consisting of a norbornene framework with an annelated dihydrophenanthrene moiety (cf. **10**). With the goal of extending this annelation method to [2.2]paracyclophane-1,9-diene, we allowed the latter to react with iodobenzene under the conditions described by *T. Jeffery*[5] ($Pd(OAc)_2$, K_2CO_3, Bu_4NBr, dimethylformamide (DMF)), which, according to our experience,[6] appeared particularly promising. Instead of 1:2 or 1:4 adducts, however, 1:3 and 1:6 coupling products were obtained. This reaction pathway is not unique to paracyclophanediene; under the same reaction conditions, it is also observed for norbornene **1** (Scheme 1).



1 **2-I** **3**

a, R=H ; **b**, R=CH_3

Scheme 1. a: $Pd(OAc)_2$, K_2CO_3, Bu_4NBr, DMF.

Independent of the relative amounts of reactants, **1** and bromobenzene (**2a**-Br) or iodobenzene (**2a**-I) yielded the norbornane derivative **3a**,[7] containing an annelated 4-phenyl-9,10-dihydrophenanthrene moiety (see Table 1). Even for a threefold excess of **1** over **2a**-X, only **3a** was found. The constitution of **3a** was established on the basis of its ^1H, ^{13}C, and ^1H-^1H correlation NMR spectra[8] and a crystal structure analysis.[9]

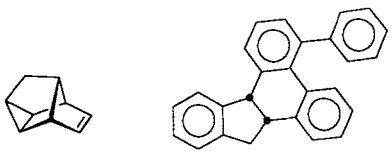
Table 1. Conditions and yields for the Pd^0-catalyzed [a] coupling of norbornene **1** with aryl halides **2**-X (see Scheme 1).

R	X	Equiv. **2**-X	*T* [°C]	*t* [h]	Yield [%] [b]	Conversion of **2**-X
H	Br	0.33	80	12	53	100
H	I	0.33	60	24	46	100
H	I	1	60	12	50	42
H	I	3	60	12	49	36
H	I	3	65	24	66 [c]	23
H	I	3	65	24	83 [d]	85
CH_3	I	1	100	6	30	100

[a] Conditions similar to [6] with 2 mol% $Pd(OAc)_2$. [b] Based on nonrecovered aryl halide **2**-X. [c] Norbornene added as an 18% solution in DMF over 24 h. [d] Norbornene added as a 20% solution in NMP over 24 h; 1 mol% $Pd(OAc)_2$ present. 3 mol% $Pd(OAc)_2$ in NMP added simultaneously over 24 h.

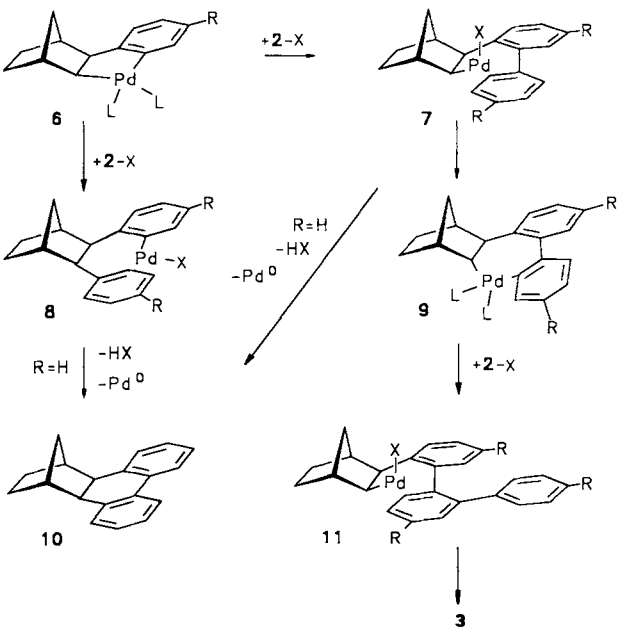
Similarly, reaction with *p*-iodotoluene (**2b**-I) affords compound **3b** as the sole low-molecular product.[7, 8] Based on recovered **2**-X, the yield is up to 53%[10] and even 83% when **1** and additional $Pd(OAc)_2$ (3 mol%), dissolved in *N*-methylpyrrolidone (NMP), are slowly added to a prepared mixture of **2a**-I and the catalyst system in NMP. In the latter case, norbornene **1** is completely consumed, in part in a still unknown competing reaction.

Deltacyclene **4** reacts analogously to **1** (25% yield based on **2a**-I), as does indene, which affords **5** in 35% yield based on **2a**-Br. The products obtained from [2.2]paracyclophanediene have similar structures containing 4-phenyl-9,10-dihydrophenanthrene moieties annelated at the bridges on one side and on both sides.[11]



4 **5**

The reaction of **1** with **2a**-I can be followed by gas chromatography. At no time could even traces of **10**[12] be detected; *Chiusoli* et al.[4] obtained this product with $Pd(Ph_3)_4$/KO*t*Bu/anisol. Although this finding indicates that **10** is not an intermediate on the way to **3a**, it still allows the metallacycle **6**, which is known to be a precursor to **10**, to lead also to **3** (Scheme 2). Whereas **10** could be formed from **7** and **8**,



Scheme 2. Mechanistic possibilities for the domino Heck coupling of iodobenzene with norbornene **1**.

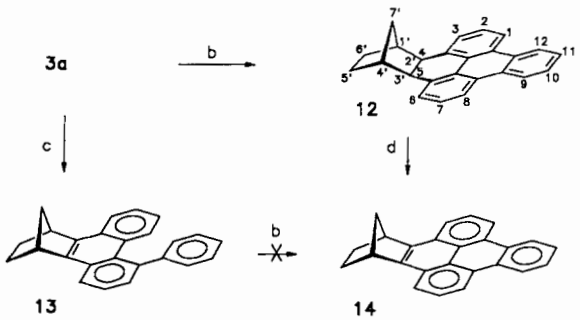
both possible products of the oxidative addition of **2**-X to a Pd–C bond in **6**, by dehydrohalogenation and reductive elimination, **3** can only be formed from **7** (via **9** and **11**). Since the use of $Pd(PPh_3)_4/K_2CO_3$/DMF/Bu_4NBr leads only to **3a**, and not to **10**, and since the addition of **2**-X to the Pd–C_{sp^2} bond in **6** to give **7** should be favored, the formation of **10** in Ref. [4] is presumably due to the more drastic reaction conditions (KO*t*Bu/anisol; 110 °C).

[*] Prof. Dr. A. de Meijere, Dipl.-Chem. O. Reiser, M. Weber
Institut für Organische Chemie der Universität
Martin-Luther-King-Platz 6, D-2000 Hamburg 13 (FRG)

[**] This work was supported by the Stiftung Volkswagenwerk and the Fonds der Chemischen Industrie as well as by Hoechst AG, Hüls AG, and Degussa AG (donation of chemicals). *O. R.* and *M. W.* thank the Studienstiftung des deutschen Volkes for fellowships.

The formation of the 1:3-coupling product **5** from indene and iodobenzene indicates that, in the first step, phenylpalladium iodide adds regioselectively to give *cis*-2-phenyl-1-indanylpalladium iodide.[13]

The domino coupling products of type **3a** offer an easy approach to the synthesis of benzo[*e*]pyrene derivatives containing annelated cycloalipatic moieties, since irradiation of **3a** in cyclohexane in the presence of iodine results in cyclization and dehydrogenation, leading smoothly to **12** (83%).[8] Further dehydrogenation with dichlorodicyanobenzoquinone (DDQ) leads to the norbornene-annelated benzo[*e*]pyrene **14** (85%).[8] If, instead, **3a** is first dehydrogenated to **13** (78%)[8] with DDQ, the photocyclization/dehydrogenation no longer takes place (Scheme 3).



Scheme 3. b: *hv*, cyclo-C_6H_{12}, I_2, N_2, 4 h. c: DDQ, $C_6H_5CH_3$, N_2, Δ, 2 h. d: DDQ, $C_6H_5CH_3$, N_2, Δ, 4 h.

In contrast to benzo[*e*]pyrene, which, like most polycyclic arenes, is only sparingly soluble, the derivative **14** dissolves readily in pentane, hexane, cyclohexane, and other solvents. Although its UV spectrum (maxima at λ_{max} (ε_{max}) = 316.5 (11520), 329.1 (19470), 343.9 nm (25320) and weak long-wavelength absorptions at λ_{max} (ε_{max}) = 365 (1000), 374 (600), 387 nm (1000)) is very similar to that of benzo[*e*]pyrene,[14] it exhibits only weak fluorescence with a quantum yield of 3.5% and emission maxima at 387, 408, and 432 nm.[15]

Received: March 30, 1989 [Z 3263 IE]
German version: *Angew. Chem. 101* (1989) 1071

[1] a) R. F. Heck, *J. Am. Chem. Soc. 90* (1968) 5518; b) R. F. Heck, J. P. Nolley, Jr., *J. Org. Chem. 37* (1972) 2320; c) H. A. Dieck, R. F. Heck, *J. Am. Chem. Soc. 96* (1974) 1133.

[2] a) R. F. Heck, *Org. React. (N.Y.) 27* (1982) 345; b) *Palladium Reagents in Organic Syntheses*, Academic Press, New York 1985; c) H. U. Reißig, *Nachr. Chem. Tech. Lab. 34* (1986) 1066.

[3] a) R. C. Larock, B. E. Baker, *Tetrahedron Lett. 29* (1988) 905; b) R. C. Larock, H. Song, B. E. Baker, W. H. Gong, *ibid. 29* (1988) 2919; c) E. Negishi, Y. Zhang, B. O'Connor, *ibid. 28* (1988) 2915; d) P. J. Harrington, K. A. DiFiore, ibid. *28* (1987) 495.

[4] M. Catellani, G. P. Chiusoli, *J. Organomet. Chem. 286* (1985) C 13; see also review: G. P. Chiusoli, *ibid. 300* (1986) 57, and references cited therein.

[5] T. Jeffery, *Tetrahedron Lett. 26* (1985) 2667.

[6] Cf. O. Reiser, S. Reichow, A. de Meijere, *Angew. Chem. 99* (1987) 1285; *Angew. Chem. Int. Ed. Engl. 26* (1987) 1277.

[7] All new compounds gave satisfactory elemental analyses.

[8] NMR data of selected compounds (*: interchangeable assignment). DEPT spectra: positive (CH or CH_3) and negative (CH_2) phases indicated by + and −, respectively; ø indicates that the signal (c) vanishes. **3a**: ^{1}H NMR: (400 MHz, $CDCl_3$, and ^{1}H-^{1}H-COSY): δ = 1.07 (d, ^2J = 9.6 Hz, 1H, 7′-H*), 1.44 (d, ^2J = 9.6 Hz, 1H, 7′-H*), 1.61–1.75 (m, 4H, 5′(6′)-H), 2.30 (s, 1′-H**), 2.45 (s, 4′-H**), 3.31 (AB system, δ_A = 3.39, δ_B = 3.23, ^3J = 10.7 Hz, 2H, 9(10)-H), 6.66 (dt, ^3J = 10.7, ^4J = 1.3 Hz, 1H), 6.85 (d, ^3J = 8.0 Hz, 1H), 6.98 (t, ^3J = 8.0 Hz, 1H), 7.05 (m, 1H), 7.12 (d, ^3J = 8.0 Hz, 1H), 7.19 (m, 2H), 7.26–7.37 (br.s, 5H, 4-Ph). ^{13}C NMR (67.92 MHz, $CDCl_3$, and DEPT): δ = 29.70 (−, C-5′*), 30.91 (−, C-6′*), 33.23 (−, C-7′), 46.80 (+, C-1′**), 47.17 (+, C-4′**), 49.25 (+, C-9***), 49.91 (+, C-10***), 124.73 (+), 126.56 (+), 126.60 (+), 128.68 (+), 128.69 (+), 129.16 (ø), 129.59 (+), 129.62 (+), 130.41 (+), 131.16 (+), 131.91 (ø), 138.91 (ø), 139.64 (ø), 140.61(ø), 145.15 (ø). – **3b**: ^{1}H NMR: (400 MHz, $CDCl_3$): δ = 1.14 (d, ^2J = 9.1 Hz, 1H, 7′-H*), 1.58 (d, ^2J = 9.1 Hz, 1H, 7′-H*), 1.74–1.80 (m, 4H, 5′(6′)-H), 1.91 (s, 3H, CH_3), 2.19 (s, 3H, CH_3), 2.43 (s, 1′-H**), 2.47 (s, 4′-H**), 2.54 (s, 3H, CH_3), 3.31 (AB system, δ_A = 3.38, δ_B = 3.24, ^3J = 10.7 Hz, 9(10)-H), 6.66 (s, 1H), 6.91 (dd, ^3J = 7.5, ^4J = 1.1 Hz, 1H), 7.13 (d, ^3J = 8.0 Hz, 1H), 7.15 (dd, ^3J = 7.5, ^4J = 1.1 Hz, 1H), 7.21 (s, 1H), 7.23 (s, 1H), 7.26 (m, 1H), 7.31 (d, ^3J = 8.0 Hz, 1H), 7.39 (d, ^3J = 8.0 Hz, 1H). ^{13}C NMR (67.92 MHz, $CDCl_3$, and DEPT): δ = 20.80 (+, CH_3), 21.11 (+, CH_3), 21.46 (+, CH_3), 30.17 (−, C-5′*), 30.57 (−, C-6′*), 33.17 (−, C-7′), 46.35 (+, C-1′**), 47.17 (+, C-4′**), 49.50 (+, C-9***), 50.08 (+, C-10***), 127.25 (+), 128.99 (+), 129.24 (+), 129.49 (+), 129.63 (+), 130.02 (+), 130.14 (+), 131.46 (ø), 132.45 (ø), 133.61 (ø), 134.70 (ø), 136.09 (ø), 136.39 (ø), 137.94 (ø), 138.85 (ø), 140.95 (ø). – **12**: ^{1}H NMR: (270 MHz, $CDCl_3$): δ = 1.07 (d, ^2J = 10.0 Hz, 1H, 7′-H), 1.39 (d, ^2J = 10.0 Hz, 1H, 7′-H), 1.75 (mc, 4H, 5′(6′)-H), 2.49 (br.s, 2H, 1′(4′)-H), 3.49 (br.s, 2H, 4(5)-H), 7.46 (d, ^3J = 7.7 Hz, 2H, 3(6)-H), 7.55 (t, ^3J = 7.7 Hz, 2H, 2(7)-H), 7.60 (XX′ part of an AA′XX′ system, ^3J = 6.2, ^4J = 3.3 Hz, 2H, 10(11)-H), 8.40 (d, ^3J = 7.7 Hz, 2H, 1(8)-H), 8.58 (AA′ part of an AA′XX′ system, ^3J = 6.2, ^4J = 3.3 Hz, 2H, 9(12)-H). ^{13}C NMR (67.92 MHz, C_6D_6, and DEPT): δ = 30.47 (−, C-5′(6′)), 33.62 (−, C-7′), 46.42 (+, C-1′(4′)), 50.60 (+, C-4(5)), 121.13 (+), 123.91 (+), 126.59 (ø), 127.26 (+), 128.32 (+), 128.42 (+), 129.48 (ø), 130.50 (ø), 137.85 (ø). – **13**: ^{1}H NMR (270 MHz, $CDCl_3$): δ = 1.32 (d, ^2J = 8.4 Hz, 2H, 5′(6′)-H*), 1.88 (AB system, δ_A = 2.00, δ_B = 1.76, ^2J = 8.4 Hz, 2H, 7′-H), 2.13 (d, ^2J = 8.4 Hz, 2H, 5′(6′)-H*), 4.08 (s, 1′-H**), 4.11 (s, 1H, 4′-H**), 7.08 (t, ^3J = 8.0 Hz, 1H), 7.50 (m, 7H), 7.64 (t, ^3J = 8.0 Hz, 1H), 7.85 (d, ^3J = 8.0 Hz, 1H), 8.01 (d, ^3J = 8.0 Hz, 1H), 8.09 (d, ^3J = 8.0 Hz, 1H). ^{13}C NMR (67.92 MHz, $CDCl_3$, and DEPT): δ = 27.42 (−, C-5′(6′)), 42.28 (+, C-1′*), 42.56 (+, C-4′*), 48.92 (−, C-7′), 123.34 (+), 125.41 (+), 125.78 (+), 126.64 (+), 127.99 (ø), 128.68 (+), 129.07 (ø), 129.25 (+), 129.36(+), 129.60 (+), 129.99 (ø), 141.26 (ø), 141.57 (ø), 141.92 (ø), 146.06(ø). – **14**: ^{1}H NMR (270 MHz, $CDCl_3$): δ = 1.32 (dd, ^2J = 7.3, ^3J = 2.2 Hz, 2H, 5′(6′)-H*), 1.82 (d, ^2J = 8.4 Hz, 1H, 7′-H**), 2.05 (d, ^2J = 8.4 Hz, 1H, 7′-H**), 2.17 (dd, ^2J = 7.3, ^3J = 2.2 Hz, 2H, 5′(6′)-H*), 4.19 (s, 2H, 1′(4′)-H), 7.72 (dd, ^3J = 6.2, ^4J = 3.3 Hz, 2H, 10(11)-H), 8.04 (t, ^3J = 8.1 Hz, 2H, 2(7)-H), 8.30 (d, ^3J = 8.1 Hz, 2H, 3(6)-H), 8.85 (m, ^3J = 6.2, ^3J = 8.1, ^4J = 3.3 Hz, 4H, 1(8,9,12)-H). ^{13}C NMR (67.92 MHz, $CDCl_3$, and DEPT): δ = 27.37 (−, C-5′(6′)), 42.40 (+, C-1′(4′)), 49.27 (−, C-7′), 119.14 (+), 121.73 (+), 123.72 (+), 125.68 (+), 127.35 (+), 127.41 (ø), 129.91 (ø), 130.50 (ø), 142.11 (ø).

[9] The crystal structure data will be published elsewhere. We thank Priv.-Doz. Dr. *J. Kopf*, Institut für Anorganische Chemie der Universität Hamburg, for help in the structure determination.

[10] In Heck couplings, the olefin component, which is usually less expensive, is most often used in a fivefold excess [1–3].

[11] Cf. A. de Meijere, A. Kaufmann, R. Lackmann, H. C. Militzer, O. Reiser, S. Schömenauer, A. Weier in G. Erker, H. Werner (Eds.): *Organometallics in Organic Synthesis II*, Springer, Heidelberg 1989, p. 255ff.

[12] Authentic **10** was prepared under the conditions described in [4].

[13] A similar regioselectivity was observed in the palladium-catalyzed hydroxyarylation of indenes: cf. H. Horino, M. Arai, N. Inoue, *Bull. Chem. Soc. Jpn. 47* (1974) 1683.

[14] *UV-Atlas organischer Verbindungen, Band 3, EG/21*, Verlag Chemie, Weinheim 1967.

[15] We thank Prof. Dr. *W. Lüttke* and Dipl.-Chem. *G. Kunz*, Göttingen, for recording the UV absorption and fluorescence spectra.

Synthesis, Characterization, and Complexation of an Unusual P_2Si_2 Bicyclobutane with Butterfly-Structure: 2,2,4,4-Tetramesityl-1,3-diphospha-2,4-disilabicyclo[1.1.0]butane **

By *Matthias Driess, Alan D. Fanta, Douglas R. Powell,* and *Robert West**

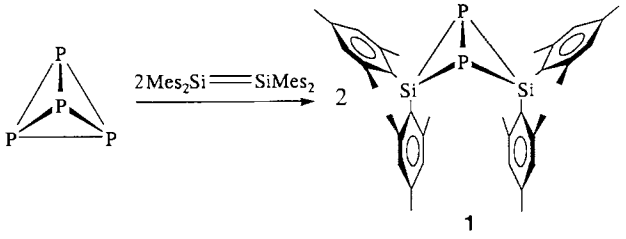
Disilenes, compounds containing silicon–silicon double bonds, are useful precursors for the synthesis of novel

[*] Prof. Dr. R. West, Dr. M. Driess [+], A. D. Fanta, Dr. D. R. Powell
Department of Chemistry, University of Wisconsin
Madison, WI 53706 (USA)

[+] Permanent Address: Anorganisch-chemisches Institut der Universität
Im Neuenheimer Feld 270, D-6900 Heidelberg (FRG)

[**] This work was supported by the Air Force Office of Scientific Research. *M. D.* thanks the Fonds der Chemischen Industrie for a Liebig fellowship grant.

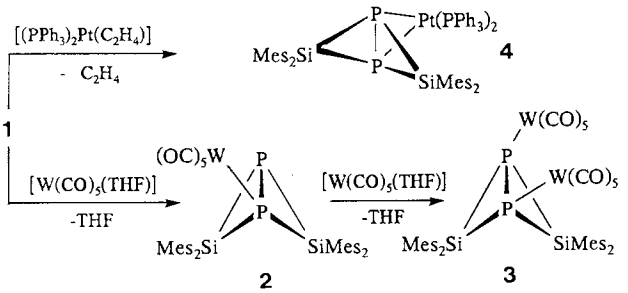
organosilicon heterocycles.[1] Of particular interest are the recent syntheses of three- and four-membered ring systems by reaction of disilenes with main group six elements O, S, Se, Te.[1,2] The products of reaction of Mes_4Si_2 (Mes = 2,4,6-$C_6H_2Me_3$) with molecular oxygen show unusual structures which present interesting problems in chemical bonding.[2,3] We have now found that Mes_4Si_2 possesses remarkable reactivity toward the group five element phosphorus as well. Tetramesityldisilene reacts with white phosphorus (40 °C, toluene, 24 h) to give an 87% yield of a yellow product having the novel butterfly-like bicyclobutane structure **1**.



1

^{31}P- and ^{29}Si-NMR spectroscopy does not show any phosphorus-rich compound as an intermediate. **1** is a pale yellow solid which is sensitive towards oxygen and moisture. Its composition was confirmed by ^1H, ^{31}P, and ^{29}Si NMR, a high resolution mass spectrum, and an elemental analysis.[4] The ^1H NMR spectrum of **1** exhibits sets of resonance signals for two chemically non-equivalent mesityl groups (*exo* and *endo* groups). The $^{31}P\{^1H\}$ NMR spectrum of **1** shows a singlet with ^{29}Si-satellites at very high field ($\delta = -324.0$), a typical region for phosphabicyclo[1.1.0]butanes with bridgehead P-atoms.[5] In the $^{29}Si\{^1H\}$ NMR spectrum a triplet resonance signal is observed at $\delta = -49.5$. The relative high value of the $J(^{29}Si\text{-}^{31}P)$ coupling constant (77 Hz) is characteristic for known silicon-phosphorus three-membered ring compounds, and is explained by a larger amount of s-character of the Si–P bond than is found in higher cyclic and acyclic Si–P compounds.[6]

1 reacts with $[W(CO)_5(THF)]$ and $[(Ph_3P)_2Pt(C_2H_4)]$ forming the crystalline transition metal complexes **2**, **3**, and **4**; the latter may have a propellane-like structure as shown, or an asterane structure, lacking the P–P bond.



Mes = 2,4,6-$C_6H_2Me_3$

The empirical formulas and structures of the metal complexes **2**–**4** are confirmed by FAB mass spectra as well as by ^1H, ^{29}Si, and ^{31}P NMR spectroscopy.[7] The ^{31}P nuclei of the Ph_3P ligand at Pt in **4** show a typically large $^1J(^{31}P\text{-}^{195}Pt)$ coupling constant (2522.6 Hz), whereas the analogous value for the bridgehead P atoms is much smaller (340.2 Hz). The remarkably low values of the $J(^{31}P\text{-}^{183}W)$ and $^1J(^{31}P\text{-}^{195}Pt)$ coupling constants, taken from the satellite peaks of the $^{31}P\{^1H\}$ NMR spectra,[7] indicates that the σ-donor bonding between the bridgehead P atom and metal includes a much smaller s-orbital contribution at phosphorus than in "normal" transition metal–phosphane complexes.[8] This finding is in accordance with MO calculations indicating that bridgehead P atoms in di-, tri-, and tetraphosphabicyclo[1.1.0]butanes possess donor orbitals with very high p-character [HOMO, HOMO-1].[9] The structure of the complex **3** in the crystal is further corroborrated by the result of an X-ray diffraction analysis (Fig. 1).[10]

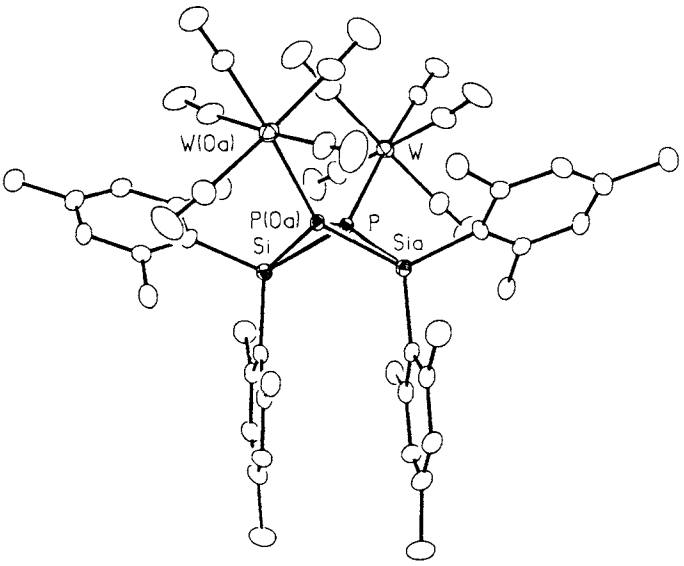


Fig. 1. Crystal structure of **3**. Important bond lengths [Å] and angles [°]: P–P 2.342(2), Si–P 2.267(2) (2.244(2)), P–W 2.560(1), Si–C 1.890(7) (1.873(5)), nonbonding Si–Si 3.244(2), P–Si–P 62.5(1), Si–P–P 58.2(1) (59.2(1)), Si–P–Si 91.9(1), C–Si–C 110.5(3).

The molecule has crystallographically determined, twofold symmetry about an axis perpendicular to the P–P bond. Each P atom lies in the center of a plane generated by the two Si atoms and one W-atom. The dihedral angle between the two three-membered Si–P–P rings is 114.6° and the torsion angle between the two P–W vectors (W–P–P–W) is 30.9°. A remarkable feature in the solid state structure of **3** is the approximately parallel conformation of the *endo*-mesityl groups.

Experimental

1: A solution of Mes_4Si_2 (500 mg, 0.94 mmol) in toluene (10 ml) was treated with white phosphorus (58.2 mg, 0.47 mmol) and the orange solution stirred for 24 h at 40 °C. The orange solution was gradually decolorized to a clear pale yellow solution. After the solution was concentrated to ca. 5 ml, benzene (5 ml) was added and **1** was recrystallized from the hot (60 °C) solvent mixture as pale yellow powder. M.p. 217–218 °C; yield: 516.8 mg (87%).

2,3: 150 mg (0.25 mmol) of **1** dissolved in 5 ml of THF was added to a freshly prepared solution of 118.7 mg (0.3 mmol) of $[W(CO)_5 \cdot THF]$ in THF and the mixture was stirred at 25 °C for 2 h. After removal of volatile components in vacuo the residue was recrystallized several times from a toluene/benzene (1:1) mixture to give **2** as yellow crystals. M.p. 192–197 °C (decomp.); yield: 142.5 mg (56%). Compound **3** was prepared in an analogous manner as **2** [150 mg, 0.25 mmol **1**; 2.5 equivalents $W(CO)_5 \cdot THF$] or by reaction of **2** with 1.5 equivalents of $W(CO)_5 \cdot THF$. Purification of **3** by recrystallization from hot

 © VCH Verlagsgesellschaft mbH, D-6940 Weinheim, 1989 0570-0833/89/0808-1039 $ 02.50/0

benzene gave orange crystals. M.p. 181–185 °C (decomp.); yield: 234.8 mg (70%).

4: A vigorously stirred solution of **1** (200 mg, 0.34 mmol) in toluene (10 ml) was treated with solid $[Pt(PPh_3)_2(C_2H_4)_2]$ (241.9 mg, 0.34 mmol) at 0 °C. Upon addition, the solution immediately turned deep brown. After the solution was allowed to warm to 25 °C and stirred for 2 h the solvent was removed in vacuo. The resulting brown oil was redissolved in benzene (3 ml) and **4** crystallized after 2–8 h as a yellow solid. M.p. 188–194 °C (decomp.); yield: 330.6 mg (74%).

Received: April 25, 1989 [Z 3305 IE]
German version: *Angew. Chem. 101* (1989) 1087

CAS Registry numbers:
1, 121654-87-3; **2**, 121674-98-4; **3**, 121674-99-5; **4**, 121675-00-1; [W(CO)$_5$THF], 36477-75-5; [Mes_4Si_2], 80785-72-4; P_4, 7723-14-0.

[1] Review: R. West, *Angew. Chem. 99* (1987) 1231; *Angew. Chem. Int. Ed. Engl. 26* (1987) 1201; G. R. Gillette, J. Maxka, R. West, *ibid. 101* (1989) 90 and *28* (1989) 54; M. Weidenbruch, B. Flintjer, S. Pohl, W. Saak, *ibid. 101* (1989) 89 and *28* (1989) 95.

[2] H. B. Yokelson, A. J. Millevolte, B. R. Adams, R. West, *J. Am. Chem. Soc. 109* (1987) 4116; M. J. Michalczyk, M. J. Fink, K. J. Haller, R. West, J. Michl, *Organometallics 5* (1986) 531. $(Mes_2Si)_2Si$ and $(Mes_2Si)_2Te$: G. R. Gillette, R. West, R. Tan, unpublished results.

[3] D. Cremer, J. Gauss, E. Cremer, *J. Mol. Struct. 169* (1988) 531.

[4] **1**: ^1H NMR (200 MHz, C_6D_6, 300 K): $\delta = 2.09$ (br. s, 12H, *p*-Me), 2.57 (s, 12H, *o*-Me), 2.80 (s, 12H, *o*-Me), 6.34 (s, 8H, $C_6H_2Me_3$); $^{29}Si\{^1H\}$ NMR (71.55 MHz, INEPT-pulse sequence, C_6D_6): $\delta = -49.50$ (t, $J = 77$ Hz); $^{31}P\{^1H\}$ NMR (202.4 MHz, C_6D_6): $\delta = -324.0$(s); MS: calcd. ($M^{\oplus}$) 594.2456, found 594.2453 (23%).

[5] E. Niecke, R. Rüger, B. Krebs, *Angew. Chem. 94* (1982) 553; *Angew. Chem. Int. Ed. Engl. 21* (1982) 544; R. Appel, B. Niemann, M. M. Nieger, *ibid. 100* (1988) 957 and *27* (1988) 957.

[6] M. Baudler, H. Jongebloed, *Z. Anorg. Allg. Chem. 458* (1979) 9; K. F. Tebbe, *ibid. 468* (1980) 202; M. Weidenbruch, M. Herrndorf, A. Schaefer, K. Peters, H. G. von Schnering, *J. Organomet. Chem. 295* (1985) 7; M. Baudler, Th. Pontzen, *Z. Anorg. Allg. Chem. 491* (1982) 27.

[7] **2**: ^1H NMR (200 MHz, C_6D_6; 300 K): $\delta = 1.97$ (s, 6H, *p*-Me), 2.16 (s, 6H, *p*-Me), 2.41 (s, 12H, *o*-Me), 2.73 (br. s, 12H, *o*-Me), 6.24 (s, 4H, $C_6H_2Me_3$), 6.67 (s, 4H, $C_6H_2Me_3$); $^{29}Si\{^1H\}$ NMR (71.55 MHz, INEPT-pulse sequence, C_6D_6): $\delta = -39.7$ (dd, $|^1J_{(^{29}Si\ PPW)}| = 80.0$ Hz, $|^1J_{(^{29}Si-PPW)}| = 34.0$ Hz); $^{31}P\{^1H\}$ NMR (202.4 MHz, C_6D_6): $\delta = -278.3$ (d, PPW, $|^1J_{(PP)}| = 106.9$ Hz, $|^1J_{(PP^{183}W)} + {}^2J_{(PP^{183}W)}| = 285.0$ Hz), -321.0 (d, *P*PW); MS (FAB, 3-$NO_2(C_6H_4)CH_2OH$ matrix): *m/z* 987 (27%, [*M* + matrix fragment]$^{\oplus}$), 891 (100%, [M–CO + 1]$^{\oplus}$); IR: $\tilde{\nu}$(CO) = 1973, 1951, 1941 cm^{-1}.—**3**: ^1H NMR (200 MHz, C_6D_6, 300 K): $\delta = 1.93$ (s, 6H, *p*-Me), 2.03 (s, 6H, *p*-Me), 2.22 (s, 12H, *o*-Me), 2.81 (br. s, 12H, *o*-Me), 6.17 (s, 4H, $C_6H_2Me_3$), 6.66 (s, 4H, $C_6H_2Me_3$); $^{29}Si\{^1H\}$ NMR (71.55 MHz, INEPT-pulse sequence, C_6D_6): $\delta = -53.7$ (t, $|^1J_{(SiP)}| = 38.2$ Hz); $^{31}P\{^1H\}$ NMR (202.4 MHz, C_6D_6): $\delta = -272.7$ (s, $|^1J_{(P^{183}W)} + {}^2J_{(P^{183}W)}| = 129.7$ Hz); MS (FAB, 3-$NO_2(C_6H_4)CH_2OH$ matrix): *m/z* 1243 (20%, [M + 1]$^{\oplus}$); IR: $\tilde{\nu}$(CO) = 1983, 1958, 1942 cm^{-1}.—**4**: ^1H NMR (500 MHz, C_6D_6/C_7D_8, 300 K): $\delta = 2.118$ (s, 6H, *p*-Me), 2.332 (s, 6H, *p*-Me), 2.761 (s, 12H, *o*-Me), 2.767 (s, 12H, *o*-Me), 6.406 (s, 4H, $C_6H_2Me_3$), 6.842 (s, 4H, $C_6H_2Me_3$), 6.933 (m, 18H, PPh_3), 7.008 (m, 12H, PPh_3); $^{29}Si\{^1H\}$ NMR (71.55 MHz, INEPT-pulse sequence, C_6D_6/C_7D_8): $\delta = -27.0$ (t, $|^1J_{(^{29}Si-P)}| = 65.0$ Hz), $^{31}P\{^1H\}$ NMR (202.4 MHz): $\delta = -119.9$ (pseudo-t, Si-*P*-Pt, $|^2J_{(P,PPh_3\,cis)} + {}^2J_{(P,PPh_3\,trans)}| = 28.3$ Hz, $|^1J_{(P,^{195}Pt)}| = 340$ Hz), $+22.5$ (pseudo-t, PPh_3; $|^1J_{Ph_3P,(^{195}Pt)}| = 2522.6$ Hz); MS (FAB, 3-$NO_2(C_6H_4)CH_2OH$ matrix): *m/z* 1346 (100%, [*M* + matrix fragment]$^{\oplus}$).

[8] J. G. Verkade, J. A. Mosbo in J. G. Verkade, L. D. Quin (Eds.): *Phosphorus–31 NMR Spectroscopy in Stereochemical Analysis*, VCH, New York/Weinheim 1987, p. 425.

[9] W. W. Schoeller, C. Lerch, *Inorg. Chem. 22* (1983) 2992; W. W. Schoeller, V. Staemmler, P. Rademacher, E. Niecke, *ibid. 25* (1986) 4382.

[10] X-ray structure analysis of **3**: orange rhombs from benzene; crystal dimensions: 0.3 × 0.45 × 0.55 mm^3, monoclinic, space group $C2/c$, $a = 17.547(4)$, $b = 14.517(3)$, $c = 20.086(4)$ Å, $\beta = 115.55(3)°$, $V = 4616.2(17)$ Å^3, $Z = 4$, $\varrho_{calcd.} = 1.788$ g cm^{-3}, $\mu = 5.262$ mm^{-1} ($Mo_{K\alpha}$); $T = 118$ K, 5330 independent reflections ($2\theta_{max} = 55.0°$), 4602 with $|F| > 2\sigma(F)$ used for the structure solution (direct methods). $R = 0.0413$ ($R_w = 0.0539$, $\omega^{-1} = \sigma F^2 + 0.0005 F^2$). Further details of the crystal structure investigation are available on request from the Fachinformationszentrum Karlsruhe, Gesellschaft für wissenschaftlich-technische Information mbH, D-7514 Eggenstein-Leopoldshafen 2 (FRG), on quoting for depository number CSD-53860, the names of the authors, and the journal citation.

N-Arylation and *N,N*-Dibenzylation of Coordinated N_2 with Organic Halides; Differences in the Reactivity of *trans*-[$Mo(N_2)_2(Me_8[16]aneS_4)$] and Its Phosphane Analogues**

By *Toshikatsu Yoshida,* Tomohiro Adachi, Tatsuo Ueda, Manabu Kaminaka, Nobuyoshi Sasaki, Taiichi Higuchi, Takayuki Aoshima, Izumi Mega, Yasushi Mizobe,* and *Masanobu Hidai**

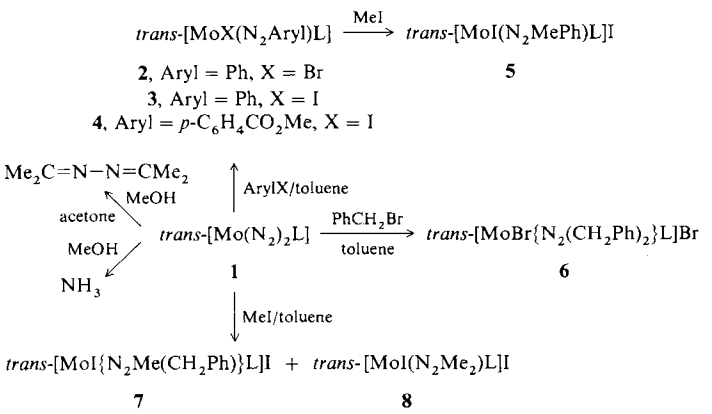
The direct formation of C–N bonds by reaction of N_2, coordinated to transition metals, with organic compounds has been the subject of intensive studies aimed at the development of new methods for the synthesis of organonitrogen compounds.[1–5] A variety of organic compounds such as RX (R = alkyl, acyl) and acid anhydrides have been found to react with Mo^0-, W^0-, and Re^I-N_2-phosphane complexes to give organo-diazenido and/or -hydrazido complexes. So far, however, no *N*-arylation or *N*-benzylation of coordinated N_2 with arylX and $PhCH_2X$ has been achieved,[2, 3] aside from the indirect *N*-arylation via a diazenido complex $[WX(N_2H)(dppe)_2]$ (dppe = $Ph_2PCH_2CH_2PPh_2$) with the very strong electrophilic aryl fluoride 2,4-$(NO_2)_2C_6H_3F$.[6, 7]

Recently, we have reported on the synthesis of a novel molybdenum(0)-dinitrogen complex *trans*-[$Mo(N_2)_2(Me_8[16]ane\text{-}S_4)$] **1** containing a quadridentate thio-crown ether ligand $Me_8[16]aneS_4$, and on its p_π electron donor properties,[10] which distinguish it from phosphanes. Compared to the phosphane analogues *trans*-[$Mo(N_2)_2(R_2PCH_2CH_2PR_2)_2$] (R = Et, Ph) **1** is very nucleophilic, as manifested by the facile *N,N*-dimethylation of the coordinated dinitrogen in **1** with MeBr under ambient conditions. We have now found the first examples of *N*-arylation and *N,N*-dibenzylation of the coordinated dinitrogen in **1** with the corresponding organic halides to give aryldiazenido and dibenzylhydrazido complexes, respectively. To clarify the difference in reactivity between **1** and the phosphane analogues further, liberation of NH_3 and acetone azine from **1** were also examined.

Reaction of **1** with two molar amounts of PhX in toluene under ambient conditions (no particular irradiation) for 10 h gave the phenyldiazenido complexes **2** (17%) and **3** (26%)[11] together with biphenyl (Scheme 1). When a more activated aryl halide *p*-$IC_6H_4CO_2Me$ was employed, **4** was obtained in a slightly better yield (32%). Formation of the aryldiazenido complexes was confirmed unequivocally by transformation of **3** into the hydrazido complex **5** on treatment with MeI at room temperature and by a single crystal X-ray structure analysis of **4** (Fig. 1).[12]

[*] Prof. Dr. T. Yoshida, T. Adachi, T. Ueda, M. Kaminaka, N. Sasaki
Department of Chemistry, Faculty of Integrated Arts and Sciences
University of Osaka Prefecture
Sakai, Osaka 591 (Japan)
Prof. Dr. T. Higuchi
Department of Chemistry, Faculty of Science
Osaka City University
Sumiyoshi, Osaka 558 (Japan)
Prof. Dr. M. Hidai, T. Aoshima, I. Mega, Dr. Y. Mizobe
Department of Synthetic Chemistry, Faculty of Engineering
Tokyo University
Hongo, Tokyo 113 (Japan)

[**] This work was supported by a Grant-in-Aid for Scientific Research (No. 61125004) from the Japanese Ministry of Education, Science, and Culture, and by the Asahi Glass Foundation for Industrial Technology (*M. H.*). – $Me_8[16]aneS_4$ = 3,3,7,7,11,11,15,15-octamethyl-1,5,9,13-tetrathiacyclohexadecane



Scheme 1. L = $Me_8[16]aneS_4$.

The complex **4** adopts a slightly distorted octahedral geometry with four S atoms in the equatorial plane and with the *p*-$N_2C_6H_4CO_2Me$ and I ligands in the *trans* axial sites. The all-up conformation of $Me_8[16]aneS_4$ in **1**[10] was retained during the *N*-arylation. The I ligand lies on the same side as the macrocyclic C atoms with respect to the 4S equatorial plane, while the N_2-*p*-$C_6H_4CO_2Me$ group lies on the opposite side. The complex has crystallographically imposed C_s symmetry with the Mo, S(1), S(9), I, N(1) and N(2) atoms and the phenyl ring as well as the CO_2 group in the symmetry plane. The bond lengths and angles of the MoN_2-*p*-$C_6H_4CO_2Me$ moiety are typical for Mo^{II} and Mo^{IV} organodiazenido complexes.[13, 14] Despite the low yield the observed facile *N*-arylation is remarkable and contrasts sharply with the failure of *trans*-[$M(N_2)_2(dppe)_2$] (M = Mo, W) to react with PhX under similar conditions and with the formation of *trans*-[$MoX_2(dppe)_2$] as sole product under forcing conditions.[15]

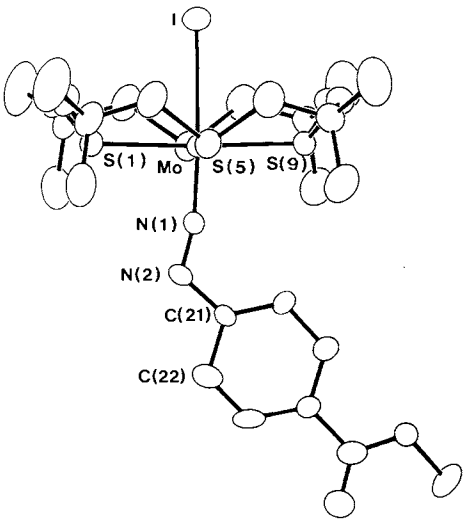


Fig. 1. Crystal structure of **4** (ellipsoids at the 50% probability level). Selected bond distances [Å] and angles [°]: Mo–S(1) 2.435(4), Mo–S(5) 2.443(3), Mo–S(9) 2.440(4), Mo–I 2.925(2), Mo–N(1) 1.775(11), N(1)–N(2) 1.257(15), N(2)–C(21) 1.369(17); S(1)–Mo–S(5) 90.0(1), S(5)–Mo–S(9) 90.0(1), I–Mo–N(1) 176.9(4), Mo–N(1)–N(2) 168.6(10), N(1)–N(2)–C(21) 117.6(11).

N,N-Dibenzylation of **1** with $PhCH_2Br$ also proceeded readily under ambient conditions in toluene to give **6** in 60% yield. A similar reaction of the dppe analogue again failed to give the corresponding diazenido or hydrazido complex, but instead *trans*-[$MoBr_2(dppe)_2$] and bibenzyl.[15] Rather surprisingly, reaction of **1** with MeI in toluene under ambient-conditions gave the *N,N*-benzyl(methyl)hydrazido complex **7** together with the expected *N,N*-dimethylhydrazido complex **8** in a 1:3 ratio. It should be noted that a similar reaction carried out in benzene afforded exclusively **8** in quantitative yield. The formation of **7** may be interpreted in terms of a radical process similar to that confirmed for the *N*-monoalkylation of *trans*-[$M(N_2)_2(dppe)_2$] (M = Mo, W) by alkyl halides.[15] Accordingly, **7** may be produced via an intermediate [$MoI(N_2CH_2Ph)Me_8[16]aneS_4$]. A decisive reaction would be an H abstraction from toluene by a methyl radical formed by an incipient reaction of **1** with MeI together with [$MoI(N_2)Me_8[16]aneS_4$]; the latter would be *N*-benzylated by the benzyl radical thus generated. Apparently the dinitrogen ligand in **1** is reactive enough to be attacked by such a stable radical as $PhCH_2^{\bullet}$.

The high nucleophilicity of **1** is further demonstrated by liberation of NH_3 on treatment with MeOH at 50 °C for 45 h (0.06 mol/Mo atom). If acetone is added to the above system, acetone azine (0.16 mol/Mo atom, 18 h; 0.40 mol/Mo atom, 40 h) is obtained. Although the generation of NH_3 and acetone azine from **1** is not so effective as observed in the corresponding reactions of *cis*-[$W(N_2)_2(PMe_2Ph)_4$] (NH_3 1.01 mol/W atom,[16, 17] $Me_2C=N-N=CMe_2$ 0.88 mol/W atom,[17] 18 h at 50 °C), molybdenum-dinitrogen complexes such as *trans*-[$Mo(N_2)_2(dppe)_2$] and *cis*-[$Mo(N_2)_2(PMe_2Ph)_4$] are known to be completely inactive for such generation of nitrogen compounds under similar conditions.[17] The novel reactivity of the coordinated dinitrogen in **1**, which probably arises from p_π electron donor ability of the crown thioether, seems to provide a basis for elucidating the role of sulfur ligands in the nitrogenase cofactor.

Received: April 5, 1989 [Z 3276 IE]
German version: *Angew. Chem. 101* (1989) 1053

[1] J. Chatt, J. R. Dilworth, R. L. Richards, *Chem. Rev. 78* (1978) 589.
[2] J. R. Dilworth, J. R. Richards in G. Wilkinson, F. G. A. Stone, E. W. Abel (Eds.): *Comprehensive Organometallic Chemistry, Vol 8*, Chap. 60, Pergamon, Oxford 1982.
[3] H. M. Colquhoun, *Acc. Chem. Res. 17* (1984) 23.
[4] M. Hidai in S. Spiro (Ed.): *Molybdenum Enzymes*, John Wiley, 1985, pp. 285.
[5] M. Hidai, Y. Mizobe in P. S. Braterman (Ed.): *Reactions of Coordinated Ligands*, Vol 2, Plenum, London 1988, pp. 53.
[6] H. M. Colquhoun, *J. Chem. Res.(S) 1979*, 325.
[7] Apart from the *N*-arylation with aryl halides, a nucleophilic *N*-phenylation of an electron-poor complex [(η^5-C_5H_5)$Mn(CO)_2(N_2)$] with PhLi and formation of aniline by reaction of titanium(IV) compounds with PhLi under high N_2 pressure are known [8, 9].
[8] M. E. Vol'pin, V. B. Shur, R. V. Kudryavster, L. A. Prodayko, *Chem. Commun. 1968*, 7038.
[9] D. Sellman, W. Weiss, *Angew. Chem. 90* (1978) 295; *Angew. Chem. Int. Ed. Engl. 17* (1978) 269.
[10] T. Yoshida, T. Adachi, M. Kaminaka, T. Ueda, T. Higuchi, *J. Am. Chem. Soc. 110* (1988) 4872.
[11] All the new compounds gave satisfactory elemental analyses except **7**, which was characterized by ^1H NMR data. Spectroscopic and physical data: **2**: yellow crystals, m.p. 262–263 °C (dec); IR (Nujol mull): $\tilde{\nu}$(N=N) 1560 cm^{-1}; ^1H NMR: δ = 1.05 (s, 12H, Me), 1.21 (s, 12H, Me), 2.60 (d, J = 11.5 Hz, 8H, CH_2S), 2.92 (d, J = 11.5 Hz, 8H, CH_2S), 7.0–7.3 (m, 5H, Ph). **3**: yellow crystals, m.p. 252–254 °C (dec); IR (Nujol mull): $\tilde{\nu}$(N=N) 1560 cm^{-1}; ^1H NMR: δ = 1.06 (s, 12H, Me), 1.20 (s, 12H, Me), 2.61 (d, J = 12.0 Hz, 8H, CH_2S), 2.98 (d, J = 12.0 Hz, 8H, CH_2S), 7.0–7.3 (m, 5H, Ph). **4**: orange crystals, m.p. 285–287 °C (dec); IR (Nujol mull): $\tilde{\nu}$((N=N) 1540, $\tilde{\nu}$(C=O) 1702 cm^{-1}; ^1H NMR: δ = 1.09 (s, 12H, Me), 1.19 (s, 12H, Me), 2.62 (d, J = 11.3 Hz, 8H, CH_2S), 2.96 (d, J = 11.3 Hz, 8H, CH_2S), 3.82 (s, 3H, CO_2Me), 7.17 (d, J = 8.8 Hz, 2H, Ar), 7.19 (d, J = 8.8 Hz, 2H, Ar). **5**: pale brown crystals, m.p. 278–281 °C (dec); ^1H NMR: δ = 1.20 (s, 24H, Me), 2.87 (d, J = 11.0 Hz, 8H, CH_2S),

3.05 (d, J = 11.0 Hz, 8H, CH_2S), 3.81 (s, 3H, NMe), 7.1–7.4 (m, 5H, Ph). **6**: pink crystals, m.p. 254 °C (dec); ^{1}H NMR: δ = 1.17 (s, 6H, Me), 1.19 (s, 6H, Me), 2.81 (d, J = 11.6 Hz, 4H, CH_2S), 2.93 (d, J = 11.6 Hz, 4H, CH_2S), 4.56 (s, 2H, NCH_2), 7.2–7.4 (m, 5H, Ph). **7**: ^{1}H NMR: δ = 1.18 (s, 12H, Me), 1.23 (s, 12H, Me), 2.86 (d, J = 11.4 Hz, CH_2S), 2.98 (d, J = 11.4 Hz, CH_2S), 3.12 (s, 3H, NMe), 4.56 (s, 2H, NCH_2), 7.15–7.40 (m, 5H, Ph). **8**: pink crystals, m.p. 297–299 °C (dec); ^{1}H NMR: δ = 1.18 (s, 6H, Me), 1.23 (s, 6H, Me), 2.84 (d, J = 11.6 Hz, 4H, CH_2S), 2.94 (d, J = 11.6 Hz, 4H, CH_2S), 3.24 (s, 3H, NMe). The ^{1}H NMR spectra show that the Me_8[16]aneS_4 ligand in **2**–**8** assumes all-up conformation.

[12] Crystal data for **4**: $C_{28}H_{47}N_2O_2S_4IMo \cdot 2\,CH_2Cl_2$, M = 964.18, orthorhombic, a = 23.353(4), b = 13.055(3), c = 13.985(4) Å, V = 4264(2) Å^3, space group *Pnam*, Z = 4, D_c = 1.50 g cm^{-3}, $\mu(Mo_{K\alpha})$ = 14.86 cm^{-1}. Crystal dimension 0.15 × 0.15 × 0.40 mm; intensity data were collected in the range $3 \leq 2\theta \leq 50°$ using the $2\theta/\omega$ scan technique; intensities were corrected for Lorentz and polarization effects. The Mo atom was located by the Patterson map and the other atoms were found by a successive Fourier method, and refined by block-diagonal least-squares procedures. One of solvent molecules (CH_2Cl_2) and the methyl group of the ester were disordered slightly, but could be modeled successfully. At final convergence, $R(R_w)$ = 0.062(0.063), S_w = 1.56 for 2218 unique reflections ($|F_o| \geq 3\sigma(F_o)$) and the final difference map showed no feature above 0.72 eÅ^{-3}. Further details of the crystal structure investigation may be obtained from the Fachinformationszentrum Karlsruhe, Gesellschaft für wissenschaftlich-technische Information mbH, D-7514 Eggenstein-Leopoldshafen 2 (FRG), on quoting the depository number CSD-53791, the names of the authors, and the journal citation.

[13] M. Sato, T. Kodama, M. Hidai, Y. Uchida, *J. Organomet. Chem. 152* (1978) 239.

[14] T.-C. Hsieh, T. Nicholson, J. Zubieta, *Inorg. Chem. 27* (1988) 241.

[15] J. Chatt, R. A. Head, G. J. Leigh, C. J. Pickett, *J. Chem. Soc. Dalton Trans. 1978*, 1638.

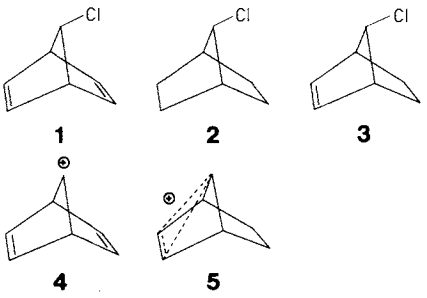
[16] J. Chatt, A. J. Pearman, R. L. Richards, *J. Chem. Soc. Dalton Trans. 1977*, 1853.

[17] A. Watanabe, T. Takahashi, D.-M. Jin, I. Yokota, Y. Uchida, M. Hidai, *J. Organomet. Chem. 254* (1983) 75.

The 7-Norbornadienyl Cation: An NMR/IGLO Validation of its ab initio Structure**

By *Matthias Bremer, Karl Schötz, Paul von Ragué Schleyer,* Ulrich Fleischer, Michael Schindler, Werner Kutzelnigg, Wolfram Koch,* and *Peter Pulay*

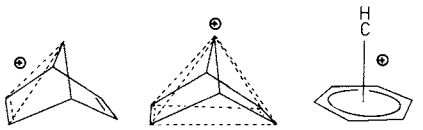
In 1960 *Winstein* et al.[1] reported a "world record for anchimeric acceleration".[2] 7-norbornadienyl chloride **1** solvolyzes 10^{14} times faster than 7-norbornyl chloride **2** and even 10^3 times faster than 7-norbornenyl chloride **3**. The exceptional stability of the 7-norbornadienyl cation **4** permitted its preparation (as the $BF_4^{\ominus}$ salt) in SO_2 solution before the days of "super acid".[3] We now present an *ab initio*/IGLO (*I*ndividual *G*auge for *L*ocalized *M*olecular *O*rbitals)[4] study on the 7-norbornadienyl cation **4** – a system important for the understanding of the electronic structure of nonclassical carbocations – which establishes the geometrical consequences of the homoaromatic interactions in **4** and in the related 7-norbornenyl cation **5**.



1 **2** **3**

4 **5**

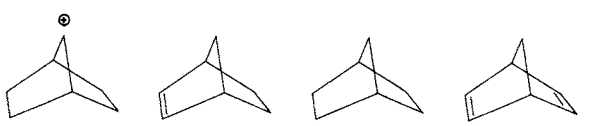
Of the three structural alternatives considered by *Winstein* for the cation intermediate **4a**–**4c**, the form with the lowest symmetry (C_s), **4a**, was indicated by NMR experiments.[3] The preference for a C_s geometry can be rationalized based on PMO arguments.[5] Tilting C7 toward the C2–C3 double bond results in better overlap and thus higher stabilization than simultaneous interaction with both double bonds in a C_{2v} arrangement. Experimentally, the barrier to bridge flipping **4a** ⇌ **4b** ⇌ **4a** was estimated to be at least 19.6 kcal mol^{-1}.[3b]



4a, C_s **4b**, C_{2v} **4c**, C_{6v}

Our *ab initio* calculations (Table 1) confirm these conclusions. The C_{2v} structure **4b** is found to be 26.6 kcal mol^{-1} (MP2-FC/6-31G*//6-31G*; the "//" means "at the geometry of") less stable than the C_s alternative **4a**. The stabilizations due to the interactions of the double bonds with the positive charges can be evaluated by isodesmic reactions [Equations (a)–(c)].

6 + norbornadiene → **4a** + norbornane (**9**) (**8**)	−20.3	(a)
6 + norbornene → **5** + **8** (**7**)	−15.0	(b)
6 + **9** → **4b** + **8**	+ 6.3	(c)



6 **7** **8** **9**

The large values found for **4a** [Eq. (a)] and for **5** [Eq. (b)] correspond to the solvolysis rate accelerations found experimentally. The situation in **4b** is interesting in view of the qualitative prediction[6] that "longicyclic" interactions in

[*] Prof. Dr. P. von R. Schleyer, Dr. M. Bremer, Dr. K. Schötz
Institut für Organische Chemie, Universität Erlangen-Nürnberg
Henkestr. 42, D-8520 Erlangen (FRG)

Dipl.-Chem. U. Fleischer, Dr. M. Schindler, Prof. Dr. W. Kutzelnigg
Lehrstuhl für Theoretische Chemie, Ruhr-Universität
Postfach 102148, D-4630 Bochum (FRG)

Dr. W. Koch
IBM Deutschland GmbH, Wissenschaftliches Zentrum Heidelberg
Tiergartenstr. 15, D-6900 Heidelberg (FRG)

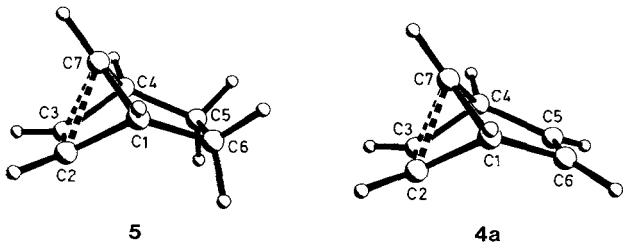
Prof. Dr. P. Pulay
Department of Chemistry and Biochemistry, University of Arkansas
Fayetteville, AR 72701 (USA)

[**] Support was provided by the Fonds der Chemischen Industrie, the Deutsche Forschungsgemeinschaft, the Convex Computer Corporation and the Regionales Rechenzentrum Erlangen. Most of the IGLO calculations were carried out on the Cyber 205 of the Rechenzentrum of the Ruhr Universität Bochum. We gratefully acknowledge a generous allocation of computer time on the IBM 3090-200 E/VF of the IBM Düsseldorf computer center. The vectorized IBM version of Gaussian 86 was used [18]. We thank *T. Laube* (Zürich) for communicating his results prior to publication.

Table 1. Total Energies [− Hartree] for **4a**, **4b**, **5** and **6–9**.

Level of calculation	**4a**	**4b**	**5**	**6**	**7**	**8**	**9**
3-21G//3-21G	267.29788	267.28200	268.49928	269.67766	269.36909	270.56656	268.16187
6-31G*//6-31G*	268.82076	268.78676	270.02099	271.17676	270.86184	272.06120	269.65251
MP2-FC/6-31G*//6-31G*	269.69686	269.65453	270.90479	272.08861	271.76737	272.97504	270.55095
6-31G*//MP2-FU/6-31G*	268.81849						
MP2-FU/6-31G*//MP2-FU/6-31G*	269.73407						
MP2-FC/6-31G*//MP2-FU/6-31G*	269.69915						

C_{2v} symmetry should be favorable. In contradiction, the isodesmic reaction (c) is *endothermic* by 6.3 kcal mol^{-1} at MP2-FC/6-31G*//6-31G*. The inductive effects of the double bonds are destabilizing.[7, 8] Despite the energy required to achieve the larger structural distortions shown in Figure 1, much greater net stabilization [20.3 kcal mol^{-1}; Eq. (a)] is gained in **4a** than in **4b** due to the bishomoaromatic interactions. Nevertheless, there is some additional stabilization by the second double bond in **4a**.[5, 6] Note the 5.3 kcal mol^{-1} difference in energies between Eqs. (a) and (b). This difference also corresponds to the faster solvolysis rates of **1** over **3**.



5 **4a**

Fig. 1. Structures of the norbornenyl cation **5** and the 7-norbornadienyl cation **4**.

Recently, the IGLO method[4] has been shown[9] to give good to excellent agreement of calculated ^{13}C NMR chemical shifts (based on *ab initio* geometries) and experimental values and thus provides a powerful tool to relate theoretical structures of carbocations to the species actually present in solution.

An advantage of such theoretical methods, for instance IGLO[4] or GIAO,[10] is that chemical shifts for experimentally *inaccessible* species can be readily calculated. It can be applied to the *ab initio* optimized transition structure **4b** as well as to the minimium **4a**. The theoretical methods are in accordance with experiment only for the C_s structure (Table 2; for comparison, results obtained with the GIAO method[10] have been included). As expected,[11] polarization functions (6-31G* basis) are needed to give an accurate description of the geometry resulting from the nonclassical interaction in **4a**. Reoptimization with electron correlation (MP2-FU/6-31G*//MP2-FU/6-31G*) does not lead to significant changes in the geometry or in the calculated chemical shifts. In contrast, the appreciable differences between the geometries of **4a** at 3-21G and at 6-31G* (Table 3) result in large differences between the calculated (IGLO) and experimental ^{13}C NMR chemical shifts (Table 2). This underscores the sensitivity of the chemical shifts as calculated by the IGLO method to geometrical changes in such carbocation systems. Calculated chemical shifts for the C_{2v} structure **4b** (Table 2) deviate widely from experiment. Hence, **4b** can clearly be ruled out as a structural alternative. Good agreement of experiment and theory is also found for the 7-norbornenyl cation **5**. Again, the 6-31G* geometry is a prerequisite for reliable results.

Table 2. Comparison of Experimental and Calculated ^{13}C-NMR chemical shifts (vs. TMS). The level of the calculation is indicated as method/basis//geometry.

4a	C1,C4	C2,C3	C5,C6	C7
Experiment [14]	63.0	122.0	114.9	36.2
IGLO/DZ//3-21G	53	135	132	96
IGLO/DZ//6-31G* [a]	55	132	120	36
IGLO/DZ//MP2-FU/6-31G*	55	134	120	30
GIAO/4-31G//6-31G* [b]	50	129	112	29
4b				
IGLO/DZ//3-21G	45	139		238
IGLO/DZ//6-31G*	42	137		218
GIAO/4-31G//6-31G*	41	135		219
5 and derivatives				
5, expt. [14]	58.0	125.9	26.7	34.0
5-7-Me, expt. [14b]	57.1	134.1	24.8	71.9
5-7-Ph, expt. [14b]	51.9	140.1	23.3	109.8
IGLO/DZ//3-21G	46	135	18	123
IGLO/DZ//6-31G*	49	127	19	33
9				
Experiment [15]	50.2	144.3		74.9
IGLO/DZ//experiment [16]	44	158		82
IGLO/DZ//3-21G	44	158		74
IGLO/DZ//6-31G*	43	150		67
GIAO/4-31G//6-31G*	43	147		68

[a] The respective shifts with larger IGLO basis sets are: IGLO/DZ + d//6-31G*: 50, 122, 108, 30; IGLO/II'//6-31G*: 49, 130, 114, 27. [b] The respective GIAO values at the GIAO/6-31G*//6-31G* level are: 47, 121, 107, 27.

Figure 1 and Tables 3 and 4 summarize the *ab initio* geometries of **4a**, **4b**, **5** and **6–9**. Relatively short C2–C7 (ca. 1.7 Å) and benzene-like C2–C3 (ca. 1.38 Å) distances characterize the three-center two-electron bonding arrangements in **4a** and **5**.[12]

Table 3. Comparison of selected geometrical parameters [Å, degrees] for the norbornadienyl cations **4a,b** and the norbornenyl cation **5** [MP2-FU/6-31G*], 6-31G*, (3-21G).

	4b, C_{2v}		**4a**, C_s			**5**, C_s	
C2-C3	1.333	(1.332)	[1.400]	1.380	(1.371)	1.380	(1.368)
C2-C7	2.190	(2.228)	[1.701]	1.719	(1.895)	1.745	(1.938)
C2-C6	2.544	(2.528)	[2.532]	2.538	(2.533)	2.577	(2.552)
C5-C6	1.333	(1.332)	[1.340]	1.316	(1.316)	1.543	(1.557)
Φ_1 [a]	119.0	(120.3)	[154.1]	152.5	(147.2)	149.4	(143.7)
Φ_2 [b]	119.0	(120.3)	[78.4]	80.2	(90.5)	83.6	(96.0)

[a] Torsion angle C6-C1-C4-C7. [b] Torsion angle C2-C1-C4-C7.

Table 4. Comparison of selected geometrical parameters [Å, degrees] for the bicyclo[2.2.1]hydrocarbons **7**–**9** [17] and the 7-norbornyl cation **6**. 6-31G* (3-21G).

	6 C_{2v}	**7**, C_s	**8**, C_{2v}	**9**, C_{2v}
C2-C3	1.562 (1.578)	1.322 (1.323)	1.557 (1.571)	1.319 (1.319)
C2-C7	2.296 (2.325)	2.345 (2.355)	2.383 (2.401)	2.338 (2.357)
C2-C6	2.534 (2.527)	2.466 (2.474)	2.503 (2.502)	2.482 (2.479)
C5-C6	1.562 (1.578)	1.557 (1.570)	1.557 (1.571)	1.319 (1.319)
Φ_1 [a]	123.3 (124.2)	120.8 (120.9)	123.5 (124.0)	122.5 (123.0)
Φ_2 [b]	123.3 (124.2)	127.1 (127.4)	123.5 (124.0)	122.5 (123.0)

[a] Torsion angle C6-C1-C4-C7. [b] Torsion angle C2-C1-C4-C7.

A combination of *ab initio* geometries, IGLO (or GIAO) calculations and NMR measurements now provide a source of structural information comparable in reliability to experimental methods.[13]

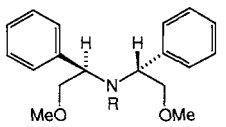
Received: March 22, 1989 [Z 3249 IE]
German version: *Angew. Chem. 101* (1989) 1063

[1] S. Winstein, C. Ordronneau, *J. Am. Chem. Soc. 82* (1960) 2084.
[2] S. Winstein, in G. A. Olah, P. von R. Schleyer (Eds.): *Carbonium Ions, Vol. III*, Wiley, New York 1972, p. 968.
[3] a) P. R. Story, M. Saunders, *J. Am. Chem. Soc. 84* (1962) 4876; b) M. Brookhart, R. K. Lustgarten, S. Winstein, *ibid. 89* (1967) 6352.
[4] a) M. Schindler, *J. Am. Chem. Soc. 109* (1987) 1020; b) W. Kutzelnigg, *Isr. J. Chem. 19* (1980) 193; c) M. Schindler, W. Kutzelnigg, *J. Chem. Phys. 76* (1982) 1919.
[5] P. Vogel, *Carbocation Chemistry*, Elsevier, Amsterdam 1985, p. 256.
[6] M. J. Goldstein, R. Hoffmann, *J. Am. Chem. Soc. 93* (1971) 6193.
[7] T. W. Bentley, B. Irrgang, H. Mayr, P. von R. Schleyer, *J. Org. Chem. 53* (1988) 3492.
[8] P. von R. Schleyer, T. W. Bentley, W. Koch, A. Kos, H. Schwarz, *J. Am. Chem. Soc. 109* (1987) 6953.
[9] a) Dehydroadamantanediyl dication: M. Bremer, P. von R. Schleyer, K. Schötz, M. Kausch, M. Schindler, *Angew. Chem. 99* (1987) 795; *Angew. Chem. Int. Ed. Engl. 26* (1987) 761; b) Bicyclo[2.1.1]hexyl cations: P. von R. Schleyer, K. E. Laidig, K. B. Wiberg, M. Saunders, M. Schindler, *J. Am. Chem. Soc. 110* (1988) 300; c) $C_4H_7^{\oplus}$ cations: M. Saunders, K. E. Laidig, K. B. Wiberg, P. von R. Schleyer, *ibid. 110* (1988) 7652; d) Cyclobutadienyl dications: M. Bremer, P. von R. Schleyer, U. Fleischer, *ibid. 111* (1989) 1147.
[10] The GIAO results were obtained with an efficient new program developed at the University of Arkansas. The details of this method will be published separately, see K. Wolinski, J. F. Hinton, P. Pulay, unpublished. For a review of methods for *ab initio* calculations of chemical shifts see D. B. Chestnut in: G. A. Webb (Ed.): *Annual Reports on NMR Spectroscopy*, Academic Press, New York 1989, p. 50.
[11] W. J. Hehre, L. Radom, P. von R. Schleyer, J. Pople: *Ab initio Molecular Orbital Theory*, Wiley, New York 1986.
[12] After this work was complete, we learned of *T. Laube*'s crystal structure determination of 2,3-dimethyl-7-phenyl-7-norbornenyl cation as $Sb_2F_{11}^{\ominus}$ salt. (Abstract A 32, Chemiedozententagung, Bielefeld 1989; T. Laube, private communication). The C2–C3 X-ray distance (1.381(10) Å) agrees well, but due to the greater degree of classical character, the C2–C7 distances (1.856(10) Å) are larger than the 6-31G* value for **5**. The experimental $\delta(^{13}C)$ values for the 7-phenyl-7-norbornenyl cation [14 b] correspond roughly with our IGLO calculations (Table 2) on the 3-21G geometry of **5** which has a C2–C7 distance of 1.94 Å (Table 3).
[13] We note in this context that IGLO chemical shifts based on the *experimental* geometry of **9** [16] are in poorer agreement with the experimental $\delta(^{13}C)$ values than those calculated using the 6-31G* geometry (Table 2).
[14] a) G. A. Olah, G. Liang, G. D. Mateescu, J. L. Riemenschneider, *J. Am. Chem. Soc. 95* (1973) 8698; b) G. A. Olah, G. Liang, *ibid. 97* (1975) 6803.
[15] G. A. Olah, S. H. Ju, *J. Org. Chem. 40* (1975) 3638.
[16] K.-H. Hellwege, A. M. Hellwege, (Eds), *Landolt-Börnstein, Zahlenwerte und Funktionen aus Naturwissenschaft und Technik, Neue Serie II/15*, Springer, Heidelberg 1987.
[17] For the STO-3G, 3-21G and 4-31G geometries of **7**–**9**, see C. R. Castro, R. Dutler, A. Rauk, H. Wieser, *J. Mol. Struc. 152* (1987) 241; see also R. Houriet, T. Schwitzguebel, P.-A. Carrupt, P. Vogel, *Tetrahedron Lett. 37* (1986) 37.
[18] M. J. Frisch, J. S. Binkley, H. B. Schlegel, K. Raghavachari, C. F. Melius, R. L. Martin, J. J. P. Stewart, F. W. Bobrowicz, C. M. Rohlfing, L. R. Kahn, D. J. DeFrees, R. Seeger, R. A. Whiteside, D. J. Fox, E. M. Fluder, J. A. Pople, *Gaussian 86*, Carnegie-Mellon University Quantum Chemistry Publishing Unit, Pittsburgh, PA, USA 1984.

A New Coordinating Chiral Lithium Amide**

By *Donald Barr, David J. Berrisford, Raymond V. H. Jones, Alexandra M. Z. Slawin, Ronald Snaith, J. Fraser Stoddart** and *David J. Williams*

Simultaneous interests in transition state molecular recognition phenomena[1] and lithium polyether[2a] and lithium amide[2b] coordination chemistry encouraged us to examine the potential of chiral lithium amides[3, 4] as enantioselective reagents. Recently, these reagents have been employed (i) as chiral bases to differentiate between enantiomerically-related hydrogen atoms in racemic substrates[5, 6] as well as to discriminate between enantiotopic hydrogen atoms of prochiral substrates,[7–10] and (ii) as chiral complexing agents to effect enantioselective alkylations,[11] carboxylations,[12] aldol condensations,[4, 13] and Michael additions[4] of lithium enolates, aldol-type condensations[14] of toluate carbanions, carbanionic rearrangements[15] of allylic propargylic ethers and asymmetric silylations[3] of certain sulfone anions. No chiral lithium amide utilized hitherto has combined the features which are desirable for wide application, i.e. C_2 symmetry[16, 17] and symmetrically-disposed coordinating groups for the lithium cation.[17, 18] Herein we wish to report on the stereospecific synthesis and characterization of the chiral amine (*R,R*)-**1**[19] and on investigations into the solid-state structure and solution behavior of the lithium amide derived therefrom, the dimer $[(R,R)\text{-}\mathbf{2}]_2$ of (*R,R*)-lithium-di(α-methoxymethylbenzyl)amide.[20]

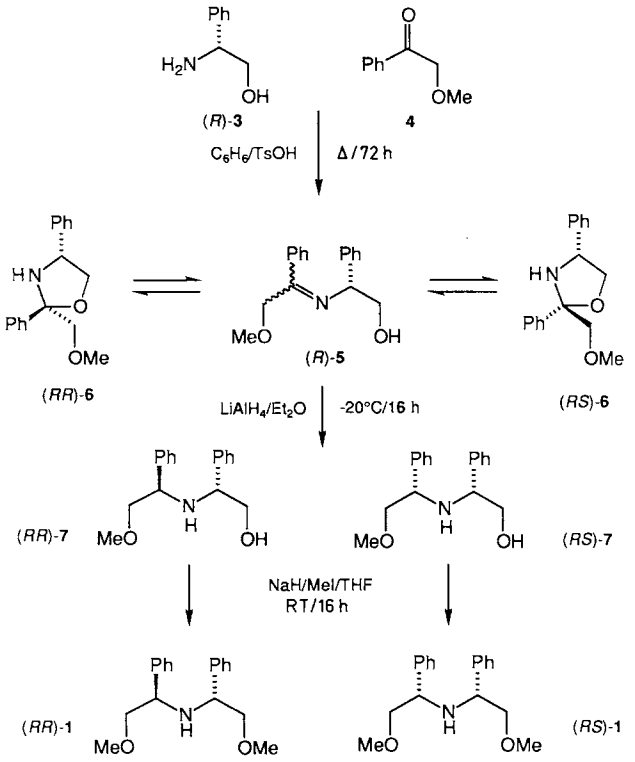


(*RR*)-**1** R = H $[(RR)\text{-}\mathbf{2}]_n$ R = Li

The new chiral auxiliary (*R,R*)-**1** can be prepared (Scheme 1) in three steps from (*R*)-phenylglycinol (*R*)-**3**.[21] Condensation of (*R*)-**3** with α-methoxyacetophenone **4**[22] affords an equilibrium mixture (in 96% yield) of the diastereoisomeric imines (*R*)-**5** and the diastereoisomeric pair (*R,R*)-**6** and (*R,S*)-**6** of the constitutionally-isomeric oxazolidines.[23] Reduction (H_2/Pd/C) of this mixture has been reported[23] to be unsuccessful. However, we have found that $LiAlH_4$ in Et_2O at low temperature (−20 °C) reduces the mixture in high yield (84%) with modest diastereoselectivity [(*R,R*)-**7**/(*R,S*)-**7** = 70/30].[24] Alternative reducing agents (for example, $NaBH_4$, $BH_3 \cdot C_5H_5N$, $BH_3 \cdot SMe_2$, $Li[CHMeCHMe_2]_3BH$, and $[(CH_3OCH_2$-

[*] Dr. J. F. Stoddart, D. J. Berrisford
Department of Chemistry, The University
Sheffield S3 7HF (UK)
Dr. R. Snaith, Dr. D. Barr
University Chemical Laboratory
Lensfield Road
Cambridge CB2 1EW (UK)
Dr. R. V. H. Jones
Process Technology Department
ICI FCMO, Earls Road
Grangemouth, Stirlingshire FK3 8XG (UK)
Dr. D. J. Williams, A. M. Z. Slawin
Chemical Crystallography Laboratory
Department of Chemistry, Imperial College
London SW7 2AY (UK)

[**] This work was supported by a Science and Engineering Research Council CASE Award and by ICI FCMO in the United Kingdom.



Scheme 1. RT = room temperature.

$CH_2O)_2AlH_2]Na$) were less effective and exhibited lower, or even opposite, diastereoselectivities.[25] The diastereoisomeric hydroxyamines (*R,R*)-**7** and (*R,S*)-**7** could be separated by *fractional crystallization* (*n*-hexane/ether) to afford initially (*R,S*)-**7** (17%) and subsequently (*R,R*)-**7** (48%). Both diastereoisomers were *O*-methylated to give (*R,S*)-**1**[26] as an oil (90%), and the C_2-symmetric dimethoxyamine (*R,R*)-**1** as a *crystalline* compound [92%, m.p. 69–70.5 °C (*n*-hexane), $[\alpha]_D = -151.4°$ ($c = 4$, $CHCl_3$)]. The configuration of the newly-generated chiral center in the crystalline compound was determined (Fig. 1) by X-ray structural analysis[27] of a single crystal of the hydrochloride, (*R,R*)-**1**·HCl.

Structural studies on the chiral lithium amide $[(R,R)\text{-}\mathbf{2}]_n$ have been performed[28] in conjunction with the investigations of its suitability and selectivity as a chiral base. Lithiation of (*R,R*)-**1** proceeds under a variety of conditions, and, in non-donor solvents, affords, upon crystallization, a dimeric amidolithium complex,[29] i.e. $n = 2$. This complex has been characterized in the solid state by X-ray crystallography[27] and in solution by NMR spectroscopy and cryoscopy. The crystal structure (Fig. 2) reveals a central, planar Li_2N_2 ring, each Li cation of which is also coordinated by two methoxy groups, one from each amido ligand.[30–34] The geometry at each Li cation is distorted tetrahedral with the largest departures from tetrahedral geometry being for the N–Li–O angles within the five-membered chelate rings.[34–36] There are similar distortions in tetrahedral geometry at each amido nitrogen, being largest within the Li_2N_2 ring. The four-membered Li_2N_2 ring has an atypical structure in which the N–Li bonds (ca. 2.06 Å) associated with one ligand are longer than those (ca. 2.02 Å) associated with the other. Usually, in dimeric amidolithium complexes, N–Li bonds on opposite sides of the Li_2N_2 ring are of near identical lengths.[37] The approximate D_2 molecular symmetry observed in the solid state represents one of the two possible constitutional isomers: the other has C_2 symmetry.[38]

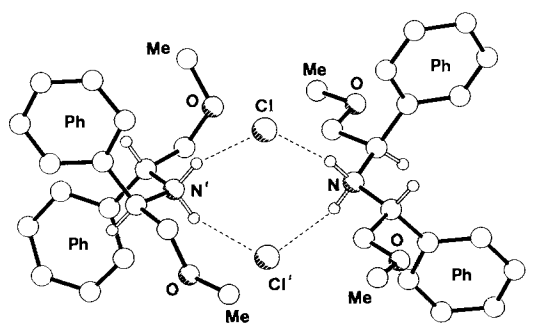


Fig. 1. Structure of (*R,R*)-**1** · HCl in the crystal. Crystal data: orthorhombic, $a = 8.247(2)$, $b = 17.333(5)$, $c = 25.384(6)$ Å, $V = 3629$ Å^3, space group $P2_12_12_1$, $Z = 8$ (2 crystallographically independent molecules), $\varrho = 1.18$ g cm^{-3}, $\mu(Cu_{K\alpha}) = 19$ cm^{-1}, 1887 independent reflections $[|F_o| > 3\,\sigma(|F_o|)$, $\theta \leq 58°]$, $R = 0.10$. The two independent molecules are bridged via hydrogen bonds between the dialkylammonium centers (N and N') and the chloride (Cl and Cl') counterions. Hydrogen bonding geometries: [N ··· Cl] 3.10, [N' ··· Cl] 3.18, [N ··· Cl'] 3.15, [N' ··· Cl'] 3.20 Å. N–H ··· Cl angles in the range, 154–166°.

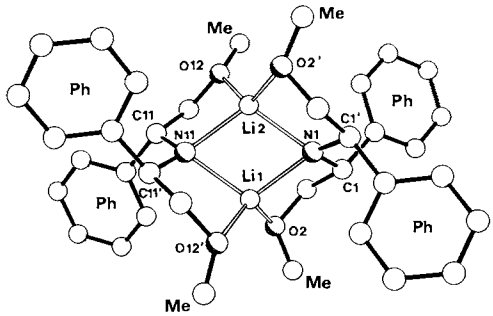


Fig. 2. Structure of $[(R,R)\text{-}\mathbf{2}]_2$ in the crystal. Crystal data: orthorhombic, $a = 10.508(4)$, $b = 15.688(4)$, $c = 20.918(5)$ Å, $V = 3448$ Å^3, space group $P2_12_12_1$, $Z = 4$, $\varrho = 1.12$ g cm^{-3}, $\mu(Cu_{K\alpha}) = 5$ cm^{-1}, 1562 independent observed reflections $[|F_o| > 3\,\sigma(|F_o|)$, $2\theta \leq 116°]$, $R = 0.077$, $R_w = 0.073$. Geometry about the Li_2N_2 ring. Bond lengths [Å]: Li(1)-N(1) 2.061(16), Li(1)-O(2) 1.977(16), Li(1)-N(11) 2.023(17), Li(1)-O(12') 1.996(16), Li(2)-N(1) 2.063(16), Li(2)-O(2') 2.017(14), Li(2)-N(11) 2.024(16), Li(2)-O(12) 1.977(14). Bond angles [°]: N(1)-Li(1)-O(2) 88.0(6), N(1)-Li(1)-N(11) 107.2(7), O(2)-Li(1)-N(11) 123.9(8), N(1)-Li(1)-O(12') 127.5(8), O(2)-Li(1)-O(12') 123.6(8), N(11)-Li(1)-O(12') 89.2(7), N(1)-Li(2)-O(2') 86.8(6), N(1)-Li(2)-N(11) 107.1(7), O(2')-Li(2)-N(11) 127.5(7), N(1)-Li(2)-O(12) 125.5(7), O(2')-Li(2)-O(12) 125.7(8), N(11)-Li(2)-O(12) 87.1(6), Li(1)-N(1)-Li(2) 72.0(6), Li(1)-N(1)-C(1) 105.8(6), Li(2)-N(1)-C(1) 133.7(6), Li(1)-N(1)-C(1') 129.6(6), Li(2)-N(1)-C(1') 107.6(6), C(1)-N(1)-C(1') 107.7(6), Li(1)-N(11)-Li(2) 73.6(6), Li(1)-N(11)-C(11) 133.2(6), Li(2)-N(11)-C(11) 105.7(6), Li(1)-N(11)-C(11') 105.4(6), Li(2)-N(11)-C(11') 130.3(6), C(11)-N(11)-C(11') 108.6. The torsion angles within the Li_2N_2 ring are, within statistical significance, all zero. The transannular Li(1) ··· Li(2) = 2.425(21) Å.

NMR (^{1}H, ^{7}Li, ^{13}C) spectroscopic studies[39] in non-donor solvents (C_6D_6, $C_6D_5CD_3$) from ambient temperature down to ca. −90 °C indicate the presence of a *single, highly symmetrical* lithium amide species. On the basis of cryoscopic measurements[40] in benzene, this species is dimeric. Therefore, there is strong evidence that the observed solid-state structure persists on dissolving in non-donor solvents, thus producing a dimer, $[(R,R)\text{-}\mathbf{2}]_2$, with averaged D_2 molecular symmetry. Knowledge of the existence of $[(R,R)\text{-}\mathbf{2}]_2$ in solution will aid the investigations of substrate deprotonations and subsequent asymmetric electrophilic additions to the derived lithium enolates.[4]

In the case of chiral lithium amides, an appreciation of their coordination chemistry is a prerequisite to understanding their roles in reagent-controlled asymmetric inductions.[41]

Experimental

(*R*)-**5**/(*R,R*)-**6**/(*R,S*)-**6**: (*R*)-phenylglycinol (*R*)-**3** (8.45 g, 98% pure, 60.4 mmol), α-methoxyacetophenone **4** (9.54 g, 95% pure, 60.4 mmol), and *p*-TsOH (115 mg, 0.6 mmol) in C_6H_6 (70 mL) were heated under reflux (N_2) with continuous removal of H_2O. After 72 h, the mixture was cooled to room temperature, diluted with Et_2O (50 mL), cooled to $-5\,^{\circ}C$, and washed sequentially with 5% aqueous $NaHCO_3$ and saturated aqueous NaCl solutions. A standard work-up procedure afforded 15.65 g (96%) of a yellow oil, which was characterized as a mixture of (*R*)-**5**, (*R,R*)-**6**, and (*R,S*)-**6**, *m/z* (CIMS): 270 for $(M + H)^{\oplus}$; ^1H NMR ($CDCl_3$): $\delta = 3.05$ (br s, 2H), 3.43–3.79, 4.14, 4.44, and 4.69 (s and m, 8H), 7.22–7.41 (m, 6H), 7.62–7.71 (m, 2H), cf. Ref. [23a]: ^{13}C NMR ($CDCl_3$) spectroscopy revealed the presence of two resonances at $\delta = 98.7$ and 99.7 characteristic of the diastereoisomerically-related quaternary carbon atoms in the oxazolidine rings of (*R,R*)-**6** and (*R,S*)-**6**.

(*R,R*)-**7** and (*R,S*)-**7**: (*R*)-**5**/(*R,R*)-**6**/(*R,S*)-**6** (15.65 g, 58.2 mmol) in dry Et_2O (50 mL) was added dropwise with stirring to a suspension of $LiAlH_4$ (2.18 g, 57.4 mmol) in dry Et_2O (10 mL) under N_2 at $-20\,^{\circ}C$. After the addition was complete, stirring was continued for 16 h at this temperature. A standard work-up procedure gave the crude product which was eluted on a short SiO_2 chromatography column (*n*-hexane/EtOAc:2/1 v/v) to give a mixture (13.25 g, 84%) of the diastereoisomeric products (*R,R*)-**7** and (*R,S*)-**7**. Fractional crystallization (*n*-hexane/Et_2O (9/1 v/v): solubility 0.1 g mL^{-1}) gave firstly fine needles of (*R,S*)-7 [2.73 g, 17%, m.p. 97.5–98 °C, $[\alpha]_D = -18.3^{\circ}$ ($c = 3$, $CHCl_3$); *m/z* (CIMS): 272 $(M + H)^{\oplus}$; ^1H NMR ($CDCl_3$): $\delta = 2.30$ (br s, 2H), 3.34 (s, 3H), 3.55 (d, 2H), 3.55–3.62 (m, 1H), 3.75–3.82 (m, 1H), 3.85–3.91 (m, 1H), 3.95 (t, 1H), 7.20–7.29 (m, 10H)] and subsequently from the mother liquors, colorless microcrystalline (*R,R*)-7 [7.55 g, 48%, m.p. 77.5–79.5 °C, $[\alpha]_D = -96.1^{\circ}$ ($c = 1.2$, $CHCl_3$); *m/z* (CIMS): 272 $(M + H)^{\oplus}$; ^1H NMR ($CDCl_3$): $\delta = 2.40$ (br s, 2H), 3.32 (s, 3H), 3.29–3.64 (m, 5H), 3.79–3.85 (m, 1H), 7.17–7.22 (m, 2H), 7.24–7.40 (m, 8H)].

(*R,R*)-**1**: (*R,R*)-**7** (4.10 g, 15.1 mmol) in dry THF (12 mL) was added dropwise with stirring over 15 min to a suspension of NaH (500 mg, 80% dispersion in oil, 16.7 mmol) in dry THF (3 mL) under N_2. The mixture was warmed to 40 °C and stirred for 30 min to give a clear solution. This was cooled to $-5\,^{\circ}C$ prior to dropwise addition of MeI (2.20 g, 15.5 mmol) in dry THF (5 mL) within 30 min. The mixture was then allowed to warm up to room temperature and stirred for 16 h. Excess of NaH was destroyed with H_2O and the product was extracted into Et_2O. Flash column chromatography on SiO_2 (*n*-hexane/EtOAc: 2/1 v/v) furnished pure (*R,R*)-**1** (3.96 g, 92%, m.p. 69–70.5 °C, crystallized from *n*-hexane). Alternatively, crystallization of the crude product directly from *n*-hexane (solubility 0.5 g mL^{-1}) afforded pure crystalline (*R,R*)-**1** [3.31 g, 77%, m.p. 69–70.5 °C, $[\alpha]_D = -151.4^{\circ}$ ($c = 4$, $CHCl_3$); *m/z* (CIMS): 286 $(M + H)^{\oplus}$; ^1H NMR ($CDCl_3$): $\delta = 2.30$ (br s, 1H), 3.29 (s, 6H), 3.38–3.57 (m, 4H), 3.64–3.70 (m, 2H), 7.22–7.37 (m, 10H); ^1H NMR (C_6D_6): $\delta = 2.99$ (s, 6H), 3.30 (br s, 1H), 3.35–3.42 (m, 4H), 3.82–3.85 (m, 2H), 7.13–7.34 (m, 10H)]. The hydrochloride (*R,R*)-**1** · HCl was prepared by dissolving (*R,R*)-**1** in methanolic HCl and evaporating in vacuo. Single crystals suitable for X-ray crystallography were obtained by the vapor diffusion method ($CHCl_3$/*n*-pentane).

(*R,S*)-**1**: (*R,S*)-7 (0.35 g, 1.3 mmol) was *O*-methylated in the manner described above for (*R,R*)-**1** to afford (*R,S*)-**1** [0.33 g, 90%, $[\alpha]_D = 0^{\circ}$ ($c = 1-5$, $CHCl_3$); *m/z* (CIMS) 286 $(M + H)^{\oplus}$; ^1H NMR ($CHCl_3$): $\delta = 2.45$ (br s, 1H), 3.34 (s, 6H), 3.51 (d, 4H), 3.94 (t, 2H), 7.14–7.27 (m, 10H)]. (*R,S*)-**1** was characterized as its hydrochloride (*R,S*)-**1** · HCl (m.p. 150.5–154 °C). Single crystals of the hydrochloride, suitable for X-ray crystallography, were obtained by the vapor diffusion method ($CHCl_3$/*n*-pentane).

[(*R,R*)-**2**]$_2$: *n*-BuLi (2.6 mL of a 1.62 M solution in hexane, 4.2 mmol) was added under N_2 to a stirred, chilled suspension of (*R,R*)-**1** (1.20 g, 4.2 mmol) in dry hexane (5 mL). Stirring caused complete dissolution of the amine. After 30 min stirring at room temperature, the mixture was stored at $-5\,^{\circ}C$ for 16 h. The resulting air sensitive, microcrystalline solid was filtered under N_2, dried in vacuo, and characterized as [(*R,R*)-**2**]$_2$ [1.0 g, 82%, m.p. 165 °C dec., Found C 74.4%, H 7.6%, N 4.8%, Li 2.5%, Calc. for $C_{18}H_{22}NLiO_2$ = C 74.2%, H 7.5%, N 4.8%; Li 2.4%; ^1H NMR ($C_6D_5CD_3$): $\delta = 3.10$ (dd, 2H), 3.15 (s, 6H), 3.65 (dd, 2H), 4.08 (br dd, 2H), 7.04–7.10 (m, 2H), 7.16 (dd, 4H), 7.30 (dd, 4H); ^1H NMR (C_6D_6): $\delta = 3.20$ (s, 6H), 3.20–3.23 (m, 2H), 3.79 (t, 2H), 4.27 (br dd, 2H), 7.15–7.23 (m, 2H), 7.31 (t, 4H), 7.47 (d, 4H); ^{13}C NMR (C_6D_6): $\delta = 58.5, 65.3, 81.3, 126.6, 128.3, 128.8, 147.8$]. Single crystals, suitable for X-ray crystallography, were isolated from a sixfold diluted solution in *n*-hexane. The crystals were sealed under N_2 in Lindemann capillary tubes prior to data collection.

Received: March 8, 1989 [Z 3218 IE]
German version: *Angew. Chem. 101* (1989) 1048

CAS Registry numbers:
(*R,R*)-**1**, 121959-66-8; (*R,R*)-**1**·HCl, 121958-26-7; (*R,S*)-**1**, 121868-98-2; (*R,S*)-**1**·HCl, 121868-99-3; [(*R,R*)-**2**] monomer, 121958-27-8; [(*R,R*)-**2**] dimer, 121886-95-1; (*R*)-**3**, 56613-80-0; **4**, 4079-52-1; (*R*)-**5**, 121868-96-0; (*R,R*)-**6**, 103621-11-0; (*R,S*)-**6**, 103621-12-1; (*R,R*)-7, 121868-97-1; (*R,S*)-**7**, 121958-25-6.

[1] For examples of enantioselective reductions and cyanohydrin formation, see J. F. Stoddart, *Biochem. Soc. Trans. 15* (1987) 1188, and references therein; for examples of trebly diastereoselective Diels-Alder reactions, see J. F. Stoddart, *Chem. Br. 24* (1988) 1203.

[2] a) S. M. Doughty, J. F. Stoddart, H. M. Colquhoun, A. M. Z. Slawin, D. J. Williams, *Polyhedron 4* (1985) 567; b) D. R. Armstrong, D. Barr, W. Clegg, S. M. Hodgson, R. E. Mulvey, D. Reed, R. Snaith, D. S. Wright, *J. Am. Chem. Soc. 111* (1989) 4719.

[3] N. S. Simpkins, *Chem. Ind. (London) 1988*, 387.

[4] D. Seebach, *Angew. Chem. 100* (1988) 1685; *Angew. Chem. Int. Ed. Engl. 27* (1988) 1624, and references therein.

[5] L. Duhamel, P. Duhamel, J.-C. Launay, J.-C. Plaquevent, *Bull. Soc. Chim. Fr. 1984*, II-421.

[6] a) H. Hogeveen, L. Zwart, *Tetrahedron Lett. 1982*, 105; b) M. B. Eleveld, H. Hogeveen, *ibid. 27* (1986) 631.

[7] a) J. K. Whitesell, S. W. Felman, *J. Org. Chem. 45* (1980) 755; b) M. Asami, *Chem. Lett. 1984*, 829; c) M. Asami, H. Kirihara, *ibid. 1987*, 389; d) S. K. Hendrie, J. Leonard, *Tetrahedron 43* (1987) 3289; M. Asami, N. Kanemaki, *Tetrahedron Lett. 30* (1989) 2125.

[8] a) N. S. Simpkins, *J. Chem. Soc. Chem. Commun. 1986*, 88; b) C. M. Cain, N. S. Simpkins, *Tetrahedron Lett. 28* (1987) 3723.

[9] a) R. Shirai, M. Tanaka, K. Koga, *J. Am. Chem. Soc. 108* (1986) 543; b) A. E. Greene, A. A. Serra, E. J. Barreiro, P. R. R. Costa, *J. Org. Chem. 52* (1987) 1169; H. Hemmerle, H.-J. Gais, *Angew. Chem. 101* (1989) 363; *Angew. Chem. Int. Ed. Engl. 28* (1989) 349.

[10] L. Duhamel, A. Ravard, J. C. Plaquevent, D. Davoust, *Tetrahedron Lett. 28* (1987) 5517.

[11] a) T. Yamashita, H. Mitsui, H. Watanabe, N. Nakamura, *Bull. Soc. Chem. Jpn. 55* (1982) 961; b) A. Ando, T. Shioiri, *J. Chem. Soc. Chem. Commun. 1987*, 656.

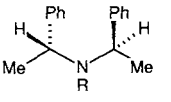
[12] H. Hogeveen, W. M. P. B. Menge, *Tetrahedron Lett. 27* (1986) 2767.

[13] a) For early related studies see: S. Brandänge, S. Josephson, L. Mörch, S. Vallén, *Acta Chem. Scand. B 35* (1981) 273; b) D. Seebach, *Proc. Robert A. Welch Found. Conf. Chem. Res. 27* ("Stereospecificity in Chemistry and Biochemistry") Houston 1983, p. 93; c) C. H. Heathcock in J. D. Morrison (Ed): *Asymmetric Synthesis, Vol. 3B*, Academic Press, New York 1984, p. 111; d) J. Mulzer, P. de Lasalle, A. Chucholowski, U. Blaschek, G. Brüntrup, I. Jibril, G. Huttner, *Tetrahedron 40* (1984) 2211; e) A. Ando, T. Shioiri, *J. Chem. Soc. Chem. Commun. 1987*, 1620; f) M. Muroaka, H. Kawasaki, K. Koga, *Tetrahedron Lett. 29* (1988) 337.

[14] A. C. Regan, J. Staunton, *J. Chem. Soc. Chem. Commun. 1983*, 764; 1987, 520.

[15] J. A. Marshall, J. Lebreton, *Tetrahedron Lett. 28* (1987) 3323; *J. Am. Chem. Soc. 110* (1988) 2925.

[16] For the synthesis of C_2-symmetric chiral secondary amines, see J. K. Whitesell, S. W. Felman, *J. Org. Chem. 42* (1977) 1663; K. E. Harding, S. R. Burks, *ibid. 46* (1981) 3920; K. E. Harding, T. H. Marman, *ibid. 49* (1984) 2838; Y. Kawanami, Y. Ito, T. Kitagawa, Y. Taniguchi, T. Katsuki, M. Yamaguchi, *Tetrahedron Lett. 25* (1984) 857; R. E. Gawley, G. Hart, M. Goicoechea-Pappas, A. L. Smith, *J. Org. Chem. 51* (1986) 3076; T. K. M. Shing, *J. Chem. Soc. Chem. Commun. 1987*, 262; R. Schlessinger, E. J. Iwanowicz, *Tetrahedron Lett. 28* (1987) 2083; R. E. Gawley, S. R. Chemburkar, A. L. Smith, T. V. Anklekar, *J. Org. Chem. 53* (1988) 5381; J. K. Whitesell, M. A. Minton, K. M. Chen, *ibid. 53* (1988) 5383; R. P. Short, R. M. Kennedy, S. Masamune, *ibid. 54* (1989) 1755. By far the most popular chiral lithium amide is (*R,R*)-**II** and its enantiomer (*S,S*)-**II**: see Refs. [3], [6], [7a], [10], [12] and [15]. The chiral amine (*R,R*)-**I** was first reported in 1961 (C. G. Overberger, N. P. Marullo, R. G. Hiskey, *J. Am. Chem. Soc. 83* (1961) 1374; see also Ref. [6]).



(*RR*)-**I** R = H

[(*RR*)-**II**]$_n$ R = Li

[17] While a number of chiral lithium amides possess these structural features (see Ref. [13c]), none have chiral centers that carry large substituents α to the N–Li bond.

[18] Intramolecular coordination not only provides transition-state rigidity but it also enhances lithium enolate-chiral amine complexation. Even in non-chelating achiral systems, the coordinated amine present, after deprotonation, exerts a profound mechanistic effect on the reactivity of a lithium enolate towards, for example, deuterium cations (T. Laube, J. D. Dunitz, D. Seebach, *Helv. Chim. Acta 68* (1985) 1373). Chiral amines, which *lack* extra intramolecular coordinating groups and are present after deprotonation of a substrate, can impart stereoselectivities upon subsequent electrophilic additions to that substrate; cf. Refs. [3], [5], [6], [12], [13a], and [15].

[19] The enantiomer (*S,S*)-**1** [m.p. 65 °C; $[\alpha]_D = 154.1^{\circ}$ ($c = 2.5$, $CHCl_3$)] has also been synthesized (D. J. Berrisford, R. V. H. Jones, D. P. Robinson, and J. F. Stoddart, unpublished results).

[20] Subscript *n* is the aggregation number of the amidolithium complex, i.e. a monomer has $n = 1$, a dimer has $n = 2$, etc.

 © VCH Verlagsgesellschaft mbH, D-6940 Weinheim, 1989 0570-0833/89/0808-1046 $ 02.50/0

[21] Both enantiomers of phenylglycinol are commercially-available. (*R*)-**3** and (*S*)-**3** can also be obtained by reduction ($BH_3 \cdot SMe_2$) of (*R*)- and (*S*)-phenylglycine, respectively (A. I. Meyers, J. Slade, *J. Org. Chem. 45* (1980) 2785).

[22] α-Methoxyacetophenone **4** (R. B. Moffett, R. L. Shriner in E. C. Horning (Ed.): *Organic Synthesis, Coll. Vol. 3*, Wiley, New York 1955, p. 562) is commercially available.

[23] M. B. Eleveld, H. Hogeveen, E. P. Schudde, *J. Org. Chem. 51*(1986) 3635. ^{1}H NMR spectrum of the product obtained after *O*-methylation. Direct integration of the mixture of hydroxyamines (*R,R*)-7 and (*R,S*)-7 was less reliable because of accidental equivalence of the resonances for the constitutionally-related protons in the diastereoisomers.

[25] Use of $[(CH_3OCH_2CH_2O)_2AlH_2]Na$/THF/ − 78 °C gave a ratio (*R,S*)-7:(*R,R*)-7 of 4:1.

[26] Solutions of both (*R,S*)-**1** and (*R,S*)-**1** · HCl in various solvents were found to be optically inactive. Unfortunately, a definitive configurational assignment was not obtained from an X-ray crystallographic study of (*R,S*)-**1** · HCl. This is probably attributable to partial rotational disorder within the structure with a pseudo C_2 axis passing through the dialkylammonium center thus producing an apparent flattening of the geometry about the two chiral carbon atoms. Crystal data: monoclinic, $a = 10.602(3)$, $b = 7.152(2)$, $c = 12.275(4)$ Å, $\beta = 103.24(2)°$, $V = 906$ Å^3, space group $P2_1$, $Z = 2$, $\varrho = 1.18$ g cm^{-3}, $\mu(Cu_{K\alpha}) = 19$ cm^{-1}. 926 independent reflections [$|F_o| > 3\,\sigma(|F_o|)$, $\theta \leq 58°$], $R = 0.097$.

[27] Nicolet R3m diffractometer, ω scans, $Cu_{K\alpha}$ radiation (graphite monochromator). The structures were solved by direct methods and refined anisotropically. Further details of these structural investigations can be obtained from the Director of the Cambridge Data Centre, University Chemical Laboratory, Lensfield Road, Cambridge CB2 1EW (England). Any request should be accompanied by the full literature citation for this communication.

[28] For a review of organolithium structural chemistry including amidolithium species, see W. N. Setzer, P. von R. Schleyer, *Adv. Organomet. Chem. 24* (1985) 353.

[29] The IR spectrum (nujol mull) of the amidolithium complex [(*R,R*)-**2**]$_2$ contained no bands characteristic of the presence of NH or LiOH. However, brief exposure to (moist) air resulted in the immediate appearance of bands at $\tilde{\nu} = 3550$ cm^{-1} (NH) and 3677 cm^{-1} (OH).

[30] The solid state structure (Fig. 2) is in accord with the structural principles underpinning amidolithium chemistry, i.e. the preferences between rings, stacks, and ladders: D. R. Armstrong, D. Barr, W. Clegg, R. E. Mulvey, D. Reed, R. Snaith, K. Wade, *J. Chem. Soc. Chem. Commun. 1986*, 869; W. Clegg, R. Snaith, K. Wade, *Inorg. Chem. 27* (1988) 3861 and references cited therein. See also Refs. [2b] and [36].

[31] The related complexes $[(PhCH_2)_2NLi \cdot Et_2O]_2$ and $[(PhCH_2)_2NLi \cdot HMPA]_2$ are dimeric ($n = 2$) and in the solid state form Li_2N_2 rings with extra coordination from the added neutral donors (see Refs. [32d] and [36]).

[32] For examples of amidolithium compounds with Li_2N_2 rings that have been characterized by X-ray crystallography, see a) M. F. Lappert, M. J. Slade, A. Singh, J. L. Atwood, R. D. Rogers, R. Shakir, *J. Am. Chem. Soc. 105* (1983) 302; b) L. M. Engelhardt, A. S. May, C. L. Raston, A. H. White, *J. Chem. Soc. Dalton Trans. 1983*, 1671; c) B. Çetinkaya, P. B. Hitchcock, M. F. Lappert, M. C. Misra, A. J. Thorne, *J. Chem. Soc. Chem. Commun. 1984*, 148 ; d) D. Barr, W. Clegg, R. E. Mulvey, R. Snaith, *ibid. 1984*, 285; e) L. M. Engelhardt, B. S. Jolly, P. C. Junk, C. L. Raston, B. W. Skelton, A. H. White, *Aust., J. Chem. 39* (1986) 1337; f) R. A. Wanat, D. B. Collum, G. Van Duyne, J. Clardy, R. T. Depue, *J. Am. Chem. Soc. 108* (1986) 3415; g) D. Barr, W. Clegg, R. E. Mulvey, R. Snaith, D. S. Wright, *J. Chem. Soc. Chem. Commun. 1987*, 716; h) R. A. Bartlett, H. Chen, H. V. Rasika Dias, M. M. Olmstead, P. P. Power, *J. Am. Chem. Soc. 110* (1988) 446.

[33] For recent examples of Li_2N_2 rings in related structures, see D. Colgan, R. I. Papasergio, C. L. Raston, A. H. White, *J. Chem. Soc. Chem. Commun. 1984*, 1708; H. Dietrich, W. Mahdi, R. Knorr, *J. Am. Chem. Soc. 108* (1986) 2462; R. Hacker, E. Kaufmann, P. von R. Schleyer, W. Mahdi, H. Dietrich, *Chem. Ber. 120* (1987) 1533; L. M. Jackman, L. M. Scarmoutzos, B. D. Smith, P. G. Williard, *J. Am. Chem. Soc. 110* (1988) 6058.

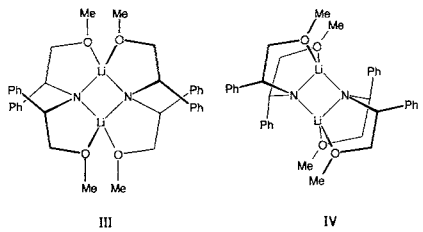
[34] In the solid state, intramolecular chelation of the ether oxygen atoms in aza-enolates has been observed to give (i) a four-membered ring (D. Seebach, W. Bauer, J. Hansen, T. Laube, W. B. Schweizer, J. D. Dunitz, *J. Chem. Soc. Chem. Commun. 1984*, 853) and (ii) a six-membered ring (D. Enders, G. Bachstädter, K. A. M. Kremer, M. Marsch, K. Harms, G. Boche, *Angew. Chem. 100* (1988) 1580; *Angew. Chem. Int. Ed. Engl. 27* (1988) 1522).

[35] Alkyllithium chemistry provides many examples of intramolecular chelation (G. W. Klumpp, *Recl. Trav. Chim. Pays-Bas 105* (1986) 1).

[36] In contrast to $[(PhCH_2)_2NLi]_3$, $[(PhCH_2)_2NLi \cdot Et_2O]_2$, and $[(PhCH_2)_2NLi \cdot HMPA]_2$ (donor:$Li^{\oplus}$ ratios 0:1, 1:1, and 1:1, respectively), no evidence has been found for an agostic C–H–M interaction in [(*R,R*)-**2**]$_n$. See D. R. Armstrong, R. E. Mulvey, G. T. Walker, D. Barr, R. Snaith, W. Clegg, D. Reed, *J. Chem. Soc. Dalton Trans. 1988*, 617. This is probably a consequence of the increased neutral donor:$Li^{\oplus}$ ion ratio of 2:1 in [(*R,R*)-**2**]$_n$.

[37] Typically, X-ray crystal structure determinations of Li_2N_2 rings reveal nonequivalence ($a \neq b$) of the N–Li bond lengths. An alternate *abab* cyclic pattern is often observed (Ref. [32]). However, [(*R,R*)-**2**]$_2$ shows a contrasting *aabb* pattern scattered around mean N–Li bond lengths (Fig. 2) that correspond with those reported.

[38] The coordination geometry of the dimeric species could be associated with either D_2 symmetry (**III**) or C_2 symmetry (**IV**). In the dimers **III** and **IV**, the two homotopic amide ligands contain, respectively, homotopic and diastereotopic 5-membered chelate rings.
The coordination geometries and ring distortions are at present being investigated by ab initio and MO calculations on model systems in collaboration with Dr. *D. R. Armstrong* (University of Strathclyde, UK).



III IV

[39] The broad-band decoupled ^{13}C NMR spectrum (63.5 MHz, C_6D_6) shows only seven signals and is therefore not at variance with a dimeric structure [(*R,R*)-**2**]$_2$ possessing averaged D_2 molecular symmetry. This conclusion is supported by variable temperature ^{7}Li NMR spectroscopy (140 MHz, $C_6D_5CD_3$, PhLi as external reference) which (i) reveals a singlet at $\delta = 0.083$ (0.062 M solution) or $\delta = 0.085$ (0.206 M solution) and (ii) produces only slight chemical shift variations on cooling down to − 90 °C. ^{1}H NMR spectroscopy (360 MHz, $C_6D_5CD_3$) reveals a single lithium amide species at ambient temperature which persists on cooling down to − 90 °C. A minor component is also observed in a proportion of < 5% which is independent of concentration (0.062–0.206 M) and temperature. This is unequivocally the parent amine (*R,R*)-**1** resulting from partial hydrolysis of the lithium amide during the experiments. No spectroscopic evidence for constitutional isomerism or aggregation equilibria is observed. We thank Dr. *D. Reed* (SERC NMR Service, University of Edinburgh) for his assistance in obtaining some of these spectra.

[40] Cryoscopic measurements were performed on a sample of [(*R,R*)-**2**]$_2$ in benzene in the concentration range 0.07–0.12 M to give a supramolecular mass of 551 ± 12, i.e. $n = 1.90 \pm 0.04$. The slight variance from $n = 2.0$ cannot arise from an amidolithium dimer-monomer equilibrium since this would be concentration dependent. The low value can be attributed to partial hydrolysis to the parent amine (*R,R*)-**1** prior to or during the measurement (see Ref. [39]).

[41] Efficient asymmetric deprotonation of 4-*tert*-butylcyclohexanone has been demonstrated using [(*R,R*)-**2**]$_n$ in toluene/HMPA. An internal enolate quench with trimethylsilyl chloride gives (*R*)-4-*tert*-butyl-1-[(trimethylsilyl)oxy]cyclohexene in 84% enantiomeric excess.

Platinum Complexes of the Anions $Se_2N_2^{2\ominus}$ and $Se_2N_2H^{\ominus}$; X-Ray Structure Analysis of $[Pt(Se_2N_2H)(PMe_2Ph)_2]Cl$

By *Paul F. Kelly, Ivan P. Parkin, Alexandra M. Z. Slawin, David J. Williams,* and *J. Derek Woollins**

We are actively involved in the preparation of metal–sulfur–nitrogen compounds since they often stabilize otherwise unknown SN anions and, as in the case of **1**

$[Pt(S_2N_2H)(PR_3)_2]X$ **1**

have solid state structures in which both the anions and cations stack.[1, 2] In contrast to SN chemistry the only known SeN heterocycle is Se_4N_4. However, in the light of the extreme stability of **1** we considered that once formed the selenium analogues of **1** would be easily handled and could lead to the development of new SeN chemistry as well as

[*] Dr. J. D. Woollins, Dr. P. F. Kelly, I. P. Parkin, A. M. Z. Slawin, Dr. D. J. Williams
Department of Chemistry, Imperial College of Science and Technology
South Kensington, London SW7 2AY (UK)

having interesting solid state properties. There has recently been a report[3] on the reaction of Se_4N_4 with WCl_6 to give $[WCl_4(NSeCl)]_2$. We have found[4, 5] that S_4N_4 reacts with **2** and **3** to give $[PtCl(S_2N_2H)(PR_3)]/[PtCl(S_3N)(PR_3)]$ and

cis-$[PtCl_2(PR_3)_2]$ **2**

$[Pt(PMe_2Ph)Cl_2]_2$ **3**

$[PtCl_2(PMe_2PH)(S_4N_4)]$, respectively. These observations prompted us to investigate reactions of Se_4N_4 with **2**, PR_3 = ½ $PPh_2CH_2CH_2PPh_2$(dppe), PPh_3, PMe_2Ph, PEt_3, and **3**. Upon refluxing a solution of Se_4N_4 and **2** in xylene at 160 °C, no reaction was observed. (**Caution:** Se_4N_4, being much more unstable than S_4N_4 explodes violently on contact with a metal spatula!)

Reaction of Se_4N_4 with **3** in refluxing $CHCl_3$, however, gave a mixture of products, including **4**,

$[PtCl(Se_3N)(PMe_2Ph)]$ **4**

which we have recently characterized by X-ray crystallography.[6] We have now been able to separate the other major product chromatographically and to identify it by mass spectroscopy as **5**.

$[PtCl(Se_2N_2H)(PMe_2Ph)]$ **5**

Unlike its sulfur analogue, **5** is not especially stable in solution and we have been unable to crystallize it. However, as was the case with the sulfur system, reaction of the crude mixture of **4** and **5** results in displacement of the halogen by phosphane to give **6** which was readily crystallized.

$[Pt(Se_2N_2H)(PMe_2Ph)_2]Cl$ **6**

The X-ray structure of **6** (Figure 1)[7] reveals an essentially planar $P_2PtSe_2N_2$ unit[8] with the expected differences in the Pt–P(1) and Pt–P(2) bond-lengths, reflecting the *trans* influence of the selenium and nitrogen substituents. The lengths of the Pt–P bonds are essentially unchanged from those in the sulfur analogue **1**.[2] The bond-lengths within the $PtSe_2N_2$ ring follow the pattern already observed, i.e. E(2)–N(2) > E(1)–N(1) > E(1)–N(2) (E = S or Se), although the differences are less marked in **6** than in **1**. There is, as expected, a small increase in the Se–Pt–N angle to accomodate the longer bonds in the $PtSe_2N_2$ ring together with a decrease in the readily deformed angles about Se(1) and Se(2); the angles at nitrogen are virtually unchanged on going from **1** to **6**. In contrast to **1** there is no longer approximate C_2 symmetry within the cations in **6**. A consequence of this is a change in the packing of the cations. Whereas in **1** (PR_3 = PMe_2Ph, X = Cl) the structure is comprised of continuous alternately stacked dimer pairs, here discrete pairs of cations pack with their $PtSe_2N_2$ rings parallel and overlapping (Fig. 2) with

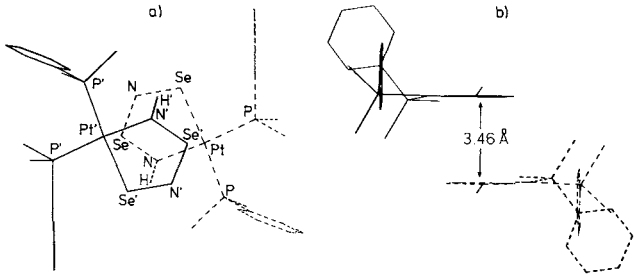


Fig. 2. (a) Plan view of **6** and (b) side view of **6** showing the stacking geometry of the dimer pairs; the Pt · · · Se′/Pt′ · · · Se distance is 3.52 Å.

an interplanar separation of 3.46 Å and a Pt · · · Se1′/Pt′ · · · Se(1) distance of 3.52 Å.[9]

A slightly surprising feature of the structure of **6** is the relative dispositions of the anions and cations. Although the $Cl^{\ominus}$ ion is available for H-bonding, lying adjacent to the N(1)–H group, the N–H · · · Cl geometry is not optimum and, indeed, the $Cl^{\ominus}$ ion lies closer to Se(1) (3.11 Å) than to N(1) (3.19 Å).

Compounds **4**–**6** are the first examples of complexes containing Se–N anions and demonstrate that the $PtSe_3N$ and $PtSe_2N_2$ rings are stable. However, the synthetic strategy described above is not completely satisfactory since Se_4N_4 is extremely hazardous and the yields are low (the overall yield of **6** is ca. 2%). We have therefore developed a new method using liquid ammonia. Thus, addition of $SeCl_4$ to liquid ammonia gives a pale orange solution and a green precipitate [**Caution:** The precipitate can explode violently at room temperature or on addition of water], which, if allowed to warm to room temperature in a pressure vessel, gives Se_4N_4. However, if **2** is added to the mixture in liquid ammonia and the reaction allowed to warm to room temperature under a stream of argon **7** is isolated in up to 70% yield. Compound

$[Pt(Se_2N_2)(PR_3)_2]$ **7**

7 can be protonated to give **8** (ca. 80% isolated yield, quantitatively by NMR). This new "one-pot" synthesis is ex-

$[Pt(Se_2N_2H)(PR_3)_2]BF_4$ **8**

tremely convenient, relatively hazard free, and allows for the preparation of reasonable amounts of metal–selenium–nitrogen compounds which may be of use in the synthesis of new heterocycles. The existence of **4**–**8** suggests that a substantial chemistry of Se–N anions awaits elucidation.

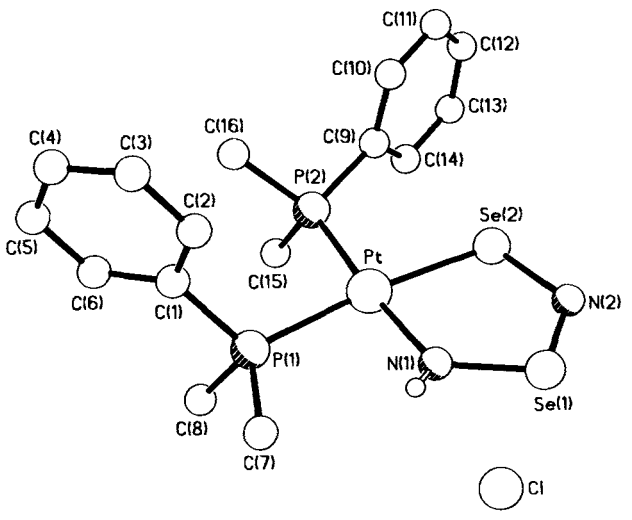


Fig. 1. The structure of **6** in the crystal. Selected bond lengths [Å] and angles: Pt–P(1) 2.305(3), Pt–P(2) 2.260(4), Pt–N(1) 2.021(10), Pt–Se(2) 2.405(1), N(1)–Se(1) 1.758(11), Se(1)–N(2) 1.718(10), N(2)–Se(2) 1.794(11); P(1)–Pt–P(2) 95.4(1), N(1)–Pt–Se(2) 87.1(3), Pt–N(1)–Se(1) 124.6(5), N(1)–Se(1)–N(2) 104.0(5), Se(1)–N(2)–Se(2) 120.6(7), N(2)–Se(2)–Pt 103.6(3).

Experimental

6: A mixture of Se_4N_4 (90 mg, 0.24 mmol) and $[PtCl_2(PMe_2Ph)]_2$ (200 mg, 0.24 mmol) in $CHCl_3$ (25 mL) was heated at $\approx 90\,^{\circ}C$ for ca. 12 h, resulting in a dark solution and a black precipitate. After removal of the solvent in vacuo the residue was extracted with CH_2Cl_2 (30 mL), and the extract filtered through celite, then concentrated and placed on a Bio-beads gel-permeation column and eluted with CH_2Cl_2. The sample resolved into three bands, the slowest moving of which (blue/purple in color) was collected and dried in vacuo to yield a crude mixture of **4** and **5** (17 mg). [At this point **4** and **5** may be separated from each other by preparative thin layer chromatography and the purple species **5** ($R_f \approx 0.2$, CH_2Cl_2 as eluent) identified as $PtCl(Se_2N_2H)(PMe_2Ph)$ by mass spectrometry (m/z 556 ($M^{\oplus}$), 426 ($[Pt(SeN)(PMe_2Ph)]^{\oplus}$) and ^{31}p NMR spectroscopy ($\delta = -26.3$ ppm $^1J(^{195}Pt,^{31}P) = 3178$ Hz).]

The mixture of **4** and **5** was dissolved in THF (20 mL) then treated with PMe_2Ph (1 mL of a 0.03 M solution in THF). Upon addition of the phosphane solution the dark purple color of the mixture immediately turned pale red then yellow/orange. After stirring for 20 minutes the volume of the solvent was reduced to 1 mL in vacuo and the crude product obtained as a pale pink/orange solid by addition of hexane. Crystals suitable for X-ray crystallography were obtained by slow hexane diffusion into a CH_2Cl_2 solution.

7, $PR_3 = \frac{1}{2}$ dppe: $SeCl_4$ (0.60 g, 19.8 mmol) was carefully added in small amounts to liquid ammonia (30 mL) at $-78\,^{\circ}C$ to produce a green solid and a pale orange solution. [$PtCl_2$ dppe] (0.21 g, 3.15 mmol) was added and the suspension stirred for 2 h at $-78\,^{\circ}C$. The solution was allowed to warm slowly to room temperature (ca. 0.5 h) with the ammonia being blown off under a stream of argon to leave a green/orange solid. Extraction with CH_2Cl_2 (50 mL) and filtration through a celite/glass wool plug afforded an orange solution which, on layering with petroleum-ether (50 mL), furnished orange crystals of the product (0.184 g, 74%). Satisfactory elemental analyses and characteristic IR, MS and ^{31}P NMR spectra were obtained ($\delta = 45.7$, 37.1; $^2J(P,P) = 10$ Hz, $^1J(PtP) = 2817$, 2627 Hz).

8, $PR_3 = \frac{1}{2}$ dppe: To a solution of **7**, $PR_3 = \frac{1}{2}$ dppe (0.057 mmol) in 10 mL of THF/benzene (1/1) was added three drops of $HBF_4 \cdot (Et_2O)_2$ (85% in ether, Aldrich). This solution was stirred at room temperature for two hours, by which time the solution had darkened from light orange to green/brown. The solution was evaporated to dryness in vacuo, dissolved in CH_2Cl_2 (5 mL) and layered with *n*-hexane to furnish green crystals of **8**, $PR_3 = \frac{1}{2}$ dppe by slow diffusion (0.040 mmol, 71%, quantitative by ^{31}P NMR). Satisfactory elemental analyses and characteristic IR, MS, and ^{31}P NMR spectra were obtained ($\delta = 48.9$, 36.2; $^2J(P,P) = 10$ Hz, $^1J(Pt,P) = 2698$, 3094 Hz).

Complexes containing other phosphanes were obtained in a similar fashion in overall yields of 25–40%.

Received: March 13, 1989 [Z 3230 IE]
German version: *Angew. Chem. 101* (1989) 1052

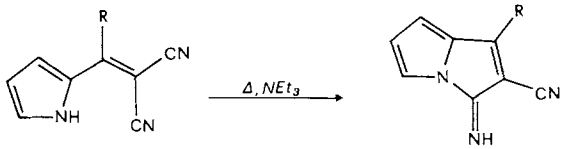
CAS Registry numbers:
3, 15699-79-3; **4**, 121810-21-7; **5**, 121810-22-8; **6**, 121810-23-9; **7**($PR_3 = 1/2$ dppe), 121810-24-0; **8**($PR_3 = 1/2$ dppe), 121810-26-2; Se_4N_4, 10102-12-2; $SeCl_4$, 10026-03-6; NH_3, 7664-41-7.

[1] R. Jones, P. F. Kelly, C. P. Warrens, D. J. Williams, J. D. Woollins, *J. Chem. Soc. Chem. Commun. 1986*, 711.
[2] R. Jones, P. F. Kelly, D. J. Williams, J. D. Woollins, *J. Chem. Soc. Dalton Trans. 1988*, 803.
[3] J. Adel, A. El-Kholi, W. Willing, U. Müller, K. Dehnicke, *Chimia 42*, (1988) 70.
[4] J. M. Jolliffe, P. F. Kelly, J. D. Woollins, unpublished.
[5] M. B. Hursthouse, M. Motevalli, P. F. Kelly, J. D. Woollins, *Polyhedron*, in press.
[6] P. F. Kelly, A. M. Z. Slawin, D. J. Williams, J. D. Woollins, *J. Chem. Soc. Chem. Commun.*, in press.
[7] Crystal data of **6**: $C_{16}H_{23}ClN_2P_2PtSe_2$, $M = 693.8$, monoclinic, $a = 24.331(10)$, $b = 10.088(5)$, $c = 19.409(5)$, $\beta = 117.35(3)^{\circ}$, $V = 4231$ Å^3, space group $I2/a$, (body-centered cell chosen because *C*-faced cell had $\beta = 131.8^{\circ}$), $Z = 8$, $\varrho_{calcd} = 2.18$ g cm^{-3}, $\mu(Cu_{K\alpha}) = 193$. Data were measured on a Nicolet R3m diffractometer with graphite monochromated $Cu_{K\alpha}$ radiation using the ω-scan routine. The structure was solved by direct methods and all the non-hydrogen atoms refined anisotropically to give an *R* value of 0.049 for 1982 independent observed absorption corrected reflections [$\theta < 50^{\circ}$, $|F_o| > 3\sigma(|F_o|)$]. Further details of the crystal structure can be obtained from the Director of the Cambridge Crystallographic Data Centre, University Chemical Laboratory, Lensfield Road, Cambridge CB2 1EW (UK). Any request should be accompanied by the full literature citation for this communication.
[8] In common with previous studies of **1** the H on N(1) lies significantly out of the PtE_2N_2 plane. We have now observed this feature in a sufficient number of instances for us to be convinced that the effect is real.
[9] In $[Pt(S_2N_2H)(PMe_2Ph)_2]Cl \cdot 0.5\,CH_2Cl_2$ the equivalent interplanar separation is 3.48 Å with Pt ··· S(1)'/Pt' ··· S(1) being 3.50 Å [2].

N-Analogues of Metal Acetylacetonates: Bis(1,2,6,7-tetracyano-3,5-diimino-3,5-dihydropyrrolizinido)metal(II), (Metal = Fe, Ni, Cu, Zn); Crystal Structure of the Copper Derivative**

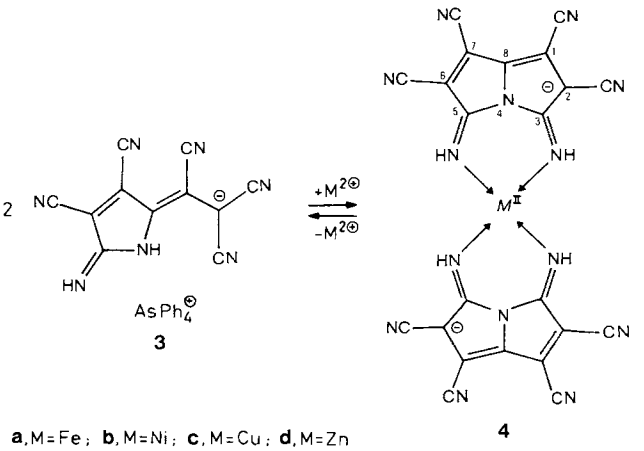
By *Mario Bonamico, Vincenzo Fares*, Alberto Flamini*, Patrizia Imperatori,* and *Nicola Poli*

The dicyanovinylpyrroles **1** readily cyclize in refluxing aqueous triethylamine to give the pyrrolizine derivatives **2**.[1]



1 **2**

In the course of our studies on the synthesis of metal complexes containing polycyano anions as ligands we have now discovered an analogous metal-promoted reaction of the anion **3**. It affords the corresponding planar symmetric β-diiminometal chelate complexes **4** with exceptional ease.



3 **4**

a, M = Fe; **b**, M = Ni; **c**, M = Cu; **d**, M = Zn

In contrast to **1**, the anion **3**[2] is stable in boiling aqueous amines, but it isomerizes promptly in the presence of a metal(II) ion at room temperature to yield the title compounds **4** (ca. 95%): the pyrrole proton attacks the adjacent nitrile nitrogen atom, and the intramolecular metal-promoted reaction proceeds with formation of the C–N bond. It is not possible to isolate the metal-free β-diimino anion, since demetalation reverses the reaction and regenerates the anion **3**.

The structure **4**, or the equivalent mesomer with the negative charge on C-6, is supported by the ^{13}C NMR spectrum of the zinc(II) compound **4d** and the X-ray crystal structure analysis of the copper(II) compound **4c** (Fig. 1).

The ESR and electronic spectra of **4c** in solution (see *Experimental*) resemble those of copper(II)-tetraazaporphy-

[*] Dr. V. Fares, Dr. A. Flamini, Prof. M. Bonamico, Dr. P. Imperatori, N. Poli
I.T.S.E.-C.N.R., Area della Ricerca di Roma
P. B. 10, 00016 Monterotondo Stazione, Roma (Italy)

[**] The Servizio NMR of Area della Ricerca di Roma is acknowledged for the ^{13}C-NMR spectra. We also thank Dr. *D. Attanasio* for the EPR spectra and Mr. *C. Veroli* for the drawings.

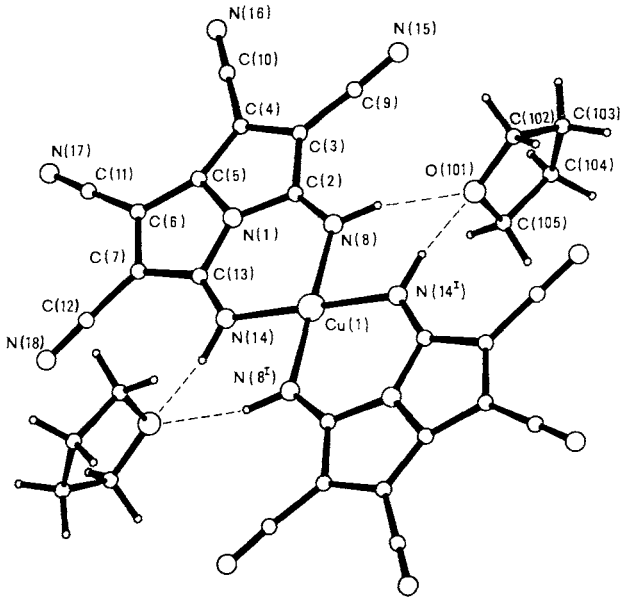
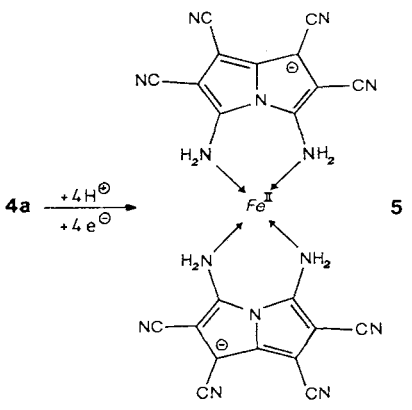


Fig. 1. Crystal structure of $Cu(C_{11}N_7H_2)_2 \cdot 2\,C_4H_8O$ **4c** · 2 THF. The labeling of the C and N atoms is identical with that of the free anionic ligand already reported [2]. *Pbca*; $a = 13.233(2)$, $b = 10.754(2)$, $c = 21.411(4)$ Å. $R = 0.054$ (1075 reflections). The copper atom completes its octahedral, tetragonally distorted coordination with two N(15) nitrogen atoms (at 2.82 Å) from two crystallographically equivalent complex units. Selected bond lengths [Å] and angles [°]: Cu–N8 1.984(5), Cu–N14 1.995(5), C2–N8 1.289(8), C13–N14 1.285(8), N1–C2 1.375(8), N1–C13 1.380(8), N1–C5 1.375(8), C2–C3 1.453(9), C7–C13 1.444(8), C3–C4 1.409(8), C6–C7 1.395(9), C4–C5 1.388(9), C5–C6 1.399(9); N8–Cu–N14 92.1(2), C2–N1–C13 133.7(5), C2–N8–Cu and C13–N14–Cu 126.2(4). Further details of the crystal structure investigation can be obtained from the Fachinformationszentrum Karlsruhe, Gesellschaft für wissenschaftlich-technische Information mbH, D-7514 Eggenstein-Leopoldshafen 2, by quoting the depository number CSD-53844, the names of the authors, and the journal citation.

rins.[3] In spite of this analogy, **4c** does not exhibit any solid state collective properties: it is a paramagnetic insulator and the extra electronic band at low energy in the reflectance spectrum arises from the transition $d_{xy} \rightarrow d_{x^2-y^2}$ confined in the chromophore CuN_4N_2.[4]

The iron(II) complex **4a** is easily reduced to the β-diamino species **5**. Therefore, **5** might undergo a Schiff condensation



with an appropriate dicarbonyl compound to yield conjugated, dianionic tetraazaannulenes, suitable for the synthesis of molecular materials.

Experimental

4b, 4c (M = Ni and Cu, resp.): A solution of **3** (0.50 g; 0.81 mmol) in acetone (50 mL) was treated with either a solution of $NiCl_2 \cdot 6\,H_2O$ (0.90 g) in water (5 mL) or a solution of $CuCl_2 \cdot 2\,H_2O$ (0.70 g; excess) in acetone (20 mL). The color immediately turned from violet to blue, and after concentration the complex **4** · 2 $(CH_3)_2CO$ separated as air-stable black (**4b**, M = Ni) or purple (**4c**, M = Cu) microcrystals (0.25 g; yield ca. 95%). Recrystallization from THF/water (9/1) afforded THF-adducts instead of acetone-adducts, as indicated by IR spectra and elemental analysis (C, H, N, O, M). **4**, characteristic IR bands (Nujol, cm^{-1}): $\tilde{\nu}$ = 3290 (m, N–H), 2220 (w, C≡N), 2210 (s, C≡N), 1640 (vs, C=N–H). Crystals of **4b** · 2 S (S = THF, acetone, EtOH) have a metallic luster; their color depends on S (purple, black and golden, respectively). The electronic transitions responsible for this behavior are not resolved in the reflectance spectra; single crystals have been grown for both reflectivity and X-ray diffraction studies. – Electronic and magnetic properties of **4c** · 2 THF: electronic spectrum in solution (THF, λ[nm], $(10^{-3}\,\varepsilon)$): 646(54), 613(52), 387(24); the reflectance spectrum shows an additional band at 950 nm; μ_{eff} = 1.85 BM at 290 K; electron paramagnetic resonance parameters (hfs in gauss units): $g_\parallel = 2.22$, $g_\perp = 2.03$, $A_\parallel = 187.5$, $A_\perp = 23$, $\langle a \rangle = 81.3$.

4d (M = Zn): this complex, which is very soluble in polar solvents, and very labile towards water, was characterized ^{13}C-NMR spectroscopically. The sample was prepared in a dry-box: A solution of 0.060 g (0.23 mmol) of $NaC_{11}N_7H_2$ (= **3**, Na instead of $AsPh_4$) in dried C_2D_5OD (1.5 mL) was treated with excess anhydrous $ZnCl_2$. The resulting blue solution was filtered into an NMR tube (∅ = 5 mm); 0.1 mL of a solution of $Cr(acac)_3$ in C_6D_6 (1.5×10^{-4} M) was added as relaxation reagent. The spectrum can be fully assigned taking into account: i) the molecular symmetry (C-8 will give the least intense peak); ii) the electronic deshielding effect (C-3, between two nitrogen atoms, will fall at lowest field), and iii) the relaxation agent effect, which will be more pronounced on the external groups (C≡N groups) of the molecule, increasing the intensity of their signals: δ = 156.9 (C-3), 125.5 (C-8), 112.4 and 110.2 (C≡N), 109.8 (C-1), 94.7 (C-2). Addition of $As(C_6H_5)_4Cl$ (0.105 g; 0.25 mmol) in water (3 mL) to the previous ethanolic solution causes the quantitative precipitation of **3** (0.14 g).

4a (M = Fe), **5**: **4a**, which is insoluble in THF was obtained in quantitative yield by reaction of **3** with anhydrous $FeCl_2$ (excess) in THF. If commercial $FeCl_2 \cdot 4\,H_2O$ is used protonation and reduction (probably at the expense of $Fe^{2\oplus}$) of the β-diimino ligand into a β-diamino ligand occur, giving **5**; this was filtered off and, after crystallization from CH_3CN/THF (1:1) under N_2, golden, moisture-sensitive crystals of composition **5** · 4 THF were obtained. A preliminary single-crystal X-ray analysis shows that this complex is six coordinated with a *trans*, tetragonally distorted, FeN_4O_2 chromophore (electronic spectrum in solution (CH_3CN, λ[nm], $(10^{-3}\,\varepsilon)$): 1040 (4.3), 880 (5.4), 730 (4.9), 617 (29), 588 (25). – The bis-β-diamino structure of **5** is supported by the IR data: the strong band of **4a** at 1640 cm^{-1}, which is due to a C=N–H stretching vibration, is absent in **5**, and the band in the N–H stretching region has two maxima (3180, 3270 cm^{-1}) indicating the presence of NH_2 groups (see also Ref. [5]).

Received: March 6, 1989;
supplemented: May 8, 1989 [Z 3216 IE]
German version: *Angew. Chem. 101* (1989) 1067

[1] K. Hartke, S. Randau, *Liebigs Ann. Chem. 1974*, 2110.
[2] G. Dessy, V. Fares, A. Flamini, A. M. Giuliani, *Angew. Chem. 97* (1985) 433; *Angew. Chem., Int. Ed. Engl. 24* (1985) 426.
[3] C. J. Schramm, B. M. Hoffman, *Inorg. Chem. 19* (1980) 383.
[4] A. B. P. Lever: *Inorganic Electron Spectroscopy*, Elsevier, Amsterdam 1984, p. 557.
[5] L. J. Bellamy: *The Infrared Spectra of Complex Molecules*, Chapman and Hall, London 1975, p. 277.

Tri-*tert*-butyl(trimethylsilyl)tricyclo[1.1.0.0^{2,4}]-butane – a Second Tetrahedrane Derivative**

By *Günther Maier** and *Dieter Born*

Dedicated to Professor Christoph Rüchardt on the occasion of his 60th birthday

Tetra-*tert*-butyltetrahedrane,[2] which was first synthesized some eleven years ago is thus far the only unequivocally identified compound with a tetrahedral C_4 ring framework.

[*] Prof. Dr. G. Maier, Dipl.-Chem. D. Born
Institut für Organische Chemie der Universität
Heinrich-Buff-Ring 58, D-6300 Giessen (FRG)

[**] Small Rings, Part 67. This work was supported by the Deutsche Forschungsgemeinschaft and the Fonds der Chemischen Industrie. – Part 66: [1].

This molecule owes its astonishing stability to a "corset effect",[2] which should also occur when the *tert*-butyl substituents are replaced by other bulky groups. This is in fact the case, as is demonstrated here for the example of tri-*tert*-butyl(trimethylsilyl)tetrahedrane **1**. In spite of the high ring strain, this molecule is stable up to 180 °C(!).

The synthesis of **1** was accomplished starting from the diazo compound **4**,[3a] the chemistry of which is unexpectedly diverse.[3b] Upon irradiation [route (b)], **4** fragments exclusively via the carbene **5** to the two acetylenes **6** and **7**.[3a] Flash thermolysis [route(c)], on the other hand, proceeds less cleanly: aside from the two acetylenes,[3a] trimethylsilyl cyanide **16** and tri-*tert*-butylazete **13**—recently described for the first time by *Regitz* et al.[4]—are also formed as cleavage products. Presumably **4** isomerizes upon heating, firstly via the betaine **8**[5a] or the diazabenzvalene **9** to the Dewar-diazabenzene **10**,[5b] which in turn serves as precursor for the azete **13** and trimethylsilyl cyanide **16**, which is in thermal equilibrium with trimethylsilyl isocyanide **17**.[6]

The thermolysis of **4** proceeds somewhat differently, both without solvent or in solution (e.g. in benzene) [route(d)]. In either case **4** isomerizes to a green compound, which, according to its spectroscopic data, has the structure **14** (whether the trimethylsilyl group is *syn* or *anti* is undecided). The formation of **14** can be explained as follows: the isonitrile **17**, which is in equilibrium with **16**, reacts with the azete **13**, present in comparable concentration, via **15**[7] to give the stable end product **14**. The reaction course discussed for the thermal excitation of **4** is supported by the isolation of the two carbonyliron complexes **11**[8] and **12**, which are formed upon heating **4** in the presence of nonacarbonyldiiron.

How does one get from the diazo compound **4** to the tetrahedrane **1**? Several experiments were necessary in order to find this out. At an earlier stage it emerged that the cyclobutadiene **2** is formed in the CuCl-catalyzed thermal decomposition of **4** [route(a)]. If, after the elimination of nitrogen, dimethyl acetylenedicarboxylate is added to the reaction mixture, the corresponding Diels-Alder adduct of **2** can be isolated.[2c, 9] Maleic anhydride and citraconic anhydride react similarly. Using the same reaction procedure with nonacarbonyldiiron leads to the cyclobutadiene complex

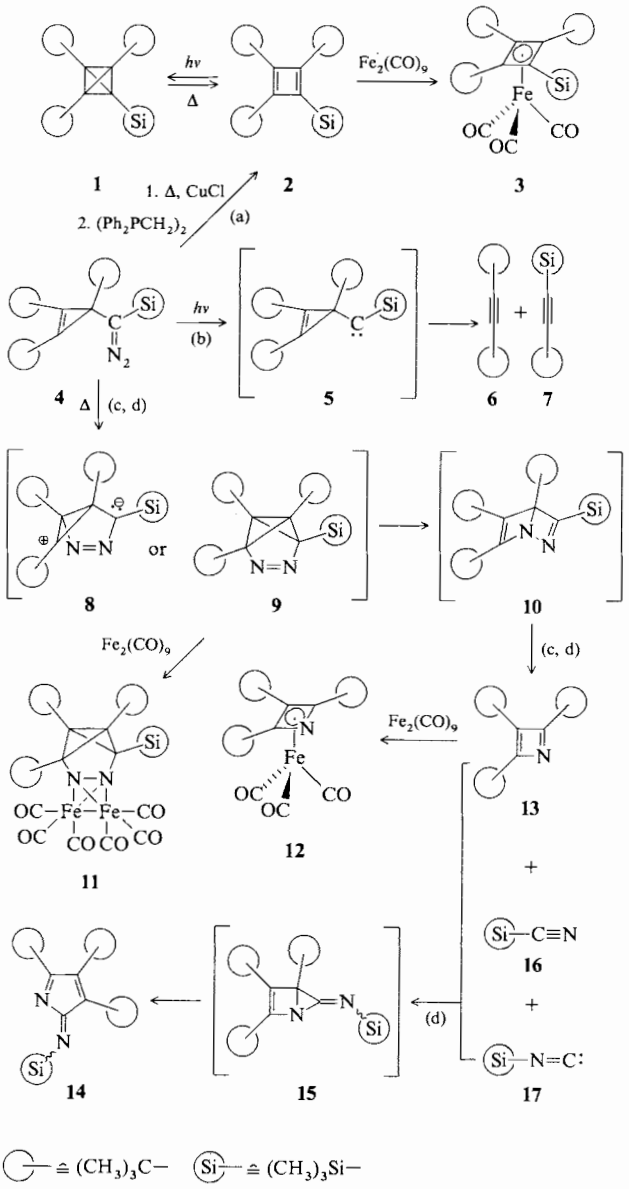


Table 1. Reaction conditions, yields, and NMR spectroscopic data of the compounds **1, 2, 3, 11, 12**, and **14**. NMR: δ values relative to TMS. **1, 3, 11** and **14** furnished correct elemental analyses.

Cpd.	Color, m.p. [°C]	Reaction-conditons	Yield [%]	δ(^{1}H), 400.1 MHz	δ(^{13}C), 100.6 MHz
1	colorless crystals, 162	see procedure	25	1.10 (s, 27H; *t*Bu), 0.12 (s, 9H; $SiMe_3$) [a]	31.09 (q; *t*Bu), 26.88 (s; *t*Bu), 13.27 (s; *C*-*t*Bu), 1.46 (q; $SiMe_3$), −23.09 (s; *C*-$SiMe_3$) [a]
2	darkred crystals, 87	see procedure	52	1.16 (s, 9H; *t*Bu), 1.15 (s, 18H; *t*Bu), 0.18 (s, 9H; $SiMe_3$) [b]	167.11 (s; 2 *C*-*t*Bu), 149.23 (s; 1 *C*-*t*Bu), 142.63 (s; *C*-$SiMe_3$), 34.05 (s; 2 *t*Bu), 32.40 (s; 1 *t*Bu), 31.43 (q; 1 *t*Bu), 30.21 (q; 2 *t*Bu), 3.64 (q; $SiMe_3$) [c]
3	yellowish white crystals, 250–254 (decomp.)	addition of $Fe_2(CO)_9$ to the solution of **2**, 6 h reflux	20	1.35 (s, 9H: *t*Bu), 1.27 (s, 18H; *t*Bu), 0.41 (s, 9H; $SiMe_3$) [a]	217.08 (s; CO), 102.83 (s; 2 *C*-*t*Bu), 102.32 (s; 1 *C*-*t*Bu), 64.92 (s; *C*-$SiMe_3$), 34.12 (q; 3 *t*Bu), 32.17 (s; 2 *t*Bu), 31.90 (s; 1 *t*Bu), 6.54 (q; $SiMe_3$) [d]
11	darkred crystals, 203–205 (decomp.)	**4** and $Fe_2(CO)_9$, benzene, 8 h 80 °C, DC-separation	2	1.39 (s, 9H; *t*Bu), 1.34 (s, 18H; *t*Bu), 0.41 (s, 9H; $SiMe_3$) [a]	211.00 (s; CO), 83.12 (s; 1 *C*-*t*Bu), 69.81 (s; 2 *C*-*t*Bu), 67.80 (s; *C*-$SiMe_3$), 34.13 (s; 1 *t*Bu), 33.64 (q; 2 *t*Bu), 32.86 (s; 2 *t*Bu), 31.09 (q; 1 *t*Bu), 2.97 (q; $SiMe_3$) [a]
12	pale yellow crystals	as in the case of **11**	30	1.23 (s, 18H; *t*Bu), 1.20 (s, 9H; *t*Bu) [b]	215.28 (s; CO), 112.77 (s; 2 *C*-*t*Bu), 97.68 (s; 1 *C*-*t*Bu), 33.38 (s; 1 *t*Bu), 32.40 (s; 2 *t*Bu), 30.50 (q; 2 *t*Bu), 30.01 (q; 1 *t*Bu) [b]
14	brown-green oil	**4**, benzene, 8 h 80 °C, GC-separation or **13** together with **16** heated to 80 °C, GC-separation	40	1.43 (s, 9H; *t*Bu), 1.29 (s, 9H; *t*Bu), 1.25 (s, 9H; *t*Bu), 0.23 (s, 9H; $SiMe_3$) [a]	171.56 (s; C=N), 170.15 (s; C=N), 163.16 (s; C=C, 125.50 (s; C=C), 35.71 (s; *t*Bu), 34.35 (s; *t*Bu), 32.25 (q; *t*Bu), 31.62 (s; *t*Bu), 31.23 (q; *t*Bu), 28.72 (q; *t*Bu), 2.07 (q; $SiMe_3$) [a]

[a] $CDCl_3$. [b] C_6D_{12}. [c] CD_2Cl_2. [d] C_6D_6.

3.[8] On the other hand, all attempts to obtain the free cyclobutadiene **2** directly from the reaction mixture failed. **2** is presumably present as a CuCl complex under the mentioned conditions. Only after addition of ethylenebis(diphenylphosphane)[10] can **2** be isolated. The structure of tri-*tert* butyl(trimethylsilyl)cyclobutadiene **2** is unequivocally confirmed by the data in Table 1.

Upon irradiation of **2** in cyclohexane or diethyl ether ($\lambda \geq 300$ nm), quantitative isomerization to the tetrahedrane **1** occurs. This second, spectroscopically confirmed[8] tetrahedrane derivative is thermally even more stable (higher barrier for the retroisomerization to the cyclobutadiene) than tetra-*tert*-butyltetrahedrane. Whereas the latter rearranges into the respective cyclobutadiene at 135 °C, **1** melts without decomposition at 162 °C to give a colorless liquid, which is converted upon reaching 180 °C with red coloration into the cyclobutadiene **2**. Since the "corset effect" in **1** is not stronger than in the tetra-*tert*-butyl analogue (longer C–Si bond), one gets the impression that the trimethylsilyl group may stabilize the tetrahedrane structure also by electronic effects.[11]

Experimental

2: A solution of 320 mg (1.00 mmol) of the diazo compound **4** in 5 mL of CH_2Cl_2 was added to 500 mg (5.06 mmol) of CuCl at 0 °C. After 14 h the mixture was warmed to room temperature and the resulting red solution added to 400 mg (1.00 mmol) of ethylenebis(diphenylphosphane) in 10 mL of CH_2Cl. The reaction mixture was heated under reflux for 2 h, the solvent evaporated off in a stream of argon, and the liberated cyclobutadiene **2** sublimed at 3×10^{-2} torr in an air-bath at about 120 °C (cf. Table 1).

1: A solution of **2** (50 mg, 0.17 mmol) in [D_{12}]cyclohexane (0.4 mL) was irradiated in a sealed NMR tube for 4 d ($\lambda \geq 300$ nm; 200W Hg high-pressure lamp). The solution was colorless during the course of irradiation, and only the signals of **1** could be observed in the ^{13}C-NMR spectrum. Chromatography on basic aluminum oxide with pentane as eluent, followed by sublimation (30 °C, 3×10^{-2} torr), afforded pure tetrahedrane **1** (cf. Table 1).

Received: April 3, 1989 [Z 3267 IE]
German version: *Angew. Chem. 101* (1989) 1085

CAS Registry numbers:
1, 120883-27-4; **2**, 120883-28-5; **3**, 120883-30-9; **4**, 97476-04-5; **11**, 120883-31-0; **12**, 120883-32-1; **14**, 120883-29-6; $Fe_2(CO)_9$, 15321-51-4.

[1] G. Maier, *Angew. Chem. 100* (1988) 317; *Angew. Chem. Int. Ed. Engl. 27* (1988) 309.

[2] a) G. Maier, S. Pfriem, U. Schäfer, R. Matusch, *Angew. Chem. 90* (1978) 552; *Angew. Chem. Int. Ed. Engl. 17* (1978) 520; b) G. Maier, S. Pfriem, U. Schäfer, K.-D. Malsch, R. Matusch, *Chem. Ber. 114* (1981) 3965; c) review: [1].

[3] a) G. Maier, K. A. Reuter, L. Franz, H. P. Reisenauer, *Tetrahedron Lett. 26* (1985) 1845; b) G. Maier, I. Bauer, D. Born, H.-O. Kalinowski, *Angew. Chem. 98* (1986) 1132; *Angew. Chem. Int. Ed. Engl. 25* (1986) 1098; among other things, a dimerization of **4** is discussed in this work.

[4] U.-J. Vogelbacher, M. Regitz, R. Mynott, *Angew. Chem. 98* (1986) 835; *Angew. Chem. Int. Ed. Engl. 25* (1986) 842.

[5] a) A. Heydt, H. Heydt, B. Weber, M. Regitz, *Chem. Ber. 115* (1982) 2965; b) P. Eisenbarth, M. Regitz, *ibid. 117* (1984) 445.

[6] M. R. Booth, S. G. Frankiss, *Chem. Commun. 1968*, 1347; b) *Spectrochim. Acta Part A 26* (1970) 859; c) J. A. Seckar, J. S. Thayer, *Inorg. Chem. 15* (1976) 501.

[7] a) 2,3,4-Tri-*tert*-butylcyclobutadiene-1-carboxylates add isonitriles in the same way: J. Fink, M. Regitz, *Chem. Ber. 119* (1986) 2159; b) According to our investigations the reaction of azete **13** with *tert*-butyl isocyanide affords an adduct analogous to **14**.

[8] We thank Dr. *R. Boese*, Gesamthochschule Essen, for the structure analyses of the complexes **3** and **11**. According to the first results by Dr. *R. Boese* the same problems of disorder occur in the case of cyclobutadiene **2** and tetrahedrane **1** as those which Prof. *H. Irngartinger*, Universität Heidelberg, had to contend with in the determination of the structure of tetra-*tert*-butylcyclobutadiene and tetra-*tert*-butyltetrahedrane (cf. discussion in Ref. [1]).

[9] I. Bauer, *Dissertation*, Universität Giessen 1986.

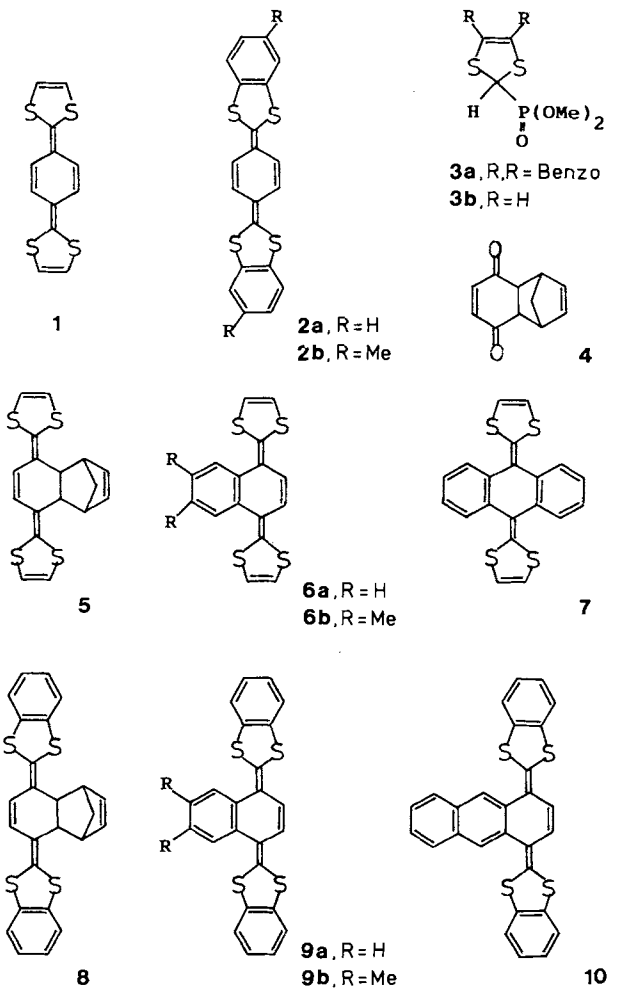
[10] Using this reagent, *Krebs* et al. have succeeded in liberating the first kinetically stabilized cyclobutadiene from its $PdCl_2$ complex: H. Kimling, A. Krebs, *Angew. Chem. 84* (1972) 952; *Angew. Chem. Int. Ed. Engl. 11* (1972) 932; A. Krebs, H. Kimling, R. Kemper, *Justus Liebigs Ann. Chem. 1978*, 431.

[11] Examples: own works cited in [1]. Theoretically, σ-donor-π-acceptor substituents can stabilize three-membered rings. J. D. Dill, A. Greenberg, J. F. Liebman, *J. Am. Chem. Soc. 101* (1979) 6814; T. Clark, G. W. Spitznagel, R. Klose, P. von R. Schleyer, *ibid. 106* (1984) 4412; D. Cremer, E. Kraka, *ibid. 107* (1985) 3811. This effect is also to be expected from a trimethylsilyl group.

p-Quinodimethane Analogues of Tetrathiafulvalene

By *Yoshiro Yamashita,* Yasuo Kobayashi,* and *Tsutomu Miyashi*

2,2′-Bis(1,3-dithiole) derivatives containing quinodimethane structures are promising electron donors for "organic metals", since the extended conjugation decreases the Coulombic repulsion.[1] However, the parent compound, 2,2′-*p*-quinobis(1,3-dithiole) **1**, was hitherto unknown, and the reported examples of derivatives as neutral donors were limited to the dibenzo derivatives **2a, b**,[2] although some dication salts were known.[3] We report here on a simple synthesis of **1** and its derivatives, and on their properties.



[*] Prof. Dr. Y. Yamashita
Institute for Molecular Science
Myodaiji, Okazaki 444 (Japan)
Y. Kobayashi, Prof. Dr. T. Miyashi
Department of Chemistry, Faculty of Science
Tohoku University
Aramaki, Sendai 980 (Japan)

We recently found the usefulness of the Wittig-Horner reaction of 2-dimethylphosphono-1,3-benzodithiole **3a** with conjugated 1,4-diketones for the preparation of 2,2′-bis(1,3-dithiole) donors.[4] We have now used the Wittig-Horner reaction of **3b**, which was synthesized by a similar method as that for **3a**,[5] to prepare **1**. In this case, a cyclopentadiene adduct of *p*-benzoquinone **4** was used as a diketone and after introduction of the 1,3-dithiole rings the cyclopentadiene was removed by a retro-Diels-Alder reaction, since the direct reaction of *p*-benzoquinone with **3b** gave a complex mixture of products without formation of **1**.

Thus, a solution of **3b** in dry THF was treated with 1.1 equivalents of *n*-butyllithium at −78 °C under nitrogen, and after stirring for 5 min, 0.43 equivalent of **4** was added. The solution was then stirred at −78 °C for a further 10 min and allowed to warm to room temperature, whereupon the bis(1,3-dithiole) derivative **5** was obtained in 27% yield. Thermolysis of **5** at 200 °C under reduced pressure furnished, via a retro-Diels-Alder reaction, dark red crystals of **1** in 54% yield.[6] The benzo derivatives **6a, b** were prepared analogously by reaction of the Diels-Alder adducts of 1,4-naphthoquinone and the corresponding methyl compound, respectively with cyclopentadiene. The dibenzo derivative **7** could be synthesized in 74% yield by direct Wittig-Horner reaction of **3b** with 9,10-anthraquinone. The dibenzotetrathiafulvalene (TTF) analogue **2a** could be prepared by a retro-Diels-Alder reaction of **8**, which was obtained in 73% yield by reaction of **3a** and **4**. **9a, b** and **10** were prepared similarly. The decomposition temperatures of the new donors are listed in Table 1. The TTF analogues **1** and **6a, b** are air sensitive, whereas the dibenzo analogues **2a, 7, 9a, b,** and **10** are stable towards air.

The oxidation potentials of the donors (Table 1) were measured by cyclic voltammetry. The values for the donors with quinoid structures are lower than those of TTF measured under the same conditions (0.28, 0.64 V vs. SCE); the parent compound **1**, in particular, is an extremely strong electron donor. This may be due to the fact that the quinoid structures form a new aromatic sextet upon oxidation.

Table 1. Decomposition temperatures and oxidation potentials [a] of the donors.

Donor	$T_{dec.}$ [°C]	$E_{1/2}$ [V]
1	230–245	−0.11, −0.04
6a	160–170	0.00
6b	190–194	−0.04
7	320–325	+0.25 [b]
9a	260–270	+0.18
9b	243–248	+0.15
10	314–317	+0.24
5	168–170	+0.17
8	260–265	+0.37

[a] 0.1 M Et_4NClO_4 in MeCN, Pt electrode, scan rate: 100 mV s^{-1}; *E* vs. standard calomel electrode (SCE). [b] Irreversible. Calculated as E_{pa} (anodic peak potential) − 0.03 V.

Other characteristic features are that the difference between the first and second oxidation potentials of **1** is very small and that two-electron oxidation waves are observed in the other new donors. Accordingly, the donors with quinoid structures form dications more readily upon oxidation, due to the decreased Coulombic repulsion. With tetracyanoquinodimethane (TCNQ), the donors **1, 6a, b, 2a,** and **9a, b** gave charge-transfer complexes which exhibit good conductivities (Table 2).

Table 2. Properties of charge-transfer complexes with TCNQ.

Donor (D)	T_{dec} [°C]	Molar ratio [a] D:A	σ[S cm^{-1}] [b]
1	> 400	3:4	5.3×10^{-4}
6a	> 360	2:3	2.9×10^{-2}
6b	> 400	2:3	1.9×10^{-2}
2a	250–253	1:1	4.1×10^{-3}
9a	245–249	3:5:3 H_2O	1.9×10^{-2}
9b	220–225	1:1.8:H_2O	2.2×10^{-2}

[a] Based on elemental analyses. [b] Electrical conductivities measured on compressed pellets by two-probe technique at room temperature.

Received: April 4, 1989 [Z 3274 IE]
German version: *Angew. Chem. 101* (1989) 1090

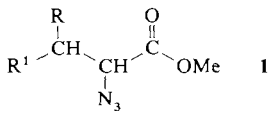
[1] P. J. L. Galigné, B. Liautard, S. Peytavin, G. Brun, M. Maurin, J. M. Fabre, E. Torreilles, L. Giral, *Acta Cryst., B36* (1980) 1109; M. R. Bryce, *J. Chem. Soc. Perkin Trans. 1, 1985,* 1675.
[2] Y. Ueno, A. Nakayama, M. Okawara, *J. Chem. Soc. Chem. Commun. 1978,* 74; M. Sato, M. V. Lakshmikantham, M. P. Cava, A. F. Garito, *J. Org. Chem. 43* (1978) 2084.
[3] Y. Ueno, M. Bahry, M. Okawara, *Tetrahedron Lett. 1977,* 4607; J.-M. Fabre, E. Torreilles, L. Giral, *ibid. 1978,* 3703; M. R. Bryce, *Mol. Cryst. Liq. Cryst. 120* (1985) 305; M. R. Bryce, A. J. Moore, *Tetrahedron Lett. 29* (1988) 1075.
[4] Y. Yamashita, T. Miyashi, *Chem. Lett. 1988,* 661.
[5] K. Akiba, K. Ishikawa, N. Inamoto, *Bull. Chem. Soc. Jpn. 51* (1978) 2674.
[6] **1** absorbs at longer wavelengths than **5**. UV (CH_2Cl_2): **1**: λ(lg ε) = 495(4.78), 469 (sh, 4.50), 257(4.07); **5**: λ(lg ε) = 440(4.65), 416(4.58), 395 (sh, 4.31).

2-Isocyanato-2-alkenoates – Synthesis and Reactions**

By *Franz Effenberger,* Christan Baumgartner,* and *Jürgen Kühlwein*

Dedicated to Professor Christoph Rüchardt on the occasion of his 60th birthday

Very few data have been quoted in the literature about 2-isocyanato-2-alkenoates; they have been detected spectroscopically as reaction intermediates,[1a, b] and in two cases have even been isolated.[1c] α-Isocyanatoacrylic acid esters have on one occasion been presumed as intermediates in the thermolysis of ethyl 1-isocyanatocyclobutane-2-carboxylate,[2a] and on another their formation and their spectroscopic detection – likewise in thermolysis reactions – have been reported in a patent.[2b]



1

In the perrhenate-catalyzed decomposition of α-azidocarboxylic acid derivatives such as **1**[3] we could successfully replace acetic anhydride by other acylating reagents, thereby providing easy access to a series of interesting *N*-substituted α,β-didehydroamino acid esters.[4a]

[*] Prof. Dr. F. Effenberger, Dr. C. Baumgartner, Dr. J. Kühlwein
Institut für Organische Chemie der Universität
Pfaffenwaldring 55, D-7000 Stuttgart 80 (FRG)

[**] This work was supported by the Deutsche Forschungsgemeinschaft and the Fonds der Chemischen Industrie.

The results which we have now found with phosgene and diphosgene as "acylating reagent" in this decomposition reaction, although hoped for, are still surprising: as reaction products, the 2-isocyanato-2-alkenoates **2** were obtained in very good yields (Table 1).[4]

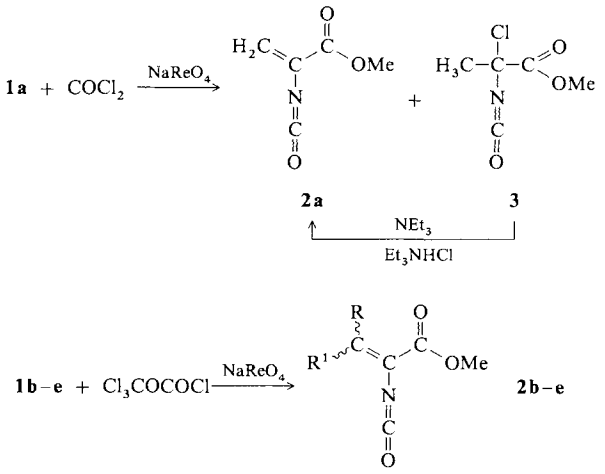
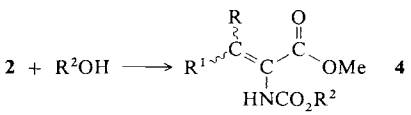


Table 1. R and R^1 in **1** and **2** and yields of **2**.

	R	R^1	Yield of **2** [%]
a	H	H	69
b	H	Me	88
c	Me	Me	82
d	H	*n*Pr	80
e	H	Ph	53

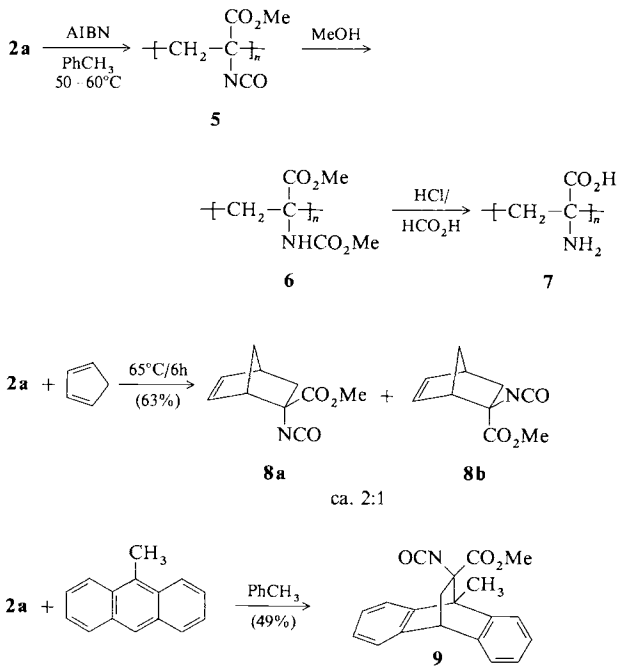
Whereas the substituted esters **2b–e** could be isolated and worked-up by distillation without any problem, the synthesis of pure α-isocyanatoacrylate **2a** at first presented great difficulties, because it was always formed in a mixture with its—distillatively—inseparable HCl-adduct **3**, and because it is exceptionally reactive, and easily polymerizes. However, the addition product **3** could be completely converted into the acrylate **2a** by careful extrusion of HCl with triethylamine in diethyl ether, so that **2a** was obtained in 69% yield—referred to **1a**—in this way.

As expected, all usual addition reactions to the isocyanato group of the compounds **2** could be carried out, which, e.g., upon using appropriate alcohols (*tert*-butyl alcohol, benzyl alcohol) yield directly the urethane-protected dehydroamino acids **4**, which are of special interest in peptide chemistry.



R^2 = *t*Bu, $PhCH_2$

The acrylic ester **2a**, which, besides the isocyanato group, has an activated and sterically unhindered C—C double bond, provides access to further, versatile reactions. In the presence of azoisobutyronitrile (AIBN) radical polymerization leads to the polymers **5**; with methanol these yield the polymeric urethanes **6**, which can be hydrolyzed to the poly(α-aminoacrylic acid) **7**. We have no explanation for the astonishingly low degree of polymerization of **5** (n = 14–15).[5] The properties of **7** are almost identical with the properties of the poly(α-aminoacrylic acid) obtained by hydrolysis of the *N*-acetyldehydroalanine polymers.[6]



That the acrylic ester **2a** is also suitable as dienophile for Diels-Alder reactions is demonstrated by the reactions with cyclopentadiene to give **8** and with 9-methylanthracene to give **9**, whereby **2a** proves to be distinctly more reactive than *N*-acetyldehydroalanine.[7] The cycloadducts **8a,b** can be further converted by alcohol addition into urethane-protected cyclic α-amino acids and by acid hydrolysis into the corresponding free cyclic α-amino acids.[8]

The previously reported reactivity sequence for Diels-Alder reactions with anthracenes is confirmed in the reactions of **2a** with anthracenes: no cycloadducts were obtained at temperatures up to 115 °C, neither with anthracene nor with 9-methoxyanthracenes. Higher reaction temperatures are not possible because of the thermolability of **2a**.

Experimental

2a: Phosgene was passed into a cold mixture of sodium perrhenate (1.0 g, 3.66 mmol) and methanesulfonic acid (0.2 g) in ethyl acetate (500 mL). After addition of 64.5 g (0.5 mmol) of **1a** and of 300 mg of hydroquinone, phosgene was condensed into the mixture such that it was always present in excess. The mixture was then heated at 70–80 °C until completion of evolution of gas, cooled down, and the whole liquid distilled rapidly under high vacuum into a cooled receiver. After evaporation of the ethyl acetate, distillation at 50 °C/12 torr furnished 69 g of a mixture of **2a** and **3** in the ratio 1:2. At 0 °C, 125 mL of diethyl ether were added, then a solution of triethylamine (in equimolar amount to **3**; 31.0 g, 310 mmol) in 125 mL of diethyl ether was added dropwise at 0 °C. After removal of precipitated triethylamine hydrochloride by filtration, the filtrate was evaporated and distilled at 44.5 °C/12 torr. Yield: 43.6 (69%) of **2a** as a colorless, viscous liquid. ^1H NMR ($CDCl_3$): δ = 3.93 (s, 3H, CH_3), 5.82, 5.50 (each s, each 1H, =CH). Correct elemental analysis (C,H,N).

Received: March 28, 1989 [Z 3258 IE]
German version: *Angew. Chem. 101* (1989) 1059

[1] a) B. W. Metcalf, P. Casara, *J. Chem. Soc. Chem. Commun. 1979*, 119; b) T. J. Nitz, E. M. Holt, B. Rubin, C. H. Stammer, *J. Org. Chem. 46* (1981) 2667; c) C. Herdeis, U. Nagel, *Arch. Pharm. (Weinheim, FRG) 317* (1984) 86.

[2] a) R. D. Miller, W. Theis, *Tetrahedron Lett. 27* (1986) 2447; b) J. F. Engel, T. J. Byerley, H. W. Christie, US Pat. 4704466 (1987), Midwest Research Institute; *Chem. Abstr. 108* (1988) 56770s.

[3] a) F. Effenberger, T. Beisswenger, *Chem. Ber. 117* (1984) 1497; b) T. Beisswenger, F. Effenberger, *ibid. 117* (1984) 1513.

[4] a) J. Kühlwein, *Dissertation*, Universität Stuttgart 1986; b) F. Effenberger, J. Kühlwein, K. Drauz, DOS 3 508 564 (1986), Degussa AG; *Chem. Abstr. 107* (1987) 354 750j.
[5] Determined in collaboration with Prof. Dr. *L. Dulog* and Dr. *R. Seidemann*, 2. Institut für Technische Chemie der Universität Stuttgart.
[6] G. Nelson, C. Chang, I. St. Pierre, *Makromol. Synth. 9* (1985) 89.
[7] H. Horikawa, T. Nishitani, T. Iwasaki, Y. Mushika, I. Inoue, M. Miyoshi, *Tetrahedron Lett. 21* (1980) 4101.
[8] A. Mielert, C. Braig, J. Sauer, J. Martelli, R. Sustmann, *Liebigs Ann. Chem. 1980*, 954.

A Polymeric Technetium Compound of the Composition $[Tc_2O_3(C_5Me_5)]_n$

By *Basil Kanellakopulos,* Bernd Nuber, Konstantinos Raptis*, and *Manfred L. Ziegler**

Dedicated to Professor Margot Becke on the occasion of her 75th birthday

The tricarboxylrhenium complex **1**[1] reacts with H_2O_2 to give the trioxo-complex **2**, which has proved to be an interesting and versatile starting compound for exploring the remarkable chemistry of rhenium in high oxidation states.[1] So far it has not been possible to carry out an X-ray structure analysis of **2** itself; however, the structure of one of its derivatives is already known, namely that of **3**, which forms discrete molecules. This might also be assumed in the case of **2**.

$[(\eta^5\text{-}C_5Me_5)Re(CO)_3]$ **1** $[(\eta^5\text{-}C_5Me_5)ReO_3]$ **2**

$[(\eta^5\text{-}C_5Me_4Et)ReO_3]$ **3** $[(\eta^5\text{-}C_5Me_5)Tc(CO)_3]$ **4** $[(C_5Me_5)Tc_2O_3]_n$ **5**

In the reaction of the tricarbonyltechnetium complex **4** with perhydrol it has now been shown that the technetium species **4** behaves differently than its rhenium homologue **1**. Elemental analysis, mass spectra, and, above all, an X-ray structure analysis yielded the empirical formula $C_{10}H_{15}Tc_2O_3$ for the product **5** in a polymeric structure. It is clear from Figure 1 that, in **5**, two Tc atoms are bridged by three μ-oxo ligands and the coordination of the Tc atoms is in each case completed by a C_5Me_5 ring (= Cp*). These Cp* rings are, however, concomitantly a component of the neighboring units, so that the above mentioned empirical formula results. The planes of the Cp* rings and of the oxo-bridge ligands are, crystallographically exactly parallel to one another, i.e. a kind of polydecker structure is formed (distances: Cp*-O_3 planes 297.3(3), Tc-O_3 plane 93.4(3), Tc-Cp* plane 204.0(4) pm). A striking feature is the unusually short distance (186.7(4) pm) between the two Tc atoms coupled by the three μ-oxo ligands (distance between the Cp*-bridged Tc atoms 407.7(4) pm); the shortest Tc–Tc distance recorded so far is 213(1) pm. Shorter metal–metal distances are found only in binuclear chromium complexes[5] with a minimum of 182.8(2) pm in $[Cr_2(2\text{-}MeO\text{-}5\text{-}MeC_6H_3)_4]$.[6]

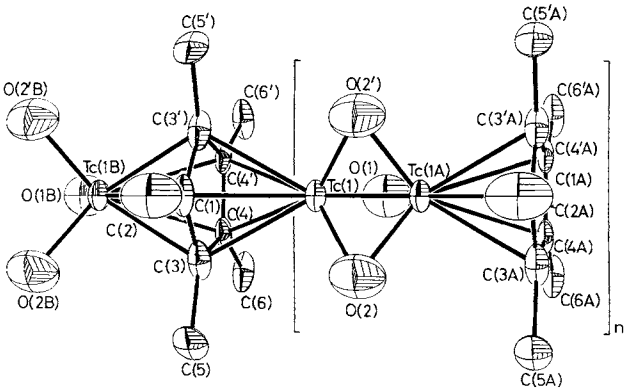


Fig. 1. Section of the polymer **5** in the crystal. The vibration ellipsoids are drawn at the 50% probability level. **5** is viewed along one of the mirror planes. Important bond lengths [pm] and angles [°]: Tc1–O1 190(2), Tc1–O2 185(2), Tc–C_{Ring} 238(2); Tc1–O1–Tc1A 58.8(8), Tc1–O2–Tc1A 60.7(6), O1–Tc1–O2 97.5(5), O2–Tc1–O2' 96.3(9).

[*] Prof. Dr. B. Kannellakopulos, Dipl.-Chem. K. Raptis
Kernforschungszentrum Karlsruhe, Institut für Heisse Chemie
Postfach 3640, D-7500 Karlsruhe (FRG)
Prof. Dr. M. L. Ziegler, Dr. B. Nuber
Anorganisch-chemisches Institut der Universität
Im Neuenheimer Feld 270, D-6900 Heidelberg (FRG)

Formally, the two technetium centers must be assigned on oxidation number of +3.5. This would mean that the ground state has the relatively rare $\sigma^2\,\pi^4\,\delta^1$ configuration and thus a bond order of 3.5.[7] This bond order together with the three μ-oxo ligands makes the extremely short Tc–Tc distance understandable.

The spectroscopic data are fully consistent with the results of the X-ray structure analysis. Thus, in the EI mass spectrum the molecular peak is clearly visible at m/z 381.6 (18%), and the Tc–O stretching vibrations appear in the IR spectrum at 909 (symmetric) and 880 cm^{-1} (antisymmetric). In the ^1H NMR spectrum the methyl protons are observed at $\delta = 1.606$.

Experimental

A solution of **4** (180 mg, 0.57 mmol) in C_6H_6 (15 mL) was treated with 5 mL of 30% H_2O_2 and the mixture stirred at room temperature. The initial concentration of **4** first started to decrease after 24 h. After 3 days, **4** could no longer be detected. After separation of the phases the organic phase was dried with Na_2SO_4 and freed of oily reaction products by chromatography (silica gel 60, 30 × 20 cm, C_6H_6). Subsequent elution with C_6H_6/diethyl ether (1/1) gave a yellow zone. After slow evaporation of solvent from the eluate (ca. 12 h), **5** was recovered in the form of needle-shaped yellow crystals. Yield: 25.0 mg (16.0%). ^{99}Tc 51.6% (calcd. 51.94%). EI-MS fragmentation (relative intensity [%] in parenthesis): $Cp^{*\oplus}$ (100); $Cp^*Tc^{\oplus}$ (36); $Cp^*TcO_3^{\oplus}$ (0.0); $Cp^*Tc_2O_3^{\oplus}$ (18). The corresponding relative intensities for **2** under similar conditions are 100, 35, 100, and 0.0%.

Received: March 8, 1989 [Z 3225 IE]
German version: *Angew. Chem. 101* (1989) 1055

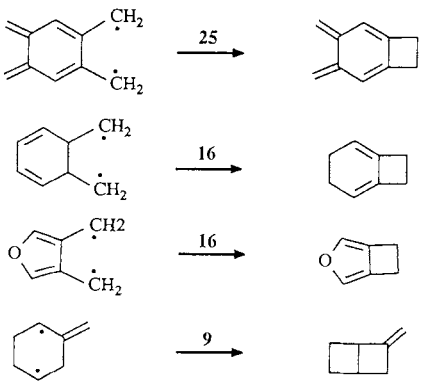
[1] W. A. Herrmann, *Angew. Chem. 100* (1988) 1269; *Angew. Chem. Int. Ed. Engl. 27* (1988) 1297, zit. Lit.; A. H. Klahn-Oliva, D. Sutton, *Organometallics 3* (1984) 1313.
[2] J. Okuda, E. Herdtweck, W. A. Herrmann, *Inorg. Chem. 27* (1988) 1254.
[3] Yellow column-shaped crystals (0.23 × 0.26 × 0.31 mm^3); a = 594.6(5), b = 869.7(4), c = 1063.0(7) pm; $V = 549.70 \times 10^6$ pm^3; $Z = 4$; space group D_{2h}^{13}–*Pmnm* (No. 59). Data collection with a Siemens-Stoe diffractometer (AED II), θ/ω scan ($3° < 2\theta < 60°$; h(min/max) 0/8, k 0/12, l 0/15), $Mo_{K\alpha}$ radiation (λ = 0.71069 Å); 969 possible reflections in the measuring range, 381 ($I > 2.0\,\sigma(I)$), 348 independent ($I > 2.25\,\sigma(I)$); empirical absorption correction (χ scans, 4 reflections $13° < 2\theta < 42°$, transmission factors (min/max) 0.74/1.00, μ = 24.41 cm^{-1}, ϱ_{calcd} = 2.3 g cm^{-3}); solution of structure by Patterson, Fourier and Difference Fourier syntheses, refinement by method of least squares (all non-hydrogen atoms anisotropic, H atoms fixed at ideal positions), $R = 0.059$, $R_w = [\sum w(|F_o| - |F_u|)^2 / \sum w\,Fo^2]^{1/2} = 0.044$, Goof $= [\sum w(|F_o| - |F_c|)^2/(\text{NO-NV})]^{1/2} = 2.19$, residual electron density 1.47/−3.13 e/Å^3, shift/esd (mean/max) 0.18/1.8. All calculations based on the program system SHELXTL. Further details of the crystal investigation are available on request from the Fachinformationszentrum Karlsruhe, Gesellschaft für wissenschaftlich-technische Information mbH, D-7514 Eggenstein-Leopoldshafen 2, on quoting the depository number CSD-53780, the names of the authors, and the journal citation.
[4] F. A. Cotton, L. D. Gage, *Nouv. J. Chim. 1* (1977) 441; F. A. Cotton, W. K. Bratton, *J. Am. Chem. Soc. 87* (1965) 921.
[5] P. O'Brien in G. Wilkinson, R. D. Gillard, J. A. McCleverty (Eds.): *Comprehensive Coordination Chemistry, Vol. 3*, Pergamon Press, Oxford 1987, p. 741 ff.
[6] F. A. Cotton, S. A. Koch, M. Miller, *Inorg. Chem. 17* (1978) 2084.
[7] M. H. Chisholm in F. A. Cotton (Ed.): *Reactivity of Metal-Metal Bonds, ACS Symp. Ser. 155* (1981).

Energy Wells of Diradicals; 4-Methylene-1,3-cyclopentanediyl**

By *Wolfgang R. Roth,* Frank Bauer, Karsten Braun,* and *Rolf Offerhaus*

Dedicated to Professor Christoph Rüchardt on the occasion of his 60th birthday

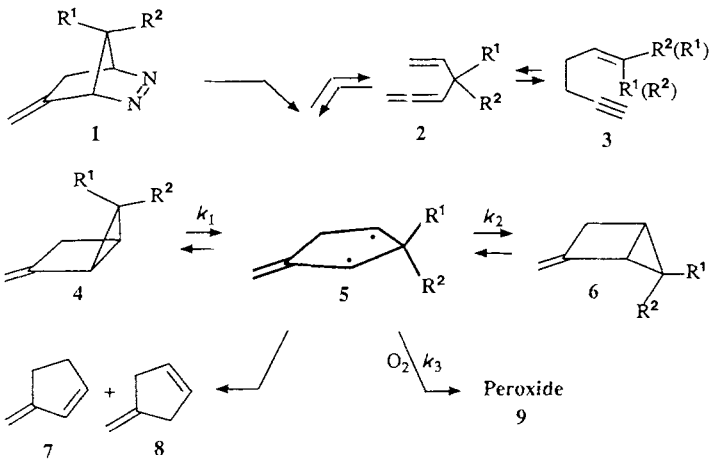
The recombination of free radicals is a collision-controlled process requiring very little activation enthalpy.[1] In the analogous intramolecular reactions the situation is far less clear, and older concepts of substantial barriers[2] have been contradicted.[3] Systematic investigations of resonance stabilized diradicals have revealed a marked dependence of the recombination barrier on the structure (see Scheme 1), which



Scheme 1. Energy wells of diradicals in kcal mol^{-1} [2].

has been explained in terms of the conformational stability of the diradicals.[4] Determination of the recombination threshold of the title compound **5** (Scheme 2) enables a critical test of this hypothesis.

In the systems outlined in Scheme 1 interaction of the unpaired electrons requires a considerable rotation of the respective orbitals, which is possible only with more or less great sacrifice of resonance stabilization. In the case of 4-methylene-1,3-cyclopentanediyl **5** the situation is completely different. Here, recombination leads to a three-membered ring, whose Walsh orbitals still allow an interaction with the



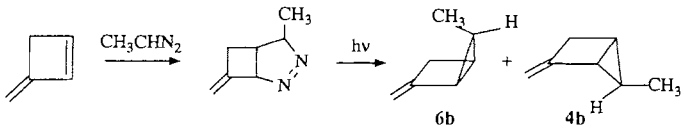
Scheme 2. **a**: $R^1 = R^2 = H$; **b**: $R^1 = H$, $R^2 = CH_3$; **c**: $R^1 = R^2 = CH_3$

[*] Prof. Dr. W. R. Roth, F. Bauer, K. Braun, R. Offerhaus
Fakultät für Chemie der Universität
Postfach 102148, D-4630 Bochum 1 (FRG)

[**] This work was supported by the Fonds der Chemischen Industrie and the Land Nordrhein-Westfalen.

exocyclic double bond even in the transition state of the reaction. The recombination enthalpy should therefore be distinctly smaller than in the homologous 2-methylene-1,4-cyclohexanediyl (see Scheme 1).

5 is accessible thermally starting from **1**,[5,6] **2**[7] and **4** or **6**,[8] and, in the case of **1** also photochemically. According to ESR investigations by *Dowd*[5] **5** has a triplet ground state. Our interest turned to the equilibrium **4** ⇌ **5** ⇌ **6**, which we have tried to detect by the mutual rearrangement **4b** ⇌ **6b**. The substrates were synthesized analogously to that of the parent compound[8a] by addition of diazoethane to methylenecyclobutene and photolysis of the resulting pyrazolines (Scheme 3). The structure of the gas-chromatographically separated isomers is confirmed by the spectroscopic data.[9]



Scheme 3.

The mutual rearrangement **4b** ⇌ **6b** was carried out in pentane at six temperatures between 20 and 60 °C. The resulting rate constants of the first order reactions (Table 1)

Table 1. Rate constants.

T [°C]	20.0	29.0	31.0	39.9	49.9	60.0	
$k_{4b,6b} \times 10^5$ [s^{-1}]	1.669		7.397	22.19	73.99	247.1	
$k_{6b,4b} \times 10^5$ [s^{-1}]	4.397	15.20		58.88	189.1	599.3	
T [°C]	175.2	185.8	195.6	206.0	216.4	226.5	236.8
$k_{4c,2c} \times 10^5$ [s^{-1}]	4.897	12.64	29.93	69.87	159.3	335.9	720.6
T [°C]	206.0	216.4	226.5	236.8	248.8	257.0	276.6	286.6
$k_{2c,3c} \times 10^5$ [s^{-1}]	0.979	2.125	4.453	9.089	18.14	34.42	112.5	211.0
T [°C]	216.4	236.8	246.8	257.0	276.6	287.6		
$k_{3c,2c} \times 10^5$ [s^{-1}]	0.224	1.032	2.227	4.118	13.68	26.64		
T [°C]	91.6	101.3	111.7	121.9	132.3	142.2	152.4	
$k_{4c,9c} \times 10^5$ [s^{-1}]	2.004	4.248	8.447	17.15	32.59	58.70	106.7	
$[O_2] \times 10^3$ [mol L^{-1}]	4.649	4.496	4.346	4.276	4.279	4.057	3.969	
$k_2 \times 10^{-12}$ [s^{-1}] [a]	1.007	1.082	1.257	1.368	1.579	1.690	1.828	
T [°C]	91.3	101.0	111.7	121.9	132.4	142.2		
$k_{4c,9c} \times 10^5$ [s^{-1}]	2.743	5.937	12.33	24.25	46.62	86.13		
$[O_2] \times 10^3$ [mol L^{-1}]	6.710	6.680	6.444	6.249	6.174	6.027		
$k_2 \times 10^{-12}$ [s^{-1}] [a]	1.034	1.121	1.276	1.415	1.604	1.713		
T [°C]	91.3	101.3	111.7	121.9	132.5	142.1		
$k_{4c,9c} \times 10^5$ [s^{-1}]	1.326	2.677	5.662	10.83	21.80	37.88		
$[O_2] \times 10^3$ [mol L^{-1}]	3.178	3.011	2.957	2.858	2.827	2.763		
$k_2 \times 10^{-12}$ [s^{-1}] [a]	1.012	1.149	1.275	1.448	1.581	1.771		
T [°C]	159.3	169.3	179.5	189.4	199.1	209.0	219.1	
$k_{4a,2a} \times 10^5$ [s^{-1}]	1.427	3.732	9.962	22.89	51.28	116.5	250.2	
$k_{4a,7} \times 10^5$ [s^{-1}]	1.656	4.250	10.32	24.79	55.60	121.8	257.2	
$k_{4a,8} \times 10^5$ [s^{-1}]	1.091	2.784	7.192	16.31	36.36	80.83	172.1	
T [°C]	248.7	258.5	268.5	278.5	288.5	308.3		
$k_{2a,3a} \times 10^5$ [s^{-1}]	21.49	38.93	71.11	126.2	222.6	589.7		
$k_{3a,2a} \times 10^5$ [s^{-1}]	62.64	111.3	201.2	351.4	609.5	1581.		
$k_{2a,7} \times 10^5$ [s^{-1}]	0.814	1.577	2.993	5.569	10.13	31.23		
$k_{2a,8} \times 10^5$ [s^{-1}]	0.585	1.085	2.128	3.899	7.094	21.68		

[a] Calculated with $k_3 = 0.5642 \times 10^{10} \times T^{1/2}$ Lmol^{-1} s^{-1}.

 © VCH Verlagsgesellschaft mbH, D-6940 Weinheim, 1989 0570-0833/89/0808-1056 $ 02.50/0

enabled calculation of the activation parameters (Table 2). For the determination of the energy well of the diradical **5** we chose the dimethyl derivative **5c**, since, in this case, the rearrangement to **7** and **8** is suppressed. The thermolysis of **4c** and **6c** led exclusively to **2c** and its secondary product **3c**. The rate of this reaction was investigated in the gas phase between 175 and 237 °C and 206 and 286 °C, respectively. The respective first order rate constants (Table 1) were ascertained by matching the reaction course simulated in Scheme 2 with the experimental data (Marquardt optimization[10]). The resulting activation parameters are listed in Table 2.

Tabelle 2. Activation parameters [a].

Reaction	E_a [kcal mol^{-1}]	A [s^{-1}]	$\Delta H^{\neq}$ [kcal mol^{-1}]	$\Delta S^{\neq}$ [cal K^{-1} mol^{-1}]
4b → **6b**	23.6 ± 0.5	$(1.7 \pm 1.4)10^{13}$	23.0 (40 °C)	0.94 (40 °C)
6b → **4b**	24.5 ± 0.3	$(2.8 \pm 1.5)10^{13}$	23.9 (40 °C)	− 0.02 (40 °C)
4c → **2c**	35.8 ± 0.2	$(4.2 \pm 1.7)10^{13}$	34.8 (206 °C)	0.85 (206 °C)
2c → **3c**	35.2 ± 0.1	$(1.1 \pm 0.3)10^{11}$	34.2 (244 °C)	− 11.0 (244 °C)
3c → **2c**	36.3 ± 1.2	$(3.9 \pm 2.6)10^{10}$	35.3 (254 °C)	− 13.2 (253 °C)
4a → **2a**	36.5 ± 0.4	$(4.1 \pm 1.9)10^{13}$	35.6 (189 °C)	0.9 (189 °C)
4a → **7**	35.8 ± 0.2	$(2.0 \pm 0.5)10^{13}$	34.9 (189 °C)	− 0.6 (189 °C)
4a → **8**	35.8 ± 0.3	$(1.3 \pm 0.5)10^{13}$	34.9 (189 °C)	− 1.3 (189 °C)
2a → **3a**	33.7 ± 0.7	$(2.7 \pm 1.7)10^{10}$	32.6 (275 °C)	− 14.0 (275 °C)
3a → **2a**	32.8 ± 0.6	$(3.5 \pm 2.0)10^{10}$	31.7 (275 °C)	− 13.5 (275 °C)
2a → **7**	36.8 ± 0.1	$(2.2 \pm 0.2)10^{10}$	35.7 (275 °C)	− 14.4 (275 °C)
2a → **8**	36.6 ± 0.5	$(1.3 \pm 0.6)10^{10}$	35.5 (275 °C)	− 15.5 (275 °C)
5c → **4c**	3.1 ± 0.2	$(5.9 \pm 1.3)10^{13}$	2.4 (118 °C)	2.5 (118 °C)

[a] All error data refer to a confidence limit of 95%.

In order to demonstrate the influence of the methyl groups on the ring opening, the thermolysis of the parent compound **4a** (= **6a**) was also investigated for comparison. As the data in Table 2 show, these differ negligibly from those of the dimethyl compound.

When the thermolysis of **4c** is carried out in the presence of oxygen, the diradical **5c** can be trapped as peroxide.[11] If one assumes that the diradical reacts collision-controlled with oxygen in analogy to the reaction of free radicals, then the rate of this reaction can be described with equation (a),[12]

$$k_3 = N_A(\sigma_a + \sigma_b)^2/4\,(8\pi kT/\mu)^{1/2}\ \mathrm{Lmol^{-1}\,s^{-1}} \qquad (a)$$

where N_A is the Avogadro number, σ_a and σ_b the collision cross-sections of the reacting molecules,[13] k the Boltzmann constant, and μ the reduced mass. Should the formation of the peroxide proceed via the triplet state an additional spin statistical factor[14] would have to be taken into account, which, however, only influences the entropy but not the enthalpy of the energy well. A singlet $\rightleftharpoons$ triplet equilibrium[15] would have the same effect. A definite statement can be made at the moment therefore only about the recombination enthalpy. The rate of formation of peroxide is—assuming a steady-state for **5**—described by equation (b).

$$k_{per} = k_1\left(1 - \frac{k_2}{k_2 + k_3[O_2]}\right) \qquad (b)$$

With this relationship, k_1 and k_2 can be determined from the dependence of the formation of peroxide on oxygen only, if the measurements are carried out in the non-linear range of the function. As the data in Table 1 show, this does not apply in the present case; owing to the limits of the apparatus used, we could only measure trapping rates up to $\leq$ 750 torr oxygen pressures. We have therefore assumed that k_1 is, to a good approximation, described by the corresponding rate konstants ($k_{\mathbf{4b,6b}}$) of the monomethyl compound. In view of the influence of the methyl substitution on the ring-opening reaction being only slight (see above) this assumption may not lead to any serious error. The resulting activation parameters for k_2 (see Table 2) clearly indicate that the oxygen pressure required for a direct determination of k_1 is ca. 1000 atm.

As already mentioned above, the available data do not allow a decision whether the determined energy well refers to the singlet or the triplet state. With a value of 2.4 kcal mol^{-1}, the well is in fact much smaller than in the case of the analogous 2-methylene-1,4-cyclohexanediyl (9 kcal^{-1}) and is practically identical with that of the parent compound (2.3 ± 0.2 kcal mol^{-1}[16]). *Closs* et al. have obtained this value from ESR measurements at low temperatures, where the reaction seems to be the result of a tunnel mechanism ($A = 10^8$ s^{-1}). Consistent with the observed A factor ($A = 5.9 \times 10^{13}$ s^{-1}) such a mechanism is ruled out under our conditions.

Received: March 3, 1989 [Z 3212 IE]
German version: *Angew. Chem. 101* (1989) 1092

[1] C. Rüchardt, H.-D. Beckhaus, *Top. Curr. Chem. 130* (1986) 1, and references cited therein.
[2] S. W. Benson, *J. Chem. Phys. 34* (1961) 521.
[3] W. von E. Doering, *Proc. Natl. Acad. Sci. USA 78* (1981) 5279.
[4] W. von E. Doering, W. R. Roth, R. Breuckmann, L. Figge, L.-W. Lennartz, W.-D. Fessner, H. Prinzbach, *Chem. Ber. 121* (1988) 1.
[5] **1a**: P. Dowd, Pittsburgh, private communication June 1988.
[6] **1c**: W. Adam, E. Günther, P. Hössel, H. Platsch, R. M. Wilson, *Tetrahedron Lett. 28* (1987) 4407.
[7] W. W. Huntsman, J. A. DeBoer, M. H. Woosley, *J. Am. Chem. Soc. 88* (1966) 5846; V. Dalacker, H. Hopf, *Tetrahedron Lett. 1974*, 15.
[8] a) G. D. Andrews, J. E. Baldwin, *J. Org. Chem. 53* (1988) 4624; b) K. Braun, Diplomarbeit, Universität Bochum 1988.
[9] ^{1}H-NMR coupling constant in the three-membered ring **6b**: 6 Hz; **4b**: 0 Hz.
[10] D. W. Marquardt, *J. Soc. Ind. Appl. Math. 11* (1963) 431.
[11] The structures of the resulting peroxides were elucidated by *Adam* et al. [6].
[12] P. J. Robinson, K. A. Holbrook: *Unimolecular Reactions*, Wiley-Interscience, London 1982, p. 164; G. B. Skinner: *Introduction to Chemical Kinetics*, Academic Press, New York 1974.
[13] $\sigma_a(O_2) = 3.6$ Å, see S. W. Benson: *Foundation of Chemical Kinetics*, McGraw-Hill, New York 1960; $\sigma_b(\mathbf{5}) = 6$ Å (estimated from models).
[14] For a two-step peroxide formation the factor is 4/9, otherwise 1/9.
[15] R. D. Small, Jr., J. C. Scaiano, *J. Am. Chem. Soc. 100* (1978) 4512; M. N. Burnett, R. Boothe, E. Clark, M. Gisin, H. M. Hassaneen, R. M. Pagni, G. Persy, R. J. Smith, J. Wirz, *ibid. 110* (1988) 2527.
[16] S. L. Buchwalter, C. L. Closs, *J. Am. Chem. Soc. 101* (1979) 4688.

Addition of Carboxamides to Alkynyl Trifluoromethyl Sulfones**

By *Michael Hanack*,* and *Bärbl Wilhelm*

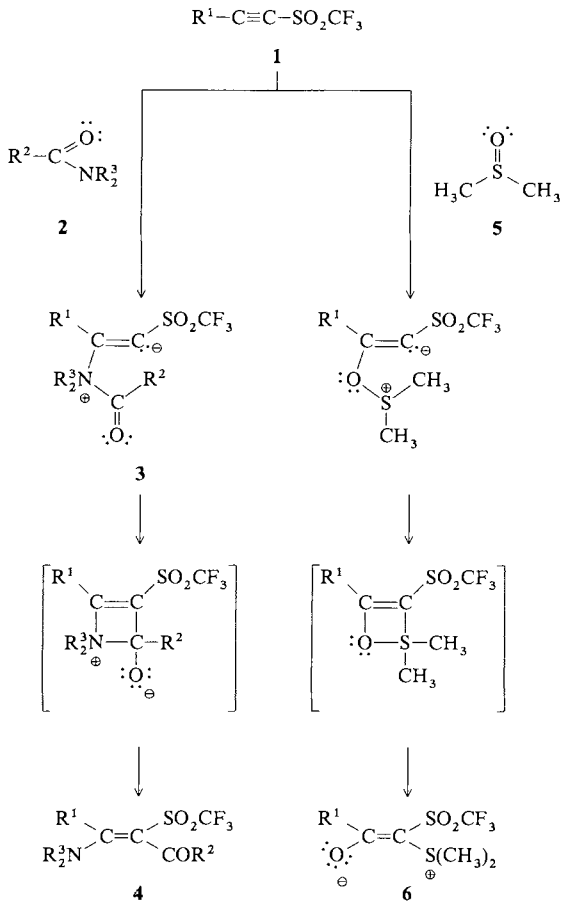
The trifluoromethylsulfonyl group is one of the strongest electron-withdrawing functional groups.[1] Olefins and alkynes bearing this substituent are highly reactive, e.g. in [4 + 2]- and 1,3-dipolar cycloadditions,[2] and are therefore of great preparative interest. We have recently reported a novel, improved method for the synthesis of alkynyl trifluoromethyl sulfones **1** from sodium acetylides and trifluoromethanesulfonic anhydride.[3] In related studies we have also investigated the addition of nucleophiles to **1**, which occurs

[*] Prof. Dr. M. Hanack, Dipl.-Chem. B. Wilhelm
Institut für Organische Chemie der Universität
Auf der Morgenstelle 18, D-7400 Tübingen (FRG)

[**] This work was supported by the Fonds der Chemischen Industrie.

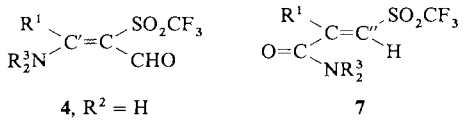
considerably more easily than in the case of comparable systems such as acetylenecarboxylic acid esters.[3,4]

On attempting to add sulfinic acids dissolved in dimethylformamide **2a** we observed an unusual addition of **2a** to the triple bond of phenylethynyl trifluoromethyl sulfone **1a** (Scheme 1). This addition is applicable to alkynyl trifluoromethyl sulfones in general: Table 1 shows the products of the reaction with several substituted carboxamides **2** and dimethyl sulfoxide (DMSO) **5**.



Scheme 1. Mechanism of the addition of carboxamides **2** and of DMSO **5** to alkynyl trifluoromethyl sulfones **1**. R^1,R^2,R^3 see Table 1.

According to the spectroscopic data, not only the structure **4** but primarily also the structure **7** had to be taken into consideration for adducts of **1a–d** and **2a–d**.



4, $R^2 = H$ **7**

In the case of **4a**,[5] for example, a singlet is observed at $\delta = 7.71$ in the ^1H NMR spectrum. This would rather point to an olefinic than to an aldehydic proton. The ^{13}C off-resonance NMR spectrum shows a singlet at $\delta = 188.7$, which could be assigned to both the carbon atom C′ in **4a** as well as to the carbonyl carbon atom in **7a** ($R^1 = C_6H_5$, $R^3 = CH_3$). A doublet appears at $\delta = 158.0$, which may arise from the aldehyde carbon atom in **4a** or from the carbon atom C″ in **7a**. In the IR spectrum the carbonyl vibration is observed at $\tilde{\nu} = 1642\ cm^{-1}$, i.e. at exceptionally low field for an aldehydic carbonyl group.

For an unequivocal elucidation of the structures of the adducts we allowed the sulfone **1a** to react with ^{13}C-labeled dimethylformamide **2a**. Due to the labeling, a doublet now appears at $\delta = 157.9$ in the ^{13}C off-resonance spectrum of the product. This rules out the structure type **7**, since the labeled carbon atom would then have to give rise to a singlet in the ^{13}C off-resonance spectrum of **7a***. Hence, the structures **4a–i** are unequivocally verified. The substituents R^3 on the nitrogen atom of the formamide adducts **4a–i** show different chemical shifts, i.e. their magnetic equivalence is removed. This is due to the interaction of the aldehyde hydrogen atoms with the lone pair on the nitrogen atom. All the addition products are sterically uniform.

Reaction of the trifluoromethyl sulfones **1a–d** with the formamides **2a–d** is quantitative. Other activated alkynes e.g. phenyl phenylethynyl sulfone, diethyl acetylenedicarboxylate and ethyl phenylpropiolate do not react with dimethylformamide **2a**, even at elevated temperatures. Owing to the low carbonyl activity, the acetamides **2e–g** are less reactive towards **1** than the formamides **2a–d** (Table 1). All

Table 1. Addition products of carboxamides **2** and of DMSO **5** with alkynyl trifluoromethyl sulfone (cf. Scheme 1).

Reactants	Product	R^1	R^2	R^3	Yield [%]
1a/2a	**4a**	C_6H_5	H	CH_3	70
1a/2b	**4b**	C_6H_5	H	i-C_3H_7	60
1a/2c	**4c**	C_6H_5	H	-$C_2H_4OC_2H_4$-	60
1a/2d	**4d**	C_6H_5	H	C_2H_5	71
1b/2d	**4e**	4-$CH_3C_6H_4$	H	C_2H_5	80
1b/2c	**4f**	4-$CH_3C_6H_4$	H	-$C_2H_4OC_2H_4$-	85
1c/2a	**4g**	n-C_4H_9	H	CH_3	50
1c/2b	**4h**	n-C_4H_9	H	i-C_3H_7	65
1d/2a	**4i**	t-C_4H_9	H	CH_3	51
1a/2e	**4j**	C_6H_5	CH_3	CH_3	19
1b/2e	**4k**	4-$CH_3C_6H_4$	CH_3	CH_3	30
1b/2f	**4l**	4-$CH_3C_6H_4$	CH_3	C_2H_5	50
1b/2g	**4m**	4-$CH_3C_6H_4$	CH_3	-$C_2H_4OC_2H_4$-	40
1a/5	**6a** [7]	C_6H_5	–	–	66
1c/5	**6b**	n-C_4H_9	–	–	90
1e/5	**6c**	c-C_6H_{11}	–	–	94

attempts to initiate reaction of **1a** with tetramethylurea or *N,N*-diethylurethane met without success. The addition of DMSO **5** to acetylenedicarboxylates is well known.[6] By way of comparison, **5** reacts much more readily with the alkynyl trifluoromethyl sulfones **1a,c,e**: even at room temperature the stable ylides **5a–c** are formed in quantitative yield[7] (Table 1).

Our results (Scheme 1) confirm a mechanism which has already been proposed[6] for the addition of DMSO **5** to acetylenecarboxylates. The structure of the acid amide adducts **4** would suggest a mechanism comparable to that for the addition of **5**: the nitrogen atom of the acid amide **2** attacks at the β-carbon atom of the alkynyl trifluoromethyl sulfone **1**, and the resulting zwitterion **3** is stabilized by cyclization and subsequent rupture of the carbon-nitrogen bond to give **4**. If this mechanism is involved in the addition, as suggested by the stereochemical uniformity of the products **4**, the latter must have *E*-configuration.

Experimental

Mixtures of the alkynes and carboxyamide **2** or dimethyl sulfoxide **5** were stirred at room temperature for 1 to 2 d. After aqueous work-up, the formamide and dimethyl sulfoxide adducts **4a–i** and **6a–c** were purified by flash chromatography (hexane/ethyl acetate); the acetamide adducts **4j–m** crystallize from the reaction mixture in analytically pure form. All the products separate

out as colorless to yellowish crystals which are stable towards air at room temperature.

Received: March 6, 1989 [Z 3217 IE]
German version: *Angew. Chem. 101* (1989) 1083

CAS Registry numbers:
1a, 52843-77-3; **1b**, 121289-99-4; **1c**, 119353-19-4; **1d**, 121290-00-4; **1e**, 119353-22-9; **2a**, 68-12-2; **2b**, 2100-30-3; **2c**, 4394-85-8; **2d**, 617-84-5; **2e**, 127-19-5; **2f**, 685-91-6; **2g**, 1696-20-4; **4a**, 121290-01-5; **4b**, 121290-02-6; **4c**, 121290-03-7; **4d**, 121290-04-8; **4e**, 121290-05-9; **4f**, 121290-06-0; **4g**, 121290-07-1; **4h**, 121290-08-2; **4i**, 121290-09-3; **4j**, 121290-10-6; **4k**, 121290-11-7; **4l**, 121290-12-8; **4m**, 121290-13-9; **5**, 67-68-5; **6a**, 121290-14-0; **6b**, 121290-15-1; **6c**, 121290-16-2.

[1] T. Gramstad, R. N. Haszeldine, *J. Chem. Soc. 1957*, 4069.
[2] a) K. Schank, in *Houben-Weyl-Müller: Methoden der Organischen Chemie, Band E11*, 4th edit., Thieme, Stuttgart 1985, p. 1281, and references cited therein; b) F. Massa, M. Hanack, L. R. Subramanian, *J. Fluorine Chem. 19* (1982) 601; c) M. Hanack, K. Laping, *Tetrahedron Lett. 1979*, 1309.
[3] M. Hanack, B. Wilhelm, L. R. Subramanian, *Synthesis 1988*, 592.
[4] E. Winterfeldt, *Angew. Chem. 79 (1967) 389; Angew. Chem. Int. Ed. Engl. 6* (1967) 423.
[5] 3-Dimethylamino-2-(trifluoromethylsulfonyl)cinnamaldehyde **4a**: colorless crystals, m.p. 100 °C. ^{1}H NMR ($CDCl_3$, 90 MHz): δ = 2.61, 3.26 (2s, 6H; $N(CH_3)_2$), 7.32–7.88 (m, 5H; aryl-H), 7.71 (s, 1H; CHO). ^{13}C NMR ($CDCl_3$, 100 MHz): δ = 41.7, 47.9 (2q; $N(CH_3)_2$), 97.3 (s; $=C$(CHO)), 120.4 (q, ^1J = 327; CF_3), 128.4, 129.8, 133.5 (3d; aryl-C), 139.3 (s; aryl-C), 158.0 (d; CHO), 188.7 (s; $=C$($N(CH_3)_2$)). IR (KBr): $\tilde{\nu}$ = 1642 (C=O), 1612 (C=C), 1359, 1159 (S=O), 1204 (C–F). MS (70 eV): *m/z* 307 (2%, $M^{\oplus}$), 238 (51, $M^{\oplus}-CF_3$), 174 (14, $M^{\oplus}-SO_2CF_3$), 131(28), 105(100), 77(80), 44(99). Correct elemental analysis.
[6] E. Winterfeldt, *Chem. Ber. 98* (1965) 1580; T. J. Chow, U.-K. Tan, S.-M. Peng, *Synth. Commun. 18* (1988) 519.
[7] (*E*)-1-Phenyl-2-trifluoromethylsulfonyl-2-dimethylsulfonium ethenolate **6a**: colorless crystals, m.p. 148 °C. ^{1}H-NMR ($CDCl_3$, 90 MHz): δ = 3.07 (s, 6H; CH_3), 7.37 (m, 5H; aryl-H). ^{13}C NMR ($CDCl_3$, 100 MHz): δ = 27.9 (q; CH_3), 76.7 (s; $=C$(SO_2CF_3)), 120.7 (q, ^1J = 326; CF_3), 127.0, 127.5, 130.2 (3d; aryl-C), 140.4 (s; aryl-C), 189.7 (s; $=C$(C_6H_5)). IR (KBr): $\tilde{\nu}$ = 1593 (C–O), 1349, 1190 (S=O), 1203 (C–F). MS (70 eV): *m/z* 312 (34%, $M^{\oplus}$), 297 (5, $M^{\oplus}-CH_3$), 243 (52, $M^{\oplus}-CF_3$), 235 (2, $M^{\oplus}-C_6H_5$), 179 (2, $M^{\oplus}-SO_2CF_3$), 105 (100, $C_7H_5O^{\oplus}$), 77 (44), 69 (2). Correct elemental analysis.

A Systematic Entry to Butterfly-Type $[M_4(CO)_{12}(\mu_4\text{-XY})]$ Clusters**

By *Harald Bantel, Bernhard Hansert, Anne K. Powell, Miklos Tasi,* and *Heinrich Vahrenkamp**

Dedicated to Professor Christoph Rüchardt on the occasion of his 60th birthday

Cluster expansion with organometal building blocks is an indispensable strategy for the systematic synthesis of multinuclear clusters.[1, 2] We are presently investigating the use of cluster-bound ligands of the type XY (X,Y = RC,RN,C,N,O) for controlling and altering the activity of such complexes[3]. Trinuclear complexes containing these ligands are fairly readily accessible, whereas their tetranuclear counterparts are largely unexplored. The unusual chemistry which, e.g., the exposed C-ligands in the clusters $[(Fe_4(CO)_{13}(\mu_4\text{-C})]$[4] and $[HFe_4(CO)_{12}(\mu_4\text{-CH})]$[5] exhibit makes further preparative and reactivity studies appear worthwhile. The clusters **1** provide simple and ideal examples for such studies; the alkyne-[6] and nitrile-complexes[7] of **1** have long been known, while the azoalkane complex[8] was first reported only recently. The current thermal methods[1] with $Fe_3(CO)_{12}$ and $Ru_3(CO)_{12}$ as fragment sources have proven unsuitable for the expansion of such clusters with $M(CO)_3$ building blocks. However, photochemical reactions[9] with $Fe_2(CO)_9$ and $Ru(CO)_5$ provided access to the tetranuclear clusters **2a** in 45%, **2b** in 42% and **2c** in 64% yield.[10]

$$\underset{\mathbf{1}}{[M_3(CO)_9(\mu_3\text{-XY})]} \xrightarrow{\text{"M(CO)}_3\text{"}} \underset{\mathbf{2}}{[M_4(CO)_{12}(\mu_4\text{-XY})]}$$

a: M = Fe, XY = Me_2C_2; **b**: M = Fe, XY = PhCN;
c: M = Ru, XY = Et_2N_2

Hitherto, only **2b**[7b] had been isolated, albeit in very small yields, and structurally characterized; the Ru-analogue[11] of **2a** was first reported somewhat earlier. The new compounds **2a** and **2c** were characterized by their spectra[12] and by structural analyses.[13] All these clusters are of the butterfly type, in which the ligand XY is located in the groove of the bicyclobutane-like folded M_4 unit.

A comparison of the structures of **2a**, **2b** and **2c** (Fig. 1) not only shows the dependence of the M_4XY skeletal geometry on the electron number of the ligand XY, but also its variability at constant electron number. Thus in **2a**, with its 4e alkyne ligand, a 60e cluster with seven skeletal electron pairs is present, which, in agreement with the Wade rules has the *closo* octahedral geometry. **2b** and **2c** are 62e clusters with eight skeletal electron pairs, since nitrile, like azoalkane, is a 6e ligand. As expected, both clusters have an open M_4XY skeleton, which however cannot be easily derived from a *nido*[7]-polyhedron. **2b** can be regarded as a capped trigonal bipyramid (with the C atom as "cap"). **2c** is best described as an *arachno*-D_{2d} dodecahedron whose vacant positions lie above the two Ru_2N_2 rectangles, a feature observed here for the first time. To a close approximation all three clusters **2** reveal the geometry of the starting cluster **1**, to which an $M(CO)_3$ has been added sideways.

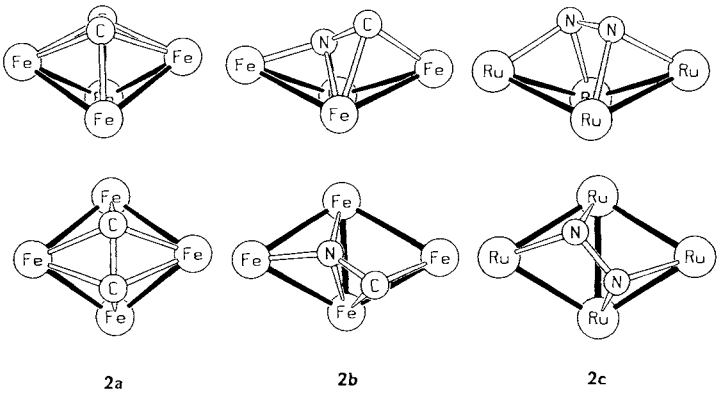


Fig. 1. Two views each of the molecular skeletons of **2a–2c**. Bond lengths in the XY ligands: **2a**, C–C 144(1); **2b**, C–N 135(1); **2c**, N–N 146(1) pm. Dihedral angle between the two M_3 units: **2a**, 115°; **2b**, 135°; **2c**, 124°.

Despite entirely different orientation of the XY ligand to the M_4 unit, all three complexes show a similar expansion of the formally X–Y multiple bond to almost the length of a single bond (Fig. 1). The weakening of this bond (reduction by coordination[3]) should correspond to a markedly modified reactivity of the XY ligands, which in **2b** and **2c** might also be increased by their exposed situation. Photochemical cluster expansion can – as long as the ligand is photochemically stable – be used generally, e.g., with other organometal

[*] Prof. Dr. H. Vahrenkamp, Dipl.-Chem. H. Bantel, Dipl.-Chem. B. Hansert, Dr. A. K. Powell, Dr. M. Tasi
Institut für Anorganische und Analytische Chemie der Universität
Albertstrasse 21, D-7800 Freiburg (FRG)

[**] This work was supported by the Stiftung Volkswagenwerk, the Fonds der Chemischen Industrie and the Rechenzentrum der Universität Freiburg.

building blocks (e.g. Cp(CO)Rh) and ligands (e.g. vinylidene).[14]

Received: February 13, 1989 [Z3176 IE]
German version: *Angew. Chem. 101* (1989) 1084

[1] H. Vahrenkamp, *Adv. Organomet. Chem. 22* (1983) 169.
[2] M. D. Vargas, J. N. Nicholls, *Adv. Inorg. Chem. Radiochem. 30* (1986) 123.
[3] H. Vahrenkamp in H. Werner, G. Erker (Hrsg.): *Organometallics in Organic Synthesis*, Springer, Heidelberg 1989, p. 235.
[4] P. L. Bogdan, C. Woodcock, D. F. Shriver, *Organometallics 6* (1987) 1377, and references cited therein.
[5] M. Tachikawa, E. L. Muetterties, *Prog. Inorg. Chem. 28* (1981) 203.
[6] J. F. Blount, L. F. Dahl, C. Hoogzand, W. Hübel, *J. Am. Chem. Soc. 88* (1966) 292.
[7] a) M. A. Andrews, H. D. Kaesz, *J. Am. Chem. Soc. 101* (1979) 7255; b) E. Keller, D. Wolters, *Chem. Ber. 117* (1984) 1572.
[8] E. J. Wucherer, H. Vahrenkamp, *Angew. Chem. 99* (1987) 353; *Angew. Chem. Int. Ed. Engl. 26* (1987) 355. For derivatives of cyclic azoalkanes cf. A. Albini, H. Kisch, *Top. Curr. Chem. 65* (1976) 105.
[9] R. D. Adams, J. E. Babin, M. Tasi, *Inorg. Chem. 25* (1986) 4514; *ibid. 26* (1987) 2807.
[10] Amounts of starting materials ca. 0.25 mmol (**2a, 2b**) or 0.03 mmol (**2c**), each in 100 mL of hexane. Irradiation with Pyrex-filtered light of an immersed Hanau TQ-150 W Hg-high pressure lamp for 48 (**2a**), 17 (**2b**), and 2.5 h (**2c**), respectively. Work-up by chromatography on silica gel with hexane, to which CH_2Cl_2 was gradually added (up to 10%).
[11] B. F. G. Johnson, J. Lewis, K. T. Schorpp, *J. Organomet. Chem. 91* (1975) C13.
[12] **2a**: IR (hexane) $\tilde{\nu} = 2055$(s), 2030(vs), 1987 cm^{-1} (w); ^1H NMR ($CDCl_3$, int. TMS): $\delta = 2.98$. **2c**: IR: $\tilde{\nu} = 2096$(vw), 2070(vs), 2036(vs), 2021 (m), 1993(sh), 1987(m), 1937 cm^{-1} (w); ^1H-NMR (CD_2Cl_2): $\delta = 3.94$ (m, 2H), 3.20 (m, 2H), 1.11 (t, $J = 7.0$ Hz, 6H).
[13] **2a**: orthorhombic, *Pnma*, $a = 1281.1(4)$, $b = 1321.6(2)$, $c = 1178.9(2)$ pm, $Z = 4$, 1602 reflections, $R = 0.049$; **2b**: monoclinic, $P2_1/n$, $a = 949.2(2)$, $b = 1764.1(4)$, $c = 1417.0(3)$ pm, $\beta = 98.34(2)°$, $Z = 4$, 3783 reflections, $R = 0.022$. Further details of the crystal structure investigations are available on request from the Fachinformationszentrum Karlsruhe, Gesellschaft für wissenschaftlich-technische Information mbH, D-7514 Eggenstein-Leopoldshafen 2 (FRG), on quoting the depository number CSD-53632, the names of the authors, and the journal citation.
[14] T. Albiez, H. Bantel, H. Vahrenkamp, unpublished.

Di(1-pyridinio)- and Di(1-bipyridindiio)-dihydrodibenzotetraaza[14]annulenes**

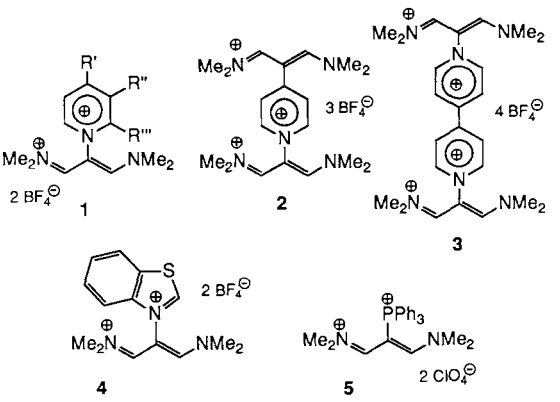
By *Florian Adams, Rudolf Gompper,** and *Eckardt Kujath*

Dedicated to Professor Christoph Rüchardt on the occasion of his 60th birthday

Derivatives and metal complexes of porphyrin[1-4] and thus of the structurally related phthalocyanine[2-5] have attracted great interest for some time as redox catalysts (inter alia for fuel cells), synthetic oxygen storage systems, molecular metals, and discotic mesophases. Porphyrins which are coupled covalently with an electron acceptor (quinone,[6] ferrocene,[7] viologen,[8] arene[9]) have recently gained special importance as models for light-induced electron transfer. The use of such systems as molecular shift registers has also been proposed.[10] Tetraaza[14]annulenes (cf. Refs. [2, 4, 11, 12]) have properties similar to those of porphyrins and phthalocyanine. Interest therefore attaches to new derivatives of these three classes of compounds because, inter alia, metal complexes of such systems which bear cationic substituents basically fulfill all the prerequisites for organic superconductors.[13] Two compounds of the porphyrin and porphyrazine series,[14] which approximate the Little models, have been investigated as catalysts for the photoreduction of water. We report here on the synthesis of dibenzotain two pyridinio- or bipyridindiio-moieties and thus are prospective redox systems for the investigation of light-prospective redox systems for the investigation of light-induced electron transfer and as models for organic superconductors.

Hitherto, only diazepines had been obtained in reactions of vinamidinium salts (which can easily be prepared with a large variety of substituents) with 1,2-diamines.[15,16] We have now found that tetraaza[14]annulenes **11** can be prepared from the 2-(1-pyridinio)vinamidinium salts **1**–**3** as well from the 2-phosphonio-vinamidinium salt **5**[17] and *o*-phenylenediamine. The 2-(1-pyridinio)-vinamidinium salts **1** and **3** (for physical data of the new compounds see Table 2) and the benzothiazoliovinamidinium salt **4** were prepared in good yields according to the method described by *Lloyd* et al.[15] for **1a** (R′ = R″ = R‴ = H)[15,18] by reaction of the corresponding *N*-carboxymethylpyridinium salts with dimethylformamide/phosphorus oxide chloride. The *N,N*′-bis(carboxymethyl)-4,4′-bipyridinediium dibromide employed for the synthesis of **3** was obtained by hydrolysis of the dimethyl ester, which in turn was prepared by reaction of 4,4′-bipyridine with methyl bromoacetate; the method of *Michaelis* and *Hill*[19] did not lead to the desired compound. No salt **1**, R″,R‴ = H, R′ = Me, could be isolated upon reaction of *N*-carboxymethyl-γ-picolinium chloride with dimethylformamide/phosphorus oxide chloride; **2** was formed directly.

As a new derivative of viologen, **3** can be reversibly reduced to a radical trication and a dication (see Table 1). Position 2 in vinamidinium salts carries a negative partial charge. It is therefore surprising that the (reversible) reduction of **3** proceeds more easily than that of methylviologen



1, 11, 12	R′	R″	R‴
a	H	H	H
b	CO_2Me	H	H
c	H	Co_2Me	H
d	$CH=CH-C_6H_5$	H	H
e	$CH=CH-C_6H_4-NO_2$ (*p*)	H	H
f	NMe_2	H	H
1g	4-pyridyl · HBF_4	H	H
11g, 12g	4-pyridyl	H	H
h	$-CH=CH-CH=CH-$		H
i	H	$-CH=CH-CH=CH-$	
11k	(1-methyl-4-pyridyl)$^{\oplus}BF_4^{\ominus}$	H	H

[*] Prof. Dr. R. Gompper, Dipl.-Chem. F. Adams, Dr. E. Kujath [+]
Institut für Organische Chemie der Universität
Karlstrasse 23, D-8000 München (FRG)
[+] Present adress: Cassella AG, Hanauer Landstrasse 526, D-6000 Frankfurt am Main 61 (FRG)

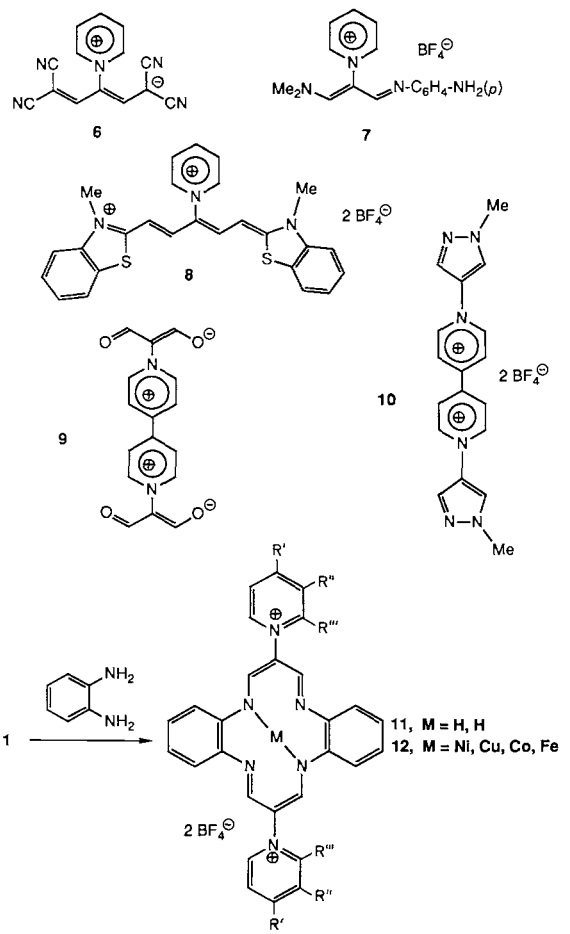
[**] This work was supported by the Deutsche Forschungsgemeinschaft and the Fonds der Chemischen Industrie.

Table 1. Redox potentials of **1g**, **3**, **9**, **11k**, **12k-Ni**, **12k-Cu** (cyclovoltammetry in (i) DMF, (ii) CH_3CN/0.1 M n-BuN_4PF_6, Pt-electrodes versus Ag/AgCl/3 M NaCl).

Cpd.	E_1 [V]	E_2 [V]	K_{com}
1g	− 0.49	− 0.12	1.9×10^6 (ii)
3	− 0.27	0.05	2.7×10^5 (ii)
9	− 0.86	− 0.45	8.9×10^6 (i)
11k	− 0.59	− 0.25	5.8×10^5 (i)
12k-Ni	− 0.59	− 0.24	8.6×10^5 (i)
12k-Cu	− 0.60	− 0.25	8.6×10^5 (i)

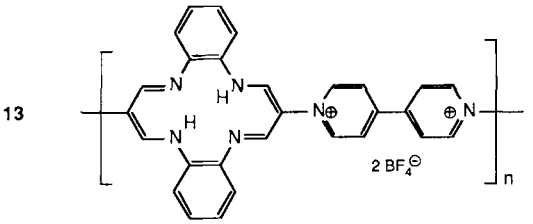
($E_1 = -0.67$ V, $E_2 = -0.26$ V; cf. Ref. [20]). One would have rather expected a similarity with **9** and bipyridinediylides[20] ($E_1 \approx -0.8$ V, $E_2 \approx -0.6$ V). In contrast, the reduction of **1g** takes place in the normal range.

Reaction of **1a** with malononitrile in the presence of Hünig base affords the orange colored ylide **6**, which should attract attention for applications in the area of nonlinear optics. Upon heating a mixture of **1a** and 2,3-dimethylbenzothiazolium tetrafluoroborate under analogous conditions the blue cyanine dye **8** is obtained. The noval viologen derivatives **9** and **10** are obtained on reaction of **3** with sodium hydroxide and methylhydrazine, respectively. Heating of **1a** with p-phenylenediamine in methanol leads to **7** and not to a polymeric condensation product.

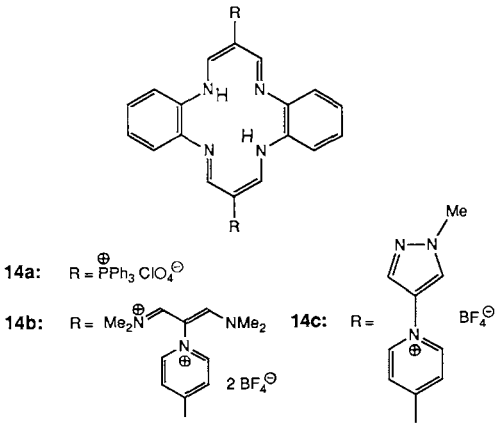


By reaction of the vinamidinium salts **1a–h** with o-phenylenediamine (**1i** reacts only under template conditions, see below), it was possible to prepare the dipyridiniodibenzotetraaza[14]annulenes **11**, which are comparable with the pyridinio-[21] and bipyridinio-substituted porphyrins.[22] **11k** is formed upon reaction of **11g** with trimethyloxonium tetrafluoroborate.

Especially interesting is the reaction of **3** with o-phenylenediamine. A practically insoluble product is formed, which, on the basis of an elemental analysis and the IR spectrum, is ascribed the structure **13**. The compounds **11** are red, whereas **13** is black.



Reaction of the phosphoniovinamidinium salt **5**[17] with o-phenylenediamine leads to formation of the [14]annulene derivative **14a**. — Of the two vinamidinium systems in **2**, only that in position 4 reacts with o-phenylenediamine, and there results the red salt **14b** in which the pyridinium ring is coupled to the [14]annulene ring via C-4 and not as in **11** via the N atom. The signals of the protons of the dimethylamino groups appear in the ^{1}H NMR spectrum of **14b** at $\delta = 2.65$ and 3.38 and thus at almost the same field as in the spectrum of **1a** (2.47, 3.40). The electronic spectrum of **14b**, like that of **1a**, shows an intense absorption maximum at 306 nm; no maxima are found in this region in the spectra of **11**–**14b** reacts with methylhydrazine (in excess) to give the dark red pyrazole derivative **14c**.



Like other dihydrodibenzotetraaza[14]annulenes,[11,23] the pyridinio derivatives **11** can be converted into their Ni-, Cu-, Co- and Fe-complexes **12** by heating with metal(II) acetates in dimethylformamide; the complexes are also formed on reaction of **1** with o-phenylenediamine in the presence of the metal acetate (cf. Ref. [24]). **12i** can be prepared only in this way. The electronic spectra of **12** show bathochromic shifts of the longest wavelength absorption maxima and of the Soret bands[23,25] at 350–400 nm compared to those of **11**.

The complexes **12** have practically the same (cyclovoltammetrically determined) redox potentials (see Table 1) as the metal-free compound **11k**, and both differ very little in this respect from methylviologen.[20] The measurement of the electrical powder conductivity[26] (4-electrode measurement, 1800 kp) shows that the complexes **12** investigated are insu-

 © VCH Verlagsgesellschaft mbH, D-6940 Weinheim, 1989 0570-0833/89/0808-1061 $ 02.50/0

Table 2. Some physical data of the new compounds.

1b: yield 71%; m.p. = 212–213 °C; UV/VIS (DMSO): λ_{max} (lg ε) = 290 nm (4.26, sh), 310 (4.49)

1c: yield 81%; m.p. = 185–186 °C

1d: yield 42%; m.p. = 242 °C; UV/VIS (CH_3CN): λ_{max} (lg ε) = 254 nm (4.14), 305 (4.61), 370 (4.57)

1e: yield 68%; m.p. = 276 °C; UV/VIS (CH_3CN): λ_{max} (lg ε) = 307 nm (4.65), 354 (4.63)

1f: yield 71%; m.p. = 276–278 °C; UV/VIS (DMSO): λ_{max} (lg ε) = 304 nm 4.68)

1g: yield 69%; m.p. = 270 °C; UV/VIS (H_2O): λ_{max} (lg ε) = 276 nm (4.53), 304 (4.59), 372 (3.26)

1h: yield 75%; m.p. = 256–257 °C

1i: yield 78%; m.p. = 260–261 °C

2: yield 69%; m.p. = 171–172 °C; ^{1}H-NMR (D_2O): δ = 2.60 (s; 6H, NMe), 3.23 (s; 6H, NMe), 3.40 (s; 6H, NMe), 3.67 (s; 6H, NMe), 7.53–9.30 (AA'BB'; 4H, pyridinio-H), 7.70 (s; 2H, C*H*NMe$_2$), 8.30 (s; 2H, C*H*NMe$_2$); UV/VIS (H_2O): λ_{max} (lg ε) = 250 nm (4.02), 302 (4.60), 351 (4.17), 397 (4.48)

3: yield 72%; m.p. = 290–292 °C; ^{1}H-NMR (D_2O): δ = 2.63 (s; 12H, NMe), 3.47 (s; 12H, NMe), 7.93 (s; 4H, C*H*NMe$_2$), 8.83–9.43 (AA'BB'; 8H, pyridinio-H); UV/VIS (H_2O): λ_{max} (lg ε) = 286 nm (4.67), 305 (4.70), 437 (3.64)

4: yield 49%; m.p. = 221–222 °C

6: yield 69%; orange needles, m.p. = 307–308 °C

7: yield 64%; red powder, m.p. = 185 °C; UV/VIS (DMSO): λ_{max} (lg ε) = 265 nm (4.09), 286 (4.11), 363 (4.35)

8: yield 83%; violet powder, m.p. = 334 °C; UV/VIS (DMSO): λ_{max} (lg ε) = 332 nm (4.27), 586 (4.81), 626 (5.23)

9: yield 61%; UV/VIS (CH_2Cl_2): λ_{max} (lg ε) = 250 nm, 489; (MeOH) = 253 (4.68), 436 (4.02); (H_2O) = 254 (4.82), 405 (3.87)

10: yield 29%; m.p. = 287–288 °C; UV/VIS (CH_3CN): λ_{max} (lg ε) = 214 nm (4.23), 235 (4.11), 295 (4.08), 357 (4.43)

11a: yield 81%; red powder, Zers. ab 355 °C; ^{1}H-NMR ([D$_6$]DMSO): δ = 7.05–7.55 (m; 8H, Benzo-H), 8.13–9.38 (m; 14H, pyridinio-H, CH=N und =CH–N), 14.59 (t, J = 7.0 Hz; 2H, NH); IR (KBr): $\tilde{\nu}$ = 1650 cm^{-1}, 1595, 1560, 1085; UV/VIS (DMF): λ_{max} (lg ε) = 360 nm (4.63, sh), 371 (4.73), 408 (4.39), 428 (4.32, sh)

11b: yield 31%; m.p. = 280–282 °C

11c: yield 74%; m.p. = 295 °C

11d: yield 88%; dark-red powder; UV/VIS (DMSO): λ_{max} (lg ε) = 360 nm (4.98), 372 (4.98), 410 (4.49), 432 (4.50), 460 (4.38)

11e: yield 37%; blue-violet crystals; UV/VIS (DMSO): λ_{max} (lg ε) = 360 nm (5.01), 428 (4.42), 490 (4.33)

11f: yield 21%; red powder; UV/VIS (DMF): λ_{max} (lg ε) = 289 nm (4.74), 362 (4.75, sh), 375 (4.82), 415 (4.27), 436 (4.23)

11g · H_2O: yield 72%; red-violet powder; UV/VIS (DMSO): λ_{max} (lg ε) = 269 nm (4.76), 360 (4.60, sh), 373 (4.70), 411 (4.36), 429 (4.37), 463 (4.20, sh)

11h: yield 30%; red powder; UV/VIS (DMF): λ_{max} (lg ε) = 356 nm (4.61), 372 (4.69), 413 (4.36), 427 (4.36)

11k · H_2O: yield 34%; dark-red powder; UV/VIS (DMSO): λ_{max} (lg ε) = 265 nm (4.79), 360 (4.60, sh), 372 (4.65), 404 (4.35), 425 (4.31), 510 (4.15)

12a-Ni: yield 62%; red powder; ^{1}H-NMR ([D$_6$]DMSO): δ = 6.95–7.80 (m; 8H, Benzo-H), 8.15–9.30 (m; 14H, pyridinio-H, CH=N und =CH–N); IR (KBr): $\tilde{\nu}$ = 1630 cm^{-1}, 1605, 1580, 1485, 1470, 1060; UV/VIS (DMF): λ_{max} (lg ε) = 308 nm (4.28), 340 (4.21), 355 (4.21), 397 (4.60, sh), 416 (4.75), 455 (4.02, sh), 489 (3.85, sh)

12a-Cu: yield 65%; brown powder

12a-Co · H_2O: yield 25%; black crystals; UV/VIS (DMSO): λ_{max} (lg ε) = 322 nm (4.25), 370 (4.29), 415 (4.39, sh), 435 (4.41)

12a-Fe: yield 96%; brown powder; UV/VIS (DMSO): λ_{max} = 390 nm, 426, 453

12c-Ni: yield 81%; dark-red crystals; UV/VIS (DMSO): λ_{max} (lg ε) = 263 nm (4.47), 305 (4.30), 350 (4.06, sh), 396 (4.47, sh), 414 (4.66), 460 (4.25), 486 (4.23, sh)

12c-Cu: yield 69%; blue-violet crystals

12d-Ni · H_2O: yield 62%; dark-red crystals; UV/VIS (DMSO): λ_{max} = 360 nm, 394, 416, 464

12d-Cu · H_2O: yield 89%; blue-violet crystals

12e-Ni: yield 96%; black-brown powder; UV/VIS (DMSO): λ_{max} (lg ε) = 355 nm (4.80), 395 (4.66), 415 (4.78), 497 (4.57)

12e-Cu: yield 98%; blue-black powder

12e-Co: yield 99%; red-brown powder

12f-Ni · H_2O: yield 72%; dark-red powder; UV/VIS (DMSO): λ_{max} (lg ε) = 289 nm (4.71), 340 (4.57), 402 (4.50), 424 (4.74), 468 (3.89), 505 (3.88)

12f-Cu · H_2O: yield 46%; blue-violet crystals

12f-Co · 2 H_2O: yield 45%; blue-black crystals

12g-Ni: yield 13%; red powder; UV/VIS (DMSO): λ_{max} = 269 nm, 397, 414, 460

12g-Cu · H_2O: yield 99%; dark-brown powder

12h-Ni · H_2O: yield 40%; red powder

12i-Ni · H_2O: yield 32%; dark-red powder

12i-Cu · H_2O: yield 25%; red-brown powder

12k-Ni · H_2O: yield 68%; red-brown powder; UV/VIS (DMSO): λ_{max} (lg ε) = 265 nm (4.72), 395 (4.44, sh), 411 (4.60), 460 (4.28), 495 (4.29)

12k-Cu · H_2O: yield 51%; brown-black powder

13: yield 26%; IR (KBr): $\tilde{\nu}$ = 1646 cm^{-1}, 1594, 1560, 1490, 1408, 1317, 1084, 830, 750

14a: yield 82%; UV/VIS (CH_3CN): λ_{max} (lg ε) = 221 nm (4.81, sh), 262 (4.64, sh), 267.5 (4.67), 273 (4.65, sh), 328 (4.41, sh), 346 (4.59, sh), 355 (4.63), 379 (4.16, sh), 397 (4.05, sh), 433 (3.32, sh)

14b: yield 85%; dark-red powder, m.p. = 324 °C; ^{1}H-NMR ([D$_6$]DMSO): δ = 2.65 (s; 12H, NMe), 3.38 (s; 12H, NMe), 7.05–7.90 (m; 8H, Benzo-H), 7.96 (s; 4H, C*H*NMe$_2$), 8.26–8.64 (AA'BB', 8H, pyridinio-H), 8.85 (br.; 4H, CH=N und =CH–N), 14.77 (br., 2H, NH); UV/VIS (DMSO): λ_{max} (lg ε) = 306 nm (4.81), 379 (4.68), 459 (4.80), 460 (4.91)

14c: yield 21%; dark-red crystals; UV/VIS (DMSO): λ_{max} (lg ε) = 345 nm (4.34, sh), 385 (4.70), 461 (4.88)

lators (**12g**-Cu: $\sigma = 1.6 \times 10^{-12}$ S/cm^{-1}; **12k**-Cu: $\sigma = 2.9 \times 10^{-10}$ S/cm^{-1}; **12k**-Ni: $\sigma = 6 \times 10^{-10}$ S/cm^{-1}); the conductivity of the metal-free compound **11k** is even greater ($\sigma = 1.9 \times 10^{-7}$ S/cm^{-1}). Also the (undoped) polymer **13** is only weakly conducting ($\sigma = 2.4 \times 10^{-7}$ S/cm^{-1}). – Table 2 lists some data of the new compounds.

Received: February 7, 1989 [Z 3162 IE]
German version: *Angew. Chem. 101* (1989) 1043
Publication delayed at author's request

[1] a) J. P. Collman, J. I. Brauman, T. J. Collins, B. L. Iverson, G. Lang, R. B. Pettman, J. L. Sessler, M. A. Walters, *J. Am. Chem. Soc. 105* (1983) 3038; b) R. D. Jones, D. A. Summerville, F. Basolo, *Chem. Rev. 79* (1979) 139; c) T. G. Traylor, *Acc. Chem. Res. 14* (1981) 102; d) B. M. Hoffman, J. A. Ibers, *ibid. 16* (1983) 15; e) C. Piechoki, J. Simon, A. Skoulios, D. Guillon, P. Weber, *J. Am. Chem. Soc. 104* (1982) 5245; f) B. Blanzat, C. Barthou, N. Tercier, J.-J. André, J. Simon, *ibid. 109* (1987) 6193; g) J. E. Baldwin, P. Perlmutter, *Top. Curr. Chem. 121* (1984) 181.

[2] H. Jahnke, *Chimia 34* (1980) 58.

[3] K. Fischer, M. Hanack, *Angew. Chem. 95* (1983) 741; *Angew. Chem. Int. Ed. Engl. 22* (1983) 724; *Angew. Chem. Suppl. 1983*, 1017.

[4] a) M. Hanack, A. Datz, R. Fray, K. Fischer, U. Keppeler, J. Koch, J. Metz, M. Mezger, O. Schneider, H.-J. Schulze in T. Skotheim (Ed.): *Handbook of Conducting Polymers*, Marcel Dekker, New York 1986; b) U. Keppeler, M. Hanack, *Chem. Ber. 119* (1986) 3363.

[5] a) D. Wöhrle, G. Meyer, *Kontakte (Darmstadt) 1985)* (3) 38; b) D. Wöhrle, *ibid. 1988* (1) 24; c) O. Schneider, M. Hanack, *Chem. Ber. 116* (1983) 2088; d) J. Koch, M. Hanack, *ibid. 116* (1983) 2109.

[6] a) A. D. Joran, B. A. Leland, G. G. Geller, J. J. Hopfield, P. B. Dervan, *J. Am. Chem. Soc. 106* (1984) 6090; b) J. A. Schmidt, A. R. McIntosh, A. C. Weedon, J. R. Bolton, J. S. Connolly, J. K. Hurley, M. R. Wasielewski, *ibid. 110* (1988) 1733; c) P. Leighton, J. K. M. Sanders, *J. Chem. Soc. Perkin Trans. 1 1987*, 2385.

[7] E. S. Schmidt, T. S. Calderwood, T. C. Bruice, *Inorg. Chem. 25* (1986) 3718.

[8] R. J. McMahon, R. Ken Forcé, H. H. Patterson, M. S. Wrighton, *J. Am. Chem. Soc. 110* (1988) 2670.

[9] F. Effenberger, H. Schlosser, P. Bäuerle, S. Maier, H. Port, H. C. Wolf, *Angew. Chem. 100* (1988) 274; *Angew. Chem. Int. Ed. Engl. 27* (1988) 281.

[10] J. J. Hopfield, J. N. Onuchic, D. N. Beratan, *Science (Washington, D.C.) 241* (1988) 817.

[11] a) H. Hiller, P. Dimroth, H. Pfitzner, *Justus Liebigs Ann. Chem. 717* (1968) 137; b) C. Reichardt, W. Scheibelein, *Z. Naturforsch. B33* (1978) 1012.

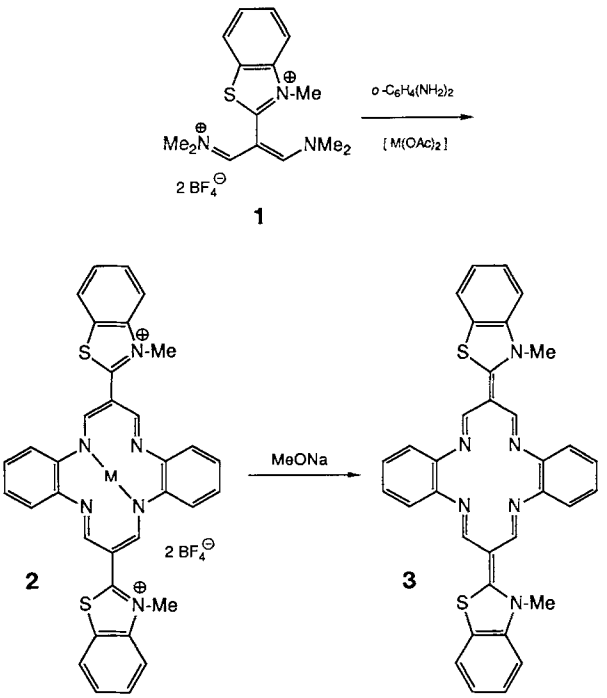
[12] a) H. Kast, DOS 2427606 (January 2, 1976) BASF AG; *Chem. Abstr. 84* (1976) 137226g; b) R. Müller, D. Wöhrle, *Makromol. Chem. 179* (1978) 2161; c) A. R. Cutler, C. S. Alleyne, D. Dolphin, *Inorg. Chem. 24* (1985) 2276, 2281; d) E. Lorch, E. Breitmaier, *Chem.-Ztg. 99* (1975) 87.
[13] W. A. Little, *Phys. Rev. A 134* (1964) 1416; b) H. J. Keller (Ed.): *Chemistry and Physics of One-dimensional Metals*, Plenum Press, New York 1977; c) W. A. Little in [13b], p. 257; d) D. Davies, H. Gutfreund, W. A. Little, *Phys. Rev. B 13* (1976) 4766; e) H. Gutfreund, W. A. Little in [13b] p. 279; f) cf. *Nachr. Chem. Tech. Lab. 24* (1976) 591.
[14] A. Harriman, G. Porter, *J. Chem. Soc. Faraday Trans. 2 75* (1979) 1532; b) A. Harriman, G. Porter, M. C. Richoux, *ibid. 2 77* (1981) 1175; c) J. R. Darwent, P. Douglas, A. Harriman, G. Porter, M. C. Richoux, *Coord. Chem. Rev. 44* (1982) 83.
[15] D. Lloyd, K. S. Tucker, D. R. Marshall, *J. Chem. Soc. Perkin Trans. 1 1981*, 726.
[16] Z. Janousek, H. G. Viehe in H. Böhme, H. G. Viehe (Eds.): *Iminium Salts in Organic Chemistry, Part 1 (Advances in Organic Chemistry: Methods and Results, E. C. Taylor (Ed.), Vol. 9)*, Wiley-Interscience, New York, 1976, p. 378.
[17] R. Gompper, E. Kujath, H.-U. Wagner, *Angew. Chem. 94* (1982) 559; *Angew. Chem. Int. Ed. Engl. 21* (1982) 543; *Angew. Chem. Suppl. 1982*, 1302.
[18] V. Kral, V. V. Semenov, M. I. Kanishchev, Z. Arnold, S. A. Shevelev, A. A. Fainzilberg, *Collect. Czech. Chem. Commun. 53* (1988) 1519.
[19] L. Michaelis, E. S. Hill, *J. Gen. Physiol. 16* (1933) 859.
[20] S. Hünig, W. Schenk, *Liebigs Ann. Chem. 1979*, 1523.
[21] a) J. Davila, A. Harriman, M.-C. Richoux, L. R. Milgrom, *J. Chem. Soc. Chem. Commun. 1987*, 525; b) W. Schuhmann, H.-P. Josel, H. Parlar, *Angew. Chem. 99* (1987) 264; *Angew. Chem. Int. Ed. Engl. 26* (1987) 241.
[22] a) L. R. Milgrom, *J. Chem. Soc. Perkin Trans. 1 1983*, 2535; b) J.-R. Fuhrhop, U. Wanja, M. Bünzel, *Liebigs Ann. Chem. 1984*, 426.
[23] K. Sakata, M. Hashimoto, N. Tagami, Y. Murakami, *Bull. Chem. Soc. Jpn. 53* (1980) 2262.
[24] a) E.-G. Jäger, *Z. Chem. 4* (1964) 437; *8* (1968) 30; *Z. Anorg. Allg. Chem. 364* (1969) 177; b) F. A., L'Eplattenier, A. Pugin, *Helv. Chim. Acta 58* (1975) 917.
[25] K. Sakata, T. Naganawa, M. Hashimoto, H. I. Ogawa, Y. Kato, *Inorg. Chim. Acta 143* (1988) 251.
[26] We thank Bayer AG (Dr. *G. Heywang*) for carrying out the conductivity measurements.

Di(4-pyridinio)-, Di(2-benzothiazolio)-, Di(2-[1,3-dithiolylio])- and Diformyltetraaza[14]annulenes and Tetraaza[14]annulenylene-Homologous Tetrathiafulvalenes **

By *Florian Adams* and *Rudolf Gompper**

Dedicated to Professor Christoph Rüchardt on the occasion of his 60th birthday

Tetrathiafulvalene (TTF) (cf. Refs. [1,2]) and bis(ethylenedithio)tetrathiafulvalene (BEDT-TTF or ET)[2,3] still have special importance as donors for the production of synthetic metals and organic superconductors, even though a whole series of derivatives, vinylogues, phenylogues, and pentalenylene homologues[4] of TTF have been sythesized in the meantime (cf., e.g., Refs. [2,3]). Metal complexes of cyclic π-electron systems such as porphyrin, phthalocyanine and dihydrodibenzotetraaza[14]annulene, bearing cationic substituents of the cyanine dye type, should according to *Little* et al.[5] have superconducting properties. As models for such compounds we have prepared 7,16-di(1-pyridinio)- and -(1-[4,4'-bipyridindio])-5,14-dihydrodibenzotetraaza[14]annulenes and some metal complexes thereof.[6] In these compounds, the (bi)pyridinio moieties are bound via the N atom to the fourteen-membered ring; an NH deprotonation could therefore only lead to zwitterions. In the case of 5,14-dihydrodibenzotetraaza[14]annulene derivatives, whose cationic substituents are attached to the ring via a C atom, the deprotonation should however lead to 7,16-bis(methylene) derivatives of tetraaza[14]annulenes, which stem from the 7,16-dihydro isomers ($C^{7/16}H$ form instead of $N^{5/14}H$ form). Ni-complexes of tetrahydro derivatives of such compounds are already known.[7] If the methylene groups were part of a 1,3-dithiole ring then such compounds would be dibenzotetraaza[14]annulene homologues of TTF. They should have interesting redox and complexation properties.



a: M = H, H ; **b**: M = Ni, Cu, Co

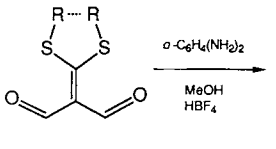
In the previous communication[6] we have only described such compounds in which two carbocation or phosphonium centers are coupled with the fourteen-membered ring (see **14** therein). A system **2a** (for physical data of the new compounds see Table 1), in which the benzothiazole rings carry the positive charges, can be obtained from the benzothiazoliovinamidinium salt[8] **1** by reaction with *o*-phenylenediamine. If the reaction is carried out in the presence of metal(II) acetates the metal complexes **2b** are formed. Deprotonation of **2a** with sodium methoxide yields the desired orange 7,16-bis(methylene)-7,16-dihydrodibenzotetraaza[14]annulene in 86% yield (the FAB mass spectrum[9] shows the required molecular mass of 582). It can be regarded as a [14]annulenylene homologue of the electron-rich 2,2'-bi(3-methyl-2,3-dihydrodibenzothiazolylidene).

Tetraaza[14]annulenylene-homologous tetrathiafulvalenes **6** are obtained by deprotonation of the dithiolylium salts **5**, which in turn are prepared by heating the methylenemalonaldehydes **4**[10] with *o*-phenylenediamine in the presence of tetrafluoroboric acid-ether in methanol. A nickel- and a copper-complex can be prepared from **6e**.

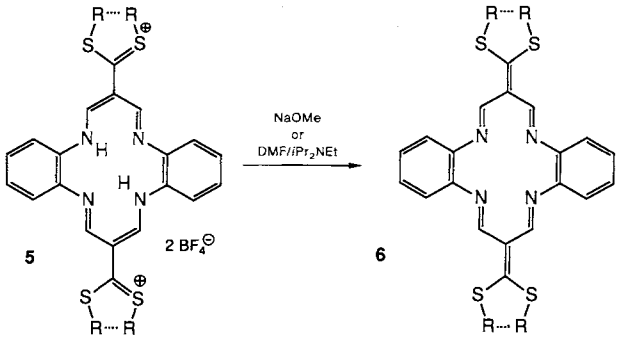
6b does not react with *p*-tetracyanoquinodimethane. This is understandable on the basis of the cyclovoltammogram of **6b** (irreversible oxidation at 0.75 eV). **6a, b, f** react with iodine to give black complexes whose elemental analyses correspond approximately to the composition $\mathbf{6} \cdot (I_3)_{1.7}$ and which have only insignificant powder electrical conductivi-

[*] Prof. Dr. R. Gompper, Dipl.-Chem. F. Adams
Institut für Organische Chemie der Universität
Karlstrasse 23, D-8000 München 2 (FRG)

[**] This work was supported by the Deutsche Forschungsgemeinschaft and the Fonds der Chemischen Industrie.



4



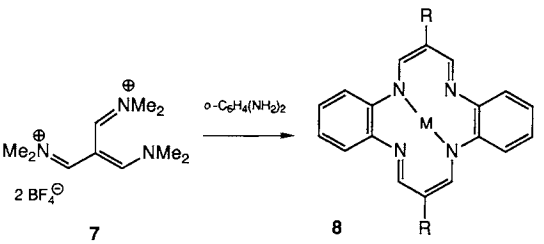
5 6

R⋯R = **a**: CH_2-CH_2 ; **b**: CH=CH ; **c**: CH=C(Ph) ; **d**: *o*-C_6H_4 ;
e: C(SMe)=C(SMe) ; **f**:



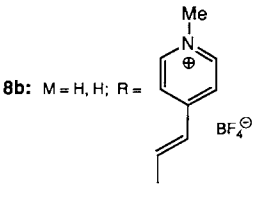
ties[11] (4-electron measurement, 1800 kp; **6a** · $(I_3)_{1.7}$: $\sigma = 1.7 \times 10^{-10}$ S/(cm^{-1}; **6b** · $(I_3)_{1.7}$: $\sigma = 2.7 \times 10^{-10}$ S/cm^{-1}; **6f** · $(I_3)_{1.7}$: $\sigma = 1.3 \times 10^{-9}$ S/cm^{-1}). — **6c, d** were synthesized in the same way.

An interesting further entry to tetraaza[14]annulenes of the structural type **2/3** and **5/6** is opened up by the diiminium salt **8a**, which can be obtained in 75% yield from the vinamidinium salt **7**[12] and *o*-phenylenediamine. **8a** can be condensed with 1,4-dimethylpyridinium tetrafluoroborate or 2,3-dimethylbenzothiazolium tetrafluoroborate to give the tetraaza[14]annulenes **8b** and **8c**, respectively. Hydrolysis of **8a** affords the dialdehyde **8d**, which can be converted into the metal complex **8e**. As the syntheses of **8b, c, e** indicate, **8a, d** could be valuable starting materials for further interesting tetraaza[14]annulene derivatives.

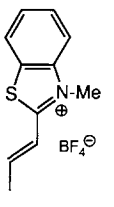


7 8

8a: M = H, H; R = -CH=⊕NMe$_2$ $BF_4^{\ominus}$



8b: M = H, H; R =



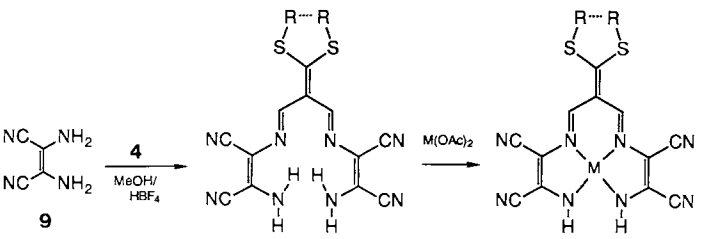
8c: M = H, H; R =

8d: M = H, H; R = -CH=O **8e**: M = Ni, Cu, Co; R = -CH=O

Attempts to prepare derivatives **5** and **6** without annelated benzene rings by reaction of diaminomaleic dinitrile **9** with **4** have thus far only led to the open-chain compounds **10**, from

Table 1. Some physical data of the new compounds.

2a:	yield 86%; red powder, m.p. = 242–243 °C; UV/VIS (DMSO): λ_{max} (lg ε) = 367 nm (4.76), 405 (4.78)
2b-Ni:	yield 57%; red powder, m.p. > 360 °C
2b-Cu · H_2O:	yield 35%; blue-violet powder
2b-Co · H_2O:	yield 20%; blue-violet crystals
3:	yield 86%; orange powder, m.p. 296 °C; UV/VIS (DMSO): λ_{max} = 373 nm, 465, 510 (sh); MS (FAB [9]): *m/z* 589 (100%, $(M + Li)^{\oplus}$)
5a:	yield 85%; red powder, m.p. = 181 °C; UV/VIS (DMF): λ_{max} (lg ε) = 275 nm (4.28), 305 (4.21), 352 (4.38), 410 (4.15, sh)
5b:	yield 45%; red-violet powder, m.p. 271–272 °C; UV/VIS (DMF): λ_{max} (lg ε) = 285 nm (4.30), 350 (4.25, sh), 385 (4.29, sh), 420 (4.36), 470 (4.33)
5c:	yield 91%; dark-red powder, m.p. 305–306 °C
5d:	yield 86%; red powder, m.p. 305–307 °C
5e:	yield 80%; red-violet powder, m.p. 284 °C
5f:	yield 82%; olive-green crystalline powder m.p. = 279–280 °C; UV/VIS (DMF): λ_{max} (lg ε) = 316 nm (4.13), 391 (3.65, sh), 509 (4.31)
6a:	yield 96%; yellow powder, m.p. 237–238 °C; UV/VIS (CH_2Cl_2): λ_{max} = 283 nm, 338, 410
6b:	yield 38%; bright-red powder, m.p. 237–238 °C; UV/VIS (CH_2Cl_2): λ_{max} (lg ε) = 230 nm (4.62), 306 (4.41), 344 (4.38), 370 (4.30), 471 (4.65); IR (KBr): $\tilde{\nu}$ = 3060 cm^{-1}, 1606, 1579, 1550, 1471, 1458, 1439, 1355, 1262, 1191, 1108, 755, 677; MS (DCI)[15]: *m/z* 489 (100%, $(M + H)^{\oplus}$)
6c:	yield 82%; bright-red powder, m.p. 262 °C
6d:	yield 76%; orange powder, m.p. 288–289 °C
6e:	yield 74%; bright-red powder, m.p. 297 °C; MS (DCI) [15]: *m/z* 673 (100%, $(M + H)^{\oplus}$)
6f:	yield 45%; red powder, m.p. 257–258 °C; UV/VIS (CH_2Cl_2): λ_{max} = 258 nm, 314, 366 (sh), 495; IR (KBr): $\tilde{\nu}$ = 2920 cm^{-1}, 1606, 1581, 1550, 1472, 1460, 1440, 1354, 1262, 1193, 755, 678
8a:	yield 75%; orange powder, m.p. 290–291 °C; UV/VIS (DMSO): λ_{max} (lg ε) = 324 nm (4.66), 354 (4.77); IR (KBr): $\tilde{\nu}$ = 1614 cm^{-1}, 1592, 1572, 1345, 1267, 1084, 761
8b:	yield 22%; red-violet powder, m.p. > 350 °C; UV/VIS (DMSO): λ_{max} (lg ε) = 273 nm (4.47), 413 (4.72), 490 (4.90)
8c:	yield 15%; brown powder, m.p. > 350 °C; UV/VIS (DMSO): λ_{max} (lg ε) = 266 nm (4.48), 405 (4.61), 529 (5.00)
8d:	yield 91%; orange needles, m.p. 346–347 °C; UV/VIS (DMSO): λ_{max} (lg ε) = 310 nm (4.70), 340 (4.61), 355 (4.68), 384 (4.35), 397 (4.29, sh); MS (EI) [9]: *m/z* 344 (100%, $(M^{\oplus})$)
8e-Ni:	yield 69%; red powder
8e-Cu:	yield 67%; red-brown crystalline powder; UV/VIS (DMSO): λ_{max} (lg ε) = 312 nm (4.65), 372 (4.48, sh), 389 (4.76), 420 (4.17, sh)
8e-Co:	yield 37%; violet crystalline powder
10a:	yield 97%; yellow powder, m.p. 300 °C (decomp.); MS (EI) [9]: *m/z* 354 (100%, $(M^{\oplus})$)
10b:	yield 98%; orange powder, m.p. 305–306 °C; UV/VIS (DMF): λ_{max} (lg ε) = 305 nm (4.22), 366 (4.37, sh), 383 (4.53), 405 (4.55), 429 (4.56), 485 (4.09), 512 (4.02)
10c:	yield 97%; dark-red powder, m.p. 265 °C (decomp.); MS (EI) [9]: *m/z* 444 (100%, $(M^{\oplus})$)
10d:	yield 76%; dark-red powder, m.p. 310–311 °C (decomp.)
11a-Ni:	yield 88%; bronze colored crystals, m.p. > 360 °C
11a-Cu:	yield 87%; olive-green crystals, m.p. 310 °C
11b-Ni:	yield 73%; brown crystals, m.p. > 360 °C
11b-Cu:	yield 63%; gold colored powder, m.p. 325 °C (decomp.); UV/VIS (DMF): λ_{max} (lg ε) = 313 nm (3.89), 365 (4.26), 388 (4.06), 480 (4.05, sh) 520 (4.24, sh), 545 (4.39), 585 (4.39)



9 10 11: M = Ni, Cu

R⋯R = **a**: CH_2-CH_2 ; **b**: CH=CH ; **c**: C(SMe)=C(SMe) ; **d**: CH=C(Ph)

which the metal complexes **11** can be obtained. The reactions of **9** with ethoxyacrolein to give dihydrotetraaza[14]annulene tetracarbonitrile[13] and of **9** with 1,3-diketones to give diazepines were first reported more than a decade ago.[14]

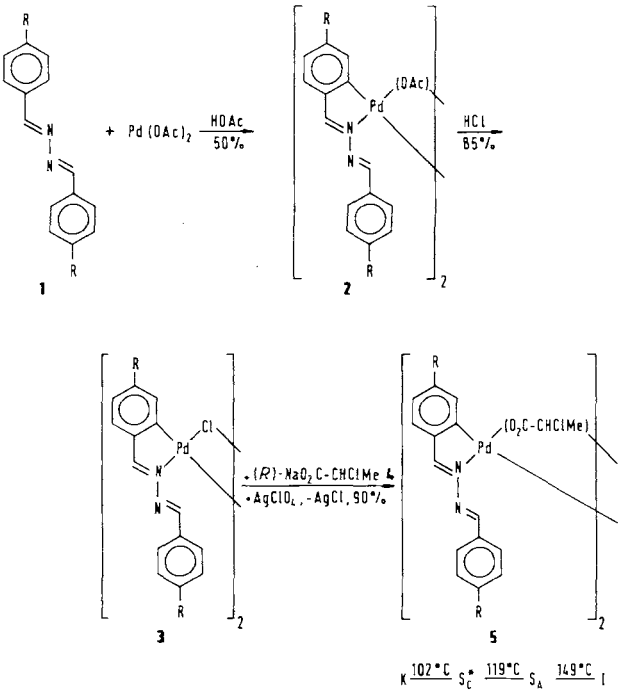
Received: February 7, 1989 [Z 3163 IE]
German version: *Angew. Chem. 101* (1989) 1046
Publication delayed at author's request

[1] a) D. O. Cowan, F. M. Wlygul, *Chem. Eng. News 64* (1986) No. 29, p. 28; b) H. Perlstein, *Angew. Chem. 89* (1977) 534; *Angew. Chem. Int. Ed. Engl. 16* (1977) 519; c) J. B. Torrance, *Acc. Chem. Res. 12* (1979) 79; d) F. Wudl, *Pure Appl. Chem. 54* (1982) 1051; *Acc. Chem. Res. 17* (1984) 227; e) M. R. Bryce, L. C. Murphy, *Nature (London) 309* (1984); f) R. L. Greene, G. B. Street, *Science (Washington) 226* (1984) 651.
[2] J. M. Williams, M. A. Beno, H. H. Wang, P. C. W. Leung, T. J. Emge, U. Geiser, K. D. Carlson, *Acc. Chem. Res. 18* (1985) 261.
[3] E. Amberger, K. Polborn, H. Fuchs, *Angew. Chem. 98* (1986) 749, 751; *Angew. Chem. Int. Ed. Engl. 25* (1986) 727, 729.
[4] W. Frank, R. Gompper, *Tetrahedron Lett. 27* (1987) 3083.
[5] a) W. A. Little, *Phys. Rev. A 134* (1964) 1416; b) H. J. Keller (Ed.): *Chemistry and Physics of One-dimensional Metals*, Plenum Press, New York 1977; c) W. A. Little in [5b], p. 257; d) D. Davies, H. Gutfreund, W. A. Little, *Phys. Rev., B 13* (1976) 4766; e) H. Gutfreund, W. A. Little in [5b], p. 279; f) cf. *Nachr. Chem. Tech. Lab. 24* (1976) 591.
[6] F. Adams, R. Gompper, E. Kujath, *Angew. Chem. 101* (1989) 1043; *Angew. Chem. Int. Ed. Engl. 28* (1989) 1060.
[7] W. P. Schammel, L. L. Zimmer, D. H. Busch, *Inorg. Chem. 19* (1980) 3159.
[8] J. R. Owen, US-Pat. Off. 890002 (September 21, 1971); *Chem. Abstr. 76* (1972) 47394r.
[9] We thank BASF AG (Dr. *W. Breitschaft*, Dr. *G. Glas*) for recording the mass spectra.
[10] F. Adams, R. Gompper, A. Hohenester, H.-U. Wagner, *Tetrahedron Lett. 29* (1988) 6921.
[11] We thank Bayer AG (Dr. *G. Heywang*) for carrying out the conductivity measurements.
[12] a) Z. Arnold, A. Holy, *Collect. Czech. Chem. Commun. 25* (1960) 1318; b) Z. Arnold, *ibid. 26* (1961) 3051; *30* (1965) 2125; c) M. Keshavarz, S. D. Cox, R. O. Angus, Jr., F. Wudl, *Synthesis 1988*, 641.
[13] I. Kohlmeyer, E. Lorch, G. Bauer, E. Breitmaier, *Chem. Ber. 111* (1978) 2919.
[14] a) R. W. Begland, D. R. Hartter, F. N. Jones, D. J. Sam, W. A. Sheppard, O. W. Webster, F. J. Weigert, Jr., *J. Org. Chem. 39* (1974) 2341; b) Y. Ohtsuka, *ibid. 41* (1976) 629.
[15] We thank Finnigan MAT GmbH, Bremen, for measuring the mass spectra.

A Novel Approach to Ferroelectric Liquid Crystals: the First Organotransition Metal Compound Displaying This Behavior **

By *Pablo Espinet, Jesús Etxebarría, Mercedes Marcos, Joaquina Pérez, Angel Remón*, and *José Luis Serrano*

Ferroelectric liquid crystals (FLC) are nowadays a major area of interest in mesogenic materials, both in basic and applied research. They are based on rodlike organic molecules with chiral centers in one of the terminal chains.[1-3] Recently, some fully organic mesogens having a "pseudo"-discotic core and helical structure have been reported[4] as a novel molecular type which could be used to obtain chiral mesogens. We have described some *ortho*-palladated dimers $[Pd_2(C,N)_2(\mu\text{-}X)_2]$ derived from the alkylidenamines $R-C_6H_4-N=CH-C_6H_4-R'$;[5] when X = acetate the molecules have a rigid roof-shaped chiral structure; however, only one of the derivatives displayed liquid crystal behavior (monotropic). We report here that similar compounds containing *ortho*-palladated azines display S_C mesophases and advantageously enable the introduction of chirality centers by means of chiral carboxylates (Scheme 1), which can



Scheme 1. Synthesis of **5** and its phase diagram. K = crystalline; S_C^* = chiral smectic C phase; S_A = smectic A phase; I = isotropic liquid; R = $H_{21}C_{10}O$.

give rise to FLC behavior. Three novel aspects may be noted: i) the unprecedented molecular shape; ii) the new way of introducing chirality; and iii) the presence of metal atoms in the molecule.

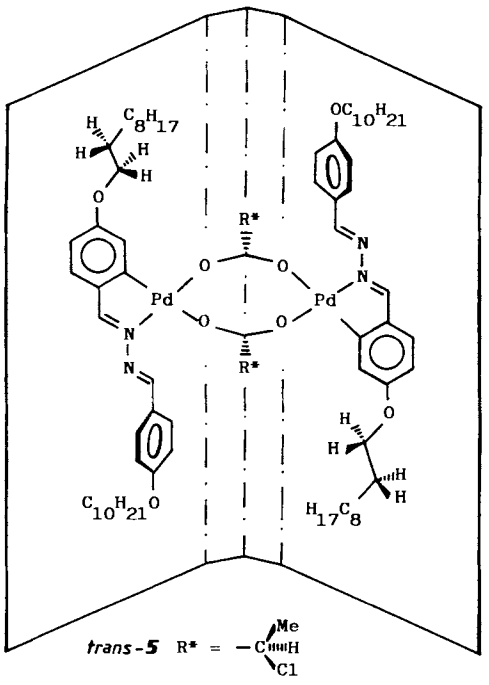
On refluxing with $Pd(OAc)_2$ in acetic acid,[6] the azine **1** was *ortho*-metalated only in one ring to give **2**.[7] Treatment of **2** in acetone with HCl (Pd/HCl = 1/1) gave **3**. Removal of the Cl bridges in **3** with $AgClO_4$, and addition of the optically active propionate **4** furnished the complex **5** in which two asymmetric carbon atoms have been introduced.

As shown by ^{1}H NMR spectroscopy, compound **5** consists of a mixture of *trans*-$\Lambda R,R$ (34%), *trans*-$\Delta R,R$ (34%) and *cis*-*R,R* (32%) isomers[8] (Fig. 1). A roof-shaped *trans* complex is chiral; since the formation of **5** is not enantioselective, *trans*-**5** must be a 1:1 mixture of Λ and Δ enantiomers. When, in addition, the two carboxylate bridges are non-racemic, the enantiomers are converted into two non-racemic diastereomers: *trans*-$\Lambda R,R$ and *trans*-$\Delta R,R$. A roof-shaped *cis* complex is not chiral on its own; the chirality introduced by the (*R*)-2-chloropropionate ligands leads to *cis*-*R,R* as the third diastereomer present in the mixture.

The hydrogens attached to the asymmetric carbon atoms of the propionato ligands give rise to distinct ^{1}H NMR signals in the three diastereomers (see Fig. 1). The two *trans* diastereomers, each containing two homotopic propionato

[*] Prof. Dr. P. Espinet, Dr. J. Pérez
Química Inorgánica, Facultad de Ciencias
Universidad de Valladolid, E-47005-Valladolid (Spain)
Dr. J. Etxebarría, Dr. A. Remón
Física de la Materia Condensada, Facultad de Ciencias
Universidad del Pais Vasco, apartado 644, E-48080 Bilbao (Spain)
Prof. Dr. J. L. Serrano, Dr. M. Marcos
Química Orgánica-ICMA, Facultad de Ciencias,
Universidad de Zaragoza-CSIC, E-50009-Zaragoza (Spain)

[**] This work was supported by the E.E.C. (Project St2J-0387-C), C.I.C.Y.T. (Spain) (Project PB86-028) and C.A.I.C.Y.T. (Spain) (Project 3282-83-C02-02).



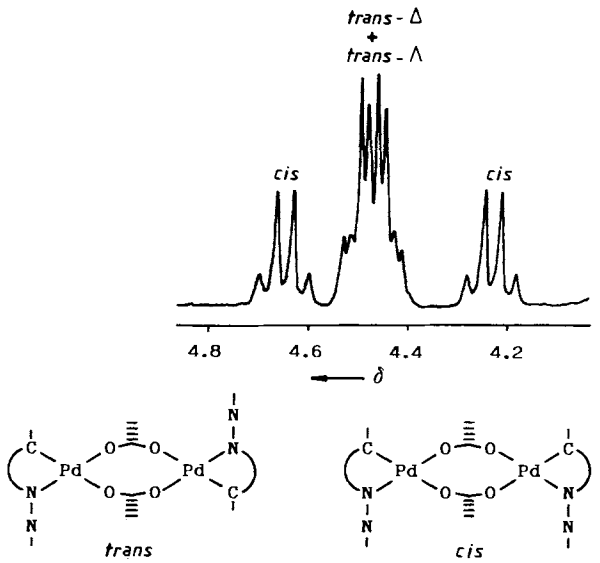


Fig. 1. Structure of *trans*-**5** and 200-MHz ^{1}H NMR spectrum of the mixture of isomers in $CDCl_3$ (*CH*ClMe signals).

ligands, give rise to two overlapped quartets at $\delta = 4.481$ ($^3J_{H,H} = 6.7$ Hz) and 4.467 ($^3J_{H,H} = 6.7$ Hz); the *cis* diastereomer, which contains two diastereotopic propionate ligands, gives rise to two additional quartets at 4.65 ($^3J_{H,H} = 6.7$ Hz) and 4.23 ($^3J_{H,H} = 6.7$ Hz) ppm.

The phase sequence and transition temperatures of **5**, studied by differential thermoanalysis and optical microscopy, are given in Scheme 1. Complex **5** possesses an enantiotropic stable smectic C phase (S_C^*) between 102 and 119 °C. A preliminary study of the physical properties of the compound concentrated on its electrooptic switching behavior.[9] When the temperature of the sample was decreased below 119 °C (entering the S_C^* phase), the material began to respond to an electric field. If the applied field is a square wave of the order of 1 Hz, the switching occurs uniformly over the sample between two states that cannot be brought to extinction between crossed polarizers. Under these conditions, the switching behavior was analyzed by recording on a digital oscilloscope the light intensity of a He–Ne laser transmitted through the sample between crossed polarizers and oriented so as to give maximum contrast. Figure 2a shows the electro-optic response of a sample region of about 2 mm^2 for a driving square voltage of ± 17 v and 0.5 Hz. The sample thickness was 11 μm. As can be seen, the optical response is about three orders of magnitude slower than that of calmitic S_C^* phases.[12] This is due to the high viscosity of the material, presumably caused by the molecular shape, which gives rise to a higher correlation between the molecules than in the calamitic case. The voltage dependence of the rise time τ is shown in Figure 2b. The parameter τ was taken as the time required for a change of transmission from 10% to 90% of the difference between the two transmission levels. Within the field region investigated[10] (11 to 17v) the results obtained fit well to a law $\tau \sim 1/U$ that is characteristic for the switching behavior of FLC.[11]

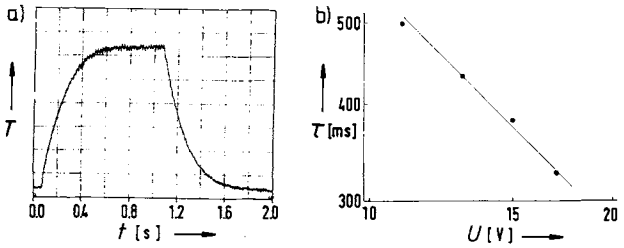


Fig. 2. a) Electrooptic response of complex **5** at a square wave voltage of ± 17v and 0.5 Hz. The sample thickness was 11 μm and the temperature 103 °C. T = transmission in arbitrary units. b) Log-log plot of the voltage dependence of the rise time of **5** at 103 °C.

Received: February 27, 1989 [Z 3203 IE]
German version: *Angew. Chem. 101* (1989) 1076

[1] R. B. Meyer, L. Liebert, L. Strzelecki, P. J. Keller, *Phys. (Paris) Lett. 36* (1975) L 69.
[2] T. M. Goodby, T. M. Leslie, *Mol. Cryst. Liq. Cryst. 110* (1984) 175.
[3] D. M. Walba, R. T. Vohra, N. A. Clark, *J. Am. Chem. Soc. 108* (1986) 7424.
[4] K. Yamamura, Y. Okada, S. Ono, M. Watanabe, I. J. Tabushi, *J. Chem. Soc. Chem. Commun. 1988*, 443.
[5] a) J. Barberá, P. Espinet, E. Lalinde, M. Marcos, J. L. Serrano, *Liquid Crystals 2* (1987) 833. b) M. A. Ciriano, P. Espinet, E. Lalinde, M. B. Ros, J. L. Serrano, *J. Mol. Struc. 196* (1989) 327.
[6] R. M. Ceder, J. Sales, X. Solans, M. J. Font-Altaba, *J. Chem. Soc. Dalton Trans. 1986*, 1351.
[7] 45 min., Pd/azine = 1/1; **2** showed a S_C phase in the range of 117.0 to 142.8 °C.
[8] Note on the nomenclature of the isomers: *cis*/*trans* refers to the orientation of the ligands relative to the (Pd-carboxylato)$_2$ ring, R describes the absolute configuration of the 2-chloropropionato ligands, Δ/Λ is used in analogy to the D/L nomenclature in octahedral complexes (see, for example, E. J. Corey, J. C. Bailar, Jr., *J. Am. Chem. Soc. 81* (1959) 2620) to distinguish the two isomers of *trans*-(*R*,*R*)-**5**.
[9] The cell used for the measurements was made of SnO_2-coated glass plates on which a thin film of nylon 6/6 was deposited. One of the plates was rubbed unidirectionaly in order to stretch the nylon film and create an anisotropic aligning surface. The material in the isotropic phase was then introduced into the cell by capillary action and cooled down slowly (0.2 °C/min) into the S_A phase. Fairly good alignment was achieved over the whole sample area.
[10] The higher field region could not be studied in further detail because the material partially deteriorates when subjected to moderate electric fields.
[11] Jin-Zhi Xue, M. A. Handschy, N. A. Clark, *Ferroelectrics 73* (1987) 305.
[12] J. W. Goodby, J. S. Patel, T. M. Leslie, *Ferroelectrics 59* (1984), and references cited therein.

Carbohydrates as Chiral Templates: Stereoselective Tandem Mannich-Michael Reactions for the Synthesis of Piperidine Alkaloids**

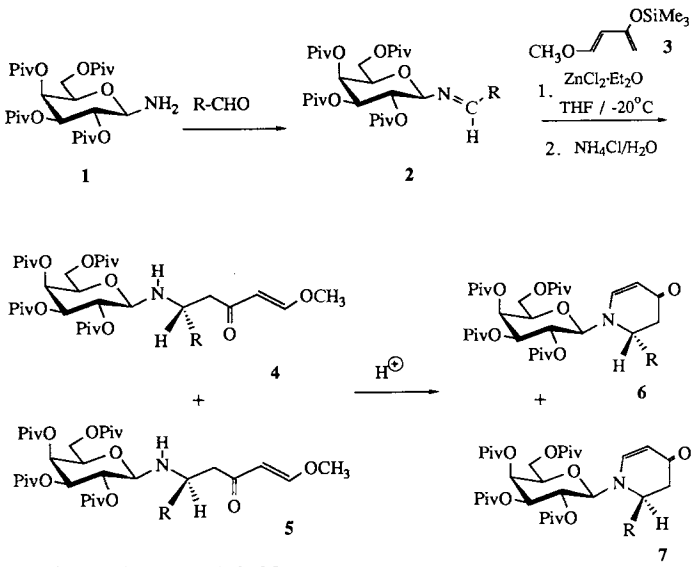
By *Horst Kunz** and *Waldemar Pfrengle*

Dedicated to Professor Helmut Ringsdorf on the occasion of his 60th birthday

O-Acyl-protected glycosylamines, particularly the 2,3,4,6-tetra-*O*-pivaloyl-β-D-galactopyranosylamine **1**,[1,2] are effective chiral auxiliaries in Strecker[1] and Ugi syntheses[2] of α-amino acids. Schiff bases **2** prepared from **1** and aldehydes, moreover, react as heterodienophiles with isoprene in aza-Diels-Alder reactions in the presence of zinc chloride at 5–20 °C, whereby chiral piperidine derivatives are formed with moderate diastereoselectivity (diastereomeric ratio ≤ 10:1).[3] An analogous reaction of the Schiff base **2d** (formed from pyridine-3-carbaldehyde and **1**) with 1-methoxy-3-trimethylsiloxybutadiene **3**,[4] first carried out for configurational assignment, turned out on closer examination to be a reaction sequence involving a Mannich reaction followed by a heteroanalogous Michael reaction and a condensation step. Since stereoselective Mannich reactions have thus far rarely been described in the literature[5] we have investigated this reaction sequence in more detail.

Aldehydes react with **1** in the presence of silica gel and a molecular sieve almost without anomerization to give the Schiff bases **2**. Conditioned by a delocalization of the C=N π-electrons in the σ* orbital of the ring C–O bond, the compounds **2** prefer a conformation in which the ring C–O bond is almost perpendicular to the plane of the double bond.[2]

In the presence of zinc chloride the Schiff bases **2** react highly selectively with the silyl dienol ether **3** in tetrahydrofuran at −20 °C to give the Mannich bases **4/5**. The diastereomeric ratios lie in the range 20–50:1 (Scheme 1 and Table 1).



Scheme 1. Piv = $(CH_3)_3C$–CO.

If the reaction is stopped after 2–12 h (T.L.C. control) with aqueous ammonium chloride solution, the Mannich compounds **4/5** can be isolated, or, in the case of the propyl derivative **4a**, detected thin-layer chromatographically. If, on the other hand, direct hydrolysis with 1 N HCl is used for work-up then the subsequent Michael addition occurs immediately followed by elimination of methanol, and the dehydropiperidones **6/7** can be isolated in high yields (≥ 90%) (Table 1).

The diastereoselectivity of these tandem Mannich-Michael reactions is fully dictated by the introductory Mannich reaction, since the Mannich bases **4/5** and the cyclization products obtained from them with dilute HCl show identical diastereomeric ratios. Direct acid hydrolysis of the reaction mixtures furnishes the piperidones **6/7** in the same diastereomeric ratio as the bases **4/5**.

In the case of **2a–2c** one equivalent of zinc chloride suffices for starting the reaction, whereas in the case of **2d** two equivalents of Lewis acid are required. It seems to be a consequence of this fact that the Mannich reaction of **2d** is stereochemically different from that of **2a–2c**, as demonstrated in the conversion of **6a** and **7d** into known piperidine alkaloids. This conversion is initiated by the reduction of the C=C double bond of **6a**[6] and **7d**[7] with L-selectride.[8]

Table 1. Diastereoselective tandem Mannich-Michael reaction of the Schiff bases **2** with 1-methoxy-3-trimethylsiloxy-1,3-butadiene in tetrahydrofuran at −20 °C according to Scheme 1.

Schiff-Base	R	Main diastereomer	Yield [%] **4(5)/6(7)** [a]	**6(7)** [b]	Diastereomeric ratio **6:7** (= **4:5**) [c]	Pure diastereomer	Yield (%)
2a	*n*-Propyl	**4a/6a**	−/90	96	97.5:2.5 (*S*):(*R*)	**6a**	81 [d] [6]
2b	*p*-Chlorphenyl	**4b/6b**	82/−	95	98:2 (*R*):(*S*)	**6b**	90 [e]
2c	2-Furyl	**4c/6c**	36/60 [e]	95	96:4 (*R*):(*S*)	**6c**	60 [e]
2d [f]	3-Pyridyl	**5d/7d**	57 [7]/−	90	4:96 (*S*):(*R*)	**7d**	86 [e] [7]

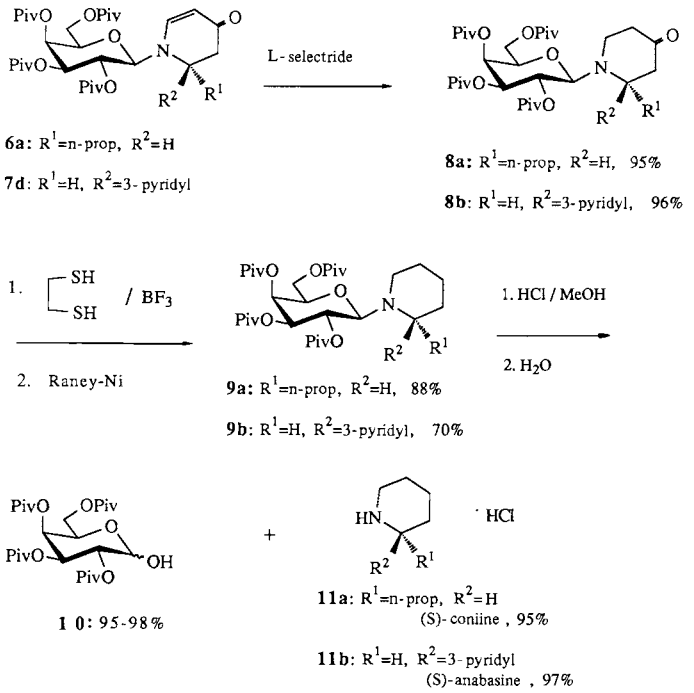
[a] After hydrolysis with aq. NH_4Cl. [b] After hydrolysis with 1 N HCl. [c] HPLC direct from the crude product. [d] Crystallization from *n*-hexane. [e] Isolation by flash chromatography in petroleum ether/acetate mixtures. [f] Reaction requires 2 equivalents $ZnCl_2$.

The *N*-galactosylpiperidones **8a** and **8b** thus formed are converted via their dithiolanes and desulfurization with Raney-Ni into the *N*-galactosylpiperidines **9a** and **9b**, respectively. Treatment of the compounds **9** with HCl in methanol leads to almost quantitative detachment of the enantiomerically pure alkaloids (*S*)-coniine **11a** and (*S*)-anabasine **11b**, respectively, from the carbohydrate template (Scheme 2). The tetrapivaloylgalactose **10** can be recovered almost completely thereby and reconverted into the starting auxiliary.

On comparing the optical rotations with the data quoted in the literature it is found that the natural (*S*)-coniine **11a** and the natural (*S*)-anabasine **11b** are obtained in enantiomerically pure form in this way. The complexing and chiral properties of the carbohydrate are crucial for the opposite, but in both cases very effective, stereoselection in the depicted Mannich syntheses **4a/5d**. For the reaction with **3**,

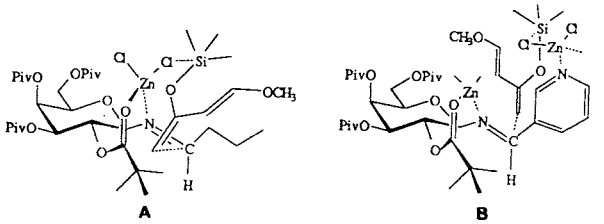
[*] Prof. Dr. H. Kunz, Dr. W. Pfrengle
Institut für Organische Chemie der Universität
Johann-Joachim-Becher-Weg 18–20, D-6500 Mainz (FRG)

[**] This work was supported by the Fonds der Chemischen Industrie. *W. P.* thanks the Fonds der Chemischen Industrie for a postdoctorate fellowship.



Scheme 2.

the Schiff bases **2** require activation by the Lewis acid. This coordinates the nitrogen and, simultaneously and in a favorable way, also the carbonyl oxygen of the pivaloyl moiety in (*Z*)-position. The Mannich reaction of this complex is thought to be initiated by liberation of the latent nucleophilicity of the silyl dienol ether **3**. The interaction of the silyl residue of **3** with a chloride ligand on the zinc—which is essential for this liberation—takes place in the case of **2a** (and **2b** and **2c**) *in front* of the plane of the C=N double bond (Formula **A**), whereby the (*S*)-diastereomer **4a** of the precursor of coniine **11a** is formed. **2d** requires two equivalents of zinc chloride for the reaction with **3**. The first is bound to the pyridine nitrogen and thus inactivated; only the second activates the C=N double bond. The zinc chloride coordinated to the more nucleophilic pyridine nitrogen should activate the silyl dienol ether **3** via its consequently more nucleophilic chloride ligands (Formula **B**). In this case, **3** is introduced *from the free back side* of **2d** and the (*S*)-configurated precursor **5d** of anabasine **11b** is formed. This



A **B**

hypothesis (reaction via **A, B**) awould explain the opposite stereochemical course of the two enantioselective syntheses of the piperidine alkaloids and the high stereocontrol of the Mannich reactions.

Received: April 12, 1989 [Z 3286 IE]
German version: *Angew. Chem. 101* (1989) 1041

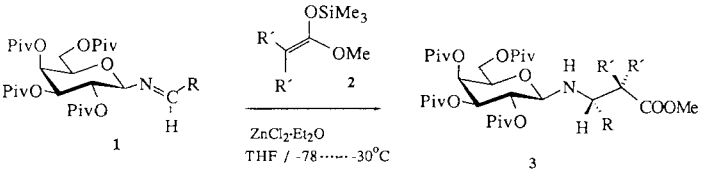
[1] H. Kunz, W. Sager, *Angew. Chem. 99* (1987) 595; *Angew. Chem. Int. Ed. Engl. 26* (1987) 557.
[2] H. Kunz, W. Pfrengle, *J. Am. Chem. Soc. 110* (1988) 651.
[3] W. Pfrengle, H. Kunz, *J. Org. Chem.*, in press; W. Pfrengle, *Dissertation*, Universität Mainz 1988.
[4] S. Danishefsky, *J. Am. Chem. Soc. 96* (1974) 7807; a diastereoselective aza-Diels-Alder reaction with such a siloxydiene, in which the stereogenic center becomes a structural element of the product, is described by S. Danishefsky, M. E. Langer, C. Vogel, *Tetrahedron Lett. 26* (1985) 5983.
[5] a) A diastereoselective synthesis of racemic Mannich bases is described by D. Seebach, C. Betschart, M. Schiess, *Helv. Chim. Acta 67* (1984) 1593; b) For a preliminary communication on stereoselective Mannich reactions see N. Risch, U. Billerbeck, A. Esser, Abstracts of the Chemiedozententagung 1988, Mainz 1988, p. 31.
[6] (*S*)-**6a**: m.p. 163 °C; $[\alpha]_D^{20} = -74.7$ ($c = 2$, $CHCl_3$); 100-MHz ^{13}C NMR ($CDCl_3$): $\delta = 91.6$ (C-1, Gal), 53.4 (C-2, piperidone). – (*R*)-**6a**: 100-MHz ^{13}C NMR ($CDCl_3$) from enriched mixture: $\delta = 90.3$ (C-1, Gal), 60.5 (C-2, piperidone). – **11a** (hydrochloride): m.p. 205 °C; $[\alpha]_D^{20} = -6.8$ ($c = 3.5$, EtOH); cf. data in [9]: m.p. 215–217 °C; $[\alpha]_D^{24} = -6.9$ ($c = 1.1$; EtOH).
[7] (*S*)-**5d**: $[\alpha]_D^{20} = -1.8$ ($c = 2$, $CHCl_3$); 400-MHz ^1H NMR ($CDCl_3$): $\delta = 7.46$ and 5.43 (each d, 1H, $J = 12.7$ Hz, methoxy-enone), 3.71 (d, 1H, $J_{1,2} = 8.4$ Hz, H-1. – (*S*)-**7d**: m.p. 176 °C; $[\alpha]_D^{20} + 19.6$ ($c = 3$, $CHCl_3$); 400-MHz ^1H NMR ($CDCl_3$): $\delta = 7.19$ and 5.13 (each d, 1H, $J = 8.0$ Hz, enamine-one), 4.49 (d, 1H, $J = 9.2$ Hz, H-1). – **11b** (*p*-nitrobenzoate): m.p. 122 °C; $[\alpha]_D^{20} = -130.8$ ($c = 1.2$, MeOH); cf. data in [10]: m.p. 127–128 °C; $[\alpha]_D^{15} = -130.0$ ($c = 3$, MeOH).
[8] H. C. Brown, S. Krishnamurthy, *J. Am. Chem. Soc. 94* (1972) 7159.
[9] W. H. Tallent, E. C. Horning, *J. Am. Chem. Soc. 78* (1956) 4467.
[10] E. Späth, F. Kesztler, *Ber. Dtsch. Chem. Ges. 70* (1937) 704.

Carbohydrates as Chiral Templates: Stereoselective Synthesis of β-Amino Acids**

By *Horst Kunz** and *Dirk Schanzenbach*

Chiral β-amino acids are of interest as constituents of antibiotics[1] and as synthetic building blocks, especially for β-lactam antibiotics.[2] In contrast to the numerous stereoselective methods for the synthesis of α-amino acids,[3] comparably few examples of methods for the symmetric synthesis of β-amino acids have been described in the literature.[4] High inductions are reported for $TiCl_4$-catalyzed reactions of the Schiff bases of valinates with silylketene acetals[5] and for a similar reaction of benzylidenaniline with the silylketene acetal of *N*-methylephedrine propionate.[6] In both cases however, *N*-substituted β-amino acids are obtained whose *N*-substituent (in the former case[5] it is the inducing group) cannot be removed at a later stage. We report here on the asymmetric synthesis of *N*-unsubstituted β-amino acids in which concomitantly high yields, very high inductions and the cleavage and recovery of the chiral auxiliary group are achieved. The basic principle of this synthesis is the effective diastereoselective Mannich reaction of Schiff bases **1** of 2,3,4,6-tetra-*O*-pivaloyl-β-D-galactosylamine.[7]

The silyl ketene acetals **2**, which are prepared in the usual way from lithium ester enolates by silylation and are distilled, react with the Schiff bases **1** in the presence of zinc chloride at −78 °C to −30 °C within 24 h to give the *N*-galactosyl-β-amino acid esters **3** (Scheme 1, Table 1).



Scheme 1. Piv = $(CH_3)_3C$-CO.

[*] Prof. Dr. H. Kunz, Dipl.-Chem. D. Schanzenbach
Institut für Organische Chemie der Universität
Johann-Joachim-Becher-Weg 18–20, D-6500 Mainz (FRG)

[**] This work was supported by the Fonds der Chemischen Industrie.

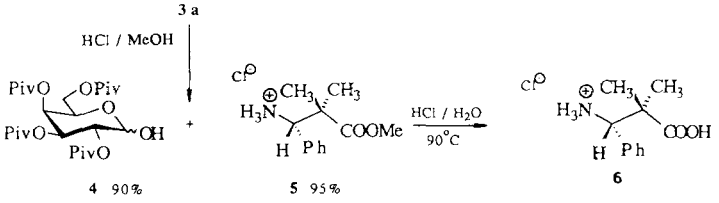
Table 1. Diastereoselective synthesis of *N*-galactosyl-β-amino acid esters **3** according to Scheme 1.

Ester	R	R′	*T* [°C]/*t* [h]	Yield [%]	(*S*):(*R*) [a]	$[\alpha]_D^{22}$ [b]
3a	C_6H_5	CH_3	−30/24	89	150:1	+16.5
3a	C_6H_5	CH_3	+30/1	90	70:1	
3b	C_6H_5	C_2H_5	−30/24	82	5:1	+13.1
3c	3-Cl-C_6H_4	CH_3	−30/24	89	200:1	+10.2
3d	2-Cl-C_6H_4	CH_3	−30/24	92	1:80 [c]	+14.2
3e	4-F-C_6H_4	CH_3	−30/24	88	105:1	+13.3
3f	2-Naphthyl	CH_3	+30/72	90	10:1	+15.4
3g	*n*-C_3H_7	CH_3	−30/24	83	250:1	+11.8

[a] Analytical HPLC (Diode array detection) on RP-18 columns in acetonitrile/water. [b] $c = 1$, $CHCl_3$. [c] The reversal of the diastereoselectivity is deceptive of the residues R, only 2-chlorophenyl has a higher priority than R'_2-C-COOMe.

The diastereoselectivity of the reaction in conversions of the silylketene acetal of methyl isobutyrate (**2**, R′ = Me) is in each case very high. The diastereomeric ratio (70–250:1) is determined directly by HPLC analysis of the reaction solution after hydrolysis with ethylenediamine tetraacetic acid (EDTA) solution. A marked stereoselectivity is still always observed even when the reaction is carried out at + 30 °C, which is necessary in the case of **1f**. In the 100-MHz ^{13}C NMR spectrum the major diastereomers of the aromatic products **3a–f** all show a signal at $\delta \approx 86.3$ for the anomeric C and a signal at $\delta \approx 71.5$ for the β-C of the amino acid moiety. In the case of the aliphatic derivative **3g** the corresponding signals appear at $\delta = 89.5$ and 59.7. The sterically demanding α-diethyl branched derivative **3b** is formed with only moderate selectivity.

In order to determine the absolute configuration of the major diastereomers, the phenyl derivative **3a** was converted into the known[8] free amino acid **6**. The removal of the β-phenyl-β-alanine ester derivative[9] from the carbohydrate template can be achieved almost quantitatively with HCl in methanol, and the auxiliary can be re-isolated in ≥ 90% yield (Scheme 2).



Scheme 2.

Comparison of the optical rotation values[10] with those quoted in the literature for the (*R*)-compound show that the (*S*)-configurated β-amino acid **6** is obtained in high enantiomeric purity by the synthesis described here. It can be concluded, therefore, that all β-amino acid derivatives prepared according to Scheme 1 are preferably formed with (*S*)-configuration. The direction of the asymmetric induction in this β-amino acid synthesis is accordingly identical to that observed in the previously described tandem Mannich-Michael reaction for the synthesis of coniine.[7]

The method presented here enables the synthesis of chiral β-amino acids in high yields and with high diastereomeric excess, and the releasing of β-amino acids without *N*-substituents from the auxiliary. The preparative scope of this method is even considerably greater when one realizes that the opposite enantiomers of the chiral β-amino acids can be obtained in the same way with 2,3,4-tri-*O*-pivaloyl-α-D-arabinopyranosylamine, as could already be demonstrated in the meantime in Ugi and Strecker syntheses.[11]

Received: April 12, 1989 [Z 3285 IE]
German version: *Angew. Chem. 101* (1989) 1042

[1] See, for example a) A. S. Khokhlov, M. M. Shemyakin, P.D. Reshetov, *Izv. Akad. Nauk SSSR 1961*, 15; b) T. Wakamiya, T. Shiba, T. Kaneko, *Bull. Chem. Soc. Jpn . 45* (1972) 3668; c) T. Yoshioka, K. Kuraoka, T. Takita, K. Maeda, H. Umezawa, *J. Antibiot. 25* (1972) 625.
[2] Y. Fukagawa, M. Okabe, T. Yoshioka, T. Ishikura, *Spec. Publ. R. Soc. Chem. 52* (1984) 163.
[3] A summary of recent developments is given in M. J. O'Donnell (Ed.), *Tetrahedron 44* (1988) 5253–5614.
[4] See H. Estermann, D. Seebach, *Helv. Chim. Acta 71* (1988) 1824, and references cited therein.
[5] I. Ojima, S. Inaba, *Tetrahedron Lett. 21* (1980) 2081, and references cited therein.
[6] C. Gennari, J. Venturini, G. Gislon, G. Schimperna, *Tetrahedron Lett. 28* (1987) 227.
[7] H. Kunz, W. Pfrengle, *Angew. Chem. 101* (1989) 1041; *Angew. Chem. Int. Ed. Engl. 28* (1989) 1067.
[8] M. Furukawa, T. Okawara, H. Noguchi, Y. Terawaki, *Heterocycles 6* (1977) 1323.
[9] **5** (hydrochloride): m.p. 184 °C (decomp.); $[\alpha]_D^{23} = -32.8$ ($c = 1.1$, 1 N HCl).
[10] **6** (hydrochloride): m.p. 248–250 °C (decomp.); $[\alpha]_D^{23} = -31.6$ ($c = 1.5$, 1 N HCl); cf. data in [8]: $[\alpha]_D^{25} = +30.6$ ($c = 1.5$, 1 N HCl).
[11] H. Kunz, W. Pfrengle, W. Sager, *Tetrahedron Lett.*, in press.

Book Reviews are written by invitation from the editor. Suggestions for books to be reviewed and for book reviewers are welcome. Publishers should send brochures or (better) books to the following address: Redaktion Angewandte Chemie, Postfach 101161, D-6940 Weinheim, Federal Republic of Germany. The editor reserves the right of selecting which books will be reviewed. Uninvited books not chosen for review will not be returned.

Solids and Surfaces: A Chemist's View of Bonding in Extended Structures. By *R. Hoffmann*. VCH Publishers, New York/VCH Verlagsgesellschaft, Weinheim 1988. x, 142 pp., hard cover, $ 24.95.—ISBN 0-89573-709-4/3-527-26905-3

Extended structures have become increasingly fashionable for study in the last two decades. Much progress has occurred towards determining and understanding chemical and physical properties of compounds of this type, whether they be solids, surfaces, or macromolecules. Theoretical models of electronic structure in such systems have also developed beyond the treatment of small molecules or small unit cells. Most recently, theoretical aspects of solid state chemistry have moved beyond the purely conceptual, e.g., as in the Zintl-Klemm rules, towards more quantitative descriptions, which have been around in solid state physics for some decades. "Solids and Surfaces: A Chemist's View of Bonding in Extended Structures" by *Roald Hoffmann* is an effective attempt to translate the language of band theory for chemists. True to his style over the years, his descriptions are highly pictorial and intuitive—an extremely useful complement to the mathematical formulation in the physics literature. Given this, one can contend that this book also teaches physicists the particular point of view of chemists for looking at such problems.

The book begins by setting up the vocabulary of band theory, i.e., Bloch functions, *k*-space, etc., in order to develop the ideas behind the construction of energy band diagrams. Such dispersion curves have no analog in molecular orbital theory, and so "to retrieve a local, chemical, or frontier orbital language in the solid state," Prof. *Hoffmann* introduces the connection between density-of-states diagrams (DOS) and molecular orbital energy level schemes—something which "chemists can sketch..., intuitively." Local descriptions fall naturally by partitioning the DOS into various components, either via atomic orbital or bond orbital contributions. COOP (crystal orbital overlap population) diagrams provide another interpretative tool that gives "a way to find bonds in the bands that a fully delocalized calculation gives." In the remainder of the book, he develops and extends these ideas using numerous examples studied in his research group over the last several years, e.g., $ThCr_2Si_2$, Chevrel phases, the NiAs → MnP transition, as well as surface structural problems involving Ni(100) with CO, and various transition metals with the methyl group. Within these examples, Prof. *Hoffmann* introduces the ideas of Peierls distortions, frontier orbital approaches, and the significance of the Fermi level, including its influence over surface reactions.

As mentioned in the preface, the material in this monograph has already appeared in two review articles, one in *Angewandte Chemie*, the other in *Reviews of Modern Physics*. One may therefore question the need for such a book. In addition, a number of other publications exist that discuss chemical bonding and electronic structure from both physical and chemical points of view. Yet, "Solids and Surfaces", through its numerous examples, combines the ideas of bonding and reactivity in molecules with those of both solids and surfaces—topics which may be too cumbersome and excessive for even a single review article.

Prof. *Hoffmann*'s self-assessment of this material is also true—the language of solid state physics is much more extensive than what is presented in his book. Yet, it represents an excellent first step for students and other chemical researchers who are not well versed in the language of electronic structure in the solid state. It may also be a valuable companion text to one which provides more quantitative descriptions for those who are interested in more of the details.

Gordon J. Miller [NB 984 IE]
Max-Planck-Institut für Festkörperforschung
Stuttgart (FRG)

The Chemistry of Sulphones and Sulphoxides. Series: The Chemistry of Functional Groups. Edited by *S. Patai, Z. Rappoport* and *C. Stirling*. Wiley, Chichester 1988. xvi, 1210 pp., bound, £ 235.00.—ISBN 0-471-91588-2

In the well-known and very useful series "The Chemistry of Functional Groups", the first volume of which appeared 25 years ago (also edited by *S. Patai*), we now have for the first time a comprehensive account of the chemistry of sulfoxides and sulfones. This not only fills a gap in the series, but also remedies a more general deficiency, as there is no recent monograph of comparable scope and standard on these classes of compounds. Such a publication was long overdue, as sulfoxides and sulfones have come to occupy an important and established place in the repertoire of organic chemistry; this is clearly shown, for example, by Chapters 12 and 16 on sulfinyl carbanions and asymmetric syntheses, Chapters 13 and 14 on rearrangement reactions, or Chapters 22 and 23 on electrochemical and electron transfer reactions.

The editors have succeeded in engaging eminent experts as authors for the individual chapters, and in addition they have, of course, the experience needed to bring the separate contributions together so as to form a consistent whole. Not surprisingly, therefore, the result is an excellent book—a handbook in the true sense, and not merely a collection of essays.

The first six chapters (165 pages altogether) deal with the theoretical and physical-chemical aspects of sulfoxides and sulfones, and also with their analysis—a very useful chapter from a practical standpoint. A separate chapter on the chirality of sulfoxides, a topic of great importance to the preparative chemist, is also included here. Next there are three substantial chapters dealing in turn with the preparation of open-chain sulfones (*K. Schank*, 68 pp.) and sulfoxides (*J. Drabowicz, P. Kielbasinski*, and *M. Mikolajczyk*, 146 pp.), and of the corresponding heterocycles (*U. Zoller*, 104 pp.). The latter chapter, in accordance with the author's own field of research, includes an especially detailed account of the unusual three-membered ring systems.

 © VCH Verlagsgesellschaft mbH, D-6940 Weinheim, 1989 0570-0833/89/0808-1070 $ 02.50/0

After two further chapters on substituent effects, hydrogen bonding and complex formation, the chemical reactions are then treated in a total of 435 pages. The chapters by *S. Oae* and *Y. Uchida* and by *G. H. Posner* on α-sulfinyl and α-sulfonyl carbanions as useful CC bond-forming reagents are of particular interest for the synthetic organic chemist; these reagents have proved to be extremely useful for asymmetric syntheses. Other chapters that are mines of information on reactions useful for preparative work are those on rearrangement reactions (*S. Bravermann*, 94 pp.)—here one thinks of the important Pummerer reaction—on reduction reactions (*J. S. Grossert*, 43 pp.), which includes a description of the interesting Julia reaction for preparing carbonyl compounds from sulfones, and on sulfinyl and sulfonyl radicals (*C. Chatgilialoglu*, 34 pp.). The last of these chapters contains, for example, (though rather inconspicuously) the SO_2 extrusion reaction which is important in cyclophane chemistry.

The numerous literature references extend up to 1987 in a few chapters, but in general only up to 1986; the long time required to produce such a book makes it very difficult to achieve a degree of topicality better than this.

This volume is, of course, essential to every library. Because of its exceptionally high quality I would also like to recommend individual organic chemists (not only sulfur chemists) to buy it, but of course the price is almost prohibitive.

Jürgen Voß [NB 947 IE]
Institut für Organische Chemie
der Universität Hamburg (FRG)

Computational Chemistry. An Emphasis on Practical Calculations. (Series: Studies in Physical and Theoretical Chemistry, Vol. 56). By *M. D. Johnston*. Elsevier, Amsterdam 1988, xviii, 680 pp., hard cover, HFl 245.00/paperback, HFl 245.00. – ISBN 0-444-42962-X/0-444-42963-8

This book is apparently based on the author's lecture notes of an introductory course on data processing for chemistry students. Its contents are arranged in a clear didactic sequence as follows: 1) basic considerations and concepts in electronic data processing, with the emphasis on personal computers (algorithms, structured programming, user-friendliness, sorting programs, text processing, preparation of tables, data banks, main-frame computers and networks, basic PC equipment, programming languages); 2) various useful application-orientated programs in analytical and numerical mathematics (factorization of rational functions; Horner scheme; useful formulas for differentiation and angular functions; complex numbers; matrices, determinants, vectors, systems of linear equations); 3) programming numerical and graphical problems of chemistry in BASIC (graphical representation of 2D and 3D functions, contour plots, simple molecular graphics, some special functions, searching for stationary points, numerical differentiation and integration, Monte-Carlo integration, matrix routines, diagonalization, differential equations, curve-fitting, regression analysis, minimization); 4) an extensive collection of useful programs for the chemist, varying greatly in length (some up to 2000 lines in length, including a molecular graphics program, a graph-plotting package, a matrix package, simplex minimization, a fast Fourier transform program, a titration curve program, and NMR spectrum simulation). Each section concludes with questions to test the reader's understanding and a few exercises.

The text is written in an easy, one might even say casual, style, such as one might use when lecturing to students so as to hold their attention. This is indeed necessary in the early part of the book, which sometimes contains long-winded general observations expressed in sentences of little factual content ("textbooks are an invaluable source of basic information"; "select the best method for the problem at hand"; "write expressions so that it is best for the actual calculation").

The teaching strategy of the book is based on illustrating the methods and enabling the reader to learn and understand by applying them himself. The theoretical background to the methods used and the programs listed is explained later (though not always adequately). This very pragmatic approach should please chemists who are not keen on theory, but it is not to everyone's taste.

The author expresses the view that some first-hand programming experience is needed in order to make effective use of the computer and pre-written programs (however, the assertion that "if you can program, the computer is your servant; otherwise you are the computer's slave" is rather an exaggeration). While it is true that programming experience is best gained by working through examples of well-written programs, the reproduction in the book of many pages of computer code appears of limited value. Would it not have been possible to supply a diskette to go with the book? Many of the comments reflect the personal tastes of the author too strongly, and should be read with a measure of skepticism ("FORTRAN is not suitable for use with microcomputers"; "In going from microcomputers (i.e. PCs) to minicomputers we gain little, if anything"; "The mouse is one of the silliest inventions which has ever captured the fancy of anyone").

The book contains much of value for a good introductory course, but there is not much on the subjects of data banks and text processing. Incidentally, it has been prepared using a *very* basic word-processing system (no special characters, no line justification, no word breaks); also the typed pages are not free of typographical errors. Students, for whom the book is no doubt intended, will surely not pay the horrendous price for this level of quality. Comparable books are available at considerably lower prices.

W. H. Eugen Schwarz [NB 959 IE]
Institut für Theoretische Chemie
der Universität-Gesamthochschule Siegen (FRG)

Two-Dimensional NMR Methods for Establishing Molecular Connectivity. A Chemist's Guide to Experiment Selection, Performance and Interpretation. By *G. E. Martin* and *A. S. Zektzer*. VCH Verlagsgesellschaft, Weinheim/VCH Publishers, New York 1988. xviii, 508 pp., hard cover, DM 126.00. – ISBN 3-527-26858-703-5/0-89573-703-5

In view of the flood of books on two-dimensional NMR spectroscopy during recent months and years, the appearance of each new book prompts one to ask whether it has a particular appeal, either with respect to the range of topics covered or the readership to which it is addressed. The book "Two-Dimensional NMR Methods for Establishing Molecular Connectivity", by *G. E. Martin* and *A. S. Zektzer*, published by VCH Verlagsgesellschaft, does in fact display such a special quality. It concentrates on a clearly defined subject area, giving a very detailed account of two-dimensional pulsed NMR methods for revealing connectivities of the two elements hydrogen and carbon, the main emphasis being on applications to organic natural products with molecular mass less than 1000. In NMR spectroscopy connectivity information is, in chemists' language, information about the molecular constitution of a compound. Questions relating to

stereochemistry or conformation are therefore excluded completely from the discussion. In accordance with this, methods for measuring such structure-related NMR parameters as coupling constants or cross-relaxation rates are not included.

The organization of the book falls clearly into seven chapters. In the introductory chapter the principles of 2D NMR spectroscopy are briefly described, and practical information and advice is given on the processing of the data, presentation of the spectra and planning of experiments (including pulse width calibration). Chapter 2 is devoted to H-H connectivities, and includes a detailed description of the basic COSY experiment and six variants of it. The chapter concludes with an account of multiple quantum NMR spectroscopy. In Chapter 3 methods for determining H-C connectivities are described. A full account of all the methods, from the first selective SPT experiments through to the most sensitive present-day pulse sequences with ^1H detection, is given. Chapter 4 is devoted to relayed experiments, including homo- and heteronuclear, single and multiple relayed experiments, and the related TOCSY experiment. Chapter 5 then deals with ^{13}C-^{13}C connectivities, with a strong emphasis on the INADEQUATE experiment. The latest variants with ^1H detection are also treated. Finally, Chapter 6 presents spectroscopic problems of structure determination in organic molecules, and solutions to these are provided in Chapter 7.

The main emphasis of the book is on the fifty or so pulse sequences that are described. The discussion of these is supported by an excellent survey of the literature, with a comprehensive bibliography which covers not only the first publication on each pulse sequence and the modifications subsequently introduced, but also many published applications. The authors give details of experimental conditions which they have themselves tested and found to give good results, and the majority of the spectra shown are their own. In many of the examples spectra recorded on the same compound using different methods are shown and discussed in order to compare the information given by each method. This gives the user a valuable impression of the advantages and disadvantages of the various methods. The descriptions of the pulse sequences include explicit information on phase cycles, although regrettably these are incorrect in some cases. Readers must therefore be warned against using these pulse sequences uncritically; instead they should compare them with the original papers.

The book does not aim to give a rigorous theoretical understanding of the pulse sequences, and the reader who is unfamiliar with "spin gymnastics" will experience some difficulty in understanding the discussions. Inevitably, therefore, certain expressions are used, such as "passive transfer", without their meaning being fully explained.

The numerous figures illustrating the techniques described are an important feature of the book. However, it is incomprehensible why the labeling of the spectra is so sparse and frequently illegible, often making the search for the spectral details discussed in the text a laborious task. The poor quality and often inadequately small scale of the figures is especially annoying in Chapters 6 and 7 which contain the spectroscopic problems. Also cross peaks are sometimes missing, so that one is forced to read the solution to the problem.

In summary it can be said that this book offers a detailed, excellently researched and unbiased account of 2D NMR methods for determining molecular constitution. For the NMR practitioner it provides very useful information and advice on planning experiments and interpreting spectra, illustrated by interesting examples from natural products chemistry. One is willing to forgive the less than perfect quality of the figures and the errors that are probably unavoidable in view of the large amount of material included.

Christian Griesinger [NB 965 IE]
Laboratorium für Physikalische Chemie
der Eidgenössischen Technischen Hochschule
Zürich (Switzerland)

Activation Analysis with Charged Particles. Ellis Horwood Series in Analytical Chemistry. By *C. Vandecasteele*. Ellis Horwood, Chichester/Halsted Press, New York 1988. 171 pp., hard cover, $ 29.95. – ISBN 0-7458-0175-7/0-470-21204-7

In contrast to neutron activation analysis (NAA), charged particle activation analysis (CPAA), mainly using protons, but also deuterons, tritons, and nuclei of helium-3 and helium-4, has found little use up to now in elemental trace analysis; consequently it has no chance of becoming a universal routine method. Nevertheless CPAA, which has very high sensitivity, can be used as a complementary method with NAA and other trace analysis methods in special types of problems. It offers higher sensitivity than the other methods, and also eliminates ambiguity in some cases, for determining light elements such as H, Be, B, C, N and O down to ppb concentrations, especially in ultra-pure metals and semiconductors. However, the acceleration of the particles for CPAA requires very expensive equipment such as a Van de Graaf generator or a cyclotron (for protons and deuterons with energies of 2 to 20 MeV), and sometimes causes complex nuclear reactions which necessitate subsequent radiochemical separation. Consequently it has great disadvantages compared with NAA and atomic spectroscopy for determining medium and heavy elements, e.g. in geochemical or biological matrices, and only in rare cases is it sensible to use it for such analyses.

The author of this first monograph on the theory, experimental requirements and applications of CPAA, who has considerable practical experience in this field, is well aware of the limitations of the method. About a half of the book is taken up by general matters, including introductions to the theoretical basis, descriptions of accelerators and irradiation techniques, the relevant nuclear reactions and data on these, and the procedures needed for calibration and avoidance of errors. In the chapters that follow describing applications to trace analysis, the practical importance of CPAA in each of the areas covered is clearly reflected by the numbers of publications cited. The most important chapter, "Determination of Light Elements", has 85 references. That on "Determination of Medium and Heavy Elements in Metals and Semiconductors" – where irradiation by protons is still the most important experimental method – has 42 references. "Analysis of Geological, Environmental and Biological Samples" has 14 references, as does the more academic "Activation Analysis using Heavy Ions". In all the chapters the literature up to the present date is covered very thoroughly and described in clear language, thus giving students, teachers and those interested in using the method an excellent picture of the capabilities of CPAA, although only a few experts will ever be able to use the method in their own laboratories. The main value of the book therefore lies in the information on when it is appropriate to use CPAA, and where to turn for help in such cases.

Günther Tölg [NB 975 IE]
Institut für Spektrochemie
Dortmund (FRG)

Industrielle Organische Pigmente. Herstellung, Eigenschaften, Anwendung. By *W. Herbst* and *K. Hunger*. VCH Verlagsgesellschaft, Weinheim 1987. xiv, 637 pp., hard cover, DM 320.00. – ISBN 3-527-26319-5

The chemistry, properties and methods of use of organic dyes and pigments as colorants for textiles, paper, leather and similar substrates have already been the subject of numerous monographs, and have also to varying degrees found their way into many organic chemistry textbooks, and thus even into undergraduate courses. However, this is not true of the second large group of organic coloring media, namely those pigments that are used mainly in the manufacture of printing inks, paints and varnishes, and as colorants for plastics. In view of the continual growth in the technological and economic importance of this latter group of products, and also the scientific problems which they present, the appearance now of a substantial and comprehensive monograph on this subject is very much to be welcomed; the book deals with all the different types of industrially manufactured pigments, mainly from the practitioner's point of view.

The general part of the book (190 pp.) begins by defining the book's subject of organic pigments, as distinct from inorganic pigments and organic dyes, then goes on to give a brief classification of the different types of pigments according to their chemical structures. The chemical and physical properties of each group, and their important behavioral characteristics when in use (e.g. color shade and strength, fastness, crystallinity, polymorphism, particle size distribution, coloring behavior), are described, together with the relevant test methods. Next the reader learns about the different areas of application of organic pigments.

The main part of the book contains a tersely written, but nevertheless almost exhaustive, description of the large class of the azo pigments (230 pp.), e.g. mono- and bis-azo, naphthol-AS, benzimidazolone, and metal complex pigments, followed by polycyclic pigments (134 pp.), such as the phthalocyanines, the quinacridones, the dioxazines, the perylene and perinone derivatives, and other types related to these in the wider sense. In every case the structures, synthetic methods, properties and applications are described, and the various commercially available products are summarized.

A further section (12 pp.) deals with the environmental aspects and toxicology of pigments, and with relevant legislation. The book ends with a set of formula schemes describing the synthetic methods used for making the most important pigments (32 pp.), together with a reference table of pigments and a subject index.

Because of its comprehensiveness, and the convenient arrangement and competent treatment of the material, the book is an almost ideal information source both for the practitioner in the field and for the reader about to enter it. The important aspects of the synthesis and applications of organic pigments are dealt with very fully, in a clear style and with a rational sub-division of the material. The excellent layout is a considerable aid to the reader, and it is a pleasure to open the book. The price seems an acceptable one for the readership envisaged by the authors, but the same does not apply for university departmental libraries or others interested in the topic.

In the reviewer's opinion, specialists in other fields who want to try something new could usefully consult this book. For example, a solid state physicist or materials scientist who, in his own studies (unrelated to pigments), wishes to investigate a range of different chemical structures, could hardly find a greater variety of easily prepared, crystallizable substances with well-defined structures than the pigments described here. To summarize, in this book by *W. Herbst* and *K. Hunger* we now have a standard work which will hold its place in the literature for a long time to come.

Wolfgang Lüttke [NB 981 IE]
Organisch-Chemisches Institut
der Universität Göttingen (FRG)

Advanced Inorganic Chemistry. 5th Edition. By *F. A. Cotton* and *G. Wilkinson*. Wiley, Chichester 1988, xvii, 1455 pp., hard cover, $ 44.95. – ISBN 0-471-84997-9

Eight years after the publication of the previous edition there is now a new "Cotton & Wilkinson" in its original English version. For a book which is aimed not only at advanced students but at everyone with interests in modern inorganic chemistry, this time interval is just about long enough for the most recent developments to be treated at a textbook distance. This already highlights one of the undoubted merits of the concept followed since the appearance of the first edition in 1962; the evidence of the authors' own productive research activities (more than 1000 scientific papers by *F. A. Cotton*) guarantees a careful selection and critical appraisal of results from the current literature.

What, then, can long-standing "subscribers" to this work and first-time readers expect to find? The manuscript deadline was mid-1987, and consequently the new superconducting materials are represented only by five lines tucked away in the chapter on copper oxides and one literature citation (*Whangbo* and *Williams*). For reasons of space, only citations later than 1979 are included, and one therefore needs to refer to previous editions for work published earlier. Although the text itself contains very few printing errors, the citations themselves are marred by some repeated annoying mistakes in German names (e.g. *Hüttner, Sherer*).

The overemphasis in "Cotton & Wilkinson" on transition metal and coordination chemistry at the expense of Main Group element and molecular compounds is perceived as such especially in the German-speaking world and is still clearly detectable despite the claim to the opposite in the book's blurb. This is apparent both from the choice of literature references and from the (too scanty) list of contents. A short introduction to coordination geometry and ligand classification is followed by a systematic treatment of the elements of the Periodic Table and their compounds; the enlarged section on Main Group elements is essentially due to the new system of classifying complex ligands under the respective coordinating atoms. In this section, moreover, the treatment is not always up-to-date; for example, the description of the photoreactivity of chlorophyll is identical to that in the third edition of 1972, and has therefore long been outdated.

In the transition metals section the compounds of the 4d and 5d elements are particularly strongly represented; furthermore, the comprehensively discussed topics of systems with metal-metal, metal-carbon and metal-hydride bonds, homogeneous catalysis, reaction mechanisms and bioinorganic chemistry are almost entirely concerned with transition metal compounds.

The still rapidly expanding field of organo-transition metal chemistry (metal carbonyl clusters, complexes containing C-ligands, catalysis) has been given increased emphasis compared with previous editions. The chapter which appeared in the fourth edition as "Transition Metal to Carbon Bonds in Synthesis" has now been given the more explicit title "Oxidative-Addition and Insertion Reactions". It would have been desirable to include a comprehensive review of the photo-

chemistry of organometallic and coordination compounds, a topic which has become increasingly important in the last few years.

The relatively small increase in size of about 60 pages compared with the previous edition gives a total of 1455 pages, still just about compact enough for convenient use. This modest increase has been achieved at the cost of excluding some "theoretical" material; as the authors note tersely in the preface, "something had to go". The original conception of "Cotton & Wilkinson" thus becomes even more strongly evident, one aspect being a consistent emphasis on experimental facts, especially on structural information, as opposed to interpretations and theoretical models; as the preface puts it, "theories come and go". However, in actual work (or examination) situations such maxims are scarcely helpful; models, even though they may change with time, are indispensable for the development of chemical knowledge (as is the process of disproving them). The approach adopted by the authors follows the current trend in the USA towards more "descriptive" chemistry; however, the book is by no means devoid of necessary theoretical discussions and popular concepts. For example, one finds the planarity of silyl amines explained in terms of unoccupied silicon d-orbitals (illustrated by a diagram), isolobal and valence electron rules are used throughout, and the coordination geometries of the elements are classified according to their not always meaningful oxidation states.

Thus "Cotton & Wilkinson" can only be recommended to the student in combination with a textbook such as "Holleman & Wiberg" in which the emphasis is on fundamentals and Main Group element chemistry; a recent serious alternative is "Greenwood & Earnshaw", which covers both fields equally well. Furthermore, using "Cotton & Wilkinson" as a work of reference has taken a certain amount of getting used to; it is true that, in contrast to the still inadequate contents list, the subject index has been enlarged by 50% compared with the previous edition, but the mixing of names with chemical formulas now results, for example, in "RHgX" being listed between "Rhenium" and "Rhodium". To sum up, however, "Cotton & Wilkinson" in this new edition will maintain, and may further extend, its unique standing as a classic work amongst the available literature for students and teachers of inorganic chemistry; being more ambitions than a conventional textbook, but now deliberately omitting the treatment of basic elementary material, this edition provides a selective "eight-year review", a bonanza of information on important results and developments which could otherwise easily be overlooked in the general deluge of publications.

Wolfgang Kaim [NB 951 IE]
Institut für Anorganische Chemie
der Universität Stuttgart (FRG)

Corrigendum

In the communication entitled "Electron Densities, Deformation Densities, and Chemical Bonding" (*Angew. Chem. Int. Ed. Engl. 28* (1989) 597), the name of one author was inadvertently omitted. The authors are W. H. Eugen Schwarz,* Klaus Ruedenberg, Lothar Mensching, Lance L. Miller, R. Jacobson, Petros Valtazanos, and Wolfgang von Niessen.

Registered names, trademarks, etc. used in this journal, even when not marked as such, are not to be considered unprotected by law.

© VCH Verlagsgesellschaft mbH, D-6940 Weinheim, 1989. – Printed in the Federal Republic of Germany by Konrad Triltsch Druck- und Verlagsanstalt Würzburg.

All rights reserved (including those of translation into foreign languages). No part of this issue may be reproduced in any form — by photoprint, microfilm, or any other means — nor transmitted or translated into a machine language without written permission from the publishers. Only single copies of contributions, or parts thereof, may be made for personal use. This journal was carefully produced in all its parts. Nevertheless, authors, editors and publisher do not warrant the information contained therein to be free of errors. Readers are advised to keep in mind that statements, data, illustrations, procedural details or other items may inadvertently be inaccurate.

Valid for users in the USA: The appearance of the code at the bottom of the first page of an article (serial) indicates the copyright owner's consent that copies of the article may be made for personal or internal use, or for the personal or internal use of specific clients. This consent is given on the condition, however, that the copier pay stated per-copy fee through the Copyright Clearance Center, Inc. (CCC), for copying beyond that permitted by Sections 107 or 108 of the U.S. Copyright Law. This consent does not extend to other kinds of copying, such as copying, for general distribution, for advertising or promotional purposes, for creating new collective works, or for resale. For copying from back volumes of this journal see 'Permissions to Photo-Copy: Publisher's Fee List' of the CCC.

Editorial office: Postfach 10 11 61, D-6490 Weinheim, Federal Republic of Germany, Telephone (06201) 60 22 55, Telex 465 516 vchwh d, Telefax (06201) 602 328.

Editor: *Peter Gölitz*

Associate editors: *D. I. Loewus, A. Stimson.* **Editorial assistant:** *E. Schweikart*

Publishers: VCH Verlagsgesellschaft mbH. (Managing Director: *Hans Dirk Köhler*), Pappelallee 3, D-6940 Weinheim, Federal Republic of Germany.

Advertising office (Advertising Manager *R. J. Roth*): Postfach 10 11 61, D-6940 Weinheim, Federal Republic of Germany, Telephone (0 62 01) 60 61 30, Telex 467 155, Telefax (0 62 01) 606 184.

ADVANCED MATERIALS

Materials Science and Engineering in Britain

Editorial Essay

By Colin Humphreys*

Mankind is poised to move into a revolutionary era: the age of new materials. For example, materials scientists are designing novel liquid crystals which will enable television sets of the future to be thin and light, so that they can be hung on a wall like a picture. We can make superconductors in which an electric current will circulate for ever with no battery required to keep it going: well known recent developments in materials chemistry have led to higher critical temperature superconductors which may ultimately result in cheaper electricity and ultrafast levitating trains. We can make materials which store information so compactly that the entire contents of the Encyclopaedia Britannica can be contained within the space occupied by this full stop →. (see Fig. 1) We can make semiconductor lasers so thin that one

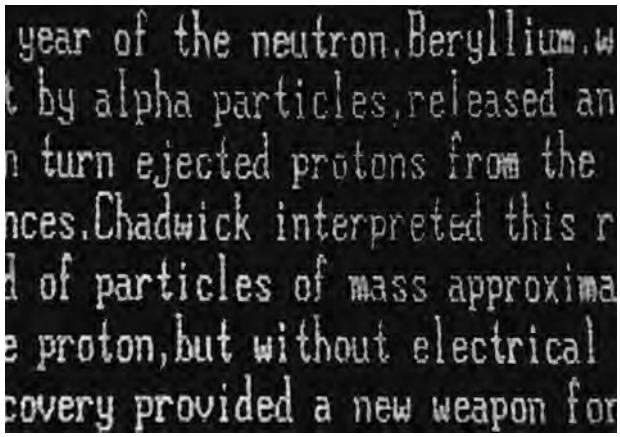


Fig. 1. A portion of the Encyclopaedia Britannica written in AlF_3 using an electron beam. The beam has a diameter of only 0.5 nm and each letter is composed of a double row of dots 4 nm in diameter. Each dot is a hole etched through the 50 nm thick AlF_3 specimen directly using the electron beam. At this scale of lithography the entire contents of the Encyclopaedia Britannica could be written on a pinhead. The potential for information storage, molecular filters, etc. is clear. The nanometer scale lithography was performed using a 100 keV electron beam in a computer controlled VG HB 501 scanning transmission electron microscope.

million of them can be stacked side-by-side within the thickness of a one penny coin, and the color of the laser light emitted can be chosen simply by varying the laser layer thickness: such lasers are being used in the latest generation of compact disc players. Laser surgery, using novel lasers developed by materials scientists, is enabling the blind to see and artificial heart valves, made from advanced materials, are giving life to some who would otherwise be dead.

Many readers of this article will require artificial hip joints in the future. Twenty years ago the average lifetime of an artificial hip joint was only three years. Today the average life time is ten years, and current research on advanced materials has improved the lifetime of the next generation of artificial hip joints to thirty years. Since the cost of an artificial hip joint is only £ 100, and the cost of the operation is about £ 3000, these recent developments in materials science and engineering are not only of benefit to the patient but also to the financial benefit of the health service. Research into artificial skin is in progress, and longer term research into an artificial pancreas so that diabetics would no longer need to inject insulin is also underway.

Novel materials are essential for use in protecting our environment in, for example, solar cell technology or in catalytic converters.

The main force driving developed nations into the age of new materials, however, is not the desire for improved health care nor for a better environment, it is that for economic growth. The economic growth argument was concisely summarized in an issue of Scientific American entirely devoted to advanced materials which stated: "Advanced materials are essential to the future growth of the aerospace, electronic device, automobile and other industries. Progress in materials science sets ultimate limits on the rate at which key sectors of the economy can grow."

For the above reason, the importance of new and improved materials is clearly recognized in developed countries. *George Keyworth*, President *Reagan*'s former chief scientific advisor, stated: "Materials science is probably the most important subject in the US today." In Japan, the Ministry of International Trade and Industry (MITI) has targeted three key areas for massive research and development: new materials, new electronic devices and biotechnology, and top of the list is new materials. In the Japanese government's Basic Technology for Future Industries Program there are eleven major projects, seven of which are in the area of new materials. About two years ago the UK government set up the Advisory Council on Science and Technology (ACOST) to advise it on priorities in science and technology. ACOST has recently identified new materials as a key enabling technology.

Materials research is a strategic research area which is essential for future industries and in which research discoveries can be transformed into market place products in a peri-

[*] Prof. C. J. Humphreys
Chairman, Materials Science and Engineering Commission,
Science and Engineering Research Council (UK)
and Head of Department of Materials Science and Engineering
University of Liverpool,
P.O. Box 17, Liverpool L69 3BX (UK)

od of typically three to twenty years. Our competitors have already realized this and overseas governments have selected new materials for priority funding in order to make their future industries competitive, to improve their future balance of trade and to reduce their future unemployment. For example, the US government invests well over £ 700 million per annum in materials research, and the Japanese government invests an estimated £ 500 million per annum. On the other hand, the UK government invests only about £ 60 million per annum in materials research of which about £ 20 million is allocated to the Science and Engineering Research Council (SERC). Last year the annual increase in spending of the Japanese government on materials research in the civil sector exceeded the total spending of the UK government in this area. With such a massive funding discrepancy in materials research between the UK and our competitors it is essential that the UK makes the best use of its limited resources, and that it invests more heavily. The UK has been slow to wake up to what has been happening in materials research in Japan, the USA and parts of Europe (notably West Germany and France). However there are now clear signs that Britain is increasingly aware of the strategic importance of materials research.

Perhaps the first evidence of this increased awareness was the decision of the SERC (which funds science and engineering research in all UK universities and polytechnics) to set up in 1987 a panel to study the funding of materials science and engineering by the SERC. The panel, chaired by Dr. *Peter Day*, reported in January 1988 that although much UK materials research is of the highest standard internationally, many areas are in rapid decline. The panel presented evidence that the funding levels are totally inadequate. Their report also stated that the administration of materials research within the SERC was very fragmented, with materials research being funded by the Physics Committee, Chemistry Committee, Materials Committee, Process Engineering Committee, etc. As a result of this report, and of further consultations, the SERC under its Chairman, Professor *Bill Mitchell*, decided to reorganize totally its funding of materials research and the Materials Science and Engineering Commission of the SERC was established in September 1988.

The Mission Statement of the Commission has recently been drawn up and is as follows:

The Commission will promote excellence of research and training in both the science and engineering of materials. It will take an integrated view of materials research from synthesis through processing to demonstrator projects. It will seek to maintain and enhance the world class materials research record of the UK. It will encourage the creation of new materials and facilitate the competitive exploitation of materials by British industry in international markets.

The breadth of the Commission can be seen from the titles of the seven committees it controls: ceramics and inorganic materials, polymers and composites, metallic and magnetic materials, semiconductors, superconductors, molecular electronics, and medical engineering and sensors. The Commission and each of its seven committees is multidisciplinary and contains chemists, physicists, materials scientists, electrical engineers, etc. Roughly half the Commission members are from universities and polytechnics and half from industry. The inherited budget of the Commission was about £ 15 m p.a., but in its first year of operation this has been increased to £ 20 m p.a. The increase is a very welcome first step to what is required.

The Commission will determine a coherent SERC strategy for the support of materials research and it will take a leading rôle in identifying national priorities in materials research. In addition to having research priority areas, the Commission fully recognizes that unpredictability is part of the fascination of research, and that many major breakthroughs have been unexpected and unplanned: it will therefore have a balance between funding priority areas and funding high quality research in any area and it will respond quickly and flexibly to the unexpected.

The Commission is very keen on fostering links with Europe and internationally in general. It has already held small scientific meetings with France, Italy and Japan. As we move into the highly competitive age of new materials, the SERC Materials Science and Engineering Commission will do its utmost to ensure that UK universities and polytechnics are at the leading edge of materials research, and that the results are transferred to industry and to medical care.



Professor Colin Humphreys obtained a B.Sc. from Imperial College, London in 1963 and a Ph.D. from Cambridge in 1967. From 1966 to 1985 he was a Research Fellow and then Lecturer in the Department of Metallurgy and Materials Science, University of Oxford. He was appointed the Henry Bell Wortley Professor of Materials Engineering and Head of the Department of Materials Science and Engineering at the University of Liverpool in 1985 and from January 1, 1990 his new address will be at the Department of Materials Science and Metallurgy, University of Cambridge. He is a Member of the Electron Diffraction Commission of the International Union of Crystallography, and a Council Member of the Science and Engineering Research Council (SERC) and of the Institute of Metals. His main research interests are electron diffraction and microscopy, semiconductors, superconductors and nanometer scale electron beam lithography. He was published over 160 papers. In 1988 he became the first Chairman of the newly formed Materials Science and Engineering Commission of the SERC.

Advanced Catalysts: Interfaces in the Physical and Biological Sciences

Heterogeneous Catalysis
Molecular Sieves
Biocatalysis
Catalyst Design
Abzymes
Ribozymes

By John M. Thomas*

1. Introduction

It has been established that catalytic materials, one way or another, now account for some 25% of the gross national product (GNP) of the USA. But catalysts have long played a central rôle in the economy of civilized nations. The ancient Greeks and Romans, for example, used biological catalysts (enzymes) for the production of wine and its conversion to vinegar and for the transformation of starch into sugar. They also used alkalis as inorganic catalysts to produce soaps from fats and oils. Nowadays, much of the food we eat and the medicines we take, many of the fabrics and building materials that keep us warm, and almost all the fuels that transport us by road, sea or air are produced by heterogeneously catalyzed reactions. The current world production of ammonia, required as an agricultural fertilizer, is about 120 million tonnes per annum. Owing to the expanding need to feed mankind, this figure is increasing at some 6% per annum. Vitamins and drugs, herbicides and pesticides, as well as a range of foodstuffs including margarine are all the products of catalysis. Catalysts are the cornerstone of the chemical industry, which, in contrast to many other sectors of the (UK) economy, continues to flourish (Figs. 1 and 2).

Most of the catalysts used for commercial processes are heterogeneous, being composed either of metals or alloys (usually supported on high area oxides), of oxides or sulfides, or of microporous, microcrystalline aluminosilicates known as zeolites. Increasingly, biocatalysts such as enzymes, immobilized on high-area solid supports, as well as appropriate micro-organisms are utilized for the production of certain key foodstuffs and pharmaceuticals (Table 1).[3]

The first patent encompassing heterogeneous catalysts was taken out by an Englishman named *Peregrine Phillips* who, in 1831, described how sulfuric acid could be manufactured by passing sulfur dioxide and oxygen over finely divid-

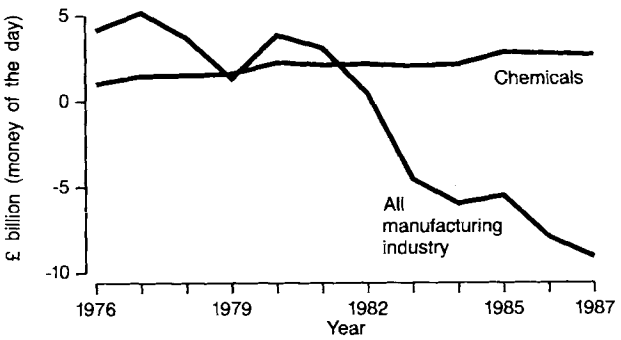


Fig. 1. U.K. Trade balance in chemicals and all manufacturing industry [1].

Table 1. Current industrial scale applications of immobilized biocatalysts [3].

Application	Enzyme	Microorganism
Steroid conversions	11-β-hydroxylase (EC 1.14.15.4)	*Curvularia lunata*
	Δ¹-dehydrogenase (EC 1.3.99.4)	*Arthrobacter simplex*
Glucose isomerization	Xylose (glucose)-isomerase (EC 53.15)	*Actinoplanes sp.* *Arthrobacter sp.* *Bacillus coagulans* *Streptomyces sp.*
Raffinose hydrolysis	α-D-galactosidase (EC 3.2.1.22)	*Mortierella vinaceae*
Starch saccharification	Glucoamylase (EC 3.2.1.3)	*Aspergillus niger*
Lactose hydrolysis	β-D-galactosidase (EC 3.2.123)	*Aspergillus niger*
6-APA from penicillin	Penicillin acylase (EC 3.5.1.11)	*Eschericia coli*
Optical resolution of α-amino acids	Amino acylase (EC 3.5.1.14)	*Aspergillus oryzae*
L-aspartic acid from fumaric acid	Aspartase (EC 4.3.1.1)	Eschericia coli (EC 3.5.2.2)
L-malic acid from fumaric acid	Fumarase (EC 4.2.1.2)	*Brevibacterium ammoniagenes*
D-phenylglycine from D,L-phenylhydantoin	Hydantoinase (EC 3.5.2.2)	*Bacillus brevis*
Acrylamide from acrylonitrile	Nitrilase (EC 3.5.5.1)	*Corynebacterium sp.*
L-phenylalanine	Transaminase (EC 3.6.1.58)	

[*] Prof. J. M. Thomas
Davy-Faraday Research Laboratory
The Royal Institution of Great Britain,
21 Albemarle St. London, W1X 4BS (UK)

[**] Based on the Presidential Address to the Chemistry Section, British Association for the Advancement of Science, Sheffield, September 1989.

I am grateful to *Barnaby Smith* for his help in preparing this paper and to the Laura Ashley Foundation for the award (to B. S.) of a school-leaver fellowship. Support from the Science and Engineering Research Council is also appreciated.

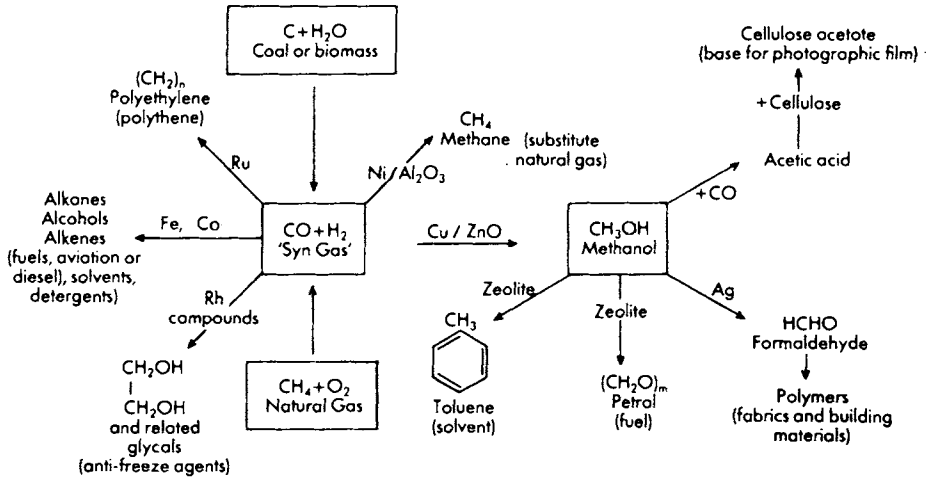


Fig. 2. Synthesis gas (abbreviated 'syngas') is a mixture of carbon monoxide and hydrogen and may be produced either by oxidizing coal or by burning methane. A wide variety of products can be generated from 'syngas' using the appropriate catalyst. Fischer-Tropsch catalysts such as Fe or Co (extreme left) promise to provide (from coal as primary feed-stock) exceptionally clean fuels [2].

ed platinum supported on clay. Platinum continues to play a pivotal rôle in modern catalysis; it serves to isomerize (reform) linear hydrocarbons, such as those initially produced by the (zeolite-catalyzed) cracking of oil, to their branched and aromatic analogs, many of which have high octane ratings. Platinum, and its congener rhodium, also finely divided and supported on alumina and ceria, are the center pieces of the automotive exhaust catalysts, which reduce emissions of undesirable gases into the environment (Table 2). Some forty million auto-exhaust catalytic units were installed on light vehicles in 1988 alone. Over a third of the world's available platinum is now used in auto-exhausts. Platinum is also of central importance in electro-catalysis which is a primary feature of the fuel cell, where electricity is generated directly by the electro-chemical combustion of hydrogen or methanol.

Table 2. Decrease in emission rates per mile driven since the introduction of auto-exhaust catalysts in the USA.

Pollutant	Percentage Decrease
Carbon Monoxide	86
Nitrogen Oxides	56
Hydrocarbons	84

2. Mechanisms of Catalysis

Much mystery still surrounds our knowledge of how heterogeneous catalysts function. The auto-exhaust catalysts that convert nitric oxide, carbon monoxide and hydrocarbons to harmless products, are less complicated than other multiphasic and multicomponent inorganic catalytic solids. The situation is also less complicated for the so-called uniform heterogeneous catalysts in which all, or almost all, of the atoms in the bulk of the solid participate directly, or are implicated indirectly, in the catalytic processes of the overall reaction.

Examples of uniform catalysts are zeolites, silico-aluminophosphates (SAPO's) – see later – as well as certain clays and pillared clays. In all these cases, the active sites are uniformly distributed in the bulk of the solid. Because of the microporosity of these structures, however, the active sites are accessible only to gaseous reactant species of the requisite size and shape. Uniform heterogeneous catalysts, primarily because their structures may be elucidated by the traditional techniques (especially X-ray crystallography) applicable to the study of bulk solids, are therefore very well characterized in comparison with heterogeneous catalysts consisting of supported or multiphasic solids.[4, 5] Detailed discussions of how catalysts function have been given elsewhere.[4, 6]

The zeolitic and SAPO-based catalysts frequently function in a dual manner. First, they provide, at specific (active) sites within the accessible pores, protons that are effectively the catalytic agents. Second, their well-defined porosity, in which the apertures in the form of cages and channels – at the internal surface of which the active sites are situated – permit access to those reactants that are of the requisite size. This shape-selectivity for the reactants, is often accompanied by a similar shape-selectivity for the products, since only those generated species that are small enough are able to diffuse out from the interior of the catalyst.

Uniform heterogeneous catalysts possessing zeolitic character are much more akin to enzymes in their mode of action than to the multiphasic inorganic solids, typified by the ammonia synthesis catalyst (which consists of iron and the oxides of potassium, silicon, aluminum and combinations thereof[7]) or by the iron–potassium based industrial cata-

lysts for the conversion of ethylbenzene to styrene. This catalyst has recently been shown[8] by in situ X-ray diffraction study to contain Fe_3O_4, $KFeO_2$ and $K_3Fe_{22}O_{34}$.

Paradoxically, much more is known about the structure of the active sites in enzymes than those in metallic or oxide catalysts, even though their overall structures and constituent parts are substantially more complicated than those of the metals and oxides in extensive industrial and laboratory-scale use. Enzymes generally have active sites which consist of pockets, or clefts, the lining of which contain the crucial set of amino acids, in the right sequence and conformation required to 'process' the reactant species.[4]

3. Trends in the Design of New Catalysts

In addition to the logical extensions and improvements that are being pursued for existing catalysts, there is also intense activity focused on the creation of radically new ones. Not only are there advances occurring in heterogeneous catalysis, which has hitherto dominated the commercial scene, there are nowadays significant developments in biocatalysis, in homogeneous catalysis and in the evolution of fundamentally new types of catalysts. Some of these are rooted in the inorganic, inanimate world, others very firmly in the biological and animate.

3.1. New Heterogeneous Catalysts

Table 3 highlights the areas currently attracting considerable attention both at the fundamental and applied level.

Table 3. Current trends in the evolution of heterogeneous catalysts.

Tailored Solids
Development of stereoselective catalysts based on pretreated metals (e.g. Ni, Pt) and on immobilized transition-metal complexes.
Membrane (e.g. metal alloy) catalysts for single-stage synthesis.
Molecular sieves in which cage and channel dimensions are controlled.
Development of new oxide-based solids capable of the sacrificial loss of structural oxygen for selective oxidation of hydrocarbons
Schottky-junction (metal on oxide) catalysts [a]
Fine-tuning of Fischer-Tropsch catalysts (based on Fe, Co, Ru) so as to generate ultra-clean hydrocarbons from CO + H_2 mixture derived from coal.
Photocatalysts
Design and preparation of solids, the electronic band-gap of which are engineered (as in the fields of semiconductor physics and opto-electronics)
Quantum solids (ultra fine particles in 20 to 500 Å diameter range) with and without enclathration.
Electrocatalysts
New designs and components for fuel cells (for energy generation).
Derivatized electrodes (for sensors and other analytical purposes).

[a] See J. C. Frost's discussion on junction effects in catalysts for methanol synthesis (*Nature London 334* (1988) 577).

Stereoselective catalysts, which are capable of producing an enantiomeric excess of a given species from a prochiral precursor, are of growing importance. Chirality, after all, holds sway in living processes and is hence of enormous relevance in the quest for catalysts needed for the generation of pharmaceuticals. Until about the early 1960s, access to enantiomerically enriched compounds from prochiral reactants was thought to be realizable only by biological or enzymatic methods.[9] However, at least a decade earlier, some fascinating Japanese work[10] had indicated that a special preparation consisting of metallic palladium supported on silk served as a heterogeneous catalyst for the asymmetric reaction involving the hydrogenation of oximes and ketones. Since that time Ziegler-Natta catalysts for the asymmetric polymerization of olefins, as well as specially modified Raney-nickel heterogeneous catalysts, have been used extensively for asymmetric conversions. Of late so-called Lindlar catalysts,[10, 11] in which the surface of the palladium is modified by the deliberately added lead 'impurities', have been extended to encompass Pd-Pb alloys, which function as efficient means of effecting stereoselective hydrogenations for the synthesis of insect sex pheromones.[12]

The scope for tailoring metal catalysts by pre-adsorbing upon their surfaces bulky organic molecules which create prochiral cavities for the incoming reactant is obviously considerable. *Wells* et al.[13] have re-examined the Orito reaction[14] in which platinum, modified by the presence of presorbed cinchonidine (a member of the cinchona alkaloids), becomes active for the stereoselective hydrogenation of an α-ketoester (e.g. methyl pyruvate) to an optically active product (e.g. *R*-(+)-methyl-lactate, Fig. 3). My colleagues

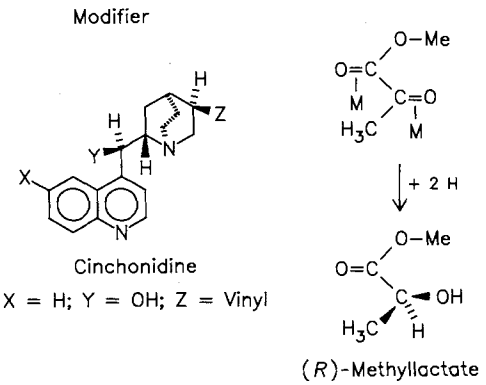


Fig. 3. Cinchonidine preadsorbed on a platinum catalyst favors the hydrogenation of a co-adsorbed α-ketoester to the optically active *R*-methyl lactate [13].

and I[15] have explored, by computer graphics (see Fig. 4), the way in which this stereoselective process might proceed. The plausible assumption here is that cinchonidine forms an ordered, well spaced out array of interstices in the sorbed layer. The interstices permit ingress of the methyl pyruvate in a preferred fashion so as to pre-ordain the formation of a given stereo product.

Membrane catalysts such as those based on palladium or on binary alloys of palladium with one of a dozen or more other metals – Al, Ti, Ni, Cu, Mo, Ru, Rh, Ag, In, W, Re and

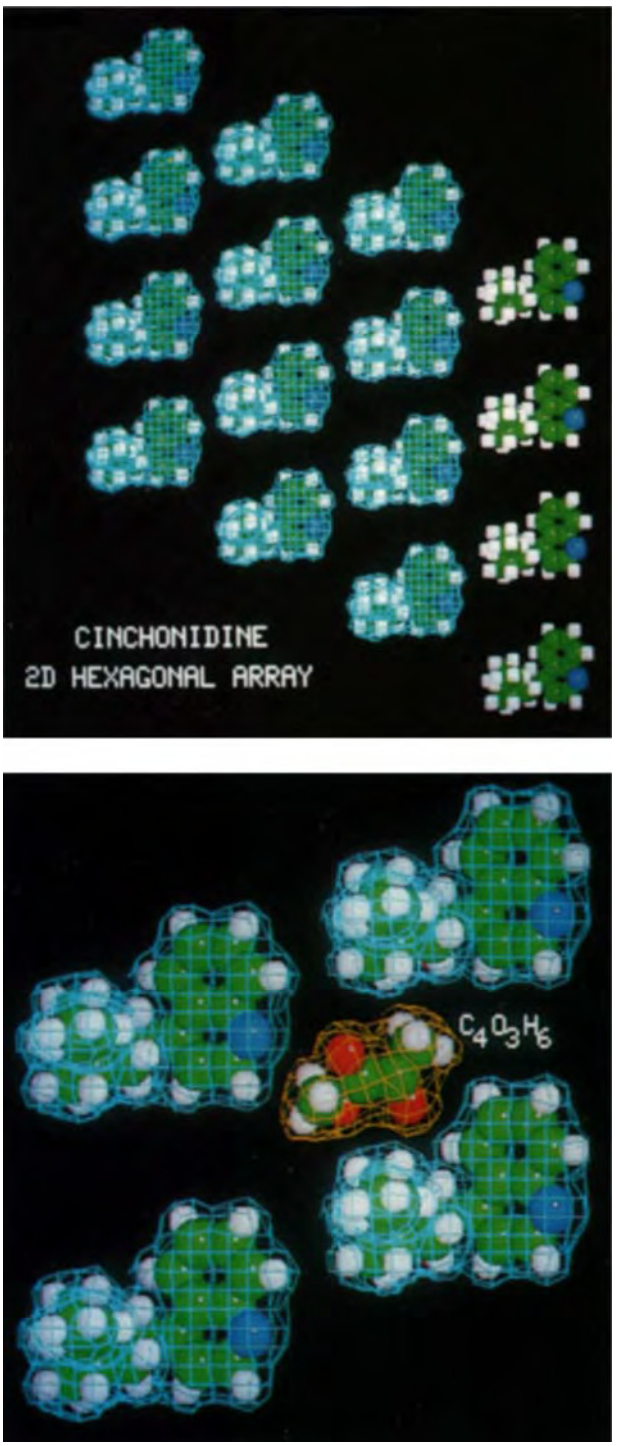


Fig. 4. (a) Schematic illustration of the way in which cavities in the ordered monolayer of cinchonidine (on a platinum surface, which is not shown) may serve as centers where a prochiral reactant may be stereo-preferentially adsorbed as in (b). This preordains the production of an enantiomeric excess of the methyl lactate formed by catalytic reduction on the modified metal surface. (After *Barnaby Smith* et al. [15]).

Pt – are permeable to hydrogen but not to the organic compounds which are to be hydrogenated. Hydrogen transfer through such membrane catalysts which are in the form of foils or thin-walled tubes, provides a new method of influencing the addition or removal of hydrogen. The Soviet scientist *Gryaznov*[16] has carried out pioneering studies of this new type of catalyst, which has already been brought to commercial use in the one-stage production of vitamin K_4, as shown in Figure 5.

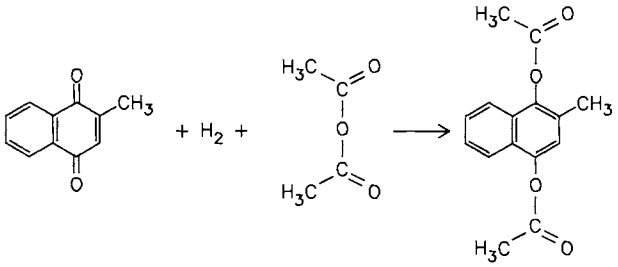


Fig. 5. One-stage production of Vitamin K_4 on a permeable palladium membrane catalyst [16].

Palladium-based binary alloys consisting of yttrium have also recently been used,[17] as membrane catalysts, for the production of hydrocarbons from synthesis gas ($CO + H_2$ mixtures). Recognizing that palladium surfaces are remarkably efficient catalysts for the trimerization of acetylene to benzene[18] and the synthesis of thiophene[19] from adsorbed acetylene and sulfur[20] (see Fig. 6), it ought to be

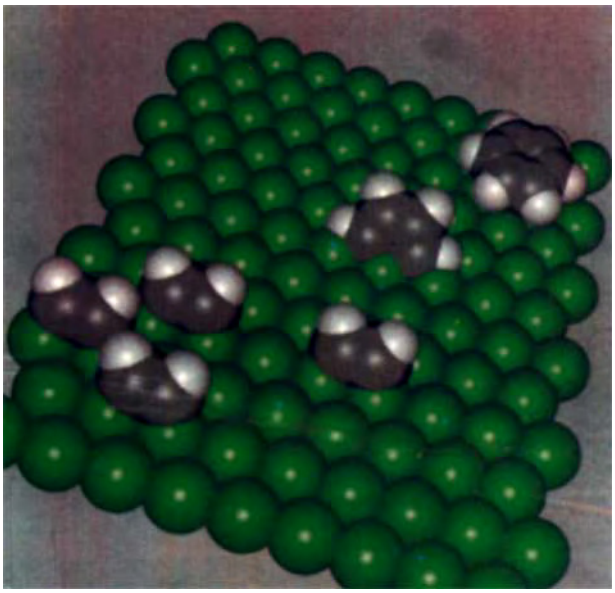


Fig. 6. Schematic illustration, after *Gellman* [19], showing how a close-packed surface of palladium metal catalyzes the trimerization of acetylene, via intermediates, to benzene.

feasible to so design a system, consisting of a membrane catalyst based on this metal, capable of selectively synthesizing partially hydrogenated aromatic and heterocyclic compounds.

Molecular sieve catalysts are already widely used[4, 20–23] in the hydrocracking of oil and petrol, in the synthesis of

petrol from methanol, in alkylations and isomerizations; and their increasing rôle in laboratory-scale synthesis and conversions continues to expand.[23–25] A selection[25–27] (taken from other publications) of interesting catalytic reactions, of value in the production of fine chemicals, is shown in Figure 7.

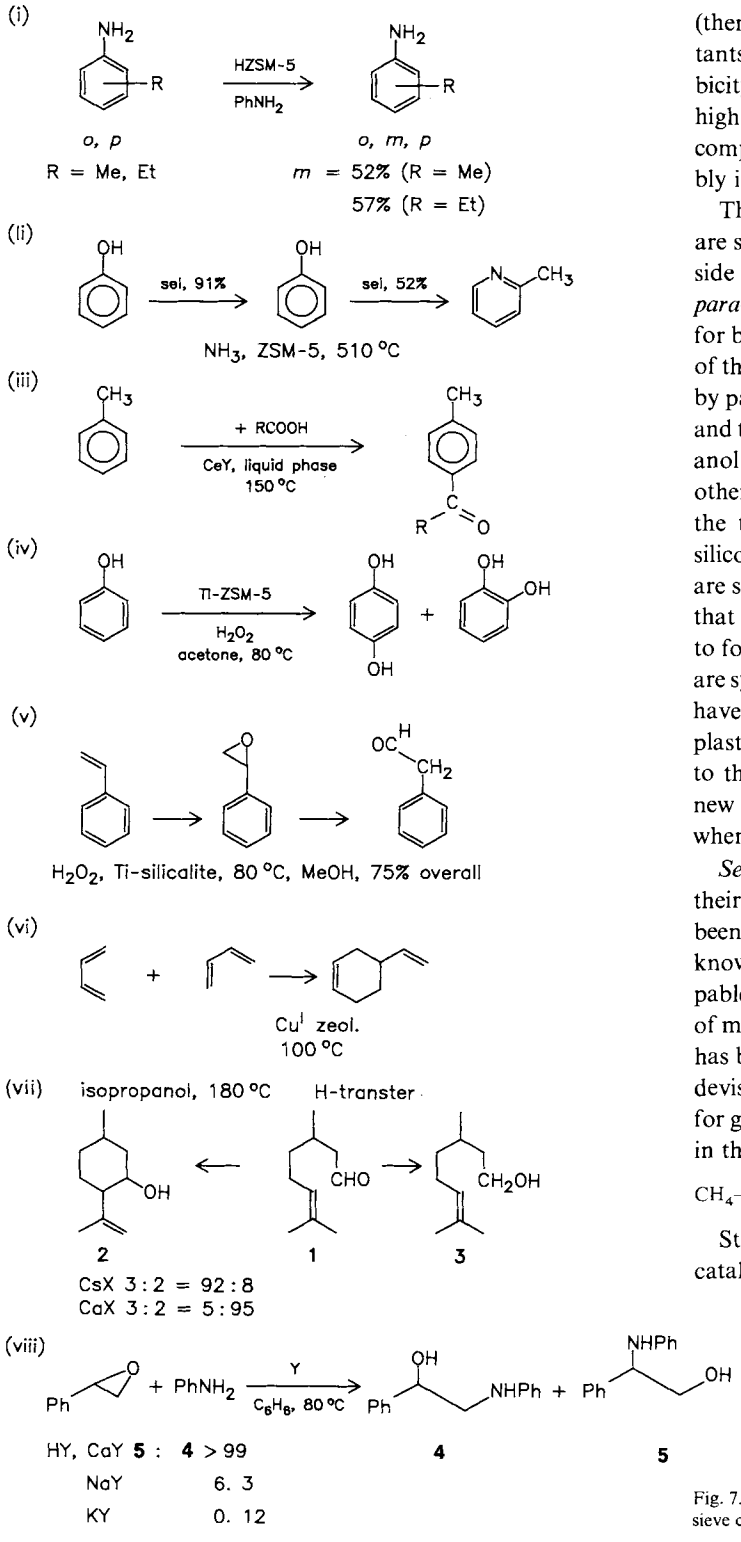


Fig. 7. A selection of some of the organic reactions catalyzed by molecular sieve catalysts. (After *Van Bekkum* [25] and *Thomas* and *Theocharis* [24])

These and other reactions, for which the appropriate microporous solid catalyst has yet to be developed, are or will be rendered possible through the special characteristics of zeolitic solids viz: a sharp, well-defined pore-size distribution; good thermostability; adjustable Brønsted or Lewis acidity; a wide range of exchangeable cations of different radius or polarizability; adjustable size and morphology (thereby allowing scope to modify diffusion times of reactants and products); adjustable hydrophilicity or hydrophobicity (according to whether the Si/Al ratio is low (1.0) or high (> 20) respectively) an ability to accommodate metal complexes, some of which are so bulky as to require assembly inside the cavities and channels.

The channel dimensions of the well-known zeolite ZSM-5 are such that, when methanol is catalytically dehydrated inside its pores, only monocyclic aromatics (benzene, toluene, *para*-xylene, etc.) are produced. The channels are too small for bicyclics such as naphthalene to form. This is the essence of the synthesis of petrol from natural gas – methane, which by partial oxidation is first converted to a $CO + H_2$ mixture and then, catalytically, over a copper-based catalyst to methanol – now operating in New Zealand.[30] By assembling another type of molecular sieve, known as SAPO-34, in which the tetrahedrally-coordinated framework constituents are silicon, aluminum and phosphorus, the channel dimensions are significantly smaller than those of ZSM-5 (see Fig. 8) so that it is not now possible for even the monocyclic aromatics to form. Instead olefins such as propene and other α-olefins are synthesized. This is an important advance as the α-olefins have a variety of end uses: components of solvents, textiles, plastics, plasticizers and surfactants. More details pertaining to the general principles of the design of new zeolites and new AlPO-based molecular sieve catalysts are given elsewhere.[4, 31, 32]

Selective oxidation catalysts, especially those that release their own structural oxygen in a sacrificial fashion, have been known for some time. Of late, however, an increased knowledge of the solid-state chemistry of solids that are capable of accommodating large, steady-state concentrations of mobile vacancies created by the loss of structural oxygen has been acquired. This will make it increasingly possible to devise novel solids capable of catalyzing reactions that have, for good reasons, been regarded as very difficult to cope with in this way. One such example is:

$$CH_4 \xrightarrow{(O)} C_2H_6 + C_2H_4 + C_2H_2 + \text{other products}$$

Strenuous efforts will continue to be made to devise new catalysts for other reactions in which there is an abundance

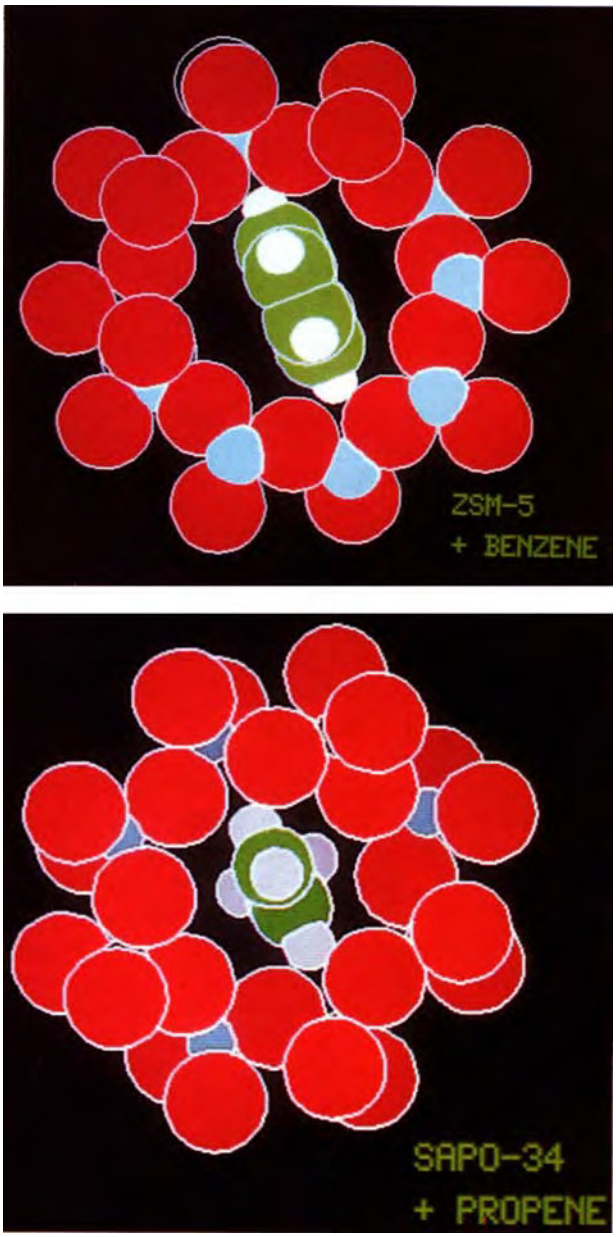


Fig. 8. When methanol is catalytically dehydrated over a molecular sieve (acid) catalyst, the nature of the products is governed by the dimensions of the channels. (a) Over a ZSM-5 catalyst, the channels are large enough to permit the formation of benzene. (b) Over a SAPO-34 (acid) catalyst, which has smaller pores, the dehydration yields only alkenes such as propene. (After *Yan Xu* and *Barnaby Smith*, unpublished).

of reactants e.g. nitrogen to nitrates, carbon dioxide to formates and fossil material to more useful hydrocarbons. Insofar as producing clean hydrocarbons (for fuels or packaging material) is concerned, there in renewed interest in Fischer-Tropsch catalysis based on iron, cobalt or ruthenium. Thus, coal or natural gas, when gasified to $CO + H_2$ mixtures, can be satisfactorily purged of sulfur, nitrogen and other environmentally harmful heteroatoms. Using catalytic systems such as the Shell middle distillate process, which by Fischer-Tropsch catalysis converts the $CO + H_2$ mixtures to a suite of hydrocarbons of controllable ranges of molecular weight, an abundance of high-quality hydrocarbons is created. Recognizing that world coal supplies will persist for many more centuries, this is an important development.

One may expect that, with our increased knowledge of the factors that influence the magnitude of the electronic band gaps of solids, and the preparative requirements for their production, important developments are likely in the field of photocatalysis. With the practice of band-gap engineering, well established in the design and preparation of solids for specific optoelectronic purposes, it would be surprising if new photocatalysts were not developed in the near future. In this connection, the realization that very finely divided solids (such as the binary III–V and II–VI semiconductors) possess band gaps larger than those of their bulk analogs offers further scope for the preparation of new photocatalysts, especially when they can be stabilized by enclathration inside zeolitic or analogous hosts.

3.2. New Homogeneous Catalysts

Whilst it is not the aim of this review to encompass homogeneous catalysts, a few comments are in order since renewed efforts are now underway to improve methods of immobilizing homogeneous catalysts on inert, durable and large surface area solids. The performance of all homogeneous catalysts could, in principle, be improved by anchoring them on to an appropriately derivatized microporous solid. More often than not, however, the support tends to diminish the effectiveness of the dispersed catalyst, either by reducing its turnover frequency or its selectivity. The supreme advantage that immobilization confers, whether it be on inorganic[33] or polymeric[34] supports, however, is the ease of separating product from reactant.

Some of the materials that ought to be relatively easy to tether to an appropriate solid surface are the metal complexes. And it is these very materials that have recently shown extraordinary efficiency as entioselective catalysts in the important field of chiral synthesis. The work of *Noyori*[9] and others[35, 36] testifies to the significance of asymmetric reactions generally. Among other things, we note that impressive entioselectivities, rivaling those attained via the use of enzymes, have been achieved using metal-complexes.

It is convenient to illustrate the strategy employed by reference to the recent elegant work of *Pfaltz*,[35] who has introduced transition-metal semicorrins, schematized in Figure 9. The C_2-symmetry of these transition-metal complexes ($M = Co^{II}$, Ni^{II}, Pd^{II} or Cu^{II}, as well as other ions) is readily apparent. The chirality elements are dictated by the size and nature of the R groups, which are in close proximity to the coordination center.

With the aid of Figures 10 and 11 we see how these semicorrin complexes function as enantioselective catalysts. Assuming that the transition state of the enantioselectivity-

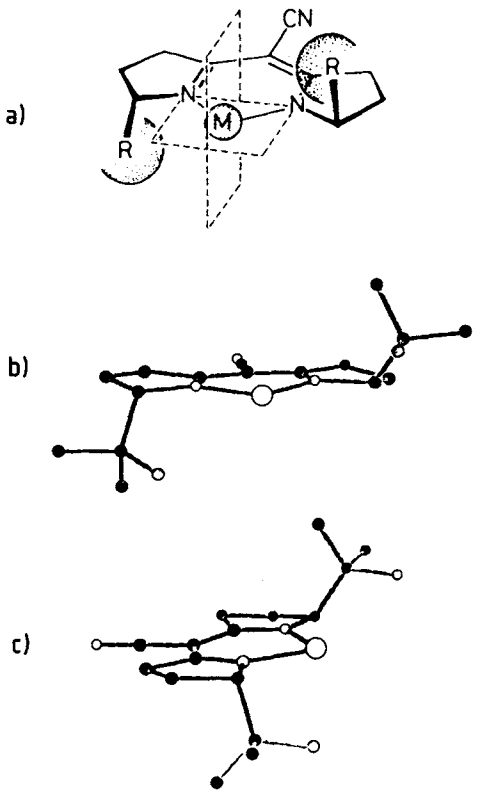


Fig. 9. The C_2-symmetry of the semicorrin ligand is illustrated in (a). The two substituents, R, at the stereogenic centres are held in close proximity to the coordination center (metal M) by the rigid framework of the semicorrin ligand. (b) and (c) represent molecular models when R is a $C(OH)(CH_3)_2$ group. (After *Pfaltz* [35]).

determining step resembles the hypothetical π-complex depicted in Figure 10, the observed selectivity may be ratio-

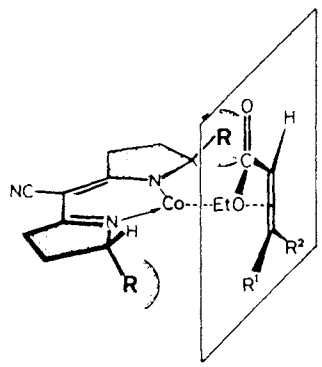


Fig. 10. The transition state for the (semicorrinato) cobalt-catalyzed reduction of α,β-unsaturated carboxylic esters is thought [35] to be of this kind.

nalized in the following manner. The ester group occupies a sterically unencumbered site of the coordination sphere, whereas the olefinic H-atom is placed in a sterically more crowded environment (Fig. 11 A). However, the transition structure leading to the opposite enantiomer (Fig. 11 B) is

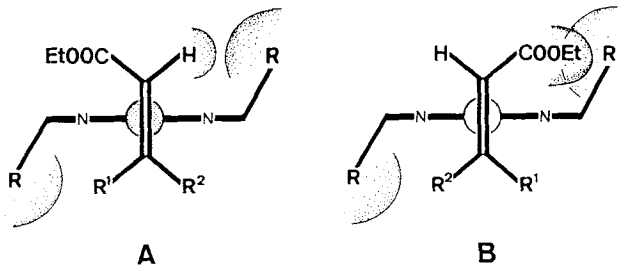


Fig. 11. Illustration of the possible origin of enantioselection. For steric reasons the transition state, represented by B, is forbidden, and that shown in A is likewise preferred [35].

expected to be considerably destabilized owing to steric repulsion between the ester group and the adjacent substituent of the semicorrin ligand.

When such elegant design can be introduced to fashion powerful homogeneous catalysts of this kind, there will be a great incentive to devise a 'tea-bag' version[37] of the immobilized catalyst, where the active catalyst may rattle around in its (molecular) container, be accessible to the reactant, and from which product may be washed away so as to regenerate the original catalyst.

3.3. Enzyme Catalysis

It has long been recognized[38, 39] that enzymes have great potential as catalysts for use in synthetic organic chemistry; and their importance in this, and other contexts, is underlined by the processes enumerated in Table 1. Increasingly, a number of small-scale syntheses of materials used in analytical procedures (such as derivatized, biological sensors), in research and as chiral building blocks (synthons) for the production of pharmaceuticals and fine chemicals, is under development. An important trend is the change in technology for the production of enzymes – partly because of improved methods from classical microbiology, and partly because of the viability of genetic engineering, in particular site-selective mutagenesis – for their stabilization and manipulation now makes these catalysts practical for far broader use than hitherto in large-scale synthetic organic chemistry.[38]

The main impetus for biotransformation studies, using enzyme catalysts as center pieces, has been the continued growth in demand for enantiomerically pure compounds. In this context, advantage is taken of the high stereospecificity of the actual reactions catalyzed. Advantage is also taken of the regioselectivity of enzyme-catalyzed reactions. Examples may be found in the selective esterification of dicarboxylic acids, the selective hydrolysis of compounds containing ester functions (e.g. sugar esters) and the selective reduction of compounds containing multiple carbonyl groups.[39]

For the materials scientist, one of the significant messages here is that enzymology is now playing a growing rôle in governing the strategies for the modification of materials

derived from fermentation synthesis. Another is the exigent need to evolve more satisfactory means of immobilizing some of the several dozen or so commercially available and useful enzymes, as well as the many more that have recently come to light but which are not yet so readily obtainable.

3.4. Trends in Biocatalysis

Because most enzymes operate effectively under mild conditions (pH usually between 6.5 and 8.5 and at around room temperature) it is often possible to assemble complex systems containing multiple enzymes operating in sequence or in parallel to achieve multi-step processing of the reactants. The work of *Knowles* and *Whitesides* et al.[40] on the synthesis of ribulose 1,5-diphosphate (RuDP), an important substrate in plant biochemistry constitutes a nice example. The point of chief technical interest here is the final conversion of 6-phosphogluconate to RuDP. The kinase that converts ribulose-5-phosphate to RuDP is oxygen sensitive. Thus, the in situ regeneration of NAD from NADH required in the conversion of 6-phosphogluconate to ribulose-5-phosphate cannot be carried out using an oxygen-based regeneration system. The regeneration is, however, conveniently carried out anaerobically using the α-ketogluconate/glutamate dehydrogenase system. This part of the synthesis requires the cooperative action of four enzymes: 6-phosphogluconate dehydrogenase and 5-phosphoribulokinase for the principal conversions, and glutamate dehydrogenase and acetate kinase for in situ regeneration of cofactors.

It may be seen, therefore, that multi-enzyme 'cocktails' constitute a useful way of producing novel biocatalysts. However, there are other ways forward; and these are summarized in Table 4.

Table 4. Current topics and trends in biocatalysis.

Use of:	(i) Multi-enzyme systems (ii) 'Whole cells' and micro-organisms, (e.g. Bacteria such as *Methylococcus capsulatus* (Bath) and baker's yeast).
Antibodies as enzymes (abzymes) [a].	
RNA as enzymes (ribozymes) [b].	
Genetic and chemical modification of enzymes (protein engineering).	
Man-made (miniature) enzymes.	

[a] See P. G. Schultz et al. *Angew. Chem. Int. Ed. Engl. 27* (1988) 1172; *Angew. Chem. 100* (1988) 1227. [b] See T. R. Cech, *Nature 339* (1989) 507, for a discussion of the idea that RNA molecules may exhibit catalytic activity.

It is often not necessary to extract an enzyme or a collection of enzymes from the living cell. The latter may be used as such; and whole cell catalysts are nowadays in quite common use, either in their suspended or immobilized state, on an inert solid (often derived from a heat-treated clay). In microbial biotechnology, one uses the microbes as such to catalyze a highly specific chemical change. Both ICI[41] and Shell[42] have put to good industrial use the microbial catalytic conversion (fermentation) of benzene and some of its derivatives to *cis*-3,5-cyclohexdiene-1,2-diol (Fig. 12).

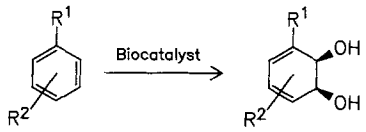


Fig. 12. The process of dioxygenation of substituted benzene (where R_1 and R_2 may, for example, be CF_3 and H respectively) is catalyzed using soil bacteria [42].

Certain enzyme systems, operating in vivo, catalyze hydrooxylations, epoxidations and related oxidation reactions with selectivities unparalleled by any other procedure. They are of great value in the oxidative functionalization of steroids and other hydrocarbons (using fungal systems).

There is a bacterium, known as *Methylococcus Capsulatus* (Bath),[43] a soluble methane monooxygenase, that converts methane to methanol at room temperature. Its mode of action, in particular its regio- and stereo-selectivity, when catalyzing the conversion of cyclohexanes consists of at least three components.

Though other microorganisms have been used to catalyze the (bio) reduction of ketones, it has recently been reported[45] that baker's yeast efficiently catalyzes the reduction of $Cr(CO)_3$-complexed aromatic ketones. Increased enantiomeric excess, over that achieved by other catalysts, and kinetic resolution of planar chiral complexes is feasible with the yeast (Fig. 13).

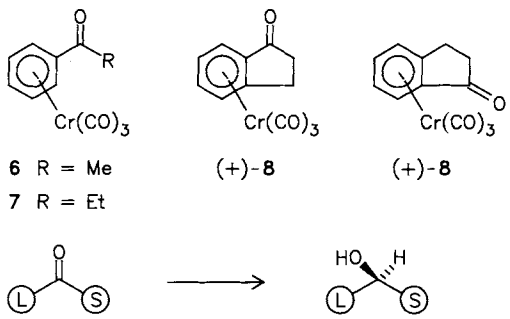


Fig. 13. Aromatic ketones, such as those shown in (1) to (3) when complexed with chromium carbonyl, undergo enantioselective reduction using baker's yeast [45]. The (*S*)-alcohol is always obtained preferentially, indicating that the reduction follows the so-called Prelog rule (Scheme 1; the large substituent L represents the aromatic group)

Abzymes (or catalytic antibodies) have appeared on the scene very recently. Their existence arises because of a question posed more than a decade ago: Can antibodies be made to serve as enzymes? (The term abzymes is a hybrid of *ant*i*b*odies and en*zymes*).

Nature, it is believed, utilizes no more than about 30 to 40 thousand enzymes to effect all the bewildering range of coupled processes responsible for the teaming manifestations of

life. So far as practical applications—outside of life cycles—are concerned, the limitation of enzymatic catalysis is that there are so few enzymes compared with the enormous numbers of scientifically important chemical reactions which one seeks to catalyze. Antibodies, like enzymes, are proteins. Their structural features complement, in a literal sense, those of the antigenic sites of intruder species. They have the ability to recognize foreign substances, and are of breathtaking diversity. The immune system, which is where antibodies are generated, is able to make over a 100 million different kinds of antibodies.

Both antibodies and enzymes exert their influences in much the same way: by binding to other molecules. The question therefore naturally arises: Can one capitalize upon the similarity of antibodies and enzymes (as molecular recognizers) to make the former act as biocatalysts? If so, the door is opened to an almost limitless range of new catalysts. However, antibodies, in their normal rôle, do not catalyze chemical transformations. The way in which they have been recently 'cultured' to function as catalysts, is by feeding the immune system with a stable structural analog of the transition-state through which a particular reactant molecule must pass to be transformed. The antibody will then bind that 'transition state' and its precursor, enabling the free energy with which antibodies bind to their targets to be harnessed in a catalytic process. This kind of abzyme chemistry is in its infancy. But it is already clear that it has a major rôle to play in biological and medical science.

Rationally modified enzymes may be produced by means of site-directed mutagenesis. Such enzymes possess significantly different surface charges, pH-activity profiles and (often) high catalytic activities as well as altered specificities compared with their parental analogs. The serine protease subtilisin (from *Bacillus amyloliquefaciens*)[46] has been 'engineered', by site-directed mutagenesis so as to effect all the above-mentioned changes. The human enzyme called tissue-type plasminogen activator has recently been modified by mutagenesis so as to increase its effectiveness in dissolving blood clots. These are pointers for directions that may be taken in the design and assembly of rationally modified enzymes, i.e. to go from the so-called wild to the mutant state.

There is a radically different route that may also be followed, and that entails the assembly of a miniature enzyme, rivaling the performance of the parent which it mimicks. *Bender* et al.[47] have constructed a miniature biological catalyst (see Fig. 14) which has a performance that closely matches that of chymotrypsin. Chymotrypsin itself is a large (MW 24,800 Daltons) and complicated (245 amino acids) enzyme, the function of which is to catalyze the hydrolysis of a variety of esters and amines. From an X-ray analysis of its structure, the constituents of its active site—the lining, as it were, of the pocket into which the reactant falls upon being bound by the catalyst—were determined. This reveals which chemical constituents are essential for the catalytic action. But an engineered miniature catalyst must also be efficient in capturing the reactant: it has to possess accessible pockets of the right size to accommodate the reactant but not too securely, for the reasons given earlier. *Bender* et al. took advantage of the carbohydrates known as cyclodextrins, which are themselves the products of enzymatic decomposition of starch. The α, β, and γ-cyclodextrins have, respectively, six, seven and eight sugar units (Fig. 14) and on a molecular scale they are like truncated cones or bottomless empty buckets. They also have remarkable receptor properties for a range of guests. It is also rather easy to graft small side-groups on to their rim. The net result is an artificial or miniature enzyme, provided the side-groups that are grafted onto the rim are those present, in the right sequence, at the active site in chymotrypsin itself.

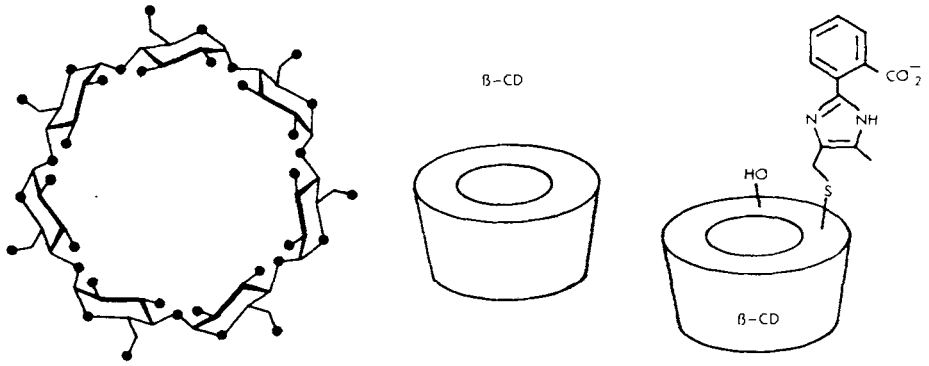


Fig. 14. A miniature enzyme, which rivals the performance of chymotrypsin, has been fashioned by *Bender* et al. [47], from a β-cyclodextrin, which consists of seven sugar units and serves as the receptacle to accommodate (recognize) the substrate molecule. The functional groups grafted on to the rim of the cyclodextrin are the same as those that line the active site of the chymotrypsin. The nature of the active site was determined by X-ray crystallography as in the classic study of lysozyme by *Phillips* [48].

The future of catalysts rests, quite clearly, not on the use of one family of structures, or on one type of catalytic system. It is instead bound up with a rich diversity of disciplines that incorporate major strands of endeavor ranging from solid-state science (physics and chemistry) on the one hand,

through to biological, and medical science (encompassing microbiology and enzymology) on the other. The materials scientist and chemical engineer confronted with the task of evolving new systems for catalytic conversion needs to be a polymathic individual capable of roaming freely, and with discrimination, through this vast field of endeavor.

Received: June 15, 1989

[1] These statistics were kindly provided by Prof. *J. I. G. Cadogan.*
[2] J. M. Thomas, *University of Wales Rev. 1* (1987) 18.
[3] M. D. Lilley: *The Complete Catalysis*, Unilever House, May 1986, p. 22.
[4] J. M. Thomas, *Angew. Chem. Int. Ed. Engl. 27* (1988) 1673; *Angew. Chem. 100* (1988) 1364.
[5] A. K. Cheetham, J. Gale, A. K. Nowak, S. D. Pickett, J. M. Thomas, *Faraday Discuss. Chem. Soc. 87* (1989) in press.
[6] G. A. Somorjai: *Chemistry in Two Dimensions* Cornell Univ. Press, Cornell, USA 1981.
[7] T. Rayment, R. Schlögl, J. M. Thomas, G. Ertl, *Nature London 315* (1985) 311.
[8] M. Muhler, R. Schlögl, A. Reller, G. Ertl, *Catal. Lett. 2* (1989) 201.
[9] R. Noyori, M. Kitamura, in R. Scheffold (Ed.): *Modern Synthetic Methods 1989*, Vol. 5, Springer Verlag, Heidelberg 1989, p. 115. R. Noyori, *Chem. Soc. Rev. 18* (1989) 187.
[10] H. Lindlar, *Helv. Chim. Acta 35* (1952) 446.
[11] J. Stachurski, J. M. Thomas, *Catal. Lett. 1* (1988) 67.
[12] J. Sobczak, T. Boleslawska, P. Pawlowska, W. Palczewska, in M. Guisnet (Ed.): *Heterogeneous Catalysis and Fine Chemicals*, Elsevier, Amsterdam 1988, p. 197.
[13] P. B. Wells, *Faraday Discuss. Chem. Soc. No. 87* (1989) in press.
[14] Y. Orito, S. Imai, S. Niva, *Nippon Kagaku Kaishi*, (1982) 137.
[15] B. Smith, S. D. Pickett, A. K. Nowak, R. H. Jones, J. M. Thomas, unpublished results.
[16] V. M. Gryaznov, *Platinum Met. Rev. 30* (1986) 68.
[17] I. T. Caga, J. M. Winterbottom, I. K. Harris, in press.
[18] T. M. Gentle, E. L. Muetterties, *J. Phys. Chem. 87* (1983) 2469.
[19] T. M. Gentle, C. T. Tsai, K. P. Walley, A. J. Gellman, *Catal. Lett. 2* (1989) 19.
[20] P. B. Weisz, *Proc. 7th Int. Congr. Catal.*, Tokyo 1980, Plenary Lecture.
[21] J. A. Rabo, *Catal. Rev. Sci. Eng. 24* (1982) 202.
[22] W. O. Haag, R. M. Lago, P. B. Weisz, *Nature London 309* (1984) 589.
[23] W. Hölderich, M. Hesse, F. Neumann, *Angew. Chem. Int. Ed. Engl. 20* (1981) 850; *Angew. Chem. 93* (1981).
[24] J. M. Thomas, C. R. Theoharis in reference 9, p. 249.
[25] H. Van Bekkum, H. W. Kouwenhoven in reference 12, p. 45.
[26] J. M. Thomas, in R. Vanselow, R. Howe (Eds): *Chemistry and Physics of Solid Surfaces VI*, Springer Verlag, Heidelberg 1986, p. 107.
[27] J. M. Thomas, W. J. Thomas: *Heterogeneous Catalysis: Theory and Practice*, Academic Press, in press.
[28] J. M. Thomas, *Proc. 8th Int. Congr. Catal. Berlin 1984*, Verlag Chemie, Weinheim, p. 31.
[29] J. M. Thomas, C. R. A. Catlow, *Progr. Inorg. Chem. 35* (1987) 1.
[30] C. J. Maiden in D. M. Bibby, C. D. Chang, R. F. Howe, S. Yunchak (Eds): *Methane Conversion*, Elsevier, Amsterdam 1988, p. 1.
[31] E. M. Flanigen, B. M. Lok, R. L. Patton, S. T. Wilson in *New Developments in Zeolite Science and Technology*, Elsevier, Amsterdam 1986, p. 103.
[32] R. J. Pellet, P. K. Coughlin, E. S. Shamshouin, J. P. Rabo, *ACS Symp. Ser. 368* (1988) (Perspective in Molecular Sieve Science), p. 512.
[33] Y. I. Yermakov in B. N. Kuznetsov, V. A. Zakharov (Eds.): *Catalysis by Supported Complexes*, Elsevier, Amsterdam 1982, p. 1.
[34] P. Hodge in D. C. Sherrington, P. Hodge (Eds.): *Synthesis and Separations Using Functional Polymers*, Wiley, Chichester 1988, p. 43.
[35] A. Pfaltz in reference 9, p. 199.
[36] S. G. Davies, J. M. Brown, A. J. Pratt, G. Fleet, *Chem. Brit. 25* (1989) 259.
[37] R. Noyori, private communication, April 28, 1989.
[38] G. M. Whitesides, C. H. Wong, *Angew. Chem. Int. Ed. Engl. 24* (1985) 617; *Angew. Chem. 97* (1985) 617.
[39] D. H. C. Crout, M. Christen in reference 9, p. 1.
[40] C. H. Wong, A. Pollak, S. D. Meburry, J. M. Sue, J. R. Knowles, G. M. Whitesides, *Methods Enzymol. 89* (1982) 108.
[41] D. G. H. Ballard, A. Courtis, I. M. Shirley, S. G. Taylor, *J. Chem. Soc. Chem. Commun.* (1983) 954.
[42] A. Fish, *Proc. R. Inst. GB. 61* (1989) in press.
[43] S. H. Staley, S. D. Prior, D. J. Leak, H. Dalton, *Biotechnol. Lett. 5* (1983) 487.
[44] D. J. Leak, H. Dalton, *Biocatalysis 1* (1987) 23.
[45] J. Gillois, D. Buisson, R. Azerad, G. Jaouen, *J. Chem. Soc. Chem. Commun. 1988*, 1224.
[46] A. J. Russell, A. R. Fersht, *Nature London 328* (1987) 496.
[47] V. T. D. Souza, K. Hanahhusa, T. O'Leary, R. C. Gradewood, M. L. Bender, *Biochem. Biophys. Res. Commun. 129* (1985) 727; see also J. M. Thomas *Nature London 322* (1986) 500.
[48] D. C. Phillips, *Proc. Nat. Acad. Sci. USA 57* (1967) 484.

Materials for the Next Millenium

By Ernest D. Hondros* and Edward Bullock*

Consumption Trends
Technico-Economics
European Performance
Materials Development

1. Introduction – The Materials Spectrum

The materials that make up the things which surround our daily lives and which are taken so much for granted are the product of a highly sophisticated and interactive chain of processes. The mineral-based materials in particular, extracted from the earth as raw ores are converted into alloys, composites and fine ceramics by techniques which call on the utmost ingenuity of man. The complexity of the basic, interactive, scientific disciplines involved in the production of modern, advanced materials is illustrated in Figure 1. The whole spectrum from the minerals in the earth to the formed material component, which has been finely tuned to closely specified properties to meet the requirements of a particular application, is shown.

The intricacy and breadth of such an interdependent chain of processes has evolved over many centuries to meet the immediate needs of society. Progress in materials utilization has largely determined the advance and ascendancy of soci-

[*] Dr. E. D. Hondros, Dr. E. Bullock
Commission of the European Communities
Joint Research Center, Petten Establishment
P.O. Box 2, 1755 ZG Petten (The Netherlands)

ADVANCED MATERIALS

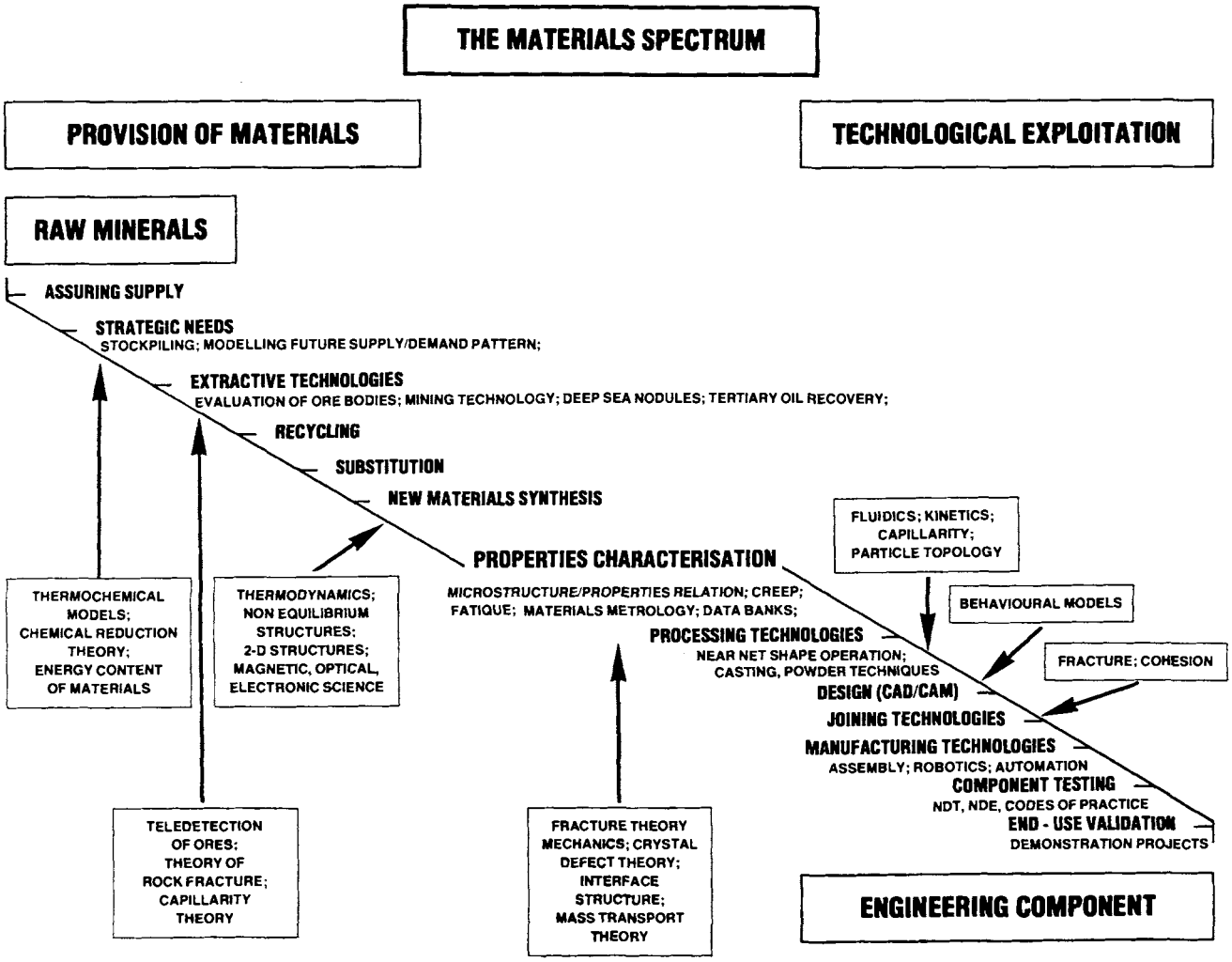


Fig. 1. The materials spectrum.

eties and has always been an issue of high priority. This situation still pertains today and will continue into the future.

As the complexity of materials processes has increased, so too has the volume of use, from the first, relatively insignificant fabrication of artifacts in the Stone Age, through the increasing demands of the Bronze and Iron Ages and accelerating during the last century to the prodigious levels of today. Concurrent with this massive expansion in volume has come a wide diversification in material types as conventional materials are developed to their physical limit and new materials are sought. Thus today in the industrially developed countries, the consumption of iron and steel, and of lead and copper have reached the top of the "S" curve of growth rate with time, while relatively new materials such as plastics, aluminum and composites are growing rapidly, and highly innovative materials, typically engineering ceramics and intermetallics are in the initial stage of slow development prior to mass exploitation.

The trend towards diversity will continue as current high growth rate materials reach their limits and saturate (including perhaps aluminum by the end of the century) to be replaced by new materials. Furthermore, as the demands for materials performance become more exacting, materials will become increasingly tailored to specific performance needs so that the trend will be for the use of combinations of highly specialized materials, each developed for a specific function within the operating system.

2. Materials Consumption Trends – The Global Responsibility

The staggering increase in utilization of the physical resources of the world, quantified in Figure 2 for the US, has led to wide concern that with such continuous growth in materials consumption, there is a danger of global exhaustion.

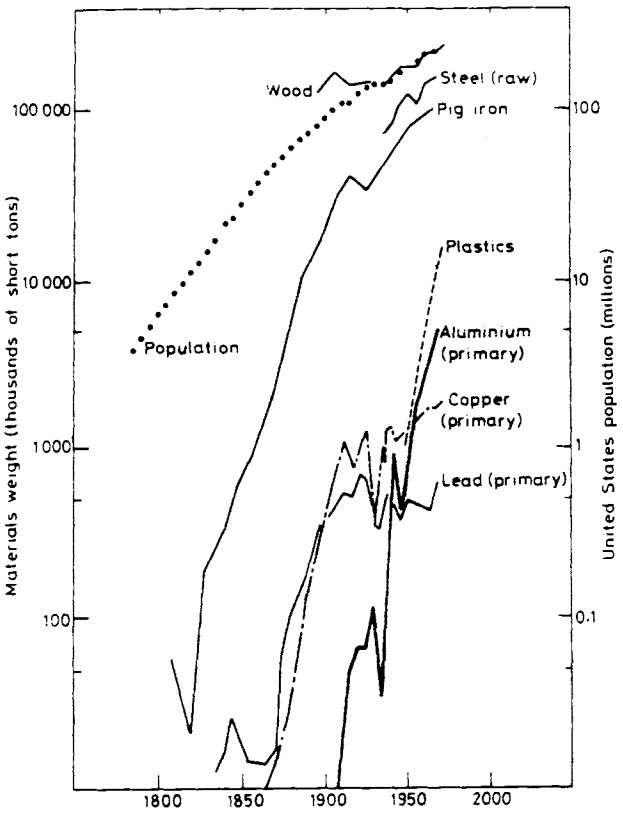


Fig. 2. Growth in usage of industrial materials in the USA compared with population growth.

Such anxieties have preoccupied the attention of strategic economic planners. There have also been signs of alarm among the industrial nations on the continuity of supply of primary materials from third world countries. The significance of the problem can be seen in Table 1 which shows the

Table 1. Import dependence of raw materials by trading areas.

	(% of consumption)			
	EEC	USA	Japan	COMECON
Aluminum	61	85	100	28
Copper	90	14	94	4
Chromium	100	91	98	2
Cobalt	100	98	100	68
Iron Ore	79	36	99	5
Lead	76	13	78	3
Nickel	100	70	100	13
Manganese	100	98	98	3
Tin	87	83	98	
Titanium	100			
Tungsten	99	52		
Zinc	91	57	74	9

amount of some principal metals imported in the form of ores and concentrates as a percentage of consumption. Among the major trading blocs, the dependence on external supplies of raw materials is most critical for Japan. The position of America is somewhat better than for example, the European Community, but nevertheless there has been considerable concern in regard to the more vulnerable strategic metals such as chromium, cobalt, tungsten and manganese, and especially fears that politico-economic movements in the Third World could produce serious restrictions to supply.

The problems of whether the growth in demand in goods and services can continue, and what constitutes the physical limit, have been the source of much agitated public debate in the past years. This was expressed perhaps in its most sensational form in the deliberations of the "Club of Rome" which led to many popular books, presenting the alarmist vision of declining natural resources.

This matter is central to any forecast of the shape of the next millenium in terms of the materials infrastructure. For this reason many analytical methodologies have been applied to the problem of forecasting the demand for raw materials throughout the world in the next century. Indeed, many of the forecast scenarios have appeared alarming.

The analysis we refer to is that of *Malenbaum*[2] who presented the outlook for demand in terms of two component elements – *the intensity of use* and *the total output of final goods and services*. He found that the intensity of use of most materials has been declining in recent years, with the exception of aluminum. The forces giving rise to a declining pattern of intensity of usage, especially in the richer waste producing countries, originate partly from technological developments, from substitutions among the raw materials and from shifts in the types of final product that consumers expect. This development, the decline in the intensity of usage, symbolizes a conscious slackening of Man's consuming appetite for raw materials.

Typical results of this type of analysis are shown in Figure 3 for three elements, chromium, tungsten and cobalt in which the intensity of usage per unit of (GDP) is plotted versus time. This indicates at least saturation in intensity of usage and even in some cases a significant reduction. The broad outcome of this analysis is that by the turn of the century the world will be consuming a volume of raw materials two to three times greater than in the previous quarter of a century. In most cases the ratios are closer to a factor of two. Compared with forecasts of equivalent ratios of five to ten made according to other models, this is an optimistic forecast.

In contrast to earlier anxieties, this represents a hopeful vision of Man and society working in close symbiosis with nature and leading to the reduction in the rates of materials consumption. It represents a conscious trend to limit the consumer appetite of Man. Since analyses of this type were made, there has been time to check on their validity and they appear to be closer to the true pattern of events. This model then is a salutary change from the Doomsday Doctrine, which suggests Man's helplessness in the face of resource exhaustion or of the deterioration of the environment. Given a certain measure of global political stability, this level of demand in raw materials can be met through existing reserves for some hundreds of years.

ADVANCED MATERIALS

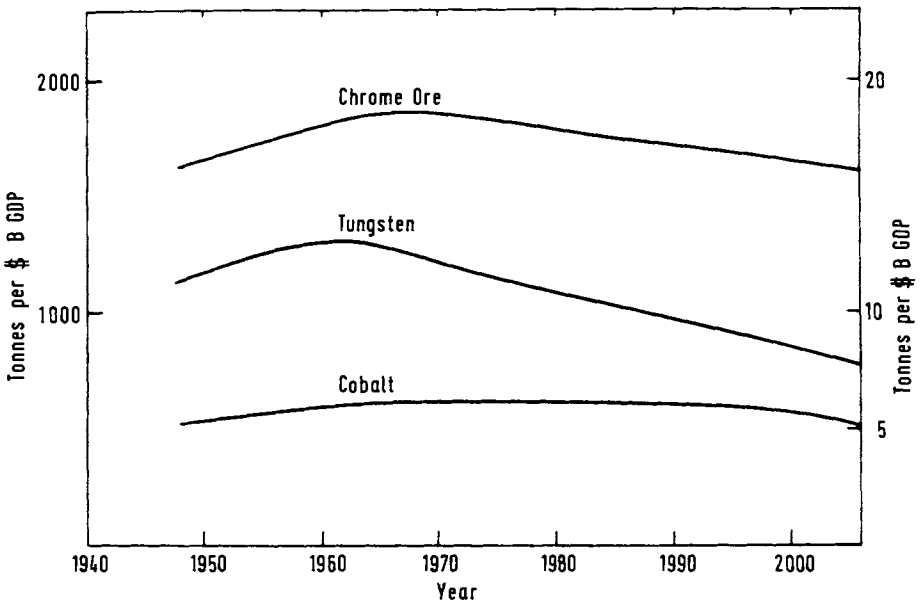


Fig. 3. Changes in intensity of use per unit GDP with time, for chromium, tungsten and cobalt.

Incidently, one conclusion from the above is that the setting of materials science and technology research objectives in terms of the substitution for scarce or unavailable materials is not a tenable assumption.

3. Materials and Future Technologies

It is now widely recognized that materials play an underpinning rôle to the major industries; they provide a substantial framework for the mechanical, chemical, building, process engineering and transport sectors. Hence, the existing euphoria about materials is partly a recognition of the fact that materials represent the rate determining step in the emergence of future technologies and for the competitivity of many existing technologies.

This is illustrated in a dramatic form in the outcome of a survey carried out by the Japanese[3a] to determine the measures that will be necessary to cope with the future requirements in industry, energy, natural resources and the environment. The question was posed as part of a systematic study of the necessary conditions for satisfying human expectations for a stable and prosperous future society. Many distinguished men and women of learning were involved in this "Delphic" type of forecasting methodology, an approach which can be considered as a process of iteration towards a consensus in games of clairvoyance. The outcome of this study, presented in Table 2, is a summary of the principal science and technology innovations for which future realization is expected. The vast amount of information collated and displayed in a chronological manner shows clearly that materials developments per se are some of the high priority items; however, the important observation is that in a large number of items in the forecast it is the materials *factor* which is implied as the rate determining step. In other words, to realize the major technological developments indicated in the table there will be a concurrent need to develop materials with specific functions.

Table 2. Technology Development Forecast (Japan).

2006	Forecasting earthquakes within one month.
2005	Super conductors with critical temperature of liquified nitrogen (77 K).
2004	Means of converting cancerous cells into normal cells.
2003	Steel production from nuclear energy.
2002	Submersible cargo ships: Aircraft and automobiles using hydrogen fuel.
2001	Drugs for arteriosclerosis.
2000	Large scale environmental purification technologies.
1999	Chemical agents for treating clotted cancer growths.
1998	Direct aluminum refining technology (direct reduction). Earthquake prediction through sea-bed crust activity.
1997	Deep sea extraction of metallic nodules. Large scale commercial nuclear fuel reprocessing plant.
1996	Engineering laboratory in space. Three dimensional memory devices.
1995	Deep sea (several hundred metres) drilling technologies. Disposal of high level radioactive wastes by solidification techniques.
1994	Super LSI – 10^9 devices per chip.
1993	Super computer (high speed devices): High efficiency thermoelectric conversion.
1992	Advanced robots for complex working environments.
1991	Long range meteorological forecasting.
1990	Large area amorphous silicon solar cell.
1989	Satellite prospecting (minerals, fishing, agricultural).

It is remarkable that in most of the categories involved in this forecast, technologies are cited which clearly depend on materials developments – thus materials related technologies are destined to be crucial in those innovations that will compose the fabric of the industries and societies of the next millenium. It seems clear that, whether in connection with

the equipment for deep sea mining or for realizing thermonuclear fusion or for replacing diseased human organs or developing large area solar conversion cells, the critical step in the realization of all these innovations will be the advent of the materials precursor.

From such a broad recognition of the rate determining rôle of materials technologies, most of the industrialized countries have recently launched programs with central government support in order to stimulate growth in materials innovations. As early as 1980 the USA in its National Materials and Minerals Policy Act highlighted the critical importance of minerals and materials to the national economy, defence and standard of living and urged the government to intervene in areas where there is a potential for high "payoff" technology. At the same time, Japan has galvanized its institutions into action and has mobilized behind advanced materials, including fine ceramics, polymers, amorphous metals and composite materials. The same note is being struck in many places and at different levels of action—in fact with a strangely repetitive beat. In the UK the *Collyear* report recommended a program of the order of a hundred million pounds over five years in new materials, equally financed by industry and government. In Germany, the German Federal Ministry for Research and Industry (BMFT) has implemented a large materials research program, to continue over about ten years, with links between the universities and the public sector in order to procure close collaboration. In France the Materials Mission has been published which is aimed at the establishment of a mobilization program to double government investment. Similarly there have been materials proposals in the Netherlands, in Belgium, more recently in Italy and currently in Spain and Portugal. In the European Community programs, materials is the pivot of the new Institute of Advanced Materials, shaped from the materials R & D activities of two establishments (Petten and Ispra) of the Joint Research Centre. Finally, materials R & D will feature strongly in collaborative cost-shared programs and in the next phase of the BRITE program, materials innovations will be closely linked with the technological end-use, particularly in the manufacturing and processing industries.

4. A Sectorial Approach

The types of materials that should be developed in the coming years in Europe are those linked to the industries in which Europe has an economic and trading ascendancy. The materials must be closely interlinked with the manufacturing industries. Hence, it might be instructive to take a glimpse at the world competitive market position of the European Community. Figure 4 shows graphically the European position. We see that the European Community has a high market share (30–40%) in a number of very high output industrial sectors, such as the chemistry sector, electrical engineering, motor manufacturing, mechanical engineering

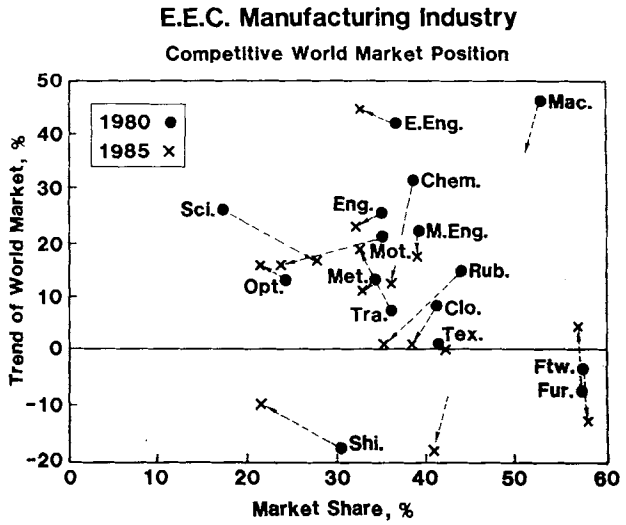


Fig. 4. EEC manufacturing industries competitive world market position.

as well as in clothing and textiles. The next point to note is the ominous drift towards a lower market share in high volume industries, in all cases except the chemical sector, mechanical engineering and textiles. The only sector which is showing a highly significant growth is that of scientific instruments, hardly a volume market. We note for example the large decline in the motor manufacturing industry, in shipping as well as in the rubber industries.

This can be compared with the Japanese position in the world market place (Fig. 5). Consistent with a total Japanese economy which is lower in volume than that of the European Community, many industrial sectors in Japan have a lower world market share. However, the targeted increases in the important sectors, notably electrical engineering, general engineering and metallurgical products are clear.

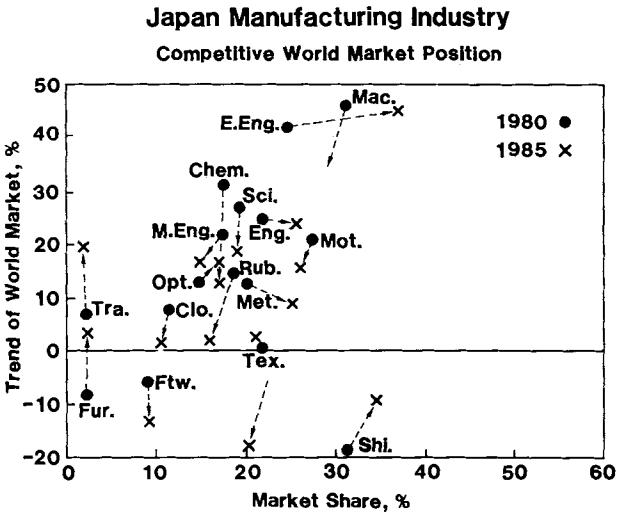


Fig. 5. Japanese manufacturing industries competitive world market position. (E.-, M.-Eng. = Electrical, Mechanical Engineering; Mot. = Motors; Rub. = Rubber; Opt. = Optics; Met. = Metals; Tra. = Tractors; Clo. = Clothing; Tex. = Textiles; Ftw. = Footware; Fur. = Furniture; Shi. = Shipping; Mac. = Machines; Chem. = Chemicals; Sci. = Science).

ADVANCED MATERIALS

The broad findings of this enquiry are that in the major sectors, although the EC and the USA hold the largest part of the world market, the EC's rate of growth is low and Japan is catching up very quickly. In all of the industrial sectors, it was noted that either the USA or Japan has the most important R & D expenditure.

Looking at it in this competitive way, which we must, the overall position is that Europe has to work harder and invest in more R & D in order to retain its market position in nearly all of the industrial sectors. This gives us a wide field of choice. The materials innovations in Europe in the coming years have to underpin a wide variety of industries, in particular those related to electrical and mechanical engineering.

5. Technico-Economic Aspects

In the western world, outside the defence sector, the future materials scene will be determined not only by the innovation and the competence of the materials scientists, but also by market forces – by the technico-economic aspects. This latter field is complex and usually neglected by the scientists. However, in a forward look such as this, it must be emphasized that the future does not depend only on the genius of the scientist and inventor.

As an example, consider the introduction of new ceramic materials into the engines of the future. We are all aware of the euphoria about advanced ceramics, and more recently, this earlier hyper-enthusiasm has been toned down to more realistic levels. Figure 6 shows an example from a worldwide

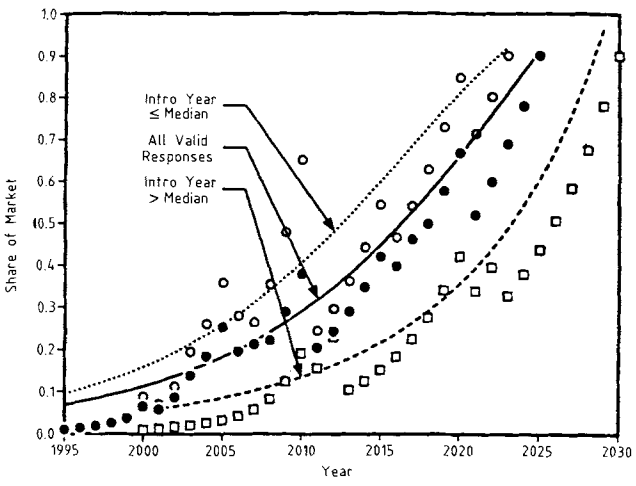


Fig. 6. Usage of ceramics in heat engines – forward look.

"Delphic" survey[3b] on the introduction of ceramics into heat engines. This was a wide, very subtle survey and the results can be treated with respect. They show the market penetration curves for ceramic engine components such as light-duty engine valves and heavy duty engine piston caps. These show reasonably good penetration prospects. The ceramics are considered to make improvements in performance through reduced fuel consumption, increased power density, reduced inertia for light duty engines and improved durability and heat insulation for heavy-duty engines.

The above scenario is highly speculative: it means that the model *could* apply, not that it is bound to apply. The realization of the above depends critically on market factors. Cost is the primary barrier; there will be a price premium for the first few years and this should inhibit manufacturers from introducing new ceramics. Are the technical advantages worth the extra cost? This is what the manufacturer has to decide – to take the risk that the public is sufficiently appreciative of the benefits.

This question throws up the whole complex subject of the strategic commitment to manufacturing among industrial firms. Enlightened industrialists are aware that in their companies, a "higher charge against the present is necessary to ensure a long term future", to quote the words of *Malpas*,[4] ex-director of B.P. research. These considerations will be essential in the introduction of advanced materials into the technologies of the next millenium. This is illustrated in the model for funds flow, (Fig. 7)[4] for a typical advanced mate-

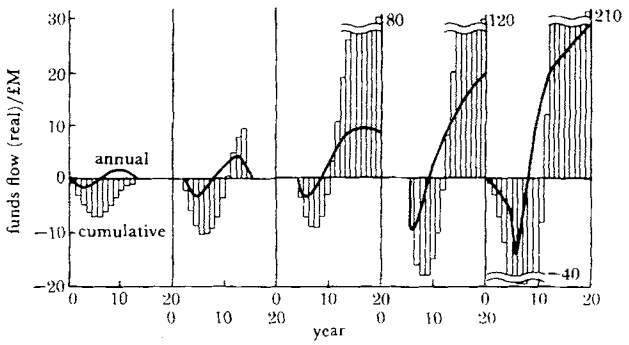


Fig. 7. Model for funds flow in a typical advanced materials business venture.

rials business venture. The first two projects represent relatively low investment; they have poor discounted cash-flow rates over the first ten years of the project life – however, they represent a sort of learning curve, leading to development markets – they are a cheap entry route into the "megabuck" business ventures, which although requiring heavy capital funding, indicate more attractive return rates. The projects 3 to 5 will be embarked upon only with the experience and "comfort factor" based on the earlier, loss making projects.

These are the vital considerations for a business with a positive strategy of long term investment, which applies in particular to high risk ventures on advanced materials.

6. The Conceptual Trends

For the materials innovations of today and the future, if there exists one grand design or overriding idea it is the

following: all materials innovations are in the direction of incorporating a greater knowledge content per unit weight of material. This important concept is shown in Figure 8, which

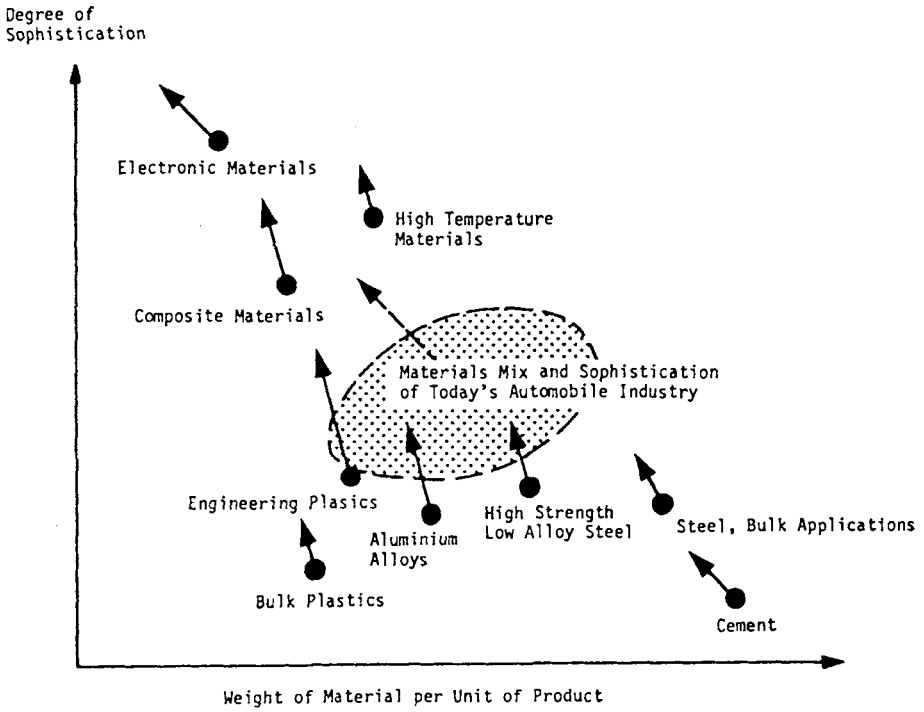


Fig. 8. Heuristic model correlating quantity of material in a given product and "information" attached to the material and its use.

is a heuristic model indicating the time dependent movement between the quantity of material in a product and information content of the material. This is derived from the work of *Altenpohl*.[5] On the diagram, each point indicates the trend for the future. In short this means that the materials innovations are increasingly incorporating a higher level of intellectual sophistication. This is consistent with the notion of the development of goods and manufactured products which have a high added value. The trend holds, whether it is for highly exotic materials for electronics applications or for bulk materials such as cement, where we see the vector moving towards improved macro-defect free cements.

Again, if we can discern a grand conception in the *means* for innovating materials for the future, it is in the ambition to design materials architectures with specific properties from basic building blocks. We are still a long way off from this, yet there are strong indicators and promising overtures in the production of two dimensional modulated structures at an atomic level which have highly specific and unique electronic properties. This grand design is the approach to the subject in terms of matter in extremely small assemblages, either two dimensional or three dimensional, these assemblages procuring properties that are completely different from those of the macroscopic forms. For example, a new type of strengthening has been suggested for an artificially produced material consisting of alternate layers of pure metals where the thickness of the layer is below a hundred nanometers. If the layers are so thin, it may not be possible for a Frank-Read source to operate in either layer, in which case the mode of plastic deformation will be by single dislocation movement.

For the development of materials for the next millenium, there are a number of conceptual trends, which can be considered as a collection of the accumulated thinking and experience among materials scientists. Here, specific themes which may exert a significant influence on materials development over the next two decades are highlighted.

7. Highlighted Themes of Future Significance

7.1. High Knowledge Content Structural Materials

In this category, the materials enable the engineering concept to be realized: the materials supply a supportive rôle. They find their value in that they permit the engineering structure to fulfil its functions and in this sense they are used to contain, to connect, to control or to display an engineering device. Here we are concerned with designing complex engineering structures to operate over a longer and more reliable lifespan, that is, we try to avoid over-design. We are concerned essentially with the benefit that is available through the incremental improvement of existing materials.

Material advances here are aimed to procure economic benefit through, for example, improved performance in the development of hexagonal boron nitride for hard coating applications or improved durability in an attempt to reduce the rates of corrosion, wear and fatigue. For example, in a recent survey[5b] it was found that in the USA some 4% of the gross national product is lost through the fracture of materials and structures.

7.2. Materials with Specific Functions

Here we are concerned with materials which in themselves constitute part of a potentially useful scientific phenomenon. They are now increasingly being referred to as 'functional' materials and their applications are typically in electronics, and optical and magnetic products. Thus, whereas in 1959 the number of transistors on a semiconductor chip was one, the increase over the last two decades has been of such enormous magnitude that in the near future we expect to have a hundred million tiny transistors on a single chip. In addition to this planar silicon technology, there are opportunities in newer, faster materials such as those provided by compounds of group III elements in the periodic table (gallium, aluminum, indium) with group V elements (antimony, arsenic, phosphorus) which offer new potential properties for opto-electronic and microwave applications. In the field of fiber optics, the traditional electric current in copper for transmitting messages is being replaced by laser light moving in a tiny glass fiber. The power of this new technology is such that each fiber can transmit the equivalent of a complete Encyclopedia Brittanica in one minute. The research opportunities here are obvious: improved fiber and better light carriers.

This is of course a very extensive and rapidly moving technological field with a large industrial infrastructure. The future will see new materials for such micro-electronics applications involving rapidly evolving techniques of fabrication, as in wafer production, epitaxial growth, sputter deposition, oxidation and diffusion of impurities, ion implantation and surface analysis techniques.

7.3. Improved Conventional Volume Materials

In spite of the slackening in the rate of consumption of traditional metals and steel in particular, these materials as well as common cement will be required in greater volumes in the future, both for advanced applications and in the more common aspects of Man's daily life such as in building materials. In particular, hydraulic cements are energy-cheap and today we see efforts being directed towards improving the strength of cement through a close study of porosity, rheology and the nature of the particle packing.

Newly innovated cements are already available, such as those known as macro-defect free cements which owe their improved strength to the removal of macroscopic voids, giving rise to cements with a bending strength of up to 70 MPa compared with the normal low strength of Portland cement of 5 MPa. In fact, a research team at ICI[6] has shown that by using combinations of high alumina cement and a copolymer of vinyl acetate and vinyl alcohol, strengths of up to 150 MPa may be achieved.

7.4. Property Design by Microstructure and Microchemistry Control

The marked influence that very small changes in chemistry or microstructure can have on bulk properties has long been recognized and exploited, as in the traditional addition of carbon to iron to make steels with highly tunable properties. In the last decade the importance of highly localized micro-environments, both chemical and structural, has been increasingly appreciated especially in the leverage effect they have on bulk mechanical properties. Examples abound; segregation to grain boundaries in metals, low melting grain boundary phases in structural ceramics, local defect populations especially in surfaces creating sites for fracture initiation, all factors controlling materials degradation and failure. Fortunately the phenomena are not exclusively deleterious and numerous opportunities to tailor the micro-environment for benefit are currently exploited; the addition of rare earth elements at trace levels to enhance the stability of corrosion protective scales on metals, the development of mechanically alloyed microstructures to enhance alloy strength, and the influence of boron in reducing brittleness in intermetallic alloys are examples.

The engineering of the micro-environment of materials has only recently begun, but is firmly founded on the basic principles that properties are in general determined by interfacial atomic interactions and that in a complex material, integrity is dependent on weakest link failure. Future exploitation of these ideas opens a promising field for materials advances, and already interesting innovative materials are emerging. Just one such example is given by the recent development of nano-crystalline structures. This novel idea of *Gleiter*[7] and his coworkers is to construct a material from nano-crystalline assemblages. This is tantamount to the production of a new state of matter, intermediate between a

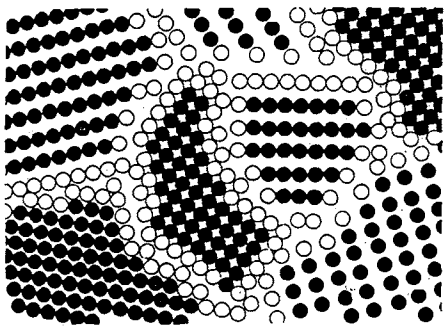


Fig. 9. Microstructural model of nanocrystalline materials.

polycrystal and a glass. The structure of the nano-crystalline metal made by evaporation on to a cold substrate followed by compaction of the fine powder is shown in figure 9. The crystal grains are so small that almost half the atoms in the metal occupy intergranular sites. As a result of the presence of a large proportion of matter in grain boundary sites, diffusion creep can operate even at low temperatures where the mass transport occurs along the grain boundary regions.

7.5. Synthesis of Non-Equilibrium Structures

The introduction of means that prevent lower free energy or ground state structures and compositions from being formed in alloys provides new opportunities for materials synthesis and property processing. More generally, the study of non-equilibrium phenomena is throwing up ideas of fundamental importance for the formation of metallurgical microstructures. The mixing of chemical species to produce alloys and ceramics has up to now been constrained by equilibrium thermodynamics – the rigid, inescapable laws of classical theory. In effect, metallurgists and solid state scientists have had to put up with a sort of tyranny of the constitutional phase diagram. By varying the processing conditions, in particular by imposing cooling rates exceeding $10^6\,^{\circ}C\,s^{-1}$, important constitutional changes can be introduced so that the retained metallurgical phases have compositions outside their equilibrium limits.[8] The resulting non-equilibrium phases may be crystalline or glassy. Such glassy materials often have unusual combinations of chemical and physical properties including strength, hardness, electric response, catalytic ability and corrosion resistance.

Already such materials have been aimed at applications, especially where combinations of extreme hardness and high corrosion resistance are required, as in cutting devices. Since these materials combine magnetic softness with mechanical hardness, they are useful for tape-recording heads. In particular ferromagnetic glasses are very easily magnetized, because magnetic domain walls move through them with ease and they therefore make excellent electric power transformers, with markedly reduced core losses. Figure 10 compares the energy losses in transformers of various sizes made by various companies. The decreases achieved by using metallic glass are quite dramatic. This is an area with enormous economic potential – it has been calculated that the introduction of metallic glass cores in the 40 million power distribution transformers in the USA could make a potential saving of a thousand million dollars per year.

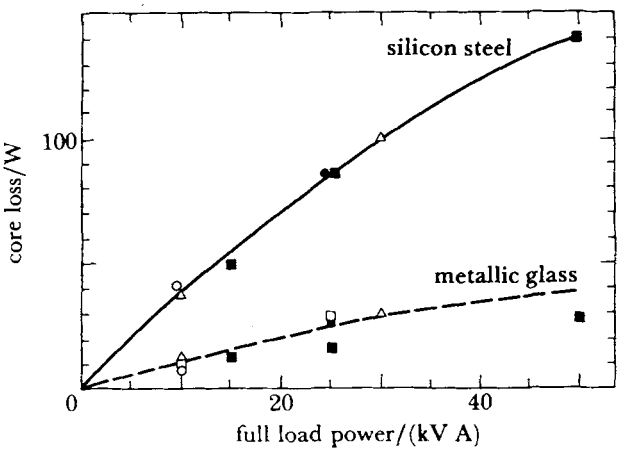


Fig. 10. Energy loss comparison in commercial transformers; with silicon steel and metallic glass cores. ○ McGraw-Edison △ Osaka □ Westinghouse ■ Allied Signal ● General Electric.

7.6. "Two-Dimensional" Phenomena

Surfaces and interfaces have long been regarded as critical regions with a fundamental importance for many solid state phenomena of technological application. Catalysis, corrosion and adhesion are some examples of surface controlled phenomena. In the past decade we have seen many advances in methods for modifying surfaces in order to control such properties. Future trends in the surface sciences of relevance to materials technologies will be the exploration of physical and chemical phenomena on and just below and just above the surface, that is, in zones with an extremely small third dimension.

Thus the introduction of ion implantation techniques, with cascade ion mixing and continuous or pulsed laser heating introduces possibilities for obtaining new types of surface phases. Alloy compositions can be produced with extended solid solubilities and with these one may manipulate basic engineering properties. A wide range of properties can be modified by these treatments. An important example of this is an improvement in wear resistance in a titanium/aluminum/vanadium alloy used for artificial hipjoints. The incorporation of nitrogen can increase the lifetime of this joint by a factor of 400.

A completely different class of "2-D" phenomena is emerging for atomically layered structures which are grown on specially prepared surfaces. By using well controlled vapor deposition and other techniques for thin film deposition, a totally new area of *artificially structured materials* is being opened up which holds great promise for the discovery of new basic phenomena. Thus for modulated metallic alloys, unusual elastic, magnetic and superconductor properties have been observed. The field of greatest interest is in optoelectronic devices made from layered structures, the chemical composition being modulated from layer to layer.

7.7. Computerized Materials Information Systems

An important future trend in the materials science is the development of computerized information systems of increasing complexity. In typical first and second generation database services they are generally specialized on a single subject, making them important for use by experts in that subject field. Already the total number of publicly available

databases of European origin is somewhat over 800. These are mostly bibliographic databases and in the non-scientific fields.

In the case of materials information systems for engineering the complex nature and high costs have hitherto hindered the construction and exploitation of factual databases of the second and third generation type aimed at the professional engineer. The future will see the development of factual data banks as an everyday tool for the materials engineer who will have access to a comprehensive, reliable and up to date data base on engineering materials.

Related to this is the trend in future materials processing now referred to as "intelligent processing" in which sensors embedded in the material while it is being formed, or non-intrusive sensors such as ultrasonic beams, will feed back information at the microstructural level during dynamic forming. Based on the physical model for the process, the computer in turn should make the adjustments or changes necessary to ensure a defect free final shape.

7.8. Micro Non-Destructive Evaluation

The value of the non-destructive evaluation of defect structures in metals, for component acceptance, for integrity evaluation of structures, welds, components in operation etc., is long established and considerable attention is being devoted to extend these techniques to the monitoring of large scale plant. The major challenge for the future will be to adapt this technology to new materials such as engineering ceramics which have intrinsically much higher defect sensitivity and have inherently high flaw population densities, arising from processing constraints. Here, critical flaw sizes are of the order of tens of micrometers. While workers in the ceramics processing technologies struggle to achieve higher reliability using finer powders, better particle size distributions and ultra-clean conditions, inevitably a proportion of a production product will contain defects of significant size, discontinuities, porosity or surface cracking, which may be detected only if the appropriate technique can be developed.

A number of possibilities are under investigation, developed from the acoustic and thermal non-destructive testing (NDT) principles of metal testing methodologies. For example, acoustic microscopy shows promise in surface crack detection and the resolution obtained using the scanning acoustic microscopy (SAM) and scanning electron acoustic microscopy (SEAM) is of the necessary order. At the current stage of development, the correct interpretation of even simple images requires a high degree of expertise and offers a major challenge to the developers of computer image identification.

8. Conclusions

The main points of this study are as follows:

- materials will increasingly grow in importance as a basic enabling technology – determining the development and innovation of other important future technologies in a variety of industrial sectors – transport, communication, etc.
- at a global level, there should be no fear of a collapse in supply of conventional materials, especially metals due to over-consumption.
- there are efforts and planning at a European level to stimulate materials R & D, to fill technology gaps and to strengthen the declining industrial sectors; here R & D cooperative networks are recognized as important.
- for making new materials into market products, innovation is necessary but not sufficient: technico-economic considerations (e.g. investment decisions) are paramount.
- a number of conceptual trends in future materials R & D can be discerned, based on the development of materials with higher "intellectual density."

Received May 16, 1989
Revised version June 7, 1989

[1] S. V. Radcliffe, *Science (Washington DC) 191* (1976) 700.
[2] W. Malenbaum: *World Demand for Raw Materials in 1985 and 2000*, National Science Foundation, Washington DC 1977.
[3] a) *Technology Development Forecast up to 2010 in Japan*, Science and Technology in Japan. (April/June 1983) p. 24. b) J. J. Duga et al.: *The Economic Effects of Fracture in the United States*, N.B.S. special publication 647-2, March 1983.
[4] R. Malpas, *Phil. Trans. R. Soc. London A 322* (1987) 347–360.
[5] a) D. G. Altenpohl, *Materials and Society 3* (1979) 315. b) R. Larson: *The Outlook for Ceramics in Heat Engines, 1990–2010*, U.S. Dept. of Energy publication, 1987.
[6] S. R. Tan, A. J. Howard, J. D. Birchall, *Phil. Trans. R. Soc. London A 322* (1987) 479–491.
[7] R. Birringer, V. Herr, H. Gleiter, *Trans. Jpn. Inst. Met.* (Nov. 1985) 25–29.
[8] H. Warlimont, *Adv. Mater. 1989*, 225; *Angew. Chem. Int. Ed. Engl. Adv. Mater. 28* (1989) 947; *Angew. Chem. Adv. Mater. 101* (1989) 971.

The following reviews will appear in future issues:

R. Zentel: Liquid Crystal Elastomers

G. W. Kriechbaum, P. Kleinschmit: Superfine Oxide Powders by Flame Hydrolysis and Hydrothermal Synthesis

R. Eidenschink: Liquid Crystals; New Compounds, New Applications

R. D. Miller: Substituted Silane Polymers

K. Bange, T. Gambke: Electrochromic Materials for Optical Switches

H. Eckert: Structural Characterization of Non Oxide Chalcogenide Glasses by Modern Solid State NMR Techniques

ADVANCED MATERIALS

Tailoring Semiconductor Crystals to Atomic Dimensions**

Molecular Beam Epitaxy
GaAs Thin Films
Film Growth Dynamics
Quantum Wells/Wires
Superlattices

By Bruce A. Joyce*

This article provides an introduction to the growth by molecular beam epitaxy (MBE) of semiconductor structures which have dimensions of the same order as interatomic distances in solids. The basic process technology is first described, followed by a brief account of surface reaction mechanisms involved in the growth of GaAs from an atomic beam of Ga and molecular beams of As_4 and As_2.

From the study of growth dynamics using electron diffraction techniques it is shown how reduced dimensionality structures can be grown and some indication is given of the effects of quantum confinement on material properties. Finally, some recent modifications of MBE based on flux interruption are described.

1. Introduction

It has become possible to fabricate semiconductor structures having dimensions of the same order as interatomic distances in solids. They are usually referred to as low dimensional systems. The movement of electrons in these structures is constrained because their dimensions are less than the electron wavelength and as a result they exhibit properties very different from those of the bulk material. The electronic confinement can be in one, two or three dimensions to produce layers, wires and dots respectively and the effects are already being exploited in novel electronic and opto-electronic devices, of which the quantum well laser is perhaps the best known example.

In this short article I will describe the technique of molecular beam epitaxy (MBE) which is one of the two major fabrication methods used to prepare low dimensional systems, indicate how the necessary levels of control and understanding have been achieved, and illustrate some of the reduced dimensionality structures which can be grown directly.

[*] Prof. B. A. Joyce
University of London
Interdisciplinary Research Centre for Semiconductor Materials
The Blackett Laboratory, Imperial College
Prince Consort Road, London SW7 2BZ (UK)

[**] The author is grateful to his ex-colleagues at Philips Research Laboratories for their invaluable contributions over the years. Particular thanks on this occasion are due to *Jon Gowers* for permission to use his micrograph of the superlattice which was grown by *David Hilton*. I also wish to thank *Steve Pringle* of VG Semicon for providing the material for Figure 1.

2. Molecular Beam Epitaxy (MBE) – The Process

The fundamental principles of MBE were established over twenty years ago, first for silicon and subsequently for III–V compounds such as gallium arsenide (GaAs). The subject has been extensively reviewed.[1-5] In this technique atomic or molecular beams are formed from Knudsen effusion cells and allowed to impinge on to a heated substrate under ultra high vacuum (UHV) conditions of $< 10^{-10}$ torr. If the conditions are correct a single crystal epitaxial film grows on the substrate, which is typically a single crystal semiconductor wafer approximately 5 cm in diameter. The cells are maintained at room temperature for gaseous sources or heated to produce an adequate vapor pressure for solid phase source material. Typical source pressures are in the range of 10^{-2} to 10^{-3} torr, which allows operation in the molecular flow, or collision-free regime, so that the first collision of a beam molecule is with the substrate. Under these conditions the molecular flux at the substrate is given by:

$$J_i = [a p_i / \pi d^2 (2\pi m_i k T)^{1/2}] \cos\theta \quad (1)$$

where J_i is the flux per unit area at a distance d from the source, which has an orifice of area a and contains molecules (atoms) of mass m_i having an equilibrium vapor pressure p_i at a temperature TK. θ is the angle between the beam and the substrate surface normal. The flux is regulated by a fast-acting shutter operating in front of each aperture.

A microcomputer is used to controll cell and substrate temperatures and all of the shutter operations, enabling any predetermined growth sequence to be achieved. Since the beams are neutral and collimated (by the aperture geometry) they are necessarily divergent and usually non-axial with respect to the substrate. To obtain uniform growth rate and composition (in the case of alloy films) over a large substrate area, the substrate stage is rotated at speeds between 0.03 and 2.0 Hz. For the growth of high quality films a substrate surface free of crystallographic and other defects and clean on an atomic scale (< 0.01 monolayers (ML) of impurities) must be prepared. This usually involves free etching by an oxidative process which removes any carbon and leaves the surface covered with a protective volatile oxide which is subsequently removed by thermal desorption in the vacuum chamber.

Experimental systems which can provide the required levels of control have become rather complex, but Figure 1 illustrates schematically the important features. The basis is

ADVANCED MATERIALS

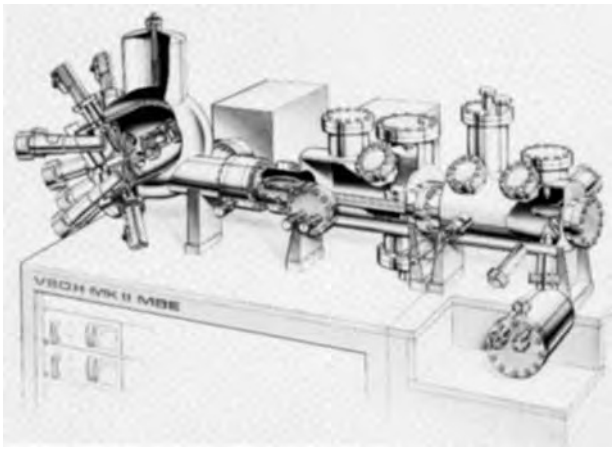


Fig. 1. Schematic illustration of an MBE system for the deposition of III–V compounds.

a two or three chamber stainless steel UHV system, usually ion- or cryo-pumped and incorporating large areas of liquid nitrogen cooled panels. An interlock system to enable the substrate to be introduced into the growth chamber without breaking the vacuum is essential if films having high quality electrical and optical properties are to be prepared.

In situ analytical facilities usually include a quadrupole mass spectrometer for residual gas analysis and a reflection high energy electron diffraction (RHEED) arrangement for assessment of surface structure and growth dynamics (see section 4). This consists of a 10–50 keV electron gun and a fluorescent screen, using a forward scattering geometry with the electron beam at a very shallow angle (1–3°) to the substrate surface. In addition, an Auger electron spectrometer may be incorporated to determine surface composition and purity. Some or all of these analytical facilities may be housed in a separate analysis/preparation chamber mounted between the sample insertion interlock and the growth chamber.

In the remainder of this article I will concentrate on films of III–V compounds, principally GaAs prepared from solid (elemental) sources, since most of our understanding of growth mechanisms and most areas of application relate to these materials, but the same basic principles apply to silicon, germanium and II–VI compounds.

3. MBE of III–V Compounds – The Basic Chemistry

The source materials used are usually elemental, and all of the group III elements produce monoatomic beams. Group V sources are rather more complex, since direct evaporation produces tetraatomic molecules (P_4, As_4, Sb_4), but dimeric molecules can be obtained by passing the tetramer flux through a high temperature stage at the front of the Knudsen cell. Dopants used are beryllium for p-type and silicon for n-type, both of which evaporate as monomers.

Growth is initiated by bringing the substrate to the appropriate temperature (typically in the range 500–700 °C) in a beam of the Group V element to prevent thermal dissociation and then opening the shutter of the group III element source. A typical growth rate is 1 μmh^{-1}, which corresponds approximately to 1 ML s^{-1}, or a flux of 5×10^{14} atoms $cm^{-2}\,s^{-1}$. The group V element flux may be between three and ten times greater, but the growth rate is entirely determined by the group III element flux.

The experimental arrangement of MBE is unique amongst epitaxial thin film preparation methods in that it allows direct in situ reaction kinetic measurements to be made using the technique of modulated beam relaxation spectroscopy (MBRS). The basic experiment is very simple; a neutral, thermal atomic or molecular beam is directed at a substrate surface and the desorbing flux detected mass spectrometrically. The problem of distinguishing between background signals and those produced by desorbing species is solved by (mechanically) modulating either the incident beam or the desorbing flux and examining the mass spectrometer signal for a correlated response. By correct choice of data acquisition and signal processing methods[6] it is possible to evaluate a wide range of kinetic parameters, including (i) thermal accommodation coefficients of molecules interacting with the surface, i.e. the nature of kinetic energy exchange processes between the surface and the incident species (ii) surface lifetimes and the energies of binding states (iii) sticking coefficients, or residence times which are long compared to the modulation frequency and (iv) orders of chemical reactions.

A good example of the power of the technique comes from its application to the interaction of Ga and As_4 beams on a GaAs(001) surface to form GaAs.[7] The presently accepted model for this is shown in Figure 2. The As_4 molecules are

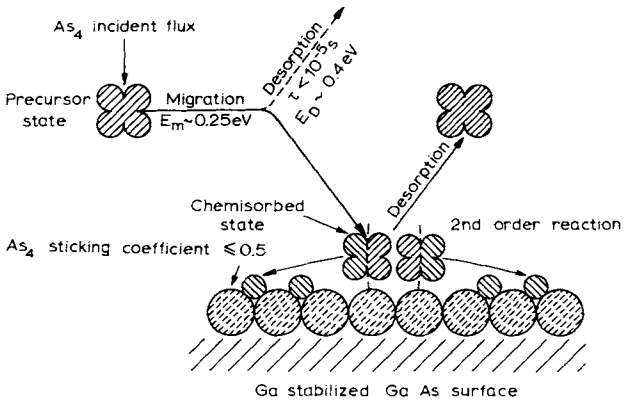


Fig. 2. Model of the growth chemistry of GaAs from molecular beams of Ga and As_4.

first adsorbed into a weakly bound mobile precursor state, in which the activation energy of migration is approximately 0.25 eV. An activation energy of desorption of ≈ 0.4 eV can be determined from the temperature dependence of the sur-

face residence time of an As_4 molecule. A crucial finding is that the sticking coefficient of As_4 never exceeds 0.5, even when the Ga flux is much higher than the As_4 flux, or when the surface is completely covered with a monolayer of Ga atoms (as in Fig. 2). Furthermore, the desorption rate is second order with respect to the incident flux. These results are explained by postulating a pairwise dissociation of As_4 molecules chemisorbed on adjacent Ga atoms, so from two As_4 molecules four As atoms go to form GaAs, while the remaining four desorb as an As_4 molecule. By contrast, in growth from As_2 the basic process for As incorporation is simple first order dissociative chemisorption on surface Ga atoms.[8]

These models are well over ten years old, but they have received some very recent experimental support from *Tsao* et al.[9] These workers also found a maximum As_4 sticking coefficient of 0.5, at which point the surface reconstruction changed from As-stable to Ga-stable. In addition, they were able to show that the chemical reaction was not the rate determining step in the growth of a GaAs film, which is an important factor in the discussion of growth dynamics (see section 4).

4. The Dynamics of Film Growth

Before embarking on a discussion of growth dynamics it is important to establish the basic concepts of the surface structure of GaAs, which can be monitored by the in situ RHEED facility. In general, semiconductor surfaces either relax by bond rotation on reconstruct, i.e. display a lower symmetry than that produced by a simple termination of the bulk lattice. In III–V compounds the form of the reconstruction is related to surface composition and stoichiometry, which can be illustrated by the GaAs(001) surface. It is a polar orientation and is ideally terminated by a complete layer of Ga or As atoms, but in practice it forms a series of surface structures, ranging from the Ga-rich 4×2, though an intermediate 3×1 to an As-stable 2×4, where $(n \times m)$ relates the surface unit cell to that of the bulk (1×1) and indicates the increase in the periodicity in two orthogonal $\langle 110 \rangle$ directions at the surface. In addition to displaying the surface symmetry the RHEED pattern can also be used to evaluate surface morphological properties such as the presence of steps, facets, antisite disorder etc.[10]

A further and extremely important application of RHEED is the direct in situ study of film growth dynamics. This has been made possible by the discovery and development of the RHEED intensity oscillation technique.[11, 12] The primary observation is that damped oscillations occur in the intensity of all features of the RHEED pattern immediately following the start of growth. Typical results for the growth of GaAs and AlAs(001) oriented films on GaAs(001) substrates are shown in Figure 3, taken using the specular spot on the 00 rod. The steady state period corresponds precisely to the growth of a single molecular layer, i.e.

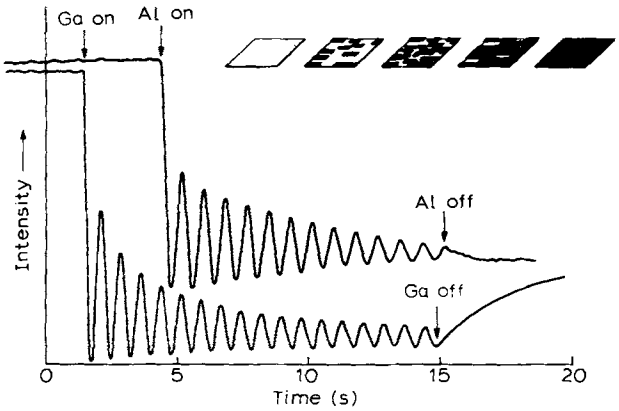


Fig. 3. Intensity oscillation of the specular beam in the RHEED pattern from AlAs and GaAs(001) 2×4 surfaces during growth. Inset shows the growth of a molecular layer in a two-dimensional mode.

a complete layer of Ga(Al) + As atoms, equivalent to $a_0/2$ in the [001] direction.

The feature common to all explanations of this oscillatory intensity response is that it occurs as a direct result of the changing surface topography associated with a layer-by-layer (two-dimensional) growth mode. On the basis of 2-D growth and a single scattering diffraction process it is a straightforward matter to construct a growth model which accounts for the RHEED results. We will deal with the specular spot for simplicity, but similar arguments can be applied to all features. If we relate intensity changes with surface roughness effects on an atomic scale, we can assume that the equilibrium surface is smooth, corresponding to a high specular intensity. When growth commences, 2-D centres are formed randomly on the surface, leading to a decrease in specular intensity (i.e. an increase in diffuse scattering). This is the expected result for a single scattering process, since the wavelength of the electrons is typically 0.1 Å whilst the GaAs monolayer step height is 2.83 Å i.e. the wavelength is more than ten times smaller than the size of the scattering centers, thus producing diffuse scattering. This will be a maximum at half-layer coverage ($\theta = 0.5$) and a minimum at the start of each layer ($\theta = 1$). The development of a monolayer is illustrated in the inset to Figure 3. In fact this model is greatly oversimplified, because electron diffraction is a multiple scattering process, but the basic tenet is correct; the oscillatory response is a manifestation of a layer-by-layer 2-D growth mode which implies significant adatom migration on the surface. In reality an intensity maximum seldom corresponds to monolayer completion because its position in the monolayer depends strongly on diffraction conditions (azimuthal and polar angles). Fortunately conditions can be chosen which ensure correspondence between intensity maxima and monolayer completion. The complexities introduced by diffraction effects have been treated extensively elsewhere[12] and need not concern us further here. The decay of the oscillations is particularly important, however, since it represents a change of growth mode from 2-D nucle-

ation to step propagation. As a result of the growth front becoming distributed over more than one layer, brought about by a second layer starting before the previous one is complete, a steady state terrace width, or step distribution is eventually established. This occurs when the mean step separation equals the surface migration distance of the group III adatoms. Under these conditions there are no intensity oscillations since statistically the surface morphology does not change during growth.

These growth mode changes which occur as a consequence of the surface migration of adatoms can be exploited in a rather simple way to establish quantitative data for the migration processes.[13] The method involves the use of a vicinal surface, which means preparing a substrate so that its surface plane is a few degrees away from a singular surface, i.e. a surface with an exact low index orientation, (001) say. To minimize its free energy, a surface of this type will break up into a formation of exact (001) terraces separated by monomolecular steps (of height $a_0/2$ in the case of III–V compounds). The mean step-free terrace width l, is given by $l = a_0/2 \tan\alpha$, where α is the angle of misorientation. As an example for $d \approx 2°$, $l \approx 80$ Å. If the migration length of the group III element is λ, for $\lambda > l$ the step edge will act as the major sink for migrating adatoms and there will be no two dimensional (2-D) growth on the terrace. Since RHEED intensity oscillations occur only as the result of 2-D growth, they will be absent for this growth mode. If, however, growth conditions are varied to the point where $\lambda < l$, 2-D growth will be re-established on the terraces and oscillations will be observed. It is consequently comparatively straight forward to study λ as a function of growth conditions. It must be emphasized, however, that in the present context surface migration refers to the transport of group III adatoms in a weakly bound precursor state before their final incorporation in a lattice site; it is migration related to growth, not surface dissociation.

Ideally, the measurements should be performed by systematically varying the extent of misorientation and hence terrace width, but in practice it is simpler to use a single substrate with a fixed misorientation and vary the migration length by changing growth parameters. A typical data set obtained by varying the substrate temperature at fixed As_2 and Ga fluxes is shown in Figure 4. The inset illustrations demonstrate the changing growth modes as the temperature changes. Clearly, as the temperature rises the migration length increases to the point where it equals the terrace width, and the RHEED intensity oscillations disappear. If surface migration is assumed to be isotropic, it is possible to determine values of the migration coefficient D_0 and the activation energy E_d using the relationships:

$$\lambda^2 = 2\,D\tau \tag{2}$$

and

$$D = D_0 \exp(-E_d/kT) \tag{3}$$

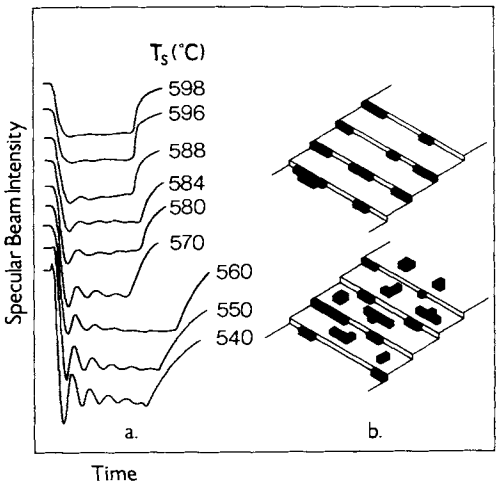


Fig. 4. Data set showing the transition from oscillation to constant response in the RHEED specular beam intensity as a function of substrate temperature, with constant gallium flux, for the growth of GaAs. Inset illustrates layer-by-layer and step propagation modes on the terraces formed from the vicinal surface.

Here λ is the mean displacement (terrace width), D the migration coefficient at a temperature T and τ the surface lifetime in the precursor state. There are some detailed analytical difficulties, but the basic principles appear to be valid.

5. Quantum Wells, Superlattices and Quantum Wires

We have seen that the fundamental growth mode on a singular surface is layer-by-layer and this enables quantum wells and superlattices to be grown. In a quantum well, a layer of one material, say GaAS, is sandwiched between two layers of material of greater band gap, say (Al,Ga)As, a III–V alloy in which some fraction of Ga is substituted by Al. More complex alternating structures are known as multiple quantum wells (MQWs). When the layers are sufficiently thin (typically < 20 Å) to allow electron coupling between them, the structure is referred to as a superlattice. Detailed consideration of the transport and optical properties of such structures are outside the scope of this article, but an excellent review has been written by *Kelly* and *Nicholas*.[14] It will perhaps be useful however to discuss briefly one example here. In semiconductors the recombination of electrons and holes causes the emission of radiation. In a quantum well structure the energy of this radiation increases (the wavelength decreases) as the well thickness is reduced. This is a quantum shift brought about by the confinement of the electrons in the well to two dimensions. The actual wavelength of emitted light is a function of the well width and this has been used to fabricate MQW lasers with emission characteristics quite different from those based on the equivalent bulk materials.

Some idea of the perfection with which two dimensional structures can be grown may be obtained from electron microscopy and this is illustrated in Figure 5. This is a cross

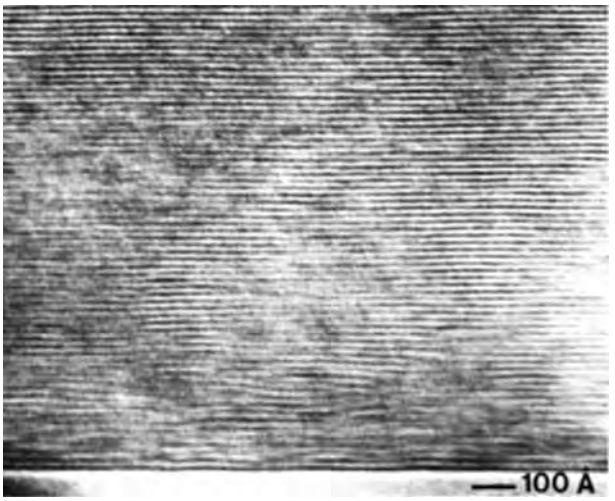


Fig. 5. Transmission electron micrograph of a GaAs (3 ML)/AlAs (3 ML) superlattice.

sectional transmission electron micrograph (TEM) of a GaAs-AlAs superlattice composed of alternate layers each 3 ML (8.5 Å) thick. It is evident that averaged over the thickness of the cross section, interfaces on a scale of < 1 ML can be produced. Similar conclusions can be drawn using X-ray diffraction and photoluminescence techniques.

Quantum well wires are low dimensional structures with quantum confinement in two dimensions. Most attempts to fabricate them have relied on high resolution lithography, but the lateral dimensions achieved have been rather too large to produce significant separation of sub-band energies. A new approach has been made possible by control of the growth mode on vicinal planes, following the principles discussed in section 4. By restricting growth to the step propagation mode and growing alternate fractional monolayers of, say, GaAs and AlAs on a GaAs(001) substrate tilted typically 2° towards (110), vertical columns of GaAs and AlAs can be grown on the terraces, which are ≈ 80 Å in width.

There is already evidence[15, 16] of some success in the growth of these structures, although it is clear that as yet they are far from ideal. Simulation studies indicate that poor quality at low substrate temperatures results from a significant amount of two-dimensional cluster formation due to restricted surface diffusion, whilst high temperature degradation is brought about by enhanced thermal fluctuations in the step edge structure.

6. Growth Process Modifications

Finally, we may consider some recently developed modifications to the growth process, which were introduced with the idea of growing more "perfect" interfaces in heterojunctions, quantum wells and superlattices, i.e. maximizing areas of single composition in the interface plane, or minimizing the number of layers normal to the plane in which compositional variations occur. They all rely on interruption of one or other or both (anion and cation) fluxes.

If growth is stopped by shutting off the group III element flux whilst maintaining constant the substrate temperatures and group V element flux, the intensity of the specular spot in the RHEED pattern recovers almost to its pre-growth value, provided correct diffraction conditions are chosen. The "recovery" or relaxation, occurs in two stages (fast and slow) and obeys an expression of the form:

$$I = A_0 + A_1 \exp(-t/\tau_1) + A_2 \exp(-t/\tau_2) \quad (4)$$

where τ_1 and τ_2 are the temperature dependent time constants of the fast and slow stage respectively. It seems probable that during the fast stage singly coordinated atoms on the peripheries of two dimensional growth centers break away to reform into more highly coordinated sites. The slow step then results from adatom clusters evolving to form the maximum number of nearest neighbor bonds.

This is the basis of the simplest modification, known as interrupted growth,[17] where the shutter controlling the cation flux is closed for periods of up to 60 s. This results in a lower step density and is more successful for lower binding energy, faster diffusing species, and it is also important for the interruption to occur close to monolayer completion. The other two modifications, known as atomic layer epitaxy (ALE)[18] and migration enhanced epitaxy (MEE)[19] both involve periodic interruptions of each flux during growth. It is claimed that as well as improving interface morphology, both techniques produce high quality material at lower substrate temperatures than is possible by conventional growth, but it is a claim which remains to be fully substantiated. It appears that both ALE and MEE depend on rapid relaxation during a short interruption period which occurs very close to monolayer completion.

It is reasonable to conclude that semiconductor structures of atomic dimensions, at least in one direction, can be reliably fabricated using MBE or one of its related alternatives. Some success has been achieved in control over two dimensions on the same scale, but much work remains to be done before successful exploitation can be claimed. Control over all three dimensions is still very much in the "ideas" stage.

Received: May 23, 1989

[1] A. Y. Cho, J. R. Arthur, *Prog. Solid State Chem. 10* (1975) 157.
[2] B. A. Joyce, *Rep. Prog. Phys. 48* (1985) 1637.
[3] K. Ploog, in H. C. Freyhardt (Ed.): *Crystals – Growth, Properties and Applications, Vol. 3*, Springer, Berlin 1980, p. 73; K. Ploog, *Angew. Chem. Int. Ed. Engl. 27* (1988) 593; *Angew. Chem. 100* (1988) 611.
[4] E. H. C. Parker (Ed.): *The Technology and Physics of Molecular Beam Epitaxy*, Plenum Press, New York 1985.
[5] M. A. Herman, H. Sitter in M. B. Panish (Ed.): *Molecular Beam Epitaxy*, Springer-Verlag Series in Materials Science, Vol. 7, 1989.

[6] C. T. Foxon, M. R. Boudry, B. A. Joyce, *Surf. Sci. 44* (1974) 69.
[7] C. T. Foxon, B. A. Joyce, *Surf. Sci. 50* (1975) 434.
[8] C. T. Foxon, B. A. Joyce, *Surf. Sci. 64* (1977) 293.
[9] J. Y. Tsao, T. M. Brennan, B. E. Hammons, *Appl. Phys. Lett. 53*, (1988) 288.
[10] B. A. Joyce, J. H. Neave, P. J. Dobson, P. K. Larsen, *Phys. Rev. B29* (1984) 814.
[11] J. H. Neave, B. A. Joyce, P. J. Dobson, N. Norton, *Appl. Phys. A31* (1983) 1.
[12] B. A. Joyce, J. H. Neave, J. Zhang, P. J. Dobson, in P. K. Larsen, P. J. Dobson (Eds.): *Reflection High-Energy Electron Diffraction and Reflection Electron Imaging of Surfaces*, Plenum Press, p. 397.
[13] J. H. Neave, P. J. Dobson, B. A. Joyce, J. Zhang, *Appl. Phys. Lett. 47* (1985) 100.
[14] M. J. Kelly, R. J. Nicholas, *Rep. Prog. Phys. 48* (1985) 1699.
[15] M. Tanaka, K. Sakaki, *Jpn. J. Appl. Phys. 27* (1988) L2025.
[16] M. Tsuchiya, J. M. Gaines, R. H. Yan, R. J. Simes, P. O. Holtz, L. A. Coldren, P. M. Petroff, *Phys. Rev. Lett. 62* (1989) 466.
[17] H. Sakaki, M. Tanaka, J. Yoshimo, *Jpn. J. Appl. Phys. 24* (1985) L417.
[18] F. Briones, L. Gongalez, M. Recio, M. Vaquez, *Jpn. J. Appl. Phys. 26* (1987) L1125.
[19] Y. Horikoshi, M. Kawashima, H. Yamaguchi, *Jpn. J. Appl. Phys. 27* (1988) 169.

Structure-Directed Synthesis of New Organic Materials**

Unnatural Products
Molecular LEGO
Solvent Sensors
Zeolitic Macropolycycles
Diels-Alder Reactions

By Franz H. Kohnke, John P. Mathias, and J. Fraser Stoddart*

1. Preamble

The time has now been reached when the chemist can make almost anything the living world has produced. Natural product synthesis has dominated the conceptual advances in synthetic organic chemistry for more than a century now. Yet, although the deep significance and fundamental importance of natural products and the life processes that sustain and characterize them are clear, they are arguably only an infinitesimally small part of the chemical scene. Compounds which are wholly unnatural comprise an infinite variety of structures which can only be conceived and constructed thanks to the knowledge, imagination, and expertise of the chemist. The reasons for making unnatural products come from many quarters – they include evaluating chemical theories, both old and new, synthesizing exotic compounds, which, more often than not have symmetry appeal, and preparing materials with some particular structural form that might perform some highly desirable physical, chemical, or biological function.

The manufacture and manipulation of structures at a molecular level raises[1] "the possibility of maneuvering things atom by atom." The prospect is one of performing physical feats on a truly microscopic scale. The question is how to construct advanced materials that express their properties at a molecular level and then to gain access to these properties, i.e. how do we make molecules and speak to them?

Recently, rigid molecular lines or strips, with nanometer scale dimensions and composed of polyacenequinone units, have been prepared[2] by repetitive Diels-Alder reactions. Their synthesis is attractive because they could provide a range of new materials capable of forming organized monolayers and molecular electronic devices of different sorts. Artificial cell bilayer membranes, and molecular barriers and sensors all rely[3] upon the formation of surface structures with the appropriate electronic characteristics. The prospect[4] that the parent polyacenes and their cyclic analogs – the cyclacenes – constitute materials with "the possibility of possessing interesting condensed phases including high temperature superconductivity and ferromagnetism" is particularly tantalizing.

Although synthetic strategies based on a repetitive Diels-Alder methodology, involving bisdienes and bisdienophiles,[5] have much to commend themselves in the synthesis of ladder polymers, there is a need to avoid ill-defined mixtures of compounds containing molecules of differing molecular weights and different stereochemistries that are not particularly amenable to purification by chromatography or by any other means.

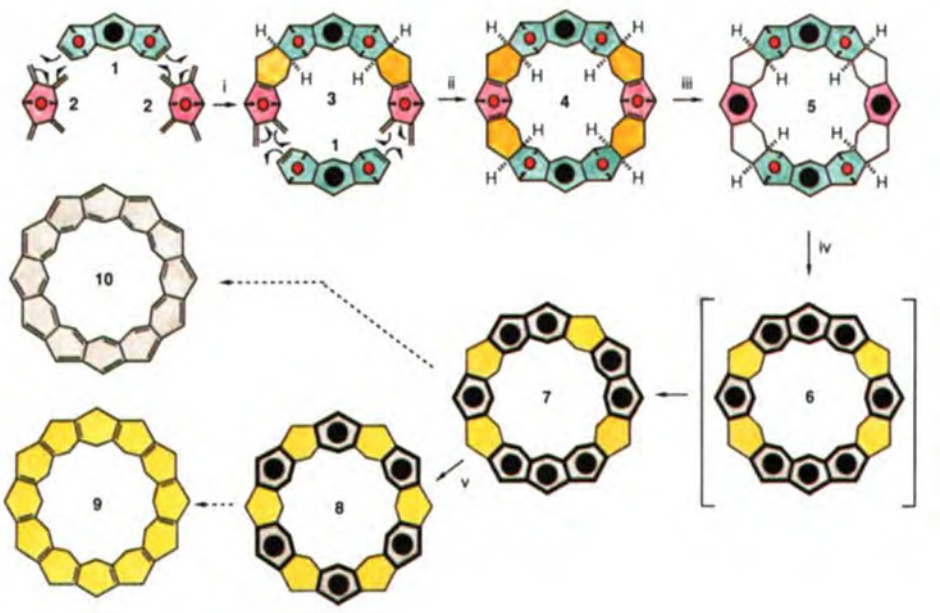
[*] Dr. J. F. Stoddart, Mr. J. P. Mathias
Department of Chemistry, The University
Sheffield S3 7HF (UK)
Dr. F. H. Kohnke
Dipartimento di Chimica Organica e Biologica
dell' Università di Messina
Salita Sperone, I-98166 Messina (Italy)

[**] We are most grateful to Dr. *N. S. Isaacs* (University of Reading) for performing all the high pressure reactions, Dr. *J. D. R. Thomas* (University of Wales College of Cardiff) for conducting the chemical sensing experiments, Mr. *P. R. Ashton* and Dr. *N. Spencer* (University of Sheffield) for recording FABMS and NMR spectra, respectively, and to Dr. *D. J. Williams* and Miss *A. M. Z. Slawin* (Imperial College London) for carrying out the X-ray crystal structure determinations. The research was supported by the University of Sheffield, the Science and Engineering Research Council, and the Ministry of Defence in the UK, and by the University of Messina in Italy. One of us (*J. F. S.*) acknowledges the award of a Research Fellowship from the Leverhulme Trust and thanks Dr. *Peter Mitchell* and Prof. *Jean-Marie Lehn* for useful discussions.

Recently, we have shown[6] that certain bisdienes and bisdienophiles, containing bicyclic ring systems, will undergo repetitive Diels-Alder reactions at their diastereotopic π-faces in a highly controllable manner,[7] not only with complete diastereoselectivity being expressed with respect to each component, but also with very high mutual diastereoselection occurring between the components, i.e. their relative reaction orientations are pre-determined. The implications of this discovery is that there are inherently simple ways of making apparently complex unnatural products from appropriate substrates. Since the pure compounds can be obtained without the need to use reagents or catalysts and result from information pre-programmed into the substrates and carried over into the products, we have referred[8, 9] to this as a form of *structure-directed synthesis*, i.e. the outcome of the reactions is dictated either by the structures of the substrates (i.e. the control is kinetic) or by the structures of the products (i.e. the control is thermodynamic). In this review, we shall outline how the principle of structure-directed synthesis can be applied to the precise and stepwise construction of new organic materials.

2. Molecular Belts

The synthesis (Scheme 1) of the macropolycycle dubbed[6] kohnkene **4** from "intelligent" substrates[10] – the bisdienophile **1** and the bisdiene **2** – is now well documented.[6, 7] The power of the synthetic approach is a double-barrelled one: a) It can be executed in discrete steps since one bisdienophile **1** will undergo cycloadditions with two bisdienes **2** under relatively mild conditions to give (78%) a discrete 2:1 adduct **3**, which can be characterized and then coaxed, under much more forcing conditions, to react remarkably efficiently (36%) in a belt-forming manner with a second bisdienophile **1**. b) Treble diastereoselectivity is expressed every time a Diels-Alder reaction occurs, such that only one product is formed after each cycloaddition step, e.g. none of the other nine configurational diastereoisomers of the 2:1 adduct **3** have been observed. It would appear that the stereoelectronic information pre-programmed into the bisdienophile **1** and the bisdiene **2** is transmitted in a domino-like fashion through all the intermediate Diels-Alder adducts to the final macropolycycle **4**. Although it has been strongly implied in the literature (see reference[7] for a discussion) that this kind of molecular recognition between bicyclic diastereofacial dienes and dienophiles is a transition state phenomenon (i.e. kinetic control is operative), the proposal remains to be vindicated or otherwise in the context of the synthesis of kohnkene **4**. Be this as it may, the practical outcome is clear: the synthetic chemist can create[7] molecular materials that are rigid, ordered, and large without having to resort to complicated multistep syntheses using expensive reagents or exotic catalysts. In this respect, unnatural product synthesis is reminiscent of prebiotic chemistry where – it has been argued[12] – certain key, relatively simple, chemical compounds served

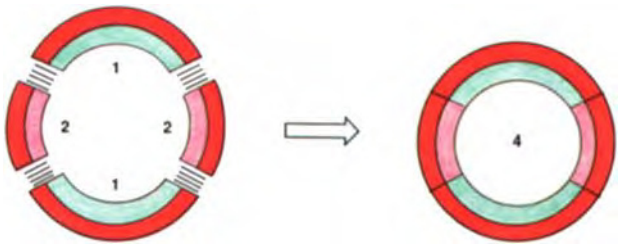


Scheme 1. The construction of kohnkene **4** from the bisdienophile **1** (blue) and the bisdiene **2** (pink) via the 2:1 adduct **3** by a stereoelectronically-programmed set of Diels-Alder reactions – leading to the formation of new cyclohexene rings (yellow) – followed by its conversion into dideoxykohnkene **5** and [12]collarene **8** via the symmetrical (?) and unsymmetrical octahydro[12]cyclacene derivatives **6** and **7**, respectively (O = solid red). In the macropolycyclic hydrocarbons, benzenoid rings are gray/black and 1,4-cyclohexadiene rings are yellow/green. Reagents and conditions: i, PhMe, reflux, 12 h; ii, CH_2Cl_2, 10 kbars, 55–60 °C, 200 h; iii, $TiCl_4$, $LiAlH_4$, THF, room temp., 18 h; iv, HCl, Ac_2O, reflux, 16 h; v, Li/NH_3, Et_2O, EtOH, – 78 °C, 45 min.

ADVANCED MATERIALS

as the building blocks for the elaboration of apparently complex biomolecules, or their biosynthetic precursors. With special structural elements of vitamin B_{12} in mind, *Eschenmoser*[11] has commented on the fact that "these outwardly complex structural elements are found to self-assemble with surprising ease under structurally appropriate preconditions". He goes on to add that "the amount of external instruction required for their formation turns out to be surprisingly small in view of the complexity of these structural elements." The prospect that the chemist might be able to create an unnatural world, using the same concepts and principles that the living world relied upon in the beginning, is an extremely exciting one indeed.

The making of kohnkene **4** has an aspect of molecular 'LEGO' about it. The rigid curved structures of the component bisdienophiles **1** and bisdienes **2**, coupled with the exclusive manner in which they interact and react with each other, dictates that a molecular-belt compound has to be the outcome. Scheme 2 is an attempt to capture visually how one



Scheme 2. A diagrammatic representation of the treble diastereoselectivity exhibited by each Diels-Alder reaction between two (blue on the concave surface) bisdienophiles **1** and two (pink on the concave surface) bisdiene **2** units in the construction of kohnkene **4**. The convex surfaces, which carry the oxygen atoms, are featured in red.

doubly "intelligent" substrate, i.e. **1**, can recognize another doubly "intelligent" substrate, i.e. **2**.

Unnatural product synthesis[13] will increasingly provide incentives for major conceptual developments in the art and science of chemical synthesis, as it relates to organometallic and inorganic materials, as well as to organic ones. A recent convincing illustration is provided by the structural features of self-assembly, cooperativity, and self-self recognition that characterize[14] the new polynuclear double-stranded helicates (trimers, tetramers, and pentamers) incorporating poly(bipyridine) strands and copper(I) cations.

One of the additional challenges in synthesizing an unnatural product is to uncover a property or demonstrate a function for the new material. X-Ray crystallography of kohnkene **4** not only reveals[6] that it is a belt-like molecule with the six oxygen atoms pointing outwards, but that the rigid cavity is of the appropriate dimensions to include a benzenoid substrate oriented orthogonally (Fig. 1) between the aromatic rings at 6 and 12 o'clock with an interplanar separation of 7.9 Å. Indeed, when a piezoelectric quartz crystal was coated with kohnkene **4**, detection of aromatic vapors

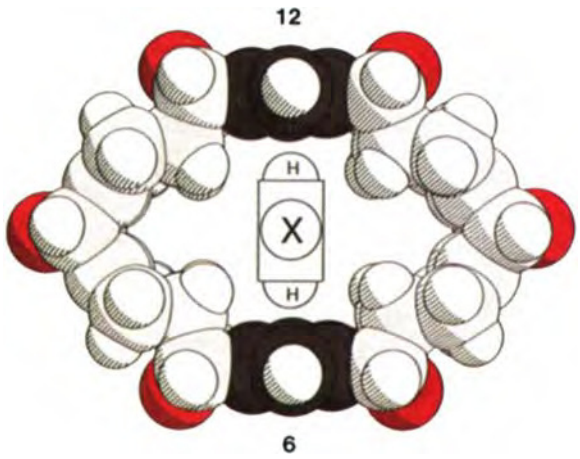


Fig. 1. Space-filling representation of the X-ray crystal structure of kohnkene **4** showing the proposed model for the rapidly-reversible inclusion of monosubstituted benzene derivatives (center) – the relative response of the piezoelectric quartz crystal is in the order, X = NO_2 > Br > Cl > H – involving stabilizing edge-to-face interactions with the aromatic rings at 6 and 12 o'clock in **4** (H = white, C = gray/black, O = red).

was achieved.[15] The response of the detection system is illustrated by a typical recorder trace for nitrobenzene (Fig. 2), the substrate for which kohnkene **4** is particularly

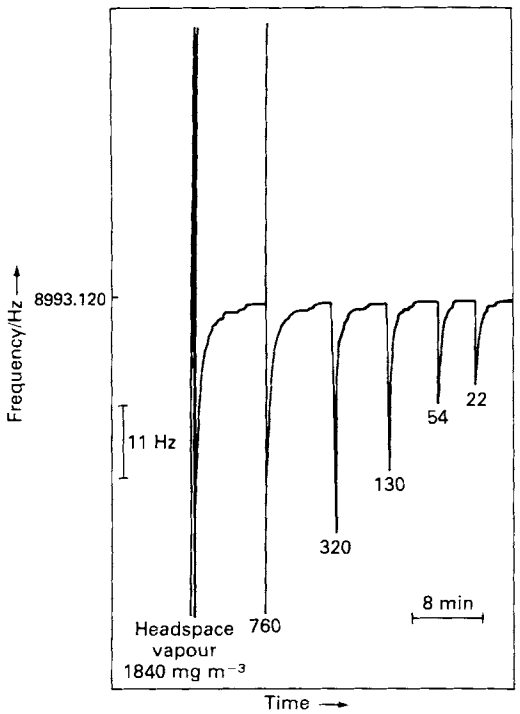


Fig. 2. A typical recorder trace of a calibration for nitrobenzene vapor using a piezoelectric quartz crystal (gold electrode) coated with kohnkene **4**. Reproduced from *Anal. Proc.* 26 (1989) 14, by permission of the publishers.

sensitive. Whatever the precise mechanism by which nitrobenzene vapor is adsorbed on to a surface of solid kohnkene **4**, the reversible association produces a change in the mass of the quartz crystal which can be monitored by changes in the

frequency of its oscillation. This extremely sensitive technique for monitoring gaseous products[16] represents one of the most immediate applications of new organic materials with zeolitic properties.

The model proposed in Figure 1 for the interaction of a monosubstituted benzene derivative with kohnkene **4** involves edge-to-face stabilizing interaction[17] between the substrate and the aromatic rings at 6 and 12 o'clock. In the case of nitrobenzene, the electron-withdrawing nitro group would only serve to enhance any stabilization through edge-to-face interactions involving slightly electron deficient – or δ^+ – hydrogen atoms on the substrate molecules and the π-electron systems of the two aromatic rings in kohnkene **4**. The dideoxy derivative **5**, obtained[18] on deoxygenation of kohnkene **4** ranks as an equally sensitive but much more universal type of sensor for a range of aromatic vapors including those of toluene, 2-nitrotoluene, 3-nitrotoluene, benzene, chlorobenzene, bromobenzene, and nitrobenzene.[15] X-Ray crystallography (Fig. 3) shows that the interplanar distance between the planes of the aromatic rings at 6 and 12 o'clock is 9.6 Å, whilst that between the planes of the aromatic rings at 3 and 9 o'clock is marginally less at 8.9 Å. The most striking feature of the solid state structure is that a disordered water molecule is positioned within its Celtic-cross like cavity such that its hydrogen atoms are more than 2.7 Å away from any potentially interactive sites within the rigid hydrophobic cavity. Attempts to reach (Scheme 1) [12]beltene[19] **9** and [12]cyclacene[20] **10** have so far only proved to be partially successful. Dehydration of dideoxykohnkene **5**, under conditions of thermodynamic control, led, not to the highly symmetrical octahydro[12]cyclacene derivative **6**, containing two benzene and two anthracene units, but rather to the much less symmetrical isomer **7** comprised of one benzene, one anthracene, and two naphthalene units. The isomer **7** was converted by means of a Birch reduction into [12]collarene **8** with six 'insulated' benzene rings. Apart from [12]cyclacene **10**, all the other hydrocarbons, i.e. **7**–**9**, in Scheme 1 are characterized by π-electron systems which are localized or delocalized in a plane perpendicular to that of the macropolycycle. Exploiting their coordination chemistry towards transition metals might uncover some novel organometallic materials.

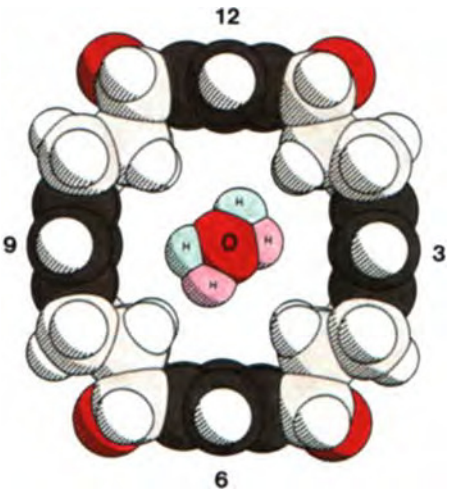
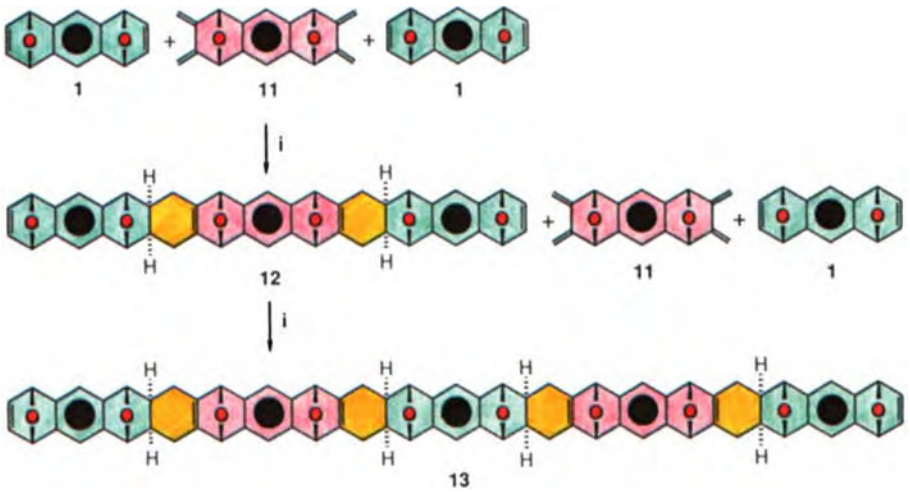


Fig. 3. Space-filling representation of the X-ray crystal structure of dideoxykohnkene **5**. In the disordered water molecule, which is included in the middle of **5**, half the molecules have their hydrogen atoms located in positions shaded pink and half in positions shaded blue (H = white, C = gray/black, O = red).

3. Molecular Strips

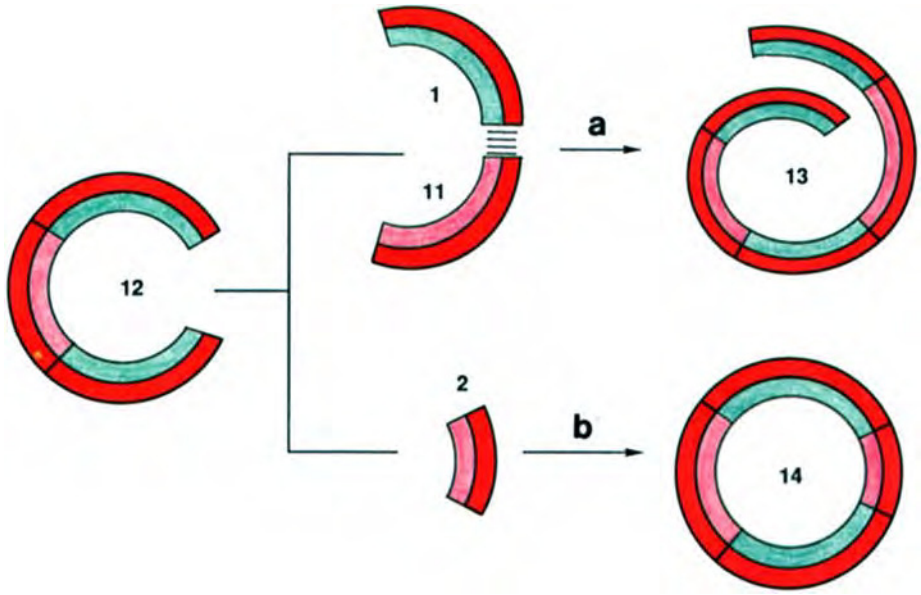
The power of any synthetic approach to new materials lies ultimately in its generality. One might ask – is it possible to replace **1** and **2** by other bisdienophiles and bisdienes and still



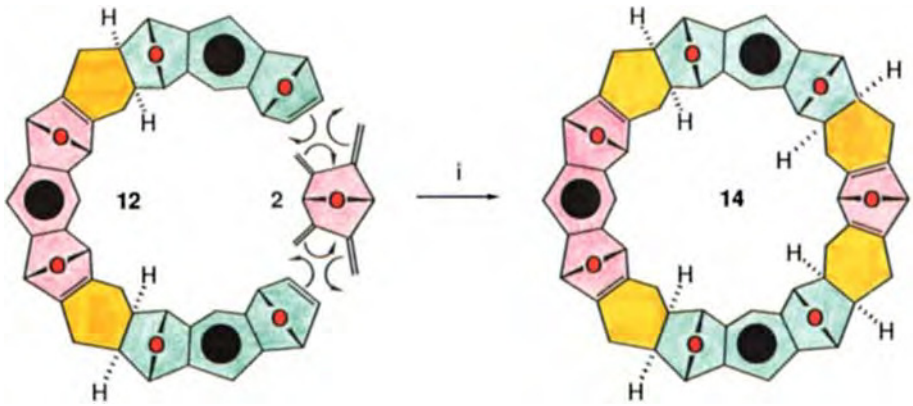
Scheme 3. The construction of the 2:1 adduct **12** and the 3:2 adduct **13** with the all-*syn* configurations from the bisdienophile **1** (blue) and the extended bisdiene **11** (pink) by repetitive Diels-Alder reactions. The newly-formed cyclohexene rings are highlighted in yellow (O = solid red). Reagents and conditions: i, CH_2Cl_2, 10 kbars, 50 °C, 6 days.

ADVANCED MATERIALS

retain stereoelectronic control of the repetitive Diels-Alder reactions? The answer is by and large – yes, but the outcome is a little different.[8] Instead of constructing molecular belts, one obtains (Scheme 3) using **1** and the extended bisdiene **11** in place of **2**, molecular strips in the form of a 2:1 adduct **12** and a 3:2 adduct **14**, which coils up like a spring – at least, so ^{1}H NMR spectroscopy in solution indicates. In Scheme 4 an attempt is made to rationalize what might be happening in this series of repetitive Diels-Alder reactions. The bisdiene **11** is obviously too large to fit into the 'gap' in the 2:1 adduct **12** and so the route to the 3:2 adduct **13** is an inevitable outcome. However, despite the fact that a [16]cyclacene derivative has not been isolated, the [14]cyclacene derivative **14**, resulting from reaction of the 2:1 adduct **12** with the smaller bisdiene **2** (Scheme 5) is formed with remarkable ease. These preliminary observations hold out the promise that it should be possible to construct molecular strips of varying sizes and shapes in a highly controlled manner. Considerable thought and effort has already been invested[2–4] in the applications to materials science of rigid molecular lines and strips.



Scheme 4. A diagrammatic representation of the construction by repetitive Diels-Alder reactions of a) the 3:2 adduct **13** from three bisdienophile **1** (blue on the concave surface) and two extended bisdiene **11** units (pink on the concave surface) and of b) the [14]cyclacene derivative **14** from the bisdiene **2** unit (pink on the concave surface) – both having the 2:1 adduct **12** as a common intermediate. The convex surfaces, which carry the oxygen atoms, are featured in red.



Scheme 5. The construction of the [14]cyclacene derivative **14** by two stereoelectronically-programmed Diels-Alder reactions from the bisdiene **2** and the 2:1 adduct **12**. Fragments derived from bisdienophile **1** units are shown in blue and those derived from bisdiene (**2** and **11**) units are shown in pink. Cyclohexene rings, resulting from Diels-Alder reactions, are highlighted in yellow (O = solid red). Reagents and conditions: i, PhMe, reflux, 17 h.

4. Molecular Cages

The relatively recent construction of carcerands[21]—hollow container-like molecules (Fig. 4), which can imprison smaller molecules to form so-called carceplexes—raises the prospect of new organic materials with exciting properties and exotic applications,[13, 21] e.g. slow release biodegradable molecular encapsulants for pharmaceuticals and agrochemicals or metabolism-resistant molecular shells, containing radiation-emitting guests, attached to immunoproteins for use in cancer therapy. Incarcerated molecules inside soluble carcerands[21] give very unusual NMR spectra. They indicate that the inside of the carcerand is a new phase—the incarcerated molecules plus 'vacuum'—whose properties are a function of the degree of occupancy of the interior of the carcerand by the imprisoned molecules. At the end of their recently-published communication, *Sherman* and *Cram*[22] speculate: "The carceplexes represent a new state of matter whose guest-mobility with respect to the host is subject to design, and whose physical properties are subject to molecular level manipulation. Several potential applications of carceplexes to materials science problems are envisioned, and are being examined."

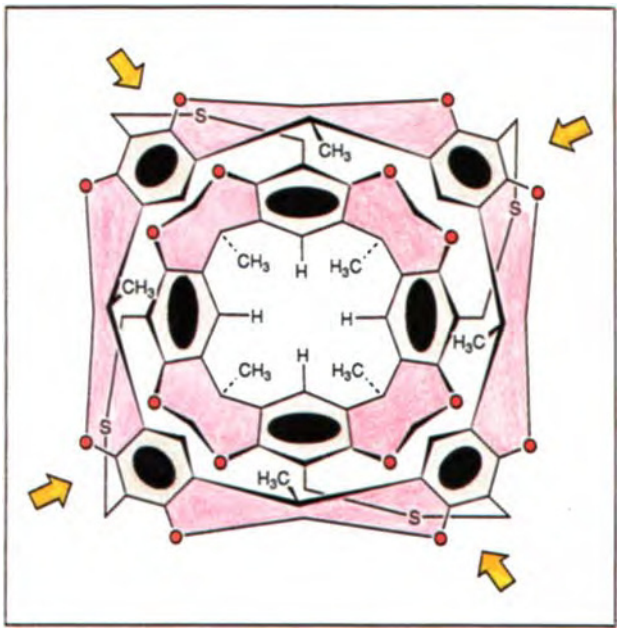
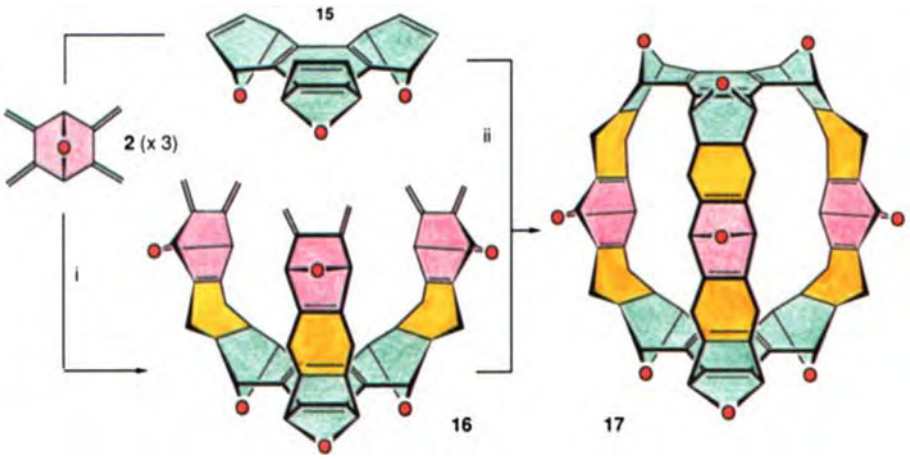


Fig. 4. Looking through the portals along the four-fold axis of the structural formula of *Cram*'s carcerand which is shaped like an American football. The arrows indicate the four carbon–sulfur bonds formed during the last step of the synthesis which brings together two cavitands each composed of alternating resorcinol (gray/black) and 8-membered acetal rings (pink) (O = solid red).

The recognition[23] that the basic carcerand topology is such that its atoms can be assembled on a minimal surface, may assist in the design and syntheses of other organic molecules. However, incentives for designing and synthesizing new materials come from many quarters. The cage compound **17**, which we have called[9] trinacrene after an old name (Trinacria) for Sicily, can be constructed via the 3:1 adduct **16** in two steps from the bisdiene **2** and the all-*syn* trisdienophile **15** (Scheme 6). The synthesis of trinacrene **17**, relying on repetitive Diels-Alder reactions as it does, is once again one that can be performed under tight stereochemical control. It is within the realms of possibility to adapt structure-directed approaches of this kind towards rational and total syntheses of carbon clusters,[24] including the C_{60} compound (Fig. 5) which has been christened buckminsterfullerene or footballene.



Scheme 6. The construction of trinacrene **17** via the 3:1 adduct **16** by a stereo-electronically-programmed set of Diels-Alder reactions from the bisdiene **2** (pink) and the all-*syn* trisdienophile **15** (blue). Newly-formed cyclohexene rings are highlighted in yellow (O = solid red). Reagents and conditions: i, PhMe, reflux, 16 h; ii, CH_2Cl_2, 10 kbars, 50 °C, 6 days.

ADVANCED MATERIALS

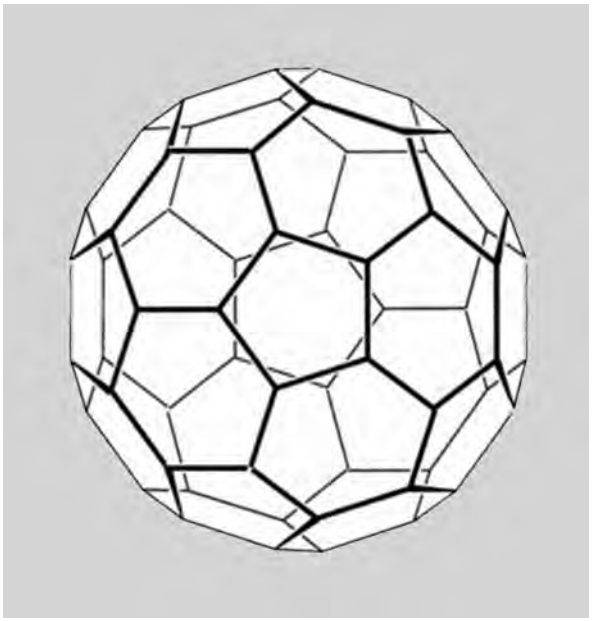


Fig. 5. The structural formula of buckminsterfullerene or footballene, a C_{60} species composed of 12 pentagonal and 20 hexagonal rings in the shape of a pentagonal dodecahedron.

neering may seem rather bizarre, but, actually, the notion that mechanical and electronic devices can operate at a molecular level has already been demonstrated in biological systems. For example, the smallest known[26] rotatory mechanical devices – either natural or artificial – are the bacterial ion-driven flagellar motors, which are unique to the fields of biology and engineering.

The form and function of unnatural products is infinite. As invention, rather than discovery, becomes more and more the hallmark of chemical research, unnatural products with form and function will result. Natural products serve only to reveal some of what is possible and they certainly do not have a monopoly on the means of realizing the possibilities. If you want to reach for the sky (Fig. 6) then wings – but without feathers – might be all you need to help you on your way.

Received: June 2, 1989



Fig. 6. Birds in flight – natural and unnatural forms functioning.

5. Outlook

The structure-directed synthesis of unnatural products is set to undergo rapid development during the next few years. It will provide a relatively straightforward means for the creation of a vast number of very large, organized, and functional structures. Opportunities beckon presently for the production of molecules with form – that look like ball bearings, beads and threads, belts, cages, chains, chimneys, clefts, coils, collars, knots, ladders, nets, springs, stacks, strips, washers, and wires – and concurrently and subsequently for molecules with function – that work like abacuses, capacitors, catalysts, circuits, clocks, conductors, dynamos, membranes, motors, nuts and bolts, resistors, screws, semiconductors, sensors, shuttles, superconductors, and switches.[25] Some of these postulated developments in molecular engi-

[1] R. P. Feynman, *Saturday Reviews 432* (1960) 45.
[2] P. W. Kenny, L. L. Miller, *J. Chem. Soc. Chem. Commun. 1988*, 84; P. W. Kenny, L. L. Miller, S. F. Rak, T. H. Jozekiak, W. C. Christopfel, J.-H. Kim, R. A. Uphaus, *J. Am. Chem. Soc. 110* (1988) 4445 and references therein.
[3] I. Rubenstein, S. Steinberg, Y. Tor, A. Shanzer, J. Sagiv, *Nature London 332* (1988) 426.
[4] S. Kivelson, O. L. Chapman, *Phys. Rev. B28* (1983) 7236.
[5] K. Blatter, A.-D. Schlüter, G. Wegner, *J. Org. Chem. 54* (1989) 2396.
[6] F. H. Kohnke, A. M. Z. Slawin, J. F. Stoddart, D. J. Williams, *Angew. Chem. Int. Ed. Engl. 26* (1987) 892; *Angew. Chem. 99* (1987) 941; J. F. Stoddart, *Chem. Br. 24* (1988) 1203; *J. Incl. Phenom. 7* (1989) 227; L. Milgrom, *New Sci. 1641* (3 Dec. 1988) p. 61.
[7] P. Ellwood, J. P. Mathias, J. F. Stoddart, F. H. Kohnke, *Bull. Soc. Chim. Belg. 97* (1988) 669; F. H. Kohnke, J. F. Stoddart, *Pure Appl. Chem. 61* (1989) 1581.
[8] P. R. Ashton, N. S. Isaacs, F. H. Kohnke, J. P. Mathias, J. F. Stoddart, *Angew. Chem. Int. Ed. Engl. 28* (1989) in press; *Angew. Chem. 101* (1989) in press.
[9] P. R. Ashton, N. S. Isaacs, F. H. Kohnke, G. Stagno d'Alcontres, J. F. Stoddart, *Angew. Chem. Int. Ed. Engl. 28* (1989) in press; *Angew. Chem. 101* (1989) in press.

[10] C. Mahaim, P.-A. Carrupt, J.-P. Hagenbuch, A. Florey, P. Vogel, *Helv. Chim. Acta 63* (1980) 1149; H. Hart, N. Raja, M. A. Meador, D. L. Ward, *J. Org. Chem. 48* (1983) 4357.
[11] S. L. Miller, L. E. Orgel: *The Origin of Life on the Earth*, Prentice-Hall, Englewood Cliffs, New Jersey, USA 1974; for a contemporary view on the origin of life, see G. Wächtershäuser, *Microbiol. Rev. 52* (1988) 452.
[12] A. Eschenmoser, *Angew. Chem. Int. Ed. Engl. 27* (1988) 5; *Angew. Chem. 100* (1988) 5.
[13] J. F. Stoddart, *Nature London 334* (1988) 10.
[14] J.-M. Lehn, A. Rigault, J. Siegel, J. Harrowfield, B. Chevier, D. Moras, *Proc. Nat. Acad. Sci. USA 84* (1987) 2565; J.-M. Lehn, A. Rigault, *Angew. Chem. Int. Ed. Engl. 27* (1988) 1095; *Angew. Chem. 100* (1988) 1121.
[15] M. A. F. Elmosalamy, G. J. Moody, J. D. R. Thomas, F. H. Kohnke, J. F. Stoddart, *Anal. Proc. London 26* (1989) 12.
[16] G. G. Guilbault, J. Ngeh-Ngwainbi in G. G. Guilbault, M. Mascini (Eds.): *Analytical Uses of Immobilised Biological Compounds for Detection, Medical, and Industrial Uses (NATO ASI Ser., Ser. C; Math. Phys. Sci. Vol. 226)* Reidel, Lancaster 1988, p. 187.
[17] S. K. Burley, G. A. Petsko, *Science Washington DC 229* (1985) 23; *J. Am. Chem. Soc. 108* (1986) 7995.
[18] P. R. Ashton, N. S. Isaacs, F. H. Kohnke, A. M. Z. Slawin, C. M. Spencer, J. F. Stoddart, D. J. Williams, *Angew. Chem. Int. Ed. Engl. 27* (1988) 966; *Angew. Chem. 100* (1988) 981.
[19] R. W. Alder, R. B. Sessions, *J. Chem. Soc. Perkin Trans. 2 (1985)* 1849.
[20] A. T. Balaban, *Pure Appl. Chem. 52* (1980) 1409.
[21] D. J. Cram, S. Karbach, Y. H. Kim, L. Baczynskyj, K. Marti, R. M. Sampson, G. W. Kalleymeyn, *J. Am. Chem. Soc. 110* (1988) 2554.
[22] J. C. Sherman, D. J. Cram, *J. Am. Chem. Soc. 111* (1989) 4527; see also M. W. Browne, *The New York Times*, 21 March 1989.
[23] Z. Blum, S. Lidin, *Acta Chem. Scand. B42* (1988) 332.
[24] H. W. Kroto, *Science Washington DC 242* (1988) 1139.
[25] J.-M. Lehn, *Angew. Chem. Int. Ed. Engl. 27* (1988) 89; *Angew. Chem. 100* (1988) 91.
[26] P. Mitchell, *FEBS Lett. 176* (1984) 287.

Metal Organic Chemical Vapor Deposition (MOCVD) Perspectives and Prospects**

High Purity Semiconductors
Heteroepitaxy
Low-Dimensional Structures
Precursors for III–V Growth
Electronic Ceramics
Thin Films

By John O. Williams*

1. Introduction

This paper reviews the progress that has been made over the past decade in the use of metal organic chemical vapor deposition (MOCVD) for the preparation of high purity, epitaxial layers of a wide range of semiconductor materials: it also considers an extension of the technique to the preparation of thin film electronic ceramics and archetypal high temperature oxide superconductors.

It is now over a decade since the pioneering work of *Manasevit* and coworkers[1, 2] gave rise to the remarkable interest subsequently shown in processes that use metal-organic compounds for the production of semiconductor materials. Since 1981 four international conferences have been held on the topic,[3] numerous workshops have been organized and nowadays, for certain key III–V materials systems (and to a lesser extent narrow band gap II–VI analogs), MOCVD or metal organic vapor phase epitaxy (MOVPE) is an accepted production technique yielding novel electronic and optoelectronic devices.[4–6] In many of these cases, MOVPE compares favorably with molecular beam epitaxy (MBE) and for certain materials particularly those containing phosphorus, MOVPE can produce superior materials. MOVPE is capable of producing thin layered structures – the so-called quantum wells and superlattices – and the technique can be used for atomic layer epitaxy (ALE)[7] and in the preparation of layered crystals (LC).[8]

One area where MOCVD has not developed to the same extent as MBE is the in situ monitoring of the deposition reactions. Despite recent progress[9, 10] our understanding of the basic processes occurring in MOCVD is not very advanced and monitoring techniques are only currently being developed unlike in the case of, for example, reflection high energy electron diffraction (RHEED) in MBE to monitor and control atomic layer deposition.[11] In addition, since compounds are used as precursors in MOCVD, a great effort has to be expended in order to achieve the required levels of high purity and safety/convenience of the growth process. Many innovative preparation and purification routes have been developed[12, 13] for the most common precursors and over the past two years, safer and less toxic chemicals have been studied as alternative starting materials.[14, 15] With an improved understanding of the growth mechanisms, we can look forward to a period of considerable innovation in the use of the MOCVD technique and it is interesting to note

[*] Prof. J. O. Williams
Solid State Chemistry Group
Department of Chemistry
UMIST, PO Box 88
Manchester M60 1QD (UK)

[**] I would like to thank members of the UMIST Solid State Chemistry Group and the UK JOERS Consortium on InP-based materials for numerous stimulating discussions. The financial support of the SERC, US Air Force, Thorn EMI CRL, Air Products Ltd. and Johnson Matthey Ltd. is also gratefully acknowledged.

ADVANCED MATERIALS

that this is already happening in the fields of both electronic ceramics e.g. $PbTiO_3$[16, 17] and high-T_c oxide superconductors of the family $YBa_2Cu_3O_x$ (x:6 to 7).[18, 19]

2. Attainment of High Purity in Semiconductor Materials

Most advances in semiconductor devices rely on the availability and subsequent doping of high purity materials. In recent years there have been significant advances in this field. MOCVD has its own difficulties in this area additional to those of other conventional preparative techniques since the precursors that are used do not lend themselves to ready purification: they are often pyrophoric, hazardous chemicals. It is now possible to analyze directly the metal organic precursors for elemental impurities at the ppb level using variants of inductively coupled plasma (ICP) analysis.[20]

Parallel studies to characterize impurities in the grown epitaxial layers by such techniques as secondary ion mass spectrometry (SIMS) and low temperature photoluminescence (PL) allow correlation between impurities in the starting materials and those in the epitaxial layers.[21–23] This relationship may be illustrated by reference to some recent work on the growth of GaAs. Two batches of trimethyl gallium (TMGa) were used with the same, high purity, arsine source. The ICP analysis of the TMGa showed different amounts of common impurities as shown in Table 1. The

Table 1. ICP analysis for impurities in TMGa1 and TMGa2*.

Elements	TMGa1	TMGa2
Si	0.2 ppm	0.05 ppm ND
Zn	0.6 ppm	0.3 ppm ND
Sn	< 0.5 ppm ND	0.5 ppm ND
Mg	0.05 ppm	0.05 ppm ND
Mn	< 0.05 ppm ND	0.05 ppm ND
Fe	< 0.3 ppm ND	0.3 ppm ND

* ND = not detected

level of Si and Zn, recognized n- and p-type impurities respectively in GaAs, is lower in source TMGa2 than in TMGa1. The electrical characteristics of GaAs grown from TMGa2 and arsine are much improved over those from TMGa1 and the same arsine. The low temperature (77 K) electron mobility and concentration are higher and lower, respectively, and for TMGa2 the lowest carrier concentration and highest mobility are obtained at the lower growth temperature of 600 °C (Figure 1). This low growth temperature can

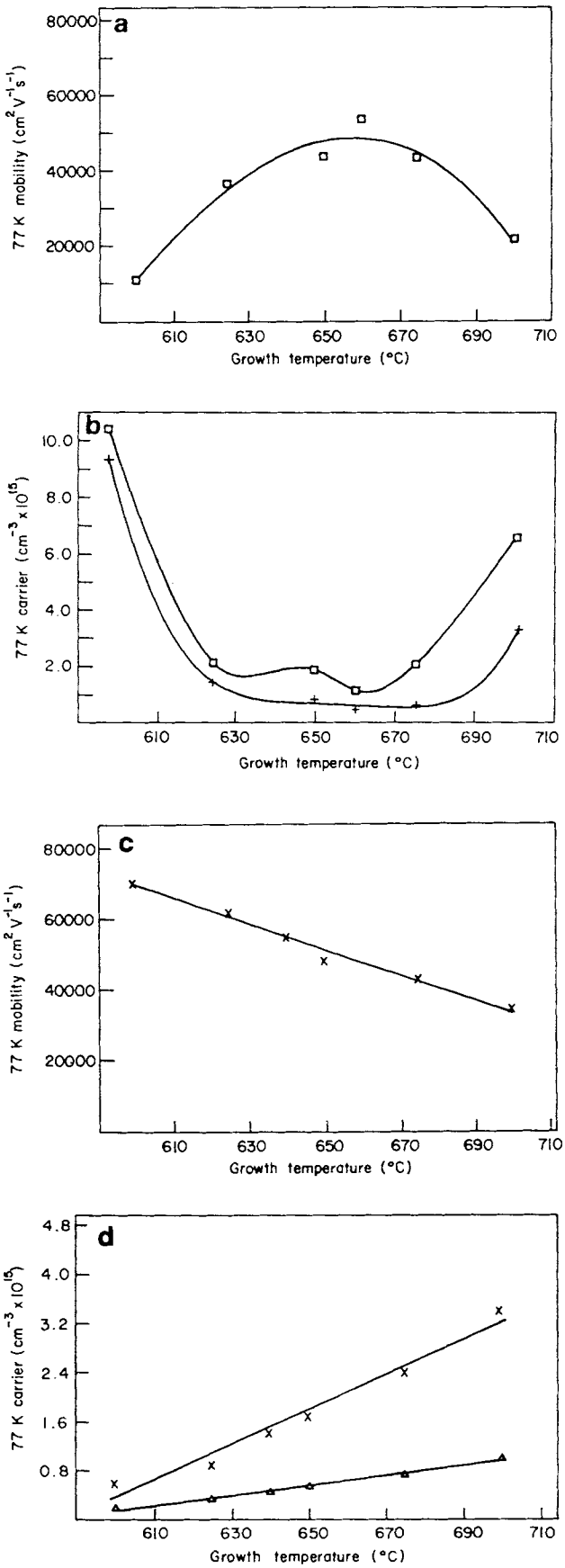


Fig. 1. a) 77 K Hall mobility variation with growth temperature for GaAs grown from TMGa1 at constant V/III ratio of 75:1. b) 77 K Hall carrier concentration yielding values of (□) N_D and (+) N_A plotted against growth temperature for GaAs grown from TMGa1 at constant V/III ratio of 75:1. c) 77 K Hall mobility variation with growth temperature for GaAs grown from TMGa2 at constant V/III ratio of 75:1. d) 77 K Hall carrier concentration yielding values of (X) N_D and (△) N_A plotted against growth temperature for GaAs grown from TMGa2 at constant V/III ratio of 75:1.

be adventitious for good morphology and crystallinity of the epilayers. The electrical properties are dominated by the Si and the activated incorporation of this impurity is consistent with doping studies using disilane.[24]

A similar situation is observed in the case of InP preparation by MOCVD where Si is again found to be the dominant impurity in the highly purified organometallic precursor, trimethylindium (TMIn). The presence of this impurity in the grown layers has been confirmed by depth profiling studies and analysis of low temperature photoluminescence spectra.[21] Figure 2a shows the electron concentration as a function of depth through the InP epilayers grown with increasing temperatures. The corresponding silicon profile in SIMS is shown in Figure 2b. Low temperature (4 K) PL spectra confirm the presence of donors, and measurements in a magnetic field (where the donor related transitions are resolved) indicate the presence of S and Ge impurities in addition to the Si. Removal of Si yields extremely high quality InP material with theoretical values of electron mobility and concentration reached for epilayers ca. 10 μm in thickness. Indeed, one of the highest reported electron mobility values for InP ca. 400.000 $cm^2 V^{-1}$ at 60 K has been reported for MOCVD material using purified TMIn.[25] The two examples cited are for binary materials. There have also, as a result of this success with GaAs and InP, been significant improvements in the purity of ternary and quaternary materials. This will not be covered in this review, but the interested reader is referred to the recent literature.[26]

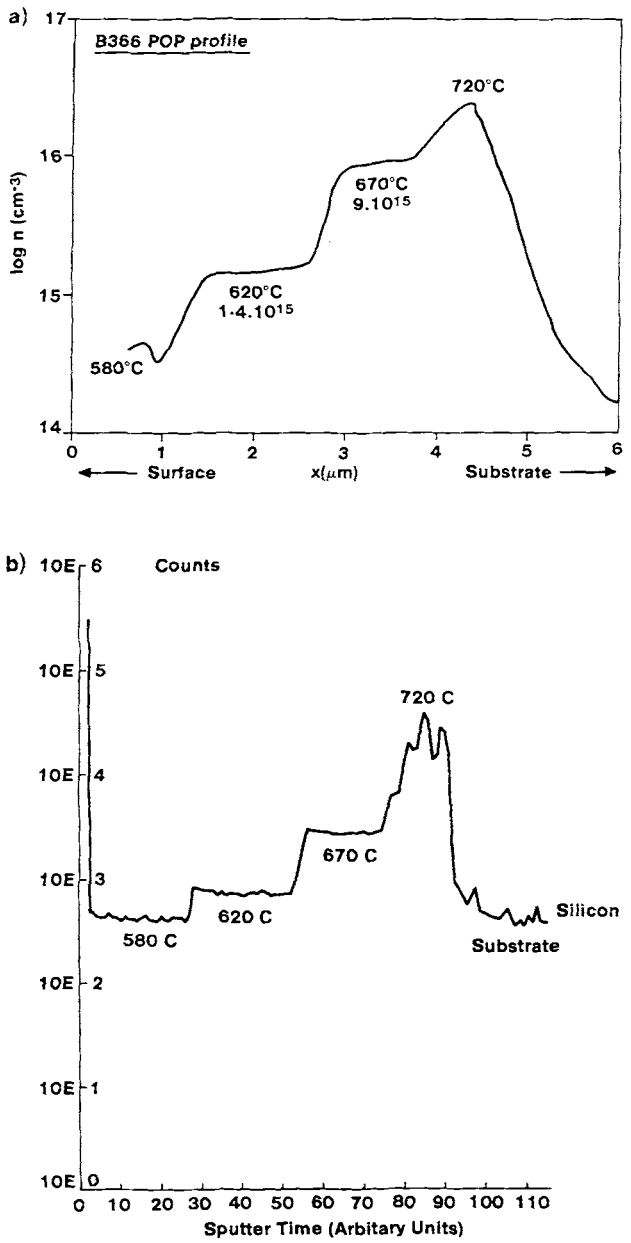


Fig. 2. a) Undoped MOCVD InP-variation of doping level with growth temperature. b) Undoped MOCVD InP-variation of silicon content with growth temperature (SIMS Profile).

3. Heteroepitaxy

Heteroepitaxy describes the situation where an epitaxial layer of one material is grown upon another in strict crystallographic registry. In addition to providing considerable fundamental scientific interest such materials combinations have enormous technological significance. Table 2 summarizes the properties of a few simple heteroepitaxial systems which are prepared by MOCVD. The list is confined to binary and elemental materials although, as we shall see later in sections 4 and 5, systems including ternary and quaternary materials may also be classified as heteroepitaxial.

Table 2. Simple heteroepitaxial systems.

Material	Crystal Structures	Unit Cell dimension a_0/pm	Lattice Mismatch $[\Delta a/a]_0 \times 10^2$	Band Gap /eV
GaAs (e)	sphalerite (fcc)	0.565331	+4.09	1.35
Si (s)	diamond	0.543072		1.14
GaAs (e)	sphalerite (fcc)	0.565331	−3.68	1.35
InP (s)	sphalerite	0.586928		1.29
ZnSe (e)	sphalerite (fcc)	0.56670	+0.24	2.67
GaAs (s)	sphalerite (fcc)	0.565331		1.35

(e) epitaxial layer; (fcc) face-centered cubic; (s) substrate: $[\Delta a/a]_0$ is the measurement for a stress free epitaxial layer and is defined as $(a_0 - a_s)/a_s$ where a_s is the unit cell dimension of the substrate.

It is instructive to consider these pairs of materials in turn. Since Si dominates the commercial semiconductor market, there has been interest in preparing GaAs on Si. There appear to be significant advantages if this could be done properly including: the relative cheapness of Si substrates as compared to GaAs, the better thermal conductivity of Si with relevance to power devices, the ability to combine high speed GaAs devices with high density Si circuits and the possibility for fabrication of GaAs opto-electronic devices in combina-

ADVANCED MATERIALS

tion with Si integrated circuits. However, two major difficulties arise. First the two materials differ in the symmetry of their respective crystal structures, and second, the unit cell dimensions differ leading to a "lattice mismatch" at the interface between epilayer and substrate. The symmetry difference (sometimes referred to as different color symmetry) leads to the formation of anti-phase boundaries (APB) when growth proceeds on substrate surfaces of particular orientations with catastrophic consequences for electrical behavior at the interfaces. Because of these difficulties it is now accepted that any devices made in the GaAs/Si system and relying on the GaAs must utilize material well away from the interface unless the APBs and other defects can be eliminated. Furthermore, these limitations are likely to preclude the development of devices that utilize both Si and GaAs simultaneously. Considerable progress has been made recently in the MOCVD growth of GaAs on Si without necessarily employing buffer layers to accommodate the lattice mismatch.

Preparation of Si surfaces prior to growth is a prerequisite and a complex series of nucleation and crystal growth steps appear necessary for the preparation of GaAs with acceptable crystallinity. Figure 3 illustrates how surface preparation, nucleation and growth temperature affect the crystallinity of GaAs grown on accurately oriented (100)Si substrates. Experiments to reduce interfacial defects have also been carried out employing substrate surfaces deviating from (100) orientation and good properties obtained at 4° off towards (110).[27] In addition to the problems encountered in the GaAs/Si system the other two pairs of materials referred to in Table 2 suffer the disadvantage of possible interdiffusion of elements with catastrophic consequences if it occurs to an appreciable extent. The situation is worst for ZnSe/GaAs since Zn acts as a p-type dopant in GaAs and Ga as an n-type dopant in ZnSe. Excellent quality ZnSe has been grown on (100)GaAs surfaces by reduced and atmospheric pressure MOVPE.[28] Room temperature photoluminescence is observed indicating the low concentrations of shallow and deep centers, but the structural, electrical and optical properties are highly dependent on epilayer thickness and the distance away from the interface. The X-ray and PL data for ZnSe epilayers grown on GaAs and varying in thickness from 0.5 μm to 8.0 μm are given in Figure 4. In the thinnest layers, deep center emission appears in the PL and in the X-ray data the ZnSe diffraction maxima are shifted to lower 2θ values. SIMS analysis on the ZnSe reveals the presence of Ga diffusion from the substrate (Fig. 4c) and cross sectional transmission electron microscopy (Fig. 4d) confirms the defective nature of the interface. It is unlikely that the ZnSe/GaAs interface can be made sufficiently good to support efficient devices relying on optical/electronic properties. However, the ternary $ZnSe_{0.95}S_{0.05}$ grown on GaAs[29] offers a lattice-matched system, and studies following MOCVD growth indicate that its properties are superior to those of ZnSe/GaAs and adequate to support devices. The distortion at the interface of ZnSe/GaAs renders the structure tetragonal as opposed to cubic[30] and this has been

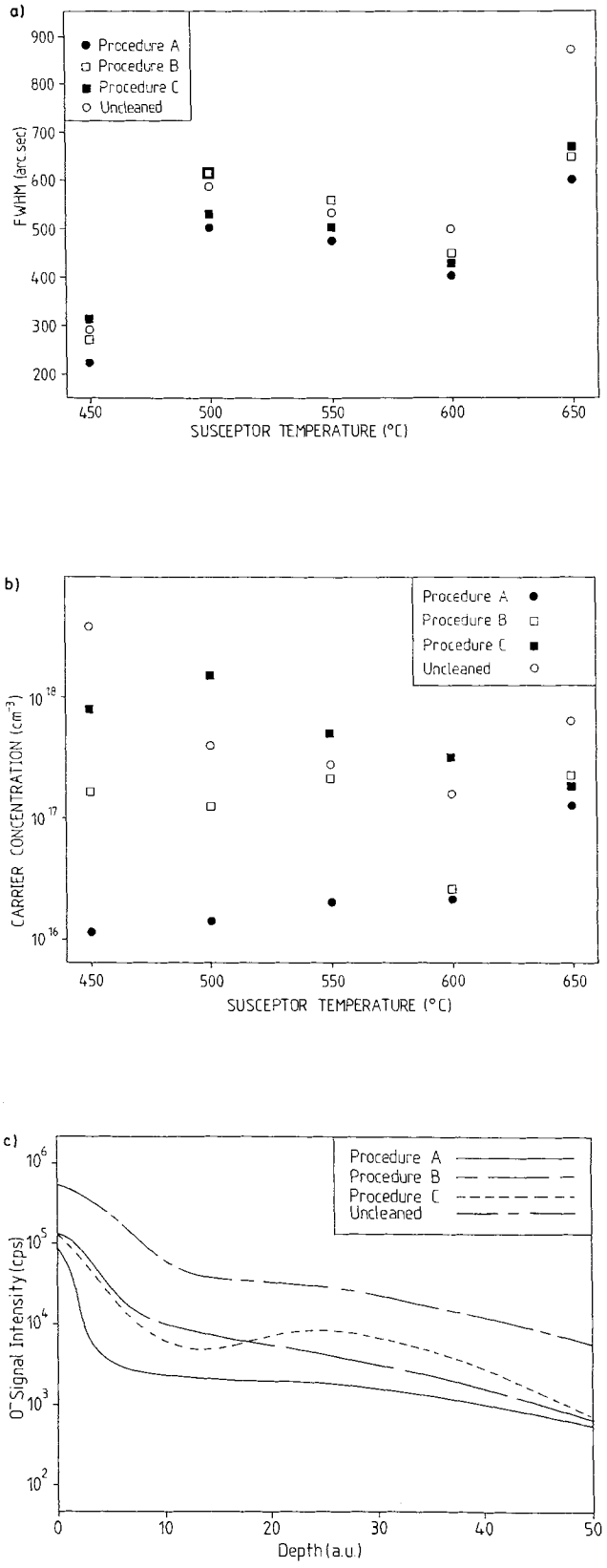


Fig. 3. a) X-Ray rocking half widths vs. susceptor temperature for each Si(100) surface. b) Background carrier (electron) concentration vs. susceptor temperature. c) Dynamic SIMS spectra showing surface oxide thickness for each Si(100) surface.

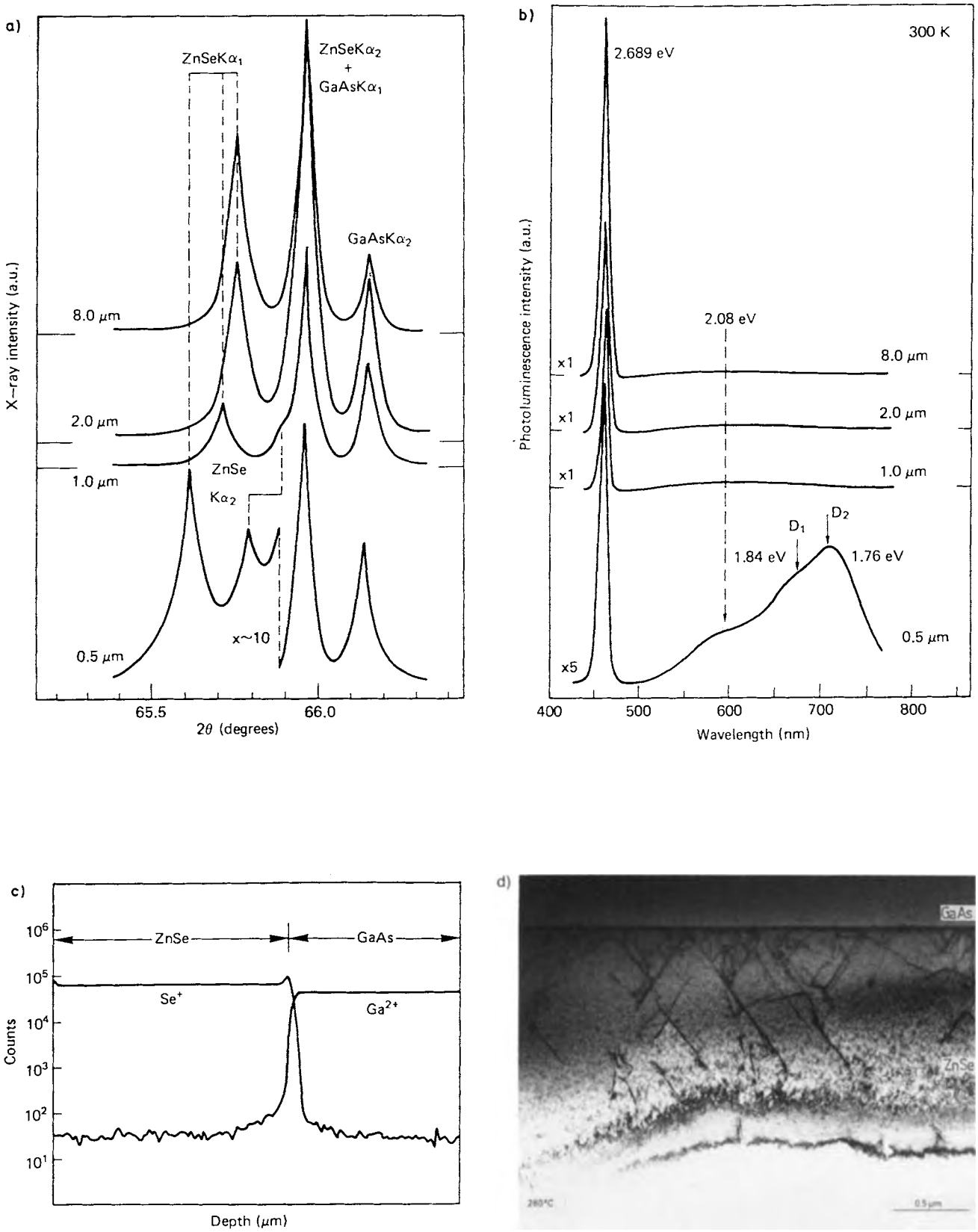


Fig. 4. a) Variation of X-ray rocking curve data for ZnSe/GaAs with layer thickness. b) Variation of 300 K PL spectra for ZnSe/GaAs with layer thickness. c) Secondary ion mass spectrometry (SIMS) profiles for $Se^{\oplus}$ and $Ga^{2\oplus}$ in ZnSe/GaAs. Note the tail in the $Ga^{2\oplus}$ profile. d) Cross-sectional TEM for ZnSe/GaAs grown by MOVPE at 280 °C showing dislocation structure close to the interface.

confirmed recently by electron spin resonance studies of Mn-doped ZnSe using the $Mn^{2\oplus}$ ions to probe the local symmetry.[31]

GaAs has been grown successfully on InP substrates[32] and efficient devices such as solar cells and MESFETS have been fabricated. As with the other two heteroepitaxial systems these do not rely on charge carrier transport across the interface or on optical generation of carriers in that region. We can, therefore, conclude that in these three heteroepitaxial systems we have important building blocks for the development of integrated opto-electronic devices that will combine important electronic and optical functions on a common substrate i.e. Si, GaAs or InP.

4. Ternary and Quaternary Materials

Figure 5 shows how the band gap of III–V materials varies with the lattice constant and composition. Such diagrams are often referred to as phase diagrams and they aid the crystal grower in his choice of material system appropriate to a particular electronic/optical requirement. (The term band gap engineering is commonly used to describe this approach). The tie-lines represent ternary compositions e.g., $Ga_{1-x}In_xAs$ and $InAs_{1-y}P_y$ and areas on the diagram contained within points of four binary compounds represent quaternary materials e.g., $Ga_{1-x}In_xAs_{1-y}P_y$. It is apparent that one particular ternary composition will have the same lattice constant as a binary compound and this may be found by drawing vertical lines through the binary point to intercept the tie-line for that particular ternary e.g. $Ga_{0.47}In_{0.35}As$ is lattice matched to InP (dotted line). Similarly, a range of quaternary compositions e.g. $Ga_{1-x}In_xAs_{1-y}P_y$ with $0 < x < 1$ and $0 < y < 1$ will be matched to InP and will be represented by the same vertical dotted line. Almost the entire range of III–V direct band gap, ternary and quaternary materials have been prepared by MOCVD. For many of these the problem of compositional uniformity both within the bulk and across the surface of the grown layers has been solved and lattice matching is achieved with good morphology and crystallinity of the grown layers. One of the most important III–V ternary systems is $Ga_{1-x}Al_xAs$/GaAs and the other is $Ga_{1-x}In_xAs$/InP. The "AlGaAs" system is unique in that lattice-matching to GaAs is retained for a wide range of x values since the radii of Al (1.43 Å) and Ga (1.41 Å) are similar. In contrast only one composition of "InGaAs" is lattice-matched to InP. Double crystal X-ray rocking curve analysis confirms that a

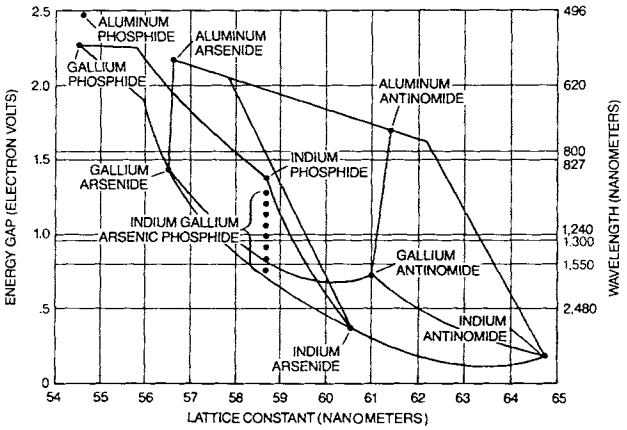


Fig. 5. Band-gap engineering of a semiconductor can be done by varying the elemental components of the semiconductor alloy in a controlled way. Here the energy across the band gap is plotted against the lattice constant, or the dimension of the basic unit of the crystalline lattice. The lines that connect points on the graph show how the band gap and the lattice constant vary for mixtures of the binary compounds to which the points correspond. Such mixtures are ternary compounds. For example, the ternary compound gallium aluminum arsenide can be made to have any band gap between about 1.4 and 2.2 electron volts by varying the ratio of gallium to aluminum between the band-gap extremes represented by gallium arsenide and aluminum arsenide. Materials of differing composition that have roughly the same lattice constant, such as these two binary compounds, can be deposited in alternating layers to create a single crystal lattice. Operating wavelengths for three important optical communications systems are 800, 1300 and 1550 nm [55].

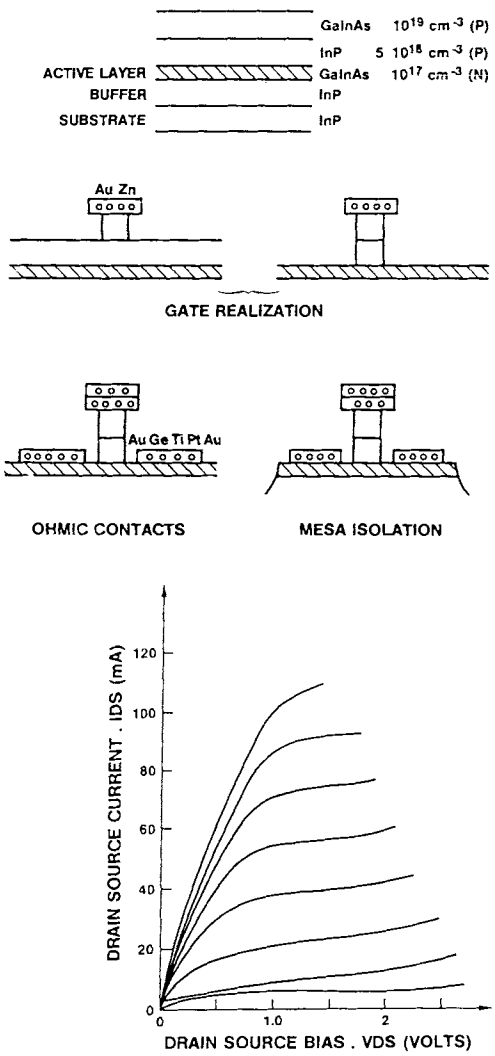


Fig. 6. (Top) Schematic diagram of the JFET fabrication process. (Bottom) JFET DC characteristics.

lattice mismatch $[\Delta a/a]_0$ of less than 8×10^{-5} may be routinely obtained with a full width at half maximum (FWHM) of < 40 arc/sec for this system. Several device structures including junction field effect transistors (JFETs) and double heterostructure pindiodes have been fabricated with excellent characteristics. Figure 6 gives details of the structure, fabrication, uniformity and characteristics of a typical JFET structure grown by MOCVD.[33]

The quaternary system $Ga_{1-x}In_xAs_{1-y}P_y$ covering the entire composition range has also been prepared by MOCVD[34] and the field has been reviewed recently.[6] There are also important advances presently being made with ternary and quaternary materials containing antimony.[35]

Over the past three years, *Dupuis* and collaborators have made significant advances in the fabrication of low threshold, high efficiency $Al_{1-x}Ga_xAs/GaAs$ double heterostructure injection lasers directly on Si substrates.[36] As mentioned in section 3, this is another example of heteroepitaxy but in this work, the lattice mismatch has been accommodated by the preparation of Si/Ge buffer layers. Four types grown by MBE have been used (i) single Ge layers (1 μm thick) deposited on Si (ii) a single Ge layer grown on Ge/Si strained layer superlattice, (iii) a Ge layer deposited on linearly graded Ge/Si alloy buffer layer, (iv) a combination of (ii) and (iii). It is found that the best device performance is obtained using procedure (i)[37] and this work illustrates the sophistication of layered structures that can be prepared by a combination of MBE and MOCVD.

5. Low-Dimensional Structures and Devices

Over the past decade there has been considerable progress in the study of low dimensional structures prepared by both MOCVD and MBE. It is not my intention in this review to compare the two techniques and the task of presenting a comprehensive account of 'LDS/LDD' is an impossible one because of the enormity of the subject area. I shall, therefore, be highly selective in my choice of topics and will attempt to address particular materials problems. The interested reader is referred to three recent excellent reviews which cover other aspects.[38, 39, 54]

Initial studies dealt with the "AlGaAs/AlAs" or "AlAs/GaAs" quantum well and multiple quantum well structures. Here GaAs acts as the well material and AlAs or AlGaAs as the material in the barrier layers. Lasers operating in the red spectral region ca. 850 nm are now in commercial use. A particularly interesting structure is that of a graded refractive index separate confinement heterostructure single quantum well laser (GRINSCH SQW laser). The laser consists of a 500 nm GaAs buffer layer, 1 μm $Al_{0.6}Ga_{0.4}As$ cladding, 340 nm graded "AlGaAs" confinement region within an 8 nm thick GaAs SQW active layer, 500 nm $Al_{0.6}Ga_{0.4}As$ cladding and 100 nm GaAs contact layer. This type of laser gives continuous wave (CW) operation at room temperature with a broad area threshold current density of ca. 300 Acm^{-2} and a single longitudinal mode operation at 843 nm with a peak width of less than 1 nm.[32]

The advent of devices such as high electron mobility transistors (HEMTs) based on a two dimensional electron gas (2 DEG) formed in the "AlGaAs"/GaAs system has further emphasized the dimensionality of these thin layer structures. Figure 7a is a schematic diagram of a typical heterojunction structure grown by MOCVD. The two dimensional electron gas is formed in the undoped GaAs layer just below the thin ca. 15 Å undoped "AlGaAs" layer and sustains a high electron mobility in two dimensions (Figure 7b). The doping in the upper "AlGaAs" layer is achieved using selenium. A

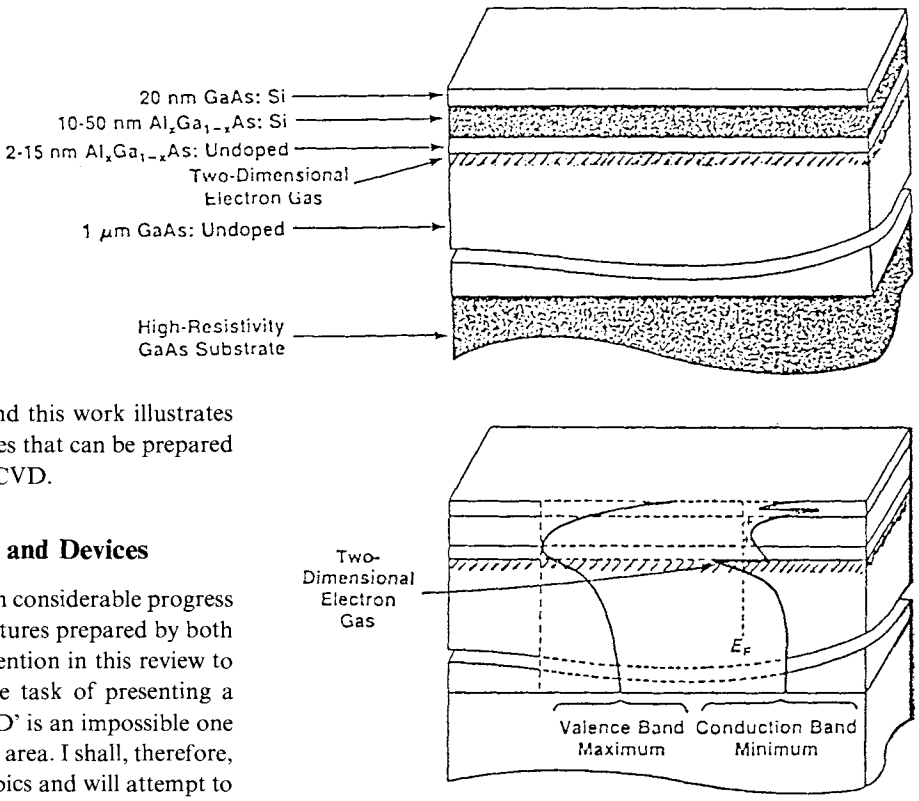


Fig. 7. a) Cross section of a modulation doped heterojunction. b) Energy band diagram for structure of (a). The two dimensional electron gas formed in the structure is ideal for the conducting channel of a FET.

ADVANCED MATERIALS

HEMT structure requires good doping uniformity, low carrier concentration in undoped material and sharp interfaces. These requirements can be met by MOCVD. Multiple quantum well structures in InP-based ternary and quaternary materials have also been prepared by MOCVD. Figure 8 shows the actual structure grown and the corresponding photoluminescence spectra for the GaInAsP/InP system. It should be noted that each quaternary well yields a PL emission peak which shifts to lower wavelengths as the well width decreases.

Examination of Figure 8 allows us to understand the concept of strained layer superlattices (SLS) and pseudo-

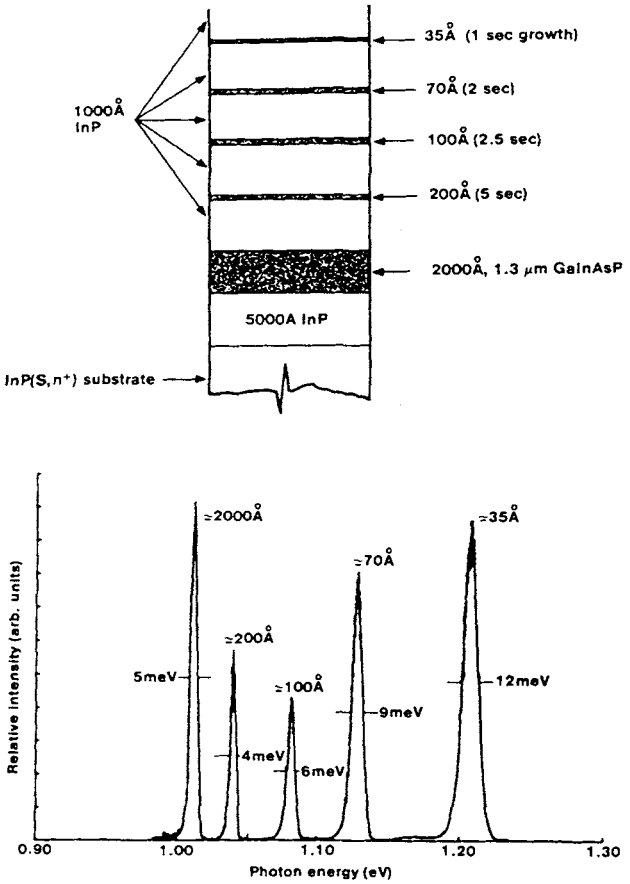


Fig. 8. a) GaInAsP/InP quantum wells grown to assess epitaxy and interface quality. b) Photoluminescence spectrum of a GaInAsP multiquantum well sample, emission from each of the four different wells and from the bulk epitaxial material can be observed. $T = 4.2$ K, 25 mV, 40 mW, 0.18 W cm^{-2}.

morphic structures. It has been shown that dislocations in ternary materials grown on binary semiconductors can be confined to the interfacial regions when the layers are thin ca. ≤ 200 Å.

Furthermore, the effective lattice-matched composition of the ternary can be achieved by growing successively thin layers of different binary compounds of the required thickness. Thus, the composition $Ga_{0.47}In_{0.53}As$ can be built up of GaAs and InAs layers of appropriate relative thickness. In a similar way, the quaternary of a given composition can be equivalent to two ternaries, neither of which is lattice-matched to the substrate. Typical materials combinations that have been grown successfully by MOCVD are indicated in Table 3. In order to achieve uniform compositions and sharp interfaces, careful control of reactor geometry is required.

Table 3. Typical materials combinations.

GaAs	–	$Al_{1-x}Ga_xAs$
GaAs	–	$In_{1-x}Ga_xAs$
GaAs	–	InAs
GaAs	–	$GaAs_{1-y}Sb_y$
GaAs	–	$In_{1-x}Ga_xP-In_{1-x}Al_xP$
InP	–	$In_{1-x}Al_xAs-In_{1-x}Ga_xAs$
InP	–	$In_{1-x}Ga_xAs_{1-y}P_y$
InP	–	InAs–GaAs
GaSb	–	InAs
GaSb	–	$InAs-AlAs_{1-y}Sb_y$
GaSb	–	AlSb
GaSb	–	$In_{1-x}Ga_xAs_{1-y}Sb_y-Al_{1-x}Ga_xAs_{1-y}Sb_y$

6. Novel Precursors for III–V Growth

Conventional group III organometallic and group V hydrides used as precursors for MOCVD suffer severe disadvantages despite the fact that good quality epitaxial layers can be produced in the majority of cases. These disadvantages arise from the toxic and hazardous nature of arsine and phosphine, for example, and the pyrophoric nature of TMGa and TMIn. TMIn suffers further limitations due to its crystalline nature which can severely reduce the levels of compositional uniformity that can be obtained in several ternary and quaternary systems.

Another important consideration when preparing complex systems is the relative thermal behavior of a pair of group III and/or group V precursors. Arsine and phosphine, for example, decompose in the gas phase and, as far as is known, at GaAs and InP substrate surfaces, with very different rates. Such considerations have prompted several research groups worldwide to seek alternative precursors. Table 4 lists alternative precursors for arsine that have been

Table 4. A selection of alternative As precursors used with TMGa to produce GaAs.

Compound	Vapor Pressure	GaAs n_{77K}/cm^{-3}	electrical data Ref μ_{77K}/cm^2 V^{-1} s^{-1}
Trimethylarsine (TMAs)	235 Torr at 20 °C	p ~ 10^{17}	–
Triethylarsine (TEAs)	5 Torr at 20 °C	n ~ 5×10^{15}	13.000
Diethylarsine (DEAs)	0.8 Torr at 18 °C	n ~ 3×10^{14}	64.000
Tertiarybutylarsine (TBAs)	96 Torr at −10 °C	n ~ 1×10^{15}	53.000
Phenylarsine	2 Torr at 20 °C	n ~ 1×10^{15}	40.000

examined in recent years for GaAs growth by MOCVD. With most of these reagents carbon incorporation is a major problem and hitherto only two precursors, tertiarybutylarsine (TBAs) and phenylarsine (PAS) have shown real promise. Both of these are liquids under normal conditions. GaAs with relatively high electron mobilities (ca. 40.000 $cm^2 V^{-1} s^{-1}$ at 77 K) and low donor concentration for nominally undoped material ($n \leq 1 \times 10^{15} cm^{-3}$) has been reported.[14] For the case of InP growth, liquid tertiarybutylphosphine (TBP) has also shown promise.[15] It may be no accident that these liquid precursors, with hydrogen atoms linked directly to the group V element, yield epitaxial layers relatively free of carbon impurities, in contrast to those precursors that contain no group V–H bonds, e.g. trimethyl- and triethylarsine (TMAs and TEAs respectively). It appears that As–H and/or As–H_2 units are required in order to react with methyl radicals from TMGa to form GaAs without resulting in carbon formation, although final details await mechanistic investigations currently underway in several laboratories. PAS is also being used to grow InAs.

From time to time in the MOCVD field, there has been interest in developing adduct precursors or "magic compounds" where the group III–group V bond has already been formed.[40] Thermal dissociation would simply detach side groups leaving behind the III–V binary compounds, a process that would be safe and cheap. However, progress in this area has been disappointing for several reasons. First, the adducts cannot be purified sufficently: second, they require the presence of other group III or group V sources in order to produce stoichiometric material and third, they cannot alone provide ternary and quaternary materials of variable composition.

7. Crystallography – Controlled Growth

The manufacture of the current generation of electronic devices with features of the order of several microns involves complex etching and lithographic processes which are both inefficient and time consuming. Therefore, considerable interest is being shown in local or selected area deposition where the semiconductor material is deposited only where it is required, e.g. in the active region. There have been several approaches to achieving selected area deposition using MOCVD. One has involved "photo-assisted" deposition using, for example, laser radiation and capitalizing on photonic or thermal effects to deposit the desired material. Several review articles have appeared covering these aspects.[41, 42] A much more recent and novel approach is to use precursors selectively to deposit on particular surfaces but not on others. The acronym CODE, compound and orientation dependent epitaxy, has been used to describe this technique.[46] Such growth surfaces would vary in their composition and/or structure and crystallography. It is also desirable to use MOCVD to overgrow contoured substrates in order to isolate component function, and for interfacing. The work of *Hersee* et al.,[43] *Demeester* et al.,[44] *Yoshikawa* et al.,[45] *Scott* et al.[46] and *Garrett* and *Thrush*[47] covering both GaAs and InP based systems should be consulted for further details. Much of this work has been concerned with the ability of MOCVD to deposit over mesa-type structures and into channels of given crystallography.

Such capabilities would assist in the fabrication of buried heterostructure lasers, waveguides and active/passive waveguide interfaces by single step epitaxy. A common technique to study the behavior over contoured substrates is to employ a multi-heterostructure growth technique to follow the time evolution of the growing surfaces, i.e. to grow a superlattice whose individual layer thickness is much less than the total thickness of the grown layer. Although the precise distortion of the growth process introduced by the creation of the superlattice is uncertain, some general preliminary conclusions can be drawn in relation to the preference for growth on certain crystallographic planes in the InGaAs/InP and AlGaAs/GaAs systems: (i) InGaAs is reluctant to nucleate on either (111)A or (111)B surfaces, whereas InP grows on all available crystal planes. AlGaAs/GaAs on the other hand nucleates on (111)A surfaces but not on (111)B surfaces. (ii) For both systems nucleation and growth on (100) and (110) surfaces appears to be better than for (111) surfaces. Clearly, the growths are controlled by surface free energies, preferential adsorption, differential sticking coefficients etc. and it will be interesting to see the results of controlled experiments involving, for example, different precursors for the group III elements.

8. Electronic Ceramics and Oxides

Over the past two years, there has been growing interest in the so-called high-T_c oxide superconductors typified by the composition $YBa_2Cu_3O_{7-x}$ where $0.1 < x < 0.2$.[48] Superconducting transition temperatures around 90 K have been obtained for compressed, polycrystalline samples prepared by sintering and annealing the constituent oxides in specific proportions. In addition, other compositions based on Bi, Tl, Sc etc. have shown promise.[49] In order to be compatible with electronic and other types of device structures and the complete range of processing technologies it is desirable to prepare these materials as thin films. There have been various reports of successes using, for example, vacuum evaporation, sputtering, MBE, spray pyrolysis and screen printing. MOCVD has also been used with variable success.[50] Hitherto, metal chelate precursors such as 2,2,6,6-tetramethyl-3,5-heptanedione (thd) derivatives have been used, but the process has been unreliable and the thermal growth has to be followed in most cases by either a high temperature treatment or an annealing process under controlled conditions. The main difficulties arise from the choice of precursor and substrate material and these have not been optimized. In general, the following conditions are typical:

ADVANCED MATERIALS

(i) precursors kept at ca. 150 °C to 300 °C
(ii) substrate materials such as MgO or yttrium stabilized zirconia
(iii) growth temperatures in the range 600–900 °C
(iv) subsequent annealing in O_2 or high temperature treatment at ca. 900 °C
(v) reduced pressure operation (10–100 Torr) with heated lines from precursor containers to the growth chamber.

Thin films of "YBCO" have been obtained with preferred orientation (*c* axis normal to film plane) and variable composition, exhibiting superconducting transition temperatures over the range 30 to 80 K. Recently, we have improved the compatibility of precursors by using fluorinated β-diketones of the three metals Y, Ba and Cu and this appears also to improve the reproducibility of the MOCVD process.[51] We have demonstrated control over the composition as measured by energy dispersive X-ray analysis (EDAX) and the perovskite structure can be obtained by careful choice of processing temperature and substrate material/orientation. Future work in this area should address the understanding of the basic deposition process in order to remove the empiricism currently prevailing, and photo-assisted techniques should be investigated.

Four years ago, we proposed MOCVD routes for the preparation of electronic ceramic and ferroelectric oxides typified by $PbTiO_3$ and $Pb(La,Zr)TiO_3$. In recent years this has proven possible for $PbTiO_3$, in particular, using alkoxide and β-diketone derivatives of Pb and Ti and some success has been obtained with $Pb(La,Zr)TiO_3$. In addition, the work of *Brierley* et al.[52] using a range of precursors has demonstrated the preparation by MOCVD of $PbTiO_3$ and $Pb(Sc,Ta)O_3$ thin films. The stoichiometry and thickness of the films may be controlled by adjusting the temperatures of the precursors, the flow rate of the carrier gas and the deposition time. As with the "YBCO" system, post-growth heat treatments and/or annealing are necessary to achieve the required crystalline structure (phase). The reader could well ask what are the advantages of MOCVD for these two materials systems. The main one overcomes the inability of sputtering to maintain stoichiometry in these complex oxides and the other removes the need with spray pyrolysis to perform the deposition sequentially in order to build up film thickness. Also in this context, our experiences with laser ablation from single targets of $PbTiO_3$ and/or $Pb(La,Zr)TiO_3$ have demonstrated that it is extremely difficult to retain film stoichiometry and obtain the pervoskite phase.[53]

9. Conclusion

In this review, I have attempted to cover certain materials aspects of MOCVD. What is readily apparent is the tremendous versatility of the MOCVD processes and their applicability to the preparation of a wide range of important materials systems. Thin film epitaxial structures of widely varying but controlled compositions and thicknesses can be prepared with complete certainty and we appear to be confined at present only by the limited range and purity of available precursors. We are also beginning to understand the fundamentals of the growth processes that involve complex combinations of gas phase and surface phenomena. Progress in this area will remove the empiricism currently dominating our quest for better and novel starting materials. The entire field appears to have an exciting future and should contribute to the development of advanced materials for many years to come.

Received: June 14, 1989

[1] H. M. Manasvelt, *Appl. Phys. Lett. 12* (1968) 136.
[2] H. M. Manasvelt, W. I. Simpson, *J. Electrochem. Soc. 116* (1969) 1725.
[3] a) ICMOVPE-I Ajaccio, France 1981, *J. Cryst. Growth 55* (1981). b) ICMOVPE-II Sheffield, England 1984, *J. Cryst. Growth 68* (1984). c) ICMOVPE-III California, USA 1986, *J. Cryst. Growth 77* (1986). d) ICMOVPE-IV, Hakone, Japan 1988, *J. Cryst. Growth 93* (1988).
[4] P. D. Dapkus, *J. Cryst. Growth 68* (1984) 345.
[5] P. H. Manuel, M. Defour, C. Grattepain, F. Omnes, O. Archer, G. Timms, M. Razeghi, *Chemtronics 4* (1989) 40.
[6] M. Razeghi: *The MOCVD Challenge*, Vol. 1, A. Hilger, Bristol 1989.
[7] H. Sasaki, M. Tanaka, J. Yoshino, *Jpn. J. Appl. Phys. 24* (1985) 417.
[8] T. Fukui, H. Saito, *Jpn. J. Appl. Phys. 24* (1985) L774.
[9] R. Luckerath, P. Balk, M. Fischer, D. Grundmann, A. Hertling, W. Richter, *Chemtronics 2* (1987) 199.
[10] J. O. Williams, R. D. Hoare, M. J. Parrott, *Phil. Trans. R. Soc. (Lond.)* 1989, in press.
[11] B. A. Joyce in P. M. Dryburgh, B. Cockayne, K. G. Barraclough, (Eds.): *Advanced Crystal Growth*, Prentice Hall 1987, p. 337.
[12] A. H. Moore, M. D. Scott, J. I. Davies, D. C. Bradley, M. M. Faktor, H. Chudzynska, *J. Cryst. Growth 47* (1989) 15.
[13] A. C. Jones, *Chemtronics 4* (1989) 15.
[14] G. T. Muhr, D. A. Bohling, T. R. Omsbead, S. Brandon, K. F. Jensen, *Chemtronics 4* (1989) 26.
[15] G. B. Stringfellow, *J. Electron. Mater. 17 (4)* (1988) 327.
[16] J. O. Williams, B. Gould, unpublished results.
[17] C. J. Brierley, C. Trundle, L. Considine, R. W. Whatmore, F. W. Ainger, private communication.
[18] J. O. Williams, N. I. Dunhill, unpublished results.
[19] H. Yamane, H. Kurosawa, H. Iwasaki, H. Masumoto, T. Hirai, N. Kobayashi, Y. Muto, *Jpn. J. Appl. Phys. 27 (7)* (1988) L1275.
[20] A. C. Jones, G. Wales, P. J. Wright, P. E. Oliver, *Chemtronics 2* (1987) 83.
[21] N. D. Gerrard, D. J. Nicholas, J. O. Williams, A. C. Jones, *Chemtronics 3* (1988) 17.
[22] N. Hunt, J. O. Williams, *Chemtronics 2* (1987) 145.
[23] A. T. T. Briggs, B. R. Butler, *J. Cryst. Growth 85* (1987) 535.
[24] T. F. Kuech, E. Veuhoff, B. S. Meyerson, *J. Cryst. Growth 68* (1984) 48.
[25] J. M. Boud, M. A. Fisher, D. Lancefield, A. R. Adams, E. J. Thrush, C. G. Cureton, *Inst. Phys. Conf. Series* No. 91, 1987, p. 801.
[26] See e.g. R. J. M. Griffiths in *Abstracts of 3rd European Workshop on MOVPE*, Montpellier, France, 5–7 June 1989, p. 16.
[27] R. W. Kaliski, C. R. Ho, D. G. McIntyre, M. Feng, K. B. Kim, R. Bean, K. Zznio, K. C. Hsieh, *J. Appl. Phys. 64* (1988) 1196.
[28] J. O. Williams, *Chemtronics 2* (1987) 43.
[29] H. M. Yates, J. O. Williams, *Appl. Phys. Lett. 51* (1987) 809.
[30] J. E. Potts, H. Cheng, S. Mohapatra, T. L. Smith, *J. Appl. Phys. 63* (1987) 333.
[31] A. H. Reddoch, D. J. Northcott, J. M. Park, J. O. Williams, unpublished results.
[32] P. Demeester, A. Ackart, M. Van Ackere, F. DePestel, C. Eckhout, Y. Grigase, D. Lootens, I. Moerman, G. Van den Bossche, R. Baets, M. Bottle, P. Van Daele, P. Lagasse, *Chemtronics 4* (1989) 44.
[33] M. A. diForte-Poisson, C. Brylinski, *Chemtronics 4* (1989) 3.
[34] P. L. Maurel, M. DeFour, D. Grattepain, F. Omnes, O. Acher, G. Timms, M. Razeghi, J. C. Portal, *Chemtronics 4* (1989) 40.
[35] i) S. K. Haywood, private communication. ii) S. K. Haywood, A. B. Henriques, D. F. Howell, N. J. Mason, R. J. Nicholas, P. J. Walker, *Inst. Phys. Conf. Ser. 91* (1988) 271.

[36] R. D. Dupuis, J. P. Van der Ziel, R. A. Logan, J. M. Brown, C. J. Pinzone, *Appl. Phys. Lett. 50* (1987) 407.
[37] R. D. Dupuis, J. C. Bean, J. M. Brown, A. T. Macrander, R. C. Miller, L. C. Hopkins, *J. Electron. Mater. 16* (1987) 69.
[38] J. W. Orton, *Chemtronics 3* (1988) 129.
[39] M. J. Kelly in M. J. Kelly, C. Weisbuch (Eds.): *The Physics and Fabrication of Microstructures and Microdevices*, Springer Verlag, Berlin 1986, p. 174.
[40] A. H. Cowley, B. L. Benac, J. G. Ekerdt, R. A. Jones, K. B. Kidd, J. Y. Lee, J. E. Miller, *J. Am. Chem. Soc. 110* (1988) 628.
[41] W. E. Johnson, L. A. Schlie, *Appl. Phys. Lett. 40(a)* (1982) 798.
[42] D. J. Ehrlich, J. Y. Tsao, C. O. Bozler, *J. Vac. Sci. Technol. B3(1)* (1985) 1.
[43] S. D. Hersee, E. Barbier, R. Blondeau, *J. Cryst. Growth 77* (1986) 310.
[44] P. Demeester, P. Van Daele, R. Baets, *J. Appl. Phys. 63* (1988) 2284.
[45] A. Yoshikawa, A. Yamamoto, M. Hirose, T. Sugino, G. Kana, I. Teramoto, *IEEE J. Quantum Electron. QE-23(6)* (1987) 725.
[46] M. D. Scott, J. R. Riffat, I. Griffith, J. I. Davies, A. C. Marshall, *J. Cryst. Growth 93* (1988) 820.
[47] B. Garrett, E. J. Thrush, *J. Cryst. Growth* (1989) in press.
[48] See e.g. *Chemtronics 2* (1987) 106–140.
[49] *MRS Bulletin xiv(i)* (1989) 20–67.
[50] H. Yamane, H. Kurosawa, H. Iwasaki, H. Masumoto, T. Hirai, N. Kobayshi, Y. Muto, *Jpn. J. Appl. Phys. 27(7)* (1988) L1275.
[51] J. O. Wiliams, N. J. Dunhill, *Chemtronics 4* (1989) in press.
[52] C. J. Brierley, private communication.
[53] J. O. Williams, J. Simpson, unpublished observations.
[54] B. A. Joyce, *Adv. Mater. 1989*, This issue; *Angew. Chem. Int. Ed. Engl. Adv. Mater. 28* (1989) No. 8; *Angew. Chem. Adv. Mater. 101* (1989) No. 8.
[55] Taken from J. M. Rowell, *Sci. Am.* (Oct. 1986) p. 132.

Communications

Manuscripts intended for publication as communications should be sent to ADVANCED MATERIALS PO Box 101161, D-6940 Weinheim, FRG. Authors are requested to consult the "Instructions to Authors" which are reproduced in the January issue of the journal or are available from the editorial office on request.

Siloxane Copolymers with Laterally and Terminally Attached Mesogenic Side Chains**

By *G. W. Gray**, *J. S. Hill* and *D. Lacey*

In view of the demand for liquid crystal polymers of different types[1] with certain specific physical characteristics, many workers have considered how this could be met through synthesizing copolymers containing two or more terminally attached mesogenic side chains, and tuning the properties of the polymers by variation of the type and ratio of the side chains. In this way, using the smectic-depressing properties of a lateral methyl substituent, a nematic side-chain polysiloxane with a proportion (but only up to 32%) of terminal cyano-groups and positive dielectric anisotropy was first produced.[2]

Acrylate polymers containing mesogenic groups attached laterally to the backbone were first reported by *Finkelmann*,[3] and analogous polysiloxanes have since been reported by *Gray* et al.[4] and *Keller* et al.[5] These are predominantly nematic materials, and by synthesizing a series of novel siloxane copolymers containing varying amounts of terminally *and* laterally attached mesogenic groups, we now show that a further degree of flexibility is provided for the development of liquid crystal polymers with defined physical characteristics for applications in areas such as integrated optics,[6] optical storage,[1,7] gas liquid chromatography,[1] and NCAP displays,[8] e.g. nematic polysiloxanes containing 80–85% of cyanosubstituted side chains, and having a range of dielectric properties of technological interest.

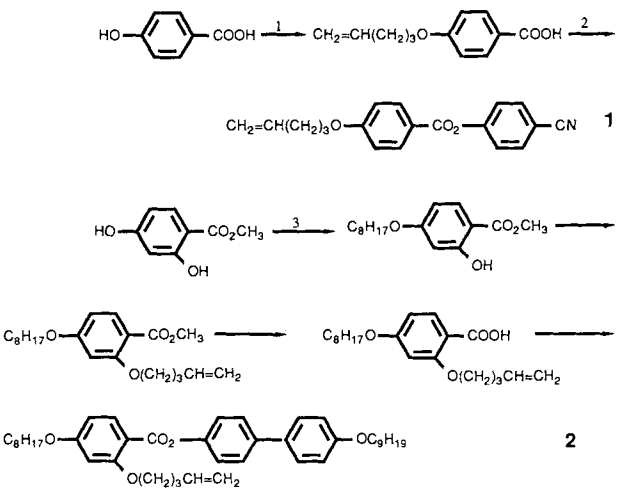
[*] Prof. G. W. Gray, Dr. J. S. Hill, Dr. D. Lacey
School of Chemistry, The University of Hull,
Hull, HU6 7RX (UK)

[**] The authors thank the Science and Engineering Research Council for financial support of the research of which this work was a part.

Experimental

For the precursor of the *terminally* attached moiety we chose the alkene **1**, which gives a crystalline smectic homopolymer with relatively high melting and clearing points. Most laterally attached polysiloxanes which have been prepared to date are nematogenic and have a glass transition. We chose as the *lateral* comesogenic precursor the alkene **2** which has been prepared in our laboratories, and gives a typically low T_g, low T_{N-I} homopolymer.

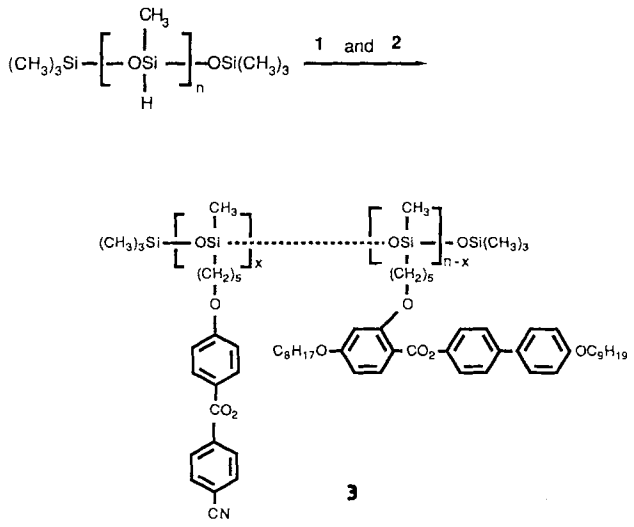
The synthesis of those compounds using standard procedures is shown in scheme 1.



Scheme 1.

The copolymers were prepared by hydrosilylation of the alkenes in toluene at 70 °C for 18–24 h (Scheme 2), using poly(hydrogenmethylsiloxane) obtained from Wacker Chemie (DP ~46, $\gamma \sim 2.2$); a 1.1 molar excess of the mixture of alkenes was used, with platinum divinyltetramethyl disiloxane as the catalyst. Purification was effected by repeated precipitation of the polymers from dichloromethane solution with 3:2 v:v methanol:ether, and subsequent centrifugation. The pure polymers were dried in vacuo in the isotropic state.

ADVANCED MATERIALS



Scheme 2.

The relative proportions of the mesogenic side chains in each polymer were determined by ^{1}H NMR. The terminal-lateral ratio in each copolymer was found to be greater than the ratio of the alkene precursors used in the feedstock for the original reaction. This implies that the overall rate of hydrosilylation is greater for the terminal than for the lateral mesogen, and is probably explained by the greater steric hindrance to the approach of the lateral moiety to the reaction site.

The thermal properties of the polymers were determined by differential scanning calorimetry and optical microscopy. The results are summarized in Table 1, and a graphical illustration of these results is given in Figure 1.

Table 1. Transition temperatures (°C) and enthalpies of transition (ΔH, in brackets, cg^{-1}) for polymers of structure **3**

% terminal	% lateral	K–S_A maximum	T_g midpoint	S_A–I maximum	S_A–N maximum	N–I maximum
100	0	107		184		
98	2	95.0		174.9		
		(1.18)		(0.86)		
95	5	62.0		139.8		
		(1.5)		(0.68)		
92	8		11.5	134.8		
				(0.56)		
86	14		13.5		130.8	134
84	16		10.8			116.6
						(0.4)
80	20		10.9			108.3
						(0.31)
70	30		1.9			72.7
						(0.26)
58	42		6.3			69.2
						(0.17)
44	56		10.7			58.9
						(0.11)
19	81		9.9			59.3
						(0.20)
0	100		4.8			58.0
						(0.17)

K = crystal; S_A = smectic A; N = nematic; I = isotropic liquid

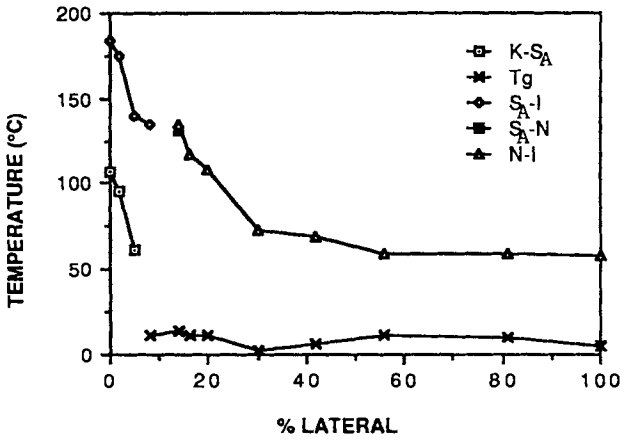


Fig. 1. Thermal properties of siloxane copolymers w.r.t. the proportion of laterally attached mesogens.

The main features of this copolymer system are summarized below.

(a) The introduction of only small amounts of the lateral side-chain component into the predominantly terminally cyano-substituted polymer has been shown for the first time to have very striking effects, whereas introduction of small amounts of the terminal side-chain component into the predominantly laterally substituted polymer has very little effect.

(b) Very low concentrations (2–5%) of the laterally attached side chain decreased both T_m and T_{S-I}, and with $\geq 8\%$, glass transitions were observed.

(c) On increasing the lateral side-chain content to 14%, a narrow range nematic phase appeared to be introduced (DSC) above the S_A phase, and with $\geq 16\%$, the polymers exhibited nematic phases only.

(d) The marked increases in the isotropization temperatures ceased with $\geq 30\%$ of lateral side-chain component, and the T_{N-I} values became fairly constant. Apart from minor fluctuations, the T_g values remained about the same for $\geq 8\%$ of lateral side-chain component.

X-ray diffraction studies (University of Bristol) and dielectric studies (University of Swansea) are currently being undertaken on these copolymers.

Through this system, we have demonstrated the possibility of tuning the thermal and mesomorphic properties of conventional siloxane polymers with terminally attached side chains by the introduction of a laterally attached comesogenic component. This is exemplified by the introduction of a glass transition, and the change from a purely smectic to a purely nematic polymer system.

At the same time, we have shown that one may introduce both small and large (up to 70%) amounts of mesogenic side chains containing cyano-groups into a laterally attached side chain polymer so that the dielectric properties may be changed considerably without significantly affecting the thermal properties of the original polymer.

This method of using mixed lateral-terminal side-chain copolymers to tune properties may be extended to other side-chain liquid crystal polymer systems such as polyacrylates and condensation polymers.

Received May 11, 1989

[1] C. B. McArdle (Ed.): *Side Chain Liquid Crystal Polymers*, Blackie, Glasgow 1989.
[2] P. A. Gemmell, G. W. Gray, D. Lacey, *Mol. Cryst. Liq. Cryst. 122* (1985) 205.
[3] F. Hessel, H. Finkelmann, *Polym. Bull. 14* (1985) 375.
[4] G. W. Gray, J. S. Hill, D. Lacey, M. S. K. Lee, G. Nestor, K. J. Toyne, M. S. White, *12th. Int. Liq. Cryst. Conf.* Freiburg, FRG, August 15 1988, Abstract P003.
[5] P. Keller, F. Hardouin, M. Mauzac, M. F. Achard, *Mol. Cryst. Liq. Cryst. 155* (1988) 171.
[6] H. Finkelmann, *Adv. Mater. 1988*, 1019; *Angew. Chem. Int. Ed. Engl. 27* (1988) 987; *Angew. Chem. 100* (1988) 1019.
[7] T. Nakamura, T. Ueno, C. Tani, *Mol. Cryst. Liq. Cryst. 169* (1989) 167.
[8] P. Drzaic, K. Verner, *Inf. Disp. 5* (1989) 6.

Polymers with a High Refractive Index and Low Optical Dispersion

By *Hans-U. Simmrock, Alfred Mathy, Ligia Dominguez, Wolfgang H. Meyer** and *Gerhard Wegner*

Materials for use in optics are usually characterized in terms of their refractive index n_D and their Abbe number ν_D which describes the wavelength dependence of the refractive index, the optical dispersion ($\nu_D = (n_D - 1)/(n_F - n_C)$ where n_D, n_F and n_C are the refractive numbers of the material at the wavelengths of the spectral lines of Na, F and C respectively).

In the n_D vs. ν_D diagram the regime of materials which combine high refractive indices with high Abbe numbers used to be exclusively occupied by inorganic glasses. Transparent polymers range from $n_D = 1.33$ to $n_D = 1.73$. However, polymers with high n_D values usually have low ν_D values and vice versa. For example, the data corresponding to two optically extreme polymers are: $n_D = 1.675$ and $\nu_D = 19$ for poly-*N*-vinylcarbazole and $n_D = 1.345$ and $\nu_D = 83$ for Teflon FEP (Fig. 1). Thus, the combination of high refractive index with low optical dispersion in polymers appeared until now to be unachievable.[1]

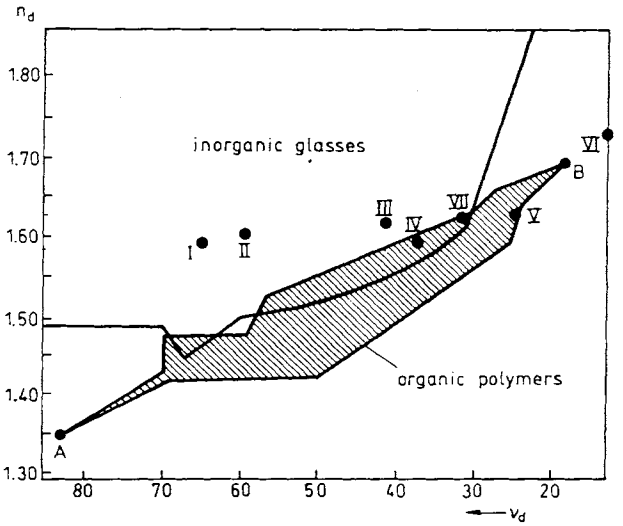


Fig. 1. Refractive indices and optical dispersion of ionenes and other materials: n_D vs. ν_D diagram. I, II, III, IV, V, VI and VII: Ionenes are defined in Table 1. A: Teflon FEP, B: Poly-*N*-vinylcarbazole.

[*] Dr. W. H. Meyer, Prof. G. Wegner,
Dr. L. Dominguez, Dr. A. Mathy, Dr. H.-U. Simmrock
Max Planck Institute for Polymer Research,
P.O. Box 3148, D-6500 Mainz (FRG)

Numerous efforts have been made in the past to extend the polymer regime towards higher indices and lower dispersion. We report here a successful approach using polyelectrolytes, in which the optical parameters can be adjusted by varying the structure of the polymer *and* by the proper choice of the counterions.[2] We use polyelectrolytes of the type **1**, which are also known as "Ionenes" (Io), with the main chain segments R^1, R^2 and the side chains R^3, R^4 being organic moieties (e.g. aliphatic groups), and X = monovalent (q = 1) or divalent (q = 0.5) counterions. The solid state properties of such polyelectrolytes are usually scorned as being "salt-like". Indeed, ionenes with R^1 and R^2 being relatively short aliphatic segments, due to their high charge density, are highly crystalline materials with physical and chemical properties resembling those of inorganic salts.[3]

1 $\quad \dagger R^1-N(R^3)_2-R^2-N(R^4)_2\dagger_n 2 \cdot n \cdot q \cdot X$

However, ionenes where R^1 and R^2 are larger organic components with low charge density have more polymer-like properties. They can be processed from the melt or from solution to form glassy films with excellent optical transmission in the visible and near-UV (Fig. 2). In such ionene glasses ionic conductivity has been recently demonstrated.[4]

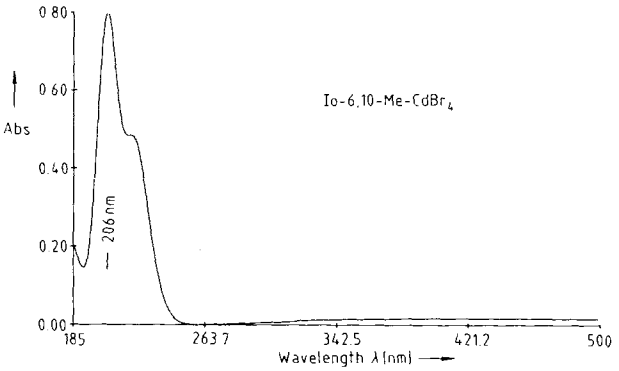


Fig. 2. UV-VIS-Absorption spectrum of a typical ionene-film (thickness: 1 μm; Io-6, 10-Me-$CdBr_4$ defined as in Table 1).

Recrystallization can be suppressed and long-term stability of the glassy state can be obtained by introducing a certain amount of irregularity along the polymeric structure such as in copolymers ($R^1 \neq R^2$) by using isomeric mixtures and by combining rigid and flexible chain segments. By these means the thermal behavior and the processibility of the materials can also be greatly influenced. For example: the glass transition temperature of Io-10-Et-BF_4 ($R^1 = R^2 = (CH_2)_{10}$; $R^3 = R^4$ = ethyl; X = BF_4) is $-22\,^\circ C$, while that of Io-Do,Pip-Me-$CdBr_4$ ($R^1 = -CH_2-CH=CH-CH_2-$; $R^2 = -cyclo\text{-}NC_5H_9-(CH_2)_3-cyclo\text{-}C_5H_9N-$; $R^3 = R^4$ = methyl; X = $CdBr_4$) is $+191\,^\circ C$. The thermal properties and relaxation phenomena in glassy ionenes have recently been discussed in detail elsewhere.[4]

ADVANCED MATERIALS

In contrast to ordinary polymers the counterions in polyelectrolytes provide an additional parameter by which the material properties can be influenced. With respect to the optical properties of ionenes the choice of counterion, turned out to be decisive: Due to the relatively simple structure of the polymer backbone a refractive index without counterions of only about 1.5 can be expected, while by the proper choice of X n_D can be shifted to 1.7 and higher.

Different counterions can be introduced into ionenes by metathetical ion exchange in solution following one of the experimental procedures described in detail elsewhere.[5] By these means materials with purities better than 99% with respect to the counterions can be obtained. Another possible method for counterion exchange in the glassy material are concentration or electrochemically driven diffusion processes.

For the optical measurements about 1 μm thick transparent films were obtained by spincoating from dimethylformamide (DMF) solutions. The optical parameters of the films were determined with a prism coupler as described in detail by *Ulrich* and *Torge*.[6, 7] The prism coupler can be used to determine the refractive index and the thickness of a light-guiding thin film. Both parameters can be obtained simultaneously and with good accuracy (n_D better than $\pm$ 0.0005) by measuring the coupling angles at the prism and fitting them to a theoretical dispersion curve. Using laser light of different wavelengths, the wavelength dependence of the refractive index and thus the Abbe-numbers can also be determined.

The optical parameters of a selection of different ionenes are compiled in Table 1 and displayed in Figure 1.

Obviously, with refractive indices between 1.58 and 1.72 and Abbe-numbers up to 65 the ionenes have intruded into the regime of inorganic glasses. When comparing ionenes with polymers with identical backbone structures but different counterions the influence of the polarizability of X on the refractive index can be substantiated: e.g. Io-6,10-Me-$CdBr_4$ exhibits an $n_D = 1.5858$, while the corresponding ionene combined with the more polarizable CdI_2Br_2 exhibits an $n_D = 1.6250$.

Similarly, the absorption of the counterions plays a rôle in the dispersion: a couterion absorbing in the UV such as $CdBr_4$ gives rise to a relatively low dispersion, whereas a counterion absorbing closer to the visible such as CdI_2Br_2 gives rise to a higher dispersion.

With the determination of the optical parameters by the prism coupler method the applicability of polyelectrolyte glasses as waveguiding material has been demonstrated. Since the choices are so manifold for the backbone structures and the counterions, a great variety of materials with tailor-made optical and other physical as well as chemical properties can be made. Therefore, the application of this class of materials in optics appears to be very promising.

Table 1. Chemical structures and optical properties of selected ionenes.

No. [a]	Ionene	R^1 [b]	R^2 [b]	R^3 [b]	R^4 [b]	X [b]	n_D	ν_D
I	Io-Do,10-Me-$ZnBr_4$	$CH_2-CH=CH-CH_2$	$(CH_2)_{10}$	CH_3	CH_3	$ZnBr_4$	1.5911	65.0
II	Io-Do,Pip-Me-$CdBr_4$	$CH_2-CH=CH-CH_2$	*cyclo*-$NC_5H_9-(CH_2)_3-$ *cyclo*-C_5H_9N	CH_3	[c]	$CdBr_4$	1.6018	59.7
III	Io-Do,Pip-Me-BPh_4	$CH_2-CH=CH-CH_2$	*cyclo*-$NC_5H_9-(CH_2)_3-$ *cyclo*-C_5H_9N	CH_3	[c]	BPh_4	1.6142	41.0
IV	Io-6,10-Me-$CdBr_4$	$(CH_2)_6$	$(CH_2)_{10}$	CH_3	CH_3	$CdBr_4$	1.5858	37.6
V	Io-6,10-Me-CdI_2Br_2	$(CH_2)_6$	$(CH_2)_{10}$	CH_3	CH_3	CdI_2Br_2	1.6250	24.6
VI	Io-6,Do-Et-HgI_4	$CH_2-CH=CH-CH_2$	$(CH_2)_6$	CH_2CH_3	CH_2CH_3	HgI_4	1.7245	13.2
VII	Io-6,10-Me-ZnI_2Br_2	$(CH_2)_6$	$(CH_2)_{10}$	CH_3	CH_3	ZnI_2Br_2	1.6260	31.6

[a] Numbers corresponding to Fig. 1. [b] Defined as in structure **1**. [c] Due to cyclic structure only one CH_3 group.

Received June 14, 1989

[1] H. Dislich, *Angew. Chem. Int. Ed. Engl. 18* (1979) 49; *Angew. Chem. 91* (1979) 52.
[2] German patent application P 39 12 244.7 (1989).
[3] L. Dominguez, W. H. Meyer, *Solid State Ionics 28/30* (1988) 941.
[4] F. Kremer, L. Dominguez, W. H. Meyer, G. Wegner, *Polymer*, in press.
[5] L. Dominguez, W. H. Meyer, G. Wegner, *Makromol. Chem. Rapid Commun. 8* (1987) 151.
[6] R. Ulrich, R. Torge, *Appl. Opt. 12* (1973) 2901.

[7] The authors are indebted to Dr. *Christoph Bubeck* for the optical equipment.

In future issues, regular series will be run in the Research News section on Biomaterials (G. Heimke), Interfaces and Joining (G. Partridge), Surface Analysis (J. Rabe), Diamond Films (P. Bachmann) and Polymers (M. Ballauff) amongst others. Further contributions on any new developments in materials science are welcome, the articles (4–5 pages manuscript plus 1 or 2 figures) being assessed by the Editorial Advisors and the Editorial Staff. Manuscripts should be sent to ADVANCED MATERIALS P.O. Box 101161 D-6940 Weinheim, FRG.

ADVANCED MATERIALS

Research News

Gauge Theory – A New Outlook on Solid State Dynamics

By Stanley Clough *

Occasionally in science a new outlook arises which radically changes perceptions and genuinely deserves the overworked description "breakthrough". Such an event has occurred recently in the recognition of the fact that the dynamics of condensed matter must be described by gauge theory.[1-3] A consequence has been to throw new light on the hitherto dark and mysterious relationship between the quantum and classical descriptions of solid state dynamic processes. A sound basis is provided for classical models and attention is now focused on new phenomena which can be expected when neither pure quantum nor pure classical descriptions are appropriate. The most important consequence however, is that the incorrect procedure and concepts which have been commonly used are highlighted.

One of the problems about understanding the properties of materials is the need to choose either a quantum mechanical or classical description, when the relationship between the two descriptions can be quite obscure. This is in spite of the existence of phenomena which are clearly quantum mechanical at low temperature but better described classically at high temperatures. A hybrid theory which would encompass both regimes has never existed. Its non-existence has even been part of a dogma which insists that only the mysterious Copenhagen interpretation links the two types of theory. It is as if we had to use two different languages in the north and the south of a country with no guidance about what to do in the middle. Nature, we were told, is like that. Now it appears that nature is more sensible. We were leaving out key features called symmetry breaking and *Berry*'s phase. Now the two languages are revealed as different dialects of the same language and one merges smoothly into the other. The hybrid theory that spans both quantum and classical regimes exists. It is gauge theory.

Berry's discovery was that there are two ways in which the phase of an eigenfunction can advance, not one as previously supposed. Quantum mechanics had been structured to handle the motion of one system but not two, and the phase associated with one system driving another had been overlooked. Not for the first time, science had mistaken a special case for the general one. The analysis of most problems of condensed matter involves a decomposition of the whole sample into two parts, a subsystem whose motion is to be described and a thermal heat bath where the effect of the latter on the former is crucial to the description. Regarding the subsystem to be isolated leads to a set of eigenstates and eigenvalues for the subsystem with the latter controlling the evolution of the phase of the wave function. When the interaction with the heat bath is switched on, the state of the subsystem changes and a new way in which the phase of its wave function can change comes into play.

The idea which makes these statements tangible is symmetry breaking. In order to swim a spherical creature must deform to create a paddle. In the same way, the symmetry of an isolated system is broken when it interacts, and one or more new coordinates are created through the interaction. Symmetry breaking is a common occurrence throughout physics and is usually discussed by means of a schematic diagram like Figure 1. This represents a potential energy surface with the shape of the bottom of a wine bottle, i.e., a central maximum surrounded by a circular trough. Superimposed on the central maximum is a deep minimum which

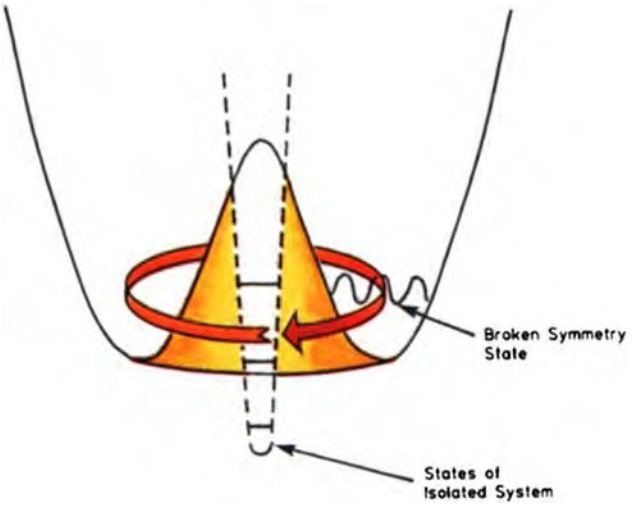


Fig. 1. A schematic representation of symmetry breaking and the consequent appearance of a new quasi-classical coordinate. An isolated system is represented by the central minimum. The state of a thermally interacting system is described by a wave packet in the circular trough, combining both quantum and quasi-classical features, the latter arising from the *Berry*'s phase associated with motion around the trough.

[*] Prof. S. Clough
Department of Physics
University of Nottingham
Nottingham NG7 2RD (UK)

represents the isolated system with its set of energy levels. When the interaction with the surroundings is turned on, the symmetry breaks and the wine bottle potential comes into play. The state of the subsystem is now a wave packet located in the circular trough and the new coordinate generated by the interaction is the position in the trough. The interacting environment drives the wave packet around the trough and this is the motion which leads to the acquisition of *Berry*'s phase. The dynamics therefore require specification of the wave packet as a linear combination of the states of the isolated system, and also the driven motion around the trough. At high temperatures the wave packet is a mixture of many states of the isolated system, averaging out the quantum motion, and the wave packet becomes localized so that its motion in the trough acquires a classical particle-like character. In this way there is a smooth progression from the almost pure quantum behavior of a weakly driven system at low temperature, when the energy levels determine the dynamics, to the quasi-classical behavior of a thermally driven system at high temperature. In the light of this description it is easy to see how earlier discussions, which attempted to describe the temperature dependence only in terms of the states of the isolated system (being unaware of the symmetry breaking, the motion associated with the new coordinate(s) and *Berry*'s phase) were handicapped.

The history of gauge theory and how it finally arrived in solid state physics is an interesting story. Its origin is the most radical idea of the century, *Einstein*'s geometrization of gravitation in his theory of general relativity. *Newton*'s force of gravity was replaced by a curvature of space into time. The notion that other forces might be represented (or replaced) by curved spaces was immediately taken up by *Weyl* in 1919 in the first gauge theory which was an example of an idea before its time. Its somewhat unhelpful name dates from this period. The problem was that no other space could be imagined into which the xyz space could be curved. It was not until the advent of quantum mechanics, when the phase of a wavefunction could be identified as a kind of additional particle coordinate in an intangible "internal" space, that the nature of the curvature in *Weyl*'s theory could be recognized. Two sub-spaces may be said to be curved into each other if a displacement through one entails a shift in the other. Thus moving a clock in a gravitational field results in a change of its time rate because space-time is curved. The gravitational field determines the magnitude of the effect and is a measure of the curvature. Similarly, a quantum particle moving in a region in which the external xyzt space time is curved into the "internal" space, experiences a change in the internal coordinate, i.e. the phase of the wave function. This provided a brilliantly simple description of electromagnetism and the foundation for particle physics theories. However, gauge theory became associated with the intangible "internal" spaces and its application to the more mundane problems of condensed matter was overlooked.

The wave function of a charged particle moving through a space–time vector dr experiences a phase change q (A. dr) where A is the electromagnetic vector potential. Thus electromagnetism can be recognized as a gauge theory arising from the existence of a very simple internal charge space. The six components of the electromagnetic field, E_x, E_y, E_z, B_x, B_y and B_z represent the curvature of the internal space into xyzt measured in the planes xt, yt, zt, yz, zx, and xy, respectively. The internal charge space is experienced only by particles carrying electric charge and can be visualized as a circle of values between 0 and 2π. All electromagnetism follows from this. The curvature is due to the presence of other charges, so that the interaction between charges occurs as each charge modifies the curvature of the space through which other charges move.

The elaboration of the theory for more complex internal spaces laid the foundation for theories of the nuclear forces between fundamental particles, which resulted later in the spectacular successes of the electro-weak theory for the unified electromagnetic and weak nuclear interactions, and quantum chromodynamics for the strong interaction. In these theories the curvature is quantized with the appearance of exchange particles like the photon in electromagnetism. A further element in the argument was required to account for the mass of the exchange particles associated with the weak interaction. This crucial element is symmetry breaking.

Solid state physics remained largely isolated from these developments of the 60's and 70's. There were warning signals that it had adopted some false concepts, but there were also standard explanations which covered up the contradictions. Then in 1984/5 the term *Berry*'s phase (or the topological phase) began to be heard and to become very common in titles in Physical Review Letters. *Berry*'s innovation[1] was to consider the evolution of the wave function of a driven system rather than a dynamically isolated one. He showed that it acquired an extra phase (*Berry*'s phase) dependent on the geometry of the driven trajectory. *Simon*[2] saw at once that this phase was a consequence of the trajectory of the driven system occurring on a curved space, and *Wilczek* and *Zee*[3] recognized the mathematical structure of gauge theory. It had finally arrived in solid state physics.

It should have been no surprise. Most problems in the solid state require a division into a subsystem P and its thermal environment Q. If subsystem P drives subsystem Q then the coordinates of the two subspaces P and Q cannot remain pure. The spaces are curved into each other and the curvature replaces the forces which each exerts on the other. Space Q acts as an "internal" space for P, and vice versa. The interaction of such systems is described by gauge theory. This means that the differential momentum operator $\partial/\partial x^P$ is replaced by the covariant derivative $D = ((\partial/\partial x^P) + iA)$. This is the prescription for differentiating on a curved x^P surface. A is a vector potential which describes (through the derived field) the curvature of the surface. It depends on the state of the interacting subsystem Q and therefore allows one subsystem (the heat bath) to drive the other (the system under examination). The curvature introduced by the inter-

action changes the space of the isolated system and is responsible for symmetry breaking.

The story so far can be summarized by saying that gauge theory is the universal description for forces between interacting systems. To understand its importance for condensed matter science, it is necessary to appreciate the bad state the latter has fallen into because of the lack of awareness of curvature. Briefly, solid state physics exists in curved spaces which have been treated as flat. Some of the consequences of curvature have been introduced in an ad hoc way and some left out. Naturally this has caused confusion. The confusion has been concealed by a set of concepts which have been developed to make physical sense out of false theoretical structure. Gauge theory with symmetry breaking blows away this conceptual smoke-screen and replaces the rather abstract mysteries by a much simpler set of ideas.

The simplest example of solid state dynamics which illustrate these matters is the hindered rotation of symmetrical molecular groups like CH_3 or NH_4 in crystals. At low temperature these exhibit clear quantum mechanical tunneling motions and at high temperatures their rotation can be described in terms of classical hopping between the wells of the hindering potential. The discrete quantum phenomena at low temperature can be accounted for by the cyclic boundary condition $\psi(\Phi) = \psi(\Phi + 2\pi)$, where Φ is the rotation coordinate. This is normally justified by the statement that the wavefunction must be single valued. In fact it only applies to the special case where the group is dynamically isolated. If it interacts with the environment so that the two move together in a correlated way then the boundary condition takes the form $\psi(\Phi) = \psi(\Phi + 2\pi)\exp(iy)$ where y is connected with the movement of the environment. The phase factor y is *Berry*'s phase and for a methyl group it is connected with the thermally activated rotation rate. At low temperatures y is small and the effect of the boundary condition is to allow only a small number of rotational states. For the methyl group these are three in number known as A, E^a and E^b, the latter pair being degenerate. The energy difference between the A and E levels is the tunnel splitting. This determines the frequency whose reciprocal specifies a time during which an additional phase y is acquired. At higher temperatures the root mean square value of y grows. When it is of the order π, the boundary condition has lost its restrictive character and a broad band has replaced the discrete levels. In short, thermal broadening has occurred clearly related to the rate of driven rotation. The magnitude of the broadening becomes identifiable as the reciprocal of the correlation time for the driven rotation as assumed in purely classical theories.

The intervention of the environment in defining $\Phi + 2\pi$ relative to Φ curves the one dimensional Φ space which may be regarded as being changed from a flat circle into a helix. This symmetry breaking is the key to an understanding of how classical mechanics can emerge from quantum mechanics. Symmetry breaking is an inevitable consequence of interactions, as for example, when two previously spherical atoms form a chemical bond. Methyl rotation is just the simplest example but the conclusions apply quite generally. The effect of the environment breaks the symmetry of the isolated system, introduces new coordinates which are embryonic versions of the classical ones, and as the fluctuations of the environment come to dominate, a smooth transition from quantum to classical behavior occurs.

How has solid state physics managed so long without these concepts? Without the broken symmetry and its quasi-classical coordinate and associated *Berry*'s phase, the attempt has been made to explain quantum damping or motional broadening only in terms of the levels in the central minimum of Figure 1. The observable broadening now attributable to *Berry*'s phase was wrongly accounted for by life time broadening of the levels due to incoherent transitions between them, though how the rate of thermal transitions between levels could be measured in thermal equilibrium was not explained. Since vibrational excitation clearly has nothing to do with rotation, it led to a curious doctrine of separation. This supposed there to be two kinds of concept, quantum and classical, and asserted that no theory should contain both. Thus rotation is a classical concept, along with torque, and according to this doctrine should not figure in a quantum theory. This made the absence of driven rotation into a principle, which was reassuring but wrong. In the central minimum there is no motion clockwise or anticlockwise because time-reversal symmetry remains unbroken, but the quantum motion can be described as a kind of bidirectional motion, both clockwise and anticlockwise simultaneously. It was then argued that the Copenhagen interpretation meant that the apparent bidirectional motion was to be interpreted statistically as either clockwise or anticlockwise rotation. This introduced rotation but it had nothing to do with the broadening and nothing to do with the lattice. Using such devices, a conceptual gap was concealed for many years. The new insights of gauge theory solve many problems simultaneously and carry the weight of established success in relativity, electromagnetism and particle physics. The new developments represent a long delayed achievement of a unified approach to interactions across the whole of Physics.

[1] M. V. Berry, *Proc. R. Soc. A 392* (1984) 45.
[2] B. Simon, *Phys. Rev. Lett. 51* (1983) 2167.
[3] F. Wilczek, A. Zee, *Phys. Rev. Lett. 52* (1984) 2111.

ADVANCED MATERIALS

Imaging Organic Molecules with the Scanning Tunneling Microscope

By Jürgen P. Rabe*

Atomic resolution has become a common feature in Scanning Tunneling Microscopy (STM) of inorganic semiconductor surfaces, both in vacuum and in a number of fluid ambients. A review has been given recently in this journal.[1] Moreover, the physics involved in the imaging process for these materials is well enough understood to allow detailed electron-spectroscopic investigations on an atomic scale to be performed. For organic materials, however, the method is much less developed. Clearly, this cannot be attributed to a lack of interest but rather to the characteristics of organic systems; above all the lack of electrical conductivity. In an attempt to circumvent this particular problem the imaging of single organic molecules as they are adsorbed on a conducting substrate has been attempted, since in this case the distance required for the probing electrons to tunnel is minimized. However, for these systems another typical feature of organic materials, molecular mobility, may still remain a problem. To date, due to these difficulties, only few systems have successfully been imaged by STM and it is this lack of experimental data which contributes to a third problem, namely the lack of a good understanding of the contrast mechanism in STM imaging of organics. Therefore, it is of particular interest that recently a number of new organic systems have been imaged.

In Figure 1 an STM image of Cu-phthalocyanine on Cu(100) is shown as obtained under ultra-high vacuum conditions by *Lippel* et al.[2] It shows isolated Cu-phthalocyanine molecules adsorbed flat with two different rotational orientations. Notably, studies of the same adsorbate on Ag(111), Au(111) and Si(111) 7×7 surfaces gave considerably less clear and stable images, indicating that the STM can resolve the internal structure of a flat isolated molecule, provided that the interaction between adsorbate and substrate is strong enough to sufficiently reduce molecular motion. The important question of contrast generation is also addressed by the authors. They interpret their images as representing the charge distributions of free molecule states near to the Fermi level. Like in the case investigated earlier[3] of benzene and carbon monoxide coadsorbed on Rh(111), the authors favor this explanation rather than an adsorbate induced change of the local work function.

In Figure 2 another high resolution STM image obtained by *J. K. Spong* et al.[4] is shown: The adsorbate layer at the interphase between a conducting solid substrate (graphite) and a liquid crystalline ambient (5-nonyl-2-*n*-nonoxylphenylpyrimidine). This example is representative of a whole

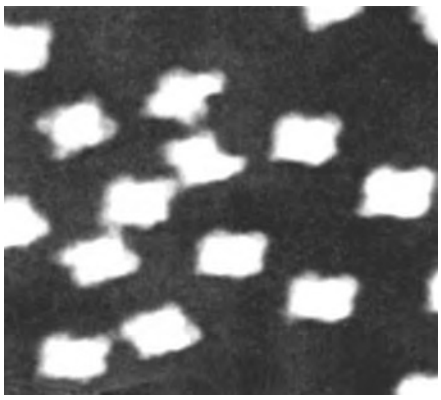


Fig. 1. STM image of Cu-phthalocyanine on Cu(100), as obtained by *P. H. Lippel* et al. [2]. The isolated molecules are adsorbd flat with two different rotational orientations. The scan dimensions are 15 nm × 15 nm.

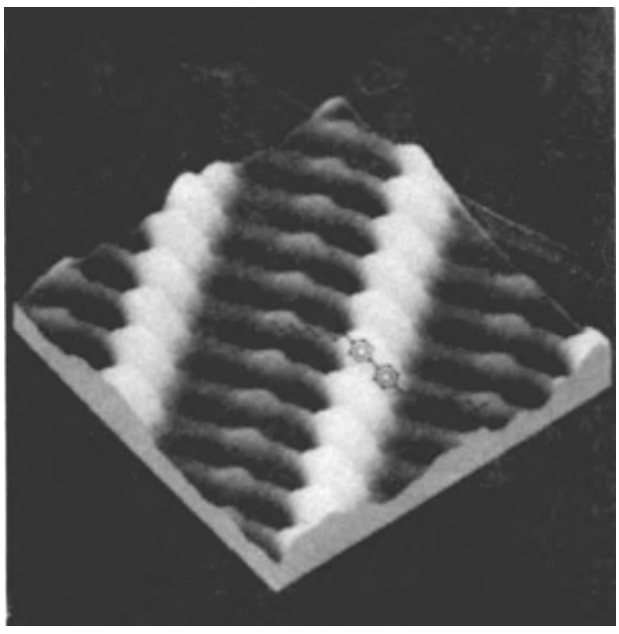


Fig. 2. Three dimensional display of an STM image of 5-nonyl-2-*n*-nonoxylphenylpyrimidine on graphite, as obtained by *J. K. Spong* et al. [4]. The scan dimensions are 4.3 nm × 5.2 nm. The image has been unit cell averaged.

[*] Dr. J. P. Rabe
Max-Planck-Institut für Polymerforschung
Postfach 3148, D-6500 Mainz (FRG)

class of liquid crystalline materials on graphite.[4, 5] Evidently, the molecules are imaged as they are adsorbed flat on graphite, quite like the phthalocyanine rings on copper. However, in this case no isolated molecules, but rather an ordered array is imaged. The intermolecular interaction within the monolayer may stabilize the position of any particular molecule, thereby reducing molecular motion sufficiently for STM imaging. The contrast is attributed in this case to the modulation of the local work function of the substrate by the polarizable molecular adsorbates. Indeed, functional groups which are electronically as dissimilar as benzene and cyclohexane can have similar contrast when imaged by the STM. This is explained by their comparable polarizability. However, it should be noted that alkane residues also have similar polarizabilities but give a different contrast in the STM. Obviously, the issue of contrast generation still remains a matter of debate.

A quite general way to reduce molecular motion is to increase the number of segments per molecule interacting with the substrate, a feature typical in polymer adsorption. Interestingly, high resolution STM images of DNA and double stranded RNA have recently been obtained by *T. P. Beebe* et al.[6] and *G. Lee* et al.[7] Both groups could resolve, minor and major grooves of the double helices adsorbed on graphite. However, the pitch periodicity was found to vary considerably. This can be attributed to the combined forces of the surface, partial dehydration and possibly intercalation with ionic species. To draw conclusions about the contrast mechanism is very difficult in these cases, since the samples were prepared by allowing buffer solutions of DNA and RNA to evaporate on graphite and the STM investigation was performed in air immediately after the last amounts of water were observed to evaporate. It cannot be excluded, therefore, that traces of electrolyte may contribute to the conductivity. Furthermore, it should be mentioned that due to the thickness of the molecule it is more complicated to interpret high resolution images of this material, than it was in the examples given before.

Our understanding of the processes involved in imaging organic adsorbates is considerably improving. This is both stimulating and encouraging for those working in this research area.

[1] J. P. Rabe, *Adv. Mater. (1989)* 13; *Angew. Chem. Int. Ed. Engl. Adv. Mater. 28* (1989) 117; *Angew. Chem. Adv. Mater. 101* (1989) 117.
[2] P. H. Lippel, R. J. Wilson, M. D. Miller, C. Wöll, S. Chiang, *Phys. Rev. Lett. 62* (1989) 171.
[3] H. Ohtani, R. J. Wilson, S. Chiang C. M. Mate, *Phys. Rev. Lett. 60* (1988) 2398.
[4] J. K. Spong, H. A. Mizes, L. J. LaComb Jr., M. M. Dovek, J. E. Frommer, J. S. Foster, *Nature 338* (1989) 137.
[5] J. S. Foster, J. E. Frommer, *Nature 333* (1988) 542.
[6] T. P. Beebe Jr., T. E. Wilson, D. F. Ogletree, J. E. Katz, R. Balhorn, M. Salmeron, W. J. Siekhaus, *Science 243* (1989) 370.
[7] G. Lee, P. G. Arscott, V. A. Bloomfield, D. F. Evans, *Science 244* (1989) 475.

Phase Equilibria under Stress

By Robert W. Cahn*

Ever since the Phase Rule was first formulated more than a century ago, it has been recognized that hydrostatic pressure is a variable that must affect phase equilibria; the normal neglect of this variable in the construction of ordinary metallurgical equilibrium diagrams is merely a recognition that atmospheric pressure is minimal, and a flourishing research field is centered upon the investigation of new polymorphs and new transition temperatures under large pressures. Nevertheless, in the last few years the whole field has been given a quite new impetus by a small group of thermodynamics theorists who have examined the whole issue afresh.

Before we look at these new developments, let us dispose of some of the other ways in which an applied stress can affect phase dispositions. Here the major interest attaches, not to hydrostatic pressure but to uniaxial stress – a simple tension or compression. One important category is that of martensitic transformations, as in ordinary carbon steel. Here, a phase transforms by combining a macroscopic shear with more complex localized strains. When a cubic crystal transforms, it can typically form 24 crystallographically equivalent orientations or variants. An applied stress in the elastic range will favor a few of these orientations, or even a single one, over all the others. This has often been experimentally confirmed (e.g. by *Kochendörfer* and *Müller*,[1] who in this way created virtually a single crystal of a martensitic phase). This same phenomenon is crucially involved in the much studied family of shape-memory alloys, which return to an 'imprinted' shape on gentle heating.[2]

Again, when a single crystal of a cubic disordered phase is cooled so as to create a non-cubic superlattice, then a very small applied compression can pick out one of the, e.g., three

[*] Prof. R. W. Cahn
University of Cambridge
Department of Materials Science and Metallurgy
Pembroke St., Cambridge CB2 3QZ (UK)

ADVANCED MATERIALS

possible variants to the complete exclusion of the others: this was demonstrated for the ordering transition of CuAu (cubic → tetragonal) by *Arunachalam* and *Cahn*.[3] More recently, those who study superalloys, the family of materials used in the construction of jet engines, have found that internal stresses within a two-phase alloy, resulting from a slight mismatch between the lattice parameters of the two epitactically intergrown 'coherent' phases, can modify the shapes of the dispersed phase particles. This effect can be substantial enough to cause dangerous deterioration of creep resistance. A very recent example of such an observation[4] refers to a dispersion of a phase with B2 order in a matrix with a Heusler ($L2_1$) type of order. The disperse particles form an array of tiny parallel cuboids, but on prolonged annealing a structural change takes place, a population of dislocations arises which winds down the internal stresses and the microstructure changes radically. The topic has been more generally treated by *Johnson* et al.[5]

The most recent work of this kind is also in some ways the most surprising. The long established and practically very important theory of Ostwald ripening—the coarsening of large precipitates at the expense of small ones in a nonuniform dispersion—has proved to be vulnerable. *Johnson* et al.[6] have shown that coherent misfit stresses can drastically alter the kinetics of Ostwald ripening, and can even lead to an inversion of the process, in the sense that smaller particles will grow at the expense of larger ones. One impatiently awaits experimental verification!

All of these diverse phenomena seem peripheral: in all of them, the orientation or morphology of a phase is affected by stress, but the volume fractions and compositions of the constituent phases should not at first sight be affected. A phase equilibrium is altered only when these two linked variables are changed. This is the issue addressed by the seminal work of my American namesake, *John Cahn*, and his French collaborator *Larché*.[7] They consider in quantitative detail the situation of a coherent two-phase solid in which the kind of elastic mismatch referred to above arises. In fact, as they show, both the magnitude of the lattice parameter mismatch and the detailed geometry of the two phases affect the Gibbs free energy of each phase. What this implies is that the Gibbs free energy of each phase is affected by the amount and morphology of the other phase. However, the classical tangent construction (see Figure) in which the composition and volume fraction of each phase is determined by drawing the common tangent in an isothermal plot of the Gibbs free energies of the two phases, depends on the absolute nature of these free energy plots. If the free energy of phase *A* of a certain composition depends on the volume fraction and disposition of phase *B*, then the tangent construction loses its validity. This has a striking consequence: in a binary alloy, a two-phase field is not what we are used to. Conventionally, all alloys within a two-phase field at a given temperature consist of differing proportions of two phases which always have the same compositions. Where the new theory of coherent stress-sensitive equilibria is valid, the compositions

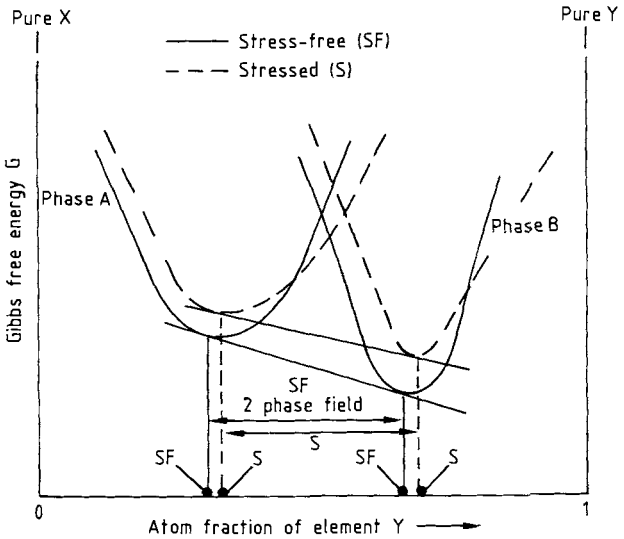


Fig. 1. Schematic diagram of the possible effect of non-hydrostatic stress (internal and external) on the free energies of two coexisting phases in the absence or presence of stress. Stress modifies the two-phase field. Only under very special conditions can the common tangent construction of free energy curves be used to depict phase equilibria in non-hydrostatically stressed solids [11].

of the two constituent phases change as the two-phase field is traversed, and the ordinary lever rule can no longer be employed to compute the volume fractions of the two phases. Somewhat similar ideas were put forward the same year[8] by the Russian theorist *Roitburd* (who is now settled in America).

These radical ideas due to *Cahn* and *Larché* have been further developed recently by two Americans, *Johnson* and *Voorhees*,[9, 10] who are making the running in this field at present. One of their conclusions is that a sort of catastrophic instability may arise so that more than one stable state is possible for the same two-phase alloy when it is subject to self-generated internal stress. The theory has also been applied to the practically important case of elastically stressed heteroepitaxial thin films,[11, 12] where the crucial rôle of coherency stresses in affecting electronic properties has been recognized for some time. The theoretical treatments have focused on elastic self-stresses (i.e., those due to lattice mismatch); the possible rôle of externally applied stresses has still to be addressed. It is clear that theory has run a long way ahead of experimental verification; it is possible that systematic experiments involving intentionally applied external stresses might go some way towards testing the theorists' predictions. Such experiments may also reveal parallels between the older work outlined at the beginning of this article and the more recent theories.

In parallel with the metallurgical literature, indeed somewhat ahead of it in point of time, has been a vigorous debate within the geological/mineralogical community concerning the rôle of non-hydrostatic stresses in phase equilibria in rocks. Phenomena such as pressure solution phenomena, crystallization under stress (the geologists call this recrystallization), shear transformations in rocks such as quartzite,

and diffusion under applied stress, and special phenomena such as the growth of Dauphiné twins in quartz crystals, are all of interest in particular to petrologists, and there has been much disagreement about the magnitude and even the sign of some of these effects. One of the leaders of this community, the Australian rock-mechanics expert *Mervyn Paterson*, some years ago wrote a masterly overview[13] of the whole field (he calls it non-hydrostatic thermodynamics) in which he sought to inject rigor into what had sometimes been a hand-waving discussion. *Paterson* does discuss coherent transitions, e.g., the α/β transition in quartz, but not from the viewpoint later developed by *Cahn, Larché, Johnson* and *Voorhees*. He is concerned here by such matters as the change in transition temperature occasioned by a uniaxial stress and how that change depends upon the crystallographic direction of that stress in a highly anisotropic crystal. It may be that the time is now ripe for a convergence of the metallurgists' and geologists' approaches.

[1] A. Kochendörfer, H.-G. Müller, *Arch. Eisenhüttenwes. 26* (1955) 291.
[2] K. Shimizu, *Trans. Jpn. Inst. Metals 27* (1986) 907.
[3] V. S. Arunachalam, R. W. Cahn, *Proc. 3rd. AIME Bolton Landing Conf.*, (Claitor's Publishing Div., Baton Rouge) 1970.
[4] L. A. Bendersky, P. W. Voorhees, W. J. Boettinger, W. C. Johnson, *Scripta Metall. 22* (1988) 1029.
[5] W. C. Johnson, M. B. Berkenpas, D. E. Laughlin, *Acta Metall. 36* (1988) 3149.
[6] W. C. Johnson, P. W. Voorhees, D. E. Zupon, *Acta Metall. 37* (1989) in press.
[7] J. W. Cahn, F. C. Larché, *Acta Metall. 32* (1984) 1915.
[8] A. L. Roitburd, *Sov. Phys. Solid State Engl. Transl. 26* (1984) 1229.
[9] W. C. Johnson, *Metall. Trans. 18A* (1987) 1093.
[10] W. C. Johnson, P. W. Voorhees, *Metall. Trans. 18A* (1987) 1213.
[11] W. C. Johnson, C. S. Chiang, *J. Appl. Phys. 64* (1988) 1155.
[12] C. S. Chiang, W. C. Johnson, *J. Mater. Res. 4* (1989) 678.
[13] M. S. Paterson, *Rev. Geophys. & Space Phys. 11* (1973) 355.

Networks Composed of Rigid Rod Polymers

By Matthias Ballauff*

The physics and chemistry of networks of rubbers is a subject of long-standing interest in polymer science. To illustrate the tremendous technical importance of this field it suffices to mention the tire industry. Considerable profit is made from the advantageous properties of materials exhibiting rubber elasticity. All network polymers used for technical purposes are composed of flexible macromolecules, and the physics of rubber elasticity has been developed based on the fact that flexible chains are crosslinked.[1, 2] In two recent publications[3, 4] *Vilgis, Boué* and *Edwards* for the first time set up a theory of rubber elasticity for networks composed of rigid rod polymers.

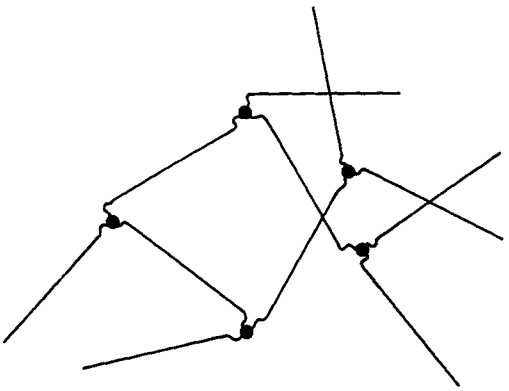


Fig. 1. Schematic representation of a network of rods connected by flexible hinges.

Figure 1 schematically depicts a rubber consisting of rods connected by flexible hinges. The first question to be asked when looking at Figure 1 is what is the degree of freedom of such a structure? More than one hundred years ago *Maxwell*[5] showed that there is a limiting functionality m_c (or an upper critical dimension) given by $m_c = 2\,d$ with d being the space dimension. This can be exemplified by considering two-dimensional networks in a simple square lattice configuration (see Fig. 2).

The functionality is four in this case which exactly corresponds to the limiting functionality in two dimensions

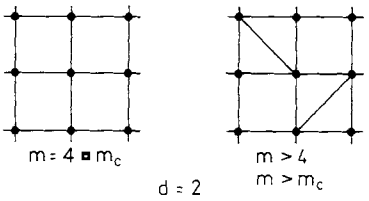


Fig. 2. Critical functionality for two dimensional networks: $m = 4 = m_c$: network can be deformed by shearing (left hand side); $m > 4$, i.e., $m > m_c$: rigid network (right hand side).

($d = 2$). This network can be deformed by shearing. If one increases the functionality beyond four by putting down rods on some diagonals (see Fig. 2) the lattice becomes entirely rigid and the elasticity is no longer of entropic nature but of a purely energic nature, i.e., deformation of this network requires the bending and elongation of bonds. The same

[*] Dr. M. Ballauff
Max-Planck-Institut für Polymerforschung
Postfach 3148
D-6500 Mainz (FRG)

argument applies in three dimensions in the case of simple cubic topology. Here the limiting functionality is $m_c = 6$.

The above named authors succeeded in elaborating a theory of rubber elasticity for rigid rod networks with $m < m_c$. The method applied is rather involved and will not be discussed here. The principal result of the calculation is shown in Figure 3.

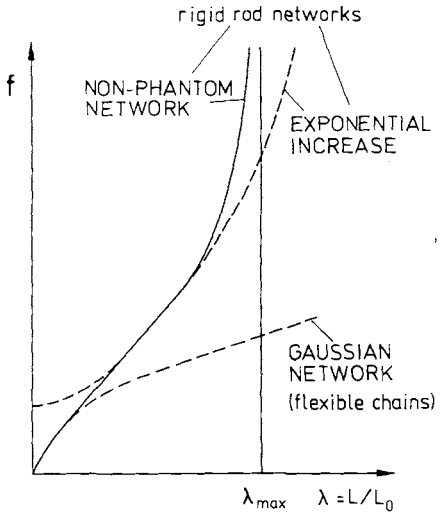


Fig. 3. Theoretical stress–strain relation of a rod network.

Here the stress per unit area f is plotted as a function of strain λ, where λ denotes the linear extension divided by the length at rest ($\lambda = L/L_0$). At low extensions the behavior resembles the results found for conventional networks.[1,2] At larger deformations the stress–strain relation crosses over to an exponential increase. Here obviously the rod-like nature of the chains within the network comes into play. It has to be noted that these results were derived for phantom networks, i.e., for systems without entanglement constraints. The authors also succeeded in including the latter effect into the model. Here theory predicts a maximum deformation at which the stress, as a function of strain, will diverge. This maximum deformation is a function of the concentration at the formation of the rod network. The physical argument leading to this divergence is again quite obvious: Due to the entanglement constraint the rods cannot move through each other but exert a mutual steric hindrance. With increasing extension of the network more and more rods will intersect and decrease the number of degrees of freedom of the system until the critical strain is reached.

This theory is the first attempt to tackle the problem of rigid rod networks. It is a mean-field approach and treats only isotropic systems. Such networks can be synthesized by simultaneous polymerization and cross-linking reaction. A totally different situation arises if cross-linking is effected in ordered liquid crystalline solutions or melts of rod-like polymers. Here the cross links would fix the liquid crystalline order even when the solvent is removed or the temperature is raised beyond the point of phase stability. This obviously provides numerous opportunities to design a whole class of new polymeric materials. The present work by *Vilgis, Boué* and *Edwards* thus could become an example for an interesting technical development preceded by theoretical ideas.

[1] P. J. Flory, *Polym. J. (Tokyo) 17* (1985) 1.
[2] T. A. Vilgis in G. Allen, J. C. Bevington, (Eds.): *Comprehensive Polymer Science*, Vol. 6, Pergamon, Oxford 1989, p. 227.
[3] F. Boué, S. F. Edwards, T. A. Vilgis, *J. Phys. 49* (1988), 1635.
[4] T. A. Vilgis, F. Boué, S. F. Edwards in C. Picot (Ed.): *The Molecular Basis of Networks*, Springer, Heidelberg 1989, in press.
[5] J. C. Maxwell, *Trans. R. Soc. Edinburgh 26* (1870), 1.

Books received:

Topics in Applied Physics, Vol. 62. – Photorefractive Materials and Their Applications II. Ed. by P. Günter and J.-P. Huignard Springer, Berlin 1989. xviii, 367 pp., bound, DM 124.— ISBN 3-540-19202-6. **Applied Superconductivity.** By A. M. Wolsky et al. Noyes, Park Ridge, USA 1989. Clothbound, USD 59. – ISBN 0-11-8155-1191-4. **Analysis of Polymers, An Introduction.** By T. R. Crompton. Pergamon, Oxford 1989. viii, 362 pp., bound, DM 165.— ISBN 0-08-033942-5. **High Temperature Corrosion of Ceramics.** By J. R. Blachere and F. S. Pettit. Noyes, Park Ridge 1989. ix, 188 pp., bound, USD 39.— ISBN 0-8155-1188-4. **The Effects of Radiation on High-Technology Polymers.** Ed. by J. H. O'Donnell and E. Reichmanis. A.C.S., Washington 1988. xi, 293 pp., bound, USD 65.95.— ISBN 0-8412-1558-8. **Epoxy Resin Chemistry II.** Ed. by R. S. Bauer. ACS, Washington 1983. x, 310 pp., bound, USD 44.95.— ISBN 0-8412-0077-1. **Ultra-Fast Silicon Bipolar Technology.** Ed. by L. Treitinger and M. Miura-Mattausch. Springer, Heidelberg 1989. ix, 167 pp., bound, DM 59.— ISBN 3-540-50638-1.

STOP PRESS: Interdisciplinary scientists sought: The Royal Society of Chemistry is inviting nominations for its 1989 Interdisciplinary Awards. The aim of the awards is to draw attention to the importance of interdisciplinary studies, particularly those of public interest, involving chemistry and one or more other science and to reward and publicize such work.There are no age or nationality restrictions but nominees should be domiciled in the UK or Republic of Ireland.

The closing date for nominations is *2 October 1990*. Further details from Dr. J. F. Gibson, RSC, Burlinton House, London WIV 0BN (UK).

Neuchatel Switzerland: The Third International Conference on Surface Modification Technologies will be held at CSEM (Centre Suisse d'Electronique et de Microtechnique) Neuchatel, Switzerland from August 28 to September 1, 1989. The Conference is jointly sponsored and organized by the Minerals, Metals, Material Society (TMS), USA, the Metallurgical Society of AIME, and the CSEM. General Meeting Information is available from M. Karl; TMS, 420 Commonwealth Drive, Warrendale, PA 15086, USA, Tel. 412-776-9050.

Conference Reports

Joining Ceramics, Glass and Metal in Bad Nauheim

By Graham Partridge*

The third international conference on joining ceramics, glass and metal was held from 26.–28. April 1989 in Bad Nauheim, a spa town in the Federal Republic of Germany. This is a very pleasant town (although it rained for much of the period of the conference. Normally, this could be expected in England but, somehow it is assumed that the Germans would do better, even with the weather). The conference itself was held in the Kurhaus (Congress Center) which is very well equipped for conferences of this type. Furthermore, the many hotels meant that no delegate need be more than a few minutes away from the Kurhaus.

The conference was organized by the Deutsche Gesellschaft für Metallkunde (DGM), together with the Deutsche Glastechnische Gesellschaft (DGG), the Deutsche Keramische Gesellschaft (DKG) and the Deutsche Verband für Schweisstechnik (DVS) and was the third in a series of conferences targeted at technical developments in joining ceramic, glass and metal. The conferences are held at four-yearly intervals which permits significant developments to take place in this broad, important field between meetings.

For convenience the conference was divided into four themes, namely

Active brazing
Diffusion bonding
Friction welding, Reaction bonding and other joining methods
Properties and testing

Oral papers were presented in each group, including an initial plenary paper by an appropriate expert on the particular theme. In addition, poster contributions reinforced and expanded the technological areas covered.

During the course of the conference, three short (1 h 20 m) workshops were held in parallel on the themes of

Active brazing/Testing methods
Diffusion bonding/Interlayers
Design of bonded systems/Applications

A total of 232 participants were recorded as attending the conference. As would be expected, more than 50% were from the Federal Republic of Germany although the majority of the European countries were well represented and there were also participants from as far afield as Australia, China and Japan. Interestingly, no attendees from the USA were recorded.

The technical sessions were always well attended (in spite of the attractions of Bad Nauheim) and the poster area was crowded during poster discussion periods. The workshops attracted 50–60 participants each and the discussions were lively and informative.

The standard of oral presentation and of the posters was high. This presented a problem for many of the speakers and poster designers since the conference was held in English with no facilities for parallel translation. It says a great deal for those who spoke and who discussed their posters in what was not their native language that they were able to make their points well and answer questions put to them. Each oral presentation allowed time for a few questions following the paper.

Inevitably, there was some overlap in the chosen themes, for example, property determinations were presented in all sessions.

The following review covers highlights (in the author's opinion only) and does not hope to cover all the many and varied aspects of this highly stimulating international conference.



1. Active Brazing

The papers in this session were concerned with brazes which contained titanium. The presence of Ti enabled the braze to wet and bond to the ceramic surface. It was shown

[*] Mr. G. Partridge
GEC Engineering Research Centre
P.O. Box 30, Lichfield Road, Stafford ST17 4LN (UK)

by *M. Nicholas* that wetting became progressively more difficult in the series oxide–nitride–carbide–boride although good wetting was not always essential to achieve a good bond, especially if pressure were applied across the join. Shear strengths of bonds involving ceramics were seen to be generally stronger with the strongest ceramics.

A number of presentations covered the difficulties of brazing ceramics to metals where a wide disparity in thermal expansion coefficients leads to high stress in the join and ceramic. The use of interlayers, such as Mo and Cu was shown to be beneficial in reducing stress levels and leading to strength improvements in the joins. Mo appeared to be particularly beneficial for SiC and Si_3N_4 (*E. Lugscheider* et al.) and useful for Graphite to stainless steel (*P. Jacquot* et al.). Design of the joints was important—a high ratio of ceramic to metal thickness in the join influenced residual stress in the ceramic and decreased shear strength (*Weise* et al.) and the use of a ductile metal filler was also helpful.

2. Diffusion Bonding

The diffusion bonding of ceramics to metal, resulting from interactions at the ceramic-metal interface at elevated temperatures was discussed by a number of lecturers covering a range of ceramic to metal systems. The plenary lecture was given by *J. J. Klomp* and he set the scene admirably. It is clear that diffusion bonding requiring transport of metal can lead to reaction products which may be disadvantageous. Ideal contact surfaces are not generally available and pores produced in the contact zones are removed by creep and vacancy diffusion. Bonding time and pressure are helpful in this respect (*B. Gibbesch* et al.) as applied to Nb and Cu bonds to sapphire. It was noted by *B. Derby* that joint strength and toughness had to be clearly distinguished when characterising the mechanical properties of diffusion bonds between ceramic and metal. Comparison of brazing and diffusion joins of SiC to metal was made by *Batfalsky* et al. who indicated that diffusion joins should be capable of higher temperature operation. Diffusion barriers and interlayers such as copper were often necessary (*J. Schiepers, J. P. Krugers* et al.) to enable expansion mismatches to be tolerated. Silicides which influence bond integrity were formed at the ceramic interface. The use of hot isostatic pressing for joins of Si_3N_4 to steel was shown to be advantageous (*M. Corbiere* et al.) and tungsten was the preferred "stress relieving material" adjacent to the ceramic. The use of TiH_2 powder interlayers, sintered simultaneously during Al_2O_3–Ti bonding (*S. Prech*) was interesting and further development of Cu to Al_2O_3 bonds was discussed by *W. Wlosinki* et al.

3. Friction Welding, Reaction Bonding and other Joining Methods

This section covered aspects of less well known methods for joining ceramics to metals. *D. Hann*, in his plenary address, covered a number of tasks which engineers must undertake in developing a reliable join, with particular emphasis on the problems occurring in lapped joins. As with a number of other applications discussed in other presentations, finite elemental analysis was seen to be useful in determining stresses which were strongly influenced by the geometry and thickness of the bonded parts. Shear strength testing was said to give general, relative information but other tests were also necessary to give critical information. *G. Partridge* et al. dealt with the joining of glass-ceramics directly to metals, either in bulk joining processes or by coating application and this latter aspect was amplified by *Ashcroft* et al. in a poster presentation. Generally, these forms were matched in expansion, so stresses were low. The development of unusual crystal phases in the glass-ceramic at the interface were discussed and problems arising from the competing diffusion processes of bond development (essentially via the metal oxide layer) and crystallization of the precursor glass were outlined. *W. Schaefer* et al. discussed bonding of high temperature zirconia electrochemical cells using a variety of joints (glass, welding, clamping) in the overall stack. Aluminophosphate mortars were described by *A. Hesse* et al. to join reaction bonded SiSiC and it was seen that the mortar itself was the weak link in the bonded assembly. Friction welding (*Weiss* et al.) was an unusual technique successfully used to join ceramic to metal. Initially metallization of the ceramic was seen to occur as the bond developed. The use of nickel foil, converting to nickelous oxide at the interface was shown to be a useful way of joining MgO to itself or to metals (*K. Atarashiya* et al.) and also for joining Al_2O_3 to Ti-6Al-4V alloys (*Y. Ito* et al.).

4. Properties and Testing

The plenary paper by *G. Gnirss* et al. discussed the properties of ceramic to metal joins with respect to design considerations and further looked at failure mechanisms in the joins. The general experience was that the bonding zone or adjacent ceramic were the weakest points and the lifetime of components was determined by creep and fatigue controlled sub-critical crack growth as well as temperature and time dependent degradation within the bonding zone. Optimization of the bonding process requires new bonding media, reduction of thermally induced stresses and improvement in the reproducibility of high quality ceramics. To some extent this latter might be met by improvements in powder processing and by composite developments. *M. Turwill* et al. discussed joining of ceramics to metals for various applications generally with reasonably close thermal expansion matching of the ceramic and metal parts. Finite element analysis of stresses in joins was discussed by *B. T. J. Stoop* et al. and *K. J. Ferenc* et al. It was found by *Stoop* that both tensile and shear stresses are maximum in the ceramic in the vicinity of the ceramic-metal interface. Elementary bending theory may also be used to determine residual thermal stress distributions in an asymmetrical ceramic/solder/metal plate as shown

by *O. T. Iancu* et al. The determination of stress in a ceramic to metal join is not easy. Optical methods using polarized light cannot generally be used owing to lack of transparency. However, in some cases X-ray diffraction techniques (*B. Ergermann* et al.) can be employed to determine residual surface stresses and triboelectric effects or light emission under stress may also be used (*H. Teodorescue* et al.).

In many cases ceramic to metal joins may be subjected to environmental conditions likely to cause weakening. *K. Suganamu* et al. discussed stress corrosion failure, in particular, the influence of water on Si_3N_4 joins where stress corrosion of the Si_3N_4 itself can take place. However, the results obtained showed that the joins can maintain high integrity over a long period of time. Several workers addressed the bonding of copper to Al_2O_3, an important bond in the microelectronics field. Fracture toughness values of K_{ic} up to 4 MPa $m^{1/2}$ were obtained by *L. J. Bostelaar* et al. and *A. Otszyna* et al. showed that the bonds to α-Al_2O_3 were stronger than those to β-Al_2O_3. *N. Klein* et al. also showed that thermal cycling led to deterioration in the Cu to Al_2O_3 bond owing to shear stresses in the join, but control of the crystallite orientation in the Al_2O_3 could beneficially influence thermal endurance.

The majority of the papers and posters presented have been drawn together in a volume entitled "Joining Ceramics, Glass and Metal", edited by *W. Kraft* and published by the DGM.

The conference was highly successful and provided not only an excellent venue for the dissemination of research results but also the opportunity to meet fellow workers in this wide and disparate field.

Magnetic and Magneto-Optic Thin Films and Multilayers in San Diego

By Ernesto Marinero* and Takao Suzuki*

The spring meeting of the Materials Research Society (MRS) in San Diego, April 24th to 29th, 1989, was host for two major symposia dealing with magnetic and magneto-optical materials. The symposium on "Growth Characterization and Properties of Ultrathin Magnetic Films and Multilayers" comprised 11 invited talks and 42 contributed papers over three and a half days and provided a unique and interactive forum in which to discuss recent advances in low dimensional magnetism, diluted magnetic semiconductors, epitaxial overlayers and the utilization of in situ and ex situ techniques to characterize their microstructure and electronic and magnetic properties. The other symposium on "Materials for Magneto-Optic Data Storage" was the first dedicated entirely to materials aspects of the rapidly emerging magneto-optic data technology. This symposium lasted for two days and was particularly successful in providing a well balanced forum between the industrial applications of the technology and fundamental materials research. Thirty seven papers were presented, including outstanding invited lectures, which covered the entire spectrum of materials issues relating to magneto-optical recording media. This included the magneto-optic active layers, dielectric layers and substrates. Emphasis was placed, in particular, on rare earth transition metal amorphous films, such as TbFeCo, GdTbFeCo, from the fundamental as well as the applicational point of view.

[*] Dr. E. Marinero, Dr. T. Suzuki
IBM Research Division, Almaden Research Center
650 Harry Road, San Jose, CA 95120-6088 (USA)

Growth, Characterization and Properties of Ultrathin Magnetic Films and Multilayers

The study of ultrathin magnetic structures is a rapidly expanding field of materials research whose growth is synergistically driven by an increasing appreciation of the degree to which the magnetic properties depend on interfacial processes and by the utilization of growth techniques which permit the fabrication of multilayer structures with novel electronic and magnetic properties. Equally important is the fact that atomic level control of the microstructure of these layers offer new opportunities to elucidate the physics of magnetism, to rigorously test theoretical models and, in some cases, to synthesize new materials.

The symposium opened with an invited talk by *Roy Richter*, General Motors (GM) who presented recent theoretical results on the temperature dependence of the spin anisotropy of a monolayer of Fe. Changes in the magnitude of the perpendicular anisotropy as a function of temperature were attributed to changes in the Fe monolayer band structure. *Mayer* and *Gutierrez* (Johns Hopkins) presented experimental results on Fe(110)/Ag(111) superlattices (SL) grown by molecular beam epitaxy (MBE). No out-of-plane magnetization was observed for this particular system. *Krebs* (NRL), on the other hand, found that Fe(001)/Ag(001) superlattice grown on thick Ag(001)/ZnSe(001) substrates exhibited strong perpendicular anisotropy for Fe layers < 3 ML. The importance of interface roughness was highlighted by *Albert Fert* (University Paris-Sud) who reported

on the measurement of giant magnetoresistance in Fe(001)/Cr(001) SL. This roughness leads to electron scattering processes at the Fe/Cr interface, and the increase in magnetoresistance for Cr < 20 Å is ascribed to a change from parallel to antiparallel orientations for the magnetization of neighboring Fe layers. In turn, the interface electron scattering is enhanced by the antiparallel orientation. Similar effects are predicted for other transition metals.

Growth of Fe (Nd, Dy, Y) SL's was reviewed by *Teruya Shinjo* (Kyoto University) who observed that for Fe < 20 Å, the Fe/Nd SL is amorphous and exhibits perpendicular anisotropy. For thicker Fe layers (30 Å) bcc ferromagnetic structures are obtained with in-plane magnetization. The growth of hcp Fe/Ru superlattices was reported for the first time by *Maurer* et al. (CNRS) with evidence for strong interactions through the Ru layers. Co/M (M = Pd, Au, Cu) SL's were also discussed and *Hoving* (Philips) pointed out significant magnetic differences between Pd/Co single crystals and polycrystalline multilayers. In particular, the anisotropy is perpendicular in the single crystal only for Co thickness of 1–2 ML vs. 8 Å for the polycrystalline system. In the case of Co/Au, *Lee* (University of Michigan) reported a transition from out to in-plane anisotropy for Co ~ 20 Å.

In situ techniques to characterize magnetic properties of thin film systems are rapidly developing. *Dan Pierce* (NIST) described the SEMPA technique (Scanning Electron Microscopy with Polarization Analysis) which permits domain imaging with intensity directly proportional to the magnetization and resolution presently ~ 400 Å. He speculated that the STM would be the ultimate magnetic tool of sensitivity to spin could be derived. An elegant demonstration of the use of STM to study ultrathin films was given by *P. N. First* (NIST) who showed images of 0.1 Å Fe layers grown on GaAs which exhibited 3D growth of 20–30 Å diameter islands at 300 K. Similarly, spin-resolved photoemission and Brillouin scattering are powerful tools to study spin-split electronic band structure as reported by *Guntherodt* (Aachen) for the case of Fe/Ni. *Eric Kay* (IBM Almaden Research Center) utilizing secondary electron spin-polarization analysis, showed that 0.1 ML of an adsorbate can alter the Curie point by as much as 30% in the case of permalloy thin films.

A combination of spectroscopies and in situ magnetic measurements were utilized in the MBE growth of Fe/Ag, Fe/Ni and Ni/Fe by *Heinrich* and collaborators (Simon Fraser University). They showed, for example, that in the case of Fe/Ni, Ni grows bcc (RHEED, REELFS) up to 6 ML. A structural transformation occurs for thicker layers giving rise to large magnetic anisotropies which from FMR studies are attributed to growth defects. The effect of strain on magnetic properties was discussed by *Farrow* (IBM) for the case of LaF_3/Dy/LaF_3 and by *Florczak* (University of Minnesota) for epitaxial (100) Fe films.

The use of ex situ techniques such as EXAFS, X-ray scattering and TEM were described by *Cargill* (IBM Watson Research Center) and *Li* (Arizona State University) to study microstructural properties of thin films. FMR and NMR studies have been applied by *de Gronckel* (Eindhoven) to Co/Pd multilayers to investigate the behavior of the anisotropy as a function of Co and Pd thickness. The spin-echo NMR studies indicate that as the Co layer thickness is decreased, structural changes take place that result in an expansion of the Co lattice. The observed magnetic changes are attributed to this structural transformation.

Werner Keune (University of Duisburg) presented results on UHV CEMS (Conversion Electron Mössbauer Spectroscopy) of fcc Fe(100) films on Cu(100) and showed that the para-, ferro- and antiferro-magnetic properties strongly depend on growth temperature. These results were discussed in terms of thickness dependent lattice relaxation.

A search for an experimental manifestation of the universality hypothesis was described by *Pescia* (Julich) who utilized spin-polarized electron scattering to measure the order parameter in < 3 ML Fe films on Au(100). It is found that although the Curie temperature exhibits a thickness dependence, the critical exponent β of the power law $M \sim (1 - T/T_c)^{\beta}$, is essentially independent of thickness. M is the order parameter. This is explained by the fact that as long as the film is thin enough, the system remains two-dimensional and therefore has a single set of critical exponents which are independent of the strength of the interaction.

Furdyna (Notre Dame), *Gunshor* (Purdue University) and *Jonker* (NRL) reviewed recent progress on diluted magnetic semiconductors (DMS). A typical material set belonging to this class are the $A_{1-x}Mn_xB$ alloys (where A = Zn, Cd and B = Se, Te). *Furdyna* indicated that DMS multilayer structures may be grown with pronounced field-dependent effects. Examples of such structures include, multiple quantum well structures in which the wells consist of a DMS material, or magnetic field-induced SL's. *Gunshor* reported on the intercalation of ZnTe monolayers in ZnSe/MnSe quantum wells which dramatically altered the optical emission due to excitonic self-trapping at Te sites. *Jonker* described ongoing work at NRL on Fe and Co-based DMS materials, indicating that their properties (magneto-optic, electronic) are strongly influenced by the ground state of the magnetic ion used and the energy levels it introduces relative to those of the host semiconductor. The electron-ion and ion-ion exchange parameters for the Fe- and Co-based materials are significantly larger than for the Mn-based counterparts.

In summary, the symposium was an excellent event in which the structural, electronic and magnetic properties of ultrathin magnetic materials were discussed. It brought together a dynamic collection of leading materials scientists from Europe, Japan and the USA, and it is apparent that state-of-the art growth and characterization techniques are widening our understanding of magnetic phenomena at an atomic level.

Materials for Magneto-Optic Data Storage

In the keynote talk, *M. Kryder* of Carnegie Mellon University reviewed the current status of the magneto-optical

recording media based on amorphous rare earth (RE)-transition metal (TM) thin films. He pointed out that to maximize Kerr rotation, anisotropy, corrosion resistance and reflectivity, the sputtering conditions should be selected to produce so-called Zone T featureless films. *F. Lin* of IBM Almaden Research Center described in his invited talk the property requirements for the magneto-optic active and dielectric layers that are needed in order to realize high performance recording and reliable data storage. He emphasized the importance of understanding the micromagnetics and controlling the regularity of the written domains in order to achieve a high carrier to noise ratio (CNR).

While the properties of TbFeCo media appear adequate for today's MO storage devices, their rather weak magneto-optic activity at shorter wavelengths (less than 500 nm) may restrict their extension to high storage densities. One approach that has been taken in order to overcome this disadvantage involves alloying TbFeCo with a light rare earth element such as Nd and Pt which both have enhanced M-O activity due to their highly spin polarized 4f states. However, the origin of this enhancement was challenged in a paper by *D. Weller* of Siemens. He presented a systematic study using XPS and Kerr spectroscopy, to characterize in situ RE-FeCo films deposited in ultra high vacuum. His main conclusion is that the 4f-excitations of RE ions are not expected to contribute more than few tenths of a degree to Kerr rotation.

The study of the magneto-optic and magnetic properties of multilayered and exchange coupled films as candidates for higher MO activity has been gaining in interest. *D. J. Sellmyer*, University of Nebraska, and *C. Falco*, University of Arizona, discussed in detail the origin of perpendicular magnetic anisotropy and magneto-optic properties in Fe/Nd, Dy/Co, Pd/Co and other alloy systems of RE-TM. *Sellmyer* concluded that single-ion anisotropy is the major contributor except in Gd. *Falco* discussed the structure of multilayered films made by MBE in conjunction with those made by sputtering. *P. F. Carcia* of E.I. du Pont presented a paper on the wavelength dependence of Kerr activity in Co/Pt multi-layer films. The enhancement in Kerr rotation at short wavelength was shown to be due to the high M-O effect in the very thin Co layers. *S. D. Bader* of Argonne National Laboratory presented an invited talk on surface magneto-optic Kerr effect (SMOKE) of ultrathin ferromagnetic films. The result showed a dramatic example of a metallic reflector enhancement effect due to the nonmagnetic Au underlayer.

Another approach for enhancing magneto-optic activity is to use exchange coupled two-layered films. In such a film structure, optimization of Kerr rotation can be done in one layer and magnetic properties in the other. *R. Gambino* of IBM Thomas Watson Research Center and *H. Wakabayashi* of IBM Almaden Research Center discussed the mechanism for exchange coupling in CoPd/TbFeCo and Co/TbFeCo films. *Gambino* pointed out that properly designed exchange coupled films appear to provide a viable approach to high density storage media. Further extensive discussion was given on multi-layered films of TbFe, Cu/Co and Pd/Co in papers presented by *Krishnan* of CNRS, and *England* of the University of Arizona.

Bi-substituted garnet films are attracting increasing attention due to their very high Faraday activity. The Faraday signal at about 500 nm is almost one order of magnitude larger than the MO activity for RE-TM films with similar thickness. However, a large readback noise results from grains and surface roughness in these polycrystalline films. *M. Gomi* (Tokyo Institute of Technology) discussed the possibility for controlling the grain boundary structure so as to provide better domain regularity and less domain noise by using additives such as W at concentrations of less than 1 atom-%. *K. Shono* of Fujitsu presented data on the recording performance of (Bi-Dy) substituted garnet disks where 57 dB and 54 dB at 5 and 1.4 μ bit length, respectively, were achieved. Such results are encouraging for the eventual use of these materials as a future high density storage media. In addition to these technology oriented talks, *P. Wigen* of the Ohio State University described evidence for partially spin polarized Bi^3 in $Bi_3Fe_5O_{12}$ where a moment of 0.25 μ_B is formed at the Bi ion sublattice while the moment on the tetrahedral iron sublattice decreases by 0.5 μ_B.

Dielectric layers are important for MO recording media because they provide the optical enhancement of Kerr rotation and protection from oxidation for the MO active layers. The dielectric layers for these purposes require a high refractive index, stability to the environment and low internal stress. *K. Hashima* of Mitsubishi Electric Co. described a new dielectric material based on AlGeN which exhibits high refractive index (2.4–2.5) with a very small internal stress (less than 10^9 dyne/cm^2).

Polycarbonate (PC) is the most widely used substrate for MO disks. However, PC can have relatively large optical retardation depending on injection molding conditions and it also absorbs water which alters the mechanical tolerances of the disk. *Y. Togami*, Mitsui Petrochemical Ind. Co., and *M. Yamazaki* of Nippon Zeon Co. described the properties of amorphous polyolefins which overcome these drawbacks.

The oxidation and corrosion behavior of TbFeCo has been a key concern because of the high reactivity of Tb. *A. Lee* of the University of Arizona discussed the interaction of H_2O on UHV clean TbFeCo surfaces using AES, XPS and RBS. Also, *D. Majundar* of Eastman Kodak Co. described the effect additive elements such as Pt and Zr have on the oxidation in TbFeCo. Both papers suggest that such additives can reduce the reactivity of TbFeCo films.

Besides these materials oriented talks, the symposium also covered a key performance disadvantage of MO technology; that is, the lack of direct overwrite capability. *N. Imamura* of TOSOH Co., and *N. Ohta* of Hitachi discussed the current status of the direct overwrite technology. *O. Ishii* of NTT presented the new approach of the direct overwrite using a magnetic head for writing and a laser beam for reading in a two-layered film.

The symposium "Materials for Magneto-Optic Data Storage" was a very successful and exciting meeting.

ADVANCED MATERIALS

Book Reviews

Sol-Gel, Drug Release, Superconductors and Liquid Crystals

Sol-Gel Technology for Thin Films, Fibers, Preforms, Electronics and Specialty Shapes. Edited by *L. C. Klein*. Noyes Publications, New Jersey, USA 1988. xxi, 407 pp., bound, US$ 72.–ISBN 0-8155-1154-X

Sol-gel technology has been a popular subject in materials science and engineering for some four decades. Its promise for the preparation of controlled and homogeneous compositions and for the fabrication of various forms such as powders, fibers, coatings and monoliths has made it the potential answer for many of the problems which have been identified by people working with the processing of ceramics and glass. The technology has proved difficult to apply to some of the more classical sectors of ceramics such as powder and monolith preparation but notable successes have been achieved particularly where precise performance is required in components of limited dimensions (films, coatings, fibers).

The present book performs the valuable function of summarizing the technical advances that have been made in the subject to the end of 1987. In 17 chapters contributed by 27 authors and co-authors drawn from the United States, from Europe and from Japan, sol-gel technology is reviewed with emphasis on examples where progress in applications has been achieved. The editor has been successful in building the book around a logical arrangement which allows the different sectors of the technology to be systematically treated; there is throughout an emphasis on processing methods and on applications and this together with the concentration on topics where commercial success has been reached or can be foreseen, makes the book a valuable and instructive guide for those wishing to find their way in what has become a complex subject.

The opening section of the book contains three introductory chapters which review the preparation of glass using sol-gel methods, the contribution which has been made by molecular dynamics theory to the understanding of the sol-gel process and the subject of phase transformations in gels; in the latter, emphasis is given to the differences that can be identified between the behavior of gel derived and conventional glasses.

The second part of the book relates to the preparation of coatings and thin films by the sol-gel process. As pointed out in the opening chapter on film preparation, such coatings directly exploit the advantages of the sol-gel process; they have reached commercial application in large quantities and they in fact predate much of the fashionable interest of recent years. Specialized treatments of anti-reflective films and of oxynitride films are given in separate chapters. The third part of the book describes the use of sol-gel methods for the preparation of fibers by drawing, blowing or by unidirectional freezing. Following a review of such developments, more detailed treatments are given of the aluminoborosilicate system and of the preparation of continuous fibers.

The fourth section of the book describes the use of sol-gel procedures for monolith formation. The treatment is in terms of glass products and this indeed reflects a general tendency in the book; where appropriate, discussions are included of the polycrystalline products which can stem from sol-gel methods but the major attention is given to glasses and amorphous systems. This section also includes descriptions of thermal insulation, of the manufacture of ultrapure glass and of particulate gels and glasses. The book concludes with a section devoted to specific applications of the technology. Following a short chapter on the fabrication of electronic ceramics, there are treatments of superionic conducting systems (both glass and crystalline, with emphasis on sodium and lithium conductors) of the fabrication of hollow glass microspheres and of filters and membranes.

The editor is to be congratulated on having assembled a timely and authoritative text around a subject which has caused a certain degree of confusion. The emphasis on practical aspects and on applications will be of particular value for those who are trying to clarify the precise contribution to be expected from this much debated technology.

Richard Brook
Max-Planck-Institut für Metallforschung
Stuttgart (FRG)

Controlled Release of Drugs: Polymers and Aggregate Systems. Edited by *M. Rosoff*, VCH Verlagsgesellschaft, Weinheim, 1989, xi, 315 pp., bound, DM 132.–ISBN 3-527-26797-2

This book is the first in a designated series intended to provide topical reviews in various areas of controlled release technology as well as from other pertinent disciplines where advances may contribute to the field of controlled release. The series itself is designed to consolidate, across a wide breadth of topics, a rapidly expanding primary literature database; each volume within the series supposedly allowing substantial review of specific current areas while emphasizing the more subjective exploration of ideas and speculation for future directions from the authors of each chapter. The overall goal of such a strategy is to provide a relevant overview of controlled release issues, problems and progress aiming at broad readership, practical utility and volume longevity. To achieve this the editors of each volume have collected an impressive set of advisory editors to assure and

endorse coherency of content as a whole as well as accuracy and quality within each chapter.

Chapters 1, 2 and 9 deal specifically with issues concerning the use of polymeric materials as matrices for the controlled release of drugs while the remaining six chapters are devoted to dispersed or aggregated system technology – emulsions, dispersions, liposomes, liquid crystals, micelles and microemulsions. I was pleasantly surprised to find so much information compiled on "organized systems" – those utilizing organizing principles which are involved in the field of lyotropic liquid crystals – directed towards controlled release technologies. In this sense, I find the term "aggregated" used in the title to be misleading as, in my opinion, lyotropic liquid crystals "organize" instead of "aggregate". It is, in fact, this organization which is critical to their use in controlled release technology. Aggregation is correctly applied in terms of microcapsules and microspheres. However, were it aggregation per se that compelled lyotropic phases to form and transform, I would believe that the anisotropy so critical to function would not exist. This may be a matter of semantics.

This is one of the few books on controlled release I have read where nine different approaches to the same problem are uniquely presented – each in the style, interests, and scope of each author with little discontinuity or repetition. Each author starts and ends his reviews and discussions within the bounds of his assigned topic which I find refreshing. In addition, each author makes an attempt to break the reader in gently to the topic at hand with short but generally adequate introductions to developments and concepts within each chapter. In this way and considering the effective, relatively straight-forward method with which theory, concept, and applications are developed and focused, the volume qualifies well as a text for newcomers to the field, persons in neighboring fields, and graduate students exposed to these ideas for the first time.

Specifically with regard to the text, chapter 1 addresses the development of models for drug release from various porous polymer matrices. Models for the classical cases of steady-state flow-through and diffusion-controlled release from macro-porous membranes are presented. Closer analyses of tortuosity, corrugation, percolation models, admittedly borrowed originally from other fields, along with various simulation procedures using Monte Carlo and other numerical methods are well formulated and digestible for the neophyte. Microporous systems, where drug and pore size are comparable, are also analyzed at length and in general concepts are well formulated and adequately presented within the constraint of the chapter length.

Chapter 2 discusses controlled drug release from biodegradable polymers. Starting from a review that contrasts polymeric controlled release with conventional drug therapies, the author continues to describe and develop ideas within the scope of biodegradeable polymer matrices. Matrix erosion and resulting release profiles for diffusion-controlled, reservoir and hydrogel devices as well as enterically-coated and covalently-bound drug matrices are addressed. A short overview of the various factors affecting polymeric biodegradation, both chemically and physically, is also given. In addition, factors considered in biodegradable device formulation, administration, and evaluation are briefly presented. Finally, mechanisms of the chemical degradation of polymers currently in use are outlined. Again, the information supplied is stimulating and heavily referenced.

Chapter 3 moves away from polymer matrices to discuss dispersed systems for injectable (parental) drug carrier systems. Materials and device formation techniques for microspheres and microcapsules are given, following an introduction to parental systems and their degradation. The author then moves on to non-polymeric dispersions – liposomes, nonionic surfactant vesicles (niosomes) and loaded erythrocytes as alternative parental vehicles. Two last sections deal with parental emulsions and nanoparticles (polymeric). I enjoyed the review and was satisfied with the content and referenced material.

Chapter 4 discusses liquid crystals and their role in dispersion stabilization and briefly, drug delivery applications. I was excited to see such a chapter because of the applicability of such molecular dynamics and organization to controlled release. However, I soon became bogged down in differentiating arrays of photomicrographs and phase diagrams that the chapter barely has room to detail. Although I did get a lot out of most sections qualitatively (liquid crystal nomenclature and properties, emulsifier associations and stabilization issues), I felt that the sections on l.c. phase behavior and applications to drug delivery lacked sufficient detail and significance and detracted from the quality of the majority. This is particularly clear after reading other chapters dealing with emulsion stabilization by other methods where applications are much more fully discussed. More importantly, I could not discriminate after all was said and done, if liquid crystals had any future in drug delivery or if they should better be left alone. Aside from these issues, I found the content of this chapter, for the most part, interesting.

Chapter 5 goes on to describe and support the weaknesses from Chapter 4 (which may indicate that Chapter 4 was an essential and fully adequate foundation to build upon). The concepts of multiple emulsions, their construction and stability, are fully detailed and referenced. Transport mechanisms for solutes, although not well understood, are developed for both micelles and facilitated transport. A final section on the in vivo administration of emulsions as parental drug delivery systems highlights current interests and levels of understanding for these systems.

Chapter 6 is structured much like Chapter 5 except that it deals with microemulsions. Two differences are notable in this interesting and well written account: namely, that unlike emulsions, microemulsions form spontaneously without external agitation, and that, unlike emulsions, the pharmaceutical value of microemulsions has not yet been adequately

assessed. The authors detail very effectively the requirements and stability of microemulsions and then explain that very little has been done in drug delivery with these systems. From the optimistic description of the basic research undertaken it seems like a ripe research opportunity.

Chapter 7 details liposomal formulations from a more commercial perspective with emphasis on macromolecular drug delivery. An array of materials and methods for the construction of liposomal vehicles having various properties are first described rather extensively. Issues concerning the various routes to delivery are reviewed, touching briefly on trouble-shooting clearance and RES uptake problems. Finally, a short section mentions the specific case of liposomes as macromolecular carriers. Issues in formulation stability and internalization by cells were not addressed to any significant extent. Nevertheless, the chapter gives a very current, well-informed review of a topic that has received much attention in the last decade.

Chapter 8 presents data on the inclusion of nucleic acids into reverse micelles. DNA and RNA of various sizes and types are shown to be solubilized into reverse micelles much smaller than the dimensions of the DNA and RNA themselves. This chapter could have been formatted more effectively in the same style as all others chapters but was instead kept in a classical journal format: Introduction, Experimental, Results, Discussion. It seems to be one of the few mistakes made by the editor. Not only is this format inappropriate for this type of literature review of applied techniques, but reader appeal becomes problematic for anyone unfamiliar with this type of work due to the less-generalized, non-conceptualized style of presentation. Not that this detracts from the quality of the data presented; it simply makes it less comprehensible. Data from spectrometric studies (UV and CD) of the inclusion of biopolymers of DNA and RNA into reverse micelles are given and explained. How this relates to controlled release drug delivery issues is mentioned in a small, speculative section at the end of the chapter.

Chapter 9 returns to polymeric matrices with a well presented review of transdermal delivery systems and models, problems in the development of these systems, and explanations about what can be done to deliver more drugs with this strategy. Less attention is paid to actual materials as is to the design of devices for specific functions, characteristics, and properties, e.g., skin or device rate control and skin permeability enhancement for desired kinetics of delivery. Strategies include diffusion and rate controlling membranes for desired release parameters, examples from current commercial products, and factors to consider in future designs. Modeling analysis include skin depot effects, permeability measurements and predictions, and rate control. This chapter is easy to read and understand and presents most essential and pertinent considerations for transdermal delivery.

David W. Grainger
Institut für Organische Chemie der
Universität Mainz (FRG)

Superconductors: The Breakthrough. By *R. M. Hazen*, Unwin Hyman Ltd., London, 1988, xxviii, 271 pp., bound, £ 12.95. – ISBN 0-04-440288-0

A review of this book from 1988 is still worthwhile just in case someone has missed it. In writing this book in such a popular style the author is running the risk of having his leg pulled by colleagues, not least for employing such a modest title. However, he should be congratulated most warmly for doing so.

This is the story of the discovery of superconductivity at temperatures above the boiling point of nitrogen, the temperature above which commercial exploitation of the effect becomes a viable proposition.

The Preface, Foreword and the first Prologue all give a historical overview and set the scene, explaining the reason for, and the potential importance of the research in the area up until the first indications of success in January 1986 from *Bednorz* and *Müller* at IBM Zürich (who were eventually awarded the Nobel Prize in Physics for their work).

The book is structured in three main sections. The first details the work in the laboratory of Prof. "*Paul*" *Chu* in Houston where the complex-metal oxide synthesis work was done and where, by switching ingredient elements from the original *Bednorz/Müller* recipe ($T_c \sim 30$ K) possibly the first indications of superconductivity above 77 K were seen. One has to say possibly, because, after the initial announcement of the IBM team there were many groups from many nations suddenly devoting their full resources to the problem.

The second section follows the work in which the author was directly involved, that of solving the structures of the two crystalline phases, work carried out at the National Geophysical Lab. in Washington DC in collaboration with *Chu*. The interactions of the multidisciplinary teams are highlighted and even espionage, betrayal and unethical publishing are hinted at.

The third section describes the intense excitement which was generated by the race to be recognized as the pioneer of high-T_c superconductivity above the all important 77 K which culminated in the New York meeting of the American Physical Society which has become known as the "Woodstock of Physics" where representatives of the various competing groups came together resulting in the most memorable scientific meeting in years.

An erroneously spelt erroneous, along with a few other minor defects are counteracted by pictures of the important participants and by lines such as "A good X-ray peak has a silhouette that soars like a futuristic skyscraper; our peaks looked more like melting igloos" which emphasize humorously the sort of problems and disappointments which were overcome on the way to success while bringing a smile to the lips of the more knowing.

The book is written with a humor which can be appreciated both by the scientist and the more general public and a good effort is made to explain enough of basic physics and chemistry to capture the attention of the non specialist, to

involve him in the excitement of discovery and to keep him reading to the end.



Anyone with an ounce of the scientist romantic in him will love a story which rivals Star Wars for fantasy and Gone With The Wind for romance. It is the sort of book which brings science to the attention of the general public and gives it a good name.

Peter Gregory
Advanced Materials
Weinheim (FRG)

Side Chain Liquid Crystal Polymers. Edited by *C. B. McArdle*. Blackie and Son Ltd., London 1989. 448 pp., bound, £ 75.–ISBN 0-216-92503-7 (USA: 0-412-01761-X)

This book presents an overview of thermotropic side chain liquid crystalline polymers, one of the rapidly growing innovative fields in liquid crystalline materials research. The book is made up of clearly structured contributions from acknowledged experts in the field. Within 14 chapters, theoretical concepts, structural and synthetic aspects, characterization methods and properties, and a discussion of potential applications are covered. Since the book is exclusively dedicated to thermotropic side chain liquid crystalline polymers it is certainly more than an extension to the existing reviews.

In an introductory chapter the editor *McArdle* summarizes the scope and potential for thermotropic side chain liquid crystalline polymers, focusing on applications based on electro-thermo-optical effects. The second chapter on the physical principles of the polymers is written by *M. Warner* and the syntheses and different structural principles of liquid crystalline polymers containing mesogenic side groups are covered by *Percec* and *Pugh*. The authors not only describe the 'classical' side chain systems, but also novel types of structural modifications. The following chapter by *Gray* deals in detail with the synthesis and properties of side chain liquid crystal polysiloxanes. The placing of liquid crystalline polysiloxanes into a separate chapter is questionable, as it overlaps and repeats some parts of the previous chapter. *Le Barny* and *Dubois* describe the scope and potential of chiral smectic C liquid crystal side chain polymers, which are currently under extensive investigation because of their potential applications. The following three chapters 6–8 summarize the characterization of side chain liquid crystalline polymers. The chapter by *Noel* covers, with well chosen examples, macroscopic structural characterization, by DSC, optical microscopy, miscibility studies and X-ray methods. The chapters on dielectric relaxation spectroscopy (*Haws, Clark* and *Attard*) and on NMR methods used to study molecular order and motions (*Böffel* and *Spiess*) treat the theoretical background and give experimental results. The contribution on cholesteric side chain polymers (*Shibaev* and *Freidzon*) discusses especially their optical properties and demonstrates features of cholesteric materials. Side chain liquid crystalline elastomers are described by *Gleim* and *Finkelmann*. The properties of side chain liquid crystalline polymers in an electric and a magnetic field are summarized by *Haase*. Chapters 12 and 13 are concerned with two potential applications of side chain liquid crystalline polymers; as optically nonlinear media (*Möhlmann* and *van der Vorst*) and as materials for optical data storage (*McArdle*). Both contributions also cover theoretical aspects and compare side chain liquid crystalline materials with low molar mass liquid crystals and inorganic materials. The last chapter by *Janini, Laub, Purnell* and *Tyagi* treats theoretical aspects as well as experimental results concerning the use of side chain liquid crystalline polysiloxanes as the stationary phase in gas-liquid chromatography.

The book demonstrates the interactions which are necessary in such an interdisciplinary research area. All chapters are distinctly structured and well written. Figures, formulas and tables are uniform and clearly incorporated within the text. The more general introductions into each specific topic and the extensive up to date (1988) literature references are very valuable. However, the organization of the chapters is not entirely convincing. In addition, more specific cross references to other chapters would be helpful. Nevertheless, the book is highly recommended to academic and industrial researchers in the field of liquid crystals and is also of general interest to physicists and chemists working in linear and nonlinear optics, optoelectronics and molecular electronics.

Hans-Werner Schmidt
Fachbereich Physikalische Chemie – Polymere
der Philipps-Universität Marburg (FRG)

Conference Calendar

The black hand symbol ☛ denotes new entries into the calendar. Send information concerning conferences to the editorial office

September 1989

7–9 **Biomaterials**
8th Eur. Congr.
Heidelberg (Fed. Rep. Germany)
Contact: Dr. U. Soltesz, Fraunhofer-Institut für Werkstoffmechanik, Wöhlerstr. 11, D-7800 Freiburg, FRG

10–11 **Ceramics in Medicine**
2nd Int. Symp.
Heidelberg (Fed. Rep. Germany)
Contact: Dtsch. Keram. Gesellsch., Frankfurter Str. 196, D-5000 Köln 90, FRG

10–12 **Colloidal Dispersions**
Faraday Discussion 90
Bristol (UK)
Contact: Prof. R. H. Ottewill, School of Chemistry, Univ. of Bristol, Bristol BS8 1TS, UK

10–14 ☛ **Electronics Packaging**
9th Annu. Int. Conf.
San Diego, CA (USA)
Contact: W. D. Ashman, Int. Electronics Packaging Soc. Inc., IEPS, 114 North Hale St., Wheaton, IL 60187, USA, Tel. 312-260-1044

10–14 **Optical Communications**
15th Eur. Conf.
Gothenburg (Sweden)
Contact: P. A. Andrekson, Dept. of Optoelectronics, Chalmers Univ. of Technol., S-41296 Gothenburg, Sweden

10–15 **Materials and Fluid Sciences in Microgravity**
Eur. Conf.
Oxford (UK)
Contact: Dr. H. U. Walter, Eur. Space Agency, Microgravity Office, 8–10 rue Mario-Nikis, F-75738 Paris Cedex 15, France

10–23 **Molecular Dynamics of Liquid Crystals**
NATO Adv. Study Inst.
Il Ciocco, Lucca (Italy)
Contact: Prof. C. A. Veracini, Dipartimento di Chimica, Universita di Pisa, Viale Risorgimento 35, I-56100 Pisa, Italy



11–13 ☛ **Thin Solid and Liquid Films**
Int. Symp. Bristol (UK)
Contact: Conf. Secr., Society of Chem. Industry, 14/15 Belgrave Square, London SW1X 8PS, UK

11–13 **Charge Transfer in Polymeric Systems**
RSC, Faraday Div.
Contact: Dr. J. F. Gibson, Royal Soc. of Chemistry, Burlington House, Piccadilly, London W1V 0BN, UK

11–13 **Holographic Systems, Components and Applications**
2nd Int. Conf.
Bath (UK)
Contact: Inst. of Electronic and Radio Eng., Conf. Dept., Savoy Hill House, London WC2R 0JD, UK

11–13 **Surface Analysis Techniques and Applications**
Manchester (UK)
Contact: E. Wellingham, Conf. Secretariat, Field End House, Bude Close, Nailsea, Bristol BS19 2FQ, UK

13–15 ☛ **Physical Aspects of Polymer Science**
Reading (UK)
Contact: G. R. Mitchell, Polymer Sci. Centre, J. J. Thomson Physical Lab., Univ. of Reading, Whiteknights, Reading RG6 2AF, UK, Tel. 7034-318573, Fax 0734-750203

13–15 **Microscopy**
150th Anniversary Commemorative Mtg.
London (UK)
Contact: Microscopical Soc., 37–38 St. Clements, Oxford OX4 1AJ, UK

17–22 **Optics and Optical Engineering**
Cambridge Symp.
Cambridge (USA)
Contact: Soc. of Photo-Optical Instrumentation Eng. (SPIE), P.O. Box 10, Bellingham WA 98227, USA

18–22 **Quantum Electronics**
9th Natl. Conf.
Oxford (UK)
Contact: Mrs. M. Sherwen, Rutherford Appleton Lab., Chilton, Didcot, Oxon OX11 0QX, UK

19–21 **High-T_c Superconductors**
Birmingham (UK)
Contact: Dr. C. Greaves, School of Chemistry, Univ. of Birmingham, POB 363, Birmingham B15 2TT, UK, Tel. 021/414-4397

19–21 **Superconductivity and Applications**
3rd Annu. Conf.
Buffalo (USA)
Contact: NYSIS, 330 Bonner Hall, State Univ. of New York, Buffalo, NY 14260, Tel. 716/636-3463

19–22 **Structure and Dynamics of Colloidal Systems**
3rd Eur. Coll. and Interface Soc. Conf. and ILL Workshop
Basel (Switzerland)
Contact: Dr. M. Zulauf, c/o F. Hoffmann-La Roche + Co., ZFE 65–509, CH-4002 Basel, Switzerland, Tel. 0041/616885746, Fax 0041/616919391

20 **Properties and Applications of CVD Diamond Thin Films**
MRS Symp.
University Park, PA (USA)
Contact: R. Messier, Pennsylvania State Univ., 265 Materials Res. Lab., University Park, PA 16802, USA, Tel. 814-865-3704

20–22 **Structural Adhesives in Engineering**
SAE II '89
Bristol (UK)
Contact: J. Herriot, SAE II '89, Butterworth Scientific Ltd., P.O. Box 63, Westbury House, Bury St., Guildford, Surrey GU2 5BH, UK

20–22 **Manmade Fibers**
Int. Congr.
Dornbirn (Austria)
Contact: Austrian Manmade Fibers Inst., Plossigasse 8, A-1041 Vienna, Austria

21–22 **Fire Retardant Polymers**
Torino (Italy)
Contact: Prof. L. Costa, Dipl. di Chim. dell'Università di Torino, Via P. Giuria, 7, 10125 Torino, Italy

22–25 **Defect Recognition and Image Processing in Semiconductors.**
3rd Int. Symp. (DRIP 3)
Tokyo (Japan)
Contact: T. Ogawa, Dept. of Physics, Gakushuin Univ., Mejiro, Tokyo 171, Japan, Tel. 03-986-0221, Fax 03-590-2602

24–28 **Metallization of Polymers**
Int. Colloquium
Montreal (Canada)
Contact: Ed. Sacher, Ecole Polytechnique, Université de Montreal, Quebec H3C 3A7, Canada

25–26 **Additive Approaches to Improved Polymer Performance**
Toronto (Canada)
Contact: Jeff Hood, Stochem. Inc., 106 Summerlea Rd., Brampton, Ontario L6T 4X3, Canada

25–27 **Structure Formation in Polymer Solutions**
22nd Europhysics Conf.
Leuven (Belgium)
Contact: Prof. H. Berghmans, Lab. for Polymer Res., Katholieke Univ. Leuven, Celestijnenlaan 200F, B-3030 Leuven, Belgium, Tel. 16/200656, Fax 16/201215

25–27 **Surface Engineering with High Energy Beams**
2nd Int. Seminar
Lisbon (Portugal)
Contact: Secretariat of ISHT '89 Seminar, Ctr. of Mech. and Mater. of the Tech. Univ. Lisbon (CEMUL), 1096 Lisboa Codex, Portugal

25–27 **Industrial Applications of Advanced Materials**
Staffordshire (UK)
Contact: J. Robson, Staffordshire Design and Techn. Centre, Keele Sci. Park, Univ. of Keele, Staffordshire ST5 5BG, UK, Tel. 0785-52331

25–27 **Sensors**
Canterbury (UK)
Contact: Inst. of Physics, 47 Belgrave Sq., London SW1X 8QX, UK, Tel. 01-235-6111, Fax 01-259-6002

25–29 **GaAs and Related Compounds**
16th Int. Symp.
Karuizawa (Japan)
Contact: T. Katoda, Res. Center for Adv. Sci. and Techn., Univ. of Tokyo, 4-6-1 Komaba, Meguro-ku, Tokyo 154, Japan

25–29 **Ceramics' 89 "C89"**
4. Int. Conf. Limoges (France)
Contact: Comité Régional D'Expansion Economique du Limousin (CREEL), 27, Boulevard de la Corderi, F-87000 Limoges, France, Tel. 0033/55451830, Fax 0033/55797789

25–29 **Vacuum Solid Surfaces**
IVC-11/CSS-7
11th Int. Conf./7th Int. Conf.
Cologne (Fed. Rep. Germany)
Contact: D. A. Benninghoven, Physikalisches Inst. der Univ. Münster, Wilhelm-Klemm-Str. 10, D-4000 Münster, FRG

25–30 **Epitaxial Crystal Growth**
Int. Conf.
Budapest (Hungary)
Contact: Dr. E. Lendfay, Hung. Acad. of Sci., Inst. for Techn. Physics, Ujpest 1, POB 76, H-1325 Budapest, Hungary

26–28 **Optical Memory**
Int. Symp. (ISOM '89)
Kobe (Japan)
Contact: ISOM '89 Secretariat, Business Ctr. for Academic Soc. Japan, 3-23-1 Hongo, Bunkyo-ku, Tokyo 113, Japan

26–28 **Microcircuit Engineering '89**
Int. Conf. on Microlithography
Cambridge (UK)
Contact: R. A. McMahon, Conf. Sec. ME 89, Cavendish Lab. Madingley Rd., Cambridge CB3 OHE, UK

26–28 **SAMPE**
21st Int. Techn. Conf.
Atlantic City (USA)
Contact: SAMPE, 843 W. Glentana, P.O. Box 2459, Covina, CA 91722, USA, Tel. 818-331-0616

26–29 **Structure and Dynamics of Colloidal Systems**
3rd Eur. Colloid and Interface Conf.
Basle (Switzerland)
Contact: Dr. M. Zulauf, F. Hoffmann-La Roche & Co, ZFE 65-509, CH-4002 Basel, Switzerland

27–29 **Polymer Reaction Engineering**
3rd Berlin Int. Workshop
Berlin (West)
Contact: Prof. Dr. K.-H. Reichert, Inst. f. Techn. Chemie, TU Berlin, Straße des 17. Juni 135, D-1000 Berlin 10

27–29 **New Polymers**
1st Materials Symp.
Regensburg (Fed. Rep. Germany)
Contact: OTTI-Fortbildung, Martin-Luther-Straße 10, D-8400 Regensburg, FRG

28–29 **Biosensors '89**
Int. Conf.
Cambridge (U.K.)
Contact: Mrs. R. Duke, IBC Techn. Services Ltd., Bath Hse., (3rd Floor), 56 Holborn Viaduct, London EC1A 2EX, UK, Tel. 01-236-4080, Fax 01-489-0849

29 **Biomaterials**
3rd Colloq.
Aachen (Fed. Rep. Germany)
Contact: W. Breuers, Klinikum der RWTH-Aachen, Inst. f. Pathologie, Pauwelstr., D-5100 Aachen, FRG, Tel. 0241-80-88392

30–4 **High-T_c Thin Films and Single Crystals**
Int. Conf.
Ustron (Poland)
Contact: M. W. Gutowski, Inst. of Physics, ON-3 Polish Acad. of Sci., Al. Lotnikow 32/46, PL-02668 Warszawa, Poland

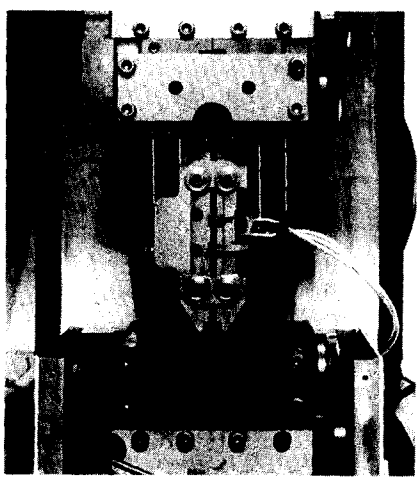
October 1989

1–4 **Interfaces in Condensed Systems Equilibria and Dynamic Phenomena**
Annu. Mtg. Dtsch. Kolloid-Gesellsch. Bochum (Fed. Rep. Germany)
Contact: Prof. Dr. G. H. Findenegg, Physikal. Chem. II, Ruhr-Univ., P.O. Box 102148, D-4630 Bochum 1, FRG, Tel. 0234/7004229

1–5 **The Metallurgical Society**
Fall Mtg.
Indianapolis (USA)
Contact: Mtgs. Dept., TMS, 420 Commonwealth Dr., Warrendale, PA 15086, USA

1–5 **Halide Glasses**
6th Int. Symp.
Clausthal (Fed. Rep. Germany)
Contact: Prof. G. Frischat, Techn. Univ. Clausthal, Fak. für Bergbau, Hütten- und Maschinenwesen, Adolf-Römer-Str. 2A, D-3392 Clausthal-Zellerfeld, FRG

Mechanical Testing of Composites



Zwick offer a wide range of Universal Testing Machines from 2 kN to 500 kN, for tensile, compression and flexural tests, plus:

- High Resolution Dual Strain Sensor Transducers (Temperature −70° to +270° C)
- Strain Measurement for thread and composite fibre bundles
- Transverse Strain Measurement for Poissons Ratio
- Compression and stabilising rigs
- Temperature Chambers (−150° to +400° C)

In addition, machine control and data storage is fully PC compatible.

Zwick is your reliable partner for testing composites in aerospace or any other high-tech industry

Interkama: Hall 01, Booth 1B 06;
K '89: In own Pavilion near hall 15

Zwick

Materials Testing

Zwick Testing Machines Ltd.
Leominster HR6 0QH, Tx 35692
Zwick Italia s.r.l.
I-31033 Castelfranco V, Tx 223422
Zwick Scandinavia
S-161 15 Bromma, Tx 14441
Zwick GmbH & Co.
D-7900 Ulm, Tx 712830

9.12.1.61

2–3 **Makromoleculares Symposium**
Hamburg (Fed. Rep. Germany)
Contact: Prof. Dr. W. Kaminsky, Inst. f. Techn. u. Makromol. Chemie, Univ. Hamburg, Bundesstr. 45, D-2000 Hamburg 13, FRG

2–4 **Electron and Optical Beam Testing of Integrated Circuits**
2nd Eur. Conf.
Duisburg (Fed. Rep. Germany)
Contact: E. Kubalek, Werkstoffe der Elektronik, Univ. Duisburg, Kommandanten-Str. 60, D-4100 Duisburg 1, FRG

2–4 **High Temperature Polymers**
Cleveland (USA)
Contact: Vivian E. Malpass, Ferro Corp., Technical Ctr., 7500 East Pleasant Valley Rd., Independence, OH 44131, USA

2–5 **Materials Week**
Technical Conf.
Indianapolis (IN, USA)
Contact: Technicol Dept. Marketing, ASM Int., Metals Park, OH 44073, USA

3–6 **Composite Materials**
4th Techn. Conf.
Blacksburg, VA (USA)
Contact: M. W. Hyer, ESM Dept., Virginia Tech., Blacksburg, VA 24061, USA, Tel. 703-231-5372

4–6 **Fabrication and Characterization of Semiconductor Optoelectronic Devices and Integr. Circuits**
1st Int. Mtg.
Tokyo (Japan)
Contact: Univ. of Tokyo, Dept. of Electronic Eng., Hongo, Bunkyo-ku, Tokyo 113, Japan

8–11 **Organometallic Vapor Phase Epitaxy**
4th Biennial Workshop
Monterey (USA)
Contact: B. Kamperman, TMS, 420 Commonwealth Dr., Warrendale, PA 15086, USA, Tel. 412/776-9050, Fax 412/776-3770

8–13 **Microelectronic Integrated Processing**
Symp.
Santa Clara, CA (USA)
Contact: SPIE, POB 10, Bellingham, WA 98227-0010, USA, Tel. 206-676-3290, Fax 206-647-1445

9–10 **Quasicrystals**
DFG-workshop
Bad Honnef (Fed. Rep. Germany)
Contact: Dr. J. Tobolski, Dtsch. Forschungsgem., Bad Godesberg, Kennedyallee 40, D-5300 Bonn 2, FRG

9–11 **German Ceramics Society Annu. Mtg. 1989**
Coblenz (Fed. Rep. Germany)
Contact: Dtsch. Keramische Gesellsch., Frankfurter Str. 196, D-5000 Köln 90, FRG, Tel. 02203-69069, Fax 02203-69301

9–13 **Defect Engineering in Semiconductor Technology**
3rd Int. Mtg.
Castle Garzau (German Dem. Rep.)
Contact: M. Kittler, Inst. of Semiconductor Physics, Acad. of Sciences of the GDR, POB 409, Frankfurt 1200, East-Germany

10–13 **Ion Beams in Materials Research and Technology**
4th Europhysics Ind. Workshop Bad Honnef (Fed. Rep. Germany) Contact: G. Thomas, Eur. Physical Soc., POB 69, CH-1213 Petit-Lancy 2, Switzerland

11–13 **Materials for Electrochemistry**
Stuttgart (Fed. Rep. Germany)
Contact: Prof. F. von Sturm, Jahnstr. 26, D-8901 Biberbach, FRG

11–13 **Surface Technology Forum**
SURTEC '89
Berlin (West)
Contact: AMK Berlin, M 3/Surtec, Messedamm 22, D-1000 Berlin 19

15–18 **Unconventional Photoactive Solids**
4th Int. Conf.
San Jose (USA)
Contact: Dr. C. G. Willson, IBM Almaden Research Ctr., 650 Harry Road, San Jose, CA 95120, USA

16–19 **High-Tech-Coating**
Congr. and Exhibition
Wiesbaden (Fed. Rep. Germany)
Contact: Demat Exposition Managing, P.O. Box 110611, D-6000 Frankfurt, FRG

17–18 **Optics in Computing**
Int. Symp.
Toulouse (France)
Contact: Secretariat Des Conferences, OPTO-Informatique, ONERA-CERT, BP 4025, F-31055 Toulouse Cedex, France

17–18 **Superconductivity: the Manufacturing Challenge**
Oak Brook (USA)
Contact: K. L. Kammerer, SME, Techn. Committee, Projects Dept., 1 SME Drive, POB 930, Dearborn, MI 48121-0930, USA, Tel. 313/271-1500/542

17–19 **Optical Storage for Large Systems**
4th Annu. Conf.
New York, (USA)
Contact: Rothchild Consult., 256 Laguna Honda Blvd., San Francisco, CA 94116-1496, USA

18–20 **Crystal Growth**
3rd Conf.
Atlantic City, NJ (USA)
Contact: J. C. Jacco, Ferroxcube Div., Amperex Electronic Corp., 5083 Knigs Hwy., Sangerties, NY 12477, USA, Tel. 914-246-2811

22–28 **Solid-State and Integrated Circuit Technology**
2nd Int. Conf.
Beijing (P.R. China)
Contact: Continuing Education in Eng., Univ. Extension, Univ. of California, 2223 Fulton St., Berkeley CA 94720, USA

23–24 **Modern Aspects of Superconductivity**
Int. Conf.
Paris (France)
Contact: Dr. R. Suryanarayanan, Lab. de Physique des Solides, 1, Place Aristide Briand, 92195 Meudon, France, Fax 1/45344696

23–24 **High-T_c Superconductors and Crystal Chemistry III**
Bad Honnef (Fed. Rep. Germany)
Contact: Dr. J. Debrus, Physikzentrum, Hauptstr. 5, D-5340 Bad Honnef 1, FRG

24–25 **Critical Currents in High-T_c Superconductors**
Karlsruhe (Fed. Rep. Germany)
Contact: M. Vukovojac, Conf. Organizer, Butterworth Scientific Ltd., POB 63, Westbury Hse., Bury St., Guildford, Surrey GU2 5BH, UK, Tel. 0483-300966, Fax 0483-301563

24–29 **Applications of Surface and Interface Analysis**
Eur. Conf. (ECASIA '89)
Antibes (France)
Contact: J. Fauvet, Soc. Français du Vide, 19, rue du Renard, F-75004 Paris, France

November 1989

5–8 **Solid State Ionics**
7th Int. Conf.
Hakone (Japan)
Contact: Dr. Y. Saito, Res. Lab. of Engineering Materials, Tokyo Inst. of Technol., 4259 Nagatsuta-cho, Midori-ku, Yokohama 227, Japan

14–15 **Polypropylene**
Madrid (Spain)
Contact: D. Varley, Plastics and Rubber Inst., 11 Hobart Place, London SW1W 0HL, UK

14–17 **Superconductivity**
2nd Int. Symp.
Ibaraki (Japan)
Contact: ISS '89 Secr., ISTEC, Eishin Kaihatsu Bldg., 34-3, Shimbaski 5-chome, Minato-ku, Tokyo 105, Japan, Tel. 03/431-4002, Fax 03/431-4044

22–24 **Euromat '89**
Eur. Conf. on Materials
Aachen (Fed. Rep. Germany)
Contact: Dtsch. Gesellsch. Metallkd., Adenauerallee 21, D-6370 Oberursel, FRG

23–24 **Superconductivity**
Int. Conf.
Paris (France)
Contact: Dr. R. Suryanarayam, Lab. de physique des solides de Bellevue, CNRS, F-92195 Meudon, France

27–29 **Electronic Packaging**
55th WE-Heraeus-Seminar
Bad Honnef (Fed. Rep. Germany)
Contact: Dr. V. Schäfer, WE-Heraeus-Stift., Heraeusstr. 12–14, D-6450 Hanau, FRG

27–2 **MRS Fall Mtg.**
Boston (USA)
Contact: A. Wagner, Materials Research Soc. (MRS), 9800 McKnight Rd., Suite 327, Pittsburgh, PA 15237, USA



27–2 **Electrical, Optical and Magnetic Properties of Organic Solid State Materials**
Boston (USA)
Contact: P. Chaikin, Dept. of Physics, Princeton Univ., Princeton, NJ 08544, USA, Tel. 609/452-4338

December 1989

4–5 **Advanced Materials by Sol-Gel Techniques, Eurogel '89**
Eur. Conf.
Strasbourg (France)
Contact: Fraunhofer-Inst. f. Silicatforsch., "Eurogel '89", Neunerplatz 2, D-8700 Würzburg, FRG

11–13 **CBE/MOMBE and Related Growth Techniques**
2nd Int. Conf.
Houston, TX (USA)
Contact: H.-D. Shih, Univ. of Houston, Sci. and Res. One, 4800 Calhoun Rd., Houston, TX 77004, USA, Tel. 713-749-3701, Fax 713-747-7724

11–16 **Physics of Semiconductor Devices**
5th Int. Workshop
New Delhi (India)
Contact: Dr. S. K. Sharma, IWPSD-89, Nat. Physical Lab., Dr. K. S. Krishnan Rd., New Delhi-110012, India, Tel. 586087

12–15 **Pacific Polymer**
Hawaii (USA)
Contact: J. C. Vogl, Pacific Polym. Federation, Polytechnic Univ., 333 Jay St., Brooklyn, NY 11201, USA

January 1990

10–14 **Superconductivity**
Int. Conf.
Bangalore (India)
Contact: Prof. S. V. Subramanyam, ICSC, Dept. of Physics, Indian Inst. of Sci., Bangalore 560012, India, Tel. 91-812-344411, Fax 91-812-341683

22–26 **Recrystallization in Metallic Materials**
Int. Conf.
Wollongong (Australia)
Contact: T. Chandra, Dept. of Metallurgy and Materials Eng., Univ. of Wollongong, Wollongong NSW 2500, Australia, Tel. 042-270008, Fax 042-270477

February 1990

4–7 **Ceramic Powder Processing**
3rd Int. Conf.
San Diego, CA (USA)
Contact: G. L. Messing, Pennsylvania State Univ., University Park, PA 16802, USA, Tel. 814-865-2262, Fax 814-865-2917

4–8 **18th Australian Polymer Symposium**
Bendigo, Vic. (Australia)
Contact: Dr. J. D. Wells, Bendigo College of Adv. Education, Bendigo, Victoria 2550, Australia

19–22 **Advanced Metals & Ceramics**
1990 TMS Annu. Mtg.
Int. Conf.
Anaheim, CA (USA)
Contact: M. Karl, TMS, Meetings Dept., 420 Commonwealth Drive, Warrendale, PA 15086, USA, Tel. 412-776-9050, Fax 412-776-3770

25–27 **Interphase Reactions and Interactions**
Freiburg (Fed. Rep. Germany.)
Contact: Prof. Dr. H.-J. Cantow, Hermann-Staudinger-Haus, Stefan-Meier-Str. 31, D-7800 Freiburg, FRG

March 1990

12–16 **American Physical Society Meeting**
Anaheim, CA (USA)
Contact: W. W. Havens, J., APS, 335 E., 45th St., New York, NY 10017, USA

Registered names, trademarks, etc. used in this journal, even when not marked as such, are not to be considered unprotected by law.

© VCH Verlagsgesellschaft mbH, D-6940 Weinheim, 1989. – Printed in the Federal Republic of Germany by Konrad Triltsch Druck- und Verlagsanstalt Würzburg.

All rights reserved (including those of translation into foreign languages). No part of this issue may be reproduced in any form — by photoprint, microfilm, or any other means — nor transmitted or translated into a machine language without written permission from the publishers. Only single copies of contributions, or parts thereof, may be made for personal use. This journal was carefully produced in all its parts. Nevertheless, authors, editors and publisher do not warrant the information contained therein to be free of errors. Readers are advised to keep in mind that statements, data, illustrations, procedural details or other items may inadvertently be inaccurate.

Valid for users in the USA: The appearance of the code at the bottom of the first page of an article (serial) indicates the copyright owner's consent that copies of the article may be made for personal or internal use, or for the personal or internal use of specific clients. This consent is given on the condition, however, that the copier pay stated per-copy fee through the Copyright Clearance Center, Inc. (CCC), for copying beyond that permitted by Sections 107 or 108 of the U.S. Copyright Law. This consent does not extend to other kinds of copying, such as copying, for general distribution, for advertising or promotional purposes, for creating new collective works, or for resale. For copying from back volumes of this journal see 'Permissions to Photo-Copy: Publisher's Fee List' of the CCC.

Editorial office: Postfach 10 11 61, D-6490 Weinheim, Federal Republic of Germany, Telephone (06201) 60 22 55, Telex 465 516 vchwh d, Telefax (06201) 602 328.

Editor: *Peter Gölitz*

Associate Editor: *Peter Gregory*. **Editorial Assistant:** Susanne Stoll

Publishers: VCH Verlagsgesellschaft mbH. (Managing Director: *Hans Dirk Köhler*), Pappelallee 3, D-6940 Weinheim, Federal Republic of Germany.

Advertising office (Advertising Manager *R. J. Roth*): Postfach 10 11 61, D-6940 Weinheim, Federal Republic of Germany, Telephone (0 62 01) 60 61 30, Telex 467 155 vchwh d, Telefax (0 62 01) 606 184.

The Active Sites in Manganese-Containing Metalloproteins and Inorganic Model Complexes

By Karl Wieghardt*

Manganese is an essential trace element, forming the active sites of a number of metalloproteins. Several metalloproteins contain two or more manganese ions per subunit. The structural properties of these enzymes and the experimental evidence for their proposed structures are described. Parallel to the efforts of biochemists, who are seeking to understand the function of these enzymes on a molecular level, inorganic chemists have been investigating the coordination chemistry of bi- and polynuclear complexes of manganese which contain O,N donor atoms and a variety of bridging O,N ligands. A large number of such complexes have been synthesized, their X-ray structures determined and their magnetic and spectroscopic properties studied in detail. In some instances the electronic and spectroscopic properties of these model compounds are amazingly similar to those of the biomolecules. This has led to a deeper understanding of the structure and sometimes of the function of the metalloproteins. Research on manganese metalloproteins with polynuclear active sites represents a fascinating example of interdisciplinary cooperation between physicists, biochemists and inorganic chemists.

1. Introduction

Manganese is an essential trace element. Typical defficiency symptoms in human beings are growth disorders, bone deformations, abnormalities in membrane formation and defects in the connective tissues. The amount of manganese in a grown man (75 kg) is only about 10–20 mg, in comparison to the 3–4 g of iron.[1] Plants and many bacteria also require minute amounts of manganese for a healthy existence. In its divalent form manganese can be an enzyme activator or, alternatively, it can form the active site of the metalloprotein.

Up to now relatively few manganese-containing metalloproteins have been isolated pure and structurally sufficiently well characterized to determine the nature of the active sites. The resolution of a single crystal X-ray determination is rarely sufficient to reveal the bonding characteristics of the manganese center (ca. 1.8–2.2 Å is required). The exact coordination geometry of the manganese atom in the protein is, however, required to give a deeper understanding of the respective functions of the enzymes.

When manganese is in the relevant physiological oxidation states +II, +III, +IV (and possibly +V) with "normal" coordination of the oxygen and nitrogen atoms from the protein (possible coordination numbers being 4, 5 and above all 6), it forms a paramagnetic centre: Mn^{II} high spin (h.s.) d^5-electronic configuration (five unpaired electrons), Mn^{III} d^4 (h.s.) (four unpaired electrons), Mn^{IV} d^3 (three unpaired electrons), Mn^{V} d^2. This means that such metalloproteins can be investigated particularly well using physical methods. For example:

1) Electron spin resonance (ESR) spectroscopy: very sensitive and informative for Mn^{II}[2] and for polynuclear complexes in which the manganese ions are in different oxidation states (mixed valence complexes, e.g. $Mn^{II}Mn^{III}$ or $Mn^{III}Mn^{IV}$).

2) Electron spectroscopy (UV-VIS spectroscopy):[3] particularly informative in the case of Mn^{III} and Mn^{IV} complexes due to (d-d) and charge-transfer (CT) absorption bands in the visible region.

3) Measurement of the magnetic susceptibility: allowing the study of the coupling of the electrons in neighboring manganese centers and thereby yielding an estimate of the distance between them.

4) Resonance Raman spectroscopy: affording information about the first coordination sphere of the Mn atoms.

5) X-ray absorption spectroscopy (EXAFS: *e*xtended *X*-ray *a*bsorption *f*ine *s*tructure, XANES: *X*-ray *a*bsorption *n*ear *e*dge *s*tructure): likewise giving information about the nature of the surrounding atoms and the oxidation state of the manganese ions.

However, each of these methods gives limited structural information only. Frequently, the combination of spectroscopic results on biomolecules and available knowledge of the spectroscopic and coordination properties of low molecular weight manganese complexes can lead to reasonable and likely structural proposals. On the other hand, in many cases spectroscopic results are obtained which are not understood by comparison with those of known manganese complexes. Here the coordination chemist needs to synthesize new relatively simple model complexes whose structures must be established in order to study their spectroscopic properties. Comparison of these results with the properties of the metal centers in biomolecules can then give information as to whether more such complexes are needed or if it is necessary for the biochemist to modify his proposed structure. This interdisciplinary cooperation between theoretical, physical and inorganic chemists on the one hand and biochemists on the other has over the last two or three decades been coined "bioinorganic chemistry".

For the inorganic chemists, in this context, metalloproteins with two or even more manganese atoms per subunit are particularly interesting. These Mn atoms can be relatively close to one another (Mn–Mn distance < 6 Å) and, consequently, inorganic chemists can conceive the

[*] Prof. Dr. K. Wieghardt
Lehrstuhl für Anorganische Chemie I der Universität
Postfach 102148, D-4630 Bochum (FRG)

biomolecule as a binuclear complex where the two Mn centers are ligated by a very large chelating ligand, namely the apoprotein. These metalloproteins are described in the first part of this review. Emphasis is laid on the structural aspects of their active sites and the evidence for published proposals, which are often based on a comparison of the spectroscopic properties of the metalloprotein with those of the synthesized model complexes whose structural and electronic properties are well defined. In the second part the chemistry of these manganese complexes is discussed and its relevance to biochemistry demonstrated. The characteristics of the model complexes[4] are discussed in order to show their enormous potential in determining the nature of the active sites of metalloproteins.

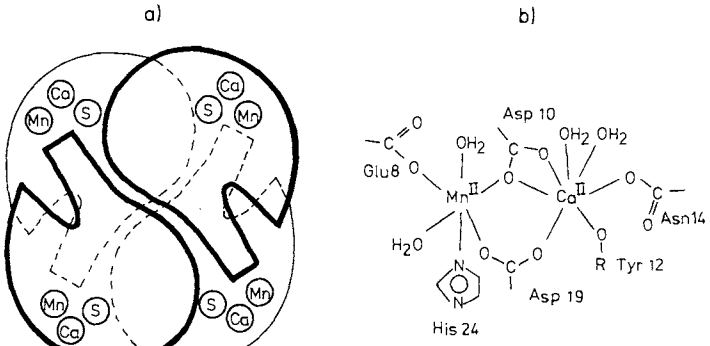


Fig. 1. a) Schematic representation of concanavalin A tetramers. The manganese and calcium binding sites are given as well as the saccharide binding site (S) near the metal atoms [6f]. b) Structure of the metal centers in concanavalin A.

2. Biomolecules with Binuclear Active Sites

2.1. Concanavalin A

This manganese and calcium metalloprotein belongs to the lectin group. It is a vegetable protein that was first isolated from jack beans, *Canavalia enisformis*;[5] subsequently animal forms were also found in mammalian cells. Its biological function is unknown but it has specific binding sites for small carbohydrates (α-D-mannopyranose, α-D-glucopyranose). Its activity is regulated by the coordination of divalent metal ions (the apoprotein does not have a large affinity for these molecules).

An X-ray structure determination, in which the resolution of the three-dimensional electron density was 2.0 Å, revealed the structure of the active site of concanavalin A, schematically illustrated in Figure 1.[6] It consists of four similar subunits at pH > 7, with a molecular weight of 25500 per unit. It forms dimeric species at pH < 6. To each subunit is bound a Mn^{II}-(S1 'transition metal binding site') and a calcium ion (S2 'calcium binding site'), which are 4.25 Å apart. The two metals are symmetrically and unsymmetrically bridged by the carboxylate groups of the aspartic acid moieties 19 and 10, and each binds two H_2O molecules. The N atom from the imidazole ring from Histidine 24 and an O atom from the $-CO_2^{\ominus}$- group of glutamate 8 are also coordinated to the Mn^{II} center; it is therefore in an octahedral environment ($MnNO_5$ coordination).

As well as being bound to the previously mentioned bridging carboxylate ligands the $Ca^{2\oplus}$ is also ligated by a carboxylate group and a phenolate group from aspartinate 14 and tyrosinate 12 and the second O atom of the asymmetrically bridging carboxylate group from aspartate 10: it exhibits a seven coordinate environment (distorted octahedral +1 coordination; CaO_7). The binuclear complex can be regarded approximately as two octahedra connected by a common edge. The structure of the apoprotein is also known, the subunits probably exhibit a different conformation than in the protein.

The metal binding sites S1 and S2 show different affinities for the divalent metal cations. This makes it feasible to selectively exchange the more weakly bound $Ca^{2\oplus}$ ion for divalent transition metal cations. The reaction of the apoprotein with Mn^{II} in the presence of methyl-α-D-mannopyranoside (α-MDM) leads to a ternary complex, which contains *two* manganese ions per subunit. The ESR spectra[7] of the Ca/Mn form without bound α-MDM (SCMPL form) and the metabolized Mn_2^{II} form with two Mn^{II} ions and bound α-MDM (SMMPL form) are completely different at 77 K. The SCMPL form shows a six-line spectrum (separation 92 G) at $g = 2.0$ typical for a Mn^{II} ion octahedrally coordinated by oxygen atoms, whereas a series of overlapping signals each split into eleven lines due to hyperfine coupling (altogether at least 32 resonances were observed) were found at $g = 1.927$ (77 K) for the SMMPL form. The hyperfine splitting was only 47 G, half the value of the SCMPL form (Fig. 2). The coordination of the two Mn^{II} ions in the SMMPL form is therefore different, and the spin systems are antiferromagnetically coupled: $H = -2JS_1S_2$ ($S_1 = S_2 = 5/2$) with a



Karl Wieghardt was born in Göttingen in 1942. He studied chemistry in Hamburg and Heidelberg from 1962–1967. After graduation he remained in Heidelberg studying under the supervision of Prof. Hans Siebert, receiving his doctorate in 1969. He spent the following years carrying out postdoctoral research with Prof. Siebert, and finally with Prof. A. G. Sykes in Leeds (1972). On returning to Germany he first took up an appointment as Lecturer at the University of Heidelberg (1974–1975) and then as Professor at the Technical University of Hannover (1976–1980) before accepting the offer of a chair in chemistry at the University of Bochum. Prof. Wieghardt's research interests include inorganic reaction mechanisms (redox chemistry), complex chemistry with macrocycles, preparative coordination chemistry, and bioinorganic chemistry.

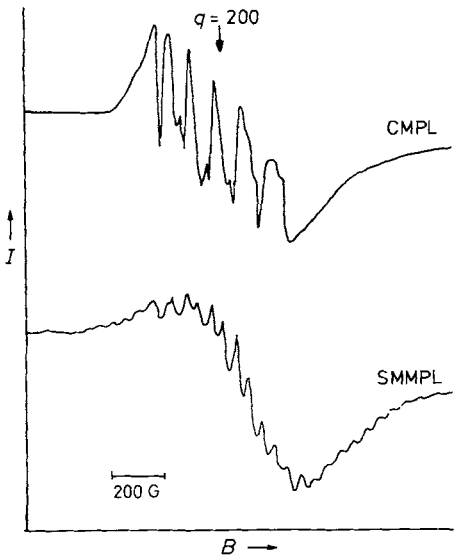


Fig. 2. X-band ESR spectra of the CMPL and SMMPL forms of concanavaline A at 77 K. CMPL is the $Ca^{2\oplus}/Mn^{II}$-containing form *without* an additional bound saccharide. The SMMPL form contains *two* neighboring Mn^{II} centers and a bound saccharide (α-MDM) [7]. B = magnetic field strength; I = first derivation of the ESR signal; g = 2.00.

spin exchange coupling constant of $J = -0.9\ cm^{-1}$ (weak antiferromagnetic coupling). The intensity of the signal of the SMMPL form decreases considerably between 1.4 and 4 K because the ground state ($S = 0$) is reached, in contrast to the SCMPL signal which remains strong ($S = 5/2$ ground state). These results were confirmed by measuring the magnetic susceptibility of the apoprotein (to obtain the diamagnetic correction) and the two differing manganese-containing forms of concanavalin A.[7b]

2.2. Further Metalloproteins with Neighboring Mn^{II} Ions

The enzymes to be described below are structurally less well characterized; no X-ray structural analyses are available to date. They all contain at least two metal cations of which one or both can be Mn^{II}. In vivo these cations can be $Mg^{2\oplus}$, $K^{\oplus}$ or $Ca^{2\oplus}$, but in vitro they can be replaced by Mn^{II}, making an ESR investigation possible. Metalloproteins which bind several metal ions and which can be investigated using Mn^{II} ions as a probe, include: pyruvate-kinase,[42] *S*-adenosylmethionine-synthetase,[8] phosphoribosylpyrophosphate-synthetase,[43] enolase,[12] inorganic pyrophosphatase,[44] and carbamylphosphate-synthetase.[45]

Some of these enzymes will be described in more detail since they demonstrate the use of ESR spectroscopy in structural investigations.

S-Adenosylmethionine-synthetase,[8] which is isolated from *Escherichia coli*, requires two metal cations (in vivo $Mg^{2\oplus}$ and $K^{\oplus}$) per enzyme subunit (it is a tetramer in its active form) to achieve optimum activity. It binds two Mn^{II} ions per subunit in the presence of a nucleotide substrate (adenylimidophosphate) or of pyrophosphate product. In the absence of nucleotides only one Mn^{II} ion per subunit is coordinated. The two Mn^{II} centers in the ternary complex must be located next to each other since weak spin exchange coupling is observed in the ESR spectrum.[8d] This coupling is caused by a magnetic superexchange through at least one bridging ligand. There are two different Mn binding sites per subunit; one is formed from the ligands of the protein component, the other can only be used if nucleotides or pyrophosphates are present. The second binding site for the Mn^{II} ion is thought to be in the phosphate component of the nucleotide. The two sites in the ternary complex are bridged by either the α-phosphoryl group of the nucleotide or by a functional group (carboxylate?) from another part of the protein.

Glutamine-synthetase, which is also isolated from the *Escherichia coli* shows very similar characteristics. It consists of twelve identical subunits and catalyzes different reactions, including the biosynthesis of glutamine from glutamate, ammonia and ATP.[9] In vivo, the enzyme requires two Mn^{II} cations to achieve catalytic activity. In the absence of ATP two Mn^{II} ions are bound at two different sites, S_1 and S_2 with differing affinities. The first $Mn^{2\oplus}$ ion is coordinated at S_1 within the protein in the absence of the substrate (a nucleotide), inducing thereby a conformational change, the second $Mn^{2\oplus}$ then occupies the S_2 site and facilitates a connection between the second $Mn^{2\oplus}$ in S_2 and the incoming substrate nucleotide. ESR investigations have shown[9h] that the distances between the S_1 and S_2 sites vary between 8 and 10 Å according to the nucleotide bound. The manganese containing enzyme with a Mn^{II} in the S_1 only was treated with a Cr^{III} containing nucleotide,[10] which acts kinetically as a 'dead end' inhibitor of the enzyme activity. The electronic interaction between the paramagnetic Cr^{III} ion in S_2 and the Mn^{II} (d^5 h.s.) in S_1 was investigated.[9h] Using the dipolar electronic spin relaxation theory of *J. S. Leigh*[11] the distance between S_1 and S_2 can be estimated from the spin-spin interaction.[11] Figure 3 shows the current proposal for the active site in glutamine synthetase in the presence of a Co^{III}-ATP complex.

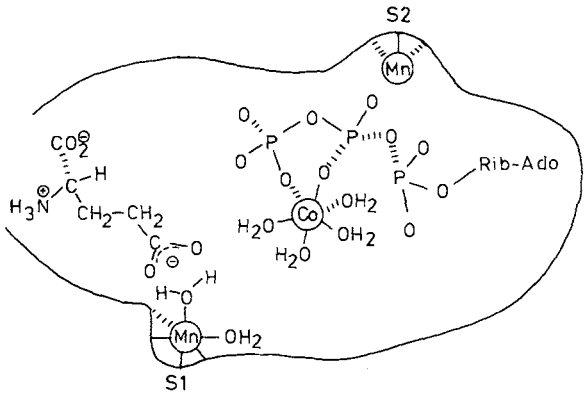


Fig. 3. Current proposal for the manganese binding site in glutamine synthetase in the presence of Co^{III}-ATP [1c].

Different binding sites for two $Mg^{\oplus}$ and Mn^{II} per subunit were discovered in a *yeast enolase* (phosphoenolpyruvate-hydratase) from *Escherichia coli 4.2.1.11*.[12] Additional Mn^{II} binding sites were also detected by ESR spectroscopy when the ratio $[Mn^{II}]/[enolase]$ was > 2. Weak spin-spin exchange interactions ($J = -0.0043\ cm^{-1}$) indicate that these sites must be near a Mn^{II} center that is strongly bound to the protein.

Finally, a manganese-containing catalase from *Thermophilium album*, a thermophilic bacteria, has been isolated. It has a molecular weight of 141 000[13] and is tetrameric with 1.4 ± 0.4 Mn^{II} ions per subunit. It is not clear if this enzyme contains one or two manganese centers per subunit. The enzyme is colorless; no absorption band has been found in the visible region, which may indicate the presence of Mn^{II} rather than Mn^{III} ions.

2.3. Metalloproteins with Mn^{III} Centers

Among the best characterized manganese containing proteins of this type are the superoxide dismutases (SODs), catalases and pseudocatalases.[14] The former catalyze the decomposition of $O_2^{\ominus}$-radicals [Eq. (a)] and the latter two the decomposition of H_2O_2 [Eq. (b)].

$$2\,O_2^{\cdot\ominus} + 2\,H^{\oplus} \rightarrow H_2O_2 + O_2 \qquad (a)$$

$$2\,H_2O_2 \rightarrow 2\,H_2O + O_2 \qquad (b)$$

These SODs are red and contain only one Mn^{III} ion per subunit. The metal ion is surrounded by N- and O-donor atoms from the amino acids of the polypeptide chain. The Mn^{III} ions are substantially more firmly bound than the Mn^{II} in the metalloproteins described in Sections 2.1 and 2.2. They show no ESR signals but a characteristic absorption spectrum with an intense maximum in the visible region ($^5E_g \rightarrow {}^5T_{2g}$ in O_h symmetry).

The SOD isolated from *Thermus thermophilus HB8* has been structurally characterized by X-ray diffraction.[15] It consists of four similar subunits. The resolution (2.4 Å) was good enough to allow the first coordination sphere of the Mn^{III} ion to be determined.[15b] Figure 4 shows the active

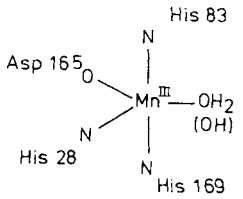


Fig. 4. Schematic representation of the active site of the superoxide dismutase from *Thermus thermophilus* bacteria.

site; four donor atoms (three N atoms, and one carboxylate-O atom) from the protein and a coordinated H_2O molecule (or $OH^{\ominus}$) give the Mn center a trigonal bipyramidal coordination geometry.

2.3.1. The Catalase from Thermus Thermophilus (HB8 strain)

Unlike all other known catalases, this catalase is very heat resistant. It consists of two Mn^{III} ions per subunit (MW = 33 000–37 000) and is a hexamer. A red single crystal was subjected to an X-ray analysis.[16] Figure 5 shows schematically the arrangement of the six subunits and a sketch of one subunit, in which the two neigboring Mn^{III}

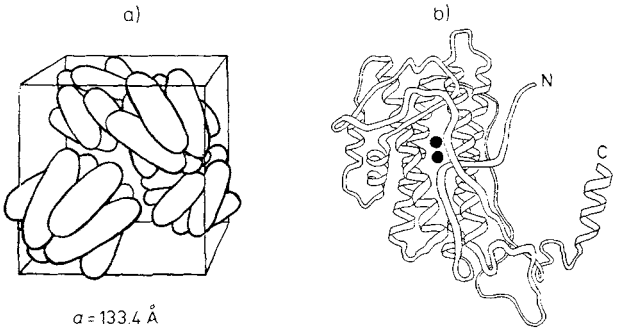
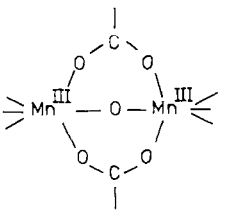


Fig. 5. Catalase from *Thermus thermophilus* (HBB strain): schematic representation a) of the quarterary structure of the hexamer in the crystal, b) a subunit. The black circles represent two manganese atoms separated by 3.6 Å [16].

centers can be clearly seen (Mn · · · Mn 3.6 Å). Due to the low resolution (3 Å) it is not possible to clearly establish the nature of the first coordination sphere of the metal centers. The manner in which the bridging ligands connect the two Mn centers is, therefore, also uncertain.

Each subunit consists of a polypeptide chain of about 300 amino acids; the sequence being unknown. Four large parallel α-helices of 25–30 amino acids form most of the quarternary structure of a subunit. The Mn ions are situated in the center of the four α-helices. This metalloprotein belongs to the group of four α-helix proteins, to which the iron-containing protein hemerythrin[17] also belongs. In this protein two Fe^{III} ions form a μ-oxo-bis(μ-carboxylato)diiron(III) structural unit to which N atoms from histidine moieties are bound. The structural relationship between some iron-containing[18] and some manganese-containing proteins will be encountered frequently further on. The duality of Fe^{III} and Mn^{III} is often referred to in the literature, since in some cases a metalloprotein can be reconstituted from the apoprotein using either Fe^{III} or Mn^{III}. Sometimes even the enzymatic activity is retained.

Interestingly, the electronic spectrum of this form shows an intense absorption band at 450 nm with a shoulder at 500 nm. As I will show later (Section 4.2) these bands are characteristic of the μ-oxo-bis(μ-carboxylato)dimanganese(III) structural unit (Scheme 1).



Scheme 1.

Khangulov et al. have shown in an elegant piece of work[16d,e] that a series of more complicated but also more informative ESR spectra are observed, if the Mn_2^{III} form is changed to Mn_2^{II}, $Mn^{II}Mn^{III}$ and $Mn^{III}Mn^{IV}$ forms by external reductants or oxidants. Particularly diagnostic is the ESR spectrum of the mixed valence form $Mn^{III}Mn^{IV}$, which shows a sixteen line pattern (50–70 K). This is characteristic for a strongly antiferromagnetic coupled (Mn^{III} $S = 2$, Mn^{IV} $S = 3/2$) oxo-bridged dimer with a $S = 1/2$ ground state.

2.3.2. The Pseudocatalase from Lactobacillus Plantarum

In concentrated solutions this catalase is pink. It has a molecular weight of 172000 and consists of five similar subunits (MW 34000), which each have two Mn^{III} ions.[19] The term pseudocatalase was introduced in order to indicate that the catalase activity is not inhibited by azide or cyanide ions, unlike in the case of other known catalases. The use of the prefix 'pseudo' has been criticized because it could imply that the catalase activity is impaired, disrupted or different, and this is not the case.

The existence of two manganese centers in close proximity was first concluded from the electronic spectrum (Fig. 6b).[61] In the visible region, a band was observed at 470 nm with shoulders at 398 and 500 nm. The molar absorption coefficient (ca. 1.3×10^3 L mol^{-1} cm^{-1}) are distinctly larger than they would normally be for monomeric octahedral Mn^{III} complexes. The synthesis of simple model complexes showed that such absorption bands are typical of complexes with the structural unit μ-oxo-bis(μ-carboxylato)dimanganese(III) or μ-oxo-bis(μ-carboxylato)manganese(III)-manganese(IV).[81,82]

This more 'indirect' evidence was recently confirmed by the discovery of a 16-line ESR spectrum of the biomolecule (Fig. 6a).[20] The manganese ions therefore form a mixed valence $Mn^{II}Mn^{III}$ or more likely a $Mn^{III}Mn^{IV}$ unit. In acid solution the manganese ions disproportionate, forming substitutionally labile Mn^{II}, which leaves the active site as $Mn(OH_2)_6^{2\oplus}$.

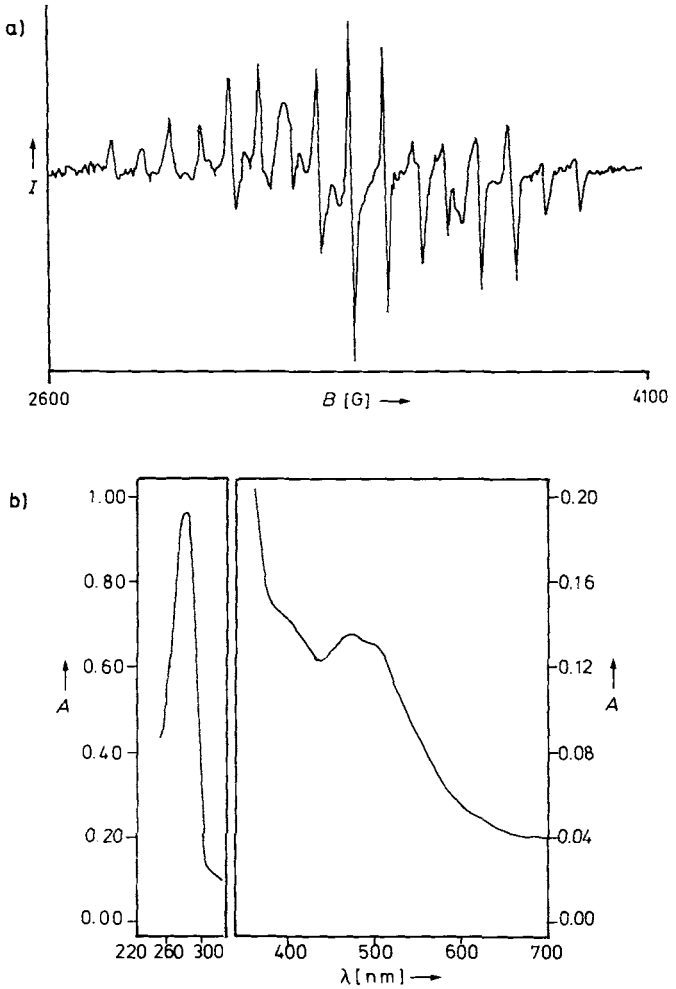
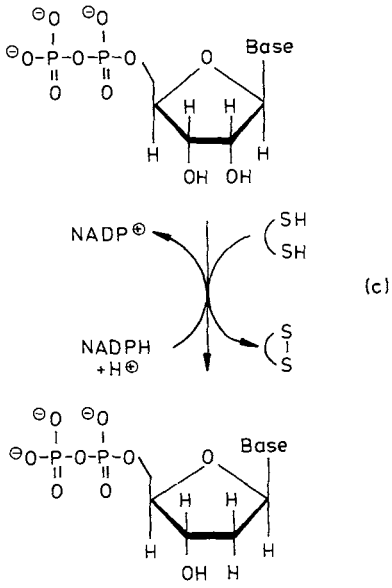


Fig. 6. Pseudocatalase from *Lactobacillus plantarum*: a) ESR spectrum at 6 K (6–10 μM [Mn]) [20]. b) Electronic spectrum at pH = 7.0 (left: 0.88, right: 17.52 mg enzyme per mL) [19]. *A* = absorption.

2.3.3. Ribonucleotide Reductase (RR) from Brevibacterium Ammoniagenes

The reduction of ribonucleotides to the corresponding 2'-deoxyribonucleotide, the building block of DNA, is one of the most important reactions for the existence and propagation of all life forms.[21] This enzymatically controlled reaction is shown in Equation (c). It appears simple enough, but the mechanistic details are by no means fully understood.



(c)

Three RR-enzymatic systems have been characterized, of which those containing iron but no heme groups are of great interest, because the active site consists of μ-oxo bridged Fe^{III} centers.[18]

Auling et al.[22] have recently shown that there is also a manganese-containing RR which was isolated from the gram-positive *brevibacterium ammoniagenes* (ATCC 6872). The enzyme consists of two protein subunits, namely a nucleotide binding protein B1 (MW = 80000) and the catalytically active protein B2 (MW = 100000). The latter is composed of two polypeptides (MW 50000) which are both necessary for enzymatic activity.

The manganese content has not yet been determined, but the electronic spectrum displaying two absorption maxima in the visible region (455 and 485 nm) is again typical of the μ-oxo-bis(μ-carboxylato)dimanganese(III) structural unit. The spectrum is shown in Figure 7 (the molar absorption coefficients are not known).

2.3.4. Further Metalloproteins with Probable Binuclear Mn_2^{III} Active Sites

The chemist is trained to determine the composition of a purified compound by an elemental analysis before describing its physical or chemical properties. This is trivial. How-

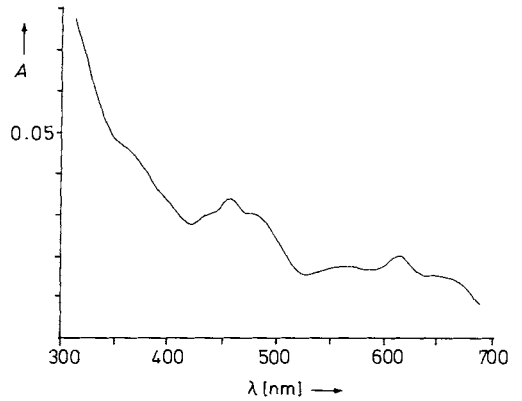


Fig. 7. Electronic spectrum of ribonucleotide reductase from *Brevibacterium ammoniagenes* at pH = 6.6 [22].

ever, the biochemist faces a series of problems in the process of purification to homogeneity of a new metalloprotein, which can often put into question the value of elemental analyses.

1) The isolation and purification of a metalloprotein is a complex multistep process. The metal content is very small and can only be determined by modern spectroscopic methods such as atomic absorption spectroscopy, ICP atomic emission spectroscopy (ICP inductively coupled plasma) or in the case of Mn^{II} containing proteins, quantitative ESR spectroscopy. Mn^{II} ions are kinetically labile and the stability constants of the binding sites are often quite small. Consequently, Mn^{II} ions are frequently washed out during the purification procedure or replaced by other divalent cations ($Ca^{2\oplus}$, $Mg^{2\oplus}$, $Fe^{2\oplus}$ etc.), which are inadvertantly introduced by the chemicals used.

2) The redox potential of the manganese cations in the oxidation states +II, +III and +IV are often close to one another. Thus, during isolation unintended changes in oxidation states can result in a formerly inert Mn center in higher oxidation state being washed out as labile Mn^{II} ions.

3) Binuclear manganese complexes tend to undergo pH dependent disproportionation reactions such as that shown in Equation (d). This process is discussed in more detail later in Section 4.2.

$$2\,Mn_2^{III} \rightarrow Mn^{II}Mn^{III} + Mn^{IV}Mn^{III} \qquad (d)$$

This reaction can again be the cause of too small a Mn content, since the Mn^{II} centers can leave the enzyme's active sites during purification.

4) Finally, sometimes even the qualitative determination of the nature of the metal in the active site can be a problem. The coordination chemistry of Fe^{III} and Mn^{III} is so similar in aqueous medium that unintended substitution of one metal cation by accidental presence of the other metal cation can lead to the wrong description of a metalloprotein. For instance:

One source of the so called *purple acid phosphatase* are the tubers of the sweet potatoes from Japan (Kokei No. 14 or Kontoki). This metalloprotein was originally described as a manganese-containing enzyme.[23] The MW is 110000 with two subunits (MW 55000). It was estimated to have one Mn^{III} ion per molecule of enzyme. *Averill* et al. have recently shown that this is probably an error.[24] They obtained a higher purity grade, with 14-fold higher activity, by slight modifications of the original purification procedure and have shown that there are two Fe^{III} ions per molecule enzyme and only traces of manganese. Purple acid phosphatase from uteroferrin and bovine spleen has a binuclear Fe^{III}–O–Fe^{III} active site.[18] However, in the present case it has been suggested that the enzyme from sweet potatoes has a mononuclear active Fe site.[24] It is conceivable that the Japanese group actually had a manganese form of the enzyme in their hands, whereas the American scientists purified an iron form. I think it highly improbable that iron was mistaken for manganese or vice versa by one or other group; more likely the duality of these two trivalent cations is the cause of the discrepancy.

In a further example, I would like to point out that the analytically determined manganese content could possibly be wrong. In 1984, *Reinards, Altdorf* and *Ohlenbusch* reported a manganese superoxide dismutase, which they purified from the procaryotic microorganism *Acholeplasma Laidlawii*.[25] It has a MW of 41500 and is formed from two subunits. The manganese content was given as 0.51 ± 0.05 Mn atoms per subunit (atomic absorption spectroscopy). The published electronic spectrum, however, appears to be remarkably like that of the spectrum of a μ-oxo-bis(μ-carboxylato)dimanganese(III) structural moiety. This would lead to the conclusion that the active site of this SOD is a binuclear Mn_2^{III} complex. Further investigation of this enzyme will be of interest.

3. The Active Site of Photosystem II

One of the fundamental processes in biology is the visible light driven oxidation of water, which occurs in a complex molecular 'apparatus' in the thylakoid membrane of chloroplasts of green plants, in algae and in some cyanobacteria. This 'apparatus', called photosystem II (PS II), has a manganese-containing active site which can oxidize coordinated water molecules[49] to oxygen [Eq. (e)].

$$2\,H_2O \rightarrow O_2 + 4\,H^{\oplus} + 4\,e^{\ominus} \qquad (e)$$

The manganese is the essential component, but $Ca^{2\oplus}$ and $Cl^{\ominus}$ ions are also necessary for the activity of PS II ($F^{\ominus}$ ions for example are effective inhibitors). Large acetate concentrations likewise inhibit O_2 evolution, but this effect is reversible; the activity is regenerated once the acetate ions have been washed out.[69]

From elemental analysis it appears that four manganese centers make up the active site;[40] whether all four are involved in the redox process is not clear. The arrangement of these four[37] manganese ions relative to one another in PS II and the mechanism of the water oxidation have been intensively investigated for many years. There have been many, in part controversial, suggestions and our understanding of the mechanism at the molecular level is still far from perfect.

I am not going to describe the spatial arrangement of PS II or the details of the photochemistry,[32,33] the electron[41] and proton transport.[46] These aspects are covered in many excellent reviews, of which only a selection is cited.[26–38]

The recent review of *Renger*'s in this Journal is particularly comprehensive in this respect.[26]

I would now like to briefly outline some features of our knowledge of the structure of the active site and some ideas for the reaction mechanisms involved in photosynthesis.

From *Joliot*'s[47] observation that periodic O_2 evolution occurs from dark-adapted chloroplasts when they are irradiated with a series of short light flashes, *Forbush, McGloin* and *Kok* have identified five states (oxidation states) during water oxidation.[48] These have been designated, S_0–S_4. In each case the absorption of one quantum of light raises the oxidation level by one unit (releasing one electron each time) and drives the system from S_0 to S_4. In the step $S_4 \rightarrow S_0$, O_2 is finally evolved and the S_0 state is regenerated (Fig. 8a).

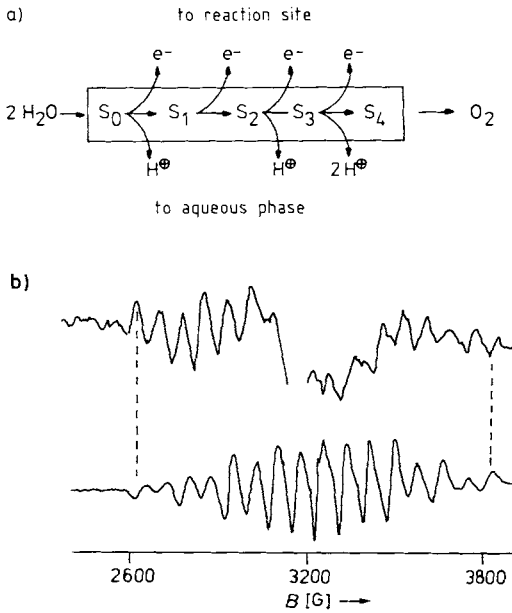


Fig. 8. a) The S-state model for water oxidation in photosynthetic membranes. b) Comparison of the ESR spectra of PS II membranes (top, at 300 K, cooled to 200 K and measured at 10 K in the dark) with that of the mixed-valence $Mn^{III}Mn^{IV}$ analogue of the borato complex **11** (Fig. 14) [61] (bottom).

The stoichiometry and sequence of the movement of protons in the cycle has been investigated by *Förster* et al.[46] *Dismukes*,[41a,b] in a pioneering observation, showed that the PS II particles are ESR active in the S_2 state. The discovery of a complex 16- to 19-line spectrum at $g = 2.0$ (Fig. 8b) and later a further signal at $g = 4.1$ [41e–k] as well as the recently discovered tyrosine radical[50] has given a large impulse to clearing up the nature of the active site. The derivation of its structure from ESR measurements, whose reproducibility under different experimental conditions and in different laboratories is not discussed here (this is a problem!), depends critically on the development of the theory of paramagnetic polynuclear manganese centers.

The only method that to date has been able to probe directly the surroundings of the manganese atoms in PS II is EXAFS spectroscopy. The method was developed for this problem bei *Klein* et al.[51] The interpretation of the spectra obtained from PS II particles in the states S_0, S_1, S_2 and recently S_3[52] proves the following:

1) The oxidation level of the manganese cluster increases stepwise from S_0 to S_2, without the structure significantly changing; the transition from S_2 to S_3 does *not*, however, bring about a change in oxidation state at the manganese center.[54] This is an important result, because up to now it has been assumed that the four electrons came successively from the manganese cluster. An organic radical must arise somewhere in the $S_2 \rightarrow S_3$ transition (oxidized histidine?).[55]

2) The first coordination sphere of all Mn atoms consists of oxygen and/or N atoms (probably more O atoms than N atoms).

3) No chloride coordination was found within 2.2 Å of the Mn atoms. The activity of PS II is $Cl^{\ominus}$ dependent and coordination of $Cl^{\ominus}$ has often been discussed but not experimentally proven. The EXAFS spectra can not exclude the possibility that there is a Mn · · · Cl distance >2.2 Å.

4) Of great significance is the observation of a Mn · · · Mn distance at 2.7 Å and probably another Mn · · · Mn distance at 3.3 Å.[51–53]

The most recent EXAFS measurements from *Cramer* et al.[53] with polarized, synchroton radiation on orientated chloroplasts shows that the manganese cluster has a Mn · · · Mn vector of 2.7 Å and a further one of 3.3 Å arranged almost vertically to the membrane. The authors conclude that the active site could be made up from two differing binuclear units, one with two μ-oxo bridges and connected to the other with carboxylato bridges. Alternatively, however, an unsymmetrical tetranuclear structure is conceivable.[39]

Figures 9, 10 and 11 give three speculative suggestions for the structure and reaction mechanism; these reflect current knowledge and have been particularly stimulating to the in-

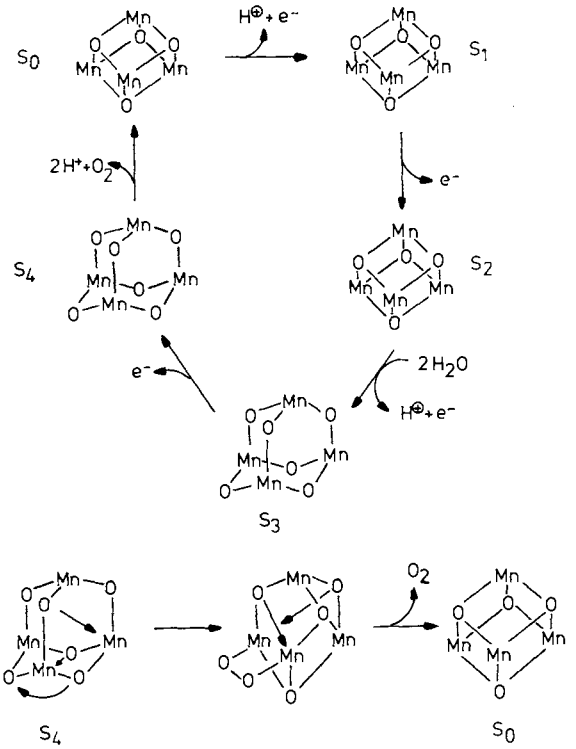


Fig. 9. Speculative reaction mechanism for the water oxidation in PS II, in which a structural change is proposed to take place between the regular cubane framework $\{Mn_4O_4\}$ and the adamantane skeleton $\{Mn_4O_6\}$ (after *Brudvig* and *Crabtree* [56]).

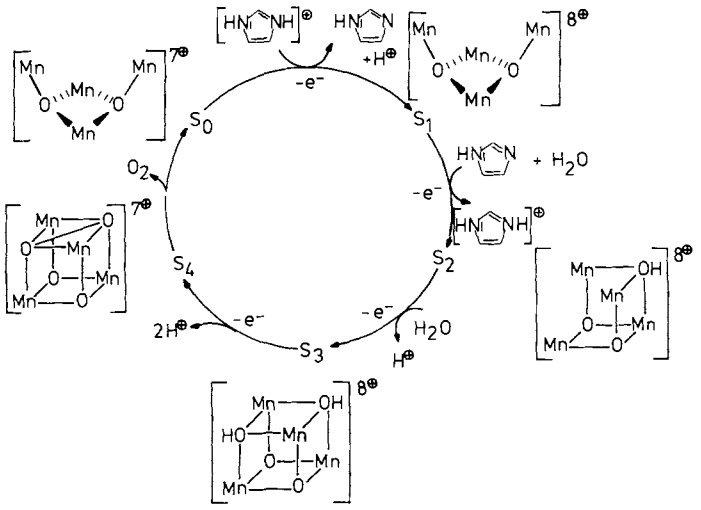


Fig. 10. Speculative mechanism for water oxidation in PS II with $\{Mn_4O_2\}$ and $\{Mn_4O_3\}$ structural units (after *Vincent* and *Christou* [57]).

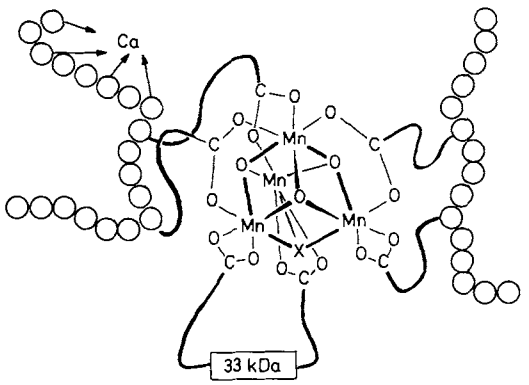


Fig. 11. Structural proposal from *Dismukes* [36a] for the active site of PS II. The circles symbolize polypeptide chains which have carboxylato groups available for bonding (the amino acid sequence is known); X is a μ_3-Cl bridge (Mn–Cl 2.6 Å). At the bottom a protein subunit (MW 33000) is sketched, which has two carboxylato groups bound to the Mn center. This protein component can be easily removed, making two Mn centers very labile.

organic chemist. Mechanistically, the minimal model, in which two H_2O ligands are oxidized at a binuclear center (*Witt* et al.,[32] *Renger*,[59] *Vänngard* et al.,[49] *Kambara* et al.[58] etc.) is still just as reasonably valid as the more complex schemes introduced by *Brudvig* and *Crabtree*[56] on the one hand and by *Vincent* and *Christou*[57] on the other. *Dismukes*' model[36] (Fig. 11) is an aesthetically pleasing combination of experimental facts, thoughtful deduction, and a lot of imagination. Thus, the mechanism could be like this but also quite different. These suggestions have been strongly influenced by more recent developments in the inorganic coordination chemistry of manganese, whereby the synthesis of low molecular weight bi-, tri- and tetranuclear complexes of manganese has stimulated many ideas.

4. Model Complexes of Manganese[60, 68]

In all the previously described biomolecules, the manganese ions were bound by O and N donor atoms from within the protein. Functional groups include, for example, carboxylato, alkoxy and phenoxy groups and the imidazole N atom from histidine. Sulfur coordination was not observed in any of our examples. Consequently, I shall describe the classical coordination chemistry (Werner type) of manganese with O and N ligands.

Complexes of Mn^V in an octahedral environment were until recently unknown. The occurrence of this high oxidation state in biological systems has not been established as yet, but due to recent preparative results it can be no longer viewed as being as exotic as it was several years ago. *Buchler* et al.[62] and *Hill* et al.[63] prepared the first diamagnetic nitridoporphyrinatomanganese(v) complex. Its structure has been determined by X-ray diffraction and has a fivefold MnN_5 coordination geometry. A very reactive oxochloroporphyrinatomanganese(v) complex with octahedral coordination of the Mn^V ion[64] has also been reported. Electrochemical and spectroelectrochemical investigations of the $Mn^V \equiv N$ unit have been published recently.[65] *Okawa* et al.[66] reported a synthesis of a probable octahedral, paramagnetic complex ($\mu_{eff} = 2.83\ \mu_B$) $K[MnL_2]$ (L is the trianion of *N*-(2-hydroxyphenyl)salicylamide), which can be recrystalized without decomposition from water. Once more it is demonstrated that 'unusual' oxidation states can be stabilized readily by the correct choice of suitable ligands. *Calvin*[67] and *Brudvig*[56] have therefore quite rightly considered Mn^V as a possible oxidation state in PS II.

4.1. Binuclear Mn^{II} Complexes

Carboxylato groups show a pronounced inclination to bind to manganese in either a monodentate or a bidentate manner; in the latter case with the formation of a symmetrical μ-carboxylato bridge. These complexes model the bonding characteristics of biomolecules with two neighboring Mn^{II} ions, since polypeptides often have unbound $-COO^{\ominus}$ groups, which can be utilized in coordination to metal ions. Figure 12 shows four structural types, which have all been characterized by X-ray crystallography. Complexes **1**,[70] **2**,[71] **3**[72] and **4**[73] contain one to four bridging acetate

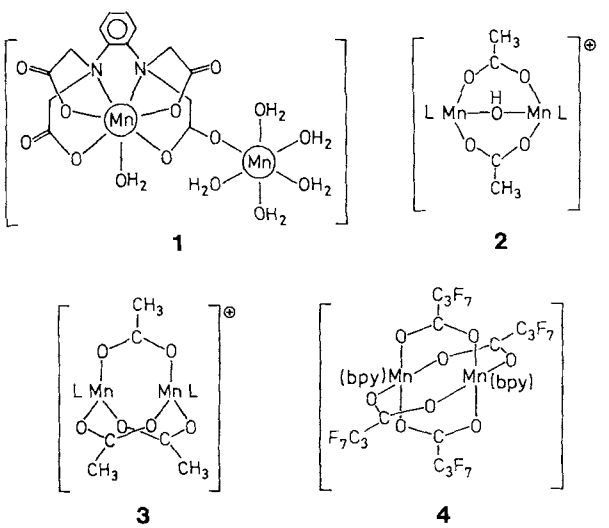
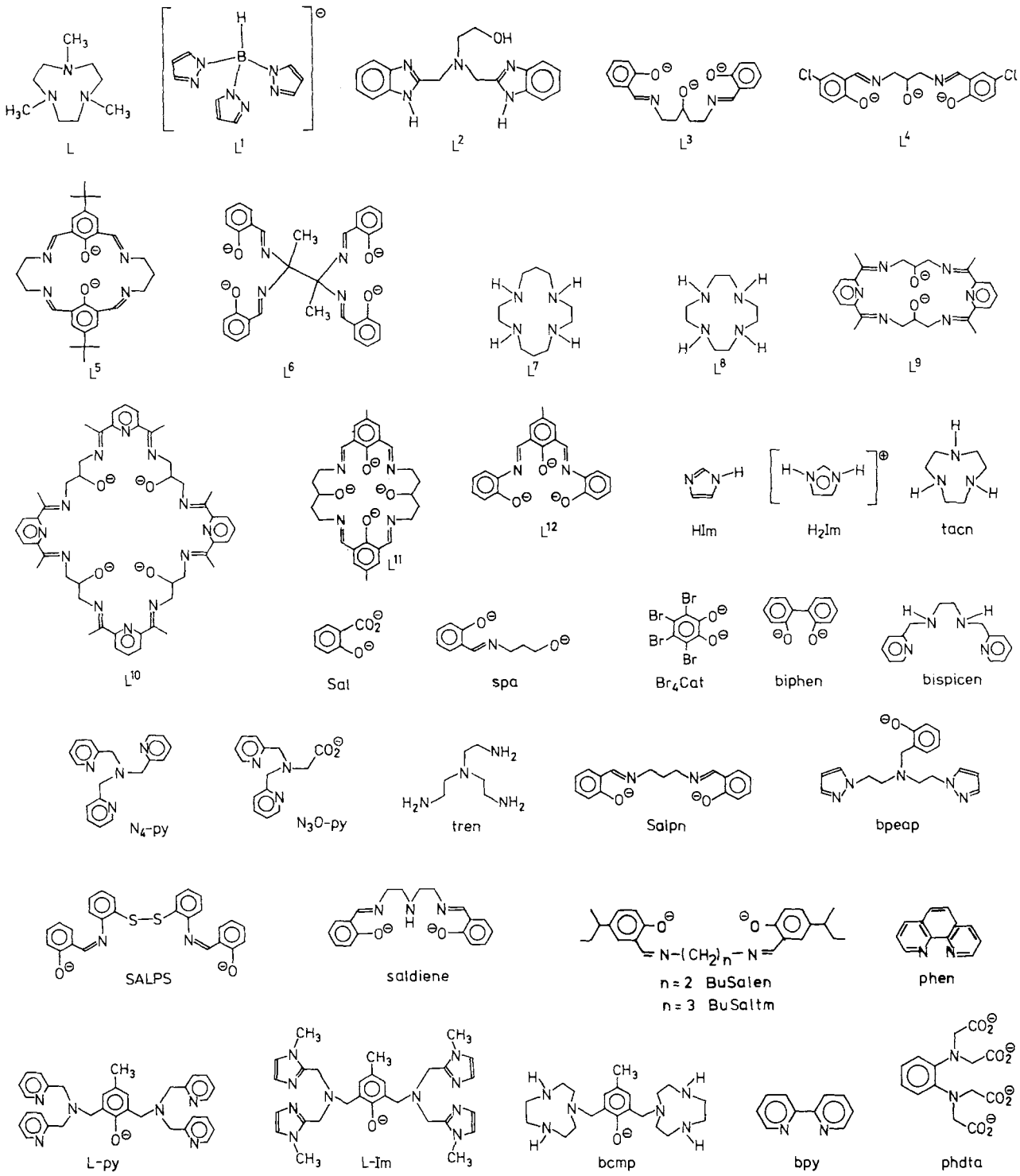


Fig. 12. The binuclear Mn^{II} complexes **1**–**4**. For ligands see Scheme 2. The counterions in **2** and **3** are $PF_6^{\ominus}$ and $BPh_4^{\ominus}$, respectively.



Scheme 2. O, N ligands and their abbreviations.

ligands. Their Mn · · · Mn distances and magnetic properties are listed in Table 1. Intramolecular weak antiferromagnetic spin exchange coupling of both high spin Mn^{II} ions is observed, occurring either through space in **3** and **4** or via a superexchange mechanism in **2**. Interestingly, the OH bridged species **2** shows the strongest coupling, i.e. μ-OH groups are good mediators for the superexchange mechanism, whereas carboxylato groups are rather poor in this respect.

A further potential ligand for Mn^{II} is the phenoxy group from tyrosine in the polypeptide. Phenoxy groups frequently link two metal ions in simple molecular complex chemistry. The complexes **5**,[74] **6**[75] and **7**[76] (Fig. 13) are examples of this; **5** and **6** have been structurally characterized by X-ray diffraction. In both cases the two octahedra are edge-linked and have relatively short Mn · · · Mn distances. In each case weak antiferromagnetic coupling is observed (Table 1).

Compounds **6**, **7** and **8**[78] show complex ESR spectra with distinct hyperfine splitting. Instructive discussions have been reported by *Hendrickson* et al.[76] and *Dismukes* et al.[78] ESR spectroscopy is a good method for distinguishing between monomeric and dimeric structures, if the spin ex-

change coupling constant J is substantially larger than the ^{55}Mn hyperfine coupling constant a.[77] The separation of the signals for a dimer is then $a/2$, half the value of the corresponding monomeric species. These investigations confirm and extend the argument for use of ESR measurements for biomolecules with two neighboring Mn^{II} ions.

The complex **8** is particularly interesting, because it serves as a functional model for the catalases from *Lactobacillus plantarum* and *Thermus thermophilus*. It decomposes H_2O_2 catalytically, the initial rate being proportional to $[H_2O_2]^2$.[8] An analogous but monomeric Mn^{II} complex is inactive. The first step in this reaction is proposed as being the formation of a μ-oxo-bridged dimanganese(III) intermediate, which then reacts with a further molecule of H_2O_2, releasing O_2 and thus being reduced [Equations (f) and (g)].

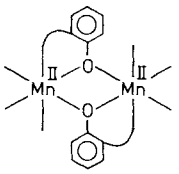
$$H_2O_2 + Mn^{II}_2 + 2\,H^{\oplus} \rightarrow Mn^{III}_2 + 2\,H_2O \qquad (f)$$

$$Mn^{III}_2 + H_2O_2 \rightarrow Mn^{II}_2 + O_2 + 4\,H^{\oplus} \qquad (g)$$

Table 1. Mn · · · Mn separation and spin exchange coupling constants in the binuclear Mn^{II} complexes **1**–**8** (Fig. 12, 13).

Complex	Mn · · · Mn [Å]	J[cm^{-1}] [a]	Ref.
1	6.16	not known	[70]
2	3.35	− 9	[71]
3	4.03	− 1.7	[72]
4	3.68	− 2.6	[73]
5	3.26	− 0.18	[74]
6	3.30	− 1.88	[75]
7	not known	− 0.65	[76]
8	3.3	weakly ferromagnetic $J \sim 1$ cm^{-1}	[78]

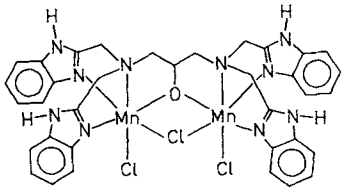
[a] From $H = -2\,J\,S_1\,S_2$ with $S_1 = S_2 = 5/2$.



$[Mn_2(bpeap)_2(THF)_2](ClO_4)_2$ **5**

$[Mn_2(SALPS)_2]$ **6**

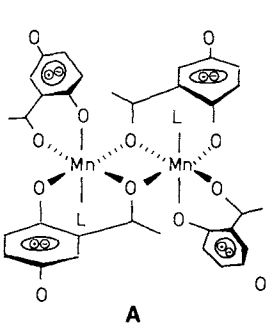
$[Mn_2(saldiene)_2]$ **7**



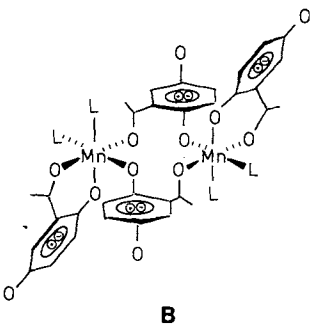
8

Fig. 13. The binuclear μ-aryloxo or μ-alkoxo bridged Mn^{II} complexes **5**–**8**. For ligands see Scheme 2.

In order to study spin-spin interactions, some binuclear Mn^{II} complexes were studied, containing coordinated organic radicals. This is a very important aspect, since in PS II the transition from the ESR active S_2 state to the ESR inactive S_3 state does not involve a change in oxidation state at the manganese centers. This means that an organic radical must extinguish the ESR signal in the S_3 state. Examples include the manganese complexes with catechol and semiquinone ligands.[79, 80] The semiquinone complex with structure A or B[79] shows, in solution, that the coordination of paramagnetic ligands results in a ferromagnetic coupling between the two Mn^{II} ions. A($S = 3$) ground state was found for the dimer with four semiquinone radicals, which couple antiferromagnetically with the Mn^{II} ions.



A

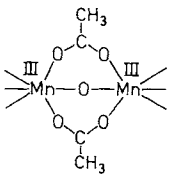


B

Hendrickson et al.[80] described a green tetrameric complex $[Mn_4(3,5\text{-DBSQ})_8]$ (3,5-DBSQ = 3,5-di-*tert*-butyl-1,2-benzoquinone) with four Mn^{II} ions and semiquinone ligands, which are weakly coupled ($\mu_{eff} = 5.1\ \mu_B$ per Mn at 295 K).

4.2. Binuclear Mn^{III} Complexes

The discovery of a series of iron-containing metalloproteins which contain the binuclear structural unit μ-oxo-bis(μ-carboxylato)diiron(III), led to the synthesis of simple binuclear molecular complexes of this type.[18] This synthesis is amazingly simple, occurring by 'spontaneous self-assembly'.[4b, c] This suggests that the formation in solution of this structural unit from labile mononuclear metal cations, polydentate and bridging ligands is favored given the correct conditions of concentration, temperature and solvent. Once these conditions had been found, complexes of this type were prepared for most trivalent metal ions of the first row transition series, including manganese(III).[81–84] In Figure 14 all



$[(tacn)_2Mn_2(\mu\text{-}O)(\mu\text{-}CH_3CO_2)_2]^{2\oplus}$ **9**

$[L_2Mn_2(\mu\text{-}O)(\mu\text{-}CH_3CO_2)_2]^{2\oplus}$ **10**

$[L^1_2Mn_2(\mu\text{-}O)(\mu\text{-}CH_3CO_2)_2]$ **11**

$[(bpy)_2Mn_2(\mu\text{-}O)(\mu\text{-}CH_3CO_2)_2(H_2O)_2]^{2\oplus}$ **12**

$[L^2_2Mn_2(\mu\text{-}O)(\mu\text{-}CH_3CO_2)_2]^{2\oplus}$ **13**

Fig. 14. The binuclear Mn^{III} complexes **9**–**13** with μ-oxo-bis(μ-acetato)dimanganese(III) core. For ligands see Scheme 2.

such complexes structurally characterized by X-ray diffraction are given. Complex **13** is the only one without a structural analysis.

As in the case of the Fe^{III} complexes of this type, it was quickly recognized that the analogous Mn^{III} complexes are excellent model complexes for the electronic characteristics of the Mn^{III} centers in the biomolecules discussed in Section 2.3:

1) The electronic spectrum in the visible is characteristic for a μ-oxo-bis(μ-carboxylato)dimanganese(III) unit. Almost independent of the nature of the remaining ligands two very intense bands between 400 and 600 nm ($\varepsilon > 600$ L mol^{-1} cm^{-1}) are observed (Fig. 15). These are not simple

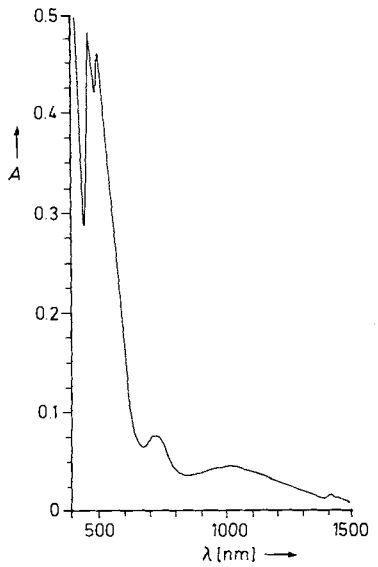


Fig. 15. Electronic spectrum of **10** in CH_3CN ([**10**] = 7.2×10^{-4} M, 1-cm cell) [81].

d–d transitions of octahedrally coordinated Mn^{III} ions and their nature is not yet fully understood. They could be due to the so called 'simultaneous pair excitation' (*Gray* et al.[91] and *Güdel* et al.[92]), in which it is suggested that two electrons per dimer (one for each Mn^{III} center) are excited simultaneously by one photon. This would mean that the observation of such absorptions in the active centers of the biomolecules described in Section 2.3 would prove their dimeric character. Interestingly, these bands are *not* observed in metalloenzymes with *mononuclear* centers. e.g. SODs.

2. Unlike the complexes with Fe^{III}–O–Fe^{III} units which exhibit strongly antiferromagnetically coupled Fe^{III} ions, the complexes **9**–**13** have Mn^{III} ions that are only very weakly coupled (ferromagnetic for **9**, **10** and **13**, antiferromagnetic in **12** and uncoupled in **11**; Table 2).

Table 2. Mn · · · Mn separation and spin exchange coupling constants in the binuclear Mn^{III} complexes **9**–**19** (Fig. 14, 17).

Complex	Mn · · · Mn [Å]	J [cm^{-1}]	Ref.
9	3.084	ferromagnetic	[81, 72]
10		+ 9	[72]
11	3.159	− 0.5	[82]
12	3.132	− 3.4	[83]
13	unknown	+ 1.72	[84a]
14	3.247	antiferromagnetic	[93]
15	2.869	− 19.1	[85]
16	2.931	− 19.6	[87]
17	3.533	not coupled	[89]
18	2.72	not reported	[86]
19	3.808	− 3.6	[90]

3. The ESR spectroscopic behavior of these complexes is still controversial. We found that **9**, **10** and **11** are ESR inactive in anhydrous solutions in the temperature range 4–290 K. *Nishida*[84b] reported a 16-line spectrum for **9** and **13** at 77 K. I think this is an artefact caused by H_2O catalyzed disproportionation of the Mn_2^{III} dimers to the $Mn^{II}Mn^{III}$ and $Mn^{III}Mn^{IV}$ dimers. The latter species show the usual 16-line spectrum. The disproportionation of **9**, **10** and **11** has been established.[71, 72]

4) The electrochemical behavior of **9**, **10**[71, 72, 81] and **11**[82] models the redox behavior of the catalase enzymes and PS II. In anhydrous solutions they can undergo reversible one-electron reduction and oxidations, giving binuclear $Mn^{II}Mn^{III}$, $Mn^{III}Mn^{IV}$ and Mn_2^{IV} complexes [Eq. (h)] without the structure rearranging.

$$Mn^{II}Mn^{III} \underset{+e^-}{\overset{-e^-}{\rightleftharpoons}} Mn^{III}Mn^{III} \underset{+e^-}{\overset{-e^-}{\rightleftharpoons}} Mn^{III}Mn^{IV} \underset{+e^-}{\overset{-e^-}{\rightleftharpoons}} Mn^{IV}Mn^{IV} \quad \text{(h)}$$

The hydroxy bridged species **2** can likewise be electrochemically oxidized twice giving μ-OH bridged complexes of $Mn^{II}Mn^{III}$ and Mn_2^{III}, respectively [Eq. (i), Fig. 16].

$$Mn^{II}Mn^{II} \underset{+e^-}{\overset{-e^-}{\rightleftharpoons}} Mn^{II}Mn^{III} \underset{+e^-}{\overset{-e^-}{\rightleftharpoons}} Mn^{III}Mn^{III} \quad \text{(i)}$$

In aqueous acidic solution, **10**, can be protonated at the μ-oxo bridge giving a μ-hydroxy bridged species; both compounds are related by the pH dependent equilibrium illustrated in Equation (j)

$$Mn^{III}\text{–}O\text{–}Mn^{III} \overset{H^{\oplus}}{\rightleftharpoons} Mn^{III}\text{–}OH\text{–}Mn^{III} \quad \text{(j)}$$

Figure 16 illustrates that due to their respective redox potentials the protonated form of **10** can oxidize the unproto-

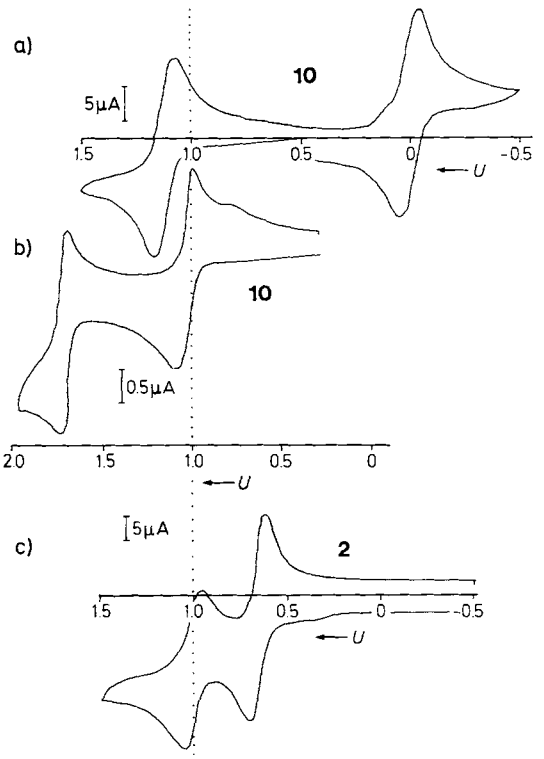


Fig. 16. Cyclic voltammogram of **10** · $(PF_6)_2$, a) in CH_3CN, b) in liquid SO_2 and c) of **2** (PF_6)·CH_3OH in CH_3CN [72].

nated form. Consequently, in aqueous acidic solution **10** disproportionates according to Equation (k).

$$Mn^{III}(OH)Mn^{III} + Mn^{III}OMn^{III} \rightarrow Mn^{II}(OH)Mn^{III} + Mn^{III}OMn^{IV} \quad \text{(k)}$$

The reduced $Mn^{II}(OH)Mn^{III}$ form decomposes to mononuclear complexes in aqueous solution but the oxidized form Mn^{III}–O–Mn^{IV} can be isolated in crystalline form and displays a 16-line ESR spectrum at 70 K. Complex **44** in Section 4.5 has been characterized by X-ray diffraction.[71b]

This acid dependent disproportionation reaction was also found for the pseudocatalase of *Lactobacillus plantarum*.[20] This could be the cause for *Nishida*'s ESR spectrum of **11** and **13**.[84]

5. The Mn · · · Mn distances in the μ-oxo- and μ-hydroxo-bis(μ-carboxylato)dimanganese model complexes vary according to the oxidation state of the metal centers and are in the range of ca. 3.1–3.4 Å. They are therefore about the same as those distances found in *Thermus thermophilus* and PS II (second vector).

Some hydroxy, alkoxy and phenoxy bridged binuclear complexes of Mn^{III} have been synthesized and their structures determined.[85–93] Figure 17 again shows a representative cross-section, and Table 2 lists their magnetic properties. The spin coupling of the high spin Mn^{III} ions in these complexes is small. Comparing the Mn–O bond lengths in the μ-oxo bridged complexes to those of the μ-OH, μ-alkoxy and μ-phenoxy bridged complexes, it can be seen that the Mn–O_{oxo} bonds are always substantially shorter (ca. 1.80 Å as opposed to 1.95 Å).

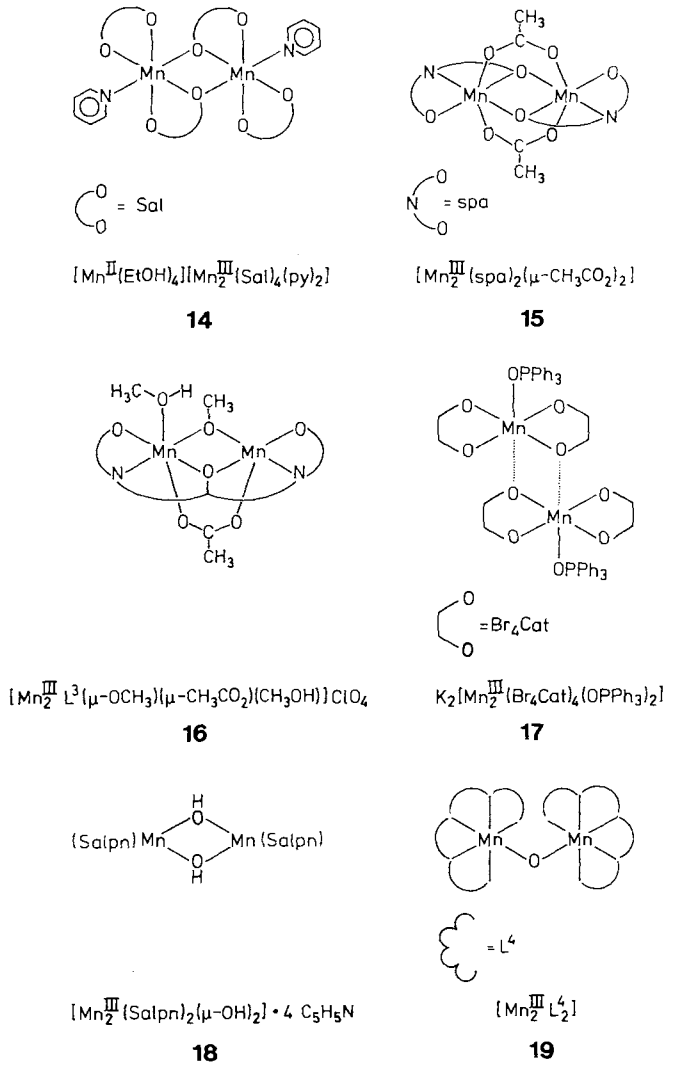
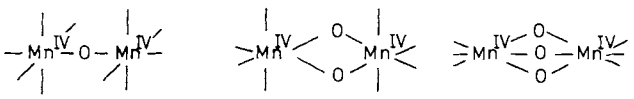


Fig. 17. The binuclear Mn^{III} complexes **14–19.** For ligands see Scheme 2.

4.3. Binuclear Mn^{IV} Complexes

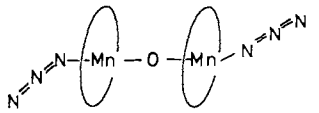
Binuclear complexes of manganese(IV) can contain one, two or three μ-oxo bridges; two octahedrally coordinated Mn^{IV} centers are connected in such a manner that the two octahedra are corner-, edge- or face-sharing as shown in structures **C, D** and **E**.



C **D** **E**

Typical examples are given in Figure 18 and Table 3. The magnetic properties of these complexes differ considerably from those of the hydroxy and alkoxy bridged complexes of Mn^{II} and the corresponding bridged compounds of Mn^{III}: the Mn^{IV} ions are strongly intramolecularly antiferromag-

Typ **C**:



20

$[Mn^{IV}_2(O)(N_3)_2(tetraphenylporphyrinato)_2]$

Typ **D**:

$[Mn^{IV}_2(\mu\text{-}O)_2(bpy)_4]^{4\oplus}$ **21**

$[Mn^{IV}_2(\mu\text{-}O)_2(C_2O_4)_4]^{4\ominus}$ **22**

$[Mn^{IV}_2(\mu\text{-}O)_2(phen)_4]^{4\oplus}$ **23**

$[Mn^{IV}_2(\mu\text{-}O)_2(BuSalen)_2]$ **24**

$[Mn^{IV}_2(\mu\text{-}O)_2(BuSaltm)]$ **25**

$[Mn^{IV}_2(\mu\text{-}O)_2(OH)_2(tacn)_2]^{2\oplus}$ **26**

Typ **E**:

$[L\,Mn^{IV}(\mu\text{-}O)_3Mn^{IV}L]^{2\oplus}$ **27**

Fig. 18. The binuclear Mn^{IV} complexes **20–27.** For ligands see Scheme 2.

Table 3. Mn–O and Mn · · · Mn distances and spin exchange coupling constants in the binuclear Mn^{IV} complexes **20–27** [a].

Complex	Mn–O [Å]	Mn · · · Mn [Å]	J [cm^{-1}]	Ref.
20	1.743; 1.794	3.54	2.0 μ_B/dimer (25 °C)	[94]
21	n.r.	n.r.	st. antifer.	[96]
22	n.r.	n.r.	st. antifer.	[97]
23	1.805; 1.80	2.75	− 144	[95, 96]
24	n.r.	n.r.	st. antifer.	[98]
25	n.r.	n.r.	st. antifer.	[98]
26	1.82	2.625	st. antifer.	[72]
27	1.82	2.296	− 390	[72]

[a] st. antifer. = strongly antiferromagnetic; n.r. = not reported.

netically coupled ($S = 0$ ground state). The face sharing tris(μ-oxo)dimanganese(IV) complex **27** has a coupling constant of $J = -390\ cm^{-1}$ ($H = -2JS_1S_2$; $S_1 = S_2$ 3/2). It has a magnetic moment of 0.8 μ_B per dimer at room temperature and an extremely short Mn · · · Mn distance of 2.296 Å.

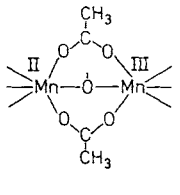
Octahedral Mn^{IV} complexes with d^3 electronic configuration have empty antibonding e_g^* orbitals, and therefore the Mn–N and Mn–O bond lengths are distinctly shorter than in the analogous Mn^{III} or Mn^{II} complexes. The Mn^{IV}–O_{oxo} bond lengths are about 1.74–1.82 Å, whereas the Mn^{III}–O_{oxo} bond lengths are 1.81–1.83 Å. The intramolecular Mn · · · Mn distances in compounds of type **C**, **D** and **E** are 3.54, 2.6, and 2.296 Å respectively. Compounds of type **D** therefore model the short Mn · · · Mn distance in PS II.

The edge-sharing compounds **21** and **23** with the di-μ-oxo-dimanganese core **D** and phenanthroline and bipyridyl ligands, respectively, have been thoroughly investigated. They can be electrochemically reversibly reduced to the corresponding $Mn^{III}Mn^{IV}$ species and to the Mn_2^{III} dimer.[99] This redox behavior has already been described for complexes containing the μ-oxo-bis(μ-carboxylato)dimanganese structural unit.[72] The corresponding binuclear Mn^{IV} complexes of this latter type are strong oxidizing agents and have still not been isolated in crystalline form. They are, however, estimated to have a Mn · · · Mn distance of 3.1–3.4 Å and thus can be viewed as model complexes for the longer Mn · · · Mn distance of 3.3 Å in PS II.[53]

None of the above compounds are ESR active at low temperature ($S = O$ ground state).

4.4. Mixed Valence Binuclear $Mn^{II}Mn^{III}$ Complexes

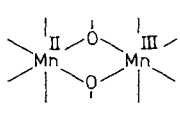
Mixed valence binuclear $Mn^{II}Mn^{III}$ complexes were synthesized and structurally characterized only in recent years (Fig. 19, Table 4). With a variety of binucleating ligands they



$[Mn_2(L\text{-}py)(\mu\text{-}CH_3CO_2)_2]^{2\oplus}$ **28**

$[Mn_2(L\text{-}Im)(\mu\text{-}CH_3CO_2)_2]^{2\oplus}$ **29**

$[Mn_2(bcmp)(\mu\text{-}CH_3CO_2)_2]^{2\oplus}$ **30**



$[Mn_2L^5(\mu\text{-}Cl)Cl\ Br]$ **31**

$[Mn_2(biphen)_2(biphenH)(bpy)_2]$ **32**

$[Mn_2L^6(OH)(OH_2)]$ **33**

Fig. 19. The mixed valence binuclear $Mn^{II}Mn^{III}$ complexes **28–33.** For ligands see Scheme 2. The bridging O is in each case a phenoxide O atom of these ligands.

form stable products and are generated from binuclear Mn^{II} precursors by air oxidation.

Dismukes et al.[102] have obtained a $Mn^{II}Mn^{III}$ complex by air oxidation of the mononuclear tetraphenylporphyrinatomanganese(II) in chlorobenzene. This compound has either a peroxo- or oxo-bridge, but in solution it converts slowly into a μ-oxo-bridged $Mn^{III}Mn^{IV}$ complex. Both forms

Table 4. Structural and magnetic properties of the mixed-valence binuclear $Mn^{II}Mn^{III}$ complexes **28–33.**

Complex	Mn · · · Mn [Å]	Mn^{II}–OR [Å] [a]	Mn^{III}–OR [Å] [a]	J [cm^{-1}]	Ref.
28	3.447	2.193	1.903	− 6.0	[103–105]
29	3.540	2.258	1.887	− 4.5	[106]
30	3.422	2.170	1.957	− 7.7	[107]
31	3.168	2.386; 2.129	1.941; 1.931	− 1.7	[105, 109]
32	3.182	2.120	1.960	+ 0.89	[108]
33	n.b.	n.b.	n.b.	− 6.0	[100]

[a] Mn–O distance for the μ-aryloxo bridge.

are ESR active, showing in each case 16 ^{55}Mn hyperfine signals at $g \approx 2.0$. The hyperfine coupling constants are different and hence the magnitude of these constants provides a method for determining the oxidation state in this case. *Hendrickson* et al.[101] have, however, previously pointed out that the knowledge of hyperfine constants is *alone* not enough to unequivocally determine oxidation states.

From the investigations of the complexes in Table 4 the following conclusions can be drawn:

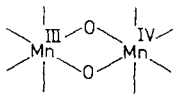
1. The oxidation states of the manganese ions are localized. Therefore X-ray structural analysis can distinguish between the Mn^{II} and Mn^{III}, provided that there is no disorder.[104–109] A possible exception could be *Kida*'s complex **33**,[100] which exhibits an intervalence band at 1300 nm in its electron spectrum. In the absence of a structural analysis this complex has been tentatively assigned to Class II in *Robin* and *Day*'s[110] scheme of mixed valence complexes.

2. The spins of the Mn^{II} and Mn^{III} ions in complexes **28–30** with a μ-phenoxy-bis(μ-carboxylato)dimanganese(II/III) core are weakly antiferromagnetically coupled ($S = 1/2$, ground state). Due to dependence on the symmetry of the coordination geometry, the ESR spectra show complicated ^{55}Mn hyperfine splitting. The spectrum of **28** measured at 15 K shows 29 hyperfine signals at $g \approx 2.0$ and at higher temperature a broad signal at $g \approx 4$ arising from an excited state ($S = 3/2$).[105, 109] Compound **32** is the only $Mn^{II}Mn^{III}$ complex with ferromagnetic spin-spin coupling; it has a $S = 9/2$ ground state.[108] The ESR spectrum at 7.5 K shows accordingly a signal at $g = 12.0$, a signal with hyperfine structure at 5.1, and two weak signals at $g = 2.01$ and 1.47.

3. The μ-phenoxy-bis(μ-carboxylato)dimanganese(II/III) complexes undergo both reversible one electron reduction and oxidation forming the corresponding Mn_2^{II} and Mn_2^{III} dimers [Eq. (i)]. Unlike the μ-OH bridged complex **2**, no disproportionation occurs in aqueous solution, since the μ-phenoxy bridges are preserved.

4.5. Mixed Valence Binuclear $Mn^{III}Mn^{IV}$ Complexes

Three types of these complexes have been structurally characterized by X-ray diffraction (Fig. 20; Table 5): a) Compounds **34–41** with the di-μ-oxo-dimanganese(III/IV) core (edge-sharing octahedra), b) the μ-acetato-di-μ-oxo-dimanganese(III/IV) complexes **42** and **43**, c) Complex **44** containing the μ-oxo-bis(μ-acetato)dimanganese(III/IV) structural unit. In crystals which are not disordered the Mn^{III} and Mn^{IV} ions can be clearly distinguished (**42** and **44** are disordered). The valences are therefore localized. The Mn^{III} ions frequently show Jahn-Teller distortions (elongated or com-



$[Mn_2(bpy)_4(\mu\text{-}O)_2]^{3\oplus}$ **34**

$[Mn_2(phen)_4(\mu\text{-}O)_2]^{3\oplus}$ **35**

$[Mn_2(bispicen)_2(\mu\text{-}O)_2]^{3\oplus}$ **36**

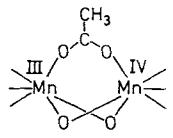
$[Mn_2(N_4\text{-}py)_2(\mu\text{-}O)_2]^{3\oplus}$ **37**

$[Mn_2\,L^7_2\,(\mu\text{-}O)_2]^{3\oplus}$ **38**

$[Mn_2\,L^8_2\,(\mu\text{-}O)_2]^{3\oplus}$ **39**

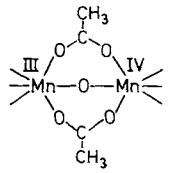
$[Mn_2(N_3O\text{-}py)_2(\mu\text{-}O)_2]^{\oplus}$ **40**

$[Mn_2(tren)_2(\mu\text{-}O)_2]^{3\oplus}$ **41**



$[Mn_2(tacn)_2(\mu\text{-}O)_2(\mu\text{-}CH_3CO_2)]^{2\oplus}$ **42**

$[Mn_2(bpy)_2Cl_2(\mu\text{-}O)_2(\mu\text{-}CH_3CO_2)]$ **43**



$[Mn_2\,L_2\,(\mu\text{-}O)(\mu\text{-}CH_3CO_2)_2]^{3\oplus}$ **44**

Fig. 20. The mixed valence binuclear $Mn^{III}Mn^{IV}$ complexes **34–44.** For ligands see Scheme 2.

Table 5. Structural and magnetic properties of the mixed-valence binuclear $Mn^{II}Mn^{IV}$ complexes **34–44.**

Complex	Mn · · · Mn [Å]	Mn^{III}–O_{oxo} [Å]	Mn^{IV}–O_{oxo} [Å]	J [cm^{-1}]	Ref.
34	2.716	1.854	1.784	− 150	[111, 112]
35	2.695	1.855	1.784	− 148	[112, 95]
36	2.695	1.833	1.793	–	[113]
37	2.643	1.837	1.776	− 159	[114]
40	2.656	1.820	1.790	− 151	[116]
41	2.679	1.851	1.774	− 146	[117]
42	2.588	[a]	[a]	− 220	[118]
43	2.667	1.840	1.798	− 114	[108]
44	3.230	[a]	[a]	− 40	[71b]

[a] Not differentiable due to disorder.

pressed octahedra), which is typical for the high spin d^4 electron configuration.

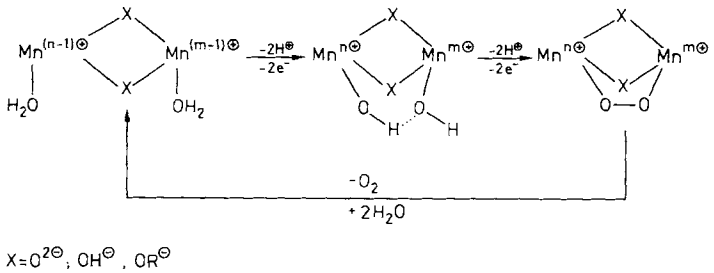
The spins of the Mn^{III} and Mn^{IV} ions in complexes of type a) and b) are intramolecularly strongly antiferromagnetically coupled ($S = 1/2$ ground state). Complex **44** shows comparatively weaker coupling (face-sharing octahedra).

Below ca. 70 K in frozen solutions complexes **34–44** all display the typical 16-line ESR spectrum with ^{55}Mn hyperfine structure at $g \approx 2.0$. This was also observed in the biomolecules of the catalase (Section 2.3.1) and the pseudocatalase (Section 2.3.2).

Complexes **34–41** are excellent models for the short Mn · · · Mn vector of 2.7 Å in PS II. They can all undergo reversible one electron oxidations and reductions giving Mn^{IV}_2 and Mn^{III}_2 dimers respectively. This has been discussed already for the complexes **9, 10** and **11** [Eq. (h)]. The redox potentials, not surprisingly, depend strongly on the nature of the ligands.

4.6. Water Oxidation by Binuclear Manganese Complexes

The manganese catalyzed oxidation of water to molecular oxygen and protons in PS II [Eq. (e)] presents a series of mechanistic problems. It seems plausible to accept that the process cannot follow from a single synchronous, concerted four-electron step. However, this poses several questions. Which intermediates are formed and how and when is the first covalent bond between the two oxygen atoms from the two H_2O molecules generated? Almost all models assume that the two H_2O molecules are coordinated to neighboring Mn atoms forming the active site of the precursor complex and that oxygen is formed stepwise by the formation of a peroxodimanganese complex, which then releases oxygen by intramolecular reduction of the manganese centers. Scheme 3 shows such a representation, which is based on the

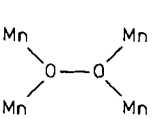


$X = O^{2\ominus}$; $OH^{\ominus}$, $OR^{\ominus}$

Scheme 3. Model representation of the mechanism of water oxidation in PS II.

known coordination chemistry of peroxo, aqua, hydroxy and oxygen ligands. It is a simple model that only shows two Mn ions participating in the redox process.

It is surprising how little reliable experimental evidence is available for the ability of simple manganese complexes to oxidize water. Until recently, peroxo complexes of manganese were almost unknown.[129, 130] There have been many manganese(II) complexes reported that can reversibly bind O_2,[128, 131] but the products have not been fully characterized. Only two peroxo complexes of manganese have been fully structurally characterized. These are the mononuclear complex $[Mn^{III}(tpp)O_2]$ (tpp = tetraphenylporphyrinate)[129] with 'side-on' bound $O_2^{2\ominus}$ and the trinuclear complex $[Mn^{III}_3(dien)_3(\mu\text{-}CH_3CO_2)_2(\mu_3\text{-}O)(\mu\text{-}O_2)]I_3 \cdot H_2O \cdot 0.33\,CH_3OH$ (dien = diethylenetriamine) with a bridging $O_2^{2\ominus}$ ligand.[130] Recently, the coordination of an $O_2^{2\ominus}$ ligand to all *four* manganese ions in PS II has been suggested (see Scheme 4). *Lippard* et al. have characterized such a compound of iron(III) with a planar $\{Fe_4(\mu\text{-}O_2)\}$ group by X-ray diffraction.[127]



Scheme 4.

Sporadic reports have appeared of stoichiometric water oxidation and even of catalytic oxidation.[121–126] Oxidation of alcohols to aldehydes has also been reported.[119, 120, 129, 133] *McAuliffe* et al.[122–124] have found that a large number of probably binuclear manganese(III) com-

plexes with Schiff base type ligands evolve O_2 upon irradiation in aqueous solution in the presence of *p*-benzoquinone. *Sawyer* et al.[132] have described a series of such binuclear complexes, which in highly oxidized form can oxidize H_2O to O_2. Mononuclear dichloromanganese(IV) complexes with Schiff base ligands react with H_2O evolving O_2,[134] as do the oxidized mononuclear tris(picolinato)- or tris(acetonato)manganese(III) complexes.[135]

The mixed valence complexes **34** and **35** do not react with H_2O yielding O_2[125, 126] in homogeneous aqueous phase, not even on irradiation, but in heterogeneous phase in the presence of Ce^{IV} O_2 is evolved.[121] Complexes **38** and **39** in their oxidized Mn_2^{IV} forms should oxidize H_2O.[115] The above examples represent only the beginning of the development of functional models for the photosynthetic process.

4.7. Tetranuclear Manganese Complexes

The possibility that a tetranuclear cluster forms the active site in PS II, has in the last five years stimulated synthetic chemists to prepare and study the properties of complexes of this nuclearity. There has been much success in this area. The structurally characterized examples are shown in Figure 21. Important data of these complexes are listed in Table 6.

The first report of a crystallographically characterized tetranuclear manganese cluster was that of complex **45** in 1983. This relatively symmetric complex has an $[Mn_4^{IV}O_6]^{4\oplus}$ adamantane skeleton.[72, 136] Recently, *Armstrong* et al.[152] have shown that in acidic solution one of the oxo bridges can be protonated; they isolated and characterized **46** with a $\{Mn_4^{IV}O_5(OH)\}^{5\oplus}$ core. The magnetic properties of **45** and **46** are interesting: **45** shows weak ferromagnetic coupling of the four Mn^{IV} ions which changes on protonation to weak antiferromagnetic interaction in **46**.[137] In 1985, *McKee* et al. showed that a macrocyclic 'tetranucleating' ligand (L^{10}, Scheme 2) forms a Mn^{II} complex **47** with a cubane structure.[138a]

The synthesis of these simple molecular complexes showed at least that the intermediates suggested by *Brudvig* and *Crabtree* in their detailed mechanism (Fig. 9) could exist. However, there are a number of factors which disfavor this aesthetically pleasing suggestion. Namely, complexes **45** and **47** have no short Mn · · · Mn vector of ca. 2.7 Å (Table 6) – this has been unequivocally proven by the EXAFS spectrum of **45**, which is not like that of the PS II measurement.[52] Also **45** and **46** are clearly not mixed valence complexes. XANES measurements on PS II particles had suggested[51] that the oxidation states of the manganese centers in the S_1 and S_2 states resemble those of the model complexes with Mn^{III} and Mn^{IV} ions. Temperature dependent ESR measurements likewise suggest that they could be the mixed valence $Mn_3^{III}Mn^{IV}$ or $Mn^{III}Mn_3^{IV}$ clusters.[41] *Christou* suggested a $Mn_3^{III}Mn^{II}$ for the S_0 state. The actual oxidation states of the Mn ions in the S_0–S_4 states are still controversial, but the existence of a mixed valence form is not disputed. Better structural models should therefore feature two different Mn · · · Mn distances at 2.7 and 3.3 Å as well as different oxidation states of the manganese ions.

Christou et al.[140] were able in 1987 to fulfill both these criteria in a model complex. **49** represents an unsymmetric complex with a butterfly structure; it has two different nonbonding Mn · · · Mn distances of 2.848(5) and 3.299(3.384) Å, but all four manganese atoms are still in the same +III oxidation state. The same group subsequently synthesized **50**.[141] This complex comprises two Mn^{II} and two Mn^{III} ions and again two different Mn · · · Mn distances are observed, which are comparable to those in PS II. Complex **52**[143] has a similar structure, but the coordination sphere of all four metals ions consists exclusively of oxygen atoms. This was the conclusion drawn for PS II also from EXAFS measurements. In spite of this synthetic success it must be emphasized that the EXAFS spectrum of **49** does not concur particularly well with that of PS II.[52] Of course complexes **49**, **50** and **52** form the basis for the proposed reaction mechanism shown in Figure 10.

Christou has been able to continue his fascinating run of success by looking at the problem of chloride coordination in the PS II. Complexes **51**[144] and **53**[142] both have terminal Mn–Cl groups as well as a μ_3-chloro bridge to three manganese centers; the corresponding Mn–Cl distances are 2.2–2.3 Å and 2.63 Å. The EXAFS spectra of PS II had eluded to there being *no* chloride coordinated within 2.2 Å; either because there is only a small amount of $Cl^{\ominus}$ bound to the cluster or because the Mn–Cl distance is larger than 2.2 Å. A Mn–Cl distance of 2.63 Å would not be unequivocally identified because of the Mn · · · Mn bond length of 2.7 Å in the EXAFS spectrum. Complexes **51** and **53** have naturally served as models for *Dismukes*' structural proposal (Fig. 11). The oxidation level of **51** and **53** is described as $Mn^{IV}Mn_3^{III}$. Complex **53** has the rare ground state S = 9/2 and no low-lying excited states. The ESR spectra of **51** and **53** are very similar to that of the S_2 state of PS II, as a comparison of Figures 22 and 8 shows.

Both these complexes model best the known physical properties of the manganese cluster in PS II. They are still,

Table 6. Important data of the tetranuclear manganese complexes **45**–**54**.

Complex		Mn · · · Mn (short) [Å]	Mn · · · Mn (long) [Å]	Oxidation state	Ref.
$[(tacn)_4Mn_4O_6]^{4\oplus}$	**45**	–	3.220	$(Mn^{IV})_4$	[72, 136]
$[(tacn)_4Mn_4O_5(OH)]^{5\oplus}$	**46**	–	3.250; 3.450	$(Mn^{IV})_4$	[137]
$[Mn_4(L^{10})]^{4\oplus}$	**47**	–	3.320	$(Mn^{II})_4$	[138a]
$[Mn_4(HL^9)(L^9)(NCS)_4]NCS$	**48**	3.135	?	$(Mn^{II})_4$	[138b]
$[Mn_4O_2(CH_3CO_2)_7(bpy)_2]^{\oplus}$	**49**	2.845	3.312; 3.385; 3.299	$(Mn^{III})_4$	[140]
$[Mn_4O_2(CH_3CO_2)_6(bpy)_2]$	**50**	2.779	3.288; 3.481	$(Mn^{II})_2(Mn^{III})_2$	[141]
$[H_2Im]_2[Mn_4O_3Cl_6(HIm)(CH_3CO_2)_3]$	**51**	2.818; 2.806	3.323; 3.285	$(Mn^{III})_3(Mn^{IV})$	[144]
$[Mn_4O_2(O_2CCPh_3)_6(OEt_2)_2]$	**52**	2.770	3.265	$(Mn^{II})_2(Mn^{III})_2$	[143]
$[Mn_4O_3Cl_4(CH_3CO_2)_3(py)_3]$	**53**	2.815	3.272	$(Mn^{III})_3(Mn^{IV})$	[142]
$[Mn_4O(L^{11})(CH_3CO_2)_3Cl(CH_3OH)]$	**54**	–	3.158; 3.442; 3.016	$(Mn^{II})_2(Mn^{III})_2$	[139]

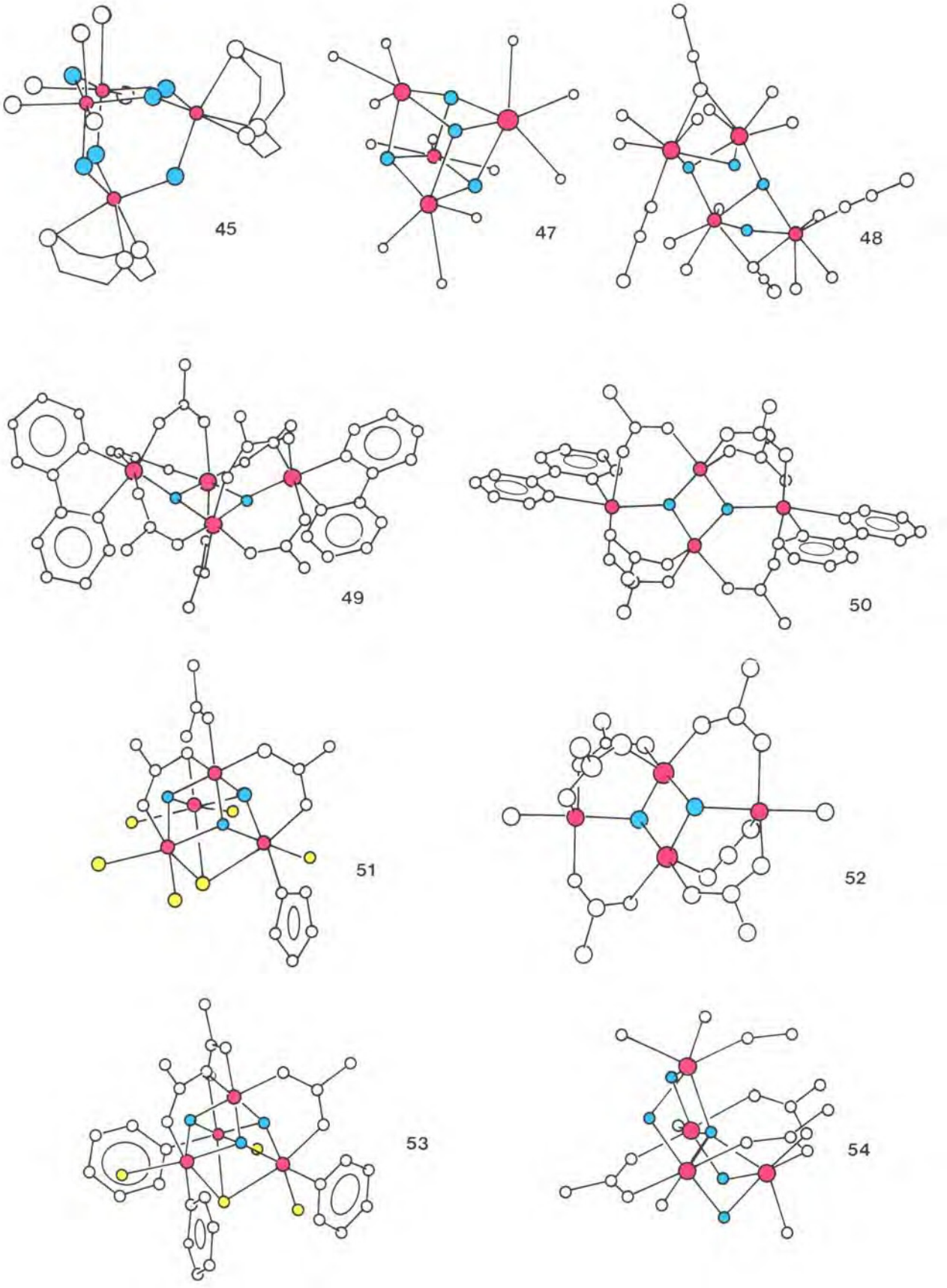


Fig. 21. Structures of the tetranuclear manganese clusters **45** and **47–54** (some ligands are omitted for clarity). Red circles: manganese atoms; yellow: chloride ligands; blue: oxygen atoms of μ-oxo-, μ-aryloxo or μ-alkoxo bridged ligands.

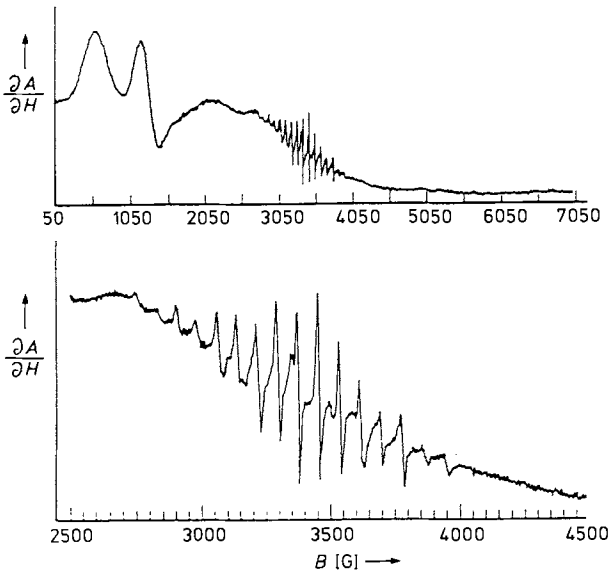


Fig. 22. X-band ESR-spectrum of **51** in frozen-in DMF/toluene at 60 K (above) and expansion of the region around $g = 2.0$ (below) [144].

however, not functional models and cannot oxidize H_2O to O_2 despite the high oxidation level of $Mn^{IV}Mn^{III}_3$.

Complex **48**[138b] is a good model for the suggestion that the manganese atoms in PS II form two neighboring dimeric pairs. The oxidation state, however, (four Mn^{II} ions) is too small and the Mn · · · Mn distances are too large.

4.8. Polynuclear Manganese Complexes

In the search for suitable synthetic methods for di- and tetranuclear manganese clusters with biological relevance, more and more complexes of higher nuclearity have been found. These molecules are of great interest to inorganic and theoretical chemists since the aggregation of paramagnetic centers leads to novel electronic and magnetic properties. Up to now, however, they have been of no biological significance, with the possible exception of the trinuclear complexes, and so in closing only a selection will be mentioned.

$Mn^{II}[Mn^{III}_4(\text{salicylhydroximate})_4(CH_3CO_2)_2(dmf)_5] \cdot 2\ dmf$
(dmf = dimethylformamide [145])
$[Mn^{III}_2Mn^{II}_4O_2(Me_3CCO_2H)(Me_3CCO_2)_{10}]$ [146]
$[Mn^{II}Mn^{III}_8(O_2CPh)_8(sal)_4(salH)_2(pyr)_4]$ (pyr = pyridine) [147]
$[Mn^{III}_4Mn^{IV}_6O_{14}\{N(CH_2CH_2NH_2)_3\}_6](CF_3SO_3)_8 \cdot 6\ CH_3CN$ **55**[148]
$[Mn_{12}O_{12}(H_2O)_4(CH_3CO_2)_{16}]$ [149]
$[Mn_{12}L^{12}_6(OH)_4(CH_3CO_2)_2]$ [150]
$[Mn_{12}O_{12}(O_2CPh)_{16}(H_2O)_4]$ **56**[151]

These complex molecules have all been characterized by X-ray diffraction (Figures 23 and 24 show two such structures, namely **55** and **56**, respectively).

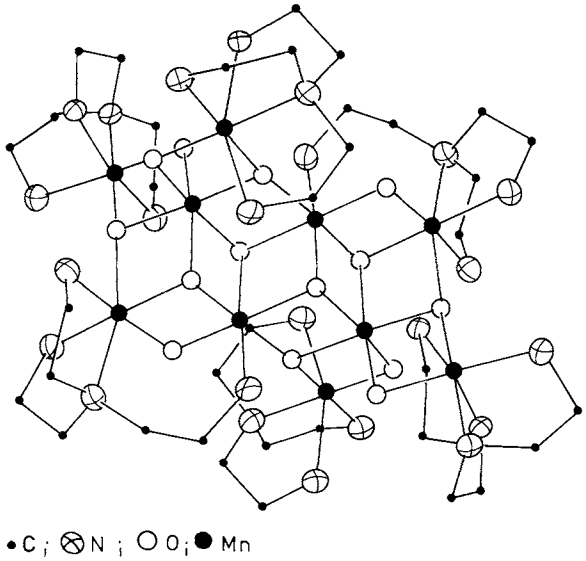


Fig. 23. The structure of the cation of **55** in the crystal [148]. It can be described as a layered inner Mn^{IV}_6 framework composed of edge-sharing MnO_6, MnO_5N and MnO_3N_3 octahedra (two of each). This layer is capped at the four corners by four $Mn^{III}O_2N_4$ octahedra (two under, two over). The cation is presumed to have antiferromagnetically coupled Mn centers.

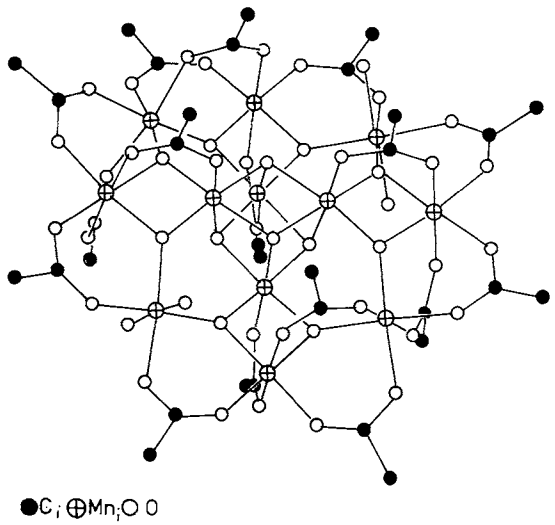


Fig. 24. The structure of **56** in the crystal [151]. The phenyl rings of the μ-benzoato bridges are not shown. Noteworthy is the central $\{Mn^{IV}_4O_4\}^{8\oplus}$ unit with a cubane core. The manganese centers are ferromagnetically coupled; the molecule has a S = 28/2 ground state (!), having eight Mn^{III} (d^4 h.s.) and four Mn^{IV} (d^3) centers.

5. Concluding Remarks

In this review, I have emphasized the modern interdisciplinary character between bio- and inorganic chemistry as exemplified by the research efforts of chemists from both camps on manganese-containing metalloproteins. The determination of the structure of their active sites and our understanding of the mechanism of their enzymatic functions is rapidly advancing by the fruitful interaction of physicists, biochemists and inorganic chemists. Structural and functional proposals from biochemistry can be scrutinized by inorganic chemists who can provide and test well characterized low molecular weight model compounds. Spectroscopic results on biomolecules are in general not readily interpreted without the availability of such compounds.

Over the last century the acquired knowledge of coordination chemistry relating to the structure, spectroscopic properties and reactivity of the essential transition metals has reached the stage where nearly all the biochemist's structural proposals can be reproduced on a simple molecular level. It

is therefore not presumptious to predict that the very complex problem of the oxygen evolution center in PS II will be better understood on a molecular basis within the next few years.

I would like to thank my co-workers for many enjoyable discussions and, of course, for their experimental prowess; their names are contained in the reference section. Frau U. Bossek deserves particular thanks for her 'golden touch' with which she so frequently crystallized tenacious materials. I thank Prof. J. Weiss and Dr. B. Nuber (Heidelberg) for friendly and invaluable cooperation over many years. I wish to thank Frau E. Padgett and Frau S. Altfeld for their help in preparing the manuscript. I am grateful to my colleagues W. H. Armstrong (Berkeley), S. P. Cramer (Brookhaven National Laboratories) and V. L. Pecarro (Ann Arbor) for providing preprints of their work prior to publication. I thank Prof. H. T. Witt (Berlin) and A. Trebst (Bochum) for their patient and comprehensive introduction into the complex world of photosynthesis. Thanks are also due to Prof. D. Sellmann (Erlangen) for critically reading the manuscript. Finally, generous financial support by the Deutsche Forschungsgemeinschaft and the Fonds der Chemischen Industrie is gratefully acknowledged.

Received: January 30, 1989 [A 731 IE]
German version: *Angew. Chem. 101* (1989) 1179

[1] a) E. Frieden (Ed.): *Biochemistry of the Essential Ultratrace Elements*, Plenum, New York 1984; b) *J. Chem. Educ. 62* (1985) 917; c) V. L. Schramm, F. C. Wedler (Eds.): *Manganese in Metabolism and Enzyme Function*, Academic Press, Orlando, FL, USA 1986.

[2] G. H. Reed, G. D. Markham, *Biol. Magn. Reson. 6* (1984) 73.

[3] A. B. P. Lever: *Inorganic Electronic Spectroscopy, 2nd edit.*, Elsevier, Amsterdam 1984.

[4] a) H. A. O. Hill, *Chem. Br. 12* (1976) 119; b) J. A. Ibers, R. H. Holm, *Science (Washington) 209* (1980) 223; c) K. Wieghardt, *Nachr. Chem. Tech. Lab. 33* (1985) 961.

[5] a) I. J. Goldstein, C. E. Hayes, *Adv. Carbohydr. Chem. Biochem. 35* (1978) 127; b) A. J. Kalb, A. Levitzki, *Biochem. J. 109* (1968) 669; c) C. F. Brewer, R. D. Brown III, S. H. Koenig, *J. Biol. Struct. Dyn. 1* (1983) 961; *Biochemistry 22* (1983) 3691.

[6] a) K. D. Hardmann, C. F. Ainsworth, *Biochemistry 11* (1972) 4910; b) G. M. Edelman, B. A. Cunningham, G. N. Reeke, Jr., J. W. Becker, M. J. Waxdal, J. L. Wang, *Proc. Natl. Acad. Sci. USA 69* (1972) 2580; c) J. W. Becker, G. N. Reeke, Jr., J. L. Wang, B. A. Cunningham, G. M. Edelman, *J. Biol. Chem. 250* (1975) 1513; d) G. N. Reeke, Jr., J. W. Becker, B. A. Cunningham, G. R. Gunther, J. L. Wang, G. M. Edelman, *Ann. N.Y. Acad. Sci. 234* (1974) 369; e) K. D. Hardmann, R. C. Agarwal, M. J. Freiser, *J. Mol. Biol. 157* (1982) 69; f) J. W. Becker, G. N. Reeke, Jr., B. A. Cunningham, G. M. Edelman, *Nature (London) 259* (1976) 407.

[7] a) G. H. Reed, M. Cohn, *J. Biol. Chem. 245* (1970) 662; b) B. C. Antanaitis, R. D. Brown III, N. D. Chasteen, J. H. Freedman, S. H. Koenig, H. R. Lilienthal, J. Peisach, C. F. Brewer, *Biochemistry 26* (1987) 7932.

[8] a) G. L. Cantoni, *Annu. Rev. Biochem. 44* (1975) 435; b) C. W. Tabor, H. Tabor, *ibid. 45* (1976) 285; c) G. D. Markham, E. W. Hafner, C. W. Tabor, H. Tabor, *J. Biol. Chem. 255* (1980) 9082; d) G. D. Markham, *ibid. 256* (1981) 1903.

[9] a) E. R. Stadtman, A. Ginsburg, *Enzymes (3rd Ed.) 10* (1974) 755; b) J. B. Hunt, A. Ginsburg, *Biochemistry 11* (1972) 3723; c) J. B. Hunt, P. Z. Smyrniotis, A. Ginsburg, E. R. Stadtman, *Arch. Biochem. Biophys. 166* (1975) 102; d) M. D. Denton, A. Ginsburg, *Biochemistry 8* (1969) 1714; e) J. J. Villafranca, D. E. Ash, F. C. Wedler, *ibid. 15* (1976) 544; f) J. J. Villafranca, M. S. Balakrishnan, F. C. Wedler, *Biochem. Biophys. Res. Commun. 75* (1977) 464; g) A. Shrake, D. M. Powers, A. Ginsburg, *Biochemistry 16* (1977) 4372; h) M. S. Balakrishnan, J. J. Villafranca, *ibid. 17* (1978) 3531.

[10] a) M. L. Pamphilis, W. W. Cleland, *Biochemistry 12* (1973) 3714; b) C. A. Janson, W. W. Cleland, *J. Biol. Chem. 249* (1974) 2567, 2572; c) K. D. Danenberg, W. W. Cleland, *Biochemistry 14* (1975) 28; d) M. S. Balakrishnan, J. J. Villafranca, *ibid. 18* (1979) 1546.

[11] J. S. Leigh, *J. Chem. Phys. 52* (1970) 2608.

[12] a) B. Malmström, *Arch. Biochem. Biophys. 46* (1953) 345; b) B. Malmström, T. Vänngard, M. Larson, *Biochim. Biophys. Acta 30* (1958) 1; c) M. Cohn, J. Townsend, *Nature (London) 173* (1954) 1090; d) M. Cohn, *Biochemistry 2* (1963) 623; e) T. Gawronski, E. W. Westhead, *ibid. 8* (1969) 4261; f) D. P. Hanlon, E. W. Westhead, *Biochim. Biophys. Acta 96* (1965) 537; *Biochemistry 8* (1969) 4247, 4255; g) J. C. W. Chien, E. W. Westhead, *ibid. 10* (1971) 3198.

[13] G. S. Allgood, J. J. Perry, *J. Bacteriol. 168* (1986) 563.

[14] a) A. M. Michelson, J. M. McCord, I. Fridovich (Eds.): *Superoxide and Superoxide Dismutases*, Academic Press, London 1977; b) A. Gärtner, U. Weser, *Top. Curr. Chem. 132* (1986) 1; c) J. V. Bannister, H. A. O. Hill (Eds.): *Chemical and Biochemical Aspects of Superoxide and Superoxide Dismutases (Dev. Biochem. 11 A* (1980)); d) L. W. Oberley (Ed.): *Superoxide Dismutase, Vol. I + II*, CRC Press, Boca Raton, FL, USA 1982.

[15] a) W. C. Stallings, K. A. Pattridge, R. K. Strong, M. L. Ludwig, *J. Biol. Chem. 260* (1985) 1624; b) B. B. Keele, Jr., J. M. McCord, I. Fridovich, *ibid. 245* (1970) 6176; c) J. A. Fee, E. R. Shapiro, T. H. Moss, *ibid. 251* (1976) 6157.

[16] a) V. V. Barynin, A. I. Grebenko, *Dokl. Akad. Nauk SSR 288* (1986) 1100; b) V. V. Barynin, A. A. Vagin, V. R. Melik-Adamyan, A. I. Grebenko, S. V. Khangulov, A. N. Popov, M. E. Andrianova, B. K. Vainshtein, *ibid. 288* (1986) 877; c) B. K. Vainshtein, V. R. Melik-Adamyan, V. V. Barynin, *Kristallografia 26* (1981) 10003; d) S. V. Khangulov, V. V. Barynin, V. R. Melik-Adamyan, A. I. Grebenko, N. V. Voevodskaya, L. A. Blumenfeld, S. N. Dobryakov, V. B. Ilyasova, *Bioorg. Khim. 12* (1986) 741; e) S. V. Khangulov, N. V. Voevodskaya, V. V. Barynin, A. I. Grebenko, V. R. Melik-Adamyan, *Biofizika 32* (1987) 960; f) B. K. Vainshtein, V. R. Melik-Adamyan, V. V. Barynin, A. A. Vagin, A. I. Grebenko, *Proc. Int. Symp. Biomol. Struct. Interactions, Suppl. J. Biosci. 8* (1985) 471.

[17] R. E. Stenkamp, L. C. Sieker, L. H. Jensen, *J. Am. Chem. Soc. 106* (1984) 618.

[18] Iron-containing metalloproteins with Fe–O–Fe active centers in their model complexes have recently been described in a review: S. J. Lippard, *Angew. Chem. 100* (1988) 353; *Angew. Chem. Int. Ed. Engl. 27* (1988) 344.

[19] a) Y. Kono, I. Fridovich, *J. Biol. Chem. 258* (1983) 6015, 13646; b) W. F. Beyer, Jr., I. Fridovich, *Biochemistry 24* (1985) 6460.

[20] R. M. Fronko, J. E. Penner-Hahn, *J. Am. Chem. Soc. 110* (1988) 7554.

[21] M. Lammers, H. Follmann, *Struct. Bonding (Berlin) 54* (1983).

[22] a) A. Willing, H. Follmann, G. Auling, *Eur. J. Biochem. 170* (1988) 603; b) J. Plönzig, G. Auling, *Arch. Microbiol. 146* (1987) 396; c) H. Follmann, A. Willing, G. Auling, J. Plönzig in A. Holmgren, et al. (Ed.): *Thioredoxin and Glutaredoxin Systems: Structure and Function*, Raven Press, New York, 1986.

[23] a) Y. Sugiura, H. Kawabe, H. Tanaka, S. Fujimoto, A. Ohara, *J. Biol. Chem. 256* (1981) 10664; b) S. Fujimoto, A. Ohara, K. Uehara, *Agric. Biol. Chem. 44* (1980) 1659; c) H. Kawabe, Y. Sugiura, M. Terauchi, H. Tanaka, *Biochim. Biophys. Acta 784* (1984) 81; d) S. Fujimoto, K. Murakami, A. Ohara, *J. Biochem. 97* (1985) 1777.

[24] S. K. Hefler, B. A. Averill, *Biochem. Biophys. Res. Commun. 146* (1987) 1173.

[25] R. Reinards, R. Altdorf, H.-D. Ohlenbusch, *Hoppe-Seyler's Z. Physiol. Chem. 365* (1984) 577.

[26] G. Renger, *Angew. Chem. 99* (1987) 660; *Angew. Chem. Int. Ed. Engl. 26* (1987) 643.

[27] W. Haehnel, *Annu. Rev. Plant Physiol. 35* (1984) 659.

[28] J. Livorness, T. D. Smith, *Struct. Bonding (Berlin) 48* (1982).

[29] Govindjee, T. Kambara, W. Coleman, *Photochem. Photobiol. 42* (1985) 187.

[30] G. Renger, Govindjee, *Photosynth. Res. 6* (1985) 33.

[31] J. Amesz, *Biochim. Biophys. Acta 726* (1983) 1.

[32] H. T. Witt, E. Schlodder, K. Brettel, Ö. Sayagin, *Ber. Bunsenges. Phys. Chem. 90* (1986) 1015.

[33] H. T. Witt, *New J. Chem. 11* (1987) 91.

[34] J. C. de Paula, W. F. Beck, G. W. Brudvig, *New. J. Chem. 11* (1987) 103.

[35] G. T. Babcock in J. Anresz (Ed.): *New Comprehensive Biochemistry Photosynthesis*, Elsevier, Amsterdam 1987, p. 125.

[36] a) G. C. Dismukes, *Chem. Scr. 28 A* (1988) 99; b) J. E. Sheats, B. C. Unni Nair, V. Petrouleas, S. Artaudi, R. S. Czernuszewicz, G. C. Dismukes, *Prog. Photosynth. Res. Proc. Int. Congr. Photosynth. 7th 1986, Vol. 1* (1987) 721; c) G. C. Dismukes, *Photochem. Photobiol. 43* (1986) 99.

[37] G. W. Brudvig, *J. Bioenerg. Biomembr. 19* (1987) 91.

[38] P. H. Homan, *J. Bioenerg. Biomembr. 19* (1987) 105.

[39] It should be pointed out that ESR spectroscopic and EXAFS investigations in particular do not rule out a trimeric cluster of three neighboring Mn centers (distance 2.7 Å) and a somewhat distant fourth Mn center (3.3 Å).

[40] a) N. Murata, M. Miyao, T. Omata, H. Matsunami, T. Kuwabara, *Biochim. Biophys. Acta 765* (1984) 363; b) G. M. Cheniae, *Annu. Rev. Plant Physiol. 21* (1970) 467.

[41] a) G. C. Dismukes, Y. Siderer, *FEBS Lett. 121* (1980) 78; *Proc. Natl. Acad. Sci. USA 78* (1981) 274; b) G. C. Dismukes, K. Ferris, P. Watnick, *Photobiochem. Photobiophys. 3* (1982) 243; c) Ö. Hansson, L.-E. An-

dréasson, *Biochim. Biophys. Acta 679* (1982) 261; d) G. W. Brudvig, J. L. Casey, K. Sauer, *ibid. 723* (1983) 361; e) J. L. Casey, K. Sauer, *ibid. 767* (1984) 21; f) A. W. Rutherford, *ibid. 807* (1985) 189; g) J. L. Zimmermann, A. W. Rutherford, *ibid. 767* (1984) 160; h) Ö. Hansson, R. Aasa, T. Vänngard, *Biophys. J. 51* (1987) 825; i) J. C. de Paula, G. W. Brudvig, *J. Am. Chem. Soc. 107* (1985) 2643; j) J. C. de Paula, W. F. Beck, G. W. Brudvig, *ibid. 108* (1986) 4002; k) J. C. de Paula, W. F. Beck, A.-F. Miller, R. B. Wilson, G. W. Brudvig, *J. Chem. Soc. Faraday Trans. 1 83* (1987) 3635.

[42] a) G. H. Reed, M. Cohen, *J. Biol. Chem. 248* (1973) 6436; b) R. K. Gupta, *ibid. 252* (1977) 5183; c) R. K. Gupta, J. L. Benovic, *ibid. 253* (1978) 8878.

[43] T. M. Li, A. S. Mildran, R. L. Switzer, *J. Biol. Chem. 253* (1978) 3918.

[44] a) D. J. Hamm, B. S. Cooperman, *Biochemistry 17* (1978) 4033; b) W. B. Knight, D. Dunaway-Mariano, S. C. Ransom, J. J. Villafranca, *J. Biol. Chem. 259* (1984) 2886.

[45] F. Ranshel, J. J. Villafranca, *Biochemistry 19* (1980) 5481.

[46] a) V. Förster, Y.-Q. Hong, W. Junge, *Biochim. Biophys. Acta 638* (1981) 141; b) V. Förster, W. Junge, *Photochem. Photobiol. 41* (1985) 183; *Chem. Scr. 28A* (1988) 111.

[47] a) P. Joliot, A. Joliot, B. Bouges, G. Barbieri, *Photochem. Photobiol. 14* (1971) 287; b) P. Joliot, G. Barbieri, R. Chabaud, *ibid. 10* (1969) 309.

[48] B. Kok, B. Forbush, M. McGloin, *Photochem. Photobiol. 11* (1970) 457.

[49] Ö. Hansson, L.-E. Andréasson, T. Vänngard, *FEBS Lett. 195* (1986) 151.

[50] a) B. A. Barry, G. T. Babcock, *Proc. Natl. Acad. Sci. USA 84* (1987) 7099; *Chem. Scr. 28A* (1988) 117; b) R. J. Debus, B. A. Barry, G. T. Babcock, L. McIntosh, *Proc. Natl. Acad. Sci. USA 85* (1988) 427.

[51] a) J. A. Kirby, A. S. Robertson, J. P. Smith, A. C. Thompson, S. R. Cooper, M. P. Klein, *J. Am. Chem. Soc. 103* (1981) 5529; b) J. A. Kirby, D. B. Goodin, T. Wydrzynski, A. S. Robertson, M. P. Klein, *ibid. 103* (1981) 5537; c) D. B. Goodin, V. K. Yachandra, R. D. Britt, K. Sauer, M. P. Klein, *Biochim. Biophys. Acta 767* (1984) 209; d) K. Sauer, R. D. Guiles, A. E. McDermott, J. L. Cole, V. K. Yachandra, J. L. Zimmermann, M. P. Klein, S. L. Dexheimer, R. D. Britt, *Chem. Scr. 28A* (1988) 87.

[52] R. D. Guiles, J. L. Zimmermann, A. E. McDermott, V. K. Yachandra, J. L. Cole, S. L. Dexheimer, R. D. Britt, K. Wieghardt, U. Bossek, K. Sauer, M. P. Klein, *Biochemistry*, in press.

[53] G. N. George, R. C. Prince, S. P. Cramer, *Science (Washington) 237* (1989) 789.

[54] a) A. N. Srinivasan, R. R. Sharp, *Biochim. Biophys. Acta 850* (1986) 211; b) A. W. Rutherford, S. Styring in S. Papa (Ed.): *Cytochrome Systems: Molecular Biology and Bioenergetics*, Plenum, New York, in press.

[55] S. Padhye, T. Kambara, D. N. Hendrickson, Govindjee, *Photosynth. Res. 9* (1986) 103.

[56] G. W. Brudvig, R. H. Crabtree, *Proc. Natl. Acad. Sci. USA 83* (1986) 4586.

[57] J. B. Vincent, G. Christou, *Inorg. Chim. Acta 136* (1987) L41.

[58] T. Kambara, Govindjee, *Proc. Natl. Acad. Sci. USA 82* (1985) 6119.

[59] G. Renger, *Chem. Scr. 28A* (1988) 105.

[60] Two excellent reviews of model complexes of manganese have appeared recently which describe the role of manganese in the PS II from the inorganic chemist's viewpoint: a) V. L. Pecoraro, *Photochem. Photobiol. 48* (1988) 249; b) G. C. Christou, J. B. Vincent in L. Que (Ed.): *Metal Clusters in Proteins (ACS Symp. Ser. 372)* (1988) 239.

[61] J. E. Sheats, R. S. Czernuszewicz, G. C. Dismukes, A. L. Rheingold, V. Petrouleas, J. Stubbe, W. H. Armstrong, R. H. Beer, S. J. Lippard, *J. Am. Chem. Soc. 109* (1987) 1435.

[62] a) J. W. Buchler, C. Dreher, K.-L. Lay, *Z. Naturforsch. B37* (1982) 1155; b) J. W. Buchler, C. Dreher, K.-L. Lay, A. Raap, K. Gersonde, *Inorg. Chem. 22* (1983) 879; c) J. W. Buchler, C. Dreher, K.-L. Lay, Y. J. A. Lee, W. R. Scheidt, *ibid. 22* (1983) 888.

[63] C. L. Hill, F. J. Hollander, *J. Am. Chem. Soc. 104* (1982) 7318.

[64] J. T. Groves, W. J. Krupper, R. C. Haushalter, *J. Am. Chem. Soc. 102* (1980) 6375.

[65] L. A. Bottomley, F. L. Neely, H.-N. Gorce, *Inorg. Chem. 27* (1988) 1300.

[66] M. Koikawa, H. Okawa, S. Kida, *J. Chem. Soc. Dalton Trans. 1988*, 641.

[67] P. A. Loach, M. Calvin, *Biochemistry 2* (1963) 361.

[68] A good review of manganese complex chemistry can be found in G. Wilkinson, R. D. Gillard, J. A. McCleverty, (Eds.): *Comprehensive Coordination Chemistry, Vol. 4*, Pergamon, New York 1987.

[69] Ö. Sayagin, G. Gerken, B. Meyer, H. T. Witt, *Photosynth. Res. 9* (1986) 71.

[70] N. Nakasuka, S. Azuma, C. Katamaya, M. Honda, J. Tanaka, M. Tanaka, *Acta Crystallogr. Sect. C41* (1985) 1176.

[71] a) K. Wieghardt, U. Bossek, B. Nuber, J. Weiss, *Inorg. Chim. Acta*, in press; b) K. Wieghardt, U. Bossek, J. Bonvoisin, P. Beauvillain, J. J. Girerd, B. Nuber, J. Weiss, J. Heinze, *Angew. Chem. 98* (1986) 1026; *Angew. Chem. Int. Ed. Engl. 25* (1986) 1030.

[72] K. Wieghardt, U. Bossek, B. Nuber, J. Weiss, J. Bonvoisin, M. Corbella, S. E. Vitols, J.-J. Girerd, *J. Am. Chem. Soc. 110* (1988) 7398.

[73] a) S. Ménage, J.-J. Girerd, unpublished results; b) S. Ménage, *Dissertation*, Université de Paris-Sud Centre d'Orsay 1988.

[74] D. J. Hodgson, B. J. Schwartz, T. N. Sorrell, *Inorg. Chem. 28* (1989) 2226.

[75] D. P. Kessissoglou, W. M. Butler, V. L. Pecoraro, *Inorg. Chem. 26* (1987) 495.

[76] a) B. Mabad, J.-P. Tuchagues, Y. T. Hwang, D. N. Hendrickson, *J. Am. Chem. Soc. 107* (1985) 2801; b) B. Mabad, P. Cassoux, J.-P. Tuchagues, D. N. Hendrickson, *Inorg. Chem. 25* (1986) 1420.

[77] J. Owen, *J. Appl. Phys. 32* (1961) 2135.

[78] P. Mathur, M. Crowder, G. C. Dismukes, *J. Am. Chem. Soc. 109* (1987) 5227.

[79] P. Mathur, G. C. Dismukes, *J. Am. Chem. Soc. 105* (1983) 7093.

[80] M. W. Lynch, D. N. Hendrickson, B. J. Fitzgerald, C. G. Pierpont, *J. Am. Chem. Soc. 106* (1984) 2041.

[81] K. Wieghardt, U. Bossek, D. Ventur, J. Weiss, *J. Chem. Soc. Chem. Commun. 1985*, 347.

[82] See Ref. [61].

[83] S. Ménage, J. J. Girerd, A. Gleizes, *J. Chem. Soc. Chem. Commun. 1988*, 431.

[84] a) Y. Nishida, N. Oshino, T. Tokii, *Z. Naturforsch. B43* (1988) 637; b) Y. Nishida, *J. Inorg. Biochem. 32* (1988) 277.

[85] a) N. Torihara, M. Mikuriya, H. Okawa, S. Kida, *Bull. Chem. Soc. Jpn. 53* (1980) 1610; b) M. Mikuriya, N. Torihara, H. Okawa, S. Kida, *Bull. Chem. Soc. Jpn. 54* (1981) 1063.

[86] H. S. Maslen, T. N. Waters, *J. Chem. Soc. Chem. Commun. 1973*, 760.

[87] Y. Nishida, N. Oshino, T. Tokii, *Z. Naturforsch. B43* (1988) 472.

[88] B. U. Nair, G. C. Dismukes, *J. Am. Chem. Soc. 105* (1983) 124.

[89] S. K. Larsen, C. G. Pierpont, G. DeMunno, G. Dolcetti, *Inorg. Chem. 25* (1986) 4828.

[90] a) J. A. Bonadies, M. J. Maroney, V. L. Pecoraro, *Inorg. Chem. 28* (1989) 2044; b) J. A. Bonadies, M. L. Kirk, M. S. Lah, D. P. Kessissoglou, W. E. Hatfield, V. L. Pecoraro, *ibid. 28* (1989) 2037.

[91] H. J. Schugar, G. R. Rossmann, C. G. Barraclough, H. B. Gray, *J. Am. Chem. Soc. 94* (1972) 2683.

[92] a) H. U. Güdel, *Comments Inorg. Chem. 3* (1984) 189; b) P. J. McCarthy, H. U. Güdel, *Coord. Chem. Rev. 88* (1988) 69.

[93] J. B. Vincent, K. Folting, J. C. Huffman, G. C. Christou, *Inorg. Chem. 25* (1986) 996.

[94] a) B. C. Schardt, F. J. Hollander, C. L. Hill, *J. Chem. Soc. Chem. Commun. 1981*, 765; b) *J. Am. Chem. Soc. 104* (1982) 3964.

[95] M. Stebler, A. Ludi, H.-B. Bürgi, *Inorg. Chem. 25* (1986) 4743.

[96] H. A. Doodwin, R. N. Sylva, *Austr. J. Chem. 20* (1967) 629.

[97] Y. Yoshino, I. Taminaga, M. Kokiso, T. Uehiro, *Bull. Chem. Soc. Jpn. 47* (1974) 2787.

[98] L. J. Boucher, C. G. Coe, *Inorg. Chem. 14* (1975) 1289.

[99] a) M. M. Morrison, D. T. Sawyer, *J. Am. Chem. Soc. 99* (1977) 257; b) K. S. Yamaguchi, D. T. Sawyer, *Isr. J. Chem. 25* (1985) 164; c) S. R. Cooper, M. Calvin, *J. Am. Chem. Soc. 99* (1977) 6623.

[100] H. Okawa, A. Honda, M. Nakamura, S. Kida, *J. Chem. Soc. Dalton Trans. 1985*, 59.

[101] B. Mabad, J.-P. Tuchagues, Y. T. Hwang, D. N. Hendrickson, *J. Am. Chem. Soc. 107* (1985) 2801.

[102] G. C. Dismukes, J. E. Sheats, J. A. Smegal, *J. Am. Chem. Soc. 109* (1987) 7202.

[103] M. Suzuki, S. Murata, A. Uehara, S. Kida, *Chem. Lett. 1987*, 281.

[104] M. Suzuki, M. Mikuriya, S. Murata, A. Uehara, H. Oshio, S. Kida, K. Saito, *Bull. Chem. Soc. Jpn. 60* (1987) 4305.

[105] H. Diril, H.-R. Chang, X. Zhang, S. K. Larsen, J. A. Potenza, C. G. Pierpont, H. J. Schugar, S. S. Isied, D. N. Hendrickson, *J. Am. Chem. Soc. 109* (1987) 6207.

[106] R. M. Buchanan, K. J. Oberhausen, J. F. Richardson, *Inorg. Chem. 27* (1988) 971.

[107] H.-R. Chang, H. Diril, M. J. Nilges, X. Zhang, J. A. Potenza, H.-J. Schugar, D. N. Hendrickson, S. S. Isied, *J. Am. Chem. Soc. 110* (1988) 625.

[108] J. S. Bashkin, A. R. Schake, J. B. Vincent, H.-R. Chang, Q. Li, J. C. Huffman, G. Christou, D. N. Hendrickson, *J. Chem. Soc. Chem. Commun. 1988*, 700.

[109] H.-R. Chang, S. K. Larsen, P. D. W. Boyd, C. G. Pierpont, D. N. Hendrickson, *J. Am. Chem. Soc. 110* (1988) 4565.

[110] M. B. Robin, P. Day, *Adv. Inorg. Chem. Radiochem. 10* (1967) 247.

[111] a) P. M. Plaskin, R. C. Staufer, M. Mathew, G. J. Palenik, *J. Am. Chem. Soc. 94* (1972) 2121; b) R. S. Nyholm, A. Turco, *Chem. Ind. (London) 1960*, 74; c) R. Usóu, *Transition Met. Chem. (Weinheim Ger.) 1* (1975) 21.

[112] a) See Ref. [99c]; b) S. R. Cooper, G. C. Dismukes, M. P. Klein, M. Calvin, *J. Am. Chem. Soc. 100* (1978) 7248.

[113] M. A. Collins, D. J. Hodgson, M. Michelsen, D. K. Towle, *J. Chem. Soc. Chem. Commun. 1987*, 1659.

[114] a) M. Suzuki, S. Tokura, M. Suhara, A. Uehara, *Chem. Lett. 1988*, 477; b) D. K. Towle, C. A. Botsford, D. J. Hodgson, *Inorg. Chim. Acta 141* (1988) 167.

[115] K. J. Brewer, A. Liegeois, J. W. Otvos, M. Calvin, L. O. Spreer, *J. Chem. Soc. Chem. Commun. 1988*, 1219.

[116] M. Suzuki, H. Senda, Y. Kobayashi, O. Oshio, A. Uehara, *Chem. Lett. 1988*, 1763.

[117] K. S. Hagen, W. H. Armstrong, H. Hope, *Inorg. Chem. 27* (1988) 969.

[118] K. Wieghardt, U. Bossek, L. Zsolnai, G. Huttner, G. Blondin, J.-J. Girerd, F. Babonneau, *J. Chem. Soc. Chem. Commun. 1987*, 651.
[119] A. Gref, G. Balavoine, H. Rivière, C. P. Andrieux, *Nouv. J. Chim. 8* (1984) 615.
[120] S. Ménage, S. E. Vitols, J.-J. Girerd, C. Cartier, M. Verdaguer, M. Mimoun, L. Saussine, P. Charpin, M. Nierlich, C. Merienne, unpublished.
[121] R. Ramarai, A. Kira, M. Kaneko, *Angew. Chem. 98* (1986) 824; *Angew. Chem. Int. Ed. Engl. 25* (1986) 825.
[122] F. M. Ashmawy, C. A. McAuliffe, R. V. Parish, J. Tames, *J. Chem. Soc. Dalton Trans. 1985*, 1391.
[123] C. A. McAuliffe, R. V. Parish, S. M. Abu-El-Wafa, R. M. Issa, *Inorg. Chim. Acta 115* (1986) 91.
[124] F. M. Ashmawy, C. A. McAuliffe, R. V. Parish, J. Tames, *J. Chem. Soc. Chem. Commun. 1984*, 14.
[125] M. Calvin, *Science (Washington) 184* (1974) 375.
[126] M. Calvin, S. R. Cooper, *Science (Washington) 185* (1974) 4148.
[127] W. Micklitz, S. G. Bott, J. G. Bentsen, S. J. Lippard, *J. Am. Chem. Soc. 111* (1989) 372.
[128] Two review articles describe this aspect of manganese chemistry: a) G. D. Lawrence, D. T. Sawyer, *Coord. Chem. Rev. 27* (1978) 173; b) W. M. Coleman, L. T. Taylor, *ibid. 32* (1980) 1.
[129] R. B. Van Atta, C. E. Strouse, L. Karle Hanson, J. S. Valentine, *J. Am. Chem. Soc. 109* (1987) 1425.
[130] R. Bhula, G. J. Gainsford, D. C. Weatherburn, *J. Am. Chem. Soc. 110* (1988) 7550.
[131] D. T. Sawyer, M. E. Bodini, *J. Am. Chem. Soc. 97* (1975) 6588.
[132] T. Matsushita, L. Spencer, D. T. Sawyer, *Inorg. Chem. 27* (1988) 1167.
[133] M. Tirant, T. D. Smith, *Inorg. Chim. Acta 121* (1986) 5.
[134] a) M. Fujiwara, T. Matsushita, T. Shono, *Polyhedron 4* (1985) 1895; b) T. Matsushita, M. Fujiwara, T. Shono, *Chem. Lett. 1981*, 631.
[135] K. Yamaguchi, D. T. Sawyer, *Inorg. Chem. 24* (1985) 971.
[136] K. Wieghardt, U. Bossek, W. Gebert, *Angew. Chem. 95* (1983) 320; *Angew. Chem. Int. Ed. Engl. 22* (1983) 328.
[137] K. S. Hagen, T. D. Westmoreland, M. J. Scott, W. H. Armstrong, *J. Am. Chem. Soc. 111* (1989) 1907.
[138] a) V. McKee, W. B. Shepard, *J. Chem. Soc. Chem. Commun. 1985*, 158; b) S. Brooker, V. McKee, W. B. Shepard, L. K. Pannell, *J. Chem. Soc. Dalton Trans. 1987*, 2555.
[139] V. McKee, S. S. Tandon, *J. Chem. Soc. Chem. Commun. 1988*, 1335.
[140] J. B. Vincent, C. Christmas, J. C. Huffman, G. Christou, H.-R. Chang, D. N. Hendrickson, *J. Chem. Soc. Chem. Commun. 1987*, 236.
[141] C. Christmas, J. B. Vincent, J. C. Huffman, G. Christou, H.-R. Chang, D. N. Hendrickson, *J. Chem. Soc. Chem. Commun. 1987*, 1303.
[142] Q. Li, J. B. Vincent, E. Libby, H.-R. Chang, J. C. Huffman, P. D. W. Boyd, G. Christou, D. N. Hendrickson, *Angew. Chem. 100* (1988) 1799; *Angew. Chem. Int. Ed. Engl. 27* (1988) 1731.
[143] R. J. Kulawiec, R. H. Crabtree, G. W. Brudvig, G. K. Schulte, *Inorg. Chem. 27* (1988) 1311.
[144] J. S. Bashkin, H.-R. Chang, W. E. Streib, J. C. Huffman, D. N. Hendrickson, G. Christou, *J. Am. Chem. Soc. 109* (1987) 6502.
[145] M. S. Lah, V. L. Pecoraro, unpublished.
[146] A. R. E. Baikie, A. J. Howes, M. B. Hursthouse, A. B. Quick, P. Thornton, *J. Chem. Soc. Chem. Commun. 1986*, 1587.
[147] C. Christmas, J. B. Vincent, J. C. Huffman, G. Christou, H.-R. Chang, D. N. Hendrickson, *Angew. Chem. 99* (1987) 934; *Angew. Chem. Int. Ed. Engl. 26* (1987) 915; *J. Am. Chem. Soc. 110* (1988) 823.
[148] K. S. Hagen, W. H. Armstrong, M. M. Olmstead, *J. Am. Chem. Soc. 111* (1989) 774.
[149] T. Lis, *Acta Crystallogr.* Sect. *B36* (1980) 2042.
[150] D. Luneau, J.-M. Savariault, J.-P. Tuchagues, *Inorg. Chem. 27* (1988) 3912.
[151] P. D. W. Boyd, Q. Li, J. B. Vincent, K. Folting, H.-R. Chang, W. E. Streib, J. C. Huffman, G. Christou, D. N. Hendrickson, *J. Am. Chem. Soc. 110* (1988) 8537.

Cyclizations via Palladium-Catalyzed Allylic Alkylations

New Synthetic Methods (79)

By Barry M. Trost*

The history of ring systems in organic chemistry parallels their synthetic accessibility. Transition-metal-catalyzed cyclizations offer a new opportunity to create carbo- and heterocyclic compounds with great facility. Among these methods, allylic alkylations catalyzed by palladium have proven unusually productive because of the extraordinary chemo-, regio-, and diastereoselectivity and the continuing possibility for the development of enantioselectivity. The rules for ring closure differ from those for non-transition-metal-catalyzed reactions. A major benefit is the ability to generate medium (eight-, nine-, ten-, and eleven-membered) and large rings in preference to normal (five-, six- and seven-membered) rings. With the appropriate substrate, efficient macrocyclizations are possible under conditions of normal concentrations. A second major benefit derives from the complementary stereochemistry of the metal-catalyzed substitution (net retention of configuration) compared to non-metal-catalyzed reactions (inversion of configuration). Further, the requirement for the substrate to conform to the transition-metal template may impose a stereochemical preference in the intermediate that ultimately translates into the thermodynamically less stable organic product regardless of the stereochemistry of the starting material. While more work has focused on carbocyclic synthesis, the possibilities for heterocyclic synthesis are just beginning to be tapped. In addition to forming heterocycles by C–C bond formation, use of a heteroatom as a nucleophile has already proven effective for oxygen and nitrogen, with other nucleophiles awaiting investigation. New dimensions for cyclization via allylic alkylation arise by generating the requisite π-allylpalladium intermediates by methods other than palladium(0)-initiated allylic ionizations. In addition, metals other than palladium will clearly expand the possibilities, but as yet remain untapped.

1. Introduction

Ring systems have fascinated organic chemists from the very beginning of the science. From its early days, the normal rings, those of five, six, or seven members, have been a major part because of their common occurrence. The year 1985 marked the one hundredth anniversary of *Adolf von Baeyer*'s "theory of ring strain" describing the existence of three- and four-membered rings.[1] Medium- and large-ring chemistry developed somewhat later, with landmark contributions exemplified by *Willstätter*'s synthesis of eight-membered rings[2] and *Ružička*'s studies into the chemistry of muscone and civetone.[3,4]

A great deal of the emphasis on cyclic compounds emanated from their biological significance. The elucidation of the structure of steroids set off a wave of studies directed toward six-membered rings. The Robinson annelation represents an early milestone.[5] The culmination of steroid synthesis by polyolefin cyclization some fifty years later systematizes cation-induced cyclizations as a good strategy for ring formation if the proper initiator and terminator are found.[6]

The discovery and structure elucidation of prostaglandins in the 1960s unleashed a fierce attack on methods for five-membered ring synthesis.[7,8] A few innovations that emanated from these studies include free radical chemistry,[9] transition-metal-promoted carbene insertion,[10] [3 + 2] cycloadditions,[11] and intramolecular carbametalations.[12]

Appreciation for the importance of macrocycles possibly began with the isolation of the first macrolide antibiotic, pikromycin, in 1950.[13] Naturally occurring macrolides may be conveniently classified according to structural type.[14] Among the diverse members are the polyoxo (e.g., pikromycin,[15] erythromycin[16]), polyene (amphotericin B,[17] tetrin A[18]), spiroketal (avermectin,[19] milbemycin[20]), ionophoric (nonactin,[21] boromycin[22]), and lactam-containing (maytansine,[23] FK 506[24]) macrolides. Macrocyclic sesquiterpenes[25] (e.g., caryophyllenes, humulenes, bazzarenes, cyclogermacranes, and germacranes), diterpenes (e.g., jatrophanes,[26] taxanes,[27] fusicoccins[28]), sesterterpenes (e.g., ophiobolins[29,30]), and miscellaneous other macrocycles (e.g., cytochalasins, esperamycin[31]/calichemicin[32]) display a broad spectrum of activity ranging from insect pheromonal to antitumor.

The study of varied ring systems closely parallels their availability. Thus, the continuing evolution of cyclization methods plays a critical role in extending our understanding and in developing the utility of carbo- and heterocyclic rings. The ability of transition-metal catalysts to exercise control in bond-forming reactions under very mild conditions makes them excellent candidates to facilitate ring formation. Indeed, cyclooligomerization of unsaturated linkages such as the nickel-catalyzed oligomerization of dienes[33] and the cobalt-catalyzed cooligomerization of triple- and/or double-bonded molecules[34] are major developments. Defined cycloadditions, as illustrated by the palladium-catalyzed

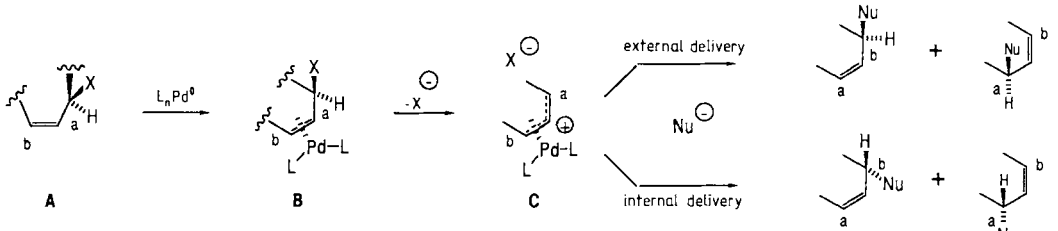
[*] Prof. Barry M. Trost
Department of Chemistry
Stanford University
Stanford, CA 94305 (USA)

[3 + 2],[11] [3 + 4],[35] and [3 + 6][36] cycloadditions, involving transfer of a trimethylenemethane unit, represent another important direction.

While such multi-bond-forming processes are attractive because of their efficiency in ring construction, the greater flexibility and diversity available from a cyclization in which only one bond is formed increases our need for improving this type of strategy. In this review, we consider the utilization of palladium-catalyzed allylic alkylations for cyclization.

2. Reaction Features

Replacing functional groups that have high intrinsic reactivity, and can therefore lead to chemical instability and potential hazards, by relatively unreactive ones, which require activation to participate in chemical reactions, may increase selectivity as well as enhance ease of handling and safety. Palladium-catalyzed allylic alkylations allow compounds **A** with relatively unreactive leaving groups (Scheme 1), including, but not limited to, carboxylate (including carbonate), phenoxide, imino ether, sulfinate, phosphonate, ammonium, sulfone, and nitro groups, to be ionized with inversion of configuration to the salt **C** via the intermediacy of an olefin–PdL_2 complex (**B**).[37] Nucleophiles attack the cationic intermediate **C** either at Ca or Cb, independent of the original position of the leaving group. The substitution proceeds with inversion by direct attack at carbon (i.e., external delivery of nucleophile) to give overall *substitution with retention of configuration* with "soft nucleophiles" (i.e., stabilized carbon and most heteroatom nucleophiles). Alternatively, the substitution may proceed by initial attack at the metal followed by reductive elimination to product (internal delivery of nucleophile) to give overall *substitution with inversion of configuration* with "hard nucleophiles" (i.e., nonstabilized carbon and some heteroatom nucleophiles).



Scheme 1. Palladium-catalyzed allylic alkylation.

The regioselectivity depends primarily upon four factors: (1) charge distribution in the intermediate π-allylpalladium cation, which favors attack at the more substituted allyl terminus; (2) steric hindrance to approach of the nucleophile, which favors attack at the less substituted allyl terminus; (3) electronic effects of substituents of the allyl unit on the S_N2 transition state, which can favor either terminus depending upon the nature of the substituent; (4) the stability of the initial olefin–palladium(0) complex generated prior to dissociation of the product from the catalyst, which favors attack at the more substituted allyl terminus. For cyclization reactions, the ring size that derives from the regioselectivity will reflect all of the above factors, as well as the effect of the tether. The presence of many competing effects represents an opportunity to fine-tune the cyclization such that ring size can be chosen at will.

Such mechanistic diversity offers great opportunity to create cyclization methods. In addition, other strategies, such as Heck additions to allenes and dienes, permit entry into the π-allylpalladium manifold and ultimately may lead to cyclization methods.

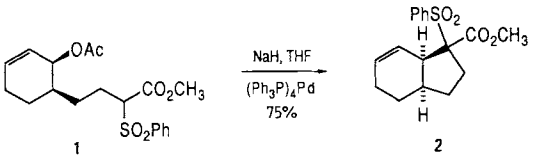


Barry M. Trost (born in 1941 in Philadelphia) obtained a B.A. in 1962 from the University of Pennsylvania and a Ph.D. in 1965 from the Massachusetts Institute of Technology. In that same year, he joined the Department of Chemistry at the University of Wisconsin as Assistant Professor, becoming Professor in 1969, Helfaer Professor in 1976, and Vilas Research Professor in 1982. In 1987, he moved to his current position at Stanford University. His research interests revolve around the theme of selectivity. Developing new reactions and reagents that are chemo-, regio-, diastereo-, and enantioselective represent the challenge. Transition metal templates serving as the equivalent of the "chemists' enzymes," main group organometallic chemistry, small ring compounds, and sulfur chemistry provide new reactions and reagents which permit creation of novel synthetic strategies employed in the total synthesis of bioactive and novel molecules. In recognition of his many contributions, Barry Trost has received a number of awards, the latest being the Arthur C. Cope Scholar Award (1989). He is a Fellow of the American Association for the Advancement of Science (1977), a Fellow of the American Academy of Arts and Sciences (1982), and a member of the National Academy of Sciences (1980).

3. Cyclization Involving Carbon Nucleophiles

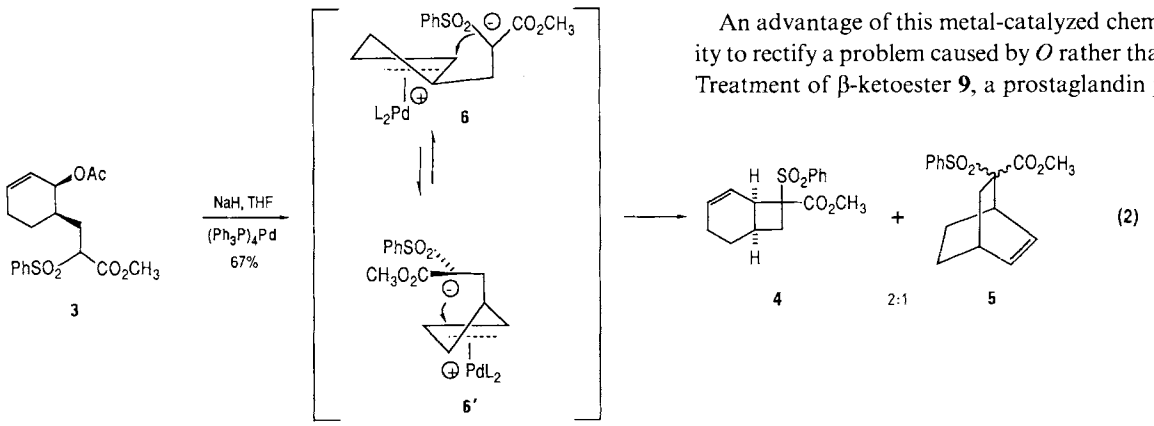
3.1. Carbocyclic Rings—Use of Soft Nucleophiles

The first example of a Pd^0-catalyzed cyclization of an allyl acetate was that of **1** [Eq. (1)]. Addition of sodium hydride



1 2 (1)

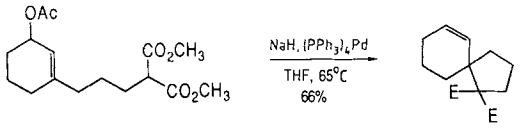
to generate the nucleophile in situ followed by 2 mol% of tetrakis(triphenylphosphane)palladium smoothly effects cyclization to form the five-membered ring product **2**. Subjecting the analogue of **1** bearing one less carbon in the side chain (**3**) to the identical conditions produces a 2:1 mixture of the four- and six-membered ring products **4** and **5**, respectively [Eq. (2)]. The predominance of the four-membered ring product may derive from the preference for the cyclization to proceed via complex **6**, in which the side chain occupies a pseudoequatorial position, rather than complex **6'**, where this chain is in a pseudoaxial orientation, in spite of the fact that an unfavorable ring size (i.e., a cyclobutane) is produced. From the outset, it became apparent that factors

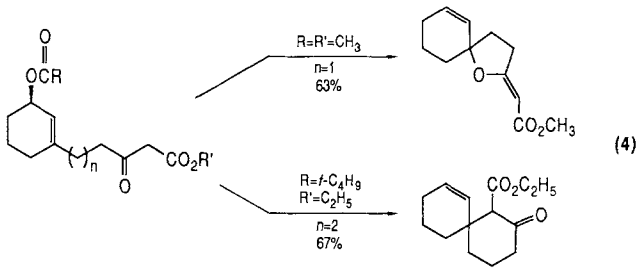


other than ring size may be most important in determining the regioselectivity of intramolecular nucleophilic attack at the two termini of a π-allylpalladium intermediate.

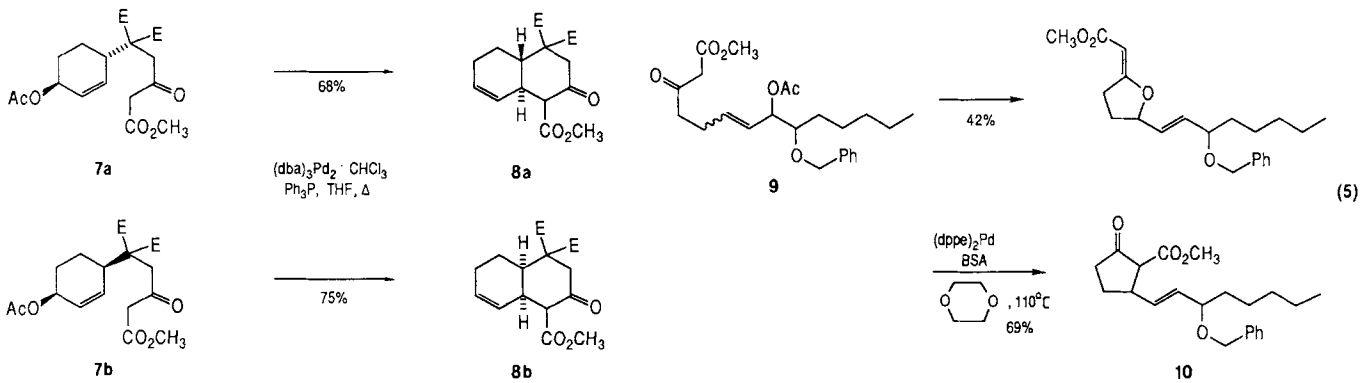
This displacement with net retention of configuration transforms the *trans* substrate **7a** into the *trans*-fused octalin **8a**, and the *cis* substrate **7b** into the *cis*-fused octalin **8b** (dba = dibenzylideneacetone).[39] Thus, this metal-catalyzed annulation complements conventional displacements which would have provided the reverse stereochemical result.

In addition to simple and fused rings, spiro rings form under these conditions [Eq. (3)].[40] Changing the nucleophile from malonate to a β-ketoester reveals the classic problem of *O* versus *C* alkylation, which mainly arises in the case of five-membered ring formation [Eq. (4); same conditions as (3)].

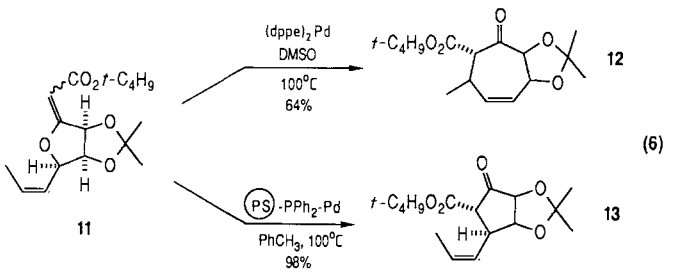


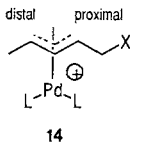


An advantage of this metal-catalyzed chemistry is its ability to rectify a problem caused by *O* rather than *C* alkylation. Treatment of β-ketoester **9**, a prostaglandin precursor, with $(PPh_3)_4Pd$ produces only the *O*-alkylated product [Eq. (5); same conditions as in (1)]. Switching to a sterically less demanding catalyst, $(dppe)_2Pd$ (dppe = 1,2-diphenylphosphinoethane), effects the equivalent of a [1,3] rearrangement to produce the desired cyclopentanone, **10** (BSA = *O*,*N*-bis(tri-



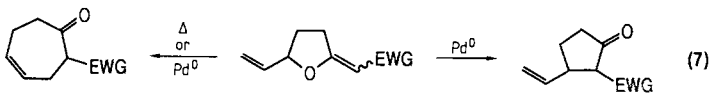
methylsilyl)acetamide).[41] Palladium-catalyzed rearrangement of allyl vinyl ethers is general and may complement their well-known thermal behavior.[42] Consider the allyl vinyl ether **11**. Use of $(dppe)_2Pd$ as catalyst led only to the seven-membered ring product [Eq. (6)]![43] This bias is observed because the inductive effect of an oxygen adjacent to an allyl system in the intermediate complex (**14**, X = OR)





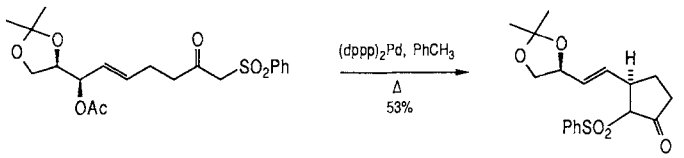
14

directs incoming nucleophiles distal to this substituent. On the other hand, increasing steric demands of the catalyst, as in the case of polymerically bound Pd^0, redirects the reaction to five-membered ring formation (**13**), since the preference for the palladium to coordinate to the less substituted allyl terminus is enhanced. As shown in Equation (7) (EWG = electron-withdrawing group), this translates into a novel reorganization of allyl vinyl ethers into either five- or seven-membered carbocycles. Full stereorelay occurs in forming both **12** and **13** with overall retention of configuration.

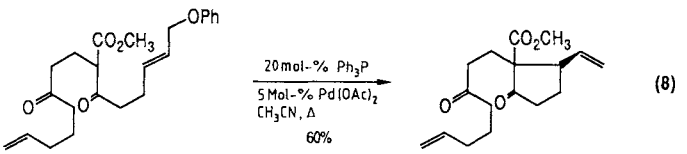


(7)

In contrast to β-ketoesters, a β-ketosulfone as the nucleophilic partner is less prone to undergo *O* compared to *C* alkylation. Excellent stereorelay accompanies this cyclopentanone synthesis (dppp = 1,3-bis(diphenylphosphino)-propane):[44]

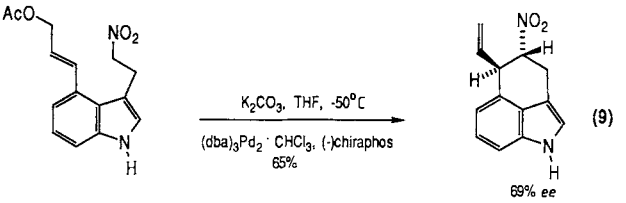


Palladium-catalyzed cyclization has formed the basis of a synthesis of the D ring of steroids in which phenoxide served as the leaving group [Eq. (8)].[45] This example illustrates a common practice in palladium-catalyzed reactions in which the catalytically active Pd^0 complex is generated in situ from a more convenient commercial Pd^{II} salt. While both palladium chloride and palladium acetate may be employed, the greater ease of reduction of the latter frequently makes it the salt of choice.

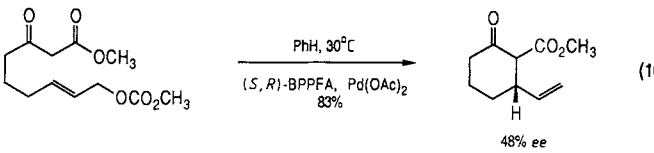


(8)

The potential for catalytic asymmetric induction constitutes a major feature of metal-catalyzed reactions. Extrapolation of the notion that chiral ligands on the metal may impart such enantioselectivity to allylic alkylations, however, is not simple. The bond-forming event occurs as far from the chiral environment as possible! Nevertheless, some modest successes have been noted in cyclizations [Eq. (9), chiraphos = 2,3-bis(diphenylphosphino)butane,[46] and (10), BPPFA = 1-[1,2-bis(diphenylphosphino)ferrocenyl]ethyldimethylamine[47]]. Equation (9) represents an asymmetric entry to the ergot alkaloids.

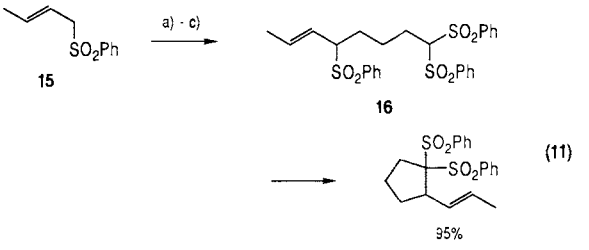


(9)



(10)

Variation of the leaving group can be important to the success of the cyclization. In some cases, use of a leaving group more reactive than acetate to allow milder conditions may be a necessity. An alternative concept considers versatility imparted by the leaving group. A sulfone stands out due to its ability to impart both nucleophilic and electrophilic properties to the adjacent carbon and has led us to describe organosulfones as chemical chameleons.[48] Equation (11) illustrates this feature.[49]

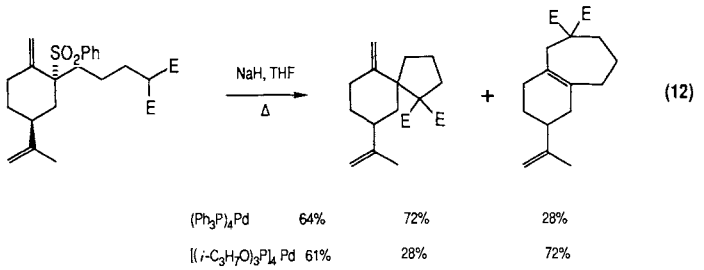


(11)

a) n-C_4H_9Li, Cl, b) NaI, c) K_2CO_3, $CH_2(SO_2Ph)_2$

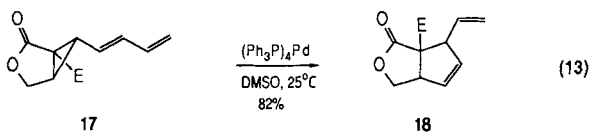
Sulfone-stabilized carbanions prepared from **15** permit easy construction of the requisite cyclization substrate **16**. Selective cyclization to the cyclopentane derivative proceeds

under standard conditions with a Pd^0 catalyst. Steric accessibility of the two termini can become important. Equation (12) reveals how a subtle change in the catalyst effects a



(12)

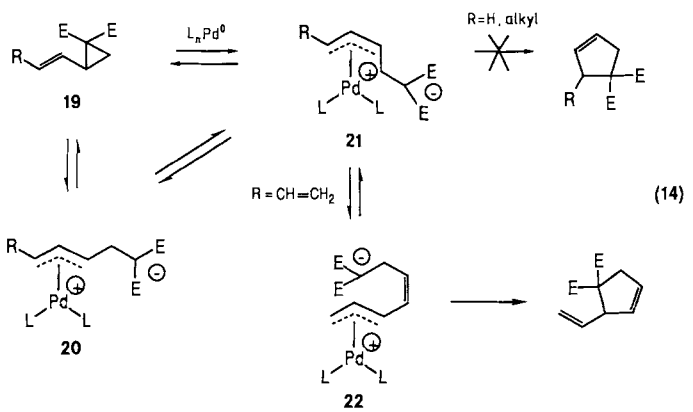
change from a charge-directed cyclization, which favors attack at the more substituted allyl terminus, to a sterically driven cyclization, which favors attack at the less substituted terminus.



(13)

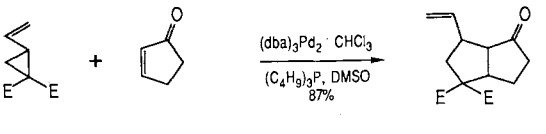
17 18

A most unusual leaving group is carbon in the form of an electron-deficient three-membered ring. The isomerization of the dienylcyclopropane **17** to the vinylcyclopentene **18** [Eq. (13)] illustrates the use of this leaving group.[50] This process also demonstrates one stereoelectronic aspect of this metal-catalyzed cyclization, since vinylcyclopropane analogues of **17** fail to give any discernible reaction. While a vinylcyclopropane such as **19** would be expected to generate the *syn* complex **20** preferentially, the *anti* complex **21** can form either directly or by well-documented isomerization processes from **20**. Cyclization of **21** requires a geometrically disfavored 5-*endo-trig* process.[51] On the other hand, the dienyl substrate **21** (R-vinyl) can isomerize to a new π-allylpalladium cation **22**, which can cyclize by a geometrically favorable 5-*exo-trig* process.

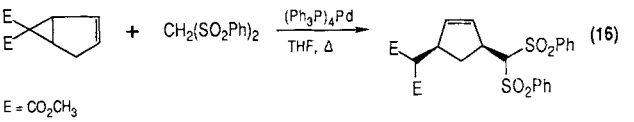


(14)

That **20** and/or **21** (R = H, alkyl) indeed form, but can only reclose to cyclopropane, has led to a novel annulation based upon the dual reactivity inherent in this zwitterion [Eq. (15)].[52] Simple diastereocontrolled alkylations are also possible [Eq. (16)].[53]



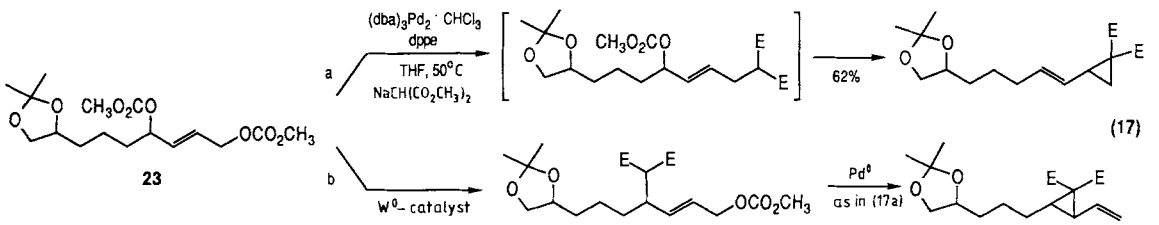
(15)



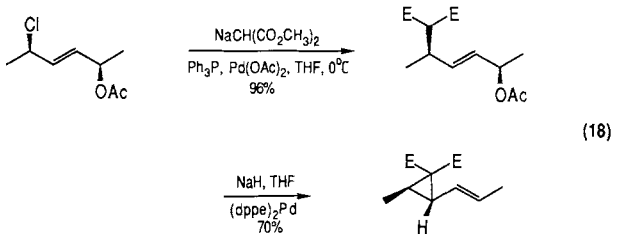
(16)

E = CO_2CH_3

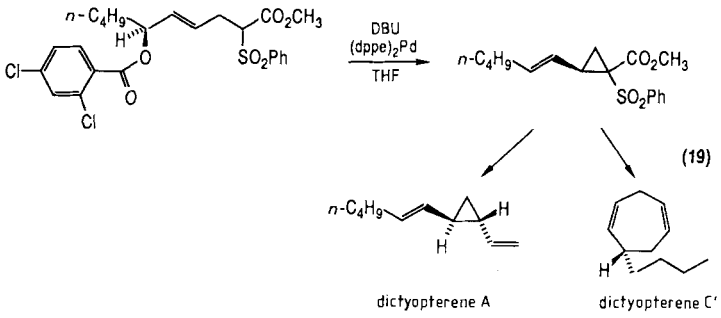
Cyclopropanes of the above type are themselves readily available by Pd-catalyzed allylic alkylations. A cyclopropanation process readily emerges as outlined in Equation (17), path a, where the bifunctional alkylating agent **23** demonstrates chemoselectivity for initial replacement of a primary leaving group in the presence of a secondary (or even tertiary) one.[54] Final Pd^0-catalyzed ring closure occurs simultaneously and produces the terminal cyclopropane. On the other hand, a regioisomeric cyclopropane may be obtained by initiating the sequence with a tungsten(0) catalyst, which allows chemoselective substitution of the secondary leaving group [Eq. (17), bath b]. Palladium(0) catalysis completes the sequence. Combining the stereochemical feature of Pd^0-catalyzed alkylations, retention of configuration, with this sequence generates a diastereocontrolled cyclopropanation [Eq. (18)].[55] To the extent that the absolute configuration of the leaving group can be controlled, the absolute configuration of the cyclopropane may also be controlled. The key step in a synthesis of dictyopterenes A and C′ employs just such a strategy [Eq. (19)].[56] Optimization of retention of stereochemistry required the use of the dichlorobenzoate leaving group. A similar strategy created the cyclopropyl steroid side chain of glaucasterol [Eq. (20)].[57] Use of achi-



(17)

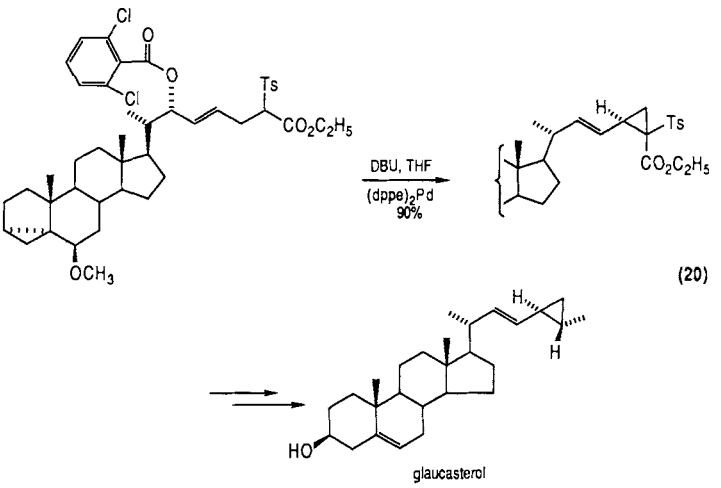


(18)



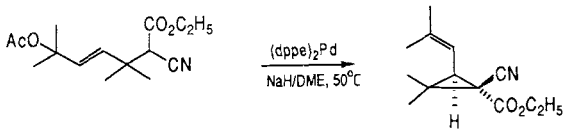
(19)

ral substrates and chiral palladium catalysts in this cyclopropanation has led to scalemic cyclopropanes, but of only modest enantiomeric excess.[58]



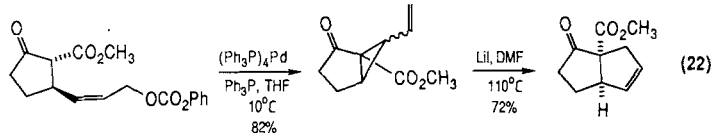
(20)

The stereochemistry at the nucleophilic carbon has been less explored, since this center is frequently nonstereogenic or its stereochemistry ultimately lost. In one cyclopropane-forming reaction [Eq. (21)], however, Pd-catalyzed cy-



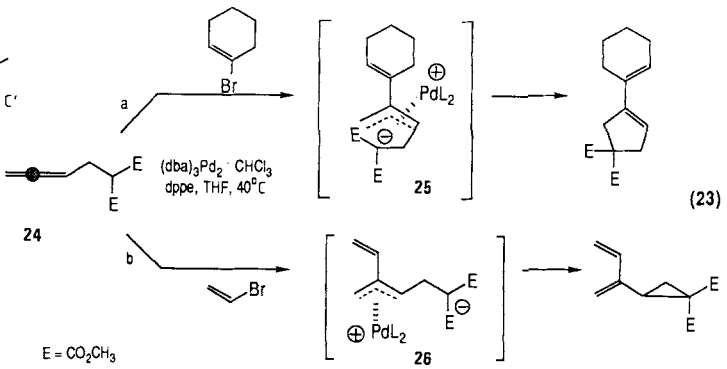
(21)

cloalkylation directed the sterically small CN group exclusively to the more hindered face of the cyclopropane, a diastereoselectivity not observed in the non-metal-catalyzed reaction.[59] Combining Pd-catalyzed cyclopropanation with a vinylcyclopropane rearrangement can create a cyclopentene synthesis [Eq. (22)].[60]



(22)

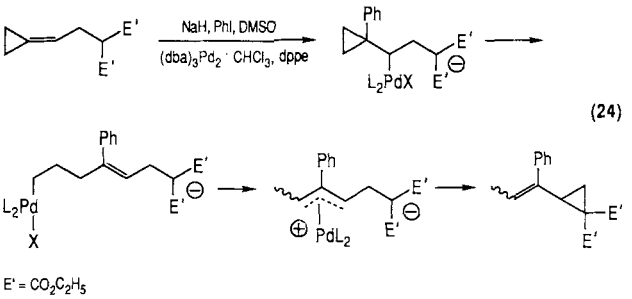
In all of the cases discussed so far, we created the reactive palladium electrophile by the addition of an allyl-X group to a Pd^0 complex. In principle, any reaction that creates a π-allylpalladium species can ultimately be followed by a reaction with a carbon nucleophile. The additions of C–Pd σ bonds to conjugated and nonconjugated dienes and to unsaturated cyclopropanes and cyclobutanes have been shown to produce stoichiometric π-allylpalladium complexes. Such addition to an appropriate allene **24** has led to a cyclization in which both a substituent C–C bond and a ring C–C bond have been formed in the same operation [Eq. (23)].[61] The



24

(23)

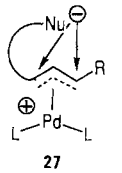
ring size depended upon the organohalide. A sterically bulky halide facilitates formation of the *anti* complex **25** as the reactive intermediate which, surprisingly, forms the cyclopentene, even though a 5-*endo-trig* cyclization is required. On the other hand, a less sterically demanding vinyl bromide leads, via the normally more stable *syn* complex **26** as the reactive intermediate, to the cyclopropane. An alkylidene cyclopropane participates in a similar sequence where the requisite reactive π-allylpalladium intermediate arises after a more complex set of reorganizations [Eq. (24)].[62]



(24)

3.1.1. Medium- and Large-Ring Carbocyclizations

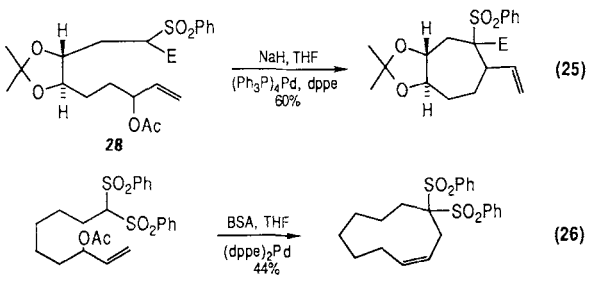
The regioselectivity of the Pd-catalyzed cyclizations determines the ring size. In the competition between three- and/or six- and eight-membered ring formation from the π-allylpalladium complex **27**, the smaller-sized ring usually predomi-



27

nates. In four-versus six-membered or five-versus seven-membered ring formation, both ring sizes appear accessible. Cyclization of the all-carbon system, in which seven- and nine-membered ring formation compete, shows how finely balanced this metal-catalyzed reaction is. Thus, cyclization of substrate **28** shows the usual propensity for seven-mem-

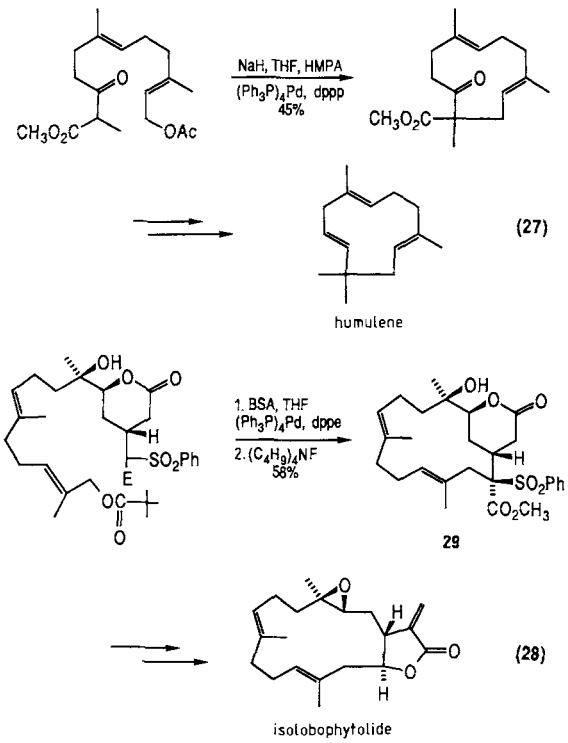
bered over nine-membered ring formation [Eq. (25)].[63] Increasing the steric hindrance of the nucleophile shifts the reaction to strongly favor nine-membered ring formation [Eq. (26)].[64] Heretofore, a plot of ring size versus yield almost always reached a minimum at nine members. The transition-metal template changes the rules to the point that the nine-membered ring is preferred over the more conventional seven-membered ring.



(25)

(26)

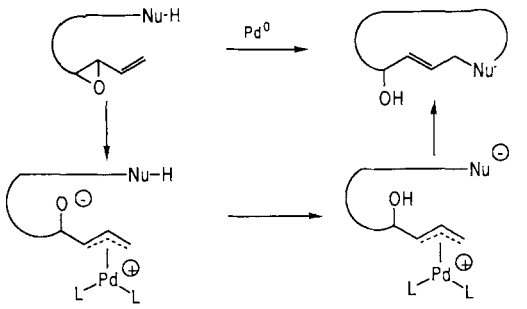
The surprising observation that nine-membered ring formation occurs easily leads to the expectation that larger rings should form even more easily—an expectation fully verified. Syntheses of the eleven-membered ring biosynthetic intermediate humulene [Eq. (27)][65] and the fourteen-membered ring cembranolide isolobophytolide [Eq. (28)][66] employ Pd^0-controlled cyclizations. The latter cyclization also exhibits high diastereoselectivity at the nucleophilic center since the macrocycle **29** was obtained as a single diastereomer.



(27)

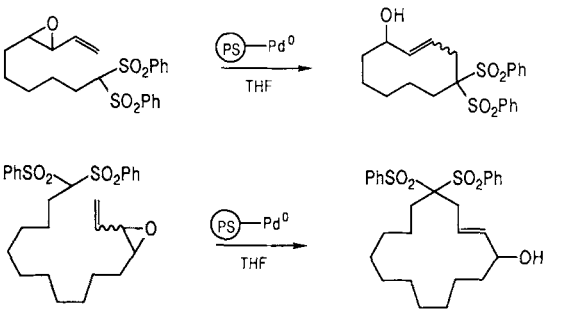
(28)

Changing the electrophilic partner in the cyclization to a vinyl epoxide has a dramatic effect on the efficacy of the macrocyclization. As illustrated in Equation (29), such cyclizations are now simple isomerizations. Such a reaction type is particularly well suited for effecting macrocyclizations at high concentration when the pseudodilution effect is exploited.[67] The reaction is compartmentalized into a storage zone, the solution of the substrate, and a reaction zone, an insoluble polymerically supported Pd^0 catalyst. The substrate, which lacks a nucleophile and a reactive electrophile in the absence of catalyst, must diffuse onto the polymer support *and* encounter an active site before it becomes reactive at all. The combined effect of having relatively few active sites and even fewer of them occupied helps ensure intramolecular reactions. The act of ionization creates the reactive electrophile in the form of a π-allylpalladium complex and a base [see Eq. (29)]. Unmasking the nucleophile re-



(29)

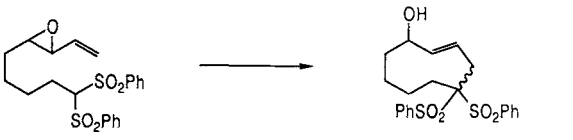
quires the pro-nucleophile to approach the base to permit proton transfer. The close proximity of the alkoxide to the π-allylpalladium cationic complex then translates into a close proximity of the nucleophile at its birth to the π-allyl unit. By operating in a nonpolar environment such as a polystyrene matrix, charge–charge attraction prevents diffusion of the nucleophile and electrophile away from each other. Simple charge neutralization then effects cyclization. In this way, ten- and fifteen-membered carbocyclic rings formed in 71% and 82% yields, respectively, at substrate concentrations of 0.1–0.5 M [Eqs. (30) and (31)].



(30)

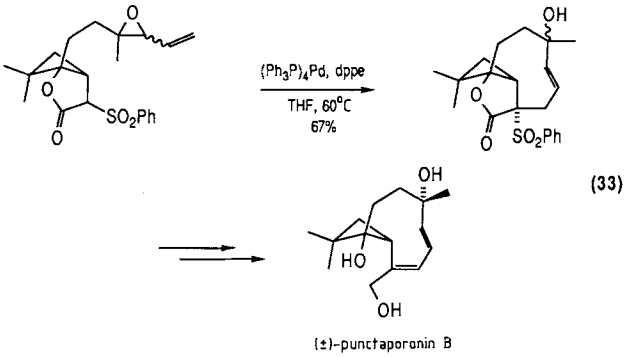
(31)

While extension to rings larger than fifteen-membered presented no problems, decreasing the ring size below ten did. Use of the pseudodilution technique provided the nine-membered ring product of Equation (32) in only low yield.



(32)

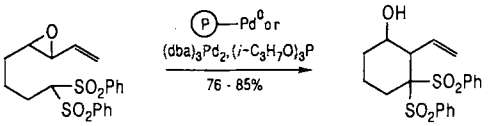
However, use of tetrakis(triisopropylphosphite)palladium at 0.01 M concentration provided the desired product in 73% yield.[68] A synthesis of the racemic form of the fungal metabolite punctaporonin B created its unusual ring system using this methodology [Eq. (33)].[69]



(±)-punctaporonin B

(33)

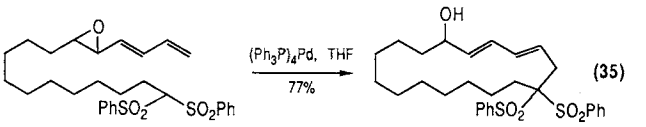
Formation of the medium- and large-sized rings in these examples derives from bond formation of the nucleophile to the less substituted terminus of the π-allylpalladium intermediate. The normal steric demands of the nucleophile are reinforced by the inductive effect of the adjacent alcohol in the intermediate complexes to direct the incoming nucleophile to the distal end of the π-allyl unit to itself. The limit of these



(34)

regiochemical control factors is reached in the analogue containing one less carbon where only the six-membered ring is observed when either polymeric heterogeneous or homogeneous catalysis is used [Eq. (34)].[68] However, this simple substrate may be an anomaly. Other work suggests that substrates with a modified tether may lead to preferential eight-membered ring formation.

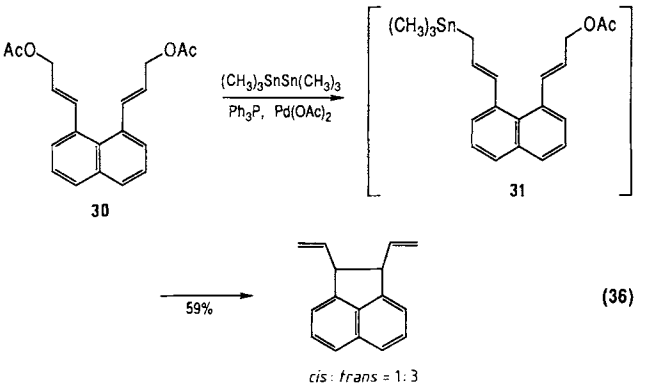
Extending the conjugation to a dienyl epoxide increased the number of possible regioisomeric products. Nevertheless, the combination of the inductive effect of the hydroxyl group and the steric preference for addition to the less hindered terminus of the allyl moiety led to only a single product [Eq. (35)].[70]



(35)

3.2. Use of Alternative Nucleophiles to Form Carbocyclic Rings

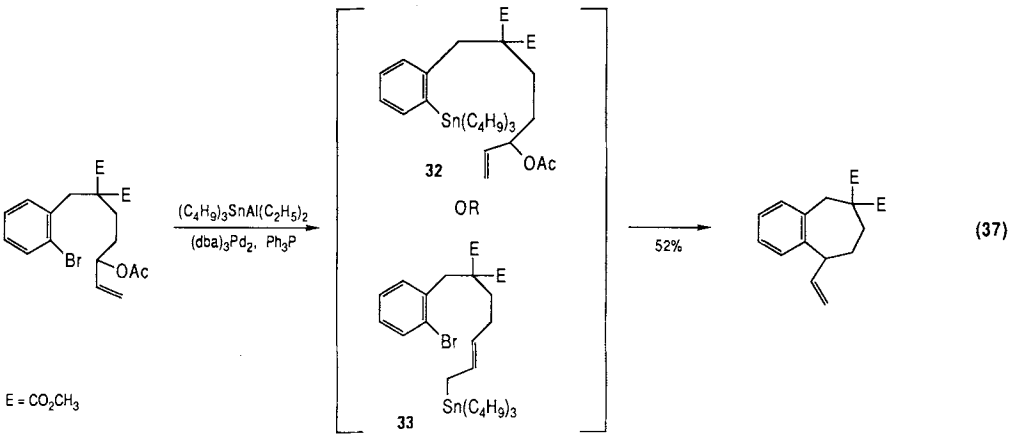
A major area yet to evolve is the employment of nucleophilic carbon partners other than stabilized carbanions. A reductive cyclization of bis(allyl acetates) such as **30** may involve an intramolecular coupling of allyl acetate **31** and an allylstannane formed in situ as shown in Equation (36).[71]



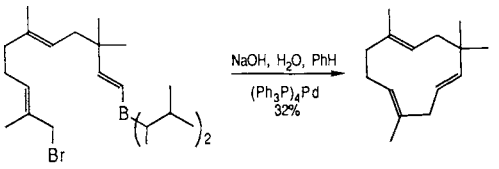
(36)

The related reductive cyclization illustrated in Equation (37) can also be envisioned to involve a Pd^0-catalyzed coupling of allyl acetate **32** and an organostannane formed in situ, although an alternative pathway via the allylstannane **33** appears more likely.[72] A clearer example of an intramolecular cross coupling via a π-allylpalladium complex involves organoboranes as the nucleophilic partner. These normally excellent nucleophilic partners in cross-coupling reactions provided only a modest yield of the eleven-membered ring product, humulene [Eq. (38)].[73]

A most interesting "nucleophile" for a π-allylpalladium complex is an olefin. Thus, Pd^0 effects cyclization of an allyl acetate onto a proximal double bond to generate five- and

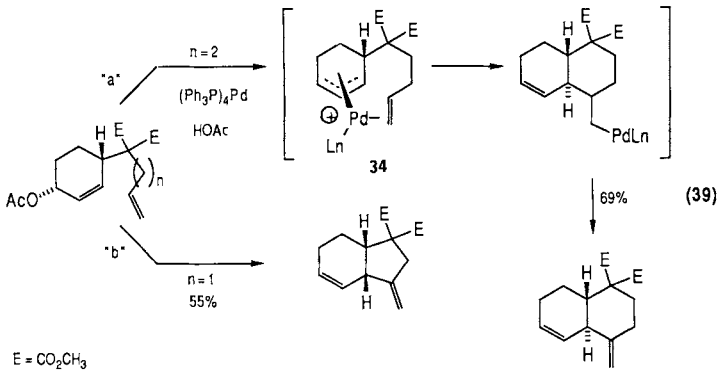


(37)



(38)

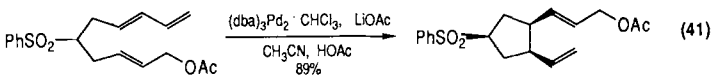
six-membered rings, the latter being illustrated in Equation (39).[74] In this reaction, coordination of the "nucleophile" to the metal (→ **34**) determines the ring sizes available and the stereochemistry of the ring closure by delivering the



(39)

olefin *syn* to palladium. Since the ionization of the allyl acetate proceeds with inversion, this metallo-ene reaction proceeded with net *inversion*—the opposite stereochemical event from cyclizations with soft nucleophiles. When the tether was too short to coordinate in a *trans* fashion, as in the case of Equation (39), path b, only the *cis* ring-fused product formed, regardless of the stereochemistry of the starting material.[75] Equilibration of the starting material occurring faster than cyclization accounts for this observation.

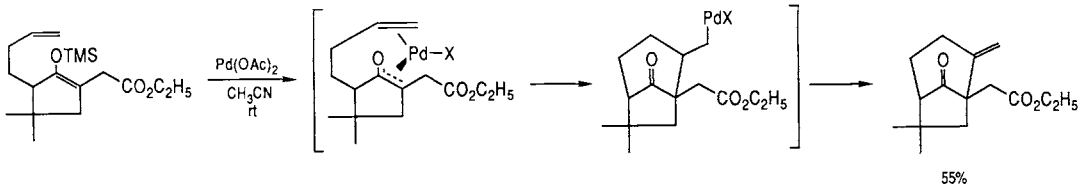
A most interesting example of cyclization via isomerization derived from the ability of the π-allylpalladium cation to add to dienes to generate a new π-allyl complex, which, in turn, may be captured by acetate to create a new allyl acetate which is simply isomeric to the starting material **35** [Eq. (40)].[76] While only the *Z* complex **36**, which derives from the *E* starting allyl acetate, can cyclize, rapid equilibration of the cyclization substrate permits the more accessible *Z* isomer to participate. Even in a conformationally non-biased system such as the acyclic substrate **37** [(Eq. (41)], only



(41)

a single diastereomeric product results under the standard Pd^0 cyclization conditions. The requirement for coordination between the π-allylpalladium cationic complex and the diene limits this cyclization to formation of five-membered rings.

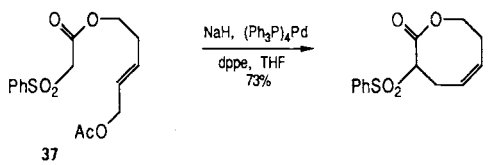
A Pd^{II}-promoted cyclization of enol silyl ethers onto olefins can be thought to involve an oxa-π-allylpalladium cationic intermediate in analogy to the reactions described above.[77–79] A synthesis of the antitimor sesquiterpene quadrone employed this novel cyclization [(Eq. (42)].[80] Evidence supporting an alternative mechanism involving nucleophilic attack on an olefin–palladium complex has been presented.[80]



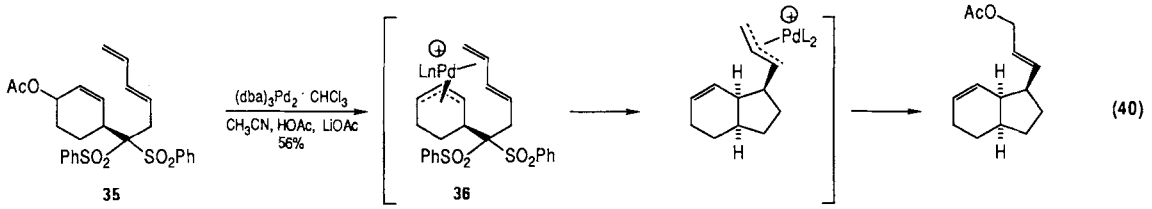
(42)

3.3. Heterocycles via C–C Bond Formation

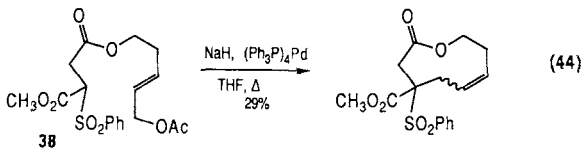
Introduction of heteroatoms into the tether connecting the cyclization termini can have a profound influence due to their conformational effects on the substrate and their coordinating ability for the metal. An early manifestation of this phenomenon was the cyclization of **37** [Eq. (43)] and **38**



(43)

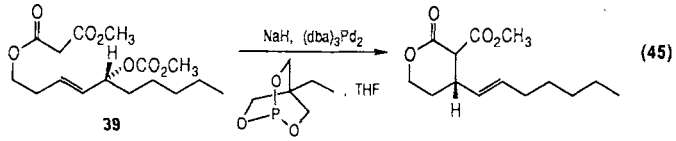


(40)



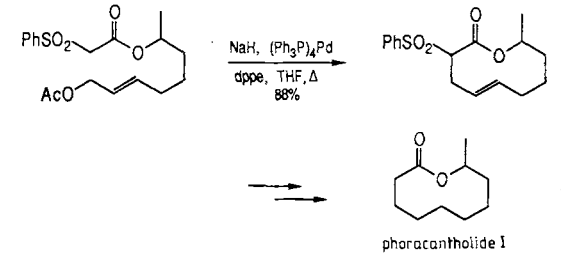
(44)

[Eq. (44)] to form the eight- and nine-membered rings preferentially or exclusively.[39, 64] The preference for eight-membered ring formation in Equation (43) in part derived from the preference for the nucleophile to attack the less substituted terminus of the allyl system. Equalizing the substitution pattern as in **39** returned the cyclization to six-membered ring formation [Eq. (45)].[81] This example also illustrates

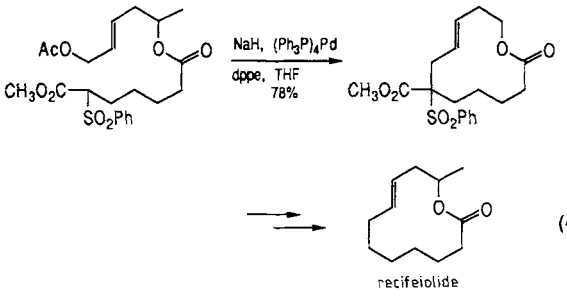


(45)

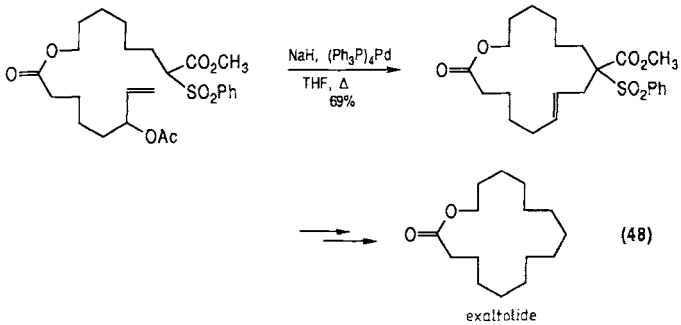
the high transfer of chirality possible in these metal-templated reactions, a feature that has previously been established in the more difficult bimolecular metal-mediated reactions.[82] The fact that the normally highly unfavorable medium-sized rings form so remarkably well implied that the larger macrolides would be readily accessible—a prediction amply fulfilled. Syntheses of the simple naturally occurring macrolides ranging from phoracantholide I [Eq. (46)] and J[39, 64] to recifeiolide [Eq. (47)][39, 83] to exaltolide [Eq. (48)][39, 84] illustrate formation of ten-, twelve-, and six-



(46)

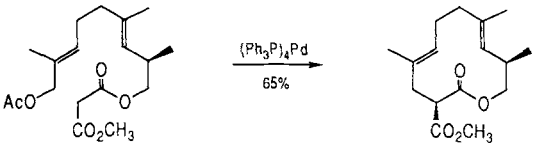


(47)



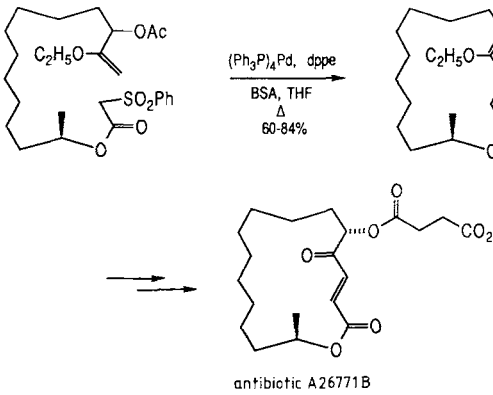
(48)

teen-membered macrolides. High diastereoselectivity with respect to the nucleophilic carbon has been observed. One example arose during the synthesis of a macrolide as an intermediate to polyether ionophores [Eq. (49)].[85]



(49)

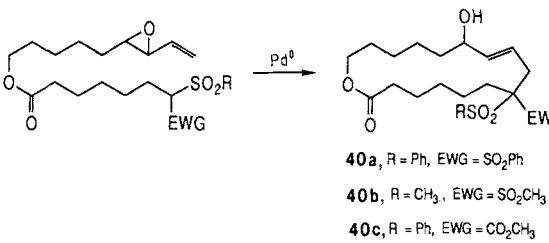
In a synthesis of antibiotic A26771B, this feature proved critical to transmit stereochemical information in creating the stereogenic center at C6 relative to that at C16 [Eq. (50)].[86] Thus, the sulfone served as a stereochemical



(50)

relay group. In both of these cases, whether the diastereoselectivity reflects kinetics or thermodynamics has not been resolved. The ability to perform the reactions with only BSA as the base, as was done for the synthesis of antibiotic A26771B [Eq. (50)], obviates problems caused by the hydroxide impurities that unavoidably accompany the hydride bases. Yields in all the other cases may be improved by this modification.

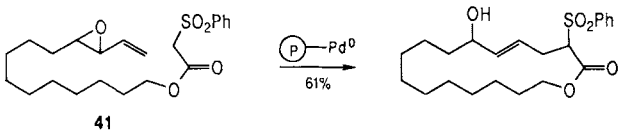
Using a vinyl epoxide permitted extension of the pseudodilution strategy of Equation (29) to macrolide formation.[87] Indeed, this variant has proved to be spectacularly successful. For example, the seventeen-membered ring macrolides **40a** and **40b** could be formed in 74–87% yields at 0.1–0.5 M concentrations [Eq. (51)]! The acidity of the hydrogen being transferred was critical. The kinetically less acidic sulfone ester substrate did not produce macrolide **40c**



(51)

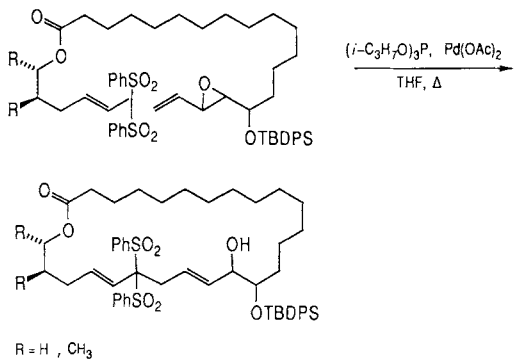
when the polymeric catalyst was used, but cyclized smoothly with the standard homogeneous Pd^0 catalyst. Restoration of a successful cyclization at high concentration with the poly-

meric Pd^0 catalyst by changing the pro-nucleophile from a methine to a methylene group as in **41** [Eq. (52)] supported the notion that the kinetic acidity of the proton being abstracted was an important feature of this high-concentration macrocyclization.



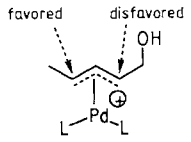
41 (52)

The choice of ligands may be important in this macrocyclization. In the homogeneously catalyzed version, the 26-membered ring model for a synthesis of the ring system of tetrin A could be formed in 92% yield by employing the better acceptor ligand triisopropylphosphite [Eq. (53)].[88]



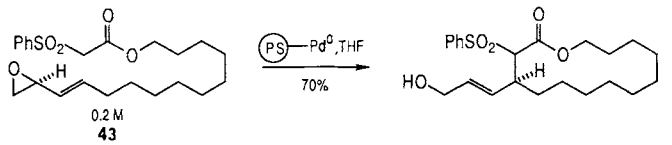
(53)

The adjacent electronegative hydroxyl group in the intermediate π-allylpalladium complex favored nucleophilic attack distal to itself as shown in **42**. This bias also dictated

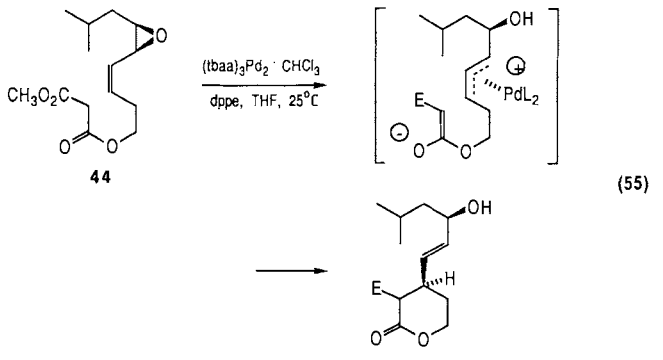


42

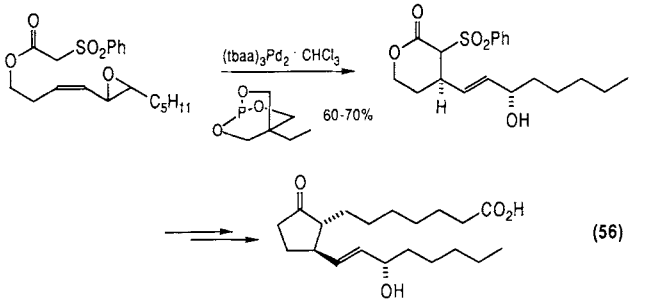
ring formation. Thus, cyclization of **43** [Eq. (54)][89] and **44** [Eq. (55)][90] generated the fourteen- and six-membered rings, respectively. In the latter case (tbaa = tris(benzylidene)acetylacetone), the transition-metal template faithfully transmitted the stereochemical information to the newly formed stereogenic center. This methodology has been employed to control the stereochemistry of C15 in prostaglandins [Eq. (56)][91] and to create the butenolide of cardenolides [Eq. (57)].[92]



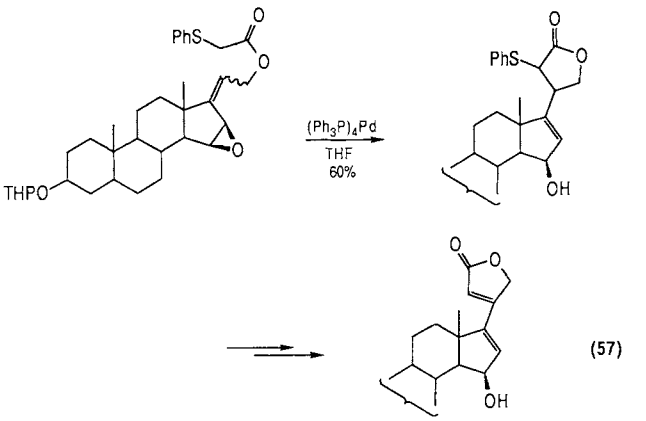
(54)



(55)

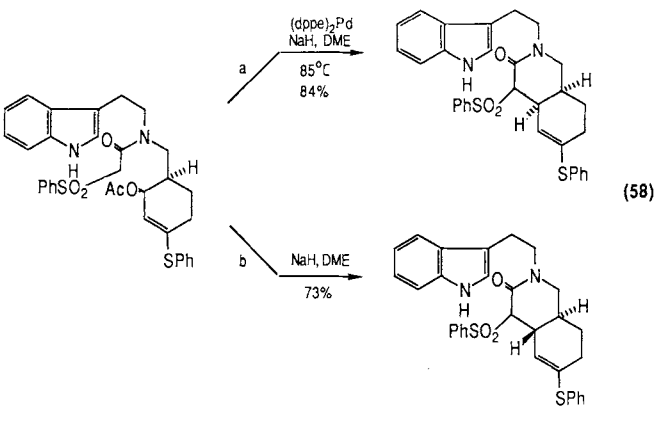


(56)



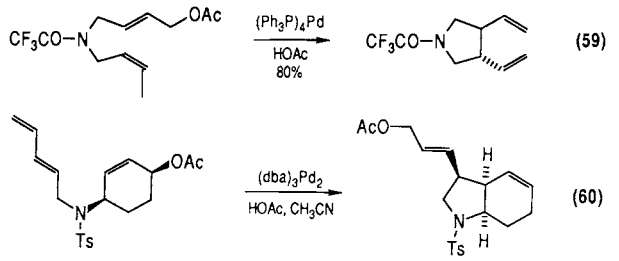
(57)

Replacing the ester linkage by an amide also led to successful heterocyclic synthesis directed to yohimbanes [Eq. (58)].[93] Comparing the Pd-catalyzed [Eq. (58), path a] and the noncatalyzed [Eq. (58), path b] reactions demonstrates the stereochemical complementarity available through metal-catalyzed reactions.



(58)

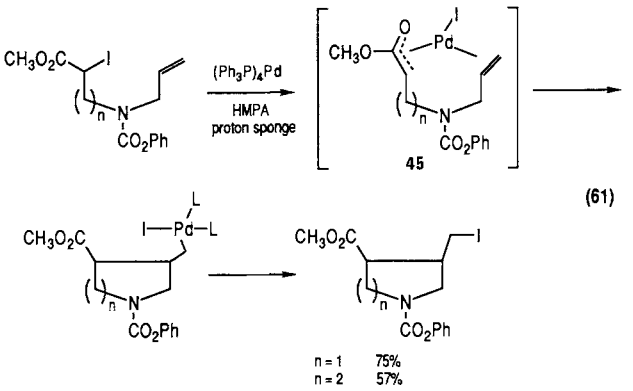
The metallo-ene reaction of π-allylpalladium intermediates derived from allyl acetates [Eq. (59)][94] and the cyclization via isomerization [Eq. (60)][95] have successfully generated nitrogen heterocycles. A version of the metallo-ene process with oxa-π-allylpalladium intermediates has been



(59)

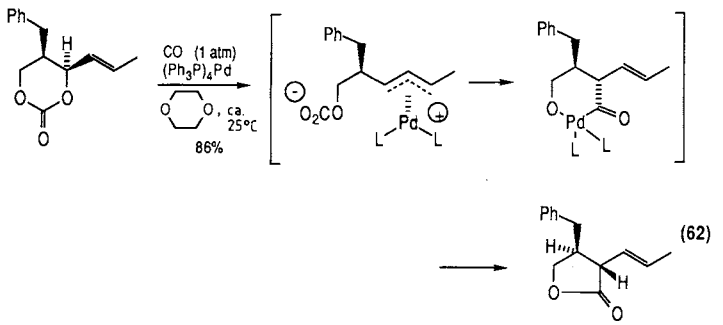
(60)

described.[96,97] The requisite intermediate **45** is formed by the oxidative addition of a Pd^0 complex to an α-iodoester. Olefin insertion followed by reductive elimination provided the pyrrolidine and piperidine products in a process which also can be described as a cyclization via isomerization (i.e., a cycloisomerization).



(61)

Intercepting the π-allylpalladium intermediate with carbon monoxide led to a novel lactone synthesis [Eq. (62)].[98] In this case, coordination of carbon monoxide to the palladium is followed by C–C bond formation with retention of configuration. Since the ionization step proceeded with inversion and the carbonylation step with retention, the overall process proceeded with inversion as depicted.

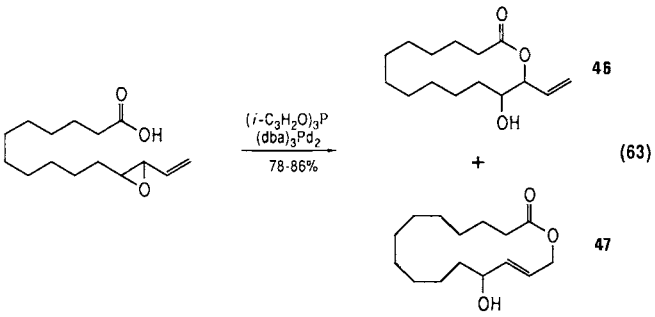


(62)

4. Cyclizations Involving Heteroatom Nucleophiles

4.1. Oxygen Nucleophiles

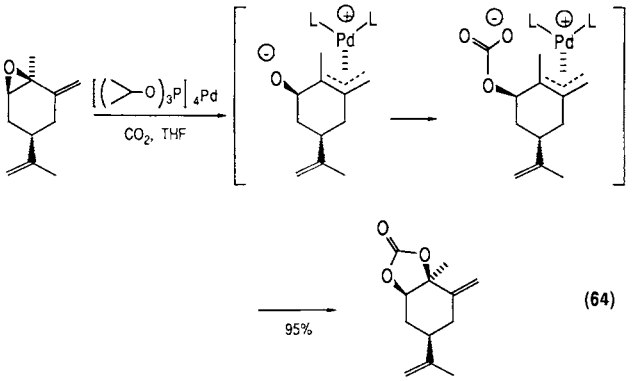
Since π-allylpalladium cations are "soft" electrophiles, "soft" nucleophiles generally react best. Thus, stabilized oxygen nucleophiles react more readily than simple alkoxides. Carboxylates represent "soft" oxygen nucleophiles, but their products with π-allylpalladium complexes are allyl carboxylates, themselves substrates for palladium. If the substrate ionizes much more rapidly with Pd^0 than the allyl carboxylate, then such nucleophiles may be employed. Macrolactonizations initiated with vinyl epoxides occurred smoothly with carboxylate anions as the nucleophiles [Eq. (63)].[68] Kinetically, this oxygen nucleophile produced equal amounts of the two macrolides **46** and **47**. The fact that the



(63)

product is subject to ionization with the catalysts used for their formation permitted equilibration at reflux, whereby the larger macrolide **47** dominated to the extent of 9:1.

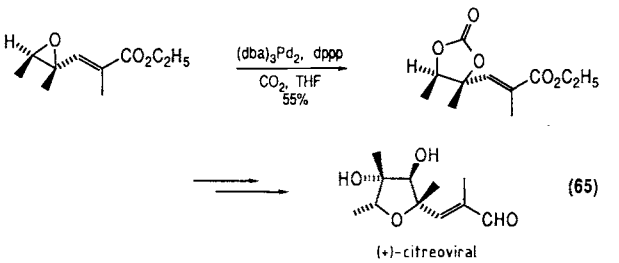
An unusual approach generates the carboxylate nucleophile in situ by capturing the oxygen leaving group in the Pd-catalyzed reactions of vinyl epoxides with carbon dioxide [Eq. (64)].[99] The tethering of the carboxylate nucleophile to



(64)

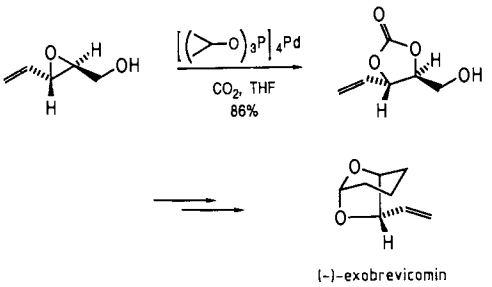
the oxygen leaving group changes the normal 1,4-addition of nucleophiles to vinyl epoxides under Pd catalysis to 1,2-addition. The ready availability of such epoxides in enantiomerically pure form makes this a practical asymmetric synthesis of vicinal diols that proved useful in a synthesis of (+)-citreoviral [Eq. (65)][100] and (−)-exo-brevicomin [Eq. (66)].[101]

Generating the π-allylpalladium complexes via routes not involving ionization of allylic leaving groups also permits



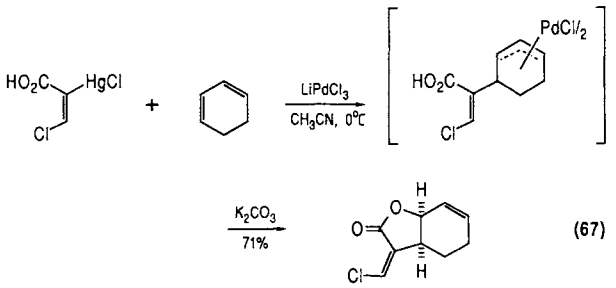
(65)

(+)-citreoviral

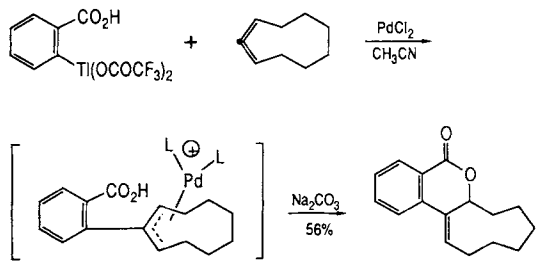


(66)

lactone formation using carboxylate nucleophiles. In situ formation of π-allylpalladium complexes by additions of σ-organopalladium intermediates, generated by transmetalations from organomercurial and organothallium compounds, to 1,3-dienes [Eq. (67)][102] and allenes [Eq. (68)][103] in the presence of stoichiometric amounts of

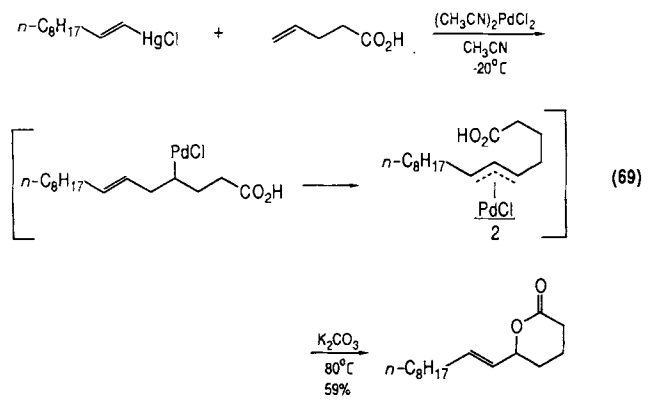


(67)



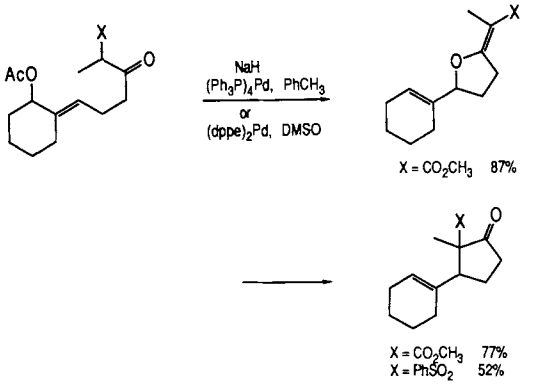
(68)

palladium produces good yields of lactones. Palladium-mediated additions of alkenyl organomercurials to unsaturated acids also produce lactones via carboxylate attack on a π-allylpalladium complex that forms after rearrangement of the kinetic adduct [Eq. (69)].[104]

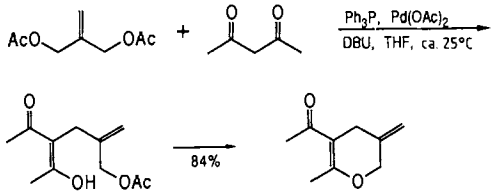


(69)

Enolates from β-ketoesters [Eq. (70)],[42,43] β-ketosulfones [Eq. (70)],[42,43] and 1,3-diketones [Eq. (71)][105] may

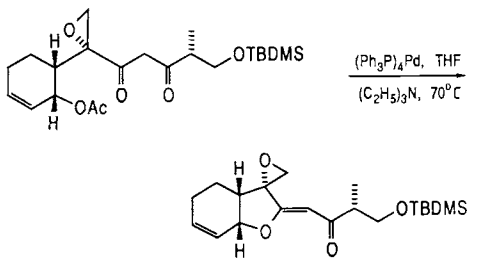


(70)

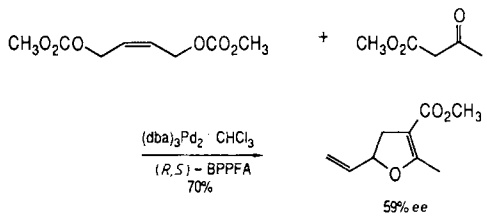


(71)

undergo preferential *O* rather than *C* alkylation. In the first two examples [Eq. (70)], prolonged treatment with the Pd^0 catalyst permuted the *O*-alkylated product to the *C*-alkylated one. The synthesis of the ring system of the aglucone of the antitumor agent phyllanthoside has been accomplished using this reaction [Eq. (72), TBDMS = *tert*-butyldimethylsilyl].[106] An asymmetric synthesis of dihydrofurans utilized a palladium catalyst bearing chiral ligands [Eq. (73)].[58] A



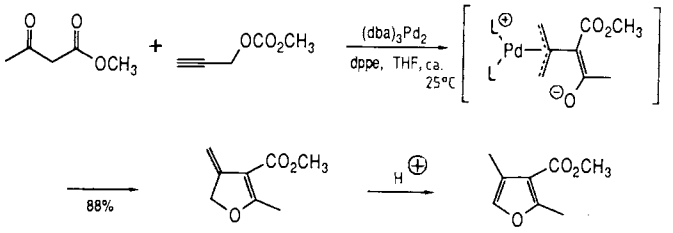
(72)



(73)

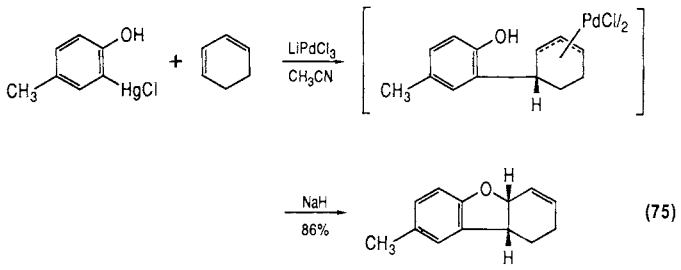
novel furan synthesis evolved from the Pd-catalyzed alkylation of β-ketoesters and 1,3-diketones with methyl propargyl carbonate.[107] The key cyclization of the oxygen nucleophile on the π-allylpalladium complex, which must have arisen by an unusual metal-promoted C–C bond formation and hydrogen shifts, involves a *5-endo-trig* attack [Eq. (74)]. Because of the geometrical constraints for such a process, the facility of this cyclization suggests that it might be viewed as an electrophilic reaction analogous to the ring closure of pentadienyl anions to cyclopentenyl anions.

Aryl oxides should also be good oxygen nucleophiles toward π-allylpalladium complexes. A synthesis of dihy-



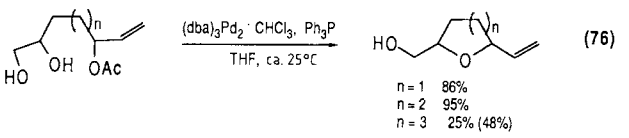
(74)

drobenzofurans involves just such a step, but utilizes stoichiometric amounts of palladium [Eq. (75)].[102] The *cis* stereochemistry of the product demands that the oxygen attack on the same face of the π-allyl unit bonded to palladium.

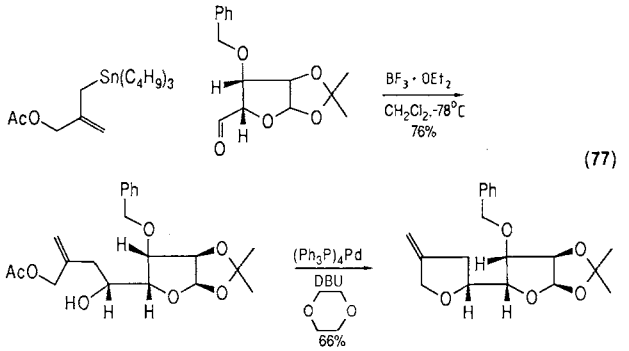


(75)

While simple alcohols are normally poor nucleophiles toward π-allylpalladium complexes in intermolecular reactions, they participate without complications in intramolecular reactions [Eq. (76)].[108] A diastereocontrolled 3-methylenetetrahydrofuran annulation employs this reaction for the ring-forming step [Eq. (77), DBU = 1,5-diazabicyclo[5.4.0]undec-5-ene].[109a]

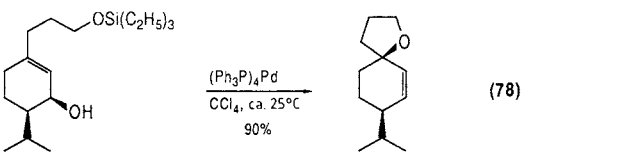


(76)



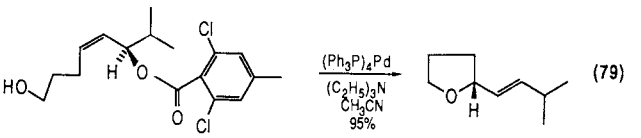
(77)

Silyl ethers have served as the nucleophiles but it is likely that desilylation to liberate a nucleophilic alkoxide occurred under the reaction conditions [Eq. (78)].[110] In addition, the



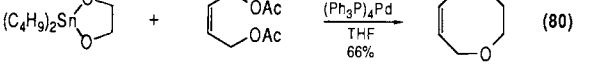
(78)

tetrakis(triphenylphosphane)palladium and carbon tetrachloride also serve to activate the allylic alcohol so that it can serve as a leaving group. The stereochemistry of the alkylation follows that associated with "soft" nucleophiles so that the leaving group departs and the nucleophile enters on the same face of the allylic unit [see Eq. (78)], in contrast to the result of Equation (75). The same stereochemistry was observed in an unconstrained acyclic substrate [Eq. (79)].[111]

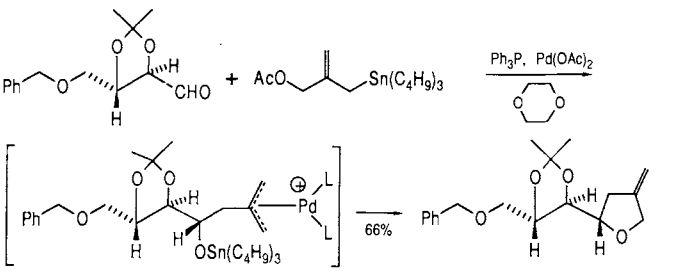


(79)

Stannyl ethers have been claimed to be excellent nucleophiles toward π-allylpalladium complexes. Indeed, medium-ring and macrocyclic polyethers form in excellent yields with such partners [Eq. (80)].[112] A [3 + 2] cycloaddition strategy to 3-methylenetetrahydrofurans takes advantage of this fact [Eq. (81)].[109b] The efficacy of the process allows a tin compound to be employed as a co-catalyst in effecting

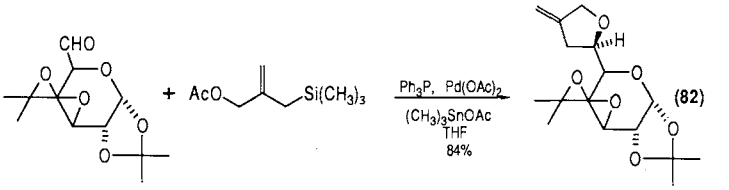


(80)



(81)

diastereocontrolled cycloadditions of aldehydes with 2-(trimethylsilylmethyl)allyl acetate [Eq. (82)].[113] The evolution of this cycloaddition strategy for the stereocontrolled synthesis of five-membered oxygen heterocycles provides additional functionality to permit further facile structural elaboration, thereby enhancing the power of this approach.

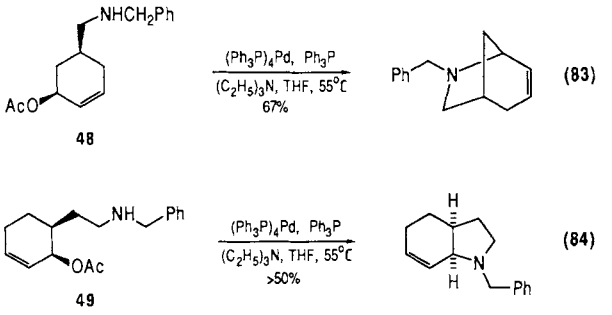


(82)

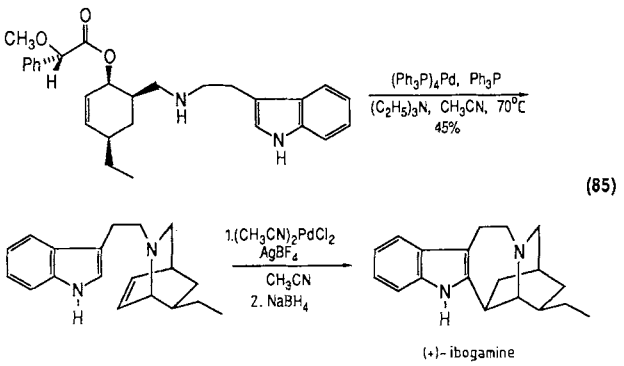
4.2. Nitrogen Nucleophiles

Amines are among the best nucleophiles for π-allylpalladium complexes. Their potency for intramolecular reactions was revealed by the simple construction of typical alkaloid skeletons represented by 6-azabicyclo[3.2.1]oct-3-ene [Eq. (83)] and 2,3,3a,4,5,7a-hexahydro-1*H*-indole [Eq.

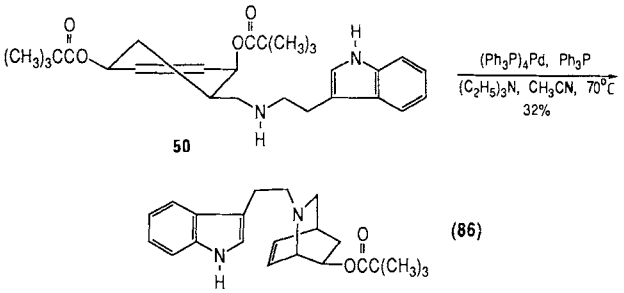
(84)].[114] The ease of availability of substrates possessing the NH and OAc functions *cis* to each other, as in substrates **48** and **49**, requires a cyclization method that permits substitu-



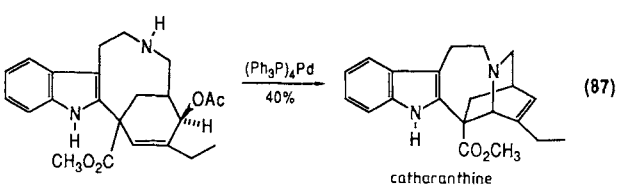
tion with *retention* of configuration, as effected by this palladium-based methodology. The Diels–Alder reaction leads to rapid construction of such substrates. An exceptionally facile synthesis of (+)-ibogamine, takes advantage of asymmetric induction in the Diels–Alder step [Eq. (85)].[115] Palladi-



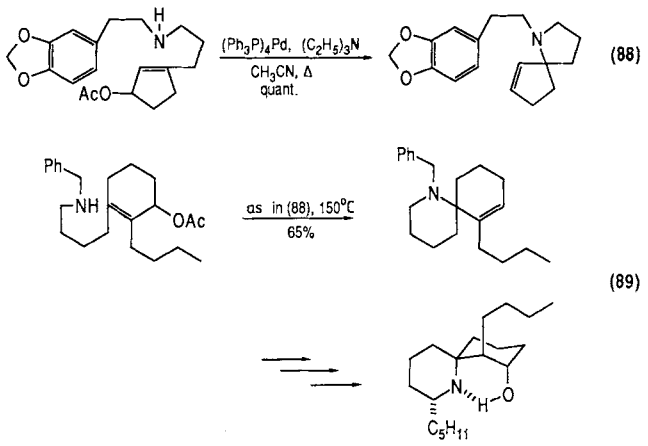
um-catalyzed ionization of the ene dicarboxylate **50**, which is chemoselective due to the steric preference of the C3 pivaloyloxy group to be in the required axial orientation, extends this methodology to the biologically significant catharanthine system [Eq. (86)].[116] An alternative strategy to



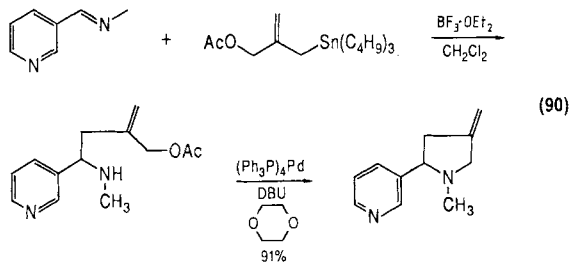
catharanthine employed the Pd-catalyzed cyclization as the final ring-forming step [Eq. (87)].[117]



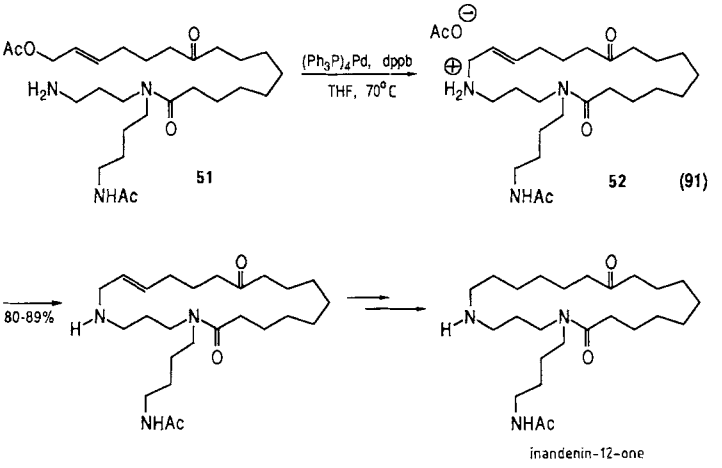
Pyrrolidine- and piperidine-containing spiroheterocycles, a core ring system of some biologically important alkaloids represented by cephalotaxine and histrionicotoxin, may be readily formed by this metal-catalyzed chemistry, as shown in a model study for the former class [Eq. (88)][118] and a formal synthesis of an analogue of the latter class, perhydrohistrionicotoxin [Eq. (89)].[119, 120] A [3 + 2] cycloaddition



strategy to 3-methylenepyrrolidines embodies this cyclization as a key step.[108] Addition of the bifunctional conjunctive reagent 2-(tri-*n*-butylstannylmethyl)allyl acetate to imines creates the proper juxtaposition of nitrogen nucleophile and electrophile [Eq. (90)]. Exposure of the adduct to a Pd^0 catalyst completes the formation of the five-membered ring nicotine analogue.

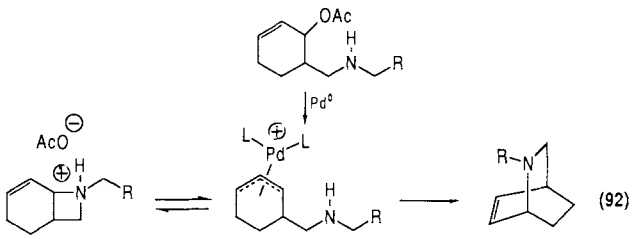


The fact that cyclization employing nitrogen nucleophiles is an isomerization facilitates macroheterocyclization. The amino acetate **51** isomerizes to the 21-membered ring ammonium acetate **52** with excellent efficiency at modest dilutions



(0.02 M) using a catalyst generated from tetrakis-(triphenylphosphane)palladium and 1,4-bis(diphenylphosphino)butane (dppb) [Eq. (91)].[121] Neutralization, hydrogenation, and acetamide hydrolysis complete the synthesis of the spermidine alkaloid inandenin-12-one.

Thermodynamic considerations may explain the observed regioselectivity and thus the ring size for the examples reported so far, in contrast to the cyclizations involving carbon and oxygen nucleophiles. The preferential formation of the bicyclo[4.2.0]octyl ring system with a carbon nucleophile [Eq. (2)], but the bicyclo[2.2.2]octyl ring system with a nitrogen nucleophile [Eq. (85)], may be an illustration of this phenomenon. Kinetically, the intermediate π-allyl complex **53** may preferentially cyclize to the azetidine [Eq. (92)] in analo-

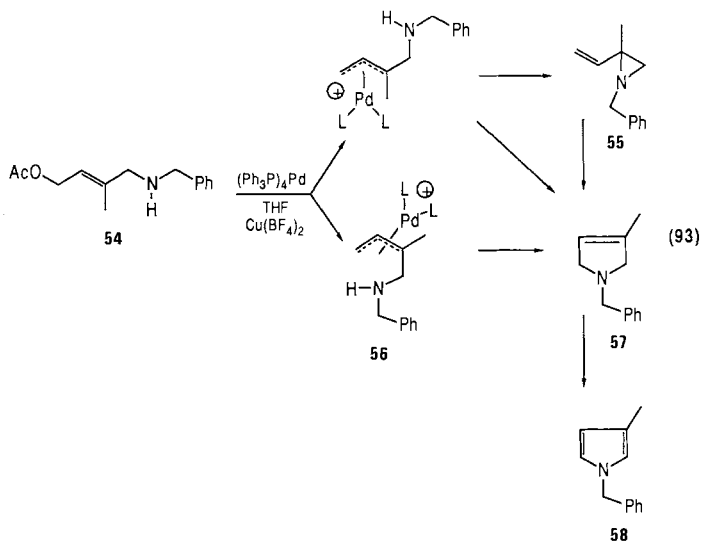


(92)

53

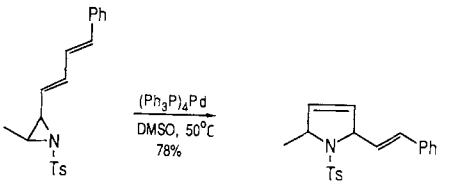
gy to the carbon case [Eq. (2)]. However, the ability of allylammonium salts to serve as substrates for Pd^0[122] permits reionization to **53**, which ultimately can collapse to the thermodynamically more stable isoquinuclidine. In support of such a suggestion, the isomerization of a *N*-tosyl-2-vinylazetidine to the six-membered ring has been reported.[123] Whereas, with carboxylate nucleophiles, both the kinetic and thermodynamic products could be obtained under cyclization conditions, only the thermodynamic product is observed with the amine nucleophiles.

A striking case is the cyclization of the amino-acetate **54**, which might have been expected to generate the vinylaziridine **55**. Instead, only the pyrrole **58**, which arises by oxidation of the initial cyclization product **57**, is obtained [Eq. (93)].[124] The attack of nitrogen on the face of the π-al-



(93)

lyl unit opposite to the palladium to form the five-membered ring in intermediate **56** is geometrically difficult. The reported failure of *N*-tosyl-2-vinylaziridine to isomerize to the 2,4-dihydropyrrole in contrast to the smooth isomerization of the dienyl analogue **59** [Eq. (94)] may be attributed to the

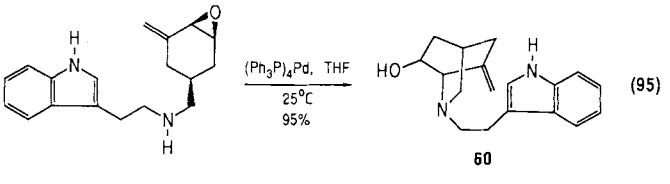


(94)

59

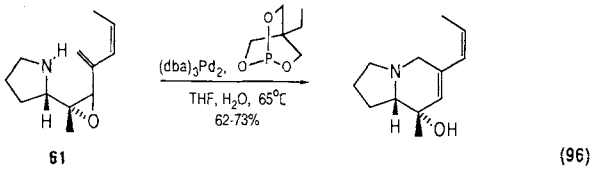
difference between a 5-*endo*- and a 5-*exo-trig* cyclization.[125] The success of the 5-*endo-trig* cyclization of **56** [Eq. (93)] may derive from a change in mechanism wherein the amine first coordinates to palladium, which then collapses by reductive elimination to give **57** (see below).

These issues become clouded when vinyl epoxides are used as electrophiles because of the propensity of the hydroxyl group adjoining the π-allyl unit to direct the regioselectivity distal to this substituent. Nevertheless, thermodynamic considerations appear to dominate. A synthesis of the enantiomerically pure isoquinuclidine **60**, a possible intermediate toward catharanthine, proceeded virtually quantitatively, even though the amine must attack proximal to the alcohol [Eq. (95)].[126] The successful cyclization of the vinyl epoxide **61** establishes the feasibility of the geometrically constrained



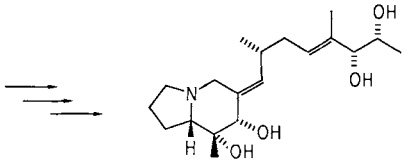
(95)

60



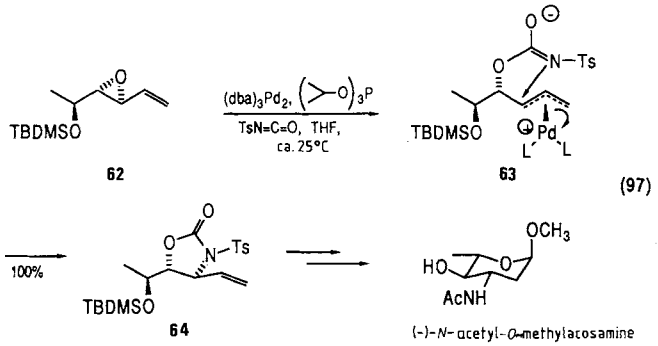
61

(96)



6-*endo-trig* cyclization.[127] Interestingly, addition of water enhances the rate of this reaction and minimizes side reactions. The effect of water may derive from its ability to solvate the epoxide oxygen, thereby enhancing its leaving group capabilities, as well as by its ability to stabilize the initial π-allylpalladium complex by protonating the forming alkoxide. For the case of vinyl epoxide substrates, the geometrical boundary for an *endo* type of cyclization lies between a five- and six-membered ring, since attempts to create a pyrrolizidine skeleton via a 5-*endo-trig* [cf. Eq. (93)] cyclization failed.[127]

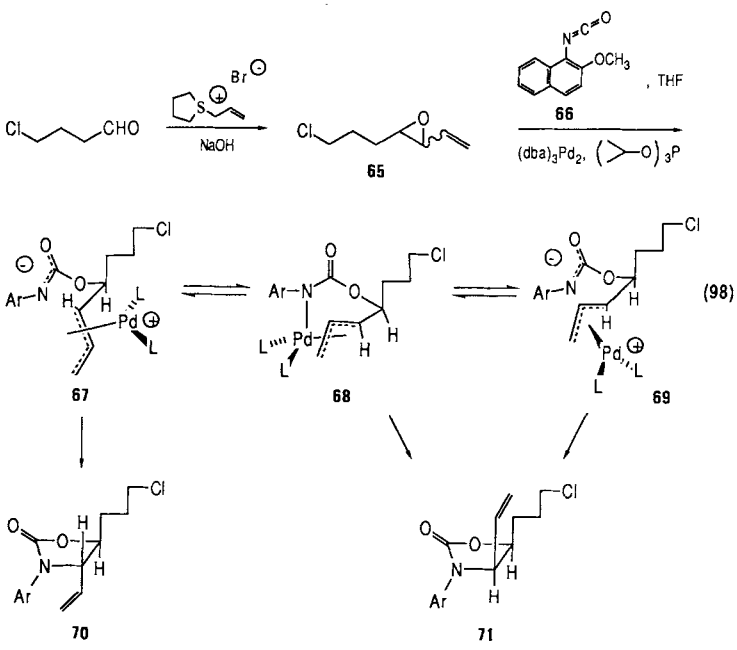
When vinyl epoxides are used, control of ring size may also be achieved by tethering the nucleophile to the epoxide oxygen in a fashion analogous to the formation of cyclic carbonates using vinyl epoxides and carbon dioxide [Eqs. (64)–(66)]. Isocyanates afford oxazolidin-2-ones, wherein ring formation occurs by nitrogen serving as a nucleophile exclusively vicinal to the oxygen, as shown in Equation (97).[128] The synthesis of the acosamine intermediate **64**



(97)

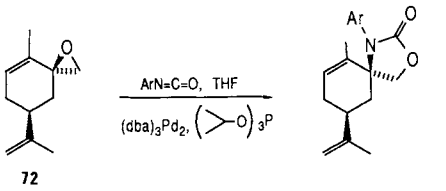
illustrates the normal stereochemical feature of substitution with net retention of configuration with *p*-toluenesulfonyl isocyanate.

Reaction of vinyl epoxides with aryl isocyanates led to a most unusual stereochemistry, which was optimized by using 2-methoxy-1-naphthyl isocyanate **66** [Eq. (98), Ar = 2-methoxy-1-naphthyl].[129] Exposing a 1:1 mixture of vinyl epoxide **65** to the isocyanate **66** under normal conditions produces a 10:1 ratio of the oxazolidin-2-one, favoring the thermodynamically less stable *Z* isomer **71**. Two explanations account for this result. In the first, kinetic generation of the normally preferred *syn* complex **67**, which generates the (*E*)-oxazolidin-2-one by the normal pathway of substitution, is followed preferentially by coordination of the nitrogen to palladium, as in **68**, and reductive elimination to give the *Z*



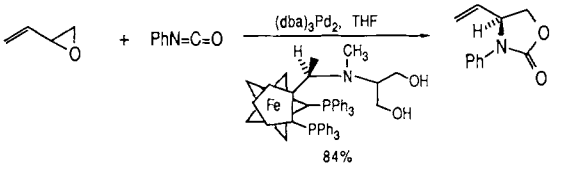
(98)

isomer. To test for this pathway, the vinyl epoxide **72** [Eq. (99)] was allowed to react with aryl isocyanates (Ar = aryl) under the usual catalytic conditions. The fact



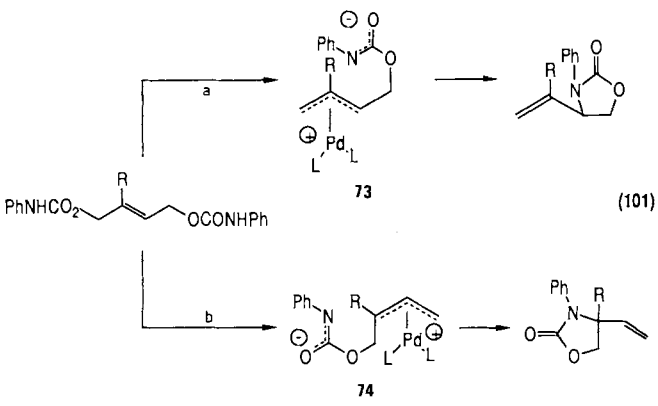
(99)

that only net retention of configuration was observed refutes the involvement of **68**.[130] An alternative explanation for the preferential formation of **71** in Equation (98) invokes rapid equilibration of the diastereomeric π-allylpalladium complexes **67** and **69**. Transition states derived from complex **69** are destabilized due to the eclipsing interaction between the vinyl and chloropropyl groups. On the other hand, the substantial interaction of the chloropropyl group with the template present in **67** may ultimately dominate. Thus, preferential formation of the *Z* isomer **71** may be an example in which the demands of the template to minimize nonbonded interactions require a product which, once released from the template, corresponds to the thermodynamically less stable one. Support for the rapid interconversion of the diastereomeric complexes **67** and **69** is provided by the observation that racemic butadiene monoepoxide reacts with phenyl isocyanate to generate the oxazolidin-2-one with 43% *ee* in the presence of enantiomerically pure ligands [Eq. (100)].[131]



(100)

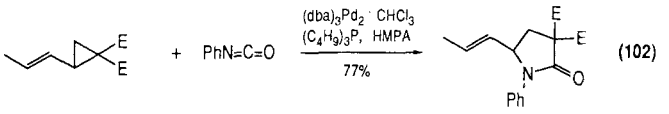
Oxazolidin-2-ones have also been formed by Pd-catalyzed cyclizations of the dicarbamates derived from 1,4-dihydroxy-2-alkenes [Eq. (101)]. Unsymmetrical substrates exhibit a remarkably high degree of chemoselectivity, favoring path a (R = *i*-C_3H_7, a:b, 96:4), which may derive from the



(101)

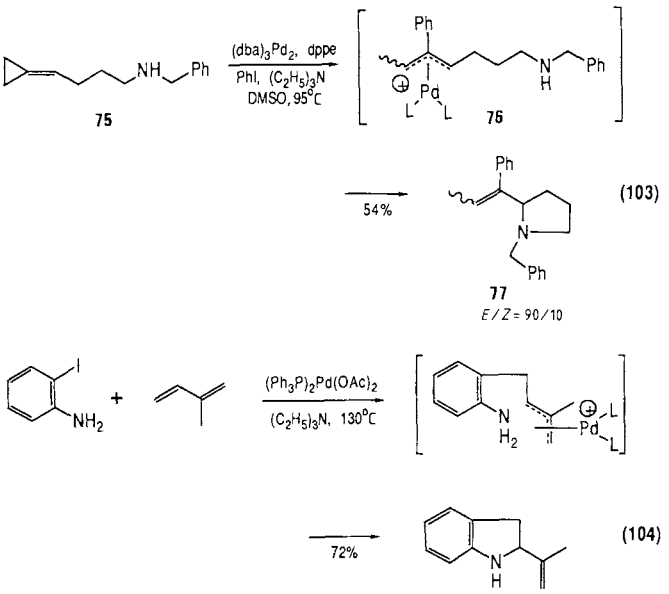
less destabilizing interactions between the organic moiety and the palladium template in intermediate **73** compared to complex **74**.[132] This same reaction with chiral ligands has led to an asymmetric induction as high as 73% *ee*.

Replacing the vinyl epoxide with a vinylcyclopropane known to undergo reversible palladium-initiated ionization in the reaction of isocyanates also successfully leads to interception of the zwitterionic intermediate [cf. Eqs. (14) and (15)] and heterocycle formation [Eq. (102)].[133] Generation

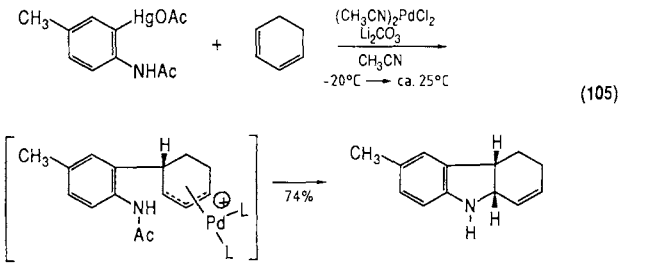


(102)

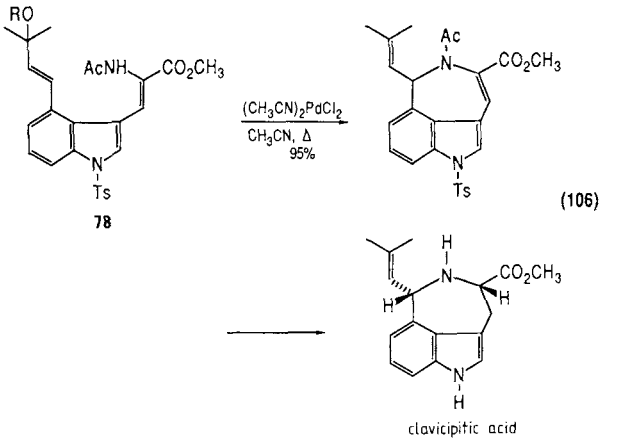
of π-allylpalladium complexes by methods other than allylic ionization in the vicinity of a nucleophilic nitrogen also can lead to nitrogen heterocycles. For example, arylation of the alkylidene cyclopropane **75** produces the pyrrolidine **77** via in situ formation of the palladium complex **76** [Eq. (103)].[62] Heck arylation of a diene with a bifunctional arylating agent leads directly to indolines [Eqs. (104)[134] and (105)[102]].



The *cis* stereochemistry in (105) arises by the amine attacking the face of the π-allyl unit proximal to the metal. It thus appears that the facial selectivity of amine nucleophiles mirrors that of oxygen. While attack may occur on the same face of the allyl unit to which the palladium is attached, the amine nucleophile generally prefers to attack the opposite side.

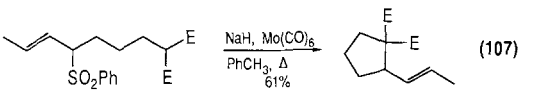


It should be noted that not all Pd-catalyzed allylic alkylations necessarily involve π-allylpalladium intermediates. An obvious candidate for cyclization via such intermediates arose in the synthesis of the ergot alkaloid clavicipitic acid. Nevertheless, any Pd^0 methodology with the substrate **78** (R = Ac or H) either failed or proceeded in very poor yields. On the other hand, **78** (R = H) cyclized nearly quantitatively using Pd^{II} complexes; the reaction apparently involves Pd-initiated amination of the olefin followed by elimination of the elements of palladium hydroxide.[135]

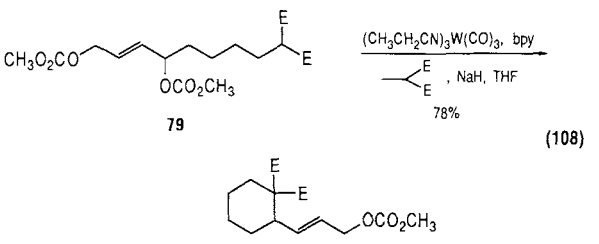


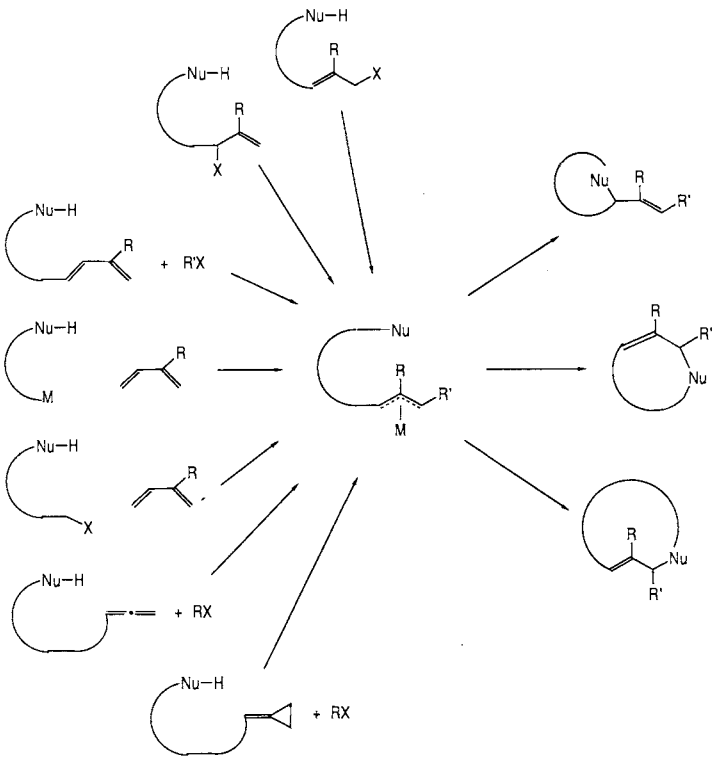
5. Conclusions

Metal-directed allylic alkylations offer a new control element for cyclizations. Chemo-, regio-, and diastereoselectivity can be totally altered. For example, the normal preference for six- and seven-membered rings can be overpowered by the metal, which may favor medium-sized (e.g., eight- and nine-membered) rings. Substitution may occur with net retention of configuration rather than inversion. Variation of the nucleophile has been very limited and clearly will expand beyond use of the stabilized carbanions or the oxygen and nitrogen nucleophiles discussed here. Other metals also catalyze allylic alkylations and will undoubtedly bring new opportunities for cyclization. Very preliminary signs establish the feasibility of this direction. A molybdenum catalyst effects the cycloalkylation of allylic sulfones [Eq. (107)].[49]



The dicarbonate **79** failed to cyclize with palladium, but smooth cyclization occurred when a tungsten catalyst was used [Eq. (108)].[136] Generating the π-allylpalladium inter-





Scheme 2. Summary of cyclizations via allylic alkylations.

mediate by methods other than allylic ionization offers great opportunities for totally new dimensions in cyclization. Scheme 2 summarizes the major routes known to date. The combinatorial possibilities assure many more will be discovered in the future. Further, the involvement of the π-allylmetal intermediate makes the metal and its attendant ligands the final arbiters in deciding the nature of the final cyclization product. One of the most important and exciting features of metal-catalyzed reactions is the development of chiral ligands for catalytic asymmetric induction—an area in which some strides have been made, but that mainly remains a prospect for the future.

I thank my many collaborators who have explored with me the utilization of abiological catalysis for synthetic selectivity. Their curiosity, intellectual and experimental skills, and enthusiasm made possible our contributions to this field. Our work has been primarily funded by the National Institutes of Health and the National Science Foundation. Merck, Sharp and Dohme Research Laboratories have provided important support for our programs. Fellowships from the Deutsche Forschungsgemeinschaft and the Alexander von Humboldt Foundation (FRG), NATO/SERC (UK), and the CNRS (France) have provided full or partial support for many of my postdoctoral associates from these countries.

Received: March 23, 1989 [A 732 IE]
German version: *Angew. Chem. 101* (1989) 1199

[1] A. von Baeyer, *Ber. Dtsch. Chem. Ges. 18* (1885) 2269; see also A. de Meijere (Ed.): *Small Ring Compounds in Organic Synthesis I, II, III (Top. Curr. Chem. 133* (1986), *135* (1987), *144* (1988)).

[2] R. Willstätter, H. Veraguth, *Ber. Dtsch. Chem. Ges. 38* (1905) 1975. For reviews see J. Sicher, *Prog. Stereochem. 3* (1962) 202; A. C. Cope, M. M. Martin, M. A. McKervey, *Q. Rev. Chem. Soc. 20* (1966) 119.

[3] L. Ružička, *Helv. Chim. Acta 9* (1926) 715, 1008.

[4] S. Coffey, (Ed.): *Rodd's Chemistry of Carbon Compounds,* 2nd ed., Vol. II, Parts A and B, Elsevier, Amsterdam 1968; M. F. Ansell, (Ed.): *Supplements to the 2nd Edition of Rodd's Chemistry of Carbon Compounds,* Vol. II, Parts A and B, Elsevier, Amsterdam 1974.

[5] E. C. du Feu, F. J. McQuillin, R. Robinson, *J. Chem. Soc. 1937,* 53.

[6] W. S. Johnson, S. J. Telfer, S. Cheng, U. Schubert, *J. Am. Chem. Soc. 109* (1987) 2517 and earlier work cited therein, Review: W. S. Johnson, *Bioorganic Chem. 5* (1976) 51; *Angew. Chem. 88* (1976) 33; *Angew. Chem. Int. Ed. Engl. 15* (1976) 9.

[7] A. Mitra: *The Synthesis of Prostaglandins,* Wiley, New York 1977; S. M. Roberts, F. Scheinmann: *New Synthetic Routes to Prostaglandins and Thromboxanes,* Academic, New York 1982; R. Noyori, M. Suzuki, *Angew. Chem. 96* (1984) 854; *Angew. Chem. Int. Ed. Engl. 23* (1984) 847; R. J. K. Taylor, *Synthesis 1985,* 364; J. E. Pike, D. R. Morton: *Chemistry of Prostaglandins and Leukotrienes,* Raven, New York 1985.

[8] See also B. M. Trost, *Chem. Soc. Rev. 11* (1982) 1419; L. Paquette, A. M. Doherty: *Polyquinane Chemistry, Syntheses and Reactions,* Springer, Berlin 1987.

[9] D. P. Curran, *Synthesis 1988,* 417, 489.

[10] For a leading reference see D. F. Taber, R. E. Ruckle, Jr., M. J. Hennessy, *J. Org. Chem. 51* (1986) 4077.

[11] B. M. Trost, *Angew. Chem. 98* (1986) 1; *Angew. Chem. Int. Ed. Engl. 25* (1986) 1; *Pure Appl. Chem. 60* (1988) 1615.

[12] E. Negishi, *Acc. Chem. Res. 20* (1987) 65; H. Yasuda, A. Nakamura, *Angew. Chem. 99* (1987) 745; *Angew. Chem. Int. Ed. Engl. 26* (1987) 723; B. M. Trost, *Phil. Trans. R. Soc., Ser. A, 326* (1988) 511. For a leading reference to the Pauson–Khand reaction see M. E. Krafft, *J. Am. Chem. Soc. 110* (1988) 968.

[13] H. Brockmann, W. Henkel, *Naturwissenschaften 37* (1950) 138.

[14] S. Masamune, G. S. Bates, J. W. Corcoran, *Angew. Chem. 89* (1977) 602; *Angew. Chem. Int. Ed. Engl. 16* (1977) 585.

[15] C. Tsai, J. J. Stezowski, R. E. Hughes, *J. Am. Chem. Soc. 93* (1971) 7286; H. Ogura, K. Furuhata, H. Kuwano, N. Harada, *ibid. 97* (1975) 1930.

[16] R. S. Egan, T. J. Perun, J. R. Martin, L. A. Mitscher, *Tetrahedron 29* (1973) 2525; J. G. Nourse, J. D. Roberts, *J. Am. Chem. Soc. 97* (1975), 4584; R. S. Egan, J. R. Martin, T. J. Perun, L. A. Mitscher, *ibid. 97* (1975) 4578.

[17] P. Ganis, G. Avitable, W. Mechlinski, C. P. Schaffner, *J. Am. Chem. Soc. 93* (1971) 4560; C. N. Chang, R. W. Richards, *Tetrahedron Lett. 1972,* 5053.

[18] R. C. Pandey, V. F. German, Y. Nishikawa, K. L. Rinehart, Jr. *J. Am. Chem. Soc. 93* (1971) 3738; K. L. Rinehart, Jr., W. P. Tucker, R. C. Pandey, *ibid. 93* (1971) 3747.

[19] G. Albers-Schönberg, B. H. Arison, J. C. Chabala, A. W. Douglas, P. Eskola, M. H. Fisher, A. Lusi, H. Mrozik, J. L. Smith, R. L. Tolman, *J. Am. Chem. Soc. 103* (1981) 4216; W. C. Campbell, M. H. Fisher, E. D. Stapley, G. Albers-Schönberg, T. A. Jacob, *Science 221* (1983) 823.

[20] H. Mishima, M. Kurabayashi, C. Tamura, *Tetrahedron Lett. 1975,* 711.

[21] K. Neupert-Laves, M. Dobler, *Helv. Chim. Acta 59* (1976) 614; M. Dobler, *ibid. 55* (1972) 1371.

[22] W. Marsh, J. D. Dunity, D. N. J. White, *Helv. Chim. Acta 57* (1974) 10.

[23] S. M. Kupchan, Y. Komoda, W. A. Court, G. J. Thomas, R. M. Smith, A. Karim, C. J. Gilmore, R. C. Haltiwanger, R. F. Bryan, *J. Am. Chem. Soc. 94* (1972) 1354.

[24] H. Tanaka, A. Kuroda, H. Marusawa, H. Hatanaka, T. Kino, T. Goto, M. Hashimoto, *J. Am. Chem. Soc. 109* (1987) 5031.

[25] J. R. Hanson, (Ed.): *Terpenoids and Steroids,* Vol. 12, The Chemical Society, London 1983 and earlier volumes in this series.

[26] S. M. Kupchan, C. W. Sigel, M. J. Matz, C. J. Gilmore, R. F. Bryan, *J. Am. Chem. Soc. 98* (1976) 2295.

[27] B. Lythgoe: *The Alkaloids, Chemistry and Physiology,* Vol. X, Academic Press, New York 1968, p. 598.

[28] K. D. Barrow, D. H. R. Barton, E. Chain, U. F. W. Ohnsorge, R. P. Sharma, *J. Chem. Soc. Perkin Trans. 1, 1973,* 1590.

[29] S. Nozoe, M. Morisaki, K. Tsuda, Y. Iitaka, N. Takahashi, S. Tamura, K. Ishibashi, M. Shirasaka, *J. Am. Chem. Soc. 87* (1965) 4968.

[30] S. W. Tanenbaum, (Ed.): *Cytochalasins, Biochemical and Cell Biological Aspects,* North Holland, Amsterdam 1978.

[31] J. Golik, G. Dubary, G. Groenewold, H. Kawaguchi, M. Konishi, B. Krishman, H. Ohkuma, K. Saito, T. W. Doyle, *J. Am. Chem. Soc. 109* (1987) 3462.

[32] M. D. Lee, T. S. Dunne, C. C. Chang, G. A. Ellestad, M. M. Siegel, G. O. Morton, W. J. McGahren, D. B. Borders, *J. Am. Chem. Soc. 109* (1987) 3466.

[33] P. W. Jolly, *Compr. Organomet. Chem. 8* (1982) 671.

[34] K. P. C. Vollhardt, *Angew. Chem. 96* (1984) 525; *Angew. Chem. Int. Ed. Engl. 23* (1984) 539.

[35] B. M. Trost, D. T. MacPherson, *J. Am. Chem. Soc. 109* (1987) 3483; B. M. Trost, S. Schneider, *Angew. Chem. 101* (1989) 215; *Angew. Chem. Int. Ed. Engl. 28* (1989) 213.

[36] B. M. Trost, P. R. Seoane, *J. Am. Chem. Soc. 109* (1987) 615.

[37] Reviews: B. M. Trost, *Tetrahedron 33* (1977) 2615; *Acc. Chem. Res. 13* (1980) 385; B. M. Trost, T. R. Verhoeven, *Compr. Organomet. Chem. 8* (1982) 799; J. Tsuji, *Organic Synthesis with Palladium Compounds*, Springer, Berlin 1980; *Tetrahedron 42* (1986) 4361; J. Tsuji, I. Minami, *Acc. Chem. Res. 20* (1987) 140.
[38] B. M. Trost, T. R. Verhoeven, *J. Am. Chem. Soc. 99* (1977) 3867; *102* (1980) 4743.
[39] J.-E. Bäckvall, J.-O. Vågberg, K. L. Granberg, *Tetrahedron Lett. 30* (1989) 617.
[40] S. A. Godleski, R. S. Valpey, *J. Org. Chem. 47* (1982) 381.
[41] B. M. Trost, L. N. Jungheim, *J. Am. Chem. Soc. 102* (1980) 7910; B. M. Trost, T. A. Runge, L. N. Jungheim, *102* (1980) 2840.
[42] B. M. Trost, T. A. Runge, *J. Am. Chem. Soc. 103* (1981) 7550.
[43] B. M. Trost, T. A. Runge, *J. Am. Chem. Soc. 103* (1981) 2485, 7559.
[44] B. M. Trost, A. D. Patten, to be published.
[45] J. Tsuji, Y. Kobayashi, H. Kataoka, T. Takahashi, *Tetrahedron Lett. 21* (1980) 3393.
[46] J. P. Genet, S. Grisoni, *Tetrahedron Lett. 29* (1988) 4543.
[47] K. Yamamoto, R. Deguchi, Y. Ogimura, J. Tsuji, *Chem. Lett. 1984*, 1657.
[48] B. M. Trost, *Bull. Chem. Soc. Jpn. 61* (1988) 107.
[49] B. M. Trost, C. A. Merlic, to be published.
[50] Y. Morizawa, K. Oshima, H. Nozaki, *Tetrahedron Lett. 23* (1982) 2871.
[51] See J. E. Baldwin, J. Cutting, W. Dupont, L. Kruse, L. Silberman, R. C. Thomas, *J. Chem. Soc. Chem. Commun. 1976*, 736.
[52] J. Tsuji, Y. Ohashi, I. Shimizu, *Tetrahedron Lett. 26* (1985) 3825.
[53] K. Burgess, *J. Org. Chem. 52* (1987) 2046.
[54] B. M. Trost, G. B. Tometzki, M.-H. Hung, *J. Am. Chem. Soc. 109* (1987) 2176.
[55] J.-E. Bäckvall, J.-O. Vågberg, C. Zercher, J. P. Genet, A. Dennis, *J. Org. Chem. 52*, (1987) 5430; J.-E. Bäckvall, J.-O. Vågberg, J. P. Genet, *J. Chem. Soc. Chem. Commun. 1987*, 159.
[56] F. Colobert, J. P. Genet, *Tetrahedron Lett. 26* (1985) 2779.
[57] J. P. Genet, J. M. Gaudin, *Tetrahedron 43* (1987) 5315.
[58] T. Hayashi, A. Yamamoto, Y. Ito, *Tetrahedron Lett. 29* (1988) 669.
[59] J. P. Genet, M. Balabane, F. Charbonnier, *Tetrahedron Lett. 23* (1982) 5027; J. P. Genet, F. Piau, *J. Org. Chem. 46* (1981) 2414. See also Y. Hanzawa, S. Ishizawa, Y. Kobayashi, *Chem. Pharm. Bull 36* (1988) 4209.
[60] S. Hashimoto, T. Shinoda, S. Ikegami, *Tetrahedron Lett. 27* (1986) 2885.
[61] M. Ahmar, B. Cazes, J. Gore, *Tetrahedron 43* (1987) 3453; *Tetrahedron Lett. 26* (1985) 3795.
[62] G. Fournet, G. Balme, J. J. Barieux, J. Gore, *Tetrahedron 44* (1988) 5821.
[63] B. M. Trost, T. R. Verhoeven, unpublished results.
[64] B. M. Trost, D. Martina, unpublished results; see also B. M. Trost, T. R. Verhoeven, *J. Am. Chem. Soc. 101* (1979) 1595.
[65] Y. Kitagawa, A. Itoh, S. Hashimoto, H. Yamamoto, H. Nozaki, *J. Am. Chem. Soc. 99* (1977) 3864.
[66] J. A. Marshall, R. C. Andrews, L. Lebroda, *J. Org. Chem. 52* (1987) 2378.
[67] B. M. Trost, R. W. Warner, *J. Am. Chem. Soc. 104* (1982) 6112.
[68] B. M. Trost, C. Brzezowski, to be published.
[69] A. S. Kende, I. Kaldor, R. Aslanian, *J. Am. Chem. Soc. 110* (1988) 6265.
[70] B. M. Trost, C. J. Urch, M. H. Hung, *Tetrahedron Lett. 27* (1986) 4949.
[71] B. M. Trost, K. M. Pietrusiewicz, *Tetrahedron Lett. 26* (1985) 4039.
[72] B. M. Trost, R. Walchli, *J. Am. Chem. Soc. 109* (1987) 3487.
[73] N. Muyaura, H. Suginome, A. Suzuki, *Tetrahedron Lett. 25* (1984) 761.
[74] W. Oppolzer, J. M. Gaudin, T. N. Birkinshaw, *Tetrahedron Lett. 29* (1988) 4705. See also W. Oppolzer, R. E. Swenson, W. Pachinger, *Helv. Chim. Acta 72* (1989) 14; E. Negishi, S. Iyer, C. J. Rousset, *Tetrahedron Lett. 30* (1989) 291.
[75] W. Oppolzer, J. M. Gaudin, *Helv. Chim. Acta 70* (1987) 1477.
[76] B. M. Trost, J. I. Luengo, *J. Am. Chem. Soc. 110* (1988) 8239.
[77] Y. Ito, H. Aoyama, T. Hirao, A. Mochizuki, T. Saegusa, *J. Am. Chem. Soc. 101* (1979) 494; Y. Ito, H. Aoyama, T. Saegusa, *ibid. 102* (1980) 4519.
[78] A. S. Kende, B. Roth, P. J. Sanfilippo, *J. Am. Chem. Soc. 104* (1982) 1784.
[79] L. E. Torres, G. L. Larson, *Tetrahedron Lett. 27* (1986) 2223.
[80] A. S. Kende, B. Roth, P. J. Sanfilippo, T. Balcklock, *J. Am. Chem. Soc. 104* (1982) 5808; A. S. Kende, R. A. Battista, S. B. Sandoval, *Tetrahedron Lett. 25* (1984) 1341.
[81] T. Takahashi, Y. Jinbo, K. Kitamura, J. Tsuji, *Tetrahedron Lett. 25* (1984) 5921.
[82] B. M. Trost, T. P. Klun, *J. Am. Chem. Soc. 101* (1979) 6756; *103* (1981) 1864; B. M. Trost, T. R. Verhoeven, *ibid. 98* (1976) 630; *100* (1978) 3435.
[83] B. M. Trost, T. R. Verhoeven, *Tetrahedron Lett. 1978*, 2275.
[84] B. M. Trost, T. R. Verhoeven, *J. Am. Chem. Soc. 99* (1977) 3867.
[85] S. L. Schreiber, T. Sammakia, B. Hulin, G. Schulte, *J. Am. Chem. Soc. 108* (1986) 2106.
[86] B. M. Trost, S. J. Brickner, *J. Am. Chem. Soc. 105* (1983) 568.
[87] B. M. Trost, R. W. Warner, *J. Am. Chem. Soc. 105* (1983) 5940.
[88] B. M. Trost, J. T. Hane, P. Metz, *Tetrahedron Lett. 27* (1986) 5695.
[89] B. M. Trost, A. dallaCort, to be published.
[90] T. Takahashi, M. Miyazawa, H. Veno, J. Tsuji, *Tetrahedron Lett. 27* (1986) 3881.
[91] T. Takahashi, H. Kataoka, J. Tsuji, *J. Am. Chem. Soc. 105* (1983) 147.
[92] J. Wicha, M. M. Kabat, *J. Chem. Soc. Perkin Trans. 1 1985*, 1601; *J. Chem. Soc. Chem. Commun. 1983*, 985.
[93] S. A. Godleski, E. B. Villhauer, *J. Org. Chem. 51* (1986) 486.
[94] W. Oppolzer, J. M. Gaudin, M. Bedoya-Zurita, J. Hueso-Rodriguez, T. M. Raynham, C. Robyr, *Tetrahedron Lett. 29* (1988) 4709; review: W. Oppolzer, *Angew. Chem. 101* (1989) 39; *Angew. Chem. Int. Ed. Engl. 28* (1989) 38.
[95] B. M. Trost, J. I. Luengo, to be published.
[96] M. Mori, N. Kanda, I. Oda, Y. Ban, *Tetrahedron 41* (1985) 5465; M. Mori, N. Kanda, Y. Ban, K. Ave, *J. Chem. Soc. Chem. Commun. 1988*, 12.
[97] M. Mori, Y. Kubo, Y. Ban, *Tetrahedron Lett. 26* (1985) 1519.
[98] Y. Tamaru, T. Bando, M. Hojo, Z. Yoshida, *Tetrahedron Lett. 28* (1987) 3497.
[99] B. M. Trost, S. R. Angle, *J. Am. Chem. Soc. 107* (1985) 6123; T. Fujinami, T. Suzuki, M. Kamiya, S. Fukuzawa, S. Sakai, *Chem. Lett. 1985*, 199. See also S. Suzuki, Y. Fujita, Y. Kobayashi, F. Sato, *Tetrahedron Lett. 27* (1986) 69.
[100] B. M. Trost, J. K. Lynch, S. R. Angle, *Tetrahedron Lett. 28* (1987) 375.
[101] S. Wershofen, H.-D. Scharf, *Synthesis 1988*, 854.
[102] R. C. Larock, L. W. Harrison, M. H. Hsu, *J. Org. Chem. 49* (1984) 3664.
[103] R. C. Larock, S. Varaprath, H. H. Lau, C. A. Fellows, *J. Am. Chem. Soc. 106* (1984) 5274.
[104] R. C. Larock, D. J. Leuck, L. W. Harrison, *Tetrahedron Lett. 28* (1987) 4977.
[105] Y. Huang, X. Lu, *Tetrahedron Lett. 28* (1987) 6219.
[106] S. Burke, Seminar at University of Wisconsin, Madison, 19. April 1984.
[107] I. Minami, M. Yuhara, H. Watanabe, J. Tsuji, *J. Organomet. Chem. 334* (1987) 225.
[108] B. M. Trost, A. Tenaglia, *Tetrahedron Lett. 29* (1988) 2927.
[109] a) B. M. Trost, P. J. Bonk, *J. Am. Chem. Soc. 107* (1985) 1778; b) *ibid. 107* (1985) 8277.
[110] S. A. Stanton, S. W. Felman, C. S. Parkhurst, S. A. Godleski, *J. Am. Chem. Soc. 105* (1983) 1964.
[111] G. Stork, J. M. Poirier, *J. Am. Chem. Soc. 105* (1983) 1073.
[112] E. Keinan, M. Sahai, Z. Roth, A. Nudelman, J. Herzig, *J. Org. Chem. 50* (1985) 3558.
[113] B. M. Trost, S. A. King, to be published. See also B. M. Trost, S. A. King, *Tetrahedron Lett. 27* (1986) 5971.
[114] B. M. Trost, J. P. Genet, *J. Am. Chem. Soc. 98* (1976) 8516.
[115] B. M. Trost, S. A. Godleski, J. P. Genet, *J. Am. Chem. Soc. 100* (1978) 3930.
[116] B. M. Trost, S. A. Godleski, J. L. Belletire, *J. Org. Chem. 44* (1979) 2052.
[117] B. Z. Andiriamialisoa, N. Langlois, Y. Langlois, *Heterocycles 14* (1980) 1457.
[118] S. A. Godleski, J. D. Meinhart, D. J. Miller, S. Van Wallendael, *Tetrahedron Lett. 22* (1981) 2247.
[119] S. A. Godleski, D. J. Heacock, J. D. Meinhart, S. Van Wallendael, *J. Org. Chem. 48* (1983) 2101.
[120] W. Carruthers, S. A. Cumming, *J. Chem. Soc. Perkin Trans. 1 1983*, 2383; *J. Chem. Soc. Chem. Commun. 1983*, 360; W. Carruthers, R. C. Moses, *J. Chem. Soc. Perkin Trans. 1 1988*, 2255.
[121] B. M. Trost, J. Cossy, *J. Am. Chem. Soc. 104* (1982) 6881.
[122] B. M. Trost, E. Keinan, *J. Org. Chem. 45* (1980) 2741.
[123] K. Fugami, Y. Morizawa, K. Oshima, H. Nozaki, *Tetrahedron Lett. 26* (1985) 857.
[124] J. P. Genet, M. Balabane, J.-E. Bäckvall, J. E. Nystrom, *Tetrahedron Lett. 24* (1983) 2745.
[125] K. Fugami, Y. Morizawa, K. Oshima, H. Nozaki, *Tetrahedron Lett. 26* (1985) 857.
[126] B. M. Trost, A. G. Romero, *J. Org. Chem. 51* (1986) 2332.
[127] B. M. Trost, T. S. Scanlan, to be published.
[128] B. M. Trost, A. R. Sudhakar, *J. Am. Chem. Soc. 109* (1987) 3792.
[129] B. M. Trost, A. R. Sudhakar, *J. Am. Chem. Soc. 110* (1988) 7933.
[130] B. M. Trost, R. Hurnaus, to be published.
[131] T. Hayashi, A. Yamamoto, Y. Ito, *Tetrahedron Lett. 29* (1988) 99.
[132] T. Hayashi, A. Yamamoto, Y. Ito, *Tetrahedron Lett. 28* (1987) 4837.
[133] K. Yamomoto, T. Ishida, J. Tsuji, *Chem. Lett. 1987*, 1157.
[134] J. M. O'Connor, B. J. Stallman, W. G. Clark, A. Y. L. Shu, R. G. Spada, T. M. Stevenson, H. A. Dieck, *J. Org. Chem. 48* (1983) 807.
[135] P. J. Harrington, L. S. Hegedus, K. F. McDaniel, *J. Am. Chem. Soc. 109* (1987) 4335.
[136] B. M. Trost, G. B. Tometzki, to be published.

The Beginnings of Organic Photochemistry

By Heinz D. Roth*

Although sunlight induced photochemistry must have occurred on the planet Earth for billions of years, the chemical changes caused by light have attracted systematic scientific scrutiny only relatively recently. How did scientists first conceive the idea that the interaction of materials with light could not only cause physical phenomena, but could also alter their chemical nature? When sunlight began to be employed as a heat source for distillation, the eventual discovery of photochemical reactions was assured. One can envision three types of changes that would have aroused the curiosity of laboratory chemists: color changes; the evolution of gas bubbles (oxygen in photosynthesis); and the precipitation of a photoproduct less soluble than its precursor. Less predictable was the observation that sunlight caused crystalline santonin to burst because it is converted into a product with a different crystal lattice. In the course of the eighteenth and nineteenth centuries a variety of photochemical reactions, some observed by chance, others uncovered in carefully planned studies, ultimately led to a major systematic investigation that established photochemistry as a viable branch of chemistry.

1. Introduction

Light induced reactions on this planet are significantly older than life itself. Sunlight induced photochemistry must have literally started as soon as the dust began to settle after the Earth's accretion phase.[1] The atmosphere of early Earth very likely was essentially free of oxygen. It may have contained chiefly a mixture of hydrocarbons and cyanocarbons, as found on Titan, the largest moon of Saturn.[2,3] In addition (or instead) it may have contained large quantities of water and carbon dioxide, as found on Mars and Venus, Earth's neighbor planets.[4] This atmosphere was exposed to radiation from a young Sun, whose spectrum very likely was quite different from the present solar spectrum, with UV fluxes one thousand times greater than the present values.[1]

Within the first one billion years plant life began to produce oxygen and to build up the atmosphere prevailing today.[5,6] At the same time it laid the foundation for seemingly inexhaustible energy resources and provided nourishment for higher forms of life. The photolysis of oxygen in the stratosphere generated the protective ozone layer, which would screen human and animal life from the high energy component of the solar spectrum.[7,8] When *homo sapiens* began to shed his hairy cover, the action of sunlight began to dimerize thymine units of human DNA and cause other changes, leading to skin cancer.[9] The human body, in turn, developed photoreactivation along with other repair processes.[9] All these photoreactions have been occurring for aeons without human intervention or, indeed, without being noticed.

How did scientists first conceive the idea that the interaction of materials with light could not only cause physical phenomena, viz. shadows, absorption, reflection, refraction, but could also alter their chemical nature? What kind of a change would be sufficiently noticeable to a chemist to whom chemical composition and appearance were the chief characteristics of a chemical substance and to whom the notion of "structure" was essentially unknown?

Numerous sunlight induced changes in the general appearance of materials or in their functionality were, indeed, noticed: the bleaching effect, exploited for the manufacture of fibers but detrimental to dyed fabrics; the preservation of oil paintings[10] and the "chalking" of exterior paint; deleterious effects on beer;[11] and the spoiling of gun cotton.[12] Aside from these matters of practical importance, three types of changes can be envisioned to arouse the curiosity of a laboratory chemist: color changes, either temporary (photochromism) or permanent; the development of gas bubbles in a liquid; and the precipitation of a photoproduct that is less soluble than its precursor.

It appears plausible that changes induced in a photochromic dye should have been the earliest photoreactions observed. Indeed, it has been claimed[13] that *Alexander the Great* exploited such an effect to coordinate the attack of his troops, which proved to be crucial for the outcome of his battles. The Macedonian troops supposedly carried rag bands around their wrists, which were impregnated with a photochromic dye. A color change caused by the exposure to sunlight thus could signal the time of attack. The device has been referred to as Alexander's Rag Time Band.[13] Alas, no scientific record of the underlying chemistry has been preserved; photochromism wasn't rediscovered until 1876.[14]

Attempts to utilize the energy of the sun are at least several thousand years old, although the fable of *Phaethon* appears to hint, that man is not meant to achieve this dream.[*] The burning mirror of *Archimedes* (Fig. 1) may well be the best known early device. More modest uses for laboratory experiments (or their outdoor equivalents) are documented as early as 1599 when *Conrad Gesner* described "The maner of

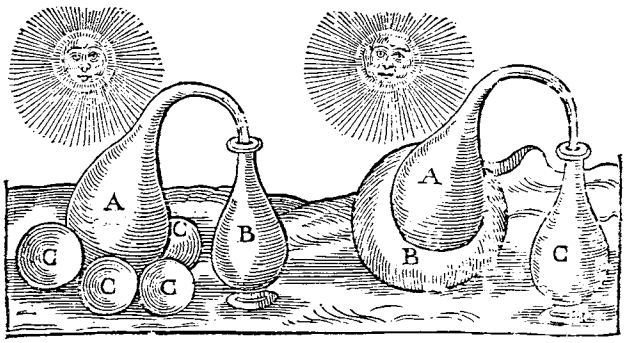
[*] Prof. Dr. H. D. Roth
Department of Chemistry, Wright Rieman Laboratories
Rutgers University
New Brunswick, NJ 08903 (USA)

[*] *Phaethon*, the son of *Helios* and the nymph *Clymene*, tried to drive his father's golden chariot. However, unable to control the powerful steeds, he let the chariot plunge to earth, burning Mt. Oeta and drying the Libyan desert. The entire universe would have perished in the conflagration, had not *Zeus* killed *Phaethon* with a bolt of lightning.



Fig. 1. Burning mirror of *Archimedes*, from "Encyclopedia", Scot, Philadelphia.

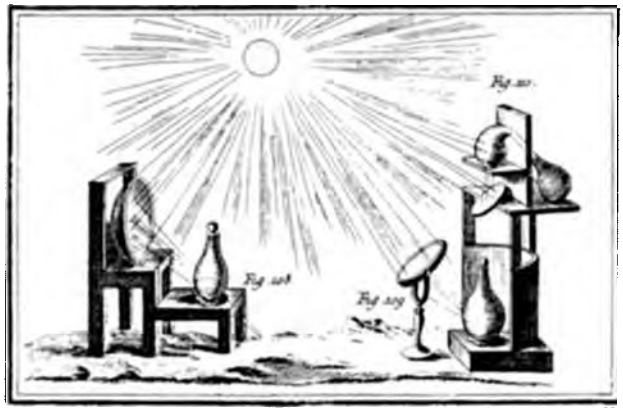
Distilling in the Sunne" in his monograph on "The practise of the new and old phisicke".[15] Some fifty years later *John French* showed two setups "to rectify spirits" (Fig. 2), which included provisions for the collection and accumulation of solar radiation, based on the heat capacity of materials such as glass, marble, or cast iron.[16]



A, *Shews the Retort.*
B, *The Receiver.*
C, *The Cryſtal Bowls...*

A, *Shews the Retort.*
B, *The Marble or Iron Mortar.*
C, *The Receiver.*

Fig. 2. Two apparatus by *John French* "to rectify spirits" [16].



108. Diſtillation ou digeſtion au ſoleil par réflexion. Libav.
109. Diſtillation ou digeſtion par réfraction. Libav.
110. Diſtillation au ſoleil par réflexion pour une cornue. Libav.

Fig. 3. A variety of distillation setups [17].

Less than fifty years later *Libavius* described several methods to focus sunlight on a designated area (Fig. 3). These methods employed mirrors or lenses and suggest an understanding of the principles of optics.[17] All uses suggested up to *Libavius'* time exploited the heat component of the sun's energy spectrum. Chemical changes were limited to combustion as a result of heating above the point of spontaneous ignition.

2. *Joseph Priestley*— Photochemistry in the Eighteenth Century

It was in a setup, similar to that of *Libavius*, that *Priestley* first encountered a comparably simple chemical conversion. In the course of his experiments on "different kinds of air" he used a twelve inch lens to focus sunlight on a sample of mercury in a closed vessel (Fig. 4).[18] He observed conversion of the mercury to a red solid with an increase in weight and a diminution of the volume of air. This pioneering experiment was correctly interpreted by *Lavoisier* as a combination of mercury with oxygen, i.e. as an oxidation.[18] Of course, this conversion is a thermal reaction.



Heinz D. Roth was born in Rheinhausen, in the Lower Rhine region of Germany, in 1936. After completing his formal education at the Universities of Karlsruhe and Köln he received a Dr. rer. nat. degree in Professor Emanuel Vogel's laboratory at the University of Köln with a dissertation on 1,6-methano[10]annulene. After two years as a postdoctoral fellow in W. von E. Doering's laboratory at Yale University he joined the Research Division of (AT&T) Bell Laboratories, Murray Hill, NJ. He has been interested in organic reaction mechanisms, particularly in the structure and reactivity of short-lived radical ions and carbenes; in electron donor-acceptor interactions and photoinduced electron transfer; and in the application of magnetic resonance techniques, especially chemically induced magnetic polarization. Since 1988 he has been Professor of Chemistry at Rutgers University, New Brunswick, NJ. In addition to his main scientific interests he pursues the historical development of the sciences as well as 16th–18th century european cartography.

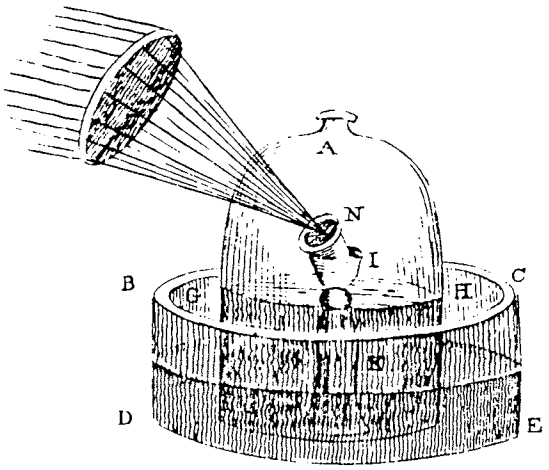


Fig. 4. Apparatus for carrying out calcinations credited to *Priestley* [18]. The metal is contained "in a porcelain cup N, placed upon the stand IK, under a jar A, in the bason BCDE, full of water; the water is made to rise up to GH by sucking out the air with a syphon, and the focus of a burning glass is made to fall upon the metal."



Fig. 5. *Joseph Priestley* (1733–1800), engraving by W. Hall – From a picture by *Gilbert Stewart*. C. Knight, London.

However, *Priestley* also was successful in observing at least two genuine photoreactions in two widely divergent fields: inorganic chemistry and photosynthesis. He exposed partially filled vials of "spirit of nitre" (nitric acid) to sunlight and observed that the liquid assumed a reddish color.[20] In follow-up experiments he ruled out a thermal reaction and established that the reddish product (nitrogen dioxide) was formed in the vapor phase and then dissolved in the liquid. "Being now satisfied that it was the action of *light* upon the *vapour* of spirit of nitre that gave it colour, I amused myself with throwing a strong light, by means of a lens, into the upper part of a phial, the lower part of which contained colourless spirit of nitre."[20]

After the initial observation these experiments were obviously well planned and executed. It must be considered the first laboratory photoreaction in the *gas* phase, although this assignment can be made only with all due apologies to its investigator. *Priestley* specifically rejected the term "gas", that had been suggested by the elder (*J. B.*) *van Helmont* (1577–1644), as unnecessary.[21a]

Priestley (Fig. 5) also deserves credit for first recognizing some facts regarding photosynthesis. In his own words, he "fully ascertained the influence of light in the production of dephlogisticated air (oxygen) in water by means of a *green substance*". When he had first observed the gas evolution, he had explained it as a light-induced reaction of water. However, in later experiments he noticed the presence of *green matter* and a colleague identified tiny plants under a microscope.[21b]

After learning of *Priestley*'s early experiments, *Jan Ingenhousz*, a Dutch physician, who practiced in England and Austria, carried out experiments of his own. He determined that the action of light on plants "improves" air and that *Priestley*'s "green matter" must be a plant.[22] *Nicholas Theodore de Saussure* (1767–1845) resolved the problem in 1804, when he grew plants in enclosed spaces that allowed him to monitor changes in the gas content quantitatively. He demonstrated that the influence of light causes plants to consume water and carbon dioxide and to generate oxygen.[23]

In concluding this brief overview of *Priestley*'s contributions to photochemistry, it is interesting to compare his views of the nature of light with those of his French contemporary *Lavoisier*. *Priestley* considered light a *"chemical principle"* and an *"important agent in the system of nature"*, although he conceded that its "effects ... are as yet but little known."[21b] *Lavoisier*, on the other hand, considered heat and light as agents capable of combining with chemical substances, causing them to expand.

About the more elusive of the two he wrote: "The combinations of light, and its mode of acting upon different bodies are still less known ... it appears to have great affinity with oxygen ..." *Lavoisier* deserves credit for the formulation of many chemical concepts, but the paucity of experimental facts was insufficient to reveal to him the nature of light. His most eloquent statement about light was of a philosophical nature: "By means of light, the benevolence of the Deity has filled the earth with organization, sensation, and intelligence. The fable of Prometheus might perhaps be considered as giving a hint of this philosophical truth even to the ancients."[24]

3. *J. W. Döbereiner* and the Light Induced Reduction of Metal Ions

An interesting laboratory experiment in photochemistry was carried out by *Döbereiner*. The August 1831 issue of *Pharmaceutisches Central Blatt* (later *Chemisches Zentralblatt*) contains an abstract, which is introduced as follows: "Prof. Döbereiner, dem die Chemie schon so viele interessante Tatsachen verdankt, theilt folgende bemerkenswerthe Beobachtungen über die chemische Wirkung des Lichts mit."[*] *Döbereiner* exposed an aqueous solution of oxalic acid and iron(III) oxide in a small glass bulb to sunlight. He observed that many tiny gas bubbles developed, which he

[*] "Professor *Döbereiner*, to whom chemistry already owes so many interesting facts, reports the following remarkable observation about the chemical effect of light."

identified as CO_2, and that a basic iron(II) oxide, humboldtite, precipitated.[25] With appropriate modifications this reaction has become the basis for ferrioxalate actinometry.[26, 27]

Döbereiner found similar reductions for salts of Pt, Ag, Ir, and ruled out the corresponding dark reactions by control experiments. However, he missed out on the first photoreaction of a ruthenium compound, because the element that has become the mainstay of so many photochemical studies was not discovered until 1844.

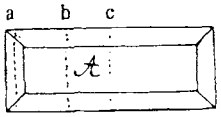
Johann Wolfgang Döbereiner (1780–1849) taught at Jena University and belonged to *J. W. von Goethe*'s circle of friends. He made important contributions in several areas: he developed a pneumatic gas lighter; he investigated oxidation reactions with "platinum black"; and he suggested (before *Faraday*) the use of simple galvanic cells for stoichiometric studies. His most important contribution to chemistry was his attempt to order the chemical elements into "triads". These considerations foreshadowed (and aided) *Mendeleev*'s and *Meyer*'s work on the periodic table. The photoreduction of metal salts in the presence of oxalate ion appears to have been *Döbereiner*'s only excursion into the field of photochemistry.

4. The Photochemistry of Santonin—*Trommsdorff, Sestini, Cannizzaro*

Perhaps the longest known photoreaction of an organic compound is that of santonin, an anthelmintic sesquiterpene lactone. It occurs in the leaves and flower buds of various species of *artemisia* and is the active ingredient of Levant wormseed which was widely used in medicine. It was first isolated in 1830 by *Kahler*[28] and by *Alms*.[29] As early as 1834, *Hermann Trommsdorff* reported the curious observation that exposure to sunlight causes santonin to turn yellow, and its crystals to burst.[30] Several years later, *Heldt* observed these changes under the microscope and was able to determine the directions of the ruptures (Fig. 6).[31] These experiments are the first dealing with solid state photochemistry.

Die Santoninkrystalle zerspringen zuerst nach Schnitten, welche normal auf die Längenaxe zugehen; die zugeschärften Endflächen werden gleichfalls durch Schnitte abgetrennt, welche die Längenaxe rechtwinklich schneiden. Die Schnittflächen sind keine Ebenen, sie haben sehr unregelmäfsige Begrenzungen.

Ist A die Oberansicht eines Krystalls, so zeigen die Linien a, b, c die Richtung der Spaltungsflächen an.



Die abgelösten Stücke zerfallen dann weiter in kleinere, an welchen eine regelmäfsige Form nicht mehr erkennbar ist.

Fig. 6. Rupture of santonin crystals upon irradiation, after *Heldt* [1]. "The santonin crystals are cleaved first along cuts normal to the long axis; the inclined crystal faces are also separated along cuts perpendicular to the long axis. The newly created surfaces are not planar but have quite irregular boundaries. If A is the top view of a crystal, the lines a, b, c, indicate the directions of cleavage. The separated pieces are then cleaved further into smaller fragments which no longer show any regular shape."

Trommsdorff came from a well established family of apothecaries; his father (*Johann Bartholomäus*) was an Editor of *Annalen der Pharmacie — Deutsche Apothekerzeitung*, which would become *Justus Liebigs Annalen der Chemie*. As an apothecary, *Trommsdorff* had ready access to santonin (or at least to Levant wormseed), and had the skill and the equipment to carry out diligent experiments.

Given this background it may not come as a surprise that *Trommsdorff* was interested in the wavelength dependence of the light induced change, and probed it with the help of a prism. He determined that "Das Santonin wird sowohl durch den unzerlegten, als durch den blauen und violetten Strahl gefärbt . . .;. . . der gelbe, grüne und rothe bringen nicht die mindeste Veränderung hervor".[30][*] This study must be considered the first to probe the wavelength dependence of an organic photoreaction, a remarkable feat over 150 years ago.

The attempts to characterize santonin and its yellow photoproduct led *Trommsdorff* to the view that these were "two isomeric modifications."[30] Similarly, *Heldt*, on the basis of elemental analyses, argued: "White and yellow santonin are identical in their composition, but different in their molecular construction."[31] The early workers, of course, did not understand the structures of santonin or its photoproduct.

About twenty years after *Heldt*'s publication an Italian chemist began an investigation of santonin, its structure, and its photochemistry.[32–36] *Fausto Alessandro Sestini* (Fig. 7)



Fig. 7. *Fausto Sestini* (1839–1904), during his year in Pisa. He became director of the Institute of Agricultural Chemistry in 1876 and founded the Institute of Toxicology in 1892. In 1911 his grateful students unveiled a bust in his honor which still graces the hall of the Faculta Agraria. *Sestini* introduced *Cannizzaro* to photochemistry and through him, *Ciamician* and *Silber*.

was a teacher in Forli and served as president of the Udine Technical Institute. In 1872 he became director of the agricultural station in Rome and, concurrently, Inspector General for technical education in the Italian Department of Agriculture. In 1876, he accepted a position at the University of

[*] "Santonin is turned yellow not only by the undivided, but also by the blue and violet ray"... whereas..."the yellow, green and red one cause not even the slightest changes."

Pisa as professor and director of the Institute for Agricultural Chemistry; later he founded an Institute of Toxicology. He was a productive chemist and has many publications to his credit, the majority dealing with agricultural products.

Sestini irradiated santonin in 65% aqueous ethanol and obtained "photosantonin", which he later recognized as a diethyl ester that could be converted into a lactone/acid (photosantonic acid). The latter was prepared directly by irradiation of santonin in 80% acetic acid. These pioneering studies provided the decisive stimulus for Italian photochemistry. When *Sestini* came to Rome, his path crossed that of *Cannizzaro* and he roused his interest in the challenging problems posed by the structure of santonin and its photoproducts. They jointly published one paper,[33] and in the following years, pursued the problems independently.

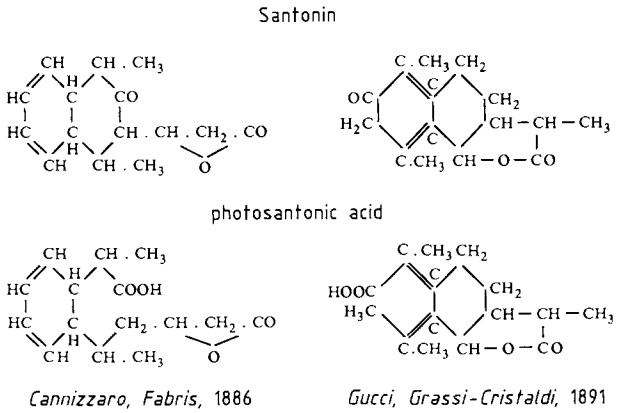
Cannizzaro (Fig. 8) and his co-workers confirmed the formation of photosantonic acid and discovered a new photo-



Fig. 8. *Stanislao Cannizzaro* (1826–1910), known for the base induced "disproportionation" reaction of benzaldehyde named after him and for the elegant treatise on molecular theory which he presented at the 1860 Karlsruhe Congress, studied the structures of santonin and two of its photoproducts, photosantonic acid and isophotosantonic acid. In his laboratory *Giacomo Ciamician* first became acquainted with photochemical experiments.

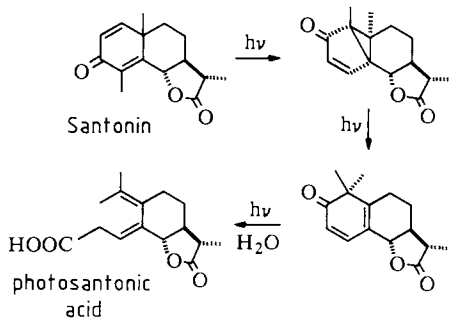
product, which they called isophotosantonic acid.[37–40] These products were well characterized by their composition, crystal properties,[41] solubilities, optical rotations,[42] and by the properties of their salts.[35] Based on these data *Cannizzaro* recognized the relation of the santonin skeleton to naphthalene, but the correct position of the functional groups in this skeleton eluded him. We illustrate the difficulty of this assignment by the structures proposed by *Cannizzaro* and *Fabris*[40] in 1886 and by *Gucci* and *Grassi-Cristaldi*[44] in 1891 (Scheme 1).

Aside from the unusual stereochemistry of the lactone ring, the latter authors assigned a large segment of the structure correctly and only failed to recognize one five-carbon fragment. However, their proposal did not enjoy a better reception than any of the alternative formulations, which deviate more substantially from the correct structure. Organic chemistry simply had not matured to a level that would have allowed an unambiguous assignment. The structural



Scheme 1.

and stereochemical complexity of santonin and the intriguing nature of its photoreactions would continue to puzzle chemists: the structure of photosantonic acid was elucidated only in 1958[45,46] and the intermediates in its formation were not identified until 1963 (Scheme 2).[47,48]



Scheme 2.

Throughout twenty years of investigating santonin and its photoproducts, *Cannizzaro* always gave *Sestini* credit for the discovery of photosantonic acid, and *Sestini* emphasized his priority.[34] *Sestini*'s importance in the history of photochemistry can hardly be overestimated: he deserves credit for having introduced *Cannizzaro* to light reactions and, through him, *Ciamician* and *Silber*.

5. Early Photodimers—Contributions by *Fritzsche* and *Liebermann*

Among the photoreactions, which first revealed themselves by the precipitation of less soluble products, dimerizations are the chief examples. The earliest laboratory photodimerization was that of anthracene, observed by *Fritzsche* in Petersburg in 1867.

Carl Julius Fritzsche (in the Russian literature *Yulii Fedorovich Fritzsche*, 1808–1871) was a student of *Mitscherlich*. After completing his studies he moved to Petersburg, where he worked for thirty-five years (1834–1869). He was concerned mainly with organic chemical problems, for example he was the first to recognize aniline as a degradation product of indigo. However, he also described the gray modification of tin (tin pest) and deserves credit for his early

work on donor-acceptor complexes. As early as 1857 he had observed and characterized 1:1 molecular complexes of picric acid with benzene, naphthalene, and anthracene.[49, 50] Remarkably, *Fritzsche* already understood these aromatics as a series of homologs:

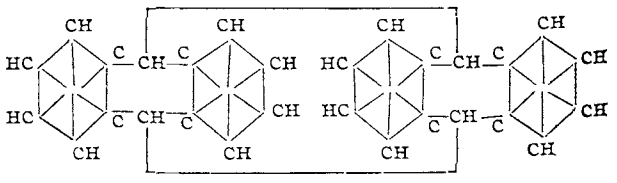
$C_4H_4 + C_8H_2$, $C_4H_4 + 2\,C_8H_2$, and $C_4H_4 + 3\,C_8H_2$

The discrepancy with today's formulation is due to the fact that carbon was assumed to have an atomic weight of six.

Fritzsche carried out detailed investigations of the components of coal tar. During these experiments, he noticed that some tar fractions lost their orange color upon exposure to sunlight. Although no specific reaction was associated with this "bleaching" effect, it is probably best understood as the formation of *endo* peroxides from polycyclic aromatic hydrocarbons. In connection with these experiments, *Fritzsche* noted that anthracene itself was light sensitive. "Gegen das Licht zeigt der Körper $C_{28}H_{10}$ ein sehr merkwürdiges Verhalten. Setzt man eine in der Kälte gesättigte Lösung desselben dem directen Sonnenlichte aus, so beginnt in derselben... die Ausscheidung von mikroskopischen Krystallen..."[*] Through appropriate control experiments, *Fritzsche* established that he was indeed dealing with a light induced reaction; he also noted that heating above the melting point regenerated anthracene.[51]

Fritzsche did not speculate in print about the chemical nature of the photoproduct, which he called the "para body". However, his colleague *Butlerov*, in an obituary address commemorating *Fritzsche*'s accomplishments, referred to the dimer as an "isomer", probably reflecting *Fritzsche*'s thoughts on the subject.[52] Apparently, this view was shared by a new generation of chemists,[53] and it prevailed for two more decades.

Twenty-five years after *Fritzsche*'s first report *Elbs* recognized the photoproduct as a dimer based on a molecular weight determination[54] by freezing point depression, a method that had been developed in the 1880's. Subsequently, *Linebarger*[55] as well as *Orndorff* and *Cameron*[56] proposed the actual structure (Scheme 3) which has been confirmed by an X-ray diffraction analysis.[57]



Scheme 3.

Another dimerization reaction was discovered in 1877 by *Liebermann* (Fig. 9) in Berlin. *Liebermann* was familiar with *Fritzsche*'s work and, like him, used exposure to sunlight to "bleach coal tar fractions", for example, in the isolation of chrysene.[58] Thus, the thought that light might cause chemical changes was not foreign to him. While working with

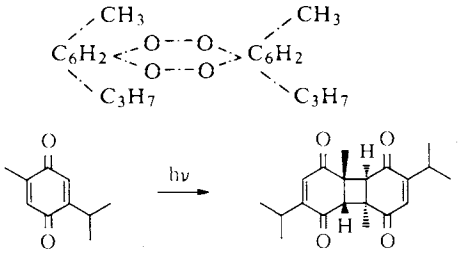
[*] "Towards light the body $C_{28}H_{10}$ shows a strange behavior. When a cold, saturated solution is exposed to sunlight, microscopic crystals begin to precipitate."



Fig. 9. *Carl Theodor Liebermann* (1842–1914), who elucidated the chemistry of many naphthalene and anthracene derivatives and had a major role in the first synthesis of alizarin as well as its industrial fabrication, carried out a greater variety of photochemical reactions than any other nineteenth century chemist.

thymoquinone, he observed that the yellow crystals under the influence of sunlight turned into a white porcelain-like mass. Through appropriate control experiments he established the conversion as a photoreaction, the first known organic [2 + 2]cycloaddition and a milestone in solid-state photochemistry.[59, 60] Of course, the elucidation of the exact structure was not achieved until much later.

Liebermann considered the compound a "polymer", a term which, at the time, would have included dimers or trimers. Concerning the structure of the photoproduct *Liebermann* noted that it was cleaved under reducing conditions. He concluded that the quinone molecules were linked through the oxygen atoms,[60] as shown below (Scheme 4). On the other hand, he had achieved the conversion of the "polymer" into a "polydioxime",[60] which suggests that the carbonyl groups are free to react and, therefore, cannot be involved in the bonding.



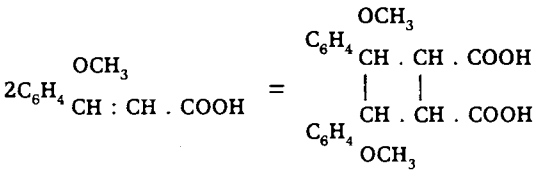
Scheme 4.

One year after *Liebermann*'s publication, *Breuer* and *Zincke* reported the isolation of a quinone, $C_{16}H_{10}O_2$, which upon exposure to sunlight gave two different "polymeric" materials.[61, 62] They did not understand the structure of the quinone, nor the nature of the photoproducts. However, they noted that one of the products readily regenerated the parent quinone upon heating, whereas the second product proved to be more stable. The quinone was later recognized as 2-phenylnaphthoquinone; the dimers likely

have cyclobutane structures.[63] A head-to-head dimer might be cleaved more readily than a head-to-tail one.

Liebermann also observed the photodimerization of styrene derivatives. In 1895, he referred to a photochemically generated "polycinnamate".[64] Also, he found that exposure of cinnamylidenemalonic acid to sunlight converted the yellow substance into a white crystalline product.[65] He suggested that this reaction was not "simply a stereoisomeric conversion" (*vide infra*) but he failed to recognize the product.

However, the credit for the first dimerization of a styrene derivative clearly belongs to *Bertram* and *Kürsten*, two industrial chemists in Leipzig.[66] Their work preceded that of *Liebermann* (though narrowly), is further reaching in its understanding, and more definitive in its conclusions. *Bertram* and *Kürsten* were working on the constituents of cassia oil when they noted that β-methylcoumaric acid slowly "polymerized" when exposed to diffuse daylight. Based upon the molecular weight they identified the product as a dimer and also recognized its structure: "this union is likely to occur by mutual saturation of the double bonds." They concluded: "Unter dem Einfluss des Lichts haben sich also zwei Moleküle der β-Methylcumarsäure zu einem Molekül der neuen Säure zusammengelagert. Diese Vereinigung wird wahrscheinlich unter Aufhebung der Doppelbindungen durch gegenseitige Sättigung stattgefunden haben, denn die polymere Säure wird nach dem Behandeln mit Brom, oder nach Einwirkung von Natriumamalgam zum grössten Theile unverändert wieder gewonnen" (Scheme 5).[*]

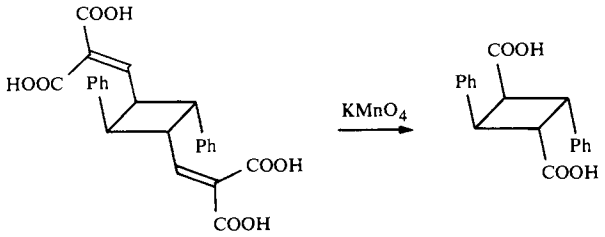


Scheme 5.

They extended their investigation to cinnamic acid and obtained an acid of melting point 274 °C, which they identified as α-truxillic acid.[66] It is remarkable that these chemists recognized the nature of the dimer, whereas *Liebermann* failed to recognize his "polycinnamate", in spite of his familiarity with truxinic and truxillic acids.

The photoproduct derived from cinnamylidenemalonic acid was recognized by *Rüber*, who reinvestigated this reaction with *Liebermann*'s encouragement.[67] He determined that the product had twice the molecular weight of the diolefin diacid. Permanganate oxidation of the product have rise to α-truxillic acid, establishing structure and stereochemistry (Scheme 6). *Rüber* also succeeded in converting cinnamic acid into (the same) α-truxillic acid[68] apparently unaware of the earlier work by *Bertram* and *Kürsten*. This earned him a reprimand by *Ciamician* and *Silber*,[69] who had begun an extensive study of photochemical reactions (see Section 11).

[*] "Under the influence of light, two molecules of β-methylcoumaric acid have associated. This union is likely to occur by mutual saturation of the double bonds; for the polymeric acid is recovered mostly unchanged after treatment with bromide or exposure to sodium amalgam."



Scheme 6.

Carl Theodor Liebermann[70, 71] spent his entire scientific career in Berlin at the Gewerbeakademie Charlottenburg, which later became the Technische Universität Berlin. In 1863 he was one of the first to join *Adolph Baeyer* as students; he received his doctorate in 1865. Together with *Carl Graebe* he elucidated the structure of alizarin, the active component of the natural dyestuff madder, and carried out the first successful synthesis of this dye with anthraquinone as starting material. This was a significant achievement as it was the first instance of a natural vegetable coloring matter having been produced artificially by a purely chemical method. Subsequently, in 1869, *Caro, Graebe,* and *Liebermann* patented a commercially promising procedure; their patent application (BP 1936) was received one day before that of *Perkin*'s (BP 1948).[72, 73]

In 1872, when *Baeyer* was offered the chemistry chair in Strassbourg, an event precipitated by the outcome of the Franco-Prussian War,[74] *Liebermann* succeeded him in Berlin, and he kept this position until his retirement in 1913 (Fig. 10). He was a founding member of the Deutsche Chemische Gesellschaft and held the office of president for two terms.



Fig. 10. The Geheime Regierungsrat *Liebermann*, in later years (after 1900), no longer actively pursued photochemical problems. However, he followed the work of *Ciamician* and *Silber* and exchanged with them unpublished results concerning the isomerization of oximes.

His scientific work is characterized by a wide range of interests. He developed the chemistry of anthracene and many derivatives, he discovered β-naphthylamine, and char-

acterized thiourethane and thiohydantoin and their derivatives. He was especially attracted to natural products occurring in plants, the coca alkaloids foremost among them. During this work he discovered the (*cis*-) stereoisomer of (*trans*-) cinnamic acid and also cinnamic acid crystals of two different crystal structures, without however recognizing them as such! *Liebermann* made several contributions to solution photochemistry, but his most important contributions were solid state photoreactions: the dimerization of quinones[59, 60] and styrene derivatives.[64, 65] He also evaluated the efficiency of several artificial light sources.[65]

6. Geometric Isomerization of Olefins—*W. H. Perkin* as a Photochemist

Geometric isomerization is one of the most general photoreactions of olefins. The credit for the first observation of this kind, in 1881, belongs to *Perkin* (Fig. 11). He was investigating 2-alkoxycinnamic acids obtained from coumarin and observed the conversion of several "α-acids" into their "β-isomers" upon exposure to sunlight.[75]



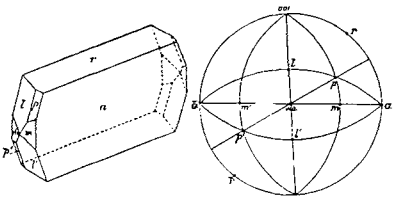
Fig. 11. *William Henry Perkin* (1838–1907), a pioneer of the synthetic dyestuff industry, was the first to observe a light-induced *cis-trans* isomerization.

Perkin's paper is distinguished by the thorough characterization of these compounds; it contains melting points and boiling points, solubility data, specific gravity at two temperatures, magneto-optical rotation data, refractive indices, and a detailed crystallographic description (Scheme 7). This is the first reference to magneto-optical rotation, which *Perkin* soon developed into an important tool for assigning structures.[76, 77]

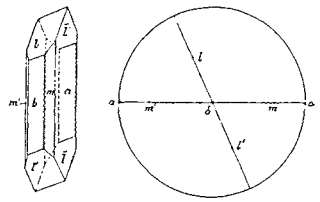
Perkin's paper is also of interest because he pronounced "the cause of isomerization of these bodies... unexplainable", and continued to discuss fumaric and maleic acid in "traditional" fashion (Scheme 8). Although he definitely was aware of *van't Hoff*'s 1874 paper, he apparently did not adopt the new concept of stereochemistry to his system.

Concerning the photochemical content, *Perkin* not only described the light-induced *cis-trans* isomerization, but he also studied the wavelength dependence of the photoreaction. In order "to see which rays of light caused the change", he used "variously colored solutions" as filters, of which he identified "sulphate of quinine" and "ammoniacal sulphate of copper". He concluded that "the alteration is due to the action of the violet and ultraviolet rays".[75]

α-methylorthoxyphenylacrylic acid



β-methylorthoxyphenylacrylic acid



Scheme 7.

	$-CH=CH-$	$-CH_2-\overset{\overset{\|\|}{}}{C}-$
Scheme 8.	fumaric acid	maleic acid

About ten years later *Liebermann* observed similar photoinduced *cis*-to-*trans* rearrangements for cinnamic and several other unsaturated acids.[78] In the course of these studies one of his coworkers tried "die für Isozimmtsäure so characteristische Umlagerung durch Jod in Schwefelkohlenstoff".[*] This led to greatly accelerated interconversions. A benzene solution of "allo"-cinnamic acid required five months of exposure to produce a 40% precipitation of cinnamic acid, whereas a solution containing iodine required only 12 days for 70% precipitation, a more than tenfold increase in rate. "Allo"-furfuracrylic acid reacted much faster, but the most rapid rearrangement was observed for "allo"-cinnamylideneacetic acid (δ-phenylpentadienoic acid), which required only one minute of exposure to produce a precipitate of the more stable isomer.[65] *Liebermann* considered the iodine assisted photoinduced isomerization a "general group reaction of the aromatic allo-acids" and suggested the most rapid conversion for a classroom demonstration.[65]

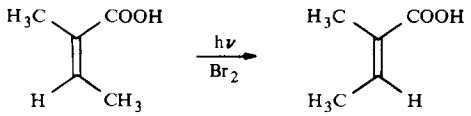
Liebermann's attempts to extend the iodine assisted photoisomerization to nonaromatic unsaturated acids did not meet with success.[65] However, *Wislicenus* (Fig. 12) achieved this interconversion. Irradiation in the presence of aqueous bromine converted isocrotonic into crotonic acid, angelic into tiglic acid (Scheme 9), and, most rapidly, maleic into fumaric acid.[79] Although *Wislicenus* is a minor contributor to the development of organic photochemistry, a few remarks about this scientist appear justifiable.

[*] "rearrangement with iodine in carbon disulfide... so characteristic for isocinnamic acid."



Fig. 12. *Johannes Wislicenus* (1835–1902), professor at Würzburg and Leipzig Universities, best known for his unsurpassed insight into stereochemical problems. His mechanism for the thermal (and light induced) isomerization of olefins is a classic of mechanistic chemistry.

Wislicenus is best known for his thorough understanding of structural and stereochemical problems. Even before the publications by *van't Hoff* and *LeBel* he had concluded: "Es muss nun unbedingt die Möglichkeit zugegeben werden, dass ... bei Körpern von *gleicher* Strukturformel ... doch noch Verschiedenheiten in gewissen Eigenschaften als Ergebnis von verschiedener *räumlicher* Anordnung der Atome ... auftreten können."[80][*]



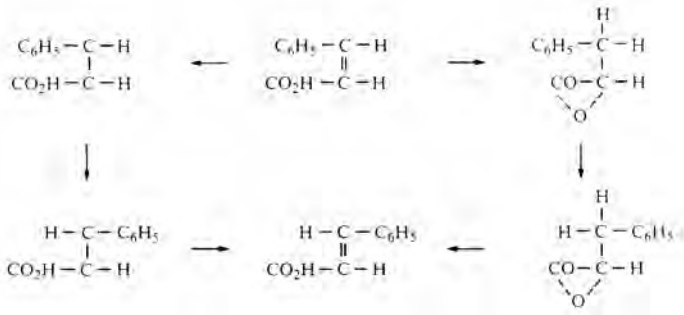
Scheme 9.

In his involvement in photochemistry he showed the same clarity of thought and the skill that characterize his entire work. He recognized that the halogen assisted reactions do not lead to a complete conversion into the more stable isomer, but that the reverse reaction could also occur, resulting in equilibrium mixtures.[79]

Wislicenus also appears to have had a superb understanding of mechanistic problems. He perceived the mechanism of heat (or light) induced geometric isomerization as follows: "dass durch die zugeführte Energie eine solche Lockerung der doppelten Bindungen eintrete, dass die vorher doppelt gebundenen Kohlenstoffatome vorübergehend dreiwerthig werden, in Folge dessen erst eine Wanderung von Atomgruppen, dann die Drehung, und hierauf ein erneuter Zusammenschluss der Kohlenstoffatome stattfinde."[81][**] To the mechanistic chemist of the 1980's this description may lack some details, but on the whole it is quite acceptable (Scheme 10).

[*] "If molecules can be structurally identical, yet possess dissimilar properties, the difference can be explained only by a different arrangement of the atoms in space."

[**] "The added energy causes a weakening of the double bond, so that the formerly doubly bonded carbon atoms become temporarily trivalent. This leads to a migration of groups, then to rotation, and then to renewed bonding of the carbon atoms."



Wislicenus, 1887 — *Liebermann*, 1890

Scheme 10.

Liebermann, on the other hand, considered this mechanism too complicated. As an alternative he proposed[78] "dass die durch die gesteigerte Energie veranlasste Lockerung der doppelten Bindung dazu führt, dass sie mit Hilfe des Carboxyls thatsächlich gelöst wird, indem dessen Wasserstoff an das eine, dessen frei gewordene Sauerstoffaffinität aber an das andere der vorher doppelt gebundenen Kohlenstoffatome tritt." ... "das innere Anhydrid" ... gibt - ... "dann Gelegenheit für die Drehung des Kohlenstoffatoms in die bevorzugte Lage und für die darauf erfolgende Rückbildung der Zimmtsäure."[*] Quite obviously, this alternative mechanism is of little but historical merit (Scheme 10).

7. Photoinduced Halogenations

In connection with the halogen induced geometric isomerizations of olefins it is of interest to mention briefly the light induced halogenation of aromatic hydrocarbons. These reactions were investigated[82–85] between 1884 and 1888 by *Julian Schramm* in Lvov, the center of eastern Galica, which was then a province of Poland.

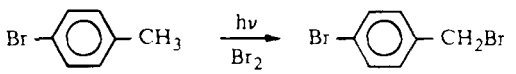
At the time it was recognized that the halogenation products of aromatic hydrocarbons varied with the reaction temperature: bromination of toluene yielded *o*- and *p*-bromotoluene in the cold, but benzyl bromide at elevated temperatures. *Schramm* systematically studied the light induced brominations of alkylbenzenes with normal and branched side chains. In the words of a contemporary reviewer "wirken ... Licht bezw. Finsterniss in derselben Richtung wie höhere bezw. niedere Temperatur."[**] *Schramm* found that direct sunlight or diffuse daylight caused side chain bromination even at low temperatures.[85]

Schramm apparently had a good knowledge of the chemical literature (which was a somewhat easier task in the 1880's than in the 1980's). He realized that *p*-bromobenzyl bromide had been isolated, though not recognized, as early as 1874 in the light induced bromination of toluene.[86] *Paul Jannasch*, in *Fittig*'s laboratory in Göttingen, tried to improve the poor yield of a dibromo derivative obtained from toluene. Ac-

[*] "... the increased energy causes the weakened double bond to be broken with the help of the carboxyl group, as its hydrogen adds to one and the freed oxygen affinity to the other carbon atom." ... "The resulting internal anhydride allows for rotation of the carbon atom into the preferred position and the regeneration of cinnamic acid."

[**] "... light and darkness work in the same way as elevated and low temperatures, respectively."

cordingly, he carried out the bromination "unter gleichzeitiger Einwirkung des directen Sonnenlichts bei Sommertemperatur."[*] In one of these experiments[86] he obtained crystals of m.p. 63 °C which *Schramm* recognized as *p*-bromobenzyl bromide (Scheme 11).



Scheme 11.

Schramm also foresaw the commercial potential of photohalogenations: "Hoffentlich wird die Methode geeignet auch zur fabrikmäßigen Darstellung der genannten Producte."[83][**] Eventually, this expectation became reality: photochlorinations have long been exploited commercially, although the reactions discovered by *Schramm* are not of industrial interest today.

8. *Heinrich Klinger*— the Photoreduction of Carbonyl Compounds

Aside from the dimerization of quinones, which is observed mainly in the solid state, photoreductions must be considered the principal light-induced reactions of quinones in solution. The credit for having observed and investigated the first reactions of this type belongs to *Heinrich Klinger*, who originated his work in *Kekule*'s institute in Bonn during an investigation of isobenzil, an assumed isomer of the long-known diketone. In an attempt to produce the supposed isomer from a solution of benzil in ether, he observed the slow precipitation of a crystalline material. However, this result was not always reproducible.[87, 88]

Among the pioneers of photochemistry, *Klinger* is the only one who relates the puzzled frustration of an experimental chemist dealing with an unknown variable and faced with seemingly irreproducible results. After "many time-consuming experiments" he finally noticed that "some of the tubes were exposed to direct sunlight in the morning hours".[88] He identified the crystals as a molecular complex of two moles of benzil with one mole of benzoin and concluded that "sunlight causes a partial reduction of benzil dissolved in wet ether".[88]

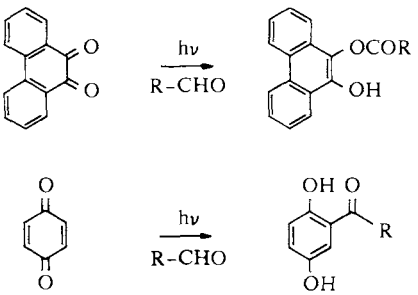
Having recognized the reducing action of sunlight on benzil, *Klinger* carried out analogous experiments with phenanthrenequinone with similar results (Scheme 12). He also began to investigate the role of the solvent and he reported the existence of preliminary results for benzoin, nitro compounds, several quinones, fuchsone, etc. *Klinger* first reported these results in preliminary form in *Sitzungsberichte der niederrheinischen Gesellschaft für Natur- und Heilkunde* in 1883 and 1885;[87] he formally published them in *Berichte* in 1886.[88] There is very little doubt that *Klinger* had priority over *Ciamician* (see Section 9), albeit by a narrow margin.



Scheme 12.

Two years later he reported an interesting extension of his work. When he replaced the ether by acetaldehyde "um dadurch die Arbeit des Sonnenlichts gleichsam zu erleichtern"...[*] he observed: "Die Wirkung des Lichts ist ... eine ganz eigenartige, synthetische, wie sie ... bisher nur in der lebenden Pflanze beobachtet wurde; ... als die beiden Substanzen sich zu einer Verbindung vereinigen, in welcher das Chinon als reducirt, der Aldehyd dagegen als oxydirt erscheint."[89][**] The product observed in this light-induced reaction, monoacetylphenanthrenehydroquinone, was indeed a new type of photoproduct.

Klinger extended the reaction to a series of aldehydes and ketones and also investigated alternative quinones. The reaction of benzoquinone with benzaldehyde proved to be particularly interesting.[90, 91] The product isolated in this reaction, 2-benzoylhydroquinone (or 2,5-dihydroxybenzophenone), established an interesting variation of the phenanthrenequinone derived product (Scheme 13). *Klinger* referred to these reactions as "Synthesen durch Sonnenlicht" (syntheses by sunlight); he must be considered the first to have exploited photochemical methods for synthetic purposes. He perceived these reactions as similar to the photosynthesis of the living plant.[90–92]



Scheme 13.

To probe this similarity further he investigated the wavelength dependence by using aqueous solutions of inorganic ions as filters, including cuprous ammonium sulfate and potassium dichromate solutions. He noted that the photochemical response of the quinones was most pronounced in the blue region, whereas green plants showed optimum response in the red region of the spectrum.[89]

Although the photoreactions discovered by *Klinger* give rise to products that appear to be widely different, it is clear that their formation is initiated by a common mechanism. The photoexcited quinone reacts with the various substrates by hydrogen abstraction, and the resulting radicals form the isolated products by recombination, disproportionation, or by free radical addition or abstraction.

Heinrich Konrad Klinger (1853–1945) studied in Leipzig and Bonn and received a doctorate in 1875 in Göttingen as

[*] "... at summer temperatures under simultaneous exposure to direct sunlight."

[**] "Hopefully, this method could prove suitable for the industrial preparation of these products."

[*] "... to facilitate the work of the sunlight."

[**] "The effect of light is a strange synthetic one ... with precedent only in the living plant ... as the two compounds are joined to form one, in which the quinone appears reduced but the acetaldehyde oxidized."

UEBER DIE

EINWIRKUNG VON PHOSPHORPENTACHLORID

AUF

PHENYLOXAMINSÄUREÄTHYLÄTHER

UND

PARATOLUYLOXAMINSÄUREÄTHYLÄTHER.

INAUGURAL-DISSERTATION

ZUR

ERLANGUNG DER PHILOSOPHISCHEN DOCTORWÜRDE

AN DER

UNIVERSITÄT GÖTTINGEN

VORGELEGT VON

HEINRICH CONRAD KLINGER

AUS

LEIPZIG

LEIPZIG,

DRUCK VON BREITKOPF UND HÄRTEL

1875.

Fig. 13. Title page of *Heinrich Klinger*'s thesis, Leipzig, 1875

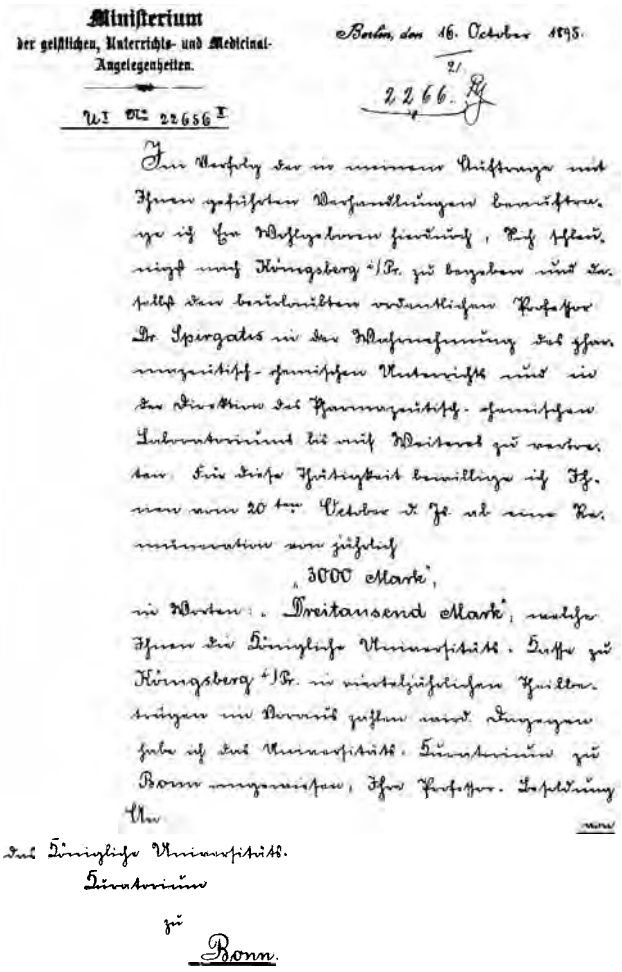
a student of *O. Wallach*. It is an interesting coincidence that *Klinger* received his doctorate (Fig. 13) in Göttingen in the same year in which *Jannasch*[86] published his light-induced experiments. We do not know whether *Klinger* knew of this work, whether he interacted with *Jannasch*, or even met him at all. He had carried out his thesis work in Bonn and received his degree in Göttingen only because his mentor had moved there.

Klinger returned to Bonn, where he rose to direct the pharmaceutical chemistry branch. In 1896 he accepted a call or, more correctly, followed a ministerial order to Königsberg (Fig. 14), where he served as director of the pharmaceutical laboratory and professor of chemistry. Following his retirement in 1922, he lived to the age of almost 92. He died on March 1, 1945 in East Prussia during the destructive climax of World War II.

9. *Ciamician* and *Silber*—an Early Episode

It was in *Cannizzaro*'s Istituto Chimico della Regia Universita in Rome that *Ciamician* and *Silber* were first introduced to photochemical reactions. It would have been hard to overlook an effort involving ... "one kilogram of santonin dissolved in 52 liters of acetic acid ... exposed to sunlight in several bottles".[40] Nevertheless, their interest was aroused only slowly. When they joined *Cannizzaro*'s group in 1881, they first focussed their attention on pyrrole chemistry. They produced a sizeable body of work, which earned *Ciamician* the Gold Medal of the Regia Accademia dei Lincei in 1887.

In the summer of 1885 *Ciamician* (Fig. 15) began some photochemical experiments[93, 94] and the following year *Silber* joined in the investigations.[95] *Ciamician* "insolated"


Ministerium
der geistlichen, Unterrichts- und Medicinal-Angelegenheiten.

Berlin, den 16. October 1895.

U I Nr. 22656 I

2266.

Ihr Gesuch vom 10. d. M. um Übertragung einer [illegible] Vertretung des [illegible] Professors Dr. Spirgatis in der Wahrnehmung [illegible] pharmaceutisch-chemischen Unterrichts und in der Direktion des pharmaceutisch-chemischen Laboratoriums bis auf Weiteres zu übertragen, [illegible] Ihre dieserhalb bewilligte Entschädigung [illegible] vom 20. October d. Js. ab eine Remuneration von jährlich

„3000 Mark",

in Worten: „Dreitausend Mark", [illegible] Ihnen die Königliche Universität [illegible] zu Königsberg i/Pr. in entsprechenden Quartalsraten [illegible] werden [illegible] Dagegen [illegible] die Universität [illegible] zu Bonn [illegible] Ihre Function [illegible]

Königliche Universität

Curatorium

zu

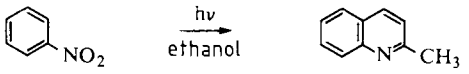
Bonn.

Fig. 14. Excerpt from the letter notifying *Klinger* of his reassignment to Königsberg. "Pursuant to negotiations carried out with you on my behalf you are ordered herewith to proceed to Königsberg i. Pr. with the utmost dispatch to substitute Professor Dr. *Spirgatus*, currently on leave of absence, in executing pharmaceutical chemistry instruction and in directing the Pharmaceutical Chemical Laboratory until further notice. For these services I grant you a remuneration of 3000 Mark annually, beginning October 20th ...".


Fig. 15. *Giacomo Ciamician* (1857–1922), during his early years in Bologna.

(exposed to sunlight) alcoholic solutions of benzoquinone. After five month's exposure he observed conversion into hydroquinone and acetaldehyde. The following year *Silber*

exposed an alcoholic solution of nitrobenzene. This reaction produced aniline and acetaldehyde, but the exceptionally skilled *Silber* also found evidence for the formation of 2-methylquinoline (quinaldine, Scheme 14).



Scheme 14.

These were interesting and promising results, and the two investigators must have had every intention to follow up these early findings. However, their first engagement in photochemical research was not destined to be of extended duration. The limitation of their initial efforts had its roots in the custom of nineteenth century chemistry that allowed a researcher to "reserve" a field for continued investigation. Most respectable scientists honored such a claim (chemistry has indeed come a long way in the last one hundred years).

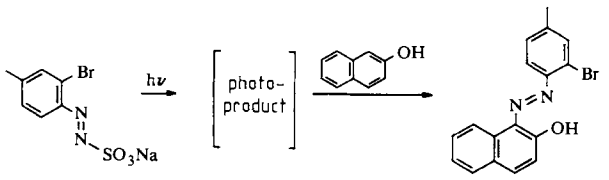
After reporting his first results in the *Rendi conti della Regia Accademia dei Lincei* on January 3, 1886,[93] *Ciamician* became aware of *Liebermann*'s 1885 publication.[60] He must have considered the potential overlap between *Liebermann*'s solid state photodimerization and his own photoreduction in solution and must have been satisfied that these two areas were sufficiently different. He rushed his work to publication in the *Gazzeta Chimica* "per acquistare il diritto di continuare le mie ricerche intraprese..."[*] even though he had not yet proven that the observed redox reaction was indeed a photoreaction ("That the conversion is indeed caused by light will be ensured by repeating the experiment in the dark").[94] However, before *Ciamician*'s *Gazzetta* paper was reviewed in *Berichte, Klinger*'s work on the reaction of phenanthrenequinone appeared, in which *Klinger* claimed this area of research for himself, including specifically the photoreduction of nitrobenzene.[88]

There is very little doubt that *Ciamician*'s experiments in Rome were carried out independent of *Klinger*'s studies in Bonn. The *Rendi conti* publication[93] appeared only a few months later than *Klinger*'s *Sitzungsbericht* of 1885.[87b] Nevertheless, *Ciamician* and *Silber* honored *Klinger*'s claim graciously. They sent a brief summary of their preliminary work to *Berichte;* it contained the previously missing control experiment for the benzoquinone photo-reduction and a brief account of the nitrobenzene reduction. They announced that, for the time being, they would not pursue the subject any further and concluded: "Wir sehen mit grossem Interesse den Resultaten der weiteren von Hrn. *Klinger* in Aussicht gestellten Untersuchungen entgegen."[95][**]

We do not know whether they took this action readily or whether they may have been persuaded by *Cannizzaro*, who had been elected to honorary membership in the Deutsche Chemische Gesellschaft in 1873. The fact remains that *Ciamician* and *Silber* did not publish another photochemical paper until fourteen years later. It also is obvious that *Ciamician* and *Silber*, having obeyed research etiquette themselves, expected similar consideration. Their major body of photochemical work in the early 1900's contains several quick rebuttals and some polemics, particularly against *Ciamician*'s compatriot *Paterno*.

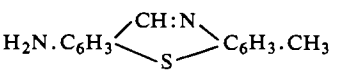
10. Photochemistry of Diazo and Diazonium Compounds

Because of their practical importance as photoresist materials and their significance as precursors for divalent-carbon species, it appears appropriate to discuss briefly the photoreactions of diazo compounds and of the somewhat related diazonium salts. This class of compounds became accessible through the pioneering studies of *Peter Griess* beginning in 1858.[96] Although it is not clear when their sensitivity to light was first noticed, attempts to utilize them for the purpose of imaging are documented as early as 1889. *Adolf Feer* noticed that irradiation of diazonium sulfonates, $R-N=N-SO_3Na$, in the presence of phenolates or arylamines led to the formation of azo dyes, presumably via the free diazonium ion. After a film containing these reagents was exposed, unreacted diazonium sulfonate could be removed by washing, leaving a colored negative (Scheme 15).[97]



Scheme 15.

Only a year later, *Green, Cross* and *Bevan* received a patent for a process generating a positive image based on the fact that irradiation converts the diazo compounds of "dehydrothiotoluidine" (primulin) into products incapable of coupling. After exposure, an image could be "developed" by converting the unreacted diazonium compound to an azo dye with an appropriate reagent (Scheme 16).[98]



Scheme 16.

It is indicative of the progress of photochemistry that in 1890 *Green* and colleagues no longer considered mere light sensitivity noteworthy. They were concerned with the practical exploitation of this property: "Von den zahlreichen Verbindungen, welche lichtempfindlich sind, erfüllen nur wenige die Bedingungen zur Erzeugung eines photographischen Bildes..."[98][*] Other imaging systems were proposed by *Andresen*,[99] *Schön*,[100] and *Ruff* and *Stein*.[101]

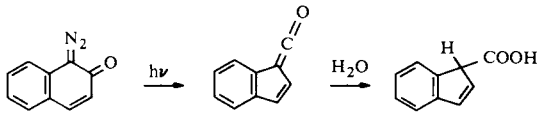
Diazoketones have been known since 1881 when *Schiff* prepared diazocamphor,[102] and by the turn of the century several such compounds were known.[103, 104] However, commercial application in diazo-type manufacture became possible only after *Kögel* and *Neuenhaus* had introduced ap-

[*] "... to ensure the unencumbered continuation of my research."

[**] "We are looking forward with great interest to the results of the further experiments delineated by *Klinger*."

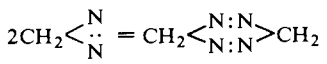
[*] "Among the many compounds that are light sensitive only a few meet the requirements for generating a photographic image..."

propriately substituted "naphthoquinone diazides" (1-diazonaphthalene-2(1*H*)-ones).[105] The nature of their photoproducts and the course of the reaction was elucidated by *Oscar Süs*,[106] who recognized that these materials undergo Wolff rearrangement with loss of nitrogen and ring contraction, generating a ketene. Reaction with adventitious water produces a carboxylic acid which can be removed by an alkaline wash (Scheme 17). The application of this photochemistry for positive photoresist materials has become a multimillion dollar industry.



Scheme 17.

Concerning other diazo compounds, despite their pronounced light sensitivity, their photoinduced decomposition was not discovered until early in the 20th century. Several diazo compounds were synthesized in the 1880's.[107–109] For example, ethyl diazoacetate was prepared by *Curtius* in 1883;[107] diazomethane was obtained by *von Pechmann* in 1894;[110] neither publication mentions any light-induced reactions.



Scheme 18.

The first reference to the irradiation of diazomethane appeared in 1901 when *Hantzsch* and *Lehmann* reported that the action of sunlight upon the diazo compound generates dihydrotetrazine (Scheme 18).[111] This interesting claim was corrected when *Curtius* et al. found only nitrogen, ethylene, and a very low yield of a greasy residue.[112] Although this paper must be considered an early report on poly(m)ethylene, it stimulated neither polymer nor carbene chemistry. We ascribe this fact to the lack of appreciation for the unique nature of divalent-carbon intermediates and to a failure to understand the relation between diazo compounds and carbenes.

11. Conclusion

At the end of the nineteenth century photochemistry was but a modest facet of the exciting and rapidly expanding science of chemistry. The principal contributors studied photochemical problems only as an aside to the work for which they were (and still are) best known. Only a limited number of reactions were known, and the sun was virtually the exclusive light source; its light was used unfocussed and unfiltered.

Only *Liebermann* experimented with alternative light sources, particularly with an arc lamp, a gas burner with a metal oxide mantle, and a magnesium flame; his results were far from promising.[65] *Trommsdorff* had evaluated the wavelength dependence of a photoreaction with the help of a prism;[30] *Perkin*[75] and *Klinger*[89] used filter solutions. *Perkin* also mentions an experiment in which "light was concentrated on..." a sample, an obvious reference to a focussing device.[75]

On the other hand, several of the general reaction types known today had been encountered. When *Liebermann* discovered the iodine mediated photoisomerization of olefins, he subjected a representative cross section of then known photoreactions to the newly found reaction conditions.[65] He surveyed three dimerizations and one rearrangement, but did not refer to abstraction or transfer reactions, such as those studied by *Klinger* and *Ciamician*; the fourth general reaction type, photocleavage, had yet to be discovered.

Organic photoreactions were being utilized for the purpose of imaging,[97–101] and *Klinger* et al.[89–91] and *Schramm*[85] had pointed out, respectively, the preparative and industrial prospects of photochemistry. All these facts suggest that the time was ripe for an outstanding scientist who would devote a major effort to organic photochemistry and establish it as a major scientific discipline.

With the advent of the twentieth century *Ciamician* (Fig. 16) and *Silber* began a systematic investigation of photochemical reactions. Their achievements far surpassed any

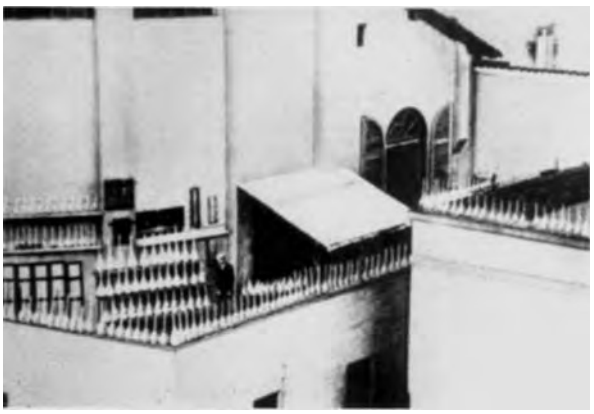


Fig. 16. *Ciamician* in his "laboratory", on the roof of the chemistry building in Bologna. The Dipartimento di Chimica "G. Ciamician" in the Via Selmi in Bologna is a fitting memorial to this pioneer of photochemistry.

previous effort and established photochemistry as a major branch of chemistry. In particular, they provided many examples of ketone photochemistry: in addition to photoreductions (vide supra) they discovered photopinacolization, intramolecular cycloadditions, and both α- and β-cleavage. These systems would later prove to be of great importance for the development of molecular photochemistry, as they revealed many fundamental principles, for example, the concepts of singlet and triplet as well as n,π* and π,π* states.

Ciamician and *Silber* reported their findings in two parallel series of thirty-seven publications entitled "Azione Chimiche della Luce" in *Gazzetta Chimica Italiana* and "Chemische Lichtwirkungen" in *Berichte der deutschen chemischen Gesellschaft*. These papers deal with an astonishing variety of systems and document unmatched skills in the separation of sometimes complex product mixtures, unprecedented understanding in the identification of the components, and unparalleled insight into the nature of photo-

chemical reactions. However, *Ciamician*'s crowning achievement was the truly astonishing lecture he delivered before the International Congress of Applied Chemistry in New York in 1912. Under the title "The Photochemistry of the Future" he summarized the status which photochemistry had attained in little more than a decade chiefly through his and *Silber*'s efforts and revealed his prediction of its future. He emphasized particularly the utilization of solar energy which he deemed second only to nuclear energy.[113] We note that *Ciamician* is not the first to have entertained the thought of solar energy conversion. *Swift* described *Gulliver*'s encounter with a Lagadoan academician "upon a project for extracting sunbeams out of cucumbers"[114] and *Goethe*'s Faust yearned for "Bäume, die sich ewig neu begrünen", a task, incidentally, which Mephisto thought achievable: "Ein solcher Auftrag schreckt mich nicht, mit solchen Schätzen kann ich dienen".[115] Of course, *Ciamician* was the first to put this dream on a rational basis. It is a testimony to *Ciamician*'s vision that more than three quarters of a century after his prophetic lecture the promise of harvesting solar energy has yet to be fulfilled.

The author is indebted to numerous colleagues for making available original literature and for stimulating discussions and helpful suggestions, especially Professor William Agosta, New York, Dr. E. A. Chandross, Murray Hill, NJ, Professor Arthur Greenberg, Newark, NJ, Professor Ned Heindel, Bethlehem, PA, Professors G. O. Schenck and K. Schaffner, Mülheim, and Ms. Thelma McCarthy, Philadelphia, PA. He also gratefully acknowledges the following for providing illustrations: Professor A. Greenberg for Figures 2 and 4; Professors F. Calderazzo, G. Lotti, and Mrs. M. G. Venditti for Figure 7; Professor W. Rettig, Berlin, for Figure 11; Dr. P. Schmidt, Archiv der Universität Bonn, for Figures 13 and 14; Professor N. D. Heindel for Figures 15 and 16. Figures 1, 3, 5, and 10 are reprinted from the collection of the author, and Figures 8, 9, 12 are reprinted courtesy of the E. F. Smith Memorial Collection, The Beckman Center for the History of Chemistry, University of Pennsylvania.

Received: October 3, 1988 [A 730 IE]
German version: *Angew. Chem. 101* (1989) 1220

[1] V. M. Canuto, J. S. Levine, T. R. Augustsson, C. L. Imhoff, M. S. Giampapa, *Nature (London) 305* (1983) 281–286.
[2] T. Owen, *Sci. Am. 246* (1982) (2) 98–109.
[3] J. P. Ferris, *Chem. Eng. News 62* (1984) (35) 22–35.
[4] H. D. Holland, B. Lazar, M. McCaffrey, *Nature (London) 320* (1986) 27–33.
[5] P. Cloud, *Am. J. Sci. 272* (1972) 537–548.
[6] L. Margulis, J. C. G. Walker, M. Rambler, *Nature (London) 264* (1976) 620–624.
[7] A. J. Blake, J. H. Carver, *J. Atmos. Sci. 34* (1977) 720–728.
[8] J. S. Levine, P. B. Hays, J. C. G. Walker, *Icarus 39* (1979) 295–309.
[9] C. S. Rupert, in A. C. Giese (Ed.): *Photophysiology, Vol. 2*, Academic Press, New York 1964, p. 283–327.
[10] D. S. Price, *J. Chem. Soc. 18* (1866) 245–249.
[11] O. Ney, *Biedermanns Zentralbl. 8* (1879) 152; quoted in *J. Chem. Soc. 38* (1880) 200.
[12] F. A. Abel, *J. Am. Chem. Soc. 20* (1867) 515–520.
[13] J. M. Beatty, *Trade Winds, Saturday Review*, 5. August 1961, p. 5; quoted by R. Dessauer, J. P. Paris, *Adv. Photochem. 1* (1963) 275–321.
[14] E. ter Meer, *Justus Liebigs Ann. Chem. 181* (1876) 1–22.
[15] C. Gesner: *The Practise of the New and Old Phisicke*, P. Short, London 1599, p. 23–24.
[16] J. French: *The Art of Distillation*, T. Williams, London 1653, p. 42.
[17] A. Libavius: *Alchymia*, 1608, reprinted in D. Diderot: *Encyclopedie*, 1766; cf. Gmelin-Institut (Ed.): *Die Alchemie des Andreas Libavius*, VCH Verlagsgesellschaft, Weinheim 1985.
[18] J. Priestley, quoted by A. Lavoisier, see [19], p. 520–521.
[19] A. Lavoisier, *Traite Elementaire de Chimie*, 1789, 2nd. edition, translated by R. Kerr, Edinburgh, 1793.
[20] a) J. Priestley: *Experiments and Observations on Different Kinds of Air*, T. Pearson, Birmingham 1790; b) see [20a], *Vol. III, Book VIII, Part I, Section XII*, p. 126–128.
[21] a) See [19], p. 9; b) see [20a], *Vol. III, Book IX, Part I, Section VII*, p. 293–305.
[22] J. Ingenhousz: *Experiments on Vegetables*, 1779.
[23] N. T. de Saussure, quoted in A. J. Ihde: *The Development of Modern Chemistry*, Harper & Row, New York 1964, p. 419–420.
[24] See [19], p. 253–254.
[25] J. F. Döbereiner, *Schweigger J. 62* (Jahr) (8) 90–96; see *Pharm. Centralbl. 2* (1831) 383–385.
[26] C. A. Parker, *Proc. R. Soc. (London) A 220* (1953) 104–116.
[27] C. G. Hatchard, C. A. Parker, *Proc. R. Soc. (London) A 235* (1956) 518–536.
[28] Kahler, *Arch. Pharm. 34* (1830) 318.
[29] Alms, *Arch. Pharm. 34* (1830) 319.
[30] H. Trommsdorff, *Ann. Chem. Pharm. 11* (1834) 190–208.
[31] W. Heldt, *Ann. Chem. Pharm. 63* (1847) 10–47.
[32] F. Sestini, *Bull. Soc. Chim. [2], 5* (1866) 202.
[33] S. Cannizzaro, F. Sestini, *Gazz. Chim. Ital. 3* (1873) 241–251.
[34] F. Sestini, *Gazz. Chim. Ital. 6* (1876) 357–369; this paper contains a reference to an earlier paper by F. Sestini; *Repert. Ital. Chim. Pharm.* (1865).
[35] F. Sestini, *Gazz. Chim. Ital. 9* (1879) 298–304.
[36] F. Sestini, L. Danesi, *Gazz. Chim. Ital. 12* (1882) 82–83.
[37] S. Cannizzaro, *Gazz. Chim. Ital. 6* (1876) 341–348.
[38] S. Cannizzaro, *Gazz. Chim. Ital. 6* (1876) 355–356.
[39] V. Villavecchia, *Ber. Dtsch. Chem. Ges. 18* (1885) 2859–2864.
[40] S. Cannizzaro, G. Fabris, *Ber. Dtsch. Chem. Ges. 19* (1886) 2260–2265.
[41] G. Struever, *Gazz. Chim. Ital. 6* (1876) 349–355.
[42] R. Nasini, *Gazz. Chim. Ital. 13* (1883) 375.
[43] S. Cannizzaro, P. Gucci, *Gazz. Chim. Ital. 23* (1893) 286–294.
[44] P. Gucci, G. Grassi-Cristaldi, *Atti R. Accad. Lincei Rend. II* (1891) 35–40; quoted in *Ber. Dtsch. Chem. Ges. 24* (1891) R 908–910.
[45] E. E. van Tamelen, S. H. Levin, G. Brenner, J. Wolinsky, P. Aldrich, *J. Am. Chem. Soc. 80* (1958) 501–502.
[46] E. E. van Tamelen, S. H. Levin, G. Brenner, J. Wolinsky, P. Aldrich, *J. Am. Chem. Soc. 81* (1959) 1666–1678.
[47] O. L. Chapman, L. F. Englert, *J. Am. Chem. Soc. 85* (1963) 3028–3029.
[48] M. H. Fisch, J. H. Richards, *J. Am. Chem. Soc. 85* (1963) 3029–3030.
[49] J. Fritzsche, *Petersb. Acad. Bull. 16* (1857) 150; reported in *Ann. Chem. Pharm. 104* (1859) 247–250.
[50] J. Fritzsche, *Petersb. Acad. Bull. 17* (1858), 68; reported in *Ann. Chem. Pharm. 104* (1859) 250–252.
[51] J. Fritzsche, *Bull. Acad. St. Petersbourg*; reported in *J. Prakt. Chemie 101* (1867) 333–343; see *Chem. Zentralbl. 38* (1867) 449–456.
[52] A. Butlerov, *Ber. Dtsch. Chem. Ges. 5* (1872) 132–136.
[53] a) C. Graebe, *Ann. Chem. Pharm. 158* (1871) 289; b) C. Liebermann, *ibid. 158* (1871) 305.
[54] K. Elbs, *J. Prakt. Chem. N.F. 44* (1891) 467–469.
[55] C. E. Linebarger, *Am. Chem. J. 14* (1892) 597–602.
[56] W. R. Orndorff, F. K. Cameron, *Am. Chem. J. 17* (1895) 658.
[57] M. Ehrenberg, *Acta Crystallogr. 20* (1966) 177.
[58] C. Liebermann, *Ann. Chem. Pharm. 158* (1871) 300.
[59] C. Liebermann, *Ber. Dtsch. Chem. Ges. 10* (1877) 2177–2179.
[60] C. Liebermann, M. Ilinski, *Ber. Dtsch. Chem. Ges. 18* (1885) 3193–3201.
[61] A. Breuer, T. Zincke, *Ber. Dtsch. Chem. Ges. 11* (1878) 1403–1407.
[62] A. Breuer, T. Zincke, *Ber. Dtsch. Chem. Ges. 13* (1880) 633–635.
[63] L. Rügheimer, M. Hankel, *Ber. Dtsch. Chem. Ges. 29* (1896) 2176–2185.
[64] C. Liebermann, *Ber. Dtsch. Chem. Ges. 28* (1895) 1438–1443.
[65] C. Liebermann, *Ber. Dtsch. Chem. Ges. 28* (1895) 1443–1448.
[66] J. Bertram, R. Kürsten, *J. Prakt. Chem. 51* (1895) 316–325; cf. *Ber. Dtsch. Chem. Ges. 28* (1895) R 386–387.
[67] C. N. Riiber, *Ber. Dtsch. Chem. Ges. 35* (1902) 2411–2415.
[68] C. N. Riiber, *Ber. Dtsch. Chem. Ges. 35* (1902) 2908–2909.
[69] G. Ciamician, P. Silber, *Ber. Dtsch. Ges. 35* (1902) 4128–4131.
[70] P. Jacobson, *Ber. Dtsch. Chem. Ges. 48* (1915) 4–5.
[71] O. Wallach, P. Jacobson, *Ber. Dtsch. Chem. Ges. 51* (1918) 1134–1204.
[72] J. W. Stadelhofer, H. Vierrath, O. P. Krätz, *Chem. Ind. (London) 1988*, 515–521.
[73] R. Meldola, *J. Chem. Soc. 93* (1908) 2214–2257; *Ber. Dtsch. Chem. Ges. 44* (1911) 911–956.
[74] R. Huisgen, *Angew. Chem. 98* (1986) 297–311; *Angew. Chem. Int. Ed. Engl. 25* (1986) 297–311.
[75] W. H. Perkin, *J. Chem. Soc. 39* (1881) 409–452.
[76] W. H. Perkin, *J. Chem. Soc. 41* (1882) 330.
[77] W. H. Perkin, *J. Chem. Soc. 45* (1884) 421–480.
[78] C. Liebermann, *Ber. Dtsch. Chem. Soc. 23* (1890) 2510–2515.
[79] J. Wislicenus, *Ber. Verh. K. Saechs. Ges. Wiss. Leipzig, Math. Phys. Kl. 1895*, 489–493; see *Ber. Dtsch. Chem. Ges. 29* (1896) R 1080.
[80] J. Wislicenus, *Justus Liebigs Ann. Chem. 166* (1873) 3–64, especially p. 47.

[81] J. Wislicenus, *Abh. K. Saechs. Ges. Wiss. Leipzig 1887*, 56, quoted by C. Liebermann in [78].
[82] J. Schramm, *Ber. Dtsch. Chem. Ges. 17* (1884) 2922–2925.
[83] J. Schramm, *Ber. Dtsch. Chem. Ges. 18* (1885) 350–355; 606–609; 1272–1279.
[84] J. Schramm, *Ber. Dtsch. Chem. Ges. 19* (1886) 212–218.
[85] J. Schramm, *Monatsh. Chem. 9* (1888) 842–853; see *Ber. Dtsch. Chem. Ges. 21* (1888) R 783–784; R 885–886.
[86] P. Jannasch, *Justus Liebigs Ann. Chem. 176* (1875) 283–290.
[87] a) H. Klinger, *Sitzungsber. Niederrhein. Ges. Natur Heilkde. 1883*, 224; b) *ibid. 1885*, 225.
[88] H. Klinger, *Ber. Dtsch. Chem. Ges. 19* (1886) 1862–1870.
[89] H. Klinger, *Justus Liebigs Ann. Chem. 249* (1888) 137–146.
[90] H. Klinger, O. Standke, *Ber. Dtsch. Chem. Ges. 24* (1891) 1340–1346.
[91] H. Klinger, W. Kolvenbach, *Ber. Dtsch. Chem. Ges. 31* (1898) 1214–1216.
[92] H. Klinger, *Justus Liebigs Ann. Chem. 382* (1911) 211–221.
[93] G. Ciamician, *Rendi Conti R. Accad. Naz. Lincei 1886*, 22–23.
[94] G. Ciamician, *Gazz. Chim. Ital. 16* (1886) 111–112; reported in *Ber. Dtsch. Chem. Ges. 19* (1886) R 551.
[95] G. Ciamician, P. Silber, *Ber. Dtsch. Chem. Ges. 19* (1886) 2899–2900.
[96] P. Griess, *Justus Liebigs Ann. Chem. 106* (1858) 123–125.
[97] A. Feer, DRP 53455 (1889).
[98] A. G. Green, C. F. Cross, E. J. Bevan, *Ber. Dtsch. Chem. Ges. 23* (1890) 3131–3133; DRP 56606 (1890).
[99] M. Andresen, *Photogr. Korresp. 32* (1895) 284.
[100] M. Schön, DRP 111416 (1899).
[101] O. Ruff, V. Stein, *Ber. Dtsch. Chem. Ges. 34* (1901) 1668–1681.
[102] R. Schiff, *Ber. Dtsch. Chem. Ges. 14* (1881) 1375–1377; *Gazz. Chim. Ital. 11* (1881) 171–173.
[103] A. Angeli, *Ber. Dtsch. Chem. Ges. 26* (1893) 1715–1719.
[104] A. Angeli, *Ber. Dtsch. Chem. Ges. 27* (1894) 590.
[105] G. Kögel, H. Neuenhaus, *Z. Wiss. Photogr. Photophys. Photochem. 24* (1926) 171; DRP 376385 (1917).
[106] O. Süs, *Justus Liebigs Ann. Chem. 556* (1944) 65–84; 85–90.
[107] T. Curtius, *Ber. Dtsch. Chem. Ges. 16* (1883) 2230–2231.
[108] T. Curtius, *Ber. Dtsch. Chem. Ges. 17* (1884) 953–959.
[109] T. Curtius, *Ber. Dtsch. Chem. Ges. 18* (1885) 1302–1304.
[110] H. vom Pechmann, *Ber. Dtsch. Chem. Ges. 27* (1894) 1888–1895.
[111] A. Hantzsch, M. Lehmann, *Ber. Dtsch. Chem. Ges. 34* (1901) 2506–2523.
[112] T. Curtius, A. Darapsky, E. Müller, *Ber. Dtsch. Chem. Ges. 41* (1908) 3161–3172.
[113] G. Ciamician, *Science 36* (Washington, D.C.) (1912) 385–394.
[114] J. Swift: Voyage to Laputa in *Gulliver's Travels*, Benjamin Motte, London 1726.
[115] J. W. von Goethe: Studierzimmer in *Faust I*, Cotta, Leipzig 1808.

Single-Source III/V Precursors: A New Approach to Gallium Arsenide and Related Semiconductors

By Alan H. Cowley* and Richard A. Jones*

Until recently, the production of gallium arsenide, indium phosphide, and related compound semiconductors has fallen in the domain of the materials scientist and the electrical engineer. By clever use of classical chemistry, exemplified by the thermal reaction of Me_3Ga and AsH_3, it is possible to make semiconductors on a commercial scale. However, there are some drawbacks associated with the existing methodology, including the environmental and health hazards of handling pyrophoric and toxic starting materials as well as stoichiometry control problems and undesirable side reactions. Can the synthetic inorganic and organometallic chemist play a useful role in this important area by designing and developing new reagents for the production of semiconductor materials? We believe the answer is yes, and in this article we discuss a new approach to the preparation of GaAs and InP thin films based on single-source precursors. These compounds feature strong σ-bonding between the group III and V elements, together with substituents that are capable of facile thermal elimination. The III/V precursors are more stable toward air and moisture and considerably less toxic than either adducts or mixtures of group III and V compounds.

1. Introduction

Group III/V semiconductors[1] have received much attention due to their usefulness in high-speed digital circuits, microwave devices, and optoelectronics. Several techniques have been employed for the preparation of thin films of these materials, including organometallic chemical vapor deposition (OMCVD) and molecular beam epitaxy (MBE).[2] The OMCVD method is often preferred for larger scale processes and typically involves the reaction of a group III trialkyl such as Me_3Ga with a group V hydride such as AsH_3 or PH_3 at elevated temperatures (600–700 °C).[3] A carrier gas such as H_2, He, or N_2 is used to sweep the volatile species through the reaction chamber. The most studied reaction is that of Me_3Ga and AsH_3 to produce GaAs [Eq. (a)].

$$Me_3Ga + AsH_3 \rightarrow GaAs + 3\,CH_4 \qquad (a)$$

There are a number of important disadvantages to the conventional OMCVD method. Alkyls of the group III elements tend to be pyrophoric and group V hydrides such as AsH_3 are extremely toxic. Apart from the potential environmental, safety, and health hazards of handling these reagents, the conventional OMCVD methodology also suffers from several other drawbacks. The high reactivity of these compounds makes them difficult to purify and handle and, once purified, they tend to react with their storage containers, thereby introducing new contaminants.[4] Other problems include carbon incorporation[5] and the difficulty in maintaining the desired film stoichiometry when growing ternary and quaternary compounds. The production of nonvolatile species via reagent prereactions has also proved to be a difficulty in the growth of InP, although this problem seems to have been overcome recently by the use of higher purity reagents.[6] Finally, the high temperatures involved in some OMCVD processes can promote interdiffusion of layers and dopants which prevents sharp heterojunctions from being achieved.

Attempts to grow superior films by modifications of the conventional OMCVD process include low-pressure,[7] plasma-enhanced,[8] and rapid thermal OMCVD systems[9] as well as hybrid MBE-OMCVD systems.[10] Several groups of workers have investigated the use of alternative sources of both the group III and group V components. Group V sources that have been investigated include Me_3P, Et_3P, $tBuPH_2$,[11] $tBuAsH_2$,[12] and Et_2AsH.[13] Group III alkyls have generally been limited to trimethyl and triethyl derivatives.[14]

The use of group III adducts has also been explored, both as direct replacements of the group III alkyls and as high-purity sources of the latter.[15] Adducts such as $Me_3In \cdot PEt_3$, for example, are less air sensitive than their components and are correspondingly easier to handle and purify.[4] A further advantage of the use of adducts is that troublesome prereactions tend to be avoided.[6] However, the donor–acceptor bonds in the adducts are generally considered to be weaker than the other bonds present (such as Ga-C or As-H).[16] As a consequence, dissociation of the adduct can occur and, typically, an excess of PH_3 or AsH_3 is necessary for the production of satisfactory III/V films.

It occurred to us that some of the problems outlined above might be overcome by the use of single-source III/V precursors of the general type $(L_nMEL'_n)_x$ which feature the desired 1:1 stoichiometry of the group III (M) and group V (E) elements. Our strategy was to cause the M–E bonds to be as strong as, or stronger than, the other bonds in the cluster by employing two-center, two-electron (σ) bonds rather than the donor–acceptor linkages found in adducts. We also sought ligands, L and L′, which are capable of facile hydrocarbon elimination. This review describes the progress which has been made with this approach.

[*] Prof. A. H. Cowley, Prof. R. A. Jones
Department of Chemistry
The University of Texas at Austin
Austin, TX 78712 (USA)

 © VCH Verlagsgesellschaft mbH, D-6940 Weinheim, 1989 0570-0833/89/0909-1208 $ 02.50/0

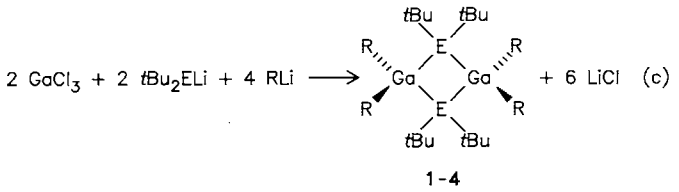
2. Synthesis of Precursors

Although this article is concerned with the heavier group III elements Ga and In, it is appropriate to mention that the trimer $[Me_2AlPMe_2]_3$ was prepared almost 50 years ago via the thermal reaction of Me_6Al_2 with Me_2PH.[17, 18] In the 1960s *Coates* et al.[19, 20] employed this alkane elimination method to prepare similar gallium and indium derivatives [Eq. (b); M = Ga, In; E = P, As; R = Me, Ph]. The aryl

$$Me_3M + R_2EH \longrightarrow \tfrac{1}{n}(Me_2MER_2)_n + CH_4 \qquad (b)$$

compounds (R = Ph) were reported to be dimeric (n = 2), while the corresponding alkyl compounds were polymeric glasses in the condensed phase, but trimeric in solution. The analogous reactions of Me_3M with primary phosphanes and arsanes afforded nonvolatile polymers.

Our initial approach to 1:1 precursor formation was to treat $GaCl_3$ with one equivalent of tBu_2ELi (E = P, As) and two equivalents of RLi (R = Me, *n*Bu) in toluene or THF solution at −78 °C [Eq. (c); salt elimination].[21] Subsequently, this method has been extended to the synthesis of the corresponding indium compounds.[22, 23]



1-4

A wide range of 1:1 precursors has now been prepared using both salt and alkane elimination methods (Table 1). As first noted by *Wells* et al.,[29] the alkane elimination method becomes very sluggish and therefore impractical when the steric bulk of the substituents increases. In such cases, silyl halide elimination methods can be very useful (Table 1). In

Table 1. III/V compounds with 1:1 stoichiometry.

Compound	Method of preparation [a]	Ref.
$[Me_2GaPMe_2]_n$	A	[20]
$[Me_2GaPEt_2]_n$	A	[20]
$[Et_2GaPEt_2]_3$	A	[24]
$[Me_2GaPPh_2]_2$	A	[19]
$[Me_2GaPtBu_2]_2$ **1**	A, B, D	[21, 22]
$[tBu_2GaPH_2]_3$ **24**	A	[25]
$[nBu_2GaPtBu_2]_2$ **2**	B	[21]
$[tBu_2GaP(H)C_5H_9]_2$ **18**	B	[26]
$[tBu_2GaP(H)tBu]_2$ **19**	A	[25]
$[(Me_3SiCH_2)_2GaPPh_2]_2$ **29**	A, B	[27]
$[Me_2GaAsMe_2]_n$	A	[20]
$[Me_2GaAsPh_2]_2$	A	[19]
$[Me_2GaAsiPr_2]_3$ **25**	A	[28]
$[tBu_2GaAsH_2]_3$ **34**	A	[25]
$[Cl_2GaAs(CH_2SiMe_3)_2]_3$	C	[29]
$[Me_2GaAs(Mesityl)_2]_n$	B	[30]
$[Cl_2GaAs(Mesityl)_2]_n$	B, C	[29, 30]
$[Me(Cl)GaAs(CH_2SiMe_3)_2]_{2,3}$ **17**	C	[31]
$[Ph(Cl)GaAs(CH_2SiMe_3)_2]_{2,3}$	C	[31]
$[Br_2GaAs(CH_2SiMe_3)_2]_3$ **26**	C	[31]
$[Ph_2GaAs(CH_2SiMe_3)_2]_2$ **20**	A	[32]
$[Me_2GaAstBu_2]_2$ **3**	A, B, D	[21, 22]
$[Et_2GaAstBu_2]_2$ **8**	D	[33]
$[nBu_2GaAstBu_2]_2$ **4**	B	[21]
$(Me_5C_5)_2GaAs(SiMe_3)_2$ **16**	B	[34]
$[Cl_2GaSbtBu_2]_3$ **7**	C	[35]
$[Me_2GaSbtBu_2]_3$ **27**	B, C	[36]
$[Me_2InPMe_2]_3$	A	[20]
$[Me_2InPEt_2]_3$	A	[20]
$[Me_2InPPh_2]_2$	A	[19]
$[Et_2InPEt_2]_3$	A	[24]
$[Me_2InPtBu_2]_2$ **5**	A, B, D	[21–23]
$[nBu_2InPtBu_2]_2$ **6**	B	[21]
$[(Me_3SiCH_2)_2InPPh_2]_2$ **23**	A, B	[27]
$[(Me_3CCH_2)_2InPPh_2]_2$ **30**	A, B	[27]
$[Me_2InAsMe_2]_3$ **28**	A	[20]
$[Me_2InAsPh_2]_2$	A	[19]

[a] A, alkane or arene elimination; B, salt elimination; C, silyl halide elimination; D, $M(EtBu_2)_3 + R_3M$.

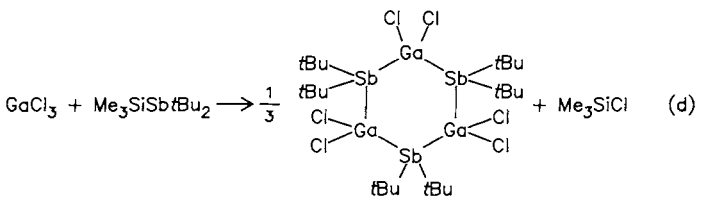




Alan H. Cowley was born in Manchester, England, in 1934. His formal education was obtained at the University of Manchester, where he received the Doctor of Philosophy in 1958. He was a Postdoctoral Fellow at the University of Florida during the period 1958–1960, and from 1962 to 1988 he was professor at The University of Texas at Austin. In 1988 and 1989 he was the Sir Edward Frankland Professor of Inorganic Chemistry at Imperial College, London. Effective September 1, 1989, he has been appointed to the Robert A. Welch Chair of Chemistry at The University of Texas at Austin. Alan Cowley has received several awards, including the Royal Society of Chemistry Award for Main-Group Element Chemistry (1980), the Centenary Medal and Lectureship of the Royal Society of Chemistry (1986), and the American Chemical Society Southwest Regional Award (1986). He was elected a Fellow of the Royal Society in 1988 and serves on the editorial boards of many journals.

Richard A. Jones was born in Abingdon, England in 1954. His university education was at the Imperial College of Science and Technology, London, where he received the Doctor of Philosophy in 1978 (supervisor Professor Sir Geoffrey Wilkinson). He joined the University of Texas at Austin in 1980 and was appointed to Full Professor in 1988. He received the 1983 Meldola Medal and Prize (awarded by the Royal Society of Chemistry in concurrence with the Society of Maccabaeans). He has authored and co-authored over 110 publications in transition-metal and main-group organometallic and coordination chemistry.

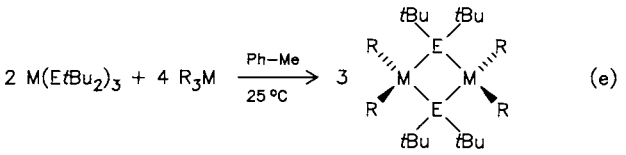
our own work we have found that the silyl elimination is preferable to salt elimination for the synthesis of antimony-containing complexes [Eq. (d)].[35] An alternative and novel



(d)

7

method for the synthesis of alkylated derivatives involves comproportionation of the $M(EtBu_2)_3$ unit accompanied by alkyl group transfer from R_3M [Eq. (e)].[22] Interestingly,



(e)

1, 3, 5, 8

the reaction of $M(EtBu_2)_3$ with less than two equivalents of R_3M leads only to mixtures of $[R_2M(\mu\text{-}EtBu_2)]_2$ and unreacted $M(EtBu_2)_3$.

Thus far, only four compounds of 1:2 stoichiometry have been prepared using either salt or silyl halide elimination methods (Table 2). Compound **9** is noteworthy since it is the first antimonido derivative of In^{III}.[37] The anion of the salt $[V_2(\mu\text{-}Cl)_3(thf)_6][Ga(PtBu_2)_2Cl_2]$ also features a 1:2 stoichiometry. This compound results from the reaction of $Ga(PtBu_2)_3$ with VCl_3 in THF solution.[38]

Table 2. III/V compounds with 1:2, 1:3, and other stoichiometries.

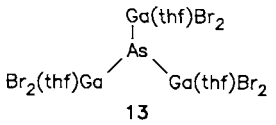
Compound	Method of preparation [a]	Ref.
1:2 stoichiometry		
$[ClGa\{As(Mesityl)_2\}_2]_n$	B, C	[29, 30]
$[ClGa\{As(CH_2SiMe_3)_2\}_2]_2$ **33**	C	[29]
$[BrGa\{As(CH_2SiMe_3)_2\}_2]_2$ **21**	C	[31]
$[ClIn(SbtBu_2)_2]_2$ **9**	C	[37]
1:3 stoichiometry		
$Ga(PtBu_2)_3$ **31**	A	[21, 22]
$Ga[P(H)(2,4,6\text{-}tBu_3C_6H_2)]_3$	B	[21]
$Ga(AstBu_2)_3$	B	[21, 22]
$Ga[As(Mesityl)_2]_3$ **15**	C	[29, 30]
$[Ga\{As(CH_2SiMe_3)_2\}_3]_2$ **22**	B	[39]
$In(PtBu_2)_3$ **32**	B	[21, 22]
$In(AstBu_2)_3$	B	[21, 22]
Other stoichiometries		
$[(PhAsH)(R_2Ga)(PhAs)_6(RGa)_4]$ **14**	A	[40]
$[Li(thf)_4][Ga(PPh_2)_4]$ **10**	B	[41]
$[Li(thf)_4][Ga(AsPh_2)_4]$ **11**	B	[41]
$[Li(thf)_4][In(PPh_2)_4]$ **12**	B	[41]
$[(thf)Br_2Ga]_3As$ **13**	C	[43]

[a] A, alkane elimination; B, salt elimination; C, silyl halide elimination.

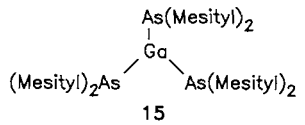
Complexes of 1:3 stoichiometry have been prepared either by salt elimination or silyl halide elimination methods (Table 2). Steric effects play a role of obvious importance because the reaction of Ph_2ELi with MCl_3 in 3:1 stoichiometry results only in intractable, apparently oligomeric, materials.[41] Interestingly, however, treatment of MCl_3 with Ph_2ELi in 1:4 stoichiometry affords the "ate" complexes **10**–**12**.[41] By contrast, it is not possible to make the corresponding "ate" complexes using the bulkier $EtBu_2$ ligands. As pointed out above, the complexes of 1:3 stoichiometry, $M(EtBu_2)_3$, are useful for synthesizing 1:1 complexes by treatment with R_3M. Such a method is also applicable to the synthesis of all six mixed metal dimers in the series $Me_2M(\mu\text{-}EtBu_2)_2M'Me_2$ (M, M' = Al, Ga, In; E = P, As) as well as heterodinuclear ethyl derivatives from Et_3Al.[42] The sole example of a 3:1 stoichiometry complex, **13**, was isolated from the reaction of $(Me_3Si)_3As$ with $GaBr_3$.[43] Finally, mention should be made of the novel complex **14** ($R = Me_3SiCH_2$), which was synthesized via the reaction of $PhAsH_2$ with $(Me_3SiCH_2)_3Ga$.[40]

3. Structural Studies

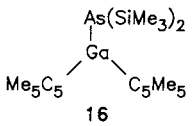
Three monomers (**13**, **15**, and **16**) have been investigated by X-ray crystallography. As expected on the basis of simple electron counting procedures, **15** and **16** exhibit approximately trigonal-planar and tetrahedral geometries at Ga and



13



15



16

As, respectively.[30, 34] Note, however, that in **15** the Ga atom is located 0.149 Å out of the As_3 plane; moreover, the geometries at the As centers depart considerably from the ideal as reflected by the wide range of Ga–As–C angles (93.1(1) to 122.1(1)°). The Ga–As bond length in **16** (2.433(4) Å) and the average Ga–As bond length in **15** (2.492(1) Å) are close to the sum of the covalent radii for Ga and As (2.46 Å).[44] In **16** the conformation is such that the As lone pair lies in the mirror plane defined by the Ga and the atoms bonded directly to it, thus obviating the possibility of As–Ga dative π-bonding. In **15** the dihedral angles between the As_3 plane and the As lone pair range from 52 to 86°, and the overall conformation corresponds to that of a staggered propeller blade arrangement. The arsenic-centered monomer **13** lies on a crystallographic C_3 axis and involves a pyramidal Ga_3As skeleton with a Ga–As–Ga bond angle of 94.4(1)° and a rather short Ga–As bond length of 2.401(4) Å.[43] The geometry at each gallium is distorted tetrahedral due to coordination of a molecule of THF.

Perusal of Table 1 reveals that compounds of empirical formula RR'MER"R'" with substituents of modest size are trimeric. Increasing the steric demands of the substituents results in dimer formation. Some compounds "on the borderline" such as **17** exhibit dimer/trimer equilibria.[31]

The available structural data for dimeric compounds are summarized in Table 3 and the structure of **3**, a typical example, is illustrated in Figure 1. Both the group III and the group V atoms adopt approximately tetrahedral geometries, consistent with a mixture of canonical forms **A** and **B**. With the exception of **22**, a weakly bonded dimer,[39] the central M_2E_2 ring is planar or nearly so. Indeed, in many of the structures the planarity of the M_2E_2 ring is imposed crystallographically. The puckered Ga_2As_2 ring of **22** resembles the Ga_2S_2 ring of the bulky thiolate complex $(i\text{PrSGaI}_2)_2$.[45] However, the fold angle along the Ga–Ga vector is considerably less in **22** than in the sulfur compound (13.6 vs. 36.7°).[39] In all the dimeric structures the endocyclic bond angle at E is larger than that at M and, typically, there are two sets of M–E bond lengths. The M ··· M and E ··· E distances are sufficiently long to preclude any cross-ring bonding interactions. The average endocyclic M–E bond lengths are somewhat longer than those found in the corresponding monomeric derivatives. This is attributable to changing the hydridization of Ga from sp^3 in the dimers to sp^2 in the monomers and/or to the possibility of dative E → M π-bonding in the latter. In a similar context, note that some of the compounds in Table 3 (e.g., **21** and **22**) feature exocyclic M–E bonds (Fig. 2) and that such bonds are always shorter than those within the M_2E_2 rings.

Table 3. Summary of structural data for the dimers $(RR'MER''R''')_2$. The average values of the bond lengths [Å] and bond angles [°] are given.

Compound	M-E	< MEM	< EME	< RMR'	< R"ER'"	Ref.
1	2.474(5)	93.5(1)	86.5(1)	106.3(5)	111.1(5)	[21]
2	2.476(5)	93.3(2)	86.7(2)	107.0(6)	109.5(7)	[21]
18 [a]	2.451(1)	98.24(3)	81.76(3)	121.0(2)	–	[26]
19	2.459(2)	101.2(1)	78.79(7)	120.1(3)	–	[25]
3	2.549(1)	95.69(2)	84.31(2)	109.3(3)	110.3(2)	[21]
8	2.544(6)	95.48(3)	84.52(2)	111.3(4)	115.5(3)	[33]
4	2.552(3)	95.07(8)	84.92(8)	110.9(7)	109.0(7)	[21]
$[(Me_3SiCH_2)_2GaAs\textit{t}Bu_2]_2$	2.589(1)	97.11(3)	82.89(3)	114.7(4)	108.8(3)	
20	2.524(1)	94.92(2)	85.08(2)	120.8(2)	104.4(2)	[32]
21 [a]	2.517(1)	95.63(2)	84.37(2)	104.3(2)	112.60(3)	[31]
22	2.555(4)	95.29(4)	83.81(4)	118.02(5)	103.8(4)	[3]
$[ClGa(Sb\textit{t}Bu_2)_2]_2$ [a]	2.831(1)	94.93(2)	85.07(2)			[37]
23	2.649(2)	97.48(8)	82.51(7)	126.8(3)	104.6(3)	[27]

[a] *anti*-isomer.

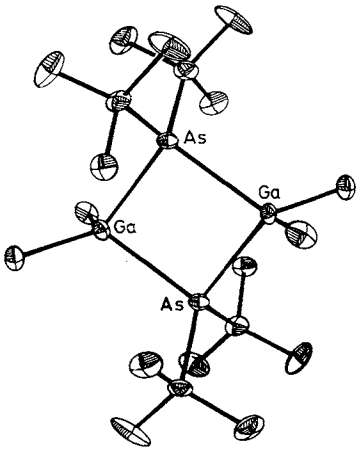
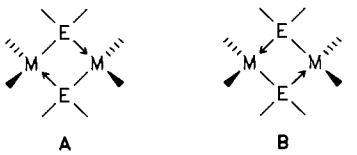


Fig. 1. Crystal structure of $[Me_2GaAs(\textit{t}Bu)_2]_2$ **3**.



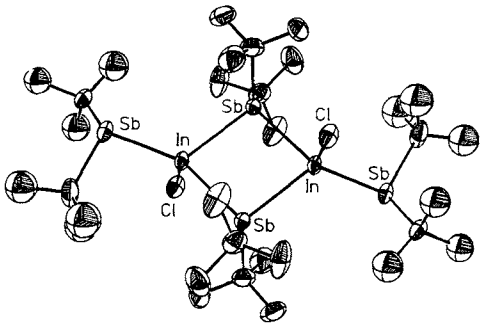


Fig. 2. Crystal structure of $[ClIn(Sb\textit{t}Bu_2)_2]_2$ **9**.

Steric effects are manifested in substantial changes in the exocyclic RMR' and R"ER'" angles. In fact, the M_2E_2 ring angles are remarkably constant. In cases where there is a choice between a bridging halide or a bridging R"R'"E moiety, the latter is always favored. The use of models indicates that this preference, together with the mutually *trans* disposition of the exocyclic R"R'"E groups, results from the minimization of steric repulsions.

It is apparent from Table 4 that several conformations of the six-membered M_3E_3 rings are close in energy. The case of

Table 4. Summary of structural data for the trimers $(R_2MER'_2)_3$. The average values of the bond lengths [Å] and bond angles [°] are given.

Compound	Conformation	M-E	< MEM	< EME	< RMR	< R'ER'	Ref.
24	planar	2.439(3)	138.5(4)	101.5(3)	122.0(7)	99.0(1) [a]	[25]
25	boat	2.517(2)	123.30(6)	105.71(6)	115.0(6)	100.6(5)	[28]
26	twist boat [b]	2.450(2)	106.67(7)	117.40(8)	112.29(9)	108.4(5)	[31]
27	twist boat	2.720(2)	121.74(5)	106.37(5)	115.8(7)	104.3(5)	[36]
7	irregular boat	2.661(2)	112.11(9)	118.6(1)	108.0(4)	110.0(1)	[35]
28	planar [c]	2.679(2)	134.26(8)	105.18(7)	123.0(1)	99.0(1)	[35]
	puckered [c]	2.669(2)	124.69(9)	96.86(8)	124.0(1)	100.0(1)	[35]
$[Me_2InSb\textit{t}Bu_2]_3$	twist boat	2.855(2)	121.64(6)	106.95(5)	117.0(1)	107.1(8)	[36]

[a] Calculated from IR data. [b] Two crystallographically independent molecules. [c] Planar and puckered froms present in same asymmetric unit.

28 is particularly interesting because of the presence of two independent conformations in the same asymmetric unit (Fig. 3).[35] One molecule adopts an approximately planar conformation, the deviations from the least-squares In_3As_3

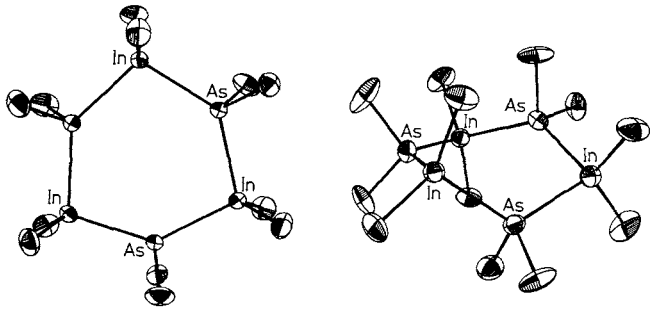


Fig. 3. Crystal structure of $[Me_2InAsMe_2]_3$. The planar conformer is shown on the left and the puckered conformer on the right.

plane ranging from 0.097(4) to −0.139(3) Å. The other molecule possesses a puckered six-membered ring. The three In atoms and one of the As atoms are virtually coplanar and the two remaining As atoms are located above and below this plane by 1.037(4) and 1.252(3) Å. Interestingly, the overall geometry of the puckered In_3As_3 core resembles those of some d-block phosphido derivatives such as $[Co\{\mu\text{-}P(C_6H_{11})_2\}(CO)_2]$.[46]

As expected on the basis of conformational flexibility, there is a wide variation in the endocyclic MEM and EME angles (Table 4). The average M–E bond lengths for the trimers are shorter than those of the corresponding dimers. In addition to the relief of steric strain in passing from the dimer to the trimer (i.e., bulky substituents lead to dimer formation), electronic effects also appear to be important. Comparing **27** and **7** (both trimers), we note that the Ga–Sb bond is longer in **27**. We attribute this to the greater electronegativity of Cl, which causes the Ga atomic radius to be smaller. Thus, the Cl and Me ligands are approximately the same size, yet the average Ga–Sb bond length in **27** is ca. 0.06 Å longer than that in **7**. Finally, we note that the In–As and In–Sb distances in Table 4 are the first such bond lengths other than those in InAs and InSb.[47]

Two further structural types have been investigated. The structures of the salts **10**–**12**[41] are of interest because GaP, GaAs, InP, and InAs all feature tetracoordinate structures of the zinc blende type.[47] The "ate" anions possess approximately tetrahedral geometries at the M and E centers (Fig. 4); however, the EME angles, for example, range from 97.3(1) to 116.0(1)°. Although the overall symmetry of these anions is C_1, in each case three of the four EPh_2 groups are related approximately by a C_3 axis. The relatively unsymmetrical structures of the $[M(EPh_2)_4]^{\ominus}$ ions contrast with those of the tetraamide and tetraphosphide transition-metal derivatives (D_{2d} skeletal symmetry).[48] The average M–E bond lengths of the group III/V anions are shorter than those of the neutral dimers (Table 3) but slightly longer than those found in GaP (2.360 Å),[47] GaAs (2.448 Å),[47] or InP (2.541 Å).[47] The structure of the "ate" complex $[V_2(\mu\text{-}Cl)_3(thf)_6][Ga(PtBu_2)_2Cl_2]$ has also been determined.[38]

The structure of the cluster **14** (R = Me_3SiCH_2) involves two nonplanar Ga_2As_3 rings.[40] These rings are linked by

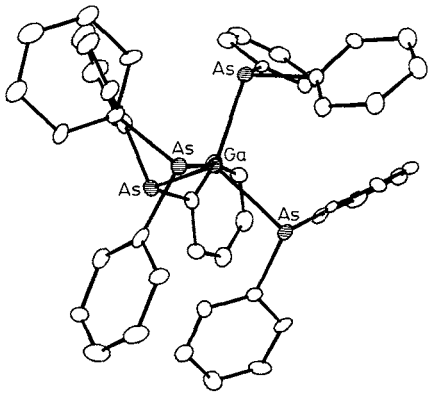


Fig. 4. View of the anion of **11** in the crystal.

two Ga–As bonds and bridged by a Ga–As unit. The average Ga–As bond length of 2.503 Å lies between the ranges found for monomeric and dimeric derivatives.

4. Spectroscopic Aspects

NMR studies have been particularly useful for discerning the structures of the III/V precursors in solution. For example, although X-ray crystallography indicates a *trans* solid-state structure for $[tBu_2GaP(H)C_5H_9]_2$ **18**, two resonances are apparent in the ^{31}P NMR spectrum at 25 °C.[26] Although specific assignments were not made, these signals were attributed to the presence of *cis* and *trans* isomers (Table 5). In the case of **21**, it was possible to assign these

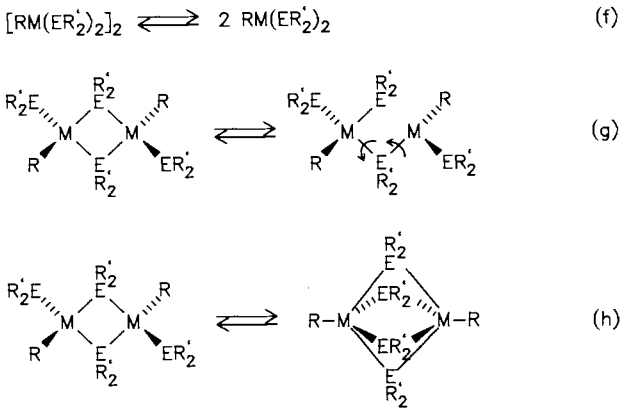
Table 5. ^{31}P NMR data.

Compound	δ	Ref.
$[Me_2GaPtBu_2]_2$ **1**	+ 28.41	[21, 22]
$[nBu_2GaPtBu_2]_2$ **2**	+ 32.9	[21]
$[Me_2InPtBu_2]_2$ **5**	+ 39.24	[21, 22]
$[tBu_2GaP(H)C_5H_9]_2$ **18**	− 90.3, − 94.5[a]	[26]
$(Me_3SiCH_2)_2GaPPh_2$	− 27.2	[27]
$[(Me_3SiCH_2)_2GaPPh_2]_2$ **29**	− 40.25	[27]
$(Me_3SiCH_2)_2InPPh_2$	− 29.15	[27]
$[(Me_3SiCH_2)_2InPPh_2]_2$ **23**	− 50.30	[27]
$(Me_3CCH_2)_2InPPh_2$	− 29.95	[27]
$[(Me_3CCH_2)_2InPPh_2]_2$ **30**	− 49.40	[27]
$[tBu_2GaPH_2]_3$ **24**		[25]
$Ga(PtBu_2)_3$ **31**	+ 54.80	[21, 22]
$In(PtBu_2)_3$ **32**	+ 70.80	[21, 22]
10	− 33.4	[41]
12	− 30.2	[41]

[a] Both *cis* and *trans* isomers are present. See text.

isomers and to estimate a *trans* → *cis* barrier of 1.3 kcal mol^{-1} using $^{13}C\{^1H\}$ NMR spectral data and assuming no difference in NOE between the *cis* and *trans* Me_3Si peaks.[31] Compounds with bridging and terminal arsenido or antimonido groups such as **9**,[37] **21**,[31] **22**,[39] and **33**[29] tend to exhibit ^1H and $^{13}C\{^1H\}$ NMR spectral equivalence of these moieties at or above ambient temperature. Simulation of the dynamic NMR spectra of **33**, for example, provided a $\Delta G^{\neq}$ value of 17.0 kcal mol^{-1} for the exchange process.[29] As pointed out by *Wells* at al.,[31] three types of process could explain the spectral observations: dissociation into and subsequent recombination of monomers [Eq. (f)]; opening of

one bridge bond, followed by rotation and formation of a new bond [Eq. (g)]; associative processes involving, for example, pentacoordinate group III metals [Eq. (h)].



(f)

(g)

(h)

A priori it might be thought that the dissociative mechanism [Eq. (f)] is a prohibitively high-energy process. For the compounds $[(Me_3SiCH_2)_2MPPh_2]_n$ (M = Ga, In) and $[(Me_3CCH_2)_2InPPh_2]_n$, however, concentration-dependent $^{31}P\{^1H\}$ NMR peaks are detectable and have been attributed to the concomitant presence of monomers and dimers (Table 5).[27]

The ^{31}P NMR chemical shifts for the anions $[M(PPh_2)_4]^{\ominus}$ of **10** and **12** (Table 5) fall within the range anticipated for terminal phosphido groups behaving as one-electron donors[41] and are similar to that of Ph_2PLi ($\delta = -38.5$).

Compounds **31** and **32** are not suitable for X-ray diffraction study.[21,22] However, the ^{31}P NMR chemical shifts (Table 5) are in a region indicative of one-electron-donor phosphido groups. Such a conclusion is consistent with the X-ray crystal structure of **15**.[30] Interestingly, upon cooling from 25 to −95 °C, the ^{31}P NMR chemical shifts of **31** and **32** change to +39.90 and +63.68, respectively.[22] This temperature sensitivity could be due to solvent interaction ([D_8]toluene) or to rapid interconversion between one- and three-electron-donor phosphido moieties.

Given the variety of conformations for the six-membered rings, trimeric compounds of the type $(R_2MER'_2)_3$ are expected to be highly fluxional. Little NMR information is available at the present time; however, dynamic ^1H NMR data for **28** indicate that equivalent In–Me environments persist to −80 °C.[35] This observation implies either rapid interconversion of the planar and nonplanar forms or a preference for the planar conformation in solution (both forms are present in the crystal; cf. Table 4).

^{71}Ga NMR spectroscopy is potentially useful for complex characterization, but information is rather sparse at the present time. The ^{71}Ga NMR chemical shifts of $[Ga(EPh_2)_4]^{\ominus}$ in **10** and **11** have been measured.[41] The signals are quite broad ($w_{1/2} \approx 3500$ Hz), presumably as a consequence of the overall C_1 symmetry at Ga.

5. Thin Film Deposition and Characterization

Initial effort has focused on III/V precursors of the general formula $[Me_2MEtBu_2]_2$ (M = Ga, In; E = P, As).

OMCVD REACTOR SYSTEM

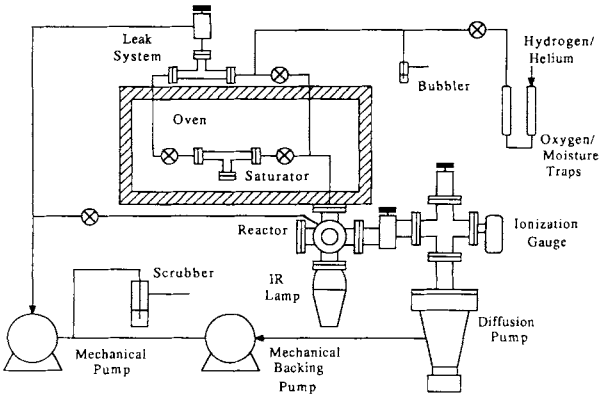


Fig. 5. Schematic drawing of a cold-wall OMCVD reactor.

Thin films of GaAs and InP have been grown using an OMCVD cold-wall reactor (Fig. 5) which is capable of operating over the pressure range 760 to 10^{-6} torr and at temperatures up to 780 °C. Several substrates have been employed for the deposition studies:[49] quartz to identify the temperatures and pressures where the precursors decompose to produce smooth, mirrored films; Si(100) 3° off toward (011) to determine GaAs sputtering rates during X-ray photoelectron spectroscopic (XPS) studies; semi-insulating GaAs(100) and Si-doped GaAs(100) to explore whether epitaxial film growth could be achieved. The optimum conditions involved a saturator temperature of 130 °C, substrate temperatures of between 450 and 700 °C, and a total system pressure of 10^{-4} torr. Use of the foregoing conditions resulted in growth rates of 0.7 to 1.0 μm h^{-1}. Interestingly, either H_2 or He can be employed as the carrier gas, thereby implying that H_2 is not involved in the thermolysis process. Similar results were obtained using the analogous indium phosphide precursor.

The films have been investigated by an array of techniques: X-ray diffraction to establish crystallinity, XPS to determine chemical composition and gross carbon contamination, secondary ion mass spectrometry (SIMS) to identify impurities, scanning electron microscopy (SEM) to observe the morphological properties, and low-temperature photoluminescence (PL) to explore the band edge. The XPS of the GaAs films exhibit signals corresponding to Ga(3d), Ga(3p), Ga(3s), As(3p), and As(3s) ionizations which match those of a single-crystal substrate (Fig. 6). No carbon was detected in the XPS experiments and, moreover, the Ga:As atomic ratio was 1:1 within experimental error. These results contrast with the somewhat high carbon levels that were reported in an OMCVD study of $[Et_2GaPEt_2]_3$.[24]

Carbon impurity levels were tested with SIMS because XPS cannot detect less than 1000 ppm of carbon. We did not have calibration standards when the SIMS profiles were taken; however, SIMS studies of the 570 °C films showed that the films did not contain any more carbon than the electronic-grade GaAs substrates. Trace amounts of the metallic impurities Na, K, Al, Si, In, Ti, Cr, and Fe were also detected. The SIMS results are significant and demonstrate that, as expected, precursor ligand loss was complete and that carbon incorporation into the films did not occur. Most of the films have

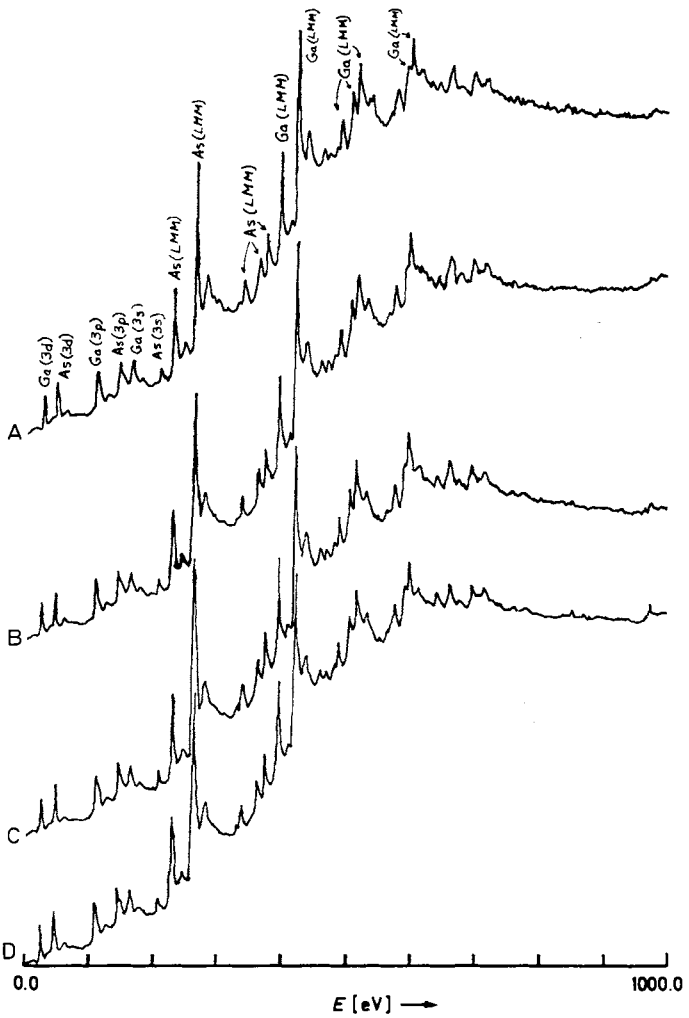


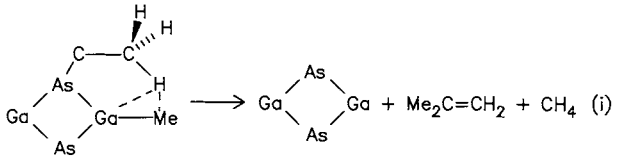
Fig. 6. X-ray photoelectron spectra of GaAs films. A: An electronic-grade sample. B: A sample grown at 700 °C with He carrier gas. C: A sample grown at 700 °C with H_2 carrier gas. D: A sample grown at 570 °C with H_2 carrier gas. E = electron binding energy.

been found to be polycrystalline by X-ray diffraction; however, of key significance are low-temperature (2 K) PL measurements on films of GaAs, grown on semi-insulating GaAs(100) and Si-doped GaAs(100) at 570 °C. These materials exhibit PL signals, thus indicating that crystalline domains are present. Although the measurements indicate degeneratively n-doped material, they also show that very good Ga:As ratios and very low levels (ca. 1 ppm) of impurities have been achieved. So far, no attempts have been made to purify the precursor compounds rigorously in order to prepare films of ultra-high electrical quality. However, we believe that this will be ultimately possible.

6. Mechanistic Considerations

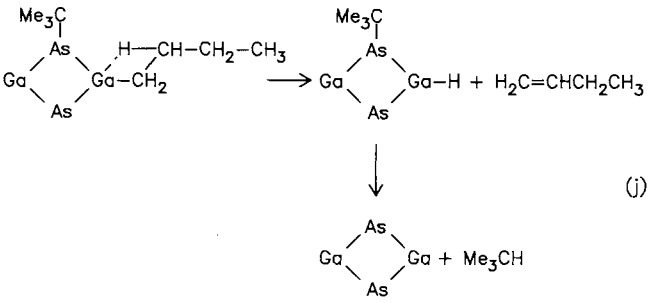
In designing the precursors, attention was paid not only to strong bonding within the skeleton but also to the necessity for substituents that are prone to facile hydrocarbon expulsion.

Substituents featuring β hydrogens such as *t*Bu, *n*Bu, *i*Pr, and Et appeared to provide the best option for facile thermal elimination of alkenes. Preliminary thermal decomposition studies of $[Me_2GaAstBu_2]_2$ **3** reveal that at 570 °C methane and isobutene are the principal hydrocarbons produced during film growth.[49] A plausible mechanism for the deposition of III/V films involves interaction of the group III metal with the C–H bond of a *t*Bu substituent, cleavage of an As–C bond to form isobutene, and the elimination of methane from Ga. This is shown for a *t*Bu and a Me substituent in Equation (i). Such a suggestion is consistent with the X-ray



crystal structure **3**.[21] Although the H atoms were not located in the X-ray experiment, placement of them in idealized positions results in a "close" Ga · · · H nonbonded distance of 2.62 Å.

Thermolysis of $[nBu_2GaAstBu_2]_2$ **4** at 250 °C results in a smooth expulsion of 1-butene and isobutane, together with smaller quantities of *n*-butane and isobutene. In this case, the primary mechanism may involve β-hydrogen transfer from an *n*Bu group giving 1-butene, followed by elimination of isobutane from a *t*BuAs moiety [Eq. (j)]. A competing path-



way, analogous to that proposed for **3**, would be responsible for the production of isobutene and *n*-butane.

Finally, low-temperature production of GaAs has been achieved using solution techniques. Treatment of **16** with *t*BuOH in pentane at ambient temperature resulted in the elimination of pentamethylcyclopentadiene and $tBuOSiMe_3$ and formation of a reddish powder [Eq. (k)].[34] The powder

$$(Me_5C_5)_2GaAs(SiMe_3)_2 \xrightarrow[-\ Me_5C_5H\ -\ tBuOSiMe_3]{tBuOH} GaAs \qquad (k)$$

16

was shown to be GaAs plus some organic impurities by elemental analysis, scanning electron microprobe analysis, and X-ray powder diffraction. However, annealing this material at 500 °C for 48 h resulted in crystalline GaAs. *Wells* et al.[50] have also produced GaAs and InAs of 88–96% and 98% purity, respectively, via the solution reaction of $(Me_3Si)_3As$ with MCl_3 (M = Ga, In), followed by heating at higher temperatures. In our laboratories, we have found that the crystalline compound $[tBu_2GaAsH_2]_3$ **34** is thermally stable at ambient temperature in the solid state. However, in solution this compound undergoes a smooth decomposition at 25 °C to finely divided, amorphous gallium arsenide.[25]

7. Addendum (August 7, 1989)

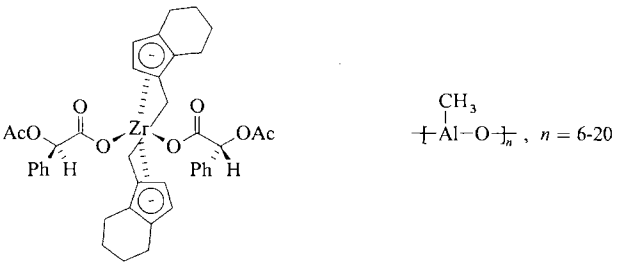
A number of important developments have occurred since the submission of this manuscript. *Bradley* et al.[51] have investigated the deposition of InP from $[Me_2InPtBu_2]_2$ using the metal-organic molecular beam epitaxy (MOMBE) technique. These authors demonstrated that indium-rich growth occurs at all substrate temperatures studied and that stoichiometric growth is only possible at 480 °C with a simultaneous incident flux of dissociated phospane. In a related publication, *Bradley* et al.[52] described the preparation of $[Me_2InPtBu_2]_2$ and $[Me_2InPPh_2]_2$ through the reaction of Me_3In with tBu_2PH and Ph_2PH, respectively. The X-ray crystal structure analysis of $[Me_2InPtBu_2]_2$ was also reported. *Wallbridge* et al.[53] have prepared $[Et_2InPtBu_2]_2$ and $In(PtBu_2)_3$ by alkane and salt elimination methods, respectively. Both compounds were investigated by X-ray crystallography. Finally, *Barron* et al.[54] have prepared polycrystalline InP by treatment of $InCl_3$ with $(Me_3Si)_3P$. The intermediates in this reaction were investigated by X-ray photoelectron spectroscopy, elemental analysis, and X-ray powder diffraction.

The work in our laboratories was carried out by the following co-workers: B. Benac, R. Geerts, D. Giolando, P. Harris, D. Heaton, K. Kidd, M. Mardones, C. Nunn, J. Power, S. Schwab, D. Westmoreland. We are also grateful for our interaction with colleagues in the Department of Chemical Engineering at the University of Texas at Austin, Professor John Ekerdt and James Miller, who have conducted the OMCVD studies. We thank Professors Ben Streetman and Al Tasch of the Department of Electrical and Computer Engineering at the University of Texas at Austin for very helpful discussions. The work has been supported by the Robert A. Welch Foundation, the National Science Foundation, and the Texas Advanced Technology Research Program.

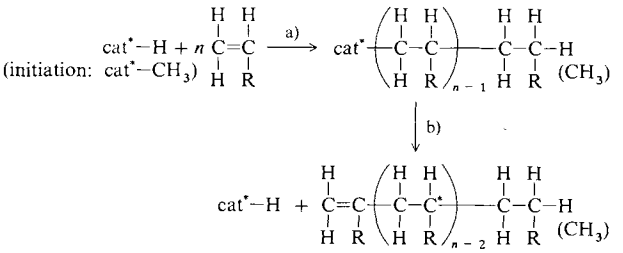
Received: March 8, 1989 [A 733 IE]
German version: *Angew. Chem. 101* (1989) 1235

[1] According to the recent IUPAC convention, groups III and V become groups 13 and 15, respectively. However, the older group III/V nomenclature is still in frequent usage in the context of semiconductor research.
[2] Some leading references: *Chem. Eng. News 64* (1986), No. 27, p. 34; *National Photovoltaics Program Five Year Plan, 1984–88*, May 1983, p. 11; A. L. Fahrenbuch, R. H. Bube: *Fundamentals of Solar Cells*, Academic Press, New York 1983, pp. 335–346; R. K. Ahrenkiel, L. L. Kazmerski, R. J. Matson, C. Osterwalf, T. P. Massopust, R. A. Michelsen, W. S. Chen, *Appl. Phys. Lett. 43* (1983) 658; J. A. Thornton, D. G. Cornog, R. B. Hall, S. P. Shea, J. D. Meakin, *Conf. Rec. IEEE Photovoltaic Spec. Conf. 17th* (1984) 781; *Chem. Eng. Prog. 81* (1985), No. 5, p. 30.
[3] H. M. Manasevit, *Appl. Phys. Lett. 12* (1968) 156; see also T. Nakanis, *J. Cryst. Growth 68* (1984) 282, and references cited therein.
[4] D. C. Bradley, M. M. Faktor, M. Scott, E. A. D. White, *J. Cryst. Growth 75* (1986) 101.
[5] See, for example, H. Heinecke, A. Brauers, H. Luth, P. Balk, *J. Cryst. Growth 77* (1986) 78.
[6] R. H. Moss, *J. Cryst. Growth 68* (1984) 78.
[7] See, for example, papers in the First International Conference on OMCVD in *J. Cryst. Growth 55* (1981) 1, and references cited therein.
[8] A. D. Huelsman, R. Reif, C. G. Fonstad, *Appl. Phys. Lett. 50* (1987) 206.
[9] S. Reynolds, D. W. Vook, J. F. Gibbons, *Appl. Phys. Lett. 49* (1986) 1720.
[10] L. M. Fraas, P. S. McLeod, L. D. Partain, R. E. Weiss, J. A. Cape, *J. Cryst. Growth 77* (1986) 386.
[11] C. H. Chen, C. A. Larsen, G. B. Stringfellow, D. W. Brown, A. J. Robertson, *J. Cryst. Growth 77* (1986) 11; C. A. Larsen, C. H. Chen, M. Kitamura, G. B. Stringfellow, D. W. Brown, A. J. Robertson, *Appl. Phys. Lett. 48* (1986) 1531.
[12] R. M. Lum, J. K. Klingert, M. G. Lamont, *Appl. Phys. Lett. 50* (1987) 285.
[13] R. Bhat, M. A. Koza, *Electronic Materials Conference* (Amherst, MA, USA 1986), Abstract B1.
[14] P. Norris, J. Black, S. Zeman, G. Lambert, *J. Cryst. Growth 68* (1984) 437; Y. Seki, K. Tanno, K. Lida, E. Echiki, *J. Electrochem. Soc. 122* (1975) 1108.
[15] The 1,2-bis(diphenylphosphino)ethane adduct of Me_3In is particularly useful in this regard. See a) D. C. Bradley, M. M. Faktor, E. A. D. White, D. M. Frigo, K. V. Young, *Chemtronics 3* (1988) 50; b) A. H. Moore, M. D. Scott, J. I. Davies, D. C. Bradley, M. M. Faktor, H. Chudzynska, *J. Cryst. Growth 77* (1986) 19.
[16] A. Zaouk, E. Salvetat, J. Sakaya, F. Maury, G. Constant, *J. Cryst. Growth 55* (1981) 135.
[17] N. Davidson, H. C. Brown, *J. Am. Chem. Soc. 64* (1942) 316.
[18] The original trimeric formulation has since been confirmed by electron diffraction. A. Haaland, J. Hougen, H. V. Volden, G. Hanika, H. H. Karsch, *J. Organomet. Chem. 322* (1987) C24.
[19] G. E. Coates, J. Graham, *J. Chem. Soc. 1963*, 233.
[20] O. T. Beachley, G. E. Coates, *J. Chem. Soc. 1965*, 3241.
[21] A. M. Arif, B. L. Benac, A. H. Cowley, R. L. Geerts, R. A. Jones, K. B. Kidd, J. M. Power, S. T. Schwab, *J. Chem. Soc. Chem. Commun. 1986*, 1543.
[22] A. M. Arif, B. L. Benac, A. H. Cowley, R. A. Jones, K. B. Kidd, C. M. Nunn, *New J. Chem. 12* (1988) 553.
[23] Professor *D. C. Bradley* and co-workers have independently synthesized $[Me_2InPtBu_2]_2$ and described its conversion to InP. For vapor pressure data see [15a]; for the deposition of InP see D. C. Bradley, M. M. Faktor, E. A. D. White, D. M. Frigo, UK Pat. Appl. 8703227 (1987).
[24] F. Maury, G. Constant, *Polyhedron 3* (1984) 581; F. Maury, M. Combes, G. Constant, R. Cartes, J. B. Renucci, *J. Phys., Colloq. 43* (1982) C1-347.
[25] A. H. Cowley, P. R. Harris, R. A. Jones, C. M. Nunn, to be published.
[26] D. E. Heaton, R. A. Jones, K. B. Kidd, A. H. Cowley, C. M. Nunn, *Polyhedron 7* (1988) 1901.
[27] O. T. Beachley, J. P. Kopasz, H. Zhang, W. E. Hunter, J. L. Atwood, *J. Organomet. Chem. 325* (1987) 69.
[28] A. H. Cowley, R. A. Jones, M. A. Mardones, C. M. Nunn, to be published.
[29] C. G. Pitt, A. P. Purdy, K. T. Higa, R. L. Wells, *Organometallics 5* (1986) 1266.
[30] C. G. Pitt, K. T. Higa, A. T. McPhail, R. L. Wells, *Inorg. Chem. 25* (1986) 2483.
[31] A. P. Purdy, R. L. Wells, A. T. McPhail, C. G. Pitt, *Organometallics 6* (1987) 2099.
[32] R. L. Wells, A. P. Purdy, A. T. McPhail, C. G. Pitt, *J. Organomet. Chem. 308* (1986) 281.
[33] A. H. Cowley, R. A. Jones, K. B. Kidd, C. M. Nunn, to be published.
[34] E. K. Byrne, L. Parkanyi, K. H. Theopold, *Science (Washington) 241* (1988) 332.
[35] A. H. Cowley, R. A. Jones, K. B. Kidd, C. M. Nunn, D. L. Westmoreland, *J. Organomet. Chem. 341* (1988) C1.
[36] A. H. Cowley, R. A. Jones, C. M. Nunn, D. L. Westmoreland, to be published.
[37] A. R. Barron, A. H. Cowley, R. A. Jones, C. M. Nunn, D. L. Westmoreland, *Polyhedron 7* (1988) 77.
[38] M. J. Benac, A. H. Cowley, R. A. Jones, C. M. Nunn, to be published.
[39] R. L. Wells, A. P. Purdy, K. T. Higa, A. T. McPhail, C. G. Pitt, *J. Organomet. Chem. 325* (1987) C7.
[40] R. L. Wells, A. P. Purdy, A. T. McPhail, C. G. Pitt, *J. Chem. Soc. Chem. Commun. 1986*, 487.
[41] C. J. Carrano, A. H. Cowley, D. M. Giolando, R. A. Jones, C. M. Nunn, J. M. Power, *Inorg. Chem. 27* (1988) 2709.
[42] B. L. Benac, A. H. Cowley, K. B. Kidd, R. A. Jones, to be published.
[43] R. L. Wells, S. Shafieezad, A. T. McPhail, C. G. Pitt, *J. Chem. Soc. Chem. Commun. 1987*, 1823.
[44] L. Pauling: *The Nature of the Chemical Bond*, Cornell University Press, Ithaca, NY, USA 1960, p. 246.
[45] C. G. Hoffmann, C. Burschka, *Angew. Chem. 97* (1985) 965; *Angew. Chem. Int. Ed. Engl. 24* (1985) 970.
[46] T. A. Albright, A. M. Arif, A. J. Bard, R. A. Jones, S. K. Kang, J. K. Leland, S. T. Schwab, *Inorg. Chem. 27* (1988) 1246.
[47] a) R. W. G. Wyckoff: *Crystal Structures*, 2nd ed., Wiley, New York 1963; b) in [47a] *Vol. 1*, pp. 108–111; c) in [47a] *Vol. 4*, p. 531.
[48] M. H. Chisholm, F. A. Cotton, M. W. Extine, *Inorg. Chem. 17* (1978) 1329; R. T. Baker, P. J. Krusic, T. H. Tulip, J. C. Calabrese, S. S. Wreford, *J. Am. Chem. Soc. 105* (1983) 6763.
[49] A. H. Cowley, B. L. Benac, J. G. Ekerdt, R. A. Jones, K. B. Kidd, J. Y. Lee, J. E. Miller, *J. Am. Chem. Soc. 110* (1988) 6248.
[50] R. L. Wells, C. G. Pitt, A. T. McPhail, A. P. Purdy, S. Shafieezad, R. B. Hallock, *Chem. Mater. 1* (1989) 4.
[51] D. A. Andrews, G. J. Davies, D. C. Bradley, M. M. Faktor, D. M. Frigo, E. A. D. White, *Semicond. Sci. Technol. 3* (1988) 1053.
[52] K. A. Aitchison, J. D. J. Backer-Dirks, D. C. Bradley, M. M. Faktor, D. M. Frigo, M. B. Hursthouse, B. Hussain, R. L. Short, *J. Organomet. Chem. 366* (1989) 11.
[53] N. W. Alcock, I. A. Degnan, M. G. H. Wallbridge, H. R. Powell, M. McPartlin, G. M. Sheldrick, *J. Organomet. Chem. 361* (1989) C33.
[54] M. D. Healy, P. E. Laibinis, P. D. Stupik, A. R. Barron, *J. Chem. Soc. Chem. Commun. 1989*, 359.

Communications may be submitted in English *or* in German. Further details regarding the submission of communications can be found in the "Notice to Authors" reproduced in the January issue of the journal. Copies thereof may be obtained from the editorial office upon request.



Scheme 1. Structural formula of (*S*)-[1,1'-ethylenebis(4,5,6,7-tetrahydro-1-indenyl)]zirconium bis(*O*-acetyl-(*R*)-mandelate) and methylalumoxane.



Scheme 2. Reaction scheme for the oligomerization of olefins with chiral zirconocene/alumoxane catalysts. a) Initiation and growth steps. b) Chain termination.

Asymmetric Oligomerization of Propene and 1-Butene with a Zirconocene/Alumoxane Catalyst

By *Walter Kaminsky,* Aurelia Ahlers,* and *Nico Möller-Lindenhof*

Dedicated to Professor Hansjörg Sinn on the occasion of his 60th birthday

Highly isotactic polymers have been prepared from propene and longer chain α-olefins with chiral transition-metal compounds such as (*R,S*)-[1,1'-ethylenebis(4,5,6,7-tetrahydro-1-indenyl)]zirconium dichloride and methylalumoxane as cocatalysts.[1–3] If, instead of the racemate, one of the two enantiomers of the transition-metal compound is used, the resulting polyolefins should exhibit practically no optical activity in solution.[4] By contrast, measurable optical rotations are expected for oligomers. Thus, *Pino* et al. were able to synthesize optically active alkanes by hydrooligomerization of propene with this catalyst system.[5, 6] Of greater preparative interest are the more reactive, optically active alkenes. However, hydrogenation cannot be used to control their molecular weights in the asymmetric oligomerization. Instead, similarly low degrees of oligomerization have to be achieved by a method that preserves the terminal double bond. This is possible by raising the catalyst concentration and simultaneously lowering the monomer concentration, thereby increasing the rate of chain termination relative to chain growth in the polymerization.

Use of (*S*)-[1,1'-ethylenebis(4,5,6,7-tetrahydro-1-indenyl)]-zirconium bis(*O*-acetyl-(*R*)-mandelate)[7] and methylalumoxane[8] (Scheme 1) thus allowed the preparation of optically active propene and 1-butene oligomers. The mandelate was employed because its activity is similar to that of the corresponding dichloride and may be obtained in purer form. In the first step, an olefin molecule undergoes insertion into a transition-metal methyl bond formed by methylation with methylalumoxane (Scheme 2). Subsequent insertions lead to chain growth. Chain termination takes place by β-hydrogen transfer to the transition-metal atom or to a complex-bound olefin, resulting in formation of the hydrido or alkyl transition-metal compound in addition to the oligomer. The former, in turn, allows new insertion steps to occur. Up to 100 molecules of propene or 1-butene undergo insertion per molecule of catalyst per hour.

Gas chromatography (Fig. 1) reveals the presence of dimers to heptamers of 1-butene. In the case of trimers and higher oligomers, the isomeric mixtures obtained consist mainly of configurational isomers. The dimer and trimer mixtures contain 88 and 78 wt%, respectively, of a main component. The tetramer fraction contains 72% of a 5:4 mixture of diastereomeric (*R,R*)/((*S,S*)- and (*R,S*)/(*S,R*)-2,4,6-triethyl-1-decenes (all four configurational isomers are presumably present since the catalyst does not function in a completely stereospecific fashion). Similarly, the main components of the pentamer fraction consist of the four possible enantiomer pairs of 2,4,6,8-tetraethyl-1-dodecene. Under comparable oligomerization conditions, propene preferentially affords pentamers and 1-butene yields trimers and tetramers (Table 1).

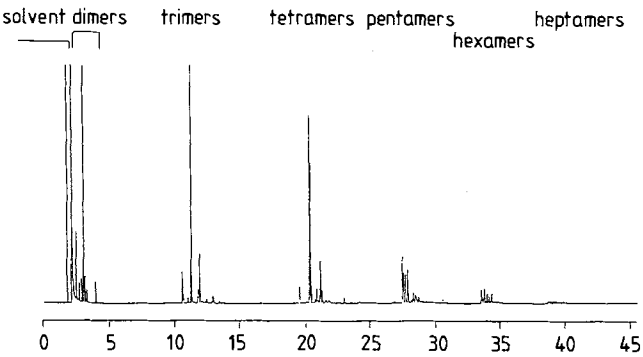


Fig. 1. Gas-chromatographic separation of the oligomerization products of 1-butene (50-m capillary column CP Sil 5 CB; 10 × 0.32 mm; d_f 0.12 μm; temperature 50–270 °C).

[*] Prof. Dr. W. Kaminsky, Dipl.-Chem. A. Ahlers, Dipl.-Chem. N. Möller-Lindenhof
Institut für Technische und Makromolekulare Chemie der Universität Bundesstrasse 45, D-2000 Hamburg 13 (FRG)

[**] This work was supported by the Volkswagen-Stiftung. We thank Prof. Dr. *H. H. Brintzinger* (Konstanz) for help in the synthesis of the optically active zirconocenes.

Table 1. Amount [wt%] of propene and 1-butene oligomers of differing degrees of oligomerization n [a].

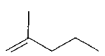
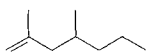
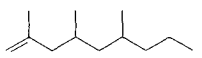
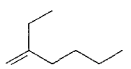
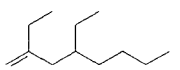
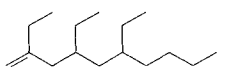
n	2	3	4	5	6	7
Propene oligomers	2.4	8.9	11.5	12.2	11.3	9.4
Butene oligomers	9.5	17.9	17.5	14.3	10.2	5.3

[a] The remaining 44.3 and 25.3 wt%, respectively, consists of higher oligomers.

The ^{1}H NMR spectrum of the mixture of 1-butene oligomers (recorded in $CDCl_3$/TMS) displays two singlets at $\delta = 4.69$ and 4.74 in the olefinic region, which, in agreement with the calculated chemical shifts[9] and the results of ^{13}C NMR spectroscopy, are assigned to 2-alkyl-substituted 1-alkenes.

The first three oligomer fractions were separated by distillation and characterized by ^{13}C NMR spectroscopy, mass spectrometry, and polarimetry (Table 2).

Table 2. Molar optical rotations $[\Phi]_\lambda^T$ of alkenes prepared by asymmetric oligomerization of propene and 1-butene.

Oligomers	Structure of the main components	$[\Phi]_{589}^{25}$	$[\Phi]_{365}^{25}$	c [a] [mg mL^{-1}]
from propene				
$n = 2$		0.0	0.0	11.5
$n = 3$		+1.1	+3.7	10.9
$n = 4$		+4.7	+14.6	10.1
from 1-butene				
$n = 2$		0.0	0.0	56.2
$n = 3$		−0.7	−2.5	61.0
$n = 4$		−2.6	−9.4	58.1

[a] Concentration in the measuring cuvette ($l = 1$ dm); solvent, toluene.

The structures of the alkenes are those expected for 1,2-insertion of the monomers. Accordingly, the number of chiral centers is always smaller by two than the degree of oligomerization. In the case of 1-butene, *König* et al.[10] succeeded in carrying out gas-chromatographic separation of the enantiomers of the trimer mixture on a modified cyclodextrin phase. The enantiomeric excess *ee* for the first diastereoselective partial reaction in 1-butene oligomerization was thereby determined to be 27%. In analogy to the results obtained in the hydrooligomerization of propene,[5] this asymmetric reaction should preferentially afford the *R* enantiomer. The stereoselectivity of the second diastereoselective partial reaction is significantly higher, since the stereocenters of the growing oligomer enhance the stereodifferentiation.[5] The diastereomer ratio (1:1.25) of the triethyl-1-decenes determined by gas chromatography reveals that the second chiral center is formed in the *R* configuration with a stereoselectivity of 80%. In agreement with this, the molar optical rotation also increases by a factor of roughly 4 (see Table 2).

Figure 2 shows the ^{13}C NMR spectrum of the trimer fraction obtained from 1-butene. Comparison of the calculated[11, 12] and the measured chemical shifts of the carbon nuclei leads to the structure shown in Figure 2, which was

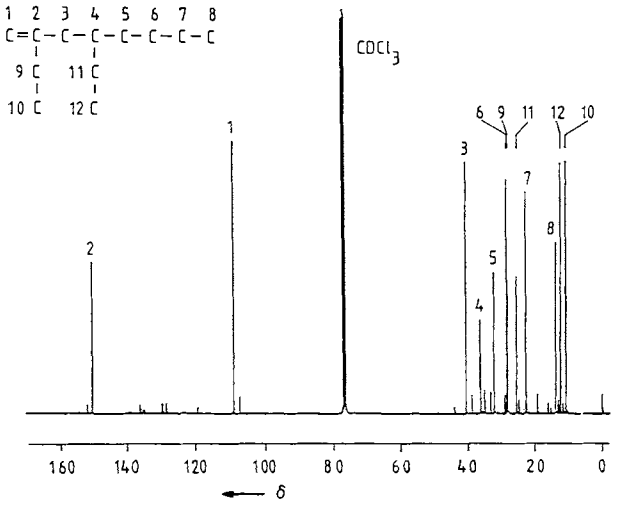


Fig. 2. 90.6-MHz ^{13}C NMR spectrum of the trimer fraction obtained in the oligomerization of 1-butene, recorded in $CDCl_3$ (main component: 2,4-diethyl-1-octene).

corroborated by mass-spectrometric data. In the mass spectrum of the trimer mixture after separation by gas chromatography (GC/MS), the molecular ion peak (m/z 168) is accompanied by peaks for $[C_nH_{2n-1}]^\oplus$ fragment ions, which are typical of alkenes, and by the peak for the product of McLafferty rearrangement (m/z 70), which is the main fragmentation product for many 2-alkyl-substituted 1-alkenes.[13]

We have thus shown that, with small amounts of optically active catalyst (10^{-4} M), it is possible to synthesize molar amounts of optically active alkenes from simple olefins. The oligomerization can be controlled so as to produce mainly dimers to pentamers. Such alkenes were previously accessible only by complicated, multistep syntheses. These oligomers may find application in the synthesis of pheromones and of chiral compounds with little functionality.

Experimental Procedure

All operations were carried out under argon. Toluene (155 mL), methylalumoxane (520 mg, 9.0×10^{-3} mol Al), and (*S*)-[1,1'-ethylenebis(4,5,6,7-tetrahydro-1-indenyl)]zirconium bis(*O*-acetyl-(*R*)-mandelate) (56.6 mg, 76×10^{-3} mol; $[\alpha]_{589}^{25} = -20.5$ ($c = 9.7$ mg mL^{-1} in toluene, $l = 1$ dm)) were placed in a 1-L glass autoclave and heated at 50 °C using a thermostat. 1-Butene (32.14 g, 0.57 mol) was then added over 16 h using a mass flow controller. Subsequently, the reaction mixture was stirred with 10% potassium hydroxide. The products were separated by fractional distillation. Yield 26.2 g (81%) of a colorless oil: $[\alpha]_{589}^{25} = -0.8$ ($c = 86.8$ mg mL^{-1} in toluene). Propene (20.4 g, 0.48 mol) was similarly added over 19 h. Yield 18.0 g (88%): $[\alpha]_{589}^{25} = +3.3$ ($c = 10.9$ mg mL^{-1} in toluene).

Received: October 27, 1988;
supplemented: June 13, 1989 [Z 3027 IE]
German version: *Angew. Chem. 101* (1989) 1304

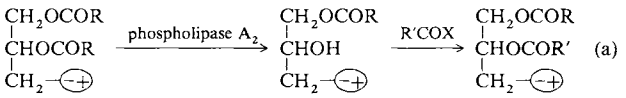
CAS Registry numbers:
2-methyl-1-pentene, 763-29-1; 2,4-dimethyl-1-heptene, 19549-87-2; 2,4,6-trimethyl-1-nonene, 55771-40-9; 2-ethyl-1-hexene, 1632-16-2; 2,4-diethyl-1-octene, 121887-29-4; 2,4,6-triethyl-1-decene, 121887-30-7; 1-butene, 106-98-9; propene, 115-07-1; (*S*)-[1,1'-ethylenebis(4,5,6,7-tetrahydro-1-indenyl)]zirconium bis(*O*-acetyl-(*R*)-mandelate), 115857-04-0.

[1] W. Kaminsky, K. Külper, H. H. Brintzinger, F. R. W. P. Wild, *Angew. Chem. 97* (1985) 507; *Angew. Chem. Int. Ed. Engl. 24* (1985) 507.
[2] J. A. Ewen, *J. Am. Chem. Soc. 106* (1984) 6355.
[3] W. Kaminsky, *Angew. Makromol. Chem. 145/146* (1986) 149.
[4] P. Pino, *Adv. Polym. Sci. 4* (1966) 393.
[5] P. Pino, P. Cioni, J. Wei, *J. Am. Chem. Soc. 109* (1987) 6189.
[6] P. Pino, P. Cioni, M. Galimberti, J. Wei, N. Piccolrovazzi in W. Kaminsky, H. Sinn, (Eds.): *Transition Metals and Organometallics as Catalysts for Olefin Polymerization*, Springer, Berlin 1988, p. 269.
[7] A. Schäfer, E. Karl, L. Zsolnai, G. Huttner, H. H. Brintzinger, *J. Organomet. Chem. 328* (1987) 87.
[8] W. Kaminsky, H. Hähnsen, Dtsch. Pat. Appl., P 32403836, procedure for the preparation of oligomeric alumoxanes (1982), Hoechst AG; *Chem. Abstr. 101* (1984) 73242u.
[9] R. J. Abraham, P. Loftus: *Proton and Carbon-13 NMR Spectroscopy*, Heyden & Son, London 1978, p. 18.
[10] a) W. A. König, *Nachr. Chem. Tech. Lab. 37* (1989) 471; b) W. A. König, S. Lutz, G. Wenz, *Angew. Chem. 100* (1988) 989; *Angew. Chem. Int. Ed. Engl. 27* (1988) 979.
[11] D. E. Dorman, M. Jautelat, J. D. Roberts, *J. Org. Chem. 36* (1971) 2757.
[12] L. P. Lindeman, J. Q. Adams, *Anal. Chem. 43* (1971) 1245.
[13] K. K. Mayer, C. Djerassi, *Org. Mass Spectrom. 5* (1971) 817.

Chain-Substituted Lipids as Substrates for Phospholipase A_2**

By *Fredric M. Menger** and *M. G. Wood, Jr.*

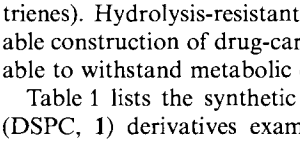
Recent monolayer,[1] calorimetric,[2] mass spectrometric,[3] biochemical,[4, 5] ^{13}C NMR,[6] and transport[7] studies of new lipid systems required the synthesis of "lysophospholipid" intermediates via phospholipase-A_2-catalyzed hydrolyses [Eq. (a)]. In the course of our work, we found that the



(a)

phospholipase gave no isolable products with phospholipids bearing certain alkyl groups on the first half of their C_{18} chains. This observation inspired further investigation owing to the possibility that the chain-substituted lipids, like related short-chain lecithins,[8] inhibit normal phospholipase-A_2 activity. Developing such inhibitors is a major goal of current chemopharmacological research[9–13] because phospholipase A_2 catalyzes the release of arachidonic acid (a precursor for prostaglandins, thromboxanes, and leukotrienes). Hydrolysis-resistant phospholipids would also enable construction of drug-carrying liposomes that are better able to withstand metabolic degradation.

Table 1 lists the synthetic distearoylphosphatidylcholine (DSPC, **1**) derivatives examined with phospholipase A_2.



1

In a typical preparative run,[14] lipid (40 μmol in 3.3 mL of 1:9 methanol/ether) was mixed with crude snake venom (1 mg *Crotalus adamanteus*[15] in 30 μL of 5 mM $CaCl_2$). After 24 hours of magnetic stirring and TLC monitoring, the reactions were quenched with 5 mL of water, after which the water layer was separated, washed with ether, and lyophilized. Reaction yields were determined by one of two methods: (1) Integrated ^1H NMR signals of the α-methylene and choline methyl groups were compared. (2) Lysophosphatidylcholine was isolated by column chromatography (silica; 8:2 $CH_3OH/CHCl_3$ as eluant).

As seen in Table 1, a yield of 97% was obtained with the parent DSPC **1**. On the other hand, *n*-propyl and *n*-butyl branching at positions 4, 6, and 8 gave 0% yields regardless of whether both chains ("1,2") or only the second chain ("2") was substituted. An *n*-butyl at a more distal locus (C-12) did not result in 0% yield but instead reduced it to 34%. Methyl groups exerted little effect on the yield (85–100%) even when they were situated close to the hydrolytic site. Yields tumbled to 5–15% with ethyl groups on carbons 4, 6, and 8. In summary, phospholipid hydrolyses are impaired by alkyl substituents, particularly large ones, located in the first half of the chains.

Table 1. Yields and rates of phospholipase-A_2-catalyzed hydrolyses of **1** and its derivatives.

Substituent	Chain(s)	Location [a]	Yield [%] [b]	Relative initial rate $v_{i,rel}$ [c]
–	–	–	97*	100
Methyl	1,2	4	95*	12
Methyl	2	4	87	20
Methyl	1,2	6	90	23
Methyl	2	6	92	48
Methyl	1,2	8	91*	45
Methyl	2	8	100	100
Methyl	1,2	12	85*	100
Ethyl	1,2	4	5	3
Ethyl	1,2	6	7	3
Ethyl	2	6	15	13
Ethyl	1,2	8	14	5
Ethyl	2	8	15	18
n-Propyl	1,2	6	0	4
n-Propyl	2	6	0	14
n-Propyl	1,2	8	0	11
n-Propyl	2	8	0	29
n-Butyl	1,2	4	0	<0.3
n-Butyl	2	4	0	3
n-Butyl	1,2	6	0	<0.3
n-Butyl	2	6	0	9
n-Butyl	1,2	8	0	2
n-Butyl	2	8	0	9
n-Butyl	1,2	12	34*	42
Phenyl	1,2	8	–	2
Phenyl	1,2	12	–	50

[a] Numbering system counts the carbonyl carbon of the fatty acid as C-1. Either both chains ("1,2") or only the second chain ("2") bears a substituent at the indicated location. [b] The percentages marked with an asterisk reflect the isolated yields after column chromatograpy. All other yields were determined in duplicate by ^1H NMR spectroscopy. [c] Rates were measured using 5.9 mM lipid substrate. Reaction conditions were different from those used to determine yields (see text). V_{max} (**1**) = 420 μmol mg^{-1} min^{-1}.

Initial rates of phospholipase-A_2-catalyzed hydrolyses (Table 1) were all measured under identical conditions: 6.0 mL of an aqueous mixture composed of 5.9 mM lipid, 20 mM Triton X-100, and 10 mM $CaCl_2$, bath-sonicated at 65 °C to produce a mixed-micellar system.[12, 16] Subsequent hydrolysis, initiated with 0.2 units of purified phospholipase from *Crotalus adamanteus* venom[17] (167 units per mg), was measured with a Radiometer pH-stat at 40.0 °C by titrating at pH = 8.0 under N_2 with 2 or 5 mM KOH.

[*] Prof. F. M. Menger, M. G. Wood, Jr.
Department of Chemistry, Emory University
Atlanta, GA 30322 (USA)

[**] This work was supported by the National Institutes of Health.

Relative rates $v_{i,rel}$ in Table 1 parallel roughly the reaction yields (an exact correspondence not being expected since conditions for obtaining the two parameters were entirely different). The following conclusions can be drawn from the $v_{i,rel}$ data: (1) The $v_{i,rel}$ values increase steadily as the methyl groups are shifted away from the carbonyl group (e.g., $v_{i,rel}$ = 12, 23, 45, and 100 for bis-methylation of carbons 4, 6, 8, and 12). (2) Methyl groups on both chains produce about a twofold lower $v_{i,rel}$ than identically positioned methyl groups on chain-2 alone. Thus, substitution need not occur on the labile fatty acid to affect the rate. (3) Ethyl and *n*-propyl groups reduce $v_{i,rel}$ from 3- to 30-fold depending on the proximity to the hydrolytic site. Interestingly, a single *n*-propyl group on C-8 of chain-2 gave a 0% yield with an ether solvent system but only a threefold rate decrease with the lipid incorporated into aqueous micelles. (4) *n*-Butyl groups induce dramatic rate decreases: DSPC bearing two *n*-butyl groups on C-4 hydrolyzes more slowly than DSPC **1** by a factor of 390 (a value that could be only approximated owing to the extreme sluggishness of the former reaction). When the butyl groups were moved to C-12, the inhibition almost disappeared. As seen from Table 1, the effect of phenyl groups is similar to that of *n*-butyl groups.

Conventional enzyme kinetics revealed details about the *n*-butyl group inhibition. Thus, micellar **1** gave K_m and V_{max} values of 3.8 mM and 420 μmol mg^{-1} min^{-1} (in satisfactory agreement with related studies on egg phosphatidylcholine[18]). The 4,4'-dibutyl derivative was shown to behave as a competitive inhibitor with K_i = 2.0 mM (Fig. 1). *n*-Butylation of the fatty acid chains, therefore, does not impair binding to the active site but instead severely impedes subsequent hydrolysis.[19]

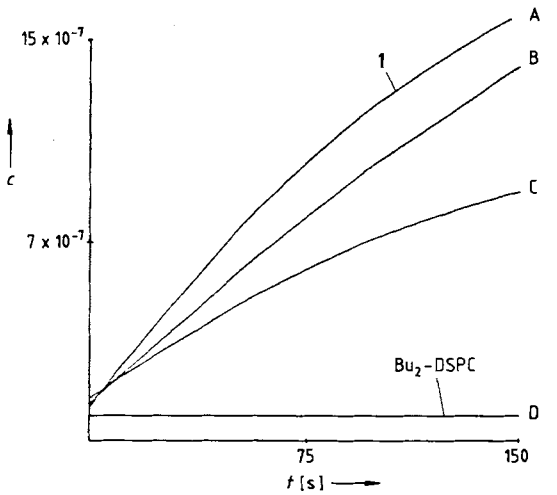


Fig. 1. Competitive inhibition of the hydrolysis of **1** by 4,4'-di-*n*-butyl-DSPC (pH-stat output; pH = 8.0, 40.0 °C). c = added equivalents of KOH. A: 0.84 mM DSPC **1**, no inhibitor. B: **1** + 1.0 mM inhibitor. C: **1** + 3.0 mM inhibitor. D: 5.9 mM 4,4'-di-*n*-butyl-DSPC alone.

On the basis of our results, chain modification of phospholipids would seem to constitute a promising method of altering lipid susceptibility to phospholipase A_2. The potential for thereby controlling prostaglandin levels, and for designing more stable drug delivery systems, should again be mentioned.[20]

Received: February 20, 1989 [Z 3182 IE]
German version: *Angew. Chem. 101* (1989) 1277

[1] F. M. Menger, M. G. Wood, Jr., S. D. Richardson, Q. Zhou, A. R. Elrington, M. J. Sherrod, *J. Am. Chem. Soc. 110* (1988) 6797.
[2] F. M. Menger, M. G. Wood, Jr., Q. Z. Zhou, H. P. Hopkins, J. Fumero, *J. Am. Chem. Soc. 110* (1988) 6804.
[3] M. J. I. Mattina, S. D. Richardson, M. G. Wood, Jr., Q. Z. Zhou, M. J. Contado, F. M. Menger, L. E. Abbey, *Org. Mass. Spectrom. 23* (1988) 292.
[4] Q. Zhou, R. L. Raynor, M. G. Wood, Jr., F. M. Menger, J. F. Kuo, *Biochemistry 27* (1988) 7361.
[5] P. A. Charp, Q. Zhou, M. G. Wood, Jr., R. L. Raynor, F. M. Menger, J. F. Kuo, *Biochemistry 27* (1988) 4607.
[6] F. M. Menger, P. Aikens, M. Wood, Jr., *J. Chem. Soc. Chem. Commun. 1988*, 180.
[7] P. Aikens, J. J. Lee, R. Persichetti, unpublished results.
[8] W. G. J. Hol, *Angew. Chem. 98* (1986) 765; *Angew. Chem. Int. Ed. Engl. 25* (1986) 767.
[9] N. S. Chandrakumar, J. Hajdu, *J. Org. Chem. 47* (1982) 2144.
[10] L. J. Reynolds, B. P. Morgan, G. A. Hite, E. D. Mihelich, E. A. Dennis, *J. Am. Chem. Soc. 110* (1988) 5172.
[11] M. H. Gelb, *J. Am. Chem. Soc. 108* (1986) 3146.
[12] W. Yuan, R. J. Berman, M. H. Gelb, *J. Am. Chem. Soc. 109* (1987) 8071.
[13] C. D. De Bose, R. A. Burns, J. M. Donovan, M. F. Roberts, *Biochemistry 24* (1985) 1298.
[14] R. L. Misiorowski, M. A. Wells, *Biochemistry 13* (1974) 4921.
[15] Sigma catalogue No. V6875.
[16] R. A. Deems, E. A. Dennis, *Methods Enzymol. 71* (1981) 703.
[17] Sigma catalogue No. P0790 (EC 3.1.1.4).
[18] C. R. Kensil, E. A. Denis, *J. Biol. Chem. 254* (1979) 5843.
[19] We cannot exclude the possibility that alkylated phosphatidylcholine modifies the micellar system, although this appears unlikely since a large excess of neutral surfactant, Triton X-100, was employed.
[20] Protein kinase C activation and inhibition by our lipid derivatives [4, 5] must be taken into consideration here.

Phosphonioboratoacetylenes: C_2 Stabilized by Donor and Acceptor Molecules

By *Hans Jürgen Bestmann,* Harald Behl,* and *Matthias Bremer*

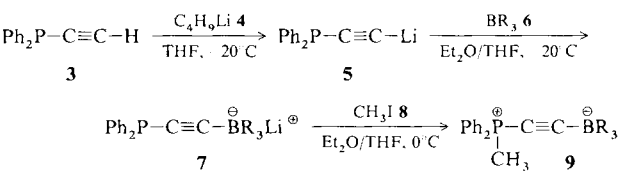
Dedicated to Professor Ernst Ruch on the occasion of his 70th birthday

Hexaphenylcarbodiphosphorane **1**[1] can be formally regarded as a "complex" consisting of two donor molecules and an electron-rich, excited carbon atom.[2] Such a purely hypothetical formulation raises the question whether the C_2 molecule[3] can be stabilized by complexation. In principle,



1 **2**

this should be possible by coordination of a donor molecule to one C atom and an acceptor molecule to the other C atom. For our investigations, we chose a phosphane as donor and a borane as acceptor. Compound **2** was used in ab initio calculations as the simplest example of this as yet unknown molecule with betaine structure. The following synthetic route led to the target molecules **9** (Scheme 1):



3 **5** **7** **9**

Scheme 1. Synthesis of **9**, **6–9**: **a**, R = Ph; **b**, R = CH_2Ph.

[*] Prof. Dr. H. J. Bestmann, Dipl.-Chem. H. Behl, Dipl.-Chem. M. Bremer
Institut für Organische Chemie der Universität Erlangen-Nürnberg
Henkestrasse 42, D-8520 Erlangen (FRG)

Ethynyldiphenylphosphane **3**[4] is transformed into the lithium acetylide **5** with butyllithium **4**. Compound **5**, in turn, reacts with triphenylboron **6a** or tribenzylboron **6b** to give the oily ate complexes **7**. Reaction of compounds **7** with methyl iodide **8** affords **9a** and **9b**, the first derivatives of **2**.[5] The overall yields of **9a** and **9b** are 64 and 53%, respectively. These very stable compounds can be recrystallized from acetonitrile: **9a**, m.p. 201 °C (dec.); **9b**, m.p. 157 °C (dec.).

The IR spectra of **9a** and **9b** display a typical C≡C valence vibrational band at 2085 cm^{-1}. The ^{13}C NMR chemical shifts[6] of C2 (**9a**, $\delta = 71.33$; **9b**, $\delta = 72.13$) and the P–C2 coupling constants (**9a**, $^1J_{PC} = 183.1$ Hz; **9b**, $^1J_{PC} = 184.6$ Hz) are similar to the values for the P-bound C atom in 1-alkynylphosphonium salts.[7] Owing to the coupling with the P atom in β position and the B atom in α position and to the short relaxation time of the latter, the signal for C1 is not observable. (Measurements at low temperatures are not possible because of the insolubility of **9**.) The ^{31}P NMR signals[6] of **9a** ($\delta = -3.63$ in D_5C_5N) and **9b** ($\delta = -5.76$) are near to the region expected for 1-alkynylphosphonium compounds.[7] The position of the ^{11}B NMR signal[6] in the same solvent (**9a**, $\delta = -11.13$; **9b**, $\delta = -14.94$) indicates the presence of a tetravalent boron atom.

The result of the X-ray structure analysis of **9a** is given in Figure 1.[8] The C1–C2 distance (121.6(5) pm) corresponds

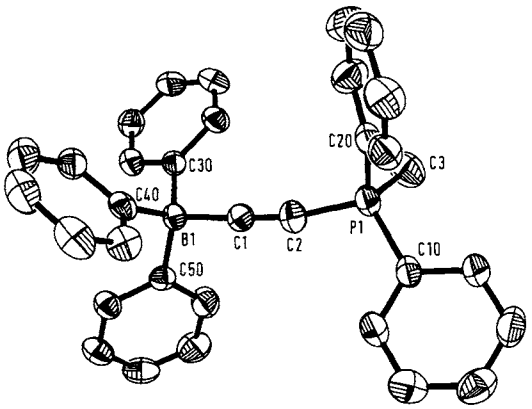


Fig. 1. Molecular structure of **9a** (ORTEP).

to a C–C triple bond. The B1–C1 distance is 159.3(5) pm and that between P1 and C2 169.9(4) pm. The molecule is not linear, the P1–C2–C1 angle being 168.9(4)°, the B1–C1–C2 angle 178.7(4)°, and the dihedral angle B1-C1-C2-P1 11.2°.

An ab initio calculation for **2** with the 3-21G basis set[9] gives bond lengths of 121.2, 159.4, and 169.4 pm for C1-C2, B1-C1, and P1-C2, respectively, in very good agreement with values found experimentally for **9a**. However, the calculation gives a linear molecule **2**. This could indicate that the bent structure of **9a** is due to a crystal packing effect.[10]

A space-filling model (Fig. 2) of **9a** shows that the C–C triple bond is very strongly shielded by the bulky groups on phosphorus (red) and boron (yellow). Indeed, **9a** and **9b** do not react, even over long periods of time, with 1,3 dipoles such as diazomethane, esters of diazoacetic acid, and phenyl azide.

As revealed in Figure 2, however, it should be easy to abstract a proton from the P-CH_3 group with methyllithium **10**. Compound **9b** thus yields phosphonium ylide **11**, which is also an ate complex (^{31}P NMR[6] (C_6D_6): $\delta = 6.76$); **11**

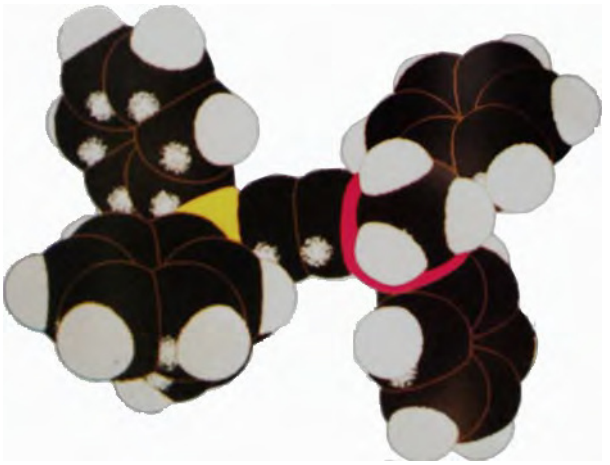
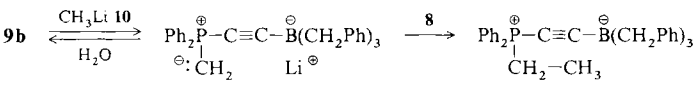


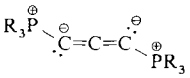
Fig. 2. Space-filling model of **9a** according to the X-ray data [8].

is transformed back into **9b** by treatment with water and reacts with methyl iodide **8** to give **12**, which, like **9**, has a betaine structure (m.p. 120 °C; NMR data[6] (D_5C_5N): ^{31}P, $\delta = 3.67$; ^{11}B, $\delta = -15.00$; ^{13}C, $\delta(C2) = 70.1$ ($^1J_{PC} = 182$ Hz); ^1H, $\delta = 1.12$ (dt, CH_3–CH_2, $^3J_{PH} = 21.61$, $^3J_{HH} = 7.3$ Hz), 2.86 (dq, CH_3–CH_2, $^2J_{PH} = 12.21$, $^3J_{HH} = 7.3$ Hz).

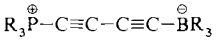


11 **12**

The successful synthesis of **9** raises the question whether the C_3 molecule might also be "stabilized". In analogy to the stabilization of a C atom in **1**, this should be possible by two donor molecules (**13**). Correspondingly, C_4 might be stabilized, as in C_2, by a donor and an acceptor molecule (**14**). We are currently investigating the synthesis of such systems.



13



14

Received: February 27, 1989;
supplemented: June 20, 1989 [Z 3195 IE]
German version: *Angew. Chem. 101* (1989) 1303

CAS-Registry-numbers:
2, 122068-87-5; **3**, 6104-47-8; **5**, 122068-86-4; **6a**, 960-71-4; **6b**, 1694-84-4; **7** R = Ph, 122068-88-6; **7** R = CH_2Ph, 122068-89-7; **9a**, 122068-90-0; **9b**, 122092-57-3; **11**, 122068-91-1; **12**, 122068-92-2; phenyl azide, 622-37-7; diazomethane, 334-88-3; diazoacetate esters, 623-73-4.

[1] Review: H. Schmidbaur, *Nachr. Chem. Tech. Lab. 27* (1979) 620.
[2] a) W. C. Kaska, D. K. Mitchell, R. F. Reichelderfer, *J. Organomet. Chem. 47* (1973) 391; b) H. Schmidbaur, *Angew. Chem. 95* (1983) 980, *Angew. Chem. Int. Ed. Engl. 22* (1983) 907.
[3] For the electronic structure of C_2 in the ground state, cf. G. Herzberg: *Atomic Spectra and Atomic Structure, Vol. I, Spectra of Diatomic Molecules*, van Nostrand, Princeton, NJ, USA 1961, p. 344.
[4] C. Charrier, W. Chodchiewicz, P. Cadiot, *Bull. Soc. Chim. Fr. 1966*, 1002.

[5] C_2 units: cf. R. Hoffmann, *Angew. Chem. 100* (1988) 1653; *Angew. Chem. Int. Ed. Engl. 27* (1988) 1593.
[6] NMR measuring frequencies: ^{13}C, 100.6 MHz; ^{1}H, 399.7 MHz; ^{31}P, 161.8 MHz; ^{11}B, 128.2 MHz.
[7] H. J. Bestmann, L. Kisielowski, *Chem. Ber. 116* (1983) 1320.
[8] **9a**: brown cubes, monoclinic symmetry, space group $P2_1/c$, $a = 988.8(2)$, $b = 1378.6(4)$, $c = 1922.9(5)$ pm, $\beta = 100.3(2)^\circ$, $V = 2579 \times 10^6$ pm^3, $\varrho_{calcd} = 1.20$ g cm^{-3}, $Z = 4$; 9372 measured reflections, 7494 unique reflections, 3865 observed reflections, ($F > 6\sigma(F)$); $R = 0.066$, $R_w = 0.081$; 318 refined parameters. Further details of the crystal structure investigation may be obtained from the Fachinformationszentrum Karlsruhe, Gesellschaft für wissenschaftlich-technische Information mbH, D-7514 Eggenstein-Leopoldshafen 2 (FRG), on quoting the depository number CSD-53823, the names of the authors, and the journal citation.
[9] 3-21G basis set: J. S. Binkley, J. A. Pople, W. S. Hehre, *J. Am. Chem. Soc. 102* (1980) 939; M. S. Gordon, J. S. Binkley, J. A. Pople, W. J. Pietro, W. J. Hehre, *ibid. 104* (1982) 2792.
[10] Bent, multiply bonded systems: cf. T. A. Albright, P. Hoffmann, E. Rossi, *Z. Naturforsch. B35* (1980) 343; G. Trinquier, J. P. Malrieu, *J. Am. Chem. Soc. 109* (1987) 5303.

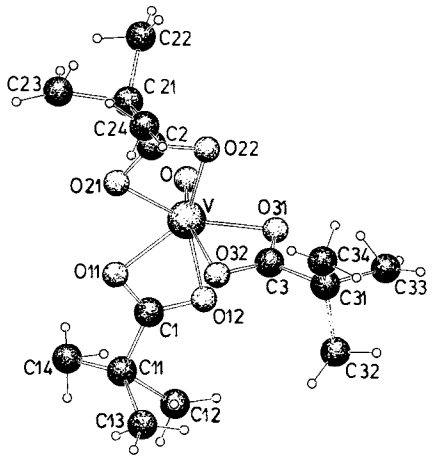


Fig. 1. Molecular structure of **1**. Selected bond lengths [pm] and angles [°]: V–O 155.7(4), V–O11 198.3(6), V–O12 220.8(4.2), V-O21 207.8(7), V–O22 201.0(4), V–O31 201.2(8), V–O32 206.4(6); O–V–O12 161.6(3), O11–V–O12 61.7(2), O21–V–O22 62.7(3), O31–V–O32 62.8(3), O11–V–O21 77.9(2), O11–V–O32 77.5(3).

$[VO(O_2CtBu)_3]$ and $[V_6O_6(\mu\text{-}O)_4(\mu\text{-}O_2CPh)_9]$: Structural Characterization of a Mononuclear V^V and a (2 + 4)-Nuclear $V^{IV}V^V_5$ Carboxylato Complex. Models for Vanadate-Dependent Peroxidases**

By *Dieter Rehder,* Wolfgang Priebsch,* and *Maren von Oeynhausen*

In recent years the bioinorganic chemistry of vanadium[1] has received increasing attention owing in part to the isolation of a vanadate(v)-dependent peroxidase from marine brown algae.[2] Haloperoxidases from knobbed wrack (*Ascophyllum nodosum*) catalyze the bromination and iodination of organic substrates with H_2O_2 and bromide or iodide, respectively. The ^{51}V NMR spectroscopic properties and the features in the XANES spectrum[3] led us to propose that the vanadium in these haloperoxidases is coordinated by six to eight ligand oxygen atoms, four to six of which belong to strained structural elements such as those formed by η^2 coordination of side-chain carboxylato groups of acidic amino acids in the protein matrix.

We have now synthesized and structurally characterized carboxylato complexes which might serve as models for the binding of vanadium in the active site of peroxidases. Simple carboxylato complexes of pentavalent vanadium, described earlier by *Preuss* et al.,[4] have still not been structurally characterized. By contrast, there exist several structurally established multinuclear acetato and benzoato complexes of vanadium with oxidation states of II, III, and IV in which the ligands serve a bridging function.[5]

The complexes $[VO(O_2CtBu)_3]$ **1**, $[VO(O_2CPh)_3]$ **2**, and $[V_6O_6(\mu\text{-}O)_4(\mu\text{-}O_2CPh)_9]$ **3**, obtained from $VOCl_3$ and the silver salts of pivalic or benzoic acid in inert solvents, form yellow (**1** and **2**) and deep red-brown (**3**) crystalline powders, which are quite stable when protected from moisture. The structures of **1** and **3**, the latter containing two molecules of CH_2Cl_2 in the unit cell ($Z = 4$), have been determined by X-ray analysis.

The mononuclear complex **1**[6] (Fig. 1) displays a pentagonal-bipyramidal structure, which is not unusual for V^V complexes of coordination number 7. All three pivalato ligands are coordinated in a bidentate fashion to vanadium, one of them being axial/equatorial with a relatively large distance of 220 pm between the vanadium atom and the axial carboxylate oxygen. The second axial ligand, in *trans* position, is a doubly bonded oxygen atom. The O–V–O12 angle is 162°; the vanadium atom is 30 pm outside the pentagonal plane. The structure of **1** found in the single crystal probably does not correspond to those of **1** and **2** in solution. The ^1H NMR and IR spectra of **1** reveal the presence of carboxylato ligands coordinated in mono- and bidentate fashion (hexacoordinated V).[4] In addition to the IR data of **1** and **2**[7] in solution, the ^{51}V NMR spectra [$\delta(^{51}V) = -597$, relative to $VOCl_3$] indicate that the chelate rings are easily opened and, on time average, contribute only partly to the overall structure.

Complex **3**,[8] shown in Figure 2, is a remarkable new type of multinuclear vanadium complex. This compound consists

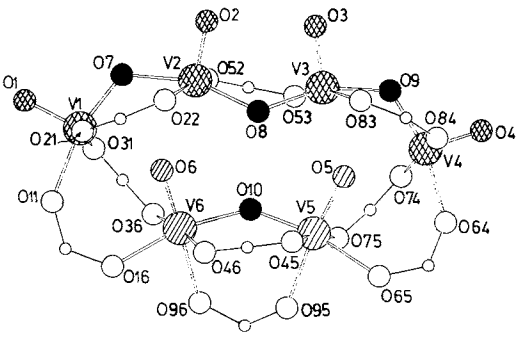


Fig. 2. Molecular structure of **3** (phenyl groups omitted). The vanadium atoms of the double bonded, terminal $O^{2\ominus}$ of the V_2 unit are hatched, those of the V_4 unit cross-hatched; $\mu\text{-}O^{2\ominus}$ shown as solid circles, carboxylate O as empty circles. The small, empty circles are the carbon atoms of the carboxylate groups. Broken lines indicate the two $\mu_3\text{-}O^{2\ominus}$. Selected bond lengths [pm] and angles [°]: V1–O1 157.3(9), V1–O7 171.0(8), V1–O11 199.8(9), V1–O21 198.9(9), V1–O31 196.4(8), V1 · · · O6 233.3(8), V2–O2 157.3(10), V2–O7 193.8(8), V2–O8 177.3(8), V2–O22 197.9(8), V2–O52 199.4(8), V2 · · · O6 243.0(8), V6–O6 161.5(8), V6–O10 185.7(7), V6–O16 199.9(8), V6–O46 200.1(7), V6–096 209.2(9), V1 · · · V2 319.5(3), V1 · · · V6 355.9(3); O1–V1–O7 102.3(4), O1–V1–O11 95.4(4), O1–V1–O21 98.8(4), O1–V1–031 99.2(4), O7–V1–O21 89.8(4), 07–V1–O31 96.1(4), O11–V1–O21 81.8(4), O11–V1–O31 86.6(4), O21–V1–O31 159.4(4), O2–V2–O7 99.7(4), O2–V2–O8 103.8(4), O7–V2–O52 80.8(3), O7–V2–O22 95.7(3), O7–V2–O2 99.7(4), O8–V2–O22 97.1(3), O8–V2–O52 89.3(3), O22–V2–O52 160.0(4), O6–V6–O10 96.4(4), O6–V6–O16 97.9(4), O6–V6–O46 94.0(3), O6–V6–O96 176.9(3), O10–V6–O36 94.0(3), O10–V6–O46 89.2(3).

[*] Prof. Dr. D. Rehder, Dipl.-Chem. W. Priebsch, M. von Oeynhausen
Institut für Anorganische und Angewandte Chemie der Universität
Martin-Luther-King-Platz 6, D-2000 Hamburg 13 (FRG)

[**] This work was supported by the Deutsche Forschungsgemeinschaft.

of one binuclear and one tetranuclear fragment, which may be regarded as mixed anhydrides of benzoic acid with divanadic and linear tetravanadic acid, respectively, the anions of which, $H_2V_2O_7^{2\ominus}$ and $HV_4O_{13}^{5\ominus}$, are known.[9] As shown by the IR spectrum (Nujol mull), compound **3** no longer contains OH groups. The V_2 and V_4 moieties in **3** are linked through four benzoate units, while the bridges within the two fragments consist of benzoate and oxo groups. The six-membered vanadium ring thereby formed adopts a flat, twist-boat conformation (puckering parameter 87.8°). The vanadium centers V5 and V6 of the V_2 unit, joined through two carboxylate bridges, have octahedral configurations. The vanadium centers V1–V4 of the tetranuclear fragment are each surrounded by five ligands, the arrangement of which corresponds to a tetragonal pyramid distorted toward a trigonal bipyramid (Fig. 3). This distortion is particularly

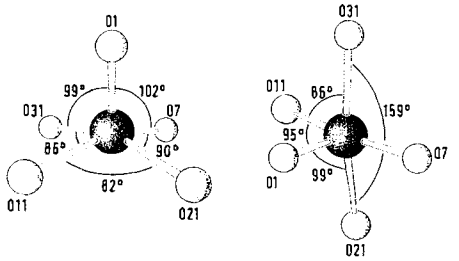


Fig. 3. Surrounding of V1 in complex **3** in the perspective of the tetragonal (left) and trigonal-bipyramidal (right) pyramids. The distance of the vanadium atom from the mean plane formed by O7, O11, O21, and O31 is 31 pm, the deviation from the trigonal plane through O1, O7, and O11 is 6.7 pm.

noticeable for the two peripheral vanadium atoms V1 and V4. This is of interest since trigonal-bipyramidal complexes of vanadium are rare.

The distances of the four vanadium centers of the V_4 unit to the vanadyl oxygen atoms O5 and O6 of the V_2 fragment (227–243 pm) lie within the range of vanadium–oxygen bonds, indicating the presence of strongly asymmetric μ_3-oxo bridges. Symmetrical μ_3-oxo bridges are commonly observed in other multinuclear vanadium complexes.[5, 10]

Of further interest is the presence of both V^{IV}[11] and V^V in **3**, as is observed in other vanadium clusters.[10] This is one more example of the frequently observed tendency of V^V to act as an oxidation agent toward organic substrates in solution.

Experimental Procedure

1: All operations were carried out under N_2 because of the high sensitivity of the compounds to moisture. A suspension of silver pivalate (6.1 g, 29.2 mmol) in 25 mL of highly purified, dry CH_2Cl_2 was slowly treated at −70 °C with a solution of $VOCl_3$ (0.84 g, 4.84 mmol) in 15 mL of CH_2Cl_2. After stirring for 60 min at this temperature, the solution was filtered to remove precipitated AgCl and the filtrate was evaporated under vacuum. The yellow, finely crystalline residue was dissolved in *n*-pentane and kept at −70 °C, resulting in the formation of suitable crystals within several hours. According to the spectroscopic data, **1** is identical with the tris(pivalato)oxovanadium(v) compound described earlier by *Preuss* et al.[4] Compound **2** was prepared similarly by reaction of $VOCl_3$ with silver benzoate at room temperature. Treatment of a solution of **2** in CH_2Cl_2 with *n*-pentane resulted, within ca. 1 week, in the crystallization of **2** along with the formation of very deep red crystals of **3** in small amounts. Compounds **1** and **2** dissolve in chlorinated solvents, the solutions turning red.

Received: March 20, 1989 [Z 3238 IE]
German version: *Angew. Chem. 101* (1989) 1295

[1] A summary of the biological functions of vanadium is found in N. D. Chasteen, *Struct. Bonding (Berlin) 53* (1983) 105.
[2] H. Vilter, *Phytochemistry 23* (1984) 1387; E. de Boer, Y. van Kooyk, M. G. M. Tromp, H. Plat, R. Wever, *Biochim. Biophys. Acta 869* (1986) 48.
[3] D. Rehder, H. Vilter, A. Duch, H. Priebsch, C. Weidemann, *Rec. Trav. Chim. PaysBas 106* (1987) 408; XANES: *X*-Ray *A*bsorption *N*ear *E*dge *S*tructure; J. Hormes, U. Kuetgens, R. Chauvistre, W. Schreiber, N. Anders, H. Vilter, D. Rehder, C. Weidemann, *Biochim. Biophys. Acta 956* (1988) 293.
[4] F. Preuss, W. Towae, J. Woitschach, *Z. Naturforsch. B35* (1980) 817.
[5] F. A. Cotton, G. E. Lewis, G. N. Mott, *Inorg. Chem. 21* (1982) 3127, 3316; *ibid. 22* (1983) 1825.
[6] a) **1**: space group $C2/C$; $a = 2761.8(5)$, $b = 897.0(2)$, $c = 2354.5(4)$ pm, $\alpha = 90.01(1)$, $\beta = 136.63(1)$, $\gamma = 89.99(1)$°, $V = 4005.6 \times 10^6$ pm^3; $\mu = 4.76$ cm^{-1}; $Z = 8$; $\varrho_{calcd} = 1.228$ g cm^{-3}; $R = 0.057$ (equal weighting) for 1869 reflections with $F > 4\sigma(F_0)$; Syntex $P2_1$ four-circle diffractometer, $Mo_{K\alpha}$ radiation (graphite monochromator), scanning range $4.5° \leq 2\theta \leq 55°$. The refinement of the structure took into consideration a threefold disorder (1:1:1) of the methyl groups on C11 and C21 and a twofold disorder (1:1:1) of the methyl groups on C31. All H atoms were placed at ideal positions. b) Further details on the crystal structure investigations may be obtained from the Fachinformationszentrum Karlsruhe, Gesellschaft für wissenschaftlich-technische Information mbH, D-7514 Eggenstein-Leopoldshafen 2 (FRG), by quoting the depository number CSD-53883, the names of the authors, and the journal citation.
[7] In the IR spectrum of **2**, dissolved in CH_2Cl_2, several bands are observed in the ν_{asym} ($CO_2^{\ominus}$) and ν_{sym} ($CO_2^{\ominus}$) regions. The $\Delta\nu$ values indicate that species with monodentate, bidentate, and bidentate-bridging carboxylate ligands are present in the equilibrium (cf. K. Nakamoto: *Infrared and Raman Spectra of Inorganic and Coordination Compounds*, 4th ed., John Wiley & Sons, New York 1986, p. 232).
[8] $3 \cdot 1/2\,CH_2Cl_2$: space group $P2_1/n$; $a = 1382.4(3)$, $b = 2391(8)$, $c = 2207.3(6)$ pm, $\alpha = 89.98(3)$, $\beta = 105.26(2)$, $\gamma = 89.98(2)$°, $V = 7038.0 \times 10^6$ pm^3; $\mu = 8.02$ cm^{-1}; $Z = 4$; $\varrho_{calcd} = 1.50$ g cm^{-3}; $R = 0.073$, $R_w = 0.063$ for 4723 reflections with $|F| > 4\sigma(F_0)$; scan range $4.5° \leq 2\theta \leq 35°$. Hydrogen atoms were calculated at ideal positions; the disorder of CH_2Cl_2 was taken into consideration with a 1:1 model [6b].
[9] L. Pettersson, B. Hedman, I. Andersson, N. Ingri, *Chem. Scr. 22* (1983) 254.
[10] A. Müller, M. Penk, E. Krickemeyer, H. Bögge, H.-J. Walberg, *Angew. Chem. 100* (1988) 1787; *Angew. Chem. Int. Ed. Engl. 27* (1988) 1719.
[11] The ESR spectrum (0.33 T) of a solution of **3** in $CHCl_3$/THF displays a complex multiline system (average spacing of the components 44 mT); an exact analysis and determination of the ESR parameters was not possible because of the extremely low solubility of **3**.

3,3′:4,4′-Bis(thieno[2,3-*b*]thiophene): A Novel Fused Heteroarene**

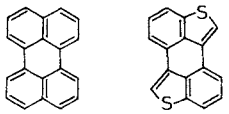
By *Yasuhiro Kono, Hisakazu Miyamoto, Yoshio Aso, Tetsuo Otsubo, Fumio Ogura,* Takanori Tanaka,* and *Masami Sawada*

The perylene–iodine complex was the first organic solid which exhibited high electrical conductivity.[1] In addition, perylene **1** formed radical-cation salts which qualified as low-dimensional organic metals.[2] The unusual properties of **1** are based on its relatively low ionization potential compared with other hydrocarbons.[3] Heteroaromatic compounds usually have lower ionization potentials than aromatic hydrocarbons. In addition, the incorporated heteroatom may induce higher polarization in the molecule and enhance intermolecular interactions. *Wudl* et al. reported an

[*] Prof. Dr. F. Ogura, Prof. Dr. T. Otsubo, Dr. Y. Aso, H. Miyamoto, Y. Kono
Department of Chemistry, Faculty of Engineering, Hiroshima University
Saijo, Higashi-Hiroshima 724 (Japan)
Prof. Dr. M. Sawada, T. Tanaka
Institute of Scientific and Industrial Research, Osaka University
Ibaraki, Osaka 567 (Japan)

[**] This work was supported in part by a grant-in-aid from the Ministry of Education, Science, and Culture, Japan.

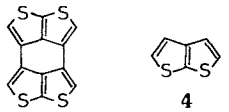
isoelectronic heterocyclic analogue of **1**, 3,4′:4,3′-bis(benzo[*b*]thiophene) **2**, which formed an iodine complex with very similar properties to those of the known perylene–iodine solid.[4]



1 **2**

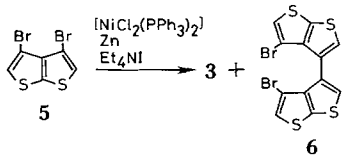
Suitable electron-donor components for organic metals must satisfy the following requirements: high symmetry, high planarity, high polarizability, low ionization potential, and strong intermolecular interaction.[5] In this connection, 3,3′:4,4′-bis(thieno[2,3-*b*]thiophene) **3**, the perimeter of which consists only of thiophene rings, might be a superior electron-donor to **1** and **2**. The unique fused structure of **3** is also interesting. Here we report the synthesis, structure, and some properties of **3**.

The simplest approach to **3** seemed to be dimerization of thieno[2,3-*b*]thiophene **4** at the two β positions. Following



3 **4**

this strategy, we attempted a reductive coupling of 3,4-dibromothieno[2,3-*b*]thiophene **5**, prepared from **4** according to a known method.[6] The conventional treatment of **5** with a catalytic amount of bis(triphenylphosphane)nickel(II) chloride, excess active zinc, and tetraethylammonium iodide in refluxing benzene[7] gave only 4,4′-dibromo-3,3′-bis(thieno[2,3-*b*]thiophene) **6** (maximum yield 28%). However, increasing the quantity of the nickel reagent resulted in formation of the desired product **3**, whose yield was optimized up to 14%.[8]



5 **6**

Compound **3**, though its molecular model reveals severe strain, was very stable and crystallized in the form of pale brown needles from carbon disulfide. It sublimed around 270 °C at atmospheric pressure and did not melt up to 300 °C in a sealed tube. The simple ^{1}H and ^{13}C NMR spectra support its highly symmetrical structure (see Table 1). Compound **3** is not so colored as perylene **1**, but the UV/VIS absorption spectrum exhibits marked bathochromic and hyperchromic shifts as compared with that of thieno[2,3-*b*]thiophene **4**; this reflects the extended π conjugation of **3**.[9]

Table 1. Some spectral data of **3**.

^{13}C NMR (67.8 MHz, [D$_6$]DMSO): δ = 121.95, 125.15, 132.98, 150.17; ^{1}H-NMR (60 MHz, CS_2): δ = 7.23(s). IR (KBr): $\tilde{\nu}$ = 3100, 1421, 819, 740, 719, 693 cm^{-1}. MS (70 eV): *m/z* (intensity [%]), 276 (100, $M^{\oplus}$), 277(16), 278(19), 279(2.7), 280(1.5). UV/VIS (THF): $\lambda_{max}(\varepsilon)$ = 242 (46400), 254 (34200), 330 nm (22000).

The structure of **3** was confirmed by an X-ray crystallographic analysis (Fig. 1).[10] The molecule is planar and has a center of symmetry. The five-membered rings suffer from considerable strain in bond angles rather than in bond lengths as compared with the structures of thiophene[11] and thieno[3,2-*b*]thiophene.[12] In conformity with this view and in contrast to perylene,[13] the central six-membered ring is somewhat deformed and different from a regular hexagon.

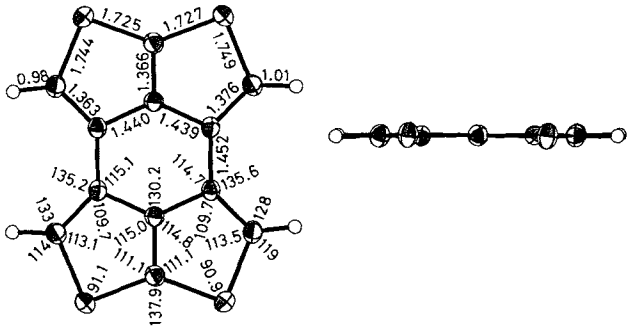


Fig. 1. Molecular structure of **3** viewed from above the plane (left) and from the side (right). The figure shows bond lengths [Å] and angles [°].

The cyclic voltammogram of **3** showed one reversible redox wave with a half-wave potential at 1.01 V versus a Ag/AgCl standard electrode.[14] This value is considerably lower than that (> 1.5 V) of **4** but equal to that (1.00 V) of **1**. Repetitive cycling soon changed the voltammogram to two redox waves at 0.74 and 1.10 V and resulted in a black polymeric deposit on the working electrode.[15] The same material was also formed by potentiostatic electropolymerization of **3** at 1.05 V in benzonitrile solution containing tetrabutylammonium perchlorate as supporting electrolyte. Since **3** has four reactive sites for polymerization, the polymer must have a complex network structure. The elemental analysis (C, 45.57; H, 1.05%) suggested that the polymer was doped with the counterion $ClO_4^{\ominus}$ (doping level 0.5). Its electrical conductivity measured on a compressed pellet at room temperature was 0.06 S cm^{-1}. Like **1** and **2**, compound **3** formed fine black crystals from chlorobenzene solution containing an equivalent amount of iodine. The complex had 1:1 stoichiometry of **3** to iodine and showed the relatively high electrical conductivity of 0.11 S cm^{-1}.

Received: March 28, 1989;
supplemented: May 23, 1989 [Z 3253 IE]
German version: *Angew. Chem. 101* (1989) 1254

CAS Registry numbers:
3, 122068-94-4; **3**-polymer, 122068-96-6; **3**·I_2, 122068-95-5; **5**, 53255-78-0; **6**, 122068-93-3.

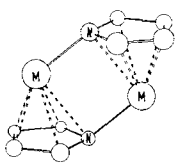
[1] H. Akamatu, H. Inokuchi, Y. Matsunaga, *Nature (London) 173* (1954) 168; *Bull. Chem. Soc. Jpn. 29* (1956) 213.
[2] H. J. Keller, D. Nöthe, H. Pritzkow, D. Wehe, M. Werner, P. Koch, D. Schweitzer, *Mol. Cryst. Liq. Cryst. 62* (1980) 181.
[3] V. D. Parker, *J. Am. Chem. Soc. 98* (1976) 98.
[4] F. Wudl, R. C. Haddon, E. T. Zellers, F. B. Bramwell, *J. Org. Chem. 44* (1979) 2491.
[5] G. Saito, J. P. Ferraris, *Bull. Chem. Soc. Jpn. 53* (1980) 2141.
[6] P. Fournari, P. Meunier, *Bull. Soc. Chim. Fr.* (1974) 583.

[7] M. Iyoda, K. Sato, M. Oda, *Tetrahedron Lett. 26* (1985) 3829, and references cited therein.
[8] Satisfactory elemental analyses were obtained for **3** and **6**. The optimal yield (14%) for **3** was obtained by refluxing a mixture of **5** (0.5 g, 1.68 mmol), bis(triphenylphosphane)nickel(II) chloride (0.54 g, 0.84 mmol), active zinc (1.42 g, 21.7 mmol), and tetraethylammonium iodide (2.76 g, 10.7 mmol) in dry benzene (15 mL) for 28 h.
[9] UV/VIS data (THF): **1**: λ_{max} [nm] (ε) = 253 (42800), 388 (12700), 410 (27900), 437 (36200); **4**: λ_{max} [nm] (ε) = 225 (25600), 248 (5020), 255 (4510), 260 (3630).
[10] Crystal data of **3**: orthorhombic, space group *Pcab*, $a = 15.029(3)$, $b = 5.179(1)$, $c = 13.380(3)$ Å, $V = 1041.0$ Å^3, $Z = 4$, $\varrho_{calcd} = 1.764$ g cm^{-3}, $\varrho_{obsd} = 1.76$ g cm^{-3}, $R = 0.033$ for 1100 unique reflections ($Mo_{K\alpha}$, $\lambda = 0.71069$ Å). Further details of the X-ray analysis can be obtained from the director of the Cambridge Crystallographic Data Centre, University Chemical Laboratory, Lensfield Road, Cambridge CB2 1EW (England), on quoting the names of the authors and the journal citation.
[11] B. Bak, D. Christensen, L. Hansen-Nygaard, J. Rastrup-Andersen, *J. Mol. Spectrosc. 7* (1961) 58.
[12] E. G. Cox, R. J. J. H. Gillot, G. A. Jeffrey, *Acta Crystallogr. 2* (1949) 356.
[13] A. Camerman, J. Trotter, *Proc. R. Soc. London Ser. A 279* (1964) 129.
[14] Cyclic voltammograms were measured with a Pt working electrode and a Pt counterelectrode at a scan rate of 100 mV sec^{-1} in benzonitrile solution containing 0.1 M tetrabutylammonium perchlorate as supporting electrolyte at room temperature.
[15] IR data (KBr) of the polymeric material obtained from **3**: 3100, 1405, 1085, 840, 735, 710, 624 cm^{-1}.

N-Cesiocarbazole · pmdta and *N*-Potassiocarbazole · pmdta (PMDTA = *N,N,N′,N″,N″*-Pentamethyldiethylenetriamine). Cation Size and Multihapto Bonding**

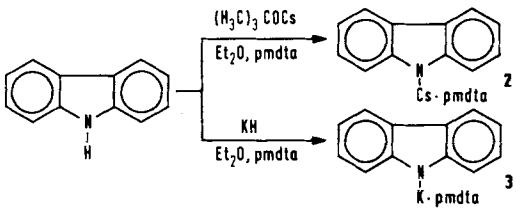
By *Karina Gregory, Matthias Bremer, Paul von Ragué Schleyer,* Peter A. A. Klusener* and *Lambert Brandsma*

We compare the solid state structures of *N*-cesiocarbazole · pmdta and *N*-potassiocarbazole · pmdta. To our knowledge,[1] these are the first single crystal diffraction analyses of a Cs-amide and of an aromatic K-amide. Compared to the rich literature on the structures of Li-amides,[2] relatively little information is available for derivatives of the heavier alkali metals.[3] Since we determined the X-ray structures of *N*-lithiocarbazole · 2 THF,[2a] and of *N*-sodiocarbazole · 2 HMPTA,[3b] we have chosen the cesium and the potassium salts as our next objectives. For *N*-lithiopyrrole (**1**, M = Li) simultaneous σ and π interactions have been predicted but are only partially achieved in the solid state structure of *N*-lithiocarbazole · 2 THF.[2a] However, multihapto bonding should become more important with increasing cation size. As the structures of the organic anion moieties are not expected to vary greatly, attention focusses on the differences in the location of the alkali metal cations and in their coordination.



1

N–Cesiocarbazole · pmdta (**2**) was prepared by treatment of a suspension of Cs-*tert*-butoxide in ether containing pmdta with a solution of carbazole in ether [Eq. (a)]. Storing for one week at -26 °C gave yellow crystals of X-ray quality. *N*–Potassiocarbozole · pmdta (**3**) was prepared in analogous manner using KH[4] as metalating agent [Eq. (b)].



The structures were solved by direct methods.[5] **2** exists as two different dimeric aggregates in the solid state. The atom numbering scheme, selected bond lengths and angles are shown in Figure 1 and 2. The asymmetric unit consists of three molecules of **2**, two of which form a dimer with C_1 symmetry. A crystallographic inversion center generates a second dimer with C_i symmetry. In each of the dimers, two chelated cesium cations bridge two organic anions differently, by making use of both σ and π interactions (π bond in this context describes the electrostatic interaction of the $Cs^{\oplus}$ cation with the π face of the carbazole system). The tridentate donor ligand PMDTA completes the $Cs^{\oplus}$ coordination sphere. In the dimer with C_i symmetry (Fig. 1), the cesium

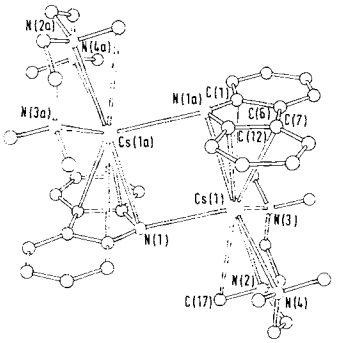


Fig. 1. Structure of the C_i-symmetric dimer of **2** in the crystal (drawn with the program XP-SHELXPLUS). Selected bond lengths [Å] and angles [°]: Cs(1)–N(1) 3.102(6), Cs(1)–N(1a) 3.335(5), Cs(1)–C(1) 3.399(6), Cs(1)–C(6) 3.511(6), Cs(1)–C(7) 3.450(5), Cs(1)–C(12) 3.343(5), Cs(1)–N(2) 3.178(5), Cs(1)–N(3) 3.200(5), Cs(1)–N(4) 3.179(7), Cs(1)–C(17) 3.473(7); Cs(1)–N(1)–Cs(1a) 91.9(2), N(1)–Cs(1)–N(1a) 88.1(2), N(1)–Cs(1)–N(2) 92.9(1).

cations are each σ bonded to one carbazole nitrogen and at the same time π bonded to the five membered ring of a second carbazole unit. The central unit, a planar $(M–N)_2$ four membered ring, also is observed in dimeric Li-amide structures.[2a–g] The Cs–C distances, indicated as close contacts in Figure 1, range from 3.3 to 3.5 Å, i.e. are shorter than the Cs–CH_3 distances (3.53 Å) found in the powder structure of methylcesium.[6] The Cs–N σ and π separations are 3.10 and 3.34 Å, respectively. The CH_3 groups on the

[*] Prof. Dr. P. von R. Schleyer, Dipl.-Chem. K. Gregory, Dr. M. Bremer
Institut für Organische Chemie der Universität Erlangen-Nürnberg
Henkestrasse 42, D-8520 Erlangen (FRG)
Prof. Dr. L. Brandsma, Mr. P. A. A. Klusener
Organisch Chemisch Laboratorium
Rijksuniversiteit Utrecht
Padualaan 8, NL-3584 CH Utrecht (The Netherlands)

[**] This work was supported by the Deutsche Forschungsgemeinschaft, the Fonds der Chemischen Industrie, the Volkswagen Stiftung, the Convex Corporation and the Netherlands Science Foundation (SON). We are indebted to Chemetall GmbH, Frankfurt a. M. (FRG) for a generous gift of cesium.

central pmdta N-atoms are bent twoards the σ bonded carbazole units, exhibiting additional metal–methyl carbon interactions at 3.47 Å. This shows again[1] that the presence of the methyl H's does not preclude short Cs–C contacts. The C_i dimer represents the ideal simultaneous combination of σ and π interactions initially predicted for *N*-lithiopyrrole (**1**, M = Li).[2a]

The dimer of **2** with C_1 symmetry (Fig. 2) has the same structural features as the C_i dimer but is distorted and exhibits significant differences. The distortion of the C_i dimer is shown by the 20.6° tilting of the carbazole units relative to one another. Hence, the central $(Cs–N)_2$ four-membered ring is non-planar. Only Cs(3) is located centrally above the five-membered ring of the carbazole anion, while Cs(2) has a reduced number of coordinative π interactions with the second anion. The Cs(2)–N(1′) and Cs(2)–(C12′) π distances (3.18 and 3.23 Å, respectively) are much shorter than in the C_i dimer. This Cs–N π distance is nearly the same as the Cs(2)–N(1″) σ separation (3.12 Å). An additional short distance of 3.43 Å between Cs(2) and the carbon atom C(17′) of the central pmdta-CH_3 group is present again. The inverted orientation of the pmdta ligand of Cs(3), compared with the C_i dimer, results in an increase of the Cs(3)–C(17″) distance (3.55 Å). Cs(3) exhibits π interactions shorter than 3.5 Å with all four carbon atoms of the central five membered ring of the carbazole unit.

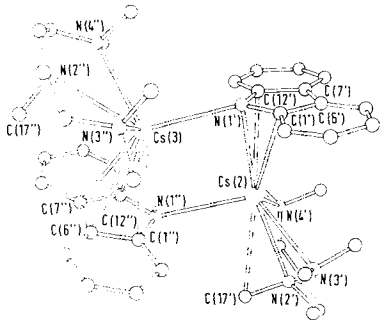


Fig. 2. Structure of the C_1-symmetric dimer of **2** in the crystal. Selected bond lengths [Å] and angles [°]: Cs(2)–N(1″) 3.116(5), Cs(2)–N(1′) 3.181(5), Cs(2)–C(1′) 3.441(5), Cs(2)–C(6′) 3.754(6), Cs(2)–C(7′) 3.625(6), Cs(2)–C(12′) 3.233(6), Cs(2)–N(2′) 3.177(5), Cs(2)–N(3′) 3.191(5), Cs(2)–N(4′) 3.149(4), Cs(2)–C(17′) 3.427(7), Cs(3)—N(1′) 3.096(5), Cs(3)–N(1″) 3.360(5), Cs(3)–C(1″) 3.396(6), Cs(3)–C(6″) 3.469(5), Cs(3)–C(7″) 3.433(6), Cs(3)–C(12″) 3.337(6), Cs(3)–N(2″) 3.198(4), Cs(3)–N(3″) 3.201(4), Cs(3)–N(4″) 3.152(5), Cs(3)–C(17″) 3.551(7); Cs(2)–N(1′)–Cs(3) 92.0(1), Cs(2)–N(1″)–Cs(3) 88.3(1), N(1′)–Cs(2)–N(1″) 90.4(1), N(1′)–Cs(3)–N(1″) 87.5(1), N(1″)–Cs(2)–N(2′) 101.3(1), N(1′)–Cs(3)–N(2″) 136.2(1).

3, the potassium analogue of **2** crystallizes as a C_i dimer and is intermediate structurally between the lithium and the cesium derivatives (Fig. 3). **3** shows similarities with both the C_i and the C_1 dimer of **2**. However, due to the smaller coordination sphere of $K^{\oplus}$, the π bonded $K^{\oplus}$ cation (K–N(1a) 2.83 Å) shows only one short K–C(12a) π contact of 3.35 Å, whereas the σ bonded (K–N(1) 2.81 Å) is shifted towards the other side of the carbazole moiety resulting in one weak carbon σ separation of 3.47 Å. The orientation of the pmdta ligands attached to the cations is the same as in the C_1 dimer of **2** at Cs(3), and therefore reversed to that in the C_i dimer of **2**. Due to the increased bending of the ligands towards the π bonded carbazole moieties, the N(1)–K–N(2) bond angle is 162.8° and the K–C(17) separation 3.33 Å. The corresponding N(1)–M–N(2) angles in **2** are 92.9° at Cs(1), 101.3° at Cs(2) and 136.2° at Cs(3).

Ab initio calculations[7] on methylcesium/potassium and the classical, nonbridging *syn*-form of allylcesium/potassium

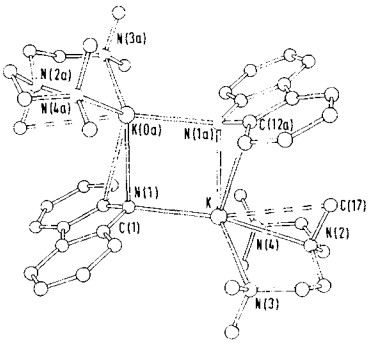
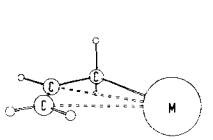
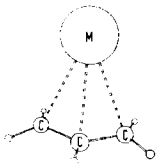


Fig. 3. Structure of the C_i-symmetric dimer of **3** in the crystal. Selected bond lengths [Å] and angles [°]: K–N(1) 2.812(3), K–N(1a) 2.827(4), K–C(12a) 3.348(4), K–C(1) 3.469(4), K–C(2) 3.521(5), K–N(2) 2.872(4), K–N(3) 2.989(4), K–N(4) 2.860(4), K–C(17) 3.327(5); K–N(1)–K(0a) 93.1(1), N(1)–K–N(1a) 86.9(1), N(1)–K–N(2) 162.8(1).

(with M in the carbon plane, **4**) gave Cs–C bond lengths of 3.073 and 3.066 Å (M = Cs) and K–C bond lengths of 2.754 and 2.750 Å (M = K), respectively. In the symmetrically bridged structure of allylcesium (**5**, M = Cs), the Cs–C distances are calculated to be somewhat longer: 3.218 Å from the Cs cation to the terminal carbon atoms and 3.210 Å to the central carbon. These values are in good agreement with the Cs–C distance of 3.29 Å in the graphite inclusion complex,[8] determined from layer spacings, and with our experimental findings for the Cs–C π separations, taking the expected effect of solvation of the cesium cations into account. Solvation in organo-lithium and -sodium compounds increases the carbon–metal distances by about 0.2 Å;[1] a similar lengthening for Cs derivatives is now indicated. The calculated bond lengths for the bridged structure of allylpotassium (**5**, M = K) are 2.888 and 2.857 Å and therefore in good agreement with the shortest K–C π separations found in the solid state structure of fluorenyl potassium · tmeda (3.04 to 3.35 Å).[9] The slightly longer K–C(12a) π bond in **3** (3.35 Å) must be due to the tridentate donor pmdta, that solvates the $K^{\oplus}$ cation more effectively than the bidentate donor tmeda in the fluorenyl compound.



4



5

The solid state structure of **2** results from the large coordination propensities of the cation. The cesium cation is stabilized via multihapto bonding with the anion, with the tridentate donor ligand, pmdta, and with the nitrogen of the second carbazole. Three of the four Cs-cations are formally nine-coordinated (taking only Cs–C separations less than 3.5 Å into account), the fourth $Cs^{\oplus}$ has only eight occupied coordination sites but with tighter interactions. The smaller coordination sphere of $K^{\oplus}$ seems to be satisfied by the pmdta ligand and the two carbazole nitrogen atoms. Only one additional K–C π contact is indicated. The corresponding dimeric solid state structures of the Li- and Na compounds[2a, 3b] differ significantly from that of *N*-cesio-carbazole. The smaller cations bridge the two anions by making use of σ and π interactions but only with the nitrogen atoms of the carbazole moieties and not with the π faces as in **2**. The smaller coordination spheres of $Li^{\oplus}$ and $Na^{\oplus}$, preclude the higher degree of multihapto bonding which is possible with

$Cs^{\oplus}$. The intermediate situation, with one M–C π contact, is presented by the potassium compound.

Experimental Procedure

Preparation of $(H_3C)_3COCs$: After opening a cold (0 °C) sealed ampule containing cesium (11.5 g, 86.5 mmol) under nitrogen, the metal was suspended in 300 ml of dried THF under argon atmosphere and warmed to 35 °C. *tert*-Butyl alcohol (5.5 g, 74 mmol) in 10 ml of THF was added in one portion under vigorous stirring. After 2 h all the alcohol had reacted, as evidenced by the formation of a light blue color. Evaporation of the solvent after filtering the reaction mixture and carefully removing unreacted metal gave $(H_3C)_3COCs$ as a white powder. The last traces of solvent were removed in vacuo at 40 °C. Yield: 13.8 g (91%).

2: $(H_3C)_3COCs$ (1.756 g, 8.5 mmol) was suspended in dried ether (20 ml) under argon atmosphere and first pmdta (3.0 ml, 14.0 mmol) and then 1.325 g of carbazole (7.9 mmol) dissolved in 20 ml of ether were added. The yellow-fluorescing reaction mixture was stored at −26 °C. After one week, yellow crystals had formed. Yield: 1.63 g (43.6%).

3: As described for **2**, using KH [4] (0.431 g, 8.5 mmol). Recrystallization gave green-yellow plates. Yield: 1.89 g (63.9%).

Received: March 28, 1989;
supplemented: June 5, 1989 [Z 3259 IE]
German version: *Angew. Chem. 101* (1989) 1261

CAS Registry numbers:
2 (without PMDTA), 73689-66-4; $(\mathbf{2})_2$, 122212-50-4; **3** (without PMDTA), 6033-87-0; $(\mathbf{3})_2$, 122189-09-7; $(H_3C)_3COCs$, 3934-09-6.

[1] C. Schade, P. von R. Schleyer, *Adv. Organomet. Chem. 27* (1987) 169.

[2] a) R. Hacker, E. Kaufmann, P. v. R. Schleyer, W. Mahdi, H. Dietrich, *Chem. Ber. 120* (1987) 1533; b) B. Cetinkaya, P. B. Hitchcock, M. F. Lappert, M. C. Misra, A. J. Thorne, *J. Chem. Soc. Chem. Commun. 1984*, 148; c) D. Barr, W. Clegg, R. E. Mulvey, R. Snaith, *ibid. 1984*, 700; d) D. Barr, W. Clegg, R. E. Mulvey, R. Snaith, D. S. Wright, *ibid. 1987*, 716; e) M. F. Lappert, M. J. Slade, A. Singh, *J. Am. Chem. Soc. 105* (1983) 302; f) D. Barr, W. Clegg, R. E. Mulvey, R. Snaith, *J. Chem. Soc. Chem. Commun. 1984*, 285; g) D. R. Armstrong, D. Barr, W. Clegg, S. M. Hodgson, R. E. Mulvey, D. Reed, R. Snaith, D. S. Wright, *J. Am. Chem. Soc 111* (1989) 4719; h) D. Mootz, A. Zinnius, B. Böttcher, *Angew. Chem. 81* (1969) 398; *Angew. Chem. Int. Ed. Engl. 8* (1969) 378; i) R. D. Rogers, J. L. Atwood, R. Grüning, *J. Organomet. Chem. 157* (1987) 229.

[3] a) K. Gregory, M. Bremer, W. Bauer, P. von R. Schleyer, E. Weiss, unpublished; b) A full paper on the structures of the alkali-metal carbazoles (M = Li, Na, K, Rb, Cs) is in preparation; c) R. Grüning, J. L. Atwood, *J. Organomet. Chem. 137* (1977) 101; d) D. J. Brauer, H. Bürger, W. Geschwandtner, G. R. Liewald, C. Krüger, *ibid. 248* (1983) 1; e) A. M. Domingos, G. M. Sheldrick, *Acta Crystallogr. Sect. B30* (1974) 517.

[4] R. Pi, T. Friedl, P. von R. Schleyer, P. Klusener, L. Brandsma, *J. Org. Chem. 52* (1987) 4299.

[5] Crystallographic data: Nicolet R3m/V diffractometer, $Mo_{K\alpha}$ radiation ($\lambda = 0.71073$ Å, graphite monochromator). $T = 200$ K. ω scan with 3 to 15°/min in ω. Solution: Direct methods (SHELXTL PLUS). Refinement: full matrix least squares, non-hydrogen atoms with anisotropic temperature factors, hydrogen atoms were included using a riding model. – **2**: $C_{21}H_{31}N_4Cs$ (monomer), $M = 469.4$, yellow columns from ether, crystal size: $0.6 \times 0.5 \times 0.5$ mm^3. Triclinic, space group $P\bar{1}$, $a = 1018.6(3)$, $b = 1331.4(4)$, $c = 2704.9(12)$ pm, $\alpha = 94.53(3)$, $\beta = 96.27(3)$, $\gamma = 108.35(2)°$, $\varrho_{calcd} = 1.37$ g cm^{-3} ($Z = 6$ monomers). 12890 reflections collected ($4° < 2\theta < 54°$); *unique: 12842; observed: 10650* ($F > 4\sigma(F)$). $R = 0.043$, $R_w = 0.047$. 706 refined parameters. – **3**: $C_{21}H_{31}N_4K$ (monomer), $M = 378.6$, yellow plates from ether, crystal size: $0.2 \times 0.4 \times 0.4$ mm^3. Triclinic, space group $P\bar{1}$, $a = 928.7(5)$, $b = 1017.7(4)$, $c = 1263.2(6)$ pm, $\alpha = 111.11(3)$, $\beta = 102.77(4)$, $\gamma = 90.30(4)°$, $\varrho_{calcd} = 1.16$ g cm^{-3} ($Z = 2$ monomers), $T = 200$ K. ω scan with 3 to 15°/min in ω. 4823 reflections collected ($4° < 2\theta < 52°$); 3865 unique; 2650 observed ($F > 5\sigma(F)$). Solution: direct methods (SHELXTL PLUS). Refinement: full matrix least squares, non-hydrogen atoms with anisotropic temperature factors, hydrogen atoms were included using a riding model. $R = 0.065$, $R_w = 0.060$. 236 refined parameters. – Further details of the crystal structure investigation are available on request from the Fachinformationszentrum Karlsruhe, Gesellschaft für wissenschaftlich-technische Information mbH, D-7514 Eggenstein-Leopoldshafen 2 (FRG), on quoting the depository number CSD-53917, the names of the authors, and the journal citation.

[6] E. Weiss, H. Köster, *Chem. Ber. 110* (1977) 717.

[7] Y.-D. Wu, P. von R. Schleyer, unpublished ab initio calculations using the 3-21G (6-31 + G) basis set and a Huzinaga DZ basis set on Cs (K), respectively.

[8] a) W. Rüdorff, *Adv. Inorg. Chem. Radiochem. 1* (1959) 223; b) S. A. Solin, *Adv. Chem. Phys. 49* (1982) 455; c) F. Levy (Ed.): *Intercalated Layered Materials*, Reidel, Dordrecht 1979.

[9] R. Zerger, W. Rhine, G. D. Stucky, *J. Am. Chem. Soc. 96* (1974) 5441.

Very Short C–C Single Bonds and Their Origin. The Central Bond Length in Bitetrahedryl**

By *Paul von Ragué Schleyer** and *Matthias Bremer*

Dedicated to Professor Christoph Rüchardt on the occasion of his 60th birthday

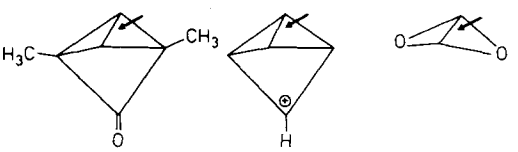
Single C–C bonds in saturated systems were once believed to be remarkably invariant in length. Compilations give 1.537(1) Å as the standard value taken from a large number of X-ray structures.[1] The C–C bond length in diamond is 1.54452 Å.[1c] However, an increasingly large number of significantly longer[2] or shorter[3–9] C–C bonds[1] are now being found, both experimentally[3–8] and calculationally.[9] The short 1.408 Å[3b] distance in **1** appears to be the experimental record in saturated systems, although the central C–C lengths are around 1.38 Å when two dicoordinate carbons are joined; e.g. in butadiyne, cyanoacetylene, and cyanogen (Table 1).

Table 1. Dicoordinate C–C bond lengths [Å].

Molecule	3-21G	6-31G*	Experimental
HCC–CCH	1.374 [a]	1.389 [b]	1.384(2) [d]
HCC–CN	1.370 [c]	1.370 [c]	1.378 [c]
NC–CN	1.368 [a]	1.397 [a]	1.387(1) [e]

[a] R. A. Whiteside, M. J. Frisch, J. A. Pople (Eds.): *The Carnegie-Mellon Quantum Chemistry Archive*, 3rd. Ed., Carnegie-Mellon University 1983. [b] This work. [c] See reference 10, Table 6.10. [d] M. Tanimoto, K. Kuchitsu, Y. Morino, *Bull. Chem. Soc. Jpn. 44* (1971) 386. [e] Y. Morino, K. Kuchitsu, Y. Mori, M. Tanimoto, *ibid. 41* (1968) 2349.

In the cation **2** corresponding to **1**, 6-31G* calculations indicate a comparable length of 1.372 Å for the central bond.[9b] Our ab initio examination of 2,4-dihetero-bicyclobutanes reveals an even greater shortening of the C–C central bond; the 6-31G* length is predicted to be only 1.338 Å in **3**.[9a] The accuracy of 6-31G* ab initio structures



	1	**2**	**3**
exp.	1.408 [3b]	-	-
3-21G	-	1.408	1.365
6-31G*	-	1.372	1.338
MP2/6-31G*	-	1.376	

Scheme 1. X-ray crystallographically determined and calculated values for the lengths of the central C–C bond [Å] in bicyclobutanes.

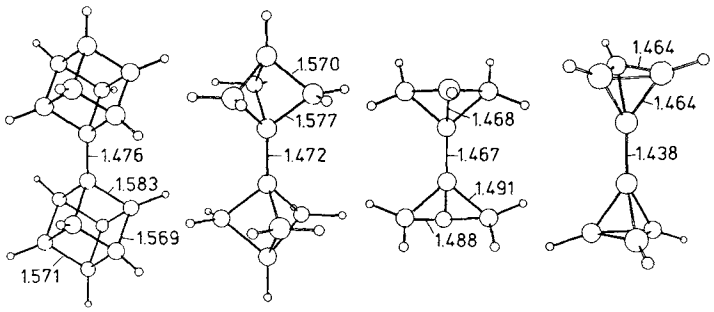
is extensively documented; average errors in C–C bond lengths are less than 0.01 Å[10] (cf. Table 1 and Scheme 2). Errors with the smaller 3-21G basis set are only somewhat greater.[10]

When two tertiary or bulky alkyl groups are bound together, the central bond lengthens, often appreciably, due to

[*] Prof. Dr. P. von R. Schleyer, Dr. M. Bremer
Institut für Organische Chemie der Universität Erlangen-Nürnberg
Henkestrasse 42, D-8520 Erlangen (FRG)

[**] This work was supported by the Fonds der Chemischen Industrie, the Convex Computer Corporation, and ARDEC, Dover, N.J., USA. We thank *B. Reindl* (Erlangen) for the calculations on **2** and Prof. *O. Ermer* (Köln) for suggestions.

steric interactions and to angular distortions.[2] When, however, the alkyl moieties are "bent back" as in the cage and bridged ring systems, bicubyl **4**, bi(bicyclo[1.1.1]pentyl) **5**, bi(bicyclo[1.1.0]butyl) **6** and bitetrahedryl **7**, appreciable shortening of the central bond results.[4] This effect has been emphasized recently;[3-7] we now provide a more detailed explanation along with calculational data for a number of these compounds including the ultimate (but experimentally inaccessible) goal, bitetrahedryl, **7**. The central bond length



	4	5	6	7
			1.468, 1.470	
exp.	1.458, 1.474	1.480	1.480, 1.480	-
MNDO	1.476	1.470	1.439	1.408
3-21G	-	1.472	1.439	1.408
6-31G*	-	-	1.467	1.438

Scheme 2. X-ray crystallographically determined and calculated values for the C–C bond lengths [Å] in **4**–**7**. The values quoted under the formulas refer in each case to the central bond.

is 1.438 Å, when optimized with the 6-31G* basis set. This basis, which contains d-type polarization functions on carbon, gives creditable agreement with experiment for the central bond lengths of **4**–**6**. The comparison given below (Scheme 2) includes the optimized distances obtained with the smaller split valence 3-21G basis set and with the semiempirical MNDO[11] method. For comparison, the C–C length in ethane at the ab initio levels used here are 1.542 Å (3-21G) and 1.528 Å (6-31G*) (the experimental value is 1.531 Å).[10]

Both these ab initio basis sets reproduce the 3 kcal mol^{-1} experimental rotation barrier in ethane satisfactorily.[10] To probe the reasons for the C–C bond length changes, we carried out a series of 3-21G optimizations of both staggered (D_{3d}) and eclipsed (D_{3h}) ethane in which all H-C-C bond angles were fixed, but the bond lengths allowed to attain their minimum energy values. The results, shown in Figure 1 for both conformations, are remarkable. When the HCC angle is widened to 150° to simulate the situation in **7**, the C–C distance in both conformers decreases to about 1.38 Å, and the rotational barrier (Fig. 2) essentially vanishes. A decrease in the HCC angle has the opposite effect, the C–C bond length increases (Fig. 1) as does the rotation barrier (Fig. 2).

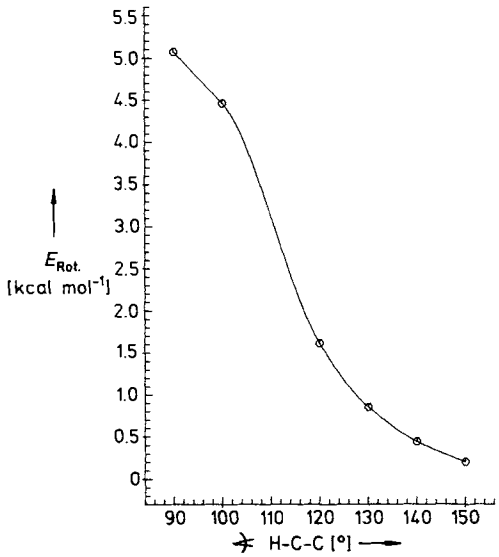


Fig. 2. The rational barrier E_{rot} for distorted ethane as a function of the H-C-C angle (3-21G).

Walsh diagrams[12] (plots of the valence orbital energies as a function of the HCC angle) provide insights. Figure 3 shows this for the D_{3d} form; the D_{3h} plot is similar. The largest change is noted for the a_{1g} orbital;[13] the energy becomes much lower at large HCC angles. This bonding sigma MO is comprised of carbon *p*-orbitals aligned with the

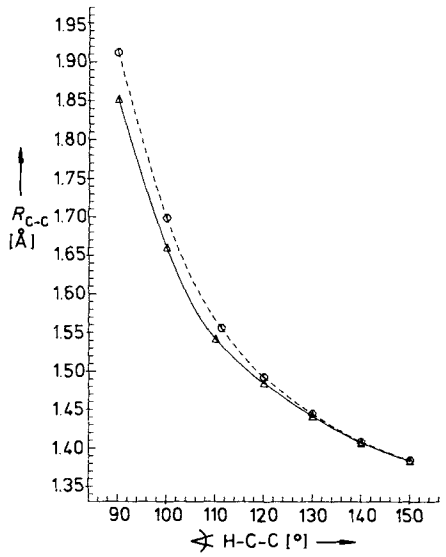


Fig. 1. The C–C bond length in distorted enthane (D_{3d}-symmetry, D_{3h} dashed) as a function of the H-C-C angle (3-21G).

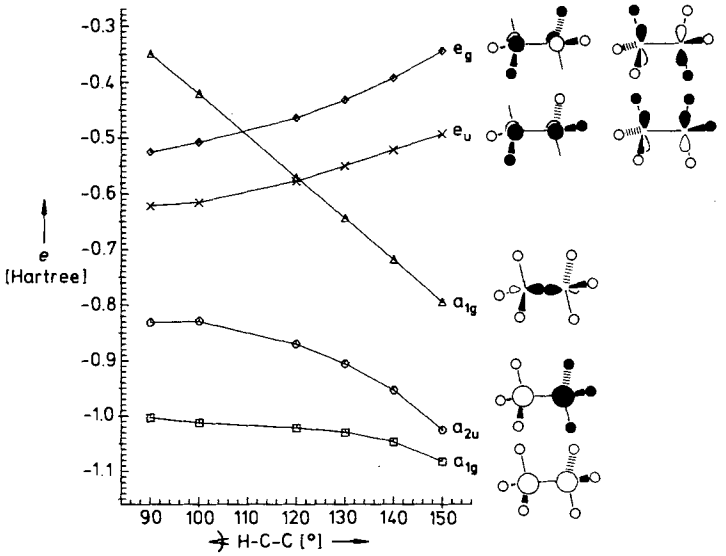


Fig. 3. Walsh diagram for distorted D_{3d}-ethane: the 3-21G orbital energies versus the HCC angle.

C–C bond. When the hydrogens are bent inward, they approach the nodes and their coefficients decrease. This means that CH bonding character is diminished. The opposite is true when the hydrogens are bent back. Not only additional CH but also enhanced CC bonding develops. The energy of the a_{2u} orbital is lower when the HCC angles are enlarged. This orbital is comprised largely of s components and has CC antibonding character. The latter is reduced on bending.

When the carbon *p*-orbitals are aligned perpendicular to the C–C bond, degenerate MO's of pseudo-π (e_u) and pseudo-π* (e_g) symmetry result. The energies of both sets of these orbitals increase at larger CCH angles since the CH bonding character is diminished. Of course, ethane distortion from the equilibrium geometry raises the overall energy, but the effects are distributed differently. A large CCH angle favors CC bonding, whereas this is decreased when this angle becomes smaller. The effects of these distortions on the CH bond energies are opposite.

Distortion also alters the hybridization. With an ethane HCC angle of 90°, the bonds to the hydrogens are nearly sp^2 hybridized, whereas very little s-character is present in the C–C bond. Conversely, a widened HCC angle increases the s-character along the C–C bond. This rehybridization effect, long familiar in cyclopropane, is more dramatic in tetrahedrane, as the external bonds have roughly sp character.[14] Hence, the central C(sp)–C(sp) bond in **7** can be compared with the central bond in 1,3-butadiyne (Table 1). Not just the hybridization in the latter, but also the conjugation and the lower coordination reduce the bond length to 1.38 Å (Table 1). Hence, the value calculated for **7** is somewhat larger.

As has been pointed out by *Ermer, Szeimies,* et al. it might be possible to prepare the hexa-*tert*-butyl derivative of **7**.[4b] They suggested that the X-ray central bond length of 1.440(2) Å in a bi-[1-tricyclo[3.1.0.0^{2,6}]hexyl] derivative might be taken as the upper limit for the C1–C1′ value in **7**. Our 6-31G* calculations agree. We predict the central bond in **7** to be 1.438 ± 0.01 Å in length. The 3-21G rotational barrier is 2.3 kcal mol^{-1}, considerably smaller than the ca. 10 kcal mol barriers for typical *tert*-butyl group rotations.[15]

Received: March 29, 1989 [Z 3261 IE]
German version: *Angew. Chem. 101* (1989) 1264

CAS Registry number:
1, 119703-39-8.

[1] Cf. a) L. E. Sutton (Ed.), *Spec. Publ. Chem. Soc. 18* (1965) 514; b) F. H. Allen, *Acta Crystallogr. B37* (1981) 890; c) L. E. Sutton (Ed.), *Spec. Publ. Chem. Soc. 11* (1958) M 102.

[2] Cf. a) E. Osawa, K. Kanematsu in J. F. Liebman, A. Greenberg (Eds.): *Molecular Structure and Energetics, Vol. 3,* VCH Verlagsgesellschaft, Weinheim 1986, p. 329; b) E. Osawa, Y. Onuki, K. Mislow, *J. Am. Chem. Soc. 103* (1981) 7475. Although long C-C distances ranging from e.g. 1.7 Å to nonbonded values (e.g. 2.0 Å in cyclobutane) are known in polycyclic systems, the largest possible *unsupported* C-C bond appears to be 1.67 Å. Sterically more crowded systems dissociate. c) C. Rüchardt, D. Beckhaus, *Top. Curr. Chem. 130* (1986) and references therein; d) See N. Yannoni, B. Kahr, K. Mislow, *J. Am. Chem. Soc. 110* (1988) 6670.

[3] a) H. Irngartinger, A. Goldmann, R. Schappert, P. Garner, P. Dowd, *J. Chem. Soc. Chem. Commun.* (1981) 455; b) H. Irngartinger, K. L. Lukas, *Angew. Chem. 91* (1979) 750; *Angew. Chem. Int. Ed. Engl. 18* (1979) 694.

[4] a) O. Ermer, J. Lax, *Angew. Chem. 99* (1987) 455; *Angew. Chem. Int. Ed. Engl. 26* (1987) 447; b) O. Ermer, P. Pell, J. Schäfer, G. Szeimies, *ibid. 101* (1989) 503; c) The bond lengths given in the structural drawings of **4**–**7** were obtained at the MNDO (**4**), 3-21G (**5**) and 6-31G* (**6**, **7**) levels of theory.

[5] R. Gilardi, M. Maggini, P. E. Eaton, *J. Am. Chem. Soc. 110* (1988) 7232.

[6] a) P. Kaszynski, J. Michl, *J. Am. Chem. Soc. 110* (1988) 5225; b) V. Bunz, K. Polborn, H.-U. Wagner, G. Szeimies, *Chem. Ber. 121* (1988) 1785. c) MNDO calculations on substituted bi(bicyclo[1.1.1]pentanes) give central bond-lengths similar to our results.

[7] J. Schäfer, K. Polborn, G. Szeimies, *Chem. Ber. 121* (1988) 2263.

[8] R. A. Alden, J. Kraut, T. G. Traylor, *J. Am. Chem. Soc. 90* (1968) 74.

[9] a) P. H. M. Budzelaar, D. Cremer, M. Wallasch, E.-U. Würthwein, P. von R. Schleyer, *J. Am. Chem. Soc. 109* (1987) 6290; b) B. Reindl and P. von R. Schleyer, unpublished calculations. Reoptimization of **2** at the correlated MP2/6-31G* level gives a distance of 1.376 Å; c) R. M. Moriarty, L. S. John, B. A. Luxon, *Tetrahedron Lett. 24* (1983) 1139.

[10] W. Hehre, L. Radom, P. von R. Schleyer, J. A. Pople, *Ab Initio Molecular Orbital Theory,* Wiley, New York 1986, Chapt. 6. For the basis set dependence of the accuracy of ab initio calculations on non-strained hydrocarbons see: G. Häfelinger, C. U. Regelmann, T. M. Krygowski, K. Wozniak, *J. Comput. Chem. 10* (1989) 329.

[11] M. J. S. Dewar, W. Thiel, *J. Am. Chem. Soc. 99* (1977) 4899, 4907. MNDO calculations on **5** are reported in reference [6 b].

[12] a) See B. M. Gimarc: *Molecular Structure and Bonding,* Academic Press, New York 1980; b) See also: K. B. Wiberg, G. B. Ellison, J. J. Wendoloski, *J. Am. Chem. Soc. 98* (1976) 1212; K. B. Wiberg, G. B. Ellison, *Tetrahedron 30* (1974) 1573.

[13] The molecular orbitals of ethane are depicted *inter alia* in W. L. Jorgensen, L. Salem; *The Organic Chemists Book of Orbitals,* Academic Press, New York 1973, p. 99–102. R. F. Hout, Jr., W. J. Pietro, W. J. Hehre: *A Pictorial Approach to Molecular Structure and Reactivity,* Wiley, New York 1984, p. 36, 40. J. M. Telder, A. Nechvatal: *Pictorial Orbital Theory,* Pitman, London 1985, p. 6–7. T. A. Albright, J. K. Burdett, M.-H. Whangbo: *Orbital Interactions in Chemistry,* Wiley, New York 1985, p. 152 f; see also Ref. [12].

[14] T. Loeyer, R. Machinek, W. Lüttke, L. W. Franz, K.-D. Malsch, G. Meier, *Angew. Chem. 95* (1983) 914; *Angew. Chem. Int. Ed. Engl. 22* (1983) 878; cf. J. Wardeimer, W. Lüttke, R. Bergholz, R. Machinek, *ibid. 94* (1982) 813 and *21* (1982) 872.

[15] Review: S. Sternhell in L. M. Jackman, F. A. Cotton (Eds.): *Dynamic Nuclear Magnetic Resonance,* Academic Press, New York 1975. The 3-21G rotational barrier (D_{3d} versus D_{3h} energy difference) for 2,2,3,3-tetramethylbutane is 8.1 kcal mol^{-1}. The central C–C bond lengths are 1.578 Å (staggered, D_{3d}) and 1.613 Å (eclipsed, D_{3h}). The experimental value is 1.583(10) Å[16]. Low rotational barriers in bicubyl derivatives have also been predicted by *Ermer* et al. [4a].

[16] L. S. Bartell, T. L. Boates, *J. Mol. Struct. 32* (1976) 379.

On the Stability of Trioxo(η^5-Cyclopentadienyl) Compounds of Manganese, Technetium, and Rhenium: An ab initio SCF Study**

By *Thomas Szyperski** and *Peter Schwerdtfeger**

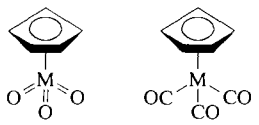
Trioxo(η^5-pentamethylcyclopentadienyl)rhenium(VII),[1] Cp*ReO_3, first prepared in 1984, has meanwhile become very important as a key compound in the synthesis of oxoalkyl- and oxoarylrhenium species.[2] The homologous trioxomanganese and -technetium, as well as the monoxo- and dioxo compounds of the scandium and vanadium groups, respectively, have not yet been isolated. The results presented in this communication suggest that the analogous trioxo(η^5-pentamethylcyclopentadienyl)technetium(VII), Cp*TcO_3, should be stable, but not the manganese con-

[*] Dr. P. Schwerdtfeger
Department of Chemistry and the Center of Information Science,
University of Auckland
Private Bag, Auckland (New Zealand)
Dipl.-Chem. T. Szyperski
Institut für Molekularbiologie und Biophysik
der Eidgenössischen Technischen Hochschule
ETH-Hönggerberg, CH-8093 Zürich (Switzerland)

[**] This work was supported by the Alexander-von-Humboldt-Stiftung and the Studienstiftung des Deutschen Volkes. We thank Prof. *Manfred L. Ziegler* (Heidelberg) for communicating his results concerning the trioxo technetium species, Prof. *W. A. Herrmann* (München), who gave the inspiration to perform this work, and *Michael Dolg* (Stuttgart) for providing the pseudopotential parameters.

gener. We also find that the fragments MO_3 (M = Tc, Re) are isolobal to CH_3, which suggests that a large number of $RTcO_3$ and $RReO_3$ compounds (R = organic or inorganic ligand) could be synthesized.

In order to study the stability of such compounds we performed Hartree–Fock (HF) calculations for the $MO_3^{\oplus}$, MO_3 (M = Mn, Tc, Re), C_5H_5 (Cp), and $C_5(CH_3)_5$(Cp*) fragments and the $CpMO_3$ compounds **1**. The $CpM(CO)_3$ compounds **2** are well characterized;[4] hence, we also performed calculations for the $M(CO)_3^{\oplus}$ and $M(CO)_3$ fragments for comparison with the oxo compounds.



1 **2**

Energy-adjusted relativistic pseudopotentials (ARPP) for Mn, Tc, and Re with a low core definition were used.[5, 6] These were tested in calculations of $MO_4^{\ominus}$.[6] Furthermore, we performed all-electron HF calculations for the manganese oxo compounds $MnO_4^{\ominus}$, $MnO_3^{\oplus}$, and MnO_3, which yield the same results as those obtained from ARPP calculations. For example, for $MnO_4^{\ominus}$ we obtain r(Mn-O) = 155 pm with both methods. All calculations were performed with a modified version of GAUSSIAN86.[7] The geometries used for rhenium compounds are those obtained from X-ray analyses.[2, 4] For the unknown manganese and technetium species, the bond distances and angles were estimated from the geometries of the $MO_4^{\ominus}$,[8] $CpM(CO)_3$,[4] and Cp^*ReO_3[3] compounds. Sufficiently large basis sets with diffuse and polarization functions were used. For example, for the fragments we used a 6-311+G* basis set for O, a valence (10s/5p/5d)/[8s/2p/4d] basis set for the metal atoms, and for C_5H_5 a 31G basis set for H and a 6-31+G basis set for C. These were slightly reduced for the $CpMO_3$ compounds.[6]

The $CpML_3$ molecular orbital (MO) interactions are usually discussed using ionic fragments $ML_3^{\oplus}$ (L = CO, O, etc.) and $Cp^{\ominus}$ (see, for example, *Burdett* et al.[9] or *Lichtenberger* and *Fenske*[10]). The calculated vertical HF ionization energies of the neutral fragments $M(CO)_3$ and MO_3 are shown in Figure 1. Compared with the rather large $M(CO)_3$ and MO_3 ionization potentials, the electron affinity for Cp is small (0.47 eV at the HF level using a 6-31+G* basis set[6, 7]). This suggests a mainly covalent Cp–M bond in **1**. Hence, the Cp–M bond should be discussed using the neutral radicals $M(CO)_3$, MO_3, and Cp rather than the ionic fragments. We can support this from Mulliken population analyses obtained for **1**, where the net fragment charges are very small: for example, + 0.05 for ReO_3 in $CpReO_3$.

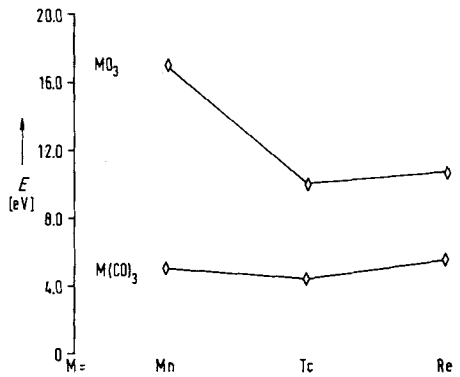
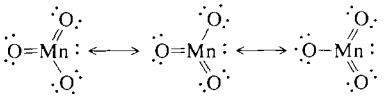


Fig. 1. Vertical ionization energies for the fragments MO_3 and $M(CO)_3$ (M = Mn, Tc, Re).

It is evident from Figure 1 that MnO_3 has an unexpectedly large ionization energy compared to all other fragments. Analyses of the molecular orbital schemes of the fragments $M(CO)_3$ (M = Mn, Tc, Re) and MO_3 (M = Tc, Re) indicate that the ground state in each case is of $^2A_1$ (C_{3v}) symmetry due to a singly occupied a_1 HOMO consisting mainly of metal s, p_z, and d_{z^2} orbitals (defining the C_3 and z axes coincident). Consistent with this result, we obtained for the $M(CO)_3^{\oplus}$ (M = Mn, Tc, Re) and $MO_3^{\oplus}$ (M = Tc, Re) ions an a_1 LUMO. For MnO_3 we obtained a $^2A_2$ ground state with a singly occupied a_2 HOMO consisting of oxygen orbitals orthogonal to the z direction, which can be simplified by the resonance structure **3**. Hence, the overlap between a_2 (MnO_3; C_{3v}) and a_2''(Cp; D_{5h}) is expected to be very small. We believe that the $a_1(MO_3)$–a_2''(Cp) interaction (M = Tc, Re) is fundamental for the stability of compounds **1**. This is not possible for MnO_3. To examine more closely this interaction, we performed HF calculations for compounds **1** (M = Mn, Tc, Re) in C_s symmetry and optimized the distance between the metal and the plane of the cyclopentadienyl ring.



3

The MO picture of the Re compound **1** is shown in Figure 2. The characters of only a few MOs are substantially different from those obtained for the fragments. As a result, the stability of the M–Cp bond is primarily described by the orbital interactions $3a_1(ReO_3) + a_2''$(Cp) (σ type) and $4e(ReO_3) + e_1''$(Cp) (π type). The $3e(ReO_3) + e''_2$(Cp) interaction is of δ type and consequently much smaller than the σ-type and the π-type linear combinations. *Lichtenberger* and *Fenske* have shown that for the $3a_1(Re(CO)_3^{\oplus}) + a_2''(Cp^{\ominus})$ interaction the overlap is small.[10] The $3a_1 + a_2''$ interaction leads to a stabilization of $\varepsilon_1 = 0.17$ Hartree for a_2'' (Cp), whereas e_1''(Cp) is stabilized only by $\varepsilon_2 = 0.05$ Hartree by the $4e + e_1''$ interaction. We therefore conclude that the linear combination $3a_1 + a_2''$ is the dominant contribution to the Cp–ReO_3 bond. This is not the case for the Cp–$Re(CO)_3$ bond, where the higher lying 5e orbitals also contribute. This is consistent with the significant bond lengthening encountered for the Re–C(Cp) bonds in the trioxo species (241 pm) when compared to the tricarbonyl species (228 pm).[3] The reason for the weak nature of the $4e + e_1''$ interaction in **1** is probably the unexpectedly high metal d character for the 4e LUMOs of ReO_3 (compared to those of $Re(CO)_3$, which are mainly of metal p character), resulting in a decreased overlap.

To obtain the relative stabilities of $CpMO_3$, we calculated the dissociation energies D_M for reaction (a) at the optimized

$$CpMO_3 \rightarrow Cp^{\cdot} + MO_3^{\cdot} \qquad \text{(a)}$$

M–Cp distance r_M: $D_{Re} = 35$ kJ mol^{-1}, $r_{Re} = 220$ pm (exp. Cp^*ReO_3 209 pm[3]); $D_{Tc} = 68$ kJ mol^{-1}, $r_{Tc} = 214$ pm (geometrical relaxation of the fragments was neglected[11]). From the Cp–MO_3 bond distance optimization, we calculat-

 © VCH Verlagsgesellschaft mbH, D-6940 Weinheim, 1989 0570-0833/89/0909-1229 $ 02.50/0

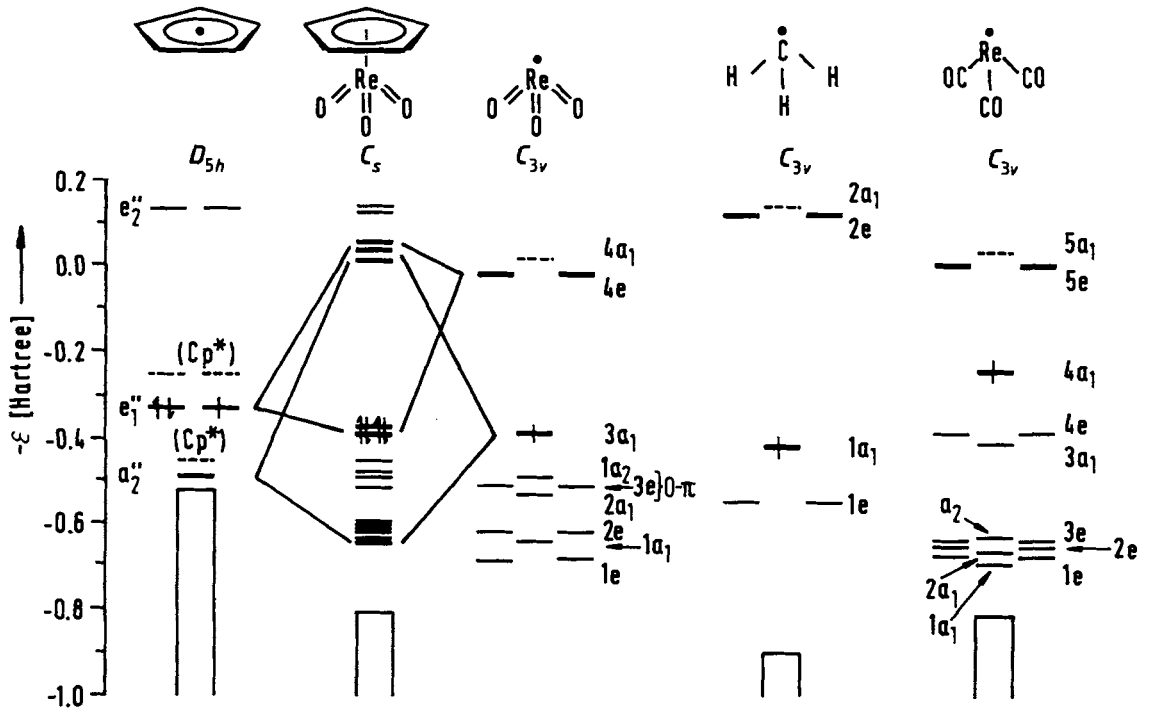


Fig. 2. Molecular orbital picture of $CpReO_3$ and the fragments Cp, Cp*, ReO_3, CH_3, and $Re(CO)_3$. Core orbitals are represented by boxes. High-lying core orbitals of Cp have been omitted from the $CpReO_3$ column for clarity. The electrons in the filled orbitals below the HOMO are not shown.

ed positive force constants for the Cp–MO_3 bond for M = Re (287.3 Nm^{-1}) and M = Tc (307.4 Nm^{-1}), whereas for M = Mn we found a Cp–MnO_3 repulsion ($\partial E/\partial r$ (for r = 200 pm) = − 1.3 kJ mol^{-1} pm^{-1}). Since the e_1'' and the a_2'' orbitals are raised in Cp* compared to Cp, the energy gaps of the interacting orbitals decrease (Fig. 2). Consequently, we expect increased thermodynamic stability for Cp*MO_3 (M = Tc, Re).

Our orbital sequence, where $e_1''(Cp) > 1a_2(ReO_3) > 3e(ReO_3) > 2a_1(ReO_3)$ (in the local symmetry of the fragments), agrees with the previously published[11] photoelectron spectrum of Cp*ReO_3. Furthermore, if we assume that the stabilization of e_1''(Cp*), due to the interaction with the $4e(ReO_3)$ LUMO, is equal to that calculated for $CpReO_3$, we get a Koopmans ionization potential of 8.1 eV (exp. 8.5 eV).[11] Very similar stabilization energies ($\varepsilon_1 = 0.16$, $\varepsilon_2 = 0.04$ Hartree) and MO picture are found for $CpTcO_3$.

Others have demonstrated that $Re(CO)_3$ (d^7-ML_3) is isolobal to $CH^{2\oplus}$ [9] and we propose that ReO_3 and TcO_3 are isolobal to $CH^{2\oplus}$ and CH_3, allowing comparisons of Cp*ReO_3 and Cp*$CH^{2\oplus}$ [13] in the first case and of the well-characterized compound CH_3ReO_3 [14] to CH_3CH_3 in the second case. Figure 2 shows that the number, symmetry properties, electron occupation, and approximate energies of the frontier orbitals of CH_3 and ReO_3 are indeed similiar. For example, compared to the a_1 HOMOs of $M(CO)_3$ (ε = 0.2 Hartree), the a_1 HOMOs of MO_3 (M = Tc, Re) are of much lower energy (0.37 Hartree for TcO_3 and 0.39 Hartree for ReO_3) and are therefore more comparible to the a_1 HOMO of CH_3 (ε = 0.43 Hartree) in C_{3v} symmetry. Additionally, the ReO_3 fragment has no high-lying metal d orbitals in contrast to $Re(CO)_3$. On the other hand, MnO_3 is not isolobal to CH_3. Consistent with this is the fact that CH_3MnO_3 is not known.

We conclude that Cp*TcO_3 (not currently known) should be a stable species if a suitable synthetic route can be developed.[15] Cp*MnO_3 is probably not stable for reasons discussed above. As a result of the isolobal analogy, we further suggest that the dinuclear species $(CO)_5M'$–$M''O_3$ (M' = Mn, Tc, Re; M'' = Tc, Re) are possibly stable.

Received: April 3, 1989 [Z 3266 IE]
German version: *Angew. Chem. 101* (1989) 1271

CAS Registry numbers:
1, M = Mn, 122093-41-8; **1**, M = Tc, 122093-42-9; **1**, M = Re, 122093-43-0.

[1] a) W. A. Herrmann, R. Serrano, H. Bock, *Angew. Chem. 96* (1984) 364; *Angew. Chem. Int. Ed. Engl. 23* (1984) 383; b) A. H. Klahn-Oliva, D. Sutton, *Organometallics 3* (1984) 1313.
[2] a) F. Bottomley, L. Sutin, *Adv. Organomet. Chem. 28* (1988) 339; b) W. A. Herrmann, *J. Organomet. Chem. 300* (1986) 111; c) W. A. Herrmann, M. Floel, J. Kulpe, J. K. Felixberger, E. Herdtweck, *ibid. 355* (1988) 297.
[3] a) W. A. Herrmann, E. Herdtweck, M. Floel, J. Kulpe, U. Küsthardt, J. Okuda, *Polyhedron 6* (1987) 1165; b) W. A. Herrmann, *Angew. Chem. 100* (1988) 1269; *Angew. Chem. Int. Ed. Engl. 27* (1988) 1297.
[4] J. Buckingham, J. Macintyre: *Dictionary of Organometallic Compounds*. Chapman & Hall, London 1984.
[5] M. Dolg, U. Wedig, H. Stoll, H. Preuss, *J. Chem. Phys. 86* (1987) 866.
[6] P. Schwerdtfeger, T. Szyperski, M. Dolg, U. Häussermann, to be published.
[7] M. J. Frisch, J. S. Binkley, H. B. Schlegel, K. Raghavachari, C. F. Melius, L. Martin, J. J. P. Stewart, F. W. Bobrowicz, C. M. Rohlfing, L. R. Kahn, D. J. DeFrees, R. Seeger, R. A. Whiteside, D. J. Fox, E. M. Fluder, J. A. Pople: GAUSSIAN86, Carnegie-Mellon Quantum Chemistry Publishing Unit, Pittsburgh, PA, USA 1984; extended for local and nonlocal pseudopotentials by *P. Schwerdtfeger* using program PSEPOT for the latter: M. Kolar, *Comp. Phys. Commun. 23* (1981) 275.
[8] a) G. J. Palenik, *Inorg. Chem. 6* (1967) 503; b) C. J. Lock, G. Turner, *Acta Crystallogr. Sect. B 31* (1975) 1764; c) G. Meyer, R. Hoppe, *Z. Anorg. Allg. Chem. 420* (1976) 40.
[9] a) T. A. Albright, J. K. Burdett, M. H. Whangbo: *Orbital Interactions in Chemistry*, Wiley, New York 1985; b) J. K. Burdett: *Theoretical Models of Inorganic Stereochemistry*, Wiley, New York 1980.

[10] D. L. Lichtenberger, R. Fenske, *J. Am. Chem. Soc. 98* (1976) 50.
[11] Reasonable dissociation energies are obtained only in CI or MP calculations including a geometry optimization, because generally HF calculations underestimate dissociation energies [12]. However, this is not practical, since a single-point HF calculation of $CpMnO_3$ using our basis set (276 primitive Gaussians contracted to 139 basis functions) yields 45 million two-electron integrals, requiring a total CPU time of about 3 hours on an IBM 3081. Nevertheless, we emphasize the striking difference between $CpMnO_3$ and $CpMO_3$ (M = Tc, Re) which, in our opinion cannot be compensated by correlation or geometrical relaxation.
[12] W. J. Hehre, L. Radom, P. von R. Schleyer, J. A. Pople: *Ab Initio Molecular Orbital Theory*, Wiley, New York 1986.
[13] a) H. Hogeveen, P. W. Kwant, *Acc. Chem. Res. 8* (1975) 413; b) H. Carnardi, C. Giordano, R. F. Heldeweg, H. Hoogeveen, E. M. G. A. van Kruchten, *Isr. J. Chem. 21* (1981) 229.
[14] I. R. Beattie, P. J. Jones, *Inorg. Chem. 18* (1979) 2318.
[15] After submission of this paper we were informed by Prof. *Manfred L. Ziegler* that the oxidation of $Cp^*Tc(CO)_3$ with H_2O_2 leads to a polymer $[Cp^*Tc_2O_3]_n$. X-ray structure determination of this compound shows, in principle, Cp^*TcO_3 units, but the three oxygen atoms serve as bridging ligands to another Tc atom [16]. This observation does not change our proposed isolobal analogy and the stability behavior discussed above.
[16] B. Kanellakopulos, B. Nuber, K. Raptis, M. L. Ziegler, *Angew. Chem. 101* (1989) 1055; *Angew. Chem. Int. Ed. Engl. 28* (1989) 1055.

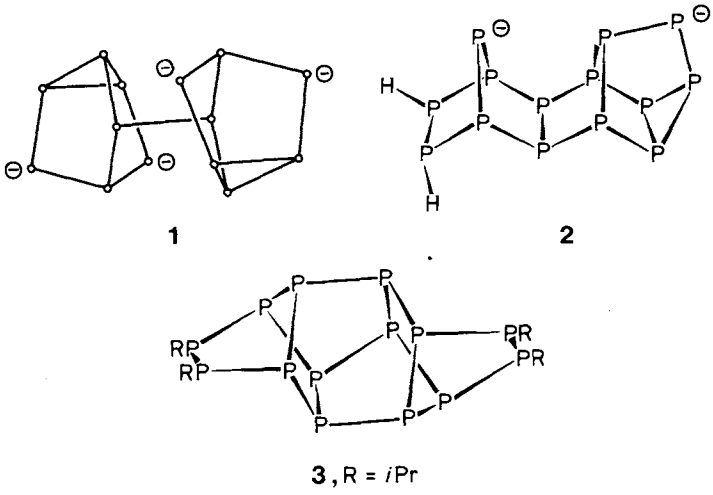
$P_{14}iPr_4$ – The First Hexacyclic Organophosphane **

By *Marianne Baudler*,* *Harald Jachow, Bernhard Lieser, Karl-Friedrich Tebbe,* and *Magda Fehér*

A large number of polycyclic phosphorus–hydrogen compounds P_nH_m ($m < n$) have been detected by mass spectrometry[1] and interest has meanwhile focused on their structural elucidation. However, the corresponding organo derivatives P_nR_m are better suited for investigation, since they are more readily soluble and crystallizable and they are easier to prepare. Accordingly, numerous bi- and tricyclic, as well as several tetra- and pentacyclic, organophosphanes have been synthesized and their structures elucidated.[1]

In 1975 *Fritz* et al.[2] reported the "inorganic" substituted tetradecaphosphane $P_{14}(SiMe_3)_4$, formed as a side product in the synthesis of $P_7(SiMe_3)_3$, but did not further characterize it structurally. The authors suggested that the compound contained the same nortricyclene-like structural element as $P_7(SiMe_3)_3$[3] and consisted of two P_7 units joined through one P atom of each unit. The corresponding $P_{14}(4)$ framework **1** was verified several years later by *von Schnering* et al.[4] by X-ray structure analysis of the polyphosphide $Na_4P_{14}(en)_6$ (en = ethylenediamine). By contrast, we found structure **2** for the tetradecaphosphide $Li_2H_2P_{14}(thf)_6$ by nuclear magnetic resonance spectroscopy.[5] The synthesis and structural investigation of a tetra*organo*tetradecaphosphane were therefore of considerable interest. We have now prepared tetraisopropyltetradecaphosphane **3**, a *hexacyclic* phosphane with an unexpected structure.

Compound **3** is formed to about 3 mol% upon thermolysis of the product mixture obtained from the reaction of dichloro(isopropyl)phosphane with white phosphorus and magnesium, which contains up to ca. 15 mol% of alkyl-rich polycyclophosphanes P_niPr_m ($n = 9-16$, $m = 6-9$). According to the mass spectrum of the thermolysis mixture, P_9iPr_3, P_9iPr_5, P_7iPr_5, $P_{11}iPr_5$, P_7iPr_3, and small amounts of P-richer isopropylcyclophosphanes are also present. Compound **3** can be enriched to about 40% by stepwise column-chromatographic separation of the thermolysis mixture and can be subsequently obtained in analytically pure form by crystallization from THF.



The tetradecaphosphane **3** forms yellow, needle-shaped, THF-containing crystals, which are stable under THF-containing inert atmosphere. They disssolve in THF and warm benzene, but not in cyclohexane or aliphatic hydrocarbons. At temperatures above 90 °C or under high vacuum, they lose THF and afford a yellow, insoluble solid (m.p. 121 °C, sealed tube). Compound **3** is sensitive toward oxidation, especially in solution. In the mass spectrum (field ionization), only the signal for the $M^{\oplus}$ ion (m/z 606) is observed.

The framework of **3** corresponds to neither **1** nor **2**, as shown by the $^{31}P\{^1H\}$ NMR spectrum (THF, 25 °C, 121.497 MHz), which displays a series of strongly overlapping multiplets between $\delta = +77$ and -25, but no signals in the high-field region typical of three-membered ring phosphorus compounds.[6] In agreement with these findings, a single-crystal structure analysis[7] identified **3** as 3,4,10,11-tetraisopropylhexacyclo[6.6.0.0^{2,6}.0^{5,14}.0^{7,12}.0^{9,13}]tetradecaphosphane (Fig. 1), present as an enantiomeric pair owing to its chirality.

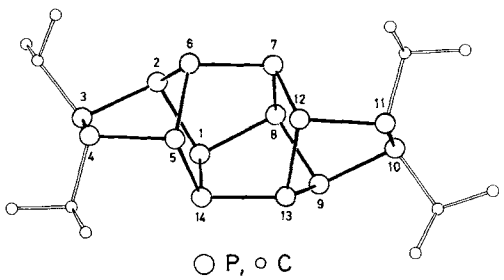


Fig. 1. Molecular structure of **3** in the crystal. Bond lengths [pm] and angles [°]: P1–P8 218.6, P8–P9 218.6, P1–P2 219.2, P2–P3 219.0, P9–P10 219.2, P3–P4 222.4, P10–P11 222.4, P13–P14 222.5, P6–P7 222.7, P7–P8 226.5, P1–P14 226.9, other P–P 220.1 to 221.2; P2–P1–P8 92.9, P1–P8–P9 93.6, P11–P12–P13 93.3, P4–P5–P6 93.4, P2–P6–P7 96.4, P9–P13–P14 97.8, P6–P7–P12 96.4, P5–P14–P13 97.1, P1–P2–P3 97.3, P8–P9–P10 98.6, P9–P13–P12 99.2, P2–P6–P5 99.7, P8–P9–P13 99.5, P1–P2–P6 99.9, other P–P–P 101.9 to 105.6.

The molecule consists of two norbornane-like P_7iPr_2 partial structures connected by three zero bridges (P1-P8, P6-P7, P13-P14) in such a way that a central six-membered ring (P5,

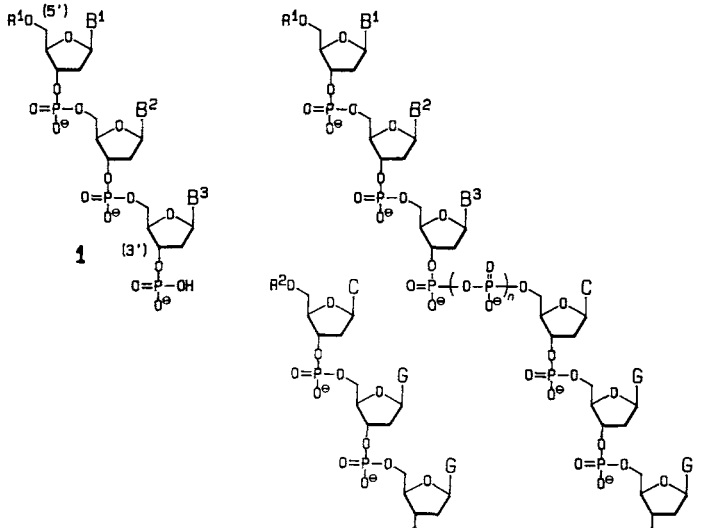
[*] Prof. Dr. M. Baudler, H. Jachow, B. Lieser, Prof. Dr. K.-F. Tebbe, Dr. M. Fehér
Institut für Anorganische Chemie der Universität
Greinstrasse 6, D-5000 Köln 41 (FRG)

[**] Contributions to the Chemistry of Phosphorus, Part 199. This work was supported by the Deutsche Forschungsgemeinschaft and the Fonds der Chemischen Industrie. Part 198: M. Baudler, C. Wiaterek, K. Kazmierczak, *Z. Anorg. Allg. Chem.*, in press.

Sequence Dependence of Template-Directed Syntheses of Hexadeoxynucleotide Derivatives with 3′–5′ Pyrophosphate Linkage**

By *Günter von Kiedrowski,* Britta Wlotzka,* and *Jörg Helbing*

Chemical models for self-replicating systems are of central interest in studies on chemical evolution.[1] Our demonstration of the autocatalytic synthesis of the self-complementary hexadeoxynucleotide **3a** from the two complementary trideoxynucleotides **1a** and **2a** in the presence of 1-ethyl-3-(3-dimethylaminopropyl)carbodiimide (EDC) as activator provided the first evidence that self-replication is possible in enzyme-free minimal systems and can be studied using the methods of bioorganic chemistry.[2] The key observation was the involvement of the hexamer **3a** with a reaction order of 1/2 in the kinetics of its own synthesis.[2] This finding has meanwhile been corroborated with a second system consisting of oligonucleotide components.[3]



1,3	R^1	B^1	B^2	B^3	n(3)
a	CH_3	C	C	G	0
b	CH_2SCH_3	C	C	C	1
c	CH_2SCH_3	G	C	C	1
d	CH_2SCH_3	C	G	C	1
e	CH_2SCH_3	G	G	C	1
f	CH_2SCH_3	C	C	G	1
g	CH_2SCH_3	G	C	G	1
h	CH_2SCH_3	C	G	G	1

2	R^2
a	H
b	$PO_3H^{\ominus}$

Here we report the first results of sequence-dependent nonenzymatic syntheses of oligodeoxynucleotides *in the presence of a self-complementary oligonucleotide as template.* The new 5′-methylthiomethyl (MTM) trideoxynucleotide 3′-phosphates[4] **1b–h** were used in these investigations. They react with the 5′-phosphorylated trimer **2b** in the presence of EDC, undergoing 3′–5′ pyrophosphate coupling to give the 5′-MTM hexadeoxynucleotides **3b–h**. The 5′–5′-coupled pyrophosphate **4**, formed by self-condensation of trimer **2b**, was also identified as a main product. The 3′–3′-coupled pyrophosphates, however, could only be detected in a few cases.

$^{3'}$pG-G-C$^{5'}$pp$^{5'}$C-G-Gp$^{3'}$

4

The reactions were carried out in 1-μL precision capillaries and followed by means of HPLC (Spherisorb 5 ODS II, 4 × 250 mm; A, 0.1 M ammonium acetate; B, acetonitrile/water 30:70 (v/v); 18–50% B within 16 min at a flow rate of 1 mL min^{-1}; detection at $\lambda = 254$ nm). Measurements of the initial rate of formation of hexamer **3f** in the presence of increasing concentrations of template **3a** showed, as observed in the system studied so far,[2] that the reaction follows the empirical rate equation (1)[5] (Fig. 1).

$$dc'/dt = a\sqrt{c} + b \qquad (1)$$

Accordingly, the synthesis of hexamer **3f** occurs via a template-dependent reaction channel, described in Figure 1 by the slope a, as well as via a template-independent channel, represented by the intercept b.

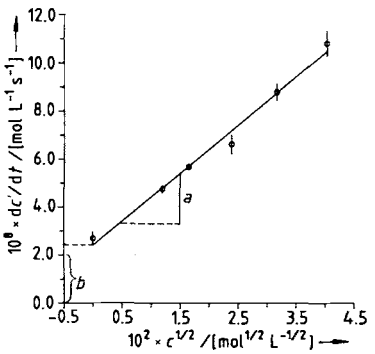


Fig. 1. Plot of the initial rate of formation of hexamer **3f** (dc'/dt) versus the square root of the initial concentration of template **3a** ($c^{1/2}$). The initial rates were determined from measurements of concentration versus time (maximum conversion 25%) by exponential regression, whereby each rate was calculated from the results of four experiments with a total of 16 HPLC runs. Initial concentrations and experimental conditions: 0.004 M **1f**, **2b**, $c = 0$–0.002 M, 0.2 M EDC, 0.1 M 2-morpholinoethanesulfonic acid (pH 6.15), 0.05 M $MgCl_2$, $T = 20$ °C, $t = 0$–12 h.

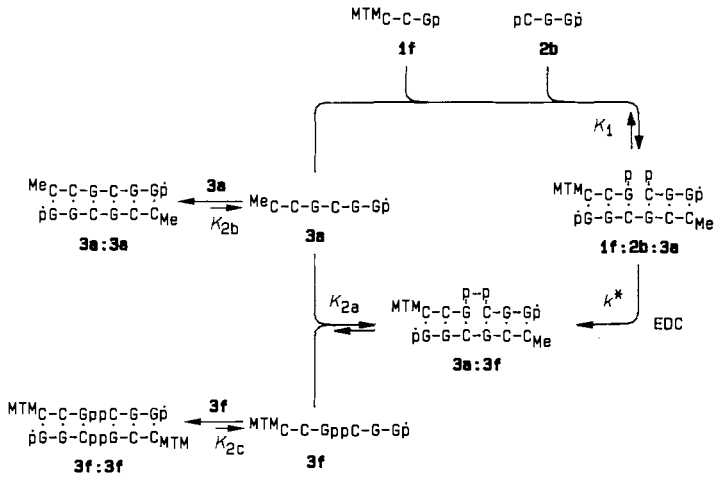
In contrast to previously studied reactions of **1a** with **2a** to give **3a**, the reaction product in this case, **3f**, differs from the template employed, **3a**, so that the constant a reflects catalysis instead of autocatalysis. Under the reaction conditions described in Ref. [2], the template-dependent synthesis of pyrophosphate **3f** is about 21 times faster than that of **3a**, whereas the rate of template-independent synthesis is only higher by a factor of 10.

According to Equation (1), catalyst **3a** participates in the rate equation for the synthesis of pyrophosphate **3f** with a reaction order of 1/2. This finding agrees with the theoretical expectation, assuming that the reaction proceeds according to the mechanism shown in Scheme 1 and three prerequisites are fulfilled:

1. The rate-determining step (k^*) is the carbodiimide-dependent formation of the 3′–5′ pyrophosphate bond within a complex formed from the template and the trimer components, **1f:2b:3a**. It is not important whether the activation by EDC takes place on the 3′-phosphate group of **1f** or

[*] Dr. G. von Kiedrowski, Dipl.-Chem. B. Wlotzka, Dipl.-Chem. J. Helbing
Institut für Organische Chemie der Universität
Tammannstrasse 2, D-3400 Göttingen (FRG)

[**] This work was supported by the Deutsche Forschungsgemeinschaft.



Scheme 1. Proposed mechanism for the template-dependent synthesis of **3f**.

the 5′-phosphate group of **2b** before or, instead, after formation of the complex. EDC-dependent pyrophosphate syntheses on a non-self-complementary template (completely complexed)[6] give an estimated half-life in the magnitude of 10^3 s for this step under the reaction conditions.

2. All single- and double-stranded oligonucleotides are in dynamic equilibrium, their concentrations being equilibrated at all times. Typical association rate constants of C/G-rich oligonucleotides give – largely temperature-independent – values of 10^6–10^7 $M^{-1}\,s^{-1}$;[7,8] the dissociation rate constants of the hexamer duplexes should be comparable to those of $(dC\text{-}G\text{-}C\text{-}G\text{-}C\text{-}G)_2$ and are presumably in the magnitude of $1\,s^{-1}$ at $T = 25\,^{\circ}C$.[8]
3. Under the reaction conditions, the majority of the template molecules are present in the form of complex **3a:3a** or **3a:3f**; a smaller number are present as complex **1f:2b:3a** and a very small number as the single-stranded species **3a**. Thermodynamic investigations on complexes with pyrophosphate-modified oligodeoxynucleotides[6] lead to the expectation that **3a:3a** should be about 1 kcal mol^{-1} more stable than **3a:3f**. Furthermore, these investigations[6] indicate that the stability of complex **1f:2b:3a** should be very similar to that of the complex consisting of **1a, 2a,** and **3a** proposed in Ref. [2]. On the other hand, a considerable difference in stability (at least 4 kcal mol^{-1}) should exist between **1f:2b:3a** and **3a:3a**. For $K_{2a} \approx K_{2b} \approx K_{2c} \gg K_1 \gg 1$, the proportionality relation (2) approximately holds for small conversions.

$$a \sim k^* K_1 K_{2b}^{1/2} \qquad (2)$$

Table 1 shows how *a* and *b* change when, instead of trinucleotide **1f**, which is fully complementary to the partial sequence C-G-G of template **3a**, trinucleotides that are not at all or only partially complementary are used. As expected, the rate of the template-dependent reaction (cf. *a*) is largest when the trinucleotide sequence optimally matches the template; mismatch sequences are incorporated 2 to 50 times more slowly under the reaction conditions. Less pronounced is the effect of the sequence on the template-independent reaction channel (cf. *b*); in this case, too, trinucleotide **1f** reacts fastest. Trinucleotides containing 3′-terminal deoxyguanosine residues react, on average, about 4 times faster than trinucleotides containing 3′-terminal deoxycytidine residues.

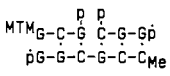
The 5′–5′-coupled pyrophosphate **4** is always formed more slowly in the presence of template **3a**, since its synthesis must

Table 1. Characteristic parameters of the template-dependent (*a*) and template-independent (*b*) syntheses of hexadeoxynucleotides **3b–h** in the presence of template **3a**; a_{rel} and b_{rel} are the values of *a* and *b* relative to **3f**. For initial concentrations and experimental conditions see Figure 1.

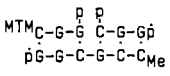
Hexamer	$10^8\,a/([M^{1/2}\,s^{-1}])$	a_{rel}	$10^9\,b/([M\,s^{-1}])$	b_{rel}
3b	15.0	0.07	2.4	0.09
3c	5.3	0.02	4.9	0.19
3d	6.4	0.03	6.2	0.25
3e	106	0.53	7.6	0.31
3f	198	1.00	24.6	1.00
3g	69.8	0.35	22.8	0.92
3h	12.8	0.06	11.5	0.46

compete with that of a 3′–5′-coupled product for activated precursors. In the absence of template **3a**, the sums of the reaction rates for the synthesis of the 3′–5′-coupled product **3** and the 5′–5′-coupled product **4** are comparable for **3b–3e,g,h** ($\Sigma = (2.18 \pm 0.16) \times 10^{-8}\,M^{-1}\,s^{-1}$), whereas the sum of rates obtained experimentally for **1f** ($\Sigma = 5.55 \times 10^{-8}\,M^{-1}\,s^{-1}$) deviates significantly.

The differences in *a* can be explained by the fact that the syntheses of hexamer pyrophosphates **3b–f** in the presence of hexamer **3a** are template-directed reactions, which proceed via complexes of the Watson–Crick type. According to Equation (2), the observable *a* is dependent on the kinetics of pyrophosphate coupling (k*) as well as on the difference in stability of the respective complex **1:2b:3a** and the template duplex **3a:3a** ($K_1 K_{2b}^{-1/2}$). The stability of the complexes **1:2b:3a** is determined by the number of C/G base pairs, the optimum value of which is only attained in complex **1f:2b:3a.** In all of the other complexes, destabilizing mismatch pairs are necessarily present, whereby G/G mismatch pairs generally cause less destabilization than C/C mismatch pairs.[7] Mismatch pairs in the vicinity of the reaction center should affect the kinetics of 3′–5′ pyrophosphate coupling more strongly than those further apart. Thus, trimer **1g**, whose complex **1g:2b:3a** contains one terminal G/G mismatch pair, reacts faster than the sequence-isomeric trimer **1h**, whose complex **1h:2b:3a** contains a G/G mismatch pair closer to the reaction center. Surprisingly, however, **1e**, the

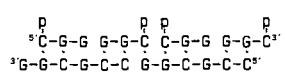


1g:2b:3a



1h:2b:3a

analogous complex of which contains three mismatch pairs, exhibits reaction behavior similar to that of **1g**. A possible explanation would be the participation of a "concatenated" complex of type **5** in which a more removed G/G mismatch pair may be formulated such as that in **1g:2b:3a**.



5

Thermodynamic data of comparable oligonucleotides[9] indicate that the trimer pair formed from **1f** and **2b** can exist and participate in the reaction as a double-stranded complex under the reaction conditions. The reaction behavior of a double-stranded complex should differ from that of single-stranded complexes in activation and hydrolysis and in pyrophosphate synthesis. We suggest that this is the reason why

both the 3′–5′-coupled pyrophosphate **3f** and the 5′–5′-coupled **4** are rapidly formed in the template-independent reaction with **1f** (cf. *b*).

The results described here offer evidence that chemical self-replication is possible even in model systems in which oligonucleotides with 3′–5′ pyrophosphate bonds are synthesized. Oligonucleotides with pyrophosphate backbones are increasingly being discussed as possible prebiotic "information molecules"; their template properties in nonenzymatic oligomerizations have been described recently.[10] Further investigations into sequence dependence will presumably show to what extent the selection values of self-replicating molecules can be understood in terms of thermodynamically and kinetically controlled selectivities in the synthesis of alternative sequences. Such studies might afford insight into the question whether a self-constitution[11] of sequential information must be considered in the later phases of chemical evolution.

Received: April 7, 1989 [Z 3280 IE]
German version: *Angew. Chem. 101* (1989) 1259

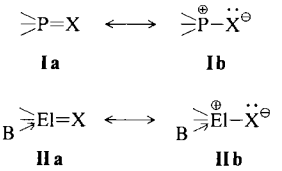
CAS Registry numbers:
1b, 122238-09-9; **1c**, 122238-10-2; **1d**, 122238-11-3; **1e**, 122238-12-4; **1f**, 122238-13-5; **1g**, 122238-14-6; **1h**, 122238-15-7; **2b**, 122238-16-8; **3a**, 122238-25-9; **3b**, 122238-17-9; **3c**, 122238-18-0; **3d**, 122238-19-1; **3e**, 122238-20-4; **3f**, 122238-21-5; **3g**, 122238-22-6; **3h**, 122238-23-7; **4**, 122238-24-8.

[1] G. F. Joyce, *Cold Spring Harbor Symp. Quant. Biol. 7* (1987) 41–51.
[2] G. von Kiedrowski, *Angew. Chem. 98* (1986) 932–934; *Angew. Chem. Int. Ed. Engl. 25* (1986) 932–935.
[3] W. S. Zielinski, L. E. Orgel, *Nature (London) 327* (1987) 346–347.
[4] The use of an MTM protecting group instead of the previously used methyl group has, in addition to logistical advantages in the synthesis of trimers, the effect that the kinetic measurements can be carried out more exactly by HPLC. Thus, **1f** reacts with the 5′-hydroxy trimer **2a** to give a hexamer, which differs from the template used, **3a**, only in the protecting group at the 5′ end, but which can be separated chromatographically from **3a**. This obviates the necessity of following the reaction by calculating differences between HPLC integrals.
[5] Equation (1) should be referred to as the "square root law", where c' is the concentration of the hexamer formed (here, **3f**), c the concentration of the added template (here, **3a**), a an empirical constant for the template-dependent synthesis of **3f**, and b the rate of the template-independent synthesis of **3f**. The constants a and b correspond to k_a and k_b in [2], K_a and K_b in [1], and α and β in [3].
[6] N. G. Dolinnaya, N. I. Sokolova, O. I. Gryaznova, Z. A. Shabarova, *Nucleic Acids Res. 16* (1988) 3721–3738.
[7] C. R. Cantor, P. R. Schimmel: *Biophysical Chemistry*, Freeman, San Francisco 1980, pp. 325, 1183 ff.
[8] S. M. Freier, D. D. Albergo, D. H. Turner, *Biopolymers 22* (1983) 1107–1131.
[9] K. J. Breslauer in H. J. Hinz (Ed.): *Thermodynamic Data for Biochemistry and Biotechnology*, Springer, Berlin 1986; S. M. Freier, A. Sinclair, T. Neilson, D. H. Turner, *J. Mol. Biol. 185* (1985) 645–647.
[10] J. Visscher, C. G. Bakker, R. van der Woerd, A. W. Schwartz, *Science (Washington) 244* (1989) 329–331.
[11] A. Eschenmoser, *Angew. Chem. 100* (1988) 5–40; *Angew. Chem. Int. Ed. Engl. 27* (1988) 5–39.

A Base-Stabilized Ge–S Double Bond

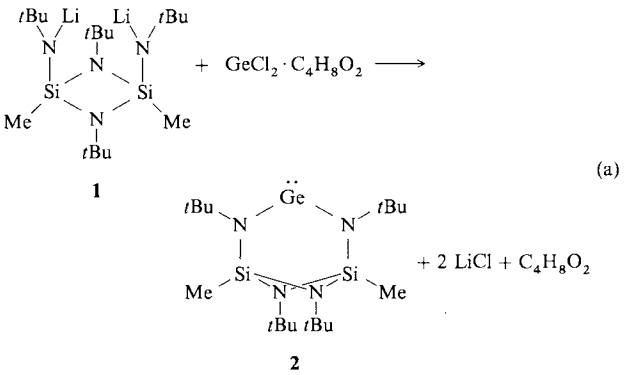
By *Michael Veith*,* *Sabine Becker*, and *Volker Huch*

Elements of higher periods (principle quantum number $n \geq 3$) apparently undergo multiple bonding with oxygen or sulfur when the d-orbitals can participate in the stabilization of the system or when resonance structures can be invoked in which the element in question carries a positive charge and the chalcogen atom a negative charge. This type of bonding is particularly common in the case of phosphorus where it is generally described in terms of the resonance structures **Ia** and **Ib**.[1] Recently, silicon-containing intermediates have also been characterized to which a structure analogous to that of the phosphorus compounds can be ascribed (Scheme 1).[2]



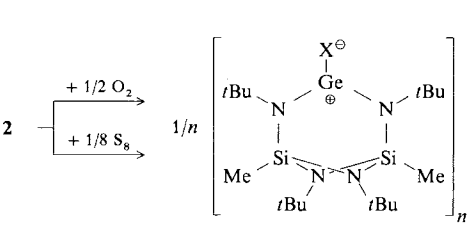
Scheme 1. X = O,S; El = Si, Ge; B = base.

We posed ourselves the question of just how far the "base-stabilization concept" can be extended to the homologous element germanium. All attempts to isolate compounds with "unprotected" Ge–O and Ge–S double bonds have previously failed, even with sterically demanding ligands on the germanium.[3–5] We wanted to achieve intramolecular addition of a base at germanium and therefore used polycyclic lithium silylamide **1** (Li bridges),[6] which apart from containing two amide nitrogen atoms also contains two amine nitrogen atoms capable of coordination.



(a)

1 reacts with the dioxane adduct of germanium(II) chloride to give the bis(amino)germanediyl **2** in high yields [Eq. (a)], which has been characterized by elemental analysis, molecular weight determination and ^{1}H NMR spectroscopy.[7] **2** can be easily converted with oxygen or sulfur into the oxidation products **3** and **4**, respectively [Eq. (b)].



(b)

3, X = O, n = 2
4, X = S, n = 1

The ^{1}H NMR spectra of **3** and **4** are identical at room temperature (in each case three resonance signals are observed for the *tert*-butyl groups,[7] indicating intramolecular chelation by one of the N-atoms of the N_2Si_2 group in solution, whereas the spectrum of **4**, in contrast to that of **3**, becomes simpler on increasing the temperature (coalescence of two *tert*-butyl signals). Apparently, in the case of **4** the

[*] Prof. Dr. M. Veith, Dipl.-Chem. S. Becker, Dr. V. Huch
Institut für Anorganische Chemie der Universität
D-6600 Saarbrücken 11 (FRG)

N–Ge donor bond then rapidly opens and closes on the NMR time scale (competition between the N-atoms in the N_2Si_2 ring). The compounds also differ greatly in their solubility: **3** precipitates as main product from the solution of **2** upon the introduction of oxygen, whereas **4** is readily soluble. X-Ray crystal structure analyses of **3** and **4** confirm that **3** is present as a dimer, whereas **4** is surprisingly, monomeric, i.e. contains a singly coordinated sulfur atom (in the crystalline state **4** still contains 1/2 molecule of benzene per formula unit).

The structures of the oxidation products **3** and **4** are shown alongside each other in Figure 1. The germanium

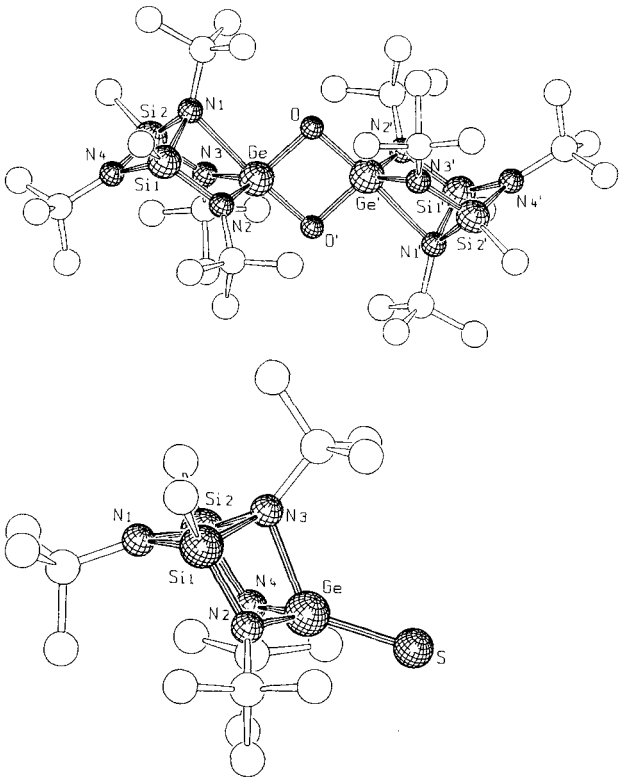


Fig. 1. The molecular structures of **3** (top) and **4** (bottom) (the carbon atoms are not labelled) [8]. Some important bond lengths [Å] and bond angles [°]: **3**: Ge–O 1.809(4), Ge–O′ 1.825(4), Ge–N1 2.370(5), Ge–N2 1.880(5), Ge–N3 1.887(5), Si–N 1.744(9) (mean); N1–Ge–O 90.5(2), N1–Ge–O′ 175.3(2), N2–Ge–O′ 108.1(2), N3–Ge–O′ 109.9(2), N2–Ge–O 119.9(2), N3–Ge–O 119.3(2), N2–Ge–N3 110.7(2), O–Ge–O′ 84.8(2), Ge–O–Ge′ 95.1(2). – **4**: Ge–S 2.063(3), Ge–N3 2.050(6), Ge–N2 1.882(6), Ge–N4 1.886(6), Si–N(1,2,4) 1.721(8) (mean), Si(1,2)–N3 1.831(5) (mean); N2–Ge–S 121.4(2), N4–Ge–S 123.0(2), N2–Ge–N4 110.6(3), S–Ge–N3 128.9(2), N2–Ge–N3 79.8(2), N4–Ge–N3 79.5(2).

atoms in **3** are coordinated almost trigonal-bipyramidally by two oxygen atoms and three nitrogen atoms, whereby the longer bonds are, as expected, the axial bonds in each case (to N1 and O′ and N1′ and O, respectively). The polycycle, with crystallographic point group $\bar{1}(C_i)$, contains two seconorcubane units (N_4Si_2Ge), which are coupled to each other via a Ge_2O_2 four-membered ring.

In **4** the germanium atom is only four coordinate. The coordination can be described as distorted tetrahedral, or better still as trigonal-planar (N2, S, N4) with an additional bond (Ge–N3), since the sum of the angles at the germanium atom for the bonds to N2,S and N4 deviates only 5° from the ideal value of 360°. Especially striking is the difference in length (0.17 Å) between the Ge–N3 bond and the other, shorter Ge–N bonds. The Ge–S distance of 2.063(3) Å is so far the shortest germanium–sulfur distance and is about 0.2 Å shorter than the value for a Ge–S single bond.[9] In the thiogermanate ion $Ge_4S_{10}^{4\ominus}$, which has an adamantane-like structure, the terminal Ge–S distances are 2.12(1) Å[10] and are thus 0.06 Å longer than in **4**. According to calculations on $H_2Ge=S$ the pπ–pπ Ge–S double bond should be 2.02 Å in length.

Accordingly, all structural data suggest that the bonding model **II** can also be applied to **4**. Compound **4** is therefore the first isolable compound with a base-stabilized double bond between sulfur and a tetravalent element of a higher period. Molecules with intramolecular base-stabilized Si–S and Ge–S bond, respectively, have recently been obtained via an entirely different route.[12] Of interest in the importance of the resonance structures **IIa** and **IIb** for the description of **4** is that a molecule isoelectronic to **4** with Ga and Cl instead of Ge and S exists[13] (see also the corresponding methylgallium derivative).[14]

Experimental

2: A solution of the dilithium compound **1** (385 mg, 1 mmol) in benzene was added dropwise within 30 min to a slurry of the dioxane adduct of germanium(II) chloride (232 mg, 1 mmol) in benzene (5 mL)[6]. After 12 hours the precipitate was filtered off, the solvent removed from the filtrate by distillation, and the resulting residue sublimed at 80 °C/10^{-3} torr; this furnished 363.3 mg (82%) of colorless, crystalline **2**.

3,4: A solution of 181.1 mg (0.41 mmol) of **2** in 2 mL of toluene was treated with a stream of oxygen diluted with nitrogen, or with 13.1 mg (0.41 mmol) of sulfur. **3** precipitated as a colorless powder, which was recrystallized from benzene; **4** could first be isolated after evaporation of the solution to dryness. Yields 112.9 mg (60%) **3**; 190.6 mg (98%) **4**.

Received: April 14, 1989 [Z 3295 IE]
German version: *Angew. Chem. 101* (1989) 1287

CAS Registry numbers:
1, 122093-34-9; **2**, 122093-35-0; **3**, [$Ge^{(IV)}$], 122093-36-1; **3**, (chelate), 122114-35-6; **4**, [$Ge^{(IV)}$], 122093-37-2; **4**, (chelate), 122093-39-4; **4** ($Ge^{(IV)}$)·1/2 benzene, 122093-38-3; **4** (chelate)·1/2 benzene, 122093-40-7; $GeCl_2$·D, 28595-67-7.

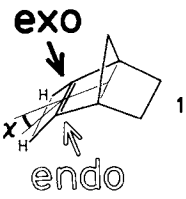
[1] M. W. Schmidt, M. S. Gordon, *J. Am. Chem. Soc. 107* (1985) 1922.
[2] N. Wiberg, G. Preiner, K. Schurz, *Chem. Ber. 121* (1988) 1407.
[3] L. Lange, B. Meyer, W. W. du Mont, *J. Organomet. Chem. 329* (1987) C17–C20.
[4] J. Barreau, G. Rima, M. El-Amine, J. Satgé, *J. Organomet. Chem. 345* (1988) 39.
[5] M. Andrianarison, C. Couret, J.-P. Declercq, A. Dubourg, J. Escudié, H. Ranaivonjatovo, J. Satgé, *Organometallics 7* (1988) 1545.
[6] M. Veith, F. Goffing, *Chem. Ber. 121* (1988) 943.
[7] ^{1}H-NMR (toluene): **2** (290 K): $\delta = 0.55$ (s, 6H, $SiCH_3$), 1.26 (s, 18H, $NC(CH_3)_3$), 1.41 (s, 18H, $NC(CH_3)_3$); **3** (290 K): $\delta = 0.71$ (s, 6H, $SiCH_3$), 1.28 (s, 9H, $NC(CH_3)_3$), 1.57 (s, 9H, $NC(CH_3)_3$), 1.73 (s, 18H, $NC(CH_3)_3$); **4** (370 K): $\delta = 0.65$ (s, 6H, $SiCH_3$), 1.34 (s, 18H, $NC(CH_3)_3$), 1.51 (s, 18H, $NC(CH_3)_3$); coalescence temperature: 307 K; **4** (290 K): $\delta = 0.58$ (s, 6H, $SiCH_3$), 1.28 (s, 9H, $NC(CH_3)_3$), 1.39 (s, 9H, $NC(CH_3)_3$), 1.52 (s, 18H, $NC(CH_3)_3$).
[8] Crystallographic data: **3**: triclinic, $P\bar{1}$, $a = 10.794(8)$, $b = 10.816(8)$, $c = 11.121(8)$ Å, $\alpha = 97.5(1)$, $\beta = 102.9(1)$, $\gamma = 97.8(1)°$, $V = 1236$ Å^3; $Z = 1$; 2064 „observed" reflections ($2\sigma_F$), 278 parameters, $R = 0.049$. – **4** · ½ C_6H_6: orthorhombic, *Pbca*, $a = 10.619(6)$, $b = 15.834(9)$, $c = 33.84(2)$ Å, $V = 5687$ Å^3; $Z = 8$; 2128 „observed" reflections ($3\sigma_F$), 305 parameters, $R = 0.051$. – Further details of the crystal structure investigation are available on request from the Fachinformationszentrum Karlsruhe, Gesellschaft für wissenschaftlich-technische Information mbH, D-7514 Eggenstein-Leopoldshafen 2 (FRG), on quoting the depository number CSD-53903, the names of the authors, and the journal citation.
[9] P. Jutzi, W. Steiner, E. König, *Chem. Ber. 111* (1978) 606; R. J. Chadha, J. E. Drake, A. B. Sarkar, *Inorg. Chem. 26* (1987) 2885.
[10] B. Krebs, S. Pohl, *Z. Naturforsch. B26* (1971) 853.
[11] G. Trinquier, M. Pelissier, B. Saint-Roch, H. Lavayssière, *J. Organomet. Chem. 214* (1981) 169.
[12] $(Me_2N\overline{-C_{11}H_8})(Ph)SiS$ and the analogous germanium compound: P. Arya, J. Boyer, R. Corriu, G. Lanneau, M. Perrot, C. Priou, *Euchem Conf. PSIBLOCS* (Paris/Palaiseau 1988).
[13] F. Goffing, *Dissertation*, Universität Saarbrücken 1988; M. Veith, F. Goffing, unpublished.
[14] M. Veith, F. Goffing, V. Huch, *Z. Naturforsch. B43* (1988) 846.

Double-Bond Geometry of Norbornene: Neutron Diffraction Measurement of a Derivative at 15 K

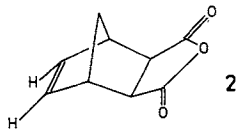
By *Otto Ermer,* Peter Bell,* and *Sax A. Mason*

Norbornene **1** is a prototypal strained olefin and as such a prominent model system of mechanistic organic chemistry. Numerous experimental and theoretical studies have shown that the reactivity of the double bond of **1** is characterized by a pronounced preference for *exo* attack. Inter alia, this has been rationalized in terms of the geometry of the double bond, which is not completely planar but bent in *endo* direction by the angle χ (*endo* pyramidalization, symmetric out-of-plane bending). The related changes in hybridization and steric factors favor *exo* attack.[1]

Despite the multitude of previous work,[1] the magnitude of the *endo* bending of the double bond of **1**, that is, the angle χ, is not reliably known. For example, from theoretical calculations applying quantum-chemical models or empirical force fields the following χ angles have been derived: 1.7° (MM2 force field),[1h] 4.2° (extended Hückel MO),[1i] 4.5° (CFF force field),[2a] 4.9° (ab initio, STO-3G).[1d,g] Furthermore, a number of X-ray analyses have been undertaken, which in most cases, however, involved unfavorable derivatives. Still worse, the light hydrogen atoms obviously can in principle not be located reliably by X-ray diffraction.



1



2

In order to place the extensive norbornene discussion on a sound basis, that is, to localize reliably the double-bond H atoms, we have performed a neutron diffraction measurement at 15 K on the simple derivative **2** (*exo-exo*-2,3-norborn-5-enedicarboxylic anhydride).[3] Norbornene itself is not suitable for such purposes: At room temperature the low-melting (m.p. 46 °C) and rather spherical hydrocarbon forms soft, deliquescent crystals of unknown structure. The present structural problem of norbornene is comparable to that of *trans*-cyclooctene, which involves a strongly nonplanar double bond and also plays the role of a prominent reference olefin. Some time ago, we reliably measured the double-bond geometry of *trans*-cyclooctene by means of neutron diffraction.[4]

Key results of the neutron diffraction measurement on the norbornene derivative **2** are collected in Figure 1.[5] Strictly

[*] Prof. Dr. O. Ermer, Dipl.-Chem. P. Bell
Institut für Organische Chemie der Universität
Greinstrasse 4, D-5000 Köln 41 (FRG)
Dr. S. A. Mason
Institut Laue-Langevin
B.P. 156X, F-38042 Grenoble Cedex (France)

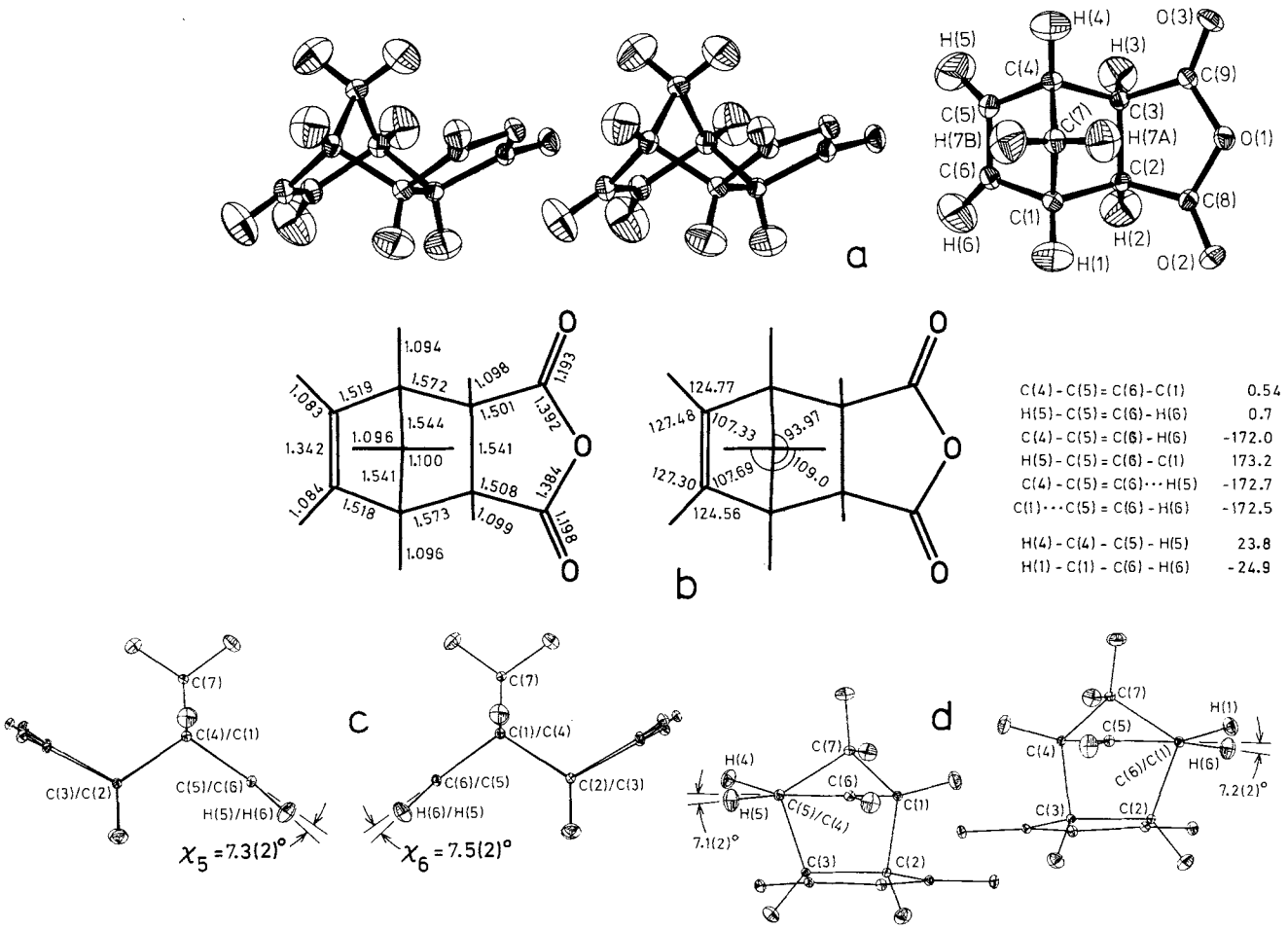


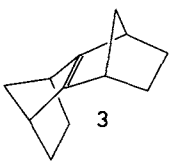
Fig. 1. Neutron diffraction results of **2**. a) Stereoview, atomic numbering, vibrational ellipsoids (90% probability). b) Bond lengths [Å], selected bond angles and torsion angles [°]; estimated standard deviations: CC,CO 0.001, CH 0.002–0.003 Å; CCC 0.06–0.07, HCC, HCH 0.2°; CCCC 0.09, HCCC 0.2, HCCH 0.3°. c) Projections down the CC double bond: illustration of the out-of-plane bending (pyramidalization) angles. d) Projections down the $C(sp^2)$–$C(sp^3)$ single bonds: influence of the double-bond bending on these partial conformations (ellipsoids 25%).

speaking, the molecules of **2** possess no symmetry in the crystal, yet are mirror-symmetric to a very good degree of approximation. The analytical description of the nonplanar double-bond deformations requires three independent geometry parameters,[4, 9] which in the present case are defined as follows: a) Twisting angle Φ_D = "torsion angle" between the p orbitals at C5 and C6 = arithmetic mean of the two double-bond torsion angles C4-C5-C6-C1 and H5-C5-C6-H6; b) out-of-plane bending (pyramidalization) angles χ_5 and χ_6 at C5 and C6 = deviation from planarity of the two dihedral angles C4-C5-C6/H5-C5-C6 and C1-C6-C5/H6-C6-C5.[10] The twisting angle Φ_D has the very small value 0.6(2)°, and the double bond is thus almost untwisted ($\Phi_D = 0°$ for exact mirror symmetry). The bending angles χ_5 and χ_6, which are at the focus of this work, amount to 7.3(2) and 7.5(2)°, respectively, and correspond to *endo* pyramidalization (Fig. 1c). In line with the approximate mirror symmetry, both bending angles are practically equal, and our neutron diffraction measurement thus affords a pyramidalization of $\chi = 1/2(\chi_5 + \chi_6) = 7.4(2)°$. This precise value turns out to be roughly twice as high as usually estimated for norbornene **1** (see above).

Like always in such cases, the question arises as to the influence of crystal packing and substituent effects on χ. In view of the absence of particularly short intermolecular contacts and the closely approximated molecular mirror symmetry, packing effects are likely to be negligible. Likewise, the rather remote anhydride moiety is expected to exert little influence on the double-bond bending; comparative quantum-chemical calculations on **1** and **2** could help settle this problem quantitatively.[2b]

Regarding other structural properties of **2**, the reader is referred to the collection of bond lengths and angles in Figure 1b. Mention is made only of the bond angle H-C7-H of 109.0(2)°, which is somewhat widened relative to the normal value of about 106–107°, since the angle C1-C7-C4 amounts to only 93.67(6)°.[11] The bond lengths C1-C2 and C3-C4 are somewhat lengthened, probably due to the anhydride group. Suffice it to say that other comparable carboxy derivatives of norbornane also show this feature, whereas we have found shortened C1–C2 bonds in ester derivatives of *exo*-2-norbornanol.

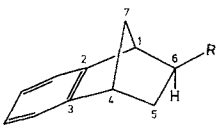
According to the simple empirical force-field models,[1h, 2a] the driving force for *endo* bending of the double bond of norbornene is to be sought in a decrease of torsional strain around both C(sp^2)–C(sp^3) single bonds, since the *endo* pyramidalizations lead to a more staggered orientation of the C(sp^2)–H bonds. The two projections of Figure 1d show quantitatively that the three torsion angles around C4-C5 and C1-C6, in which H5 and H6, respectively, participate, each assume more favorable (more staggered) values by 7.1 and 7.2° through the *endo* pyramidalizations. In the *syn*-sesquinorbornene **3**, two norbornene systems are fused



3

across the double bond such that on *endo* pyramidalization the torsional strain is lowered around four C(sp^2)–C(sp^3) single bonds as compared to two in **1**. In the light of the present norbornene results it is therefore gratifying to note that the out-of-plane bending angles χ of about 16–18° measured for a number of derivatives of **3**[12] are roughly two times larger than in norbornene. However, it is to be conceded that this very simple and more qualitative picture most likely does not convey the whole truth since the quantitative reproduction of the double-bond bendings in the force-field calculations is not satisfactory. For example, the amount of double-bond bending in **3** is probably also influenced by angle strain factors.[9a, 12e]

For benzonorbornene **4** considerably smaller pyramidalization (at C2 and C3) than in norbornene **1** may be anticipated, since the rotational barriers around C(sp^2)–C(sp^3) bonds at a benzene ring are substantially lower than around such bonds at an olefinic double bond. (Compare the sixfold rotational barrier of the methyl group in toluene of only 0.013 kcal mol^{-1}[13a] with the essentially threefold barrier in propene, which amounts to 1.98 kcal mol^{-1}.[13b]) Furthermore, pyramidalization (out-of-plane bending) at the benzene ring is energetically somewhat more costly relative to olefinic double bonds.[14] We have prepared the two crystalline benzonorbornene derivatives **5** and **6** and have sub-



4 R = H
5 R = COOH
6 R = COO-*p*-C_6H_4-NO_2

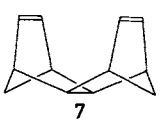
jected them to X-ray analysis.[15] The resulting average bendings χ (*endo* direction) at the C(sp^2)–C(sp^2) bond shared by the norbornene unit and the benzene ring are 2.7(3)° in **5** and 2.0(9)° in **6**. These rather similar *endo* pyramidalizations are thus indeed much smaller than observed in **2**.

Received: April 14, 1989 [Z 3290 IE]
German version: *Angew. Chem. 101* (1989) 1298

CAS Registry numbers:
2, 2746-19-2; **5**, 23537-81-7; **6**, 122144-55-2; neutrons, 12586-31-1.

[1] a) P. von R. Schleyer, *J. Am. Chem. Soc. 89* (1967) 701; b) H. C. Brown, P. Geohegan, *ibid. 89* (1967) 1522; c) S. Inagaki, H. Fujimoto, K. Fukui, *ibid. 98* (1976) 4054; d) G. Wipff, K. Morokuma, *Tetrahedron Lett. 21* (1980) 4445; e) R. Huisgen, P. H. J. Ooms, M. Mingin, N. L. Allinger, *J. Am. Chem. Soc. 102* (1980) 3951; f) A. A. Pinkerton, D. Schwarzenbach, J. H. A. Stibbard, P. A. Carrupt, P. Vogel, *ibid. 103* (1981) 2095; g) N. G. Rondan, M. N. Paddon-Row, P. Caramella, K. N. Houk, *ibid. 103* (1981) 2436 (Note that the out-of-plane bending angle chosen in that work differs from χ; cf. also [12i]); h) U. Burkert, *Angew. Chem. 93* (1981) 602; *Angew. Chem. Int. Ed. Engl. 20* (1981) 572; i) J. Spanget-Larsen, R. Gleiter, *Tetrahedron Lett. 24* (1982) 2435.

[2] a) O. Ermer, C.-D. Bödecker, H. Preut, *Angew. Chem. 96* (1984) 57; *Angew. Chem. Int. Ed. Engl. 23* (1984) 55. b) In [2a] the X-ray analysis of a derivative of tetracyclo[6.2.1.$1^{3,6}$.$0^{2,7}$]dodeca-4,9-diene **7** is described, which consists of two norbornene units fused across a single bond and



7

which has two parallel double bonds in close proximity. A relatively large *endo* pyramidalization of $\chi = 8.1(2.1)°$ was found for one of the two double bonds and ascribed to particularly strong nonbonding repulsions between the double bonds due to orbital symmetry. However, comparison with the reliable neutron diffraction results on **2** now available indicates that this influence of orbital symmetry is smaller than previously [2a] believed. More definite conclusions would necessitate diffraction measurement also on the tetracyclododecadiene derivative.

[3] A relatively crude X-ray measurement was reported earlier for **2** (photographic intensity data, $R = 0.086$, hydrogen positions constructed on the basis of a planar double bond but not refined): G. Filippini, C. M. Gramaccioli, C. Rovere, M. Simonetta, *Acta Crystallogr. B28* (1972) 2869. In order to avoid unpleasant disturbances (e.g., disorder), we performed a renewed X-ray measurement on **2** (four-circle diffractometer) before embarking upon neutron diffraction and obtained a well-refinable "clean" structure free from any unusual features ($R = 0.038$). Altogether we prepared six simple norbornene derivatives and tested their suitability for neutron diffraction by means of complete X-ray analyses, until eventually the anhydride **2** was selected.

[4] O. Ermer, S. A. Mason, *Acta Crystallogr. B38* (1982) 2200.

[5] Thick orthorhombic plates of **2** [6] were grown from acetone solution; m.p. 142 °C. Space group $P2_12_12_1$, $Z = 4$, $a = 7.362(2)$, $b = 7.968(2)$, $c = 12.500(2)$ Å, temperature 15.0(1) K. Neutron intensities of altogether 2991 reflections were measured at this low temperature on the four-circle diffractometer D9 of the Institut Laue-Langevin, Grenoble (focusing Be monochromator, two-dimensional position-sensitive detector, $\lambda = 0.8429$ Å, $\theta_{max} = 51°$, crystal size ca. $3.7 \times 3.6 \times 1.3$ mm^3). After averaging, 2687 independent observed reflections with $I > 0$ remained, which were fed into the least-squares refinements. Absorption corrections were applied with a corresponding coefficient $\mu = 1.47$ cm^{-1} adopting an incoherent scattering cross-section of 35 barns for hydrogen. The final R value after anisotropic refinement of all atoms was 0.033 ($R_w = 0.032$, $\sum w(\Delta F)^2$ minimized, $w = 1/\sigma(F_0)^2$, extinction correction, nuclear scattering lengths taken from a recent compilation of *Sears* [7]). The refined atomic nuclear coordinates and anisotropic temperature factor coefficients are given in Table 1. A list of observed and calculated neutron structure amplitudes has been deposited [8].

Table 1. Fractional atomic nuclear coordinates ($\times 10^5$) and anisotropic temperature factor coefficients (Å$^2 \times 10^4$) of **2** at 15 K with estimated standard deviations in parentheses. Temperature factor expression of the form: $\exp[-2\pi^2(U11h^2a^{*2} + \ldots + 2U12hka^*b^* + \ldots)]$.

	x	y	z	U11	U22	U33	U12	U13	U23
C1	57384(11)	-7034(9)	46895(6)	66(2)	67(2)	66(2)	-6(2)	10(2)	-1(2)
C2	75631(10)	3239(9)	46749(5)	63(2)	58(2)	51(2)	1(2)	0(2)	-1(2)
C3	82611(10)	755(9)	35239(6)	54(2)	54(2)	57(2)	1(2)	4(2)	-1(2)
C4	67375(11)	-10303(9)	29962(5)	79(2)	68(2)	52(2)	-7(2)	0(2)	-2(2)
C5	69068(11)	-27188(9)	35509(6)	93(3)	60(2)	80(2)	-4(2)	5(2)	-3(2)
C6	63220(11)	-25192(10)	45601(6)	84(3)	65(2)	74(2)	-11(2)	3(2)	10(2)
C7	50278(11)	-3283(10)	35550(6)	65(2)	74(2)	84(2)	-2(2)	-12(2)	4(2)
C8	72135(10)	21839(9)	47558(6)	72(2)	52(2)	71(2)	0(2)	4(2)	-8(2)
C9	82996(11)	18148(9)	30638(6)	64(2)	59(2)	66(2)	-3(2)	7(2)	10(2)
O1	76350(13)	29722(11)	38008(7)	94(3)	53(2)	84(3)	2(2)	9(2)	10(2)
O2	66158(14)	29811(12)	54878(7)	122(3)	81(3)	92(3)	11(3)	22(3)	-24(2)
O3	87514(14)	22667(12)	21933(7)	106(3)	94(3)	77(3)	-6(3)	24(2)	27(2)
H1	48621(31)	-4052(30)	53720(17)	203(8)	243(8)	173(7)	7(7)	78(6)	-26(6)
H2	85019(31)	-644(28)	53119(16)	208(8)	219(7)	157(6)	31(6)	-60(6)	12(6)
H3	96151(27)	-4882(27)	34438(18)	131(6)	191(7)	223(7)	41(6)	23(5)	7(6)
H4	67876(35)	-10360(30)	21213(14)	280(9)	240(8)	103(5)	-16(8)	3(6)	-1(5)
H5	75474(39)	-38172(27)	32069(19)	330(11)	149(7)	245(8)	72(8)	50(8)	-34(6)
H6	64033(39)	-34202(28)	52081(17)	324(11)	189(7)	188(7)	11(7)	2(7)	87(6)
H7A	47726(32)	10106(26)	34000(18)	214(8)	149(6)	251(8)	38(6)	-12(7)	20(6)
H7B	37989(30)	-10450(32)	33650(19)	152(7)	252(9)	257(8)	-53(7)	-37(6)	-28(7)

[6] D. Craig, *J. Am. Chem. Soc. 73* (1951) 4865.

[7] V. F. Sears in K. Sköld, D. L. Price (Eds.): *Methods of Experimental Physics (Neutron Scattering)*, Vol. 23, Part A; Academic Press, Orlando, FL, USA 1986.

[8] Further details of the crystal structure investigations are available on request from the Fachinformationszentrum Karlsruhe, Gesellschaft für wissenschaftlich-technische Information mbH, D-7514 Eggenstein-Leopoldshafen 2 (FRG), on quoting the depository number CSD-53752, the names of the authors, and the journal citation.

[9] a) O. Ermer: *Aspekte von Kraftfeldrechnungen*, Wolfgang Baur Verlag, München 1981; b) O. Ermer, S. Lifson, *J. Am. Chem. Soc. 95* (1973) 4121; c) O. Ermer, *Struct. Bonding (Berlin) 27* (1976) 161; d) O. Ermer, *Z. Naturforsch. B32* (1977) 837.

[10] These two dihedral angles may easily be evaluated as the "improper" torsion angles C4-C5-C6 ··· H5 and C1 ··· C5-C6-H6 (Fig. 1b) [9a–c].

[11] a) W. L. Duax, M. D. Fronckowiak, J. F. Griffin, D. C. Rohrer in J. Jortner, B. Pullman (Eds.): *Intramolecular Dynamics*, Reidel, Dordrecht, Holland 1982, p. 505; b) O. Ermer, J. D. Dunitz, I. Bernal, *Acta Crystallogr. B29* (1973) 2278.

[12] a) W. H. Watson, J. Galloy, P. D. Bartlett, A. A. M. Roof, *J. Am. Chem. Soc. 103* (1981) 2022; b) J.-P. Hagenbuch, P. Vogel, A. A. Pinkerton, D. Schwarzenbach, *Helv. Chim. Acta 64* (1981) 1818; c) R. Gleiter, J. Spanget-Larsen, *Tetrahedron Lett. 24* (1982) 927; J. Spanget-Larsen, R. Gleiter, *Tetrahedron 39* (1983) 3345; d) L. A. Paquette, P. Charumilind, M. C. Böhm, R. Gleiter, L. S. Bass, J. Clardy, *J. Am. Chem. Soc. 105* (1983) 3136; e) O. Ermer, C.-D. Bödecker, *Helv. Chim. Acta 66* (1983) 943; f) K. N. Houk, N. G. Rondan, F. K. Brown, W. L. Jorgensen, J. D. Madura, D. C. Spellmeyer, *J. Am. Chem. Soc. 105* (1983) 5980; g) F. S. Jörgensen, *Tetrahedron Lett. 25* (1983) 5289; h) C. A. Johnson, *J. Chem. Soc. Chem. Commun. 1983*, 1135; i) see also: W. H. Watson (Ed.): *Stereochemistry and Reactivity of Systems Containing π Electrons*, Verlag Chemie Intl., Deerfield Beach, FL, USA 1983.

[13] a) H. D. Rudolph, H. Dreizler, A. Jaeschke, P. Wendling, *Z. Naturf. A 22* (1967) 940; b) D. R. Lide, D. E. Mann, *J. Chem. Phys. 27* (1957) 868; c) see also: R. K. Harris, M. Thorley, *J. Mol. Spectrosc. 42* (1972) 407; T. Ogata, A. P. Cox, D. L. Smith, P. L. Timms, *Chem. Phys. Lett. 26* (1974) 186.

[14] a) H. B. Bürgi, E. Shefter, *Tetrahedron 31* (1975) 2976; b) R. A. Kydd, *Spectrochim. Acta 27A* (1971) 2067; c) R. L. Arnett, B. L. Crawford, *J. Chem. Phys. 18* (1950) 118; B. L. Crawford, J. E. Lancaster, R. G. Inskeep, *ibid. 21* (1953) 678.

[15] **5**: monoclinic crystals, m.p. 113 °C (from acetone); space group $P2_1/c$, $Z = 4$, $a = 5.896(1)$, $b = 6.624(2)$, $c = 24.688(16)$ Å, $\beta = 90.74(3)°$; $\varrho_{calcd} = 1.297$ g cm^{-3}. Intensity measurements at room temperature on a four-circle diffractometer ($\lambda_{Mo} = 0.71069$ Å, $\theta_{max} = 27°$); direct methods; refinement (C, O anisotropic, H isotropic) including 1529 reflections with $F_0 > 3\sigma(F_0)$; $R = 0.046$, $R_w = 0.047$ [8]. **6**: triclinic crystals, m.p. 93 °C (from pentane); space group $P\bar{1}$ assumed, $Z = 2$, $a = 8.393(2)$, $b = 9.535(4)$, $c = 10.758(5)$ Å, $\alpha = 78.14(3)$, $\beta = 68.02(3)$, $\gamma = 71.95(2)°$; $\varrho_{calcd} = 1.362$ g cm^{-3}; measuring conditions, structure solution, and refinement as for **5**; 1716 reflections with $F_0 > 4\sigma(F_0)$; $R = 0.080$, $R_w = 0.079$ [8].

$[H_2\overline{C(CH_2)_5NLi}]_6$, the First Cyclized Lithium Amide Ladder: Synthesis and Structure of Hexamethyleneimidolithium **

By *Donald Barr, William Clegg, Susan M. Hodgson, Glenn R. Lamming, Robert E. Mulvey, Andrew J. Scott, Ronald Snaith,** and *Dominic S. Wright*

Lithium amides (amidolithiums), RR'NLi, are valuable reagents in both organometallic and organic syntheses.[1] As such, solutions of these reagents are usually either bought, or prepared in situ by lithiation of amines, then used forthwith in subsequent reactions.[2] More recently, however, a selection of these materials has been isolated and they have been examined in their own right; in particular, structures have been elucidated (in the crystal by X-ray diffraction,[3] and in solution by molecular mass measurements and NMR spectroscopy[4]), and attempts have been made to rationalize the occurrence of such structures.[5] Here we describe the synthesis, solid-state structure, and solution behavior of hexamethyleneimidolithium, **1**. Most importantly, in the crystal **1** is a hexamer (n = 6), and as such it is the first uncomplexed lithium amide structure with $n > 4$ and the first which is not a simple planar $(NLi)_n$ ring.[6] Despite such novel features, the structure of **1** is consistent with the prior rationalizations of amidolithium structures: although the hexamer could be viewed as arising from two vertically stacked trimeric rings, analysis of N–Li bond lengths within it reveals that it is in fact best seen as a ladder-type structure with sufficient N–Li rings (six) that the ladder can turn back on itself and cyclize.

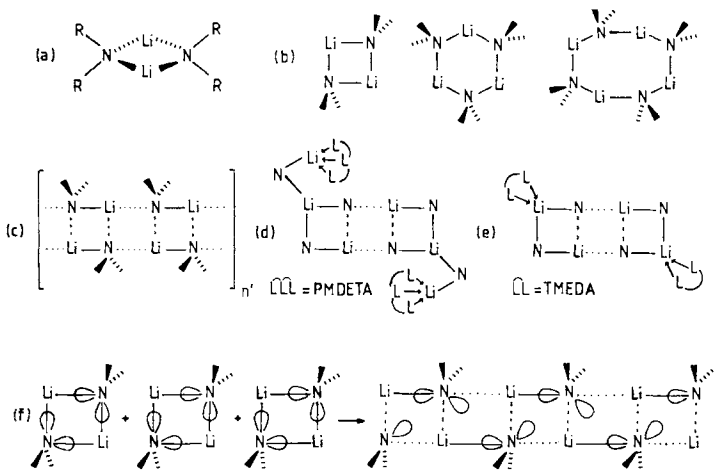
$[H_2\overline{C(CH_2)_5NLi}]_6$ **1**

The building blocks for lithium amide structures appear to be planar $(NLi)_n$ rings (Scheme 1a, shown for n = 2). In the

[*] Dr. R. Snaith, Dr. D. Barr, D. S. Wright
University Chemical Laboratory, Lensfield Road
Cambridge, CB2 1EW (UK)
Dr. W. Clegg, S. M. Hodgson, G. R. Lamming, A. J. Scott
Department of Chemistry, The University
Newcastle upon Tyne, NE1 7RU (UK)
Dr. R. E. Mulvey
Department of Pure and Applied Chemistry, University of Strathclyde
Glasgow, G1 1XL (UK)

[**] This work was supported by the U.K. Science and Engineering Research Council.

absence of donors, such ring structures have been found (with n = 2–4,[6] Scheme 1 b) usually only when R,R′ groups



Scheme 1.

are particularly bulky. More typically, lithiation of amines RR′NH in non-donor solvents produces insoluble, seemingly polymeric materials. Such continuous association cannot, it has been argued[5] have taken place vertically by stacking of rings (as occurs for most other types of organolithium compounds[7]) since their R,R′ groups project above and below the ring plane (Scheme 1 a). Rather, it must presumably have taken place laterally, by joining $(NLi)_n$ ring edges and so giving "ladders" or "fences"[8] (Scheme 1 c). Some credence has been given to such a view by the recent isolation of oligomeric ladders: thus, although lithiation in toluene solvent of pyrrolidine **2**—chosen as its R,R′ groups are both small and tied—produces an insoluble, polymeric amide **3**, lithiations in the presence of pentamethyldiethylenetriamine (PMDETA) or tetramethylethylenediamine (TMEDA) result in donor-intercepted ladders, **4** and **5** respectively (cf. Scheme 1 d and e, resp.).[9] Interestingly,

$H_2\overline{C(CH_2)_3NH}$ **2** $[H_2\overline{C(CH_2)_3NLi}]_\infty$ **3**

$\{[H_2\overline{C(CH_2)_3NLi}]_3 \cdot PMDETA\}_2$ **4**

$\{[H_2\overline{C(CH_2)_3NLi}]_2 \cdot TMEDA\}_2$ **5**

lithiation of a higher homolog of **2**, hexamethyleneimine, in the absence of a donor produces the crystalline, arene-soluble lithium amide, **1** (see Experimental). The crystal structure[10] of **1** reveals a hexamer. This could be viewed (Fig. 1) as a cyclized ladder composed of six NLi rungs, or as a stack of two six-membered, trimeric $(NLi)_3$ rings (Fig. 2). In the context of these alternatives, it has been argued on the basis of MO optimizations of $(H_2NLi)_6$ structures [a stack of two rings, $[(H_2NLi)_3]_2$, being lower in energy than a ladder of six rungs, $(H_2NLi)_6$][11] that lithium amide rings should be able to associate vertically. In the case of **1** these alternatives can be resolved by inspection of the N–Li distances (Fig. 2): these fall clearly into two sets, (i) short, 1.99(1)–2.00(2) Å, (ii) long, 2.06(1)–2.12(2) Å. A short-medium-long pattern has been observed for a series of iminolithium hexamers,[12] each structure then being readily interpretable in terms of two stacked trimeric rings, with alternating short and medium length N–Li bonds within each ring and long bonds

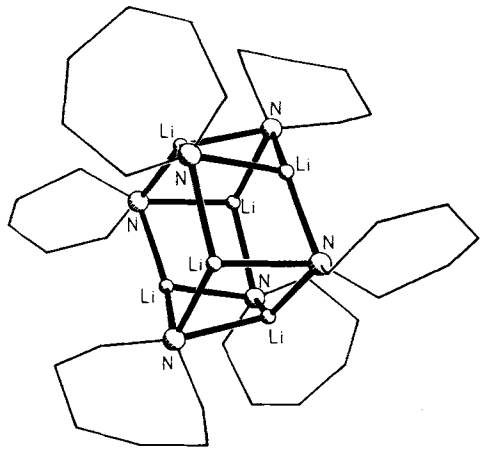


Fig. 1. Molecular structure of 1. The molecule has crystallographic inversion symmetry.

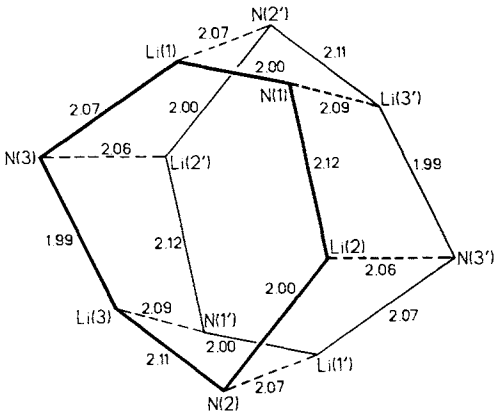


Fig. 2. Li–N bond lengths in 1 (standard deviation 0.01–0.02 Å). Hexamethylene units have been omitted for clarity.

between the rings. In the observed structure for **1**, however, the bonds between six-membered rings are not the longest; the pattern is rather one of alternating short and long bonds within the six-membered rings, which are held together by medium length bonds (though there is one instance of overlap of the medium and long distances). This implies that the structure of **1** is better viewed as a cyclized ladder (Fig. 1). As shown in Scheme 1 f, for $(RR'NLi)_2$ rings to come together laterally, one of the two lone-pair lobes on each amide $N^\ominus$ center must be redirected markedly, so to bond to two Li centers; the resulting ladder edges (N · · · Li) and rungs (N---Li) will thus be longer than the two-center edges (N-Li). A continuation of such ladder formation, and eventual cyclization, will thus produce short-long N-Li edges, with fairly constant (medium) length N–Li rungs; this is essentially the pattern observed for **1**.

In arene solutions it seems that **1** can form even higher aggregates than the hexamer found in the solid. Cryoscopic measurements on benzene solutions of **1** give association state values (n) of around 6 in relatively dilute solution, but these values increase markedly, to over 10, on concentration.[13] The ^{7}Li NMR spectra of $C_6D_5CD_3$ solutions of **1**[14] concur with the above. At ambient temperatures, a singlet is observed for each solution examined, though this broadens and moves to higher frequency (from $\delta \approx -1.1$ to $\delta \approx -0.8$) in more concentrated solutions. When the spectra are recorded at −90 °C, two signals ($\delta \approx -0.5$, -1.6) of approximately equal intensity are observed in dilute solutions; on progressive concentration, the higher frequency

singlet grows in intensity relative to the other singlet until, finally, it is the only signal observed. The implications of these cryoscopic and spectroscopic results are that there are (at least) two species present: presumably the hexamer (especially at lower concentrations; [δ (^{7}Li) ≈ -1.6] and an aggregate with n > 6 [δ (^{7}Li) ≈ -0.5].

Experimental Procedure

1: *n*BuLi (6.25 ml of a 1.60 M solution in hexane, 10 mmol) was added under N_2 to a chilled solution of hexamethyleneimine $H_2C(CH_2)_5NH$ (0.99 g, 10 mmol) in hexane/toluene (6 ml/4 ml). At room temperature, a white solid precipitated; this dissolved on warming to give a pale yellow solution. Cooling gave large colorless cube-shaped crystals which were filtered and characterized as **1**, [0.90 g, 86%, m.p. 112–115 °C; found C 68.4%, H 11.3%, Li 6.8%, N 13.4%. Calculated for $C_6H_{12}LiN$ = C 68.6%, H 11.4%, Li 6.7%, N 13.3%. ^{1}H NMR (C_6D_6, 80 MHz, 20 °C) δ = 1.71 (br s, 8H), 3.02 (br m, 4H)]. Single crystals suitable for X-ray crystallography were sealed under N_2 in Lindemann capillary tubes prior to data collection.

Received: April 12, 1989 [Z 3282 IE]
German version: *Angew. Chem. 101* (1989) 1279

[1] a) For uses in the syntheses of metal amides, see M. F. Lappert, P. P. Power, A. R. Sanger, R. C. Srivastava: *Metal and Metalloid Amides*, Wiley, Chichester 1980; b) For uses in organic syntheses, see M. Fieser: *Fieser's Reagents for Organic Synthesis, Vol. 12*, Wiley-Interscience, New York 1986 and earlier volumes.

[2] The advantages of isolating lithium amides as crystalline materials prior to subsequent reaction were first pointed out in: M. F. Lappert, M. J. Slade, A. Singh, J. L. Atwood, R. D. Rogers, R. Shakir, *J. Am. Chem. Soc. 105* (1983) 302; see also Ref. [9].

[3] For a review of organolithium X-ray structures up to 1984 (and including N–Li species) see W. N. Setzer, P. von R. Schleyer, *Adv. Organomet. Chem. 24* (1985) 353; for related reviews covering work published 1985–1987, see R. Snaith, *Prog. Chem. Annu. Rep. A82* (1986) 3; *ibid. A83* (1987) 3; *ibid. A84* (1988) 3.

[4] a) D. Reed, D. Barr, R. E. Mulvey, R. Snaith, *J. Chem. Soc. Dalton Trans. 1986*, 557; b) A. S. Galinano-Roth, E. M. Michaelides, D. B. Collum, *J. Am. Chem. Soc. 110* (1988) 2658; c) J. S. DePue, D. B. Collum, *ibid. 110* (1988) 5518, and references therein.

[5] a) D. R. Armstrong, D. Barr, W. Clegg, R. E. Mulvey, D. Reed, R. Snaith, K. Wade, *J. Chem. Soc. Chem. Commun. 1986*, 869; b) D. Barr, W. Clegg, R. E. Mulvey, R. Snaith, D. S. Wright, *ibid. 1987*, 716; see also Ref. [9] and references cited therein.

[6] Uncomplexed lithium amides (RR'NLi)$_n$ with (NLi)$_n$ ring structures are a) R = R' = Me_3Si, n = 2 (gas phase, by electron diffraction), T. Fjeldberg, P. B. Hitchcock, M. F. Lappert, A. J. Thorne, *J. Chem. Soc. Chem. Commun. 1984*, 822; b) R = R' = Me_3Si, n = 3 (crystal structure), R. D. Rogers, J. L. Atwood, R. Grüning, *J. Organomet. Chem. 157* (1978) 229; c) R = R' = $PhCH_2$, n = 3 (crystal structure), D. R. Armstrong, R. E. Mulvey, G. T. Walker, D. Barr, R. Snaith, W. Clegg, D. Reed, *J. Chem. Soc. Dalton Trans. 1988*, 617; d) RR'N = $Me_2C(CH_2)_3CMe_2N$, n = 4 (crystal structure), Ref. [2].

[7] The so-called "ring-stacking principle" is applicable to organolithium ring compounds whose R,R' groups are relatively coplanar with the (ELi)$_n$ rings (n = 2 or 3) e.g., in imidolithium compounds (RR'C = NLi)$_n$, E = N, in alkoxy- and enolatolithium compounds (ROLi)$_n$, and [R(H_2C=)COLi]$_n$ respectively, E = O, and in alkynyllithiums, (RC≡CLi)$_n$, E = C. Such relatively flat systems can thus associate vertically, giving clusters (e.g., two dimeric rings, to give a pseudocubane tetramer; two trimeric ones to give a hexamer). See a) D. Barr, W. Clegg, R. E. Mulvey, R. Snaith, K. Wade, *J. Chem. Soc. Chem. Commun. 1986*, 295; b) D. R. Armstrong, D. Barr, R. Snaith, W. Clegg, R. E. Mulvey, K. Wade, D. Reed, *J. Chem. Soc., Dalton Trans. 1987*, 1071; c) D. Barr, R. Snaith, W. Clegg, R. E. Mulvey, K. Wade, *J. Chem. Soc. Dalton Trans. 1987*, 2141, and references cited therein.

[8] The term "fences" was first used in H. Kato, K. Hirao, K. Akagi, *Inorg. Chem. 20* (1981) 3659, to describe lateral associations of (LiH)$_2$ rings within a theoretical MO study of structural options for lithium hydride.

[9] D. R. Armstrong, D. Barr, W. Clegg, S. M. Hodgson, R. E. Mulvey, D. Reed, R. Snaith, D. S. Wright, *J. Am. Chem. Soc.*, in press. See also Ref. 5a].

[10] **1**: $C_{36}H_{72}Li_6N_6$, M_r = 630.7, triclinic, space group $P\bar{1}$, a = 9.966(4), b = 10.539(4), c = 11.692(5) Å, α = 116.01(2), β = 96.76(2), γ = 108.90(2)°, V = 914.2 Å^3, Z = 1, D_c = 1.053 g cm^{-3}, F(000) = 348, $Cu_{K\alpha}$ radiation, λ = 1.54184 Å, μ = 0.41 mm^{-1}. The structure was determined by direct methods and refined from 1522 unique observed reflections measured at room temperature with a Stoe-Siemens diffractometer ($2\theta_{max}$ 110°), with anisotropic thermal parameters, and with isotropic H atoms in calculated positions; R = 0.098, R_w = 0.098, S = 1.06 for 218 parameters. Further details of the crystal structure investigation can be obtained from the Director of the Cambridge Crystallographic Data Centre, University Chemical Laboratory, Lensfield Road, Cambridge, CB2 1EW (UK). Any request should be accompanied by the full literature citation for this communication.

[11] These calculations (K. Raghavachari, A.-M. Sapse, D. C. Jain, *Inorg. Chem. 26* (1987) 2585 showed, for $(LiNH_2)_6$ as two stacked trimeric rings, two "short" Li–N bonds (1.99 Å) and one "long" bond (2.06 Å) for each triply-bridging N atom. The fact that three sets of bond lengths are found for experimental imidolithium hexamers[12] was attributed to crystal packing effects. This attribution, and the validity of comparing theoretical amidolithium structures with experimental imidolithium ones, was challenged (W. Clegg, R. Snaith, K. Wade, *ibid. 27* (1988) 3861), drawing a response from the original authors (K. Raghavachari, A.-M. Sapse, D. C. Jain, *ibid. 27* (1988) 3862).

[12] The hexameric imidolithiums, (RR'C=NLi)$_6$, R = R' = *t*$BuMe_2N$, R = Ph, R' = *t*$BuMe_2N$, display average lengths of 1.98, 2.01, and 2.05 Å for their N–Li bonds. See Refs. [7a] and [7b].

[13] Cryoscopy was carried out on benzene solution of **1**. Relative molecular mass values found (molarity of solution, M, expressed in terms of the empirical formula of **1**, n = 1), and hence association states (n) were: 564 ± 23 n(0.055 M) = 5.37 ± 0.22; 895 ± 33 n(0.113 M) = 8.52 ± 0.32; 1061 ± 53 n(0.139 M) = 10.11 ± 0.51.

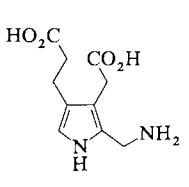
[14] Variable-temperature (25 °C, −90 °C) and variable-concentration (0.19 M, 0.25 M, 0.61 M solutions) ^{7}Li NMR spectra (139.96 MHz) were recorded for solutions of **1** in $C_6D_5CD_3$. At 25 °C each solution afforded a singlet: these were sharp (δ = −1.13, −1.24) in the relatively dilute solutions, much broader (δ = −0.80) in the concentrated one. At −90 °C, the 0.19 M and 0.25 M solutions each displayed two signals, though of differing relative integrals [δ = −0.50, −1.63 (ca. 1:1) and −0.49, −1.61 (ca. 2:1), respectively]; the 0.61 M solution spectrum consisted of just one, very broad resonance, at δ = −0.48.

Biomimetic Synthesis of an Inverted Porphyrinoid with Peripheral N Atoms**

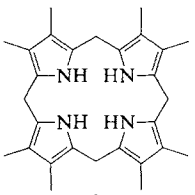
By *Karl-Heinz Schumacher* and *Burchard Franck**

Dedicated to Dr. Günther Ohloff on the occasion of his 65th birthday

A key step in the biosynthesis of all porphyrin natural products is the cyclocondensation of monopyrrole porphobilinogen **1** to give a colorless, nonconjugated porphyrinogen **2**.[2, 3] We have mimicked this biosynthetic reaction to



1



2

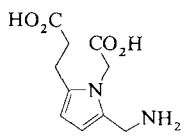
condense derivatives of **1** in vitro under acid catalysis to give novel, structurally modified porphyrinogens.[3, 4] These biomimetic[5] porphyrin syntheses excel other procedures in the low number of steps and the good overall yields.

Of particular interest is the question whether it is possible to prepare an inverted porphyrinogen **4a** by biomimetic condensation of a porphobilinogen isomer such as **3**. Here we

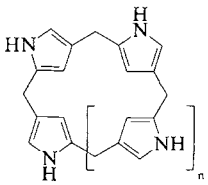
[*] Prof. Dr. B. Franck, Dr. K.-H. Schumacher [+]
Organisch-chemisches Institut der Universität
Orleansring 23, D-4400 Münster (FRG)

[+] Present address:
BASF AG, D-6700 Ludwigshafen

[**] Novel Porphyrinoids, Part 7. This work was supported by the Deutsche Forschungsgemeinschaft and the Fonds der Chemischen Industrie. Part 6: [1].



3



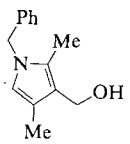
4a, n = 1
4b, n = 2

report the first biomimetic synthesis of a compound with the ring system of **4b**.

Inverted porphyrinogens, the nitrogen atoms of which are on the periphery of the molecule instead of in the interior, give rise to several questions which are important for understanding porphyrin systems:

1. Can inverted porphyrinogens be dehydrogenated to give the corresponding, possibly aromatic porphyrins?
2. Are cyclic tetrapyrroles preferentially formed in the biomimetic synthesis of inverted porphyrinogens as they are for natural porphyrinogens?
3. Does the comparison of inverted porphyrinogens with normal porphyrinogens offer evidence of transannular interactions between the N atoms of the latter?

The porphobilinogen isomer **3** and the structurally similar monopyrroles, which were initially considered as starting pyrroles for the biomimetic synthesis of an inverted porphyrinogen, proved unsuitable because of their tendency to undergo polymerization. Therefore, the better protected *N*-benzylpyrrole **5** was chosen for subsequent investigations.



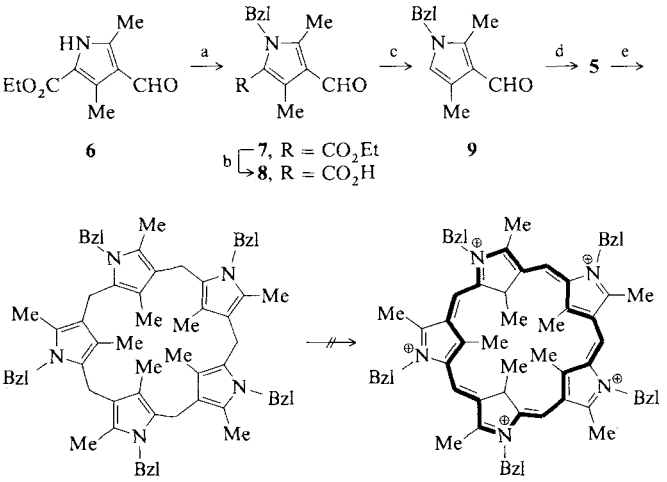
5

Although this pyrrole was expected to undergo some cyclocondensation to give products in which the *C*-methyl groups are directed toward the center of the ring, earlier experience[4a] indicated that this reaction would not interfere with the cyclization.

The synthesis of monopyrrole **5** (Scheme 1) started from the known[6] pyrrole aldehyde **6**, accessible in two steps from acetylacetone and diethylhydroxyiminomalonate by Kleinspehn condensation[7] and formylation. *N*-Benzylation to give **7**, ester saponification to give **8**, and thermal decarboxylation afforded aldehyde **9** (m.p. 64 °C), which crystallizes as needles and serves as a stable synthetic precursor.

To perform the biomimetic condensation, **9** was reduced to the reactive hydroxymethylpyrrole **5** by treatment with $NaBH_4$. Compound **5** was then treated in situ at −50 °C under oxygen-free conditions with *p*-toluenesulfonic acid/glacial acetic acid. Subsequent warming to 20 °C afforded a 71% yield of an oxygen-sensitive solid, which was pure according to thin layer chromatography. Elemental analysis and mass spectrometry ($M^{\oplus}$, *m/z* 985, 40%) gave the empirical formula $C_{70}H_{75}N_5$ for the condensation product; structure **10** was derived from the fragment peaks in the EI mass spectrum and from the ^1H NMR data.[10]

Compound **10** is the first inverted porphyrinoid. It is especially interesting that, in this biomimetic condensation, the



6 **7**, R = CO_2Et **8**, R = CO_2H **9** **10** **11**

Scheme 1. Synthesis of the inverted porphyrinoid **10** via *N*-benzyl-3-formyl-2,4-dimethylpyrrole **9**. Reaction conditions: a) BzlBr, NaH/DMF, 20 °C, 30 min; 96% **7** (m.p. 48 °C). b) 25% NaOH, 100 °C, 2 h; 86% **8** (m.p. 157–158 °C). c) Kugelrohr distillation 180 °C/0.2 mbar; 80% **9** (m.p. 64 °C). d) $NaBH_4$/MeOH, 20 °C, 15 min. e) *p*-TosOH/AcOH, −50 °C, 1 h; 71% **10** [10].

inversion of the pyrrole rings leads with high selectivity to a cyclic *penta*pyrrole instead of a tetrapyrrole. This has never been observed before in similar condensations with porphobilinogen **1**.[2] We propose the name *inverto-pentaphyrinogen* for the basic framework of **10**.[8]

Further noteworthy are the chemical reactivity and oxidation sensitivity of **10**. Whereas non-inverted porphyrinogens, like our new vinylogously enlarged porphyrinogens,[1,4d–f] are smoothly dehydrogenated by bromine and other oxidation agents to give stable, aromatic porphyrins, we failed, despite extensive attempts, to transform **10** under these conditions into a conjugated, possibly aromatic inverto-pentaphyrin such as **11**; instead, only decomposition products were obtained. A possible explanation might be that, although **11**, the hypothetical dehydrogenation product of **10**, can form an aromatic 22 π-electron perimeter, this results in a destabilizing accumulation of charge.[11]

Received: April 12, 1989 [Z 3283 IE]
German version: *Angew. Chem. 101* (1989) 1292

CAS Registry numbers:
5, 122069-36-7; **6**, 2199-64-6; **7**, 122069-33-4; **8**, 122069-34-5; **9**, 122069-35-6; **10**, 122069-37-8.

[1] G. Knübel, B. Franck, *Angew. Chem. 100* (1988) 1203–1204; *Angew. Chem. Int. Ed. Engl. 27* (1988) 1170–1172.
[2] L. Bogorad in D. Dolphin (Ed.): *The Porphyrins, Vol. 6*, Academic Press, New York 1979, pp. 125–178.
[3] B. Franck, *Angew. Chem. 94* (1982) 327–337; *Angew. Chem. Int. Ed. Engl. 21* (1982) 343–353.
[4] a) B. Franck, C. Wegner, *Angew. Chem. 87* (1975) 419–420; *Angew. Chem. Int. Ed. Engl. 14* (1975) 424; b) B. Franck, G. Bringmann, C. Wegner, U. Spiegel, *Liebigs Ann. Chem. 1980*, 263–274; c) G. Bringmann, B. Franck, *ibid. 1982*, 1272–1279; d) M. Gosmann, B. Franck, *Angew. Chem. 98* (1986) 1107–1108; *Angew. Chem. Int. Ed. Engl. 25* (1986) 1100–1101; e) B. Franck, M. Gosmann, G. Knübel, DOS 3 635 820 (1988), BASF "Vinyloge Porphyrine"; *Chem. Abstr. 109* (1988) 94748u; f) R. Timmermann, R. Mattes, B. Franck, *Angew. Chem. 99* (1987) 74–77; *Angew. Chem. Int. Ed. 26* (1987) 64–65; g) B. Franck, G. Fülling, M. Gosmann, G. Knübel, H. Mertes, D. Schröder, *SPIE Proc. Ser. 5, Vol. 997* (Symp. Adv. Photochemotherapy, Boston 1988), p. 107–112.
[5] B. Franck, *Angew. Chem. 91* (1979) 453–464; *Angew. Chem. Int. Ed. Engl. 18* (1979) 429–439.

[6] E. J.-H. Chu, T. C. Chu, *J. Org. Chem. 19* (1954) 266–269.
[7] G. G. Kleinspehn, *J. Am. Chem. Soc. 77* (1955) 1546–1548.
[8] This nomenclature proposal corresponds to the term "pentaphyrin", introduced by *Rexhausen* and *Gossauer* [9], for porphyrin-like cyclic pentapyrroles. Accordingly, the porphyrinogen analogues of cyclic pentapyrroles are called "pentaphyrinogens". Since **10** differs from these in the inversion of the five pyrrole rings, it is called an "inverto-pentaphyrinogen".
[9] H. Rexhausen, A. Gossauer, *J. Chem. Soc. Chem. Commun. 1983*, 275.
[10] The new compounds **7**–**10** were completely characterized by elemental analyses and spectroscopic data.
[11] Structure **11** may be regarded as the most likely tautomer of a dehydrogenation product of **10**. A smaller conjugated perimeter, which would enclose the inward directed methyl-substituted C atoms of all pyrrole rings, would contain 20 π electrons and thus be antiaromatic. Likewise, less charged structures, in which the outer CN double bonds not involved in the π-electron perimeter are hydrogenated, may presumably be excluded for the dehydrogenation product of **10**.

Binary Alloys of 2,5-Disubstituted DCNQI Radical Anion Salts of Copper and Their Electrical Conductivity**

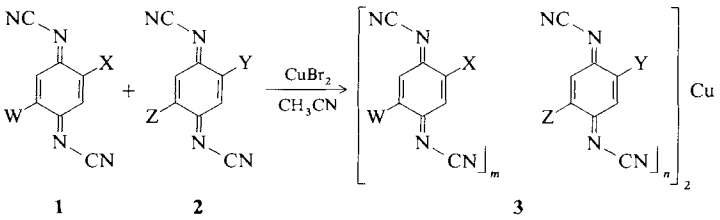
By *Peter Erk, Hans-Jörg Gross, Siegfried Hünig,* Uwe Langohr, Hubert Meixner, Hans-Peter Werner, Jost Ullrich von Schütz,* and *Hans Christoph Wolf*

Dedicated to Professor Gottfried Märkl on the occasion of his 60th birthday

N,N'-Dicyanoquinodiimines (DCNQIs),[1] particularly in the form of their 2,5-substituted benzoquinone derivatives, have proven very useful as novel acceptors in charge transfer (CT) compounds[1c, 2] and especially in radical anion salts of the type [2,5-X,Y-DCNQI]$_2$M (M = monovalent metal ion).[3] Despite wide variation of the substituents X and Y (see below) and of M (Li, Na, K, Rb, Cu, Ag, Tl,[3c] NH_4[3c, 4a] all these salts crystallize in the same structure type:[3a, 3c, 4] by tetrahedral coordination of the metal ions these are strung out like a pearl necklace and surrounded by four stacks of DCNQI units.[3a, 3c, 4a] The retainment of the same structure type despite large variation of the substituents and counterions is unknown in the case of other conductive radical salts.

The copper salts [2,5-X,Y-DCNQI]$_2$Cu play a special role, for only they show a multidimensional[5, 6] and significantly increased metallic conductivity. As in many analogous cases,[7, 8] in the salts with X,Y = Me/Cl, Me/Br, Cl/Cl, Cl/Br, Br/Br a metal-semiconductor transformation takes place on cooling as a result of a Peierls distortion.[3c, 4c, 5] Contrastingly, when X,Y = Me,Me,[3a] Me,I[3b] and MeO, MeO[4c] the conductivity steadily increases up to < 3 K, whereby values of up to 5×10^5 S cm^{-1} are achieved.[3a] So far, however, neither the substituent-dependence[9] nor the unusual pressure-dependence[10] of the phase transitions are fully understood. It was therefore considered of interest to prepare alloys of the corresponding copper salts in which two differently substituted DCNQIs are incorporated in the stack, so as to study the influence of this disturbance on the electrical conductivity and other physical properties in a fundamentally similar crystal lattice.

For the synthesis of the necessary single crystals of binary alloys of the type [(2,5-W,X-DCNQI)$_m$(2,5-Y,Z-DCNQI)$_n$]$_2$Cu **3** we first resorted to the usual method of electrocrystallization.[3a] In this way (method A), **3a–c, 3g, 3i** and **3k** (Table 1) could be obtained. However, the much simpler method of immersing a polished copper wire into a solution of the DCNQIs in acetonitrile (method B)[11] also led to well crystallized alloys, as demonstrated by the examples **3d–f, 3h, 3j, 3l,** and **3m**. The ratio of the two components in the alloy frequently deviate thereby from that obtained by electrocrystallization, even though equimolar amounts of the two DCNQIs were employed in all cases.



1 **2** **3**

The ratios $\mathbf{1}_m/\mathbf{2}_n$ in the salts **3** were ascertained from the elemental analyses and are therefore subject to the corresponding errors. All alloys crystallize isotypically to the individual components (space group $I4_{1/a}$).[12] Which factors determine the composition is still unknown. The difference ΔE in the redox potentials of the components **1** and **2** (Table 1)[2c, 3c] can only play a subordinate role; e.g. for $\Delta E = +0.21$ V corresponding to an energy difference of 4.8 k calmol^{-1}, a ratio of easily reducible to difficulty reducible components of ca. 3000:1 would be expected if thermodynamic factors alone were to be responsible. Thin (10–30 μm), black, shiny crystalline needles of ca. 1–15 mm in length are obtained by methods A and B. Their structureless IR spectrum (KBr) in the region 4000–600 cm^{-1} immediately points to high electrical conductivity.[13] This is confirmed by powder conductivities[14] of ca. 0.1–0.2 S cm^{-1} and sin-

Table 1. Binary alloys **3** of the DCNQI components **1** and **2** and copper(II) bromide in acetonitrile by electrocrystallization (method A) or immersion of a copper wire (method B). Amounts of the components **1** (*m*) and **2** (*n*) and their potential difference ΔE. Powder(P) conductivity or single-crystal(S) conductivity σ of **3** at room temperature (highest measured values).

W	X	*m*	Y	Z	*n*	Method	ΔE [V] [a]	**3**	σ [S cm^{-1}]
Me	Me	0.5	Me	Cl	1.5	A	+0.22	**a**	200 (S)
Me	Me	0.5	Me	Br	1.5	A	+0.21	**b**	200 (S)
Me	Me	0.6	Me	I	1.4	A	+0.21	**c**	200 (S)
Me	Me	1.0	Me	I	1.0	B	+0.21	**d**	0.2 (P)
Me	Me	0.8	Me	OMe	1.2	B	−0.01	**e**	0.2 (P)
Me	Me	1.0	OMe	OMe	1.0	B	−0.06	**f**	200 (S)
Me	Cl	0.8	Me	Br	1.2	A	+0.01	**g**	400 (S)
Me	Cl	1.0	Me	Br	1.0	B	+0.01	**h**	0.2 (P)
Me	Cl	1.0	Me	I	1.0	A	−0.01	**i**	400 (S)
Me	Cl	1.5	Me	I	0.5	B	−0.01	**j**	400 (S)
Me	Br	1.2	Me	I	0.8	A	±0.0	**k**	200 (S)
Me	I	0.8	Me	OMe	1.2	B	−0.22	**l**	250 (S)
Me	I	1.3	OMe	OMe	0.7	B	−0.27	**m**	200 (S)

[a] E_2 (**1**) − E_2 (**2**); cf. [2c, 3c].

[*] Prof. Dr. S. Hünig, Dr. P. Erk, Dipl.-Chem. H. Meixner
Institut für Organische Chemie der Universität
Am Hubland, D-8700 Würzburg (FRG)
Prof. Dr. H. C. Wolf, Dr. J. U. von Schütz, Dipl.-Phys. H.-J. Gross, Dipl.-Phys. U. Langohr, Dr. H.-P. Werner
3. Physikalisches Institut der Universität
Pfaffenwaldring 57, D-7000 Stuttgart (FRG)

[**] This work was supported by the Volkswagen Stiftung, the Fonds der Chemischen Industrie, and BASF AG, Ludwigshafen. – DCNQI = *N,N'*-dicyanoquinodiimine.

gle-crystal conductivities[15] of 100 to 500 S cm^{-1} which almost reach those of the components.[2b, 3, 4b, 4c]

That mixed crystals are actually present and not just mixtures with different elemental analyses is demonstrated by the following findings:

1) In several single crystals of **3k** both bromine as well as iodine could be detected.
2) The X-ray powder diagrams of **3i** show reflections which cannot be assigned to either of the two components.[12] Their large half-widths and the high noise-to-signal ratios point to a strong disorder, presumably as a result of random distribution of the components.
3) The temperature-dependence of the electrical conductivity, which is discussed in detail elsewhere,[16] deviates significantly from that of the component copper salts, whereby three different types with metallically conductive alloys can be distinguished: a) alloys which exhibit a sharp phase transition to the semiconductor between 180–120 K (**3g** and **3i**); b) alloys with a very broad phase transition to the semiconductor (**3a** and **3b**); c) alloys whose conductivity increases up to 4 K (**3c, 3f** and **3k–m**).

Remarkable is the case of **3k** (Fig. 1): although the component [2,5-Br,Me-DCNQI]$_2$Cu is characterized by a sharp

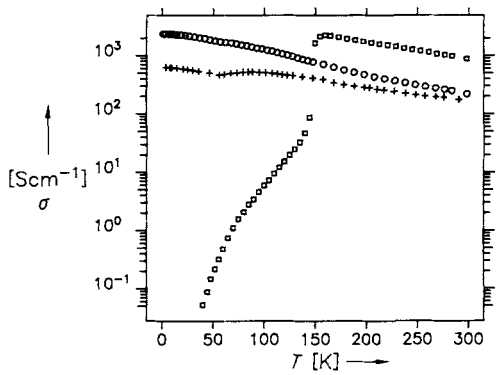


Fig. 1. Comparison of the temperature-dependent conductivities σ of [2,5-Br,Me-DCNQI]$_2$Cu (□□□) and [2,5-I,Me-DCNQI]$_2$Cu (○○○) with that of the alloy **3k** (+ + +) of both components.

phase transition to the semiconductor at 150 K,[4c, 5] the breakdown in conductivity in the mixed crystal is suppressed with [2,5-I,Me-DCNQI]$_2$Cu. The phase transition is still albeit only weakly in the temperature range 90–20 K. Upon further cooling it is apparently cancelled, so that the conductivity increases to 600 S cm^{-1} as the temperature approaches 4 K. Our studies are being extended to tertiary[16] and quaternary alloys of the same type, the first examples of which have already been synthesized.

Experimental Procedure

Method A: A mixture of 200–400 μmol each of **1** and **2** and 200–300 μmol of $CuBr_2$ in 60 mL of acetonitrile was electrolyzed galvanostatically in a three-compartment cell with Pt wire at 30–50 μA for 4–5 days at room temperature. The crystals that were filtered off were washed with acetonitrile and dried.

Method B: As described in Ref. [11] a freshly polished copper wire was immersed in a solution of 100 μmol each of **1** and **2** and 150 μmol of $CuBr_2$ in 25 mL of acetonitrile. After 3–4 days the crystals that separated (40–90%) were filtered off, washed with acetonitrile, and dried.

Received: May 13, 1989 [Z 3287 IE]
German version: *Angew. Chem. 101* (1989) 1297

[1] a) A. Aumüller, S. Hünig, *Angew. Chem. 96* (1984) 437; *Angew. Chem. Int. Ed. Engl. 23* (1984) 447; b) *Liebigs Ann. Chem. 1986*, 142; c) G. D. Andreetti, S. Bradamante, P. C. Bizzarri, G. A. Pagani, *Mol. Cryst. Liq. Cryst. 120* (1985) 309.
[2] a) A. Aumüller, E. Hädicke, S. Hünig, A. Schätzle, J. U. von Schütz, *Angew. Chem. 96* (1984) 439; *Angew. Chem. Int. Ed. Engl. 23* (1984) 449; b) A. Aumüller, P. Erk, S. Hünig, J. U. von Schütz, H.-P. Werner, H. C. Wolf, *Mol. Cryst. Liq. Cryst. 156* (1988) 215; c) A. Aumüller, P. Erk, S. Hünig, H. Meixner, J. U. von Schütz, H.-P. Werner, *Liebigs Ann. Chem. 1987*, 997.
[3] a) A. Aumüller, P. Erk, G. Klebe, J. U. von Schütz, H.-P. Werner, *Angew. Chem. 98* (1986) 759; *Angew. Chem. Int. Ed. Engl. 25* (1986) 740; b) P. Erk, S. Hünig, J. U. von Schütz, H.-P. Werner, H. C. Wolf, *ibid. 100* (1988) 286 and *27* (1988) 267; c) S. Hünig, A. Aumüller, P. Erk, H. Meixner, J. U. von Schütz, H.-J. Gross, U. Langohr, H.-P. Werner, H. C. Wolf, C. Burschka, G. Klebe, K. Peters, H.-G. von Schnering, *Synth. Met. 27* (1988) B181, and references cited therein.
[4] a) R. Kato, H. Kobayashi, A. Kobayashi, T. Mori, H. Inokuchi, *Chem. Lett. 1987*, 1579; b) *Synth. Met. 27* (1988) B263; c) A. Kobayashi, T. Mori, H. Inokuchi, R. Kato, H. Kobayashi, *ibid. 27* (1988) B275.
[5] J. U. von Schütz, M. Bair, H.-J. Gross, U. Langohr, H.-P. Werner, H. C. Wolf, D. Schmeisser, K. Graf, W. Göpel, P. Erk, H. Meixner, S. Hünig, *Synth. Met. 27* (1988) B249, and references cited therein.
[6] T. Mori, K. Imaeda, R. Kato, A. Kobayashi, H. Inokuchi, *J. Phys. Soc. Jpn. 56* (1987) 3429.
[7] Review: F. Wudl, *Acc. Chem. Res. 17* (1984) 227.
[8] Review: K. Menke, S. Roth, *Chem. Unserer Zeit 20* (1986) 1, 33.
[9] A. Kobayashi, R. Kato, H. Kobayashi, T. Mori, H. Inokuchi, *Solid State Commun. 64* (1987) 45.
[10] a) R. T. Henriques, D. Jérome, P. Erk, S. Hünig, J. U. von Schütz, *J. Phys. C: Solid State Phys. 23* (1988) L1205; b) S. Tomic, D. Jérome, A. Aumüller, P. Erk, S. Hünig, J. U. von Schütz, *Synth. Met. 27* (1988) B281.
[11] P. Erk, S. Hünig, H. Meixner, J. U. von Schütz, H. P. Werner, *Liebigs Ann. Chem. 1988*, 157.
[12] P. Batail, P. Erk, unpublished results.
[13] Cf. measurements on CT-complexes, R. C. Wheland, J. L. Gilson, *J. Am. Chem. Soc. 98* (1976) 3916.
[14] Method cf. [2c].
[15] Four-point measurement, cf. H.-P. Werner, *Dissertation*, Universität Stuttgart 1988.
[16] H. J. Gross, U. Langohr, J. U. von Schütz, H.-P. Werner, H. C. Wolf, S. Tomic, P. Jérome, P. Erk, H. Meixner, S. Hünig, *J. Phys. Les Ulis Fr.*, in press.

Structure and Properties of the Cryptophane-E/$CHCl_3$ Complex, a Stable van der Waals Molecule**

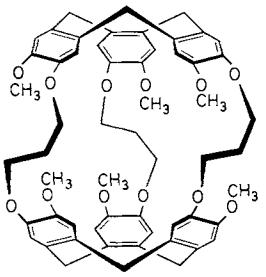
By *Josette Canceill, Michèle Cesario, André Collet,* Jean Guilhem, Liliane Lacombe, Bénédicte Lozach,* and *Claudine Pascard*

What are the driving forces leading to the formation of stable complexes between neutral host and guest molecules *in the absence of hydrophobic effects*? Examples of such complexes are the 1:1 complexes between cryptophane-E **1** and chloroform[1] or isobutane,[2] which form reversibly in 1,1,2,2-tetrachloroethane with association constants of over 10^2 M^{-1} at room temperature.[3] We report here some evidence that the above complexes may be viewed as "van der

[*] Prof. Dr. A. Collet, Dr. B. Lozach
U.M.R. C.N.R.S.-E.N.S.L. 117
Stéréochimie et Interactions Moléculaires,
Ecole Normale Supérieure de Lyon
46, allée d'Italie, F-69364 Lyon Cedex 07 (France)
Dr. J. Canceill, L. Lacombe
Equipe de Recherche du C.N.R.S. No. 285
Chimie des Interactions Moléculaires, Collège de France
11, place Marcelin-Berthelot, F-75231 Paris Cedex 05 (France)
Dr. M. Cesario, Dr. J. Guilhem, Dr. C. Pascard
Institut de Chimie des Substances Naturelles, C.N.R.S.
B.P. 1, F-91190 Gif-sur-Yvette (France)

[**] We are grateful to Région Rhône-Alpes and Société LIPHA for a grant (to *B. L.*)

Waals molecules", that is, structurally well-defined assemblies of two neutral species noncovalently bound to each other.[4] This conclusion stems from an X-ray structure determination of the **1** · $CHCl_3$ complex and from variable-temperature ^1H NMR studies of a series of complexes of **1** with neutral guest molecules of appropriate size.



1

The structure of the **1** · $CHCl_3$ complex in the crystalline state is depicted in Figure 1.[5] The host molecule is almost spherical (10 Å in diameter) and displays nearly noncrystallographic D_3 symmetry. The two cyclotriveratrylene caps are twisted with respect to each other by ca. 60° around the pseudo C_3 axis, and the benzene rings α, β, and γ of the upper cap are parallel to the rings β′, γ′, and α′, respectively, of the lower cap. The three $O(CH_2)_3O$ bridges have about the same conformation, with the pseudo C_2 axes of the D_3 group passing through the inner methylenes of the chains. One of the methoxy groups shows orientational disorder (three positions), whereas the others are roughly coplanar with the aromatic rings to which they are bound. In this conformation, they partially obstruct the windows giving access to the host cavity.

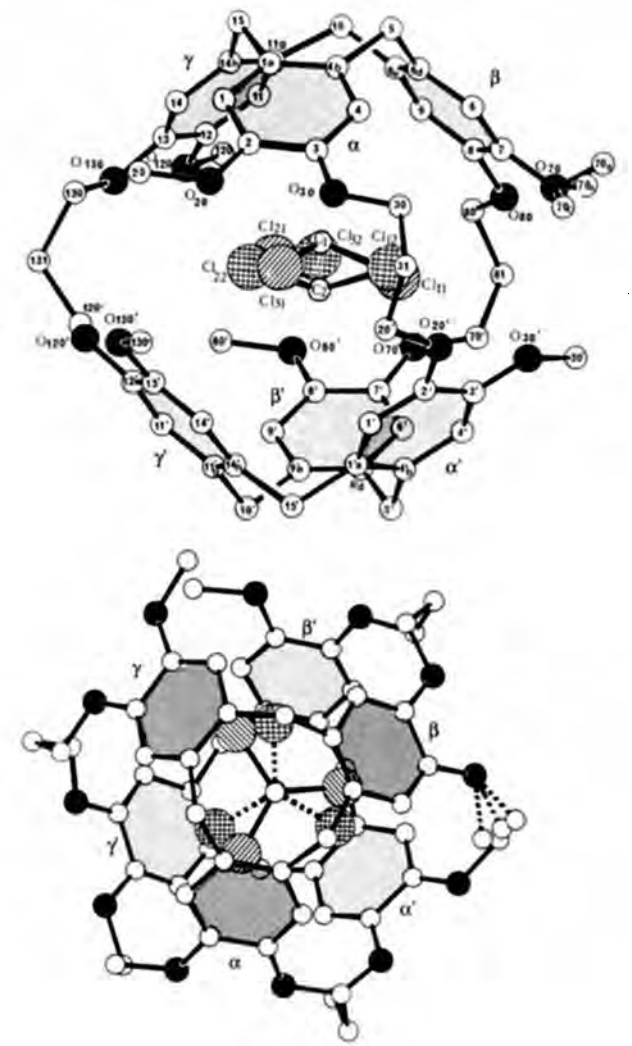


Fig. 1. Side view (top) and top view (bottom) of **1** · $CHCl_3$ in the crystal.

In the crystal, the encaged chloroform molecule exhibits two almost equivalent and equiprobable orientations, in which the chlorine atoms occupy the central equatorial plane of the host and the C–H bond points either up or down along the pseudo C_3 axis. The two positions are related by pseudo-symmetry around the C_2 axes of the host, and the two complexes are thus structurally similar. We cannot decide whether this situation is the consequence of a static disorder, where the host molecules are filled statistically with a chloroform molecule turned up or down, or of a dynamic disorder of the guest turning upside down (and possibly rotating around its C_3 axis) during the time needed for the X-ray data collection.

In ^1H NMR studies (Table 1) of complexes between **1** and various guests ranging in size from CH_3I (54.5 Å^3) to $(CH_3)_3CCl$ (93.9 Å^3) in 1,1,2,2-tetrachloro-1,2-dideuterioethane as solvent, we observed in all cases a slow exchange, on the NMR time scale, between the free and complexed guest molecules. The resonances of the latter were shifted upfield ($\Delta\delta$ = 2.9–4.5 ppm) with respect to those of the free species, as a result of the shielding effect of the six aromatic rings of the host. The $\Delta\delta$ values given in Table 1 suggest that the complexes of **1** with CHXYZ guests in solution have a structure similar to that of the chloroform complex in the crystal, with the H atom embedded in one of the cyclotriveratrylene caps ($\Delta\delta$ = 4.25–4.44 pm) and the X, Y, and Z groups in the equatorial plane ($\Delta\delta$ = 2.95 ppm for the methyl groups in isobutane).

In the $CCl_n(CH_3)_{4-n}$ complexes (n = 1–3), which are much weaker in strength than the CHXYZ complexes, the observed $\Delta\delta$ values presumably represent some averaging between axial and equatorial positions of the methyl groups. In the CCl_3CH_3 complex, the methyl $\Delta\delta$ value approaches that of an axial group, whereas in the $CCl(CH_3)_3$ complex it is close to that of isobutane, which indicates that the chlorine

Table 1. Guest van der Waals volume, upfield ^1H NMR shift of the guest in the **1** · guest complex, barrier for inclusion (ΔG_i^*), free energy, enthalpy, and entropy of complexation (ΔG_i, ΔH_i, ΔS_i); data obtained by variable temperature ^1H NMR in 1,1,2,2-tetrachloro-1,2-dideuterioethane at 200.13 MHz.

Guest	V_{vdw} [Å^3]	$\Delta\delta$	ΔG_i^* [kcal mol^{-1}] 300 K	330 K	ΔG_i [kcal mol^{-1}] 300 K	ΔH_i [kcal mol^{-1}]	ΔS_i [cal mol^{-1} K^{-1}]
CH_3I	54.5	3.70	13.6		−2.4		
CH_2Cl_2	57.6	4.19	13.3		−2.8	+1.0	+6
CH_2Br_2	65.5	4.18			−3.0		
CH_3COCH_3	70.0	3.44			−1.3		
$CHCl_3$	72.2	4.44	13.3	14.4	−3.7	−6.0	−7
$CHCl_2Br$	76.1	4.42		14.9	−3.4	−5.2	−6
$CH(CH_3)_3$	79.4	4.25 2.95	13.9		−2.8	−3.8	−3
$CHClBr_2$	80.1	4.41		14.8	−2.9	−1.5	+4
$CHBr_3$	84.0	4.35		15.1	−2.3	−1.4	+4
CCl_4	86.8				−1.2		
$C(CH_3)Cl_3$	89.2	3.55			−0.2		
$C(CH_3)_2Cl_2$	91.6	3.45			+0.1		
$C(CH_3)_3Cl$	93.9	3.18			+0.8		

atom is preferentially axial. In these two cases, the complex of higher symmetry (C_3) seems to be preferred. The fact that a single signal was observed for the methyl groups in all these complexes means that the substituents exchange their position rapidly on the NMR time scale.

In Figure 2, we have plotted the complexation free energy (ΔG_i) at 300 K as a function of the van der Waals volume

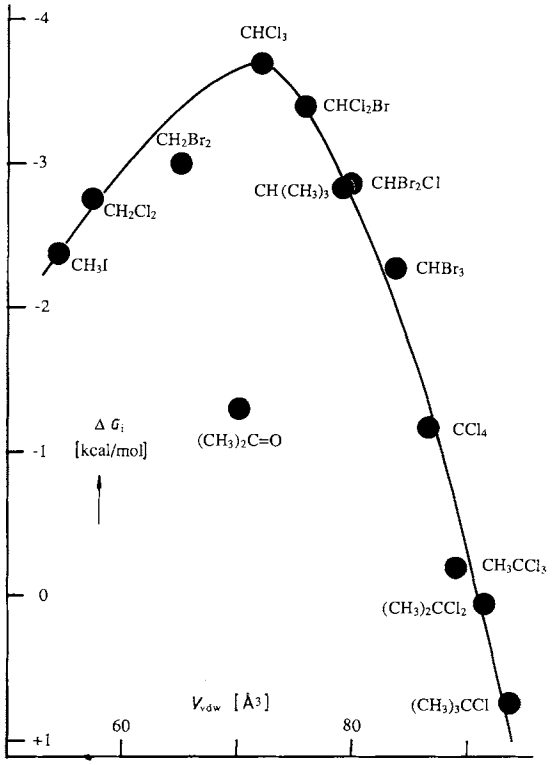


Fig. 2. Free energy of formation (ΔG_i) at 300 K of a series of complexes of **1** as a function of the size (V_{vdw}) of the guests.

(V_{vdw}) of the guest.[6] At this temperature, **1** displays a smooth and steep size recognition and, for instance, discriminates between $CHCl_3$ and $CHCl_2Br$ by 0.3 kcal mol^{-1}, an energy difference which is best appreciated by considering that the difference in volume of these two molecules is only 5%. However, **1** does not discriminate between isobutane and $CHBr_2Cl$, which have the same V_{vdw}. On the other hand, acetone is more weakly bound than chloroform although they have almost the same size. Host **1** therefore efficiently recognizes tetrahedral (sp^3) versus flat (sp^2) molecules. It is noteworthy that we did not observe any significant increase of the inclusion barrier ($\Delta G_i^{\neq}$ in Table 1) on going from the smallest (CH_3I) to the largest guest ($CHBr_3$) for which this value was measured. Therefore, the cross section of the windows does not control the selectivity, at least in this range of guest size.

From the temperature dependence of ΔG_i (over a range of at least 40 K) we obtained relatively precise[7] values of the enthalpy ΔH_i and entropy ΔS_i for guest inclusion (Table 1). These data indicate that the driving forces for complexation depend on the guest size. The complexation of $CHCl_3$ and of slightly larger substrates (at least up to isobutane) is enthalpy driven and entropy disfavored. In 1,1,2,2-tetrachloroethane, solvophobic forces[8] are probably too weak to account for the magnitude of ΔH_i for these guests (-3.8 to -6.0 kcal mol^{-1}), and the stability of these complexes should therefore be ascribed to attractive host–guest interactions, provided by dispersion forces. These interactions require a good fit between partners, which is apparently experimentally realized with CHXYZ substrates that are 70–80 Å^3 in size (a value ca. 20% smaller than that suggested by CPK models[9]). We may thus consider these complexes as examples of very stable van der Waals molecules.

By contrast, the complexation of smaller (CH_2Cl_2) or larger substrates (> $CHClBr_2$) by **1** is not enthalpy driven. These complexes therefore do not owe their stability to attractive host–guest interactions, but rather to the operation of external factors. These factors may include solvophobic effects, as well as more subtle thermodynamic contributions, such as specific heat and/or volume differences between the complexes and their separated components. Whether or not these complexes still belong to the category of van der Waals molecules is only a matter of definition.[4]

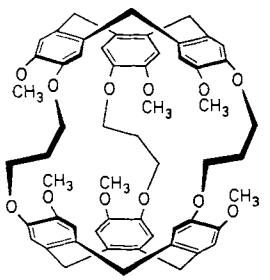
Received: April 14, 1989 [Z 3294 IE]
German version: *Angew. Chem. 101* (1989) 1249

[1] J. Canceill, L. Lacombe, A. Collet, *J. Am. Chem. Soc. 108* (1986) 4230.
[2] J. Canceill, L. Lacombe, A. Collet, *C.R. Acad. Sci. Sér. II 304* (1987) 815.
[3] For a review on the complexation of neutral molecules see: F. Diederich, *Angew. Chem. 100* (1988) 372; *Angew. Chem. Int. Ed. Engl. 27* (1988) 362.
[4] As presently accepted, the term "van der Waals molecule" only applies to species of very short life time such as He · · · He or $C_6H_6 \cdot Cl_2$ assemblies, which have been the object of numerous theoretical and experimental investigations. Here we extend this definition to supermolecules, which, in solution, may have life times of the order of several seconds at 273 K; see: A. van der Avoid, P. E. S. Wormer, F. Mulder, R. M. Berns, *Top. Curr. Chem. 93* (1980) 3; P. Hobza, R. Zahradnik, *ibid.* (1980) 53.
[5] The crystal used for the X-ray data collection was grown from chloroform/95% ethanol. The asymmetric unit consists of one $\mathbf{1} \cdot CHCl_3$ supermolecule with additional $CHCl_3$ and H_2O molecules outside in nonstoichiometric ratios, corresponding to [($C_{57}H_{60}O_{12} \cdot CHCl_3$), 0.2 $CHCl_3$, 0.2 H_2O]. Monoclinic, space group $P2_1/n$, $a = 38.262(14)$, $b = 12.441(5)$, $c = 12.748(5)$, Å, $\beta = 95.78(6)°$, $V = 6037$ Å^3, $Z = 4$, $\varrho_{calcd} = 1.192$ g cm^3. A total of 8688 independent reflections were collected on an automatic four-circle diffractometer, using graphite monochromated $Cu_{K\alpha}$ radiation (1.5418 Å); 4380 reflections were used in structure solution and refinement [$(I > 3\sigma(I)$]. Lorentz and polarization corrections were applied but no absorption corrections. The structure was solved by Direct Methods [10] and the atomic coordinates and anisotropic thermal parameters for heavy atoms (except for solvent molecules and a disordered methyl group) were refined to $R = 13.3\%$ ($R_w = 11.9\%$) using a large-blocks least-squares refinement program [11]. Hydrogen atoms were introduced at their theoretical positions (C-H 1.08 Å) and assigned the equivalent isotropic thermal factors of the C atoms to which they are bound. The electronic density analysis of the inner part of the cavity showed the chloroform molecule in two equally occupied orientations. One of the six methyl groups showed rotational disorder over three positions, with occupancy factors 0.6, 0.2, and 0.2. Fourier-difference series revealed the presence of additional molecules in the lattice vacancies, namely chloroform molecules in two mutually exclusive positions (occupation factor = 0.09 and 0.11) and a water molecule (occupation factor = 0.20). The refinement of internal and external chloroform molecule coordinates was performed in rigid groups, using a theoretical model (C-Cl = 1.73 Å, Cl-C-Cl = 111°). The highest residue on the final electronic density map is 0.58 e. Å^3. Further details of the structure analysis are available on request from the Director of the Cambridge Crystallographic Data Centre, University Chemical Laboratory, Lensfield Road, Cambridge CB2 1EW (UK), on quoting the full literature citation.
[6] A. Bondi, *Physical Properties of Molecular Crystals, Liquids and Glasses*, Wiley, New York 1968; A. I. Kitaigorodsky: *Molecular Crystals and Molecules*, Academic Press, London 1973.
[7] From least-squares linear regressions of $\ln K$ versus T^{-1} in several independent experiments we estimate the error range on ΔH_i and ΔS_i to be ± 1 kcal mol^{-1} and ± 3 cal mol^{-1} K^{-1}, respectively.
[8] This point will be discussed in more detail in a forthcoming article. For relevant discussions see: J. J. Moura Ramos, L. Dumont, M. L. Stien, J. Reisse, *J. Am. Chem. Soc. 102* (1980) 4150; G. Michaux, J. Reisse, *ibid.* (1982) 6895; M. Claessens, O. Fabre, D. Zimmermann, J. Reisse, *Bull. Soc. Chim. Belg. 93* (1984) 983; M. Ohba, K. Arakawa, *Bull. Chem. Soc. Jpn. 58* (1985) 3068.
[9] For a similar remark, see [3] and F. Diederich, K. Kick, D. Griebel, *Chem. Ber. 118* (1985) 3588.
[10] C. Riche, *Abstr. 7th Eur. Crystallogr. Mtg.*, Jerusalem, 1982, p. 25.
[11] D. Sheldrick, *SHELX76, a Program for Crystal Structure Determination*, University of Cambridge (England) 1976.

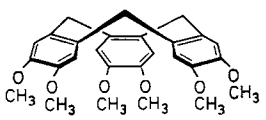
Cryptophane Radical Cations as Components of Three-Dimensional Charge-Transfer Salts**

By *Anne Renault, Daniel Talham, Josette Canceill, Patrick Batail, André Collet,* and *Janine Lajzerowicz**

Most organic donors known to date are flat molecules such as tetrathiafulvalene (TTF), which, when associated with suitable electron acceptors, tend to form charge-transfer (CT) salts of low dimensionality.[1] The use of increasingly larger inorganic anions,[2] or of electron-rich molecules that cannot achieve a flat conformation (e.g., *para*-cyclophanes)[3] has been recently considered as a way to increase the dimensionality of these materials. We report here a series of *three-dimensional* charge-transfer complexes in which a large, essentially spherical (10 Å in diameter) cryptophane molecule is employed as the donor. A cryptophane[4] such as **1**[5] is made of two electron-rich cyclotriveratrylene units **2** held together rigidly by three short chains. We anticipated that oxidation of **1** would afford radical cation species which might be stabilized by delocalization over the entire molecule.



1



2

Indeed, we found that cryptophane-E **1** in acetonitrile solution showed two reversible oxidations (Fig. 1) at 0.69 V ($\mathbf{1}/\mathbf{1}^{\oplus}$) and 0.85 V ($\mathbf{1}^{\oplus}/\mathbf{1}^{2\oplus}$) versus $Ag/Ag^{\oplus}$.[6] We also observed another oxidation ($\mathbf{1}^{2\oplus}/\mathbf{1}^{3\oplus}$), approaching chemical reversibility, at 1.11 V. The behavior of **1** contrasts markedly with that of cyclotriveratrylene itself, which, under the same conditions, shows two nonreversible waves at 0.87 and 1.03 V; irreversibility in the latter case might be due to a conformational change (crown to saddle) occurring on oxidation and leading to reactive species, as in the case of the cyclotriveratrylene cation itself;[4] such a conformational change cannot take place in cryptophane **1**.

Well-faceted, blue-green hexagonal single crystals of a series of charge-transfer salts $[(\mathbf{1}^{\bullet\oplus})(X^{\ominus})(CHCl_3)]$ were grown

[*] Prof. Dr. J. Lajzerowicz, Dr. A. Renault
Laboratoire de Spectrométrie Physique
Université Joseph Fourier-Grenoble I
B.P. 87, F-38402 Saint-Martin-d'Hères Cedex (France)
Dr. J. Canceill
Chimie des Interactions Moléculaires, E.R. C.N.R.S. 285
Collège de France
F-75231 Paris Cedex 05 (France)
Dr. D. Talham, Dr. P. Batail
Laboratoire de Physique des Solides, L.P. C.N.R.S. 02
Université Paris-Sud
Bât. 510, F-91405 Orsay Cedex (France)
Prof. Dr. A. Collet
U.M.R. C.N.R.S.-E.N.S.L. 117
Stéréochimie et Interactions Moléculaires
Ecole Normale Supérieure de Lyon
F-69364 Lyon Cedex 07 (France)

[**] We are grateful to Dr. *P. Rey* (D.R.F.-C.E.N.G.) for carrying out the spin susceptibility measurements.

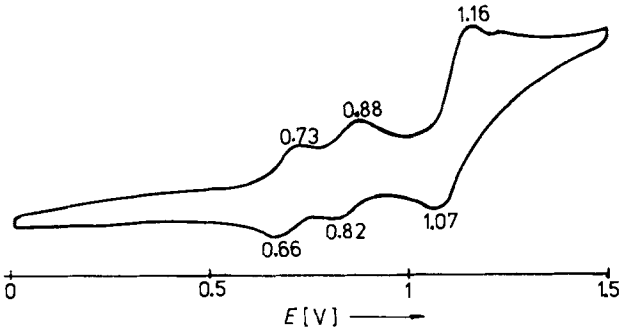


Fig. 1. Cyclic voltammogram of **1** [6]; 0.1 M nBu$_4$NPF$_6$ as electrolyte; Ag/AgNO$_3$ reference electrode in acetonitrile; scan rate 100 mV s^{-1}.

at a platinum wire anode by constant-current electrolysis (20.5 μA cm^{-2}) of a $CH_2Cl_2/CHCl_3$ (4:1) mixture containing **1** (10^{-3} M) and the tetrabutylammonium salts (10^{-1} M) of various $X^{\ominus}$ ions ($BF_4^{\ominus}$, $ClO_4^{\ominus}$, $PF_6^{\ominus}$, and $ReO_4^{\ominus}$) as supporting electrolytes. Their unit-cell parameters are similar (Table 1), which indicates that their structures are related.

Table 1. Single-crystal lattice parameters for charge-transfer complexes of $\mathbf{1}^{\bullet\oplus}$ with inorganic anions [a].

Anion	a [Å]	b [Å]	c [Å]	V [Å^3]
$PF_6^{\ominus}$	12.692(7)	12.692(6)	30.467(11)	4209
$ClO_4^{\ominus}$	12.595(7)	12.595(6)	29.783(11)	4104
$ReO_4^{\ominus}$	12.617(7)	12.617(6)	30.011(11)	4137
$BF_4^{\ominus}$	14.805(7)	14.805(7)	25.878(9)	4881

[a] Rhombohedral lattice with hexagonal cell parameters, $\alpha = \beta = 90°$, $\gamma = 120°$ for all complexes.

The stoichiometry of the salts has been determined by the crystal structure analysis[7] of $[(\mathbf{1}^{\bullet\oplus})(PF_6^{\ominus})(CHCl_3)]$ (Fig. 2). Indeed, this salt is a fully charge-transferred 1:1 complex, since the asymmetric unit consists of one oxidized cage $\mathbf{1}^{\bullet\oplus}$ and one $PF_6^{\ominus}$ ion and also contains a chloroform molecule

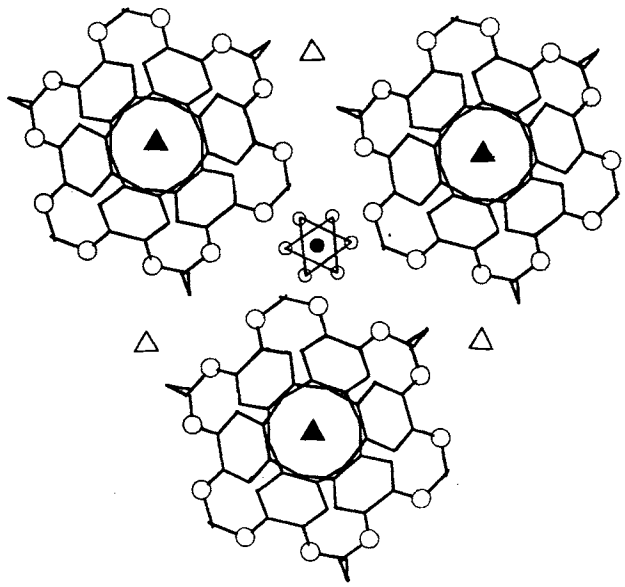


Fig. 2. Projection of the structure of $[(\mathbf{1}^{\bullet\oplus})(PF_6^{\ominus})(CHCl_3)]$ onto a plane perpendicular to the threefold axis; ▲ and △ centers of 1 at $z = 0$ and $z = 1/3$, respectively; ● center of $PF_6^{\ominus}$ at $z = 1/6$.

 © *VCH Verlagsgesellschaft mbH, D-6940 Weinheim, 1989* *0570-0833/89/0909-1249 $ 02.50/0*

accommodated within the cryptophane cavity, as in the [**1** · $CHCl_3$] complex.[8] The packing is a face-centered cubic array of the large spherical cations, with the anions (roughly thirteen times smaller) located in all the octahedral sites (at the edge centers and body centers of the cubic unit cell).[9]

ESR spectra of single crystals of $[(\mathbf{1}^{\bullet\oplus})(PF_6^{\ominus})(CHCl_3)]$ at room temperature displayed a single line with $g = 2.0030$ and with a line width of ca. 1.8–2 gauss. This further demonstrates the existence of quasi-free, delocalized π electrons. Also, the paramagnetic signal was still present when the crystals were dissolved in dichloromethane, from which we conclude that $\mathbf{1}^{\bullet\oplus}$ is a stable species.

For some single crystals of $[(\mathbf{1}^{\bullet\oplus})(PF_6^{\ominus})(CHCl_3)]$ the temperature dependence of the spin susceptibility was measured directly using a squid susceptometer in the range of 4 to 300 K and found to follow a Curie–Weiss law with a weak antiferromagnetic coupling. The corrected magnetic moment is 1.7 μ_B, corresponding to one essentially noninteracting spin ($S = 1/2$) per molecule of **1**. The observed insulating character of the complex is thus a consequence of the purely ionic nature of the salt and indicates the lack of stabilization of any intermolecular mixed valence state in the solid, presumably because of the very poor overlap between the radical cations.

In conclusion, we would like to focus on the following ideas: (1) The above results suggest that **1** and presumably other cryptophanes easily form a radical cation on oxidation and hence represent a new family of organic donors. (2) These large, spherical molecules drive the crystal structure toward three-dimensional close-packed arrays, in contrast to flat donor molecules which often stack in unidimensional columns. (3) The cryptophane cavity can accommodate relatively large guest species[4] (here, a chloroform molecule); this feature may aid in the design of new materials. (4) Finally, we wish to point out that the second oxidation wave of **1** (not investigated thus far), which is also chemically reversible, generates a dication with a potential triplet ground state (D_3 symmetry).[10]

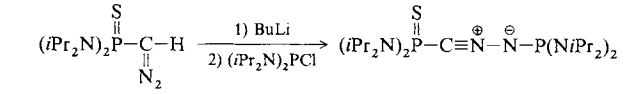
Received: April 14, 1989 [Z 3293 IE]
German version: *Angew. Chem. 101* (1989) 1251

[1] J. B. Torrance in D. Jérome and L. G. Caron (Eds.): *Low-Dimensional Conductors and Superconductors, NATO ASI ser. B: Physics, Vol. 155*, Plenum Press, New York 1987, p. 113.
[2] P. Batail, L. Ouahab, *Mol. Cryst. Liq. Cryst. 125* (1985) 205; P. Batail, L. Ouahab, J. B. Torrance, M. L. Pylman, S. S. P. Parkin, *Solid State Commun. 55* (1985) 597.
[3] A. Renault, C. Cohen Addad, J. Lajzerowicz, E. Canadell, O. Eisenstein, *Mol. Cryst. Liq. Cryst. 164* (1988) 179.
[4] A. Collet, *Tetrahedron 43* (1987) 5725, and references cited therein.
[5] For a short synthesis of **1** (cryptophane-E) see: J. Canceill, A. Collet, *J. Chem. Soc. Chem. Commun. 1988*, 582.
[6] All electrochemical criteria for reversibility are satisfied for scan speeds below 200 mV s^{-1}; for details see: A. J. Bard, L. P. Faulner: *Electrochemical Methods*, Wiley, New York 1980, p. 224.
[7] Details on these X-ray crystal structure determinations will be discussed in a forthcoming article.
[8] J. Canceill, M. Cesario, A. Collet, J. Guilhem, L. Lacombe, B. Lozach, C. Pascard, *Angew. Chem. 101* (1989) 1249; *Angew. Chem. Int. Ed. Engl. 28* (1989) 1246.
[9] Note that, since this is an fcc array of cations, it is formally an anti-NaCl type of structure. For another example of a giant charge-transfer rock salt, see: A. Pénicaud, P. Batail, S. Tomic, D. Jérome, C. Coulon, A. Perrin, to be published.
[10] T. J. LePage, R. Breslow, *J. Am. Chem. Soc. 109* (1987) 6412–6421; J. Thomaides, P. Maslak, R. Breslow, *ibid. 110* (1988) 3970–3979; J. S. Miller, A. J. Epstein, W. M. Reiff, *Acc. Chem. Res. 21* (1988) 114–120; J. B. Torrance, P. S. Bagus, I. Johannsen, A. I. Nazzal, S. S. P. Parkin, P. Batail, *J. Appl. Phys., 63* (1988), 2962–2965.

A Distillable *C*- and *N*-Silylated Nitrile Imine**

By *Florence Castan, Antoine Baceiredo,* and *Guy Bertrand**

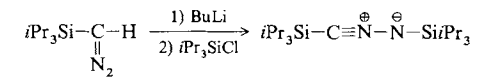
Since the famous *Huisgen* reviews[1] in 1963, 1-3 dipolar cycloadditions have been the subject of a tremendous number of papers. In this area, much work has been dedicated to the study of nitrile imines.[2] However, it was only in 1988 that the first compound of this type, (**2**), was isolated.[3]



1 **2**

It was of interest to know if the method used for synthesizing **2** was generally applicable to the preparation of other stable nitrile imines with common substituents, which could be of use for the facile synthesis of a variety of heterocycles. Here we wish to report the synthesis and reactivity of a distillable *C*- and *N*-silylated nitrile imine.

Bulky substituents are necessary in order to kinetically stabilize highly reactive species. We therefore chose to study the action of the lithium salt of triisopropylsilyldiazomethane on the triisopropysilyl chloride. The reaction occurred between $-90°$ and $-100\,°C$, in dry THF, in the presence of a crown ether, affording the desired nitrile imine **4**.[4]



3 **4**

Interestingly, compound **4** is stable enough to be purified by distillation at 90–100 °C (0.15 torr) without noticeable decomposition (80% yield) as a pale yellow oil (λ_{max} = 272 nm). The strong and broad absorption in the IR spectrum at 2120 cm^{-1} was slightly shifted compared to that observed for *N*-silylated nitrile imines in a matrix[5] but its position excluded the diazirine and isodiazirine isomers as possible products. The non-equivalence of the silicon atoms, demonstrated in the ^{29}Si NMR spectrum, excluded the four other isomers, namely the diazo compounds carbodiimide, cyanamide and isocyanamide. The ^{13}C NMR signal for the quarternary carbon is shifted downfield compared to that in the starting diazo compound **3**. This was also observed for compound **2** (Table 1).

Table 1. ^{13}C,^{29}Si, and IR spectroscopic data for the compounds **1**–**4** and **8**. The ^{13}C and ^{29}Si NMR spectra were recorded at 75.469 and 59.628 MHz, respectively, in $CDCl_3$ (**1**–**3**) and in C_6D_6 (**4**, **8**); the IR spectra in pentane.

Cpd.	^{13}C NMR δ(CN)	^{29}Si NMR δ	IR $\tilde{\nu}$ [cm^{-1}]
1	40.28		2080
2	61.04		2040 (br., s)
3	14.99	6.13	2060
4	46.73	0.71, 6.40	2120 (br., s)
8	124.25	3.60	2200 (br., s)

[*] Dr. G. Bertrand, F. Castan, Dr. A. Baceiredo
Laboratoire de Chimie de Coordination du CNRS,
associé à l'Université Paul Sabatier
205, Route de Narbonne, F-31062 Toulouse Cedex (France)

[**] This work was supported by the Pierre-Fabre-Medicaments Company. We thank *Dennis Bigg* for helpful discussions.

The influence of bulky substituents on the course of the reaction is quite obvious, and *Seyferth* et al.[6] have reported that the lithium salt of the tri*methyl*silyldiazomethane reacts with tri*methyl*silylchloride giving the bis(trimethylsilyl)diazomethane.

The silylated dipolar compound **4** reacts at room temperature, in the presence of a large excess of methyl acrylate, methyl propiolate and dimethyl fumarate, affording the expected adducts **5–7** in 20 to 30% isolated yield (Table 2).

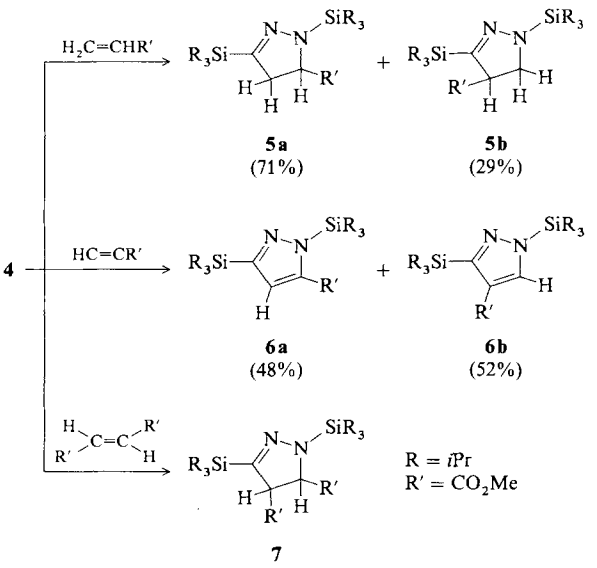
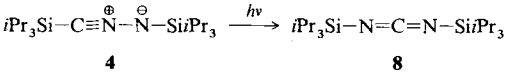


Table 2. ^{13}C and ^{29}Si NMR spectroscopic data for the adducts **5–7**. The ^{13}C NMR spectra were recorded at 50.323 MHz (**7**) and at 75.469 MHz (**5, 6**) in $CDCl_3$, the ^{29}Si NMR spectra at 39.761 MHz in $CDCl_3$.

Cpd.	^{13}C NMR δ(C=N)	δ(CCC)	δ(CCN)	^{29}Si NMR δ
5a	147.16	45.60	59.42	−1.02, 8.12
5b	142.66	56.63	45.60	−0.05, 7.40
6a	151.33	120.59	139.79	−0.92, 20.28
6b	154.11	121.42	140.17	1.70, 15.96
7	142.75	61.55	63.92	0.11, 9.39

The low yield of these reactions was probably due to some decomposition of the products on the silica gel since NMR analysis of the crude reaction mixtures indicated a nearly quantitative yield. The non-regioselectivity observed for non-symmetrical dipolarophiles has already been noted in the trapping reactions of unstable nitrile imines[7] and has been explained using molecular orbital theory.[8]

Depending on the nature of the substituents, nitrile imines thermally rearrange either by a 1,3 sigmatropic shift to form diazo compounds,[9] a 1,4 shift to form azines,[10] or cyclization.[9b, 11] Rearrangement to a carbodiimide has been detected only at very high temperature (> 500 °C) in the gas phase[10] or photochemically in a matrix along with the cleavage of the N–N bond.[12] No thermal rearrangements have been observed for **4** up to 250 °C in the gas phase, but irradiation of a pentane solution at 300 or 254 nm for 1 day quantitatively afforded bis(triisopropylsilyl)carbodiimide **8** (Table 1).



4 **8**

The facile cleavage of silicon-nitrogen and even silicon-carbon bonds makes this first bis(silylated)nitrile-imine **4** a synthetic equivalent of the parent compound (HCNNH) which should be a useful tool in organic synthesis. Moreover, these results demonstrate the wide applicability of the synthetic method used.

Received: April 17, 1989 [Z3296 IE]
German version: *Angew. Chem. 101* (1989) 1253

CAS Registry numbers:
3, 122093-27-0; **4**, 122093-28-1; **5a**, 122093-29-2; **5b**, 122093-32-7; **6a**, 122093-30-5; **6b**, 122093-33-8; **7**, 122093-31-6; **8**, 86071-46-7; iPr_3SiCl, 13154-24-0; $H_2C=CHCO_2Me$, 96-33-3; $HC\equiv CCO_2Me$, 922-67-8; $MeO_2CCH=CHCO_2Me$, 624-49-7; ^{29}Si, 14304-87-1; dibenzo[18]crown-6, 14187-32-7.

[1] a) R. Huisgen, *Angew. Chem. 75* (1963) 604, 742; *Angew. Chem. Int. Ed. Engl. 2* (1963) 565, 633.
[2] P. Caramella, P. Grünanger in A. Padwa (Ed.): *1,3 Dipolar Cycloaddition Chemistry*, Wiley Interscience, New York 1984.
[3] G. Sicard, A. Baceiredo, G. Bertrand, *J. Am. Chem. Soc. 110* (1988) 2663.
[4] **4**: A solution of triisopropylsilyldiazomethane **3** (0.40 g, 2 mmol) and dibenzo[18]crown-6 ether (0.80 g, 2 mmol) in THF (20 mL) was treated dropwise at −90 °C with a stoichiometric amount of BuLi in hexane. After stirring for 10 minutes at −90 °C, triisopropylsilyl chloride (0.39 g, 2 mmol) was added to the mixture. After warming up to room temperature, the solvent was removed by evaporation. The residue was treated with pentane and after filtration and evaporation of the solvent, **4** (0.56 g, 80% yield) was purified by distillation.
[5] C. Wentrup, S. Fischer, A. Maquestiau, R. Flammang, *Angew. Chem. 97* (1985) 74; *Angew. Chem. Int. Ed. Engl. 24* (1985) 56.
[6] D. Seyferth, T. C. Flood, *J. Organomet. Chem. 29* (1971) C25.
[7] a) W. Fliege, *Dissertation*, Universität München 1969; b) R. Huisgen, R. Sustmann, G. Wallbillich, *Chem. Ber. 100* (1967) 1786; c) R. Huisgen, W. Fliege, W. Kolbeck, *ibid. 116* (1983) 3027; d) W. Fliege, R. Huisgen, J. S. Clovis, H. Knupfer, *ibid. 116* (1983) 3039; e) J. S. Clovis, W. Fliege, R. Huisgen, *ibid. 116* (1983) 3062.
[8] a) K. N. Houk, J. Sims, C. R. Watts, L. J. Luskus, *J. Am. Chem. Soc. 95* (1973) 7301; b) K. N. Houk, J. Sims, R. E. Duke, R. W. Strozier, J. K. George, *ibid. 95* (1973) 7287; c) H. Bock, R. Dammel, S. Fischer, C. Wentrup, *Tetrahedron Lett. 28* (1987) 617.
[9] a) M. Granier, A. Baceiredo, G. Bertrand, *Angew. Chem. 100* (1988) 1397; *Angew. Chem. Int. Ed. Engl. 27* (1988) 1350; b) W. Reichen, *Helv. Chim. Acta 59* (1976) 1636; c) A. Padwa, T. Caruso, D. Plache, *J. Chem. Soc. Chem. Commun. 1980*, 1229; d) A. Padwa, T. Caruso, S. Nahm, *J. Org. Chem. 45* (1980) 4065; e) C. Wentrup, *Helv. Chim. Acta 61* (1978) 1755; f) R. Gleiter, W. Rettig, C. Wentrup, *ibid. 57* (1974) 2111; g) A. Padwa, T. Caruso, S. Nahm, A. Rodriguez, *J. Am. Chem. Soc. 104* (1982) 2865.
[10] S. Fischer, C. Wentrup, *J. Chem. Soc. Chem. Commun. 1980*, 502.
[11] a) C. Wentrup, A. Damerius, W. Reichen, *J. Org. Chem. 43* (1978) 2037; b) C. Wentrup, J. Benedikt, *ibid., 45* (1980) 1407; c) L. Garanti, A. Vigevani, G. Zecchi, *Tetrahedron Lett. 1976*, 1527; d) L. Garanti, A. Sala, G. Zecchi, *J. Org. Chem. 42* (1977) 1389; e) H. Meier, H. Heimgartner, *Helv. Chim. Acta 60* (1977) 3035; f) G. Schmitt, B. Laude, *Tetrahedron Lett. 1978*, 3727.
[12] a) N. H. Toubro, A. Holm, *J. Am. Chem. Soc. 102* (1980) 2093; b) W. Sieber, P. Gilgen, S. Chaloupka, H. J. Hansen, H. Schmid, *Helv. Chim. Acta 56* (1973) 1679; c) H. Meier, W. Heinzelmann, H. Heimgartner, *Chimia 34* (1980) 504, 506.

Hg_8 ("Mercubane") Clusters in $Rb_{15}Hg_{16}$

By *Hans-Jörg Deiseroth** and *Axel Strunck*

RbHg is so far the only compound among the alkali-metal amalgams of composition MHg (M = alkali metal) whose conditions of existence are unclear. On attempting to synthesize RbHg by a method that had proven successful in the case of several other amalgams[1] we have now unexpectedly, but reproducibly obtained gold-colored, shiny metallic single crystals of the composition $Rb_{15}Hg_{16}$ which are extremely

[*] Prof. Dr. H.-J. Deiseroth, Dr. A. Strunck
Fachbereich 8 – Anorganische Chemie der Universität-GH
Postfach 101240, D-5900 Siegen (FRG)

air-sensitive. The compound contains isolated, almost ideal cubic-shaped Hg_8 clusters ("mercubane") of a type that has hitherto never been detected in any other amalgam. Rectangular Hg_4 clusters, as have been found in the amalgams CsHg, KHg and Na_3Hg_2,[2-5] were also observed.

The tetragonal crystal structure of $Rb_{15}Hg_{16}$,[6,7] thus far only observed in this compound, is a defect variant of the CsCl type. Its structure and its lattice constants[7] can be interpreted in terms of an ensemble embodying $4 \times 4 \times 4 = 64$ CsCl unit cells (each $a \approx 410$ pm, $Rb_{64}Hg_{64}$). This large cubic cell is somewhat elongated in one direction, such that it corresponds to the real c-axis of the tetragonal unit cell of $Rb_{15}Hg_{16}$. The 64 Hg atoms of the idealized unit cell, arranged in cubic primitive geometry (d(Hg–Hg) = 410 pm) now "relax" to a real structure of a type that forms eight Hg_4 squares (32 Hg atoms) and four Hg_8 cubes (32 Hg atoms) with Hg–Hg distances of ca. 300 pm (Fig. 1).

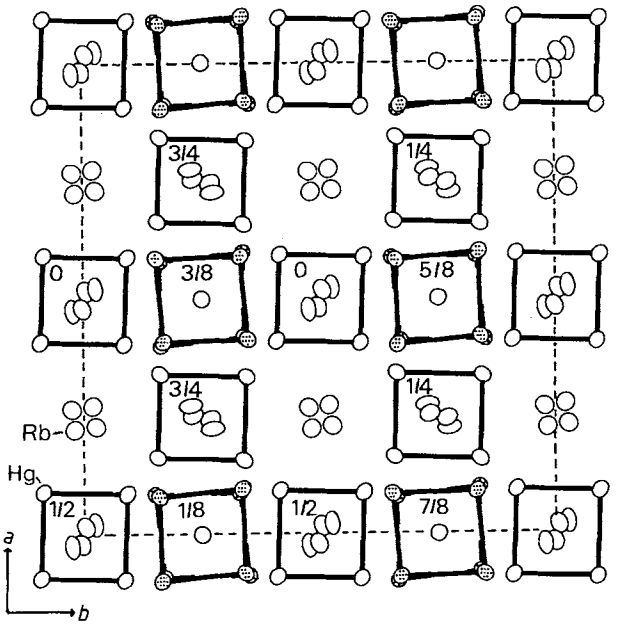


Fig. 1. Projection of the crystal structure of $Rb_{15}Hg_{16}$ along [001]; dotted Hg-atoms form Hg_8 cubes, undotted Hg_4 squares; the numbers indicate the approximate coordinate of the center of the respective square or cube in z. The Rb atoms are shown uncoupled.

The centers of the cubes occupied by rubidium atoms in the ideal structure are, as a result of the reduced Hg–Hg distance, no longer occupied in the real structure, so that the composition $Hb_{60}Hg_{64} = Rb_{15}Hg_{16} = RbHg_{1.067}$ approaches RbHg.

The distances within the mercury clusters ($d \approx 300$ pm) and between them ($d > 500$ pm) are significantly different in the compound described here. The shortest distances between the clusters (cube–cube, cube– square etc.) are 539.65 pm (Hg1–Hg4); the distances within the clusters are shown in Figure 2.

The preferred Hg–Hg–Hg angles of ca. 90°, not only in $Rb_{15}Hg_{16}$ but also in KHg, CsHg and Na_3Hg_2, are a clear indication of the presence of σ_p bonds (6p) between the Hg atoms. The bonding electrons necessary for this are provided by rubidium, which itself is present as $Rb^{\oplus}$ ion (shortest Rb–Rb distances in $Rb_{15}Hg_{16}$ 378.9 pm, in γ-Rb_2O 338 pm, in Rb metal 468 pm). This simplified picture of the chemical bond is also supported by the results of relativistic band structure calculations for NaHg, another CsCl variant.[8]

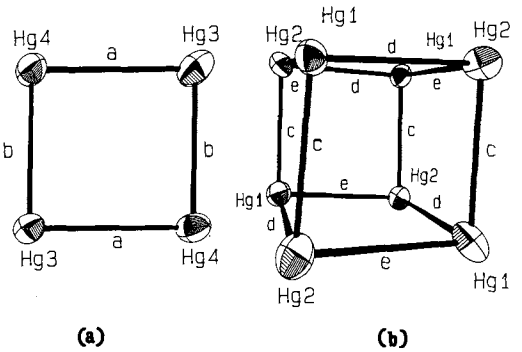


Fig. 2. Hg_4 square (a) and Hg_8 cube (b) in $Rb_{15}Hg_{16}$: distance [pm]: $a = 295.6(3)$, $b = 304.2(3)$, $c = 295.5(3)$, $d = 297.9(3)$, $e = 293.9(3)$; interatomic angles [°] at Hg1: 85.66(7), 86.38(7), 86.16(7); Hg2: 94.26(7), 93.44(8), 93.69(7); Hg3: 90.32(7); Hg4: 89.68(8).

According to these calculations the electronic states in the neighborhood of the Fermi edge are essentially dominated by Hg(6p) (small proportions of Na(3s) and Na(6s)).

The quasimolecular units Hg_8 and Hg_4 in the heavy alkali metal amalgams belong to a previously unknown class of mercury clusters. These differ from the already classical linear polycations $Hg_n^{2\oplus}$ in that σ_p bonds dominate in such clusters.[10] The chemical bonding in the polycations, on the other hand, has σ_s character. The latter is primarily realized by removal of electrons from antibonding 6s states, whereas in the former cases additional electrons (from the alkali metal) are transferred into the 6p states.

A critical interpretation of the phase diagrams determined from thermal analyses (see, e.g. Ref. [11]) would indicate the possibility of further previously unknown alkali-metal amalgams with mercury clusters in the range of composition around MHg (M = Na, K, Rb, Cs).

Received: May 2, 1989 [Z 3318 IE]
German version: *Angew. Chem. 101* (1989) 1286

CAS Registry number:
$Rb_{15}Hg_{16}$, 122469-76-5.

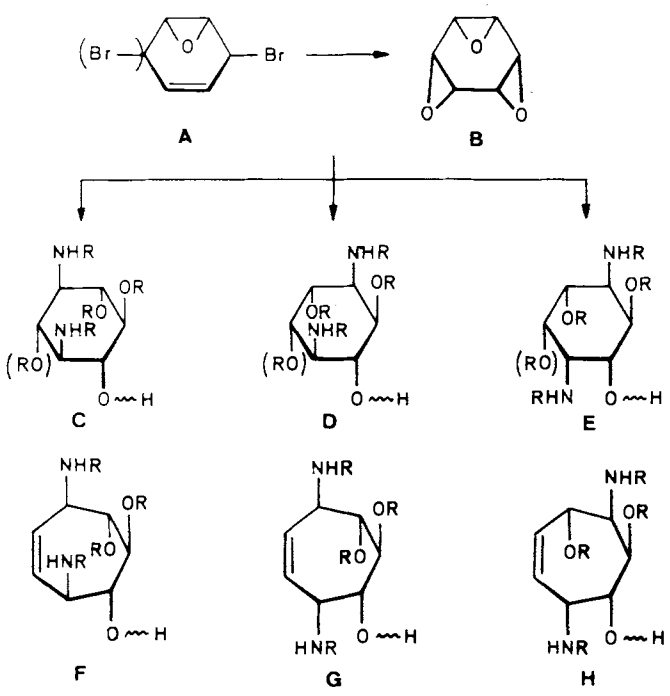
[1] H. J. Deiseroth, A. Strunck, W. Bauhofer, *Z. Anorg. Allg. Chem. 558* (1988) 128.
[2] H. J. Deiseroth, A. Strunck, *Angew. Chem. 99* (1987) 701; *Angew. Chem. Int. Ed. Engl. 26* (1987) 687.
[3] H. J. Deiseroth, A. Strunck, W. Bauhofer, *Z. Anorg. Allg. Chem.*, in press.
[4] E. J. Duwell, N. C. Baenziger, *Acta Crystallogr. 8* (1955) 705.
[5] J. W. Nielsen, N. C. Baenziger, *Acta Crystallogr. 7* (1954) 277.
[6] Sample preparation: gold colored, shiny metallic, air-sensitive single crystals (diameter a few tenths of a mm) of $Rb_{15}Hg_{16}$ were obtained from samples of the overall composition RbHg (prepared according to [1]) by tempering at 120 °C in an evacuated Duran glass ampoule ($l \approx 200$ mm, $\varnothing \approx 20$ mm); m.p. 157 °C (according to DTA investigations).
[7] Crystallographic data for $Rb_{15}Hg_{16}$: space group $I4_1/a$ (No. 88), $Z = 4$, $a = 1665(3)$, $c = 1813(4)$ pm, $\mu = 627$ cm^{-1}, CAD4 single crystal diffractometer, room temperature, $Mo_{K\alpha}$, $2\theta_{max} = 50°$, crystal dimensions: $0.30 \times 0.28 \times 0.51$ mm, 2206 observed, unique reflections, 1261 with $I > 3\sigma(I)$. Refinement factors $R_{aniso} = 0.075$, $R' = 0.128$ (calculated absorption corrections with the program DIFABS [9]). All structure calculations were carried out with the program system NRCVAX [12]. Further details of the crystal structure investigation are available on request from the Fachinformationszentrum Karlsruhe, Gesellschaft für wissenschaftlich-technische Information mbH, D-7514 Eggenstein-Leopoldshafen 2 (FRG) on quoting the depository number CSD-54014, the names of the authors, and the journal citation.
[8] H. J. Deiseroth, N. E. Christensen, A. Stupperich, unpublished.
[9] N. Walker, D. Stuart, *Acta Crystallogr. A39* (1983) 158.
[10] N. N. Greenwood, A. Earnshaw: *Chemistry of the Elements*, Pergamon, Oxford 1984, p. 1410.
[11] W. Biltz, F. Weibke, H. Eggers, *Z. Anorg. Allg. Chem. 219* (1934) 119.
[12] The NRCVAX Crystal Structure System (PC version): E. J. Gabe, F. L. Lee, Y. Le Page in G. M. Sheldrick, C. Krüger, R. Goddard (Eds.): *Crystallographic Computing 3*, Clearendon Press, Oxford 1985, p. 167–174.

Unsaturated 1,4-*cis* and 1,4-*trans*-Diaminotetradeoxycycloheptites—Enantiomerically Pure, Polyfunctionalized Tropa Derivatives by Enzymatic Hydrolysis**

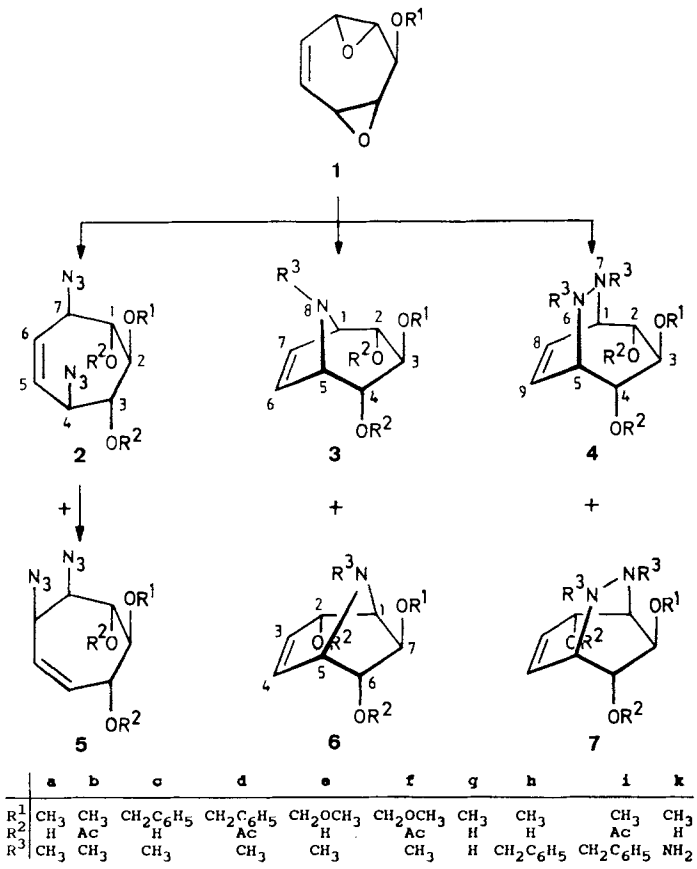
By *Manuela Falk-Heppner, Manfred Keller,* and *Horst Prinzbach**

Dedicated to Professor Christoph Rüchardt on the occasion of his 60th birthday

For the total syntheses of non-natural aminoglycoside antibiotics of the astromicin, sannamycin and sporaricin type, we have developed efficient routes to diverse chemically modified aglycone building blocks (**C**[1]**D**,[2] **E**[3]) starting from epoxycyclohexene bromides **A** or *cis*-benzene trioxide **B**. Further modification of this class of bioactive substances involves the replacement of the diaminocyclohexite units by diaminocycloheptite units.[4] We report here the syntheses of sannamine- and sporamine-analogous unsaturated *cis*-/*trans*-1,4-diaminotetradeoxycycloheptites **F** and **G**, respectively, as well as the 1,4-*trans*-diamines **H**. Starting material is generally the *anti,cis*-diepoxycycloheptene alcohol **1** (R^1 = H) that has been prepared from tropone in another context.[5] The entry to racemic *cis*-1,4-diamino aglycones of the type **F** thus is reduced to the substitution of the two allylically activated epoxide C–O bonds by suitable *N*-nucleophiles. Subsequent epimerization by inter- or intramolecular S_N2 substitution at an N-bearing site should provide access to the *trans*-1,4-diamine series **G**.



From a comprehensive study of the behavior of **1a**, **1c** and **1e** towards mono- and bifunctional *N*-nucleophiles[4, 6] the findings collected in Scheme 1 are of relevance here: with NaN_3 in fourfold excess (methanol/water, $MgSO_4$, reflux, 10 h), the 1,4-diazide **2a** (isolated as **2b**, 70–75%) was formed selectively from **1a** (30 mmol);[7] depending on the reaction conditions the *cis*-1,2-diazide *rac*-**5a** (15–20% *rac*-**5b**) resulting from S_N2'-attack or Cope rearrangement is also formed. The opening of the second epoxide ring is much more rapid, so that different *N*-substituents cannot be selectively introduced in this way. Methylamine (2 equiv., 40% aqueous solution, 80 °C) adds almost quantitatively to give a ca. 3:1 mixture of the isomeric 8-aza-bicyclo[3.2.1]octene skeletons **3a/6a** (only one invertomer detected in each case at room temperature (^{1}H NMR)) without a primary adduct being detectable (even after acetylation to **3b/6b**); by addition of Lewis acids ($LiClO_4$, $MgSO_4$, $ZnSO_4$) this ratio can be improved to ca. 4:1. With benzylamine, **3h** and **6h** are formed in the ratio 2.3:1 (isolated as **3i/6i**, 67% and 29%, respectively). Hydrazine (water, reflux) behaves as a 1,1- and 1,2-dinucleophile towards **1a**: aside from ca. 50% of the desired 6,7-diazabicyclo[3.2.2]nonene **4g**, ca. 50% of 8-azabicyclo[3.2.1]octene **3k** is formed (more than 3% of **6k** or **7g** would have been detected). 1,2-Dimethylhydrazine reacts with **1a** to give exclusively **4a** (93%).[4]



Scheme 1.

The diols (diacetates) **2**, **3**, and **4** are *meso* compounds with favorable structural prerequisites for enzyme-catalyzed esterification (hydrolysis) (relatively rigid 1,3-diol arrangement).[8] The results of the hydrolysis of some diacetates **2–4** and of **8–10** carried out with porcine liver esterase (PLE, Boehringer) in water (where necessary, with addition of up to 10% methanol or acetone) are collected in Table 1: even at total conversion and with amounts of starting material of up to ca. 15 mmol—except in the case of **10**—both the yields of monoester as well as the *ee* values (determined ^{1}H NMR

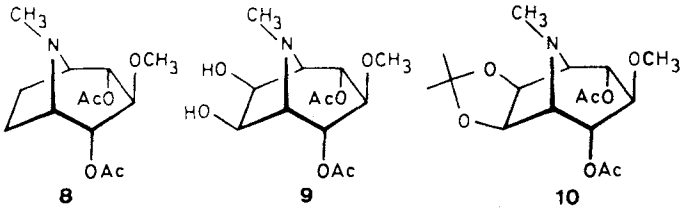
[*] Prof. Dr. H. Prinzbach, Dipl.-Chem. M. Falk-Heppner, Dr. M. Keller
Chemisches Laboratorium der Universität
Institut für Organische Chemie und Biochemie
Albertstrasse 21, D-7800 Freiburg (FRG)

[**] This work was supported by the Deutsche Forschungsgemeinschaft, the Fonds der Chemischen Industrie, and BASF AG. Special thanks are due to Dipl.-Chem. *J. Kammerer* for help with the enzymatic work, and to Prof. Dr. *H. Fritz* and Dr. *D. Hunkler* and Dr. *J. Wörth* for the NMR and MS analyses, respectively.

Table 1. PLE hydrolysis of the *meso*-diacetates.

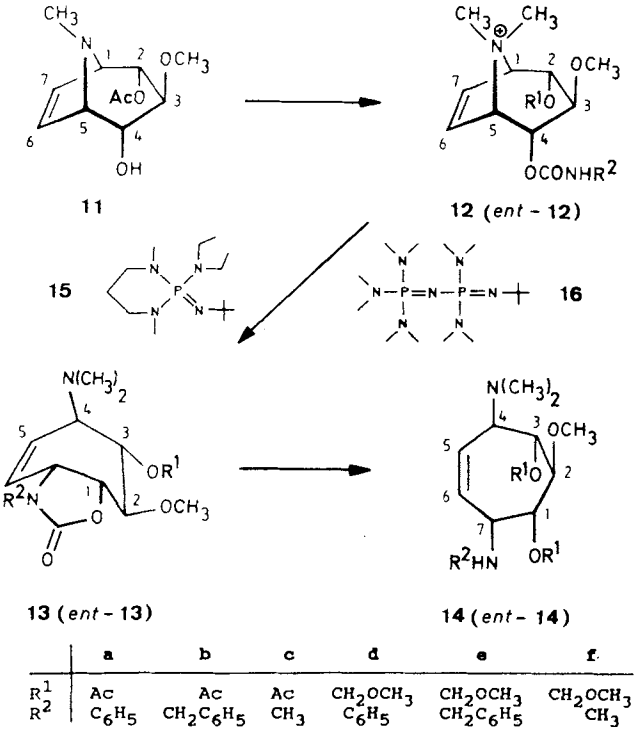
Diacetate	Amount of substance [mmol]	Monoacetate Yield [%]	*ee* [%]
2b	0.3	88	86
3b	15.0	100	>99
3d	0.3	100	>99
3f	0.5	86	>99
3i	0.4	97	>99
4b	0.5	89	>99
8	0.4	100	>99
9	0.4	73	89
10	0.3	no conversion	

spectroscopically with the (*R*)- and (*S*)-MTPA esters (MPTA = α-methoxy-α-trifluoromethylphenylacetic acid)[9] are very good to excellent. Accordingly, transesterification (racemization) is largely ruled out. It follows from the absolute configuration derived with the help of the Mosher model that the "frontal" acetate group in the illustrated formula (cf. **11**) is hydrolyzed[11] (uncertain in the case of **3i**).



8 **9** **10**

How the stereoisomeric compounds of the *trans*-diamino series can be prepared, starting from the enantiomerically pure monoacetates obtained from **3**, is illustrated by examples in Scheme 2: reaction of the monoacetate **11** (1–3 mmol) with phenyl, benzyl or methyl isocyanate in THF, if necessary in the presence of catalytic amounts of di-*n*-butyltin laurate,[12] affords the carbamates (> 95%), which can be quaternized to the ammonium salts **12a–12c** with methyl iodide (80 °C). From the vicinal J_{HH} couplings ($J_{1,2(4,5)} = 4.5$, $J_{2,3(3,4)} = 7.5$ Hz) a chair conformation of the six-membered ring with quasi-equatorial disposition of the three residues has been established for **12a–12c**. The cyclization **12** → **13** associated with the quasi-axial orientation of the carbamate residues involves complications, not unexpected because of the steric/stereoelectronic conditions. After a series of inadequately selective reactions with a variety of conventional bases (NaH, KH, lithium diisopropylamide(LDA), *t*BuOK etc.) the Schwesinger iminophosphorane bases **15** ($pK_a = 27.6$, CH_3CN) and **16** ($pK_a = 32.7$, CH_3CN)[13] eventually enabled a breakthrough: thus, with **15**, 92% of **13a** was formed from **12a** and, with the stronger base **16**, 76% of **13c** from the less acidic **12c**. After hydrolysis of the acetate residues, all functions in the resulting alcohols (**13a**, $R^1 = H$: $[\alpha]_D^{25} = -226$ ($c = 0.5$, $CHCl_3$)) are protected, except the OH group to be glycosidated. Hydrolysis of the urethanes ($Ba(OH)_2/CH_3OH/H_2O$, reflux) and subsequent acetylation quantitatively affords the unsaturated *trans*-diaminotetradeoxycycloheptite diacetates **14a–14c**. After protection of the 4-OH group in **11** (here as methoxymethyl (MOM) ether) and acetate hydrolysis, the enantiomeric series of compounds *ent*-**12d–12f** to *ent*-**14a–14c** are obtained analogously and with comparable results (*ent*-**13a**, $R^1 = H$: $[\alpha]_D^{25} = +229$ ($c = 0.1$, $CHCl_3$)). By control measurements with the camphanoic acid derivatives of **13a** and *ent*-**13d** consistently high *ee* values (> 99%) are ensured. Variations regarding *N*-substitution are possible in this way.



11 **12** (*ent*-**12**) **15** **16**

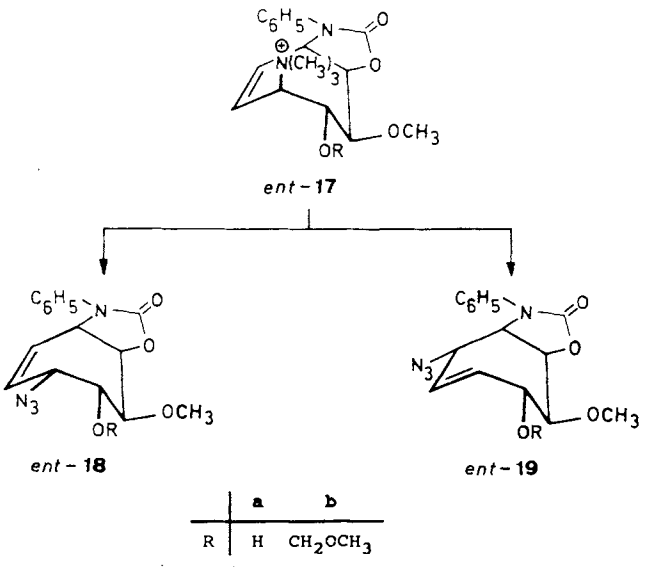
13 (*ent*-**13**) **14** (*ent*-**14**)

	a	b	c	d	e	f
R^1	Ac	Ac	Ac	CH_2OCH_3	CH_2OCH_3	CH_2OCH_3
R^2	C_6H_5	$CH_2C_6H_5$	CH_3	C_6H_5	$CH_2C_6H_5$	CH_3

Scheme 2.

Further perspectives of this project are indicated: an alternative entry to the *cis*-1,4-diamino series **F**—even with different *N*-residues—is possible via S_N2 substitution (1 mmol, dimethylformamide (DMF), 100 °C) of the allylic trimethylammonio group in the substrates *ent*-**17a,b** prepared from *ent*-**13d** ($J_{1,2} = J_{1,7} = 7.5$, $J_{2,3} = 9.5$, $J_{3,4} = 8.3$, $J_{4,5} = 5.6$, $J_{5,6} = 12.0$, $J_{5,7} = 2.3$, $J_{6,7} = 2.5$ Hz), whereby the size of the neighboring residue R significantly influences the outcome. With R = H (MOM), 70% (35%) *ent*-**18a(b)** ($J_{1,2} = J_{2,3} = 8.3$, $J_{3,4} = 4.2$ Hz) is isolated together with 21% (52%) *ent*-**19a(b)** ($J_{1,2} = 8.3$, $J_{2,3} = 9$, $J_{6,7} = 2.3$ Hz).

An efficient entry to diamines **H** based on the step **12** → **13** emerges, in that rearrangement of **12** into the less strained 8-azabicyclo[3.2.1]non-3-ene skeleton, which, depending upon the reaction conditions competes with the cyclization, can be steered selectively if not specifically with certain base systems and residues R. Thus, e.g., with *t*BuOK/*t*BuOH (25 °C), **20** ($[\alpha]_D^{25} = -62$ ($c = 0.08$, CH_3CN; $J_{1,2} = J_{4,5} =$

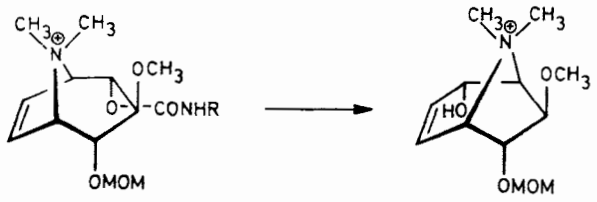


ent-**17**

ent-**18** *ent*-**19**

	a	b
R	H	CH_2OCH_3

 © VCH Verlagsgesellschaft mbH, D-6940 Weinheim, 1989 0570-0833/89/0909-1254 $ 02.50/0



ent-**12d,f** **20**

$J_{5,6} = 5.3$, $J_{1,7} = 0$, $J_{2,3} = 1.7$, $J_{3,4} = 10.5$, $J_{6,7} = 3.0$ Hz) is formed from *ent*-**12d** ($J_{1,2} = J_{4,5} = 4.5$, $J_{2,3} = J_{3,4} = 7.5$, $J_{5,6} = J_{6,7} = 1.5$ Hz) in 85% yield (along with 9% *ent*-**13d**) and from *ent*-**12f** in 100% yield (1–3 mmol).

Received: April 28, 1989 [Z 3313 IE]
German version: *Angew. Chem. 101* (1989) 1281

CAS Registry numbers:
1a, 122237-46-1; **1d**, 122237-74-5; **1f**, 122237-75-6; **2a**, 122237-47-2; **2b**, 122237-48-3; **2b** (3-OH), 122237-67-6; **3a**, 122237-51-8; **3b**, 122237-53-0; **3d**, 122237-62-1; **3d** (4-OH), 122237-69-8; **3f**, 122237-63-2; **3f** (4-OH), 122237-70-1; **3h**, 122237-55-2; **3i**, 122237-57-4; **3i** (4-OH), 122237-71-2; **3k**, 122237-60-9; **4a**, 122237-61-0; **4b**, 122237-64-3; **4b** (4-OH), 122237-72-3; **4g**, 122237-59-6; (±)-**5a**, 122237-49-4; (±)-**5b**, 122237-50-7; (±)-**6a**, 122237-52-9; (±)-**6b**, 122237-54-1; (±)-**6h**, 122237-56-3; (±)-**6i**, 122237-58-5; **8**, 122237-65-4; **8** (4-OH), 122237-73-4; **9**, 122237-66-5; **9** (4-OH), 122269-94-7; **11**, 122237-68-7; **11** (4-MOM-ether), 122237-87-0; **11** (2-OH, 4-MOM-ether), 122237-88-1; **11** (phenyl carbamate), 122237-76-7; **11** (benzyl carbamate), 122237-77-8; **11** (methyl carbamate), 122237-78-9; **12a** · $I^{\ominus}$, 122237-79-0; **12b** · $I^{\ominus}$, 122237-80-3; **12c** · $I^{\ominus}$, 122237-81-4; *ent*-**12d** · $I^{\ominus}$, 122237-88-1; *ent*-**12e** · $I^{\ominus}$, 122237-89-2; *ent*-**12f** · $I^{\ominus}$, 122237-90-5; **13a**, 122237-82-5; **13a** (R' = H), 122237-84-7; *ent*-**13a** (R' = H), 122330-77-2; **13c**, 122237-83-6; *ent*-**13d**, 122237-92-7; **14a**, 122237-85-8; *ent*-**14a**, 122330-75-0; *ent*-**14b**, 122237-91-6; **14c**, 122237-86-9; *ent*-**14c**, 122330-76-1; **15**, 98015-45-3; **16**, 111324-03-9; *ent*-**17a**, 122237-93-8; *ent*-**17b**, 122237-94-9; *ent*-**18a**, 122237-95-0; *ent*-**18b**, 122237-98-3; *ent*-**19a**, 122237-96-1; *ent*-**19b**, 122237-99-4; *ent*-**20**, 122237-97-2; PhNCO, 103-71-9; $PhCH_2NCO$, 3173-56-6; MeNCO, 624-83-9; $PhCH_2NH_2$, 100-46-9; $(H_2N)_2$, 302-01-2; $(Me_2N)_2$, 540-73-8; $MeNH_2$, 74-89-5.

[1] R. Schwesinger, W. Fritsche, H. Prinzbach, *Chem. Ber. 115* (1982) 946.
[2] J. Schubert, R. Schwesinger, L. Knothe, H. Prinzbach, *Liebigs Ann. Chem. 1986*, 2009; R. Kühlmeyer, R. Schwesinger, H. Prinzbach, *Tetrahedron Lett. 25* (1984) 3429; R. Kühlmeyer, B. Seitz, T. Weller, H. Fritz, R. Schwesinger, H. Prinzbach, *Chem. Ber.*, in press.
[3] B. Seitz, R. Kühlmeyer, T. Weller, W. Meier, C. Ludin, R. Schwesinger, L. Knothe, H. Prinzbach, *Chem. Ber.*, in press.
[4] P. Becker, *Dissertation*, Universität Freiburg 1985; C. Kaiser, *Dissertation*, Universität Freiburg 1979.
[5] C. Rücker, W. Seppelt, H. Fritz, H. Prinzbach, *Chem. Ber. 117* (1984) 1801.
[6] M. Keller, *Dissertation*, Universität Freiburg 1989.
[7] The new compounds were characterized by ^{1}H NMR (250, 400 MHz), ^{13}C NMR (100.6 MHz), IR, MS) and elemental analyses. **2b**: m.p. 88–89 °C (CCl_4); IR (KBr): $\tilde{\nu} = 1755$ (C=O), 2166 cm^{-1} (N_3); ^{1}H NMR ($CDCl_3$): $\delta = 5.64$ (d, 5,6-H), 5.01 (dd, 1,3-H), 4.20 (dd, 4,7-H), 3.49 (s, OCH_3), 3.46 (t, 2-H), 2.21 (s, 2 OAc); $J_{1,2} = J_{2,3} = 8.3$, $J_{1,7} = J_{3,4} = 9.3$, $J_{4,5} = J_{6,7} = 1.8$ Hz. – **3b**: m.p. = 98 °C (methanol); IR (KBr): $\tilde{\nu} = 1720$ (C=O), 1645 (C=C), 1235 cm^{-1} (C–O); ^{1}H NMR ($CDCl_3$): $\delta = 6.06$ (br.s, 6,7-H), 4.87 (dd, 2,4-H), 3.65 (d, 1,5-H), 3.35 (s, OCH_3), 3.26 (t, 3-H), 2.24 (s, NCH_3), 2.08 (s, 2 OAc); $J_{1,2} = J_{4,5} = 4.5$, $J_{2,3} = J_{3,4} = 7.5$ Hz; ^{13}C NMR ($CDCl_3$): $\delta = 170.2$ (C=O), 130.1 (d, C-6,7), 81.2 (d, C-3), 73.5 (d, C-2,4), 67.9 (d, C-1,5), 59.1 (q, OCH_3), 40.4 (q, NCH_3), 21.2 (q, OCO-CH_3). – **6b**: colorless oil; IR (Film): $\tilde{\nu} = 1730$ (C=O), 1645 cm^{-1} (C=C); ^{1}H NMR ($CDCl_3$): $\delta = 5.79$ (dd, 3-H), 5.67 (dt, 4-H), 5.63 (m, 2-H), 5.02 (dd, 6-H), 4.08 (d, 5-H), 3.73 (t, 1-H), 3.33 (t, 7-H), 3.32 (s, OCH_3), 2.58 (s, NCH_3), 2.14 (s, OAc), 2.09 (s, OAc); $J_{1,2} = J_{1,7} = J_{6,7} = 5.2$, $J_{2,3} = 4.2$, $J_{2,4} = J_{4,5} = 1.0$, $J_{3,4} = 10.5$, $J_{5,6} = 3.5$ Hz. – *ent*-**12d**: m.p. = 86 °C; IR (KBr): $\tilde{\nu} = 1725$ cm^{-1} (C=O); ^{1}H NMR (CD_3CN): $\delta = 8.32$ (br.s, NH), 7.52–7.05 (m, 5H), 6.44 (br.s, 6,7-H), 5.18 (dd, 2-H), 4.79 (s, OCH_2), 4.70 (dd, 1-H), 4.56 (dd, 5-H), 4.11 (dd, 4-H), 3.48 (s, OCH_3), 3.42 (s, OCH_3), 3.40 (t, 3-H), 3.29 (s, NCH_3 *syn*), 3.24 (s, NCH_3 *anti*); $J_{1,2} = J_{4,5} = 4.5$, $J_{1,7} = J_{5,6} = 1.5$, $J_{2,3} = J_{3,4} = 7.5$ Hz. – *ent*-**13d**: m.p. = 107 °C (methanol); IR (KBr): $\tilde{\nu} = 1742$ (C=O), 1673 cm^{-1} (C=C); ^{1}H NMR ($CDCl_3$): $\delta = 7.52–7.13$ (m, 5H), 5.85 (ddd, 5-H), 5.66 (dd, 6-H), 5.38 (ddd, 7-H), 4.81 and 4.76 (d, OCH_2), 4.78 (t, 1-H), 3.94 (dd, 3-H), 3.64 (s, OCH_2OCH_3), 3.52 (s, OCH_3), 3.38 (dd, 2-H), 2.85 (dd, 4-H), 2.32 (s, NCH_3); $J_{1,2} = J_{1,7} = 9.0$, $J_{2,3} = J_{CH_2} = 7.5$, $J_{3,4} = 3.7$, $J_{4,5} = 6.8$, $J_{5,6} = 11.3$, $J_{5,7} = 3.0$, $J_{6,7} = 2.6$ Hz; ^{13}C NMR ($CDCl_3$): $\delta = 154.4$ (s, C=O), 136.7 (s, C_i), 129.2 (d, 2 C_m), 128.9 (d, C-5), 128.5 (d, C-6), 124.6 (d, C_p), 120.3 (d, 2 C_o), 96.5 (t, OCH_2), 84.4 (d, C-2), 76.1 (d, C-3), 75.8 (d, C-1), 66.8 (d, C-4), 61.7 (q, OCH_3), 55.8 (d, C-7), 55.7 (q, OCH_3), 43.7 (q, $N(CH_3)_2$); MS (70 eV): *m/z* 363 ($M^{\oplus}$, 100%), 165 (50%), 88 (47%). – *ent*-**14d**: colorless oil; ^{1}H NMR ($CDCl_3$): $\delta = 7.4–7.1$ (m, 5H), 5.77 (m, 5-,6-H), 5.31 (d, 1-H), 5.04 (dd, 3-H), 4.38 (br.s, NH), 3.49 (s, OCH_3), 3.39 (m, 4-,7-H), 3.29 (m, 2-H), 2.25 (s, NCH_3), 2.07 (s, OAc), 2.02 (s, OAc); $J_{2,3} = 10.5$, $J_{3,4} = 6.9$ Hz.
[8] Y.-F. Wang, C. S. Chen, G. Girdaukas, C. J. Sih, *J. Am. Chem. Soc. 106* (1984) 3695; G. M. R. Tombo, H.-P. Schär, X. F. I. Busquets, O. Ghisalba, *Tetrahedron Lett. 27* (1986) 5707; G. Guanti, L. Banfi, E. Narisano, R. Riva, S. Thea, *ibid. 27* (1986) 4639; D. H. G. Crout, V. S. B. Gaudet, K. Laumen, M. P. Schneider, *J. Chem. Soc. Chem. Commun. 1986*, 808; K. Yamamoto, H. Ando, H. Chikamatsu, *ibid. 1987*, 334; V. Kerscher, W. Kreiser, *Tetrahedron Lett. 28* (1987) 531; M. Eberle, M. Egli, D. Seebach, *Helv. Chim. Acta 71* (1988) 1; M. Ohno, S. Kobayashi, K. Adachi in M. P. Schneider (Ed.): *Enzymes as Catalysts in Organic Synthesis*, Reidel, Dordrecht, Holland 1986, p. 123; T. Kuhn, C. Tamm, A. Riesen, M. Zehnder, *Tetrahedron Lett. 30* (1989) 693.
[9] J. A. Dale, H. S. Mosher, *J. Am. Chem. Soc. 95* (1973) 512; S. Yamaguchi ("Nuclear Magnetic Resonance Analysis Using Chiral Derivates") in J. D. Morrison (Ed.): *Asymmetric Synthesis*, Vol. 1, Academic Press, New York 1983, p. 125.
[10] J. A. Dale, H. S. Mosher, *J. Am. Chem. Soc. 90* (1968) 3732.
[11] Comparable high *ee* values were achieved in PLE hydrolyses of analogous bicyclo[3.2.1]octane di(tri)esters; e.g., the respective monoacetates were obtained in 100% yield from **21**, and in 70% yield from **22** (*ee* = 92% and > 99%, resp.).



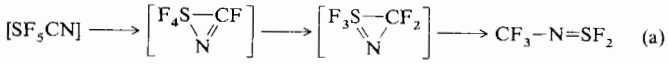
[12] T. Francis, M. P. Thorne, *Can. J. Chem. 54* (1976) 24.
[13] R. Schwesinger, *Chimia 39* (1985) 269; R. Schwesinger, H. Schlemper, *Angew. Chem. 99* (1987) 1212; *Angew. Chem. Int. Ed. Engl. 26* (1987) 1167.

Sulfur Cyanide Pentafluoride SF_5CN **

By *Oliver Lösking* and *Helge Willner**

Since the discovery of SF_5Cl,[1] the chemistry of SF_5 has developed very rapidly—a chemistry which claims special interest by virtue of the bulky, kinetically stable SF_5 group and the highly charged sulfur atom. The reactive SF_5Br and the inert S_2F_{10}, as well as numerous SF_5–C-, SF_5–N- and SF_5–O-compounds, have already been intensively studied.[2–4] The detection of the simplest SF_5 compounds containing a formal sp-hybridized C atom or N atom, SF_5CN and SF_5NC respectively, however, has thus far never succeeded.

The synthesis of SF_5CN by fluorination of methyl thiocyanate was first reported as long ago as 1959,[5] but it later turned out that the boiling point and spectroscopic data unequivocally corresponded to the isomer $CF_3-N=SF_2$.[6] All other attempts to synthesize SF_5CN, such as by the reaction of $(FCN)_3$ with SF_4 in the presence of CsF,[7] by the photochemical reaction between S_2F_{10} and $(CN)_2$[8] and by the metathesis between $CsSF_5$ and BrCN[9] also failed to give the target compound. In all cases the reactions led to the formation of, inter alia, $CF_3-N=SF_2$. On the basis of this observation it was finally concluded that SF_5CN very readily isomerizes [Eq. (a)].[9]



[*] Prof. Dr. H. Willner, Dr. O. Lösking
Institut für Anorganische Chemie der Universität
Callinstrasse 9, D-3000 Hannover 1 (FRG)

[**] This work was supported by the Deutsche Forschungsgemeinschaft and the Fonds der Chemischen Industrie. We thank Dr. *W. Hofer* of the Institut für Organische Chemie der Universität Hannover for recording the NMR spectra.

Herein we report the first successful preparation of the surprisingly stable SF_5CN; the synthesis of sulfur pentafluoride isocyanide will be described in the following communication.[10]

For the synthesis of SF_5CN a solution of dirhodane in 1,1,2-trichloro-1,2,2-trifluoroethane was allowed to react with dilute fluorine ($F_2:N_2 = 1:10$) at $-20\,^{\circ}C$. The resulting product mixture was frozen out from the gas stream at $-183\,^{\circ}C$ and separated from co-condensed solvent in vacuo by fractional condensation at $-120\,^{\circ}C$. The pre-separated mixture consisting of ca. 10% SF_5CN, 3% SF_6, 30% SF_4, 40% SOF_2, 8% NSF_3, 4% $(FCN)_3$ and 5% CF_3NSF_2 was condensed into a 2 M KOH solution and shaken for a few minutes at room temperature. The mixture thus freed of SF_4, SOF_2 and $(FCN)_3$, could then be dried over $Mg(ClO_4)_2$ and completely separated by repeated fractional condensation in a vacuo into a series of cooled traps at $-127\,^{\circ}C$, $-140\,^{\circ}C$, and $-196\,^{\circ}C$. According to the IR, Raman, UV and ^{19}F NMR spectra, the middle fraction consisted of SF_5CN with less than 1% impurities (CF_3NSF_2, NSF_3). Based on reacted $(SCN)_2$ the yield was about 5%.

Sulfur cyanide pentafluoride is a stable colorless gas at room temperature (boiling point $-25\,^{\circ}C$, triple point $-107\,^{\circ}C$). In the temperature range -100 to $-30\,^{\circ}C$ its vapor pressure curve can be described by the equation

$$\log_{10}(p/1013) = -(A/T) + B$$

where A = 1244 K and B = 5.017 (p in mbar, T in K). Noteworthy is that SF_5CN does not isomerize spontaneously to CF_3NSF_2 as was hitherto presumed. The compound does not decompose even on pyrolysis in a corundum tube at 350 °C, ca. 10^{-4} mbar with a contact time of ca. 10^{-3} s. Under the same conditions 90% of S_2F_{10} decomposes to SF_4 and SF_6 and 50% of SF_5Br to SF_4 and BrF, as demonstrated in matrix isolation experiments.

The molecular weight determination according to *Regnault* gave a value of 154 ± 2 g mol^{-1}, which agrees with the calculated molecular weight of 153.1 g mol^{-1}.

The spectrum of the gaseous substance (Fig. 1) shows the characteristic CN stretching vibration at 2235 cm^{-1}; the corresponding band of the isocyanide is observed at 2080 cm^{-1}.[10] These values are comparable with those of CF_3CN ($\tilde{\nu}_{CN} = 2278$ cm^{-1}[11]) and CF_3NC ($\tilde{\nu}_{NC} = 2133$ cm^{-1}[12]), which are somewhat higher because of the strong coupling with the XC and XN stretching vibrations, respectively. The presence of a S-C-N subunit in the new compound can be demonstrated by comparison of the measured frequency shifts of the CN stretching vibration of ^{13}C- and ^{15}N-containing isotopomers with values from model calculations (Table 1; the measured frequency shifts derived from matrix isolated SF_5CN (Ar matrix, 14 K) with natural content of ^{13}C and ^{15}N). Analogous calculations were carried out on Me_3SiCN and Me_3SiNC.[13]

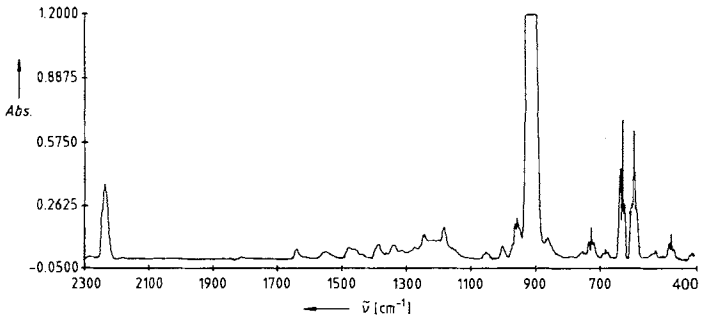


Fig. 1. IR spectra of SF_5CN in the gas phase. $p = 7$ mbar, optical path length 20 cm; Abs = absorption.

Table 1. Calculated isotopic shifts of the CN stretching vibration.

		$\tilde{\nu}$ [cm^{-1}]	Shifts $\Delta\tilde{\nu}$ [cm^{-1}] [a] ^{13}C	^{15}N
SF_5CN	$(SF_5)-C$	630	52 (51.1)	30 (29.5)
	$C\equiv N$	2235		
SF_5NC	$(SF_5)-N$	630	42.5	38
	$N\equiv C$	2235		

[a] Measured values in parenthesis.

The ^{19}F NMR spectrum (188.5 MHz, CD_2Cl_2, CCl_3F int.) of the new compound, measured at $-40\,^{\circ}C$, showed the typical AB_4 spin system of an SF_5 group with a total of nine lines for the axial fluorine atom (A) and two multiplets for the four equatorial fluorine atoms (B). The spectrum could be simulated with the parameters $\delta_A = -61.4$, $\delta_B = -80.1$; $J_{AB} = 163$, $J_{BB} = 0$ and $J_{BB'} = 2$ Hz – values which are typical for SF_5 compounds. On some lines the signals of the ^{34}S isotopomer are recognizable on the lower frequency side, thus confirming the presence of an SF_5 moiety. We are currently carrying out structure determinations by microwave spectroscopy and electron diffraction.

Received: January 19, 1989 [Z 3131 IE]
German version: *Angew. Chem. 101* (1989) 1283
Publication delayed at authors' request

[1] H. L. Roberts, N. H. Ray, *J. Chem. Soc. 1960*, 665.
[2] A. Senning (Ed.): *Sulfur in Organic and Inorganic Chemistry, Vol. 4*, Dekker, New York 1982.
[3] *Gmelin Handbuch der Anorganischen Chemie, Schwefel, Ergänzungsband 2*, Springer, Berlin 1978.
[4] *Gmelin Handbuch der Anorganischen Chemie, Schwefel-Stickstoff-Verbindungen, Band 32, Teil 1*, Springer, Berlin 1977.
[5] J. A. Attaway, R. H. Groth, L. A. Bigelow, *J. Am. Chem. Soc. 81* (1959) 3599.
[6] W. C. Smith, C. W. Tullock, R. D. Smith, V. A. Engelhardt, *J. Am. Chem. Soc. 82* (1960) 551.
[7] J. E. Griffiths, D. F. Sturman, *Spectrochim. Acta A 25* (1969) 1355.
[8] B. Cohen, A. G. MacDiarmid, *Inorg. Chem. 4* (1965) 1782.
[9] M. D. Vorob'ev, A. S. Filatov, M. A. Englin, *Zh. Obshch. Khim. 43* (1973) 1653.
[10] J. S. Thrasher, K. V. Madappat, *Angew. Chem. 101* (1989) 1284; *Angew. Chem. Int. Ed. Engl. 28* (1989) 1256.
[11] J. A. Faniran, H. F. Shurvell, *Spectrochim. Acta A 26* (1970) 1459.
[12] D. Lentz, *J. Fluorine Chem. 24* (1984) 523.
[13] H. R. Linton, E. R. Nicon, *J. Chem. Phys. 58* (1958) 990.

Sulfur-Pentafluoride Isocyanide, SF_5NC**

By *Joseph S. Thrasher** and *Krishnan V. Madappat*

Of the six possible chalcogen pentafluoride cyanates and isocyanates, four are now known ($SF_5N=C=O$, $SF_5O-C\equiv N$, $SeF_5O-C\equiv N$, and $TeF_5N=C=O$), with the latest addition being $SF_5O-C\equiv N$.[1] On the other hand, there is

[*] Prof. J. S. Thrasher, K. V. Madappat
Department of Chemistry
The University of Alabama
Tuscaloosa, AL 35487 (USA)

[**] This work was supported by the State of Alabama and the Petroleum Research Fund, administered by the American Chemical Society. We thank Dr. *Matthew Clark* for his assistance with the AM1 calculations, Dr. *Jon B. Nielsen* for technical assistance, and Prof. *Helge Willner* for sharing his research results prior to publication.

not a single correct report of a chalcogen pentafluoride cyanide or isocyanide. There are, however, both incorrect as well as unsuccessful reports on one of these materials, namely SF_5CN.[2-7] Many other research groups have also had an interest in and have made attempts to prepare SF_5CN because of the commonly held belief that it would be a better electron capture agent than SF_6[8] as well as a useful precursor for synthetic chemistry. Recently, we succeeded in preparing the first chalcogen pentafluoride isocyanide SF_5NC,[9] while the C-bonded isomer SF_5CN has been described in the preceding paper.[10]

By utilizing the chemistry developed by *Lentz* for a high yield, high purity synthesis of CF_3NC,[11] we have been able to prepare SF_5NC (Scheme 1). However, the following differences are noteworthy: first, $SF_5N{=}CCl_2$, unlike $CF_3N{=}CCl_2$,[11] does not react with magnesium in tetrahydrofuran (THF);[12] second, the $<5\%$ yield of SF_5NC in no way compares with the 65–90% yield of CF_3NC.[11] We

$$SF_5N{=}CCl_2 + 3HF \longrightarrow SF_5NHCF_3 + 2HCl^{[13]}$$

$$SF_5NHCF_3 + BBr_3 \xrightarrow{-HBr} [SF_5N(CF_3)BBr_2 \xrightarrow{-BF_3} SF_5N{=}CBr_2^{[14]}$$

$$SF_5N{=}CBr_2 \xrightarrow[-MgBr_2]{Mg/THF} SF_5NC$$

Scheme 1.

have even tried a number of reactions of $SF_5N{=}CBr_2$ with lithium reagents such as *n*-C_4H_9Li, *sec*-C_4H_9Li, *t*-C_4H_9Li, C_6H_5Li, and CH_3Li, but in each case we have obtained no more than a 5% yield of the isocyanide. Only traces of SF_5NC were produced in reactions of $SF_5N{=}CCl_2$ with these lithium reagents.

The new isocyanide SF_5NC is a colorless gas which has been characterized by its IR, ^{19}F NMR, and mass spectra as well as by a vapor-density molecular weight determination (found 154 ± 4; calc. 153.1). In the gas phase SF_5NC was unexpectedly found to isomerize to the cyanide even at room temperature and reduced pressure (<50 torr). Partial isomerization of the sample was apparent within a few hours, while complete isomerization generally took about one week. In addition, both SF_5NC and SF_5CN were observed in the product mixtures of some reactions which were carried out at approximately $-45\,^{\circ}C$ instead of colder. Thus, the stability of SF_5NC towards isomerization strongly contrasts with that of CF_3NC. Although CF_3NC is known to undergo polymerization even at $-78\,^{\circ}C$ in either the condensed phase or at pressures greater than 150 torr,[11] temperatures of almost 500 °C are required for its isomerization to CF_3CN in the gas phase in vacuo.[15] Unfortunately, both the poor yield and the instability of SF_5NC have thus far prevented us from obtaining reliable data for a vapor pressure curve; however, one can conclude that SF_5NC has a lower boiling point than SF_5CN, as a $-135\,^{\circ}C$ slush bath will stop SF_5CN while SF_5NC passes through to a $-155\,^{\circ}C$ slush bath (10^{-4} torr vacuum). Similar relative volatilities are observed for CF_3NC and CF_3CN.

The appearance of the NC stretching frequency at 2080 cm^{-1} in the infrared spectrum of SF_5NC clearly indicates that the compound is an isocyanide and not a cyanide. It is interesting to compare this stretching frequency to that observed in CF_3NC (2133 cm^{-1}).[11] Although isocyanides in general display an inverse frequency behavior (i.e., more electron-withdrawing substituents lower $\tilde{\nu}_{CN}$),[16] this alone cannot explain the large variation of 53 cm^{-1} between the two compounds. Since the isocyanide stretch is a coupled vibration, most of the variation is due instead to both differences in mass between the sulfur and carbon based groups as well as differences in the respective strengths of the S–N and C–N bonds adjacent to the isocyanide link.[16] Further support for the identity of the product from Scheme 1 as an isocyanide is found by comparison with the CN (NC) stretching frequencies of other known sulfur(VI) cyanides or isocyanides: $CF_3SF_2(CN)_2Cl$, 2210 cm^{-1};[17] FSO_2CN, 2213 cm^{-1}; CF_3SO_2CN, 2195 cm^{-1};[18] and SF_5CN, 2235 cm^{-1}.[10] We have also calculated the normal-mode vibrational frequencies of SF_5NC, SF_5CN, CF_3NC, and CF_3CN by the AM1 method:[19] SF_5NC, 2239 cm^{-1} (calc./observed 1.08); SF_5CN, 2489 cm^{-1} (1.11); CF_3NC, 2338 cm^{-1} (1.10); CF_3CN, 2566 cm^{-1} (1.13). Even though computational methods consistently give calculated frequencies which are 10–15% larger than the experimental values,[20] these results lend further credence to the correct identification of our product as the isocyanide SF_5NC.

As expected from the diamagnetic anisotropy of the isocyanide function, the axial fluorine atom in SF_5NC resonates upfield (59.1 ppm) of the equatorial fluorine atoms (77.3 ppm, $J_{ab} = 158.8$ Hz) in the ^{19}F NMR spectrum (cf. Ref. [21]). The spectrum, which was measured on a dilute solution of the isocyanide in THF, remained unchanged for more than several months while storing the sample at room temperature. The mass spectrum of SF_5NC displays the molecular ion $M^{\oplus}$ at $m/z = 153$ (3%) as well as the expected fragmentation pattern [$m/z = 134$ ($SF_4NC^{\oplus}$, 19%), 127 ($SF_5^{\oplus}$, 100%), 108 ($SF_4^{\oplus}$, 10%), 89 ($SF_3^{\oplus}$, 53%), 70 ($SF_2^{\oplus}$, 9%), 51 ($SF^{\oplus}$, 3%)].

Starting from $TeF_5N{=}CCl_2$,[22] it should also be possible to prepare TeF_5NC by the route shown in Scheme 1. In fact, we have recently prepared $TeF_5N{=}CBr_2$,[23] but we anticipate even greater problems in our efforts to isolate the product (cf. Ref. [24]) as TeF_5-substituted materials generally have 25–40° higher boiling points than do their SF_5 analogues.[22]

Experimental Procedure

In a typical reaction $SF_5N{=}CBr_2$ (2.54 g, 8.12 mmol) was condensed at $-196\,^{\circ}C$ into a 250-mL reaction vessel containing CH_3Li (10.0 mmol) in 25 mL of dry diethyl ether/tetrahydrofuran. The reaction vessel was connected to a series of traps held at $-196\,^{\circ}C$, and the entire apparatus was filled with approximately 200 torr of dry nitrogen. The reaction mixture was then warmed to $-78\,^{\circ}C$ and stirred for 4 h before being allowed to warm slowly to room temperature. After pumping off the noncondensable gases, the volatile products were distilled through a series of traps at -135, -155, and $-196\,^{\circ}C$. Repeated distillation afforded 0.06 g of SF_5NC (5%) in the $-155\,^{\circ}C$ trap.

Received: January 13, 1989;
revised: May 12, 1989 [Z 3121 IE]
German version: *Angew. Chem. 101* (1989) 1284

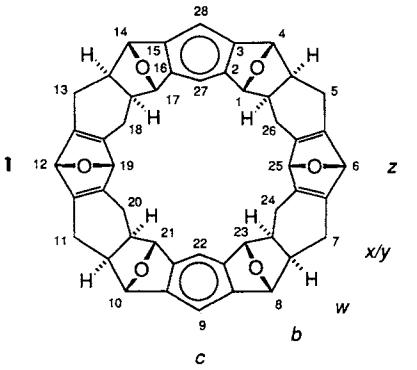
[1] A. Schmuck, K. Seppelt, *Angew. Chem. 99* (1987) 138; *Angew. Chem. Int. Ed. Engl. 26* (1987) 134.
[2] J. A. Attaway, R. H. Groth, L. A. Bigelow, *J. Am. Chem. Soc. 81* (1959) 3599.
[3] a) B. Cohen, A. G. MacDiarmid, *Chem. Ind. (London) 1962*, 1866; b) *Inorg. Chem. 4* (1965) 1782.
[4] M. D. Vorob'ev, A. S. Filatov, M. A. Englin, *Zh. Obshch. Khim. 43* (1973) 2386.
[5] a) W. C. Smith, C. W. Tullock, R. D. Smith, V. A. Engelhardt, *J. Am. Chem. Soc. 82* (1960) 551; b) J.E. Griffiths, D. F. Sturman, *Spectrochim. Acta A 25* (1969) 1355; c) A. Haas in *Gmelin-Handbook of Inorganic Chemistry, Fluorine: Perfluorohalogenoorgano Compounds of Main Group Elements, Part 9;* Springer, New York 1981, p. 13.
[6] M. D. Vorob'ev, A. S. Filatov, M. A. Englin, *Zh. Obshch. Khim. 43* (1973) 1653.
[7] H. Schachner, W. Sundermeyer, *J. Fluorine Chem. 18* (1981) 259.
[8] R. E. Eibeck, W. Mears, *Kirk-Othmer Encycl. Chem. Technol. 3rd ed. 10* (1980) 799.
[9] J. S. Thrasher, *Abstr. Pap. Am. Chem. Soc. 194th* (1987) FLUO 13.

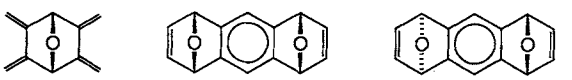
[10] O. Lösking, H. Willner, *Angew. Chem. 101* (1989) 1283; *Angew. Chem. Int. Ed. Engl. 28* (1989) 1255.
[11] D. Lentz, *J. Fluorine Chem. 24* (1984) 523.
[12] D. Lentz, private communication.
[13] C. W. Tullock, D. D. Coffman, E. L. Muetterties, *J. Am. Chem. Soc. 86* (1964) 357.
[14] $SF_5N=CBr_2$: pale yellow liquid, m.p. = −27 to −28 °C, yield: 53%. IR (gas): $\tilde{\nu}$ = 1738(wsh), 1677(s), 1611(s), 910(vs), 865(vs), 820(m), 602(ss) cm^{-1}; EI-MS (70 eV, ^{79}Br): *m/z* 292 ($M^{\oplus}-F$, 2%), 232 ($M^{\oplus}-Br$, 100), 127 (SF_5, 23); CI-MS (methane, ^{79}Br): *m/z* = 312 ($M^{\oplus}+H$, 90), 292 ($M^{\oplus}-F$, 100), 232 ($M^{\oplus}-Br$, 84), 127 (SF_5, 48); ^{19}F NMR (CCl_3F): AB_4 spectrum, δ_a = 70.4, δ_b = 62.4, J = 157.0 Hz; correct elemental analysis.
[15] H. Bock, R. Dammel, D. Lentz, *Inorg. Chem. 23* (1984) 1535.
[16] L. J. Bellamy (Ed.): *The Infrared Spectra of Complex Molecules, Vol. 2*, Chapman and Hall, New York 1980, Chap. 3.
[17] R. C. Kumar, J. M. Shreeve, *Z. Naturforsch. B36* (1981) 1407.
[18] D. D. DesMarteau, M. I. Cook, S. P. Kotun, W. Navarini, C. W. Bauknight, Jr., *Abstr. 8th Winter Fluorine Conf. Fluorine Div. Am. Chem. Soc., St. Petersburg, FL*; Am. Chem. Soc., Washington, DC, January 1987, No. 25.
[19] a) M. J. S. Dewar, E. G. Zoebisch, E. F. Healy, J. J. P. Stewart, *J. Am. Chem. Soc. 107* (1985) 3902; b) Dewar Research Group, J. J. P. Stewart, *QCPE Bull. 6* (1986) 24; c) *QCPE 506*.
[20] W. J. Hehre, L. Radom, P. von R. Schleyer, J. A. Pople: *Ab Initio Molecular Orbital Theory*; John Wiley & Sons, New York 1986, Chapter 6 and references cited therein.
[21] J. M. Canich, M. M. Ludvig, W. W. Paudler, G. L. Gard, J. M. Shreeve, *Inorg. Chem. 24* (1985) 3668.
[22] a) J. S. Thrasher, K. Seppelt, *Angew. Chem. 95* (1983) 813; *Angew. Chem. Int. Ed. Engl. 22* (1983) 789; *Angew. Chem. Suppl. 1983*, 1106; b) *Inorg. Chem. 24* (1985) 4171.
[23] $TeF_5N=CBr_2$: yellow liquid, yield: 30%. IR (Gas): $\tilde{\nu}$ = 1641(s), 1570(s), 804(s), 701(s) cm^{-1}; EI-MS (70 eV, ^{130}Te, ^{79}Br): *m/z* = 330 ($M^{\oplus}-Br$, 100%), 288 ($TeBr_2^{\oplus}$, 17), 225 ($TeF_5^{\oplus}$, 28), 187 ($TeF_3^{\oplus}$, 39), 105 ($NCBr^{\oplus}$, 47), 79 ($Br^{\oplus}$, 26); CI-MS (methane, ^{130}Te, ^{79}Br): *m/z* = 410 ($M^{\oplus}+H$, 46%), 390 ($M^{\oplus}-F$, 11), 330 ($M^{\oplus}-Br$, 26), 184 ($NCBr_2^{\oplus}$, 38), 106 ($HNCBr^{\oplus}$, 100); ^{19}F NMR (CCl_3F): AB_4X spectrum, δ_a = 42.2, δ_B = 47.5, J_{AB} = 172.4 Hz, $J(^{125}Te\text{-}A)$ = 3406, $J(^{125}Te\text{-}B)$ = 3989 Hz.
[24] D. Lentz, K. Graske, D. Preugschat, *Chem. Ber. 121* (1988) 1445.

Stereoregular Oligomerization by Repetitive Diels–Alder Reactions**

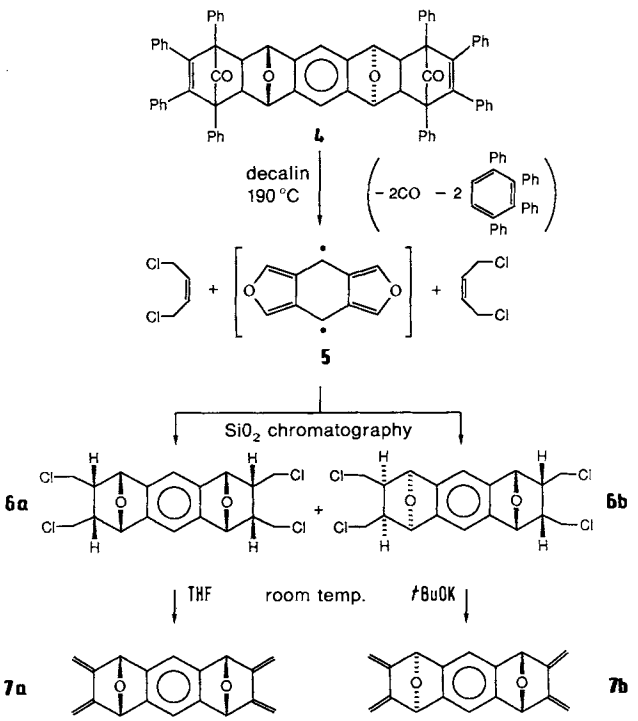
By *Peter R. Ashton, Neil S. Isaacs, Franz H. Kohnke, John P. Mathias,* and *J. Fraser Stoddart**

In recent times, linear polyacenes and their derivatives[1] have become increasingly attractive synthetic goals because of their potential applications[2,3] in science and technology. In an attempt to circumvent solubility difficulties, oxygen atoms have been introduced either into exocyclic positions, as in the polyacenequinones,[4] or into bridging endocyclic positions, as in the epoxypolyacenes.[4] Although a number of synthetic strategies may be envisaged,[5] the repetitive Diels–Alder approach[1,4,6–8] has many attractions. However, in those cases where stereogenic centers are created during reactions between dienes and dienophiles, some stereochemical uncertainty associated with isomer production and consequent oligomer/polymer heterogeneity at a configurational level is often encountered. The realization[9,10] that the [12]cyclacene derivative **1**, with its 20 stereogenic centers,[11] can be synthesized[12] in at least 28% overall yield[13] in two steps from the bisdiene **2**[14] and the bisdienophile **3a**[15] shows that it is possible to program small molecules to express themselves through their mutual reactions in unique structural fashions without reagent control and to create thereby much larger molecules that are highly ordered.[16] Treble diastereoselectivity[9,16] is exercised repetitively in the four Diels–Alder reactions that allow the construction of **1** out of a pair of bisdienes **2** and a pair of bisdienophiles **3a**. The next question was whether this high degree of stereoelectronic control can be incorporated into





oligomerizations—and hence polymerizations—to yield acyclic products through repetitive Diels–Alder reactions. Here, we report firstly the high pressure diastereoselective synthesis[17] of the novel oligomers **8b** and **9** (Scheme 2), containing 11 and 19 laterally-fused six-membered rings, respectively, from the bisdiene **7a** (Scheme 1) and the bis-



Scheme 1.

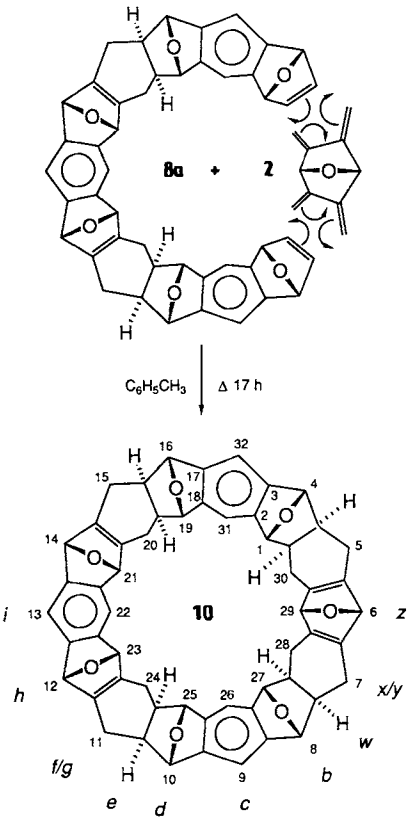
[*] Dr. J. F. Stoddart, P. R. Ashton, J. P. Mathias
Department of Chemistry, The University
Sheffield S3 7HF (UK)
Dr. N. S. Isaacs
Department of Chemistry, The University
Whiteknights, P.O. Box 224
Reading RG6 2AD (UK)
Dr. F. H. Kohnke
Dipartimento di Chimica Organica e Biologica
dell' Università di Messina
Salita Sperone, I-98166 Messina (Italy)

[**] This work was supported by the Science and Engineering Research Council and the Ministry of Defence in the United Kingdom and by the University of Messina in Italy.

dienophile **3a** and secondly the facile double Diels–Alder reaction of **8b** with the bisdiene **2** to afford the [14]cyclacene derivative **10** (Scheme 3) without, rather surprisingly, having to resort to the use of high pressure to promote the final intramolecular polymacrocyclization.

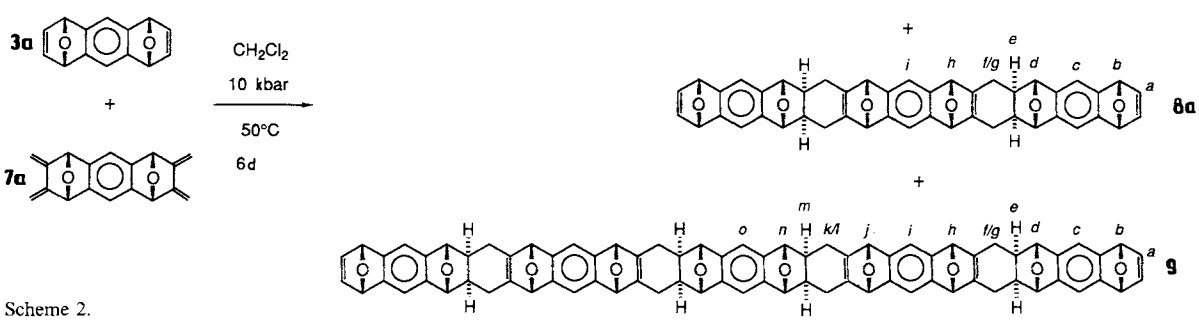
Employing a literature procedure,[18] a mixture of the *syn*- and *anti*-tetrachlorides **6a** and **6b** were obtained (Scheme 1) by reaction of *cis*-1,4-dichlorobut-2-ene with the benzo[1,2-*c*:4,5-*c'*]difuran equivalent **5**, generated in situ by the thermolytic decomposition of the bisadduct **4**, formed between the *anti* isomer **3b** of 1,4:5,8-diepoxy-1,4,5,8-tetrahydroanthracene[20] and tetraphenylcyclone. The satisfying aspect of this synthetic approach is that **3b**, obtained during the preparation[12, 15] of the desired (Scheme 2) *syn*-isomer **3a**, is also utilized. As a result of the presumed planar nature of the intermediate **5**, the relative configurations of the endoxide (and carbonyl) bridges in **4** are of no consequence[18] in the synthesis of **6a** and **6b**, which have now been separated chromatographically and characterized fully by X-ray crystallography.[19, 20] Eliminations have then been performed stereospecifically[21] on the separate and pure isomers **6a** and **6b** to afford the bisdienes **7a** and **7b** with the *syn* and *anti* configurations, respectively. Reaction (Scheme 2) of two molar equivalents of the *syn*-bisdienophile **3a** with the *syn*-bisdiene **7a** under high pressure in dichloromethane solution yields the 2:1 and 3:2 adducts **8a** and **9**, with the all-*syn* configurations, as the major products[22]: these all-*syn* adducts are believed to be the result[23] of trebly diastereoselective Diels–Alder reactions, involving exclusively *endo* and *exo* approaches with respect to the diene and dienophile units, respectively. The all-*syn* 2:1 adduct **8a** is accompanied by trace amounts[23] of the *syn-anti* 2:1 adduct **8b**, implying the existence of a minor reaction pathway where the approach is *exo* with respect to both diene and dienophile units. On account of their remarkably high solubilities in most organic solvents, **8a, 8b,** and **9** have been separated with ease by silica gel chromatography and characterized structurally by fast atom bombardment mass spectrometry (FABMS), high field ^{13}C- and ^{1}H-NMR spectroscopies, and, in the case of **8a**, by its reaction (Scheme 3) with **2** in refluxing toluene, without having to use high pressure, to give the [14]cyclacene derivative **10**.[24]

In accordance with their C_{2v} symmetries, the all-*syn* adducts **8a** and **9** exhibit 12 and 20 resonances respectively in their high resolution broad-band decoupled ^{13}C-NMR spectra. By contrast, the 2:1 adduct **8b** with the *syn-anti* configuration displays 23 peaks, in harmony with its lower C_s symmetry. The ^{1}H-NMR chemical shift data summarized in



Scheme 3.

matrix fashion in Table 1 emphasizes the structural similarities and highlights the structural differences between **8a, 8b, 9, 10** – and **1**. The assignment of the *endo* configurations to all ring junction hydrogen atoms (*e* and *m*) is supported by the very small coupling constants[1, 14] they exhibit towards the vicinal hydrogen atoms (*d* and *n*, respectively) at the neighboring bridgehead positions. Most intriguing is the appearance, at appreciably lower frequencies (shifted by ca. 0.36, 0.16 and 0.07 ppm, respectively), of the signals for protons *a, b,* and *c* (Scheme 2) in **9** relative to those for the "same" protons in **8a** and **8b**. This suggests that the 3:2 adduct **9** with the all-*syn* configuration adopts a "Swiss roll-like" conformation, wherein the six-membered rings at the termini of the oligomeric chain are forced into close proximity. In this regard, it is interesting that all attempts to effect a cyclization of **8a** with the bisdiene **7a** and thus construct a [16]cyclacene derivative have failed so far. Yet, reaction of



Scheme 2.

 © VCH Verlagsgesellschaft mbH, D-6940 Weinheim, 1989 0570-0833/89/0909-1259 $ 02.50/0

Table 1. A comparison of the ^{1}H-NMR chemical shift data (δ values) in $CDCl_3$ [a] for **1**, **8a**, **8b**, **9**, and **10** with their structural features displayed in Scheme 1.

^{1}H[b]	*q*	*p*	*o*	*n*	*m*	*k/l*	*j*	*i*	*h*	*f/g*	*e*	*d*	*c*	*b*	*a*	*w*	*x/y*	*z*
8b	6.95	5.58 or 5.56	7.06 or 7.04	4.91 or 4.90	1.70 ↓ 1.90	2.30 ↓ 2.60	5.32 or 5.31	7.07	5.31 or 5.32	2.30 ↓ 2.60	1.70 ↓ 1.90	4.90 or 4.91	7.04 or 7.06	5.56 or 5.58	6.91	—	—	—
	(m,2H)	(m,2H)	(s,2H)	(s,2H)	(m,2H)	(m,4H)	(s,2H)	(s,2H)	(s,2H)	(m,4H)	(m,2H)	(s,2H)	(s,2H)	(s,2H)	(m,2H)			
8a	—	—	—	—	—	—	—	7.08	5.32	2.35 ↓ 2.55	1.78 ↓ 1.82	4.90	7.05	5.59	6.85	—	—	—
								(s,2H)	(s,4H)	(m,8H)	(m,4H)	(s,4H)	(s,4H)	(m,4H)	(m,4H)			
9[c]	—	—	7.08	4.92	1.60 ↓ 1.67	2.35 ↓ 2.55	5.35 or 5.31	7.05	5.31 or 5.35	2.35 ↓ 2.55	1.60 ↓ 1.67	4.85	**6.98**	**5.42**	**6.52**	—	—	—
			(s,2H)	(s,4H)	(m,4H)	(m,8H)	(s,4H)	(s,4H)	(s,4H)	(m,8H)	(m,4H)	(s,4H)	(s,4H)	(m,4H)	(m,4H)			
10	—	—	—	—	—	—	—	7.12	5.31	2.30 ↓ 2.76	1.80 ↓ 1.94	4.87 or 4.92	6.95	4.92 or 4.87	—	1.58 ↓ 1.74	2.35 ↓ 2.76	5.04
								(s,2H)	(s,4H)	(m,8H)	(m,4H)	(s,4H)	(s,4H)	(s,4H)		(m,4H)	(m,8H)	(s,2H)
1	—	—	—	—	—	—	—	—	—	—	—	—	6.98	4.89	—	1.58 ↓ 1.74	2.25 ↓ 2.76	5.08
													(s,4H)	(s,8H)		(m,8H)	(m,16H)	(s,4H)

[a] The spectra were recorded at ambient temperature on either a Bruker AM250 or WH400 spectrometer using Me_4Si as an internal standard. [b] In many cases, it is not possible to differentiate with certainty assignments of protons to signals with very similar δ values. [c] The δ values (recorded in boldface) for protons *a*, *b* and *c* are all shifted to higher field relative to those for the 'same' protons in **8a** and **8b**.

8a with the smaller bisdiene **2** in refluxing toluene produced **10** (Scheme 3) in the remarkably high isolated yield of 76%. In particular, the final intramolecular Diels–Alder cyclization must be stereoelectronically favored, i.e. the reaction is enthalpically and entropically favorable.

Stereoregular oligomerizations – and hence polymerizations – by repetitive Diels–Alder reactions using "intelligent" monomers can be performed[25] by choice to give either acyclic or cyclic products. The high yielding and diastereoselective preparations of compounds such as **1**, **8a**, **8b**, **9**, and **10** are obviously *directed by the structures of the substrates and/or the products.*[26] *There are inherently simple ways of making apparently complex unnatural products*[27] *from appropriate substrates without the need for reagent control or catalysis:* call it structure-directed synthesis?

Experimental Procedure

8a/8b/9: Reaction (10 kbar, 50–55 °C, 6 days) of **3a** (1.67 g, 7.97 mmol) with **7a** (1.04 g, 3.98 mmol) in CH_2Cl_2 (45 mL) afforded, after chromatography (SiO_2/$CHCl_3$-MeOH) and in order of elution, **8b** (40 mg, 1.5%) as a white solid [*m/z* (positive ion FABMS) 682 for $M^{\oplus}$ and 705 for $[M + Na]^{\oplus}$; ^{1}H-NMR (see Table 1); ^{13}C-NMR ($CDCl_3$): δ = 26.4, 26,5, 40.3, 40.4, 82.2, 82.3, 84.6, 84.7, 86.7, 86.8, 111.9, 112.2, 112.3, 143.1, 143.4, 143.7, 147.9, 148.0, 148.2, 148.2, 148.6, 148.9, 148.9], **8a** (696 mg, 25%) [m.p. > 140 °C (decomp.), *m/z* (positive ion FABMS) 682 for $M^{\oplus}$ and 705 for $[M + Na]^{\oplus}$; ^{1}H-NMR (see Table 1); ^{13}C-NMR ($CDCl_3$): δ = 26.5, 40.4, 82.3, 84.6, 86.7, 111.9, 112.3, 143.3, 143.5, 147.9, 148.3, 148.7] and **9** (48 mg, 2%) as a white solid [*m/z* (positive ion FABMS) 1154 for $M^{\oplus}$ and 1177 for $[M + Na]^{\oplus}$, *m/z* (negative ion FABMS) 1153 for $[M - H]^{\ominus}$, ^{1}H-NMR (see Table 1); ^{13}C-NMR ($CDCl_3$): δ = 26.7, 26.7, 38.1, 41.9, 82.1, 84.8, 84.8, 86.1, 88.4, 110.4, 111.9, 112.3, 143.2, 143.6, 145.3, 146.7, 147.6, 148.1, 148.5, 149.4].

10: **2** (13 mg, 0.09 mmol) and **8a** (55 mg, 0.08 mmol) were heated under reflux (17 h) in toluene (60 mL), affording, after chromatography (SiO_2, $CHCl_3$ MeOH), the [14]cyclacene derivative **10** (51 mg, 76%) as a white solid [*m/z* (positive ion FABMS) 829 for $[M + H]^{\oplus}$, ^{1}H-NMR (see Table 1); ^{13}C-NMR ($CDCl_3$): δ = 26.3, 27.3, 40.5, 42.8, 84.3, 85.3, 86.0, 86.4, 110.3, 112.2, 144.5, 144.7, 148.1, 148.4, 151.2].

Received: March 28, 1989 [Z 3256 IE]
German version: *Angew. Chem. 101* (1989) 1266

CAS Registry numbers:
2, 53011-99-7; **3a**, 87248-22-4; **7a**, 113431-22-4; **8a**, 122270-61-5; **8b**, 122331-48-0; **9**, 122270-62-6; **10**, 122293-21-4.

[1] J. Luo, H. Hart, *J. Org. Chem. 52* (1987) 3631, 4833 and references therein.
[2] a) For speculation on the conductivity properties of polyacenes, see S. Kivelson, O. L. Chapman, *Phys. Rev. B28* (1983) 7235; b) For a description of the use of polyacenequinone derivatives in organized monolayers, see P. W. Kenny, L. L. Miller, S. F. Rak, T. H. Jozekiak, W. C. Christopfel, J.-H. Kim, R. A. Uphaus, *J. Am. Chem. Soc. 110* (1988) 4445.
[3] F. H. Kohnke, J. P. Mathias, J. F. Stoddart, *Angew. Chem. Adv. Mater. 101* (1989) 1129; *Angew. Chem. Int. Ed. Engl. Adv. Mater. 28* (1989) 1103; *Adv. Mater. 1989*, 275.
[4] T. Chiba, P. W. Kenny, L. L. Miller, *J. Org. Chem. 52* (1987) 4327; P. W. Kenny, L. L. Miller, *J. Chem. Soc. Chem. Commun. 1988*, 84 and references therein.
[5] For other synthetic approaches to polyacenes and their derivatives, see W. H. Mills, M. Mills, *J. Chem. Soc. 1912*, 2194; M. P. Satchell, B. E. Stacey, *J. Chem. Soc. (C) 1971*, 268, 269.
[6] W. J. Bailey, J. Rosenberg, *J. Am. Chem. Soc. 77* (1955) 73; W. J. Bailey, C.-W. Liao, *ibid.* 992; W. J. Bailey, E. J. Detter, J. Economy, *J. Org. Chem. 27* (1962) 3479.
[7] R. O. Angus, Jr., R. P. Johnson, *J. Org. Chem. 48* (1983) 273.
[8] H. Hart, C. Lai, G. C. Nwokogu, S. Shamouilian, *Tetrahedron 43* (1987) 5203.
[9] J. F. Stoddart, *Nature 334* (1988) 10; *Chem. Br. 24* (1988) 1203.
[10] L. Milgrom, *New Scientist No. 1641* (3. Dec. 1988) 61.
[11] In addition to having 16 chiral centers, it should be noted that **1** contains 4 pseudochiral centers at C-6, C-12, C-19 and C-25. Thus, the systematic name for the compound, referred to trivially as kohnkene [9] should be

revised from the original designation (P. R. Ashton, N. S. Isaacs, F. H. Kohnke, A. M. Z. Slawin, C. M. Spencer, J. F. Stoddart, D. J. Williams, *Angew. Chem. 100* (1988) 981; *Angew. Chem. Int. Ed. Engl. 27* (1988) 966) to rel-(1*R*,4*S*,4a*S*,6*r*,7a*R*,8*R*,10*S*,10a*S*,12*r*,13a*R*,14*R*,17*S*,19*r*,20a*R*,21*R*,23*S*,23a*S*,25*r*,26a*R*)-1,4:6,25:8,23:10,21:12,19:14,17-hexaepoxy-1,4,4a,5,6,7,7a,8,10,10a,11,12,13,13a,14,17,17a,18,19,20,20a,21,23,23a,24,25,26,26a-octocosahydro-2,16:3,15-dimethanoundecacene.

[12] F. H. Kohnke, A. M. Z. Slawin, J. F. Stoddart, D. J. Williams, *Angew. Chem. 99* (1987) 941; *Angew. Chem. Int. Ed. Engl. 26* (1987) 892.

[13] This yield should be looked upon as only a *conversion* since, in the final high pressure step [12] the production of **1** is accompanied by substantial amounts of unreacted starting materials.

[14] P. Vogel, A. Florey, *Helv. Chim. Acta 57* (1974) 200; C. Mahaim, P.-A. Carrupt, J.-P. Hagenbuch, A. Florey, P. Vogel, *Helv. Chim. Acta 63*(1980) 1149; F. H. Kohnke, J. F. Stoddart, A. M. Z. Slawin, D. J. Williams, *Acta Crystallogr. C44* (1988) 736.

[15] H. Hart, N. Raja, M. A. Meador, D. L. Ward, *J. Org. Chem. 48* (1983) 4357; F. H. Kohnke, J. F. Stoddart, A. M. Z. Slawin, D. J. Williams, *Acta Crystallogr. C44* (1988) 738, 742.

[16] P. Ellwood, J. P. Mathias, J. F. Stoddart, F. H. Kohnke, *Bull. Soc. Chim. Belg. 97* (1988) 669.

[17] N. S. Isaacs, A. V. George, *Chem. Br. 23* (1987) 47.

[18] J. Luo, H. Hart, *J. Org. Chem. 55* (1988) 1341 and also footnotes and references [6]–[12] therein.

[19] F. H. Kohnke, J. P. Mathias, J. F. Stoddart, A. M. Z. Slawin, D. J. Williams, *Acta Crystallogr.*, in press.

[20] In both **6a** and **6b**, the chloromethyl groups have the *endo* configuration with vicinal coupling constants of ca. 4 Hz for the bridgehead and *exo* methine protons being observed in their ^{1}H-NMR spectra.

[21] F. H. Kohnke, J. P. Mathias, J. F. Stoddart, A. M. Z. Slawin, D. J. Watts, D. J. Williams, *Acta Crystallogr.*, in press.

[22] The systematic names for **8a** and **9** are rel-(1*R*,4*S*,6*R*,6a*R*,8*S*,10*R*,11a*S*,12*S*,14*R*,17*S*,19*S*,19a*R*,21*S*,23*R*,24a*S*,25*S*)-1,4:6,25:8,23:10,21:12,19:14,17-hexaepoxy-1,4,6,6a,7,8,10,11,11a,12,14,17,19,19a,20,21,23,24a,25-eicosahydroundecacene and rel-(1*R*,4*S*,6*R*,6a*R*,8*S*,10*R*,11a*S*,12*S*,14*R*,14a*R*,16*S*,18*R*,19a*S*,20*S*,22*R*,25*S*,27*R*,27a*R*,29*S*,31*R*,32a*S*,33*S*,35*R*,35a*R*,37*S*,39*R*,40a*R*,41*S*)1,4:6,41:8,39:10,37:12,35:14,33:16,31:18,29:20,27:22,25-decaepoxy-1,4,6,6a,7,8,10,11,11a,12,14,14a,15,16,18,19,19a,20,22,25,27,27a,28,29,31,32,32a,33,35,35a,36,37,39,40,40a,41-hexatriacontahydrononadecacene, respectively. The systematic name for **8b** is identical to that of **8a** except for the replacement of the configurational descriptor by rel-(1*R*,4*S*,6*R*,6a*R*,8*S*,10*R*,11a*R*,12*R*,14*S*,17*R*,19*S*,19a*S*,21*S*,23*R*,24a*S*,25*S*).

[23] The 2:1 and 3:2 adducts contain, respectively, 16 and 28 chiral centers and can exist in 10 and 136 diastereoisomerically-different configurations, respectively. Analytical HPLC on a 5μ Hypersil Silica Gel Cartridge Column using 2% MeOH in CH_2Cl_2 as eluent revealed that the ratio of **8a**:**8b** in the crude high pressure reaction mixture is 16:1. We thank Mr. *I. Staton* for obtaining this result.

[24] The systematic name for **10** is rel-(1*R*,4*S*,4a*S*,6*r*,7a*R*,8*R*,10*S*,10a*S*,12*R*,14*S*,15a*R*,16*R*,19*S*,19a*S*,21*R*,23*S*,24a*R*,25*R*,27*S*,27a*S*,29*r*,30a*R*)-1,4:6,29:8,27:10,25:12,23:14,21:16,19-heptaepoxy-1,4,4a,5,6,7,7a,8,10,10a,11,12,14,15,15a,16,19,19a,20,21,23,24,24a,25,27,27a,28,29,30,30a-triacontahydro-2,18:3,17-dimethanotridecacene. Note, that in addition to 20 chiral centers, **10** contains 2 pseudochiral centers (at C-6 and C-29).

[25] "Small molecules evolve into bigger ones by eating smaller ones, although it is not always clear which is the eater and which the eaten. Little molecules eat by impact, and what emerges from their collisions is sometimes a bigger molecule"... "complex molecules emerge from simpler ones inhabiting planets; and so the specification could be simplified still further. That simplification can itself be simplified, for if you merely specify the elements, and perhaps some other things, sooner or later there will be elephants." Excerpts from P. W. Atkins: *The Creation*, Freeman, Oxford 1981, p. 3 and 4. For a recent thought-provoking analysis of the topologies of complex organic molecules in relation to periodic minimal surfaces, see Z. Blum, S. Lidin, *Acta Chem. Scand. B42* (1988) 332.

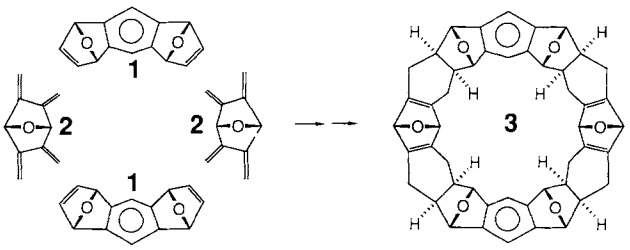
[26] Although the stereoselectivities of Diels–Alder reactions involving bicyclic dienes and bicyclic dienophiles has been discussed at length [in particular, by K. N. Houk (p. 1), L. A. Paquette (p. 41), R. Gleiter and M. C. Böhm (p. 105), and P. Vogel (p. 147) in W. H. Watson (Ed.): *Stereochemistry and Reactivity of Systems containing π-Electrons*, Verlag Chemie International, Deerfield Beech, FL (USA) 1983], it is not yet clear in th case of the present examples, what kind of controls – kinetic and/or thermodynamic – preside over the close (*endo* versus *exo*) and remote (*syn* versus *anti*) aspects of the trebly diastereoselective cycloadditions.

[27] The concept of structure-directed synthesis has already been addressed in the field of biomolecules and natural product synthesis. In analyzing the specific structural elements of vitamin B_{12}, Prof. Dr. *Albert Eschenmoser* [*Angew. Chem. 100* (1988) 5; *Angew. Chem. Int. Ed. Engl. 27* (1988) 5] has drawn attention to the fact that "these outwardly complex structural elements are found to 'self-assemble' with surprising ease under structurally appropriate preconditions; the amount of 'external instruction' required for their formation turns out to be surprisingly small in view of the complexity and specificity of these structural elements." See also G. Kansder, G. Bold, R. Lattmann, C. Lehmann, T. Früh, Y.-B. Xiang, K. Inomata, H.-P. Buser, J. Schreiber, E. Zass, A. Eschenmoser, *Helv. Chim. Acta 70* (1987) 1115. We should stress that, in extending the concept of structure-directed synthesis to the field of unnatural product synthesis, we wish to draw attention to the fact that the synthesis of complex new materials can be achieved without having to resort to the use of sophisticated reagents or exotic catalysts. It is the structures of the substrates and/or products that are important. A recently published series of communications concerning the synthesis of dodecahedrane derivatives from *Prinzbach* et al. elegantly demonstrates the point: G. Lutz, D. Hunkler, G. Rihs, H. Prinzbach, *Angew. Chem. 101* (1989) 307; *Angew. Chem. Int. Ed. Engl. 28* (1989) 298 and four communications following.

Trinacrene – a Product of Structure-Directed Synthesis**

By *Peter R. Ashton, Neil S. Isaacs, Franz H. Kohnke, Guglielmo Stagno D'Alcontres,* and *J. Fraser Stoddart**

The fact that the macropolycyclic belt-like compound kohnkene **3** can be prepared[1] stereoselectively by consecutive Diels–Alder reactions in two steps (Scheme 1) from the readily-available bisdienophile **1**[2] and bisdiene **2**[3] has led us to speculate[4] that cage compounds with barrel-like structures might be accessible starting from **2** and building blocks containing three or more rigid and suitably-disposed

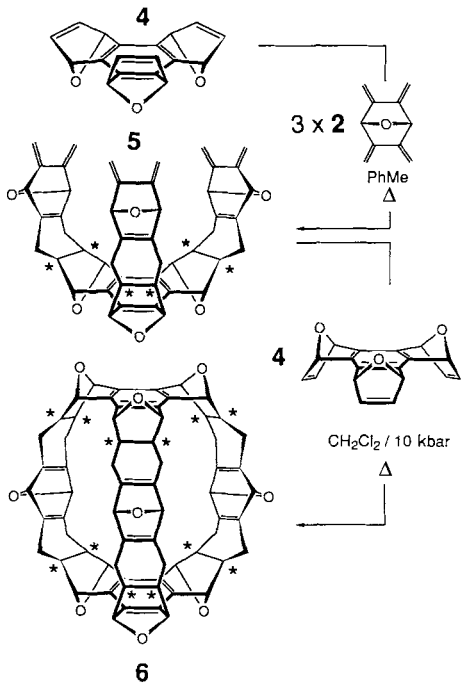


Scheme 1. The general strategy employed in the synthesis of **3**.

dienophilic units. In this communication, we firstly, establish that this speculation has become reality and announce the successful completion[5] of the stereoselective synthesis (Scheme 2) of a cage compound *trinacrene* **6**[6] from the bisdiene **2** and the trisdienophile **4**[7] via the intermediacy of trisadduct **5**, and secondly, call attention to the prospect that the concept of *structure-directed synthesis*[8] provides a new and fundamental platform from which small but stereoelectronically-programmed, molecular building blocks[9] can be elaborated through the practice of a kind of precision molecular "LEGO", into large and ordered structural arrays of organic materials.[10]

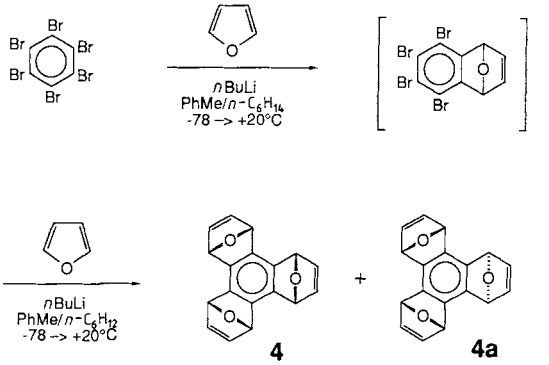
[*] Dr. J. F. Stoddart, P. R. Ashton
Department of Chemistry, The University
Sheffield S3 7HF (UK)
Dr. N. S. Isaacs
Department of Chemistry, The University
Whiteknights, PO Box 224
Reading RG6 2AD (UK)
Prof. G. Stagno d'Alcontres, Dr. F. H. Kohnke
Dipartimento di Chimica Organica e Biologica dell' Università di Messina
Salita Sperone, I-98166 Messina (Italy)

[**] This work was supported by the Agricultural and Food, and the Science and Engineering Research Councils in the United Kingdom and by the University of Messina in Italy.



Scheme 2. The two step synthesis of **6**. The H atoms at the ring junctions indicated by asterisks all have the *endo* configuration.

Hexabromobenzene was treated with a 1:1 molar equivalent of *n*BuLi and an excess of furan at −78 °C in toluene-hexane, which was allowed to warm up to room temperature before being cooled to −78 °C in preparation for the addition of a further 2.2 molar equivalents of *n*BuLi. This reaction mixture, after it had been allowed to reach room temperature for the second time and had been extracted and chromatographed repeatedly, afforded[11] two configurationally-isomeric trisdienophiles in the molar ratio 1:3[12] (Scheme 3). The relative configurations of the minor and major isomers were established unambiguously[13] as **4** and **4a** respectively on the basis of their ^{1}H-NMR spectra which can be interpreted with a knowledge of their molecular sym-



Scheme 3. The preparation of the trisdienophile **4**.

metries, viz. C_{3v} for **4** and C_s for **4a**. In particular, the C_{3v} isomer **4** shows only two equal-intensity resonances centered on δ 5.72 and 6.78 in its ^{1}H-NMR spectrum ($CDCl_3$, 400 MHz).

Reaction of **4** with 3.3 molar equivalents of **2** in toluene under reflux afforded, after chromatography, a trisadduct **5** in 48% yield along with minor amounts of a bisadduct and a monoadduct.[14] Despite the fact that there are 16 diastereoisomeric trisadducts, only *one* has been isolated and characterized. ^{1}H-NMR spectroscopy is consistent with the C_{3v} symmetry and the *endo* configurations[15] for the methine hydrogen atoms at the junctions of the newly-formed cyclohexene rings, and after subjecting equimolar amounts of **5** and **4** in CH_2Cl_2 solution to an intermolecular, followed by two intramolecular, Diels–Alder reactions under very high pressure[16] only trinacrene **6** was isolated. The positive ion fast atom bombardment mass spectrum (FABMS) of **6** revealed an intense peak at m/z 991 for $[M + H]^{\oplus}$ with little fragmentation of the molecule. Five resonances are observed in the high field ^{1}H-NMR spectrum of **6** recorded in $CHCl_3$ at δ = 1.56–1.66, 2.35–2.45, 2.76–2.88, 4.92, 5.10 (cf. the equivalent resonances at δ = 1.58–1.74, 2.25–2.40, 2.57–2.76, 4.89, 5.08 in **3**) for the five sets of heterotopic protons in the molecule with D_{3h} symmetry.

From a preliminary examination of trinacrene **6** by computer molecular graphics, it is clear that its large rigid molecular cavity could play host to a variety of organic, organometallic, metalloorganic and inorganic guest species, both neutral and charged. As with kohnkene **3**, chemical modification[1] (e.g. deoxygenation, dehydration, hydrogenation, and dehydrogenation) of **6** should permit useful steric and electronic manipulation of the structure. The synthesis of trinacrene **6** with its 24 chiral centers and 6 pseudochiral centers in two steps from **2** and **4** establishes the principle of *structure-directed synthesis* in the realm of unnatural products.[17]

Experimental Procedure

4/4a: Hexabromobenzene (33 g, 59.8 mmol) and furan (90 mL) in toluene (1.8 L) was cooled down to −78 °C and 1.1 mol equiv. of BuLi (24 mL of a 2.5 M solution in 60 mL of hexane) was added with stirring under argon during 4 h. The reaction mixture was allowed to warm up to room temperature (16 h) before being cooled down again to −78 °C prior to the addition (8 h) of a further 2.2 mol equiv. of BuLi (48 mL of a 2.5 M solution in 120 mL of hexane). After allowing the reaction mixture to warm up to room temperature, a work-up procedure, involving addition of water (50 mL), washing the organic phase with water (3 × 100 mL), drying ($CaSO_4$), and concentration, yielded a crude product, which, after chromatography (SiO_2,CH_2Cl_2/$CHCl_3$), afforded two components, both of which crystallized on addition of acetone. The compound, which was eluted first from the column, was characterized as the *anti*-isomer **4a** [300 mg, 1.8%, m.p. > 250 °C, m/z (EIMS) 276 for M$^{\oplus}$. ^{1}H-NMR ($CDCl_3$): δ = 5.68 (m, 2H), 5.69 (m, 2H), 5.75 (m, 2H), 6.72 (m, 2H), 6.88 (m, 2H), 6.89 (m, 2H); ^{13}C-NMR ($CDCl_3$): δ = 79.9, 80.0, 80.1, 134.0, 134.3, 134.6, 140.8, 140.9, 141.1] and the second compound to be eluted from the column was characterized as the all-*syn* isomer **4** [100 mg, 0.6%, m.p. > 250 °C, m/z (EIMS) 276 for M$^{\oplus}$. ^{1}H-NMR ($CDCl_3$): δ = 5.73 (m, 6H), 6.78 (m, 6H).

5: The bisdiene **2** (105 mg, 0.73 mmol) and the trisdienophile **4** (61 mg, 0.22 mmol) were heated under reflux (16 h) in toluene (20 mL) affording after chromatography (SiO_2,CH_2Cl_2/EtOAc) the trisadduct **5** [76 mg, 48%, recrystallized from CH_2Cl_2, m.p. > 250 °C, m/z (positive ion FABMS) 715 for $[M + H]^{\oplus}$, ^{1}H-NMR ($CDCl_3$): δ = 1.68–1.81 (6H, m), 2.28–2.43 (6H, m), 2.60–2.73 (6H, m), 4.98 (6H, s), 4.99 (6H, bs), 5.10 (6H, bs).

6: Reaction (CH_2Cl_2, 10 kbar, 50 °C, 6 days) of **5** (36 mg, 0.05 mmol) and **4** (14 mg, 0.05 mmol) yielded, after chromatography (SiO_2,$CHCl_3$/MeOH) **6** [ca. 2 mg, recrystallized from MeOH, m.p. > 300 °C, m/z (positive ion FABMS) 991 for $[M + H]^{\oplus}$; ^{1}H-NMR ($CDCl_3$): δ = 1.58–1.66 (12H, m), 2.35–2.45 (12H, m), 2.76–2.88 (12H, m), 4.92 (12 H, s), 5.10 (6H, s).

Received: March 28, 1989 [Z 3257 IE]
German version: *Angew. Chem. 101* (1989) 1269

CAS Registry numbers:
2, 53011-99-7; **4**, 122330-78-3; **4a**, 122330-79-4; **5**, 122238-26-0; **6**, 122269-95-8; hexabrombenzene, 87-82-1; furan, 110-00-9.

[1] F. H. Kohnke, A. M. Z. Slawin, J. F. Stoddart, D. J. Williams, *Angew. Chem. 99* (1987) 941; *Angew. Chem. Int. Ed. Engl. 26* (1987) 892; P. R. Ashton, N. S. Isaacs, F. H. Kohnke, A. M. Z. Slawin, C. M. Spencer, J. F. Stoddart, D. J. Williams, *ibid. 100* (1988) 981; and *27* (1988) 966; J. F. Stoddart, *Chem. Br. 24* (1988) 1203.

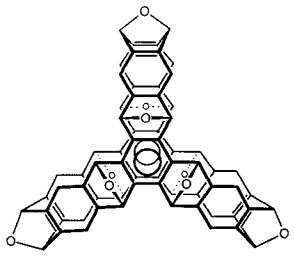
[2] H. Hart, N. Raja, M. A. Meador, D. L. Ward, *J. Org. Chem. 48* (1983) 4357; F. H. Kohnke, J. F. Stoddart, A. M. Z. Slawin, D. J. Williams, *Acta Crystallogr. C44* (1988) 738, 742.

[3] P. Vogel, A. Florey, *Helv. Chim. Acta 57* (1974) 200; C. Mahain, P.-A. Carrupt, J.-P. Hagenbuch, A. Florey, P. Vogel, *ibid. 63* (1980) 1149; F. H. Kohnke, J. F. Stoddart, A. M. Z. Slawin, D. J. Williams, *Acta Crystallogr. C44* (1988) 736.

[4] Conceptually, in structural terms, the progression from "divalent benzene", expressed as the bisdienophile **1** and used in the construction of molecular belts, to "trivalent benzene", present in the trisdienophile **4** and employed here in the assembly of a molecular cage by repetitive Diels–Alder reactions, is reminiscent of the emergence (B. Dietrich, J.-M. Lehn, J.-P. Sauvage, *Tetrahedron Lett. 1969*, 2885, 2889) of [2.2.2]cryptand from 18-crown-6 (C. J. Pedersen, *J. Am. Chem. Soc. 89* (1967) 7017) wherein two diagonally-related divalent oxygen atoms are replaced by trivalent nitrogen atoms joined together (in both cases) by $-CH_2CH_2OCH_2CH_2OCH_2CH_2-$ chains. Note that a naphthalene nucleus is potentially "tetravalent".

[5] F. H. Kohnke, G. Stagno d'Alcontres, J. F. Stoddart, *Abstr. 13th Int. Symp. Macrocyclic Chem.*, Hamburg, 4–8 September 1988, Gesellschaft Deutscher Chemiker, Frankfurt am Main 1988, p. 244.

[6] The trivial name *trinacrene* for **6** has been coined from the old name for Sicily, i.e. *Trinacria*, which according to legend refers to the three-pointed shape of the island. As if to emphasize this shape, the emblem of Trinacria became (A. Colocci, *La Trinacria Trichetria*, Catania, Italy 1908) the Trichetria, i.e. the head (of Medusa) with three legs.



Trinacrene **6**



Trichetria

[7] The trisdienophile has only been reported (M. B. Stringer, D. Wege, *Tetrahedron Lett. 21* (1980) 3831) as a mixture of the all-*syn* (**4**) and *anti* (**4a**) isomers after a low yielding stepwise synthesis starting from 3,6-dibromoanthranilic acid.

[8] The regioselective synthesis of a range of pyrrole derivatives has been accomplished (G. Ksander, G. Bold, R. Lattmann, C. Lehmán, T. Früh, Y.-B. Xiang, K. Inomata, H.-P. Buser, J. Schreiber, E. Zass, A. Eschenmoser, *Helv. Chim. Acta 70* (1987) 1115; A. Eschenmoser, *Angew. Chem. 100* (1988) 5; *Angew. Chem. Int. Ed. Engl. 27* (1988) 5) with remarkable ease in high conversions starting from substrates such as 2-amino-2-propenenitrile without the need for any reagent control. Thus, inherently simple syntheses exist for the production of apparently complex structures. Since the syntheses of **3** and **6** rely upon high diastereoselectivities in consecutive Diels–Alder reactions, which are dictated by the *structures* of the substrates and possibly the products, we have chosen (P. R. Ashton, N. S. Isaacs, F. H. Kohnke, J. P. Mathias, J. F. Stoddart, *Angew. Chem. 101* (1989) 1266; *Angew. Chem. Int. Ed. Engl. 28* (1989) 1258) to refer to this kind of *unnatural product synthesis* as being *structure-directed*.

[9] Although the bicyclic nature of **1**, **2** and **4** incorporating diene and dieneophilic units is a necessary component of their design, the bridging oxygen atoms can, in principle at least, be replaced by other atoms (e.g. S) and groups (i.e. CH_2 and NR) without necessarily sacrificing the desired diastereoselectivities in the [4 + 2] cycloadditions between the diene and dienophilic units.

[10] In principle, there is no reason to restrict the description *structure-directed synthesis* to organic compounds. The existence of clays and zeolites bears witness to the spontaneous ordering of inorganic substrates and no doubt there are also many potentially new organometallic materials where organic substrates have reacted with inorganic substrates in a highly ordered manner: see, for example, J.-M. Lehn, A. Rigault, J. Siegel, J. Harrowfield, B. Chevrier, D. Moras, *Proc. Natl. Acad. Sci. USA 84* (1987) 2565; J.-M. Lehn, A. Rigault, *Angew. Chem. 100* (1988) 1121; *Angew. Chem. Int. Ed. Engl. 27* (1988) 1095.

[11] Although hexabromobenzene is formally a trisaryne equivalent, the trisadducts **4** and **4a** are *only* formed in the very low yields of 0.6 and 1.8% respectively when a stepwise addition (Scheme 3) of reagents is employed. When 1.1, followed by 2.2, molar equivalents of *n*BuLi are added, we assume that the reaction proceeds via a monoadduct and that a small quantity of a 1,3-bisaryne is generated, following lithiation of the *para*-oriented bromine atoms and subsequent elimination of lithium bromide. Interestingly, if only 2.2 molar equivalents of *n*BuLi are employed in one step then the major reaction product is 9,10-dibromo-1,4:5,8-diepoxy-1,4,5,8-tetrahydroanthracene – the *anti*-isomer has been characterized (A. M. Z. Slawin, D. J. Williams, unpublished results) by X-ray crystallography. The polylithiation of polyhaloarenes to produce bisaryne equivalents has been investigated extensively (H. Hart, G. C. Nwokogu, *Tetrahedron Lett. 24* (1983) 5721; G. C. Nwokogu, H. Hart, *Tetrahedron Lett. 24* (1983) 5725; H. Hart, C. Lai, G. C. Nwokogu, S. Shamouilian, A. Teuerstein, B. Zlotogorski, *J. Am. Chem. Soc. 102* (1980) 6649; H. Hart, C. Lai, G. C. Nwokogu, S. Shamouilian, *Tetrahedron 43* (1987) 5203). Currently, we are investigating the use of hexahalogenobenzenes containing several different halogens in the hope of exploiting the differences in their reactivities towards lithiation in the hope of achieving trisaryne generation with high regioselectivity. An efficient synthesis of the trisdieneophile **4** is an essential prerequisite to obtaining substantial quantities of trinacrene **6**.

[12] Note that, statistically, the *anti*-isomer **4a** is three times more likely to be formed than the all-*syn* isomer **4**.

[13] Cf. P. G. Gassman, I. Gennick, *J. Am. Chem. Soc. 102* (1980) 6864.

[14] It should be noted that cycloadditions involving the "first" diene unit in **4** usually occur much faster (> 100 times) than those involving the "second" diene unit (Y. Bessière, P. Vogel, *Helv. Chim. Acta 63* (1980) 232).

[15] The fact that the bridgehead methine protons in the hexahydrotriphenylene trisendoxide resonate as a singlet establishes the *endo* configuration for the methine hydrogen atoms at the ring junctions (C. Mahaim, P.-A. Carrupt, J.-P. Hagenbuch, A. Florey, P. Vogel, *Helv. Chim. Acta 63* (1980) 1149).

[16] N. S. Isaacs, A. V. George, *Chem. Br. 23* (1987) 47.

[17] J. F. Stoddart, *Nature 334* (1988) 10.

Efficient Ion Exchangers and Receptors for Organic and Organometallic Cations**

By *Stefan Eller, Peter Brandt, Abdul K. Brimah, Peter Schwarz, and R. Dieter Fischer**

It has long been known that polymeric metal cyanides may also be ion-exchangers.[1] Whereas all previous observations have largely concerned the exchange of $H^{\oplus}$ and alkali metal cations, the Sn^{IV}-organic coordination polymers $[A(Me_3Sn)_3M^{II}(CN)_6]_\infty \triangleq [AM^{II}(\mu\text{-}CN \cdot Me_3Sn \cdot NC)]_\infty$ (M = Fe[2] and Ru) now being investigated in detail by us enable the preferred exchange of organic and organometallic cations $A^{\oplus}$. The equations (1)–(3) depict some representative and, in all cases, *quantitative* ion-exchange reactions (Route A).

$$[A(Me_3Sn)_3M(CN)_6]_\infty \xrightarrow[H_2O]{Et_4NCl} [(Et_4N)(Me_3Sn)_3M(CN)_6]_\infty + A^{\oplus}_{aq} \quad (1)$$

1a, A = Li, M = Fe[3] — **4a**, M = Fe
2a, A = NH_4, M = Fe, — **4b**, M = Ru
3a, A = Me_3Sn, M = Fe[4]
3b, A = Me_3Sn, M = Ru

$$[A(Me_3Sn)_3Fe(CN)_6]_\infty \xrightarrow[H_2O]{Me_3SnCl} [(Me_3Sn)_4Fe(CN)_6]_\infty + A^{\oplus}_{aq} \quad (2)$$

1a, 2a, 5a — **3a**

$$[A(Me_3Sn)_3Fe(CN)_6]_\infty \xrightarrow[H_2O \text{ or } EtOH]{[Cp_2Co][ClO_4]} [(Cp_2Co)(Me_3Sn)_3Fe(CN)_6]_\infty + A^{\oplus}_{aq} \quad (3)$$

2a, 3a — **6a**

5a, A = Et_3NH, M = Fe(EtOH)

That these heterogeneous reactions proceed to completion after only a few hours at room temperature[5] is more likely due to the pronounced lipophilicity of the cavities of the polymeric host lattice that are well padded by CH_3 groups than to the occasionally largely differing hydration en-

[*] Prof. Dr. R. D. Fischer, Dipl.-Chem. P. Brandt, Dipl. Chem. S. Eller, Dipl.-Chem. A. K. Brimah, P. Schwarz
Institut für Anorganische und Angewandte Chemie der Universität
Martin-Luther-King-Platz 6, D-2000 Hamburg 13 (FRG)

[**] This work was supported by the Fonds der Chemischen Industrie and by the Deutsche Forschungsgemeinschaft.

thalpies of competing cations (e.g. of $Li^{\oplus}/Cs^{\oplus}$, cf. Table 1). However, only products of the general composition $[(R_4N)_x(Me_3Sn)_{4-x}M(CN)_6]_\infty$ ($0 < x < 1$) are formed from **3** with $R_4N^{\oplus} \neq Et_4N^{\oplus}$ and $A^{\oplus} = Me_3Sn^{\oplus}$ [Eq. (1)], whereas **1a**, **2a** and **3a** show absolutely no ion-exchange with $K^{\oplus}$- or $Cs^{\oplus}$-salts. Thus, the affinity to the polymeric host system varies approximately in the following order: $K^{\oplus}$, $Cs^{\oplus} < Li^{\oplus}$, $NH_4^{\oplus} < NR_4^{\oplus}$ ($R \neq Et$), $Me_3Sn^{\oplus} < Et_3NH^{\oplus} < Cp_2Co^{\oplus}$, $Et_4N^{\oplus}$ (cf. Table 1).

Table 1. Proportion x of encapsulated cation $A^{\oplus}$ from results of elemental analyses.

$A^{\oplus}$	Route A [a]	Route B [b]	Route C [c]
$Li^{\oplus}$	0	0	1.0
$Na^{\oplus}$	0	0	1.0
$Cs^{\oplus}$	0	0	< 0.25
$NH_4^{\oplus}$	0.5	0	1.0
$Me_4N^{\oplus}$	0.7	0.3 0.8	1.0 [d]
$Et_4N^{\oplus}$	1.0	1.0 1.0	1.0
$nPr_4N^{\oplus}$	0.9	0.7 0.9	0.4
$nBu_4N^{\oplus}$	0.5	0.5 0.5	0.2

[a] Starting compound: **1a**; product $[A_xLi_{1-x}(Me_3Sn)_3Fe(CN)_6]_\infty$; standard conditions: see [5]. [b] Cf. Eq. (4); product: $[A_x(Me_3Sn)_{4-x}Fe(CN)_6]_\infty$; left: $(Me_3SnCl)/(R_4NCl)$ 1:1; right: $(Me_3SnCl)/(R_4NCl)$ 1:2. [c] product: $[A_x(Me_3Sn)_3Fe^{II}_xFe^{III}_{1-x}(CN)_6]_\infty$. [d] Estimated on the basis of relative IR intensities (ν-CN).

The topochemically favored host-guest systems **4**, with R = Et, and **5a** can also be synthesized according to Equation 4, by simple precipitation from H_2O[6] (Route B) and, with M = Fe, as for the already described[2] host-guest system $[(Cp_2Fe)(Me_3Sn)_3Fe(CN)_6]_\infty$, via the tribochemical reaction (5) (Route C).

$$\left.\begin{array}{l} 3\,Me_3SnCl + Et_4NCl + K_4[M(CN)_6] \xrightarrow[-4\,KCl]{(H_2O)} \\ 3\,Me_3SnCl + [Et_4N]_4[M(CN)_6] \xrightarrow[-3\,Et_4NCl]{(H_2O)} \end{array}\right\} \textbf{4a, 4b} \downarrow \quad (4)$$

$$[(Me_3Sn)_3Fe^{III}(CN)_6]_\infty + Et_4NI \xrightarrow[-1/2\,I_2]{\text{grinding}} [(Et_4N)(Me_3Sn)_3Fe^{II}CN)_6]_\infty \quad (5)$$

7a → **4a**

The routes A–C lead to the same products (**4**), whose superimposable X-ray powder diagrams rule out a cubic "super Prussian blue"–like host lattice.[8] With $R_4N^{\oplus}$ ($R \neq Et$), precipitated products of the complex type $[(R_4N)_x(Me_3Sn)_{4-x}M(CN)_6]_\infty$ are again formed, also via Route B, whereas with $M^{\oplus} = Li^{\oplus}$–$Cs^{\oplus}$ and $NH_4^{\oplus}$ only the compounds **3** are formed (cf. Table 1). Route C [Eq. (5)], appropriately modified,[13] also serves for the synthesis of **1a**[3] and **2a**.[7] The tribochemical reaction of R_4NI ($R \neq H$, Me, Et) and MI ($M \neq Li$, Na) with **7a** no longer proceeds to completion (Table 1). The anionic host lattice present in the host-guest systems **1a**–**6a** forms a rare example of an efficient $Et_4N^{\oplus}$ receptor: whereas molecular anionic receptors generally only form very weak complexes with tetra*alkyl*ammonium ions,[9] the likewise polymeric $R_4N^{\oplus}$/zeolite cation intercalates[11] formed in the gel synthesis of zeolites[10] (after subsequent $Na^{\oplus}/R_4N^{\oplus}$ ion exchange) appear to be best comparable with **4**. The encapsulation of metallocene cations $Cp_2M^{\oplus}$ (M = Co, Fe; cf. **6a**) in zeolites by ion exchange was first described only recently.[12]

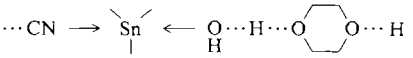
In contrast to the previously obtained coordination polymers of the general type $[(R_3Sn)_mM(CN)_n]_\infty \triangleq [M(\mu\text{-}CN \cdot R_3Sn \cdot NC)_{n/2}]_\infty$[14] where $m = n/2$, in the case of **3** $m = n/2 + 1$, so that in this instance not all four Me_3Sn groups can be incorporated in equivalent, trigonal-bipyramidally (tbp) configurated $Me_3Sn(NCM\cdots)_2$ bridges. The tempting (in view of the easy ion exchange [Eq. (1)–(3)]) assumption of one (per M atom) coordinatively extremely weakly anchored and therefore unusually mobile $Me_3Sn^{\oplus}$ ion in the lattice does not however manifest itself either in the vibrational spectra of **3**[15] or in the ^{119}Sn Mössbauer spectrum[16] of **3a**. On the other hand, the CP-MAS ^{119}Sn-NMR spectra[17] of **3a** and **3b** clearly show two widely separated ($\Delta\delta > 100$) signals.

Dioxane inhibits the spontaneous precipitation of **3** (Route B); the very slowly crystallizing novel host-guest system **8a** [Eq. (6)] now contains *all* Sn atoms in bridging tbp

$$4\,Me_3SnCl + K_4[Fe(CN)_6] \xrightarrow[-4\,KCl]{H_2O/C_4H_8O_2(1:2)} [(Me_3Sn)_4Fe(CN)_6 \cdot 2\,H_2O \cdot C_4H_8O_2]_\infty \quad (6)$$

8a

units.[18] The incorporation of the apparently more mobile $Me_3Sn^{\oplus}$ ions of **3a** into chain building blocks of the type



leads, compared to **3a**, to a drastic quenching of the $Me_3Sn^{\oplus}/Et_4N^{\oplus}$ ion exchange.[19]

The findings described here open up new possibilities for the systematic development of host-guest complexes with numerous organometallic and organic cations. Such solid state compounds with acentric space groups are especially interesting for the development of materials with high nonlinear second order effects (e.g. for frequency doubling).[20, 22]

Received: April 3, 1989;
revised: June 19, 1989 [Z 3270 IE]
German version: *Angew. Chem. 101* (1989) 1274

[1] Cf. W. E. Prout, E. R. Russell, H. J. Groh, *J. Inorg. Nucl. Chem. 27* (1965) 473.
[2] P. Brandt, A. K. Brimah, R. D. Fischer, *Angew. Chem. 100* (1988) 1578; *Angew. Chem. Int. Ed. Engl. 27* (1988) 1521.
[3] Cf. P. Brandt, R. D. Fischer, E. Sanchez Martinez, R. Diaz Calleja, *Angew. Chem. 101* (1989) 1275; *Angew. Chem. Int. Ed. Engl. 28* (1989) 1265.
[4] Cf. K. Yünlü, *Dissertation*, Universität Hamburg 1983, p. 107ff.
[5] Synthesis of **4a** and **4b** (as examples for Route A): **3** (or **1a**) (0.5 mmol) was treated with a solution of 1.0 mmol of Et_4NCl in 20 mL of H_2O. After 30 minutes of stirring at room temperature and filtration the colorless solid remaining was washed three times with 10 mL of H_2O and dried for ca. 5 h (high vacuum, ca. 30 °C). Yields > 85% in each case. Elemental analysis calculated for **4a** ($C_{23}H_{47}N_7Sn_3Fe$): C 33.14, H 5.68, N 11.76, Fe 6.70, Sn 42.72%; found: C 33.11, H 5.56, N 11.67, Fe 6.60, Sn 42.54%.
[6] Synthesis of **4b** (example for Route B): A stirred solution of 0.30 g (0.70 mmol) of $K_4[Ru(CN)_6]$ and 0.36 g (2.10 mmol) of Et_4NCl in 20 mL of H_2O was treated with a solution of 0.42 g (2.10 mmol) of Me_3SnCl in 10 mL H_2O. The spontaneously separating colorless precipitate was filtered off, washed with H_2O and dried for several hours (high vacuum, room temperature). Yield: 0.56 g (0.64 mmol) = 92%. – Alternative: Addition of a solution of 84 mg (0.423 mmol) of Me_3SnCl in 10 mL of H_2O to a solution of 110 mg (0.141 mmol) of $[NEt_4]_4[Ru(CN)_6]$ in 10 mL of H_2O. Yield after work-up as in [5]: 10 mg (0.132 mmol) = 94%. Elemental analysis calculated for **4b** ($C_{23}H_{47}N_7Sn_3Ru$): C 31.43, H 5.39, N 11.16, Sn 40.52%; found: C 31.25, H 5.30, N 10.89, Sn 39.14. Alternative: C 31.36, H 5.35, N 11.07, Sn 39.30%. **4a** can be prepared analogously. Decomp. temp.: **4a**, 283 °C; **4b**, 322 °C.
[7] Synthesis of **4a** (example for Route C): orange $(Me_3Sn)_3Fe^{III}(CN)_6$ **7a** (500 mg, 0.7 mmol) was ground for 5 minutes together with 360 mg (1.40 mmol) of Et_4NI. After washing several times with methanol (in the synthesis of **1a** and **2a** with isopropyl alcohol) the product was dried for 1 h (high vacuum, room temperature).

[8] See K. Yünlü, N. Höck, R. D. Fischer, *Angew. Chem. 97* (1985) 863; *Angew. Chem. Int. Ed. Engl. 24* (1985) 879. The host lattice of the noble gas inclusion compounds $CdPt(CN)_6 \cdot 1.046$ Kr and $CdPt(CN)_6 \cdot 1.128$ Xe, on the other hand, is cubic face centered: M. Kämper, M. Wagner, A. Weiss, *Angew. Chem. 91* (1979) 517; *Angew. Chem. Int. Ed. Engl. 18* (1979) 486.

[9] Cf. J.-M. Lehn, *Angew. Chem. 100* (1988) 91; *Angew. Chem. Int. Ed. Engl. 27* (1988) 1121; *J. Inclusion Phenom. 6* (1988) 351; M. Dhaenens, L. Lacombe, J.-M. Lehn, J.-P. Vigneron, *J. Chem. Soc. Chem. Commun. 1984*, 1097, and references cited therein; regarding the slightly more stable host-guest complexes with mono*aryl*trialkylammonium ions see: F. Vögtle, T. Merz, H. Wirth, *Angew. Chem. 97* (1985) 226; *Angew. Chem. Int. Ed. Engl. 24* (1985) 221, and references cited therein.

[10] See B. M. Lok, T. R. Cannan, C. A. Messina, *Zeolites 3* (1983) 282, and references cited therein.

[11] H. von Koningsveld, H. van Bekkum, J. C. Jansen, *Acta Crystallogr. B43* (1987) 127, and references cited therein.

[12] Cf. a) G. A. Ozin, J. Godber in A. B. P. Lever (Ed.): *Excited States and Reactive Intermediates, (ACS Symp. Ser. 307)* Am. Chem. Soc., Washington, D.C., USA 1986, p. 212ff; b) G. A. Ozin, A. Kuperman, A. Stein, *Angew. Chem. Adv. Mater. 101* (1989) 373; *Angew. Chem. Int. Ed. Engl. Adv. Mater. 28* (1989) 359; *Adv. Mater. 1989*, 69 and references cited therein.

[13] Under less mild conditions, various metal oxides also react with alkali metal iodides to give the corresponding intercalates. Cf. D. W. Murphy, P. A. Christian, F. J. DiSalvo, J. V. Waszczak, *Inorg. Chem. 18* (1979) 2800; A. K. Ganguli, L. Ganapathi, J. Gopalakrishnan, C. N. R. Rao, *J. Solid State Chem. 74* (1988) 228.

[14] See R. Uson, J. Fornies, M. A. Uson, E. Lalinde, *J. Organomet. Chem. 185* (1980) 359 ($n = 2$, M = Ag, Au; $n = 4$, M = Pd, Pt; $n = 6$, M = Fe); quotations [4] and [8] ($n = 4$, M = Ni; $n = 6$, M = Fe, Co); S. Eller, S. Dülsen, K. Yünlü, R. D. Fischer, unpublished ($n = 6$, M = Fe, Ru; $n = 8$, M = Mo, W).

[15] Comparison of the CN-vibrations of **3a**, **4a** and **6a**: IR: $\tilde{\nu} = 2052$(s), 2075(vs); 2052(vs), 2065(s); 2045(vs), 2060(s), 2075 cm^{-1} (s); Raman: $\tilde{\nu} = 2065$(m), 2087(vs), 2130(s); 2071(m), 2081(vs), 2120(s); 2066(m), 2083(s), 2124 cm^{-1}) (m).

[16] IS/IQ ([mm s^{-1}]; standard: SnO_2; 22 °C): 1.3058/3.4580 (symmetr. doublet); −200 °C, 1.2217/3.3048, 1.5258/3.3839 (two symmetr. doublets only after computer fitting). Regarding the IS/IQ data of a Me_3Sn compound with tbp- and ψ-T_d configurated Me_3Sn building blocks see R. Barbieri, A. Silvestri, F. Huber, D.-C. Hager, *Inorg. Chim. Acta 55* (1981) L13. − ^{57}Fe (standard, α-Fe, room temp.) −0.0927/0. We thank *C. Meyer, C. Mohr* and Prof. Dr. *K. Nagorny*, Hamburg, for the measurements.

[17] Unpublished results, Prof. *R. K. Harris*, Durham University (England).

[18] M. Adam, A. K. Brimah, X.-F. Li, R. D. Fischer, unpublished.

[19] Complete loss of H_2O and $C_4H_8O_2$ (high vacuum, ca. 60 °C) leads back to **4a** (control by X-ray powder diagram; renewed easy ion-exchange).

[20] Cf. D. J. Williams, *Angew. Chem. 96* (1984) 637; *Angew. Chem. Int. Ed. Engl. 23* (1984) 690; D. S. Chemla, J. Zyss (Eds.): *Nonlinear Optical Properties of Organic Molecules and Crystals*, Vol. I and II. Academic Press, New York 1987.

[21] Regarding a systematic study of numerous inclusion compounds of uncharged organometallic compounds see W. Tam, D. F. Eaton, J. C. Calabrese, I. D. Williams, Y. Wang, A. G. Anderson, *Chem. Mater. 1* (1989) 128.

Spontaneous Oxidation and in-situ Polymerization of Pyrrole in Channels of the Three-Dimensional Coordination Polymer $[(Me_3Sn)_3Fe^{III}(CN)_6]_\infty$ **

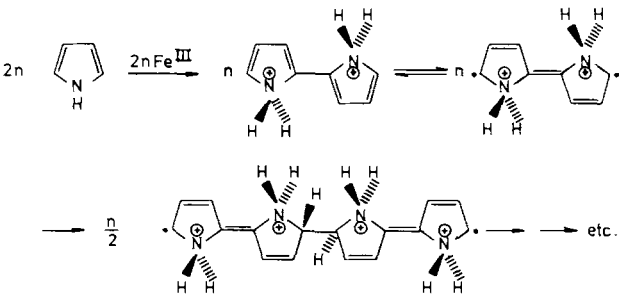
By *Peter Brandt, R. Dieter Fischer,* Enrique Sanchez Martinez* and *Ricardo Diaz Calleja**

The zeolite-like coordination polymer $[Fe^{III}(\mu\text{-}CN\cdot Me_3Sn\cdot NC)_3]_\infty \triangleq [(Me_3Sn)_3Fe^{III}(CN)_6]_\infty$ **1** oxidizes ferrocene[1] as well as numerous metal and ammonium iodides under encapsulation of the respective remaining cation $A^\oplus$ ($Cp_2Fe^\oplus$, $1/nM^{n\oplus}$, $R_4N^\oplus$ etc.) in the spacious channels[1,2] of the negatively charged host lattice afforded after reduction of its Fe^{III} ions. The resulting cation-"intercalates" of the type $[(A_x(Me_3Sn)_3Fe^{II}_xFe^{III}_{1-x}(CN)_6]_\infty$ $(1 \geq x > 0)$ – type I – are not only of interest as novel ion-exchangers and chemical storage materials,[2] but also as potential cation conductors. We describe here primarily the novel cation-encapsulation compound **2** [Eq. (1)], whose guest ions $A^\oplus$ consist of oligomerized and/or polymerized[17a] pyrrole (Ppy) units, and might therefore also give rise to a more pronounced *electronic* conductivity than e.g. **1** and type I systems with $x < 1$.[3]

$$\underset{\textbf{1 (orange)}}{[(Me_3Sn)_3Fe^{III}(CN)_6]_\infty} \xrightarrow{\text{pyrrole}} \underset{\textbf{2 (black)}}{[(Ppy)(Me_3Sn)_3Fe^{II}(CN)_6]_x} \qquad (1)$$

Ppy ≙ $[1/n(C_4H_5N)_n]^\oplus$, n = average degree of oligomerization/polymerization

1 reacts spontaneously with freshly distilled pyrrole (and also pyridine[17b]) at room temperature,[4] but not with thiophene. The salts $K_3[Fe(CN)_6]$ and $[nBu_4N]_3[Fe(CN)_6]$, which do not form inclusion compounds, oxidize neither pyridine nor pyrrole. The strict absence of $Fe^{III}(CN)_6$ units, apparent from both the ν(CN) region of the IR spectrum[5] and the diamagnetism of **2**, supports, in accordance with the elemental analyses,[6] the assumption that each pyrrole molecule transfers one electron to a Fe^{III} ion[17c] of the host after entering a channel of **1**. While the diamagnetism would at least advocate for the pairwise dimerization of all $C_4H_5N^{\cdot\oplus}$ radical cations, the deep "color" and the comparatively good conductivity of **2** suggest spontaneous oligomerization or polymerization (Scheme 1).



Scheme 1. Conceivable initial steps of the oxidative polymerization of pyrrole in channels of **1**.

The electrical conductivity σ[7] of **2** exceeds that of freshly prepared and "aged" (irradiated[8]) **1** (i.e. of **1** and **1'**, respectively) as well as that of the type I reference systems **3**–**5**[9] (cf. Table 1) by at least three orders of magnitude (Table 2

Table 1. General properties of the samples **1**–**5**.

	Sample Composition	Color	Dec.-temp. [°C]	μ_{eff} [B.M.]
1	$[(Me_3Sn)_3Fe^{III}(CN)_6]_\infty$	orange	180	2.18
1'	[a]	blue-green	ca. 110	1.08 [b]
2	$[(C_4H_5N)(Me_3Sn)_3Fe^{II}(CN)_6]_\infty$	black	ca. 250	diamagn.
3	$[Cp_2Fe^{III}(Me_3Sn)_3Fe^{II}(CN)_6]_\infty$	deep blue	ca. 80	3.65 [1]
4	$[Li_{0.3}(Me_3Sn)_3Fe^{II}_{0.3}Fe^{III}_{0.7}(CN)_6]_\infty$	yellow	ca. 200	1.54
5	$[Fe^{II}_{0.1}(Me_3Sn)_3Fe^{II}_{0.2}Fe^{III}_{0.8}(CN)_6]_\infty$	green	ca. 200	2.43

[a] Sample **1'** has the same composition as **1**; structural details are still unknown. [b] Exhaustive ageing, bright blue sample.

[*] Prof. Dr. R. D. Fischer, Dipl.-Chem. P. Brandt
Institut für Anorganische und Angewandte Chemie der Universität
Martin-Luther-King-Platz 6, D-2000 Hamburg 13 (FRG)
Prof. Dr. R. Diaz Calleja, Dr. E. Sanchez Martinez
E.T.S. Ingenieros Industriales, Universidad Polytecnica
Camino Vera, E-46071 Valencia (Spain)

[**] This work was supported by the Deutsche Forschungsgemeinschaft and the Fonds der Chemischen Industrie (*R. D. F.* and *P. B.*).

Table 2. Arrhenius parameters and room temperature conductivity of samples **1–5**.

Sample	Preexponential factor σ_0 [S cm^{-1}]	Activation energy E_a [eV]	σ [S cm^{-1}]	T [K]
1	[a]		3.74×10^{-8}	290
1'	1.21×10^{-3}	0.86	7.42×10^{-11}	300
2	1.65×10^{-1}	0.39	7.02×10^{-5}	300
3	3.0×10^{-3}	0.96	2.60×10^{-11}	300
4	10^{-1}	0.98	4.94×10^{-10}	300
5	1.5×10^{-4}	0.50	8.51×10^{-9}	300

[a] $\ln\sigma$ is not proportional to T^{-1}.

and Fig. 1). The absolute value of σ, however, rules out the presence of pure "highly conducting" polypyrrole[10] in **2**. The H-content of **2** also turns out to be too high for polymeric Ppy chains with ideally conjugated double bonds throughout. Although the IR spectra of the Ppy units of **2** and of the cation intercalate "$Ppy_{0.34}FeOCl$" **6**[11] (prepared recently

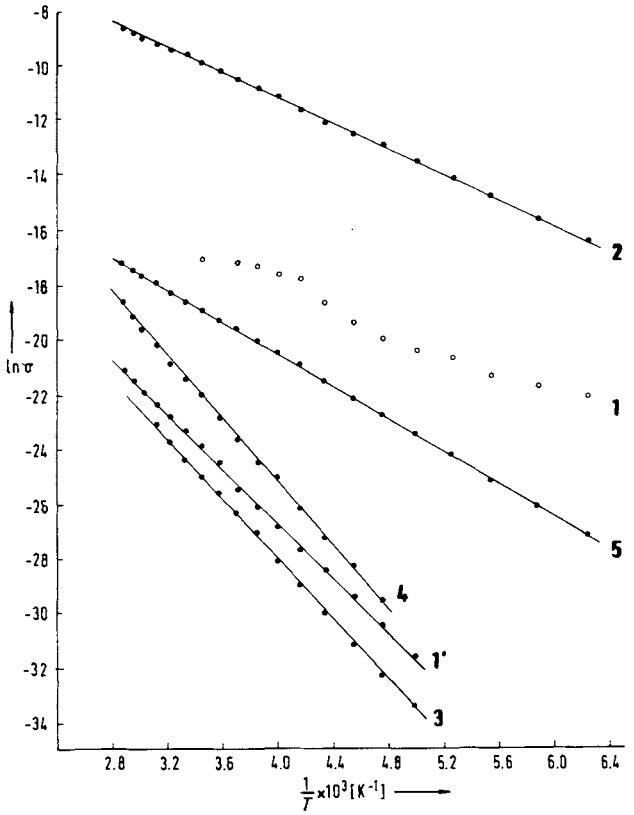


Fig. 1. Temperature dependence of ln σ of the samples **1–5** (see also Tables 1 and 2).

from pyrrole and $Fe^{III}OCl$) strongly resemble each other, the Ppy in the partially reduced FeOCl is likely to be more exhaustively oxidized than the Ppy in **2**. Thus the σ-value of **6**[11] exceeds that of **2** by a factor of 10^3. The significant deviations of the linear $\log\sigma$-vs-T^{-1} plot ($200\,K < T < 340\,K$) of **2** from the two almost parallel $\log\sigma$-vs-T^{-1} curve sections of **6** and host-free $(Ppy)(NO_3)_{0.27}$[11] make it very unlikely that the conductivity of **2** is dominated by only small amounts of non-encapsulated (i.e. externally chemisorbed) "highly conducting" Ppy.[12] It cannot be fully ruled out, however, that the enhanced semiconductivity of **2**[13] may at least in part be due to a particularly high mobility of the charge-compensating protons[14, 17b] which have only formally been attributed to N-atoms of the Ppy chain in Scheme 1.

In view of the approximate cross-section of ca. 6.8 Å of the parallel channels running through the starting compound **1**,[1] the oxidative in-situ oligomerization (or polymerization) of pyrrole in **1** should proceed without chain-branching (cross-linking) and charge transfer interactions between neighboring Ppy chains (formation of ideal "molecular wires"[15]). Some first results of similar experiments with zeolites as host systems of Ppy have most recently been reported.[16]

Received: April 3, 1989;
revised: June 19, 1989 [Z 3272IE]
German version: *Angew. Chem. 101* (1989) 1275

CAS Registry numbers:
$[(Me_3Sn)_3Fe^{III}(CN)_6]_\infty$, 117341-33-0; pyrrole, 109-97-7; polypyrrole, 30604-81-0.

[1] P. Brandt, A. K. Brimah, R. D. Fischer, *Angew. Chem. 100* (1988) 1578; *Angew. Chem. Int. Ed. Engl. 27* (1988) 1521.

[2] S. Eller, P. Brandt, A. K. Brimah, P. Schwarz, R. D. Fischer, *Angew. Chem. 101* (1989) 1274; *Angew. Chem. Int. Ed. Engl. 28* (1989) 1263.

[3] The simultaneous presence of transition metal ions in different oxidation states (e.g. in the case of type I when $x < 1$) should likewise make electron hopping possible.

[4] Synthesis of **2**: 3 g (4.3 mmol) of **1** was placed on a frit under an atmosphere of N_2 and covered with a layer of 5 mL of freshly distilled pyrrole. The undissolved solid remaining on the frit first turned green and then black. After 30 min at ca. 20 °C the excess pyrrole was filtered off and the solid product washed with CH_2Cl_2 and dried in vacuo (30 °C). Elemental analysis, calculated for $C_{19}H_{32}N_7FeSn_3$: C 29.62, H 4.19, N 12.73, Fe 7.25, Sn 46.22%; found: C 29.53, H 4.22, N 12.48, Fe 7.29, Sn 44.03%.

[5] ν(CN)-absorptions (in cm^{-1}, IR): **2**: 2050 (s, br); **1**: 2141(vs), 2080(w).

[6] The analytical data (see [4]) lead to the significant ratios H(Ppy)/N(Ppy) 6.11, C(Ppy)/N(Ppy) 4.61, Sn/N(Ppy) 3.42; cf. the values quoted for "$Ppy(ClO_4)_{0.33}$" [10b]: H/N 3.37, C/N 3.94.

[7] Cylindrical pellets of **1** to **5** (diameter: 1 cm, height: 1–2 mm) were prepared under a pressure of 5×10^8 Pa. The resistances were measured in a non-commercial apparatus (evacuated corundum pot, gilted electrodes, resistance thermometer Pt-100, Eurotherm Single Loop Communication Controller 820, Hewlett-Packard Multimeter 4329A).

[8] Synthesis of **1'**: orange-yellow **1** was exposed under air, either for several months to daylight, or just a week to a UV lamp. The color changed to green and then to blue; concomitant decrease of μ_{eff}. IR, $\tilde{\nu}$[cm^{-1}]: ν-CN, 2142(vs), 2085(vs), δ-$Fe^{II}C$, 600(w), ν-SnC, 555(s), ν-$Fe^{II}C$, 412(m). Elemental analysis: As for **1**.

[9] Synthesis of **4** and **5** according to the procedure given in Ref. [2]; correct elemental analyses (C, H, N, Fe); for **3** see [1].

[10] Cf. a) K. K. Kanazawa, A. F. Diaz, M. T. Krounbi, G. B. Street, *Synth. Met. 4* (1981) 119; b) G. B. Street, T. C. Clarke, M. Krounbi, K. Kanazawa, V. Lee, P. Pfluger, J. C. Scott, G. Weiser, *Mol. Cryst. Liq. Cryst. 83* (1982) 253, and [11] and references cited therein.

[11] M. G. Kanatzidis, L. M. Tonge, T. J. Marks, H. O. Marcy, C. R. Kannewurf, *J. Am. Chem. Soc. 109* (1987) 3797.

[12] The consideration of a conceivable increase in the conductivity (of **2**) by a percolation mechanism was initiated by a referee.

[13] Films of uncharged Ppy are practically insulating: cf. [10b].

[14] Upon evacuation, the rather "mobile", charge compensating protons in zeolites loaded with CdS apparently recombine with S^{2-} ions: $[CdS\cdot2H^{\oplus}\cdot zeol^{2\ominus}] \rightleftharpoons [Cd^{2\oplus}\cdot zeol^{2\ominus}] + H_2S$; cf. N. Herron, Y. Wang, M. M. Eddy, G. D. Stucky, D. E. Cox, K. Moller, T. Bein, *J. Am. Chem. Soc. 111* (1989) 530.

[15] Cf. a) F. Vögtle: *Supramolekulare Chemie*, B. G. Teubner, Stuttgart 1989, Chap. 10.5 and 11.1; b) G. A. Ozin, A. Kuperman, A. Stein, *Angew. Chem. Adv. Mater. 101* (1989) 373; *Angew. Chem. Int. Ed. Engl. Adv. Mater. 28* (1989) 359; *Adv. Mater. 1989*, 69.

[16] a) Cf. [15b]; b) T. Bein, P. Enzel, *197th. ACS Nat. Meet. Dallas, Tx, 9.–14. April 1989*, Abstr. INOR 135; c) *Chem. Eng. News 67* (1989) No. 17.

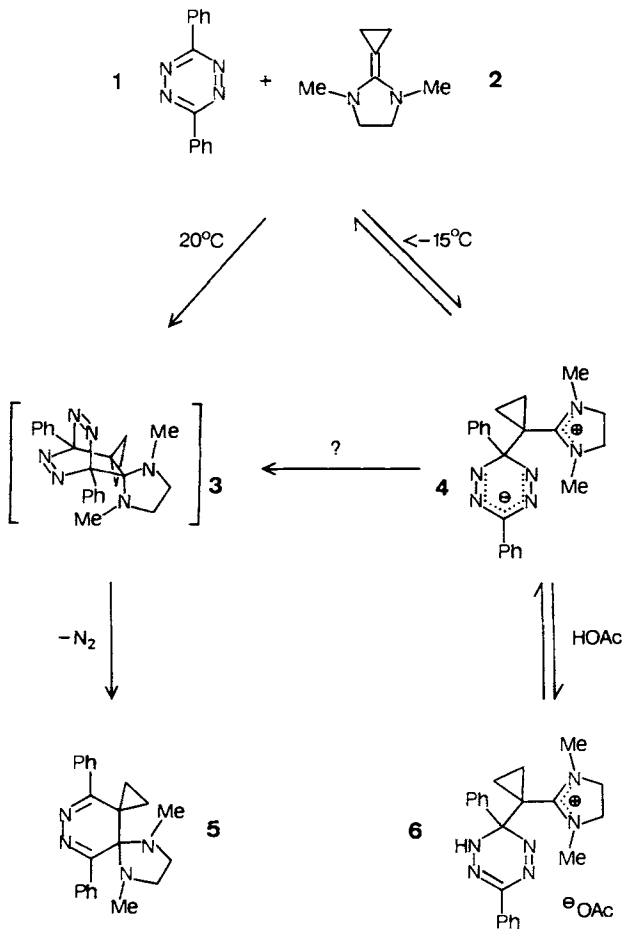
[17] Note added in proof: a) Quite unexpectedly, at least some of the Ppy encapsulated in **2** can be liberated by ion-exchange (according to Ref. [2]) without notable color change of the solid. b) The conductivity of the likewise diamagnetic, but brown reaction product of **1** with pyridine which could also contain "charge-compensating protons" is notably lower than 10^{-9} S cm^{-1}. c) In aqueous solution, a clean 1:1 (i.e. oxidant/pyrrole) oxidation of pyrrole has so far not been observed; see: S. P. Armes, *Synth. Met. 20* (1987) 365. d) First attempts to dope **2** with I_2 did not lead to a significant increase of σ.

Isolation of a Zwitterion in a Diels–Alder Reaction with Inverse Electron Demand**

By *Klaus-Peter Hartmann* and *Manfred Heuschmann**

Cycloadditions of electron-deficient tetrazines with electron-rich ketene acetals[1] have served as impressive model reactions for the chemist's understanding of Diels–Alder reactions with inverse electron demand.[2] It is generally assumed that the reaction products, functionalized pyridazines, are formed in a reaction cascade of cycloaddition, nitrogen extrusion, and elimination of alcohol, thiol or amine. Despite extensive and detailed investigations not much is known of the individual steps of the reaction. We report here on the first detectable two-step Diels–Alder reaction of a tetrazine with a ketene *N,N*-acetal.

From the high reactivity[3] of 2-cyclopropylidene-imidazolidine **2** in inverse Diels–Alder reactions it may be expected that it reacts with tetrazines even at very low temperatures and should thus enable the isolation of thermally labile intermediates. Indeed, the deep-red solution of the diphenyltetrazine **1** in [D_2]dichloromethane decolorized even at $-60\,^{\circ}C$ after addition of **2**. A yellow solid crystallized from the viscous solution; at temperatures above $10\,^{\circ}C$ this redissolved, and concomitant elimination of nitrogen resulted in the formation dihydropyridazine **5**. Small amounts of tetrazine **1** were also detectable (Scheme 1).



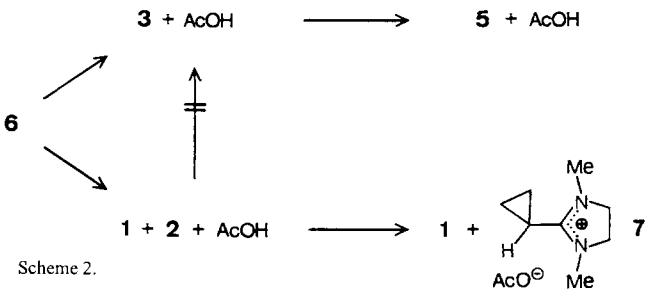
Scheme 1.

The ^1H NMR spectrum of the labile intermediate is fully consistent with the structure of the zwitterion **4**. The signals for the *N*-methyl and *N*-methylene groups[4] resemble those of the dihydroimidazolium iodide **8**[5] (cf. **7** in Scheme 2, $I^{\ominus}$ instead of $OAc^{\ominus}$) and lie markedly further downfield than in the final product **5**. On the other hand, the phenyl groups of **4** absorb further upfield than those of **5**, as might be expected for a dihydrotetrazine anion.[7] In toluene, **4** crystallized in 88% yield at $-15\,^{\circ}C$; upon warming the mixture to room temperature, we isolated **5** in 78% yield. The sparing solubility of **4** in unpolar, polar aprotic and protic solvents and its temperature sensitivity precluded an accurate spectroscopic characterization of the zwitterion.

As could be expected from the pK_A values of dihydrotetrazines,[7] acetic acid (or [D_4]acetic acid) protonates the zwitterion and leads to a salt that is readily soluble in [D]chloroform and [D_2]dichloromethane and whose ^1H and ^{13}C NMR spectra[8] confirm the structure **6**. The signals correlate well with the chemical shifts of 4,5-dihydroimidazolium ions[5] and 1,6-dihydrotetrazines.[7] The change in the spectrum as a function of the acid concentration as well as the reactivity is consistent with an equilibrium between **4** and **6**. Upon warming to room temperature, **6** also loses nitrogen but more slowly than **4**. The ^1H NMR spectrum of the resulting product was identical with that of isolated dihydropyridazine **5** in $CDCl_3/CD_3CO_2D$. In addition, we identified ca. 5–10% of the tetrazine **1**.

Two fundamentally different mechanisms can explain these observations. Either the zwitterion **4** is an intermediate of the Diels–Alder reaction and closes the ring in an intramolecular reaction to give the bicyclic adduct **3**, or **4** is formed in a reversible side reaction and splits again into the starting compounds **1** and **2**, which then form the same adduct **3** in a concerted cycloaddition. In both cases **3** then loses nitrogen in a rapid secondary [4 + 2]-cycloreversion. Zwitterions are often formed in side reactions upon reaction of tetrazines and triazines with ketene acetals,[9a,10] but all attempts to prove their participation in two-step cycloadditions have thus far failed.

Since the dihydropyridazine **5** is formed from the protonated zwitterion **6** even in the presence of an excess of acetic acid, a concerted cycloaddition, which requires a retrocleavage to the starting compounds **1** and **2**, can be ruled out: independent experiments show that the cyclopropylidene-imidazoline **2** reacts much more rapidly with acetic acid than with tetrazine **1** (Scheme 2). Both at $-30\,^{\circ}C$ as well as at



Scheme 2.

$20\,^{\circ}C$ only the dihydroimidazolium acetate **7** is formed when **2** is added dropwise to a mixture of tetrazine **1** and acetic acid (1:2) in $CDCl_3$. Even after prolonged heating of the mixture for several hours at $80\,^{\circ}C$ we could not detect any trace of the dihydropyridazine **5**. Consequently, in the conversion of **6** into **5**, which proceeds in ca. 90–95% yield, no free ketene aminal **2** can occur in the presence of acetic acid; hence, the Diels–Alder reaction proceeds in two steps.

[*] Priv.-Doz. Dr. M. Heuschmann, Dipl.-Chem. K.-P. Hartmann
Institut für Organische Chemie der Universität
Karlstrasse 23, D-8000 München 2 (FRG)

[**] This work was supported by the Deutsche Forschungsgemeinschaft and the Fonds der Chemischen Industrie.

In cycloadditions of other ketene acetals, too rapid a retrocleavage of the zwitterions to the starting compounds prevents any decision regarding two-step or concerted mechanisms.[10] Retrocleavage of the zwitterion **4** into the starting compounds is observed only as an insignificant side reaction, which with other substitutions, however, can easily become the major reaction. The ca. 14 kcal mol^{-1} higher strain energy of methylenecyclopropane[11] compared to that of cyclopropane, which must be provided for the formation of the cyclopropylidene-imidazolidine **2** from the zwitterion **4**, specifically retards this retrocleavage and thus enables the detection of the two-step mechanism. On the other hand, to a first approximation, the cyclopropyl group has no effect on the difference in the activation energies of concerted and two-step cycloaddition. One may therefore conclude that Diels–Alder reactions of ketene acetals, at least of ketene *N,N*-acetals, with tetrazines generally proceed in two steps. This provides a new basis on which to discuss previously unexplainable phenomena, e.g. the special position of the ketene *N,N*-acetals with regard to regioselectivity and its solvent dependence.[9]

Received: April 19, 1989 [Z 3301 IE]
German version: *Angew. Chem. 101* (1989) 1288

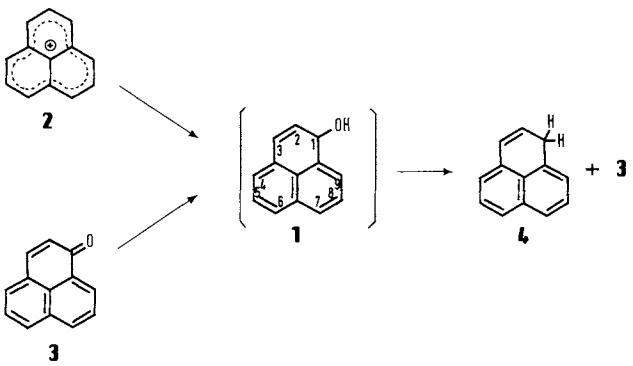
CAS Registry numbers:
1, 6830-78-0; **2**, 109153-25-5; **4**, 122172-50-3; **5**, 122172-49-0; **6**, 122188-68-5.

[1] D. L. Boger, *Chem. Rev. 86* (1986) 781–793; *Tetrahedron 39* (1983) 2869–2939.
[2] J. Sauer, R. Sustmann, *Angew. Chem. 92* (1980) 773–801; *Angew. Chem. Int. Ed. Engl. 19* (1980) 779–814; R. Sustmann, *Pure Appl. Chem. 40* (1974) 569–593.
[3] U. Gruseck, M. Heuschmann, *Tetrahedron Lett. 28* (1987) 6027–6030.
[4] **4**: ^{1}H-NMR (80 MHz, CD_2Cl_2, 10° C): δ = 0.83, 1.47 (2 m_c, *c*Pr); 3.09 (s, 2N-Me); 3.56 (s, 2N-CH_2); 6.8–7.7 (m, 2Ph).
[5] U. Gruseck, M. Heuschmann, *Chem. Ber. 120* (1987) 2053–2064.
[6] **5**: ^{1}H-NMR (80 MHz, $CDCl_3$): δ = 1.08, 1.25 (2m_c, *c*Pr); 2.32 (s, 2N-Me); 3.05 (s, 2N-CH_2); 7.2–8.1 (m, 2Ph). ^{13}C-NMR (20 MHz, $CDCl_3$): δ = 11.2 (t, *c*Pr); 36.5 (q, N-Me); 52.5 (t, N-CH_2); 21.9, 75.2, 160.8, 169.8 (4s, dihydropyridazine); 127.7, 127.9, 128.9, 129.0, 129.0, 129.1 (6d, *o*-, *m*-, *p*Ph); 135.3, 140.1 (2s, *i*Ph).
[7] A. Counotte-Potman, H. C. van der Plas, B. van Heldhuizen, *J. Org. Chem. 46* (1981) 3805–3810.
[8] **6**: ^{1}H-NMR (80 MHz, $CDCl_3$, −16 °C): δ = 1.31, 1.52 (2m_c, *c*Pr); 3.08 (s, 2N-Me); 3.78 (m_c, 2N-CH_2), 7.1–7.7 (m, 2Ph). ^{13}C-NMR (**4** + 1.1 equiv. CD_3CO_2D, 20 MHz, CD_2Cl_2, −19 °C): δ = 11.4 (t, *c*Pr); 22.7 (s, *c*Pr); 35.3 (q, N-Me); 49.9 (t, N-CH_2); 80.8, 154.8 (2s, dihydrotetrazine); 123.4, 127.8, 128.1, 128.1, 128.5, 129.6 (6d, *o*-, *m*-, *p*Ph); 134.5, 136.9 (2s, *i*Ph); 167.4 (s, imidazolium-C-2). ^{13}C-NMR (**4** + 2.1 equiv. CD_3CO_2D, 20 MHz, CD_2Cl_2, −16 °C): δ = 11.4; 21.5; 35.0; 49.9; 77.0, 153.2; 124.5, 127.4, 128.3, 128.6, 129.0, 130.0; 132.0, 133.4; 165.4.
[9] a) B. Burg, W. Dittmar, R. Reim, A. Steigel, J. Sauer, *Tetrahedron Lett. 1975*, 2897–2900; b) K. Müller, J. Sauer, *Tetrahedron Lett. 25* (1984) 2541–2544.
[10] Private communication from Prof. Dr. *J. Sauer*, Regensburg.
[11] A. Greenberg, J. F. Liebman: *Strained Organic Molecules*, Academic Press, New York 1978, pp. 66 and 94; N. C. Baird, M. J. S. Dewar, *J. Phys. Chem. 50* (1969) 1262–1274.

1-Phenalenol: Isolation and Disproportionation

By *Yoshikazu Sugihara, Hidetoshi Kawanaka,* and *Ichiro Murata**

1-Phenalenol **1** is of fundamental importance for phenalene chemistry.[1] This compound has been suggested as a probable intermediate generated in situ in the hydrolysis of the phenalenium ion **2**[2] and the hydride reduction of phenalenone **3**.[3] However, attempts to isolate and characterize **1** have so far failed, presumably owing to its marked propensity to disproportionate into phenalene **4** and phenalenone **3**.[1, 2, 3a, 3c] We wish to report for the first time the isolation of **1** through the controlled hydride reduction of **3** and the disproportionation reaction of **1**.



For the reduction of **3**, we used sodium borohydride in the presence of ceric chloride in methanol.[4] To a solution of **3** (100 mg) and ceric chloride hexahydrate (197 mg) in methanol (10 mL) was added sodium borohydride (90 mg) in small portions with ice cooling. Usual workup of the reaction mixture afforded equal amounts of **3** and **4** in a total isolated yield of 96%. When the reduction was conducted in a dilute methanol solution (80 mL) with a large excess of sodium borohydride (300 mg), however, a single new spot due to neither **3** nor **4** was detected on the thin layer chromatogram. After several attempts, a new product could be separated by the following procedures.[5] The solvent was evaporated in vacuo to give a colorless solid which was extracted into dichloromethane containing a small amount of triethylamine. The organic layer was poured into water through cotton placed on a funnel, separated, and concentrated. Recrystallization of the residue from hexane below 30 °C afforded colorless needles (m.p. 64.5–65.0 °C, 83% yield). The elemental analysis[6] and the spectral data of this compound (Table 1) are consistent with the structure of **1**, which, however, suffered a very small amount of disproportionation to **3** and **4** as detected by careful ^{1}H NMR inspection.[7]

Table 1. Spectral data of **1**.

400-MHz ^{1}H NMR ($CDCl_3$): δ = 7.74 (d, J = 8.25 Hz, H-7), 7.71 (dt, J = 7.25, 1.28 Hz, H-9), 7.66 (d, J = 8.24 Hz, H-6), 7.51 (dd, J = 8.25, 7.25 Hz, H-8), 7.35 (dd, J = 8.24, 6.96 Hz, H-5), 7.18 (d, J = 6.96 Hz, H-4), 6.74 (dd, J = 9.79, 1.10 Hz, H-3), 6.18 (dd, J = 9.79, 4.03 Hz, H-2), 5.52 (m, H-1), 2.19 (d, J = 9.16 Hz, OH)

100-MHz ^{13}C NMR ($CDCl_3$): δ = 135.6, 132.5, 129.2 (C-3a, C-6a, C-9a), 129.3 (C-2), 128.3 (C-3), 128.0 (C-6), 127.9 (C-9), 127.8 (C-7), 126.5 (C-8), 126.1 (C-9b), 126.0 (C-5), 124.7 (C-4), 66.0 (C-1)

EI-MS: *m/z* 182 ($M^{\oplus}$, 0.5%), 181 ($M^{\oplus}-H$, 3.0), 180 ($M^{\oplus}-H_2$, 100), 165 ($M^{\oplus}-OH$, 7.0), 152 ($M^{\oplus}-H_2-CO$, 15.6)

IR (CH_2Cl_2): $\tilde{\nu}$ = 3420 cm^{-1}

The disproportionation of **1** was studied by means of time-dependent ^{1}H NMR spectroscopy, labeling, and competition reactions. Compound **1** did not undergo disproportionation in deuteriochloroform. In [D_4]methanol distilled from potassium carbonate, however, **1** disproportionated slowly but cleanly into **3** and **4** with a half-life of 7 d. Since the

[*] Prof. Dr. I. Murata, Dr. Y. Sugihara, H. Kawanaka
Department of Chemistry, Faculty of Science
Osaka University, Toyonaka, Osaka 560 (Japan)

disproportionation reaction occurred in deuteriochloroform in the presence of a small amount of [D_1]acetic acid (**1**:[D_1]acetic acid = 30:1) with a half-life of ca. 30 min, protic substances are involved in the reaction. During the ^{1}H NMR measurement no signals ascribable to the reaction intermediate could be observed.

1-Deuteriophenalenol [D_1]**1** was prepared by reduction of **3** with sodium borodeuteride in [D_1]methanol followed by washing with water. When [D_1]**1** was subjected to reaction with a small amount of acetic acid in benzene, the clean disproportionation reaction was complete within 2 d. The products were separated into **3** and **4** by column chromatography with deactivated alumina (5% H_2O). ^{1}H NMR (500 MHz) spectroscopy revealed that no deuterium is incorporated into **3** whereas two deuterium atoms are present in **4** ([D_2]**4**). Since the vicinal coupling patterns of H-3, H-4, H-6, H-7, and H-9 of [D_2]**4** are the same as those of undeuterated **4**, the deuterium atoms are not located at the 2-, 5-, and 8-positions. As expected, the intensities of the ^{1}H NMR signals for H-2, H-5, and H-8 were found to be the same. From the integrated intensity of each proton with respect to that of the well-separated H-2 signal, it can be concluded that the two deuterium atoms are distributed at the 1-, 3-, 4-, 6-, 7-, and 9-positions of **4** with appreciable scrambling as shown in Figure 1. Because of the fast hydrogen migration characteristic of the phenalene skeleton,[1] the distribution of two deuteriums in [D_2]**4** could not be explained explicitly. Nevertheless, these findings mean that the deuterium introduced in [D_1]**1** is transferred directly from the 1-position of [D_1]**1** to another molecule of [D_1]**1** with the formation of [D_2]**4** together with **3** (Scheme 1).

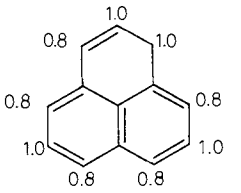
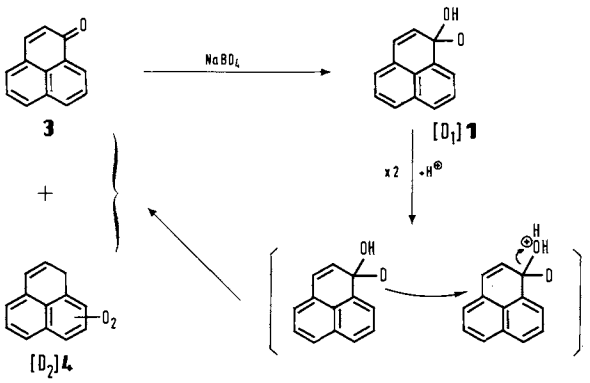


Fig. 1. Integrated intensities of the protons in [D_2] **4**.



Scheme 1. Conceivable mechanism for the disproportionation of **1**.

In the presence of carbonyl compounds (ca. 1 equivalent) such as benzophenone, 1-naphthaldehyde, and phenalanone, the disproportionation of **1** preferentially took place with a small amount of acetic acid in benzene. Alcohols, which should be produced by Meerwein–Pondorf–Verley reduction, were not found. Hydride is transferred more rapidly to phenalenium ion than to added ketone or aldehyde, since the cation has a lower reduction potential.[8]

Compound **1**, as has been inferred for a long time, undergoes very facile disproportionation in the presence of protic substances. The present work opens a possible route to the unknown cycloheptatrienol and cyclopropenol.

Received: May 8, 1989 [Z 3325 IE]
German version: *Angew. Chem. 101* (1989) 1258

CAS Registry numbers:
1, 91598-47-9; [D_1] **1**, 122114-41-4; **3**, 548-39-0; **4**, 203-80-5; [D_2] **4**, 122144-54-1.

[1] D. H. Reid, *Q. Rev. Chem. Soc. 19* (1965) 274.
[2] a) R. Pettit, *Chem. Ind. (London) 1956*, 1306; b) *J. Am. Chem. Soc. 82* (1960) 1972.
[3] a) V. Boekelheide, C. E. Larrabee, *J. Am. Chem. Soc. 72* (1950) 1240; b) R. M. Pagni, C. R. Watson, *Tetrahedron 29* (1973) 3807; c) P. Boudjouk, P. D. Johnson, *J. Org. Chem. 43* (1978) 3979.
[4] a) J. L. Luche, L. Rodriguez-Hahn, P. Crabbe, *J. Chem. Soc. Chem. Commun. 1978*, 601; b) J. L. Luche, *J. Am. Chem. Soc. 100* (1978) 2226.
[5] All experiments were carried out in argon atmosphere and the solvents used were degassed by bubbling argon through them before use.
[6] Found: C, 85.69; H, 5.55%. Calc. for $C_{13}H_{10}O$: C, 85.69; H, 5.53%.
[7] From comparison of the height of the H-2 signal (dd) of **1** with that of H-9 (d) of **3**, the amount of **3** produced by the disproportionation of **1** was roughly estimated at less than 0.6%.
[8] a) H. Adkins, F. W. Cox, *J. Am. Chem. Soc. 60* (1938) 1151; b) F. W. Cox, H. Adkins, *ibid. 61* (1939) 3364; c) R. H. Baker, H. Adkins, *ibid. 62* (1940) 3305.

Synthesis and Structure of $[(C_5H_5)_2TiS_4AsCH_3]$—a New Reagent for the Synthesis of Sulfur-Rich Heterocycles**

By *Ralf Steudel,** *Birger Holz*, and *Joachim Pickardt*

Titanocenepentasulfide, Cp_2TiS_5 **1** (Cp = η^5-C_5H_5), has proved extremely valuable as a reagent for the synthesis of sulfur- and selenium-containing homo- and heterocycles since it reacts under mild conditions with numerous sulfur and selenium halides to give the corresponding ring compounds with elimination of Cp_2TiCl_2. Twelve compounds of the types S_n and Se_xS_y ($n = 6-20$; $x = 1-3$; $x + y = 6-8$) have been prepared in this way and obtained in pure form.[1] The symmetrical binuclear complexes $Cp_4Ti_2S_4$ and $Cp_4Ti_2S_6$ also react with SCl_2, S_2Cl_2, $SeBr_2$, and Se_2Cl_2 with elimination of Cp_2TiCl_2, a mononuclear titanocene complex being the main product[2] [see, e.g., Eq. (a)]. In an analogous way, we have now obtained the first arsenic-containing titanocene polysulfide complex [Eq. (b)].

$$[Cp_2Ti(\mu\text{-}S_2)_2TiCp_2] + SCl_2 \rightarrow \underset{\mathbf{1}}{Cp_2TiS_5} + Cp_2TiCl_2 \qquad (a)$$

$$[Cp_2Ti(\mu\text{-}S_2)_2TiCp_2] + CH_3AsCl_2 \xrightarrow[CCl_4]{20\,^\circ C} \underset{\mathbf{2}}{[Cp_2Ti(\mu\text{-}S_2)_2AsCH_3]} + Cp_2TiCl_2 \qquad (b)$$

Compound **2** was obtained in 20% yield as black-red crystals, which are air-stable at 20 °C.[3] Compound **2** is readily

[*] Prof. Dr. R. Steudel, Dipl.-Chem. B. Holz, Prof. Dr. J. Pickardt
Institut für Anorganische and Analytische Chemie
der Technischen Universität, Sekr. C 2
Strasse des 17. Juni 135, D-1000 Berlin 12

[**] Sulfur Compounds, Part 128. This work was supported by the Deutsche Forschungsgemeinschaft and the Verband der Chemischen Industrie. Part 127: R. Steudel, G. Holdt, T. Göbel, *J. Chromatogr.* 475 (1989) 442.

soluble in CS_2, CH_2Cl_2, and $CHCl_3$, but less soluble in CCl_4. In the mass spectrum (17 eV, 100 °C), the signal for the molecular ion (m/z 396) is observed. In the ^1H NMR spectrum (80 MHz), recorded at 20 °C in $CDCl_3$, three singlets at $\delta = 6.35$ (Cp), 5.86 (Cp), and 0.43 (CH_3) are found.[3] Accordingly, the conformation of the metallacycle is rigid at 20 °C, as found for Cp_2TiS_5, the Cp NMR signals of which coalesce at 90 °C.[6] However, an equivalence of the Cp ligands requires not only ring inversion of the metallacycle but also simultaneous pyramidal inversion at the As atom. The two Cp proton signals in the NMR spectrum of **1** ($CDCl_3$, 80 MHz) are found at $\delta = 6.35$ and 6.09. The first value coincides exactly with that of a Cp signal in the spectrum of **2**. Therefore, this signal can be assigned to the protons of the Cp ligand furthest removed from the methyl group.

A single-crystal X-ray structure analysis[7] revealed that a chair-shaped TiS_4As ring is present in **2**, the methyl group on the arsenic atoms being in axial position (Fig. 1). The molecular structure of **2** strongly resembles that of **1**,[8] insofar as

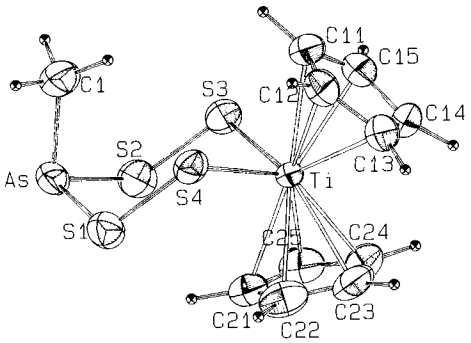


Fig. 1. Molecular structure of **2** in the crystal. Selected distances [pm] and angles [°]: C1-As 195, As-S1 226.4, As-S2 225.9, S1-S4 205.6, S2-S3 205.9, Ti-S4 241.9, Ti-S3 243.0; C1-As-S1 99.0, C1-As-S2 99.6, As-S1-S4 107.4, S1-S4-Ti 111.0, S4-Ti-S3 94.4, Ti-S3-S2 111.1, S3-S2-As 108.3, S2-As-S1 105.9.

angles and distances in the fragment Cp_2TiS_4 are nearly identical in both compounds. Thus, the average distance of the Cp carbon atoms from the titanium atom is 237.4 pm in **1** and 238.2 pm in **2** and the S–Ti–S angle is 94.6° in **1** and 94.4° in **2**. The two S–S distances in **2** (average 205.8 pm) are not only nearly identical to the corresponding distances in **1** (205.9 pm), but also to those in the likewise chair-shaped *cyclo*-hexasulfur (S_6: 206.8 pm[9]). The two As–S distances (226 pm) are somewhat longer than those in As_2S_3 (221 pm) and As_4S_4 (224 pm).[10] Although the molecules of **2** occupy general positions in the crystal, the TiS_4As ring displays nearly C_s symmetry. To a certain extent, this ring resembles that in $[Cp_2Ti(\mu\text{-}S_2)_2C(CH_3)_2]$.[5]

Compound **2** reacts rapidly and quantitatively with SCl_2 or S_2Cl_2 in CCl_4 at 20 °C to give initially Cp_2TiCl_2 and *cyclo*-arsasulfanes CH_3AsS_m, which can be separated and identified by reversed-phase (RP) HPLC and ^1H NMR spectroscopy [Eq. (c)].

$$Cp_2TiS_4AsCH_3 + S_xCl_2 \longrightarrow CH_3AsS_{4+x} + Cp_2TiCl_2 \quad (c)$$
$$x = 1,2$$

The two new compounds CH_3AsS_5 and CH_3AsS_6,[11] along with the known CH_3AsS_7,[12] form a homologous series of heterocyclic compounds, since their ^1H NMR shifts are very similar and their HPLC retention times, expressed as $\ln k'$, are linearly dependent on the ring size $m + 1$, as for sulfur homocycles (Table 1). Therefore, it is very likely that

Table 1. Retention times t_R of CH_3AsS_m and S_n under the same chromatographic conditions ($k' = (t_R - t_0)/t_0$; t_0 = dead time = 1.20 min [13]). The correlation coefficients of the linear regression were better than 0.995.

Ring size		6	7	8	9
CH_3AsS_m:	t_R (min):	2.71	3.19	3.67	–
S_n:	t_R (min):	3.17	3.72	4.80	6.38

$\ln k'_1 = 0.246\,(m+1) - 1.236$; $\ln k'_2 = 0.326\,n - 1.492$.

the structure of CH_3AsS_6 is similar to that of S_7.[15] In contrast to the synthesis of CH_3AsS_7, which is formed from CH_3AsCl_2 and Cp_2TiS_5 in CS_2 under reflux in a reaction whose mechanism is not yet understood, the synthesis according to Equation (c) affords *cyclo*-arsasulfanes of defined ring size.

CH_3AsS_6 undergoes decomposition upon exposure to sunlight in CCl_4 solution with formation of homologous CH_3AsS_m molecules and sulfur rings S_n. Both CH_3AsS_6 and CH_3AsS_7 react slowly with S_2Cl_2 at 20 °C in CCl_4 according to Equation (d).

$$CH_3AsS_m + S_2Cl_2 \longrightarrow CH_3AsCl_2 + S_{m+2} \quad (d)$$
$$m = 6,7$$

In this way it was possible to determine the ring size of the arsasulfanes, since the resulting sulfur rings S_{m+2} could easily be identified by their HPLC retention times (Table 1 and Ref. [14]). CH_3AsCl_2 was identified by ^1H NMR spectroscopy. Since reaction (d) partly takes place during reaction (c), the reaction products always contain, besides CH_3AsS_m, some S_8, especially when S_2Cl_2 is used in excess.[11]

Received: April 28, 1989 [Z 3312 IE]
German version: *Angew. Chem. 101* (1989) 1301

CAS Registry numbers:
2, 122093-47-4; $Cp_2Ti(\mu\text{-}S_2)_2TiCp_2$, 106162-08-7; CH_3AsS_5, 122093-44-1; CH_3AsS_6, 122093-45-2; CH_3AsS_7, 122093-46-3; CH_3AsCl_2, 593-89-5; SCl_2, 10545-99-0; S_2Cl_2, 10025-67-9.

[1] S_6, S_7, S_9, S_{10}, S_{11}, S_{12}, S_{13}, S_{15}, S_{20}, SeS_5, Se_2S_5, and Se_3S_5 have been prepared; see M. Schmidt, B. Block, H. D. Block, H. Köpf, E. Wilhelm, *Angew. Chem. 80* (1968) 660; *Angew. Chem. Int. Ed. Engl. 7* (1968) 632; M. Schmidt, E. Wilhelm, *J. Chem. Soc. Chem. Commun. 1970*, 1111; T. Sandow, J. Steidel, R. Steudel, *Angew. Chem. 94* (1982) 782; *Angew. Chem. Int. Ed. Engl. 10* (1982) 794; R. Steudel, E.-M. Strauss, *ibid. 96* (1984) 356 and *23* (1984) 362; R. Steudel, R. Strauss, *J. Chem. Soc. Dalton Trans. 1984*, 1775; R. Steudel, R. Strauss, D. Jensen, *Chem.-Ztg. 109* (1985) 349; R. Steudel, J. Steidel, T. Sandow, *Z. Naturforsch. B41* (1986) 958; R. Strauss, R. Steudel, *ibid. 43* (1988) 1151.

[2] R. Steudel, D. Jensen, M. Papavassiliou, *Phosphorus Sulfur Silicon 41* (1989) 349, and unpublished results.

[3] $Cp_4Ti_2S_4$ (1.2 g, 2.48 mmol) [4], suspended in 200 mL of CCl_4, was stirred for 10 min and treated with CH_3AsCl_2 (0.214 mL, 2.40 mmol). After ca. 15 h at 20 °C, the precipitate was separated by filtration from Cp_2TiCl_2 and excess starting material, the filtrate was evaporated to dryness, and the residue (0.6 g) was dissolved in CH_2Cl_2. The solution was fractionated by column chromatography on silica gel 40 F_{254} (95 g, column length 55 cm: eluant CH_2Cl_2) (side products: Cp_2TiS_5, S_8, and others). The fractions containing **2** (monitored by HPLC) were combined, evaporated to dryness in vacuo, dissolved in a small amount of CH_2Cl_2, and chromatographically fractionated again (eluent: CCl_4/diethyl ether 70/30 v/v). The fractions with **2** were evaporated and the product was recrystallized from 10 mL of hot CCl_4. Yield: 190 g **2** (0.48 mmol), m.p. 155 °C (dec.). The CH analysis agrees with that calculated. The mass spectrum shows the signal for the molecular ion ($M^{\oplus}$) at m/z 396 and signals for the fragment ions at m/z 332 ($M^{\oplus}$-S_2), 317 ($M^{\oplus}$-S_2CH_3), 276 ($As_2(CH_3)_2S_3$), 261 ($As_2CH_3S_3$), 242 (Cp_2TiS_2), 210 (Cp_2TiS),197 (As_2CH_3S), 178 (Cp_2Ti), and 154 ($AsCH_3S_2$). IR (KBr disc): $\tilde{\nu} = 3090$(m), 2930–2860(w), 1435(m), 1380(w), 1360(w), 1220(w-m), 1025–1018(m), 860(m), 835(vs), 815(sh), 580(m), 490(m), 430(m), 385(sh), 370(m), 340(m), 325(m) cm^{-1}.

[4] D. Giolando, T. B. Rauchfuss, A. L. Rheingold, S. R. Wilson, *Organometallics 6* (1987) 667.

[5] D. M. Giolando, T. B. Rauchfuss, *Organometallics 3* (1984) 487.
[6] H. Köpf, B. Block, M. Schmidt, *Chem. Ber. 101* (1968) 272.
[7] Crystal structure analysis of **2**: space group $P2_1/c$ (Nr. 14): $a = 1333.7(7)$, $b = 809.8(9)$, $c = 1448.4(9)$ pm, $\alpha = 90$, $\beta = 115.13(6)$, $\gamma = 90°$, $V = 1416.25\ 10^6$ pm^3, $Z = 4$, $\varrho_{X\ ray} = 1.86$ g cm^{-3}, $\mu(Mo_{K\alpha}) = 33.47$ cm^{-1}, Syntex $P2_1$ diffractometer, room temperature, $Mo_{K\alpha}$ radiation ($\lambda = 71.069$ pm), $2\theta \leq 50°$; 2088 unique reflections, 1935 with $I \geq 2\sigma(I)$, empirical absorption correction, structure solution with Patterson methods, refinement with anisotropic temperature factors for all atoms except hydrogen, the CH bonds were calculated and not refined: 159 parameters, $R = \Sigma(||F_o| - |F_c||)/\Sigma|F_o| = 0.0643$. Further details of the crystal structure investigation may be obtained from the Fachinformationszentrum Karlsruhe, Gesellschaft für wissenschaftlich-technische Information mbH, D-7514 Eggenstein-Leopoldshafen 2 (FRG), on quoting the depository number CSD-54021, the names of the authors, and the journal citation.
[8] E. F. Epstein, I. Bernal, H. Köpf, *J. Organomet. Chem. 26* (1971) 229.
[9] J. Steidel, J. Pickardt, R. Steudel, *Z. Naturforsch. B33* (1978) 1554.
[10] Review: D. B. Sowerby in I. Haiduc, D. B. Sowerby (Eds.): *The Chemistry of Inorganic Homo- and Heterocycles*, Vol. 2, Academic Press, London 1987, p. 713.
[11] In a typical experiment, **2** (560 mg, 1.41 mmol) was dissolved in 60 mL of CCl_4 and treated with a solution of S_2Cl_2 in CCl_4 (1 mmol S_2Cl_2/mL) added in portions. The initially dark red solution turned bright red and a red precipitate (Cp_2TiCl_2) formed. After each S_2Cl_2 addition, a chromatogram was recorded. A maximum of 2 mol S_2Cl_2 per mole of **2** was used. The ratio of the heights of the peaks assigned to S_8 and CH_3AsS_6 steadily increased with increasing molar ratio of S_2Cl_2:**2**; for a molar ratio of 1:1, the peak ratio was 0.05. ^{1}H NMR spectrum of CH_3AsS_6(CCl_4/$CDCl_3$): singlet at $\delta = 1.85$.
[12] I. Pauli, *Dissertation*, Universität Würzburg 1987: CH_3AsS_7 forms a crown-shaped eight-membered ring with the methyl group in equatorial position. We have been able to reproduce this synthesis. ^{1}H NMR spectrum (CCl_4/$CDCl_3$): singlet at $\delta = 1.80$.
[13] Eluant, methanol: column, 10C18 Radial-Pak (Waters) UV detector (254 nm); for further details see [14]. When methanol/water (90/10 v/v) was used as eluant, the best separation of the sulfur homocycles from the arsasulfanes was achieved.
[14] R. Steudel, H.-J. Mäusle, D. Rosenbauer, H. Möckel, T. Freyholdt, *Angew. Chem. 93* (1981) 402; *Angew. Chem. Int. Ed. Engl. 20* (1981) 394; R. Strauss, R. Steudel, *Fresenius' Z. Anal. Chem. 326* (1987) 543.
[15] R. Steudel, J. Steidel, J. Pickardt, F. Schuster, R. Reinhardt, *Z. Naturforsch. B35* (1980) 1378.

Nitrogenase Model Compounds: $[\mu\text{-}N_2H_2\{Fe(\text{“}N_HS_4\text{”})\}_2]$, the Prototype for the Coordination of Diazene to Iron Sulfur Centers and Its Stabilization through Strong N-H · · · S Hydrogen Bonds**

By *Dieter Sellmann,* Wolfgang Soglowek, Falk Knoch,* and *Matthias Moll*

Biological N_2 fixation is one of the fundamental synthetic processes of nature. It is catalyzed by nitrogenases, and the elucidation of the structure and function of these enzymes constitutes a major task in chemistry and biochemistry. The dominating metal in all nitrogenases is iron in a coordination sphere of sulfur. Most nitrogenases also include molybdenum and some of them vanadium.[1] Recently, however, a nitrogenase type was characterized which contains exclusively iron.[2] This casts doubt on the presumption prevalent for many years that the heterometal centers Mo or V ought to be the N_2 bonding site in Mo/Fe or V/Fe nitrogenases;[1] it rather demonstrates that the iron centers could very well be the N_2 bonding site in all nitrogenases. Hence, iron complexes with biologically occurring donors, e.g. thiolate, thioether or amine ligands, are of major importance as model compounds for nitrogenases, especially when they possess binding sites for N_2 and its reduction products. In this context, the coordination of diazene, HN=NH, is as equally important as that of molecular nitrogen. In the course of N_2 reduction, diazene should be regarded as the product of the first $2e^\ominus$ reduction step.[3]

$$N_2 + 2e^\ominus + 2H^\oplus \rightarrow N_2H_2$$

It is, however, extremely unstable in the free state ($\Delta H_f^{298} = 212$ kJ/mol[4]). Thus, the question arises by what means it is stabilized in nature at the metal centers of nitrogenase in order to avoid insurmountably high energy barriers in the course of N_2 reduction.

An answer is provided by the diazene complex **1**, which was prepared from a hydrazine complex.[5]

$$[Fe(N_2H_4)(\text{“}N_HS_4\text{”})] + O_2 \xrightarrow[DMF]{-60\,^\circ C} \underset{\mathbf{1}}{[\mu\text{-}N_2H_2\{Fe(\text{“}N_HS_4\text{”})\}_2]} + \text{other products}$$

$$\text{“}N_HS_4\text{”} - H_2 = o\text{-}HS-C_6H_4-S-CH_2CH_2-NH-CH_2CH_2-S-C_6H_4-SH(o)$$

1 is a prototype model compound for enzymatic N_2 fixation in several respects: 1) **1** is the first example for the coordination of diazene to iron. 2) Being ligated by $\text{“}N_HS_4\text{”}^{2\ominus}$, the iron center is exclusively coordinated by biologically occurring donor atoms. 3) The diazene is stabilized not only by coordination to iron and by considerable steric shielding but also by strong tricentric (forked) N−H · · · S hydrogen bridges. Therefore, **1** meets, for the first time, all the functional (coordination and stabilization of N_2H_2) *and* structural (Fe centers and donor atoms) requirements for such model complexes.

An X-ray structure analysis[6] revealed that **1** possesses a center of inversion at the midpoint of the N=N bond (Fig. 1). The *trans* N_2H_2 ligand bridges two iron atoms, each of which are pseudo-octahedrally coordinated by the additional amine nitrogen and four sulfur donor atoms.

The N_2H_2 protons were located by a difference Fourier synthesis. N_2H_2, Fe and S(thiolate) atoms form a plane (±3 pm). The N–N distance of 130.0(7) pm and the trigonal-

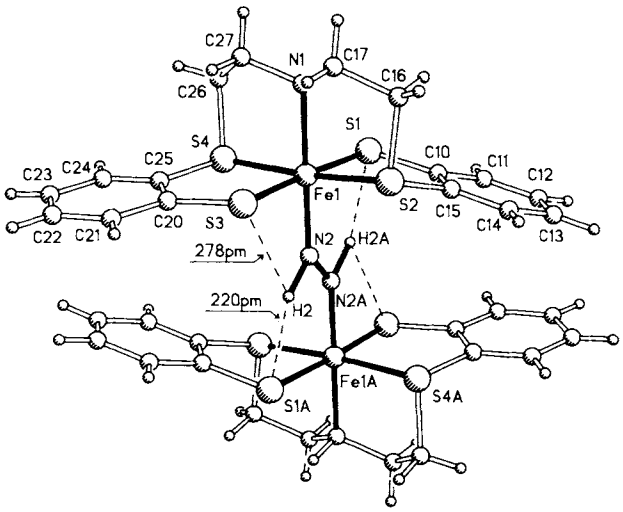


Fig. 1. Molecular structure of **1**. Important distances [pm] and angles [°]: N2–H2 116.2(54), N2–N2A 130.0(7), Fe1–N2 186.7(4), S1A–H2 220.1, S3–H2 278.0, Fe1–N1 203.7(4), Fe1–S1 231.8(2), Fe1–S2 223.4(1), Fe1–S3 228.8(2), Fe1–S4 225.1(1); Fe1–N2–N2A 132.2(5), N2A–N2–H2 103.1, Fe1–N2–H2 124.7, N1–Fe1–N2 179.5(2), S1–Fe1–N2 91.5(1), S2–Fe1–N2 93.1(1), S3–Fe1–N2 87.7(1), S4–Fe1–N2 93.4(1).

[*] Prof. Dr. D. Sellmann, Dipl.-Chem. W. Soglowek, Dr. F. Knoch, Dr. M. Moll
Institut für Anorganische Chemie der Universität Erlangen-Nürnberg
Egerlandstrasse 1, D-8520 Erlangen (FRG)

[**] Transition Metal Complexes with Sulfur Ligands, Part 48. This work was supported by the Deutsche Forschungsgemeinschaft and the Fonds der Chemischen Industrie. – Part 47: D. Sellmann and I. Barth, *Inorg. Chim. Acta 164* (1989) 171. – $\text{“}N_HS_4\text{”}$-H_2 = 2,2'-bis(2-mercaptophenylthio)diethylamine).

ly planar N atoms characterize the N_2H_2 unit as a diazene ligand. The Fe–N(diazene) distance (186.7(4) pm) is significantly shorter than the Fe–N(amine) distance (203.7(4) pm). These results and the intense color of **1** (λ_{max} = 573.6 nm) indicate a 4c-6e$^{\ominus}$-π bond in the Fe $\doteq$ N $\doteq$ N $\doteq$ Fe core.[7] The steric shielding of the N_2H_2 ligand between the [Fe("N_HS_4")] fragments becomes particularly evident from the space-filling model of **1** (Fig. 2). The N_2H_2 entity is protected by the [Fe("N_HS_4")] fragments (Fig. 2a) as though by the shells of a bivalve; however, it is not totally encapsulated, as shown by the side view (Fig. 2b). In fact, **1** reacts rapidly with bases.[8]

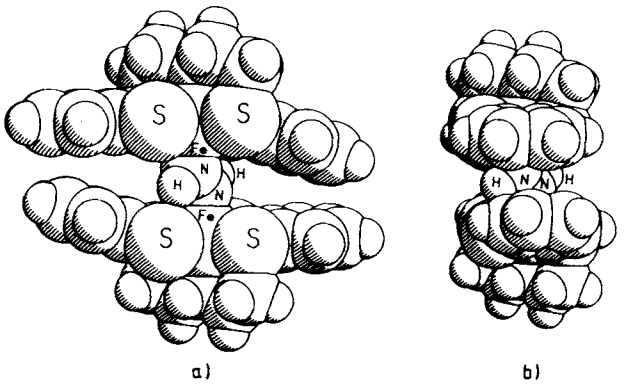


Fig. 2. Space-filling model of **1**; a) front view, b) side view.

The stabilization of the diazene ligand by N–H $\cdots$ S hydrogen bridges follows from the distances (Fig. 1). X–H $\cdots$ S bridges (X = O, N, S) are generally weak (ΔH_f^{298} (HSH $\cdots$ SH_2) = 7.7 kJ/mol).[9] In special cases, as, e.g., (amide)NH $\cdots$ S(cysteine) bridges in ferredoxines, however, they can exhibit substantially higher bonding energies up to 80 kJ/mole.[10]

As follows from the short distances (Fig. 1) the N–H $\cdots$ S bridges of **1** must have considerable strength. As far as we are aware, 220 pm is the shortest H $\cdots$ S distance ever reported; a length of 278 pm for the longer branch of the tricentric H bond is still distinctly less than the sum of the van der Waals radii of H and S (285–305 pm).[11] The important role of the H bridges follows also from the stereochemistry of **1**. The [Fe("N_HS_4")] fragment can form several isomers;[12] in **1**, only that isomer is found which allows the maximum number of N–H $\cdots$ S(thiolate) bridges. When account is taken of the ΔH_f(N—H $\cdots$ S) values calculated for ferredoxines, a total energy of at least 70 kJ/mol may be estimated for the H bridges in **1**. Thus, alone by forming H bridges $\Delta H_f(N_2H_2)$ could be reduced by ca. 30%. Consequently, in nitrogenases complexation and stabilization via 4c-π bond, steric hindrance and H bridges should favor the formation of a diazene in accord with Figure 3. The stabilization by H bridges is of major significance because such H bridges are not to be expected for a precursor N_2-complex and have never been observed in isolable N_2-complexes.

If in nitrogenase centers the same structural principles are realized as are found in **1**, these results show that the $N_2 \rightarrow N_2H_2$ conversion, the most difficult step of N_2 fixation, should be facilitated and possibly even become exoenergetic.

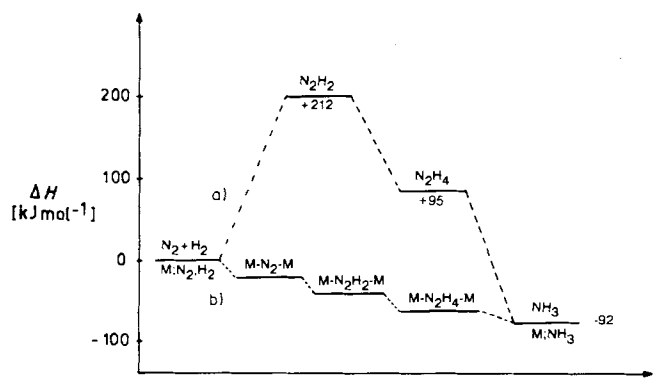


Fig. 3. Energy diagram for reactions between N_2 and H_2; a) in gas phase without metals, b) proposal for a reaction pathway via metal-stabilized intermediates.

Received: May 2, 1989 [Z 3317 IE]
German version: *Angew. Chem. 101* (1989) 1244

[1] F. J. Bergersen, J. R. Postgate (Eds.): *A Century of Nitrogen Fixation Research*, The Royal Society, London 1987.
[2] J. R. Chisnell, R. Premakumar, P. E. Bishop, *J. Bacteriol. 170* (1988) 27.
[3] Cf. D. Sellmann, *Angew. Chem. 86* (1974) 692; *Angew. Chem. Int. Ed. Engl. 13* (1974) 639, and references cited therein.
[4] S. N. Foner, R. L. Hudson, *J. Chem. Phys. 68* (1978) 3162.
[5] *Experimental Procedure*: All operations were carried out under nitrogen using Schlenk techniques. 70 mL of air was injected in small portions into a brown-yellow solution of 480 mg (1.09 mmole) [Fe(N_2H_4)("N_HS_4")] [12] in 20 mL of DMF at −60 °C by means of a syringe. The solution turned deep blue. After standing for 1 h it was covered with a layer of 20 mL of methanol and stored at −30 °C for 7 days. Yellow microcrystals of [Fe(CH_3OH)("N_HS_4")] and black crystals of **1** precipitated; these were filtered off and washed with 25 mL of DMF and 10 mL of methanol. Analytically pure **1** (80 mg, 17%) remained.
[6] X-ray structure analysis of **1**: Nicolet R3m/V, T = 200 K, λ($Mo_{K\alpha}$) graphite monochromator, ω-scan, $4° < 2\theta < 54°$, direct methods (SHELXTL-PLUS). 4166 reflections measured, 3490 unique, and 2787 with $F > 4\sigma(F)$. Non-hydrogen atoms were refined isotropically, N_2H_2 hydrogen atoms were located by a difference Fourier synthesis and refined isotropically. 212 parameters refined, R = 5.5%, R_w = 4.1%. – $P2_1/c$, a = 1198.9(3), b = 1332.2(3), c = 1187.9(3) pm, β = 108.99(2)°, $V = 1794(1) \times 10^6$ pm^3, ϱ_{calc} = 1.56 g/cm^3, Z = 2. Further details of the X-ray crystal structure investigation may be obtained from the Fachinformationszentrum Karlsruhe, Gesellschaft für wissenschaftlich-technische Information mbH, D-7514 Eggenstein-Leopoldshafen 2 (FRG), on quoting the depository number CSD-53837, the names of the authors, and the journal citation.
[7] Cf. D. Sellmann, E. Böhlen, M. Waeber, G. Huttner, L. Zsolnai, *Angew. Chem. 97* (1985) 984; *Angew. Chem. Int. Ed. Engl. 24* (1985) 981, and references cited therein.
[8] The products have not yet been characterized. This reaction of **1**, however, is of importance regarding the base-catalyzed disproportionation of N_2H_2-complexes. Cf. D. Sellmann, A. Brandl, R. Endell, *J. Organomet. Chem. 90* (1975) 309.
[9] P. Schuster, G. Zundel, C. Sandorfy (Eds.): *The Hydrogen Bond*, North Holland, Amsterdam 1976; R. C. Kerns, L. C. Allen, *J. Am. Chem. Soc. 100* (1978) 6587.
[10] R. P. Sheridan, L. C. Allen, C. W. Carter, *J. Biol. Chem. 256* (1981) 5052.
[11] L. Pauling, *Die Natur der chemischen Bindung*, Verlag Chemie, Weinheim 1968; A. Bondi, *J. Phys. Chem. 68* (1964) 441.
[12] D. Sellmann, H. Kunstmann, F. Knoch, M. Moll, *Inorg. Chem. 27* (1988) 4183.

A New Class of DNA-Cleaving Molecules: pH-Dependent DNA Cleavage by Propargylic and Allenic Sulfones**

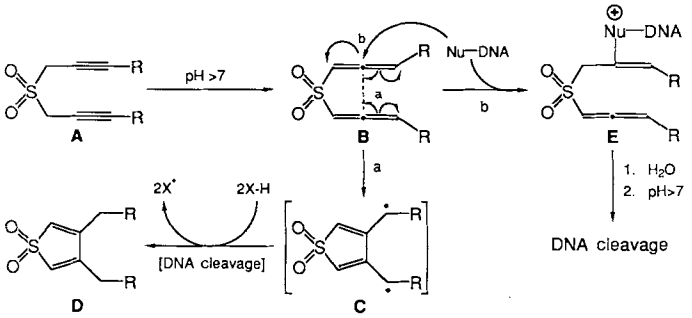
By *K. C. Nicolaou,* G. Skokotas, P. Maligres, G. Zuccarello, E. J. Schweiger, K. Toshima,* and *S. Wendeborn*

Molecules that cleave DNA are of considerable interest from the points of view of molecular biology[1] and drug

[*] Prof. K. C. Nicolaou, G. Skokotas, P. Maligres, G. Zuccarello, E. J. Schweiger, K. Toshima, S. Wendeborn
Department of Chemistry, University of Pennsylvania
Philadelphia, PA 19104-6323 (USA)

[**] This work was supported by the National Science Foundation, the National Institutes of Health, and the University of Pennsylvania.

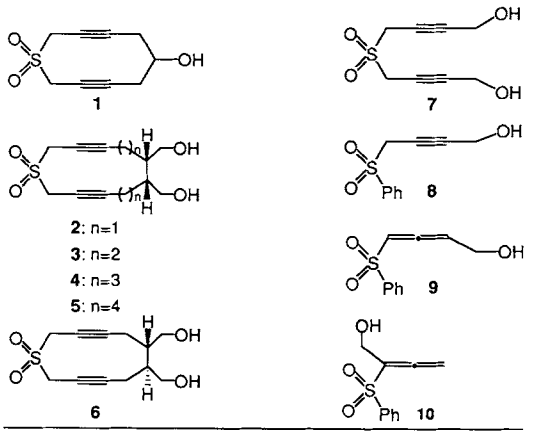
design.[2] In this communication we report the design, synthesis, and activity of a new class of DNA-cleaving compounds equipped with a propargylic or allenic sulfone moiety.[3]



Scheme 1. Hypothesis for DNA cleavage by bis(propargyl) sulfones via the Garrat–Braverman reaction sequence [4, 5]. For paths a and b, see text.

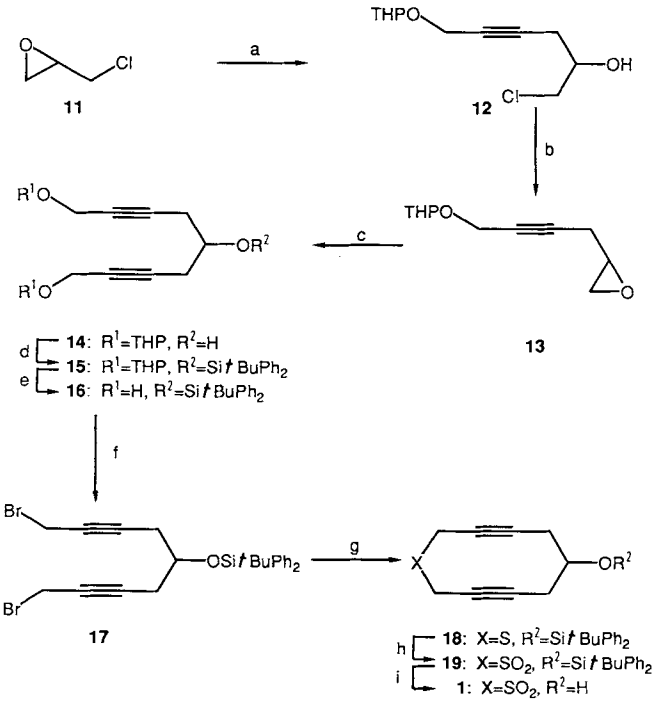
Scheme 1 depicts the mechanistic rationale that led to the design of the first active compounds in this series. Specifically, it was hypothesized that the Garratt[4]–Braverman[5] reaction sequence (Scheme 1) would proceed in aqueous solutions at pH > 7, transforming a bis(propargylic) sulfone **A** first to bis(allenic) sulfone **B** and subsequently to the diradical **C**[6] (path a), which might then initiate DNA strand scission.[7] Alternatively, nucleophilic attack (path b) by nitrogen nucleophiles from DNA on the conjugated allenic acceptor **B** could lead to structures such as **E**, which were then expected to undergo Maxam–Gilbert[8] type chemistry leading to clean DNA rupture as depicted in Scheme 1. To test this hypothesis, compounds **1**–**7** (Table 1) were designed

Table 1. Unsaturated sulfones **1**–**10** with DNA-cleaving properties.



and synthesized as potential DNA-cleaving agents. These compounds were chosen so as to allow subsequent attachment of a variety of appendages to probe the effect of molecular shape on the DNA interaction and to study reaction rates as a function of ring size.

The synthesis of the 10-membered ring bis(propargylic) sulfone **1** is shown in Scheme 2.[9] Thus, opening of epichlorohydrin **11** with the anion of propargyl tetrahydropyranyl ether in the presence of $BF_3 \cdot Et_2O$ resulted in the formation of compound **12**, which was converted into the epoxide **13** by base treatment. Reiteration of the epoxide opening as above then gave the diacetylene **14**, from which



Scheme 2. Synthesis of **1**: Reagents and conditions. a) 2.2 equiv. $THPO-CH_2C\equiv CH$, 2.0 equiv. *n*BuLi, 2.0 equiv. $BF_3 \cdot Et_2O$, THF, $-78 \rightarrow 25\,^{\circ}C$, 12 h, 94%; b) 1.1 equiv. NaOMe, MeOH, 25 °C, 12 h, 74%; c) 2.0 equiv. $THPO-CH_2C\equiv CH$, 2.2 equiv. *n*BuLi, 2.2 equiv. $BF_3 \cdot Et_2O$, THF, $-78 \rightarrow 25\,^{\circ}C$, 2 h, 58%; d) 1.2 equiv. *t*$BuPh_2SiCl$, 2.0 equiv. imidazole, DMF, 25 °C, 12 h, 44%; e) 0.2 equiv. pyridinium *p*-toluenesulfonate, MeOH, 25 °C, 12 h, 92%; f) 2.2 equiv. CBr_4, 2.7 equiv. $P(Oct)_3$, Et_2O, $0 \rightarrow 25\,^{\circ}C$, 4 h, 84%; g) 2.0 equiv. $Na_2S \cdot Al_2O_3$ [10], CH_2Cl_2:EtOH (5:2), 25 °C, 2 h, 55%; h) 4.0 equiv. *m*-chloroperbenzoic acid, CH_2Cl_2, $0 \rightarrow 25\,^{\circ}C$, 3 h, 87%; i) 48% aqueous HF:CH_3CN (1:5), 25 °C, 16 h, 30%.

Table 2. Properties of selected compounds.

1: $R_f = 0.14$ (SiO_2, 80% Et_2O in petroleum ether). ^1H NMR (250 MHz, CD_3OD): $\delta = 4.07$ (dt, $J = 16.7$, 2.1 Hz, 2H, SO_2CH_2), 3.96 (dt, $J = 16.7$, 2.2 Hz, 2H, SO_2CH_2), 3.87 (m, CH-OH), 2.38 (m, 4H, $C\equiv C-CH_2$), 1.18 (br. s, 1H, OH). IR ($CHCl_3$): $\tilde{\nu}_{max} = 3680$, 3620, 3010, 2970, 2890, 2390, 1220, 1045 cm^{-1}; MS (CI): *m/z* calculated for $C_9H_{11}O_3S$ ($M^{\oplus}-H$): 199.043, found 199.042

2: $R_f = 0.25$ (SiO_2, 10% MeOH in CH_2Cl_2). ^1H NMR (250 MHz, CD_3OD): $\delta = 4.04$ (m, 4H, SO_2CH_2), 3.58 (dd, $J = 10.7$, 6.4 Hz, 2H, CH_2OH), 3.51 (dd, $J = 10.7$, 7.8 Hz, 2H, CH_2OH), 2.36 (dd, $J = 17.1$, 7.9 Hz, 2H, $C\equiv C-CH_2$), 2.20 (d, $J = 16.9$ Hz, 2H, $C\equiv C-CH_2$), 1.82 (m, 2H, CH); IR (Nujol): $\tilde{\nu}_{max} = 3560$, 3380, 2900, 2240, 1315 cm^{-1}. MS (CI): *m/z* calculated for $C_{12}H_{17}O_4S$ ($M^{\oplus}-H$): 257.085, found 257.084

7: $R_f = 0.50$ (SiO_2, EtOAc). ^1H NMR (500 MHz, $CDCl_3$): $\delta = 4.35$ (s, 4H, CH_2OH), 4.08 (s, 4H, SO_2CH_2), 2.08 (br. s, 2H, OH); IR (neat): $\tilde{\nu}_{max} = 3200$, 2960, 2920, 1330, 1130 cm^{-1}. MS (CI): *m/z* calculated for $C_8H_{11}O_4S$ ($M^{\oplus}-H$): 203.038, found 203.037

8: $R_f = 0.16$ (SiO_2, 80% Et_2O in petroleum ether). ^1H NMR (250 MHz, $CDCl_3$): $\delta = 7.95$ (m, 2H, phenyl), 7.60 (m, 3H, phenyl), 4.23 (dt, $J = 6.2$, 2.1 Hz, 2H, CH_2OH), 3.99 (t, $J = 2.1$ Hz, 2H, SO_2CH_2). 2.15 (t, $J = 6.2$ Hz, 1H, OH); IR ($CHCl_3$): $\tilde{\nu}_{max} = 3600$, 3500, 3020, 2910, 1450, 1320, 1140 cm^{-1}. MS (CI): *m/z* calculated for $C_{10}H_{11}O_3S$ ($M^{\oplus}-H$): 211.043, found 211.043

9: $R_f = 0.48$ (SiO_2, 10% MeOH in CH_2Cl_2). ^1H NMR (250 MHz, $CDCl_3$): $\delta = 7.91$ (m, 2H, phenyl), 7.58 (m, 3H, phenyl), 6.31 (dt, $J = 5.7$, 2.9 Hz, 1H, SO_2CH), 6.02 (dt, $J = 5.7$, 5.6 Hz, 1H, CH_2CH), 4.29 (m, 2H, CH_2OH), 2.35 (br. s, 1H, OH). IR ($CHCl_3$): $\tilde{\nu}_{max} = 1960$, 1320, 1146 cm^{-1}. MS (CI): *m/z* calculated for $C_{10}H_{11}O_3S$ ($M^{\oplus}-H$): 211.043, found 211.041

24: $R_f = 0.43$ (SiO_2, Et_2O). ^1H NMR (250 MHz, $CDCl_3$): $\delta = 9.38$ (m, 2H, aromatic), 8.77 (s, 1H, aromatic), 8.06 (dd, $J = 8.4$, 0.7 Hz, 2H, aromatic), 7.69 (m, 2H, aromatic), 7.55 (m, 2H, aromatic) 4.34 (t, $J = 2.1$ Hz, 2H, SO_2CH_2), 3.92 (dt, $J = 6.3$, 2.1 Hz, 2H, CH_2OH), 1.21 (t, $J = 6.3$ Hz, 1H, OH). IR ($CHCl_3$): $\tilde{\nu}_{max} = 3595$ (m), 3020 (m), 1320 (s), 1160 (m), 1145 (m), 1125 (s) cm^{-1}; UV/VIS ($CHCl_3$): $\lambda_{max} = 414$ (sh), 394, 377, 365, 348 (sh), 262 nm; MS (CI): *m/z* calculated for $C_{18}H_{14}O_3S$ ($M^{\oplus}$): 310.066, found 310.063

compounds **15–17** were sequentially generated by standard methods. The reagent[10] derived from Na_2S and Al_2O_3 reacted smoothly with dibromide **17** in CH_2Cl_2/EtOH at 25 °C, producing the cyclic sulfide **18** in 55% yield. Finally, oxidation of **18** with *m*-chloroperbenzoic acid to the corresponding sulfone **19**, followed by disilylation, gave the requisite target **1**. The synthesis of the remaining compounds in Table 1 was performed by standard methods.

Compounds **1–7** (Tables 1 and 2) cleaved double-stranded DNA in alkaline solution. Thus, incubation of **1–7** (1000 μM) with supercoiled ΦX174 DNA (form I) aerobically at pH 8.5 and 37 °C produced DNA rupture, leading initially to form II and finally to form III DNA, as shown in Figure 1 (lanes 1–7). Of interest is the more extensive scission produced by the two 11-membered ring sulfones **2** and **6** and the acyclic bis(propargylic) sulfone **7** as compared to the 10-membered ring compound **1** and the higher ring sulfones **3–5** under the same conditions. As expected, the saturated analogue of sulfone **2** produced no DNA cleavage under similar conditions (Fig. 1, lane 11).

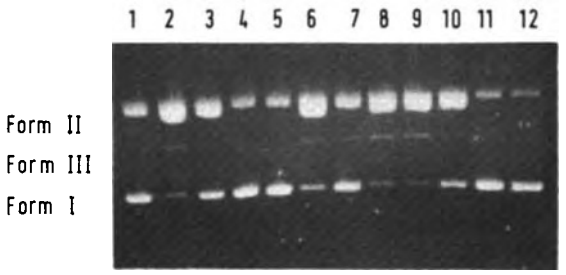


Fig. 1. ΦX174 form I DNA (50 μM per base pair) was incubated for 24 h with various compounds (1000 μM) in buffer(Tris-acetate, pH 8.5, 50 mM) and analyzed by electrophoresis (1% agarose gel, ethidium bromide stain). Lanes 1–11, compounds **1, 2, 3, 4, 5, 6, 7, 8, 9, 10**, and the saturated analogue of **2**, respectively; lane 12, DNA alone. For forms II and III, see text.

Further investigations demonstrated that a series of monopropargylic and monoallenic sulfones (e.g., **8–10**, Table 1) exhibited DNA-cleaving properties (Fig. 1, lanes 8–10) under similar conditions. DNA cleavage by the propargylic and even the allenic sulfones exhibited a striking pH dependence as shown in Figure 2 for the case of **2**. It is worth noting that the DNA-cleaving action of a 10-membered ring enediyne recently reported from these laboratories[3a] showed no such pH dependence. As Figure 2 shows, optimum cleavage occurred at around pH 8.5, whereas little cleavage was observed at pH < 7 or > 10. Although less, considerable rupture was also observed at pH 7 and pH 10 (Fig. 1).

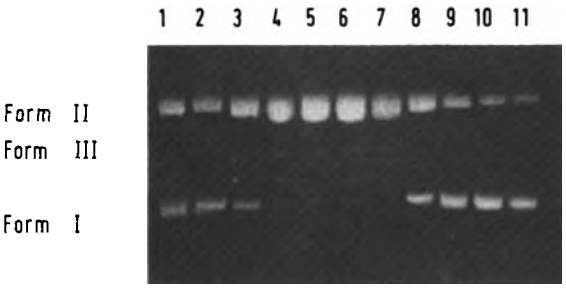
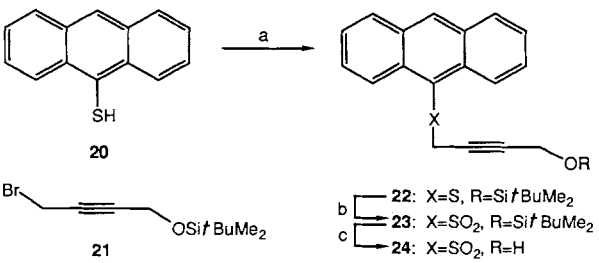


Fig. 2. ΦX174 form I DNA (50 μM per base pair) was incubated for 24 h with compound **2** (1000 μM) in various pH buffers (50 mM) and analyzed as described under Fig. 1. Lanes 1–10 correspond to pH 5.0, 6.0, 7.0, 7.4, 8.0, 8.5, 9.0, 9.5, 10.0, and 10.7, respectively; lane 11, DNA alone at pH 8.5. For forms II and III see text.

The expectation that DNA intercalators and other DNA binding moieties would enhance the potency of these compounds as DNA cleavers was born out in preliminary experiments. Thus, the anthryl sulfone **24** (Scheme 3, Table 2)[11] synthesized by standard chemistry from thiol **20**[11] and bromide **21**,[12] exhibited much higher potency as a DNA cleaving agent (at concentrations as low as 0.1 μM) than any of the compounds of Table 1. Figure 3 demonstrates the action of **24** and some of its relatives on supercoiled ΦX174 DNA. Noteworthy is the ca. 100-fold loss of activity in the sulfoxide derivative of **24** (Figure 3, lane 5) and the even further loss of activity in the corresponding sulfide (Fig. 3, lane 6).[13] Not surprisingly, the saturated analogue of **24** was devoid of any DNA-cleaving properties (Fig. 1, lane 4).



Scheme 3. Synthesis of **24**: Reagents and conditions. a) 1.1 equiv. NaH, 0.75 equiv. **21**, DMF, 0 → 25 °C, 0.5 h, 100%; b) 3.0 equiv. *m*-chloroperbenzoic acid, CH_2Cl_2, 0 → 25 °C, 4 h, 75%; c) 48% aqueous HF:CH_3CN (1:5), 0 → 25 °C, 0.25 h, 90%.

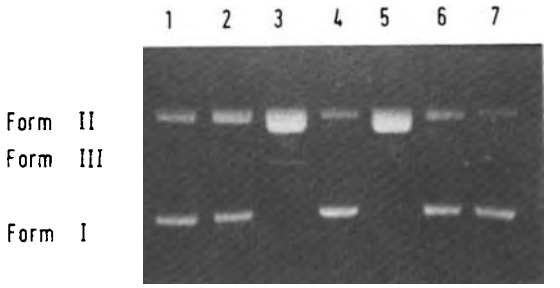


Fig. 3. ΦX174 form I DNA (50 μM per base pair) was incubated for 24 h with various compounds and at various concentrations in buffers (Tris-acetate, pH 8.5, 50 mM) and analyzed as described under Fig. 1. Lane 1, **24**, 0.1 μM; lane 2, **24**, 1 μM; lane 3, **24**, 10 μM; lane 4, saturated analogue of **24**, 1000 μM; lane 5, sulfoxide of **24**, 1000 μM; lane 6, sulfide of **24**, 1000 μM; lane 7, DNA alone. For forms II and III see text.

Studies currently in progress include gathering information on structure-activity relationships, experiments designed to elucidate the precise mode of action (e.g., nucleophilic versus radical addition, Scheme 1)[7] of these molecules and the design of sequence-specific DNA-cleaving systems and anticancer agents.

Received: May 12, 1989 [Z 3338 IE]
German version: *Angew. Chem. 101* (1989) 1255

[1] a) P. B. Dervan, *Science (Washington, D.C.) 232* (1986) 464; b) H. O. Smith, ibid. 205 (1979) 455; c) D. Natans, H. O. Smith, *Annu. Rev. Biochem. 44* (1975) 273.

[2] a) W. A. Remers (Ed.), *Antineoplastic Agents*, Wiley, New York 1984; b) S. Neidle, M. J. Waring, (Eds.): *Molecular Aspects of Anti-Cancer Drug Action*, Verlag Chemie, Weinheim 1983; c) C. Chagas, B. Pullman (Eds.):

Molecular Mechanisms of Carcinogenic and Antitumor Activity, Adenine Press, Schenectady 1987.
[3] For other recent reports on DNA-cleaving molecules see a) K. C. Nicolaou, Y. Ogawa, G. Zuccarello, H. Kataoka, *J. Am. Chem. Soc. 110* (1988) 7247, and references cited therein; b) S. A. Strobel, H. E. Moser, P. B. Dervan, *J. Am. Chem. Soc. 110* (1988) 7927; c) J. P. Sluka, S. J. Horvath, M. F. Braist, M. I. Simon, P. B. Dervan, *Science (Washington, D.C.) 238* (1987) 1129; d) R. N. Zuckermann, P. G. Schultz, *J. Am. Chem. Soc. 110* (1988) 6592; e) C.-H. B. Chen, D. S. Sigman, *ibid. 110* (1988) 6570; f) S. C. Kim, A. Podhajska, W. Szybalski, *Science (Washington, D.C.) 240* (1988) 504.
[4] a) P. J. Garratt, S. B. Neoh, *J. Org. Chem. 44* (1979) 2667; b) Y. S. P. Cheng, P. J. Garratt, S. B. Neoh, V. M. Rumjanek, *Isr. J. Chem. 26* (1985) 101.
[5] a) S. Braverman, D. Segev, *J. Am. Chem. Soc. 96* (1974) 1245; b) S. Braverman, Y. Duar, D. Segev, *Tetrahedron Lett. 1976*, 3181.
[6] J. C. Sciano, V. Wintgens, A. Bedell, J. A. Berson, *J. Am. Chem. Soc. 110* (1988) 4050.
[7] Consideration of C–H bond dissociation energies for allylic (diradical **C**) and aliphatic positions (DNA) argue against the potential capability of diradical **C** to abstract an H· from the CH_2 group of DNA, although, as part of a cascade, it may still serve as a DNA-damaging species due to equilibria shifting. The observed DNA-cleaving properties of the monofunctional compounds **8–10** and **24** suggest, however, the nucleophilic mechanism indicated in Scheme 1 (path b).
[8] A. M. Maxam, W. Gilbert, *Methods Enzymol. 65* (1980) 499.
[9] All new compounds exhibited satisfactory spectral and analytical and/or exact mass data. Yields have not been maximized and refer to spectroscopically and chromatographically homogeneous materials.
[10] This reagent was prepared by mixing $Na_2S \cdot 9\,H_2O$ (51 g) dissolved in H_2O and Al_2O_3 (basic, 49 g) followed by solvent removal under vacuum.
[11] W. Conway, D. S. Tarbell, *J. Am. Chem. Soc. 78* (1956) 2228.
[12] Bromide **21** was prepared from 3-*tert*-butyldimethylsiloxyprop-1-yne (A. K. Samantha, S. K. Bose, S. B. Mahato, *J. Antibiot. 37* (1984) 733) by standard methods.
[13] This loss of potency in the series sulfone → sulfoxide → sulfide was observed in other systems such as compounds **2** and **7** (Table 1).

Dithia Dications from Cyclic and Acyclic Precursors by Gas-Phase Oxidation ("Charge Stripping") of 3e/2c-Radical Cations**

By *Thomas Drewello, Carlito B. Lebrilla, Klaus-Dieter Asmus,* and *Helmut Schwarz**

Dedicated to Professor Christoph Rüchardt on the occasion of his 60th birthday

Two-center three-electron bonds (2c/3e) have attracted considerable interest in recent years.[1] They are formed in cationic, neutral and anionic radicals generated from heteroatom-containing compounds. The most extensively studied group of such species are the sulfur-centered radical cations. Detailed investigations have been carried out in the gas phase,[2] in liquids[3] and in solid matrixes.[4] Experimental results as well as theoretical calculations have unambiguously shown the formation of homo- and heteronuclear binding structures of the general types **1** and **2** (X,Y: fragments with sulfur, selenium, nitrogen, phosphorus, halogen, oxygen etc.).

1 $X \cdot\cdot X^{\oplus}$ $\quad$ $X \cdot\cdot Y^{\oplus}$ **2**

[*] Prof. Dr. H. Schwarz, Dr. C. B. Lebrilla, Dr. T. Drewello
Institut für Organische Chemie, Technische Universität Berlin, Strasse des 17. Juni 135, D-1000 Berlin 12
Prof. Dr. K.-D. Asmus
Hahn-Meitner Institut Berlin G.m.b.H., Bereich Strahlenchemie
Postfach 39 01 28, D-1000 Berlin 39

[**] This work was supported by the Deutsche Forschungsgemeinschaft, the Fonds der Chemischen Industrie, and the Gesellschaft von Freunden der Technischen Universität Berlin. We thank *Dr. E. Anklam* for synthesizing some of the dithia compounds.

The 2c/3e bond (with a formal bond order of 0.5) is characterized by two electrons located in a σ-orbital and one electron in an antibonding σ*-orbital. The actual bond strength is essentially determined by the extent of orbital interaction between the heteroatoms (X,X or X,Y), i.e. by the overlap or in general by structural parameters and by the electronic nature of the substituents at the heteroatoms. For example, the experimentally determined S···S bond strength in $[(CH_3)_2S \cdot\cdot S(CH_3)_2]^{\oplus}$ is ca. 25 kcal/mol,[2b, 3j, 3l] in very good agreement with theoretical calculations.[1b, c, d]

An indication of the strength of the 2c/3e bond is given by the optical absorption spectrum. The maxima of the UV/VIS bonds are proportional (at least to a first approximation) to the difference between the σ and σ* energy levels and can thus be directly correlated with the extent of orbital interaction between X,Y in **1** and **2**.[1] Accordingly, any increase in bond strength shows up as a blue-shift in λ_{max}, while bond weakening in a 2c/3e system results in a corresponding red shift of the absorption band.[3e, k]

Considering that one of the electrons in a 2c/3e bond is antibonding in nature, it can be expected that the removal of this σ*-electron, e.g. via ionization, requires considerably less energy than the removal of a bonding electron from the σ-bond. Chemically, such a process constitutes an oxidation of **1** or **2** to the respective paramagnetic dications **3** and **4**.

$X^{\oplus}-X^{\oplus}$ **3** $\quad$ $X^{\oplus}-Y^{\oplus}$ **4**

This should be accompanied by a shortening of the X–X and X–Y bonds[5] which has experimentally verified very convincingly in a number of cases, particularly for nitrogen-centered systems.[4a, 6]

Dications could also be generated by the oxidation of quite a number of cyclic di- and polythia compounds in solution.[3c, d, 7] So far, however, it has not been possible to detect any dications from acyclic dithia compounds, not even as short-lived transients. This is considered to be mainly due to the fact that such 2c/3e radical cations are powerful oxidants. Therefore they generally act as electron acceptors rather than to suffer loss of an electron. But, even if formed, any such dications would probably undergo fast charge transfer reactions or solvent assisted deprotonation processes, particularly in polar solvents like water.

A much more suitable environment for the stabilization of sulfur-centered dications is expected to be the gas phase. This is indeed the case, as will be demonstrated in this paper, for a series of cyclic as well as acyclic dithia compounds. All of these substrates yield 2c/3e radical cations via intramolecular (transannular) stabilization after one-electron oxidation. The respective dications can then be generated if these 2c/3e species (**5–14** in Table 1) are subjected to a "charge stripping" experiment.[8] One of the interesting parameters such experiments reveal is the vertical ionization energy IE_v for the underlying general process $M^{\oplus} \rightarrow M^{2\oplus} + e^{\ominus}$.

The electron to be removed from the 2c/3e bond upon oxidation (i.e. from $M^{\oplus}$), on energetic grounds, is expected to be the antibonding σ*-electron. Considering that the energy of this σ*-electron depends on the σ/σ* separation a direct correlation should exist between IE_v and the extent of X,X (X,Y) orbital interaction. The experimental results on IE_v and λ_{max} as listed in Table 1 clearly substantiate this assumption.

Considering species **5–10** it is noted that an increasing sulfur-p-orbital interaction, as facilitated by increasingly favorable sterical structures, results in an increasing σ/σ* separation and a corresponding blue-shift in λ_{max}.[3e, m] As the

Table 1. Vertical ionization energies, IE_v, and λ_{max} values [a] of the dithia radical cations **5**–**14**.

Radical cations		IE_v [eV]	λ_{max} [nm]	ΔE (σ^*/σ) [eV]
	**5**	15.0 ± 0.3	650	1.91
	**6**	14.1 ± 0.4	600	2.07
	**7**	13.3 ± 0.2	525	2.36
	**8**	13.2 ± 0.2	470	2.64
	**9**	12.7 ± 0.3	450	2.76
	**10**	12.3 ± 0.3	440	2.82
	**11**	15.3 ± 0.3	[b]	–
	**12**	14.3 ± 0.4	650	1.91
	**13**	15.2 ± 0.2	≈ 650 [c]	≈ 1.9
	**14**	13.3 ± 0.2	610	2.30

[a] λ_{max} values taken from Ref. [3e, f, m]. [b] The lifetime of **11** in solution is too short for accurate measurement of λ_{max}; the latter presumably lies in the near IR. [c] A large error limit has to be allowed for λ_{max} of the radical cation **13** owing to its short lifetime and low yield.

σ^* energy rises to higher levels the measured IE_v values decrease continuously from 15.0 to 12.3 eV.

While **10** constitutes one extreme in our series, species **11** represents the other. In the latter, sulfur-p-orbitral interaction is practically prevented by the rigid and almost planar structure of the 1,3-dithiacyclopentane moiety. Accordingly, this system has a particularly low-lying σ^* level, if any, and correspondingly exhibits the highest IE_v value for the ionization of the primarily formed radical cation.

The observed correlation between the blue-shift in λ_{max} and the decrease in IE_v for species **11, 12** and **14** can also be explained in steric terms. Substitution of hydrogen by methyl at the C(2) position, particularly in the case of geminal dialkylation, changes the molecular geometry in favor of p-orbital interaction.[3m] This results in a strengthening of the 2c/3e bond, a rise of the σ^* level and a decrease in IE_v. The opposing, i.e. bond-weakening effect caused by electron induction from the methyl substituent cannot compete with this structural factor for C(2) substitution. It becomes apparent, however, in the case of methylation at C(4) (species **13**), which exerts no further structural changes on the 1,3-dithiacyclopentadiene moiety. Electron donation is now the only factor to affect the σ/σ^* splitting in **13** as compared to **12**. The resulting decrease in the strength of the 2c/3e bond is reflected in a comparatively higher IE_v.

It is interesting to note that this latter effect does not show up in the optical measurements, which are rather insensitive for the weak 2c/3e bonds absorbing at $\lambda_{max} \approx 600$ nm. (Here is a large error limit of ca. ± 30 nm due to broadness of the absorption band, low yields and low kinetic stability.) The expected differences between **12** and **13** are clearly reflected, however, in the respective IE_v values.

The remarkable correlation between the optical data and IE_v values obtained for the three-electron bonded radical cations renders "charge stripping" an excellent complementary method to pulse radiolysis, particularly for the investigation of weak 2c/3e bonds.

Received: May 2, 1989 [Z 3319 IE]
German version: *Angew. Chem. 101* (1989) 1247

[1] a) N. C. Baird, *J. Chem. Ed. 54* (1977) 291; b) T. Clark, *J. Comput. Chem. 2* (1981) 261; c) T. Clark, *J. Am. Chem. Soc. 110* (1988) 1672; d) P. M. W. Gill, L. Radom, *ibid. 110* (1988) 4931; e) for examples and special literature concerning 2c/3e bonds in hydrazines see: H. Bock, W. Kaim, H. Nöth, A. Semkow, *J. Am. Chem. Soc. 102* (1980) 4421.

[2] a) T. Drewello, C. B. Lebrilla, H. Schwarz, L. J. de Koning, R. H. Fokkens, N. M. M. Nibbering, E. Anklam, K.-D. Asmus, *J. Chem. Soc. Chem. Commun. 1987*, 1381; b) A. J. Illies, P. Livant, M. L. McKee, *J. Am. Chem. Soc. 110* (1988) 7980.

[3] Selected references: a) T. Gillbro, C. M. L. Kerr, F. Williams, *Mol. Phys. 28* (1974) 1225; b) K. Nishikawa, F. Williams, *Chem. Phys. Lett. 34* (1975) 302; c) W. K. Musker, P. B. Roush, *J. Am. Chem. Soc. 98* (1976) 6745; d) W. K. Musker, T. L. Wolford, P. B. Roush, *ibid. 100* (1978) 6416; e) K.-D. Asmus, *Acc. Chem. Res. 12* (1979) 436; f) K.-D. Asmus, D. Bahnemann, C.-H. Fischer, D. Veltwisch, *J. Am. Chem. Soc. 101* (1979) 5322; g) M. Bonifačić, K.-D. Asmus, *J. Chem. Soc. Perkin Trans. 2 1980*, 758; h) T. G. Brown, A. S. Hirschon, W. K. Musker, *J. Phys. Chem. 85* (1981) 3767; i) S. A. Chaudhri, K.-D. Asmus, *Angew. Chem. 93* (1981) 690, *Angew. Chem. Int. Ed. Engl. 20* (1981) 672; j) R. Wilbrandt, N. H. Jensen, P. Pagsberg, A. H. Sillesen, K. B. Hansen, R. E. Hester, *J. Raman Spectrosc. 11* (1981) 24; k) M. Göbl, M. Bonifačić, K.-D. Asmus, *J. Am. Chem. Soc. 106* (1984) 5984; l) J. Mönig, R. Goslich, K.-D. Asmus, *Ber. Bunsenges. Phys. Chem. 90* (1986) 115; m) M. Bonifačić, K.-D. Asmus, *J. Org. Chem. 51* (1986) 1216; n) H. Mohan, K.-D. Asmus, *J. Chem. Soc. Perkin Trans. 2 1987*, 1795; o) S. Mahling, K.-D. Asmus, R. S. Glass, M. Hojjatie, G. S. Wilson, *J. Org. Chem. 52* (1987) 277; p) X.-Z. Quin, Q. Meng, F. Williams, *J. Am. Chem. Soc. 109* (1987) 6778; q) M. C. R. Symons, H. Chandra, R. W. Alder, *J. Chem. Soc. Chem. Commun. 1988*, 844; r) E. Anklam, H. Mohan, K.-D. Asmus, *J. Chem. Soc. Perkins Trans. 2 1988*, 1297.

[4] a) R. W. Alder, A. G. Orpen, J. M. White, *J. Chem. Soc. Chem. Commun. 1985*, 949; b) S. F. Nelsen, *Mol. Struct. Energ. 3* (1986) 1; c) B. Frleć, D. Gauter, L. Golić, I. Leban, *Acta Crystallogr. B37* (1981) 666.

[5] The effect that successive electron removal from an AB system may result in a strengthening and shortening of the A–B bond was clearly recognized as early as 1933 by *Pauling* and later substantiated by *Dunitz* and *Ha*: a) L. Pauling, *J. Chem. Phys. 1* (1933) 56; b) J. D. Dunitz, T. K. Ha, *J. Chem. Soc. Chem. Commun. 1972*, 568.

[6] a) W. J. Bouma, L. Radom, *J. Am. Chem. Soc. 107* (1985) 345; b) T. Drewello, C. B. Lebrilla, H. Schwarz, D. Stahl, *Int. J. Mass Spectrom. Ion Processes 77* (1987) R3.

[7] a) H. Fujihara, R. Akaishi, N. Furukawa, *J. Chem. Soc. Chem. Commun. 1987*, 930; b) F. Iwasaki, N. Toyoda, R. Akaishi, H. Fujihara, N. Furukawa, *Bull. Chem. Soc. Jpn. 61* (1988) 2563. c) For a recent high level ab initio MO calculation of $H_2SSH_2^{2\oplus}$, see: P. M. W. Gill, L. Radom, *J. Am. Chem. Soc. 111* (1989) 4613.

[8] All experiments were performed on a ZAB-HF-3F triple-sector mass spectrometer under the following conditions: the radical cations $m^{\oplus}$ were generated by 70 eV electron impact ionization of the corresponding neutral molecules and mass selected by means of B(1). Charge stripping was brought about by collision of an 8 keV beam of $m^{\oplus}$ with oxygen (pressure ca. 10^{-4} torr) in a collision chamber located between the magnetic (B) and electric sector E. Dications $M^{2\oplus}$ formed in the collision experiment are detected by scanning the electric sector voltage at ca. $E/2$, where E corresponds to the voltage necessary to transmit the primary ion beam $m^{\oplus}$. The ionization energy necessary for the oxidation of $m^{\oplus}$ is provided by the kinetic energy of $m^{\oplus}$ with the consequence that the "charge stripping" signal of the reaction $m^{\oplus} + O_2 \rightarrow m^{2\oplus} + O_2 + e^{\ominus}$ is not recorded at exactly $E/2$ but is shifted to a smaller value ($E/2 - \delta$). The energy deficit (Q_{min}) of the reaction, after calibration of the energy scale determined from the "onset" of the signals, in a first approximation corresponds to the vertical ionization energy IE_v of $m^{\oplus}$ (Ref. [9]). Oxidation of toluene radical cations was employed for the calibration of the energy scale (F. M. Dorman, J. D. Morrison, *J. Chem. Phys. 35* (1961) 575).—For further details, see: T. Drewello, *Dissertation D83*, Technische Universität Berlin 1989.

[9] Reviews and special literature: a) R. G. Cooks, T. Ast, J. H. Beynon, *Int. J. Mass Spectrom. Ion Phys. 11* (1973) 490; b) T. Ast, *Adv. Mass Spectrom. 10* (1986) 471; c) K. Levsen, H. Schwarz, *Mass Spetrom. Rev. 2* (1983) 77; d) T. Ast, C. J. Porter, C. J. Proctor, J. H. Beynon, *Glas. Hem. Drus. Beograd 46* (1981) 135; e) W. Koch, F. Maquin, D. Stahl, H. Schwarz, *Chimia 39* (1985) 376; f) W. Koch, H. Schwarz, in P. Ausloos, S. G. Lias (Eds.): *Structure/Reactivity and Thermochemistry of Ions*, Reidel Publishing Company, Dordrecht, 1987, p. 413 ff; g) H. Schwarz, *Pure Appl. Chem. 61* (1989) 685.

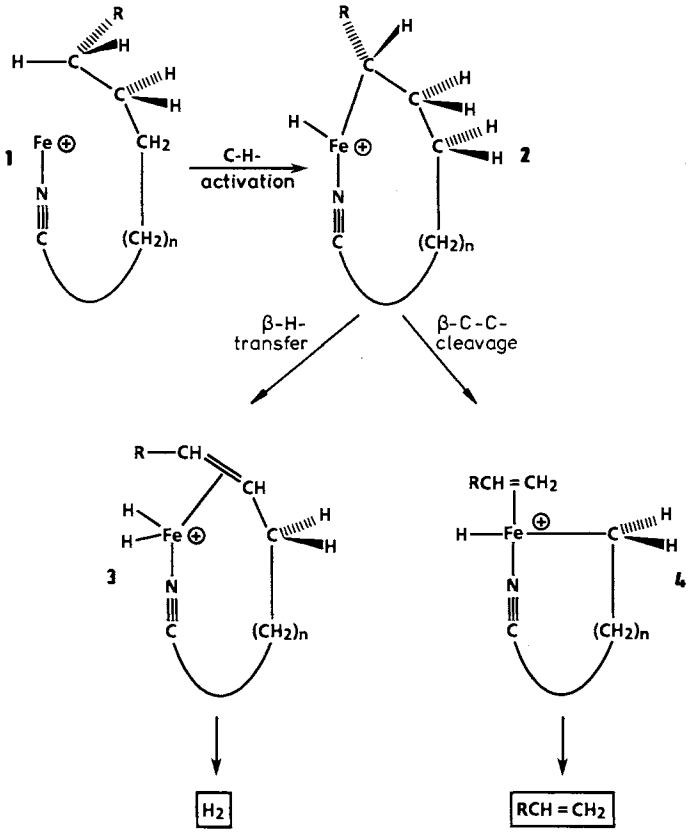
Multiple "Remote Functionalization" of Different Sites in Flexible Molecules by "Anchored" Bare Fe^{I} Ions**

By *Gregor Czekay, Karsten Eller, Detlef Schröder,* and *Helmut Schwarz**

Dedicated to Dr. Günther Ohloff on the occasion of his 65th birthday

The direct functionalization of *remote* C–H or C–C bonds, i.e. several carbon atoms away from an activating group, represents a great challenge. While such processes are common to enzymes, which "anchor" a functional group and *geometrically* select a specific segment of the substrate, only a few cases are reported[1] for relatively rigid molecules where a similar principle seems to be operative. *Breslow*[1a,b] has coined the term "remote functionalization" for this method of coordination of a functional group followed by selective reactions at sites away from the complexed functionality.

We[2] and later others[3] have demonstrated that a similar principle holds true in the gas phase for quite a variety of *flexible* organic substrates including aliphatic nitriles,[2,3] isonitriles,[4] amines,[5] alcohols,[6] ketones,[7] alkynes[8] and allenes,[9] respectively. For example, the chemistry of the $Fe^{\oplus}$-complexes of unbranched nitriles e.g. **1** (Scheme 1) is unique, in that *selective C-H activation occurs only at positions remote from the CN group*. The results of detailed studies[2] are compatible with a mechanism in which the reaction commences with the formation of an "end-on" complex **1**. For nitriles containing four to seven carbon atoms, the "anchored" transition-metal ion, $Fe^{\oplus}$, activates exclusively the C–H bond of the terminal methyl group (R = H) by oxidative addition (**1** → **2**). The insertion is followed by competitive β-hydrogen transfer (**2** → **3**) or β-cleavage of the C–C bond (**2** → **4**) to generate intermediates from which eventually neutral ethylene and molecular hydrogen are eliminated. If the carbon chain is lengthened, activation of internal C–H bonds is also observed. While the previous studies[2–9] permitted a detailed insight into many mechanistic details, no examples are known for the operation of *multiple* "remote functionalizations" of different sites in flexible molecules. Here, for the first time, evidence will be presented for the existence of such a reaction, which is also without precedence in condensed phase chemistry.



Scheme 1.

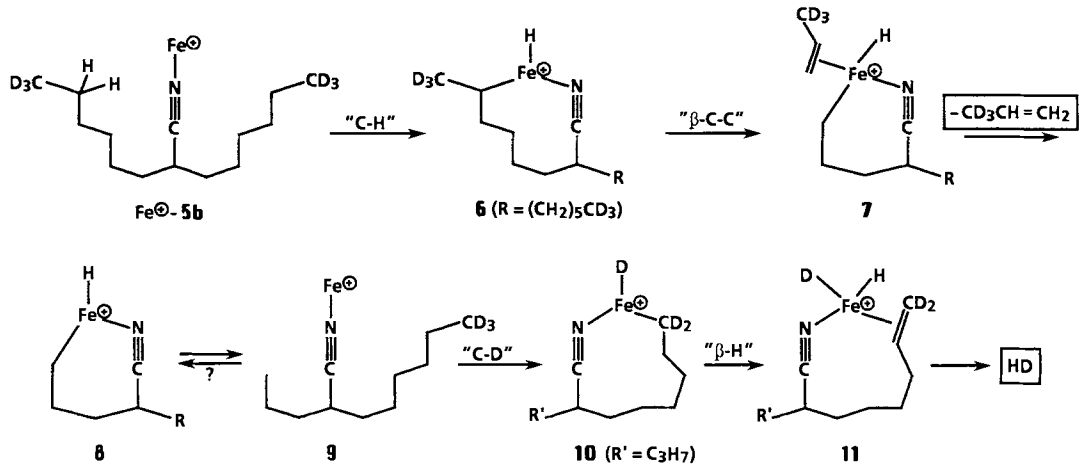
The metastable ion (MI) mass spectrum of mass-selected $(CH_3(CH_2)_5)_2CHCN/Fe^{\oplus}$ (**5a**-$Fe^{\oplus}$)[10] contains in addition to signals corresponding to the loss of neutral H_2 (46%), C_2H_4 (30%), C_3H_6 (15%) and C_4H_8 (3%), two signals which can be ascribed to the production of C_2H_6 and C_3H_8 (3% each). While the genesis of molecular hydrogen and of the alkenes[11] can be accounted for in terms of the traditional concept,[2] there exist two pertinent questions related to the formation of C_2H_6 and C_3H_8: (i) Do the neutral compounds correspond to genuinely formed alkanes C_nH_{2n+2} or are the observed mass differences due to the combined production of $C_nH_{2n}H_2/H_2$? (ii) If the latter is true, are both species formed from the same alkyl chain, or do the neutral fragments originate from both alkyl chains, and what sequence prevails?

The experimental findings are unambiguously in favor of the second alternative. This is evidenced by a study of the $Fe^{\oplus}$-complex of $(CD_3(CH_2)_5)_2CHCN$ (**5b**). If ethane and propane would be generated from **5b** according to the established pathway,[2,12] complex **5b**-$Fe^{\oplus}$ should undergo losses of CD_3CH_3 (Δm = 33) and $CD_3CH_2CH_3$ (Δm = 47). These two mass differences are *not* observed; rather, one finds Δm = 33 and 48. Moreover, if one selects, in a tandem experiment,[13] the $[M-28]^{\oplus}$ and $[M-42]^{\oplus}$ species unimolecularly generated from **5a**-$Fe^{\oplus}$ and studies their MI mass spectra, the *only* product formed corresponds to the production of H_2. While the latter experiment leaves no doubt that actually no alkanes but rather alkenes and molecular hydrogen are formed,[14] the labeling experiment proves for the C_3 neutral (and, by analogy, the same is presumed for the C_2-neutral) that *both* alkyl chains are involved in the $Fe^{\oplus}$-mediated C—H and C–C bond activation processes. For the formation of $C_3H_4D_4$, i.e. sequential losses of $CD_3CH=CH_2$ and HD, a mechanism is depicted in Scheme 2.

While for the nitrile complex **5a**-$Fe^{\oplus}$ the double remote functionalization constitutes a relatively minor decomposition path, the situation is very different for the $Fe^{\oplus}$-complex of 5-nonanone (**12a**-$Fe^{\oplus}$). The MI mass spectrum of this complex consists of three signals which are due to the losses of H_2 (31%), C_2H_4 (17%) *and* C_2H_6 (52%). The study[15] of the isotopomers **12a–h** leaves no doubt that molecular hydrogen and ethylene are formed in a process analogous to Scheme 1 ("remote functionalization"). However, the "alkane" generated from **12a**-$Fe^{\oplus}$ does *not* correspond to authentic ethane; rather it is due to the combined eliminations of ethylene and molecular hydrogen which are formed from the two alkyl chains in an unambiguous manner involving the $\omega/(\omega-1)$ and $\omega'/(\omega'-1)$ positions. This is evidenced by the data given in Table 1.[16] In addition, tandem experiments with the $[M-C_2H_4]^{\oplus}$- and $[M-H_2]^{\oplus}$-species prove

[*] Prof. Dr. H. Schwarz, Dipl.-Chem. G. Czekay, Dipl.-Chem. K. Eller, Dipl.-Chem. D. Schröder
Institut für Organische Chemie der Technischen Universität
Strasse des 17. Juni 135, D-1000 Berlin 12

[**] This work was supported by the Volkswagen-Stiftung, the Fonds der Chemischen Industrie, and the Gesellschaft von Freunden der Technischen Universität Berlin.



Scheme 2.

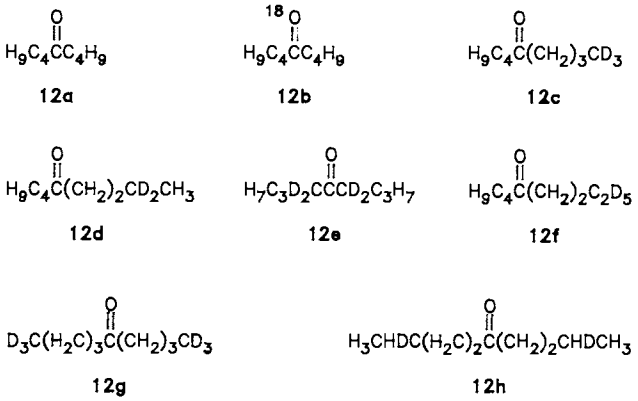


Table 1. Unimolecular elimination of molecular hydrogen, ethylene and "ethane" [a] from the $Fe^{\oplus}$-complexes of 5-nonanone isotopomers **12a–h**.

Δm [b]	12a	12b	12c	12d	12e	12f	12g	12h
2	31	25	26	18	23	15	–	15
3	–	–	12	6	–	–	18	6
4	–	–	–	–	–	3	–	–
28	17	20	10	16	17	20	–	–
29	–	–	–	–	–	–	–	23
30	52	55	7	8	60	–	27	–
31	–	–	23	27	–	–	–	40
32	–	–	22	25	–	34	–	16
33	–	–	–	–	–	–	55	–
34	–	–	–	–	–	28	–	–

[a] See text; "ethane" actually corresponds to the consecutive losses of ethylene and molecular hydrogen. [b] Δm corresponds to the mass differences with regard to the $Fe^{\oplus}$-complexes of **12a–h**; data are given in %, Σ fragment ions = 100%.

once more that the reaction follows the sequence **12a**-$Fe^{\oplus}$ → C_2H_4 → H_2 and not the reverse one.

To the best of our knowledge, the present results demonstrate for the first time beyond any doubt that an "anchored" transition-metal ion is capable of consecutively activating different sites of flexible molecules.

Received: May 8, 1989 [Z 3328 IE]
German version: *Angew. Chem. 101* (1989) 1306

[1] a) R. Breslow, *Chem. Soc. Rev. 1* (1972) 553; b) R. Breslow, *Acc. Chem. Res. 13* (1980) 170; c) R. Breslow, A. Adams, T. Guo, J. Hunger, *Lect. Heterocycl. Chem. 9* (1987) 43; d) U. Kerb, M. Stahnke, P. E. Schulze, R. Wiechert, *Angew. Chem. 93* (1981) 89; *Angew. Chem. Int. Ed. Engl. 20* (1981) 88.

[2] a) C. B. Lebrilla, C. Schulze, H. Schwarz, *J. Am. Chem. Soc. 109* (1987) 98; b) T. Drewello, K. Eckart, C. B. Lebrilla, H. Schwarz, *Int. J. Mass Spectrom. Ion Processes 76* (1987) R1; c) C. B. Lebrilla, T. Drewello, H. Schwarz, *ibid. 79* (1987) 287; d) C. B. Lebrilla, T. Drewello, H. Schwarz, *J. Am. Chem. Soc. 109* (1987) 5639; e) T. Prüsse, C. B. Lebrilla, T. Drewello, H. Schwarz, *ibid. 110* (1988) 5986; f) T. Prüsse, T. Drewello, C. B. Lebrilla, H. Schwarz, *ibid. 111* (1989) 2857; g) G. Czekay, T. Drewello, H. Schwarz, *ibid. 111* (1989) 4561; h) For review: H. Schwarz, *Acc. Chem. Res.*, in press.

[3] R. M. Stepnowski, J. Allison, *Organometallics 7* (1988) 2097.

[4] K. Eller, C. B. Lebrilla, T. Drewello, H. Schwarz, *J. Am. Chem. Soc. 110* (1988) 3068.

[5] a) S. Karraß, K. Eller, C. Schulze, H. Schwarz, *Angew. Chem. 101* (1989) 634; *Angew. Chem. Int. Ed. Engl. 28* (1989) 607. b) S. Karraß, T. Prüsse, K. Eller, H. Schwarz, *J. Am. Chem. Soc.*, in press.

[6] T. Prüsse, H. Schwarz, *Organometallics*, in press.

[7] D. Schröder, H. Schwarz, unpublished.

[8] a) C. Schulze, H. Schwarz, D. A. Peake, M. L. Gross, *J. Am. Chem. Soc. 109* (1987) 2368; b) C. Schulze, H. Schwarz, *J. Am. Chem. Soc. 110* (1988) 67; c) C. Schulze, T. Weiske, H. Schwarz, *Organometallics 7* (1988) 898.

[9] N. Steinrück, H. Schwarz, *Organometallics 8* (1989) 759.

[10] The experimental set-up has been described in detail in earlier papers [2, 4–9]. Briefly, $Fe^{\oplus}$ is generated from $Fe(CO)_5$ by electron impact ionization (100 eV) and reacted with the organic substrate of interest in a chemical ionization source of a VG Instruments ZAB-HF-3F triple sector mass spectrometer. (For a description of the machine, see: a) T. Weiske, Dissertation D83, Technische Universität Berlin (1985); b) J. K. Terlouw, T. Weiske, H. Schwarz, J. L. Holmes, *Org. Mass. Spectrom. 21* (1986) 665). The organometallic complexes corresponding to RCN/$Fe^{\oplus}$ and ketone-$Fe^{\oplus}$, respectively, and having 8 keV kinetic energy, are mass-selected and focused with B(1)E (B stands for magnetic and E for electrostatic sector). Unimolecular reactions occurring in the field-free region between E and B(2) were recorded by scanning B(2). MS/MS/MS experiments, performed in order to prove the multi-step decomposition of **5a**-$Fe^{\oplus}$ and **12a**-$Fe^{\oplus}$, were conducted by mass-selecting **5a**-$Fe^{\oplus}$ and **12a**-$Fe^{\oplus}$ by means of B(1); the products due to metastable losses of H_2 or alkenes were "isolated" by using E; fragment ions originating from further dissociations of $[M-H_2]^{\oplus}$ or $[M-C_nH_{2n}]^{\oplus}$ were recorded by scanning B(2). The signal-to-noise ratio was improved by using signal averaging techniques employing the VG 11/250 data system.

[11] A detailed discussion of the mechanisms by which these species are formed, is given in: G. Czekay, T. Drewello, K. Eller, W. Zummack, H. Schwarz, *Organometallics*, in press.

[12] For the transition metal ion mediated alkane formation in most cases reported it is, strictly speaking, not possible to distinguish between the two reaction sequences, i.e. 1) insertion of the metal ion in a C–C bond followed by β-hydrogen transfer, or 2) oxidative addition of a C–H bond followed by β-alkyl migration to the metal center. Both variants generate the same intermediate from which eventually reductive elimination of RH occurs.

[13] a) F. W. McLafferty (Ed.): *Tandem Mass Spectrometry*, Wiley Interscience, New York (1983); b) K. L. Busch, G. L. Glish, S. A. McLuckey: *Mass Spectrometry/Mass Spectrometry: Techniques and Applications of Tandem Mass Spectrometry*, VCH, Weinheim (1988).

[14] The reverse sequence, i.e. loss of H_2 followed by elimination of $RCH=CH_2$ (R = H, CH_3), does *not* contribute to the formation of "alkanes". This is evidenced by studying the mass-selected $[M-2]^{\oplus}$ species formed from **5a**-$Fe^{\oplus}$; no signals due to loss of $RCH=CH_2$ are present in this spectrum.

[15] D. Schröder, *Diploma Thesis*, Technische Universität Berlin (1989).

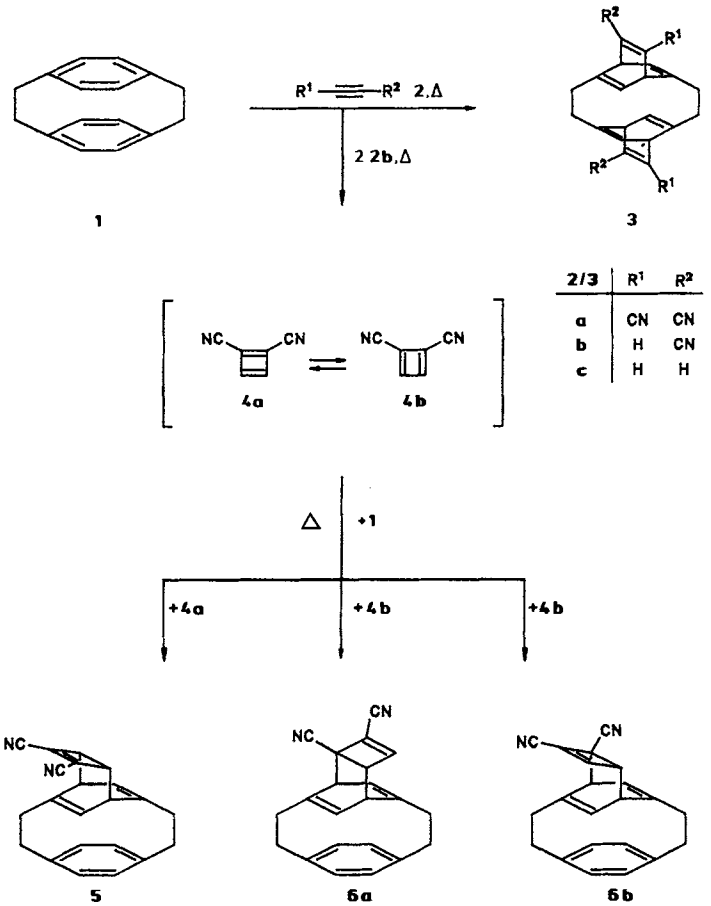
[16] A full discussion of these and other data, together with a detailed analysis of the kinetic isotope effects associated with the generation of molecular hydrogen, ethylene and "ethane", is given in [7, 15].

Does Cyanoacetylene Dimerize Thermally to 1,3-Cyclobutadiene-1,2-dicarbonitrile?**

By *Bernhard Witulski, Ludger Ernst, Peter G. Jones,* and *Henning Hopf**

Dedicated to Professor Virgil Boekelheide on the occasion of his 70th birthday

Strained aromatic compounds such as [2.2]paracyclophane **1** and its multiply bridged homologues undergo [2 + 4] cycloadditions under much milder reaction conditions than benzene and its methyl derivatives.[1] In 1967 *Ciganek*[2] found that **1** reacted with dicyanoacetylene **2a** in benzene at 130 °C to give a 1:2 cycloadduct, to which he assigned structure **3a**.[3] Since **3a** is a tetracarbonitrile derivative of a still unknown $C_{20}H_{20}$ hydrocarbon (**3c**, "double barrelene"), which might exhibit interesting rearrangement reactions (access to other $C_{20}H_{20}$ isomers such as dodecahedrane[4] or pagodane[5]?), we have reexamined the reaction of **1** with cyanoacetylenes. To minimize the number of further required steps (**3b** → **3c**), however, we used the mononitrile **2b** instead of **2a** (Scheme 1).



Scheme 1.

To our surprise, instead of compounds **3b** (isomeric mixture) analogous to *Ciganek*'s adduct, we obtained 2:1 adducts of a completely different type. [2.2]Paracyclophane **1** reacts with an excess of **2b** at 160 °C in benzene (sealed ampoule) within 22 h to give a complex mixture of products. Column chromatography (silica gel/dichloromethane) and recrystallization (chloroform/pentane) afforded a 47% recovery of starting material together with two main fractions in 6% and 21% yield, respectively. According to the ^{1}H NMR spectrum, the second fraction consists of two isomers in a ratio of 2.5:1. Further recrystallization (chloroform/pentane) allowed two of the three adducts to be obtained in analytically pure form. According to X-ray structure analysis and spectroscopic data, these adducts are compounds **5** (6%) and **6a** (15%). Because of limited space, only a summary of the crystallographic data (Fig. 1), together with the ^{1}H and ^{13}C NMR spectroscopic data (Table 1), is presented[6] for only one of the two compounds.

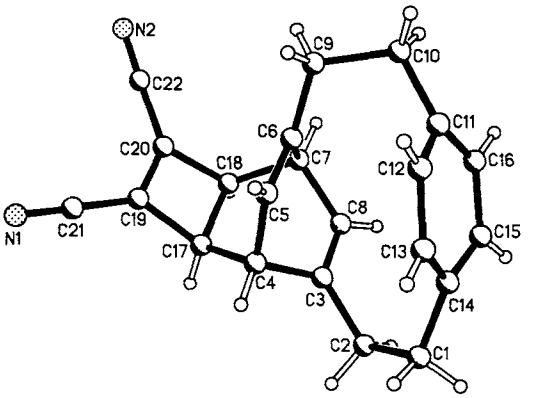


Fig. 1. Molecular structure of **5** (arbitrary atomic radii). Crystal data for **5**: $C_{22}H_{18}N_2$, $M_r = 310.4$, monoclinic, space group $P2_1$, $a = 779.2(3)$, $b = 760.3(3)$, $c = 1402.2(6)$ pm, $\beta = 96.13(3)°$, $V = 0.8259$ nm^3, $Z = 2$, $\varrho_{calcd} = 1.25$ Mg m^{-3}, $\lambda = 71.069$ pm ($Mo_{K\alpha}$), $\mu = 0.07$ mm^{-1}, $F(000) = 328$. Colorless plates, $0.8 \times 0.7 \times 0.15$ mm. Nicolet R3 diffractometer, $2\theta_{max} = 55°$, 3946 reflections, 3800 unique ($R_{int} = 0.009$), $3518 > 4\sigma(F)$. Orientation matrix refined on the basis of 50 reflections in the range $2\theta = 20$–$23°$. Structure solution by direct methods. Refinement to $R = 0.036$ for 216 parameters (hydrogen atoms positioned geometrically and refined using a riding model). Further details of the crystal structure investigation may be obtained from the Fachinformationszentrum Karlsruhe, Gesellschaft für wissenschaftlich-technische Information mbH, D-7514 Eggenstein-Leopoldshafen 2 (FRG), on quoting the depository number CSD-53941, the names of the authors, and the journal citation. The crystals of **6a** were of relatively poor quality (thin, weakly scattering plates with broad, irregular reflection profiles). Nonetheless, an X-ray structure analysis, which confirmed the connectivity of the molecule, could be carried out. In view of the low accuracy, only the crystal data are given: further details are available as described above. Crystal data for **6a**: orthorhombic, space group *Pbca*, $a = 1432.4(3)$, $b = 1235.4(5)$, $c = 1857.4(6)$ pm, $V = 3.287$ nm^3, $Z = 8$, $\varrho_{calcd} = 1.25$ Mg m^{-3}, $\mu(Mo_{K\alpha}) = 0.07$ mm^{-1}, $F(000) = 1312$. $R = 0.105$ for 1466 reflections.

The formation of cycloadducts **5** and **6** can be explained most simply by answering the title question in the affirmative. Thus, head-to-head coupling of two molecules of **2b** would form 1,3-cyclobutadiene-1,2-dicarbonitrile, which should exist as an equilibrium mixture of the valence tautomers **4a** and **4b**. In a subsequent step, these products would be trapped by **1** to give the [2 + 4] adducts (Scheme 1), which are derivatives of the Nenitzescu hydrocarbon. Whereas **6a, b** could also be formed by a Diels–Alder addition of **2b** to **1** followed by a [2 + 2] cycloaddition, there is no analogous route for the formation of **5**. Whatever reaction mechanism ultimately proves operative, it is clear that

[*] Prof. Dr. H. Hopf, B. Witulski
Institut für Organische Chemie der Technischen Universität
Hagenring 30, D-3300 Braunschweig (FRG)
Prof. Dr. L. Ernst
NMR-Laboratorium der Chemischen Institute
der Technischen Universität Braunschweig (FRG)
Prof. Dr. P. G. Jones
Institut für Anorganische und Analytische Chemie
der Technischen Universität Braunschweig (FRG)

[**] Cyclophanes, Part 31. Part 30: Z. Pechlivanidis, P. G. Jones, H. Hopf, *Z. Naturforsch. B 44b* (1989) 860.

Table 1. ^{13}C and ^{1}H NMR data for **5** [a].

Position	δ(C)	δ(H) [b]	Position	δ (C)	δ(H)
1	33.1	2.86, 2.75	12	132.5	6.92
2	33.8	2.23, 2.53	13	128.6	6.86
3	141.0	–	14	138.9	–
4	43.91	2.84	15	132.3	6.90
5	127.7	5.10	16	128.4	6.85
6	136.9	–	17	47.0	2.68
7	43.87	2.83	18	46.6	2.65
8	131.5	5.43	19, 20	132.8	–
9	34.1	2.56, 2.12		132.6	–
10	33.1	2.77, 2.87	21, 22	111.0	–
11	139.5	–		110.8	–

[a] At 400.1 and 100.6 MHz, respectively, in $CDCl_3$/TMS. Atom numbering as in Fig. 1. The first δ(H) value for CH_2 groups refers to the proton *cis* to H-4 on the ring C1–C6, C9–C14–C1. [b] H,H coupling constants J(H-12,13) = J(H-15,16) = 7.8, J(H-12,16) = 1.9, J(H-13,15) = 1.8, J(H-4,5) = J(H-7,8) = 6.3, J(H-5,9c) = J(H-2t,8) = 1.5 Hz (c,t rel. to H-4); the remaining J(H,H) could not be assigned or are involved in higher order spin systems. The ^{13}C and ^{1}H NMR spectra of **5** and **6a** [8] were assigned using $^{1}H\{^{1}H\}$ NOE difference spectra, decoupling experiments, and two-dimensional techniques (H,H and C,H COSY and C,H COLOC) [9]. A notable feature of the ^{13}C data is that the shifts of the aromatic carbon atoms C-12 and C-15, which are found below the sp^2-hybridized atoms C5 and C-8, respectively, are similar to those in **1** (δ = 133.1), whereas C-13 and C-16, under the sp^3-hybridized bridgeheads C-4 and C-7, respectively, are shielded by about 4 ppm relative to C-12 and C-15. A correlation of the inter-ring C–C distances in **1** (309 pm) [10], **5** [1/2 ($r_{5,12}$ + $r_{8,15}$) = 303 pm, 1/2 ($r_{4,13}$ + $r_{7,16}$) = 361 pm] and in [3.3]paracyclophane **7** (330 pm) [11] with the chemical shifts of the corresponding arene carbon atoms in **1** (δ_C = 133.1), in **5** [1/2 (δ_{C-12} + δ_{C-15}) = 132.4, 1/2 (δ_{C-13} + δ_{C-16}) = 128.5], and in **7** (δ_C = 129.7) indicates that this phenomenon is probably due more to the larger nonbonding distances $r_{4,13}$ and $r_{7,16}$ in **5** than to the changed hybridization of C-4 and C-7. In the ^{13}C spectrum of **6a**, the same effect is observed as in the spectrum of **5**.

cyanoacetylene **2b** behaves as an equivalent of the cyclobutadienes **4** under these reaction conditions.[7]

Received: May 10, 1989 [Z 3331 IE]
German version: *Angew. Chem. 101* (1989) 1290

[1] A. E. Mourad, J. Kleinschroth, H. Hopf, *Angew. Chem. 92* (1980) 388; *Angew. Chem. Int. Ed. Engl. 19* (1980) 389, and references cited therein.
[2] E. Ciganek, *Tetrahedron Lett. 1967*, 3321.
[3] In the structure shown, **3a**, the two dicycanoethene bridges are parallel to each other. Besides this adduct, an isomer with mutually orthogonal (crossed) bridges is also conceivable. The preferred mode of addition was not originally determined [2], though the second alternative seems more probable, since *N*-phenylmaleimide reacts to give a crossed 2:1 product, as shown by X-ray structure analysis: K. Matsumoto, T. Okamoto, A. Sera, K. Itoh, K. Hameda, *Chem. Lett. 1987*, 805.
[4] Summary: L. Paquette in T. Lindberg (Ed.): *Strategies and Tactics in Organic Synthesis, Vol. 1*, Academic Press, Orlando 1984, p. 175ff.
[5] R. Pinkos, J.-P. Melder, H. Fritz, H. Prinzbach, *Angew. Chem. 101* (1989) 319; *Angew. Chem. Int. Ed. Engl. 28* (1989) 310, and previous publications as well as references cited therein.
[6] **5**, m.p. 163–64 °C; **6a**, m.p. 212 °C. The other spectroscopic data and elemental analyses are also in agreement with the structures suggested above for **5** and **6a**. Repetition of the experiment at lower temperatures (130 °C) afforded traces of adduct **5** and a mixture of **6a/b** in 4% yield together with 90% recovery of **1**. There is no indication that a 1:1 adduct is formed between **1** and **2b**.
[7] As by-products in the cycloadditions described here, varying amounts of 1,2,4- and 1,2,3-tricycanobenzene were also formed. These products can likewise be explained in terms of intermediates of type **4**. In the 1960's *Viehe* et al. observed that *tert*-butylfluoroacetylene underwent oligomerization in solution in an exothermic reaction to give trimers and tetramers: H. G. Viehe, R. Merenyi, J. F. M. Oth, J. R. Senders, P. Valange, *Angew. Chem. 76* (1964) 922; *Angew. Chem. Int. Ed. Engl. 3* (1964) 755. The trimers are Dewar benzene and benzvalene derivatives, which may have been formed via the corresponding cyclobutadienes. Although trapping experiments were carried out (cf. H. G. Viehe, *ibid. 77* (1965) 768 and *4* (1965) 746) they were unsuccessful (personal communication from Prof. *Viehe* on June 27, 1989). Cyanoacetylene **2b** belongs to the class of highly unsaturated compounds that have recently been detected in interstellar space: G. Winnewisser, *Top. Curr. Chem. 99* (1981) 39; molecules such as **4a/b** may also be stable under these extreme conditions.
[8] **6a**: ^{13}C NMR (100.6 MHz, $CDCl_3$, standard TMS)/^{1}H NMR (400.1 MHz, $CDCl_3$, standard TMS): δ_C/δ_H = 155.4/6.68, 51.7/2.84 (CH in four-membered ring); 111.1, 46.8 (C in four-membered ring); 118.8, 118.7 (CN); 132.5/6.91, 132.4/6.92, 128.5/6.89, 128.2/6.84 (CH_{ar}); 139.4, 139.0 (C_{ar}); 133.2/5.61, 127.5/5.15, 47.2/3.03, 44.8/2.81 (CH in cyclohexadiene ring); 139.9, 138.5 (C in cyclohexadiene ring); 34.4/2.67,2.33 and 34.1/2.46,1.99 (CH_2 bonded to C=C); 33.0/2.91,2.76 and 33.0/2.85,2.72 (CH_2 bonded to aryl). Isomer **6b** has not yet been obtained free of **6a**. The structural assignment given in the scheme is based above all on the similarity of the nuclear magnetic resonance spectra of the two adducts **6**. The distinct ^{1}H NMR signals of **6b** in the **6a/b** mixture show the same splitting pattern and similar shifts as the corresponding absorptions of **6a**. **6b**: ^{1}H NMR (400.1 MHz, $CDCl_3$, standard TMS): δ = 6.66 (=C*H* in the four-membered ring), 5.56, 5.06, 3.04 (three of the four C*H* units in the cyclohexadiene ring), 2.25, 2.16 (part of the CH_2 bonded to C=C).
[9] Summary of recent NMR techniques: a) J. K. M. Sanders, B. K. Hunter: *Modern NMR Spectroscopy*, Oxford University Press, Oxford 1987; b) A. E. Derome: *Modern NMR Techniques for Chemistry Research*, Pergamon Press, Oxford 1987.
[10] H. Hope, J. Bernstein, K. N. Trueblood, *Acta Crystallogr. B28* (1972) 1733.
[11] P. K. Gantzel, K. N. Trueblood, *Acta Crystallogr. 18* (1965) 958.

Book Reviews are written by invitation from the editor. Suggestions for books to be reviewed and for book reviewers are welcome. Publishers should send brochures or (better) books to the following address: Redaktion Angewandte Chemie, Postfach 101161, D-6940 Weinheim, Federal Republic of Germany. The editor reserves the right of selecting which books will be reviewed. Uninvited books not chosen for review will not be returned.

Chromatographic Enantioseparation—Methods and Applications. (Ellis Horwood Series in Analytical Chemistry). By *S. G. Allenmark*. Halsted Press, New York/Wiley, Chichester 1988. 224 pp., hard cover, £ 38.50.—ISBN 0-85312-988-6/0-470-21080-X.

Research on chiral chromatographic separations is at a peak at the present time, about 25 years after the feasibility of direct resolution of chiral phases by modern techniques was first demonstrated. The variety of systems now known to display stereoselectivity is considerable, and new developments are constantly emerging. However, the understanding of the mechanisms involved in chiral recognition lags behind practical achievements. Also, comparative studies of different procedures recommended for the solution of a certain problem are scarce.

Under these circumstances, it is not easy to summarize satisfactorily and comprehensively the state of the art. The author is to be commended on having attempted to do so, although, in the opinion of the reviewer, he has only succeeded in part.

The best chapters are those dealing with "Chiral Liquid Chromatography" and with "Analytical Applications in Academic Research and Industry"; they represent about half of the book. This is not surprising, as the direct experience of the author seems to have been mainly in these areas. Even so, some interesting recent contributions to chiral LC have not been included, and in the applications chapter there is no mention of geochemical, cosmochemical and archaeometric analyses, or the study of the configuration of bacterial cell wall constituents, and of racemization of proteins in living (including human) beings.

The summary treatment of chiral GC does not do justice to the importance of this mode of chromatography, nor does the section on resolution via diastereomers. Such interesting procedures as the precolumn derivatization of amino acids by *o*-phthaldialdehyde plus *N*-acetyl-L-cysteine (D. W. Aswad, *Anal. Biochem.*, 1984) and the resolution of olefins through Pt complexes coordinated to chiral ligands (M. Goldman et al., *J. Am. Chem. Soc.*, 1981) are disregarded.

Chiral TLC is not referred to, to say nothing of techniques related to chromatography, such as droplet counter-current chromatography and capillary electrophoresis, which have lately been shown to produce effective enantioseparations.

Some topics, such as the use of cyclodextrins as selectors, would already have to be largely rewritten one year after the appearance of the book. This is also true, to some extent, of the brief chapter on "Preparative Scale Enantioseparations".

The author has not discussed available spectroscopic evidence for some proposed chiral recognition models, nor the results of any relevant calculations of favored conformations of selectors likely to be involved in the recognition process. Such material might perhaps be outside the scope of a book which is essentially practically orientated. However, certain of the examples of models of chiral recognition that are shown would have been more instructive if accompanied by some additional critical comments. For instance, in Fig. 7.15 the nature, and indeed the necessity, of involving a $-CH\cdots O=C-$ hydrogen bond in the intermediate stereoselective complex should have been discussed; and for the model in Fig. 7.16, possible alternatives to the proposed C_5-C_5 hydrogen bonded association should have been given (C_7-C_5 association or intercalation between two selector molecules).

Though the text is, in general, lucid, there are instances in which the original papers have not been accurately quoted or are better formulated. All statements are, however, referenced and can be readily checked. The legends and annotations of the figures taken from the literature have not always been adapted to the new text, and the data listed in the tables are not always complete.

In spite of the above shortcomings, the monograph should be useful to many readers, particularly as it is at present the only book covering a relatively wide range of the subject. It will provide a good idea of the potential of the approach for researchers in academia, and analysts in industry dealing with optically active compounds. The copious bibliography (more than 600 references) will be of great value to the reader.

There are almost no printing errors in the text; the structure given in Fig. 3.3 is drawn incorrectly.

Emanuel Gil-Av [NB 980 IE]
Organic Chemistry Department
Weizmann Institute of Science
Rehovot (Israel)

Theory and Methods of Calculation of Molecular Spectra. By *L. A. Gribov* and *W. J. Orville-Thomas*. Wiley, Chichester 1988. xxvii, 636 pp., hard cover, £ 85.00.—ISBN 0-471-91882-2

It is appropriate and welcome that the authors have written a comprehensive book on the theory of molecular spectra and methods of calculation at the present time. The attractive presentation of this book, the generality of its title, and its size (more than 600 pages) thus raise high expectations on the part of potential readers. However, there is a little disappointment on discovering that the book concentrates mainly on the traditional forms of spectroscopy (IR, Raman, and vibrational excitations caused during electronic transitions).

The book treats molecular vibrations with great thoroughness, and addresses some interesting aspects and problems. Thus, for example, the kinetic energy of vibrational motions—including internal rotations—is treated in detail and illustrated by numerous applications. The expression for the

kinetic energy, in the form appropriate for large amplitude vibrations, is simplified in stages by introducing the relevant approximations according to different problem situations. An appropriate amount of space in the book is devoted to normal coordinate analysis and the treatment of anharmonicities, including suggestions for numerical methods suitable for computer calculations, together with examples. The theory of band intensities in infrared and Raman spectra is treated in two separate chapters.

A topic which I found especially interesting was the "inverse spectral problem", which is referred to frequently in the book. This is the problem of using experimental spectra to derive information about the molecule and its physical parameters. The authors describe models which allow simulation of an experimental spectrum, with successive modifications of the model to improve the matching.

Several chapters are concerned with the theory of electronic states and methods for calculations thereon. These chapters have little relevance to the central theme of molecular vibrations, and do not seem to fit well into the book. They are too long to provide just a brief survey of this area, while at the same time being insufficiently detailed and consistent to give the reader a proper understanding. Many books dealing with this topic are already available.

Although the treatment of some of the topics is very thorough, the work is not suitable for use as a student textbook. Considerable parts of it can only be fully understood with the help of supplementary reading, and many of the papers cited are only available in Russian. It is noticeable that recent publications from authors in the Western world are rarely cited, and it is disconcerting to find that about 25% of the references are to the authors' own papers. Three particularly striking examples of this appear in Chapters 9, 12 and 15. Chapter 9, "The Potential Function of a Polyatomic Molecule and its Properties", contains references to work by authors from the West only up to 1971, despite the considerable more recent progress in this field (which is even covered in textbooks). Chapter 12, "Characteristic Vibrations of Polyatomic Molecules", begins with a reference to the authors' own work and contains only two citations. Chapter 15, on the important and much discussed topic of Raman intensities, contains only three references, two to the authors' own work and one to a 1954 paper by *W. Heitler*.

Although this book deals with many interesting and important problems, and is of the right length to provide an accurate but nevertheless easily readable account of the subject, I find that I have to express my disappointment with the result. The discussions and derivations are often lengthy but, despite this, not easy to understand. The literature coverage is infuriating, the nomenclature is rather unfortunate in some places (e.g. the well-known Wilson G- and F-matrices have been renamed), and certain modern concepts such as local modes and vibrations in short-lived electronic states are not discussed. The authors in their preface say that criticisms are welcomed. I hope that the comments offered here will be taken as constructive.

Lorenz S. Cederbaum [NB 976 IE]
Physikalisch-Chemisches Institut
der Universität Heidelberg (FRG)

Corrigenda

In the communication entitled "Flexible Syntheses of Optically Active Isocarbacyclins" by H. Hemmerle and H.-J. Gais (*Angew. Chem. Int. Ed. Engl. 28* (1989) 349), the R^1-containing side chain of **12** should have one additional CH_2 group.

The communication entitled "Are Lithiosulfones Configurationally Stable?" by H.-J. Gais, G. Hellmann, H. Günther, F. Lopez, H. J. Lindner, and Sigmar Braun (*Angew. Chem. Int. Ed. Engl. 28* (1989) 1025) contained several inadvertent mistakes. The sentence beginning on line 30, page 1026, should read: "A linear relation between $\ln \alpha$ and t ..." In reference [11], the equation should read: $k_{rac} = 2\,k_{enan}$.

Registered names, trademarks, etc. used in this journal, even when not marked as such, are not to be considered unprotected by law.

© VCH Verlagsgesellschaft mbH, D-6940 Weinheim, 1989. – Printed in the Federal Republic of Germany by Konrad Triltsch Druck- und Verlagsanstalt Würzburg.

All rights reserved (including those of translation into foreign languages). No part of this issue may be reproduced in any form — by photoprint, microfilm, or any other means — nor transmitted or translated into a machine language without written permission from the publishers. Only single copies of contributions, or parts thereof, may be made for personal use. This journal was carefully produced in all its parts. Nevertheless, authors, editors and publisher do not warrant the information contained therein to be free of errors. Readers are advised to keep in mind that statements, data, illustrations, procedural details or other items may inadvertently be inaccurate.

Valid for users in the USA: The appearance of the code at the bottom of the first page of an article (serial) indicates the copyright owner's consent that copies of the article may be made for personal or internal use, or for the personal or internal use of specific clients. This consent is given on the condition, however, that the copier pay stated per-copy fee through the Copyright Clearance Center, Inc. (CCC), for copying beyond that permitted by Sections 107 or 108 of the U.S. Copyright Law. This consent does not extend to other kinds of copying, such as copying, for general distribution, for advertising or promotional purposes, for creating new collective works, or for resale. For copying from back volumes of this journal see 'Permissions to Photo-Copy: Publisher's Fee List' of the CCC.

Editorial office: Postfach 10 11 61, D-6490 Weinheim, Federal Republic of Germany, Telephone (06201) 60 22 55, Telex 465 516 vchwh d, Telefax (06201) 602 328.

Editor: *Peter Gölitz*

Associate editors: *D. I. Loewus, A. Stimson.* **Editorial assistant:** *E. Schweikart*

Publishers: VCH Verlagsgesellschaft mbH. (Managing Director: *Hans Dirk Köhler*), Pappelallee 3, D-6940 Weinheim, Federal Republic of Germany.

Advertising office (Advertising Manager *R. J. Roth*): Postfach 10 11 61, D-6940 Weinheim, Federal Republic of Germany, Telephone (0 62 01) 60 61 30, Telex 4 67 155, Telefax (0 62 01) 606 184.

ANGEWANDTE CHEMIE
International Edition in English
Volume 28 · Number 10
October 1989
Pages 1283–1444

Catalytic Antibodies

By Peter G. Schultz*

The vast binding repertoire of the immune system has been exploited for the generation of tailor-made biological catalysts. A number of strategies have been developed to generate catalytic antibodies that carry out a wide range of reactions with exquisite specificities. The generation and characterization of these novel catalysts is not only providing new insights into the nature of biological recognition and catalysis, but may also lead to novel catalysts for applications in chemistry, biology, and medicine.

1. Introduction

The synthesis of catalysts with tailored specificities and catalytic properties is a challenging problem to both chemists and biologists alike. A key element in the design of enzymelike catalysts is the rational generation of receptors capable of discriminating ligands with high selectivity. To date, most efforts in this regard have focused on either the synthesis and functionalization of relatively small cavity-containing hosts or the alteration of the natural specificity of enzymes by chemical modification or oligonucleotide-directed mutagenesis.

With the advent of hybridoma technology[1] it has become possible to generate homogeneous, high-affinity antibody binding sites that selectively recognize a large number of structurally diverse ligands. Antibodies have been generated against large biopolymers such as nucleic acids, peptides, and polysaccharides, natural products such as steroids and prostaglandins, and small synthetic molecules such as phenylphosphonates and benzylamines. The immune system's ability to selectively generate antibodies against virtually any molecule of interest has resulted in the widespread use of antibodies (1) as therapeutic and imaging agents, (2) as diagnostic agents, and (3) as probes for isolating and unraveling the structures of complex biological molecules.[1b, 2]

Because antibodies can be generated against virtually any molecule of interest, the development of general strategies for introducing catalytic activity into antibody combining sites should lead to a new class of enzymelike catalysts *with tailored specificities*. Catalytic antibodies could have considerable value as biochemical or molecular-biological tools, as therapeutic agents, or in the synthesis of pharmaceuticals and novel materials. To date, two general approaches have been pursued for the generation of catalytic antibodies. The steric and electronic complementarity of an antibody to its corresponding hapten (the ligand against which the antibody is elicited) has been exploited to generate combining sites that (1) are complementary to the rate-determining transition state, (2) act to overcome the entropy requirements involved in orienting reaction partners, (3) contain an appropriately positioned catalytic amino-acid side chain, or (4) contain cofactor binding sites. Alternatively, catalytic groups can be introduced directly into the combining site of an antibody by chemical modification or by site-directed mutagenesis or genetic selection. The ability to generate antibody combining sites with specific catalytic groups and/or

[*] Prof. P. G. Schultz
Department of Chemistry, University of California
Berkeley, CA 94720 (USA)

 © VCH Verlagsgesellschaft mbH, D-6940 Weinheim, 1989 0044-8249/89/1010-1283 $ 02.50/0

microenvironments should, in addition to affording selective catalysts, also help dissect the contribution of various factors involved in enzymatic catalysis, including transition-state stabilization, general acid–base catalysis, nucleophilic catalysis, ground-state strain, and proximity effects.

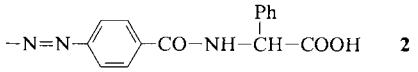
2. Antibody Generation, Structure, and Function

2.1. Antibody–Ligand Interaction

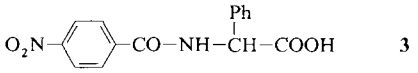
Much of our current knowledge of the nature of antibody–ligand interactions is based on measurements of the binding affinities of heterogeneous polyclonal antibodies to a series of haptens (substances which are not immunogenic until coupled to a carrier molecule) of defined structure.[3] The high specificity of antihapten antibodies can be illustrated by the following experimental examples. Polyclonal antibodies were elicited to the "*p,p'*-azophenylazobenzoate" group **1**

$$(p)\text{-}N{=}N\text{-}C_6H_4\text{-}N{=}N\text{-}C_6H_4\text{-}COO^{\ominus}\text{-}(p) \quad \mathbf{1}$$

conjugated to the carrier protein bovine serum albumin.[4] Relative average binding affinities of a series of hapten analogues to the anti-*p,p'*-azophenylazobenzoate antibodies were then determined by precipitation inhibition assays.[5] These antibodies effectively discriminated aryl rings substituted with sulfonate ($-SO_3^{\ominus}$), phosphonate ($-PO_3H^{\ominus}$), and arsonate ($-AsO_3H^{\ominus}$) groups as well as the neutral hydroxyl (-OH) group relative to the planar carboxylate monoanion. In addition, neither acetate nor cyclohexanecarboxylate inhibits the precipitation reaction, indicating antibody specificity for the flat aryl ring. *Karush* has demonstrated that polyclonal antibodies directed against the D isomer of **2** bind the L isomer of **3** with approximately 200-fold lower affinity than the D isomer.[4b]



2



3

Electrostatic interactions play an important role in ligand recognition by antibodies. Chemical modification experiments by *Pressman* and co-workers have revealed the presence of positively charged arginine and lysine residues in the combining sites of antibodies to the "*p*-azobenzoate" group, $(p)\text{-}N{=}N\text{-}C_6H_4\text{-}COO^{\ominus}$, and, conversely, the presence of carboxylate groups in antibodies specific to the *p*-trimethylammoniophenylazo ("*p*-azobenzenetrimethylammonium") group.[6] Hydrophobic and hydrogen-bonding interactions also play an important role in antibody–ligand recognition. For example, NMR experiments have shown that a tryptophan π-stacks with the aryl ring in the anti-2,4-dinitrophenyl (DNP) antibody MOPC 315.[7] X-ray crystallography has revealed that hydrogen-bonding interactions are important in the recognition of lysozyme by an antilysozyme antibody[8] and in the recognition of phosphorylcholine by the antibody McPC 603.[9]

Antibodies bind ligands ranging in size from about 6 to 34 Å with association constants in the range of 10^4 to 10^{14} M^{-1}.[3] The rate constants for the forward reaction of hapten with antibody are typically in the range of 1×10^7 to 1×10^8 $M^{-1}\,s^{-1}$,[10] whereas the rate k_{off} of the reverse reaction can vary considerably; for example, k_{off} is 1.1 s^{-1} for ε-DNP-lysine with anti-DNP antibody and 1300 s^{-1} for DNP-glycine with MOPC 315.[10]

2.2. Antibody Structure

Antibodies are large proteins (ca. 150 000 daltons for an IgG monomer) that consist of four polypeptide chains: two identical heavy chains of ca. 50 000 daltons and two identical light chains of ca. 25 000 daltons, cross-linked by disulfide bonds.[11] The light chains are divided into two domains, V_L (variable) and C_L (constant), while the heavy chains consist of V_H, C_{H1}, C_{H2}, and C_{H3} domains. Amino-acid sequencing has shown that light and heavy chains of the same antigenic class possess a constant amino-acid sequence in the C_L and C_H regions, while the V_L and V_H regions are unique and highly polymorphic for each immunoglobulin (Ig). The ligand combining site of immunoglobulins consists of six hypervariable regions, that is, regions of extensive amino-acid diversity, located in roughly the first 110 amino acids of



Peter G. Schultz received his Ph.D in 1983 under Prof. Peter Dervan (California Institute of Technology) and was an NIH postdoctoral fellow with Prof. Christopher Walsh (Massachusetts Institute of Technology) in 1984. He joined the faculty in the Department of Chemistry at the University of California, Berkeley, in 1985 and was promoted to Associate Professor in 1987 and Professor of Chemistry in 1989. His research program focuses on the study of the mechanisms of molecular recognition and catalysis and the applications of these studies to the design of highly selective catalysts for applications in chemistry, biology, and medicine. His research includes the generation and characterization of catalytic antibodies, the development and application of new mutagenesis methods for selectively introducing unnatural amino acids into proteins and the design of sequence-specific nucleases for large RNAs and DNAs. Peter G. Schultz has received a number of awards including the ACS Nobel Laureate Signature Award, the NSF Waterman Award, and the ACS Award in Pure Chemistry. He is an NSF Presidential Young Investigator, Searle Scholar, and Alfred P. Sloan Fellow. He is also a founding scientist of the Affymax Research Institute, a novel drug discovery effort.

the light (V_L) and heavy (V_H) polypeptide chains of the Ig[11] (Fig. 1). Combinatorial joining of the gene segments encoding the V_L and V_H genes and combinatorial association of different light and heavy chains generate a minimum of 10^8 different antibody molecules; mutations expand this baseline repertoire of receptors still further.[12] Cleavage of immunoglobulins with papain results in the formation of an F_{ab} fragment containing the light chain as well as the V_H and C_{H1} regions of the heavy chain (Fig. 1).

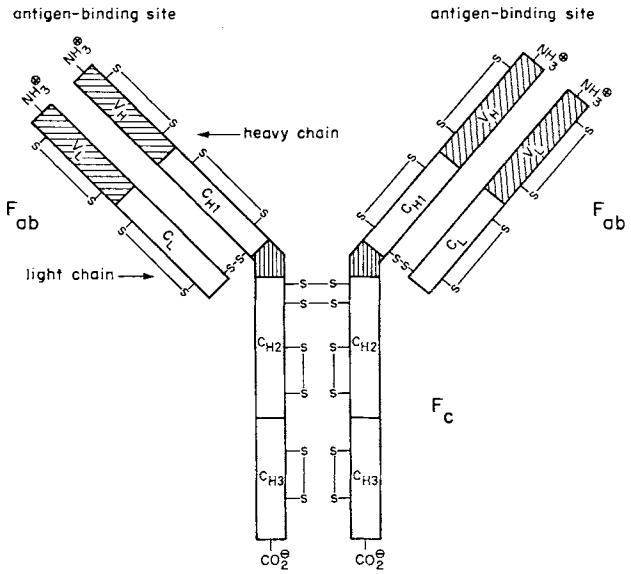


Fig. 1. The schematic structure of immunoglobulins (antibodies).

The structural basis for antibody binding affinity and specificity has been probed by X-ray crystallography, ESR and NMR studies of spin-labeled haptens, and affinity-labeling studies. High-resolution X-ray diffraction studies have led to three-dimensional structures for a number of antibody F_{ab} fragments, including those of the F_{ab} fragment of the myeloma protein McPC 603 with phosphorylcholine,[9] the F_{ab} fragment of human protein New with a vitamin K derivative,[13] the F_{ab} fragment of two immunoglobulins with lysozyme,[8] an F_{ab} fragment with the viral protein neuraminidase,[14] and the F_{ab} fragment Kol.[15]

2.3. Generation of Monoclonal Antibodies

Work on catalytic antibodies to date has focused entirely on the generation of monoclonal antibodies. A monoclonal antibody is a single molecule with defined affinity and specificity for a hapten.[1] A polyclonal antibody preparation, on the other hand, contains a variety of antibody molecules directed against the same antigen. These antibodies can differ in affinity and specificity, and the composition of the preparation may vary. Consequently, it is more straightforward (and meaningful) to characterize a monoclonal catalytic antibody rather than the average properties of a polyclonal mixture. Moreover, monoclonal antibodies can be generated *reproducibly* and on a gram scale.

The protocol for preparing monoclonal antibodies is outlined in Figure 2.[1] After an antigenic response to the desired immunogen is achieved, antibody-producing plasma cells

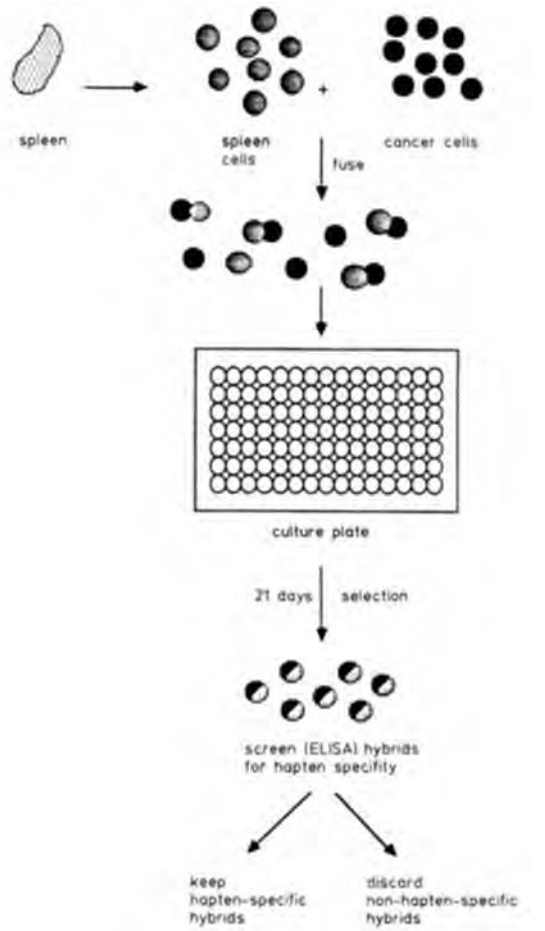


Fig. 2. The production of monoclonal antibodies.

from the spleen are fused (or hybridized) to an immortal myeloma cell line. This step insures that the antibody-producing cells can be cultured and caused to multiply indefinitely. The hybridomas are then cloned or separated into colonies of cells which produce a single antibody. The resulting cells are screened by an ELISA (enzyme-linked immunosorbent assay) for their ability to generate antibodies that bind selectively and with high affinity to the ligand of interest (Fig. 3).[16]

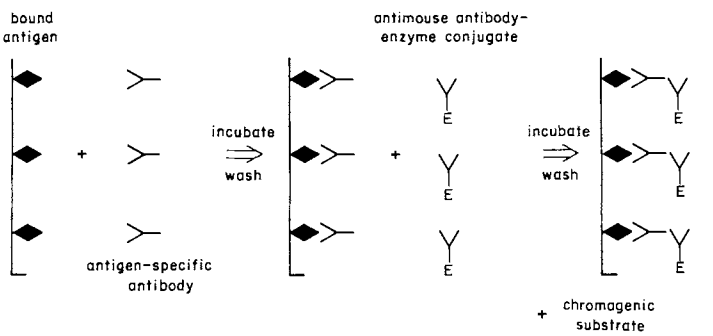


Fig. 3. Enzyme-linked immunosorbent assay (ELISA) for screening antibodies for selectivity and high affinity.

Since small haptens are not immunogenic unless coupled to a carrier molecule, all of the haptens described in this review were coupled to the carrier protein bovine serum albumin (BSA) and keyhole limpet hemocyanin (KLH). The length of the spacer arm between the hapten and carrier is in the range of 6 to 8 Å, which should preclude any steric interference with carrier side chains.[17] The haptens were typically coupled to BSA and KLH via *N*-(3-dimethylaminopropyl)-*N'*-ethylcarbodiimide or the *N*-hydroxysuccinimide ester at pH 5.5 in water.[17] Other coupling strategies have included disulfide exchange reactions, electrophilic aromatic substitution with diazonium salts, and reductive amination.[17] Hapten-to-carrier ratios typically ranged between 8 and 15 haptens per carrier.

Balb/c, Swiss Webster, or AJ1 mice were immunized with the KLH–hapten conjugate emulsified in complete Freund's adjuvant.[18] Fusions were carried out by standard methods with Sp2/0 myeloma cells as fusion partners.[19] Antibodies were screened by ELISA for cross-reactivity with the BSA–hapten conjugate, for inhibition of binding to the BSA–hapten conjugate by free hapten, and for lack of cross-reactivity with KLH. IgG's were purified from ascites fluid by protein A affinity chromatography[20] or Mono Q cation-exchange chromatography and judged to be homogeneous by 12% sodium dodecyl sulfate polyacrylamide gel electrophoresis.

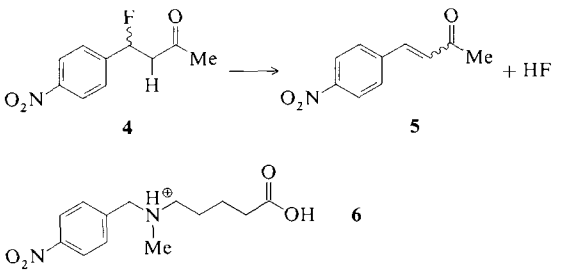
The purity of monoclonal antibodies is tremendously important, especially when an enzyme is known to catalyze the reaction of interest. For example, if k_{cat} for a catalytic (IgG) antibody is $1\ min^{-1}$ and a natural enzyme has a k_{cat} of $3 \times 10^4\ min^{-1}$, contamination of the antibody with 6×10^{-5}% (mol/mol) of the natural enzyme would lead one to believe that the antibody is catalytic, when, in fact, contaminating enzyme is responsible for the rate-enhancement observed. Kinetic analysis, specificity, or inhibition data cannot always distinguish between catalysis by an antibody and catalysis by an enzyme impurity. Rigorous checks of specific activity must therefore be performed after each purification step, along with a comparison between different methods of purification and a comparison of whole antibody versus isolated Fab. For example, we have found it very difficult, even after considerable purification (including affinity chromatography), to remove glycosidase, adenosine deaminase, and ribonuclease impurities from what appears by gel electrophoresis to be homogeneous antibody.

3. Catalytic Antibodies

3.1. Generation of Antibody Combining Sites Containing Catalytic Amino-Acid Side Chains

3.1.1. Hapten–Antibody Complementarity

A β-Elimination Reaction. One strategy for inducing catalytic residues, such as basic or acidic amino-acid side chains, in the combining site of an antibody involves generating antibodies to a hapten whose structure is complementary to that catalytic group. In fact, an important goal in the design of catalytic antibodies is the development of general rules relating hapten structure to the corresponding catalytic groups or microenvironment in the antibody combining site. One such example involves the use of electrostatic complementarity between a hapten and antibody to generate an amino-acid side chain that catalyzes the β-elimination reaction **4** → **5**.[21] This reaction, which involves C–H proton



abstraction, is a member of an important class of reactions including elimination and isomerization reactions and aldol and Claisen condensations. Proton abstraction in enzymes that catalyze these reactions is often performed by the carboxylate side chain of glutamic or aspartic acid. These residues typically display higher than normal pK_a values in the hydrophobic active sites of enzymes.[22]

Aspartate and glutamate residues have been generated in the combining sites of antibodies by taking advantage of charge complementarity between haptens and the corresponding antibodies.[6] Consequently, we reasoned that an antibody combining site could be generated that contains a carboxylate within bonding distance of an abstractable substrate proton by using the appropriate positively charged hapten. Importantly, the position of the charged group in the hapten should reflect that of the target C–H group in the substrate. Hapten **6** contains a positively charged ammonium ion replacing the α-CH_2 group of substrate **4**. The fact that the hapten and substrate share a common recognition element, the *p*-nitrophenyl group, should insure reasonable binding affinity of substrate to the antibodies. Moreover, replacement of hapten by substrate in the antibody combining site should lead to an increase in the pK_a of the catalytic carboxylate group since a stabilizing salt-bridge interaction is lost.

Of six antibodies generated against the KLH conjugate of **6**, four catalyzed the β-elimination reaction **4** → **5**. The IgG 43D4-3D3 obeyed the classical Michaelis–Menten expression [Eq. (1)] ($k_{cat} = 0.2\ min^{-1}$, $K_m = 182\ \mu M$ at 37 °C, pH 6.0), demonstrated substrate specificity, and was competitively inhibited by hapten ($K_i = 290\ nM$). Chemical

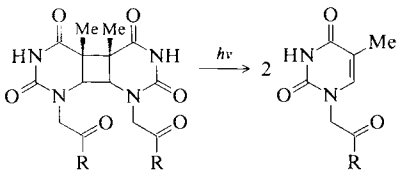
$$\mathrm{Ig} + \mathrm{S} \underset{k_{-1}}{\overset{k_1}{\rightleftharpoons}} \mathrm{Ig{\cdot}S} \xrightarrow{k_{cat}} \mathrm{Ig} + \mathrm{P}$$

$$v = \frac{k_{cat}[E_T][S]}{K_m + [S]}, \quad K_m = \frac{k_{-1} + k_{cat}}{k_1} \qquad (1)$$

modification experiments with the carboxylate-specific reagent diazoacetamide, in the presence and absence of bound hapten, demonstrated that a glutamate or aspartate residue was responsible for catalysis. Determination of k_{cat} as a function of pH revealed that the carboxylate had a pK_a of 6.2 in the presence of bound substrate. The increased pK_a of the carboxylate side chain is consistent with loss of a salt-bridge interaction when hapten **6** is replaced by substrate in the

antibody combining site. The rate enhancement obtained by introduction of the carboxylate residue in the antibody combining site, compared to acetate free in solution, is 8.80×10^4 at pH 6.0. This value is similar to the rate acceleration of about 10^4 attributable to the bases Glu 43 in staphylococcal nuclease[23] and Asp 102 in trypsin.[24]

A [2 + 2] Cycloreversion Reaction. A second example in which hapten structure was used to induce a catalytic side chain in an antibody combining site involves the generation of antibodies which catalyze the light-dependent [2 + 2] cycloreversion reaction of thymine dimer **7a**.[25] Thymine dimers are the predominant DNA photolesion produced by UV light. Model studies have shown that photosensitizers such as indoles, quinones, or flavins can reversibly transfer an electron to or accept an electron from a thymine dimer, resulting in facile cleavage of the intermediate thymine-dimer radical.[26–28] These results suggest that an antibody combining site specific for a thymine dimer and containing an appropriately positioned sensitizer should act as a photorepair enzyme. It seemed reasonable to us that antibodies generated against the polarized π system of a pyrimidine dimer might contain a complementary tryptophan residue in the combining site, much as antibodies generated against positively charged haptens contain complementary aspartate and glutamate residues.[3] In order to test this strategy, antibodies were generated against *cis,syn* thymine dimer **7b**.



7a: R = OH
7b: R = $NHCH_2COOH$

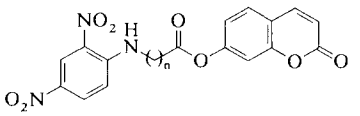
Five out of six antibodies generated against the KLH conjugate of dimer **7b** catalyzed the photoreversion of dimer **7a** to the corresponding monomer when irradiated with 300-nm monochromatic light. The k_{cat} of the IgG 29E5 was 1.2 min^{-1} (under conditions of nonsaturating light), *close to the k_{cat} of 3.4 min^{-1} for thymine-dimer cleavage by the repair enzyme Escherichia coli DNA photolyase.*[29] The quantum yield of the photocleavage reaction, corrected for the number of tryptophans, was $\Phi \geq 0.75$, compared to the quantum yield of approximately 1.0 for DNA photolyase. The antibody did not catalyze the cleavage of the corresponding *N,N'*-dimethyl substrate, consistent with the high specificity of antibodies. The wavelength dependence of the photocleavage quantum yield as well as fluorescence quenching experiments demonstrated the involvement of a tryptophan in catalysis. Pulse radiolysis experiments have shown that dimethyl and tetramethyl thymine-dimer radical anions decay to the corresponding monomers with a frequency of 0.05.[30] Since the quantum yield of the antibody-sensitized reaction is significantly higher than 0.05, the antibody appears to partition the breakdown of the intermediate radical anion. Further experiments are being carried out to precisely define the mechanism of this antibody-catalyzed reaction.

In the two examples described above, a high percentage of the antibodies isolated were catalytic. This result may reflect the generality of using electrostatic and π-stacking interactions to elicit complementary combining-site residues. The generation of antibodies with rate accelerations on the order of 10^8 or greater will likely involve the simultaneous application of two or more strategies for introducing catalytic activity into antibodies. Clearly then, strategies, such as that described above, that yield a high percentage of catalytic antibodies relative to the total number of hapten-specific antibodies isolated are the most desirable and generalizable. One can imagine many other reactions which can be catalyzed by antibodies using this strategy (or this strategy in conjunction with those detailed in Section 3.1.2), including aldol reactions (a β-aminophosphonate hapten), ester/amide hydrolysis (an *N*-oxide hapten), and oxy-Cope rearrangements (an aminocyclohexane hapten). It should also be noted that monoclonal antibodies have been reported that fortuitously contain nucleophilic residues that react in a stoichiometric fashion with an activated ester analogue of the hapten.[31]

3.1.2. Site-Directed Mutagenesis

An alternative approach for the introduction of catalytic groups into an antibody combining site involves site-specific mutagenesis. This approach has also been applied to the antibody MOPC 315,[32] which binds substituted 2,4-dinitrophenyl ligands with association constants ranging from 10^3 to 10^7 M^{-1}.[33, 34] The combining site has been characterized by spectroscopic methods (UV, fluorometry, NMR), chemical modification, and amino-acid sequencing of the variable region. Moreover, earlier affinity-labeling studies with reagents of varying structures[35] defined a number of reactive amino-acid side chains in the vicinity of the combining site.

In the absence of an X-ray crystal structure of MOPC 315, *chemical modification experiments* were used to guide the mutagenesis. Despite the presence of 14 potentially reactive side chains in the hypervariable region (2 histidines, 2 lysines, 3 arginines, and 7 tyrosines), DNP-containing affinity labels alkylate primarily two residues, tyrosine 34L and lysine 52H.[35] Tyrosine 34L was chosen as the initial target for mutagenesis since it appeared that a histidine at residue 34 would be situated to catalyze the hydrolysis of esters **8a–c**. The role of tyrosine 34L in DNP binding has not been clearly established; affinity labeling of the tyrosine to form the 5-mercapto-2-oxopentyl ether prevents binding of ligands,[35] perhaps by sterically blocking the entrance to the site. Nitration of the tyrosine ring has no effect.[36] Phenylalanine was also substituted to assess the contribution of the tyrosine hydroxyl group to hapten binding.



8a: n = 2
8b: n = 4
8c: n = 5

In order to generate mutants of MOPC 315, we chose to express the variable region (F_v) of the antibody in *E. coli*. MOPC 315 IgA can be proteolyzed with pepsin to yield functional F_{ab} or F_v fragments.[37] The F_v fragment (26 kD) is a heterodimer consisting of two peptides, V_H (14 kD) and V_L

(12 kD) (cf. Fig. 1), and contains all the sequences necessary for folding of the binding domain and recognition of the DNP hapten. Reduced and separated V_H and V_L peptides of MOPC 315 and several other antibodies can be recombined to form a stable F_V (Fig. 4).[37] The single disulfide bond in

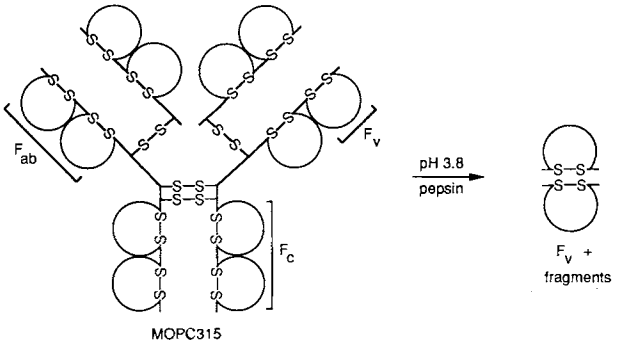


Fig. 4. The schematic structure of the antibody MOPC 315 and its cleavage by pepsin.

V_H or V_L can be efficiently formed by oxidation of the reduced forms prior to reconstitution.[37] The simplicity and efficiency of reconstitution makes the F_V fragment a desirable target for expression of an antibody combining site in *E. coli*. We have exploited this property to produce a hybrid F_V fragment, in which recombinant V_L produced in *E. coli* is reconstituted with V_H derived from MOPC 315 IgA. Functional F_V and F_{ab} fragments of other antibodies have been previously expressed in *E. coli*.[38] A gene encoding the 115 *N*-terminal amino acids of MOPC 315 light chain was chemically synthesized and expressed in *E. coli* as a fusion with the lambda cII gene.[39] The resulting hybrid protein was cleaved at one site with Factor Xa, the liberated V_L peptide was reconstituted with V_H, and the resulting F_V fragment was purified by gel filtration and affinity chromatography.

Wild-type F_V (F_V(315)) and the phenylalanine mutant (F_V(Y 34 F_L)) bound DNP-L-lysine with similar affinities at pH 6.8 ($K_D = 250 \pm 20$ nM), while the histidine mutant (F_V(Y 34 H_L)) bound DNP-lysine with sixfold lower affinity ($K_D = 1400 \pm 200$ nM). The histidine mutant F_V fragment accelerated hydrolysis ($k_{cat}/K_M/k_{4-MeIm}$) of ester **8b** $6.0 \pm 3.0 \times 10^5$ fold over the reaction with 4-methylimidazole at pH 6.8. The initial rate of ester cleavage is 50 times faster than that of wild-type F_V or the F_V(Y 34 F_L) mutant. In addition, the hydrolyses of the homologous esters **8a** and **8c** were not significantly accelerated, consistent with the postulated location of the His 34 side chain in the active site.

Site-directed mutagenesis should prove a powerful tool for augmenting the rate enhancements of catalytic antibodies generated via other strategies and for the stepwise evolution of catalytic activity in antibodies to produce efficient selective catalysts. In addition, genetic selection or screening might also be used to generate a catalytic residue in the combining site of an antibody already specific for the substrate (or transition-state analogue) of interest.

3.2. Generation of Antibodies Complementary to Transition-State Analogues

An antibody generated to a haptenic group resembling the transition-state configuration of a given reaction should lower the free energy of activation of the reaction by stabilizing the corresponding transition-state relative to reactants or products.[40] In fact, the active sites of many enzymes are complementary in structure and electronic distribution to rate-limiting transition states, as evidenced by studies of enzyme active sites[41] as well as enzyme inhibition by transition-state analogues.[42] Antibodies elicited to transition-state analogues have been demonstrated to catalyze a variety of reactions (see Sections 3.2.1 to 3.2.3), including carbonate, ester, and amide hydrolysis, the Claisen rearrangement of chorismic acid to prephenic acid, bimolecular amide bond formation, a six-membered ring lactonization reaction, and peptide bond formation.

3.2.1. *Carbonate, Ester, and Amide Hydrolysis*

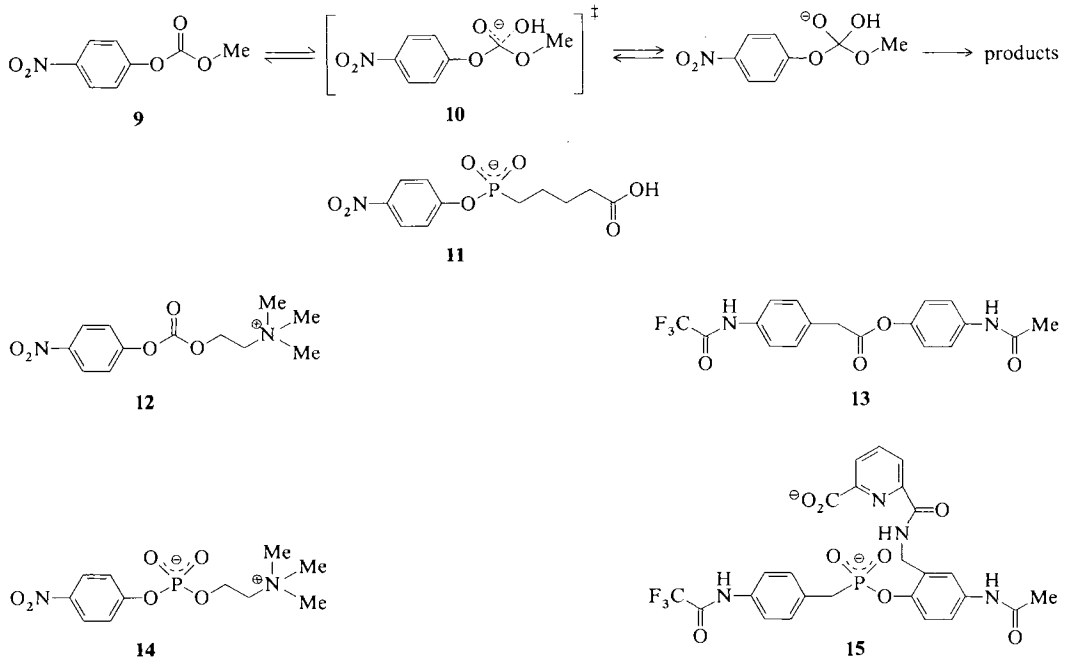
The first examples of catalytic antibodies specific for transition-state (TS) analogues bound tetrahedral, negatively charged phosphate and phosphonate TS analogues for the hydrolysis of carbonates and esters.[43,44] A number of factors were considered in the design of this first generation of catalytic antibodies. Carbonates and esters undergo substantial structural and electronic changes on the reaction pathway from substrate to product, making possible differential binding and stabilization of the transition state. Moreover, the tetrahedral transition states for these hydrolytic reactions have been successfully mimicked with tetrahedral phosphonate, α,α-difluorocarbonyl, and hydroxymethylene groups. Hydrolytic reactions do not necessarily require catalytically active side chains (such as a nucleophilic serine); they can also take place by simple attack of a water molecule on the polarized carbonyl of the substrate in the binding site. Additional considerations included the desirability of common recognition elements in both substrate and transition state, as well as diminished affinity of the antibody for the reaction products.

Monoclonal antibodies specific for tetrahedral transition-state analogues **11**, **14**, and **15** were found to selectively catalyze the hydrolysis of the corresponding substrates **9** (transition state **10**), **12**, and **13**, respectively, with kinetics consistent with the Michaelis–Menten rate expression [Eq. (1)].[43,44] The antibody-catalyzed reactions were competitively inhibited by their corresponding transition-state analogues. In each case, the inhibition constant (K_i) is substantially lower than the corresponding K_m of the substrate, suggesting that transition-state stabilization plays a role in catalysis. A comparison of the rates of the antibody-catalyzed reactions [Eq. (2)] with the rates of hydroxide-dependent hydrolysis [Eq. (3)] afforded antibody rate accelerations in the range of 10^3 to 10^5.[43] These accelerations are in the

$$v_{Ig} = k_{Ig}[Ig \cdot S][OH] \quad (2)$$

$$v_{OH} = k_{OH}[S][OH] \quad (3)$$

same range as those attributable both experimentally and theoretically to transition-state stabilization in hydrolytic enzymes. For example, a triple mutant of the enzyme subtilisin, in which each amino acid of the catalytic triad of His, Ser, and Asp is replaced by an alanine residue, hydrolyzes a *p*-nitroanilide peptide substrate 3000-fold more rapidly than the corresponding uncatalyzed reaction, which gives an esti-



9 10 11 12 13 14 15

mate of the extent of catalysis that can be achieved by stabilization of the transition state by binding determinants other than the catalytic triad.[45] In all cases the antibodies also displayed high substrate specificity.

The three-dimensional structure of the antibody McPC603, which is highly homologous to the catalytic phosphorylcholine-binding antibodies T15 and MOPC167, has been solved. The crystal structure makes possible direct identification of the combining-site residues responsible for catalysis (Fig. 5).[9] The hapten is bound in the cavity of

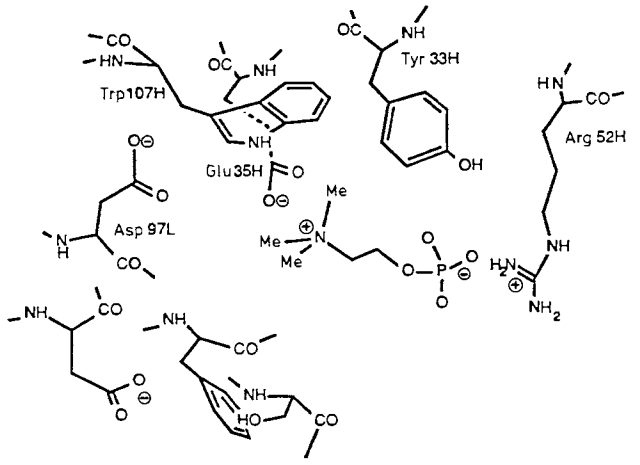
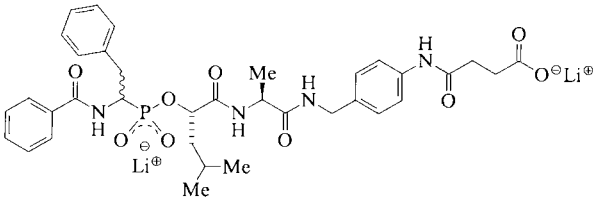


Fig. 5. Phosphorylcholine in the combining site of the antibody McPC603.

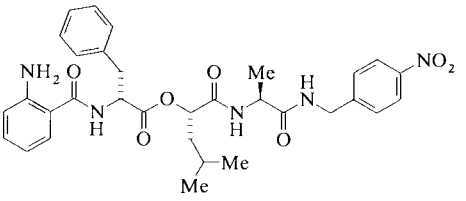
McPC603 with the choline group deep in the interior and the phosphate toward the exterior, in contact with aqueous solvent. The heavy-chain residues Tyr33H and Arg52H, which are invariant in all of the phosphorylcholine-binding Ig's sequenced to date,[46] bind the phosphate through hydrogen bonding and electrostatic interactions with the phosphoryl oxygen atoms. The combining site of McPC603 is both sterically and electronically complementary to the tetrahedral, negatively charged phosphate moiety of phosphorylcholine. Inasmuch as this tetrahedral phosphate mimics the transition state for the hydroxide-ion-catalyzed hydrolysis of carbonate **12**, the phosphorylcholine antibodies should be capable of polarizing the bound carbonyl group of **12** for attack of hydroxide ion in the rate-determining step. In light of the fact that the ground-state structure of **12** differs substantially from the transition-state configuration (cf. **10**), the differential binding affinity of the Ig to these two species should be reflected in a lowered free energy of activation for reaction. In fact, the transition-state analogue 4-nitrophenyl phosphorylcholine **14** is bound more tightly than the corresponding substrate by both MOPC167 and T15[46] (K_i = 5 μM, K_m = 208 μM for MOPC167). However, the differential binding of T15 and MOPC167 to carbonate **12** and the transition-state analogue **14** does not fully account for the magnitude of the rate accelerations. Therefore, although the crystallographic and binding data strongly suggest that T15 and MOPC167 selectively stabilize the transition-state configuration and thereby reduce the barrier to reaction, other factors are contributing to the rate acceleration. Site-directed mutagenesis is currently being used to characterize the catalytic roles of various amino acids in the active site of phosphorylcholine-specific antibodies. Biophysical studies and chemical modification experiments suggest that tyrosine and arginine also play a catalytic role in the antibodies specific for hapten **11**.[43] Again, these residues can act to stabilize the tetrahedral transition state. Histidine or tyrosine is thought to be involved in catalysis by antibodies specific for **15**.[44] It is not yet clear what catalytic role these residues play.

Antibodies have also been generated to phosphonate transition-state analogues that catalyze the stereospecific hydrolysis of unactivated alkyl esters under mild conditions.[43f]Antibodies were generated against hapten **16**, a tripeptide transition-state analogue for the hydrolysis of ester **17** under basic conditions. Note that the hapten also contains analogues of the fluorogenic groups at the amino

and carboxy termini of substrate **17**. These groups allow hydrolysis of the substrates to be monitored by observing the fluorescence increase which occurs when the fluorescent 2-aminobenzoyl group is separated from the quenching 4-nitrobenzylamide in the reaction.[47] This sensitive assay may allow direct screening of ELISA plates for catalytic activity, facilitating the production of catalytic antibodies.



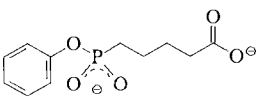
16



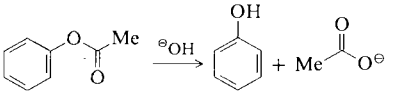
17

The antibody-catalyzed hydrolyses were 50- to 300-fold faster than reaction with hydroxide ion. With relatively large transition-state analogues such as tripeptides **16**, the tetrahedral phosphonate probably contributes proportionally less to the overall binding energy of the hapten to the antibody and, consequently, the rate acceleration observed is less than those of antibodies raised to smaller transition-state analogues. Interestingly, all 18 antibodies (out of 25) found to accelerate the hydrolysis of ester **17** were selective for the D-phenylalanine-containing diastereomer, although a mixture of diastereomers was used to generate the antibodies.[48] With three of the five IgG's, the ratio of the rate of hydrolysis of the L-phenylalanine-containing ester to that of the D-phenylalanine-containing ester was less than 0.5%. The antibodies also show a high degree of substrate specificity. Esters containing nitrophenylalanine, leucine, or tryptophan in place of phenylalanine are not hydrolyzed by any of the antibodies. Antibodies of this sort may prove useful in the chiral resolution of amino acids and alcohols.[49] *Benkovic* and co-workers have reported antibodies with lipase activity, *R* or *S* substrate specificity, and rate accelerations of 8×10^4 fold.[49]

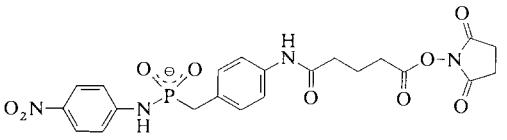
Antibodies can also carry out reactions on water-insoluble organic substrates. Antibodies specific for the phenylphosphonate transition-state analogue **18** were capable of catalyzing the hydrolysis of phenyl acetate in reverse micelles.[50] The k_{cat} and K_m values of the antibody solubilized in isooctane in reverse micelles were 3.74 min^{-1} and 650 μM, respectively [Wo value (water to detergent ratio) of 23], compared to the corresponding values of 18.8 min^{-1} and 157 μM in aqueous solution. The optimal value of Wo is significantly higher than that previously reported for enzymes, consistent with the increased molecular weight of IgG molecules. The ability of antibodies to function in reverse micelles should significantly expand the versatility of antibodies in catalysis and immunoassays.



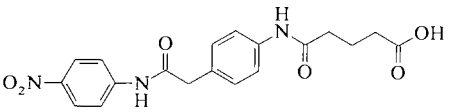
18



More recently, antibodies have been generated against the KLH conjugate of arylphosphonamidate **19**. One antibody was found to catalyze the hydrolysis of the nitroanilide **20**[51] with a k_{cat} of 0.08 min^{-1} and a K_m of 562 μM. The antibody-catalyzed reaction is characterized by high specificity and a rate enhancement of 2.5×10^5 relative to the uncatalyzed reaction. The difference in binding of the phosphonamidate transition-state analogue (K_i) and substrate (K_m) ($\Delta\Delta G^{\neq} = -2.2$ kcal mol^{-1}) does not account for the magnitude of the rate acceleration. Therefore, other factors such as acid or base catalysis or ground-state destabilization must be involved in catalysis. Generation of an antibody combining site with these additional catalytic interactions may have simply been the result of immunological diversity (one IgG out of 44 was found to be catalytic) or could be a consequence of hapten structure. The P-NH and P-O groups



19



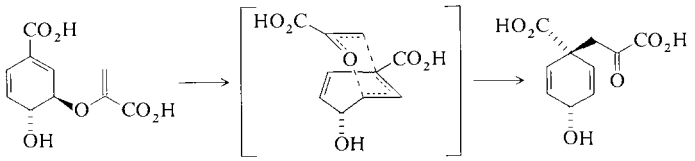
20

each have a lone pair that can act as a hydrogen-bond acceptor, whereas only the P-NH group can act as a hydrogen-bond donor. It is not clear, however, how this difference in hydrogen bonding pattern would affect the nature of the combining site. Mechanistic analysis of this antibody-catalyzed reaction should provide important insight into the generation of antibodies that catalyze the related, but considerably more energetically demanding hydrolysis of peptide bonds. One can also imagine transition-state analogues for the hydrolysis of glycosidic (nojirimycin derivatives) and phosphodiester (nucleoside vanadyl complexes) bonds.

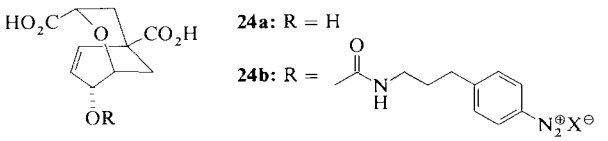
3.2.2. A Claisen Rearrangement

It should also be possible to generate antibodies which increase reaction rates by reducing entropic barriers to reactions. The binding energy in this case acts to reduce translational and rotational motions for reaction by properly orienting the reactants in the antibody combining site. This approach should be applicable to intramolecular reactions such as macrocyclic lactonization reactions or intermolecular reactions such as peptide bond formation or Diels–Alder reactions.

We have used these ideas to guide us in the generation of antibodies that carry out the formal Claisen rearrangement of chorismic acid **21** to prephenic acid **23**.[52] This thermal 3,3-sigmatropic rearrangement occurs through an asymmetric chairlike transition state (**22**) in which the carbon–oxygen bond is substantially broken while carbon–carbon bond formation has not occurred to any appreciable extent.[53] The activation entropy and enthalpy of reaction have been determined to be -12.85 cal K^{-1} mol^{-1} and 20.7 kcal mol^{-1}, respectively.[53] The unimolecular rearrangement is catalyzed approximately 10^6-fold by the enzyme chorismate mutase at the branch point in the biosynthesis of aromatic amino acids in bacteria and plants.[54] Although the enzymatic reaction has also been demonstrated to proceed through a chairlike transition state, the mechanism by which chorismate mutase accelerates the rearrangement remains poorly understood.[55]



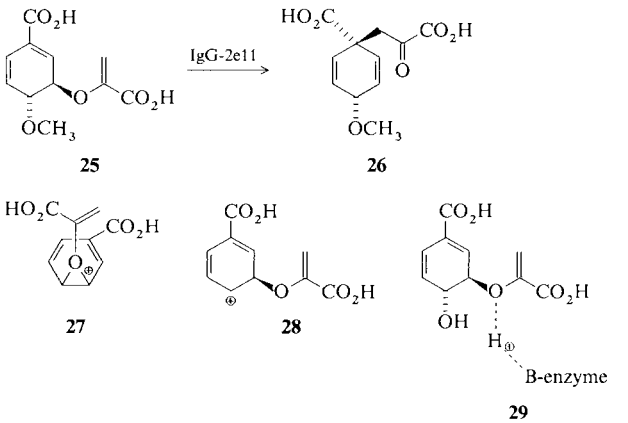
21 **22** **23**



24a: R = H

24b: R =

One might expect that an antibody combining site, complementary to the conformationally restricted transition-state configuration, but presumably lacking catalytic side chains, could accelerate the Claisen rearrangement of chorismic acid to prephenic acid. Monoclonal antibodies were elicited to the *endo* bicyclic transition-state analogue **24a**, the most potent known inhibitor of chorismate mutase with a K_i of 0.15 μM.[56] One of eight antibodies (IgG) generated to the KLH conjugate of **24b** was found to catalyze the Claisen rearrangement **21** → **23**, with initial rates consistent with the Michaelis–Menten rate expression [Eq. (1)] (k_{cat} = 2.7 min^{-1}, K_m = 260 μM at 10 °C). The rate of the antibody-catalyzed reaction can be directly compared with that of the uncatalyzed unimolecular thermal rearrangement, affording a value of k_{cat}/k_{uncat} of 1×10^4 at 10 °C and pH 7.0. This factor can be compared with the 3×10^6-fold acceleration by chorismate mutase from *E. coli* under the same conditions. Of the various mechanisms put forth for the enzymatic rearrangement, most can be ruled out for the antibody-catalyzed process. For example, the fact that the (±) methyl ether of chorismic acid, **25**, is converted into the (±) ether of prephenic acid, **26**, argues against mechanisms involving loss of the 4-hydroxyl group (such as formation of **27** or a C-4 cation such as **28**). Moreover, the observation of a D_2O solvent isotope effect of 1 on the antibody-catalyzed reaction excludes general acid or base catalysis (cf. **29**) in the rate-limiting step. One is left with the appealing mechanistic alternative that the antibody catalyzes the reaction by providing an environment complementary to the conformationally restricted transition state. Consistent with this



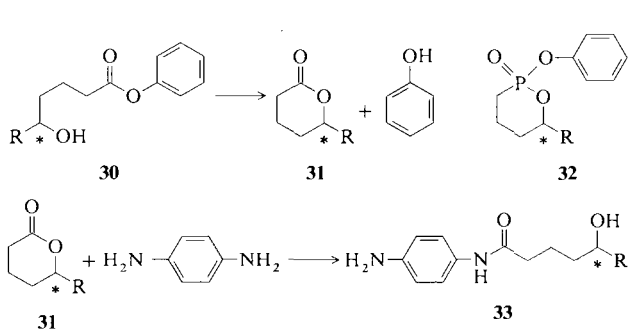
25 **26** **27** **28** **29**

notion, the $\Delta H^{\neq}$ and $\Delta S^{\neq}$ for the antibody-catalyzed reaction are 18.3 kcal mol^{-1} and -1.2 cal K^{-1} mol^{-1}, respectively.[57]

A second antibody, independently generated against an ester-linked analogue of **24a**, also catalyzed the rearrangement of chorismic acid to prephenic acid, but at a 100-fold lower rate.[58] In this case the ratio K_i/K_m corresponds roughly with the observed rate enhancement consistent with preferential binding of the transition-state analogue by the antibody. The stabilization was shown to be largely enthalpic in nature. In addition, catalysis was shown to be highly regioselective; only the (−) isomer of chorismic acid was a substrate for the antibody.[58]

3.2.3. *Transacylation Reactions*

The constraints imposed by the antibody binding pocket should also accelerate an intramolecular cyclization by reducing rotational entropy.[59] *Benkovic* and co-workers have demonstrated that an antibody elicited to transition-state analogue **32**, which is representative of a six-membered ring lactonization reaction, acts as a catalyst for the cyclization of the substrate **30** to give lactone **31**.[60] The rate of the antibody-catalyzed reaction relative to that of the uncatalyzed reaction was 167. Again, the antibody-catalyzed reaction was competitively inhibited by the corresponding cyclic phosphonate. The antibody cyclization reaction was stereoselective, permitting isolation of the lactone **31** in an enantiomeric excess of 94%.[60] Antibodies specific for **32** also catalyzed the stereospecific formation of amide **33** from



30 **31** **32** **31** **33**

racemic lactone **31** and 1,4-diaminobenzene.[61] The antibody bound 1,4-diaminobenzene and lactone **31** with K_m values of 1.2 mM and 4.9 mM, respectively, and the transition-state analogue **32** with a K_i of 75 nM. The acceleration of

the antibody-catalyzed reaction relative to the uncatalyzed reaction was 16 M, which compares with a $K_m \cdot K_m/K_i$ value of 155 M. A second phosphonamidate-specific antibody was also shown to catalyze bimolecular amide bond formation with an effective molarity of 10.5 M (in this case the hapten did not incorporate the leaving group, an important element of the transition state).[62] These values are considerably below the value of 10^8 M, which is thought to represent an approximate upper limit for an antibody-catalyzed reaction compared to its bimolecular counterpart.[63] Nonetheless, the demonstration that an antibody can catalyze bimolecular reactions offers the possibility of antibody-catalyzed peptide bond formation, Diels–Alder reactions, macrolide synthesis, or transglycosylation reactions. Recently, an antibody has been generated that catalyzes peptide bond ligation.[74]

3.3. Introduction of Chemical Catalysts into Antibody Combining Sites

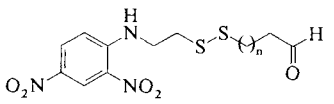
3.3.1. Semisynthetic Antibodies

One strategy whereby catalytic groups can be introduced into antibody combining sites involves the selective chemical modification of antibodies with natural or synthetic catalysts such as transition-metal complexes, cofactors, bases, or nucleophiles. *Kaiser* and co-workers demonstrated that enzymes can be selectively modified with cofactors to afford semisynthetic enzymes with new properties.[64] This approach has recently been extended to antibodies, making it possible to combine the exquisite binding specificity of the immune system with the efficient diverse catalysts available from synthetic chemistry.[65, 66]

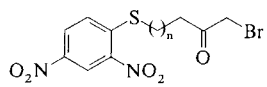
The key to the generation of semisynthetic catalytic antibodies is the development of mild methods for selectively introducing derivatizable groups of unique reactivity into or near the combining site. These groups can then be modified in a second step to incorporate the chemical functionality (cofactor, metal–ligand complex, fluorophore, etc.) of interest. One such derivatizable group is a free thiol, which, by virtue of its high nucleophilicity and ease of oxidation, can be selectively modified via disulfide exchange or electrophilic reactions. Moreover, introduction of a nucleophilic thiol into an antibody combining site might directly afford a catalytic antibody. We have used cleavable affinity labels to selectively modify the antibody combining site of the IgA MOPC315 with a nucleophilic thiol.[65] Importantly, this method does not require knowledge of the three-dimensional structure of the antibody and should therefore be applicable to a large number of proteins of interest.

Cleavable affinity-labeling reagents were synthesized that contain the DNP group linked to an electrophilic aldehyde or α-bromoketone via cleavable disulfide or sulfide linkages (cf. **34** and **35**, respectively).

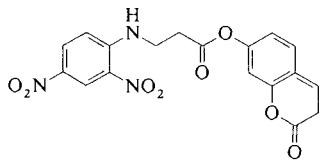
The distance between the DNP group and electrophilic moiety of the affinity labels was varied, since the position of a nucleophilic Lys, His, or Tyr side chain in the combining site was not precisely known. Covalent attachment of the label to the antibody, followed by cleavage of the cross-link and removal of the free ligand, resulted in site-specific incorporation of a free thiol into the antibody combining site (cf. **36a**, Fig. 6). Affinity labeling of the antibody with the aldehyde labeling reagent **34b** in the presence of $NaCNBH_3$ provides, after cleavage of the disulfide linkage, homogeneous antibody containing a free thiol attached to Lys 52H[65] (bromoketone **35b** selectively modified the antibody at Tyr 34L). The binding affinity of this modified antibody to *N*-DNP-glycine was similar to that of native MOPC315. The thiol itself is appropriately positioned to act as a nucleophile in the thiolysis of coumarin ester **8a**.[65] The semisynthetic



34a: n = 1
34b: n = 2



35a: n = 1
35b: n = 2
35c: n = 3



8a

antibody demonstrated saturation kinetics and was competitively inhibited by *N*-DNP-glycine with a K_i of 8 μM. The rate acceleration by the thiol-containing antibody relative to dithiothreitol was 6×10^4 for ester **8a**. This value is quite similar to that found in the antibody-catalyzed β-elimination reaction and suggests that proximity of a base or nucleophile to a complexed substrate can lower $\Delta G^{\neq}$ for reaction by up to 7.0 kcal mol^{-1}.

Importantly, the thiol also acted as a handle to introduce other synthetic chemical functionality into the antibody combining site.[65, 66] Imidazole was incorporated in greater than 90% yield by treatment of the pyridyl disulfide adduct of the antibody with 4-(mercaptomethyl)imidazole[66] (Fig. 6). The resulting semisynthetic antibody of type **36c** catalyzed the hydrolysis of coumarin ester substrate **8a** with

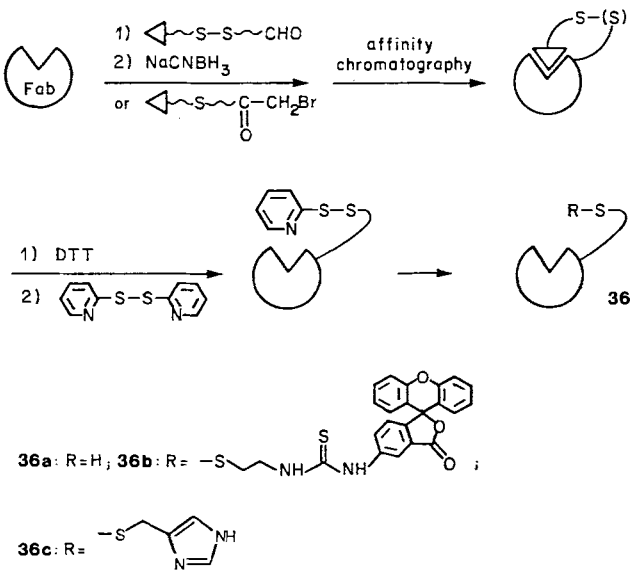


Fig. 6. The incorporation of synthetic catalysts in the combining site of antibodies. DTT = dithiothreitol.

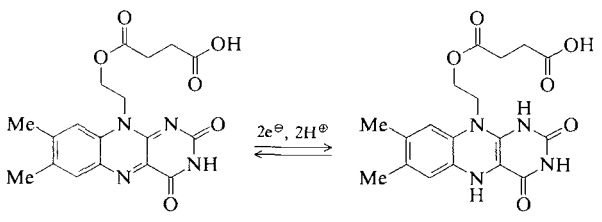
a rate 10^3 times faster than the rate of catalysis by 4-methylimidazole. Presumably, imidazole is acting as a general base or nucleophile in the hydrolysis of **8a**. The slower rate with this antibody is likely due to the increased flexibility of the imidazole side-chain linkage. The semisynthetic antibody showed specificity for the 3-(DNP-amino)proprionate ester **8a** versus the *N*-DNP-glycine or 4-(DNP-amino)butyrate ester.

It is interesting to compare catalysis by $F_V(Y34H_L)$ (see Section 3.1.2) and by chemically modified MOPC315, containing imidazole linked to lysine 52 of the heavy chain through a flexible eight-bond tether.[8] $F_V(Y34H_L)$ hydrolyzes **8a** approximately 16 times more rapidly than the imidazole-modified F_{ab} fragment. This difference is likely due to the decreased number of degrees of freedom of the histidine-34 side chain imposed by the protein backbone and surrounding side chains. In addition, the imidazole may be better aligned for attack on the carbonyl or for activation of a water molecule.

The thiol-containing antibody could also be modified with a fluorophore.[65] Addition of the ligand *N*-DNP-glycine to the adduct **36b** resulted in a decrease in fluorescein fluorescence, providing a direct assay of ligand binding. The binding constant obtained from quenching of fluorescein fluorescence was identical within experimental error to that reported in the literature for unmodified MOPC315.[34] Semisynthetic antibodies of this sort may prove useful as sensors and in diagnostics. Derivatization of antibodies with other groups ($Zn^{2\oplus}$– or $Co^{3\oplus}$–ligand complexes, flavins, pyridoxamine, etc.) should enable us to generate semisynthetic antibodies with a variety of novel catalytic activities. Therapeutic agents can also be incorporated proximate to the antibody combining site via this strategy.

3.3.2. *Cofactor Binding Sites*

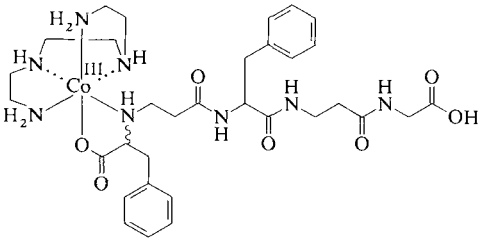
Another strategy whereby catalytic groups can be introduced into antibody combining sites involves generating, in addition to the substrate binding site, a cofactor (either natural or synthetic) binding site.[67] To this end, antibodies have been generated to flavin **37**. Because flavin **37** and the 1,5-dihydroflavin **38** have substantially different electronic



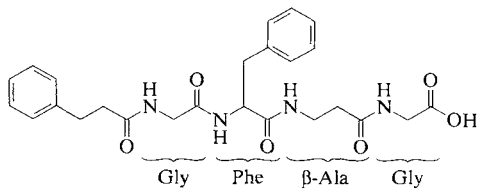
37 **38**

and conformational properties,[68] antibodies generated specifically to **37** preferentially bind **37** with 4×10^4 higher affinity than 1,5-dihydroflavin **38**. This differential stabilization of the oxidized and reduced forms of the cofactor by the antibody combining site makes the Ig·**38** complex a substantially stronger reducing agent than free **38** in solution; the reduction potential of **37** bound to antibody is −342 mV, representing a lowering of the reduction potential ($E_m = -206$ mV) by approximately 5 kcal mol^{-1}. Because the Ig·**38** complex is a stronger reducing agent than free **38**, the substrate Safranine T ($E_m = -289$ mV) could be rapidly reduced by Ig·**38**, but not by **38** itself. The antibody–flavin complex is able to mediate redox processes not thermodynamically accessible to free flavin. Incorporation of a substrate binding site into these antibodies may lead to catalytic antibodies which can carry out stereocontrolled chemical reductions.

An exciting recent result in the area of catalytic antibodies has been the generation of antibodies that bind a metal-complex cofactor and catalyze the specific hydrolysis of a Gly–Phe bond of peptide substrate **40** at neutral pH.[69] The



39



40

antibodies were produced by immunizing with hapten **39**, a Co^{III}–peptide complex containing the triethylenetriamine ("trien") ligand. These antibodies as a group are capable of binding trien complexes not only of Co^{III} but also of numerous other metals. The antibody–trien–metal complex selectively cleaved the Gly–Phe amide bond of peptide **40**. One antibody was studied in detail, and cleavage was observed for **40** with the trien complexes of Zn^{II}, Ga^{III}, Fe^{III}, In^{III}, Cu^{II}, Ni^{II}, Lu^{III}, Mg^{II}, or Mn^{II} as cofactors. A turnover number of 6×10^{-4} s^{-1} was measured. Interestingly, the amide bond hydrolyzed is one removed from the bond one might have expected to be cleaved based on model chemistry by *Buckingham* and others.[70] Nonetheless, this work is a starting point for the generation of sequence-specific peptidases, "restriction enzyme" equivalents for proteins.

The generation of antibody combining sites that bind natural and synthetic cofactors should prove a general powerful approach for the generation of new catalytic antibodies for hydrolytic and redox reactions. It should be noted that a number of years ago *Stollar* et al. attempted to generate antibodies with pyridoxamine binding sites that catalyze Schiff base formation and transamination.[71] Their lack of success may have been due to the fact that polyclonal antibodies were used.

4. Related Applications in Organic Chemistry

Antibodies may find a number of other applications in organic chemistry. For example, antibodies have recently

been used as templates to control the stereochemical outcome of photoaddition reactions.[72] Antibodies to cyclic peptides might be used to evaluate binding contributions of conformational restriction in drug design. Antibodies to a covalently linked electron donor and acceptor might be used as a scaffold to probe through-bond versus through-space effects on electron-transfer rates. And antibodies to azoalkanes might be used to probe environmental effects on radical reactions. Clearly, the ability to generate a tailored chemical microenvironment in the form of a monoclonal antibody should provide organic chemists with exciting new opportunities.

5. Conclusion

In the short period of time which has elapsed since the first reports of antibody catalysis in 1986,[43, 44] a considerable number of different reactions have been catalyzed using antibodies. The specificities of catalytic antibodies are high and rate enhancements approaching those of enzymes have been demonstrated. A number of general strategies have also evolved for generating catalytic antibodies. The development of antibodies with 10^8-fold or higher rate enhancements will require careful mechanistic analysis of those factors affecting antibody catalysis and the generation of antibodies which *combine several of these features*. This process will not only provide new insight into the nature of molecular recognition and catalysis, but may also afford tailor-made catalysts for applications in chemistry, biology, and medicine.

The author gratefully acknowledges the invaluable contributions of all co-workers named in the citations as well as support of this work by the Office of Naval Research, the National Science Foundation, the Department of Energy, and the National Institutes of Health.

Received: May 26, 1989 [A 737 IE]
German version: *Angew. Chem. 101* (1989) 1336

[1] a) G. Kohler, C. Milstein, *Nature (London) 256* (1975) 495; b) F. R. Seiler, P. Gronski, R. Kurrle, G. Lüben, H.-P. Harthus, W. Ax, K. Bosslet, H.-G. Schwick, *Angew. Chem. 97* (1985) 141; *Angew. Chem. Int. Ed. Engl. 24* (1985) 139; c) J. W. Goding: *Antibodies: Principles and Practice*, Academic Press, New York 1986.

[2] a) R. C. Nowinski, M. R. Tam, L. C. Goldstein, L. Strong, C.-C. Kuo, L. Corey, W. E. Stamm, H. H. Handsfield, J. S. Knapp, K. K. Holms, *Science (Washington, D.C.) 219* (1983) 637; b) E. S. Vitetta, K. A. Krulick, M. Miyama-Inaba, W. Cushley, J. W. Uhr, *ibid. 219* (1983) 644.

[3] a) D. Pressman, A. Grossberg: *The Structural Basis of Antibody Specificity*, Benjamin, New York 1968; b) J. W. Goodman in M. Sela (Ed.): *The Antigens, Vol. 3*, Academic Press, New York 1985; c) A. Nisonoff, J. Hopper, S. Spring: *The Antibody Molecule*, Academic Press, New York 1975.

[4] a) K. Landsteiner: *The Specificity of Serological Reactions*, Harvard University Press, Cambridge 1944; b) F. Karush, *J. Am. Chem. Soc. 78* (1956) 5519; c) L. Pauling, D. Pressman, A. Grossberg, *ibid. 66* (1944) 784.

[5] A. Nisonoff, D. Pressman, *J. Am. Chem. Soc. 79* (1957) 1616.

[6] a) A. L. Grossberg, D. Pressman, *Biochemistry 7* (1968) 272; b) M. H. Freedman, A. L. Grossberg, D. Pressman, *ibid. 7* (1968) 1941; c) D. Pressman, M. Siegel, *J. Am. Chem. Soc. 75* (1953) 686.

[7] a) R. Dwek, S. Wain-Hobson, S. Dower, P. Gettins, B. Sutton, S. J. Perkins, D. Givol, *Nature (London) 266* (1977) 31; b) S. Dower, R. Dwek, *Biochemistry 18* (1979) 3668.

[8] a) A. G. Amit, R. A. Mariuzza, S. E. Phillips, R. J. Poljak, *Science (Washington, D.C.) 233* (1986) 747; b) S. Sheriff, E. W. Silverton, E. A. Padlan, G. H. Cohen, S. J. Smith-Gill, B. C. Finzel, D. R. Davies, *Proc. Natl. Acad. Sci. USA 84* (1987) 8075.

[9] a) D. Segal, E. Padlan, G. Cohen, S. Rudikoff, M. Potter, D. Davies, *Proc. Natl. Acad. Sci. USA 71* (1974) 4298; b) E. Padlan, G. Cohen, D. Davies, *Ann. Inst. Pasteur (Paris) 126* (1985) 271; c) E. Padlan, *Q. Rev. Biophys. 10* (1977) 35; d) E. Padlan, *J. Mol. Biol. 190* (1986) 593.

[10] a) L. A. Day, J. M. Sturtevant, S. Singer, *Ann. N.Y. Acad. Sci. 103* (1963) 611; b) A. Froese, A. H. Sehon, M. Eigen, *Can. J. Chem. 40* (1962) 1786; c) J. Pecht, D. Givol, M. Sela, *J. Mol. Biol. 68* (1972) 241.

[11] L. Amzel, R. Poljak, *Annu. Rev. Biochem. 48* (1979) 961.

[12] S. Tonegawa, *Nature (London) 302* (1983) 575.

[13] L. Amzel, R. Poljak, F. Saul, J. Varga, F. Richards, *Proc. Natl. Acad. Sci. USA 71* (1974) 1427.

[14] P. M. Colman, W. G. Laver, J. N. Varghese, A. T. Baker, P. A. Tulloch, G. M. Air, R. G. Webster, *Nature (London) 326* (1987) 358.

[15] M. Marquart, J. Deisenhofer, R. Huber, N. Palm, *J. Mol. Biol. 141* (1980) 369.

[16] E. Engvall, *Meth. Enzymol. 70* (1980) 419.

[17] a) B. Erlanger, *Meth. Enzymol. 70* (1980) 85; b) T. Nishima, A. Tsuji, D. Fukushima, *Steroids 24* (1974) 861.

[18] B. Hurn, S. Chantler, *Meth. Enzymol. 70* (1980) 104.

[19] a) R. Sugasawara, C. Prato, J. Sippel, *Infect. Immun. 42* (1983) 863; b) E. Engvall, J. Perlmann, *J. Immunol. 109* (1972) 129.

[20] G. Kronvall, H. Grey, R. Williams, *J. Immunol. 109* (1972) 129.

[21] K. M. Shokat, C. J. Leumann, R. Sugasawara, P. G. Schultz, *Nature (London) 338* (1989) 269.

[22] C. T. Walsh: *Enzymatic Reaction Mechanisms*, Freeman, New York 1978.

[23] a) D. W. Hilber, J. A. Gerlt, *Fed. Proc. Fed. Am. Soc. Exp. Biol. 45* (1986) 1875; b) E. H. Serpersu, D. Shortle, A. S. Mildvan, *Biochemistry 26* (1987) 1289.

[24] C. S. Craik, S. Roczniak, C. Largman, W. J. Rutter, *Science (Washington, D.C.) 237* (1988) 909.

[25] A. G. Cochran, R. Sugasawara, P. G. Schultz, *J. Am. Chem. Soc. 110* (1988) 7888.

[26] a) C. Helene, M. Charlier, *Photochem. Photobiol. 25* (1977) 429; b) J. R. Van Camp, T. Young, R. F. Hartman, S. D. Rose, *ibid. 45* (1988) 365.

[27] H. D. Roth, A. Lamola, *J. Am. Chem. Soc. 94* (1972) 1013.

[28] a) S. E. Rotika, C. T. Walsh, *J. Am. Chem. Soc. 106* (1984) 4589; b) M. S. Jorns, *ibid. 109* (1987) 3133.

[29] M. S. Jorns, G. B. Sancar, A. Sancar, *Biochemistry 24* (1985) 1856.

[30] A. A. Lamola, *Mol. Photochem. 4* (1972) 107.

[31] a) F. Kohen, J. B. Kim, H. R. Lindner, Z. Eshbar, B. Green, *FEBS Lett. 111* (1980) 427; b) F. Kohen, J. B. Kim, G. Barnard, H. R. Lindner, *Biochim. Biophys. Acta 629* (1980) 328.

[32] E. Baldwin, P. Schultz, to be published.

[33] D. Haselkorn, S. Friedman, D. Givol, I. Pecht, *Biochemistry 13* (1974) 2210.

[34] a) R. A. Dwek, S. Wain-Hobson, S. Dower, P. Gettins, B. Sutton, S. J. Perkins, *Nature (London) 266* (1977) 31; b) S. K. Dower, R. A. Dwek, *Biochemistry 18* (1979) 3668; c) K. Kumar, D. J. Phelps, P. R. Carey, N. M. Young, *Biochem. J. 175* (1978) 727; d) D. A. Kooistra, J. H. Richards, *Biochemistry 17* (1978) 345; e) E. J. Goetzl, H. Metzger, *ibid. 9* (1970) 3862; f) D. Givol, *ibid. 10* (1971) 3461; g) P. H. Strausbauch, Y. Weinstein, M. Wilchek, S. Shaltiel, D. Givol, *ibid. 10* (1971) 4342.

[35] J. Haimovich, H. N. Eisen, E. Hurwitz, D. Givol, *Biochemistry 11* (1972) 2389.

[36] R. Leatherbarrow, W. Jackson, R. Dwek, *Biochemistry 21* (1982) 5124.

[37] a) J. Hochman, D. Inbar, D. Givol, *Biochemistry 12* (1973) 1130; b) J. Hochman, M. Gavish, D. Inbar, D. Givol, *ibid. 15* (1977) 2706.

[38] a) A. Skerra, A. Plückthun, *Science (Washington, D.C.) 240* (1988) 1038; b) M. Bette, et al., *ibid. 240* (1988) 1041.

[39] K. Nagai, H. Thogersen, *Nature (London) 309* (1984) 8110.

[40] a) L. Pauling, *Am. Sci. 36* (1948) 51; b) W. Jencks: *Catalysis in Chemistry and Enzymology*, McGraw-Hill, New York 1969.

[41] a) T. J. Borgford, T. E. Gray, N. J. Brand, A. R. Fersht, *Biochemistry 26* (1987) 7246; b) C. C. Blake, *Proc. R. Soc. London B167* (1967) 378.

[42] a) R. Wolfenden, *Annu. Rev. Biophys. Bioeng. 5* (1976) 271; b) P. Bartlett, C. Marlowe, *Biochemistry 22* (1983) 4168.

[43] a) S. J. Pollack, J. W. Jacobs, P. G. Schultz, *Science (Washington, D.C.) 234* (1986) 1570; b) S. J. Pollack, P. G. Schultz, *Cold Spring Harbor Symp. Quant. Biol. 234* (1987) 1570; c) J. Jacobs, P. G. Schultz, R. Sugasawara, M. Powell, *J. Am. Chem. Soc. 109* (1987) 2174; d) J. Jacobs, P. G. Schultz, in J. F. Liebman, A. Greenberg (Eds.): *Environmental Influences and Recognition in Enzyme Chemistry*, VCH Publishers, New York 1988, Chap. 11, pp. 303–335; e) P. G. Schultz, *Science (Washington, D.C.) 240* (1988) 426; f) S. J. Pollack, P. Hsuin, P. G. Schultz, *J. Am. Chem. Soc.*, in press (1989).

[44] a) A. Tramontano, K. Janda, R. Lerner, *Science (Washington, D.C.) 234* (1988) 1566; b) A. Tramontano, A. Ammann, R. A. Lerner, *J. Am. Chem. Soc. 110* (1988) 2282; c) A. Tramontano, K. Janda, A. O. Napper, S. Benkovic, R. A. Lerner, *Cold Spring Harbor Symp. Quant. Biol. 52* (1987) 91; d) R. A. Lerner, A. Tramontano, *Sci. Am. 258* (1988) 58.

[45] P. Carter, J. A. Wells, *Nature (London) 332* (1988) 564.

[46] P. J. Gearhart, N. D. Johnson, R. Douglas, L. Hood, *Nature (London) 291* (1981) 29.

[47] N. Nishino, J. C. Powers, *J. Biol. Chem. 255* (1980) 3482.

[48] I. Schechter, M. Sela, *Biochemistry 6* (1967) 897.
[49] The observation of catalytic antibodies that stereospecifically hydrolyze unactivated esters of chiral alcohols was also recently reported: K. D. Janda, S. J. Benkovic, R. A. Lerner, *Science (Washington, D.C.) 244* (1989) 437.
[50] C. N. Durfor, R. J. Bolin, R. J. Sugasawara, R. J. Massey, J. W. Jacobs, P. G. Schultz, *J. Am. Chem. Soc. 110* (1988) 8713.
[51] K. D. Janda, D. Schloeder, S. J. Benkovic, R. A. Lerner, *Science (Washington, D.C.) 241* (1988) 1188.
[52] D. Y. Jackson, J. W. Jacobs, R. Sugasawara, S. H. Reich, P. A. Bartlett, P. G. Schultz, *J. Am. Chem. Soc. 110* (1988) 4841.
[53] a) S. D. Copley, J. R. Knowles, *J. Am. Chem. Soc. 107* (1985) 5306; b) K. Addadi, E. K. Jaffe, J. R. Knowles, *Biochemistry 22* (1983) 4494; c) R. M. Coates, B. D. Rogers, S. J. Hobbs, D. R. Peck, D. P. Curran, *J. Am. Chem. Soc. 109* (1987) 1160; d) P. R. Andrews, G. D. Smith, I. G. Young, *Biochemistry 12* (1973) 3492; e) J. J. Gajewski, J. Jurayi, D. Kimbrough, M. E. Gande, B. Ganem, B. K. Carpenter, *J. Am. Chem. Soc. 109* (1987) 1170.
[54] a) H. Gorisch, *Biochemistry 17* (1978) 3700; b) E. Halsam: *The Shikimate Pathway*, Wiley, New York 1974; c) B. Ganem, *Tetrahedron 34* (1978) 3353; d) G. L. Koch, D. C. Shaw, F. Gibson, *Biochim. Biophys. Acta 258* (1972) 719.
[55] a) S. G. Sogo, T. S. Widlanski, J. H. Hoare, C. E. Grimshaw, G. A. Berchtold, J. R. Knowles, *J. Am. Chem. Soc. 106* (1984) 2701; b) W. J. Guilford, S. D. Copley, J. R. Knowles, *ibid. 109* (1987) 5013.
[56] P. A. Bartlett, C. R. Johnson, *J. Am. Chem. Soc. 107* (1985) 7792.
[57] D. Y. Jackson, P. G. Schultz, unpublished results.
[58] a) D. Hilvert, S. H. Carpenter, K. D. Nared, M. T. M. Auditor, *Proc. Natl. Acad. Sci. USA 85* (1988) 4953; b) D. Hilvert, K. D. Nared, *J. Am. Chem. Soc. 110* (1988) 5593.
[59] a) T. C. Bruice, U. K. Pandit, *Proc. Natl. Acad. Sci. USA 46* (1960) 402; b) D. W. Griffiths, M. L. Bender, *J. Am. Chem. Soc. 95* (1973) 1679; c) M. I. Page, W. P. Jencks, *Proc. Natl. Acad. Sci. USA 68* (1971) 1678.
[60] A. D. Napper, S. J. Benkovic, A. Tramontano, R. A. Lerner, *Science (Washington, D.C.) 237* (1987) 1042.
[61] S. J. Benkovic, A. D. Napper, R. A. Lerner, *Proc. Natl. Acad. Sci. USA 85* (1988) 5355.
[62] K. D. Janda, R. A. Lerner, A. Tramontano, *J. Am. Chem. Soc. 110* (1988) 4835.
[63] W. P. Jencks, *Adv. Enzymol. Relat. Areas Mol. Biol. 43* (1975) 219.
[64] E. T. Kaiser, D. S. Lawrence, *Science (Washington, D.C.) 226* (1984) 505; E. T. Kaiser, *Angew. Chem. 100* (1988) 945; *Angew. Chem. Int. Ed. Engl. 27* (1988) 913.
[65] a) S. J. Pollack, G. R. Nakayama, P. G. Schultz, *Science (Washington, D.C.) 242* (1988) 1038; b) S. J. Pollack, G. R. Nakayama, P. G. Schultz, *Methods Enzymol.*, in press.
[66] S. J. Pollack, P. G. Schultz, *J. Am. Chem. Soc. 111* (1989) 1929.
[67] K. M. Shokat, C. H. Leumann, R. Sugasawara, P. G. Schultz, *Angew. Chem. 100* (1988) 1227; *Angew. Chem. Int. Ed. Engl. 27* (1988) 1172.
[68] a) F. Muller, *Top. Curr. Chem. 108* (1983) 71; b) V. Massey, P. Hemmerich, *Biochem. Soc. Trans. 8* (1980) 246.
[69] B. L. Iverson, R. A. Lerner, *Science (Washington, D.C.) 243* (1989) 1184.
[70] D. A. Buckingham, D. M. Foster, A. M. Sargeson, *J. Am. Chem. Soc. 92* (1970) 6151.
[71] W. Raso, B. Stollar, *Biochemistry 14* (1975) 584.
[72] A. Balan, B. Doctor, B. S. Green, M. Torter, H. Ziffer, *J. Chem. Soc. Chem. Commun. 1988*, 106.
[73] It should be noted that this experiment was carried out with serum, not purified antibody.
[74] Schultz et al., unpublished results.

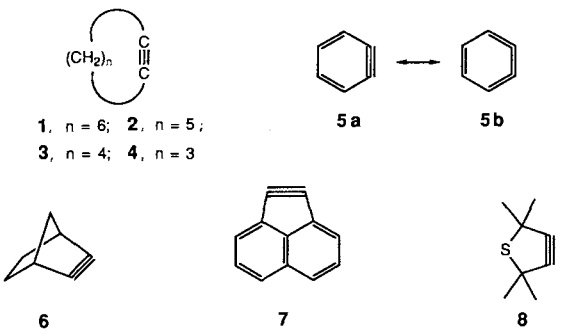
Metal Complexes of Small Cycloalkynes and Arynes

By Martin A. Bennett* and Heinz P. Schwemlein*

Cyclooctyne is the smallest unsubstituted cycloalkyne that can be isolated in the free state and it is more reactive than acyclic alkynes towards transition metal complexes. Smaller cycloalkynes such as cycloheptyne, cyclohexyne, benzyne and cyclopentyne, which are transient molecules in the free state, can be stabilized by coordination either to mononuclear, electron-rich, transition metal-containing fragments, e.g. $[ZrCp_2(PMe_3)]$ and $M(PR_3)_2$ (M = Ni, Pt), or by formation of dinuclear or polynuclear metal complexes, e.g. $[Os_3H_2(CO)_9(C_6H_4)]$ and $[Pt_2(\mu\text{-}PPh_2)(\mu\text{-}C_5H_6)(PPh_3)_3]$. The alkynes can donate between two and four π-electrons to the metal centers, the higher number being favored for the early transition metals. The metal–cycloalkyne and metal–aryne bonds in the mononuclear complexes readily insert molecules containing C=O, C=C, C≡C and C≡N bonds, a feature that may be useful in organic synthesis. The highly unsaturated species 1,4-benzdiyne acts as a bridging ligand between two metal centers in $[\{Ni(Cy_2PCH_2CH_2PCy_2)\}_2(\mu\text{-}C_6H_2)]$.

1. Introduction

Although cyclooctyne **1** is the smallest unsubstituted carbocyclic alkyne that can be isolated in the free state, it is well established that its smaller homologues cycloheptyne **2**, cyclohexyne **3**, and cyclopentyne **4** exist as transient, highly reactive molecules which oligomerize readily in the absence of a suitable trapping agent. Undoubtedly the most extensively studied member of this class is benzyne (1,2-didehydrobenzene) **5**, whose fleeting existence was first established by the classic studies of *Wittig* and *Roberts* in the 1950's, and which can now be regarded as a standard organic reagent. Although the main evidence for the intermediacy of benzyne and small cycloalkynes came initially from trapping and kinetic studies, some of these species have been generated in matrices at low temperature or in the gas phase at low pressure and have been studied by appropriate spectroscopic techniques. Not surprisingly, the lifetime of the cycloalkynes becomes shorter with decreasing ring size, although it can be increased by methyl substitution adjacent to the triple bond. Thus, 3,3,7,7-tetramethylcycloheptyne can be isolated, although 3,3,6,6-tetramethylcyclohexyne cannot. In addition to cyclopentyne, other five-membered ring cycloalkynes that are believed to exist as short-lived intermediates are norbornyne (bicyclo[2.2.1]hept-2-yne) **6**, acenaphthyne **7**, and 2,2,5,5-tetramethyl-1-thiacyclopentyne **8**. However, there is no evidence for the independent existence of the smaller rings cyclobutyne and cyclopropyne. Authoritative reviews on the chemistry of benzyne and cycloalkynes are available.[1–11]



The first attempts to form transition metal complexes of benzyne were made by *Wittig* and *Bickelhaupt* in 1958.[12] They treated 1,2-dilithiobenzene with various transition metal salts but could only isolate biphenyl and polyphenyls. More recent work has shown that benzyne and cycloalkynes form complexes with both early and late transition elements, some of which are stable and can be isolated; others are reactive intermediates. The complexes, not surprisingly, show markedly different chemistry from that of the parent hydrocarbons, and some of them are promising reagents in synthetic organic chemistry. Before discussing these developments, it is useful for purposes of comparison to summarize current views on the bonding in the organic ligands themselves.

2. Structure and Properties of Benzyne and Cycloalkynes

Benzyne in its ground state can be represented as a resonance hybrid of the cycloalkyne structure **5a** and the cumulene structure **5b**, and has been subjected to theoretical calculations at various levels of sophistication.[13–20] Figure 1 shows bond lengths and angles obtained from an ab-initio

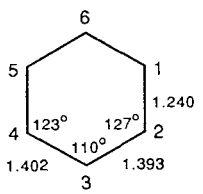


Fig. 1. Calculated bond lengths [Å] and angles [°] in benzyne. [19]

[*] Dr M. A. Bennett, Dr H. P. Schwemlein [+]
Research School of Chemistry
Australian National University
Canberra, ACT 2601 (Australia)
[+] Present address: Ciba Geigy AG
Entwicklungszentrum Agro
CH 4333 Münchwilen AG (Switzerland)

6-31G*-based calculation;[19] the former are corrected values based on the standard C=C and C≡C bond lengths of 1.334 Å and 1.203 Å respectively. The acetylenic bond length C1–C2 generally falls in the range 1.22–1.25 Å and is thus only slightly longer than a normal C≡C bond; there is some disagreement about the trend in the other C–C distances.

The microwave spectrum of benzyne in the gas phase can be simulated using the ab-initio geometry; the predicted and observed rotational constants agree to within 1%.[21] The IR spectrum of benzyne, measured in an argon matrix,[22] shows a C≡C stretching band at 2085 cm^{-1}, which is only slightly lower than the value of ca. 2200 cm^{-1} in acyclic alkynes. However, the C1–C2 bond length of 1.344 Å derived from a force-constant analysis of the IR spectrum[23a] is larger than those obtained from the most recent calculations.[23b]

Structural determinations and spectroscopic studies on isolable seven- and eight-membered cycloalkynes are summarized in Ref. [11], from which most of the following information is taken. In cyclooctyne **1**, the C≡C bond length of 1.23 Å found by electron diffraction is significantly greater than that found in cyclononyne (1.21 Å). The internal C≡C–C bond angle of 158.5° is close to the value of 159.3° determined by X-ray analysis of 1,5-cyclooctadiyne **9**. The



9

corresponding angles in cycloheptyne **2**, cyclohexyne **3**, and cyclopentyne **4** have been calculated as 150.4°/145°, 130.6° and 116.2°, respectively. The IR C≡C stretching frequencies of **1** (measured as a liquid) and **2** (measured in an argon matrix) are 2260/2206 cm^{-1} and 2121 cm^{-1} respectively. The corresponding value for free 3,3,7,7-tetramethylcycloheptyne (2190/2170 cm^{-1}) is higher than for cycloheptyne.

One consequence of *cis*-bending of an alkyne moiety is that the in-plane and out-of-plane π-orbitals are no longer degenerate. The splitting is not detectable by photoelectron spectroscopy in the case of eight-membered rings such as cyclooctyne and 1,5-cyclooctadiyne, but is measured as about 0.3 eV for the more strained seven-membered rings 3,3,7,7-tetramethylcycloheptyne and 3,3,6,6-tetramethylthiacycloheptyne.[25, 26] For cyclohexyne, the splitting is predicted to be ca. 1 eV.[26] Ab-initio calculations on cyclohexyne[27, 28] and cyclopentyne[29] confirm that these species in their ground states should be regarded as highly strained alkynes having diradical character, corresponding to partial breakage of the in-plane π-bond. The predicted values for the C≡C stretching frequencies in **3** are 2003 cm^{-1}[27] or 2169 cm^{-1}[28]; as expected, the predicted value for **4** is much lower (1828 cm^{-1}).[29] The last value can be compared with the frequency of 1930 cm^{-1} tentatively assigned to the C≡C stretching frequency of matrix-isolated acenaphthyne **7**.[30]

A second consequence of *cis*-bending of an alkyne, which is evident from ab-initio calculations of the frontier MO's, is a marked lowering of the LUMO; this is due to efficient mixing of the π*-orbital with a σ*-orbital lying only slightly higher in energy.[31] There is only a small effect on the HOMO. This feature accounts for the characteristic electrophilicity of benzyne and small cycloalkynes e.g. their ready reaction with alcohols, amines, thiols, water, and carbanions, because there is a strong interaction of the benzyne or cycloalkyne LUMO with the HOMO of the nucleophile. In contrast, the benzyne or cycloalkyne HOMO–electrophile LUMO interaction will be normal.

3. Metal Complexes of Small Cycloalkynes

3.1. Cyclooctyne and Related Eight-Membered Rings

Even though it can be isolated, cyclooctyne (C_8H_{12}) is considerably more reactive than acyclic alkynes or larger cycloalkynes, as is shown, for example, by its reactions with



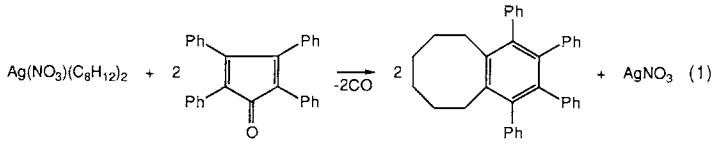


Martin Bennett was born in Harrow, near London, England on August 11, 1935. He graduated from Imperial College of Science, London in 1957 and obtained a Ph.D. from the same institution in 1960 for his work on olefin and carbonyl complexes of transition metals under the direction of Sir Geoffrey Wilkinson. After a postdoctoral year with Professor Arthur Adamson at the University of Southern California, he returned to London as a Turner and Newall Fellow to work with the late Sir Ronald Nyholm at University College London and was appointed to a lectureship there in 1963. In 1967 he moved to the newly formed Research School of Chemistry of the Institute of Advanced Studies at the Australian National University, Canberra, where he is now a Professorial Fellow. He has a long-standing interest in the activation of organic and inorganic molecules by transition metal compounds, especially those of the platinum metals. His work has appeared in about 170 publications. Since 1980 he has been a Fellow of the Australian Academy of Science. He received an award from the Royal Society of Chemistry (1981) as well as the H. G. Smith Medal (1977) and the G. J. Burrows Award (1987) of the Royal Australian Chemical Institute. With the support of the Alexander von Humboldt Foundation, he spent two six-month periods in the Federal Republic of Germany at the Max-Planck-Institut für Kohlenforschung in Mülheim/Ruhr in 1973 and at the Institut für Anorganische Chemie in Würzburg in 1981.

Heinz Schwemlein was born in Balingen, West Germany on June 20, 1955. He studied chemistry at the University of Konstanz (1975–1981), where he received his Diplom degree in 1981 and his Ph.D. in 1985 working with Professor H. H. Brintzinger on ansa metallocenes. He then joined the group of M. A. Bennett at the Research School of Chemistry, ANU, as a postdoctoral fellow. Since 1988 he has been working as a chemist at the analytical center of the Development Center Agro, Ciba-Geigy AG, Switzerland.

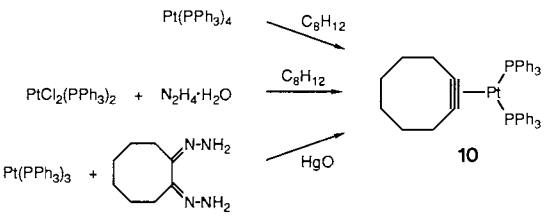
Diels–Alder reagents at room temperature. This enhanced reactivity is also evident in its transition metal chemistry. Thus, cyclooctyne metal complexes are more stable with respect to dissociation of the ligand than the complexes of acyclic alkynes. Cyclooctyne also undergoes cyclooligomerization in the presence of transition metal compounds far more readily than do acyclic alkynes.

Whereas 4-octyne does not form stable complexes with the univalent coinage metals, cyclooctyne forms air-stable, solid complexes $[CuBr(C_8H_{12})_n]$ (n = 1,2),[32] $[AgNO_3(C_8H_{12})_2]$,[33] and $[AuBr(C_8H_{12})_2]$.[32] These compounds are labile in solution and react with tetracyclone to give the adduct derived from cyclooctyne [Eq. (1)].



(1)

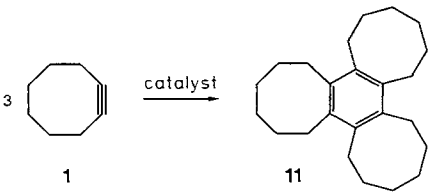
The more stable platinum(0) complex **10** can be prepared in high yield by direct reaction of cyclooctyne at room temperature either with $Pt(PPh_3)_4$[34] or with ethanolic *cis*-$[PtCl_2(PPh_3)_2]$ in the presence of hydrazine hydrate.[32] **10** is formed in lower yield when cyclooctyne is generated in situ by mercuric oxide oxidation of 1,2-cyclooctanedionebis(hydrazone) in the presence of $Pt(PPh_3)_3$[35] (Scheme 1). The



Scheme 1. Synthesis of cyclooctynebis(triphenylphosphane)platinum **10**.

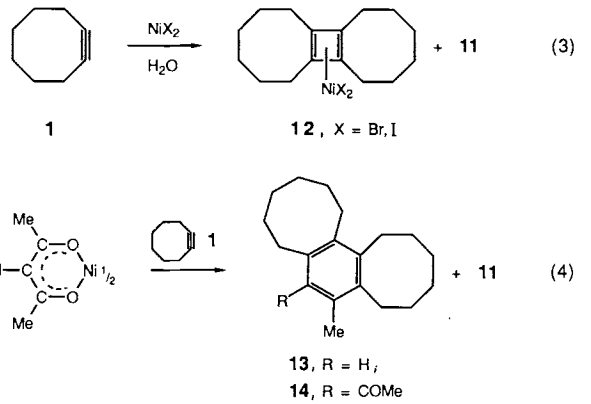
triphenylphosphane ligands of **10** can be replaced by dppe [dppe = ethane-1,2-diylbis(diphenylphosphane)] to give $[Pt(dppe)(C_8H_{12})]$. However, attempts to prepare analogues of **10** by reaction of cyclooctyne with the two-coordinate complexes PtL_2 (L = tBuPh$_2$P, tBu$_2$PhP) were unsuccessful, presumably because of steric hindrance by the bulky phosphanes.[36] In contrast to 4-octyne and other acyclic alkynes, cyclooctyne is not readily displaced from its $Pt(PPh_3)_2$ complex, and **10** does not react with typical Diels–Alder reagents.

Although cyclooctyne is thermally fairly stable in the absence of catalysts, it undergoes cyclotrimerization to tris(hexamethylene)benzene **11** in the presence of many transition metal compounds, including $TiCl_4$,[37] nickel compounds NiX_2 (X = Br, I, CN),[38] nickel(II) acetylacetonate,[38] bis(acrylonitrile)nickel,[32] $Fe(CO)_5$,[39] and $Mo(CO)_6$[40] [Eq. (2)]. The $TiCl_4$-promoted reaction occurs



(2)

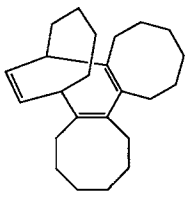
cleanly and rapidly at room temperature, while that with $Ni(CN)_2$ occurs in boiling THF. When the reaction between cyclooctyne and nickel(II) halides is carried out in the presence of small amounts of water, bis(hexamethylene)cyclobutadiene-nickel(II) complexes **12** are obtained in low yield, in addition to **11** [Eq. (3)].[38] Also, in the reaction of cyclooctyne with nickel(II) acetylacetonate, small amounts of the bis(hexamethylene)aromatic compounds **13** and **14** are formed [Eq. (4)].[38] These are presumably derived by a



(3)
(4)

metal-promoted condensation of two cyclooctyne molecules with one of the β-diketonato ligands and subsequent loss of water or acetic acid, since cyclooctyne does not react with free acetylacetone. It is noteworthy that, although the cyclooligomerization of acyclic alkynes can be catalyzed by Ni^0 and Ni^{II} compounds, only strained cycloalkynes such as cyclooctyne can give isolable cyclobutadiene complexes by direct reaction with nickel(II) halides.

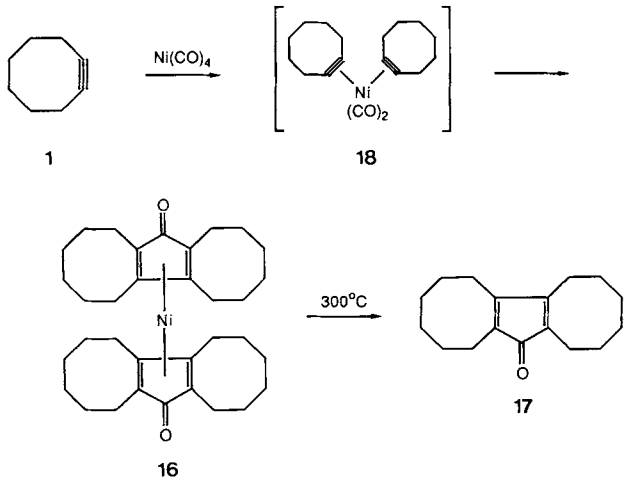
Reaction of $[Pt(PPh_3)_2(C_8H_{12})]$ **10** with cyclooctyne in a 1:1 mol ratio at 75 °C gives a non-aromatic cyclotrimer for which structure **15** has been suggested;[32] when the relative amount of cyclooctyne is increased, a mixture of **11** and **15** is formed. Since $[Pt(PPh_3)_2$(acenaphthylene)] catalyzes only the formation of **11** from cycloctyne, **10** is clearly the species responsible for the generation of **15**, but the topic deserves further investigation.



15

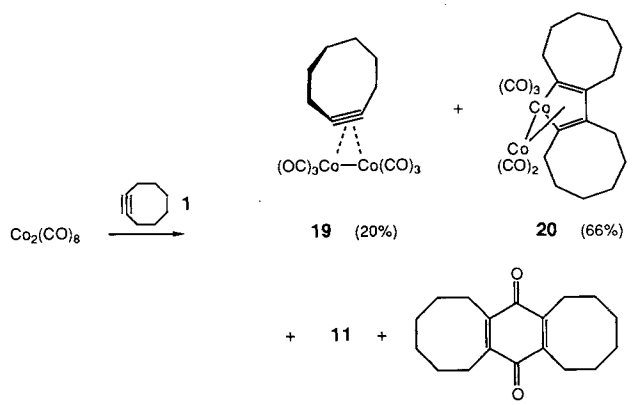
The reactions of cyclooctyne with metal carbonyl compounds are characterized by the ready oligomerization of the alkyne with CO. Thus, the final product from the reaction with $Ni(CO)_4$ in ether is the cyclopentadienone complex **16**, from which dodecahydrocyclopentadicycloocten-13-one (**17**) is liberated at 300 °C (Scheme 2).[38] There is evidence for an intermediate bis(cyclooctyne) complex **18**.

In the dark, both $Fe(CO)_5$ and $Mo(CO)_6$ slowly catalyze the formation of **11** from cyclooctyne. Under UV irradiation, $Fe(CO)_5$ and cyclooctyne form mainly the $Fe(CO)_3$ complex of **17** and dodecahydrobenzo[1,2:4,5]dicyclo-



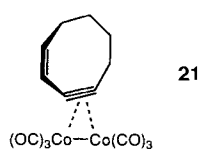
Scheme 2. Formation of dodecahydrocyclopentadicycloocten-13-one **17**.

octene-7,14-dione.[39] Under similar conditions reaction of cyclooctyne with $Mo(CO)_6$ gives mainly **11** and dodecahydrobenzo[1,2:4,5]dicyclooctene-7,14-diol, together with smaller amounts of the quinone and a complex $[Mo(CO)(C_8H_{12})_3]$.[40] Cyclooctyne reacts with $Co_2(CO)_8$ in ether or pentane at room temperature to give the μ-alkyne complex **19** of the usual type, together with a complex of empirical formula $[Co_2(CO)_5(C_8H_{12})_2]$, which was shown by X-ray crystallography to be a cobaltacyclopentadiene **20** (Scheme 3).[41] Such complexes have not been observed hith-



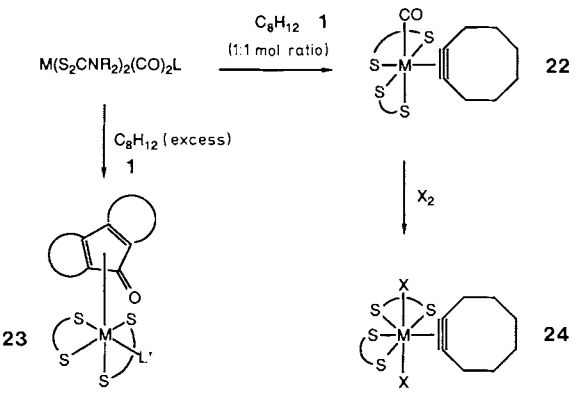
Scheme 3. Reaction of octacarbonylcobalt with **1**.

erto in the reactions of $Co_2(CO)_8$ with acyclic alkynes, though they may be precursors to the well-known "fly-over" complexes $[Co_2(CO)_4(alkyne)_3]$ that are formed under forcing conditions.[42] Both **19** and **20** separately catalyze cyclotrimerization of cyclooctyne to **11**. The formation of **20** and other oligomerization products can be largely suppressed by adding $Co_2(CO)_8$ to cyclooctyne in a 1:1 molar ratio, and **19** can then be isolated in 71% yield.[43] The $Co_2(CO)_6$ complex of the even more highly strained *cis*-cyclooct-1-en-3-yne **21** has been made similarly, but



attempts to liberate the alkyne from the complex by ceric ion oxidation led to polymerization, even at −40 °C.[43]

Cyclooctyne forms stable complexes with molybdenum and tungsten in oxidation states +2 and +4. Deep green dialkyldithiocarbamato complexes **22** are obtained upon reaction of cyclooctyne with $[M(S_2CNR_2)_2(CO)_2L]$ (M = Mo, L = PPh_3; M = W, L = CO) in a 1:1 mol ratio (Scheme 4).[44] The highly deshielded alkyne ^{13}C resonances and the



Scheme 4. Reactions of cyclooctyne-molybdenum and -tungsten complexes. L = CO, PPh_3; L' = CO, C_8H_{12}; $\widehat{S\,S}$ = Me_2NCS_2, Et_2NCS_2; X = Br, I; M = Mo, W.

failure of the complexes to react with CO and tertiary phosphanes suggest that in **22** cyclooctyne donates four electrons from its orthogonal π-orbitals to the metal atom. In this respect, complexes **22** resemble the corresponding acyclic alkyne complexes. The latter, however, react only under forcing conditions with an excess of alkyne (CO being displaced) to give the bis(alkyne) complexes $[M(alkyne)_2(S_2CNR_2)_2]$. In contrast, complexes **22** react readily with an excess of cyclooctyne, with retention of CO, to give complexes **23** (Scheme 4).[45] Further, complexes **22** are readily oxidized by iodine or bromine to give the cyclooctyne complexes **24** of molybdenum(IV) or tungsten(IV),[44] the acyclic alkyne analogues of which are unknown. Likewise, the cyclooctyne molybdenum(IV) complexes $[MoO(S_2CNR_2)_2(C_8H_{12})]$ (R = Me, Et) do not readily lose their coordinated alkyne, in contrast to the behavior of the corresponding complexes of C_2H_2, PhC_2H and PhC_2Ph.

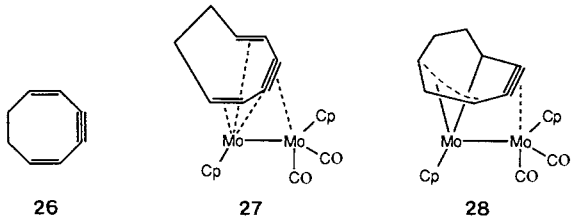
Cyclooctyne also forms divalent metal-tertiary phosphane complexes **25** [Eq. (5)], but attempted halogenation of these compounds led only to decomposition.

$$[MBr_2(CO)_n(PEt_3)_2] \xrightarrow{C_8H_{12},\ 1} [MBr_2(CO)(PEt_3)_2(C_8H_{12})] \quad (5)$$

M = Mo, n = 2; M = W, n = 3 — **25**

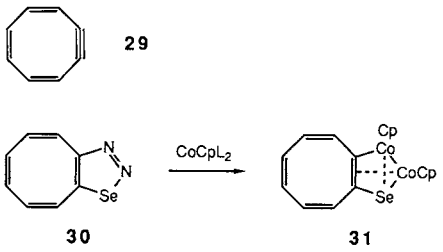
The unknown 1,5-cyclooctadien-3-yne **26** can be stabilized in the form of a purple dimolybdenum complex **27**, which is formed by heating $[\{Mo(Cp)(CO)_3\}_2]$ with cyclooctatetraene in *n*-octane.[46] The alkyne unit lies across a Mo–Mo bond, the two C=C bonds being coordinated to one of the molybdenum atoms. Clearly the formation of **27** requires hydrogen migration in the C_8H_8 ring, and such a process also occurs when **27** is dissolved in polar solvents. The product is the

thermodynamically stable isomer **28** in which the bridging alkyne unit is retained but there is now a η^1, η^3-interaction of the remaining C=C bonds with one of the molybdenum atoms.



26 **27** **28**

An attempt to stabilize the unknown 1,3,5-cyclooctatrien-7-yne (**29**) by metal complexation was unsuccessful. Treatment of the 1,2,3-selenadiazole **30** with $CoCpL_2$ (L = PPh_3, C_2H_4) gave a green-black complex **31** in which a C_8H_6Se fragment is attached to a Co_2Cp_2 unit [Eq. (6)].[47]

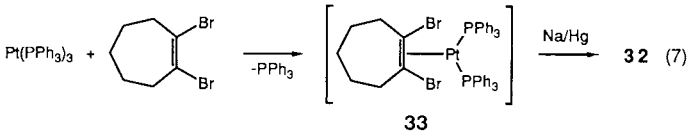


29

30 **31** (6)

3.2. Cycloheptyne and Related Seven-Membered Rings

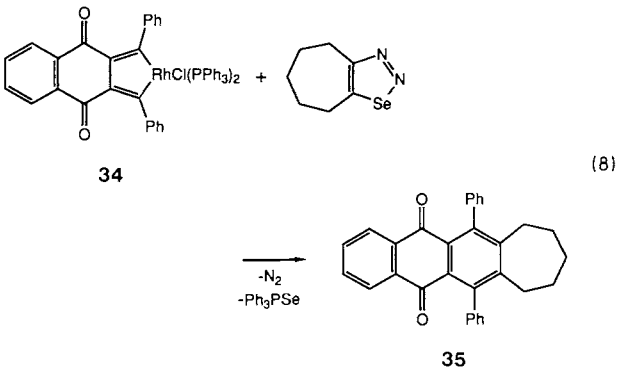
Although free cycloheptyne, C_7H_{10}, cannot be isolated, its platinum(0) complex **32** has been made in 20% yield by mercuric oxide oxidation of 1,2-cycloheptanedionebis(hydrazone) in the presence of $Pt(PPh_3)_3$, and in 80% yield by reaction of $Pt(PPh_3)_3$ or $Pt(PPh_3)_4$ with 1,2-dibromocycloheptene in the presence of 1% sodium amalgam (Scheme 5).[35,48] The first reaction undoubtedly involves trapping of transient cycloheptyne by $Pt(PPh_3)_3$. This may hold also for the second reaction, since cycloheptyne can be generated by alkali- or alkaline-earth metal reduction of 1,2-dibromocycloheptene. Recent work (Sections 3.3, 3.4), however, suggests that a more likely mechanism is reduction of a transient complex **33** [Eq. (7)]. Chelating phosphanes



33 **32** (7)

$R_2PCH_2CH_2PR_2$ (R = Ph, Me) displace PPh_3 from **32** without removing the cycloalkyne (Scheme 5).

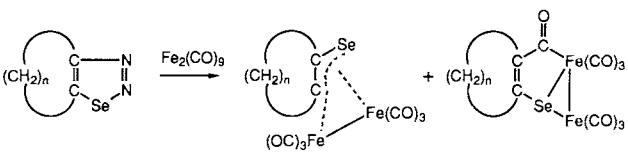
The palladium(0) analogue of **32** has been made from $Pd(PPh_3)_4$, 1,2-dibromocycloheptene, and 1% Na/Hg, but there have been no other reported attempts to form cycloheptyne metal complexes by generating the cycloalkyne in the presence of low-valent metal complexes. Clearly, a low-valent metal complex may not survive the drastic thermal or oxidizing conditions necessary to generate the cycloalkyne and, in addition, trapping by the complex must compete with oligomerization. Nevertheless, cycloheptyne, generated by the thermal decomposition of 4*H*-5,6,7,8-tetrahydro-1-selena-2,3-diazaazulene, does insert into the rhodium–carbon bonds of the metallacyclopentadiene **34** to give the anthraquinone **35** in 47% yield[49] [Eq. (8)]. The selenadiazoles



34 (8)

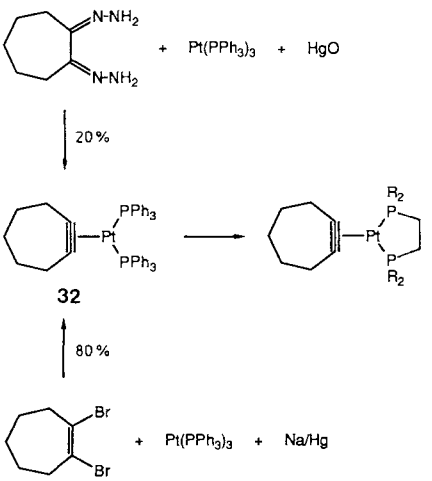
35

themselves react with metal-carbonyls to give stable complexes which still contain selenium (Scheme 6).[50]



Scheme 6. Reaction of selenadiazoles with $Fe_2(CO)_9$.

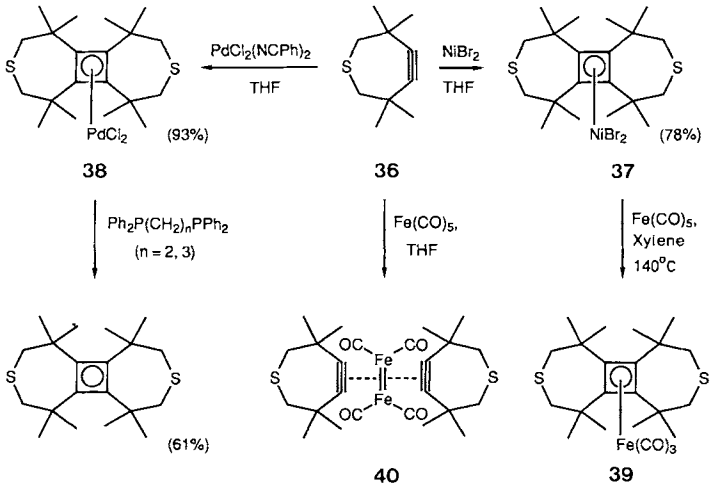
The isolable strained cycloalkyne 3,3,6,6-tetramethylthiacyclohept-4-yne **36** dimerizes on reaction with anhydrous $NiBr_2$ or $[PdCl_2(NCPh)_2]$ to give deep violet and yellow crystals, respectively, of the corresponding monomeric cyclobutadiene metal dihalide complexes **37** and **38** in high yields[51,52] (Scheme 7). The cyclobutadiene can be transferred from Ni to Fe by heating with $Fe(CO)_5$[53] and can be displaced from **38** (but not from **37**) by heating with $Ph_2P(CH_2)_nPPh_2$ (n = 2,3). As expected, the free cyclobuta-



Scheme 5. Synthesis of cycloheptyne-platinum(0) complexes. R = Ph, Me.

diene has alternating long and short C–C bonds (1.600, 1.344 Å),[54] whereas the C–C bond lengths in **38**[55] and in the $Fe(CO)_3$ complex **39**[53] are almost equal at ca. 1.45–1.48 Å.

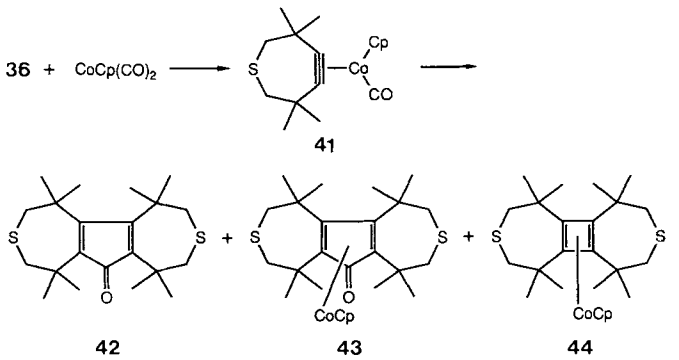
Direct reaction of $Fe(CO)_5$ with **36** gives complex **40**, in which two cycloalkyne units lie across an $Fe_4(CO)_4$ unit; the



Scheme 7. Reactions of 3,3,6,6-tetramethylthiacyclohept-4-yne **36** with transition metal compounds.

remarkably short Fe–Fe distance, 2.225(3) Å, indicates the presence of a double bond between the metal atoms.[56]

At low temperatures **36** reacts with $[CoCp(CO)_2]$ to give a mono-alkyne complex **41** almost quantitatively; on heating, a mixture of the cyclopentadienone **42**, its CoCp complex **43**, and the cyclobutadiene complex **44** is formed, presumably via **41** as intermediate (Scheme 8).[57]

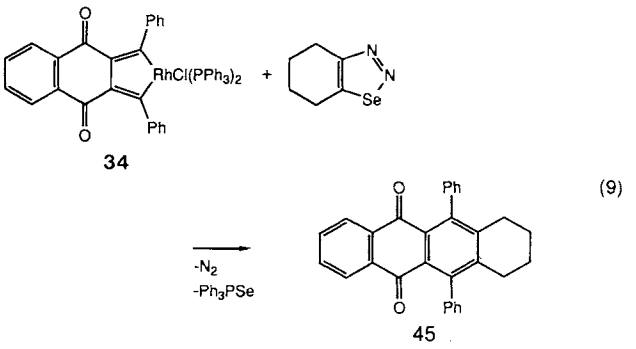


Scheme 8. Reaction of 3,3,6,6-tetramethylthiocyclohept-4-yne **36** with the complex $CoCp(CO)_2$.

3.3. Cyclohexyne and Related Six-Membered Rings

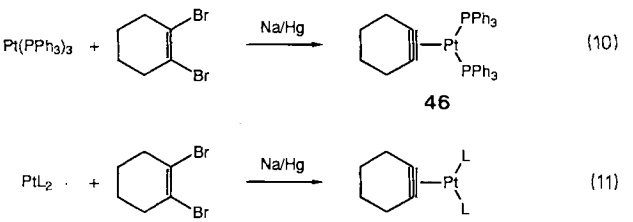
Cyclohexyne is much shorter-lived than cycloheptyne and most attempts to form metal complexes by generating it in the presence of a low-valent metal complex have been unsuccessful. However, thermally generated cyclohexyne inserts into the Rh–C bonds of **34** to give the anthraquinone **45** in 38% yield [Eq. (9)].[49]

The cyclohexyne-platinum(0) complex **46** can be obtained as colorless, air-stable crystals in 70–90% yield by reaction of 1,2-dibromocyclohexene, 1% sodium amalgam, and



(9)

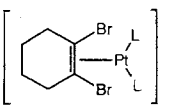
$Pt(PPh_3)_3$ [Eq. (10)].[35,48] The corresponding complexes $PtL_2(C_6H_8)$ (L = P-*t*Bu_2Ph, P-*t*$BuPh_2$) are formed similarly in ca. 30% yield by a similar reaction employing the two-coordinate complexes PtL_2 in place of $Pt(PPh_3)_3$ [Eq. (11)].[36] The cyclohexyne-palladium(0) complex $[Pd(PPh_3)_2(C_6H_8)]$ has been prepared similarly in 25% yield from $Pd(PPh_3)_4$.[35]



(10)

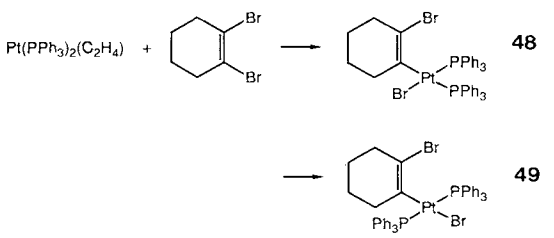
(11)

These reactions probably do not proceed via the free cycloalkyne but by rapid reduction of a transient 1,2-dibromocyclohexene complex **47** (see Section 3.4).



47

In the absence of sodium amalgam, 1,2-dibromocyclohexene reacts at room temperature with the ethylene complex $[Pt(PPh_3)_2(C_2H_4)]$ to give the *cis*-oxidative addition product **48** which isomerizes slowly to the *trans*-compound **49** [Eq. (12)]. Presumably **48** is formed via **47**, though the latter



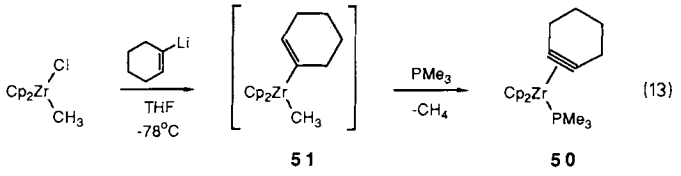
(12)

has not been detected. Neither **48** nor **49** are reduced by 1% sodium amalgam to **46**.[58]

The phosphane ligands of **46** can be replaced without affecting the coordinated cyclohexyne by diphenylmethylphosphane and by various ditertiary bisphosphanes

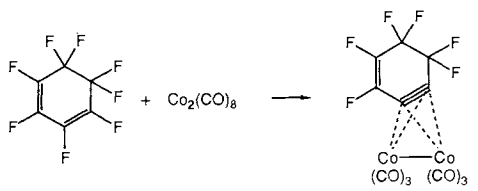
e.g. $Ph_2P(CH_2)_nPPh_2$ (n = 2,3,4), (*Z*)-$Ph_2PCH=CHPPh_2$, and $Me_2PCH_2CH_2PMe_2$.[35, 36, 59]

So far, only one other transition element, zirconium, has been reported to form a mononuclear cyclohexyne complex. Treatment of [ZrClMe(η-Cp)$_2$] with 1-cyclohexenyllithium at low temperature and subsequent addition of trimethylphosphane gives the cyclohexyne-zirconium complex **50** in 60% yield as an air- and moisture-sensitive solid.[60] The reaction proceeds by elimination of methane from the (1-cyclohexenyl)(methyl)zirconocene **51** to give a coordinatively unsaturated zirconocene cyclohexyne, [Zr(η-C_5H_5)$_2$(C_6H_8)], which is trapped by PMe_3 [Eq. (13)].



51 50 (13)

A remarkable example of stabilization of a small cycloalkyne by coordination is provided by the reaction of octafluoro-1,3-cyclohexadiene, C_6F_8, with $Co_2(CO)_8$ at 80 °C. The resulting dinuclear complex **52** (15% yield) contains hexafluorocyclohex-1-en-3-yne bound to two cobalt atoms by its triple bond, which is oriented at right-angles to the Co-Co axis in the usual way [Eq. (14)].[61]

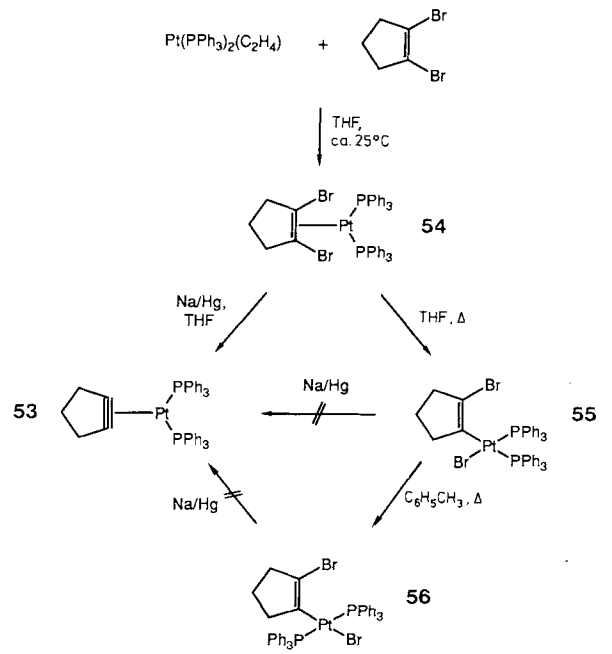


52 (14)

Other metal-carbonyl or organometallic precursors tested did not react similarly with C_6F_8 and no attempts to extend this interesting reaction have been reported.

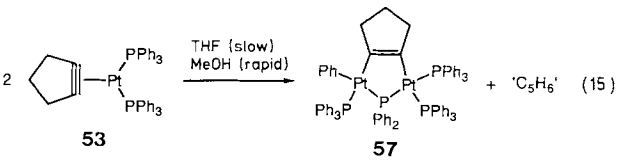
3.4. Cyclopentyne and Related Five-Membered Rings

Early attempts to prepare cyclopentynebis(triphenylphosphane)platinum **53** similarly to the cyclohexyne analogue **46** by treating a mixture of 1,2-dibromocyclopentene and $Pt(PPh_3)_3$ with 1% sodium amalgam were unsuccessful.[35] Recently, however, **53** has been isolated as a colorless, very reactive solid as shown in Scheme 9.[58] Reaction of ethylene bis(triphenylphosphane)platinum with 1,2-dibromocyclopentene gives the olefin complex **54**, which isomerizes successively to the *cis*- and *trans*-oxidative addition products **55** and **56**, respectively. This process is slow at room temperature, so that **54** (in contrast to the corresponding 1,2-dibromocyclohexene complex **47**, cf. Section 3.3) can be isolated. Reduction of **54** with 1% sodium amalgam in THF at room temperature gives **53**, which has been fully characterized by ^1H, ^{13}C, and ^{31}P NMR spectroscopy (Section 3.5). This complex loses a C_5H_6 fragment (slowly in THF, rapidly in methanol at room temperature) and undergoes P–Ph bond



Scheme 9. Synthesis of cyclopentynebis(triphenylphosphane)platinum **53**.

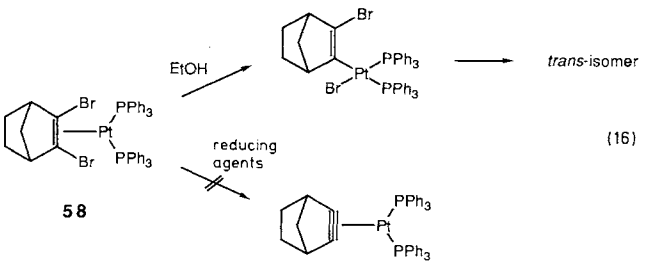
cleavage, presumably according to Equation (15), to give the dinuclear complex **57** containing bridging cyclopentyne (or cyclopentene-1,2-diyl) and PPh_2 groups, as shown by X-ray crystallography.[62]



53 57 (15)

Complexes **55** and **56** are not reduced to **54** by 1% sodium amalgam. Similar lack of reactivity is found in the six-membered ring series (Section 3.3), so that these oxidative addition products cannot be intermediates in the formation of the cycloalkyne complexes. The results in the five-membered ring series strongly suggest that the six- and seven-membered ring analogues of **54**, i.e. **47** and **33**, are intermediates in the formation of the corresponding cycloalkyne complexes **46** and **32**, though they have not been detected or isolated.

Attempts to stabilize norbornyne (**6**) by a similar method have been unsuccessful.[63] Reaction of 2,3-dibromobicyclo[2.2.1]hept-2-ene with $Pt(PPh_3)_3$ or [$Pt(PPh_3)_2(C_2H_4)$] gives the olefin complex **58**, which, like **53**, rearranges slowly to the *cis*- and, finally, the *trans*-oxidative addition products [Eq. (16)]. Unlike **53**, however, **58** is unaffected by sodium amalgam, naphthalenesodium, or *n*-butyllithium.



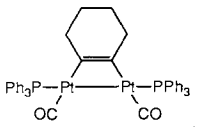
58 (16)

3.5. Reactivity of Cycloalkyne-Metal Complexes

The preparative results show clearly that six- to eight-membered ring cycloalkynes, in general, are less easily displaced from their metal complexes than are the corresponding acyclic alkynes. Chelating ditertiary phosphanes replace only PPh_3 from the $Pt(PPh_3)_2$ complexes of cyclohexyne, cycloheptyne, and cyclooctyne (**46**, **32** and **10**, respectively).[35, 59] The only π-acceptor ligands that seem to be able to displace cyclohexyne completely from **46** are PF_3 and tetracyanoethylene (TCNE) [Eq. (17)], and the fate of the cyclohexyne has not been established.

$$Pt(PF_3)_2(PPh_3)_2 \xleftarrow{PF_3} \mathbf{46} \xrightarrow{TCNE} Pt(TCNE)(PPh_3)_2 \qquad (17)$$

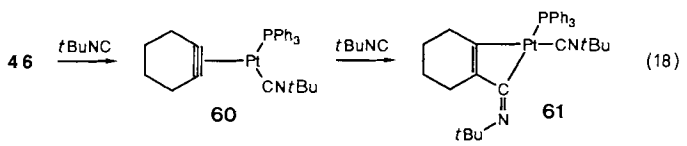
Interestingly, carbon monoxide is inert towards the cycloheptyne complex **32**, but it reacts with the cyclohexyne complex **46** to form the dinuclear μ-cyclohexyne- or cyclohexene-1,2-diyl-platinum(I) complex **59**, together with unidentified carbonyltriphenylphosphane platinum(0) complexes. Again,



59

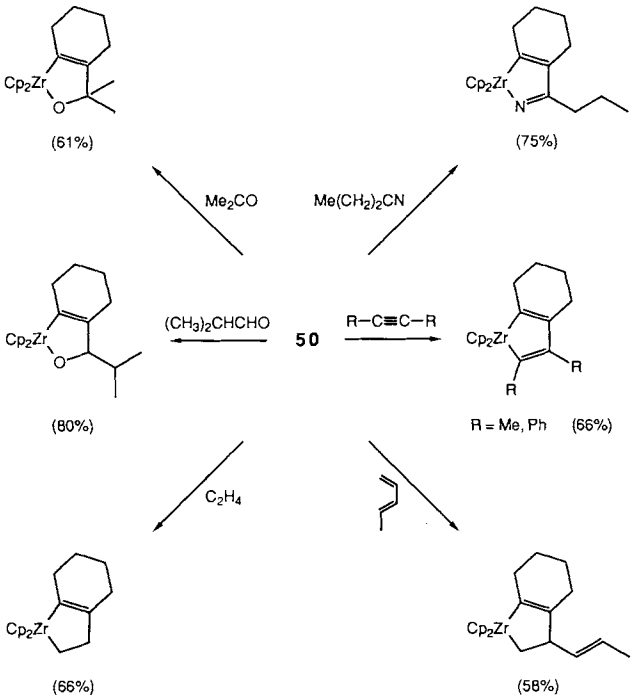
the fate of the displaced cyclohexyne is unknown.[35] The reaction is reminiscent of the formation of the cyclopentene-1,2-diylcomplex **57** from cyclopentynebis(triphenylphosphane)platinum **53**. It suggests that mononuclear metal complexes of the smaller cycloalkynes are strained and, at least in the case of platinum, that the strain can be relieved by formation of a four-membered dimetallacycle containing two M–C σ-bonds.

One consequence of this strain is that simple unsaturated molecules readily insert into the cycloalkyne-metal bond. Thus, **47** reacts with *tert*-butyl isocyanide at room temperature to give first the substitution product **60** and then the insertion product **61** [Eq. (18)]; **32** does not react similarly.[35]



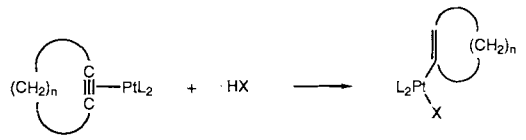
(18)

The cyclohexyne-zirconium complex **50** undergoes insertion reactions of this type with many substrates, including alkenes, alkynes, aldehydes, ketones and nitriles, towards which the platinum complex **46** is inert (Scheme 10). Probably, in the first step, the trimethylphosphane ligand of **50** is displaced by the unsaturated molecule, and coupling then occurs. In some cases the same result can be achieved by generating $[Zr(\eta\text{-}Cp)_2(C_6H_8)]$ in situ at low temperature and treating it with the unsaturated compound.[60]



Scheme 10. Insertion reactions of $[ZrCp_2(PMe_3)(C_6H_8)]$ **50**.

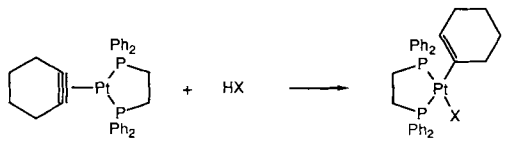
The bis(triphenylphosphane)platinum(0) complexes of cyclohexyne (**46**) and cycloheptyne (**32**), and their ditertiary bisphosphane analogues, are readily protonated by strong acids HX (X = Cl, CO_2CF_3) to give η^1-cycloalkenylplatinum(II) complexes [Eq. (19)]. Excess of acid cleaves the Pt–C σ-bond to give PtX_2L_2.



(19)

n = 4, 5

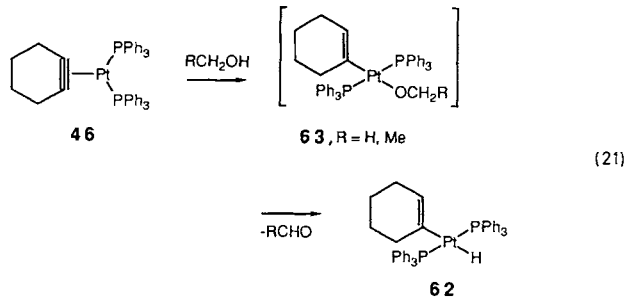
Similar reactions are well-known for acyclic alkyne-platinum(0) complexes. However, the cyclohexyne compounds are unique in this series in being protonated irreversibly even by weak acids. For example, $[Pt(dppe)(C_6H_8)]$ reacts with thiophenol, *p*-cresol, nitromethane, acetonitrile, phenylacetonitrile, carboxamides, and (in the presence of water) methyl ketones [Eq. (20)].[35, 59]



(20)

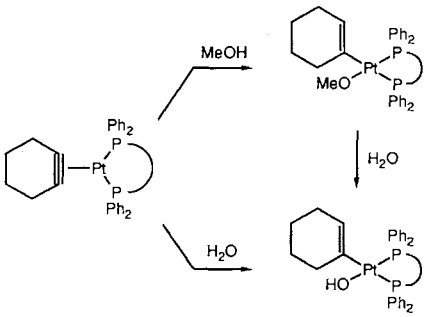
X = SPh, *p*-OC_6H_4Me, CH_2NO_2, CH_2CN, CH(Ph)CN

46 also reacts readily with methanol or ethanol under reflux to form the η^1-cyclohexenyl hydrido complex **62**. Initially **46** is probably protonated to give an alkoxide **63** which then undergoes β-hydride migration and elimination of aldehyde [Eq. (21)]. The corresponding complexes



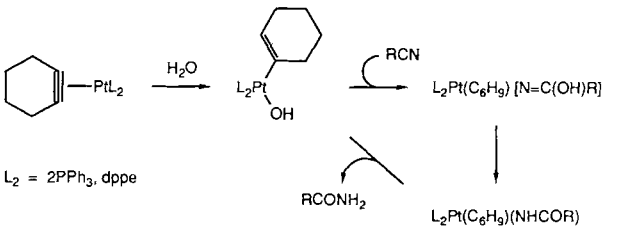
(21)

[Pt(P⌒P)(C$_6$H$_8$)] with ditertiary bisphosphane ligands (P⌒P) react with methanol to give isolable methoxoplatinum(II) species [Pt(OMe)(P⌒P)(C$_6$H$_9$)] that do not undergo β-elimination even on prolonged heating. They are readily hydrolyzed to monomeric hydroxo complexes [Pt(OH)(P⌒P)(C$_6$H$_9$)], which can also be obtained directly from [Pt(P⌒P)(C$_6$H$_8$)] and water (Scheme 11).[35, 48, 59]



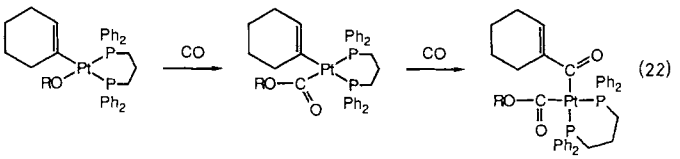
Scheme 11. Reactions of [Pt(P⌒P)(C$_6$H$_8$)] with water and methanol.

The ability of **46** and [Pt(C$_6$H$_8$)(dppe)] to catalyze the formation of carboxamides from nitriles and water undoubtedly depends on the initial formation of hydroxoplatinum(II) complexes (Scheme 12),[64] even though [Pt(OH)(C$_6$H$_9$)(PPh$_3$)$_2$] has never been isolated from the reaction of water with **46**.



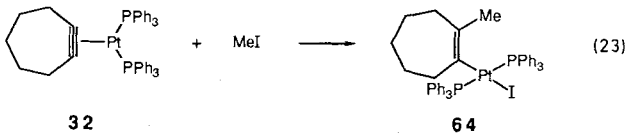
Scheme 12. Catalysis of the synthesis of carboxamides from water and cyanides by cyclohexyne-platinum(0) complexes.

The discovery of these hydroxy compounds has led to the preparation of many monomeric alkyl- or aryl-hydroxoplatinum(II) complexes whose chemistry is outside the scope of this review.[64] We note here that the η^1-cyclohexenylhydroxy- and methoxy-platinum(II) complexes readily insert CO to give the corresponding hydroxycarbonyl and methoxycarbonyl complexes. Further, when the ditertiary phosphane is Ph$_2$P(CH$_2$)$_3$PPh$_2$, insertion of CO into the Pt–C σ-bond also takes place to give acyl cyclohexenyl complexes [Eq. (22)].[65]



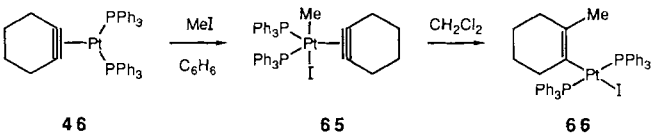
(22)

Electrophiles such as methyl iodide and iodine also add to cycloalkyne-PtL$_2$ complexes.[66] Thus, methyl iodide reacts with **32** to give the 2-methylcycloheptenyl complex **64** as the main product [Eq. (23)] together with a small amount of *trans*-[PtIMe(PPh$_3$)$_2$]. The latter is the only organoplatinum compound obtained from [Pt(PPh$_3$)$_2$(PhC$_2$Ph)] and methyl iodide.



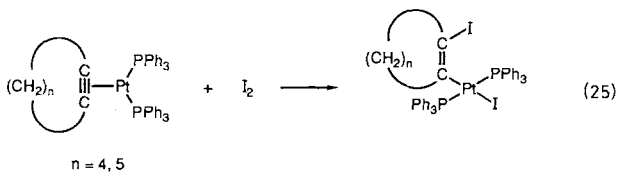
(23)

The first step in this "insertion" reaction is probably oxidative addition of methyl iodide to the metal atom. In the case of the reaction of methyl iodide with the cyclohexyne complex **46** in benzene, the oxidative addition product **65** can be isolated; it rearranges to the 2-methylcyclohex-1-enyl complex **66** in dichloromethane [Eq. (24)].



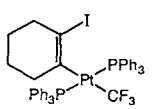
(24)

Iodine reacts similarly with **33** and **47** to give mainly the *trans*-2-iodocycloalk-1-enyl complexes [Eq. (25)], whereas [Pt(C$_6$H$_8$)(dppe)] and [Pt(C$_7$H$_{10}$)(dppe)] give mainly PtI$_2$(dppe).



(25)

Trifluoromethyl iodide acts as a source of positive iodine in its reaction with **46**: the product is the 2-iodocyclohex-1-enyl complex **67**.[66]



67

3.6. Structure, Spectroscopic Properties and Bonding of Some Cycloalkyne-Metal Complexes

Important parameters obtained from X-ray structural analyses of cycloalkyne-metal complexes are summarized in Table 1. The basic geometry and structural parameters relating to the MC_2 unit of the cycloalkyne-$Pt(PPh_3)_2$ complexes **10**, **32** and **46**[48, 67–69] are very similar to those of the complex $[Pt(PPh_3)_2(Ph-C\equiv C-Me)]$ **68**.[70] All four complexes have an almost planar coordination geometry. The C≡C distances in all four complexes (1.28–1.30 Å) do not differ significantly and are longer than a normal C≡C bond. The bend-back angle of the substituents at the alkyne carbon atom is very similar (34–41°) for **10**, **32** and **68**, but the smaller ring in **46** causes an increase to 53°. Similarly large bend-back angles are observed in **50**[60] and **52**.[61] The C–C–C bond angles in the six-membered rings of **46** and **50**, and in the eight-membered ring of **10**, are close to the expected tetrahedral value; this probably indicates release of strain when the cycloalkyne is bound to the metal atom. Surprisingly, however, some of the ring C–C–C bond angles in the cycloheptyne complex **32** are considerably distorted and some of the C–C distances are substantially shorter than normal C–C single bonds.

Table 1. Selected structural parameters for the alkyne metal complexes $[Pt(PPh_3)_2(C_8H_{12})]$ **10**, $[Pt(PPh_3)_2(C_7H_{10})]$ **32**, $[Pt(PPh_3)_2(C_6H_8)]$ **46**, $[Pt(PPh_3)_2(PhC_2Me)]$ **68**, $[ZrCp_2(PMe_3)(C_6H_8)]$ **50** and $[Co_2(CO)_6(C_6F_6)]$ **52**.

Cpd.	d(C≡C) [Å]	Bend-back-angle [°]	C-M-C angle [°]	d(M-C) [Å]	Ref.
10	1.279(13)	34.0	36.6	2.036(9) [a]	[68, 69]
32	1.283(5)	41.3	36.5	2.050(4) [a]	[48, 67]
46	1.297(8)	52.7	37.1	2.039(5) [a]	[67]
68	1.277(25)	38(Me) 41(Ph)	36.7	2.014(16)(Me) 2.044(17)(Ph)	[70]
50	1.295(25)	54.4	32.1	2.204(13)	[60]
52	1.36	59		1.92	[61]

[a] Average value.

The bonding in mononuclear alkyne-metal complexes can be described similarly to that in alkene-metal complexes.[71, 72] Forward donation from the filled alkyne $\pi_{\parallel}$ orbital into a vacant metal orbital is supplemented by back donation from a filled metal π^* orbital to an empty π^* orbital of the alkyne. In contrast to alkenes, an additional pair of electrons is available from the orthogonal $\pi_{\perp}$ orbital, so that alkynes can donate up to four electrons, especially to earlier transition elements, which have suitable vacant d-orbitals.[73] Infrared C≡C stretching frequencies[72] and the ^{13}C chemical shifts of the alkyne carbon atoms (δ_c)[74] are useful qualitative indicators of the nature of alkyne–metal bonding. The shift $\Delta\tilde{\nu}$(C≡C) relative to $\tilde{\nu}$(C≡C) of the free alkyne gives a rough estimate of the extent to which the C≡C bond is modified by coordination.[72] For cyclooctyne complexes (Table 2), the $\Delta\tilde{\nu}$(C≡C) values range from ca. 150–600 cm^{-1}, being lowest for the labile complexes of Cu^I, Ag^I and Au^I. The chemical shifts of the alkyne carbon atoms correlate qualitatively with the number of π-electrons donated by the alkyne to the metal, ranging from $\delta = 100-140$ for two-electron donors to $\delta = 200-240$ for four-electron donors.[74] The cyclooctyne complexes of molybdenum and tungsten provide a good illustration of the trend. Thus, in the complexes **22** (R = Me, Et) and **25**, cyclooctyne should donate four π-electrons if the metal atoms are to reach the 18 electron configuration, and this is borne out by the ^{13}C chemical shifts (Table 2). In contrast, cyclooctyne behaves as a two π-electron donor in the complexes **23**. In the oxomolybdenum(IV) complexes $[MoO(S_2CNR_2)_2(C_8H_{12})]$, cyclooctyne has to compete with the strongly π-donor oxo-ligand for the vacant metal d_{xy}-orbital, and the ^{13}C chemical shift suggests that cyclooctyne donates about three π-electrons in this compound.[44]

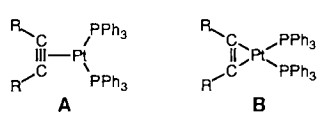
Table 2. IR and ^{13}C NMR data for the C≡C units of some cyclooctyne-metal complexes.

Compound	$\tilde{\nu}$(C≡C) [cm^{-1}]	$\delta(^{13}C)$	Ref.
$[CuBr(C_8H_{12})]$	2060	–	[32]
$[CuBr(C_8H_{12})_2]$	2085	–	[32]
$[AuBr(C_8H_{12})_2]$	2035	–	[32]
$[Pt(PPh_3)_2(C_8H_{12})]$ **10**	1810/1793	–	[32, 35]
$[Pt(dppe)(C_8H_{12})]$	1775	–	[35]
$[M(S_2CNR_2)_2(CO)(C_8H_{12})]$ (M = Mo, W) **22**	[a]	216.3 ± 1.9 128.2 ± 0.5	[44]
$[M(S_2CNR_2)_2\{(C_8H_{12})_2CO\}-(C_8H_{12})]$ **23**	1835–1870	120.5 [b] 130.4 ± 0.4 140.0 ± 0.6 [c]	[45]
$[MX_2(S_2CNR_2)_2(C_8H_{12})]$; (M = Mo,W) **24**	1720–1750	227.4 ± 6.9	[44]
$[MoO(S_2CNR_2)_2(C_8H_{12})]$	1851	145.7 ± 0.2	[44]
$[MBr_2(CO)(PEt_3)_2(C_8H_{12})]$ **25**	–	236.0 [b] 227.8 [c]	[44]
$[Mo(CO)(C_8H_{12})_3]$	1585	95.0, 106.8	[40]
$[Co_2(CO)_6(C_8H_{12})]$ **19**	1625	99.9	[41, 43]

[a] Not located. [b] M = Mo. [c] M = W.

The complex $[Mo(CO)(C_8H_{12})_3]$[40] seems to be exceptional. For the 18-electron configuration to be achieved, each alkyne should donate on average 3⅓ electrons to the metal, but the reported ^{13}C chemical shifts (δ = 95.0, 106.8) are more typical of a two-electron donor and are very different from those of the hex-3-yne complex $[W(CO)(EtC_2Et)_3]$ (δ = 170.8, 191.1).[74]

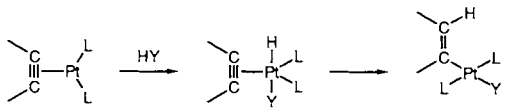
The $Pt(PPh_3)_2$ complexes of acyclic alkynes show $\tilde{\nu}$(C≡C) frequencies of ca. 1800 cm^{-1} and their C≡C ^{13}C NMR signals lie in the range $\delta = 100-120$, so they can be classified as 16-electron platinum(0) complexes **A** in which the alkyne is a two-electron donor. Alternatively, the alkyne can be considered to bind to the metal atom by two σ-bonds giving a dicarbanion of platinum(II) or a platinacyclopropene **B**. It can be shown that the two formulations are equivalent when



the metal-alkyne interaction is very strong.[71, 75] The bending-back from linearity of the alkyne substituents on coordination (ca. 40°) is believed to be a consequence of back-bonding and gives an indication of the extent to which the alkyne is perturbed on coordination.[75, 76] In the case of

small cycloalkynes, the substituents suffer less distortion relative to the free ligand on coordination to $Pt(PPh_3)_2$ (ca. 12° for cyclohexyne, cycloheptyne and cyclooctyne, based on the C–C≡C angles for the free ligands given in Section 2.1). This must be an important factor that contributes to the great stability of the complexes.

The bend-back angle from linearity of 53° in cyclohexyne complexes probably indicates exceptionally strong metal–ligand back-bonding. For **46** this probably is due to good overlap of the low-lying LUMO of cyclohexyne (Section 2) with the HOMO of $Pt(PPh_3)_2$ (mainly $d_{x^2-y^2}$ in character), while the σ-bond is formed by overlap of the energetically higher HOMO of cyclohexyne with the LUMO of $Pt(PPh_3)_2$ comprising $6p_y$, $6p_z$ and 6s orbitals. It is not yet clear why the cyclohexyne-platinum(0) complexes should be so reactive towards weak acids. For acyclic alkyne complexes, protonation with HCl or CF_3CO_2H probably occurs first at the metal atom to give a hydridoplatinum(II) species **69**; the hydride then migrates to the coordinated alkyne [Eq. (26)].[77] Back-bonding to the alkyne in the corresponding hydrido intermediate [Eq. (26)] may be strong enough to



(26)

69

allow attachment of strongly electron-donating anions derived from weak acids.

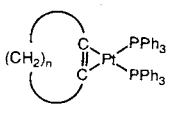
The chemical shifts of the alkyne C atoms and the coupling constants $^1J_{PtC}$ are greater in $[Pt(PPh_3)_2(cycloalkyne)]$ than in $[Pt(PPh_3)_2(MeC_2Me)]$, and both increase with decreasing ring size (Table 3). The trend in $^1J_{PtC}$ is consistent

Table 3. Comparison of IR and NMR data for the C≡C units of the cyclic and acyclic alkyne complexes $[Pt(PPh_3)_2(C_7H_{10})]$ **32**, $[Pt(PPh_3)_2(C_6H_8)]$ **46**, $[Pt(PPh_3)_2(C_5H_6)]$ **53**, $[Pt(PPh_3)_2(MeC_2Me)]$, $[Pd(PPh_3)_2(C_7H_{10})]$ and $[Pd(PPh_3)_2(C_6H_8)]$.

Cpd.	IR $\tilde{\nu}$ (C≡C) [cm^{-1}]	IR $\Delta\tilde{\nu}$ (C≡C) [cm^{-1}]	^{13}C NMR $\delta(^1J_{PtC}$ [Hz])	^{31}P NMR $\delta(^1J_{PtP}$ [Hz])	Ref.
32	1770	351	124.0 (318)	29.4 (3420)	[35, 58]
46	1721	448, 282	131.6 (395)	28.3 (3406)	[35, 58]
53	1630	198	155.5 (436)	28.1 (3437)	[58]
[a]	1812	458	113.1 (274)	31.2 (3454)	[78]
[b]	1848	273	–	–	[35]
[c]	1780	389, 223	–	–	[35]

[a] $[Pt(PPh_3)_2(MeC_2Me)]$. [b] $[Pd(PPh_3)_2(C_7H_{10})]$. [c] $[Pd(PPh_3)_2(C_6H_8)]$.

with increasing Pt 6s-character in the σ-bonding orbital used in the alkyne–metal bond, i.e. the metallacyclopropene structure **70** becomes increasingly important for the smaller rings. This correlates with the increasing diradical character of the smaller rings in the free state (Section 2).



70

Despite the constancy of the C≡C distances in **10**, **32** and **46**, there is a steady decline in $\tilde{\nu}$(C≡C) along the series from ca. 1800 cm^{-1} to ca. 1700 cm^{-1}, and there is a further drop to ca. 1630 cm^{-1} for **53**. This trend correlates well with increasing metallacyclopropene character, though it may arise from different degrees of coupling of the C≡C stretch with other ring vibrations. The values of $\Delta\tilde{\nu}$(C≡C) generally decrease for the smaller cycloalkynes and are less than those for acyclic alkynes, reflecting the fact that the former are less perturbed on coordination than the latter.

4. Mononuclear Metal Complexes of Benzyne

Many benzyne complexes are dinuclear or polynuclear, the C_6H_4 unit being attached to two metal atoms by two σ-bonds or by σ- and π-bonds to three or four metal atoms. For mononuclear benzyne complexes, as for other alkyne complexes, two limiting modes of coordination, **C** and **D**, can be considered.

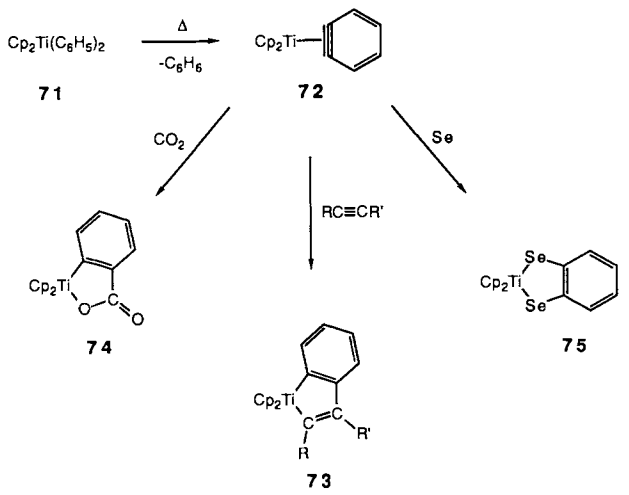


C **D**

Some authors refer to the σ-bonded compounds (whether mononuclear or polynuclear) as *o*-phenylene derivatives (**C**) and to the π-bonded mononuclear compounds as benzyne complexes (**D**). At least for mononuclear compounds, the representations are equivalent when the metal-ligand interaction is strong, and it is difficult to distinguish between the terms benzyne and o-phenylene in this context.

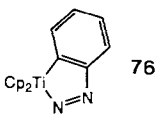
4.1. Complexes of Early Transition Metals (Ti, Zr, Nb, Ta, Mo, W, Re) and Actinoid Elements (U, Th)

A benzyne-chromium complex is one of the suggested intermediates in the hydrolytic σ- to π-rearrangement of $[Cr(C_6H_5)_3(thf)_3]$ to $[Cr(C_6H_6)_2]^{\oplus}$ (the classic Hein reaction)[79] and, in general, benzyne complexes are strongly implicated as reactive intermediates in the thermal decomposition of perphenyl derivatives of the early transition elements, and of uranium and thorium; they can sometimes be isolated from such reactions. When $[TiCp_2(C_6H_5)_2]$ **71** is heated in the solid state or in hydrocarbon solvents, the main organic product is benzene. Almost no biphenyl is formed, so free phenyl radicals are not involved. The benzene is formed mainly by elimination of one phenyl group with a hydrogen atom from the *ortho*-position of the other phenyl group, although there is a minor pathway in which a hydrogen atom is abstracted from one of the Cp rings.[80–82] Similar processes occur on heating titanium complexes with substituted aryl groups, and the presumed intermediates e.g. **72** can be trapped by reaction with alkynes,[83–85] CO_2[86] or selenium[87] to give the expected titanacycles **73**–**75** (Scheme 13). **72** is probably also formed when $TiCl_2Cp_2$ is treated with *o*-bromofluorobenzene and magnesium, for in the presence of diphenylacetylene the titanacycle **73** (R = R′ = Ph) can be isolated in 15% yield.[88]



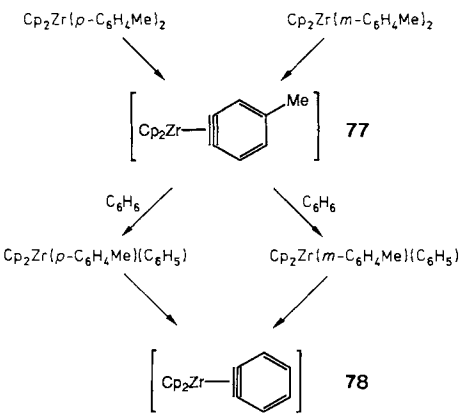
Scheme 13. Generation and trapping of $[TiCp_2(C_6H_4)]$ **72**.

When **71** or its *m*- or *p*-tolyl analogues are heated in benzene or ether at 80–130 °C under nitrogen (100 atm) and the solution is subsequently hydrolyzed, small amounts of aniline (or the appropriate toluidine) are formed in addition to the main product, ammonia. Aniline is also formed from $TiCl_2Cp_2$, *o*-bromofluorobenzene and magnesium under N_2 (100 atm). These results are thought to indicate that **72** reacts with N_2 to give the insertion compound **76**. The aromatic amines are not formed in the corresponding zirconium systems.[89]



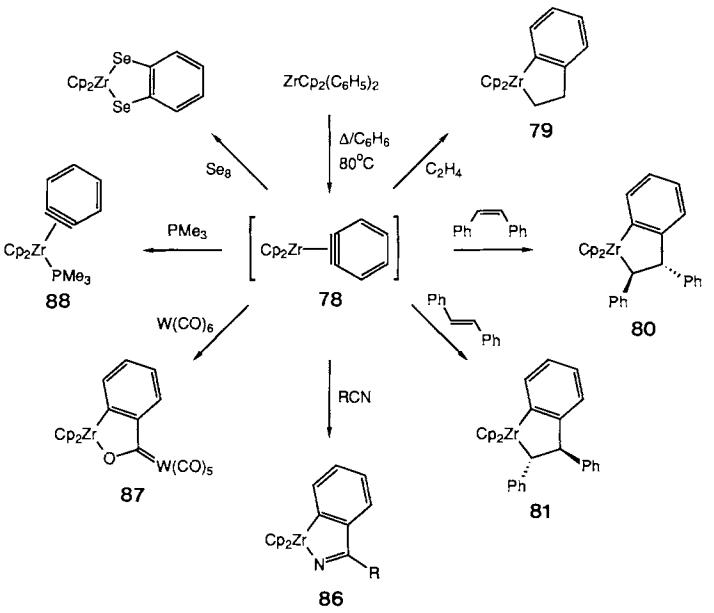
76

On heating in aromatic solvents, zirconium complexes $ZrCp_2(Aryl)_2$ undergo successive replacements of their aryl groups by aryl groups from the solvent (Scheme 14).[90] This behavior is suggestive of a 16-electron, coordinatively unsaturated aryne-metal intermediate (e.g. **77**). The trapping reactions of aryne-zirconocene complexes formed in this way with multiply bonded molecules have been studied more



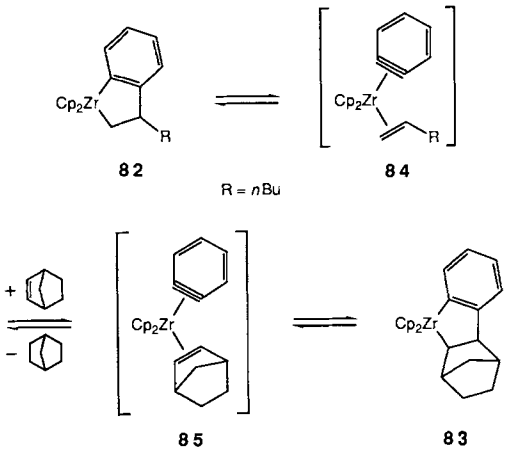
Scheme 14. Aryl group exchange in $[ZrCp_2(Aryl)_2]$.

intensively than those of the titanium system, possibly because Cp ligands are not cleaved so easily from the heavier element, so there is less net decomposition.[90b] Typical reactions of $[ZrCp_2(C_6H_4)]$ **78** are summarized in Scheme 15.



Scheme 15. Reactions of $[ZrCp_2(C_6H_4)]$ **78**.

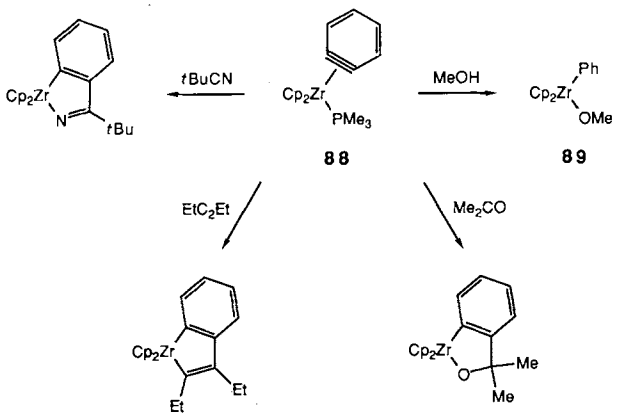
Ethylene inserts to give the zirconaindan **79**[91] and the substituted derivatives **80** and **81** are formed stereospecifically from *cis*- and *trans*-stilbene respectively.[92] The zirconaindan **82** formed from **78** and 1-hexene undergoes olefin exchange on heating with norbornene to give a new zirconaindan **83** (Scheme 16), suggesting that **82** and **83** are in equilibrium with their respective zirconocene benzyne olefin complexes **84** and **85**.[91]



Scheme 16. Olefin exchange in zirconaindan complexes.

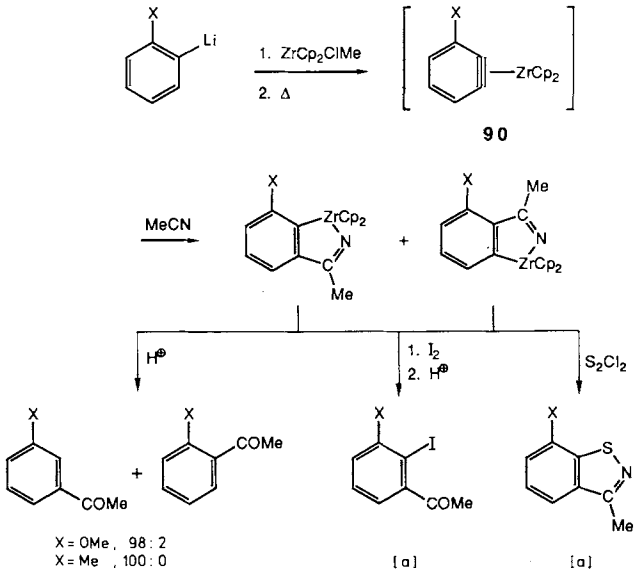
78 also reacts with cyanides to give dimeric azazirconacyclopentenes **86** which can be hydrolyzed to ketones.[93] The marked oxophilicity of the Cp_2Zr unit is demonstrated by the reaction of **78** with $W(CO)_6$ to give the zirconaoxycarbene complex **87**.[94] **78** can be trapped almost quantitatively in the form of its stable trimethylphosphane adduct **88** which

contains η^2-benzyne, as shown by X-ray crystallography.[95] The trimethylphosphane is readily displaced by other ligands in solution, so **88** represents a convenient alternative source of **78**. High-yield insertion reactions of **88** with *tert*-butyl cyanide, 3-hexyne and acetone have been carried out; methanolysis of **88** gives the stable methoxy-complex **89** (Scheme 17).



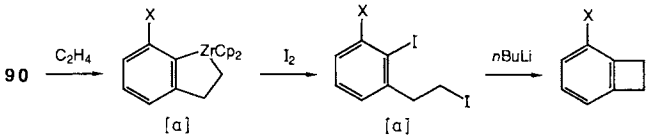
Scheme 17. Reactions of $[ZrCp_2(PMe_3)(C_6H_4)]$ **88**.

A more general route to aryne-zirconocene complexes is to treat the chloro(methyl) complex $[ZrCp_2Cl(Me)]$ with an aryllithium.[96] The resulting complex $[ZrCp_2(Aryl)(Me)]$ loses methane on heating and the transient aryne complex **90** can be trapped with cyanides or ethylene (Scheme 18). This



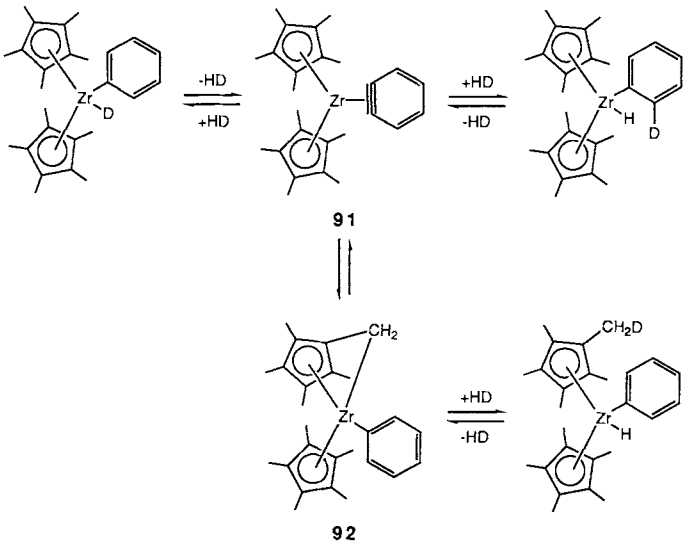
Scheme 18. Synthesis and reactions of $[ZrCp_2(aryne)]$ **90**. [a] Only isomer observed for X = OMe, Me.

procedure can be used to produce 3-substituted benzyne complexes which would otherwise be inaccessible; zirconocene complexes containing two *o*-substituted aryl ligands cannot be prepared, probably because of steric crowding. The zirconacycles can be converted, without being isolated, into organic products such as aromatic ketones and *o*-iodophenylketones, isothiazoles (Scheme 18) and dihydrocyclobutabenzenes (Scheme 19). Steric hindrance by the substituents X to the approach of the trapping agent is probably responsible for the high regiospecificity observed in the reaction of cyanides with 3-substituted benzyne zirconocenes.



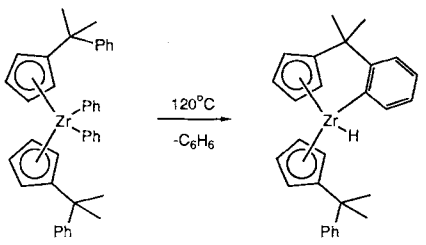
Scheme 19. Synthesis of dihydrocyclobutabenzenes from aryne-zirconocene complexes **90**. [a] Mixture of regioisomers.

Phenyl derivatives of bis(pentamethylcyclopentadienyl)-zirconium,[97,98] -uranium[98] and -thorium[99] also undergo phenyl group exchange with aromatic solvents, and the intermediate benzyne complexes can be trapped with ethylene or diphenylacetylene. A solution of $[ZrCp_2^*D(Ph)]$ in C_6D_6 incorporates deuterium in both the *ortho*- positions of the phenyl ring and in the Cp* methyl groups at room temperature; these processes probably proceed via the benzyne complex **91** (Scheme 20). When either $ZrCp_2^*Ph_2$



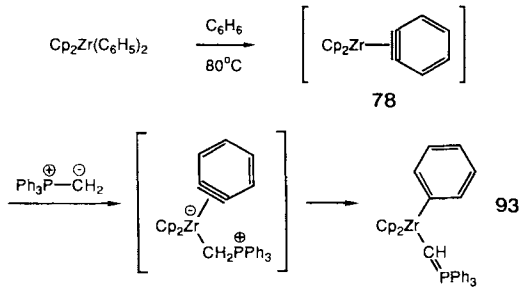
Scheme 20. H/D exchange in $[ZrCp_2^*D(Ph)]$.

or $[ZrCp_2^*H(Ph)]$ is heated in benzene, the cyclometalated complex **92** is formed by hydrogen transfer from a Cp* methyl group to the coordinated benzyne.[97,98] Similar processes occur on heating the substituted Cp complexes $[Zr(\eta^5\text{-}C_5H_4CMe_2Ph)_2Ph_2]$ and $[Zr(\eta^5\text{-}C_5H_4CMe_3)_2Ph_2]$; in the first case, a phenyl C–H bond of the CMe_2Ph substituent is cleaved preferentially [Eq. (27)].[100]



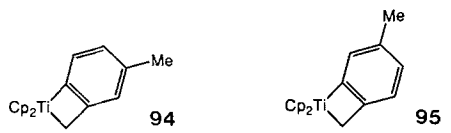
(27)

When $Ph_3P{=}CH_2$ reacts with $ZrCp_2(C_6H_4)$ **78** a hydrogen atom is transferred from the ylide to coordinated benzyne to give the phenylzirconium(IV) complex **93**, probably via an intermediate zirconium(II) complex (Scheme 21).

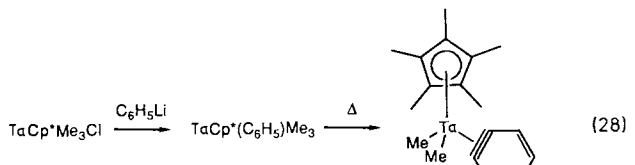


Scheme 21. Reaction of $[ZrCp_2(C_6H_4)]$ **78** with methylenetriphenylphosphorane.

Similarly, the 4-methylbenzyne complex **77** reacts with $Ph_3P{=}CH_2$ to form a mixture of 3- and 4-tolyl derivatives in the ratio 2:3.[101] The titanium analogue of **77** behaves similarly, but in this case there is a competing reaction in which PPh_3 is eliminated and CH_2 inserts into the titanium–aryne bond to give isomeric titanacyclobutanes **94** and **95**.[102]

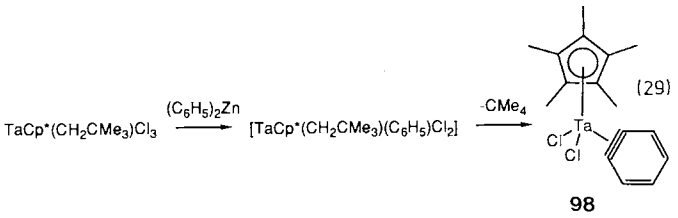


The elimination of benzene from two adjacent σ-phenyl groups, or of an alkane from adjacent σ-phenyl and σ-alkyl groups, has been used to prepare benzyne complexes of niobium, tantalum, molybdenum, tungsten and rhenium, but the chemistry of most of these compounds has received little attention. Treatment of $[TaCp^*Me_3Cl]$ with phenyllithium (1:1 mol ratio) gives $[TaCp^*(C_6H_5)Me_3]$ which, on heating in chlorobenzene at 120°, loses methane to give the pale yellow, fairly air-stable benzynetantalum(III)- complex **96** [Eq. (28)].[103] This was the first mononuclear benzyne com-



(28)

plex to be characterized structurally.[103, 104] The niobium analogue **97** can be made similarly. Both **97** and **98** undergo insertion with ethylene to form the expected benzometallacyclopentene complexes. The dichlorotantalum compound **98** can be made directly by the action of diphenylzinc on $[TaCp^*(CH_2CMe_3)Cl_3]$ [Eq. (29)], the presumed intermediate neopentyl-phenyl complex being undetected.[103]



(29)

Treatment of $TaCp^*_2Cl_2$ with phenyllithium (1:2 mol ratio) gives directly the hydrido(benzyne) tantalum(III) complex $[TaCp^*_2H(C_6H_4)]$, which is shown by variable temperature NMR spectroscopy to be in equilibrium with the σ-phenyl complex $[TaCp^*_2(C_6H_5)]$. At 50 °C the free energy of activation for the β-hydride migration is 70.6 kJ mol^{-1}.[105]

Sarry et al.[106–111] have shown that pentahalides of tantalum, niobium, tungsten and molybdenum react with an excess of phenyllithium (or aryllithium) in ether to form a remarkable series of complexes of general formula $[Li(Et_2O)]_n[M(C_6H_4)_2(C_6H_5)_4]$ in which two benzyne units are coordinated to each transition metal atom. The compounds described to date are given in Table 4, together with

Table 4. Anionic bis(aryne) complexes isolated from reactions of early transition metal pentahalides with aryllithium reagents.

Reactants	Products	Oxidation state, d^n C_6H_4 neutral (C_6H_4 dianion)	Ref.
$NbBr_5/PhLi/Et_2O$	**99** (black) [a]	Nb^0, d^5 (Nb^{IV}, d^1)	[108, 110]
$TaBr_5/PhLi/Et_2O$	**100** (black) [b]	Ta^0, d^5 (Ta^{IV}, d^1)	[107, 110]
$TaBr_5/PhLi/Et_2O$	**101** (bright green) [c]	Ta^I, d^4 (Ta^V, d^0)	[107, 110]
$MoCl_5/PhLi/Et_2O$	**102** (black) [d]	Mo^0, d^6 (Mo^{IV}, d^2)	[107]
$WBr_5/PhLi/Et_2O$	**103** (black) [e]	W^0, d^6 (W^{IV}, d^2)	[108, 110]
WBr_5/p-TolLi/Et_2O	**104** (violet-black) [e]	W^0, d^6 (W^{IV}, d^2)	[111]
$NbCl_5/PhLi/THF$	**105** (dark blue) [f]	Nb^{-I}, d^6 (Nb^{III}, d^2)	[112]
$TaCl_5/PhLi/THF$	**106** (yellow) [g]	Ta^I, d^4 (Ta^V, d^0)	[112]

[a] Thermally unstable; $\mu_{eff} = 1.81\ \mu_B$. [b] $\mu_{eff} = 1.68\ \mu_B$. [c] Intermediate in the synthesis of **100**. [d] Diamagnetic/paramagnetic equilibrium in solution; broad ^1H NMR signals at room temperature. [e] Diamagnetic. [f] Contains five-coordinate Nb. [g] Contains six-coordinate Ta.

$[Li(Et_2O)]_4[Nb(C_6H_4)_2(C_6H_5)_4]$ **99** $[Li(Et_2O)]_4[Ta(C_6H_4)_2(C_6H_5)_4]$ **100**

$[Li(Et_2O)]_3[Ta(C_6H_4)_2(C_6H_5)_4]$ **101** $[Li(Et_2O)]_4[Mo(C_6H_4)_2(C_6H_5)_4]$ **102**

$[Li(Et_2O)]_4[W(C_6H_4)_2(C_6H_5)_4]$ **103** $[Li(Et_2O)]_4[W(C_6H_3Me)_2(p\text{-}Tol)_4]$ **104**

$[Li(thf)]_4[Nb(C_6H_4)_2(C_6H_5)_3][C_6H_5Li(thf)]\cdot 0.5\ THF\cdot 0.5\ C_6H_{14}$ **105**

$[Li(thf)]_2[Li_4Cl_2(thf)_{10}][Ta(C_6H_4)_2(C_6H_5)_4]$ **106**

the formal oxidation states and electron configurations of the metal atoms; these have been calculated on the assumption that benzyne acts either as a neutral donor or as a dianionic ligand. The products isolated from these reactions are very sensitive to slight changes in experimental conditions and to the reagents used. In the cases of tantalum and niobium, different compounds in which the oxidation states of the metal atoms differ by one can be obtained from similar reaction mixtures. The compounds themselves are generally very sensitive to heat, air and moisture and they tend to lose ether, so the proportions of ether in **99**–**104** are approximate.

In early work, the compounds of W, Ta and Nb were formulated[106–108] as hexaphenylmetalates

$[Li(Et_2O)]_n[M(C_6H_5)_6]$ by analogy with the known chromium(III) complex. Compounds of this type are undoubtedly precursors to the bis(benzyne) complexes and can be isolated in some cases. For example, $MoCl_5$ reacts with phenyllithium (1:10 mol ratio) to give the bis(benzyne) complex **102**, whereas under the same conditions *p*-tolyllithium gives the hexa(*p*-tolyl)molybdate complex $[Li(Et_2O)]_3[Mo(C_6H_4Me)_6]$. In contrast, WBr_5 reacts with *p*-tolyllithium to give the bis(4-methylbenzyne) complex **104**.[111] The strongly basic aryllithium evidently abstracts *ortho*-protons from the aryl groups, but the exact conditions and mechanism have not been elucidated.

Recently, the crystal structures have been determined of complexes with the empirical formulas **105** and **106**, which have been isolated in low yield from the reactions of $NbCl_5$ and $TaCl_5$, respectively, with phenyllithium in THF.[112] The niobium atom in **105** has an approximately trigonal bipyramidal coordination sphere comprising two η^2-benzyne ligands and a σ-phenyl group in equatorial positions and two σ-phenyl groups in axial positions. The tantalum atom in **106** is coordinated in approximately octahedral fashion by mutually *cis*-η^2-benzyne ligands and four σ-phenyl groups (Fig. 2). Alternatively, if C_6H_4 is regarded as a dianionic

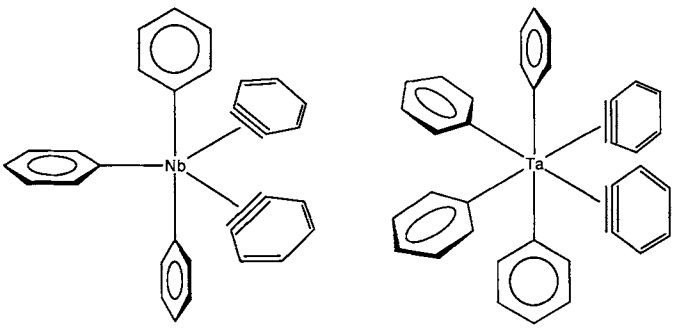
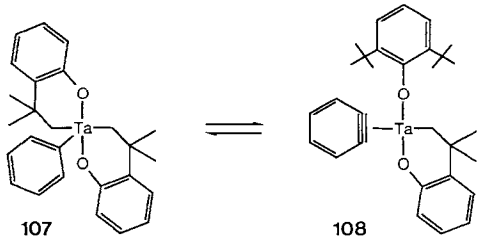


Fig. 2. Primary coordination spheres of the anions of complexes **105** and **106**.

ligand, the coordination geometries of **105** and **106** could be described as approximately pentagonal bipyramidal (seven-coordinate) and square antiprismatic (eight-coordinate), respectively. Both anions contain a complicated secondary coordination sphere in which there are extensive interactions between solvated lithium ions and carbon atoms of the benzyne and phenyl rings. These interactions are important for stabilizing the structures.

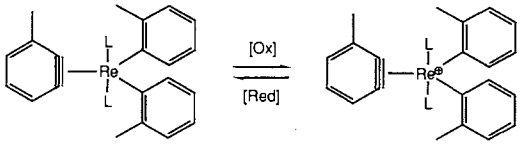
There is one other example of a benzyne-tantalum complex as an intermediate which is not stabilized by the presence of Cp, Cp* or PMe_3 ligands. At 120 °C the phenyl-substituted metallaspiro complex **107** is in equilibrium with the benzyne complex **108**, a hydrogen atom being transferred



107 108 (30)

reversibly from the phenyl group to the Ta–CH_2 group of the metallacycle [Eq. (30)].[113, 114]

Treatment of tetra-*o*-tolylrhenium with two equivalents of PMe_3 or PMe_2Ph(L) at −40 °C causes rapid elimination of toluene and formation of dark red 3-methylbenzyne complexes **109**, which are paramagnetic (one unpaired electron) and very stable to air and heat [Eq. (31)].[115] They readily undergo reversible oxidation to the diamagnetic cations **110**,



109 110 (31)

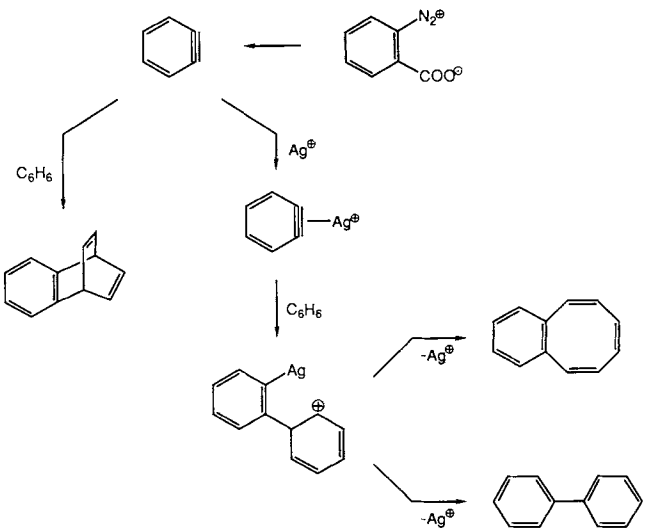
[Ox] = $[FeCp_2]^{\oplus}$, I_2, $Co_2(CO)_8$, $Ag[CF_3SO_3]$, CF_3SO_3H;

[Red] = $Li[Et_3BH]$, Me_3SiCH_2MgCl

which can be isolated as $PF_6^{\ominus}$, $CF_3SO_3^{\ominus}$, $BPh_4^{\ominus}$, and $I_5^{\ominus}$ salts. The X-ray structure analyses of **109** (L = PMe_2Ph) and **110** (L = PMe_3; $I_5^{\ominus}$ salt) show that both species are approximately trigonal-bipyramidal, if the C_6H_4 unit is assumed to occupy one coordination site; the tertiary phosphane ligands are in axial positions. Both **109** and **110** are remarkably inert towards a variety of substrates, including CO, H_2, olefins, acetylenes, acetonitrile, and acetone.

4.2. Complexes of Late Transition Metals (Ag, Ni, Pt)

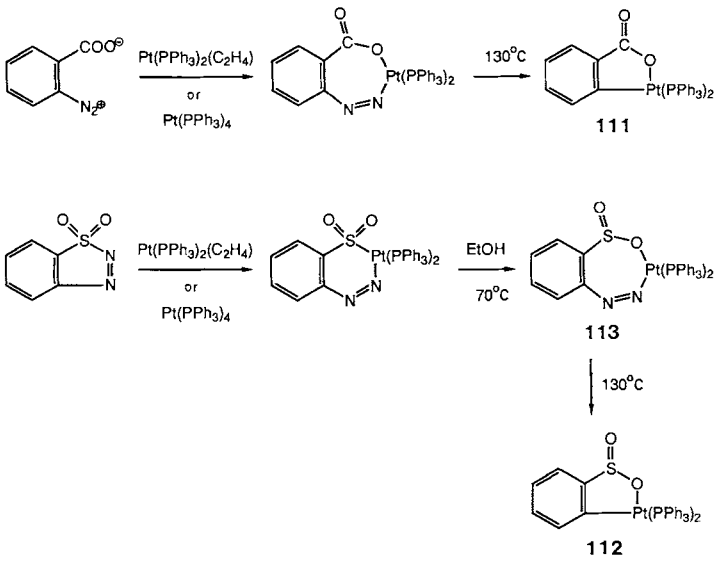
The first indication of complex formation between benzyne and a d^{10} metal atom was the observation that the cycloaddition of benzyne to benzene is strongly influenced by the presence of traces of silver ion. The normal 1,4-cycloaddition to give benzobarrelene is suppressed and the main products become benzocyclooctene and biphenyl. *Friedman*[116] proposed that a silver-benzyne complex is formed which is more electrophilic than benzyne itself (Scheme 22).



Scheme 22. Influence of $Ag^{\oplus}$ on the cycloaddition of benzyne to benzene.

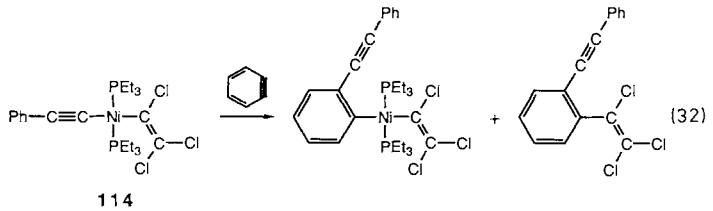
Similar effects are observed in other cycloadditions of benzyne.[117]

An early attempt to prepare $[Pt(PPh_3)_2(C_6H_4)]$ by treating 1,2-dilithiobenzene with *cis*-$[PtCl_2(PPh_3)_2]$ failed.[118] Efforts to trap benzyne, generated from suitable precursors, by zerovalent platinum complexes have also been unsuccessful. Thus, thermal decomposition of 2-diazoniobenzoate or benzo-1,2,3-thiadiazole *S*,*S*-dioxide in the presence of $[Pt(PPh_3)_2(C_2H_4)]$ or $Pt(PPh_3)_4$ gives the metallacyclic platinum(II) complexes **111** and **112**, respectively, as the final products (Scheme 23).[34, 119, 120] These will not eliminate

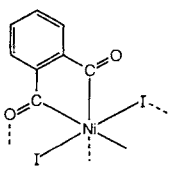


Scheme 23. Reaction of benzyne precursors with Pt^0 complexes.

CO_2 or SO_2 to give $[Pt(PPh_3)_2(C_6H_4)]$, although UV irradiation of **113**, a precursor to **112**, does generate free benzyne which can be trapped with furan or tetracyclone.[34, 120] Free benzyne also inserts into the acetylide-metal bond of the nickel(II) complex **114** [Eq. (32)].[121]

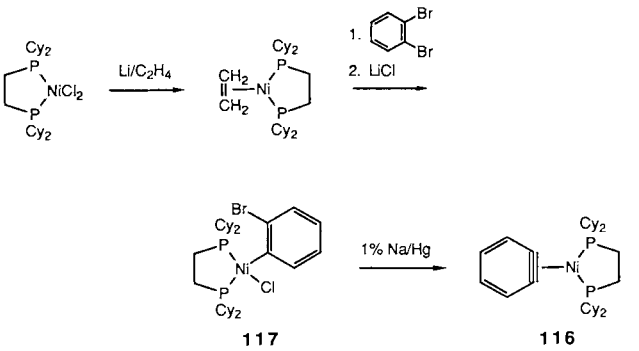


Although $Ni(CO)_4$ was claimed to react with *o*-diiodobenzene to give a benzyne complex, this was subsequently shown to be a polymeric nickel(IV) complex **115** containing a tridentate benzene-1,2-dicarbonyl group.[122]



115

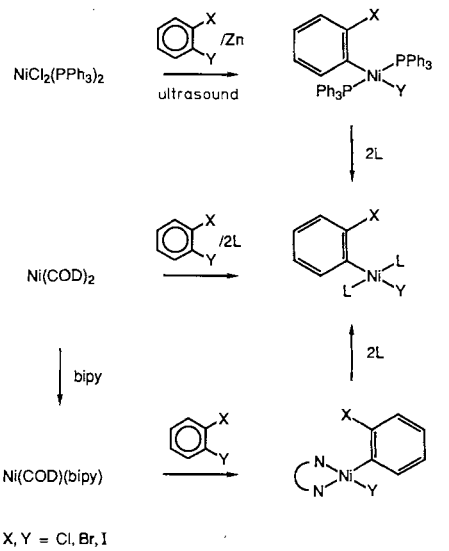
The first mononuclear benzyne-nickel(0) complex **116** was obtained as a yellow, crystalline solid by reduction of the (2-bromophenyl)chloronickel(II) complex **117** with 1% sodium amalgam (Scheme 24), and its structure was confirmed



Scheme 24. Preparation of $[Ni(Cy_2PCH_2CH_2PCy_2)(C_6H_4)]$ **116**.

by X-ray crystallography.[123] The complexes $NiL_2(C_6H_4)$ (L = PCy_3, $PiPr_3$; Cy = cyclohexyl) have been obtained in a similar way,[124] although the PEt_3 complex has been assigned a dimeric μ-*o*-phenylene structure (cf. Section 6).[125] Reduction of **117**, Ph instead of Cy, with various alkali-metal reducing agents, gave only $Ni(dppe)_2$ instead of the expected benzyne complex.[124]

Unfortunately, **116** or its analogues cannot be made similarly to the zirconium compound **78** by heating diphenyl- or methyl(phenyl)-nickel(II) complexes, because the σ-bonded carbon ligands on nickel(II) generally undergo reductive elimination rather than hydrogen abstraction.[126] It is therefore necessary to have convenient high-yield syntheses of the (2-halogenphenyl)nickel(II) halide precursors, and these are summarized in Scheme 25.[124]

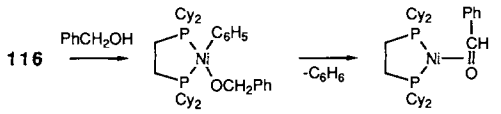


Scheme 25. Preparation of (2-halogenphenyl)nickel(II) halides. COD = cyclooctadiene, bipy = bipyridine.

Mononuclear benzyne-platinum(0) complexes $PtL_2(C_6H_4)$ (2L = $2PEt_3$, $2PCy_3$, $2PiPr_3$, $Cy_2PCH_2CH_2PCy_2$) have been prepared similarly to their thermally less stable nickel analogues, 43% sodium amalgam being the best reducing

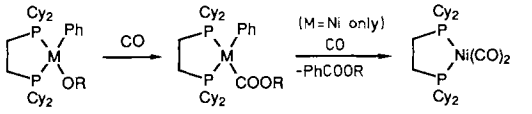
agent.[124] Attempts to prepare $ML_2(C_6H_4)$ (M = Ni, Pt; L = PMe_3, PPh_3) by the reduction method have not been successful. However, the triisopropylphosphane ligands in $[M(PiPr_3)_2(C_6H_4)]$ can be substituted, partially or completely, by less bulky tertiary phosphanes, reaction being more rapid and complete in the case of nickel. Compounds that have either been isolated or identified by NMR spectroscopy include $[M(PMe_3)_2(C_6H_4)]$ (M = Ni, Pt) and $[Pt(PiPr_3)L(C_6H_4)]$ (L = PMe_3, PEt_3, PPh_3, PMe_2Ph, $PMePh_2$).[124]

The benzyne-nickel and -platinum complexes are even more sensitive to water, alcohols, and other protonic solvents than the cyclohexyne complex **46**. The nickel complex **116** reacts rapidly with primary and secondary alcohols to give alkoxides; these are unstable at room temperature and eliminate benzene with formation of a nickel(0) complex of the corresponding aldehyde or ketone [e.g. Eq. (33)].



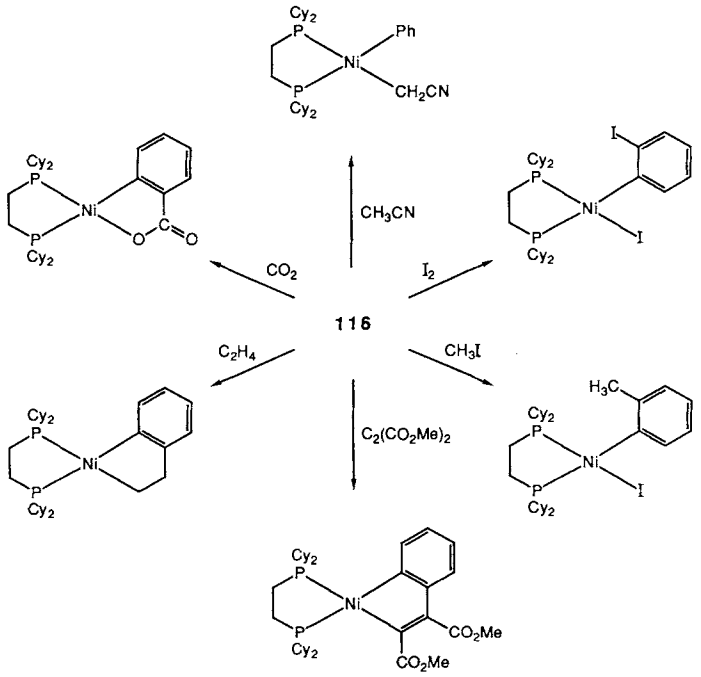
(33)

The Pt^{II} methoxide $[Pt(OMe)(C_6H_5)(Cy_2PCH_2CH_2PCy_2)]$ is thermally stable but is rapidly hydrolyzed by traces of water to the corresponding hydroxide. The M–O bonds in these alkoxides of nickel(II) and platinum(II) readily insert CO, but only in the case of platinum can the insertion product be isolated; in the case of nickel, both σ-bonded groups undergo reductive elimination [Eq. (34)].[124]



(34)

The benzyne–nickel bond in **116** is attacked by other electrophiles such as iodine and methyl iodide and undergoes insertions with CO_2, ethylene, and dimethyl acetylenedicarboxylate to give metallacycles (Scheme 26).[123] Whereas acetonitrile inserts into the benzyne-zirconocene complex **78**,[93] it is deprotonated by **116**.[124] Also in contrast with **78**, **116** does not undergo insertion with diphenylacetylene; instead, the benzyne is displaced to give $[Ni(Cy_2PCH_2CH_2PCy_2)(PhC_2Ph)]$.[123]



Scheme 26. Reactions $[Ni(Cy_2PCH_2CH_2PCy_2)(C_6H_4)]$ **116**.

4.3. Structure, Spectroscopic Properties and Bonding of Benzyne Complexes

Table 5 compares the benzyne C–C bond lengths determined by X-ray crystallography in various complexes with those in free benzyne as obtained by an ab-initio calculation.[119] In all cases the "acetylenic" bond (C1–C2) is lengthened on coordination; the remaining C–C bonds are of about the same length as, or slightly shorter than, those in free benzyne.

Table 5. Comparison of C–C bond lengths in metal benzyne complexes with those in free benzyne [a].

	C_6H_4 [b]	**116**	**88**	**96**	**105**	**106**	**109**	**110**
C1-C2	1.240	1.332(6)	1.364(8)	1.364(5)	1.419(7)	1.384(8)	1.34(1)	1.39(2)
					1.410(7)	1.402(8)		
C2-C3	1.393	1.386(6)	1.389(8)	1.410(5)				
C3-C4	1.402	1.383(7)	1.383(9)	1.362(2)				
C4-C5	1.421	1.390(8)	1.380(9)	1.403(6)	1.388(8)–	1.380(9)–	1.37(1) –	1.36(2)–
C5-C6	1.402	1.383(7)	1.377(9)	1.375(6)	1.416(7) [c]	1.404(9) [c]	1.43(1)	1.44(2)
C6-C1	1.393	1.389(6)	1.406(8)	1.408(6)				

[a] Carbon atoms numbered as in Fig. 1. [b] Values from Ref [19]. [c] C4-C5 is the shortest bond.

In **116**, benzyne is considered to be a two-electron donor, similar to alkynes in the 16e ML_2(alkyne) (M = Ni, Pt) complexes. The C1–C2 bond length of 1.332 Å is greater than the value of 1.29 Å typical of most ML_2(alkyne) complexes, but the lengthening on coordination relative to the free ligand (Δr = 0.08–0.09 Å) is about the same. Correspondingly, the $\tilde{\nu}$(C≡C) value of ca. 1580 cm^{-1} in $ML_2(C_6H_4)$ (M = Ni, Pt) complexes is less than the value of ca. 1700 cm^{-1} found in ML_2(alkyne) complexes, but the decrease relative to the free ligand is of the same order ($\Delta\tilde{\nu}$ = 400–500 cm^{-1}) in both series.

Electron-counting suggests that benzyne should behave as a 2e donor in **88**, since the zirconium atom then achieves its 18e configuration, but the C1–C2 distance (1.364 Å) is significantly greater than in **116**. The other benzyne C–C distances in **88** and **116** are almost equal, suggesting that the delocalized benzometallacyclopropene structure **118** is a reasonable representation in these cases.



118 **119**

If benzyne is regarded as a 2e donor, the tantalum atom in **96** has only 14 valence electrons and is thus highly electron-deficient. The C1–C2 distance in **96** is similar to that in

88, but the remaining C–C distances in the six-membered ring of **96** show a small but distinct long-short alternation. Also, the benzyne ligand in **96** is oriented perpendicular to the plane of the Cp* ring, whereas in the ethylene complex $[TaCp^*Me_2(C_2H_4)]$ the olefin is parallel to this plane. These observations have led to the suggestion that both sets of orthogonal benzyne π-orbitals are involved in bonding to the metal.[103, 104] Thus, benzyne in **96** may donate up to four π-electrons and the bonding could be represented simplistically as in **119**.

The benzyne ^{13}C chemical shifts provide some support for this idea. The δ values for C1 and C2 in **116** and **96** are 145.2 and 230.5 respectively, the latter being in the region expected for alkynes acting as four π-electron donors (Section 3.6). The former value is somewhat higher than expected for a typical two π-electron donor alkyne, but the difference can probably be attributed to the small ring which increases the contribution from the metallacyclopropene structure **118** (Table 3). The chemical shifts of the nonequivalent C1 and C2 atoms of **88** (δ = 154.1, 174.3) are intermediate between those of **116** and **96**.

The NMR spectra of **88, 110** and **116** indicate that in these complexes the benzyne ligand is rigid on the NMR time scale, whereas the benzyne ligand in **96** is apparently rotating rapidly about the metal–ring axis ($\Delta G^{\neq} \leq 37.8$ kJ mol^{-1}). At first sight this seems incompatible with the idea that benzyne donates more than two π-electrons, but the fluxional process may be associated with a pseudorotation of the formally pseudotetragonal pyramidal structure of **96**.

A feature of the structures of **105,106, 109** and **110** is that the M–C(aryne) bonds are shorter by 0.07–0.14 Å, and presumably stronger, than the σ–M–C(aryl) bonds. The C1–C2 distances in the anions of **105** and **106** [1.414(8) Å (av.) and 1.393(8) Å respectively] are slightly larger than in **96** and **88**; the same trend is apparent in the remaining benzyne C–C bond lengths, which also are reported to show some evidence for bond alternation. The general bond lengthening has been attributed[112] to the good σ-donor and poor π-acceptor properties of the σ-phenyl co-ligands and to the extensive interactions of the anions with lithium ions.

5. Metal Cluster Complexes of Benzyne and Small Cycloalkynes

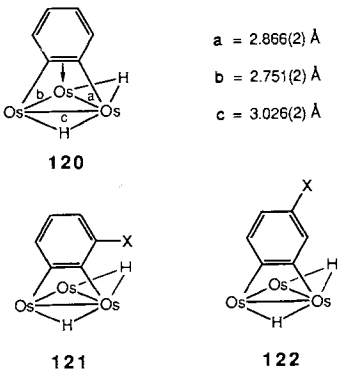
By far the largest number of known benzyne complexes are those based on the trinuclear osmium carbonyl framework.[127] These compounds can be generated by cleavage of aromatic carbon-element (commonly C–H) bonds in simple aromatic compounds. Most interest has concentrated on the structures adopted and on their fluxional behavior; little attention has been paid to their chemistry.

The parent compound $[Os_3H_2(CO)_9(\mu_3\text{–}C_6H_4)]$ **120** (Scheme 27) is obtained as yellow crystals in ca. 30% yield by heating benzene with $Os_3(CO)_{12}$ at 194 °C[128] or, more conveniently, with $[Os_3(CO)_{10}(MeCN)_2]$ under reflux.[129] Other methods of preparation are the thermal decarbonylation of $[Os_3H(\mu_2\text{-}COPh)(CO)_{10}]$[130] or $[Os_3H(OCH_2Ph)(CO)_{10}]$[131] which are obtained by heating $Os_3(CO)_{12}$ with benzaldehyde and benzyl alcohol, respectively, and the photoinduced isomerization of the face-capping benzene complex $[Os_3(CO)_9(\mu_3\text{–}\eta^1\text{:}\eta^2\text{:}\eta^1\text{–}C_6H_6)]$.[132]

X-ray analysis of **120** shows that the C_6H_4 unit lies over a triangle of bonded Os atoms, the dihedral angle between the two planes being 64° or 69° (two independent molecules).[129] The benzyne donates four electrons to the Os_3 triangle, being bound by σ-bonds to two metal atoms and by a π-bond to the third. The cluster has 48 valence electrons and each Os atom has the 18e configuration, assuming three Os–Os bonds to be present.

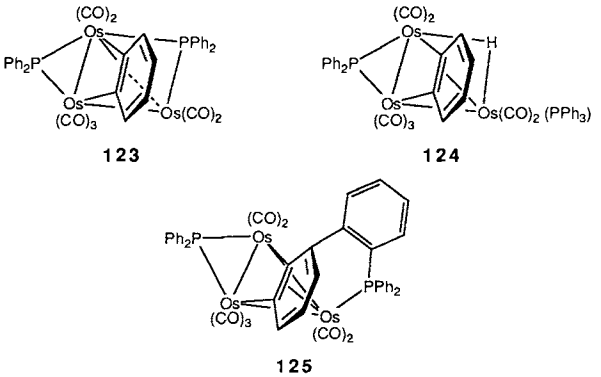
The ring C–C distances do not vary significantly from the mean [1.43(7) Å]. The hydride ligands in **120** are equivalent on the NMR time scale at room temperature, probably because of rapid rotation or flipping of the C_6H_4 unit and rapid reversible hydride migration between the metal triangle and the C_6H_4 ring.[133]

Analogues of complex **120** have been made from $[Os_3(CO)_{10}(MeCN)_2]$ and mono- and di-substituted arenes. The complexes derived from toluene and chlorobenzene exist in solution as mixtures of positional isomers **121** and **122** (Scheme 27).[129]



Scheme 27. Structures of the trinuclear osmium complexes **120**–**122**. X = CH_3, Cl; CO ligands omitted for clarity.

When $Os_3(CO)_{12}$ is treated with arylphosphanes or arylarsanes in high-boiling solvents or, more conveniently, when the ligand substitution products of $Os_3(CO)_{12}$ are first isolated and then thermolyzed, P–C (or As–C) and C–H bonds are cleaved to give a range of products, including μ_3-benzyne complexes. These are isolated, usually in poor yield, after chromatographic separation. Thus, from the reaction of $Os_3(CO)_{12}$ with PPh_3 in refluxing xylene, or from thermolysis of $[Os_3(CO)_{10}(PPh_3)_2]$, the μ_3-benzyne compounds **123, 124** and **125** have been isolated and structurally character-



ized.[134–136] The X-ray structure of the ruthenium analogue of **123**, obtained from $[Ru_3(CO)_9(PPh_3)_3]$ in refluxing decalin or mesitylene[137] has also been determined.[138]

Complex **125** apparently arises by "insertion" of coordinated C_6H_4 into a cyclometalated triphenylphosphane.

Complexes derived similarly from PMe_2Ph or $AsMe_2Ph$ and $Os_3(CO)_{12}$ include **126, 127** (E = P, As) **128** and **129**. In **126**, which is analogous to **123**, variable temperature NMR

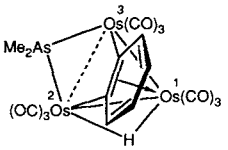
$Os_3(CO)_7(EMe_2)_2(C_6H_4)$ **126**

$Os_3H(CO)_9(EMe_2)(C_6H_4)$ **127**

$Os_3H(CO)_8(PMe_2Ph)(PMe_2)(C_6H_4)$ **128**

$Os_3H(CO)_8(PMe_2)(Me_2PC_6H_4C_6H_3)$ **129**

studies suggest that the C_6H_4 ligand executes two independent 60° rotational processes about the Os_3 triangle.[127, 139, 140] Complexes **127** and **128** each contain one more two-electron donor ligand than the otherwise similar compound **124**; likewise **129** differs from **125** only by the presence of an additional CO group. To account for this, it was initially suggested[139] that in **127** C_6H_4 donates only two electrons to the cluster. However, the X-ray structure of **127** (E = As) shows that, in contrast to **124**, the triangle of metal atoms contains only two Os–Os bonds.[140] The four-electron donor C_6H_4 unit is π-bonded to Os 1 and σ-bonded to the two non-bonded Os atoms [Os 2, Os 3], which are bridged by $AsMe_2$.



127

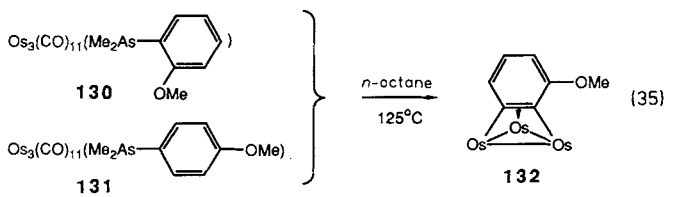
Os 1 - Os 2 2.95Å

Os 1 - Os 3 2.84Å

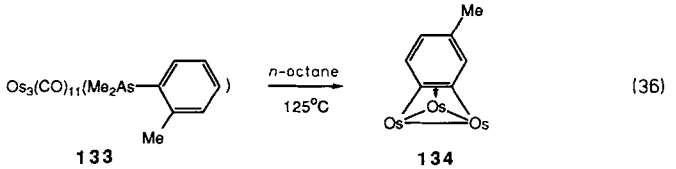
Os 2 - Os 3 3.93Å

∠ Os 2 - Os 1 - Os 3 85.5°

The ^1H and ^{13}C (CO) NMR spectra of **127** between −60 °C and +27 °C have been interpreted in terms of hydride migration from one Os–Os bond to the other accompanied by angular reorganization of the CO groups.[140] As in **120**, the hydride ligand also migrates reversibly between the metal atoms and the six-membered ring. Thus, both **130** and **131** in *n*-octane at 125 °C give the *same* 3-methoxybenzyne complex **132** [Eq. (35)], and the *o*-tolyldimethylarsane complex **133** gives only the 4-methylbenzyne complex **134** instead of the expected 3-isomer [Eq. (36)].[141]



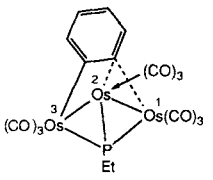
130 **131** **132** (35)



133 **134** (36)

A complex similar to **127** containing SMe in place of $AsMe_2$ has been prepared in low yield from the reaction of $Os_3(CO)_{12}$ with methyl phenyl sulfide. Variable temperature NMR studies show that, in addition to hydride migration between the Os–Os bonds, there is a higher energy process involving inversion at sulfur.[142]

Other modes of interaction of benzyne with metal clusters have been found. In the yellow complex **135**, which is formed in high yield on heating $[Os_3(CO)_{11}(PPh_2Et)]$ in nonane, one benzyne carbon atom is σ-bonded to one osmium atom while the other carbon atom bridges the other two osmium atoms.[143] The PEt group bridges all three osmium atoms but, as in **127**, there are only two Os–Os bonds, so that C_6H_4 again contributes four electrons to the cluster. An interesting feature of **135** is the distance between the benzyne carbon atoms of 1.53(5) Å, typical of a single bond. The complexes are highly fluxional, probably owing to a rocking motion of the six-membered ring such that the two benzyne carbon atoms become equivalent.



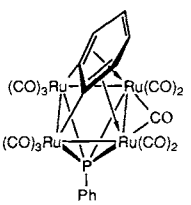
135

Os 1 - Os 2 2.789(2)Å

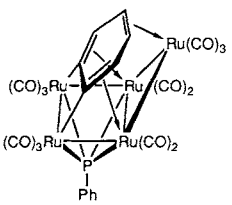
Os 2 - Os 3 2.929(2)Å

∠ Os 1 - Os 2 - Os 3 89.1°

When $[Ru_3(CO)_{11}(PPh_3)]$ is heated in toluene, the complexes $[Ru_3(CO)_7(\mu\text{-}PPh_2)_2(C_6H_4)]$, **136**, and **137** are formed.[144] In **136** benzyne bridges four ruthenium atoms in a square plane and donates six electrons to them. The same structural unit is found in **137**, but an additional $Ru(CO)_3$ group replaces one bridging carbonyl group and is attached to the remaining double bond of C_6H_4, so that benzyne now acts as an eight-electron donor. This mode of coordination provides a model for the activation of two *ortho*–C–H bonds of benzene at a step site on a (111) metal surface.[132, 144]

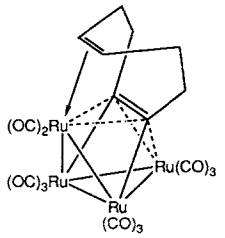


136

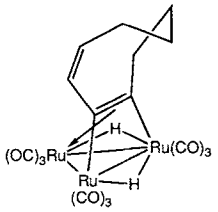


137

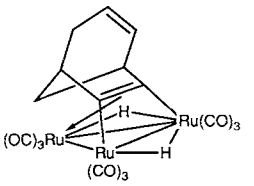
Cycloolefins undergo dehydrogenation similarly to benzene on reaction with carbonyls of ruthenium and osmium. The complexes $[Os_3H_2(CO)_9(\text{cycloalkyne})]$ obtained from $Os_3(CO)_{12}$ and cyclopentene[128] or cyclooctene[145, 146] are structurally similar to the benzyne complex **120**. They show two hydride resonances at low temperatures but these coalesce above room temperature owing to hydride migration between the Os–Os bonds and rotation of the organic ligand. Reaction of indene with $Os_3(CO)_{12}$ leads to the indyne complex $[Os_3H_2(CO)_9(C_9H_6)]$ whose hydride ligands are derived from the five-membered ring.[147] Cyclopentadiene similarly gives ca. 2% yield of $[Os_3H_2(CO)_9(C_5H_4)]$, which is believed to contain cyclopent-1-en-3-yne.[148] Reaction of either 1,5- or 1,3-cyclooctadiene with $[Ru_4H_4(CO)_{12}]$ or $[Ru_4H_2(CO)_{13}]$ gives a mixture of products in low yield, including



138



139



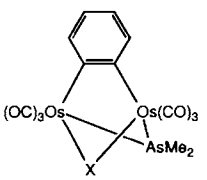
140

the black C_8H_{10}-complex **138**.[145] This contains cyclooct-1-en-5-yne bound to four metal atoms in a butterfly arrangement, as shown by X-ray crystallography.[149] 1,3-Cyclooctadiene and 2,6-bicyclo[3.2.1]octadiene undergo dehydrogenation on reaction with $Ru_3(CO)_{12}$ to give the complexes **139** and **140**, respectively.[145, 150]

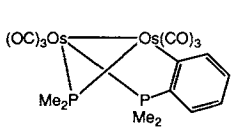
6. Dinuclear μ_2-Benzyne (μ-*o*-Phenylene) Complexes

In compounds of this class the C_6H_4 group is bound by two σ-bonds to two metal atoms. No systematic synthetic methods have been developed, although in principle the compounds could serve as precursors both to mononuclear η^2-benzyne complexes and to higher nuclearity clusters containing bridging C_6H_4 groups.

When $[Os_3(CO)_{10}(AsMe_2Ph)_2]$ is heated, small amounts of the dinuclear μ_2-C_6H_4 complexes **141** and **142** are formed in addition to the trinuclear μ_3-C_6H_4 species **126** and **127**; **142** is also produced on heating $[Os_3(CO)_{11}(AsMe_2Ph)]$.[139] Unlike the trinuclear complexes, **141** and **142** show temperature-invariant NMR spectra. Analogous dinuclear complexes are not formed in the corresponding PMe_2Ph system; treatment of $[Os_3(CO)_7(PMe_2)_2(C_6H_4)]$ **126** with CO in refluxing nonane induces coupling of the C_6H_4 ligand with one of the PMe_2 groups to give the dinuclear complex **143**.

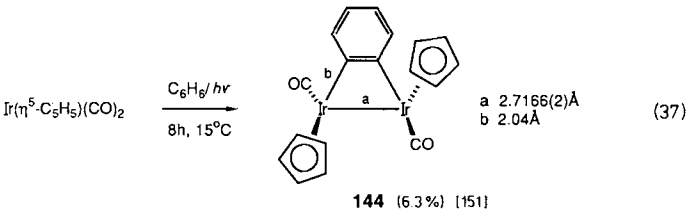


141, X = $AsMe_2$
142, X = H



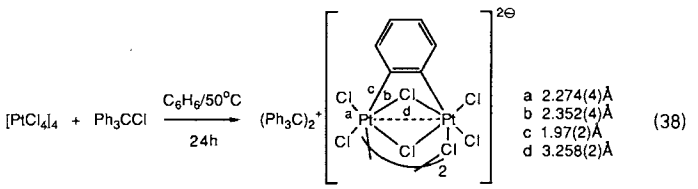
143

Other μ-*o*-phenylene complexes (**144**–**149**) have been obtained by various routes and in varying yields as summarized in Equations (37)–(40) and Schemes 28 and 29.[125, 151–156] Complex **144** is formed in poor yield upon irradiation of



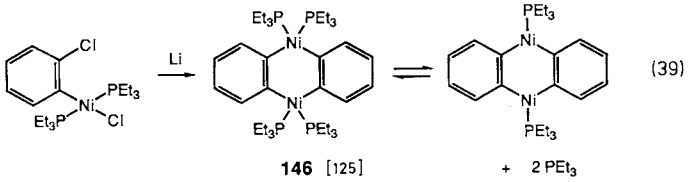
144 (6.3%) [151]

(37)



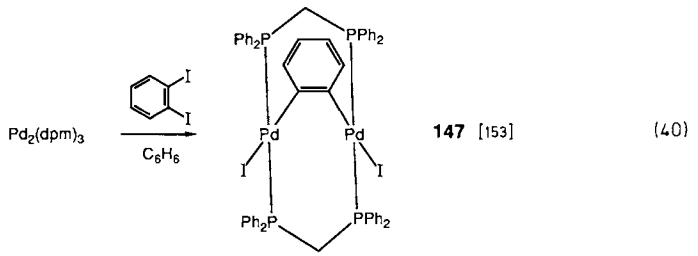
145 (5%) [152]

(38)



146 [125] + 2 PEt_3

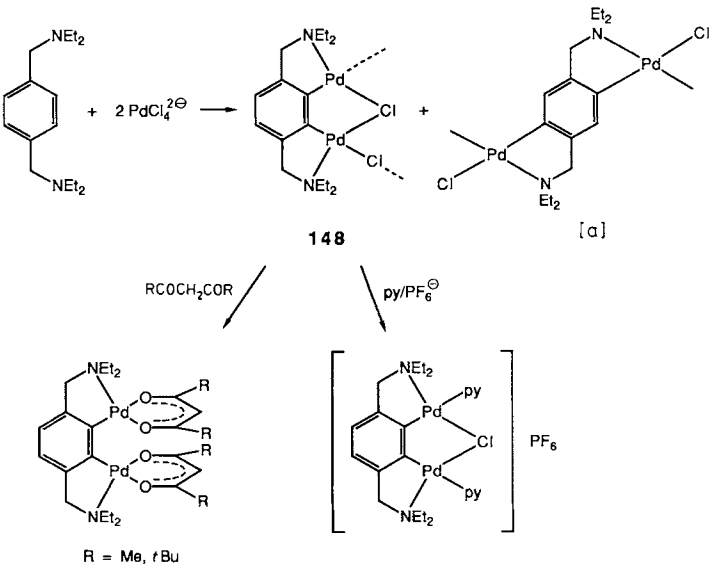
(39)



147 [153]

(40)

[$IrCp(CO)_2$] in benzene via an unstable intermediate hydrido(phenyl) complex [$IrCp(C_6H_5)(CO)$].[151] The palladium(II) complexes **147** and **148** are formed, respectively, by double oxidative addition of *o*-diiodobenzene to a dipalladium(0) complex [Eq. (40), dpm = dipivaloylmethane][153] and by cyclometalation (Scheme 28).[154] Complex **149** (Scheme 29) is apparently formed by direct trapping of

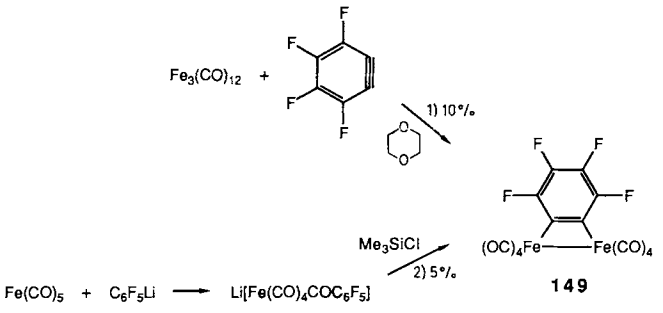


148

[a]

R = Me, *t*Bu

Scheme 28. Formation of some substituted μ-*o*-phenylenepalladium(II) complexes; [154] py = pyridine. [a] Insoluble.

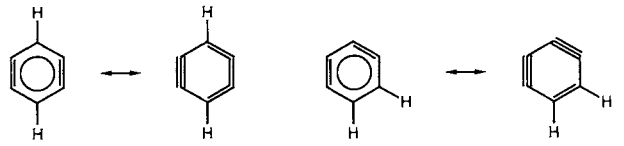


Scheme 29. Synthesis of $[\{Fe(CO)_4\}_2(\mu\text{-}C_6F_4)]$ [155, 156]

tetrafluorobenzyne, generated by decomposition of C_6F_5MgBr in dioxane, with $Fe_3(CO)_{12}$.[155, 156] A similar reaction using $Co_2(CO)_8$ in place of $Fe_3(CO)_{12}$ gives a tetranuclear species $[Co_4(CO)_{10}(C_6F_4)]$, but using $Pt(PPh_3)_4$ does not give $[Pt(PPh_3)_2(C_6F_4)]$.[155]

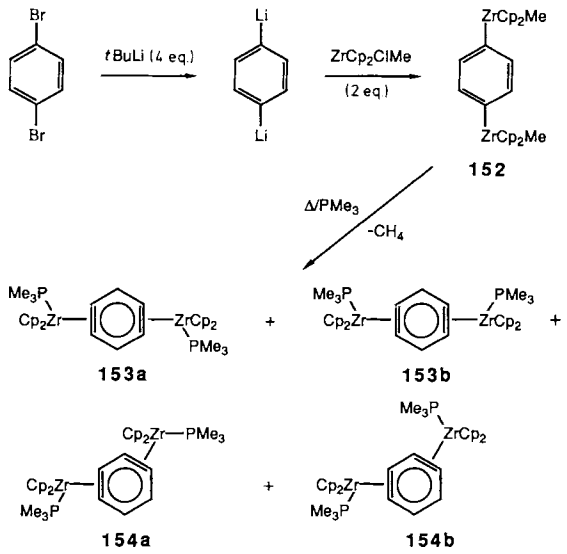
7. Metal Complexes of Tetradehydrobenzene and Dimethoxytetradehydrobenzene

Recent work has shown that the more highly unsaturated analogues of benzyne, 1,4-benzdiyne (1,2,4,5-tetradehydrobenzene) **150** and 1,3-benzdiyne (1,2,3,4-tetradehydrobenzene) **151** can be stabilized as dinuclear metal complexes. The free molecules have never been observed, and theoretical calculations suggest that their ring-opening to give HC≡C–C≡C–C≡CH will be more favorable than the corresponding process for benzyne to give HC≡CH and HC≡C–C≡CH.[20] However, 1,2,4,5- and 1,2,3,4-tetrabromoarenes behave as useful benzdiyne synthons, because on treatment with two equivalents of an organolithium reagent in the presence of a suitable diene, the Diels–Alder bis-adducts are formed.[157]

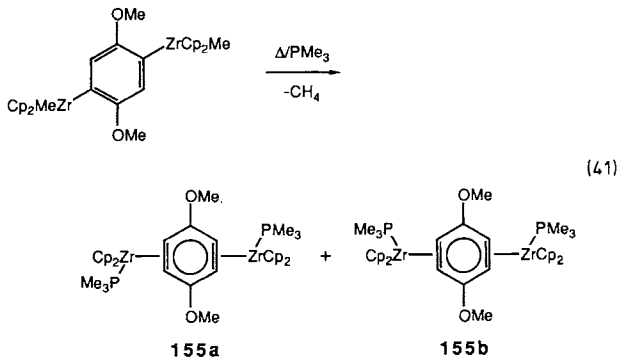


The zirconocene complexes of **150** and **151** have been prepared by an extension of the procedure used to synthesize the benzyne complex **88** (Scheme 30).[158] Treatment of 1,4-dilithiobenzene with two equivalents of $[ZrCp_2ClMe]$ gives the *p*-phenylenezirconium complex **152** which, on heating, eliminates CH_4 to give a mixture of two pairs of isomers. One pair (**153a, 153b**) contains 1,4-benzdiyne bound to two $ZrCp_2(PMe_3)$ units, the other (**154a, 154b**) contains 1,3-benzdiyne, also bound to two $[ZrCp_2(PMe_3)]$ units. The isomers in each pair differ in having *anti*- or *syn*-arrangements of the PMe_3 ligands.

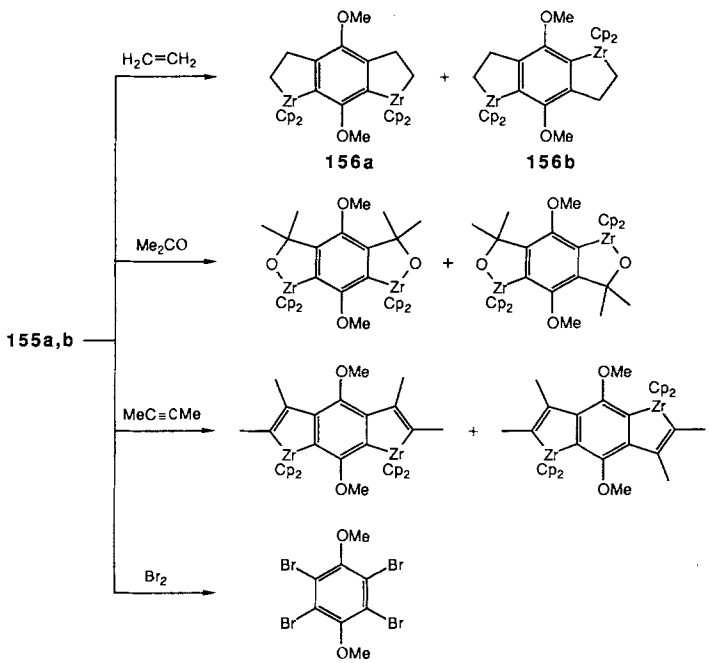
Upon heating with trimethylphosphane, the 1,4-dimethoxy-substituted analogue of **152** gives a pair of isomers **155a** and **155b** containing 1,4-dimethoxy-2,5-benzdiyne [Eq. (41)]. The *anti*-isomer **155a** crystallizes from the reaction mixture and its structure has been confirmed by



Scheme 30. Synthesis of the benzdiyne-zirconocene complexes **153a, b** and **154a, b**.

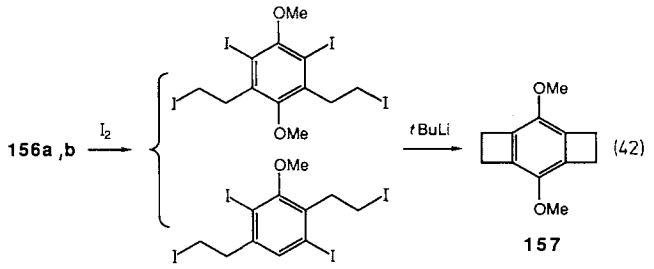


X-ray crystallography.[158] It undergoes insertions with unsaturated organic molecules e.g. acetone, 2-butyne and ethylene to give bis(metallacycles) (Scheme 31). The com-



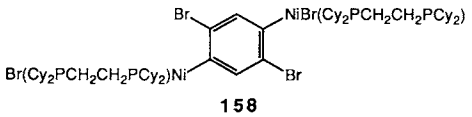
Scheme 31. Reactions of the benzdiyne-biszirconocene complexes **155a, b**.

pounds derived in this way from ethylene (**156a, 156b**) give, on successive treatment with iodine and *tert*-butyllithium, the tetrahydrodicyclobutabenzene **157** [Eq. (42)].

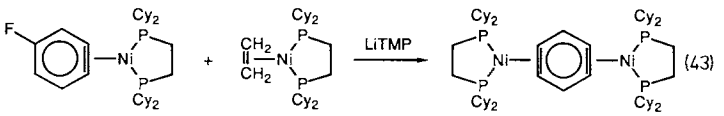


(42)

For reasons discussed in Section 4.2, a different approach is necessary to make a dinickel(0) complex of 1,4-benzdiyne. In principle, alkali metal reduction of the dinickel(II) complex **158** could be expected to give the 1,4-benzdiyne dinickel(0) complex **159**, but all attempts to make **158** or its analogues by double oxidative addition of 1,2,4,5-tetrabromobenzene to nickel(0) precursors have failed. However, treatment of the 4-fluorobenzyne nickel(0) complex **160** with a large excess of lithium tetramethylpiperidide (LiTMP) in the presence of $[Ni(Cy_2PCH_2CH_2PCy_2)(C_2H_4)]$ gives **159** as a yellow solid in ca. 60–70% yield [Eq. (43)].[159]



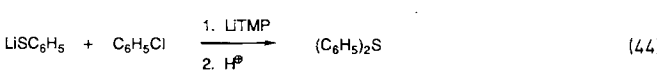
158



(43)

160 **159**

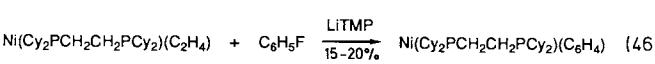
The success of this synthesis is based on the following observations: If chlorobenzene is treated with a powerful, poorly nucleophilic base such as LiTMP, the resulting benzyne can be trapped either by added nucleophiles such as C_6H_5SLi [Eq. (44)][160] or as a Diels–Alder adduct by e.g. 1,3-diphenylisobenzofuran [Eq. (45)].[161] If the nickel(0) complex $[Ni(Cy_2PCH_2CH_2PCy_2)(C_2H_4)]$ is used as trapping reagent in this type of reaction, the benzyne-nickel(0) complex **116** can be detected spectroscopically [Eq. (46)], but the



(44)



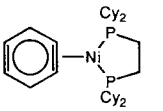
(45)



(46)

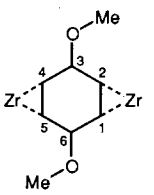
116

yields are poor (15–20%), and there are other unidentified products. We assume that in the first step of Equation (44) the *mononuclear* benzdiyne complex **161** is formed by the reaction of LiTMP with **160** and that **161** is intercepted by the ethylene nickel(0) complex to give **159**. The surprisingly high yield of **159** suggests that **161** may be longer-lived than benzyne.

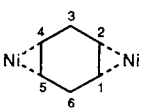


161

The structural analyses of **155a** and **159** show the same features, the coordination geometries being similar to those of the corresponding benzyne complexes **88** and **116**. In both cases the metal atoms are displaced slightly from the plane of the aromatic ring [0.17 Å (**155a**), 0.08 Å (**159**)]. The "acetylenic" C1–C2 bond length in **155a** is slightly greater than in **159** (Fig. 3); the same trend is evident on comparison of **88** and **116**.



Bond lengths [Å]		Bond angles [°]	
C1 - C2	1.345(11)	∠ C1 - C2 - C3	121.1(6)
C2 - C3	1.398(11)	∠ C2 - C3 - C4	118.8(7)
C3 - C4	1.401(10)	∠ C6 - C1 - C2	120.1(6)



C1 - C2	1.313(12)	∠ C1 - C2 - C3	124.1(9)
C2 - C3	1.402(13)	∠ C2 - C3 - C4	112.2(8)
C3 - C4	1.417(13)	∠ C6 - C1 - C2	123.6(9)

Fig. 3. Comparison of the bond lengths [Å] and angles [°] of the 1,2,4,5-tetradehydrobenzene (1,4-benzdiyne) ligands in **155a** and **159**.

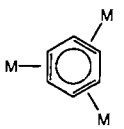
8. Summary and Outlook

Methods have been developed for the synthesis of thermally stable but highly reactive mononuclear complexes of small cycloalkynes and arynes. These compounds are formed mainly with low-valent, early transition elements, e.g. Zr, Nb, Ta, Mo, W, and with low-valent, late (d^{10}) transition elements (Ni, Pt). Unsaturated molecules readily insert into the benzyne–metal bonds of e.g. $[ZrCp_2(PMe_3)(C_6H_4)]$ and $[Ni(Cy_2PCH_2CH_2PCy_2)(C_6H_4)]$ to form new metallacycles that may be useful in organic synthesis. The aryne zirconium compounds show particular promise in this respect because they can be prepared from aromatic monohalides, whereas the nickel compounds require less easily accessible *o*-dihaloarenes. Few mononuclear benzyne or small cycloalkyne complexes of the mid-transition elements are known, and new synthetic methods may be needed for these compounds.[162–165] One possibility is to transfer an aryne or cycloalkyne unit from zirconium or nickel to another metal center. This could give new mononuclear aryne or cycloalkyne complexes or, if transfer is incomplete, it could

give interesting heterobinuclear or heteropolynuclear bridging aryne or cycloalkyne complexes.

A potentially valuable reaction is the generation of coordinated arynes or cycloalkynes directly from arenes or cycloolefins by hydrogen transfer to a metal system. So far this has been achieved in moderate yield only with $Os_3(CO)_{12}$ or its derivatives. Undoubtedly the modest yields, the expense of the metal, and the reversibility of the hydrogen transfer have limited synthetic applications.

In principle, there seems to be no reason why the methods developed so far should not be applicable to the synthesis of a range of metal-stabilized heteroarynes and polynuclear arynes. The isolation of the first complexes of 1,4-benzdiyne also suggests that even more highly unsaturated cyclic molecules could be similarly stabilized, and an obvious synthetic target is 1,3,5-benztriyne (C_6) coordinated to three metal atoms (**162**).[166]



162

One of the authors (M.A.B.) wishes to thank the Institute of Molecular Science, Okazaki, Japan for the award of a three-month Visiting Professorship which enabled much of this review to be written, and Professor Hidemasa Takaya (now at the University of Kyoto) and his group for their kindness and hospitality.

Received: February 7, 1989;
supplemented: May 5, 1989 [A 735 IE]
German version: *Angew. Chem. 101* (1989) 1349

[1] G. Wittig, *Pure Appl. Chem. 7* (1963) 173.
[2] G. Wittig, *Angew. Chem. 77* (1965) 752; *Angew. Chem. Int. Ed. Engl. 4* (1965) 731.
[3] R. W. Hoffmann, *Dehydrobenzene and Cycloalkynes*, Academic Press, New York 1967.
[4] a) H. Viehe (Ed.): *Chemistry of Acetylenes*, Marcel Dekker, New York 1969; b) R. W. Hoffmann in [4a], pp. 1063–1148.
[5] A. Krebs in [4a], pp. 987–1062.
[6] H. Meier, *Synthesis 1972*, 235.
[7] E. K. Fields in S. P. McManus (Ed.): *Organic Reactive Intermediates*, Academic Press, New York 1973, pp. 448.
[8] M. G. Reinecke in R. A. Abramovitch (Ed.): *Reactive Intermediates, Vol. 2*, Plenum Press, New York 1982, pp. 367–414.
[9] M. Nakagawa in S. Patai (Ed.): *The Chemistry of Functional Groups: The Chemistry of the Carbon-Carbon Triple Bond, Part 2*, Wiley, New York 1978, pp. 635–712.
[10] T. L. Gilchrist in S. Patai, Z. Rappoport (Eds.): *The Chemistry of Functional Groups, Supplement C: The Chemistry of Triple Bonded Functional Groups, Part 1*, Wiley, New York 1983, pp. 383–419.
[11] A. Krebs, J. Wilke, *Top. Curr. Chem. 109* (1983) 189.
[12] G. Wittig, F. Bickelhaupt, *Chem. Ber. 91* (1958) 883.
[13] M. D. Newton, H. A. Fraenkel, *Chem. Phys. Lett. 18* (1973) 244.
[14] M. J. S. Dewar, W.-K. Li, *J. Am. Chem. Soc. 96* (1974) 5569.
[15] K. Yamaguchi, A. Nishio, S. Yabushita, T. Fueno, *Chem. Phys. Lett. 53* (1978) 109.
[16] J. O. Noell, M. D. Newton, *J. Am. Chem. Soc. 101* (1979) 51.
[17] W. Thiel, *J. Am. Chem. Soc. 103* (1981) 1420.
[18] M. J. S. Dewar, G. P. Ford, C. H. Reynolds, *J. Am. Chem. Soc. 105* (1983) 3162.
[19] C. W. Bock, P. George, M. Trachtman, *J. Phys. Chem. 88* (1984) 1467.
[20] L. Radom, R. H. Nobes, D. J. Underwood, W.-K. Li, *Pure Appl. Chem. 58* (1986) 75.
[21] R. D. Brown, P. D. Godfrey, M. Rodler, *J. Am. Chem. Soc. 108* (1986) 1296.
[22] O. L. Chapman, C.-C. Chang, J. Kolc, N. R. Rosenquist, H. Tomioka, *J. Am. Chem. Soc. 97* (1975) 6586; O. L. Chapman, K. Mattes, C. L. McIntosh, J. Pacansky, G. V. Calder, G. Orr, *ibid. 95* (1973) 613.
[23] a) J. W. Laing, R. S. Berry, *J. Am. Chem. Soc. 98* (1976) 660. b) Recent calculations on benzyne [20, 23c, d] suggest that the bond length C1–C2 is in fact 1.25–1.26 Å and that the C–C stretching frequency of this bond is only 1965–2010 cm^{-1}; a band at 1860 cm^{-1} in the gas phase photodetachment spectrum has been assigned to the same mode [23e]. The more recent work suggests that the band at 2085 cm^{-1} in the IR spectrum of matrix-isolated benzyne, which has been confirmed experimentally by several groups, [23f] is due to some other species. The question is obviously wide open; c) I. Hillier, M. A. Vincent, M. F. Guest, W. von Niessen, *Chem. Phys. Lett. 134* (1987) 403; d) A. C. Scheiner, H. F. Schaefer III, B. Liu, *J. Am. Chem. Soc. 111* (1989) 3118; e) D. G. Leopold, A. E. S. Miller, W. C. Lineberger, *J. Am. Chem. Soc. 108* (1986) 1379; f) I. R. Dunkin, J. G. McDonald, *J. Chem. Soc. Chem. Commun.* (1979) 772; H-H. Nam, G. E. Leroi, *J. Mol. Struct. 157* (1987) 301; C. Wentrup, R. Blanch, H. Briehl, G. Gross, *J. Am. Chem. Soc. 110* (1988) 1874.
[24] A. Krebs, W. Cholcha, M. Müller, T. Eicher, H. Pielartzik, H. Schnöckel, *Tetrahedron Lett. 25* (1984) 5027.
[25] G. Bieri, E. Heilbronner, E. Kloster-Jensen, A. Schmelzer, J. Wirz, *Helv. Chim. Acta 57* (1974) 1265.
[26] H. Schmidt, A. Schweig, A. Krebs, *Tetrahedron Lett. 1974*, 1471.
[27] S. Olivella, M. A. Pericàs, A. Riera, A. Solé, *J. Org. Chem. 52* (1987) 4160.
[28] J. Tseng, M. L. McKee, P. B. Shevlin, *J. Am. Chem. Soc. 109* (1987) 5474.
[29] S. Olivella, M. A. Pericàs, A. Riera, A. Solé, *J. Am. Chem. Soc. 108* (1986) 6884.
[30] O. L. Chapman, J. Gano, P. R. West, M. Regitz, G. Maas, *J. Am. Chem. Soc. 103* (1981) 7033.
[31] R. W. Strozier, P. Caramella, K. N. Houk, *J. Am. Chem. Soc. 101* (1979) 1340; N. G. Rondan, L. N. Domelsmith, K. N. Houk, A. T. Bowne, R. H. Levin, *Tetrahedron Lett. 1979*, 3237; W. F. Maier, G. C. Lau, A. B. McEwen, *J. Am. Chem. Soc. 107* (1985) 4724.
[32] G. Wittig, S. Fischer, *Chem. Ber. 105* (1972) 3542.
[33] G. Wittig, H.-L. Dorsch, *Justus Liebigs Ann. Chem. 711* (1968) 46.
[34] T. L. Gilchrist, F. J. Graveling, C. W. Rees, *J. Chem. Soc. Chem. Commun. 1968*, 821.
[35] M. A. Bennett, T. Yoshida, *J. Am. Chem. Soc. 100* (1978) 1750.
[36] M. A. Bennett, H.-G. Fick, unpublished work.
[37] H. Meier, J. Heiss, H. Suhr, E. Müller, *Tetrahedron 24* (1968) 2307.
[38] G. Wittig, P. Fritze, *Justus Liebigs Ann. Chem. 712* (1968) 79.
[39] H. Kolshorn, H. Meier, E. Müller, *Tetrahedron Lett. 1971*, 1469.
[40] H. Kolshorn, H. Meier, E. Müller, *Tetrahedron Lett. 1972*, 1589.
[41] M. A. Bennett, P. B. Donaldson, *Inorg. Chem. 17* (1978) 1995.
[42] R. S. Dickson, P. J. Fraser, *Adv. Organomet. Chem. 12* (1974) 323.
[43] H. Petersen, H. Meier, *Nouv. J. Chim. 4* (1980) 687.
[44] M. A. Bennett, I. W. Boyd, *J. Organomet. Chem. 290* (1985) 165.
[45] M. A. Bennett, I. W. Boyd, G. B. Robertson, W. A. Wickramasinghe, *J. Organomet. Chem. 290* (1985) 181.
[46] R. Goddard, S. A. R. Knox, F. G. A. Stone, M. J. Winter, P. Woodward, *J. Chem. Soc. Chem. Commun. 1976*, 559.
[47] J. Knebel, C. P. Morley, G. Wilke, C. Krüger, J. M. Wallis, *J. Organomet. Chem. 334* (1987) C39.
[48] M. A. Bennett, G. B. Robertson, P. O. Whimp, T. Yoshida, *J. Am. Chem. Soc. 93* (1971) 3797.
[49] E. Müller, G. Odenigbo, *Justus Liebigs Ann. Chem. 1975*, 1435.
[50] K. H. Pannell, A. J. Mayr, R. Hoggard, R. C. Pattersen, *Angew. Chem. 92* (1980) 650; *Angew. Chem. Int. Ed. Engl. 19* (1980) 632.
[51] H. Kimling, A. Krebs, *Angew. Chem. 84* (1972) 952; *Angew. Chem. Int. Ed. Engl. 11* (1972) 932.
[52] A. Krebs, H. Kimling, R. Kemper, *Justus Liebigs Ann. Chem. 1978*, 431.
[53] H. Irngartinger, H. Kimling, A. Krebs, R. Mäusbacher, *Tetrahedron Lett. 1975*, 2571.
[54] H. Irngartinger, H. Rodewald, *Angew. Chem. 86* (1974) 783; *Angew. Chem. Int. Ed. Engl. 13* (1974) 740.
[55] H. J. Schmitt, K. Weidenhammer, M. L. Ziegler, *Chem. Ber. 109* (1976) 2558.
[56] H. J. Schmitt, M. L. Ziegler, *Z. Naturforsch. B28* (1973) 508.
[57] A. Krebs, B. Jessel, unpublished results cited in Ref. [11].
[58] M. A. Bennett, G. F. Warnock, unpublished work.
[59] M. A. Bennett, A. Rokicki, *Aust. J. Chem. 38* (1985) 1307.
[60] S. L. Buchwald, R. T. Lum, J. C. Dewan, *J. Am. Chem. Soc. 108* (1986) 7441.
[61] N. A. Bailey, M. R. Churchill, R. L. Hunt, R. Mason, G. Wilkinson, *Proc. Chem. Soc. (London) 1964*, 401; R. L. Hunt, G. Wilkinson, *Inorg. Chem. 4* (1965) 1270.
[62] E. K. Ditzel, G. B. Robertson, unpublished work.
[63] P. G. Gassman, I. G. Cesa, *Organometallics 3* (1984) 119.
[64] M. A. Bennett, T. Yoshida, *J. Am. Chem. Soc. 95* (1973) 3030; for a recent review, see: H. C. Bryndza, W. Tam, *Chem. Rev. 88* (1988) 1163.

[65] M. A. Bennett, A. Rokicki, *J. Organomet. Chem. 244* (1983) C41; *Organometallics 4* (1985) 180.
[66] T. G. Appleton, M. A. Bennett, A. Singh, T. Yoshida, *J. Organomet. Chem. 154* (1978) 369.
[67] G. B. Robertson, P. O. Whimp, *J. Am. Chem. Soc. 97* (1975) 1051; *J. Organomet. Chem. 32* (1971) C69.
[68] G. B. Robertson, P. O. Whimp, *Aust. J. Chem. 33* (1980) 1373.
[69] L. Manojlovič-Muir, K. W. Muir, R. Walker, *Acta Crystallogr. Sect. B35* (1979) 2416.
[70] B. W. Davies, N. C. Payne, *J. Organomet. Chem. 99* (1975) 315.
[71] D. M. P. Mingos in G. Wilkinson, F. G. A. Stone, E. W. Abel (Eds.): *Comprehensive Organometallic Chemistry, Vol. 3*, Pergamon, Oxford 1982, Chapter 19, p. 59.
[72] S. Otsuka, A. Nakamura, *Adv. Organomet. Chem. 14* (1976) 245.
[73] J. L. Templeton, P. B. Winston, B. C. Ward, *J. Am. Chem. Soc. 103* (1981) 7713; K. Tatsumi, R. Hoffmann, J. L. Templeton, *Inorg. Chem. 21* (1982) 466.
[74] J. L. Templeton, B. C. Ward, *J. Am. Chem. Soc. 102* (1980) 3288.
[75] F. R. Hartley in G. Wilkinson, F. G. A. Stone, E. W. Abel (Eds.): *Comprehensive Organometallic Chemistry, Vol. 6*, Pergamon, Oxford 1982, Chapter 39, pp. 614, 691.
[76] S. D. Ittel, J. A. Ibers, *Adv. Organomet. Chem. 14* (1976) 33.
[77] Cf. [75], Chapter 39, p. 702.
[78] N. M. Boag, D. M. Grove, J. A. K. Howard, J. L. Spencer, F. G. A. Stone, *J. Chem. Soc., Dalton Trans. 1980*, 2170.
[79] R. P. A. Sneeden, *Organochromium Compounds*, Academic Press, New York 1975, p. 284.
[80] J. Dvorak, R. J. O'Brien, W. Santo, *Chem. Commun. 1970*, 411.
[81] C. P. Boekel, J. H. Teuben, H. J. de Liefde Meijer, *J. Organomet. Chem. 81* (1974) 371; *102* (1975) 161.
[82] V. N. Latyaeva, L. I. Vyshinskaya, V. P. Mar'in, *J. Gen. Chem. USSR (Engl. Transl.) 46* (1976) 627.
[83] H. Masai, K. Sonogashira, N. Hagihara, *Bull. Chem. Soc. Jpn. 41* (1968) 750.
[84] J. Mattia, M. B. Humphrey, R. D. Rogers, J. L. Atwood, M. D. Rausch, *Inorg. Chem. 17* (1978) 3257.
[85] M. D. Rausch, E. A. Mintz, *J. Organomet. Chem. 190* (1980) 65.
[86] I. S. Kolomnikov, T. S. Lobeeva, V. V. Gorbachevskaya, G. G. Aleksandrov, Yu. T. Struchkov, M. E. Vol'pin, *Chem. Commun. 1971*, 972.
[87] B. Gautheron, G. Tainturier, S. Pouly, F. Théobald, H. Vivier, A. Laarif, *Organometallics 3* (1984) 1495.
[88] V. B. Shur, E. G. Berkovitch, M. E. Vol'pin, B. Lorenz, M. Wahren, *J. Organomet. Chem. 228* (1982) C36.
[89] E. G. Berkovitch, V. B. Shur, M. E. Vol'pin, B. Lorenz, S. Rummel, M. Wahren, *Chem. Ber. 113* (1980) 70.
[90] a) G. Erker, *J. Organomet. Chem. 134* (1977) 189; b) for a recent review, see: S. L. Buchwald, R. B. Nielsen, *Chem. Rev. 88* (1988) 1047.
[91] G. Erker, K. Kropp, *J. Am. Chem. Soc. 101* (1979) 3659.
[92] K. Kropp, G. Erker, *Organometallics 1* (1982) 1246.
[93] S. L. Buchwald, A. Sayers, B. T. Watson, J. C. Dewan, *Tetrahedron Lett. 28* (1987) 3245.
[94] G. Erker, U. Dorf, R. Mynott, Y.-H. Tsay, C. Krüger, *Angew. Chem. 97* (1985) 572; *Angew. Chem. Int. Ed. Engl. 24* (1985) 584.
[95] S. L. Buchwald, B. T. Watson, J. C. Huffman, *J. Am. Chem. Soc. 108* (1986) 7411.
[96] S. L. Buchwald, B. T. Watson, R. T. Lum, W. A. Nugent, *J. Am. Chem. Soc. 109* (1987) 7137.
[97] L. E. Schock, C. P. Brock, T. J. Marks, *Organometallics 6* (1987) 232.
[98] F. D. Miller, R. D. Sanner, *Organometallics 7* (1988) 818.
[99] P. J. Fagan, J. M. Manriquez, E. A. Maatta, A. M. Seyam, T. J. Marks, *J. Am. Chem. Soc. 103* (1981) 6650.
[100] G. Erker, T. Mühlenbernd, *J. Organomet. Chem. 319* (1987) 201.
[101] G. Erker, P. Czisch, R. Mynott, Y.-H. Tsay, C. Krüger, *Organometallics 4* (1985) 1310.
[102] H. J. R. de Boer, O. S. Akkerman, F. Bickelhaupt, G. Erker, P. Czisch, R. Mynott, J. M. Wallis, C. Krüger, *Angew. Chem. 98* (1986) 641; *Angew. Chem. Int. Ed. Engl. 25* (1986) 639.
[103] S. J. McLain, R. R. Schrock, P. R. Sharp, M. R. Churchill, W. J. Youngs, *J. Am. Chem. Soc. 101* (1979) 263.
[104] M. R. Churchill, W. J. Youngs, *Inorg. Chem. 18* (1979) 1697.
[105] G. Parkin, E. Bunel, B. J. Bunger, M. S. Trimmer, A. van Asselt, J. E. Bercaw, *J. Mol. Catal. 41* (1987) 21.
[106] B. Sarry, V. Dobrusskin, H. Singh, *J. Organomet. Chem. 13* (1968) 1.
[107] B. Sarry, M. Schön, *J. Organomet. Chem. 13* (1968) 9.
[108] B. Sarry, H. Grossmann, *Z. Anorg. Allg. Chem. 359* (1968) 234; previous reports with wrong formulations: H. Funk, W. Hanke, *Angew. Chem. 71* (1959) 408; B. Sarry, *ibid. 71* (1959) 776.
[109] B. Sarry, H. Singh, B. Hahn, R. Schaffernicht, *Z. Anorg. Allg. Chem. 456* (1979) 181.
[110] B. Sarry, R. Schaffernicht, *Z. Naturforsch. B36* (1981) 1238.
[111] B. Sarry, P. Velling, *Z. Anorg. Allg. Chem. 500* (1983) 199.
[112] R. A. Bartlett, P. P. Power, S. C. Shoner, *J. Am. Chem. Soc. 110* (1988) 1966.
[113] L. R. Chamberlain, I. P. Rothwell, *J. Am. Chem. Soc. 105* (1983) 1665.
[114] L. R. Chamberlain, J. L. Kerschner, A. P. Rothwell, I. P. Rothwell, J. C. Huffman, *J. Am. Chem. Soc. 109* (1987) 6471.
[115] J. Arnold, G. Wilkinson, B. Hussain, M. B. Hursthouse, *J. Chem. Soc. Chem. Commun. 1988*, 704; *Organometallics 8* (1989) 415.
[116] L. Friedman, *J. Am. Chem. Soc. 89* (1967) 3071.
[117] E. Vedejs, R. A. Shepherd, *Tetrahedron Lett. 1970*, 1863; L. A. Paquette, *Chem. Commun. 1971*, 1076; P. Warner, *Tetrahedron Lett. 1971*, 723.
[118] H. J. S. Winkler, G. Wittig, *J. Org. Chem. 28* (1963) 1733.
[119] C. D. Cook, G. S. Jauhal, *J. Am. Chem. Soc. 90* (1968) 1464.
[120] T. L. Gilchrist, F. J. Graveling, C. W. Rees, *J. Chem. Soc. C 1971*, 977.
[121] R. G. Miller, D. P. Kuhlman, *J. Organomet. Chem. 26* (1971) 401.
[122] E. W. Gowling, S. F. A. Kettle, G. M. Sharples, *Chem. Commun. 1968*, 21; N. A. Bailey, S. E. Hull, R. W. Jotham, S. F. A. Kettle, *ibid. 1971*, 282.
[123] M. A. Bennett, T. W. Hambley, N. K. Roberts, G. B. Robertson, *Organometallics 4* (1985) 1992.
[124] M. A. Bennett, J. S. Drage, T. Okano, R. Milczarek, N. K. Roberts, H. P. Schwemlein, unpublished work.
[125] J. E. Dobson, R. G. Miller, J. P. Wiggen, *J. Am. Chem. Soc. 93* (1971) 554.
[126] A. Yamamoto, *Organotransition Metal Chemistry*, Wiley, New York 1986, Chapter 6, p. 243.
[127] A. J. Deeming, *Adv. Organomet. Chem. 26* (1986) 1.
[128] A. J. Deeming, M. Underhill, *J. Chem. Soc. Dalton Trans. 1974*, 1415.
[129] R. J. Goudsmit, B. F. G. Johnson, J. Lewis, P. R. Raithby, M. J. Rosales, *J. Chem. Soc. Dalton Trans. 1983*, 2257.
[130] K. A. Azam, A. J. Deeming, I. P. Rothwell, *J. Chem. Soc. Dalton Trans. 1981*, 91.
[131] K. A. Azam, C. Choo Yin, A. J. Deeming, *J. Chem. Soc. Dalton Trans. 1978*, 1201.
[132] M. A. Gallop, B. F. G. Johnson, J. Lewis, A. McCamley, R. N. Perutz, *J. Chem. Soc. Chem. Commun. 1988*, 1071.
[133] H.-J. Kneuper, J. R. Shapley, *Organometallics 6* (1987) 2455.
[134] C. W. Bradford, R. S. Nyholm, G. J. Gainsford, J. M. Guss, P. R. Ireland, R. Mason, *J. Chem. Soc. Chem. Commun. 1972*, 87.
[135] G. J. Gainsford, J. M. Guss, P. R. Ireland, R. Mason, C. W. Bradford, R. S. Nyholm, *J. Organomet. Chem. 40* (1972) C70.
[136] C. W. Bradford, R. S. Nyholm, *J. Chem. Soc. Dalton Trans. 1973*, 529.
[137] M. I. Bruce, G. Shaw, F. G. A. Stone, *J. Chem. Soc. Dalton Trans. 1972*, 2094.
[138] M. I. Bruce, J. M. Guss, R. Mason, B. W. Skelton, A. H. White, *J. Organomet. Chem. 251* (1983) 261.
[139] A. J. Deeming, R. E. Kimber, M. Underhill, *J. Chem. Soc. Dalton Trans. 1973*, 2589.
[140] A. J. Deeming, I. P. Rothwell, M. B. Hursthouse, J. D. J. Becker-Dirks, *J. Chem. Soc. Dalton Trans. 1981*, 1879.
[141] A. J. Arce, A. J. Deeming, *J. Chem. Soc. Dalton Trans. 1982*, 1155.
[142] R. D. Adams, D. A. Katahira, L.-W. Yang, *Organometallics 1* (1982) 235.
[143] S. C. Brown, J. Evans, L. E. Smart, *J. Chem. Soc. Chem. Commun. 1980*, 1021; A. J. Deeming, S. E. Kabir, N. I. Powell, P. A. Bates, M. B. Hursthouse, *J. Chem. Soc. Dalton Trans. 1987*, 1529.
[144] S. A. R. Knox, B. R. Lloyd, A. G. Orpen, J. M. Viñas, M. Weber, *J. Chem. Soc. Chem. Commun. 1987*, 1498.
[145] A. J. Canty, B. F. G. Johnson, J. Lewis, *J. Organomet. Chem. 43* (1972) C35; A. J. Canty, A. J. P. Domingos, B. F. G. Johnson, J. Lewis, *J. Chem. Soc. Dalton Trans. 1973*, 2056.
[146] J. Evans, B. F. G. Johnson, J. Lewis, T. W. Matheson, *J. Organomet. Chem. 97* (1975) C16.
[147] A. J. Deeming, *J. Organomet. Chem. 150* (1978) 123.
[148] A. P. Humphries, S. A. R. Knox, *J. Chem. Soc. Dalton Trans. 1975*, 1710.
[149] R. Mason, K. M. Thomas, *J. Organomet. Chem. 43* (1972) C39.
[150] A. J. P. Domingos, B. F. G. Johnson, J. Lewis, *J. Organomet. Chem. 36* (1972) C43.
[151] M. D. Rausch, R. G. Gastinger, S. A. Gardner, R. K. Brown, J. S. Wood, *J. Am. Chem. Soc. 99* (1977) 7870.
[152] P. M. Cook, L. F. Dahl, D. W. Dickerhoof, *J. Am. Chem. Soc. 94* (1972) 5511.
[153] A. L. Balch, C. T. Hunt, C.-L. Lee, M. M. Olmstead, J. P. Farr, *J. Am. Chem. Soc. 103* (1981) 3764.
[154] S. Trofimenko, *J. Am. Chem. Soc. 93* (1971) 1808; *Inorg. Chem. 12* (1973) 1215.
[155] D. M. Roe, A. G. Massey, *J. Organomet. Chem. 23* (1970) 547.
[156] M. J. Bennett, W. A. G. Graham, R. P. Stewart, Jr., R. M. Tuggle, *Inorg. Chem. 12* (1973) 2944.
[157] H. Hart, C.-Y. Lai, G. Nwokogu, S. Shamouilian, A. Teuerstein, C. Zlotogorski, *J. Am. Chem. Soc. 102* (1980) 6649; H. Hart, S. Shamouilian, Y. Takehira, *J. Org. Chem. 46* (1981) 4427; H. Hart, S. Shamouilian, *ibid. 46* (1981) 4874; H. Hart, N. Raju, M. A. Meador, D. L. Ward, *ibid. 48* (1983) 4357.
[158] S. L. Buchwald, E. A. Lucas, J. C. Dewan, *J. Am. Chem. Soc. 109* (1987) 4396.
[159] M. A. Bennett, J. S. Drage, K. D. Griffiths, N. K. Roberts, G. B. Robertson, W. A. Wickramasinghe, *Angew. Chem. 100* (1988) 1002; *Angew. Chem. Int. Ed. Engl. 27* (1988) 941.

[160] R. A. Olofson, C. M. Dougherty, *J. Am. Chem. Soc. 95* (1973) 582.
[161] K. L. Shepard, *Tetrahedron Lett. 1975*, 3371.
[162] The first example of such a complex has been synthesized and characterized by X-ray crystallography [163]. Treatment of *cis*-[RuClMeL$_4$] (L = PMe$_3$) with C_6H_5MgBr gives *cis*-[Ru(C_6H_5)MeL$_4$], which, on heating in benzene at 110 °C, eliminates methane to give the η^2-benzyne ruthenium(0) complex [RuL$_4$(η^2-C_6H_3)] **161a**. The coordinated C-C bond length in **161a** is 1.355(3) Å. Compound **161a** resembles the d^{10} metal-benzyne complexes in its high basicity, but it also undergoes C-H and C-C activation reactions, e.g. with acetophenone it forms the cyclometalated species, $L_4\dot{R}u$-*o*-$C_6H_4\bar{C}(=\bar{C}H_2)\ddot{O}$ **161b**, presumably by elimination of C_6H_6 from an intermediate phenyl(*O*-enolate) [L_4Ru(C_6H_5){OC(CH_2)Ph}]. Remarkably, **161b** is also formed from **161a** and acetone, a reaction in which the C-C bond of acetone is cleaved and methane is eliminated.
The ion [FeC_6H_4]$^{\oplus}$ has been generated in the gas phase by reaction of $Fe^{\oplus}$ with chlorobenzene [164] and its reactions with alkanes have been studied by FT-mass spectrometry [165].
[163] J. F. Hartwig, R. A. Andersen, R. G. Bergman, *J. Am. Chem. Soc. 111* (1989) 2717.
[164] T. G. Dietz, D. S. Chatellier, D. P. Ridge, *J. Am. Chem. Soc. 100* (1978) 4905.
[165] Y. Huang, B. S. Freiser, *J. Am. Chem. Soc. 111* (1989) 2387.
[166] A first attempt to synthesize such a complex was described recently: S. L. Buchwald, E. A. Lucas, W. M. Davis, *J. Am. Chem. Soc. 111* (1989) 397.

Organic Dications: Gas Phase Experiments and Theory in Concert

By Koop Lammertsma,* Paul von Ragué Schleyer,* and Helmut Schwarz*

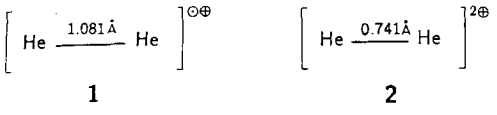
Dedicated to Professor Christoph Rüchardt on the occasion of his 60th birthday

Knowledge of structure and bonding are integral parts in the understanding of the chemistry of neutral, radicaloid and positively or negatively charged species. The interplay of molecular bonding and the inherent electrostatic repulsion in doubly-charged molecules expands our insight in the versatility of bonding in electron deficient molecules. Small organic dications are now routinely detected in the gas phase by a variety of mass spectrometric techniques. Ab initio molecular orbital theory has advanced to the stage of accurately predicting potential energy surfaces. This review highlights the symbiotic relationship between gas-phase ion and computational studies and gives a rationale for the salient bonding features in doubly-charged organic cations.

1. Introduction

Whereas polycharged species were first recorded over half a century ago,[1] only the recent developments in mass spectrometric techniques now permit organic dications to be observed routinely in the gas phase. Simultaneously, computational studies have provided an understanding of the structures and energies of these doubly charged species. Both these sources of information complement the already extensive data on the larger dications that are observable in solution.[2] This review combines the information available from the theoretical and experimental gas phase studies on the newly emerging classes of organic dications. The two approaches are complementary: mass spectrometric studies reveal the existence of small dications, whereas ab initio MO calculation (on species in isolation) provide structural details—comparisons of observed and calculated energies provide a calibration of the agreement between experiment and theory. Previous reviews focused on more specific aspects of dications.[3]

As illustrated by the recent detection of $He_2^{2\oplus}$,[4] virtually any dication can be generated in the gas phase. The smallest two-electron diatomic dication, $He_2^{2\oplus}$ has a surprisingly large 33.2 kcal/mol barrier to dissociation despite the 200 kcal/mol exothermicity.[5] This kinetic stability also is emphasized by the very short He–He bond of 0.741 Å, even 0.037 Å shorter than the H–H bond in the hydrogen molecule. The He–He distance contracts upon successive removal of electrons from the neutral He-dimer to $He_2^{\odot\oplus}$, **1**, and then to the dication **2**. The observation of $He_2^{2\oplus}$ highlights what *Pauling*[6a] already envisioned in the 1930s, as substantiated later by *Dunitz* and *Ha*,[6b] that bonding interactions can counteract strong electrostatic charge-charge repulsions sufficiently to result in kinetically stable species (Fig. 1). Consequently, the number of observable dications is virtually unlimited. Hence, we will not discuss each dication exhaustively, but will emphasize common trends. We do not consider di- and polycations based on diatomics, noble gas and other clusters, organometallics, and polycyclic aromatics, and we limit ourselves mainly to ab initio calculations, as the available semiempirical methods have not been calibrated for such species.



1 **2**

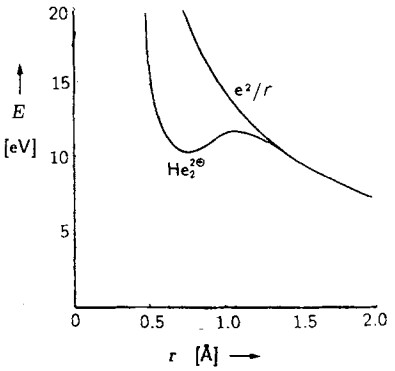


Fig. 1. The potential energy surface of $He_2^{2\oplus}$ and the Coulomb repulsion curve. [6a]

The ground states of organic dications, that have been detected in the gas phase, are revealed by theory to have remarkable properties. We discuss briefly the different mass spectrometic techniques and the theoretical methods that are commonly used. Throughout we concentrate on the formalisms of double oxidations, diprotonations, and charge-transfer complexes as bases for understanding the chemistry of gas phase dications. These can result from ionizations of monocations. Although we focus on gaseous species, implications for the dications observable under stable ion solution

[*] Prof. K. Lammertsma
Department of Chemistry, University of Alabama at Birmingham
UAB Station, Birmingham, AL 35294 (USA)
Prof. P. von R. Schleyer
Institut für Organische Chemie der Universität Erlangen-Nürnberg
D-8520 Erlangen (FRG)
Prof. H. Schwarz
Institut für Organische Chemie der Technischen Universität
Strasse des 17. Juni 135, D-1000 Berlin 12

conditions are drawn. We first document and analyze the very small dications. Then we consider the effects of substituents. A "building block" approach is used to highlight the common structural rules for organic dications.

2. Methods

The two gas phase techniques commonly employed to detect small dications are *c*harge-*s*tripping (CS) and *d*oubly *c*harged *i*on (DCI) mass spectrometry. These methods differ fundamentally in their approach, and are complemented by the charge-separation technique. This provides energetic information on metastable (decomposing) dications. Other mass spectrometric techniques (e.g., photoionization, *p*hoto*i*on-*p*hoto*i*on *c*oincidence (PIPICO), and *i*on *k*inetic *e*nergy *s*pectra (IKES)) which give or can be applied to dications are less important.

2.1. Charge-Stripping Mass Spectrometry [3d, 7, 8, 9]

This technique uses a double-focusing mass spectrometer, preferentially of reversed geometry (BE configuration). Most studies have been conducted on a VG Micromass ZAB-2F. The singly charged positive ions $M^{\oplus}$, which can be generated with a variety of ionization methods (typically *e*lectron *i*mpact, EI) or ion molecule reactions (when no suitable neutral precursors are available as for example $CH_5^{\oplus}$, $H_3O^{\oplus}$, etc.)) are mass selected by means of a magnetic field (*B*) before interacting with a target gas G (e.g., nitrogen, helium, or oxygen) in the collision cell located in the second field-free region. As the charge-stripping process [Eq. (1)] takes place in an isolated system, the energy necessary to drive the reaction is provided by the translational energy of $M^{\oplus}$ (typically several keV).

$$M^{\oplus} + G \rightarrow M^{2\oplus} + G + e^{\ominus} \quad (1)$$







Koop Lammertsma was born in Makkum, the Netherlands, in 1949. He received his M.Sc. in 1974 from the University of Groningen and his Ph.D. in organic chemistry in 1979 from the University of Amsterdam (with H. Cerfontain). After postdoctoral work with Professors F. Sondheimer, P. von R. Schleyer, and G. A. Olah, he joined the University of Alabama at Birmingham in 1983. His present research interests include the study of structures and reactivities of carbocations, electron deficient systems, strained hydrocarbons, small clusters, and lately the chemistry of phosphinidenes.

Paul von Ragué Schleyer was born in 1930 in Cleveland, Ohio, USA and was educated at Princeton University (B.A. 1951) and at Harvard University (M.A. 1956, Ph.D. 1957). He joined the Chemistry Department of Princeton University becoming Full Professor in 1965 and Eugene Higgins Professor of Chemistry in 1969. In 1976 Schleyer accepted his present position in Erlangen, West Germany. Among his many honors are the degree Honoris Causa bestowed by the Université de Lyon, France, in 1971, the Adolf von Baeyer Prize of the German Chemical Society (1986), the James Flack Norris Award in Physical Organic Chemistry of the American Chemical Society (1987), and the C.K. Ingold Medal and Lectureship of the Royal Society of Chemistry, London (1988). Schleyer is a Fellow or member of numerous scientific organizations. Seven books dealing with carbonium ions, the norbornyl cation, and ab initio molecular orbital theory, and over five hundred research publications are to his credit. His research contributions include the discovery of simple ways of synthesizing adamantane and other cage molecules by rearrangement, elucidation of solvolysis mechanisms, reactive intermediates, and a broad range of physical organic, organo-metallic, inorganic and theoretical topics. The discovery of basically new molecular structures by computer, particularly those involving lithium, is one of his major achievements.

Helmut Schwarz, born in Nickenich, Eifel, West Germany, worked for four years as a technician in chemical industry before beginning his studies at the Technical University in Berlin in 1966. In 1972 he was awarded a Ph.D. while working with F. Bohlmann and habilitated two years later. Post doctoral work with J. Seibl (Zurich), K. Biemann (MIT), and D. H. Williams (Cambridge, UK) led him to work in mass spectrometry. Since 1983 he has occupied a chair in Organic Chemistry at the Technical University in Berlin. He is co-editor of the International Journal of Mass Spectrometry and Ion Processes. He has been a guest Professor at the universities of Cambridge, Lausanne, Jerusalem and Haifa. His work on the gas phase chemistry and physics of ions has led to 400 scientific papers and has been recognized by the award of a "Dozentenstipendium" by the Fonds der Chemischen Industrie and the Otto-Klung Prize for Chemistry. In November he will receive the Otto-Baeyer Prize of Bayer AG, Leverkusen.

Charge-stripping peaks are obtained by scanning the electric sector voltage (E) around $E/2$, where E represents the electric voltage required to transmit stable $M^{\oplus}$ ions. The resulting spectra are known as $E/2$ spectra. The displacement of the peak from $E/2$ reflects the translational energy loss in the charge-stripping process and corresponds in a first approximation to the (presumably) vertical ionization energy of the monocation $M^{\oplus}$ if both $M^{\oplus}$ and $M^{2\oplus}$ are in their electronic ground states [eq. 2 and 3] and the collisions are

$$E_{obs} = (E - Q_{min})/2 \quad (2)$$

$$Q_{min} = IE(M^{\oplus} \rightarrow M^{2\oplus}) \quad (3)$$

inelastic. The minimum translational energy loss (Q_{min}) is measured from the high-energy side of this charge-stripping peak by extrapolation to the base line (Fig. 2).[7] While it

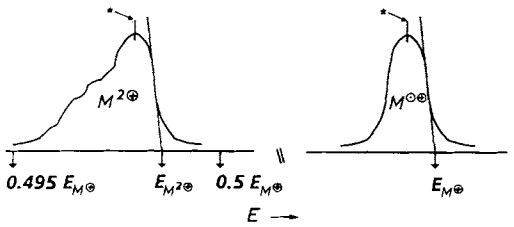


Fig. 2. Illustration of the method used to determine Q_{min} from a charge-stripping spectrum.

has been recognized that the cross-section for process (1) is affected by the nature of the collision gas, the ionization energies (IE) are considered to be independent of the collision gas used and can be compared with theoretically calculated vertical IE_v and adiabatic IE_a. Interference from singly charged ions can occur in cases in which a $M^{\oplus}$ dissociates to $(M/2)^{\oplus}$. Moreover, an experimental complication results from isotopic species due to naturally occurring isotopes. For example, high resolution mass spectrometry is required to distinguish between the $^{12}CH^{\oplus}$ and $^{13}C^{\oplus}$ cations and to make sure which "m/z 13" species is probed in the C.S. experiment (see below). The two different calibration methods that are in use for the determination of Q_{min} complicate comparisons with theoretical values. *Schwarz, Stahl,* and coworkers[3e] advocate a multiplicative calibration, whereas *Ast* and *Beynon*[3d, 7] employ an additive correction factor,

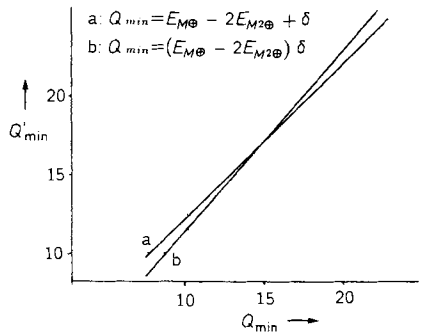


Fig. 3. Illustration of the additive a) and multiplicative b) calibration methods for determining Q_{min} values. Method (a) is used by the *Beynon/Ast* groups and method (b) by the *Stahl/Schwarz* groups. Both methods often use the value of 15.7 eV of toluene as standard for calibration.

both using toluene as calibrant with $Q_{min} = 15.7\,eV$[10] for $C_7H_8^{\odot\oplus} \rightarrow C_7H_8^{2\oplus}$. The values obtained in this manner become significantly different when the measured Q_{min} values are much larger (or much lower) than that of toluene as summarized in Figure 3. The results only are comparable when the measured Q_{min} value is similar in magnitude to that of the reference compound.

Charge-stripping mass spectrometry is a two step process in which the dications are generated in the second step through ionization of monocations that are thermally relaxed (lifetime $> 10^{-5}$ s). As a consequence, dications (like $CH_4^{2\oplus}$) can be detected that are not observable from direct double (vertical) ionization methods (EI) which may generate species above the dissociation threshold (Fig. 4).[11]

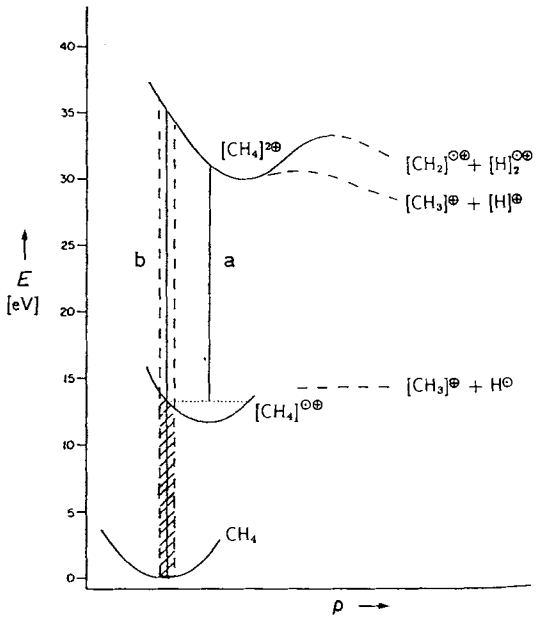


Fig. 4. Calculated MINDO/3 hypersurface for CH_4, $CH_4^{\odot\oplus}$, and $CH_4^{2\oplus}$. [11] The vertical lines represent the Franck-Condon transitions. The charge-stripping from $CH_4^{\odot\oplus}$ to $CH_4^{2\oplus}$ is indicated by a. Electron impact ionization of CH_4, shown by b gives an excited $CH_4^{2\odot}$ that lies above the dissociation asymptote.

2.2. Doubly-Charged Ion Mass Spectrometry[3d, 9b, 12, 13]

With this technique doubly charged ions, generated in the ion source, are fully accelerated into the first field-free region where the dications $M^{2\oplus}$ undergo single electron transfer with a target gas G [Eq. (4)].

$$M^{2\oplus} + G \rightarrow M^{\oplus} + G^{\oplus} \quad (4)$$

In this collision the momentum of the charged species is maintained. Thus, the resulting monocation product $M^{\oplus}$ has essentially the same velocity as the fast dication reactant $M^{2\oplus}$. The fast singly charged ions are transmitted through an electric sector operated at twice the normal voltage ($2E$) and subsequently through the magnetic sector for momentum analysis. The electric sector, set at $2E$, acts as a kinetic filter and discriminates against fast singly charged ions $M^{\oplus}$, formed by electron impact, and unreacted dications. A variant of this technique employs a reversed geometry instrument where the charge exchange reaction [Eq. (4)] occurs in

the second field-free region to momentum-analyzed ions. Similarly, the electric sector is set at twice the normal value required to transmit ions. The results are known as $2E$ spectra. A typical example is shown in Figure 5. *Beynon* has

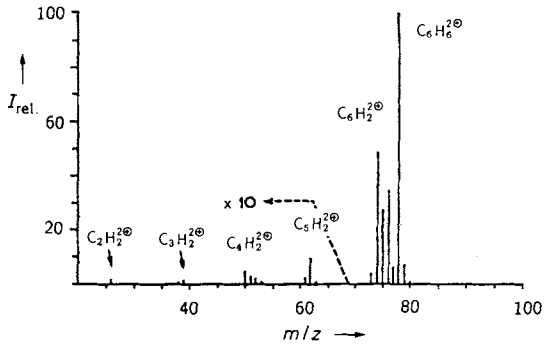


Fig. 5. Doubly-charged ion mass spectrum of benzene. [13b]

advocated the use of charge exchange for higher resolution of charge-stripping peaks in a multi-sector mass spectrometer.[14]

2.3. Charge Separation Mass Spectrometry[3d, 13a, 15]

Unimolecular fragmentations of dications [Eq. (5)] may occur in the second field-free region between the magnet and the electrostatic sector. Such processes ("Coulomb explosions"[*]) can be recorded by scanning the voltage across the sector from E to $2E$. The charge-separation peaks are typically steep sided and severely dished (Fig. 6). The width of a dished metastable peak is determined by the spread of total translational energy release E_T (in eV) of the ions. The release of this kinetic energy has been related to the release of Coulombic repulsion between two point charges in the fragmenting dication, separated by the intercharge distance R. Although the calculated value of R [Eq. (6)] is fictitious because of charge delocalization, it is inter alia used to discriminate between linear and cyclic dication structures. It must also be recognized that the determined kinetic energy release E_T refers to the transition state for the Coulomb explosion and may not necessarily be related to a ground state species.



Fig. 6. Unimolecular Mass-Selected-Ion-Kinetic-Energy (MIKE) spectrum of $C_4H_2^{2\oplus}$ ions. Peaks are due to charge-separation reactions: a–a from reaction $C_4H_2^{2\oplus} \rightarrow C_3H_2^{\odot\oplus} + C^{\odot\oplus}$ and b–b from reaction $C_4H_2^{2\oplus} \rightarrow C_3H^{\oplus} + CH^{\oplus}$.

[*] The "Coulomb explosion" in mass spectrometry should not be confused with the physical phenomena that one observes when high speed charged particles (with kinetic energy on the order of MeV) are accelerated through a thin solid film, at which process all the electrons are stripped from the nucleus. The resulting aggregate of positive ions (lifetime $<10^{-14}$ s) explodes due to the enormous Coulomb repulsion. All the velocity components of all the emerging fragment ions are measured precisely with a detector. From this on obtains a "picture" of $M^{\oplus}$ before the charge stripping. The most impressive example is that of $C_2H_3^{\oplus}$; it can be shown that the vinyl cation $H_2C=\overset{\oplus}{C}H$ has the non-classical bridged structure $HC(H^{\oplus})=CH$ instead of the open structure. For reviews see Z. Vagar, R. Naaman, E. P. Kanter in J. P. Maier (Ed.): *Ion and Cluster Ion Spectroscopy and Structure*, Elsevier, Amsterdam 1989, p. 1–26; *Science (Washington) 244* (1989) 426.

$$M^{2\oplus} \rightarrow M_1^{\oplus} + M_2^{\oplus} \quad (5)$$

$$R \text{ (in Å)} = 14.40/E_T \text{ (in eV)} \quad (6)$$

2.4. Computational Methods

Most but not all of the ab initio calculations referred to in this review have been carried out with the GAUSSIAN series of programs, developed by *Pople* et al.[16] The strategy for ab initio calculations[16] and the available basis sets[16, 17] are well documented. However, a short synopsis may be useful. For electron deficient species, the minimal STO-3G basis set is inadequate. Typically, most studies start with a split-valence basis set like 3-21G at the Restricted (for singlets) or Unrestricted (for triplets) Hartree-Fock (HF) level of theory. The more flexible 6-31G* basis set includes valence d-functions to provide for polarization of the "heavy" (non-hydrogen) elements. The 6-31G** basis set also includes p-functions to describe H-polarization. The most complete basis set we refer to is 6-311G**, which has single zeta core, triple zeta valence, and polarization functions on all atoms.

Of the various ways to include the effect of electron correlation in energy evaluations, we refer mainly to the use of Møller-Plesset (MP) perturbation theory. The most common level is MP2, this refers to the second order treatment which occasionally is included in geometry optimizations. However, only single point calculations are feasible with MP4(SDTQ); this full fourth order treatment includes contributions from single, double, triple, and quadruple substitutions. Such calculations are denoted MP4(SDTQ)/6-311G**//HF/6-31G*, where "//" means "at the geometry of."

Generally, geometries are fully optimized at the (Un)Restricted Hartree-Fock level under specified symmetry constraints. Throughout the text we refer to HF/6-31G* optimized geometries unless indicated otherwise. A geometry is fully characterized as an equilibrium structure (or minimum) if the Hessian (force constant) matrix of its stationary point (identified by a gradient of zero) has only positive eigenvalues; such a structure has only real harmonic frequencies. A transition structure is characterized by one imaginary frequency, whose normal mode indicates the reaction coordinate.

3. Observed and Calculated Gaseous Dications

In order to appreciate the structural features that are common to gaseous dications, we focus on small carbodications.

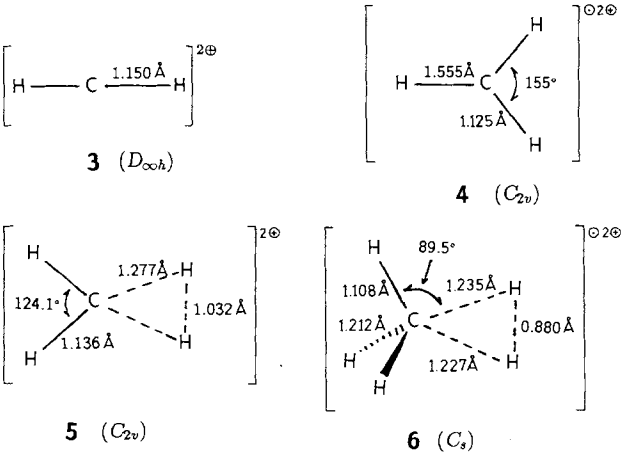
Virtually all are known. Both the larger carbodications and the heterodications display similar structural trends.

3.1. One Heavy Atom Dications, $XH_n^{2\oplus}$

Described in the following and listed in Table 1 are the observed and calculated dication hydrides containing the heavy elements C, Si, N, P, O, and S.

3.1.1. C_1-Dications

Charge-stripping of methane[7, 8, 18] produces the $CH_4^{2\oplus}$ **5**, $CH_3^{\odot 2\oplus}$ **4**, $CH_2^{2\oplus}$ **3**, and $C^{2\oplus}$ dications, but not $CH^{\odot 2\oplus}$. In contrast to the charge-stripping (and PIPICO)[19] experiments, the $2E$ spectrum[11] of methane does not show a trace of its $CH_4^{2\oplus}$ dication. Figure 4 presents a rationale for this observation (see also section 2.1.). Ionization of the methonium ion $CH_5^{\oplus}$ leads to $CH_5^{\odot 2\oplus}$ **6**.[20] The experimental and



theoretical ionization energies (Q_{min}) of the corresponding monocations are given in Table 1, in which the barriers for deprotonation and thermodynamic stabilities of the dications are also tabulated. The reported data for $CH^{\odot 2\oplus}$, a controversial species (see below), also are given.

The experimental and theoretical adiabatic ionization energies listed in Table 1 appear to be in good agreement. Differences can be attributed to the occurrence of excited monocations which give lower experimental values. The discrepancies in most experimental ionization energies result from different calibration methods (see comment in section 2.1.).

The odd-electron species $CH^{\odot 2\oplus}$ is the smallest and most controversial diatomic carbodication. Initial studies by *Beynon* et al. claimed its observation by charge-transfer using N_2 as collision gas.[7, 18] However, the first theoretical study showed the $CH^{\odot 2\oplus}$ energy potential to be repulsive.[21] *Mathur* et al.[22] have subsequently supported the experimental finding. *Wetmore* et al.'s theoretical study[23] using multireference CI-DZP calculations gave a kinetic stability for $CH^{\odot 2\oplus}$ of 0.01 eV. However, *Koch* et al. (using O_2, which is known to have the highest cross-section for charge stripping) have found no experimental evidence for $CH^{\odot 2\oplus}$ nor did they find a minimum on the potential energy surface of the three lowest $^2\Sigma^{\oplus}$ states of $CH^{\odot 2\oplus}$ using CISD (five electrons correlated) on the large 6s6p3d1f/4s3p1d Slater-type basis set.[24] They conclude that there is no metastable $CH^{\odot 2\oplus}$ radical dication and attribute the earlier erroneous

Table 1. Theoretical (IE_a) and experimental (Q_{min}) ionization energies of $XH_n^{\oplus}$ (n = 1–6) cations and the kinetic and thermodynamic stabilities (in kcal/mol) toward deprotonation of the corresponding dications $XH_n^{2\oplus}$.

Species	Q_{min} [eV]	[a]	Lit.	IE_a [eV]	Deprotonation Barrier	Deprotonation Stability	Lit.
$CH^{\odot 2\oplus}$ [b]	22.8	–	[7, 8, 24]	–	–	–	[24]
$CH_2^{2\oplus}$	19.6		[7, 8]	21.1	30.8	−71.4	[21]
$CH_3^{\odot 2\oplus}$	18.9		[7, 8]	23.5	2.9	−108.5	[21]
$CH_4^{2\oplus}$	17.9	18.9	[7, 8, 20]	19.7			
$CH_5^{\odot 2\oplus}$	20.3	21.6	[7, 8, 20]	21.9	23.7	−86.6	[20]
$CH_6^{2\oplus}$					35.4	−63.0	[27]
$SiH^{\odot 2\oplus}$	18.7	18.8	[33, 37a]	18.2	24.7	−33.0	[37c]
$SiH_2^{2\oplus}$	17.7	16.7	[33, 37a]	16.5		−20.0	[37a]
$SiH_3^{\odot 2\oplus}$		15.4	[37a]	15.9		−48.0	[37a]
$SiH_4^{2\oplus}$						−26.1	[37a]
$SiH_5^{\odot 2\oplus}$						−13.4	[37a]
$NH^{2\oplus}$ [b]	25.0		[8]	26.4	2.2	−136.3	[39]
$NH_2^{\odot 2\oplus}$	23.3		[8]	23.2	9.8	−108.1	[39]
$NH_3^{2\oplus}$	22.2		[8]	23.3	35.2	−62.9	[39]
$NH_4^{\odot 2\oplus}$	24.5		[8]	24.0	7.8	−116.5	[39]
$PH^{2\oplus}$				18.7	64.5	−16.9	[38a]
$PH_2^{\odot 2\oplus}$				19.2		−51.6	[38a]
$PH_3^{2\oplus}$				18.0	60.9	−25.9	[38a]
$PH_4^{\odot 2\oplus}$				20.3	17.0	−69.0	[38a]
$OH^{\odot 2\oplus}$	29.0		[8]	–			
$OH_2^{2\oplus}$	23.4		[8]	23.5/24.5	1.5	−128.8	[40a]
$OH_3^{\odot 2\oplus}$	22.5	23.5	[8, 40a]	23.2	20.7	−89.6	[40a]
$OH_4^{2\oplus}$					[39].6	−59.0	[40]
$SH^{\odot 2\oplus}$	21.2		[8]	21.9	36.3	−69.7	[38a]
$SH_2^{2\oplus}$	21.0		[8]	20.8	[39].3	−61.8	[38a]
$SH_3^{\odot 2\oplus}$	21.4		[8]	19.6	40.5	−53.5	[38a]
$SH_4^{2\oplus}$							[41]

[a] First column: 5 keV accelerating voltage, N_2 as collision gas, *Beynon/Ast* calibration. Second column: 8 KeV, O_2, and *Stahl/Schwarz* calibration. [b] See text.

conclusion to experimental artifacts possibly led by incomplete separation of the isotopic $^{13}C^{\oplus}$ and $^{12}CH^{\oplus}$ species in the earlier experiments.

Oxidation of the methyl cation leads to $CH_3^{\odot 2\oplus}$ **4** with a C_{2v} geometry, that can be viewed as a complex between $CH_2^{2\oplus}$ and a hydrogen atom.[21] Charge-stripping of $CH_5^{\oplus}$, the parent "non-classical" ion, gives the methonium radical dication $CH_5^{\odot 2\oplus}$ with a similar C_s geometry.[20]

Because of the two-electron difference, dications display structural trends that differ from their neutral precursors. This is already evident in the parent C_1-dications. For example, the methylene dication, $CH_2^{2\oplus}$ **3**, is linear ($D_{\infty h}$) with a divalent, dicoordinate sp-hybridized carbon atom[21] similar to the isoelectronic BeH_2, whereas singlet methylene, $:CH_2$ (C_{2v}), contains a sp^2-carbon. The methane dication, $CH_4^{2\oplus}$ **5**, has a planar C_{2v} symmetry with a planar, trivalent, tetracoordinated "sp^2-hybridized" carbon and an empty p-orbital orthogonal to the plane of the molecule,[25] while neutral methane (T_d) is sp^3-hybridized. A molecular orbital diagram (Fig. 7) shows that removal of two electrons from the triply degenerate methane HOMO results in a planar dication structure due to the Jahn–Teller effect. Because there are only six valence electrons available to bond four hydrogens to carbon, the best bonding arrangement results with two regular CH bonds and one 3 center 2 electron (3c–2e) CHH bond. Consequently, the methane dication can be viewed as a $CH_2^{2\oplus}$–H_2 complex where the hydrogen molecule interacts in an "side-on" fashion with one of the vacant p-orbitals of the methylene dication.[25] Earlier studies at lower theoretical levels indicated a square planar D_{4h} structure for $CH_4^{2\oplus}$[21, 26].

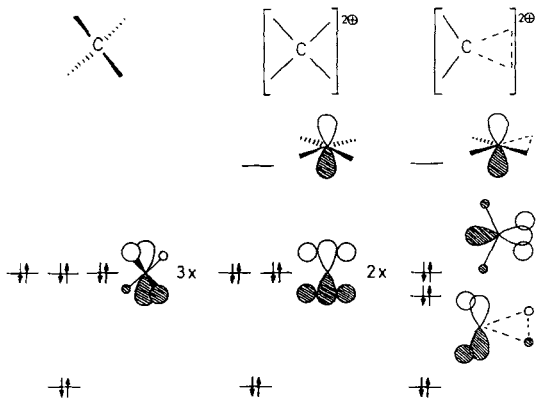
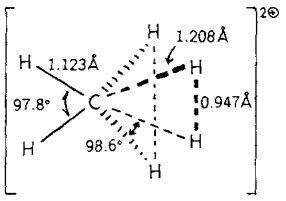


Fig. 7. MO diagram of methane and the planar D_{4h} and C_{2v} dications.

Both $CH_2^{2\oplus}$ and $CH_4^{2\oplus}$ units can be used as building blocks in the structural analysis of larger dications, as the ylid dications and the cation-substituted methonium ions, (see section 3.3.6). The methane dication, the simplest example of anti-van't Hoff stereochemistry, already represents a $CH_2^{2\oplus}$-H_2 complex. Diprotonated methane $CH_6^{2\oplus}$ **7** contains

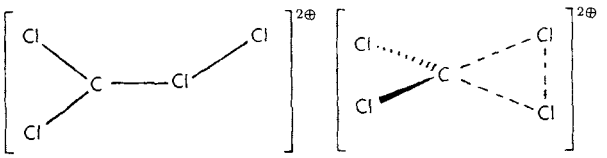


7 (C_s)

a tetravalent, hexacoordinate sp^3-hybridized carbon atom with two elongated 3c–2e ligands and can be pictured as a $CH_2^{2\oplus}$ dication complexed with two hydrogen molecules.[27] $CH_6^{2\oplus}$ has not been observed experimentally. As $CH_4^{2\oplus}$ and $CH_6^{2\oplus}$ illustrate, there is no simple monocation analogy with regard to "classical" and "non-classical" carbodications.

3.1.2. Halogenated C_1-Dications

Oxidation of carbon tetrachloride to its dication, accomplished by electron impact (EI) ionization, has been shown by *m*ass-selected *i*on *k*inetic *e*nergy spectrometry (MIKE).[28a] In sharp contrast to the methane dication which prefers a planar $CH_2^{2\oplus}$–H_2 complex conformation, planar $CCl_4^{2\oplus}$ does not correspond to a stationary point. The planar "end-on" complex between $CCl_2^{2\oplus}$ and Cl_2 **8** is 39 kcal/mol more stable than $CCl_4^{2\oplus}$ **9** which represents a transition structure (C_{2v}).[29] At HF/4-31G the ylid dication $Cl_2CClCl^{2\oplus}$ **8** is the global $CCl_4^{2\oplus}$ minimum, but appears to be very unstable thermodynamically (> 100 kcal/mol)

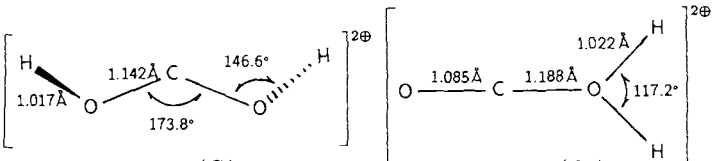


8 (C_s) **9** (C_{2v})

toward all fragmentations.[29] Interestingly, $CCl_4^{2\oplus}$ can not be generated by charge-stripping from the $CCl_4^{\odot\oplus}$ radical cation (distorted C_{2v}) nor from the $Cl_2CClCl^{\odot\oplus}$ distonic radical cation that is generated by the decarbonylation of $CCl_3COCl^{\oplus}$.[28] However, a double charge transfer experiment gave a double ionization energy for CCl_4 of 29.3 eV.[30]

The $CCl_3^{\odot 2\oplus}$ and $CCl_2^{2\oplus}$ dications have been observed in several EI studies.[31] Their appearance energies (AE) have been determined to be 30.4 and 31.8 eV, respectively.[31a] The coincidence method has been applied to the $CCl_4^{2\oplus}$ and $CF_4^{2\oplus}$ dications.[32] The latter shows three dissociations, e.g. the fragmentation to $CF_3^{\oplus} + F^{\oplus}$ releases 5.0 eV of kinetic energy. Similarly, the $CH_3I^{2\oplus}$ dication releases 5.1 eV kinetic energy during the dissociation into $CH_3^{\oplus} + I^{\oplus}$.

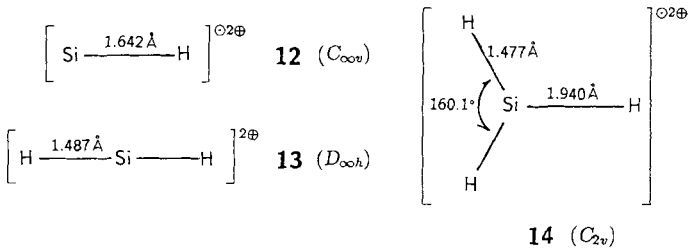
A variety of halogenated $CX^{\odot 2\oplus}$ and $CX_2^{2\oplus}$ dications (X = F, Cl, Br, and I) has been observed by charge-stripping.[33] The bond lengths in these $D_{\infty h}$ ground states are remarkably short,[34] but relatively long in the transition structures for dissociation.[35] The C–F bond of 1.146 Å (MP2/6-31G*) in $CF^{\odot 2\oplus}$ is extremely short.[34] Similarly, the C–F bond of 1.166 Å in $CF_2^{2\oplus}$ is 0.149 Å shorter than in neutral CF_2. Also the C–O bonds in the dihydroxycarbene dication $C(OH)_2^{2\oplus}$ are relatively short (1.142 Å).[36] Comparison with *neutral* $C(OH)_2$ is appropriate. This structure **10** has a near linear OCO geometry and is 11 kcal/mol (MP4/6-311G**) more stable than the H_2O–CO dication complex **11**. No experimental data on $CH_2O_2^{2\oplus}$ have been reported.



10 (C_2) **11** (C_{2v})

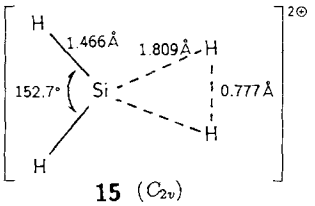
3.1.3. Heterodications

Charge-stripping experiments have afforded the silicodications $SiH^{\odot 2\oplus}$ **12**, $SiH_2^{2\oplus}$ **13** and $SiH_3^{\odot 2\oplus}$ **14**.[33, 37] In sharp contrast to $CH^{\odot 2\oplus}$, the $SiH^{\odot 2\oplus}$ radical dication has a remarkable kinetic stability toward deprotonation of

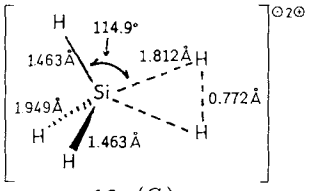


12 ($C_{\infty v}$) **13** ($D_{\infty h}$) **14** (C_{2v})

1.06 eV as calculated by MRDCI (multireference CI) and CASSCF (*c*omplete *a*ctive *s*pace SCF).[37c] As a result of the lower electronegativity and higher polarizability of silicon, the calculated (thermodynamic) deprotonation energies of the silicon dications are markedly less exothermic than that of the corresponding carbodications.[37a] The $SiH_4^{2\oplus}$ **15** and $SiH_5^{\odot 2\oplus}$ **16** dications are kinetically stable, but have not been



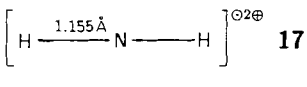
15 (C_{2v})



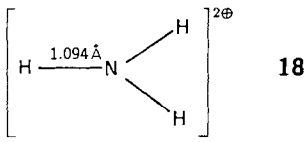
16 (C_1)

observed in the gas phase due to lack of suitable precursor ions. Both dications can be viewed as hydrogen complexes of $SiH_2^{2\oplus}$ and of $SiH_3^{2\oplus}$, respectively,[37a] having sets of short two electron and of long 3c–2e Si–H bonds.

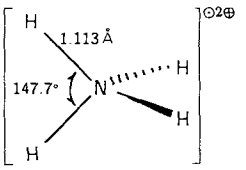
Of the $NH_n^{2\oplus}$ series, only the $NH_2^{\odot 2\oplus}$ **17** and $NH_3^{2\oplus}$ **18** dications are accessible by charge-transfer mass spectrometry.[8, 38] $NH^{2\oplus}$ has a repulsive potential energy surface.[38, 39] The ammonium dication, $NH_4^{\odot 2\oplus}$ **19**, is kinetically stable, but vertical ionization leads to an energy state above the threshold for deprotonation.[38, 39] In contrast to the $NH_n^{2\oplus}$ dications, no experimental data are available for $PH_n^{2\oplus}$. A theoretical study shows that all these phosphodications (n = 1–4, (**20**–**23**)) are kinetically stable, with a deprotonation barrier for $PH^{2\oplus}$ as high as 64.5 kcal/mol.[38a] Also the $NH_5^{2\oplus}$ (C_{4v}) and $PH_5^{2\oplus}$ (C_s) are calculated to be kinetically stable species.[39b]



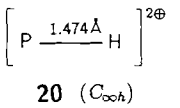
17 ($D_{\infty h}$)



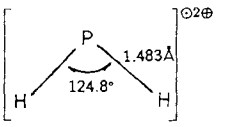
18 (D_{3h})



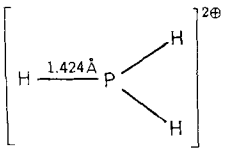
19 (D_{2d})



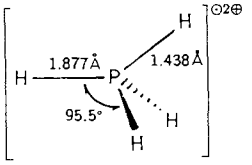
20 ($C_{\infty h}$)



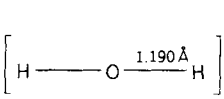
21 (C_{2v})



22 (D_{3h})

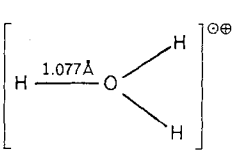


23 (C_{3v})

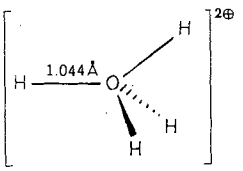


(triplet)

24 ($D_{\infty h}$)

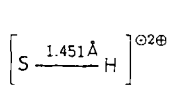


25 (D_{3h})

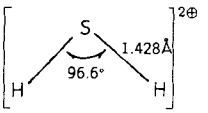


26 (T_d)

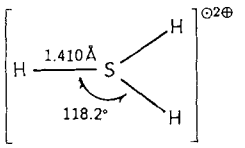
it has eluded gas phase detection due to the lack of a suitable precursor, but was inferred from H/D exchange in the protonation of $H_3O^{\oplus}$ in super acid media.[40b] The diatomic $OH^{\odot 2\oplus}$ has a repulsive potential energy surface.[38a, 40a] Similarly, evidence has been presented for the existence of $SH_4^{2\oplus}$ **30** under stable-ion solution conditions[41] and $SH_n^{2\oplus}$ (n = 1–3, (**27**–**29**)) in charge-stripping experiments.[8] All sulfodications have high barriers for deprotonation.[38a, 41]



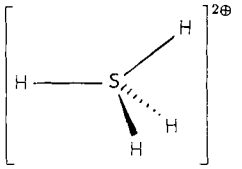
27 ($C_{\infty h}$)



28 (C_{2v})



29 (C_{3v})



30 (T_d)

3.2. Two Heavy Atom Dications

This section is mainly limited to carbon based dications. Few other two heavy atom systems have been studied.

3.2.1. C_2-Dications

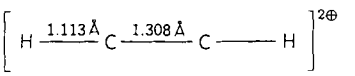
The $C_2H_n^{2\oplus}$ dications with n = 1–6 have been observed in the gas phase by charge-stripping from ethane and ethyl halides.[7, 18] The second ionization energies Q_{min} ($M^{\oplus} \rightarrow M^{2\oplus}$) are given in Table 2.

Table 2. Experimental (Q_{min}) ionization energies of C_2-cations and theoretical stabilities (in kcal/mol) of the corresponding dications.

Monocations	Q_{min} [eV] [a]		Dications	Deprotonation Barrier	Deprotonation Stability
$C_2H^{\oplus}$	20.4	21.6	$C_2H^{2\oplus}$		
$C_2H_2^{\odot\oplus}$	20.5	20.8	$C_2H_2^{2\oplus}$	65	−9.8 [b]
$C_2H_3^{\oplus}$	20.1	21.3	$C_2H_3^{\odot 2\oplus}$		
$C_2H_4^{\odot\oplus}$	17.8	20.0	$C_2H_4^{2\oplus}$	69	−16 [c]
$C_2H_5^{\oplus}$	19.1	20.2	$C_2H_5^{\odot 2\oplus}$		
$C_2H_6^{\odot\oplus}$	19.4	18.4	$C_2H_6^{2\oplus}$	57	−105 [d]
$C_2H_7^{\oplus}$	20.5	–	$C_2H_8^{2\oplus}$	–	−100 [e]

[a] First column: 5 keV accelerating voltage, N_2 as collision gas. *Beynon*'s calibration. [7, 18, 45, and 49] Second column: 8 KeV, O_2, *Stahl*'s calibration, unpublished data by *D. Stahl* and [47]. [b] Ref. [42]. [c] Ref. [43]. [d] Ref. [48], the barrier for demethylation is 32 kcal/mol (MP4/6-311G**). [e] Ref. [27b].

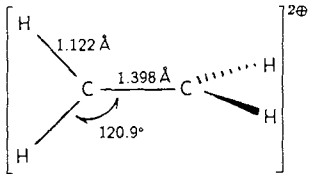
The acetylene dication $C_2H_2^{2\oplus}$ **31** is linear with a triplet electronic configuration and can be viewed as dioxidized acetylene, with oxidation occurring from its degenerate π-or-



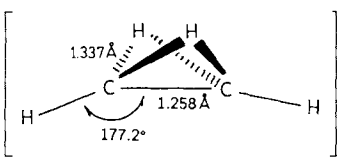
31 ($D_{\infty h}$)

bitals.[42] The short C–C bond length of 1.308 Å (HF/6-31G*) in the $C_2H_2^{2\oplus}$ dication is only 0.123 Å longer than that in neutral acetylene. The dication has a higher barrier of 62 kcal/mol deprotonation, which is only 9.8 kcal/mol exothermic.

The ethylene dication $C_2H_4^{2\oplus}$ (**32**, D_{2d}) also has a relatively short C–C single bond, 1.398 Å (MP2/6-31G*).[43] In the planar form this bond lengthens to 1.587 Å and the energy increases by 28 kcal/mol. The short C–C bond results from significant hyperconjugation of each monocation center with its neighboring CH_2 group i.e., *cross-hyperconjugation*.[3a] This effect is maximized in the doubly-H-bridged structure **33**, which can be viewed as diprotonated acetylene; the C–C bond length is 1.258 Å. However, this non-classical species is 12 kcal/mol (MP4/6-311G**) less stable than the classical D_{2d} isomer.[43c,d] The hyperconjugative stabilization in the ethylidene dication CH_3–$CH^{2\oplus}$ (**34**, C_{3v}) also results in a short C–C single bond distance, 1.297 Å,[43c,d] although this species is 22 kcal/mol higher in energy.

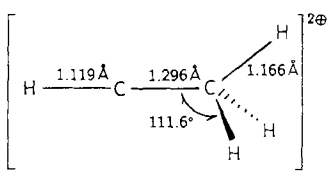


32 (D_{2d})



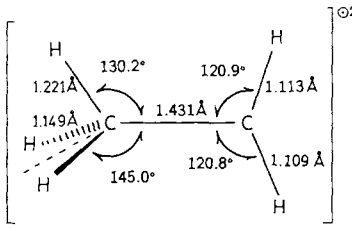
33 (C_{2v})

∠HCCH=104.3°

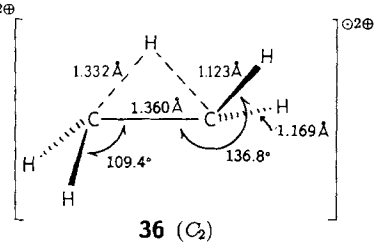


34 (C_{3v})

The ethyl dication $C_2H_5^{\odot 2\oplus}$ **35** has an open (classical) structure with a C–C bond length of 1.431 Å (MP2/6-31G*), this is 6.5 kcal/mol more stable than the hydrogen-bridged (nonclassical) transition structure **36**.[44] The calculated[44] second adiabatic ionization energy of 19.7 eV is in reasonable agreement with the experimental[7,45] values of 19.1 and 20.2 eV.

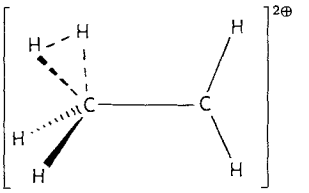


35 (C_s)

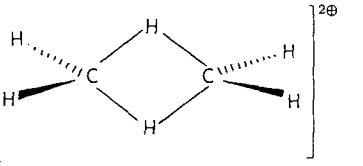


36 (C_2)

The ethane dication $C_2H_6^{2\oplus}$ has been the subject of several theoretical studies.[27b,46] Charge stripping of the ethane cation radical with O_2 (but not N_2)[7,45] as collision gas resulted in the detection of a minute amount of $C_2H_6^{2\oplus}$.[47] Although it has been argued that the observed species is $^{13}CCH_5^{\odot 2\oplus}$,[45b] the detection of both these dications has now been achieved.[48] Two $C_2H_6^{2\oplus}$ minima have been identified by theory.[27b,46,48] The $C_2H_6^{2\oplus}$ dication was observed in a collision-induced MIKE spectrum of $C_2H_6^{\odot\oplus}$; an IE of 19.4 eV was reported.[49] The most stable $C_2H_6^{2\oplus}$ structure is a carbenium-carbonium dication **37**, which can be viewed as a hydrogen molecule complex of the ethylene (D_{2d}) dication **32**.[27b] This isomer is 12 kcal/mol (MP4/6-311G**) more stable than the "diborane" form **38**. The energetically preferred pathway for dissociation of the ethane dication $C_2H_6^{2\oplus}$ is homolytic cleavage into the two methyl cations ($\Delta\Delta H_f^\circ$ = 32 kcal/mol). It is likely that the process involves the diborane structure.[48] The deprotonation barrier for this dication is much higher, 52 kcal/mol.



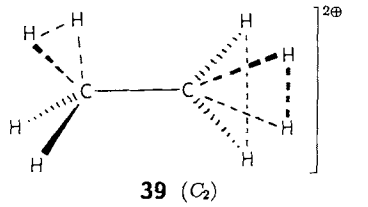
37 (C_s)



38 (D_{2h})

The $C_2H_7^{\odot 2\oplus}$ radical dication has been observed in a collision-induced MIKE spectrum of $C_2H_7^{\oplus}$. An ionization energy of 20.5 eV is reported.[49] No theoretical data are available on $C_2H_7^{\odot 2\oplus}$.

Diprotonated ethane, $C_2H_8^{2\oplus}$ **39**, has only been studied theoretically.[27b] Its structure resembles a di-hydrogen complex of the ethylene dication ($C_2H_4^{2\oplus}$, D_{2d}, **32**). The likely dissociation route is the formation of $CH_5^{\oplus}$ + $CH_3^{\oplus}$.



39 (C_2)

3.2.2. *Halogenated C_2-Dications*

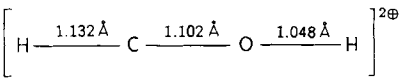
Several fluoro substituted ethylene dications $C_2H_nF_{4-n}$ (n = 0–3) have been observed and have been studied by theory.[50] The measured second ionization energies (Q_{min})[50c] are for some systems in reasonable agreement with the theoretical values[50a] (given in parentheses); 18.7 (19.1) eV for $H_2CCHF^{\odot\oplus}$, 18.7 (19.0) eV for $H_2CCF_2^{\odot\oplus}$, 20.4 (18.4) eV for $HFCCF_2^{\odot\oplus}$, and 19.0 (18.2) eV for $F_2CCF_2^{\odot\oplus}$. In contrast with the ethylene dication, $C_2F_4^{2\oplus}$ prefers the planar D_{2h} structure over the D_{2d} form by 2.3 kcal/mol.[50a,b] Its long C–C and short C–F bond lengths

of 1.587 and 1.199 Å, respectively, result from effective interactions between the fluorine lone pairs and the cationic centers.

3.2.3. Substituted Methylene Dications, $HCX^{2\oplus}$

The methyl derivative of the doubly charged methylene carbene, the ethylidene dication $HCCH_3^{2\oplus}$ **34**[43] was discussed above.

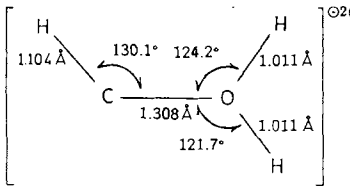
The hydroxymethylene dication $H–C–OH^{2\oplus}$ **40**, but not the isomeric formaldehyde dication $H_2CO^{2\oplus}$, has been ob-



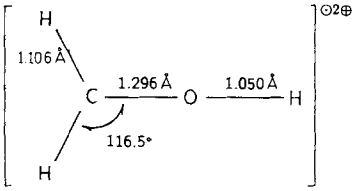
40 ($C_{\infty h}$)

served in the gas phase.[51] The calculated ionization energies[52] of 18.9 (IE_v, vertical) and 17.2 (IE_a, adiabatic) eV are in reasonable agreement with the experimental Q_{min} value of 17.7 eV.[51] Theory confirms dication **40** to be the global minimum with a 20 kcal/mol barrier for deprotonation to $H–CO^{\oplus}$.[52] The intercharge distance R for this process is 4.0 Å as estimated from $E_T = 3.6$ eV.[51] We note that the calculated H,H-separation in the corresponding transition structure is 4.104 Å at MP2/6-31G*.[52]

Although the oxoniomethylene radical dication $H–C–OH_2^{\odot 2\oplus}$ **41** is 22.7 kcal/mol (MP2/6-31G**) more stable than the hydroxymethyl radical dication $H_2C–OH^{\odot 2\oplus}$ **42**,



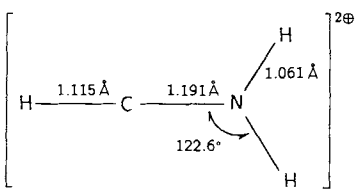
41 (C_s)



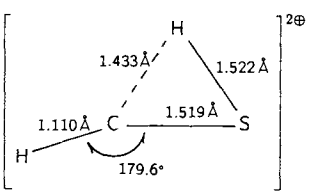
42 (C_{2v})

they are separated by a barrier of 24 kcal/mol. This prevents rapid interconversion.[53a] In fact, only the higher energy isomer is observed in the charge stripping of $H_2C–OH^{\oplus}$. The experimental Q_{min} of 22.5 eV, is in good agreement with the theoretical ionization energy, $IE_v = 22.2$ eV.[53a]

The most stable $H_3CN^{2\oplus}$ species, the aminomethylene dication $H–C–NH_2^{2\oplus}$ **43**, resides in a deep potential well. The barrier for deprotonation is 42 kcal/mol (MP4/6-311G**).[53b] Its estimated ionization energies are IE_v = 18.7 eV und IE_a = 17.3 eV, but due to the lack of a suitable precursor no experimental data are available. The halogenated carbene dications $H–C–F^{2\oplus}$ (C–F = 1.138 Å, IE_v =



43 (C_{2v})



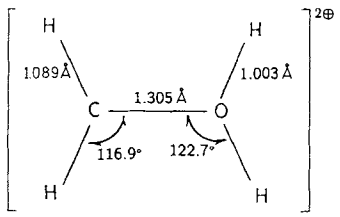
44 (C_s)

21.0 eV), $HC–Cl^{2\oplus}$ (C–Cl = 1.459 Å, IE_v = 17.8 eV), and the H-bridged $CH_2S^{2\oplus}$ **44** are predicted by theory (MP3/6-31G**) to be experimentally observable.[43d]

3.2.4. Ylid Dications, $H_2C–XH^{2\oplus}$

Structures of the type $H_2C–XH^{2\oplus}$ (X = halogen, OH, SH, NH_2) can be viewed as dioxidized ylids. Formal removal of the free electron pair of the ylid carbon strengthens the bond between the carbon and the heteroatom. While the interaction between methylene and XH in the neutral ylid is at best weak,[54] the dication strongly prefers a tight structure.

The $CH_4O^{2\oplus}$ ylid dication results from charge-stripping of $H_2COH_2^{\odot\oplus}$,[55] and also from the methanol radical cation $CH_3OH^{\odot\oplus}$, if oxygen is used as collision gas.[55c] The $CH_3OH^{2\oplus}$ dication is purely repulsive.[55c] The theoretical vertical ionization energy for $H_2COH_2^{\odot\oplus}$, 16.6 eV, is in good agreement with the experimental Q_{min} value of 16.5 eV.[55c] A short C–O bond length of 1.314 Å (MP2/6-31G*) is calculated for this planar methyleneoxonium dication **45**,[56] which



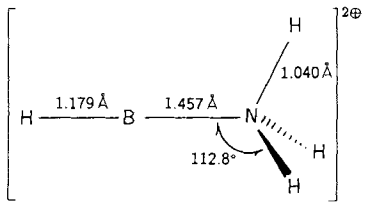
45 (C_{2v})

is isoelectronic with ethylene. In contrast, the C–O distance in the hydrated methylene ylid (C_s) is 1.805 Å (MP2/6-31G*).[54c]

Vertical ionization energies (Q_{min}) have also been obtained by charge-stripping experiments[55c] and theory[56] for related ylids. They are, (with the theoretical values in parentheses): 19.8 (15.7) eV for $H_2CSH_2^{\odot\oplus}$, 18.9 (16.2) eV for $H_2CNH_3^{\odot\oplus}$, 17.9 (18.8) eV for $H_2CFH^{\odot\oplus}$, 17.5 (17.2) for $H_2CClH^{\odot\oplus}$, 17.6 eV for $H_2CBrH^{\odot\oplus}$, and 16.3 eV for $H_2ClH^{\odot\oplus}$. The discrepancies between the theoretical and experimental data for the sulfonium and ammonium ylids are significant and are as yet unexplained. Theoretical studies show that these ylid dications have high barriers for both deprotonation and homolytic cleavage to $CH_2^{\odot\oplus} + XH^{\odot\oplus}$. The HF/6-31G* calculated C–X bond distances are 1.420 Å for $H_2C–NH_3^{2\oplus}$, 1.738 Å for $H_2C–SH_2^{2\oplus}$, 1.348 Å $H_2C–FH^{2\oplus}$, and 1.673 Å for $H_2C–ClH^{2\oplus}$.[56] The bond lengths in all these dications are shorter than in the neutral ylids. The calculated phosphonium ylid dication (C–P = 1.879 Å)[56] has not yet been observed experimentally.

3.2.5. Heterodications

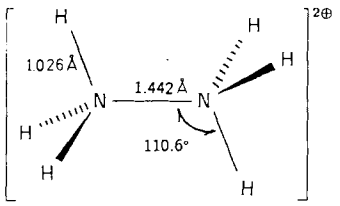
Aminoborane is isoelectronic with ethylene. Charge-stripping shows the formation of a $BNH_4^{2\oplus}$ dication from the radical cation precursor. The observed Q_{min} value of 15.2 eV is in reasonable agreement with the IE_v value of 15.8 eV (MP4/6-311G**) calculated for the ammonia borene $H_3NBH^{2\oplus}$ **46**; the 0.6 eV energy difference results since oxi-



46 (C_{3v})

dation occurs from the excited aminoborene $HB{-}NH_3^{\odot\oplus}$.[57] The structural preference for $H_3N{-}BH^{2\oplus}$ (isoelectronic with the high-energy ethylene dication isomer $H_3C{-}CH^{2\oplus}$ **34**), over the aminoborane dication $H_2N{-}BH_2^{2\oplus}$ (cf. $H_2C{-}CH_2^{2\oplus}$) is attributed to the strong donor–acceptor interaction (see section 3.3.6) between the $BH^{2\oplus}$ and NH_3 fragments.

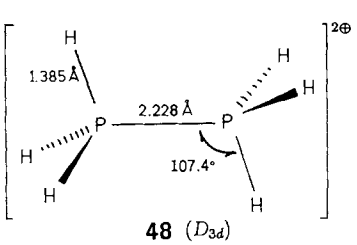
The hydrazinium dication **47** has been subject to a variety of spectrometric studies. An X-ray structure on the $N_2H_6F_2$



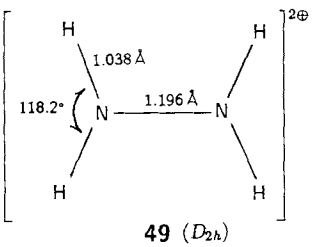
47 (D_{3d})

salt is available.[58] The calculated short N–N bond of 1.442 Å (HF/6-31G*)[56] is in agreement with the geometry in the crystal. Theory predicts that the dication should not be accessible by charge-stripping, because vertical ionization of the $H_3NNH_3^{\odot\oplus}$ radical cation with its long N–N bond of 2.164 Å would lead to dissociation.[59] Even though protonation of $N_2H_5^{\oplus}$ is exothermic, this is not possible in the gas phase, due to the barrier resulting from electrostatic repulsion. Dissociation of the dication **47** into two $NH_3^{\odot\oplus}$ radical cations (33 kcal/mol) has a 41 kcal/mol barrier (MP4/6-311G**).[60] The staggered form of $P_2H_6^{2\oplus}$ **48** also is calculated to reside in a deep potential well. In contrast, $H_2OOH_2^{2\oplus}$, $H_2SSH_2^{2\oplus}$, $HFFH^{2\oplus}$, and $HClClH^{2\oplus}$ have small dissociation barriers.[60]

The hydrazine dication $H_2NNH_2^{2\oplus}$ **49** is isoelectronic with ethylene and has a planar D_{2h} structure with a N–N bond



48 (D_{3d})



49 (D_{2h})

only 1.196 Å in length (HF/6-31G*). The calculated IE_v of 16.2 eV agrees well with the observed Q_{min} value of 15.8 eV for the gas phase oxidation of ionized hydrazine.[61]

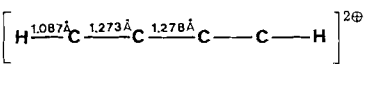
3.3. The Building Block Approach

The dications discussed so far reveal structural features applicable to larger systems. To elaborate this theme, we now discuss classes of larger gaseous dications. Because the $C_nH_2^{2\oplus}$, $C_nH_4^{2\oplus}$, and $C_nH_6^{2\oplus}$ carbodications are ubiquitous in doubly charged ion mass spectra,[3d,62] we will employ these species to illustrate common features and building blocks that can be used more generally to describe dication structures.

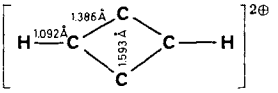
3.3.1. The $C_nH_2^{2\oplus}$ Carbodications

Doubly-charged species with n = 2–9, have been the subject of several studies.[63–66] Expectantly, linear acetylene-like structures $H{-}C_n{-}H^{2\oplus}$ are found for all, but $C_4H_2^{2\oplus}$ is an exception (see below).[64] The different fragmentation patterns observed[64] in the charge-separation reactions of $C_nH_2^{2\oplus}$ ions with even and with odd numbers of carbon atoms qualitatively confirm the theoretical prediction that these doubly-charged ions prefer, respectively, singlet and triplet states. The deprotonation of $C_nH_2^{2\oplus}$ with n = even has been ascribed to formation of excited dications; the ground state deprotonations for all $C_nH_2^{2\oplus}$ dications (n > 2) are endothermic.[65]

$C_4H_2^{2\oplus}$ and Inverted Tricoordinate Carbons: Two charge-separation reactions are observed for $C_4H_2^{2\oplus}$ i.e., to give $C_3H^{\oplus} + CH^{\oplus}$ and to give $C_3H_2^{\odot\oplus} + C^{\odot\oplus}$.[64] Formation of the latter fragments is considered to result from a cyclic form. The two processes have different translational energies E_T, corresponding to a difference in intercharge distance R of 0.4 Å.[64] A theoretical study[67] on $C_4H_2^{2\oplus}$ shows the linear triplet **50** to be only 13.3 kcal/mol (MP3/6-31G*) more stable than its rhombic D_{2h} isomer **51**. The energies of the two observed $C_4H_2^{2\oplus}$ fragmentations are in agreement with experiment. Dissociation of $CH^{\oplus}$ from the linear structure is endothermic by 36.7 kcal/mol, while loss of $C^{\odot\oplus}$ from the rhombic isomer "costs" 14.7 kcal/mol.[67]



50 ($D_{\infty h}$)



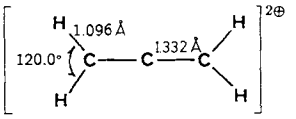
51 (D_{2h})

Rhombic $C_4H_2^{2\oplus}$ **51** can be viewed as diprotonated rhombic C_4 and is of considerable interest because of its two inverted tricoordinate carbons.[68] Its stability arises from π-electron aromatic delocalization. This balances the high ring-strain which is augmented by the "non-bonding" σ-orbital between the two bridgehead carbons. The transannular and ring C–C bond distances, 1.593 and 1.386 Å (HF/6-31G*), respectively, are remarkably short for a doubly charged cyclic species.[67,68]

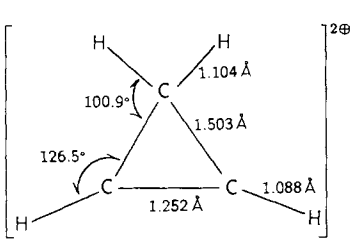
3.3.2. The $C_nH_4^{2\oplus}$ Carbodications

These dications, present in high abundance in the 2*E* spectra of a variety of hydrocarbons,[62,69] also have been studied theoretically several times.

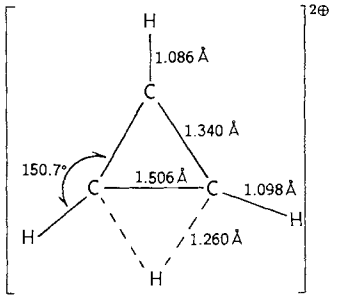
The methane $CH_4^{2\oplus}$ and ethylene $C_2H_4^{2\oplus}$ dications already have been discussed above. A kinetic energy release E_T of 4.44 eV for the $C_3H_4^{2\oplus}$ dication has been determined for the charge separation involving loss of a proton.[70] Since this translates into an intercharge distance of 3.24 Å (significantly less than the $R = 4.29$ Å (from $E_T = 3.36$ eV) measured in the same study for $C_3H_2^{2\oplus}$), a cyclic $C_3H_4^{2\oplus}$ structure has been suggested.[70] Collisional activation (CA) and charge-stripping of three $C_3H_4^{\odot\oplus}$ isomers (allene, propyne, cyclopropene) suggest the existence of isomeric dications.[71] A study using the coincidence method also suggests the presence of two isomers.[72] $C_3H_4^{2\oplus}$ dications have also been observed in $2E$ spectra; an appearance potential of 30.2 eV is reported in an EI study.[73] In strongly acidic media H/D exchange has been observed for donor-stabilized cyclopropenium ions, and has been suggested to occur through C-protonation.[74] Our recent ab initio study[75] on the parent $C_3H_4^{2\oplus}$ indicates the existence of a protonated cyclopropenium ion to be unlikely. Instead, the linear allene dication **52** with a planar (D_{2h}) structure is found to be the global minimum. This lies in a deep potential well with a deprotonation barrier of 83 kcal/mol and barriers of ca 15 kcal/mol (all MP4/6-31G*) for both hydrogen and carbon scrambling **53**, **54**.



52 (D_{2h})

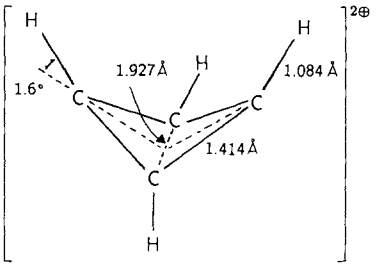


53 (C_{2v})



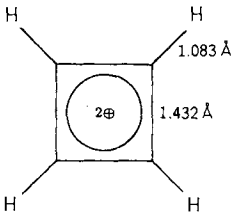
54 (C_{2v})

The cyclic $C_4H_4^{2\oplus}$ isomer has attracted interest since it is the smallest Hückel aromatic dication. *Olah* et al. succeeded in generating a variety of long-lived substituted cyclobutadiene dications substituted with F, CH_3, and/or phenyl groups in superacid media, but the parent $C_4H_4^{2\oplus}$ was not observed.[76] Calculations on this $C_4H_4^{2\oplus}$ dication show the puckered (D_{2d}) isomer **55** to be the global minimum.[77, 78] The energy difference between the puckered **55** and planar **56** forms is 9.6 kcal/mol (MP4/6-31G*).[78] Also the tetramethyl substituted dication prefers a puckered structure according to ab initio data.[77c, 78] Using the IGLO method[79] and the HF/6-31G* geometry the calculated ^{13}C NMR chemical shifts are remarkably similar to those observed experimentally ($\delta = 18.8$ and 209.7 ppm).[78] Hence, the long-lived tetramethylcyclobutadiene dication has a puckered conformation.[78]



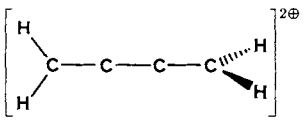
55 (D_{2d})

∠CXC=137.4°

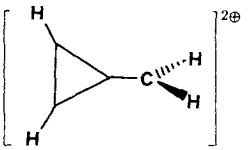


56 (D_{4h})

$C_4H_4^{2\oplus}$ has been observed in gas phase studies from a variety of precursors including aromatic substrates.[62a] Charge-stripping experiments give a Q_{min} value of 16.5 eV;[7] no theoretical second IE is available. The $2E$ spectrum of *n*-butane gives an appearance potential of 32.6 eV for $C_4H_4^{2\oplus}$.[69] Although no structural analyses were conducted, the $C_4H_4^{2\oplus}$ dication was assumed to have a cumulene-like structure.[3d] However, an ab initio study shows linear D_{2d} structure **57** to be 19.7 kcal/mol (estimated MP2/6-31G*) less stable than the puckered cyclobutadiene dication **55** and to have a rotational barrier of 19.1 kcal/mol (same level).[77a] In contrast, the methylenecyclopropene dication **58**, which also benefits from aromatic delocalization, is only 9.1 kcal/mol (same level) less stable than the global $C_4H_4^{2\oplus}$ minimum.

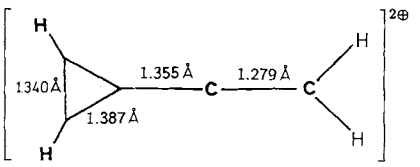


57 (D_{2d})

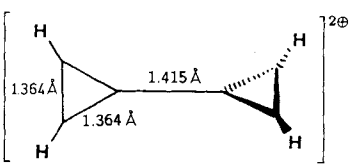


58 (C_{2v})

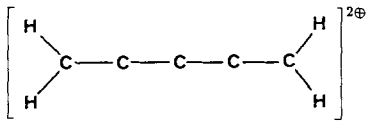
The preference for 2π-electron aromatic species is also evident from a theoretical study on the $C_5H_4^{2\oplus}$ and $C_6H_4^{2\oplus}$ dications, which indicate the vinylidenecyclopropenium **59** and trifulvalene **60** structures to be the global minima, respectively.[80] Derivatives of the trifulvalene dication have been characterized in solution.[81] The cumulene dications are higher energy isomers i.e., only 9.4 kcal/mol (MP2/6-31G*) for $C_5H_4^{2\oplus}$ **61** but 16.1 kcal/mol (HF/6-31G*) for $C_6H_4^{2\oplus}$ **62**.[80] Common methyl substituted acetylenic structures, CH_3–$C_{(n-1)}$-$H^{2\oplus}$, have been suggested for the $C_nH_4^{2\oplus}$



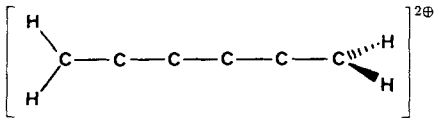
59 (C_{2v})



60 (D_{2d})



61 (D_{2h})



62 (D_{2d})

dications observed in the gas phase.[3d] This is very unlikely for $C_5H_4^{2\oplus}$ and $C_6H_4^{2\oplus}$ as these dications are high energy isomers i.e., $\Delta E = 55.6$ and 77.2 kcal/mol, respectively.[80] Charge-stripping gives a Q_{min} value of 15.6 eV for $C_5H_4^{2\oplus}$ and 15.0 eV for $C_6H_4^{2\oplus}$.[7] Both dications are common in the $2E$ spectra of a series of *n*-alkanes,[69] olefins,[62b] and aromatics.[62a]

It appears that no common structure represents all $C_nH_4^{2\oplus}$ dication global minima. Plots of Q_{min} (from charge-stripping) vs carbon number show a smooth curve for $C_nH_4^{2\oplus}$, but a jagged line (lowest values for n = odd) for the $C_nH_2^{2\oplus}$ dications, with linear acetylenic-like structures (Fig. 8).[7] Additional detailed experimental data are needed to confirm the theoretical analyses. Interestingly, the $C_nH_4^{2\oplus}$ dications have the lowest Q_{min} values among the $C_nH_m^{2\oplus}$ (n = 1–9, m = 0–8) dications.[7]

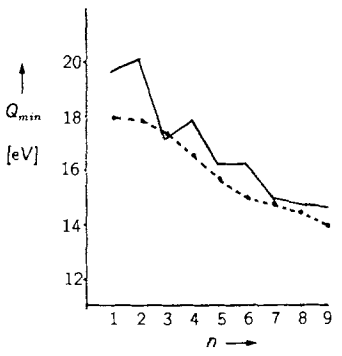
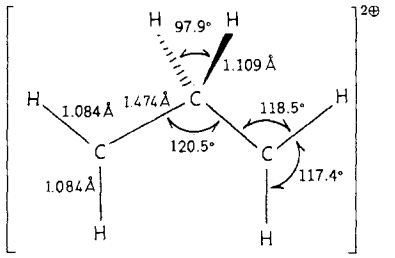


Fig. 8. Dependence of Q_{min} on the number of carbon atoms C_n for carbodications containing two (——) and four (– – –) hydrogens. [7]

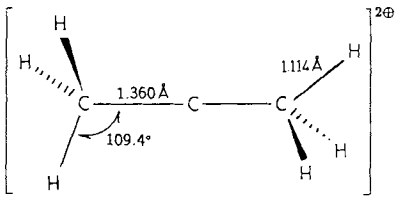
3.3.3. The $C_nH_6^{2\oplus}$ Carbodications

Many mass spectrometric observations of $C_nH_6^{2\oplus}$ dications from a variety of precursor molecules have been reported.[3d, 62, 69, 82] The $C_2H_6^{2\oplus}$ dication was discussed above. The following Q_{min} values (in eV) have been determined,[7a] using N_2 as collision gas in charge-stripping experiments: $C_3H_6^{\odot 2\oplus}$, 18.2; $C_5H_6^{\odot 2\oplus}$, 16.0; $C_6H_6^{2\oplus}$, 16.4; $C_7H_6^{\odot 2\oplus}$, 14.7; $C_8H_6^{2\oplus}$, 15.4; $C_9H_6^{\odot 2\oplus}$, 14.6. Appearance potentials obtained from $2E$ spectra depend on the precursor substrate.[62] Because the $C_nH_6^{2\oplus}$ dications loose $CH_3^{\oplus}$ readily with large intercharge distances, a common linear H_3C–$C_{(n-2)}$-$CH_3^{2\oplus}$ structure has been proposed.[3d] The corresponding kinetic energy releases (with *R* values in parentheses), $C_6H_6^{2\oplus}$ 2.6 (5.5 Å) and $C_8H_6^{2\oplus}$ 2.0 eV (7.3 Å), probably refer to the decomposition of high energy isomers.[3d] $C_8H_6^{2\oplus}$ also fragments into $C_5H_3^{\oplus} + C_3H_3^{\oplus}$ with an E_T of 3.0 eV, giving an *R* value of 4.8 Å.[13a] Theoretical studies do not support a common $C_nH_6^{2\oplus}$ dication structure.

Our recent ab initio study[83] of $C_3H_6^{2\oplus}$ isomers indicated the global minimum to be the central-protonated allyl cation **63** with the two charges formally on the terminal carbons. The CCC angle of 120.5° and the relatively short C–C bond distances, 1.474 Å (HF/6-31G*), resemble those of the allyl cation. These geometrical parameters reveal the importance of *bishyperconjugation*, i.e., the combined hyperconjugative effect on the same C–H bond(s) by two adjacent cation centers. The propylidene dication **64**, where the central carbon formally (but only formally) bears both charges, has virtual-



63 (C_{2v})



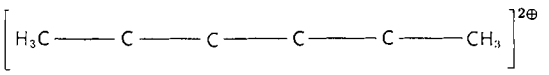
64 (D_{3d})

ly the same energy (MP4/6-31G* + ZPE). Its very short C–C bond lengths of 1.360 Å can be compared with those of the ethylene (**32**, 1.289 Å) and of the ethylidene dication (**34**, 1.398 Å) and are attributed to *cross-hyperconjugation*, i.e., hyperconjugation occurring in two orthogonal planes. The preferred fragmentations into $CH_3^{\oplus} + C_2H_3^{\oplus}$ and into $H_3^{\oplus} + C_3H_3^{\oplus}$ are both exothermic by ca. 60 kcal/mol (MP3/6-31G*), but are assumed to have sizable barriers.

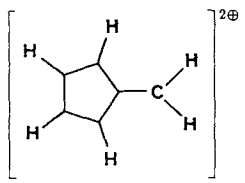
The calculated IE_a of 15.9 eV for the "protonated" allyl cation **63** from the cyclopropane radical dication differs significantly from the measured[7] Q_{min} value of 18.2 eV for $C_3H_6^{2\oplus}$. This discrepancy, once again, may reflect an experimental vertical ionization to an excited dication. The suggested cyclic structure, based on $R = 2.36$ Å for the deprotonation of $C_3H_6^{2\oplus}$ ($E_T = 6.1$ eV),[70] also does not agree with the theoretical predictions. Clearly, more detailed mass spectrometric studies are needed for experimental characterization of the gaseous $C_3H_6^{2\oplus}$ dications.

The $C_6H_6^{2\oplus}$ Ions: The best known species in this family is the hexamethyl derivative $C_6(CH_3)_6^{2\oplus}$ synthesized by *Hogeveen* and *Kwant*.[84] A pyramidal geometry with a hexacoordinate apical carbon was assigned to this dication based on synthetic routes, spectrometric methods, trapping experiments, and theoretical calculations.[84] The nature of the bonding in this symmetrical pentagonal pyramid has been extensively discussed.[85, 86] In contrast, less information is available for the parent gaseous $C_6H_6^{2\oplus}$ dication.[7, 62, 82] Mass spectrometric studies initially focused on the fragmen-

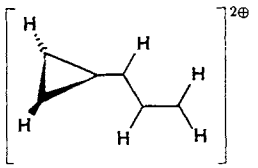
tation yielding $C_5H_3^{\oplus} + CH_3^{\oplus}$. The dimethylacetylenic structure for $CH_3CCCCCH_3^{2\oplus}$ was assigned based on the calculated $R = 5.5$ Å ($E_T = 2.6$ eV).[3d] However, our ab initio study[85a] showed this (triplet) isomer **65** to be 45.1 kcal/mol (3-21G) higher in energy than the global minimum, the fulvene dication **66**. The latter is stabilized over the two allylcyclopropenium ion isomers **67**, **68** by only 5–6 kcal/mol. Calculations at higher theoretical levels are needed to determine the energy difference between the fulvene **66** and the non-classical "Hogeveen" dication **69**, (29 kcal/mol at HF/3-21G). Due to its degenerate π HOMO, dioxidation



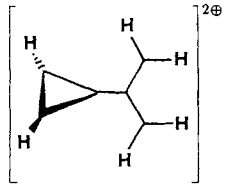
65 (D_{3d})



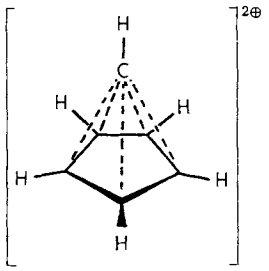
66 (C_{2v})



67 (C_s)



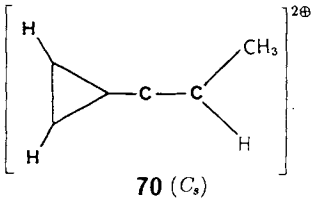
68 (C_{2v})



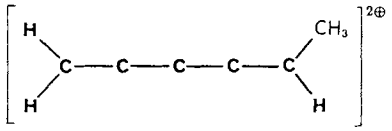
69 (C_{5v})

from benzene results in a D_{6h} triplet $C_6H_6^{2\oplus}$ dication, which is estimated to be 17.5 kcal/mol less stable than the fulvene dication (3-21G with triplet correction). The singlet benzene dication, which is virtually of the same energy as the triplet form, is subject to Jahn–Teller distortion. An elongated cyclic double-allyl D_{2h} geometry is calculated at HF/3-21G to have C–C bond distances of 1.418 (4×) and 1.525 Å (2×).[85a] MINDO/3 favors a C_{2h} chair conformation for this species.[86a] A surface-induced collision study suggests that the $C_6H_6^{2\oplus}$ ions generated from benzene by electron impact have the same cyclic structure as singly ionized benzene.[82a]

In order to interpret the observed dissociation of metastable $C_6H_6^{2\oplus}$ into $CH_3^{\oplus} + C_5H_3^{\oplus}$, several methyl group containing structures were calculated.[85a] Two possible candidates, the methyl substituted ethynylcyclopropenium **70** and the C_5-cumulene **71** dications, lose $CH_3^{\oplus}$ exothermically by 47 and 25 kcal/mol (HF/3-21G), respectively. Assuming that the fragmentation requires only a modest activation energy, then the energy of the former process (47 kcal/mol) is in reasonable agreement with the experimental translational energy release of ca. 60 kcal/mol (2.6 eV). However, we note that (U)HF/3-21G, MINDO/3, and MNDO give very large differences in calculated relative $C_6H_6^{2\oplus}$ energies. The fact that different structures are deduced from experiments in solution and in the gas phase while still others are indicated by MO theory (3-21G and MINDO/3) indicates the need for more detailed investigations.



70 (C_s)

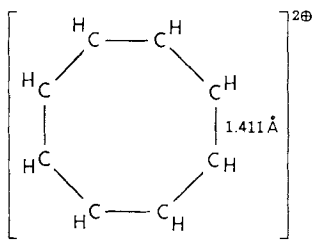


71 (C_s)

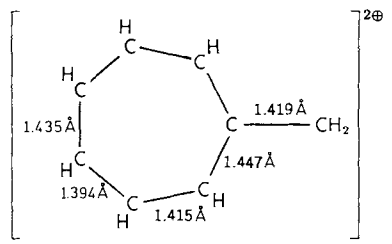
3.3.4. The $C_nH_8^{2\oplus}$ Ions

Little information is available on these dications other than that the $C_6H_8^{2\oplus}$, $C_7H_8^{2\oplus}$, $C_8H_8^{2\oplus}$, $C_{10}H_8^{2\oplus}$, and $C_{12}H_8^{2\oplus}$ dications are ubiquitous in the 2E spectra of n-alkanes and aromatic hydrocarbons.[62, 69, 82]

MINDO/3 calculations on a series of (bi)cyclic and cage structures gave as most stable $C_8H_8^{2\oplus}$ isomer the cyclooctatetraene dication.[87] Di- and tetra-substituted methyl and phenyl derivatives of this isomer have been observed under stable-ion solution conditions.[88] The isomeric octamethyldihydro-pentalene and bis(tetramethylhomocyclopropenyl) dications have also been observed.[88] It has not been possible to observe the parent cyclooctatetraene dication **72** in solution. Ab initio calculations at the STO-3G level found this species to be 25 kcal/mol less stable than the planar heptafulvene dication **73**.[89] The 2E spectra of a variety of hydrocarbons show the presence of $C_8H_8^{2\oplus}$.[90] Collisional activation spectra of the ions results in dissociation into $C_5H_3^{\oplus} + C_3H_5^{\oplus}$ ($E_T = 2.4$ eV), $C_6H_5^{\oplus} + C_2H_3^{\oplus}$ ($E_T = 3.3$ eV), and $C_7H_5^{\oplus} + CH_3^{\oplus}$ ($E_T = 3.2$ eV). It was suggested that all $C_8H_8^{2\oplus}$ dications have cyclic structures.[91]



72 (D_{8h})



73 (C_{2v})

3.3.5. The anti-van't Hoff Rule

According to the stereochemical rules determined by *van't Hoff* in 1875,[92] cumulenes with an even number of double bonds and an odd number of carbons, (e.g., methane, allene and pentatetraene), prefer perpendicular (D_{2d}) arrangements (methane of T_d symmetry), while cumulenes with an odd number of double bonds and an even number of carbons, (e.g., ethylene und butatriene), prefer planar (D_{2h}) struc-

tures. Removal of two electrons to give a cumulene dication reverses the van't Hoff stereochemistry: perpendicular neutral species become planar dications and vice versa.[80] The same applies to structures where a terminal cumulene carbon is replaced by an allyl or a cyclopropenium cation group. Figure 9 shows representative examples of planar and perpendicular dications.

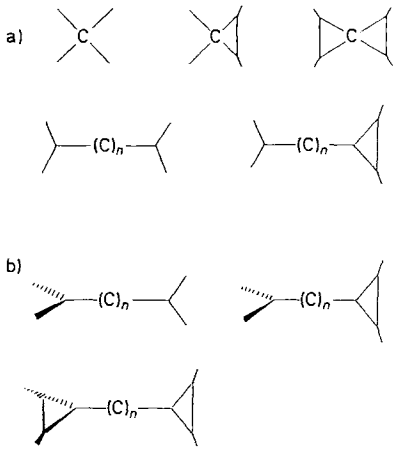


Fig. 9. Anti van't Hoff dication structures. a) Planar dications, n = odd. b) Dications with allene type arrangement of the substituents, n = 0, even.

3.3.6. The $CH_2^{2\oplus}$ and $CH_4^{2\oplus}$ Building Blocks

Saturated hydrocarbons and their derivatives have C-chains that are terminated by methyl groups. This is precluded in cationic systems when a charge is located at a terminal position. Maintaining single C–C or C–X bonds, the terminus can either be a $CH_2^{\oplus}$ group formally derived from hydride abstraction from CH_3, or $CH_4^{\oplus}$, formally a protonated methyl group. Hence, many dications can be considered to be comprised of a $CH_2^{2\oplus}$ or $CH_4^{2\oplus}$ dication joined to a neutral molecule. Using such a building block approach, donor-acceptor complexes can be formed and used didactically to explain bonding patterns in doubly charged species.[3a–c, e, f, 43, 48, 53, 93, 94] The acceptor molecule is either the linear $CH_2^{2\oplus}$ or the planar $CH_4^{2\oplus}$, both having an empty p-orbital perpendicular to the axis/plane of the molecule. The two-electron donor interactions with σ-, π-, and n-donor molecules X can be deduced from Figure 10.

Also note that CH_2–$X^{2\oplus}$ and CH_4–$X^{2\oplus}$ dications differ by only one H_2-molecule. Thus, the substituted methonium dication CH_4–$X^{2\oplus}$ represents a hydrogenated ylid dication CH_2–$X^{2\oplus}$ (Fig. 10).[93] The CH_4–$X^{2\oplus}$ dication is a methonium ion $CH_5^{\oplus}$ with one H-ligand replaced for a cation substituent $X^{\oplus}$. The 3c–2e bonding in pentacoordinate tetravalent $CH_5^{\oplus}$ arises via a 40 kcal/mol favorable interaction between $CH_3^{\oplus}$ and H_2. CH_4–$X^{2\oplus}$ should be analogous.[93]

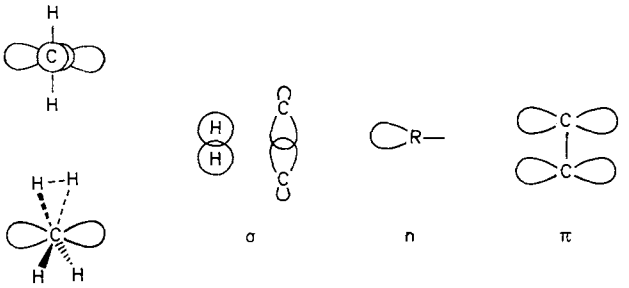
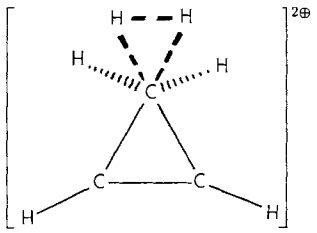


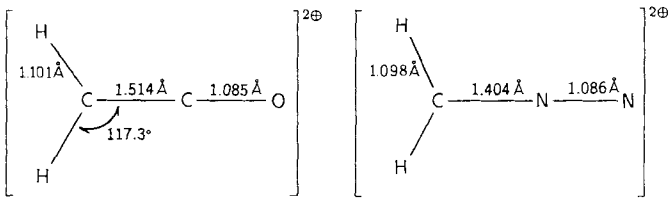
Fig. 10. Donor–acceptor interactions for carbodications. The carbocations $CH_2^{2\oplus}$ and $CH_4^{2\oplus}$ (left) interact with the σ-, n-, and π-two electron donors (right).

The ethane dication discussed above illustrates these arguments nicely. First, we build the familiar D_{2d} ethylene dication **32** from the interaction of neutral $:CH_2$ and the $CH_2^{2\oplus}$ dication **3**. One of the resulting $CH_2^{\oplus}$ termini can then be hydrogenated to give the carbonium-carbenium CH_4–$CH_2^{2\oplus}$ dication **37**. The same species results conceptually both from "complexation" of neutral $:CH_2$ with the planar methane dication **5** and from replacement of a hydrogen in $CH_5^{\oplus}$ by a $CH_2^{\oplus}$-ligand. Other illustrations are the ylid dications above discussed, which can be considered to be complexes between $CH_2^{2\oplus}$ and a neutral n-donor molecule, like FH, ClH, OH_2, SH_2, and NH_3.[94] Other unfamiliar and sometimes high energy structures can be understood on the same basis. For example, interaction with π donors, $CH_2^{2\oplus}$ with ethylene and $CH_4^{2\oplus}$ with acetylene, give three-membered ring $C_3H_6^{2\oplus}$ transition structures **53**, **74**.[83] Similarly, interaction of atomic C with $CH_4^{2\oplus}$ gives CH_4–$C^{2\oplus}$, which is an exotic high energy isomer of the ethylene dication.[43c]



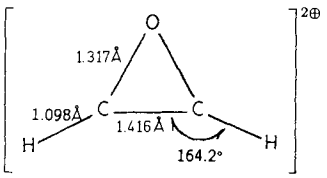
74 (C_{2v})

The CH_n-$XY^{2\oplus}$ (n = 2,4) Dications: The ketene **75** and diazomethane **76** dications also illustrate this approach when viewed as complexes of the $CH_2^{2\oplus}$ dication and carbon



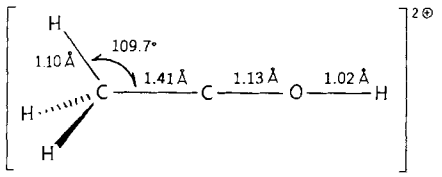
75 (C_{2v}) **76** (C_{2v})

monoxide and nitrogen, respectively.[93] The dioxygen complex is similar, and there is perfect agreement between the Q_{min} value determined for $C_2H_2O^{2\oplus}$ and the calculated IE_v (MP2/6-31G*). Both are 18.6 eV.[95] The ketene dication **75** is the global $C_2H_2O^{2\oplus}$ minimum. The isomeric oxirene dication **77**, 27 kcal/mol (MP2/6-31G*) less stable, lacks experimental confirmation since no suitable gas phase precursors are available.[95] In contrast, the isomeric hydroxyacetylene dication, which is 59 kcal/mol (same level) less stable, has been observed.[96] The same is true for the isoelectronic aminoacetylene dication, $HCCNH_2^{2\oplus}$. The reported Q_{min} value of 17.9 eV is in good agreement with theory.[97]

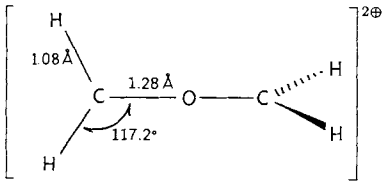


77 (C_{2v})

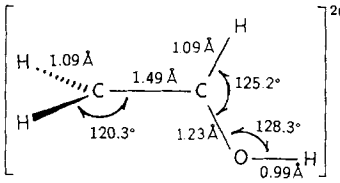
The $C_2H_4O^{2\oplus}$ dications have been studied by charge-stripping mass spectrometry and ab initio theory.[98] Because of the isoelectronic relationship between $C_2H_4O^{2\oplus}$ and the $C_3H_6^{2\oplus}$ dications, similarities are expected and confirmed. The global $C_2H_4O^{2\oplus}$ minimum is the hydroxy substituted ethylidene dication CH_3–C–$OH^{2\oplus}$ **78**. This is 14.7 kcal/mol (MP2/6-31G*//HF/4-31G) more stable than the ring-opened ethylene oxide dication **79**, which can be



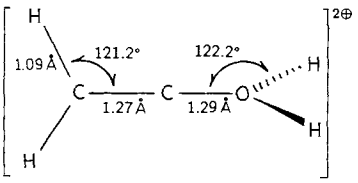
78 (C_{3v})



79 (D_{2d})



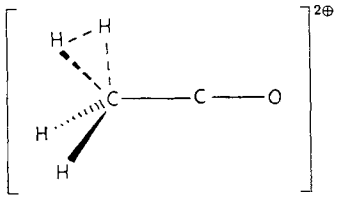
80 (C_s)



81 (C_{2v})

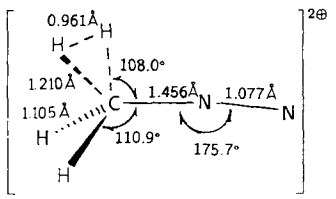
viewed as the complex between $CH_2^{2\oplus}$ and formaldehyde.[98] This stability order differs from that for the $C_3H_6^{2\oplus}$ carbodications, which shows the related dication isomers to be of virtually equal stability at MP4/6-31G*//HF/6-31G*; note that the propylidene dication is bent whereas the H_2C–O–$CH_2^{2\oplus}$ structure **79** has a linear D_{2d} geometry.[83] Other stable $C_2H_4O^{2\oplus}$ isomers are dioxidized vinyl alcohol **80** and the H_2C–C–$OH_2^{2\oplus}$ structure **81**, which is reminiscent of allene.[83] Charge-stripping experiments[98] on $CH_2OCH_2^{\odot\oplus}$ and $CH_2CHOH^{\odot\oplus}$ gave Q_{min} values of 16.3 (15.6) and 17.1 (17.2) eV, respectively, in good agreement with the theoretical IE_v values that are given in parentheses.[83] Charge-stripping from $CH_3COH^{\odot\oplus}$ gave a too low abundance for determination of the Q_{min} value. Derivatives of $C_2H_4O^{2\oplus}$ are discussed in section 3.4.2.

A different $C_2H_4O^{2\oplus}$ structural type results when $CH_4^{2\oplus}$ and CO are used as building blocks.[93] The resulting species can be viewed as a hydrogenated ketene dication **82**. However, this CH_4–$CO^{2\oplus}$ isomer is 24.6 kcal/mol (HF/6-31G*) less stable than CH_3–C–$OH^{2\oplus}$ **78**. Nevertheless, the relatively modest energy difference between the O- and C-protonated forms of the acetyl cation may render experimental verification under stable ion-solution conditions feasible. The trends discussed for these O-containing dications are also reflected in the $C_2OH_3^{\odot 2\oplus}$ radical dications.[99] Thus, the charge stripping from the 1-hydroxyvinyl cation gives a Q_{min} of 18.7 eV, but the 29 kcal/mol (MP2/6-31G*) less stable acetyl radical dication could not be generated from the corresponding cation.[99b, c]

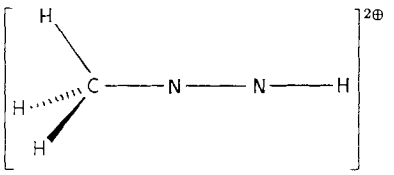


82 (C_s)

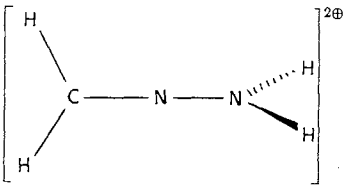
$C_2H_4O^{2\oplus}$ and the diazomethane dication are similar, but the latter has not yet been studied by charge-stripping mass spectrometry. The dioxidized diazomethane dication $CH_2N_2^{2\oplus}$ **76** can be considered as a complex of $CH_2^{2\oplus}$ **3** and dinitrogen. Formal complexation of the $CH_4^{2\oplus}$ dication **5** with nitrogen results in CH_4–$N_2^{2\oplus}$ **83**, which can be viewed as hydrogenated CH_2–$N_2^{2\oplus}$ dication as well as di-*C*-protonated diazomethane.[93] Although **83** is 12 kcal/mol (HF/3-21G) more stable than the *N*-protonated methyl diazonium ion (**84**, a transition structure), it is 49.5 kcal/mol (HF/6-31G*) less stable than the di-*N*-protonated isomer $H_2C{=}N{=}NH_2^{2\oplus}$ **85**.[93] This is in agreement with a stable ion-solution study.[100]



83 (C_s)



84 (C_{3v})



85 (C_{2v})

3.4. Special Types of Dications

The structures of many observed and calculated simple dications can be understood on the basis of their electronic properties. Dication structures typically are very different

from those of their neutral homologues. We now consider the next question. Can dications be as versatile as the many intriguing monocations that have fascinated chemists for decades? Highlights of recent carbodication chemistry are discussed in the remainder of this review.

3.4.1. Classical versus Non-Classical Carbodications

Part of the richness of carbocation chemistry arises from the ability of the electron deficient center to gain stabilization through hypercoordination. This non-classical behavior results in more efficient charge distribution throughout the molecule. Thus, all primary and most secondary and many tertiary cations tend to form non-classical ions, or ions with significant non-classical character.[101] This characteristic also applies to carbodications, but is more restricted due to the Coulombic repulsion of charges. Hence, in a non-classical dication the two formally charged centers compete to a greater extent for charge delocalization than is the case in a classical structure. However, charge-charge repulsion may be countered with effective π-delocalization as in e.g., the Hogeveen **69** and dehydroadamantanediyl dications **104** (see section 3.4.3.). Of the many possible examples, the ethylene and ethane dications can be used to illustrate σ-delocalized systems.

The classical D_{2d} ethylene dication **32**, with its two neighboring cation centers oriented in an orthogonal fashion, is 12 kcal/mol (MP4/6-311G**) more stable than the non-classical bis-hydrido bridged structure **33**.[43c] This is due to the less effective charge distribution in the latter diprotonated acetylene structure. That charge-charge repulsion is the dominant factor is also indicated by the isoelectronic B_2H_4, where the di-H-bridged structure is only 1.5 kcal/mol (MP2/6-31G**) less stable than the D_{2d} isomer.[102] In contrast, both the singly charged ethyl and vinyl cations prefer H-bridged structures.[103]

Similarly, the open ethane CH_4–$CH_2^{2\oplus}$ dication structure (**37**, C_s), is 7 kcal/mol (MP4/6-31G**) more stable than the doubly bridged diborane-like isomer **38**.[48] Most of the positive charge resides on the hydrogens, and in **37**, these are as far apart as possible. Consequently, protonation of a C–H bond of the ethyl cation is preferred over that of a C–C bond.

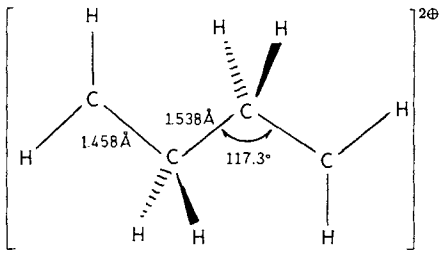
3.4.2. Proximity of Cation Centers

It is of interest to examine in more detail the structural and energetic effect of one cation center on the other. Again, we recall some of the already discussed dications. In the D_{2d} ethylene dication **32**, the charged centers are located next to each other; the resulting *crosshyperconjugation* yields a formal C–C single bond that is 0.14 Å shorter than that of a regular aliphatic hydrocarbon. Several ethylene dications with aryl substituents have been observed under stable ion-solution conditions. An X-ray study[104a] of the dichloroiodate salt of the tetra-*t*-anisylethylene dication reveals a 41° twist around the 1.43 Å short central C–C bond (compare 1.432 Å for $C_2H_4^{2\oplus}$, HF/6-31G*). Also crystals (no X-ray) have been obtained for a related species in which two neighboring tetrakis(dimethylamino)-allyl cation units are connected via their central carbons.[104b]

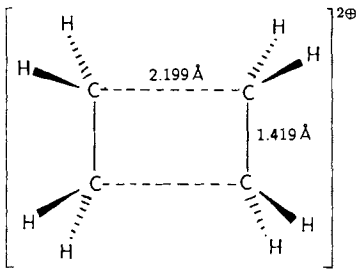
Separating the charges with one CH_2-unit as in the protonated allyl cation (**63**, $C_3H_6^{2\oplus}$) still yields short C–C bonds now because of *bishyperconjugation* i.e., the combined hyperconjugative effects on the central CH_2-group. Attempts to prepare a 1,1,3,3-tetramethyl derivative under stable ion-solution conditions failed because of deprotonation and disproportionation reactions.[105] However, experimental and theoretical studies on diprotonated 1,6-methano[10]annulene confirm the bishyperconjugative effect.[106] This species contains the cyclopropyl-1,1-diallenyl dication fragment in a frozen conformation that shows significant C–C bond lengthening in the cyclopropane ring (1.602 Å, HF/6-31G*) enabling conjugation between the two allylic units. Isoelectronic replacement of the central CH_2-group in $C_3H_6^{2\oplus}$ for oxygen results in a larger number of experimentally characterized dications of the type R_2C–O–$CR_2^{2\oplus}$ (R = NH_2, $N(CH_3)_2$, $C_5H_{10}N$, C_6H_5) and R–O–$R^{2\oplus}$ (R = cyclopropenylium, tropenylium, pyridinium, etc.); X-ray structures are known for some of the dication ether triflates R–O–$R^{2\oplus}$.[107] The determined C–O–C angles are for R = 1,2-bis(dimethylamino)-3-cyclopropenyliumyl 116.7°,[107a] for R = bis(dimethylamino)carbinyl 122.4°,[107b] for R = tropenyliumyl 125.3°,[107f] and for R = 1,3-dimethyl-2-imidazoliniumyl 120.3°.[107e] These experimental angles are very similar to the calculated angle of 120.5° (HF/6-31G*) for the corresponding $C_3H_6^{2\oplus}$ isomer.[83] The calculated energy differences between the bent and linear R–O–$R^{2\oplus}$ forms is small; MINDO/3 gives a 3.3 kcal/mol preference for a linear bistropenyliumyl ether dication in contrast to the X-ray crystal structure.[107g] The parent ether dication H_2C–O–$CH_2^{2\oplus}$ prefers a linear D_{2d} structure.[98]

Under stable ion-solution conditions several acyclic aryl substituted and the tetramethyl ($R_2C^{\oplus}$–CH_2CH_2–$CR_2^{\oplus}$) dications have been generated. The CH_2–CH_2-unit separates the cation centers.[105] The vicinal 1,2-(diphenylcarbinyl)-cyclopropane has also been generated in solution.[105] Recent theoretical studies on a series of $C_4H_8^{2\oplus}$ dications (**86, 87, 88**)[108a] show the parent 1,4-butanediyl dication **86**, C_i to be the global energy minimum. This structure, like the corresponding $C_3H_6^{2\oplus}$ dication, also shows significant hyperconjugation of both cation centers with their neighboring CH_2-groups. This is evident from the C–C–C angles of 117.3°, the C–$C^{\oplus}$ bond lengths of 1.454 Å, and the C–C bond length of 1.539 Å (HF/6-31G*).

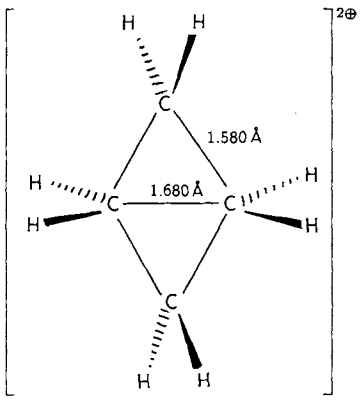
Several cyclic and polycyclic aliphatic carbodications have been probed by experiment and theory for the through-space proximity of the two cation centers. The [1.1.1]-, [2.2.2]-, and [3.3.3]propellanes enable the study of such dications, where the charged centers are connected through C_1, C_2, and C_3 bridges, respectively. The highly strained [1.1.1]propellane has been extensively studied. Since theoretical studies give a central C–C separation ranging from 1.543 Å (HF) to 1.592 Å (MP2 (Full)/6-31G*)[109a–c] and show the HOMO to be of "non-bonding" σ-character,[109d] removal of its two electrons (dioxidation) should not have a major structural impact other than that resulting from charge-charge repulsion. Although this $C_5H_6^{2\oplus}$ dication **89** has not yet been studied neither by theory nor by charge-stripping techniques, the isoelectronic diborabicyclo[1.1.1]pentane $C_3H_6B_2$ **90** has been calculated to have a B–B separation of only 1.61 Å (HF/4-31G), a length equal to the C–B bonds.[109d] Alternative to the dioxidation diprotonation would yield the bicyclo[1.1.1]pentane dication $C_5H_8^{2\oplus}$ which



86 (C_i)

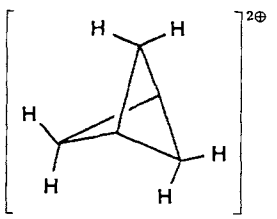


87 (D_{2h})

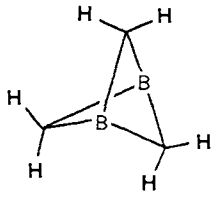


88 (D_{2h})

is calculated to have a short C1–C3 distance (1.452 Å, 6-31G*) in D_{3h} symmetry. The corresponding nonbonded distance is 1.869 Å (6-31G*) in bicyclo[1.1.1]pentane. However, an ab initio study of this $C_5H_8^{2\oplus}$ species[108b] shows not to be a minimum on the potential energy surface.

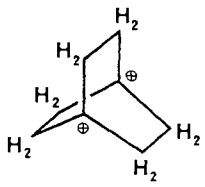


89

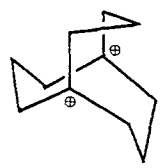


90

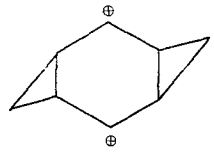
Despite the favorable electronic structure of the 1,4-bicyclo[2.2.2]octanediyl dication $C_8H_{12}^{2\oplus}$ **91**, as first indicated by MINDO/3, claims of its experimental observation under stable ion-solution conditions could not be confirmed.[110] The calculated distance between the bridgehead cation centers is 1.990 Å (MINDO/3),[110b] 2.147 Å (3-21G), and 2.118 Å (6-31G*),[110c] while a value of 1.512–1.57 Å (HF and TCSCF/6-31G*) is reported for neutral [2.2.2]propellane.[109a–c] Furthermore, IGLO chemical shift calculations on **91**[110c] rule out the possibility that this species was observed experimentally. In contrast, a "stable" species is observed when the charged centers are connected through propylene bridges as in the 1,5-bicyclo[3.3.3]-undecanediyl (manxyl) dication $C_{11}H_{18}^{2\oplus}$ **92**.[111] This is not the case when the three bridges are *vic*-substituted cyclopropanes,[112a] even though MINDO/3 calculations predicted such dications to be stabilized up to 12 kcal/mol, relative to **91**.[112b] However, dications are observed under stable ion-solution conditions when the cation centers are bridged by only two cyclopropane rings as in substituted 2,6-antitricyclo[5.1.0.$0^{3,5}$]-octanediyl dications **93**.[113] Even 1,4-diaryl-1,4-cyclohexanediyl dications **94** have been studied by NMR spectroscopy.[114] In the observed 2,5-diaryl-2,5-norbornanediyl dication **95** the charged centers are separated by two C_2-units.[114]



91



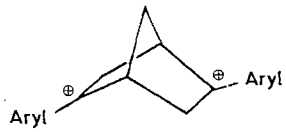
92



93

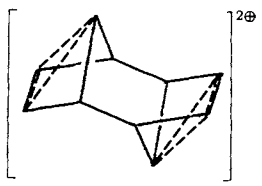


94



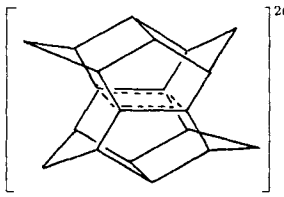
95

A Sandwiched Bishomoaromatic Dication: The anti-tricyclo[4.2.1.$1^{2,5}$]deca-3,7-diene-9,10-diyl dication $C_{10}H_{10}^{2\oplus}$ **96** has been generated under stable ion-solution conditions and studied by NMR spectroscopy.[115] This dication represents a sandwiched bishomoaromatic system. The two monocations, each delocalized in a bishomoaromatic 3c-2e interaction, are linked together by two C_2-units. The NMR data suggest that the two cation systems are essentially independent of one another. Neither theoretical nor gas phase studies have been reported on this or related dications.

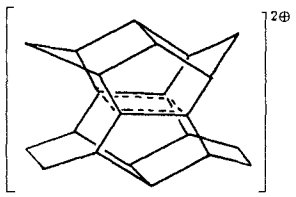


96

$C_4H_8^{2\oplus}$ and the Pagodane Dication. Oxidation of [1.1.1.1]pagodane[116] under stable ion-solution conditions generates a dication **97** that has been characterized by NMR spectroscopy and quenching experiments.[117] Charge-stripping mass spectrometry has shown the formation of dications from [1.1.1.1]-**97** and [2.2.1.1]pagodane **98**, $C_{20}H_{20}^{2\oplus}$ and $C_{22}H_{24}^{2\oplus}$, respectively.[118] Unfortunately, the corresponding Q_{min} values of 13.4 (± 0.7) and 13.2 (± 1.0) eV have large uncertainties such that in this case charge-stripping does not



97



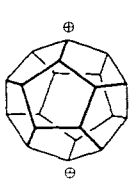
98

discriminate between structurally closely related hydrocarbon radical cation isomers.[118] MNDO and ab initio calculations (STO-3G and 3-21G) suggest that the pagodane cage structure contains a substituted rectangular D_{2h} cyclobutane dication. Rather than being of σ-aromatic nature,[117, 118] the 2.21 Å (3-21G) separation[108a] (2.58 Å MNDO) for **97** suggests the interaction of the two olefin radical cation moieties to be weak.

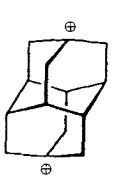
A recent theoretical study on several parent $(CH_2)_4^{2\oplus}$ structures shows the open C_i *trans*-tetramethylene dication **86** (minimum, see above) to be 22.4 kcal/mol (MP2/6-31G*) more stable than the rectangular D_{2h} cyclobutane **87**.[108a] The C–C bonds in the latter structure are 1.419 and 2.199 Å (HF/6-31G*). There is only 2.3 kcal/mol energy difference between this cyclic isomer and the less stable (classical) open C_{2v} *cis*-tetramethylene dication, which has C–C bond lengths of 1.477 (2×) and 1.632 Å; however, both structures have 3 imaginary frequencies (HF/3-21G) indicating that they are neither minima nor transition structures! An interesting D_{2h} cyclobutane dication **88** is calculated with four C–C peripheral bonds of 1.580 Å and a transannular C–C bond of 1.680 Å (HF/6-31G*). This species is a candidate for the transition structure (15.1 kcal/mol, MP2/6-31G**) for dyotropic rearrangement of the open **86** tetramethylene dication,[108a] but it has two imaginary frequencies at MP2/6-31G*.

The 1,16-Dodecahedryl Dication, $C_{20}H_{18}^{2\oplus}$. The pentagonal dodecahedrane[119] has the highest symmetry I_h of all organic molecules. Ionization with subsequent protonation of chlorododecahedrane[120] under stable ion-solution condition affords the apical/apical 1,16-dodecahedryl dication **99**.[121] NMR analysis shows the positive charges to be localized at opposite sides of the hydrocarbon cage. This conclusion is supported by MNDO calculations.[121] No charge-stripping experiments have been performed on the $C_{20}H_{18}^{2\oplus}$ dication.

The 4,9-dication of diadamantane $C_{14}H_{20}^{2\oplus}$ **100**,[122] generated in solution from the corresponding dichloro precursor, also has its charged centers located at opposite bridgehead positions.[84] The diminished C–C hyperconjugation as compared to monocations was attributed to charge–charge repulsion. Neither gas phase nor theoretical studies have been performed on this dication. We conclude that charge–charge repulsion is important in these saturated hydrocarbon cages, especially when stabilization mechanisms to disperse or delocalize charge over the carbon framework are lacking.



99



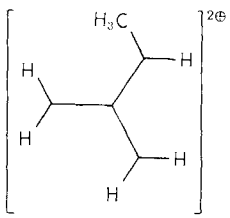
100

3.4.3. Aromatic Dications

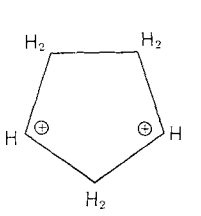
Many dioxidized or diprotonated aromatic compounds and (4n + 2) Hückel annulene aromatic dications, studied under stable ion conditions in solution, have been reviewed elsewhere.[2] Here, we consider less common two-electron aromatic dications.

We have discussed two-σ electron systems, i.e., the [1.1.1.1]-pagodane dication, and σ-π delocalized systems already. The latter bishyperconjugated dications can also be viewed as mixed σ,π Y-aromatic species. Aromatic π systems, satisfying the (4n + 2) rule, can be classified into three topological groups, i.e., ring systems, systems with a node, and three-dimensional (or cage) systems. The cyclobutadienyl dication, a member of the first class, has already been discussed in detail.

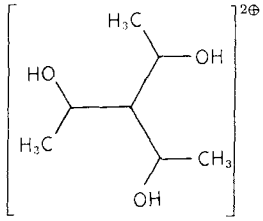
The planar trimethylene methane dication $C_4H_6^{2\oplus}$ is the parent molecule for Y-aromaticity.[123] Although of considerable theoretical interest, this dication has eluded experimental gas phase verification. MNDO calculations indicated that doubly charged Y-conjugated systems may even be more stable than their cyclic aromatic counterparts.[124] Recent calculations on the $C_5H_8^{2\oplus}$ potential energy surface[108b] show the methyl-trimethylene methane dication **101** to be the global minimum, 0.9 kcal/mol (HF/6-31G*) more stable than the cyclopentanediyl dication **102**. Whereas attempts to generate methyl and phenyl substituted trimethylene methane dications proved unsuccessful, a trimethyl-trihydroxy derivative **103** has been observed under stable ion-solution conditions.[125]



101

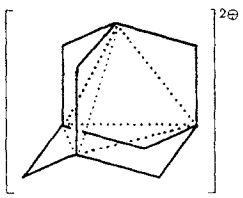


102



103

The Didehydroadamantanediyl Dication, $C_{10}H_{12}^{2\oplus}$: The long sought after 1,3-dehydro-5,7-adamantanediyl dication **104**[122] was synthesized recently by ionization of the difluorodehydroadamantane precursor.[126] This species is a prime



104

example of three-dimensional aromaticity. The four p-orbitals of the adamantane bridgehead carbons all point inwards and overlap appreciably. Occupancy of this bonding orbital with two interstitial electrons is favorable. Theoretical calculations preceded the experimental realization and predicted a tetrahedral aromatic unit in the hydrocarbon cage.[126] The calculated C–C interbridge distances of this tetrahedron are 2.052 Å (HF/6-31G*). The dication structure with its 1.504 Å C–C bonds and flattened bridgeheads is more condensed than adamantane itself. The dication contains a $C_4^{2\oplus}$ tetrahedron with each of its six edges bridged by an aliphatic CH_2-unit. No gas phase data related to this species are available.

4. Conclusion

The detection and the characterization of small organic dications have flourished in the last decade. There is a symbionic relationship between gas phase experiments and ab initio molecular orbital studies. Generally good agreement is found between measured and calculated ionization energies of monocations from which dications are formed. The combined experimental and theoretical approach has provided detailed understanding of small dications. The salient features that confer kinetic (and even thermodynamic) stability to dications are now recognized. As a consequence, the structural changes, often quite large, in going from neutral molecules to di-charged cations can now be understood. The small gaseous dications are often related to the substituted and the thermodynamically more stable dications that are observable in solution. With the advance of new mass spectrometric techniques and computational methods (e.g. IGLO) it is inevitable that the relationship between gas phase, solution, and theoretical studies is even further strengthened. Clearly, the chemistry of multiply charged cations has a bright future.

This work was supported by the Fonds der Chemischen Industrie, the Deutsche Forschungsgemeinschaft, the Petroleum Research Fund, administered by the American Chemical Society, and Research Corporation. K. L. thanks the Deutscher Akademischer Austauschdienst (DAAD) for a Science Exchange Award.

Received: April 17, 1989 [A736 IE]
German version: *Angew. Chem. 101* (1989) 1313

[1] E. Friedlander, H. Kalmann, W. Lasareff, B. Rosen, *Z. Phys. 76* (1932) 60, 70; R. Conrad, *ibid. 31* (1930) 888; W. Bleakney, *Phys. Rev. 36* (1936) 1303.

[2] G. K. S. Prakash, T. N. Rawdah, G. A. Olah, *Angew. Chem. 95* (1983) 356; *Angew. Chem. Int. Ed. Engl. 95* (1983) 356; R. M. Pagni, *Tetrahedron 40* (1984) 4161; G. A. Olah, G. K. S. Prakash, K. Lammertsma, *Rev. Chem. Intermed.*, in press.

[3] a) K. Lammertsma, *Rev. Chem. Intermed. 9* (1988) 141; b) W. Koch, H. Schwarz in P. Ausloos, S. G. Lias (Eds.): *Structure/Reactivity and Thermochemistry of Ions*, Reidel, Dordrecht 1987, page 413; c) P. von R. Schleyer, *Adv. Mass. Spectrom. 10* (1986) 287; d) T. Ast, *ibid. 8A* (1980) 555; *ibid. 10* (1986) 471; e) W. Koch, F. Maquin, D. Stahl, H. Schwarz, *Chimia 39* (1985) 376; f) P. von R. Schleyer *Am. Chem. Soc. Div. Pet. Chem. Prepr. 28* (1983) 413.

[4] M. Guilhaus, A. G. Brenton, J. H. Beynon, M. Rabrenović, P. von R. Schleyer, *J. Chem. Soc. Chem. Commun. 1985*, 210; *J. Phys. B17* (1984) L605.

[5] L. Radom, P. M. W. Gill, M. W. Wong, R. H. Nobes, *Pure Appl. Chem. 60* (1988) 183; H. Yagisawa, H. Sato, T. Watanabe, *Phys. Rev. A16* (1977) 1352.

[6] a) L. Pauling, *J. Chem. Phys. 1* (1933) 56; b) J. D. Dunitz, T. K. Ha, *J. Chem. Soc. Chem. Commun. 1972*, 568.

[7] a) M. Rabrenović, C. J. Proctor, T. Ast, C. G. Herbert, A. G. Brenton, J. H. Beynon, *J. Phys. Chem. 87* (1983) 3305; b) S. Singh, R. K. Boyd, F. M. Harris, J. H. Beynon, *Proc. R. Soc. A402* (1985) 373.

[8] C. J. Proctor, C. J. Porter, T. Ast, P. D. Bolton, J. H. Beynon, *Org. Mass Spectrom. 16* (1981) 454.

[9] a) R. G. Cooks, T. Ast, J. H. Beynon, *Int. J. Mass Spectrom. Ion Processes 11* (1973) 490; b) J. Durup, J. Appell, F. C. Fehsenfeld, P. Fournier, *J. Phys. B5* (1972) L110, 1810; c) D. L. Kemp, R. G. Cooks in R. G. Cooks (Ed.): *Collision Spectroscopy*, Plenum, New York 1978, S. 257; d) T. Ast, C. J. Porter, C. J. Proctor, J. H. Beynon, *Glas. Hem. Drus. Beograd 46* (1981) 135; e) K. Levsen, H. Schwarz, *Mass Spectrom. Rev. 2* (1983) 77.

[10] F. H. Dorman, J. D. Morrison, *J. Chem. Phys. 35* (1961) 575.

[11] A. M. Hanner, T. F. Moran, *Org. Mass Spectrom. 16* (1981) 512.

[12] B. P. Mathur, L. E. Abbey, E. M. Burgess, T. F. Moran, *Org. Mass Spectrom. 15* (1980) 312.

[13] a) T. Ast, J. H. Beynon, R. G. Cooks, *Org. Mass Spectrom. 6* (1972) 749; b) J. H. Beynon, A. Mathias, A. E. Williams, *ibid. 5* (1971) 303; c) T. Ast, J. H. Beynon, *ibid. 7* (1973) 503; d) H. Sakurai, A. Tatematsu, H. Nakata, *ibid. 7* (1973) 1109; e) T. Blumenthal, J. H. Bowie, *ibid. 6* (1972) 1083.

[14] E. E. Kingston, A. G. Brenton, J. H. Beynon, R. Flammang, A. Maquestiau, *Int. J. Mass Spectrom. Ion Processes 62* (1984) 317.

[15] J. H. Beynon, R. M. Caprioli, W. E. Baitinger, J. W. Amy, *Org. Mass Spectrom. 3* (1970) 455.

[16] W. J. Hehre, L. Radom, P. von R. Schleyer, J. A. Pople: *Ab Initio Molecular Orbital Theory*, Wiley-Interscience, New York 1986.

[17] E. R. Davidson, D. Feller, *Chem. Rev. 86* (1986) 681.

[18] M. Rabrenović, C. G. Herbert, C. J. Proctor, J. H. Beynon, *Int. J. Mass Spectrom. Ion Phys. 47* (1983) 125; T. Ast, C. J. Porter, C. J. Proctor, J. H. Beynon, *Chem. Phys. Lett. 78* (1981) 439.

[19] S. Leach, *J. Mol. Struct. 141* (1986) 43; *ibid. 157* (1986) 197.

[20] D. Stahl, F. Maquin, T. Gäumann, H. Schwarz, P.-A. Carrupt, P. Vogel, *J. Am. Chem. Soc. 107* (1985) 5049.

[21] J. A. Pople, B. Tidor, P. von R. Schleyer, *Chem. Phys. Lett. 88* (1982) 533.

[22] D. Mathur, C. Badrinathan, F. A. Rajgara, U. T. Raheja, *Chem. Phys. 103* (1986) 447; D. Mathur, C. Badrinathan, J. Phys. *B20* (1987) 1517; M. Hamdan, A. G. Brenton, D. Mathur, *Chem. Phys. Lett. 144* (1988) 387.

[23] R. W. Wetmore, R. K. Boyd, R. J. LeRoy, *Chem. Phys. 89* (1984) 329.

[24] W. Koch, B. Liu, T. Weiske, C. B. Lebrilla, T. Drewello, H. Schwarz, *Chem. Phys. Lett. 142* (1987) 147.

[25] M. W. Wong, L. Radom, *J. Am. Chem. Soc. 111* (1989) 1155.

[26] P. E. M. Siegbahn, *Chem. Phys. 66* (1982) 443.

[27] a) K. Lammertsma, G. A. Olah, M. Barzaghi, M. Simonetta, *J. Am. Chem. Soc. 104* (1982) 6851; b) K. Lammertsma, M. Barzaghi, G. A. Olah, J. A. Pople, P. von R. Schleyer, M. Simonetta, *ibid. 105* (1983) 5258.

[28] a) C. Guenat, F. Maquin, D. Stahl, W. Koch, H. Schwarz, *Int. J. Mass Spectrom. Ion Processes 63* (1985) 265; b) T. Drewello, T. Weiske, H. Schwarz, *Angew. Chem. 97* (1985) 855; *Angew. Chem. Int. Ed. Engl. 24* (1985) 869.

[29] T. Drewello, W. Koch, T. Weiske, H. Schwarz, D. Stahl, *Int. J. Mass Spectrom. Ion Processes 72* (1986) 313.

[30] W. J. Griffiths, F. M. Harris, *Rapid. Commun. Mass Spectrom. 2* (1988) 29.

[31] a) K. Leiter, K. Stephan, E. Märk, T. D. Märk, *Plasma Chem. Plasma Processes 4* (1984) 235 and references cited; b) T. Gäumann, C. Guenat, F. Maquin, D. Stahl, *Spectra 2000 11* (1983) 17.

[32] D. M. Curtis, J. H. D. Eland, *Int. J. Mass Spectrom. Ion Processes 63* (1985) 241.

[33] C. J. Porter, C. J. Proctor, T. Ast, J. H. Beynon, *Croat. Chem. Acta 54* (1981) 407.

[34] W. Koch, G. Frenking, *Chem. Phys. Lett. 114* (1985) 178.

[35] P. M. W. Gill, L. Radom, *Chem. Phys. Lett. 147* (1988) 213; *ibid. 136* (1987) 294.

[36] W. Koch, H. Schwarz, *Chem. Phys. Lett. 125* (1986) 443.

[37] a) W. Koch, G. Frenking, H. Schwarz, F. Maquin, D. Stahl, *J. Chem. Soc. Perkin Trans. 2 1986*, 757; b) W. Koch, G. Frenking, H. Schwarz, *J. Chem. Soc. Chem. Commun. 1985*, 1119; c) W. Koch, G. Frenking, C. C. Chang, *J. Chem. Phys. 84* (1986) 2703; d) C. J. Porter, C. J. Proctor, T. Ast, J. H. Beynon, *Int. J. Mass Spectrom. Ion. Phys. 41* (1982) 251; e) M. Rabrenović, F. M. Harris, G. A. Keenan, J. H. Beynon, *Chem. Phys. Lett. 102* (1983) 263.

[38] a) S. A. Pope, I. H. Hillier, M. F. Guest, *Faraday Symp. Chem. Soc. 19* (1984) 1; b) S. A. Pope, I. H. Hillier, M. F. Guest, J. Kendric, *Chem. Phys. Lett. 95* (1983) 247; c) R. K. Boyd, S. Singh, J. H. Beynon, *Chem. Phys. 100* (1985) 297; d) M. Hamdan, A. G. Brenton, *Int. J. Mass Spectrom. Ion Processes 84* (1988) 211.

[39] a) W. Koch, H. Schwarz, *Int. J. Mass Spectrom. Ion Processes 68* (1986) 49; b) J. A. Pople, P. von R. Schleyer, preliminary calculations; R. A. Whiteside, M. J. Frisch, J. A. Pople: *The Carnegie-Mellon Quantum*

Chemistry Archive, 3rd ed., Carnegie-Mellon University, Pittsburgh, PA, USA 1983.
[40] a) W. Koch, N. Heinrich, H. Schwarz, F. Maquin, D. Stahl, *Int. J. Mass Spectrom. Ion Processes 67* (1985) 305; b) G. A. Olah, G. K. S. Prakash, M. Barzaghi, K. Lammertsma, P. von R. Schleyer, J. A. Pople, *J. Am. Chem. Soc. 108* (1986) 1032.
[41] G. A. Olah, G. K. S. Prakash, M. Marcelli, K. Lammertsma, *J. Phys. Chem. 92* (1988) 878.
[42] J. A. Pople, M. J. Frisch, K. Raghavachari, P. von R. Schleyer, *J. Comput. Chem. 3* (1982) 468. For a detailed comparison of C_2H_2, $C_2H_2^{\odot\oplus}$ and $C_2H_2^{2\oplus}$, see A. T. Balaban, G. R. de Maré, R. A. Poisier, *J. Mol. Struct. (THEOCHEM) 183* (1989) 103.
[43] a) K. Lammertsma, M. Barzaghi, G. A. Olah, J. A. Pople, A. J. Kos, P. von R. Schleyer, *J. Am. Chem. Soc. 105* (1983) 5252; b) M. J. S. Dewar, C. H. Reynolds, *Theochem 29* (1986) 209; c) R. H. Nobes, M. W. Wong, L. Radom, *Chem. Phys. Lett. 136* (1987) 299; d) M. W. Wong, B. F. Yates, R. H. Nobes, L. Radom, *J. Am. Chem. Soc. 109* (1987) 3181; e) T. Ohwada, K. Shudo, *ibid. 111* (1989) 34.
[44] M. W. Wong, J. Baker, R. H. Nobes, L. Radom, *J. Am. Chem. Soc. 109* (1987) 2245.
[45] a) M. Rabrenović, J. H. Beynon, *Int. J. Mass Spectrom. Ion Processes 54* (1983) 79; b) E. E. Kingston, J. H. Beynon, T. Ast, R. Flammang, A. Maquestiau, *Org. Mass Spectrom. 20* (1985) 546.
[46] S. D. Peyerimhoff, R. J. Buenker, *J. Chem. Phys. 49* (1968) 312; G. A. Olah, M. Simonetta, *J. Am. Chem. Soc. 104* (1982) 330; P. von R. Schleyer, A. J. Kos, J. A. Pople, A. T. Balaban, *ibid. 104* (1982) 3771; G. C. Shields, T. F. Moran, *Org. Mass Spectrom. 21* (1986) 479.
[47] D. Stahl, F. Maquin, *Chimia 37* (1983) 87.
[48] K. Lammertsma, F. Maquin, P. von R. Schleyer, D. Stahl, Y.-D. Wu, unpublished. Whereas the $C_2H_6^{\odot\ominus}$ radical cation has been claimed to be detected in the gas phase (M. Rabrenović, J. H. Beynon, *J. Chem. Soc. Chem. Commun. 1983*, 1043) a theoretical study indicated its stability in the $CH_2CH_4^{\odot\oplus}$ (methylene methonium) form to be marginal i.e., J. Baker, E. E. Kingston, W. J. Bouma, A. G. Brenton, L. Radom, *ibid. 1985*, 1625.
[49] M. Rabrenović, J. H. Beynon, *Int. J. Mass Spectrom. Ion Processes 56* (1984) 85.
[50] a) G. Frenking, W. Koch, H. Schwarz, *J. Comput. Chem. 7* (1986) 406; b) W. Koch, G. Frenking, F. Maquin, D. Stahl, H. Schwarz, *J. Chem. Soc. Chem. Commun. 1984*, 1187; c) F. Maquin, D. Stahl, unpublished results.
[51] D. Stahl, F. Maquin, *Chem. Phys. Lett. 106* (1984) 531.
[52] Reference 43d. For earlier references on $COH_2^{2\oplus}$, see: W. J. Bouma, L. Radom, *J. Am. Chem. Soc. 105* (1983) 5484; P. Cremaschi, M. Simonetta, *Theor. Chim. Acta 43* (1977) 351; N. L. Summers, J. Tyrrell, *J. Am. Chem. Soc. 99* (1977) 3960.
[53] a) W. Koch, F. Maquin, H. Schwarz, D. Stahl, *J. Am. Chem. Soc. 107* (1985) 2256; b) W. Koch, N. Heinrich, H. Schwarz, *ibid. 108* (1986) 5400.
[54] a) C. Wesdemiotis, R. Feng, P. O. Danis, E. R. Williams, F. W. McLafferty, *J. Am. Chem. Soc. 108* (1986) 5847; b) J. A. Pople, K. Raghavachari, M. J. Frisch, J. S. Binkley, P. von R. Schleyer, *ibid. 105* (1983) 6389; c) B. F. Yates, W. J. Bouma, L. Radom, *ibid. 109* (1987) 2250.
[55] a) J. L. Holmes, F. P. Lossing, J. K. Terlouw, P. C. Burgers, *J. Am. Chem. Soc. 104* (1982) 2931; b) J. L. Holmes, F. P. Lossing, J. K. Terlouw, P. C. Burgers, *Can. J. Chem. 61* (1983) 2305; c) F. Maquin, D. Stahl, A. Sawaryn, P. von R. Schleyer, W. Koch, G. Frenking, H. Schwarz, *J. Chem. Soc. Chem. Commun. 1984*, 504.
[56] B. F. Yates, W. J. Bouma, L. Radom, *J. Am. Chem. Soc. 108* (1986) 6545.
[57] T. Drewello, W. Koch, C. B. Lebrilla, D. Stahl, H. Schwarz, *J. Am. Chem. Soc. 109* (1987) 2922.
[58] See for example B. Frlec, D. Gantar, L. Golič, I. Leban, *Acta Crystallogr., Sect. B 37* (1981) 666 and references cited. For leading references see ref. 14, 34 und 37 in [59].
[59] W. J. Bouma, L. Radom, *J. Am. Chem. Soc. 107* (1985) 345.
[60] P. M. W. Gill, L. Radom, *J. Am. Chem. Soc 111* (1989) 4613.
[61] T. Drewello, C. B. Lebrilla, H. Schwarz, D. Stall, *Int. J. Mass Spectrom. Ion Processes 77* (1987) R3.
[62] a) B. P. Mathur, E. M. Burgess, D. E. Bostwick, T. F. Moran, *Org. Mass Spectrom. 16* (1981) 92; b) J. R. Appling, K. M. Musier, T. F. Moran, *ibid. 19* (1984) 412.
[63] B. Brehm, U. Fröbe, H.-P. Neitzke, *Int. J. Mass Spectrom. Ion Processes 57* (1984) 91.
[64] M. Rabrenović, J. H. Beynon, *Int. J. Mass Spectrom. Ion Processes 54* (1983) 87.
[65] G. W. Burdick, G. C. Shields, J. R. Appling, T. F. Moran, *Int. J. Mass Spectrom. Ion Processes 64* (1985) 315; J. R. Appling, T. F. Moran, *Chem. Phys. Lett. 118* (1985) 188; J. R. Appling, G. C. Shields, T. F. Moran, *Org. Mass Spectrom. 21* (1986) 69; G. C. Shields, T. F. Moran, *Theor. Chim. Acta 69* (1986) 147.
[66] P. A. Carrupt, F. Maquin, D. Stahl, *Adv. Mass Spectrom. 10* (1986) 775.
[67] K. Lammertsma, J. A. Pople, P. von R. Schleyer, *J. Am. Chem. Soc. 108* (1986) 7; *Theochem. 7* (1986) 183.
[68] K. Lammertsma, *J. Am. Chem. Soc. 108* (1986) 5127.
[69] B. E. Jones, L. A. Abbey, H. L. Chatham, A. W. Hanner, L. A. Teleshefsky, E. M. Burgess, T. F. Moran, *Org. Mass Spectrom. 17* (1982) 10.
[70] R. E. March, *Org. Mass Spectrom. 22* (1987) 545.
[71] A. A. Mommers, P. C. Burgers, J. L. Holmes, J. K. Terlouw, *Org. Mass Spectrom. 19* (1984) 7.
[72] B. Brehm, G. De Frênes, *Adv. Mass Spectrom. 8A* (1980) 138.
[73] J. L. Franklin, A. Mogenis, *J. Phys. Chem. 71* (1967) 2820.
[74] R. Weiss, H. Kölbl, C. Schlierf, *J. Org. Chem. 41* (1976) 2258; T. Clark, R. Weiss, *ibid. 45* (1980) 1790.
[75] P. von R. Schleyer, K. Lammertsma, unpublished results.
[76] G. A. Olah, J. S. Staral, *J. Am. Chem. Soc. 98* (1976) 6290; G. A. Olah, J. S. Staral, R. J. Spear, G. Liang, *ibid. 97* (1975) 5489; G. A. Olah, G. D. Mateescu, *ibid. 92* (1970) 1430; G. A. Olah, J. M. Bollinger, A. M. White, *ibid. 91* (1969) 3667.
[77] a) J. Chandrasekhar, P. von R. Schleyer, K. Krogh-Jespersen, *J. Comput. Chem. 2* (1981) 356; b) K. Krogh-Jespersen, D. Cremer, J. D. Dill, J. A. Pople, P. von R. Schleyer, *J. Am. Chem. Soc. 103* (1981) 2589; c) K. Krogh-Jespersen, P. von R. Schleyer, J. A. Pople, D. Cremer, *ibid. 100* (1978) 4301; d) B. A. Hess, C. S. Ewig, L. J. Schaad, *J. Org. Chem. 50* (1985) 5869.
[78] M. Bremer, P. von R. Schleyer, V. Fleischer, *J. Am. Chem. Soc. 111* (1989) 1147.
[79] W. Kutzelnigg, *Isr. J. Chem. 19* (1980) 193; M. Schindler, W. Kutzelnigg, *J. Chem. Phys. 76* (1982) 1919; For a typical application on carbocations, see: M. Schindler, *J. Am. Chem. Soc. 109* (1987) 1020.
[80] K. Lammertsma, P. von R. Schleyer, *J. Phys. Chem. 92* (1988) 881.
[81] H. Wolf, R. Weiss, *Chem. Ber. 113* (1980) 1746; R. Gompper, E. Bartmann, *Angew. Chem. 90* (1978) 490; *Angew. Chem. Int. Ed. Engl. 17* (1978) 456; Z.-I. Yoshida, H. Konishi, S.-I. Sawada, H. Ogoshi, *J. Chem. Soc. Chem. Commun. 1977*, 850.
[82] a) M. J. Hayward, Md. A. Mabud, R. G. Cooks, *J. Am. Chem. Soc. 110* (1988) 1343; b) K. Vékey, A. G. Brenton, J. H. Beynon, *J. Phys. Chem. 90* (1986) 3569; c) R. G. Kingston, M. Guilhaus, A. G. Brenton, J. H. Beynon, *Org. Mass Spectrom. 20* (1985) 406; d) M. Guilhaus, R. G. Kingston, A. G. Brenton, J. H. Beynon, *ibid. 20* (1985) 424, 565; e) J. R. Appling, G. W. Burdick, M. J. Hayward, L. E. Abbey, T. F. Moran, *J. Phys. Chem. 89* (1985) 13; f) R. Engel, D. Halpern, B.-A. Funk, *Org. Mass Spectrom. 7* (1973) 177; g) J. H. Beynon, A. E. Fontaine, *J. Chem. Soc. Chem. Commun., 1966*, 717; h) W. Higgins, K. R. Jennings, *ibid. 1965*, 99; i) M. Rabrenović, A. G. Brenton, T. Ast, *Org. Mass Spectrom. 10* (1983) 587.
[83] K. Lammertsma, O. F. Güner, A. F. Thibodeaux, P. von R. Schleyer, *J. Am. Chem. Soc.*, in press.
[84] H. Hogeveen, P. W. Kwant, *Tetrahedron Lett. 1973*, 1665; Idem, *J. Am. Chem. Soc. 96* (1974) 2208; *Acc. Chem. Res. 8* (1975) 413; C. Giordano, R. F. Heldeweg, H. Hogeveen, *J. Am. Chem. Soc. 99* (1977) 5181; H. Hogeveen, E. M. G. A. van Kruchten, *J. Org. Chem. 46* (1981) 1350.
[85] a) K. Lammertsma, P. von R. Schleyer, *J. Am. Chem. Soc. 105* (1983) 1049; b) H. Schwarz, *Angew. Chem. 93* (1981) 1046; *Angew. Chem. Int. Ed. Engl. 20* (1981) 991.
[86] a) M. J. S. Dewar, M. K. Holloway, *J. Am. Chem. Soc. 106* (1984) 6619; b) T. W. Bentley, C. A. Wellington, *Org. Mass Spectrom. 16* (1981) 523; c) H. T. Jonkman, W. C. Nieuwpoort, *Tetrahedron Lett. 1973*, 1671; d) E. D. Jemmis, P. von R. Schleyer, *J. Am. Chem. Soc. 104* (1982) 4781.
[87] G. W. Klumpp, J. Fleischhauer, W. Schleker, *Recl. Trav. Chim. Pays-Bas 101* (1982) 208.
[88] G. A. Olah, J. S. Staral, G. Liang, L. A. Paquette, W. P. Melega, M. J. Carmody, *J. Am. Chem. Soc. 99* (1977) 3349; G. A. Olah, G. Liang, L. A. Paquette, W. P. Melega, *ibid. 98* (1976) 4327; G. A. Olah, J. S. Staral, L. A. Paquette, *ibid. 98* (1976) 1267.
[89] T. Clark, P. von R. Schleyer, *Nouv. J. Chim. 2* (1978) 665; L. Radom, H. F. Schaefer III, *J. Am. Chem. Soc. 99* (1977) 7522; M. Bremer, *Dissertation*, Erlangen, 1989.
[90] J. R. Appling, K. M. Musier, L. E. Abbey, T. F. Moran, *Org. Mass Spectrom. 19* (1984) 524.
[91] F. Borchers, K. Levsen, *Org. Mass Spectrom. 10* (1975) 584.
[92] J. H. van't Hoff: *La Chimie dans l'Espace*, Bazendyk, Rotterdam 1875; *The Arrangement of Atoms in Space*, 2nd ed., Longmans, Green, and Co., New York 1898, p. 103–105.
[93] K. Lammertsma, *J. Am. Chem. Soc. 106* (1984) 4619.
[94] W. Koch, G. Frenking, J. Gauss, D. Cremer, *J. Am. Chem. Soc. 108* (1986) 5808.
[95] W. Koch, F. Maquin, D. Stahl, H. Schwarz, *J. Chem. Soc. Chem. Commun. 1984*, 1679.
[96] B. van Baar, T. Weiske, J. K. Terlouw, H. Schwarz, *Angew. Chem. 98* (1986) 275; *Angew. Chem. Int. Ed. Engl. 25* (1986) 282.
[97] B. van Baar, W. Koch, C. B. Lebrilla, J. K. Terlouw, T. Weiske, H. Schwarz, *Angew. Chem. 98* (1986) 834; *Angew. Chem. Int. Ed. Engl. 25* (1986) 827.
[98] W. Koch, G. Frenking, H. Schwarz, F. Maquin, D. Stahl, *Int. J. Mass Spectrom. Ion Processes 63* (1985) 59.
[99] a) L. A. Teleshefsky, B. E. Jones, L. E. Abbey, D. E. Bostwick, E. M. Burgess, T. F. Moran, *Org. Mass Spectrom. 17* (1982) 481; b) W. Koch, H.

Schwarz, F. Maquin, D. Stahl, *Int. J. Mass Spectrom. Ion Processes 67* (1985) 171; c) Recent results prove that charge stripping of $CH_3CO^{\oplus}$ gives rise to the formation of $H_2C=C-OH^{\odot 2\oplus}$. T. Drewello, H. Schwarz, *ibid. 87* (1989) 135.

[100] J. F. McGarrity, D. P. Cox, *J. Am. Chem. Soc. 105* (1983) 3961.

[101] W. Koch, B. Liu, P. von R. Schleyer, *J. Am. Chem. Soc. 111* (1989) 3474; P. von R. Schleyer, J. W. de M. Carneiro, W. Koch, K. Raghavachari, *ibid. 111* (1989) 5475; P. von R. Schleyer, W. Koch, B. Liu, U. Fleischer, *J. Chem. Soc. Chem. Commun. 1989*, 1098; P. von R. Schleyer, J. W. de M. Carneiro, W. Koch, D. A. Forsyth, unpublished.

[102] R. R. Mohr, W. N. Lipscomb, *Inorg. Chem. 25* (1986) 1053.

[103] K. Raghavachari, R. A. Whiteside, J. A. Pople, P. von R. Schleyer, *J. Am. Chem. Soc. 103* (1981) 5649.

[104] a) N. C. Baenziger, R. E. Buckles, T. D. Simpson, *J. Am. Chem. Soc. 89* (1967) 3405; b) R. Gompper, J. Schelble, C. S. Schneider, *Tetrahedron Lett. 1978*, 3897.

[105] G. A. Olah, J. L. Grant, R. J. Spear, J. M. Bollinger, A. Serianz, G. Sipos, *J. Am. Chem. Soc. 98* (1976) 2501.

[106] K. Lammertsma, H. Cerfontain, *J. Am. Chem. Soc. 102* (1980) 3257; K. Lammertsma, O. F. Güner, S.-W. Yang, W. Koch, B. W. Liu, unpublished results.

[107] a) T. Gramstad, S. Husebye, J. Saebø, *Tetrahedron Lett. 24* (1983) 3919; b) T. Gramstad, S. Husebye, K. Maartman-Moe, J. Saebø, *Acta Chem. Scand. Ser. B39* (1985) 35; c) P. J. Stang, G. Maas, T. E. Fisk, *J. Am. Chem. Soc. 102* (1980) 6361; d) P. J. Stang, G. Maas, D. L. Smith, J. A. McCloskey, *ibid. 103* (1981) 4837, e) G. Maas, P. J. Stang, *J. Org. Chem. 48* (1983) 3038; f) R. F. Childs, R. Faggiani, C. J. L. Lock, C. V. Rogerson, *ibid. 48* (1983) 3043; g) Y. Apeloig, D. Arad, *J. Am. Chem. Soc. 103* (1981) 4258.

[108] a) P. von R. Schleyer, R. Herges, unpublished results; b) K. Lammertsma, O. F. Güner, M.-F. Burkart, P. von R. Schleyer, unpublished results.

[109] a) K. B. Wiberg, R. F. W. Bader, C. D. H. Lau, *J. Am. Chem. Soc. 109* (1987) 985; b) K. Lammertsma, O. F. Güner, R. F. W. Bader, unpublished results; c) D. Feller, E. R. Davidson, *J. Am. Chem. Soc. 109* (1987) 4133; d) J. E. Jackson, L. C. Allen, *ibid. 106* (1984) 591.

[110] a) A. de Meijere, O. Schallner, P. Gölitz, W. Weber, P. von R. Schleyer, G. K. S. Prakash, G. A. Olah, *J. Org. Chem. 50* (1985) 5255; b) G. A. Olah, G. Liang, P. von R. Schleyer, E. M. Engler, M. J. S. Dewar, R. C. Bingham, *J. Am. Chem. Soc. 95* (1973) 6829; c) M. Bremer, P. von R. Schleyer, U. Fleischer, unpublished calibrations; d) M. Bremer, *Dissertation*, Universität Erlangen-Nürnberg 1989.

[111] G. A. Olah, G. Liang, P. von R. Schleyer, W. Parker, C. I. F. Watt, *J. Am. Chem. Soc. 99* (1977) 966.

[112] a) A. de Meijere, O. Schallner, C. Weitemeyer, W. Spielmann, *Chem. Ber. 112* (1979) 908; b) A. de Meijere, O. Schallner, G. A. Mateescu, P. Gölitz, P. Bischof, *Helv. Chim. Acta 68* (1985) 1114.

[113] G. K. S. Prakash, A. P. Fung, T. N. Rawdah, G. A. Olah, *J. Am. Chem. Soc. 107* (1985) 2920.

[114] G. A. Olah, G. K. S. Prakash, T. N. Rawdah, *J. Am. Chem. Soc. 102* (1980) 6127.

[115] G. K. S. Prakash, M. Farnia, S. Keyanian, G. A. Olah, H. J. Kuhn, K. Schaffner, *J. Am. Chem. Soc. 109* (1987) 911.

[116] W.-D. Fessner, G. Sedelmeier, P. R. Spurr, G. Rihs, H. Prinzbach, *J. Am. Chem. Soc. 109* (1987) 4626; H. Prinzbach, B. A. R. C. Murty, W.-D. Fessner, J. Mortensen, J. Heinze, G. Gescheidt, F. Gerson, *Angew. Chem. 99* (1987) 488; *Angew. Chem. Int. Ed. Engl. 26* (1987) 457.

[117] G. K. S. Prakash, V. V. Krishnamurthy, R. Herges, R. Bau, H. Yuan, G. A. Olah, W.-D. Fessner, H. Prinzbach, *J. Am. Chem. Soc. 108* (1986) 836; *ibid. 110* (1988) 7764.

[118] T. Drewello, W.-D. Fessner, A. J. Kos, C. B. Lebrilla, H. Prinzbach, P. von R. Schleyer, H. Schwarz, *Chem. Ber. 121* (1988) 187.

[119] R. J. Ternansky, D. W. Balogh, L. A. Paquette, *J. Am. Chem. Soc. 104* (1982) 4503; L. A. Paquette, R. J. Ternansky, D. W. Balogh, G. Kentgen, *ibid. 105* (1983) 5446; W.-D. Fessner, B. A. R. C. Murty, J. Wörth, D. Hunkler, H. Fritz, H. Prinzbach, W. D. Roth, P. von R. Schleyer, A. B. McEwen, M. F. Maier, *Angew. Chem. 99* (1987) 484; *Angew. Chem. Int. Ed. Engl. 26* (1987) 452.

[120] L. A. Paquette, J. C. Weber, T. Kobayashi, *J. Am. Chem. Soc. 110* (1988) 1303.

[121] G. A. Olah, G. K. S. Prakash, T. Kobayashi, L. A. Paquette, *J. Am. Chem. Soc. 110* (1988) 1304; G. A. Olah, G. K. S. Prakash, W.-D. Fessner, T. Kobayashi, L. A. Paquette, *ibid. 110* (1988) 8599.

[122] G. A. Olah, G. K. S. Prakash, J. G. Shih, V. V. Krishnamurthy, G. D. Mateescu, G. Liang, G. Sipos, V. Buss, T. M. Gund, P. von R. Schleyer, *J. Am. Chem. Soc. 107* (1985) 2764.

[123] P. Gund, *J. Chem. Educ. 49* (1972) 100.

[124] a) T. Clark, D. Wilhelm, P. von R. Schleyer, *Tetrahedron Lett. 23* (1982) 3547; b) M. Bremer, P. von R. Schleyer, unpublished results, find a different order at ab initio levels.

[125] K. Schötz, T. Clark, H. Schaller, P. von R. Schleyer, *J. Org. Chem. 49* (1984) 733.

[126] M. Bremer, P. von R. Schleyer, K. Schoetz, M. Kausch, M. Schindler, *Angew. Chem. 99* (1987) 795; *Angew. Chem. Int. Ed. Engl. 26* (1987) 761.

Communications may be submitted in English *or* in German. Further details regarding the submission of communications can be found in the "Notice to Authors" reproduced in the January issue of the journal. Copies thereof may be obtained from the editorial office upon request.

Metal-Induced Reduction of Sulfur Dioxide to Sulfur Monoxide and Sulfur**

By *Armin Neher* and *Ingo-Peter Lorenz**

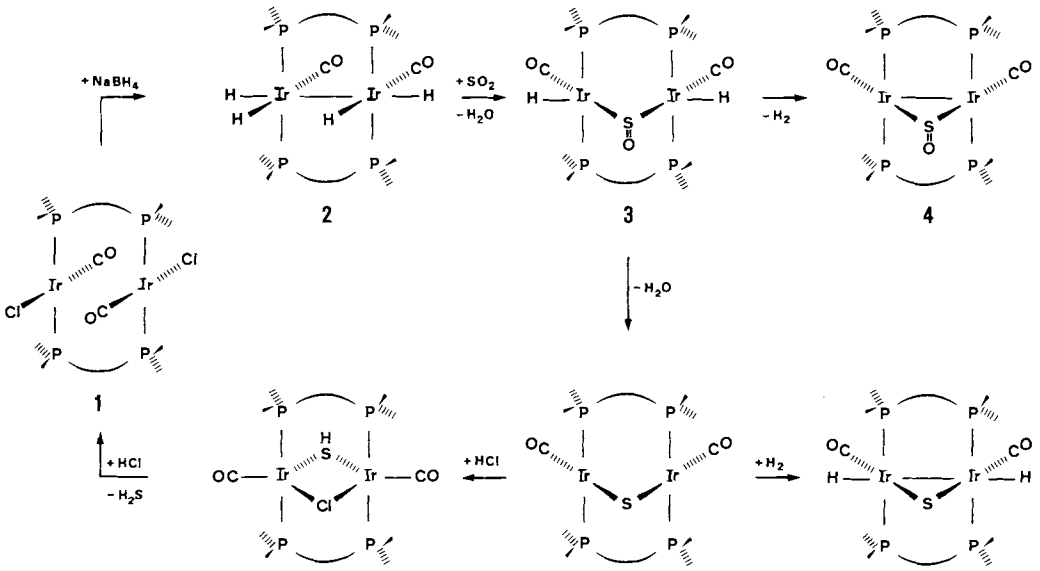
Sulfur dioxide is an important and versatile reagent in the chemistry of transition-metal complexes. Free SO_2 can be added to or inserted into complexes: coordinated SO_2 can undergo elimination, substitution, addition, oxidation, and reduction reactions. A focus of interest is the reduction of SO_2, particularly the development of model systems for the reductive removal of SO_2 from flue gas and, in bioinorganic chemistry, for the active center of sulfite reductase. Transition-metal-mediated reductions of SO_2 have so far afforded disulfido,[1] thiosulfato,[2] and dithionito complexes[3]—the latter via the metallosulfinic acids.

In our investigations of sulfur monoxide as a complex ligand, we succeeded in deoxygenating free SO_2 to complex-bound sulfur monoxide and sulfur. To reduce SO_2, we used the tetrahydrido complex $[Ir(CO)(dppm)H_2]_2$ **2** (dppm = $Ph_2PCH_2PPh_2$), which is more easily obtained from the dichloro complex **1**[4] and $NaBH_4$ in refluxing ethanol than according to the literature procedure.[5]

When SO_2 is bubbled through a solution of **2** in toluene, the very unstable μ-SO complex **3**, containing two hydrido ligands, is initially formed. Complex **3** gives two decomposition products upon chromatographic workup on silica gel: loss of H_2 or H_2O leads to the μ-SO complex **4** or the μ-S complex **5**. Bubbling SO_2 for at least 30 min through a solution of **2** in toluene results in a red solution containing mainly **5** along with a small amount of **4**. The μ-S complex **5** was identified by analytical and spectroscopic comparison with an authentic sample, accessible by reaction of **1** with sodium sulfide.[6] Analogous reactions in CH_2Cl_2 or THF afforded smaller yields of **5**.

To carry out the reaction catalytically, we attempted to reduce **5** further in the hope of liberating the μ_2-sulfur as H_2S. However, we failed to obtain the expected hydrido complex **2** either by simply bubbling H_2 through solutions of **5** (cf. Ref. [7]) or by treating **5** with H_2 in an autoclave (80 bar, 60 °C). Instead, we obtained the known[6] isomeric mixture of **6** with an iridium:hydride ratio of 1:1; this product is also obtained by controlled reduction of **5** with $NaBH_4$ in ethanol (Scheme 1).

As a further possibility for liberating H_2S from **5**, we investigated the stepwise protonation of the μ_2-sulfur ligand. Admission of HCl gas to a solution of **5** in THF results in formation, after only a few minutes, of the mixed bridged complex **7**. Only after 5 d of stirring is the SH bridge gone.



Scheme 1.

The product thereby obtained is the purple starting material **1**. Thus, the cycle shown in Scheme 1 is complete. These stoichiometric reactions indicate that **1** might be used catalytically in the reduction of SO_2 (cf. Scheme 2). If reduction

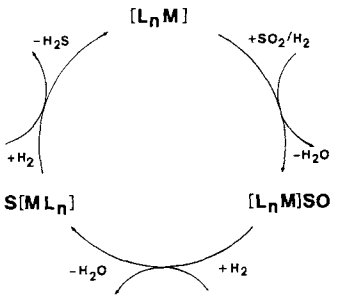
1	+	3 H_2	⟶	**2**	+	2 HCl
2	+	SO_2	⟶	**5**	+	2 H_2O
5	+	2 HCl	⟶	**1**	+	H_2S
3 H_2	+	SO_2	⟶	2 H_2O	+	H_2S

Scheme 2.

[*] Prof. Dr. I.-P. Lorenz, Dipl.-Chem. A. Neher
Institut für Anorganische Chemie der Universität
Auf der Morgenstelle 18, D-7400 Tübingen (FRG)

[**] This work was supported by the Deutsche Forschungsgemeinschaft, the Fonds der Chemischen Industrie, and Degussa AG. *A. N.* thanks the Fonds der Chemischen Industrie for a doctoral fellowship.

of **1** to **2** is possible with H_2 instead of $NaBH_4$, a catalytic reaction as shown in Scheme 3 would be conceivable. We are currently investigating this possibility.



Scheme 3.

Complexes **1–7** were characterized by IR and $^{31}P\{^1H\}$ NMR spectroscopy and by FAB mass spectrometry (Table 1). The CO complexes **1** and **7**, which have *trans* configurations, show only one ν(CO) absorption band in the IR

Table 1. Important spectroscopic data for complexes **1–7**.

Compd	IR $\tilde{\nu}$ [cm^{-1}] [a] ν(CO)/ν(SO)	$^{31}P\{^1H\}$ NMR [b] δ	FAB MS *m/z*	Color
1	1953 sst	2.3, s	–	purple [4]
2	1890 sst, 1933 st	−4.8, s	1210, $(M-4)^{\oplus}$	orange [5]
3	1950 m, 2020 sst/1135	−1.4, m −20.2, m	1258, $(M-2)^{\oplus}$	yellow
4	1962 sst, 1990 st/1150	−9.0, s	1258, $(M)^{\oplus}$	red
5	1905 sst 1920 st	3.6, s	1242, $(M)^{\oplus}$	red [6]
6	1921 st 1980 sst	−6.6, m −18.8, m	1242, $(M-2)^{\oplus}$	yellow [7]
7	2030 sst	−12.6, s	1278, $(M)^{\oplus}$	gray

[a] Solid, KBr. [b] In CH_2Cl_2 at −40 °C.

spectrum: by contrast, the two ν(CO) absorptions of complexes **2–6** indicate a *cis* arrangement of the CO ligands. The relatively high wavenumber of the ν(SO) bands of the two SO complexes **3** and **4** indicates a four-electron donor function of the SO bridging ligand, which hinders polarization of the $S^{\delta\oplus}=O^{\delta\ominus}$ bond and increases the SO bond order. Accordingly, **3** and **4** are 18-electron compounds. The very similar ^1H NMR spectra of these complexes provide little information; those of the hydrido complexes **2, 3** and **6** display multiplets at −10 to −12 ppm. Resolution of the signals and isomer assignment, as in Ref. [7], has not yet been accomplished. As the $^{31}P\{^1H\}$ NMR spectra show, the hydrido species **3** and **6** consist of mixtures of isomers (only one isomer of each species is shown in Scheme 1; cf. Ref. [7]). Thus, depending on the coordination of the hydride ligands, both singlet and multiplet signals are observed for the phosphorus atoms of the dppm ligand, whereas the other, symmetrically bridged complexes **2, 4, 5** and **7** each show only singlets. On the other hand, similar compounds of rhodium exhibit complicated splitting patterns.[8] The FAB mass spectrum of each compound, except for the hydrido complexes **2, 3,** and **6**, always contains the molecular ion peak.

The reaction of **2** with SO_2 confirms that a direct transition-metal-promoted reduction of sulfur dioxide via sulfur monoxide to sulfur is possible. The four hydrogen atoms required for the reduction are present at the reaction center and the individual intermediates can be identified. As the results for the palladium[9] and rhodium[8] systems have already shown, the relatively stable A-frame complexes play an important role in these reactions. At the same time, this work offers an alternative synthesis of SO complexes.[10]

Experimental Procedure

2: A suspension of **1** (200 mg, 0.156 mmol) and $NaBH_4$ (48 mg, 1.25 mmol) in 15 mL of ethanol was refluxed for 15 min, the color changing from purple to orange. After cooling, the reaction mixture was filtered and the product was washed with ethanol and dried under vacuum. Yield: 134 mg (71%).

3: A weak stream of SO_2 was bubbled for 3 min through a solution of **2** (92 mg, 0.076 mmol) in 15 mL of toluene. The yellow precipitate of **3** thereby formed was completely precipitated by addition of *n*-hexane, filtered, and dried under vacuum. Yield: 76 mg (78%).

4, 5: a) Chromatography of **3** on silica gel with THF as eluant afforded two red fractions containing **4** and **5**. Yield: 29 mg (38%) **4** and 33 mg (44%) **5** (R_f = 0.65 (**4**), 0.79 (**5**)). b) SO_2 was bubbled for 30 min through a solution of **2** (85 mg, 0.07 mmol) in 15 mL of toluene; concentration of the reaction solution to about 2 mL and chromatography on silica gel afforded **5** as the first red fraction. Yield: 70 mg (80%).

6: Hydrogenation reactions: a) H_2 was bubbled for 30 min through a solution of **5** in CH_2Cl_2. b) 3 h under H_2 in an autoclave at 60 °C and 80 bar. c) A solution of **5** (30 mg, 0.024 mmol) and $NaBH_4$ (38 mg, 0.173 mmol) in 5 mL of ethanol was stirred for 2 h. In each case, an isomeric mixture of **6** was obtained.

7: After HCl was bubbled for 10 min through a solution of **5** (60 mg, 0.048 mmol) in 10 mL of THF, a marked color change from red to yellow occurred. Addition of 20 mL of *n*-hexane resulted in the precipitation of **7** as a gray powder, which was filtered, washed and dried under vacuum. Yield: 58 mg (95%). When HCl was bubbled through the yellow solution of **7** for 30 min, the solution gradually turned red; after 5 d of stirring, 30 mg (50%) of **1** was obtained.

Received: April 28, 1989 [Z 3311 IE]
German version: *Angew. Chem. 101* (1989) 1389

[1] C. R. Brulet, S. S. Isied, H. Taube, *J. Am. Chem. Soc. 95* (1973) 4758.
[2] G. J. Kubas, R. R. Ryan, *Inorg. Chem. 23* (1984) 3181.
[3] G. J. Kubas, H. J. Wassermann, R. R. Ryan, *Organometallics 4* (1985) 2012.
[4] B. R. Sutherland, M. Cowie, *Inorg. Chem. 23* (1984) 2324.
[5] R. McDonald, B. R. Sutherland, M. Cowie, *Inorg. Chem. 26* (1987) 3333.
[6] C. P. Kubiak, C. Woodcock, R. Eisenberg, *Inorg. Chem. 19* (1980) 2733.
[7] B. A. Vaarstra, K. N. O'Brien, R. Eisenberg, M. Cowie *Inorg. Chem. 27* (1988) 3668.
[8] A. Neher, O. Heyke, I.-P. Lorenz, *Z. Anorg. Allg. Chem.*, in press; A. Neher, *Dissertation*, Universität Tübingen, 1989.
[9] G. Besenyei, C.-L. Lee, J. Gulinski, S. J. Rettig, B. R. James, D. A. Nelson, M. A. Lilga, *Inorg. Chem. 26* (1987) 3622.
[10] W. A. Schenk, *Angew. Chem. 99* (1987) 101; *Angew. Chem. Int. Ed. Engl. 26* (1987) 98.

From the Bicyclo[3.3.0]octane Framework to Multiply Bridged [12]Annulenes and Semibullvalenes**

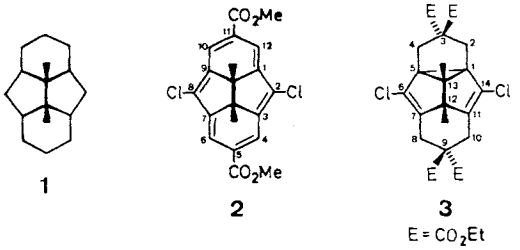
By *Harald Kohnz, Bernhard Düll,* and *Klaus Müllen**

The previously unknown tetracycle **1** (12,13-*cis*-dimethyltetracyclo[9.2.1.0^{5,13}.0^{7,12}]tetradecane) is the basic framework of attractive target compounds. Generation of cyclic π conjugation would lead to an ethanediylidene-[12]annulene and suitable transformation of the central bicyclo[3.3.0]octane unit would lead to a long-sought doubly

[*] Prof. Dr. K. Müllen, Dr. H. Kohnz, Dipl.-Chem. B. Düll
Institut für Organische Chemie der Universität
Johann-Joachim-Becher-Weg 18–22, D-6500 Mainz 1 (FRG)

[**] This work was supported by the Deutsche Forschungsgemeinschaft and the Fonds der Chemischen Industrie.

bridged semibullvalene. We report here on compounds **2** and **3**, the first examples of the two title compounds. Annulene **2** can serve as a conformationally rigid 12π analogue of cyclooctatetraene for studying electron-transfer processes, and the strained semibullvalene **3** is of interest for investigating extremely rapid Cope rearrangements.



1 **2** **3**
E = CO_2Et

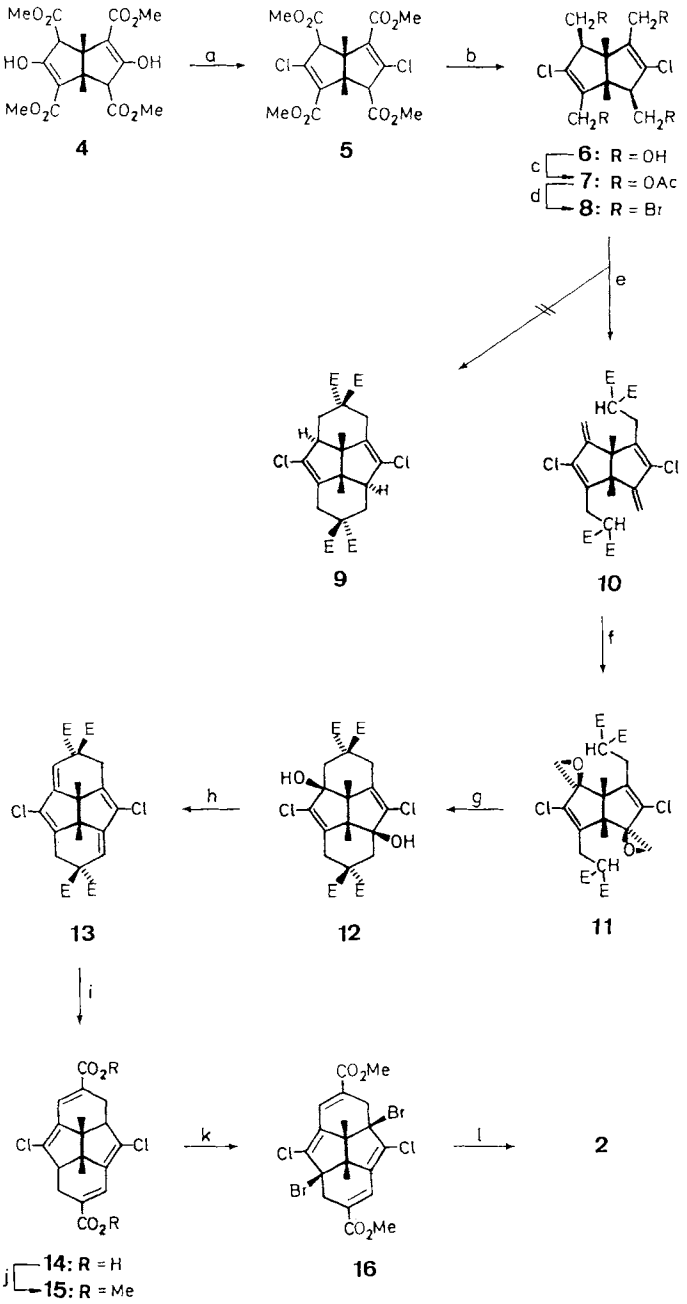
The readily accessible tetraester **4**[1] is a convenient starting material for the synthesis of **2** and **3**, since it already contains 14 of the 16 required C atoms (of **1**) in the topologically correct arrangement.[2] The synthetic strategy (Scheme 1) envisioned the coupling of two malonate moieties with a tetrafunctional electrophile derived from **4**. In order to preserve the double bonds of the "bis-enol" **4** and to establish their *anti* arrangement, dichloride **5** was generated by treatment of **4** with phosphorus pentachloride and re-formation of the allyl ester functions, which were also attacked. Tetrol **6**, formed by reduction of **5**, was transformed into the tetrafunctional bromide **8** via the tetraacetate intermediate **7**.

Direct incorporation of a malonate ester (with formation of **9**) is not possible for steric reasons. Treatment of **8** with potassium diethyl malonate leads instead to **10**. Therefore, a new electrophile (**11**) with "inverted" configuration at C-4 and C-8 was generated by regioselective and *exo*-stereoselective epoxidation of the exocyclic double bonds of **10** with *m*-chloroperbenzoic acid in diethyl ether. After deprotonation with potassium *tert*-butoxide, double ring closure occurs to give diol **12**. The routes leading to annulene **2** and semibullvalene **3** (Scheme 3) branch at this point.

Diol **12** cannot be isolated without decomposition. However, the tetrahydro[12]annulene **13**, formed by acidic dehydration, is stable. Saponification and decarboxylation of the malonate ester moieties afford dicarboxylic acid **14** under mild conditions. Compound **14** is converted into its dimethyl ester **15** by treatment with diazomethane in ether. Dibromide **16** is formed by selective Wohl–Ziegler bromination and can be dehydrobrominated with potassium acetate in acetonitrile to give **2**.

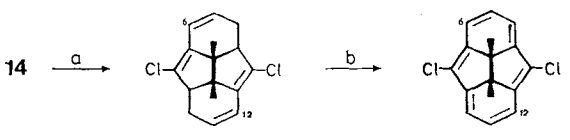
The presence of (alkoxycarbonyl and chloro) substituents in **2** is important, since, on the one hand, they contribute to stabilization of the $4n\pi$ annulene and, on the other hand, they allow coupling of several annulene units and therefore oligomerization of redox-active $4n\pi$ systems.[3] Compound **14** can be decarboxylated to **17**, which, in turn, may be transformed into the [12]annulene **18** by bromination/dehydrobromination (Scheme 2).

The [12]annulene **2** [^{1}H NMR (200 MHz, [D$_8$]THF: δ = 2.51 (CH_3), 3.69 (OCH_3), 5.95 (H-4,6,10,12)][4] forms green-black crystals (m.p. 140–142 °C), which dissolve in organic solvents to afford orange-brown solutions. Comparison of the ^{1}H NMR chemical shifts of annulenes **2** and **18** [^{1}H NMR (200 MHz, $CDCl_3$): δ = 2.58 (CH_3), 5.1–5.5 (m, CH)] with those of the model compounds **15** and **17**, which are not cyclically conjugated, reveals significant shielding of



Schema 1. a) 1. 6 PCl_5, $CHCl_3$, Δ, 5 h; 2. MeOH/H$^\oplus$, 65%. b) $LiAlH_4$, ether, Δ, 4 h. c) Ac_2O, pyridine, 100 °C, 2 h, b + c: 65%. d) HBr 33% in AcOH, 85 °C, 2 d, 88%. e) 4 $KCH(CO_2Et)_2$, DME/THF, RT, 80%. f) *m*-Chloroperbenzoic acid, ether, RT, 18 h. g) KO*t*Bu, THF, 0 °C → RT, 2 h. h) *p*-CH_3–C_6H_4–SO_3H, $CHCl_3$, Δ, 2 h, f–h: 30%. i) KOH, MeOH/H_2O. j) CH_2N_2, ether, i + j: 81%. k) 2 *N*-Bromosuccinimide/CCl_4, 85%. l) KOAc, acetonitrile, Δ, 12 h, 50%.

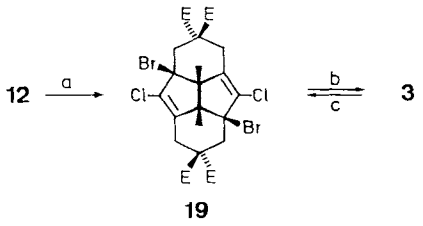
the ring protons of **2** and **18** [**2/15**, $\Delta\delta_H$ (H-6) = 1.40; **18/17**, $\Delta\delta_H$ (H-6) = 1.02) as well as deshielding of the methyl protons (**2/15**: $\Delta\delta_H$ = 1.43; **18/17**, $\Delta\delta_H$ = 1.53). These findings can only be explained in terms of the paratropism of the cyclic $4n\pi$ system.[5, 6]



17 **18**

Scheme 2. a) Cu_2O, quinoline, 210 °C, 2 h, 46%. b) 1. *N*-Bromosuccinimide/CCl_4; 2. diazabicycloundecene, THF, 0 °C.

Reaction of the crude diol **12** with phosphorus tribromide leads instantaneously to a semibullvalene precursor, the *exo, exo* dibromide **19**. Reductive dehalogenation of **19** with magnesium, in a reaction monitored by NMR spectroscopy,[7] generates **3**.[8] A chemical structural proof for **3** is provided by its reaction with bromine, which results in reformation of **19**[3, 9] (Scheme 3).



19

Scheme 3. a) PBr_3, $CHCl_3$, 0 °C, 35% based on **10**. b) Mg, THF, quant. c) Br_2, CCl_4, −78 °C, 63%.

The attractivity of semibullvalene is due to its particularly strained divinylcyclopropane structure, which allows a degenerate Cope rearrangement to occur with extremely low activation energy. Attempts to further accelerate the Cope rearrangement have involved substitution[10–13] and the introduction of nitrogen atoms,[14, 15] but the extreme case of a "bishomoaromatic" ground state has not yet been attained. Simple bridging of the semibullvalene framework, as in **20a**,[16] leads to nonequivalence of the valence isomers **20a/20b**. In the first doubly bridged semibullvalene **3**, the Cope rearrangement of which is again degenerate, the two bridges should increase the strain in the ground state more than in the transition state, thus further lowering the activation barrier of the Cope rearrangement.[17] In a ^{13}C NMR



20a **20b**

X = e.g., CH_2, $(CH_2)_2$, $(CH_2)_3$, O, S, NR, CH_2–O–CH_2, CH_2–S–CH_2

measurement [50 MHz, dimethyl ether:[D$_8$]THF (5:1)], the averaged signal for the terminal centers C-1,5,7,11 of the allyl systems in **3** revealed no significant line broadening even at −160 °C. Therefore, the Cope rearrangement is rapid on the NMR time scale even at this temperature. From the Eyring relationship, an upper limit of ca. 15 kJ mol^{-1}[18] for the free energy of activation $\Delta G^{\ddagger}_{93}$ can be estimated for **3**; this value is considerably less than the value for semibullvalene $\Delta G^{\ddagger}_{93}$ = 23 kJ mol^{-1}).[19, 20]

Received: April 24, 1989 [Z 3304 IE]
German version: *Angew. Chem. 101* (1989) 1375

CAS Registry numbers:
2, 122425-03-0; **3**, 122425-04-1; **4**, 79150-94-0; **5**, 122442-94-8; **6**, 122442-95-9; **7**, 122442-96-0; **8**, 122442-97-1; **10**, 122425-05-2; **11**, 122425-06-3; **12**, 122425-07-4; **13**, 122425-08-5; **14**, 122425-09-6; **15**, 122425-10-9; **16**, 122442-98-2; **17**, 122425-11-0; **18**, 122425-12-1; **19**, 122425-13-2; potassium diethyl malonate, 37892-24-3.

[1] U. Weiss, J. M. Edwards, *Tetrahedron Lett. 1968*, 4885; S. H. Bertz, J. M. Cook, A. Gawish, U. Weiss, *Org. Synth. 64* (1986) 27.
[2] The configurations could be determined by a homonuclear NOE experiment.
[3] H. Kohnz, M. Krauss, K. Müllen, to be published.
[4] All new compounds gave correct elemental analyses. Selected spectroscopic data for **2**: ^{13}C NMR (50 MHz, [D$_8$]THF): δ = 18.4 (CH_3), 52.4 (OCH_3), 57.0 (C-13,14), 116.5 (C-2,8), 119.7 (C-4,6,10,12), 131.9 (C-1,3,7,9), 155.7 (C-5,11), 164.7 (C=O); MS (*m/z*): 390 (100%, $M^{\oplus}$). IR (KBr): $\tilde{\nu}$ = 2940, 2870, 1705, 1235, 755 cm^{-1}. UV (CH_2Cl_2): λ = 244 nm (lg ε 5.30), 310 (5.46), 411 (4.63).
[5] E. Vogel, H. Königshofen, K. Müllen, J. F. M. Oth, *Angew. Chem. 86* (1974) 229; *Angew. Chem. Int. Ed. Engl. 13* (1974) 281.
[6] K. Hafner, V. Kühn, *Angew. Chem. 98* (1986) 648; *Angew. Chem. Int. Ed. Engl. 25* (1986) 632.
[7] B. Düll, *Diplomarbeit*, Universität Mainz 1987.
[8] **3**: Colorless, air-sensitive solid: ^1H NMR (200 MHz, [D$_8$]THF): δ = 1.10 (CH_3), 1.222, 1.224 (OCH_2CH_3), 2.85 (H-2,4,8,10), 4.08, 4.13 (OCH_2). ^{13}C NMR (50 MHz, [D$_8$]THF): δ = 9.6 (C-CH_3), 14.26, 14.31 (OCH_2CH_3), 30.0 (C-2,4,8,10), 61.8 (C-3,9), 62.1 (OCH_2), 70.8 (C-12,13), 100.4 (C-1,5,7,11), 121.4 (C-6,14), 170.6 (C=O). MS (*m/z*): 568 (15%, $M^{\oplus}$). IR (KBr): $\tilde{\nu}$ = 2984, 1734, 1275, 1261, 750 cm^{-1}. Compound **3** is stable in degassed ether solvents even at 80 °C; exposure to oxygen or moisture, however, results in rapid decomposition.
[9] L. A. Paquette, G. H. Birnberg, J. Clardy, B. Parkinson, *J. Chem. Soc. Chem. Commun. 1973*, 129; R. Askani, H. Sönmez, *Tetrahedron Lett. 1973*, 1751.
[10] R. Askani, M. Littmann, *Tetrahedron Lett. 23* (1982) 3651.
[11] H. Quast, J. Christ, Y. Görlach, W. von der Saal, *Tetrahedron Lett. 23* (1982) 3653; H. Quast, J. Christ, E.-M. Peters, K. Peters, H. G. von Schnering, *Chem. Ber. 118* (1985) 1154.
[12] L. S. Miller, K. Grohmann, J. J. Dannenberg, L. Todaro, *J. Am. Chem. Soc. 103* (1981) 6249.
[13] D. Paske, R. Ringshandl, I. Sellner, H. Sichert, J. Sauer, *Angew. Chem. 92* (1980) 464; I. Sellner, H. Schuster, H. Sichert, J. Sauer, H. Nöth, *Chem. Ber. 116* (1983) 3751.
[14] R. Gompper, H. Nöth, P. Spes, *Tetrahedron Lett. 29* (1988) 3639.
[15] C. Schnieders, H.-J. Altenbach, K. Müllen, *Angew. Chem. 94* (1982) 638; *Angew. Chem. Int. Ed. Engl. 21* (1982) 637; *Angew. Chem. Suppl. 1982*, 1353.
[16] L. A. Paquette, R. L. Burson, *Tetrahedron 34* (1978) 1307, and references cited therein.
[17] R. V. Williams, H. A. Kurtz, *J. Org. Chem. 53* (1988) 3626.
[18] A shift difference of 4500 Hz was assumed for the signals of C-1 and C-7 in the slow exchange domain. This value corresponds to the shift difference for C-2 and C-4 of unsubstituted semibullvalene. A value of −180 °C was chosen for the coalescence temperature T_c. Based on experience with other semibullvalenes [19] with respect to the temperature range in which dynamic processes result in line-shape changes, however, T_c is presumably considerably lower.
[19] D. Moskau, R. Aydin, W. Leber, H. Günther, H. Quast, H.-D. Martin, K. Hassenrück, K. Grohmann, *Chem. Ber.*, in press. We thank Prof. *Günther* and Prof. *Quast* for providing us with unpublished data.
[20] The fastest degenerate Cope rearrangement ($\Delta G^{\ddagger}_{115}$ = 13.0 kJ mol^{-1}) was observed for 1,5-dimethylsemibullvalene-2,6-dicarbonitrile.

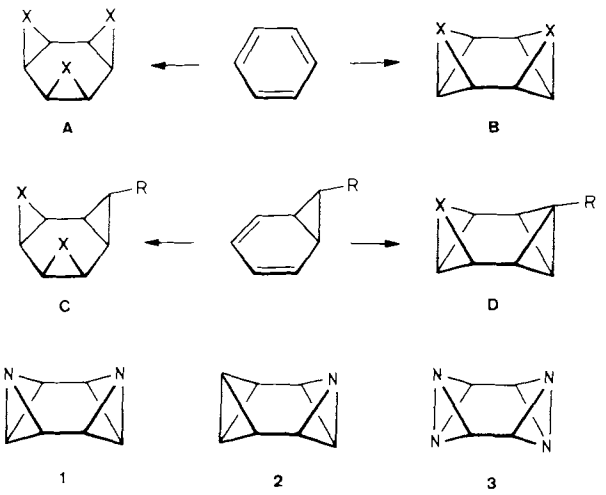
Azaoctabisvalenes**

By *Björn Trupp, Hans Fritz,* and *Horst Prinzbach**

Our syntheses of the preparatively challenging and theoretically intriguing carbo- and heterocyclic all-*cis*-tris-σ-homobenzenes **A** and **C** are based ultimately on benzene[1] and substituted cycloheptatrienes,[2] respectively. The readily accessible intermediates involved in these syntheses provided the main impulse for our work on the highly strained octabisvalenes **B** and **D**.[3] Here we describe the synthesis of diazaoctabisvalene (**B**, X = N) and azaoctabisvalenecarbonitrile (**D**, X = N, R = CN). Like the framework of the still unknown tetraaza analogue **3**,[4] the heterocyclic frameworks **1** and **2**, with their azabicyclobutane subunits,[5] should have a strain energy on the order of that

[*] Prof. Dr. H. Prinzbach, Dipl.-Chem. B. Trupp, Prof. Dr. H. Fritz
Chemisches Laboratorium der Universität,
Institut für Organische Chemie und Biochemie
Albertstrasse 21, D-7800 Freiburg (FRG)

[**] This work was supported by the Deutsche Forschungsgemeinschaft, the Fonds der Chemischen Industrie, and BASF AG. We would like to thank Dr. *D. Hunkler* and Dr. *J. Wörth* for the NMR and MS analyses, respectively.



(E_{st} = 154 kcal mol^{-1} [3]) calculated for the recently reported $(CH)_8$ parent framework **B** (X = CH).[6]

A key intermediate in the synthesis of *cis*-trioxide **A** (X = O) is the *anti-cis*-dibromoepoxycyclohexene **4**.[1] Its facile conversion to the *muco*-diazido- and *muco*-diamino-dideoxyinositols **5a** and **6a**, respectively, has been described.[7, 8] The use of suitably functionalized derivatives reduces the preparation of **1** to the intramolecular substitution of the four OR leaving groups *trans*-vicinal to the *N* functions (**4** → **5** (**6**) → **7** → **8** → **10** → **1**). A potential complication was the competing cyclization of monoaziridine **7** ⇄ **7′** to 1,4-bis(aziridine) **9**.

Also uncertain was whether **1**, with its highly reactive C4(8)–N bonds and acidic C4(8) hydrogens, would withstand the conditions required for the final bond formation, which, according to calculations, involves a significant increase in strain. After unsatisfactory results with the diamino tetraesters **6b, c**, we focused our efforts on the diazido tetramesylate **5b**.[9] Compound **5b** was first treated with $LiAlH_4$ under the conditions used for the preparation of *cis*-tris(imine) **A** (X = NH) (THF, 10 → 25 °C, 2 h).[10] In agreement with the explanation given there for the selective course of the reaction, we were unable to obtain satisfactory results, despite wide variation of the reaction conditions. By contrast, treatment of **5b** with triphenylphosphane/acetonitrile[11] afforded the unstable bis(aziridine) **8a** in 65–70% yield (20-mmole scale) as a crystalline solid; the intermediate monoaziridine **7** was not isolated. Repeated, careful monitoring of the reaction (TLC, ^{1}H NMR) revealed no evidence of bis(aziridine) **9a**. This competing reaction, which adversely affects the synthesis of the analogous carbocyclic compounds,[12] is presumably suppressed by the enormous repulsion of the nitrogen lone pairs oriented in an *endo, endo* fashion in the boatlike transition state leading to **9a**. According to the ^{1}H NMR spectrum (cf. Table 1) **8a** (**b, c**) has C_s symmetry at room temperature; this reflects the equilibration between the equivalent 5e,6a and 5a,6e half-chair conformations.

Owing to the relatively weak acidity of the aziridine *N* protons, which engage in hydrogen bonding, very strong bases are required for the two deprotonation steps leading from **8a** to **1**. Therefore, a potentially competing reaction was β-elimination to give **11**. The best result so far has been achieved by treating **8a** (2–3 mmol) with 2.2 equivalents of *n*BuLi/THF (−78 → + 25 °C). The unstable, ambiphilic, volatile $C_6H_6N_2$ pentacycle **1** (*Z*-3,7-diazapentacyclo[5.1.0.0^{2,4}.0^{3,5}.0^{6,8}]octane) was easily isolated as a pure crystalline solid in 45–55% yield by ether extraction of the solid residue (containing **1** as the only monomeric component according to TLC and ^{1}H NMR). Attempts to obtain the tetracyclic intermediate **10** by use of ca. 1 equivalent of base provided, in addition to starting material (ca. 18%) and traces of **1**, mainly polymeric material along with ca. 3% of the 1,4-dihydro-1,4-diazocine **12**[13] derived from the *cis*-diaza bis-σ-homobenzene **11**; according to the ^{1}H NMR data, **12** is planar-diatropic. The mono-N-"anion" derived from **8a** is presumably stabilized by an internal hydrogen bond, only the bis-N-"anion" cyclizing via **10** to **1**. Control experiments showed that, under the conditions used here, **1** is slowly metalated at C-4(8) and thereby slowly lost as polymer. Crystalline **1** exhibits high thermal stability; it sublimes upon heating above ca. 95 °C and melts (on a preheated hot plate) at ca. 136 °C with decomposition. In the ^{1}H and ^{13}C NMR spectra (Fig. 1), the two signals are shifted downfield relative to those of the C_8H_8 framework;[6] the ^{13}C,H coupling constants differ only slightly, whereas the H,H coupling constants (determined for **1** by spectral simulation) and ^{13}C, ^{13}C coupling constants differ significantly. The ^{15}N shift, mea-

Table 1. Physical data for selected compounds.

(1α,2α,4α,5α,6α,7α)-3,8-Benzoyl-3,8-diazatricyclo[5.1.0.0^{2,4}]octane-5,6-diyl bismethanesulfonate **8c**: m.p. 182–183 °C ($CHCl_3$/ether); ^{1}H NMR ($CDCl_3$): δ = 8.04 (m, 4*o*-H), 7.60 (m, 2*p*-H), 7.46 (m, 4*m*-H), 5.37 (m, 5-,6-H), 3.41 (m, 1-,2-H), 3.25 (s, 2 CH_3), 3.23 (br.m, 4-,7-H)

7-Acetyl-3,7-diazatetracyclo[4.1.1.0^{2,4}.0^{3,5}]octan-8-yl acetate **13c**: m.p. 118–120 °C (subl.); ^{1}H NMR ($CDCl_3$): δ = 5.01 (dd, 8-H), 4.51 (m, 1-H)*, 4.42 (m, 6-H)*, 3.54 (dd, 4-H), 3.23 (m, 2-H)**, 3.18 (m, 5-H)**, 2.19 (s, CH_3), 2.13 (s, CH_3); $J_{1,8} \approx 4.5$, $J_{2,4} \approx 1.5$, $J_{4,5} \approx 1.5$, $J_{6,8} \approx 4.5$ Hz; ^{13}C NMR ($CDCl_3$): δ = 174.8 (C=O), 170.4 (C=O), 71.0 (C-8), 62.8 (C-1)*, 60.6 (C-6)*, 56.4 (C-2)**, 55.9 (C-5)**, 38.5 (C-4), 20.7 (CH_3), 19.9 (CH_3); MS (CI, isobutane): *m/z* 209 ($M^{\oplus}$ + 1, 100%), 208 ($M^{\oplus}$, 5%), etc.

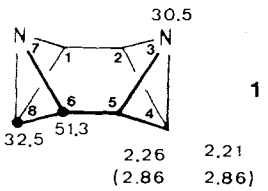
5-Benzyl-10-phenyl-1,5,9-triazapentacyclo[5.3.0.0^{2,6}.0^{3,9}.0^{4,8}]decane **16**: oil; ^{1}H NMR ($CDCl_3$): δ = 7.2–7.5 (m, 10 H), 4.78 (s, 10-H), 4.26 (m, 4-,6-H), 4.18 (m, 7-,8-H), 3.92 (m, 2-,3-H), 3.31 (s, CH_2); ^{13}C NMR ($CDCl_3$): δ = 137.6, 134.9 (2C), 128.7, 128.5, 128.3, 127.8, 127.6, 127.5 (10C), 95.4 (C-10), 70.2 (C-7,-8), 68.8 (C-2,-3), 65.0 (C-4,-6), 52.5 (CH_2); MS (CI, NH_3): *m/z* 302 ($M^{\oplus}$ + 1, 100%), 301 ($M^{\oplus}$, 2%), etc.

DL-(1α,6α,7α)-*Z*-3-Cyano-8-azatetracyclo[5.1.0.0^{2,4}.0^{3,5}]oct-6-yl methanesulfonate **21b**: dec. >105 °C (methanol/ether); ^{1}H NMR ([D_5]pyridine): δ = 5.29 (d, 6-H), ≈ 3.85 (br.s, N-H), 3.39–3.58 (m, 2-,5-H), 3.45 (s, CH_3), 2.97 (dd, 4-H), 2.35 (m, 1-, 7-H); $J_{2,4}$ = 3.0, $J_{4,5}$ = 3.0, $J_{5,6}$ = 3.5, $J_{6,7} \approx 0$ Hz

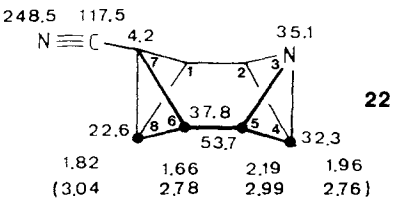
8-Benzyl-2,8-diazatetracyclo[4.3.0.0^{3,9}.0^{4,7}]nonane-5-*endo*-carbonitrile **26**: m.p. 82 °C (ether); ^{1}H NMR ($CDCl_3$): δ = 7.2–7.4 (m, 5H), 4.67 (m, 7-H), 4.48 (m, 9-H), 3.80 (m, 1-,3-H), 3.34 (s, CH_2), 2.91 (s, 5-H), 2.78 (m, 4-,6-H), 1.99 (br.s, N-H; $J_{1,6} \approx 3.5$, $J_{1,9} \approx 2.5$, $J_{4,5} \approx 2.5$, $J_{7,9} \approx 2.5$ Hz; ^{13}C NMR ($CDCl_3$): δ = 137.4, 128.8, 128.6, 127.6 (6C), 122.2 (CN), 77.5 (C-9), 75.0 (C-7), 61.4 (C-1,-3), 52.3 (CH_2), 43.1 (C-4,-6), 22.2 (C-5); MS (EI, 70 eV): *m/z* 237 ($M^{\oplus}$, 2%), 91 ($C_7H_7^{\oplus}$, 100%), etc.

sured for the first time for an azabicyclobutane, deviates considerably from that of aziridine.[14]

Compound **1** behaves like azabicyclobutanes[5] and octabisvalenes[3, 6] toward nucleophiles (1-mmole scale): $ZnSO_4$-catalyzed addition of water leads, via the nonobservable



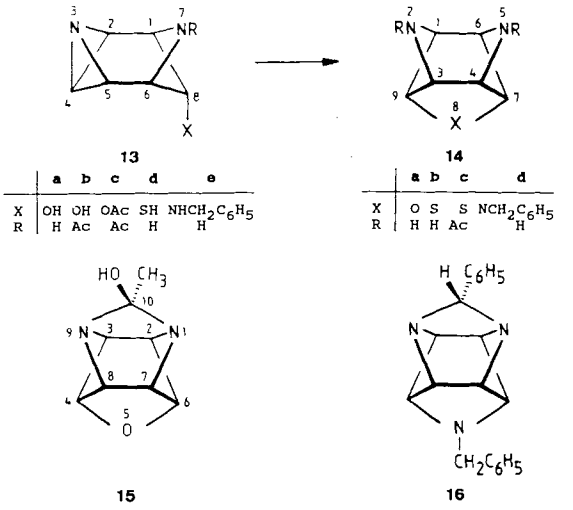
1



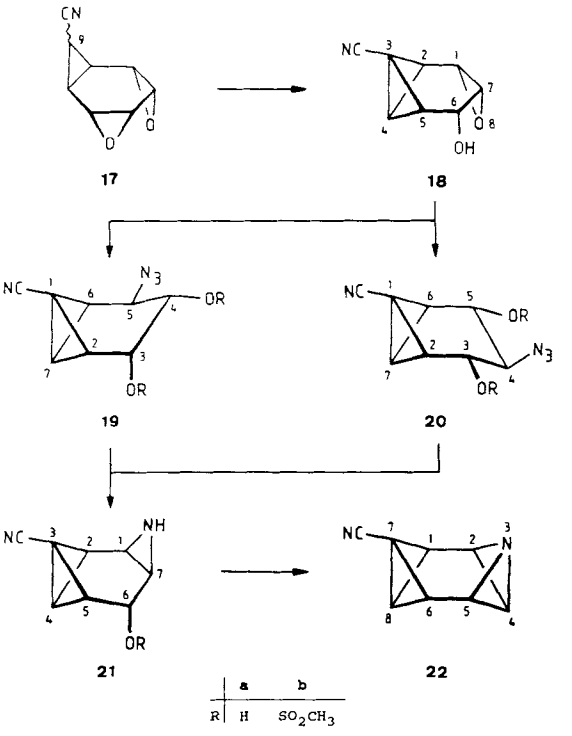
22

Fig. 1. Selected spectral data for **1** and **22** (in [D_6]benzene and, in parentheses, $CDCl_3$). **1**: $J_{1,2}$ = 4.65, $J_{1,6}$ = 4.41, $J_{1,8}$ = 1.40 Hz; $J_{C1,H}$ = 168, $J_{C4,H}$ = 209, $J_{C1,C8}$ = 29.2, $J_{N,4H} \approx 8$ Hz. MS (EI, 70 eV): *m/z* 106 ($M^{\oplus}$, 3%), 52 (100%), etc. **22**: $J_{1,2} \approx 4$, $J_{1,8} \approx 3$, $J_{2,4} \approx 1.5$ Hz; $J_{C1,H}$ = 164, $J_{C2,H}$ = 170, $J_{C4,H}$ = 209, $J_{C8,H}$ = 212 Hz. MS (EI, 70 eV): *m/z* 130 ($M^{\oplus}$, 21%), 129 ($M^{\oplus}-1$, 100%), etc.

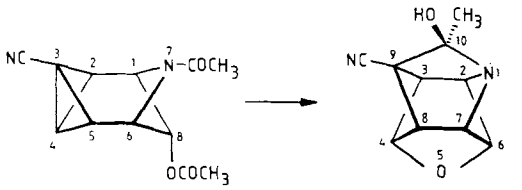
13a, to oxadiazatetracycle **14a** (which, in water, is complexed with $Zn^{2\oplus}$ according to ^{1}H NMR). Similarly, reaction with the nucleophiles Na_2S (*t*BuOH/50 °C/1 d) and benzylamine/BF_3 (*t*BuOH/50 °C/1 d) selectively leads, via **13d/e**, to the analogous thiadiaza- and triazatetracycles **14b(c)** (ca. 90%) and **14d** (ca. 85%), respectively. The piperazine boat in tetracycles **14** is ideally suited for transannular *N,N* bridging. Thus, **13c**, prepared by treatment of **1** with acetic anhydride, reacts with weak bases (NH_3, Na_2CO_3) to afford a nearly quantitative yield of oxadiazapentacycle **15**; triazapentacycle **16** is likewise obtained from **14d** and benzaldehyde.



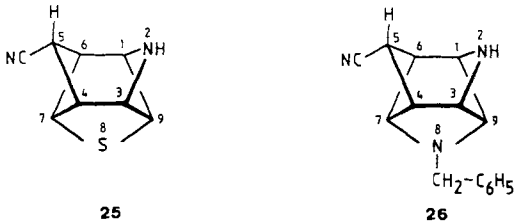
A mixture of epimeric *trans*-dioxatris-σ-homobenzenecarbonitriles **17**,[2] which has proved useful for syntheses in the **C** series,[1] is a readily accessible starting material for monoazaoctabisvalenes **2**. Compound **17** is sufficiently acidic at C-9 to be deprotonated without affecting the epoxide functions and to be regioselectively cyclized (three-membered ring formation) to **18** (0.15 M scale, 1 equiv. lithium-bis(trimethylsilyl)amide/THF, 0–20 °C, 50–60%; m.p. 135–136 °C, $J_{1,2} \approx 3.5$, $J_{1,7} \approx 4$, $J_{2,4} \approx 3.5$, $J_{2,5} \approx 3.5$, $J_{4,5} \approx 3.5$ Hz). In the reaction of **18** (50 mmol) with sodium azide/$MgSO_4$ (5 equiv., H_2O, 40 °C, ca. 5 d) – substitution at C-4 does not compete – the product (90–95% overall yield) consisted of a mixture of azidodiols **19a** (78%) und **20a** (7%) along with three (characterized) diazides arising therefrom (in toto 5–10%): the main components could be sepa-



rated without material loss by flash chromatography. The bismesylates **19b/20b**, prepared under standard conditions in 85–90% yield, can be converted into the tetracyclic aziridine **21b** (70–85%) under the conditions used for **5b** (10 mmol, triphenylphosphane/THF). Cyclization of **21b** to **22** proceeds under the optimized conditions found for **1** (5 mmol, 1.05 equiv. *n*BuLi/THF, $-78 \rightarrow +20\,^{\circ}C$) without any competition by the base-induced reactions typical of bicyclobutanecarbonitriles[15] and azabicyclobutanes. Trituration of the crude product with ether affords a practically quantitative yield of crystalline **22** (*Z*-3-azapentacyclo-[5.1.0.0^{2,4}.0^{3,5}.0^{6,8}]octane-7-carbonitrile), which remains unchanged up to its melting point (128 °C). The NMR data (Fig. 1) are characteristic for cyanocyclobutane and azabicyclobutane moieties.



23 **24**



25 **26**

Saponification of **23**, obtained by treatment of **22** with acetic anhydride, leads "directly" to oxaazapentacycle **24**: reaction of **22** with Na_2S (CH_2Cl_2/*t*BuOH, reflux) and with benzylamine/BF_3 (CH_2Cl_2/*t*BuOH, 50 °C) gives heterocycles **25** and **26**, respectively (55–60%, not optimized).

Received: April 28, 1989 [Z 3314 IE]
German version: *Angew. Chem. 101* (1989) 1381

CAS Registry numbers:
1, 122846-98-4; **5b**, 122847-01-2; **7**, 122847-02-3; **8a**, 122873-97-6; **8c**, 122874-00-4; **10**, 122847-03-4; **11**, 122847-04-5; **13c**, 122847-05-6; **14a**, 122847-06-7; **14b**, 122846-99-5; **14d**, 122847-00-1; **15**, 122847-07-8; **16**, 122873-99-8; (±)-**17**, 122921-39-5; (±)-**18**, 122847-08-9; (±)-**19a**, 122847-09-0; (±)-**19b**, 122873-98-7; (±)-**20a**, 122847-10-3; (±)-**20b**, 122841-13-6; (±)-**21b**, 122847-11-4; (±)-**22**, 122847-12-5; **24**, 122847-14-7; **25**, 122847-15-8; **26**, 122847-16-9; **A**, 52851-26-0; PhCHO, 100-52-7.

[1] R. Schwesinger, H. Fritz, H. Prinzbach, *Chem. Ber. 112* (1979) 3318, and references cited therein.
[2] B. Zipperer, K.-H. Müller, B. Gallenkamp, R. Hildebrand, M. Fletschinger, D. Burger, M. Pillat, D. Hunkler, L. Knothe, H. Fritz, H. Prinzbach, *Chem. Ber. 121* (1988) 757, and references cited therein.
[3] H. Bingmann, *Dissertation*, Universität Freiburg 1978; C. Rücker, H. Prinzbach, *Angew. Chem. 97* (1985) 426; *Angew. Chem. Int. Ed. Engl. 24* (1985) 411; C. Rücker, H. Prinzbach, H. Irngartinger, R. Jahn, H. Rodewald, *Tetrahedron Lett. 27* (1986) 1565; T. Netscher, R. Schwesinger, B. Trupp, H. Prinzbach, *ibid. 28* (1987) 2115; D.-R. Handreck, *Dissertation*, Universität Freiburg 1989.
[4] R. Krieger, *Diplomarbeit*, Universität Freiburg 1989.
[5] A. G. Hortmann, D. A. Robertson, *J. Am. Chem. Soc. 89* (1967) 5974; A. G. Hortmann, J. E. Martinelli, *Tetrahedron Lett. 1968*, 6205; W. Funke, *Angew. Chem. 81* (1969) 35; *Angew. Chem. Int. Ed. Engl. 8* (1969) 70; W. Funke, *Chem. Ber. 102* (1969) 3148; J. L. Kurz, B. K. Gillard, D. A. Robertson, A. G. Hortmann, *J. Am. Chem. Soc. 92* (1970) 5008; A. G. Hortmann, D. A. Robertson, *ibid. 94* (1972) 2758; R. Bartnik, Z. Cebulska, A. Laurent, *Tetrahedron Lett. 24* (1983) 4197; B. Mauze, *ibid. 25* (1984) 843; S. Calet, H. Alper, *ibid. 27* (1986) 2739; R. Bartnik, Z. Cebulska, A. Laurent, B. Orlowska, *J. Chem. Res. 1986*, 5.
[6] C. Rücker, *Chem. Ber. 120* (1987) 1629; C. Rücker, B. Trupp, *J. Am. Chem. Soc. 110* (1988) 4828; C. Rücker, H. Fritz, *Magn. Reson. Chem. 26* (1988) 1103.
[7] J. Schubert, R. Keller, R. Schwesinger, H. Prinzbach, *Chem. Ber. 116* (1983) 2524.
[8] B. Trupp, *Dissertation*, Universität Freiburg 1989.
[9] The new compounds were characterized by their spectra (^{1}H NMR (250, 400 MHz), ^{13}C NMR (100.6 MHz), IR, MS) and by elemental analysis (Table 1).
[10] R. Schwesinger, M. Breuninger, B. Gallenkamp, K.-H. Müller, D. Hunkler, H. Prinzbach, *Chem. Ber. 113* (1980) 3127.
[11] P. Pöchlauer, E. P. Müller, *Helv. Chim. Acta 67* (1984) 1238, and references cited therein.
[12] W.-D. Braschwitz, C. Rücker, H. Fritz, H. Prinzbach, *manuscript in preparation*; cf. W.-D. Braschwitz, T. Otten, C. Rücker, H. Fritz, H. Prinzbach, *Angew. Chem.* 101 (1989) 1383; *Angew. Chem. Int. Ed. Engl. 28* (1989) 1348.
[13] M. Breuninger, R. Schwesinger, B. Gallenkamp, K.-H. Müller, H. Fritz, D. Hunkler, H. Prinzbach, *Chem. Ber. 113* (1980) 3161; M. Fletschinger, B. Zipperer, H. Fritz, H. Prinzbach, *Tetrahedron Lett. 28* (1987) 2517; H. J. Altenbach, H. Stegelmeier, E. Vogel, *ibid. 1978*, 3333.
[14] G. J. Martin, M. L. Martin, J.-P. Gouesnard: *^{15}N-NMR Spectroscopy*, Springer, Berlin 1981, p. 115.
[15] K. H. Hall, E. P. Blanchard, Jr., S. C. Cherkofsky, J. B. Sieja, W. A. Sheppard, *J. Am. Chem. Soc. 93* (1971) 110.

Stabilized *cis*-Tris-σ-homobenzenes: Syntheses, [σ2 + σ2 + σ2] Cycloreversions**

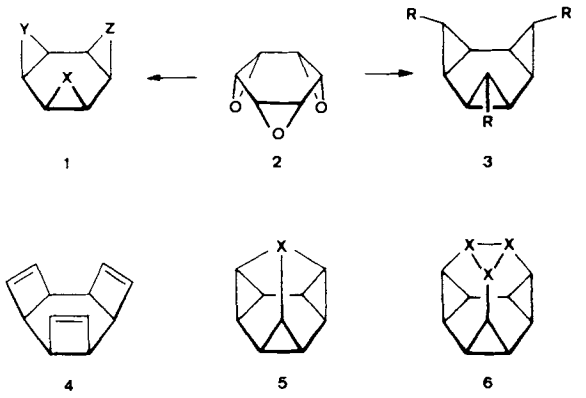
By *Wolf-Dieter Braschwitz, Thomas Otten, Christoph Rücker,* Hans Fritz,* and *Horst Prinzbach**

Extensive variation of the X, Y, and Z positions of the carbo- and heterocyclic *cis*-tris-σ-homobenzenes **1** is of interest from both mechanistic and preparative points of view.[1] Such carbocyclic frameworks have so far been rare[2, 3]—in part because of their inherent steric properties and their pronounced tendency to undergo [σ2 + σ2 + σ2] cycloreversion (estimated/calculated E_a value for the still unknown C_9H_{12} framework **3** (R = H), 24–28/37 kcal mol^{-1}[4–6]). Triple oxirane → aziridine and oxirane → thiirane transformations, starting from the readily accessible *cis*-benzene trioxide **2**, provided us with an efficient approach to compounds **1**, X,Y,Z = NR or S.[1] However, the analogous construction of carbocyclic frameworks (**2** → **3**) by triple oxirane → cyclopropane transformation met with severe complications.[3] Here we describe an efficient synthesis, based on **2**, of 3,6,9-tris-acceptor-substituted *cis*-tris-σ-homobenzenes **3**. This special kind of substitution should provide kinetic stability and facilitate the transformation of **3** to the ring-expanded compound **4** and, still more important, to bridged structures of the diademane type **5** (X = CH)[4, 5] and the semiregular Archimedian polyhedron **6** (X = CH, "truncated tetrahedron"[7]).[8]

The synthetic pathway shown in Scheme 1 is based on the following findings and assumptions: (1) The starting material, *scyllo*-tripropargyltriol **7b** (see Table 1), was obtained in 60–65% yield by triple epoxide opening of trioxide **2** with the reagent [(*i*Pr)$_3$SiC≡CCH$_2$(2-thienyl)Cu(CN)Li$_2$][9] to give **7a** followed by desilylation.[3, 10] (2) Tritosylate **7c** (all-equatorial) preferentially gave elimination products upon treatment with bases.[3, 11] However, elimination reactions should be suppressed by restricting the CH_2R^1/OR^2 sub-

[*] Prof. Dr. H. Prinzbach, Dr. C. Rücker, Dipl.-Chem. W.-D. Braschwitz, Dipl.-Chem. T. Otten, Prof. Dr. H. Fritz
Chemisches Laboratorium der Universität,
Institut für Organische Chemie und Biochemie
Albertstrasse 21, D-7800 Freiburg (FRG)

[**] This work was supported by the Deutsche Forschungsgemeinschaft, the Fonds der Chemischen Industrie, and BASF AG. We would like to thank Dr. *D. Hunkler* and Dr. *J. Wörth* for the NMR and MS measurements, respectively.



Scheme 1.

stituents to axial positions such as in **8** and **9**. (3) In **9** and **11**, R = CO_2Alkyl, the α-methylene groups should be metalated faster than the cyclopropane rings; cyclization of **9** to **10** and **11** and of **11** to **13** should therefore be favored over cyclization to **14** and **15**, respectively.[12] (4) The isopropyl ester groups in **8d** hinder self-condensation.[13]

Table 1. Physical data for selected compounds.

(1α,2β,3α,4β,5α,6β)-2,4,6-Tris(prop-2-ynyl)cyclohexane-1,3,5-triol **7b**: m.p. 172 °C (EtOH/petroleum ether); ^{1}H NMR ($CDCl_3$): δ = 3.93 (br.d, 3 OH), 3.54 (m, 1-,3-,5-H), 2.64 (t, 6H), 2.02 (t, 3H), 1.50 (m, 2-,4-,6-H); $J_{1,2}$ = 10.5, $J_{2,CH2}$ = 3.5, $J_{CH,CH2}$ = 3, $J_{1,OH}$ = 5 Hz; ^{13}C NMR ($CDCl_3$): δ = 81.4 (3 C), 71.0 (3 CH), 69.0 (C-1,-3,-5), 48.8 (C-2,-4,-6), 17.1 (3 CH_2)

[(1α,2β,3α,4β,5α,6β)-2,4,6-Tris(methoxycarbonylmethyl)cyclohexane-1,3,5-triyl]phosphate **8c**: m.p. 158 °C (ethyl acetate/cyclohexane 1/1); ^{1}H NMR ($CDCl_3$): δ = 4.85 (m, 1-,3-,5-H), 3.76 (s, 3 CH_3), 3.39 (t, 2-,4-,6-H), 2.56 (d, 3 CH_2); $J_{1,2}$ = 3, $J_{2,CH2}$ = 10, $J_{P,1}$ = 19 Hz; ^{13}C NMR ($CDCl_3$): δ = 170.0 (3 CO), 79.9 (C-1,-3,-5), 57.6 (3 OCH_3), 37.3 (C-2,-4,-6), 33.1 (3 CH_2); $J_{P,1(3,5)}$ = 6.5, $J_{P,2(4,6)}$ = 3.5 Hz.

DL-[(1α,2α,4α,5α,6β,7α,8α)-6-Isopropoxycarbonylmethyl-3,8-bis(isopropoxycarbonyl)tricyclo[5.1.0.0^{2,4}]oct-5-yl] dimethyl phosphate **11a**: m.p. 123 °C (ethyl acetate); ^{1}H NMR ($CDCl_3$): δ = 5.05 (sept., 2H), 4.9 (sept., 1H), 3.77 (OCH_3), 3.74 (OCH_3), 3.61 (m, 5-H), 2.74 (dd, 9-H), 2.48 (m, 6-H), 2.22 (dd, 9-H), 2.05 (1-,2-H), 1.80 (m, 7-H), 1.59 (m, 4-H), 1.38 (m, 3-H), 1.22 (s, CH_3), 1.2 (m, 8-H); $J_{4,5}$ = 3.5, $J_{5,6}$ = 9, $J_{6,7}$ = 4.5, $J_{6,9}$ = 3.5, $J_{6,9'}$ = 10, $J_{9,9'}$ = 15 Hz, $J_{P,5}$ = 12, $J_{P,6}$ = 0, $J_{P,OMe}$ = 11 Hz; ^{13}C NMR ($CDCl_3$): δ = 171.8 (CO), 171.4 (CO), 171.3 (CO), 76.5 (C-5), 68.3 (CH), 68.3 (CH), 68.0 (CH), 54.5 (OCH_3), 54.3 (OCH_3), 36.4 (C-9), 34.3 (C-6), 27.4 (C-7), 24.5 (C-3), 23.3 (C-4), 21.8 (2 CH_3), 21.7 (2 CH_3), 20.1 (C-1), 19.1 (C-2), 18.8 (C-8); $J_{P,5}$ = 6, $J_{P,6}$ = 9, $J_{P,OCH3}$ = 6 Hz.

Triisopropyl (1α,2α,3α,4α,5α,6α,7α,8α,9α)-tetracyclo[6.1.0.0^{2,4}.0^{5,7}]nonane-3,6,9-tricarboxylate **3a** (see also Fig. 1): m.p. 132 °C (cyclohexane): ^{1}H NMR ($CDCl_3$): δ = 4.99 (3 C*H*Me_2), 1.83 (6H), 1.25 (6 CH_3), 0.52 (3H); ^{13}C NMR ($CDCl_3$): δ = 172.8 (3 CO), 66.4 (3 CH), 21.8 (6 CH_3), 21.6 (3 C), 15.5 (6 C).

Triisopropyl *cis,cis,cis*-cyclonona-2,5,8-triene-1,4,7-tricarboxylate **17a**: ^{1}H NMR ($CDCl_3$): δ = 5.54 (6H), 5.02 (3 CHMe_2), 4.61 (3H), 1.23 (6 CH_3); ^{13}C NMR (C_6D_6): δ = 171.4 (CO), 126.6 (6 C), 68.5 (3 CH), 43.6 (3 C), 21.5 (6 CH_3)

Treatment of triol **7b** (20 mmol) with $POCl_3$/pyridine (80 °C) affords the crystalline adamantoid phosphate **8a** (m.p. 207 °C; $J_{1,2}$ = 3, $J_{2,CH2}$ = 10, $J_{P,1}$ = 19 Hz) in at least 60% yield (along with oligomers). Oxidative cleavage of the three alkyne functions of **8a** to give triacid **8b** was best accomplished with RuO_2/$NaIO_4$ in CH_3CN/CCl_4/H_2O (2:2:3).[14] The yield, after esterification of **8b** with diazomethane to give **8c**, was over 90%. Triple transesterification of **8c** to triisopropyl ester **8d** (m.p. 210 °C) proceeded smoothly with Ti[OCH(CH_3)$_2$]$_4$[15] (3.5 equiv., 80 °C, 4 h, 94%). In reactions of **8c** or **8d** (5-mmole scale) with various bases, including lithiumdiisopropylamide (LDA), NaH, and *n*BuLi, the combination **8d**/LDA(THF) gave the best results: (1) At −70 °C, **8d** does not react with base (1.1 equiv.; no H/D exchange); warming the reaction mixture to room temperature, followed by hydrolysis and esterification with diazomethane, gave a crude product, which, according to TLC and ^{1}H NMR monitoring, consisted of unreacted **8d** and the monocyclic compound **9a** (50%; 1:1 mixture of diastereomeric phosphates). The ^{1}H NMR analysis of **9a** ($J_{1,2} \approx 0$, $J_{2,3} \approx 3$, $J_{3,4} \approx J_{4,5} \leq 1$, $J_{5,6} = J_{6,1} = 9$, $J_{6,7} = J_{7,1} = 4.5$ Hz, etc.) revealed a half-chair conformation with the 7-ester group in α position, quasi-*trans*-diaxial CH_2R/phosphate moieties, and a chairlike phosphate ring. (2)

Reaction of **8d** with an excess of base (5(10) equiv. LDA, $-50 \rightarrow +20\,^{\circ}C$), followed by the same workup (CH_2N_2), gave a 7:3 mixture (TLC, ^1H NMR) of the bicyclopropa compound **11a** (m.p. 123 °C) and the C_s isomer **10a** (oil) in ca. 75% yield; the two products could be separated by chromatography (silica gel, cyclohexane/ethyl acetate 7:3). Compound **3a** was not detected, in agreement with the low nucleofugality of the phosphate dianion substituent in **11** ($-OPO_3^{2\ominus}$). 3,6,9-Triisopropyl ester **3a** was obtained in 85% yield by treatment of trialkyl phosphate **11a** with 3.0 equivalents of LDA ($-30 \rightarrow +20\,^{\circ}C$, THF, 30 min); **3a** was then converted, via triacid **3b**, into trimethyl ester **3c**. Compounds **3a,c** isomerize (**17a,c**) upon melting (130–132 °C).

Synthesis of the 3,6,9-trinitrile **3e**, which was of special interest for preparative purposes, was first attempted via triamide **3d**. This approach was unsuccessful, however, owing to the kinetic lability of the intermediates. Trinitrile **7g** was easily obtained from triamide **7f**. Despite wide variation of the reaction conditions, however, the phosphate ester **8f** could not be satisfactorily prepared from **7g** (< 10%; the same is true for **7d** → **8c**). A route to **3e**, which was surprisingly efficient in view of the complexity of the reactions involved, emerged from the rather vague notion, based on the regioselectivity observed in the preparation of **7a** from **2**,[3, 16] that it should be possible to ensure conformations with leaving groups in axial positions in the "triscarbanion"[16] of **7h**, as well as in the intermediates (with deprotonated three-membered rings), by lithium cluster formation (**12/13**[17]). Indeed, after treatment of **7h** (1 mmol, THF, $-78 \rightarrow +20\,^{\circ}C$) with at least 5 equivalents of lithium-diisopropylamide and complete conversion, **3e** emerged as the only monomeric component along with polymers (TLC, ^1H NMR) and could be easily isolated (filtration through silica gel) as a crystalline solid in 35% yield (m.p. 239 °C (dec.)). Diverse control experiments support a reaction path starting from the **7h** "triscarbanion"; for example, use of only 1 equivalent of base led neither to **3e** nor to intermediate or competition products (cf. **10, 11, 14, 15**).

Informative with respect to the spectroscopic and kinetic data of *cis*-tris-σ-homobenzenes **3a,c,e** is the comparison with the analogously substituted oxa compounds **16a,b**.[18] ^1H and ^{13}C NMR data (Fig. 1) confirm the presence of pla-

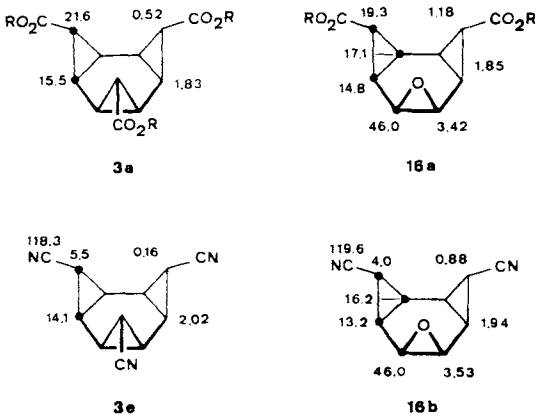
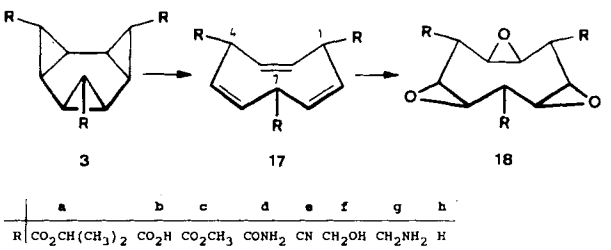


Fig. 1. Selected NMR data ($CDCl_3$) for *cis*-tris-σ-homobenzenes **3a,e** and **16a,b**.

nar, C_{3v}-symmetric structures. Compounds **3a** ($\Delta G^{\neq}$ (C_6D_6, 142 °C) = 28.5 kcal mol^{-1}) and **3e** ($\Delta G^{\neq}$ ($CDCl_3$), 142 °C) = 29.0 kcal mol^{-1}) are thermally more labile than **16a,b** ($\Delta G^{\neq}$ (benzene, 140 °C) = 32.1 and 32.4 kcal mol^{-1}, respectively), in agreement with the "additive" contribution of the respective three-membered ring components to the activation barrier for these [σ2 + σ2 + σ2] cycloreversions.[1] According to NMR analysis, the *cis,cis,cis*-cyclononatriene derivatives **17a,c,e**, which are stable under the thermolysis conditions, prefer a C_{3v} crown conformation with outward directed R groups. Triester **17a** is oxidized stereospecifically to the *exo,exo,exo*-trioxide **18a** (98%) by treatment with



benzoylperoxycarbamic acid in excess (benzene, 80 °C).[19] Attempted reduction of **3a,e** to **3f,g** (precursor to **4**) with $LiAlH_4$ ($-50 \rightarrow$ ca. 0 °C) only led to the corresponding π isomers **17f,g** (80–85%).[4, 5]

Trihomobenzenes **3a–c,e** are now available in gram quantities for preparative use.[8]

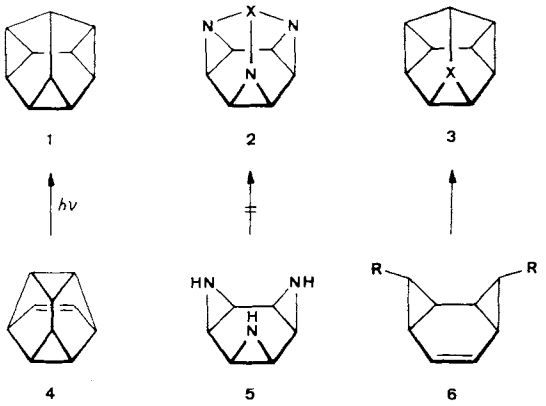
Received: April 28, 1989 [Z 3315 IE]
German version: *Angew. Chem. 101* (1989) 1383

[1] S. Kagabu, C. Kaiser, R. Keller, P. G. Becker, K.-H. Müller, L. Knothe, G. Rihs, H. Prinzbach, *Chem. Ber. 121* (1988) 741; B. Zipperer, K.-H. Müller, B. Gallenkamp, R. Hildebrand, M. Fletschinger, D. Burger, M. Pillat, D. Hunkler, L. Knothe, H. Fritz, H. Prinzbach, *ibid. 121* (1988) 757, and references cited therein.
[2] H.-W. Whitlock, Jr., P. F. Schatz, *J. Am. Chem. Soc. 93* (1971) 3837.
[3] C. Rücker, H. Prinzbach, *Tetrahedron Lett. 24* (1983) 4099, and references cited therein.
[4] H. Prinzbach, D. Stusche, J. Markert, H.-H. Limbach, *Chem. Ber. 109* (1976) 3505.
[5] A. de Meijere, D. Kaufmann, O. Schallner, *Tetrahedron Lett. 1973*, 553; D. Kaufmann, H.-H. Fick, O. Schallner, W. Spielmann, L.-U. Meyer, P. Gölitz, A. de Meijere, *Chem. Ber. 116* (1983) 587.
[6] J. Spanget-Larsen, R. Gleiter, *Angew. Chem. 90* (1978) 471; *Angew. Chem. Int. Ed. Engl. 17* (1978) 441.
[7] H. J. Schiwek, Universität Freiburg, private communication 1972; I. Hargittai, M. Hargittai, *Symmetry through the Eyes of a Chemist*, VCH Verlagsgesellschaft, Weinheim 1986, p. 70; J. M. Schulman, R. L. Disch, M. L. Sabio, *J. Am. Chem. Soc. 108* (1986) 3258.
[8] D.-R. Handreck, D. Hunkler, H. Prinzbach, *Angew. Chem. 101* (1989) 1386; *Angew. Chem. Int. Ed. Engl. 28* (1989) 1351.
[9] B. H. Lipshutz, J. A. Kozlowski, D. A. Parker, S. L. Nguyen, K. E. McCarthy, *J. Organomet. Chem. 285* (1985) 437.
[10] The new compounds were characterized by their spectra (^1H NMR (250, 400 MHz), ^{13}C NMR (100.6 MHz), IR, MS) and by elemental analysis.
[11] W.-D. Braschwitz, *Dissertation*, Universität Freiburg 1989.
[12] a) Z. Rappoport: *The Chemistry of the Cyclopropyl Group*, Wiley, New York 1987; b) M. A. Battiste, J. M. Coxon in [12a], p. 255; c) H.-U. Reißig in [12a], p. 375; d) G. Boche, H. M. Walborsky in [12a], p. 701; e) C. Rücker, *Chem. Ber. 120* (1987) 1629; C. Rücker, B. Trupp, *J. Am. Chem. Soc. 110* (1988) 4828.
[13] H. W. Pinnick, Y.-H. Chang, S. C. Foster, M. Govindan, *J. Org. Chem. 45* (1980) 4505; R. Häner, T. Maetzke, D. Seebach, *Helv. Chim. Acta 69* (1986) 1655.
[14] P. H. J. Carlsen, T. Katsuki, V. S. Martin, K. B. Sharpless, *J. Org. Chem. 46* (1981) 3936.
[15] D. Seebach, E. Hungerbühler, R. Naef, P. Schnurrenberger, B. Weidmann, M. Züger, *Synthesis 1982*, 138.
[16] C. Rücker, *J. Organomet. Chem. 310* (1986) 135.
[17] J. Kaneti, P. von R. Schleyer, T. Clark, A. J. Kos, G. W. Spitznagel, J. G. Andrade, J. B. Moffat, *J. Am. Chem. Soc. 108* (1986) 1481; G. Boche, *Angew. Chem. 101* (1989) 286; *Angew. Chem. Int. Ed. Engl. 28* (1986) 277, and references cited therein.
[18] H. Prinzbach, H.-P. Böhm, S. Kagabu, V. Wessely, H. V. Rivera, *Tetrahedron Lett. 1978*, 1243.
[19] H. Prinzbach, V. Wessely, H. Fritz, *Tetrahedron Lett. 1976*, 2765.

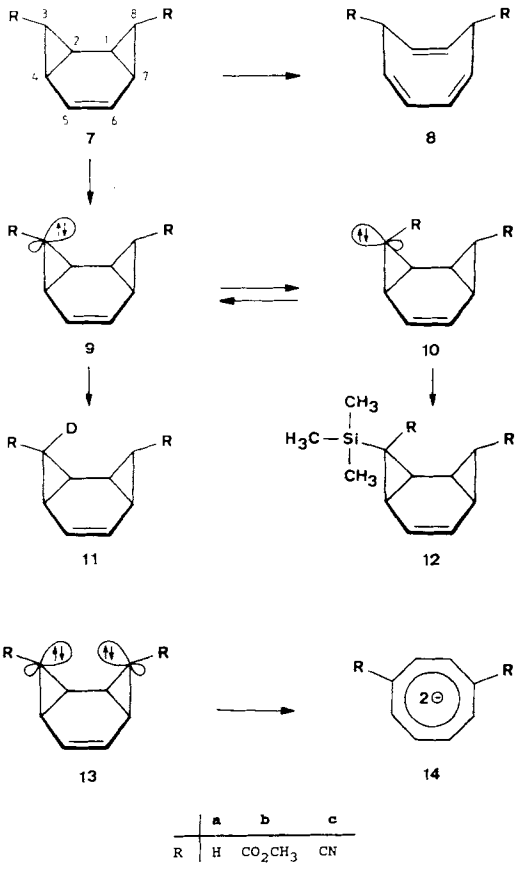
Bridged *cis*-Tris-σ-homobenzenes: Heterodiademanes**

By *Dirk-Rainer Handreck, Dieter Hunkler,* and *Horst Prinzbach**

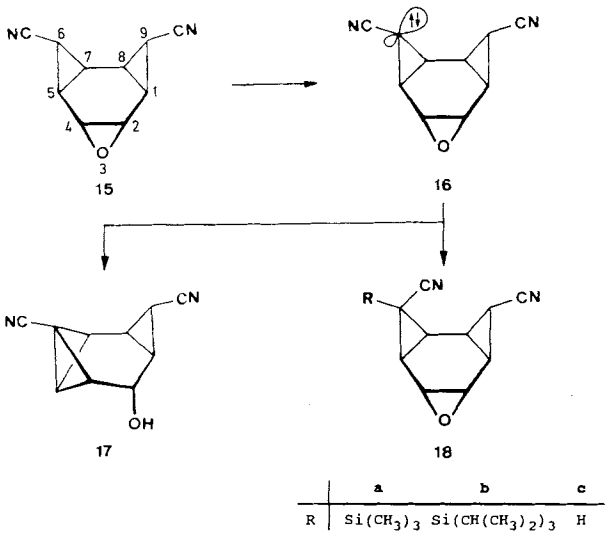
Attempts to prepare the highly interesting triply bridged *cis*-tris-σ-homobenzenes (cf. **5** and **6**)[1,2]—as carbocycles or with N atoms in diverse positions—have been of limited success so far. The $(CH)_{10}$ framework **1** ("diademane"[3] ("mitrane")[4]) and a C_{11} "homologue"[3] are known; however, the photochemical [π2 + σ2] step **4** → **1** is not efficient. Moreover, our efforts to obtain the triaza analogues **2** by bridging *cis*-trisimine **5** were unsuccessful.[5,6] Here we describe an approach to heterodiademanes of type **3** ("heterohexadehydroadamantanes"), which is based on bridge formation in *cis*-bis-σ-homobenzenes **6** and features some variability.



The following preliminary findings[9] were crucial for planning the reaction sequence[7] presented in Scheme 1: (1) The *cis*-bis-σ-homobenzene diester **7b**[10] and the dinitrile **7c**[11]—obtainable from cyclooctatetraene in decigram quantities by a meanwhile improved procedure[12]—are considerably more stable (**7c** → **8c**, $t_{1/2}$ (38 °C) ca. 520 min)[11,12] than the parent compound **7a** (**7a** → **8a**, $t_{1/2}$ (− 22 °C) ca. 38 min).[13] (2) Compounds **7b,c** are deprotonated practically instantaneously at C-3[8] with lithiumdiisopropylamide (LDA)/THF (1.0–1.2 equiv.) at −78 °C. Of the resulting, rapidly inverting "carbanions"[14] **9b,c/10b,c**, only that of the dinitrile can be trapped, with D_2O preferentially as the *endo* product **11c**, with bulky trimethylsilyl chloride (2 equiv. added to the reaction solution) nearly quantitatively as the *exo* product **12c**. (3) "Dianions" **13b,c**, generated with an excess of base (2–5 equiv.), cannot be detected, presumably owing to their expected, very rapid cycloreversion to the 10π aromatic dianions **14b,c**. (4) Monoanion **16**, generated from **15**[11] with LDA/THF at −78 °C, undergoes regioselective substitution at C-4 above − 60 °C to give **17** (C2–C6 bond formation does not compete). After inversion, **16** reacts rapidly at −78 °C with trimethylsilyl chloride to give **18a**.[15] (5) In contrast to **7c**, the silylated derivative **12c** is oxidized by trifluoroperacetic



acid in an *exo*-specific fashion to give the *trans*-oxa tris-σ-homobenzene **18a** (see Table 1).



Compound **18a** (3–5 mmol) reacts with 1.1 equivalents of LDA at −78 °C (THF) rapidly and completely (**19a**); the three components identified after addition of pH 7 buffer (TLC, ^1H NMR) and isolated in pure form by chromatography are the desilylated, epimeric (reusable) dinitriles **15** and **18c** (no **24a**) and the pentacyclic, crystalline imine **20a**, obtained as an *E*/*Z* pair (3:1) (up to 35%; optimization in favor of **20a** has not yet been carried out). The sterically bulky triisopropylsilyl group in **18b** does not significantly control the product ratio (ca. 35% **20** (R = triisopropyl, 8:1

[*] Prof. Dr. H. Prinzbach, Dr. D.-R. Handreck, Dr. D. Hunkler
Chemisches Laboratorium der Universität,
Institut für Organische Chemie und Biochemie
Albertstrasse 21, D-7800 Freiburg (FRG)

[**] This work was supported by the Deutsche Forschungsgemeinschaft and the Fonds der Chemischen Industrie; we would like to thank BASF AG for cyclooctatetraene, Prof. *H. Fritz* for special NMR measurements, and Dr. *J. Wörth* for MS measurements.

Table 1. Physical data for selected compounds.

DL-(1α,2β,4β,5α,6β,7α,8α,9α)-6-Trimethylsilyl-3-oxatetracyclo[6.1.0.0^{2,4}.0^{5,7}]-nonane-6,9-dicarbonitrile **18a**: m.p. 129–130 °C (ether); IR (KBr): $\tilde{\nu}$ = 2240 (CN), 2205 (CN) cm^{-1}. ^{1}H NMR ($CDCl_3$): δ = 3.48 (m, 4-H*), 3.39 (m, 2-H*), 3.00 (dd, 9-H), 2.09 (m, 8-H), 1.97 (dd, 1-H), 1.6 (m, 5-,7-H), 0.19 (s, 3 CH_3); $J_{1,2}$ = 4.5, $J_{1,8}$ = 8.5, $J_{1,9}$ = 4.5, $J_{2,4}$ = 3.9, $J_{4,5}$ = 4.5, $J_{8,9}$ = 4.8 Hz.

DL-(1α,2α,3β,5β,6α,7α)-9-Imino-4-oxapentacyclo[5.3.0.0^{2,10}.0^{3,5}.0^{6,8}]decane-8-carbonitrile **20b**: m.p. 134–150 °C (ether); IR (KBr): $\tilde{\nu}$ = 3234 (=N–H), 2230 (CN), 1630 (C=N) cm^{-1}; ^{1}H NMR ($CDCl_3$): δ = 9.94 (br.s, NH), 3.66 (m, 3-,5-H), 2.91 (ddd, 7-H), 2.43 (ddd, 6-H), 2.3 (m, 1-,10-H), 1.90 (ddd, 2-H); $J_{1,2}$ = 9.0, $J_{1,6}$ = 1.0, $J_{1,7}$ = 5.6, $J_{2,3}$ = 3.0, $J_{2,7}$ = 1.0, $J_{2,10}$ = 8.5, $J_{3,5}$ = 4.0, $J_{5,6}$ = 3.0, $J_{6,7}$ = 8.5 Hz.

DL-8-Hydroxy-1-*methoxy*-2-trimethylsilyl-10-azapentacyclo[4.4.0.0^{2,4}.0^{3,9}.0^{5,7}]-decane-6-carbonitrile **22a**: m.p. 129–131 °C (ether); IR (KBr): $\tilde{\nu}$ = 3274 (NH), 3212 (OH), 2214 (CN) cm^{-1}; ^{1}H NMR ($CDCl_3$): δ = 4.11 (dd, 8-H), 3.65 (ddd, 9-H), 3.55 (s, OCH_3), 2.56 (dd, 5-H), ≈2.1 (br.s, NH, OH), 1.87 (ddd, 7-H), 1.69 (dd, 4-H), 1.54 (dd, 3-H), 0.0 (s, 3 CH_3); $J_{3,4}$ = 7.0, $J_{3,9}$ = 6.5, $J_{4,5}$ = 5.0, $J_{5,7}$ = 8.5, $J_{7,8}$ = 4.5, $J_{7,9}$ = 1.5, $J_{8,9}$ = 4.5 Hz.

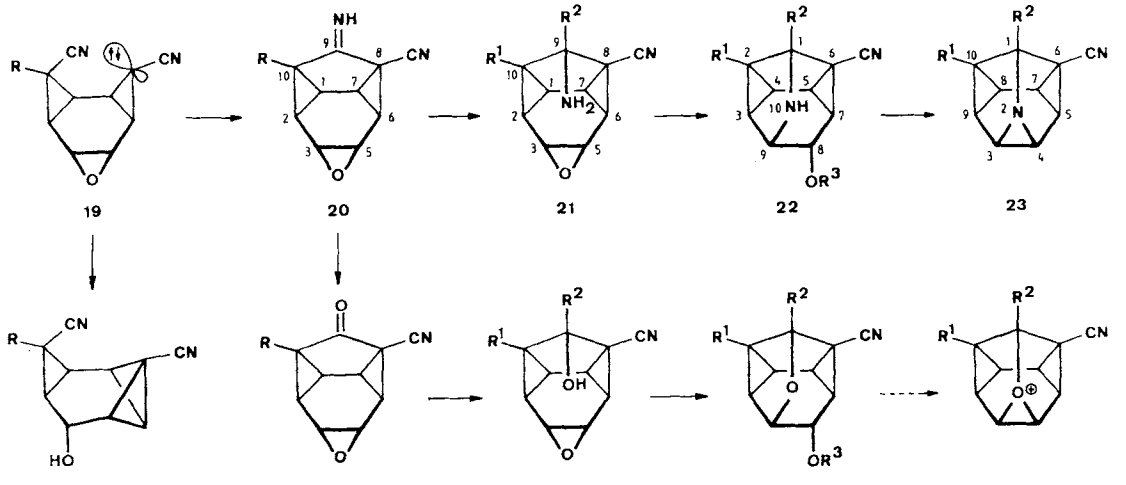
DL-(1α,2α,3β,5β,6α,7α)-9-Oxo-4-oxapentacyclo[5.3.0.0^{2,10}.0^{3,5}.0^{6,8}]decane-8-carbonitrile **25b**: m.p. 188–189 °C (methanol); IR (KBr): $\tilde{\nu}$ = 2225 (CN), 1730 (C=O). ^{1}H NMR ($CDCl_3/C_6D_6$, 250 MHz): δ = 2.91 (ddd, 3-H), 2.73 (ddd, 5-H), 2.00 (ddd, 7-H), 1.62 (dd, 6-H), 1.60 (dd, 10-H), 1.37 (dddd, 1-H), 1.03 (ddd, 2-H); $J_{1,2}$ = 9.0, $J_{1,3}$ = 1.0, $J_{1,7}$ = 6.0, $J_{1,10}$ = 6.6, $J_{2,3}$ = 3.0, $J_{2,7}$ = 0.7, $J_{2,10}$ = 9.0, $J_{3,5}$ = 4.8, $J_{5,6}$ = 3.1, $J_{5,7}$ = 0.7, $J_{6,7}$ = 8.7 Hz.

DL-(7α,8α)-8-Hydroxy-10-oxapentacyclo[4.4.0.0^{2,4}.0^{3,9}.0^{5,7}]decane-6-carbonitrile **27c**: oil; IR (neat/NaCl): $\tilde{\nu}$ = 2212 (CN) cm^{-1}. ^{1}H NMR ($CDCl_3$): δ = 4.96 (d, 1-H), 4.46 (ddd, 9-H), 4.19 (dd, 8-H), 3.08 (ddd, 2-H), 2.63 (dd, 5-H), ≈2.2 (br.s, OH), 2.04 (dddd, 4-H), 1.95 (ddd, 7-H), 1.88 (ddd, 3-H); $J_{1,2}$ = 4.0, $J_{2,3}$ = 8.7, $J_{2,4}$ = 8.7, $J_{3,4}$ = 7.5, $J_{3,9}$ = 5.4, $J_{4,5}$ = 5.3, $J_{4,9}$ = 1.0, $J_{5,7}$ = 8.7, $J_{7,8}$ = 4.7, $J_{7,9}$ = 1.0, $J_{8,9}$ = 4.5 Hz.

mixture)). The importance of the Si moiety in the transannular C–C bond formation to give **20** is manifested by the fact that **20b** could not be obtained from **15** (which instead afforded a nearly quantitative yield of **18c**). Slow chromatographic workup of **20a** (silica gel) or careful hydrolysis results in formation of ketone **25a** with practically no material loss. Removal of the Si "auxiliary groups" in **20a** (→ **20b**) and **25a** (→ **25b**) was accomplished with tetra-*n*-butylammonium fluoride · 3 H_2O, whereby partial hydrolysis of **20b** to **25b** has to be accepted: the use of dry reagents leads to a mixture of the epimeric dinitriles **15** and **18c** from **20a**. The desired *exo* attack on the C=N bond in **20a**, that is, the introduction of an *endo* NH_2 group in **21a**, should be sterically favored according to models.

Indeed, the addition of methanol to **20a** in methanol/ammonium acetate (20 °C) is highly selective; however, the product, isolated in ca. 90% yield and crystallized from ether, is not the amino epoxide **21a**, but rather the alcohol **22a**[16] arising from regioselective substitution at C-3. Proton catalysis should in fact favor this epoxide opening over that at C-5. The NH and OR^3 groups in **22** have the quasi-axial orientation (**22b**: $J_{8,9}$ = 4.5 Hz) needed for the subsequent cyclization. After (as yet unselective) esterification of **22a** to **22b** (ca. 15%, along with *N*-mono- and *O,N*-disulfonates), treatment with triethylamine at room temperature effects rapid and exclusive substitution to give azadiademane **23a** (1-methoxy-10-trimethylsilyl-2-azahexacyclo[4.4.0.0^{2,4}.0^{3,9}.0^{5,7}.0^{8,10}]decane-6-carbonitrile). Attempts to synthesize only doubly (singly) substituted **23b** (**c**) by reaction of **20a** (**b**) with "mild" hydride sources such as $LiBH_3CN$, $NaBH_3CN$,[17] and $KBH(OiPr)_3$[18] (to avoid attack at the CN and epoxide groups) have not afforded satisfactory results so far. Thus, **20a** was unreactive toward $KBH(OiPr)_3$, whereas **20b** underwent opening to **18c**, a notorious behavior of the imide anion. Selective reduction of the ketone function in **25b** is best accomplished with $KBH(OiPr)_3$/THF (1 equiv., 0 → 20 °C). The reproducible yield of epoxy alcohol **26c**, together with varying amounts of **27c** depending on the workup,[16] is 85%. The isomerization **26c** → **27c** occurs rapidly and cleanly on silica gel. The intermediacy of oxoniadiademanes **28a, b** in the solvolysis of ester sulfonates **27b, d** has not yet been elucidated.

The ^{1}H and ^{13}C NMR data for **23a** (Fig. 1), especially the H/H coupling constants between the three-membered rings, are of the magnitude known for "mixed" *C,N-cis*-tris-σ-homobenzene frameworks.[19] Distortions of the six-membered ring are revealed by the calculated H/H interplanar angles. Also noteworthy is the fragmentation pattern upon electron impact (EI, 70 eV: *m/z* 257 ($M^{\oplus}$ – 1, 0.8%), 154 ($M^{\oplus}$ – $Si(CH_3)_3$, – OCH_3, 100%), 128 ($M^{\oplus}$ – $Si(CH_3)_3$, – OCH_3, – CN, 14%)). Compound **23a** behaves differently from hydrocarbon **1** upon thermolysis: In 10^{-2} M



Scheme 1.

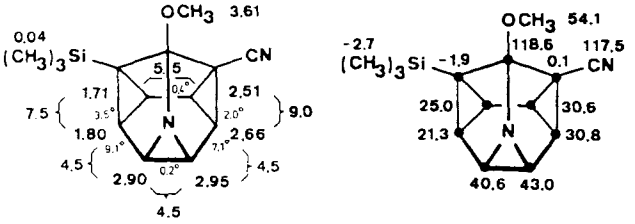
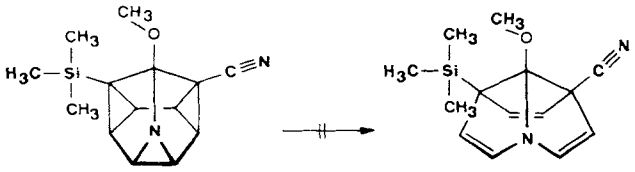


Fig. 1. ^{1}H and ^{13}C NMR shifts ($CDCl_3$), H,H coupling constants and calculated interplanar angles of **23a**.

degassed $CDCl_3$ solution, **23a** does not undergo any change upon heating to 150 °C for several hours; ^{1}H NMR monitoring of the rapid decomposition occurring above 180 °C revealed polymer, but no azatriquinacene **29**. This consider-

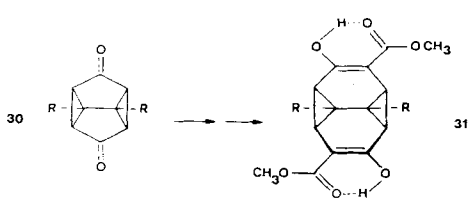


ably higher kinetic stability of **23a** as compared with **1** (E_a = 32.3 ± 0.7 kcal mol^{-1} [3]) mirrors primarily the influence of the cyano group and the steric compression accompanying the [σ2 + σ2 + σ2] cycloreversion **23a** → **29**.

Received: April 28, 1989 [Z 3316 IE]
German version: *Angew. Chem. 101* (1989) 1386

CAS Registry numbers:
(±)-**15**, 122922-68-3; (±)-**18a**, 122876-38-4; (±)-**18b**, 122876-37-3; (±)-**18c**, 122922-69-4; (±)-**19a**·Li⊕, 122923-77-7; (±)-**20** (R = *i*-Pr_3Si), 122876-36-2; (±)-**20a**, 122876-39-5; (±)-**20b**, 122876-47-5; (±)-**22a**, 122876-40-8; (±)-**22b**, 122876-42-0; (±)-**23a**, 122876-41-9; (±)-**25a**, 122876-43-1; (±)-**25b**, 122876-46-4; (±)-**26c**, 122876-44-2; (±)-**27c**, 122876-45-3.

[1] W.-D. Braschwitz, T. Otten, C. Rücker, H. Fritz, H. Prinzbach, *Angew. Chem. 101* (1989) 1383; *Angew. Chem. Int. Ed. Engl. 28* (1989) 1348.
[2] For doubly bridged examples, see H. Prinzbach, H. Fritz, H. Hagemann, D. Hunkler, S. Kagabu, G. Philippossian, *Chem. Ber. 107* (1974) 1971; H. Prinzbach, S. Kagabu, H. Fritz, *Angew. Chem. 86* (1974) 522; *Angew. Chem. Int. Ed. Engl. 13* (1974) 482; S. Kagabu, H. Prinzbach, *Tetrahedron Lett. 1975*, 29.
[3] W. Spielmann, H.-H. Fick, L.-U. Meyer, A. de Meijere, *Tetrahedron Lett. 1976*, 4057; D. Kaufmann, H.-H. Fick, O. Schallner, W. Spielmann, L.-U. Meyer, P. Gölitz, A. de Meijere, *Chem. Ber. 116* (1983) 587.
[4] H. Prinzbach, D. Stusche, *Helv. Chim. Acta 54* (1971) 755; cf. A. Nickon, E. F. Silversmith: *The Name Game*, Pergamon Press, New York 1987, p. 20.
[5] W. Fritsche-Lang, P. Wilharm, E. Hädicke, H. Fritz, H. Prinzbach, *Chem. Ber. 118* (1985) 2044; R. Hildebrand, *Dissertation*, Universität Freiburg 1986.
[6] We are attempting to carry out an X-ray structure analysis of the "Al triazadiademane" **2**, X = $AlCl_3$, the presumed intermediate in the synthesis of **5**. (R. Schwesinger, M. Breuninger, B. Gallenkamp, K.-H. Müller, D. Hunkler, H. Prinzbach, *Chem. Ber. 113* (1980) 3127).
[7] In exploring an alternative route to frameworks of the "truncated tetrahedron" type (cf. **6** in [1]), we have found that the tetracyclo[4.4.0.0^{2,10}.0^{5,7}]decadiene derivative **31**, generated from **30** and stabilized by hydrogen bonding, is stable up to at least 100 C (cf. $\Delta H^{\neq}$ = 21 kcal mol^{-1} for the $(CH)_{10}$ parent framework [8]).
[8] J. J. Gajewski: *Hydrocarbon Thermal Isomerizations*, Academic Press, New York 1981, p. 351; S. Masamune, R. T. Seidner, H. Zenda, M. Wiesel, N. Nakatsuka, G. Gigam, *J. Am. Chem. Soc. 91* (1970) 1810; cf. other stabilized derivatives: D. Ginsburg: *Propellanes*, Verlag Chemie, Weinheim 1975, p. 81 ff; cf. H. D. Carnadi, P. Hildenbrandt, J. Richter, G. Schröder, *Liebigs Ann. Chem. 1978*, 2074; M. J. Goldstein, S. A. Kline, *Tetrahedron Lett. 1973*, 1085, 1089.
[9] The new compounds were characterized by their spectra (^{1}H NMR (250, 400 MHz), ^{13}C NMR (100.6 MHz), IR, MS) and by elemental analysis (Table 1).
[10] G. Kaupp, K. Rösch, *Angew. Chem. 88* (1976) 185; *Angew. Chem. Int. Ed. Engl. 15* (1976) 163; R. C. Kerber, H. Müller, *J. Organomet. Chem. 329* (1987) 357.
[11] H.-P. Böhm, *Dissertation*, Universität Freiburg 1978; H. Prinzbach, H.-P. Böhm, S. Kagabu, V. Wessely, H. V. Rivera, *Tetrahedron Lett. 1978* 1243.
[12] W.-D. Braschwitz, *Dissertation*, Universität Freiburg 1989; D.-R. Handreck, *Dissertation*, Universität Freiburg 1989.
[13] P. Schal, *Dissertation*, Universität Freiburg 1980.
[14] H. M. Walborsky, J. M. Motes, *J. Am. Chem. Soc. 92* (1970) 2445, and references cited therein; G. Boche, K. Buckl, D. Martens, D. R. Schneider, H. U. Wagner, *Chem. Ber. 112* (1979) 2961; B. Halton, M. G. Banwell in Z. Rappoport *The Chemistry of the Cyclopropyl Group*, Wiley, New York 1987, p. 1223 ff; G. Boche, *Angew. Chem. 101* (1989) 286; *Angew. Chem. Int. Ed. Engl. 28* (1989) 277.
[15] Compound **17** and its *O*-phenylsulfonate offer an approach to octabisvalene-3,7-dicarbonitrile (*Z*-pentacyclo[5.1.0.0^{2,4}.0^{3,5}.0^{6,8}]octane-3,7-dicarbonitrile [12].
[16] The corresponding pentacyclic $C_{10}C_{12}$ framework is known as "2,4,6,9-tetradehydroadamantane": H. W. Geluk, T. I. deBoer, *Tetrahedron 28* (1972) 3351.
[17] R. F. Borch, M. D. Bernstein, H. D. Durst, *J. Am. Chem. Soc. 93* (1971) 2897; H. C. Brown, S. Krishnamurthy, *Tetrahedron 35* (1979) 567.
[18] H. C. Brown, J. S. Cha, B. Nazer, S.-C. Kim, S. Krishnamurty, C. A. Brown, *J. Org. Chem. 49* (1984) 885.
[19] B. Zipperer, K.-H. Müller, B. Gallenkamp, R. Hildebrand, M. Fletschinger, D. Burger, M. Pillat, D. Hunkler, L. Knothe, H. Fritz, H. Prinzbach, *Chem. Ber. 121* (1988) 757.



Diels–Alder Adducts on the *b* Side of Naphthalene: Rapid Cycloreversion of *o*-Quinodimethanes**

By *Wolfram Grimme,* Peter Höner, Heinz Theo Kämmerling, Robert Waldraff,* and *Jakob Wirz**

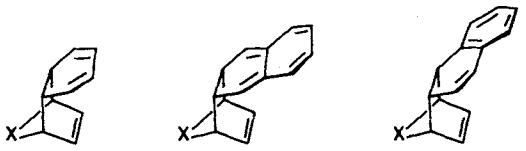
Cycloreversions are a fascinating type of reaction both mechanistically and preparatively, since their rates can be varied over 18 orders of magnitude by structural changes and since their first-order kinetics allow them to be carried out both in the gas phase and in glass matrices.

The cycloreversion of benzene–arene adducts is accompanied by a considerable increase in resonance energy. For adducts of type **1b, c,** *one* isolated or fused benzene ring is formed in each of the cleavage products. We have found that the free energies of activation $\Delta G^{\neq}$ for six of these adducts, derived from kinetic data, depend linearly[1] on the gain in resonance energy ΔE calculated according to the method of *Dewar* and *de Llano*.[2] The fastest cycloreversion in this series occurs for *o,p*-dibenzene **1b**, which forms two isolated benzene rings. Also conceivable, however, are Diels–Alder adducts of arenes that, upon cleavage, regain the *entire* resonance energy of a fused-ring aromatic system: for example,

[*] Prof. Dr. W. Grimme, P. Höner, Dr. H. T. Kämmerling, Dr. R. Waldraff
Institut für Organische Chemie der Universität
Greinstrasse 4, D-5000 Köln 41 (FRG)
Prof. Dr. J. Wirz
Institut für Physikalische Chemie der Universität
Klingelbergstrasse 80, CH-4056 Basel (Switzerland)

[**] This work was supported by the Fonds der Chemischen Industrie, BASF AG, Ludwigshafen, and the Swiss National Science Foundation.

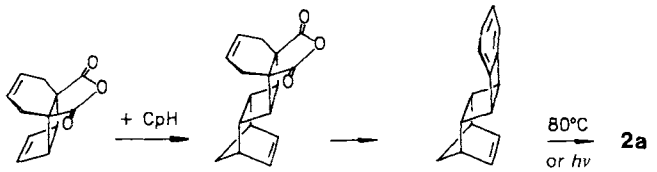
compounds of type **2**, the synthesis of which formally involves the *b* side of naphthalene as the dienophile. According to the linear dependence of ΔG^{+} on ΔE, cycloreversion of these adducts should proceed much faster than that of the isomeric adducts **3**, involving the *a* side of naphthalene, and even faster than that of the benzene adducts **1**.



1 **2** **3**

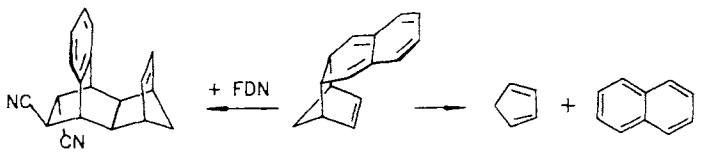
a: X = CH_2; **b**: X =  ; **c**: X =

To synthesize adducts **2**, we chose the benzobicyclo[2.2.0]hexene unit as precursor for their *o*-quinodimethane structural element. This strategy made tetracycle **6**, prepared via **4**[3] and **5**, the immediate precursor of adduct **2a** with cyclopentadiene (CpH). We obtained **6** by electrolytic bisdecarboxylation of the initially formed cycloadduct **5** followed by dehydrogenation with dichlorodicyanobenzoquinone (DDQ).



4 **5** **6**

The benzobicyclo[2.2.0]hexene unit in **6** opens at 80 °C, affording the naphthalene–CpH adduct **2a**, which, in a very rapid and quantitative subsequent reaction, undergoes cleavage to its components. In the presence of excess fumarodinitrile (FDN) in refluxing benzene 0.04 M, however, **2a** is trapped almost completely as Diels–Alder adduct **7**. When the concentration of FDN is decreased to 0.005 M, addition to the *o*-quinodimethane moiety of **2a** competes with retro-Diels–Alder reaction of **2a**, leading to formation of a 1:1 mixture of **7** and the FDN adduct with CpH.



7 **2a**

After a control experiment had shown that **6** could also be opened by photolysis at $\lambda = 254$ nm, we attempted to use flash photolysis to determine the rate of cycloreversion of **2a**. However, we found that the cycloreversion did not follow first-order kinetics in degassed hexane and, moreover, was influenced by the intensity of the light used ($\lambda = 400$ nm, $t_{1/2}$ on the order of minutes). The rate constants of cycloreversion were therefore determined indirectly by addition of FDN. For the kinetic measurements, a solution of **6** (0.001 M) and FDN (0.005 M) in hexane was exposed in a quartz photolysis cell to flashes of light generated by capacitor discharge. From the observed first-order rate constants ($k = k_2$[FDN] = 1.12 and 1.25 s^{-1} at 29.9 °C: 0.71, 0.61, and 0.69 s^{-1} at 20.1 °C; 0.47 and 0.40 at 11.8 °C), we calculated the Arrhenius parameters for the cycloaddition of FDN to **2a**: $E_a = (9.54 \pm 0.80)$ kcal mol^{-1} and $A = (1.74 \pm 1.02) \times 10^9$ M^{-1} s^{-1}. The rate constant of addition k was calculated to be (11 ± 5) s^{-1} for the above competition between the cycloreversion of **2a** and its addition to FDN. (80 °C, [FDN] = 0.005 M). That of cycloreversion is of the same magnitude. Table 1 contains important physical data for the new compounds.

Table 1. Selected physical data for compounds **2b**, **3a**, **4**, **6–9**, **13**, and **14**. ^{1}H NMR spectra recorded at 90 MHz (**7**, **14**) or 300 MHz (**13**) in $CDCl_3$ or CCl_4 (**3a**, **6**), TMS as standard.

2b: UV (EPA glass [a] at 77 K): λ_{max}[nm] = 397, 423, 453

3a: m.p. −10 °C; ^{1}H NMR: δ = 7.2–6.7 (m, 4H), 6.0 (m, 2H), 5.7 (m, 2H), 3.39 (AB, $\Delta\nu$ = 28, ^3J = 11 Hz, 2H), 3.0 (m, 2H), 1.42 (t, 2H; CH_2). UV(*n*-hexane): λ_{max}[nm] (ε) = 263 (6400), 273 (6300), 285 (4000, sh), 294 (800, sh), 308 (200, sh)

4: m.p. 158 °C; ^{1}H NMR: δ = 6.48 (d, 2H), 5.70 (d, 2H), 3.63 (d, 2H), 2.51 (AB, $\Delta\nu$ = 30.1, ^2J(A,B) = 18 Hz, 4H; 2 CH_2)

6: m.p. 38 °C; ^{1}H NMR: δ = 7.01 (AA'BB', 4H), 6.31 (t, 2H), 3.22 (s, 2H), 3.0 (m, 2H), 2.7 (m, 2H), 1.45 (AB, $\Delta\nu$ = 31.6, ^2J = 13.6 Hz, 2H; CH_2)

7: m.p. 189 °C; ^{1}H NMR: δ = 7.04 (AA'BB', 4H), 4.82 (m, 2H), 3.39 (m, 2H), 2.88 (AB, $\Delta\nu$ = 35.6, ^3J(A,B) = 5.4 Hz, 2H), 2.8 (m, 4H), 1.26 (t, 2H; CH_2)

8: m.p. 56 °C; ^{1}H NMR: δ = 7.6–7.1 (m, 4H), 5.64 (dAB), $\Delta\nu$ = 41, ^3J(A,B) = 6.3 Hz, 2H), 3.46 (dAB, $\Delta\nu$ = 70, ^3J(A,B) = 6.3 Hz, 2H), 3.31 (m, 1H), 3.18 (m, 1H), 1.73 (t, 2H; CH_2). UV(*n*-hexane): λ_{max}[nm] (ε) = 285 (2300), 297 (2550), 312 (200), 328 (260), 343 (240). IR (neat): $\tilde{\nu}$[cm^{-1}] = 1703 (C=O)

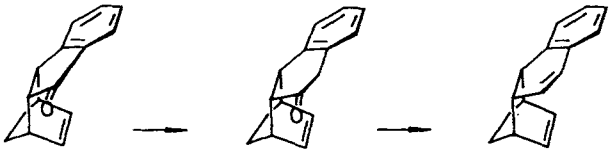
9: ^{1}H NMR: δ = 7.6 (m, 4H), 5.99 (dAB, $\Delta\nu$ = 28, ^3J(A,B) = 6 Hz, 2H), 3.88 (m, 1H), 3.5–3.0 (m, 5H), 1.57 (t, 2H; CH_2); IR (neat): $\tilde{\nu}$[cm^{-1}] = 1708 (C=O)

13: m.p. 93 °C; ^{1}H NMR: δ = 7.08 (AA'BB', 4H), 6.47 (t, 2H), 6.36 (t, 2H), 3.72 (m, 2H), 3.22 (s, 2H), 2.27 (s, 2H); 75.5 MHz ^{13}C NMR. δ = 148.37, 134.97, 134.11, 107.03, 121.97, 45.58, 45.01, 40.34. UV(*n*-hexane): λ_{max}[nm] (ε) = 263 (1600), 269 (2600), 275 (2600)

14: ^{1}H NMR: δ = 7.5–7.1 (m, 5H), 7.0 (AA'XX' partial spectrum, 2H), 6.5 (AA'XX' partial spectrum, 2H), 6.4 (t, 2 H), 5.25 (dd, 2H), 4.5 (m, 2H), 3.5 (m, 2H), 3.2 (m, 2H), 2.25 (m, 2H)

[a] EPA is a 5:5:1 mixture of Et_2O, $Me_2CHCH_2CH_3$, and EtOH.

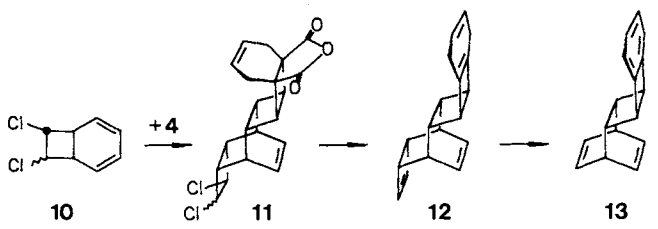
The synthesis of the CpH adduct **3a**, isomeric to **2a**, started from the CpH adduct of indenone, **8**,[4] which was allowed to react with dibromomethane and base to give the ring-expanded ketone **9**.[5] After reduction with sodium borohydride and esterification with methanesulfonyl chloride, reaction with alumina (activity I) in ether at room temperature gave **3a**. The cycloreversion of **3a** in *n*-decane was monitored continuously between 80 and 92 °C in a thermostated quartz cell at $\lambda = 311$ nm; the reaction is first order with the kinetic parameters $E_a = (25.77 \pm 0.72)$ kcal mol^{-1} and $A = (1.03 \pm 1.04) \times 10^{12}$ s^{-1}. The rate constant k at 80 °C is 1.0×10^{-4} s^{-1}; thus, **2a** undergoes cycloreversion 10^5 times faster than the isomer **3a** and 2×10^3 times faster than the benzene adduct **1a**[2]!



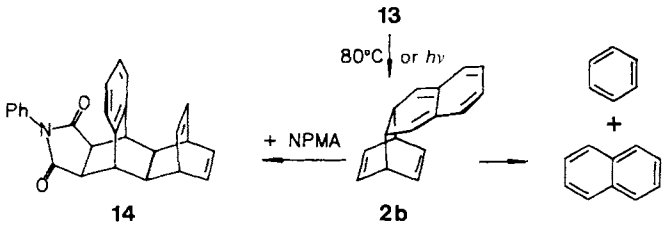
8 **9** **3a**

 © VCH Verlagsgesellschaft mbH, D-6940 Weinheim, 1989 0570-0833/89/1010-1354 $ 02.50/0

To obtain Diels–Alder adducts with even higher rates of cycloreversion, we synthesized the adduct of benzene with the *b* side of naphthalene in an analogous way; the precursor was the tetracycle **13**. By cycloaddition of anhydride **4** to a stereoisomeric mixture of 8,9-dichlorobicyclo[4.2.0]octadiene **10**, we obtained adducts **11**; two further double bonds were introduced by electrolytic bisdecarboxylation and dechlorination with sodium in ammonia. Treatment of the resulting hexacyclic compound **12** with DDQ led to aromatization. Finally, photolysis of the *o*-chloranil adduct removed the cyclobutene ring to give **13**.



The benzobicyclo[2.2.0]hexene moiety in **13** also opens at 80 °C, affording the naphthalene–benzene adduct **2b**, which immediately undergoes cycloreversion to its components. Compound **2b** could no longer be trapped with fumarodinitrile, but only with the more reactive *N*-phenylmaleimide (NPMA). In the presence of an excess of this dienophile in benzene (1.18 M), **2b** afforded, after 48 h at 80 °C, cycloadduct **14** in addition to naphthalene in a ratio of 1:4.4. The



rate constant for the trapping reaction can be estimated under two assumptions: (1) The *o*-quinodimethane units in **2a** and **2b** add FDN at the same rate; (2) At 80 °C, NPMA and FDN differ in reactivity toward the *o*-quinodimethane unit by a factor of 22, the value determined by *Sauer* et al.[6] for CpH. Under these two assumptions, the rate constant for the trapping reaction giving **14** is $5 \times 10^4\ s^{-1}$ and that for the cycloreversion $2 \times 10^5\ s^{-1}$.

The benzobicyclo[2.2.0]hexene moiety in **13** can also be opened by photolysis at $\lambda = 254$ nm. At room temperature, only naphthalene and benzene are obtained. At 77 K in an EPA glass, however, **2b** is thermally stable and can be identified by UV spectroscopy.[7] Since **2b** undergoes further cleavage photochemically, its concentration remains small; the photocleavage is completed by irradiation at $\lambda =$ 436 nm. Laser flash photolysis (248 nm) of **13** in air-saturated hexane solution (0.0013 M, 24 °C) allows the cycloreversion of the **2b** formed to be followed by UV spectroscopy. Analysis of the transient recorded at 430 nm gives a first-order rate constant k of $(6 \pm 0.5) \times 10^3\ s^{-1}$. This value is in agreement with that found by competition experiments at 80 °C; the free energy of activation for cycloreversion of **2b** obtained from both values is $\Delta G^{\neq} = 12.2$ kcal mol^{-1}. This value, which makes **2b** the least stable alicyclic Diels–Alder adduct, and the calculated gain in resonance energy, $\Delta E = 50.5$ kcal mol^{-1}, agree with the linear relation established earlier.

The free energies of activation $\Delta G^{\neq}$ for the [2 + 4] cycloreversions of compounds **1–3** are listed in Table 2. As observed

Table 2. Free energies of activation, $\Delta G^{\neq}$, and calculated gain in resonance energy, ΔE [2], for the [4 + 2] cycloreversion of arene adducts.

	2b	**1b**	**1c**	**2a**	**1a**	**3a**
$\Delta G^{\neq}$ [a]	12.2	15.7	20.8	19.1	24.4 [9]	27.1
ΔE [b]	50.5	40.0	30.5	30.5	20.0	10.5

a) At 80 °C, in kcal mol^{-1}. b) In kcal mol^{-1}.

for the arene–arene adducts, a linear relation between the free energy of activation and the gain in resonance energy is found again for the arene–CpH adducts **1a**, **2a**, and **3a**, in agreement with the hypothesis of a synchronous process.

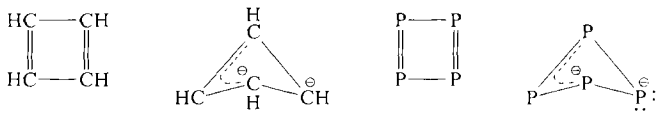
Received: May 8, 1989 [Z 3324 IE]
German version: *Angew. Chem. 101* (1989) 1390

[1] A. Bertsch, W. Grimme, G. Reinhardt, *Angew. Chem. 98* (1986) 361; *Angew. Chem. Int. Ed. Engl. 25* (1986) 377.
[2] M. J. S. Dewar, C. de Llano, *J. Am. Chem. Soc. 91* (1969) 789.
[3] Compound **4** is obtained from bicyclo[4.4.0]deca-3,8-diene-1,6-dicarboxylic anhydride by bromination of one double bond, double dehydrobromination, and photochemical ring closure.
[4] H. H. Szmant, R. Nanjundiah, *J. Org. Chem. 43* (1978) 1835.
[5] H. Taguchi, H. Yamamoto, H. Nozaki, *J. Am. Chem. Soc. 96* (1974) 6510.
[6] J. Sauer, H. Wiest, A. Mielert, *Chem. Ber. 97* (1964) 3183.
[7] The longest-wavelength UV absorption band of **2** displays a bathochromic shift of ca. 40 nm compared with the other *o*-quinodimethanes [8]. Its vibrational fine structure corresponds to that of other *o*-quinodimethanes.
[8] R. D. Miller, J. Kolc, J. Michl, *J. Am. Chem. Soc. 98* (1976) 8510.
[9] A. R. Rye, D. Wege, *Aust. J. Chem. 27* (1974) 1943.

Tetraphosphacyclobutadiene as Complex Ligand**

By *Otto J. Scherer,* Jürgen Vondung,* and *Gotthelf Wolmershäuser*

Of the *cyclo*-P_x compounds[1] isoelectronic to the carbocyclic $(CH)_x$ π systems, x = 3–6, *cyclo*-P_4 has not yet been reported. Structures **C** and **D** may be postulated for the phosphorus analogues of cyclobutadiene **A**[2] and its dianion **B**.[3]



C_4H_4 **A** $C_4H_4^{2\ominus}$ **B** P_4 **C** $P_4^{2\ominus}$ **D**

The P_x complexes **2–4** have now been prepared photochemically under very mild conditions starting from $[Cp^*Nb(CO)_4]$ **1** and white phosphorus.

[*] Prof. Dr. O. J. Scherer, Dipl.-Chem. J. Vondung, Dr. G. Wolmershäuser [†]
Fachbereich Chemie der Universität
Erwin-Schrödinger-Strasse, D-6750 Kaiserslautern (FRG)
[†] X-ray structure analyses
[**] This work was supported by the Fonds der Chemischen Industrie.

$$[Cp^*Nb(CO)_4] \xrightarrow[n\text{-}C_6H_{14},\ ca.\ 20\,^\circ C]{P_4,\ h\nu} [Cp^*(CO)_2Nb(\eta^4\text{-}P_4)] + [\{Cp^*(CO)Nb\}_2(P_4)] + [\{Cp^*Nb\}_2(P_6)]$$

1 **2** **3** **4a**

$Cp^* = \eta^5\text{-}C_5Me_5$

Complex **2** forms yellow crystals, **3** pink microcrystals, and **4a** dark red needles, which are readily soluble in dichloromethane, moderately soluble in benzene, and sparingly soluble in pentane (in each case, **3** is less soluble than **2** and **4a**). All of the compounds can be handled for a short time in the air; **2** and **3** are appreciably more air sensitive in solution than **4**.

The $^{31}P\{^1H\}$ NMR spectrum of **2**[4] at room temperature displays a broad singlet, which, at 223 K, splits into the well-resolved signals of an AMX_2 spin system.[4] This finding reveals hindered rotation of the *cyclo*-P_4 ligand. The $^{31}P\{^1H\}$ NMR, ^1H NMR, and IR spectra as well as the mass spectrum of **3**[4] indicate the presence of *trans*-$[\{Cp^*(CO)Nb(\mu,\eta^2\text{-}P_2)\}_2]$, which formally requires a Nb–Nb double bond to attain an electron count of 18 valence electrons per Nb atom.

The crystal structure analysis of **2**[5a] (Fig. 1) shows that the molecule exhibits nearly C_s symmetry. The four P atoms

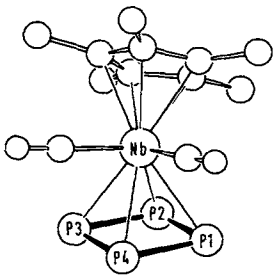


Fig. 1. Molecular structure of **2**. Selected distances [Å] and angles [°]: P1-Nb 2.639(1), P2-Nb 2.607(1), P3-Nb 2.631(1), P4-Nb 2.634(1), P1-P2 2.136(2), P2-P3 2.141(2), P3-P4 2.181(2), P4-P1 2.178(2), Nb-Cp*(center) 2.084, Nb-P_4(center) 2.139; P1-P2-P3 92.6(1), P2-P3-P4 88.4(1), P3-P4-P1 90.4(1), P4-P1-P2 88.6(1), Cp*(center)-Nb-P_4(center) 142.0.

are coplanar and form a slightly distorted (kite-shaped) square (P3-P4 = 2.181(2), P4-P1 = 2.178(2), P1-P2 = 2.136(2), P2-P3 = 2.141(2) Å); the P2–Nb bond (2.607(1) Å) is slightly shorter than the other three P–Nb bonds (average 2.635 Å).

These findings can be explained in terms of an allyl-like, distorted *cyclo*-$P_4^{2\ominus}$ ligand **D** (d^2-Nb) or a *cyclo*-P_4 ligand **C** (d^4-Nb), whose slight distortion is possibly due to the different ligands on the Nb atom. Compared with **2**, complex **5**[6] displays a more pronounced lack of symmetry in the metal–

$[(Me_3P)_2ClRh(P_2C_2tBu_2)]$ **5**

heterocyclobutadiene distances, at least for the C atoms. The flattening of the *cyclo*-$P_4^{2\ominus}$ ligand in **2** would be in agreement with the geometry calculated for $Li^{\oplus}C_4H_4^{2\ominus}$.[3] The Wade–Mingos electron counting rules[7] give seven electron pairs for the slightly distorted square pyramid P_4Nb of **2**, in accordance with a *nido* structure.

A crystal of **4a** suitable for X-ray structure analysis has not yet been obtained; however, X-ray data are available for the triple-decker complex $[\{Cp'Nb\}_2(P_6)]$ **4b** (dark red crystals, Cp′ = $\eta^5\text{-}C_5Me_4Et$; for NMR data, see Ref. [4]), the "decks" of which are planar and mutually parallel.[8] A noteworthy structural feature of the 26-valence-electron complex **4b**[5b] (Fig. 2) is the *cyclo*-P_6 middle deck, which can be

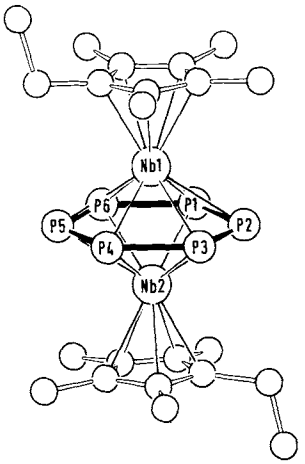
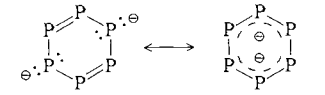


Fig. 2. Molecular structure of **4b**. Selected distances [Å] and angles [°]: Nb1-Nb2 2.791(2), Nb1-P1 2.581(5), Nb1-P2 2.573(6), Nb1-P3 2.619(5), Nb1-P4 2.581(5), Nb1-P5 2.574(5), Nb1-P6 2.630(5), Nb2-P1 2.585(5), Nb2-P2 2.567(6), Nb2-P3 2.620(5), Nb2-P4 2.579(5), Nb2-P5 2.578(6), Nb2-P6 2.628(5), P1-P2 2.241(10), P2-P3 2.181(9), P3-P4 2.149(9), P4-P5 2.243(9), P5-P6 2.157(9), P6-P1 2.140(9), Nb1(2)-Cp′(center) 2.080(2.072), Nb1(2)-P_6-(center) 1.395(1.396); P1-P2-P3 120.6(3), P2-P3-P4 118.3(3), P3-P4-P5 120.5(3), P4-P5-P6 121.0(3), P5-P6-P1 118.8(3), P6-P1-P2 120.7(3), Nb1-P-Nb2 64.1(1)–65.8(1) (average 65.1), Cp′(center)-Nb1(2)-Nb2(1) 179.4 (178.5), P_6(center)-Nb1(2)-Cp′(center) 179.4(178.1), Nb1-P_6(center)-Nb2 179.1. The figure shows one of the two rotationally disordered conformers.

regarded formally as consisting of two allyl-like $P_3^{\ominus}$ units joined to form the *cyclo*-$P_6^{2\ominus}$ ligand. There are two long (P1-P2 = 2.241(10), P4-P5 = 2.243(9) Å) and four short

E  **F**

(2.140(9)–2.181(9), average 2.157 Å) P–P distances. In agreement with this, the Nb1(2)–P3 distances (2.619(5) and 2.620(5) Å) and the Nb1(2)–P6 distances (2.630(5) and 2.628(5) Å) are significantly longer than the remaining eight Nb–P distances (2.567(6)–2.585(5) Å, average 2.577 Å). Thus, **4b** may be formulated as $[Cp'Nb(\mu,\eta^3,\eta^3\text{-}P_6)NbCp']$. Such a distortion has also been discussed for the 26-valence-electron triple-decker complex $[\{CpV\}_2(C_6H_6)]$ containing C_6H_6 as a 2 × 3-electron ligand.[9] The differences in the P–P bonds (two short, four long) found for **6**[10] may be inter-

$[Cp'V(\mu,\eta^6\text{-}P_6)VCp']$ **6**

preted in terms of a preference for the resonance structure **E**. LCAO-MO calculations[11] for the series *cyclo*-$P_6^{n\ominus}$ (n = 0, 2, 4, 6) indicate that *cyclo*-$P_6^{2\ominus}$ (idealized symmetry 6/mmm) is most stable.

The synthesis of **2** and **4** establishes a further bridge between the molecular and solid-state chemistry of polyphosphides.[12]

Experimental Procedure

A solution of **1** (400 mg, 1.18 mmol) [13] and P_4 (150 mg, 1.21 mmol) in 250 mL of hexane was irradiated at room temperature for 7 min with UV light (150-W high-pressure mercury lamp, Quarzlampen GmbH, Hanau, FRG). After removal of the solvent under oil-pump vacuum, the residue was chromatographed at ca. −50 °C on silanized silica gel (Merck, particle size 63–200 μm, column 100 × 3 cm). Unreacted **1** (50 mg, 12%) was eluted with petroleum ether as a red-orange fraction. The following yellow fraction contained **2** along with small amounts of **4a** (crude yield 69 mg, containing ca. 5% **4a**); the products were separated by recrystallization (twice) from CH_2Cl_2/hexane (1:1). Yields: 12 mg (3% based on reacted **1**) of **2** as yellow crystals and 1 mg (0.15%) of **4a** as dark red needles [8]. Toluene as eluant afforded a pink fraction, which, at the end, overlapped with a green fraction. A second chromatographic separation (basic Al_2O_3, activity II, column 25 × 3 cm, watercooled) with petroleum ether/toluene (10:1) gave a pink fraction (crude yield: 25 mg, 4%). Recrystallization from CH_2Cl_2/hexane (2:1) afforded pink **3**. Toluene eluted traces of a green fraction, the exact composition of which is still unknown. Partial decomposition with formation of a brown residue occurred during both chromatographic separations.

Received: May 18, 1989 [Z 3346 IE]
German version: *Angew. Chem. 100* (1989) 1395

CAS Registry numbers:
1, 80432-28-6; **2**, 122647-47-6; **3**, 122647-48-7; **4a**, 122647-49-8; **4b**, 122647-50-1; **C**, 10544-46-4.

[1] Reviews: O. J. Scherer, *Comments Inorg. Chem. 6* (1987) 1; M. Di Vaira, P. Stoppioni, M. Peruzzini, *Polyhedron 6* (1987) 351.

[2] Recent review: G. Maier, *Angew. Chem. 100* (1988) 317; *Angew. Chem. Int. Ed. Engl. 27* (1988) 309; for theoretical studies on *cyclo*-P_4, see G. Ohanessian, P. C. Hiberty, J.-M. Lefour, J.-P. Flament, S. S. Shaik, *Inorg. Chem. 27* (1988) 2219.

[3] B. A. Hess, Jr., C. S. Ewig, L. J. Schaad, *J. Org. Chem. 50* (1985) 5869.

[4] $^{31}P\{^1H\}$ NMR (162 MHz, 85% H_3PO_4 ext.): **2** (333 K, $CDCl_3$), δ = 89.2(s); **2** (223 K, CD_2Cl_2): AMX_2 spin system (A,M = P2,P4, X = P1,P3), $\delta(P_A)$ = 133.3(t), $^1J(AX)$ = 313 Hz, $\delta(P_M)$ = 76.8(t), $^1J(MX)$ = 248 Hz, $\delta(P_X)$ = 53.0(dd); **3** (293 K, $CDCl_3$), δ = 290.0(s); **4a,b** (293 K, $CDCl_3$), δ = 123.2(s), 126.0(s). ^1H NMR (200 MHz, $CDCl_3$, 293 K, TMS int.): **2**: δ = 2.37(s); **3**: δ = 2.10(s); **4a**: δ = 1.50(s); **4b**: δ = 1.49(s, 24H), 1.76(q, 4H), 0.62(t, 6H), $^3J(HH)$ = 7.4 Hz. IR (hexane): $\tilde{\nu}$(CO) [cm^{-1}]: **2**, 1997(s), 1957(s); **3**: 1932(s, br). – EI-MS of **2** (70 eV, 150 °C): *m/z* 408 ($M^{\oplus}$, 15%), 380 ($M^{\oplus}$ − CO, 28), 352 ($M^{\oplus}$ − 2 CO, 66), 124 ($P_4^{\oplus}$, 24), 62 ($P_2^{\oplus}$, 11), 28 ($CO^{\oplus}$, 100) and other fragments. EI-MS of **3** (70 eV, 160 °C): *m/z* 636 ($M^{\oplus}$, 3%), 608 ($M^{\oplus}$ − CO, 22), 580 ($M^{\oplus}$ − 2 CO, 100) and other fragments, but no P_x fragments.

[5] a) **2**: orthorhombic, $P2_12_12$; a = 8.9833(3), b = 20.7335(7), c = 8.7097(4) Å; Z = 4; 1958 unique reflections ($Mo_{K\alpha}$; 1.5° < θ < 27°), 1836 observed with $I \geq 2\sigma(I)$; 188 parameters, R = 0.023, R_w = 0.029 [5c]; b) **4b**: monoclinic, $P2_1/n$; a = 9.006(1), b = 20.442(2), c = 15.243(1) Å, β = 94.34(1)°; Z = 4; 3271 unique reflections ($Mo_{K\alpha}$; 1.5° < θ < 25°), 2140 observed with $I \geq 2\sigma(I)$; 280 parameters, R = 0.064, R_w = 0.064 [5c]; c) Solution and refinement of the structures was accomplished with the programs SHELX 76, SHELXS 86. In the crystal of **4b**, the Nb2-bonded Cp′-ring is oriented in such a way that the ethyl group occupies two neighboring positions with 55% and 45% probability. Further details of the crystal structure investigation may be obtained from the Fachinformationszentrum Karlsruhe, Gesellschaft für wissenschaftlich-technische Information mbH, D-7514 Eggenstein-Leopoldshafen 2 (FRG), on quoting the depository number CSD-53948, the names of the authors, and the journal citation.

[6] P. Binger, B. Biedenbach, R. Mynott, C. Krüger, P. Betz, M. Regitz, *Angew. Chem. 100* (1988) 1219; *Angew. Chem. Int. Ed. Engl. 27* (1988) 1157.

[7] See for example K. Wade, *Adv. Inorg. Chem. 18* (1976) 1; D. M. P. Mingos, *Acc. Chem. Res. 17* (1984) 311.

[8] Reaction of [RNb(CO)$_4$] (R = Cp* or Cp′) and P_4 in decalin at ca. 170 °C (ca. 4 h) gives **4a** or **4b**, respectively, in ca. 23% yield: O. J. Scherer, J. Vondung, R. Winter, unpublished.

[9] K. Angermund, K. H. Claus, R. Goddard, C. Krüger, *Angew. Chem. 97* (1985) 241; *Angew. Chem. Int. Ed. Engl. 24* (1985) 237, and references cited therein.

[10] O. J. Scherer, J. Schwalb, H. Swarowsky, G. Wolmershäuser, W. Kaim, R. Gross, *Chem. Ber. 121* (1988) 443.

[11] H. G. von Schnering, T. Meyer, W. Hönle, W. Schmettow, U. Hinze, W. Bauhofer, G. Kliche, *Z. Anorg. Allg. Chem. 553* (1987) 261. For extended Hückel calculations on triple-decker complexes with *cyclo*-P_x middle decks, see W. Tremel, R. Hoffmann, M. Kertesz, *J. Am. Chem. Soc. 111* (1989) 2030; E. D. Jemmis, A. C. Reddy, *Organometallics 7* (1988) 1561. For sandwich complexes, see: M. C. Kerins, N. J. Fitzpatrik, M. T. Nguyen, *Polyhedron 8* (1989) 1135.

[12] H. G. von Schnering, W. Hönle, *Chem. Rev. 88* (1988) 243.

[13] W. A. Herrmann, W. Kalcher, H. Biersack, I. Bernal, M. Creswick, *Chem. Ber. 114* (1981) 3558.

Aurophilicity as Concerted Effect: Relativistic MO Calculations on Carbon-Centered Gold Clusters**

By *Notker Rösch,** *Andreas Görling, Donald E. Ellis,* and *Hubert Schmidbaur**

A strong attractive interaction has been observed between gold atoms with d^{10} configuration and + 1 oxidation state in numerous polynuclear gold compounds.[1–6] It is manifested in molecular conformations with relatively close Au · · · Au contacts (2.9–3.0 Å)[1,2] or discrete Au–Au bonds,[3,4] whose strength has been estimated from spectroscopic data to be 6–8 kcal mol^{-1}.[3] Noteworthy is the tendency of polyaurated organogold compounds to bond further gold(I) units, $[LAu]^{\oplus}$ (L = R_3P), to a carbon center.[1,2] The term aurophilicity has been coined for this phenomenon.[5] Particularly striking examples of this interaction are provided by the recently synthesized carbon-centered gold-cluster cations $[\{(C_6H_5)_3PAu\}_nC]^{(n-4)\oplus}$ (n = 5,6).[5,6] The X-ray structure analyses of these compounds revealed an only slightly distorted highly symmetric arrangement of the gold atoms (trigonal-bipyramidal for n = 5,[6] octahedral for n = 6[5]) around a central carbon atom. Accordingly, these clusters offered an ideal starting point for a more detailed theoretical study of aurophilic interactions,[7] the results of which are presented here. Although this investigation focused on the analysis of the electronic structure of the carbon-centered gold cluster $[\{(C_6H_5)_3PAu\}_6C]^{2\oplus}$, our goal was to arrive at general conclusions on the bonding in polyauriomethanes.

The MO structure of the quasi-octahedral cluster is best derived through fragment analysis, proceeding from the uncomplexed cluster $[Au_6]^{2\oplus}$ via the carbon-centered cluster $[Au_6C]^{2\oplus}$ to the complete cluster $[(LAu)_6C]^{2\oplus}$. Any discussion of the electronic structure of a "centered" metal cluster has to take into consideration the interplay of tangential bonds within the metal polyhedron and of radial bonds to both the central atom and the outer ligands,[7,8] since this influences the hybridization of the metal atoms. Furthermore, it is important to bear in mind that the 6s orbitals of gold are lowered in energy owing to the relativistic increase in mass;[9,10] sp hybridization with 6p orbitals is thereby made more difficult, whereas sd hybridization with 5d orbitals is facilitated. In the following MO analysis, all three features of the bonding in gold clusters are treated together theoretically for the first time. Starting from the reference configuration d^{10}, for which a (weakly) repulsive interaction between gold(I) atom pairs is assumed,[8,11] we used the *extent of disruption of the closed 5d valence shells* as a criterion for the strength of a possible aurophilic interaction. This approach considers only one, though important, aspect of the Au–Au interaction; the bonding picture so obtained must therefore be augmented by an analysis of orbital interactions[7] (see Fig. 1 and the accompanying text).

The calculations for the systems $[Au_6]^{2\oplus}$, $[Au_6C]^{2\oplus}$, and $[(LAu)_6C]^{2\oplus}$, as well as for $[Au_5]^{\oplus}$ and $[Au_5C]^{\oplus}$, were performed using the discrete variational (DV) Xα method,[12] a

[*] Prof. Dr. N. Rösch, Dipl.-Chem. A. Görling, Prof. D. E. Ellis [+], Ph. D. Lehrstuhl für Theoretische Chemie der Technischen Universität München Lichtenbergstrasse 4, D-8046 Garching (FRG)
Prof. Dr. H. Schmidbaur
Anorganisch-chemisches Institut der Technischen Universität München Lichtenbergstrasse 4, D-8046 Garching (FRG)

[+] Guest from the Department of Physics and Astronomy, Northwestern University, Evanston, IL 60201 (USA)

[**] This work was supported by the Deutsche Forschungsgemeinschaft (Sonderforschungsbereich 128 (*N.R.*) and Leibniz-Programm (*H.S.*)), the Bund der Freunde der Technischen Universität München (*N.R.*), and the Fonds der Chemischen Industrie.

self-consistent LCAO–MO method within the framework of density functional theory;[13] both nonrelativistic and relativistic versions of the computer program are available, the latter based on four-component Dirac spinors. Symmetry-adapted molecular orbitals were constructed from atomic orbitals, numerically determined for the atomic configurations present in the cluster by a self-consistent Mulliken population analysis.[12] The DV Xα method takes into consideration all electrons, but only the valence electrons were included in the self-consistent process. To simplify the calculations still further, we selected a model with SH_2 instead of Ph_3P ligands, so that the assumed symmetry of the resulting cluster was appreciably higher (point group T_h). However, because of its nonbonding orbital perpendicular to the molecular plane and the associated interaction, SH_2 is not a fully adequate model for Ph_3P.[14] An idealized octahedral structure was assumed in these calculations (d(Au-Au) = 3.005,[5] d(Au-C) = 2.125, d(Au-S) = 2.270, d(S-H) = 1.345 Å, $\sphericalangle$ (H-S-H) = 90°).

We found that the use of a relativistic MO method is essential for a *complete* theoretical description of the aurophilic interactions. This is shown in Table 2 by the Mulliken populations of the gold and carbon valence orbitals and the resulting atomic charges. In *all* systems studied, the relativistic treatment yields the expected increase (by about 0.2) in the Au 6s population, the Au 5d population decreasing by nearly the same amount. Compared with the inert d^{10} configuration, the deficit in the Au 5d population of the Au_6 cluster calculated relativistically is practically twice as large as the deficit calculated nonrelativistically. The tendency toward Au–Au interaction should correspondingly increase, in accordance with the criterion given above ("disruption of the closed 5d valence shell"). (Even nonrelativistic calculations on the cluster $[Au_6]^{\oplus}$, with a 5d population of 9.80, revealed a deficit of 0.20, so that the Au 5d orbitals can make a definite, though small, contribution to the Au–Au bond.) The radial bonds of the gold cluster (to the central carbon atom as well as to the outer ligands) lead to a further reduction in the Au 5d population, thereby improving the possibility of an aurophilic interaction. The central carbon atom is of crucial importance for the stability of the complete cluster (see below), though its direct contribution to further disruption of the Au 5d shell of (relativistically described) gold(I) units, $[LAu]^{\oplus}$, is likely to be small.

Table 1. Mulliken valence orbital populations and resulting atomic charges Q [|e|] from nonrelativistic (nr) and relativistic (r) DV Xα MO calculations for the clusters $[Au_6]^{2\oplus}$, $[Au_6C]^{2\oplus}$, and $[(LAu)_6C]^{2\oplus}$ (L = SH_2) as well as for the clusters $[Au_5]^{\oplus}$ and $[Au_5C]^{\oplus}$ [a].

		Au				C		
		6s	6p	5d	Q	2s	2p	Q
$[Au_6]^{2\oplus}$	nr	0.58	0.29	9.80	+0.33	–	–	–
	r	0.80	0.27	9.59	+0.33	–	–	–
$[Au_6C]^{2\oplus}$	nr	0.48	0.24	9.72	+0.56	1.52	3.81	−1.33
	r	0.69	0.19	9.53	+0.59	1.47	4.08	−1.54
$[(LAu)_6C]^{2\oplus}$ [b]	nr	0.61	0.27	9.45	+0.68	1.59	4.21	−1.81
	r	0.82	0.31	9.29	+0.58	1.46	4.22	−1.69
$[Au_5]^{\oplus}$ [c]	nr	0.69	0.25	9.87	+0.20	–	–	–
	r	0.93	0.20	9.67	+0.20	–	–	–
$[Au_5C]^{\oplus}$ [c]	nr	0.61	0.24	9.72	+0.43	1.54	3.61	−1.15
	r	0.85	0.18	9.52	+0.45	1.41	3.85	−1.26

[a] Because of the largely systematic agreement between the results obtained for the pentanuclear and the corresponding hexanuclear clusters, we did not carry out the relatively involved calculation on the cluster $[(LAu)_5C]^{\oplus}$. [b] Q(L) = −0.04 (nr); +0.04(r). [c] Values determined for the axial and equatorial Au atoms.

Comparison of the results presented above with those obtained for the systems $[Au_5]^{\oplus}$ and $[Au_5C]^{\oplus}$ shows that it should be possible to extend this analysis to other gold clusters. There is clear agreement of the charge distribution with those of the corresponding octahedral systems, especially for the population of the Au 5d orbitals and for the changes found upon relativistic treatment. Noteworthy, however, is the higher Au 6s population for the Au_5 clusters and the fact that the charge on the central carbon atom is reduced in nearly direct proportion to the number of ligands.

We have thus shown that the use of a relativistic MO method yields the correct contributions of the Au 6s orbitals to the disruption of the d^{10} configuration. In the following discussion, we present a qualitative orbital interaction analysis of the systems $[Au_6]^{2\oplus}$, $[Au_6C]^{2\oplus}$, and $[(LAu)_6C]^{2\oplus}$ based on nonrelativistic calculations, since they offer the advantage of symmetry classification according to the normal point groups. This analysis obviates the interpretation of the much more complex relativistic orbitals and thus the necessity of using double groups with their lower number of irreducible representations. A further complication encountered in relativistic calculations is caused by appreciable spin–orbit interaction in gold atoms, which can be neglected in a qualitative discussion of the bonding. In the following, only orbitals of symmetry a_{1g} and t_{1u} (point group O_h) are analyzed, since the valence orbitals of the central carbon atom only encompass these irreducible representations (Fig. 1). A population analysis of the corresponding orbitals of the cluster $[(LAu)_6C]^{2\oplus}$ is given in Table 2.

In previous discussions[5, 6, 8] of the electronic structure of Au_6 clusters, the closed d^{10} shells were neglected and only

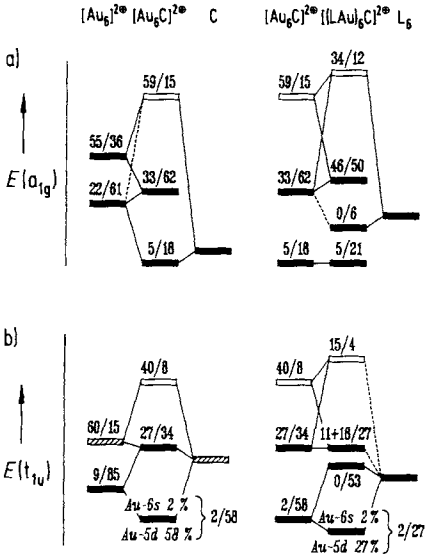


Fig. 1. Schematic interaction diagram of orbitals with the irreducible representations a_{1g} (a) and t_{1u} (b) – or 1_g and t_u in T_h – for the systems $[Au_6]^{2\oplus}$-C and $[Au_6C]^{2\oplus}$-L_6, derived by self-consistent DV Xα calculations. For clarity, only orbitals containing dominant contributions from the carbon atom or from the ligands L (=SH_2) are represented (the latter limited to the σ interaction with the Au_6 cluster). Furthermore, the diagram focuses on the 6s–5d hybridization of the gold atoms: the numbers on the energy levels give the gold 6s and gold 5d populations [%] (in this order). The populations for the Au-6p, C, and L orbitals are omitted (they are listed in Table 2). Unoccupied orbitals are drawn as empty bars; the two hatched bars represent energy levels partially filled with two electrons each. In the bar labeled 11 + 18/27, the orbitals $3't_{1u}$ and $3t_{1u}$ are summarized from Table 2; the 5d orbital population in the $3't_{1u}$ orbital is not given since these orbitals are largely of π character with respect to Au–L bonding. For the selection of the orbitals of symmetry type t_u, see text [7].

Table 2. Energies and Mulliken populations [%] for those molecular orbitals of the cluster $[(LAu)_6C]^{2\oplus}$ ($L = SH_2$) that make essential contributions to the radial bonds (nonrelativistic calculations). See also Figure 1.

Energy [eV]	Symmetry [a]	Au 6s	Au 6p	Au 5d	C 2s	C 2p	L
−19.36	$2a_g$ ($1a_{1g}$)	5	0	21	70	–	4
−16.44	$3t_u$ ($1t_{1u}$)	2	1	27	–	7	63
−15.62	$3a_g$ ($2a_{1g}$)	0	3	6	9	–	82
−14.29	$4t_u$ ($2t_{1u}$)	0	−1	53	–	27	21
−12.20	$4a_g$ ($3a_{1g}$)	46	0	50	0	–	4
−12.07	$7t_u$ ($3't_{1u}$) [b]	11	1	72	–	2	14
−9.23 [c]	$9t_u$ ($3t_{1u}$) [b]	18	12	27	–	28	15
−4.77	$6a_g$ ($4a_{1g}$)	34	0	12	12	–	42
−3.75	$11t_u$ ($4t_{1u}$)	15	4	4	–	16	61

[a] Numbering based on all valence orbitals of the cluster, irreducible representations of the point group T_h; the corresponding representations for idealized octahedral symmetry are given in parentheses with only those orbitals included that contribute to Au–C and Au–L bonding. [b] Interaction distributed over two orbitals. [c] HOMO.

the six (6sp) hybrid orbitals considered. The direct interaction between Au 5d orbitals is relatively weak, but cannot be neglected. The following values for the Au 5d overlap integrals S can be derived from the DV Xα orbitals:[7] $S(\sigma) = 0.039$, $S(\pi) = 0.026$, $S(\delta) = 0.002$. These values are about twice as large as those assumed in earlier calculations.[8] In the octahedron, the σ(sp) hybrid orbitals span orbitals of symmetry types a_{1g}, t_{1u}, and e_g (in order of increasing energy). The highest occupied orbital (HOMO) of $[Au_6]^{2\oplus}$, the $2t_{1u}$ σ(sp) level, contains two electrons. However, the $2a_{1g}$ σ(sp) orbital shows a significant Au 5d population (36%, cf. Fig. 1) and lies energetically within the "band" of the 5d level. Correspondingly, the $1a_{1g}$ level, formally ascribed to the Au 5d cluster orbitals, displays 39% sp character. In the relativistic calculation, this energetically *lowest-lying* valence orbital of the cluster ($1a_{1g}$) has to be identified as the Au σ(sp) level (6s, 57%; 6p, 21%; 5d, 22%), whereas the $2a_{1g}$ orbital is formally ascribed to the Au 5d cluster orbitals.[10] The interaction with the central carbon atom leads to the expected charge transfer Au → C. Formally, the $2a_{1g}$ and $2t_{1u}$ levels of the cluster $[Au_6]^{2\oplus}$ are emptied in favor of the $2t_{1u}$ HOMO of the carbon-centered cluster $[Au_6C]^{2\oplus}$. However, the HOMO is localized to a considerable extent on the gold atoms (6s, 27%; 5d, 34%). In the complete cluster, $[(LAu)_6C]^{2\oplus}$, the character of the HOMO changes only slightly. Nonetheless, since the reduction of the Au_6–ligand interaction to a minimum number of involved energy levels for the symmetry type t_u (point group T_h) is incomplete, the choice of the orbitals is not unambiguous[7] (cf. Fig. 1 and Table 2).

For the orbitals formally ascribed to the Au 5d manifold, the radial (essentially σ-like) interactions of the Au_6 cluster both with the central carbon atom and with the outer six ligands L lead to changes that can be interpreted in terms of a classical perturbational approach[15] (cf. Fig. 1). Examples are the orbitals $1a_{1g}$ of $[Au_6]^{2\oplus}$ and $2a_{1g}$ of $[Au_6C]^{2\oplus}$; although they are largely nonbonding with respect to the Au–Au interaction, energetically higher-lying orbitals of the respective starting cluster can "mix" into them through the interaction partner C or L.[11] Since these higher-lying orbitals display a stronger Au 6s character and a correspondingly weaker Au 5d population, this mixing disrupts the "closed" Au 5d shell and establishes the orbital-dependent prerequisite for aurophilic interaction. The effect of the outer ligands exceeds that of the central carbon atom, as revealed by the charge balance (Table 1) and the character of the individual orbitals (Fig. 1 and Table 2).

Received: May 24, 1989 [Z 3357 IE]
German version: *Angew. Chem. 101* (1989) 1410

[1] F. Scherbaum, B. Huber, G. Müller, H. Schmidbaur, *Angew. Chem. 100* (1988) 1600; *Angew. Chem. Int. Ed. Engl. 27* (1988) 1542.
[2] H. Schmidbaur, F. Scherbaum, B. Huber, G. Müller, *Angew. Chem. 100* (1988) 441; *Angew. Chem. Int. Ed. Engl. 27* (1988) 419.
[3] H. Schmidbaur, W. Graf, G. Müller, *Angew. Chem. 100* (1988) 439; *Angew. Chem. Int. Ed. Engl. 27* (1988) 417; *Helv. Chim. Acta 69* (1986) 1748; H. Schmidbaur, A. Schier, G. Reber, G. Müller, *Inorg. Chim. Acta 147* (1988) 143.
[4] H. Schmidbaur, C. Hartmann, G. Reber, G. Müller, *Angew. Chem. 99* (1987) 1189; *Angew. Chem. Int. Ed. Engl. 26* (1988) 1146.
[5] F. Scherbaum, A. Grohmann, B. Huber, C. Krüger, H. Schmidbaur, *Angew. Chem. 100* (1988) 1602; *Angew. Chem. Int. Ed. Engl. 27* (1988) 1544.
[6] F. Scherbaum, A. Grohmann, B. Huber, C. Krüger, H. Schmidbaur, *Angew. Chem. 101* (1989) 464; *Angew. Chem. Int. Ed. Engl. 101* (1989) 463.
[7] A. Görling, N. Rösch, D. E. Ellis, G. L. Goodman, H. Schmidbaur, unpublished.
[8] D. M. P. Mingos, *J. Chem. Soc. Dalton Trans. 1976*, 1163.
[9] P. Pyykkö, *Chem. Rev. 88* (1988) 563.
[10] R. Arriata-Perez, G. L. Malli, *Chem. Phys. Lett. 125* (1986) 143.
[11] P. K. Mehrota, R. Hoffmann, *Inorg. Chem. 17* (1978) 2187; Y. Jiang, S. Alvarez, R. Hoffmann, *ibid. 24* (1985) 749; K. M. Merz, Jr., R. Hoffmann, *ibid. 27* (1988) 2120.
[12] D. E. Ellis, G. S. Painter, *Phys. Rev. B 2* (1970) 2887; A. Rosén, D. E. Ellis, *J. Chem. Phys. 62* (1975) 3039; A. Rosén, D. E. Ellis, A. Adachi, F. W. Averill, *ibid. 65* (1976) 3629.
[13] J. P. Dahl, J. Avery (Eds.): *Local Density Approximations in Quantum Chemistry and Solid State Physics*, Plenum, New York 1984; S. B. Trickey (Ed.): *Adv. Quantum Chem. 20* (1989), in press.
[14] Calculations are currently being performed on a cluster $[(LAu)_6C]^{2\oplus}$ with $L = PH_3$. However, these calculations are more extensive owing to the reduced symmetry (maximum D_{3d}). We will report elsewhere on the results of this study.
[15] T. A. Albright, J. K. Burdett, W. M.-H. Whangbo: *Orbital Interactions in Chemistry*, Wiley, New York 1985.

Synthesis and Pharmacological Properties of a Novel Cardioactive Steroid**

By *Ulrich Werner, Uwe Möller, Petra Wagner, Peter Welzel,* Christa Zylka, Siegfried Mechmann, Hermann Pusch,* and *Helfried Günther Glitsch**

The $Na^{\oplus}$ pump of animal cells generates and maintains the $Na^{\oplus}$ and $K^{\oplus}$ gradients across the cell membrane. These ion gradients are essential for the electrical excitability of the plasma membrane. In addition, the $Na^{\oplus}$ gradient serves as an energy source for the transmembrane transport of specific substances: for example, sugar and amino-acid import and $Ca^{2\oplus}$ transport out of the cell.[1]

Cardioactive glycosides inhibit the $Na^{\oplus}$ pump, thereby raising the intracellular $Na^{\oplus}$ concentration. The resulting decrease in the $Na^{\oplus}$ gradient across the sarcolemma reduces the energy available for transport of $Ca^{2\oplus}$ out of the cell by

[*] Prof. Dr. P. Welzel, Dr. U. Werner,
Dipl.-Chem. U. Möller, Dipl.-Chem. P. Wagner
Fakultät für Chemie der Universität
Postfach 102148, D-4630 Bochum (FRG)
Prof. Dr. H. G. Glitsch, Dr. H. Pusch,
Dr. S. Mechmann, Dipl.-Biol. C. Zylka
Fakultät für Biologie der Universität
Postfach 102148, D-4630 Bochum (FRG)

[**] This work was supported by the Deutsche Forschungsgemeinschaft (We 595/12-3, researcher group "Konzell") and the Fonds der Chemischen Industrie.

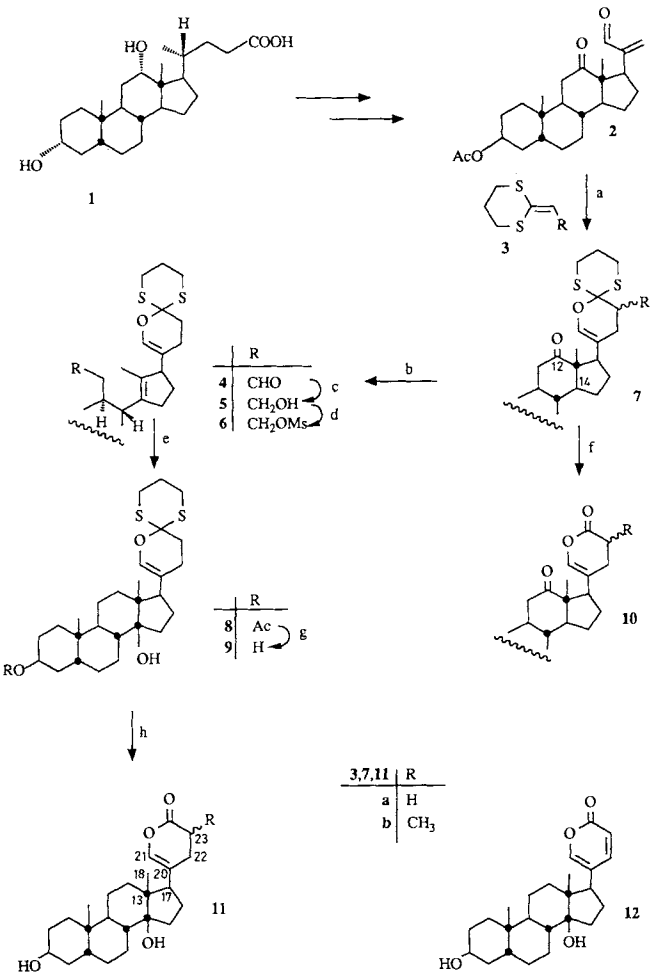
$Na^{\oplus}/Ca^{2\oplus}$ exchange. This ultimately leads to the (medicinally used) positive inotropic effect of these substances.[2]

The molecular basis of the $Na^{\oplus}$ pump is a $Mg^{2\oplus}$-dependent $Na^{\oplus}$-and $K^{\oplus}$-activated ATPase in the plasma membrane. This ATPase consists of a large catalytic α subunit and a smaller β subunit whose function is still unknown. The complete amino-acid sequence of the α subunit was recently determined.[1] The protein chain presumably spans the plasma membrane eight times. At least four of the extracellular regions are assumed to be involved in binding the steroid moiety of the cardiac glycosides; however, the precise site of binding and the mode(s) of binding have not yet been determined.[1] To localize the lactone binding site of the ATPase by affinity labeling,[3] we have attempted to develop a general route to cardioactive steroids containing a (latently) reactive group in the lactone ring. The target compounds were the previously unknown bufenolides of type **11**, which differ from the classical bufadienolides—for example, bufalin **12**—in the absence of a double bond between C-22 and C-23.

The unsaturated aldehyde **2**,[4] accessible in five steps from deoxycholic acid **1**, underwent $Eu(fod)_3$-catalyzed[6] reaction with *Seebach*'s ketene acetal **3a**[5] to give the [4 + 2] cycloadduct **7a** in 96% yield. Similarly, **7b** was obtained from **2** and **3b**.[5] According to ^1H NMR analysis, **7b** was a 3:1 mixture of two diastereomers. $Cu^{2\oplus}$-catalyzed hydrolysis transformed **7a** and **7b** into the enol lactones **10a**[7] and **10b**,[8] respectively. Product **10b** was also a 3:1 diastereomeric mixture. NMR analysis[9] revealed that in the main component the 23-methyl group occupies an axial position; however, the configuration at C-23 could not be determined, even by means of circular dichroism ($\lambda_{max}(\Delta\varepsilon) = 286$ (+ 0.88), 234 (+ 5.6), 202 nm (− 0.5).

To introduce the 14β-OH group, we used a procedure recently developed by us.[10] The method consists of four steps: (1) photochemical rearrangement of a 12-oxo-14α-steroid to an unsaturated secoaldehyde (here: **7** → **4**); (2) reduction of the secoaldehyde (**4** → **5**); (3) mesylation (**5** → **6**); (4) ring closure under solvolysis conditions (**6** → **8**). The orthoester group in **7** has the advantage that there is no interfering overlap between its UV absorptions[11] and the n → π* band of the keto group at 300 nm.[12] On the other hand, the aldehyde group in secoaldehydes such as **4** also absorbs at 300 nm and undergoes an H-transfer reaction in the excited state.[13] The photochemical rearrangement **7** → **4** was therefore carried out in the presence of a selective reducing agent that immediately reduces the newly formed aldehyde **4** to **5** without attacking the keto group in **7**. Lithium tri-*tert*-butoxyhydridoaluminate was well-suited for this purpose, and **5** was obtained in 59% yield (based on **7**). Mesylation (**5** → **6**) and subsequent solvolysis then led to **8** (49%). Finally, the protecting groups were removed: first, the 3-OH group was deprotected (**8** → **9**),[14] then the enol lactone (**9** → **11a**). Cleavage of the thioacetal function in **9** could not be accomplished by a number of commonly used procedures;[15] only the conditions given in Scheme 1 led to a good yield of **11a** (93%). Careful NMR analysis showed that the side chain of **11a** (in $CDCl_3$ solution) adopts a conformation in which the torsional angle (17-H)C-17–C-20(C-21) is ca. 30° (NOE effects between CH_3-18 ⤳ 21-H and 17-H ⤳ 21-H.

The positive inotropic effect of 22,23-dihydrobufalin **11a** was investigated with guinea-pig papillary muscles and the inhibition of the $Na^{\oplus}$ pump with Purkinje fibers of sheep heart by electrophysiological methods. Some details of the contraction measurements are found in the caption to Figure 1. The example in Figure 1 shows that **11a** has a markedly positive inotropic effect on guinea-pig heart. The effect is



Scheme 1. All yields are based on consumed starting material. The reaction mixtures were purified, after workup (distribution between water and CH_2Cl_2, drying of the organic phase, solvent evaporation), by column-chromatography on silica gel with petroleum ether/ethyl acetate or petroleum ether/acetone mixtures of suitable polarity. a) **2** + 3.9 equiv. **3a** and 0.05 equiv. $[D_{27}]$-$Eu(fod)_3$, $CHCl_3$, 20 °C, 18 h; 96%. b, c) **7** + 1.9 equiv. $LiAlH(OtBu)_3$, toluene/*t*BuOH (4/1), *hv* (Philips HPK 125, Pyrex filter), −20 °C, 22 h; 59%. d) **5** + 2.5 equiv. NEt_3, 2.5 equiv. MsCl, CH_2Cl_2, −78 °C, 10 min. e) **6** + 24 equiv. aqueous oxalic acid (0.2 mol L^{-1}), acetone, 50 °C, 2 h; 55% (based on **5**). f) **7** + 4.7 equiv. CuO, 3.2 equiv. $CuCl_2$, acetone/H_2O (10/1), 20 °C, 22 h; 78%. g) **8** + 5.5 equiv. LiOH · H_2O, THF/H_2O (7.5/1), 20 °C, 2 d; 97%. h) **9** + 4.6 equiv. CuO, 3.2 equiv. $CuCl_2$, acetone/H_2O (10/1), 20 °C, 42 h; 93%. **11a**: ^1H NMR (400 MHz, $CDCl_3$): $\delta = 0.81$ (s, 3H, CH_3-18), 0.92 (s, 3H, CH_3-19), 1.20 (m, 6β-H), 1.23–1.31 (m, 4-H, 7-H, 11β-H), 1.24 (m, 12α-H), 1.42 (m, 12β-H), 1.48 (m, 8-H), 1.50 (m, CH_2-2), 1.52 (m, 9-H), 1.56 (m, 15-H), 1.63 (m, 7-H, 11α-H), 1.70 (m, 5-H), 1.74 (m, 16-H), 1.85 (m, 6α-H), 1.92 (m, 16-H), 1.94 (m, 4-H), 1.98 (m, 15-H), 2.25–2.34 ("t", 1H, 17-H), 2.32–2.41 (m, 1H, 22-H), 2.48–2.62 (m, 3H, 22-H, CH_2-23), 4.10 (m, 1H, $W_{1/2} = 7.3$ Hz, 3α-H), 6.33 (m, 1H, $W_{1/2} = 3$Hz, 21-H). ^{13}C NMR (100.6 MHz, $CDCl_3$): $\delta = 15.67$ (CH_3, C-18), 20.65 (CH_2, C-22), 21.38 (CH_2, C-7), 21.42 (CH_2, C-11), 23.75 (CH_3, C-19), 25.47 (CH_2, C-16), 26.53 (CH_2, C-6), 27.89 (CH_2, C-2), 28.64 (CH_2, C-23), 29.62 (CH_2, C-1), 32.73 (CH_2, C-15), 33.26 (CH_2, C-4), 35.36 (C_q, C-10), 35.64 (CH, C-9), 35.98 (CH, C-5), 41.21 (CH_2, C-12), 42.45 (CH, C-8), 48.40 (C_q, C-13), 53.16 (CH, C-17), 66.85 (CH, C-3), 85.06 (C_q, C-14), 122.48 (C_q, C-20), 138.07 (CH, C-21), 169.56 (C_q, C-24).

dose dependent and reversible. After a control period, the muscle is bathed in a solution containing 10^{-6} mol L^{-1} of **11a**. The contractile force increases and, after a few minutes, reaches a new steady state. When **11a** is washed out, the contractile force returns to the control value. A smaller concentration of **11a** effects a smaller positive inotropic effect, which is also reversible (see Fig. 1). Figure 2 shows the dose–response curve for 22,23-dihydrobufalin **11a**, as well as for **12**, which, for comparison, was studied on the same muscle. The ordinate gives the contractile force of the muscle relative

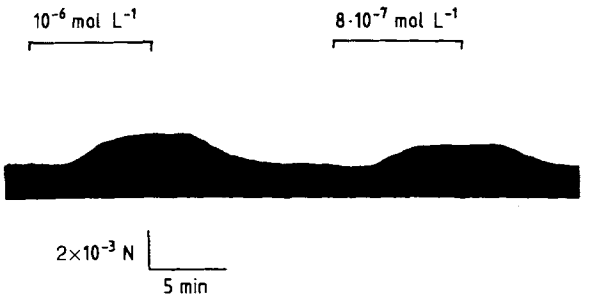


Fig. 1. Positive inotropic effect of **11a** (two concentrations) on a guinea-pig papillary muscle. The bracketed regions represent times during which the muscle was bathed in solution containing **11a** (bathing fluid, Tyrode solution containing 2.7×10^{-3} mol L^{-1} KCl and 1.8×10^{-3} mol L^{-1} $CaCl_2$; pH 7.4, 35 °C). The contractions were induced by square-wave electrical pulses (stimulus potential, twice the threshold potential; pulse duration 4 ms; frequency, 1.2 Hz) and recorded with a mechano-electrical transducer (Endevco, model 8107-20) on a recorder (Schwarzer Physiopolygraph Varioscript; units in Newton).

to that during the preceding control period; the abscissa gives the logarithmic concentrations of **11a** and **12**. The linear parts of the curves reveal that **11a** is less active than **12** by a factor of 10. Spontaneous activity of **12** (toxic effect) is observed at a concentration of 5×10^{-6} mol L^{-1}, whereas **11a** shows no toxic effect at a concentration of 4×10^{-6} mol L^{-1}. Increasing the extracellular $K^{\oplus}$ concentration leads to a rightward shift of the two dose–response curves (not shown). Similar results were obtained with two other papillary muscles.

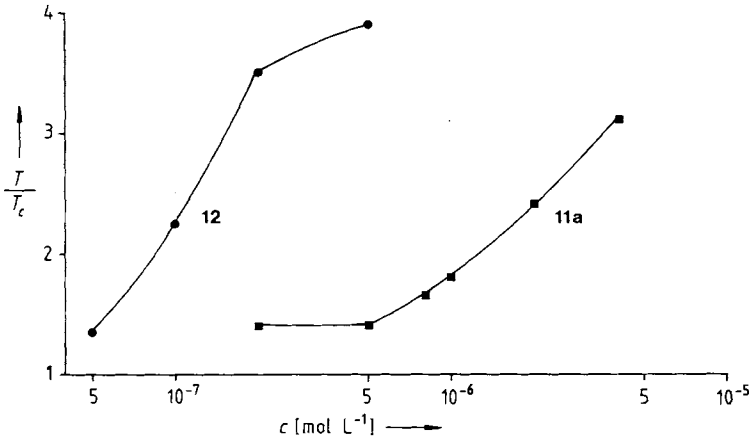


Fig. 2. Dose–response curves of the positive inotropic effect of steroids **11a** (■) and **12** (●) on a guinea-pig papillary muscle. Ordinate: contractile force (T) relative to the contractile force of muscle during the preceding control period (T_c). Abscissa: concentrations (logarithmic). Note that the numbers 5 on the abscissa stand for 5×10^{-8}, 5×10^{-7}, and 5×10^{-6}.

Compound **11a** also inhibits the $Na^{\oplus}$ pump current of sheep Purkinje fibers (measured as described previously[16]) in a dose-dependent fashion: At **11a** concentrations of 5×10^{-8}, 1×10^{-7}, and 5×10^{-7} mol L^{-1}, the transient outward (pump) current decreased by 27.5, 38.6, and 62%, respectively. Apparently, **11a** is active on sheep Purkinje fibers at lower concentrations than those required for guinea-pig papillary muscle, in agreement with similar results obtained for three cardiac glycosides.[17]

The results described here show that 22,23-dihydrobufalin **11a** exhibits the characteristic pharmacological properties of cardioactive steroids: it displays positive inotropic activity and inhibits active $Na^{\oplus}/K^{\oplus}$ transport. We plan to extend these investigations to compounds of type **11** whose R group is suitable for affinity labeling of the ATPase.

Received: June 2, 1989 [Z 3372 IE]
German version: *Angew. Chem. 101* (1989) 1417

[1] E. M. Price, J. B. Lingrel, *Biochemistry 27* (1988) 8400–8408, and references cited therein.
[2] a) Review: D. G. Allen, D. A. Eisner, S. C. Wray, *Nature (London) 316* (1985) 674–675; b) recent pharmacological studies: J. Yamahara, S. Tanaka, H. Matsuda, T. Sawada, H. Fujimura, *Nippon Yakurigaku Zasshi 88* (1986) 413–423.
[3] Earlier investigations of photoaffinity labeling: a) B. M. Anner, *Biochem. J. 227* (1985) 1–11, and references cited therein; b) T. Deffo, D. S. Fullerton, M. Kihara, R. H. McParland, R. R. Becker, B. M. Simat, A. H. From, K. Ahmed, M. I. Schimerlik, *Biochemistry 22* (1983) 6303–6309, c) K. Ahmed, R. McParland, R. Becker, A. From, D. S. Fullerton, *Fed. Proc., Fed. Am. Soc. Exp. Biol. 46 (part 3)* (1987) 1983.
[4] H. W. Hoppe, M. Kaiser, D. Müller, P. Welzel, *Tetrahedron 43* (1987) 2045–2057.
[5] D. Seebach, M. Kolb, B.-T. Gröbel, *Chem. Ber. 106* (1973) 2277–2290.
[6] M. Bednarski, S. Danishefsky, *J. Am. Chem. Soc. 105* (1983) 3716–3717; S. J. Danishefsky, W. H. Pearson, *J. Org. Chem. 48* (1983) 3865–3866; S. Castellino, J. J. Sims, *Tetrahedron Lett. 25* (1984) 2307–2310; M. M. Midland, R. S. Graham, *J. Am. Chem. Soc. 106* (1984) 4294–4296.
[7] Alternative preparation of **10a**: H.-W. Hoppe, B. Stammen, U. Werner, H. Stein, P. Welzel, *Tetrahedron 45* (1989) 3695–3710.
[8] Related investigations of the synthesis of enol lactones: S. E. Denmark, J. A. Sternberg, *J. Am. Chem. Soc. 108* (1986) 8277–8279; K. Vogt, R. R. Schmidt, *Tetrahedron 44* (1988) 3271–3280.
[9] ^1H, ^{13}C NMR, $^1H/^1H$ COSY, $^1H/^{13}C$ COSY, NOE difference spectra, $^1H/^1H$ decoupling experiments.
[10] H.-W. Hoppe, P. Welzel, *Tetrahedron Lett. 27* (1986) 2459–2462, and references cited therein.
[11] E. A. Braude, *Annu. Rep. Prog. Chem. 42* (1945) 105–130; J. D. Willet, J. R. Grunwell, G. A. Berchtold, *J. Org. Chem. 33* (1968) 2297–2302.
[12] Detailed discussion of this problem: U. Werner, H.-W. Hoppe, P. Welzel, G. Snatzke, R. Boese, *Tetrahedron 45* (1989) 1703–1710.
[13] P. E. Hammann, G. G. Habermehl, *Z. Naturforsch. B42* (1987) 781–782.
[14] E. J. Corey, I. Székely, C. S. Shiner, *Tetrahedron Lett. 1977*, 3529–3532; E. J. Corey, K. Narasaka, M. Shibasaki, *J. Am. Chem. Soc. 98* (1976) 6417–6418.
[15] B.-T. Gröbel, D. Seebach, *Synthesis 1977*, 357–402.
[16] H. G. Glitsch, H. Pusch, T. Schumacher, F. Verdonck, *Pflügers Arch. 394* (1982) 256–263.
[17] I. S. Cohen, N. B. Datyner, G. A. Gintant, N. K. Mulrine, P. Pennefather, *J. Physiol. (London) 383* (1987) 251–267.

Complexes with an η^2-μ_2-SiO Bridge. Structure of the Bimetallic Complex $[Fe(CO)_3\{\mu\text{-}Si(OMe)_2\overline{OMe}\}(\mu\text{-dppm})PdCl]$-(*Fe-Pd*)**

By *Pierre Braunstein,* Michael Knorr, Antonio Tiripicchio,* and *Marisa Tiripicchio Camellini*

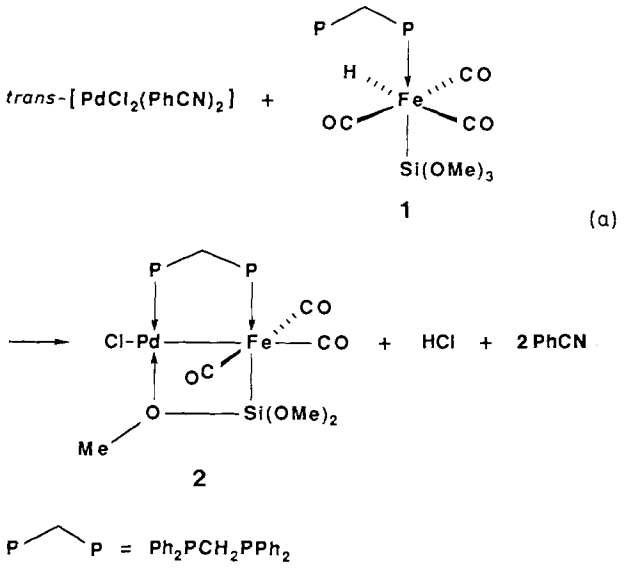
Interest in the synthesis and study of molecular clusters having iron–palladium bonds largely stems from their still relatively small number[1] and their successful use as precursors of SiO_2-supported heterogeneous catalysts, in particular

[*] Dr. P. Braunstein, Dr. M. Knorr
Laboratoire de Chimie de Coordination UA 416 CNRS
Université Louis Pasteur
4 rue Blaise Pascal, F-67070 Strasbourg Cédex (France)
Prof. A. Tiripicchio, Prof. M. Tiripicchio Camellini
Istituto di Chimica Generale ed Inorganica
Università di Parma, Centro di Studio per la Strutturistica
Diffrattometrica del CNR
Viale delle Scienze, I-43100 Parma (Italy)

[**] Financial support from the CNRS (Paris), CNR (Rome), the "Commission of the European Communities" (Contract No. ST2J-0347-C), and the Deutsche Forschungsgemeinschaft (to *M.K.*) are gratefully acknowledged.

for highly selective reductive carbonylation reactions.[2] Moreover, there is a renewed interest in the chemistry of silicon-containing transition-metal compounds.[3] In attempts to combine these two facets, we have sought to prepare Pd–Fe–Si systems and report here the first complexes in which a siloxy ligand acts as an η^2-μ_2-SiO bridge between two metal centers, thus forming novel $\overrightarrow{MM'SiO}$ four-membered ring structures.

Reaction of the *mer* hydrido complex **1**[4] with $[PdCl_2(PhCN)_2]$ in toluene was expected to afford a bimetallic complex resulting from HCl elimination and dppm-assisted metal–metal bond formation [Eq. (a)] (dppm = bis(diphenylphosphino)methane). In addition, the structure of the



product **2**, fully elucidated by X-ray diffraction methods, shows an unprecedented η^2-μ_2-siloxy bridging ligand (Fig. 1).

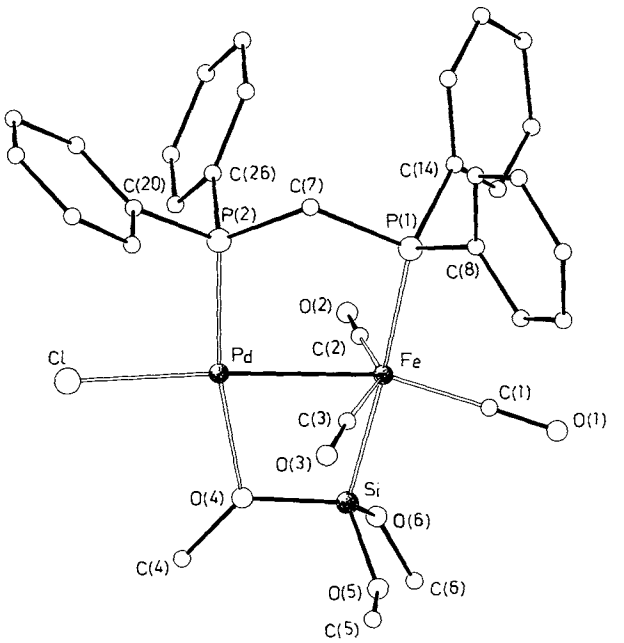
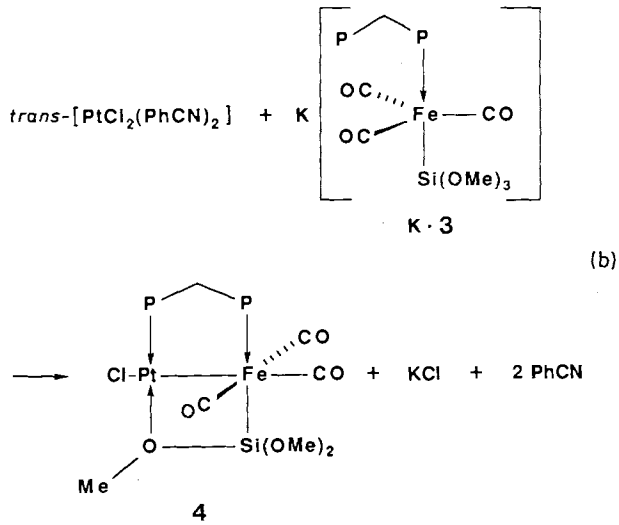


Fig. 1. Perspective view of the molecular structure of **2**. Selected bond lengths [Å] and angles [°]: Fe-Pd 2.582(1), Fe-P(1) 2.241(2), Fe-Si 2.275(2), Fe-C(1) 1.758(5), Fe-C(2) 1.776(7), Fe-C(3) 1.782(6), Pd-P(2) 2.185(1), Pd-Cl 2.303(2), Pd-O(4) 2.100(4), Si-O(4) 1.659(4), Si-O(5) 1.630(6), Si-O(6) 1.627(5); Pd-Fe-P(1) 100.4(1), Pd-Fe-C(1) 162.1(2), Pd-Fe-C(2) 77.8(2), Pd-Fe-C(3) 71.5(2), Pd-Fe-Si 76.2(2), Cl-Pd-P(2) 94.0(1), P(2)-Pd-Fe 90.6(1), O(4)-Pd-Fe 79.7(1), Cl-Pd-O(4) 95.3(1), Pd-O(4)-Si 103.2(2), O(4)-Si-Fe 100.8(2).

The Fe atom in **2** has an octahedral environment which retains the *trans*-P–Fe–Si arrangement found in the precursor. The square-planar geometry about the Pd atom is achieved by oxygen coordination of one of the Si-OMe groups (the O(4) atom deviates by 0.114(5) Å from the mean plane passing through the Pd, Fe, P(2), Cl, and O(4) atoms). The PdFeSiO(4) four-membered ring is almost planar (the Pd–Fe–Si–O(4) torsion angle is 1.5(2)°) and nearly coplanar with the P(1)FeP(2)Pd moiety, the dihedral angle between the two mean planes being 3.8(1)°).

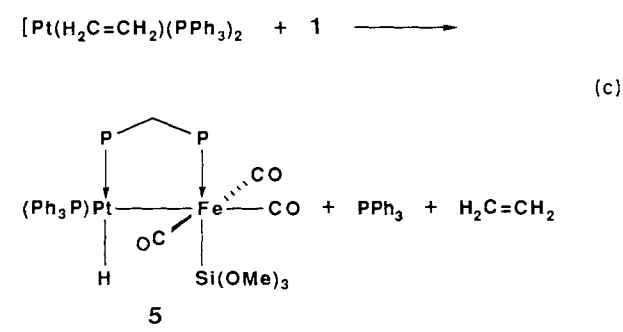
Reaction of the trigonal-bipyramidal anion **3** with $[PdCl_2(PhCN)_2]$, $[PdCl_2(PPh_3)_2]$, or $[PdCl_2(dppm)]$ also leads to **2**. In the latter case, it is noteworthy that no bis-dppm complex was formed.[5] The entropically favored intramolecular η^2-μ_2-SiO bridge formation wins over intermolecular nucleophilic displacement by a donor ligand such as CO (acetone, 20 min) or PPh_3 at room temperature. The Fe–Pt complex **4**, analogous to **2**, was prepared according to Equation (b).



In solution, Pd–O dissociation readily occurs in **2**, as shown by the presence of only one signal for all nine OMe protons in the ^1H NMR spectrum. The Pt–O bond in **4** is less labile and two signals are observed for the methoxy protons in a 2:1 ratio, the latter resonance showing coupling with phosphorus ($^4J_{PH}$ = 2.5 Hz).

The oxidative addition reaction of the Fe–H bond of **1** to Pt^0, shown in Equation (c), affords the hydrido bimetallic complex **5**, in which there is no evidence for a Pt–O interaction. Spectroscopic data support the structure drawn.

The new η^2-μ_2-SiO bonding mode presented here opens the possibility of using the "hemilabile" behavior of the $Si(OR)_3$ ligand in solution for the stabilization of unsaturated, catalytically active polynuclear systems. It also provides



a new structural model for the bonding of small metal clusters or aggregates onto silica, a dominant theme in heterogeneous catalysis.[2a, 2b, 6] The additional bonus in dealing with heterometallic systems is further exemplified here by their ability to display selective metal–ligand interactions.

Experimental Procedure

Satisfactory elemental analyses were obtained for all new compounds. ^{1}H NMR signals of phenyl protons not given. **2**: Method A: A mixture of $[PdCl_2(PhCN)_2]$ (384 mg, 1 mmol) and **1** (646 mg, 1 mmol) in 40 mL of toluene was stirred at -20 °C for 1 h. The solution became dark red at room temperature. After solvent evaporation to ca. 10 mL under reduced pressure, **2** precipitated as a red-orange powder. Addition of ca. 40 mL of hexane completed the precipitation. Filtration and recrystallization from CH_2Cl_2/hexane gave 378 mg (48%) of **2** as red crystals. IR (nujol) $\tilde{\nu}$(CO)[cm^{-1}]: 1985 m, 1925 s, 1905 s. FT IR (polyethylene): $\tilde{\nu}$(PdCl)[cm^{-1}] = 270. ^{1}H NMR (200 MHz, [D$_6$]acetone, TMS, 20 °C): δ = 3.74 (s, 9H, OMe), 4.36 (t, 2H, CH$_2$, ^2J(PH) = 11 Hz). ^{31}P{^{1}H} NMR (81.02 MHz, C_6D_6/CH_2Cl_2, 20 °C): AX spin system: δ_A = 34.9 (d, P(Pd), J(PP) = 55 Hz); δ_X = 48.0 (d, P(Fe)).

2: Method B: A solution of K·**3** (685 mg, 1 mmol) in 20 mL of THF was added dropwise at -40 °C to a suspension of $[PdCl_2(PPh_3)_2]$ (701 mg, 1 mmol) in 25 mL of THF. Upon slowly warming to room temperature, the solution turned dark red. After 10 h agitation, the solution was filtered (to remove KCl) and concentrated to ca. 5 mL under reduced pressure. Complete precipitation of **2** was achieved by addition of hexane. PPh_3 was eliminated by extraction with Et_2O/hexane. Yield: 510 mg (65%).

4: A solution of K·**3** (685 mg, 1 mmol), prepared by the reaction of **1** with KH in THF (for the PPh_3 analogue, see Ref. [7]), in 20 mL of THF was added dropwise (1 h) at room temperature to a suspension of $[PtCl_2(PhCN)_2]$ (472 mg, 1 mmol) in 30 mL of THF. After stirring for 12 h, the dark red solution was filtered (to remove KCl) and concentrated to ca. 10 mL under reduced pressure. Addition of 40 mL of hexane induced precipitation of **4** as a yellow-brown powder. Subsequent recrystallizations from CH_2Cl_2/pentane afforded yellow microcrystals of **4**. Yield: 210 mg (24%). IR(THF) $\tilde{\nu}$(CO) [cm^{-1}] = 1995 m, 1935 s, 1910 m, sh. ^{1}H NMR (200 MHz, [D$_6$]acetone, TMS, 20 °C): δ = 3.74 (s, 6H, Si(OMe)$_2$), 3.80 (d, 3H, Pt-OMe, ^4J(PH) = 2.5 Hz), 4.04 (t with ^{195}Pt satellites, 2H, CH$_2$, ^2J(PH) = 11, ^3J(PtH) = 66 Hz). ^{1}H NMR (200 MHz, C_6D_6, TMS, 20 °C): δ = 3.25 (t, 2H, CH$_2$, ^2J(PH) = 11 Hz), 3.74 (s, 6H, Si(OMe)$_2$), 3.90 (d, 3H, Pt-OMe, ^4J(PH) = 2.5 Hz). ^{31}P{^{1}H} NMR (81.02 MHz, [D$_6$]acetone, 20 °C): δ = 7.7 (d with ^{195}Pt satellites, P(Pt), J(PP) = 47 Hz, ^1J(PPt) = 4756 Hz), 52.9 (d, P(Fe)).

5: A solution of $[Pt(C_2H_4)(PPh_3)_2]$ (751 mg, 1 mmol) in 20 mL of toluene was allowed to react at room temperature with successive fractions of **1** (total 646 mg, 1 mmol). Each time, gas evolution was noted. At the end of the reaction (ca. 0.5 h, IR monitoring), the yellow solution was concentrated to ca. 5 mL, 20 mL of hexane was added, and the colorless precipitate of **5** was washed with Et_2O/hexane to remove free PPh_3. Yield: 905 mg (82%). Compound **5** may be recrystallized from CH_2Cl_2/hexane IR(KBr): $\tilde{\nu}$(PtH)[cm^{-1}] = 2149 w. IR(CH_2Cl_2): $\tilde{\nu}$(CO)[cm^{-1}] = 1965 m, 1900 s, 1870 s. ^{1}H NMR (200 MHz, CD_2Cl_2, TMS, 20 °C): δ = -4.51 (dt with ^{195}Pt satellites, 1H, PtH, ^2J(P$_{trans}$H) = 197.6, ^2J(PH) = 13.9 ^1J(PtH) = 686 Hz), 3.56 (s, 9H, OMe), ca. 3.5 (2H, CH$_2$, overlapping with OMe signal). ^{31}P{^{1}H} NMR (81.02 MHz, C_6D_6/toluene, 20 °C): ABX spin system: δ = 29.4 (d with ^{195}Pt satellites, P(Pt), J[PP(Fe)] = 130, ^1J(PtP) = 2074 Hz), 32.0 (t with ^{195}Pt satellites, PPh_3, ^3J(PP) = 10, ^1J(PtP) = 3478 Hz), 72.2 (dd with ^{195}Pt satellites P(Fe), J(pp) = 130.10, ^2J(PtP) = 88 Hz).

Crystal structure determination of **2**: monoclinic, $C2/c$, Z = 8, a = 24.644(8), b = 15.839(5), c = 17.795(5) Å, β = 112.95(2)°; V = 6396(4) Å^3; M_r = 787.32; ϱ_{calcd} = 1.635 g cm^{-3}; F(000) = 3184, μ(Mo$_{K\alpha}$) = 12.69 cm^{-1}. Siemens AED diffractometer, $\theta/2\theta$ scan technique and Nb-filtered Mo$_{K\alpha}$ radiation (λ = 0.71073 Å), $3 < \theta < 25°$, 6075 unique reflections, 3722 observed with $I > 2\sigma(I)$. The structure was solved by Patterson and Fourier methods and refined by the full-matrix least-squares method with anisotropic thermal parameters for all non-hydrogen atoms. The SHELX system of computer programs was used (G. M. Sheldrick, *Program for Crystal Structure Determination*, Cambridge 1976). Some hydrogen atoms were clearly located and refined isotropically, the others were placed at their geometrically calculated positions and introduced in the final structure-factor calculation with fixed isotropic thermal parameters. R = 0.0285, R_w = 0.0354. Further details of the crystal structure analysis may be obtained from the Fachinformationszentrum Karlsruhe, Gesellschaft für wissenschaftlich-technische Information mbH, D-7514 Eggenstein-Leopoldshafen 2 (FRG) on quoting the depository number CSD-54012, the names of the authors, and the journal citation.

Received: May 30, 1989 [Z 3363 IE]
German version: *Angew. Chem. 101* (1989) 1414

[1] a) M. I. Bruce, *J. Organomet. Chem. Libr. 17* (1985) 399; b) P. Braunstein, C. de Méric de Bellefon, M. Ries, J. Fischer, *Organometallics* 7 (1988) 332; G. B. Jacobsen, B. L. Shaw, *J. Chem. Soc., Dalton Trans. 1987*, 2005.

[2] a) P. Braunstein, J. Rosé in I. Bernal (Ed.): *Stereochemistry of Organometallic and Inorganic Compounds, Vol. 3*, Elsevier, Amsterdam 1989, in press; b) B. C. Gates, L. Guczi, H. Knözinger (Eds.): *Metal Clusters in Catalysis*, Elsevier, New York 1986; c) P. Braunstein, J. Kervennal, J.-L. Richert, *Angew. Chem. 97* (1985) 762; *Angew. Chem. Int. Ed. Engl. 24* (1985) 768; d) P. Braunstein, R. Devenish, P. Gallezot, B. T. Heaton, C. J. Humphreys, J. Kervennal, S. Mulley, M. Ries, M. *ibid. 100* (1988) 972 and *27* (1988) 927.

[3] a) K. M. Mackay, B. K. Nicholson in G. Wilkinson, F. G. A. Stone, E. W. Abel (Eds.): *Comprehensive Organometallic Chemistry*, Pergamon, Oxford 1982, chapter 43; b) U. Schubert, *J. Organomet. Chem. 358* (1988) 215; c) C. Zybill, *Nachr. Chem. Tech. Lab. 37* (1989) 248; d) T. D. Tilley in S. Patai, Z. Rappoport (Eds.): *The Chemistry of Organic Silicon Compounds*, Wiley, New York 1988, chapter 26; e) J. Powell, J. F. Sawyer, M. Shiralian, *Organometallics 8* (1989) 577.

[4] P. Braunstein, M. Knorr, U. Schubert, unpublished.

[5] P. Braunstein, N. Guarino, C. de Méric de Bellefon, J.-L. Richert, *Angew. Chem. 99* (1987) 77; *Angew. Chem. Int. Ed. Engl. 26* (1987) 88.

[6] a) S. J. Tauster, *Acc. Chem. Res. 20* (1987) 389; b) R. T. K. Baker, S. J. Tauster, J. A. Dumesic, *Strong Metal-Support Interactions (1986) ACS Symp. Ser. 298*.

[7] U. Schubert, E. Kunz, M. Knorr, J. Müller, *Chem. Ber. 120* (1987) 1079.

Two Novel Polyoxomolybdates Containing the $(MoNO)^{3\oplus}$ Unit: $[Mo_5Na(NO)O_{13}(OCH_3)_4]^{2\ominus}$ and $[Mo_6(NO)O_{18}]^{3\ominus}$ **

By *Pierre Gouzerh,* Yves Jeannin, Anna Proust,* and *Francis Robert*

The chemistry of polyoxometalates is under active investigation because of their use for imaging in metal oxide surface chemistry. A few organopolyoxomolybdate derivatives structurally related to $[Mo_6O_{19}]^{2\ominus}$ [1] with a terminal oxo group replaced by a nitrogen-ligated group such as a diazenido, hydrazido, imido, or nitrido ligand have been recently reported.[2] A number of dinuclear,[3] tetranuclear,[4] and octanuclear[5] diazenidomolybdenum species are also known. Despite the obvious analogy between $RN_2^{\oplus}$ and $NO^{\oplus}$ [6] and extensive studies of the reaction of hydroxylamine with oxomolybdenum compounds,[7, 8] nitrosyl derivatives of polyoxomolybdates were hitherto unknown. The reductive nitrosylation of oxomolybdenum complexes was found to produce either mononuclear[7] or polynuclear[8] molybdenum(II) complexes containing the $(MoNO)^{3\oplus}$ unit. Here we report the first polynuclear species containing both $(Mo^{II}NO)^{3\oplus}$ and $(Mo^{VI}O)^{4\oplus}$ units.

$(NBu_4)_2[Mo_4O_{12}\{NC{-}CH{=}CH{-}C(NH_2)NO\}_2]$ **1**

$(NBu_4)_2[Mo_5Na(NO)O_{13}(OCH_3)_4]\cdot 4CH_3OH$ **2**

Treatment of complex **1** [9] with hydroxylamine in refluxing methanol and cooling the solution led to the formation of violet crystals, which were identified as complex **2** by chemical analysis and X-ray structure determination.[10] The crystals readily lose solvent. Their structure (cf. Fig. 1) derives from the Lindqvist structure. One MoO group is missing and is replaced by a sodium cation interacting with four terminal oxygen atoms of the polyanion and one methanol molecule. The linear $(MoNO)^{3\oplus}$ group is opposite to sodium, and four methoxo ligands asymmetrically bridge Mo^{II} to its four Mo^{VI} neighbors. Formal molybdenum oxida-

[*] Prof. Dr. Y. Jeannin, Dr. P. Gouzerh, A. Proust, F. Robert
Laboratoire de Chimie des Métaux de Transition
Université Pierre et Marie Curie
4 place Jussieu, 75252 Paris Cedex 05 (France)

[**] This work was supported by the Centre National de la Recherche Scientifique under contract URA 419.

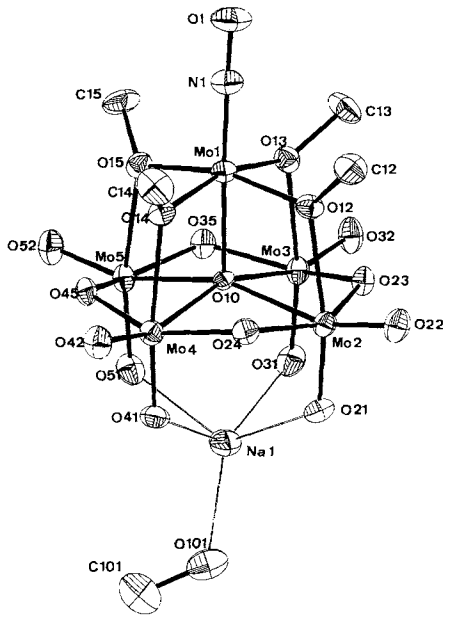


Fig. 1. Molecular structure of **2** Selected bond distances [Å] and angles [°]: Mo1-N1 1.75(1), N1-O1 1.22(1), Mo1-O10 2.122(5), Mo2-O10 2.343(5), Mo3-O10 2.363(5), Mo4-O10 2.319(5), Mo5-O10 2.348(5), Na-O10 3.191(7); Mo1-N1-O1 178(1). Asymmetrical OCH_3 bridges with averaged distances: Mo1-O(12-15) 1.995(6), Mo(2-5)-O 2.279(7); Mo1-O-Mo 106.8(3). Na-O(21-24) 2.379(9) (averaged).

tion states may be inferred from the polyanion charge; this polymolybdate contains localized Mo^{II} and Mo^{VI} atoms.

When **2** is dissolved in dichloromethane or acetonitrile, it spontaneously transforms into another polymolybdate, **3**. The X-ray study[10] revealed another Lindqvist structure type and confirmed the formula obtained by chemical analysis. The unit cell contains two independent $[Mo_6(NO)O_{18}]^{3\ominus}$ anions located on inversion centers. The disorder of both anions influences the observed interatomic distances. Since this disorder might also result from a statistical distribution of $[Mo_6(NO)_2O_{17}]^{4\ominus}$ and $[Mo_6O_{19}]^{2\ominus}$, an electrochemical

$(NBu_4)_3[Mo_6(NO)O_{18}]$ **3**

study was undertaken; cyclic voltammetry in CH_2Cl_2 on a Pt electrode in the range -1.0 to $+1.0$ V vs. SCE reveals only one quasi-reversible one-electron oxidation process at $+0.87$ V; pure $[Mo_6O_{19}]^{2\ominus}$ shows a reversible reduction process at -0.29 V. Therefore, the occurrence of $[Mo_6O_{19}]^{2\ominus}$ is ruled out and the species is a mononitrosylhexamolybdate derived from $[Mo_6O_{19}]^{2\ominus}$ by replacing one MoO group by one $(MoNO)^{3\oplus}$ group. Compound **3** is another member of the family $[Mo_6O_{18}L]^{n\ominus}$.[2]

Compounds **2** and **3** are the first examples of polyoxomolybdates containing an $(MoNO)^{3\oplus}$ unit. Moreover, **2** is the first example of a lacunar Lindqvist structure.

Experimental Procedure

2: In a typical experiment, **1** [9] (32 g, 25 mmol) in 20 mL of methanol was mixed with 80 mL of 1 M NH_2OH in methanol (the hydroxylamine was prepared from $NH_2OH \cdot HCl$, which was poured into a methanolic solution of sodium methoxide; NaCl was then removed by filtration). The suspension was refluxed for 3 h. After standing ca. 12 h at room temperature, the solution afforded 5 g of violet crystals (yield: 18%).

3: Compound **2** (5 g, 3.7 mmol) was dissolved in hot acetonitrile (30 mL) and the solution was refluxed for 5 h. Cooling the solution gave 2.3 g of brown crystals (yield: 38%). IR(KBr): $\tilde{\nu}$(NO): **2**, 1630; **3**, 1575 cm^{-1}.

Received: April 28, 1989;
supplemented: July 3, 1989 [Z 3310 IE]
German version: *Angew. Chem. 101* (1989) 1377

[1] O. Nagano, Y. Sazaki, *Acta Crystallogr. Sect. B35* (1979) 2387.
[2] a) T. C. Hsieh, J. Zubieta, *Polyhedron 5* (1986) 1655; b) S. Bank, S. Liu, S. N. Shaikh, X. Sun, J. Zubieta, P. D. Ellis, *Inorg. Chem. 27* (1988) 3535; c) H. Kang, J. Zubieta, *J. Chem. Soc. Chem. Commun. 1988*, 1192.
[3] a) D. Carrillo, P. Gouzerh, Y. Jeannin, *Nouv. J. Chim. 9* (1985) 749; b) V. Chilou, P. Gouzerh, Y. Jeannin, G. Olivarès, F. Robert, T. C. Hsieh, J. Zubieta, *Polyhedron 8* (1989) 29.
[4] a) T. C. Hsieh, J. Zubieta, *Polyhedron 5* (1986) 305; b) S. N. Shaikh, J. Zubieta, *Inorg. Chim. Acta 121* (1986) L43.
[5] T. C. Hsieh, J. Zubieta, *J. Chem. Soc. Chem. Commun. 1985*, 1749.
[6] a) A. P. Gaughan, B. L. Haymore, J. A. Ibers, W. H. Myers, T. E. Nappier, D. W. Meek, *J. Am. Chem. Soc. 95* (1973) 6859; b) D. Sutton, *Chem. Soc. Rev. 4* (1975) 443.
[7] a) A. Müller, S. Sarkar, N. Mohan, R. G. Bhattacharyya, *Inorg. Chim. Acta 45* (1980) L245; b) R. Bhattacharyya, G. P. Bhattacharjee, *J. Chem. Soc. Dalton Trans. 1983*, 1593; c) K. Wieghardt, W. Holzbach, J. Weiss, B. Nuber, B. Prikner, *Angew. Chem. 91* (1979) 582; *Angew. Chem. Int. Ed. Engl. 18* (1979) 548; d) K. Wieghardt, V. Holzbach, *ibid. 91* (1979) 583 and *18* (1979) 549; e) K. Wieghardt, V. Holzbach, B. Nuber, J. Weiss, *Chem. Ber. 113* (1980) 629; f) K. Wieghardt, G. Backes-Dahmann, W. Swiridoff, J. Weiss, *Inorg. Chem. 22* (1983) 1221.
[8] a) A. Müller, W. Eltzner, N. Mohan, *Angew. Chem. 91* (1979) 158; *Angew. Chem. Int. Ed. Engl. 18* (1979) 168; b) A. Müller, W. Eltzner, H. Bögge, S. Sarkar, *ibid. 94* (1982) 555 and *21* (1982) 535; *Angew. Chem. Suppl.* 1982, 1167; c) A. Müller, W. Eltzner, H. Bögge, E. Krickemeyer, *Angew. Chem. 95* (1983) 905; *Angew. Chem. Int. Ed. Engl. 22* (1983) 884.
[9] This compound was prepared as described for acetamidoxime: V. Chilou, P. Gouzerh, Y. Jeannin, F. Robert, *J. Chem. Soc. Chem. Commun. 1987*, 1469.
[10] **2**: monoclinic, $P2_1/a$, $M_r = 1477.93$ g, $Z = 4$, $a = 23.325(7)$, $b = 15.917(5)$, $c = 18.433(7)$ Å, $\beta = 105.82(6)°$, $V = 6584(8)$ Å^3, $\varrho_{calcd} = 1.49$ g cm^{-3}, $2 < \theta < 23°$, $\lambda(Mo_{K\alpha}) = 0.71069$ Å, $\mu = 9.73$ cm^{-1}, $R = 0.059$, $R_w = 0.063$. 7286 unique reflections collected; direct methods; 5281 reflections ($I > 3\sigma(I)$) were used for least-squares refinement; 642 refined parameters. **3**: monoclinic, $P2_1/a$, $M_r = 1621.04$ g, $Z = 4$, $a = 16.688(3)$, $b = 17.210(3)$, $c = 24.267(4)$ Å, $\beta = 97.44(1)°$, $V = 6910(4)$ Å^3, $\varrho_{calcd} = 1.56$ g cm^{-3}, $1 < \theta < 23°$, $\lambda(Mo_{K\alpha}) = 0.71069$ Å, $\mu = 10.9$ cm^{-1}, $R = 0.055$, $R_w = 0.063$. 9575 unique reflections collected; direct methods; 3436 ($I > 3\sigma(I)$) were used for least-squares refinement; 707 refined parameters. For both structures, final refinement was carried out with anisotropic thermal parameters for all atoms; hydrogen atoms not introduced. Further details of the crystal structure investigations may be obtained from the Fachinformationszentrum Karlsruhe, Gesellschaft für wissenschaftlich-technische Information mbH, D-7514 Eggenstein-Leopoldshafen 2 (FRG), on quoting the depository number CSD-53953, the names of the authors, and the journal citation.

$HoAl_3Cl_{12}$ in Crystalline Form**

By *Dietmar Hake* and *Werner Urland**

The chemical transport of metal halides is only possible through the formation of gas-phase complexes with, for example, $AlCl_3$, $GaCl_3$, or $FeCl_3$.[1] Thus, the relatively nonvolatile trichlorides of the lanthanoids ($LnCl_3$) can be transported with $AlCl_3$;[2,3] spectroscopic studies reveal the formation of gaseous complexes of empirical formulas $LnAl_3Cl_{12}$ and $LnAl_4Cl_{15}$,[4] in which the lanthanoid ion, depending on its size, is probably nona- or hexacoordinated.[5] Here we report, for the first time, the synthesis and crystal structure of $HoAl_3Cl_{12}$.

$HoAl_3Cl_{12}$ was synthesized by reaction of commercially available holmium oxide with aluminum trichloride followed by chemical transport;[6] the analytical composition was determined by ICP analysis and argentometric titration with potentiometric indication.[7] The salmon-colored compound is sensitive to moisture and decomposes within a few minutes upon exposure to air.

[*] Prof. Dr. W. Urland, Dipl-Chem. D. Hake
Institut für Anorganische Chemie der Universität
Callinstrasse 9, D-3000 Hannover 1 (FRG)

[**] This work was supported by the Fonds der Chemischen Industrie.

The result of the X-ray structure analysis[8] is shown in Figure 1. The structure type presented here is, to our knowledge, the first in which a cation is surrounded by chlorine

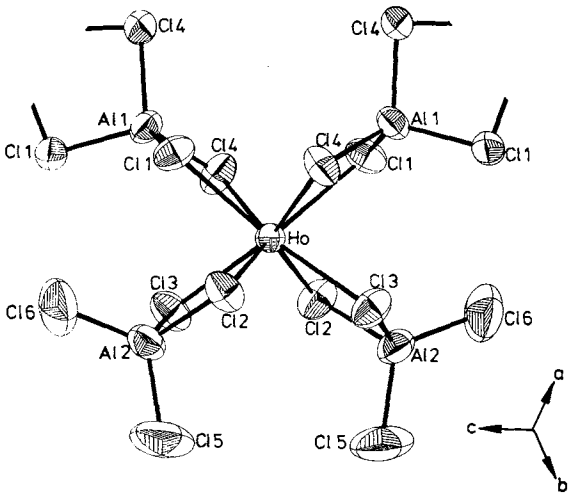


Fig. 1. ORTEP view of $HoAl_3Cl_{12}$ with the coordination polyhedron for $Ho^{3\oplus}$. Selected bond lengths [pm]: Ho-Cl1 281.7(2), Ho-Cl2 273.4(2), Ho-Cl3 270.8(2), Ho-Cl4 287.7(2), Al1-Cl1 212.4(2), Al1-Cl4 213.6(3), Al2-Cl2 218.9(3), Al2-Cl3 220.0(3), Al2-Cl5 206.9(3), Al2-Cl6 206.7(4), Ho-Al1 368.2(1), Ho-Al2 366.8(2).

atoms in such a way as to form a square antiprism. Usually, a trigonal bicapped prism is formed for octacoordinated lanthanoid trichlorides.[9, 10] The square antiprism found here is edge-linked with four $AlCl_4$ tetrahedra, two of which are linked to the next $HoCl_8$ polyhedron. This linkage leads to a screw-shaped chain along [001]. The Ho–Cl distances within the antiprism vary from 270.8 to 287.7 pm. The antiprism is slightly distorted; this is especially revealed in the slightly bent faces, which, ideally, are square planar (Fig. 1). The terminal Al–Cl distances (206.7 and 206.9 pm) are significantly shorter than the Al–Cl bridging distances, in agreement with the results of a crystal structure analysis of $PdAl_2Cl_8$.[11]

The synthesis and X-ray structure analysis of $HoAl_3Cl_{12}$ and of analogous compounds is of particular interest in connection with the determination of thermodynamic data for a better understanding of chemical transport and with respect to the role of these substances in high-pressure discharge lamps.[12]

Received: June 7, 1989 [Z 3383 IE]
German version: *Angew. Chem. 101* (1989) 1416

[1] H. Schäfer, *Angew. Chem. 88* (1976) 775; *Angew. Chem. Int. Ed. Engl. 15* (1976) 713.
[2] H. Schäfer, M. Binnewies, W. Domke, J. Karbinski, *Z. Anorg. Allg. Chem. 403* (1974) 116.
[3] H. Gunsilius, W. Urland, R. Kremer, *Z. Anorg. Allg. Chem. 550* (1987) 35.
[4] H. A. Øye, D. M. Gruen, *J. Am. Chem. Soc. 91* (1969) 2229.
[5] G. N. Papatheodorou, G. M. Kucera, *Inorg. Chem. 18* (1979) 385.
[6] Ho_2O_3 (378 mg, 1 mmol) and $AlCl_3$ (475 mg, 3.5 mmol) were placed in a cylindrical transport ampoule made of Duran glass. The ampoule was sealed under inert gas and the reaction was initiated with a burner. Transport was then carried out in a two-zone oven with a temperature gradient from 250 °C to 160 °C (transport time: three days). The salmon-colored product was deposited on the cooler side in the form of trigonal trapezoids.
[7] Determination of the analytical composition (Ho and Al by inductively coupled plasma (ICP) analysis, Cl by argentometry): Ho 25.5% (calcd 24.6%), Al 12.2% (calcd 12.0%), Cl 60.4% (calcd 63.4%).
[8] $HoAl_3Cl_{12}$: $P3_112$, $a = 1050.04(7)$, $c = 1562.24(9)$ pm (25 °C), $V = 1491.73 \times 10^6$ pm^3, $Z = 3$; Siemens AED-2 diffractometer, $Mo_{K\alpha}$ radiation, graphite monochromator, measuring range $3° \leq 2\theta \leq 50°$, ω-2θ scan, 5915 measured reflections, 1770 unique reflections, absorption correction with ψ scan, anisotropic refinement, $R = 0.035$ for 74 refined parameters. $R_w = 0.025$. Further details of the crystal structure investigation may be obtained from the Fachinformationszentrum Karlsruhe, Gesellschaft für wissenschaftlich-technische Information mbH, D-7514 Eggenstein-Leopoldshafen 2 (FRG), on quoting the depository number CSD-53974, the names of the authors, and the journal citation.
[9] H. Gunsilius, H. Borrmann, A. Simon, W. Urland, *Z. Naturforsch. B43* (1988) 1023.
[10] D. Hake, W. Urland, *Z. Kristallogr. 186* (1989), in press.
[11] W. Lenhard, H. Schäfer, H.-U. Hürter, B. Krebs, *Z. Anorg. Allg. Chem. 482* (1981) 19.
[12] C. Hirayama, P. M. Castle, C. S. Liu, R. J. Zollweg, *J. Illum. Eng. Soc. 6* (1977) 209.

Synthesis, Structure and Magnetic Properties of a Dinuclear Manganese(II) Complex with One μ-Aqua and Two μ-Carboxylato Bridges **

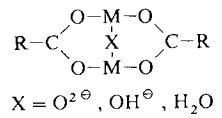
By *Andrea Caneschi, Fabrizio Ferraro, Dante Gatteschi,* Maria Chiara Melandri, Paul Rey,* and *Roberta Sessoli*

Polynuclear manganese complexes are currently of great interest owing to their relevance to many important naturally occurring processes. In particular, a cluster of four manganese ions is known to be involved in the photosynthetic water-oxidizing complex,[1] and two manganese ions per protein subunit are present in the pseudo-catalase from *Lactobacillus plantarum*.[2]

During our efforts to synthesize magnetic materials by using manganese(II) and stable organic radicals comprising two equivalent NO groups,[3] we isolated the dinuclear complex **1**, L = 2-ethyl-4,4,5,5-tetramethyl-3-oxo-4,5-dihydro-

$[Mn_2(F_5C_2COO)_4(H_2O)_3L_2]$ **1**

1*H*-imadazolyl-1-oxyl (see Table 1).[4] Complex **1** contains one μ-H_2O and two μ-carboxylato bridges with a structure of the $Mn_2(\mu\text{-}H_2O)(\mu\text{-}O_2CR)_2$ core analogous to that observed in hemerythrin,[5] the marine invertebrate oxygen transport protein, and in various metal complexes.[6]



Scheme 1. Framework of complexes **1**–**7** (Table 1).

Complex **1** is the first such manganese compound in which X is water (see Scheme 1), although similar structures are known for ruthenium, cobalt, and nickel compounds[7] (an iron analogue does not exist). This provides the opportunity to compare the efficiency of the three X groups in transmitting exchange interactions between the two d^5 ions.

[*] Prof. Dr. D. Gatteschi, Dr. A. Caneschi, F. Ferraro, M. C. Melandri, Dr. R. Sessoli
Università degli Studi di Firenze
Dipartimento di Chimica
Via Maragliano 77, I-50144 Firenze (Italy)
Dr. P. Rey
Laboratoire de Chemie, UA 1194 CNRS
Département de Recherche Fondamentale, C.E.N.G.
F-38041 Grenoble (France)

[**] This work was supported by the Italian Ministry of Public Education and by CNR.

The X-ray analysis[8] of compound **1** reveals that the two nonbridging carboxylates are monodentate and bind to the two metal ions (Fig. 1). The distances of the noncoordinated

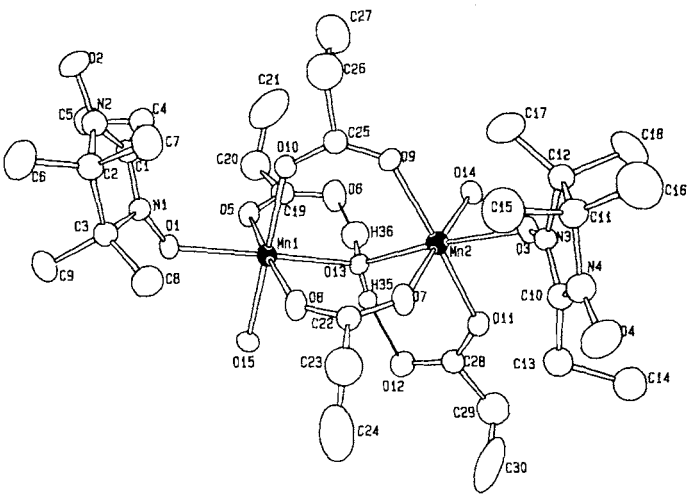


Fig. 1. Molecular structure (ORTEP) of complex **1** . The fluorine atoms are omitted for the sake of clarity. Selected bond distances [Å] and angles [°]: Mn1-Mn2 3.739(2); Mn1-O1 2.164(6); Mn1-O5 2.210(6), Mn1-O8 2.146(7), Mn1-O10 2.114(8), Mn1-O13 2.228(7), Mn1-O15 2.137(9), Mn2-O3 2.158(6), Mn2-O7 2.099(8), Mn2-O9 2.141(7), Mn2-O11 2.226(7), Mn2-O13 2.214(7), Mn2-O14 2.166(9), O1-N1 1.309(10), O3-N3 1.326(9), O6-H36 1.33(8), O12-H35 1.75(7), O13-H35 0.87(7), O13-H36 1.29(9); Mn1-O13-Mn2 114.6(3), Mn1-O1-N1 127.1(5), Mn2-O3-N3 128.3(5), H35-O13-H36 106(7). The hydrogen bonds O6-H36 and O12-H35 are drawn as solid lines.

oxygen atoms to the oxygen of the μ-H_2O bridge (O6-O13 2.55, O12-O13 2.56 Å) clearly indicate the presence of hydrogen bond interactions, which certainly contribute to stabilizing the dinuclear structure. A similar geometry around the bridging water molecule was found in a Ru^{II} dimer with one μ-H_2O and two μ-carboxylato bridges.[7b] Each radical L is bound through one of its oxygen atoms to a manganese ion, whose octahedral coordination environment is completed by one water molecule. The lengths of the N–O bonds confirm that the radical nature of the ligand is preserved. The two radicals are magnetically well separated from each other; the shortest distance between noncoordinated NO groups is about 5 Å.

The temperature dependence of the magnetic susceptibility is shown in Figure 2 in the form $\chi_m T$ versus T. The product $\chi_m T$ decreases slowly in the range 300–100 K, but decreases dramatically at lower temperatures. This finding suggests that the four spins are antiferromagnetically coupled with a large and a small coupling constant. This prediction is confirmed by a quantitative calculation for a cluster of four spins, coupled as shown in Scheme 2.

NO′(ligand)—$\overset{J'}{}$Mn—$\overset{J}{}$Mn—$\overset{J'}{}$NO′(ligand)

Scheme 2.

The best-fit curve ($R = 4.6 \times 10^{-4}$) is shown in Figure 2; the corresponding parameters are $J' = 113(1)\ cm^{-1}$, $J = 3.3(0.2)\ cm^{-1}$, and $g = 2.02$. We use the spin Hamiltonian in the form $\boldsymbol{H} = J\boldsymbol{S}_1 \cdot \boldsymbol{S}_2$. The value of J' is slightly smaller than those reported for other manganese(II) complexes with similar NO·-containing ligands,[9] presumably due to the longer Mn–O distance in **1**.

The coupling constant J, which reflects the manganese–manganese interaction, is determined in principle by the three bridges between the two metal ions. However, it is

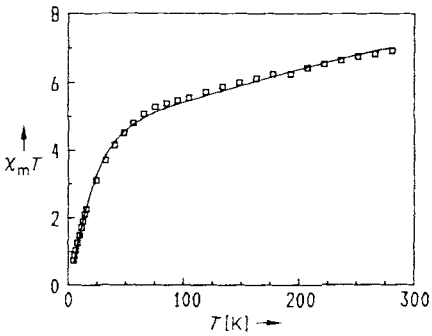
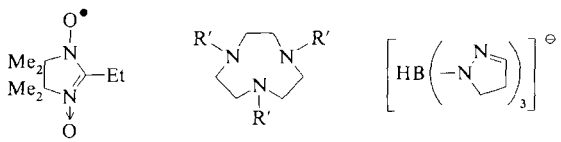


Fig. 2. Temperature dependence of the magnetic susceptibility of **1** in the form $\chi_m T$ vs. T. □: experimental value. The solid line represents the best-fit calculated values. Ordinate: $\chi_m T$ in [$cm^3\ mol^{-1}\ K$].

Table 1. Magnetic coupling constants J (see Scheme 2) in dinuclear $M_2(RCOO)_2X$ moieties of the complexes **1**–**7** (see Scheme 1). M = Mn^{II}, Fe^{III}; X = $O^{2\ominus}$, $OH^{\ominus}$, H_2O.



L L′: R′ = Me; L″: R′ = H L‴

Complex	J [cm^{-1}]	Ref.
1 $[Mn_2F_3C_2COO)_4(H_2O)_3L_2]$	3.3	
2 $[Mn_2(CH_3COO)_2(OH)L'_2](ClO_4)$	18	[10]
3 $[Fe_2(CH_3COO)_2(OH)L''_2]^{\oplus}$	34	[11]
4 $[Fe_2(CH_3COO)_2OL'_2](PF_6)_2$	190, 238	[12, 6]
5 $[Fe_2(CH_3COO)_2OL'_2](ClO_4) \cdot H_2O$	238	[6]
6 $[Fe_2(CH_3COO)_2L''_2]I_2 \cdot 0.5\,NaI \cdot 3\,H_2O$	168	[12, 13]
7 $[Fe_2(CH_3COO)_2OL''_2]$	242	[14]

generally assumed[6] that the carboxylates are rather ineffective in transmitting the exchange interaction, and that the X group (see Scheme 1) governs the coupling. Accordingly, the differences in the magnetic coupling in complexes with X = $O^{2\ominus}$, $OH^{\ominus}$, and H_2O must be ascribed entirely to the X group. The values of the coupling constants J for some $M_2(RCOO)_2X$ clusters are given in Table 1. A direct comparison cannot be performed because no μ-oxo manganese(II) species has been reported. However, since the μ-hydroxo manganese(II) and iron(III) species have comparable J values, it is apparent that on going from $O^{2\ominus}$ to $OH^{\ominus}$ to H_2O, J decreases by roughly one order of magnitude at each step. The decrease of J in the series $O^{2\ominus} > OH^{\ominus} > H_2O$ is perfectly in line with the decrease in bonding interaction between ligand and metal on decreasing the charge on the ligand. This result confirms the possibility that azidodeoxyhemerythrin, which has a paramagnetic ground state, has indeed a μ-aqua bridge.[6, 15, 16]

Received: May 22, 1989 [Z 3354 IE]
German version: *Angew. Chem. 101* (1989) 1408

[1] a) L. Schramm, F. C. Wedler (Eds.): *Manganese in Metabolism and Enzyme Function*, Academic Press, New York 1980; b) G. C. Dismukes: *The Organization and Function of Manganese in the Water Oxidizing Complex of Photosynthesis*, Academic Press, New York 1986, chapter 16, p. 275.
[2] a) Y. Kono, I. Fridovich, *J. Biol. Chem. 258* (1983) 6015; b) W. F. Beyer, Jr., I. Fridovich, *Biochemistry 2* (1985) 6460.
[3] C. Benelli, A. Caneschi, D. Gatteschi, P. Rey in P. Delhaes, M. Drillon (Eds.): *Organic and Inorganic Low Dimensional Crystalline Materials*, Plenum, New York 1987, p. 385.
[4] Manganese(II) pentafluoropropionate · 2 H_2O was dissolved in dichloromethane and the radical L (see text and Table 1) was added in a 1:1 ratio

in *n*-heptane. After standing in a refrigerator for 2 d at 4 °C, the solution afforded ruby-red crystals of **1**, which gave a satisfactory elemental analysis.
[5] I. M. Klotz, D. M. Kurtz, Jr., *Acc. Chem. Res. 17* (1984) 16.
[6] J. A. R. Hartman, R. L. Rardin, P. Chaudhuri, K. Pohl, K. Wieghardt, B. Nuber, J. Weiss, G. C. Papaefthymiou, R. B. Frankel, S. J. Lippard, *J. Am. Chem. Soc. 109* (1987) 7387.
[7] a) U. Turpeinen, *Finn. Chem. Lett. 1976*, 173; *1977*, 36; b) M. O. Albers, D. C. Liles, E. Singleton, J. E. Yates, *J. Organomet. Chem. 272* (1984) C62; c) M. O. Albers, D. C. Liles, E. Singleton, J. E. Stead, *Acta Crystallogr. Sect. C42* (1986) 1299; d) U. Turpeinen, R. Hamalainen, J. Reedijk, *Polyhedron 6* (1987) 1603.
[8] X-ray structure analysis: $C_{30}H_{40}N_4O_{15}F_{20}Mn_2$; $M_r = 1186.4$; monoclinic, space group $P2_1/c$, $a = 12.985(2)$, $b = 25.155(8)$, $c = 15.711(5)$ Å, $\beta = 105.90(2)°$, $Z = 4$, $\varrho_{calcd} = 1.597\ g\,cm^{-3}$, Enraf-Nonius CAD4 diffractometer, room temperature, $Mo_{K\alpha}$ radiation, $5 \le 2\theta \le 46$, 5684 independent reflections, 3330 with $F_o \ge 6\,\sigma(F_o)$. Solution by Patterson and Fourier synthesis for all non-hydrogen atoms as well as the hydrogen atoms of the water molecules. Disorder and/or anisotropic thermal motion was found in the CF_3-CF_2 groups. The final refinement, including the other hydrogen atoms in idealized positions, converged to $R = 0.070$. Further details of the crystal structure investigation are available on request from the Fachinformationszentrum Karlsruhe, Gesellschaft für wissenschaftlich-technische Information mbH, D-7514 Eggenstein-Leopoldshafen 2 (FRG), on quoting the depository number CSD-54127, the names of the authors, and the journal citation.
[9] A. Caneschi, D. Gatteschi, J. Laugier, L. Pardi, P. Rey, C. Zanchini, *Inorg. Chem. 27* (1988) 2027.
[10] K. Wieghardt, U. Bossek, J. Bonvoisin, P. Beauvillain, J. J. Girerd, B. Nuber, J. Weiss, J. Heinze, *Angew. Chem. 98* (1986) 1026; *Angew. Chem. Int. Ed. Engl. 25* (1986) 1030.
[11] W. H. Armstrong, S. J. Lippard, *J. Am. Chem. Soc. 106* (1984) 4632.
[12] K. Wieghardt, K. Pohl, D. Ventur, *Angew. Chem. 97* (1985) 415; *Angew. Chem. Int. Ed. Engl. 24* (1985) 392.
[13] K. Wieghardt, K. Pohl, W. Gebert, *Angew. Chem. 95* (1983) 739; *Angew. Chem. Int. Ed. Engl. 22* (1983) 727.
[14] W. H. Armstrong, A. Spool, G. C. Papaefthymiou, R. B. Frankel, S. J. Lippard, *J. Am. Chem. Soc. 106* (1984) 3653.
[15] M. J. Maroney, D M. Kurtz, Jr., J. M. Nocek, L. L. Pearce, L. Que, Jr., *J. Am. Chem. Soc. 108* (1986) 6871.
[16] R. Reem, E. I. Solomon, *J. Am. Chem. Soc. 109* (1987) 1216.

Synthesis and Crystal Structure of a Phospholyl Anion**

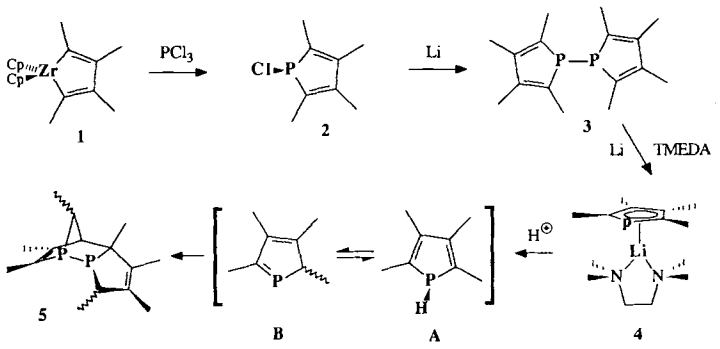
By *Trevor Douglas* and *Klaus H. Theopold**

The study of phospholes is an active research area of heterocyclic chemistry.[1] However, the available synthetic routes to these five-membered rings can be of very low yield and generally produce derivatives with aryl or alkyl groups on phosphorus. Here we report simple procedures for the synthesis of a chlorophosphole and a phospholyl anion in high yields as well as the first crystal structure determination of a phospholyl anion.

Fagan et al. have recently reported the synthesis of several main-group heterocycles by transfer of the organic ligand of the easily prepared zirconacyclopentadienes to various main-group electrophiles.[2] We have now found that reaction of $Cp_2ZrC_4Me_4$ **1** with PCl_3 yields the permethylated chlorophosphole **2** (Scheme 1). Compound **2** is a volatile yellow oil, which was isolated in 85% yield by sublimation at 0 °C.[3] It slowly decomposes at room temperature but can be stored at − 20 °C for months without any signs of decomposition.

[*] Prof. K. H. Theopold, T. Douglas
Department of Chemistry, Baker Laboratory, Cornell University
Ithaca, NY 14853 (USA)

[**] This research was supported by grants from AKZO Corporate Research America Inc. and the New York State Science and Technology Foundation.



Scheme 1.

The common synthetic route to phospholyl anions involves the reductive cleavage of 1-phenylphospholes and is stricken with the concomitant generation of phenyllithium, which may interfere in subsequent reactions of the phospholyl anion.[1] Several strategies (involving selective removal of the phenyllithium) have been devised to overcome this problem.[4] However, reduction of the chlorophosphole **2** with excess lithium (in THF at room temperature, excess tetramethylethylenediamine (TMEDA) added) cleanly yielded the lithium salt of the phospholyl anion, $Li(tmeda)PC_4Me_4$ **4**, which was isolated as colorless needles in 80% yield by recrystallization from ether.[5] The crystal structure of **4** is shown in Figure 1.[6]

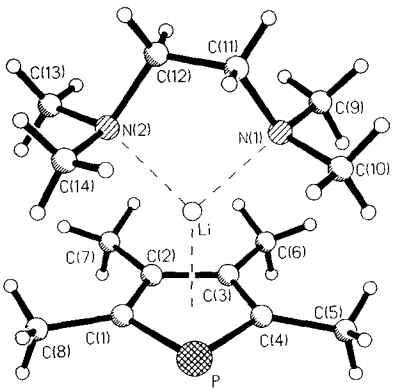


Fig. 1. The molecular structure of $Li(tmeda)PC_4Me_4$. Selected bond distances [Å] and angles [°]: P-C(1) 1.750(5), P-C(4) 1.752(4), C(1)-C(2) 1.396(5), C(2)-C(3) 1.424(7), C(3)-C(4) 1.396(7), P-Li 2.531(7), C(1)-Li 2.373(8), C(2)-Li 2.373(8), C(3)-Li 2.398(8), C(4)-Li 2.425(8), N(1)-Li 2.136(9), N(2)-Li 2.127(8); C(1)-P-C(4) 90.5(2), P-C(1)-C(2) 112.2(4), C(1)-C(2)-C(3) 112.6(4), C(2)-C(3)-C(4) 112.2(4), C(3)-C(4)-P 112.4(4), N(1)-Li-N(2) 85.2(3).

The crystal features a monomeric molecule with η^5 coordination of the heterocycle to lithium. The coordination sphere of the alkali metal is completed by a chelating TMEDA ligand. Carbon atoms C(11) and C(12) of the diamine exhibit large thermal ellipsoids, probably indicating disorder, but the configuration shown in Figure 1 is the predominant one. The carbon–carbon bond distances within the heterocycle [C(1)-C(2) 1.396, C(2)-C(3) 1.424, C(3)-C(4) 1.396 Å] are very similar, indicating a high degree of delocalization. Similarly, the phosphorus–carbon bonds [P-C(1) 1.750, P-C(4) 1.752 Å] are significantly shorter than P–C single bonds (ca. 1.83 Å), consistent with partial double-bond character. These structural features are direct evidence for the highly aromatic nature of the phospholyl anion, in accord with theoretical studies.[7] Calculations have also suggested considerable negative charge density on the phosphorus, and a comparison of the lithium–phosphorus distance of 2.531 Å and the lithium–carbon distances (average 2.39 Å) with the respective sums of the covalent radii (Li-P

2.29, Li-C 2.00 Å) indeed suggests that the lithium is displaced toward the phosphorus atom. A comparison with the structurally characterized transition-metal derivative $(PC_4Me_4)_2ZrCl_2$ revealed no significant differences between the bond distances or angles of the heterocyclic anion in the two structures.[8]

When the reduction of **2** was carried out in the absence of TMEDA (in THF), donor-free $LiPC_4Me_4$ was isolated as a white solid.[9] In addition, **2** could be reduced with potassium; in the presence of 1.0 equivalent of 18-crown-6, the salt $K(18\text{-crown-6})PC_4Me_4$ was isolated as colorless crystals in 89% yield.[10] Monitoring of the lithium reduction of **2** in [D$_8$]THF by ^{1}H or ^{31}P NMR allowed the detection of an intermediate, which could be isolated and identified as the 1,1′-biphospholyl **3**.[11] This dimer was presumably formed by a fast reaction of phospholyl anion with remaining chlorophosphole starting material. No NMR resonances of $LiPC_4Me_4$ were observed until all of the chlorophosphole had been consumed. In a separate experiment $LiPC_4Me_4$ was allowed to react with **2**. Even at −78 °C this reaction was too fast to be followed by NMR and yielded **3** cleanly.

Protonation of the phospholyl anion (with NH_4BF_4 or HBF_4) yielded a new compound which exhibited a fairly complex ^{1}H NMR spectrum. The spectroscopic data of this material are consistent with a dimer (**5** in Scheme 1)[12] formed by a Diels–Alder reaction of the 2*H*-phosphole **B**, which is in equilibrium with the 1*H*-phosphole **A**. This transformation is well precedented.[13]

Zirconacyclopentadienes similar to **1** are easily prepared with a wide variety of ring substituents.[14] The transformations reported here thus represent a convenient synthetic entry to phosphole chemistry. The isolation of pure phospholyl anions in particular should facilitate the use of these nucleophiles in further reactions. We are currently employing **4** in the synthesis of various organometallic derivatives and we are also investigating the extension of this chemistry to other group 15 elements.

Experimental Procedure

NMR: Bruker WM 300 spectrometer (300 MHz for ^{1}H, 75.47 for ^{13}C, and 121.49 for ^{31}P). Shifts are reported relative to TMS for ^{1}H and ^{13}C and relative to an external PCl_3 reference ($\delta = 219$) for ^{31}P. MS: Kratos MS 890. IR: Mattson Alpha Centauri FT-IR. X-ray: Nicolet R3$_m$/V. M.p. uncorrected.

2: Cp_2ZrCl_2 (13.5 g, 46.2 mmol) was reduced using 46.2 mL of a 2.0 M solution of *n*-butyllithium (92.4 mmol) at −78 °C in THF. After addition of 2-butyne (5.0 g, 92.4 mmol), the reaction mixture was allowed to warm to room temperature and then stirred for 16 h. The mixture was filtered, the solvent evaporated, and the zirconium metallacycle **1** crystallized from pentane at − 30 °C (93.8% yield). Compound **1** (3.2 g, 9.7 mmol) was dissolved in pentane, and PCl_3 (1.3 g, 9.7 mmol) was added. An immediate color change from deep red to yellow was observed. Following filtration of the reaction mixture and evaporation of the solvent, the residue was sublimed at 0 °C and the chlorophosphole **2** was collected as an air-sensitive yellow oil (85% yield).

4: Excess lithium dispersion was added to a THF solution of **2** (300 mg, 0.17 mmol), containing an excess of TMEDA. After stirring for 1 h, the reaction mixture was filtered and the solvent was evaporated. The phospholyl anion was recrystallized from ether at − 30 °C and isolated as colorless crystals (80% yield).

Received: May 9, 1989 [Z 3330 IE]
German version: *Angew. Chem. 101* (1989) 1394

CAS Registry numbers:
1, 84101-39-3; **2**, 122762-50-9; **3**, 122762-51-0; **4**, 122762-53-2; **5**, 122762-52-1; Cp_2ZrCl_2, 1291-32-3; $LiPC_4Me_4$, 112549-01-6; $K(18\text{-crown-6})PC_4Me_4$, 122762-55-4; 2-butyne, 503-17-3.

[1] Review: F. Mathey, *Chem. Rev. 88* (1988) 429.
[2] P. J. Fagan, W. A. Nugent, *J. Am. Chem. Soc. 110* (1988) 2310.
[3] **2**: ^{1}H NMR (C_6D_6): $\delta = 1.85$ (d, J(PH) = 9.9 Hz; 6H), 1.42 (d, J(PH) = 5.2 Hz; 6H). ^{13}C NMR (C_6D_6): $\delta = 11.67$ (d, J(PC) = 24.2 Hz), 13.46(s), 136.04 (d, J(PC) = 19.6 Hz), 144.95 (d, J(PC) = 9.7 Hz). ^{31}P NMR (C_6D_6): $\delta = 80.69$(s). IR (neat): $\tilde{\nu}$ = 2998(s), 2911(s), 2839(s), 2723(w), 1442(s), 1373(m), 1297(m), 1067(m), 782(s) cm^{-1}. MS for $C_8C_{12}ClP$: calcd 174.0365, found 174.0369; $(M + 2)^{\oplus}$: calcd 176.0336, found 176.0344. The observation of a 1-bromophosphole intermediate by NMR spectroscopy has been reported: C. Charrier, H. Bonnard, F. Mathey, D. Neibecker, *J. Organomet. Chem. 231* (1982) 361.
[4] a) G. Muller, H. Bonnard, F. Mathey, *Phosphorus Sulfur 10* (1981) 175; b) R. M. G. Roberts, J. Silver, A. S. Wells, *Inorg. Chim. Acta 119* (1986) 1; c) J.-M. Alcaraz, E. Deschamps, F. Mathey, *Phosphorus Sulfur 19* (1984) 45.
[5] **4**: ^{1}H NMR ([D$_8$]THF): $\delta = 1.86$ (s; 6H), 2.06 (d, J(PH) = 10.3 Hz; 6H), 2.09 (s; 12H), 2.21 (s; 4H). ^{13}C NMR ([D$_8$]THF): $\delta = 14.03$(s), 16.29(d, J(PC) = 29.4 Hz), 45.15(s), 56.12(s), 125.17(s), 135.09(d, J(PC) = 33.2 Hz); ^{31}P NMR ([D$_8$]THF): $\delta = 64.66$(s). IR (Nujol): $\tilde{\nu}$ = 2720(w), 1289(s), 1249(w), 1184(w), 1161(m), 1130(m), 1102(w), 1067(w), 1038(s), 1018(m), 946(m), 892(w), 789(m) cm^{-1}. M.p. 101–104 °C. Correct elemental analysis.
[6] Colorless crystals from pentane, monoclinic, $P2_1/n$, $a = 8.927(2)$, $b = 15.857(3)$, $c = 12.704(2)$ Å, $\beta = 108.870(14)°$, $Z = 4$, $R = 0.072$. Further details of the crystal structure investigation may be obtained from the Fachinformationszentrum Karlsruhe, Gesellschaft für wissenschaftlich-technische Information mbH, D-7514 Eggenstein-Leopoldshafen 2 (FRG), on quoting the depository number CSD-53940, the names of the authors, and the journal citation.
[7] a) G. Kaufmann, F. Mathey, *Phosphorus 4* (1974) 231; b) C. Guimon, G. Pfister-Guillouzo, F. Mathey, *Nouv. J. Chim. 3* (1979) 725; c) N. M. Kostic, R. F. Fenske, *Organometallics 2* (1983) 1008.
[8] F. Nief, F. Mathey, L. Ricard, F. Robert, *Organometallics 7* (1988) 921.
[9] $LiPC_4Me_4$: ^{1}H NMR ([D$_8$]THF): $\delta = 1.87$ (s; 6H), 2.07 (d, J(PH) = 10.2 Hz; 6H); ^{31}P NMR ([D$_8$]-THF): $\delta = 62.94$(s). This compound was previously prepared in situ: C. Charrier, F. Mathey, *Tetrahedron Lett. 28* (1987) 5025 (see also Ref. [8]).
[10] $K(18\text{-crown-6})PC_4Me_4$: ^{1}H NMR ($C_6D_6$): $\delta = 2.50$ (s; 6H), 2.87 (d, J(PH) = 10.6 Hz; 6H), 3.13 (s; 24H); ^{31}P NMR (C_6D_6): $\delta = 74.16$(s), M.p. 210–212 °C.
[11] **3**: ^{1}H NMR ([D$_8$]THF): $\delta = 1.74$ (t, J(PH) = 5 Hz; 12H), 1.82 (s; 12H); ^{13}C NMR ([D$_8$]THF): $\delta = 13.20$ (t, J(PC) = 11.3 Hz), 13.78(s), 134.17 (t, J(PC) = 3.3 Hz), 142.63 (t, J(PC) = 5.6 Hz). ^{31}P NMR ([D$_8$]THF): $\delta = -9.40$(s), IR (Nujol): $\tilde{\nu}$ = 2717(w), 1598(m), 1316(m), 1260(m), 1143(s), 1067(s), 1020(s), 958(m), 904(m), 786(m) cm^{-1}. Correct elemental analysis.
[12] **5**: ^{1}H NMR (CD_2Cl_2): $\delta = 0.83$ (dd, J = 7.0, 15.4 Hz; 3H), 1.10 (dd, J = 7.4, 19.7 Hz; 3H), 1.19 (s; 3H), 1.43 (t, J = 0.9 Hz; 3H), 1.45 (d, J = 18.7 Hz; 3H), 1.54 (s; 3H), 1.65 (dd, J = 0.9, 2.0 Hz; 3H), 1.78 (dd, J = 0.9, 10.1 Hz; 3H), 1.85 (m; 1H), 2.05 (m; 1H); ^{13}C NMR (CD_2Cl_2): $\delta = 12.77$ (dd, J(PC) = 9.2, 15.7 Hz), 13.19(s), 14.29(s), 14.82(s), 17.02(s), 17.78 (d, J(PC) = 26.6 Hz), 21.73 (dd, J(PC) = 4.9, 31.4 Hz), 23.49 (d, J(PC) = 33.9 Hz), 36.77 (d, J(PC) = 15.6 Hz), 50.05 (dd, J(PC) = 5.1, 9.7 Hz), 61.85 (d, J(PC) = 24.2 Hz), 68.42(s), 135.69(s), 136.35(s), 146.95(s); ^{31}P NMR (C_6D_6): $\delta = -26.90$ (d, J(PP) = 203 Hz), 4.75(d). IR (Nujol): $\tilde{\nu}$ = 2712(w), 1612(m), 1304(w), 1276(w), 1202(m), 1144(m), 1123(m), 1108(w), 1086(s), 1063(s), 1025(s), 987(m), 758(m), 738(m), 698(s) cm^{-1}. MS: 280 ($M^{\oplus}$, 1.6%), 140 (100%). M.p. = 87–90 °C. Correct elemental analysis.
[13] C. Charrier, H. Bonnard, G. de Lauzon, F. Mathey, *J. Am. Chem. Soc. 105* (1983) 6871. Stable 2-alkylphospholes have been reported: F. Zurmühlen, M. Regitz, *J. Organomet. Chem. 332* (1987) C1.
[14] a) E. Negishi, T. Takahashi, *Aldrichimica Acta 18* (1985) 31; b) W. A. Nugent, D. L. Thorn, R. L. Harlow, *J. Am. Chem. Soc. 109* (1987) 2788.

Comments on the Molecular Structure and Bonding in $[W_4Cl(O)(O\mathit{i}Pr)_9]$ and $[W_4(O)(O\mathit{i}Pr)_{10}]$. Analogies with Tetranuclear Carbonyl Clusters

By *Malcolm H. Chisholm,* Kirsten Folting, Charles E. Hammond, John C. Huffman,* and *James D. Martin*

The cluster **1** was discovered as a minor product formed in the preparation of $[W_4(H)_2(O\mathit{i}Pr)_{14}]$ from the reactants $[W_2(O\mathit{t}Bu)_6]$, $NaO\mathit{i}Pr/\mathit{i}PrOH$, and $Me_2NH_2^{\oplus}Cl^{\ominus}$.[1] Com-

[*] Prof. M. H. Chisholm, Dr. K. Folting, C. E. Hammond, Dr. J. Huffman, J. D. Martin
Department of Chemistry and Molecular Structure Center,
Indiana University
Bloomington, IN 47405 (USA)

[**] This work was supported by the Department of Energy, Office of Basic Sciences, Chemistry Division.

pound **1** is very soluble in hexane and is readily obtained as orange crystals from Et_2O. This allows it to be isolated in analytically pure form and easily separated from $[W_4(H)_2(O\mathit{i}Pr)_{14}]$ and $[W_4(O\mathit{i}Pr)_{12}]$, which are present in the reaction mixture. The reaction pathway leading to **1** is not known.

$[W_4Cl(O)(O\mathit{i}Pr)_9]$ $[W_4(O)(O\mathit{i}Pr)_{10}]$
1 **2**

The cluster **2** is observed as a minor product in the thermal decomposition of $[W_4(O\mathit{i}Pr)_{12}]$ in hydrocarbon solvents and is also formed upon addition of H_2O (0.5 equiv.) to solutions of $[W_2(O\mathit{t}Bu)_6]$ in hexane/*i*PrOH. Compound **2** forms analytically pure, dark red-brown crystals from Et_2O and reacts with $Me_2NH_2^{\oplus}Cl^{\ominus}$ (1 equiv.) to generate **1**.

The ^1H NMR spectra of **1** and **2** suggest that they are structurally related, having five types of O*i*Pr ligands. In **2** these form five pairs with one having nondiastereotopic methyl groups, whereas in **1** they are in the integral ratio 2:2:2:2:1 with the methyl groups of the unique isopropyl ligand being nondiastereotopic. Evidently both molecules have one plane of symmetry.

The molecular structure of **1**, deduced from an X-ray study,[2] is shown in Figure 1. A WCl(O*i*Pr) unit caps a W_3 triangle that is supported by two bridging O*i*Pr ligands and one bridging oxo group. The geometry about each tungsten atom in the basal plane corresponds to a square plane formed by two terminal O*i*Pr ligands and two oxygen atoms from either two bridging alkoxide ligands or one bridging alkoxide and one oxo ligand. Of particular note are the short W–W distances of ca. 2.50 Å from the tungsten atoms of the W_3 unit to the capping WCl(O*i*Pr) unit and the longer W–W distances in the basal plane (2.85–2.96 Å). In a localized valence bond (V.B.) description, these are suggestive of a significant contribution of resonance form **B** relative to the fully delocalized form **A** for a 12-electron M_4 unit.

The ^1H NMR spectrum of **1** is entirely consistent with the structure observed in the solid state and the structure of **2** can most reasonably be formulated as being related to that of **1** by the formal replacement of Cl by O*i*Pr. In solution, however, there must be facile rotation of the $W(O\mathit{i}Pr)_2$ unit of **2** above the W_3 fragment.

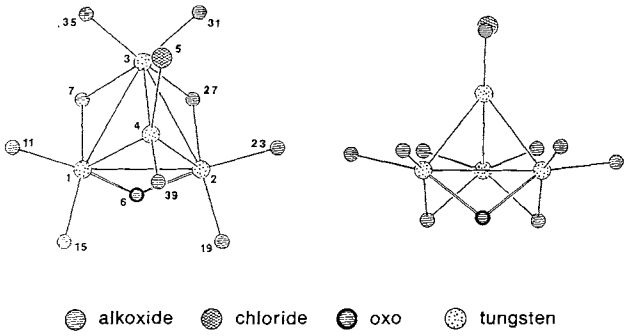
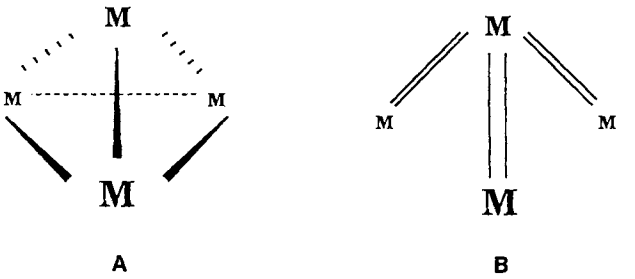


Fig. 1. Two views of the central $W_4Cl(O)_{10}$ skeleton of $[W_4Cl(O)(O\mathit{i}Pr)_9]$. Pertinent distances [Å] and angles [°]: W1-W2 2.847(2), W1-W3 2.958(2), W1-W4 2.484(1); W2-W3 2.965(2), W2-W4 2.470(1), W3-W4 2.547(1), W4-Cl5 2.462(4), W-O (terminal) 1.88(2) (averaged), W-O (oxo) 1.92(1), W-O (μ-OR) 2.01–2.07; Cl5-W4-O39 85.8(4).



The bonding in **1** is best understood from a fragment molecular orbital analysis.[3] We consider the cluster to be formed from the fragments WCl(OR) and $W_3(O)(OR)_8$ and have investigated the bonding by using the method of *Fenske* and *Hall*[4] for the model compound $[W_4Cl(O)(OH)_9]$. An OH bond distance of 0.96 Å was used; otherwise, bond distances and bond angles for the model compound were taken from the solid-state molecular structure of **1** and idealized to C_s symmetry. The important interactions are shown in Figure 2.

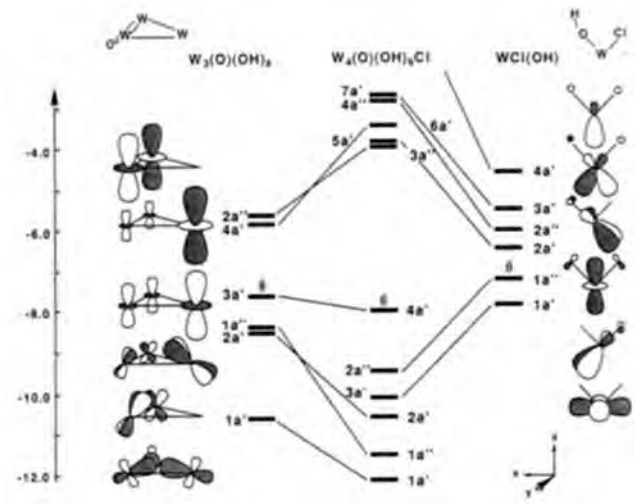


Fig. 2. Frontier orbital interactions showing the formation of $[WCl(O)(OH)_9]$ from the fragments WCl(OH) and $W_3(\mu\text{-}O)(\mu\text{-}OH)_2(OH)_6$. Ordinate: E[eV].

The molecular orbitals of the $W_3(O)(OH)_8$ fragment are similar to those seen in the $W_3(OR)_9$ fragment[5] of $[W_3(OR)_9(\mu_3\text{-}CMe)]$,[6] though the presence of the bridging oxo group results in a reduction of symmetry from C_{3v} to C_s and a loss of one electron from the M_3 cluster fragment. The orbitals of the WCl(OH) fragment are reminiscent of those expected for an ML_2 fragment except for the notable mixing of the 1a″ and 2a″ orbitals so as to minimize the π antibonding between the tungsten d_π and oxygen p_π electrons.

On combining the fragments, the filled 1a′ and 1a″ orbitals of WCl(OH) find their match with unoccupied 4a′ and 2a″ nonbonding orbitals of the tritungsten fragment. Similarly, the 1a′, 2a′, and 1a″ W–W bonding orbitals and the 3a′ occupied nonbonding orbital of the W_3 fragment, made up of the in-phase combinations of tungsten z^2 orbitals, interact strongly with the respective 2a′, 2a″, 3a′, and 4a′ unoccupied orbitals of the ML_2 cap. Placing electrons into M_3 nonbonding (or weakly antibonding) orbitals and withdrawing electrons from the M_3 bonding orbitals causes the Mulliken atomic charges to be −0.631 for the capping tungsten atom and 1.407, 1.407, and 1.343 for the tungsten atoms in the

basal plane. This results in a severe weakening of the M–M bonding in the basal plane and leads to M–M multiple bonding to the capping tungsten atom.[7] The importance of the V.B. description depicted by resonance structure **B**, relative to that of **A**, is apparent. A slightly weaker interaction would be obtained were the WCl(O) fragment rotated by 180° such that the Cl was directed toward the bridging oxo group owing to an increased population of the W–O π^* orbitals.

We have previously discussed[5] the relationships between d^3-$W(OR)_3$ and d^9-$Co(CO)_3$ and their respective clusters of formula $M_3X_9(\mu_3\text{–}Y)$ (M = W, X = OR, Y = CR[6] or P[8]). Aspects of the bonding in **1** are reminiscent of the hypothetical cluster **3** discussed by *Hoffmann*,[9] where the

$[O_3(CO)_9(\mu_3\text{-}PtL_2)]^{2\ominus}$ **3** $[Os_3Pt(H)_2(CO)_{10}(PR_3)]$ **4**

hydrides of **4**[10] are treated as protons. We suggest here that the $Os_3(CO)_9^{2\ominus}$ fragment is related to the $Co_3(CO)_9$ fragment in a similar fashion as $W_3(O)(OR)_8$ is to $W_3(OR)_9$. Furthermore, we suggest an internal isolobal analogy relates the yz and z^2 orbitals of the d^4-WCl(OH) fragment to the xz and sp hybrid orbitals of the d^{10}-PtL_2 fragment. From this simple analysis, we conclude that the orientation of the respective ML_2 fragments to the M_3 plane should be rotated by 90° for the early and late cluster elements, W versus Os, as indeed is observed by X-ray crystallography. Nonetheless, the orthogonal sets of orbitals in both ML_2 and M_3X_9 fragments allow facile rotation of the capping ML_2 groups, as seen here from the ^{1}H NMR spectrum of **2** in [D_8]toluene at 22 °C.

Received: May 16, 1989 [Z 3339 IE]
German version: *Angew. Chem. 101* (1989) 1399

[1] M. H. Chisholm, J. C. Huffman, C. A. Smith, *J. Am. Chem. Soc. 108* (1986) 222; M. Akiyama, M. H. Chisholm, D. A. Haitko, D. Little, F. A. Cotton, M. W. Extine, *J. Am. Chem. Soc. 101* (1979) 2504.

[2] Crystal data for $[W_4(Cl)(O)(O/Pr)_9]\cdot 1/2\,(Et_2O)$ at −146 °C: a = 41.172(18), b = 9.185(2), c = 22.718(8) Å, β = 97.15(2)°, Z = 8, ϱ_{calcd} = 2.113 g cm^{-3}, space group $C2/c$. Of 6513 reflections collected ($Mo_{K\alpha}$), $6° < 2\theta < 45°$), 5594 were unique and the 4851 reflections having $F > 3\sigma(F)$ were used in the full least-squares refinement. The asymmetric unit contains one W_4 complex and one half molecule of ether (solvent) located at a twofold axis. All the hydrogen atoms, except those on the solvent were introduced in fixed calculated positions. The full-matrix least-squares refinement was completed using anisotropic thermal parameters on the atoms in the W_4 complex and isotropic thermal parameters on the solvent atoms (O(43) through C(45)) and fixed hydrogen atoms. The final residuals are R = 0.051 and $R_w(F)$ = 0.050. Further details of the crystal strueture investigations may be obtained from the Fachinformationszentrum Karlsruhe, Gesellschaft für wissenschaftlich-technische Information mbH, D-7514 Eggenstein-Leopoldshafen 2 (FRG), on quoting the depository number CSD-53966, the names of the authors, and the journal citation.

[3] R. Hoffmann, *Angew. Chem. 94* (1982) 725; *Angew. Chem. Int. Ed. Engl. 21* (1982) 711; T. A. Albright, J. K. Burdett, M. H. Whangbo: *Orbital Interactions in Chemistry*, Wiley, New York 1985.

[4] M. B. Hall, R. F. Fenske, *Inorg. Chem. 11* (1972) 768.

[5] M. H. Chisholm, D. L. Clark, M. J. Hampden-Smith, D. M. Hoffman, *Angew. Chem. 101* (1989) 446; *Angew. Chem. Int. Ed. Engl. 28* (1989) 432; M. H. Chisholm, B. K. Conroy, J. D. Martin, unpublished.

[6] M. H. Chisholm, K. Folting, J. A. Heppert, D. M. Hoffman, J. C. Huffman, *J. Am. Chem. Soc. 107* (1985) 1234.

[7] For comparison: W–W = 2.732(2) Å in $[W_3(\mu_3\text{-}CMe)(O/Pr)_9]$ from [6]) and 2.757(1) Å in $[W_3(\mu_3\text{-}P)(O/Pr)_9]$ from [8]).

[8] M. H. Chisholm, K. Folting, J. W. Pasterczyk, *Inorg. Chem. 27* (1988) 3057.

[9] B. E. R. Shilling, R. Hoffmann, *J. Am. Chem. Soc. 101* (1979) 3456.

[10] L. J. Farrugia, J. A. K. Howard, P. Mitrprachachon, J. L. Spenser, F. G. A. Stone, P. Woodward, *J. Chem. Soc. Chem. Commun. 1978*, 260.

Complexation of a Novel Organoytterbium(II) Ligand with Dimethylplatinum(II): Crystal Structure of the Resulting Heterobimetallic Complex **

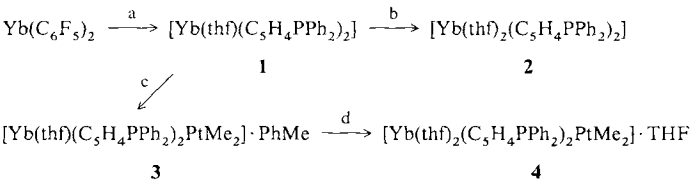
By *Glen B. Deacon,* Andreas Dietrich, Craig M. Forsyth,* and *Herbert Schumann**

Dedicated to Professor Friedo Huber on the occasion of his 60th birthday

Heterobimetallic complexes (see, e.g. Ref. [1]) have attracted attention because of the possibility of unusual catalytic activity, including redox catalysis due to cooperative reactivity involving both metal centers. We now report a new organoytterbium(II) ligand **1**, as well as the preparation and crystal structure of a derived heterobimetallic complex **4** with Yb^{II} and Pt^{II} centers. The present example is novel among organolanthanoid d-block-element bimetallic complexes[2–4] in having the lanthanoid in the donor rather than the acceptor part of the molecule.

Metalation of diphenylphosphinocyclopentadiene[5] with bis(pentafluorophenyl)ytterbium[6] gives the phosphinoytterbocene **1** as a green air-sensitive solid[7] (Scheme 1). Dissolution of **1** in THF gives a wine-red solution from which orange-red **2** is isolated. The distinctive identities of **1** and **2** are evident from solid-state visible spectra.[7] The chemical shift of the single ^{31}P NMR resonance of **1** in THF[7] is indicative[1] of equivalent uncoordinated phosphane groups. This result, together with the similarity of the visible spectra of **1** in THF and solid **2**, suggests no P → Yb coordination in the latter, but such bonding cannot be ruled out for solid **1**. Thus, **2** probably has pseudo-tetrahedral eight coordination for ytterbium as observed in **4** (see below).

Reaction of a suspension of **1** in toluene with $PtMe_2$(cod) (cod = *cis,cis*-cycloocta-1,5-diene) results in displacement of cyclooctadiene and formation of the air-sensitive heterobimetallic complex **3**[8] (Scheme 1). Coordination of the



Scheme 1. Reagents and conditions: a) 2 $C_5H_5PPh_2$, THF/OEt_2, 20 °C, 40 h, evaporation to dryness, then 80 °C, vacuum for 2 h, followed by toluene, 20 °C, 24 h; b) THF, 20 °C, 10 min; c) $PtMe_2$(cod), toluene, 20 °C, 22 h; d) slow cooling of a saturated solution in hot THF.

phosphane groups is evident from the single ^{31}P NMR resonance[8], which shows the expected[1] downfield shift from that of the free ligand **1**, and from the P–Pt coupling,[8] which is similar in magnitude to that (1856 Hz) of *cis*-$PtMe_2(PEt_3)_2$.[9] Crystallization of **3** from THF yielded single crystals of **4** (Scheme 1). An X-ray crystal structure

[*] Dr. G. B. Deacon, C. M. Forsyth
Chemistry Department, Monash University
Clayton, Victoria 3168 (Australia)
Prof. Dr. H. Schumann, Dipl.-Chem. A. Dietrich
Institut für Anorganische und Analytische Chemie
der Technischen Universität
Strasse des 17. Juni 135, D-1000 Berlin 12

[**] Organolanthanoids, Part 16, and Organometallic Lanthanoid Compounds, Part 51. This work was supported by the Australian Research Council, the Fonds der Chemischen Industrie, and the Deutsche Forschungsgemeinschaft. Part 15: G. B. Deacon, D. L. Wilkinson, *Aust. J. Chem. 42* (1989) 845. Part 50: H. Schumann, P. R. Lee, J. Loebel, *Chem. Ber.*, in press.

determination[10] revealed that the bis(diphenylphosphino)ytterbocene acts as a chelating phosphane ligand to platinum (Fig. 1). Ytterbium has pseudo-tetrahedral eight coordination (two staggered cyclopentadienyl ligands and two tetrahydrofuran oxygens), while platinum has approximately square-planar stereochemistry. The Pt···Yb distance (5.01 Å) precludes any interaction. There is a marked similarity between the ytterbium geometry of **4** and that of $[Yb(thf)_2(C_5H_4SiMe_3)_2]$[12] and between the platinum stereochemistry in **4** and that for other *cis*-$PtMe_2P_2$ complexes.[13] Thus, coordination of the organoytterbium ligand **1** to the dimethylplatinum(II) complex to give **4** does not cause major disruption of the parent structures.

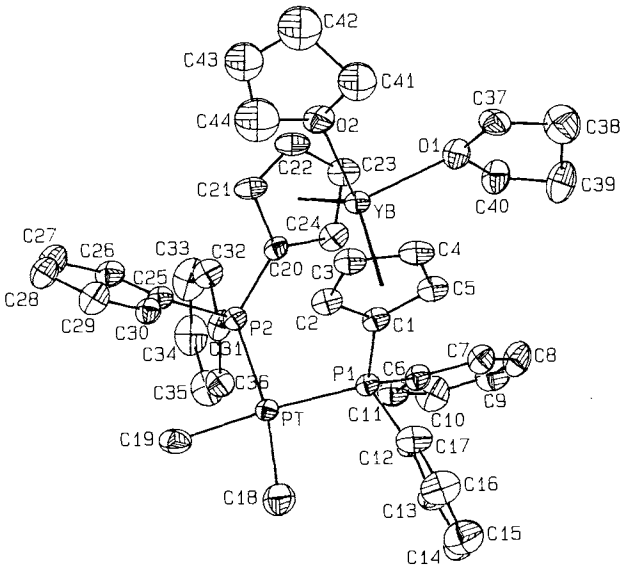


Fig. 1. Crystal structure of **4** (H atoms and THF of solvation omitted for clarity). Selected bond distances [Å] and angles [°] (CT1 and CT2 denote the centroids of cyclopentadienyl rings C1-C5 and C20-C24, respectively): Yb-CT1 2.422(8), Yb-CT2 2.434(9), mean Yb-C (C1-C5, C20-C24) 2.71, Yb-O1 2.428(8), Yb-O2 2.379(6), Pt-P1 2.288(3), Pt-P2 2.290(3), Pt-C18 2.10(1), Pt-C19 2.12(1); CT1-Yb-CT2 133.6(3), O1-Yb-O2 93.7(3), CT1-Yb-O1 104.3(3), CT1-Yb-O2 106.5(3), CT2-Yb-O1 106.2(4), CT2-Yb-O2 105.5(4), C18-Pt-C19 82.2(5), P1-Pt-P2 99.4(1), C18-Pt-P1 92.1(4), C19-Pt-P1 174.2(4), C18-Pt-P2 168.5(4), C19-Pt-P2 86.3(4).

Received: April 19, 1989 [Z 3300 IE]
German version: *Angew. Chem. 101* (1989) 1374

CAS registry numbers:
1, 122425-14-3; **2**, 122425-15-4; **3**, 122425-16-5; **4**, 122443-09-8; **4** (without THF), 122425-17-6; $Yb(C_6F_5)_2$, 66080-22-6; $C_5H_5PPh_2$, 58109-48-1; $PtMe_2(cod)$, 12266-92-1.

[1] D. L. Dubois, C. W. Eigenbrot, A. Miedaner, J. C. Smart, R. C. Haltiwanger, *Organometallics 5* (1986) 1405; R. M. Bullock, C. P. Casey, *Acc. Chem. Res. 20* (1987) 167 and references therein.

[2] H. Schumann, *Angew. Chem. 96* (1984) 475; *Angew. Chem. Int. Ed. Engl. 23* (1984) 474.

[3] W. J. Evans, *Polyhedron 6* (1987) 403.

[4] C. J. Burns, R. A. Andersen, *J. Am. Chem. Soc. 109* (1987) 915.

[5] F. Mathey, J. P. Lampin, *Tetrahedron 31* (1975) 2685.

[6] G. B. Deacon, W. D. Raverty, D. G. Vince, *J. Organomet. Chem. 135* (1977) 103.

[7] **1** (yield 46%) and **2** (yield 80%) were characterized by elemental analysis and spectroscopy. UV/VIS: **1** (Nujol): λ_{max} = 430, 590 nm, (THF): 400, 520 nm; **2** (Nujol): 390, 510 nm; ^1H NMR: **1** (C_4D_8O, TMS int.): δ = 5.87 (t, br., C_5H_4P), 5.95 (t, J = 3 Hz, C_5H_4P), 7.17 (m, br., Ph); $^{31}P\{^1H\}$ NMR: **1** (THF, 85% H_3PO_4 ext.): δ = −20.5.

[8] **3** (yield 79%) was characterized by elemental analysis and spectroscopy. ^1H NMR (C_4D_8O, TMS int.): δ = 0.22 (t, $^3J(HP)$ = 8 Hz, $^2J(HPt)$ = 68 Hz, MePt), 2.30 (s, *Me*Ph), 5.74 (s, br., C_5H_4P), 5.81 (s, br., C_5H_4P), 7.08–7.21 (m, PhP + *Ph*Me), 7.49 (t, $^3J(HH)$ = 8 Hz, PhP), $^{31}P\{^1H\}$ NMR (THF, 85% H_3PO_4 ext.): δ = 17.1 (t, $^1J(PtP)$ = 1920 Hz.

[9] T. G. Appleton, H. C. Clark, L. E. Manzer, *Coord. Chem. Rev. 10* (1973) 335.

[10] **4**, air-sensitive red plates, $C_{48}H_{58}O_3P_2PtYb$, M_r = 1113.1, triclinic, space group $P\bar{1}$, a = 14.181(4), b = 14.927(5), c = 12.701(3) Å, α = 100.34(2), β = 106.87(2), γ = 112.78(3)°, V = 2238.6 Å^3, Z = 2, ϱ_{calcd} = 1.651 g cm^{-3}, $F(000)$ 1096, $Mo_{K\alpha}$ radiation 0.71069 Å, graphite monochromator, $\theta-2\theta$ scans in the range $1 \le 2\theta \le 52°$ at 140(5) K, 8462 independent reflections, 6798 observed ($F_0 \ge 4\sigma(F_0)$). Data corrected for Lorentz and polarization effects, and an empirical absorption correction applied (min./max. transmission 0.88/1.17). Solution by Patterson and Fourier techniques and refinement by blocked-matrix least-squares methods. One coordinated THF (O2, C41–C44) is disordered with two preferred positions for C41, C42, C41–C44 and other non-hydrogen atoms were refined with isotropic and anisotropic temperature factors, respectively. Hydrogen atoms were inserted in calculated (d(C–H) = 1.08 Å) positions with a common isotropic temperature factor. Unit weights were used throughout the refinement (maximum ratio of shift to error, 0.014) giving R = 0.038. Two peaks of 3.64 and 3.56 e/Å^3 electron density in the final difference Fourier map are associated with the THF molecule of solvation. Calculations with SHELX-76 and anomalous dispersion terms applied [11]. Further details of the crystal structure investigation may be obtained from the Fachinformationszentrum Karlsruhe, Gesellschaft für wissenschaftlich-technische Information mbH, D-7514 Eggenstein-Leopoldshafen 2 (FRG), on quoting the depository number CSD-54051, the names of the authors, and the journal citation.

[11] G. M. Sheldrick: *SHELX-76 Program for Crystal Structure Determination*, University of Cambridge (UK).

[12] M. F. Lappert, P. I. W. Yarrow, J. L. Atwood, R. Shakir, J. Holton, *J. Chem. Soc. Chem. Commun. 1980*, 987.

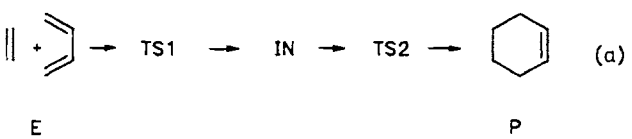
[13] J. M. Wisner, T. J. Bartczuk, J. A. Ibers, *Organometallics 5* (1986) 2044.

Mechanism of the Hetero-Diels–Alder Reaction of Oxadienes and Alkenes: Calculation of the Acrolein/Ethene System**

By *Lutz F. Tietze,* Jens Fennen,* and *Ernst Anders**

Dedicated to Professor Christoph Rüchardt on the occasion of his 60th birthday

The Diels–Alder reaction is still—more than 60 years after its discovery—of special preparative value, since it not only offers an approach to carbocyclic compounds, but also to a variety of heterocycles. Furthermore, it is often characterized by high selectivity. The theoretical discussion of this reaction has focused above all on whether it proceeds by a synchronous, a concerted two-stage, or a two-step mechanism involving diradicals or zwitterions as intermediates.[1] Since the temporal sequence of bond breaking and bond formation is difficult to determine experimentally, quantum-chemical calculations have been used to analyze the mechanism of the Diels–Alder reaction.[2] The ab initio calculations carried out for the butadiene/ethene system [Eq. (a)] by

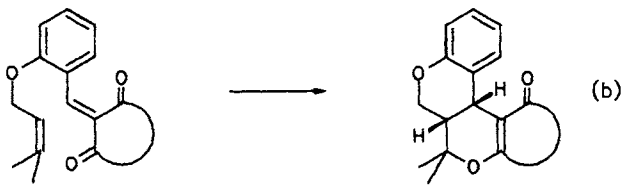


[*] Prof. Dr. L. F. Tietze, J. Fennen
Institut für Organische Chemie der Universität
Tammannstrasse 2, D-3400 Göttingen (FRG)
Prof. Dr. E. Anders
Institut für Organische Chemie der Universität Erlangen-Nürnberg
Henkestrasse 42, D-8520 Erlangen (FRG)

[**] Inter- and Intramolecular Hetero-Diels–Alder Reactions, Part 27. This work was supported by the Deutsche Forschungsgemeinschaft and the Fonds der Chemischen Industrie. We thank Prof. Dr. *P. von R. Schleyer*, Dr. *T. Clark* (Universität Erlangen-Nürnberg), and Prof. Dr. *M. C. Zerner* (University of Florida, Gainsville, USA) for helpful discussions. Part 26: M. Buback, W. Tost, T. Hübsch, E. Voß, L. F. Tietze, *Chem. Ber. 122* (1989) 1179–1186.

Houk et al.,[2b] *Ortega* et al.,[2c] *Bernardi* et al.,[2d] and *Gajewski* et al.[2e] gave a symmetrical transition state, whereas *Dewar* et al.,[2f] using the semiempirical AM1/CI method (half electron approximation), found an unsymmetrical diradicaloid intermediate. Calculations for Diels–Alder reactions of heterodienes such as acrolein have been performed only once, without considering the problem of diradicaloid intermediates.[3]

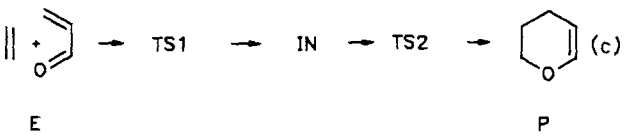
In our studies of intramolecular Diels–Alder reactions[4] of heterodienes such as **1**, readily accessible in situ by condensation of an aldehyde with a 1,3-dioxo compound, we were able to show that cycloaddition to give **2** [Eq. (b)] very



(b)

1 **2**

likely proceeds in a concerted fashion without the intermediacy of diradicaloids.[5] Moreover, we obtained the first experimental proof that this type of reaction proceeds via an unsymmetrical transition state.[6] Here we present the results of a theoretical study, using the AM1 method, of the intramolecular cycloaddition of acrolein and ethene [Eq. (c)],



E P

the parent reaction of (b), and we compare the results with those obtained for the butadiene/ethene system [Eq. (a)]. Our goal was to develop a theoretical framework for understanding the stereoselectivity of the reaction. The most important results of the calculations for reaction (c) are summarized in Table 1.

The assessment of the radicaloid character of intermediates requires quantum-chemical methods capable of treating open-shell systems. In carrying out these calculations, we found it advantageous to determine approximately the geometries of the transition states TS or intermediates IN by using an MMX force field[7a] and to use the results as starting points for the restricted Hartree–Fock (RHF) optimization of the geometries with initially fixed C–C and C–O bond lengths. This approach saves CPU time and proved to be widely applicable.

The enthalpies of formation ΔH_f of starting materials E and products P were calculated by using the AMPAC[7b] or VAMP program package.[7c] All structures were completely optimized without symmetry restrictions. After the RHF optimization of the geometry, the RHF transition state TS was completely calculated (NS01A routine[7d] of the VAMP program package). Its structure then served as the starting geometry for calculating the two unrestricted Hartree–Fock (UHF) transition states TS1 and TS2. The determination of the configuration interaction (CI) transition states TS1 and TS2 is generally straightforward when the UHF transition states are known and the NS01A routine is used. The NS01A geometries were refined[7e] and then characterized by a FORCE calculation.[7f] NS01A and SADDLE routines[7g] were generally found to give nearly identical results. For relatively long partial bonds (starting at ca. 240 pm) and only insignificantly differing heats of formation, NS01A afforded somewhat deviating structural parameters. This may be explained by the overall very flat potential energy surfaces close to the first transition state TS1.

For the two reactions (a) and (c), both the UHF and the CI approximation revealed the existence of an intermediate IN and thus indicated a two-step mechanism. However, the energy profiles of reactions (a) and (c) are fundamentally different both qualitatively and quantitatively (Fig. 1, left and right, respectively).

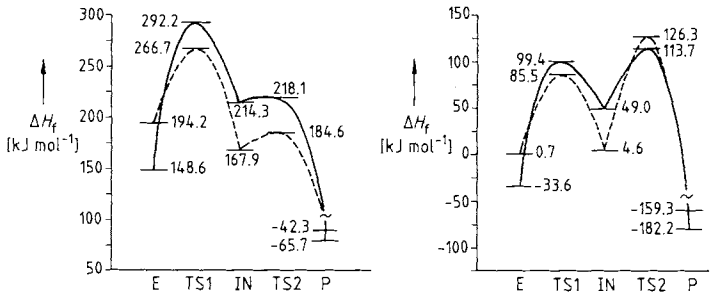


Fig. 1. Reaction profile for cycloaddition calculated with the semiempirical methods AM1/UHF (– – –) and AM1/CI (—). Left: Reaction (a) [2f]. Right: Reaction (c).

Table 1. Characteristic data for the hetero-Diels–Alder systems acrolein/ethene; AM1 results for reaction (c).

Method	Species	ΔH_f [kJ mol^{-1}]	r(C-C) [pm]	r(C-O) [pm]	S^2	Coefficients of the configurations [a] a^1b^1	a^2	b^2
RHF	TS [b]	126.3	198.7	200.8	–	–	–	–
UHF	E	0.7	–	–	–	–	–	–
	TS1	85.5	194.7	354.5	0.836	–	–	–
	IN	4.6	152.2	364.2	1.050	–	–	–
	TS2	126.3	198.7	200.8	0.000	–	–	–
	P	−159.3	148.2	137.7	0.000	–	–	–
CI	E	−33.6	–	–	–	–	–	–
	TS1	99.4	184.0	265.8	–	0.055 [c]	0.953	−0.298
	IN	49.0	151.7	358.3	–	0.319 [c]	−0.686	0.654
	TS2	113.7	198.6	200.9	–	0.041 [c]	0.989	−0.142
	P	−182.2	148.1	137.1	–	0.014	0.985	−0.172

[a] a indicates the HOMO, b the LUMO. [b] Dipole moment, 2.104 D; charge separation; arcolein/ethene, −0.13/+0.13. For comparison, butadiene/ethene [2f]: 0.560 D, −0.00/+0.00. [c] For comparison, a^1b^1 values for butadiene/ethene [2f]: TS1, 0.055; IN, 0.872; TS2, −0.241.

Thus, the second transition state in (c) is higher in energy than the first and therefore rate-determining. In reaction (a), the first—nonradicaloid—transition state initially appears to be rate-determining owing to its higher energy. The ΔH_f value of the second transition state must be corrected, however, because of its radicaloid character (see below);[2g] the resulting increased importance of TS2 in reaction (a) makes it impossible to determine which transition state is rate-determining.

The ΔH_f values calculated by the two open-shell approximations (UHF and CI) differ by only ca. 13 kJ mol^{-1} for both TS1 and TS2 in reaction (c); this value is much smaller than that calculated for cycloaddition (a) (Fig. 1, left, $\Delta\Delta H_f$(TS1) = 25.5, $\Delta\Delta H_f$(TS2) = 33.5 kJ mol^{-1}; the higher value in each case was obtained from the CI calculation[2g]). The C–C bonds being formed in the two transition states

TS 1 and TS 2 of reaction (c) are more similar in length (184.0 and 198.6 pm, respectively) than those of reaction (a) (193 and 153.2 pm, respectively). The C–O bond being formed in TS 1 of (c) is only 265.8 pm, a very short value compared with that of the second C–C bond in TS 1 of (a) (498.9 pm). Comparison of the TS 2 bond lengths in cycloadditions (c) and (a) shows that the rate-determining transition state TS 2 of (c) (r(C-C) = 198.6 pm, r(C-O) = 200.9 pm) is surprisingly "symmetric" (TS 2 of (a): r(C-C) = 153.2 and 290.3 pm).

The involvement of radicaloids in reaction (c) is usually expressed by the coefficient contributions to the singlet CI eigenfunction, composed of the configurations a^1b^1, a^2, and b^2 (Table 1), though there are a number of other criteria for determining the extent of mixing of singly excited states;[8] the a^1b^1 coefficient is particularly suitable. The rate-determining transition state TS 2 ($a^1b^1 = 0.041$) in (c), in contrast to TS 2 of (a) ($a^1b^1 = -0.241$), displays almost no radicaloid character, but does exhibit a certain degree of polarity, as revealed by comparison of the dipole moments of the RHF transition states (footnote [b] in Table 1). An only slightly higher a^1b^1 contribution (0.055) is obtained for transition state TS 1 of (c), whereas the radicaloid character of intermediate IN is pronounced ($a^1b^1 = 0.319$). Since the stability of these species is overestimated by the use of such calculation methods, however, it is necessary to correct the calculated heats of formation to a more positive value.[2f] Although the amount of this correction is somewhat uncertain,[2b, 2f] even an increase of only a few kJ mol^{-1} in the heat of formation of IN in (c) decreases its importance as a sufficiently long-lived and therefore significant intermediate for the reaction.[9] Our experimental finding that the configuration of the dienophilic moiety of **1** is retained in the intramolecular hetero-Diels–Alder reaction (b) may thus be explained on the basis of this AM 1 study.

The essential difference between reactions (a) and (c) lies in the finding that the total course of the hetero-Diels–Alder reaction (c) is governed by the structural and energetic properties of transition state TS 2. Of particular importance is the fact that, in contrast to reaction (a), all methods employed here (RHF, UHF, CI) gave very similar results for TS 2 of (c). Therefore, the much less time-consuming RHF method may be used for calculating the hetero-Diels–Alder reaction of oxadienes. Thus, it should also be possible to describe—at least roughly—more complex transition-state structures containing substituents of practical relevance with the RHF method.

Received: June 8, 1989 [Z 3386 IE]
German version: *Angew. Chem. 101* (1989) 1420

CAS Registry numbers:
acrolein, 107-02-8; ethene, 74-85-1.

[1] J. Sauer, R. Sustmann, *Angew. Chem. 92* (1980) 773–801; *Angew. Chem. Int. Ed. Engl. 19* (1980) 779–807.

[2] a) R. Sustmann, P. Daute, R. Sauer, W. Sicking, *Tetrahedron Lett. 29* (1988) 4699–4702; b) K. N. Houk, Y. Lin, F. K. Brown, *J. Am. Chem. Soc. 108* (1986) 554–556; c) M. Ortega, A. Oliva, J. M. Lluch, J. Bertrán, *Phys. Lett. 102* (1983) 317–326; d) F. Bernardi, A. Bottoni, M. A. Rott, M. J. Field, I. H. Hillier, M. F. J. Guest, *J. Chem. Soc. Chem. Commun. 1985*, 1051–1052; e) J. J. Gajewski, K. B. Peterson, J. R. Kagel, *J. Am. Chem. Soc. 109* (1987) 5545–5546; f) M. J. S. Dewar, S. Olivella, J. J. P. Stewart, *ibid. 108* (1986) 5771–5779.

[3] I. Lee, E. S. Han, J. J. Choi, *J. Comput. Chem. 5* (1984) 606–611; see also X. Balcells, M. Duran, A. Ledós, J. Bertrán, *J. Mol. Struct. (THEOCHEM) 149* (1987) 153–160.

[4] Review: L. F. Tietze in W. Bartmann, B. M. Trost (Eds.): *Selectivity—A Goal for Synthetic Efficiency*, Verlag Chemie, Weinheim 1984, p. 299; see also D. L. Boger, S. M. Weinreb, *Hetero-Diels-Alder Methodology in Organic Synthesis*, Academic Press, New York 1987; L. F. Tietze, G. von Kiedrowski, K. Harms, W. Clegg, G. Sheldrick, *Angew. Chem. 92* (1980) 130–131; *Angew. Chem. Int. Ed. Engl. 19* (1980) 134–135.

[5] L. F. Tietze, M. Bratz, R. Machinek, G. von Kiedrowski, *J. Org. Chem. 52* (1987) 1638–1640.

[6] L. F. Tietze, T. Brumby, S. Brand, M. Bratz, *Chem. Ber. 121* (1988) 499–506.

[7] a) MMX: K. Steliou, unpublished; b) AMPAC: J. J. P. Stewart, QCPE No. 506; c) VAMP (T. Clark, Universität Erlangen-Nürnberg, unpublished) is a "vectorized" version of AMPAC 1.0, updated for MOPAC 4.0 and the CONVEX-C computer series; d) NS01A is a gradient optimization routine described by *M. J. D. Powell* and modified by *J. Chandrasekar, P. H. M. Budzelaar*, and *T. Clark* (Universität Erlangen-Nürnberg) for the VAMP program package; e) PRECISE option of the AMPAC and VAMP program package; f) only one negative eigenvalue (frequency analysis) is obtained for all the transition states described here; compare J. W. McIver, A. Kormonicki, *J. Am. Chem. Soc. 94* (1972) 2625–2633, g) M. J. S. Dewar, E. F. Haley, J. J. P. Stewart, *J. Chem. Soc. Faraday Trans. 2 80* (1984) 227–333.

[8] P. M. Lahti, A. S. Ichimura, J. A. Berson, *J. Org. Chem. 54* (1989) 958–965.

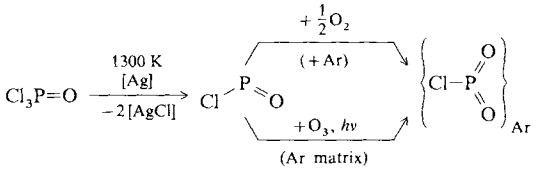
[9] On the basis of ab initio calculations, *L. Salem* et al. obtained a comparable result for substituted reactants in reaction (a). In this case, too, the existence of an experimentally hardly detectable, radicaloid intermediate cannot be ruled out; see R. E. Townshend, G. Ramunni, G. Segal, W. J. Hehre, L. Salem, *J. Am. Chem. Soc. 98* (1976) 2190–2198, the statement on page 2197.

Generation and Ionization Pattern of the Iso(valence)electronic Compounds $ClP(=O)_2$ and $ClP(=S)_2$**

By *Manfred Meisel,* Hans Bock,* Bahman Solouki,* and *Matthias Kremer*

Dedicated to Professor Christoph Rüchardt on the occasion of his 60th birthday

According to the "classical" Walsh rules[1] tetraatomic chalcogen-element halides $Hal_2E{=}X$ and $HalE(=X)_2$ with 24 valence electrons are planar, and in the case of the main group elements E they form a link between the likewise planar iso(valence)electronic molecules F_3B and SO_3. In spite of their fundamental importance as π/σ bond models, only the (diamagnetic) neutral compounds $Hal_2C{=}O$ (Hal = F,Cl,Br),[2] $Hal_2C{=}S$ (Hal = F,Cl),[2] $F_2C{=}Se$[2] and $HalN(=O)_2$ (Hal = F,Cl)[2] have thus far been characterized by their ionization patterns, since unsaturated derivatives such as $F_2Si{=}O$[3a] tend to oligomerize and can frequently only be generated and investigated in noble gas matrices at low temperatures. The same applies for $ClP(=O)_2$, which previously had to be either cold-trapped from rather non-selective gas reactions[3b] or generated from $ClP{=}O$ by photolyzing[3c] ozone in a joint matrix[3d] (Scheme 1).

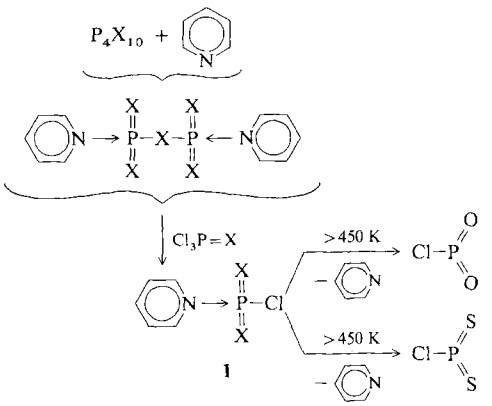


Scheme 1.

[*] Prof. Dr. M. Meisel
Zentralinstitut für Anorganische Chemie
der Akademie der Wissenschaften
Rudower Chaussee 5, DDR-1199 Berlin
Prof. Dr. H. Bock, Dr. B. Solouki, Dipl.-Chem. M. Kremer
Institut für Anorganische Chemie der Universität
Niederurseler Hang, D-6000 Frankfurt am Main 50 (FRG)

[**] Gas-Phase Reactions, Part 76. This work was supported by the Deutsche Forschungsgemeinschaft, the Fonds der Chemischen Industrie, and by the Land Hessen. Part 75: H. Bock, M. Bankmann, *Angew. Chem. 101* (1989) 950; *Angew. Chem. Int. Ed. Engl. 28* (1989) 911.

In contrast, pyridinium betaines which are readily accessible from pyridine and P_4O_{10} or P_4S_{10} and $Cl_3P{=}O$ or $Cl_3P{=}S$ provide an easy access to dioxophosphorus(v) chloride $ClP(=O)_2$ and the previously unknown $ClP(=S)_2$ (Scheme 2).



Scheme 2.

According to the PE spectra (Fig. 1), evaporation under a pressure of about 10 Pa already leads to the dissociation into the respective betaine components. The energies of the radical cation states of $ClP(=O)_2$ and $ClP(=S)_2$ can be "extracted" from the recorded ionization band patterns of the dissociation mixtures by digital subtraction of the computer-stored spectrum of pyridine (Fig. 1: hatched); they can then be assigned by Koopmans' correlation with MNDO eigenvalues, supported by characteristic band shapes and by comparison of the iso(valence)electronic molecules (Fig. 1).

The unexpectedly readily accessible "textbook" compounds, $ClP(=O)_2$ and $ClP(=S)_2$, not only extend the scope of preparative phosphorus chemistry but, at the same time, constitute a "missing link" in the discussion of planar tetraatomic molecules with 24 valence electrons. This will be discussed in greater detail for a series of such compounds based on their structures,[6] their π-radical cation states (see Fig. 1 and Ref. [7]), and their total- and π-charge densities calculated by the semiempirical MNDO method,[8] starting from the self-consistent Koopmans' assignment of the $ClPO_2^{\cdot\oplus}$ and $Cl_2PS_2^{\cdot\oplus}$ states (Fig. 2).

Obviously (Fig. 2), the structures of the planar 24 valence electron molecules Hal_3E, Hal_2EX, $HalEX_2$ and EX_3 are largely comparable; regarding the different EX bond lengths, reference is made to the various covalent radii, r_E and r_X.[6a] All of them possess six π electrons, so that in the case of D_{3h} symmetry the $M^{\cdot\oplus}$ states $1e'' < 1a_2''$ are to be expected, and on removal of the threefold axis in C_{2v} the sequence $1a_2 < 2b_1 < 1b_1$ (Fig. 2; exception $Cl_2C{=}S$ with $2b_1 < 1a_2$ (···) as a result of the readily ionizable π_{CS} group). A correlation according to dominant $M^{\cdot\oplus}$ contributions immediately demonstrates the influence of the effective nuclear charges: $\pi(1b_1)$ decreases from −14.7 to −18.1 eV (!) upon exchanging S → O and P → N; at the same time the $M^{\cdot\oplus}(1a_2)$ states, which might be used as "π-standard" because of their nodal plane through the bond Cl–E, unequivocally allow to read off $\alpha_S^\pi = 9.8$ eV or $\alpha_O^\pi \approx 12$ eV as respective parameters. Various interactions are superposed, which, for example, for the molecules $ClE(=X)_2$ can be discussed in terms of second order perturbations[9] $\beta^2_{Cl/PX2}/\Delta\alpha_{Cl/PX2}$ and are reflected in different $M^{\cdot\oplus}$ charge distributions: thus, the accompanying MNDO calculations for $ClP(=S)_2$ in its $\pi(2b_1)$ and $\pi(1b_1)$ states assign about 50% each Cl and PS_2 contributions, whereas for $ClP(=O)_2$ in $\pi(2b_1)$ 85% and—vice versa—in $\pi(1b_1)$ 88% PO_2 are obtained ($ClN(=O)_2$: $\pi(2b_1)$ 95% Cl and $\pi(1b_1)$ 94% NO_2). The charge distributions calculated by MNDO (Fig. 2) are also consistent with the π ionization patterns. In all cases except for the thio derivatives the positively charged center E is surrounded in a star-like fashion by negatively charged centers (Fig. 2; Q_μ^{MNDO}), whose "π back-bonds"—beginning with Cl_3B which in contrast to $(H_3B)_2$ is monomeric—lead to considerable π-electron densities (Fig. 2: $q_{\mu\pi}^{MNDO}$) at the centers E. Based on the general comparability of the tetraatomic molecules with 24 valence electrons, the following trend in polarization in accord with the effective nuclear charges and total electron densities becomes particularly evident:

$$\overleftarrow{B{-}Cl} > \overrightarrow{C{-}S} \quad \text{or} \quad \overrightarrow{P{-}S} < \overrightarrow{P{-}O} < \overrightarrow{N{-}O} \ll \overrightarrow{S{-}O}$$

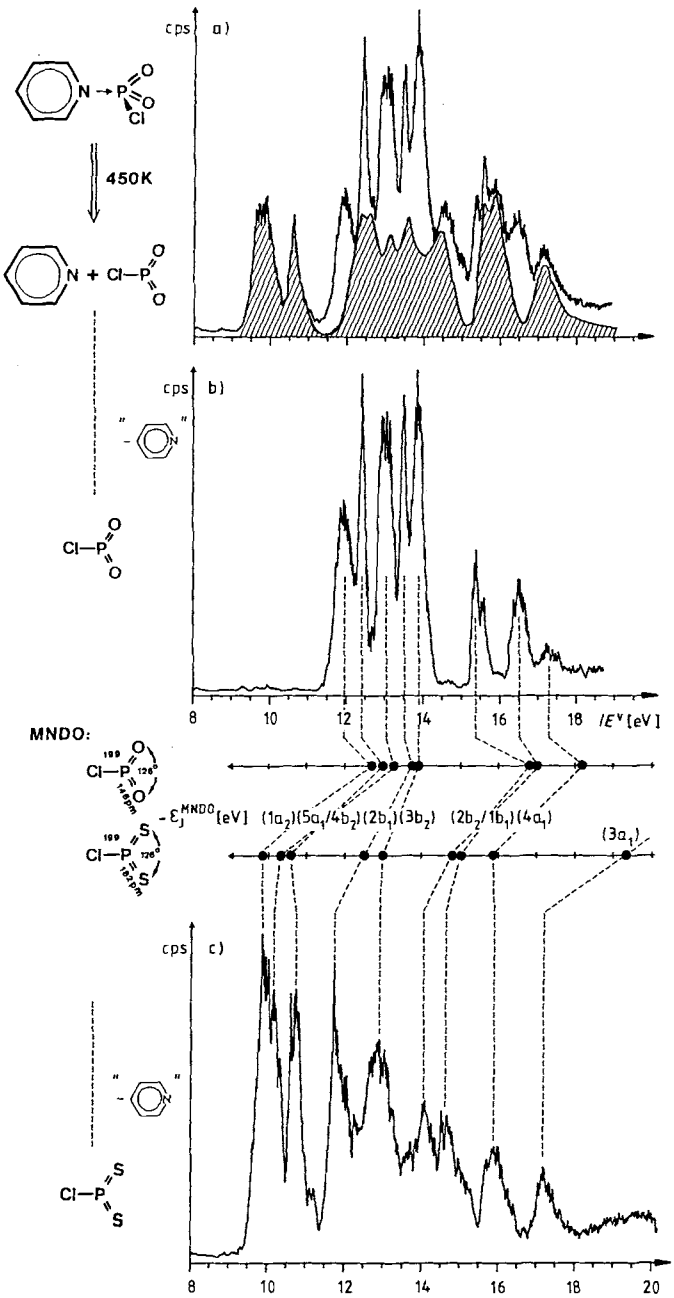


Fig. 1. He(I) PE spectra of the mixture formed upon dissociation of the betaines I at 450 K [5] in pyridine and $ClP(=O)_2$ (a) and of dioxophosphorus(v) chloride (b) and dithiophosphorus(v) chloride (c), extracted by digital subtraction of the computer-stored pyridine band pattern (hatched) [5] together with their Koopmans' assignment on the basis of MNDO eigenvalues.

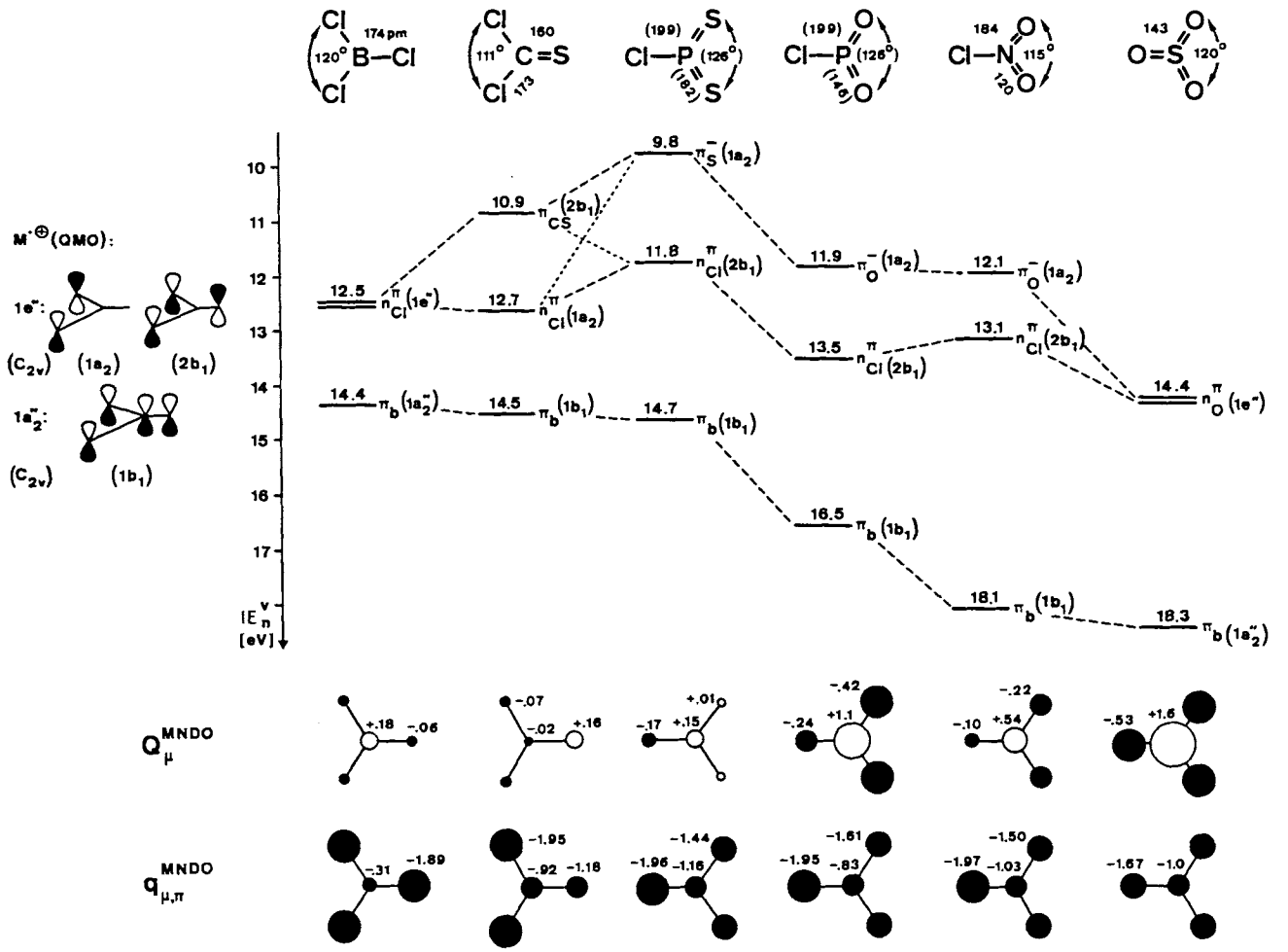
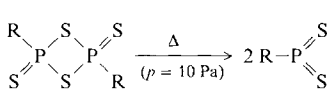


Fig. 2. Structures [6] of Cl_3B, $Cl_2C{=}S$, $ClP(=S)_2$, $ClP(=O)_2$, $ClN(=O)_2$ and SO_3, their vertical π-ionization energies [7] with $M^{+\bullet}$-state characterization by dominant contributions and (in brackets) the respective irreducible representations as well as total- and π-charge densities from geometry-optimized MNDO calculations [8] (cf. text).

Thus, the extreme π-back bonding in SO_3, for whose S center MNDO calculations yield the total charge +1.6 (!) (Fig. 2: Q_μ^{MNDO}) and which formally provides three of the six π electrons, partially replenishes the substantial electron deficit in the σ skeleton.

The preceding discussion of the PES data, supported by the calculated charge distributions, also enlightens various aspects regarding the still unknown reactivity of $ClP(=O)_2$ and $ClP(=S)_2$. For illustration, the suitability of $RP(=S)_2$ derivatives as novel complex ligands is pointed out, which can be expected because of the low first ionization energy (Fig. 1) and the electron distribution (Fig. 2). The reactive methyl and ethyl derivatives are easily synthesized by heating the preparatively accessible dimers in vacuum.[10]



R = CH_3, C_2H_5

With these molecules as well as $ClP(=S)_2$, the class of phosphorus(v) compounds $Y{-}P(=X)_2$ with three-coordinate phosphorus is further extended. The first prototype of this class, $(R_3Si)_2N{-}P(=NSiR_3)_2$,[11a] which is kinetically stabilized by steric encapsulation, has in the meantime been succeeded by numerous Y,X-substituted derivatives[11b] including the supermesityl compound $tBu_3C_6H_2P(=S)_2$[11c] and the trithiometaphosphate $[(H_5C_6)_4As]^{\oplus}[PS_3]^{\ominus}$.[11d]

Received: April 26, 1989 [Z 3306 IE]
German version: *Angew. Chem. 101* (1989) 1378

[1] A. D. Walsh, *J. Chem. Soc. 1953*, 2301; cf. R. J. Buenker, S. D. Peyerimhoff, *Chem. Rev. 74* (1974) 127; B. M. Gimarc, *J. Am. Chem. Soc. 100* (1978) 2346 and references cited therein.

[2] Cf. summary by K. Wittel, H. Bock: "*Photoelectron Spectra of (Organic) Halogen Compounds*" in S. Patai, Z. Rappoport (Eds.): *The Chemistry of Functional Groups, Supplement D*, Wiley, Chichester 1983, p. 1499–1603, and references cited therein. The PE spectrum of $F_2C{=}Se$ is given in H. Bock, S. Aygen, P. Rosmus, B. Solouki, E. Weissflog, *Chem. Ber. 117* (1984) 187.

[3] Cf. a) H. Schnöckel, *J. Mol. Struct. 65* (1980) 115; b) M. Binnewies, *Z. Anorg. Allg. Chem. 507* (1983) 77; $ClPO_2$ is formed only in small concentration [3c] together with e.g. Cl_3PO, ClPO or P_4O_{10}; c) R. Ahlrichs, C. Ehrhardt, M. Lakenbrink, S. Schunk, H. Schnöckel, *J. Am. Chem. Soc. 108* (1986) 3596: a stream of Ar containing ClPO, generated from Cl_3PO and Ag at 1300 K, was passed over solid O_3 at 84 K and the frozen-out Ar-matrix first photolyzed with hν = 310 nm and then with broad-band radiation; d) ClPO can be obtained PE spectroscopically pure by passage of $Cl_3P{=}O$ over Ag wool heated to 1100 K, cf. M. Binnewies, B. Solouki, H. Bock, R. Becherer, R. Ahlrichs, *Angew. Chem. 96* (1984) 704; *Angew. Chem. Int. Ed. Engl. 23* (1984) 731; not mentioned in Ref. [3c].

[4] Syntheses: a) $H_5C_5N \rightarrow PO_2Cl$ (G. U. Wolf, M. Meisel, *Z. Chem. 22* (1982) 54): a total of 73.3 g of P_4O_{10} was added portionwise to 200 mL of anhydrous pyridine and heated to reflux after each addition. The white powder recovered after filtration under N_2 was washed with CCl_4 and dried over P_4O_{10} in vacuo; yield 138 g (96%). A mixture of 20 g of this powder, 100 g Cl_3PO and 5 g of pyridine was heated under reflux for 3 h. The needle-like crystals recovered upon cooling the mixture were filtered

off, washed with ether, and dried in vacuo; yield 27 g. b) $H_5C_5N \rightarrow PS_2Cl$ (M. Meisel, H. Grunze, *Z. Anorg. Allg. Chem. 360* (1968) 277): a solution of 13.7 g of P_4S_{10} in 180 mL of anhydrous pyridine was heated under reflux for 2 h; subsequent cooling of the solution furnished 124 g (53%) of pale yellow crystals, 3.81 g of which were added, together with 5.1 g Cl_3PS, to 10 mL of pyridine, and the mixture heated to boiling for 30 min; after cooling and filtration, 3.8 g (63%) of crystals (m.p. 115–120°C) were recovered. Cf. also E. Fluck, H. Binder, *ibid. 354* (1967) 113.

[5] PE spectrometer Leybold-Heraeus UPG 200 equipped with short-path pyrolysis-electron impact furnace connected via an Apple IIe computer to a VAX11/750. Cf. also the review by H. Bock, B. Solouki, S. Aygen, M. Bankmann, O. Breuer, R. Dammel, J. Dörr, M. Haun, T. Hirabayashi, D. Jaculi, J. Mintzer, S. Mohmand, H. Müller, P. Rosmus, B. Roth, J. Wittman, H.-P. Wolf, *J. Mol. Struct. 173* (1988) 31–49, and references cited therein.

[6] Structures a) BCl_3 and SO_3: cf. A. F. Wells: *Structural Inorganic Chemistry*, 4th edit., Clarendon Press, Oxford 1975; b) $Cl_2C=S$: N. Nakata, T. Fukyama, K. Kuchitsu, *J. Mol. Struct. 81* (1982) 121; c) $ClP(=O)_2$ and $ClP(=S)_2$: geometry optimized MNDO calculations, which, e.g., give $d_{CCl} = 173$ pm, $d_{CS} = 166$ pm and $\sphericalangle ClCCl = 111°$ for $Cl_2C=S$; d) $ClNO_2$: T. Tanaka, J. Morino, *ibid. 32* (1969) 430, and references cited therein.

[7] Vertical π-ionization energies a) BCl_3: [2] and references cited therein; b) $Cl_2C=S$: K. Wittel, A. Haas, H. Bock, *Chem. Ber. 105* (1972) 3685 with the alternative assignment $(1b_1) < (4a_1)$ quoted therein; c) $ClP(=X)_2$: Fig. 1; d) $ClN(=O)_2$: D. C. Frost, S. T. Lee, C. A. McDowell, N. P. C. Westwood, *J. Electron Spectrosc. Relat. Phenom. 7* (1975) 331 with an alternative CNDO assignment quoted therein, which is confirmed by geometry-optimized MNDO calculations; e) SO_3: R. L. DeKock, D. R. Lloyd, *J. Chem. Soc. Dalton Trans. 1973*, 526.

[8] M. J. S. Dewar, W. Thiel, *J. Am. Chem. Soc. 89* (1977) 4899, 4970. For increased clarity, the total charge densities in Figure 2 are represented by circles with radius $r_\mu = (Q_\mu^{MNDO})^{1/2}$ and the π-charge densities with $r_\mu = (q_{\mu,\pi}^{MNDO})^{1/2}$.

[9] Cf. e.g. E. Heilbronner, H. Bock: *Das HMO-Modell und seine Anwendung, Bd. 1*, 2nd edit. Verlag Chemie, Weinheim 1978, p. 168f, or H. Stafast, H. Bock, *Z. Naturforsch. B28* (1973) 746.

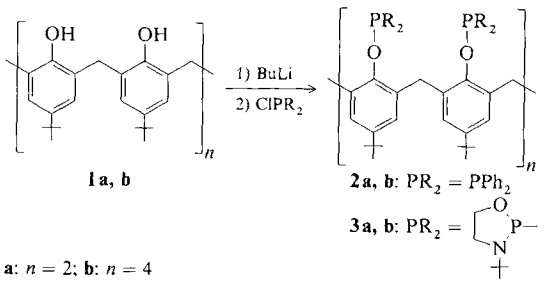
[10] M. Binnewies, H. Bock, B. Solouki, M. Kremer, *Phosphorus Sulfur*, in press.

[11] a) E. Niecke, W. Flick, *Angew. Chem. 86* (1974) 128; *Angew. Chem. Int. Ed. Engl. 13* (1974) 134; S. Pohl, E. Niecke, B. Krebs, *ibid. 87* (1975) 284 and *14* (1975) 261; O. J. Scherer, N. Kuhn, *Chem. Ber. 107* (1974) 2123; b) cf. the summaries by J. I. Cadogan, P. K. G. Hodgson, *Phosphorus Sulfur 30* (1987) 3; F. H. Westheimer, *Chem. Rev. 81* (1981) 313; c) R. Appel, F. Knoch, H. Kunze, *Angew. Chem. 95* (1983) 1008; *Angew. Chem. Int. Ed. Engl. 22* (1983) 1004; J. Navech, J. P. Majoral, R. Kraemer, *Tetrahedron Lett. 24* (1983) 5885; M. Yoshifuji, K. Toyota, K. Ando, N. Inamato, *Chem. Lett. 1984*, 317; d) H. W. Roesky, R. Ahlrichs, S. Brode, *Angew. Chem. 98* (1986) 91; *Angew. Chem. Int. Ed. Engl. 25* (1986) 82.

Aggregation of Metal Ions with Functionalized Calixarenes: Synthesis and Structure of an Octanuclear Copper(I) Chloride Complex**

By *Carlo Floriani,* Denis Jacoby, Angiola Chiesi-Villa,* and *Carlo Guastini*

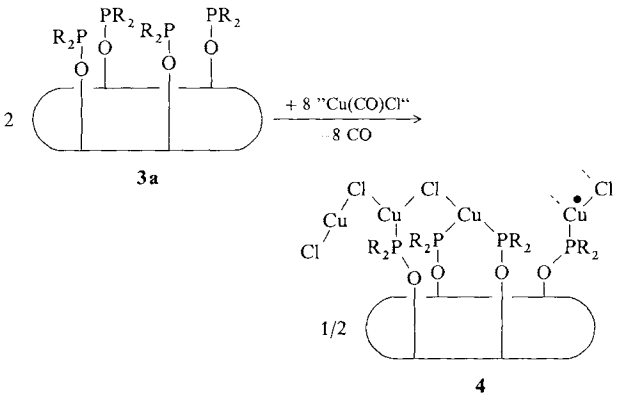
A number of peculiarities, such as the simultaneous presence of a hydrophobic and a hydrophilic site, a receptor cavity, and the possible functionalization of donor atoms, make calixarenes[1] a very attractive class of molecules for binding metal ions[2] in the form of aggregates. In such metal derivatives both the cavity and the metal ions may act synergetically for the fixation and activation of certain substrates. Accordingly, we converted *p-tert*-butyl-calix[4]arene **1a**[3] and *p-tert*-butyl-calix[8]arene **1b**[3] using the 3-*tert*-butyl-2-chloro-1,3,2-oxazaphospholidine and the chlorodiphenylphosphane, into the corresponding multidentate phosphorus ligands[4] **2a,b** and **3a,b**, respectively. (Scheme 1).



Scheme 1.

Compounds **2a,b** and **3a,b** can be isolated in pure, crystalline form in very good yields (see Experimental Procedure). Crystals suitable for X-ray analysis are often difficult to obtain due to the tendency of the crystals to decompose by loss of solvent molecules. A further significant problem existing in calixarene chemistry is the possibility of various conformations. However, a "frozen" conformation can be obtained by adding bulky groups to the oxygen atoms.[1] In this work, cone conformation for calixarenes is supported by both NMR spectroscopy and X-ray structural analysis for **2a** and **4**, a metal derivative of **3a**.

We used $[Cu(CO)Cl]_n$[5] as a source of copper(I) which has a high affinity for phosphorus-containing ligands. The reaction of **3a** with $[Cu(CO)Cl]_n$ gave a polymetal species containing one copper ion per phosphorus atom. Only half of the symmetric dimer is shown in Scheme 2.



Scheme 2. The dot marks the center of symmetry.

This result was proven by analytical data (see Experimental Procedure) and is exemplified by the structure of **4**[6] (Fig. 1). Complex **4** is a centrosymmetric molecule, in which the eight phosphorus donor atoms derived from two *p-tert*-butyl-calix[4]arenes define a binding surface for six copper atoms. The mode of aggregation of such a polymetallic unit depends on a) the coordination requirements of the metal, b) the proximity of the phosphorus within the calixarene geometry, and c) the binding mode of the chloride ligand. The four copper atoms of the half-molecule are arranged in an irregular metal chain determined by the factors cited above. Since the reaction was carried out with a specific

[*] Prof. Dr. C. Floriani, Dr. D. Jacoby,
Section de Chimie, Université de Lausanne
Place du Château 3, CH-1005 Lausanne (Switzerland)
Prof. Dr. A. Chiesi-Villa, Dr. C. Guastini
Istituto di Strutturistica Chimica
Centro di Studio per la Strutturistica Diffrattometrica del CNR
Università di Parma
I-43100 Parma (Italy)

[**] This work was supported by the Fonds National Suisse de la Recherche Scientifique (S.N.F. 2000-005536).

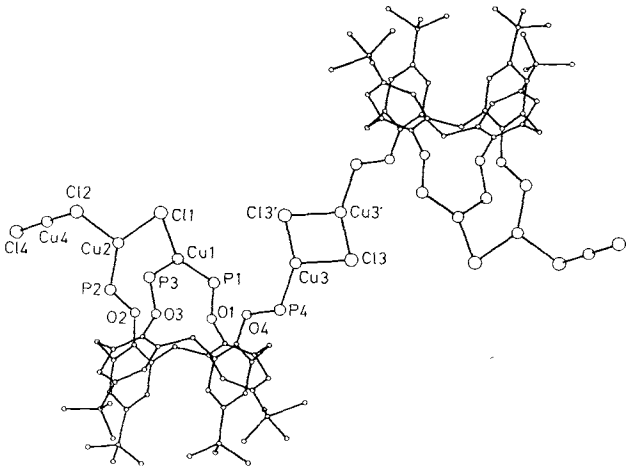


Fig. 1. Structure of complex **4** in the crystal. The oxazaphospholidine rings and the related structural parameters have been omitted for clarity. Bond lengths [Å] and angles [°]: Cu1-Cl1 2.251(5), Cu1-P1 2.210(4), Cu1-P3 2.233(6), Cu2-Cl1 2.275(5), Cu2-Cl2 2.295(5), Cu2-P2 2.167(5), Cu3-Cl3 2.217(6), Cu3-Cl3' 2.253(6), Cu3-P4 2.137(6), Cu4-Cl2 2.120(8), Cu4-Cl4 2.077(8), P1-O1 1.621(11), P2-O2 1.638(10), P3-O3 1.605(10), P4-O4 1.671(10); P1-Cu1-P3 129.5(2), Cl1-Cu1-P3 114.7(2), Cl1-Cu1-P1 114.6(2), Cl2-Cu2-P2 120.0(2), Cl1-Cu2-P2 136.7(2), Cl1-Cu2-Cl2 103.2(2), Cl3-Cu3-P4 148.0(3), Cl3'-Cu3-P4 111.2(2), Cl3-Cu3-Cl3' 99.3(2), Cl2-Cu4-Cl4 178.8(3). Prime indicates a transformation of x, $-y$, $1-z$.

stoichiometry and in the absence of any other good ligand for copper(I), the metal centers maintain low coordination numbers. The main structural features of complex **4** can be summarized as follows: 1) the conformation of half a molecule corresponds to the cone conformation of calix[4]arenes, the oxygen atoms almost forming a plane on one side of the molecule. They are arranged to form an irregular ellipse having the principal axes O1···O3 and O2···O4 equal to 3.536(13) and 5.994(12) Å, respectively, the other O···O distances ranging from 3.255(11) to 3.897(11) Å; 2) the P1, P2, P3 atoms are at the vertices of an approximate isosceles triangle (nearly parallel to the O1, O2, O3, O4 plane) with the two shorter edges P1···P3 [4.019(6) Å] and P2···P3 [4.115(7) Å] respectively chelating and bridging the Cu1 and Cu2 copper atoms. P1···P2 equals 4.457(6) Å, while the P···P distances involving P4 (displaced by 1.864(6) Å from the P1, P2, P3 plane) range from 5.504(7) to 8.995(6) Å; 3) the aggregation mode appears to be the result of a compromise between the flexibility of the ligand and the coordination needs of copper. The bridging capability of chlorine is relevant not only in causing dimerization but also in satisfying the coordination geometry of adjacent copper atoms which show a great adaptability, adopting digonal (Cu4), and trigonal (Cu1, Cu2, Cu3) coordination, and binding chlorine atoms at very different distances (see Fig. 1); 4) the Cu···Cu separations being the result of geometric constraints imposed by the ligand, varying from 2.930(3) [Cu1···Cu2] and 2.960(4) [Cu3···Cu3'] to 3.342(4) Å [Cu2···Cu4].

Experimental Procedure

2a, b and **3a, b**: The detailed procedure is given for **2a**, all the other compounds being synthesized by the same method. Yields are between 70 and 85% based on recrystallized products. Analytical and spectroscopic data agree with the proposed formulas. Spectroscopic and analytical measurements were carried out on crystals rigorously dried in vacuo. A hexane solution (77.5 mL) of *n*BuLi (1.6 M, 0.125 mol) was added at room temperature to a THF suspension (300 mL) of **1a** (20.0 g, 0.031 mol). An orange solution, containing some insoluble white solid formed, and then $ClPPh_2$ (22.8 mL, 0.125 mol) was added, keeping the suspension at 0 °C. The resulting light-brown solution was heated at 60 °C for 2 h. The solvent was evaporated and the residue dissolved in toluene (300 mL). LiCl was removed by filtration, and 75% of the toluene was evaporated. The slow addition of CH_3CN gave a light-yellow crystalline solid (31.0 g, 72%) which could be recrystallized from a toluene–acetonitrile mixture as white crystals and dried in vacuo (m.p. 225–227 °C). ^1H NMR (200 MHz, CD_2Cl_2): $\delta = 1.03$ (s, 9H, *t*Bu), 2.14 (d, 1H, $J_{HH} = 13.3$ Hz, CH_2), 4.00 (d, 1H, $J_{HH} = 13.3$ Hz, CH_2), 6.58 (s, 2H, C_6H_2), 7.07–7.44 (m, 10H, C_6H_5).

4: A THF suspension (300 mL) of CuCl (0.74 g, 7.70 mmol) reacted with carbon monoxide gave a suspension of the white microcrystalline "CuCOCl".[5] The ligand **3a** (2.28 g, 1.86 mmol) was then added as a solid at room temperature and rapid evolution of carbon monoxide was observed. The suspension was heated for 1 h at 50 °C, and a little insoluble solid was removed by filtration. The solvent was evaporated to a third of its original volume, causing a microcrystalline white solid to form (2.60 g, 86%). Crystals suitable for X-ray analysis were obtained from the mother liquor. The two solids are identical. Analysis was performed on crystals whose solvent of crystallization had been removed in vacuo. The amount of solvent determined by G.C. and ^1H NMR was ca. 2.5 THF molecules per calix[4]arene unit. Solvent molecules are only weakly bound. ^1H NMR (200 MHz, CD_2Cl_2): $\delta = 0.57$–1.81 (series of singlets, 18H, *t*Bu), 3.12–4.10 (series of multiplets, 6H, CH_2), 6.64–7.17 (m, 2H, C_6H_2). This ^1H NMR spectrum can be compared with that of the free ligand. $\delta = 0.966$–1.303 (singlets, 18H, *t*Bu), 2.97–5.31 (multiplets, 6H, CH_2), 6.64–6.94 (multiplets, 2H, C_6H_2).

Received: June 21, 1989;
supplemented: July 20, 1989 [Z 3406 IE]
German version: *Angew. Chem. 101* (1989) 1430

[1] C. D. Gutsche *Prog. Macrocyclic Chem.* **3** (1987) 93.

[2] For complexes having a metal bonded to the calixarene oxygen centers, see: a) B. M. Furphy, J. M. Harrowfield, D. L. Kepert, B. W. Skelton, A. H. White, F. R. Wilner, *Inorg. Chem. 26* (1987) 4231; b) S. G. Bott, A. W. Coleman, J. L. Atwood, *J. Chem. Soc. Chem. Commun. 1986*, 610; c) M. M. Olmstead, G. Sigel, H. Hope, X. Xu, P. P. Power, *J. Am. Chem. Soc. 107* (1985) 8087; d) G. E. Hofmeister, F. E. Hahn, S. F. Pedersen, *ibid. 111* (1989) 2318; e) G. D. Andreetti, G. Calestani, F. Ugozzoli, A. Arduini, E. Ghidini, R. Ungaro, *J. Inclusion Phenom. 5* (1987) 123.

[3] C. D. Gutsche, B. Dhawan, K. Hyun No, R. Muthukrishnan, *J. Am. Chem. Soc. 103* (1981) 3782.

[4] B. L. Tumanskii, T. E. Kron, S. P. Solodovnikov, N. N. Bubnov, M. I. Kabashnik, *Izv. Akad. Nauk SSSR Ser. Khim. 1982*, 2692; S. D. Pastor, J. L. Hyun, P. A. Odorisio, R. K. Rodebaugh, *J. Am. Chem. Soc. 110* (1988) 6547.

[5] M. Pasquali, C. Floriani, A. Gaetani-Manfredotti, *Inorg. Chem. 20* (1981) 3382.

[6] Structure of **4**: $C_{136}H_{208}Cl_8Cu_8N_8O_{16}P_8 \cdot 5C_4H_8O$, $M_r = 3611.5$, triclinic, space group $P\bar{1}$, $a = 18.175(2)$, $b = 22.033(2)$, $c = 15.523(1)$ Å, $\alpha = 106.19(1)$, $\beta = 112.29(1)$, $\gamma = 89.66(1)°$, $V = 5488.62(10)$ Å^3, $Z = 1$, $\varrho_{calcd} = 1.093$ g cm^{-3}, $\lambda(Cu_{K\alpha}) = 1.54178$ Å, $\mu(Cu_{K\alpha}) = 26.87$ cm^{-1}; crystal dimensions $0.30 \times 0.46 \times 0.55$ mm^3. The structure was solved by the heavy atom method (Patterson and Fourier synthesis) and refined by full-matrix least-squares. For 6285 unique observed structure amplitudes [$I > 2\sigma(I)$, corrected for absorption] collected at room temperature on a Siemens AED diffractometer in the range $6 < 2\theta < 120°$, the R value is 0.089. Five independent residues in regions far from the complex molecule, corresponding to five "partial" THF molecules were found from successive difference Fourier syntheses and isotropically refined trying different site occupation factors. The best fit was found for s.o.f's corresponding to a dimer/THF molar ratio of 1/5. The hydrogen atoms were ignored. Rigid body constraints were applied to the benzene rings and THF molecules. All calculations were carried out using SHELX 76. Further details of the crystal structure investigation are available from the Director of the Cambridge Crystallographic Data Centre, University Chemical Laboratory, Lensfield Road, Cambridge CB2 1EW (England) on quoting the full journal citation.

$[Ir_2(\mu\text{-}CH_2)(CO)_4(Me_2PCH_2PMe_2)_2][CF_3SO_3]_2$, an Unprecedented Electrophilic Methylene Complex; $H^{\ominus}$ Addition to Prepare a Bridging Methyl Complex **

By *Mark K. Reinking, Phillip E. Fanwick,* and *Clifford P. Kubiak**

The first stable CH_2-bridged transition metal complex was prepared by *Herrmann* et al. in 1975.[1] Since then, numerous μ-alkylidene complexes have been reported.[2] "Herrmann

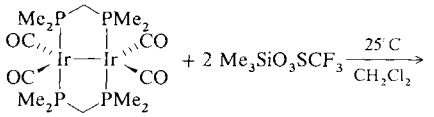
[*] Prof. C. P. Kubiak [†], M. K. Reinking, P. E. Fanwick
Department of Chemistry, Purdue University
West Lafayette, IN 47907 (USA)

[†] Research Fellow of the Alfred P. Sloan Foundation, 1987–1989.

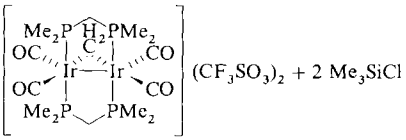
[**] This work was supported by the NSF (CHE-8707963). NSF support of the X-ray Diffraction Facility at Purdue and a generous loan of $IrCl_3$ from Johnson-Matthey Inc. is gratefully acknowledged.

carbenes" have been regarded to be similar to "Schrock carbenes", displaying significant reactivity toward electrophiles.[2] We describe here the preparation and chemistry of the di-iridium methylene complex $[Ir_2(\mu\text{-}CH_2)(CO)_4(dmpm)_2][CF_3SO_3]_2$ **1** (dmpm = bis(dimethylphosphino)methane) which does *not* react with electrophiles. The μ-CH_2 group of **1** however readily adds nucleophiles, e.g. $H^{\ominus}$, to yield the μ-methyl complex $[Ir_2(\mu\text{-}CH_3)(CO)_2(dmpm)_2][CF_3SO_3]$ **2**.

Addition of $CF_3SO_3SiMe_3$ (2 equiv.) to the iridium complex $[Ir_2(CO)_4(dmpm)_2]$[3] in CH_2Cl_2 affords **1** in 70% yield [Eq. (a)]. A quintet in the ^1H NMR spectrum at $\delta = 5.05$



(a)



1

($J_{PH} = 8.5$ Hz) is assigned to the μ-CH_2 protons. Two dmpm methylene multiplets ($\delta = 3.25, 2.99$) and two methyl signals ($\delta = 2.12, 2.10$) are indicative of a *trans,trans* dmpm bridged structure.[4] The structure of **1** was confirmed by X-ray crystallography (Fig. 1).[5a, c] The μ-CH_2 group symmetrically bridges the two Ir atoms and exhibits metrical parameters (Ir1-CB 2.11(1) Å, Ir2-CB 2.10(1) Å; Ir1-CB-Ir2 81.5(5)°) essentially identical to those of the only other structurally characterized $Ir_2(\mu\text{-}CH_2)$ complex.[6]

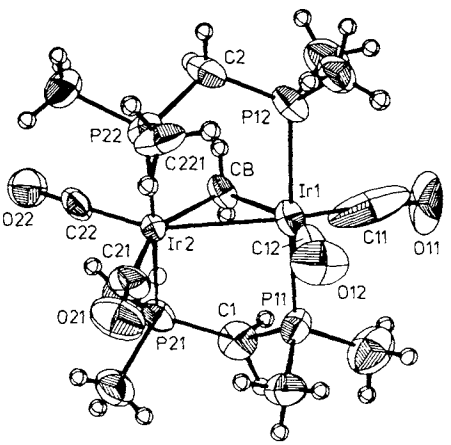
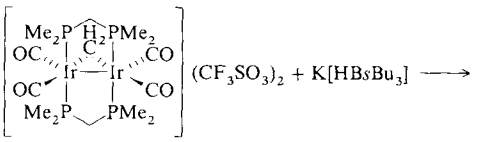


Fig. 1. Structure of $[Ir_2(\mu\text{-}CH_2)(CO)_4(dmpm)_2]^{2\oplus}$ in the crystal (ORTEP). Selected distances [Å] and angles [°]: Ir1-Ir2 2.7534(9), Ir1-CB 2.11(1), Ir2-CB 2.10(1), Ir-P(ave) 2.360(5); Ir1-CB-Ir2 81.5(5), Ir1-Ir2-CB 49.4(4), Ir2-Ir1-CB 49.1(4), P11-Ir1-P12 174.2(2), P21-Ir2-P22 175.3(1), CB-Ir1-C11 106.9(8), CB-Ir1-C12 149.2(7), CB-Ir2-C21 151.5(7), CB-Ir2-C22 100.4(7).

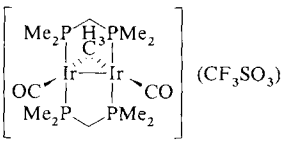
Bridging methylene ligands are generally considered to possess significant formal negative charge.[2, 7] Indeed, most Herrmann carbene complexes react readily with electrophiles.[1, 2] Remarkably, complex **1** is *completely unreactive* toward aqueous 1 M CF_3SO_3H. Similarly, reaction of **1** with Br_2 and I_2 does not result in formation of dihalomethanes.

However, the μ-CH_2 group of complex **1** is reactive toward nucleophiles. Addition of tri-*sec*-butyl borohydride (K-selectride, 1 equiv.) to a THF solution of **1** produces the methyl complex **2** [Eq. (b)].



1

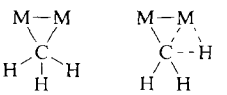
(b)



2

The IR spectrum of **2** exhibits two $\tilde{\nu}$(CO) bands at 1948(s) and 1915(s) cm^{-1} and a single dmpm $\tilde{\nu}$(P-C) band.[8] **2** has further been characterized by ^1H, 2D-NOESY ^1H, and $^{31}P\{^1H\}$ NMR studies, as well as by X-ray crystallography.[5b, c] The ^1H NMR spectrum of **2** shows a quintet at $\delta = 3.34$ ($J_{PH} = 4.7$ Hz), a multiplet at $\delta = 2.84$ and a singlet at $\delta = 1.85$. The quintet is assigned to the μ-CH_3 fragment.

Shapley et al. have employed equilibrium isotope effects to distinguish between symmetrical (**I**) and "agostic" (**II**) C···H···M interactions.[9]



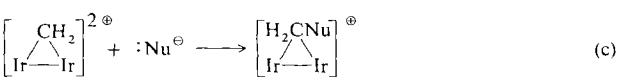
I **II**

The partially deuterated complex $[Ir_2(\mu\text{-}CD_2H)(CO)_2(dmpm)_2][CF_3SO_3]$ $[D_2]$-**2** was prepared from $[D_2]$-**1** and K[HB*s*Bu$_3$]. The ^1H NMR spectrum of complex $[D_2]$-**2** at 25 °C however did not show a discernible difference in the μ-CHD_2 chemical shift compared to **2**. These data suggest that the μ-CH_3 group of **2** symmetrically bridges the metal centers in solution and that there are no significant C···H···Ir interactions at 25 °C (see [10]).

The structure of **2** is that of a symmetrically methyl-bridged "A-frame" complex (Fig. 2). A noteworthy feature of the structure is the overall "boat" conformation of the $Ir_2(PCH_2P)_2$ ring and close μ-$CH_3 \cdots CH_2(PMe_2)_2$ interactions (C31···C2, 3.24(4) Å, C31···C1, 3.11(4) Å). We have investigated the possibility of a μ-$CH_3 \leftrightarrow CH_2(PMe_2)_2$ exchange by 2D-NOESY ^1H NMR spectroscopy and find that if exchange does occur, the exchange rate constant, k_{ex}, is $< 1\ s^{-1}$. The extreme thermal sensitivity of **2** in various solvents at temperatures above −78 °C has so far frustrated our attempts to study the chemistry of **2** in more detail.

Complex **1** adds other nucleophiles to the μ-CH_2 group. For example, addition of NaOPh to a solution of **1** produces the cation $[Ir_2(CH_2OPh)(CO)_4(dmpm)_2]^{\oplus}$.[11]

The unprecedented reactivity of **1** toward nucleophiles is most likely due to a combination of factors which have not



(c)

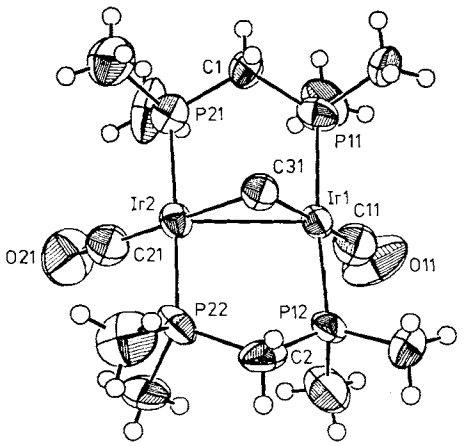


Fig. 2. Structure of $[Ir_2(\mu\text{-}CH_3)(CO)_2dmpm)_2]^{\oplus}$ in the crystal (ORTEP). Selected distances [Å] and angles [°]: Ir1-Ir2 2.885(1), Ir1-C31 2.19(2), Ir2-C31 2.17(2), Ir-P(ave) 2.328(8), Ir-C(ave) 1.95(4); Ir1-C31-Ir2 82.8(8), Ir2-Ir1-C31 48.3(6), Ir1-Ir2-C31 48.8(6), P11-Ir1-P12 171.0(3), P21-Ir2-P22 171.7(3), C11-Ir1-C31 173(1), C21-Ir2-C31 178(1).

been encountered previously. The dicationic nature of the complex effectively limits the metal electron density available for donation to the vacant p-orbital of the methylene fragment.[12] The presence of four carbonyl ligands diminishes the electron density on the μ-CH_2 group further.

Experimental Procedure

1 was prepared from $[Ir_2(CO)_4(dmpm)_2]$ (0.14 g, 0.18 mmol) in CH_2Cl_2 by reaction with 2 equivalents of $CF_3SO_3SiMe_3$ (0.073 mL) for 12 h. Yield: 0.14 g (70%). Me_3SiCl was identified as the only coproduct. $CF_3SO_3SiMe_3$ alone does not react with CH_2Cl_2.[13] ^1H NMR (CD_3CN): $\delta = 5.05$ (quint., 2H), 3.25 (m, 2H), 2.99 (m, 2H), 2.12 (s, 12H), 2.10 (s, 12H). $^{31}P\{^1H\}$ NMR (CD_3CN): $\delta = -45.8$(s), IR (KBr): $\tilde{\nu}$[cm^{-1}] = 2071 (s, CO), 2033 (s, CO), 945 (s, PC). The corresponding μ-CD_2 complex was prepared from CD_2Cl_2 in place of CH_2Cl_2. ^1H NMR (CD_3CN): $\delta = 3.16$ (m, 4H), 2.08 (s, 24H). $^{31}P\{^1H\}$ NMR (CD_3CN): $\delta = -45.8$(s). IR (KBr): $\tilde{\nu}$[cm^{-1}] = 2065 (s, CO), 2033 (s, CO).

2 was prepared by addition of K-Selectride (0.07 mL of 1.0 M of tri-*sec*-butylborohydride in THF) to **1** (0.072 g, 0.066 mmol) in THF at -78 °C. The solution was immediately placed under vacuum and after 0.5 h the solution was allowed to slowly warm to room temperature under vacuum. Pure **2** was carefully removed and recrystallized from THF/hexane. Yields of this reaction were not consistent and varied from 0 to 80%. Numerous other attempts to synthesize **2** were made. The use of other $H^{\ominus}$ sources (catecholborane, sodium trimethoxyborohydride), different reaction and recrystallization solvents (C_6F_6, C_6H_6, CH_3CN, Et_2O), and higher reaction temperatures were not successful. ^1H NMR (CD_3CN): $\delta = 3.34$ (quint., 3H), 2.84 (m, 4H), 1.85 (s, 24H). $^{31}P\{^1H\}$ NMR (CD_3CN): $\delta = -37.2$(s). IR (KBr): $\tilde{\nu}$[cm^{-1}] = 1948 (s, CO), 1915 (sh, CO), 945 (s, PC).

Received: April 21, 1989 [Z 3303 IE]
German version: *Angew. Chem. 101* (1989) 1431.

CAS Registry numbers:
1, 122647-93-2; **1**·CH_3CN, 122647-99-8; **2**, 122647-95-4; **3**, 121920-65-8; $[Ir_2(CH_2)(CO)_4(dmpm)_2][BPh_4]_2$, 122647-96-5; $[Ir_2(CH_2OPh)(CO)_4(dmpm)_2][BPh_4]$, 122647-98-7; $Me_3SiO_3SCF_3$, 27607-77-8; NaOPh, 139-02-6.

[1] W. A. Herrmann, B. Reiter, H. Biersack, *J. Organomet. Chem. 97* (1975) 245.

[2] a) W. A. Herrmann, *Adv. Organomet. Chem. 20* (1982) 159; b) J. E. Hahn, *Prog. Inorg. Chem. 31* (1984) 205; c) A. L. Balch, C. T. Hunt, C.-L. Lee, M. M. Olmstead, J. P. Farr, *J. Am. Chem. Soc. 103* (1981) 3764; d) M. P. Brown, J. R. Fisher, R. J. Puddephatt, K. R. Seddon, *Inorg. Chem. 18* (1979) 2808; e) H. H. Murray, J. P. Fackler, A. M. Mazany, *Organometallics 3* (1984) 1310.

[3] M. K. Reinking, J. Ni, P. E. Fanwick, C. P. Kubiak, *J. Am. Chem. Soc. 111* (1989) 6459.

[4] M. L. Kullberg, C. P. Kubiak, *Inorg. Chem. 25* (1986) 26.

[5] a) Crystal data for **1**: $Ir_2S_2P_4F_6O_{10}NC_{10}H_{33}$, $M_r = 1121.9$, orthorhombic, space group $P2_12_12_1$, $a = 23.744(5)$, $b = 11.812(3)$, $c = 12.682(3)$ Å, $V = 3557(2)$ Å^3, $Z = 4$, $\varrho_{calc} = 2.095$ g cm^{-3}. Crystal dimensions: $0.66 \times 0.30 \times 0.17$ mm^3. The structure was solved by MULTAN-least-squares-Fourier methods and was refined to R and R_w values of 0.036 and 0.047, respectively, for 397 variables and 3074 observations with $I > 3.0\,\sigma(I)$ with $Mo_{K\alpha}$ radiation. Data were corrected for absorption empirically, $\mu = 78.12$ cm^{-1}. b) Crystal data for **2**: $Ir_2SP_4F_3O_5C_{14}H_{31}$, $M_r = 876.8$, monoclinic, space group $P2_1/n$ with $a = 14.726(3)$, $b = 9.254(2)$, $c = 20.145(5)$ Å, $\beta = 91.25(2)$ Å, $V = 2745(2)$ Å^3, $Z = 4$, $\varrho_{calc} = 2.122$ g cm^{-3}. Crystal dimensions: $0.56 \times 0.22 \times 0.17$ mm^3. The structure was solved by MULTAN-least-squares-Fourier methods and is refined to R and R_w values of 0.050 and 0.058, respectively, for 247 variables and 1718 observations with $I > 3.0\,\sigma(I)$ with $Mo_{K\alpha}$ radiation. Data were corrected for absorption empirically, $\mu = 99.95$ cm^{-1}. c) Further details of the two crystal structure investigations can be obtained from the Fachinformationszentrum Karlsruhe, Gesellschaft für wissenschaftlich-technische Information mbH, D-7514 Eggenstein-Leopoldshafen 2 (FRG), by quoting the depository number CSD-53963, the names of the authors and the journal citation.

[6] M. El Amane, A. Maisonnat, F. Dahan, R. Pince, R. Poilblanc, *Organometallics 4* (1985) 773.

[7] D. C. Calabro, D. L. Lichtenberger, W. A. Herrmann, *J. Am. Chem. Soc. 103* (1981) 6852; D. A. Clemente, B. Rees, G. Bandoli, M. Cingi Biagini, B. Reiter, W. A. Herrmann, *Angew. Chem. 93* (1981) 920; *Angew. Chem. Int. Ed. Engl. 20* (1981) 887.

[8] J. Wu, P. E. Fanwick, C. P. Kubiak, *J. Am. Chem. Soc. 110* (1988) 1319; *ibid 111* (1989), in press.

[9] R. B. Calvert, J. R. Shapley, *J. Am. Chem. Soc. 100* (1978) 7726.

[10] G. M. Dawkins, M. Green, A. G. Orpen, F. G. A. Stone, *J. Chem. Soc. Chem. Commun. 1982*, 41; G. F. Schmidt, E. . Muetterties, M. A. Beno, J. M. Williams, *Proc. Natl. Acad. Sci. USA 78* (1981) 1318.

[11] $[Ir_2(CH_2OPh)(CO)_4(dmpm)_2][BPh_4]$ was prepared from 0.045 g of $[Ir_2(\mu\text{-}CH_2)(CO)_4(dmpm)_2][BPh_4]_2$ and 0.0081 g NaOPh in 2 mL of CH_3CN. Solids were obtained by slow diffusion of toluene into the CH_3CN. ^1H NMR (CD_2Cl_2): $\delta = 7.00$ (m, 25H), 2.74 (m, 4H), 1.80 (s, 12H), 1.69 (s, 12H), 0.52 (m, 2H). $^{31}P\{^1H\}$ NMR (CD_3CN): $\delta = -39.4$(s), IR (KBr): $\tilde{\nu}$[cm^{-1}] = 2009 (m, CO), 1961 (sh, CO), 1943 (s, CO), 1914 (m, CO), 941 (s, PC).

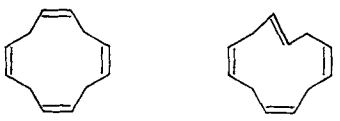
[12] M. A. Gallop, W. R. Roper, *Adv. Organomet. Chem. 25* (1986) 121.

[13] G. A. Olah, A. Husain, B. C. Balaram Gupta, G. F. Salem, S. C. Narang, *J. Org. Chem. 46* (1981) 5212.

all-*cis*-1,4,7,10-Cyclododecatetraene—X-Ray Structure Analysis and Photoelectron Spectrum**

By *Alfred Krause,* Hans Musso* †, *Wilhelm Boland, Reinhart Ahlrichs,* Rolf Gleiter,* Roland Boese,** and *Michael Bär*

The title compound **1** was recently isolated for the first time as a colorless liquid which solidifies on collection in a cooling trap;[1] it is formed together with the main product **2** in the intramolecular cyclization of all-*cis*-dodeca-3,6,9-



1 **2**

[*] Dipl.-Chem. A. Krause, Prof. Dr. H. Musso †, Prof. Dr. W. Boland
Institut für Organische Chemie der Universität
Richard-Willstätter-Allee, D-7500 Karlsruhe (FRG)
Prof. Dr. R. Ahlrichs, Dipl.-Chem. M. Bär
Institut für Physikalische Chemie der Universität
Richard-Willstätter-Allee, D-7500 Karlsruhe (FRG)
Prof. Dr. R. Gleiter
Institut für Organische Chemie der Universität
Im Neuenheimer Feld 270, D-6900 Heidelberg 1 (FRG)
Dr. R. Boese
Institut für Anorganische Chemie der Universität-Gesamthochschule
Universitätsstrasse 3-5, D-4300 Essen 1 (FRG)

[**] This work was supported by the Fonds der Chemischen Industrie. We thank *A. Kuiper, P. Lang, E. Fischer, I. Süss, U. Tanger* and *A. Flatow* for numerous analytical and spectroscopic data.

trienedial under McMurry conditions.[2] After complete separation from **2** (colorless liquid) the cyclic hydrocarbon **1** crystallizes as colorless needles with a melting point of 35.5 °C.[3] **1** is of special interest as a tetrahomo-8π-system, when all four π-bonds are so arranged that maximum interaction is guaranteed. This arrangement is realized with the crown conformation[4] **1a**, which according to force-field calculations (MM2)[5] is predicted to be about 17.6 kJ mol^{-1} less in energy than the chair conformation **1b** (Fig. 1). The

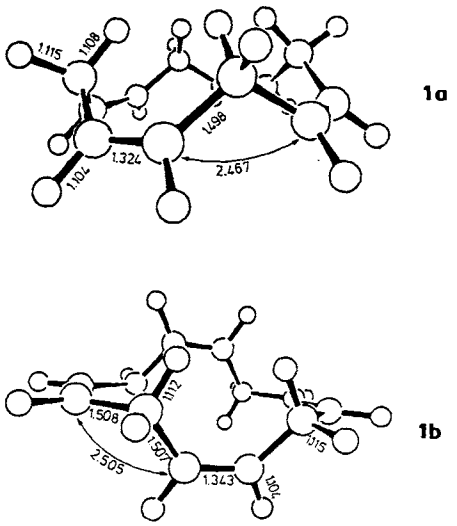


Fig. 1. MM2-optimized crown conformation **1a** and chair conformation **1b**; distances in Å. Calculated enthalpies of formation ΔH_f (strain energies SE) in kJ mol^{-1}: **1a**, 235.0(53.5); **1b**, 252.6(71.1).

X-ray structure analysis of **1** at 120 K[6] confirms the conformation **1a** in the solid state (Fig. 2), whereby eight independent molecules crystallize in the space group *Pbca*, and, within the limits of error, have C_{4v} symmetry. The C=C bond lengths (mean 1.324 Å) correspond approximately to those in the planar 1,4-cyclohexadiene **3** (1.318 Å),[7] whereas the single bonds (mean 1.503 Å) are somewhat longer then in **3** (1.486 Å). The distance between the CH_2-bridged sp^2 centers is on average 2.48 Å. As a result of the interactions between neighboring hydrogen atoms that are directed towards the center of the ring and whose separation, with a mean distance of 2.01 Å, is clearly shorter than the sum of the van der Waals radii of 2.4 Å (the C–H distances were expanded from the observed hydrogen positions to the standard value of 1.09 Å), all the C–C–C bond angles are widened (mean value: C(sp^2) 127.4°, C(sp^3) 111.2°). The intramolecular hydrogen distances agree astonishingly well with those obtained by ab-initio calculations on **1a** (HF–SCF, dz basis),[8] just as do the bond lengths and angles (maximum deviation 0.007 Å and 0.8°, resp.) as well as the torsion angles (experimental averages C–C–C=C 117.3, C–C=C–C 1.9°, calculated 116.5 and 0°, resp.).

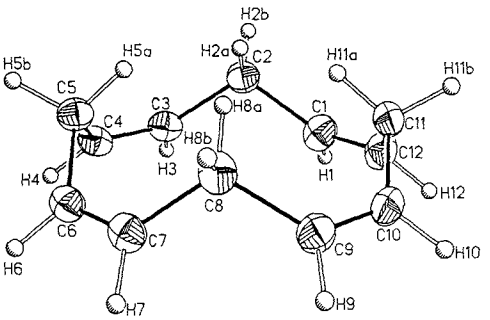


Fig. 2. Structure of **1** in the crystal (not systematically numbered) [6]. Distances [Å] and angles [°], standard deviation in parenthesis: C1-C12 1.323(2), C3-C4 1.326(2), C6-C7 1.325(2), C9-C10 1.321(2), C1-C2 1.506(2), C2-C3 1.503(2), C4-C5 1.501(2), C5-C6 1.507(2), C7-C8 1.506(2), C8-C9 1.503(2), C10-C11 1.505(2), C11-C12 1.495(2); C2-C1-C12 127.1(1), C2-C3-C4 127.5(1), C5-C6-C7 127.2(1), C8-C9-C10 126.8(1), C3-C4-C5 127.3(1), C6-C7-C8 127.7(1), C9-C10-C11 127.5(1), C1-C12-C11 127.5(1), C1-C2-C3 111.7(1), C4-C5-C6 110.3(1), C7-C8-C9 112.0(1), C10-C11-C12 110.8(1); C1···C3 2.489(1), C4···C6 2.469(1), C7···C9 2.495(1), C10···C12 2.470(1).

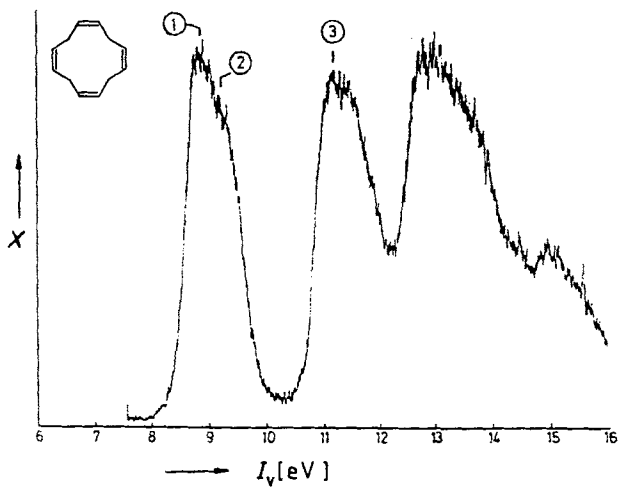


Fig. 3. PE spectrum of **1** [14]. x = count rate.

Table 1. Comparison of measured vertical ionization energies I_{vj} [eV] and calculated orbital energies ε_j [eV] of **1**.

	I_{vj}	Assignment	$-\varepsilon_j$ (HF–SCF)	$-\varepsilon_j$ (MINDO/3)
		$5b_1$	9.27	9.09
①	8.9	11e	9.43	9.29
②	9.3	$5a_1$	9.85	9.46
		$6b_2$	12.57	10.79
③	11.2	$3a_2$	12.84	10.89
		10e	12.99	10.90

The lower homologue all-*cis*-1,4,7-cyclononatriene **4**[9] is likewise present in the crown conformation, and its PE spectrum indicates a homoconjugative interaction of the three double bonds.[10] According to the concept of *Winstein* et al.[11] **4** is a trishomobenzene; however, the results of more recent investigations are inconsistent with a homoaromatic stabilization of the ground state.[12] Homoantiaromatic interactions have been observed in the monohomo-8π-system of 3*H*-cyclonona[*def*]biphenylene.[13] Therefore, it was to be expected that **1a** should be destabilized and thus **1b** be energetically more favorable. In order to establish incidental electronic interactions in **1**, the He(I) photoelectron spectrum[14] of this compound was recorded (cf. Fig. 3 and Table 1). It shows a broad band at 8.9 eV with a shoulder at 9.3 eV.

On the basis of semiempirical (MINDO/3)[15] and ab-initio calculations (HF–SCF, dz basis)[8] on **1a**, we assign to the first peak (①, ②) four ionizations from the π-MOs $5b_1$, $11e$, and $5a_1$. The small half-width of this peak contradicts a homoconjugative interaction. A similar bandwidth is found for **2** (I_{v1} = 9.1 eV). The results of a population analysis[16] for **1a**, SEN (C1···C3) = 0.06, likewise show that a significant homoconjugation is missing.

Our investigations show that **1**, in contrast to cyclooctatetraene, prefers a conformation in which all double bonds are coplanar. We attribute this to the absence of a homoantiaromatic destabilization.

Experimental Procedure

A mixture of 15.76 g (102.5 mmol) of $TiCl_3$ and 18.7 g of Zn/Cu couple in 1000 mL of dimethoxyethane (DME) was heated under reflux for 3 h in an inert atmosphere (Ar). A solution of 2.0 g (10.2 mmol) of *all,cis*-dodeca-3,6,9-trienedial[11] in 800 mL of DME was then added dropwise for 40 h and the mixture kept under reflux for a further 5 h before cooling and filtering over Florisil. The filtrate was evaporated to 50 mL using a 20-cm Vigreux column, treated with 250 mL of water, and extracted several times with pentane. The combined organic phases were washed with water, dried over Na_2SO_4, and concentrated to ca. 5 mL with a column. After chromatography on silica gel/pentane (2: R_f = 0.38; 1: R_f = 0.2) and removal of solvent by distillation, the enriched fractions of **1** and **2** were further purified by preparative gas chromatography,[17] at 115 °C (injector 200 °C). 150 mg (9.0%) of **2** (retention time 35 min) and 38 mg (2.3%) of **1** (retention time 45 min) were obtained. Colorless needles with a melting point of 35.5 °C (uncorrected) were obtained by careful sublimation of **1** at room temperature/50 torr.

Received: May 17, 1989 [Z 3343 IE]
German version: *Angew. Chem. 101* (1989) 1401

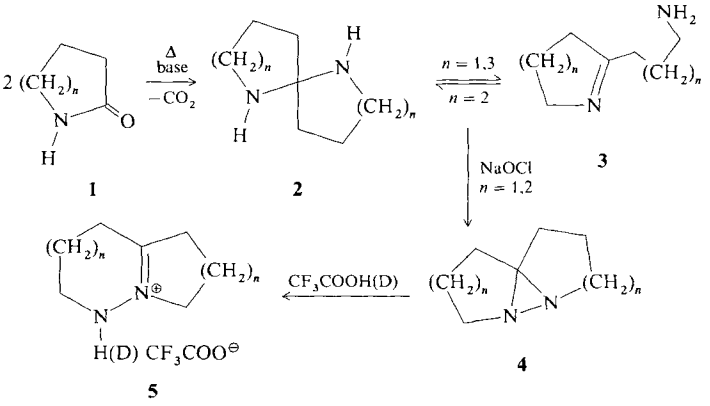
CAS Registry numbers:
1, 112681-65-9; **2**, 112790-14-4; all-*cis*-dodeca-3,6,9-triendial, 112681-64-8.

[1] M. Brudermüller, H. Musso, *Angew. Chem. 100* (1988) 267; *Angew. Chem. Int. Ed. Engl. 27* (1988) 298.
[2] J. E. McMurry, M. P. Flemming, K. L. Kees, L. P. Krepski, *J. Org. Chem. 43* (1978) 3255.
[3] A. Krause, unpublished results.
[4] J. Dale, *Top. Stereochem. 9* (1976) 199.
[5] N. Burkert, N. L. Allinger, *ACS Monogr. 177* (1982) 1.
[6] Crystal dimensions 0.59 × 0.21 × 0.20 mm³, orthorhombic, space group *Pbca*. a = 7.913(1), b = 14.569(2), c = 17.280(2) Å, V = 1992.2(4) Å³, Z = 8, 120 K, $Mo_{K\alpha}$ radiation, ϱ_{calcd} = 1.068 g cm⁻³, 2930 unique reflections, 2192 observed reflections, 181 parameters, R = 0.047, R_w = 0.048, $w^{-1} = \sigma^2(F_o) + 0.0005F^2$. Further details of the crystal structure investigation are available on request from the Fachinformationszentrum Karlsruhe, Gesellschaft für wissenschaftlich-technische Information mbH, D-7514 Eggenstein-Leopoldshafen 2 (FRG), on quoting the depository number CSD-53929, the names of the authors, and the journal citation.
[7] A. Jeffrey, J. Buschmann, C. W. Lehmann, P. Luger, *J. Am. Chem. Soc. 110* (1988) 7218.
[8] The calculations were carried out on an IRIS-4D Workstation (Silicon Graphics) using a DSCF program developed in Karlsruhe.
[9] K. G. Untch, R. J. Kurland, *J. Am. Chem. Soc. 85* (1963) 346; W. R. Roth, W. B. Bang, P. Göbel, R. L. Sass, R. B. Turner, A. P. Yü, *ibid. 86* (1964) 3178.
[10] P. Bischof, R. Gleiter, E. Heilbronner, *Helv. Chim. Acta 53* (1970) 1425.
[11] S. Winstein, *J. Am. Chem. Soc. 81* (1959) 6524; *Q. Revs. Chem. Soc. 23* (1969) 141; P. Radlich, S. Winstein, *J. Am. Chem. Soc. 85* (1970) 344.
[12] J. F. Liebmann, L. A. Paquette, J. P. Peterson, D. W. Rogers, *J. Am. Chem. Soc. 108* (1986) 8267; L. T. Scott, M. J. Cooney, D. W. Rogers, K. Dejroongruang, *ibid. 110* (1988) 7244; M. A. Miller, J. M. Schulman, R. L. Dish, *ibid. 110* (1988) 7681; and references cited therein.
[13] C. F. Wilcox, D. A. Blain, J. Clardy, G. Van Duyne, R. Gleiter, M. Eckert-Maksic, *J. Am. Chem. Soc. 108* (1986) 7693.
[14] The He(I)PE spectra were recorded with a Perkin-Elmer PS-18 spectrometer at room temperature and calibrated with argon.
[15] R. Bingham, M. J. S. Dewar, D. H. Lo, *J. Am. Chem. Soc. 97* (1975) 1285; P. Bischof, *ibid. 98* (1976) 6844.
[16] R. Heinzmann, R. Ahlrichs, *Theor. Chim. Acta 42* (1976) 33.
[17] 20% diethylene glycol succinate (DEGS) on Chromosorb W-AW, 80–100 mesh, 3 m × 3/8".

The First Tricyclic Diaziridines—a Simple Synthetic Route**

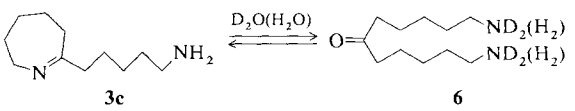
By *Sergej N. Denisenko, Eva Pasch,* and *Gerd Kaupp**

Diaziridines are of special interest with regard to the synthesis of anticancer drugs[1] and psychopharmaceuticals.[2] Numerous bicyclic representatives have been described,[3] but tricyclic condensed diaziridines were hitherto unknown. We report here on simple syntheses of **4a** and **4b** and on their ring-opening reactions leading to bicyclic protonated azomethine imines.



a: n = 1, **b:** n = 2, **c:** n = 3

When the lactams **1** are heated in the presence of LiOH, NaOH or CaO under strictly controlled reaction conditions, a complex reaction involving elimination of CO_2 takes place, leading to formation of the spiroaminals/iminoamines **2/3** in moderate to good yields which can be purified by distillation.[4–6] This provides an attractive preparative entry to **2/3**, because the starting materials are inexpensive. By-products are olefins and tar, and, in the case of **2b**, 2-methylpiperidine.[7] According to the NMR spectra (Table 1) in $CDCl_3$ and D_2O the plausible equilibria **2/3** lie either completely on the right-hand side (**3a, c**) or completely on the left-hand side (**2b**). Only **3c** is hydrolyzed to the diaminoketone (82% **6** at 25 °C in D_2O)—presumably due to ring strain effects. In the case of the isomeric pairs **2a/3a** and **2b/3b**, semiempirical AM1 calculations[8] give comparable energy values for the geometrically most favorably optimized conformations, so that prediction of this surprising behavior was not possible. Also hydrolysis equilibria can rarely be predicted reliably as yet.



Reaction of **3a** and **2b** with *tert*-butyl hypochlorite, or more conveniently sodium hypochlorite, leads respectively

[*] Prof. Dr. G. Kaupp, Dr. S. N. Denisenko [+], Dipl.-Chem. E. Pasch
Fachbereich Chemie – Organische Chemie I – der Universität
Postfach 2503, D-2900 Oldenburg (FRG)
[+] Permanent address:
Division of TOONS,
Department of Chemical Technology
Prospect Gagarina 8, SU-320640 Dnepropetrovsk (USSR)

[**] This work was supported by the Deutsche Forschungsgemeinschaft, the Fonds der Chemischen Industrie, the Bundesminister für Forschung und Technologie (Project 10 IVS325) and by a DAAD grant (1988–1989) for *S.N.D.*

Table 1. Important physical and spectroscopic data of the compounds **2, 3, 4, 5, 6,** and **7**. UV spectra in CH_3OH, 300 MHz ^1H NMR and 75 MHz ^{13}C NMR spectra in $CDCl_3$, 25 °C, TMS internal; (high-resolution) 70 eV mass spectra; FT-IR spectra.

3a: b.p. 83 °C 14 torr; $n_D^{20} = 1.4852$; IR (film): $\tilde{\nu}$ [cm^{-1}] = 3362, 3287 (NH_2), 1642 (C=N); ^1H NMR: $\delta = 3.9 - 3.7$(2H), 2.8 – 2.65(2H), 2.55 – 2.3(4H), 1.95 – 1.65(4H), 1.25(br.s., $\Delta\nu_{1/2} = 4$ Hz, 2H); (D_2O): $\delta = 3.55$ (br.s, 2H), ca. 2.5 (br.s, 2H), 2.3 (br.s, 4H), 1.65 (br.s, 4H); ^{13}C NMR: $\delta = 176.6$(C=N), 59.6, 40.8, 36.1, 29.9, 29.2, 21.5; (D_2O): $\delta = 182.0$(C=N); 59.4, 40.6, 37.1, 30.6, 28.7, 22.1; MS: *m/z* 126($M^{\oplus}$, 1%), 110(2), 108(4), 96(50), 83(100), 82(47), 68(11); $M^{\oplus}$ at 126.1157 (calc. 126.1147)

2b: b.p. 84 °C 14 torr; $n_D^{20} = 1.5305$; ^1H NMR: $\delta = 2.75$ (br.s., $\Delta\nu_{1/2} = 7.5$ Hz, 4H), 1.85 (br.s, $\Delta\nu_{1/2} = 6.5$ Hz, 2H), 1.7 – 1.3 (12H); (D_2O): $\delta = 2.5$ (br.s, 4H), 1.35 (br.s, 12H); ^{13}C NMR: $\delta = 64.2$, 39.5(2C), 36.0(2C), 25.5(2C), 19.5(2C); (D_2O): $\delta = 64.8$ (quat. C), 39.0, 36.0, 24.7, 19.2; MS: *m/z* 154 ($M^{\oplus}$, 23%), 110(52), 97(100), 82(27); $M^{\oplus}$ at 154.1470 (calc. 154.1481)

3c: b.p. 94 °C 1 torr; $n_D^{20} = 1.4981$; IR (Film): $\tilde{\nu}$ [cm^{-1}] = 3364, 3288 (NH_2), 1659 (C=N); ^1H NMR: $\delta = 3.85 - 3.5$ (2H), 2.69 (t, $J = 6.8$ Hz, 2H), 2.4 – 2.3 (2H), 2.3 – 2.2 (2H), 1.78 (quint, $J = 5.8$ Hz, 2H); 1.7 – 1.3 (10H), 1.21 (br.s, $\Delta\nu_{1/2} = 4.5$ Hz, 3H); ^{13}C NMR: $\delta = 177.2$(C=N), 50.6, 41.6, 40.98, 38.97, 32.5, 32.0, 30.5, 25.6, 25.4, 24.9, 22.5; MS: *m/z* 182 ($M^{\oplus}$, 5%), 166(8), 152(20), 138(12), 124(58), 111(100), 96(37), 83(35); $M^{\oplus}$ at 182.1783 (calc. 182.1782)

4a: b.p. 52–54 °C 15 torr; $n_D^{20} = 1.4828$; ^1H NMR: $\delta = 3.05$–3.19 (2H), 2.86 – 2.69 (2H), 2.22 – 2.11 (2H), 1.93 – 1.50 (6H); ^{13}C NMR: $\delta = 78.7$ (N–C–N), 52.78 (2C), 27.18 (2C), 21.50 (2C); MS: *m/z* 124 ($M^{\oplus}$, 16%), 123 (84), 109(9), 107(10), 106(14), 97(47), 96(100), 95(20), 94(16), 83(32), 81(32); $M^{\oplus}$ at 124.1001 (calc. 124.1004)

4b: b.p. 83–85 °C 15 torr; $n_D^{20} = 1.4952$; ^1H NMR: $\delta = 3.25 - 3.14$ (2H), 3.05 – 2.92 (2H), 2.10 – 1.99 (2H), 1.70 – 1.57 (2H), 1.57 – 1.40 (4H), 1.39 – 1.11 (4H); ^{13}C NMR: $\delta = 58.6$ (N–C–N), 49.6 (2C), 30.5 (2C), 20.6 (2C), 17.6 (2C); MS: *m/z* 152 ($M^{\oplus}$, 8%), 151(5), 124(26), 123(100), 110(10), 97(32), 96(18), 81(20); $M^{\oplus}$ at 152.1314 (calc. 152.1314)

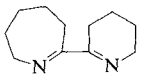
5a: ^1H NMR: $\delta = 4.0 - 3.8$ (2H), 3.15 – 3.0 (2H), 2.8 – 2.7 (2H), 2.5 – 2.4 (2H), 2.0 – 1.9 (2H), 1.8 – 1.6 (2H); ^{13}C NMR: $\delta = 166.8$, 160.0 (q, $J =$ 46 Hz), 115.0 (q, $J = 287$ Hz), 60.0, 43.2, 35.4, 23.7, 16.3, 15.7; UV: $\lambda_{max} =$ 238 nm

5b: ^1H NMR: $\delta = 4.07$ (t, $J = 5.5$ Hz, 2H), 3.1 – 3.05 (2H), 2.9 – 2.75 (4H), 2.65 – 2.55 (2H), 2.05 – 1.95 (2H), 1.85 – 1.75 (4H); ^{13}C NMR: $\delta = 177.9$, 160.6 (q, $J = 46$ Hz), 115.0 (q, $J = 287$ Hz), 54.8, 48.7, 35.9, 32.6, 28.3, 21.1, 19.1, 16.5; UV: $\lambda_{max} = 246$ nm

6: IR (D_2O solution): $\tilde{\nu}$ [cm^{-1}] = 1688 (C=O); ^1H NMR (D_2O): $\delta = 2.49$ (t, $J = 7.0$ Hz, 4H), 1.6 – 1.1 (m, 16H); ^{13}C NMR (D_2O): $\delta = 217.3$ (C=O), 41.0 (2C), 32.3 (2C), 26.5 (2C),26.3 (2C), 23.7 (2C)

7: b.p. 72 °C 0.1 torr; IR (film): $\tilde{\nu}$ [cm^{-1}] = 1668, 1636 (C=N); ^1H NMR: $\delta = 3.9 - 3.7$ (4H), 2.95 – 2.85 (2H), 2.6 – 2.45 (2H), 1.9 – 1.3 (10H); ^{13}C NMR: $\delta = 175.6$, 167.8, 52.5, 50.1, 31.4, 26.2, 26.0, 24.8, 23.3, 21.8, 19.3

to the diaziridines **4a** and **4b**. In contrast, no corresponding derivative **4c** could hitherto be obtained from **3c** because of a high tendency to polymerization and hydrolysis. After distillation, however, labile **7** could be isolated in 10% yield.



7

The highly strained tricyclic derivatives **4a, b** can be distilled without decomposition. Their structure is unequivocally established by the number and position of the signals in the ^1H and ^{13}C NMR spectra. On steric grounds, which are confirmed by AM1 calculations (with geometry optimization), they must be present in the *trans*-configuration (Fig. 1). Nevertheless, their stability is remarkable in view of the abnormal calculated bond angles at the quaternary carbon ($\sphericalangle$ CC_qC, CC_qN, NC_qN for **4a**: 121.5, 111.7, 57.3°; for **4b**: 112.5, 121.8, 57.3°). The bond angles calculated for *trans*-tetramethyldiaziridine (109.8, 123.1, 57.5°) are taken as normal.

The much greater strain in **4a** also manifests itself in large differences in the δ values of the quaternary carbon atoms

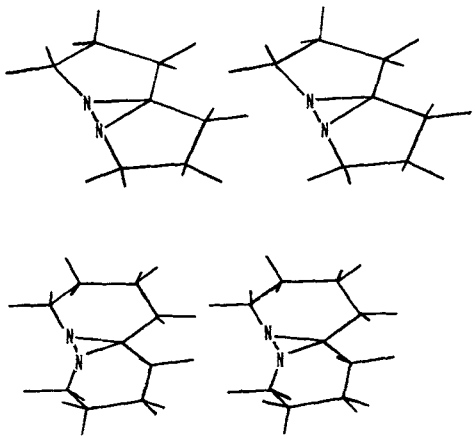


Fig. 1. Stereoplots of the optimized AM1 geometries of **4a** (top) and **4b** (bottom) (lowest energy symmetric conformation).

($\Delta\delta = 20$!) (see Table 1). The strain, however, is not released even by a conceivable ring opening to the isomeric azomethine imines (**5a/b**-CF_3COOH) upon distillation. In contrast, such ring openings very readily take place upon protonation.[9] Thus, the trifluoroacetates **5a** and **5b** of the azomethine imines are formed immediately upon dissolution in [D]trifluoroacetic acid. These are remarkably stable; even upon prolonged heating with concentrated HCl the protonated azomethine imines are not hydrolyzed to the expected ketohydrazines.[10]

The compounds **4a, b** should be very suitable for theoretical studies because of the restricted molecular mobilities, which are reflected in the spectroscopic data when the ring size is varied. Further physical measurements and quantum chemical calculations would be desirable.[11] For practical applications, nucleophilic substitutions at the quaternary C atom and cycloadditions with the tricyclic diaziridines appear attractive.

Experimental Procedure

2b: A mixture of **1b** (10 g, 100 mmol) and $LiOH \cdot H_2O$ (2.1 g, 50 mmol) was heated to 200 °C in order to distil off the water. Thereafter the crude product was driven over by heating to 320 °C. The crude mixtures from two batches were fractionated on a heatable rotary band column; yield 7.2 g (36%) **2b**.

3a [5] and **3c** [6] were prepared according to procedures given in the literature. Yields after rotary band column distillation: 88% and 55%, respectively.

4a: A mixture of **3a** (5.2 g, 41 mmol) and NaOH (3.0 g, 75 mmol) in water (70 mL) was treated with 30 mL of a 15% NaOCl solution at 5 °C. After 10 h stirring at 20 °C, 10 g of NaOH was added and the mixture extracted with CH_2Cl_2 and distilled at 14 torr over a Vigreux column; yield 3.8 g (74%) of **4a**. Compounds **4b** and **2b** were obtained analogously and purified by distillation. Yield 66%. Both diaziridines evolve iodine from aqueous HI. Reaction of **2b** with *t*BuOCl and NEt_3 in diethyl ether afforded 32% **4b**, while reaction of **3c** with *t*BuOCl and Na_2CO_3 in dichloromethane furnished 10% **7**.

Solvolyses of **4a** and **4b**: 100 mg of the respective diaziridine was dissolved with cooling in 1 mL of CF_3COOD and the ^1H NMR spectra were measured immediately. After evaporation of the solutions to dryness the ^1H and ^{13}C NMR spectra were measured in $CDCl_3$ and the UV spectra in CH_3OH. The same UV spectra were obtained after 1 h and ca. 2 min, when dilute solutions of **4a** and **4b** in CH_3OH were treated with one drop of 2N H_2SO_4 (1 mm cell).

Received: May 5, 1989 [Z 3333 IE]
German version: *Angew. Chem. 101* (1989) 1397

CAS Registry numbers:
1b, 675-20-7; **2b**, 7174-73-4; **3a**, 18548-39-5; **3c**, 5960-99-6; **4a**, 122951-79-5; **4b**, 122951-84-2; **5a**, 122951-81-9; **5b**, 122951-86-4; **6**, 122951-82-0; **7**, 122951-83-1.

[1] S. Takase, M. Watanabe, O. Shiratori, Y. Hata, *Biochem. Biophys. Res. Commun. 104* (1982) 746; G. Sosnovsky, J. Lukszo, *Z. Naturforsch. B38* (1983) 884; *J. Cancer Res. Clin. Oncol. 107* (1984) 217; further biological actions in [3b].

[2] R. G. Kostyanovskii, G. V. Shustov, O. G. Nabiev, S. N. Denisenko, S. A. Sukhanova, E. F. Lavretskaya, *Khim.-Farm. Zh. 20* (1986) 671; *Chem. Abstr. 106* (1987) 27665q.
[3] a) G. V. Shustov, S. N. Denisenko, R. G. Kostyanovskii, *Izv. Akad. Nauk SSSR Ser. Khim. 1986*, 1831; *Chem. Abstr. 107* (1987) 39017p; G. V. Shustov, S. N. Denisenko, I. I. Chervin, N. L. Asfandiyarov, R. G. Kostyanovskii, *Tetrahedron 41* (1985) 5719; E. Schmitz in A. R. Katritzky, C. W. Rees (Eds.): *Comprehensive Heterocyclic Chemistry, Vol. 7*, Pergamon Press, Oxford 1984, Chapter 5.08; b) H. W. Heine in A. Weissberger, E. C. Taylor (Eds.): *The Chemistry of Heterocyclic Compounds*, Wiley, New York 1983, Chap. 2.
[4] **3a** [5] and **3c** [6] are described in patents, and **3b** is mentioned but is not accessible. It is possible instead to prepare **2b** (see Experimental Procedure).
[5] a) K. Teramoto, R. Harada, Jpn. Kokai 7307, 432 (March 5, 1973), Toray Industries, Inc.; *Chem. Abstr. 79* (1973) 31861s; b) Farbenfabriken Bayer AG, Br. Pat. 922275 (March 27, 1963); *Chem. Abstr. 59* (1963) 11261e.
[6] T. Setsuda, H. Aizawa, T. Kimura, Jpn. Kokai No. 79125654 (Sept. 29, 1979), Toray Industries, Inc.; *Chem. Abstr. 92* (1980) 163854v.
[7] E. Wenkert, B. Chauncy, K. G. Dave, A. R. Jeffecat, F. M. Schell, H. P. Schenk, *J. Am. Chem. Soc. 95* (1973) 8427.
[8] QCPE-program MOPAC version 3.10 from N. E. Heimer, J. T. Swanson, J. J. P. Stewart, F. J. Seiler Research Laboratory United States Air Force Academy Colorado Springs, CO 80840; M. J. S. Dewar, E. G. Zoebisch, E. F. Healy, J. J. P. Stewart, *J. Am. Chem. Soc. 107* (1985) 3902.
[9] E. Schmitz, *Chem. Ber. 95* (1962) 676.
[10] E. Schmitz, D. Habisch, *Chem. Ber. 95* (1962) 680; C. Szántay, E. Schmitz, *ibid. 95* (1962) 1759.
[11] G. Kaupp, J. A. Döhle, K. Burger, P. Rademacher, R. Poppek, *J. Phys. Org. Chem. 1* (1988) 267; R. Gleiter, C. Sigwart, H. Irngartinger, S. Gisies, W. Marterer, O. Klingler, H. Prinzbach, *Tetrahedron Lett. 29* (1988) 185; H. Irngartinger, D. Kallfaß, H. Prinzbach, O. Klingler, *Chem. Ber. 122* (1989) 175; J. Kaneti, L. Hoesch, A. S. Dreiding, *Helv. Chim. Acta 69* (1986) 1461.

Indium 2,4,6-Tris(trifluoromethyl)phenoxide—a Dimer with the Coordination Number Two at the Indium Atoms**

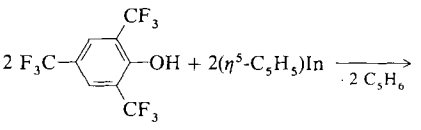
By *Mario Scholz, Mathias Noltemeyer,* and *Herbert W. Roesky**

Dedicated to Professor Kurt Issleib on the occasion of his 70th birthday

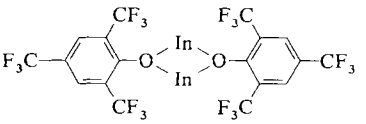
Compounds containing low-coordinate boron have been the subject of numerous investigations just recently.[1] However, in the case of aluminum the number of structurally characterized compounds is not large, even with three-coordinate Al centers.[2]

We describe here the first synthesis of an indium(I) compound with two-coordinate indium atoms. 2,4,6-tris(trifluoromethyl)phenoxide appeared suitable as ligand to stabilize indium(I), for it is sterically demanding and has electron-attracting properties. 2,4,6-tris(trifluoromethyl)phenol **1**, prepared from bis(trimethylsilyl)peroxide and 2,4,6-tris(trifluoromethyl)phenyllithium,[3] reacts with cyclopentadienylindium[4] in *n*-hexane to give indium 2,4,6-tris(trifluoromethyl)phenoxide **2**. The title compound is formed in good yield (67%) as a white solid which is unstable towards air and water. In the FI-mass spectrum the molecular peak (*m/z* 824) is observed with low relative intensity (4%).

Single crystals suitable for an X-ray structure analysis[5] were obtained from *n*-hexane. Owing to the random arrangement of the CF_3 groups, the molecule has no crystallographic symmetry; the two phenyl groups, however, lie almost in one plane (2.9° deviation) and very nearly at right angles (within ± 2.5 pm) to the planar four-membered In_2O_2 ring.



1



2

The number of structurally investigated indium(I) compounds is small. Notable examples are $(\eta^5\text{-}C_5Me_5)In$[6] and the arene complexes investigated by *Schmidbaur* et al.,[7] which, however, are hexameric or polymeric in the solid state.

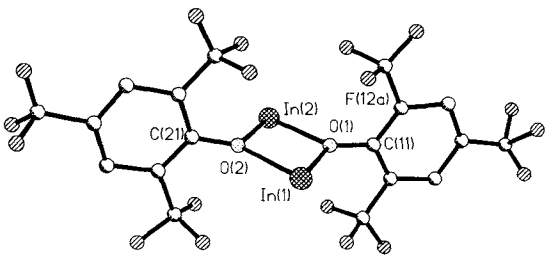


Fig. 1. Crystal structure of the dimer **2**.

The average In–O distance in **2** is 232.0 pm; this value can best be compared with that in complex **3** (217.1 pm).[8]

$[L_2In_2(MeCO_2)_4(\mu\text{-}O)] \cdot 2\ NaClO_4$ **3**, L = 1,4,7-triazacyclononane

At the same time, however, it must be taken into account that the indium atoms in **3** have the formal oxidation state + 3 and are octahedrally coordinated. The covalent radii of In (144 pm) and O (66 pm) would give an In–O distance of only 210 pm.[7]

Thus, the 2,4,6-tris(trifluoromethyl)phenoxide ligand appears to be preferentially suitable for the stabilization of metals with lower coordination numbers.[3]

Experimental Procedure

2: A solution of **1** (2.5 g, 8.3 mmol) in *n*-hexane (30 mL) was added dropwise to a suspension of $(\eta^5\text{-}C_5H_5)In$ (1.5 g, 8.3 mmol) in 30 mL of *n*-hexane at room temperature. The resulting colorless, slightly cloudy solution was allowed to stand for 12 h and then was filtered through a thin layer of celite. The filtrate was evaporated down to half its original volume and, upon cooling to 4 °C, **2** crystallized as a colorless solid. Yield: 2.3 g (67%) **2**. ^1H NMR (80 MHz, C_6D_6, TMS ext.): δ = 7.8 (s, Aryl-H). $^{19}F\{^1H\}$ NMR (75.39 MHz, C_6D_6, $CFCl_3$ ext.): δ = − 60.5 (s, *o*-CF_3), − 61.9 (s, *p*-CF_3). MS (70 eV): *m/z* 824 ($M^{\oplus}$, 4%). IR (Nujol): $\tilde{\nu}$[cm^{-1}] = 1630 m, 1580 w, 1310 w, 1290 m, 1260 m, 1200 m, 1150 m, 1120 m, 915 m, 840 m, 790 m.

[*] Prof. Dr. H. W. Roesky, M. Scholz, Dr. M. Noltemeyer
Institut für Anorganische Chemie der Universität
Tammannstrasse 4, D-3400 Göttingen (FRG)

[**] This work was supported by the Deutsche Forschungsgemeinschaft and the Fonds der Chemischen Industrie.

Received: June 5, 1989 [Z 3376 IE]
German version: *Angew. Chem. 101* (1989) 1419

[1] Selected examples: H. Nöth, *Angew. Chem. 100* (1988) 1664; *Angew. Chem. Int. Ed. Engl. 27* (1988) 1603; P. Paetzold, *Adv. Inorg. Chem. 31* (1987) 123; M. Pilz, J. Allwohn, R. Hunold, W. Massa, A. Berndt, *Angew. Chem. 100* (1988) 1421; *Angew. Chem. Int. Ed. Engl. 27* (1988) 1370; H. V. R. Dias, P. P. Power, *ibid. 99* (1987) 1320 and *26* (1987) 1270.

[2] For example K. M. Waggoner, H. Hope, P. P. Power, *Angew. Chem. 100* (1988) 1765; *Angew. Chem. Int. Ed. Engl. 27* (1988) 1699; J. J. Jerius, J. M. Hahn, A. F. M. M. Rahman, O. Mols, W. H. Ilsley, J. P. Oliver, *Organometallics 5* (1986) 1812; W. Uhl, *Z. Naturforsch. B43* (1988) 1113.

[3] H. W. Roesky, M. Scholz, M. Noltemeyer, F. T. Edelmann, *Inorg. Chem.*, in press.

[4] E. O. Fischer, H. P. Hofmann, *Angew. Chem. 69* (1957) 639.

[5] Crystal structure analysis of **2**: space group $P2_1/c$, $a = 1113.8(6)$, $b = 1695.3(14)$, $c = 1408.0(9)$ pm, $\beta = 109.72(4)°$, $V = 2.5027$ nm^3, $Z = 4$, $\varrho_{calc} = 2.19$ Mg m^{-3}, $\mu(Mo_{K\alpha}) = 1.96$ mm^{-1}. 6062 measured reflections up to $2\theta_{max} = 45°$; empirical absorption correction, 2191 symmetry independent reflections with $|F_o| > 3\sigma(|F_o|)$ used for solution of the structure and refinement. $R = 0.078$ ($R_w = 0.065$. Weighting scheme $w^{-1} = [\sigma^2(|F_o|) + 0.0004|F_o|^2)$. Further details of the crystal structure investigation are available on request from the Fachinformationszentrum Karlsruhe, Gesellschaft für wissenschaftlich-technische Information mbH, D-7514 Eggenstein-Leopoldshafen 2 (FRG), on quoting the depository number CSD-53976, the names of the authors, and the journal citation.

[6] O. T. Beachley, Jr., M. R. Churchill, J. C. Fettinger, J. C. Pazik, L. Victoriano, *J. Am. Chem. Soc. 108* (1986) 4666.

[7] J. Ebenhöch, G. Müller, J. Riede, H. Schmidbaur, *Angew. Chem. 96* (1984) 367; *Angew. Chem. Int. Ed. Engl. 23* (1984) 386.

[8] K. Wieghardt, M. Kleine-Boymann, B. Nuber, J. Weiss, *Inorg. Chem. 25* (1986) 1654.

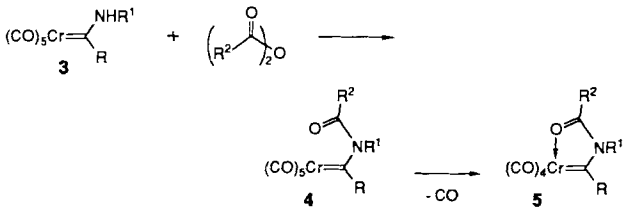
Activated Aminocarbene Complexes of the Fischer Type: Synthesis, Structure, and Annelation Reactions**

By *Karl Heinz Dötz,* Douglas Grotjahn*, and *Klaus Harms*

The annelation of Fischer type alkoxycarbene complexes[1] **1** (M = Cr, Do = OR) with alkynes leads to 4-alkoxyphenols[2] and is also of interest in natural product synthesis[3] because of its regioselectivity and the mild reaction conditions. The corresponding aminocarbene complexes (**1**: Do = NR_2) require higher temperatures (90–125 °C) and are annelated exclusively *without* incorporation of a CO ligand.[4] Apparently the better donor nitrogen strengthens the metal–CO bond and thus slows down the incorporation of the alkyne **1** or hinders a CO insertion in **2**/**2'**. We have now tried to weaken the marked donor character of the nitrogen-carbene substituent by its acylation and hoped at the same time that the amide function favored a decarbonylation of **1** (Do = NC(=O)R) with formation of a tetracarbonyl-chelate carbene complex. Chelate carbene complexes have already proven to be excellent starting materials for carbene annelation.[5]

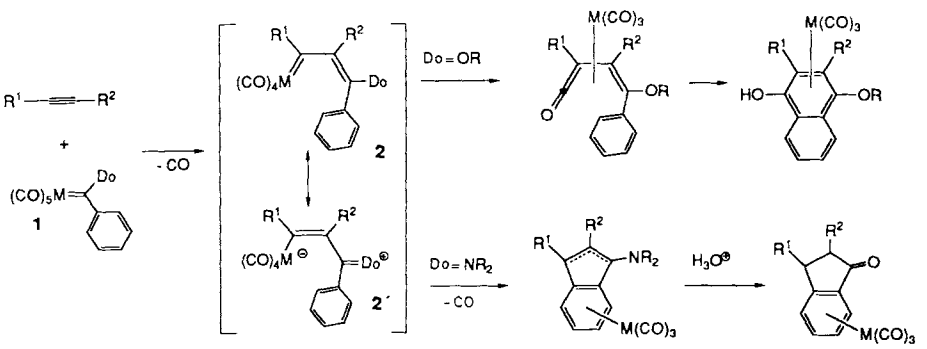
After preliminary experiments with carboxylic acid chlorides, which immediately led via the expected *mono-N*-acyl species **4** to the *bis*acylation product,[6] we found that di-*tert*-butyl dicarbonate $(t\text{BuOCO})_2\text{O}$ is a selective monoacylating agent, which, in the presence of 4-dimethyl-aminopyridine (DMAP), is suitable for both amino- and *N*-alkylamino-carbene complexes (Table 1). Under the reaction conditions, predominantly the tetracarbonyl-chelate compounds **5** are formed directly via the pentacarbonyl(acylaminocarbene) complexes **4**, which can be detected during the reaction by IR spectroscopy and thin-layer chromatography. The decarbonylation is slower in the case of *alkyl*aminocarbene complexes than in the case of the *aryl* homologues; thus, in a CO-saturated solution **4f** is obtained as major product from **3e** together with only small amounts of the corresponding complex **5**. When less than 2 equivalents of di-*tert*-butyl dicarbonate and 0.1 equivalents of DMAP are used, the reaction does not go to completion. Only *N*-unsubstituted aminocarbene complexes (**3a**) react smoothly with Ac_2O/NEt_3/DMAP.

Table 1. Acylation of aminocarbene complexes. Conditions: 2.0 equivalents $(t\text{BuOCO})_2\text{O}$, 0.1 equivalents DMAP, Et_2O, 25 °C, 8–16 h.



	R	R^1	R^2	Product	Yield [%]
3a	*p*-Tolyl	H	*t*BuO	**5a**	83
3a	*p*-Tolyl	H	CH_3	**5b**	60 [a]
3b	*p*-Tolyl	Benzyl	*t*BuO	**5c**	76 [b]
3c	Phenyl	CH_3	*t*BuO	**5d**	57 [c]
3d	1-Cyclohexenyl	Benzyl	*t*BuO	**5e**	76 [b]
3e	CH_3	H	*t*BuO	**4f**	80 [d]

[a] In the presence of $(CH_3CO)_2O$ (1.49 equiv.) and NEt_3 (1.46 equiv.) instead of $(t\text{BuOCO})_2\text{O}$. [b] Total yield including aminolysis, based on the corresponding methoxycarbene complex. [c] Only 1.3 equiv. of $(t\text{BuOCO})_2\text{O}$ was used. [d] Under 1 bar CO.



[*] Prof. Dr. K. H. Dötz, Dr. D. Grotjahn, Dr. K. Harms
Fachbereich Chemie der Universität
Hans-Meerwein-Strasse, D-3550 Marburg (FRG)

[**] Reactions of Complex Ligands, Part 37. This work was supported by the Deutsche Forschungsgemeinschaft and the Fonds der Chemischen Industrie. *D.G.* thanks the National Science Foundation for a grant. – Part 36: K. H. Dötz, H.-G. Erben, K. Harms, *J. Chem. Soc. Chem. Commun. 1989*, 692.

The chelate complexes **5** form brown needle-like crystals that are briefly stable in air. The X-ray structure analysis[7] of **5a** (Fig. 1) shows a planar five-membered chelate ring with a short chromium–carbene bond (1.985(4) Å) and a

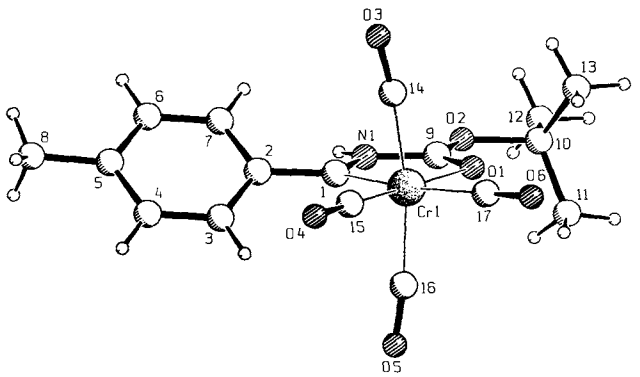
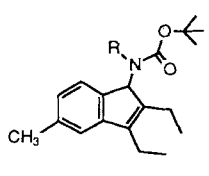


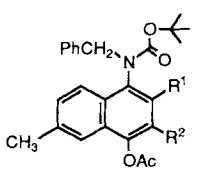
Fig. 1. Crystal structure of **5a**. Important bond lengths [Å] and angles [°]: Cr1-C1 1.985(4), Cr-O1 2.144(3), C1-N1 1.374(5), C9-O1 1.230(5), C9-O2 1.311(5), C9-N1 1.363(6); C1-Cr1-O1 77.8(1), N1-C9-O1 119.7(4), N1-C9-O2 114.0(4), O1-C9-O2 126.3(4), C1-N1-C9 116.7(3), C1-N1-H 120(2), C9-N1-H 123(2).

relatively long chromium–oxygen distance (2.144(3) Å).[8] In the ^{13}C NMR spectra the signals for the carbene carbon ($\delta = 311-330$) are shifted markedly downfield compared to that in aminocarbene complexes ($\delta \approx 280$) (for comparison: alkoxycarbene complexes $\delta = 330-350$). Above 0 °C, a rapid exchange on the NMR time scale is observed for the four CO ligands. This may indicate the formation of a fluctional coordinatively unsaturated tetracarbonyl-carbene fragment[9] and thus an easy opening of the chelate ring.

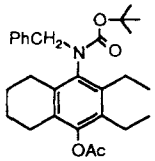
From the NMR spectroscopic and structural characteristics the arylcarbene chelate complexes appear to be suitable as starting materials for an aminocarbene annelation. Thus **5a, c, e** react with alkynes to give the aminoindenes **6, 7** and/or with insertion of CO to give the aminophenol derivatives **8–10**, whereby the non-alkylated complex **5a** affords primarily the five-membered ring compound **6**, whereas the benzyl complex **5c** furnishes mainly the six-membered ring compounds **8, 9**. As has been demonstrated by IR spectroscopy, $Cr(CO)_3$-coordinated annelation products are formed initially, which, however, are partly demetalated under the reaction conditions. Complete demetalation was



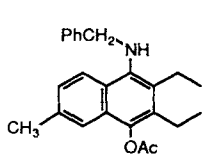
6: R = H
7: R = CH_2Ph



8: $R^1 = R^2 = Et$
9: R^1 = H, $R^2 = (CH_2)_4CH_3$



10



11

5a + EtC≡CEt ----------> **6** (54%)
5c + EtC≡CEt ----------> **7** (11%) + **8** (56%)
5c + $CH_3(CH_2)_4C{\equiv}CH$ ----> **9** (46%)
5e + EtC≡CEt ----------> **10** (67%)

effected with Fe^{III} after in-situ acetylation of the aminonaphthols. The ready cleavage of the $Cr(CO)_3$ fragment is not unexpected, at least in the case of the benzyl-substituted annelation products **8–10**: herein the benzyl hydrogen atoms in the ^1H NMR spectrum are diastereotopic, indicating a sterically determined tilting of the amino substituents from the aminophenol plane, which in turn favors a demetalation. Terminal alkynes are incorporated with the regioselectivity known from the alkoxycarbene annelation: during the formation of five- and six-membered ring products the carbene carbon is preferentially added at the sterically less shielded alkyne carbon atom. By activation with the readily recleavable *tert*-butyloxycarbonyl (Boc) protecting group,[11] also aminocarbene complexes undergo selective annelation reactions under mild reaction conditions and open up – for example by an intramolecular variant – a new route to the synthesis of azapolyheterocycles.

Experimental Procedure

Example of an acylation: A solution of pentacarbonyl methoxy (4-methylphenyl)carbene chromium (1.20 g, 3.68 mmol) in 4 mL of ether was treated dropwise with 0.412 mL (3.77 mmol) of benzylamine. Upon completion of addition the solution boiled and, within 5 min, was decolorized. After 30 min the solution was concentrated in high vacuum and the viscous liquid residue was dissolved in a solution of 1.64 g (7.51 mmol) of $(tBuO_2C)_2O$ in 10 mL of ether. After addition of 45 mg (0.37 mmol) of DMAP the mixture was stirred at RT for 16 h. Subsequent workup by column chromatography on silica gel (– 20 °C, ether/petroleum ether 1/4 to 1/2) afforded **5c** as fine brown needles (1.33 g, 76%). – IR (KBr): $\tilde{\nu}$ = 2014, 1951, 1893, 1863 [$Cr(CO)_4$], 1660 cm^{-1} (NC=O); ^{13}C NMR (– 40 °C, CD_3COCD_3, 100.6 MHz): δ = 326.0 (Cr=C), 235.5, 230.6, 216.0 [1:1:2, $Cr(CO)_4$], 161.0 (NC=O), 145.5, 139.2, 137.1, 129.5, 129.4, 128.2, 126.7, 123.0, 89.5 ($OC(CH_3)_3$), 53.4 (NCH_2Ph), 27.3 [$OC(CH_3)$], 21.0 (CH_3 aryl); EI-MS: *m/z* 473 ($M^{\oplus}$, 1.65%).

Example of a carbene annelation: A degassed solution (triple sequence of freezing, evacuating and thawing, – 196 °C to RT, "freeze-pump-thaw") of 0.189 g (0.408 mmol) of **5e** and 0.093 mL (0.82 mmol) of 3-hexyne in 1.6 mL of toluene in a screw-capped vessel was heated to 55 °C for 4 h. The solution was then treated at RT with Et_3N (0.114 mL, 0.82 mmol), Ac_2O (0.069 mL, 0.73 mmol) and DMAP (4.8 mg, 0.020 mmol). After 3.5 h the mixture was oxidized with 0.6 g (2.2 mmol) of $FeCl_3 \cdot 1.5$ DMF.[12] After 20 min, filtration of the mixture with ether/petroleum ether (1/1) over silica gel and subsequent radial chromatography on silica gel with ether/petroleum ether (1/3) afforded 0.123 g (67%) of **10** as a viscous oil. Its NMR data showed the presence of two rotamers in the ratio 3:1. – Main rotamer: ^1H NMR (C_6D_6, 300 MHz): δ = 7.25–7.3 and 7.0–7.2 (m, 5H), 4.71 and 4.61 (each d, *J* = 13.9 Hz, each 1H, NCH_2Ph), 2.0–2.8 (m, 8H, CH_2 aryl), 1.85 (s, 3H, OAc), 1.35 [s, 9H, $C(CH_3)_3$], 1.3–1.6 (m, 4H), 1.15 and 1.07 (each t, *J* = 7.5 Hz, each 3H, 2 CH_2CH_3); secondary rotamer: distinct signals at δ = 4.47 and 4.44 (each d, *J* = 14.5 Hz, each 1H, NCH_2Ph), 1.85 (s, 3H, OAc), 1.54 [s, 9H, $C(CH_3)_3$]; IR (NaCl, CH_2Cl_2): $\tilde{\nu}$ = 1759 (OAc), 1696 cm^{-1} (NC=O); EI-MS: *m/z* 451 ($M^{\oplus}$, 6%).

Spectroscopic characterization of a five-membered ring annelation product: **6**: IR (NaCl, CH_2Cl_2): $\tilde{\nu}$ = 1699 cm^{-1} (NC=O); ^1H NMR (C_6D_6, 300 MHz): δ = 7.08 (d, *J* = 7.6 Hz, 1H), 7.05 (s, 1H), 7.00 (d, *J* = 7.5 Hz, 1H), 5.6 (br. s, 1H, NH), 3.26 (dd, *J* = 4.2, 5.4 Hz, 1H, CHN), 2.52 (dq, *J* = 7.5, 15 Hz, 1H), 2.25 (s, 3H, CH_3 aryl), 2.0–2.2 (m, 1H), 1.85 (ddq, *J* = 4.2, 7.4, 14.7 Hz, 1H), 1.64 (ddq, *J* = 5.4, 7.4, 14.7 Hz, 1H), 1.42 [s, 9H, $C(CH_3)_3$], 1.01 (t, *J* = 7.5 Hz, 3H), 0.54 (t, *J* = 7.4 Hz, 3H); ^{13}C NMR and multiplicity test (C_6D_6, 75.5 MHz): δ = 153 (br, NC=O), 145.2 (C), 141.7 (C), 140.9 (C), 134.0 (C), 127.3 (CH), 123.8 (CH), 118.3 (CH), 79.5 [$OC(CH_3)_3$], 48.2 (CH,CN), 28.4 [$C(CH_3)_3$], 22.8 (CH_2), 21.6 (CH_3 aryl), 19.9 (CH_2), 13.6 (CH_3), 8.5 (CH_3); MS: *m/z* 301.2059 ($M^{\oplus}$, 26%, calculated for $C_{19}H_{27}NO_2$: 301.2076).

Received: June 22, 1989 [Z 3407 IE]
German version: *Angew. Chem. 101* (1989) 1425

[1] K. H. Dötz, H. Fischer, P. Hofmann, F. R. Kreissl, U. Schubert, K. Weiss: *Transition Metal Carbene Complexes*, Verlag Chemie, Weinheim 1983.
[2] K. H. Dötz, *Angew. Chem. 87* (1975) 672; *Angew. Chem. Int. Ed. Engl. 14* (1975) 644; recent reviews: K. H. Dötz, *Angew. Chem. 96* (1984) 573; *Angew. Chem. Int. Ed. Engl. 23* (1984) 587; W. D. Wulff, P.-C. Tang, K.-S. Chan, J. S. McCallum, D. C. Yang, S. R. Gilbertson, *Tetrahedron 41* (1985) 5813.
[3] Recent examples from the anthracycline series: K. H. Dötz, M. Popall, *Chem. Ber. 121* (1988) 665; W. D. Wulff, Y.-C. Xu, *J. Am. Chem. Soc. 110* (1988) 2312.

[4] K. H. Dötz, I. Pruskil, *Chem. Ber. 111* (1978) 2059; A. Yamashita, *Tetrahedron Lett. 27* (1986) 5915.
[5] Review: K. H. Dötz, M. Popall, G. Müller, *J. Organomet. Chem. 334* (1987) 57.
[6] K. H. Dötz, D. Grotjahn, unpublished results; R. Aumann, S. Althaus, C. Krüger, P. Betz, *Chem. Ber. 122* (1989) 357.
[7] a) Crystallographic data for **5a** ($C_{17}H_{17}CrNO_6$): monoclinic, space group $C2/c$ (No. 15), $a = 23.355(5)$, $b = 11.187$, $c = 15.629$ Å, $\beta = 111.66(1)°$, $V = 3795$ Å^3, $M_r = 303.32$, $\varrho_{calcd} = 1.342$ g cm^{-3}, $F(000) = 1504$ e, $\mu(Cu_{K\alpha}) = 53.0$ cm^{-1} A crystal with the dimensions $0.3 \times 0.3 \times 0.5$ mm was measured at room temperature on an Enraf-Nonius CAD 4 diffractometer ($Cu_{K\alpha}$ radiation, graphite monochromator). Of 2429 measured reflections (ω scans, 2–55°) 2120 are unique; 1864 with $F_o > 4\sigma(F_o)$ were regarded as observed. Solution by the automatic Patterson method in SHELXS-86 [7b], refinement with SHELX-76 [7c], H atoms with fixed isotropic temperature factors, with exception of N–H at calculated positions, all other atoms anisotropic, $R = 0.042$, $wR = 0.034$ ($w = 1/\sigma^2$), 241 parameters. The absorption was corrected empirically with DIFABS [7d]. All calculations were carried out on a MICRO-VAX II [7e–g]. b) G. M. Sheldrick, SHELX-86, Program for Crystal Structure Solution, Göttingen 1986; c) G. M. Sheldrick, SHELX-76, Program for Crystal Structure Determination, Cambridge 1976; d) N. Walker, D. Stuart, *Acta Crystallogr. Sect. A 39* (1983) 158; e) A. L. Spek, Platon 88, Program for Geometrical Analysis of Crystal Structures, Utrecht 1988; f) E. Keller, SCHAKAL-88B, A FORTRAN Program for the Graphic Representation of Molecular and Crystallographic Models, Freiburg 1988. g) Further details of the crystal structure determination are available on request from the Fachinformationszentrum Karlsruhe, Gesellschaft für wissenschaftlich-technische Information mbH, D-7514 Eggenstein-Leopoldshafen 2 (FRG) on quoting the depository number CSD-320007, the names of the authors, and the journal citation.
[8] Cf. H. G. Alt, G. S. Herrmann, H. E. Engelhardt, R. D. Rogers, *J. Organomet. Chem. 331* (1987) 329.
[9] C. P. Casey, M. C. Cesa, *Organometallics 1* (1982) 87.
[10] K. H. Dötz, J. Mühlemeier, U. Schubert, O. Orama, *J. Organomet. Chem. 247* (1983) 187.
[11] The Boc protecting group was removed from **8** with HCl/ether with formation of **11** · HCl (79%).
[12] S. Tobinaga, E. Kotani, *J. Am. Chem. Soc. 94* (1972) 309.

Chlorocarbon Activation: Catalytic Carbonylation of Dichloromethane and Chlorobenzene**

By *Marc Huser, Marie-Thérèse Youinou,* and *John A. Osborn**

Chlorocarbons are of interest as intermediates but suffer from their relatively inert character (C–Cl bond energy ≈ 80 kcal mol^{-1}), and consequently catalytic functionalization of halocarbons has almost exclusively involved the use of the more reactive but expensive bromo- and iodo-compounds.

Dichloromethane is known to be activated by strong nucleophiles[1] or by oxidative addition (thermal[2] and photochemical[3]). Our initial objective was the monoactivation of CH_2Cl_2 using a mononuclear complex, allowing access in a catalytic process to chloromethyl organic products (e.g. $ClCH_2COOR$). Two conditions appeared necessary for monoactivation: a) an extremely electron-rich metal center and b) sufficiently sterically bulky ligands to impede further attack on the M–CH_2Cl unit. It was eventually found that Pd^0 complexes with strongly donating, but voluminous phosphanes, e.g. PCy_3 and $PiPr_3$, have the required properties. The complex **1a** reacts rapidly with CH_2Cl_2 at 25 °C, yielding after recrystallization the colorless chloromethyl complex **2a.**

$[Pd(PCy_3)_2(dba)]$ **1a**
dba = dibenzylideneacetone, Cy = cyclohexyl
trans-$[Pd(PCy_3)_2(CH_2Cl)Cl]$ **2a**
trans-$[Pd(PCy_3)_2(CH_2Br)Br]$ **2b**

Its ^1H NMR spectrum shows a triplet at $\delta = 3.92$ (2H, $^3J_{HP} = 8$ Hz) for the Pd–CH_2Cl resonance, as well as the cyclohexyl resonances. In the analogous bromomethyl complex **2b** prepared similarly from CH_2Br_2, the ^1H resonance of Pd–CH_2Br is shifted to $\delta = 3.70$. The $^{31}P\{^1H\}$ NMR (80 MHz, CD_2Cl_2) shows the expected singlet resonance at $\delta = 24.0$ (**2a**) and $\delta = 23.5$ (**2b**). Notably in the infrared spectra, the absorption at 650 cm^{-1} (assigned to νC–Cl) in **2a** is replaced by an absorption at 585 cm^{-1} (νC–Br). Similar observations have been made using $PiPr_3$ as ligand, but in contrast complexes with less basic ligands (e.g. $P(CH_2Ph)_3$, PPh_3 and PPh_2Cy) do not react with CH_2Cl_2.

When **2a** is treated with CO (30 bar) in C_6D_6 at 25 °C, the NMR spectra (^1H and ^{31}P) show the formation of the complex **3** and diketene **4**; the ^1H NMR signals appearing at $\delta = 4.56$ (1H), 3.92 (1H) and 2.88 (2H) are characteristic for diketene. Two feasible mechanisms (**A, B**) for this reaction are shown in Figure 1, both of which have analogues in the literature.[5, 6] We note that stable Pt^{II} ketene complexes (of type **5**) have recently been synthesized.[6c]

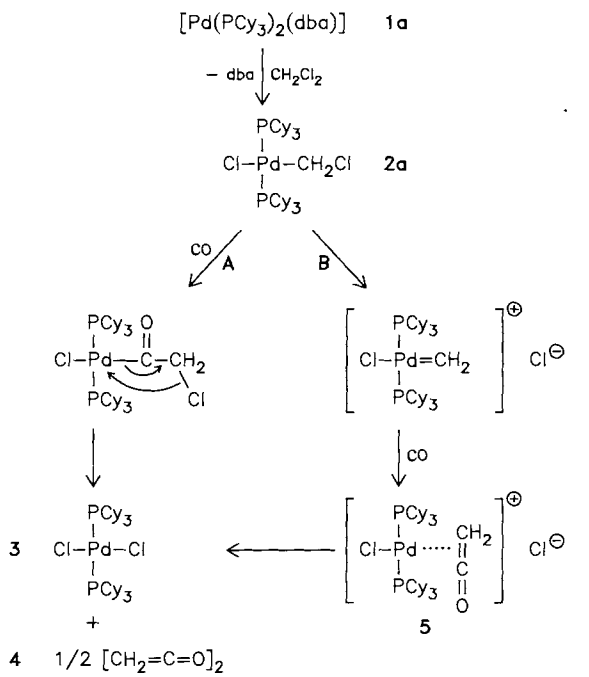


Fig. 1. Possible mechanisms **A** and **B** for the formation of ketene by carbonylation of **2a**.

Chlorobenzene activation by Ni,[7] Pd[8] or Pt[8c, 9] complexes has been reported, but a catalytic functionalization has so far not been observed. We have now found that solutions of the complexes **1** in chlorobenzene turn from orange to yellow at 60 °C and white crystalline phenyl complexes **6** can be isolated in good yields. Unexpectedly, under the same conditions neither the Pd^0 complexes with basic but more bulky phosphane ligands ($PtBu_3$, $PtBu_2Ph$) nor those of lower basicity but similar steric volume (PPh_2Cy, $P(m\text{-tol})_3$)

[*] Prof. Dr. J. A. Osborn, Dr. M. T. Youinou, Dr. M. Huser [+]
Laboratoire de Chimie des Métaux de Transition et de Catalyse, UA au CNRS n° 424, Université Louis Pasteur, Institut Le Bel
4, rue Blaise Pascal, F-67000 Strasbourg (France)
[+] Present address: Max-Planck-Institut für Kohlenforschung
Postfach 01 13 25, D-4330 Mülheim a.d. Ruhr (FRG)

[**] Rhône-Poulenc is thanked for a Graduate Fellowship (*M.H.*) and for financial support.

yield phenyl complexes of type **6**. Further, **6a**, can be rapidly carbonylated (25 °C, 30 bar CO) to yield **7a**; the reaction is reversible at 60 °C under argon.

$[Pd(PR_3)_2(dba)]$ **1**, $PR_3 = PCy_3$ (**1a**), PCy_2Ph, $P(CH_2Ph)_3$, $PiPr_3$
trans-$[Pd(PR_3)_2(C_6H_5)Cl]$ **6**, $PR_3 = PCy_3$ (**6a**)
trans-$[Pd(PR_3)_2(COC_6H_5)Cl]$ **7**, $PR_3 = PCy_3$ (**7a**)

The substituted chlorobenzenes, p-RC_6H_5Cl ($R = OCH_3$, NO_2, COOEt) also react to form complexes analogous to **7a**, the rate of reaction decreasing in the order $R = NO_2 > COOEt \gg H > OCH_3$. The X-ray structure analysis of the adduct, **6a**,[10] confirms the *trans* arrangement of the phenyl- and chloro-ligands (Fig. 2).

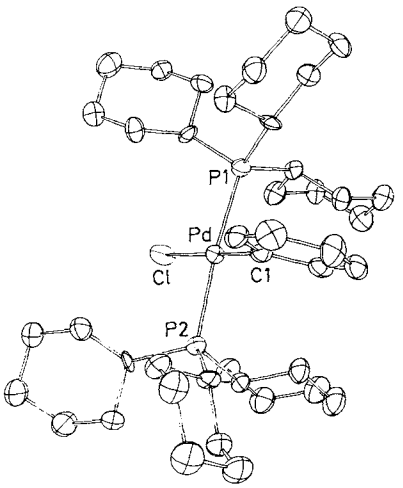


Fig. 2. Structure (ORTEP) of complex **6a**. Principal bond distances [Å]: Pd-P1 2.343(1), Pd-P2 2.347(1), Pd-Cl 2.403(1), Pd-C1 2.004(6); selected bond angles [°]: P1-Pd-P2 173.98(5), C1-Pd-Cl 177.5(2), Cl-Pd-P1 90.07(5), Cl-Pd-P2 90.05(5), C1-Pd-P1 90.4(1), C1-Pd-P2 89.8(1).

Under suitable conditions, the activation and functionalization of these chlorocarbons can be carried out catalytically with **1a**. Thus, the carbonylation of CH_2Cl_2 to ketene (or its derivatives) is possible if the complex **3** formed from **1a** can be reduced to regenerate the active species $Pd(PCy_3)_2$. This has been carried out using H_2 and a base B to trap the HCl formed as $BH^{\oplus}Cl^{\ominus}$. However, B must be a) a poor nucleophile (e.g. sterically hindered) to minimize chloride displacement in **2a** and quaternization of CH_2Cl_2, but b) more basic than PCy_3 to prevent protonation of the phosphane. Excess PCy_3 is used to maintain $Pd(PCy_3)_2$ as the predominant species of Pd^0 even under CO pressure. To illustrate the catalytic formation of ketene, NCy_2H was used as base so as to trap ketene by its reaction with the N–H function to form CH_3CONCy_2, which is stable under the reaction conditions and readily quantified. Hence, using **1a**/PCy_3 (1:3), CH_2Cl_2 (25 equiv.) and NCy_2H (50 equiv.) in toluene at 180 °C under CO/H_2 (30 bar, 1/1) a 40% yield of CH_3CONCy_2 and CH_3NCy_2 (1/1) is formed over 2.5 hours. Using $NEtiPr_2$ as base under the same conditions, both $CH_3CONiPr_2$ and $CH_3CONEtiPr$ were produced at a turnover rate of 5 (mol Pd)$^{-1}$ h^{-1}.

With chlorobenzene, two catalytic reactions were studied: alkoxycarbonylation and hydrocarbonylation with **1** or **6** as catalyst. The equations (a) and (b) show examples.

$$C_6H_5Cl + CO + ROH + B \rightarrow C_6H_5COOR + BH^{\oplus}Cl^{\ominus} \quad (a)$$

$$C_6H_5Cl + CO + H_2 + B \rightarrow C_6H_5CHO + BH^{\oplus}Cl^{\ominus}. \quad (b)$$

B = base

Typical conditions for these reactions are presented in the Experimental Section, but we note:

1) Significant catalytic activity is found only with phosphanes which are *both strongly basic* ($pK_a > 6.5$[11]) and with *well defined steric volume*, i.e. the cone angle θ[12] must exceed ca. 160° but be less than 180°. Hence in alkoxycarbonylation [Eq. (a)], only PCy_3 (pK_a 9.7, $\theta = 179°$) and $PiPr_3$ (pK_a 8.7, $\theta = 160°$) gave active catalysts, complexes involving smaller (PEt_3, pK_a 8.7, $\theta = 130°$), larger ($PtBu_3$, pK_a 10.3, $\theta = 182°$) or less basic phosphanes ($P(CH_2Ph)_3$, pK_a 6.0, $\theta = 165°$; PPh_3, pK_a 2.9, $\theta = 145°$) being totally inactive. Using methanol, both C_6H_5COOMe and C_6H_5COOEt were observed, the latter resulting from metathetical alkyl exchange with the base NEt_3. No double carbonylation products were detected.[13] In hydrocarbonylation [Eq. (b)], the use of PCy_3 and $PiPr_3$ again gave the highest activity, other phosphanes studied giving either inactive (PPh_3, $P(m\text{-tol})_3$, PPh_2Bu, $P(CH_2Ph)_3$) or poorly active (PEt_3, $PnBu_3$, $PtBu_3$) catalyst systems. The only products detected were C_6H_5CHO (ca. 90%) and C_6H_6 (ca. 10%).

2) On addition of *excess phosphane* to the catalyst system a) the Pd catalyst is more stable to decomposition and b) the rate of catalysis increases until a certain phosphane concentration is reached. Further addition of phosphane beyond this optimum value causes a decrease in the reaction rate. Thus, on using **6a** as catalyst, addition of 3 equiv. of PCy_3 increased the rate of hydrocarbonylation fourfold. However, if a further 5 equiv. of PCy_3 are added, the rate now observed is only twice that found initially. The optimum concentration of phosphane depends on the conditions used and, in general, increases with increasing CO pressure.

3) The *nature* and *concentration* of the *base* B are both important. The base must have a pK_a higher than that of the phosphane used if the phosphane is not to serve as proton acceptor. Further, the rate of hydrocarbonylation increases with increasing concentration of base used. Hence on doubling the base concentration under standard conditions, the catalytic rate increases from 1.9 to 3.4 (mol Pd)$^{-1}$ h^{-1}, the selectivity for C_6H_5CHO remaining constant.

The observation that a maximum rate occurs for a certain phosphane concentration can be related to two opposing effects. Firstly, an increase in phosphane concentration will increase the concentration of the C–Cl activating species, $Pd(PR_3)_2$, with a concomitant decrease in inactive carbonyl-containing species. A rate increase is thus expected but will only occur if the phosphane is sufficiently bulky to prevent further formation of less reactive $Pd(PR_3)_n$ (n = 3,4) species. Secondly, the rate limiting step in such reactions is the base-assisted alcoholysis[13] or hydrogenolysis of **7** which is inhibited by phosphane, addition of which will thereby cause a decrease in rate.

In conclusion, although the catalytic reactions of bromo- and iodo-aromatics are well known,[13] the analogous chloro-derivatives have resisted functionalization except when coactivated by coordination to a tricarbonylchromium moiety.[14] The molecular Pd complexes reported here show a well defined window of reactivity imposed by the electronic and steric properties of the phosphane ligands. Further, despite our preconceptions, the C–Cl activation of CH_2Cl_2 and C_6H_5Cl is not rate limiting in the catalytic process and, unexpectedly, is comparatively facile.

Experimental Procedure:

Synthesis of **2a**: 186 mg (0.2 mmol) of **1a** were dissolved in CH_2Cl_2 (10 mL). After 15 min, the red solution had turned yellow. The solvent was removed, and the recovered solid washed with 2×10 mL Et_2O and recrystallized from 1:1 $(CH_3)_2CO/Et_2O$ to yield colorless microcrystals. Yield 95 mg (65%). ^1H NMR (200 MHz, C_6D_6): $\delta = 3.92$ (t, $^3J(P-H) = 8$ Hz, 2H, Pd-CH_2Cl), 1.20–2.66 (m, 66H, C_6H_{11}P); $^{31}P\{^1H\}$ NMR (80 MHz, C_6D_6): $\delta = 24.0$(s); IR (nujol) $\tilde{\nu}$[cm^{-1}] = 650 (C–Cl); MS: $m/z = 715$ ($M^{\oplus} - Cl$), 701 ($M^{\oplus} - CH_2Cl$).

Synthesis of **6a**: 1.3 g (1.44 mmol) **1a** were dissolved in C_6H_5Cl (100 mL) and the solution heated at 60 °C for 2 h and filtered to remove traces of metallic Pd. After evaporation of the filtrate, the resultant colorless solid was washed with ether (50 mL) to extract free dba. Yield 850 mg (76%). Crystals suitable for an X-ray structure determination were obtained from toluene solutions. ^1H NMR (200 MHz, C_6D_6): $\delta = 7.74$ (d, 2H, H *ortho*), 7.13 (t, 2H, H *meta*), 7.00 (t, 1H, H *para*), 1.2–2.35 (m, 66H, C_6H_{11}, P); $^{31}P\{^1H\}$ NMR (80 MHz, C_6D_6): $\delta = 22.9$(s). Satisfactory microanalyses (C,H,P,Cl) were obtained. Similar procedures were used for other phosphane complexes **6**, and substituted chlorobenzenes.

Carbonylation of **2a**: a solution of 400 mg **2a** in C_6D_6 (10 mL) was stirred at room temperature under CO (30 bar). Sample were analyzed periodically by ^1H and $^{31}P\{^1H\}$ NMR. The reaction was complete after 48 h, giving **3** and diketene **4** quantitatively.

Catalytic experiments were carried out in a 125 mL autoclave (Hastelloy HB2): A typical experiment used: Pd complex (1 mmol), PCy_3 (total 5 mmol), CO (15 bar), C_6H_5Cl (50 mmol), NEt_3 (55 mmol), in toluene (total volume 30 mL), 180 °C. In reaction a) CH_3OH (50 mmol) was added; in reaction b) H_2 (15 bar) was used. The Pd catalysts originally used were **1** or **6** with 3 equiv. of PR_3 in addition, but their generation in situ under the appropriate conditions by use of $Pd(CH_3COO)_2$ with 5 equiv. of phosphane was found to give similar behavior. Products from a) were C_6H_5COOR where $R = CH_3$ or C_2H_5 with turnover rates of ca. 1.2 (mol Pd)$^{-1}$ h^{-1}. Products from b) were C_6H_5CHO and C_6H_6 (selectivity ca. 9:1) with a turnover rate of 1.9 (mol Pd)$^{-1}$ h^{-1}. Using no excess PCy_3, a rate of 0.5 (mol Pd)$^{-1}$ h^{-1} was observed. Using 110 mmol NEt_3, the rate of 3.4 (mol Pd)$^{-1}$ h^{-1} was measured.

Received: May 8, 1989
revised: July 19, 1989 [Z 3326/3327 IE]
German version: *Angew. Chem. 101* (1989) 1427

CAS Registry numbers:
1a, 122744-44-9; **2a**, 122700-57-6; **2b**, 122700-59-8; **3**, 78655-99-9; **4**, 674-82-8; **6a**, 122700-58-7; **7a**, 122700-60-1; CH_2Cl_2, 75-09-2; C_6H_5Cl, 108-90-7; CH_2Br_2, 74-95-3; NCy_2H, 101-83-7; CH_3CONCy_2, 1563-91-3; CH_3NCy_2, 7560-83-0.

[1] a) Y. C. Lin, J. C. Calabrese, S. S. Wreford, *J. Am. Chem. Soc. 105* (1983) 1679; b) M. J. Krause, R. G. Bergman, *ibid. 107* (1985) 2972.

[2] a) A. L. Balch, C. T. Hunt, C. L. Lee, M. M. Olmstead, J. P. Farr, *J. Am. Chem. Soc. 103* (1981) 3764; b) P. Jandik, U. Schubert, H. Schmidbaur, *Angew. Chem. 94* (1982) 74; *Angew. Chem. Int. Ed. Engl. 21* (1982) 73; *Angew. Chem. Suppl. 1982*, 1; c) H. H. Murray, J. P. Fackler, A. M. Mazani, *Organometallics 3* (1984) 1310; d) B. Kellenberger, S. J. Young, J. K. Stille, *J. Am. Chem. Soc. 107* (1985) 6105; e) T. Yoshida, T. Ueda, T. Adachi, K. Yamamoto, T. Higuchi, *J. Chem. Soc. Chem. Commun. 1985*, 1137; f) T. B. Marder, W. C. Fultz, J. C. Calabrese, R. L. Harlow, D. Milstein, *ibid. 1987*, 1543.

[3] a) W. L. Olson, D. A. Nagaki, L. F. Dahl, *Organometallics 5* (1986) 630; b) J. A. Labinger, J. A. Osborn, N. J. Coville, *Inorg. Chem. 19* (1980) 3236; c) J. V. Caspar, H. B. Gray, *J. Am. Chem. Soc. 106* (1984) 3029; d) O. J. Scherer, H. Jungmann, *J. Organomet. Chem. 208* (1981) 153; e) L. Chassot, A. von Zelewsky, *Helv. Chim. Acta 69* (1986) 1855.

[4] M. Huser, J. A. Osborn, unpublished results.

[5] For path **A** see: S. I. Hommeltoft, M. C. Baird, *Organometallics 5* (1986) 190.

[6] For path **B** see: a) A. Miyashita, R. H. Grubbs, *Tetrahedron Lett. 22* (1981) 1255; b) A. Miyashita, H. Shitara, H. Nohira, *J. Chem. Soc. Chem. Commun. 1985*, 850; c) *Organometallics 4* (1985) 1463; d) B. Cetinkaya, P. Dixneuf, M. F. Lappert, *J. Chem. Soc. Chem. Commun. 1973*, 206; e) T. W. Bodnar, E. J. Crawford, A. R. Cutler, *Organometallics 5* (1986) 947; f) C. A. Ghilardi, S. Midollini, S. Moneti, A. Orlandini, J. A. Ramirez, *J. Chem. Soc. Chem. Commun. 1989*, 304.

[7] a) M. Hidai, T. Kashiwagi, T. Ikeuchi, Y. Uchida, *J. Organomet. Chem. 30* (1971) 279; b) M. Hidai, Y. Uchida, I. Ogato, *Organotransition Met. Chem. Proc. Jpn-Am. Semin. 1st* (1974) 265; *Chem. Abstr. 86* (1977) 42729; c) S. Otsuka, K. Tani, I. Kato, O. Teranaka, *J. Chem. Soc. Dalton Trans. 1974*, 2216; d) M. Uchino, K. Asagi, A. Yamamoto, S. Ikeda, *J. Organomet. Chem. 84* (1975) 93; M. Uchino, A. Yamamoto, S. Ikeda, *ibid. 24* (1970) C63; e) M. Foa, L. Cassar, *J. Chem. Soc. Dalton Trans. 1975*, 2572; f) P. E. Garrou, R. F. Heck, *J. Am. Chem. Soc. 98* (1976) 4115; g) M. Troupel, Y. Rollin, S. Sibille, J. F. Fauvarque, J. Perichon, *J. Chem. Res. Synop. 1980*, 24, 147; h) T. T. Tsou, J. K. Kochi, *J. Am. Chem. Soc. 101* (1979) 6319; i) D. R. Fahey, J. E. Mahan, *ibid. 99* (1977) 2501; j) A. Morvillo, A. Turco, *J. Organomet. Chem. 208* (1981) 103.

[8] a) D. R. Coulson, *J. Chem. Soc. Chem. Commun. 1968*, 1530; b) P. Fitton, E. A. Rick, *J. Organomet. Chem. 28* (1971) 287; c) R. D. Rieke, A. V. Kavaliunas, *J. Org. Chem. 44* (1979) 3069; d) J. V. Caspar, *J. Am. Chem. Soc. 107* (1985) 6718.

[9] a) D. H. Gerlach, A. R. Kane, G. W. Parschall, J. P. Jesson, E. L. Muetterties, *J. Am. Chem. Soc. 93* (1971) 3543; b) R. S. Paonessa, A. L. Prigano, W. C. Trogler, *Organometallics 4* (1985) 647; c) J. Fornies, M. Green, J. L. Spencer, F. A. Gordon, *J. Chem. Soc. Dalton Trans. 1977* 1006.

[10] Crystal structure analysis of **6a**: $C_{49}H_{79}P_2ClPd$; $P2_1/c$; $a = 17.686(6)$, $b = 9.656(4)$, $c = 27.845(9)$ Å, $\beta = 101.04(2)°$, $V = 4667.3$ Å^3 and $Z = 4$, $\varrho_{calc} = 1.241$ g cm^{-3}, $\mu(Cu_{K\alpha}) = 4.7$ cm^{-1}. Philips PW 1100/16 diffractometer; 173 K; 5312 measured reflections, averaged to 5195, of which 3827 observed ($I \geq 3\sigma(I)$; $R = 0.054$, $R_w = 0.075$).

[11] W. A. Henderson, Jr., C. A. Streuli, *J. Am. Chem. Soc. 82* (1960) 5791.

[12] C. A. Tolman, *J. Am. Chem. Soc. 92* (1970) 2956.

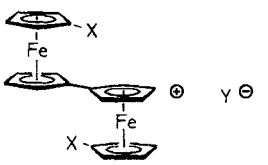
[13] See F. Ozawa, N. Kawasaki, T. Yamamoto, A. Yamamoto, *Organometallics 6* (1987) 1640, and references cited therein.

[14] R. Mutin, C. Lucas, J. Thivolle-Cazat, V. Dufaud, F. Dany, J. M. Basset, *J. Chem. Soc. Chem. Commun. 1988*, 896.

Pronounced Anion Dependence of Valence Detrapping Temperature in Mixed-Valence 1′,1‴-Disubstituted Biferrocenium Salts**

By *Robert J. Webb, Arnold L. Rheingold, Steven J. Geib, Donna L. Staley,* and *David N. Hendrickson**

The study of intramolecular electron-transfer events in mixed-valence metal complexes[1] in the solid state has given fundamental information about environmental effects on rates of electron transfer. The lowest-energy electronic states are vibronic[2] and as a result mixed-valence complexes are very sensitive to their environments. The sensitivity to solvate molecules (S) has been demonstrated for mixed-valence μ-oxo-centered $[Fe_3O(O_2CCH_3)_6(py)_3] \cdot S$ complexes.[3] However, little is known of what effect a change in counterion has on the rate of intramolecular electron transfer in binuclear or trinuclear mixed-valence complexes. In this paper we report dramatic changes in the temperature of valence detrapping which occur for the mixed-valence 1′,1‴-diiodobiferrocenium and related cations as the anion is changed (see **1**).



1

X = I, Br, Cl, $CH_2C_6H_5$
Y = I_3, SbF_6, PF_6

Detailed physical data have been presented[4] for the $I_3^{\ominus}$ and Br–I–Br$^{\ominus}$ salts of various 1′,1‴-disubstituted biferrocenium cations. The $I_3^{\ominus}$ salts of the 1′,1‴-dibromo- and 1′,1‴-diiodobiferrocenium cations are valence detrapped (one

[*] Prof. Dr. D. N. Hendrickson
Department of Chemistry, D-006
University of California at San Diego
La Jolla, CA 92093 (USA)
Prof. Dr. A. L. Rheingold, S. J. Geib, D. L. Staley
Department of Chemistry, University of Delaware
Newark, DE 19716 (USA)
R. J. Webb
School of Chemical Sciences, University of Illinois
Urbana, IL 61801 (USA)

[**] This work was supported by the U.S. National Institutes of Health (HL 13652).

doublet) on the ^{57}Fe Mössbauer time scale at 4.2 K. This has been attributed[4d,f,g,i] to rapid tunneling ($> 10^9\ s^{-1}$ at 4.2 K) between the two vibronic states of the cation which are at equal energy as a result of the site symmetry of the cation in the crystal. On the other hand, the analogous 1′,1‴-dichlorobiferrocenium salt is valence trapped to 340 K, a fact attributed[4d] to an asymmetric positioning of the anion relative to the nearest cation. In this case one of the two vibronic states for the cation is at lower energy and the cation is valence trapped in this one state.

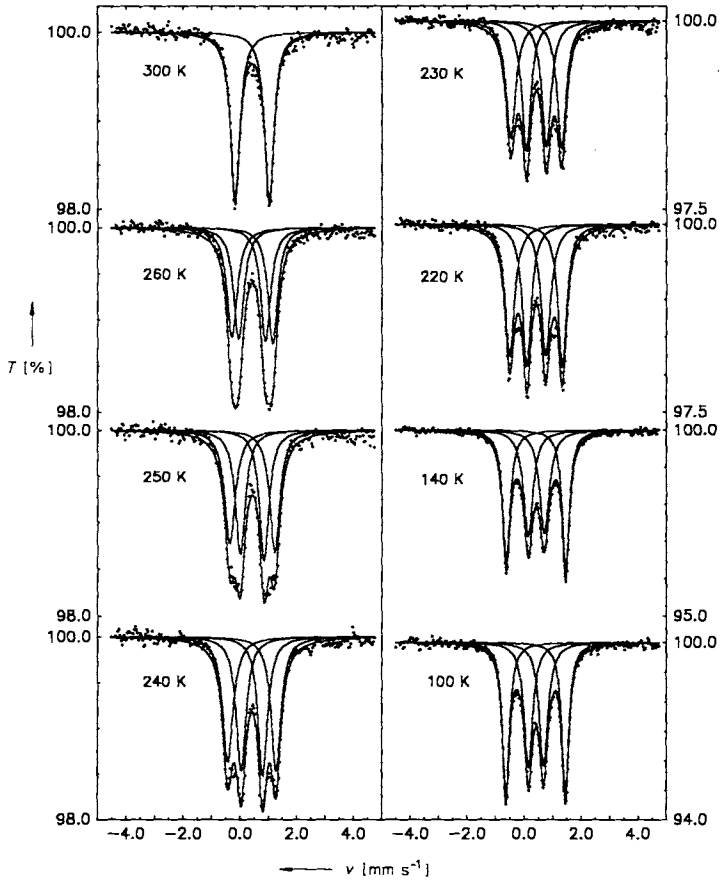


Fig. 1. Variable-temperature ^{57}Fe Mössbauer spectrum of a polycrystalline sample of 1′,1‴-diiodobiferrocenium hexafluoroantimonate. The solid lines result from least-squares fits of the data to Lorentzian lineshapes. T = transmission; v = rate.

It was surprising to find that changing from $I_3^\ominus$ to $PF_6^\ominus$ for the 1′,1‴-diiodobiferrocenium counteranion leads to a change from valence detrapped (one doublet) at 4.2 K to valence trapped at 350 K (two doublets) on the Mössbauer time scale. Furthermore, it was found that the $SbF_6^\ominus$ salt of this same cation begins to convert from trapped to detrapped at ca. 230 K and is completely converted by ca. 300 K (Fig. 1). It must be emphasized that the mixed-valence cation in all of these salts does have a potential-energy barrier for electron transfer, as evidenced by IR data where the ⊥ C–H bending mode is oxidation-state dependent.[5] The $I_3^\ominus$ salt has Fe^{II} and Fe^{III} bands at 820 and 845 cm^{-1}, respectively; the corresponding bands are found at 814 and 853 cm^{-1} for the $SbF_6^\ominus$ salt. A large IR band associated with the $PF_6^\ominus$ anion obscures this region, but it is clear from the Mössbauer data that this salt has a barrier. The cations in the $PF_6^\ominus$ and $SbF_6^\ominus$ salts are indicated to be electronically quite similar from their 7 K powder EPR signals: $g_{||} = 3.306$ and $g_\perp = 1.886$ for the $PF_6^\ominus$ salt and $g_{||} = 3.362$ and $g_\perp = 1.817$ for the $SbF_6^\ominus$ salt. These signals are characteristic of species which are trapped on the EPR time scale. 1′,1‴-Diiodobiferrocenium triiodide exhibits at 4.2 K quite a different powder EPR signal ($g_x = 1.97$, $g_y = 2.01$, and $g_z = 2.75$) which indicates it is also valence detrapped at 4.2 K on the EPR time scale.[4] The X-ray structure[4d] of the $I_3^\ominus$ salt shows that the cation does have the trans conformation found for the other compounds and the cation is relatively isolated from other cations.

Pronounced anion sensitivity of the valence-detrapping temperature has been observed for several other 1′,1‴-disubstituted biferrocenium compounds, yet there is no systematic response as the anion is changed from $I_3^\ominus$ to $PF_6^\ominus$ to $SbF_6^\ominus$. For example, the $I_3^\ominus$ salt of 1′,1‴-dibromobiferrocenium cation is detrapped at 4.2 K as with isostructural 1′,1‴-diiodobiferrocenium triiodide. However, in the case of the 1′,1‴-dibromobiferrocenium cation it is the $SbF_6^\ominus$ salt which remains trapped up to 345 K, whereas, the $PF_6^\ominus$ salt is detrapped down to at least 100 K.

For all twelve 1′,1‴-disubstituted biferrocenium compounds for which there is an X-ray structure[5–7] the mixed-valence cation assumes a *trans* conformation where the central ligand is essentially planar and remains so independent of temperature. Such is the case for 1′,1‴-dibenzylbiferrocenium $PF_6^\ominus$ and 1′,1‴-dibenzylbiferrocenium $SbF_6^\ominus$ salts of which we determined the 299 K X-ray structures.[8] These two compounds crystallize in sheets of 1′,1‴-dibenzylbiferrocenium cations separated by the anions. Figure 2 illustrates the packing in the $PF_6^\ominus$ salt. The mixed-valence cation has a center of inversion and the $PF_6^\ominus$ ion is disordered in two orientationally related positions. The inversional symmetry of the cation at 299 K is consistent with the observation that the cation becomes detrapped at ca. 165 K on the Mössbauer time scale. The two iron ions of the cation in the $SbF_6^\ominus$ salt are crystallographically inequivalent at 299 K. The Fe-ring ligand distances [Fe1-ring = 1.697(8) Å, Fe2-ring = 1.644(5) Å], as well as the Fe-Sb distances to the nearest $SbF_6^\ominus$ ion [Fe1-Sb = 5.649(8) Å, and Fe2-Sb = 6.166(9) Å] indicate Fe^{III} and Fe^{II} metallocene moieties for Fe1 and Fe2, respectively. Despite this asymmetry the $SbF_6^\ominus$ salt does de-

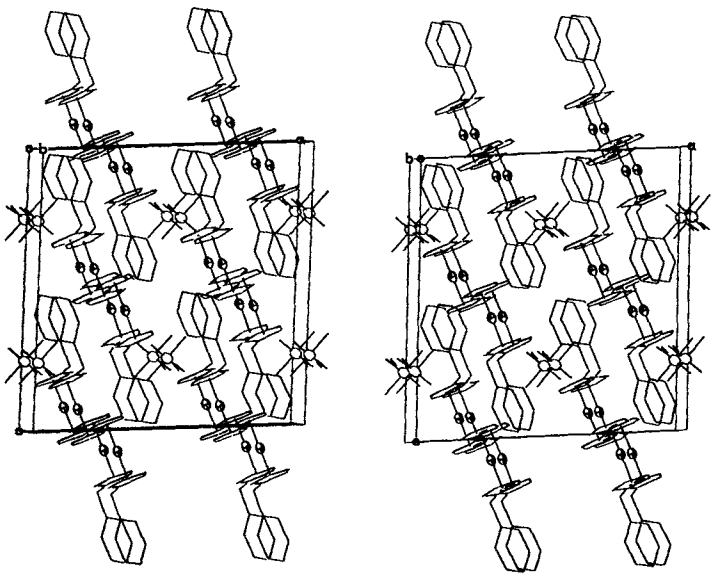


Fig. 2. Stereoview of the packing in $C2/c$ symmetry 1′,1‴-dibenzylbiferrocenium hexafluorophosphate. The viewing direction is approximately parallel to the b-axis.

 © VCH Verlagsgesellschaft mbH, D-6940 Weinheim, 1989 0570-0833/89/1010-1389 $ 02.50/0

trap in the vicinity of 200 K; however, in contrast to the $PF_6^\ominus$ salt the Mössbauer spectrum at high temperatures is a superposition of two valence-detrapped signals. The $SbF_6^\ominus$ complex is the first documented case of a binuclear mixed-valence complex with two crystallographically different metal ions which becomes detrapped as the temperature is increased. The two vibronic states for the cation are at different energies, but the difference in energy must be small enough to permit extremely fast thermally activated tunneling on the Mössbauer time scale. It appears that it is the coulombic interaction between the cation and its neighboring anions which dictate the rate of oscillation of the mixed-valence cation between its two vibronic states (i.e., electron-transfer rate).

It is the crystalline environment about a mixed-valence cation which is the most important factor controlling the rate of intramolecular electron transfer in complexes which have a potential energy barrier. It is not too surprising that the rate of electron transfer in chemical and biological systems can be sensitively controlled by subtle environmental conditions.[9] Understanding how the specificity of electron flow is controlled in biological electron transport chains is important.[10]

Received: June 30, 1989 [Z 3417 IE]
German version: *Angew. Chem. 101* (1989) 1422

[1] P. Day, *Int. Rev. Phys. Chem. 1* (1981) 249; D. B. Brown (Ed.): *Mixed-Valence Compounds, Theory and Applications in Chemistry, Physics, Geology and Biology*, Reidel, Bost 1980; C. Creutz, *Prog. Inorg. Chem. 30* (1983) 1; D. E. Richardson, H. Taube, *Coord. Chem. Rev. 60* (1984) 107.

[2] I. B. Bersuker: *The Jahn-Teller Effect and Vibronic Interactions in Modern Chemistry*, Plenum Press, New York 1984; K. Y. Wong, P. N. Schatz, *Prog. Inorg. Chem. 28* (1981) 369.

[3] H. G. Jang, S. J. Geib, Y. Kaneko, M. Nakano, M. Sorai, A. L. Rheingold, B. Montez, D. N. Hendrickson, *J. Am. Chem. Soc. 111* (1989) 173, and references cited within.

[4] a) T.-Y. Dong, M. J. Cohn, D. N. Hendrickson, C. G. Pierpont, *J. Am. Chem. Soc. 107* (1985) 4777; b) M. J. Cohn, T.-Y. Dong, D. N. Hendrickson, S. J. Geib, A. L. Rheingold, *J. Chem. Soc. Chem. Commun. 1985*, 1095; c) T.-Y. Dong, D. N. Hendrickson, K. Iwai, M. J. Cohn, A. L. Rheingold, H. Sano, I. Motoyama, S. J. Nakashima, *J. Am. Chem. Soc. 107* (1985) 7996; d) T.-Y. Dong, D. N. Hendrickson, C. G. Pierpont, M. F. Moore, *ibid. 108* (1986) 963; e) M. F. Moore, S. R. Wilson, M. J. Cohn, T.-Y. Dong, U. T. Müller-Westerhoff, D. N. Hendrickson, *Inorg. Chem 24* (1985) 4559; f) T.-Y. Dong, T. Kambara, D. N. Hendrickson, *J. Am. Chem. Soc. 108* (1986) 4423; g) *ibid. 108* (1986) 5857; h) M. Sorai, A. Nishimori, D. N. Hendrickson, T.-Y. Dong, M. J. Cohn, *ibid. 109* (1987) 4266; i) T. Kambara, D. N. Hendrickson, T.-Y. Dong, M. J. Cohn, *J. Chem. Phys. 86* (1987) 2362.

[5] J. A. Kramer, D. N. Hendrickson, *Inorg. Chem. 19* (1980) 3330.

[6] M. Konno, H. Sano, *Bull Chem. Soc. Jpn. 61* (1988) 1455.

[7] M. Konno, S. Hyodo, S. Iijima, *Bull Chem. Soc. Jpn. 55* (1982) 2327.

[8] X-ray structure data: 1′,1‴-dibenzylbiferrocenium hexafluorophosphate ($Fe_2C_{34}H_{30}PF_6$), monoclinic, $C2/c$, $a = 14.640(2)$, $b = 12.938(2)$, $c = 15.463(3)$ Å, $\beta = 93.70(1)°$, $V = 2922.7(8)$ Å^3, $Z = 4$; $R = 0.048$ and $R_w = 0.055$ for 2139 observed reflections ($I_0 > 3\sigma(I_0)$) on a Nicolet R3 diffractometer ($Mo_{K\alpha}$, 296 K). – 1′,1‴-dibenzylbiferrocenium hexafluoroantimonate ($Fe_2C_{34}H_{30}SbF_6$), monoclinic, $P2_1$, $a = 10.899(2)$, $b = 11.969(3)$, $c = 12.145(5)$ Å, $\beta = 102.88(2)°$, $V = 1544(1)$ Å^3, $Z = 2$; $R = 0.039$ and $R_w = 0.047$ for 1955 observed reflections ($I_0 > 2.58\sigma(I_0)$) on an Enraf-Nonius CAD4 diffractometer ($Mo_{K\alpha}$, 299 K). Further details for both of these structure determinations are available on request from the Director of the Cambridge Crystallographic Data Centre, University Chemical Laboratory, Lensfield Road, Cambridge CB2 1EW (UK), on quoting the complete journal citation.

[9] R. D. Cannon: *Electron Transfer Reactions*, Butterworths, Boston 1980; K. V. Middelsen, M. A. Ratner, *Chem. Rev. 87* (1987) 113; R. A. Marcus, N. Sutin, *Biochim. Biophys. Acta 811* (1985) 265.

[10] D. DeVault: *Quantum-Mechanical Tunneling in Biological Systems, 2nd Ed.*, Cambridge University Press, Cambridge 1984; J. Jortner, *Biochim. Biophys. Acta 594* (1980) 193; G. Williams, G. R. Moore, R. J. P. Williams, *Comments Inorg. Chem. 4* (1985) 55; R. J. P. Williams, D. Concar, *Nature 332* (1986) 213; B.P.S.N. Dixit, J. M. Vanderkooi, *Curr. Top. Bioenerg. 13* (1984) 159.

Novel Nickel Clusters with Se and Cp′ as Ligands: $[Ni_4Se_2(CO)BrCp'_3]$, $[Ni_6Se_4Cp'_5]$, $[Ni_{15}Se_{10}(CO)_3Cp'_8]$, and $[Ni_{15}Se_{10}(CO)Cl_2Cp'_8]$ **

By *Dieter Fenske** and *Achim Hollnagel*

Complexes of transition metal halides containing allyl-, cyclopentadienyl- or phosphane-ligands react with silyl derivatives of the elements P, As, S, Se, and Te to give metal-rich cluster complexes.[1,2] Our investigations, so far, show that the structures of the compounds formed are influenced by the solvent and the ligand bound to the transition metal atom. For example, upon reaction of $[NiCl_2(PPh_3)_2]$ with $Se(SiMe_3)_2$ mixtures of clusters are obtained containing 2,4,6,8,9,12,15 and 34 nickel atoms. In contrast, upon reaction of [NiCp(PPh$_3$)Cl] (Cp = cyclopentadienyl) with the same selenium reagent only tetranuclear complexes such as $[Ni_4Se_2Cp_4]$ **1** and $[Ni_4Se_2Cp_4(PPh_3)_2]$ are formed.[3]

If the complex [NiCp′(CO)Br][4] presumably formed in the reaction of $[NiCp'(CO)]_2$ (Cp′ = methylcyclopentadienyl) with Br_2 is allowed to react with $Se(SiMe_3)_2$ in diethyl ether, CO is evolved, and a finely crystalline black precipitate of **2**, **3** and **4** separates. After filtration of the reaction mixture black crystals of **2**, **3** and **4** can be isolated from the filtrate after several days standing. If the reaction is carried out in the presence of solid $NiCl_2$, **5** is also formed. Compounds **2**–**5** are only sparingly soluble in THF, acetone and dichloromethane, but cannot be recrystallized from these solvents without decomposition.

$[Ni_4Se_2(CO)BrCp'_3]$ **2** $[Ni_6Se_4Cp'_5]$ **3**

$[Ni_{15}Se_{10}(CO)_3Cp'_8]$ **4** $[Ni_{15}Se_{10}(CO)Cl_2Cp'_8]$ **5**

The IR spectra of **2**–**5** are almost identical, with the exception of the bands observable for the CO stretching vibrations in **2**, **4** and **5** [**2**: $\tilde{\nu} = 2004$ cm^{-1}; **4**: 1992, 1975(sh); **5** = 2001 (in KBr). The ^{1}H NMR spectra of the diamagnetic compounds **2**, **4** and **5** show characteristic signals for the Cp′ ligands.

To elucidate the molecular structures we carried out X-ray structure analyses on **2**–**5**.[5] Accordingly, **2** (Fig. 1) is a

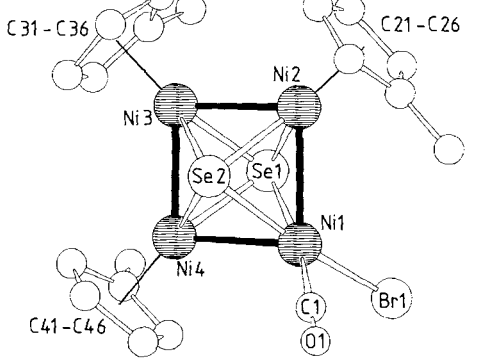


Fig. 1. Structure of **2** in the crystal. Important bond lengths [pm] and angles [°]: Ni1-Ni2 263.1(2), Ni1-Ni4 259.7(2), Ni2-Ni3 255.1(2), Ni3-Ni4 252.8(2), μ_4-Se-Ni 235.0–239.1(2), Ni1-Br1 237.2(2), Se1···Se2 301.3(2), Ni1-C1 192.4(1.7), Ni-C(Cp′) 210.5–216.1(1.2); Ni-Ni-Ni 87.6–91.4(1), Ni-Se-Ni 64.9–67.6 and 100.4–101.3(1), Se2-Ni1-Br1 171.8(1), Se1-Ni1-Br1 94.0(1), Se1-Ni1-C1 171.3(4), Se2-Ni1-C1 96.6(4), C1-Ni1-Br1 91.3(4).

[*] Prof. Dr. D. Fenske, Dipl.-Chem. A. Hollnagel
Institut für Anorganische Chemie der Universität
Engesserstrasse, Geb. Nr. 30.45, D-7500 Karlsruhe (FRG)

[**] Cp′ = $C_5H_4CH_3$. – This work was supported by the Deutsche Forschungsgemeinschaft and the Fonds der Chemischen Industrie.

square planar Ni_4 cluster in which Ni2, Ni3 and Ni4 are each bound to a η^5-Cp′ ring and Ni1 is coordinated by one $Br^{\ominus}$ ligand and one CO ligand. The Ni_4 square is additionally bridged by two μ_4-Se ligands. If one assumes that $Se^{2\ominus}$-, $Cp'^{\ominus}$- and $Br^{\ominus}$-ligands are present then Ni has the formal oxidation number + 2.

In contrast to the 68e-cluster $[Ni_4Se_2Cp_4]$ **1** (Ni–Ni 257–258 pm), the 66e-cluster **2** (Ni–Ni 252.8–263.1 pm) contains only two electrons more than one would expect according to the 18-electron rule. Complex **2** must be considered as a reactive intermediate for the synthesis of larger clusters. If, for example, **2** is allowed to react with [NiCp′(CO)Br] and $Se(SiMe_3)_2$ in THF the hexanuclear cluster **3** (Fig. 2) is formed by reaction at Ni1.

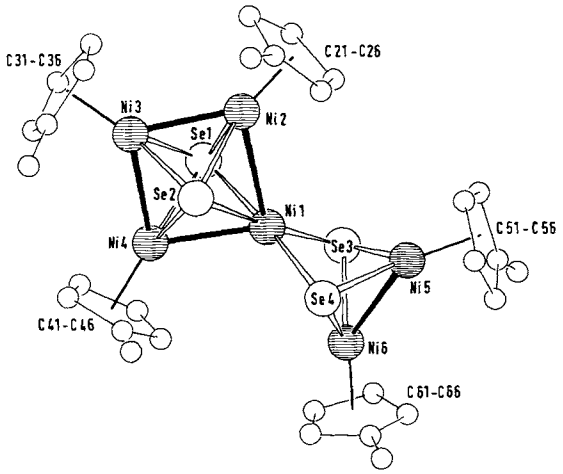


Fig. 2. Structure of **3** in the crystal. Important bond lengths [pm] (error ± 0.3 pm) and angles [°] (error ± 0.1°): Ni1-Ni2 262.9, Ni2-Ni3 251.4, Ni3-Ni4 250.2, Ni1-Ni4 261.3, Ni1-Ni5 319.4, Ni1-Ni6 319.3, Ni5-Ni6 253.1, Se1-Ni-(1–4) 236.8–238.2, Se2–Ni(1–4) 234.1–238.0, Se3–Ni(1,5,6) 227.1–230.7, Se4-Ni(1,5,6) 229.4–232.2, Se1 ··· Se2 304.6, Se3 ··· Se4 302.0; Ni-Ni-Ni (Ni_4-ring 88.1–93.1, Ni-μ_4-Se-Ni 63.6–67.3 bzw. 99.2–100.2, Ni-μ_3-Se-Ni 66.5–88.5.

Complex **3** also contains a planar Ni_4-ring, which is bridged by two μ_4-Se ligands. This Ni_4-ring is joined by two μ_3-Se ligands (Se3, Se4) to a Ni_2-dumbbell. With the exception of Ni1, which is planar coordinated by four Se atoms, all Ni atoms are bound to an η^5-Cp′ ligand; the Ni-μ_3-Se bonds (227.1–232.3 pm) are significantly shorter than the Ni-μ_4-Se bonds (234.1–238.2 pm). The Ni–Ni distances in the four-membered ring of **3** are comparable with those in **2**. In the same way, the distance Ni5–Ni6 (253.1 pm) can also be compared with the Ni–Ni bonding that has been found in other Ni clusters.[1, 6, 9, 11] If one assumes that five Ni–Ni single bonds are present in **3** the paramagnetic 101e-cluster contains three electrons more than would be expected according to the 18-electron rule.

In **2** and **3** the distance between the μ_4-Se and μ_3-Se ligands (301.3–304.6 pm) lies significantly below the van-der-Waals distance that has been found in Se_n and $Se_8^{2\oplus}$ [7] – possibly there is a weak interaction between the Se ligands, as has already been discussed for the μ_4-E ligands in $[Co_4(CO)_{10}(\mu_4\text{-}E)_2]$ (E = S, Te).[8]

The molecular structures of **4** and **5** (Fig. 3) are practically identical: In **4**, three Ni atoms (Ni10, Ni13, Ni15) are bound to CO ligands, and in **5**, two of these ligands (C1-O1 and C2-O2) are replaced by Cl1 and Cl2. The structures of **4** and **5** depicted in Figure 3 show that a previously unknown cluster condensation principle exists. Accordingly, **4** consists of

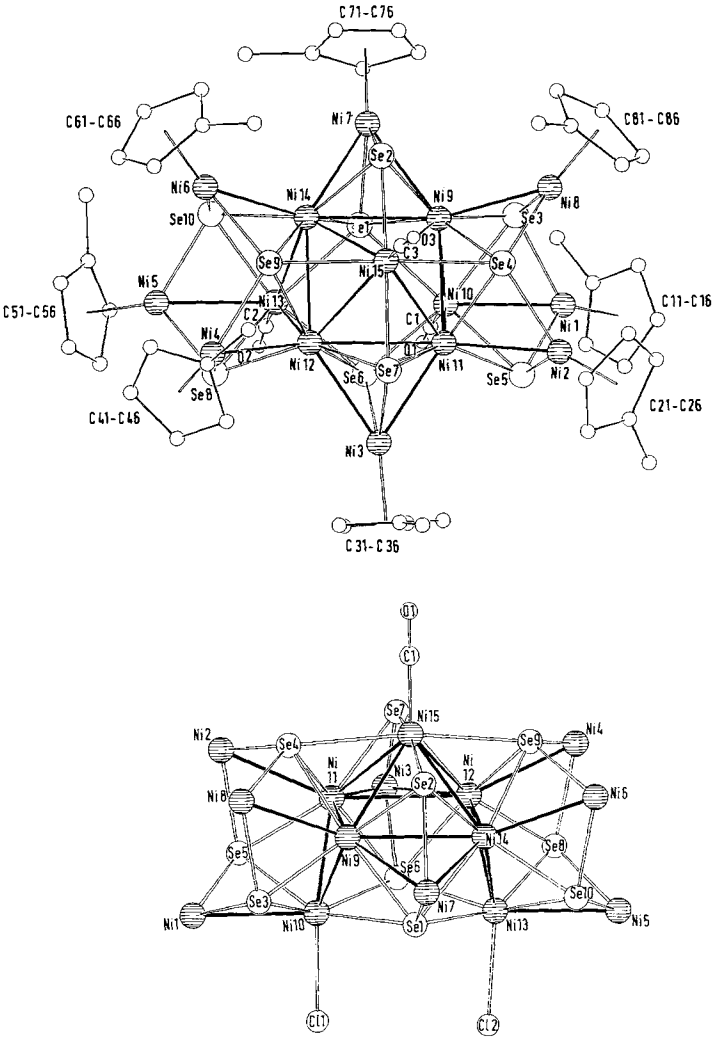


Fig. 3. Top: Structure of **4** in the crystal. Important bond lengths [pm] and angles [°] in **4** (error ± 0.2 pm and ± 0.1°, resp.): Ni1-Ni10 259.6, Ni2-Ni11 259.6, Ni3-Ni 261.3–265.9, Ni4-Ni12 252.3, Ni5-Ni13 259.0, Ni6-Ni14 257.2, Ni7-Ni 265.9–268.3, Ni8-Ni9 254.5, Ni9-Ni11 282.0, Ni11-Ni12 294.8, Ni12-Ni14 283.0, Ni9-Ni14 291.1, Ni15-Ni 271.8–273.5, Ni9-Ni10 259.5, Ni10-Ni11 259.0, Ni12-Ni13 258.5, Ni13-Ni14 259.0, μ_4-Se-Ni 228.3–248.6; μ_5-Se-Ni 232.7–258.2, Ni-C(carbonyl) 180–184(1), C-O: 108–113(2); ✳ □ (Ni9, Ni11, Ni12, Ni14) 89.2–91.0, Ni-Ni15-Ni 62.3–64.7, △ (Ni7, Ni9, Ni14) 56.6–66.0, △(Ni12, Ni13, Ni14) 56.9–66.3, △(Ni3, Ni11, Ni12) 55.3–66.3, Ni-(μ_4-Se)-Ni on Se2 and Se7 67.8–76.7 and 125.5–126.4, on Se3, Se5, Se8 and Se10 64.9–68.5 and 107.0–119.2, Ni-(μ_5-Se)-Ni on Se1 and Se6 63.5–95.9 and 117.0–126.7, resp., on Se4 and Se9 63.5–106.8 and 120.7–125.3, resp. Bottom: Structure of **5** in the crystal (without Cp′ groups). The bond lengths and angles in **5** differ by ±4 pm and ±2° maximally from those in **4**.

a central square Ni_5-pyramid (Ni9, Ni11, Ni12, Ni14, Ni15), in which the Ni–Ni distances in the Ni_4 base [**4**: 282–294.8; **5**: 278.9–289.9 pm] are distinctly longer than the distances to the pyrimid apex Ni15 [**4**: 271.8–273.5; **5**: 270.3–273.9 pm]. Eight further Ni atoms are bound to the Ni_5 cluster (Ni2–4, Ni6–8, Ni10, Ni13), whose distances from each another are 252.3–268.3. The cluster is completed by the atoms Ni1 and Ni5 bound to Ni10 and Ni13, respectively (Ni–Ni 259.0–261.5 pm). Eight η^5-Cp′ groups are bound to the peripheral Ni atoms 1–8 of **4** and **5**, and all faces of the Ni_{15} polyhedron are capped by Se ligands, which either function as μ_4-Se-ligands (Se2, Se3, Se5, Se7, Se8, Se10) or as μ_5-Se-ligands (Se1, Se4, Se6, Se9). The Ni–Se distances in **4** and **5** compare with the values which we have already found in other cluster complexes (Ni-μ_4-Se: 227.7–248.6, Ni-μ_5-Se: 233.1–257.8 pm).[9] The unusual μ_5-coordination of Se

atoms as in **4** and **5** was first observed quite recently in the complex ion $[Co_8Se_8(PPh_3)_6]^{\oplus}$.[10]

One could alternatively consider the structure of the Ni_{15} cluster consisting of four Ni_3 triangles (Ni1, Ni2, Ni8; Ni9, Ni10, Ni11; Ni12, Ni13, Ni14; and Ni4, Ni5, Ni6). The Ni–Ni distances in the outer rings (Ni1, Ni2, Ni8 and Ni4, Ni5, Ni6) are very long (368–378 pm), and in the inner rings (Ni9, Ni10, Ni11, Ni12, Ni13, Ni14) they are 258.5–283.0 pm, i.e. in the range for Ni–Ni bonds. The cluster core is completed by the atoms Ni3, Ni7 and Ni15.

If it is assumed that $Se^{2\ominus}$ and $Cp'^{\ominus}$ ligands are present in **4**, and $Se^{2\ominus}$, $Cp'^{\ominus}$ and $Cl^{\ominus}$ ligands in **5**, then the Ni_{15} clusters in **4** and **5** have the formal charges + 28 and + 30, respectively. Moreover, assuming that the Ni–Ni bonds depicted in Figure 3 are single bonds, it is surprising to note that the valence-electron concentration (226e) in **4** (236e) and **5** (234e) predicted according to the 18-electron rule is relatively well fulfilled. The 18-electron rule is rigidly fulfilled in the case of **5**, even if the long Ni–Ni distances in the central Ni_4 ring (282–294 pm) are interpreted as non-bonding contacts.

Also other authors have already reported on the synthesis of multinuclear nickel complexes with Cp ligands. Examples of such compounds are $[Ni_6Cp_6]^{n\oplus}$ (n = 0, + 1), $[Ni_5Cp_4S_4]$ and $[Ni_3Cp_3S_2]$.[11] Investigations currently under way, however, clearly demonstrate that a direct variation of the Cp ligands can lead to metal-rich cluster compounds with novel structures.

Experimental Procedure

A solution of $[NiCp'(CO)]_2$ (2.2 g, 6.63 mmol) in 35 mL of diethyl ether was treated with 0.34 mL (6.60 mmol) of Br_2 at − 80 °C. After 30 min, a solution of 1.41 mL (6.60 mmol) of $Se(SiMe_3)$ in 10 mL of diethyl ether was added dropwise. Evolution of CO was observed, and at the same time a black crystalline precipitate separated out which consisted of a mixture of **2**, **3** and **4**. After 24 h the residue was filtered off and the filtrate was allowed to stand for several days. A mixture of **2** (black needles), **3** (black hexagons) and **4** (black rhombuses) crystallized from the filtrate. When the reaction described above was carried out in the presence of 0.2 g of solid $NiCl_2$, **5** (black columns) was also formed. Yields: 30% **2**, 20% **3**, 20% **4**, and 30% **5**.

Received: May 26, 1989 [Z 3360 IE]
German version: *Angew. Chem. 101* (1989) 1412

[1] D. Fenske, J. Ohmer, J. Hachgenei, K. Merzweiler, *Angew. Chem. 100* (1988) 1300; *Angew. Chem. Int. Ed. Engl. 27* (1988) 1277.

[2] P. G. Maué, D. Fenske, *Z. Naturforsch. B43* (1988) 1213; *ibid.*, in press; D. Fenske, P. G. Maué, K. Merzweiler, *ibid. B42* (1987) 928.

[3] D. Fenske, A. Hollnagel, K. Merzweiler, *Angew. Chem. 100* (1988) 978; *Angew. Chem. Int. Ed. Engl. 27* (1988) 965.

[4] W. Kläui, L. Ramacher, *Angew. Chem. 98* (1986) 107; *Angew. Chem. Int. Ed. Engl. 25* (1986) 97; E. O. Fischer, C. Palm, *Chem. Ber. 91* (1958) 1725.

[5] X-ray structure analyses: Stoe-Stadi IV diffractometer, $Mo_{K\alpha}$ radiation, empirical absorption correction; solution of structure: Patterson methods, all atoms refined anisotropically. – **2**: $C_{19}H_{21}BrNi_4OSe_2$; lattice constants (190 K): a = 941.6(5), b = 951.7(6), c = 1368.1(11) pm, α = 97.13(4), β = 100.72(3), γ = 112.81(4)°; space group $P\bar{1}$, Z = 2, $\mu(Mo_{K\alpha})$ = 85.6 cm^{-1}; data collection and refinement: ω-Scan, 2 θ_{max} = 50°, 4073 reflections, 2584 with $J > 2\sigma(J)$, 244 parameters without H atoms; R_1 = 0.060, R_2 = 0.064. **3**: $C_{30}H_{35}Ni_6Se_4$; lattice constants (190 K): a = 1336.4(5), b = 1931.1(9), c = 1399.6(6) pm, β = 115.08(3)°; space group $P2_1/c$, Z = 4, $\mu(Mo_{K\alpha})$ = 44.73 cm^{-1}; data collection and refinement: profile analysis, ω-Scan, 2 θ_{max} = 54°, 7666 reflections, 5235 with $J > 2\sigma(J)$, Cp' rings disordered, 384 parameters without H-atoms; R_1 = 0.086, R_2 = 0.084. **4**: $C_{51}H_{56}Ni_{15}O_3Se_{10}$; lattice constants (190 K): a = 1108.9(7), b = 1948.7(12), c = 2927.1(14) pm, β = 90.41(4)°; space group $P2_1/n$, Z = 4, $\mu(Mo_{K\alpha})$ = 100.98 cm^{-1}; data collection and refinement: profile analysis, ω-Scan, 2 θ_{max} = 52°, 13531 reflections, 10860 with $J > 2\sigma(J)$, 713 parameters without H-atoms; R_1 = 0.056, R_2 = 0.062. **5**: $C_{49}H_{56}Cl_2Ni_{15}OSe_{10}$, **5** crystallized with 1 mol diethyl ether/formula unit; lattice constants (190 K): a = 1062.8(5), b = 1408.2(6), c = 2387.0(11) pm, α = 99.40(3), β = 98.17(4), γ = 102.85(4)°; space group $P\bar{1}$, Z = 2, $\mu(Mo_{K\alpha})$ = 95.3 cm^{-1}; data collection and refinement: profile analysis, ω-Scan, 2 θ_{max} = 54°, 15560 reflections, 11715 with $J > 2\sigma(J)$, 715 parameters without H-atoms; R_1 = 0.049, R_2 = 0.064. – Further details of the crystal structure investigations are available on request from the Fachinformationszentrum Karlsruhe, Gesellschaft für wissenschaftlich-technische Information mbH, D-7514 Eggenstein-Leopoldshafen 2 (FRG), on quoting the depository number CSD-53965, the names of the authors, and the journal citation.

[6] J. C. Calabrese, L. F. Dahl, A. Cavalieri, P. Chini, G. Longoni, S. Martinengo, *J. Am. Chem. Soc. 96* (1974) 2616; F. Cecconi, C. A. Ghilardi, S. Midollini, *Inorg. Chem. 22* (1983) 3802.

[7] E. H. Henninger, R. C. Buschert, L. Heaton, *J. Chem. Phys. 46* (1967) 586; R. K. MacMullan, D. J. Prince, J. D. Corbett, *Inorg. Chem. 10* (1971) 1749.

[8] R. C. Ryan, L. F. Dahl, *J. Am. Chem. Soc. 97* (1975) 6904; C. H. Wei, L. F. Dahl, *Cryst. Struct. Commun. 4* (1975) 583.

[9] D. Fenske, J. Ohmer, *Angew. Chem. 99* (1987) 155; *Angew. Chem. Int. Ed. Engl. 26* (1987) 148.

[10] D. Fenske, J. Ohmer, K. Merzweiler, *Z. Naturforsch. B42* (1987) 803.

[11] M. S. Paquette, L. F. Dahl, *J. Am. Chem. Soc. 102* (1980) 6621; H. Vahrenkamp, L. F. Dahl, *Angew. Chem. 81* (1969) 152; *Angew. Chem. Int. Ed. Engl. 8* (1969) 144; H. Vahrenkamp, V. A. Uchtmann, L. F. Dahl, *J. Am. Chem. Soc. 90* (1968) 3272.

X-Ray Structure Analysis of α-Lithiophenylacetonitrile·Lithium Diisopropylamide·2 Tetramethylethylenediamine— a "Quasi-Dianion Complex"**

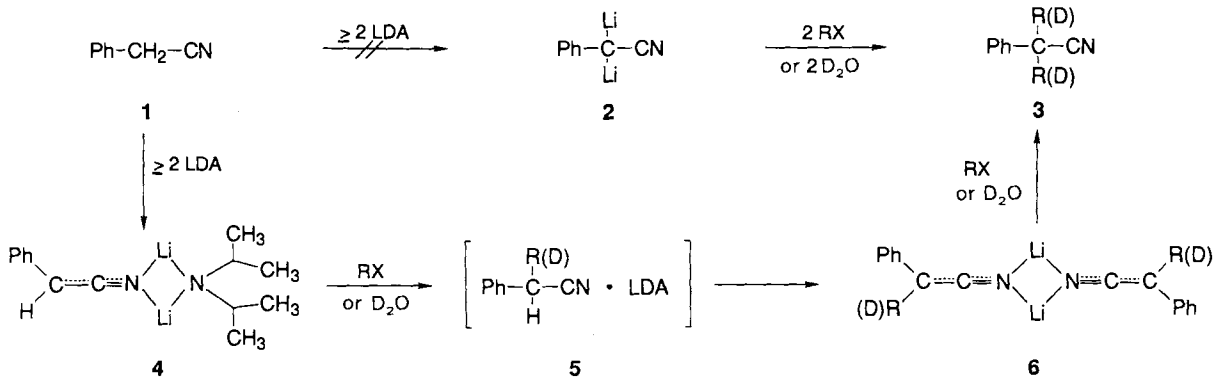
By *Wolfgang Zarges, Michael Marsch, Klaus Harms,* and *Gernot Boche**

The reaction of phenylacetonitrile **1** (or other CH-acidic compounds with acceptor substituents) with 2 mol equivalents of a base such as lithium bis(trimethylsilyl)amide, *n*-butyllithium or lithium diisopropylamide (LDA) misled one to the assumption that "dianions" of the type **2** were formed, since the subsequent alkylation with 2 mol equivalents of RX or the deuteriation with 2 mol equivalents of D_2O afforded dialkylated and dideuteriated products **3**, respectively, in ca. 80% yield.[1]

The complex $(CH_3)_3SiCCNLi_2$ recently characterized by us as a true geminal dianion by an X-ray structure analysis actually reacts with methyl iodide to give 2-methyl-2-trimethylsilylpropiononitrile in 86% yield.[2] However, *Meth-Cohn, Wakefield* et al. recently showed, on the basis of ^{13}C NMR investigations, that in the case of phenylacetonitrile under the aforementioned conditions, monoanions are formed which should be present, with a molecule of base, in the form of "quasi-dianion complexes (QUADACs)" having the structure **4**.[5] If this is the case, then the subsequent reaction of **4** is as follows: 1. RX or D_2O(!) reacts selectively with the PhCHCNLi moiety of **4**, whereby **5** is formed;[6] 2. **5** must be present as the LDA-adduct, since only a reprotonation within an adduct to give the anion **6** can compete with the intermolecular reaction of LDA with RX or D_2O(!).[7] In the subsequent alkylation (deuteriation) of **6**, **3** is formed. The assumption that PhCR(D)CNLi should be present as dimer **6**,[5] was confirmed by the solid state structure of $(PhCHCNLi \cdot TMEDA)_2 \cdot C_6H_6$ **7** (Scheme 1, structure without cocrystallizing C_6H_6).[8] In the following we demonstrate, on the basis of the solid state structure of **4** · 2 TMEDA,[9] that also the assumption of QUADACs was correct. Figure 1 shows the complexation via a Li–N–Li–N four-membered ring of the kind also found in the dimer **7**

[*] Prof. Dr. G. Boche, Dipl.-Chem. W. Zarges, M. Marsch, Dr. K. Harms
Fachbereich Chemie der Universität
Hans-Meerwein-Strasse, D-3550 Marburg (FRG)

[**] This work was supported by the Fonds der Chemischen Industrie and by the Deutsche Forschungsgemeinschaft. *W.Z.* gratefully acknowledges a "Graduiertenstipendium".



(and in other α-lithionitriles[2b]). The bond lengths Li1–N2 and Li2–N2 in the four-membered ring of **4** · 2 TMEDA (203.5(8) and 203.5(9) pm, respectively) compare very closely with those in the four-membered ring of **7** (mean value: 204(3) pm); the distances Li1–N1 (207.5(9) pm) and Li2–N1 (210.9(8) pm) are slightly longer. Since also the bond lengths in the PhCHCN moiety of **4** · 2 TMEDA and **7** are largely comparable, e.g. d(C1-C2) = 138.3(8) compared with 137.8(8) pm and d(C2-N1) = 117.3(7) compared with 117.9(8) pm, the PhCHCN anions in **4** · 2 TMEDA and **7** are similarly structured and bound to lithium. In contrast, the bonds from the TMEDA molecules to lithium differ completely in the two compounds. Thus, the mean value of the Li–N(TMEDA) distances in **7** (205(4) pm) is normal, and the TMEDA molecules are located at practically equal distances from both PhCHCN anions. In **4** · 2 TMEDA, on the other hand, the Li–N(TMEDA) distances are considerably longer [220(1), 220.6(9), 232.0(9) and 234.7(8) ppm[17]]. The TMEDA molecules are concomitantly bent away from the iPr$_2$N moiety towards the PhCHN moiety. The N1–Li1–N3 and N2–Li1–N3 angles (100.1(3)° and 135.2(4)°, respectively) demonstrate this very nicely. The sterically demanding isopropyl groups are undoubtedly responsible for the long Li–N(TMEDA) distances, and also for the bending away of the TMEDA molecules.[18, 19]

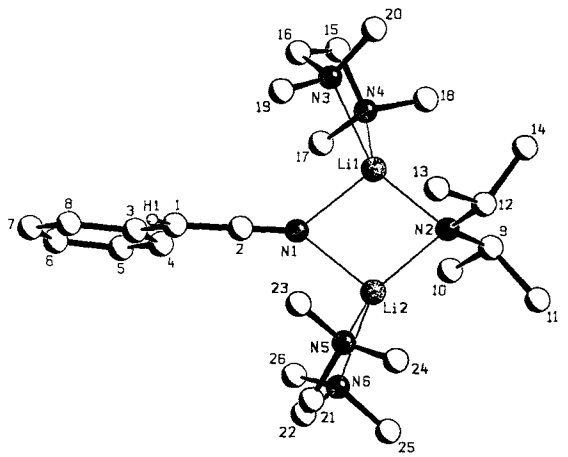
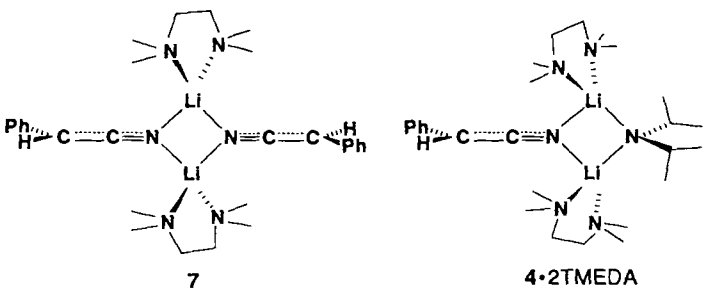


Fig. 1. Asymmetric unit of the structure of **4** · 2 TMEDA in the crystal [10]. Important bond lengths [pm] and angles [°]: Li1-N1 207.5(9), Li1-N2 203.5(8), Li1-N3 234.7(8), Li1-N4 220.6(9), Li2-N1 210.9(8), Li2-N2 203.5(9), Li2-N5 220(1), Li2-N6 232.0(9), C1-C3 143.2(8), C1-C2 138.3(8), C2-N1 117.3(7); C1-C2-N1 179.5(7), N1-Li1-N2 99.2(3), Li1-N2-Li2 82.7(3), N2-Li2-N1 98.1(4), Li2-N1-Li1 80.0(3), N1-Li1-N3 100.1(3), N2-Li1-N3 135.2(4) N1-Li1-N4 111.3(3), N2-Li1-N4 126.8(4), N1-Li2-N5 107.0(4), N2-Li2-N5 128.4(4), N1-Li2-N6 100.2(3), N2-Li2-N6 137.6(4).



4 · 2 TMEDA represents the first adduct of the QUADAC type to be structurally characterized.[20] Preliminary reactions with electrophiles confirm the reaction sequence outlined at the outset. Further details of the reaction, from which it follows that adducts such as **4** · 2 TMEDA have quite other properties than the two anions from which they form, will be reported later.

Received: June 23, 1989 [Z 3411 IE]
German version: *Angew. Chem. 101* (1989) 1424

[1] Review article: E. M. Kaiser, J. D. Petty, L. A. Knutson, *Synthesis 1977*, 509.
[2] a) W. Zarges, M. Marsch, K. Harms, G. Boche, *Chem. Ber. 122* (1989) 1307; b) Review: G. Boche, *Angew. Chem. 101* (1989) 286; *Angew. Chem. Int. Ed. Engl. 28* (1989) 277; see also [3, 4].
[3] Dilithioacetonitrile: G. A. Gornowicz, R. West, *J. Am. Chem. Soc. 93* (1971) 1714.
[4] NMR data for lithium-sodium-malononitrile: H. H. Vogt, R. Gompper, *Chem. Ber. 114* (1981) 2884.
[5] P. J. Crowley, M. R. Leach, O. Meth-Cohn, B. J. Wakefield, *Tetrahedron Lett. 27* (1986) 2909.
[6] Even though the pK_a values of **1** [21.9 in DMSO, F. G. Bordwell, G. E. Drucker, G. J. McCullum. *J. Org. Chem. 47* (1982) 2505] and diisopropylamine [35.7 in THF, R. R. Fraser, T. S. Mansour, *Tetrahedron Lett. 27* (1986) 331] are not directly comparable, there is a great difference in basicity in any case between the two corresponding bases, so that at least the selective deuteriation is astonishing.
[7] a) For similar unusual protonation and deprotonation reactions see: R. Polt, D. Seebach *J. Am. Chem. Soc. 111* (1989) 2622; b) review: D. Seebach, *Angew. Chem. 100* (1988) 1685; *Angew. Chem. Int. Ed. Engl. 27* (1988) 1624.
[8] G. Boche, M. Marsch, K. Harms, *Angew. Chem. 98* (1986) 373; *Angew. Chem. Int. Ed. Engl. 25* (1986) 373; see also [2b].
[9] Synthesis of **4** · 2 TMEDA: A solution of 1.9 mmol of LDA (prepared from 200 mg of diisopropylamine and 1.2 mL of a 1.6 M solution of *n*-butyllithium in hexane) in 3.5 mL of diethyl ether was treated with 100 mg (0.85 mmol) of **1** and 230 mg (2.0 mmol) of TMEDA at 20 °C. Single crystals of **4** · 2 TMEDA could be isolated after 6–8 h at 6 °C; yield 0.12 g (31%).
[10] Structural data of **4** · 2 TMEDA: $C_{26}H_{52}N_6Li_2$, M = 462.62; triclinic, space group $P\bar{1}$, a = 9.968(2), b = 11.966(3), c = 14.171(2) Å, γ = 77.24(2), β = 73.47(1), α = 87.16(2)°, Z = 2, ϱ_{calcd} = 0.972 g cm^{-3}, μ(Cu$_{K\alpha}$) = 4.1 cm^{-1}. 4235 reflections were measured on an Enraf-Nonius CAD4 dif-

fractometer ($Cu_{K\alpha}$ radiation, graphite monochromator, $T = -10\,^{\circ}C$), of which 3955 were unique and 2732 with $F_0 > \sigma(F_0)$ regarded as observed. Solution by direct methods (SHELXS-86 [11]), refinement (SHELX-76 [12]) to $R = 0.084$, $R_w = 0.062$, non-hydrogen atoms anisotropic, H atoms with fixed isotropic temperature factors, with exception of H1 at calculated positions. 311 parameters. Correction of data with the program DIFABS [13]. All calculations were carried out on a Micro-VAX II [14–16].

[11] G. M. Sheldrick, SHELXS-86, Program for Crystal Structure Solution, Göttingen 1986.

[12] G. M. Sheldrick, SHELX-76, Program for Crystal Structure Determination, Cambridge 1976.

[13] N. Walker, D. Stuart, *Acta Cryst. A 39* (1983) 158.

[14] A. L. Spek, Platon 88, Program for Geometrical Analysis of Crystal Structures, Utrecht 1988.

[15] E. Keller, SCHAKAL-88 B, A FORTRAN Program for the Graphic Representation of Molecular and Crystallographic Models, Freiburg 1988.

[16] Further details of the crystal structure investigation are available on request from the Fachinformationszentrum Karlsruhe, Gesellschaft für wissenschaftlich-technische Information mbH, D-7514 Eggenstein-Leopoldshafen 2 (FRG), on quoting the depository number CSD-320008, the names of the authors, and the journal citation.

[17] The Li–N (TMEDA) distances in **4** · 2 TMEDA [232.0(9) and 234.7(9) pm] are the longest hitherto known. In three of the 97 Li-TMEDA compounds on the Cambridge Data Files, distances of between 230 and 231 pm were found: a) D. Seebach, R. Amstutz, T. Laube, W. B. Schweizer, J. D. Dunitz, *J. Am. Chem. Soc. 107* (1985) 5403; b) P. von R. Schleyer, R. Hacker, H. Dietrich, W. Mahdi, *J. Chem. Soc. Chem. Commun. 1985*, 622; c) W. Bauer, G. Müller, R. Pi, P. von R. Schleyer, *Angew. Chem. 98* (1986) 1130; *Angew. Chem. Int. Ed. Engl. 25* (1986) 1103.

[18] The long Li–N(TMEDA) distances were also attributed to "local overcrowding" in Ref. [17a].

[19] The space-filling of the isopropyl groups in the dimer $[(LDA)_2(THF)_2]$, in which the isopropylamide anions are likewise coupled via a Li–N–Li–N four-membered ring, leads to only *one* more THF molecule being bound to the only three-coordinate Li(P. G. Williard, cited as [81] in [7b]); a comparable situation is found in $[\{(Me_3Si)_2NLi\}_2 \cdot 2\,OEt_2]$ [M. F. Lappert, M. J. Slade, A. Singh, J. L. Atwood, R. D. Rodgers, R. Shakir, *J. Am. Chem. Soc. 105* (1983) 302].

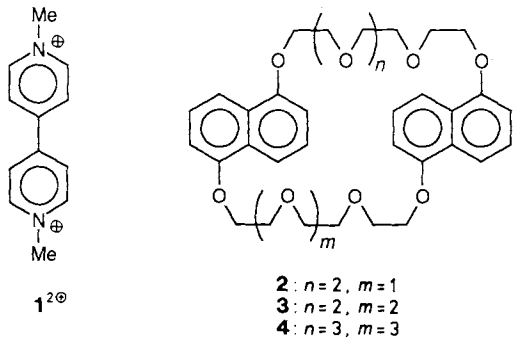
[20] A mixed complex of the lithium enolate of 5-(*tert*-butyldimethylsiloxy)-3,3-dimethylpentan-2-one and LDA has been described: P. G. Williard, M. J. Hintze, *J. Am. Chem. Soc. 109* (1987) 5539.

A Polymolecular Donor–Acceptor Stack Made of Paraquat and a 1,5-Dihydroxynaphthalene-Derived Crown Ether **

By *Jean-Yves Ortholand, Alexandra M. Z. Slawin, Neil Spencer, J. Fraser Stoddart,** and *David J. Williams*

Our interest[1] in the rôle of dispersive forces in determining the complexing abilities and supramolecular structures of macrocyclic receptors containing π-electron rich aromatic units with π-electron deficient substrates (e.g. Paraquat $\mathbf{1}^{2\oplus}$) has led us to investigate the effect of varying both the macrocyclic ring size and the nature of the π-donor. Since a major contributing factor in complex formation is undoubtedly the presence and constitutional disposition of the aryl oxygen atoms associated with the π-donor, we have examined[2] the effect of replacing benzo with naphtho units in the macrocyclic polyether cyclophanes.

We have already established[2] that macrocycles, such as **2** and **3**, containing two 1,5-dihydroxynaphthalene residues will form 1:1 inclusion complexes with Paraquat $\mathbf{1}^{2\oplus}$. Furthermore, solution studies[3] on **4** also provide evidence for



$\mathbf{1}^{2\oplus}$

2: $n = 2$, $m = 1$
3: $n = 2$, $m = 2$
4: $n = 3$, $m = 3$

the formation of a 1:1 inclusion complex with $\mathbf{1}^{2\oplus}$. However, a single crystal X-ray investigation[4] has revealed not a 1:1 inclusion complex but – for the first time – a 2:1 stoichiometry[5] with the formation of a continuously stacked π-donor/π-acceptor structure with Paraquat dications alternately included within and sandwiched between adjacent macrocycles (Fig. 1). As in the case of the adduct $[\mathbf{3} \cdot \mathbf{1}]^{2\oplus}$, in the solid

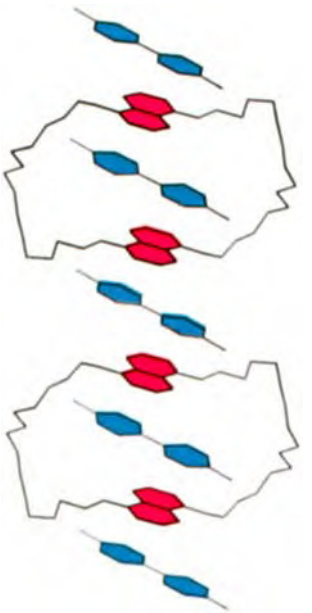


Fig. 1. Structure of $[\mathbf{4} \cdot 2\,(\mathbf{1})]_n^{4n\oplus}$ in the crystal (Paraquat = blue, 1/5 dinaphtho unit = red). Crystal data for $[\mathbf{4} \cdot 2\,(\mathbf{1})][PF_6]_4$. Me_2CO: triclinic, $a = 11.160(5)$, $b = 13.187(7)$, $c = 15.466(9)$ Å, $\alpha = 97.33(4)$, $\beta = 105.47(4)$, $\gamma = 107.86(4)^{\circ}$, $V = 2033$ Å^3, space group $P\bar{1}$, $Z = 1$ (the molecule is disposed about a center of symmetry), $\varrho = 1.41$ g cm^{-3}, $\mu(Cu_{K\alpha}) = 19$ cm^{-1}. 3603 independent observed reflections with $[|F_0| > 3\sigma(|F_0|), 2\theta \leq 116^{\circ}]$, $R = 0.110$, $R_w = 0.120$.

state structure of $[\mathbf{4} \cdot 2\,(\mathbf{1})]^{4\oplus}$, a Paraquat dication[6] is positioned (Fig. 2) about a crystallographic center of symmetry and sandwiched within the macrocycle between the parallelly-aligned naphtho residues and oriented so as to maximize overlap between the two π-electron rich naphtho units and each pyridinium ring of the π-electron deficient dication. The second Paraquat dication[6] is also positioned (Fig. 1) about a crystallographic center of symmetry between parallel lattice-translated complexes and nearly perfectly co-aligned with its included counterparts. In contrast with $[\mathbf{3} \cdot \mathbf{1}]^{2\oplus}$, the interplanar separation between the naphtho units in the $[\mathbf{4} \cdot \mathbf{1}]^{2\oplus}$ complex[2] is reduced significantly from 7.1 to 6.8 Å with a consequent reduction in the receptor-substrate separation. The same interplanar separation is present between adjacent complexes and the intercalated Paraquat dications. Clearly, this continuous alternating arrangement

[*] Dr. J. F. Stoddart, J. Y. Ortholand, Dr. N. Spencer
Department of Chemistry, The University
Sheffield S3 7HF (UK)
A. M. Z. Slawin, Dr. D. J. Williams
Chemical Crystallography Laboratory
Department of Chemistry, Imperial College
London SW7 2AY (UK)

[**] This work was supported by the Agricultural and Food, and Science and Engineering Research Councils in the United Kingdom

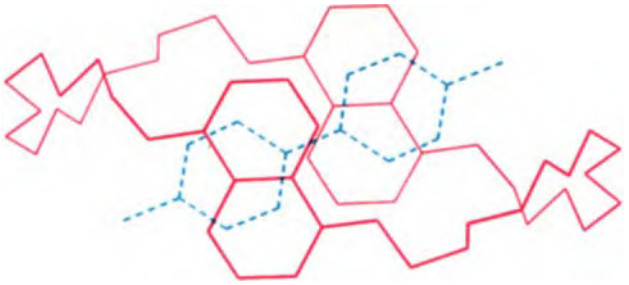


Fig. 2. Side-on view (normal to the mean plane of the Paraquat dication) of the skeletal representation of the $[\mathbf{4}\cdot\mathbf{1}]^{2\oplus}$ complex (Paraquat = blue, **4** = red).

of π-donors and π-acceptors in the solid state merits further investigation, particularly in regard to potential conductivity properties.[7]

Since an important feature in the design of a molecular receptor targeted towards a specific substrate is the presence or absence of a pre-organized[8] receptor geometry, we have also investigated the solid state structure[4] (Fig. 3) of **4**[9].

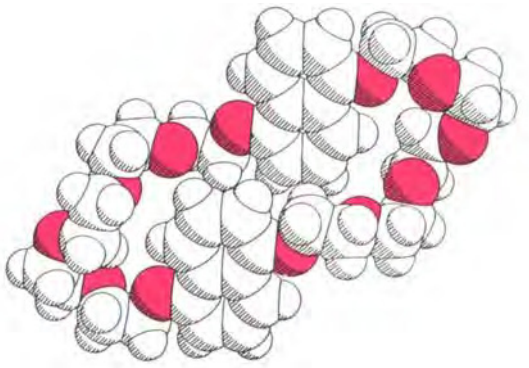
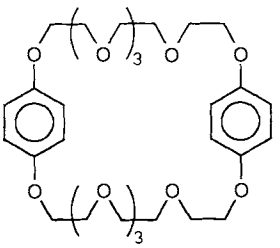


Fig. 3. Space-filling representation of the solid state structure of **4** (O = red). Crystal data for **4** · 7X where X corresponds to unidentified solvent fragments of scattering approximately equal to C atoms: monoclinic, $a = 8.750(3)$, $b = 15.056(4)$, $c = 16.270(5)$ Å, $\beta = 90.51(3)°$, $V = 2143$ Å^3, space group $P2_1/a$, $Z = 2$ (the molecule is disposed about a center of symmetry), $\varrho = 1.25$ g cm^{-3}, $\mu(Cu_{K\alpha}) = 7$ cm^{-1}. 2031 independent observed reflections with $[|F_o| > 3\sigma(|F_o|), 2\theta \leq 100°]$, $R = 0.095$, $R_w = 0.098$.

This shows that this free macrocycle has a gross conformation highly reminiscent[10] of the crown ether **5**, which contains polyether chains of the same length. **4** is also self-filling and, unlike **2**,[2] does not display any intramolecular naph-



5

tho-naphtho stabilizing interactions. However, investigation of the crystal packing shows that the intermolecular face-to-face[11] and edge-to-face[12] interactions[13] are present.

Experimental Procedure

4: Partial benzylation [K_2CO_3 (1 mol equiv.)/DMF/rt/18 h] of 1,5-dihydroxynaphthalene with $PhCH_2Br$ (1 mol equiv.) afforded the monobenzylether (m.p. 136–138 °C) in 21% yield after chromatography (SiO_2:$CHCl_3$). Reaction [NaH(0.5 mol equiv.)/DMF/70 °C/12 h] of this naphthol with $Ts(OCH_2CH_2)_5OTs$ (0.5 mol equiv.) gave 1,14-bis-(5′-benzyloxynaphthoxy)-3,6,9,12-tetraoxatetradecane (70%, m.p. 90–92 °C) after chromatography [SiO_2:CH_2Cl_2/Et_2O (98:2)]. Deprotection (H_2/Pd on C, MeOH/$CHCl_3$), followed by reaction [NaH (3 mol equiv.)/THF/66 °C/96 h] of the derived dinaphthol with $Ts(OCH_2CH_2)_5OTs$ (1 mol equiv.) afforded **4** (39%, m.p. 89–91 °C) after chromatography [SiO_2:$CHCl_3$/Et_2O/MeOH (68.5:30:1.5)]. EI-MS: *m/z* 724; ^{1}H NMR (CD_3COCD_3): $\delta = 3.61$ (s, 8H), 3.63 (m, 8H), 3.69 (m, 8H), 3.89 (m, 8H), 4.12 (m, 8H), 6.75 (dd, 4H), 7.29 (t, 4H), 7.79 (dd, 4H); ^{13}C NMR (CD_3COCD_3): $\delta = 68.9, 70.4, 71.5, 71.5, 71.7, 106.6, 115.1, 126.0, 127.7, 155.3$.

Received: May 22, 1989 [Z 3352 IE]
German version: *Angew. Chem. 101* (1989) 1402

[1] J. F. Stoddart, *Pure Appl. Chem. 60* (1988) 467 and references therein.
[2] P. R. Ashton, E. J. T. Chrystal, J. P. Mathias, K. P. Parry, A. M. Z. Slawin N. Spencer, J. F. Stoddart, D. J. Williams, *Tetrahedron Lett. 28* (1987) 6367.
[3] By employing the charge-transfer band as a quantitative spectroscopic probe ($\lambda_{max} = 416$ nm) at 25 °C, and subjecting the data to a modified (R. Foster, D. L. Hammick, A. A. Wardley, *J. Chem. Soc. 1953*, 3817; R. Foster: *Organic Charge-Transfer Complexes*, Academic Press, London 1969, p. 125) Benesi–Hildebrand treatment (H. A. Benesi, J. H. Hildebrand, *J. Am. Chem. Soc. 71* (1949) 2703) using experimental procedures recommended (W. B. Person, *J. Am. Chem. Soc. 87* (1965) 167; D. A. Deranleau, *ibid. 91* (1969) 4044) for weak complex formation (substrate concentration range, 1.0–9.1 mM), 1:1 stoichiometry was established in MeCN solution for the interaction between **4** and Paraquat $\mathbf{1}^{2\oplus}$. The value of 317 ± 5 M^{-1} obtained for K_a corresponds to $\Delta G^0 = -3.41$ kcal mol^{-1}. The receptor concentration was held constant at 1.8 mM and the substrate concentration was varied accordingly to ensure that UV/VIS absorption data were obtained in those regions of the "saturation curve" where errors are minimal. The data were corrected for a very weak absorption ($\varepsilon_{\lambda(max)} = 4.3$) in the 460–500 nm range. The inclusion nature of the 1:1 complex was confirmed by FAB-MS and ^{1}H NMR spectroscopy. **4** (5 mg, 6.9×10^{-3} mmol) was dissolved in $CHCl_3$ (< 1 mL) and **1** $[PF_6]_2$ (3.3 mg, 6.9×10^{-3} mmol) in Me_2CO (< 3 mL) was added. The red crystalline sample, obtained on evaporation of the solvent, was examined on a Kratos MS80RF mass spectrometer using argon. From a 3-nitrobenzylalcohol matrix, the crystals afforded a strong $[\mathbf{1}\cdot\mathbf{4}\cdot PF_6]^{\oplus}$ ion at *m/z* 1055 as a result of loss of one $[PF_6]^{\ominus}$ counterion from the 1:1 complex. The crystalline 1:1 complex was redissolved in CD_3COCD_3 for ^{1}H NMR spectroscopic studies. Relative to spectra recorded for free **4** and free Paraquat $\mathbf{1}^{2\oplus}$, chemical shift changes ($\Delta\delta$) of up to −0.29 were observed for the naphtho protons (H-3/H-7) in the receptor with $\Delta\delta$ values of −0.30 and −0.55 for the protons α and β to nitrogen in Paraquat $\mathbf{1}^{2\oplus}$.
[4] Nicolet R3m diffractometer, ω-scans, $Cu_{K\alpha}$ radiation (graphite monochromator). The structures were solved by direct methods and refined anisotropically. Further details of crystal structure investigations can be obtained from the Cambridge Crystallographic Data Centre, University Chemical Laboratory, Lensfield Road, Cambridge CB2 1EW (England). Any request should be accompanied by the full literature citation of this communication.
[5] When the CD_3COCD_3 solution of $[\mathbf{1}\cdot\mathbf{4}][2PF_6]$, employed (Experimental Procedure) in the NMR spectroscopic studies, was subjected to vapor diffusion with iPr_2O, deep red colored single crystals, with a stoichiometry for **1**-$[PF_6]_2$:**4** of 2:1 and suitable for X-ray crystallography, were obtained.
[6] In contrast to the situation in previously characterized Paraquat inclusion complexes with macrocyclic polyethers, where stabilizing [C-H · · · O] receptor substrate interactions have been evident (see [1]), here (Fig. 1 and 2) there is a distinct absence of any such interactions. The shortest contact between any of the polyether oxygen atoms and the carbon atoms α to the nitrogen atoms in the Paraquat dications is a long 3.51 Å.
[7] Currently, experiments to obtain crystals of a size [at least 0.5 mm along the (110) direction] adequate for conductivity measurements are in progress.
[8] D. J. Cram, *Angew. Chem. 100* (1988) 1041; *Angew. Chem. Int. Ed. Engl. 27* (1988) 1009; *Science (Washington, DC) 240* (1988) 760.
[9] Single crystals, suitable for X-ray crystallography, were grown by vapor diffusion of iPr_2O into a solution of **4** in Me_2CO.
[10] A. M. Z. Slawin, N. Spencer, J. F. Stoddart, D. J. Williams, *J. Chem. Soc. Chem. Commun. 1987*, 1070.
[11] The interplanar separation for the face-to-face interaction is 3.80 Å, with the shortest intermolecular six-membered ring centroid-centroid distance being 4.83 Å.
[12] For the edge-to-face interaction, the shortest centroid-centroid distance is 5.17 Å, with the associated vector inclined at 71° to one of the six-membered ring planes.
[13] R. O. Gould, A. M. Gray, P. Taylor, M. D. Walkinshaw, *J. Am. Chem. Soc. 107* (1985) 5921; S. K. Burley, G. A. Petsko, *Science (Washington DC) 229* (1985) 23; *J. Am. Chem. Soc. 108* (1986) 7995.

A [2]Catenane Made to Order**

By *Peter R. Ashton, Timothy T. Goodnow, Angel E. Kaifer, Mark V. Reddington, Alexandra M. Z. Slawin, Neil Spencer, J. Fraser Stoddart,* Cristina Vicent,* and *David J. Williams*

Our discovery[1] of the ability of bisparaphenylene-34-crown-10 to form (Fig. 1) a 1:1 inclusion complex **1** with the paraquat dication ($PQT^{2\oplus}$) in both solution and the solid state by virtue of electron donor-acceptor interactions led[2, 3] to the successful realization that the donor-acceptor rôles of receptor and substrate could be reversed, giving rise to the 1:1 supramolecular complex **2** of cyclobis(paraquat-*p*-phenylene) with 1,4-dimethoxybenzene. The observation,[4] that a continuous alternating electron donor-acceptor stack is formed in crystals containing 1,5-dinaphtho-44-crown-12 and $PQT^{2\oplus}$ in a molar ratio of 1:2, suggested to us the possibility (Fig. 1) of combining the features of **1** and **2** to create the novel [2]catenane **3**. This communication reports 1) the highly efficient one-step template-directed synthesis (Scheme 1) of **3** from the bis(pyridinium) salt **4** · $2PF_6$, 1,4-bis(bromomethyl)benzene **5**,[5] and bisparaphenylene-34-crown-10 **6**,[1] 2) the crystal structure of **3** as its tetrakis(hexafluorophosphate) and MeCN adduct, 3) its dynamic ^1H NMR spectroscopic behavior, and 4) its intriguing electrochemical properties in solution.

When **4** · $2PF_6$ was stirred in acetonitrile at room temperature with 1.0 molar equivalent of **5**[5] and a 2.5 molar excess of **6**,[1] copious amounts of a red precipitate emerged from a highly colored solution. The 70% yield (see Experimental Procedure) takes no account of any product which remains in solution, i.e. a highly efficient reaction has ensued. Following the isolation of the crude product and its conversion into the tetrakis-(hexafluorophosphate), positive-ion FAB-MS revealed peaks at *m/z* 1491 and 1347 corresponding to loss of one and two $PF_6^{\ominus}$ counterions respectively from **3** · $4PF_6$. The complete lack of fragmentation ions thereafter down to *m/z* 810 for the loss of two $PF_6^{\ominus}$ counterions from the parent cyclobis(paraquat-*p*-phenylene) tetrakishexafluorophosphate substantiated the view that a [2]catenane had indeed been formed.[6] This deduction was confirmed by obtaining good quality single crystals, which were subjected to X-ray crystallographic analysis.[7, 8] This has exposed (Fig. 2 and 3) the elegantly ordered structural arrangement with the tetracationic cyclobis(paraquat-*p*-phenylene) intimately interlocked with the bisparaphenylene-34-crown-10. As anticipated, the dominant noncovalent bonding interactions are the electrostatic and dispersive forces associated with the mutual sandwiching of 1) a hydroquinol unit between parallelly-aligned bipyridinium moieties and of 2) a bipyridinium moiety between parallelly-aligned hydroquinol units. An important structural feature (Fig. 4) is the existence of an identical orientation within the tetracation of one of the hydroquinol units in **6** to that observed[3] in **2** for 1,4-dimethoxybenzene. In contrast to **1**, however, where the

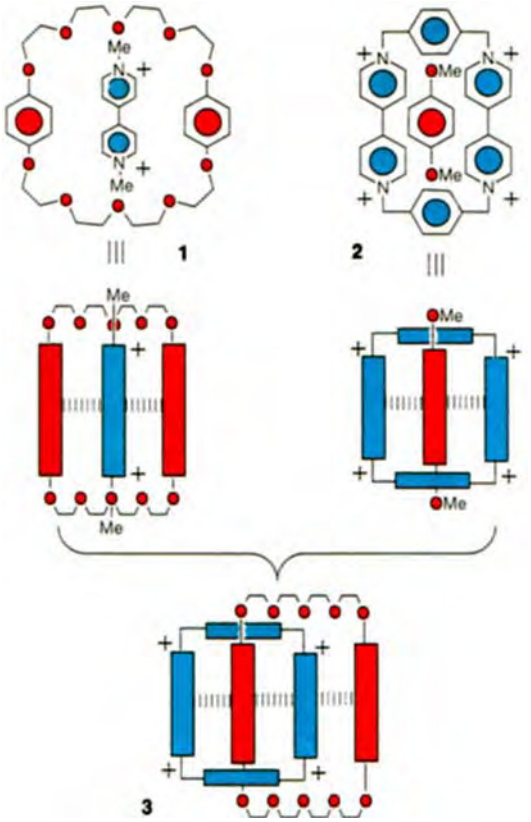
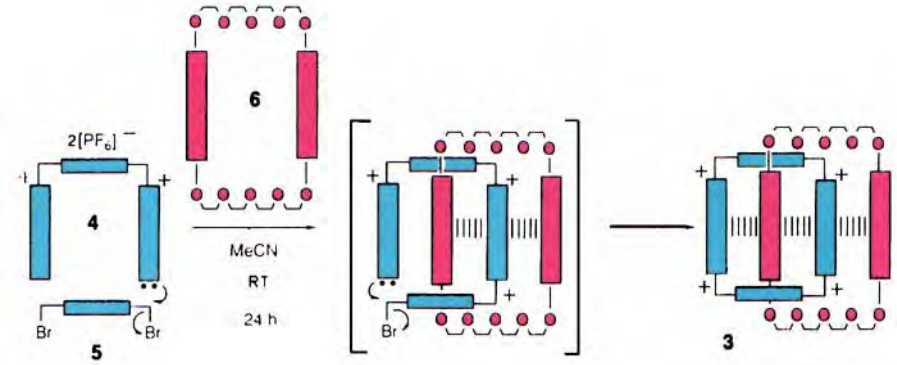


Fig. 1. Schematic representation of the design concept behind the fabrication of the [2]catenane **3**. Donors are red and acceptors are blue.



Scheme 1.

[*] Dr. J. F. Stoddart, M. V. Reddington, Dr. N. Spencer, P. R. Ashton
Department of Chemistry, The University
Sheffield S3 7HF (UK)
T. T. Goodnow, Prof. A. E. Kaifer
Department of Chemistry,
University of Miami, Coral Gables, FL 33124 (USA)
C. Vicent
Instituto de Quimica Organica General, CSIC
Juan de la Cierva 3, 28006 Madrid (Spain)
A. M. Z. Slawin, Dr. D. J. Williams,
Chemical Crystallography Laboratory
Department of Chemistry, Imperial College
London SW7 2AY (UK)

[**] This work was supported by Shell Research Limited, The Royal Society, and the Agricultural and Food, and Science and Engineering Research Councils in the United Kingdom and by the University of Miami Research Council in the United States.

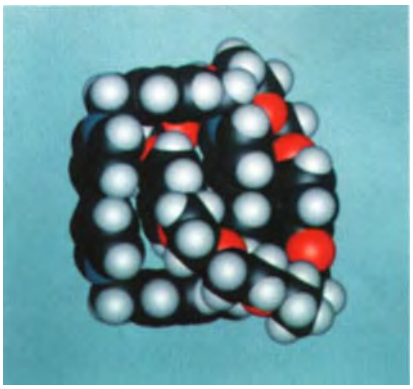


Fig. 2. Computer generated space-filling representation of the [2]catenane **3**.

macrocyclic polyether possesses[1] crystallographic C_i symmetry with its consequent alignment of the hydroquinol units, in **3**, they are no longer so oriented, probably as a result of their different stereoelectronic environments "in-

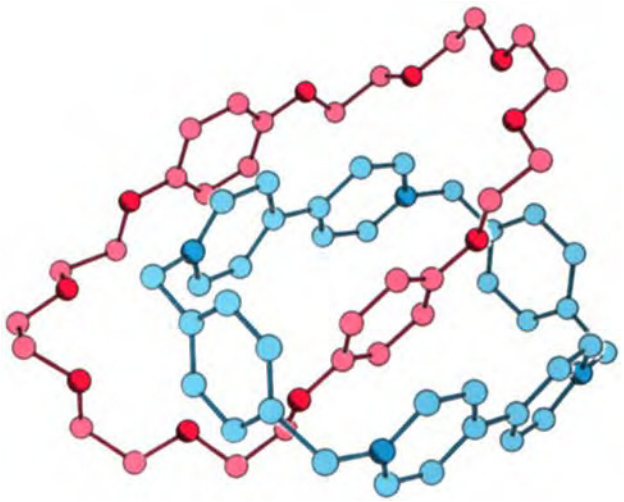


Fig. 3. Structure of **3** in the crystal with the donor and acceptor macrocycles shaded red and blue respectively. O atoms are dark red and N atoms are dark blue.

side" and "alongside" the tetracation. The effective interplanar separations between the two hydroquinol units and their associated bipyridinium moieties are, in all cases, ca. 3.5 Å. As observed previously,[3] there is a small twist angle of ca. 6° between the pyridinium rings within each bipyridinium moiety. Furthermore, the weak electrostatic edge-to-face

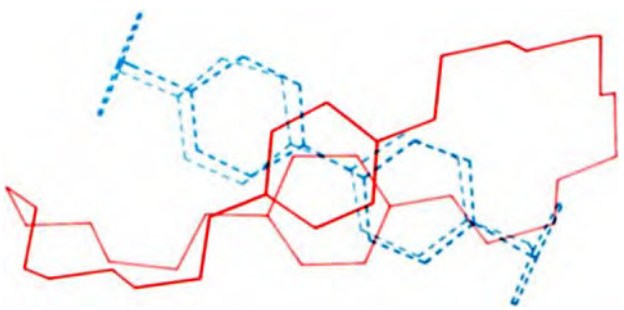


Fig. 4. Skeletal representation of **3** viewed normal to the plane of the hydroquinol ring lying within the tetracationic cavity. The donor is red and the acceptor is blue.

interactions, noted[3] in **2** between the orthogonally-aligned *para*-phenylene units in the tetracation and an included 1,4-dimethoxybenzene molecule, are also present in **3**.

Investigation of the packing[9] of the anions, tetracations, and solvent (MeCN) molecules uncovered the existence of continuously-stacked catenane entities aligned along the crystallographic *b* direction (Fig. 5). This alternating pattern

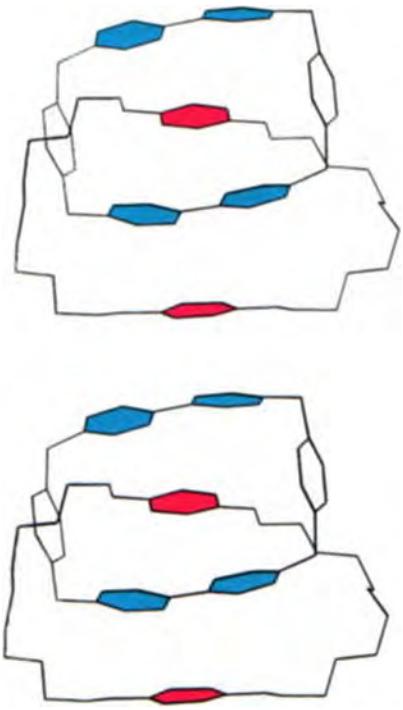


Fig. 5. Part of the continuous sequence of [2]catenanes **3** in the crystal. Donors are red and acceptors are blue.

of overlapping π-electron rich and deficient components is directly analogous to the solid state structure[4] of 1,5-dinaphtho-44-crown-12 incorporating two paraquat dications, one included within the macrocycle and the other sandwiched between adjacent 1:1 complexes. The approximate interplanar separation between overlapping π-electron rich and deficient components in adjacently stacked catenane entities is ca. 3.5 Å. Not only does the obvious possibility exist for investigating the conductivity in a suitably grown single crystal, but this polymolecular array provides a prototype for the design of a new generation of highly ordered electron donor-acceptor polymer chains.

Most importantly, the ordered arrangement of the [2]catenane **3** in the solid state is retained in solution. Dynamic ^{1}H NMR spectroscopy of $\mathbf{3}\cdot 4PF_6$ reveals (Fig. 6) the occurrence of temperature dependent processes operating both below (in CD_3COCD_3) and above (in CD_3CN or CD_3SOCD_3) room temperature. At + 25 °C, two equal intensity singlets are observed in CD_3CN at $\delta = 3.45$ and 6.16, which may be assigned respectively to the protons on the hydroquinol ring located "inside" the cavity of the tetracation and those on the hydroquinol ring associated with the face "alongside" one of the bipyridinium units of the tetracation (Fig. 7). The coalescence temperature (T_c) of + 81 °C observed at 250 MHz can be employed,[10] along with the limiting chemical shift difference ($\Delta\nu$) of 678 Hz between the singlets for the slowly exchanging protons, to obtain a $\Delta G_c^{\neq}$ value of 14.0 kcal mol^{-1} from the first order rate constant (k_c) of 1500 s^{-1} for the site exchange process. The free ener-

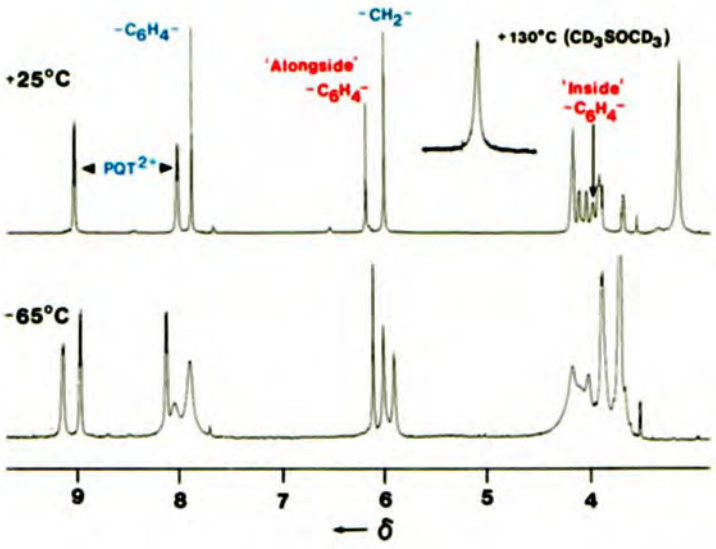


Fig. 6. The ^{1}H NMR spectra of $3 \cdot 4PF_6$ recorded in CD_3COCD_3 at -65 °C and at $+25$ °C. The signal for the phenylene protons in the bis(phenylene)-34-crown-10 portion of **3** is also shown recorded in CD_3SOCD_3 at $+130$ °C.

gy of activation ($\Delta G_c^{\ddagger}$) is for the degenerate supramolecular process (I) involving passage of the bisparaphenylene-34-crown-10 macrocycle through the center of the tetracation, leading to exchange of the hydroquinol rings (A and B) between "inside" and "alongside" environments. The other degenerate supramolecular process (II), which involves the exchange of the bipyridinium rings (A and B) of the tetracation between "inside" and "alongside" environments with respect to bisparaphenylene-34-crown-10, requires one hydroquinol ring in the macrocycle to sweep round the external periphery of the tetracation by pirouetting about the O–C_6H_4–O axis of the other hydroquinol ring. A $\Delta G_c^{\ddagger}$ value of 12.2 kcal mol^{-1} was obtained for this process from the temperature dependence of the signal for the benzylic methylene protons of the tetracation in the ^{1}H NMR spectrum of **3** in CD_3COCD_3, which resonates as a singlet at $+25$ °C but separates[11] out into two equal intensity singlets at -65 °C

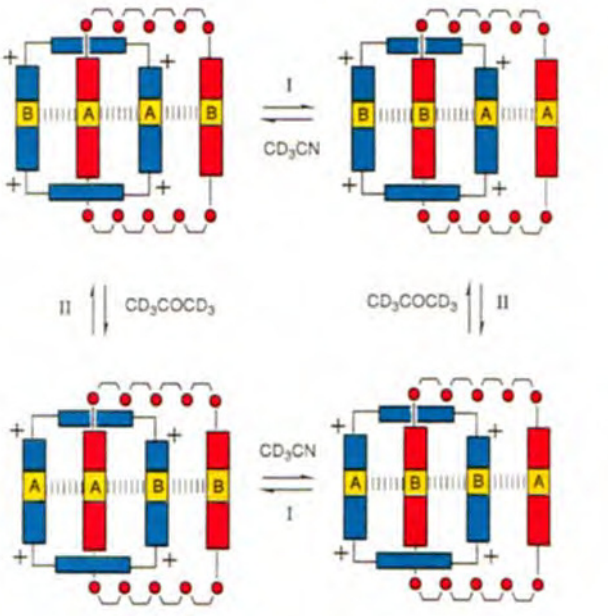


Fig. 7. A diagrammatic scheme showing the degenerate rearrangements (processes I and II) involving aromatic rings labelled A and B between "inside" and "alongside" positions for both donor (red) and acceptor (blue) macrocycles.

with $\Delta\nu = 46$ Hz giving[10] $k_c = 102\ s^{-1}$ at $T_c = -23$ °C. The ordering of the tetracationic [2]catenane **3** in solution suggests strongly that its remarkably efficient production[12] is templated (Scheme 1) during its formation from the dicationic starting material **4** via, presumably,[13] a complexed tricationic intermediate. Moreover, the non-covalent bonding responsible for this templating action "lives on" in **3**, distinguishing this [2]catenane from any of its predecessors.

Cyclic voltammetry of free cyclobis(paraquat-*p*-phenylene) in 0.1 M nBu$_4$PF$_6$/MeCN reveals two redox couples (Fig. 8a). The first monoelectronic reduction ($PQT^{2\oplus}/PQT^{\oplus}$) of both paraquat moieties appears as a single reduction process ($E^{0\prime} = -0.279$ V) and so does the second redox process ($PQT^{\oplus}/PQT$, $E^{0\prime} = -0.703$ V). This is the expected behavior for a molecule having two identical and independent paraquat units that undergo electron transfer at similar potentials.[5] In contrast with this, $3 \cdot 4PF_6$ shows three well resolved redox couples (Fig. 8b). The $PQT^{2\oplus}/PQT^{\oplus}$ process

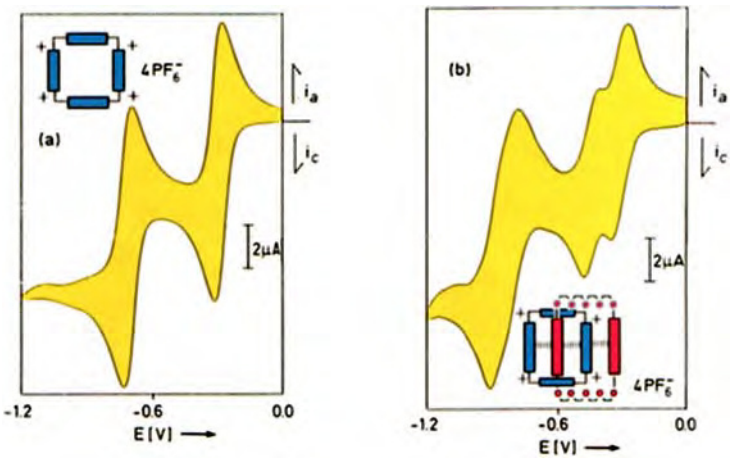


Fig. 8. Cyclic voltammetry at 25 °C of 0.5 mM solutions of a) free cyclobis-(paraquat-*p*-phenylene) and b) $3 \cdot 4PF_6$ in 0.1 M nBu$_4$NPF$_6$/MeCN. Scan rate: 20 mV s^{-1}. Donors are red and acceptors are blue.

is split into two distinct couples having $E^{0\prime}$ values of -0.307 and -0.438 V, respectively. The ensuing reduction of the paraquat units appears as a single redox process at $E^{0\prime} = -0.841$ V although the shape of the waves suggests two close but unresolved redox steps. The splitting of the first reduction process may result from the topological differences between the "inside" and "alongside" paraquat units in the catenane. The "inside" paraquat is more strongly stabilized by the interactions with the two adjacent hydroquinol units than the "alongside" paraquat which interacts with only one of these. Thus, the "alongside" $PQT^{2\oplus}$ is reduced more easily than the "inside" $PQT^{2\oplus}$ (see Fig. 9). In the next reduction step, the differences between the two paraquat units are not so marked because the strength of their interaction with the hydroquinol groups is probably diminished by the decreased acceptor character of the $PQT^{\oplus}$ units. An alternative interpretation of the splitting of the $PQT^{2\oplus}/PQT^{\oplus}$ redox process can be offered if one assumes that the electronic communication between the two paraquat units is greatly enhanced in the catenane by the intervening hydroquinol moiety. One-electron reduction of the catenane would then yield a cation radical having the spin density delocalized through the two paraquat units and, perhaps, the hydroquinol group. This possibility is currently under investigation using EPR spectroscopy. In any instance, the electro-

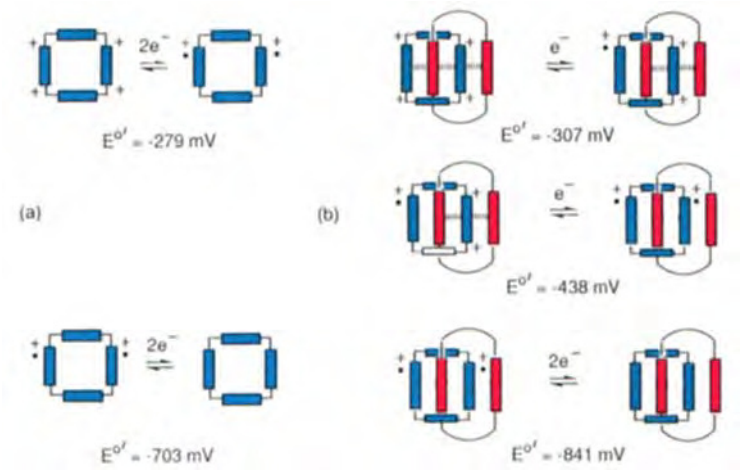


Fig. 9. A diagrammatic scheme comparing the redox processes of $3 \cdot 4PF_6$ and free cyclobis(paraquat-*p*-phenylene). Donors are red and acceptors are blue.

chemical properties of $3 \cdot 4PF_6$ are very intriguing since they suggest that either an electrochemical gradient between the two paraquat units exists in the catenane or that both reducible subunits are electronically coupled in a highly efficient manner.

The preparation of the [2]catenane **3**, involving repetitive nucleophilic substitution reactions, is another example[15] of a synthesis of an unnatural product[16] which is *structure-directed*.[17] The exploitation of this principle looks set to create many new molecular ensembles.

Experimental Procedure

$3 \cdot 4PF_6$: $4 \cdot 2PF_6$ (140 mg, 0.2 mmol) was dissolved in dry MeCN (5 mL) and then added to a solution of **6** (280 mg, 0.52 mmol) in dry MeCN (5 mL) under N_2 with stirring. A deep yellow color was formed immediately and **5** (56 mg, 0.2 mmol), dissolved in dry MeCN (5 mL), was added. After 4 h, the reaction mixture had become deep red and overnight a red precipitate formed. After stirring at room temperature for 48 h, the precipitate was filtered off, washed with $CHCl_3$ to remove excess of **6**, dissolved in H_2O, and filtered to remove a small amount of insoluble material. An aqueous solution of NH_4PF_6 was added until no further precipitation occurred. The precipitate was filtered off, washed (H_2O), and dried. Recrystallization from $MeCN/H_2O$ gave $3 \cdot 4PF_6$ (230 mg, 70%) as a pink solid, m.p. > 280 °C. Single crystals, suitable for X-ray crystallography, were grown by vapor diffusion of iPr_2O into a solution of $3 \cdot 4PF_6$ in MeCN.

Received: May 22, 1989 [Z 3353 IE]
German version: *Angew. Chem. 101* (1989) 1404

CAS Registry numbers:
$3 \cdot 4PF_6^{\ominus}$, 122801-13-2; $3 \cdot 4PF_6^{\ominus} \cdot 5MeCN$, 122801-14-3; $4 \cdot 2PF_6^{\ominus}$, 108861-20-7; **5**, 623-24-5; **6**, 53914-95-7.

[1] B. L. Allwood, H. Shariari-Zavareh, N. Spencer, J. F. Stoddart, D. J. Williams, *J. Chem. Soc. Chem. Commun. 1987*, 1064.
[2] B. Odell, M. V. Reddington, A. M. Z. Slawin, N. Spencer, J. F. Stoddart, D. J. Williams, *Angew. Chem. 100* (1988) 1605; *Angew. Chem. Int. Ed. Engl. 27* (1988) 1547.
[3] P. R. Ashton, B. Odell, M. V. Reddington, A. M. Z. Slawin, J. F. Stoddart, D. J. Williams, *Angew. Chem. 100* (1988) 1608; *Angew. Chem. Int. Ed. Engl. 27* (1988) 1550.
[4] J.-Y. Ortholand, A. M. Z. Slawin, N. Spencer, J. F. Stoddart, D. J. Williams, *Angew. Chem. 101* (1989) 1402; *Angew. Chem. Int. Ed. Engl. 28* (1989) 1394.
[5] W. Geuder, S. Hünig, A. Suchy, *Angew. Chem. 95* (1983) 501; *Angew. Chem. Int. Ed. Engl. 22* (1983) 489; *Tetrahedron 42* (1986) 1665.
[6] The first fragmentation of the bisparaphenylene-34-crown-10 ring in **3**, which will lead to its mechanical disconnection with the intact tetracationic macrocycle by an unthreading process, is expected to give subsequent fragmentations that are characteristic of the component rings. This distinctive behavior has been observed in the mass spectra of other catenanes: see, for example, W. Vetter, E. Logemann, G. Schill, *Org. Mass Spectrom. 12* (1977) 351; C. O. Dietrich-Buchecker, J.-P. Sauvage, J. M. Kern, *J. Am. Chem. Soc. 106* (1984) 3043.
[7] Crystal data for $3 \cdot 4PF_6 \cdot 5MeCN$: triclinic, $a = 13.847(6)$, $b = 13.998(4)$, $c = 26.584(15)$ Å, $\alpha = 84.36(4)$, $\beta = 80.91(4)$, $\gamma = 60.79(3)°$, $V = 4440$ Å^3, space group $P\bar{1}$, $Z = 2$, $\varrho = 1.38$ g cm^{-3}, $\mu(Cu_{K\alpha}) = 17$ cm^{-1}, 5188 independent observed reflections with [$|F_o| > 3\sigma(|F_o|)$, $2\theta \leq 100°$], refined to a current $R = 0.141$, $R_w = 0.136$.
[8] Nicolet R3m diffractometer, ω-scans, $Cu_{K\alpha}$ radiation (graphite monochromator). The structure was solved by direct methods and refined anisotropically. Further details of the crystal structure investigation can be obtained from the Cambridge Crystallographic Data Centre, University Chemical Laboratory, Lensfield Road, Cambridge CB2 1EW (England). Any request should be accompanied by the full literature citation of this communication.
[9] There is extensive solvtion of the crystals by acetonitrile molecules, there being 3 at full weight, 2 at three-quarters, and 1 at half weight per $3 \cdot 4PF_6$. The counterions and these solvent molecules are intercalated between layers of catenanes.
[10] Values for k_c were obtained (I. O. Sutherland, *Annu. Rep. NMR Spectrosc. 4* (1971) 71) using the approximate expression, $k_c = \pi(\Delta\nu)/(2)^{1/2}$, and the Eyring equation was then used to calculate $\Delta G_c^{\ddagger}$ values at T_c.
[11] The signals for the protons α to the nitrogen atoms on the bipyridinium rings also separated (Fig. 6) out into equal intensity signals in the ^1H NMR spectrum of **3** recorded in CD_3COCD_3 at −65 °C.
[12] For a historical perspective and a discussion of the early research carried out on catenanes, see G. Schill: *Catenanes, Rotaxanes and Knots*, Academic Press, New York 1971. More recently, an excellent review by *C. O. Dietrich-Buchecker* and *J. P. Sauvage* (*Chem. Rev. 87* (1987) 795) has surveyed the different routes to catenanes, which had been devised and exploited up to 1986. Previously, macrocyclic polyethers have been incorporated into catenanes by statistical threading (G. Agam, D. Graiver, A. Zilkha, *J. Am. Chem. Soc. 98* (1976) 5206) and by using transition metals as covalent templates (C. O. Dietrich-Buchecker, J. P. Sauvage, *Tetrahedron Lett. 24* (1983) 5095; C. O. Dietrich-Buchecker, J. P. Sauvage, J. M. Kern, *J. Am. Chem. Soc. 106* (1984) 3043; J. P. Sauvage, *Nouv. J. Chim. 9* (1985) 299; *D. K. Mitchell, J. P. Sauvage, Angew. Chem. 100* (1988) 985; *Angew. Chem. Int. Ed. Engl. 27* (1988) 930). The most recent communication from the Strasbourg group relates to a synthetic molecular trefoil knot (C. O. Dietrich-Buchecker, J. P. Sauvage, *Angew. Chem. 101* (1989) 192; *Angew. Chem. Int. Ed. Engl. 28* (1989) 189.
[13] Experiments to assess the nature and the strength of the binding of the bisparaphenylene-34-crown-10 with the tricationic compound, obtained by reaction of the bis(pyridinium) salt $4 \cdot 2PF_6$ with *para*-methylbenzyl bromide, are in progress.
[14] Electrochemical experiments were performed with a Princeton Applied Research Model 175 universal programmer, a Model 173 potentiostat, and a Model 179 digital coulometer equipped with positive feedback circuitry for IR compensation. Voltammograms were recorded on a Soltec VP-6423S X-Y recorder. A glassy carbon disk electrode (0.080 cm^2), Pt flag, and sodium chloride saturated calomel (SSCE) were used as the working, auxiliary, and reference electrodes, respectively. All solutions for the voltammetric experiments were deoxygenated by sparging with nitrogen gas; a nitrogen atmosphere was maintained above the solution during the experiments.
[15] In a structure-directed synthesis, no reagent or catalyst is required (P. Ellwood, J. P. Mathias, J. F. Stoddart, F. H. Kohnke, *Bull. Soc. Chim. Belg. 97* (1988) 669).
[16] J. F. Stoddart, *Nature 334* (1988) 10.
[17] P. R. Ashton, N. S. Isaacs, F. H. Kohnke, J. P. Mathias, J. F. Stoddart, *Angew. Chem. 101* (1989) 1266; *Angew. Chem. Int. Ed. Engl. 28* (1989) 1258; P. R. Ashton, N. S. Isaacs, F. H. Kohnke, G. Stagno d'Alcontres, J. F. Stoddart, *ibid. 101* (1989) 1269 and *28* (1989) 1261.

(4*RS*,5*R*)- and (4*RS*,5*S*)-4-Methoxy-5-methyloxazolidin-2-one Derivatives of Threonine—Interesting Chiral Amidoalkylating Reagents**

By *Christiane Herborn, Andrea Zietlow,* and *Eberhard Steckhan**

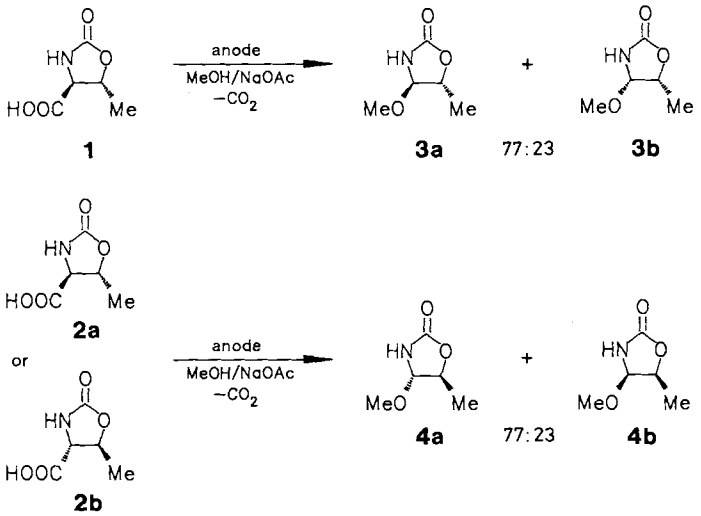
The electrochemical substitution of the carboxyl group of an *N*-acyl-α-aminocarboxylic acid or of an *N*-acylaminoma-

[*] Prof. Dr. E. Steckhan, Dipl.-Chem. C. Herborn, A. Zietlow
Institut für Organische Chemie und Biochemie der Universität
Gerhard-Domagk-Strasse 1, D-5300 Bonn 1 (FRG)

[**] This work was supported by the Deutsche Forschungsgemeinschaft, the Fonds der Chemischen Industrie, BASF AG, and DEGUSSA AG (donation of chemicals). We thank Prof. Dr. *E. Breitmaier* (Bonn) for carrying out NMR shift and NOE experiments. Communicated in part in lectures delivered at the 20th European Peptide Symposium (Tübingen, September 4–9, 1988) and the 7th EUCHEM Conference on Electrochemistry (Assisi, April 17–22, 1989).

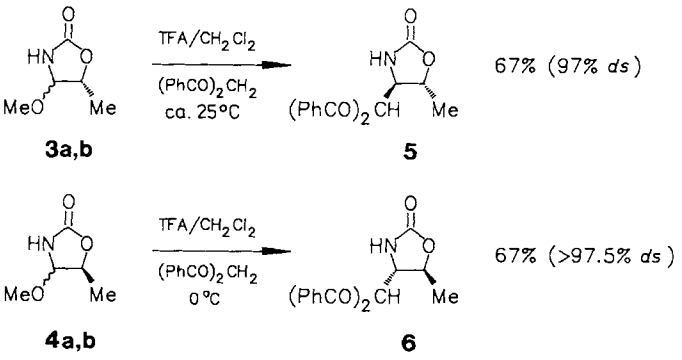
lonic acid half ester by a methoxy group (non-Kolbe reaction) is readily carried out and leads to interesting synthetic building blocks.[1-6] Remarkable, however, is that the anodic methoxylation usually proceeds with a diastereoselectivity of maximally only 2:1.[3,4] Replacement of the methoxy group by nucleophiles shows the highest diastereoselectivity when the C atom in the α-position to the methoxy group is part of a cyclic system, as for example in a (4*R*)-4-hydroxy-2-methoxypyrrolidine derivative.[4] In some cases, however, even the chelate effect, brought about by $TiCl_4$, leads to practicable diastereoselectivities.[5] The anodic decarboxylation of cyclic systems such as (2*R*,4*S*)-2-(*tert*-butyl)oxazolidine-4-carboxylic acid with introduction of an acetoxy group already proceeds with good diastereoselectivity in the electrochemical step.[5a,6]

We have now found that anodic decarboxylation of the (4*S*,5*R*)-, (4*S*,5*S*)-, and (4*R*,5*S*)-5-methyl-2-oxooxazolidine-4-carboxylic acids **1** and **2a, b** as starting substances in methanol affords the (4*R*,5*R*)- and (4*S*,5*S*)-4-methoxy-5-methyloxazolidin-2-ones **3a** and **4a** respectively with 77% *ds* in each case.



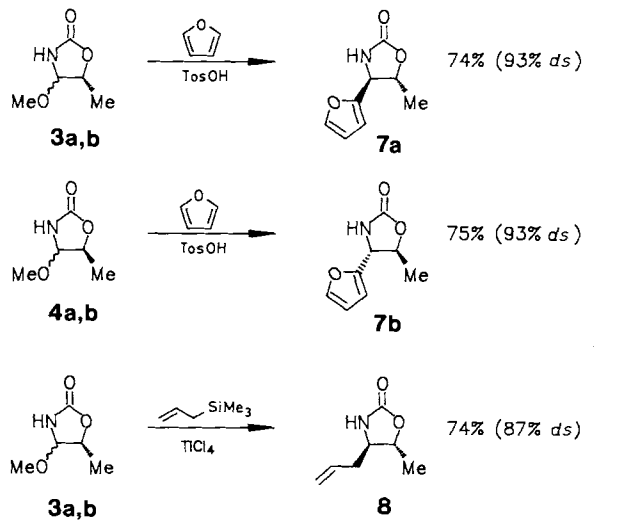
1 and **2a, b** are readily obtainable in 75% yield by cyclization of L-threonine, L-allothreonine and D-threonine, respectively, with methyl chloroformate. The electrolyses of the carboxylic acids (divided cell, methanol) in the presence of sodium acetate proceed almost quantitatively (95% isolated yields of **3a, b** and **4a, b**, respectively). Even in undivided cells using graphite electrodes and the same electrolyte the diastereomeric mixture **3a, b** is obtained in 89% yield after consumption of 3 Faraday mol^{-1}. The diastereomeric mixture can be separated by column-chromatography (silica gel, ether). Thus, starting from L-threonine or D-threonine **3a** and **4a**, respectively, have been obtained enantiomerically pure (**4a**: $[\alpha]_D^{20} = -140.7°$, $c = 1.025$, $CHCl_3$; **3a**: $[\alpha]_D^{20} = +144.1°$, $c = 1.025$, $CHCl_3$). In each case, however, the diastereomeric mixture itself can be used for further reactions.

Thus, **3** and **4** are readily accessible precursors for α- and β-chiral β-aminoalcohols and their derivatives. According to the findings of *Ben-Ishai* et al.,[7] *Shono* and *Irie* et al.,[8] *Speckamp* et al.,[9] and our own,[10] the methoxy groups in **3** and **4** can be replaced by nucleophiles, either under the conditions of proton catalysis or catalysis by Lewis acids. The reactions involve intermediary formation of *N*-acyliminium ions. Reaction of the diastereomeric mixtures **3a, b** or **4a, b** with dibenzoylmethane in trifluoroacetic acid affords the *trans*-derivatives **5** ($[\alpha]_D^{20} = -24.9°$, $CHCl_2$, $c = 0.5$) and **6** ($[\alpha]_D^{20} = +26.1°$, CH_2Cl_2, $c = 0.5$), respectively, as pure enantiomers with 97% and >97.5% *ds*.



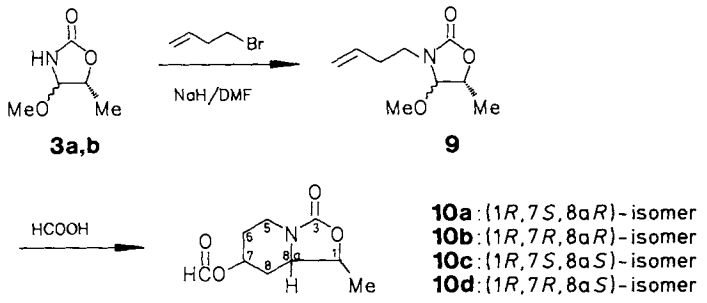
Reaction of furan with **3a, b** in the presence of 10 mol-% *p*-toluenesulfonic acid at room temperature furnishes the (4*S*,5*R*)-*trans*-isomer **7a** ($[\alpha]_D^{20} = +40.2$, $CHCl_3$, $c = 1.025$, after diastereomeric separation) with 93% *ds* whereas **4a, b** affords the (4*R*,5*S*)-*trans*-isomer **7b** ($[\alpha]_D^{20} = -41.6°$, $CHCl_3$, $c = 1.025$, after diastereomeric separation) with the same diastereoselectivity. The diastereomers were separated by flash chromatography on silica gel, and their enantiomeric purity was determined by NMR spectroscopy with chiral shift reagents. The oxazolidine-2-one ring in **7** can easily be opened with NaOH (1.25 M in EtOH:H_2O 70:30) to give the corresponding amino alcohol.

Reaction of allyltrimethylsilane with **3a, b** in the presence of $TiCl_4$ (CH_2Cl_2, 0 °C; $TiCl_4$:**3a, b**:allyltrimethylsilane = 1.2:1:1.2) affords the (4*R*,5*R*)-*trans*-isomer **8** with 87% *ds*. *Kano* et al.[11] have reported analogous reactions with *N*-alkylated 4-alkoxyoxazolidin-2-ones as being completely diastereoselective.



N-alkylation of **3a, b** with homoallyl bromide affords **9**, which in accordance with the findings of *Speckamp* et al.[9] and *King* et al.[12] can be cyclized with formic acid. **10** is formed in 65% yield as a mixture of four diastereomers in the ratio **a:b:c:d** = 8.5:2:3:1. By flash chromatography on silica gel (eluent: diethyl ether), the enantiomerically

pure (1*R*,7*S*,8a*R*)-1-methyl-3-oxo-1,5,6,7,8,8a-hexahydro-oxazolo-[3,4-*a*]-pyrid-7-yl formate **10a** ($[\alpha]_D^{20} = -8.59°$, CH_2Cl_2, $c = 0.8$; 1.7% contamination by the other diastereomers) can be isolated in 36% yield. In **10a** the six-membered ring is coupled *trans* to the methyl group, and the formate residue is oriented equatorially, whereas the formate residue in **10b** assumes the axial position. **10c** and **10d** are



the *cis*-coupled diastereomers with equatorial and axial arrangement of the formate residue. The ratio of *trans*- to *cis*-coupling is 2.6:1 and is thus substantially higher than in comparable cyclizations with diastereomeric ratios of 1:1[13] and 1.5:1.[14] The diastereoselectivity of the ring closure via *N*-acyliminium ions can be drastically increased if the double bond is terminally substituted.[13, 14]

The configurations of the products were determined by ^1H NMR spectroscopy and NOE measurements. All the compounds were characterized by IR, NMR, and mass spectra and elemental analyses. The replacement of the methoxy group by other nucleophiles and the preparation of interesting amino alcohols are currently the subject of intensive investigation.

Received: May 8, 1989;
supplemented: June 30, 1989 [Z 3329 IE]
German version: *Angew. Chem. 101* (1989) 1392

[1] T. Iwasaki, H. Horikawa, K. Matsumoto, M. Miyoshi, *Bull. Chem. Soc. Jpn. 52* (1979) 820.
[2] H. Horikawa, T. Iwasaki, K. Matsumoto, M. Miyoshi, *Tetrahedron Lett. 1976*, 191; T. Iwasaki, H. Horikawa, K. Matsumoto, M. Miyoshi, *J. Org. Chem. 42* (1977) 2419.
[3] P. Renaud, D. Seebach, *Synthesis 1986*, 424.
[4] P. Renaud, D. Seebach, *Helv. Chim. Acta 69* (1986) 1704.
[5] a) P. Renaud, D. Seebach, *Angew. Chem. 98* (1986) 836; *Angew. Chem. Int. Ed. Engl. 25* (1986) 843; b) D. Seebach, R. Charczuk, C. Gerber, P. Renaud, *Helv. Chim. Acta 72* (1989) 401.
[6] D. Seebach, G. Stucky, P. Renaud, *Chimia 42* (1988) 176.
[7] a) D. Ben-Ishai, J. Altmann, Z. Bernstein, N. Peled, *Tetrahedron 34* (1978) 67; b) D. Ben-Ishai, I. Sataty, N. Peled, R. Goldshare, *ibid. 43* (1987) 439.
[8] T. Shono, *Tetrahedron Lett. 40* (1984) 811; T. Shono, Y. Matsumura, K. Tsubata, K. Uchida, *J. Org. Chem. 51* (1986) 2590; T. Shono, Y. Matsumura, O. Onomura, M. Sato, *ibid. 53* (1988) 4118; K. Irie, K. Aoe, T. Tanaka, S. Saito, *J. Chem. Soc. Chem. Commun. 1985*, 633.
[9] W. N. Speckamp, H. Hiemstra, *Tetrahedron 41* (1985) 4367; W. N. Speckamp, *Recl. Trav. Chim. Pays-Bas 100* (1981) 345.
[10] K. D. Ginzel, P. Brungs, E. Steckhan, *Tetrahedron 45* (1989) 1691.
[11] S. Kano, Y. Yuasa, S. Shibuya, *Heterocycles 26* (1987) 373; S. Kano, Y. Yuasa, T. Yokomatsu, S. Shibuya, *J. Org. Chem. 53* (1988) 3865.
[12] M. S. Hadley, F. D. King, R. T. Martin, *Tetrahedron Lett. 24* (1983) 91.
[13] S. Kano, T. Yokomatsu, Y. Yuasa, S. Shibuya, *Heterocycles 24* (1986) 621.
[14] B. P. Wijnberg, W. N. Speckamp, *Tetrahedron Lett. 21* (1980) 1987.

BOOK REVIEWS

Book Reviews are written by invitation from the editor. Suggestions for books to be reviewed and for book reviewers are welcome. Publishers should send brochures or (better) books to the following address: Redaktion Angewandte Chemie, Postfach 101161, D-6940 Weinheim, Federal Republic of Germany. The editor reserves the right of selecting which books will be reviewed. Uninvited books not chosen for review will not be returned.

Advances in Boron and the Boranes. (Series: Molecular Structure and Energetics). Series editors: *J. F. Liebman* and *A. Greenberg;* volume editors: *J. F. Liebman, A. Greenberg* and *R. E. Williams*. VCH Verlagsgesellschaft, Weinheim/VCH Publishers, New York 1988. xx, 547 pp., hard cover, DM 195.00. – ISBN 3-527-26624-0/0-89573-272-6

Whereas most of the nine volumes published so far in this series have titles ("Physical Measurement", "Studies of Organic Molecules", "Structure and Reactivity", etc.) that are as general and non-specific as the series title, this volume treats a more clearly defined subject area, that of molecular compounds of boron. It excludes the important area of solid compounds of boron, and thus does not deal with the oxide, nitride and carbide ceramic phases nor with the metal oxoborates and metal borides. The hundred or so full-time molecular boron chemists throughout the world look to *Alfred Stock* as their spiritual ancestor. The scientific legacy which he left was continued mainly in the USA, where a center of boron chemistry was built up during the 1930s around *Schlesinger* at Chicago University. One of the most important representatives of this group is *Anton B. Burg*. To celebrate his eightieth birthday the Loker Hydrocarbon Institute arranged a symposium in Los Angeles on 14 March 1985. Because of this location most of the boron chemists who took part were American. The symposium proceedings resulted in this volume, in which only one chapter of the 22 contributions is of non-American origin. The articles are largely concerned with boron cluster chemistry and therefore with electron-deficient compounds formed by "non-classical" multicenter bonding.

The first chapter contains the text of *Burg*'s birthday lecture. Although *Burg* has still continued to publish important papers even after his eightieth birthday (the one-time cham-

pion high-jump athlete having kept himself young), this chapter is mainly one of historical reminiscence. As well as having unrivalled knowledge and experience, he is as original in his writing, embellished with verse, as he has always been in his personal style. As, for example, when in his younger days he would make a standing leap over other researchers seated in the departmental library, a useful form of exercise for a high-jumper but a startling experience for the others; or later when, as a professor at UCLA, he cycled along the Californian highways wearing a gas mask, a symbol not so much of public protest but more of the constructive and pragmatic attitude which experimental chemistry teaches us.

It is therefore not surprising that quite a number of the chapters that follow have a historical theme running through them, and seek to show general relationships. *R. E. Williams*, the organizer of this symposium and one who has played a prominent part in the systematization of boron cluster chemistry, in a joint paper with *G. K. S. Prakash, L. D. Field* and no less than *G. A. Olah*, reports that there is a proportional relationship between the NMR chemical shifts of boron and carbon nuclei at equivalent positions in two isoelectronic cluster molecules; conversely, one can infer isoelectronic analogies in cases where such a proportionality is observed. For example, this method has shown that the carbocation $C_3H_7^{\oplus}$ formed by protonation of cyclopropane in a superacid is isoelectronic with the familiar anion $B_3H_8^{\ominus}$. If one now regards protonated nortricyclanes, such as the norbornyl cation whose structure was at one time hotly disputed, as derivatives of the basic $C_3H_7^{\oplus}$ structure, the earlier discussions are at last seen in a systematic light: evidently we have here a non-classical cation, rather than a case of valence tautomerism between two enantiomeric classical cations, and this is now just as obvious as, for example, the rejection of a valence tautomerism between two cyclohexatriene molecules as a model for the structure of benzene. Using the same proportionality rule the cation $Me_2CBH_4^{\oplus}$ can be shown to be isoelectronic with 1,1-dimethylborane, and $MeC_2BH_7^{\oplus}$ with the anion $MeB_3H_7^{\ominus}$, which amounts to a proof that anomalous CHB bridges are formed as a result of the action of $Me_2CH^{\oplus}$ on BH_3.

R. N. Grimes appropriately points out that synthetic boron cluster chemistry (in contrast to the analytical chemistry of these compounds) is now at a stage of development similar to that of organic chemistry during last century (the "hunter and gatherer" stage, as one might say). Nevertheless, *Grimes* himself makes notable contributions towards passing beyond this stage, e.g. in achieving structure doubling by the oxidative fusion of two halves of a cluster, or η-bonding of the metal atom of a metallacarbaborane to aromatic compounds such as C_6H_6, $C_7H_7^{\oplus}$, $C_8H_8^{2\ominus}$ or paracyclophane. Another contribution which deals mainly with syntheses is that by *S. G. Shore*, who is more at home with the pure boron hydrides than virtually anyone else. In collaboration with *J. R. Wermer* he reports here, amongst other topics, on efficient syntheses of higher hydrides of boron and boron hydride anions from pentaborane(9), and on an anion $B_{10}H_{14}I^{\ominus}$ with an unusual structure. The Czech authors *B. Stibr, J. Plesek* and *S. Hermanek* report results on the preparation of nona-, deca- and undecaboranes and -borates containing C, N, S or Se as heteroatoms, and in some cases also Fe, Co, Ni or Pt. In the area of boron clusters with three to six atoms, *G. Kodama* has prepared some further electron-rich *hypho* species by the addition of Lewis bases, while *J. A. Morrison* gives a useful account of the chemistry of the boron subhalides, which are extremely electron-deficient ("electron-hyperdeficient"), the main ones being B_4Cl_4, B_8Cl_8 and B_9Cl_9, and reports several new reactions. *N. S. Hosmane* and *J. A. Maguire* give a detailed enumeration of all those carbaboranes which contain, in addition to carbon, skeletal heteroatoms of heavy elements belonging to Main Groups 3 or 4. Concluding this section, *L. J. Todd, A. Arafat, J. Baer* and *J. C. Huffman* report on the area of the thiaboranes and the scarcely developed azaboranes.

Anyone wishing to remedy the present lack of a unified systematization of synthetic methods cannot avoid becoming involved in elucidating reaction mechanisms. *D. F. Gaines*, in collaboration with *D. E. Coons* and *J. E. Heppert*, has incorporated a ^{10}B atom into 2-methylpentaborane(9) and has shown by NMR spectroscopy that a base-induced rearrangement of the B_5 skeleton occurs. *T. B. Fehlner* has used a molecular beam mass spectrometer to investigate the mechanisms of the reactions between the unstable basic borane unit BH_3 and various organic molecules, as well as the structure and reactivity of the BH_3 unit in the cluster molecule $[HFe_3(CO)_9(BH_3)]$. *T. Onak* devotes his paper to the mechanism of the isomerization of mono- and dihalogen derivatives of *closo*-dicarbaheptaborane. *L. Sneddon* and *E. W. Corcoran* have investigated the catalytic effect of $PdBr_2$ in the alkenylation of cluster molecules, and that of $PtBr_2$ in the formation of BB linkages. Conversely, *M. F. Hawthorne*, the doyen of metallacarbaborane chemistry, has used a rhodadicarbadodecaborane as a catalyst for the shifting or hydrogenation of double bonds in alkenes.

R. A. Beaudet summarizes the epoch-making history of the structure of diborane. The prejudice in favor of an ethane-type structure persisted until the middle of this century, despite the intuitively correct suggestion by *Dilthey* in 1921 and *Burg*'s pointers in the late 1930s. Eventually, however, the belief in the predominance of two-electron two-center bonding had to be modified, and the model extended to include non-classical multicenter bonding, both on the basis of incontrovertible experimental data (first from infrared spectroscopy and electron diffraction, and later from X-ray diffraction), and on theoretical grounds. It took the chemical community at large longer to accept multicenter σ-bonding than it had taken to accept multicenter π-bonding, perhaps because the familiar canonical forms that were in use in the fifties and sixties for describing conjugated π-electron systems led the theoretically inexperienced to believe that fixed two-electron two-center bonds were present. *Beaudet* also gives a detailed review of the known structures of neutral boron hydrides and carbaboranes, and lists some structural problems that remain to be solved. In the appendix he collects together in the form of a table the atomic coordinates for 31 crystalline compounds.

S. H. Bauer, the doyen of electron diffraction and *Burg*'s colleague for more than half a century, gives an excellent review of the preparation and the thermodynamic and spectroscopic properties of highly reactive boron-containing molecules, and of the kinetics of some of their elementary reactions with small molecules and with oxygen and nitrogen atoms. *J. F. Liebman, J. S. Chickos* and *J. Simons* have developed simple rules for predicting thermodynamic parameters, especially enthalpies of vaporization, and applied them to boron compounds of all kinds. Only the future can tell us whether or not the "plemeioelectronic relationship" of a substance will gain acceptance as a useful concept. In collaboration with *Z. S. Hermann, L. Pauling* applies his latest statistical theory of non-synchronized resonance in covalent compounds to elemental boron (unfortunately, though, to the so-called "tetragonal boron", which does not exist in its pure form) and to the simpler boron hydrides.

One of the papers on topics other than boron clusters is that by *D. S. Matteson* on the asymmetric synthesis of alco-

hols of the types R–CHMe–OH and R–CHMe–CHMe–OH using the pinandiolatoboryl group as an auxiliary group. *K. Niedenzu* describes the preparation and properties of 76 "pyrazaboles", i.e. the six-membered ring cyclo-dimers of the unstable (1-pyrazolyl)borane. *A. R. Siedle* begins by reviewing the well-known Brønsted acidity of certain of the hydrogen atoms in boron hydrides, then discusses bis(fluorosulfonyl)methane and bis(fluorosulfonyl)amine as strong protonic acids. *B. F. Spielvogel* summarizes the numerous chemotherapeutic properties of amino-acid homologs of the $L-BH_2-COOR$ and $L-BH_2-CONEt_2$ types ($L = NH_xMe_{3-x}$), but these have been found unsuitable for use in neutron capture therapy.

Several monographs on the molecular chemistry of boron, and in particular on boron cluster chemistry, are now available, such as the 1982 monograph by *R. N. Grimes* on "Metal interactions with Boron Clusters", published in the "Modern Inorganic Chemistry" series. The rapid progress in the field is also reviewed every three years in reports dealing with the main papers presented at the IUPAC conferences on boron chemistry. The present volume should be regarded as something intermediate between a monograph and a progress report. The emphasis laid on chemical history or on reviewing particular topics or on presenting new results in a given field varies from chapter to chapter. The careful preparation by the publishers and good typographical presentation make this book a must for all boron chemists, and it can be recommended to everyone working in the field of cluster compounds, and also to those who are only concerned with the field as a fringe interest, or who are interested in the recent history of chemistry. Every library which aims to be well equipped in the area of inorganic molecular chemistry should buy this book.

Peter Paetzold [NB 967 IE]
Institut für Anorganische Chemie
der Technischen Hochschule Aachen (FRG)

Chaos und Ordnung: Die komplexe Struktur des Lebendigen. By *F. Cramer*. Deutsche Verlagsanstalt, Stuttgart 1988. 320 pp., hard cover, DM 48.00. – ISBN 3-421-02753-6

It is a privilege to review this exceptional book, which gives a unique account of the problems we face at the end of this century in the vast domain extending from science to philosophy. The book contains nine chapters dealing mainly, but not solely, with biological problems. Each chapter is preceded by a dialogue, whose hero in most cases is *Georg Christoph Lichtenberg*, and ends with a poem; a quite unusual structure indeed, which reflects the wide range of interests and artistic tastes of Professor *Cramer*.

As is the case in great works of art, this book refers to multiple levels of reality. The world around us is full of aspects which seem contradictory: the regularity of planetary motion, the long-range unpredictability of the weather, the static structure of crystals, the dynamic and self-organizing properties of living systems. Nevertheless, we have to find a way of incorporating these various aspects into a coherent view of nature. For all who are interested in trying to obtain such an overall picture, Professor *Cramer*'s book will be an excellent guide, Obviously, we are far from a final, all-encompassing answer. However, great strides have been made and we may today propose solutions to these apparent contradictions which only a few years ago would have been impossible even to formulate.

This book is first and foremost an excellent introduction to the main problems of modern molecular biology. The author's constant concern is to put these problems into the context of the progress that has recently been achieved in the theory of nonlinear systems far from equilibrium. In recent years the ideas of order and disorder have gone through a radical revision. For a long time, equilibrium structures such as crystals were considered as ideal ordered systems, while hydrodynamic flow and chemical reactions were associated with ideas of randomness and disorder. This is no longer so today. We now know that nonequilibrium can be the source of order. Self-organization is no longer outside the scope of science.

Classical dynamics was associated with time-reversible and deterministic behavior, as is indeed the case for planetary motion. But we now know that this description applies only to a restricted class of dynamic systems. The fascinating properties of unstable dynamic systems which may lead to chaos, to the generation of information, are now studied from the perspectives of an ever-increasing number of disciplines which include physics, chemistry and biology, as well as economics and social sciences. *Cramer*'s presentation is clear and accurate, and will assist the interested reader in finding his way through the labyrinth of these new concepts developed in recent years.

Professor *Friedrich Cramer* is well known for his own original contributions to molecular biology; but characteristically, he uses his insights in this field as a starting point for trying to develop an overall picture of the great questions which have always fascinated men: the position of *Homo sapiens* in relation to other living things, the position of life in relation to matter, and that of matter in our evolving universe.

It is unavoidable that some of Professor *Cramer*'s conclusions will not be shared by everybody. For example, on pages 250–252, he states that the famous "Big Bang" gives us a kind of cosmic horizon, that the question of what time and space would be before the Big Bang is meaningless. Nevertheless, many physicists try to give a physical meaning to the Big Bang, and therefore also to the state of the universe preceding its present structure. This, I think, is unavoidable. Science does not deal with unique events; we have to categorize the Big Bang within some class of grand-scale cosmic phenomena. There is, of course, a wide variety of opinions ranging from *Hawking*'s introduction of a cosmic wave function to models which I favor, in which the Big Bang corresponds to an entropy-producing instability whereby the gravitational field is transformed into matter.

The dialogues placed at the start of each chapter relate its content to the global history of ideas. It is remarkable to read that *Goethe* (page 76) writes of "bewegliche Ordnung" – a kind of dynamic nonequilibrium state. It is also interesting that *Goethe* emphasized that "creation" is still going on. This seems to clash with the ideas of *Newton* as presented on page 219, where *Cramer* appears to state that *Darwin* would be the father of the evolutionary picture of nature. This is, however, not in agreement with historical evidence. What we call the Newtonian or mechanistic concept of nature was not *Newton*'s personal view. He believed in a world which would decay if God did not intervene to repair the damage. Indeed, this is the main theme of controversy between *Newton* and *Leibnitz* as documented by the correspondence between *Leibnitz*, who favored a static view of the universe, and *Clarke*, writing for *Newton*.

"Chaos und Ordnung" is the work of a man who rejects a fragmented view of the universe, who refuses to be a prisoner of preconceived doctrines. There is a feeling of excitement, a

feeling that we are living at a unique moment in the history of science. The world appears to us at the same time as more strange, but also more connected and more harmonious, than to any of the generations which have preceded us. I can only hope that *Cramer*'s book will inspire many readers and will receive the international acclaim it fully deserves.

Ilya Prigogine [NB 985 IE]
Faculté des Sciences
Université Libre de Bruxelles
Brussels (Belgium)
and Department of Statistical Mechanics
and Thermodynamics
University of Texas
Austin, TX (USA)

Ab Initio Calculation of the Structures and Properties of Molecules. By *C. E. Dykstra*. Elsevier, Amsterdam 1988. x, 275 pp., hard cover, HFl 210.00. – ISBN 0-444-43013-X

The development of useful approximate methods and the enormous progress made in computer technology have enabled quantum chemical ab initio methods to become an equal partner alongside experimental methods in determining structures and properties of molecules in the gas phase. However, it is difficult for the non-specialist to assess the credibility and reliability of results obtained from a particular calculation, despite the fact that the subtle factors which determine the accuracy that can be achieved for a given problem are generally well understood in quantum chemistry. The author of this book has set himself the commendable objectives of equipping the non-specialist with the knowledge needed to make such a judgement, and providing him with a survey of the capabilities of modern ab initio methods. This has confronted him with the difficult task of conveying in a condensed form the required knowledge of the methods and the terminology used. *Dykstra* tackles this in a descriptive manner with the authority of an experienced quantum chemist (Chapter 3, 40 pp.). Whether or not this presentation is informative even for the non-specialist will be tested by the verdict of this reader.

In Chapter 1 (10 pp.) the nature of the task of theoretically determining molecular structures is illustrated by five examples from astrophysics. After an explanation of the fundamental concept of the potential surface (and that of the property surface) as applied in the Born-Oppenheimer approximation, Chapter 4 (21 pp.) gives a systematic account of ab initio structures. Chapters 6 to 8 deal in turn with molecular vibrations (18 pp.), electrical properties (44 pp.) and magnetic properties (22 pp.). The 390 literature references, which extend up to the beginning of 1988, are arranged alphabetically in the form of a bibliography, and it is pleasing that they also include the titles of the papers cited. An author index and a subject index are also included, although regrettably the latter does not include details of which molecules are covered in the text.

The compilation and discussion of results is not comprehensive. It deals almost exclusively with molecules and molecular complexes which contain two or three atoms of elements of Period 2 together with some hydrogen atoms (only two pages are devoted to heavy elements). The author, who naturally draws mainly on results in his own field of research, has consciously applied this restriction. Nevertheless, it is difficult to understand why there are no references to earlier books on the same subject, such as those of *Hehre, Radom, Schleyer* and *Pople* (1986)[*], *Mulliken* and *Ermler* (1981), and *Carsky* and *Urban* (1980), nor to relevant review articles. The author's special area of interest also accounts for the relatively large amount of space given to the rather formal description of the role of analytical derivations in quantum chemistry (Chapter 5, 26 pp.), and to the "Polymatrix Approach for SCF and Local Space SCF" (11 pages in Chapter 9).

The book is well written, and its production and presentation are such that it is pleasing to read. The number of printing errors is within acceptable limits, and they only alter the meaning in a few cases, e.g. on page 118 where "quartic" has become "quadratic". All quantum chemists will welcome the compilation of important results which this volume contains. On the other hand, the non-specialist will need to supplement his reading with other monographs, review articles and original papers in order to get a full and balanced view of the capabilities of ab initio methods and the results that it has given up to now, especially as quantum chemists themselves have still not reached agreement on the usefulness of some of the approximate methods (e.g. those for taking account of electron correlation in structure determination).

Joachim Sauer [NB 968 IE]
Zentralinstitut für Physikalische Chemie
der Akademie der Wissenschaften der DDR
Berlin (GDR)

[*] See W. Kutzelnigg, *Angew. Chem. 100* (1988) 312; *Angew. Chem. Int. Ed. Engl. 27* (1988) 862.

Registered names, trademarks, etc. used in this journal, even when not marked as such, are not to be considered unprotected by law.

© VCH Verlagsgesellschaft mbH, D-6940 Weinheim, 1989. – Printed in the Federal Republic of Germany by Konrad Triltsch Druck- und Verlagsanstalt Würzburg.

All rights reserved (including those of translation into foreign languages). No part of this issue may be reproduced in any form — by photoprint, microfilm, or any other means — nor transmitted or translated into a machine language without written permission from the publishers. Only single copies of contributions, or parts thereof, may be made for personal use. This journal was carefully produced in all its parts. Nevertheless, authors, editors and publisher do not warrant the information contained therein to be free of errors. Readers are advised to keep in mind that statements, data, illustrations, procedural details or other items may inadvertently be inaccurate.

Valid for users in the USA: The appearance of the code at the bottom of the first page of an article (serial) indicates the copyright owner's consent that copies of the article may be made for personal or internal use, or for the personal or internal use of specific clients. This consent is given on the condition, however, that the copier pay stated per-copy fee through the Copyright Clearance Center, Inc. (CCC), for copying beyond that permitted by Sections 107 or 108 of the U.S. Copyright Law. This consent does not extend to other kinds of copying, such as copying, for general distribution, for advertising or promotional purposes, for creating new collective works, or for resale. For copying from back volumes of this journal see 'Permissions to Photo-Copy: Publisher's Fee List' of the CCC.

Editorial office: Postfach 10 11 61, D-6490 Weinheim, Federal Republic of Germany, Telephone (06201) 60 22 55, Telex 465 516 vchwh d, Telefax (06201) 602 328.

Editor: *Peter Gölitz*

Associate editors: *D. I. Loewus, A. Stimson.* **Editorial assistant:** *E. Schweikart*

Publishers: VCH Verlagsgesellschaft mbH. (Managing Director: *Hans Dirk Köhler*), Pappelallee 3, D-6940 Weinheim, Federal Republic of Germany.

Advertising office (Advertising Manager *R. J. Roth*): Postfach 10 11 61, D-6940 Weinheim, Federal Republic of Germany, Telephone (0 62 01) 60 61 30, Telex 4 67 155, Telefax (0 62 01) 606 184.

ADVANCED MATERIALS

The European Ceramic Society (ECerS)

Editorial Essay

By Rudi Metselaar*

The European Ceramic Society was founded in 1987 as a federation of the ceramic societies of eleven European countries: Belgium, France, Federal Republic of Germany, Italy, The Netherlands, Norway, Portugal, Spain, Sweden, the United Kingdom, and Yugoslavia. Important goals of the Society are to improve mutual communication between ceramists within European countries, to maintain a calendar of meetings and to coordinate international meetings. Until now conferences were organized independently in different countries, sometimes leading to unfortunate timetable clashes. Now, meetings are planned by the ECerS, not only within Europe, but also on a global scale. Examples of topical meetings are the Conference on Ceramic Powder Processing Science organized in an alternating manner in Europe and the USA, and the Symposium on Ceramic Materials and Components for Engines organized in a similar way in Europe and Japan.

The need for a larger meeting covering the whole field of ceramics was also recognized. In June this year we organized the 1st Conference and Exhibition of the ECerS, in Maastricht, The Netherlands. It was the aim of this conference to bring together scientists, engineers and technicians with an interest in all fields of ceramics and this first conference was certainly a great success. A total number of 1400 participants and over 450 technical papers are clear evidence of the enthusiasm, and the interest from outside Europe was also great, 38 countries being represented. The papers presented covered basic science, engineering ceramics, bioceramics, electronic ceramics, and silicate ceramics and an exhibition of scientific equipment, raw materials and products was organized to run simultaneously. Special attention has been paid in order to make the Society and its activities attractive to young people. For example, student poster contests have been organized for those having just finished their masters or Ph.D. degrees. It was decided to continue this series of conferences in 1991 under the direction of the new president of the Society, *Hans Hausner* (Berlin) in the Federal Republic of Germany and in 1993 in Spain. From then on the conference will probably be organized annually, although the presidency of the Society will continue to change hands (and country) every two years.

During the meeting in Maastricht another important achievement was announced. As a result of discussions between the ceramic societies of Europe, Australia, USA, China, Canada, Japan, South Africa, USSR and South America it was decided to establish a world federation under the name International Ceramic Federation. I will be the first president of the Federation, and Dr. *McLaren* of the American Ceramic Society will occupy the post of Secretary. The role that the Society played in the establishment of the ICF is clear evidence of the influence and strength of the European Ceramic Society. Another important development is the founding of the Society's new journal. The first issue of the *Journal of the European Ceramic Society* which is set up as a scientific journal with high standards appeared in June this year. Indeed, there has been a great need for such a journal in Europe, as until now, the results of European research in ceramic science and engineering have been scattered over many different journals. From now on it will be possible to present the European research effort in a coherent way. In view of the rapid developments in technical ceramics and the correspondingly strong competition, we consider this an important achievement. Readers of *Advanced Materials* may wonder if it is useful to start a discipline-oriented society at a time when everywhere else more general materials societies are being founded. The answer, in my opinion, is partly given above. Both the speed of the scientific and technological developments and the competitive nature of the materials industry produce the need for dedicated journals and specialist meetings.

[*] Prof. Dr. R. Metselaar
Centre for Technical Ceramics, Eindhoven University of Technology
P.O. Box 513, 5600 MB Eindhoven (The Netherlands)



Rudi Metselaar (born 1936) studied chemistry at the University of Amsterdam, The Netherlands, obtaining a Ph.D. in molecular spectroscopy of solids at the same university. From 1967–1977 he worked as a research scientist on magnetic materials at Philips Research Laboratories in Eindhoven. Since 1977 he has been professor of physical chemistry at the Eindhoven University of Technology and has been scientific director of the Centre for Technical Ceramics at the university since it was founded. He has just finished a two year term as the first president of the European Ceramic Society and is now chairman of the International Ceramic Federation.

The future of ceramics in Europe requires a joint (international) effort. This does not mean that the ceramists want to stay in an isolated position and are not interested in developments in other fields of materials science. On the contrary, in some areas there is so much overlap of interests that a cooperation with for instance, metallurgists or polymer chemists is certainly necessary and fruitful. For ceramists this is not new, since ceramics has always been an interdisciplinary science practised by chemists, physicists and metallurgists and now, as a result, the European Society is always open for discussions with other societies or for bilateral meetings.

In this respect cooperation in education should be encouraged in order that European materials science and technology will in the future hold a strong position in the world of advanced materials. The ECerS is ready to contribute and participate.

[1] For a Conference Report see R. J. Brook, *Adv. Mater. 1989* No. 11; *Angew. Chem. Int. Ed. Engl. Adv. Mater. 28* (1989) No. 11; *Angew. Chem. Adv. Mater. 101* (1989) No. 11.

Liquid Crystalline Elastomers

By Rudolf Zentel*

Crosslinkable Polymers
Chiral Phases
Piezo Electric Effects
Mechanical Orientability
Rubber-Like Elasticity

Today, material science is directed towards the development of multifunctional and oriented structures. One example of such supramolecular systems are liquid crystalline (LC) elastomers which combine the properties of LC phases (the combination of order and mobility) with rubber elasticity, one of the most typical polymer properties. Their most outstanding characteristic is their mechanical orientability; strains as small as 20% are enough to obtain a perfectly oriented LC monodomain. This orientability, if LC elastomers with chiral phases are used, leads, for example, to elastomers with chiral smectic C* phases which are likely to show piezo-electric behavior.

1. Introduction

LC Phases combine the long range order of crystals with the mobility of liquids. Their formation from molecules with anisotropic forms, the so called "mesogenic" groups, has long been known for low molar mass compounds and structure-property relationships are well established.[1,2] These LC Phases are thermodynamically stable phases that exist in a temperature range between the crystalline phase and the isotropic melt. For rod-like mesogenic groups, these phases can be subdivided into the nematic phase, for which the long range order is only caused by the – more or less – parallel orientation of the mesogenic groups, and into different smectic phases, in which the molecules are additionally arranged in layers. Different orientations of the mesogenic groups with respect to the layers, which can be perpendicular or tilted, are the basis for a further discrimination between smectic A and smectic C phases (Fig. 1). The transitions among the different phases can be detected by, for example, differential scanning calorimetry (DSC) which measures the latent heat associated with the phase transitions. The most prominent property of these phases is their orientability in electric and magnetic fields.

LC Polymers[3–5] combine the self organization of the mesogenic groups into the ordered structure of LC phases with some typical polymer properties, such as the freezing of the disorder of the polymer chain at the glass transition temperature. Thus, in most cases, the LC phases also freeze glassy on cooling. In addition, an induced orientation can be frozen-in. LC Polymers can be prepared by incorporating the anisotropic mesogenic groups into polymeric systems. Three different ways (Fig. 2) to do this will be discussed, the first two of which are most commonly used. First, the mesogenic groups can be linked to the polymer chain as side groups, to produce LC side group polymers. Second, they

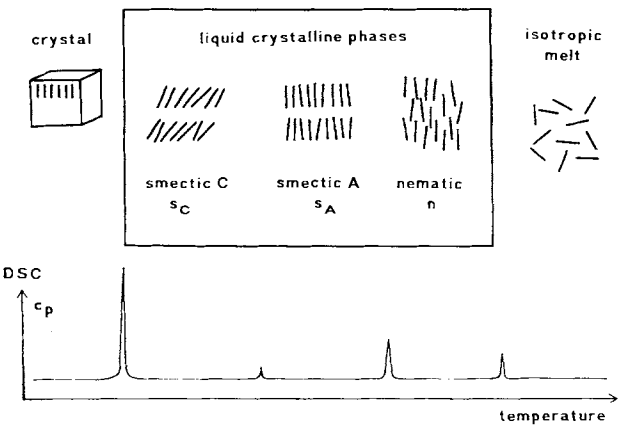


Fig. 1. Schematic representation of different LC phases that exist at temperatures between the crystalline and the isotropic phase. The transitions between these phases show up as peaks in Differential Scanning Calorimetry (DSC) mesurements (C_p vs. temperature).

[*] Priv. Doz. Dr. R. Zentel
Institut für Organische Chemie
Universität Mainz, J.-J. Becher-Weg 18–20
D-6500 Mainz (FRG)

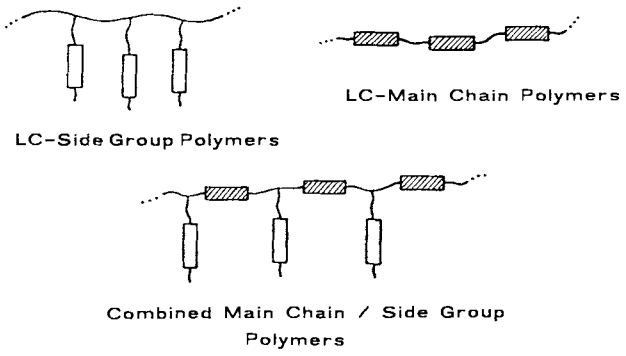


Fig. 2. Different types of LC polymers [5].

can be incorporated into the polymer chain, to obtain LC main chain polymers. Third, both structural principles can be combined, to prepare combined main chain/side group polymers ("combined" LC polymers).[5]

LC Elastomers (Fig. 3) combine the properties already discussed, with rubber elasticity. In these systems a macroscopic deformation of the crosslinked sample (above the glass transition temperature) leads to a corresponding equilibrium deformation of the polymer chains. Different degrees of orientation of the polymer chains can be achieved by stretching the macroscopic sample to different degrees. Afterwards an orientation of the mesogenic groups, which results due to interactions of polymer chains and mesogenic groups, can be determined under equilibrium conditions. In uncrosslinked LC polymers however, non equilibrium orientations resulting from flow above the glass transition temperature have to be frozen-in below T_g. Therefore LC elastomers seem to be ideal systems in which to investigate the interaction of the orientation of the polymer chains (induced by mechanical fields) and that of the mesogenic groups (induced by electric fields). As polymer networks, which are not liquid crystalline, cannot be swollen with mesogenic groups in the LC phase due to incompatibility,[6] the mesogenic groups must be linked covalently to the polymer chains (Fig. 4) to prevent a demixing.

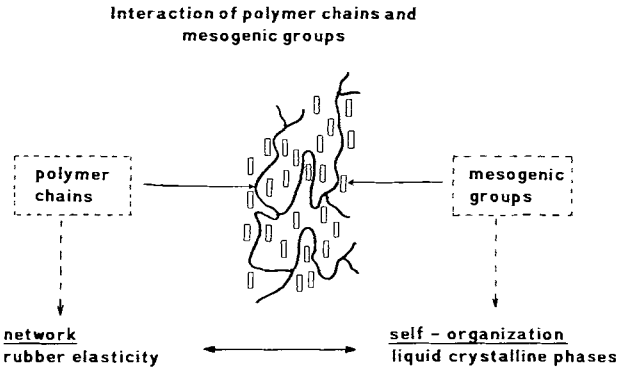


Fig. 3. Schematic representation of a crosslinked LC elastomer. The linkage between polymer chains and mesogenic groups is not yet specified.

In the following, ways to prepare differently structured LC elastomers (see Section 2.1.), as well as their properties, will be discussed. This will be done for achiral LC elastomers (see Section 2.2.) which have been studied most intensively, and then for the new elastomers with chiral LC phases (see Section 2.3.) which are interesting because of their optical and electrical properties.

2. Liquid Crystalline Elastomers

2.1. Structural Variation of Achiral Elastomers

Densely crosslinked thermosets with a liquid crystalline structure that remains unchanged up to the decomposition temperature of the polymer have been known for some time.[7, 8] Slightly crosslinked LC polymers, however, which show reversible phase transitions on heating and cooling and which show elastic properties, are relatively new. The first to be prepared were based on crosslinked side-group polymers (Fig. 4) with a polysiloxane backbone.[9–12] This work has been summarized by *Finkelmann* et al.[13] Shortly afterwards the work on LC elastomers was extended to crosslinked side group polymers with polyacrylate and polymethacrylate backbones[14–18] and also to slightly crosslinked main chain polymers and "combined" polymers (Fig. 4).[14, 19, 20] A comparative investigation of LC elastomers of these different structures is interesting because the behavior of the two "subsystems" (network of the polymer chains – mesogenic groups) in each case should be different. Thus the coupling between the orientation of polymer chains and mesogenic groups should differ significantly for the different types (Fig. 4). For crosslinked side group polymers the orientation



Rudolf Zentel (born 1953) studied chemistry at the University of Mainz, FRG, obtaining his Diploma in 1980 and his Ph.D. in 1983 after working with Professors G. Strobl and H. Ringsdorf. After this, he spent one year as a post-doctoral fellow at the University of Freiburg with Professor H.-J. Cantow, and then returned to Mainz in 1984 to start work on "Liquid Crystalline Elastomers". In April 1989 he finished his Habilitation and obtained the "Venia Legendi" in Organic Chemistry. Since July 1989 he has been at the IBM Almaden Research Center in San Jose (USA) as a Visiting Scientist working on materials for optical data storage. He has published 27 papers on various topics in polymer chemistry.

of the mesogenic groups is relatively free with respect to the polymer chain, since they are decoupled by a flexible spacer. In crosslinked main chain polymers, however, the mesogenic groups are directly incorporated into the polymer chains. Crosslinked "combined" polymers may behave in an intermediate manner because one half of the mesogenic groups are incorporated into the polymer chains, while the other half are linked to the polymer backbone as side groups via a flexible spacer. Both types of mesogens must, however, interact cooperatively to form an LC phase (both types of mesogens orient parallel to each other (Fig. 4)).[19]

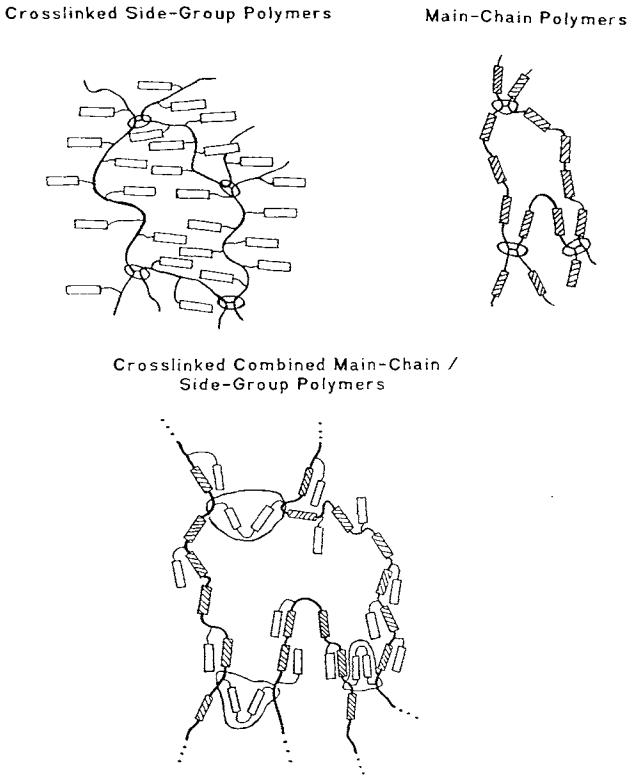
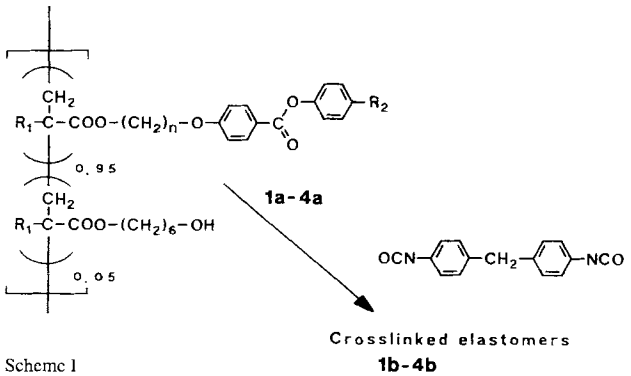


Fig. 4. Schematic representation of different types of LC elastomers.

Some of the LC elastomers derived from side group polymers are presented in Scheme I and Table 1. Due to the use



Scheme I

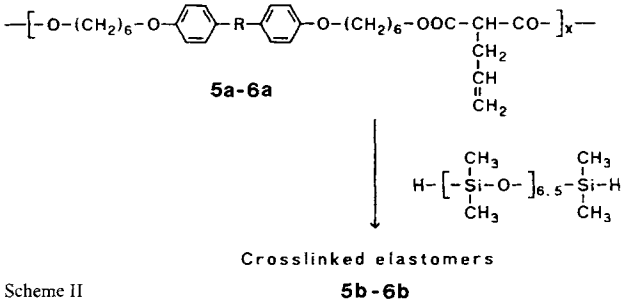
Table 1. Phase transitions of uncrosslinked (**a**) and crosslinked (**b**) LC side group polymers [14, 17] (see Scheme I).

No.	R_1	n	R_2	Molecular weight (GPC)	Cross linker (mol.-%)	Phase transitions[a]/K
1a	CH_3	6	OCH_3	> 100000	–	g313 n379 i
1b	CH_3	6	OCH_3	–	0.5	g315 n379 i
2a	CH_3	6	$O-(CH_2)_3CH_3$	> 100000	–	g318 s_A375 n379 i
2b	CH_3	6	$O-(CH_2)_3CH_3$	–	3.5	g318 s_A377 n382 i
3a	H	6	OCH_3	45000	–	g299 s_A355 n383 i
3b	H	6	OCH_3	–	2.5	g304 s_A353 n384 i
4a	H	2	OCH_3	> 100000	–	g329 n368 i
4b	H	2	OCH_3	–	2.5	g336 n376 i

[a] g: glassy frozen liquid crystal, s_A: smectic A, n: nematic, i: isotropic melt.

of functionalized polymethacrylates (**1a–2a**) and polyacrylates (**3a–4a**) of a high molecular weight, small amounts of diisocyanates are sufficient to prepare crosslinked samples (**1b–4b**). For the preparation of crosslinked polysiloxanes, however,[9–12] much higher amounts of crosslinker are necessary, due to the lower molecular weight of the precursor polymers.

Some of the LC elastomers derived from main chain polymers are presented in Scheme II and Table 2. In this case the



Scheme II

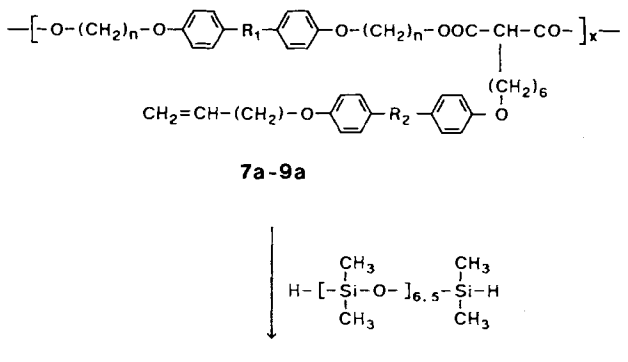
Table 2. Phase transitions of uncrosslinked (**a**) and crosslinked (**b**) LC main chain polymers [14, 19] (see Scheme II).

No.	R	Molecular weight (GPC)	Cross-linker (mol.-%)	Phase transitions[a]/K
5a	–	> 80000	–	c334 s_B368 s_A386 i
5b	–	–	5	c329 s_B368 s_A389 i
6a	–N=N–	20000	–	c307 S_A405 i
6b	–N=N–	–	10	c304 s_A401 i

[a] c: crystalline, s_A: smectic A, s_B: smectic B, i: isotropic melt

crosslinking is performed by reaction of some of the olefinic double bonds of the polymer with the Si-H groups of an α, ω difunctionalized oligosiloxane.[14, 20] Thus crosslinked polymers with different smectic phases can be obtained.

In Scheme III and Table 3 some of the LC elastomers derived from "combined" polymers are presented. Again the



Scheme III

Table 3. Phase transitions of uncrosslinked (**a**) and crosslinked (**b**) combined LC polymers [14, 19, 20] (see Scheme III).

No.	R_1	R_2	Molecular weight (GPC)	Cross linker (mol.-%)	Phase transitions[a]/K
7a	$-N=N-$	–	> 80000	–	c397 s_C423 s_A427 i
7b	$-N=N-$	–	–	10	c392 s_C421 i[b]
8a	$-N=N-$	$-N=N-$	45000	–	c383 s_C405 s_A411 n433 i
8b	$-N=N-$	$-N=N-$	–	10	c379 s_C397 n424 i[b]
9a	$-N(O)=N-$	$-N=N-$	52000	–	g293 s_C399 s_A407 n437 i
9b	$-N(O)=N-$	$-N=N-$	–	10	g293 s_C395 s_A403 n434 i

[a] c: crystalline or highly ordered smectic phase, s_C: smectic C, s_A: smectic A, n: nematic, i: isotropic melt. [b] the transitions s_C-s_A and s_A-n or i are not resolved.

crosslinking is done by a hydrosililation reaction between the Si-H groups of the oligosiloxane and some of the double bonds at the end of the mesogenic side groups.[14, 19, 20] The "combined" LC polymers show a strong polymorphism (Tab. 3, see also[5b]) which means that different LC phases are often found for one polymer at different temperatures.

2.2. Properties of Achiral LC Elastomers

The basic properties of LC elastomers – such as: phase behavior, elasticity and orientability – are independent of their molecular structure (see Scheme I–III and Fig. 4).

The LC phase is retained for the crosslinked elastomers. X-Ray measurements performed with the uncrosslinked and the slightly crosslinked polymers (see Tab. 1–3) show the same LC phases.[14, 17–20] Only for higher crosslinking densities are changes of the X-ray pattern sometimes observed.[12] Thus the crosslinking reaction, which transforms a soluble polymer into a soft solid and prevents diffusion of the polymer chains, does not influence the LC order.

As long as the crosslinking density is low, the phase transition temperatures are not shifted significantly.[9, 13–17] Only a slight increase or decrease (±5 K) is observed (see Tab. 1–3 and Fig. 5) by DSC-measurements. A decrease of the phase transition temperature derives from the presence

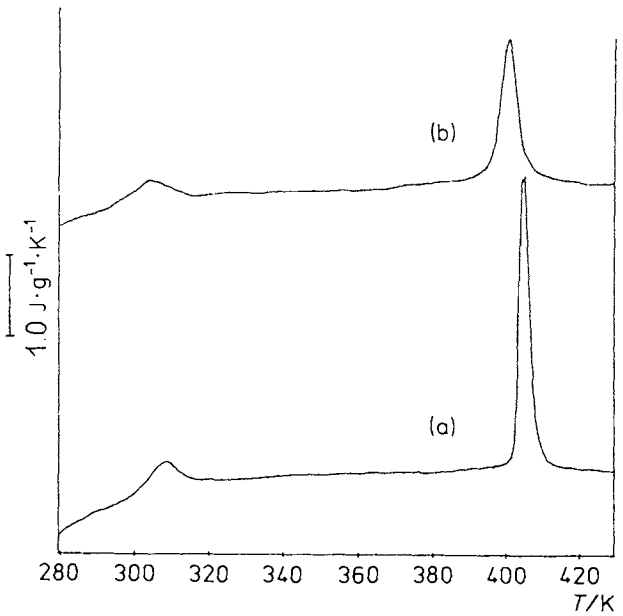


Fig. 5. DSC-measurements of the uncrosslinked main chain polymer **6a** (a) and the crosslinked elastomer **6b** (b) (Tab. 2), figure taken from ref. [14].

of the crosslinking molecules (diisocyanates or oligosiloxanes) at the netpoints, which are not mesogenic by themselves and disturb the LC order. An increase of the phase transition temperature may result from an increase of the molecular weight associated with the crosslinking reaction (an increase of the molecular weight increases the phase transition temperatures for uncrosslinked polymers).[21] Theory further predicts that the state of order during the crosslinking reaction (LC or isotropic phase) should influence the phase transition temperatures of the final network,[22] because the distribution of the netpoints should stabilize the state of order experienced during the crosslinking reaction.

All slightly crosslinked LC polymers show elastic properties (LC elastomers) both in the isotropic and in the LC phase. This is shown for one crosslinked side group polymer with a polymethacrylate chain by the mechanical-dynamical measurements shown in Figure 6[23] (the results of the crosslinked polysiloxanes are described elsewhere).[10, 12, 13, 24, 25] This behavior is also found for crosslinked main chain and "combined" polymers.[23, 26]

In the isotropic phase a "normal" rubber-like behavior is observed.[12, 13, 23–26] This is evident from the (rubber)-plateau in the real part of the compliance (J') at low frequencies (Fig. 6a). The plateau compliance is the same as that of slightly crosslinked elastomers that are not liquid crystalline. The decrease of J' at high frequencies, which is associated with a maximum in J'', is due to the dynamic glass process and the slippage of entanglements. The presence of LC phases at lower temperatures only shows up in a strong increase of the stress optical coefficient[10–13] at temperatures close to the transition into the nematic phase (pretransitional effects).

ADVANCED MATERIALS

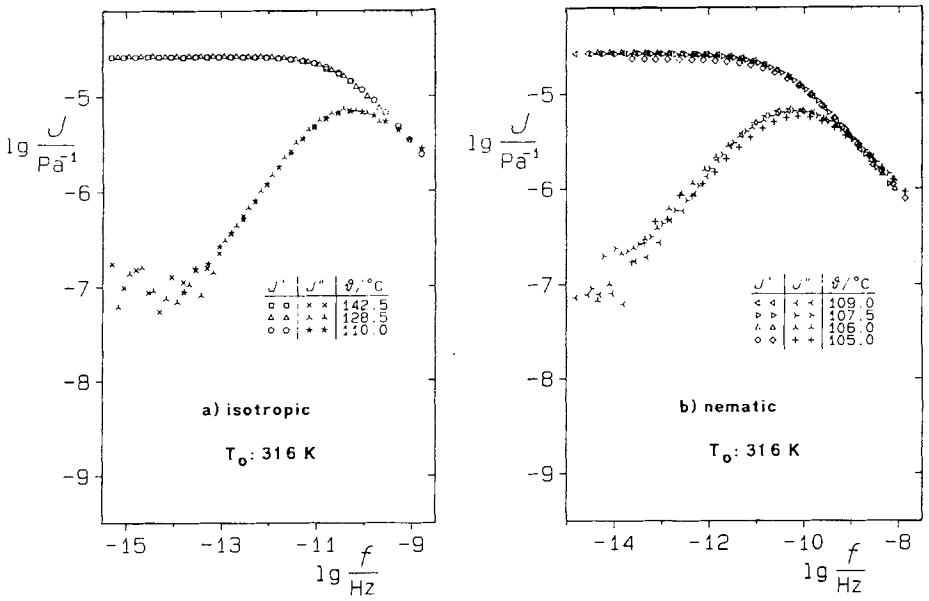


Fig. 6. Mastercurve obtained for the LC side group elastomer **2b** (Tab. 1). The real (J') and the imaginary (J'') part of the complex mechanical compliance is plotted. The measurements were performed in the isotropic (a) and in the unoriented nematic (b) phase (frequencies between 10^{-6} 10^{-2} Hz) and shifted to a reference temperature of 316 K. Measurement performed by *Hanus* and *Pechhold* [23].

In the nematic phase the plateau compliance is the same as in the isotropic phase (see Fig. 6b). This proves that the chain conformation is not significantly changed at the transition to the nematic phase.[27] This result is consistent with the results obtained by neutron scattering of uncrosslinked LC polymers of a similar structure,[28] which show that the radius of gyration is slightly anisotropic in the nematic phase, but the averaged value is the same as in the isotropic phase. At the transition into the smectic A phase (layer structure), the plateau compliance is reduced, but the material remains elastic.

Care has to be taken in interpreting the mechanical measurements in the LC phase, because different properties are found for macroscopically unoriented samples (this corresponds more to the isotropic phase) and for LC monodomains (anisotropic elastic properties). These monodomains show—in addition—changed dimensions in the stress-free state,[12, 25, 29] leading to a stress relaxation during formation. They can be produced—quite accidentally—by small strains during the measurement[10–14, 17–19, 24–26, 29] and sometimes they form spontaneously[12, 24] in highly crosslinked networks.

The mechanical orientability is the most prominent property of LC elastomers.[10–14, 17–19, 24–26, 29] If the network does not orient spontaneously in the LC phase (that means, if the ground state is macroscopically unoriented), then small strains (about 20%) are enough for the reversible formation of an LC monodomain (Fig. 8).[13, 25, 29] This orientation is achieved under equilibrium conditions far above the glass transition temperature. It is not necessary to freeze-in an orientation induced by flow, as in uncrosslinked LC polymers. *Schätzle* et al. were able to determine a threshold stress[25] for the reversible orientation of LC elastomers. Also a small shift of the phase transition temperatures of about 2 K can be induced by stretching[13, 25] and has been theoretically explained.[22, 30] The orientation induced by the same strain is orders of magnitude smaller if the elastomer is in the isotropic phase. This corresponds to the situation in non LC elastomers, for which strains up to 1000% are necessary to obtain a very well oriented sample. Such behavior is found for all types of LC elastomers (Fig. 4) independent of their molecular structure.[29] Differences that are expected e.g. between crosslinked side group and main chain polymers (Fig. 4), may be hidden behind differences in the crosslinking density and the network topology.

The measurement of the strain induced orientation is done with the help of birefringence measurements[10, 12, 25] (only isotropic phase), measurements of the IR-dichroism[11, 25] and X-ray measurements[17–19, 29] (isotropic and LC phase). In this way X-ray measurements, as presented in Figure 7 (polymer **3b** of Tab. 1) were obtained. This X-ray pattern can be used for an accurate assignment of the LC

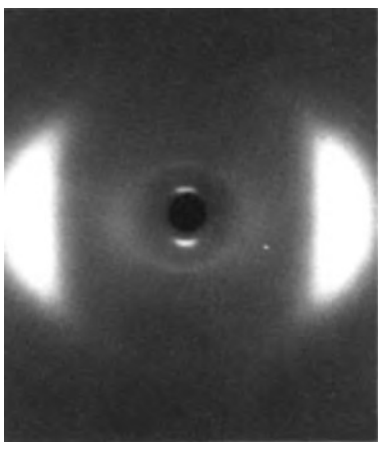


Fig. 7. Fiber pattern of elastomer **3b** (Tab. 1) in the smectic A phase (room temp.), strain $\Delta l/l_0 = 0.73$, fiber axis vertical, figure taken from ref. [17].

phases and, in addition, for a determination of the macroscopic orientation of the sample, as done by *Mitchell* et al.[18] for a similar elastomer (Fig. 8). The orientation, which is reached at an extension ratio of 1.3, corresponds to a monodomain of a nematic polymer. It can be frozen-in below the glass transition temperature.

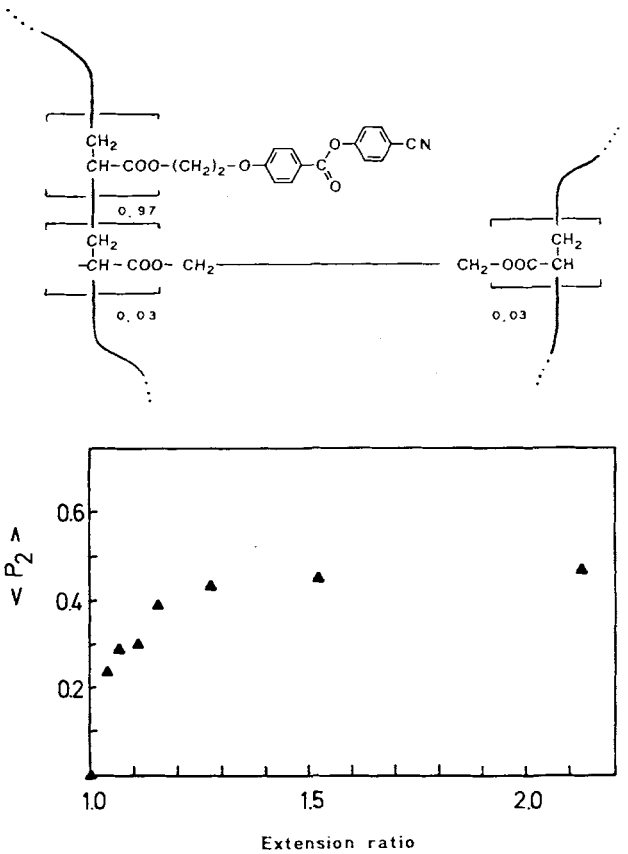


Fig. 8. A plot of the orientation parameter $\langle P_2 \rangle$ for the LC elastomer presented above; the ordinate corresponds to the extension applied. Figure taken from ref. [18] (*Mitchell* et al.).

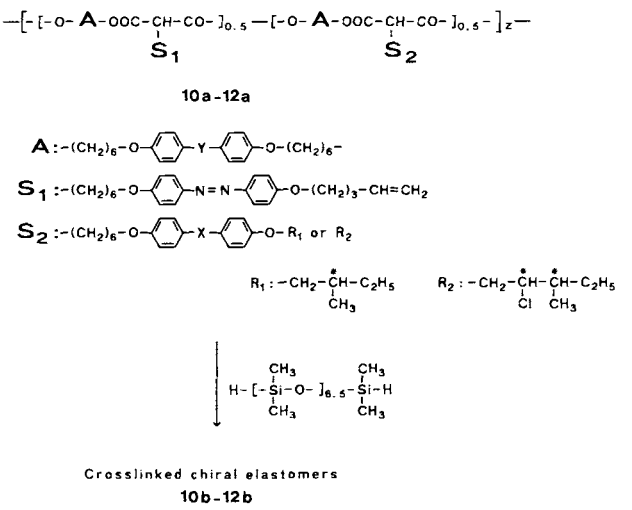
The mechanical orientability of the LC elastomers is presumably due to the anisotropic conformation, which the polymer chains adopt in the LC phase[28] (Fig. 3). Therefore the average distance between two crosslinks in a network does not only depend on the chain length between them, but also on the orientation relative to the long axis of the mesogenic groups. This leads to a coupling of the preferred orientation of polymer chains and mesogenic groups, which has been described theoretically by various authors.[22, 30]

The reversible mechanical orientability of LC elastomers is of considerable interest for the following reasons: For most applications LC phases must be well aligned. LC elastomers thus offer a simple way to do this under equilibrium conditions. The aligned samples can then be used e.g. for an accurate phase assignment by X-ray measurements (Fig. 7),[19, 26] for the determination of the orientation of polymer chains and mesogenic groups with respect to each other[10, 12, 17] or because of their optical properties. Their application as wave guides seems possible,[31] because the local orientation and thus the birefringence can be changed by local strains. In addition, the orientation of an unoriented LC sample into a monodomain transforms reversibly a highly turbid sample into a transparent one. Therefore applications as mechanical-optical switches may be considered.

The anisotropic dielectric properties should also be considered. The stretching of a sample leads to orientation and changes the effective dielectric constant. This can be detected dielectrically. In turn, the action of electric fields on the material can lead to shape variations of the sample,[15] because the elastomers (soft solids) try to orient the axis of their maximal dielectric constant parallel to the electric field.

2.3. Chiral LC Elastomers

Bearing in mind the mechanical orientability of LC elastomers, it seems interesting to look for elastomers which show very drastic changes of their properties during orientation. In this context LC elastomers which combine the properties already discussed with the properties of chiral phases (cholesteric or chiral smectic C* phases) are of considerable interest. These phases, prepared from chiral mesogens, are the chiral modifications of the nematic and the smectic C phase. They possess very special properties, which are: selective reflection of light (cholesteric phase)[1, 2, 32] and ferroelectric properties (chiral smectic C* phase)[33] (see Fig. 9). Besides low molar mass liquid crystals, polymers with the same phases[34, 35] have also been prepared. Since these properties are linked to the helical superstructure of the phases (Fig. 9a and c) it can be asked if it is possible to use a typical elastomer property – the orientability by stretching (mechanical field) – to untwist the helix (repeating distance: 0.2–2 μm). Such a possibility has been predicted theoretically.[30] In low molar mass liquid crystals[32, 33] the helical



Scheme IV

ADVANCED MATERIALS

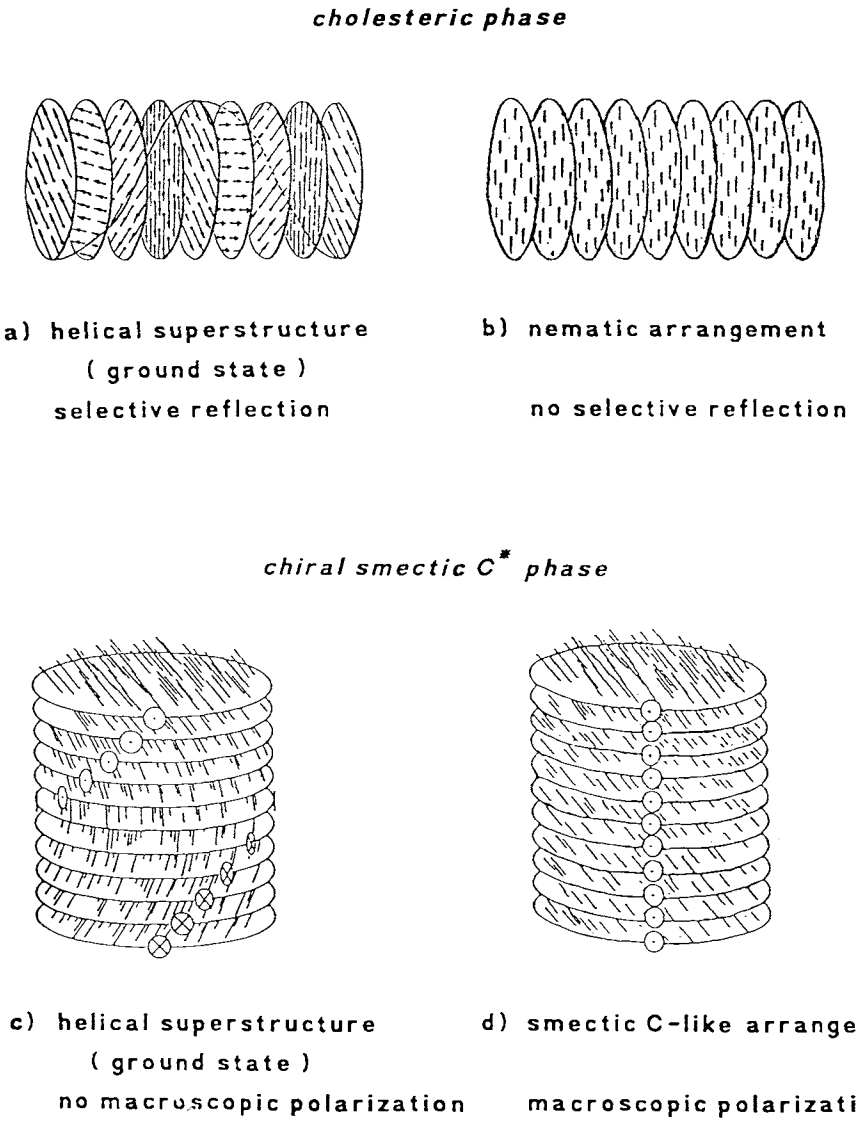


Fig. 9. Schematic representation of the cholesteric (a) and the chiral smectic C* (c) phase. Both phases have a helical superstructure in the ground state. The nematic arrangement (b) or the smectic C like arrangement (d) (untwisted states) can be induced by electric or magnetic fields or by stretching (LC elastomer).

structure can be untwisted by strong electric or magnetic fields, thus transforming the helical cholesteric phase (with selective reflection) into a nematic structure (without selective reflection, Fig. 9a and b) or the chiral smectic C* phase (without a macroscopic polarization) into a smectic C like structure (with a macroscopic polarization, Fig. 9c and d).

In order to investigate elastomers with these properties, a series of chiral crosslinkable polymers have been prepared (Tab. 4 and Scheme IV).[36, 37] For this purpose combined polymers were selected because they form broad smectic and nematic phases (see Tab. 3) if they are achiral, and cholesteric and chiral smectic C* phases[38] if they are chiral. The polymers thus prepared show cholesteric and chiral smectic C* phases in the uncrosslinked and crosslinked state (Tab. 4).

The phase assignment of these polymers was done by polarizing microscopy and by X-ray measurements,[37] proving that cholesteric and different smectic phases were present. The ferroelectric properties of the chiral smectic C* phase

Table 4. Phase transitions of uncrosslinked (**a**) and crosslinked (**b**) chiral combined polymers [37] (see Scheme IV).

No.	Y	X_1	X_2	R	Molecular weight	Crosslinker (mol.-%)	Phase transitions[a]/K
10a	–N=N–	–N=N–	–N=N–	R_1	60000	–	c382 s_c*397 n*422 i
10b	–N=N–	–N=N–	–N=N–	R_1	–	10	c372 s_c*387 n*414 i
11a	–N(O)=N–	–N=N–	–N=N–	R_1	47000	–	g297 s_c*388 n*422 i
11b	–N(O)=N–	–N=N–	–N=N–	R_1	–	10	g298 s_c*383 n*420 i
12a	–N(O)=N–	–	–	R_2	17000	–	g293 s_c*397 n*403 i
12b	–N(O)=N–	–	–	R_2	–	20	g292 s_c*383 n*396 i

[a] c: crystalline or highly ordered smectic phase, g: glassy frozen phase, s_c*: chiral smectic C*, n*: cholesteric phase, i: isotropic melt

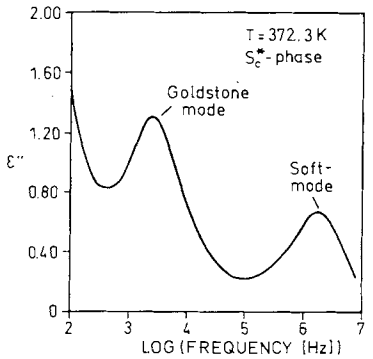


Fig. 10. A plot of the dielectric loss ε'' versus frequency for a thin (10 μm) and aligned sample of polymer **12a** (Tab. 4) measurement performed by *Vallerien* and *Kremer* [40].

can be determined by dielectric relaxation measurements.[39] The results obtained from polymer **12a** are presented in Figure 10.[40] In the chiral smectic C* phase, two very intensive dielectric loss processes are found, which are not present in the isotropic phase. Due to their high intensity and their temperature dependence, they cannot be local relaxation processes.[39] In analogy to low molar mass liquid crystals, these dielectric loss processes can be assigned as the soft mode and the Goldstone mode,[41] which are typical for chiral smectic C* phases (Fig. 9c). They correspond to fluctuations of the spontaneous electric polarization due to changes of the tilt angle (soft mode) or due to changes of the tilt direction at constant tilt angle (Goldstone mode, distortion of the helical structure).

The first X-ray measurements performed on the chiral elastomers prove that the helical superstructure in the cholesteric and chiral smectic C* phase can be untwisted by stretching.[37] This is presented in Figure 11 for the chiral smectic C* phase of elastomer **11b**. For small strains, a fiber pattern as presented in Figure 11a is obtained. They correspond to an oriented chiral smectic C* phase with a helical superstructure (Fig. 9c). For higher strains (about 400%) fiber pattern as presented in Figure 11b could be obtained. In this case it was necessary to cool the stretched sample down to the glass transition temperature in order to prevent a tearing of the sample during the measurement. These fiber patterns correspond to a smectic C like monodomain (Fig. 9d) without a helical superstructure. Therefore the sample should not have a macroscopic polarization for small strains (Fig. 9c and 11a) due to its helical superstructure, but it should have a macroscopic electric polarization (Fig. 9d and 11b) if it is highly strained.

Most of the work on chiral LC elastomers still remains to be done. For the future it is necessary to prepare e.g. elastomers with a still higher spontaneous polarization in the chiral smectic C* phase. In addition it should be possible to stretch the elastomers more highly (> 400%) and to obtain in this way a uniform orientation over the whole sample[37] (otherwise the polarizations arising from differently oriented domains will compensate each other). Despite these limitations the results of the X-ray measurements show that the chiral LC elastomers have the potential to act like a device that transforms a mechanical signal (the strain) into an optical signal (cholesteric phase, Fig. 9a and b) or an electrical signal (chiral smectic C* phase, Fig. 9c and d). In the last case (chiral smectic C* phase) the elastomer should behave like a piezo-element.

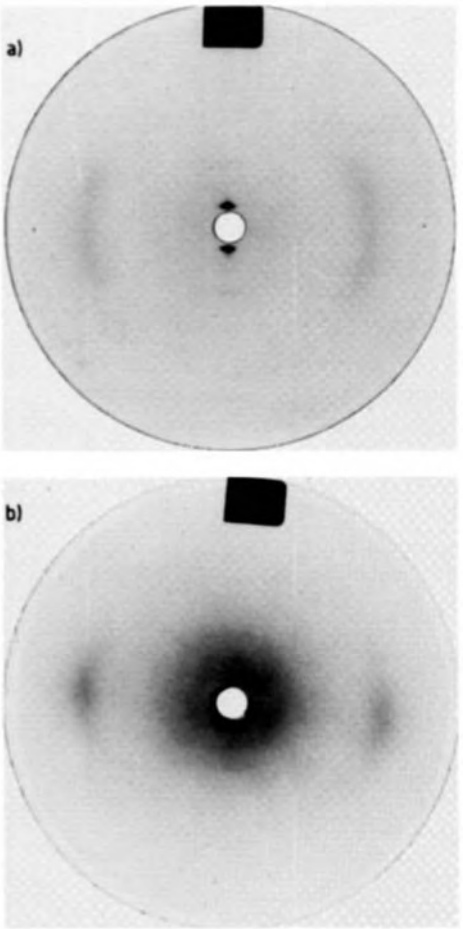


Fig. 11. X-Ray fiber pattern of the chiral elastomer **11b** (Tab. 4) in the chiral smectic C* phase [37], fiber axis vertical. a) a strain of 300% applied, temperature 363 K. b) a strain of more than 400% was applied at 360–370 K, the measurement was performed at room temperature. The wide angle reflections correspond to 4.4 Å and the small angle reflections correspond to 26–27 Å.

3. Summary and Outlook

Starting from a search for a detailed understanding of "classical" materials, such as liquid crystals, polymers and rubbers, material science today is directed to the investigation of more complex systems that combine different properties and functions with ordered structures. The interest in these more complex systems is twofold. On one hand new properties are expected, and on the other hand the study of the interaction of the different subsystems (e.g. polymer chains and mesogenic groups) is fascinating.

ADVANCED MATERIALS

LC elastomers belong to this group of materials. They combine a wide variety of properties such as: i) the mechanical orientability of rubbers, ii) the ordered structure and the mobility of LC phases and iii) the possibility as in polymers to freeze-in an induced orientation below T_g.

LC elastomers with different molecular structures can be prepared by crosslinking LC polymers, while retaining the LC phases. Their elasticity is comparable to "classical" networks. While the understanding of the interaction of the liquid crystalline and the rubber properties in LC elastomers is still at an early stage their mechanical orientability makes them interesting for academic research (phase assignment, structure investigation) and also for applications such as optical switches (turbid–clear) or as wave guides.

The combination of these properties with chiral phases (chiral LC elastomers) yields materials that transform mechanical strain into optical or electrical signals and elastomers with chiral smectic C* phases are likely to show piezo electric properties.

Received May 17, 1989

[1] P. G. de Gennes: *The Physics of Liquid Crystals*. Clarendon Press, Oxford 1975.

[2] R. Steinsträßer, H. Krüger in E. Bartholomé et al. (Eds.): *Ullmanns Encyklopädie Technischer Chemie, 4. Aufl. 11*, Verlag Chemie 1976, p. 657.

[3] H. J. Cantow (Ed.): *Adv. Polym. Sci. 59–61* (1984).

[4] H. Finkelmann, *Angew. Chem. Int. Ed. Engl. 26* (1987) 816; *Angew. Chem. 99* (1987) 840.

[5] a) H. Ringsdorf, B. Schlarb, J. Venzmer, *Angew. Chem. Int. Ed. Engl. 27* (1988) 113; *Angew. Chem. 100* (1988) 117. b) B. Reck, H. Ringsdorf, *Makromol. Chem. Rapid Commun. 6* (1985) 291.

[6] F. Brochard, *J. Phys. (Les Ulis, Fr.) 40* (1979) 1049.

[7] Strzelecki, L. Liebert, *Bull. Soc. Chim. Fr. (1973)* 597.

[8] S. N. Bhadani, D. G. Gray, *Mol. Cryst. Liq. Cryst. Lett. 120* (1984) 255.

[9] H. Finkelmann, H.-J. Kock, G. Rehage, *Makromol. Chem. Rapid. Chommun. 2* (1981) 317.

[10] H. Finkelmann, H.-J. Kock, W. Gleim, G. Rehage, *Makromol. Chem. Rapid Commun. 5* (1984) 287.

[11] J. Schätzle, H. Finkelmann, *Mol. Cryst. Liq. Cryst. 142* (1987) 85.

[12] W. Gleim, H. Finkelmann, *Makromol. Chem. 188* (1987) 1489.

[13] W. Gleim, H. Finkelmann in C. B. McArdle (Ed.): *Side Chain Liquid Crystal Polymers*, Blackie & Son, Glasgow 1989, p. 287.

[14] R. Zentel, G. Reckert, *Makromol. Chem. 187* (1986) 1915.

[15] R. Zentel, *Liq. Cryst. 1* (1986) 589.

[16] F. J. Davis, A. Gilbert, J. Mann, G. R. Mitchell, *J. Chem. Soc., Chem. Commun. (1986)* 1333.

[17] R. Zentel, M. Benalia, *Makromol. Chem. 188* (1987) 665.

[18] G. R. Mitchell, F. J. Davis, A. Ashman, *Polymer 28* (1987) 639.

[19] R. Zentel, G. F. Schmidt, J. Meyer, M. Benalia, *Liq. Cryst. 2* (1987) 651.

[20] S. Bualek, R. Zentel, *Makromol. Chem. 189* (1988) 791.

[21] V. Percec, C. Pugh in C. B. McArdle (Ed.): *Side Chain Liquid Crystal Polymers*, Blackie & Son, Glasgow 1989, p. 30; H. Finkelmann, G. Rehage, in ref. [3], p. 99; V. P. Shibaev, N. A. Platé, in ref. [3], p. 173.

[22] M. Warner, K. P. Gelling, T. A. Vilgis, *J. Chem. Phys. 88* (1988) 4008.

[23] K.-H. Hanus, *Ph. D. thesis*, University of Ulm, FR-Germany 1989; K.-H. Hanus, B. Stoll, W. Pechhold, University of Ulm, FR-Germany in cooperation with R. Zentel, unpublished.

[24] W. Oppermann, K. Braatz, H. Finkelmann, W. Gleim, H.-J. Kock, G. Rehage, *Rheol. Acta 21* (1982) 423.

[25] J. Schätzle, *Ph. D. Thesis*, University of Freiburg, FR-Germany 1989; J. Schätzle, W. Kaufhold, H. Finkelmann, *Makromol. Chem.* (1989) submitted.

[26] K.-H. Hanus, W. Pechhold, F. Soergel, B. Stoll, R. Zentel, *Coll. & Polym. Sci.* (1989) submitted.

[27] L. R. G. Treloar: *The Physics of Rubber Elasticity*. Clarendon Press, Oxford 1975.

[28] R. G. Kirste, H. G. Ohm, *Makromol. Chem. Rapid Commun. 6* (1985) 179; F. Moussa, J. P. Cotton, F. Hardouin, P. Keller, M. Lambert, G. Pepy, M. Mouzak, H. Richard, *J. Phys. (Les Ulis, Fr.) 48* (1987) 1079.

[29] S. Bualek, H. Kapitza, J. Meyer, G. F. Schmidt, R. Zentel, *Mol. Cryst. Liq. Cryst. 155* (1988) 47.

[30] H. Brand, *Makromol. Chem. Rapid Commun. 10* (1989) 57.

[31] H. Finkelmann, J. Schätzle, W. Kaufhold, L. Pohl, *18. Freiburger Arbeitstagung Flüssigkristalle*, 15.–17. März 1989, Abstracts of Communications.

[32] S. Chandrasekhar: *Liquid Crystals*, Cambridge University Press, Cambridge 1977.

[33] J. W. Goodby, T. M. Leslie, *Mol. Cryst. Liq. Cryst. 110* (1984) 175.

[34] N. A. Platé, R. V. Talroze, Ya. S. Freidzon, V. P. Shibaev, *Polymer J. 19* (1987) 135; H. Finkelmann, G. Rehage, in ref. [3], p. 99.

[35] P. LeBarny, J. C. Dubois in C. B. McArdle (Ed.): *Side Chain Liquid Crystal Polymers*, Blackie & Son, Glasgow 1989, p. 130.

[36] R. Zentel, G. Reckert, B. Reck, *Liq. Cryst. 2* (1987) 83.

[37] R. Zentel, *Liq. Cryst. 3* (1988) 531; R. Zentel, G. Reckert, S. Bualek, H. Kapitza, *Makromol. Chem.*, (1989) in press.

[38] H. Kapitza, R. Zentel, *Makromol. Chem. 189* (1988) 1793.

[39] S. U. Vallerien, R. Zentel, F. Kremer, H. Kapitza, E. W. Fischer, *Makromol. Chem. Rapid Commun.* (1989) in press.

[40] S. U. Vallerien, F. Kremer, MPI- für Polymerforschung, Mainz, FR-Germany, in cooperation with R. Zentel, unpublished.

[41] J. Musevic, R. Blinc, B. Zeks, C. Filipic, M. Copic, A. Seppen, P. Wyder, A. Levanyuk, *Phys. Rev. Lett. 60* (1988) 1530; S. U. Vallerien, F. Kremer, H. Kapitza, R. Zentel, W. Frank, *Phys. Lett. A 138* (1989) 219.

The following review articles will be published in future issues:

H. Sixl et al.: Polymer Systems for Optoelectronics.

F. Aldinger, J. Huber et al.: High Performance Silicon Nitride Materials.

R. D. Miller: Substituted Silane Polymers—A New Look at Some Old Materials.

H. Eckert: Structural Characterization of Non-Oxide Chalcogenide Glasses Using Modern Solid State NMR Techniques.

K. Bange, T. Gambke: Electrochromic Materials for Optical Switching Devices.

ADVANCED MATERIALS

Superfine Oxide Powders—Flame Hydrolysis and Hydrothermal Synthesis

Nanocrystalline Ceramics
Powder Processing
Clean Room Technology
Sintering

By Gangolf W. Kriechbaum * and Peter Kleinschmit *

1. Introduction

The excitement surrounding the technical potential of ceramic materials has gained new support since the surprising physical properties of so-called nanocrystalline materials have been observed.[1] *Gleiter* and coworkers were able to show that a thin ceramic plate of TiO_2 with a nanocrystalline microstructure could be plastically deformed at a temperature as low as 180 °C. This behavior opens the way to new ceramic processing and forming techniques.

In the last decade a lot of research activities have been focused on the development of new synthetic methods for the production of sinter-active submicron ceramic powders. The state of the art of powder synthesis has been reviewed by several authors.[2–6]

This paper describes flame hydrolysis and hydrothermal synthesis, two techniques with the potential to yield superfine powders with a particle size in the nanometer range, and discusses problems involved with the synthesis and handling of superfine materials.

The step from conventional ceramics to high performance ceramics can be described as a change in size range. Conventional technical ceramics with grain sizes between 5 to more than 100 microns and flaw sizes in a similar range are made out of powders prepared by classical mixing-calcining-milling methods or out of refined minerals. High performance ceramics with grain sizes between 0.2 to less than 1 micron need chemically prepared powders in a submicron size range and processing techniques which prevent flaw sizes much bigger than the grain size. By far the most ceramic powders are still produced by conventional techniques but high performance ceramic applications are gaining in importance and therefore the share of chemically prepared powders increases.

Reducing the particle size and increasing the chemical and morphological homogeneity of the powders has led to some specific problems in synthesis and processing.

The need to work in clean rooms or in closed production lines in order to avoid contamination by dust and other particles which are omnipresent in normal unfiltered air is just one example of the required changes for submicron processing.

By improving powder quality and processing techniques and by the design of new microstructures, e.g. the development of toughening concepts like transformation toughening in ZrO_2, a tremendous improvement of strength, toughness and reliability has been accomplished in modern ceramic materials. The nanophase ceramics which go a further step in size reduction are a new challenge to both fields, powder synthesis and processing science.

2. Problems Involved in Processing Superfine Powders

Before synthesis of nanosized powders is discussed, a short description of possible problems involved with the synthesis and handling of fine powders will be given.

2.1. Processing Environment

An overview of the sizes of different airborne particulates is given in Figure 1. To obtain optimal strength and reliability data, maximum flaw sizes in ceramics should be in the range of the grain size. Taking into account that normal air contains between 10^7 to 10^8 particles/m^3 in the micron range, it becomes obvious, that a clean environment is one of the key requirements for submicron processing. This is necessary not only during synthesis but also during handling and shaping. For nanophase materials this becomes even more necessary but clean room techniques are very limited in a particle size range smaller than 0.1 micron.

2.2. Agglomerates and Aggregates

The tendency of fine powders to form uncontrolled agglomerates and aggregates has a strong influence on synthesis and processing. Interparticle cohesion increases strongly with decreasing particle size because of the greater significance of short range, weak forces like electrostatic forces and van der Waals forces, with the result that the strength of agglomerates increases with decreasing particle size. In powders with particle sizes below 50 nanometers strong agglom-

[*] Dr. G. W. Kriechbaum, Dr. P. Kleinschmit
Degussa AG, ZN Wolfgang, Rodenbacher Chaussee 4,
D-6450 Hanau 11 (FRG)

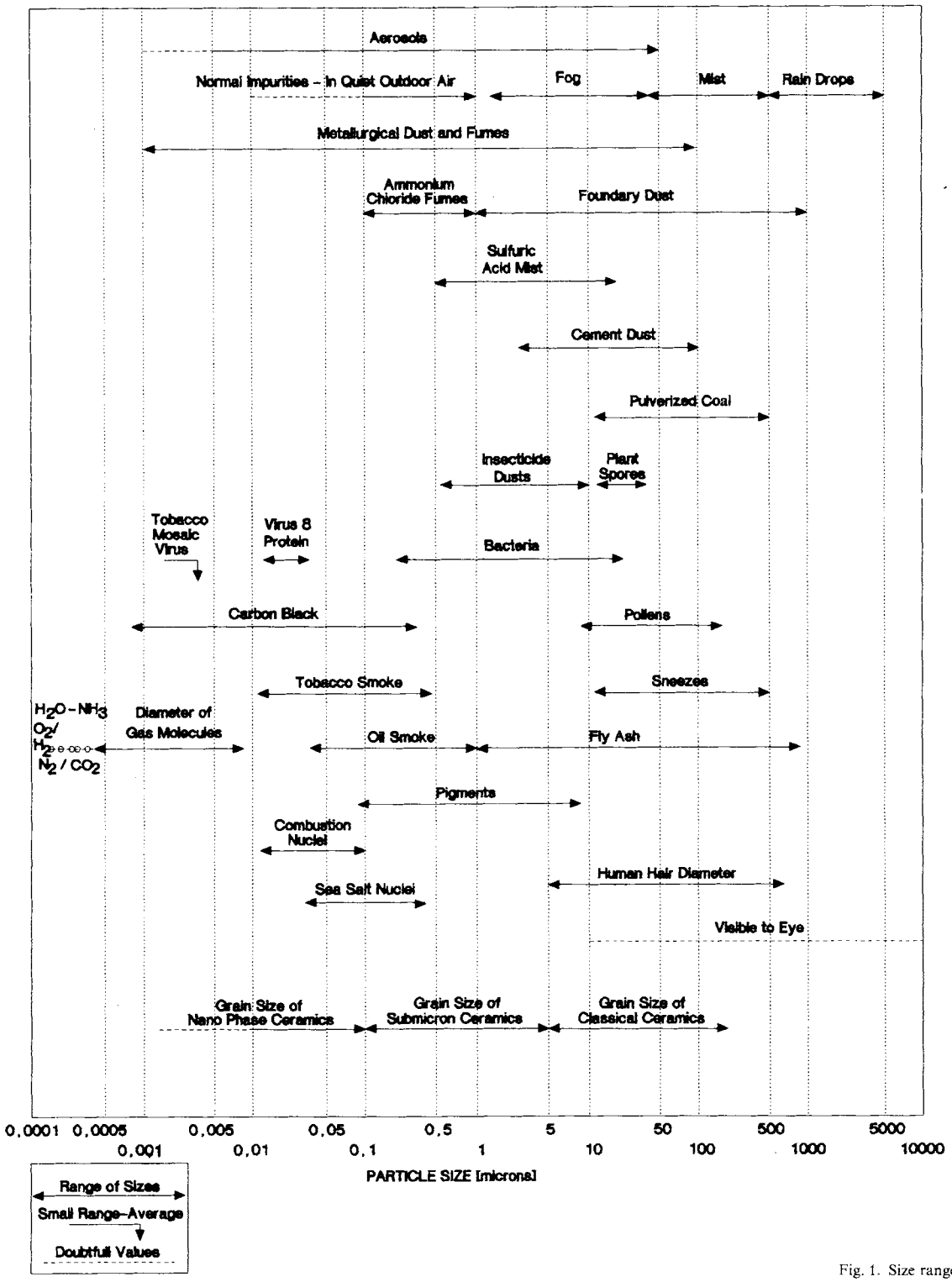


Fig. 1. Size ranges of airborne particulates.

erates can hardly be avoided because of the significance of the van der Waals attraction in this size region.[7] In addition, the increasing specific surface area resulting from the decreasing particle size leads to a greater tendency for vapor condensation on particle contacts. This causes bonds to form between particles and so further strengthens the existing agglomerates.[8] The negative effect of strong agglomerates on powder packing and morphological homogeneity of the green body is well described in the literature.[9-11] Inhomogeneities in the green body lead to structural flaws in the sintered product and increase the necessary sintering temperature because intra-agglomerate sintering occurs at lower

Table 1. Concepts for controlling agglomerates [14].

I Possible ways to influence agglomerate characteristics during their formation
  1. Optimization of precipitation conditions
  2. Special treatment of precipitates before or during drying
     - Removal of anions
     - Washing with organic liquids
     - Freeze-drying
     - Drying in controlled humidity
     - Hydrothermal treatment
  3. Optimization of calcination

II Possible ways to eliminate or destroy agglomerates after their formation
  1. Sedimentation
  2. Milling
  3. Ultrasonic treatment
  4. Dispersing agents
  5. High forming pressure

temperatures than inter-agglomerate sintering.[12, 13] In addition strength, toughness and reliability are decreased. Several concepts have been developed to improve particle agglomeration in submicron powders.

Recently, techniques for agglomeration control in wet-chemical powder synthesis have been reviewed by *Roosen* and *Hausner*.[14] Table 1 lists the techniques proposed for controlling agglomerate characteristics. To avoid agglomerates during synthesis or to destroy or eliminate agglomerates formed already are the two fundamental possibilities.

Destroying agglomerates after their formation by milling or sedimentation is limited to powders with agglomerate sizes bigger than 0.1 micron. For nanosized powders, ways to influence agglomerate characteristics during their formation have to be found. This is rather difficult to achieve because the main advantage of superfine particles, their very high sintering activity, becomes a major disadvantage during synthesis. Synthetic methods where high temperatures are involved, promote the formation of aggregates by forming solid bridges on particle contacts.

Therefore low temperature methods like gas-condensation techniques or small particle concentrations during high temperature treatment in a dispersed phase – gas phase or liquid phase – are necessary for the synthesis of weakly agglomerated nanosized powders.

2.3. Forming

The nanocrystalline TiO_2 plate mentioned earlier which showed ductile behavior[11] was shaped by in situ compaction of the powder by dry pressing with a pressure as high as 1.4 GPa.[15] No value of the achieved green density is given nor is it explained why a high pressure far beyond the usual pressure range, was applied. Poor packing of the synthesized powders may be one of the reasons. To obtain homogeneous, dense sintered structures from superfine powders, green bodies with a uniform pore size distribution are required. Since weak forces dominate the packing of dry ultrafine particles, dry forming techniques are not favored.

Wet forming processes like colloidal filtration[16] may be more successfull. Packing of fine powders in suspension can be improved substantially by the use of the appropriate pH range and by organic dispersants. *Sacks* has investigated the packing behavior of fine silica spheres and found that by proper control of the particle dispersion, sintering temperatures can be decreased by increasing the homogeneity of green compacts.[17]



Peter Kleinschmit was born in 1938 in Leipzig (GDR) and studied chemistry at the Universities of Hannover (FRG) and Vienna (Austria) gaining a Ph.D. for a study of "Chemistry in Molten Salts" in 1968. Since then he has occupied various positions with Degussa, starting as a Research Chemist and becoming a Board Assistant in 1970, a Plant Manager in 1973 and the Head of the Inorganic Research Department in 1975.



Gangolf Kriechbaum was born in Nürnberg (FRG) in 1953 and studied chemistry at both the University of Regensburg (FRG) gaining his Diploma in 1981, and the University of Frankfurt (FRG) where he gained a Ph.D. for his work on the "Reactivity of Metal-Metal Multiple Bonds" in the group of Prof. W. Herrmann in 1983. He then spent a year working with Prof. A. Cotton at Texas A & M University (USA) before joining Degussa as a Research Scientist in 1984.

ADVANCED MATERIALS

3. Synthesis of Superfine Powders

The nanophase TiO_2 ceramic described by *Gleiter* and coworkers was made out of a powder which had been synthesized by the so called gas-condensation method.[15] The principle of this synthetic technique is the evaporation of titanium metal in an oxygen free vacuum by resistance heating and the decomposition of the metal vapor on a liquid nitrogen cooled cold finger. Controlled oxidation of the deposited metal powder by introducing oxygen to the reactor finally produces titanium dioxide. The advantage of this method is that it works in a very clean, easily controlled environment.

On the other hand, gas-condensation is limited to very few chemical systems which are not necessarily in the focus of ceramic interest. Also, the turnover limits this technique to small scale operation and therefore other synthetic routes to nanosized powders have to be developed.

Because of their potential to yield superfine powders, flame hydrolysis and hydrothermal synthesis are synthetic routes which are promising for the preparation of suitable powders on an industrial scale.

3.1. Flame Hydrolysis

The reaction of volatizable compounds like for example $TiCl_4$ or $SiCl_4$ in an oxygen-hydrogen flame leads to highly dispersed oxides. This technique, called flame hydrolysis or the AEROSIL process, was originally developed by *Klöpfer*[18] and has been designed to make highly-dispersed silica. Meanwhile, flame hydrolysis has been used to produce a variety of different compounds, some of which are listed in Table 2.[19–21] A flow sheet of the process is shown in Figure 2. Silica, alumina and titania are produced on a commercial scale and have found numerous industrial applications, for example, as fillers and thickeners.[19]

Table 2. List of pyrogenic products [18].

Product	Raw Material	b.p. [°C]
SiO_2 [1]	$SiCl_4$	57
Al_2O_3 [1]	$AlCl_3$	180 [3]
TiO_2 [1]	$TiCl_4$	137
ZrO_2 [2]	$ZrCl_4$	331 [3]
ZrO_2/Al_2O_3 [2]	$ZrCl_2/AlCl_3$	331 [3]/180 [3]
ZrO_2/TiO_2 [2]	$ZrCl_2/TiCl_4$	331 [3]/137
Al_2O_3/TiO_2 [2]	$AlCl_3/TiCl_4$	180 [3]/137
$AlBO_3$ [2]	$AlCl_3/BCl_3$	180 [3]/12
$AlPO_4$ [2]	$AlCl_3/PCl_3$	180 [3]/74
Bi_2O_3 [2]	$BiCl_3$	441
Cr_2-O_3 [2]	CrO_2Cl_2	117
Fe_2O_3 [2]	$FeCl_3$	319
	$Fe(CO)_5$	103
GeO_2 [2]	$GeCl_4$	84
NiO [2]	$Ni(CO)_4$	42
MoO_3 [2]	$MoCl_5$	268
SnO_2 [2]	$SnCl_4$	114
V_2O_5 [2]	$VOCl_3$	127
WO_3 [2]	WCl_6	346
	$WOCl_4$	228

[1] commercial. [2] laboratory product. [3] sublimation point.

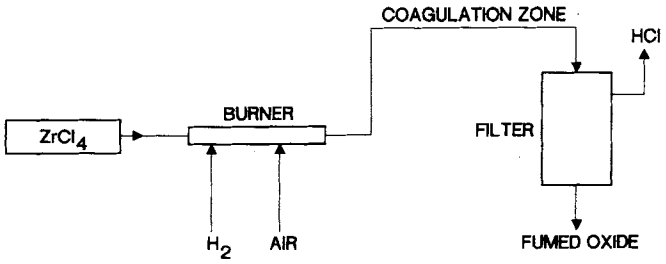


Fig. 2. General flow sheet for the preparation of ZrO_2 by flame hydrolysis [22].

The major advantages of flame hydrolysis are the high purity of the compounds, its chemical flexibility, and the possibility to synthesize mixed oxides which are homogeneous even on a molecular scale. In addition, powder properties like specific surface area and particle size can be easily controlled by varying the reaction conditions. The most important disadvantage for ceramic use is the very low bulk density of pyrogenic materials. Figure 3 shows transmission electron micrographs of some of the commercially available silica powders. Powders with particle sizes between 7 and 50 nanometers and specific surface areas between 50 and 380 M^2/g can be synthesized. For ceramic applications the chemical systems ZrO_2,ZrO_2–Al_2O_3, Al_2O_3–ZrO_2 and Al_2O_3–TiO_2 are of interest.

Promising results have been obtained on zirconia powders, synthesized by flame hydrolysis.[22] Powders with specific surface areas between 20 and 100 m^2/g and a particle size between 10 and 50 nm have been prepared. X-Ray diffraction (XRD) analysis showed that the pyrogenic ZrO_2 crystallizes in the tetragonal phase with only a small monoclinic part. The "as prepared" powder has a very low bulk density of about 150 g/l and therefore precompaction is necessary. The sintering experiments were performed on powders which were yttria doped and precompacted by spray drying. Densities of about 99% of theory were achieved at a sintering temperature of 1450 °C. The relatively high sintering temperature caused grain growth so that grain sizes of about 0.2 micrometers were obtained. The originally nanosized powder only preserves its size range when the applied sintering temperature is much lower.

The same authors have made silica stabilized aluminum titanate powders by cohydrolysis of $SiCl_4$, $AlCl_3$ and $TiCl_4$. The transmission electron micrograph of the powder shows spherical particles in a size range between 20 and 100 nanometers (Fig. 4).

Cold isostatically pressed compacts were densified at a temperature as low as 1300 °C to a density of more than 3.6 g/cm^3 and showed a grain size of much below 1 micron, which is rather small for aluminum titanate (Fig. 5). By flame hydrolysis with a specially designed burner nanosized zirconia powders have been coated with alumina.[23] The synthesized Al_2O_3–ZrO_2 particles have a size between 40 and 100 nm. Data on the sintering behavior of this material have not been published.

Pyrogenic aluminas differ fundamentally in their properties from other aluminas which are prepared by precipitation

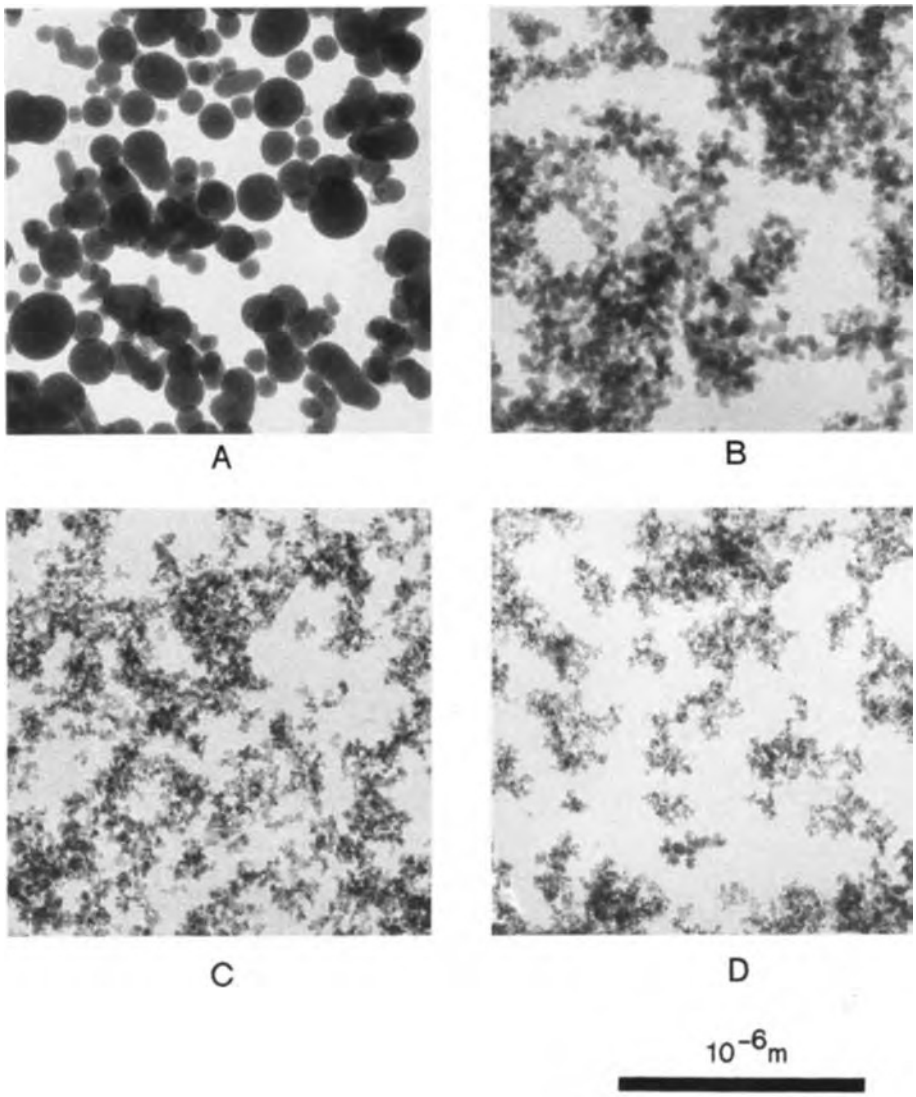


Fig. 3. Transmission electron micrographs of commercial silica powders prepared by flame hydrolysis with different specific surface areas. A: 50 m^2/g, B: 130 m^2/g, C: 300 m^2/g, D: 380 m^2/g. Mag. 1:50000.

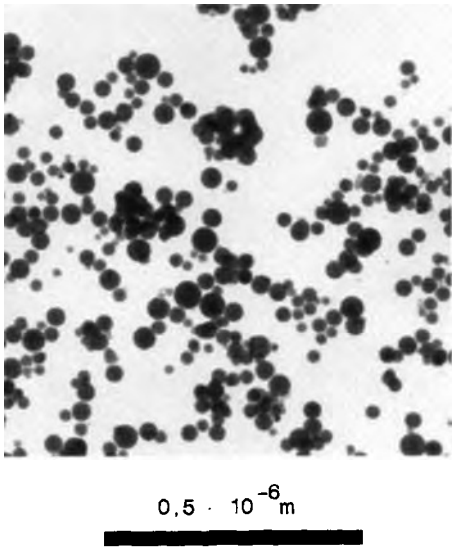


Fig. 4. Transmission electron micrograph of a pyrogenic Al_2O_3–TiO_2 powder (Mag. × 100000).

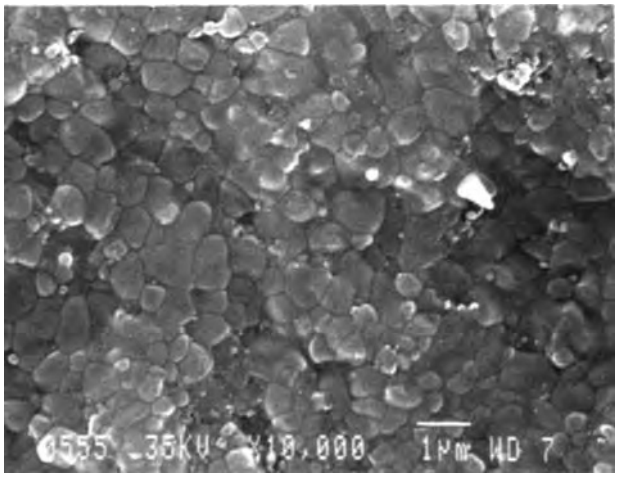


Fig. 5. Scanning electron micrograph of a fracture surface in sintered Al_2TiO_5 prepared from pyrogenic powders (Sintering temp. 1300 °C, 2 h).

ADVANCED MATERIALS

and/or solid state reactions. They have a primarily gamma structure with traces of delta and have a particle size of about 15 to 20 nm with a specific surface area of about 100 m^2/g.[19] Sintering of the "as prepared" powder is not very successful because of the phase transformation to α-alumina during the sintering process. A high sintering activity has been reported by *Kato* et al. when the chemical vapor deposition CVD derived Al_2O_3 powder was precalcinated at 1200 °C to 1350 °C. During the calcination process particle growth occurs and powders with particle sizes between 0.1 to 0.5 are obtained.[24] It has not been reported that nanosized alumina can be synthesized in its α-form by flame hydrolysis.

3.2. Hydrothermal Synthesis

Reactions in water above its boiling point and therefore under pressure, are called hydrothermal reactions. This very general definition illustrates that a variety of very different chemical processes are categorized under the heading hydrothermal reactions.

Historically the first hydrothermal experiments were performed by *Schafhäuptl*[38] who synthesized quartz crystals from amorphous silica although nature used hydrothermal reactions long before for the formation of numerous minerals. Although hydrothermal processing is a familiar technique very few examples of commercialization are known. Most important is the Bayer-process which includes a hydrothermal leaching step to form soluable sodium aluminates for separation from remaining solids. The synthetic and hardware aspects of hydrothermal synthesis have been reviewed by *Rabenau*.[26] This paper is limited to hydrothermal processes connected to superfine ceramic raw materials.

The different hydrothermal reaction types described in the literature are decomposition, oxidation, crystallization, precipitation, sintering, and leaching. For the synthesis of superfine ceramic oxides only hydrothermal precipitation and hydrothermal crystallization have to be considered. General flow sheets of both techniques are shown in Figure 6. While hydrothermal precipitation starts from clear metal salt solutions, hydrothermal crystallization uses hydroxide gels or sols. Hydrothermal synthesis yields oxide suspensions of crystalline metal oxides which in some cases can even be used for ceramic processes without a calcination step. A variety of different oxides have been synthesized by hydrothermal techniques (Table 3). For structural ceramics, zirconia, alumina, titania and mixed powders like Al_2O_3–ZrO_2, ZrO_2–Y_2O_3 and Al_2O_3–TiO_2 are the most relevant systems. As already mentioned, the major advantage of hydrothermal

Table 3. Oxides prepared by hydrothermal synthesis [29].

Oxides	Mixed Oxides	Complex Oxides
ZrO_2	ZrO_2–Y_2O_3	$BaFe_{12}O_{19}$
SiO_2	ZrO_2–Y_2O_3–MgO	$BaTiO_3$
Al_2O_3	ZrO_2–MgO	
TiO_2	ZrO_2–Al_2O_3	

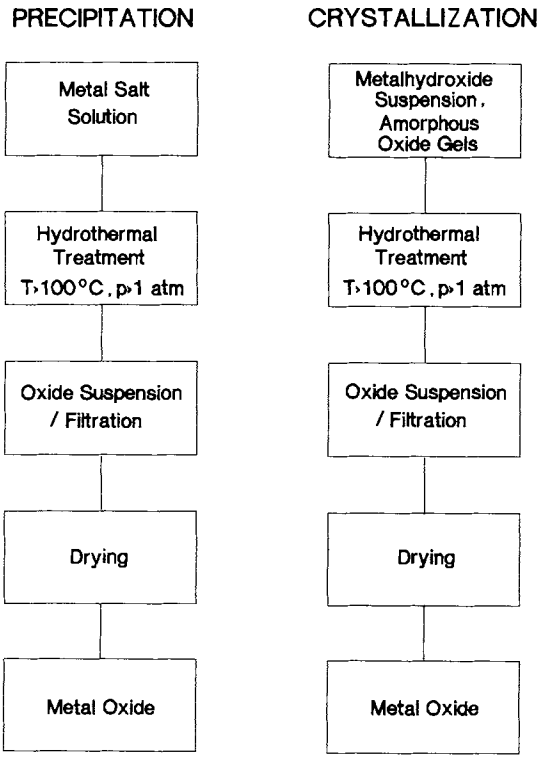


Fig. 6. General flow sheet for hydrothermal precipitation and crystallization.

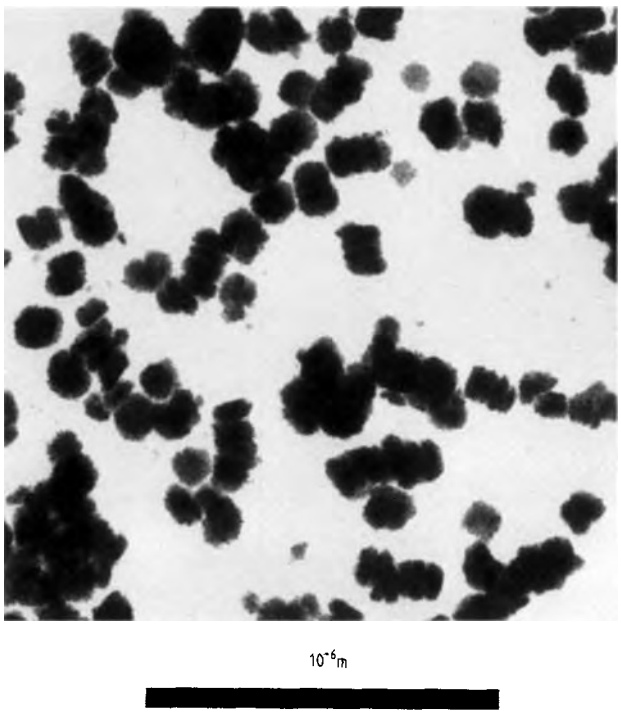


Fig. 7. Transmission electron micrograph of a ZrO_2 powder synthesized by hydrothermal precipitation from a $ZrOCl_2$ solution ($T = 200$ °C). Mag. 1:100000.

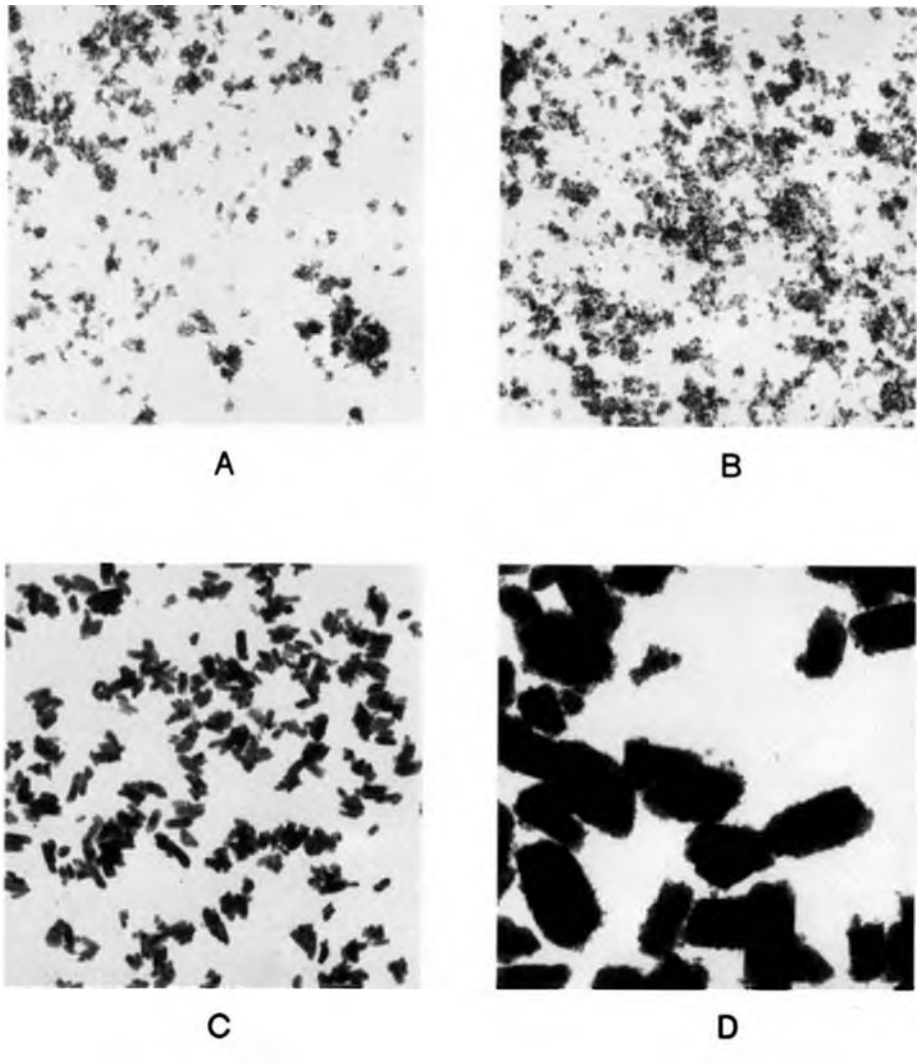


Fig. 8. Transmission electron micrographs of hydrothermally prepared Y_2O_3 doped ZrO_2 powders, synthesized at the same temperature but different NaOH-concentrations. (A: NaOH = 10^{-3} Mol, B: NaOH = 10^{-2} Mol, C: NaOH = 10^{-1} Mol, D: NaOH = 1 Mol) Mag. 1:100000.

processing is that high temperature calcination is not needed to form oxides.[27] Having no solid state calcination step the formation of hard agglomerates and aggregates can be more easily avoided which is not the case in sol-gel or coprecipitation methods where nanosized particles are formed which are also enlarged and aggregated when solid state crystallization to the oxide is performed.

One of the most promising candidates for hydrothermal synthesis is ZrO_2. The formation of highly dispersed ZrO_2 by hydrothermal precipitation from zirconium oxychloride or other zirconium salt solutions has been described by several authors.[27-31] Depending on the reaction conditions anhydrous monoclinic ZrO_2 with particle sizes between 3 and 10 nanometers and surface areas as high as 180 m^2/g can be obtained.

The very fine primary particles are agglomerated into regular shaped clusters in the narrow size range between 0.1 and 0.25 μm (Fig. 7).[32] For use in structural ceramics pure ZrO_2 has to be doped with Y_2O_3. To synthesize homogeneously doped zirconia the described precipitation method has to be modified because Y_2O_3 is not precipitated under acidic conditions.[33]

Using a thermally unstable compound like urea which decomposes at elevated temperatures and so changes the pH to higher values, is one of the possibilities to succeed in synthesizing Y_2O_3–ZrO_2 powders by hydrothermal precipitation.[34] Problems with material corrosion caused by the changing pH values during the reaction may limit this method to small scale production where teflon lined autoclaves can be easily used.

An alternative way to prepare superfine yttria-doped zirconia powders is the hydrothermal crystallization of hydrous zirconium and yttrium oxides.[33] The particle size of the synthesized powders can be varied according to the reaction conditions between 10 to about 500 nanometers.[32, 35] Figure 8 shows transmission electron micrographs of yttria-zirconia powders (3 mol-% Y_2O_3) synthesized at different pH values. With increasing $^{\ominus}OH$ concentration, particle size can be increased. Besides size, particle shape can also be controlled by the addition of mineralizers.[36]

ADVANCED MATERIALS

The published sintering results[32, 36] indicate that theoretical densities have almost been obtained with hydrothermal ZrO_2–Y_2O_3 powders. The dilatometer investigation shown in Figure 9, where the sintering behavior of a hydrothermal

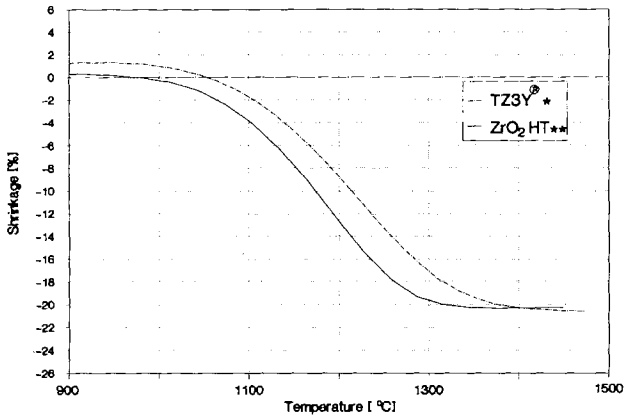


Fig. 9. Shrinkage vs. temperature of two Y_2O_3 doped ZrO_2 powders, one prepared by coprecipitation, (* Tosoh Co.) the other hydrothermally (** Degussa AG)

oxide powder is compared with a powder obtained by coprecipitation, clearly indicates that a decrease of sintering temperature can be achieved.[37] Necessary sintering temperatures are still too high to prevent grain growth during sintering and a grain size of 0.2 micrometer in the dense body is observed.

Hydrothermal crystallization can also be used for the synthesis of CaO,[38] MgO[39] and MgO–Y_2O_3[39] doped zirconia. The synthesis of Al_2O_3 and Al_2O_3–TiO_2 powders by hydrothermal crystallization has also been reported.[36] Published results show however that the powders obtained are not in the nanosized range.

4. Outlook

The synthesis of nanosized powders can be achieved by flame hydrolysis and hydrothermal synthesis. The poor packing of the fine powders is responsible for the fact that the advantages of these super fine materials with respect to sinterability and the possibility of yielding nanocrystalline materials have not been fully exploited. Research is needed to develop appropriate processing techniques for the compaction and the shaping of superfine powders.

Both discussed synthetic routes have already proved that upscaling is possible. If progress in the development of better handling and processing methods is achieved, flame hydrolysis and hydrothermal synthesis will become important techniques for the production of super fine oxidic ceramic raw materials which in turn will further improve the performance of ceramic materials.

Received June 23, 1989

[1] J. Karch, R. Birringer, H. Gleiter, *Nature 330* (1987) 556.
[2] D. W. Johnson, *Adv. Ceram. 21* (1987) 3.
[3] E. Matijevic in L. L. Hench, D. R. Ulrich (Eds.): *Ultrastructure Processing of Ceramics, Glasses and Composites*, J. Wiley, New York 1984.
[4] P. Vincencini (Ed.): *Ceramic Powders, materials science monographs 16*, Elsevier, Amsterdam 1983.
[5] H. Hausner in W. Bunk, H. Hausner (Eds.): *Ceramic Materials and Components for Engines*. Dt.-Keram. Gesell. 1986, p. 27.
[6] H. Hausner, *Ber. Dt. Keram. Gesell. 55* (1978) 194.
[7] W. A. Gray: *The packing of Solid Particles*. Chapman and Hall, London 1968.
[8] R. W. German: *Particle Packing Characteristics*. Metal powder Industries. Princeton, NY 1989.
[9] D. E. Niesz, R. Benett in G. Y. Onoda, L. L. Hench (Eds.): *Ceramic Processing before Firing*, Wiley, New York 1978, p. 61.
[10] T. Vasilos, W. W. Rhodes in J. J. Burke, N. L. Reed, V. Weiss (Eds.): *Ultrafine-Grain Ceramics*, Syracuse University, Syracuse, New York 1970.
[11] F. W. Dynys, J. W. Halloran, *J. Am. Ceram. Soc. 66* (1983) 396.
[12] K. D. Reeve, *Am. Ceram. Soc. Bull. 42* (1963) 452.
[13] A. G. Evans, *J. Am. Ceram. Soc. 65* (1982) 497.
[14] A. Roosen, H. Hausner, *Adv. Cer. Mater. 3* (1988) 131.
[15] R. W. Siegel, S. Ramasamy, H. Hahn, L. Zongquan, L. Ting, *J. Mater. Res. 3* (1988) 1367.
[16] J. A. Aksay, F. F. Lange, B. I. Davis, *J. Am. Ceram. Soc. 66* (1983) C 190.
[17] M. D. Sacks in L. L. Hench, D. R. Ulrich (Eds): *Science of Ceramic Chemical Processing*, Wiley, New York 1986, p. 522.
[18] Degussa, DE 762 723 (1942).
[19] Degussa, Frankfurt, *Tech. Bull. Pigments 56* (1982).
[20] A. T. Liu, P. Kleinschmit in R. W. Davidge (Ed.): *Novel Ceramic Fabrication Processes and Applications*, Institute of Ceramics, Shelton 1986, p. 1.
[21] E. Wagner, H. Brunner, *Angew. Chem. 72* (1960) 744.
[22] W. Hartmann, A. T. Liu, D. Peuckert, P. Kleinschmit, *Mater. Sci. Eng.* (1989) 243.
[23] S. Hori, *US Pat.* 4 491 482 (1985).
[24] S. Kato, T. Iga, H. Inoue, *Jpn. Pat.* 7 489 911 (1974).
[25] Schafhäuptl, *Gelehrter Anzeiger Bayer. Akad. 20* (1845) 557.
[26] A. Rabenau, *Angew. Chem. Int. Ed. Engl. 24* (1985) 1026; *Angew. Chem. 97* (1985) 1017.
[27] W. J. Dawson, *Ceram. Bull. 67* (1988) 1673.
[28] E. P. Stammbaugh, R. A. Foos, *US Pat.* 3 090 770 (1963).
[29] E. P. Stammbaugh, J. F. Miller, *Proc. 1st Symp. Hydrothermal Reactions* (1983) 859.
[30] E. Morgan, *J. Am. Ceram. Soc. 67* (1984) C 204.
[31] Y. Murase, E. Kato, *J. Cryst. Growth 50* (1980) 509.
[32] G. W. Kriechbaum, P. Kleinschmit, D. Peuckert, *Proc. Symp. Ceram. Powder Science 1*, Orlando, Florida (1988).
[33] A. R. Burkin, H. Sacrimen, B. C. H. Steele, *Trans. Br. Ceram. Soc. 79* (1980) 105.
[34] S. Somiya, M. Yoshimura, Z. Nakai, K. Hishinuma, T. Kuma, *DOS* 3 714 911 (1987).
[35] E. Tami, M. Yoshimira, S. Somiya, *J. Am. Ceram. Soc. 64* (1981) 181.
[36] G. W. Kriechbaum, W. Hartmann, D. Peuckert, in *Proc. Symp. Materialforschung*, KFA Jülich, (1988) 592.
[37] G. W. Kriechbaum, unpublished results.
[38] K. Haberko, W. Pyda in N. Claussen, M. Rühle, A. H. Heuer (Eds.): *Adv. Ceram. 12. Am. Ceram. Soc. Columbus*, OH, USA 1984, p. 774.
[39] E. P. Stammbaugh, J. H. Adair, J. Sekercioglu, R. R. Wills, *US Pat.* 4 619 817 (1987).

ADVANCED MATERIALS

Liquid Crystals— New Compounds, New Applications

Thermotropic Phases
Disk-Like Nematics
Electrooptical Devices
Laser Optics

By Rudolf Eidenschink *

1. Introduction

Fluidity and long range molecular orientational order are the common characteristics of liquid crystal phases. Depending on temperature and pressure, rod-like molecules can form the well known nematic and various smectic phases which have an additional positional order.[1] Optically active molecules form special helical phases, the cholesteric phase formed being closely related to the nematic phase and its helical structure gives rise to temperature dependent selective reflection. Quite recently a new helical smectic phase, named the S_A^* phase, with an unusual structure has been found.[2]

Fluidity and order can be realized with disk-like molecules in a similar way.[3] In the so-called phasmids, for example, the rod-like core and the half-disk ends of the molecules generate mesophases structurally different from known phases.[4a] Polarization microscopy aided by differential scanning calorimetry and X-ray diffraction have been the main tools used for structural classification. Now, scanning tunnelling microscopy of liquid crystal layers on graphite is offering some exciting details of molecular arrangement.[4b, 4c] The patterns of molecular order of the above mentioned phases can be transferred to polymers with a huge applicational potential.

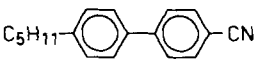
Until now the technical application of low molecular weight thermotropic liquid crystals has been almost restricted to electrooptical displays using nematic and smectic phases although nematic phases are of scientific interest as anisotropic solvents in NMR spectroscopy and foils with encapsulated cholesteric liquid crystals have found a small field of application in thermometry.[5]

In the case of polymers, fibers with high tensile liquid strength have reached a state of industrial production and lyotropic phases, colloid disperse systems being formed by lamellae or nonspherical micelles, are of fundamental importance for biological processes. In some novel compounds and mixtures the characteristics of thermotropic and lyotropic phases overlap. In the following article some main points of this fast developing field shall be touched upon, the emphasis being on nonpolymer thermotropic materials with a potential for new technical application.

[*] Dr. R. Eidenschink
Nematel
Galileo-Galilei-Str. 10
D-6500 Mainz 42 (FRG)

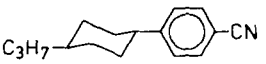
2. Nematogenic Compounds

Since their first application in displays some twenty years ago there has been an intensive search for new nematogenic compounds. Compounds **1** to **4** are examples of technologi-



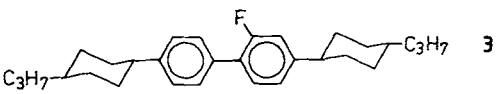
1

C 23 N 35 I



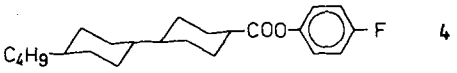
2

C 45 N 46 I



3

C 51 S_B 103 S_A 131 N 296 I



4

C 74 N 178 I

cally important species (C = crystalline, S_A = smectic A, etc., N = nematic, I = isotropic, transition temperatures in °C.

A nematic phase used for the twisted nematic cell[6] nowadays often contains 12 or more compounds in order to match the values of the parameters required: transition temperature from the nematic to the isotropic phase (T_{NI}), melting temperature, viscosity coefficients, elastic constants, optical and dielectric anisotropies and specific ohmic resistivity. A precondition for applicability is the long term stability of the compounds.

By now seemingly all simple molecular building elements permitting linear linking in order to obtain long shaped molecules have been applied.[7, 8, 9] An important task of research in this field is the fine tuning of special physical parameters of known classes of compounds. A good example is the systematic introduction of fluorine atoms.[8, 9, 10]

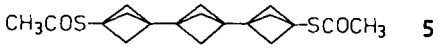
The newly introduced 1,3-bicyclo[1.1.1]pentylene moiety leads to a number of interesting compounds, exemplified by

ADVANCED MATERIALS

5. It was found, however, that the corresponding 1,4-bicyclo[2.2.2]octylene or 1,4-phenylene compounds generally have higher T_{NI} values.[12]

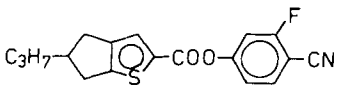
Replacing one 1,4-disubstituted six membered ring of a nematogenic molecule by a 1,3-disubstituted carbocyclic or heterocyclic five membered ring often yielded compounds with interesting physical properties. However, the decrease in the transition temperatures was prohibitive. To overcome this drawback, fused ring systems such as indanes[13] and s-hydrindacenes without a conventional ring system[14] have been synthesized. A particularly interesting example is the propanothiophen carboxylate **6**.[15]

New aspects of the field are opened up by some nematic transition metal complexes of Au, Ag, Pt, Pd and Ni[16], e.g. the platinum complex of 4'-pentylbiphenyl-4-carbonitrile **7**.



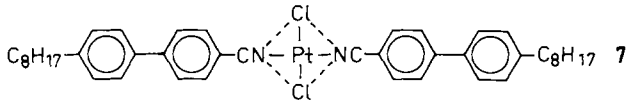
5

C 137 S_G 167 N 192 I



6

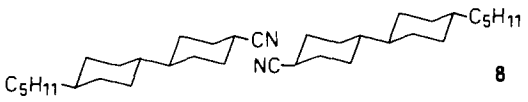
C 48 N 92 I



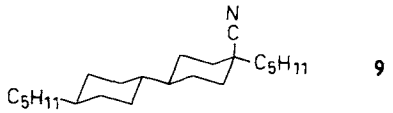
7

C 165 N 180 I

Some deviations from the usual building principle have become known. The fact that *trans,trans*-4'-alkylbicyclohexyl-4-carbonitriles like **8** are nematic has been explained in terms of association via the carbonitrile groups. It turns out, however, that bicyclohexyl compounds like **9** which do not undergo association because of steric deshielding are also nematic.[17]



8

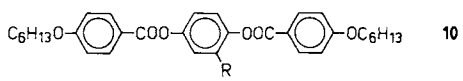


9

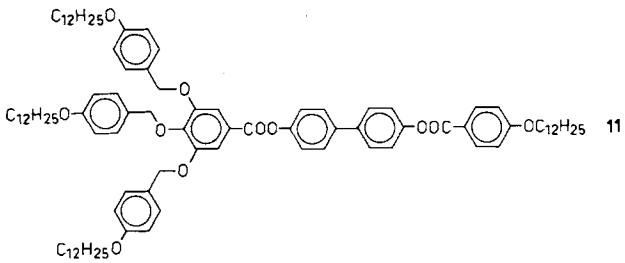
C 25 S_B 30 N 66 I

If in esters of type **10**, R = H is substituted by n-C_nH_{2n+1}, T_{NI} decreases.[18] The fact that the nematic state can be observed even with very long alkyl chains (up to n = 16!) has been explained in terms of an energetically preferred conformation permitting this chain to run parallel to the rigid core.[9]

The free rotation around the longest molecular axis of the biphenyldiol-dibenzoate **11** is obviously restricted. This



10



11

compound is the first example of a biaxial thermotropic nematic phase found among nonpolymer compounds.[19]

Today it is widely assumed that the occurrence of a thermotropic nematic phase is due to a combination of the at-

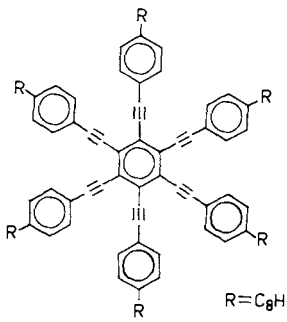


Rudolf Eidenschink worked as an engineer on selenium diodes and electroplating before moving to chemistry, completing a Doctoral Thesis in synthetic uses of anionic 1,3-cycloadditions at the University of Münster, FRG. After a postdoctoral fellowship at the University of Sussex, UK, he joined the company Merck in Darmstadt, FRG where he was responsible for the discovery and exploitation of a number of classes of liquid crystals, for example those known by the acronyms PCH, BCH, CCH, CBC, and CCN. In 1987 he left the group he had built up at Merck to found his own company, Nematel, which is situated in Mainz, FRG.

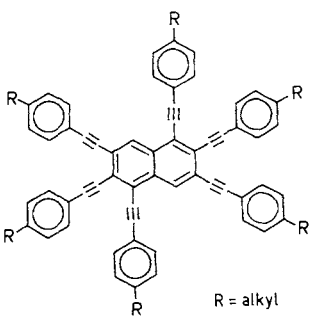
tracting dispersion forces and the hard core repulsion interactions, both of which are enhanced by the anisotropic shape. In the generalized van der Waals theory of *M. Cotter* and *W. M. Gelbart*[20] the first order phase transition from the isotropic to the nematic state at T_{NI} depends on the molecular package density and on a term for the attractive forces. The package density in a fluid can be assumed to depend on the ratio of molecular length over width.[9] Here—as with any molecular theory dealing with T_{NI}—the question of the conformation equilibrium is essential. In this context it was shown by ^{13}C-NMR of *trans*-1-alkoxy-4-alkoxy-carbonyl-cyclohexanes[21] that a distinct anomeric effect influences the concentration of the long shaped equatorial, equatorial-form in the conformational equilibrium. The hypothesis that the uncertainty of the local assignment of energy quanta passing between parallel molecules leads to an orientational effect was helpful in correlating chemical bonding parameters with T_{NI}.[22]

Hexaalkynylbenzenes like **12**[23] being the first disk-like nematic (N_D) hydrocarbons have no permanent dipole moment. The dielectric anisotropy of **12** due to electronic polarizibility made possible the realization of an electrooptical cell.[24]

Despite the long term instability of **12** this result gives impetus towards the development of displays with discotic phases proposed earlier.[25] In this context it is worth noting also that the 1,2,3,5,6,7-hexakis[phenylethynyl]naphthalenes **13**[26] form discotic phases with sequences comprised of



12

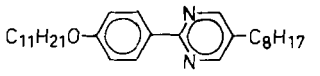


13

different columnar phases and the disk-like nematic phase in an order opposite to that usually observed.

3. Compounds Forming Smectic C Phases

The invention of the surface stabilized ferroelectric liquid crystal displays (SSFLC)[27] in 1980 initiated the search for stable compounds with broad temperature ranges of S_C phases. Compounds forming this phase with a tilt of the molecules in the smectic layers have at least two aromatic rings,[28] with a few exceptions (see, for example, compound **16**). A perpendicular dipole, off center, combined with a polarizable center are the general features of such molecules and the phenylpyrimidines **14**[29] which have this feature are often used as basic components of S_C phases.

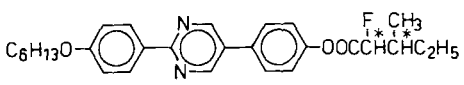


14

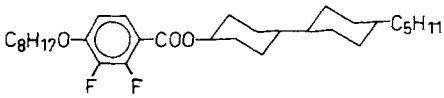
C 45 S_C 60 S_A 67 N 69 I

The environment of a molecule in an S_C phase can be described as monoclinic, with a 2-fold axis of symmetry and a mirror plane. To generate ferroelectricity, and to form a smectic S_C^* phase the mirror plane has to be removed. This is done by doping with an optically active compound, in most cases with an enantiotropic S_C^* phase. The spontaneous polarization P of thin layers (2 μm) can be expected to be high if high transverse dipole moments are connected as rigidly as possible to the chiral center and if intermolecular interactions impede the rotation around the long molecular axis. Compound **15**[30] synthesized from L(+)-isoleucine has a very high P of 400 nAs · cm^{-2}.

For low switching times in displays a small value of the coefficient of rotational viscosity[31] is advantageous. Here difluorobenzoates of the type **16**[32] are very useful.



15

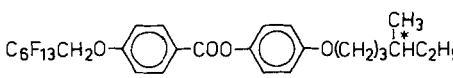


16

C 90 S_C 98 N 170 I

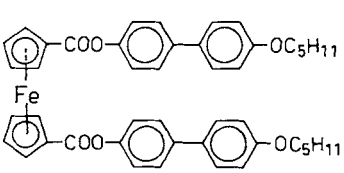
It has been long known that substitution in the alkyl chains of a mesogenic compound by several fluorine atoms leads to an enhancement of smectic phases (mostly S_A) over the nematic phase. In the case of simple phenyl benzoates[33] S_C phases could be induced by special substitution patterns, as shown in **17**.

The ferrocene derivative **18** is another example of the integration of a transition metal complex into a mesogenic struc-



17

C 52 S_C^* 78 S_A 89 I



18

C 129 S_C 140 I

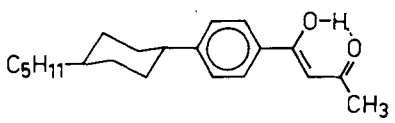
ADVANCED MATERIALS

ture. Despite the participation of four 1,4-phenylene units the transition temperature to the isotropic state is relatively low. This is explained by the presence of different geometric isomers.[34]

4. Compounds with Hydrogen Bonds

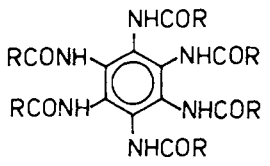
Compounds forming hydrogen bonds provide a variety of aspects not only for the well known aqueous lyotropics but more and more for thermotropic liquid crystals. *Trans*-4-alkylcyclohexane-carboxylic acids[35] and 1-(4-*trans*-4-alkylcyclohexyl-phenyl)-alkane-1,3-diones[36] being predominantly in their keto-enol form (**19**) have already been proposed for technical application in displays. Solutions of the high melting amide **20** in alkanes, chloroform or toluene are lyotropic nematic and can be oriented uniformly by a magnetic field.[37] This is probably due to the formation of intra and intermolecular hydrogen bonds.

The relatively low melting amides **21**[38] and **22**[39] have broad temperature ranges of thermotropic mesophases.



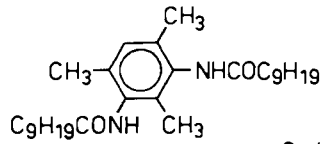
19

C 83 N 97 I



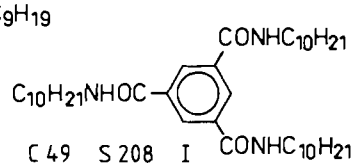
20

$R = C_6H_{13}$



C 126 S 168 N 211 I

21

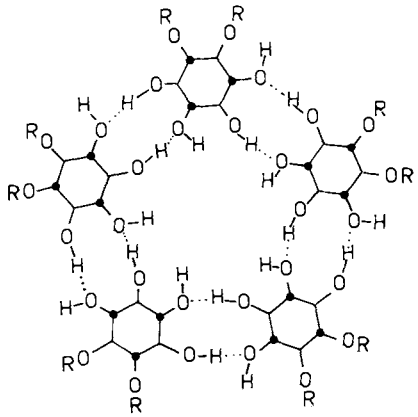


C 49 S 208 I

22

Although it was only 23 years after the synthesis of the liquid crystalline cholesteryl benzoate by *Reinitzer* in 1888 that the first 1-alkyl-o-glucosides with liquid crystal properties were synthesized,[40] the systematic search for liquid crystal derivatives of natural products in general and carbohydrates in particular is beginning[41,42,43] only now.

Interesting examples that exploit H-bonding are the columnar discotic phases formed by ionosite derivatives possibly having the supramolecular structure of **23** (R = alkyl).[44]



23

Also of interest are the 2-(*trans*-4-alkylcyclohexyl)-1,3-propandiols that form intermolecular hydrogen bonds in their S_A phases.[45] This molecular arrangement suggests the equivalent conductivity for $H^{\oplus}$ ions to be anisotropic. It was shown that diols are able to incorporate water that in certain concentrations enhances the thermodynamic stability of the S_A phase.[46] Generally speaking, with compounds forming intermolecular H-bonds, the characteristics of thermotropic and lyotropic liquid crystals begin to overlap.

5. Applications

5.1. New Electrooptical Devices

Today most of the liquid crystal displays are still twisted nematic cells. Recently major improvements have been made in the multiplexibility by using various techniques[6] which have a higher twist angle of the nematic layer (up to 270°) in common. The ratio of the elastic constants is regarded more and more as an important parameter for phases used in data screens. For pocket television screens the technique of an active matrix is favored, where one thin film transistor for every pixel switches a simple twisted nematic layer. The materials must be of very low viscosity and must have a high value for the product of dielectric constant and specific ohmic resistivity in order to limit the decrease of voltage at the pixels during the addressing cycle.[47] The above mentioned SSFL holds promise for a more economic realization.

A new and elegant technique to switch light using an electric field are the polymer dispersed liquid crystals (PDLC).[48,49] Droplets (2 to 5 μm in diameter) of a low molecular weight nematic phase are dispersed in an isotropic polymer (e.g. epoxy resin). Without an electric field the preferred direction of the nematic molecules is a statistical one

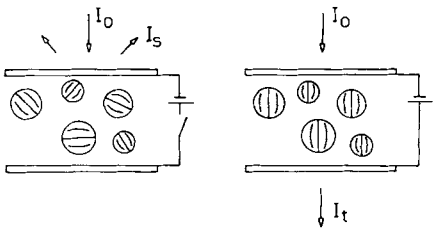


Fig. 1. Principle of PDLC films. I_0 = incident light, I_s = scattered light, I_t = transmitted light.

(Fig. 1). Incident light is scattered in all directions because of the mismatch of the refractive indices at the phase barriers. In an electric field the molecules have a preferred orientation because of their dielectric anisotropy. If the refractive index of the polymer is equal to the ordinary refractive index of the nematic phase the foil appears transparent. The PDLC is of interest for displays as well as solar control windows.

5.2. Laser Optics

The molecular order provided by the liquid crystal state makes possible some new applications of laser optics. Grids and other optical elements produced by a laser in a nematic phase can be used to switch another laser.[50] It has been claimed that switching times of fractions of nanoseconds can be achieved,[51] the molecular orientational movement in the laser field being the limiting factor.

To obtain materials with nonlinear optical properties, i.e. high values for the macroscopic hyperpolarizabilities ($X^{(1)}$) the integration of moieties with strong molecular hyperpolarizabilities (X) as side-chains of a liquid crystal polymer has been considered.[47] This might be exploited to build e.g. frequency doublers (high $X^{(2)}$) or to switch light by an electric field (high $X^{(3)}$, Pockels-effect). For high values of $X^{(2)}$ the moieties have to be ordered in an antiparallel way. To create a material with this feature, thin film techniques seem particularly suitable. Thin films being deposited as monomolecular layers of lyotropic lamellae onto a substrate[53] also have a good future in lithographics and antifriction layers. The molecular self organization in such layers is of fundamental significance in material science as well as in biology.[54]

5.3. Reaction Media

Influencing the kinetics of a chemical reaction by using anisotropic reaction media has in the past inspired many chemists. In recent times the possibilities have been substantiated. In the case of thermotropic liquid crystals[55] improvement of enantioselectivity in cholesteric phases and photochemical reactions are preferred topics. For technical application, lyotropic aqueous phases generally have a better perspective. A dramatic change of the rates of the acid-catalyzed hydrolysis of phosphinate esters in surfactant solutions has been observed going from a disk-like to a rod-like nematic phase.[58]

5.4. Engineering

The change of viscosity—a tensor quantity in mesomorphic phases—during phase transitions has some interesting aspects in engineering.[57, 58] The fast and reversible transitions accomplished by a change of temperature or pressure make possible a new method of construction of mechanical elements such as clutches, brakes, slide bearings and hydraulic devices.

6. Summary and Outlook

The growing interest in nonpolymer liquid crystal compounds in the past 20 years is attributed to the upswing in uses of liquid crystal displays. Synthetic chemistry and applied physics have promoted each other in a fruitful way. Besides some technologically important phases formed by rod-like molecules it has also become apparent that disk-like and so called phasmidic molecules exhibit fluidity and order. The building elements of molecular architecture are being extended to transition metal chemistry and hydrogen bonding, the latter with the potential to bridge the gap between thermotropic phases and the lyotropic liquid crystals which are of fundamental importance to biology. The technical exploitation of the special physical and physicochemical properties of the liquid crystal state can be regarded as being still in its initial state.

Received May 9, 1989
Revised version June 23, 1989

[1] General reference: G. Vertogen, W. H. de Jeu: *Thermotropic Liquid Crystals, Fundamentals*, Springer Series in Chemical Physics, Vol. 45, Springer, Berlin 1988.
[2] J. W. Goodby, M. A. Waugh, S. M. Stein, E. Chin, R. Pindak, J. S. Patel, *Nature 337* (1989) 449.
[3] C. Destrade, P. Foucher, H. Gasparoux, Nguyen Huu Tinh, A. M. Levelut, J. Malthete, *Mol. Cryst. Liq. Cryst. 106* (1984) 121.
[4] a) Nguyen Huu Tinh, C. Destrade, A. M. Levelut, J. Malthete, *J. Phys. 47* (1986) 553, and lit. cited. b) J. S. Foster, J. E. Frommer, *Nature 333* (1988) 542. c) D. P. E. Smith, H. Hörber, C. Gerber, G. Binnig, *Science 245* (1989) 43.
[5] D. G. McDonnell in G. W. Gray (Ed.): *Thermotropic Liquid Crystals*, Wiley, New York 1987, p. 120–144.
[6] M. Schadt, *Mol. Cryst. Liq. Cryst. 165* (1988) 405, and lit. cited.
[7] G. W. Gray, *Mol. Cryst. Liq. Cryst. 63* (1981) 3.
[8] R. Eidenschink, *Mol. Cryst. Liq. Cryst. 123* (1985) 57.
[9] D. Demus, *Mol. Cryst. Liq. Cryst. 165* (1988) 45.
[10] K. J. Toyne in G. W. Gray (Ed.): *Thermotropic Liquid Crystals*, Wiley, New York 1987, p. 28–63.
[11] U. Finkenzeller, A. Kurmeier, E. Poetsch, *18. Freiburger Arbeitstagung Flüssigkristalle 1989*, paper 17, IAF, Freiburg.
[12] P. Kaszinski, A. C. Friedli, J. Michl, *Mol. Cryst. Liq. Cryst. Lett. 6* (1988) 27.
[13] T. Korishima, Y. Kumai, *Jpn. Kokai Tokkyo Koko* Jp 87, 181, 247.
[14] E. Praß, R. Eidenschink, H. Kolshorn, *18. Freiburger Arbeitstagung Flüssigkristalle 1989*, paper 19, IAF, Freiburg.

[15] J. Krause, A. E. F. Wächtler, B. S. Scheuble, G. Weber, *DE Pat.* 3734322.
[16] H. Adams, N. A. Bailey, D. W. Bruce, D. A. Dunmur, E. Lalinde, M. Marcos, C. Ridgeway, A. J. Smith, P. Styring, P. M. Maitlis, *Liq. Cryst. 2* (1987) 381, and lit. cited.
[17] R. Eidenschink, G. Haas, M. Römer, B. S. Scheuble, *Angew. Chem. Int. Ed. Engl. 23* (1984) 147; *Angew. Chem. 96* (1984) 151.
[18] W. Weißflog, D. Demus, *Cryst. Res. Technol. 19* (1984) 55.
[19] J. Malthete, L. Liébert, A. M. Levelut, Y. Galerne, *C.R. Acad. Sc. Paris, Ser. II 303* (1986) 1073.
[20] M. A. Cotter, Philos, *Trans. R. Soc. London A 309* (1983) 217, and lit. cited.
[21] E. Kleinpeter, H. Köhler, C. Tschierske, H. Zaschke, *J. Prakt. Chem. 330* (1988) 484.
[22] R. Eidenschink, *Kontakte 1* (1987) 15.
[23] B. Kohne, K. Praefcke, *Chimia 41* (1987) 196.
[24] G. Heppke, H. Kitzerow, F. Oestreicher, S. Quentel, A. Ranft, *Mol. Cryst. Liq. Cryst. Lett. 6* (1988) 71.
[25] C. Vaucher, A. Zann, P. LeBarny, J. C. Dubois, J. Billard, *Mol. Cryst. Liq. Cryst. 66* (1981) 103.
[26] K. Praefcke, B. Kohne, K. Gutbier, N. Johnen, D. Singer, *Liq. Cryst. 4* (1989) in print.
[27] N. A. Clark, S. T. Lagerwall, *Appl. Phys. Lett. 36* (1980) 899.
[28] J. W. Goodby, T. M. Leslie, *Mol. Cryst. Liq. Cryst. 110* (1984) 175.
[29] H. Zaschke, *J. Prakt. Chem. 317* (1975) 617.
[30] J. Bömelburg, G. Heppke, A. Ranft, *Z. Naturforsch. B*, in press.
[31] C. Escher, T. Geelhaar, E. Böhm, *Liq. Cryst. 3* (1988) 469.
[32] V. Reiffenrath, J. Krause, H. J. Plach, G. Weber, *Liq. Cryst. 5* (1989) 159.
[33] E. P. Janulis, J. C. Novack, G. A. Papapolymerou, M. Tristani-Kendra, W. A. Huffmann, *Ferroelectrics 85* (1988) 375.
[34] J. Bhatt, B. M. Fung, K. M. Nicholas, C. D. Poon, *J. Chem. Soc. Chem. Commun. 1988*, 1439.
[35] D. Demus, H. Zaschke: *Flüssigkristalle in Tabellen*, VEB Deutscher Verlag für die Grundstoffindustrie, Leipzig 1974, p. 34.
[36] R. Eidenschink, L. Pohl, *DE Pat.* 2918775.
[37] B. Kohne, K. Praefcke, T. Derz, H. Hoffmann, B. Schwandner, *Chimia 40* (1986) 171.
[38] Y. Matsunaga, M. Terada, *Mol. Cryst. Liq. Cryst. 141* (1986) 321.
[39] Y. Matsunaga, Y. Nakaysu, S. Sakai, M. Yanenaga, *Mol. Cryst. Liq. Cryst. 141* (1986) 327.
[40] E. Fischer, B. Helferich, *Liebigs Ann. Chem. 383* (1911) 68; C. R. Noller, W. C. Rockwell, *J. Am. Chem. Soc. 60* (1938) 2076.
[41] G. A. Jeffrey, *Acc. Chem. Res. 19* (1986) 168.
[42] A. Eckert, B. Kohne, K. Praefcke, *Z. Naturforsch. 43b* (1988) 878.
[43] K. Praefcke, A. M. Levelut, B. Kohne, A. Eckert, *Liq. Cryst.* in print.
[44] K. Praefcke, B. Kohne, P. Marquardt, P. Psaras, W. Stephan, A. Eckert, A. M. Levelut, *18. Freiburger Arbeitstagung Flüssigkristalle 1989*, paper 22, IAF, Freiburg.
[45] S. Diele, S. Geißler, H.-M . Vorbrodt, H. Zaschke, *Mol. Cryst. Liq. Cryst. Lett. 102* (1984) 181.
[46] C. Tschierske, H. Zaschke, *Tetrahedron Lett. 29* (1988) 5359.
[47] T. Shimasaki, S. Mizushima, S. Minezaki, K. Yano, M. Hijikigana, *Proc. Jpn. Disp.*, Tokyo, Sept. 1988, p. 78.
[48] J. L. Fergason, *WO Pat.* 83/01016.
[49] J. L. West, *Mol. Cryst. Liq. Cryst. 157* (1988) 427.
[50] I. C. Khoo, Y. R. Shen, *Opt. Eng. 24* (1985) 579.
[51] H. J. Eichler, R. Macdonald, unpublished.
[52] D. J. Williams in D. S. Chemla, J. Zyss (Eds.): *Nonlinear Optical Properties of Organic Molecules and Crystals*, Vol. 1, Academic Press, New York (1987).
[53] G. G. Roberts, *Adv. Phys. 34* (1985) 475.
[54] H. Ringsdorf, B. Schlarb, J. Venzmer, *Angew. Chem. Int. Ed. Engl. 27* (1988) 113; *Angew. Chem. 100* (1988) 117.
[55] R. G. Weiss, *Tetrahedron 44* (1988) 3413.
[56] V. Ramesh, M. M. Labes, *J. Am. Chem. Soc. 110* (1988) 738.
[57] R. Eidenschink, *Angew. Chem. Int. Ed. Engl. Adv. Mater. 27* (1988) 1579; *Angew. Chem. Adv. Mater. 100* (1988) 1639.
[58] A. G. Milaev, I. G. Gumenchuk, *Khim. Tekhnol. Topl. Masel* (1988) 18, *Chem. Abstr.* 110:117 926n.

Research News

High Resolution Solid State NMR of Quadrupolar Nuclei

By Bernhard Blümich*

Nuclear magnetic resonance spectroscopy is a standard technique used for the structural analysis of liquid and dissolved samples. The information about the molecular structure is contained in narrow resonance lines at various isotropic chemical shift values, which can be assigned to different segments of a molecule. In solids, however, the chemical shift information is hidden under overlapping wide lineshapes. As a result of the reduced molecular mobility in the solid state, a number of orientation dependent spin interactions such as the quadrupolar and the dipolar couplings and the anisotropy of the chemical shielding (chemical shift) dominate the resonance. For spin 1/2 nuclei, for instance ^{13}C, ^{29}Si and ^{31}P, there is no quadrupolar interaction, but even under dipolar decoupling from the protons, the NMR spectrum typically shows many overlapping chemical shielding powder patterns, each of which can be a few kilohertz wide. The standard approach to high resolution solid state spectra for spin 1/2 nuclei then is magic angle spinning (MAS). The sample is packed into a gas-driven turbine which is spun at a rotation frequency of 3 to 10 kHz with the rotation axis inclined against the magnetic field by the magic angle of $\Phi_m = 54.7°$. In this case liquid-like high resolution spectra are obtained, which at slow spinning rates exhibit side bands at integer multiples of the rotation frequency away from the isotropic chemical shifts.[1]

[*] Priv. Doz. Dr. B. Blümich
Max-Planck-Institut für Polymerforschung
P.O. Box 3148, D-6500 Mainz (FRG)

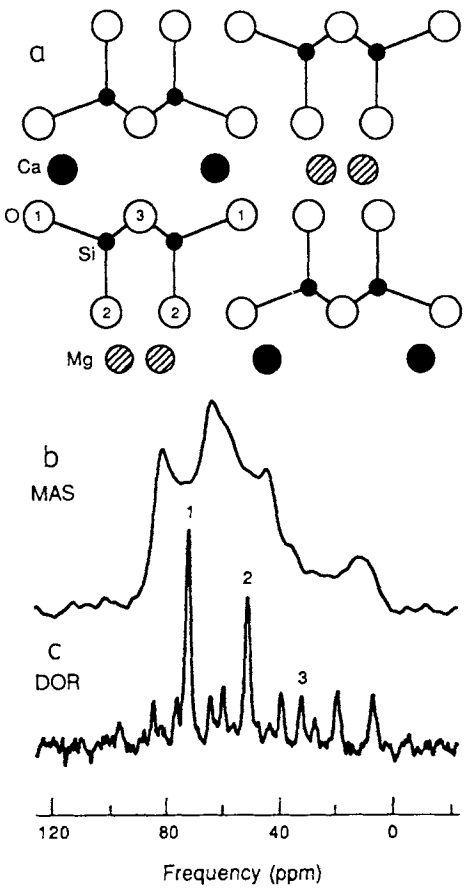


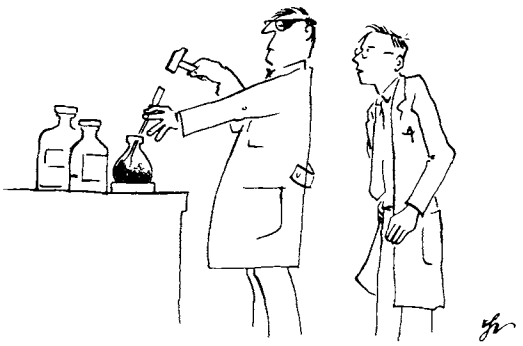
Fig. 1. a) Structure of diopside, $CaMgSi_2O_6$. Oxygen is represented by open circles with the three distinct sites labeled. b) MAS spectrum of ^{17}O in a sample of diopside. c) DOR spectrum with the outer rotor spinning at 680 Hz. (Adapted from ref. 4)

However, MAS is unable to fully remove the broadening of the central transition $(1/2 \leftrightarrow -1/2)$ of half-integer quadrupolar spins like ^{11}B, ^{17}O, ^{23}Na and ^{27}Al, because the linewidth is limited by second order quadrupolar broadening. Instead of just the second order Legendre polynomial, which determines the magic angle, the fourth order term also has to be eliminated.[2] This requires sample spinning around two axes, one at $\Phi_1 = 37.38°$ and the other at $\Phi_2 = 79.19°$. At first sight this seems impossible, but it can be done either in a 2D experiment with successive rotation around both axes involving flipping of the spinning axis (dynamic angle spinning: DAS) or by simultaneous rotation around both axes (double rotation: DOR).[3-5] Both experiments have recently been realized. A DAS probe is already available commercially with a flipping time of less than 40 ms.[6] However, the T_1 relaxation time must be longer than the flipping time for the experiment to work. The DOR experiment works with an ingeneously constructed rotor assembly, where a small rotor is embedded in a large rotor, each of the rotors spinning at one of the two angles Φ_1 and Φ_2.[3]

Figure 1 gives an example with the ^{17}O resonance of a powder of crystalline diopside.[4] The sample contains three distinct oxygen sites (a), which give rise to overlapping MAS powder patterns (b). With the DOR technique the wide line spectrum is broken down into narrow sideband resonances (c), where the isotropic centerband peaks can be assigned to the numbered oxygen sites. The linewidths are of the order of 100 Hz. This technique opens up a whole new area of NMR spectroscopy, where *high resolution spectra* can now be obtained for many nuclei of interest in ceramics, catalysis, geophysics and high temperature superconductivity.

[1] C. S. Yannoni, *Acc. Chem. Res. 15* (1982) 201.
[2] A. Llor, J. Virlet, *Chem. Phys. Lett. 152* (1988) 248.
[3] A. Samoson, E. Lippmaa, A. Pines, *Mol. Phys. 65* (1988) 1013.
[4] B. F. Chmelka, K. T. Mueller, A. Pines, J. Stebbins, Y. Wu, J. W. Zwanziger, *Nature 339* (1989) 42.
[5] K. T. Mueller, B. Q. Sun, G. C. Chingas, J. W. Zwanziger, T. Terao, A. Pines, *J. Magn. Reson.* (1989) in press.
[6] Doty Scientific, Inc., 600 Clemson Road, Columbia, S. C. 29223, USA.

Call for Short Communications · Call for Short Communications · Call for Short Communications



... doesn't melt, won't dissolve, just can't be broken down – let's send it to ADVANCED MATERIALS!

ADVANCED MATERIALS

Biomaterials Highlights III

Bone Replacements: Implant Materials and the Modes of Implant Fixation**

By Günther Heimke*

1. Introduction

During the last three decades the success rates of hard tissue replacements have increased considerably and have, thus, become a standard way of treatment. Based on early experiences, and taking advantage of the progress in material technology,[1, 2, 3] most of the directly material related reasons for reoperations could be either excluded completely or confined to extreme situations, like, for example, accidents in which the natural bone concerned would also have suffered severely. The causes for the remaining necessity for reintervention are essentially implant loosening or, in other words, failure of the implant fixing method.

This demonstrates that the kind of implant anchorage used is the key issue for any further improvement of the success rates of permanent orthopedic and dental implants. Many different ways of implant anchorage have been, and still are discussed, tested in-vitro and in animal experiments, and studied clinically. Some of them have successfully contributed to the improvements mentioned above and to the understanding of the remodeling reactions and the processes controlling them. A systematic survey of the modes of implant fixation[4] can facilitate the understanding of some of the different success rates and may even help to prevent some waste of effort and failure.

2. The Material Aspect of Implant Fixation

Like in all other fields, there are many viewpoints from which the materials used for a particular purpose can be surveyed and categorized. For implant materials a grouping according to the tissue reaction they stimulate in their environment can be regarded as adequate, as shown in Table 1.

The three terms characterizing the tissue reactions indicate some of possibilities of implant fixation in a bony environment. The list of influences on the sequence of reaction of the adjacent tissue, however, is not yet complete. Besides the essentially biochemical reactions mentioned in Table 1, there are nonmaterial-controlled influences on the remodeling of the bony tissue around implants. In addition to general aspects like age, health, and previous operations, the mechanical situation along the implant to bone interface plays an important role.[6, 7, 8] There is some similarity to fracture healing: a complete and stable union along a fracture site can be achieved only if the two surfaces can be brought together and maintained sufficiently motionlessness relative to each other during the healing period. The lack of rest along the interface will inevitably result in the formation of a soft tissue layer essentially consisting of bundles of collagen fibers mostly oriented parallel to the surfaces and containing only a few cells. Such creation of an artificial joint results in an additional mobility which, of course, is highly undesirable in this kind of treatment.

In fracture healing, the required motionlessness can be achieved by the application of a cast around the fractured bone, and if possible the two adjacent joints. Because of the remaining relative mobility of the two surfaces, the essential steps of fracture healing do not procede until a callus has been formed around the fracture site which provides the required additional stability. Another possibility is that the fragments are stabilized by pins (or so called nails) intro-

Table 1. Classification of implant materials according to the material influenced reactions in the surrounding bony tissue.

Class of material	Kind of influence	Tissue reaction	Typical materials in this class
biotolerant	ions and/or monomers go into solution, biochemical effects on differentiation and proliferation	distance osteogenesis[a]	stainless steels, polymethylmethacrylate (PMMA bone cement) Co based alloys, polyethylene
bioinert	no matter influencing the adjacent tissue goes into solution	contact osteogenesis[a]	Al_2O_3-ceramic, carbon, titanium
bioactive	bond formation by not yet completely understood processes	bonding osteogenesis[a]	Ca-phosphate based ceramics and Ca-phosphate containing glasses and glass-ceramics

a) These termes and definitions have been coined by Osborn [5].

[*] Prof. G. Heimke
Department of Engineering, College of Engineering
Clemson University, Clemson, SC 29634-0905 (USA)

[**] For Part II see *Adv. Mater. 1989, 234; Angew. Chem. Int. Ed. Engl. Adv. Mater. 28* (1989) 956; *Angew. Chem. Adv. Mater. 101* (1989) 980.

duced into the medullary canal or by plates screwed onto the bone parts, if possible in a way in which the fracture site is under compression (pressure osteosynthesis).

Because the trauma caused by the insertion of an implant into a bony environment can be expected to be similar to that at a fracture site, the sequence of reactions along an implant to bone interface following this trauma cannot be expected to be more favorable than in fracture healing. However, there are additional handicaps for implants as nearly all their mechanical properties are different from those of bone. Thus, even after the most favorable healing processes, the differences of the mechanical compliances will result in a lasting discontinuity along all bone to implant interfaces.

Besides biochemical and mechanical compliance, two further material dependent aspects must be considered which influence the reliability of implant anchorage: the enzyme controlled immune response of the host tissue, and long term systemic effects. This latter point of view has been dealt with in the previous contribution (Biomaterials Highlights II[9]).

3. Mechanical Aspects of Implant Fixation

The forces acting along the bone to implant interfaces must be considered in two stages: first, for the healing period until a reliable equilibrium between the bone forming and the bone resorbing processes has been achieved around the implant and, second, for the rest of the lifetime of the implant which, hopefully, will be identical with the lifetime of the patient.

During the first stage, optimum conditions for fracture healing must be provided for all those interfaces along which a close bone to implant contact is vital for the correct functioning of the implant. The easiest way to realize this requirement is to keep the implant unloaded during this period. However, this is possible only in exceptional cases. The main problems of the second stage are the different mechanical compliances of the bony tissue, or tissues, and the implant. The possibilities and limitations for the design of implants resulting from these mechanical considerations have been dealt with in detail elsewhere[6, 7, 8] and have recently been summarized.[10]

The essential statement is: if all other influences are, or can be, excluded it is the stress and strain field created in the bony tissue around an implant that controls the interface remodeling. If, thus, the implant can be designed allowing for motionlessness along all those interfaces which are necessary for a stable anchorage, usually all load bearing interfaces, the conditions for fracture healing as well as for long term stability can be met.

4. The Modes of Implant Fixation

Table 2 summarizes the modes of implant fixation either realized, attempted, or aimed at in bone and joint surgery, and dental implantology.

Table 2. Modes of fixation for bone and joint replacements and dental implants.

Mode	Kind of interface	Kind of load transmission	Comments
Soft tissue encapsulation	identical with non-union of a fracture site	via soft tissue deformation	not reliable, but successful in exceptional cases for up to 20 yrs
Mechanical interlocking			
a) macroscopic porous coatings	partially soft, partially direct bony tissue contact	mixed, via direct bone contact partially only	not reliable, some severe difficulties in implant removal
b) microscopic surface porosity (flame sprayed powders)	direct bone contact	via direct bone contact	reliable and stable anchorage
c) controlled surface undulations	direct bone contact	via direct bone contact	reliable and stable anchorage
Isoelasticity	soft tissue encapsulation	via a soft tissue layer	not reliable
Bond formation via bioactivity	direct bone contact	via direct bone contact	fatigue of bioactive materials

4.1. The soft tissue mode

The reasons for soft tissue encapsulation are twofold: either the implant material is only partially biotolerant and the differentiation and proliferation of the bone forming cells is prevented or disturbed, or the shape of the implant does not provide sufficiently large surfaces along which relative movements can be prevented. The correlation between a soft tissue interlayer and implant failure has been clearly established for dental implants.[11] The stability of a soft tissue layer around total joint replacements anchored via the polymethylmethacrylate bone cement (PMMA) suffers severely from interactions with polyethylene wear particles resulting from the articulation between the polyethylene sockets and metal balls. The use of ceramic balls[2] can reduce the production of such wear debris considerably and, thus, extend the life expectancy of these implants.

4.2. Mechanical fixation modes

A mechanical interlocking between the bony tissue and the implant surfaces can be achieved in different ways with very different results:

4.2.1. Macroscopic porous coatings

Porous coatings mostly consisting of one or more layers of metal spheres sintered or otherwise attached to the surface of CoCrMo-alloys allow for the on- and ingrowth of load bearing bony structures as deeply as the stress and strain field reaches and, of course, only at interfaces along which a sufficient motionlessness can be provided during the healing

period. This mode of implant fixation has reached relatively wide application in the US. It has been stated recently that the success rates of such knee replacements are no better than with cemented devices.[12] Some initially very successful femoral components of hip prostheses had to be abandoned because of the severe destruction necessary for their removal.[13]

4.2.2. Coatings of sprayed powders

Coatings consisting of microscopic titanium powder particles flame or plasma sprayed onto the surfaces of the anchoring portions of several dental implants have achieved very high success rates in more than ten years of application. These implants are kept completely unloaded during the healing period by initially placing them underneath the gingiva and supplying them with a superstructure only after about three months. Figure 1 shows an example.

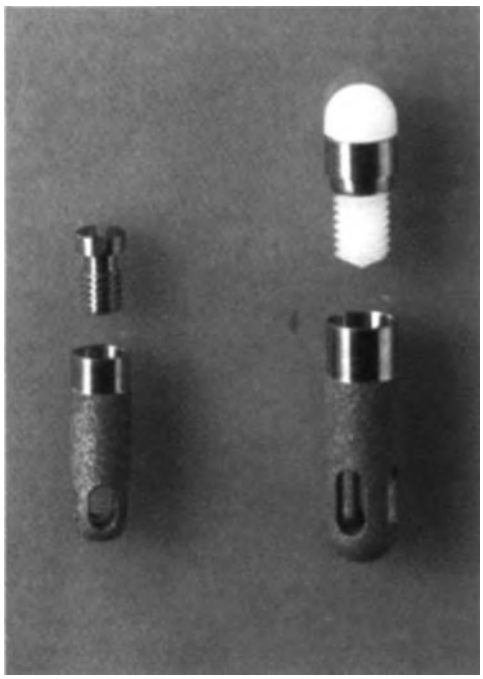


Fig. 1. Titanium dental implant (IMZ-implant) with Ti-powder particles flame sprayed onto the cylindrical surface. Note the openings for bony ingrowth and additional stabilization.

4.2.3. Controlled surface undulations

Controlled surface undulations can be regarded as a combination of shape elements of an implant which allow the control of the stress and strain field in the adjacent bone in order to minimize the effect of the differences in stiffness, and an optimization of the concept of porous coatings by providing the biomechanically favorable shape of the surface undulations (Fig. 2). This can result in an interlocking by which a close bone contact can be achieved[8] and maintained even along tangentially loaded interfaces.[8, 14]



Fig. 2. BMO- (biomechanically optimized-) Stepped Stem of the femoral component of the FRIALIT total hip replacement system made of the vanadium free TiAlFe alloy. Note the macroscopic steps and additional fine surface undulations providing for an interlocking along otherwise tangentially loaded interfaces.

4.2.4. The interfacial bonding mode

The anchorage of implants via an interfacial bond made possible by bioactive materials would very much facilitate implant design, the operation procedure, and, if it enhances bone formation, the post-operative treatment. Unfortunately, none of the bioactive materials have been found stable enough to withstand many years of shear loading. The same reactivity that allows for the bond formation obviously also accounts for the high mechanical fatigue. Presently, many attempts are underway to overcome these handicaps by coating the bioactive glasses, glass-ceramics, and ceramics onto mechanically strong substrate materials. Whether the aging and dissolution phenomena of such coatings can be overcome remains to be seen.

5. The Concept of Isoelasticity

The concept of the so-called isoelastic prosthesis is another attempt to avoid the problems resulting from the large differences of the mechanical performance of all metals and ceramics as compared to bony tissue. At a first glance, it might appear a reasonable approach to make the implant as

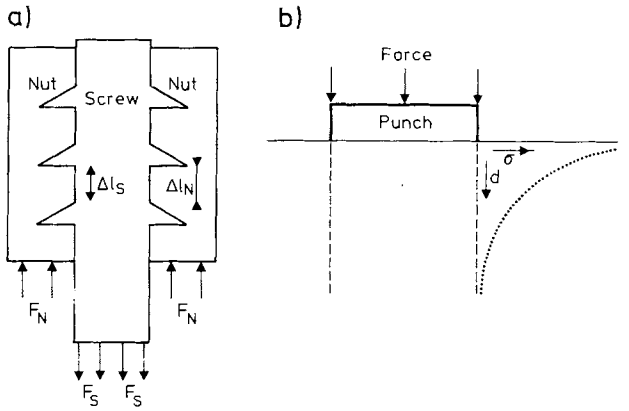


Fig. 3. a) The "nut and bolt" of identical materials results in a severe stress concentration on the first thread. Δl_S = elongation, Δl_N = compression. If the cross sections are equal $|\Delta l_S| = |-\Delta l_N|$, $\sum F_S = \sum F_N$. The cylinder underneath the circular punch (b) represents the situation of complete isoelasticity and of an ideal bonding to its environment within this half space. The dotted curve shows the stresses along the dashed interface between this cylinder and the environment and the extreme stress concentration towards the surface. It is this stress concentration that allows for all punching processes! σ stresses along d, d distance along dotted line.

stiff as the surrounding bone. As such an implant can be realized only with fiber reinforced plastics, this idea has found much attention in chemically oriented research groups. This concept, however, violates very basic and old rules of mechanical engineering. This has already been shown previously for two special cases[15, 16] and is explained on general terms in Figure 3.

6. Final Remark

The application of bone forming stimulants along implant to bone interfaces might be beneficial during part of the healing phase. As the stability of implant fixation essentially depends on the load pattern in the adjacent bony tissue and on the biochemical influences of the implant materials, hardly any contribution of such extracts can be expected for long term implant reliability.

The recent observation[17] of a particularly favorable adhesion of fibroblasts onto controlled surface undulations with dimensions in the one to two microns range can be regarded as a means to understand the bond formation on the Ti-powder coated surfaces. It appears that further results from this ongoing study will provide deeper insights into such surface mediated responses of cells and, thus, allow for further improvements of implant anchorage.

[1] M. Lorenz, M. Semlitsch, B. Panic, H. Weber, H. G. Willert, *Eng. Med. 7* (1978) 241.
[2] M. Semlitsch, M. Lehmann, H. Weber, E. Dörre, H.-G. Willert, *J. Biomed. Mater. Res. 11* (1977) 537.
[3] G. Heimke, P. Griss, *Arch. Orthop. Traumat. Surg. 98* (1981) 165.
[4] G. Heimke, in G. Heimke (Ed.): *Osseo-Integrated Implants*, CRC-Press, Inc., Boca Raton, FL. 1989 (in press).
[5] J. F. Osborn: *Implant Material Hydroxylapatite Ceramic. Basic Considerations and Clinical Applications*, Quintessenz-Verlag, Berlin 1985.
[6] G. Heimke, P. Griss, E. Werner, G. Jentschura, *J. Biomed. Eng. 3* (1981) 209.
[7] G. Heimke, W. Schulte, P. Griss, G. Jentschura, P. Schulz, *J. Biomed. Mater. Res. 14* (1980) 537.
[8] G. Heimke, W. Schulte, B. D'Hoedt, P. Griss, D. Stock, *J. Artificial Organs 5* (1982) 207.
[9] G. Heimke, *Adv. Mater. 1989*, 234; *Angew. Chem. Int. Ed. Engl. Adv. Mater. 28* (1989) 956; *Angew. Chem. Adv. Mater. 101* (1989) 980.
[10] G. Heimke, *Adv. Mater. 1989*, 7; *Angew. Chem. Int. Ed. Engl. Adv. Mater. 28* (1989) 111; *Angew. Chem. Adv. Mater. 101* (1989) 113.
[11] H. Spiekermann, in G. Heimke (Ed.): *Dental Implants*, Hanser, München 1980, p. 49.
[12] J. N. Insall, *Clin. Orthop. 226* (1988) 38.
[13] G. A. Lord, in *Proc. Symp. Uncemented Total Joint Replacement*, Phoenix, AZ, Harrington Arthrites Research Center, (Nov. 1984) p. 49.
[14] B. d'Hoedt, C. M. Büsing, *Fortschr. Zahnärztl. Implantol. 1* (1985) 150.
[15] R. Scholten, H. Röhrle, in S. K. Gupta (Ed.): *Trends in Biomedical Engineering*, CBME Publications, New Delhi, 1978, p. 148.
[16] R. Huiskes, in P. Ducheyne, G. Van der Perre, A. E. Aubert (Eds.): *Biomaterials and Biomechanics*, Elsevier, Amsterdam 1984, p. 7.
[17] C. E. Campbell, A. F. von Recum, *J. Investigative Surg.*, (1989) in print.

Conference Reports

Graphite Intercalation Compounds in Berlin

By Ralph Setton *

The fifth international symposium on graphite intercalation compounds sponsored by the Freie Universität Berlin, was held in Berlin (West), on May 22.–25., 1989. It was attended by 137 scientists from 17 countries, with West Germany, France, Japan and the United States contributing about 85% of the participants. Fourteen invited talks were presented, as well as 41 other papers and 73 posters. Following a well-established custom of these symposia, seventeen

[*] Dr. R. Setton
Solides à Organisation Cristalline Imparfaite
Centre National de la Recherche Scientifique
45071 Orléans (France)

presentations were not directly related to graphite but involved other low-dimensional solids such as chalcogenides, conducting polymers, or layered hydroxides.

It has often been said that whoever wants to learn all about solid-state chemistry or physics need only study the graphite intercalation compounds (GICs), as shown by the following summary of the presentations.

The synthesis of graphite-like materials of composition BC_3, C_5N and BC_2N was described by *N. Bartlett*, Berkeley. In another plenary lecture, *J. Rouxel*, Nantes, discussed the design and synthesis of a large variety of low-dimensional compounds, whereas *T. J. Pinnavaia*, East Lansing, presented various synthetic layered pillared structures.

The thermodynamic requisites of intercalation were exposed by *A. Hérold*, Nancy, and *W. Metz*, Hamburg, discussed nucleation processes and threshold pressures. *P. Lagrange*, Nancy, described the intercalation of Cs–Sb and Cs–As alloys while co-intercalation from the vapor phase of potassium and rare earth elements was presented by *H. Suematsu*, Tokyo. A 1st-stage CoC_{14} was obtained electrochemically by *P. Touzain*, Grenoble, by reduction of a $CoCl_2$ GIC, whereas high pressure was used by *I. T. Belash*, Moscow, to synthesize 'super-rich' GICs of Li, Na, or K, all of them metastable at normal temperature and pressure.

Intercalate exchange was shown by *E. Stumpp*, Clausthal, and by *H. P. Boehm*, Munich, to be capable of yielding hitherto unknown metal halide GICs and *M. Inagaki*, Toyohashi, detailed the preparation of metal halide GICs from molten salts. New GICs of Nb or Ta fluorides, in which the valence state of the metal is not V but III or IV, were announced by *A. Hamwi*, Clermont, while *T. Nakajima*, Kyoto, described a series of GICs of various stages containing fluorides of Ti, V, Nb or Ta with excess fluorine, or the volatile oxyfluorides WO_2F_2 or WOF_4. GICs of molybdenum oxynitrate and of Ce, Hg, Pt or Au nitrates were described by *E. Stumpp*.

D. Guérard, Nancy, has completed the series of ternary GICs with alkali metals and hydrogen, some of them showing unexpected stability towards air and water. Similarly, the ternary alkaline earth-NH_3 GICs prepared by *E. Stumpp* complete the series started in 1955 by the late *W. Rüdorff*. In the ternary GICs prepared by *J. O. Besenhard*, Münster, *D. Billaud*, Nancy, or *K. Lüders*, Berlin, water or nitromethane is the third component solvating the intercalated anion. The ternary GIC studied by *F. Béguin*, Orléans, contains an organic molecule physisorbed at room temperature.

Somewhat similar to the ternary GICs, the bi-intercalation compound presented by *H. Suematsu* contains sequential layers of potassium and $MoCl_5$. Other structural determinations addressed phase transitions induced by pressure (*K. Syassen*, Stuttgart, *S. Matsuzaki*, Kumamoto, *O. E. Andersson*, Umeå, *I. T. Belash*) or by temperature (*F. Rousseaux*, Orléans, *P. Lagrange*, *P. Behrens*, Konstanz). Charge transfer between host lattice and guest was discussed by *S. Flandrois*, Bordeaux, *W. Metz*, *S. Ikehata*, Tokyo, *A. Métrot*, Reims, *R. Setton*, Orléans, and *H. Zabel*, Urbana. Closely related to these problems are the EXAFS and XANES measurements carried out by *W. Metz*, *A. Tressaud*, Bordeaux, and *G. Wortmann*, Berlin, while band structure calculations and experimental verifications of some of their features were given by *S. Rabii*, Philadelphia, *W. Berthold*, Dortmund, *K. Nakao*, Tsukuba, and *A. Charlier*, Metz. Problems of lattice dynamics were studied by *S. A. Solin* and by *S. D. Mahanti*, both from East Lansing, *H. C. Gupta*, New Delhi, *W. Lassmann*, Hannover, *J. E. Fischer*, Philadelphia, and new experimental methods for their study were presented by *Y. Yacoby*, Jerusalem.

Some physical methods of investigation, such as resistivity measurements or X-ray diffraction, are now so commonplace in solid-state studies that there is no point in detailing the cases in which they are used. It is interesting however to note that *W. Metz* showed that a new correction factor must be used to obtain good agreement between calculated and experimentally determined intensities of the X-ray spectra. Magnetic properties, both static and dynamic, also seem to be used so extensively (over 20 papers!) that individual presentation of the papers is impossible, in spite of the numerous interesting results thus obtained. More spectacular are the 'pictures' obtained by Scanning Tunneling Microscopy of the atoms on the external surfaces of GICs presented by *R. Wiesendanger*, Basel.

It is worth noting that increasing attention is paid to applications of GICs: as electrochemical sensors for charge in Pb batteries (*H. Krohn*, Duisburg), as catalysts for the synthesis of NH_3 (*K. Kalucki*, Szczecin), in rechargeable Li batteries (*M. Endo*, Nagano), in the separation of the isotopes of hydrogen (*T. Terai*, Tokyo), etc.

The Fifth International Symposium on Graphite Intercalation Compounds was a highly successful meeting in which the latest expertise in the field was made available and for which the organizers, Professors *K. Lüders* and *R. Schöllhorn*, are to be highly congratulated.

Books received:

The Vibrational Spectroscopy of Polymers. By D. I. Bower and W. F. Maddams. Cambridge University Press, Cambridge 1989. xiii, 326 pp., bound, US $ 89.50. – ISBN 0-521-24633-4. **Handbook of Ion Beam Processing Technology.** Ed. by J. J. Cuomo et al. Noyes Publications, Park Ridge 1989. xviii, 438 pp., bound, US $ 72. – ISBN 0-8155-1199-X. **Corrosion Handbook, Vol. 4.** Ed. by D. Behrens. VCH Verlagsgesellschaft, Weinheim 1989. x, 392 pp., bound, DM 775. – ISBN 3-527-26655-0. **Materials Testing for the Metal Forming Industry.** By K. Pöhlandt. Springer-Verlag, Berlin 1989. xi, 240 pp., bound, DM 108. – ISBN 3-540-16722-6. **Quantitative Image Analysis of Microstructures.** Edited by H. E. Exner and H. P. Hougardy. DGM Informationsgesellschaft Verlag, Oberursel 1988. 235 pp., bound, DM 95. – ISBN 3-88355-132-5. **Transmission Electron Microscopy.** By L. Reimer. Springer-Verlag, Berlin 1989. xiii, 547 pp., soft cover, DM 128. – ISBN 3-540-50499-0.

Solids: Dynamics and Kinetics in Siegen

By Hermann Schmalzried *

German physical chemists are organized in the "Deutsche Bunsengesellschaft". Their annual meetings on varying topics of current interest and importance are held each year at a different university, this year's, the 88th, being held from May 4.–6. in Siegen. The physical chemistry of solids links the two basic solid state sciences, chemistry and physics. The dramatic increase in effort and progress in the solid state sciences has been triggered by the growing need of materials in our technical civilization. As a response, this year's main topic of the "Bunsen-meeting" was formulated as "Solids: Dynamics and Kinetics".

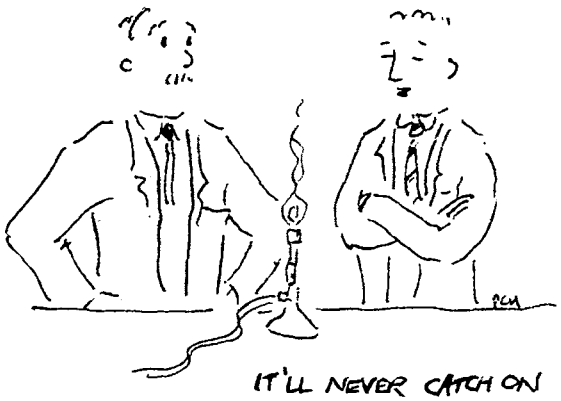
Solid state kinetics deal with chemical processes in solids and particularly with their behavior within time. These processes occur under the influence of thermodynamic driving forces which act on the atomic particle ensembles of the solid. An example is the widely studied oxidation of metals in a tarnishing process.

Solid state dynamics deals with the restricted, and often correlated motions of localized atomic particles, an example of which is the vibration of an atom or a group of atoms in a crystal. Traditionally, kinetics is more the domain of the chemist, whereas dynamics has rather been investigated by the physicist.

The key problem in the physical chemistry of solids is the explanation of the parameters of phenomenological kinetic theory in terms of solid state dynamics. In line with this theme, the three plenary lectures of the Bunsen-meeting started with a contribution by *H. Stiller* (Jülich/Berlin, FRG), discussing in detail individual and collective local particle motions in crystalline solids. *J. W. Cahn* (Washington, USA), whose theme was the physical chemistry of stressed solids, pointed out the fundamental differences between solids and fluids when it comes to the formulation of driving forces for solid state reactions: Solids can store elastic energies stemming from nonhomogeneous stresses. *G. Petzow* (Stuttgart, FRG) illustrated how to produce new materials with desired (mechanical) properties which are based on kinetic processes, through structure design; his examples were essentially taken from the field of nonmetallic inorganic compounds.

In addition to these plenary lectures, five more invited speakers gave progress reports on various topics of solid state research: *S. Clough* (Nottingham, UK) dealt with "Gauge theory and molecular rotation in crystals",[1] *K. Funke*'s (Münster, FRG) topic was "Transport and relaxation in ionic crystals", and *J. Rouxel* (Nantes, France) discussed "Reactivity and phase transitions in the chemistry of low dimensional compounds". The current state of solid state electrochemistry was reviewed by *A. R. West* (Aberdeen, UK) in his report on "Solid electrolytes", and the final contribution of *H. Sixl* (Frankfurt, FRG) dealt with "Organic solids: possible applications in optics and electronics".[2]

More than twenty oral presentations in three sessions and forty poster contributions from different research groups and various research fields clearly illustrated the breadth of solid state research and the interdisciplinary character of solid state physical chemistry. Physicists, chemists, polymer scientists, ceramists, and metallurgists all demonstrated the impact that basic research can have in helping to solve practical problems in material science.



Physical chemistry is, to a large extent, an experimental science. It is therefore interesting to review the main experimental methods applied in current research, as reflected in this meeting. One notes that solid state electrochemistry in its broad sense, and its classical experiments, still plays an important role, particularly when it comes to interfaces. Structure and dynamics are largely explored using neutron techniques, because their advantage of energy discrimination overrides in importance the general availability of X-rays. Solid state NMR, Mössbauer-effect, PAC-experiments and related experimental methods that probe the charge or spin density of the atomic surroundings are indispensable if one studies motion and transport on an atomic and a macrosopic

[*] Prof. Dr. H. Schmalzried
Institut für Physikalische Chemie und Elektrochemie
der Universität Hannover, Callinstrasse 3-3A
D-3000 Hannover 1 (FRG)

ADVANCED MATERIALS

scale, although the more classical methods of sensing electromagnetic interactions between radiation and matter are being used continuously. In kinetic research it is found that in situ experiments, which for solids often mean high temperature experiments, are absolutely necessary. However, this makes the application of IR and visible light spectroscopy a most difficult task.

In a way it was interesting to note that electron microscopy is not used more by solid state physical chemists – at least in Germany. After all it is the (periodic) structure that distinguishes the solid from the fluid state and determines most of its properties including the kinetic and the dynamic ones, and high resolution electron microscopy offers spatial resolution on an atomic scale. Therefore it seems clear that electron microscopy will increasingly help us to understand the basis of solid state kinetics: the defect in the solid state. Additionally, modern chemical analysis results in a much better characterization of the solids under investigation than ever before. This is most important with regard to the fact that it is always the crystal defect, including chemical impurities, that (as is well known in semiconductor technology) govern many of the crystal properties.

In conclusion: The Bunsen-meeting has again illustrated the interdisciplinary character of physical chemistry and has fulfilled its role of promoting the exchange of ideas, this year in particular between the different groups which work in the broad field of solid state science.

[1] S. Clough, *Adv. Mater. 1989*, 296; *Angew. Chem. Int. Ed. Engl. Adv. Mater. 28* (1989) 1124; Angew. Chem. Adv. Mater. *101* (1989) 1150.
[2] H. Sixl, W. Groh, D. Lupo, *Adv. Mater. 1989*, No. 11; *Angew. Chem. Int. Ed. Engl. Adv. Mater. 28* (1989) No. 11; *Angew. Chem. Adv. Mater. 101* (1989) No. 11.

Sol–Gel Processing in Bad Honnef

By Hans Reuter *

The 52nd seminar of the Dr. *Wilhelm Hereaus* and *Else Hereaus* Foundation entitled "Sol–Gel Processing for Glasses, Ceramics and Inorganic–Organic Polymers" was held from Monday, May 22nd, through Wednesday, May 24th, 1989 at the Physikzentrum in Bad Honnef, FRG.

Basically the expression "Sol–Gel Process" means the formation of an amorphous solid, the gel, starting from a homogeneous liquid, a molecular dispersion or colloidal solution. The great amount of scientific and technological interest devoted to this process ranges from molecular chemistry to material science. One aim of the seminar was to bring together, in a small circle, scientists from these different fields to discuss in an interdisciplinary manner the numerous aspects of sol–gel-processing. Twenty invited speakers and about thirty further participants attended the meeting coming from both university laboratories and industry.

An instructive overview of the present industrial application of the sol–gel technique was given in the paper "Sol–Gel 1969–1989, Paths of Development and Products, Especially the Newer Ones" from *H. Dislich* (FRG), who also showed some remarkable examples of industrially fabricated, sol–gel derived products. Complementing this, *D. R. Uhlmann* (USA) illustrated in his lecture "General View of Sol–Gel Technologies" not only the present state of the art developments and the numerous unsolved problems but also the future possibilities of the technology.

One main problem is, that there is only little known about the chemistry which happens during the sol to gel transformation. This was analyzed in two papers. In the first one, "Monoorgano Tin Compounds as Model Substances for the Investigation of the Sol–Gel Process", *M. Jansen* (FRG) showed that with organometallic precursors it is possible to isolate crystalline oligomers, which can be studied by X-ray structure analysis in order to see directly how i.e. the solvent may influence the reaction path. In the second paper "Sol–Gel Chemistry of Transition Metal Oxides", *C. Sanchez* (France) demonstrated, using titanium alkoxides as an example, not only the role of solvent molecules but also that of other chemical additives like catalysts, stabilizing agents or drying control chemical additives.

The processes following gel formation, like drying and densification, were reviewed in the lectures of *G. W. Scherer* (USA) who talked about "Hypercritical Drying", "Aging and Syneresis" and "Sintering of Gels", while *D. J. Brinker* (USA) discussed the "Fundamentals of Thin Film Formation from Sol–Gel Solution" and the "Spinnability of Silica Sols: Structural and Rheological Criteria" dealing with the more practical aspects.

New experimental paths were pointed out by *C. Rüssel* (FRG) "Non-Oxide Ceramics by Sol–Gel Techniques" mak-

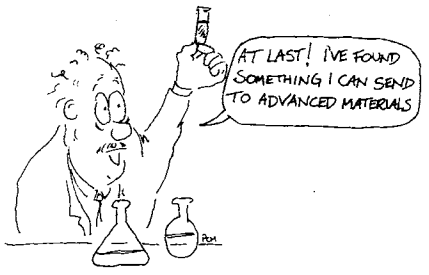
[*] Dr. H. Reuter
Institut für Anorganische Chemie
Universität Bonn, Gerhard-Domagk-Strasse 1
D-5300 Bonn 1 (FRG)

ing AlN by anodic dissolution of the metal in amines, by *U. Schubert* (FRG) "Sol–Gel Processing of Transition Metal Complexes" describing materials in which a transition metal complex moiety is bound by an inert spacer and an anchoring group to a silica gel matrix, and by *H. Schmidt* (FRG), who gave in his paper "Inorganic–Organic Polymers by Sol–Gel Techniques" first impressions about the manifold possibilities of organic modified silicates.

Many of the papers dealt with the possible applications of sol–gel derived materials. *J. Fricke* (FRG) "SiO_2-Aerogels—Structure, Properties, Applications" demonstrated that aerogels, due to their porosity, have very unusual but useful properties. Another example was presented in the paper "Oxide Gels, New Materials for Micro-Ionics" from *J. Livage* (France) who gave examples of systems which are good candidates for making "all-gel" derived micro-ionic devices.

On the whole, one can say that the goal of the meeting, of discussing the fundamental and applicationally oriented aspects of sol–gel processing with respect to material preparation, technology and structure/property relationships, was fulfilled, much to the credit of *H. Schmidt* from the Frauenhofer-Institut für Silicatforschung (Würzburg, FRG), who had composed this most interesting scientific program. This positive impression was not altered by the recognition that the great hopes for sol–gel technology have been somewhat overdone: today it is possible to make coatings by this method in considerable variety but until we succeed in making bulk materials on an industrial scale there will be much to do.

Materials Forum



Durable Thermometer for Molten Metals

Conventional thermometers used to measure the temperature of, for example, molten steel are usually destroyed very quickly by the environment and provide data for only 1–3 seconds.

A new thermometer, developed by Nippon Steel and the Asahi Glass Co. has a functioning lifetime of over 40 hours. This increased durability is achieved by encasing the thermometer in a tube made from the advanced ceramic zirconium boride which has a melting point of 3060 °C allowing continuous measurement of temperatures up to 1600 °C.

Continuous monitoring of the temperature enables the effects of defect inclusions to be located precisely, processing abnormalities to be prevented and energy to be saved.

Further information is available from the Nippon Steel Corporation, Königsallee 30, Düsseldorf 4, FRG.

Laser Microscope for Surfaces

Zygo has introduced the Maxim 3D three-dimensional noncontact laser microscope for the measurement of surface structure. Its optical design allows it to measure coated carbon surfaces as easily as polished aluminum substrates.

Combining the capabilities of an optical microscope with the measurement resolution of phase-measuring interferometry, the Maxim 3D can perform vertical, lateral, angular and positional measurements to 6 Å vertical resolution and less than 0.5-micrometer lateral resolution. Three-dimensional measurements allow accurate analysis of surface defects, which can be located at low magnification, then measured at higher magnification by rotating the turret. Details from Zygo Corporation, Laurel Brook Road, Middlefield, Connecticut 06450, USA.

Field Emission Scanning Electron Microscope

International Scientific Instruments of California, USA have introduced a new field emission scanning electron microscope called the DS-130F which offers high resolution and large-sample handling capability. It is a dual stage microscope which provides nanometer resolution in its top stage and maintains 2 nm resolution in the bottom stage even with a large sample (up to 6 inches diameter).

The DS-130F operates in the 10^{-8} torr range and even at an electron beam energy of 1 kV provides resolution in the top and bottom stages of 4 and 10 nm respectively. Further features are a new condenser lens system, a high brightness thermal field emission gun and the high stability of the emission current, which makes tip flashing unnecessary.

More details are available from International Scientific Instruments, 1457 McCarthy Boulevard, Milpitas, California 95035, USA.

New Generation of Turbomolecular Vacuum Pumps

TURBOVAC 150, 360 and 1000 V and H (see figure) from Leybold AG are universal turbomolecular pumps with continuous oil lubrication. The modular design of the pumps makes them suitable for various kind of applications including normal high vacuum research or demanding industrial tasks such as plasma etching. The pumps are highly reliable due to a well proven oil lubrication system. The bearings are continuously lubricated with filtered oil and any particles which beat the filter are flushed out by the oil.



The V-versions (vertical) are designed for upright installation only, while the H-version (horizontal) can be incorporated between the vertical and horizontal. With a modification kit the V-version can be converted at a later time for horizontal use.

Special Features: Inert gas seal system for the protection of the lubricant and bearings; Integral vent port to ensure "clean venting" of the pump; Simple oil level control and oil changing; Water or optional air-cooling; Inlet flanges in ISO-K, CF and ASA in different sizes available.

For more information contact Otmar Reuter, Leybold AG, Bonner Strasse 498, D-5000 Cologne 51, FRG. Tel. (0221)347-1556.

Intelligent Liquids

Liquids, whose viscosity can be dramatically altered in a fraction of a second by the application of an electric field have been developed by Bayer. Silicone oils mixed with aluminum silicate form the basis of the new materials whose aggregation state is regulated by the applied voltage which ranges up to 2000 V (with very low current).

Although Bayer have not yet developed market-ready applications for these "intelligent liquids", uses can be envisaged, for example, in shock absorbers in cars which can react immediately to every road contour. Other properties include thermal stability, an ignition point of over 250 °C and compatibility with elastomeric materials. Further details available from Bayer AG, Bayerwerk, D-5090 Leverkusen, FRG. Tel. (0214) 30-72215.

Superconductivity

The nature of the Fermi-liquid electronic states in the high-T_c uperconductor $Bi_2CaSr_2Cu_2O_8$ has, until recently, been a matter of controversy. Some workers have attributed the existence of these states to the 2p orbitals of the BiO plane and others to those of the CuO_2 plane.

If the Fermi-liquid states were supplied by the BiO plane, which is not present in other copper-oxide superconductors, then the mechanisms for superconductivity based on the Fermi-liquid states would lose there experimental basis.

Using scanning tunneling spectroscopy (STS), an extention of scanning tunneling microscopy (STM), combined with photoemission (PES) and inverse photoemission (IPES) spectroscopies, *Tanaka* et al., *Nature 339* (1989) 691, have shown, reassuringly, that the Fermi-liquid states reside not in the BiO planes but in the CuO_2 planes and this description of the states should provide an experimental basis on which models of high-T_c conductivity in the copper oxide materials can be built.

New Polyamide Curing Agent

Industrial Copolymers Limited (ICL), manufacturers of speciality resins, based in Preston, UK, has added a further product to its innovative range. The company announces the introduction of INCOREZ 147LV, a new polyamide curing agent for water dispersed epoxies which it claims, according to the Gardner scale, is the lowest color polyamide curing agent presently on the market.

INCOREZ 147LV is a major step forward in technology allowing formulators to achieve white coatings comparable in color with solvent based counterparts. INCOREZ 147LV also has a faster cure rate and is capable of being infinitely diluted with water, retains a high solids content of 75% and can be formulated into matt, semi-gloss and full gloss coatings.

A variety of coating markets is envisaged including solvent sensitive areas, abrasion resistant applications and primers for concrete. Additionally, the product can be used in cementitious screeds to improve chemical resistance and adhesion to damp substrates.

For more information contact *P. Mileham,* ICL, P.O. Box 7, London Road, Preston PR1 4AJ, Lancashire, UK. Tel. (0772) 59781.

K' 89

The 11th International Plastics and Rubber Trade Fair (Kunststoffe '89, K '89) runs from November 2.–9. 1989 in Düsseldorf, FRG. With over 220.000 visitors and 1700 exhibitors in 1986 the "K" is one of the biggest materials trade fairs and this year is expected to be even bigger. Approximately 50% of both the visitors and the exhibitors are from West Germany, the other half coming from more than 40 countries making it a truly international exhibition.

The fair is aimed at the innovative users of plastics and rubbers in for example automotive construction, electrical engineering, electronics and aerospace, exhibitors representing everything from raw materials producers to applications engineers.

Book Reviews

NLO, SiN, GaAs, CVD, Acronyms, and Abbreviations

Photorefractive Materials and Their Applications I: Fundamental Phenomena. By *P. Guenter* and *J.-P. Huignard.* Springer-Verlag, Berlin 1988. xvi, 295 pp., hard cover, DM 119.—ISBN 3-540-18332-9

The field of nonlinear optics has received quite a dramatic increase in interest lately from research groups both in industry and in academia. This development was initiated in the mid-seventies when it was recognized that reversible laser induced material changes, as observed in nonlinear optics, can actually be utilized to modify and process one light beam with another. Applications in optical signal processing, optical computing and realtime holography became feasible, and widespread technical use of the effects in image processing and fiber-optic switching can be envisaged in the not too distant future.

Photorefractive materials have played a key role in these developments and many important demonstrations of principles have been made with photorefractive crystals, e.g. in phase conjugation, pattern recognition and neural optical processing. The photorefractive effect is generally observed in doped inorganic single crystals, mainly $LiNbO_3$, $BaTiO_3$, $Bi_{12}SiO_{20}$, $KNbO_3$, InP or GaAs. Its main virtue is that relatively low light powers can induce large material changes, sources being for example helium–neon, diode or small argon lasers, at the expense, however, of relatively slow response times (milliseconds to hours). Being a rather complicated multistep process, the photorefractive effect was subject to a substantial body of material-centered research which is reviewed in this volume.

Generally the following sequential steps are involved: excitation of charge carriers from impurity centers upon light absorption, migration of these carriers to other impurities outside the illuminated area, and trapping there. The resulting space-charge field changes the refractive index via the electro-optic effect and hence modifies the optical properties of the material. Several theoretical models for this effect have been developed, with the band transport model of *N. V. Kukhtarev* being currently the most versatile and widely used.

The editors, both leading European researchers and pioneers in the field, have brought together a well balanced mixture of articles (four from the USA, two from the USSR and three from Europe) covering virtually all aspects of the above described process. After a very brief introduction, they summarize effects and materials mainly from an experimental point of view. A detailed treatment of the photorefractive effects in dielectric crystals by *G. Valley* and *J. Lam* follows, and all theoretical aspects of the band transport model are very clearly described by *N. V. Kukhtarev*. He also demonstrates the predictive power of his model. Spectroscopic investigations of photorefractive centers using optical techniques as well as ESR and Mössbauer spectroscopy are reviewed by *E. Kraetzig* and *O. F. Schirmer*. *R. A. Mullen* presents justification for the charge hopping model, which is the main theoretical model competing with the band transport model, and outlines boundaries between both descriptions as she summarizes the measurement of physical parameters of the material.

The following two articles describe two specific classes of photorefractive materials in more detail. *M. B. Klein* summarizes the properties of $BaTiO_3$, the material with the largest known photoinduced refractive index changes. The study of this material has been restricted to relatively few groups due to the difficulties in obtaining poled single crystals of good optical quality. A relatively recent development (since 1984) are photorefractive semiconductors which are reviewed by *A. M. Glass* and *J. Strait*. GaAs-Cr and InP-Fe are particularly interesting as they operate in the near infrared, close to the wavelengths of interest for fiber optic communications.

Finally, *S. I. Stepanov* and *M. P. Petrov* describe moving photoinduced gratings and their applications in coherent amplification and phase conjugation, leading naturally to the second volume of the series which is on applications of photorefractives. In reading the book, it becomes apparent that most of the research is actually prompted by the applications, and therefore the separation between materials and applications seems artificial in many places. The general level of understanding reached at the time of writing (late 1987) is such that the development of new improved photorefractive materials can be expected. New centers and host crystals should be predictable, and photorefractive organic polymeric composites seem also feasible in the view of the authors.

The reading of the book requires a fundamental knowledge of solid state physics, as well as some classical background in holography, image processing, phase conjugation or nonlinear optics. To this end the previous reading of selected chapters of the book "Laser-induced Dynamic Gratings" co-authored by *P. Guenter* (Springer Ser. Opt. Sci. Vol. 50) might be beneficial, especially to the inexperienced reader.

General conclusions: a very thorough overview from a materials point of view, quite complex in places, mainly for researchers entering or already active in nonlinear optics or related fields. The book is likely to become a standard reference for further research on photorefractive effects and materials.

Werner Blau
Department of Pure and Applied Physics
Trinity College, Dublin 2 (Ireland)

Electronic Structure and Optical Properties of Semiconductors. By *M. L. Cohen* and *J. R. Chelikowsky*. Springer-Verlag, Berlin 1988, xii, 264 pp., hard cover, DM 98,— ISBN 3-540-18818-5

In the preface to this book the authors state that they tried to strike a compromise between a reference text and an textbook. The authors have achieved their goal. It contains much compiled information on the optical properties of semiconductors, and whether one is interested in the technologically important semiconductors, such as Si, Ge and GaAs, or the obscure such as $ZnGeP_2$, the desired information is there. In the back of the book there are over fifty pages of references, so the active researcher can quickly find detailed information in a subject of interest.

The book should also be of considerable use to the newcomer to the area as it provides a very nice introduction to the theory of band structure calculations. The authors begin with the nearly-free electron and tight binding models to demonstrate the basic properties of electrons in a periodic potential and point out that these two methods represent the two extreme views of electrons in solids and therefore, the augmented plane wave and the orthogonal plane wave methods have been developed to more realistically describe the electronic structure of solids.

Although the authors give a completely adequate introduction to the theoretical methods, they spend most of the time describing the pseudopotential method and its variations. This is not surprising, considering that the authors have made contributions in this area for more than twenty years. They begin the chapter on pseudopotentials with the mathematical formalism, and go on to explain the empirical, self consistent and the ab initio variations not only providing details of the mathematical formalism, but also describing in detail the computational philosophy used in each pseudopotential variation.

The three chapters that follow are those that make this book quite special. In these chapters the authors explain how, once you have completed a band structure calculation, the results can be compared to experiments. When one experimentally measures the optical properties of a semiconductor, one does not measure the band structure but some property related to it. In these chapters the authors go through in detail the process of calculating response functions.

They then compare how the pseudopotential calculations and experimental determined values agree. This is the section of the book that truly sets it apart from other theoretical books on solid state physics. Numerous experimental methods and how they can be used to further understand the band structure of solids are described. These include not only optical methods, such as electroreflectance, but also surface analysis techniques, such as X-ray photoemission and ultraviolet photoemission spectroscopy.

The last section in the book, which consists of almost one hundred pages, is devoted to describing the optical properties of numerous semiconductors. This is an excellent reference section for anyone working in the field of semiconductor physics or optoelectronics. It begins with the elemental semiconductors Si, Ge and Sn and then goes on to describe the III-V and II-VI semiconductors. Not only are the optical properties of the zinc blende and diamond structure semiconductors described, but detailed information on the wurtzite semiconductors is also included.

This is a very fine book on the optical and electronic properties of semiconductors and should find a place on the bookshelf of everybody who is involved in the areas of semiconductor physics or optoelectronics.

Robert N. Bicknell-Tassius
Department of Physics, University of Würzburg
Am Hubland, D-8700 Würzburg (FRG)

Silicon-nitride in Electronics. By *V. J. Belyi* et al. Elsevier Science Publishers, Amsterdam 1988. viii, 340 pp., bound, US$ 100.— ISBN 0-444-42689-2

This book, originally written in Russian, describes the technology of silicon nitride film preparation on a silicon wafer. This subject is not new and therefore the authors intent is to present a collection of the properties and physical-chemical aspects, which govern the production.

In the first chapters, the reaction theories of all the gaseous production techniques are discussed. This is done in a style which is typical for a Russian theoretical book. However, one clearly recognizes that the formulas characterizing the process steps dramatically define the properties of the silicon nitride layer. In contrast to solid-state silicon nitride, which is widely resistant against chemical attack, a silicon nitride film, produced by vapor deposition techniques can be structurized by normal photolithographic techniques. The reader who is interested in a deep understanding of the fundamental parameters of the process would certainly read this chapter with interest. On the other side, the practical point of view is not forgotten. The process of the layer-deposition is described in detail.

In the following chapters, the basic principles of the deposition-process are emphasized more than the manufacturing techniques. Pictures of furnaces or other types of processing hardware, which are common to a book of this kind, are not given. However, a nearly complete literature list is provided.

The properties of the different types of films, produced using the different types of processes are discussed in detail. Curves and diagrams will help the reader, who is not so familiar with the formula-language. A more theoretically oriented user however, will be deeply impressed by the equations and the data, which can help him to calculate his process and compare the results to the electrical data given in this book. This collection of data explaining the influence of process parameters on the electrical properties is helpful to any producer of silicon nitride layers on silicon.

The data is presented in a format oriented for a semiconductor technologist. Band-diagrams and energy representa-

tions are given. These can be used by the circuit designer as input to his calculations on an integrated circuit. In the last chapter the applications for silicon nitride films are reviewed, including LOCOS process, EPROM devices, pH sensors, etc. This is done only briefly but a reader who needs more information can use the comprehensive literature list.

In summary, this book collects all the theoretical and practical aspects of the production of a silicon nitride film on a silicon-wafer. A user, who is working on this process and this material will certainly welcome this book as a process handbook or dictionary of the silicon nitride preparation process.

H. Gernoth
Department of Materials Research
Hoechst AG P.O. Box 800320, D-6230 Frankfurt (FRG)

Textile Structural Composites. Edited by *T.-W. Chou* and *F. Ko*. Elsevier Science Publishers, Amsterdam 1988. xiii, 480 pp., bound, US$ 155.25. – ISBN 0-444-42992-1

Textile composites can be defined as the combination of a resin system with a textile fiber, yarn or fabric system. The various textile composite systems are described with reference to chopped fiber and filament yarn constructions, the different fabric and non-woven fabric structures, behavior, and related composites.

Basic principles of the mechanics of tensile deformation and theories describing the non-linear stress-strain relations of fabrics are covered, concentrating on the two basic structures, plain woven and plain knitted fabrics.

The characteristics of the braiding process, the wide composite applications, and mechanical performance along with the structure, formation, properties and analysis of 3-D fabrics are reviewed.

Dr. *S. M. Bishop* discusses the properties of carbon fiber fabric laminates. Woven fabrics combined with unidirectional tape structures are investigated and their advantages in terms of tensile, compressive, impact and fatigue properties are described. Prof. *T.-W. Chou* presents analytical and calculational models for determining the thermal and mechanical properties of woven fabric laminates. The fabrics studied are either made of one material or are hybrid fabrics. The properties determined, such as stiffness, strength and thermal expansion, are partly compared with experimental data. The paper by Prof. *I. M. Yang* and Prof. *T.-W. Chou* deals with the thermo-elastic analysis of triaxial woven fabrics and the laminates made therefrom. This theoretical study also covers non-orthogonal fabrics, which are compared with triaxial fabrics.

Dr. *S. R. Moghe* describes the development of a mathematical model for designing woven fabric laminates taking into account the different material properties and process parameters. The calculated values are presented.

Additional materials covered are flexible composites and coated fabrics.

The book on the whole gives a good and up-to-date account of the theoretical and practical aspects of textile intermediates and their behavior in composites.

K. Hillermeier
Enka AG P.O. Box 100149
D-5600 Wuppertal 1, FRG

PARAT. Index of Acronyms and Abbreviations in Electrical and Electronic Engineering. Compiled by *Büro Scientia*, Berlin. VCH Verlagsgesellschaft, Weinheim 1989. 538 pp., bound, DM 224. – ISBN 3-527-26842-1

The book lists about 45000 acronyms and abbreviations with their associated definitions. In an attempt to facilitate the use of the book the entries have been standardized by printing the acronyms and abbreviations in capital letters while the full texts of the comments appear in lower case. This is certainly helpful. Looking up terms is made easy by the large and clear print. The solid binding promises to stand well the heavy usage one expects for a reference book of this kind.

A German-speaking reader will look in vain for the explanation of BTX, DIN, EVU, or the like since only English terms are listed. This could be indicated in the title of the book by changing it to: "Index of English Acronyms...".

The book contains a wealth of valuable entries that are not restricted only to the area of electric and electronic engineering but that go far beyond. The terms reach from ACELSCO (associated civil engineers and land surveyors of santa clara county) on page 6 to YST (yukon standard time) on page 563. Of course, the reader will find most of the expressions he would look for in a book on electric and electronic terms e.g. CPU, TV, CRT, LCD, VHF, VLSI, WATS, ISDN, and many more. But one would also expect to see terms like MODEM or AI, and a materials scientist would be interested in MOS or HTSC (high-temperature superconductivity) all of which are not (yet) listed.

Many of the terms are related to computer technology or to military applications. Unavoidably many abbreviations have multiple meanings, for some of them, e.g. SP, MS, CC, or MC more than 50 different interpretations are listed. To show the broad scope of the book, here are some examples selected at random: referring to organizations/institutions/company names one finds entries like FCCN, CBO, ISO, IBM, PAA down to SAAD (san antonio air depot). Relating to projects/products there are ILLIAC, STAIRS or LLM (lunar landing mission or module). And among the more general concepts are listed DEPT, VAT, SQRT (square root), and PAYE (pay as you earn).

Keeping in mind that it is impossible to please everybody, the editors did a good job in selecting the material and in including many "exotic" terms that are rarely found elsewhere. Altogether this volume is a comprehensive and up-to-date reference tool for the individual scientist or engineer as

well as a valuable addition to any collection of reference books.

Hermann J. Graml
Siemens AG P.O. Box 830953
D-8000 München 83 (FRG)

Fiber Reinforcement for Composite Materials. Edited by *A. R. Bunsell*, Elsevier, New York 1988, ix, 538 pp., bound, US$ 171.– ISBN 0-444-42801-1

This book is the second volume of a publication series on composite materials edited by *R. B. Pipes* (Center of Composite Materials, University of Delaware). It deals with various types of synthetic fibers used as reinforcements in advanced composite materials. This volume is subdivided into various chapters giving a clear description of the manufacture, structures and applications of the different fibers, as well as a brief compilation of characterizing methods for single fibers. The chapters are authored by internationally well-known experts and arranged as follows: Chapter 1. *A. R. Bunsell:* Fiber development for composite materials. Chapter 2. *P. K. Gupta:* Glass fibers for composite materials. Chapter 3. *E. Fitzer, M. Heine:* Carbon fiber manufacture and surface treatment. Chapter 4. *A. Oberlin, M. Guigon:* The structure of carbon fibers. Chapter 5. *G. Calundann, M. Jaffe, R. S. Jones, H. Yoon:* High performance organic fibers for composite reinforcement. Chapter 6. *H. H. Yang:* Aramid fibers. Chapter 7. *P. Bouriot:* Polyester and polyamide fibers for elastomeric matrix composite materials. Chapter 8. *F. E. Wawner, Jr:* Boron and silicon carbide/carbon fibers. Chapter 9. *A. R. Bunsell, G. Simon, Y. Abe, M. Akiyama:* Ceramic fibers. Chapter 10. *R. Hagege, A. R. Bunsell:* Testing methods for single fibers.

The book gives a clear overview over the current "state of the art" and is very informative. However, the subdivision into CVD- and ceramic fibers is astonishing because the presented CVD-fibers are counted as ceramic fibers as well. The main interest of this volume is concerned with carbon, glass and organic fibers although fibers of interest in ceramic matrix composites have not been sufficiently covered. This is probably due to recent improvements of the known fibers and the development of new fibers. In summary this book is of great interest for scientists working with reinforcing components.

A. Hölscher, K. Schulte
Deutsche Forschungsanstalt
für Luft- und Raumfahrt, P.O. Box 906058,
D-5000 Cologne 90 (FRG)

Conference Calendar

The black hand symbol ☛ denotes new entries into the calendar. Send information concerning conferences to the editorial office



November 1989

11–14 **Solid-State Devices**
☛ 19th Eur. Conf.
Berlin (West)
Contact: H.-C. Petzold, Fraunhofer-Inst. f. Mikrostrukturtechnik, Dillenburger Str. 53, D-1000 Berlin 33.

14–15 **Polypropylene**
Madrid (Spain)
Contact: D. Varley, Plastics and Rubber Inst., 11 Hobart Place, London SW1W 0HL, UK

14–17 **Superconductivity**
2nd Int. Symp.
Ibaraki (Japan)
Contact: ISS '89 Secr., ISTEC, Eishin Kaihatsu Bldg., 34-3, Shimbaski 5-chome, Minato-ku, Tokyo 105, Japan, Tel. 03/431-4002, Fax 03/431-4044

22–24 **Euromat '89**
Eur. Conf. on Materials
Aachen (Fed. Rep. Germany)
Contact: Dtsch. Gesellsch. Metallkd., Adenauerallee 21, D-6370 Oberursel, FRG

23–24 **Superconductivity**
Int. Conf.
Paris (France)
Contact: Dr. R. Suryanarayam, Lab. de physique des solides de Bellevue, CNRS, F-92195 Mendon, France

27–29 **Electronic Packaging**
55th WE-Heraeus-Seminar
Bad Honnef (Fed. Rep. Germany)
Contact: Dr. V. Schäfer, WE-Heraeus-Stift., Heraeusstr. 12–14, D-6450 Hanau, FRG

27–2 **MRS Fall Mtg.**
Boston (USA)
Contact: A. Wagner, Materials Research Soc. (MRS), 9800 McKnight Rd., Suite 327, Pittsburgh, PA 15237, USA

27–2 **Electrical, Optical and Magnetic Properties of Organic Solid State Materials**
Boston (USA)
Contact: P. Chaikin, Dept. of Physics, Princeton Univ., Princeton, NJ 08544, USA, Tel. 609/452-4338

28–1 **New Materials**
1st Int. Symp.
Chiba (Japan)
Contact: Nikkan Kogyo Shimbun, 8–10 Kudan Kita 1-chome, Chiyoda-ku, Tokyo 102, Japan

28–1 **Magnetism and Magnetic Materials**
34th Annu. Conf.
Boston, MA (USA)
Contact: D. Suiters, Courtesy Assoc. Inc., 655 15th St., NW, Suite 300, Washington, DC 20005, USA

29 **Polymer Blends**
Baden-Baden (Fed. Rep. Germany)
Contact: VDI-Gesellsch. Kunststofftechnik, POB 1139, D-4000 Düsseldorf 1, FRG, Tel. 0211-6214-527

December 1989

4–5 **Advanced Materials by Sol-Gel Techniques, Eurogel '89**
Eur. Conf.
Strasbourg (France)
Contact: Fraunhofer-Inst. f. Silicatforsch., "Eurogel '89", Neunerplatz 2, D-8700 Würzburg, FRG

11–13 **CBE/MOMBE and Related Growth Techniques**
2nd Int. Conf.
Houston, TX (USA)
Contact: H.-D. Shih, Univ. of Houston, Sci. and Res. One, 4800 Calhoun Rd., Houston, TX 77004, USA, Tel. 713-749-3701, Fax 713-747-7724

11–16 **Physics of Semiconductor Devices**
5th Int. Workshop
New Delhi (India)
Contact: Dr. S. K. Sharma, IWPSD-89, Nat. Physical Lab., Dr. K. S. Krishnan Rd., New Delhi-110012, India, Tel. 586087

12–15 **Pacific Polymer**
Hawaii (USA)
Contact: J. C. Vogl, Pacific Polym. Federation, Polytechnic Univ., 333 Jay St., Brooklyn, NY 11201, USA

20–22 **Thin Films and Multilayers**
Mtg.
Warwick (UK)
Contact: Inst. of Physics, Magnetism Group, 47, Belgrave Sq., London SW1X 8QX, UK

31–2 **Corrosion-Erosion-Wear of Materials at Elevated Temperatures**
4th Int. Conf.
Berkeley, CA (USA)
Contact: A. V. Levy, Lawrence Berkeley Lab., MS 62-203, Univ. of Calif., Berkeley, CA 94720, USA, Tel. 415-486-5822

January 1990

10–14 **Superconductivity**
Int. Conf.
Bangalore (India)
Contact: Prof. S. V. Subramanyam, ICSC, Dept. of Physics, Indian Inst. of Sci., Bangalore 560012, India, Tel. 91-812-344411, Fax 91-812-341683

14–19 **Electro Optics**
Conf.
Los Angeles, CA (USA)
Contact: SPIE, POB 10, Bellingham, WA 98227-0010, USA, Tel. 206-676-3290, Fax 206-647-14445

Registered names, trademarks, etc. used in this journal, even when not marked as such, are not to be considered unprotected by law.

© VCH Verlagsgesellschaft mbH, D-6940 Weinheim, 1989. – Printed in the Federal Republic of Germany by Konrad Triltsch Druck- und Verlagsanstalt Würzburg.

All rights reserved (including those of translation into foreign languages). No part of this issue may be reproduced in any form — by photoprint, microfilm, or any other means — nor transmitted or translated into a machine language without written permission from the publishers. Only single copies of contributions, or parts thereof, may be made for personal use. This journal was carefully produced in all its parts. Nevertheless, authors, editors and publisher do not warrant the information contained therein to be free of errors. Readers are advised to keep in mind that statements, data, illustrations, procedural details or other items may inadvertently be inaccurate.

Valid for users in the USA: The appearance of the code at the bottom of the first page of an article (serial) indicates the copyright owner's consent that copies of the article may be made for personal or internal use, or for the personal or internal use of specific clients. This consent is given on the condition, however, that the copier pay stated per-copy fee through the Copyright Clearance Center, Inc. (CCC), for copying beyond that permitted by Sections 107 or 108 of the U.S. Copyright Law. This consent does not extend to other kinds of copying, such as copying, for general distribution, for advertising or promotional purposes, for creating new collective works, or for resale. For copying from back volumes of this journal see 'Permissions to Photo-Copy: Publisher's Fee List' of the CCC.

Editorial office: Postfach 10 11 61, D-6490 Weinheim, Federal Republic of Germany, Telephone (06201) 60 22 55, Telex 465 516 vchwh d, Telefax (06201) 602 328.

Editor: *Peter Gölitz*

Associate Editor: *Peter Gregory*. **Editorial Assistant:** *Susanne Stoll*

Publishers: VCH Verlagsgesellschaft mbH. (Managing Director: *Hans Dirk Köhler*), Pappelallee 3, D-6940 Weinheim, Federal Republic of Germany.

Advertising office (Advertising Manager *R. J. Roth*): Postfach 10 11 61, D-6940 Weinheim, Federal Republic of Germany, Telephone (0 62 01) 60 61 30, Telex 467 155 vchwh d, Telefax (0 62 01) 606 184.

ANGEWANDTE CHEMIE
International Edition in English
Volume 28 · Number 11
November 1989
Pages 1445–1600

Materials for Optical Data Storage

By Michael Emmelius*, Georg Pawlowski *, and Hansjörg W. Vollmann*

Dedicated to Professor Wolfgang Hilger on the occasion of his 60th birthday

The outstanding feature of materials research in the eighties has been the convergence of basic research and practical application, leading to ever shorter cycles of innovation. This is especially true of materials which form the basis of key technologies. The mass storage units of the next generations of computers will be based on optical processes having a storage density which exceeds that of all hitherto known storage techniques that are practicable from the technical standpoint. In view of the fact that since 1982 read-only memories in the form of compact discs (CD-ROM) have become very successful in the field of audio electronics, research and development are now concentrated on materials for write-once (WORM) and erasable (EDRAW) storage systems. Suitable materials for optical data storage are substances in which data markings can be recorded and deleted respectively using semiconductor lasers. Materials development is centered on the synthesis of infrared-absorbing dyes for WORM memories and the production of rare earth/transition metal alloys for magneto-optical data recording. An introduction to CD-ROM technology will be followed by an overview of the state of development of the most important storage materials which are currently available commercially, and then the properties of these materials will be discussed with reference to selected examples.

1. Introduction

The storage of biological information represents one of the basic explanations for the existence of highly differentiated living organisms. The biological information medium DNA (*d*eoxyribo*n*ucleic *a*cid) is the substrate for numerous enzymes which, at the molecular level, store, read and erase genetic data. Combinations of the basic building blocks of DNA (uracil, adenine, cytosine and guanine) provide the code for protein amino-acids as well as addresses on the DNA for starting and stopping the DNA replication. Replication, which is equivalent to storage, commences at primer-formatted DNA segments. Because of corrective mechanisms, for appoximately every 10^{10} nucleotides combined, a maximum of one unit is incorrectly positioned. Erasure of genetic information occurs either during regulation of cell metabolism or as a result of chemical mutations of the base pairs. On considering the interrelationships of molecular biology from this rather formal point of view, parallels with the function of technical data stores are immediately evident. At the same time it is clear that what is involved here is a

[*] Dr. M. Emmelius, Prof. Dr. H. W. Vollmann
Hoechst Aktiengesellschaft
Geschäftsbereich Informationstechnik
Werk Kalle/Albert
D-6200 Wiesbaden (FRG)
Dr. G. Pawlowski
Hoechst Aktiengesellschaft
Zentralforschung I
Hauptlaboratorium
D-6230 Frankfurt/Main 80 (FRG)

fundamental principle,[1] which is implemented in nature and to which the physical structuring of information systems can be traced.[2]

Not only do biological and technical information carriers differ in numerous fundamental respects; they differ, above all, as regards the physical size and arrangement of their data units. The genetic information of a DNA molecule corresponds to an information density of 10^{21} bit cm^{-3} (three-dimensional storage), while technical memories of the highest information density hold approximately 10^{8} bit cm^{-2} (two-dimensional storage) (Fig. 1). In spite of the high rate at which miniaturization is progressing, as well as the use of new storage processes, it appears dubious whether the limit to storage at a molecular level can be overcome in the near future.[*] However, optical memories represent an important step in this direction, since they exceed the storage densities of hitherto well-established information media.

Research has been in progress on optical memories since the end of the sixties. However, it was not until 1982 that the breakthrough finally came with the audio compact disc; this was closely linked with the availability of new semiconductor lasers as light sources. In the field of consumer electronics, the conventional playback processes lost considerable ground, since it was not possible to achieve comparable levels of quality of reproduction using any other medium. Accordingly, it was an obvious step to utilize the potential of

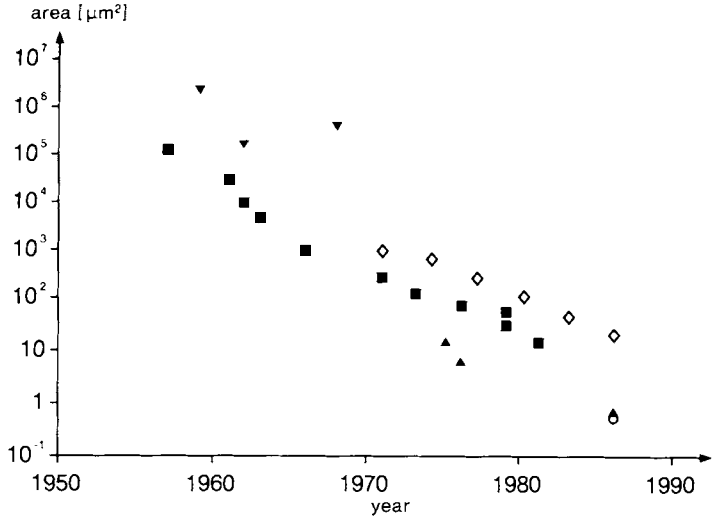


Fig. 1. Trend toward higher storage density for various media. Reduction of area A required to store one bit of information (after [2c]). ■ disk file, ▲ magnetic bubble, ▼ thin film memory, ○ optical disk, ◇ semiconductor.

[*] See also the Editorial Essay by *D. Haarer* in the *Advanced Materials* part of this issue.



Michael Emmelius was born in 1954 and studied chemistry and medicine at the University of Mainz, where he was awarded his doctorate for studies in the field of macromolecular chemistry under Professor H. Ringsdorf. In 1986 he joined the research department of the Information Technology Division at Hoechst AG and was entrusted with the development of photoresists. In 1988 he became assistant to the director of R&D in information technology. Since September 1989 he has been concerned with technical marketing. His scientific interest pivots around the physicochemical problems of materials research.



Georg Pawlowski was born in 1952 and studied chemistry at the University of Tübingen where he completed his doctoral work on conductive polymers under Professor M. Hanack. In 1981 he joined the research department of the Information Technology Division at Hoechst AG where his work was primarily concerned with "photoreactive polymers". In 1987 he became assistant to the director of R&D in information technology. He is at present leader of the photochemistry group in the central research department at Hoechst AG. His interest centers on the development of new radiation-sensitive materials.



Hansjörg W. Vollmann was born in 1933 and studied chemistry in Cologne, Bonn and Stuttgart. After gaining his doctorate for studies in preparative organic chemistry under Professor H. Brederek he worked for a short while as research chemist at Cassella AG. In 1964 he joined the central research department at Hoechst AG and worked in the area of intermediates and dyestuffs. In 1970 he was appointed in charge of the construction and direction of the central research department of the American Hoechst Corp. (now Hoechst Celanese Corp.) in Rhode Island, USA. Since 1978 he has been head of research and development in the Information Technology division at Hoechst AG. He is honorary professor for Industrial Chemistry at the University of Würzburg. His main scientific interest focuses on the products, processes and applications of photochemistry in information technology.

optical memories for the greatly expanding computer technology, since it is mainly the requirements of modern microelectronics which stimulate the search for faster and more powerful mass storage units. Circuits exhibiting very large scale integration permit access to 4MByte DRAM (*D*ynamic *R*andom *A*ccess *M*emory) from semiconductor memories and to the management of sophisticated software, which require permanent storage of increasing quantities of data. At the same time, there is a trend towards information storage in a more compact and robust, i.e. user-friendly, form. Accordingly, recent years have seen a broadly based advance in the development of appropriate materials, which has led to the initial marketing of optical data memories.

The present paper is concerned with the development of materials for optical data storage and gives special consideration to systems which can be applied on a technical scale and which are of commercial interest. An introduction to the most important concepts and processes will be followed by a discussion of the principles of Compact Disc and CD-ROM (*C*ompact *D*isc *R*ead *O*nly *M*emory) technology. The broad principles of optical readout and of the production of polymer storage discs with impressed information will be summarized in Section 3. Sections 4 and 5 give an overview of the most important materials and their properties for write-once (*W*rite *O*nce *R*ead *M*any, WORM) and erasable (*E*rasable *D*irect *R*ead *A*fter *W*rite, EDRAW) storage media. The main items covered are organic dyes for WORM systems and alloys of rare earth elements and transition metals for EDRAW systems.

There will be no discussion of metal coatings for WORM memories. More extensive references deal with compact disc and CD-ROM memories[1-5, 7] and with general aspects of optical memories,[5c] applications for optical data stores[8] and recording media for WORM and EDRAW memories.[6, 9-18]

2. Optical Memories

Audio and video CDs are optical memories which are based on a principle similar to that of gramophone records: information items are encoded in a structural pattern, from which the original information can be regained by means of a playback unit. In contrast to gramophone records, the readout takes place by a noncontact method using laser light. The information is impressed into a plastic plate and cannot be altered. CDs have meanwhile been used for other fields of application as well, outside the field of consumer electronics. The term CD-ROM has established widespread usage in connection with this type of information storage. This term signifies Compact Disk Read Only Memory (Data disk with k, in contrast to the audio/video disc with c). Write-once optical memories are designated as WORM systems. In contrast to the CD-ROM, it is possible for the user to record information. The principle of all WORM memories is based on an irreversible physical transformation of the recording medium, which is initiated by the irradiation of laser light. The following processes have been described:[5] formation of pits, bubbles, bumps, changes to the surface texture, phase change, switching of liquid-crystal phases, alloying of metal films and photochromic color change. In most cases, the reflectivity of the recording medium is altered by the marking process. This takes place locally at positions heated by the laser beam so that data spots are created, which are distinguished from the surrounding medium by their reflectivity. The physical marking process of EDRAW media is reversible, and thus enables the user to erase data which have been inscribed. EDRAW memories have been developed on the basis of magneto-optical materials, reversible phase transformations and photochromic dyes. In the first case, use is made of the magneto-optical effect: the rotation of the plane of polarization on reflection or transmission of laser light on or through magnetized material, in order to detect magnetic domains as data spots. The reversible phase change between crystalline and amorphous phases leads to an alteration of the reflectivity of the storage medium. The photochromic effect permits the marking of data on the basis of the differing absorption of a tautomeric dye molecule. Thus, in contrast to the two previously described storage methods, photochromic systems require the use of two laser sources. In addition, there exists a series of other reversible storage processes to which no technical significance is yet, however, ascribed.

The development of optical data storage is closely connected with the progress made in microelectronics. This applies both to the production of semiconductor lasers and also to the entire process technology which is necessary in order to produce structures in the μm range. The photoresists used for this purpose were primarily developed for the semiconductor industry, as were numerous vacuum coating processes for the preparation of metallic films. Accordingly, it was possible to use the know-how in vacuum technology for the construction of appropriate production plants for optical storage disks (Fig. 2).



Fig. 2. Vacuum coating machine for the production of magneto-optic disks. To reach the required clean room conditions the room is air conditioned with laminar flowing air, which is fed in through a filter in the roof and out through a floor grating.

The problems which are connected with particle contamination and its effect on production output are common to both the production of optical storage disks and the semiconductor industry. Both cases require processes with ex-

tremely stringent purity demands and acceptable particulate concentration tolerances.

3. Compact Disc Technology (CD-ROM)

Not only has CD-ROM technology laid the foundations, in terms of process technology, for optical information storage it has in addition stimulated the development of other storage systems (WORM, EDRAW) which are advanced and therefore in many ways significant for the future. The key to all optical processes resides in the availability of suitable radiation sources which, for mass production, must above all be small and cheap. With this background, it was the progress made in laser technology which, together with the development of semiconductor lasers, fulfilled all prerequisites for the successful marketing of optical storage systems. The experience gained from microelectronics made it possible to achieve miniaturization and the availability of a process technology for lasers which are suitable in terms of quality and price. A point of prime importance in the technology for the production of compact discs is the multiplication of the original information, in a manner similar to that used in the stamping of gramophone records. In the case of the CD, however, the size of the impressed structures—which is 0.5 to 2 μm—is several orders of magnitude smaller than those of a gramophone record. In order to produce corresponding dies and to use them in special injection molding processes, it was therefore necessary to find appropriate techniques which could be developed so as to include methods and materials known in the semiconductor industry. The outstanding quality of reproduction, which is highly important to the purchasers, and the decreasing cost have helped this new technology to achieve great market successes, especially in the audio sector.

This is not yet true of the CD-ROM data disk, which can store up to 650 Mbytes of information. A whole series of data banks are supplied in the form of CD-ROM disks, but in many cases there is no compatibility with the current operating systems and the standardization of interfaces and peripherals is proceeding only slowly. In spite of significant cost advantages (Fig. 3), certain technical problems such as,

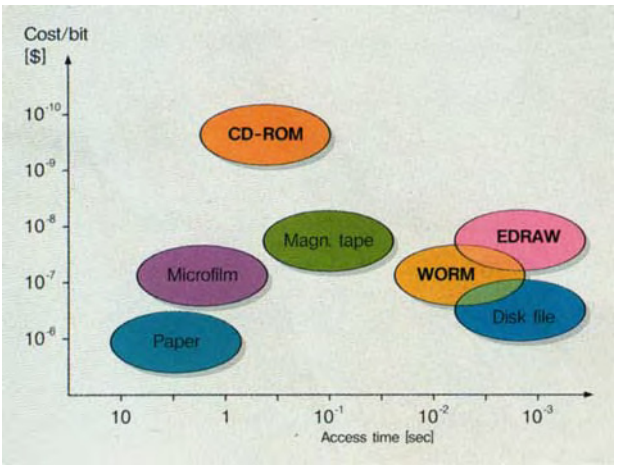


Fig. 3. Cost (US $) per bit and access times of classical and modern storage media [8e].

for example, the long access time of approximately 0.5 to 1 s, are still preventing widespread acceptance on the market.

Philips and Sony have initiated a joint project for the purpose of increasing the attractiveness of the data CD, and in 1987 specified the CD-I (Compact-Disk Interactive Media) in the so-called "Green Book" (forum for publication of standards). This amounts to a closed system which, using the multitasking operating system OS-9, is designed for microprocessors of the 68 family. As yet, there is no compatibility with MS-DOS. A further step in this direction is represented by the "Extended Architecture" which was first designed by Philips, Sony and Microsoft in August 1988 (CD-ROM XA). Using this system, it is also possible to use the data CD to store digital audio data and graphics in a similar manner as the CD-I is used but on a system-independent basis. While it is probable that new playback systems will be necessary for the CD-ROM XA, a different format can be operated with the CD players previously available: DVI (*D*igital *V*ideo *I*nteractive), which is based on a 100:1 data compression and decompression for digital video and should facilitate the PC-assisted processing of images. The beginnings of the technology of optical data storage go back as far as the late fifties; marketing in the form of the audio compact disc did not start until after 1982, as a result of the collaboration of Philips (basic research and disk development) and Sony (optics and playback unit). Following the immense market success of the new audio technology, several companies have become established as CD manufacturers, and joint efforts are meanwhile being made in the development of this technology by large companies: in 1985, Philips and DuPont founded PDO (*P*hilips *D*uPont *O*ptical), a joint venture company which is concerned with research and development of optical storage disks and which operates with Polygram (Hannover, FRG), the largest CD production site in the world.

The progress made in laser technology was tremendously important for the development of optical data storage. The first CD players were, in some cases, still operated using He-Ne or argon ion lasers. Since that time, all players have been equipped with semiconductor lasers, which can be produced inexpensively and in a more compact form. The widespread technical use of semiconductor lasers (emission wavelength ca. 780–840 nm) became possible only with their continuous operation at room temperature and long service lives.[19] To this end, it was necessary to reduce the threshold current of the lasers: the electrical power which is expended until the laser threshold is reached is lost in the form of heat and rapidly leads to the destruction of the optical system. The availability of appropriate semiconductor materials and the progress which has been made in the field of production engineering have created a situation in which semiconductor lasers can nowadays be supplied at very favorable prices (ca. US $ 3 each).

3.1. Digital Data Storage and Reproduction

Audio CDs and video CDs contain data in digitalized form which are read by means of a playback system (CD player consisting of disk drive and optical system) and are transmitted via analog-digital conversion to the output unit (loudspeaker and/or screen). The information carriers are

pits which are impressed into the surface of a plastic disk and are separated by the relief positions, the land (Fig. 4a). The pits, which are arranged in sequence and which have a depth of approximately 0.5 μm and a width of 0.8 μm, form tracks at a spacing of approximately 1.6 μm.[3,4] The disk consists of an injection-molded polycarbonate or polymethyl methacrylate substrate (diameter 12 cm) and is coated on the information-carrier side with a highly reflective aluminum film, which is protected against mechanical damage by a polymer layer.

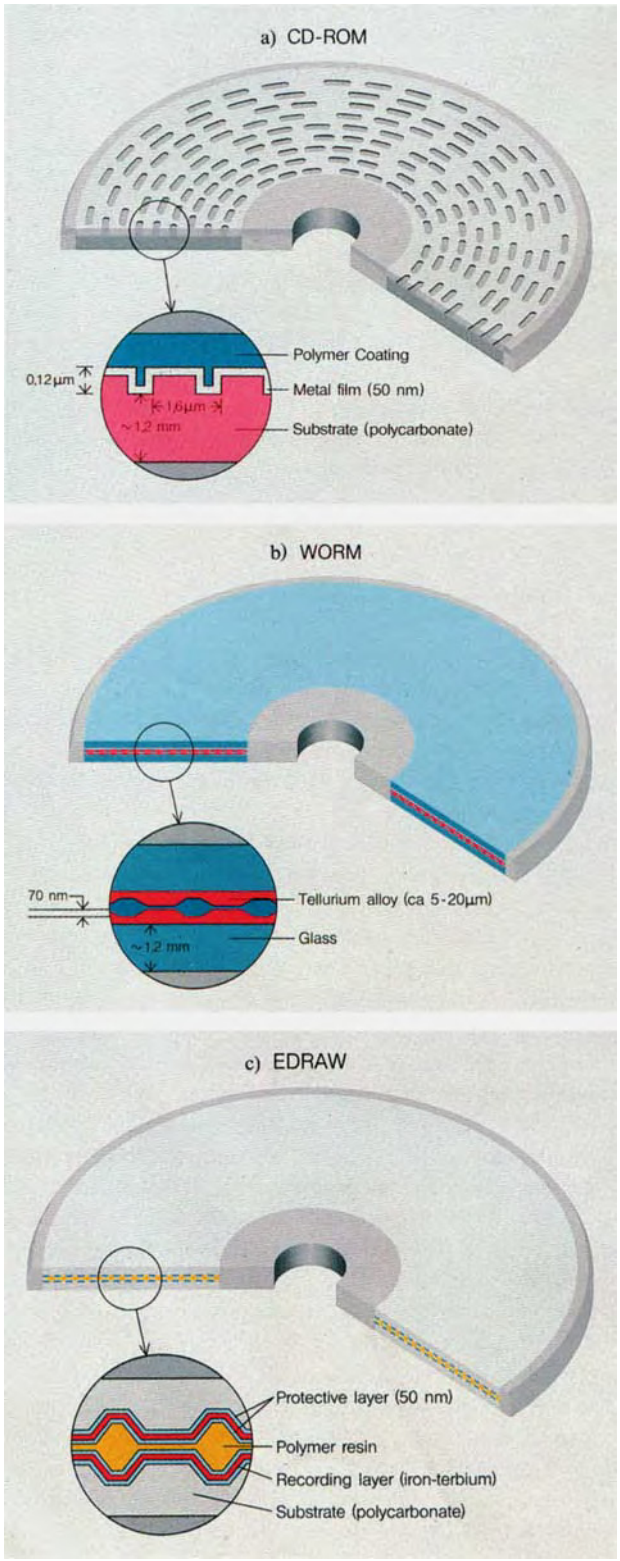


Fig. 4. Schematic representation of the construction of optical disks. a) CD-ROM disk. b) WORM disk as air-sandwich construction with a tellurium alloy as recording layer. c) EDRAW disk as three layer construction with a magneto-optic terbium-iron alloy as storage layer.

The playback unit includes an optical system which is located on a pivotable arm and is tracked to follow the pit track. The optical system focuses the light beam of the laser through the substrate onto the plane of the pits; the beam has a diameter of approximately 1 μm on the disk. The light reflected by the aluminum mirror is passed to a photodetector. When a pit is swept over, the signal intensity of the laser beam decreases significantly since the light is scattered by the pit structures. The optimal reflection conditions are on the land situated between the pits. In this way, it is possible to read binary data which are encoded in accordance with specified algorithms: reflection results in a high signal intensity and is recorded for example as 1; a signal intensity which is reduced by scattering represents 0.

The binary data form of the analog original sound recording is obtained by a frequency-dependent recording in audio channels: the signal level of each channel is given as a binary code word of 16 bits, to which error correction processing bits are also added. This gives rise to a bit stream encoding the sound recording. On playback of a CD disk, the decoding of the square-wave signal takes place in the electronic system of the recorder. Using electronic filters, the bit stream is broken down into the individual signals for sound (audio CD) and also for picture and color (video CD). In the case of a video CD, the picture is encoded by means of the spatial frequency of the pits along the track, while color and sound are encoded by modulation of the ratio of pit length to repetition rate. The signal fulfills additional functions which are essential for the recorder to operate properly. Disk rotation speed as well as focusing and tracking of the laser beam must be measured continuously and, where appropriate, automatically readjusted.[20] These servo functions avoid situations in which the laser beam, for example, "deviates" on the disk, jumps between pit tracks or "overlooks" pits. By means of special photodetectors, consisting of four subquadrants and each delivering a respective signal, several signals are generated electronically from the intensity/time progression of a laser beam, and these signals are available for servo functions. Another possibility consists in three beams being produced optically from a laser source, and then being used to scan the disk surface. These three additional signals are thus available for adjusting the optical system and the disk. Finally, it is necessary to constantly regulate the intensity of the laser light in order to maintain the optimal signal-to-noise ratio, and thus to obtain the same conditions for reading the information when the disk is played back at any position.

The compact disc system developed by Philips and Sony has meanwhile become a world standard, and has been licensed to many other companies. There are as yet no standardized formats for the WORM and EDRAW data disks. This applies both to the disk construction and to the write/read unit. One construction for the WORM data disk and one for the EDRAW data disk are shown in Figures 4b and 4c respectively. These represent some of the numerous systems which are currently at the development stage.

As far as the data disks are concerned, the main difference from the CD format is that the substrates are provided with one or more guide tracks which, using a laser beam, permit

orientation on the initially uninscribed disk. The impressing of the guide track, also referred to as a groove or track, creates elevated regions to receive the data markings. A series of possible formats are distinguished according to the mode of rotation of the disk and the form of the guide track:[3, 4] CLV (*C*onstant *L*inear *V*elocity), CAV (*C*onstant *A*ngular *V*elocity), spiral and concentric track arrangement. Where the speed of rotation of the disk is constant (CAV), the disk has linear speeds which are different inside and outside, and the data markings are larger outside than inside. Constant pit size requires constant linear velocity, and in this case the speed of rotation must be regulated as a function of the radius. For orientation purposes, marks are used within the guide track system, which divide the disk into sectors. If the marks are set at constant intervals beside a spiral track, this is referred to as the "sampled servo" format. In the continuous composite format tracking is achieved by direct evaluation of the signal reflected from the tracks. Due to the division of the CDs into sectors, the data file can be stored in a similar way to that applicable with the magnetic disk memories, not only on a serial basis but also in a dispersed configuration (sector offset with interleave factors). The format of a disk controls the maximum attainable storage density, so that the storage density is increased by appropriate changes to the formatting. For this purpose, it is, e.g., possible to write data directly by using track grooves. The second-order reflected beam then reproduces the information from only one side of the groove.[21]

The air-sandwich design (Philips) is shown in Figure 4b[22a] as an example of the design of a write-once data disk. The recording layer, a tellurium alloy, is coated onto the substrate which is provided with track grooves. Using appropriately dimensioned spacers at the center of the disk and at the edge of the disk, the size of the air gap is regulated when two disks are welded together. The composition of the gas in the gap can be chosen so that the air-sensitive layers are protected. However, it is still possible for the recording layer to be subjected to attack as a consequence of failures in the sealing of the disk construction; accordingly, in another design the air gap is filled with an inert polymer mixture.[22b] In addition to the direct coating of the substrate disk with a light-sensitive write layer, it is also possible to apply the information layer to a flexible fabric which is firmly clamped in a suitable disk construction (*S*ealed *D*isk *A*ssembly, SDA; Kodak).[22c] When data disks rotate (approximately 1800 rpm), in some cases relatively large forces act, and these have the effect of bending the flat substrate (radial run out); this can lead to difficulties in focusing and tracking the laser beam (cross talk). Thus, the suspension of a light-sensitive lightweight layer achieves the greatest possible mechanical decoupling between disk and layer.

The construction of magneto-optical storage systems[23, 24] (EDRAW, see Fig. 4c) is similar to that of WORM disks. A recording film made from rare earth elements and transition metals is located on a substrate provided with track grooves, between two protective layers consisting of amorphous silicon nitride or aluminum nitride. Encapsulation is necessary for the purpose of protecting the storage medium from oxidation. A polymer adhesive is applied to the outer protective layer in order to produce, by combination with a further substrate, a disk which can be inscribed on both sides. In addition to the protective function, amorphous nitride films also have the function of effecting the coupling-in and coupling-out of the laser light for optical writing, reading and erasure.

In the case of magneto-optical memories, two disk formats are currently under development: 3.5″ (approximately 130 MByte) and 5.25″ disks (approximately 300 MByte). The two formats will probably be used for different markets. 3.5″ disks and disk drives could be used for personal computers. The optical storage disk can fulfill two functions at the same time which previously would still have required separate components: the hard disk function as mass memory and the floppy disk function as exchangeable data file. The 5.25″ system will mainly be used for data archiving and data exchange at very high data rates.

In the case of the optical WORM and EDRAW systems, the operations of data encoding and decoding correspond to a large extent to the principles applied in magnet technology. Accordingly, in the field of computer operating systems it is necessary to make changes on introducing the optical storage technique only insofar as they relate to the matching of the interfaces to the optical disk drive. All data disk systems which are currently exhibited are to a large extent compatible with existing systems.

3.2. Production of Substrates

One of the prerequisites for the acceptance of new mass-produced products is high quality production, as well as high output in short periods of time at the lowest prices possible. Accordingly, the development of CD disk production was pursued, from the outset, with particular regard to these conditions, and has made a contribution to the success and commercial attractiveness of the CD technology.

There are essentially three processes for the multiple production of flat molded components: stamping, injection molding and injection stamping. The first represents a process which is widely used in the gramophone record industry, but which is not suitable for use in CD production since the requirements as regards dimensions and mold tolerances are more stringent by an order of magnitude (the submicron range). Injection molding and injection stamping can be used to achieve the desired structural interrelationships, injection stamping representing the most demanding technique. Both processes are used in the production of CD audio and video discs and in the production of substrates for WORM and EDRAW disks. The production is divided into the fabrication of the master and the preparation of substrates. Injection-molding dies are cast in a multistage process (mastering)[28, 30] which involves the latest technologies of microelectronics (Fig. 5). The mastering process begins with the cleaning and polishing of a glass disk which is required to construct the master. An adhering layer is applied by vapor deposition using an agent creating water-repellent properties, e.g. hexamethyldisilazane (HMDS), which coats the surface with a positive photoresist. The surface is exposed to a UV argon ion laser, which inscribes the pit structure in accordance with the digital information as played back from the master magnetic tape.[25] During subsequent development the exposed resist is dissolved away. At this stage it is

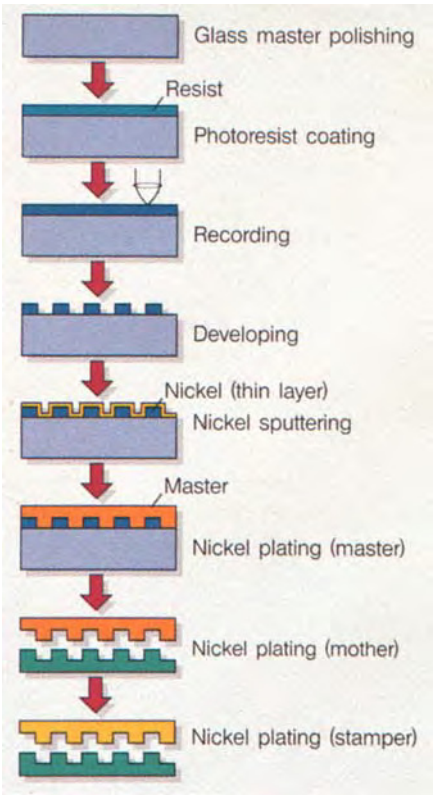


Fig. 5. Mastering process of the stamper for the injection molding optical disk. [30]

necessary to precisely control the development process since the geometry of the pits is influenced unfavorably by underdevelopment or over-development; this also applies, in the same way, to the imaging of the track guide grooves in WORM and EDRAW mastering.[29] The photoresist and the glass surface are then coated with a layer of metal (nickel in most cases) approximately 50–100 nm, either by vacuum vapor deposition or by sputtering. In this way, the master surface can be visually monitored before further processing and can be directly played back in a disk drive; an initial quality control is possible by comparing master and the master magnetic tape.

Further metallic layering to form the actual metal master is carried out using a currentless or electrolytic process.[26] After separating the master from the glass base, parent masters are produced by electroplating, and the individual injection-molding masters are formed from these parent masters by means of a second electroplating operation. By setting up such a "family of masters", it is possible to prepare new ones immediately without repeating the costly mastering process.[26] The mastering process specifies the quality of the finished disk, and accordingly numerous attempts have been made to improve critical process steps.[31]

Within narrow tolerances, the substrate materials for optical data storage systems must exhibit properties which are mainly determined by the nature of the data storage and reproduction. In most cases, the information is read through the disk, i.e. the laser beam must pass through the substrate material without loss of intensity and—in the particular case of magneto-optical systems—without change of polarization. This requires a substrate material of high optical homogeneity, purity and optical transmission and low birefringence. Bubbles, gel particles, inclusions, surface defects, and zones of turbidity due to impurities can give rise to scattering and absorption effects which cannot be compensated by the servo functions of the electronic and optical systems. Significant properties of the disk materials with regard to mechanics, optics, environment and productivity are represented in Figure 6 for polycarbonate (PC), polymethyl methacrylate (PMMA), polycarbonate–polystyrene blend (PC/PST) and

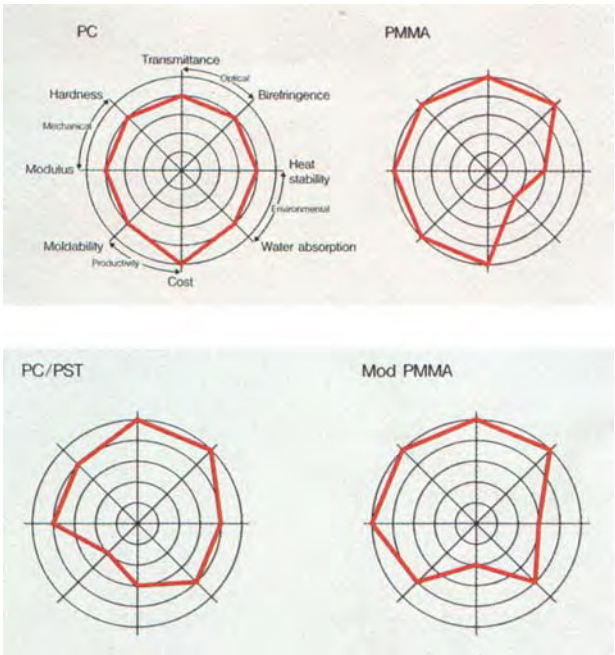


Fig. 6. Properties of polymeric substrate materials [32]. Parameters are represented regarding optical, mechanical and environmental properties and productivity of polycarbonate, polymethyl methacrylate, polycarbonate-polystyrene blend and modified polymethyl methacrylate. The performance of a polymer improves from the inner to the outer circle.

modified polymethyl methacrylate (Mod. PMMA).[32] A further criterion for the selection of a substrate material is its absorption of water, since swelling and thus distortion of the disks can arise as a result of water vapor. The sensitivity to moisture of certain recording media is very great, so that the water absorption of the substrate may be the limiting factor with respect to its use.[33] The severity of this problem may be reduced by the use of protective layers; however, it can represent a latent uncertainty regarding the long-term stability of data archives. It is possible to measure such effects quite well by accelerated storage tests; the manufacturers give their guarantees on the basis of these tests (required long-term stability: 10 years).

The birefringence of the flat polymer disks must be as small as possible; for example, it is specified at ± 50 nm for the Compact Disc. Birefringence occurs where a light wave in a medium propagates at differing velocity.[36, 37] Prerequisite for this is an anisotropic polarizability of the medium. In the case of a polycarbonate, this preferred direction of the polarizability is parallel to the polymer chain. Accordingly, the resultant birefringence is referred to as orientation birefringence. When forces act on a molded component of polycarbonate the birefringence alters in consequence of the movement of chain segments. In the course of the production

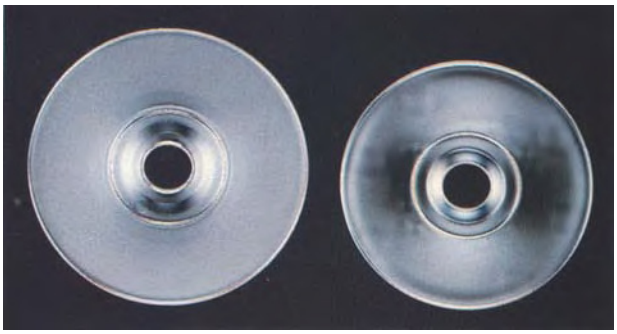


Fig. 7. Birefringence of injection molded polycarbonate substrates. The left disk fulfills the specification for an optical disk, the right disk is useless because of inhomogeneities.

process, for example by injection molding, it is possible for deformations to be frozen in as internal stresses. The resulting stress birefringence remains operative at room temperature; it may decrease or entirely disappear only at higher temperatures and on reaching the glass point.[34] The process of molding storage disks must accordingly be adapted to the specific birefringence properties of the polymer; in addition to this, it is necessary to include the effects of other production steps. The uniformity of the birefringence of disks can easily be monitored visually, for example, by placing substrates between two polarizing foils (Fig. 7). Reduction of the birefringence of substrate disks may be achieved by the use of polymer blends which consist of polymers having different anisotropic polarizabilities. Thus polycarbonate/polystyrene,[39] polyphenylene ether/polystyrene,[27] polymethyl methacrylate/polyvinylidene fluoride[38] and polymethyl methacrylate/polyvinyl chloride[39] blends can be prepared which are suitable for the production of disks. New types of polymers such as cyclic polyolefins, compounds with very low water absorption, are now being used for the production of substrates.

Instead of using injection molding or injection stamping, it is also possible to produce CD disks by a process developed by Philips (Fig. 8).[30, 40–43] In this "2P Process" (*photopolymerization*) a base plate is fixed at a defined spacing on a nickel stamper and the gap is filled with a photopolymerizable mixture. The mass is hardened by means of UV radiation and removed from the stamper together with the base plate as a completely structured disk. An advantageous feature of this process is the precise structural imaging, since the curable mixture can flow into every fine pit of the stamper. This process may be carried out using simple devices, and the quality of the raw liquid material is controlled at low costs. Moreover, the wear and tear of the stamper in this pressureless technique is considerably less than in other processes, whereby additional costs can be saved. The photopolymerizable mixture is composed, for example, of ethylene acrylates or ethylene methacrylates and photoinitiators.[35]

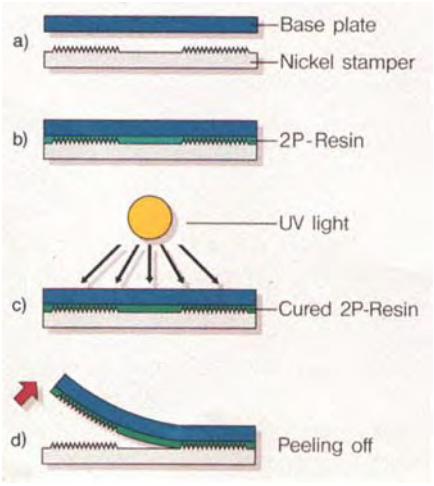


Fig. 8. 2P process for disc replication (2P = photopolymerization). [30] a) Production of plate and stamper. b) Filling with 2P polymer. c) Photopolymerisation. d) Separation of disk from stamper.

The problems associated with this process reside in long exposure times involved in the photopolymerization. The cycle times of injection molding machines are in the region of five seconds for the molding of a disk, but the UV curing of a mixture demands considerable optimization to achieve exposure times of similar brevity. Monomers and photoinitiators must virtually be 100% consumed in order to eliminate subsequent complications by diffusion into the storage medium. In the course of polymerization, a decrease in volume usually takes place as a result of the combination of the monomers, and the molded component shrinks accordingly. In the case of the 2P process a considerable proportion of the process-technology know-how is specifically based on keeping the volume shrinkage to a minimum.

4. Write-Once Storage Disks

The development work carried out on write-once optical storage disks has led to the first commercially available products which are marketed in combination with appropriate write/read systems. Write-once optical storage media are designated as WORM or DRAW (*D*irect *R*ead *A*fter *W*rite) systems; common to these is that they accept information from the user and can make this available again within short access times. WORM and DRAW systems differ from each other in that the latter can compare the stored with the specified information immediately after each inscription process, and thus correct readability is guaranteed.

A typical field of application for WORM memories is the archiving of data. Their objective is thus to replace the documentary or microfilm archiving which is customary nowadays in offices. With a diameter of 5.25 inches, commercially available storage disks offer a storage capacity of approximately 2×400 MBytes, which corresponds to the information content of approximately 150000 typed A4 pages. This mode of office filing, which is still unusual, will create new possibilities for information processing in view of the increase in direct electronic communication via telefax and electronic mail. Furthermore, write-once optical storage disks, just like CD-ROMs, may be used as data banks for reference works. In this case, the mixing of pictures, texts and data is possible. In addition, compact and fast-access "analog" image storage in the video field is also possible with these storage systems.[44]

While the advantages of write-once optical storage disks as compared with conventional filing (long access time, great

bulkiness, labor-intensive), microfilming (long access time, no freely selectable sorting facility, costly setting-up procedure) and storage by means of magnetic tapes (medium access time, inadequate data security, limited data service life) are clearly evident, they find in the magnetic disk systems, which are likewise under rapid development and which have exceptionally short access times, a genuine competition over which they have, to date, not yet been able to acquire precedence.

In order to compete against the magnetic storage technology, the following fundamental requirements must be placed on write-once optical storage disks: high storage capacity ($>10^8$ bit/cm^2), fast access times ($<10^{-2}$ s), low storage costs ($<10^{-7}$ DM/bit), high data service life (>10 years), high write sensitivity (<1 nJ/bit), reliable reproduction as a result of a high signal-to-noise ratio (>55 dB), low defect density ($<10^{-13}$ bit after correction) and easy handling of the entire system.

4.1. Principles of the Write/Read Mechanism

The selective, thermally induced and irreversible deformation, as well as the phase change of an active layer, the so-called recording layer, have become established as preferred methods for the inscription of write-once optical storage disks. In practice, radiation from semiconductor lasers having emission maxima between 780 and 840 nm is used. This absorption of energy results in a locally specific chemical-physical change of the active layer. As a result of this change, which is limited to a very small area and which is unambiguously defined, it is possible by means of a suitable reading mechanism to detect digital information and to convert it into a bit sequence.

The most widespread technique is based on an aperture-forming mechanism (ablative recording) (Fig. 9a). The active layer converts the closely concentrated irradiated laser light into thermal energy, which at approximately 1700 °C initiates complex physical processes.[45] This leads to the formation of a pit with the simultaneous localized alteration of the optical properties of the layer which are detected by means of the intensity variation of a weak laser beam. In order to convert the laser light into heat, the recording layer must consist of a material which absorbs radiation of the prescribed wavelength. Possible materials used are metals or amorphous dye films.

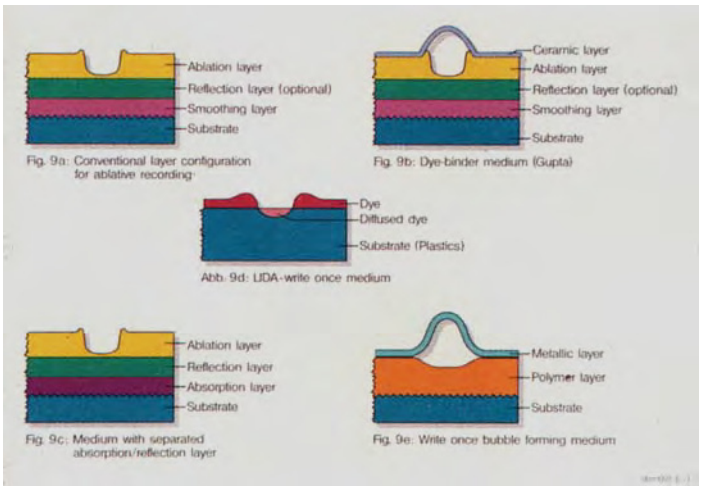


Fig. 9. Conventional layer configuration for ablative recording.

The basic structure of this type of write-once storage disks consists of a disk-shaped molded substrate unit, which is in most cases solid in structure and usually made of glass, aluminum, polymethyl methacrylate or polycarbonate. The recording layer is applied to this substrate unit and covered with a protective layer. Occasionally, an additional layer is introduced between substrate and recording medium; this improves the adhesion properties, reduces the microporosity of the substrate, and, where appropriate, prevents the diffusion of components of the active layer into the substrate. The microstructure of the substrate has a substantial influence on the background noise and thus on the quality of reproduction of a disk, which is characterized by the signal-to-noise ratio (SNR).

The active layer consists of a metallic or dye film, which has a thickness of approximately 50–200 Å and which, depending upon the material, is applied by sputtering, sublimation, or spin-coating from a solvent mixture, which is financially preferred but is only possible with soluble dye systems.[46] The long-term stability and optical constancy of pure dye films[47] is frequently limited as a result of agglomerate formation and the tendency to crystallize. These effects can be circumvented by using mixtures of the dyes with special polymers,[48] which not only considerably improve the stability of the recording layer but also the quality of the pit formation (dye-in-polymer (DIP) concept).[49] In addition to these, recording layers consisting of special polymer composites are also used.[50] *Gupta* modified the DIP configuration by applying a thin transparent ceramic layer to the recording layer[51] (Fig. 9b). In the course of the writing process, a pit is formed in the active layer and gas is evolved. The ceramic layer is likewise heated and bows as a result of the internal pressure generated in the pit. The bubble formed above the pit leads to a unification of the pit geometry and the still intact ceramic layer prevents thermally induced ejection of material. Both effects result in an outstanding signal-to-noise ratio of the medium (>65 dB).

Another variant consists in a separation of the functions of the recording layer into an absorption layer and a film forming pits (Fig. 9c).[52] This arrangement permits a fine optimization of the respective layer with regard to its specific task. A disadvantage of these multi-layer variants is that the additional layers lead to an increase in the layer defects and thus an increased bit error rate (BER) and rejection rate.

The LIDA concept (*L*aser *I*nduced *D*ye *A*mplification)[53] is based on the diffusion—brought about by laser light and thermally induced—of a dye into the substrate polymer (Fig. 9d). The resulting difference in the optical properties between pure dye film and molecularly dispersed dye is used for signal differentiation.[54]

Alternatively, it is possible to apply a temperature-sensitive layer beneath a metallic absorbing layer which is irreversibly expanded by the irradiation, for example by the evolution of a gas, and thus leads to bubble formation[55] (Fig. 9e). The altered light scattering of the reading beam is produced by the deformation of the film surface. A write-once storage disk using this arrangement has been exhibited by Thomson CSF under the designation of Gigadisk.

The formation of pits or bubbles has the effect of altering various optical properties of the recording layer, e.g. extinction, transmission, reflection or light scattering. In most cases, the readout of the information takes place by the write laser operating with relatively low radiative power, or occasionally by a read laser emitting at a different wavelength. In order to be able to inscribe and to read an optical storage disk on both sides, use is made of the altered reflection behavior of the active layer. The signal contrast can be considerably improved by the use of an additional thin, metallic reflective layer beneath the active layer. The mechanisms of pit and bubble formation in the active layer have been intensively investigated; the initial studies date back to *Mayden*[56] and *Kivits* et al.[57], who used thin tellurium films. According to *Kivits* et al.[58], the pit formation takes place in several stages. When the laser pulse strikes the metal foil, optical energy is converted into thermal energy; and within the narrowly defined irradiation region, temperatures are reached which are close to the boiling point of the metal. The duration of the absorption of energy during the laser pulse is so short that it is not possible for any thermal equilibria to become operative (superheating). The temperature profile occurring in the molten metal leads to surface tension gradients (Marangoni effect),[45,49b] as well as inhomogeneous pressure, bubble formation, and vaporization zones which lead to flow of the material and thereafter to a local broadening of the active layer with pit formation. As a result of the rapid cooling of the material after termination of the laser pulse this condition is frozen in, and the pit and edge geometry is determined. Comparable interrelationships may also be utilized regarding the pit formation in active layers based on organic materials.[15,45,49b] The dye molecules which undergo electron excitation upon irradiation convert the absorbed energy into vibrational, translational and rotational energy, resulting in thermal energy. On account of the low thermal conductivity of organic compounds, the heating is limited to a narrow local region. This heating leads to melting and vaporization or even decomposition of the molecule. The pit formation in organic materials is discussed controversially and is associated with thermally induced surface tension and melt viscosity phenomena,[59] the optical density of the recording layer[60] or the rheological properties of the active layer.[61]

In this case, it is necessary to find a compromise between film thickness and dye loading on the one hand and pit formation on the other, since the growth increases the absorption capacity, but in order to form pits, more material has to be discarded.

As compared with metal films, recording layers containing organic dyes which absorb IR radiation have numerous advantages, such as an increased resistance to atmospheric influences and lower toxicity.[13,15] In addition to this, especially in the DIP configuration, they combine high physicochemical stability, low thermal conductivity and relatively low melting or sublimation temperatures.

4.2. Dye Systems and Dye/Polymer Systems

The traditional task of dyes consisted in generating the coloration of requisites found in daily life. Consequently, the efforts put into their synthesis in the past were in particular directed towards providing dyes having absorption maxima in the visible range, i.e. between 420 and 700 nm, while dyes for absorption in the near infrared (NIR range) became of technical interest only with the advent of infrared photography. Accordingly, it is no surprise that virtually all dyes manufactured on a large industrial scale are of no interest for the purposes of optical data storage, since they exhibit no or only slight absorptions in the NIR range, while these absorptions are necessary when using diode lasers to achieve the pit formation temperatures in the write process and signal contrast levels in the readout process. However, considerable progress has been made in the meantime specifically in the synthesis of NIR-sensitive dyes.

If dyes are used as absorbers in write-once disks, then the following general requirements must be met: high absorption capacity for semiconductor laser radiation (780–840 nm), in order to require low write energies; a commensurate threshold value, which permits a distinction between the write and read process at the same wavelength; low thermal conductivity in order to achieve pits of sharply defined shape; good film formation; high stability in relation to light, heat and moisture; low toxicity; high thermal stability (for sublimates).

Depending upon their structure, dyes may be applied to a substrate by sublimation or spin-coating. Thus, without reference to the material concerned, it may be stated that according to the hitherto published results systems which have been applied by sublimation are superior to spin-coated dye solutions as regards stability towards atmospheric effects and the quality of pit formation, but are inferior in terms of signal-to-noise ratio. With frequent reading, the latter is caused by sublimation and leads, as a result of deposits, to a surface roughness which reduces the uniformity of the reflectivity of the layer.

4.3. Dyes for WORM Memories

The initial investigations on write-once disks based on dyes were carried out using non-directly-modulable gas lasers, for example argon ion lasers emitting at 488 nm, owing to the lack of NIR-sensitive dyes. Even at that time, the benefit of this technology became known and was protected under patent law. The dyes which were used included azo dyes,[62] ketocoumarins,[49b] quinones,[53b] fluorescein,[63] polyester yellow,[48,49a,60] or diethoxythioindigo.[64] Phthalocyanines,[65] naphthoquinones,[66] simple squarylium[67] and cyanine dyes[68] or triarylmethane dyes[69] proved to be suitable for recording information by means of helium–neon lasers (633 nm). The practical significance of these storage media is slight. Nevertheless, it should not be overlooked that it is possible to achieve a reduction of the pit geometry and thus, in principle, a higher storage density of the disk by light of shorter wavelength. The first paper which described the use of semiconductor lasers as write lasers was published in 1981 by *Jipson* and *Jones* (IBM).[47a] They used a hydroxysquarylium derivative (Fig. 10) as the recording layer, which was applied to the substrate by sublimation. This compound has good thermal and optical stability prop-

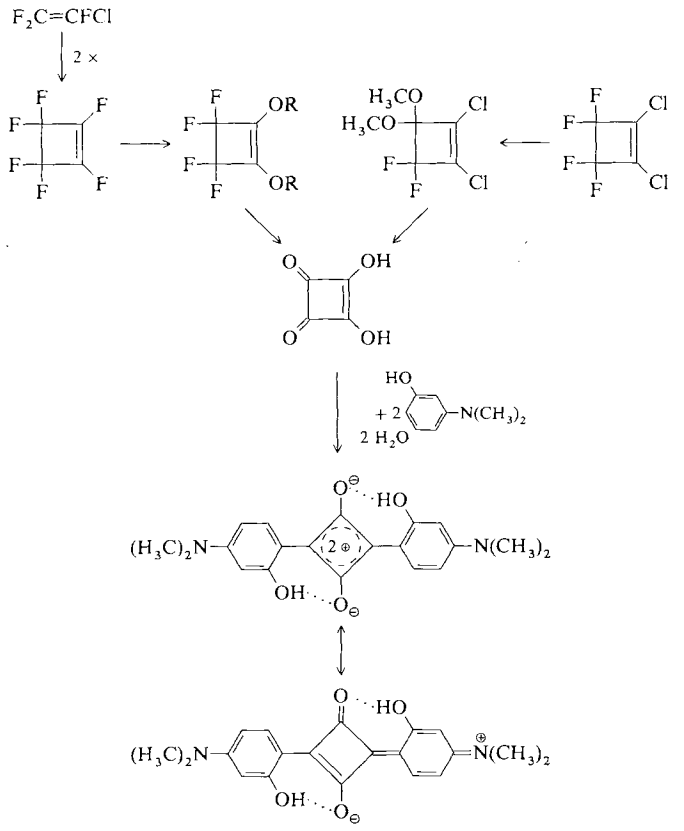


Fig. 10. Syntheses for squaric acid and a hydroxysquarylium derivative.

erties. The pit formation proceeded in a reproducible manner and is ascribed to pure sublimation processes.

However, such films are unsuitable for practical application since the sensitivity in the NIR range proved to be too low and the long-term stability proved to be inadequate in consequence of the tendency towards crystallization. In addition to this, the dye film did not demonstrate any threshold value for pit formation, as a result of which, following frequent read out, a loss of the data was observed. Similar results have been reported by *Kivits* et al.,[70] who used recording layers consisting of vanadylphthalocyanine. The number of NIR-sensitive dyes has greatly increased during recent years. In practical terms, four categories of dyes have, in particular, achieved significance: 1. methine dyes, 2. phthalocyanine derivatives, 3. specific condensed arenes, and 4. metal complexes. There are also many other examples of dyes which do not fall into this subclassification; some of these will be outlined after the discussion of the four classes of substances.

4.3.1. Methine Derivatives

The first compounds of this category to be investigated were heptamethine cyanines, with benzoxazole, benzothiazole, (benzoannelated) indole or quinoline moieties as terminal groups.[71] In addition to having high absorption coefficients, these compounds exhibit excellent reflection properties (up to 40% at 800 nm) and thus yield materials with good SNR values and high signal contrast. Indole derivatives are particularly preferred on account of their favorable solubility properties.[71a-d] Cyanine dye films are almost exclusively produced by application from solution. In order to coat the substrate with the dye, the latter must be soluble in solvents which do not attack the substrate material. Propanol, ethyl acetate and—less preferred—acetonitrile have proven to be suitable solvents. While the absorption maxima of the monomeric methine dyes in solution are relatively sharply localized, the half-width of the signals becomes broader in a polymer matrix with the formation of new maxima. This broadening of the signal is ascribed to dye aggregation.[54a, 72] The following properties distinguish the methine dyes as absorbers for write-once disks: they have a high molar extinction coefficient and require only small energies to form sharp and intense pits (approximately 0.5 nJ/pit), and a favorable signal-to-noise ratio results from the high reflectivity (> 30%). Methine dyes are photooxidized by singlet oxygen in the presence of light. The reaction is bimolecular and proceeds under unsensitized conditions relatively slowly on account of small quantum yields; however, it is accelerated by suitable sensitizers. The rate of decomposition increases with increasing methine chain length, and may be influenced by substituents in the heterocycle. The photodecomposition begins with 1,2-addition of $^1O_2$ to an exocyclic CC double bond.[73]

An increase in the stability may be achieved by the introduction of electron-withdrawing substituents, for example halogens or cyano groups, as a result of which a slight bathochromic shift of the absorption maximum takes place in consequence of a reduction of the LUMO (*L*owest *U*noccupied *M*olecular *O*rbital).[74] There are other possibilities for stabilization by introduction of a cyclic unit (Fig. 11) into the methine group.[75] It has been shown that particularly

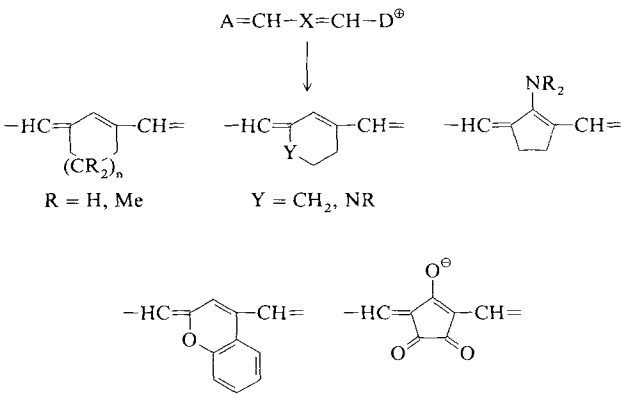


Fig. 11. Stabilization of methine dyes sensitive to oxidation by introduction of cyclic moieties. A = acceptor, D = donor.

suitable compounds are those derivatives which contain squarylium[76] or croconium groups[77] like those shown in Figure 11 (bottom right) in the methine chain. These have been combined with the most widely varying terminal groups such as azulenium,[78] pyrylium,[79] benzo or naphthothiapyrylium,[80] naphtholactam[81] or oxoindolizine heterocycles.[82] Furthermore, storage media consisting of polymeric cyanine derivatives[83] or of tetra(dialkylaminophenyl)cyanines[84] have been proposed. The latter exhibit good solubility properties, but are inferior to the cyanines in their optical properties. However, they are more stable towards

singlet oxygen, and the addition of radical traps increases their stability.

The sensitivity to oxidation of the above indicated methine dyes may also be reduced by the addition of an oxygen trap.[85] Examples of suitable compounds are dithiolato complexes of platinum, cobalt and nickel[86] (see also Section 4.3.4) or aminium derivatives,[87] which can be obtained as salts. They are added to the mixture or directly attached to the dye.[88] Alternatively, salts with a cyanine dye as a cation and a radical trap as an anion can be used, e.g. a dithiolato derivative. These salts tend to be highly stable.[89]

A particularly intensively investigated group of methine dye derivatives comprises the squarylium dyes, which have been developed by Philips and Kodak.[84d, 84e] The compound SQS (Fig. 12) which forms an inner salt can be spin-

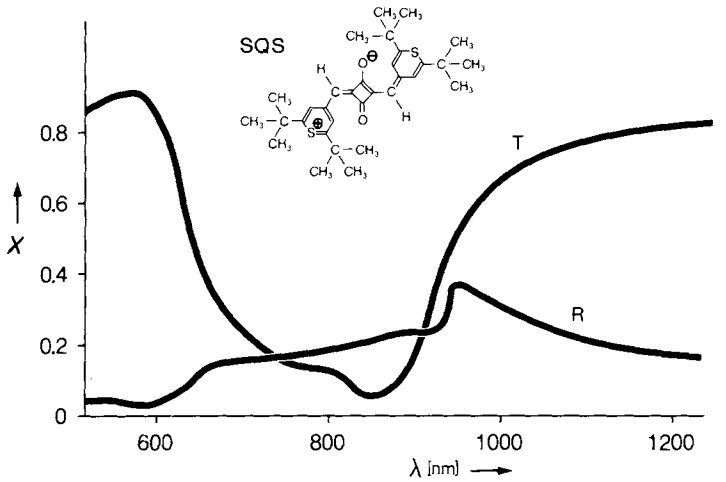


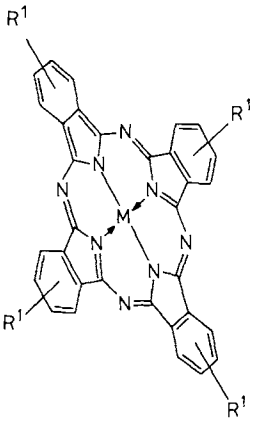
Fig. 12. Transmission (T) and reflection (R) spectra of a 90 nm thick film of the squarylium dye SQS suitable for a WORM medium. X = relative transmission or reflection [84d].

coated as a dye solution (approximately 50 g/L *n*-propanol), on account of the *tert*-butyl groups which increase the solubility. At 800 nm (Kr ion laser), an SQS film having a thickness of 90 nm reflects approximately 20%, and transmits approximately 10% (Fig. 12). Transmission and reflection are functions of the layer thickness; transmission decreases exponentially with layer thickness, while reflections are at a maximum at approximately 90 nm layer thickness in the case of SQS dye. The signal-to-noise ratio is a function of the irradiated energy.

A decisive factor regarding the suitability as archiving material is the aging behavior of the dye layer. When stored for relatively long periods at 90 °C, pure SQS films tend to crystallize, leading to a change in the optical properties (e.g. doubling of transmission after 20 days at 90 °C). This can, however, be controlled by the addition of small quantities of a polymer. At room temperature, the pure film also exhibits virtually no change. In the Z/AD test (temperature change between 25 and 65 °C with relative atmospheric humidity of 93%), the transmission of SQS varies by a factor of 2 after 40 days. SQS is rather stable towards light; this was tested at 40 °C and 65% atmospheric humidity using white light having an intensity of 1000 $W m^{-2}$; the SQS films showed varying stabilities, depending upon the environment. While water and oxygen alone generated only very slight changes in the optical properties of the recording layer, in the presence of both water and oxygen peroxides were formed and relatively large changes were observed. A reading test using a commercial NIR write/read laser revealed that after 10^8 reading processes no change in the optical properties was detected provided that a certain energy threshold value was not exceeded.[84d, 84e, 90]

4.3.2. *Phthalocyanine Derivatives*

Phthalocyanine (H_2Pc), a tetraaza[18]annulene or tetrabenzotetraazaporphyrin,[91] has proven to be a useful dye for write-once optical storage disks. In $Pc^{2\ominus}$, four isoindole units are cyclically connected to one another by nitrogen bridges. The two protons of the metal-free substance may be replaced by numerous metal atoms (MPc)[92] with valency three or higher. In this case axial residues situated perpendic-



λ_{max} = 600–800 nm
M = $Cu^{2\oplus}$, $VO^{2\oplus}$, Al(OAlkyl)$^{2\oplus}$, Si(OAlkyl)$_2^{2\oplus}$, Ge(OAlkyl)$_2^{2\oplus}$
R^1 = H, 4F, OAlkyl, CH_2O-Alkyl

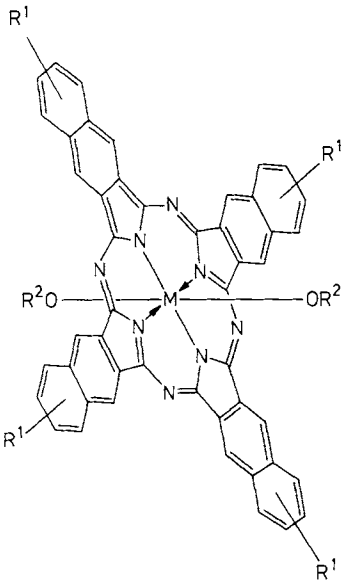
Fig. 13. Peripherally substituted phthalocyanine derivatives for WORM media.

ularly to the Pc plane can be introduced leading to a considerable improvement in the solubility of the virtually insoluble original substance[93] (Fig. 13). In the presence of peripheral substituents,[94, 95] the solubility in aqueous solutions or organic solvents is increased. Unsubstituted phthalocyanines (Pc) are easily synthesized in high yield and are compounds of high chemical stability. More important, phthalocyanines are attractive as optical recording media: they have high absorption coefficients $\varepsilon > 10^5$, they are thermally stable, they exhibit virtually no toxicity, they show an excellent stability towards atmospheric effects and they may be applied to the substrate by sublimation or, with appropriate substitution, by spin-coating. Their absorption properties are determined by the rigid, internal 18π electron system as a chromophore. They absorb especially well in the range of HeNe laser radiation (633 nm). In 1981, *Kivits* et al.[70] were the first to propose the use of phthalocyanines as absorbers in storage disks of the WORM type and to expand the range of spectral sensitivity of the particularly suitable vanadylphthalocyanine (VOPc), the absorption maximum

of which is at 730 nm, by thermal treatment;[96] this results in a broadening of the long-wavelength absorption band beyond 800 nm. Using this material, it became possible to produce a recording medium with a weak SNR with the use of a krypton laser (799 nm). A bathochromic shift and broadening of the longest-wavelength absorption maximum of phthalocyanines, e.g. in the case of MgPc, AlClPc, InClPc[97] or TiClPc,[98] may also be achieved by a THF or CH_2Cl_2 solvent or vapor treatment.

It is possible to achieve a bathochromic shift of the longest-wavelength absorption band by the use both of strongly electron-donating and -withdrawing substituents. Thus, in particular, hexadecafluoro derivatives of $Cu^{2\oplus}$, $Zn^{2\oplus}$, $Pb^{2\oplus}$ or $SnCl_2^{2\oplus}$ show high absorptions above 800 nm and are suitable for irradiation with semiconductor lasers.[99] Similar structural modifications, for example by the introduction of peripheral azo or thiol radicals, have been documented in numerous patent applications, predominantly by Japanese companies.[100]

Apart from these few exceptions, the influence of peripheral substituents on the absorption behavior proved to be minimal. However, if the conjugated system is enlarged by benzoannelation to give the naphthalocyanines (Nc) (Fig. 14), then a substantial bathochromic shift of the long-



λ_{max} = 720–820 nm
M = Si, Ge
R^1 = H, *t*-C_4H_9, $(OCH_2-CH_2)_n-O$Alkyl, COOAlkyl
R^2 = Si(Alkyl)$_3$, Si(Alkyl)$_2$–O–Alkyl

Fig. 14. Peripherally and axially substituted naphthalocyanine derivatives for WORM media.

wavelength absorption band may result. While the absorptions of the 1,2-naphthalic acid derivatives show, in this case, a slight bathochromic shift by 20 nm,[101] in the case of the 2,3-naphthalic acid derivatives shown in Figure 14 this effect is significantly more marked: displacements by more than 100 nm to 752 (PdNc) to 855 ($MnNc(OCOCH_3)$) have been observed.[102] However, by enlarging the π-system, the derivatives are less thermally stable and considerably difficult to synthesize.

The naphthalocyanines are even less soluble than the phthalocyanine compounds, and in most cases cannot be sublimed. In order to increase their range of application, soluble naphthalocyanine derivatives were therefore tested for their suitability as absorbers for write-once disks; this is possible, as with the MPc compounds, by peripheral or axial substitution. The solubility is increased by adding peripheral substituents, e.g. the bulky *tert*-butyl group.[103] Meanwhile, there have been reports of numerous naphthalocyanine derivatives which obtain their solubility by peripheral voluminous or long-chain alkyl radicals,[104] carboxylic acid esters of long-chain alcohols[105] or long-chain polyethers.[106]

The biaxial derivatives of silicon-naphthalocyanine ($SiNc^{2\oplus}$) (Fig. 15)[107] have been noted for their economical

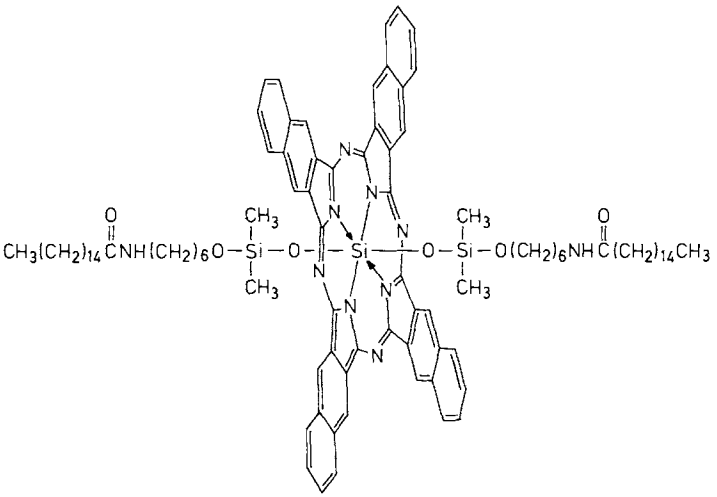


Fig. 15. Bisaxially substituted silicon-naphthalocyanine for WORM media.

synthetic properties as well as their outstanding optical properties. The axial substituents can be selected so that they guarantee adequate solubility as well as representing a type of polymeric matrix preventing the tendency towards crystallization or reagglomeration. Compounds of this type exhibit high absorptions in the range of 780–830 nm, a reflectivity exceeding 30% and a signal-to-noise ratio of > 50 dB.[107b] The use of a soluble, axially substituted aluminum-naphthalocyanine has been reported; in this case, at a write wavelength of 830 nm a sensitivity of 0.7 nJ/per pit, a reflectivity of 25%, a signal-to-noise ratio of 55 dB and a reduction of the signal-to-noise ratio after 1.5×10^6 reading cycles by less than 1 dB (1 mW readout energy at 830 nm) have been observed.[108] The derivatives must be extremely pure in order to reproduce signals without considerable output loss. The most recent patent applications claim naphthalocyanine derivatives for WORM memories, which are both axially and also peripherally substituted.[109] The synthesis of the naphthalocyanine system by peripheral substitution becomes very expensive since the corresponding 2,3-dicyanonaphthalene derivatives must be produced as intermediates. The expenditure and the raw material costs may be reduced by the use of phthalonaphthalocyanines.[110]

The naphthalocyanine derivatives represent an interesting alternative to methine dyes as absorbers of diode laser radi-

ation. Initial prototypes of WORM disks based on naphthalocyanines have already been put on the market.

4.3.3. Quinoid Polynuclear Aromatic Compounds

A further category of dyes to which reference is frequently made in the literature and which can be used as an absorber layer for WORM storage disks comprises the quinoid polynuclear aromatic compounds. The use of these compounds is based on a different concept: the dye molecules are rather small, generally of low solubility and, in contrast to the methine dyes, uncharged, so that they may be applied to the substrate by means of vapor deposition techniques (Figs. 16 and 17).

Although this method of coating is more complex and, in general, more costly, it also has its advantages. For example, where sublimation is carried out, any dissolution of a polymeric substrate is avoided, and the possibilities of providing the substrate with a polymeric intermediate layer to improve the total properties increase.

The most widely investigated group of dyes are amino derivatives of the 1,4-naphthoquinone type (Fig. 16), which have already been known for a long time in the dyeing industry as pigments with a broad color spectrum.[111] In terms of their reflectivity and sensitivity properties, they are less attractive than the known cyanine dye systems but offer higher chemical stability and give storage media with long service life of the data. The systematic examination of 1,4-naphthoquinone derivatives[112] absorbing in the NIR range was extended by *Matsuoka* et al. to anthraquinone, phenothiazinequinone and phenoselenazinequinone derivatives (Fig. 17)[113] and previously developed synthetic strategies by means of PPP molecular orbital computations.[114] In this case, it became evident that the long-wavelength absorption maximum was influenced both by a change in the donor- and in the acceptor-moieties, since the coloration of these compounds is generated by an intramolecular charge transfer. Derivatives of the type shown in Figure 16 contain the combination of a suitable donor and strong acceptors. In solution, they absorb at approximately 770 nm, with high molecular extinction coefficients, and respond to the radiation of commercial laser diodes. At a signal-to-noise ratio > 50 dB, an acceptable reflectivity of up to 25% was observed at 830 nm.[115] The substitution of the free amino group by alkyl or aryl radicals leads to a further bathochromic shift. In 1985, NEC announced a WORM storage disk based on the ethyl ether (Fig. 16, R = C_2H_5). Although these ethers exhibit optical properties which are on the whole acceptable, they have the disadvantage of high output losses on vacuum coating.

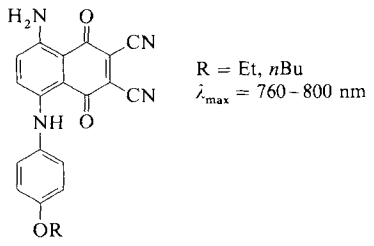


Fig. 16. 5,8-Diamino-1,4-naphthoquinones absorbing in the near infrared.

An improvement in the chemical and thermal stability (and thus in the sublimation properties) has been achieved by the phenothiazine or selenazinequinone derivatives (Fig. 17) and their isomers.[116] These compounds form homogeneous films with smooth surfaces.[117] Their absorption range is between 750 and 850 nm, and strongly electron-withdrawing substituents have a strong bathochromic effect.[118] Structurally related compounds used include specific indanthrene derivatives[119a,b] violanthrones,[119c] and amino-substituted phthaloylacridones.[120]

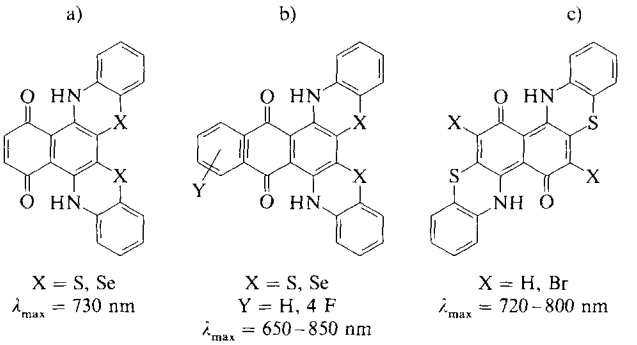


Fig. 17. Infrared absorbing phenothiazine and phenoselenazine derivatives with benzoquinone (a), naphthoquinone (b) and 1,4-diketo units (c).

4.3.4. Metal Complexes

While the phthalocyanine ligand ($Pc^{2\ominus}$) is itself a chromophore, there is a series of colorless, in most cases sulfur-containing ligands which absorb in the visible or near infrared range only as a result of 2:1 complexing by means of a metal ion. The long-wavelength absorption occurs due to the formation of a 10 π electron system in the complex. A typical example is represented by the dithiolatonickel complexes (Fig. 18), which can be isolated as salts or neutral complexes and exhibit absorption bands between 715 and 1300 nm in solution.[121] Other suitable metals are palladium, platinum or alternatively cobalt, copper, zinc and cadmium. In DIP

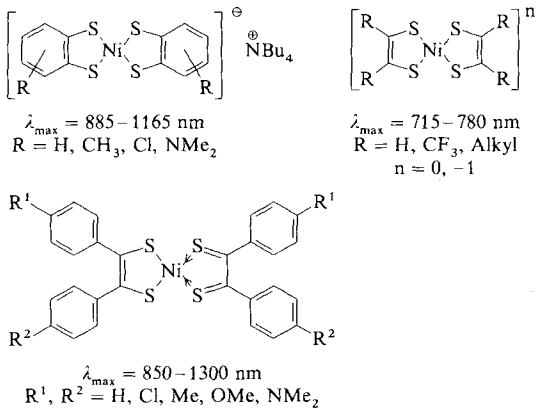


Fig. 18. Infrared absorbing dithiolatonickel complexes.

configurations, an additional bathochromic shift by 20–60 nm is observed, which limits the use of numerous compounds of this type in WORM storage disks.[122] The solubility of the easily accessible original substances[123] in organic solvents is moderate, but can be increased by appropriate substituents so that they can be spin-coated from solvents. However, the reflectivity values observed are distinctly inferior to those of cyanine dyes. For this reason, they probably will not be used alone as absorbers in WORM storage disks.

It has already been pointed out, in connection with the cyanines, that dithiolato complexes are very efficient oxygen traps and thus considerably increase the stability of cyanine absorber layers. In 1985, almost 60 patent applications were filed in which such combinations are claimed. At the present time, there is no precise concept concerning the protection mechanism. Closely related classes of compounds include α,α-diimino-*cis*-1,2-ethylenedithiolatonickel derivatives[124] or complexes in which aromatic *o*-diamines, *o*-aminothiols or *o*-selenols (λ_{max} = 780–900 nm),[125] indoanilines[126] or quinolinediones[127] are used as ligands.

4.3.5. Other Dyes

In addition to the most important classes of compounds which have been outlined in Sections 4.3.1–4.3.4, the patent literature also discloses a whole series of other NIR-absorbing compounds. These include specific aminoarylpentafulvenedicarbonitriles (λ_{max} = 680–785 nm),[128] ethynevinyl di- and triphenylcyclopropanes (λ_{max} = 530–820 nm),[129] and triquinocyclopropanes ($\lambda_{max} \approx$ 770 nm),[130] which can be applied by sublimation or, with appropriate substitution, by spin-coating, polypyrrole (1 nJ/pit at 830 nm)[131] and intermolecular charge transfer complexes with 5-nitro-2,3-dicyanonaphthoquinone as acceptor ($\lambda_{max} <$ 740 nm).[132]

5. Reversible Data Storage

The set of requirements imposed on erasable optical data stores is prescribed by the current specifications of the conventional magnet technology (Winchester disk drives), since the two technologies are designed for the same range of application. The storage densities of the EDRAW media which are in an initial marketing phase, currently amount to approximately 10^8 bit cm^{-2}, while hard disks on average achieve 10^6 bit cm^{-2}.[133–135] An increase in the bit density of magnetic hard disks to 10^7 bit cm^{-2} is under investigation by the use of special preparations of γ-Fe_2O_3 or new types of cobalt alloys.[141, 149] The direction of magnetization for a recording is not altered in the plane of the disk (longitudinal), but perpendicular to it so that magnetic domains <1 μm can be inscribed.[137]

In magnetic high-performance disk drives, the aerodynamic write/read head is guided at a height of approximately 0.1 μm,[136] and therefore it is possible for "head crash" to occur as a result of dust particles and vibrations. The disk-drive must therefore be mounted rigidly as well as protected from dust and other foreign particles. In contrast in the optical process, the corresponding components are situated at a non-critical spacing, which gives substantial insensitivity to particles, as well as no encapsulation of the disk and, in consequence thereof, an exchange facility and secure handling.

In optical data carriers, the density of the guide tracks (8000–9000 tracks cm^{-1}) is higher than with magnetic carriers (1000–1500 tracks cm^{-1}),[138] so that the storage capacity of optical systems is greater by a factor of 10 than that of the Winchester disks.[139, 140] On the other hand, data access via hard disks is considerably faster (8–20 ms) than with optical disks (30–50 ms) and the data rate, approximately 12 Mbyte s^{-1}, is two to three times greater than with optical recording processes. By increasing the speed of rotation to 4000 rpm and using a laser diode array, the data rates for optical media may be increased to 6 Mbyte s^{-1} or $>$10 Mbyte s^{-1}.[142, 143] It is expected that by about 1995 the access times may even be reduced to a value of 20 to 25 ms.[144] General requirements to be imposed on reversible storage media include bit error rates of approximately 10^{-12} (after correction), application cycles exceeding 10^7 and the "direct overwrite" of stored information. In a similar way to the write-once memories, a defined threshold value or a steep progression of the energy/sensitivity curve is required for the reversible types of marking of the EDRAW media. Other conditions include long-term stability of up to 10 years for the archiving of information and compatibility with existing hardware and software.

Several different materials may be used for reversible data storage, but only a few are at the stage of industrial application. It is required that the information can be easily read and erased, and this leads to a conflict which can be resolved only in circumstances in which a material at room temperature exhibits two conditions which can be selectively addressed and switched. However, many materials which are in principle appropriate are altered in their condition of marking when a laser beam is frequently used for readout.

The development of reversibly operating magneto-optical memories and phase transformation media has progressed to a stage at which marketing is imminent. The overview given below therefore concentrates on a description of these processes.

5.1. The Magneto-Optical Effect

The magneto-optical (M/O) effect can be used for the readout of data, since a rotation of the plane of polarization takes place as a result of the interaction of a polarized light beam with magnetic material (Fig. 19).[145] In this way, it is possible to read data markings in reflection (M/O Kerr effect) or in transmission (M/O Faraday effect). Writing and erasure by means of a laser beam is based on the temperature dependency of the magnetization (Fig. 19). A recording medium magnetized perpendicular to the disk is heated at definite positions, and the magnetization is flipped over into the opposite direction by a magnetic field. There are three categories of recording materials used: crystalline intermetallic compounds, amorphous rare earth/transition metal alloys (RETM), and ferrites.

The progression of the magnetization of alloys of rare earths and transition metals is shown as a function of the temperature in Figure 20.[10] The RETM alloys are included

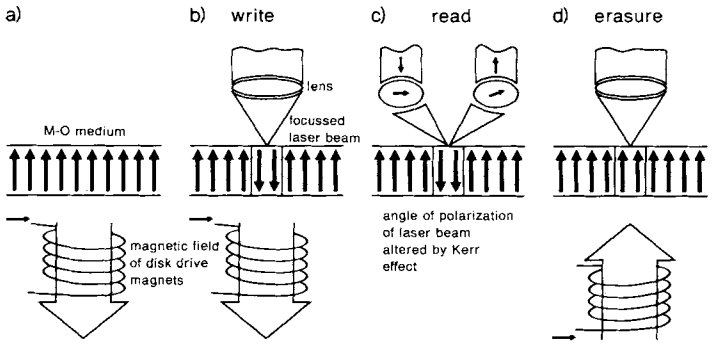


Fig. 19. Principle of magneto-optic (MO) data storage [145]: a) the perpendicular magnetization of the MO-medium is unaffected by magnetic field at room temperature; b) recording via heating by laser beam and turnover of the magnetization via a magnetic field; c) reading via Kerr effect; d) erasing via heating by laser beam and turnover of the magnetization according to original direction.

among the ferrimagnetic substances. The magnetic structure is characterized by the presence of various subunits, which are magnetically coupled and assume an antiparallel orientation. The temperature dependence of the magnetization of the subunits differs, so that the difference represents the spontaneous magnetization of the entire system. In this case, the orientation is perpendicular to the plane of the recording medium (perpendicular magnetic anisotropy). At low temperatures, the magnetic moment of the rare earth atoms is greater; at a higher temperature, the magnetic moment of the transition metal atoms predominates. Accordingly, as a result of the antiparallel configuration, the temperature progression of the total magnetization is characterized by two temperatures. The point of compensation is marked by the temperature (T_{comp}) at which the magnetizations are equal, and the net magnetization of the alloy becomes zero. In the event of an increase in temperature, the magnetic moments of both species of atoms disappear at the Curie point (T_{Curie}) and the alloy material becomes paramagnetic from this temperature upwards.

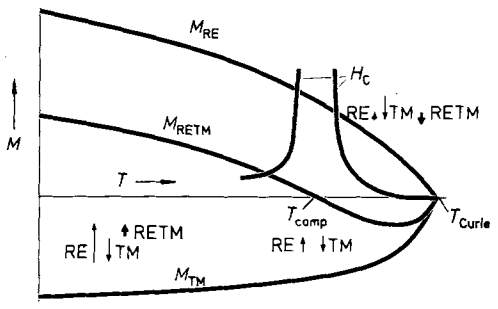


Fig. 20. Temperature dependence of magnetization M and coercitivity H_c of an alloy RETM of rare earth element (RE) and transition metal (TM) [10].

The preferred direction of the total magnetization is given by external magnetic fields. The stronger the external field and the lower the temperature, the more completely the external magnetic field forces the orientation of the elemental magnets in the field direction. On account of the high perpendicular anisotropy, the maximum attainable magnetization, i.e. the saturation magnetization, can be changed only in circumstances in which the external magnetic field reaches a threshold value, i.e. the coercive field strength (H_c). At the compensation temperature, the coercivity of a ferrimagnetic alloy is theoretically infinitely large, so that due to large magnetic coupling, the direction of the magnetization cannot be altered by external fields. Above T_{comp}, the coercive field strength falls again to small values and at the Curie point becomes zero.

Depending upon the writing temperature, a distinction is made between compensation point or Curie point writing. For compensation point writing, T_{comp} is set by the composition of the alloy to room temperature. The writing process takes place with simultaneous heating of the recording medium by a laser beam and application of an antiparallel external field by means of the disk drive magnet. As a result of heating, the coercive field strength diminishes and the direction of magnetization is flipped over in the heated area—the data bit—by application of an external field and read out by means of the Kerr effect. Curie point writing involves the heating of the metallic layer to achieve the elimination of the magnetic order at T_{Curie} and setting of the new preferred direction by an external magnetic field. The erasure process is distinguished from writing only by the direction of the field of the disk drive magnet.

In comparison with the magnet technology, the smaller data rates of the M/O technology are determined by an additional disk rotation, which is required for erasure, in order to create the orginal magnetic orientation on the disk. Thus, a total of two disk rotations must be executed for the writing of new data. Accordingly, M/O disk drives of the next generations will be provided with a direct overwrite device.[146, 147, 149] One possibility is the use of a magnetic head, the field of which switches the data spots heated by the laser in accordance with the bit stream (Magnetic Field Modulation Method). In this way, data rates exceeding 10 Mbyte s^{-1} have been achieved.[148] The distance between the head and the disk is 2–5 μm, so that conditions are not as critical as with the Winchester disk drives.

The layered structure of a storage medium is of prime importance for the optical properties. However, the RETM media adopt a certain special position, since they must be encapsulated with protective layers on account of their sensitivity to oxidation. The protective layers fulfill several functions: a barrier against oxygen, water vapor, substrate, and protective polymer lacquer, an antireflection layer for coupling in the laser light, and thermal insulation of the recording layer in order to keep the temperature of the substrate constant. In most cases, use is made of multilayer structures which, depending upon the construction and layer thicknesses, influence the maximum attainable signal intensity and sensitivity. Thus, reports have been given, for example, not only of simple systems consisting of an M/O layer, antireflection layer and metal mirror, but also of constructions consisting of a barrier film, two different M/O layers and an antireflection layer.[6, 23] In this way, the reflectivity of a RETM medium may be varied between approximately 4 and 30%. The materials used for barrier layers or dielectric layers are in most cases amorphous films of SiN, AlSiN, or BN.[153] Additionally, investigations have been carried out on TiO, TiON, TiN, AlSiON, SiO, AlN, SiON, ZnS and SiO_2.[151] For the setting of an optimal SNR, the materials

of barrier layers must exhibit amorphous structure, low birefringence, high transparency at the laser wavelength, low thermal conductivity, and must by easy to manufacture. The Kerr angle can be increased by appropriate selection of refractive index and layer thickness of the barrier film.[150, 152]

A prerequisite for the magneto-optical data storage is a perpendicular magnetic anisotropy of the recording medium. The causes of the anisotropy have, to date, not been fully clarified; it is generally assumed that three phenomena may occur: spin-orbit coupling, magnetic dipole interaction and magnetostriction.[156, 177, 222–225] However, it has been verified that a relationship exists between magnetic anisotropy and the process of preparation of the RETM layer. Amorphous RETM alloys can be produced by a multiplicity of vacuum coatings: thermal[154a] and electron-beam vapor deposition,[154b] ion-beam sputtering,[154c], RF sputtering,[154d] and DC magnetron sputtering[154e] have all been used with success. Certain properties of the materials can be influenced by the coating process to a far greater extent than by controlling the layer composition.[155] M/O films consisting of RETM alloys are produced by DC magnetron sputtering for the production of data stores.[157]

5.2. Magneto-Optical Materials

The interest in M/O materials for data recording dates back to work by *Williams* in 1956 in the Bell Laboratories; a hot needle was used to inscribe magnetic domains into a manganese/bismuth film which were read out by means of the Faraday effect.[158] Curie point writing using an electron beam was demonstrated in 1958 by *Mayer*,[159] and the Kerr effect was used for the first time for the detection of magnetic domains in 1960.[188] Compensation point writing was attempted in 1965 on $Gd_3Fe_5O_{12}$, a magnetic garnet.[160] Lasers were developed parallel to this work and gained increasing acceptance as a radiation source for writing, reading and erasure. These first M/O materials exhibit a series of properties which prevented large-scale technical use as storage media[161, 162] and led to the development of the RETM alloys, which are today the most important materials for M/O memories.

Chaudhari et al. were the first to show that gadolinium-cobalt and gadolinium-iron films exhibit spontaneous perpendicular magnetic anisotropy.[163] The variation of the compensation point between $-233\,^{\circ}C$ and $+230\,^{\circ}C$ was achieved by the selection of the $Gd_{1-x}Co_x$ composition. At the compensation point the coercivity showed a maximum, which was greatly dependent upon the method of production. In initial writing attempts at the compensation point, it was possible to inscribe data markings. In further investigations, it emerged that the stability of small magnetic domains is very low.

A fundamental disadvantage of GdCo resides in the difficulty of obtaining homogeneous layers with a constant compensation point. The compensation point decreasing from the center towards the edge is based on irregularities of oxygen traces in the layer.[169–173] In terms of magnetic properties, oxidizied gadolinium behaves differently from pure gadolinium; accordingly, the relative proportion of cobalt is increased, and as a result of this the compensation point drops. A difference of 2 atom-% in the cobalt content causes a change of T_{Curie} by approximately 50 K[188] (Fig. 21). It is possible to produce homogeneous GdCo films by applying a negative bias voltage to the substrate.[169, 174] It is assumed that the oxygen content of the film is reduced by increased argon ion bombardment.[169] In this case, an anisotropic distribution of Gd and Co is generated by selective resputtering of gadolinium atoms, and thereby the perpendicular magnetic anisotropy is built up as a function of the bias voltage.[175] A columnar structure is generated in the layer by the processes taking place during sputtering.[176] In other investigations, gadolinium was replaced by holmium[164] ($T_{comp} = 46\,^{\circ}C$) with the composition $Ho_{35}Co_{65}$. The coercive field strength of HoCo films is greater than the comparable GdCo layers, and it was possible to write stable data bits.

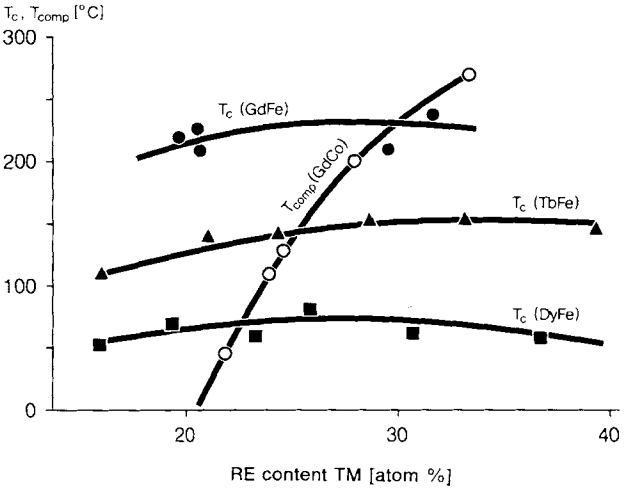


Fig. 21. Curie temperature T_C as a function of rare earth content of GdFe, TbFe, and DyFe alloys and compensation temperature T_{comp} of GdCo as a function of Gd content [188].

In Gd alloys, the replacement of cobalt by iron leads to the lowering of the Curie temperature (T_{Curie})[178–180] and Kerr angle.[181] The coercivity of GdFe alloys is, like that of GdCo, relatively small.[182] The properties of GdFe compounds can also be modified by alloying with other metals: yttrium increases H_c and reduces T_{Curie}; bismuth,[185] tin[186] and lead[187] increase the Faraday and Kerr effects; bismuth and tin cause the lowering of T_{Curie} and T_{comp}.[185, 186] If gadolinium is used in place of terbium in REFe alloys, materials of which the Curie temperatures are approximately 100 K below those of GdFe[188, 189] (Fig. 21) are formed. On going from gadolinium to terbium to dysprosium, the progressions of the T_{Curie} curves are displaced in almost constant intervals by 50–100 K in each case. The Curie temperatures of iron alloys are significantly less sensitive with respect to variation of the rare earth element content (Fig. 21).

In the case of the iron and cobalt alloys of gadolinium, compensation temperature writing is employed; in the case of terbium and dysprosium alloys, Curie point marking is mostly used. On comparing coercive force and spontaneous

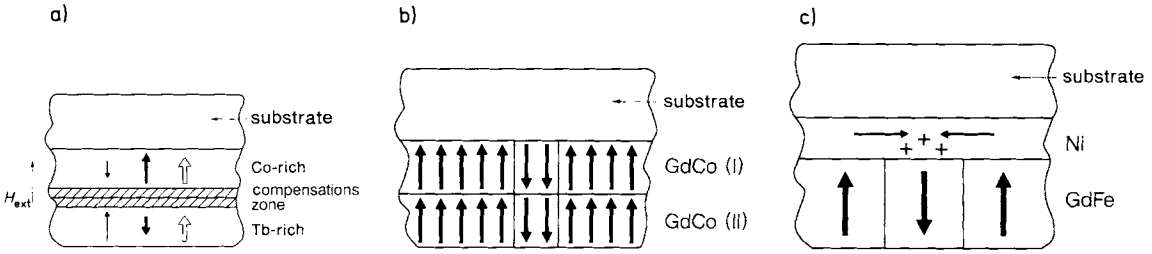


Fig. 22. Principle of MO layers for recording of small domains: a) double layer of TbCo alloy with Co enrichment in the upper and Tb enrichment in the lower film. The arrows indicate the preferred directions of the magnetic moments of the Tb (→) and Co atoms (⇒) as well as of the resulting magnetic netto moment of the layer (→); b) two GdCo layers (I and II) with compensation temperatures $T_{comp}(II) < T_{comp}(I) <$ room temperature; c) small magnetic domains in GdFe via exchange coupling with a nickel layer.

magnetization as a function of the temperature, similar marked differences are found as for the Curie points in the case of the iron alloys with the heavier rare earth metals (RE = Gd, Tb and Dy). GdFe alloys exhibit the already mentioned low coercive field strengths, which lead to instabilities on writing small bit domains. TbFe and DyFe are characterized by coercive field strengths of a few 100 000 A m^{-1} and steep temperature dependence of the magnetization; this is desired for the writing of small domains.

The methods by which the TbFe films are prepared determines to a great extent their properties. Uniaxial anisotropy K_u and saturation magnetization of TbFe films can be varied as a function of the substrate temperature;[190] in contrast, the perpendicular anisotropy of GdFe is almost independent of the substrate temperature. Using X-ray scattering, it was found that during the coating an oxidation of terbium to the suboxide takes place, which causes, at a relatively high temperature, the large drop in the saturation magnetization in terbium-rich films.

The magnetic and magneto-optical characteristic quantities of TbFe layers can, moreover, also be modified by the variation of the film thickness[191] and the pressure of the sputtering gas,[192] and can be optimized by selection of a suitable layer construction with respect to their dynamic write/read/erase properties.[193]

The mechanical conditions applicable to the substrate material can also have an effect on the magnetic anisotropy constant, and can generate orientation effects by anisotropic stresses (magnetostriction), for example in foils as carrier material for magneto-optical layers. Attempts at coating TbFe films onto Kapton foils by RF sputtering led to recording media with a high magnetic anisotropy, which could possibly be used as M/O tapes.[194]

The RETM alloys are particularly oxygen-sensitive and must be protected from the atmosphere for long-term storage. Within the individual alloy systems there are, however, significant differences. RECo films are far less subject to oxidation than REFe layers[165] and exhibit higher thermal stabilities.[167] The write sensitivity is very high in the region of the compensation composition on account of the sharp decline of H_c, so that it is possible to write using lasers of low energy; therefore the stability is greater upon frequent reading.[165]

Alloys of terbium and cobalt have been tested; unlike GdCo, these alloys are more stable and do not contain inhomogeneities of the layer when gadolinium is replaced by terbium. Using homogeneous TbCo films, it was not possible to achieve this;[195] by modulating the terbium/cobalt ratio within a film, it was possible to increase magnetic coercivity and resistance to oxidation.[196] Using bias RF sputtering, cobalt-rich films have been produced at a bias voltage of 100 V and terbium-rich ones without a bias (Fig. 22a). At a negative bias voltage, it is assumed that terbium is preferentially resputtered, so that a relative increase in the cobalt content results. The lattice positions which have become free in consequence of terbium resputtering are clearly occupied by the sputtering gas; this leads to a more porous microstructure and easier oxidizability than in the case of films sputtered without. In this way, films with up to 36 layers may be prepared; these have an average thickness between 80 and 100 Å. Between the layers, compensation zones are formed which result in a homogeneous layer only from a film thickness of approximately 40 Å. By appropriate selection of the layer composition of the terbium-rich layer, the compensation temperature has been set above room temperature so that in consequence of exchange coupling of the magnetic moments between the two layers, a high coercive field strength (ca. 320 000 A m^{-1} and above) is achieved. The Faraday rotation of TbCo media read out in reflection is mainly based on the cobalt sublattice and is less due to the influence of terbium,[197] in contrast to the TbFe alloys, in which both components contribute to the Faraday effect.[198] Effects of the exchange coupling of heterogeneously structured RETM films have also been investigated on GdFe/DyFe and GdFe/TbFe layers.[184]

In many cases the requirement for high write sensitivity is incompatible with the requirement for high domain stability, bit density and a high SNR both for T_{Curie} and T_{comp} writing. By decoupling the writing and reading processes onto two separate layers these weak points are avoided.[184] The write film should ideally exhibit high coercive field strength at a low Curie temperature in order to achieve high sensitivity and domain stability. The read layer must be coupled by means of exchange coupling to the spin moments of the write layer and also exhibit a high Curie temperature and coercive field strength for the transfer of written domains from the write onto the read layer. TbFe and DyFe layers were tested as write films in conjunction with deposition of a GdFe layer as read film.[184] In the case of TbFe/GdFe structures, coercive field strengths increased to a few 100 000 A m^{-1}, and an associated domain stability of up to approximately 1 μm were found. Accordingly, the properties of monofilms consisting of GdCo or GdFe were exceeded.

Another method for writing small magnetic domains consists in the use of two layers of GdCo with differing composition[165-167] (Fig. 22b). The compensation temperature T_{comp} of the upper layer (I) is set by the ratio of Gd to Co to be somewhat below room temperature, and T_{comp} of the lower layer (II) is below T_{comp} of the upper film. This means that at room temperature the saturation magnetization M_s and the demagnetizing field H_d of the upper layer are small (the field lines of an upwardly directed magnetic domain penetrate the surrounding layer in the reverse direction and therefore act in the sense of a demagnetizing field), while M_s and H_d are greater in the lower layer. In this way, domains of the upper film are stabilized. This also applies to the case in which the preferred direction of the anisotropic magnetization is not exactly vertical, but tilted.[168]

Small magnetic domains in the μm range can also be written with the aid of a layer of ferromagnetic material[183, 184] (Fig. 22c). It is assumed that by vapor deposition of a nickel film on the GdFe recording layer a written magnetic domain is stabilized by the formation of a locally closed domain in the longitudinally magnetized Ni film. The coercivity of the entire GdFe–Ni structure becomes greater and a higher magnetic field strength is required to switch the data bit.

Ternary and quaternary alloys of rare earths and transition metals open up a multiplicity of design possibilities for structure/property relations. The search for technically suitable M/O materials extends on a preferential basis to alloys of such transition elements as iron and cobalt with the heavy lanthanoids gadolinium, terbium, dysprosium, holmium, erbium, neodymium, praseodymium and samarium[10, 189] (Fig. 23a). In addition, films of the most widely varying

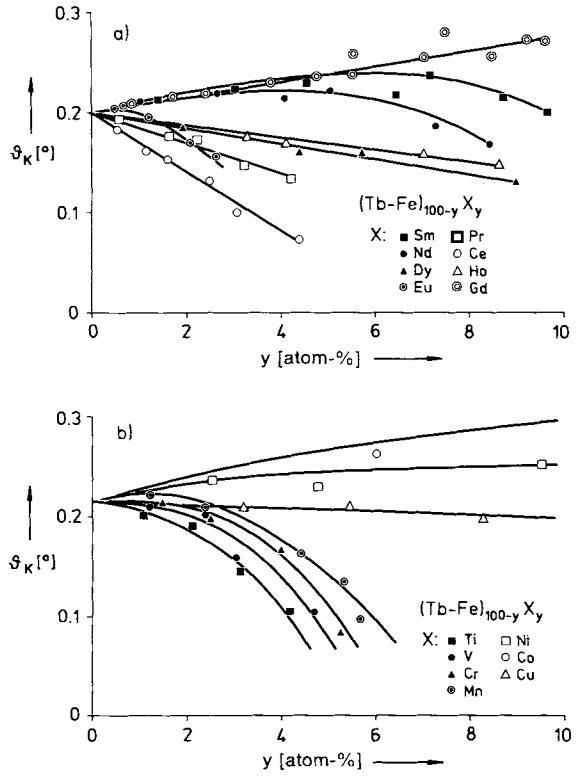


Fig. 23. Kerr rotation angle ϑ_K of $(FeTb)_{100-y}X_y$ alloys as a function of the composition. a) X = rare earth element. b) X = transition metal [189].

ternary and quaternary alloys have been described: with cerium, promethium and europium as rare earth elements,[189] and titanium, vanadium, chromium, manganese, nickel and copper as transition metals[199] (Fig. 23b), as well as various doping elements such as bismuth,[185] tin,[200] lead,[187] germanium,[201] molybdenum, gold,[202] silver, palladium, platinum[199] and uranium.[203a] In Figure 23 the Kerr angle ϑ_k of some ternary Tb-Fe alloys are shown as a function of the content of the third alloying component.

The number of the most promising alloys is, however, for marketable products, relatively small, and restricted to the GdTbFe, TbFeCo systems and their four component alloys with dysprosium and neodymium respectively. By using ternary GdTbFe alloys, it is possible to combine the properties of TbFe and GdFe:[206] the Kerr angle (ca. 0.30°) is about the same (TbFe 0.25°, GdFe 0.30°; at $\lambda = 800$ nm),[155] the Curie temperature (between 150–180 °C) is reduced as compared to GdFe (200–250 °C),[204] and the coercivity is increased.[203b]

Dynamic memories and reading experiments with GdTbFe films[205-207] demonstrate the usefulness of this ternary alloy system. In initial experiments, bit error probabilities of 10^{-3}–10^{-4} and 10^7 intact write cycles were obtained.[207] The magneto-optical rotation was optimized using different metal reflection layers (Au, Cu, Ag) and dielectric films (SiO_2).[208] By using a quaternary alloy of GdTbFe with dysprosium, it was possible to increase the signal from 0.7 (at 800 nm) to 1.7 (at 700 nm). By replacing gadolinium by dysprosium in ternary RETbFe alloys, the Kerr angle (Fig. 23a) and the Curie temperature are reduced.[208] The Kerr effect can be increased by a three-layer structure of Cu reflection layer, DyTbFe, and SiO_2 dielectric. The write process was executed with an 8 mW semiconductor laser. The optical transmission of the write/read/erase head showed approximately 44% power loss, so that it was possible to measure 4.5 mW write power and 2 mW read power on the disk. The prerequisites for the writing of magnetic domains < 1 μm were satisfied by a coercive field strength of ca. 80000 A m^{-1}, and the erasure of data bits could be performed by means of a 12000 A m^{-1} magnetic field.[208] The bit density of this system was quoted as being 1.5×10^7 bit cm^{-2}.

As shown for the binary REFe alloys, together with an increase in the order number of the lanthanoids it was possible to detect a lowering of the Curie temperature, even for ternary alloy systems (Fig. 24).[16] This applies in the same

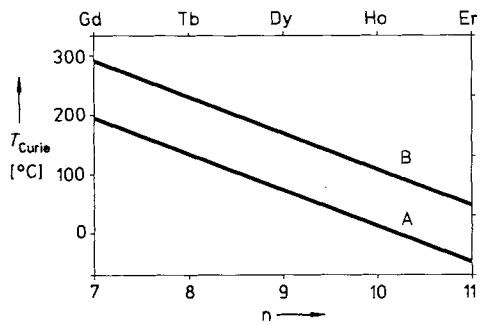


Fig. 24. Variation of Curie temperature T_{Curie} with substitution of rare earths for Tb in $(Tb_{1-x}Y_x)_{0.2}Fe_{0.8}$ (curve A) and in $(Tb_{1-x}Y_x)_{0.2}(Fe_{0.9}Co_{0.1})_{0.8}$ (curve B) where x is determined by the average number of 4f electrons in the alloy; $0 < x < 0.1$ [209].

way to iron and cobalt alloys; the Curie temperatures of the cobalt compounds are generally higher. The particular influence of the cobalt is also shown in comparison with the other transition elements. The curves in Figure 25 indicate the change in the Curie temperature of the amorphous Tb-Fe-

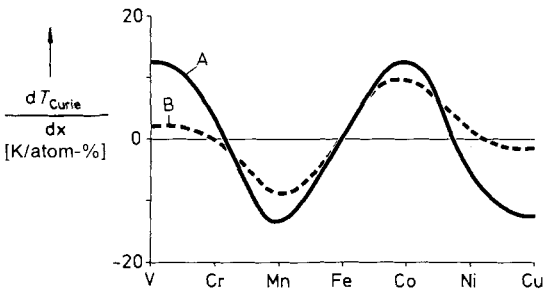


Fig. 25. Variation of Curie temperature T_{Curie} with substitution of small amounts of various transition metals (TM) in amorphous $Tb_{0.2}(Fe_{1-x}TM_x)_{0.8}$ (curve A) and in crystalline $Fe_{1-x}TM_x$ (curve B), respectively; $0 < x < 0.1$ [16].

transition metal alloys (A) and crystalline Fe-transition metal compounds (B) as a function of the transition metal (up to 10 atom-%) for several transition metals. Thus, with a fixed lanthanoid content, the Curie temperature can be set by the ratio of two transition elements.

The temperature dependencies of spatial arrangement, electron interaction, spin moment and exchange coupling give the interelations between magnetization, Curie temperature and Kerr effect.[209, 210] Figure 26 shows a plot of the

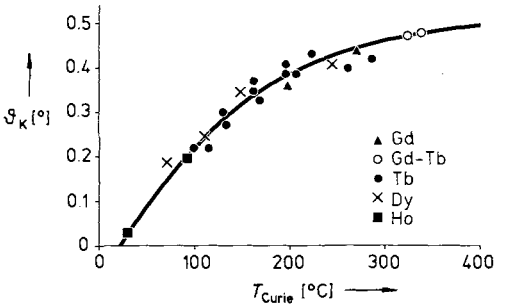


Fig. 26. Kerr rotation angle ϑ_k versus Curie temperature T_{Curie} for various rare earth substituted FeCo-alloy films. [209]

Kerr angles of several rare earth element-substituted FeCo alloys versus their Curie points. It is evident that for a magnetization which is higher at room temperature a larger Kerr angle results. In the case of alloying cobalt with TbFe and GdFe, the Kerr angles increase. The effect is particularly marked in the case of TbFe: in a $Tb_{16}Fe_{84}$ alloy, the Kerr angle increases from 0.18° to 0.37° for $Tb_{16}(Fe_{0.7}Co_{0.3})_{84}$; at the same time, the Curie temperature increases 4 K/atom-% Co.[211]

TbFeCo films are used in the majority of commercial storage disks,[212] accordingly, they have been extensively investigated. The properties of a M/O layer consisting of TbFeCo may be varied by the ratios of the components within very wide limits. $Tb_{28}Fe_{60}Co_{12}$ (RE-rich) and $Tb_{22}Fe_{68}Co_{10}$ (TM-rich) films were investigated for their use as storage media and were characterized with respect to their magneto-optical parameters.[213] Both layers exhibit a Curie temperature of 200 °C; however, there are differences in the saturation magnetization and coercive field strength. The storage layer with the larger iron content shows a higher saturation magnetization than the terbium-rich film. The marked magnetic domains become larger with increasing laser power and external field strength as a result of the dissipation of thermal energy and the consequent profile of the coercive field strength H_c in the layer. The domain size can be computed from the temperature progression in the film, assuming a gaussian distribution for the intensity of the laser beam, and to a first approximation is given by Equation (a) where

$$T(r)\ [°C] = 120 \exp(2r^2/0.6^2) + 80 \qquad (a)$$

r [μm] is the distance from the focal point to the laser source. This term is based on the assumption that at the focus the Curie temperature of 200 °C is reached and the laser beam has a radius of 0.6 μm.

With the aid of this equation and of the temperature dependence of H_c, the distribution of the coercive field strength $H_c(r)$ in the layer can be computed (Fig. 27). The domain

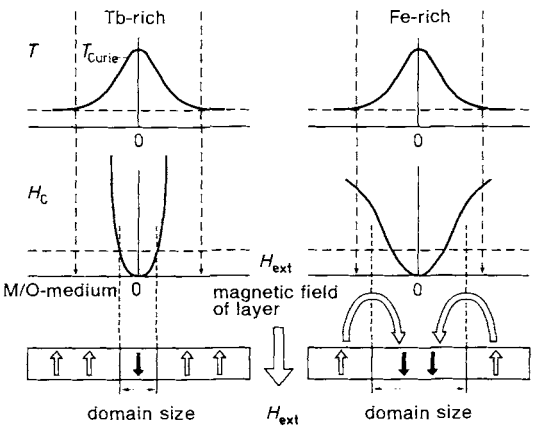


Fig. 27. Domain formation model for MO recording. [213] The profil of temperature T and coercivity H_c are represented for a Tb-rich ($Tb_{28}Fe_{60}Co_{12}$) and an Fe-rich ($Tb_{22}Fe_{68}Co_{10}$) film. The domain size in a Tb-rich film is smaller than in an Fe-rich film due to differences in saturation magnetization. The vertical dashed arrows in the upper part of the figure demonstrate the width of the laser beam. The horizontal dashed lines indicate the initial niveaus of T and H_c of the films.

radius r_s is then obtained from the balance of the magnetic fields in the layer [Equations (b) and (c)] as radius of the

$$H_c(r_s) = H_{ext} + H_d \qquad (b)$$

$$M_s = \chi \mu_0 H_d \qquad (c)$$

$$H_c(r_s) > H_{ext} + H_d \qquad (d)$$

circle in which (d) applies. χ is the magnetic susceptibility, μ_0 the magnetic induction constant and M_s the saturation magnetization. H_{ext} is the external magnetic field which is applied to switch the heated data spot and together with the magnetic field H_d generated by the recording layer must be greater

than the coercive field strength $H_c(r_s)$, in order to mark a pit (see Fig. 27).[213]

In consequence of the high saturation magnetization of the iron-rich layer, the demagnetizing magnetic field H_d of the $Tb_{22}Fe_{68}Co_{10}$ film is greater than that of the terbium-rich $Tb_{28}Fe_{60}Co_{12}$ film. In the case of an equal external magnetic field H_{ext}, the progression of $H_c(r_s)$ in the iron-rich layer is substantially broader due to the differing H_d fields, so that larger domains are written. This can be an advantage when the storage disk is rotated at high speeds and the temperature profile generated in the recording layer becomes narrower (high speed recording).

Media with a write characteristic comparable with that of the terbium-rich film are particularly suited for high recording densities. The demagnetizing field H_d generated by the magnetization of the magneto-optical film can, if the composition is suitable, become so large that the coercive field strength of the heated data spot is exceeded and writing can take place without an external magnetic field H_{ext}; this is true, for example, of $Tb_{22}Fe_{69}Co_9$ and $Tb_{26}Fe_{59}Co_{15}$. The form of the data spots is dependent upon the ratio of the individual magnetic fields on writing and erasure respectively and has an effect on the signal-to-noise ratio;[214-218] heat dissipation in the layer structure of the storage medium represents a significant boundary condition. The laser beam propagates heat, and therefore heat sinks in the form of insulating dielectric layers are introduced, which are located between the metallic reflection layer and the storage medium.[208] The dimensioning of such multi-layer structures consisting of an antireflection layer, a storage layer and a reflection layer as well as dielectric, requires considerable optimization. The radial temperature distribution in magneto-optical media has accordingly been the subject of numerous investigations, especially from the point of view of influencing the SNR.[216]

The modulation noise N_{mod} is the noise difference before and after writing, which can be measured on scanning the data markings and is a measure of the regularity of the magnetic domains. The smaller N_{mod} the greater is the optimally attainable SNR. As a result of an inhomogeneous temperature distribution (caused in consequence of fluctuation of the layer composition or within the laser beam) in a heated data spot, differences in the magnetization may arise between the center and the edge zone. Under particular conditions, these differences may become so large that instead of punctiform domains annular ones are written. These irregularly shaped data spots increase the modulation noise and reduce the SNR.

By way of analogy with the binary alloys, the SNR can be increased by specific layer structures. TbFeCo was used to produce layered films by means of sputtering, with which high SNRs were attainable.[217] The optimization of the signal-to-noise ratio, which is proportional to $\vartheta_k\sqrt{R}$ (R = reflectivity, ϑ_k = Kerr angle), was described for three-layer storage systems using TbFeCo and DyFeCo alloys.[218] The most suitable layer thicknesses for the dielectric film are those given at the largest possible Kerr angle and low reflectivity. Using $(Nd_{13}Dy_{87})_{30}(Fe_{84}Co_{16})_{70}$ films, data rates of 10 MByte s^{-1} for 5.25″ disks at 50 dB for the SNR value were achieved in dynamic write tests.[221] Moreover, investigations were carried out on quaternary RETM alloys of the TbXFeCO[219] and GdXFeCo type,[220] where X = Dy, Ho, and Er, in order to modify Curie temperature, coercive field strength, Kerr angle and magnetic anisotropy.

In contrast to the amorphous RETM alloys, ferrites are air-stable M/O materials which are capable of being used without costly protective layers. Recently, these oxides gained renewed importance after having lost significance for reasons associated with the difficult process technology and inadequate quality of reproduction.[239] Ferrites are mixed oxides consisting of trivalent iron and various metal cations which crystallize with spinel, garnet or hexagonal type structures.

In the field of data stores, hexagonal ferrites have been recognized as hard magnetic pigments for the magnetic technology.[226] As far as M/O storage is concerned, barium ferrites $BaFe_{12}O_{19}$ with a magnetoplumbite structure are of special interest. The barium ions can be replaced by strontium, lead or in some cases calcium ions, or alternatively by equimolar quantities of M^I (Na, K, Rb etc.) and M^{III} (La, Pr, Gd etc.). There are five magnetic sublattices with differing spin orientation of the $Fe^{3\oplus}$ ions. At a wavelength of 788 nm, $BaFe_{12}O_{19}$ shows a Kerr rotation of 0.22° which increases on partial replacement of the $Fe^{\oplus}$ by $Co^{2\oplus}$/$Ti^{4\oplus}$.[227] The coating of the substrate with a ferrite film can take place by epitaxy from the melt[228] or by reactive sputtering on glass disks at substrate temperatures above 550 °C.[229]

Ferrites having a spinel structure have the general composition MFe_2O_4 (M = $Co^{2\oplus}$, $Mn^{2\oplus}$, $Ni^{2\oplus}$, $Zn^{2\oplus}$ etc.). At 700 nm, chromium-substituted and rhodium-substituted cobalt spinels $CoM'_xFe_{2-x}O_4$(M′ = Cr, Rh) exhibit Kerr angles of approximately 0.3–0.5°. The Curie temperature of the cobalt spinel (x = 0) is 520 °C. The very high rate of heat loss, which arises in the course of the Curie point writing of thin layers of these materials, can be reduced by incorporation of a dielectric layer into a three-layer structure of the storage medium.[231] As a result of the incorporation of chromium or rhodium, the Curie temperature of the cobalt spinel is reduced: $M'_x = Rh_1$, $T_c = 62$ °C; $M'_x = Rh_{1.5}$, $T_{Curie} = -113$ °C; $M'_x = Cr_1$, $T_{Curie} = 107$ °C.[230] On account of the high saturation magnetization, domains are marked at T_{Curie} without an external magnetic field. In order to improve the magneto-optical properties, the combination of ferrites in mutually superimposed film layers was also tested, and, for example, using $NiFe_2O_4$ and $CoFe_2O_4$,[232] it is possible to produce aluminum-cobalt ferrites $CoAl_xFe_{2-x}O_4$ as film by sintering at 1250 °C; as the aluminum content rises, the Curie temperature falls from approximately 500 °C (x = 0.1) to 150 °C (x = 1.0).[233]

Ferrites having a garnet structure—$M_3Fe_5O_{12}$ (M = Y, Gd, Dy, Ga, Tb; $M_3 = M^IM^{II}M^{III}$)—are similar to the rare earth/transition metal alloys. In garnets of the type $Gd_{3-x}Bi_xFe_5O_{12}$, a displacement of the compensation temperature was measured as a function of x; $\Delta T_{comp} = 135$ K per atom-% Bi.[234] The sublattice of the $Gd^{3\oplus}$ ions couples antiparallel to the $Fe^{3\oplus}$ sublattice. At low temperatures, the moment of the rare earths is greatest, while at higher temperatures that of the iron ions is predominant. In the middle temperature range, a compensation temperature occurs.

In a similar way to the case of the RETM alloys, the magnetic anisotropy constant K_u is dependent on the condi-

tions of the film preparation, which can vary widely when the layers are prepared by liquid-phase epitaxy on the one hand and by sputtering on the other.[235] In spite of their outstanding physical and chemical stability, magneto-optical films consisting of ferrites are at present not yet suitable for industrial application in commercial products since the Curie temperatures are too high and light absorption and surface smoothness are too low. As a result of the crystalline structure, the signal noise is very high compared to that of the amorphous RETM materials. The possible coating methods for magneto-optical oxides require high temperatures ($>500\,^{\circ}C$), so that the use of polymeric substrates demands the development of special processes. $(GdBi)_3(FeAlGa)_5O_{12}$ could be sputtered by using a garnet target while maintaining a substrate temperature of 100 °C using an RF magnetron.[236] Composite films of RETM alloys and garnets have been produced, with the objective of combining sensitivity and storage density of amorphous compounds with the large Kerr angles of the crystalline ferrites. $(BiY)_3(FeGa)_5O_{12}$ layers have been covered with DyFe[237] and TbFe.[238] The Kerr angles of the composite layers were greater by a factor of 10 compared to the values of the amorphous compounds.

5.3. Materials for Reversible Phase Change

Reversible phase change of inorganic materials is the second alternative to the magnet technology which is currently under intensive investigation. Transitions between light-scattering crystalline and highly reflective amorphous phases permit the switching. The crystalline materials—alloys of elements of the fifth and sixth main group—change into an amorphous phase after pulsed laser irradiation from the melt with rapid cooling. The crystalline phase is formed again by extended heating beyond the glass point. The advantages of this storage technique are the simple optical system of the disk drive and high stability of the medium. Disadvantages are the incomplete recrystallization in the event of frequent overwriting, thus deforming the atomic lattice and destabilizing the inscribed information on repeated reading.[146, 240] This can be reduced by matching the laser energy to the number of cycles.[241]

The reversible properties of amorphous tellurium alloys were observed for the first time by *Ovshinsky*.[242] Using electron microscopy, it was found that amorphous and crystalline phases respectively are present which differ in their reflectivity.[243] The rates of crystallization from the amorphous condition were investigated on various materials and were ascribed to crystallization effects intensified by photons.[244] Other authors have not confirmed this finding.[246] In principle, the possibilities exist of writing either by the change from amorphous to crystalline or from crystalline to amorphous. *Von Gutfeld* et al. were the first to propose the phase change from crystalline to amorphous as a writing mode[245] which is also referred to as RM (*R*everse *M*ode) recording.

The advantage of this mode of data marking is that the crystallization rate limits the switching speed in the amorphous-crystalline mode. This is of importance with regard to computer application with the shortest possible write times; where erasure from amorphous to crystalline is concerned, longer switching times can be tolerated. Figure 28 represents the temperatures and pulse times for writing, reading and erasure in the case of RM recording. Before being used, the storage medium is heated by a floodlight (approximately

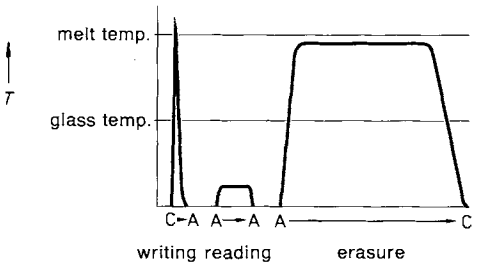


Fig. 28. Principle of reverse mode recording with amorphous (A) to crystalline (C) phase change materials [6]. The width of the signals corresponds to the pulse duration.

1–10 μs), in order to crystallize the film for the starting condition. Using short pulses—approximately 100 nsec and shorter—the marking of the amorphous domains takes place at high laser power. In this case, the material is melted briefly so that the crystalline arrangement is destroyed. After the pulse, the medium cools down at cooling rates of 10^9–$10^{11}\,K\,s^{-1}$, whereby the formation of a regular crystal lattice is prevented. The read beam has only a fraction of the energy of the write beam, in order to permit the appearance of changes even at very high numbers of cycles ($>10^6$). The energy of the erasure beam is selected so that the storage medium is heated beyond the glass point and recrystallization commences.

The particular objective of current developments is to increase the speed of switching (crystallization) and the stability at room temperature in order to guarantee data security. However, the improvement of the stability is also in most cases associated with longer crystallization times and results in longer pulse times for erasure. Within these conflicting requirements there resides a fundamental difficulty regarding the development of phase-change materials which can be used on a technical scale. The extension of the crystallization can, for example, follow from a phase separation taking place simultaneously during the crystallization since in this case diffusion-controlled transport processes limit the speed of crystallization.

Reference will be made herein to some current materials. High linear bit densities of 0.63 μm per bit were achieved with a PbTeSe alloy, which permitted, in a specific practical form, an increase in the density to 0.50 μm per bit.[247] In this way, it is possible to store approx. 1 GByte data capacities per side on a 5.25″ disk. Depending upon the tellurium content, indium-containing films of the $In_{50-x}Sb_{50}Te_x$ type may be switched very rapidly: with x = 1, 2, 5, 10 and 20, a pulse width of 50, 70, 90, 300 ns and 1 μs respectively was measured for the recrystallization from the amorphous phase.[248]

InSeTlCo alloys show a rapidly switchable phase change from amorphous to crystalline: the phase transformation takes place in 60 ns at a laser power of 14 mW[249] (Fig. 29). Based on a crystallization temperature of 320 °C and an acti-

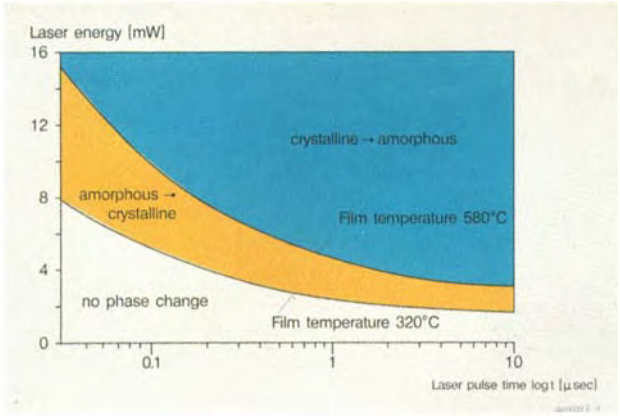


Fig. 29. Laser energy and pulse duration for the reversible phase transformation of an InSeTlCo alloy at two film temperatures [249].

vation energy of 3 eV, the result is approximately 100 years for the lifetime of amorphous domains. During recent times, progress has been reported regarding GeTeSn,[250] GeTeTi,[251] and InSePb[252] alloys.

6. Summary and Outlook

As a result of the success of CD technology, the development of write-once (WORM) and reversible (EDRAW) storage disks to the stage of marketing readiness has become a matter of prime importance in industry during recent years. The IR emission of the semiconductor lasers employed as light source makes the synthesis of novel IR-absorbing dyes necessary for WORM recording media. Specific compounds of the category of the polymethines, phthalo- and naphthalocyanines and dithiolatonickel complexes have already been used with success. In addition, metal alloys have been recognized to permit storage by means of a phase change. WORM memories are mainly used for data archiving; accordingly, a high degree of data security over long periods of time is required. Due to the sensitivity to oxidation of the inorganic WORM layers, there are some advantages of the dye media.

The most highly developed EDRAW memories are represented by the magneto-optical films consisting of rare earth/element/transition metal alloys. It is expected that they will be able to replace the currently dominant mass memories on the basis of magnet technology within broad fields. Their advantages are relatively high storage density, insensitivity to mechanical stress, and easy exchangeability and thus they follow the development trends of computer technology.

Developments of new optical disk drives will be a great incentive with regard to storage media. The use of optical reading systems based on laser arrays, of integrated optical systems together with polymeric optical waveguides, and of lasers with frequency doubling to generate smaller wavelengths will open up possibilities for further increasing the data rates and storage densities. In the near future, this will also initiate the production of novel recording layers. Alternatives to the memories discussed above could be represented by storage media which are based on photochromic dyes,[253] liquid-crystal polymers,[254] Langmuir–Blodgett films,[255] demixing effects in polymers,[256] crystallization effects in doped polymer matrices,[257] specific fluorescence dyes,[258] luminescence in doped aluminum oxide,[259] or storage processes utilizing the piezoelectric or pyroelectric effects,[260] scanning tunneling microscopy,[261] the birefringence relaxation of stretched dye–polymer films,[262] and the LIESST effect (*L*ight *I*nduced *E*xcited *S*pin *S*tate *T*rapping).[263] With other recording processes, the information densities of the industrially produced optical memories may even be exceeded: photochemical hole burning 10^{11} bit cm^{-2},[264] electron beam solid state memories 10^{12} bit cm^{-2}[265] and holographic memories 10^{14} bit cm^{-2}.[265] These recording media and processes have no practical significance yet; however, they form part of intensive research and development efforts as is evident from a research program of the Japanese MITI[266] and more recent publications in the field of photochemical hole burning.[267]

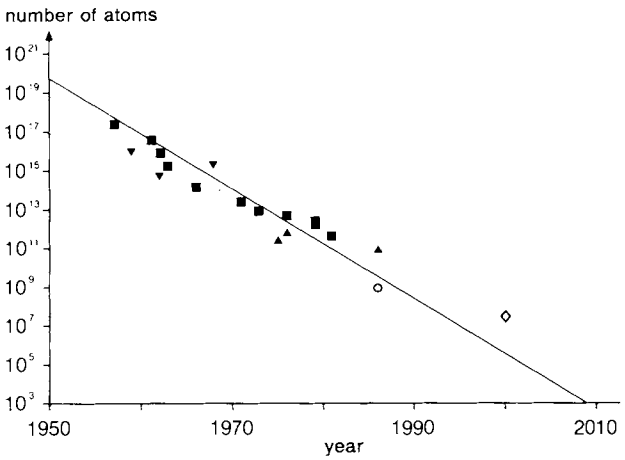


Fig. 30. Comparison for different storage technologies of number of atoms used to store a bit; the line represents the development of future technologies (after [2c]). ■ = Fixed disk, ▲ = magnetic bubble memory, ▼ = thin layer technique, ○ = optical memory, ◇ = molecular storage.

Projects which are concerned with the construction of molecular switches and molecular storage elements are framed in terms of molecular dimensions.[268] This work is concerned with the construction and the characterization of isolated simple models for investigating fundamental phenomena and the further development of model concepts concerning possible modes of operation of molecular memories.

In this connection, conceptual considerations take account of the significance of molecular order and supramolecular structures. Against this background, attempts have been made to utilize phenomena of self-organization in order to generate orientation and structure. Thus, there are parallels with the biological information system, which is characterized by the formation of highly ordered molecular systems. It appears that even future information systems can be developed using concepts which are based on principles realized in nature.

We express our thanks to Dr. B. Fischer, Dr. B. Löhr, and Dr. W. Wiedemann (Information Technology Division of Hoechst

AG, Wiesbaden) for helpful discussions, to Mrs. P. Sendelbeck, Mrs. S. Nink, Mrs. E. Himburg, Mrs. U. Jensen and Mrs. U. Kletschke for typing the article, and to Mrs. G. Wettlaufer and Mr. M. Utermark for the graphical material.

Received: June 21, 1989 [A 738 IE]
German version: *Angew. Chem. 101* (1989) 1475

[1] H. Kuhn, *IBM J. Res. Dev. 32* (1988) 37.
[2] a) R. Landauer, Phys.1971 *Plenarvortr. Physikertag. 36th 1971* 286; b) H. Kuhn, *Ber. Bunsenges. Phys. Chem. 80* (1976) 1209; c) R. W. Keyes, *IBM J. Res. Dev. 32* (1988) 24.
[3] G. Bouwhuis, J. Braat, A. Huijser, J. Pasman, G. van Rosmalen, K. Schouhamer-Immink: *Principles of Optical Disc Systems*, Adam Hilger, Bristol, UK 1985.
[4] J. Isailovic: *Videodisc and Optical Memory Systems*, Prentice-Hall, Englewood Cliffs, NJ, USA 1985.
[5] a) R. A. Sprague, (Ed.), *Proc. SPIE Int. Soc. Opt. Eng. 329* (1982); b) D. Chen (Ed.), *ibid. 382* (1983); c) E. V. La Budde (Ed.), *ibid 421* (1983); d) R. A. Sprague (Ed.), *ibid. 529* (1985); e) D. A. Carlin, Y. Tsunoda, A. A. Jamberdino (Ed.), *ibid. 899* (1988); f) G. R. Knight, C. N. Kurtz (Ed.), *ibid. 1078* (1989).
[6] A. E. Bell in M. J. Weber (Ed.): *Handbook of Laser Science and Technology, Vol. 5, Part 3*, CRC Press, Boca Rota, FL, USA 1987, p. 65.
[7] a) H. H. Hopkins, *J. Opt. Soc. Am. 69* (1979) 4; b) M. G. Carasso, J. B. M. Peek, J. P. Sinjou, *Philips Tech. Rev. 40* (1982) 151; c) J. P. J. Heemskerk, K. A. Schouhamer-Immink, *ibid. 40* (1982) 157; d) L. J. Laub, *IEEE Trans. Consum. Electron. CE-22* (1976) 258.
[8] a) G. C. Kenney, *IEEE Trans. Consum. Electron. CE-22* (1976) 327; b) I. Sebestyen, *Electron. Pub. Rev. 2* (1982) 41; c) C. M. Goldstein, *Science (Washington) 215* (1982) 862; d) M. Noordenbos, *Mikrodok.* (FBO-Fachverlag; ISSN 0344-8010) *14* (1988) 8; e) R. P. Freeze, *IEEE Spectrum 25* (1988) 41; f) D. Caruso, *Electronics 58* (1985) 26.
[9] A. E. Bell, *SID Proc. 24* (1983) 17.
[10] M. H. Kryder, *J. Appl. Phys. 57* (1985) 3913.
[11] G. Kaempf, H. Loewer, M. W. Witman, *Polym. Eng. Sci. 27* (1987) 1421.
[12] F. E. Luborsky, *Mater. Res. Soc. Symp. Proc. 80* (1987) 375.
[13] J. E. Kuder, *J. Imaging Technol. 12* (1986) 140.
[14] J. E. Kuder, *J. Imaging Technol. 32* (1988) 51.
[15] J. M. Pearson, *CRC Crit. Rev. Solid State Mater. Sci. 13* (1986) 1.
[16] D. S. Bloomberg, G. A. Neville Connell in C. D. Mee, E. D. Daniel (Ed.): *Magnetic Recording, Vol. 2*, McGraw-Hill, New York 1988; p. 304.
[17] M. Fujimoto, G. Sato, *Shikizai Kyokaishi 61* (1988) 215.
[18] F. J. A. M. Greidanus, S. Klahn, *Angew. Chem. Adv. Mater. 101* (1989) 243; *Angew. Chem. Int. Ed. Engl. Adv. Mater. 28* (1989) 229; *Adv. Mater. 1989*, 45.
[19] a) N. Grote, *Phys. Unserer Zeit 8* (1977) 103; b) K. J. Ebeling, *Laser Optoelektr. 16* (1984) 176; c) W. T. Tsang, *Appl. Phys. Lett. 42* (1983) 650; d) C. H. Good: *Injection Electroluminescent Devices*, Wiley, New York 1973.
[20] a) A. Watabe, K. Katoh, H. Ukita, *Proc. SPIE Int. Soc. Opt. Eng. 529* (1985) 150; b) O. Ito, K. Yoshimoto, I. Watanabe, T. Kubo, *ibid. 529* (1985) 145; c) R. Miller, C. Abate, *ibid. 529* (1985) 140; d) Y. Tsunoda, S. Horigome, Z. Tsutsumi, *ibid. 382* (1983) 24; e) C. Bricot, J. Cornet, J.-L. Gerad, F. Le Carvennec, *ibid. 329* (1982) 94; f) I. Prikryl, *ibid. 1078* (1989) 244; g) K. Katoh, A. Watabe, M. Yamamoto, *ibid. 899* (1988) 24.
[21] M. Nagashima, *Appl. Phys. Lett. 42* (1983) 144.
[22] a) A. T. Eventoff, G. C. Kenney, *Proc. SPIE Int. Soc. Opt. Eng. 329* (1982) 252; b) D. H. Davies, *ibid. 420* (1983) 53; c) D. B. Kay, *ibid. 382* (1983) 97.
[23] K. Ohta, A. Takahashi, T. Deguchi, T. Hyuga, S. Kobayashi, H. Yamaoka, *Proc. SPIE Int. Soc. Opt. Eng. 382* (1983) 252.
[24] R. N. Gardner, T. Rinehart, L. H. Johnson, R. P. Freese, R. A. Lund, *Proc. SPIE Int. Soc. Opt. Eng. 420* (1983) 242.
[25] J. H. T. Pasman, H. F. Olijhoek, R. Verkaik, *Proc. SPIE Int. Soc. Opt. Eng. 529* (1985) 62.
[26] C. M. Rodia, *Proc. SPIE Int. Soc. Opt. Eng. 529* (1985) 69.
[27] K. Manabe, M. Niwano, M. Isohe, S. Shimokihara, *Polym. Prepr. (Am. Chem. Soc. Div. Polym. Chem.) 29* (1988) 230.
[28] P. E. J. Legierse, *Galvanotechnik 79* (1988) 3246.
[29] J. G. Dil, C. A. Weshop, *Appl. Opt. 18* (1979) 3198.
[30] Y. Okino, K. Sano, T. Kashihara, *Proc. SPIE Int. Soc. Opt. Eng. 329* (1982) 236.
[31] M. J. Brekner, *Polym. Prepr. (Am. Chem. Soc. Div. Polym. Chem.) 29* (1988) 234.
[32] J. Hennig, *Jpn. J. Appl. Phys. 26, Suppl. 24–4* (1987) 9.
[33] J. Hennig, *Kunststoffe 75* (1985) 425.
[34] M. Nakada, M. Saitoh, K. Toki, H. Gokan, *Jpn. J. Appl. Phys. 26, Suppl. 24–4* (1987) 95.
[35] N. A. Peppas, C. N. Bowman, A. L. Carver, S. L. Kennett, M. M. Williams, *Polym. Prepr. (Am. Chem. Soc. Div. Polym. Chem.) 29* (1988) 204.
[36] W. G. Driscoll (Ed.): *Handbook of Optics*, McGraw-Hill, New York 1978.
[37] A. Nussbaum, R. A. Philips: *Comtemporary Optics for Scientists and Engineers*, Prentice Hall, Englewood Cliffs, NJ, USA 1976.
[38] B. R. Hahn, J. H. Wendorff, *Polymer 26* (1985) 1619.
[39] M. Isobe, S. Imai, *Sumitomo Chem. Co., Ltd., Ehime Res. Lab. 1986*, 79
[40] K. Compaan, P. Kramer, *Philips Tech. Rev. 33* (1973) 178.
[41] R. G. Gossink, *Angew. Makromol. Chem. 145/146* (1986) 365.
[42] H. C. Haverkorn, P. E. J. Legierse, G. E. Thomas, *Philips Tech. Rev. 40* (1982) 287.
[43] J. G. Kloosterboer, G. J. M. Lippits, H. C. Meinders, *Philips Tech. Rev. 40* (1982) 298.
[44] H. Völz, *Nachrichtentech. Elektron. 37* (1987) 164.
[45] J. J. Wrobel, A. B. Marchant, D. G. Howe, *Appl. Phys. Lett. 40* (1982) 928.
[46] D. Meyerhofer, *J. Appl. Phys. 49* (1978) 3993.
[47] a) V. B. Jipson, C. R. Jones, *J. Vac. Sci. Technol. 18* (1981) 105; b) A. E. Bell, F. W. Spong, *IEEE J. Quantum Electron. QE 14* (1978) 487.
[48] K. Y. Law, P. S. Vincett, R. O. Loufty, L. Alexandru, M. A. Hopper, J. H. Sharp, G. E. Johnson, *Appl. Phys. Lett. 36* (1980) 884.
[49] a) K. Y. Law, P. S. Vincett, G. E. Johnson, *Appl. Phys. Lett. 39* (1981) 718; b) D. G. Howe, J. J. Wrobel, *J. Vac. Sci. Technol. 18* (1981) 92.
[50] a) T. W. Smith, D. Wychik, *J. Phys. Chem. 84* (1980) 1621; b) J. Drexler, *J. Vac. Sci. Technol. 18* (1981) 87.
[51] M. C. Gupta, *Appl. Opt. 23* (1984) 3950.
[52] M. Mitsuya, M. Terao, T. Kaku, K. Shigematsu, M. Akagi, *J. Appl. Phys. 54* (1983) 3710.
[53] a) V. Novotny, L. Alexandru, *J. Appl. Phys. 50* (1979) 1215; b) *J. Appl. Polym. Sci. 24* (1979) 1321.
[54] a) L. Alexandru, M. A. Hopper, R. O. Loufty, J. H. Sharp, P. S. Vincett, G. E. Johnson, K. Y. Law, *Polym. Prepr. (Am. Chem. Soc. Div. Polym. Chem.) 25* (1984) 305; b) L. Alexandru, M. A. Hopper, R. O. Loufty, J. H. Sharp, P. S. Vincett, G. E. Johnson, K. Y. Law in A. Davidson (Ed.): *Materials for Microlithography (ACS Symp. Ser. 219* (1983)).
[55] a) J. A. Cornet, *Proc. SPIE Int. Soc. Opt. Eng. 420* (1983) 86; b) US-Pat. 4 360 895 (1982), Thomson CSF S.A.; c) J. Cornet, J. C. Lehureau, H. Magna, EP-A 33 046 (1981), Thomson CSF S.A.; d) K. N. Mafitt, W. B. Robbins, R. F. Williams, US-Pat. 4 430 659 (1984), Minnesota Mining & Mfg. Comp.
[56] D. Mayden, *Bell Syst. Tech. J. 50* (1971) 1761.
[57] P. Kivits, R. de Bont, *Appl. Phys. 24* (1981) 307.
[58] a) P. Kivits, R. de Bont, P. Zalm, *Appl. Phys. 24* (1981) 273; b) P. Kivits, R. de Bont, B. Jacobs, P. Zalm, *Thin Solid Films 87* (1982) 215.
[59] T. S. Chung, *J. Appl. Phys. 60* (1986) 55.
[60] K. Y. Law, G. E. Johnson, *J. Appl. Phys. 54* (1983) 4799.
[61] M. F. Molaire: *The Influence of Melt Viscosity on the Writing Sensitivity of Organic Dye-Binder Optical Disk Recording Media (OSA Top. Meet. Opt. Data Storage, Stageline, NV, USA 1987*, Abstr. ThA 4-1.
[62] a) A. Bloom, R. A. Bartolini, A. E. Bell, US-Pat. 4 023 185 (1977), RCA Corp.; b) H. T. Thomas, J. J. Wrobel, US-Pat. 4 380 769 (1983), Eastman Kodak Comp.; c) S. R. Gerfast, US-Pat. 4 365 257 (1982), Minnesota Mining & Mfg. Comp.; d) B. Albert, P. Neumann, G. Hansen, K. D. Schomann, DOS 34 28 458 (1986), BASF AG.
[63] A. E. Bell, R. A. Bartolini, US-Pat. 4 195 312 (1980), RCA Corp.
[64] A. Bloom, R. A. Bartolini, US-Pat. 4 218 689 (1980), RCA Corp.
[65] A. Kuroiwa, K. Namba, S. Asami, T. Aoi, K. Takahashi, S. Nakagawa, *Jpn. J. Appl. Phys. Part 1 22* (1983) 340.
[66] M. Kunikane, Jpn. Kokai Tokkyo JP 58-112 793 (1983), Ricoh Co., Ltd.; *Chem. Abstr. 99* (1983) 167101.
[67] Jpn. Kokai Tokkyo Koho JP 56-46 221 (1981), Nippon Telegraph and Telephone Public Corp.; *Chem. Abstr. 95* (1981) 178630.
[68] Jpn. Kokai Tokkyo Koho JP 58-112 790 (1983), Ricoh Co., Ltd.; *Chem. Abstr. 99* (1983) 167102.
[69] M. Kunikane, M. Abe, Jpn. Kokai Tokkyo JP 58-112 791 (1983), Ricoh Co., Ltd.; *Chem. Abstr. 99* (1983) 131425.
[70] P. Kivits, R. de Bont, J. van der Veen, *Appl. Phys. A 26* (1981) 101.
[71] a) M. Kunikane, M. Abe, M. Umehara, US-Pat. 4 460 665 (1984), Ricoh Co., Ltd.; b) K. Namba, S. Asami, A. Kuroiwa, A. Nakagawa, Jpn. Kokai Tokkyo JP 59-55 795 (1984), TDK Corp.; *Chem. Abstr. 102* (1985) 87717; c) Jpn. Kokai Tokkyo JP 59-85 791 (1984), Ricoh Co., Ltd.; *Chem. Abstr. 101* (1984) 181296; d) Jpn. Kokai Tokkyo JP 59-24 690 (1984), TDK Corp.; *Chem. Abstr. 100* (1984) 219114; e) Jpn. Kokai Tokkyo JP 59-67 092 (1984), TDK Corp.; *Chem. Abstr. 102* (1985) 36849; f) H. Oba, Y. Ueda, T. Sato, M. Umehara, M. Abe, H. Funakoshi, S. Kobayashi, GB-Appl. 2 165 658 (1986), Ricoh Co., Ltd.
[72] a) E. Daltrozzo, G. Scheibe, K. Gschwind, F. Haimerl, *Photogr. Sci. Eng. 18* (1974) 441; b) T. M. Herz, *ibid. 18* (1974) 323.
[73] G. W. Byers, S. Gross, P. M. Henrichs, *Photochem. Photobiol. 23* (1976) 37.
[74] H. Oba, T. Sato, M. Umehara, M. Abe, Jpn. Kokai Tokkyo JP 61-248 789 (1986), Ricoh Co., Ltd.; *Chem. Abstr. 107* (1987) 49658.

[75] a) Jpn. Kokai Tokkyo JP 58-195 595 (1983), Canon KK; *Chem. Abstr. 101* (1984) 238217; b) Jpn. Kokai Tokkyo JP 58-220 792 (1983), Canon KK; *Chem. Abstr. 101* (1984) 81726; c) Jpn. Kokai Tokkyo JP 58-219 091 (1983), Canon KK; *Chem. Abstr. 101* (1984) 81727; d) Jpn. Kokai Tokkyo JP 59-150 795 (1984), Ricoh Co., Ltd.; *Chem. Abstr. 102* (1985) 70330.

[76] a) K. Miura, T. Ozawa, J. Iwanami, Jpn. Kokai Tokkyo JP 60-228 448 (1986), Mitsubishi Chemical Industries *Chem. Abstr. 104* (1986) 129641; b) Jpn. Kokai Tokkyo JP 61-167 680 (1986), Mitsubishi Chemical Industries; *Chem. Abstr. 106* (1987) 50042; c) Jpn. Kokai Tokkyo JP 61-167 681 (1986), Mitsubishi Chemical Industries; *Chem. Abstr. 106* (1986) 50044; d) T. Ozawa, S. Maeda, Y. Kurose, Jpn. Kokai Tokkyo JP 62-138 459 (1987), Mitsubishi Chemical Industries; *Chem. Abstr. 107* (1987) 226072.

[77] a) Jpn. Kokai Tokkyo JP 58-217 391 (1983), Asahi Chemical Industry Co., Ltd.; *Chem. Abstr. 102* (1985) 36847; b) Jpn. Kokai Tokkyo JP 58-173 696 (1983), Canon KK; *Chem. Abstr. 100* (1984) 94591; c) Jpn. Kokai Tokkyo JP 59-14 150 (1984), Canon KK; *Chem. Abstr. 102* (1985) 15216.

[78] a) W. Schrott, B. Albert, P. Neumann, H. Benthack-Thoms, DE-OS 37 03 985 (1988), BASF AG; b) T. Hioki, Y. Inagaki, M. Yabe, DE-OS 38 06 181 (1988), Fuji Photo Film Co., Ltd.; c) T. Ozawa, S. Maeda, Y. Kurose, Jpn. Kokai Tokkyo JP 62-130 890 (1987), Mitsubishi Chemical Industries; *Chem. Abstr. 107* (1987) 226074.

[79] a) M. Dust, P. Neumann, DE-OS 36 22 138 (1988), BASF AG; b) Y. Ma, S. Ishikawa, T. Arita, K. Sakai, M. Maikara, Jpn. Kokai Tokkyo JP 59-84 249 (1984), Canon KK; *Chem. Abstr. 102* (1985) 103493.

[80] K. Sakai, S. Ishikawa, T. Arita, M. Mabuchi, S. Umehara, US-Pat. 4 501 808 (1985), Canon KK.

[81] a) M. Dust, P. Neumann, E. Schefczik, H. Benthack-Thoms, H. Barzynski, K. D. Schomann, H. Kuppelmaier, E. Köster, DE-OS 36 08 214 (1987), BASF AG; b) M. Dust, P. Neumann, P. Hauser, G. Wagenblast, H. Benthack-Thoms, H. Barzynski, K. D. Schomann, H. Kuppelmaier, E. Köster, DE-OS 36 31 843 (1988), BASF AG.

[82] a) G. L. Fletcher, S. L. Bender, D. H. Wadsworth, US-Pat. 4 577 024 (1986), Eastman Kodak Comp.; b) D. H. Wadsworth, H. T. Thomas, G. L. Fletcher, C. H. Weidner, US-Pat. 4 446 223 (1984), Eastman Kodak Comp.; c) M. F. Molaire, US-Pat. 4 499 165 (1984), Eastman Kodak Comp.

[83] M. A. Elmasry, WO 86/05504 (1986), Minnesota Mining & Mfg. Comp.

[84] a) M. Thomas, P. Neumann, DE-OS 34 13 940 (1985), BASF AG; b) H. Berneth, R. Raue, DE-OS 37 04 263 (1988), Bayer AG; c) Jpn. Kokai Tokkyo JP 58-219 090 (1983), Canon KK; *Chem. Abstr. 101* (1984) 81728; d) D. J. Gravesteijn, J. van der Veen, *Philips. Tech. Rev. 41* (1983/1984) 325; e) D. J. Gravesteijn, C. Steenbergen, J. van der Veen, *Proc. SPIE Int. Soc. Opt. Eng. 420* (1983) 327.

[85] a) K. Namba, Jpn. Kokai Tokkyo JP 60-159 087 (1985), TDK Corp.; *Chem. Abstr. 104* (1986) 120089; b) Jpn. Kokai Tokkyo JP 60-163 243 (1985), TDK Corp.; *Chem. Abstr. 106* (1987) 11249; c) Jpn. Kokai Tokkyo Koho JP 59-55 795 (1984), TDK Corp.; *Chem. Abstr. 102* (1985) 87717; d) Jpn. Kokai Tokkyo Koho JP 59-67 092 (1984), TDK Corp.; *Chem. Abstr. 102* (1985) 36849.

[86] a) Jpn. Kokai Tokkyo Koho JP 59-55 794 (1984), TDK Corp.; *Chem. Abstr. 102* (1985) 70319; b) Jpn. Kokai Tokkyo Koho JP 59-81 194 (1984), TDK Corp.; *Chem. Abstr. 102* (1985) 140964; c) S. Yamamuro, M. Abe, Y. Ueda, T. Sato, M. Umehara, Jpn. Kokai Tokkyo Koho JP 60-257 290 (1985) Ricoh Co., Ltd.; *Chem. Abstr. 105* (1986) 15357; d) Jpn. Kokai Tokkyo Koho JP 59-83 695 (1984), TDK Corp.; *Chem. Abstr. 102* (1985) 70323.

[87] a) P. V. Susi, DE-OS 18 16 247 (1969), American Cyanamid Corp.; b) P. V. Susi, N. A. Weston, FR-Appl. 1 398 240 (1965), American Cyanamid Corp.; c) T. Sato, M. Umehara, M. Abe, H. Oba, Y. Ueda, GB-Appl. 2 155 811 (1985), Ricoh Co., Ltd.; d) T. Sato, S. Shindo, T. Numa, M. Sumiya, Jpn. Kokai Tokkyo Koho JP 62-32 132 (1987), Nippon Kayaku Co., Ltd.; *Chem. Abstr. 107* (1987) 24277; e) T. Sato, M. Umehara, M. Abe, H. Oba, Y. Ueda, DE-OS 35 03 995 (1988), Ricoh Co., Ltd.

[88] a) K. Namba, EP-A 147 083 (1985), TDK Corp.; b) K. Namba, S. Asami, T. Aoi, K. Takahashi, A. Kuroiwa, Jpn. Kokai Tokkyo Koho JP 61-8 384 (1986), TDK Corp.; *Chem. Abstr. 105* (1986) 70213; c) S. Yamamuro, H. Oba, M. Abe, T. Sato, Y. Ueda, M. Umehara, Jpn. Kokai Tokkyo Koho JP 61-72 586 (1986), Ricoh Co., Ltd.; *Chem. Abstr. 106* (1987) 58998.

[89] a) T. Sato, T. Sakaeda, K. Ichinose, Jpn. Kokai Tokkyo Koho JP 62-193 891 (1987), Ricoh Co., Ltd.; *Chem. Abstr. 109* (1988) 160675; b) T. Sato, DE-PS 35 21 915 (1985), Ricoh Co., Ltd.; c) K. Namba, *1st Int. Symp. Chem. Funct. Dyes,* Kinki Chemical Society, Osaka, Japan 1989; d) H. Flohr, J. Jesse, B. Albert, P. Neumann, DE-OS 35 20 109 (1986), BASF AG; e) T. Sato, T. Eida, K. Ichinose, DE-OS 37 24 981 (1988), Ricoh Co., Ltd.

[90] Neth. Appl. NL 83 00 155 (1984), Philips Gloeilampenfabrieken.

[91] a) F. H. Moser, A. L. Thomas: *The Phthalocyanines, Vol. I, II,* CRC Press, Boca Rota, FL, USA 1983; b) A. B. P. Lever, *Adv. Inorg. Chem. Radiochem. 7* (1965) 27; c) D. Wöhrle, G. Meyer, *Kontakte (Darmstadt) 1985,* No. 3, p. 38.

[92] a) F. H. Moser, A. L. Thomas: *Phthalocyanine Compounds,* Reinhold, New York; Chapman and Hall, London 1968; b) L. J. Boucher in G. A. Meslon (Ed): *Coordination Chemistry of Macrocyclic Compounds,* Plenum, New York 1979; Chapter 7.

[93] a) A. R. Kane, J. F. Sullivan, D. H. Kenney, M. E. Kenney, *Inorg. Chem. 9* (1970) 1445; b) B. L. Wheeler, G. Nagasubramanian, A. J. Bard, L. E. Schechtman, D. R. Dininny, M. E. Kenney, *J. Am. Chem. Soc. 106* (1984) 7404.

[94] a) M. Hanack, J. Metz, G. Pawlowski, *Chem. Ber. 115* (1982) 2836; b) D. Wöhrle, G. Meyer, B. Wahl, *Makromol. Chem. 181* (1980) 2127; c) C. Piechocki, J. Simon, A. Skoulios, D. Guillon, P. Weber, *J. Am. Chem. Soc. 104* (1982) 5245.

[95] a) S. Higaki, K. Hanabusa, H. Shirai, N. Hojo, *Makromol. Chem. 183* (1984) 691; b) G. Pawlowski, M. Hanack, *Synthesis 1980,* 287.

[96] Y. Goto, N. Kohino, H. Goto, K. Ogawa, EP-A 83 991 (1983), Fujitsu Ltd.

[97] a) A. M. Hor, R. O. Loufty, *Thin Solid Films 106* (1983) 291; b) R. O. Loufty, A. M. Hor, G. DiaPaola, C. K. Hsiao, *J. Imaging Sci. 29* (1984) 116.

[98] Jpn. Kokai Tokkyo Koho JP 59-16 785 (1984), Sumitomo Chemical Co., Ltd.; *Chem. Abstr. 100* (1984) 148595.

[99] a) K. Tanikawa, US-Pat. 4,458,004 (1984, Ricoh Co., Ltd.); b) O. Kaieda, I. Okitaka, H. Ito, Jpn. Kokai Tokkyo Koho JP 63-30 566 (1988), Nippon Shokubai KK Co., Ltd.; *Chem. Abstr.* 109 (1988) 75212; c) I. Okitaka, H. Ito, O. Kaieda, Jpn. Kokai Tokkyo Koho JP 63-141 342 (1988), Nippon Shukobai KK Co., Ltd.; *Chem. Abstr. 110* (1988) 77513.

[100] a) A. Kuroiwa, N. Namba, T. Kamijo, Jpn. Kokai Tokkyo Koho JP 61-152 685 (1986), TDK Corp.; *Chem. Abstr. 106* (1987) 20 000; b) Jpn. Kokai Tokkyo Koho JP 61-246 091 (1986), TDK Corp.; *Chem. Abstr. 106* (1987) 224577; c) S. Ehashi, S. Miyazaki, M. Sakamoto, Jpn. Kokai Tokkyo Koho JP 63-37 991 (1988), Toyo Ing. Mfg. Co., Ltd.; *Chem. Abstr. 109* (1988) 119826; d) M. Sakamota, S. Miyazaki, T. Sato, S. Ehashi, *1st Int. Symp. Chem. Funct. Dyes,* Kinki Chemical Society, Osaka, Japan 1989; e) H. Shibano, H. Yamazaki, K. Morikawa, Jpn. Kokai Tokkyo Koho JP 63-39 388 (1988) Kao Corp.; *Chem. Abstr. 109* (1988) 46307.

[101] a) S. A. Mikhalenko, E. A. Lukyanets, *Zh. Obshch. Khim. 39* (1969) 2129; b) H. Itoh, S. Takahara, M. Matsumoto, *1st Int. Symp. Chem. Funct. Dyes,* Kinki Chemical Society, Osaka, Japan 1989.

[102] S. A. Mikhalenko, E. A. Lukyanets, *Zh. Obshch. Khim. 39* (1969) 2554.

[103] E. I. Kovshev, E. A. Lukyanets, *Zh. Obshch. Khim. 42* (1972) 696.

[104] a) K. Y. Law, G. E. Johnson, J. W. P. Lin, US-Pat. 4 492 750 (1985), Xerox Corp.; b) S. Hirose, K. Abe, H. Ozawa, Y. Hosono, EP-A 188 331 (1986), Mitsui Toatsu Chemicals, Inc.

[105] S. Tai, S. Hayashida, N. Hayashi, Y. Iwakabe, S. Numata, N. Kinjo, S. Era, S. Kobayashi, A. Mukoh, Y. Sato, EP-A 284 370 (1988), Hitachi Chemical Co., Ltd./Hitachi, Ltd.

[106] S. Maeda, Y. Kurose, Y. Wada, EP-A 279 426 (1988), Mitsubishi Kasei Corp.

[107] a) S. Hayashida, S. Tai, EP-A 254 553 (1988), Hitachi Ltd./Hitachi Chemical Ltd. Co., Ltd. b) R. S. Jones, D. E. Nikles, M. E. Kenney, EP-A 279 426 (1986), Celanese Corp.; c) T. Seiji, S. Hayashida, H. Hagiwara, M. Katayose, K. Kamijima, T. Akimoto, S. Era, S. Kobayashi, A. Mukoh, EP-A 296 876 (1988), Hitachi Chemical Co., Ltd.

[108] T. Kanno, H. Watanabe, S. Nozaki, *Proc. 34th Conf. Soc. Appl. Phys. 1987,* 720.

[109] a) K. Morikawa, H. Shibano, H. Yamazaki, Jpn. Kokai Tokkyo Koho JP 62-223 287 (1987), Kao Corp.; *Chem. Abstr. 109* (1988) 46307; b) S. Hirose, H. Ozawa, K. Abe, Y. Hosono, Jpn. Kokai Tokkyo Koho JP 63-57 287 (1988), Mitsui Toatsu Chemicals, Inc.; *Chem. Abstr. 109* (1988) 83689; c) S. Era, S. Kobayashi, A. Mukoh, EP-A 279 501 (1988), Hitachi Ltd.

[110] B. Albert, H. Kuppelmaier, G. Wagenblast, DE-A 37 11 762 (1988), BASF AG.

[111] a) E. Merian, *Chimia 13* (1959) 181; b) *Am. Dyest. Rep. 48* (1959) 31.

[112] a) K. Y. Chen, J. Griffiths, *J. Chem. Res. Miniprint 1978,* 2319; b) K. Takagi, M. Matsuoka, Y. Kubo, T. Kitao, *Dyes Pigm. 6* (1985) 75.

[113] a) M. Itoh, S. Esho, K. Nakagawa, M. Matsuoka, *Proc. SPIE Int. Soc. Opt. Eng. 420* (1983) 332; b) K. Takagi, M. Kawabe, M. Matsuoka, T. Kitao, *Dyes Pigm. 6* (1985) 177; c) S. H. Kim, M. Matsuoka, Y. Kubo, T. Yoshida, T. Kitao, *ibid. 7* (1986) 93; d) S. H. Kim, S. Minami, M. Matsuoka, T. Kitao, *Chem. Express 2* (1987) 73.

[114] a) Y. Kogo, H. Kikuchi, M. Matsuoka, T. Kitao, *J. Soc. Dyers Colour. 96* (1980) 475; b) M. Matsuoka, K. Takagi, H. Obayashi, K. Wakasugi, T. Kitao, *ibid. 99* (1983) 257.

[115] a) Jpn. Kokai Tokkyo Koho JP 58-112 793 (1983), Ricoh Co., Ltd.: *Chem. Abstr. 99* (1983) 167101; b) Jpn. Kokai Tokkyo Koho JP 59-76 296 (1984), NEC Corp.; *Chem. Abstr. 102* (1985) 103688; c) Jpn. Kokai Tokkyo Koho JP 59-76 297 (1984), NEC Corp.; *Chem. Abstr. 102* (1985) 140967; d) S. Esho, M. Itoh, M. Matsuoka, Jpn. Kokai Tokkyo Koho JP 59-5 096 (1984) TDK Corp.; Chem. Abstr. 100 (1984) 148588.

[116] S. H. Kim, M. Matusoka, T. Kitao, *Chem. Lett. 1985,* 1351.

[117] a) S. Edokoro, M. Itoh, M. Matsuoka, Jpn. Kokai Tokkyo Koho JP 61-22-4 588 (1986), NEC Corp.; *Chem. Abstr. 107* (1987) 49663; b) Jpn.

Kokai Tokkyo Koho JP 61-246 092 (1986), NEC Corp.; *Chem. Abstr. 107* (1987) 49665.
[118] S. H. Kim, M. Matsuoka, T. Yodoshi, T. Kitao, *Chem. Express 1* (1986) 129.
[119] a) Jpn. Kokai Tokkyo Koho JP 58-169 152 (1983), Ricoh Co., Ltd.; *Chem. Abstr. 106* (1987) 147206; b) Jpn. Kokai Tokkyo Koho JP 58-224 448 (1984), TDK Corp.; *Chem. Abstr. 101* (1984) 238255; c) W. Schrott, P. Neumann, B. Wolff, A. Stange, DE-OS 3726 458 (1989), BASF AG.
[120] a) I. L. Boguslavskaya, V. I. Gudzenko, *J. Org. Chem. USSR 4* (1968) 96; b) H. Shibano, K. Morikawa, H. Yamazaki, Jpn. Kokai Tokkyo JP 62-81 082 (1988), Kao Corp.; *Chem. Abstr. 109* (1988) 160749.
[121] a) M. J. Baker-Hawkes, E. Billig, H. B. Gray, *J. Am. Chem. Soc. 88* (1966) 4870; b) H. Shiozaki, H. Kakazumi, Y. Nakado, T. Kitao, *Chem. Lett. 1987*, 2393.
[122] a) M. Suzuki, M. Kawamura, K. Kato, M. Takahashi, T. Morishita, K. Nakayama, A. Nakatsuka, EP-A 278 257 (1987), Seitetsu Kagaku Co., Ltd.; b) W. Schrott, P. Neumann, B. Albert, EP 193 774 (1986) BASF AG; c) W. Schrott, P. Neumann, B. Albert, M. Thomas, H. Barzynski, K. Schomann, H. Kuppelmaier, DE-OS 3505 751 (1986), BASF AG; d) K. Sasagawa, E. Noda, M. Imai, WO 83/02428 (1983), Mitsui Toatsu Chemicals, Inc.
[123] G. N. Schrauzer, V. P. Mayweg, *J. Am. Chem. Soc. 87* (1965) 1483.
[124] Y. Suzuki, G. Hayashi, DE-OS 3726 013 (1988), Fuji Photo Film Co., Ltd.
[125] S. H. Kim, M. Matsuoka, M. Yomoto, Y. Tsuchiya, T. Kitao, *Dyes Pigm. 8* (1987) 381.
[126] Y. Kubo, K. Sasaki, K. Yoshida, *Chem. Lett. 1987*, 1563.
[127] K. Yoshida, M. Ishiguro, Y. Kubo, *Chem. Lett. 1987*, 2057.
[128] H. Junek, G. Uray, G. Zuschnig, *Dyes Pigm. 9* (1988) 137.
[129] a) S. Akiyama, S. Nakatsuji, K. Nakashima, M. Watanabe, *J. Chem. Soc. Chem. Commun. 1987*, 710, 1240; b) S. Akiyama, S. Nakatsuji, K. Nakashima, S. Yamasaki, *Dyes Pigm. 9* (1988) 459.
[130] a) R. West, D. C. Zecher, *J. Am. Chem. Soc. 92* (1970) 155; b) W. Schrott, P. Neumann, DE-OS 3507 379 (1986), BASF AG.
[131] H. Barzynski, H. Naarmann, EP-A 230 240 (1987), BASF AG.
[132] M. Matsuoka, T. Yodoshi, L. Han, T. Kitao, *Dyes Pigm. 9* (1988) 343.
[133] G. Kämpf, *Ber. Bunsenges. Phys. Chem. 89* (1985) 1179.
[134] A. E. Bell, *Proc. SPIE Int. Soc. Opt. Eng. 382* (1983) 2.
[135] A. S. Haogland, *Proc. SPIE Int. Soc. Opt. Eng. 382* (1983) 16.
[136] S. Yoshii, O. Oshii, S. Hattori, T. Nagakawa, G. Ishida, *J. Appl. Phys. 53* (1982) 2256.
[137] G. J. Akashi, *J. Telev. Eng. 40* (1986) 466.
[138] D. C. Hsieh, E. V. La Budde, R. J. Johnson, *Proc. SPIE Int. Soc. Opt. Eng. 329* (1982) 814.
[139] E. W. Pugh, D. L. Critchlow, R. A. Henle, L. S. Russell, *IBM J. Res. Dev. 25* (1981) 585.
[140] J. M. Harker, D. W. Brede, R. E. Pattison, G. R. Santana, S. G. Taft, *IBM J. Res. Dev. 25* (1981) 677.
[141] a) A. Kunimoto, M. Kato, T. Masuda, S. Ohmuma, T. Masumoto, *IEEE Trans. Magn. MAG-23* (1987) 2803; b) T. Osaka, N. Kasai, I. Koiwa, F. Goto, Y. Suganuma, *J. Electrochem. Soc. 130* (1983) 568.
[142] J. P. van der Ziel, R. A. Logan, R. M. Mikulyak, *Appl. Phys. Lett. 41* (1982) 9.
[143] D. Boetz, J. C. Connolly, C. B. Gilbert, M. G. Harvey, M. Ettenberg, *Appl. Phys. Lett. 41* (1982) 1040.
[144] J. McLeod, *Electronics 10* (1988) 70.
[145] M. L. Levene, *Proc. SPIE Int. Soc. Opt. Eng. 899* (1988) 279.
[146] M. Ojima, N. Ohta, *Hitachi Rev. 37* (1988) 139.
[147] F. Tanaka, *Jpn. J. Appl. Phys. 26* (1987) 231.
[148] T. Nakao, *Jpn. J. Appl. Phys. 26, Suppl. 26-4* (1987) 149.
[149] I. Koiwa, M. Toda, T. Osaka, *J. Electrochem. Soc. 133* (1986) 597.
[150] T. Niihara, N. Ohta, K. Kaneko, Y. Sugita, S. Horigome, *IEEE Trans. Magn. MAG-22* (1986) 1215.
[151] M. Asano, M. Kobayashi, Y. Maeno, K. Oishi, K. Kawamura, *IEEE Trans. Magn. MAG-23* (1987) 2620.
[152] H. Oda, S. Ozaki, *Jpn. J. Appl. Phys. 22* (1983) 1930.
[153] T. K. Hatwar, S. C. Shin, *IEEE Trans. Magn. MAG-22* (1986) 946.
[154] a) J. W. M. Biesterbos, A. G. Dirks, M. A. P. J. Farla, P. J. Grundy, *Thin Solid Films 58* (1979) 259; b) R. Hasegawa, R. C. Tylor, *J. Appl. Phys. 46* (1975) 3606; c) Y. Mimura, N. Jamamura, T. Kobayashi, *IEEE Trans. Magn. MAG-12* (1976) 779; d) J. M. E. Harper, R. J. Gambino, *J. Vac. Sci. Technol. 16* (1979) 1901; e) R. B. van Dover, *J. Appl. Phys. 59* (1986) 1291.
[155] H. Heitmann, M. Hartmann, M. Rosenkranz, H. J. Tolle, *J. Phys. Colloq. 1985*, 9.
[156] F. E. F. E. Luborsky, *Ts'ai Liao K'o Hsueh 19* (1987) 1987.
[157] K. Arita (Ed.): *Development of Optical Recording Disk in Daicel Chemical Industries*, Daicel Chemical Industries, Tokyo 1987.
[158] H. J. Williams, R. C. Sherwood, R. F. G. Foster, E. M. Kelleg, *J. Appl. Phys. 28* (1957) 1181.
[159] L. Mayer, *J. Appl. Phys. 29* (1958) 1003; 1454.
[160] J. T. Chang, J. F. Dillon, M. F. Gianola, *J. Appl. Phys. 36* (1965) 1100.
[161] a) D. Chen, W. E. Stutius, *IEEE Trans. Magn. MAG-10* (1974) 581; b) S. Esho, S. Noguchi, Y. Oho, M. Nagao, *Appl. Opt. 13* (1974) 779; c) D. Chen, G. N. Otto, F. M. Schmidt, *IEEE Trans. Magn. MAG-9* (1973) 66; d) D. Chen, *Appl. Opt. 13* (1974) 767; e) H. E. Haskal, G. Bernal, D. Chen, *ibid. 13* (1974) 866; f) S. Honda, T. Nomura, T. Kusuda, *IEEE Trans. Magn. MAG-9* (1973) 467.
[162] W. K. Unger, E. Wolfgang, H. Harms, H. Handek, *J. Appl. Phys. 43* (1972) 2875.
[163] a) P. Chaudhari, J. J. Cuomo, R. J. Gambino, *Appl. Phys. Lett. 22* (1973) 337; b) *IBM J. Res. Dev. 17* (1973) 66.
[164] S. Matsushita, K. Sunago, *Jpn. J. Appl. Phys. 14* (1975) 1851.
[165] Y. Togami, K. Kobayashi, M. Kajiura, K. Sato, T. Teranishi, *Proc. SPIE Int. Soc. Opt. Eng. 329* (1982) 208.
[166] Y. Togami, K. Kobayashi, M. Kajiura, K. Sato, T. Teranishi, *J. Appl. Phys. 53* (1982) 2335.
[167] Y. Togami, *Appl. Phys. Lett. 32* (1978) 673.
[168] S. Honda, K. Meda, T. Kusuda, *J. Appl. Phys. 52* (1981) 2295.
[169] S. Tatsuoke, Y. Togami, *Kino Zairyo 3* (1983) 9.
[170] Y. Kobayashi, Y. Togami, T. Teranishi, *Jpn. J. Appl. Phys. 19* (1980) 581.
[171] Y. Togami, K. Kobayashi, *Jpn. J. Appl. Phys. 19* (1980) 1457.
[172] Y. Togami, K. Kobayashi, I. Yanagida, *Jpn. J. Appl. Phys. 19* (1980) 1663.
[173] Y. Hoshi, M. Naoe, S. Yamanaka, *J. Appl. Phys. 53* (1982) 2344.
[174] M. Ohkoshi, O. Ryoji, K. Inoue, S. Honda, K. Tetsuzo, *Jpn. J. Appl. Phys. 19* (1980) 1807.
[175] S. Yasugi, S. Honda, M. Ohkoshi, T. Kuzuda, *J. Appl. Phys. 52* (1981) 2298.
[176] A. G. Dirks, H. J. Leamy, *J. Appl. Phys. 49* (1978) 1735.
[177] T. Katayama, M. Hirano, Y. Koizumi, K. Kawanishi, *IEEE Trans. Magn. MAG-13* (1977) 1603.
[178] G. A. N. Conell, R. Allen, *J. Magn. Magn. Mater. 31-34* (1983) 1516.
[179] P. Hansen, *J. Appl. Phys. 63* (1988) 2364.
[180] S. Tsunashima, S. Masui, T. Kobayashi, S. Uchiyama, *J. Appl. Phys. 53* (1982) 8175.
[181] Y. Mimura, N. Imamura, T. Kobayashi, *Jpn. J. Appl. Phys. 17* (1978) 2007.
[182] Y. Mimura, N. Imamura, T. Kobayashi, *J. Appl. Phys. 47* (1976) 368.
[183] S. Honda, K. Ueda, T. Kuzuda, *J. Appl. Phys. 52* (1981) 2295.
[184] S. Tsunashima, M. Tsuji, T. Kobayashi, S. Uchiyama, *IEEE Trans. Magn. MAG-17* (1981) 2840.
[185] P. Hansen, M. Urner-Wille, *J. Appl. Phys. 50* (1979) 7471.
[186] M. Urner-Wille, P. Hansen, K. Witter, *IEEE Trans. Magn. MAG-16* (1980) 1188.
[187] M. Hartmann, P. Hansen, P. Willich, *J. Appl. Phys. 56* (1984) 2870.
[188] N. Imamura, *Oyo Butsuri 50* (1981) 1225.
[189] N. Imamura, S. Tanaka, F. Tanaka, Y. Nagao, *IEEE Trans. Magn. MAG-21* (1985) 1607.
[190] H. Kobayashi, T. Ono, A. Tsushima, *Appl. Phys. Lett. 43* (1983) 389.
[191] T. Chen, M. Mansuripur, R. Malmhäll, *Proc. SPIE Int. Soc. Opt. Eng. 382* (1983) 260.
[192] T. Chen, R. Malmhäll, G. B. Charlan, *J. Appl. Phys. 53* (1982) 2356.
[193] T. Chen, D. Treves, *Proc. SPIE Int. Soc. Opt. Eng. 329* (1982) 264.
[194] R. Krishnan, M. Porte, M. Tessier, J. P. Vitton (Eds.), *Polym. Prepr. (Am. Chem. Soc. Div. Polym. Chem.) 29-2* (1988) 232.
[195] T. Tokunaga, M. Harada, M. Ohkoschi, S. Honda, T. Kuzuda, *INTERMAG Conf. 1986*, FC-08.
[196] S. Honda, M. Ohkoschi, T. Kuzuda, *IEEE Trans. Magn. MAG-22* (1986) 1221.
[197] T. R. McGuire, *IEEE Trans. Magn. MAG-22* (1986) 1224.
[198] M. Hartmann, T. R. McGuire, *Phys. Rev. Lett. 51* (1985) 1194.
[199] S. Tanaka, Y. Nagao, F. Tanaka, *Kinzoku Hyomen Gijutsu 38* (1987) 439.
[200] Y. Togami, *IEEE Trans. Magn. MAG-18* (1982) 1233.
[201] Y. Kudo, A. Muto, N. Hara, M. Birukawa, H. Kawabata, *Jpn. Natl. Tech. Rep. 1988*, 28.
[202] J. J. Cuomo, R. J. Gambino, *J. Vac. Sci. Technol. 12* (1975) 79.
[203] a) J. F. Dillon, R. B. van Dover, M. Hong, E. M. Gyorgy, S. D. Alliston, *J. Appl. Phys. 61* (1987) 1103; b) Y. Nagao, S. Tanaka, F. Tanaka, N. Imamura, *Jpn. J. Appl. Phys. 21* (1982) L 509.
[204] N. Imamura, *Proc. 3rd Int. Conf. Ferrites Kyoto 1980*, 798 (Center for Academic Publications Japan, Tokyo 1981.
[205] D. Jeanniot, J. Desserre, *J. Appl. Phys. 54* (1983) 2820.
[206] S. Tanaka, N. Imamura, *J. Magn. Magn. Mater. 35* (1983) 205.
[207] a) I. Sander, M. Urner-Wille, *Proc. SPIE Int. Soc. Opt. Eng. 382* (1983) 240; b) K. Ohta, A. Takahoshi, T. Deguchi, T. Hyuga, S. Kobayashi, H. Yamaoka, *ibid. 382* (1983) 252.
[208] T. Deguchi, T. Hyuga, S. Kobayashi, A. Takahashi, K. Ota, H. Yamaoka, *Shapu Giho 22* (1982) 57.
[209] S. Uchiyama in Y. Sakurai (Ed.): *Magneto-optic Properties of Ternary and Quarternary Rare Earth-Transition Metal Amorphous Films* (*Jpn. Annu. Rev. Electron. Comput. Telecommun. 12* (1986)).
[210] a) A. P. Malozemof, A. R. Williams, K. Terakura, V. L. Moruzzi, K. Fukamichi, *J. Magn. Magn. Mater. 35* (1983) 192; b) G. A. N. Connell, *ibid. 54-57* (1986) 1561; c) G. A. N. Connell, S. J. Oh, J. Allen, R. Allen, *J. Non-Cryst. Solids 61 & 62* (1984) 1061.

[211] H. Tzujimoto, M. Shoiyi, A. Suito, S. Matsushita, Y. Sakuai, *J. Jpn. Appl. Magn. Soc. 7* (1988) 119.
[212] D. Harzberg (Ed.): *Optical Memory News December 1988,* Rothchild Consultants.
[213] M. Takahashi, N. Okta, S. Takayama, Y. Sugita, M. Yoshihiro, K. Shigematsu, *IEEE Trans. Magn. MAG-22* (1986) 931.
[214] S. Takayama, T. Niihara, K. Kaneko, Y. Sugita, M. Ojima, *J. Appl. Phys. 61* (1987) 2610.
[215] P. Hansen, *J. Appl. Phys. 62* (1987) 216.
[216] a) B. G. Huth, *IBM J. Res. Dev. 18* (1987) 100; b) M. Mansuripur, G. A. N. Connell, *J. Appl. Phys. 55* (1984) 3049; c) *Proc. SPIE Int. Soc. Opt. Eng. 420* (1983) 222; d) M. Mansuripur, M. F. Ruane, *IEEE Trans. Magn. MAG-22* (1986) 33.
[217] M. Sato, K. Habu, T. Oyama, *IEEE Trans. Magn. MAG-23* (1987) 2614.
[218] F. Tanaka, Y. Nagao, N. Imamura, *IEEE Trans. Magn. MAG-20* (1984) 1033.
[219] M. Akihira, T. Satch, J. Tada, T. Satoh, *IEEE Trans. Magn. MAG-22* (1986) 928.
[220] S. Takayama, F. Kirino, Y. Suzuki, S. Okamine, N. Ohta, *IEEE Trans. Magn. MAG-23* (1987) 2611.
[221] M. Sato, S. Tatsukawa, N. Tsukane, T. Mitani, M. Toba, *Jpn. J. Appl. Phys. 26* (1987) 19.
[222] Y. Suzuki, S. Takayama, F. Kirino, N. Ohta, *IEEE Trans. Magn. MAG-23* (1987) 2275.
[223] S. Chikazumi: *Physics of Magnetism,* Wiley, New York 1964.
[224] M. Mansuripur, M. F. Ruane, M. N. Hormstein, *Proc. SPIE Int. Soc. Opt. Eng. 529* (1985) 25.
[225] a) Y. Nishihura, T. Katayama, Y. Yamaguchi, S. Ogawa, T. Tsushina, *Jpn. J. Appl. Phys. 17* (1978) 1083; b) R. B. van Dover, E. M. Gyorgy, R. P. Frankenthal, M. Hong, D. J. Siconolfi, *J. Appl. Phys. 59* (1986) 1291; c) T. Mizoguchi, G. S. Cargill, *ibid. 50* (1979) 3570.
[226] H. Hibst, *Angew. Chem. 94* (1982) 263; *Angew. Chem. Int. Ed. Engl. 21* (1982) 270.
[227] A. Watada, H. Nakamura, H. Machida, *IEEE Trans. Magn., Mag. 23* (1987) 2961.
[228] H. L. Glas, J. H. W. Liaw, *J. Appl. Phys. 49* (1978) 1578.
[229] M. Matsuoko, Y. Hoshi, M. Naoe, S. Yamanaka, *IEEE Trans. Magn. MAG-18* (1982) 1119.
[230] R. Ahrenkiel, T. Coburn, *IEEE Trans. Magn. MAG-11* (1975) 1103.
[231] J. W. D. Martens, A. B. Voermaus, *IEEE Trans. Magn. MAG-20* (1984) 1007.
[232] H. Matsuda, H. Iwasaki, M. Kaneko, K. Aso, Jpn. Kokai Tokkyo Koho JP 63-47 908 (1988); Sony Corp.; *Chem. Abstr. 109* (1988) 203 521.
[233] J. W. D. Martens, W. L. Peters, P. Q. J. Nederpel, *J. Appl. Phys. 55* (1984) 1100.
[234] P. Hansen, J.-P. Krumme, *Thin Solid Films 114* (1984) 69.
[235] W. Tolkdorf, C.-P. Klages, *Thin Solid Films 114* (1984) 33.
[236] J.-P. Krumme, V. Doormann, P. Willich, *J. Appl. Phys. 57* (1985) 3885.
[237] Y. Yokoyama, S. Tsukahara, T. Tanaka, *J. Magn. Magn. Mater. 35* (1983) 175.
[238] Y. Yokoyama, S. Tsukahara, T. Tanaka, *IEEE Trans. Magn. MAG-20* (1984) 1039.
[239] a) M. Abe, M. Gomi, *Oyo Butsuri 57* (1988) 723; b) K. Inomata, *Denshi Zairyo 27* (1988) 40.
[240] B. R. Brown, *Appl. Opt. 13* (1974) 761.
[241] A. W. Smith, *Appl. Opt. 13* (1974) 795.
[242] S. R. Ovshinsky, US-Pat. 3 530 441 (1970), Energy Conversion Devices Incorp.
[243] a) S. Asai, E. Maruyama, *Suppl. Jpn. J. Appl. Phys. 40* (1971) 172; b) A. Hamada, T. Kuroso, M. Saito, M. Kikuchi, *Appl. Phys. Lett. 20* (1972) 9; c) P. Chaudhari, S. Herd, D. Ast, M. H. Brodsky, R. J. von Gutfeld, *J. Non-Cryst. Solids 8–10* (1972) 900.
[244] J. Feinleib, J. de Neuville, S. C. Moss, S. R. Ovshinsky, *Appl. Phys. Lett. 18* (1971) 254.
[245] R. J. von Gutfeld, P. Chaudhari, *J. Appl. Phys. 43* (1972) 4688.
[246] K. Weiser, R. J. Gambino, J. A. Reinhold, *Appl. Phys. Lett. 22* (1973) 48.
[247] A. Saito, T. Maeda, H. Sugiyama, Y. Tsumoda, *Appl. Opt. 27* (1988) 4274.
[248] K. Suzuki, DE-OS 38 02 679 (1988), Toshiba Corp.
[249] M. Ojima, T. Nakao, H. Sukeda, N. Okta, H. Yasuoka, T. Nishida, M. Terao, *Proc. SPIE Int. Soc. Opt. Eng. 899* (1988) 154.
[250] M. Chen, K. A. Rubin, *Proc. SPIE Int. Soc. Opt. Eng. 1078* (1989) 150.
[251] P. K. Raychaudhuri, *Proc. SPIE Int. Soc. Opt. Eng. 1078* (1989) 157.
[252] F. S. Jiang, L. S. Hau, F. X. Gyan, *Proc. SPIE Int. Soc. Opt. Eng. 1078* (1989) 165.
[253] a) S. C. Stinson, *Chem. Eng. News 66* (1988) No. 42, p. 30; b) W. J. Tomlinson, *Appl. Opt. 23* (1984) 3990; c) J. Hibino, E. Ando, Jpn. Kokai Tokkyo Koho JP 63-273 688 (1988), Agency of Industrial Science and Technology; *Chem. Abstr. 110* (1989) 222 674; d) K. Ichimura, N. Morii, M. Sakuragi, N. Aaki, Jpn. Kokai Tokkyo Koho JP 63-222 174 (1988), Agency of Industrial Science and Technology; *Chem. Abstr. 110* (1989) 125 523.
[254] a) M. Eich, B. Reck, H. Ringsdorf, J. H. Wendorff, *Proc. SPIE Int. Soc. Opt. Eng. 682* (1987) 93; b) S. Tazuke, *Kokagaku 12* (1988) 85.
[255] *Proc. Int. Symp. Future Electronic Devices* (Bioelectric and Molecular Electric Devices), Tokyo 1985.
[256] W. Siol, U. Terbrack, DE-OS 37 08 428 (1988), Röhm GmbH.
[257] W. Dabisch, P. Kuhn, S. Müller, K. Narayanan, DE-OS 29 07 352 (1980), Graficor.
[258] T. Potrawa, H. Langhals, *Chem. Ber. 120* (1987) 1075.
[259] G. Hollingsworth, J. D. Barrie, B. Dunn, J. I. Zink, *J. Am. Chem. Soc. 110* (1988) 6569.
[260] a) W. J. Merz, J. R. Anderson, *Bell Lab. Rec. 33* (1955) 335; b) M. Nützuma, R. Sato, *Ferroelectrics 34* (1980) 37.
[261] K. Dransfeld, R. Pott, G. Kämpf, EP 275 881 (1988), Bayer AG.
[262] P. S. Murthy, K. A. Klingensmith, J. Michl, *J. Appl. Polym. Sci. 31* (1986) 2331.
[263] P. Gütlich, S. Decurtins, H. Spiering, A. Mauser, DE-OS 36 220 005 (1988), Bayer AG.
[264] J. Friedrich, D. Haarer, *Angew. Chem. 96* (1984) 96; *Angew. Chem. Int. Ed. Engl. 23* (1984) 112.
[265] E. Krätzig, R. Orlowski, V. Doormann, M. Rosenkranz, *Proc. SPIE Int. Soc. Opt. Eng. 164* (1979) 33.
[266] *Jpn. High-Technol. Monitor 7* (1989) 14.
[267] a) A. Renn, R. Locher, A. Meixner, M. P. Wild, *J. Lumin. 38* (1987) 37; b) Y. Jino, T. Tani, M. Sakuda, M. Nakahara, K. Fukuda, *Chem. Phys. Lett. 140* (1987) 76; c) M. P. Wild, A. Renn, *Proc. SPIE Int. Soc. Opt. Eng. 910* (1988) 61.
[268] H. Sixl in M. Borrisov (Ed.): *Molecular Electronics,* Singapore Press 1987, p. 11.

The Crystal Chemistry of High-Temperature Oxide Superconductors and Materials with Related Structures

By Hanskarl Müller-Buschbaum*

Dedicated to Professor Wolfgang Hilger on the occasion of his 60th birthday

Never before in human history has a chemical substance been the object of collaborative research by so many scientists of different disciplines as in the case of the first high-temperature (HT_c) oxide superconductor $La_{2-x}Sr_xCuO_4$. If the importance of a class of materials is measured by the number of papers published in a given period, the new superconductors hold the all-time record; moreover, this flood of publications also reflects the high expectations that are held worldwide for this class of substances. Every day seems to bring further surprises. From the two phases of HT_c oxide superconductors that were recognized at the outset there have developed within a period of scarcely two years a series of new materials which all show superconductivity at temperatures above the boiling point of liquid nitrogen; this property is undoubtedly closely related to the crystal chemistry of the individual phases and compounds. This article will report and discuss the resemblances and differences between the HT_c superconductors and materials with related structures.

1. Introduction

Twelve years ago when, in this journal,[1] I reported the crystal chemistry of oxometalates with planar coordination, despite taking a speculative view of these compounds I did not dare to guess that one of them, La_2CuO_4,[2, 3] with slight modifications, was to be the cause of a revolution.[4]

The original work on compounds of the general formula A_2MO_4, which form crystals of the same type as K_2NiF_4 (see structure in Fig. 1a), was concerned with the elongation of the MO_6 octahedra along the tetragonal c axis. An increase in the Cu–O or Ni–O interatomic distance is also observed in the compounds La_2CuO_4 (cf. Fig. 1b) and Nd_2NiO_4, whose structures are orthorhombically distorted variants of the K_2NiF_4 type.[5] In compounds of the formula A_2MO_4 where M is a Jahn–Teller-active ion such as Ni^{3+}, Mn^{3+}, or Cu^{2+}, the observed elongations of the MO_6 octahedra parallel to the c axis are 15% for $SrLaNiO_4$,[6] 21% for $SrNdMnO_4$,[7] and 29% for La_2CuO_4.[4, 8] When the Ni^{3+}, Mn^{3+}, or Cu^{2+} ions with octahedral coordination are replaced by Jahn–Teller-inactive ions such as Cr^{3+}, Al^{3+}, Co^{3+}, or Ni^{2+}, it is found that the MO_6 octahedra are also stretched along the [001] direction. The experimentally determined values of the octahedral stretching (M–O distances along the [001] direction relative to the M–O distances in the a/b plane) are 4% for $SrNdCrO_4$,[7] 11% for $SrNdAlO_4$,[9] $SrCeAlO_4$,[9] and $SrSmAlO_4$,[8] 5 to 11% for La_2CoO_4 and Sm_2CoO_4,[10] and 11% for Nd_2NiO_4.[5] These examples show that oxometalates with the K_2NiF_4

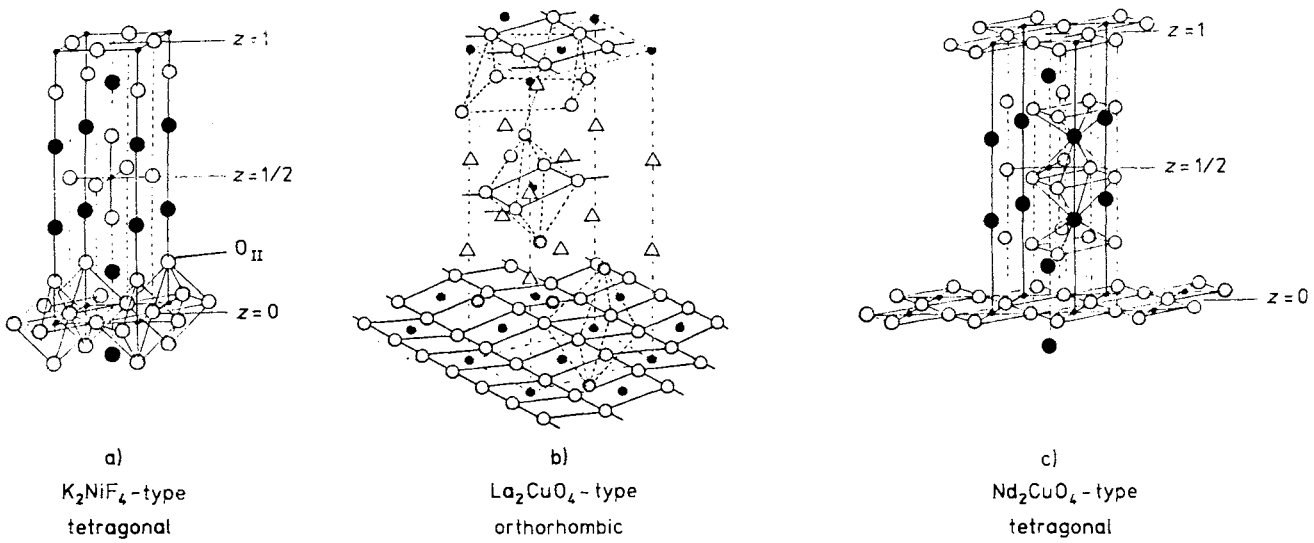


Fig. 1. Structure of compounds with the general formula A_2MO_4. z is a positional parameter. O_{II} denotes oxygen at lattice position II. a) K_2NiF_4-type structure. ● = K^+ (≙ A^{y+}), • = Ni^{2+} (≙ M^{x+}), ○ = F^- (≙ O^{2-}); $2y + x = 8$. The octahedra around the small ion M are shown. b) La_2CuO_4-type structure △ = La^{3+}, ● = Cu^{2+}, ○ = O^{2-}. The octahedra around Cu (small filled spheres) are shown by broken lines. c) Nd_2CuO_4-type structure with planar CuO_4 coordination. ● = Nd^{3+}, • = Cu^{2+}, ○ = O^{2-}.

[*] Prof. Dr. Hk. Müller-Buschbaum
Institut für Anorganische Chemie der Universität
Olshausenstrasse 40–60, D-2300 Kiel (FRG)

structure or the orthorhombically distorted La_2CuO_4 structure exhibit an octahedral stretching which depends on the structural type. They also show that Jahn–Teller-active ions cause a significant increase in this elongation. This effect is largest for Cu^{2+}.

Naturally there was interest in discovering the cause of the structure-dependent octahedral stretching, especially since it seemed to bring the comparatively widely separated upper and lower apical oxygen atoms of the MO_6 octahedron (O_{II} in Fig. 1a) much too close to the bulky A atoms in A_2MO_4. The calculated lattice energy as a function of the z parameters of O_{II} and A (at the point $00z$ in each case) is shown in Figure 2 in the form of an energy surface diagram. There is

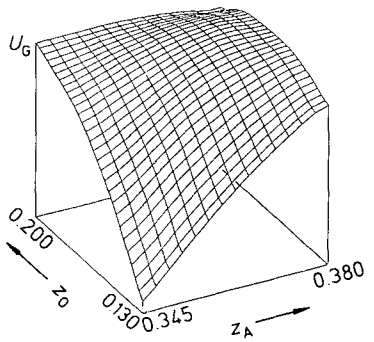


Fig. 2. Lattice energy U_G as a function of the parameters z_O (O_{II}, see Fig. 1a) and z_A in A_2MO_4 compounds (K_2NiF_4 type).

an optimum lattice energy at a position which is in good agreement with the experimentally determined z parameters of the O_{II} and A atoms. The octahedral stretching found in every case is therefore a consequence of the minimization of lattice energy. Before the discovery of the oxide superconductors, there was also interest in the electronic structures and magnetic properties of oxometalates of the K_2NiF_4 type,[11–23] and in structures of this type formed by substituting other atoms in place of A and at the same time altering the valence of the ion M.[24–30]

X-ray diffraction studies on microcrystalline samples initially suggested that all compounds with the general formula Ln_2CuO_4 (Ln = lanthanoid) crystallized with the K_2NiF_4-type structure.[31–34] However, a structure determination on single crystals gave the surprising result that the Cu^{2+} ions in Nd_2CuO_4 were coordinated not in an octahedral but in a planar fashion. This structure is shown in Figure 1c alongside the orthorhombic La_2CuO_4 structure (Fig. 1b) and the tetragonal K_2NiF_4 structure (Fig. 1a). This discovery stimulated further work which soon revealed that all the other lanthanoid elements capable of forming compounds of the general formula Ln_2CuO_4 (i.e., Sm, Eu, and Gd) give compounds with Cu^{2+} in a planar environment.[4] The same also applies to mixed crystals such as $NdGdCuO_4$, $NdSmCuO_4$,[36] and $LaNdCuO_4$.[37] Also relevant here is a study of the magnetic properties of the compounds Ln_2CuO_4 (Ln = Nd or Pr),[38] in which the remarkable assumption was made that the strongly reducing ion Pr^{3+} was present alongside Cu^{2+}. In summary, it should be emphasized that La_2CuO_4 is the only lanthanoid oxocuprate, Ln_2CuO_4, in which Cu^{2+} is coordinated in a (stretched) octahedral fashion.

2. The First HT_c Oxide Superconductor: $La_{2-x}Sr_xCuO_4$

The discovery of the first HT_c oxide superconductor[39] was followed by an unprecedented flood of publications on the physical properties of superconducting phases with the general formula $Ln_{2-x}M_xCuO_4$ in relation to their methods of synthesis, chemical constitution, and structure. The earliest papers[40–60] were concerned with replacing the lanthanoid ions by other metal ions M^{3+} with the same charge or by ions of alkaline-earth metals. The temperature region of the transition to the superconducting state was investigated as a function of the degree of substitution, the elements involved, the oxygen partial pressure, and the transition from orthorhombic symmetry (La_2CuO_4-type structure) to tetragonal symmetry (K_2NiF_4-type structure). At temperatures $T < 150$ K, $La_{1.85}Sr_{0.15}CuO_4$ undergoes a phase transition from tetragonal to orthorhombic.[61] When the La^{3+} ions in La_2CuO_4 are partly replaced by divalent ions to give $La_{2-x}M_xCuO_4$, where M = Ca^{2+}, Sr^{2+}, or Ba^{2+}, a compensating fraction of the Cu^{2+} ions become Cu^{3+} ions. For larger values of the doping coefficient x an O^{2-} deficit appears in the oxygen partial lattice. An early investigation of this behavior was reported in 1981,[58] but there are also more recent publications on the superconducting phases $Ln_{2-x}M_xCuO_{4-y}$, a few examples of which are listed in the references.[62–66] A recent publication[67] classifies the



Hanskarl Müller-Buschbaum was born in Thüringen in 1931. He studied chemistry and physics at the Universität Greifswald, where he received his doctorate in 1960 under H. Witzmann on UV-photoexcited borate luminophores. He then worked at Siemens in Munich on hard superconductors. In 1962, Müller-Buschbaum resumed his academic career under Wilhelm Klemm at the Universität Münster and, in 1965, he moved to the Universität Gießen, where he completed his "Habilitation" under Rudolf Hoppe on the generation of high temperatures with the low-pressure high-frequency plasma burner and its use in high-temperature solid-state reactions. In 1969, he accepted a "Lehrstuhl" in the Department of Inorganic Chemistry at the Universität Kiel. His work focuses on solid-state chemical reactions at high temperatures involving high-frequency plasma discharges and on the synthesis of entropy-supported metastable materials by CO_2 laser methods.

different phases so far observed in the La_2O_3–SrO–CuO system. Concurrent investigations have included calculations on the electronic structure,[68–74] a study on electron–electron correlation in $La_{2-x}Sr_xCuO_4$,[75] and several studies of the mechanism of superconductivity in the new copper oxide compounds.[76–80]

An annoying aspect of the early papers on $La_{2-x}M_xCuO_4$ (M = an alkaline-earth metal) was that several authors, in discussing the question whether the symmetry was orthorhombic or tetragonal, completely disregarded the fact that all the lanthanoid species except those with La^{3+} crystallize not with the La_2CuO_4-type structure but with the Nd_2CuO_4-type structure, which has planar-coordinated copper. Assuming that the superconduction took place in the planar Cu/O grid,[78, 79] it appeared very doubtful whether, in the preparation of microcrystalline samples by cosintering—a process almost reminiscent of alchemy—the Cu^{2+} ions had a stretched octahedral coordination. As was stated in Section 1, the existence of the upper and lower apical oxygen atoms O_{II} of the CuO_6 octahedra can only be proved unambiguously by neutron diffraction or single-crystal X-ray studies. The focus of interest in our investigations was therefore not so much the question of the orthorhombic distortion of the tetragonal K_2NiF_4 structure, but rather that of whether the Cu^{2+} or Cu^{3+} ions in the superconducting phase have a planar or a stretched octahedral coordination. Using improved techniques, several research groups[81–83] have succeeded in preparing single crystals of $La_{2-x}Sr_xCuO_4$ (x = 0.12 to 0.15) and unambiguously determining the position of the controversial oxygen atom (O_{II} in Fig. 1a). These investigations showed that the Cu^{2+} ion definitely occupies a markedly elongated octahedron and that the elongation along the [001] direction decreases with increasing introduction of Sr^{2+} ions at the La^{3+} positions.[83] Determining the symmetry is not so easy, since the question whether or not the higher tetragonal symmetry is present depends on detecting very small deviations of the atomic parameters from the tetragonal position 00z and slight differences in the temperature factor of the upper and lower apical oxygen atoms. However, recent work has succeeded in growing large single crystals of $La_{2-x}Sr_xCuO_4$ up to 10 mm long.[84]

The following question then arose: Why do oxocuprates of the Nd_2CuO_4 type not show superconducting properties? Could this be attributed to the paramagnetism of the ions in the series Pr^{3+} to Gd^{3+} or to the planar-coordinated copper (which would have been inconsistent with some of the proposed mechanisms), or was the Nd_2CuO_4-type structure much less favorable energetically than the orthorhombic La_2CuO_4 structure? To estimate the stabilities of the two crystal structures, the Coulomb contribution to the lattice energy (MAPLE value[85, 86]) was calculated for both the K_2NiF_4-type and the La_2CuO_4-type structures and also for a stepwise transition of the upper and lower apical oxygen atoms (O_{II} in Fig. 1a) from the 00z position ($z = 0.176$) to the position 0; ½; ¼ in the Nd_2CuO_4 structure. Figure 3 shows the MAPLE values for the oxygen atoms as a function of the O_{II} positional parameters. The result is surprising, since the two extreme situations in the stepwise shift of O_{II} from the K_2NiF_4-type to the Nd_2CuO_4-type have virtually identical Coulomb contributions to the lattice energy, and,

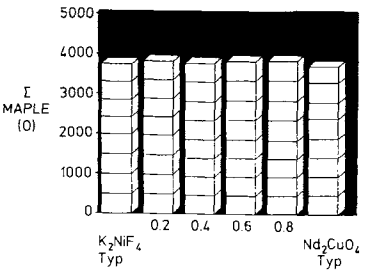


Fig. 3. Contributions of the Coulomb term (MAPLE) to the lattice energy for the K_2NiF_4- and Nd_2CuO_4-type structures, with stepwise transition from octahedral to planar coordination of the upper and lower apical oxygen ions. Ordinate: Sum of the MAPLE values for all oxygen atoms. Abscissa: Change in the positional parameter z for O_{II}.

furthermore, the shift of the O_{II} atoms gives no reduction in the Coulomb term at the hypothetical intermediate positions. Thus, energy considerations are not inconsistent with a planar Cu/O grid in the Nd_2CuO_4-type structure. The only possible conclusions were either that all lanthanoid ions that form Nd_2CuO_4-type structures (namely, Ce^{3+}, Pr^{3+}, Nd^{3+}, Sm^{3+}, and Gd^{3+}) suppress superconductivity owing to their magnetic properties or that superconductivity is not possible in oxocuprates with exclusively planar-coordinated copper.

In the field of oxide superconductors, however, new theories seem to become rapidly obsolete, for a paper then appeared[87] reporting superconductivity in cerium-doped oxocuprates $Ln_{2-x}Ce_xCuO_4$ (Ln = Pr^{3+}, Nd^{3+}, Sm^{3+}) which have the Nd_2CuO_4-type structure with planar-coordinated copper. This result provoked a number of theoretical considerations based on the idea that the addition of a fifth or sixth oxygen atom to planar CuO_4 grids leads to the formation of stretched tetragonal pyramids, or, as in La_2CuO_4, stretched octahedra. The other HT_c superconductors yet to be discussed also have these 4 + 1 or 4 + 2 oxygen polyhedra as a characteristic feature of their structures. Interestingly, the question whether pure La_2CuO_4 is also a superconductor has since received a positive answer. It had already been shown in 1973 that La_2CuO_4 is a metallic conductor.[88] Other authors found only semiconducting behavior,[89] but more recent publications reported superconductivity, both at particle boundaries[90] and in bulk.[91, 92] If La_2CuO_4 is partly fluorinated, thereby introducing a charge deficit in the anion partial lattice ($La_2CuO_{4-x}F_x$), a superconducting material with a T_c value of about 35 K is obtained.[93]

The crystal chemistry of the superconducting phases $La_{2-x}M_xCuO_4$ and $Nd_{2-x}Ce_xCuO_4$ fits into the pattern of previously known compounds. This relationship is shown in Figure 4. The K_2NiF_4-type structure in the center leads, by a small orthorhombic distortion, to the La_2CuO_4 structure. A doped La_2CuO_4 with the constitution $La_{1.8}Sr_{0.2}CuO_4$ was the first known HT_c superconductor. In Figure 4, two oxygen positions (O_I and O_{II}) in the K_2NiF_4-type structure have been marked. If, for example, O_{II} is moved from the 00z position ($z = 0.176$) to the position 0; ½; ¼, this gives, with no change in chemical constitution, the Nd_2CuO_4 structure with planar Cu/O grids. A derivative of this structure leads to the most recently discovered superconducting material, $Nd_{2-x}Ce_xCuO_4$, with $T_c = 35$ K. Here, for the first time in a superconducting material, the planar Cu/O polygons do not have O^{2-} neighbors to extend the network. In early research on oxide HT_c superconductors, great hopes were held out for

the compounds Sr_2CuO_3[94] and $SrCuO_2$.[95] If the trivalent lanthanum ion in La_2CuO_4 is formally replaced by Sr^{2+}, there is a deficit of two positive charges. Nature responds to this situation with a rearrangement from the K_2NiF_4-type structure to the Sr_2CuO_3 structure. If the oxygen atoms marked O_I in the K_2NiF_4-type structure in Figure 4 are removed, this gives Cu^{2+} a planar oxygen environment. The crystal structure has isolated chains of planar Cu/O polyhedra, joined at their corners; this is a characteristic feature of the Sr_2CuO_3-type structure. If an SrO group is formally removed from Sr_2CuO_3, the compound $SrCuO_2$ is obtained.[95] Figure 4 shows that, when Sr_2CuO_3 is transformed by an $a/2:c/2$ translation, the isolated $[CuO_3]_n^{4-}$ chains coalesce to form $[CuO_2]_n^{2-}$ double chains consisting of CuO_4 squares joined at their edges.

Also formally derived from the K_2NiF_4-type structure is a long-known fluorooxoferrate(III) with the formula Sr_2FeO_3F.[96] In this structure one of the original apical oxygen positions is occupied by randomly distributed O^{2-} and F^- ions. The evidence for this oxygen/fluorine distribution is based on plausible argument, since X-ray diffraction methods cannot distinguish between O^{2-} and F^-. An interesting feature of the structure is the FeO_5F octahedron, which is asymmetrically distorted. It is again stretched in the direction of the c axis in relation to the randomly occupied octahedral apical sites. If the O_{II} atoms in oxometalates of the K_2NiF_4 type are completely replaced by halogen ions, one obtains, for example, the halogenooxocuprate(II) compounds with the general formula $Sr_2CuO_2X_2$ ($X = Cl^-$,[97] Br^-[98]) or $Ca_2CuO_2X_2$ ($X = Cl^-$, Br^-[99]). In the search for new oxide superconductors, the partially halogenated materials will attract more interest[93] if preparative routes can be found which avoid the formation of the stable fluorite structures SrF_2 or BaF_2 when superconducting phases are reacted with fluorine or fluorides.

Although copper has up to now been an essential constituent of HT_c superconductors, as in $Ln_{2-x}M_xCuO_4$ and $Ln_{2-x}Ce_xCuO_4$, there has recently been renewed interest in

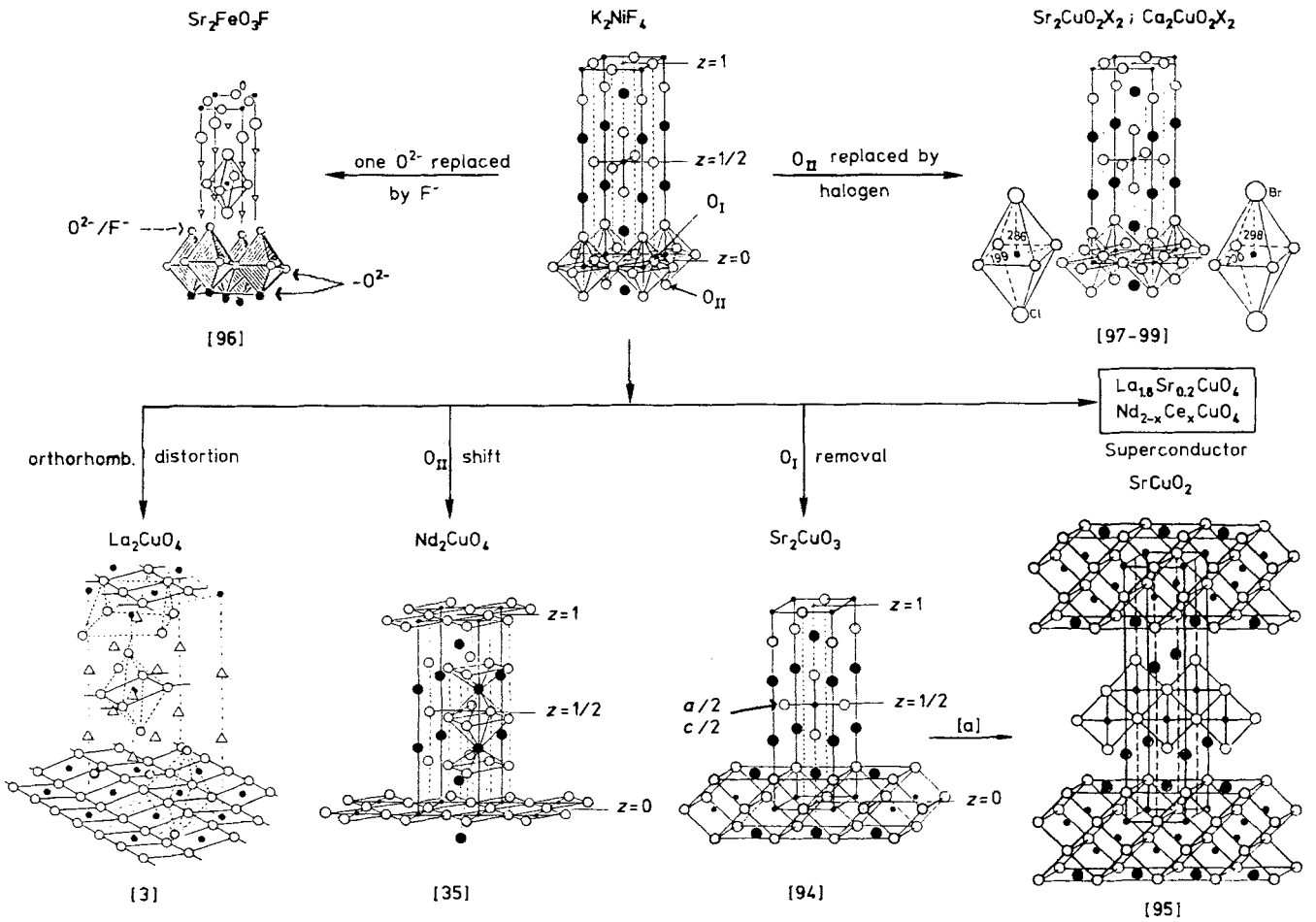


Fig. 4. Relationships between the K_2NiF_4-type structure and compounds with related structures. Step [a]: Remove SrO, shift by $a/2$ and $c/2$ (see text).

the formally similar oxonickelates.[5, 8, 100–103] One approach is to replace Cu^{2+} by Ni^{2+}.[104] A recent investigation using single crystals showed that in $Nd_2(Cu,Ni)O_4$[105] the orthorhombically distorted K_2NiF_4-type structure is formed in preference to the planar Nd_2CuO_4 type. Obviously Ni^{2+} stabilizes the octahedral mode of coordination, despite the fact that, as an element with a d^8 electronic configuration, it prefers planar coordination. A comparable situation is also found in $Nd_{1.5}Sr_{0.5}(Cu,Al)O_4$.[105] On the other hand, when Cu^{2+} is replaced by Al^{3+} it is easier to understand the formation of octahedral $(Cu,Al)O_6$ coordination, since a planar oxygen environment around Al^{3+} would be very surprising. Pt^{4+} also stabilizes the octahedral mode of coordination of Cu. Single crystals of

$La_{1.5}Sr_{0.5}(Cu_{0.75}Pt_{0.25})O_4$ have been prepared;[83] they have a structure practically identical to the K_2NiF_4 type (i.e., the orthorhombic distortion is extremely small). Our own experiments aimed at replacing as many La^{3+} ions as possible in $La_{2-x}Sr_xCuO_4$ by Sr^{2+} confirmed the finding by others[84] that the substitution fraction x can only be significantly increased by using a large excess of SrO. However, if Pt^{4+} is incorporated at the Cu^{2+} sites along with Cu^{2+}, the material reacts completely with whatever fraction of SrO is added to the mixture.[81] This supports results from other studies which showed that when La^{3+} in La_2CuO_4 is replaced by Sr^{2+} only a limited amount of conversion from Cu^{2+} to Cu^{3+} occurs.[58, 64, 65]

3. The Yttrium Superconductors

3.1. $YBa_2Cu_3O_{6+x}$

The real breakthrough in the discovery and development of superconducting oxide phases came with the very early identified $YBa_2Cu_3O_{6+x}$ system.[106, 107] Transition temperatures in the region of 90 to 93 K brought superconductivity for the first time within the range accessible with liquid nitrogen, which is cheaper than liquid helium by a factor of about 1000. The new material became known to many physicists and chemists as the "YBACU" superconductor, or the 1-2-3 superconductor[*] (1 Y, 2 Ba, 3 Cu), from its formula $YBa_2Cu_3O_{6+x}$. Thus, it was this compound that further stimulated the unprecedented increase in experiments and publications in this field. All these efforts were directed towards shifting the transition to still higher temperatures and to understanding the phenomenon of superconductivity in oxides. In this article it will only be possible to cite a limited selection from the wealth of publications. With regard to the early work on the Y 1-2-3 superconductor, it is sufficient to list only a few publications[108–119] which themselves contain references to many further papers. Naturally, a considerable amount of space in the bibliography is given to papers reporting experiments on substitution. In view of the fact that, starting from $La_{2-x}Sr_xCuO_4$, the successive replacement of La^{3+} by Y^{3+} and of Sr^{2+} by Ba^{2+} had led to $YBa_2Cu_3O_{6+x}$, it was hoped that further modification of the chemical constitution might result in higher T_c values. Many of these publications report on the replacement of Y^{3+} by other trivalent lanthanoid ions.[120–135] Some investigators have aimed to replace Ba^{2+} or Y^{3+} by ions of other alkaline-earth metals, and Cu^{2+} by other metals of the same subgroup.[136–145]

Quite a lot of research has been done on the dependence of the properties on synthesis and structure. It was quickly recognized that the occurrence of superconductivity, the sharpness of the transition from metallic conduction to superconductivity, and the relation to current density depend critically on the preparation conditions. Usually the starting materials ($BaCO_3$/$Ba(OH)_2 \cdot 8H_2O$, Y_2O_3, CuO) are first heated to a relatively high temperature (950–1000 °C); superconductivity is then achieved by processing the material in an oxygen-containing atmosphere. A number of papers[146–164] discuss important details such as the evolution of oxygen as the temperature is increased, the reorganization of the superconducting crystal lattice at moderate temperatures, and a phase transition which can occur depending on the chemical constitution and the temperature. Superconductivity in $YBa_2Cu_3O_{6+x}$ only begins to appear when $x > 0.5$. Some of the divalent copper must therefore be converted to the trivalent oxidation state. Since the ideal constitution $YBa_2Cu_3O_{7.0}$ cannot quite be reached with one Cu^{3+} ion and Cu^+ ions are also present, it has been suggested that charge neutrality is maintained by the presence of some oxygen in the -1 oxidation state. The publications cited here[165–171] refer to various studies of the oxidation state of copper. The superconducting phase $YBa_2Cu_3O_{6+x}$ ($0.5 < x < 0.93$) has an oxygen deficit, which depends on the thermal treatment in the presence of oxygen. It was therefore of interest to find out whether the O^{2-} vacancies in the oxygen partial lattice occur in an ordered or a disordered fashion. A related problem is the usual formation of twinned crystals, which cause difficulties in determining the structure by diffraction methods. For this reason $YBa_2Cu_3O_{6+x}$ crystals have also been studied by high-resolution transmission electron microscopy.[172–179]

The earlier studies using diffraction methods have been reviewed.[171, 180–184] Other publications[185, 186] review studies of crystal twinning. Neutron diffraction results that include temperature dependence have also been reported.[187–191] The key feature in all these diffraction experiments is the ordering of the vacancies, as well as its influence on the crystal structure and on T_c.[192–196] An investigation using Raman spectroscopy was recently reported;[197] by this method regions of the crystals unaffected by twinning could be clearly identified. Shortly afterwards, an untwinned single crystal of $YBa_2Cu_3O_{6.9}$ was isolated and studied by X-ray diffraction at different temperatures.[198] Also relevant here are two papers reporting measurements on the superconducting properties of single crystals,[199, 200] which contain references to other work on this topic.

Figure 5 shows a perspective drawing of the coordination polyhedra around the Cu, Y, and Ba ions. In Figures 5a and 5b the tetragonal pyramids of O^{2-} ions around Cu_{II} are indicated by hatching. The CuO_5 pyramids are joined at their base corners to form an infinite two-dimensional network of quasi-planar CuO_4 squares. The fifth oxygen (the apex of the pyramid) is considerably more removed in the [001] direction. These Cu^{2+} ions must therefore be regarded as having a 4 + 1 coordination. Figures 5a and 5b also indicate the square-planar coordination around Cu_I. One-dimensional infinite chains of Cu/O squares joined at their corners extend through the crystal in the direction of the *b* axis, as had also been found previously in Sr_2CuO_3.[94] Many of the papers on the replacement of Y^{3+}, Ba^{2+}, and especially Cu^{2+}/Cu^{3+}, which are cited here, were concerned with the question whether the superconducting properties were especially affected by replacing either the copper ions in the isolated chains or those with 4 + 1 coordination. Our calculations of the Coulomb contribution to the lattice energy using the MAPLE method[85, 86] show that, if we assume that Cu^{2+} is partially converted to Cu^{3+}, the Cu^{3+} ions should occur in the isolated chains.

[*] Owing to the growing number of superconducting systems, this nomenclature inevitably leads to errors unless a symbol denoting the particular system is included, in this case Y1-2-3.

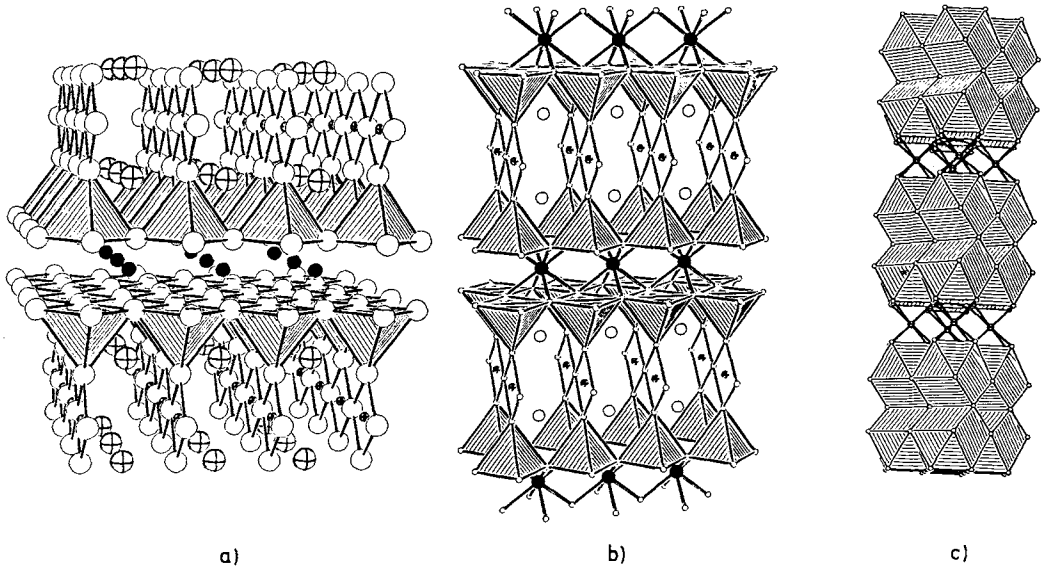


Fig. 5. Structure of $YBa_2Cu_3O_{6+x}$. a) Coordination of Cu^{2+}/Cu^{3+}. The tetragonal pyramids around Cu_{II} are hatched. ● = Y^{3+}, ⊕ = Ba^{2+}, ⊛ = Cu^{2+}, ○ = O^{2-}. b) Coordination of Cu^{2+}/Cu^{3+}, symbols as in a) with the $Y^{3+}-O^{2-}$ bonds also shown. ● = Y^{3+}, O = Ba^{2+}, ⊛ = Cu^{2+}, ○ = O^{2-}. The isolated CuO_4 chains (containing the Cu^{3+} ions) are indicated. c) Coordination of Ba^{2+} (see text). ⊖ = Y^{3+}, o = O^{2-}.

Figure 5b also reveals how the Y^{3+} ions are arranged between the layers of CuO_5 pyramids. Each Y^{3+} ion is surrounded by eight O^{2-} ions in the form of a slightly stretched cube. The coordination of the bulky Ba^{2+} ions is relatively complicated, with a geometry as shown in Figure 5c. The Ba^{2+} ion occupies a distorted rectangular antiprism with markedly different faces in the [001] direction.

From a crystallographic standpoint this HT_c superconductor is also related to other known compounds. Directly related compounds are $Sr_3Ti_2O_7$,[201] the compounds and solid phases with the general formula $La_{2-x}A_{1+x}Cu_2O_{6-x/2}$ (A = Ca or Sr),[202] and $Ln_{2-x}Sr_{1+x}Cu_2O_{6-x/2}$ (Ln = Sm–Gd).[203] Also belonging to this class are the barium oxoindates which were studied in the early 1980s; the system $BaO-In_2O_3$[204,205] gives rise to a series of compounds,[206,207] whose structures have only been determined very recently. Other compounds directly related to the $YBa_2Cu_3O_{6+x}$ superconductor are $Ba_3In_2O_6$,[206,207] $Ba_2SrIn_2O_6$,[208] and $BaSr_2In_2O_6$.[209] $Ca_3In_2O_6$[210] and $SrCa_2In_2O_6$,[211] although they have similar molecular formulas, are metastable compounds with their own unique crystal chemistry. The phases $La_{2-x}Sr_{1+x}Cu_2O_{6-x/2}$ and $Ba_3In_2O_6$, which are isotypes, can also be regarded as variants of the $Sr_3Ti_2O_7$-type structure.[201] These relationships are illustrated in Figure 6. The $Sr_3Ti_2O_7$ type (Fig. 6a) is an extension of the K_2NiF_4 structure shown in Figure 4. The

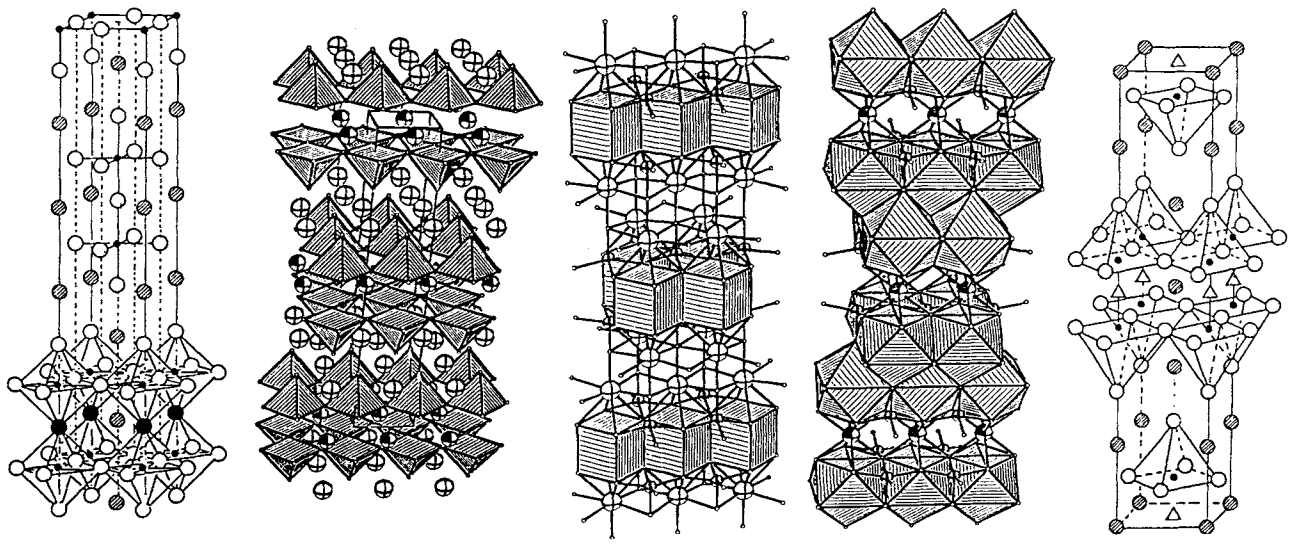


Fig. 6. Transition from the $Sr_3Ti_2O_7$-type structure (a) to $Ba_3In_2O_6$ (b)–(d) or $La_{2-x}A_{1+x}Cu_2O_{6-x/2}$ (e) (A = Ca, Sr; shown for A = Sr, x = 0) by removing the oxygen ions (O_{II}) marked by large filled circles. The InO_5 and CuO_5 pyramids are clearly shown in b) and e), respectively. In c), the stretched BaO_8 "cube" is shown and in d) the rectangular antiprism with a ninth O^{2-} neighbor. a) ◍ = Sr^{2+}, • = Ti^{4+}, ○ = O^{2-}; b) ⊕ = Ba^{2+}, InO_5 pyramids hatched, o = O^{2-}; c) ⊕ = Ba^{2+}, BaO_8 polyhedra hatched, ⊛ = In^{3+}; d) ⊕ = Ba^{2+}, ⊛ = In^{3+}, o = O^{2-}; e) ◍ = La^{3+}, △ = Sr^{2+}, ● = Cu^{2+}, ○ = O^{2-}.

essential difference between these two structures is that $Sr_3Ti_2O_7$ has a double layer of octahedra instead of a single two-dimensional layer as in K_2NiF_4. The spaces in the octahedral double layers shown in Figure 6a are occupied by alkaline-earth ions (hatched spheres); thus, in this region of the $Sr_3Ti_2O_7$ structure a perovskite layer is formed, with Sr^{2+} at the 12-coordinated sites and Ti^{4+} in the octahedral oxygen-coordinated sites. From this it is clear why these materials are referred to as perovskite-type superconductors. If the two Ti^{4+} ions of $Sr_3Ti_2O_7$ are replaced by two In^{3+} ions, the resulting positive charge deficit is corrected by loss of an O^{2-} ion, giving a crystal structure of the $Ba_3In_2O_6$ type (Fig. 6b–d). If, instead, two Sr^{2+} ions and the two Ti^{4+} ions are formally replaced by two La^{3+} ions and two Cu^{2+} ions, respectively, one obtains compounds such as $La_2SrCu_2O_6$ (Fig. 6e).[202,203] From Figure 6a it can be seen that the oxygen ions indicated by filled circles and lying between the layers of octahedra leave the crystal lattice, and the octahedra surrounding the Ti^{4+} ions in $Sr_3Ti_2O_7$ lose one of their shared apexes to form tetragonal pyramids around the In^{3+} ions of $Ba_3In_2O_6$ (Fig. 6b). When the marked oxygen ions are removed (cf. Fig. 6c), the 12-fold coordination around the alkaline-earth ion in $Sr_3Ti_2O_7$ is reduced to an 8-fold coordination, which can be described as a stretched cube. In the change from the $Sr_3Ti_2O_7$ structure to the $Ba_3In_2O_6$ structure, one part is left completely unaffected, namely, that part of the structure which also remained unaltered in the transition from the K_2NiF_4 type to the $Sr_3Ti_2O_7$ type. Consequently, the bulky alkaline-earth ions in this part of the structure, which lies between the layers of octahedra, have the 8 + 1 coordination characteristic of the K_2NiF_4 type.

From the relationships between $Sr_3Ti_2O_7$, $La_2SrCu_2O_6$, and $Ba_3In_2O_6$ it is possible to show how the latter two materials are structurally related to the superconductor $YBa_2Cu_3O_{6+x}$. Figure 7 illustrates the series of formal changes needed to transform the structure of, for example, the compound $Ba_3In_2O_6$ into that of the Y1-2-3 HT_c superconductor, $YBa_2Cu_3O_{6+x}$. In the $Ba_3In_2O_6$ and $La_2SrCu_2O_6$ structures the structural type is retained when Ba^{2+} is replaced by Sr^{2+}[209], although the process of filling the quasi-cubic holes in the lattice involves an interplay between the sizes of the ions and holes and the lattice energy. In the compounds $Ba_2SrIn_2O_6$ and $BaSr_2In_2O_6$, this means that the smaller Sr^{2+} ion prefers to occupy the quasi-cubic coordination sites between the layers of InO_5 pyramids. In $YBa_2Cu_3O_{6+x}$ similar layers of tetragonal CuO_5 pyramids are present, with Y^{3+} as the linking ion in the cubelike polyhedra. If, in $Ba_2SrIn_2O_6$, we formally replace all the In^{3+} ions by Cu^{2+} or Cu^{3+}, and all the Sr^{2+} ions by Y^{3+}, this already brings us very close to the structure of the Y1-2-3 superconductor. At the positions marked by arrows in Figure 7, a layer of CuO_5 pyramids undergoes shifts of $a/2$ and $b/2$, bringing the apexes

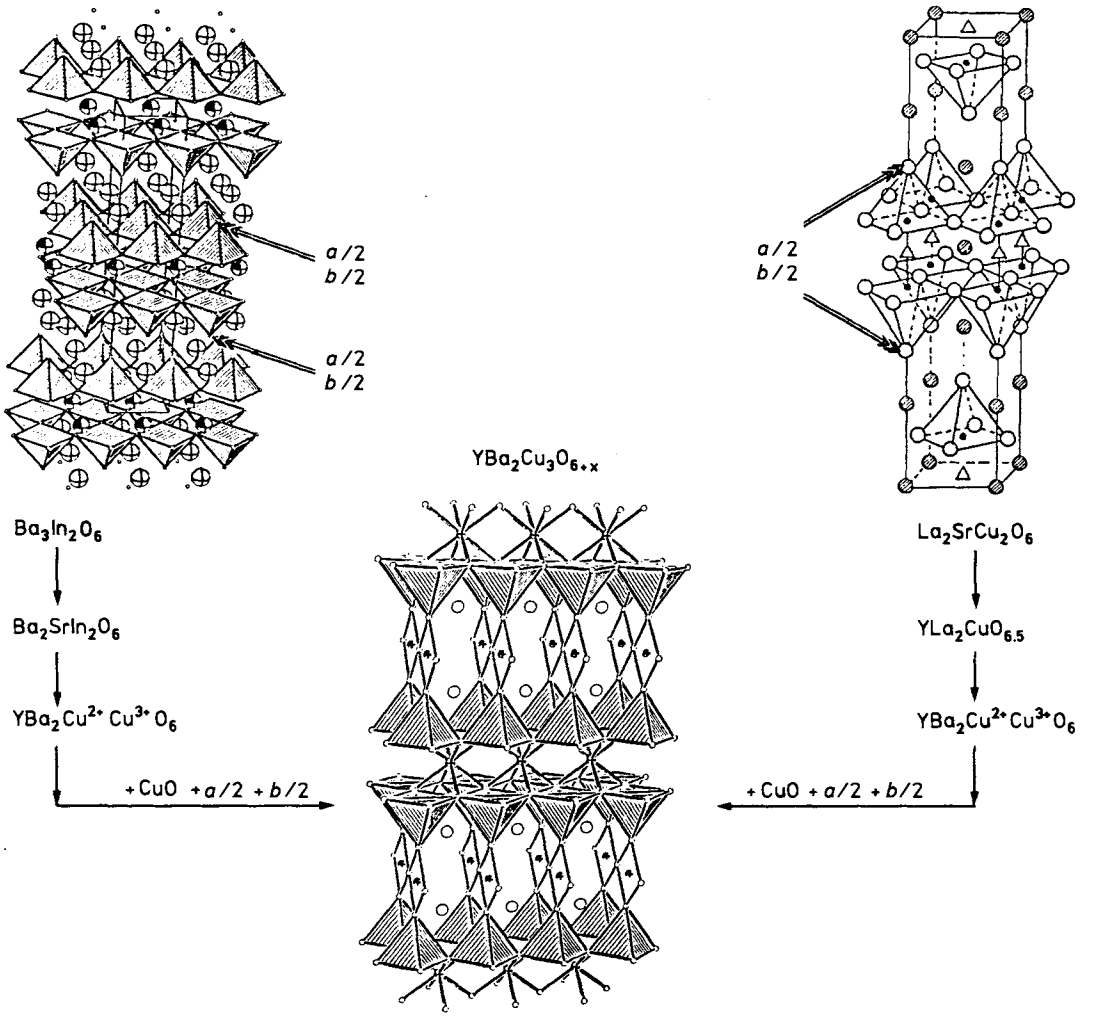


Fig. 7. Crystallographic relationships between $La_{2-x}A_{1+x}Cu_2O_{6-x/2}$ (A = Sr, x = 0), $Ba_3In_2O_6$, and the superconductor $YBa_2Cu_3O_{6+x}$.

of the pyramids into alignment. Incorporation of CuO leads to the square-planar polyhedra in $YBa_2Cu_3O_{6+x}$, which, by linking the apexes of the pyramids, give the isolated chains along the [001] direction as shown. Thus, $La_2SrCu_2O_6$ and $Ba_3In_2O_6$ (as well as $Ba_{3-x}Sr_xIn_2O_6$) have a close structural relationship to the HT_c superconductor $YBa_2Cu_3O_{6+x}$.

The Ba–Y–Cu–O system has been intensively studied;[212–215] spectroscopic methods have been used to investigate optical transitions,[216–220] and calorimetric measurements[221] have provided evidence of antiferromagnetism. Moreover, the electronic structure, bonding, and valence fluctuation in this system[222–226] and the mechanism of superconductivity in $YBa_2Cu_3O_{6+x}$ have also been studied.[227–229] Also of interest are further experiments on fluorination,[227,229] which at first seemed to offer great hopes of achieving considerably higher transition temperatures ($T_c > 150$ K).[230–232]

Our experiments along these lines showed that BaF_2 is preferentially formed, even when YOF or CuF_2 is used. Other authors have reported similar results.[233] It therefore seems very unlikely that the oxidation state in the anion partial lattice can be changed by incorporating fluorine.

3.2. $Y_2Ba_4Cu_7O_{14+x}$

In the course of measuring the effects of pressure and temperature on the quasi-binary system $YBa_2Cu_3O_{6+x}$-O_2,[234] a new phase with the chemical constitution $Y_2Ba_4Cu_7O_{14+x}$ was identified. The crystal structure of this new superconducting phase ($T_c \approx 40$ K) was determined by X-ray measurements on single crystals.[235] In Figures 8a and 8b this rather complex structure is shown as a ball-and-stick model and in the form of hatched polyhedra, respectively. There is an obvious resemblance to the structure of the $YBa_2Cu_3O_{6+x}$ superconductor. In this new phase, too, the Cu^{2+} and Cu^{3+} ions display a tetragonal-pyramidal coordination to O^{2-}. Copper is present at several different crystallographic positions. For Cu_{III} the CuO_5 pyramids are in parallel layers with their apexes facing each other. In contrast to $YBa_2Cu_3O_{6+x}$, however, the pyramid apexes in $Y_2Ba_4Cu_7O_{14+x}$ are laterally shifted relative to each other by a distance $b/2$. The main difference compared with the Y1-2-3 superconductor lies in the Cu/O double chains of Cu_{IV} (Fig. 8b), which consist of planar CuO_4 squares joined at their edges. These planar chains attached to the apexes of the Cu_{III} pyramids correspond exactly to the chains in $SrCuO_2$[95] (cf. Fig. 4), except that here the CuO_4 squares are slightly distorted. The layers of pyramids around Cu_{II} have their bases facing those of the Cu_{III} layer and are linked together by Y^{3+} ions, an arrangement which is similar to that in $YBa_2Cu_3O_{6+x}$. As revealed by Figure 8a, Cu_I can be regarded as being in a dumbbell configuration (i.e., with a linear coordination to oxygen). The O–Cu–O dumbbells link the pyramid apexes of the $Cu_{II}O_5$ polyhedra. The dumbbell-type coordination of Cu_I is only present so long as the sites O_{VIII} and O_{IX} are unoccupied. However, X-ray structural analysis indicates that these two sites have a 10% and 20% occupancy by oxygen, respectively. This can be interpreted to mean that in a micro-domain having 100% occupation at O_{VIII} and zero occupation at O_{IX}, Cu_I would have square-planar coordination. The resulting chains of planar

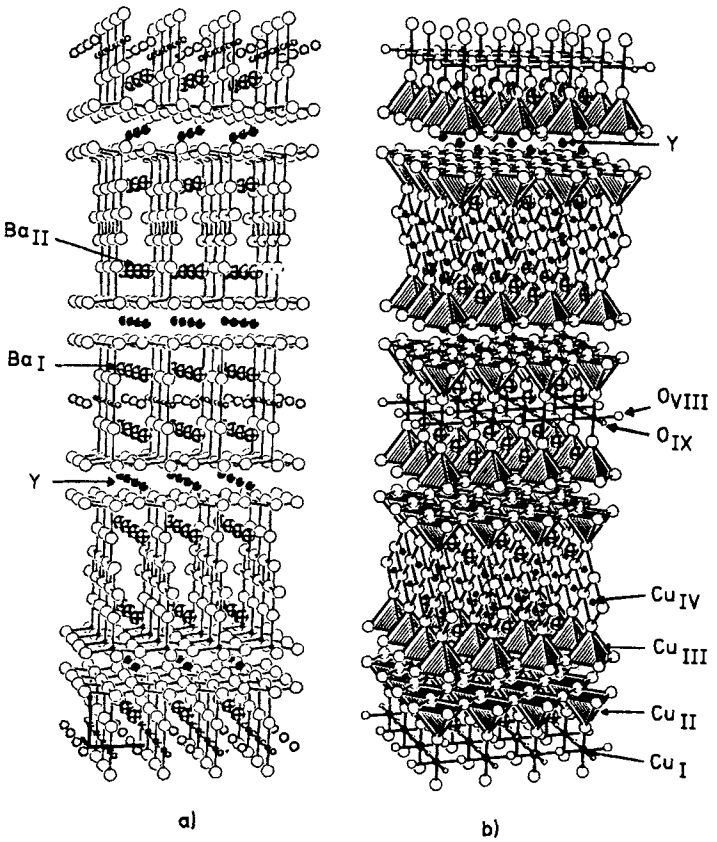


Fig. 8. Structure of $Y_2Ba_4Cu_7O_{14+x}$. a) Ball-and-stick model: ● = Y^{3+}, ⊕ = Ba^{2+}, • = Cu^{2+}, ○ = O^{2-}. b) The polyhedra around Cu_{II} and Cu_{III} are indicated by hatching. Cu_I is shown in an octahedral coordination (see text). Symbols as in a).

CuO_4 polygons run in a direction perpendicular to the Cu_{IV} double chains already described. If, instead, we consider the hypothetical case where only the O_{IX} sites are occupied, we again find that Cu_I has a square-planar coordination, giving corner-linked chains which run in the same direction as the Cu_{IV} double chains. If both the O_{VIII} and O_{IX} sites were fully occupied, Cu_I would have the octahedral coordination shown in Figure 9b. From this it can be concluded that, in the actual situation, dumbbells, planar polygons and octahedra are present in a statistical distribution with probabilities of 72%, 26%, and 2%, respectively.

Y^{3+} is surrounded by eight O^{2-} ions in the form of a cube. The O^{2-} ions forming the YO_8 polyhedra belong to the coordination spheres of Cu_{II} and Cu_{III}. This Y^{3+} environment corresponds to the coordination in $YBa_2Cu_3O_{6+x}$. The oxygen environment of the Ba^{2+} ions is more complex. Ba_I is surrounded by eight O^{2-} ions, if the O_{VIII} and O_{IX} sites are unoccupied, forming a rectangular antiprism with Ba^{2+} not quite in the center. If the O_{VIII} and O_{IX} positions are partly occupied, a distorted close-packed 12-fold coordination must be assumed. For example, Ba_{II} then lies in the region of the planar Cu/O double chain and the Cu_{III} pyramids. It has tenfold coordination, again with a rectangular antiprism and two extra O^{2-} ions. These extra neighbors belong to the coordination sphere of Cu_{IV}. Thus, the crystal structure of $Y_2Ba_4Cu_7O_{14+x}$ is made up of $YBa_2Cu_3O_{6+x}$ blocks with corner-linked planar CuO_4 chains and blocks with the constitution $YBa_2Cu_4O_8$,[235] which include edge-linked CuO_4 double chains.

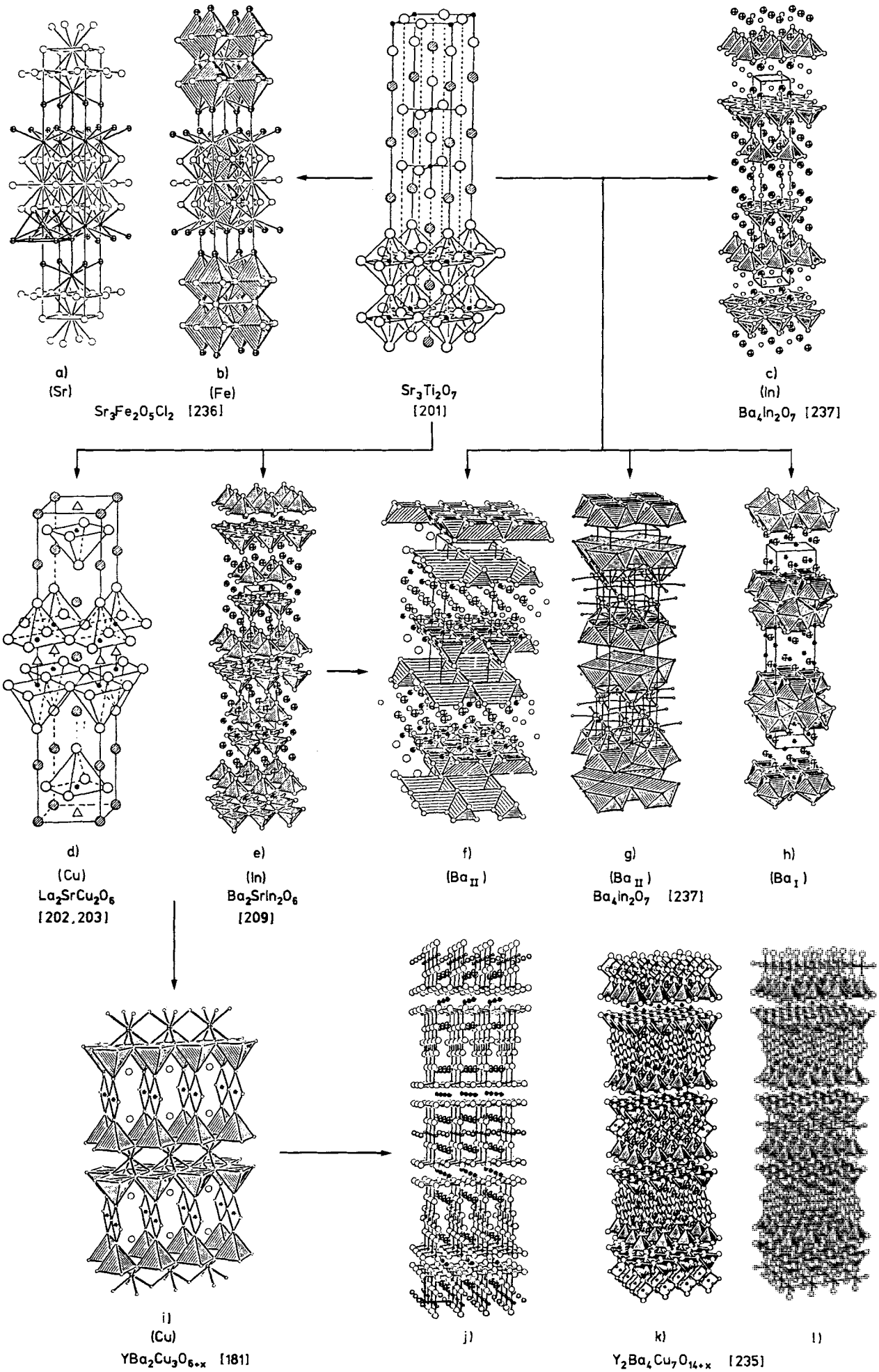


Fig. 9. Relationships between the $Sr_3Ti_2O_7$-type structure, the superconductors $YBa_2Cu_3O_{6+x}$ and $Y_2Ba_4Cu_7O_{14-x}$ and compounds with related crystal chemistry.

To conclude the discussion of the yttrium superconductors, it is appropriate to compare these with other related structures. Figure 9 shows some of these relationships, starting from the $Sr_3Ti_2O_7$-type structure.[201] Directly related to the latter is again a halogenooxoferrate, $Sr_3Fe_2O_5Cl_2$,[236] which contains Fe^{3+} in an octahedral coordination (Fig. 9a). Here there is a Cl^- ion at each of the apexes of the octahedra along the [001] direction which does not form a common linking point in the double layer of octahedra. Interestingly, the O^{2-} apexes forming the links in the double layer of octahedra are compressed, whereas the Cl^- corners of the CuO_5Cl octahedra (*trans* position) are stretched. From the $Sr_3Ti_2O_7$-type structure are derived the phases $La_{2-x}Sr_{1+x}Cu_2O_{6-x/2}$ ($x = 0$ in Fig. 9)[202,203] and the compound $Ba_2SrIn_2O_6$. As was already discussed in Section 3.1 (Fig. 7), $YBa_2Cu_3O_{6+x}$ (Fig. 9i) is directly related to the phase shown in Figure 9d and to the compound $Ba_2SrIn_2O_6$ (Fig. 9e).[209] Figures 9j-l show that the $Y_2Ba_4Cu_7O_{14+x}$ structures are also closely related to $YBa_2Cu_3O_{6+x}$ (Fig. 9i). Every second planar Cu/O chain is formally replaced by a double chain. Figure 9k, in contrast to Figure 8b, shows Cu_I in a planar O^{2-} coordination, which is conceivable for a micro-domain.

From the $Sr_3Ti_2O_7$ type one can also derive $Ba_4In_2O_7$.[237] Figure 9c shows the In/O environment for this compound. In this barium-rich oxoindate, In^{3+} again has five O^{2-} neighbors in the form of a tetragonal pyramid. The arrangements and linkages in the crystal structure correspond to the InO_5 coordination sphere of $Ba_3In_2O_6$. The extra BaO group spreads out the layers of pyramids, which are arranged with their bases facing each other. This increased spreading of the pyramid layers is one of the main differences between this structure and that of $Y_2Ba_4Cu_7O_{14+x}$ (compare Fig. 9c with Figs. 9k and 9l). The BaO polyhedra in $Ba_4In_2O_7$ are shown in Figures 9f–h. As in all these crystallographically related compounds, the BaO polyhedra are unaffected by changes in the crystal lattice. Thus, Ba_I has the 8 + 1 coordination which is characteristic of the K_2NiF_4- and $Sr_3Ti_2O_7$-type structures (cf. Figs. 5c and 6b–d). Ba_{II}, on the other hand, has a coordination sphere with one unoccupied oxygen site, which means that in the micro-domain Ba_{II} has a trigonal-prismatic coordination (Fig. 9f). The orientation of the elongated edge of the prism is alternately parallel to the *a* and *b* axes, which explains why the crystal does not cleave readily at this position. If the O_{II} sites mentioned above were fully occupied, Ba_{II} would have a rectangular antiprism of O^{2-} ions, with a considerably elongated rectangular face.[237]

4. The Bismuth Superconductors

Starting from $La_{2-x}Sr_xCuO_4$, the replacement of La^{3+} by Y^{3+} and of Sr^{2+} by Ba^{2+} led to the superconducting phase $YBa_2Cu_3O_{6+x}$. An urgent task, therefore, was to pursue such substitution reactions further in order to discover still more superconducting phases. The first high-T_c superconductor that contained neither yttrium nor a lanthanoid was found in the Bi-Sr-Cu-O system.[238] The fact that superconductivity had already been observed at about 20 K with the same mixture of components a year earlier[89] was almost overlooked. A number of subsequent studies[239–252] confirmed the original observation of at least two superconducting phases with transition temperatures between about 85 K and 108 K. Considerable efforts were put into elucidating the dependence of T_c on the preparation conditions,[253–259] the substitution,[260–262] and the crystal structure. Thus, electron and X-ray diffraction experiments were carried out on both microcrystalline material and single crystals, and, as in the case of $YBa_2Cu_3O_{6+x}$, high-resolution transmission electron microscopy was also used.[263–265] It was not long before a paper appeared reporting single-crystal X-ray diffraction results in combination with neutron diffraction,[266] and giving a complete description of the two superconducting phases, namely, $Bi_2(Sr_{1-x}Ca_x)_2CuO_{8-y}$ (I, Bi2-2-1) and $Bi_2(Sr_{1-x}Ca_x)_3Cu_2O_{10-y}$ (II, Bi2-3-2). Figure 10 shows a perspective view of the different coordination polyhedra surrounding Cu, Bi, and Sr/Ca in phase I. In Figure 10a the CuO_6 octahedra, stretched along the [001] direction, are indicated by hatching. The Cu^{2+} and Cu^{3+} ions have the same

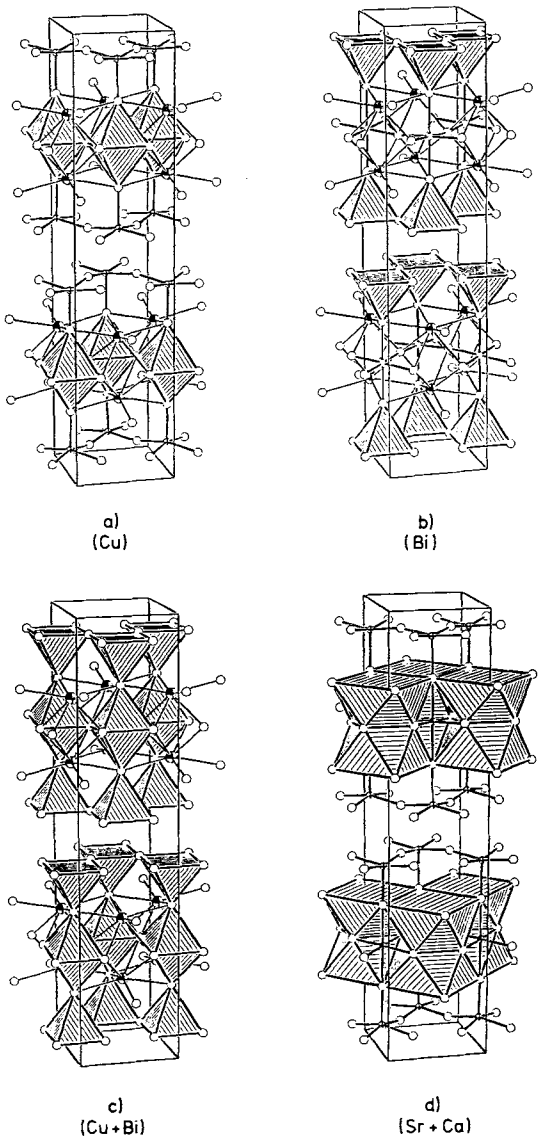


Fig. 10. Coordination polyhedra in the superconductor $Bi_2(Sr,Ca)_2CuO_{8-x}$ ("phase I"). a) Octahedral coordination around the copper ions indicated by hatching. b) Idealized BiO_5 polyhedra with ball-and-stick model of the Cu/O coordination. c) Linking between the CuO_6 octahedra and the idealized BiO_5 pyramids. d) The rectangular antiprism around the alkaline-earth ions.

coordination as in $La_{2-x}Sr_xCuO_4$. The bismuth ion occupies a tetragonal-pyramidal environment, which is shown in an idealized representation in Figure 10b. In preparing single crystals of phases I and II[266] it was found that, depending on the thermal treatment, crystals varying from black to brown were produced, although with no detectable effect on the structure; these also varied in their ability to oxidize HCl (liberation of Cl_2). The authors attribute this to defects in the $Bi_2O_{4-\delta}$ partial structure which were shown by neutron diffraction to be present. From this it appears that oxygen deficits can occur in the pyramid bases of the BiO_5 polyhedra. Figure 10c shows the typical corner linkage of the BiO_5-CuO_6-BiO_5 polyhedra along the [001] direction. The alkaline-earth ions (Sr^{2+} in the single crystal investigated here) are arranged within the Cu/Bi/O crystal packing (Fig. 10d), although not in the form of links between the layers of pyramids like the Y^{3+} ions in $YBa_2Cu_3O_{6+x}$. The coordination polyhedra of these alkaline-earth ions consist of highly distorted rectangular antiprisms (see Fig. 10d).

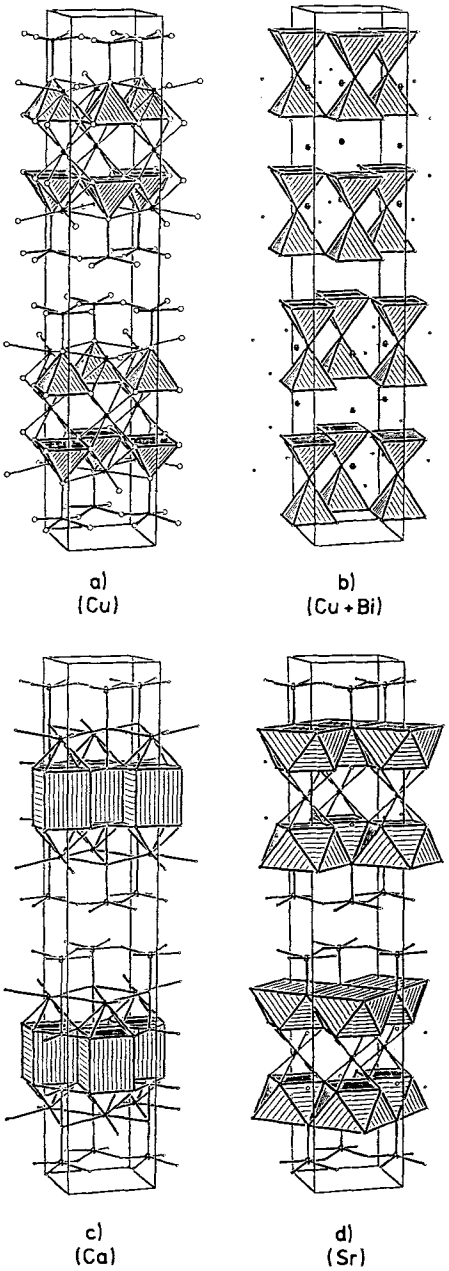


Fig. 11. Coordination polyhedra in the superconductor $Bi_2(Sr,Ca)_3Cu_2O_{10-x}$ ("phase II"). a) Tetragonal-pyramidal coordination of Cu^{2+}/Cu^{3+} by O^{2-}. The BiO_5 environment is shown in a ball-and-stick model. b) Linking of the CuO_5 and BiO_5 polyhedra. The BiO_5 pyramids are shown in an idealized representation. c) Coordination of Ca^{2+} by O^{2-}. d) Coordination of Sr^{2+} by O^{2-}.

The structure of the second superconducting phase, $Bi_2(Sr_{1-x}Ca_x)_3Cu_2O_{10-\delta}$, is derived from that of phase I. The coordination polyhedra are shown in Figure 11 in a perspective drawing. In Figure 11a the tetragonal pyramids of O^{2-} ions around Cu^{2+} and Cu^{3+} are indicated by hatching; Figure 11b shows in addition the tetragonal pyramids around Bi^{3+} and Bi^{5+}, which are linked to those of Figure 11a. In the Cu/O partial lattice one recognizes exactly the same structural units as in $YBa_2Cu_3O_{6+x}$, $La_{2-x}Sr_{1+x}Cu_2O_{6-x/2}$, and the indates $Ba_{3-x}Sr_xIn_2O_6$ (cf. Fig. 7), with the same spatial arrangement. These resemblances between phase II and the substances mentioned also apply to the Ca^{2+} ions intercalated between the layers of CuO_5 pyramids; as can be seen in Figure 11c, these have a stretched cubic coordination. The bulky Sr^{2+} ions occupy rectangular antiprisms in this case (see Fig. 11d), with the same distortion of the square faces along the [001] direction as was described earlier for the K_2NiF_4-type structure. In phase II, which contains less bismuth, Bi again undergoes valence changes depending on the oxygen treatment, resulting in varying degrees of oxygen deficiency in the Bi/O partial lattice. Details of compounds with orthorhombic symmetry, in which the Bi ions are bent out of the square face of the pyramid, can be found in the literature.[266]

5. The Thallium Superconductors

Research on the bismuth superconductors was followed by the discovery of further superconducting oxide phases based on thallium.[267, 268] Within a few months after this discovery, a succession of publications[191, 196, 269–284] reported several different types of thallium superconductors. The superconducting properties were evidently structure-dependent, and numerous studies on the crystal structures of these materials were therefore carried out; some examples are cited here.[285–292] Here again the elucidation of the crystal chemistry was helped by high-resolution transmission electron microscopy (cf. Refs. [293–295]). Two series of materials are now recognized, and a few examples will be described here.

5.1. Superconductors with One Thallium Atom per Unit

This group of materials has the general formula $TlBa_2Ca_{n-1}Cu_nO_{2n+3}$ with n = 2, 3, or 4 (cf. Refs. [283, 287–289, 292]). The three values of n give materials with the following constitutions, listed here with the commonly used abbreviations: (1) $TlBa_2CaCu_2O_{7+x}$ = 1-2-1-2 (specifically, Tl1-2-1-2), (2) $TlBa_2Ca_2Cu_3O_{9+x}$ = 1-2-2-3 (Tl1-2-2-3), and (3) $TlBa_2Ca_3Cu_4O_{10.5+x}$ = 1-2-3-4 (Tl1-2-3-4). In this article the Tl1-2-2-3 superconductor will be described. Figures 12a–c show the different coordination spheres around copper and thallium. The copper coordination is indicated in Figure 12a. Here we see the tetragonal-pyramidal environ-

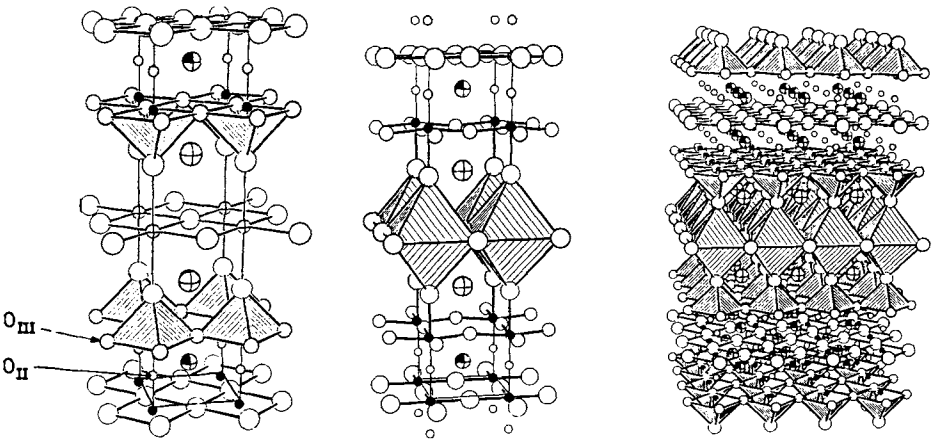


Fig. 12. Coordination polyhedra in the thallium superconductor $TlBa_2Ca_2Cu_3O_{9+x}$. a) Coordination around Cu^{2+}, with the tetragonal pyramids shown by hatching. Position O_{III} is shown in an idealized representation (i.e., fully occupied). O_{II} has a very low occupancy and is ignored here from a coordination standpoint. o = Tl^{3+}, ⊕ = Ba^{2+}, ⊕ = Ca^{2+}, ● = Cu^{2+}, ○ = O^{2-}. b) The octahedra around Tl^{3+} are indicated by hatching. Symbols as in a). c) Linking of the Cu/Tl-O^{2-} polyhedra. Symbols as in a).

ment (hatched) and, at the two ends of the unit cell, a square-planar CuO_4 coordination. The tetragonal CuO_5 pyramids are oriented with their distorted bases parallel to the *a/b* plane, linked at all their corners within this plane. The apexes of the pyramids are also stretched by about 11% in comparison with the interatomic distances of the base. These apexes are shared with the coordination spheres of the thallium ions and will be discussed again later. The planar CuO_4 squares are also oriented parallel to the *a/b* plane and are linked at their corners to form an infinite two-dimensional grid. This arrangement resembles the planar linking often found in oxocuprate(II) structures, for example in Nd_2CuO_4.[35] However, this description needs to be qualified, since there are some vacant oxygen sites in $TlBa_2Ca_2Cu_3O_{9+x}$.[287] In particular, the site marked O_{II} in Figure 12a has an unusually low occupancy. The position O_{III}, also marked, has an occupancy of about 80%. Consequently, Cu_{II}, whose coordination is shown in Figure 12a as tetragonal-pyramidal, can also have octahedral coordination in micro-domains, and the CuO_5 pyramids can also be oriented perpendicular to the plotted direction. Cu_I, at the position $x = 0$, $y = 0$, $z = 0$, also has pyramidal coordination in micro-domains of the crystal lattice owing to the partial occupancy of site O_{II}. However, since point position O_{II} only has an occupancy of about ⅓, the statistical probability of octahedral coordination around Cu_I is quite low.

As already mentioned, the thallium polyhedra are linked to the tetragonal pyramids of the CuO_5 environment. Figure 12b shows that the apex of each pyramid is also a corner of an octahedron of O^{2-} ions surrounding a Tl^{3+} ion. The TlO_6 octahedra are hardly distorted. It should be noted that the TlO_6 octahedra are joined by their edges in the *a/b* plane, and they do not have an oxygen deficit at any position.

The alkaline-earth ions are incorporated in an ordered pattern into the crystal structure. The Ca^{2+} ions are confined within the Cu–O partial lattice, with a cubic coordination to eight O^{2-} ions. The experimentally determined site occupancy factors[287] show that the Tl sites are partly vacant, and some of the Ca^{2+} sites are also occupied by Tl^{3+} ions. As shown in Figure 12c, the Ba^{2+} ions lie between the Tl and Cu polyhedra. Their coordination can be described as 8 + 3, since the partial vacancy of the O_{III} sites means that 12-fold coordination is not quite reached. Further work will improve our knowledge of these crystal structures. One of the older papers,[283] and also one recent paper,[292] report different occupancies, and even different positions, for the light ions.

5.2. Superconductors with Two Thallium Atoms per Unit

The second series of thallium oxide superconductors is described by the general formula $Tl_2Ba_2Ca_nCu_{n+1}O_{2n+6}$ with n = 0, 1, or 2. Up to now two forms with n = 0, having the constitution $Tl_2Ba_2CuO_6$, are known, and these are identified in the literature as o-2-2-0-1 (o-Tl2-2-0-1) and t-2-2-0-1 (t-Tl2-2-0-1) (o = orthorhombic, t = tetragonal). Figure 13a gives an overall picture of the structure, showing all the atoms in several unit cells. The coordination sphere of the copper ions is indicated by hatching. The stretching of the CuO_6 octahedra, amounting to about 39%, is clearly seen. The CuO_6 octahedra are joined at their corners to form a two-dimensional grid, which corresponds to the Cu/O coordination in $La_{2-x}Sr_xCuO_4$. In the orthorhombically distorted form[291] the apexes of the octahedra are slightly displaced. Figure 13b shows the oxygen environment of the Tl^{3+} ions, which is also octahedral. The Tl/O partial lattice consists of double layers of octahedra joined at their edges, with their bases tilted out of the common plane. The layers of CuO_6 octahedra are linked to the Tl/O double layers by common corners along the [001] direction. Adjacent CuO_6 and TlO_6 octahedron bases are inclined at 45° relative to each other. The linking pattern in this part of the crystal structure is therefore not of the perovskite type. The spaces in the $Tl_2CuO_6^{4-}$ lattice are occupied by Ba^{2+} ions; according to the experimentally determined distances, the Ba^{2+} ion has a coordination number C.N. = 9.

Inserting the value n = 1 into the general formula $Tl_2Ba_2Ca_nCu_{n+1}O_{2n+6}$ gives $Tl_2Ba_2CaCu_2O_{8+x}$ (Tl2-2-1-2),

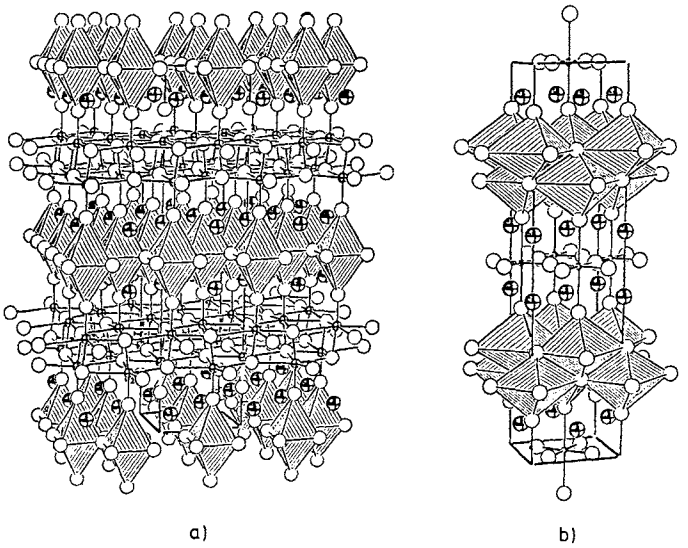


Fig. 13. Coordination polyhedra in Tl_2BaCuO_6. a) The octahedra around Cu^{2+} are shown by hatching. b) Double layers of compressed TlO_6 octahedra indicated by hatching. ⊕ = Ba^{2+} and ○ = O^{2-}.

which has the crystal structure shown in Figure 14. In Figure 14a the coordination around the copper ions in a unit cell is indicated. The Cu^{2+} and Cu^{3+} ions are again surrounded by O^{2-} in a tetragonal-pyramidal coordination, with the pyramid apexes oriented along the [001] direction showing an unusually large stretching of up to 40%. The arrangement of the pyramids corresponds to that in, for example, $YBa_2Cu_3O_{6+x}$. Figure 14b shows, over a larger region, the linking of the CuO_5 polyhedra to the double layer of TlO_6 octahedra formed by the joining of the latter at their edges. Certain regions of the crystal structure are identical to the structure of Tl_2BaCuO_6, as shown in Figure 13b. It should

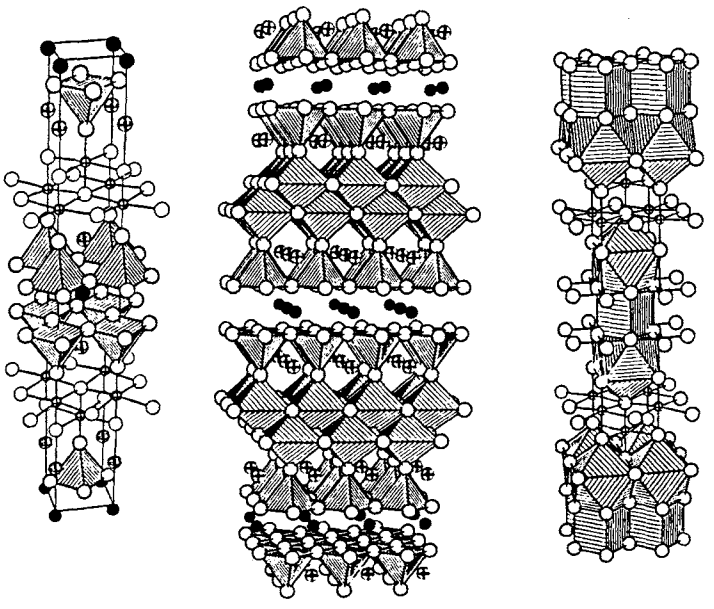


Fig. 14. Coordination polyhedra in $Tl_2Ba_2CaCu_2O_{8+x}$. a) The tetragonal pyramids around copper are shown hatched. ⊕ = Ba^{2+}, ⊛ = Tl^{3+}, ● = Ca^{2+}. b) Linking of the CuO_5 pyramids with the double layers of TlO_6 octahedra. Symbols as in a). c) Coordination around Ca^{2+} (cubic) and Ba^{2+} (a rectangular antiprism extended by neighboring ions).

be noted that in Figure 14 O_{III} is shown in an idealized representation. The experimentally observed split positional coordinates (16n) of $x = 0.104$, $y = 0$, $z = 0.782$ were idealized (4e) to $x = 0$, $y = 0$, $z = 0.782$ in order to show the crystal structure more clearly. Finally, Figure 14c shows the environment of the alkaline-earth ions.

The smaller Ca^{2+} ions have a cubic coordination, like Y^{3+} in $YBa_2Cu_3O_{6+x}$ or Sr^{2+} in $BaSr_2In_2O_6$ (cf. Figs. 5b and 6c). Ba^{2+} has a coordination number C.N. = 8 + 1, corresponding to a rectangular antiprism with one extra ion.

The third of these thallium-rich superconducting phases is well known and has the highest transition temperature of this series (T_c = 125 K); it has n = 2 and thus the formula $Tl_2Ba_2Ca_2Cu_3O_{10+x}$ (Tl2-2-2-3). Figures 15a–c show the coordination polyhedra around Cu, Tl, and Ca. In Figure 15a the tetragonal-pyramidal coordination of the copper ion is indicated by hatching. As in all the superconductors with CuO_5 polyhedra described up to now, the bases of the pyramids are oriented parallel to the *a*/*b* plane and are linked at all four base corners. The apexes of the pyramids are stretched to an unusual extent: 39% relative to the distances in the base of the pyramid. Figure 15a shows that there are further CuO polyhedra at $z = 0$ and $z = ½$, and, as in the oxocuprates (e.g., Nd_2CuO_4[35]), these are joined to form infinite two-dimensional grids. Within the crystal structure there are regions where copper ions are crowded together. Figure 15b shows the polyhedra around thallium. These compressed octahedra are joined together to form a double layer as in the other thallium superconductors. Along the [001] direction the CuO_5 pyramids and the TlO_6 octahedra are joined at their corners by shared oxygen ions, thus forming the spaces which contain the Ca^{2+} ions (small spheres with a quadrant) and the Ba^{2+} ions (larger spheres with a cross). The alkaline-earth ions are packed into the crystal lattice in an ordered pattern. Ba^{2+} has the 8 + 1 coordination which has already been described several times and is typical of the K^+ ions in the K_2NiF_4-type structure. Ca^{2+}, which is present only in the spaces of the Cu/O structure, again has a stretched cubic coordination, as shown, for example, in Figures 6b and 11c for $Ba_3In_2O_6$ and $Bi_2(Sr,Ca)_3Cu_2O_{10-x}$.

The structure of $Tl_2Ba_2Ca_2Cu_3O_{10+x}$ contains some detailed features which it is not possible to show in Figure 15. One such feature relates to the oxygen sites (16-fold lattice position marked by arrows in Figure 15b), which are in fact occupied by only four O^{2-} ions. The statistical distribution of four O^{2-} ions between 16 equivalent sites gives four possible positions for each one, located around the points marked in the figure. The actual positional coordinates, namely, $x = 0.100$, $y = 0$, $z = 0.775$, were idealized in Figures 15a–c by using the values $x = 0$, $y = 0$, $z = 0.775$. The experimentally observed split positions of the marked oxygen ions cause a distortion of the TlO_6 polyhedra, but without any bending out of the *a*/*b* plane.

We have just completed a determination of the structure[296] of the compound $Ba_8In_6O_{17}$, which is crystallographically related to the thallium-rich superconductor $Tl_2Ba_2Ca_2Cu_3O_{10+x}$. This structure is shown in Figures 16a and 16b alongside that of $Tl_2Ba_2Ca_2Cu_3O_{10+x}$ (Fig. 15a). The structure of $Ba_8In_6O_{17}$ is interesting because it belongs to the same family as the K_2NiF_4 and $Sr_3Ti_2O_7$ structures.

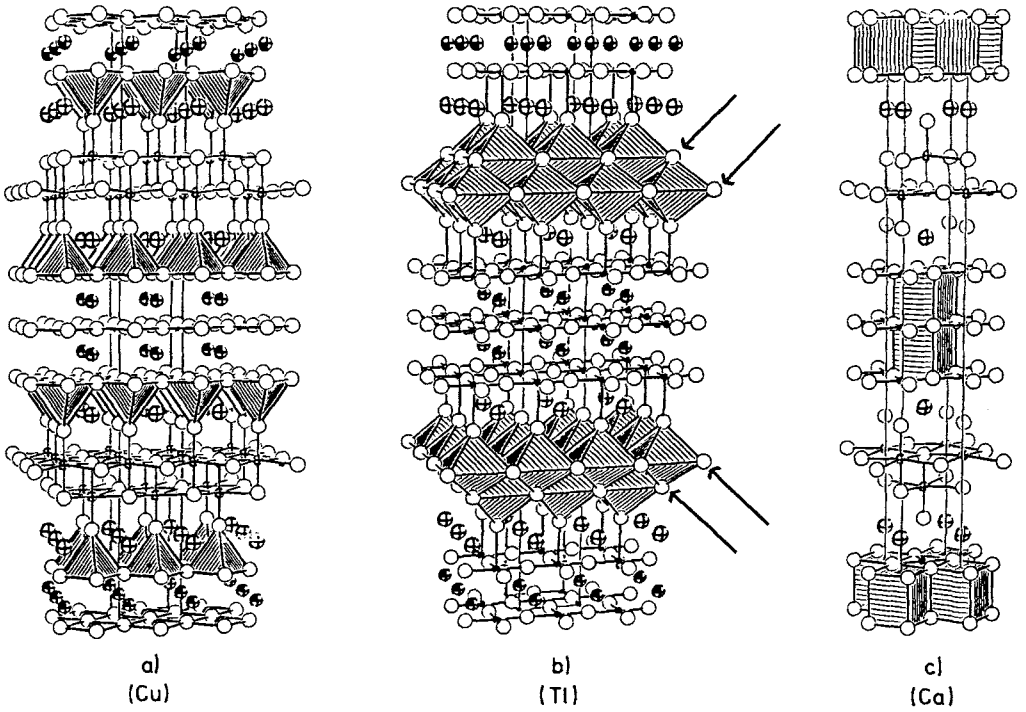


Fig. 15. Coordination polyhedra in $Tl_2Ba_2Ca_2Cu_3O_{10+x}$. a) CuO_5 pyramids around copper (hatched) and planar polygons at the beginning and middle of the unit cell. ⊕ = Ba^{2+}, ◐ = Ca^{2+}, partly substituted by Tl^{3+}, ○ = O^{2-}. b) Double layers of TlO_6 octahedra, shown hatched. The oxygen sites indicated by the arrows are only 25% occupied, and these positions are shown with idealized parameters (see text). Symbols as in a). c) Coordination polyhedra around Ca/Tl. Symbols as in a).

If the latter are extended by one layer of octahedra, the $Sr_4Ti_3O_{10}$-type structure is obtained.[201] This is shown for comparison in Figure 16c. If Ti^{4+} is replaced by In^{3+} and Sr^{2+} by Ba^{2+} in two formula units of $Sr_4Ti_3O_{10}$, one arrives at the constitutional formula $Ba_8In_6O_{17}$. In each of the octahedron base planes of the $Sr_4Ti_3O_{10}$ structure, marked by arrows in Figure 16c, there is half an O^{2-} ion missing per unit cell, so that in micro-domains of $Ba_8In_6O_{17}$ there are two InO_5 pyramids per octahedron layer per unit cell. An important property of these InO_5 pyramids is that their square faces are never oriented parallel to the *a*/*b* plane. The InO_5 pyramids occurring in the octahedron layer are not shown in Figure 16a; instead, the structure is shown with the idealized oxygen occupancy corresponding to the hypothetical formula "$Ba_8In_6O_{20}$". It is clearly evident that the middle octahedron in $Ba_8In_6O_{17}$ is stretched on both sides; this is a novel feature in indium chemistry. The outer octahedra, which adjoin the middle layer of octahedra, are both stretched and compressed, in a similar way to the FeO_5Cl octahedra in $Sr_3Fe_2O_5Cl_2$[236] (cf. Fig. 9b). The step from this to the thallium-rich superconductor $Tl_2Ba_2Ca_2Cu_3O_{10+x}$ (cf. Fig. 15a) shows that the entire Cu/O region, for example in the middle of the unit cell, can be constructed from triple layers of corner-linked octahedra (perovskite blocks), as in $Sr_4Ti_3O_{10}$ (Fig. 16c). If the upper and lower apical oxygen ions are removed from the middle layer of octahedra in the $Sr_4Ti_3O_{10}$-type structure, we obtain a planar MO_4-coordinated system bounded by two layers of pyramids. Thus, it is possible to derive the structure of the superconductor $Tl_2Ba_2Ca_2Cu_3O_{10+x}$ from the $Sr_4Ti_3O_{10}$ type, although here, in contrast to $YBa_2Cu_3O_{6+x}$, there is no chain of planar CuO_4 polyhedra between the apexes of the pyramids in the outer layer of octahedra, but instead a double layer of TlO_6 octahedra is inserted. In the formula $Tl_2[Ba_2Ca_2Cu_3O_{6+x}]O_3$, the partial structure inside the brackets is practically of the same type as $Sr_4Ti_3O_{10}$, with Cu^{2+} inserted into the layers of octahedra in place of Ti^{4+}.

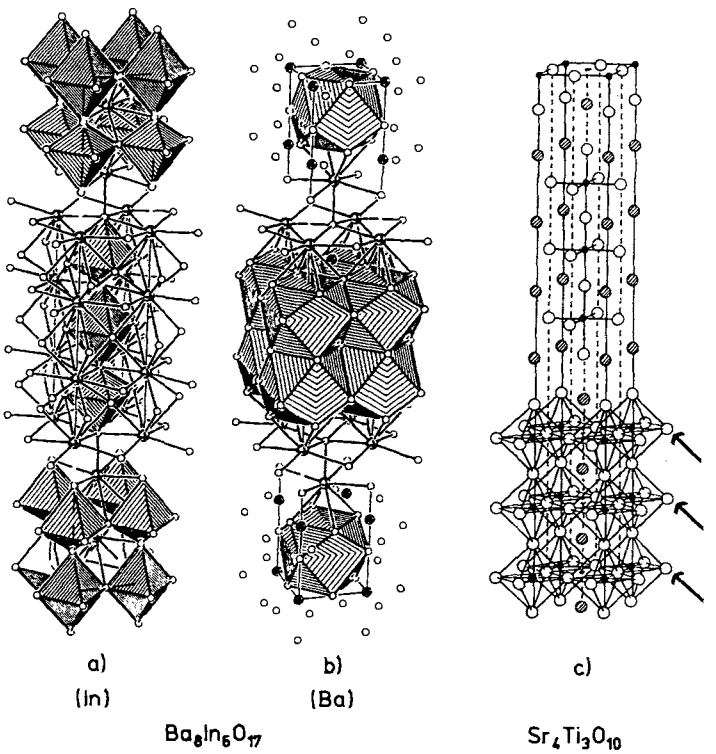


Fig. 16. Relationships between the $Sr_4Ti_3O_{10}$-type structure, $Ba_8In_6O_{17}$, and the superconductor $Tl_2Ba_2Ca_2Cu_3O_{10+x}$ (see Fig. 15a for CuO_5 pyramids around Cu in the superconductor). a) "InO_6" polyhedra in $Ba_8In_6O_{17}$. The octahedra shown here only occur in limited numbers (see text). b) Coordination of Ba^{2+} in $Ba_8In_6O_{17}$ assuming fully occupied oxygen sites. c) Incomplete unit cell of the $Sr_4Ti_3O_{10}$-type structure. The arrows indicate the O^{2-} layers in which $Ba_8In_6O_{17}$ has an oxygen deficiency. ◍ = Sr^{2+}, ● = Ti^{4+}, ○ = O^{2-}.

In the sequence from $Sr_4Ti_3O_{10}$ through $Sr_3Ti_2O_7$ to Sr_2TiO_4[201] (K_2NiF_4 type), the perovskite structure persists, though becoming a smaller proportion of the whole. These examples show that nature uses building blocks of the perovskite structure in many different superconducting phases.

6. The Lead Superconductor

The lead superconductors to be described here are not the classical perovskites such as $BaPb_{1-x}Bi_xO_3$[297] and their later derivatives (see, e.g., Ref. [298]), nor the materials obtained by partial substitution of the bismuth superconductors (see, e.g., Refs. [299, 300]), even though transition temperatures as high as 132 K have been reported[300] for the $(Bi_{1.9-x}Pb_xSb_{0.1})Sr_2Ca_2Cu_3O_y$ system with x = 0.3 and 0.4. The $Pb_2Sr_2ACu_3O_{8+x}$ system (A = Ln, Ca, Ln + Sr) and the phase $Pb_2Sr_{2.24}Nd_{0.76}Cu_3O_{8+x}$,[301] which will be described here, with a T_c of about 68 K, are interesting from a crystal chemical point of view. Figure 17 shows the structure of the latter system; in Figure 17a the tetragonal pyramids around the copper ions are indicated by hatching. This superconductor again fits into the general pattern in having CuO_5 polyhedra joined together in a two-dimensional grid. As in $YBa_2Cu_3O_{6+x}$ or $Tl_2Ba_2CaCu_2O_{8+x}$, the pyramids are aligned with their bases facing each other to form capped octahedra. The CuO_5 pyramids are all elongated up to 18%. The sites between the bases of the pyramids are occupied by strontium and neodymium ions in a random distribution. The coordination polyhedron is of the cubic type, which has already been described several times. Figure 17b shows PbO_5 polyhedra in addition to the CuO_5 pyramids. Although the CuO_5 and PbO_5 polyhedra share a common apex, the base planes of the two types of polyhedra are inclined at 45° to each other. The effect of this tilting is to alter the linking between the PbO_5 pyramids so that they are joined through all their edges to form a grid parallel to the *a*/*b* plane. An interesting feature of the lead superconductor structures is seen here, namely, the O–Cu–O dumbbells with monovalent copper which are aligned along the [001] direction in the middle of the structure. This twofold coordination, which is characteristic of Cu^+, forms a link along the direction of the *c* axis joining the bases of the PbO_5 pyramids.

Sr^{2+}, as the larger of the ions, occurs only in the gaps between the CuO_5 and PbO_5 pyramids. The polyhedron that is shown surrounding the large sphere marked with a quadrant is a rectangular antiprism extended by two neighboring ions.

7. Superconductor Byproducts

During the course of the innumerable experiments aimed at synthesizing superconductors almost every research group has come across new compounds, which have become known as "superconductor byproducts".

Since these byproducts represent reactions which compete with those leading to the superconductors, and therefore need to be eliminated from the solid-state reactions by a suitable choice of reaction conditions, it is very important to identify and understand them. A few examples, which also lead to some interesting conclusions about the crystal chemistry of HT_c superconductors will be described here. The compounds concerned are usually oxocuprates, but also occasionally oxoplatinates, which are formed by side reactions involving the platinum of the reaction vessel. Space will only allow these byproducts to be described briefly here.

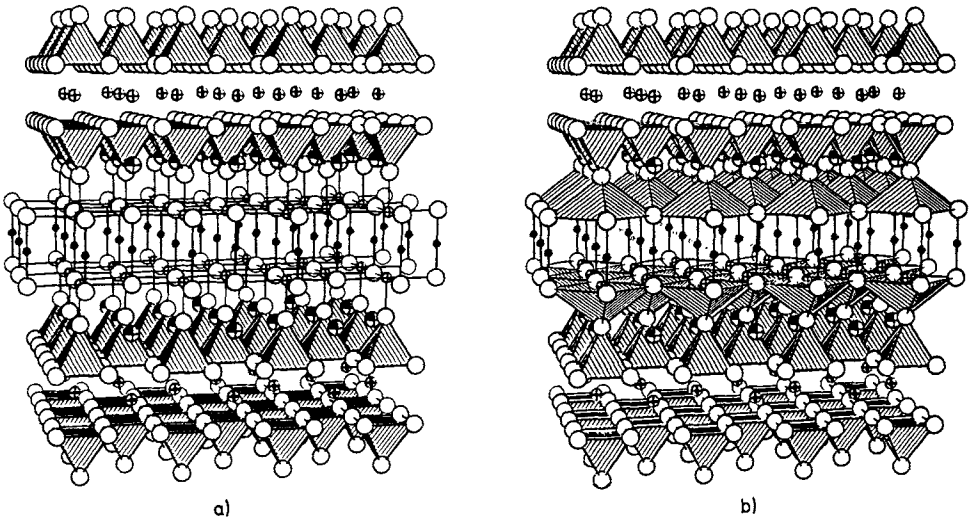


Fig. 17. Coordination polyhedra in $Pb_2Sr_{2.24}Nd_{0.76}Cu_3O_{8+x}$. a) Tetragonal pyramids around copper ions are shown hatched. ⊕ = Sr^{2+}, ⊕ = Sr^{2+}/Nd^{3+}; ● = Cu^+; ○ = O^{2-}. b) CuO_5 pyramids linked to PbO_5 pyramids, both shown hatched. The O–Cu^+–O dumbbells between the PbO pyramids are clearly shown. Symbols as in a).

7.1. Oxocuprates as Superconductor Byproducts

It should first be mentioned that, in the course of work on $YBa_2Cu_3O_{6+x}$, a well-known compound, $BaCuY_2O_5$,[302, 303] was rediscovered.[107, 304] The crystal structure of $BaCuY_2O_5$ was also refined by further measurements.[305] The $BaCuLn_2O_5$-type structure on which this is

based, with the characteristic isolated CuO_5 tetragonal pyramids, is formed by many of the lanthanoid elements.[304, 306, 307] It is interesting that Ni^{2+}, with octahedral coordination in the original $BaNiLn_2O_5$ structure, also crystallizes in the $BaCuLn_2O_5$-type structure with the smallest of the lanthanoid ions, Yb^{3+} and Lu^{3+}.[307–309] In contrast to the copper compounds, the Ni^{2+} ion in the NiO_5 tetragonal pyramid is surrounded by five equidistant O^{2-} ions.

7.1.1. $Sr_2CuO_2(CO_3)$

The compound $Sr_2CuO_2(CO_3)$ was a surprising discovery.[308] This dark gray substance is apparently an intermediate phase arising when $SrCO_3$ and CuO are allowed to react in the solid state to give the well-known compound Sr_2CuO_3.[94] The structure of Sr_2CuO_3, shown in Figure 4, is a variant of the K_2NiF_4 type.

It consists of isolated infinite one-dimensional chains made up of planar polyhedra linked at their corners. As Figure 18 shows, the Cu^{2+} ions in $Sr_2CuO_2(CO_3)$ also have

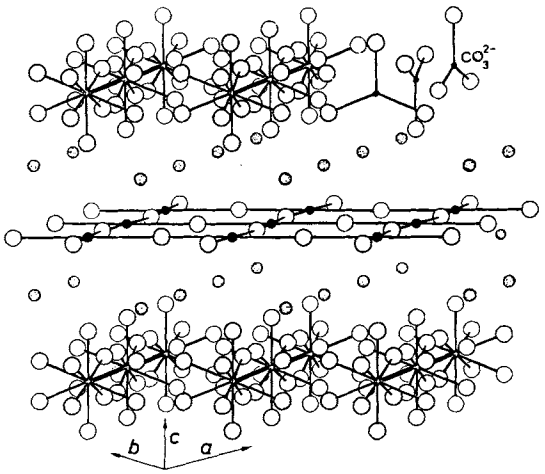


Fig. 18. Coordination polyhedra in $Sr_2CuO_2(CO_3)$ [306]. The planar grids of CuO squares and the orientations of the CO_3^{2-} groups are shown. ○ = Sr^{2+}, ● = Cu^{2+}, ○ = O^{2-}.

a square-planar coordination, in infinite two-dimensional layers of $[CuO_2]_n^{2-}$ units linked at the corners; these layers are combined with Sr^{2+} ions above and below to form $[Sr_2CuO_2]^{2+}$ blocks. These blocks in turn are joined by CO_3^{2-} groups. Figure 18 also shows that the carbonate groups exhibit an orientational disorder, with four equivalent orientations in the [110] planes.

7.1.2. $Sr_{14}Cu_{24}O_{38-\delta}$ and $La_6Ca_8Cu_{24}O_{39}$

These recently investigated crystal structures[310, 311] contain Cu^{2+} in a square-planar coordination. The overall structures can be regarded as made up of a tightly knit framework of $[Sr_2Cu_2O_3]^{2+}$ units enclosing a second partial structure of $[CuO_{2-\delta}]^{2-}$ units. Figure 19 shows that the outer framework contains $^2_\infty[Cu_2O_3\blacksquare]$ grids, where the solid square denotes defects. Inside this framework are arranged four isolated chains of edge-linked $CuO_{4-\delta}$ polyhedra, each shifted in phase relative to the others. The type of phase shift

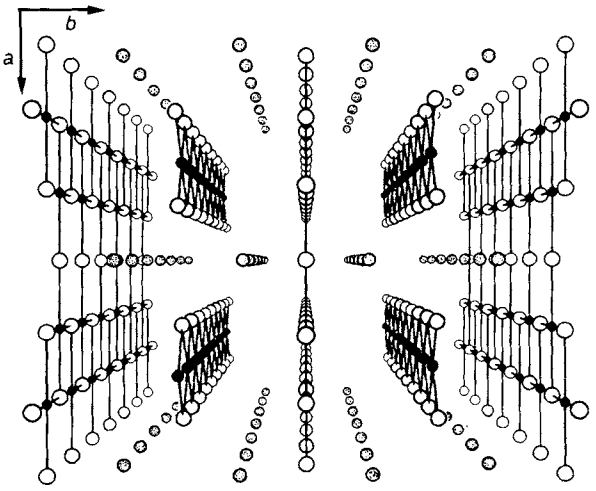


Fig. 19. Perspective view of the structure of $M_{14}Cu_{24}O_{38-\delta}$. ○ = M^{2+}, ● = Cu^{2+}, ○ = O^{2-}.

in each case determines the differences in structure between $Sr_{14}Cu_{24}O_{38-\delta}$ and $La_6Ca_8Cu_{24}O_{38}$. The recently published paper on these structures[312] is in good agreement with previous studies except for some significant differences in the stoichiometry. If an ideal situation with all the O^{2-} sites occupied is assumed, the formula $M_{14}Cu_{24}O_{41}$ is obtained. It has been shown[312] that the oxygen content in the crystal lattice is a function of the oxygen partial pressure during the synthesis of this substance. By varying the oxygen content, with otherwise identical preparative conditions, crystals with different oxygen occupancy have been prepared with formulas varying from $Sr_{14}Cu_{24}O_{38}$ to $Sr_{14}Cu_{24}O_{33}$.

7.1.3. $La_{8-x}Sr_xCu_8O_{20-x/2}$ and $La_4BaCu_5O_{13+x}$

Phases with the constitution $La_{8-x}Sr_xCu_8O_{20-x/2}$ with values of x varying from 1.28 to 1.92 have recently been described[313] and their metallic conduction properties have been investigated.[314] A typical region of the crystal structure is shown in Figure 20a. The octahedral coordination around Cu_I is indicated by hatching; it is interesting that the distances from Cu to the apical oxygens show a compression of about 5%. A second crystallographic copper site, Cu_{II}, has planar coordination to O^{2-}. In Figure 20a, the one-di-

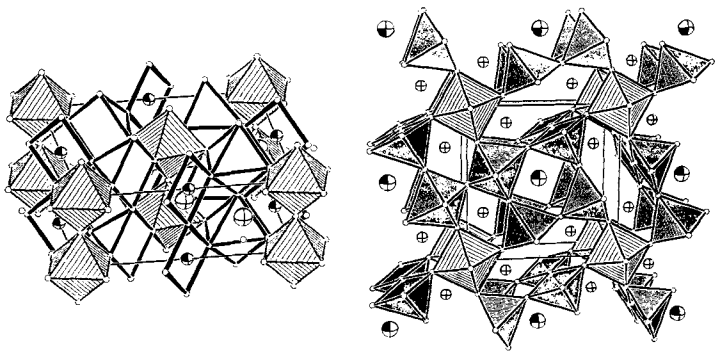


Fig. 20. a) Cu/O polyhedra in $La_{8-x}Sr_xCuO_{20-x/2}$. The octahedra around Cu^{2+} are shown hatched and the planar CuO_4 squares are indicated by thicker lines. The CuO_5 pyramids are shown in open form. ⊕ = Cu^{2+}. b) Cu/O polyhedra in $La_4BaCu_5O_{13+x}$. The CuO_6 octahedra are shown hatched and the CuO_5 pyramids are gray to black.

mensional chains of CuO_4 squares run through the crystal structure along the [001] direction in the middle of the unit-cell faces. The third site, Cu_{III}, has the tetragonal-pyramidal O^{2-} environment which is also often found in the superconductors. In Figure 20a, the CuO_5 polyhedra are shown by thicker lines. The authors[313] point out the resemblance to $La_4BaCu_5O_{13+x}$,[315,316] which also has CuO_5 polyhedra linked at their corners to CuO_6 octahedra to form a tunnel structure.

The structure of $La_4BaCu_5O_{13+x}$ is illustrated in Figure 20b. The most noticeable difference compared with $La_{8-x}Sr_xCu_8O_{20-x/2}$ is the absence of the Cu/O chains of planar corner-linked squares. Attempts to confirm the existence of an oxygen deficit in the lattice by more accurate determination of the occupancy factors, taking as an example a phase with the constitution $La_{6.4}Sr_{1.6}Cu_8O_{19.84}$, were unsuccessful. The oxygen deficiency is presumably shared equally between all the sites in the anion partial lattice. Further details are given in the original papers.[313,315]

7.1.4. $M_{10}Cu_{17}O_{29}$

In the course of preparing well-formed prismatic single crystals of the bismuth superconductor, an interesting new phase with the constitution $Bi_{0.31}Ca_{5.64}Sr_{4.05}Cu_{17}O_{29}$ was obtained.[317] It is essentially a bismuth-doped mixed crystal $M_{10}Cu_{17}O_{29}$, where M denotes alkaline-earth metals. The Cu/O coordination is shown in Figure 21. Planar-coordinated copper is present, for example in the form of isolated one-dimensional chains of edge-linked CuO_4 squares. Similar structural units have also been found in alkali-metal oxocuprates,[318-320] and in compounds with the constitution $M_{14}Cu_{24}O_{38-\delta}$ (M = alkaline-earth metal)[310-312] (cf. Fig. 19). The special feature of these chains compared with previously known oxocuprates is a torsional deformation within the square CuO_4 units, that is, a transition to tetrahedral coordination. The Cu/O regions at the beginning and middle of the unit cell are identical to the Cu/O partial lattice in $CaCu_2O_3$.[321] It is therefore useful from a crystallographic point of view to rewrite the formula $M_{10}Cu_{17}O_{29}$ as $M_{10}[(CuO_2)_7][(Cu_2O_3)_5]$. In the crystal structure the larger M ions occupy the spaces above the distorted oxygen squares shown in Figure 21.

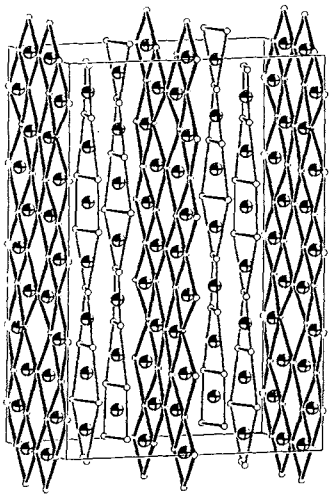


Fig. 21. The Cu/O coordination in $M_{10}Cu_{17}O_{29}$, as exemplified by $Bi_{0.31}Ca_{5.64}Sr_{4.05}Cu_{17}O_{29}$. ⊕ = Cu, ○ = O^{2-} (see text).

7.2. Oxocuprates and Oxoplatinates as Superconductor Byproducts

Superconducting phases prepared in corundum reaction vessels readily take up Al^{3+}, which usually has a deleterious effect on the superconductivity. This can be avoided by using crucibles of other materials such as platinum. However, platinum has only limited resistance to oxygen in alkaline media; it is therefore not surprising that various platinum-containing compounds or the oxoplatinates themselves have been found as by-products in research on superconductivity. One such substance, $La_{1.5}Sr_{0.5}(Cu_{0.75}Pt_{0.25})O_4$, has already been mentioned in Section 2;[83] it is not of interest here since it crystallizes with the well-known K_2NiF_4- type structure.

7.2.1. $Ba_2Y_2CuPtO_8$ and $Ba_2Er_2Cu_{1+x}Pt_{1-x}O_8$

Both these substances have the same crystal structure and they were studied almost at the same time.[322,323] To supplement the structural representations of $Ba_2Y_2CuPtO_8$ given in the literature,[322] the platinum and copper coordination is shown in Figure 22 from a different perspective. The octahedral coordination of Pt^{4+} to O^{2-} is indicated by hatching. This is a normal coordination sphere for Pt^{4+}. Cu^{2+} is again coordinated by O^{2-} in a tetragonal-pyramidal fashion, and we again find that the apex of the pyramid is stretched (by 6%). The Cu^{2+} ion lies practically in the base plane of this tetragonal pyramid. PtO_6 octahedra and CuO_5 pyramids are joined in a *cis* configuration at the corners of the octahedra, forming double chains along the direction of the *b* axis. The literature on this structure[322] draws attention to its relationship to $KPbCr_2F_9$.

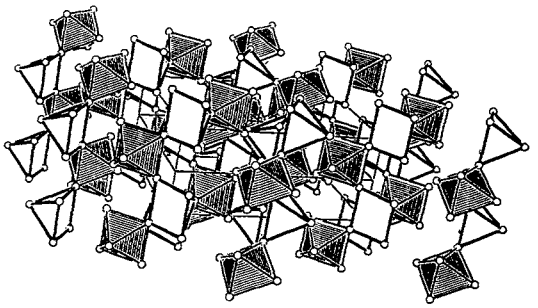


Fig. 22. Cu/O and Pt/O coordination in $Ba_2Y_2CuPtO_8$ and $Ba_2Er_2Cu_{1+x}Pt_{1-x}O_8$. The hatched octahedra are the polyhedra around Pt^{4+}, and the open tetragonal pyramids are the polyhedra around Cu^{2+}.

7.2.2. $Ba_3Ln_2PtCu_2O_{10}$ (Ln = Y, Ho)

Shiny metallic crystals, which appear dark green in transmitted light, were found to form from a reaction mixture consisting of Y_2O_3, $BaCO_3$, and CuO (0.5:2:3) in contact with the walls of a platinum crucible in air at about 600–700 °C.[324] X-ray diffraction studies gave a crystal structure with the coordination polyhedra shown in Figure 23. The structural features shown in Figures 23a–d, respectively, consist of capped trigonal prisms around Y^{3+}, a 12-fold

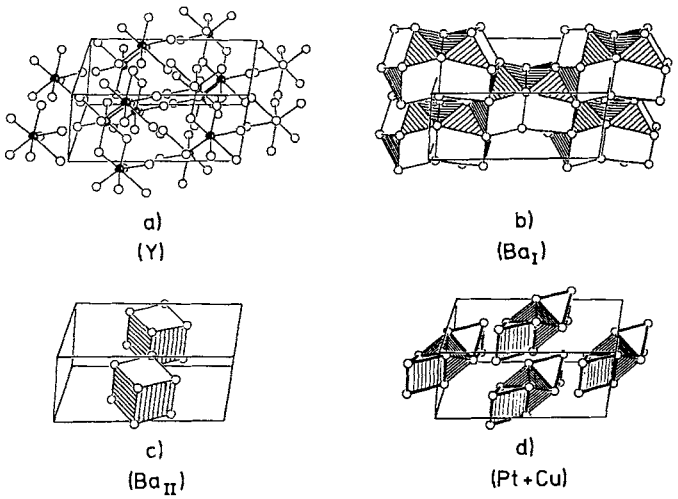


Fig. 23. Separate diagrams of the different polyhedra in $Ba_3Ln_2PtCu_2O_{10}$. a) Polyhedra around $Ln = Y^{3+}$. b) and c) Polyhedra around Ba^{2+}. d) Octahedra (finely hatched) around Pt^{4+} and tetragonal pyramids (partly hatched) around Cu^{2+}.

coordination around Ba_I, cubic coordination around Ba_{II}, and PtO_6 octahedra with CuO_5 pyramids. The corners of the unit cells in Figure 23c are also occupied by Ba_{II} in a cubic coordination, which is not shown here. The complete structure is obtained by superimposing all these partial structures. The main interest here is in the CuO_5 polyhedra, which are joined to the PtO_6 octahedra at their edges. This is a novel feature which sets the compound apart from other substances occurring in copper/platinum oxochemistry.

7.2.3. $Ba_8Pt_4Y_3O_{17.5}$

This section will conclude by describing a byproduct found in our own research. During the preparation of single crystals of the yttrium superconductor $YBa_2Cu_3O_{6+x}$ it was observed that at 1000 °C within 48 hours appreciable quantities of the platinum crucible material had coreacted.[325] The interesting structural feature of the new substance thus formed, $Ba_8Pt_4Y_3O_{17.5}$, is the discovery that Pt^{2+} and Pt^{4+} are present together. Here the divalent platinum ion in the oxoplatinate has the same role as the divalent copper ion in the mixed oxocuprate-oxoplatinates, but, in contrast to the chemistry of the oxocuprate, it forces the formation of isolated square-planar polyhedra around Pt^{2+}.[326] Figure 24 (cf. Ref. [327]) shows the characteristic coordination polyhedra around Y^{3+}, Pt^{4+}, and Pt^{2+}. The isolated PtO_4 squares rest on the centers of the faces of the cubic unit cells. The unit cells have $Pt^{4+}O_6$ octahedra at their corners, and the YO_6 octahedra are attached at the middle of each edge.

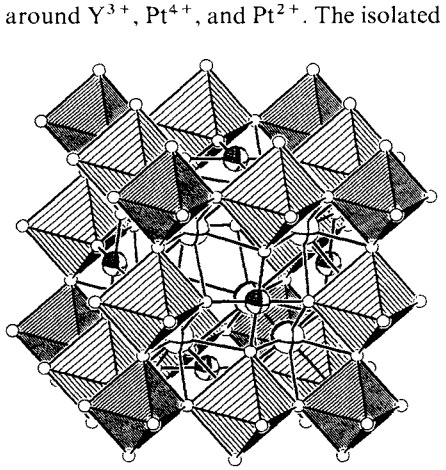


Fig. 24. Coordination polyhedra in $Ba_8Pt_4Y_3O_{17.5}$. Octahedra (hatched) around Y^{3+}, octahedra (gray) around Pt^{4+}; ⊕ = Ba^{2+}, ⊕ = Pt^{2+}, ○ = O^{2-}.

If the Pt^{2+} ions also had octahedral coordination and the centers of the unit cells were occupied by Ba^{2+} ions instead of being empty, $Ba_8Pt_4Y_3O_{17.5}$ would have been classified as a perovskite structure. Since Pt^{5+} is definitely not present in this structure, there must be a deficit in the oxygen partial lattice. A striking feature of the structure of $Ba_8Pt_4Y_3O_{17.5}$ is the fact that the center of the unit cell is unoccupied. This space is essentially due to the planarity of the Pt^{2+} coordination.

8. Concluding Remarks

The numerous studies carried out on oxide superconductors, with their widely differing chemical constitutions, show that all superconducting materials have certain common features, and superconductivity does not occur when these are absent. For example, all the materials have copper as part of their crystal structures, and, except for $Nd_{2-x}Ce_xCuO_4$, the coordination around Cu^{2+} or Cu^{3+} is always of a stretched tetragonal-pyramidal (C.N. = 4 + 1) or stretched octahedral (C.N. = 4 + 2) type. These are interesting observations for chemists involved in research on oxocuprates. From the standpoint of crystal chemistry the oxide superconductors and some of the byproducts described reveal Cu^{2+} in a new light. In the past I have promulgated the view that Cu^{2+} in oxocuprates has planar coordination, even when it forms part of the anionic partial lattice.[1] According to this view, the only circumstance in which Cu^{2+} could instead have octahedral coordination is as a cationic component of the oxometalates with severely stretched octahedra. Taking into account the superconductors and byproducts, this view now needs to be revised. The crystal structures described above show that copper is just as likely to be found in a tetragonal-pyramidal coordination to O^{2-}. In all the examples with pyramidal coordination the distance between Cu^{2+} and the apex of the pyramid is proportionately greater than the Cu–O distances in the square base. Since tetragonal pyramids can be regarded as capped octahedra, it seems as though Cu^{2+} is able to "remember" its role in an octahedron with tetragonal Jahn–Teller distortion. Apparently, the planar arrangement of oxygen around copper is not confined to Cu^{2+} with its d^9 configuration; instead, it seems that very small proportions of Cu^{3+} (d^8 configuration) in oxocuprates, whose presence was not previously recognized, quite generally induce the adoption of a planar oxygen environment. Research on the HT_c superconductors has also shown that Cu^{2+} is never present in isolation, but is accompanied by Cu^{3+} (and Cu^+), so that the properties of these materials are affected by mixed valences. This recognition has generated a reawakened interest in this long-familiar area of crystal chemistry.

The question of what changes would be seen in our world if the transition from metallic conduction to superconductivity could be shifted up to room temperature has already inspired much speculation. There is indeed still a long way to go in the direction of increased transition temperatures, and it may even require a breakthrough in a completely new direction, comparable with the step from the older metallic

superconductors to the new HT_c oxide superconductors. Extrapolating from the results of previous research, we may assume that with increasing transition temperatures the chemical substances used will become ever more complex and sensitive and it will be even more difficult to achieve the correct balance between the valence states of the metal ions and the oxygen deficit. New methods must therefore be found for carrying out syntheses with the necessary degree of control over the crystal lattice, if one is to have any chance at all of building into the lattice, according to a predetermined design, the structures which give superconductivity. But also the discovery of a high-T_c superconductor that does not contain copper would be a major step forward in the understanding of superconductivity in oxide systems.

Even if, in the 1990s, we are bound to reach an upper limit to T_c (as was the case for the metallic superconductors in the 1960s), no one who has been involved in this field of research would have wished to miss experiencing the enthusiasm that has driven it forward. It is to be hoped that other chemical substances to be discovered in the future will similarly stimulate collaboration between scientists on a worldwide scale.

Some of the studies carried out in my own laboratory and mentioned here were supported by the Fonds der Chemischen Industrie, the Deutsche Forschungsgemeinschaft, and the Bundesministerium für Forschung und Technologie. I and my collaborators express our thanks for this support. I am also grateful to some of my colleagues, Dr. Teske, graduate chemists Gutau, Lalla, Lang, Mader, and in particular to final-year student Hansen, for their help in preparing the figures which were produced using a modified ORTEP program[328, 326] at the University of Kiel computer center.

Received: March 23, 1989 [A 739 IE]
German version: *Angew. Chem. 101* (1989) 1503
Translated by *Jack Becconsall*, Pwllheli, UK

[1] Hk. Müller-Buschbaum, *Angew. Chem. 89* (1977) 704; *Angew. Chem. Int. Ed. Engl. 16* (1977) 674.
[2] J. M. Longo, P. M. Raccah, *J. Solid State Chem. 6* (1973) 526.
[3] B. Grande, Hk. Müller-Buschbaum, M. Schweizer, *Z. Anorg. Allg. Chem. 428* (1977) 120.
[4] J. G. Bednorz, K. A. Müller, *Angew. Chem. 100* (1988) 757; *Angew. Chem. Int. Ed. Engl. 27* (1988) 735.
[5] U. Lehmann, Hk. Müller-Buschbaum, *Z. Naturforsch. B35* (1980) 389.
[6] H. Pausch, Hk. Müller-Buschbaum, *Z. Naturforsch. B34* (1979) 378.
[7] K. Sander, U. Lehmann, Hk. Müller-Buschbaum, *Z. Anorg. Allg. Chem. 480* (1981) 153.
[8] U. Lehmann, Hk. Müller-Buschbaum, *Z. Anorg. Allg. Chem. 447* (1978) 47.
[9] H. Pausch, Hk. Müller-Buschbaum, *Z. Naturforsch. B27* (1972) 888.
[10] U. Lehmann, Hk. Müller-Buschbaum, *Z. Anorg. Allg. Chem. 480* (1980) 59.
[11] J. B. Goodenough, G. Demazeau, M. Pauchard, P. Hagenmuller, *J. Solid State Chem. 8* (1973) 325.
[12] J. L. Soubeyroux, P. Courbin, L. Fournes, D. Fruchart, G. Le Flem, *J. Solid State Chem. 31* (1980) 313.
[13] N. Nguyen, M. Vlasse, M. Perrin, G. Le Flem, *J. Solid State Chem. 32* (1980) 1.
[14] J. C. Bouloux, J. L. Soubeyroux, G. Le Flem, P. Hagenmuller, *J. Solid State Chem. 38* (1981) 34.
[15] J. C. Joubert, A. Collomb, D. Elmaleh, G. Le Flem, A. Daoudi, G. Olivier, *J. Solid State Chem. 2* (1970) 343.
[16] J. C. Bouloux, J. L. Soubeyroux, A. Daoudi, G. Le Flem, *Mater. Res. Bull. 16* (1981) 860.
[17] G. Demazeau, P. Courbin, G. Le Flem, M. Pouchard, P. Hagenmuller, *Nouv. J. Chim. 3* (1979) 171.
[18] G. Demazeau, M. Pouchard, M. Thomas, *Mater. Res. Bull. 15* (1980) 451.
[19] J. B. Goodenough, S. Rameseshan, *Mater. Res. Bull. 17* (1982) 383.
[20] G. Le Flem, *C. R. Seances Acad. Sci. Ser. 2 294* (1982) 29.
[21] G. Le Flem, G. Demazeau, P. Hagenmuller, *J. Solid State Chem. 44* (1982) 82.
[22] G. Demazeau, M. Pouchard, P. Hagenmuller, *J. Solid State Chem. 18* (1976) 159.
[23] R. Berjoan, J. P. Courtures, G. Le Flem, M. Saux, *J. Solid State Chem. 42* (1982) 75.
[24] J. M. Moreau, G. Olivier, *J. Solid State Chem. 10* (1974) 51.
[25] A. Daoudi, G. Le Flem, *J. Solid State Chem. 5* (1972) 57.
[26] A. F. Reid, A. E. Ringwood, *J. Solid State Chem. 1* (1970) 557.
[27] K. Lukaszevics, *Rocz. Chem. 33* (1959) 239.
[28] R. Weiss, R. Faivre, *C. R. Hebd. Seances Acad. Sci. 248* (1959) 106.
[29] H. Stoll, R. Hoppe, *Z. Anorg. Allg. Chem. 548* (1987) 165.
[30] V. A. Fotiev, G. V. Baznev, *Russ. J. Inorg. Chem. (Engl. Transl.) 26* (1981) 471.
[31] M. Foex, A. Nancheron, M. Line, *C. R. Hebd. Seances Acad. Sci. 250* (1960) 3028.
[32] M. Foex, *Bull. Soc. Chim. Fr. 1961*, 109.
[33] R. Frushour, K. S. Vorres, *A.E.C. Accession No. 46–245 Rept. Bo. TID-22-207* Paper E (1965); *Chem. Abstr. 65* (1966) 6697f.
[34] V. F. Savshenko, Ya. S. Rubinchik, *Vestn. Akad. Nauk Beloruss. SSR Ser. Khim. 1969*, 44; *Chem. Abstr. 72* (1970) 94051d.
[35] Hk. Müller-Buschbaum, W. Wollschläger, *Z. Anorg. Allg. Chem. 414* (1975) 76.
[36] B. Knieriemen, *Diplomarbeit*, Universität Kiel 1987.
[37] O. Harneit, *Diplomarbeit*, Universität Kiel 1988.
[38] R. Saez Puche, M. Norton, T. R. White, W. S. Glausinger, *J. Solid State Chem. 50* (1983) 281.
[39] J. G. Bednorz, K. A. Müller, *Z. Phys. B Condens. Matter 64* (1986) 189.
[40] J. G. Bednorz, M. Takashige, K. A. Müller, *Europhys. Lett. 3* (1987) 379.
[41] R. J. Cava, R. B. Van Dover, B. Batlogg, E. A. Rietman, *Phys. Rev. Lett. 58* (1987) 408.
[42] S. J. Uchida, H. Takagi, K. Kitazawa, S. Tanaka, *Jpn. J. Appl. Phys. 26* (1987) L1.
[43] K. Fukuda, M. Sato, S. Shamoto, M. Onoda, S. Hosoya, *Solid State Commun. 63* (1987) 811.
[44] C. W. Chu, P. H. Hor, R. L. Meng, L. Gao, Z. J. Huang, Y. Q. Wang, *Phys. Rev. Lett. 58* (1987) 405.
[45] C. Politis, J. Geerk, M. Dietrich, B. Obst, *Z. Phys. B Condens. Matter 66* (1987) 141.
[46] P. Ganguly, R. A. Mohan Ram, K. Sreedhar, C. N. R. Rao, *Solid State Commun. 62* (1987) 807.
[47] I. Felner, *Solid State Commun. 62* (1987) 791.
[48] M. Sato, H. Hosoya, S. Shamoto, M. Onoda, K. Imaeda, H. Inokuchi, *Solid State Commun. 62* (1987) 85.
[49] J. G. Bednorz, K. A. Müller, M. Takashige, *Science (Washington, D.C.) 236* (1987) 73.
[50] G. M. Phatak, A. M. Umariji, J. V. Yakhmi, L. C. Gupta, K. Gangadnaran, *Solid State Commun. 63* (1987) 905.
[51] J. M. Tarascon, L. H. Greene, W. R. McKinnon, G. W. Hull, *Solid State Commun. 63* (1987) 499.
[52] M. B. Maple, K. N. Yang, M. S. Tarikachvili, J. M. Ferreira, I. J. Neumeier, H. Zhon, Y. Dalichaouch, B. W. Lee, *Solid State Commun. 63* (1987) 635.
[53] A. K. Grover, S. K. Dhar, P. L. Paulose, V. Nagarajan, E. V. Sampathkumaran, R. Nagarajan, *Solid State Commun. 63* (1987) 1003.
[54] E. Osquiguil, R. Decca, G. Nieva, L. Civale, F. de la Cruz, *Solid State Commun. 65* (1988) 491.
[55] G. Chiodelli, G. Campari-Viganó, V. Massarotti, G. Flor, *Z. Naturforsch. A44* (1989) 26.
[56] L. Mihály, Gy. Hutiray, S. Pekker, G. Kriza, *Solid State Commun. 63* (1987) 133.
[57] W. K. Kwok, G. W. Crabtree, D. G. Hinks, D. W. Capone, J. D. Jorgensen, K. Zhang, *Phys. Rev. B35* (1987) 5343.
[58] N. Nguyen, J. Choisnet, M. Hervieu, B. Raveau, *J. Solid State Chem. 39* (1981) 120.
[59] G. A. Held, P. M. Horn, C. C. Tsuei, S. J. La Placa, J. G. Bednorz, K. A. Müller, *Solid State Commun. 64* (1987) 75.
[60] D. J. Jorgensen, H.-B. Schüttler, D. G. Hinks, D. W. Capone, K. Zhang, M. B. Brodsky, D. J. Scalapino, *Phys. Rev. Lett. 58* (1987) 1024.
[61] M. Francois, K. Yvon, P. Fischer, M. Decroux, *Solid State Commun. 63* (1987) 35.
[62] Y.-C. Zahng, J.-H. Lin, K. Dwight, P. H. Rieger, A. Wold, *Solid State Commun. 63* (1987) 765.
[63] K. Sreedhar, T. V. Ramakrishnan, C. N. R. Rao, *Solid State Commun. 63* (1987) 835.
[64] M. W. Shafer, T. Penney, B. L. Olson, *Phys. Rev. B36* (1987) 4047.
[65] E. H. Appelman, L. R. Morss, A. M. Kini, U. Geiser, A. Umezawa, G. W. Crabtree, K. D. Carlson, *Inorg. Chem. 26* (1987) 3237.
[66] W. Schäfer, J. Meier-Rosenkranz, S. Lösch, R. Kiemel, W. Wischert, S. Kemmler-Sack, H. Kneisel, B. Elschner, *J. Less-Common Met. 142* (1988) 25.
[67] D. M. de Leeuw, C. A. H. A. Mutsaers, G. P. J. Geelen, C. Langereis, *J. Solid State Chem.*, in press.
[68] N. Nücker, J. Fink, B. Renker, D. Evert, C. Politis, P. J. W. Weijs, J. C. Fuggle, *Z. Phys. B Condens. Matter 67* (1987) 9.
[69] L. F. Mattheis, *Phys. Rev. Lett. 58* (1987) 1028.

[70] M.-H. Whangbo, M. Evain, M. A. Beno, J. M. Williams, *Inorg. Chem. 26* (1987) 1829.
[71] K.-H. Schwarz, *Solid State Commun. 64* (1987) 421.
[72] R. A. de Groot, H. Gutfreund, M. Weger, *Solid State Commun. 63* (1987) 451.
[73] A. Fujimori, E. Takajama-Muromachi, Y. Uchida, *Solid State Commun. 63* (1987) 857.
[74] B. Batlogg, A. P. Ramirez, R. J. Cava, R. B. Van Dover, E. A. Rietman, *Phys. Rev. B35* (1987) 5340.
[75] R. L. Greene, H. Maletta, T. S. Plaskett, J. G. Bednorz, K. A. Müller, *Solid State Commun. 63* (1987) 379.
[76] H. Aoki, H. Komimura, *Solid State Commun. 63* (1987) 665.
[77] R. P. Messmer, *Solid State Commun. 63* (1987) 405.
[78] A. Simon, *Chem. Unserer Zeit 22* (1988) 1.
[79] A. Simon, *Angew. Chem. 99* (1987) 602; *Angew. Chem. Int. Ed. Engl. 26* (1987) 579.
[80] M. J. S. Dewar, *Angew. Chem. 99* (1987) 1313; *Angew. Chem. Int. Ed. Engl. 26* (1987) 1273.
[81] H. H. Wang, U. Geiser, R. J. Thorn, K. D. Carlson, M. A. Beno, M. R. Monaghan, T. J. Allen, R. B. Proksch, D. L. Stupka, W. K. Kwok, G. W. Crabtree, J. M. Williams, *Inorg. Chem. 26* (1987) 1192.
[82] G. Collin, R. Comes, *C.R. Acad. Sci. Ser. 2 304* (1987) 1159.
[83] Hk. Müller-Buschbaum, A. Teichert, *J. Less-Common Met.*, in press.
[84] C. Chen, B. E. Watts, B. M. Wanklyn, P. Thomas, *Solid State Commun. 66* (1988) 611.
[85] R. Hoppe, *Angew. Chem. 78* (1966) 52; *Angew. Chem. Int. Ed. Engl. 5* (1966) 95.
[86] R. Hoppe, *Adv. Fluor. Chem. 6* (1970) 387.
[87] Y. Tokura, H. Takagi, S. Uchida, *Nature (London) 337* (1989) 345.
[88] T. Kenjo, S. Yajima, *Bull. Chem. Soc. Jpn. 46* (1973) 1329.
[89] C. Michel, M. Hervieu, M. M. Borel, A. Grandien, F. Deslandes, J. Provost, B. Raveau, *Z. Phys. B Condens. Matter 68* (1987) 421.
[90] W. Kang, G. Collin, M. Ribault, J. Friedel, D. Jerome, J. M. Bassat, J. P. Coutures, P. Odier, *J. Phys. (Les Ulis, Fr.) 48* (1987) 1181.
[91] J. Beille, B. Chevalier, G. Demazeau, F. Deslandes, J. Etourneau, O. Laborde, C. Michel, P. Lejay, J. Provost, B. Raveau, A. Sulpice, J. L. Tholence, R. Tournier, *Physica B (Amsterdam) 146* (1987) 307.
[92] J. Beille, R. Cabanel, C. Chaillout, B. Chevalier, G. Demazeau, F. Deslandes, J. Etourneau, P. Lejay, C. Michel, J. Provost, B. Raveau, A. Sulpice, J. L. Tholence, R. Tournier, *C. R. Acad. Sci. Ser. 2 304* (1987) 1097.
[93] B. M. Tissue, K. M. Cirillo, J. C. Wright, M. Daeumling, D. C. Labalestier, *Solid State Commun. 65* (1988) 51.
[94] C. L. Teske, Hk. Müller-Buschbaum, *Z. Anorg. Allg. Chem. 371* (1969) 325.
[95] C. L. Teske, Hk. Müller-Buschbaum, *Z. Anorg. Allg. Chem. 379* (1970) 234.
[96] F. Galasso, W. Darby, *J. Phys. Chem. 67* (1963) 1451.
[97] B. Grande, Hk. Müller-Buschbaum, *Z. Anorg. Allg. Chem. 417* (1975) 68.
[98] B. Grande, Hk. Müller-Buschbaum, *Z. Anorg. Allg. Chem. 433* (1977) 152.
[99] B. Grande, Hk. Müller-Buschbaum, *Z. Anorg. Allg. Chem. 429* (1977) 88.
[100] D. J. Buttrey, J. M. Honig, C. N. R. Rao, *J. Solid State Chem. 64* (1986) 287.
[101] M. Sayer, P. Odier, *J. Solid State Chem. 67* (1987) 26.
[102] J. Choisnet, J. M. Bassat, H. Pilliere, P. Odier, *Solid State Commun. 66* (1988) 1245.
[103] Z. L. Ming, G. Demazeau, M. Pouchard, J. M. Dance, P. Hagenmuller, *J. Solid State Chem. 78* (1989) 46.
[104] K. K. Singh, P. Ganguly, C. N. R. Rao, *Mater. Res. Bull. 17* (1982) 493.
[105] Hk. Müller-Buschbaum, O. Harneit, *Z. Anorg. Allg. Chem.*, in press.
[106] M. K. Wu, J. R. Ashburn, C. J. Torng, P. H. Hor, R. L. Meng, L. Gav, Z. J. Huang, Y. Q. Wang, C. W. Chu, *Phys. Rev. Lett. 58* (1987) 908.
[107] R. J. Cava, B. Batlogg, R. B. Van Dover, D. W. Murphy, S. Sunshine, T. Siegrist, J. P. Remeika, E. A. Rietman, S. Zahurak, G. P. Espinosa, *Phys. Rev. Lett. 58* (1987) 1676.
[108] C. Michel, F. Deslandes, J. Provost, P. Lejay, R. Tournier, M. Hervieu, B. Raveau, *C.R. Acad. Sci. Ser. 2 304* (1987) 1059.
[109] Z.-W. Dong, H. Cheng Li, R. L. Wang, D. Li, *Solid State Commun. 63* (1987) 197.
[110] A. M. Kini, U. Geiser, H.-C. J. Kao, K. D. Carlson, H. H. Wang, M. R. Monaghan, J. M. Williams, *Inorg. Chem. 26* (1987) 1836.
[111] J. K. Schuller, D. G. Hinks, M. A. Beno, D. W. Capone II, L. Soderholm, J.-P. Locquet, Y. Bruynseraede, C. U. Segre, K. Zhang, *Solid State Commun. 63* (1987) 385.
[112] B. Jayaram, S. K. Agarwal, A. Gupta, A. V. Narlikav, *Solid State Commun. 63* (1987) 713.
[113] F. I. Kedves, S. Mészáros, K. Vad, G. Halász, O. Keszei, L. Mihaly, *Solid State Commun. 63* (1987) 991.
[114] D. W. Murphy, S. Sunshine, R. B. Van Dover, R. J. Cava, B. Batlogg, S. M. Zahnrak, *Phys. Rev. Lett. 58* (1987) 1888.
[115] J. Z. Sun, D. J. Webb, M. Naito, K. Char, R. M. Hahn, J. W. P. Hsu, A. D. Kent, D. B. Mitzi, B. Oh, M. R. Beasley, T. H. Geballe, R. M. Hammond, A. Kapitulnik, *Phys. Rev. Lett. 58* (1987) 1574.
[116] B. Fisher, E. Polturak, G. Koren, A. Kessel, R. Fisher, L. Harel, *Solid State Commun. 64* (1987) 87.
[117] J. G. Gopalakrishnan, J. V. Yakhmi, R. M. Iyer, *Nature (London) 328* (1987) 604.
[118] X. Cai, R. Joynt, D. C. Larbalestier, *Phys. Rev. Lett. 58* (1987) 2798.
[119] E. M. Engler, V. Y. Lee, A. I. Nazzal, R. B. Beyers, G. Lim, P. M. Grant, S. S. P. Parkin, M. L. Ramirez, J. E. Vazquez, R. J. Savoy, *J. Am. Chem. Soc. 109* (1987) 2848.
[120] C. Michel, F. Deslandes, J. Provost, P. Lejay, R. Tournier, M. Hervieu, B. Raveau, *C.R. Acad. Sci. Ser. 2 304* (1987) 1169.
[121] F. Garcia-Alvarado, E. Moran, M. Vallet, J. M. Gonzalez-Calbet, M. A. Alario, M. T. Pérez-Friaz, J. L. Vincent, S. Ferrer, E. Garcia-Michel, M. C. Asensio, *Solid State Commun. 63* (1987) 507.
[122] K. N. Yang, Y. Dalichaonch, J. M. Ferreira, B. W. Lee, J. J. Neumeier, M. S. Torikachvili, H. Zhou, M. B. Maple, R. R. Hake, *Solid State Commun. 63* (1987) 515.
[123] C. Ning, D. Zhanguo, S. Xiuyu, Z. Jiagi, R. Qize, L. Jinxiang, C. Yinchuan, H. Desen, F. Hui, C. Xichen, G. Weiyan, *Solid State Commun. 63* (1987) 965.
[124] G. Xiao, F. H. Streitz, A. Gavrin, C. L. Chin, *Solid State Commun. 63* (1987) 817.
[125] Z. Qi-rui, Q. Yi-tai, C. Zu-yao, G. Wei-yan, Z. Yong, Z. Hang, C. Lie-zhao, X. Jian-cheng, P. Guo-qiang, Z. Min-jian, S. Shi-fang, Y. Dao-qi, H. Z. Hui, *Solid State Commun. 63* (1987) 961.
[126] M. Hervieu, N. Nguyen, C. Michel, F. Deslandes, B. Raveau, *C.R. Acad. Sci. Ser. 2 305* (1987) 1063.
[127] Y. Maeno, T. Tomita, M. Kyogoku, S. Awaji, Y. Aoki, K. Hoshino, A. Minami, T. Fujita, *Nature (London) 328* (1987) 512.
[128] L. Soderholm, K. Zhang, D. G. Hinks, M. A. Beno, J. D. Jorgensen, S. U. Segre, I. K. Schuller, *Nature (London) 328* (1987) 604.
[129] Y. Xu, Z. Li, C. Li, H. Wang, W. Li, X. Lin, *Phys. Status Solidi A 103* (1987) K 113.
[130] J. van den Berg, C. J. van der Beek, P. H. Kes, J. A. Mydosh, G. J. Nieuwenhuys, L. J. de Jongh, *Solid State Commun. 64* (1987) 699.
[131] X. Obradors, A. Labarta, J. Tejada, F. Garcia-Alvarado, E. Morán, M. Vallet, J. M. González-Calvet, M. A. Alario, *Solid State Commun. 64* (1987) 707.
[132] R. J. De Angelis, J. W. Brill, M. Chung, W. D. Arnett, X.-D. Xiang, G. Minton, L. A. Rice, C. E. Hamrin, Jr., *Solid State Commun. 64* (1987) 1353.
[133] L. E. Conroy, A. Nørlund Christensen, J. Bøttiger, *Acta Chem. Scand. Ser. A 41* (1987) 501.
[134] P. Millet, R. Enjalbert, J. Galy, C. Faulmann, P. Cassoux, H. Rakoto, S. Askenazy, *C.R. Acad. Sci. Ser. 2 306* (1988) 407.
[135] M. Hervieu, B. Domenges, F. Deslandes, C. Michel, B. Raveau, *C.R. Acad. Sci. Ser. 2 307* (1988) 1441.
[136] M. Ausloos, C. Laurent, H. W. Vanderschueren, A. Rulmont, P. Tarte, *Solid State Commun. 68* (1988) 539.
[137] S. K. Malik, C. V. Tomy, D. T. Adroja, S. K. Dhar, R. Nagarajan, R. Prasad, N. C. Soni, *Solid State Commun. 67* (1988) 521.
[138] S. K. Blower, C. Greaves, *Solid State Commun. 68* (1988) 765.
[139] R. F. Jardin, S. Gama, O. F. de Lima, S. Zacarelli, *Solid State Commun. 68* (1988) 835.
[140] A. Manthiram, S.-J. Lee, J. B. Goodenough, *J. Solid State Chem. 73* (1988) 278.
[141] K. Tsuchida, Y. Miura, H. Tsudo, A. Kato, *J. Less-Common Met. 146* (1989) L 19.
[142] E. M. McCarron III, M. K. Crawford, J. B. Parise, *J. Solid State Chem. 78* (1989) 192.
[143] D. Cahen, M. Schwartz, S. Reich, I. Felner, *Inorg. Chem. 26* (1987) 3653.
[144] G. Ferey, A. Le Bail, Y. Laligant, M. Hervieu, B. Raveau, A. Sulpice, R. Tournier, *J. Solid State Chem. 73* (1988) 610.
[145] P. H. Hor, R. L. Meng, Y. Q. Wang, L. Gao, E. J. Huang, J. Bechtold, K. Forster, C. W. Chu, *Phys. Rev. Lett. 58* (1987) 1891.
[146] Y. K. Huang, K. Kadowaki, M. van Sprang, A. C. Moleman, A. A. Menovsky, *J. Less-Common Met. 136* (1987) 169.
[147] I.-Wei Chen, S. J. Keating, C. Y. Keating, X. Wu, J. Xu, P. E. Reyes-Morel, T. Y. Tien, *Solid State Commun. 63* (1987) 997.
[148] P. Strobel, J. J. Capponi, C. Chaillout, M. Marezio, J. L. Tholence, *Nature (London) 327* (1987) 306.
[149] R. Provencher, M. E. Brett, M. G. Townsend, *Phys. Status Solidi A 103* (1987) K 107.
[150] C. C. Torrardi, E. M. McCarron, P. E. Bierstedt, A. W. Sleight, D. E. Cox, *Solid State Commun. 64* (1987) 497.
[151] P. Strobel, J. J. Capponi, M. Marezio, P. Monod, *Solid State Commun. 64* (1987) 513.
[152] Z. Gabelica, G. Demortier, G. Deconninck, F. Bodert, A. A. Lucas, M. Renier, P. Lambin, J. P. Vigneron, E. G. Devuane, *Solid State Commun. 64* (1987) 1137.
[153] Z. Gabelica, E. G. Derouane, J. P. Vigneron, P. Lambin, M. Renier, A. A. Lucas, G. Deconninck, F. Bodart, G. Demortier, *Solid State Commun. 64* (1987) 1221.

[154] H. Eickenbusch, W. Paulus, E. Gocke, J.-F. March, H. Koch, R. Schöllhorn, *Angew. Chem. 99* (1987) 1201; *Angew. Chem. Int. Ed. Engl. 26* (1987) 1188.
[155] S. R. Dharwadkar, V. S. Jakkal, J. V. Yakhmi, I. K. Gopalakrishnan, R. M. Iyer, *Solid State Commun. 64* (1987) 1429.
[156] W. E. Farneth, R. K. Bordia, E. M. McCarron, M. K. Crawford, R. B. Flippen, *Solid State Commun. 66* (1988) 953.
[157] G. M. Lin, Q. Z. Huang, J. X. Zhang, G. G. Siu, M. J. Stokes, *Solid State Commun. 68* (1988) 639.
[158] S. Kemmler-Sack, R. Kiemel, W. Schäfer, W. Wischert, A. Radak, B. Elschner, *J. Less-Common Met. 138* (1988) L 21.
[159] P. K. Gallagher, H. M. O'Bryan, S. A. Sunshine, D. W. Murphy, *Mater. Res. Bull. 22* (1987) 995.
[160] H. U. Krebs, R. Wördenweber, *J. Appl. Phys. 63* (1988) 1642.
[161] C. L. Teske, Hk. Müller-Buschbaum, *Z. Naturforsch. A 43* (1988) 965.
[162] T. Graf, J. L. Jorda, J. Muller, *J. Less-Common Met. 146* (1989) 49.
[163] H. R. Khan, C. J. Raub, *J. Less-Common Met. 146* (1989) L 1.
[164] I. Haller, M. W. Shafer, R. Figat, D. B. Goland, *Pure Appl. Chem.*, in press.
[165] H. Verweij, *Solid State Commun. 64* (1987) 1213.
[166] D. C. Harries, T. A. Hewston, *J. Solid State Chem. 69* (1987) 182.
[167] R. Liu, C. Thomson, M. Cardona, Hj. Mattausch, *Solid State Commun. 65* (1988) 67.
[168] D. D. Sarma, C. N. R. Rao, *Solid State Commun. 65* (1988) 47.
[169] T. Iwazumi, I. Nakai, M. Izumi, H. Oyanagi, H. Sawada, H. Ikeda, Y. Saito, Y. Abe, K. Takita, R. Yoshizaki, *Solid State Commun. 65* (1988) 213.
[170] W. Schäfer, J. Maier-Rosenkranz, R. Kiemel, S. Kemmler-Sack, *J. Less-Common Met. 138* (1988) L 25.
[171] A. W. Hewat, J. J. Capponi, C. Chaillout, M. Marezio, E. A. Hewat, *Solid State Commun. 64* (1987) 301.
[172] A. Ourmazd, J. A. Rentschler, J. C. H. Spence, M. O'Keeffe, R. J. Graham, D. W. Johnson, Jr., W. W. Rhodes, *Nature (London) 327* (1987) 328.
[173] G. Van Tendeloo, H. W. Zandbergen, T. Okabe, S. Amelinckx, *Solid State Commun. 63* (1987) 969.
[174] H. W. Zandbergen, G. Van Tendeloo, T. Okabe, S. Amelinckx, *Phys. Status Solidi A 103* (1987) 45.
[175] C. Boulesteix, M. Ben Salem, R. Mokrani, O. Monnereau, J.-P. Sorbier, B. Dubois, J.-M. Bassat, P. Odier, D. Morin, S. Nitsche, *C.R. Acad. Sci. Ser. 2 305* (1987) 1059.
[176] M. Hervieu, B. Domenges, C. Michel, J. Provost, B. Raveau, *J. Solid State Chem. 71* (1987) 263.
[177] J.-H. Müller, V. Plies, R. Gruehn, *Naturwissenschaften 75* (1988) 194.
[178] J. Y. Henry, P. Burlet, A. Bourret, G. Roult, P. Bacher, M. J. G. M. Jurgens, J. Rossat-Mignod, *Solid State Commun. 64* (1987) 1037.
[179] L. Ganapathi, A. K. Ganguli, R. A. Mohan Ram, C. N. R. Rao, *J. Solid State Chem. 73* (1988) 593.
[180] E. F. Paulus, G. Kämpf, H. Schmidt, W. Höhnle, *Z. Kristallogr.*, in press.
[181] G. Calestani, C. Rizzoli, *Nature (London) 328* (1987) 606.
[182] M. F. Garbanskas, R. H. Arendt, J. S. Kasper, *Inorg. Chem. 26* (1987) 3191.
[183] M. François, E. Walker, J.-L. Jorda, K. Yvon, P. Fischer, personal communication (April 15, 1989).
[184] Y. Hoydoo, R. K. McMullan, J. D. Axe, D. E. Cox, J. Z. Liu, G. W. Crabtree, D. J. Lam, *Solid State Commun. 64* (1987) 739.
[185] W. Höhnle, H. G. von Schnering, *Z. Kristallogr.*, in press.
[186] J. L. Hodeau, C. Chaillout, J. J. Capponi, M. Marezio, *Solid State Commun. 64* (1987) 1349.
[187] M. A. Beno, L. Soderholm, D. W. Capone II, D. G. Hinks, J. D. Jorgensen, I. K. Schuller, C. U. Segre, K. Zhang, J. D. Grace, *Appl. Phys. Lett. 51* (1987) 57.
[188] J. J. Capponi, C. Chahaillont, A. W. Hewat, P. Lejay, M. Marezio, N. Nguyen, B. Raveau, J. L. Soubeyroux, J. L. Tholence, R. Tournier, *Europhys. Lett. 3* (1987) 1301.
[189] F. Izumi, H. Asano, T. Ishigaki, E. Takayama-Muromachi, Y. Uchida, N. Watanabe, *J. Appl. Phys. 26* (1987) L 1193.
[190] A. Seyneira, H. Rajagopal, L. Ganapathi, C. N. R. Rao, *J. Solid State Chem. 76* (1988) 235.
[191] O. K. Antosn, P. E. Hiismäki, H. O. Pöyry, A. T. Tiita, K. M. Ullakko, V. A. Trunov, V. A. Ul'yanov, *Solid State Commun. 64* (1987) 757.
[192] E. G. Derouane, Z. Gabelica, J.-L. Bredas, J.-M. Andre, P. Lambin, A. A. Lucas, J.-P. Vigneron, *Solid State Commun. 64* (1987) 1061.
[193] A. Renault, J. K. Burdett, J.-P. Pouget, *J. Solid State Chem. 71* (1987) 587.
[194] Z. Bukowski, R. Horyn, K. Rogacki, I. Filatow, C. Sulkowski, M. Wolcyrz, J. Klamut, *J. Less-Common Met. 144* (1988) 153.
[195] C. Chaillout, M. A. Alario-Franco, J. J. Capponi, J. Chenavas, P. Strobel, M. Marezio, *Solid State Commun. 65* (1988) 283.
[196] W. L. Lechter, M. S. Osofsky, R. J. Soulen, Jr., V. M. Le Tourneau, E. F. Skelton, S. B. Qadri, W. T. Elam, H. A. Hoff, R. A. Hein, L. Humphreys, C. Skowronek, A. K. Singh, J. V. Gilfrich, L. E. Toth, S. A. Wolf, *Solid State Commun. 68* (1988) 519.
[197] C. Thomsen, M. Cardona, R. Liu, B. Gegen, A. Simon, *Phys. Rev. B 37* (1988) 9860.
[198] A. Simon, J. Köhler, H. Borrmann, B. Gegenhamer, R. Kremer, *J. Solid State Chem. 77* (1988) 200.
[199] L. F. Schneemeyer, J. V. Waszczak, T. Siegrist, R. B. Van Dover, L. W. Rupp, B. Batlogg, R. J. Cava, D. W. Murphy, *Nature (London) 328* (1987) 601.
[200] T. K. Worthington, W. J. Gallagher, T. R. Dinger, *Phys. Rev. Lett. 59* (1987) 1160.
[201] S. N. Ruddlesden, P. Popper, *Acta Crystallogr. 11* (1958) 54; cf. also [27].
[202] N. Nguyen, L. Er-Rakho, C. Michel, J. Choisnet, B. Raveau, *Mater. Res. Bull. 15* (1980) 891.
[203] N. Nguyen, J. Choisnet, B. Raveau, *Mater. Res. Bull. 17* (1982) 567.
[204] T. A. Kalinina, L. N. Lykova, L. M. Kovba, M. G. Melnikova, N. V. Porotnikov, *Russ. J. Inorg. Chem. (Engl. Transl.) 28* (1983) 259.
[205] L. M. Kovba, L. N. Lykova, T. A. Kalinina, *Russ. J. Inorg. Chem. (Engl. Transl.) 25* (1980) 397.
[206] W. Kwestro, H. C. A. Van Gerven, C. Langereis, *Mater. Res. Bull. 12* (1977) 157.
[207] K. Mader, Hk. Müller-Buschbaum, *Z. Anorg. Allg. Chem. 559* (1988) 89.
[208] A. Lalla, *Dissertation*, Universität Kiel 1989.
[209] A. Lalla, Hk. Müller-Buschbaum, *Rev. Chim. Miner. 24* (1987) 605.
[210] R. von Schenck, Hk. Müller-Buschbaum, *Z. Anorg. Allg. Chem. 398* (1973) 15.
[211] Hk. Müller-Buschbaum, W. Muschick, *Z. Anorg. Allg. Chem. 412* (1975) 209.
[212] Z. X. Zhao, L. Q. Chen, Q. S. Yang, Y. Z. Huang, G. H. Chen, R. M. Tang, G. R. Liu, C. G. Cui, L. Chen, L. H. Wang, S. Q. Guo, S. L. Li, *Kexue Tongbao 32* (1987) 661.
[213] G. C. Che, J. K. Liang, W. Chen, Q. S. Yang, G. H. Chen, Y. M. Ni, *J. Less-Common Met. 138* (1988) 137.
[214] H. Fjellvag, P. Karen, A. Kjekshus, *Acta Chem. Scand. Ser. A 41* (1987) 283.
[215] P. H. Hor, L. Gao, R. L. Meng, Z. J. Huang, Y. Q. Wang, K. Forster, J. Vassilious, C. W. Chu, M. K. Wu, J. R. Ashburn, C. J. Torng, *Phys. Rev. Lett. 58* (1987) 911.
[216] R. Liu, R. Merlin, M. Cardona, Hj. Mattausch, W. Bauhofer, A. Simon, F. Garcia-Alvarado, E. Moran, M. Vallet, J. M. Gonzales-Calbet, M. A. Alario, *Solid State Commun. 63* (1987) 839.
[217] Y. Chang, M. Quellion, D. W. Niles, R. Joynt, G. Margaritondo, N. G. Stoffel, J. M. Tarascon, *Solid State Commun. 63* (1987) 717.
[218] R. M. Mcfarlane, H. Rosen, H. Sek, *Solid State Commun. 63* (1987) 831.
[219] L. Genzel, A. Wittlin, J. Kühl, Hj. Mattausch, W. Bauhofer, A. Simon, *Solid State Commun. 63* (1987) 843.
[220] M. Cardona, L. Genzel, R. Liu, A. Wittlin, Hj. Mattausch, F. Garcia-Alvarado, E. Garcia-Gonzalez, *Solid State Commun. 64* (1987) 727.
[221] J. C. Ho, P. H. Hor, R. L. Meng, C. W. Chu, C. Y. Huang, *Solid State Commun. 63* (1987) 711.
[222] L. F. Mattheiss, D. R. Hamann, *Solid State Commun. 63* (1987) 395.
[223] M.-H. Wangbo, M. Evain, M. A. Beno, J. M. Williams, *Inorg. Chem. 26* (1987) 1834.
[224] J. Friedel, *C.R. Acad. Sci. Ser. 2 305* (1987) 543.
[225] J. Hauck, *Solid State Commun. 64* (1987) 1217.
[226] L. A. Curtiss, T. O. Brun, D. M. Gruen, *Inorg. Chem. 27* (1988) 1421.
[227] W. Urland, *Angew. Chem. 99* (1987) 1316; *Angew. Chem. Int. Ed. Engl. 26* (1987) 1275.
[228] Z. Goumeng, D. Zhanguo, C. Ning, L. Hongcheng, *Solid State Commun. 63* (1987) 151.
[229] V. Bayot, F. Delannay, C. Dewitte, J.-P. Erauw, X. Gonze, J.-P. Issi, A. Jonas, M. Kinany-Alaoui, M. Lambricht, J.-P. Michenaud, J.-P. Minet, L. Piraux, *Solid State Commun. 63* (1987) 983.
[230] S. R. Ovshinsky, R. T. Young, D. D. Allred, G. DeMaggio, G. A. Van der Leeden, *Phys. Rev. Lett. 58* (1987) 2579.
[231] R. N. Bhargava, S. P. Herku, W. N. Osborne, *Phys. Rev. Lett. 59* (1987) 1468.
[232] P. K. Davies, J. A. Stuart, D. White, C. Lee, P. M. Chaikin, M. J. Naughton, R. C. Yu, R. L. Ehrenkaufer, *Solid State Commun. 64* (1987) 1441.
[233] H. H. Wang, A. M. Kini, H.-C. I. Kao, E. H. Appelman, A. R. Thompson, R. E. Botto, K. D. Carlson, J. M. Williams, M. Y. Chen, J. A. Schlueter, B. D. Gates, S. L. Hallenbeck, A. M. Despotes, *Inorg. Chem. 27* (1988) 5.
[234] J. Karpinski, C. Beeli, E. Kaldis, A. Wisard, E. Jilek, *Physica C (Amsterdam) 153* (1988) 830.
[235] P. Bordet, C. Chaillout, J. Chenavas, J. L. Hodeau, M. Marezio, J. Karpinski, E. Kaldis, *Nature (London) 334* (1988) 596.
[236] W. Leib, Hk. Müller-Buschbaum, *Z. Anorg. Allg. Chem. 518* (1984) 115.
[237] A. Lalla, Hk. Müller-Buschbaum *Z. Anorg. Allg. Chem.*, in press.
[238] H. Maeda, Y. Tanaka, M. Fukotomi, T. Asano, *Jpn. J. Appl. Phys. 27* (1988) L 209.
[239] J.-P. Locquet, J. Vanacken, M. d'Halle, C. Van Haesendonck, Y. Bruynseraede, J. K. Schuller, *Solid State Commun. 66* (1988) 393.
[240] J. B. Torrance, Y. Tokura, S. J. LaPlaca, T. C. Huang, R. J. Savoy, A. I. Nazzal, *Solid State Commun. 66* (1988) 703.
[241] S. Xie, J. Q. Huang, W. Chen, G. C. Che, J. K. Liang, Y. L. Zhang, X. R. Cheng, Z. X. Zhao, *Solid State Commun. 66* (1988) 1211.

[242] J. M. Tarascon, Y. Le Page, P. Barboux, B. G. Bagley, L. H. Greene, W. R. McKinnon, G. W. Hull, M. Giroud, D. M. Hwang, *Phys. Rev. Lett.*, in press.
[243] K. Sugiyama, Y. Waseda, K. Moroishi, A. Inoue, T. Masumoto, *Z. Naturforsch. A 43* (1988) 517.
[244] H. Takagi, H. Eisaki, S. Uchida, A. Maeda, S. Tajima, K. Uchinokura, S. Tanaka, *Nature (London) 332* (1988) 236.
[245] Y. Oka, N. Yamamoto, A. Yuba, H. Kitaguchi, J. Takada, *Jpn. J. Appl. Phys. 27* (1988) L 1429.
[246] W. Korczak, S. Z. Korczak, P. Mazurek, K. I. Wysokinski, *Solid State Commun. 66* (1988) 971.
[247] J. L. Tallon, R. G. Buckley, P. W. Gilberd, M. R. Presland, I. W. M. Brown, M. E. Bowden, L. A. Christian, R. Goguel, *Nature (London) 333* (1988) 153.
[248] Z. Zhanchun, F. Minghu, X. Jiansheng, X. Zhuan, Z. Yong, S. Dunming, C. Zuyao, Q. Vitai, Z. Qirui, *Solid State Commun. 67* (1988) 101.
[249] J. M. Tarascon, W. R. McKinnon, P. Barboux, D. M. Hwang, B. G. Bagley, L. H. Greene, G. Hull, Y. LePage, N. Stoffel, M. Giroud, *Phys. Rev. B*, in press.
[250] C. W. Chu, J. Bechtold, L. Gao, P. H. Hor, Z. J. Huang, R. L. Meng, Y. Y. Sun, Y. Q. Wang, Y. Y. Xue, *Phys. Rev. Lett. 60* (1988) 941.
[251] R. M. Hazen, C. T. Prewitt, R. Angel, N. L. Ross, L. W. Finger, C. G. Hadidiacos, D. R. Veblen, P. J. Heaney, P. H. Hor, R. L. Meng, Y. Y. Sun, Y. Q. Wang, Y. Y. Xue, Z. J. Huang, L. Gao, J. Bechtold, C. W. Chu, *Phys. Rev. Lett. 60* (1988) 1174.
[252] D. R. Veblen, P. J. Heaney, R. J. Angel, L. W. Finger, R. M. Hazen, C. T. Prewitt, N. L. Ross, C. W. Chu, P. H. Hor, R. L. Meng, *Nature (London) 332* (1988) 334.
[253] H. Sato, W. Zhu, T. Ishiguro, *J. Solid State Chem. 75* (1988) 207.
[254] T. Kajitani, M. Hirabayashi, M. Kikuchi, K. Kusaba, Y. Syono, N. Kabayashi, H. Iwasaki, Y. Muto, *Jpn. J. Appl. Phys. 27* (1988) L 1453.
[255] U. Endo, S. Koyama, T. Kawai, *Jpn. J. Appl. Phys. 27* (1988) L 1476.
[256] Y. Ando, K. Fukuda, S. Kondoh, M. Sera, M. Onoda, M. Sato, *Solid State Commun. 67* (1988) 815.
[257] R. L. Meng, P. H. Hor, Y. Y. Sun, Z. J. Huang, L. Gao, Y. Y. Xue, Y. Q. Wang, J. Bechtold, C. W. Chu, R. M. Hazen, C. T. Prewitt, R. J. Angle, N. C. Ross, *Mod. Phys. Lett. B 2* (1988) 543.
[258] M. A. Subramanian, C. C. Torardi, J. C. Calabrese, J. Gopalakrishnan, K. J. Morrisey, T. R. Askew, R. B. Flippen, U. Chowdry, A. W. Sleight, *Science (Washington, D.C.) 239* (1988) 1016.
[259] S. Jin, R. C. Sherwood, T. H. Tiefel, G. W. Kammlott, R. A. Fastnacht, M. E. Eavis, S. M. Zahurak, *Appl. Phys. Lett. 52* (1988) 1628.
[260] S. Kemmler-Sack, A. Ehmann, R. Kiemel, S. Lösch, W. Schäfer, L. Kan, B. Elschner, *J. Less-Common Met. 144* (1988) L 1.
[261] W. A. Groen, H. W. Zandbergen, *Solid State Commun. 68* (1988) 527.
[262] L. Ganapathi, S. Krishna, K. Murthy, R. Vijayaraghavan, C. N. R. Rao, *Solid State Commun. 67* (1988) 967.
[263] H. W. Zandbergen, Y. K. Huang, M. J. V. Menken, J. N. Li, K. Kodowaki, A. A. Menovsky, G. Van Tendeloo, S. Amelinckx, *Nature (London) 332* (1988) 620.
[264] E. A. Hewat, M. Dupuy, P. Bordet, J. J. Capponi, C. Chaillout, J. L. Hodeau, M. Marezio, *Nature (London) 333* (1988) 53.
[265] O. Eibl, *Solid State Commun. 67* (1988) 703.
[266] H. G. von Schnering, L. Walz, M. Schwarz, W. Becker, M. Hartweg, T. Popp, B. Hettig, P. Müller, G. Kämpf, *Angew. Chem. 100* (1988) 604; *Angew. Chem. Int. Ed. Engl. 27* (1988) 574.
[267] Z. Z. Sheng, A. M. Hermann, *Nature (London) 332* (1988) 55.
[268] S. Kondoh, Y. Ando, M. Onoda, M. Sato, J. Akimitsu, *Solid State Commun. 65* (1988) 1329.
[269] Z. Z. Sheng, A. M. Hermann, A. El. Ali, C. Almasan, J. Estrada, T. Datta, R. J. Matson, *Phys. Rev. Lett. 60* (1988) 937.
[270] Z. Z. Sheng, A. M. Hermann, *Nature (London) 332* (1988) 138.
[271] L. Gao, Z. J. Huang, R. L. Meng, P. H. Hor, J. Bechtold, Y. Y. Sun, C. W. Chu, Z. Z. Sheng, A. M. Hermann, *Nature (London) 332* (1988) 623.
[272] Y. C. Zahng, G. C. Che, J. K. Liang, X. R. Chen, Q. S. Yang, D. N. Zheng, J. H. Wang, J. Q. Huang, S. L. Iia, Y. M. Ni, Z. X. Zhao, D. H. Shen, S. S. Xie, *Supercond. Sci. Technol. 1* (1988) 92.
[273] M. Sera, S. Kondoh, Y. Ando, K. Fukuda, S. Shamoto, M. Onoda, M. Sato, *Solid State Commun. 66* (1988) 707.
[274] S. Sato, I. Nakada, T. Kohara, Y. Oda, *Acta Crystallogr. Sect. C 44* (1988) 11.
[275] Z. Z. Sheng, W. Kiehl, J. Bennett, A. El Ali, D. Marsh, G. D. Mooney, F. Arammarsh, J. Smith, D. Viar, A. M. Hermann, *Appl. Phys. Lett. 52* (1988) 1738.
[276] A. M. Hermann, Z. Z. Seng, D. C. Vier, S. Schultz, S. B. Oseroff, *Phys. Rev. B 37* (1988) 9742.
[277] R. M. Hazen, L. W. Finger, R. J. Angel, C. T. Prewitt, N. L. Ross, C. G. Hadiacos, P. J. Heaney, D. R. Veblen, Z. Z. Sheng, A. El Ali, A. M. Hermann, *Phys. Rev. Lett. 60* (1988) 1657.
[278] M. Zhenghong, C. Lquan, C. Xi, C. Shufan, H. Yuzhen, D. Daoyang, X. Zili, Z. Dongning, Z. Zhongxian, *Supercond. Sci. Technol. 1* (1988) 94.
[279] Z. Z. Sheng, A. M. Hermann, D. C. Vier, S. Schultz, S. B. Oseroff, D. J. George, R. M. Hazen, *Phys. Rev. B 38* (1988) No. 10.
[280] K. Takahashi, M. Nakao, D. R. Dietrich, H. Kumakura, K. Togano, *Jpn. J. Appl. Phys. 27* (1988) L 1457.
[281] M. Itoh, R. Liang, K. Urabe, T. Nakamura, *Jpn. J. Appl. Phys. 27* (1988) L 1672.
[282] R. Sugise, M. Hirabayashi, N. Terada, M. Jo, T. Shimomura, H. Ihara, *Jpn. J. Appl. Phys. 27* (1988) L 1709.
[283] S. S. Parkin, V. Y. Lee, A. I. Nazzal, R. Savoy, R. Beyers, S. J. La Placa, *Phys. Rev. Lett. 61* (1988) 750.
[284] C. C. Torardi, M. A. Subramanian, J. C. Calabrese, J. Gopalakrishnan, K. J. Morrissey, T. R. Askew, R. B. Flippen, U. Chowdry, A. M. Sleight, *Science (Washington D.C.), 240* (1988) 631.
[285] S. S. Parkin, V. Y. Lee, E. M. Engler, A. I. Nazzal, T. C. Huang, G. Gorman, R. Savoy, R. Beyers, S. J. La Placa, *Phys. Rev. Lett. 60* (1988) 2539.
[286] M. A. Subramanian, J. C. Calabrese, C. C. Torardi, J. Gopalakrishnan, T. R. Askew, R. B. Flippen, K. J. Morrissey, U. Chowdry, A. W. Sleight, *Nature (London) 332* (1988) 420.
[287] C. Martin, C. Michel, A. Maignan, M. Hervieu, B. Raveau, *C.R. Acad. Sci. Ser. 2 307* (1988) 27.
[288] M. Hervieu, A. Maignan, C. Martin, C. Michel, J. Provost, B. Raveau, *J. Solid State Chem. 75* (1988) 212.
[289] P. Haldar, K. Chen, B. Mahreswaran, A. Roig-Janicki, N. K. Jaggi, R. S. Markiewicz, B. C. Giessen, *Science (Washington, D.C.) 241* (1988) 1198.
[290] H. H. Otto, T. Zetterer, K. F. Renk, *Naturwissenschaften 75* (1988) 509.
[291] J. B. Parise, J. Gopalakrishnan, M. A. Subramanian, A. W. Sleight, *J. Solid State Chem. 76* (1988) 432.
[292] M. A. Subramanian, J. B. Parise, J. C. Calabrese, C. C. Torardi, J. Gopalakrishnan, A. W. Sleight, *J. Solid State Chem. 77* (1988) 192.
[293] M. Hervieu, C. Michel, A. Maignan, C. Martin, B. Raveau, *J. Solid State Chem. 74* (1988) 428.
[294] A. K. Ganguli, K. S. N. Swamy, G. N. Subbana, A. M. Umarji, S-V. Bhat, C. N. R. Rao, *Solid State Commun. 67* (1988) 39.
[295] M. Hervieu, C. Martin, J. Provost, B. Raveau, *J. Solid State Chem. 76* (1988) 419.
[296] K. Mader, Hk. Müller-Buschbaum, *J. Less-Common Met.*, in press.
[297] A. W. Sleight, J. L. Gillson, P. E. Bierstedt, *Solid State Commun. 17* (1975) 27.
[298] M. Hikada, H. Fujii, Y. Horie, S. Mase, *Phys. Status Solidi B 145* (1988) 649.
[299] C. Chen, J. Q. Li, Y. S. Yao, X. M. Huang, Z. X. Zhao, W. K. Wang, *Solid State Commun. 68* (1988) 749.
[300] L. Hongbao, C. Liezhav, Z. Ling, M. Zhiqiang, Z. Weijie, L. X. Xiaoxian, Y. Zhidong, X. Bai, M. Xianglei, Z. Guien, R. Yaozhong, C. Zhaojia, Z. Yuheng, *High Tc Update 2*, (1988) No. 24.
[301] R. J. Cava, B. Batlogg, J. J. Krajenski, L. W. Rupp, L. F. Schneemeyer, T. Siegrist, R. B. Van Dover, P. Marsh, W. F. Peck, Jr., P. K. Gallagher, S. H. Glarum, J. H. Marshall, R. C. Farrow, J. V. Waszczak, R. Hull, P. Trevor, *Nature (London) 336* (1988) 211.
[302] C. N. R. Rao, P Ganguly, A. K. Roychaudhuri, R. A. Moham Ram, K. Sreedhar, *Nature (London) 326* (1987) 856.
[303] C. Michel, B. Raveau, *J. Solid State Chem. 43* (1982) 73.
[304] C. Michel, B. Raveau, *Rev. Chim. Miner. 21* (1984) 85.
[305] S. F. Watkins, F. R. Fronczek, *Acta Crystallogr. Sect. C 44* (1988) 3.
[306] S. Schiffler, Hk. Müller-Buschbaum, *Monatsh. Chem. 117* (1986) 465.
[307] S. Schiffler, Hk. Müller-Buschbaum, *Z. Anorg. Allg. Chem. 540* (1986) 243.
[308] H.-G. von Schnering, T. Popp, M. Hartweg: *Jahresbericht des MPI für Festkörperforschung Stuttgart* (1988).
[309] Hk. Müller-Buschbaum, I. Rüter, *Z. Anorg. Allg. Chem.*, in press.
[310] E. M. McCarron, III, M. A. Subramanian, J. C. Calabrese, R. L. Harlow, *Mater. Res. Bull. 23* (1988) 1355.
[311] T. Siegrist, L. F. Schneemeyer, S. A. Sunshine, J. V. Waszczak, *Mater. Res. Bull. 23* (1988) 1429.
[312] T. Popp, M. Hartweg, H. G. von Schnering, *Z. Kristallogr. 286* (1988) 238.
[313] L. Er-Rakho, C. Michel, B. Raveau, *J. Solid State Chem. 73* (1988) 514.
[314] C. Michel, L. Er-Rakho, B. Raveau, *J. Phys. Chem. Solids 49* (1988) 451.
[315] C. Michel, L. Er-Rakho, B. Raveau, *Mater. Res. Bull. 20* (1985) 667.
[316] C. Michel, L. Er-Rakho, M. Hervieu, J. Pannetier, B. Raveau, *J. Solid State Chem. 68* (1987) 143.
[317] K. Kato, E. Takayama-Muromachi, K. Kosuda, Y. Uehida, *Acta Crystallogr. Sect. C 44* (1988) 1881.
[318] K. Hestermann, R. Hoppe, *Z. Anorg. Allg. Chem. 367* (1969) 249.
[319] K. Hestermann, R. Hoppe, *Z. Anorg. Allg. Chem. 367* (1969) 261.
[320] R. Hoppe, H. Rieck, *Z. Anorg. Allg. Chem. 379* (1970) 157.
[321] C. L. Teske, Hk. Müller-Buschbaum, *Z. Anorg. Allg. Chem. 370* (1969) 134.
[322] Y. Laligant, G. Ferey, M. Hervieu, B. Raveau, *Europhys. Lett. 4* (1987) 1023.
[323] K. Ukai, T. Shishido, T. Fukuda, *Acta Crystallogr. Sect. C 44* (1988) 958.
[324] U. Geiser, L. C. Porter, H. H. Wang, T. A. Allen, J. M. Williams, *J. Solid State Chem. 73* (1988) 243.
[325] W. Gutau, Hk. Müller-Buschbaum, *Eur. J. Solid State Inorg. Chem. 25* (1988) 231.
[326] K.-B. Plötz, *Dissertation*, Universität Kiel 1982.
[327] W. Gutau, *Dissertation*, Universität Kiel, planned 1990.
[328] C. K. Johnson, *Oak Ridge Nat. Lab. Rep. ORNL-3794 1965.*

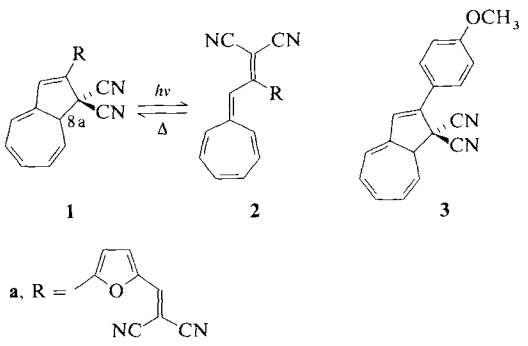
Communications may be submitted in English *or* in German. Further details regarding the submission of communications can be found in the "Notice to Authors" reproduced in the January issue of the journal. Copies thereof may be obtained from the editorial office upon request.

Light-Sensitive Molecular Building Blocks with Electron Transfer Activity: Synthesis and Properties of a Photochemically Switchable, Dicyanovinyl-Substituted Furan**

By *Jörg Daub,* Josef Salbeck, Thomas Knöchel, Christian Fischer, Horst Kunkely,* and *Knut M. Rapp*

Photochromic groups have the potential for serving as an "antenna" function; that is, they can be used to trigger photoinduced reactions in which the molecular structure, electronic structure, and physical characteristics of a substrate are reversibly altered. Such reactions are particularly easily demonstrated in the case of photochromic groups bound to polymers.[1–3] Multifunctional compounds with photochromic characteristics can thus behave as photochemically activated switches and sensors, the precise characteristics of which depend upon the nature of the functional groups. The magnitude of such an effect is governed by the extent to which the various groups interact.

We have previously demonstrated a significant influence of substituents upon the switchable photochromic system dihydroazulene **1** ⇄ vinylheptafulvene **2**, a system activated by visible light.[4] These studies have now been extended to include oligofunctional compounds in an attempt to examine the mutual influences exerted by a photochemically switchable substrate and various covalent or non-covalent functional groups[5a] or macromolecules.[5b, 6] Here we report results on the light-sensitive and electron-transfer-active reactant pair **1a** ⇄ **2a**. In these compounds the photochromic dihydroazulene unit is attached covalently to a dicyanovinyl substituent, which provides the electron-transfer capability. The connecting link is a 2,5-furandiyl residue. That the latter is capable of serving as an efficient transmitter of substituent effects is further demonstrated by the electron-transfer chemistry of **4**.



In contrast to **3**,[4a] room-temperature irradiation with visible light of a solution containing **1a** does not lead directly to observable photochromism. The only immediate change is the appearance of a weak absorption band in the electronic spectrum at 550 nm, suggesting that a small amount of **1a** has been converted to **2a**. However, if irradiation is conducted at −50 °C the originally orange solution changes to blue. The UV/VIS spectrum reveals a decrease in absorption at 440 nm and an intensification of the new band at 548 nm, which can be assigned unambiguously to the vinylheptafulvene **2a** (Fig. 1). These observations indicate that in the case of furan-substituted compounds of the type **1** ⇄ **2**, particularly if there are −M substituents in the furan ring, the reverse thermal reaction **2** → **1** is so rapid that room-temperature photochromism is prevented.

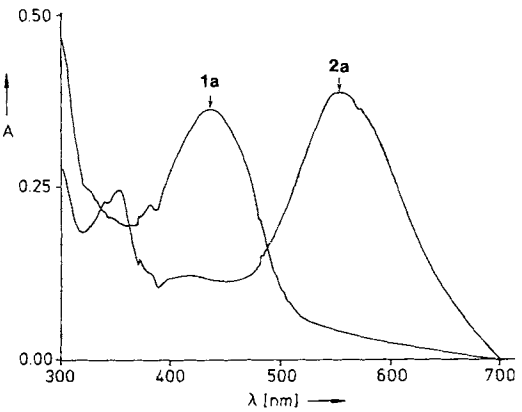


Fig. 1. Electronic spectrum of the photochromic system **1a** ⇄ **2a** at −50 °C in ethanol. Irradiation: ethanol film, mercury lamp (Osram HBO 100 W/2); Balzers filter K2 (420–480 nm); 30 s. Isosbestic points at 335, 362, and 468 nm. Ordinate: arbitrary units.

The reductive portion of the cyclic voltammogram for **1a** [in acetonitrile, tetrabutylammonium hexafluorophosphate as supporting electrolyte, vs. ferrocene (FOC)] reveals a signal ($E_{p,irr}$) at −1185 mV that clearly indicates irreversible formation of the radical anion $\mathbf{1a}^{\bullet\ominus}$. The model compound **4**, containing two dicyanovinyl groups, behaves differently; both cyclic voltammetry and UV/VIS spectroelectrochemistry suggest reversible conversion of **4** (yellow) into the radical anion $\mathbf{4}^{\bullet\ominus}$ (blue, $E_{1/2}$ = −890 mV vs. FOC) and the dianion $\mathbf{4}^{2\ominus}$ (orange, $E_{1/2}$ = −1240 mV vs. FOC) (Fig. 2). The locations of the most intensive absorption bands are: for the neutral compound **4**, 392 nm with a shoulder at 409 nm; for the radical anion $\mathbf{4}^{\bullet\ominus}$, 599 nm; and for the dianion $\mathbf{4}^{2\ominus}$, 493 nm with a shoulder at 467 nm. In the case of the benzoid analogue of **4** [i.e., a benzene ring bearing *p*-bis(dicyanovinyl) groups], both the radical anion and the dianion rapidly undergo further chemical reactions.[7, 8]

[*] Prof. Dr. J. Daub, Dr. J. Salbeck, Dr. T. Knöchel, Dipl.-Chem. C. Fischer, Dr. H. Kunkely
Institut für Organische Chemie der Universität
Universitätstrasse 31, D-8400 Regensburg (FRG)
Dr. K. M. Rapp
Südzucker A.G. Mannheim/Ochsenfurt, Zentrallaboratorium
D-6718 Grünstadt (FRG)

[**] This work was supported by the Volkswagen-Stiftung, the Bundesminister für Forschung und Technologie, and the Deutsche Forschungsgemeinschaft.

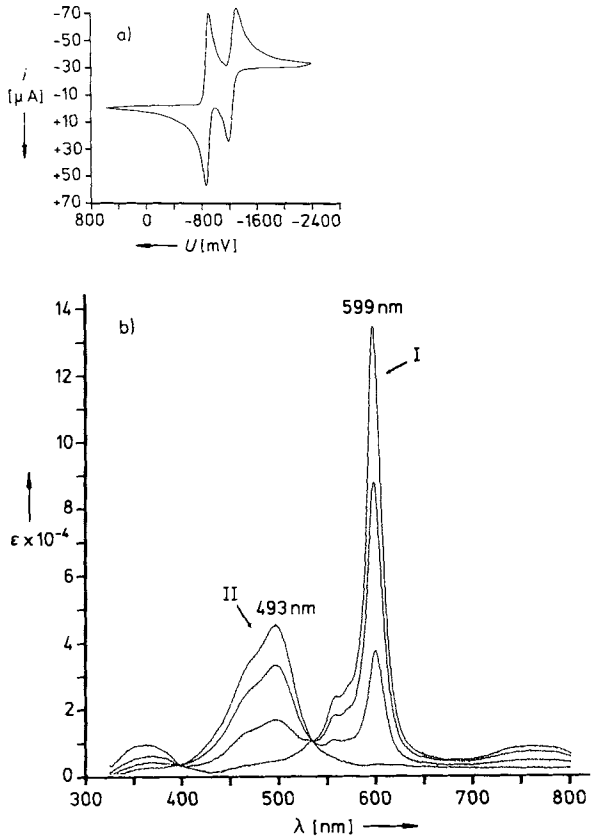
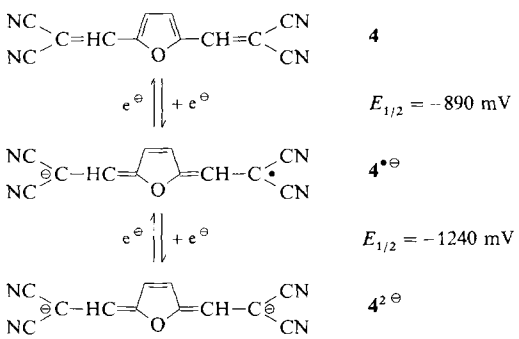


Fig. 2. (a) Cyclic voltammogram of the model compound **4** in acetonitrile ($c = 4 \times 10^{-3}$ M), 0.1 M tetrabutylammonium hexafluorophosphate as supporting electrolyte, potential data vs. ferrocene (FOC). (b) UV/VIS spectroelectrochemistry of **4** in acetonitrile ($c = 1 \times 10^{-3}$ M). Measurement conditions for curve I: -1000 mV vs. FOC (formation of $\mathbf{4}^{\bullet\ominus}$); for curve II: -1400 mV vs. FOC (formation of $\mathbf{4}^{2\ominus}$). Isosbestic points at 391 and 530 nm.

Photoelectrochemical experiments were carried out in a specially constructed cell[9] that permits irradiation of a solution of **1a** in acetonitrile with simultaneous detection of



current flow. Figure 3 shows the results in the form of a current/time curve for a sample subjected to a series of light pulses (5-sec duration) from a high-pressure xenon-mercury lamp (XBO). Current was measured as a function of the pulse train, maintaining a working potential of -1050 mV (vs. FOC). At this potential **1a** is inert, but **2a** is reduced to the radical anion $\mathbf{2a}^{\bullet\ominus}$, as is apparent from a comparison with the half-cell potential $E_{1/2}$ for $\mathbf{4}/\mathbf{4}^{\bullet\ominus}$. The intensity of the electrochemical signals diminishes with time, an indication that under these reaction conditions the radical anion $\mathbf{2a}^{\bullet\ominus}$

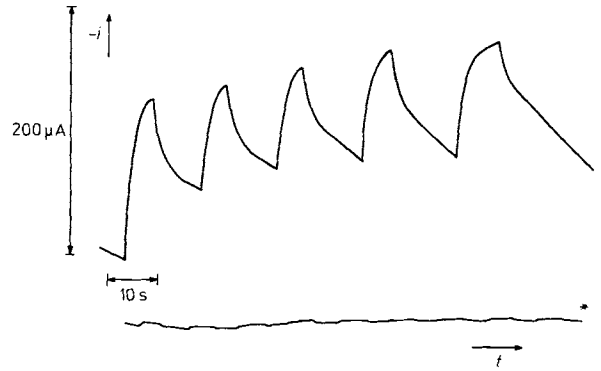
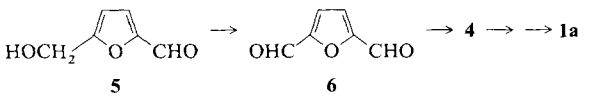


Fig. 3. Upper curve: photochemical switching effect upon irradiation of **1a** in acetonitrile ($c = 1 \times 10^{-3}$ M) at a potential of -1050 MV vs. FOC. Lower curve: no switching effect at a potential of -800 mV vs. FOC.

is subject to further transformations. Apparently the heptafulvene fragment in $\mathbf{2a}^{\bullet\ominus}$ lowers its chemical stability.

The observed results may be interpreted with respect to the electron-transfer characteristics of compounds **1a** and **2a** as follows: the bis(dicyanovinyl)furan derivative **2a** that arises from light-induced ring opening of **1a** is more readily reduced than **1a** itself. Therefore, establishment of an appropriate electrochemical potential permits detection of a cathode current.[10]

Compound **1a** was synthesized in part from substances of plant origin and in part from petrochemical reagents. The



electron-transfer portions of **1a** and **2a** were derived from D-fructose by way of the intermediate 5-(hydroxymethyl)furfural **5**.[11] Oxidation of **5** produced the dialdehyde **6** (barium manganate, 1,2-dichloroethane).[12] Knoevenagel condensation of **6** to **4** was carried out as a solid-state reaction (trituration of **6** in a mortar with malononitrile and neutral aluminum oxide, 70% yield).[13] [8+2] cycloaddition with 8-methoxyheptafulvene[15] and subsequent elimination of methanol (P_2O_5) produced the photochromic dihydroazulene **1a** in good yield.[4b, 16]

Received: June 14, 1989;
supplemented version: August 4, 1989 [Z 3395 IE]
German version: *Angew. Chem. 101* (1989) 1541

CAS Registry numbers:
1, 123077-83-8; **2**, 123077-84-9; **3**, 88694-82-0.

[1] Recent review of photochromic compounds: H. Dürr, *Angew. Chem. 101* (1989) 427; *Angew. Chem. Int. Ed. Engl. 28* (1989) 413.
[2] F. Ciardelli, C. Carlini, R. Solaro, A. Altomare, O. Pieroni, J. L. Houben, A. Fissi, *Pure Appl. Chem. 56* (1984) 329.
[3] I. Cabrera, F. Shyartsman, O. Veinberg, V. A. Krongauz, *Science (Washington, D.C.) 226* (1984) 341.
[4] a) J. Daub, T. Knöchel, A. Mannschreck, *Angew. Chem. 96* (1984) 980; *Angew. Chem. Int. Ed. Engl. 23* (1984) 960; b) J. Daub, S. Gierisch, U. Klement, T. Knöchel, G. Maas, U. Seitz, *Chem. Ber. 119* (1986) 2631; c) S. Gierisch, J. Daub, *ibid. 122* (1989) 69; d) S. Gierisch, W. Bauer, T. Burgemeister, J. Daub, *ibid.*, im Druck.
[5] a) Excerpts from J. Daub, J. Achatz, S. Gierisch, T. Knöchel, J. Salbeck, *Seventh International Conference on Photochemical Conversion and Storage of Solar Energy*. Evanston, IL (USA) 1988, Abstr. S. 60; b) J. Daub, *Naurod-Treffen "Optische und elektronische Phänomene in organischen Festkörpern"*, Wiesbaden-Naurod, May 1989.
[6] Related studies: J. Anzai, A. Ueno, T. Osa, *J. Chem. Soc. Chem. Commun. 1984*, 688; H. Tachibana, T. Nakamura, M. Matsumoto, H. Komizu, E. Manda, H. Niino, A. Yabe, Y. Kawabatta, *J. Am. Chem. Soc. 111* (1989) 3080.

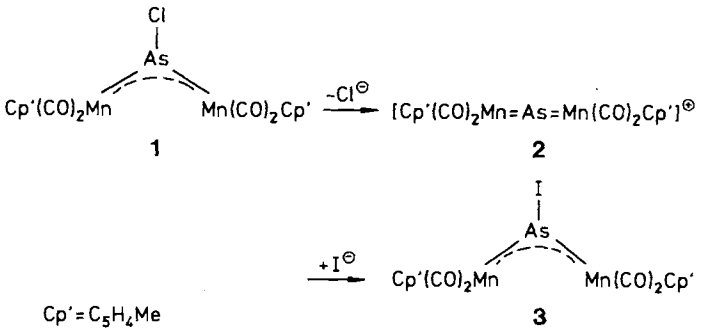
[7] J. Daub, *Nachr. Chem. Tech. Lab. 36* (1988) 896.
[8] R. O. Loufty, C. K. Hsiao, B. S. Ong, B. Keoshkerian, *Can. J. Chem. 62* (1984) 1877.
[9] J. Salbeck, C. Fischer, unpublished results.
[10] Photochemical production of heptafulvene was demonstrated through cyclic voltammetry studies with a model compound based on **3**, one in which the $-OCH_3$ group was replaced by $-CN$. The signal obtained prior to irradiation had a peak potential of -1540 mV vs. FOC. This may be ascribed to formation of a short-lived radical anion of **3** ($-CN$ in place of $-OCH_3$). Irradiation led to a new signal with a peak potential of -1235 mV vs. FOC. This signal corresponds to irreversible formation of the radical anion derived from the heptafulvene that results from photochemical ring opening (C. Fischer, unpublished results). Technical difficulties have so far prevented similar experiments with **1/2**.
[11] Cf. H. Schiweck, K. Rapp, M. Vogel, *Chem. Ind. (London) 1988*, 228.
[12] a) H. Firouzabadi, E. Ghaderi, *Tetrahedron Lett. 1978*, 839; b) A. F. Oleinik, K. Yu. Novitskii, *J. Org. Chem. USSR (Engl. Transl.) 6* (1970) 2643; T. El Hajj, A. Masroua, J.-C. Martin, G. Descotes, *Bull. Soc. Chim. Fr. 1987*, 855.
[13] Cf. F. Texier-Boullet, A Foucaud, *Tetrahedron Lett. 23* (1982) 4927.
[14] Cf. K. Yu. Novitskii, V. P. Volkov, Yu. K. Yur'ev, *Zhur. Obshch. Khim. 31* (1961) 538; *Chem. Abstr. 55* (1961) 23485h.
[15] Synthesis of dihydroazulenes: J. Daub, S. Gierisch, T. Knöchel, E. Salbeck, G. Maas, *Z. Naturforsch. B41* (1986) 1151.
[16] Additional spectroscopic and analytical data: **1**: mp = 172–173 °C; MS (70 eV): *m/e* 322 (M^+, 100%), 295 (*M*-HCN, 31%); IR (KBr): $\tilde{\nu}$ [cm^{-1}] = 2220; ^1H NMR (250 MHz, $CDCl_3$): δ = 3.8 (m, 1H; 8a-H), 5.8 (dd, J = 10.6, 3.8 Hz, 1H; 8-H), 7.5 [s, 1H; CH = $C(CN)_2$]; correct elemental analysis obtained. – **4**: mp = 195–197 °C; IR (KBr): $\tilde{\nu}$ [cm^{-1}] = 2220; ^1H NMR (250 MHz, [D_6]DMSO): δ = 7.7 (s, 2H), 8.5 (br.s, 2H); correct elemental analysis obtained. A mp = 207–208 °C has been reported for **4** prepared by a different method [14].

[{Cp'(CO)$_2$Mn}$_2$PbS*t*Bu]$^\ominus$; Completion of an Isoelectronic Series of Binuclear Complexes Containing Trigonal-Planar Coordinated Main Group Elements**

By *Frank Ettel, G. Huttner,** and *Laszlo Zsolnai*

Dedicated to Professor Margot Becke-Goehring on the occasion of her 75th birthday

The relationship between dimetalla-allene systems and "inidene"-complexes[1] was recently demonstrated with the reaction sequence **1** → **2** → **3**[2, 3] for elements of the fifth main group as central atom.



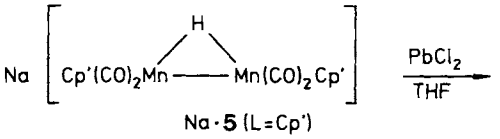
Since the bonding pattern found in "inidene" complexes for elements of the fifth main group can also be realized with elements of the sixth main group, e.g. **4**,[4]

[{Cp(CO)$_2$Mn}$_2$SPh]$^\oplus$ **4**

we were encouraged to check for this bonding pattern also with elements of the fourth main group as bridge ligands by reaction of the corresponding heterocumulenes with Lewis bases.

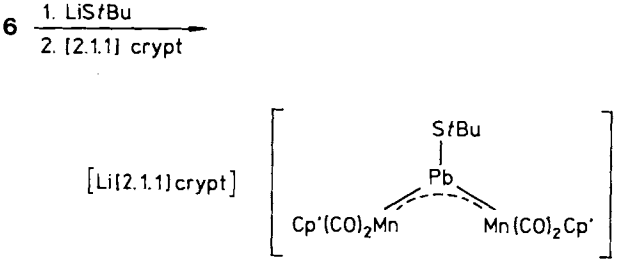
The heterocumulenes [L(CO)$_2$Mn=X=Mn(CO)$_2$L] (L = Cp, Cp') were first described by *E. Weiss* et al. (X = Ge)[5, 6] and *W. A. Herrmann* et al. (X = Pb).[7] In the reaction of the hydrido complex **5**[8] with $PbCl_2$ or $GeCl_4$ we have now found a preparatively productive novel entry to these complexes, which serve as the necessary starting materials in this study.

The Pb-derivative **6** reacts spontaneously with alkali-metal thiolates to give anionic adducts (bathochromic shift of



[Cp'(CO)$_2$Mn=Pb=Mn(CO)$_2$Cp'] **6**

the ν_{CO} vibrations by ca. 30 cm^{-1}). By addition of cryptands to the reddish-brown solutions, the corresponding salts can be obtained in crystalline form.



For the derivative **7**, the expected trigonal-planar coordination of the lead atom could be confirmed by an X-ray structure analysis[9] (Fig. 1).

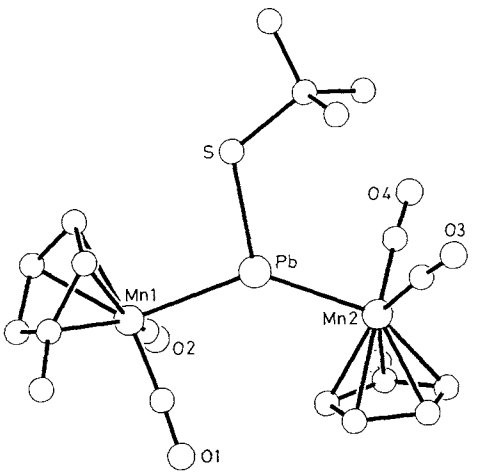


Fig. 1. Structure of **7** in the crystal.

[*] Prof. Dr. G. Huttner, Dipl.-Chem. F. Ettel, Dr. L. Zsolnai
Anorganisch-chemisches Institut der Universität
Im Neuenheimer Feld 270, D-6900 Heidelberg (FRG)

[**] This work was supported by the Fonds der Chemischen Industrie and by the Deutsche Forschungsgemeinschaft (SFB 247).

The maximum deviation from the best plane through the two Mn atoms, the S atom of the S*t*Bu substituent and the lead atom is 2.6 pm, and the Mn–Pb–Mn angle (135.5(1)°) is in good agreement with the corresponding angles in other compounds of the "inidene" type.[10]

The Pb–Mn bonds in **7** (257.4(3) pm) are somewhat longer than in the cumulene **6** with Cp instead of Cp′ (246.3(1) pm[7]). This change in bond length corresponds qualitatively to the changes which have been observed in the isoelectronic pair of arsenic compounds **1**/**2** and **3**/**2**.[2, 11]

The orientation of the S*t*Bu residue allows for a π-interaction between the S atom and the three-center 4π-electron system[10] of the Mn–Pb–Mn fragment: the *ipso*-C atom of the S*t*Bu substituent is located only 7 pm outside of the coordination plane of the lead atom. The observed orientation of the S*t*Bu substituent (Fig. 1) leads by necessity to a repulsive interaction with the $Cp'(CO)_2Mn$ fragment nearer to the *t*Bu group: the S–Pb–Mn2 angle is correspondingly large (123.98(1)° vs. S–Pb–Mn1 100.6(1)°). The π interaction between S and the Mn_2Pb unit is also manifested in a short Pb–S distance of 257.4(4) pm (cf. $[Cp'(CO)_2MnPb(SMes)_3]^{\ominus}$: Pb–S 260.3(6) pm[12]).

7 is the first "inidene" complex with a heavy element of the fourth main group as bridge atom (Fig. 2). The main group

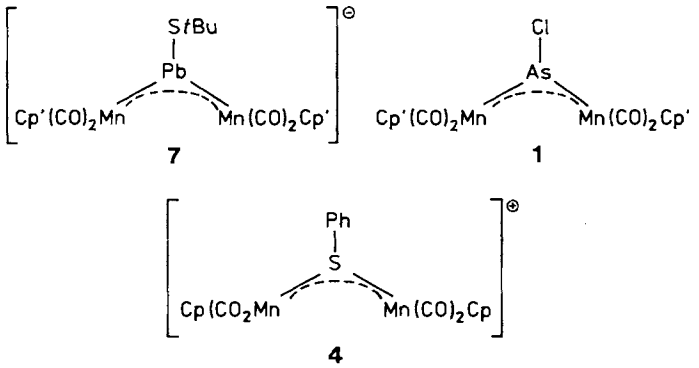
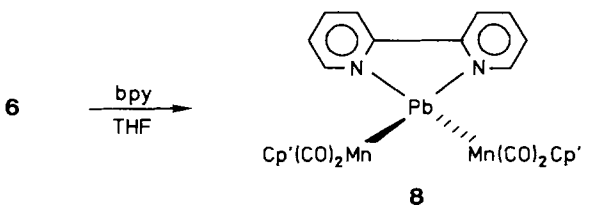


Fig. 2. Inidene complexes of elements of the fourth, fifth [10], and sixth [4] main groups.

atoms in such compounds are coordinatively unsaturated and can therefore add bases. In compounds with bridge elements from the fifth main group this unsaturated behavior is substantiated by many reactions.[10] The base adducts obtained are especially stable if the basic center is anchored via a chelate bridge on the main group element.[13]

Fully consistent with this, **6** forms neutral chelate complexes such as **8** upon reaction with neutral chelate ligands such as tmeda,[12] 1,10-phenanthroline(phen)[12] and 2,2′-bipyridine(bpy).



An X-ray structure analysis of **8** revealed (Fig. 3) that the lead atom has a distorted tetrahedral coordination geometry and that the Pb–Mn bonds (252.8(3) pm) are longer than in the starting compound **6**.

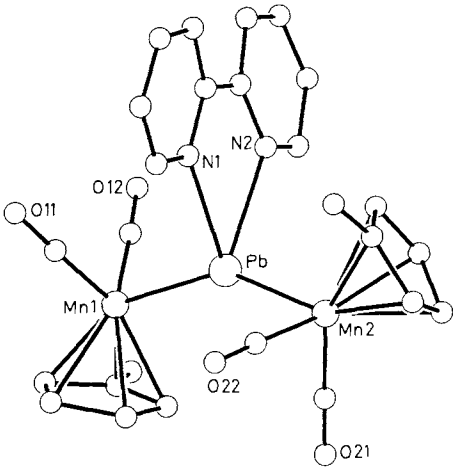


Fig. 3. Structure of **8** in the crystal.

The Mn–Pb–Mn angle with a value of 146.9(1)° lies in the range that is characteristic for isoelectronic chelate complexes of elements of the fifth main group.[13] The Pb–N bonds are comparatively long (255.9(9) pm);[14] however, Pb^{IV} centers are present in the reference compounds whereas **8**, like **6** and **7**, contains lead in the formal oxidation state 0. With respect to the coordination of the main group element, the silicon compound $[(hmpa)_2Si\{Fe(CO)_4\}_2]$[15] and the anionic base adduct complex of thallium $[Et_4N][\{Fe_2(CO)_8\}TlL]$ (L = tmeda, phen, bpy, ene)[16] are analogous to base adducts such as **8**.[16] The coordinatively unsaturated parent compounds of these analogues of **8** $[(L_nM)_2XR]^{n\ominus}$ (X = Si, n = 1; X = Tl, n = 2) and $[(L_nM)_2X]^{m\ominus}$ (X = Si, m = 0, X = Tl, n = 1) are so far unknown.

Experimental

All operations were carried out with freshly purified and distilled solvents under N_2. The silica gel (0.05–0.2 mm, J. T. Baker Chemicals) used for the chromatography was freed of oxygen in a vacuum for 3d and stored under N_2. IR spectra: Perkin Elmer 983G.

6: A solution of Na·**5** (L = Cp′; 1.0 g, 2.5 mmol) in 100 mL THF was treated with 2.0 g (10 mmol) of dry $PbCl_2$ and then stirred for 1 h at room temperature. The initially red solution turned dirty brown, and a grey precipitate formed. After passage through kieselgur on a frit and collection on silanated silica gel, column chromatography (silica gel, *l* = 25 cm, ∅ 2 cm) with pentane afforded a yellow zone ($[MnCp(CO)_3]$) and with toluene/pentane 1/2 a green zone ($[(\mu_3\text{-}Pb)\{Cp'(CO)_2Mn\}_3]$). Subsequent elution with diethyl ether afforded a dark-red zone, which after removal of the solvent furnished 370 mg (0.63 mmol) of **6**. Yield: 25% referred to **5**; characterization by comparison with authentic **6** (IR(THF): $\tilde{\nu}$ [cm^{-1}] = 1925 m, 1899 vs, 1860 vs, 1860 s [7].

[Li[2.1.1]crypt]-**7**: A solution of **6** (100 mg, 0.17 mmol) in THF (5 mL) was treated with 16.4 mg of Li*t*Bu in 5 mL of THF. The red color of the solution immediately deepened; the reaction is quantitative. Crystals of **7** were obtained as follows: after addition of 30 mg of [2.1.1]crypt the solution was concentrated to about 5 mL. Upon covering the red solution with a layer of 10 mL of Et_2O, Li[2.1.1]crypt **7** precipitated out within 5 d in the form of analytically pure, red needles. Yield: 38 mg (20% referred to **6**); m.p. 100 °C (decomp); correct C,H,S analysis. IR(THF): $\tilde{\nu}$ [cm^{-1}] = 1897 m, 1873 vs, 1837 s.

8: To a solution of **6** (100 mg, 0.17 mmol) in 5 mL of THF was added a solution of 26.5 mg (0.17 mmol) of bpy in 5 mL of THF. Immediately after the addition the IR spectrum showed the ν_{CO} bands of **8**. Deep-dark red, analytically pure crystals of **8** were obtained as follows: THF was removed from the solution at −20 °C until clouding was observed. The cloudy solution was then covered with a layer of 10 mL of Et_2O at 25 °C and diffusion allowed to take place for 5d. Yield: 38 mg (30% referred to 6); m.p. 130 °C (decomp); correct C,H,N analysis. IR(THF): $\tilde{\nu}$ [cm^{-1}] = 1925 w, 1899 s, 1887 vs, 1860 m, 1846 s.

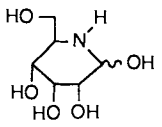
Received: May 23, 1989 [Z 3356 IE]
German version: *Angew. Chem. 101* (1989) 1525

[1] The terms arsinidene and stibinidene are used here instead of the IUPAC recommended terms arsanediyl and stibanediyl, respectively.
[2] A. Strube, G. Huttner, L. Zsolnai, *Angew. Chem. 100* (1988) 1586; *Angew. Chem. Int. Ed. Engl. 27* (1988) 1529.
[3] A. Strube, G. Huttner, unpublished.
[4] H. Braunwarth, G. Huttner, L. Zsolnai, *Angew. Chem. 100* (1988) 731; *Angew. Chem. Int. Ed. Engl. 27* (1988) 698.
[5] W. Gäde, E. Weiss, *J. Organomet. Chem. 213* (1981) 451.
[6] D. Melzer, E. Weiss, *J. Organomet. Chem. 263* (1984) 67.
[7] W. A. Herrmann, H. J. Kneuper, E. Herdtweck, *Chem. Ber. 122* (1989) 445.
[8] P. Oltmanns, D. Rehder, *J. Organomet. Chem. 345* (1988) 87; K. Plößl, G. Huttner, L. Zsolnai, *Angew. Chem. 101* (1989) 482; *Angew. Chem. Int. Ed. Engl. 28* (1989) 446.
[9] [Li[2.1.1]crypt]7: $a = 11.771(5)$, $b = 12.165(4)$, $c = 15.472(5)$ pm, $\alpha = 82.69(3)$, $\beta = 67.85(2)$, $\gamma = 71.17(3)^\circ$, space group $P\bar{1}$, $Z = 2$, $R_1 = 0.045$, $R_2 = 0.039$. – **8**: $a = 11.141(5)$, $b = 9.093(3)$, $c = 25.760(1)$ pm, $\alpha = 90.00(3)$, $\beta = 105.04(3)$, $\gamma = 90.00(3)^\circ$, space group $P2_1/c$, $Z = 4$, $R_1 = 0.061$, $R_2 = 0.049$. Measurement on a Nicolet(Syntex) P3 diffractometer, graphite monochromator, $Mo_{K\alpha}$ radiation, solution and refinement of the structure with the program system SHELXTL (G. Sheldrick, SHELXTL, Revision 4, Göttingen 1984). Further details of the crystal structure investigation are available on request from the Fachinformationszentrum Karlsruhe, Gesellschaft für wissenschaftlich-technische Information mbH, D-7514 Eggenstein-Leopoldshafen 2 (FRG), on quoting the depository number CSD-53922, the names of the authors, and the journal citation.
[10] G. Huttner, K. Evertz, *Acc. Chem. Res. 19* (1986) 406; G. Huttner, *Pure Appl. Chem. 58* (1986) 585.
[11] J. von Seyerl, B. Sigwarth, H. G. Schmid, G. Mohr, A. Frank, M. Marsili, G. Huttner, *Chem. Ber. 114* (1981) 1392.
[12] F. Ettel, G. Huttner, unpublished.
[13] H. Lang, L. Zsolnai, G. Huttner, *Z. Naturforsch. B40* (1985) 500; A. Lombard, G. Huttner, *J. Organomet. Chem. 352* (1988) 303; J. von Seyerl, B. Sigwarth, G. Huttner, *Chem. Ber. 114* (1981) 1407.
[14] R. Allmann, A. Waskowska, R. Hohfeld, J. Lorberth, *J. Organomet. Chem. 198* (1980) 155; T. N. Tarkova, E. V. Chuprunov, L. E. Nicolaeva, M. A. Simonov, *Sov. Phys. Crystallogr. (Engl. Transl.) 23* (1978) 281.
[15] C. Zybill, D. L. Wilkinson, G. Müller, *Angew. Chem. 100* (1988) 574; *Angew. Chem. Int. Ed. Engl. 27* (1988) 583.
[16] J. M. Cassidy, K. H. Whitmire, *Inorg. Chem. 28* (1989) 1435.

Total Synthesis of Allonojirimycin (5-Amino-5-deoxy-D-allopyranose)**

By *Yves Auberson* and *Pierre Vogel**

The substitution of the ring oxygen of furanoses and pyranoses by nitrogen[1,2] leads to a class of powerful and specific glycosidase inhibitors whose chemotherapeutic potential is now recognized.[3] Among the 5-amino-5-deoxyhexopyranoses the derivatives of D-glucose (gluconojirimycin),[1,4] D-mannose (mannojirimycin),[5] D-galactose (galactonojirimycin)[6,7] and L-altrose[3,8] have been described. Their 1-deoxy derivatives[3,8] as well as 5-amino-1,5-dideoxy-L-fucose[3,9] are also known. We present a short, total synthesis of the yet unknown allonojirimycin **1** (5-amino-5-deoxy-D-allopyranose) starting with the Diels–



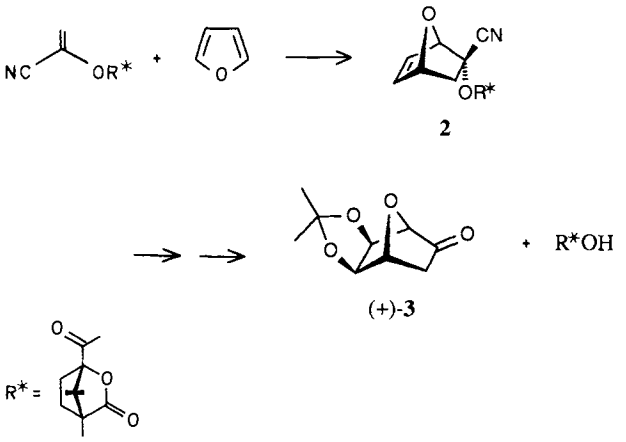
1

Alder adduct **2** of furan and (–)-(1-cyanovinyl)-(1*S*)-camphanate.[10]

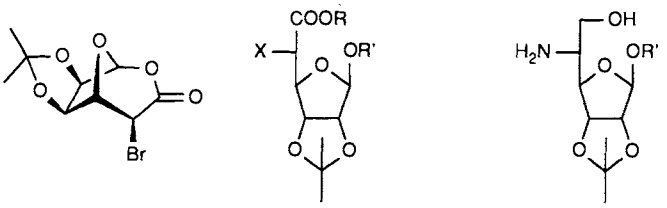
[*] Prof. P. Vogel, Y. Auberson
Section de chimie de l'Université
rue de la Barre 2, CH 1005 Lausanne (Switzerland)

[**] This work was supported by the Swiss National Science Foundation, the Fonds Herbette (Lausanne), and Hoffmann-La Roche & Cie, AG (Basel).

Double hydroxylation of **2** and protection of the glycol as an acetonide followed by saponification gives optically pure ketone (+)-**3** (60%) and (1S)-camphanic acid (recovery of the chiral auxiliary).[11] Ketone (+)-**3** is tranformed (three



steps, 72% overall) into bromolactone (–)-**4** as already described.[12] Treatment with allylic alcohol and CH_3SO_3H at 20 °C gives (–)-**5** (66%). Saponification of (–)-**5** (and other ester derivatives) with K_2CO_3, KOH or NH_3 leads to epimerization at C5 of the uronate. Selective hydrolysis of the allylic ester (–)-**5** into acid (–)-**6** (87%) is achieved by heating in $EtOH/H_2O$ 9:1 in the presence of 0.1 equiv. of $[Rh(PPh_3)_3Cl]$ and 0.2 equiv. of 1,4-diazabicyclo [2.2.2] octane (DABCO). The allyl ether → prop-1-enyl ether isomerization[13] is not observed under these conditions. Treatment of the potassium salt of (–)-**6** with NaN_3 (DMF, 60 °C, 8 h) affords azide (–)-**7** (90%) with retention of configuration.[14]



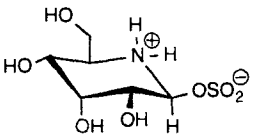
(–)-**4**

(–)-**5**:X=Br, R=R'= allyl
(–)-**6**:X=Br, R=H, R'= allyl
(–)-**7**:X=N_3, R=H, R'= allyl
(–)-**9**:X=N_3, R=Bn, R'= allyl

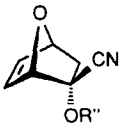
8:R'=*n*Pr
(–)-**10**:R'= allyl

Catalytical hydrogenation of (–)-**7** (H_2, Pt/C, EtOH) followed by reduction of the acid group with $BH_3 \cdot Me_2S$ (THF) furnishes **8** which affords the hydrochloride **1** · HCl (ca. 15%) on treatment with aqueous 1 N HCl. A better procedure was found by converting the cesium salt of (–)-**6** into the corresponding benzylic ester (–)-**9** (83%, based on (–)-**5**) by treatment first with CsN_3 and then with $PhCH_2Br$ in DMF. Reduction of (–)-**9** with $LiAlH_4$ in THF gives (–)-**10** (61%) which affords **1** · HCl on treatment with 1 N HCl. Its 360-MHz ^1H NMR spectrum is typical of allopyranose (^3J(H-C1,H-C2) = 9 Hz, ^3J(H-C4,H-C5) = 10.5 Hz) and not of talopyranose derivatives,[12] thus confirming the retention of configuration in reaction (–)-**6** + NaN_3 → (–)-**7** and the absence of epimerization at C5. Compound **1** · HCl is not stable in water and undergoes decomposition into pyridine derivatives at 20 °C. However, the bisulfite (–)-**11** (54%) obtained by treatment of (–)-**10** with SO_2/H_2O (50 °C, 3 d), then with SO_2/EtOH (0 °C), is a

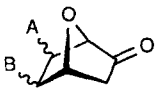
stable, crystalline compound which could be fully characterized. Its 250-MHz ^{1}H NMR spectrum is similar to that of **1**·HCl and confirmed the pyranose structure (−)-**11** in D_2O.



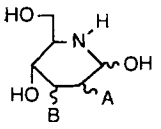
(−)-**11**



12



13



14

Since the Diels–Alder adduct **12** [R″ = (1*R*)-camphanoyl] is also readily available, our synthesis can be applied to the preparation of 5-amino-5-deoxy-L-allopyranose. We have shown[15] that 7-oxabicyclo[2.2.1]hept-5-en-2-yl derivatives **2, 12** and their enones can be substituted at C5 and C6 with high regio- and stereoselectivity with various groups A and B giving systems **13**. Thus our synthetic approach should allow one, in principle, to obtain all kinds of 5-amino-5-deoxy-hexopyranose derivatives **14** readily.

Experimental Procedure

(−)-**5**: A mixture of (−)-**4** [12] (0.5 g, 1.54 mmol), allyl alcohol (10 mL) and CH_3SO_3H (90 μL) was kept at 20 °C for 18 h. After addition of saturated aqueous solution of $NaHCO_3$ (20 mL), the solvent was evaporated and the residue taken with CH_2Cl_2 and dried ($MgSO_4$). Filtration on silica gel (AcOEt/petroleum ether 1:2, R_f = 0.69) gave 426 mg (66%) colorless oil. $[\alpha]_D^{20} = -58$ (c = 1.55, CH_2Cl_2); IR (KBr): $\tilde{\nu}$ = 2980, 1740 cm^{-1}. [16]

(−)-**6**: A mixture of (−)-**5** (265 mg, 0.7 mmol), EtOH (18 mL), H_2O (2 mL), [$Rh(Ph_3P)_3Cl$] (70 mg, 0.07 mmol) and DABCO (18 mg, 0.14 mmol) was heated under reflux for 5 h. After addition of aq. 0.5 N KOH (20 mL) and solvent evaporation to ca. 20 mL, the mixture was washed twice with CH_2Cl_2 (20 mL). The aqueous phase was acidified with 1 N HCl (20 mL) and extracted four times with CH_2Cl_2 (25 mL). After drying ($MgSO_4$) and solvent evaporation 214 mg (87%) of a colorless oil was obtained. $[\alpha]_D^{20} = -74$ (c = 0.63, CH_2Cl_2); IR ($CDCl_3$): $\tilde{\nu}$ = 2980, 2940, 1720 cm^{-1}. [16]

(−)-**7**: The solution of the crude potassium salt of (−)-**6** (143 mg of acid, 0.42 mmol) was evaporated to dryness; the residue was dissolved in DMF (2.5 mL) and NaN_3 (61 mg, 0.92 mmol) was added. The solution was heated to 60 °C for 8 h. After dilution with 0.5 N NaOH (20 mL), the mixture was washed with CH_2Cl_2 (10 mL), then acidified with 1 N HCl (20 mL) and extracted three times with CH_2Cl_2 (10 mL). The extracts were combined, dried ($MgSO_4$) and the solvent evaporated, yielding 114 mg (90%) yellowish oil. IR ($CHCl_3$): $\tilde{\nu}$ = 2990, 2105, 1720 cm^{-1}. [16]

(−)-**9**: 378 mg of (−)-**6** (1 mmol) were neutralized by 182 mg of Cs_2CO_3 in 5 mL anhydrous DMF. After stirring at 20 °C for 15 min, CsN_3 (403 mg, 2.2 mmol) was added and the mixture heated to 60 °C for 8 h. After cooling to 20 °C, $PhCH_2Br$ (500 μL) was added. After stirring at 20 °C for 10 min, 1 N HCl (40 mL) was added and the mixture extracted three times with CH_2Cl_2 (20 mL). The organic phases were combined, washed with saturated aqueous solution of NaCl (20 mL) and dried ($MgSO_4$). After solvent evaporation, the residue was filtered on silica gel (AcOEt/petroleum ether 1:4, R_f = 0.5), yielding 419 mg (96%) yellowish oil. Purification by column chromatography on silica gel afforded an analytical sample of (−)-**9** (58%). $[\alpha]_D^{20} = -41$ (c = 0.96, CH_2Cl_2); IR ($CDCl_3$): $\tilde{\nu}$ = 2990, 2940, 2100, 1740 cm^{-1}; ^{1}H NMR (250 MHz, $CDCl_3$): δ = 7.39 (m; 5H), 5.75 (dddd, ^3J = 17, 10.5, 6, 5 Hz; 1H), 5.30, 5.22 (2 d, ^2J = 12 Hz), 5.18 (dm; 1H), 5.15 (dm; 1H), 5.11 (s; H-C1), 4.88 (dd, ^3J = 6.0, 1.0 Hz; H-C3), 4.63 (d, ^3J = 6 Hz; H-C2); 4.48 (dd, ^3J = 9.0, 1.0 Hz; H-C4), 4.06, 3.78 (2 ddt), 3.85 (d, ^3J = 9.0 Hz; H-C5), 1.48, 1.31 (2 s; 2 Me).[16]

(−)-**10**: A mixture of (−)-**9** (50 mg, 0.13 mmol), $LiAlH_4$ (14 mg) and anhydrous THF (2 mL) was stirred at 20 °C for 1 h. After addition of 1 N HCl (10 mL), the mixture was washed twice with CH_2Cl_2 (10 mL), then 2 N NaOH (10 mL) was added and the solution extracted twice with CH_2Cl_2 (10 mL). The extracts were combined, dried ($MgSO_4$) and the solvent evaporated to yield 21 mg (61%) colorless oil that solidifies slowly. $[\alpha]_D^{20} = -46.5$ (c = 0.72, CH_2Cl_2); IR (KBr): $\tilde{\nu}$ = 3380, 3300, 2990, 2940, 2860, 1378, 1080 cm^{-1}.

(+)-**10**, obtained from (±)-**3** as described above, is a colorless solid, m.p. = 83.5–84.5 °C.

1·HCl: A mixture of (−)-**10** (100 mg, 0.38 mmol) and 1 N HCl (2 mL) was kept at 20 °C for 18 h. Solvent evaporation gave an unstable, white solid. ^{1}H NMR (360 MHz, CD_3OD): δ = 4.59 (d, J = 9 Hz; H-C1), 4.14 (t, J = 2.5 Hz; H-C3), 3.96 (d, J = 3.5 Hz; H_2C6), 3.82 (dd, J = 10.5, 2.5 Hz; H-C4), 3.71 (dd, J = 9.0, 2.5 Hz; H-C2), 3.49 (dt, J = 10.5, 3.5 Hz; H-C5).

(−)-**11**: SO_2 was bubbled through a solution of (−)-**10** (100 mg, 0.38 mmol) in H_2O (2 mL) at 55 °C for 3 d. EtOH (2 mL) was added and the solution saturated with SO_2 at 0 °C. The precipitate was collected, yielding 54 mg (54%) colorless crystals. m.p. = 104–106 °C (dec.). $[\alpha]_D^{20} = -3.8$ (c = 1.55, H_2O); IR (KBr): $\tilde{\nu}$ = 3420, 3060–3020, 1570, 1425, 1210, 1065, 1045 cm^{-1}; ^{1}H NMR (250 MHz, D_2O): δ = 4.19 (d, J = 11 Hz; H-C1), 4.13 (dd, J = 2.5, 1.5 Hz; H-C3); 4.05 (dd, J = 11.0, 2.5 Hz; H-C2), 3.94, 3.84 (2 dd, ^2J = 13, ^3J = 2.5 Hz, H_2C6), 3.84 (dd, J = 11.0, 1.5 Hz, H-C4), 3.40 (dt, J = 11.0, 2.5 Hz, H-C5); ^{13}C NMR (90.55 MHz, CD_3OD/D_2O 1:4): δ = 71.8 (d, ^1J(C,H) = 151 Hz), 68.4 (d, ^1J(C,H) = 150 Hz), 68.3 (d, ^1J(C,H) = 150 Hz), 66.1 (d, ^1J(C,H) = 142 Hz; C1, C2, C3, C5), 58.5 (t, ^1J(C,H) = 146 Hz; C6), 57.5 (d, ^1J(C,H) = 164 Hz; C4). Satisfactory elemental analysis was found. Racemic (±)-**11**, m.p. = 143–145 °C (dec.).

Received: June 19, 1989 [Z 3402]
German version: *Angew. Chem. 101* (1989) 1554

CAS Registry numbers:
(−)-**1**·HCl, 123237-48-9; (−)-**4**, 123149-52-0; (−)-**5**, 123149-53-1; (−)-**6**, 123149-54-2; (−)-6 potassium salt, 123168-76-3; (−)-**6**, cesium salt, 123168-77-4; (−)-**7**, 123149-55-3; (−)-**7**, R = n-propyl, 123149-56-4; **8**, 123149-57-5; (−)-**9**, 123149-58-6; (−)-**10**, 123168-75-2; (±)-**10**, 123149-60-0; (−)-**11**, 123149-59-7; (−)-(1-cyanovinyl)-(1S)-camphanic ester, 123149-61-1; allyl alcohol, 107-18-6.

[1] H. Paulsen, A. Todt, *Angew. Chem. 78* (1966) 501; *Angew. Chem. Int. Ed. Engl. 5* (1966) 495; *Adv. Carbohydr. Chem. Biochem. 23* (1968) 115.
[2] L. E. Fellows, *Chem. Br. 1987*, 842, and references cited therein.
[3] G. W. J. Fleet, *Chem. Br. 1989*, 287, and references cited therein.
[4] S. Inouye, T. Tsuruoka, T. Niida, *Tetrahedron 24* (1968) 2125; E. Truscheit, W. Frommer, B. Junge, L. Müller, D. Schmidt, W. Wingender, *Angew. Chem. 93* (1981) 738; *Angew. Chem. Int. Ed. Engl. 20* (1981) 744; B. Rajanikanth, R. Seshadri, *Tetrahedron Lett. 30* (1989) 755.
[5] G. Legler, E. Jülich, *Carbohydr. Res. 128* (1984) 61; T. Niwa, T. Tsuruoka, H. Goi, Y. Kodama, J. Itoh, S. Inouye, Y. Yamada, T. Niida, M. Nobe, Y. Ogawa, *J. Antibiotics 37* (1984) 1579.
[6] G. Legler, S. Pohl, *Carbohydr. Res. 155* (1986) 119.
[7] Y. Miyako, M. Ebata, *J. Antibiotics 40* (1987) 122.
[8] A. Richardson, L. Hough, D. Hendry, *Tetrahedron Lett. 28* (1987) 4601; G. Fleet, N. Ramsden, D. Witty, *Tetrahedron 45* (1989) 319, 327.
[9] G. W. J. Fleet, A. Shaw, S. Evans, L. E. Fellows, *J. Chem. Soc. Chem. Commun. 1985*, 841; H. Paulsen, M. Matske, *Liebigs Ann. Chem. 1988*, 483.
[10] E. Vieira, P. Vogel, *Helv. Chim. Acta 66* (1983) 1865; A. Warm, P. Vogel, *J. Org. Chem. 51* (1986) 5348.
[11] J. Wagner, E. Vieira, P. Vogel, *Helv. Chim. Acta 71* (1988) 624; see also R. R. Schmidt, C. Beitzke, A. K. Forrest, *J. Chem. Soc. Chem. Commun. 1982*, 909; E. Vieira, P. Vogel, *Helv. Chim. Acta 65* (1982) 1700.
[12] Y. Auberson, P. Vogel, *Helv. Chim. Acta 72* (1989) 278.
[13] E. Corey, J. Suggs, *J. Org. Chem. 38* (1973) 3224.
[14] E. Grunwald, S. Winstein, *J. Am. Chem. Soc. 70* (1948) 841.
[15] K. A. Black, P. Vogel, *J. Org. Chem. 51* (1987) 5341; C. LeDrian, P. Vogel, *Helv. Chim. Acta 70* (1986) 1703; J.-L. Reymond, P. Vogel, *Tetrahedron Lett. 29* (1988) 3695.
[16] All other spectral data as well as the elemental analyses confirmed the structures of the new compounds; Y. Auberson, P. Vogel, unpublished results.

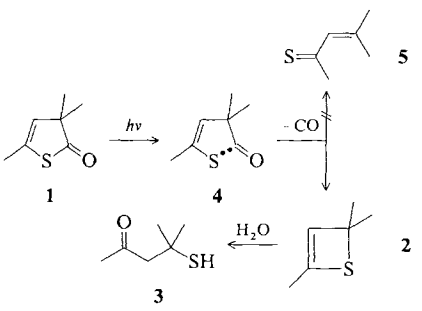
Formation of 2,4,4-Trimethylthiete by Photodecarbonylation of 3,3,5-Trimethyl-2(3*H*)-thiophenone

By *Heiko Hinrichs* and *Paul Margaretha**

Irradiation of the carbonyl tautomers of hydroxythiophenes, for example, 2(5*H*)- and 3(2*H*)-thiophenones,[1,2] as well as their 1-oxides,[3] results in selective formation of new

[*] Prof. Dr. P. Margaretha, Dipl.-Chem. H. Hinrichs
Institut für Organische Chemie der Universität
Martin-Luther-King-Platz 6, D-2000 Hamburg 13 (FRG)

and interesting organosulfur compounds. Here we report that the previously uninvestigated 2(3*H*)-thiophenones react similarly. Thus, irradiation[4] of 3,3,5-trimethyl-2(3*H*)-thiophenone **1**[5] in MeOH, MeCN, or CH_2Cl_2 leads to a single (GC)[6] product, **2**, which was identified as a thiete on the basis of its spectroscopic data[7] and its quantitative transformation to 4-mercapto-4-methylpentan-2-one **3** upon addition of small amounts of water. A very small number of thietes have so far been prepared from 3-(*N*,*N*-dialkylamino)thietanes by Hofmann elimination.[8–10] The mercaptoketone **3**, isolated in 70% yield (based on **1**),[11] was identified on the basis of its ^{1}H NMR spectrum[12] and by comparison with an authentic sample.[13]



Noteworthy is the formation of only the *cyclic* product **2** upon decarbonylation of **4** (the known α,β-unsaturated thioketone **5** dimerizes to give a stable thiine,[14] which was not observed here). By contrast, preliminary findings indicate that 2(3*H*)-furanones[15] and 3-cyclopentenones[16] give exclusively *open-chain* products (α,β-unsaturated ketones and 1,3-dienes, respectively). This differing behavior of thiolactone **1** (or diradical **4**) was not predicted from CNDO calculations on model compounds.[17]

Received: June 5, 1989 [Z 3374 IE]
German version: *Angew. Chem. 101* (1989) 1546

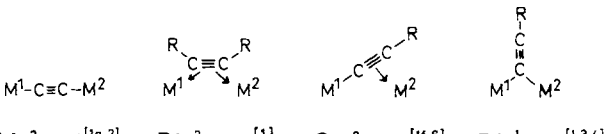
CAS Registry numbers:
1, 33687-83-1; **2**, 123265-62-3; **3**, 19872-52-7.

[1] R. Kiesewetter, P. Margaretha, *Helv. Chim. Acta 72* (1989) 83.
[2] E. Anklam, S. Lau, P. Margaretha, *Helv. Chim. Acta 68* (1985) 1129.
[3] R. Kowalewski, P. Margaretha, *Angew. Chem. 100* (1988) 1437; *Angew. Chem. Int. Ed. Engl. 27* (1988) 1374.
[4] λ = 300 nm, Rayonet RPR 100 photoreactor, Ar-degassed solution.
[5] Synthesis according to [18]; workup was carried out by addition of water and ether, repeated extraction of the aqueous phase with ether, drying of the organic phase ($MgSO_4$), removal of the solvent under vacuum, chromatography of the residue (SiO_2, pentane/ether 49:1), and kugelrohr distillation (70 °C, 15 torr). Yield: 24%. ^{13}C NMR (100.63 MHz, $CDCl_3$): δ = 212(s), 131(s), 127(d), 58(s), 24, 18, 17(q). UV (CH_3CN): λ_{max} = 270 nm (lg ε = 3.16).
[6] SE 30 capillary column (25 m); the relative retention times (isothermal, 100 °C) were: **1**, 3.36 min; **2**, 3.03 min; **3**, 2.88 min.
[7] ^{1}H NMR (400 MHz, CD_3OD): δ = 5.45 (q, 1H) 1.98 (d, 3H) 1.63 (s, 6H); MS (70 eV): 114 ($M^{\oplus}$, 21%), 99 (40%), 59 (40%), 41 (100%). Enrichment by preparative GC gives a 4:1 mixture of **2** and **3**, the latter presumably formed partly by hydrolysis of **2** upon GC purification. A distillative separation of the solvent from **2** is only partly possible owing to the ready volatility of **2**; however, isolation of homologues with R > CH_3 should be easy to carry out by chromatography.
[8] D. C. Dittmer, T. C. Sedergramm in A. Hassner (Ed.): *Small Ring Heterocycles, Part 3*, Wiley, New York 1985, p. 512.
[9] B. H. Patwardhan, E. J. Parker, D. C. Dittmer, *Phosphorus Sulfur 7* (1979) 5.
[10] D. C. Dittmer, P. L. Chang, F. A. Davis, M. Iwamani, I. Stamos, K. Takahashi, *J. Org. Chem. 37* (1972) 1111.
[11] A solution of **1** (2.84 g, 0.02 mol) in 19 mL of MeOH and 1 mL of H_2O was irradiated for 40 h. The solution was poured into pentane/water, the organic phase separated, and the aqueous phase extracted twice more with pentane. After drying of the organic phase ($MgSO_4$) and distillation of the pentane through a Vigreux column, 1.84 g (70%) of **3** was obtained by distillation. (b.p. 52–57 °C, 15 torr).
[12] ^{1}H NMR ($CDCl_3$): δ = 2.72 (s, 2H), 2.38 (s, 1H), 2.11 (s, 3H), 1.43 (s, 6H).
[13] F. Asinger, M. Thiel, W. Höringklee, *Justus Liebigs Ann. Chem. 610* (1957) 1.
[14] P. Beslin, D. Lagain, J. Vialle, *Bull. Soc. Chim. Fr. 1979*, 2677.
[15] R. Martinez-Utrilla, M. A. Miranda, *Tetrahedron 37* (1981) 2111.
[16] P. S. Engel, H. Ziffer, *Tetrahedron Lett. 1969*, 5181.
[17] J. P. Snyder, *J. Org. Chem. 45* (1980) 1341.
[18] J. Brunet, D. Paquer, P. Rioult, *Phosphorus Sulfur 3* (1977) 377.

Triorganolead Cations Stabilized by Side-on Coordination to the C≡C Bond in Alkynylborates**

By *Bernd Wrackmeyer,** *Klaus Horchler*, and *Roland Boese*

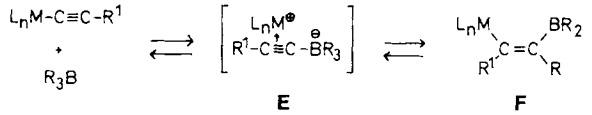
The many-faceted coordination chemistry of the C≡C bond (Scheme 1) is particularly well documented in the case of transition metals.[1] Apart from the η^1-bond in $L_nM-C\equiv C-R^1$,[2] main group elements mainly form dimers [e.g. $(R_2M-C\equiv C-Ph)_2$ with M = Be,[3a] Al,[3b] and Ga;[3c] there is also a gradual transition between structures of type **C** and **D**[3d]], oligomers (lithium alkynides,[4] Type **D**) or ionic acetylides (e.g. CaC_2[5]).



A [$\eta^2\{\sigma,\sigma\}$][1g,2] **B** [$\eta^2\{\pi,\pi\}$][1] **C** [$\eta^2\{\sigma,\pi\}$][1f,6] **D** [$\eta^1\{\sigma,\sigma\}$][1,3,4]

Scheme 1.

There are, however, few compounds in which the alkynide ligand bridges both a transition metal and a main group element as in **C** or **D**,[6] and such a bridging of two different main group elements was previously unknown. In many reactions of the alkynides $L_nM-C\equiv C-R^1$ with triorganoboranes, the M–alkynyl bond is cleaved (Scheme 2). Structure **E**, which is reminiscent of alkynylborates, has been suggested as an intermediate in the formation of **F**.[7] In **E**, which is similar to **C**, the cationic fragment is coordinated side-on to the C≡C bond.

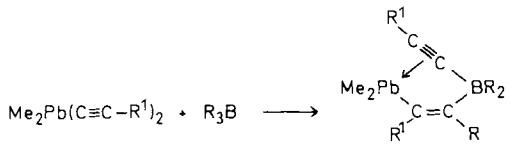


Scheme 2. L_nM = Me_3Si, Me_3Sn, Me_3Pb, $(Et_3P)_2(MeC\equiv C)Pt$; R = alkyl; R^1 = H, alkyl, aryl, L_nM.

We have now been able to detect the intermediates **3** analogous to **E** in the reaction of bis(alkynyl)dimethyl-

[*] Prof. Dr. B. Wrackmeyer, Dipl.-Chem. K. Horchler
Laboratorium für Anorganische Chemie der Universität
Postfach 10 12 51, D-8580 Bayreuth (FRG)
Dr. R. Boese
Institut für Anorganische Chemie der Universität-Gesamthochschule
Universitätsstrasse 5–7, D-4300 Essen 1 (FRG)

[**] This work was supported by the Deutsche Forschungsgemeinschaft and the Fonds der Chemischen Industrie.



(1)

1a: R^1 = Me
1b: R^1 = Bu
1c: R^1 = *t*Bu
1d: R^1 = Ph

2a: R = Et
2b: R = *i*Pr

3a: R^1 = Me, R = Et
3b: R^1 = Me, R = *i*Pr
3c: R^1 = Bu, R = Et
3d: R^1 = Bu, R = *i*Pr
3e: R^1 = *t*Bu, R = Et
3f: R^1 = Ph, R = Et

plumbanes **1** with trialkylboranes **2** [Eq. (1)] by NMR spectroscopy in solution (see Table 1); in addition, we characterised **3b**[8] by X-ray structural analysis[9] (Fig. 1).

Table 1. $^{13}C[J(^{207}Pb^{13}C)]$, ^{11}B and ^{207}Pb NMR data [a] for **3a**, **3b** and **6**–**8**.

	3a [b]	**3b**	**6**	**7**	**8**
Pb–*C*≡	146.1	147.1	150.7	144.0	141.7
	[640.9]	[672.7]	[660.0]	[379.3]	[462.1]
B–*C*≡	181.4	184.0	177.7	164.9	163.8
	[~ 260(br)]	(br)	(br)	(br)	(br)
Pb–*Me*	19.6	18.1	20.8	− 1.4	2.9
	[60.5]	[105.7]	[74.1]	[c]	[119.4]
B–*R*	18.8, 13.0	20.5, 22.4	17.9, 21.0	26.2, 20.8	26.6, 19.8
	br)	(br) 22.6 [d]	(br) 21.2 [d]	(br)	(br)
B–*C*≡*C*–	108.7, 106.6	107.0, 108.5	– [e]	–	–
	(br) [28.0]	(br) [30.0]			
B–C≡C–*R*^{1}	4.2	4.1	–	–	–
	[10.9]	[10.0]			
=C–*R*^{1}	22.5	26.2	27.2	23.5	24.3
	[307.4]	[316.6]	[278.0]	[93.7]	[126.5]
=C–*R*	28.4, 14.5	36.2, 22.1	34.2, 21.7	31.1, 23.0	32.0, 22.6
	[262.7] [28.9]	[304.1] [20.7]	[281.2] [22.9]	[113.4] [10.4]	[136.2] [9.8]
^{11}B	− 8.6	− 2.6 [f]	8.2	76.5	85.2
^{207}Pb	722.7	667.2 [f]	664.1	− 195.0	− 121.8

[a] 10–15% solutions in C_6D_6, Bruker AC 300, 26–28 °C, δ-values vs. Me_4Si (^{13}C) [$\delta(C_6D_6) = 128.0$], Et_2O-BF_3 (^{11}B) and Me_4Pb (^{207}Pb), in each case external; coupling constants $^nJ(^{207}Pb^{13}C)$ in Hz; (br) refers to broad ^{13}C NMR signals from carbons bonded to boron. [b] In [D_8]toluene at −20 °C [$\delta(C_6D_5CD_3) = 20.4$]. [c] Signal broad, since at room temperature the ring inversion is slow on the NMR timescale. [d] The methyl groups are diastereotopic. [e] $\delta(^{13}C(OMe)) = 51.7$ [3.3]. [f] After addition of pyridine (ratio **3b**/pyridine 1/1.5): $\delta(^{11}B) = -6.3$; $\delta(^{207}Pb) = 464.0$ (25 °C), 417 (0 °C), 384 (−20 °C), 363 (−40 °C), 353 (−60 °C).

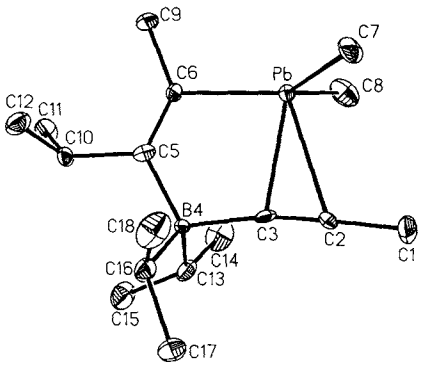
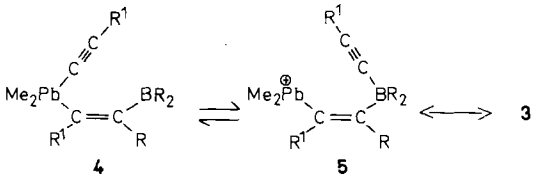


Fig. 1. Structure of **3b** in the crystal (hydrogen atoms not shown). Selected bond lengths [Å] and angles [°]: Pb-C2 2.648(6), Pb-C3 2.467(6), Pb-(mid point C2, C3) 2.487, Pb-C6 2.203(3), Pb-C7 2.222(7), Pb-C8 2.206(7), C1-C2 1.481(10), C2-C3 1.210(10), C3-B4 1.640(10), B4-C5 1.648(8), C5-C6 1.334(9); C6-Pb-C3 81.3(2), C6-Pb-C2 108.3(2), C6-Pb-C7 123.7(2), C6-Pb-C8 118.6(3), C7-Pb-C8 113.4(3), C1-C2-C3 177.3(7), C6-Pb-(mid point C2, C3) 96.5, C8-Pb-(mid point C2, C3) 99.1, C2-C3-B4 169.5(6), C3-B4-C5 111.2(5), B4-C5-C6 125.6(6), C5-C6-Pb 115.6(4), B4-C3-Pb-C6 6.8, C3-C2-Pb-C6 5.8, C3-B4-C5-C6 3.8, B4-C5-C6-Pb 2.7.

The first step of the reaction (formation of **4**, analogous to the transformation of **E** into **F**) is followed by a rapid intramolecular transfer of the alkynyl residue from the lead to the boron atom, giving the alkynylborate anion and the triorganolead cation, i.e. the mesomeric structure **5** (Scheme 3).

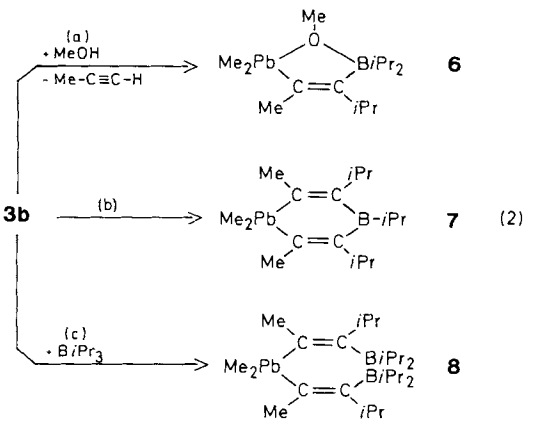


Scheme 3.

The cationic center in **5** is stabilized by the asymmetric side-on coordination of the lead atom to the C≡C bond; the lead atom thus achieves a distorted tetrahedral geometry, and the resulting ring is nearly planar. This confirms experimentally the mechanistic ideas presented earlier[7] for the 1,1-organoboration reaction and should thus be a suitable model for other borations,[10] as well as for many reactions of alkynyltriorganoborates with electrophiles.[11] The relative stability of the zwitterionic intermediate (Type **E**) as a function of the groups L_nM, R^1 and R provides an explanation for the reversibility of the 1,1-organoboration previously observed (where **F** reverts to **E** and to the starting materials).[7b]

The presence of **3** is demonstrated qualitatively by the ^{207}Pb NMR spectra of the reaction mixtures (δ_{Pb}^{207} = 630–750, shifted by $\Delta\delta$ 600–800 to lower field with respect to tetraorganoplumbanes[12]). The δ_B^{11} values are typical for tetracoordinated boron,[13] while the δ_C^{13} (C≡C) values are characteristic of the B–C≡C–R^1 group, the signal for the carbon atom bound to boron being extremely broad.[13] The agreement between the positions of the ^{13}C and ^{207}Pb signals of **3b** in solution and in the solid state[14] shows that the main features of the structure are retained in solution.

Compounds **3** decompose on warming above 40 °C (lead is deposited from **3a** even at 10–20 °C) and are very reactive; thus **3b** reacts with methanol to give **6**,[15a] undergoes intramolecular rearrangement to **7**,[15b] and yields **8** on treatment with further triisopropylborane[15c] [Eq. (2a)–(2c)]. The electrophilic nature of the lead atom is made clear by the interaction of **3b** with pyridine: the ^{207}Pb resonance of the complex is shifted by more than $\Delta\delta$ = 200 to lower frequencies.



(2)

The clean formation of **8** confirms that **3** is produced reversibly. With the exception of R^1 = *t*Bu and R = Et, it is

not possible to observe the formation of intermediates in reactions between BR_3 and bis(alkynyl)dimethylstannanes **1**, where Sn is used instead of Pb. In such reactions we only observe products corresponding, for example, to **7**[16b] and **8**.[16c]

Received: July 5, 1989 [Z 3426 IE]
German version: *Angew. Chem. 101* (1989) 1563.

CAS Registry numbers:
1a, 35369-90-5; **1b**, 123100-83-4; **1c**, 123100-84-5; **1d**, 123100-85-6; **2a**, 97-94-9; **2b**, 1776-66-5; **3a**, 123100-89-0; **3b**, 123100-90-3; **3c**, 123100-91-4; **3d**, 123100-92-5; **3e**, 123100-93-6; **3f**, 123100-94-7; **6** [B^{III}], 123100-88-9; **6** (chelate), 123100-95-8; **7**, 123100-86-7; **8**, 123100-87-8; ^{207}Pb, 14119-29-0; ^{11}B, 14798-13-1.

[1] a) R. Nast, *Coord. Chem. Rev. 47* (1982) 89; b) A. J. Carty, *Pure Appl. Chem. 54* (1982) 113; c) G. Consiglio, F. Morandini, *Chem. Rev. 87* (1987) 761, d) E. Sappa, A. Tiripicchio, P. Braunstein, *Coord. Chem. Rev. 65* (1985) 219; e) G. Erker, W. Frömberg, R. Mynott, B. Gabor, C. Krüger, *Angew. Chem. 98* (1986) 456; *Angew. Chem. Int. Ed. Engl. 25* (1986) 463; f) P. M. Fritz, K. Polborn, M. Steinmann, W. Beck, *Chem. Ber. 122* (1989) 889; g) H. Ogawa, K. Onitsuka, T. Joh, S. Takahashi, Y. Yamamoto, N. Yawasaki, *Organometallics 7* (1988) 1257.

[2] a) B. Schubert, U. Behrens, E. Weiss, *Chem. Ber. 114* (1981) 2640; b) A. Meller, W. Maringgele, G. Elter, D. Bromm, M. Noltemeyer, G. M. Sheldrick, *ibid. 120* (1987) 1437.

[3] a) N. A. Bell, I. W. Nowell, H. M. M. Shearer, *J. Chem. Soc. Chem. Commun. 1982*, 147; b) G. D. Stucky, A. M. McPherson, W. E. Rhine, J. J. Eisch, J. L. Considine, *J. Am. Chem. Soc. 96* (1974) 1941; c) B. Tecle, W. H. Ilsley, J. P. Oliver, *Inorg. Chem. 20* (1981) 2335; d) P. N. V. P. Kumar, E. D. Jemmis, *J. Am. Chem. Soc. 110* (1988) 125.

[4] M. Geissler, J. Kopf, M. Schubert, E. Weiss, W. Neugebauer, P. von R. Schleyer, *Angew. Chem. 99* (1987) 569; *Angew. Chem. Int. Ed. Engl. 26* (1987) 587.

[5] N.-G. Vannerberg, *Acta. Chem. Scand. 15* (1961) 769; *ibid. 16* (1962) 1212.

[6] A. Sebald, B. Wrackmeyer, C. R. Theocharis, W. Jones, *J. Chem. Soc. Dalton Trans.* (1984) 747.

[7] a) B. Wrackmeyer, *Rev. Silicon Germanium Tin Lead Compds. 6* (1982) 75; b) B. Wrackmeyer in S. Hermanek (Ed.): *Boron Chemistry*, World Scientific, Singapore 1987, pp. 387–415; c) B. Wrackmeyer, *J. Organomet. Chem. 364* (1989) 331; d) *Organometallics 3* (1984) 1; e) *J. Chem. Soc. Chem. Commun.* (1988) 1624.

[8] General preparation of **3** as for **3b**: a solution of 1.96 g (6.2 mmol) **1a** in 25 mL hexane/benzene (3:1) is cooled to −40 °C, treated with 0.88 g (6.3 mmol) **2b** and allowed to warm slowly to room temperature with constant stirring. Solvents and traces of excess **2b** are removed in vacuo. The colorless crystalline residue is recrystallized from a small amount of hexane. Yield of **3b** 2.75 g (97%), mp = 50 °C (dec.) ^{1}H NMR ... (300 MHz, C_6D_6): $\delta(^1H)$ [$^nJ(^{207}Pb^1H)$] = 0.88 [26.5] (s, 6H; $PbMe_2$), 1.23 m, 1.29(d), 1.35 (d, 14H; $BiPr_2$), 1.46 [10.0] (s, 3H; ≡C-Me), 1.86 [218.5] (s, 3H; =C-Me), 2.87 [30.0] (Sept), 1.39 [12.4] (d, 7H; =C-*i*Pr). $\delta(^{207}Pb)/\delta(^{11}B)$ **3c**: 751.0/−8.2; **3d**: 715.0/−3.1; **3e**: 632.0/−3.2; **3f**: 668.0/−5.7.

[9] X-ray structure analysis of **3b** at 110 K: monoclinic, $P2_1/n$, a = 8.961(2), b = 15.065(2), c = 14.328(2) Å β = 103.78(1)°, V = 1878.7(5) Å^3, Z = 4, ϱ_{ber} = 1.610 g cm^{-3}, μ = 90.4 cm^{-1}. $Mo_{K\alpha}$ irradiation (graphite monochromator), 4286 independent reflexions, for 3766 of which $F_o > 4.\sigma(F_o)$, $2^\circ \le 2\theta \le 55^\circ$, empirical absorption correction, min./max. transmission 0.45/1.00, 221 parameters, R = 0.040, R_w = 0.038. Further details of the crystal structure analysis can be obtained from the Fachinformationszentrum Karlsruhe, Gesellschaft für wissenschaftlich-technische Information GmbH, D-7514 Eggenstein-Leopoldshafen 2, on quoting the deposition number CSD-54078, the authors and the journal citation.

[10] a) H. Klusik, C. Pues, A. Berndt, *Z. Naturforsch. B 39* (1984) 1042; b) R. J. Binnewirtz, H. Klingenberger, R. Welte, P. Paetzold, *Chem. Ber. 116* (1983) 1271.

[11] a) R. Köster, *Pure Appl. Chem. 49* (1977) 765; b) A. Pelter, *Chem. Soc. Rev. 11* (1982) 191; c) A. Suzuki, *Acc. Chem. Res. 15* (1982) 178; d) K. K. Wang, K.-H. Chu, Y. Lin, J.-H. Chen. *Tetrahedron 45* (1989) 1105.

[12] B. Wrackmeyer, K. Horchler, *Annu. Rep. NMR Spectrosc. 22*, in press.

[13] a) B. Wrackmeyer, R. Köster in *Houben-Weyl-Müller: Methoden der Organischen Chemie, Band XIII/3c*, 4th ed., Thieme, Stuttgart 1984, pp. 377–611; b) B. Wrackmeyer, *Annu. Rep. NMR Spectrosc. 20* (1988) 61.

[14] 75.5-MHz ^{13}C and 62.8-MHz ^{207}Pb CP/MAS NMR spectra (Bruker MSL 300) of **3b**; we thank Dr. *A. Sebald* for measurement.

[15] a) **6**: after 12 h at room temperature in hexane, **3b** and methanol (ratio 1:1.5) yield **6** as a colorless solid after removal of volatile materials. (dec. 82 °C). ^{1}H NMR: (300 MHz, C_6D_6): $\delta(^1H)$[$^nJ(^{207}Pb^1H)$] = 0.87 [33.5] (s, 6H; $PbMe_2$), 1.05 (m), 1.09 (d, 14H; $BiPr_2$), 2.02 [204.7] (s, 3H; =C-Me), 2.79 (sept), 1.26 [10.0] (d, 7H; =C-*i*Pr), 3.20 [6.2] (s, 3H;OME); b) **7**: when a solution of **3b** in hexane is heated to 65 °C for 4 h, a cloudy yellow solution is obtained and lead is deposited. After filtration and removal of volatile materials in vacuo, the residue is isolated as a yellow oil consisting of ca. 85% **7** (plus unidentified organic products). ^{1}H NMR: (300 MHz, C_6D_6): $\delta(^1H)$[$^nJ(^{207}Pb^1H)$] = 0.78 [56.0] (br s, 6H; $PbMe_2$), 1.70 (sept). 1.08 (d, 7H; B-*i*Pr), 2.22 [94.3] (s, 6H; =C-Me), 2.84 [7.2] (sept), 1.21 [4.1] (d, 14H; =C-*i*Pr); c) **8**: stirring a solution of **3b** in hexane in the presence of excess **2b** at room temperature for 24 h leads to the quantitative formation of **8** obtained as a colorless oily liquid on removal of volatile materials. ^{1}H-NMR (300 MHz, C_6D_6): $\delta(^1H)$[$^nJ(^{207}Pb^1H)$] = 0.63 [46.3] (s, 6H; $PbMe_2$), 1.41 (sept), 1.09 (d, 28H; $BiPr_2$), 2.19 [102.0] (s, 6H; =C-Me), 2.60 (sept), 1.08 (d, 14H; =C-*i*Pr).

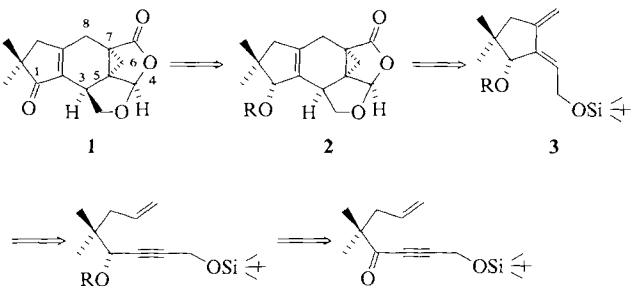
[16] a) L. Killian, B. Wrackmeyer, *J. Organomet. Chem. 148* (1978) 137; b) *ibid. 153* (1978) 153; c) S. Kerschl, B. Wrackmeyer, *Z. Naturforsch. B 39* (1984) 1037.

The Effect of Acetylene Substituents on a Pd^{II}-Catalyzed Cycloisomerization. Total Synthesis of (−)-Sterepolide and Assignment of Absolute Stereochemistry

By *Barry M. Trost,* Philip A. Hipskind, John Y. L. Chung, and Chuen Chan*

The curious biological and biochemical questions posed by sesquiterpenoid fungal metabolites enhance interest in their absolute stereochemistry and synthesis. The biosynthesis of cyclopentane-containing sesquiterpenes indicates that different classes arise by enantiomeric folding of farnesyl pyrophosphate by the various sesquiterpene synthetases.[1] Among the cyclopentane sesquiterpenes, the isolactaranes,[2] represented by isolactarorufin,[3] merulidial,[4] and sterepolide **1**,[5] constitute a relatively rare class compared to the more common and frequently co-occurring lactaranes. We therefore undertook an asymmetric synthesis of **1**[6] in order to develop a facile strategy to enantiomerically pure members of this family—a strategy which also might be modified to apply to related families such as marasmanes, illudanes, and sterpuranes—as well as to establish its absolute configuration.

In considering a strategy based upon an enyne cyclization as outlined in Scheme 1, we envision an intermediate **2** in



1 **2** **3** **4** **5**

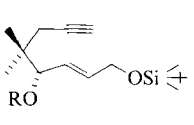
Scheme 1. R = *p*-methoxybenzyl.

[*] Prof. B. M. Trost, P. A. Hipskind, J. Y. L. Chung, C. Chan
Department of Chemistry, Stanford University
Stanford, CA 94305 (USA)
and
Department of Chemistry, University of Wisconsin
Madison, WI 53706 (USA)

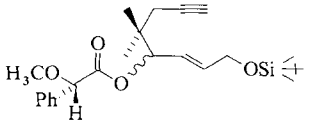
[**] We thank the National Institutes of Health, General Medical Sciences, for their generous support of our programs. We are specially grateful to Prof. *W. Ayer* for an authentic sample of (−)-sterepolide. Mass spectra were gratefully provided by the Mass Spectrometry Facility, University of California, San Francisco, supported by the NIH Division of Research Resources.

which C-1 becomes a stereogenic center. All the stereogenic centers of **1** are derived by propagation of the stereogenic center of diene **3** via a diastereoselective Diels–Alder reaction. The success of this sequence depends upon the ease of accessibility of enantiomerically pure diene **3**. The excellent enantioselective reductions of acetylenic ketones (cf. **5**)[7] made the enyne **4** the substrate of choice for a Pd^{II}-catalyzed cycloisomerization.

In our synthesis of racemic **1**,[6] we employed the related enyne substrate **6**, since our early work showed that substrates bearing alkyl substituents at the acetylenic terminus



6



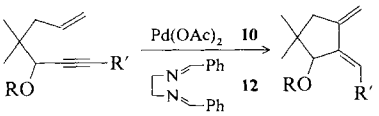
7: (*S*)
8: (*R*)

failed to react.[8] The awkwardness of a scalemic[9] synthesis via an enyne such as **6**, because of the difficulties in carrying out an asymmetric synthesis except through a resolution of the *O*-methylmandelate esters **7** and **8**, led us to reconsider the feasibility of expanding the scope of our Pd^{II}-catalyzed enyne cyclization to substrates containing disubstituted acetylenes.[10] The formation of 1,3-dienes, substrates for subsequent cycloaddition chemistry, provides further impetus for this study.

The substrate **9** offers a convenient template to explore the effect of the acetylene substituent on the efficacy of the cyclization. With palladium acetate **10** or bis(triarylphosphane)palladium acetate **11** as catalyst, poor reactions

$Pd(OAc)_2$ **10** $[Pd(Aryl_3P)_2(OAc)_2]$ **11**

occur with $R' = CH_3$, $SiMe_3$, Cl, SPh, CH_2SPh. When R′ is a strong electron-withdrawing group like acetyl, cyclization



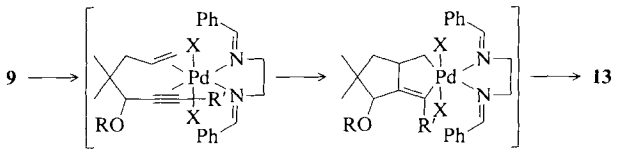
9 **13**

$R = p\text{-}H_3COC_6H_4CH_2$

a: $R' = COCH_3$, **b**: $R' = CH_2OCH_3$, **c**: $R' = CH_2CH_2OCH_3$, **d**: $R' = SiMe_3$, **e**: $R' = CH_3$, **f**: $R' = OC_2H_5$

proceeds with **11** (aryl = phenyl or *o*-tolyl) but in only 20–40% yield.[11] Decreasing the electron-withdrawing capability of the substituent by switching to methoxymethyl or even more so by switching to methoxyethyl still affords low yields of **13**, and mixtures of isomeric products result. Furthermore, the rate of the reaction depends critically on the quality of complex **11**.

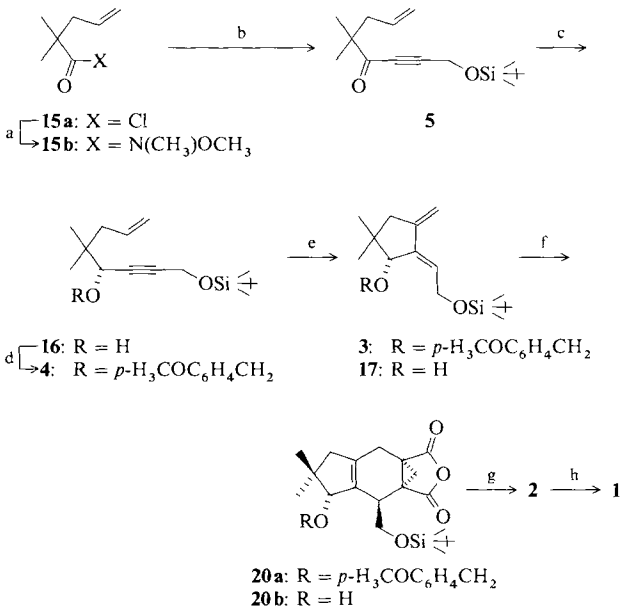
A dramatic change in the prospects of this cycloisomerization occurs by changing the ligands to *N*,*N*′-bis(benzylidene)ethylenediamine **12**.[12] For the acetyl substrate **9a**, the yield of **13a**[13] jumped to 67%. Most importantly, the other substrates, which either failed to react or led to mixtures of isomeric products, smoothly cyclize (substrate, % yield of cyclization product: **9b**, 77%; **9c**, 96%; **9d**, 89%; **9e**, 88%; **9f**, 32%).[13] In a typical reaction, a 0.2 M solution of substrate in benzene containing 5–15 mmol% each of **12** and palladium acetate **10** is heated at 60 °C. After complete reaction, the mixture is directly chromatographed to give **13**. A possible rationale for the remarkable role of ligand **12** on the efficacy of the cyclization compared to phosphane ligands invokes a mechanism (Scheme 2) in which this ligand can be thought to stabilize a Pd^{IV} species[14] much more effectively than the triarylphosphane ligands.[15]



14a **14b**

Scheme 2. R = *p*-methoxybenzyl; for R′ see above.

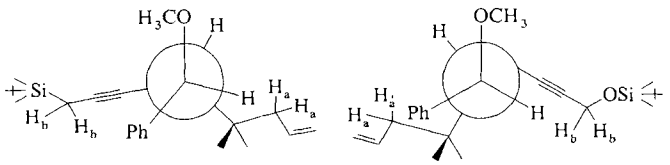
The successful cyclization of disubstituted acetylenic substrates led to a scalemic synthesis of the requisite diene **3** from the known acid chloride **15a** (Scheme 3).[16] Addition



Scheme 3. Synthesis of (−)-sterepolide **1**. a) $CH_3NHOCH_3 \cdot HCl$, pyridine, $CHCl_3$, 0 °C → RT, 96%. b) $LiC{\equiv}CCH_2OSiMe_2tBu$, THF, −78 °C, 98%. c) $LiAlH_4$/Darvon alcohol complex, ether, −100 °C, 100%, >98% *ee*. d) NaH, *p*-H_3C-$C_6H_4CH_2Br$, cat. Bu_4NI, THF, RT, 82%. e) 5% $Pd(OAc)_2$ **10**, 10% **12**, benzene, 70 °C, 81%. f) 1) 2-Bromomethylmaleic anhydride, benzene, 80 °C; 2) DBU, benzene, RT, 81%. g) Two steps (see [6]), 64%. h) Dichlorodicyano-*p*-benzoquinone, CH_2Cl_2, H_2O, then Pd/C, CH_2Cl_2, 85%.

of a 1.9 M solution of ketone **5** in ether to a 0.095 M solution of the $LiAlH_4$/Darvon alcohol complex at −100 °C at a rate of 10 mL h^{-1} gave a quantitative yield of the alcohol **16**. Assessment of the enantiomeric excess as >98% (NMR and VPC) and assignment of absolute configuration as *R* (NMR) rests upon analysis of the *O*-methylmandelate esters **18** and **19** of the two protected enantiomeric alcohols **4** (Scheme 4) which are shown in extended Newman projections (**18**, $\delta = 2.05$ (H_a), 4.23 (H_b); **19**, $\delta = 1.79$ (H_a), 4.34 (H_b)).[17] The assignment of the *R* configuration also derives from ample precedent in the Mosher reduction of acetylenic ketones.[7]

Gratifyingly, the **12**–$Pd(OAc)_2$ complex smoothly catalyzes the cycloisomerization of **4** to enantiomerically pure



18 19

Scheme 4. Esters **18** and **19**.

diene **3**.[13] Propagation of the stereochemical information of the carbinol center of **3** to the stereogenic centers of sterepolide **1** depends upon the diastereofacial selectivity of the Diels–Alder reaction, which we suspected would depend upon the choice of O substituent. Based upon the notion of a possible (but controversial) π-stacking interaction to direct the dienophile on the face of the diene distal to oxygen,[18] we chose the *p*-methoxybenzyl group. Indeed, cycloaddition with diene **3** followed by cyclopropyl ring closure produces a single diastereomeric tetracyclic anhydride **20a**. On the other hand, a similar sequence from diene **17** produces a 5:4:1 ratio of diastereomeric tetracyclic products. Completion of the synthesis following the protocol in the racemic series[6] produces (−)-**1**/m.p. 226–227 °C, $[\alpha]_x^{28}$ ($c = 0.56$, $CDCl_3$), x = Na D line, −112.7°; x = 557 nm, −113.2°; x = 546 nm, −130.4°; x = 435 nm, −234.3°; x = 405 nm, −275.4°).

Since the rotation of the natural product had not been recorded, we measured its rotation on a sample kindly supplied by *W. Ayer*. The excellent agreement of its rotation ($[\alpha]_D^{28}$ −111.4° ($c = 0.63$, $CDCl_3$)) with that of our synthetic sample, as well as a sharp mixed melting point (227–227.5 °C), confirm the identity of the two samples and establishes the absolute configuration depicted in Scheme 1. This assignment indicates that the isolactaranes derive from the same enantiomeric folding of the farnesyl pyrophosphate as has been established for the sterpuranes, illudanes, and marasmanes.

This facile route produces enantiomerically pure (−)-sterepolide **1** in 11 steps and 34% overall yield. In this strategy, a carbinol center, whose stereochemistry is ultimately destroyed in the final product, becomes a convenient stereochemical control element since its stereochemistry readily derives from asymmetric carbonyl reductions. Most importantly, the development of the *N,N'*-bis(benzylidene)ethylenediamine ligand **12** greatly extends the scope of this novel palladium-catalyzed cycloisomerization. The l-substituted dienes **13**, especially those bearing the l-ethoxy (**13f**) and l-trimethylsilyl (**13d**) substituents, are particularly valuable building blocks for further ring construction via cycloadditions.

Received: June 26, 1989 [Z 3413 IE]
German version: *Angew. Chem. 101* (1989) 1559

[1] For a review see D. E. Cane, *Acc. Chem. Res. 18* (1985) 220; for some recent papers see D. E. Cane, D. B. McIlwaine, P. H. M. Harrison, *J. Am. Chem. Soc. 111* (1989) 1152; C. Abell, A. P. Leech, *Tetrahedron Lett. 29* (1988) 4337.
[2] W. A. Ayer, L. M. Browne, *Tetrahedron 37* (1981) 2199; W. Steglich, *Pure Appl. Chem. 53* (1981) 1233.
[3] W. M. Daniewski, M. Kocor, S. Thoren, *Polish J. Chem. 52* (1978) 561.
[4] (a) B. Giannetti, B. Steffan, W. Steglich, W. Quack, T. Anke, *Tetrahedron 12* (1986) 3579; (b) The 8 *S* configuration for merulidial has been suggested by using *Horeau's* method.
[5] W. A. Ayer, M. H. Saeedi-Ghomi, *Tetrahedron Lett. 22* (1981) 2071.
[6] A racemic synthesis has been previously recorded. B. M. Trost, J. Y. L. Chung, *J. Am. Chem. Soc. 101* (1985) 4586. For the desilylation of **20**, we now prefer tetrabutylammonium fluoride in THF, at room temperature and the subsequent disiamylborane reduction is best performed in ether.
[7] S. Yamaguchi, H. S. Mosher, *J. Org. Chem. 38* (1973) 1870; R. S. Brinkmeyer, V. M. Kapoor, *J. Am. Chem. Soc. 99* (1977) 8339. Also see P. A. Wender, N. C. Ihle, C. R. D. Correia, *J. Am. Chem. Soc. 110* (1988) 5904.
[8] (a) B. M. Trost, M. Lautens, *J. Am. Chem. Soc. 107* (1985) 1781. (b) M. Lautens, *Ph. D. Thesis*, University of Wisconsin, 1985.
[9] C. H. Heathcock, B. L. Finkelstein, E. T. Jarvi, P. A. Radel, C. R. Hadley, *J. Org. Chem. 53* (1988) 1922. As referenced by *Heathcock*, the term "scalemic", suggested by *Brewster*, denotes unequal mixtures of enantiomers.
[10] For an alternative approach see B. M. Trost, D. C. Lee, *J. Am. Chem. Soc. 110* (1988) 7255.
[11] In preliminary work, the viability of a substrate bearing a methoxycarbonyl group has been established; see [8b].
[12] B. M. Trost, D. J. Jebaratnam, *Tetrahedron Lett. 28* (1987) 1611.
[13] All new compounds have been fully characterized spectrally and their elemental compositions have been established by high-resolution mass spectroscopy and/or combustion analysis.
[14] While the mechanism of this reaction has yet to be established, at least two pathways are feasible, one of which invokes an intermediate analogous to **14b**. See B. M. Trost, G. J. Tanoury, *J. Am. Chem. Soc. 109* (1987) 4753; B. M. Trost, D. C. Lee, F. Rise, *Tetrahedron Lett. 30* (1989) 651.
[15] For a recent claim of nitrogen ligands facilitating formation of Pd^{IV}, see P. K. Byers, A. J. Canty, *J. Chem. Soc. Chem. Commun. 1988*, 639.
[16] D. J. Hart, T. Yang, *J. Org. Chem. 50* (1985) 235.
[17] B. M. Trost, J. L. Belletire, S. Godleski, P. McDougal, J. M. Balkovec, J. J. Baldwin, M. E. Christy, G. S. Ponticello, S. L. Varga, J. P. Springer, *J. Org. Chem. 51* (1986) 2370.
[18] This concept has been quite controversial. See B. M. Trost, D. O'Krongly, J. L. Belletire, *J. Am. Chem. Soc. 102* (1980) 7595; D. A. Evans, K. T. Chapman, J. Bisaha, *J. Am. Chem. Soc. 110* (1989) 1238; C. Siegel, E. R. Thornton, *Tetrahedron Lett. 29* (1988) 5225.

Application of the Dimethyl(phenyl)silyl Group as a Masked Form of the Hydroxy Group in the Synthesis of an L-*glycero*-α-D-*manno*-heptopyranoside-Containing Trisaccharide from the Dephosphorylated Inner Core Region of *Neisseria meningitidis***

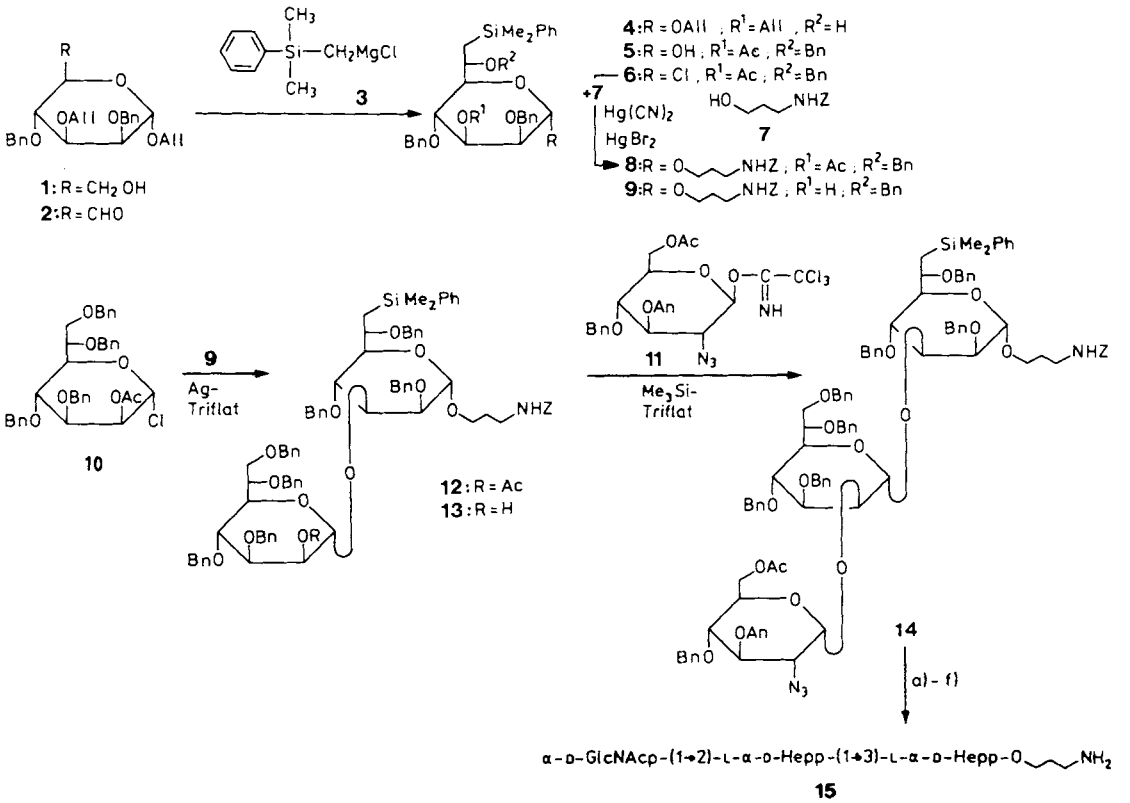
By *G. J. P. H. Boons, M. Overhand, G. A. van der Marel,* and *J. H. van Boom**

Recently, the structures of the largest dephosphorylated oligosaccharides of the L2, L3 and L5 serotype lipopolysaccharides (LPS) of *Neisseria meningitidis* have been elucidated.[1] It was illustrated that the core region consisted of a structurally invariant outer core lacto-N-neotetraose unit and an inner core region showing microheterogeneity. Immunological studies indicated[2] that the determinants responsible for LPS serotype specificity and LPS cross-reactivity resided largely in the inner core of oligosaccharides and, further, that the presence of ethanolamine phosphate substituents in native LPS is not a major serological factor. In order to study the antigenicity of the inner core region and the specificity of antibodies raised against this antigenic region, we report the synthesis of an inner core dephosphorylated L5 trisaccharide containing a spacer suitable for conjugation with macromolecular carriers (Scheme 1).

An essential element in a synthetic route to **15** is the availability of suitably protected L-*glycero*-D-*manno*-heptopyranoside (L-D-Hepp) building blocks. Earlier studies indicated[3] that the diastereoselective hydroxymethylene extension of allyl α-D-*manno*-hexodialdo-1,5-pyranoside **2**

[*] Prof. Dr. J. H. van Boom, Drs. G. J. P. H. Boons, M. Overhand, Dr. G. A. van der Marel
Gorlaeus Laboratories
P.O. Box 9502, NL-2300 RA Leiden (The Netherlands)

[**] This work was supported by the WHO Program for Vaccine Development.



Scheme 1. a) Dioxane, CH_3OH, 4N NaOH (29:9:2, v/v), 3 h, 50 °C. b) Pyridine, $(CH_3CH_2)_3N$, H_2O (30:10:1, v/v), H_2S, 18 h, 20 °C. c) Ac_2O, pyridine (1:1, v/v), 3 h, 20 °C. d) AcOH, AcOOH, NaOAc, KBr, 2 h, 10–20 °C. e) CH_3OH, $NaOCH_3$. f) PdC, 18 h, 1 bar. Ag- and Me_3Si-triflate = silver and trimethylsilyl trifluoromethanesulfonate, respectively. All = allyl, Bn = benzyl, An = anisoyl, Z = benzyloxycarbonyl.

with the Grignard reagent **3** could be expected to give access to the key L-D-Hepp derivative **4** having at C-7 the dimethyl(phenyl)silyl group as a masked form of the hydroxy group. Thus Swern oxidation of **1**, prepared in an overall yield of 30% starting from allyl α-D-mannopyranoside,[4] and subsequent treatment of **2** with **3** afforded **4** in very good diastereomeric purity[3] (≥95%) and in 70% yield [$[\alpha]_D^{20} = +26.9$ ($c = 0.99$, $CHCl_3$)]. The latter was converted into **5** (overall yield of 42%) by the following well-established procedures: benzylation,[5] one-step deallylation,[6] acetylation and finally regioselective deacetylation.[7] Treatment of **5** with the Vilsmeier reagent[8] (chlorodimethylformamidinium chloride) furnished **6** which was coupled in situ with **7**, under Helferich conditions[9] in ether, to afford **8** [76% yield $[\alpha]_D^{20} = +32.4$ ($c = 1.05$, $CHCl_3$); 300 MHz ^1H NMR ($CDCl_3$, TMS): $\delta = 4.90$ (1-H, $J_{1,2} = 3.0$ Hz), 5.17 (3-H, $J_{2,3} = 2.0$ Hz, $J_{3,4} = 7.5$ Hz), 1.35 (7a-H and 7b-H)]. Zemplén deacetylation of **8** resulted in the quantitative isolation of **9**.

Ag-triflate[10] promoted glycosidation (in the absence of base) of acceptor **9** with donor **10**, obtained by a similar[11] silane-mediated hydroxymethylene process, furnished disaccharide **12** [72% yield, $[\alpha]_D^{20} = +19.8$ ($c = 1.0$, $CHCl_3$); 300 MHz ^1H NMR ($CDCl_3$, TMS): $\delta = 5.12$ (1-H, $J_{1,2} = 1.5$ Hz), 4.87 (1-H, $J_{1,2} = 2.0$ Hz), 1.36 (7a-H and 7b-H)].

Glycosyl imidate donor **11** was prepared in three steps (overall yield of 73%) by acetolysis[12] of 1,6-anhydro-2-azido-2-deoxy-3-*O*-anisoyl-4-*O*-benzyl-β-D-glucopyranose[13] followed by deacetylation[7] at C-1 and subsequent treatment[14] with trichloroacetonitrile in the presence of potassium carbonate.

Disaccharide **12** was converted to **13** by Zemplén deacetylation and coupled in the presence of trimethylsilyltriflate[15] and 4 Å molecular sieves (CH_2Cl_2) with the glycosyl donor **11**, to afford the fully-protected trisaccharide **14** [92% yield, $[\alpha]_D^{20} = +83.8$ ($c = 1.0$, $CHCl_3$); 300 MHz ^1H NMR ($CDCl_3$, TMS): $\delta = 5.27$ (1′-H, $J_{1,2} = 1.5$ Hz), 4.79, 4.71 (1″-H, $J_{1,2} = 3.0$), 1.36 (7a-H and 7b-H)].

For the deblocking of **14** the base labile groups are cleaved with NaOH. Subsequent reduction of the azido group with H_2S[16] is then followed by reacetylation of the amine and the two hydroxy functions with acetic anhydride. The Ph-Me_2Si moiety at C-7 is now unmasked[17] in the dark with KBr and AcOOH, and the two *O*-acetyl groups are subsequently removed under Zemplén conditions. Finally, the benzyloxycarbonyl and benzyl groups are cleaved hydrogenolytically in *tert*-butyl alcohol-water-acetic acid (5:1:1), and crude **15** thus obtained is purified on Sephadex LH-20. The overall yield of this six-step conversion from **14** to the deblocked and α-glycosidically linked trisaccharide **15** is 30% [$[\alpha]_D^{20} = +103.7$ ($c = 1.0$ H_2O); 300 MHz ^1H NMR (D_2O, referred to HDO, $\delta = 4.75$): $\delta = 5.34$ (1′-H, $J_{1,2} = 1.5$ Hz), 5.07 (1″-H, $J_{1,2} = 3.5$ Hz), 4.81 (1-H, $J_{1,2} = 1.5$ Hz)]. These values agree with the data of other L-D-Hepp containing oligosaccharides obtained via a different route[18] and with those of the natural product which, apart from the artificial spacer, contain this sequence.[1b]

The example demonstrates that the dimethyl(phenyl)silyl masking group is not only compatible with manipulations frequently applied in sugar chemistry to achieve selective protection of hydroxy groups, but also with reliable and highly stereoselective glycoside coupling procedures.

Received: June 7, 1989 [Z 3381 IE]
German version: *Angew. Chem. 101* (1989) 1538

CAS Registry numbers:
1, 123149-75-7; **2**, 123149-76-8; **3**, 107735-20-6; **4**, 123149-77-9; **5**, 123149-78-0; **6**, 123149-79-1; **7**, 34637-22-4; **8**, 123149-80-4; **9**, 123149-81-5; **10**, 116302-70-6; **11**, 123149-82-6; **12**, 123149-83-7; **13**, 123149-84-8; **14**, 123149-85-9; **15**, 123149-86-0; 1,6-anhydro-2-azido-2-desoxy-3-*o*-anisoyl-4-*o*-benzyl-β-D-glucopyranose, 123149-87-1; trichloroacetonitrile, 545-06-2.

[1] a) H. J. Jennings, M. Beurret, A. Gamian, F. Michon, *Antonie van Leeuwenhoek 53* (1987) 519; b) H. J. Jennings, K. G. Johnson, L. Kenne, *Carbohydr. Res. 121* (1983) 233; c) J. McLeod Griffis, H. Schneider, R. E. Mandrell, R. Yamasaki, G. A. Jarvis, J. J. Kim, B. W. Gibson, R. Hamaden, M. A. Apicella, *Rev. Infect. Dis. 10* (suppl. 2), (1988) S287.

[2] H. J. Jennings, C. Lugowski, F. E. Ashton, *Infect. Immun. 43* (1984) 407.

[3] G. J. P. H. Boons, G. A. van der Marel, J. H. van Boom, *Tetrahedron Lett. 30* (1989) 229.

[4] A. Y. Chernyak, A. B. Levinsky, B. A. Dmitriev, N. K. Kochetkov, *Carbohydr. Res. 128* (1984) 269.

[5] S. Czernecki, G. Georgoulis, C. Provelenghion, *Tetrahedron Lett. 1976*, 3535.

[6] R. Boss, R. Scheffold, *Angew. Chem. 88* (1976) 578; *Angew. Chem. Int. Ed. Engl. 15* (1976) 558.

[7] G. Excoffier, D. Gagnaire, J.-P. Utille, *Carbohydr. Res. 39* (1975) 368.

[8] H. H. Bossard, R. Mory, M. Schmidt, H. Zollinger, *Helv. Chim. Acta 42* (1959) 1653.

[9] B. Helferich, W. Olst, *Chem. Ber. 95* (1962) 2612; b) H. M. Flowers, *Methods Carbohydr. Chem. 6* (1972) 474.

[10] S. Hanessian, J. Banoub, *Carbohydr. Res. 53* (1977) C13–C16.

[11] G. J. P. H. Boons, P. A. M. van der Klein, G. A. van der Marel, J. H. van Boom, *Recl. Trav. Chim. Pays-Bas 107* (1988) 507; Compound **10** was prepared earlier by *Paulsen* et al. (see [18a]) via a different route.

[12] H. Paulsen, O. Lockhoff, *Chem. Ber. 114* (1981) 3102.

[13] M. Kloosterman, M. P. de Nijs, J. H. van Boom, *J. Carbohydr. Chem. 5* (1986) 215.

[14] R. R. Schmidt, J. Michel, M. Roos, *Liebigs Ann. Chem. 1984*, 1343.

[15] W. Kinzy, R. R. Schmidt, *Liebigs Ann. Chem. 1985*, 1537.

[16] P. J. Garegg, M. Haraldsen, H. Lönn, T. Norberg, *Glycoconjugate J. 4* (1987) 231.

[17] I. Flemming, P. E. J. Sanderson, *Tetrahedron Lett. 28* (1987) 4429.

[18] a) H. Paulsen, A. C. Heitmann, *Liebigs Ann. Chem. 1988*, 1061; b) H. Paulsen, A. Wulff, A. C. Heitmann, *ibid. 1988*, 1073; c) K. Driewiszek, A. Banaszek, A. Zamojski, *Tetrahedron Lett. 28* (1987) 1569.

The Acetonitrile(pentafluorophenyl)xenon(II) Cation, $[MeCN–Xe–C_6F_5]^{\oplus}$: The First Structural Characterization of a Xenon–Carbon Bond**

By *Hermann Josef Frohn,* Stephanus Jakobs,* and *Gerald Henkel*

Since the synthesis of the first noble-gas compound in 1962,[1,2] xenon compounds containing Xe–F, Xe–O, and Xe–N bonds have been unambiguously characterized. The first Xe–C compound, $Xe(CF_3)_2$, reported by *Lagow* et al.[3] in 1979, has not been satisfactorily characterized by physical and spectroscopic data, nor is its identity supported by chemical reactions. In 1988 we isolated the Xe^{II} compound $[(C_6F_5Xe]^{\oplus}[C_6F_5BF_3]^{\ominus}$, characterized it in solution by ^{129}Xe and ^{19}F NMR spectroscopy, and verified the Xe–C bond by specific reactions.[4] Here we describe the synthesis, the molecular structure, the ^{129}Xe, ^{19}F, ^{13}C, and ^{11}B solution NMR spectra, and the reactivity of **1**, a further Xe–C compound. For the first time, we have succeeded in determining a Xe–C bond length and the distance between Xe^{II} and the nitrogen atom of a coordinated N base.

$[MeCN–Xe–C_6F_5]^{\oplus}[(C_6F_5)_2BF_2]^{\ominus}$ **1**

Low-temperature reaction of XeF_2 with $B(C_6F_5)_3$ in noncoordinating solvents affords $[C_6F_5Xe]^{\oplus}[(C_6F_5)_2BF_2]^{\ominus}$ as a sparingly soluble colorless solid, which readily dissolves in MeCN to form **1**. The Xe–C bond can be identified in MeCN solution by ^{129}Xe, ^{19}F, and ^{13}C NMR spectroscopy. The ^{129}Xe NMR spectrum contains a triplet at $\delta = -1956$ (standard, XeF_2; coupling with the *ortho* fluorine atoms of the aryl moiety, $^3J_{Xe,F} = 68.8$ Hz). Further couplings cannot be determined unambiguously from the ^{129}Xe NMR spectrum, since the signal halfwidth is 25.1 Hz. The $^3J_{F,Xe}$ coupling in the corresponding signal of the ^{19}F NMR spectrum is 68.6 Hz. One additional fluorine–xenon coupling, $^4J_{F,Xe} = 18.7$ Hz, was determined. A further indication for the Xe–C bond is the $^1J_{C,Xe}$ coupling of 119.0 Hz in the ^{13}C NMR spectrum. The chemical shifts of the $[C_6F_5Xe]^{\oplus}$ ion in MeCN also provide interesting information. In comparison with the isoelectronic C_6F_5I molecule, the *m*- and *p*-F signals in the ^{19}F NMR spectrum are shifted significantly downfield by Xe^{II} ($\Delta\delta_m = 5.4$, $\Delta\delta_p = 11.6$). The position of the *p*-F signal, which is extremely low-field for that of the C_6F_5 group, is comparable to the situation in C_6F_5Br(III and V) and C_6F_5I(III and V) compounds,[5–7] in which resonance interactions between the aryl moiety and the positive halogen atom through the *p*-F atom of the C_6F_5 group can be detected. With respect to the Xe^{II} system, this means that the aryl moiety reduces the charge density at Xe^{II} by back-bonding. The same argument explains the strikingly high-field position of the ^{129}Xe resonance compared with that of XeF_2. In this case, however, the solvation of the cation by MeCN can enhance the effect. In contrast to most known pentafluorophenyl element compounds, the C4 resonance is found at lower field than the C2,6 resonance in the ^{13}C NMR spectrum (see Table 1). Compound **1** and some pentafluorophenyl compounds of polyvalent halogens share this property.

Table 1. ^{129}Xe, ^{19}F, ^{13}C, and ^{11}B NMR data [a] for **1** in MeCN at −30 °C.

Nucleus	Chemical shifts [δ values] with assignment and coupling constants [Hz]
$[C_6F_5Xe]^{\oplus}$	
^{129}Xe	−1956 (t; 68.8 Hz; HWB 25.1 Hz) [$\delta(XeF_2) \equiv 0$]
^{19}F	−125.15 (*o*-F; dm; $^3J_{F,Xe} = 68.6$ Hz; rel. int. 2) [$\delta(CCl_3F) \equiv 0$]
	−142.00 (*p*-F; tt; $^3J_{F,F} = 20.6$ Hz; $^4J_{F,F} = 5.3$ Hz; rel. int. 1)
	−154.71 (*m*-F; dm; $^4J_{F,Xe} = 18.7$ Hz; rel. int. 2)
^{13}C	144.65 (C4; dtt; $^1J_{C,F} = 261.4$ Hz; $^2J_{C,F} = 14.0$ Hz; $^3J_{C,F} = 5.1$ Hz)
	143.20 (C2,6; ddm; $^1J_{C,F} = 259.6$ Hz; $^2J_{C,F} = 14.2$ Hz)
	137.62 (C3,5; dm; $^1J_{C,F} = 263.2$ Hz)
	82.77 (C1; dtm; $^1J_{C,Xe} = 119.0$ Hz; $^2J_{C,F} = 25.8$ Hz)
$[(C_6F_5)_2BF_2]^{\ominus}$	
^{19}F	−136.47 (*o*-F; m; rel. int. 4), −144.6 (BF_2; br. q; rel. int. 2), −160.53 (*p*-F; tt; $^3J_{F,F} = 19.8$ Hz; rel. int. 2), −165.34 (*m*-F; m; rel. int. 4)
^{13}C	146.94 (C2,6; dm; $^1J_{C,F} = 239.1$ Hz), 138.26 (C4; dtt; $^1J_{C,F} = 244.5$ Hz; $^2J_{C,F} = 14.2$ Hz; $^3J_{C,F} = 7.0$ Hz), 135.94 (C3,5; dm; $^2J_{C,F} = 246.0$ Hz), 120 (C1; s, HWB ca. 250 Hz)
^{11}B	5.54 (BF_2; t; $^1J_{B,F} = 57.6$ Hz) [$\delta(BF_4^{\ominus}) \equiv 0$]

[a] Measured on a Bruker WP 80 SY (^{13}C NMR spectrum with a Bruker WM 300). HWB = halfwidth.

The constitution of the $[(C_6F_5)_2BF_2]^{\ominus}$ ion was confirmed in solution by ^{19}F and ^{11}B NMR spectroscopy. In the ^{19}F NMR spectrum, the signal of the BF_2 group appears as a broadened quartet at $\delta = -144.6$; in the ^{11}B NMR spectrum, a broadened triplet with a $^1J_{B,F}$ coupling of 57.6 Hz is found at $\delta = 5.54$ (standard: $[BF_4]^{\ominus}$).

Single crystals, grown from MeCN solution, were investigated by X-ray crystallography[8] and showed that no signif-

[*] Priv.-Doz. Dr. H. J. Frohn, Dipl.-Chem. S. Jakobs, Prof. Dr. G. Henkel
Fachgebiet Anorganische Chemie der Universität
Lotharstrasse 1, D-4100 Duisburg (FRG)

[**] This work was supported by the Fonds der Chemischen Industrie.

icant fluorine bridges were present between cation and anion (shortest intermolecular Xe–F distance 3.135(5) Å), such as are found, for example, in $[(FSO_2)_2NXe]^{\oplus}[Sb_3F_{16}]^{\ominus}$ [9] (2.457(8) Å). The $[C_6F_5Xe]^{\oplus}$ ion (Fig. 1) is coordinated by

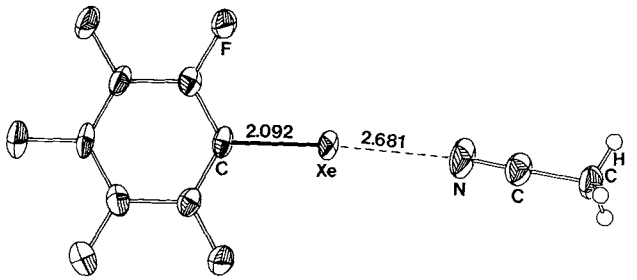


Fig. 1. Molecular structure of the $[MeCN–Xe–C_6F_5]^{\oplus}$ ion with thermal ellipsoids at 50% probability (150 K) and important Xe–ligand bond distances (standard error 0.008 Å). The C–Xe–N bond angle is 174.5(3)°.

the nitrogen atom of a MeCN molecule (C–Xe–N bond angle: 174.5(3)°). An additional MeCN molecule per formula unit is disordered and displays no contact to the cation. The Xe–C distance (2.092(8) Å) is comparable to the I–C distance in $C_6F_5I(O_2CC_6F_5)_2$ (2.072(4) Å).[10] Structural data for C_6F_5I, isoelectronic with $[C_6F_5Xe]^{\oplus}$, have not been reported. The coordination of $[C_6F_5Xe]^{\oplus}$ with MeCN (Xe–N distance 2.681(8) Å) lowers the effective charge density at Xe^{II} and is partly responsible for the extremely high-field position of the ^{129}Xe NMR signal. The measured Xe–N distance is significantly longer than those of the previously described Xe–N single bonds in $[(FSO_2)_2NXe]^{\oplus}$ [9] (2.02(1) Å) and $FXeN(SO_2F)_2$ [11] (2.200(3) Å). The coordination in **1** is presumably similar to that in the fluoro(nitrile)xenon(II) cations (in solution) described by *Schrobilgen* et al.[12]

Warming **1** above 14 °C results in slow decomposition. Perfluorobiphenyl and $(C_6F_5)_2BF$ were identified as the decomposition products. The thermal stability in MeCN solution is similar. Within 5 h at 0 °C, 30% of the Xe–C bonds have reacted; at 35 °C, 50% of the cations have reacted within 20 min. Pentafluorobenzene and oxidation products of this arene are found as additional decomposition products in solution.

Compound **1** is a typical electrophile, allowing C_6F_5 groups to be transferred to soft bases.[4] The formation of perfluorobiphenyl in the thermolysis may be regarded as an electrophilic pentafluorophenyl transfer to the nucleophilic aryl moiety in the anion. The anion can undergo exchange with Lewis acids such as BF_3 or AsF_5 [reaction (a)]. The previously unknown $(C_6F_5)_2BF$ is obtained as a coproduct and could be identified from its ^{19}F NMR spectrum [δ = −136.1 (*o*-F; m; rel. intensity 4), −156.4 (*p*-F, tt; 2), −164.0 (*m*-F; m; 4), −176.0 (BF; br. s; 1)].

$$\mathbf{1} + AsF_5 \xrightarrow[\leq -20\,^{\circ}C]{MeCN} [C_6F_5Xe]^{\oplus}[AsF_6]^{\ominus} + (C_6F_5)_2BF \qquad (a)$$

Experimental Procedure

All operations were performed under rigorously dried atmosphere (argon) in FEP apparatus.

1: A solution of $B(C_6F_5)_3$ (512 mg, 1 mmol) in CH_2Cl_2 at −40 °C was added dropwise to a solution of sublimed XeF_2 (339 mg, 2 mmol) in CH_2Cl_2 at −40 °C. After 10 min, a colorless solid precipitated. After 6 h, the precipitate was collected by filtration, washed at −78 °C with CH_2Cl_2, and dried under high vacuum at −40 °C. Yield: 627 mg (0.92 mmol, 92%) $[C_6F_5Xe]^{\oplus}[(C_6F_5)_2BF_2]^{\ominus}$. Single crystals were grown from saturated MeCN solution and washed with CH_2Cl_2. IR (AgCl): $\tilde{\nu}$[cm^{-1}]: 1647s, 1533sh, 1516vs, 1470vs, 1392m, 1368m, 1283s, 1093vs, 1004sh, 993sh, 978vs, 961vs, 933s, 814m, 794s, 760m, 741s, 715vw, 695vs, 668vw, 608w, 577vw, 485vw.

Received: May 26, 1989 [Z 3361 IE]
German version: *Angew. Chem. 101* (1989) 1534

CAS Registry numbers:
1, 123168-24-1; XeF_2, 13709-36-9; $B(C_6F_5)_3$, 1109-15-5; $[C_6F_5Xe]^{\oplus}[(C_6F_5)_2BF_2]^{\ominus}$, 123168-25-2; $(C_6F_5)_2BF$, 123168-21-8; $[C_6F_5Xe]^{\oplus}[AsF_6]^{\ominus}$, 123168-26-3; AsF_5, 7784-36-3; perfluorobiphenyl, 434-90-2.

[1] N. Bartlett, *Proc. Chem. Soc. (London) 1962*, 218.
[2] R. Hoppe, W. Dähne, H. Mattauch, K. M. Rödder, *Angew. Chem. 74* (1962) 903; *Angew. Chem. Int. Ed. Engl. 1* (1962) 599.
[3] L. J. Turbini, R. E. Aikman, R. J. Lagow, *J. Am. Chem. Soc. 101* (1979) 5833–5834.
[4] a) W. Breuer, H. J. Frohn, M. Giesen, S. Jakobs, *12th Int. Symp. Fluorine Chem.*, Santa Cruz, CA, USA 1988 ("Aryl-Fluorine-Metathesis Reactions on Halogen Fluorides and Xenon Difluoride: a Comparison of Preparative Results"). At the same symposium, *D. Naumann* and *W. Tyrra* reported the observation of $[C_6F_5Xe]^{\oplus}[(C_6F_5)_3BF]^{\ominus}$ in solution. b) H. J. Frohn, S. Jakobs, *J. Chem. Soc., Chem. Commun. 1989*, 625–627; c) D. Naumann, W. Tyrra, *ibid. 1989*, 47–50.
[5] H. J. Frohn, M. Giesen, *J. Fluorine Chem. 24* (1984) 9–15.
[6] W. Breuer, H. J. Frohn, *J. Fluorine Chem. 34* (1987) 443–451.
[7] H. J. Frohn, *Chem.-Ztg. 108* (1984) 146–147.
[8] Crystal structure analysis: Syntex $P2_1$ four-circle diffractometer, $Mo_{K\alpha}$ radiation, graphite monochromator, scintillation counter, T = 150 K, empirical absorption correction, EXTL and SHELXTL programs, direct methods, least-squares refinement; monoclinic, space group $P2_1/n$, a = 11.690(3), b = 12.956(3), c = 16.591(4) Å, β = 90.47(2)°, V = 2512.7 Å^3, Z = 4, ϱ_{calcd} = 2.018 g cm^{-3}, $\mu(Mo_{K\alpha})$ = 15.1 cm^{-1}; crystal dimensions ca. 0.30 × 0.24 × 0.21 mm^3, θ-2θ-Scan, 2θ_{max} = 50°, 4601 unique reflections, $R(R_w)$ = 0.063 (0.075) for 3858 reflections with $F_0 > 3.92\,\sigma(F_0)$ (410 parameters, H atoms of the coordinated MeCN molecule refined as an ideal rigid group with a common isotropic temperature factor; all other atoms were refined individually with anisotropic temperature factors; H atoms of the disordered MeCN molecule not included, one scaling factor. Further details of the crystal structure investigation may be obtained from the Fachinformationszentrum Karlsruhe, Gesellschaft für wissenschaftlich-technische Information mbH, D-7514 Eggenstein-Leopoldshafen 2 (FRG), on quoting the depository number CSD-54019, the names of the authors, and the journal citation.
[9] R. Faggiani, D. K. Kennepohl, C. J. L. Lock, G. J. Schrobilgen, *Inorg. Chem. 25* (1986) 563–571.
[10] H. J. Frohn, J. Helber, A. Richter, *Chem.-Ztg. 107* (1983) 169–172.
[11] J. F. Sawyer, G. J. Schrobilgen, S. J. Sutherland, *Inorg. Chem. 21* (1982) 4064–4072.
[12] A. A. A. Emara, G. J. Schrobilgen, *J. Chem. Soc., Chem. Commun. 1987*, 1644–1646.

$[P_4Aryl_6][Me_3SnF_2]_2$ (Aryl = 2,6-$(MeO)_2C_6H_3$): An Unusual Ion Pair Consisting of a Planar 2,4-Diphospha-1,3-diphosphoniacyclobutane Dication and the Difluorotrimethylstannate Anion **

By *Lutz Heuer, Ludger Ernst, Reinhard Schmutzler,** and *Dietmar Schomburg**

Dedicated to Professor Kurt Issleib on the occasion of his 70th birthday

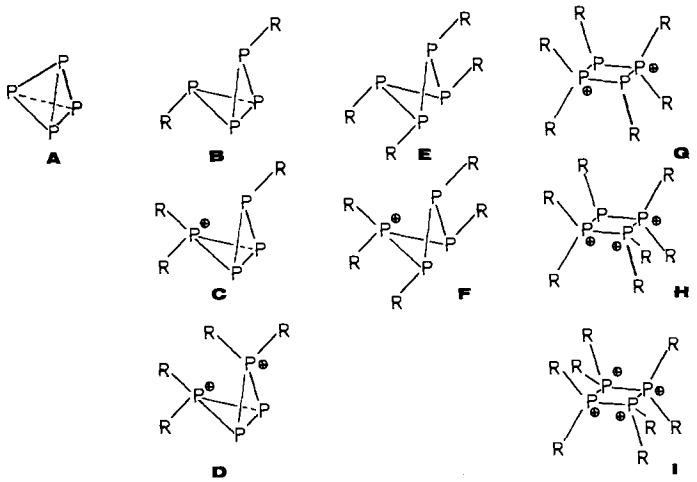
The degradation of white phosphorus, P_4, is thought to occur by successive addition of nucleophiles and elec-

[*] Prof. Dr. R. Schmutzler, Prof. Dr. L. Ernst, Dr. L. Heuer
Institut für Anorganische und Analytische Chemie der Technischen Universität
Hagenring 30, D-3300 Braunschweig (FRG)
Dr. habil. D. Schomburg
Gesellschaft für Biotechnologische Forschung
Mascheroder Weg 1, D-3300 Braunschweig (FRG)

[**] This work was supported by BASF AG, Bayer AG, Chemetall GmbH, Degussa AG, Hoechst AG, and Stauffer Chemical Co. and by the Fonds der Chemischen Industrie. *L. Heuer* thanks the Land Niedersachsen for a graduate fellowship and for computer time at the computer center of the Technische Universität Braunschweig. We would like to thank Dr. *H.-M. Schiebel* (EI and FAB mass spectrometry) and Dr. *D. Böhler*, Göttingen (FD mass spectrometry), for their help.

trophiles to the PP bond[1] and to proceed via structures of types **B**[2,3] and **E**[4] (Scheme 1). Addition of further electrophiles to these cyclophosphanes gives the cationic species **C**, **D**, and **F**[5,6] to **I**. Structures **C** and **D** are unlikely to be stable, since P–P bond cleavage would presumably take place. The synthesis of cation **F** has been described as being difficult.[6] A dication of type **G** has not yet been isolated.

Here we describe the unusual formation of a dication of type **G**. Reaction of 2,6-dimethoxyphenyl(trimethyl)stannane with chlorodifluorophosphane—in an attempt to synthesize 2,6-dimethoxyphenyl(difluoro)phosphane[8] by an alternative route—gave 1,1,2,3,3,4-hexakis(2,6-dimethoxyphenyl)-2,4-diphospha-1,3-diphosphoniacyclobutane difluorotrimethylstannate **1**, isolated as colorless crystals. Since MOPAC calculations predict that species of types **H** and **I** should be relatively unstable,[7] the dication in **1** presumably represents the final synthetically accessible member of the series **A** to **I**.



Scheme 1.

The dication in **1** is isoelectronic with 1,3-diphosphetanes, the hexasubstituted CPCP four-membered rings of which are also planar.[9] In the ^1H and ^{13}C NMR spectra[10] of **1**, the 2,6-dimethoxyphenyl substituents of the dication give rise to two sets of signals in a ratio of 1:2, corresponding to two aryl groups on the λ^3P atoms and four aryl groups on the λ^4P atoms. Thus, the λ^3P-bound substituents are *trans* to each other. The ^{31}P NMR spectrum of **1** consists of an A_2B_2 spin system,[11] like that observed by *Fluck* et al.[3] for a compound of type **B** with R = 2,4,6-tri(*tert*-butyl)phenyl. In the field desorption (FD) mass spectrum,[12] the dication in **1** could only be observed with ca. 1% intensity owing to rapid decomposition upon exposure to air. The structural parameters, important for understanding the λ^3P–λ^4P bonding, were determined by an X-ray diffraction study (Fig. 1).

Compound **1** crystallizes in the space group $P2_1/c$ with $Z = 2$.[13] The cation is crystallographically centrosymmetric and displays a planar four-membered ring, in which λ^3P and λ^4P atoms alternate and the substituents on the λ^3P atoms are *trans* to each other. The only slight anisotropy of the temperature factors (U_{ii} for P1, 0.034 to 0.038; for P2, 0.039 to 0.050) reveals that the ring is indeed planar and that apparent planarity is not caused by crystallographic disorder. All phosphorus atoms exhibit very short distances to three or four oxygen atoms (P1···O6 276 pm, P1···O12 278 pm, P1···O2 307 pm, P1···O8 305 pm, P2···O2′ 291 pm, P2···O18 279 pm, P2···O14 303 pm). Such short distances, which, in this case, are obviously also made possible by the positions of the *ortho* substituents on the phenyl ring, necessitate the assumption of attractive interactions between phosphorus and oxygen atoms (compare the sums of the van der Waals radii (328 pm[14])). This assumption is supported by the relatively rigid orientation of the nonbonding electron pairs on the oxygen atoms toward the phosphorus atoms (torsion angle C-O-C-C(-P) 166.8° to 178.9°; average 173.9°). The observed electrophilicity of the λ^3P atoms has also been described for other compounds.[15] The stability of the dication in **1** is also clearly due to the increase in the coordination number at the phosphorus atom. The P–P bond lengths (223.1 and 223.2 pm) and the P–C bond lengths (178.3–180.9 pm) lie in the usual ranges.

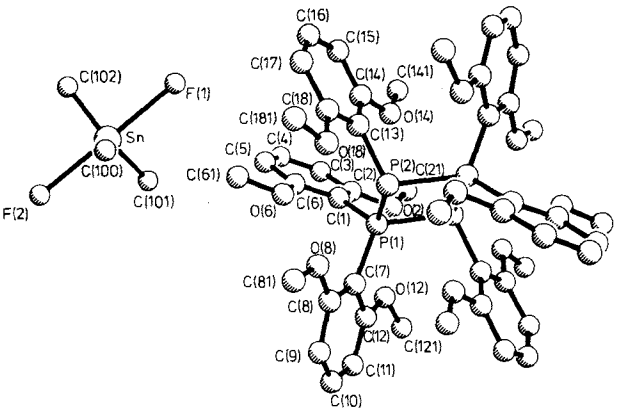


Fig. 1. Molecular structure of **1**.

The structure of an $[R_3SnF_2]^{\ominus}$ ion has not yet been described;[16] the anion in **1**, $[Me_3SnF_2]^{\ominus}$ (Fig. 2), displays an

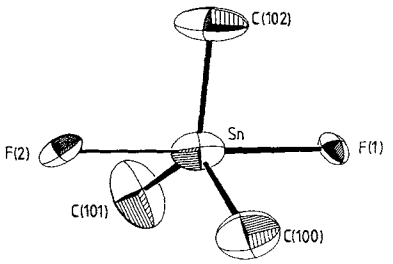


Fig. 2. Molecular structure of $[Me_3SnF_2]^{\ominus}$

only slightly distorted trigonal-bipyramidal geometry with axial fluorine atoms (maximum deviation from the ideal bonding angle, 1.8°). Owing to the negative charge, the Sn–F distances (259.6 and 260.7 pm) and the Sn–C distances (213.8–215.5 pm) are somewhat longer than those in the pentacoordinated tin compound fluorotris(trimethylsilylmethyl)stannane, $[(Me_3SiCH_2)_3SnF]$ (Sn-F 256.5 pm, Sn-C 210.1 pm),[17] which is present in the crystal as a fluorine-bridged polymer. Compared with the Sn-F bond (244.8 pm) in the tetracoordinated tin compound tri(cyclohexyl)fluorostannane,[18] the Sn-F bonds in **1** are lengthened by 15 and 16 pm owing to the increased coordination number and to the negative charge.

Experimental Procedure

1: Under inert atmosphere, 2,6-dimethoxyphenyl(trimethyl)stannane [19] (6.0 g, 0.02 mol) and iodine (ca. 5 mg) in 6 g of resorcinol dimethyl ether were placed in a thick-walled glass tube equipped with a Teflon stopcock, and PF_2Cl (4.5 g, 0.04 mol) was then condensed into the solution at $-196\,^{\circ}C/10^{-2}$ Torr. The reaction mixture was filtered after 50 days at 70 °C and the colorless crystals were washed with ca. 5 mL of CH_3CN and dried, affording 81 mg of **1** (m.p. 224–227 °C). Analysis: calculated (found), C 48.0 (47.5), H 5.4 (5.6). Com-

pound **1** spontaneously decomposes upon dissolution in $CDCl_3$ and is both air- and moisture-sensitive [21].

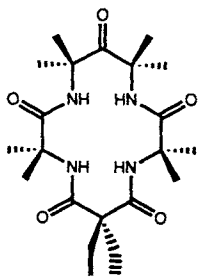
Received: May 29, 1989 [Z 3362 IE]
German version: *Angew. Chem. 101* (1989) 1549

[1] C. Brown, R. F. Hudson, G. A. Wartew, *Phosphorus Sulfur 5* (1978) 67.
[2] E. Niecke, R. Rüger, B. Krebs, *Angew. Chem. 94* (1982) 553; *Angew. Chem. Int. Ed. Engl. 21* (1982) 544; R. Riedel, H.-D. Hausen, E. Fluck, *ibid. 97* (1985) 1050 and *24* (1985) 1056.
[3] E. Fluck, R. Riedel, H.-D. Hausen, G. Heckmann, *Z. Anorg. Allg. Chem. 551* (1987) 85.
[4] L. Heuer, M. Sell, R. Schmutzler, D. Schomburg, *Polyhedron 6* (1987) 1295.
[5] K. Issleib, B. Mitscherling, *Z. Naturforsch. B 15* (1960) 267.
[6] L. Maier, *Fortschr. Chem. Forsch. 8* (1967) 1.
[7] The MOPAC, MNDO 2.04, program of *J. J. P. Stewart*, University of Texas at Austin, Austin, TX 78712 (USA), was used. The MNDO calculations indicated that the P_4 ring of *trans* derivatives of $[P_4R_6]^{2\oplus}$ (R = H, Me) should be planar. Furthermore, the rhomboid shape of the P_4 ring was confirmed. The heats of formation of higher-substituted species such as $[P_4H_7]^{3\oplus}$ and $[P_4H_8]^{4\oplus}$ ($[P_4H_6]^{2\oplus}$ 469, $[P_4H_7]^{3\oplus}$ 907, $[P_4H_8]^{4\oplus}$ 1454 kcal mol^{-1}) make their existence unlikely.
[8] L. Heuer, R. Schmutzler, *J. Fluorine Chem. 39* (1988) 197.
[9] G. Becker, W. Uhl, *Z. Anorg. Allg. Chem. 475* (1981) 35; R. Appel, C. Casser, F. Knoch, *Chem. Ber. 117* (1984) 2693; R. Appel, V. Winkhaus, F. Knoch, *ibid. 119* (1986) 2466.
[10] Atom numbering for the NMR data shown in Fig. 1a. ^{1}H NMR (400 MHz, CD_3CN, 22 °C, CHD_2CN as standard, $\delta = 1.93$): two sets of signals a/b (ratio 2:1); set a: $\delta = 7.34$ (t, ^3J(H,H) = 8.4 Hz; H-4,10), 6.71 (dt, ^3J(H,H) = 8.4, ^4J(P,H) = 3.0 Hz; H-3,9*), 6.17 (dt, ^3J(H,H) = 8.4, ^4J(P,H) = 2.8 Hz; H-5,11*), 4.15 and 3.18 (both s; OCH_3); set b: $\delta = 7.40$ (tt, ^3J(H,H) = 8.4, ^5J(P,H) = 1.6 Hz; H-16), 6.85 (m; H-15**), 5.98 (d, ^3J(H,H) = 8.4 Hz; H-17**), 4.18 and 2.91 (both s; OCH_3); $\delta = 0.62$ (s; satellites with ^2J(Sn,H) = 67.8 (^{117}Sn) and 70.9 Hz (^{119}Sn); $SnCH_3$). ^{1}H assignment by ^{31}P decoupling and H,H COSY [20]. ^{13}C NMR (101 MHz, CD_3CN, 25 °C, CD_3CN as standard, $\delta = 1.3$): set a: $\delta = 136.7$ (s; C-4,10), 106.1 (t, ^3J(P,C) = 3.7 Hz; C-3,9*), 104.2 (t, ^3J(P,C) = 3.2 Hz; C-5,11*), 56.6 and 56.5 (both s; OCH_3); set b: $\delta = 137.7$ (t, ^4J(P,C) = 2.0 Hz; C-16), 105.7 (t, ^3J(P,C) ≈ 1.5 Hz; C-15**), 104.6 (t, ^3J(P,C) ≈ 1.5 Hz; C-17**), 57.6 and 55.9 (both s; OCH_3); signals at $\delta = 162-161$ for C-2,6,8,12 and C-14,18 not assignable with certainty; resonances not observed for C-1,7 and C-13; $\delta = 6.6$ (s; $SnCH_3$). The tripletlike ^{1}H and ^{13}C signals are the X parts of $AA'B_2X$ spin systems. Simulation gives $^2J(P_A,P_{A'}) > 25$ Hz. The line spacings in the triplets are half of the J(P,H) and J(P,C) values given above. The multiplicities given for the ^{13}C NMR spectrum refer only to ^{31}P splitting.
[11] ^{31}P NMR (81 MHz, CD_3CN, ext. H_3PO_4): A_2B_2 spectrum with $\delta_A = 41.19$ and $\delta_B = 2.17$, $|J_{AB}| = 287.0$ Hz; analyzed iteratively, error between calculated and observed transitions 0.03 Hz, all lines assigned.
[12] Mass spectra (Ar = 2,6-dimethoxyphenyl): EI mass spectrum (70 eV; 175 °C): $Ar_5P_3^{\oplus}$ 778 (1%); $[Ar_5P_3-H]^{\oplus}$ 777 (2%); $Ar_4P_2^{\oplus}$ 610 (8%); $Ar_3P_2^{\oplus}$ 473 (98%); $[Ar_3P_2-Me]^{\oplus}$ 458 (78%); $Ar_2P^{\oplus}$ 305 (95%); $[SnMe_3F+H]^{\oplus}$ 185 (34%). FD(+) mass spectrum (transferred to the emitter as a solution in CH_3CN): $[Ar_6P_4-Me]^{\oplus}$ 931 (20%); $Ar_5P_3^{\oplus}$ 778 (100%); $Ar_4P_2^{\oplus}$ 610 (10%); $Ar_6P_4^{2\oplus}$ 473 (1%).
[13] Crystals obtained from reaction mixture. $a = 1073.52(10)$, $b = 1379.26(8)$, $c = 2184.55(13)$ pm, $\beta = 94.27(2)°$, $\varrho_{calcd.} = 1.39$ g cm^{-3}, 4080 reflections, ($Mo_{K\alpha}$, $3° \le 2\theta \le 50°$), $R = 0.070$. Further details of the crystal structure investigation may be obtained from the Fachinformationszentrum Karlsruhe, Gesellschaft für wissenschaftlich-technische Information mbH, D-7514 Eggenstein-Leopoldshafen 2 (FRG), on quoting the depository number CSD-53991, the names of the authors, and the journal citation.
[14] A. Bondi, *J. Phys. Chem. 68* (1964) 441.
[15] L. Heuer, D. Schomburg, R. Schmutzler, *Phosphorus Sulfur Silicon Relat. Elem. 45* (1989) 217.
[16] The stability constants for $[Me_3SnF_2]^{\ominus}$ were measured in aqueous solution: A. Cassol, L. Magon, B. Barbieri, *Inorg. Nucl. Chem. Lett. 3* (1967) 25; A. Cassol, L. Magon, *Gazz. Chim. Ital. 97* (1967) 1724, 1752 (*Chem. Abstr. 67* (1967) 15433a and 15435c). A fluoro complex of pentacoordinated tin is known: R. R. Holmes, S. Shafieezad, V. Chadrasakhar, A. C. Sau, J. M. Holmes, R. O. Day, *J. Am. Chem. Soc. 110* (1988) 1168.
[17] L. N. Zakharov, Yu. T. Struchkov, E. A. Kuz'min, B. I. Petrov, *Kristallografiya 28* (1983) 271.
[18] S. Calogera, P. Ganis, V. Peruzzo, G. Tagliavini, G. Valle, *J. Organomet. Chem. 220* (1981) 11.
[19] H. J. Kroth, H. Schumann, H. G. Kuivila, C. D. Schaeffer, J. J. Zuckerman, *J. Am. Chem. Soc. 97* (1975) 1754.
[20] A. Bax, R. Freeman, *J. Magn. Reson. 44* (1981) 542.
[21] Dichloro(2.6-dimethoxyphenyl)phosphane, Me_3SnCl, and $PF_6^{\ominus}$ were identified by NMR spectroscopy (^{1}H, ^{31}P) as further products. In addition, a number of unidentified products were formed.

The First Macrocyclic Square-Planar Cobalt(III) Complex Relieves Ring Strain by Forming a Nonplanar Amide**

By *Terrence J. Collins** and *Erich S. Uffelman*

We are developing a series of oxidation-resistant macrocyclic tetraamide ligands to support highly oxidized and/or highly oxidizing middle and later transition-metal centers. Here we report that the tetradeprotonated form of the macrocycle, H_4-**1**, coordinates to cobalt to give a macrocyclic square-planar cobalt(III) complex.[1] This complex



H_4-**1**

contains one significantly nonplanar amide group. The source of the nonplanarity appears to be ring strain derived from a mismatch of the geometrical features of the macrocycle and the structural requirements of the square-planar metal center, a unique case of amide nonplanarity in inorganic chemistry.

Square-planar cobalt(III) complexes remain rare[1] and Li[Co(η^4-**1**)] is the first such macrocyclic complex. Although its ^{1}H NMR spectrum (Fig. 1) shows the paramagnetically shifted signals characteristic[1f, j, k] of square-planar cobalt(III), the solid-state structure is distorted from square-planar geometry. [Me_4N][Co(η^4-**1**)] crystallizes as two dis-

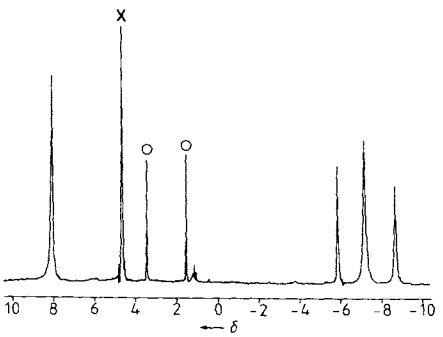


Fig. 1. ^{1}H NMR spectrum (300 MHz, D_2O) of Li[Co(η^4-**1**)] $\delta = 8.10$ (br, 12H), −5.85 (br, 4H), −7.19 (br, 12H), −8.66 (br, 6H) o = HOD (used as reference), x = THF.

[*] Prof. T. J. Collins [+], E. S. Uffelmann [++]
Department of Chemistry, Carnegie Mellon University
4400 Fifth Avenue, Pittsburgh, PA 15213 (USA)

[+] *T.J.C.* is a Dreyfus Teacher-Scholar (1986–1990) and an Alfred P. Sloan Research Fellow (1986–1989).

[++] On leave from the California Institute of Technology.

[**] Support by the National Science Foundation (Grant No. CHE-8714720) is gratefully acknowledged. *E.S.U.* wishes to thank *Sonny Lee* and *Carla Slebodnick* for useful discussions and the National Science Foundation for a Predoctoral Fellowship (1984–1987).

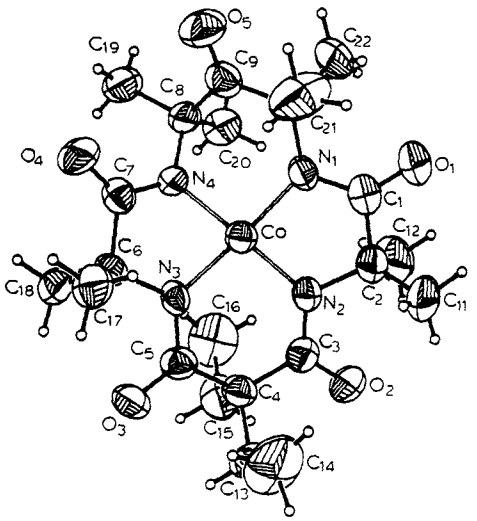


Fig. 2. Molecular structure of anion 1 of $[Me_4N][Co(\eta^4\text{-}\mathbf{1})]$. ORTEP drawing with all nonhydrogen atoms drawn to encompass 50% of electron density. Selected bond distances [Å] and angles [°]: Co-N1 1.865(5), Co-N2 1.837(5), Co-N3 1.845(5), Co-N4 1.844(5); N1-Co-N2 87.6(2), N1-Co-N3 163.5(3), N1-Co-N4 94.6(2), N2-Co-N3 96.8(2), N2-Co-N4 167.4(3), N3-Co-N4 84.6(2).

tinct anions (Fig. 2).[2] For each anion, the Dunitz amide nonplanarity parameters[3, 4] show that the amide ligand most shifted from the CoN_4 plane is substantially distorted from planarity (Table 1).

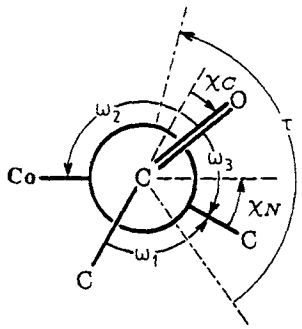


Table 1. Dunitz amide nonplanarity parameters [3, 4].

Amide	$\bar{\tau}$	X_N	X_C
N1-C1-O1 (anion 1)	4.65	16.17	2.49
N2-C3-O2 (anion 1)	9.96	11.61	0.87
N3-C5-O3 (anion 1)	6.68	5.46	5.91
N4-C7-O4 (anion 1)	−22.31	−23.82	−0.60
N1-C1-O1 (anion 2)	18.64	16.87	4.84
N2-C3-O2 (anion 2)	4.26	4.18	6.34
N3-C5-O3 (anion 2)	8.70	11.97	0.22
N4-C7-O4 (anion 2)	−6.13	13.55	0.39

This result enrichens the class of ring-constrained nonplanar amido-*N* ligands.[5] Whereas, in other examples, an unstrained amide-containing chelate ring is forced into a strained configuration by the geometrical demands of additional ligands,[5e, f] this is the first example where the amido-*N* nonplanarity arises in the absence of ancillary ligand effects. The controlling ring-strain term appears to be similar to that of the medium-ring lactams of organic chemistry.[5a]

Although there is voluminous literature on macrocyclic polyamines and Schiff bases, only one example of a complex of a macrocyclic tetraamido ligand (a cyclic tetrapeptide) has been previously reported.[6a, b, 7] The copper(III) complex of that study proved susceptible to degradation via α-hydrogen (α to amido-*N*) abstraction.[6b] This problem has been solved in both acyclic[6c, 5e, 8] and macrocyclic systems by peralkylation or aromatization of the relevant ligand positions, steps that are proving to be significant in attaining oxidation-resistant ligands. The distortion at the metal from square planarity and the amide distortions observed in $[Co(\eta^4\text{-}\mathbf{1})]^{\ominus}$ highlight the subtlety encountered in designing ligand systems for highly oxidized metal centers. Macrocyclic tetraamide ligands have been used by us to afford structurally characterized manganese(V) oxo complexes.[9]

Experimental Procedure

$[Me_4N][Co(\eta^4\text{-}\mathbf{1})]$. H_4-**1** was dissolved in dry, deoxygenated THF, and a stoichiometric amount of *tert*-butyllithium was added to the frozen solution under nitrogen. $CoCl_2$ was added under nitrogen as soon as the THF finished thawing (−108 °C). As the suspension warmed to room temperature, a yellow-green precipitate (presumably a cobalt(II) complex) collected on the flask walls. After 30 min at room temperature, air was admitted and a bright red solution rapidly developed with concomitant disappearance of the yellow-green precipitate. Crude $Li[Co(\eta^4\text{-}\mathbf{1})]$ was obtained in 95% yield. The $[Me_4N]^{\oplus}$ salt was obtained by adding excess $[Me_4N][Cl]$ in water to an aqueous solution of the complex. The water was removed in vacuo, and a CH_2Cl_2/CH_3CN solution of the residue was treated with pentane to precipitate the LiCl and excess $[Me_4N][Cl]$. Bright red rectangular parallelepipeds, characterized by X-ray analysis, were obtained by diffusion of pentane into a $CH_2Cl_2/CHCl_3$ solution of $[Me_4N][Co(\eta^4\text{-}\mathbf{1})]$.

Received: June 14, 1989;
supplemented version: August 17, 1989 [Z 3393 IE]
German version: *Angew. Chem. 101* (1989) 1552

[1] For other examples of the rare Co^{III} square-planar geometry see; a) R. Eisenberg, Z. Dori, H. B. Gray, J. A. Ibers, *Inorg. Chem. 7* (1968) 741; b) M. J. Baker-Hawkes, E. Billig, H. B. Gray, *J. Am. Chem. Soc. 88* (1966) 4870; c) J. R. Dorfman, C. P. Rao, R. H. Holm, *Inorg. Chem. 24* (1985) 453; d) R. Fikar, S. A. Koch, M. M. Millar, *ibid. 24* (1985) 3311; e) C. P. Rao, J. R. Dorfman, R. H. Holm, *ibid. 25* (1986) 428; f) P. J. van der Put, A. A. Schilperoord, *ibid. 13* (1974) 2476; g) J. J. Bour, P. T. Beurskins, J. J. Steggerda, *J. Chem. Soc. Chem. Commun. 1972* 221; h) P. J. M. W. L. Birker, J. J. Bour, J. J. Steggerda, *Inorg. Chem. 12* (1973) 1254; i) P. J. M. W. L. Birker, P. T. Beurskins *Recl. Trav. Chim. Pays-Bas 93* (1974) 218; j) J. C. Brewer, T. J. Collins, M. R. Smith, B. D. Santarsiero, *J. Am. Chem. Soc. 110* (1988) 423; k) T. J. Collins, T. G. Richmond, B. D. Santarsiero, B. G. R. T. Treco, *ibid. 108* (1986) 2088. For a discussion of the low affinity of these compounds for "typical" axial σ-donor ligands, see reference [1j]. Square-planar cobalt(III) complexes have been made with "innocent" and potentially "noninnocent" ligands. The ligand system used here is innocent. For a discussion of these terms see F. C. Anson, T. J. Collins, T. G. Richmond, B. D. Santarsiero, J. E. Toth, B. G. R. T. Treco, *J. Am. Chem. Soc. 109* (1987) 2974. References [1a–f] concern aliphatic and aromatic thiolate ligands. References [1g–i] concern innocent biuret ligands. References [1j, k] discuss aromatic and innocent aliphatic tetradentate diamide dialkoxide ligands.

[2] Crystal data: Single crystals of $[(CH_3)_4N][Co(\eta^4\text{-}\mathbf{1})]$. H_2O at 20 ± 1 °C, monoclinic, space group $P2_1/C-C_{2h}^5$ (No. 14) with $a = 17.221(3)$, $b = 19.075(6)$, $c = 21.797(6)$ Å, $\beta = 109.74(2)°$, $V = 6739(3)$ Å^3, $Z = 8$, $\varrho_{calcd} = 1.137$ g cm^{-3}; $\mu_a(Cu_{K\alpha}) = 5.2$ mm^{-1}). A total of 9248 independent absorption-corrected reflections having $2\theta(Cu_{K\alpha}) < 115.0°$ (the equivalent of 0.6 limiting $Cu_{K\alpha}$ spheres) were collected on a computer-controlled Nicolet autodiffractometer using θ-2θ scans and Ni-filtered $Cu_{K\alpha}$ radiation. The structure was solved by direct methods with the Nicolet SHELXTL software package as modified at Crystalytics Company. The structural parameters were refined to convergence (R_1(unweighted) = 0.054 for 4033 independent reflections having $2\theta_{CuK\alpha} < 115.0°$ and $I > 3\sigma(I)$) using counter-weighted cascade block-diagonal least-squares techniques and a structural model which incorporated anisotropic thermal parameters for 88 nonhydrogen atoms and isotropic thermal parameters for all hydrogen atoms. The 28 methyl groups were included in the refinement as idealized sp^3 rigid rotors. The remaining hydrogen atoms were fixed at idealized sp^3-hybridized positions with a C–H bond length of 0.96 Å. The calculated density is exclusive of disordered halocarbon solvent in the lattice. Further details of the crystal structure investigation are available on request from the Director of the Cambridge Crystallographic Data Centre, University Chemical Laboratory, Lensfield Road, Cambridge CB2 1EW (UK), on quoting the full journal citation.

[3] a) J. D. Dunitz, F. K. Winkler, *J. Mol. Biol. 59* (1971) 169; b) *Acta Crystallogr., Sect. B: Struct. Crystallogr. Cryst. Chem. B 31* (1975) 251; c) A. Walshal, M. Levitt, S. Lifson, *J. Mol. Spectrosc. 33* (1970) 84.

[4] The twist angle τ and the pyramidalization terms χ_C and χ_N were obtained from the primary torsion angle data ω_1, ω_2, and ω_3 as follows: $\tau = (\omega_1 + \omega_2)/2$; $\chi_N = (\omega_2 - \omega_3 + \pi) \bmod 2\pi$; $\chi_C = (\omega_1 - \omega_3 + \pi) \bmod 2\pi$. Here we use the modified twist angle, $\bar{\tau}$: $\bar{\tau} = (\tau) \bmod \pi$ [5a]. $\bar{\tau}$ maximizes at $\pm 90°$ and can be interpreted as the angle between the idealized positions of the pπ orbitals on C and N. The pyramidalization terms maximize at $\pm 60°$.

[5] The other two classes are (1) cases where nonplanar amido-*N* ligands are thermodynamically favored over planar analogues accessible by isomerization at the metal center and (2) cases where steric effects can be identified as the principal cause of nonplanarity. a) T. J. Collins, R. J. Coots, T. T. Furutani, J. T. Keech, G. T. Peake, B. D. Santarsiero, *J. Am. Chem. Soc. 108* (1986) 5333, and references cited therein; b) F. C. Anson, T. J. Collins, S. L. Gipson, J. T. Keech, T. E. Krafft, G. T. Peake, *ibid. 108* (1986) 6593; c) T. J. Collins, T. Lai, G. T. Peake, *Inorg. Chem 26* (1987) 1674; d) T. J. Collins, J. M. Workman, *Angew. Chem. 101* (1989) 924; *Angew. Chem. Int. Ed. Engl. 28* (1989) 912; e) F. C. Anson, J. A. Christie, T. J. Collins, R. J. Coots, T. T. Furutani, S. L. Gipson, J. T. Keech, T. E. Krafft, B. D. Santarsiero, G. H. Spies, *J. Am. Chem. Soc. 106* (1984) 4460; f) C. J. Barner, T. J. Collins, B. E. Mapes, B. D. Santarsiero, *Inorg. Chem. 25* (1986) 4322.

[6] a) D. W. Margerum, J. S. Rybka, *Inorg. Chem. 19* (1980) 2784; b) J. S. Rybka, D. W. Margerum, *ibid. 20* (1981) 1453; c) L. L. Diaddario, W. R. Robinson, D. W. Margerum, *ibid. 22* (1983) 1021.

[7] For a summary of work performed with macrocyclic ligands containing one, two, or three amide groups see E. Kimura, *J. Coord. Chem. 15* (1986) 1.

[8] T. J. Collins, S. W. Gordon-Wylie, *J. Am. Chem. Soc. 111* (1989) 4511.

[9] T. J. Collins, R. D. Powell, C. Slebodnick, E. S. Uffelman, to be published.

The First Example of an *Ethylene*-Selective Soluble Ziegler Catalyst of the Zirconocene Class

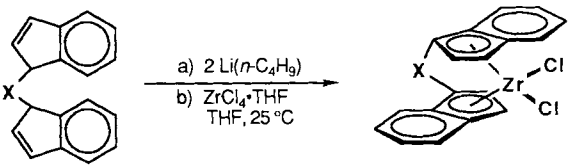
By *Wolfgang A. Herrmann,* Jürgen Rohrmann,* Eberhardt Herdtweck, Walter Spaleck,* and *Andreas Winter*

Dedicated to Professor Wolfgang Hilger on the occasion of his 60th birthday

Combination of chiral, sterically rigid metallocene derivatives containing metals of the fourth subgroup with methylalumoxane (as cocatalyst) gives highly active, stereospecific catalysts for the polymerization of α-olefins.[1-4] The chiral complexes may be used as racemates. For instance, highly isotactic polypropylene with a narrow molecular-weight distribution can be prepared with the catalyst *rac*-[ethylene-1,2-(bis-4,5,6,7-tetrahydroindenyl)]zirconium dichloride **1**;[1] however, the average molecular weights of such polymers are too low for practical applications. Our goal was therefore to improve the catalyst properties by stepwise modification of the ligand system. In an initial approach, we have introduced silyl groups to vary the bridging of the two indenyl ligands.

Conversion of the bis(indenyl) systems **2a, b**, accessible from indenyllithium and the corresponding dichlorosilanes, to the dilithio compounds followed by reaction with zirconium tetrachloride (Scheme 1) yielded the new silyl-bridged complexes **3** and **4** as pure racemates. The similarly obtained *meso* forms could be *quantitatively* separated owing to their differing solubilities. Complete separation of the *meso* forms is necessary because the propylene polymerization otherwise leads to undesired atactic polymer.

The dimethylsilyl-bridged complex **3** exhibits particularly high activity in the polymerization of propylene in liquid monomer (bulk polymerization) with methylalumoxane as cocatalyst (Table 1) and affords polypropylene with an average molecular weight nearly twice as high as that obtained with **1**, the narrow molecular-weight distribution and high isotacticity being maintained. Surprisingly, metallocene **4** (with a longer bridge) is *completely inactive toward propylene*. To determine whether this drastic effect is due to the size of the olefin, we carried out polymerization experiments with ethylene for comparison and observed a fully unexpected *high activity of 4 toward ethylene*. This activity is lower than that of **3** by a factor of only 3 (Table 1). The lower ethylene activity of the two compounds in comparison with the propylene activity is due to the different polymerization procedures. The bis(indenyl) complex **4** is thus an *ethylene-selective catalyst*. Since the cause of this phenomenon presumably lies in the molecular structure of **4**, we characterized both metallocenes by X-ray structure analyses (Fig. 1).[6]



2a,b *rac*-**3**: X = $Si(CH_3)_2$

rac-**4**: X = $(CH_3)_2SiCH_2CH_2Si(CH_3)_2$

Scheme 1.

Table 1. Polymerization of propylene (bulk polymerization) and ethylene (suspension polymerization) at 65 °C.

Metallocene	Activity [(kg polymer) (mmol Zr)$^{-1}$ h^{-1}]	
	Propylene	Ethylene
3	110	19.3
4	0	6.5

As shown in Figure 1, top, the structure of the dimethylsilyl-bridged complex **3** (racemate) is similar to that of the ethylene-bridged derivative **1**, which has a C_2-symmetric ligand system.[5] This results in similar catalytic properties. The only salient difference is the larger angle between the two halves of the ligand system in **3** (62° compared with 55° in **1**) due to the one-atom bridge. The resulting increase in the accessibility of the $ZrCl_2$ group, the actual reaction center, is reflected in the high catalytic activity of **3**. By contrast, **4** displays an unsymmetrical arrangement of the ligand system. As shown in Figure 1, bottom, in which the $ZrCl_2$ unit is viewed from the same direction, the much longer Si–C–C–Si bridge is no longer found in the back of the molecule, but rather bulges to one side. As a result, the indenyl rings are twisted with respect to each other. The angle between the two halves of the ligand is 54°. The catalytic inactivity of metallocene **4** toward propylene is therefore due to shielding of the reaction center of the catalyst by the bulky bridge and by the indenyl ligand directed toward the $ZrCl_2$ function (Fig. 1, bottom, "upper" ligand). These structural features are less detrimental for the sterically less demanding ethylene molecule. For ethylene, therefore, the polymerization activity dramatically increases. These structural differences are also reflected in the colors of the complexes: **3** is orange, **4** yellow.

The findings presented here show that the selectivity of olefin polymerization catalysts of the zirconocene class can

[*] Prof. Dr. W. A. Herrmann, Dr. E. Herdtweck
Anorganisch-chemisches Institut der Technischen Universität München
Lichtenbergstrasse 4, D-8046 Garching (FRG)
Dr. J. Rohrmann, Dr. W. Spaleck, Dr. A. Winter
Hoechst Aktiengesellschaft
Brüningstrasse 50, D-6230 Frankfurt am Main 80 (FRG)

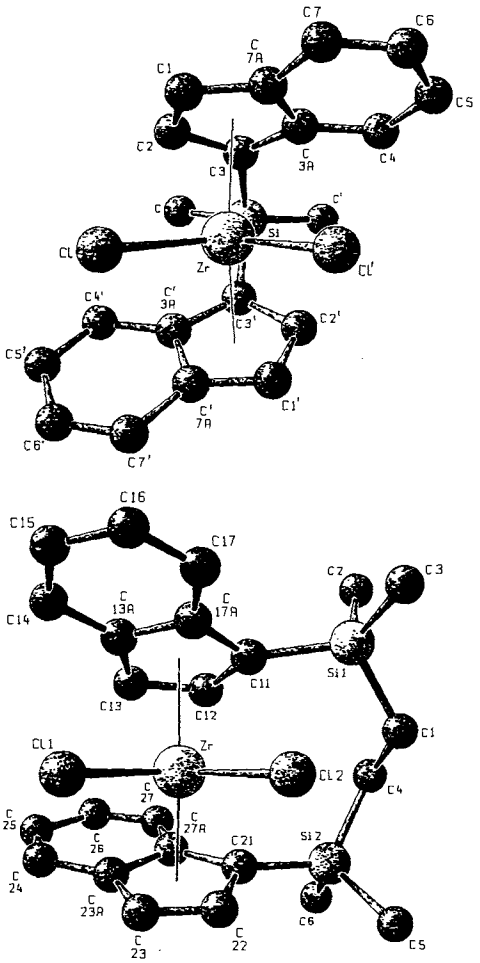


Fig. 1. Top: Molecular structure (SCHAKAL) of *rac*-**3**. Selected bond lengths [pm] and angles [°]: Zr-Cl 243.1(<1), Zr-Cp*(1) 229.3, Si-C3 187.1(1); Cl,Zr,Cl' 98.76(1), Cp*(1),Zr,Cp*(2) 119.04, C3,Si,C3 94.57(6), C,Si,C' 111.2(1) (Cp*: centroid of the C_5 moiety of the C_9 ligands). Bottom: Molecular structure (SCHAKAL) of *rac*-**4**. Selected bond lengths [pm] and angles [°]: Zr-Cl1 244.6(1), Zr-Cl2 242.5(1), Zr-Cp*1 223.3, Si1-C11 188.2(3), Si2-C21 187.5(4); Cl1,Zr,Cl2 94.82(4), Cp*1,Zr,Cp*2 128.81, C1,Si1,C11 111.9(1), C2,Si1,C3 108.8(2), C4,Si2,C21 117.2(2), C5,Si2,C6 109.2(2) (Cp*: centroid of the C_5 moiety of the C_9 ligands).

be dramatically varied by structural and conformational changes.

Experimental Procedure

All operations were performed under argon atmosphere.

rac-**3**: A solution of **2a** [7] (5.60 g, 19.4 mmol) in 40 mL of THF was treated at room temperature with 15.5 mL (38.8 mmol) of *n*-butyllithium (2.5 M, *n*-hexane). After 2 h, the deep red solution was added dropwise over 4–6 h to a suspension of $ZrCl_4 \cdot 2$ THF (7.30 g, 19.4 mmol) in 60 mL of THF. The resulting reaction mixture was stirred for 2 h and the orange precipitate was collected by filtration and recrystallized from CH_2Cl_2, affording 1.20 g (14%) of *rac*-**3** as orange crystals, which slowly decompose above 200 °C. Correct elemental analyses and mass spectra ($m/z = 448$). ^{1}H NMR (400 MHz, $CDCl_3$, 28 °C): $\delta = 7.04$–7.60 (m, 8H, arom. H), 6.90 (dd, 2H, β-IndH), 6.08 (d, 2H, α-IndH), 1.12 (s, 6H, $SiCH_3$).

rac-**4**: A solution of **2b** (4.30 g, 12.5 mmol), prepared from indenyllithium and 1,2-bis(chlorodimethylsilyl)ethane, in 40 mL of THF was treated as described above with *n*-butyllithium (9.3 mL, 23.2 mmol) and $ZrCl_4 \cdot 2$ THF (4.40 g, 11.6 mmol). Cooling of the reaction solution to −35 °C led to the crystallization of *rac*-**4** (1.50 g, 25%) as yellow crystals, which melt at 246–249 °C. Correct elemental analyses and mass spectra ($m/z = 523$). ^{1}H NMR (270 MHz, $CDCl_3$, 28 °C): $\delta = 7.2$–7.9 (m, 8H, arom. H), 6.80 (dd, 2H, β-IndH), 5.58 (d, 2H, α-IndH), 0.99–1.29 (m, 4H, C_2H_4), 0.53 (s, 6H, $SiCH_3$), 0.23 (s, 6H, $SiCH_3$).

Propene polymerization: a) A dry 16-L steel reactor equipped with a thermostat was flushed with nitrogen and charged at 30 °C with 10 L of liquid propene. A solution (30 mL) of methylalumoxane in toluene (40 mmol Al; average molecular weight, cryoscopic, 900 g mol^{-1}) was then added. At the same time, *rac*-**3** (4.5 mg, 0.01 mmol) was dissolved in 20 mL of the same methylalumoxane solution in toluene (27 mmol Al) and allowed to stand for 15 min to "preactivate" it. The orange-red solution was then placed in the reactor, which was heated to 65 °C and kept at this temperature for 1 h. After the reactor had cooled to 20 °C and the pressure was released, the product was dried under vacuum. Yield: 1.10 kg polypropylene ($M_w = 44\,300$ g mol^{-1}; $M_w/M_n = 2.2$; II = 96.2%, ^{13}C NMR). b) In a similar experiment in which *rac*-**4** (62.1 mg, 0.12 mmol) was used, no polymer was isolated; the reactor contained only the propylene and the toluene used and decomposition products arising from the methylalumoxane.

Ethylene polymerization: a) The procedure was the same as that employed in propene polymerization. Instead of liquid propene, 10 L of a purified hydrocarbon fraction (100–120 °C) was used. After addition of methylalumoxane solution, ethylene (5 bar) was admitted. After termination of the polymerization, the product was collected by filtration and dried under vacuum. If 6.4 mg (0.014 mmol) of *rac*-**3** is used, 0.27 kg of polyethylene ($M_w = 201\,000$ g mol^{-1}; $M_w/M_n = 2.8$) is obtained. b) In a similar experiment in which *rac*-**4** (48.8 mg, 0.091 mmol) was used, 0.59 kg of polyethylene ($M_w = 480\,000$ g mol^{-1}, $M_w/M_n = 3.7$) was obtained.

Received: May 31, 1989 [Z 3364 IE]
German version: *Angew. Chem. 101* (1989) 1536

CAS Registry numbers:
3, 121009-93-6; **3**, 121009-93-6; **4**, 123485-92-7; polypropylene, 9003-07-0; polyethylene, 9002-88-4.

[1] W. Kaminsky, K. Külper, H. H. Brintzinger, F. R. W. P. Wild, *Angew. Chem. 97* (1985) 507; *Angew. Chem. Int. Ed. Engl. 24* (1985) 507.
[2] J. A. Ewen, *J. Am. Chem. Soc. 106* (1984) 6355.
[3] J. A. Ewen, L. Haspeslagh, J. L. Atwood, H. Zhang, *J. Am. Chem. Soc. 109* (1987) 6544.
[4] P. Pino, P. Chioni, J. Wei, *J. Am. Chem. Soc. 109* (1987) 6189.
[5] a) F. R. W. P. Wild, M. Wasicionek, G. Huttner, H. H. Brintzinger, *J. Organomet. Chem. 288* (1985) 63; b) S. Collins, B. A. Kuntz, N. J. Taylor, D. G. Ward, *ibid. 342* (1988) 21.
[6] R. E. Schmidt, M. Birkhahn, W. Massa, P. Kiprof, E. Herdtweck: STRUX-II program system for analyzing X-ray data, Universität Marburg 1980/ Technische Universität München 1985–1987. Compound *rac*-**3**: Orange-red prisms from chloroform. The systematic absences (*hkl*, $h + k = 2n + 1$; *h0l*, $l = 2n + 1$) are consistent with the monoclinic space groups *C*2/*c* and *Cc*. The lattice constants were refined to $a = 1651.9(2)$, $b = 1214.4(1)$, $c = 1109.6(1)$ pm, $\beta = 122.45(1)°$; $V = 1878 \times 10^6$ pm^3; formula, $C_{20}H_{18}Cl_2SiZr$; $Z = 4$; $\varrho_{calcd} = 1.586$ g cm^{-3}. The centrosymmetric space group *C*2/*c* was confirmed in the calculations. The measurement was performed on a four-circle CAD4 diffractometer (Enraf-Nonius) with $Mo_{K\alpha}$ radiation ($\lambda = 71.073$ pm; graphite monochromator) at $T = 23 \pm 1$ °C in the measuring range $2.0° \leq \theta \leq 25.0°$ (ω scan) for variable scan width and measuring time $t_{max} = 90$ s. Of 3636 measured reflections, 1572 (NO) unique reflections with $I > 1.0\,\sigma(I)$ and 144 (NV) parameters were used in the full matrix least squares refinement after averaging and correction for slight decomposition. $R = \sum||F_o| - |F_c||/\sum|F_o| = 0.017$; $R_w = [\sum w(|F_o| - |F_c|)^2/\sum w|F_o|^2]^{1/2} = 0.022$; GOF $= [\sum w(|F_o| - |F_c|)^2/(\text{NO-NV})]^{1/2} = 3.960$, $w = 1/\sigma^2(F_o)$. The structure solution was carried out by the Patterson method and difference Fourier technique; empirical absorption correction ($\mu = 9.2$ cm^{-1}). The hydrogen positions were taken from difference Fourier syntheses and refined with collective (methyl group) or individual (indenyl group) isotropic temperature factors. Anomalous dispersion was taken into consideration; residual electron density after the final cycle of refinement $+0.22$ $e_0^{\ominus}$ Å^{-3}, shift/err < 0.00.

Compound *rac*-**4**: Lemon-yellow prisms from chloroform/*n*-hexane. The observed systematic absences (*h0l*, $l = 2n + 1$; *0k0*, $k = 2n + 1$) are consistent with the monoclinic space group $P2_1/n$. The lattice constants were refined to $a = 1851.6(3)$, $b = 804.3(4)$, $c = 1768.8(4)$ pm, $\beta = 112.58(2)°$; $V = 2432 \times 10^6$ pm^3; formula, $C_{24}H_{28}Cl_2Zr$; $Z = 4$; $\varrho_{calcd} = 1.460$ g cm^{-3}. The measurement was carried out on a four-circle CAD4 diffractometer (Enraf-Nonius; $Mo_{K\alpha}$ radiation ($\lambda = 71.073$ pm; graphite monochromator) at $T = 24 \pm 1$ °C in the measuring range $2.0° \leq \theta \leq 22.5°$, ω scan, variable scan width, measuring time $t_{max} = 60$ s. Of 6867 measured reflections, 2548 (NO) unique reflections with $I > 1.0\,\sigma(I)$ and 262 (NV) parameters were refined by the full matrix least squares method after averaging and correction for slight decomposition. $R = 0.036$; $R_w = 0.030$; GOF $= 2.259$. The structure solution was carried out by the Patterson method and difference Fourier technique; empirical absorption correction ($\mu = 7.7$ cm^{-1}). The hydrogen positions were taken from difference Fourier syntheses and refined with collective isotropic temperature factors. Anomalous dispersion was taken into consideration. After the final cycle of refinement, the residual electron density was $+0.41$ $e_0^{\ominus}$ Å^{-3} for a shift/err < 0.00. Further details of the crystal structure investigations may be obtained from the Fachinformationszentrum Karlsruhe, Gesellschaft für wissenschaftlich-technische Information mbH, D-7514 Eggenstein-Leopoldshafen 2 (FRG), on quoting the depository number CSD-53960, the names of the authors, and the journal citation.
[7] E. Maréchal, J. P. Tortai, *C.R. Acad. Sci. Paris 267* (1968) 467.

Counterion Dependent Structural Diversity in Silver Polyselenides; Structures of the New Complex Anions $[Ag(Se_4)]_4^{4\ominus}$, $[Ag(Se_5)]_n^{n\ominus}$ and $[Ag_4(Se_4)_3]^{2\ominus}$ **

By *Mercouri G. Kanatzidis** and *Song-Ping Huang*

The chemistry of metal-polychalcogenide compounds particularly with heavier chalcogens, lately is attracting considerable interest.[1] The main reasons for this are the potential of using these compounds as precursors to solid state electronic materials[2, 3] and the fascinating and thus far unpredictable structural chemistry exhibited by the heavier polychalcogenides which often does not parallel that of the corresponding polysulfides.[1, 4] Recently, we have reported on a new homologous family of Group 11 polychalcogenides with the general formula $[M(Q_x)]_n^{n\ominus}$ (x = 4, M = Cu, Q = S[5] and M = Ag, Q = Se[6]) all of which have distinct one-dimensional structures. For example, $[Ag(Se_4)]_n^{n\ominus}$ crystallizes from a dimethylformamide (DMF) solution of $Ag^{\oplus}$ and $Se_x^{2\ominus}$ with $Ph_4P^{\oplus}$ as the cation. Since the lability of $Ag^{\oplus}/Se_x^{2\ominus}$ mixtures in strong polar solvents is high, with a variety of species participating in complex equilibria,[7] we thought that such a system might be particularly influenced to yield different final crystallization Ag/Se products by varying important crystallization factors such as the counterion. Indeed, we found a significant influence. We report here the syntheses and structures[8] of two new members of the $[M(Q_x)]_n^{n\ominus}$ family, $[Et_4N]_4[Ag(Se_4)]_4$ **1** and $\{[Me_4N][Ag(Se_5)]\}_n$ **2**, as well as of $[n\mathrm{Pr}_4N]_2[Ag_4(Se_4)_3]$ **3**. The latter compound does not belong to the $[M(Q_x)]_n^{n\ominus}$ family. To date none of these compounds find corresponding sulfur analogs.

The compounds **1** and **2** were obtained upon reaction of $AgNO_3$ and R_4NCl (R = Et, Me) with Na_2Se_5 in DMF according to Equation (a).

$$AgNO_3 + Na_2Se_5 + R_4NCl \rightarrow [(R_4N)Ag(Se_x)]_n + NaCl + NaNO_3 \quad \text{(a)}$$
$$x = 4,\ n = 4$$
$$x = 5,\ n = \infty$$

The structure of $[Ag(Se_4)]_4^{4\ominus}$ which is situated on a crystallographic inversion center, is shown in Figure 1 top. This is a discrete tetramer featuring two different kinds of $Ag^{\oplus}$ coordination. A planar rhombus of four silver atoms, symmetrically disposed around the inversion center, is "glued" together by four $Se_4^{2\ominus}$ ligands. Two of the silver atoms, Ag1 and Ag1′, are tetrahedrally coordinated while the other two, Ag2 and Ag2′, possess a trigonal planar coordination. The bridging $Se_4^{2\ominus}$ ligands are not equivalent and are divided into two sets. In one set, two $Se_4^{2\ominus}$ ligands are bridging three silver atoms, Ag1, Ag1′ and Ag2 with atoms Se1 and Se4 being μ_2 type. In the other set the two $Se_4^{2\ominus}$ ligands are bridging two silver atoms with only one terminal atom, Se8 being μ_2 type. The tetrahedral geometry around Ag1 is highly distorted with one very long "bond", Ag1-Se1 at 2.901(1) Å, a long Ag1-Se1′ bond at 2.708(1) Å and two normal bonds Ag1-Se8 and Ag1-Se4 at 2.641(1) and 2.644(1) Å respectively. The Ag1 atom is displaced from the center of the Se1 Se4 Se8 Se1′ tetrahedron towards the Se1 Se4 Se8 face. The angles around Ag1 deviate dramatically from the ideal tetrahedral angles (Fig. 1 top). The Ag1 atom lies 1.868(1) Å above the Se1′ Se4 Se8 plane. The geometry around Ag1 is best described as intermediate between trigonal planar and tetrahedral. The Ag···Ag distances in this cluster are as follows, Ag1-Ag1′ 2.917(1) Å, Ag1-Ag2 3.178(1) Å, Ag1-Ag2′ 3.482(1) Å. The $Se_4^{2\ominus}$ ligand chelating the Ag1 atom adopts a twist boat conformation while the corresponding ligand chelating the Ag2 atom is best described by an envelop conformation. The molecular structure of the anion in **1** is unique and bears no analog in metal polychalcogenide chemistry.

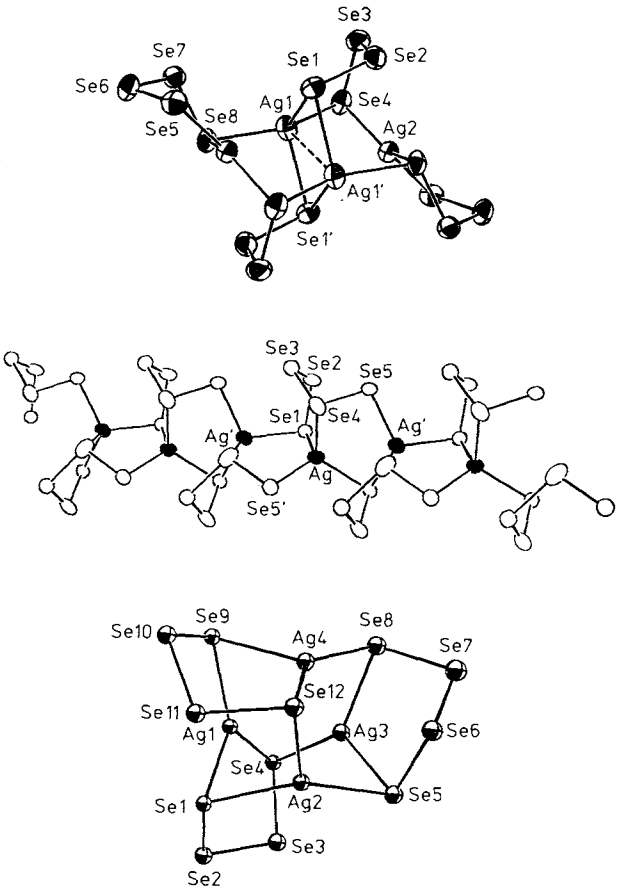


Fig. 1. Top: The structure of $[Ag(Se_4)]_4^{4\ominus}$ in the crystal. Distances [Å]: Ag2-Se4 2.583 (1), Ag2-Se5 2.596 (1), Ag2-Se8 2.616 (1), Se1-Se2 2.331 (2), Se2-Se3 2.341 (2), Se3-Se4 2.343 (2), Se5-Se6 2.340 (2), Se6-Se7 2.336 (2), Se7-Se8 2.350 (2). Angles [°]: Se1-Ag1-Se1 117.44 (4), Se1-Ag1-Se4 95.47 (4), Se1′-Ag1-Se4 100.43 (4), Se1-Ag1-Se8 94.76 (4), Se1′-Ag1-Se8 111.82 (4), Se8-Ag1-Se4 136.47 (4), Se5-Ag2-Se4 118.27 (4), Se4-Ag2-Se8 134.52 (4), Se5-Ag2-Se8 106.21 (4). Middle: The structure of $[Ag(Se_5)]_n^{n\ominus}$ in the crystal. Distances [Å]: Ag-Se1 2.633 (2), Ag′-Se1 2.670 (3), Ag-Se4 2.756 (2), Ag-Se5 2.648 (3), Se1-Se2 2.334 (3), Se2-Se3 2.329 (3), Se3-Se4 2.362 (4), Se4-Se5 2.324 (4). Angles [°]: Se1-Ag-Se1′ 115.40 (7), Se1-Ag-Se4 101.86 (8), Se1-Ag-Se5 122.34 (8), Se1-Ag-Se4′ 110.62 (8), Se1-Ag-Se5′ 109.49 (8), Se4-Ag-Se5 94.03 (7), Ag-Se1-Ag′ 91.11 (7). Bottom: The structure of $[Ag_4(Se_4)_3]^{2\ominus}$ in the crystal. Distances [Å] (standard deviation 0.001 Å): Ag1-Ag2 3.005, Ag1-Ag3 3.074, Ag2-Ag3 3.022, Ag2-Ag4 3.193, Ag3-Ag4 2.990, Ag4-Ag1 3.017, Ag1-Se1 2.621, Ag1-Se4 2.614, Ag1-Se9 2.554, Ag2-Se1 2.588, Ag2-Se5 2.552, Ag2-Se12 2.710, Ag3-Se4 2.545, Ag3-Se5 2.680, Ag3-Se8 2.589, Ag4-Se8 2.567, Ag4-Se9 2.634, Ag4-Se12 2.592, Se1-Se2 2.371, Se2-Se3 2.311, Se3-Se4 2.357, Se5-Se6 2.352, Se6-Se7 2.306, Se7-Se8 2.366, Se9-Se10 2.367, Se10-Se11 2.316, Se11-Se12 2.361. Angles [°] (standard deviation 0.02°): Se1-Ag1-Se4 104.52, Se1-Ag1-Se9 122.47, Se4-Ag1-Se9 132.97, Se1-Ag2-Se5 146.58, Se1-Ag2-Se12 101.15, Se5-Ag2-Se12 112.03, Se5-Ag3-Se4 119.72, Se5-Ag3-Se8 105.79, Se4-Ag3-Se8 134.14, Se8-Ag4-Se9 117.59, Se8-Ag4-Se12 136.83, Se9-Ag4-Se12 105.40. Average Ag-Se-Ag: 72 (2).

Contrary to the discrete molecular nature of **1**, the structure of **2** is composed of non-interacting $Me_4N^{\oplus}$ cations and one-dimensional, non-centrosymmetric $[Ag(Se_5)]_n^{n\ominus}$ macroanions (Fig. 1 middle). The structure of $[Ag(Se_5)]_n^{n\ominus}$ differs

[*] Prof. M. G. Kanatzidis, S.-P. Huang
Department of Chemistry and
Center for Fundamental Materials Research
Michigan State University
East Lansing, MI 48824 (USA)

[**] This work was supported by the Donors of the Petroleum Research Fund (administered by the American Chemical Society) and by the Center for Fundamental Materials Research at Michigan State University.

from the previously reported $[Ag(Se_4)]_n^{n\ominus}$[6] **4** in two ways. First, in **2** $Se_5^{2\ominus}$ instead of $Se_4^{2\ominus}$ ligands are present with distinct mode of ligation compared to those in **4**; second, the $Ag^{\oplus}$ atom in **2** assumes a tetrahedral geometry, compared to a trigonal planar one in **4**. The $Se_5^{2\ominus}$ ligands bridge three $Ag^{\oplus}$ atoms in an unprecedented fashion. In this bonding mode, the chelation of the $Se_5^{2\ominus}$ ligand occurs through the first and the fourth Se atoms forming a five-membered ring. The fifth terminal Se atom is then bonded to a neighboring $Ag^{\oplus}$ atom. The entire $[Ag(Se_5)]_n^{n\ominus}$ chain can be viewed as being made of fused five-membered $AgSe_4$ and Ag_2Se_3 rings. The structure of $[Ag(Se_5)]_n^{n\ominus}$ is also different from those recently reported for α- and β-$[Cu(S_4)]_n^{n\ominus}$[5] and represents a new structural motif for a one-dimensional material.

Interestingly when the counterion was changed to $nPr_4N^{\oplus}$, a different stoichiometry was adopted to yield **3** with the anion $[Ag_4(Se_4)_3]^{2\ominus}$. This complex anion features a tetrahedral array of $Ag^{\oplus}$ atoms held together by three $Se_4^{2\ominus}$ ligands forming a highly distorted Ag_4Se_6 central adamantane-like core in which all $Ag^{\oplus}$ ions assume a trigonal planar coordination (Fig. 1 bottom). The chelating mode of the $Se_4^{2\ominus}$ ligands is similar to that found in the isostructural series $[M_4(Q_4)_x(Q_5)_{3-x}]^{2\ominus}$ (M = Cu, Q = S,[9] Se;[10] M = Ag, Q = Se[10]). Contrary to the structural disorder encountered in the polyselenide ligands in $[Ag_4(Se_4)_x(Se_5)_{3-x}]^{2\ominus}$[10] (which crystallizes with $Ph_4P^{\oplus}$), **3** crystallizes with only $Se_4^{2\ominus}$ ligands and no disorder.

From the results reported here it is clear that a trend of the dependence of the $Ag^{\oplus}$ coordination sphere on the size of the counterion appears to emerge. Large cations such as $Ph_4P^{\oplus}$ and $nPr_4N^{\oplus}$ effect a lower $Ag^{\oplus}$ coordination number (i.e. trigonal planar in **3** and **4**) while small ones such as $Me_4N^{\oplus}$ favor a higher coordination number (i.e. tetrahedral in **1**). Apparently, intermediate size counterions such as $Et_4N^{\oplus}$ stabilize an intermediate average coordination number of 3.5 (both trigonal planar and tetrahedral). Such systematic correlation of counterion size/coordination number of coinage metals has been observed previously in the $R_4N^{\oplus}/M^{\oplus}$/halide systems,[11] M = $Cu^{\oplus}$, $Ag^{\oplus}$, and more recently recognized in other metal/ligand systems.[12]

At this stage, there is no apparent reason for these effects to be limited to the $Ag^{\oplus}/Se_x^{2\ominus}$ systems. We expect similar, although not necessarily analogous results with other congeners in this system (i.e. $Cu^{\oplus}$, $Au^{\oplus}$ and $S_x^{2\ominus}$, $Te_x^{2\ominus}$). Certainly the metal coordination numbers (CN) found in α- and β-$KCuS_4$[5] (CN = 4), $[Ph_4P]_2[NH_4][Cu_3(S_4)_3]$[13a] (CN = 3), $[Ph_4P]_2[Au_2S_8]$[9] (CN = 2), $[Ph_4P]_4[M_2S_{20}]$ (M = Cu,[13b] Ag[14a]) (CN = 3), $[Ph_4P]_2[Ag_2(S_6)_2]$[14b] (CN = 2), $[(Ph_3P)_2N][Ag(S_9)] \cdot S_8$[14c] (CN = 2) and $[Ph_4As][Au(S_9)]$[15] (CN = 2) are consistent with this contention.

Experimental Procedure

All manipulations were carried out in a glove-box under inert atmosphere. Na_2Se_5 was prepared dissolving the stoichiometric amount of the elements in liquid ammonia. Satisfactory elemental analyses were obtained from all compounds.

1 and **2**: The reaction of 0.30 mmol $AgNO_3$ with 2 equiv. of Na_2Se_5 in 50 mL DMF in the presence of 1 equiv. Et_4NCl and Me_4NCl respectively yields a dark brown solution which after filtration and dilution with ether affords red needles of **1** (96%) and **2** (93%) respectively.

3: The reaction of 0.60 mmol $AgNO_3$ with 1 equiv. of Na_2Se_5 in 50 mL DMF in the presence of 1 equiv. nPr_4NCl yields a dark brown solution which after filtration and dilution with ether affords red needles of **3** (75%).

Received: June 15, 1989 [Z 3396 IE]
German version: *Angew. Chem. 101* (1989) 1556

[1] a) R. W. M. Wardle, S. Bhaduri, C.-N. Chau, J. A. Ibers, *Inorg. Chem. 27* (1988) 1747–1755; b) W. A. Flomer, S. C. O'Neal, A. W. Cordes, D. Jetter, J. W. Kolis, *ibid. 27* (1988) 969–971; c) W. A. Flomer, S. C. O'Neal, W. T. Pennington, D. Jeter, A. W. Cordes, J. W. Kolis, *Angew. Chem. 100* (1988) 1768–1769; *Angew. Chem. Int. Ed. Engl. 27* (1988) 1702–1703; d) R.-W. M. Wardle, C. H. Mahler, C.-N. Chau, J. A. Ibers, *Inorg. Chem. 27* (1988) 2790–2795; e) S. C. O'Neal, J. W. Kolis, *J. Am. Chem. Soc. 110* (1988) 1971–1973; f) W. A. Flomer, J. W. Kolis, *197th ACS Natl. Mtg.*, Dallas TX, USA 1989, Abstr. INOR 327; g) J. Adel, F. Weller, K. Dehnicke, *Z. Naturforsch. B 43* (1988) 1094–1100; h) B. W. Eichhorn, R. C. Haushalter, F. A. Cotton, B. Wilson, *Inorg. Chem. 27* (1988) 4085–4094; i) H. Strasdeit, B. Krebs, G. Henkel, *Inorg. Chim. Acta 89* (1984) L11.

[2] a) M. L. Steigerwald, *Chem. Mater. 1* (1989) 52–57; b) M. L. Steigerwald, C. E. Rice, *J. Am. Chem. Soc. 110* (1988) 4228–4231; c) M. L. Steigerwald, C. R. Sprinkle, *Organometallics 7* (1988) 245–246; d) M. L. Steigerwald, C. R. Sprinkle, *J. Am. Chem. Soc. 109* (1987) 7200–7201.

[3] a) R. C. Haushalter, D. P. Goshorn, M. G. Sewchok, C. B. Roxlo, *Mater. Res. Bull. 22* (1987) 761–768; b) R. C. Haushalter, C. M. O'Connor, J. P. Haushalter, A. M. Umarji, G. K. Shenoy, *Angew. Chem. 96* (1984) 147–148; *Angew. Chem. Int. Ed. Engl. 23* (1984) 169–170; c) R. C. Haushalter, C. M. O'Connor, A. M. Umarji, G. K. Shenoy, C. K. Saw *Solid State Commun. 49* (1984) 929–933.

[4] a) A. Müller, E. Diemann, *Adv. Inorg. Chem. Radiochem. 31* (1987) 89–122; b) M. Draganjac, T. B. Rauchfuss, *Angew. Chem. 97* (1985) 745; *Angew. Chem. Int. Ed. Engl. 24* (1985) 742–757; c) A. Müller, *Polyhedron 5* (1986) 323–340.

[5] M. G. Kanatzidis, Y. Park, *J. Am. Chem. Soc. 111* (1989) 3767–3769.

[6] M. G. Kanatzidis, S.-P. Huang, *J. Am. Chem. Soc. 111* (1989) 760–761.

[7] DMF solution spectroscopic data such as UV/VIS and ^{77}Se NMR obtained from these compounds are identical with corresponding data from $Se_x^{2\ominus}$ solutions and indicate complete dissociation into $Ag^{\oplus}$ and $Se_x^{2\ominus}$.

[8] a) Crystal data for $[Et_4N]_4[Ag(Se_4)]_4$ **1**: monoclinic $P\,2_1/n$, $Z = 2$, $a = 16.229(3)$, $b = 11.480(5)$, $c = 17.171(3)$ Å, $\beta = 106.06(1)^\circ$, $V = 3074$ Å^3 at 25 °C. $2\theta_{max}(Mo_{K\alpha}) = 45^\circ$. Number of data measured 8020. Number of unique data 4260. Number of data having $F_{o^2} > 3\sigma(F_{o^2})$: 2510. Number of variables 253. Number of atoms 68. An empirical absorption correction was applied. $\mu = 106.5$ cm^{-1}. The minimum and maximum correction was 0.40 and 0.99 respectively. Final $R = 0.028$ and $R_w = 0.030$. b) Crystal data for $\{[Me_4N][Ag(Se_5)]\}_n$ **2**: monoclinic Cc, $Z = 4$, $a = 11.350(2)$, $b = 18.764(3)$, $c = 7.434(1)$ Å, $\beta = 124.59(1)^\circ$, $V = 1303.4$ Å^3 at 25 °C. $2\theta_{max}(Mo_{K\alpha}) = 44^\circ$. Number of data measured 1935. Number of data having $F_{o^2} > 3\sigma F_{o^2}$): 1397. Number of variables 98. Number of atoms 23. An empirical absorption correction was applied. $\mu = 90.4$ cm^{-1}. The minimum and maximum correction was 0.66 and 0.99 respectively. Final $R = 0.052$ and $R_w = 0.057$. c) Crystal data for $[nPr_4N]_2[Ag_4(Se_4)_3]$ **3**: monoclinic $P2_1/n$, $Z = 4$, $a = 10.493(2)$, $b = 24.573(3)$, $c = 17.499(1)$ Å, $\beta = 93.84(1)^\circ$, $V = 4502$ Å^3 at −125 °C. $2\theta_{max}(Mo_{K\alpha}) = 46^\circ$. Number of data measured 6829. Number of unique data 6428. Number of data having $F_{o^2} > 3\sigma(F_{o^2})$: 4255. Number of variables 387. Number of atoms 98. An empirical absorption correction was applied. $\mu = 113.3$ cm^{-1}. The minimum and maximum correction was 0.83 and 0.99 respectively. Final $R = 0.033$ and $R_w = 0.040$. All structures were solved with SHELXS-86 and were refined with the SDP package of crystallographic programs. Further details of the crystal structure investigations are available on request from the Director of the Cambridge Crystallographic Data Centre, University Chemical Laboratory, Lensfield Road, Cambridge CB2 1EW (UK), on quoting the full journal citation.

[9] A. Müller, M. Römer, H. Bögge, E. Krickemeyer, K. Schmitz, *Inorg. Chim. Acta 85* (1984) L39–L41.

[10] J. Cusick, M. L. Scudder, D. C. Craig, I. G. Dance *Polyhedron 8* (1989) 1139–1141.

[11] a) S. Andersson, S. Jagner, *Acta Chem. Scand. Ser A 42* (1988) 691–697; b) *ibid. A 41* (1987) 230–236; c) *ibid. A 40* (1986) 52–57; d) S. Jagner, S. Olson, R. Stomberg, *ibid. A 40* (1986) 230–232; e) S. Andersson, S. Jagner, *ibid. A 40* (1986) 210–217; f) *ibid. A 39* (1985) 423–428; g) *ibid. A 39* (1985) 799–812; h) *ibid. A 39* (1985) 515–521; i) M. Asplund, S. Jagner, M. Nilsson, *ibid. A 39* (1985) 447–451; j) S. Andersson, S. Jagner, *ibid. A 39* (1985) 181–186; k) M. Asplund, S. Jagner, *ibid. A 39* (1985) 47–51; l) S. Andersson, S. Jagner, *ibid. A 39* (1985) 177–181.

[12] S. Pohl, R. Lotz, W. Saak, D. Haase, *Angew. Chem. 101* (1989) 355–356; *Angew. Chem. Int. Ed. Engl. 28* (1989) 344–345.

[13] a) A. Müller, F.-W. Baumann, H. Bögge, M. Römer, E. Krickemeyer, K. Schmitz, *Angew. Chem. 96* (1984) 607–608; *Angew. Chem. Int. Ed. Engl. 23* (1984) 632–633; b) A. Müller, F.-W. Baumann, H. Bögge, K. Schmitz, *Z. Anorg. Allg. Chem. 521* (1985) 89–96.

[14] a) A. Müller, M. Römer, H. Bögge, E. Krickemeyer, F.-W. Baumann, K. Schmitz, *Inorg. Chim. Acta 89* (1984) L7–L8; b) A. Müller, E. Krickemeyer, M. Zimmermann, M. Penk, K. Schmitz, *ibid. 90* (1984) L69–L71; c) A. Müller, M. Römer, H. Bögge, E. Krickemeyer, M. Zimmermann, *Z. Anorg. Allg. Chem. 534* (1986) 69–76.

[15] G. Marbach, J. Strähle, *Angew. Chem. 96* (1984) 229–230; *Angew. Chem. Int. Ed. Engl. 23* (1984) 246–247.

Side-chain Homologues of 20-Hydroxyecdysone: Synthesis, Configurational Assignment, and Biochemical Characterization**

By *Udo Hedtmann, Kurt Hobert, Ralf Klintz, Peter Welzel,* Jadwiga Frelek, Magdalena Strangmann-Diekmann, Antje Klöne,* and *Olaf Pongs**

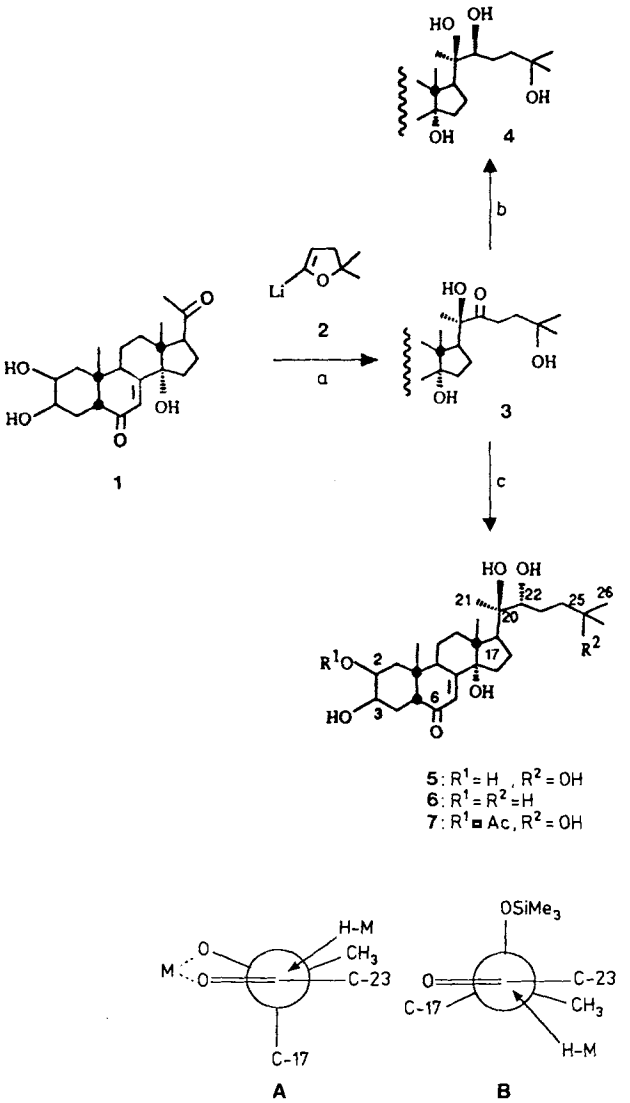
The postembryonic development of insects and crustaceans is controlled by the steroid hormone 20-hydroxyecdysone **5**.[1] Like steroid hormones in vertebrates, 20-hydroxyecdysone probably regulates the expression of specific genes via an interaction of the steroid receptor complex with DNA and/or chromatin.[2] In contrast to vertebrate steroid hormone receptors,[3] the ecdysteroid receptor in invertebrates remains virtually uncharacterized.[4]

The low concentration of the receptor in target cells (e.g., cytoplasm and nuclei in the case of *Drosophila melanogaster* at various stages of development, or Kc cells), as well as the limited stability of the hormone–receptor complex in extracts from insect tissue, are probably responsible for the difficulties in the biochemical characterization of the ecdysteroid receptor.[4] If one were able to prepare a derivative of 20-hydroxyecdysone that a) contained a reactive functional group, b) was radioactively labeled, and c) proved biologically active, it would then be possible to a) use the reactive group to covalently bind the compound to the receptor, thereby permitting its identification[5] (affinity labeling[3b]) and b) attach it to a matrix in order to concentrate or even isolate the receptor through affinity chromatography.[6]

Unfortunately, essentially all the functional groups in **5** are required to ensure full biological activity,[7, 8] and cannot be used to attach a potential coupling group. In contrast, structural changes at the end of the side-chain appear not to cause a loss of activity (cf. ponasterone A **6**[8] and ref.[5a, c]).

We report here a flexible approach to the synthesis of ecdysteroids with substituents at C-26 (and C-27), together with the biological properties of the new compounds. One of these compounds meets the requirements of a ligand for affinity labeling and affinity chromatography experiments.

Poststerone **1** reacts with an excess of the lithium compound **2**, prepared from 2,2-dimethyl-2,3-dihydrofuran, to give an addition product the enol ether group of which can be cleaved with 0.1 N HCl producing **3** (Scheme 1). Reduction of **3** with $LiAlH(OtBu)_3$ leads to a 16:1 mixture of **4** and **5**.[9] This stereochemical result can be explained using the cyclic Cram model (cf. Scheme 1, **A**). By contrast, silylation of all the OH groups of **3** with trimethylsilyl triflate,[10] reduction of the keto groups at C-22 and C-6 with diisobutylaluminum hydride (DIBAH), oxidation of the allylic OH group at C-6 with MnO_2, and fluoride-induced removal of the silyl groups leads in an overall yield of 50% to a 39:1 mixture of **5** and **4**.[11] Thus, when the neighboring 20-OH group is silylated, the 22-CO group can be reduced with high Cram-selectivity (cf. Scheme 1, **B**). This approach to the synthesis of **5** from **3** is superior to the one we reported previously[9] in terms both of much higher diastereoselectivity and more reliable reproducibility.[12]



Scheme 1. a: 0.1 N HCl, THF/H_2O, 20 °C, 30 min.[9] b: $LiAlH(OtBu)_3$.[9] c: 1) 16 equiv. 2,6-dimethylpyridine, 8 equiv. trimethylsilyl triflate, THF, 20 °C, 1 h, 78%; 2) 7.5 equiv. DIBAH (1.2 M in toluene), THF, −78 → 0 °C, 4 h, extractive workup (water/diethyl ether) followed by careful drying; 3) 65 equiv. MnO_2, CH_2Cl_2, 20 °C, 16 h, 83% (for steps 2,3); 4) 6.5 equiv. Bu_4NF, THF, 1 h, 80%. Diastereomeric ratio determined by HPLC (5 μm RP-18, 25 cm × 0.4 cm, methanol/water = 3:4).

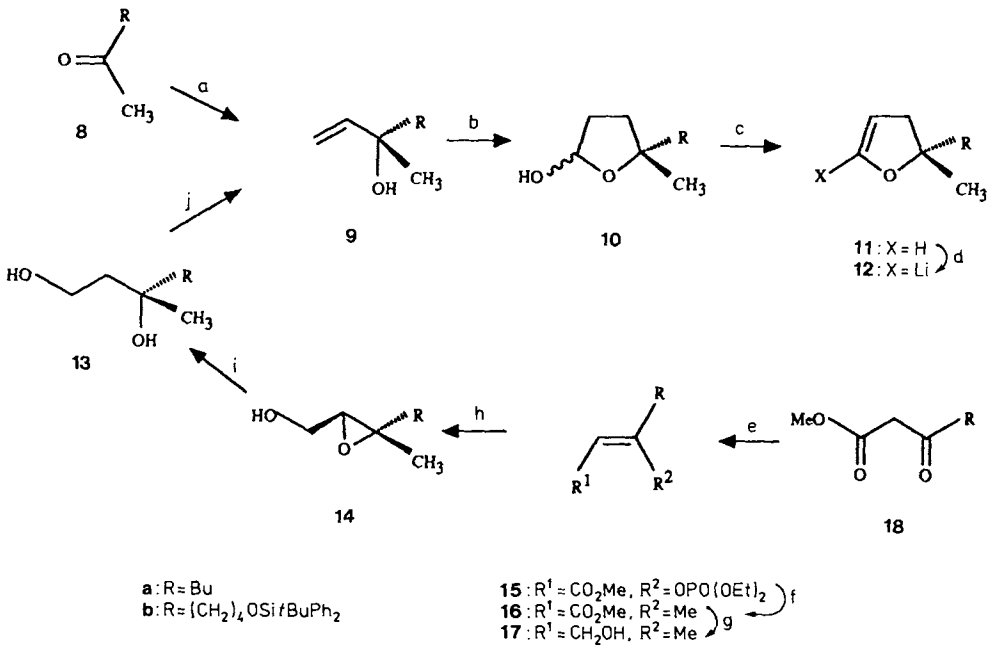
The 2,2,-disubstituted 2,3-dihydrofurans *rac*-**11a** and *rac*-**11b** required for preparing side-chain homologues of **5** were synthesized in three steps from ketones **8a** and **8b**, respectively,[13] guided by the procedure of *Botteghi*.[14] The dehydration step (**10** → **11**) is critical, and the reaction conditions listed in Scheme 2 must be followed meticulously. Enol ethers **11** react with *tert*-butyllithium to give the lithium compounds **12** (Scheme 2).

The 1:1 mixture of diastereomers **19a** and **20a** obtained from poststerone **1** and *rac*-**12a** (Scheme 3) could not be separated. On the other hand, the reduction products **21a** and **22a** from direct reduction of **19a** and **20a** with $LiAlH(OtBu)_3$ were separable by preparative HPLC, as were the derivatives **19b** and **20b** obtained from **19a** and **20a** by silylation. In order to establish the configurational relationships linking **21a** and **22a** with **19a** and **20a** the silyl groups

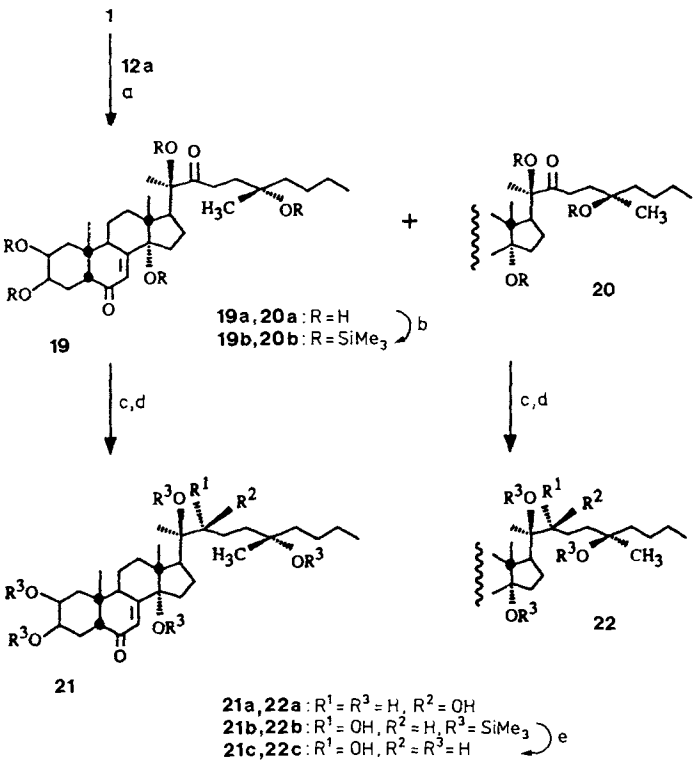
[*] Prof. Dr. P. Welzel, Dr. U. Hedtmann, Dr. J. Frelek,[+] Dipl.-Chem. R. Klintz, Dipl.-Ing. K. Hobert, Prof. Dr. O. Pongs, Dipl.-Chem. M. Strangmann-Diekmann, Dipl.-Chem. A. Klöne
Fakultät für Chemie der Universität
Postfach 102148, D-4630 Bochum (FRG)

[+] Permanent address:
Department of Chemistry, Warszawa University
ul.Pasteura 1, PL-02-093 Warszawa (Poland)

[**] This work was supported by the Deutsche Forschungsgemeinschaft, the Fonds der Chemischen Industrie, and the Minister für Wissenschaft und Forschung des Landes Nordrhein-Westfalen.



Scheme 2. a: 2 equiv. vinylmagnesium bromide, THF, reflux, 2 h; 77%. b: 7×10^{-4} equiv. $Rh(PPh_3)_3(CO)Cl$, 0.75 equiv. NEt_3, C_6H_6, CO/H_2 1:1, 5 MPa, 70% **10a**, 89% **10b**. c: **11a**: quartz apparatus, 270 °C, 5.3 kPa, Al_2O_3 (Woelm, neutral, for TLC), 72%. **11b**: quartz apparatus, 270 °C, 13 Pa, 6.2 wt-% Al_2O_3 (Woelm, neutral, for TLC), mixed with 200 wt.-% sea sand, 77%, $[a]_D$ (*ee* > 86%) = −18.1 (*c* = 0.70, $CHCl_3$). d: *t*BuLi, THF, −78 °C → −20 °C, 2 h. e: **18b** → **15b**: NaH, $ClPO(OEt)_2$, [16] 100%. **18b** was prepared from methyl acetoacetate as follows: 1) 1.1 equiv. NaH, THF, 0 °C, 15 min; 2) 1.1 equiv. *n*BuLi, 2 equiv. HMPT, 0 °C, 15 min; 3) 0.5 equiv. 1-(*tert*-butyldiphenylsilyloxy)-3-iodopropane, 0 → 20 °C, 1.5 h, 77%. f: MeMgCl, MeCu, [17] 81%. g: 7 equiv. DIBAH, CH_2Cl_2, −78 °C, 7 min, 93%. h: Sharpless epoxidation, [18] (L-(+)-diethyl tartrate as auxiliary), $[a]_D$ (*ee* > 86%) = −2.6 (*c* = 0.67, $CHCl_3$). i: 2 equiv. Red-Al®, THF, 0 °C, 6 h, 92% based on **17**, $[a]_D$ (*ee* > 86%) = +1.0 (*c* = 0.98, $CHCl_3$). j: Grieco elimination, [21] 77%, $[a]_D$ (*ee* > 86%) = +7.7 (*c* = 0.79, $CHCl_3$).



Scheme 3. a: cf. a in Scheme 1, [9] 85% of a 1:1 mixture of **19a** and **20a**. b: cf. c1) in Scheme 1, followed by preparative HPLC (5 μm Si 100, 2,2,4-trimethylpentane/dioxane/isopropanol = 200:0.20:0.25), 35% **19b**, 34% **20b**. c: **19a/20a** → **21a/22a**: cf. b in Scheme 1, [9] followed by preparative HPLC (5 μm RP-18, methanol/water = 1:1), 34% **21a**, 34% **22a**. d: **19b** → **21b** and **20b** → **22b**: cf. c1)–c3) in Scheme 1, 77% **21b**, 71% **22b**. e: **21b** → **21c** and **22b** → **22c** (and determination of the diastereomeric excess): cf. c4) in Scheme 1, 83% **21c**, 83% **22c**.

were removed from **19b** (**19b** → **19a**) and the resulting *pure* **19a** was reduced with $LiAlH(OtBu)_3$, leading to **21a**.

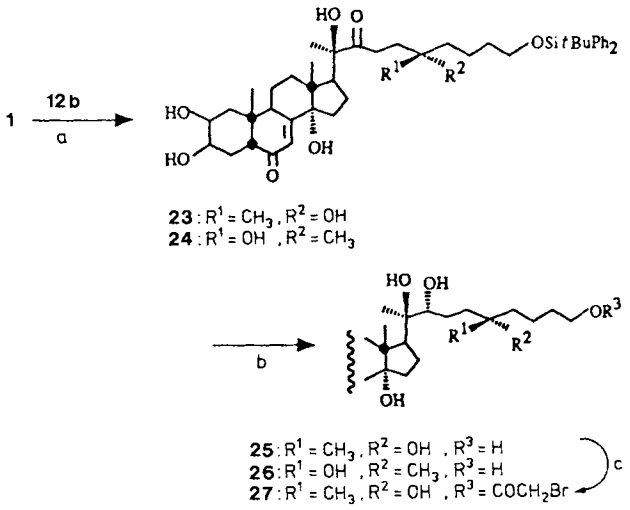
Reduction of **19b** and **20b** with DIBAH and subsequent re-oxidation of the 6-OH group with MnO_2 produced **21b** and **22b**, respectively, each contaminated with traces of the corresponding 22*S* isomer. Cleavage of the silyl ether groups followed by HPLC showed the diastereomeric excess in the DIBAH reduction step to be 94%.

The configurations at C-22 of **21a,c** and **22a,c** were established by the method of *Snatzke* et al. [CD analysis of the in situ complexes of optically active 1,2-diols with $Mo_2(OAc)_4$ [15]]. Details of this analysis will be reported elsewhere. The results are consistent with those of the ^{1}H-NMR studies, as summarized in Table 1. Thus, as in the case of **4** and **5**, for the pairs **21a/21c** and **22a/22c** the 21-CH_3 groups in the 22*S* isomers **a** are more deshielded. The configuration at C-25 in the compounds **19**–**22** has not yet been clarified, and is depicted arbitrarily in Scheme 3.

Table 1. ^{1}H-NMR signals for the 21-CH_3 groups of compounds **4**, **5**, **21a,c**, **22a,c**, **25**, and **26** (in [D_5]pyridine).

Config.	δ-Values (21-CH_3)			
22*S*	1.71 (**4**)	1.73 (**21a**)	1.73 (**22a**)	
22*R*	1.60 (**5**)	1.61 (**21c**)	1.61 (**22c**)	1.59 (**25**, **26**)

In analogy to the experiments described above, compounds **25** and **26** were prepared from **1** and *rac*-**12b** via the 22-ketones **23** and **24**, which could be separated by HPLC (Scheme 4).



Scheme 4. a: **1** + *rac*-**12b**: cf. a in Scheme 1, [9] followed by preparative HPLC (5 μm Si 100; 2,2,4-trimethylpentane/$CHCl_3$/ethanol = 15:5:1), 35% **23**, 32% **24**; **1** + **12b**: 50% **23** and **24** in the ratio > 93:7 (determined by HPLC). b: **23** → **25** and **24** → **26** cf. c in Scheme 1, 43% **25**, 40% **26**. c: 0.9 equiv. $BrCH_2COOH$, 1 equiv. dicyclohexylcarbodiimide, 0.1 equiv. 4-(dimethylamino)pyridine, THF, −20 °C, 3 h, 64%.

Table 2. Relative receptor-binding affinity (RBA) and relative puff induction (RPI) of ecdysone and the ecdysteroids **3**–**7**, **19a**, **20a**, **21c**, **22c**, and **25**–**27**.[a]

Compound	RBA	RPI
6	1000	1000
Ecdysone	0.3 ± 0.3	0.2 ± 0.2
3	5.3 ± 2	5 ± 3
4	inactive	inactive
5	14.0 ± 3	14 ± 4
7 [29]	1.0 ± 0.4	0.6 ± 0.4
19a	1.4 ± 0.4	0.8 ± 0.3
20a	1.4 ± 0.4	1 ± 0.3
21c	8.0 ± 0.4	8 ± 1
22c	11.3 ± 3	8 ± 2
25	5.3 ± 2	6 ± 1
26	8.0 ± 2	8 ± 2.5
27	15.0 ± 2	not tested

[a] RBA-values were determined by the method of *Ojasoo* et al.[25] The RBA-value for **6** was taken to be 1000. Binding constant at 4 °C for [$^3H_2$]-ponasterone A, [$^3H_2$]-**6**, with the ecdysteroid receptor preparations (ca. 200 fmol receptor/mg protein) from nuclei or cytoplasm: $(4.2 \pm 0.3) \times 10^{-9}$ M; for [$^3H_4$]-**5**: $(3.0 \pm 1.5) \times 10^{-7}$ M. The constants were established by the method of *Scatchard* [30] (average of three independent measurements). The ecdysteroid concentration producing half-maximum puff induction at 74 EF and 75B on salivary gland chromosomes of third instar *Drosophila* larvae was determined by the method of *Ashburner*.[28] The required concentration of **6** was taken to be 1000 and corresponding concentrations for the other ecdysteroids were based on this value, permitting computation of relative puff induction values (RPI). Reported values are averages taken over four measurements.

The *R*-configuration at C-22 follows from the reduction procedure employed and is supported by the chemical shift of the CH_3-21 protons (cf. Table 1). The configuration at C-25 was established by a stereochemically unambiguous synthesis. Thus, the dianion of methyl acetoacetate[16] was alkylated to give **18b** (cf. Scheme 2) from which trisubstituted alkene **16b** was stereoselectively prepared via the enol phosphate **15b** by the method of *Weiler* et al.[17] Reduction of the ester function with DIBAH led to allylic alcohol **17b**, the *E* configuration of which could be confirmed with an NOE experiment. **17b** was converted to the epoxy alcohol **14b** by Sharpless epoxidation (catalytic variant,[18] L-(+)-diethyl tartrate as auxiliary). Reduction with Red-Al[19] gave diol **13b**, a Mosher ester analysis of which revealed that the enantiomeric excess of the Sharpless epoxidation was at least 86%.[20] Grieco elimination[21] provided the desired optically active allylic alcohol (*S*)-**9b**, which was converted to (*S*)-**11b** by the method described above. The reaction of **1** with **12b**, prepared from (*S*)-**11b**, resulted almost exclusively in **23** (cf. Scheme 4).

As expected, the primary OH group in **25** could be esterified selectively with bromoacetic acid to give the bromoacetyl derivative **27**.[22] Biochemical properties of the various ecdysteroids are summarized in Table 2.

A salt extract of nuclei from *Drosophila* embryos (maximum age twelve hours)[23] and a lysate of cytoplasm from *Drosophila* pupae[24] were used to determine *in vitro* relative binding affinities (RBA)[25] to the ecdysteroid receptor. The RBA values were established by competition with either [23,23,24,24-$^3H_4$]-**5** or [24,25-]/[25,26-$^3H_2$]-**6** for binding to the ecdysteroid receptor proteins. Since there was essentially no difference between data obtained with the receptor preparations from nuclei and cytoplasm, only a single value is included in Table 2 for each ecdysteroid. The RBA values for ecdysone, **5**, and **6** are consistent with previously reported binding constants.[26, 27]

In addition, the extent of puff induction by the ecdysteroids on polytene chromosomes from the salivary glands of third instar *Drosophila* larvae was established.[28] This puff induction was determined quantitatively and, in analogy to RBA values, relative puff induction (RPI) values are reported corresponding to the ecdysteroid concentration required for half-maximal puff induction at loci 74EF and 75B on the third chromosome.

A comparison of the RBA and RPI values in Table 2 shows that there is no significant difference between the activity of the ecdysteroids to bind in vitro to the receptor and to induce in vivo puffs. We conclude, therefore, that the biological activity of the ecdysteroids is a consequence of their affinity to the receptor. Table 2 also confirms that the OH groups in ring A and in the side-chain are essential for complete biological activity. Ecdysone (lacking the OH group at C-20) and the 2-*O*-acetyl compound **7**[29] show only a fraction of the activity of **5**. The (22*S*)-isomer **4** is completely inactive, and the activity of the 22-ketone **3** is reduced to ca. 30%. It is also instructive to compare the values for **5** with those for **21c**, **22c**, **25**, and **26**. Elongation of the side-chain at C-26 apparently has little effect on the biological activity, and inversion of the configuration at C-25 does not result in a change in activity (cf. the values for **21c** and **22c**). This part of the steroid apparently does not interfere with the binding site of the receptor protein.[5a]

With respect to the problem posed in the introduction, it has now been shown that **27** (radioactively labeled in the bromoacetyl group) is a compound that is appropriate for affinity labeling of ecdysteroid receptors and for the preparation of an affinity matrix. Experiments along these lines are currently in progress.

Received: July 10, 1989 [Z 3431 IE]
German version: *Angew. Chem. 101* (1989) 1543

[1] P. Karlson, *J. Cell. Comp. Physiol. 66* (1965) 69–76; J. Hoffmann, M. Porchet (Eds.): *Biosynthesis, Metabolism and Mode of Action of Invertebrate Hormones*, Springer, Berlin 1984.

[2] Reviews: K. R. Yamamoto, *Annu. Rev. Genet. 19* (1985) 209–252; G. Ringold, *Annu. Rev. Pharmacol. Toxicol. 25* (1985) 529–566.

[3] a) Reviews: S. Green, P. Chambon, *Nature (London) 324* (1986) 615–617; b) H. Gronemeyer (Ed.): *Affinity Labelling and Cloning of Steroid and Thyroid Hormone Receptors*, Ellis Horwood, VCH, Chichester/Weinheim, 1988.

[4] O. Pongs, *Eur. J. Biochem. 175* (1988) 199–204.

[5] For recent experiments of this type see a) D. Guédin-Vuong, Y. Nakatani, B. Luu, G. Ourisson, *Tetrahedron Lett. 26* (1985) 5959–5962; D. Guédin-Vuong, Y. Nakatani, G. Ourisson, *Croat. Chim. Acta 58* (1985) 547–557; b) B. A. Sage, D. H. S. Horn, T. M. Landon, J. D. O'Connor, *Arch. Insect. Biochem. Physiol. 1986*, 25–33; c) P. Cherbas, L. Cherbas, S.-S. Lee, K. Nakanishi: *Proc. Natl. Acad. Sci. USA 85* (1988), 2096–2100.
[6] M. Lombest, M. Claire, P. Lustenberger, A. Michaud, M.-E. Rafestin-Oblin, *J. Biol. Chem. 262* (1987) 8121–8127, and references cited therein.
[7] P. Cherbas, D. A. Trainor, R. J. Stonard, K. Nakanishi, *J. Chem. Soc. Chem. Commun. 1982*, 1307–1308.
[8] Review: R. Bergamasco, D. H. S. Horn in J. A. Hoffmann (Ed.): *Progress in Ecdysone Research*, Elsevier/North Holland Biomedical Press, Amsterdam 1980, S. 299–324.
[9] U. Hedtmann, P. Welzel, *Tetrahedron Lett. 26* (1985) 2773–2774.
[10] E. J. Corey, H. Cho, C. Rücker, D. H. Hua, *Tetrahedron Lett. 22* (1981) 3455–3458.
[11] The literature describing previous syntheses of 20-hydroxyecdysone has been summarized in [9]; cf. also T. Kametani, M. Tsubuki, K. Higurashi, T. Honda, *J. Org. Chem. 51* (1986) 2932–2939.
[12] The conversion of **3** to **5** by reaction with *N,O*-bis(trimethylsilyl)-acetamide, reduction with $LiAlH(OtBu)_3$, and subsequent silyl ether cleavage [9] could be performed only with a single specimen of the reducing agent.
[13] **8a** was synthesized from 1-(*tert*-butyldiphenylsilanyloxy)-3-iodopropane and acetone dimethylhydrazone using the method of E. J. Corey, D. Enders, *Chem. Ber. 111* (1978) 1337–1361; cf. also C. H. Heathcock, E. F. Kleinman, E. S. Binkley, *J. Am. Chem. Soc. 104* (1982) 1054–1068.
[14] C. Botteghi, *Gazz. Chim. Ital. 105* (1975) 233–245.
[15] J. Frelek, Z. Majer, A. Perkowska, G. Snatzke, I. Vlahov, U. Wagner, *Pure Appl. Chem. 57* (1985) 441–451.
[16] S. N. Huckin, L. Weiler, *J. Am. Chem. Soc. 96* (1974) 1082–1087.
[17] M. Alderdice, C. Spino, L. Weiler, *Tetrahedron Lett. 25* (1984) 1643–1646.
[18] R. M. Hanson, K. B. Sharpless, *J. Org. Chem. 51* (1986) 1922–1925.
[19] Sodium bis(2-methoxyethoxy)dihydridoaluminate: S. M. Viti, *Tetrahedron Lett. 23* (1982) 4541–4544; J. M. Finan, Y. Kishi, *ibid. 23* (1982) 2719–2722.
[20] The enantiomeric excess was established employing the 3-CH_3 signals (^{1}H-NMR, 400 MHz, $CDCl_3$ at $\delta = 1.12$, $\Delta\delta = 0.0085$) of the Mosher esters of **13b** and *rac*-**13b**, cf. J. A. Dale, D. L. Dull, H. S. Mosher, *J. Org. Chem. 34* (1969) 2543–2549.
[21] P. A. Grieco, S. Gilman, M. Nishizawa, *J. Org. Chem. 41* (1976) 1485–1486.
[22] B. M. Trost, J. L. Belletire, S. Godleski, P. G. McDougal, J. M. Balkovec, *J. Org. Chem. 51* (1986) 2370–2374; A. Hassner, V. Alexanian, *Tetrahedron Lett. 1978*, 4475–4478; M. K. Dhaon, R. K. Olsen, K. Ramasamay, *J. Org. Chem. 47* (1982) 1962–1965.
[23] R. Heiermann, O. Pongs, *Nucleic Acid Res. 13* (1985) 2709–2730.
[24] F. Kreklau, *Diplomarbeit*, Universität Bochum, 1985.
[25] T. Ojasoo, J. P. Raynaud, *Cancer Res. 38* (1978) 4186–4198.
[26] P. Maroy, R. Dennis, C. Beckers, B. A. Sage, J. D. O'Connor, *Proc. Natl. Acad. Sci. USA 75* (1978) 6035–6038.
[27] M. A. Yund, D. S. King, J. W. Fristrom, *Proc. Natl. Acad. Sci. USA 75* (1978) 6039–6043.
[28] M. Ashburner, *Dev. Biol. 35* (1973) 47–61.
[29] H. Moriyama, K. Nakanishi, *Tetrahedron Lett. 1968*, 1111–1112; M. N. Galbraith, D. H. S. Horn, *Aust. J. Chem. 22* (1969) 1045–1057.
[30] G. Scatchard, *Ann. N.Y. Acad. Sci. 51* (1949) 660–672; vgl. auch D. L. Osterbur, M. A. Yund, *J. Cell. Biochem. 20* (1982) 277–282.

Reaction of Decamethylsilicocene with Sulfur, Selenium, and Tellurium: From a p_π–p_π System to New Heterocycles

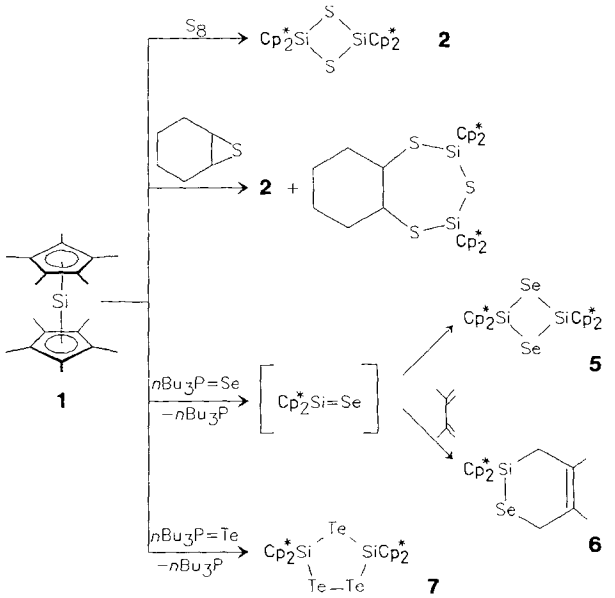
By *Peter Jutzi,* Andreas Möhrke, Achim Müller,* and *Hartmut Bögge*

Decamethylsilicocene **1** is the first stable compound of divalent silicon.[1] According to our earlier investigations, this π complex reacts as a dialkylsilanediyl: for example, **1** undergoes insertion into element–hydrogen bonds[2] and [2+1] cycloadditions with double-bond systems of the type $X=C=Y$.[3] This behavior is due to the facile η^5–η^1 haptotropic rearrangement of the pentamethylcyclopentadienyl (Cp^*) ligands. An η^1-bonded Cp^* ligand at silicon has been shown to be very bulky.[4] For this reason, we decided to investigate whether simple combination of **1** with electron-sextet fragments X might offer an approach to kinetically stabilized p_π–p_π systems of the type $Cp^*_2Si=X$ [Eq. (a)]. In particular, we studied the reaction of **1** with sulfur, selenium, and tellurium sources (X = S, Se, Te).

$$R_2Si: + :\ddot{X} \rightarrow R_2Si=\ddot{X} \qquad \text{(a)}$$

Compound **1** reacts in benzene at room temperature with *cyclo*-S_8 in a nearly quantitative fashion to give 2,2,4,4-tetrakis(pentamethylcyclopentadienyl)-1,3,2,4-dithiadisiletane **2** (Scheme 1). The conceivable silathione intermediate, $Cp^*_2Si=S$, has not been detected so far; for example, trapping experiments with 2,3-dimethylbutadiene have been unsuccessful. If cyclohexene sulfide is used as the sulfur source, higher reaction temperatures are required. In addition to **2**, the novel bicyclic compound **3** was unexpectedly obtained. We were able to show that **3** is not formed from cyclohexene sulfide and **2**.

Reaction of **1** with tri-*n*-butylphosphane selenide[5] in benzene at room temperature led, again nearly quantitatively, to formation of diselenadisiletane **5**, which is analogous to **2**.[6] If the reaction is carried out in the presence of 2,3-dimethylbutadiene, the heterocycle **6** is obtained in good yield. Thus, it was possible to trap the intermediate silaselone **4** by [2+4] cycloaddition.[7] Apparently, however, **4** is not kinetically stable enough to be isolated under normal conditions.



Scheme 1. Reactions of **1** with sulfur, selenium, and tellurium.

The reaction of **1** with tri-*n*-butylphosphane telluride proceeds in an unexpected way.[5] At room temperature, or even at −30 °C, the dark red 1,2,4,3,5-tritelluradisilole **7** is formed. Intermediates have not yet been detected. Compound **7** is the first neutral silicon–tellurium heterocycle. The molecular structure of **7**, determined by X-ray analysis,[8] is shown in Figure 1 together with selected bond distances and angles. No X-ray structure data were previously available for molecular silicon–tellurium systems, though X-ray struc-

[*] Prof. Dr. P. Jutzi, Dipl.-Chem. A. Möhrke, Prof. Dr. A. Müller [+], Dr. H. Bögge [+]
Fakultät für Chemie der Universität
Universitätsstrasse, D-4800 Bielefeld (FRG)
[+] X-ray structure analysis

tures have been determined for $K_6Si_2Te_6$,[9] $Na_6Si_2Te_6$,[10] and $K_4Si_4Te_{10}$.[11] Noteworthy in the structure of **7** are the large C–Si–C angles (approximately 118°), caused by the bulky Cp* ligands. The Te–Si–Te angles (approximately 104°) are correspondingly smaller than expected for tetrahedrally coordinated silicon. The Te–Te distance (2.681 Å) is comparatively[12] short; the dihedral angle Si1-Te1-Te2-Si2 is 51°. The Si–Te distances in **7** (2.529 Å) are slightly longer than the terminal Si–Te distances in the tellurosilicates above. For comparison, the Pauling method,[13] that is, the sum of the tetrahedron radii for covalent single bonds, gives a distance of 2.49 Å.

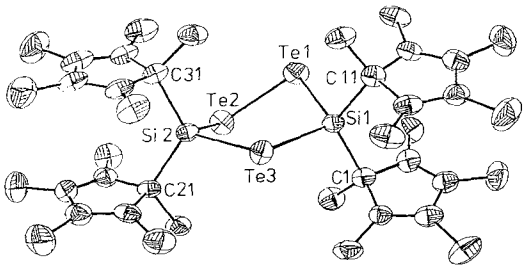


Fig. 1. Molecular structure of **7**. Important bond lengths [Å] and angles [°]: Si1–Te1 2.529(2), Si1-Te3 2.529(3), Te1-Te2 2.681(1); Te2-Te1-Si1 99.4(1), Te1-Te2-Si2 97.8(1), Si1-Te3-Si2 106.8(1), Te1-Si1-Te3 104.3(1), Te2-Si2-Te3 104.4(1).

The identity of the other new compounds (**2, 3, 5, 6**) was established by spectroscopic and analytical data. The functionality offered by the Cp* ligands[4] makes these compounds, as well as the heterocycle **7**, very interesting preparatively.

It remains to be determined whether the formation of **2, 3,** and **7** proceeds via double-bond systems of the type $Cp^*_2Si=X$. Detection of the silaselone **4**, however, should encourage reaction of other electron-sextet fragments with decamethylsilicocene **1** in order to synthesize compounds with (p–p)π bonds to silicon.

Experimental Procedure

2: A solution of **1** (1.2 g, 4.02 mmol) in 20 mL of benzene was treated with sulfur (640 mg) and the reaction mixture was stirred for 16 h at room temperature. The solvent was removed under vacuum and the residue was washed with carbon disulfide. Crystallization from toluene afforded 1.12 g (84%) of **2** (m.p. 330 °C). ^{1}H NMR (300.133 MHz, $CDCl_3$): $\delta = 1.45$, 1.69, 1.84 (each s, 12H:24H:24H; $C_5(CH_3)_5$). MS (CI isobutane): *m/z* 660 ($M^{\oplus}$, 31%), 525 ($M^{\oplus}-Cp^*$, 100).

2/3: **1** (1.66 g, 5.56 mmol) and cyclohexene sulfide (790 mg, 6.92 mmol) in 15 mL of toluene were heated at 105 °C for 2.5 h. After removal of the solvent by vacuum distillation, 20 mL of *n*-hexane was added to the colorless residue to form a suspension. Insoluble **2** (1.2 g, 65%) was separated. Concentration of the *n*-hexane phase gave **3** (400 mg, 19%) as colorless needles (m.p. 251 °C, dec.). ^{1}H NMR (300.133 MHz, $CDCl_3$): $\delta = 1.18$ (s, 6H; $C_5(CH_3)_5$), 1.28 (m, 4H; $-CH_2-CH_2-CH=$), 1.39, 1.66, 1.74, 1.76, 1.82, 1.90, 1.99, 2.03 (each s, 6H:12H:6H:6H:6H:6H:6H:6H; $C_5(CH_3)_5$), 2.31 (m, 4H; $-CH_2-CH_2-CH=$), 3.48 (m, 2H, $=CH-S-$). ^{29}Si NMR (59.595 MHz, $CDCl_3$): $\delta = 14.9$; MS (CI isobutane): 774 ($M^{\oplus}$). MS (EI, 70 eV): *m/z* 639 ($M^{\oplus}-Cp^*$, 39%), 505 [$M^{\oplus}$-($Cp^* + C_5(CH_3)_4CH_2$), 3], 309 [$(C_6H_{10}S_2Si\text{-}Cp^*)^{\oplus}$, 100].

5: **1** (500 mg, 1.7 mmol) was treated with tri-*n*-butylphosphane selenide (560 mg, 2.0 mmol) in 10 mL of benzene. The solution was stirred for 12 h at room temperature and the solvent then removed under vacuum. The residue was washed with *n*-pentane. Crystallization from toluene gave 560 mg (89%) of **4** as colorless needles (m.p. 335 °C). ^{1}H NMR (300.133 MHz; $CDCl_3$): $\delta = 1.55$, 1.68, 1.85 (each s, 12H:24H:24H; $C_5(CH_3)_5$). MS (70 eV): *m/z* 756/754 ($M^{\oplus}$, 1%), 621/619 ($M^{\oplus}-Cp^*$, 10), 487/485 [$M^{\oplus}-(Cp^* + C_5(CH_3)_4CH_2$), 41], 163 ($Cp^*Si^{\oplus}$, 100).

6: **1** (640 mg, 2.1 mmol) was dissolved in 5 mL of toluene and 5 mL of 2,3-dimethyl-1,3-butadiene. Tri-*n*-butylphosphane selenide (620 mg, 2.2 mmol) was added and the resulting solution was stirred for 18 h at room temperature. The solvent was removed under vacuum and the residue was recrystallized from a small amount of *n*-pentane, affording 586 mg (58%) of **4** (m.p. 121 °C). ^{1}H NMR (300.133 MHz, C_6D_6): $\delta = 1.13$ (s, 6H; $C_5(CH_3)_5$), 1.71 (s, 15H; $C_5(CH_3)_5/C=C-CH_3$), 1.85 (s, 9H; $C_5(CH_3)_5/C=C-CH_3$), 1.89 (s, 2H; Si–CH_2–), 1.97 (s, 6H; $C_5(CH_3)_5$), 2.84 (s, 2H; Se–CH_2–). ^{29}Si NMR (59.595 MHz, $CDCl_3$): $\delta = 25.2$. MS (70 eV): *m/z* 460 ($M^{\oplus}$, 5%), 325 ($M^{\oplus}-Cp^*$, 73), 243 [$M^{\oplus}-(Cp^* + C_6H_{10})$, 69], 135 ($Cp^{*\oplus}$, 100).

7: A solution of tri-*n*-butylphosphane telluride (1.32 g, 4.0 mmol) in 10 mL of toluene was added dropwise over 1 h to a solution of **1** (1.2 g, 4.0 mmol) in 15 mL of toluene at room temperature. The dark red solution was concentrated to dryness under vacuum and the residue was washed with a small amount of *n*-pentane. Crystallization from refluxing toluene afforded 1.49 g (76%) of **7** as dark red prisms (m.p. 227 °C, dec.). ^{1}H NMR (300.133 MHz, $CDCl_3$): $\delta = 1.25$, 1.72, 1.92 (each s, broad; 12H:24H:24H, $C_5(CH_3)_5$). ^{29}Si NMR (59.595 MHz, $CDCl_3$): $\delta = 13.0$. ^{125}Te NMR (94.714 MHz, $CDCl_3$): $\delta = -564$, -255. MS (70 eV): *m/z* 846 ($M^{\oplus}-Cp^*$, 4%), 711 ($M^{\oplus}-2Cp^*$, 4), 163 ($Cp^*Si^{\oplus}$, 100).

Received: June 8, 1989 [Z 3385 IE]
German version: *Angew. Chem. 101* (1989) 1527

[1] P. Jutzi, D. Kanne, C. Krüger, *Angew. Chem. 98* (1986) 163; *Angew. Chem. Int. Ed. Engl. 25* (1986) 164.
[2] P. Jutzi, U. Holtmann, H. Bögge, A. Müller, *J. Chem. Soc. Chem. Commun. 1988*, 305.
[3] P. Jutzi, A. Möhrke, *Angew. Chem. 101* (1989) 769; *Angew. Chem. Int. Ed. Engl. 28* (1989) 762.
[4] P. Jutzi, *Comments Inorg. Chem. 6* (1987) 133.
[5] Compound **1** reacts at higher temperatures with elemental selenium or tellurium, resulting in the formation of complex mixtures.
[6] Only a few diselenadisiletanes have been reported: a) M. N. Bochkarev, L. P. Sanina, N. S. Vyazankin, *Zh. Obshch. Khim. 39* (1965) 135; b) D. P. Thompson, P. Bondjouk, *J. Chem. Soc. Chem. Commun. 1987*, 1466.
[7] For the intermediacy of an $R_2Si=Se$ system, see [6b].
[8] Compound **7** forms triclinic crystals $P\bar{1}$, $a = 8.886$, $b = 15.794$, $c = 15.749$ Å, $\alpha = 69.92(3)$, $\beta = 88.29(3)$, $\gamma = 79.91(3)°$, $V = 2042.9$ Å^3, $Z = 2$, $\varrho_{calcd.} = 1.59$ g cm^{-3}; structure solution by the heavy-atom method (SHELXTL), $R = 0.067$ for 6658 unique reflections with $F_o > 3.92\,\sigma(F_o)$, Syntex $P2_1$ four-circle diffractometer, $Mo_{K\alpha}$ radiation, graphite monochromator. Further details of the crystal structure investigation may be obtained from the Fachinformationszentrum Karlsruhe, Gesellschaft für wissenschaftlich-technische Information mbH, D-7514 Eggenstein-Leopoldshafen 2 (FRG), on quoting the depository number CSD-54136, the names of the authors, and the journal citation.
[9] G. Dittmar, *Angew. Chem. 89* (1977) 566; *Angew. Chem. Int. Ed. Engl. 16* (1977) 554; *Acta Crystallogr. B34* (1978) 2390.
[10] B. Eisenmann, H. Schäfer, *Z. Anorg. Allg. Chem. 491* (1982) 67.
[11] B. Eisenmann, H. Schwerer, H. Schäfer, *Z. Naturforsch. B36* (1981) 1538.
[12] Compare with the Te–Te distance of 2.710 Å in *cis*-3,5-dibenzylidene-1,2,4-tritellurole: M. V. Lakshmikantham, M. P. Cava, M. Albeck, L. Engman, P. Carrol, I. Bergman, F. Wudl, *Tetrahedron Lett. 22* (1981) 4199.
[13] L. Pauling: Die Natur der chemischen Bindung, Verlag Chemie, Weinheim 1962, p. 237; The Nature of the Chemical Bond, 3rd ed., Cornell University Press, Ithaca, NY, 1960.

Water-Soluble Porphyrin Diglycosides with Photosensitizing Properties**

By *Gerd Fülling, Doris Schröder,* and *Burchard Franck**

Since the mid-1970s, photosensitizing porphyrins have been used in tumor therapy.[1] This photodynamic therapy (PDT) is based on the fact that suitable porphyrins become concentrated in tumor tissue and, upon subsequent irradiation with visible light in the presence of oxygen, specifically

[*] Prof. Dr. B. Franck, Dr. G. Fülling [+], Dipl.-Chem. D. Schröder
Organisch-chemisches Institut der Universität
Orleansring 23, D-4400 Münster (FRG)
[+] Present address:
Hoechst AG
D-6000 Frankfurt am Main 80 (FRG)

[**] Novel Porphyrinoids, Part 8. This work was supported by the Deutsche Forschungsgemeinschaft and the Fonds der Chemischen Industrie. Part 7: K.-H. Schumacher, B. Franck, *Angew. Chem. 101* (1989) 1292; *Angew. Chem. Int. Ed. Engl. 28* (1989) 1243.

destroy the tumor. A porphyrin mixture obtained from hemin **1**, the red pigment of blood, is most often used; it consists of hematoporphyrin **3** and related porphyrins and is called "hematoporphyrin derivative" (Hpd). Of topical interest is the use of Hpd to kill viruses in transfusion blood.[2]

The wider application of PDT requires photosensitizing porphyrins that are chemically pure, readily accessible, and structurally related to naturally occurring porphyrins. Furthermore, they should be rapidly excreted from the body after therapy. This property may be favored by improved water solubility of the porphyrins.

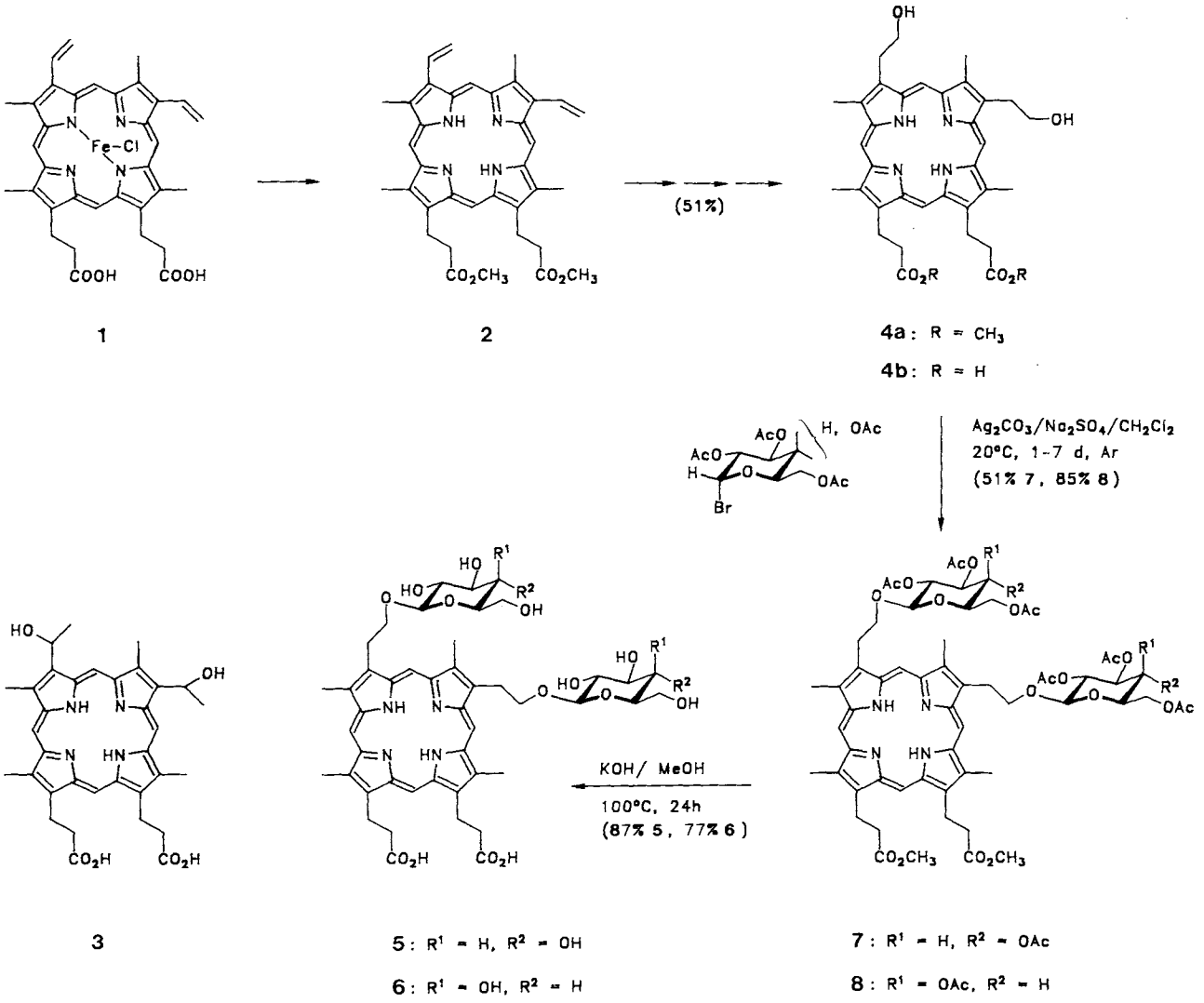
Here we report the first synthesis of porphyrin diglycosides that exhibit excellent water solubility and are efficient photosensitizers—namely, the diglucoside **5** and the digalactoside **6** of isohematoporphyrin **4b**.

In contrast to **3** and Hpd, compound **4b** is both chemically and sterically pure owing to its primary hydroxyl groups. Its dimethyl ester **4a** can be obtained from protoporphyrin dimethyl ester **2** in three steps (51% overall yield) as described by *Kenner* et al.[3] Diastereoselective *O*-glycosylation was accomplished in nonpolar solvents with a solid, surface-active silver catalyst and neighboring-group-active acetyl groups, affording stable β-diglycosides (Scheme 1).

The glycosylation with α-D-acetobromoglucose or α-D-acetobromogalactose, carried out at room temperature with TLC monitoring, was complete in 1–7 days depending on the quality of the freshly prepared silver carbonate.[5] Column chromatography with CH_2Cl_2:MeOH 50:1 on silica gel gave the octaacetylporphyrin diglucoside **7** (m.p. 118 °C) or digalactoside **8** (m.p. 100 °C) in 51 and 85% yield, respectively.[4] The β configuration at the glycosidic C atoms is unambiguously established by comparison of the ^{13}C NMR signals ($CDCl_3$) of C1 and C5 in the sugar moieties of **7** and **8** with those of the acetylated α- and β-methylglycosides of D-glucose and D-galactose.[6]

Conversion of the octaacetylporphyrin diglycosides **7** and **8** to the water-soluble, free diglycosides **5** and **6**, respectively, was accomplished by alkaline saponification. According to TLC monitoring, reaction was complete after refluxing with KOH/aqueous MeOH for 24 h (87 and 77% yield, respectively). These conditions show that the bis(D-glucosyl)isohematoporphyrin **5** and the bis(D-galactosyl)isohematoporphyrin **6** are extremely stable.

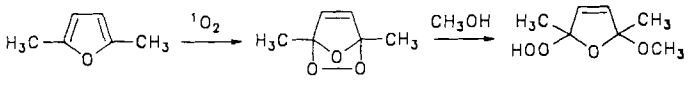
Diglucoside **5** exhibits a water solubility of 4%, which is unusually good for a porphyrin derivative: **5** is therefore a promising candidate for physiological investigations. The water solubility of digalactoside **6** is similarly high. The two isohematoporphyrin diglycosides **5** and **6** are both easily accessible from inexpensive hemin **1** in six steps (overall yields of 16 and 23%, respectively). Compounds **5**–**8** offer derivatives of a porphyrin natural product with a wide range of distribution coefficients and membrane interactions.



Scheme 1. Synthesis of isohematoporphyrin diglycosides **5** and **6** from isohematoporphyrin dimethyl ester **4a** [4].

With respect to medicinal applications of the isohematoporphyrin diglycosides **5–8**, it was important to know whether the polar sugar moiety would affect the photosensitizing activity. Of particular interest was the formation of singlet oxygen, which is thought to be involved in the antitumor activity of Hpd.[7]

The trapping reaction with 2,5-dimethylfuran **9**[8] under standard conditions proved suitable for comparative, quantitative determination of the amount of $^1O_2$ formed.[9]



9 **10** **11**

The results in Table 1 show that the new porphyrin diglycosides **5–8** are efficient photosensitizers. Each produces roughly a hundredfold amount of chemically reacted $^1O_2$ in 20 min. Thus, they are almost as efficient as the well-known photosensitizer Rose Bengal.

Table 1. Comparison of $^1O_2$ formation under standard conditions: 2,5-dimethylfuran **9** as trapping agent; quantitative determination (after methanolysis) of the amount of crystalline hydroperoxide **11** formed. Ca. 0.005 mmol of photosensitizer and 1.44 g (15 mmol) of **9** in 160 mL of benzene:MeOH (3:1); irradiation with a 150-W halogen lamp while O_2 is bubbled through the solution (20 min, 0 °C).

Sensitizer ([mg])	Yield of **11** based on **9** [%]
Isohematoporphyrin dimethyl ester **4a** (3.0)	18
Hematoporphyrin **3** (3.0)	30
Octaacetylporphyrin diglucoside **7** (4.8)	46
Octaacetylporphyrin digalactoside **8** (4.6)	19
Isohematoporphyrin diglucoside **5** (4.1)	22
Isohematoporphyrin digalactoside **6** (4.4)	28
Rose Bengal (5.4)	50
Control without sensitizer	–

Detailed investigations of the photophysical properties of the isohematoporphyrin diglucoside **5** and vinylogous porphyrinoids[10, 11] will soon be reported.[12]

Experimental Procedure

7: α-D-Acetobromoglucose (1.6 g, 3.9 mmol), sodium sulfate (3 g), and freshly prepared silver carbonate [5] (1.6 g) were added under argon to a solution of isohematoporphyrin dimethyl ester **4a** (172 mg, 0.27 mmol) in 250 mL of degassed, dry dichloromethane and the reaction mixture was stirred in the dark at room temperature for 24 h (TLC monitoring, chloroform:methanol 50:1, silica gel TCL plates F_{254}, Merck). The reaction mixture was then filtered through Celite and the filtrate was evaporated under vacuum. Column chromatography of the residue on 200 g of silica gel (Merck, particle size 0.063–0.2 mm) with chloroform gave 180 mg (51%) of red, microcrystalline octaacetylisohematoporphyrin diglucoside dimethyl ester **7**, m.p. 118 °C. EI-MS: *m/z* 1287 (100%, $M^{\oplus}$), 1200 (6, $M^{\oplus}-CH_2CH_2COOCH_3$), 927 (60, $M^{\oplus}-CH_2O$-glucose acetate). UV/VIS ($CHCl_3$): λ_{max} (log ε) = 400 (5.25), 499 (4.15), 533 (3.98), 568 (3.80), 595 (3.11), 622 nm (3.64). ^1H NMR (300 MHz, $CDCl_3$): $\delta = -3.84$ (s, 2H; NH), 9.99, 10.01, 10.08, 10.10 (4s, 1H each; *meso*-H). ^{13}C NMR (75.47 MHz, broadband-decoupled, $CDCl_3$): δ = 11.67, 11.75, 11.84 (pyrrole CH_3), 19.44, 19.52, 20.46, 20.51, 20.65 (acetyl-CH_3), 51.70 (ester CH_3), 61.99 (Glu-C6), 68.44 (Glu-C4), 71.06 (Glu-C2), 71.96 (Glu-C5), 72.87 (Glu-C3), 101.23 (Glu-C1), 96.41, 96.63, 96.75, 96.90 (*meso*-C).

8 was synthesized analogously.

5: A solution of **7** (51 mg, 0.04 mmol) and potassium hydroxide (80 mg) in 75 mL of methanol and 6 mL of distilled water was refluxed for 24 h. The reaction mixture was then allowed to cool to room temperature and neutralized by addition of acetic acid. Evaporation under vacuum afforded an oily residue, which was applied with a 10-mL syringe to a SEP-PAK C_{18} cartridge (Waters, Part. No. 51910), previously washed with methanol followed by water. The porphyrin diglucoside **5** was completely adsorbed on the cartridge and retained, so that inorganic components could be removed by washing with water and **5** could be subsequently eluted with methanol. Evaporation of the eluate gave 32 mg (87%) of red **5**, m.p. 180 °C. FD-MS: *m/z* 923 (100%, $M^{\oplus}$), UV/VIS (MeOH): λ_{max} (log ε) = 396 (5.00), 498 (3.77), 532 (3.62), 569 (3.46), 620 nm (3.26). ^1H NMR (300 MHz, [D_6]acetone, solution prepared by the SEP-PAK cartridge method, see above): $\delta = -4.0$ (s, 2H; NH), 9.92, 10.01, 10.07, 10.10 (4s; *meso*-H). ^{13}C NMR (75.47 MHz, broadband-decoupled, D_2O): δ = 9.2 (pyrrole CH_3), 61.0, 61.1 (Glu-C6), 69.7, 69.9 (Glu-C4), 73.5 (Glu-C2), 76.1, 76.2 (Glu-C3, Glu-C5), 95 (br., *meso*-C), 102.1, 102.8 (Glu-C1), 179 (COOH).

Received: June 6, 1989 [Z 3378 IE]
German version: *Angew. Chem. 101* (1989) 1550

CAS Registry numbers:
3, 14459-29-1; **4a**, 33070-12-1; **4b**, 3819-29-2; **5**, 122744-60-9; **6**, 122744-61-0; **7**, 122744-62-1; **8**, 122744-63-2; **9**, 625-86-5; **10**, 45722-89-2; **11**, 13249-74-6; α-D-acetobromogalactose, 3068-32-4; α-D-acetobromoglucose, 572-09-8.

[1] T. J. Dougherty, *Proc. SPIE Int. Soc. Opt. Eng. Ser. 5, Vol. 997* (1988) 2–7; A. Andreoni, R. Cubeddu (Eds.): *Porphyrins in Tumor Therapy*, Plenum Press, New York 1984.
[2] J. L. Matthews, J. T. Newman, F. Sogandares-Bernal, M. M. Judy, H. Skiles, J. E. Leveson, A. J. Marengo-Rove, T. C. Chanh, *Transfusion (Philadelphia) 28* (1988) 81–83.
[3] G. W. Kenner, S. W. McCombie, K. M. Smith, *Justus Liebigs Ann. Chem. 1973*, 1329–1338.
[4] The new compounds **5–8** were completely characterized by elemental analysis and spectroscopic data.
[5] C. M. McCloskey, G. H. Coleman, *Org. Synth. Coll. Vol. 3* (1955) 435.
[6] K. Bock, H. Thorgerson in G. A. Webb (Ed.): *Annu. Rep. NMR Spectrosc. 13* (1982) 2–57.
[7] K. R. Weishaupt, L. J. Gomer, T. J. Dougherty, *Cancer Res. 36* (1976) 2326–2329.
[8] C. S. Foote, M. T. Wuesthoff, S. Wexler, I. G. Burstain, R. Denny, G. O. Schenck, K.-H. Schulte-Elte, *Tetrahedron 23* (1967) 2583–2599.
[9] B. Franck, M. Dust, A. Stange, P. P. Hoppe, *Naturwissenschaften 69* (1982) 401–402.
[10] M. Gosmann, B. Franck, *Angew. Chem. 98* (1986) 1107–1108; *Angew. Chem. Int. Ed. Engl. 25* (1986) 1100–1101; B. Franck, M. Gosmann, G. Knübel, DOS 3635820 (28. April 1988) BASF AG; *Chem. Abstr. 109* (1988) 94748u.
[11] G. Knübel, B. Franck, *Angew. Chem. 100* (1988) 1203–1204; *Angew. Chem. Int. Ed. Engl. 27* (1988) 1170–1172.
[12] G. Schermann, R. Schmidt, A. Völker, H.-D. Brauer, H. Mertes, B. Franck, *Photochem. Photobiol.* in press.

Thermal and Electrocatalytic Epimerization at Iron as the Chiral Center**

By *Henri Brunner,* Konrad Fisch, Peter G. Jones,* and *Josef Salbeck*

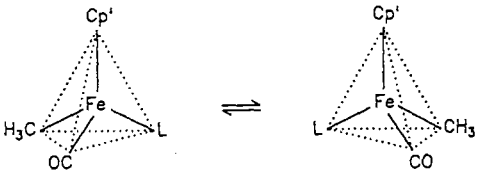
Optically active transition metal compounds in which the transition metal is the chiral center can be synthesized with the optically active aminophosphane ligands L and L'.[1]

(*S*)-(+)-$(C_6H_5)_2P$-N(CH_3)-CH(CH_3)C_6H_5 L
(*S*)-(−)-$(C_6H_5)_2P$-NH-CH(CH_3)C_6H_5 L'

[*] Prof. Dr. H. Brunner, Dipl.-Chem. K. Fisch
Institut für Anorganische Chemie der Universität
Universitätsstrasse 31, D-8400 Regensburg (FRG)
Prof. Dr. P. G. Jones
Institut für Anorganische und Analytische Chemie der
Technischen Universität Braunschweig
Dr. J. Salbeck
Institut für Organische Chemie der Universität Regensburg

[**] Optically active transition metal complexes. Part 96. This work was supported by the Deutsche Forschungsgemeinschaft, the Fonds der Chemischen Industrie and BASF AG, Ludwigshafen. Part 95: P. Bladon, P. L. Pauson, H. Brunner, R. Eder, *J. Organomet. Chem. 355* (1988) 449.

Examples are the acetyl iron compounds (*RS*)- and (*SS*)-$[CpFe(CO)(L)COCH_3]$ (Cp = η-C_5H_5) and their analogues containing the ligand L′. In all cases, the epimerization at the iron atom occurs via dissociation of L and L′; because of the participation of chiral dihapto-acyl intermediates and the achiral rearrangement product $[CpFe(CO)_2CH_3]$, it is difficult to analyze this process.[2–4] Such complications do not occur in the epimerization of the methyl iron compounds **1**[5] and **2**.



$(-)_{436}$-($R_{Fe}S_C$)-**1a** $(+)_{436}$-($S_{Fe}S_C$)-**1b**
$(-)_{436}$-($R_{Fe}S_C$)-**2a** $(+)_{436}$-($S_{Fe}S_C$)-**2b**
1, Cp′ = Cyclopentadienyl (Cp); **2**, Cp′ = Indenyl (In)

The photochemical reaction of the prochiral compounds $[Cp'Fe(CO)_2CH_3]$, Cp′ = cyclopentadienyl or indenyl, with L proceeds via exchange of one of the two enantiotopic CO groups to give the compounds **1a,b**[5] and **2a,b**; the diastereomeric ratio is 50:50 in each case.[6] The isomers can be separated by preparative liquid chromatography and by fractional crystallization.[7] The absolute configurations of **1a** and **2a** have been determined by X-ray structural analysis;[8] these compounds take up remarkably similar conformations in the crystal (Fig. 1).

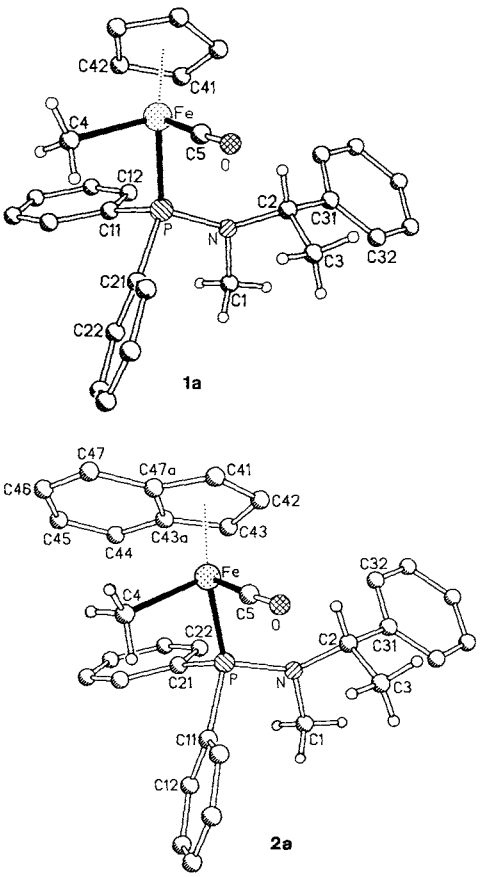


Fig. 1. Structures of $(-)_{436}$-($R_{Fe}S_C$)-**1a** and $(-)_{436}$-($R_{Fe}S_C$)-**2a** in the crystal.

The thermal epimerization of **1a** and **2a** in C_6D_6 is first order;[9] in both cases it was followed by baseline-separated ^1H NMR signals.[10] The rate of epimerization is not changed measurably when L is added, while in the presence of L′, a complete phosphane exchange occurs which is also first order. The epimerization of **2a** was shown to have a large positive entropy of activation (75 $J\,K^{-1}\,mol^{-1}$).[11]

These results suggest a dissociative epimerization mechanism whose rate-determining step is the cleavage of the Fe–L bond. The kinetic data for this process indicate that the intermediate or transition state is an achiral species.[12]

The indenyl complex **2a** ($t_{1/2}$ = 37 min, 50.0 °C) epimerizes 10–20 times faster than the cyclopentadienyl complex **1a** ($t_{1/2}$ = 70 min, 70.0 °C). We suggest that this relatively small acceleration is due to the increased steric interaction between the indenyl and aminophosphane ligands which favors phosphane dissociation. The absence of an "indenyl effect" (higher reactivity of the indenyl system compared to the analogous Cp system because of ring slippage[13, 14]) must be due to the absence of associative processes.

Significant differences were observed in the electrocatalytic configuration transformation of the iron complexes **1a** and **2a**, depending on the pentahapto-bonded π ligand. While the indenyl complex **2a** is epimerized completely within one minute at −35 °C in THF using sodium amalgam as the reducing agent,[15] the Cp compound **1a** surprisingly does not epimerize either at −35 °C or at +20 °C under the same conditions. In contrast to the Cp compound **1a**, the indenyl compound **2a** undergoes electron transfer to give a 19e-species which loses phosphane. The resulting 17e-radical anion changes its configuration before phosphane association and transfer of the electron back to the catalyst or substrate completes the catalytic cycle.

When the epimerization of **2a** is oxidatively induced with 50 mol-% $[Cp_2Fe][PF_6]$, it is incomplete at +20 °C in THF after 30 min; however, under the same conditions the epimerization of **1a** establishes thermodynamic equilibrium **1a**:**1b** = 62:38 after five minutes.

The cyclovoltammograms of **1a** and **2a** are in agreement with the behavior of the complexes with respect to the starting reagents used; while the reduction of **2a** shows an irreversible reduction wave at a peak potential of −2185 mV vs. SCE, no corresponding behavior is observed for **1a** up to the commencement of the reduction of the solvent at −2570 mV. The reduction of the indenyl compound **2a** is accompanied by a further rapid reaction. The voltammograms are however almost identical for the oxidation of **2a** (+240 mV) and **1a** (235 mV); in each case these are irreversible oxidation processes followed by other rapid reactions.[16] All observed oxidation and reduction potentials lie within the potential range of the starting reagents used for the electrocatalysis.

Thus, in the case of the oxidatively or reductively induced epimerization of **1a** and **2a**, we have detected for the first time a configuration transformation induced by electron transfer[17] which is accelerated enormously in comparison with the thermal reaction.

Received: June 21, 1989;
revised: August 2, 1989 [Z 3405 IE]
German version: *Angew. Chem. 101* (1989) 1558

CAS Registry numbers:
1a, 59727-90-1; **1b**, 59568-04-6; **2a**, 123075-70-7; **2b**, 123163-87-1.

[1] H. Brunner, *Adv. Organomet. Chem. 18* (1980) 183.
[2] H. Brunner, H. Vogt, *Chem. Ber. 114* (1981) 2186.
[3] H. Brunner, H. Vogt, *J. Organomet. Chem. 191* (1980) 181.

[4] H. Brunner, B. Hammer, *Organometallics 2* (1983) 1595.
[5] H. Brunner, H. Vogt, *J. Organomet. Chem. 210* (1981) 223.
[6] The indenyl complex **2a,b** was prepared analogous to the Cp complex **1a,b**. [5] **2a,b** is chromatographed on Al_2O_3 in the absence of air; after removal of the starting materials, **2a,b** is eluted with pentane–diethyl ether (4:1) as a brown zone. Removal of the solvents yields **2a,b** as a powder.
[7] The diastereomers **1a** and **1b** were separated as previously described. [5] The separation of **2a** and **2b** was carried out as follows: 1 g of the 1:1 mixture was stirred rapidly in 10 mL pentane. The mother liquor was removed and the extraction of the residue repeated with 5 mL pentane. The residue remaining contains 300 mg of the diastereomer **2a** in optically pure form.
[8] *Crystal structure analysis of* **1a**: $C_{28}H_{30}FeNOP$, $M_r = 483.1$, space group $P2_12_12_1$, $a = 1238.5(2)$, $b = 1387.0(2)$, $c = 1395.5(2)$ pm, $Z = 4$. Structure solved using direct methods. Anisotropic refinement up to $R = 0.028$, $R_w = 0.029$ for 3967 absorption-corrected reflexions up to $2\theta \leq 50°$ ($Mo_{K\alpha}$ irradiation). Absolute configuration determined by η-refinement: $\eta = +1.04(3)$ [4]. *Crystal structure analysis of* **2a**: $C_{32}H_{32}FeNOP$, $M_r = 533.4$, space group $P2_12_12_1$, $a = 1050.4(2)$, $b = 1152.0(1)$, $c = 2245.4(2)$ pm, $Z = 4$. The structure was solved using direct methods. Anisotropic refinement up to $R = 0.051$, $R_w = 0.041$ for 3775 absorption-corrected reflexions up to $2\theta \leq 50°$ ($Mo_{K\alpha}$ irradiation). Absolute configuration determined by η-refinement; $\eta = +0.99(4)$. Further details regarding the crystal structures can be obtained from the Fachinformationszentrum Karlsruhe, Gesellschaft für wissenschaftlich-technische Information mbH, D-7514 Eggenstein-Leopoldshafen 2 (FRG), on quoting the deposition number CSD-54028, the authors and the literature reference.
[9] *Kinetic data for the epimerization of* **1a**: $T = 70.0\,°C$; $k(\mathbf{1a}) = (1.66 \pm 0.03) \times 10^{-4}\,s^{-1}$; $RS/SS_{eq} = 62/38$; $K_{eq} = 0.61$. **1a** + L: $T = 70.0\,°C$; $c(\mathbf{1a}) = c(L) = 0.1\,mol\,L^{-1}$; $k(\mathbf{1a} + L) = (1.66 \pm 0.03) \times 10^{-4}\,s^{-1}$. **2a**: $T = 50.0\,°C$; $k(\mathbf{2a}) = (3.19 \pm 0.10) \times 10^{-4}\,s^{-1}$; $RS/SS_{eq} = 62/38$; $K_{eq} = 0.61$. **2a** + L: $T = 50.0\,°C$; $c(\mathbf{2a}) = c(L) = 0.1\,mol\,L^{-1}$; $k(\mathbf{2a} + L) = (3.10 \pm 0.10) \times 10^{-4}\,s^{-1}$. **2a** + L': $T = 50.0\,°C$; $c(\mathbf{2a}) = 0.1$ mol L^{-1}, $c(L') = 0.3\,mol\,L^{-1}$; $k(\mathbf{2a} + L') = (1.81 \pm 0.06) \times 10^{-4}\,s^{-1}$.
[10] ^1H NMR: **1a** und **1b** see [4]. **2a** (**2b**) (C_6D_6, TMS int., 250 MHz): $\delta = -0.71$ (−0.62) (d, 3H, $J = 5.5$ Hz, Fe-CH_3), 1.52 (1.27) (d, 3H, $J = 7$ Hz, C-CH_3), 2.05 (2.09) (d, 3H, $J = 7.5$ Hz, N-CH_3), 4.50 (4.43) (d, 2H, H-41, H-43), 4.83 (4.73) (t, 1H, H-42), 5.86 (5.35) (m, 1H, H-2), 5.93–7.63 (6.13–7.63) (m, 19H, phenyl and indenyl H).
[11] $\Delta S^* = +(75 \pm 5)\,J\,K^{-1}\,mol^{-1}$; $\Delta H = (119 \pm 6)\,kJ\,mol^{-1}$. The activation parameters were determined between 45.0–55.0 °C.
[12] P. Hofmann, *Angew. Chem. 89* (1977) 551; *Angew. Chem. Int. Ed. Engl. 16* (1977) 536.
[13] M. E. Rerek, F. Basolo, *J. Am. Chem. Soc. 106* (1984) 5908.
[14] M. E. Rerek, F. Basolo, *Organometallics 2* (1984) 740.
[15] **2a** undergoes slight decomposition, as detected by the formation of free phosphane. The degree of decomposition increases with increasing reaction temperature and reaction time.
[16] In the case of **2a**, a second reduction wave is observed at low feed rates during the recording of the cyclovoltammogram in the opposite direction.
[17] D. Astruc, *Angew. Chem. 100* (1988) 662; *Angew. Chem. Int. Ed. Engl. 27* (1988) 643.

Versatile Modes of Allene Bonding in the Structures of $[W_2(OtBu)_6(C_3H_4)]$, $[W_2(OtBu)_6(C_3H_4)(CO)_2]$, and $[W_2(OtBu)_6(C_3H_4)_2]$

By *Roger H. Cayton, Stephanie T. Chacon, Malcolm H. Chisholm,* Mark J. Hampden-Smith, John C. Huffman, Kirsten Folting, Paul D. Ellis,* and *Beth A. Huggins*

The compounds $[M_2(OR)_6](M \equiv M)$ provide templates for developing organometallic chemistry.[1] In particular, the dinuclear center and the M≡M bond allow novel modes of coordination and reactivity. We report here three different modes of allene bonding in compounds **1–3**.

$[W_2(OtBu)_6(C_3H_4)]$ **1** $[W_2(OtBu)_6(C_3H_4)(CO)_2]$ **2** $[W_2(OtBu)_6(C_3H_4)_2]$ **3**

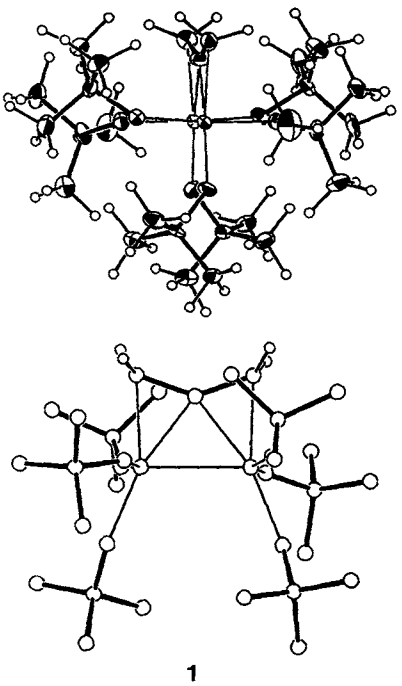
We recently reported the preparation of **1** from $[W_2(OtBu)_6]$ and allene in hydrocarbon solvents.[2] On the basis of NMR spectroscopic data, we proposed a μ-perpendicular allene coordination in which the C_3H_4 moiety had rehybridized to resemble that predicted[3] on theoretical grounds for the transition state for allene racemization.

Compound **1** reacts with CO (>2 equiv.) in hydrocarbon solvents to give complex **2**, which shows two CO stretching frequencies (1900 and 1830 cm^{-1}) in the IR spectrum and four *t*Bu groups in the ^1H and ^{13}C NMR spectra in the ratio 1:2:2:1. For the allene methylene groups one ^{13}C NMR signal and two ^1H NMR signals are observed.

Compound **1** and excess allene react in hydrocarbon solvents at <22 °C to give complex **3**, which, by NMR spectroscopy, has six different O*t*Bu groups, eight allenic protons, and six allenic carbon atoms. The allenic proton resonances form two separate ABCD spin systems.

We have been able to obtain crystals suitable for an X-ray analysis for **1–3** and find, contrary to our earlier prediction,[2] that the allene is aligned parallel to the W–W axis in **1**, whereas complexes **2** and **3** display other modes of bonding.[4]

Two views of compound **1** are shown in Figure 1. The structural parameters associated with the central W_2C_3 moiety indicate an extensive degree of $Wd_\pi - C_3p_\pi$ orbital mixing. Indeed, the C–C distance of 1.47(1) Å is essentially identical to a $C_{sp^2} - C_{sp^2}$ single-bond distance.[5]



1

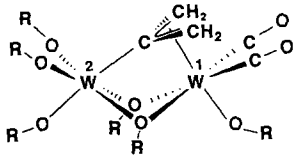
Fig. 1. Two drawings of complex **1** emphasizing the μ-parallel mode of allene-to-W_2 bonding. Pertinent distances [Å] (average) and angles [°]; W-W 2.583(1), C-C (allene) 1.47(1), W-CH_2 2.13(1), W-C 2.09(1), W-O 1.90(2); C-C-C 141(1).

The molecular structure of **2** is shown by a line drawing. The allene ligand, which may be viewed as part of a tungstaallyl(2−)moiety, is σ-bonded to one tungsten and

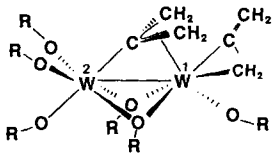
[*] Prof. M. H. Chisholm, Dr. R. H. Cayton, S. T. Chacon, Dr. M. J. Hampden-Smith Dr. J. C. Huffman, Dr. K. Folting
Department of Chemistry and Molecular Structure Center
Indiana University
Bloomington, IN 47405 (USA)
Prof. P. D. Ellis, B. E. Huggins
Department of Chemistry, University of South Carolina
Columbia, SC 29208 (USA)

[**] This work was supported by the Department of Energy, Office of Basic Sciences, Chemistry Division, and by the National Science Foundation.

$\pi(\eta^3)$-bonded to the other.[6] The formal oxidation states of the two tungsten atoms are then +6 and +2 with the two CO ligands being bound to the d^4 W^1 center. The W–W distance is 3.0 Å, a nonbonding distance. The $W(CO)_2$ moiety in **2**, with its low values of $\tilde{\nu}$(CO) and small C–W–C angle (79°), is reminiscent of that in the Mo complex $[Mo(OtBu)_2(py)_2(CO)_2]$.[7]



2



3

The molecular structure of **3**, also shown by a line drawing, reveals a μ-tungstaallyl moiety similar to that found in the structure of **2** and, in addition, a terminal η^2-C_3H_4 ligand which formally may be viewed as replacing the *cis* carbonyl groups in **2**. However, the geometry about W1 is rather different in the two compounds. In **2** the coordination geometry approximates a distorted octahedral unit with the μ-C_3 ligand occupying one site, whereas in **3**, if the η^2-C_3H_4 ligand is considered to take up one position at the metal center, the local geometry corresponds to a square pyramid with the μ-C_3 ligand in the apical position. The W–O bond *trans* to the η^2-C_3H_4 ligand in the basal plane is very long (2.306(7) Å). The long C–C distance of the η^2-C_3H_4 moiety (1.44(1) Å), together with the long W–W distance (2.855(1) Å), indicates extensive Wd_π-to-Cπ^* back-bonding. The NMR data obtained for **3** in solution are entirely consistent with the observed molecular structure in the solid state and require that the η^2-C_3H_4 moiety and the other ligands are not fluxional.

Since the observed molecular structure of **1** is at variance with the previously proposed structure, we compared the bonding between a bent allene fragment and $[W_2(OtBu)_6]$ in the parallel and perpendicular modes. Moreover, we considered the possibility of a facile interconversion of μ-parallel and μ-perpendicular conformers. Such a process would allow the four allenic protons and three carbon atoms to "see" the two tungsten atoms as time-averaged and equivalent and thereby readily account for the observed satellite spectra arising from ^{183}W coupling (^{183}W, $I = ½$ 14.3% natural abundance).

Figure 2 shows the results from Fenske–Hall calculations[8] on the hypothetical molecule $[W_2(OH)_6(C_3H_4)]$ with the structural parameters taken from the structure of **1** (shown on the left side) and with the C_3 moiety rotated about the molecular C_2 axis of symmetry.

The μ-parallel moiety is found to be lower in energy. The extensive mixing of Wd_π–Wd_π and allene p_π orbitals is largely responsible for the lengthening of the C–C and W–W bonds. In particular, this is seen in the bonding of the $2a_1$ orbital, which favors the μ-parallel mode. The rotation of the C_3H_4 moiety about the pseudo-C_2 axis of symmetry is, however, a symmetry-allowed process with only filled–filled crossings being trivially avoided. An analysis of the HOMO and LUMO orbitals during rotation reveals that they do not exhibit an avoided crossing.

The possibility that the μ-allene in **1** was fluxional even in the solid state was investigated by recording the ^2H solid-state nonspinning NMR spectra[9] for $[W_2(OtBu)_6(C_3D_4)]$ ($[D_4]$**1**). The major spectral feature at 19° and −45 °C was a classic Pake doublet with a quadrupole coupling constant of 182.5 ± 0.5 kHz and an asymmetry parameter of 0.06 ± 0.2. The temperature independence and ease of saturation of this line shape are consistent with ^2H nuclei *not* undergoing significant molecular motion in the solid state on the ^2H NMR time scale (i.e., μs range). The observation of only one powder spectrum is consistent with the equivalent ^2H nuclei observed in the solid-state X-ray structure of $[D_4]$ **1**.

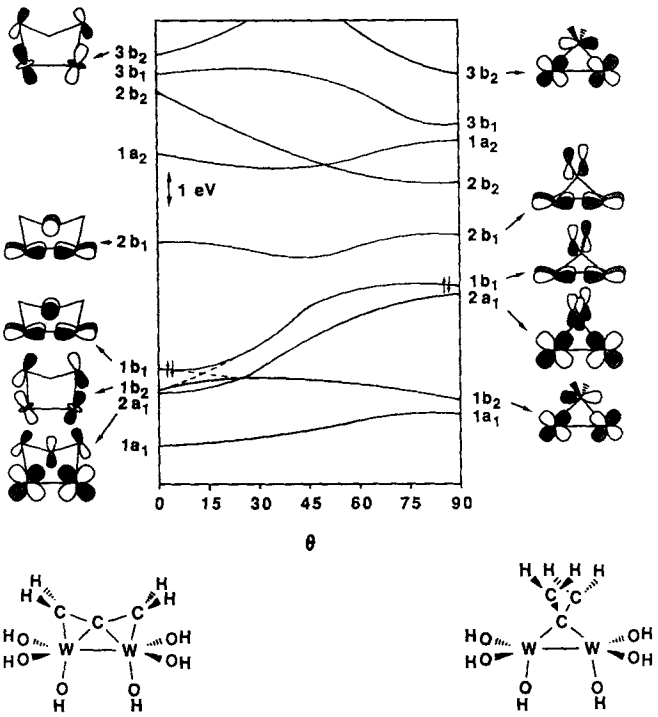


Fig. 2. A Walsh diagram depicting the variations in frontier orbital energies of $[W_2(OH)_6(C_3H_4)]$ obtained by rotating the allene moiety from a μ-parallel to a μ-perpendicular bonding mode. θ refers to the torsional angle between the C_3 plane and the W–W vector (in degrees). The arrows indicate the HOMO.

The bonding modes of allene in compounds **1**–**3** provide prime examples of the flexible modes of coordination available to unsaturated hydrocarbons in their ligation to $[M_2(OR)_6]$ compounds. In each compound the allene-to-tungsten bonding is different from that in the complex $[Cp_2Mo_2(CO)_4(C_3H_4)]$.[10] Whereas the μ-allene coordination in **2** and **3** has been seen before, that in **1**, involving the μ-parallel coordination, is unprecedented.[11] Evidently, μ-parallel–μ-perpendicular interconversions are not rapid in the solid state; whether they occur in solution remains a matter for further study.

Received: April 19, 1989 [Z 3299 IE]
German version: *Angew. Chem. 101* (1989) 1547

CAS Registry numbers:
1, 114907-28-7; **2**, 123099-08-1; **3**, 123123-91-1; $[W_2(OH)_6(C_3H_4)]$, 123123-92-2; allene, 463-49-0.

[1] M. H. Chisholm, D. L. Clark, M. J. Hampden-Smith, D. M. Hoffman *Angew. Chem. 101* (1989) 446; *Angew. Chem. Int. Ed. Engl. 28* (1989) 432.
[2] R. H. Cayton, M. H. Chisholm, M. J. Hampden-Smith *J. Am. Chem. Soc. 110* (1988) 4438.
[3] P. Voltazanos, S. T. Elbert, K. Rudenberg, *J. Am. Chem. Soc. 108* (1986) 3147.
[4] Crystal data for **1** at −144 °C: $a = 11.676(1)$, $b = 16.771(2)$, $c = 17.116(2)$ Å, $\beta = 90.39(1)°$, $Z = 4$, $\varrho_{calcd} = 1.68$ g cm^{-3} space group $P2_1/n$. Of 8830 reflections collected, 4397 were unique and the 4035

having $F > 3\sigma(F)$ were used in the full least-squares refinement. The hydrogen atoms on the allene were located in a difference map. Refinement was completed using anisotropic thermal parameters on the hydrogen atoms. The final residuals are $R(F) = 0.031$ and $R_w(F) = 0.030$. Crystal data for **2** at $-155\,^{\circ}C$: $a = 15.823(4)$, $b = 18.807(5)$, $c = 22.457(6)$ Å, $\beta = 90.93(1)^{\circ}$, $Z = 8$, $\varrho_{calcd} = 1.75\ gm^{-3}$, space group $P2_1/c$. Because of difficulties caused by the presence of a significant "pseudo-cell", no attempt was made to refine anisotropically any atoms except the W atoms. Of the 9384 reflections collected, 8714 were unique and the 3500 reflections with $F > 2.33\sigma(F)$ were used in the refinement, giving final residuals of $R(F) = 0.071$ and $R(F) = 0.071$ and $R_w(F) = 0.072$. The X-ray analysis of the structure can be considered sufficient to uniquely define the basic coordination geometry of **2**. Crystal data for **3** at $-155\,^{\circ}C$: $a = 9.516(3)$, $b = 19.114(7)$, $c = 19.438(6)$ Å, $\beta = 103.32(2)^{\circ}$, $Z = 4$, $\varrho_{calcd} = 1.715\ g\,cm^{-3}$, space group $P2_1/c$. Of the 5957 reflections collected ($6 < 2\theta < 45^{\circ}$, $Mo_{K\alpha}$) 4503 were unique and the 3867 having $F > 2.33\sigma(F)$ were used in the refinement. The hydrogen atoms were refined isotropically and the nonhydrogen atoms anisotropically in the final cycles leading to residuals of $R(F) = 0.038$ and $R_w(F) = 0.037$. For general operating procedures see M. H. Chisholm, K. Folting, J. C. Huffman, C. C. Kirkpatrick *Inorg. Chem. 23* (1984) 1021. Further details of the crystal structure investigation may be obtained from the Fachinformationszentrum Karlsruhe, Gesellschaft für wissenschaftlich-technische Information mbH, D-7514 Eggenstein-Leopoldshafen 2 (FRG), by quoting the depository number CSD-54211, the name of the authors, and the journal citation.

[5] K. Kuchitsa *MTP. Rev. Sci. Phys. Chem. Ser. One 11* (1972) 221.

[6] This type of $M_2(\mu\text{-}\eta^1,\eta^3)$ bonding was first seen for allene in the molecular structure of $[Fe_2(CO)_6(PPh_3)(C_3H_4)]$: R. E. Davies *J. Chem. Soc. Chem. Commun. 1968*, 248.

[7] M. H. Chisholm, J. C. Huffman, R. L. Kelly *J. Am. Chem. Soc. 101* (1979) 7615.

[8] M. B. Hall, R. F. Fenske, *Inorg. Chem. 11* (1972) 768.

[9] C. A. Fyfe: *Solid State NMR for Chemists*, C.F.C. Press, Guelph, Ontario (Canada) 1983. The ^2H NMR spectra were recorded on a Varian XL-400 spectrometer at 61.4 MHz. Each spectrum was an accumulation of 10000 transients, separated by a 10 s–1.7 μs–90° pulse. A solid echo (90°-τ-90°) pulse sequence was used.

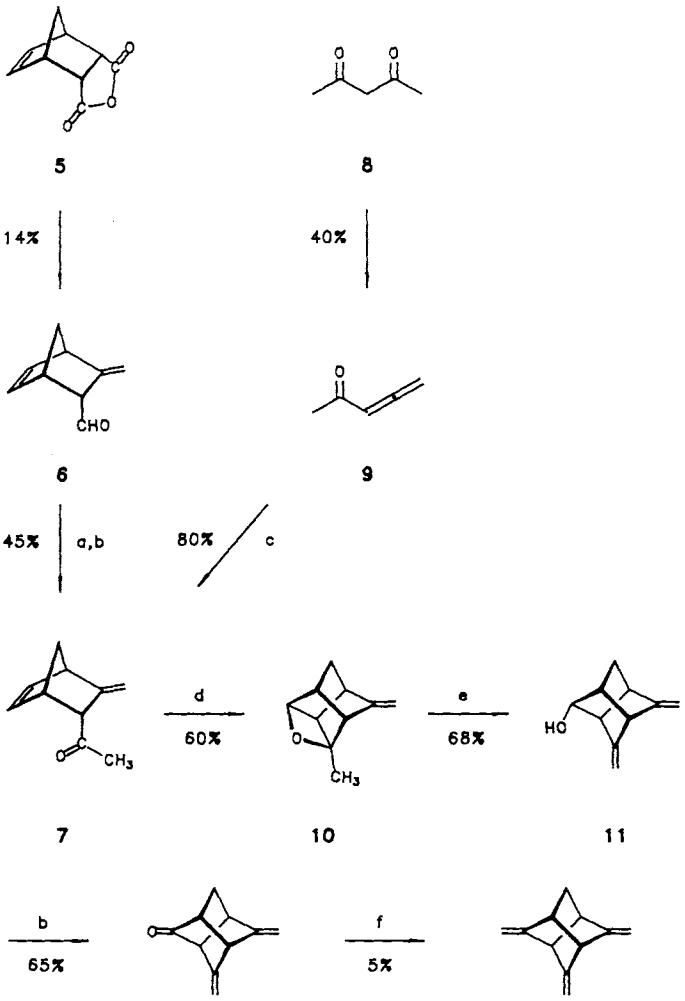
[10] W. I. Bailey, M. H. Chisholm, F. A. Cotton, C. A. Murillo, L. A. Rankel *J. Am. Chem. Soc. 100* (1978) 802.

[11] The alignment of the C–C–C vector with the W–W axis is reminiscent of the carbodiimide adduct $[W_2(O^tBu)_6(RNCNR)]$, R = p-tolyl: F. A. Cotton, W. Schwotzer, E. S. Shamshoum, *Organometallics 4* (1985) 461.

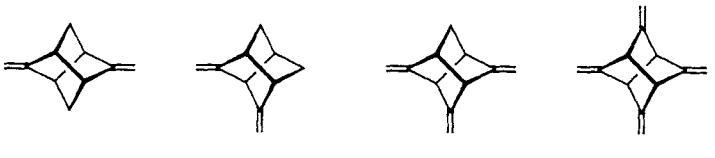
4 6-Dimethylenetricyclo[3.3.0.0^{3,7}]octane-2-one and 2,4,6-Trimethylenetricyclo[3.3.0.0^{3,7}]octane**

By *Rolf Gleiter,* Christoph Sigwart,* and *Bernd Kissler*

The methylene substituted tricyclo[3.3.0.0^{3,7}]octane derivatives **1**–**4**[1] are not only appealing because of their molecular symmetry, they are also of interest with respect to the electronic interaction of the double bonds. Furthermore one must consider possible rearrangements due to the strained ring-skeleton. While the synthesis and properties of **1** and **2** have been reported recently,[2, 3] stellatriene **3**[1] and stellatetraene **4**[1] were unknown species at that time. Now the synthesis of **3** has been achieved along two paths, as shown in Scheme 1. Our first approach started with the aldehyde **6**,[4] which is available in four steps from the *endo* adduct of cyclopentadiene with maleic anhydride **5**. The second path which is shorter and more economic sets out with acetylallene **9** which may be prepared in two steps from acetylacetone **8**.[5] The key intermediate for both routes is the norbornene derivative **7** which yields the oxetane **10** in an intramolecular Paterno–Büchi reaction.[6] Treatment of **10** with lithium diisopropylamide (LDA) affords the regioselective cleavage of the oxetane ring to yield the alcohol **11**, which can be oxidized[7] to 4,6-dimethylenetricyclo-[3.3.0.0^{3,7}]octane-2-one **12**[8]. Stellatriene **3** is obtained from **12** by a Wittig reaction with "instant-ylide" at $-10\,^{\circ}C$.



Scheme 1. a) CH_3MgI/Et_2O; b) $CrO_3 \cdot 2py/CH_2Cl_2$; c) $C_5H_6/CH_2Cl_2/ZnCl_2$; d) $h\nu/C_6H_6$; e) LDA/THF; f) $[(C_6H_5)_3PCH_3]Br/NaNH_2$/THF, $-10\,^{\circ}C$.



The dienone **12** and the triene **3** contain—in a highly strained system—one and two 1,5-hexadiene units, respectively. Both systems react in a [3,3]sigmatropic rearrangement to the corresponding tricyclo[5.2.1.0^{4,10}]deca-1,6-diene derivatives **14**[8] and **13**[8], respectively ($\tau_{1/2}(50\,^{\circ}C) = 31$ min for **12**, $\tau_{1/2}(30\,^{\circ}C)$ ca. 30 min for **3**). Characteristic spectroscopic data of **3** and **12**–**14** are given in Table 1. **12** rearranges to **14** in a process following first order kinetics in [D_6]benzene with the activation parameters lg $A = 16.5$ and $E_a = 29.4$ kcal mol^{-1}. In contrast, **2** is not affected by this

[*] Prof. Dr. R. Gleiter, Dipl.-Chem. C. Sigwart, Dr. B. Kissler
Organisch-chemisches Institut der Universität
Im Neuenheimer Feld 270, D-6900 Heidelberg (FRG)

[**] This work was supported by the Deutsche Forschungsgemeinschaft, the Fonds der Chemischen Industrie and the BASF AG, Ludwigshafen.



X=CH_2 **3** X=CH_2 **13**
X=O **12** X=O **14**

Table 1. Spectroscopic data for **3**, **12**, **13**, and **14**.

3: ^{1}H NMR (CD_2Cl_2, 200 MHz, 263 K): δ = 4.46 (2H, s, br), 4.45 (2H, s, br), 4.36 (2H, s, br), 2.94–2.91 (2H, m), 2.78–2.74 (2H, m), 1.59–1.56 (2H, m); ^{13}C NMR (CD_2Cl_2, 50.32 MHz, 263 K): δ = 159.19 [a] (s), 156.44 (s), 94.80 [a] (t), 94.33 (t), 50.51 [a] (d), 44.9 [a] (d), 42.58 (t)
12: ^{1}H NMR (CD_2Cl_2, 300 MHz): δ = 4.80 (1H, s), 4.73 (1H, s), 4.70 (1H, s), 4.65 (1H, s), 3.22–3.18 (1H, m), 3.02–2.98 (1H, m), 2.76–2.72 (1H, m), 2.59–2.55 (1H, m), 1.79 (1H, d, J = 11.06 Hz), 1.72 (1H, d, J = 11.06 Hz); ^{13}C NMR ($CDCl_3$, 75.46 MHz): δ = 205.58 (s), 155.49 (s), 148.27 (s), 101.00 (t), 97.76 (t), 53.16 (d), 49.62 (d), 48.72 (d), 43.63 (d), 36.50 (t)
13: ^{1}H NMR (C_6D_6, 300 MHz, 283 K): δ = 5.69 (1H, s, br), 5.06–5.04 (1H, m), 4.90 (1H, s, br), 4.77 (1H, s, br), 3.55 (1H, s, br), 3.22–3.08 (2H, m), 2.38–2.13 (5H, m)
14: ^{1}H NMR ($CDCl_3$, 200 MHz): δ = 5.74–5.72 (1H, m), 5.09–5.07 (1H, m), 3.71 (1H, s, br), 3.12–2.68 (5H, m), 2.56–2.37 (2H, m); ^{13}C NMR ($CDCl_3$, 50.32 MHz): δ = 212.54 (s), 186.74 (s), 144.81 (s), 125.24 (d), 120.16 (d), 61.79 (d), 46.23 (d), 38.74 (t), 29.32 (6), 26.43 (t)

[a] Double intensity.

rearrangement even when heated to 100 °C for 15 min in a sealed tube.[9] To rationalize these findings we assume that the Cope rearrangement proceeds in two steps. In the rate determining step the central C–C single bond is broken first, forming the diradicals **15** and **16** in the case of **3** and **12**, respectively.[10] In the second step the products **13** and **14** are formed.

Species **17** would be the corresponding diradical intermediate in the case of **2**. A concerted process seems very unlike-



X=CH_2 **15**
X=O **16**

17

ly because the C=CH_2 moieties in **3** and **12** are pointing away from each other. Furthermore the rather high value for the preexponential factor supports also our view of a stepwise mechanism.

In line with these arguments are the results of force-field calculations (MMX[11]). These calculations predict an energy difference between **3** and **15** of only 1.20 kcal mol^{-1} while the energy difference between **2** and **17** is calculated to be 10.13 kcal mol^{-1}.[12] We ascribe this difference to two effects caused by the additional double bond in **3**: a) the increase in strain energy in **3** compared to **2** and b) an additional stabilization of **15** (one allyl-, one pentadienyl moiety) with respect to **17** (two allyl moieties).

Received: June 28, 1989 [Z 3415 IE]
German version: *Angew. Chem. 101* (1989) 1561

[1] We propose for tricyclo[3.3.0.0^{3,7}]octane the trivial name "stellane" and for the methylene derivatives correspondingly: **1** pseudo *para* stelladiene, **2** pseudo *ortho* stelladiene, **3** stellatriene, and **4** stellatetraene.

[2] B. Kissler, R. Gleiter, *Tetrahedron Lett. 26* (1985) 185; R. Gleiter, B. Kissler, *ibid. 28* (1987) 6151.
[3] R. Gleiter, B. Kissler, C. Ganter, *Angew. Chem. 99* (1987) 1292; *Angew. Chem. Int. Ed. Engl. 26* (1987) 1252.
[4] M. Nakazaki, K. Naemura, H. Harada, H. Narutaki, *J. Org. Chem. 47* (1982) 3470.
[5] G. Buono, *Synthesis 1981*, 872.
[6] R. R. Sauers, J. A. Whittle, *J. Org. Chem. 34* (1969) 3579; R. R. Sauers, K. W. Kelly, *ibid. 35* (1970) 498, R. R. Sauers, W. Schinski, M. M. Mason, *Tetrahedron Lett. 1969*, 79.
[7] J. C. Collins, *Tetrahedron Lett. 1968*, 3363.
[8] Satisfactory elemental analysis have been obtained for **12**, **13** and **14**.
[9] B. Kissler, unpublished results.
[10] According to MINDO/3 calculations the central bonds of **3** are 1.61 Å long.
[11] J. J. Gajewski, Serena Software, Bloomington, IN, USA.
[12] We are grateful to Professor *Klärner*, Bochum, FRG, for helpful discussions.

The Structure of $BrF_6^{\ominus}$ and Related Compounds**

By *Ali Reza Mahjoub, Andrzej Hoser, Joachim Fuchs,* and *Konrad Seppelt**

Gaseous xenon hexafluoride has a flexible C_{3v} structure[1] and can be described on the basis of the electron-pair repulsion model; i.e., the non-bonding electron pair exercises a steric effect.[2] The only information previously available about the structure of the isoelectronic anions $IF_6^{\ominus}$ and $BrF_6^{\ominus}$ was that they were different, a conclusion drawn from powder diagrams and vibrational spectroscopic studies.[3–5] We have now succeeded in growing single crystals of $CsBrF_6$ from BrF_5 solutions at 80 °C. According to an X-ray structural analysis, the $BrF_6^{\ominus}$ ion exists as a nearly perfect octahedron in the space group $R\bar{3}$ (Fig. 1), and is therefore not consistent with the electron pair repulsion model. Consideration of crystallographic alternatives (e.g., disordered $R3$, $R3$, inversion-twinned $R3$) resulted in the same structure but with slightly less favorable characteristics. A comparison with the $BrF_4^{\ominus}$ ion, which is known to be square planar, demonstrated that the vibrational amplitudes of the fluorine atoms in $BrF_6^{\ominus}$ are not abnormal (Fig. 2).[6] The same structure of $BrF_6^{\ominus}$ is obtained from neutron diffraction of powdered $CsBrF_6$. Bond lengths and angles are virtually the same both at room temperature and at 5 K.

The observed octahedral symmetry cannot be simply a consequence of crystal lattice forces, because $BrF_6^{\ominus}$ dissolved in acetonitrile has been shown by vibrational spectroscopy also to be octahedral, although little can be said about the possibility of static or dynamic deviations.[7] In this sense $BrF_6^{\ominus}$ differs from such anions as $SeCl_6^{2\ominus}$, $TeCl_6^{2\ominus}$, and $SnCl_6^{4\ominus}$. The latter are apparently subject to dynamic distortions. Lattice forces distort these anions depending upon the type of lattice involved.[8] It is noteworthy that the ion $TeF_6^{2\ominus}$ has not been unequivocally observed thus far.

The reason for the structural differences between XeF_6 and $BrF_6^{\ominus}$ may lie in the fact that s electrons on bromine are strongly bound to the nucleus due to the incomplete shielding of the nucleus, caused by the first filled d shell. As a

[*] Prof. Dr. K. Seppelt, Dipl.-Chem. A. R. Mahjoub, Prof. Dr. J. Fuchs
Institut für Anorganische und Analytische Chemie der Freien Universität
Fabeckstrasse 34–36, D-1000 Berlin 33
Dr. A. Hoser
Hahn-Meitner-Institut Berlin GmbH
Glienicker Strasse 100
D-1000 Berlin 39

[**] This work was supported by the Deutsche Forschungsgemeinschaft and the Fonds der Chemischen Industrie.

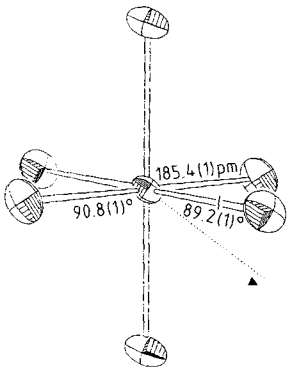


Fig. 1. Structure of the anion of $CsBrF_6$ in the crystalline state. The vibrational ellipsoids represent 50% probability. Dotted lines: three-fold crystallographic axes of rotation. $a = 522.7(1)$ pm, $\alpha = 96.501(2)°$, $R\bar{3}$ (No. 148), $Z = 1$. 2016 measured reflections between $2° \leq \Theta \leq 40°$, 580 independent reflections, 572 reflections with $I \geq 3\sigma(I)$, $R = 2.1\%$, $R_w = 2.8\%$. The crystals were obtained within a week from sealed PFA tubes containing excess BrF_5 and maintained at 80 °C. Such crystals are often twinned in the sense $x' = -x$, $y' = -y$, $z' = -z + (x + y) \cdot \cos\alpha$. A single crystal ($0.03 \times 0.04 \times 0.1$ mm) was embedded in paraffin oil at ca. −50 °C under nitrogen and measured at −160 °C with a CAD-4 diffractometer;[13] graphite monochromator, $Mo_{K\alpha}$ irradiation. Intensity measurements with speed varied as a function of I and maximum possible precision, $\omega\delta$ scan. Programs: SHELX, XTAL, SFLS;[14] least squares, full matrix.[15] Neutron diffraction: measured at the Institut Laue Langevin (Grenoble) on $CsBrF_6$ powder at 258 and 5 K. Bond lengths [pm] and angles [ ]: 298 K: Br-F 184.7(1), F-Br-F 91.3, 88.7, $R = 9.2\%$, $R_w = 13.1\%$. 5 K: Br-F 187.7(1), F-Br-F 90.7, 89.3, $R = 10.990$, $R_w = 17.4\%$.

result, the Br−F bond would be expected to show mainly p character. The substantial differences in bond length between $BrF_6^{\ominus}$ [185.4(1) pm] and the comparably octahedral cation $BrF_6^{\oplus}$ [ca. 169 pm[9]] would thus be explained by assuming that the nuclear charge in the anion is shielded by the centrosymmetric non-bonding electron pair. This difference also verifies the fact that the octahedral structure is not of steric origin, since the Xe−F bond length in XeF_6 (189.0 pm) is essentially identical to the Br−F bond length in $BrF_6^{\ominus}$.[10]

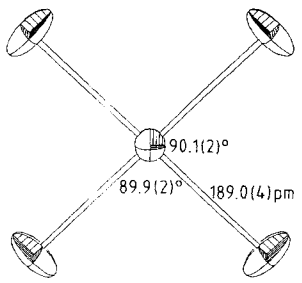


Fig. 2. Structure of the anion of $RbBrF_4$ in the crystalline state. The vibrational ellipsoids represent 50% probability. $a = 635.1(6)$, $c = 1148.9(10)$ pm, $I4/mcm$ (no. 140), $Z = 4$. 704 measured reflections between $2° \leq \Theta \leq 30°$, 204 independent reflections, 157 reflections with $I \geq 3\sigma(I)$, $R = 4.5\%$, $R_w = 4.4\%$, −60 °C. [15] $RbBrF_4$ was formed as a byproduct in the course of attempts to crystallize $RbBrF_6$.

Based on these considerations, $IF_6^{\ominus}$—like XeF_6—should not be octahedral. Unfortunately, crystallization experiments have in this case proven unsuccessful. In the system CsF/IF_5 the crystalline product obtained is CsI_3F_{16} (cf. [4]), and similarly in the system KF/IF_5 the only single crystals isolated had the composition $KI_3F_{16}^{\ominus}$. The anion $I_3F_{16}^{\ominus}$ has the same structure in both salts (Fig. 3), resembling a segment of the crystalline tetrameric XeF_6.[11] An analogy with $CsF \cdot 3XeOF_4$ is also appropriate.[12]

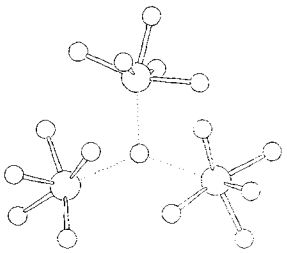


Fig. 3. Structure of the anions of CsI_3F_{16} and KI_3F_{16} in the crystalline state. CsI_3F_{16}: $a = 1379.0(11)$ pm, $P\bar{4}3n$ (no. 218), $Z = 8$. 4896 reflections, $2° \leq \Theta \leq 25°$, 521 independent reflections, 362 reflections with $I \geq 3\sigma(I)$, $R = 3.2\%$, $R_w = 2.8\%$, −60 °C. Bond lengths [pm] and angles [°]: I-F_{ax} 181(2), I-F_{eq} 185–190, $I\cdots F^{\ominus}$ 252.4(7), F_{ax}-I-F_{eq} 79–81, $F^{\ominus}\cdots$I-F_{ax} 146.8(8), $I\cdots F^{\ominus}\cdots I$ 118.7(4). [15] CsI_3F_{16} bears a crystallographic and structural resemblance to the salt $Cs[Xe_3O_3F_{13}]$. However, the latter crystallizes in the space group $Pa3$ (No. 203). [13] KI_3F_{16}: $a = 1353.5(5)$, $b = 1363.8(2)$, $c = 1342.1(4)$ pm, $\beta = 90.49°$ (3), $P2_1/c$ (no. 14), $Z = 8$. 7941 reflections between $2° \leq \Theta \leq 30°$, 7180 independent reflections, 6559 with $I \geq 3\sigma(I)$, $R = 6.0\%$, $R_w = 5.9\%$, −150 °C. Bond lengths [pm] and angles [°]: I-F_{ax} 182.5–185.2, I-F_{eq} 187.3–193.0, $I\cdots F^{\ominus}$ 247.7–251.4, F_{ax}-I-F_{eq} 77.8–82.0, $F^{\ominus}\cdots$I-F_{ax} 141.4–149.0, $I\cdots F^{\ominus}\cdots I$ 114.6–122.4 [15].

The anion $I_3F_{16}^{\ominus}$ is comprised of three square-pyramidal IF_5 molecules whose bond lengths and angles are essentially the same as those in gaseous IF_5. These three IF_5 molecules are joined by a bridging fluoride ion. The latter does not occupy the sixth coordination site on the iodine octahedron but is instead displaced somewhat to the side, an observation that provides additional indirect evidence for the steric effect of the non-bonding electron pair in IF_5.

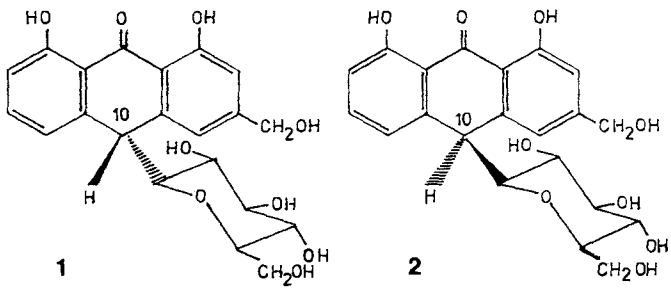
Received: June 12, 1989 [Z 3391 IE]
German version: *Angew. Chem. 101* (1989) 1528

[1] For comprehensive discussion of the structural problems related to gaseous XeF_6 see: S. Y. Wong, L. L. Lohr jr., *J. Chem. Phys. 60* (1974) 3901; *ibid. 61* (1974) 4110; K. S. Pitzer, C. S. Bernstein, *ibid. 63* (1975) 3849; W. E. Falconer, F. A. Stevie, *ibid. 66* (1977) 5335.
[2] R. J. Gillespie, R. S. Nyholm, *Q. Rev. Chem. Soc. 11* (1957) 339; R. J. Gillespie, *Angew. Chem. 79* (1967) 885; *Angew. Chem. Int. Ed. Engl. 6* (1967) 819.
[3] R. Bougon, P. Charpin, M. Soriano, *C.R. Acad. Sci. Ser. C 272* (1971) 565.
[4] K. O. Christe, *Inorg. Chem. 11* (1972) 1215.
[5] H. Klamm, H. Meinert, P. Reich, K. Witke, *Z. Chem. 8* (1968) 393, 469.
[6] S. Siegel, *Acta Crystallogr. 9* (1956) 493; W. G. Sly, R. E. Marsh, *Acta Crystallogr. 10* (1957) 378.
[7] K. O. Christe, *Winter Fluorine Conf. 8th* St Petersburg, FL, USA 1989.
[8] W. Abriel, *Acta Crystallogr. B 42* (1986) 449.
[9] Bond lengths estimated on the basis of calculated force constants for $[BrF_6][AsF_6]$ [K. O. Christe, D. D. Wilson, *Inorg. Chem. 14* (1975) 694].
[10] R. M. Gavin jr., L. S. Bartell, *J. Chem. Phys. 48* (1968) 2460.
[11] R. D. Burbank, G. R. Jones, *Science (Washington D.C.) 168* (1970) 248; *ibid. 171* (1971) 485; *J. Am. Chem. Soc. 96* (1974) 43.
[12] J. H. Holloway, V. Kaucic, D. Martin-Rovet, D. R. Russell, G. J. Schrobilgen, H. Selig, *Inorg. Chem. 24* (1985) 678.
[13] M. Veith, H. Bärnighausen, *Acta Crystallogr. B 30* (1974) 1806; H. Schumann, W. Genthe, E. Hahn, M. B. Hossain, D. von der Helm, *J. Organomet. Chem. 299* (1986) 67.
[14] Program for computing twinned crystals: H. Bärnighausen, *Z. Kristallogr. 170* (1985) 5; M. Eitel, *Dissertation*, Universität Karlsruhe 1985.
[15] Further details of the crystal structure investigation are available on request from the Fachinformationszentrum Karlsruhe, Gesellschaft für wissenschaftlich-technische Information mbH, D-7514 Eggenstein-Leopoldshafen 2 (FRG) by quoting the depository number CSD-50341 the names of the authors, and the journal citation.

Establishment of Configurations for the Two Diastereomeric *C*-Glucosylanthrones Aloin A and Aloin B

By *Hans W. Rauwald,* Karsten Lohse*, and *Jan W. Bats*

Aloin [10-(β-D-glucopyranosyl)-1,8-dihydroxy-3-hydroxymethyl-9(10*H*)-anthracenone] is the principal component and principal active ingredient in the world-wide used pharmaceutical agents *Aloe barbadensis and Aloe capensis*. It is known to be present in at least 68 aloe species.[1] Aloin was first isolated in 1851,[2] but the correct molecular formula was not established until 1945,[3] and only in 1952 was the compound shown to be a *C*-glucosylanthrone derivative.[4] The suggestion that aloin might exist in stereoisomeric forms[4] was confirmed by HPLC separation into the two diastereomers aloin B (**1**) and aloin A (**2**) in 1979.[5, 6] Partial synthesis[6] and ^{1}H NMR analysis[7] proved that the anthrone system is attached β with respect to the D-glucosyl residues in both aloins. It follows that **1** and **2** must differ



only with respect to the configuration at C10 itself. Recent exhaustive studies have demonstrated that a configurational assignment like that described in[6] and based on ^{1}H NMR data is not possible with the aloins because spectra of the two compounds show no significant differences in either chemical shifts or coupling constants.[7] It thus became necessary to establish the configurations by X-ray analysis.[7] Since aloin A and aloin B are readily separable in quantity by droplet countercurrent chromatography (DCCC),[8] large-scale crystallization experiments were feasible with both. The work had to be performed quickly, however, since the aloins are unstable in solution, where they are subject to interconversion via the tautomeric anthranol. Experiments with aloin A **2** resulted in needle-shaped crystals, but these were too slender to utilize for X-ray analysis. By contrast, aloin B **1** gave crystals that were quite adequate in size. In vivo experiments on the biosynthesis of the aloins have shown that **1** is actively synthesized by plants, whereas the isomer **2** arises in a secondary way through transformations of **1**.[9] Structural analysis on crystalline **1** provided unambiguous proof of the configurations at C10 for both diastereomers.

Figure 1 shows the molecular structure[10] of **1** in the crystalline state. Since the glucose is bound to the anthrone system as a β-D-glucosyl residue, the absolute configuration of **1** can be assigned as 10*R*, 1′*S*. The glucosyl residue has a chair conformation in which all substituents are equatorial

[*] Prof. Dr. H. W. Rauwald, K. Lohse
Institut für Pharmazeutische Biologie der Universität
Georg-Voigt-Strasse 16, D-6000 Frankfurt am Main 11 (FRG)

Dr. J. W. Bats
Institut für Organische Chemie der Universität
Niederurseler Hang, D-6000 Frankfurt am Main 50 (FRG)

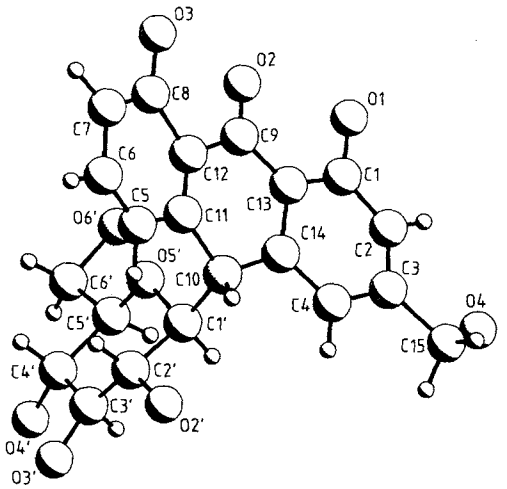


Fig. 1. Perspective drawing of the molecular structure of crystalline aloin B.

and all hydrogen atoms are axial. The A and C rings in the 1,8-dihydroxyanthrone system may be described as planar within the limits of experimental accuracy. Ring B, on the other hand, has a "sofa" or "envelope" conformation, in which C10 is raised out of the plane of the other five ring atoms by 0.29(2) Å. The glucopyranosyl residue at C10 is in axial, the hydrogen atom in equatorial position. The nonplanarity of ring B results in an angle of 16(2)° between rings A and C. This nonplanarity of the anthrone skeleton is a consequence of substitution at C10: unsubstituted 1,8-dihydroxyanthrone itself is planar.[11] The observed deviation from planarity in 1,1′,8,8′-tetrahydroxy-10,10′-bis-anthrone corresponds to that in aloin B **1**[12]. The torsion angles about the C10-C1′ bond [C14-C10-C1′-O5′: −79(2)°; C11-C10-

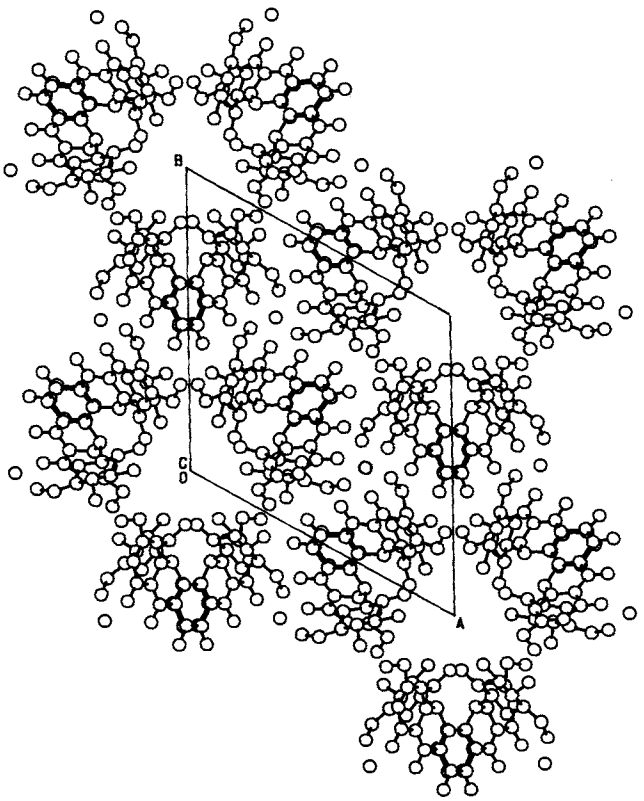


Fig. 2. Projection of the crystal structure of aloin B onto (001). The channels in the direction of the *c* axis contain disordered solvent.

C1'-O5': 48(2)°; H10-C10-C1'-O5':158°] reveal deviations from the staggered arrangement of about 15°, which may be a result of repulsion between H5 and H2'.

The crystal packing (Fig. 2) shows channels at least 4 Å in diameter along the *c* axis, where no atoms were found. The volume defined by such a channel is sufficient to permit incorporation of at least five positionally disordered water molecules. The resulting disorder within the channel is transmitted to some extent to adjacent atoms in the aloin B molecule (C15,C3',O2',O3', and O4').

Establishment of the configuration at C10 of aloin B as *R* simultaneously defines the configuration of aloin A (10*S*,1'*S*). Since the two substances may be regarded as parent structures for other naturally occuring diastereomeric 10-glucosylanthrones they should prove useful for making future comparisons within this class of compounds.

Received: June 7, 1989 [Z 3382 IE]
German version: *Angew. Chem. 101* (1989) 1539

[1] Q. J. Groom, T. Reynolds, *Planta Med. 53* (1987) 345–348.
[2] T. Smith H. Smith, *Pharm. J. 11* (1851) 23.
[3] R. Eder, W. Zinn, *Pharm. Acta Helv. 20* (1945) 410, 485.
[4] H. Mühlemann, *Pharm. Acta Helv. 27* (1952) 17.
[5] M. Grün, G. Franz, *Pharmazie 34* (1979) 669.
[6] H. Auterhoff, E. Graf, G. Eurisch, M. Alexa, *Arch. Pharm 313 (Weinheim, Ger.)* (1980) 113.
[7] H. W. Rauwald, K. Roth, *Arch. Pharm. (Weinheim, Ger.) 317* (1984) 362.
[8] H. W. Rauwald, *Arch. Pharm. (Weinheim, Ger.) 315* (1982) 769.
[9] M. Grün, G. Franz, *Arch. Pharm. (Weinheim, Ger.) 315* (1982) 231–241.
[10] Details related to the crystal structure analysis of aloin B **1** ($C_{21}H_{22}O_9$): yellow-brown, trigonal crystals from water/methanol, space group *P*321, $a = 17.67(1)$, $c = 11.381(4)$ Å, $V = 3079(5)$ Å^3, $Z = 6$. Enraf-Nonius-CAD4 diffractometer, $Cu_{K\alpha}$ radiation, 1474 independent reflections to $2\Theta = 110°$, very broad reflections, ω scan with $\Delta\omega = 9°$, $R(F) = 0.164$, $R_w(F) = 0.146$ for 1187 reflections with $I > \sigma(I)$, structure determination by direct methods (SHELXS-86), hydrogen atoms on C-atoms calculated, those on O-atoms not localized, SDP program system. The high *R* values are a consequence of disordered solvent. The residual density is less than 0.6 e Å^{-3}. Further details of the crystal structure investigation are available on request from the Fachinformationszentrum Karlsruhe, Gesellschaft für wissenschaftlich-technische Information mbH, D-7514 Eggenstein-Leopoldshafen 2 (FRG), on quoting the depository number CSD-53855, the names of the authors, and the journal citation.
[11] F. R. Ahmed, *Acta Crystallogr. B36* (1980) 3184.
[12] M. Whitefield, K. Henrich, P. G. Owston, *Acta Crystallogr. B38* (1982) 1248; F. R. Ahmed, G. A. Neville, *ibid. B38* (1982) 2930.

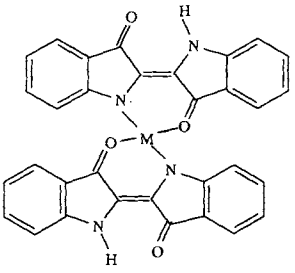
Indigo-Metal Complexes: Synthesis and Structure of Pd^{II} and Pt^{II} Compounds Containing the Anions of Indigo and Octahydroindigo as Mono- and Bis-Chelate Ligands**

By *Wolfgang Beck*, Christoph Schmidt, Rolf Wienold, Manfred Steimann,* and *Barbara Wagner*

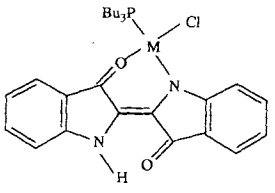
Dedicated to Professor Wolfgang Lüttke on the occasion of his 70th birthday

It was *Adolf von Baeyer*, who, in Munich in 1883, firmly established the structure of indigo[1a] in what has been described as "probably the most difficult structure proof to that point accomplished".[1b] The existence of chelate complexes ML_2 **1** (M = $Ni^{2\oplus}$, $Co^{2\oplus}$, $Cu^{2\oplus}$, $Zn^{2\oplus}$; L = monoanion of indigo and certain derivatives) was demonstrated by *Kunz*[2] as well as by *Kuhn* and *Machemer*.[3] So far as we are aware, however, little attention has been paid to these complexes since 1930.[4]

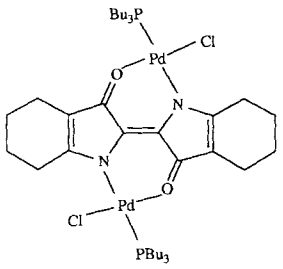
The complexes **1** show little solubility in organic solvents. Despite numerous attempts we were unable to prepare crystals that were suitable for X-ray analysis. The synthesis of soluble, crystalline indigo complexes was finally accomplished by introduction of the ligand tri(*n*-butyl)phosphane. Green chelate complexes **2** and **3**, respectively, result from



1



2a : M = Pd
2b : M = Pt



3

treatment of chlorine-bridged palladium(II) and platinum(II) compounds $[(nBu_3P)(Cl)M(\mu\text{-}Cl)]_2$ (M = Pd,Pt) with indigo or octahydroindigo in THF in the presence of sodium hydride or silver acetate.

Absorption bands in the UV/VIS spectrum of the complexes **2a** and **3** show bathochromic shifts relative to those of indigo itself.[5] According to X-ray structural analyses, the atoms palladium, imide nitrogen, and keto oxygen in **2a** (Fig. 1) and **3** (Fig. 2) lie in nearly planar six-membered rings (average deviation from planarity: 11 and 13 pm in **2a** and **3**, respectively). The monoanion of indigo functions as a monochelate ligand in **2a**, the dianion of octahydroindigo as a bischelate ligand in **3**. The four ligand atoms together with the central Pd deviate from planarity up to 6 pm (**2a**) and 30 pm (**3**), respectively. The two planar five-membered chelate rings are twisted out of the plane of the central C=C bond by 9.6° (**2a**) and 15° (**3**). Replacement of the bridging hydrogen atoms in indigo[6] by Pd produces virtually no change in the bond lengths in the five-membered rings or in the coordinated carbonyl groups (Table 1). The same is true of a structurally related Pd^{II} chelate complex of an a,β-ketoiminate.[7]

It is interesting to note that the bond of the free carbonyl group in **2a** [C2-O1 122.4(9) pm] is shorter than those of the coordinated carbonyl groups in **2a**, **3**, and indigo itself. This suggests that the inter- and intramolecular N–H···O bridging in free indigo[8a] has been disrupted. Crystals of **2a** con-

[*] Prof. Dr. W. Beck, Dipl.-Chem. C. Schmidt, R. Wienold, M. Steimann [†], Dipl.-Chem. B. Wagner [†]
Institut für Anorganische Chemie der Universität
Meiserstraße 1, D-8000 München 2

[†] X-ray structure analysis

[**] This work was supported by the Deutsche Forschungsgemeinschaft and the Fonds der Chemischen Industrie. We thank Prof. *W. Lüttke*, Göttingen, for valuable suggestions and encouragement; *H. Schönmann*, Consortium für elektrochemische Industrie GmbH, München, for "Computer Molecular Modeling"; and BASF AG, Ludwigshafen, for chemicals.

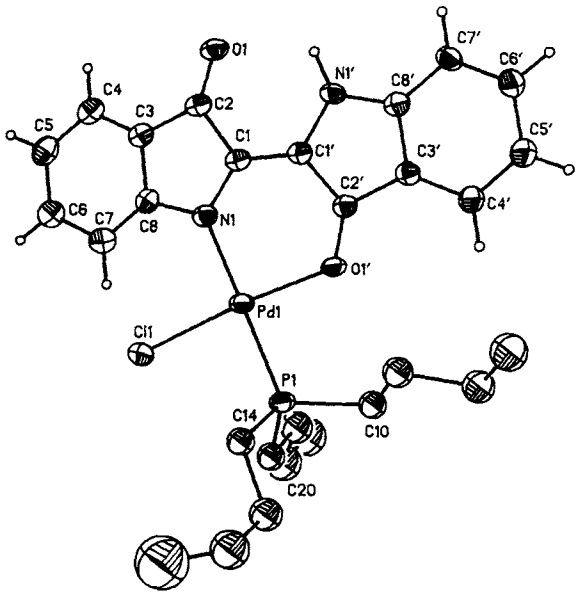


Fig. 1. Molecular structure of **2a** at 21 °C in the crystal, 20% probability level. $P2_1/n$, $a = 1248.5(4)$, $b = 1372.1(3)$, $c = 1691.7(5)$ pm, $\beta = 98.87(2)°$, $V = 2.863(1)$ nm^3, $Z = 4$, $\mu(Mo_{K\alpha}) = 0.81$ mm^{-1}, Wyckoff scan, $\Delta\omega = 1.2°$, $4 \le \dot{\omega} \le 30°$ min^{-1}, $4 \le 2\Theta \le 50°$; 9918 reflections measured, of which 5021 were unique and 4141 observed [$I \ge 2\sigma(I)$], 257 parameters. Empirical absorption correction (Psi scan, using 10 reflections, 36 measurements each). $R = 0.075$, $R_w = 0.079$, $w = [\sigma^2(F_o) + 0.0007\,F_o^2]^{-1}$. Maximum of residual electron density 1.33×10^{-6} e pm^{-3}. Hydrogen atoms in calculated positions. Programs used: SHELX 86, SHELX 76 and SHELXTL-Plus. [10]

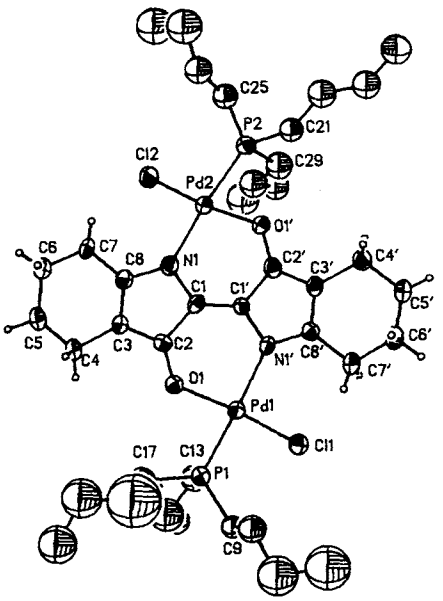


Fig. 2. Molecular structure of **3** at 21 °C in the crystal, 20% probability level. $P\bar{1}$, $a = 1274(1)$, $b = 1384(1)$, $c = 1489(1)$ pm, $\alpha = 63.85(7)$, $\beta = 77.42(7)$, $\gamma = 82.07(8)°$, $V = 2.297(4)$ nm^3, $Z = 2$, $\mu(Mo_{K\alpha}) = 0.99$ mm^{-1}, ω scan, $\Delta\omega = 1.4°$, $6 \le \omega \le 30°$ min^{-1}, $4 \le 2\Theta \le 50°$; 12359 reflections measured, of which were 7228 unique and 3696 observed [$I \ge 2\sigma(I)$], 338 parameters. Empirical absorption correction (Psi scan, using 11 reflections, 36 measurements each). $R = 0.077$, $R_w = 0.081$, $w = [\sigma^2(F_o) + 0.0007\,F_o^2]^{-1}$. Maximum of residual electron density 1.30×10^{-6} e pm^{-3}. Hydrogen atoms in calculated positions. The bond angles of the C atoms in one of the nBu$_3$P ligands (high U values) were fixed. Programs used: SHELX 86, SHELX 76 and SHELXTL-Plus. [10]

tain pairs of coplanar molecules that are rotated relative to each other by 180°, thereby eliminating the possibility of intermolecular N–H···O bridges. Apparently the twisting of the two five-membered rings about the central double bond in the indigo anion also interferes with conditions that are necessary for N–H···O bridging. The absence of such bridges is apparent from IR spectra (Table 2). Thus, the sharp ν_{NH} and ν_{CO} bands of the non-coordinated carbonyl groups in **1** and **2a** are shifted to higher wavenumbers relative to the corresponding bands of indigo.[8a]

Table 1. Selected bond lengths [pm] for indigo, **2a**, and **3**.

	Indigo [6c]	**2a**	**3**
Pd-Cl	-	230.9(2)	229.5(6)
Pd-P	-	225.2(2)	224.9(3)
Pd-N	-	211.8(5)	213.8(9)
Pd-O	-	203.8(5)	202.2(12)
C1-C1′	134.2(5)	137.0(10)	134.4(22)
C1-N1	138.2(6)	135.4(9)	141.8(22)
C1′-N1′	138.2(6)	139.5(9)	137.8(21)
C1′-C2′	145.9(5)	144.8(9)	147.8(21)
C1-C2	145.9(5)	151.3(9)	151.4(16)
C2′-O1′	124.0(5)	127.6(8)	132.2(21)
C2-O1	124.0(5)	122.4(9)	128.6(20)

Table 2. IR data for indigo, octahydroindigo, and **1**–**3** in Nujol ($\tilde{\nu}$ [cm^{-1}]).

	ν(NH)	ν(CO), ν(C=C)
Indigo	3270 (br)	1625, 1610, 1580
1, M = Cu	3398	1680 [a], 1635, 1610, 1595, 1575
2a	3350	1675 [a], 1650, 1610, 1595, 1575
Octahydroindigo	3340 (br)	1630, 1550, 1460, 1440, 1415
3	-	1635, 1570, 1455, 1415, 1395

[a] Non-coordinated C=O.

Additional complexes of indigo and related systems will be prepared in order to investigate their potential as energy transfer agents or catalysts.

Experimental Procedure

All work was conducted under nitrogen and in anhydrous solvents.

2a: A suspension of 24 mg (1 mmol) of NaH and 350 mg (1.33 mmol) of indigo (Fluka) in 10 mL of THF was heated for 15 min under reflux. After cooling the green suspension, 380 mg (0.5 mmol) of $[Cl_2PdP\textit{n}Bu_3]_2$ was added. The reaction solution was stirred for 3 h at room temperature and then filtered (glass frit, G4). Removal of the THF in vacuo left a dark residue that was dissolved in 5 mL of dichloromethane. This solution was filtered, and solvent was again removed in vacuo. **2a** was obtained as a dark, granular material; yield 300 mg (50%). Crystallization from dichloromethane/pentane. VIS spectroscopy ($CHCl_3$): $\lambda_{max} = 748$ nm, log $\varepsilon = 4.0$. ^{31}P NMR (109 MHz, CD_2Cl_2): $\delta = 23.47$. ^{1}H NMR (270 MHz, CD_2Cl_2): $\delta = 0.99$ (t,9H), 1.52–1.93 (m,18H), 6.9 (q,2H), 7.18 (d,1H), 7.37 (q,2H), 7.47 (d,1H), 7.58 (d,1H), 8.46 (d,1H), 9.07 (s,NH).

3: To a stirred suspension of 140 mg (0.5 mmol) of octahydroindigo[9] and 168 mg (1 mmol) of silver acetate in 10 mL of THF were added 500 mg (0.66 mmol) of $(Cl_2PdP\textit{n}Bu_3)_2$. The reaction mixture was stirred for 12 h at room temperature and filtered through a glass frit (G4). Solvent was removed in vacuo. The residue was taken up in 15 mL of ether and again filtered. Unreacted starting complex was precipitated by addition of 15 mL of pentane and cooling to −15 °C (3d). The cold solution was decanted and solvent was removed in vacuo. **3** was obtained as a dark green powder; yield 360 mg (75%). VIS spectroscopy ($CHCl_3$): $\lambda_{max} = 663$ nm, log $\varepsilon = 3.5$. ^{31}P NMR (109 MHz, CD_2Cl_2): $\delta = 21.6$. ^{1}H NMR (90 MHz, CD_2Cl_2): $\delta = 0.9$ (t, 18H), 1.4–1.8 (m,44H), 2.1 (t,4H); 3.0 (t,4H).

Received: March 29, 1989 [Z 3251 IE]
Publication was delayed at the authors' request.
German version: *Angew. Chem. 101* (1989) 1532

[1] a) A. von Baeyer, *Ber. Dtsch. Chem. Ges. 33(3)* (1900) supplement IV, p. LI; b) R. Huisgen, *Angew. Chem. 98* (1986) 297; *Angew. Chem. Int. Ed. Engl. 25* (1986) 297.

[2] K. Kunz, *Ber. Dtsch. Chem. Ges. 55* (1922) 3688.
[3] R. Kuhn, H. Machemer, *Ber. Dtsch. Chem. Ges. 61* (1928) 118; H. Machemer, *J. prakt. Chem. 127* (1930) 109.
[4] A compound isolated from the reaction of pentacarbonyliron and indigo, reported to be extremely sensitive to oxygen (a property we have confirmed), was introduced as a "Breathing Model of Indigo Blue": K. Kunz, A. J. Kreß, *Ber. Dtsch. Chem. Ges. 60* (1927) 367; W. Hieber, F. Sonnekalb, *ibid. 61* (1928) 565. However, it has been shown that O_2 uptake by this indigo-iron complex is irreversible: L. F. Larkworthy, *J. Chem. Soc. 1961*, 4025. Rhodium(III) compounds of indigo carmine (5,5'-indigodisulfonic acid disodium salt), which were not further characterized, catalyze the hydroformylation of olefins: V. A. Avilov, E. G. Chepaikin, M. L. Khidekel, *Izv. Akad. Nauk. SSSR Ser. Khim. 1974*, 2559; *Chem. Abstr. 82* (1975) 105808. The thermal behavior of indigo carmine-transition metal compounds has been investigated: J. M. Salas-Peregrin, J. Suarez-Varela, *Therm. Anal. 29* (1984) 515.
[5] MO calculations (Dr. *H. U. Wagner*) are in progress. For MO calculations on indigo cf. M. Klessinger, W. Lüttke, *Tetrahedron Suppl. 2* (1963) 315; M. Klessinger, *Chem. Unserer Zeit 12* (1978) 1.
[6] a) A. Reis, W. Schneider, *Z. Kristallogr. Mineral. 68* (1928) 543; b) H. von Eller, *Bull. Soc. Chim. Fr. 106* (1955) 1426; c) for a recent, precise crystal structure analysis of indigo (with localization of H atoms) see: P. Süsse, M. Steins, V. Kupcik, *Z. Kristallogr. 184* (1988) 269.
[7] H. Wanjek, U. Nagel, W. Beck, *Chem. Ber. 121* (1988) 1021.
[8] a) W. Lüttke, M. Klessinger, *Chem. Ber. 97* (1964) 2342; M. Klessinger, W. Lüttke, *ibid. 99* (1966) 2136; b) H. Meier, W. Lüttke, *Liebigs Ann. Chem. 1981*, 1303.
[9] G. Pfeiffer, H. Bauer, *Justus Liebigs Ann. Chem. 1976*, 383; *Liebigs Ann. Chem. 1980*, 564.
[10] Further details of the crystal structure investigation are available on request from the Fachinformationszentrum Karlsruhe, Gesellschaft für wissenschaftlich-technische Information mbH, D-7514 Eggenstein-Leopoldshafen 2 (FRG), on quoting the depository number CSD-53930, the names of the authors, and the journal citation.

Stack-Type Redox Systems: Synthesis via Repeated Carbanion Alkylation and Electron Transfer Studies**

By *Jürgen Alexander, Marianne Ehrenfreund, Jürgen Fiedler, Walter Huber,* Hans-Joachim Räder,* and *Klaus Müllen**

Dedicated to Professor Wolfgang Lüttke on the occasion of his 70th birthday

Stack-type π-systems such as multiply layered phanes[1, 2] or radical cation salts[3] can be used as models for studying one-dimensional charge transport.[4] We recently reported the preparation of **3a** and **3b**, members of a new class of two-layer π-systems[5a] in which the disk-shaped subunits are bridged [14]-annulenes; in contrast to the phanes, the subunits are linked by bridging groups "within" the π-system, and the distance between the layers can readily be varied. We have now been able to synthesize *multiply layered* homologues of **3** with up to five single layers by means of a "one-pot" reaction in which the pyrene isomer **1**[5b, 6, 7] undergoes reductive alkylation. The multilayer redox systems are constructed from separate electroactive groups and can be subjected to successive electron transfer reactions.[5c–e]

[*] Prof. Dr. K. Müllen, Dipl.-Chem. J. Alexander, Dr. J. Fiedler, Dipl.-Chem. H.-J. Räder
Institut für Organische Chemie der Universität
J.-J.-Becher-Weg 18–22, D-6500 Mainz 1 (FRG)
Priv.-Doz. Dr. W. Huber [+], Dipl.-Chem. M. Ehrenfreund
Institut für Physikalische Chemie der Universität
Klingelbergstrasse 80, CH-4056 Basel (Switzerland)
[+] Present address:
Hoffmann-La Roche & Co AG, CH-4002 Basel (Switzerland)

[**] Reductive transformations, Part 13. This work was supported by the Deutsche Forschungsgemeinschaft and the Fonds der Chemischen Industrie. Part 12: D. Bender, M. Przybylski, K. Müllen. *Makromol. Chem.*, in press.

The energies of interaction between the charged subunits and the nature of the charge distribution are important for the redox steps formed, and have been determined by cyclovoltammetry and ESR spectroscopy, respectively.

The synthesis of the two-layer compound **3** is made possible by the fact that **1** can be alkylated in a regioselective manner at the two central carbon atoms via the dilithium salt **2**.[5d, 6] It is thus, for example, possible to obtain the nucleophile **4a** and the electrophile **5a**; these can then undergo coupling to give **3a** in 95% yield[5a] (see Scheme 1, route I).[7]

Analogues with more than two layers should be available from a reaction in which the bifunctional nucleophile **2** ($=\mathbf{1}^{2\ominus}/2\,Li^{\oplus}$) is treated with bifunctional electrophiles such as **6**; the resulting monoalkylation products **7** are both electro- *and* nucleophilic and can in principle form stack-type compounds in a *poly*reaction. If, however, **2** is treated with 1,3-dichloropropane **6a**, the intermediate **7a** (X = Cl) reacts mainly via intramolecular cyclisation to give **8**. Stack-type molecules are not formed, and the expected diadduct **9a** is also only formed as a by-product, even if an excess of the alkylating agent is used (molar ratio **8**:**9a** = 5:3).[6] The bifunctional electrophile **9a** is, however, formed in 70% yield when 1-chloro/bromo-3-(trifluoromethylsulfonyloxy)-propane **6b** is used, since in this case **2** reacts only with the more reactive electrophilic group.

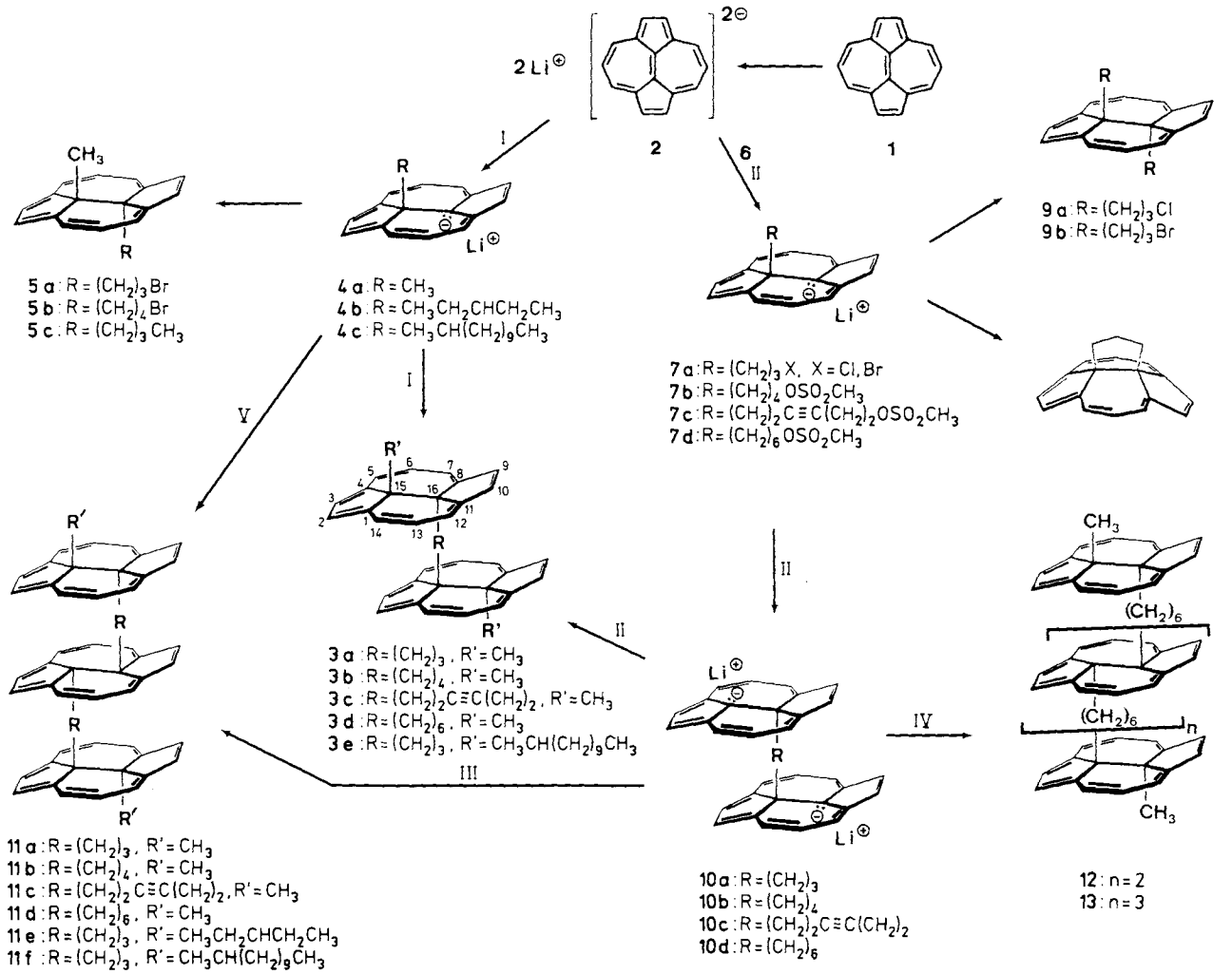
XRX'
6a: X = X' = Cl, R = $(CH_2)_3$
6b: X = Cl(Br), X' = OSO_2CF_3, R = $(CH_2)_3$
6c: X = X' = OSO_2CH_3, R = $(CH_2)_4$
6d: X = X' = OSO_2CH_3, R = $(CH_2)_2C{\equiv}C(CH_2)_2$
6e: X = X' = OSO_2CH_3, R = $(CH_2)_6$

The intramolecular cyclization of **7** to **8** can be prevented by variation of the alkylating agent; while the use of **6d** with a hex-3-ynediyl unit naturally prevents cyclization, the analogous hexanediyl (**6e**) and even the butanediyl (**6c**) agents also show no tendency to cyclization. When **6c** is allowed to react with 2.5 equivalents of **2**, followed by a trapping reaction with the monofunctional electrophile dimethyl sulfate, the double layer compounds **3b–d** are obtained in 32, 50 and 50% yield, respectively (after chromatography and recrystallization). The intermediates **7b–d** apparently react preferentially with **2** to form the dianions **10b–d**, which then undergo double methylation. Compounds **3** can thus be readily obtained via two routes (I,II).

It is significant that the "triple-decker" compounds **11c** and **11d**[8] are formed as by-products of the formation of the new systems **3c** and **3d** in yields of ca. 10%. This makes it certain that the dianions **10c** and **10d** can undergo further alkylation by **6d** or **6e** prior to the termination reaction with dimethyl sulfate (route III). The short-chain system **10b**, in contrast, is precipitated from the solution and thus cannot undergo further reactions.

We expect that the triply or multiply layered products will be formed in preference to the double layers **3** if a molar ratio of **2** to **6c–e** of 1:1 rather than 2.5:1 is used; in this case the nucleophilic positions of **10** will be alkylated by **6**, so that the alkylation sequence is continued. The reaction of **2** and **6e** (1:1, THF, 20 °C, 24 h) does indeed give a mixture of soluble oligomers in 70% yield (10% of **3d** are also formed); mass spectrometry indicates the mixture to contain the three, four- and five-layer systems **11d**, **12** and **13** which can be distinguished by ^1H NMR spectroscopy (routes III, IV).

It would be particularly attractive for studies of electron hopping processes between the annulene units in **3** and **11** to



Scheme 1.

be able to make the distances between the layers short: however, as we have seen, the formation of multilayer systems is hindered in the case of propanediyl bridges by the rapid cyclization of **7a** to give **8**, and in the case of butanediyl bridges by the low solubility of the intermediate **10b**.

These problems suggest an alternative procedure for stack formation: during the reaction of the bifunctional electrophile **9b** with **2** it might be possible to achieve repetitive attachment of layers without cyclization occurring. However, an electron transfer reaction between **2** and **9b** to give reoxidation of **2** is in fact the main reaction observed. Comparable reactions have been described for sterically hindered carbanion alkylation with *t*BuBr.[9] One possible solution is the use of the monoanion **4** (which is less redox-active than the dianion **2**) as the nucleophile, although in this case the number of π-systems which can be linked is limited to three. However, for the synthesis of compounds with short interlayer distances the solubility of the products must be increased by replacing the methyl group in the nucleophile **4** by a residue R with a longer chain (3-pentyl or 2-dodecyl). It is indeed possible to synthesize the soluble "triple-deckers" **11e** and **11f** with the shortest interlayer distance from **9b** and **4b** or **4c**[10] (see route V).

As expected from the diatropism of the annulene units, the ring protons in the multilayer compounds are deshielded, while the protons within the bridge are strongly shielded because they lie within the sphere of influence of several annulene layers. In **11e** the methylene protons in positions neighboring the central annulene unit absorb at $\delta = -7.17$ (see[8]).

In spite of the large interlayer distance, the protons of the methyl groups in the double-layer compound **3b** are surprisingly more strongly shielded than in the model system **5c** [$\delta(CH_3) = -4.84$ and -4.50, respectively]. The shielding also increases within the homologous series **3d, 11d, 12** and **13** [$\delta CH_3) = -4.72$ (**3d**), -4.74 (**11d**), -4.75 (**12**), -4.755 (**13**)]. The members of the series can thus clearly be distinguished.

The question as to whether such a stack constructed from separate electrophores is suitable for use as an electron storage system was first investigated by cyclovoltammetry (THF, nBu$_4$N as conducting salt, 0 °C, $v = 100$ mV s^{-1}) for **9c** ("monomer", R = CH$_3$CHCH$_2$CH$_3$), **3e** ("dimer") and **11f** ("trimer"). Compound **9c** is reduced reversibly to the radical anion at -2.16 V; **3e** shows two very close redox steps at ca. -2.18 V, which are due to uptake of one electron by each layer;[11] the half-wave potentials of these were determined by simulation to be -2.13 and -2.24 V. After correction for the entropy term[12] (two independent redox centers) the potential difference $E^1_{1/2} - E^2_{1/2} = 110$ mV gives an interaction energy of 1.78 kcal mol^{-1}. The cyclovoltammogram of **11f** also shows only two cathodic peak potentials with a shoulder in the anodic reoxidation peak. Computer simulation of the curve indicates a two-electron transfer at

-2.18 ($E^1_{1/2} - E^2_{1/2} < 20$ mV) and a one-electron transfer at $E^3_{1/2} = -2.30$ V. The corrected potential differences at 0 °C then give interaction energies of <0.24 ($1 \rightarrow 2$) and 1.80 kcal mol^{-1} ($2 \rightarrow 3$). The excess charges are apparently localized in the two outer redox centers in the dianion of **11f**. This "decoupling" corresponds to that in the "dimer" with a large interlayer distance.[11] Formation of the trianion requires the inner layer to become charged, and thus leads to an electrostatic interaction between the three neighboring subunits. However, the energy of 1.80 kcal mol^{-1}, which corresponds to two interlayer interactions in **11f**, is considerably smaller than would have been expected from the repulsion term in **3e**. The takeup of charge by higher oligomers should be describable in a manner completely analogous to that for **11f**.

The question occurs as to whether the unpaired electron in the radical anion which is the primary product of the reduction remains localized, or whether an intramolecular electron transfer which is fast with respect to the time-scale of ESR/ENDOR experiments leads to an effective delocalization over all the subunits. The rate of electron transfer depends on the distance between the electrophoric groups and the stability of the various ion pairs. In order to be able to study both contact ion pairs and solvent-separated ion pairs, the radical ions **11d–f** (with $K^{\oplus}$ as counterion) were prepared in several solvents (see Table 1). The size and multiplicity of the ESR hyperfine coupling constants were used as experimental criteria for distinguishing between spin localization and delocalization.[5a, c]

Table 1. ESR Coupling Constants [mT] for the radical monoanions **11d**$^{\bullet\ominus}$, **11e**$^{\bullet\ominus}$ and **11f**$^{\bullet\ominus}$ (in each case with $K^{\oplus}$ as counterion)[a, b].

11d$^{\bullet\ominus}$ all solvents	**11e**$^{\bullet\ominus}$ [c] all solvents		**11f**$^{\bullet\ominus}$ [c] DME/HMPT	**11f**$^{\bullet\ominus}$ DME
0.480(2H)*	0.471*	0.200● [d]	0.208● [d]	0.480(2H)*
0.156(4H)*	0.156*	0.072●	0.069●	0.156(4H)*
0.092(4H)*	0.146*	0.042●	0.042●	0.091(4H)*
0.010*	0.105*	0.010●	0.010●	0.010*
	0.084*			

[a] Solvent: 2-methyltetrahydrofuran, THF, DME, HMPT and mixtures of DME and THF or HMPT; temperature: −80 °C. [b] Coupling constants typical for a localized or delocalized form of the radical monoanion are denoted by * or ●, respectively. [c] The ESR spectra are not resolved, so that the multiplicity of the coupling constants could not be determined. [d] Broad ENDOR signal (ca. 0.03 mT); probably corresponds to several non-equivalent coupling constants.

Under all the experimental conditions used, the unpaired electron in the radical anion **11d**$^{\bullet\ominus}$ with the largest interlayer distance is localized within a single redox unit: the number of coupling constants observed indicates this to be the inner annulene layer. The radical anion **11f**$^{\bullet\ominus}$ in which the interlayer distance is shorter shows the same behavior in dimethoxyethane (DME). When however mixtures of DME and hexamethylphosphoric acid triamide (HMPA) are used, in which solvent-separated ion pairs are favored, the four coupling constants observed in the ENDOR spectrum are considerably smaller than those observed in DME. In addition, the largest coupling constant is much smaller than for a spin delocalization over two annulene layers as in **3a**$^{\bullet\ominus}$.[5a] Thus when the redox centers approach one another, and when the interaction between the anion and the counterion is weak, rapid electron transfer leads to an effective spin delocalization over all the annulene layers.

The situation in **11e**$^{\bullet\ominus}$ is even more complex, because under all the various experimental conditions spectra are obtained which point to the existence of both spin-localized *and* spin-delocalized forms.

Further reduction of the radical monoanions leads in all cases to triplet states. The mean distances between the unpaired electrons estimated from the zero-field parameters [D = 8.85 mT (**11e**$^{2\ominus}$/2 $K^{\oplus}$), 5.05 mT (**11d**$^{2\ominus}$/2 $K^{\oplus}$)] are ca. 650 and 820 pm respectively; they are thus in agreement with the cyclovoltammetric results indicating the localization of the excess charges on the outer π-units. Additional electron transfer processes then generate more highly charged radical anions, the coupling constants of which indicate a localization of the unpaired electron at single redox centers.

Received: March 22, 1989;
supplemented: August 11, 1989 [Z 3247 IE]
German version: *Angew. Chem. 101* (1989) 1530

[1] S. Misumi in P. M. Keehn, S. M. Rosenfeld (Eds.): *Cyclophanes, Vol. II*, Academic Press, New York 1983, p. 573 ff.
[2] S. El-Tamany, F.-W. Raulfs, H. Hopf, *Angew. Chem. 95* (1983) 631; *Angew. Chem. Int. Ed. Engl. 22* (1983) 633.
[3] V. Enkelmann, B. S. Morra, C. Kröhnke, G. Wegner, J. Heinze, *Chem. Phys. 66* (1982) 303.
[4] J. B. Torrance in D. Jérome, L. G. Caron (Eds.): *Low-Dimensional Conductors and Superconductors*, Plenum Press, New York 1987, p. 113 ff.
[5] a) W. Irmen, W. Huber, J. Lex, K. Müllen, *Angew. Chem. 96* (1984) 800; *Angew. Chem. Int. Ed. Engl. 23* (1984) 818; b) K. Müllen, *ibid. 99* (1987) 192 and *26* (1987) 204; c) W. Huber, H. Unterberg, K. Müllen, *ibid. 95* (1983) 239 and *22* (1983) 242; d) J. Fiedler, W. Huber, K. Müllen, *ibid. 98* (1986) 444 and *25* (1986) 443; e) W. Huber, J. Lex, T. Meul, K. Müllen, *ibid. 93* (1981) 401 and *20* (1981) 391.
[6] W. Huber, W. Irmen, J. Lex, K. Müllen, *Tetrahedron Lett. 23* (1982) 3889.
[7] Apart from coupling between two molecules of **7**, multilayer compounds can also be formed by attack of the dianion **2** or of the bifunctional electrophiles **6** on **7**.
[8] NMR-spectroscopic data of some new compounds: **3c**: deep red needles (CH_2Cl_2), m.p. > 350 °C; ^{1}H-NMR (400 MHz, $CDCl_3$): δ = 8.64 (4 H; H-2,3), 8.59 (4 H; H-5,14), 8.53 (4 H; H-7,12), 8.52 (4 H; H-9,10), 7.87 (4 H; H-6,13), −1.63 (4 H; H-2'), −4.72 (6 H; CH_3), −4.93 (4 H; H-1'); ^{13}C-NMR (100 MHz, $CDCl_3$): δ = 152.4, 149.2 (C-1,4,8,11), 136.6, 135.7 (C-2,3,9,10), 119.8, 119.4, 119.1 (C-5,6,12,13,14), 77.7 (C-3'), 46.4, 43.1 (C-15,16), 24.9 (C-2'), 14.7 (CH_3), 10.3 (C-1'). **11c** (numbering of the central annulene unit 1–16, of the terminal annulene units 1'–16' and the bridging group 1''–6'', starting from the center: light green microcrystals, m.p. > 350 °C; ^{1}H-NMR (400 MHz, $CDCl_3$): δ = 8.61 (4 H; H-2',3'), 8.56 (4 H); H-5',14'), 8.54 (4 H; H-7',12'), 8.49 (4 H; H-9',10'), 8.40 (4 H; H-2,3,9,10), 8.32 (4 H; H-5,7,12,14), 7.84 (4 H; H-6',13'), 7.66 (2 H; H-6,13), −1.68 (4 H; H-5''), −1.76 (4 H; H-2''), −4.75 (6 H; H-CH_3), −4.98 (4 H-6''), −5.13 (4 H; H-1''); ^{13}C-NMR (100 MHz, $CDCl_3$): δ = 151.9, 148.9, 148.6 (C-1,4,8,11,1'4'8'11'), 136.4, 136.0, 135.2 (C-2,3,9,10,2'3'9'10'), 119.4, 119.2, 119.0, 118.7 (C-5,6,7,12,13,14,5',6',7',12',13',14'), 77.5 (C-3'', 4''), 46.1, 46.0, 42.6 (C-15,16,15',16'), 24.4 (C-5''), 23.9 (C-2''), 14.4 (C-CH_3), 10.1 (C-6''), 10.1 (C-6''), 9.7 (C-1''). **11e**: light green microcrystals, m.p. > 350 °C; ^{1}H-NMR (200 MHz, 20 °C, $CDCl_3$): δ = 8.34 − 8.21 (16 H; H-2',3'9',10' and H-5',7',12',14'), 8.06 (4 H; H-2,3,9,10), 7.94 (4 H; H-5,7,12,14), 7.58 (4 H; H-6',13'), 7.36 (2 H; H-6,13), −0.91 (12 H; (CH_3CH_2)$_2$CH), −2.33, −2.60 (8 H; (CH_3CH_2)$_2$CH), −4.94 (2 H; (CH_3CH_2)$_2$C*H*), −5.59 (4 H; H-2''), −7.11 (4 H; H-3''), −7.17 (4 H; H-1'').
[9] T. Lund, H. Lund, *Acta Chem. Scand. Ser. B42* (1988) 269.
[10] The monoanionic intermediate **4** can be prepared from **2** and 1 equivalent of the alkylating agent, since the dianion **2** is much more reactive than **4**. However, the yield of **4** depends to a great extent on the nature of the electrophile. With comparatively reactive reagents such as primary alkyl halides and secondary alkyl tosylates the main products are the dialkyl adducts. **4b** was thus prepared using the less reactive 3-bromopentane.
[11] A. J. Fry, T. A. Powers, K. Müllen, W. Irmen, *Tetrahedron Lett. 26* (1985) 4879.
[12] J. B. Flanagan, S. Margel, A. J. Bard, F. C. Anson, *J. Am. Chem. Soc. 100* (1978) 4248; F. Ammarand, J.-M. Saveant, *J. Electroanal. Chem. 47* (1973) 215.

Book Reviews are written by invitation from the editor. Suggestions for books to be reviewed and for book reviewers are welcome. Publishers should send brochures or (better) books to the following address: Redaktion Angewandte Chemie, Postfach 101161, D-6940 Weinheim, Federal Republic of Germany. The editor reserves the right of selecting which books will be reviewed. Uninvited books not chosen for review will not be returned.

The Chemistry of Macrocyclic Ligand Complexes. By *L. F. Lindoy*. Cambridge University Press, Cambridge 1989. viii, 269 pp., hard cover, £ 45.00. – ISBN 0-521-25261-X.

Bless them—macrocycles have been an excellent vehicle for the reunification of chemistry during these past three decades. Chemists, trained in research in the erstwhile parochial camps that also happened to rely upon macrocyclic compounds to achieve their rather limited ends, have begun to abandon their feudal practices and rediscover the power and satisfaction of the scientific method when it is applied to solving some of the "big problems" around in science today. *Len Lindoy*'s monograph captures much of the spirit and joy of this renaissance. Written through the eyes of someone who has largely seen macrocycles as ligands for transition metals, it devotes the best part of three chapters (3–5) to crown ethers, their lariat variants, and related synthetic receptors; it emphasizes their abilities to complex with organic cations, neutral organic molecules, inorganic anions, and metallo-organic guests, as well as with alkali metal and alkaline earth metal cations—including those intriguing situations where "alkalides" and "electrides" are generated; it features their applications in separation science (enantiomer differentiation by chiral hosts to cite but one example), in making simple devices and systems that are photochemically driven (e.g. membrane ion-transporters), and in promoting chemical reactions efficiently and selectively, i.e. behaving as phase-transfer catalysts and enzyme mimics. Room has also been found to extol the virtues of other wholly-synthetic molecular receptors (e.g. picket fence porphyrins and bisporphyrins, spherands, calixarenes, and cyclophanes) as well as one of nature's gifts—the cyclodextrins—both in their unadulterated forms and, after varying degrees of structural change, in search of enzyme-like catalytic activities, substrate specificities, and reaction selectivities. All this and more leads up to a discussion of the biomimetic chemistry of many (e.g. antibiotics, ionophores, vitamin B_{12}, chlorophyll, hemoglobin, myoglobin, and the cytochromes including P450) of nature's other macrocycles in the final chapter (9).

These topics are highlighted alongside an authoritative treatment (Chapters 1–3) of macrocycles—containing heteroatom-wise, nitrogen only, nitrogen and sulfur, nitrogen and phosphorus, and a very few, all-phosphorus and all-arsenic—intended for the complexation of cobalt, copper, and nickel for the most part. Their metal- and ligand-centered redox properties are discussed in Chapter 8 in the light of a detailed consideration in the preceding two chapters (6 and 7) of the thermodynamics and kinetics of complexation/decomplexation processes. The template effect is analyzed from both viewpoints. There are some gems of information that just have to make a lasting impression on any reader. What about this one as an example? Under acidic conditions, square-planar $[Ni(cyclam)]^{2\oplus}$ dissociates with a half-life of approximately 30 years! Sometimes these metals can be devils to get out of these macrocycles, but ways can be found at the end of Chapter 2 to demetallate. Stereochemical issues and mechanistic proposals keep surfacing, helping as they do to put some meaning into popular terms, such as chelate and macrocycle effects.

All in all, this monograph is the work of a scholar for scholars, be they practising "macrocyclists" or "those seeking an introduction to the field" to borrow a word and a phrase from the Preface. It represents one of the first courageous attempts by a single author to integrate the presentation of a multidisciplinary field. He is to be congratulated for taking up the challenge and then meeting it so successfully. The outcome is a trend-setter which is destined to become a classic in its time. It will suffer little from the literature "black-out" from 1986 onwards that unfortunately characterizes it—provided its readers get the "take-home" message, i.e. this is an area of chemistry that is on the move, so much so, that, sooner or later, it will be much bigger than macrocycles alone. As Professor *Lindoy* notes at the end of Chapter 7, "similar effects may occur for non-cyclic systems in which the donor atoms are constrained by attachment to a rigid backbone. That is, it has become increasingly apparent that many of the properties associated with simple macrocyclic systems also occur for metal ions bound in structurally rigid sites which are found, for example, in metalloenzymes." Has the time not come as well for "macrocyclists" to look beyond macrocycles?

J. Fraser Stoddart [NB 1018 IE]
Department of Chemistry
The University of Sheffield
(United Kingdom)

Stereochemical Applications of Gas-Phase Electron Diffraction. Edited by *I. Hargittai* and *M. Hargittai*. VCH Verlagsgesellschaft, Weinheim/VCH Publishers, New York 1988. **Part A: The Electron Diffraction Technique.** xviii, 563 pp., hard cover, DM 210.00. – ISBN 3-527-26691-7/0-89573-337-4; **Part B: Structural Information for Selected Classes of Compounds.** xviii, 511 pp., hard cover, DM 210.00. – ISBN 3-527-26790-5/0-89573-292-0.

This title comprises two volumes which are quite different in content. The sub-title of Part A is "The Electron Diffraction Technique", that of Part B "Structural Information for Selected Classes of Compounds". The two books are remarkable in several respects. Most research groups presently active in the field have contributed to produce an exhaustive, up-to-date overview of the field in approximately 1100 pages. The kernel of the book is an accurate notion of molecular structure including both its static and dynamic aspects. Electron diffractionists have contributed significantly to this notion, in exemplary cooperation with specialists in related fields: rotational and vibrational spectroscopy, X-ray diffraction, ab initio and molecular mechanics calculations, to name but a few.

On the whole the editors have coordinated the various contributions well. A certain degree of redundancy can probably not be avoided in a book of this kind and, in fact, is probably necessary in order to display the multitude of approaches that has developed around *Mark*'s orginal experiment done about 60 years ago. The books are typeset and illustrated with high quality pictures. They deserve a readership far beyond the immediate (rather small) electron diffraction community and are recommended to anyone interested in molecular structure, both for the information and inspiration which they offer.

Part A. The Electron Diffraction Technique. In an introductory survey *I. Hargittai* describes the gas-phase electron diffraction (GED) technique of molecular structure determination for the benefit of those who need to use the structural information but are not familiar with the technique. He explains, among other things, the bewildering variety of structural parameters (e.g. r_g, r_a, r_z, r_c) used in the literature to take into account vibrational effects. The chapter sets the stage for a review by *Kuchitsu, Nakata* and *Yamamoto* on the joint use of GED and high resolution rotational spectroscopy – the respective results being affected differently by molecular vibrations – for accurate structure determination. In many cases the weaknesses of one technique are at least partially compensated for by the strengths of the other, and joining the two has led to a renaissance of both. From this success it is a small step to integrating other types of data into the interpretation of GED data. Two chapters describe the concerted use of GED and quantum chemical calculations (by *Schäfer, Ewbank, Siam, Chiu* and *Sellers*, and by *Geise* and *Pyckhout*). The limited information obtainable from low resolution rotational spectroscopy is shown to provide useful constraints for the interpretation of GED data, especially on mixtures of conformers (*Bohn*). In spite of differences in the state of aggregation, liquid crystal NMR results may often be combined with GED results (*Rankin*). Three of the chapters deal explicitly with dynamic aspects: vibrational information obtained from GED (*Spiridonov*), large amplitude motion (*Lowrey*) and the temperature dependence of GED structural parameters (*Fink* and *Kohl*). Another article discusses temperature dependent experiments in relation to conformational mixtures in the gas phase and associated thermodynamic quantities (*Hedberg*). *Bartell* reviews the status of electron scattering theory with respect to accuracy in structural analyses. Two chapters address small angle electron scattering and the information on electron distribution in very small molecules obtainable from such experiments (*Konaka* and *Shibata, Hirota*). The fact that both EXAFS and GED results are often represented as radial distribution curves provoked a discussion on common ground between the two (*Beagley*). Modern synchrotron sources have given a new impetus, not only to EXAFS studies, but also to gas phase X-ray diffraction investigations of electron distributions in small molecules (*Jijima, Nishikawa*, and *Mitsuhashi*). Experimental aspects of GED are summarized by *Tremmel* and *Hargittai*. The book has an author and a formula index which give ready access to the abundance of primary literature quoted in each chapter.

Part B. Structural Information for Selected Classes of Compounds. The second volume contains chapters on boron and silicon compounds (*Mastryukov*), nitrogen and phosphorus compounds (*Vilkov, Sadova*), oxygen and sulfur compounds (*Naumov*), fluorine derivatives (*Oberhammer*), saturated organic molecules (*Montgomery*), unsaturated organic molecules (*Traetteberg*), substituted benzene derivatives (*Domenicano*), organometallic compounds of main group elements (*Haaland*) and metal halides (*M. Hargittai*). It concludes with a discussion of the interaction of theoretical chemistry with GED (*Boggs*). An author and a formula index give access to molecular structure determinations of approximately 1500 compounds.

This volume is encyclopedic in character, especially the first six chapters. They are not easy to read, but the treasures of information encourage browsing. The choice of structural parameters reported in numerous tables is subjectively selective. The reader interested in detailed and complete information has to consult the primary literature. One would hope that sometime in the future the encyclopedic material of this and analogous previous books[*] will be available in a critically edited, computer readable data base, in order to make more room for discussion of the results.

The chapter on saturated organic molecules summarizes some of the assumptions necessary for analysis of large molecules with low symmetry, and thereby illustrates some limitations of GED. Another caveat is discussed with respect to organometallic compounds and metal halides which are often unstable and reactive; thus their identity cannot always be taken for granted. A further limitation of GED is that it measures averages of similar distances quite accurately but not their differences; from quantum chemical calculations, on the other hand, differences are much better determined than absolute distances. Similarly, ratios of force constants, but not their absolute values, may be computed by ab initio methods and combined with experimental frequencies to gain a better understanding of the vibrational aspects of molecular structure. The chapters mentioned here will help the non-specialist reader to gain a critical appreciation of GED structures.

The discussion of benzene derivatives is, in a way, the most interesting chapter. Not only does it critically discuss the reliability of the GED structures but it also addresses the problems of structural substituent effects and chemical bonding, by comparing all available and reliable information on the gas and crystalline phases.

H. B. Bürgi [NB 979 IE]
Laboratorium für chemische und
mineralogische Kristallographie
der Universität Bern (Switzerland)

Organic High Pressure Chemistry. Edited by *W. J. LeNoble*. Elsevier, Amsterdam 1988, xii, 489 pp., hard cover, HFl 320.00. – ISBN 0-444-43023-7

Following the appearance recently of numerous review articles on various aspects of organic reactions at high pressure, this monograph attempts to provide a comprehensive overview of the topic. As the editor indicates in his preface, this is not an easy task, since the number of high pressure laboratory systems, and consequently also the numbers of high pressure experiments published, have grown considerably in very recent times. As a result high pressure chemistry is developing from being a specialized field of work, accessible to only a few, into a widely used research method; pressure, as one of the variables in optimizing reaction conditions, thereby assumes an importance similar to that of temperature and solvent, for example.

[*] An extensive compilation complementary to this one has recently been published (Vilkov, Mastryukov and Sadova, *Determination of the Geometrical Structure of Free Molecules*, English translation, MIR Publishers, Moscow 1983).

In the book's 14 chapters the different subdivisions of the topic are described by 15 expert authors, who have themselves made important contributions to research in these fields. The latest developments in high pressure apparatus are not reported, however. Following an introduction written by the editor (Chapter 1, 18 pp.), which briefly outlines the main physical-chemical principles underlying the effects of pressure on reactions in compressed solutions, *O. Exner* in Chapter 2 (31 pp.) introduces empirical group increments for calculating molar volumes of many types of aliphatic, carbocyclic and heterocyclic compounds; these are as simple to use as the Benson increments for calculating enthalpies of formation. With the help of these molar volumes it is a simple matter to estimate the reaction volumes which are important for assessing pressure effects.

Chapters 3 (50 pp., *S. D. Haman*) and 4 (23 pp., *M. Sasaki* and *J. Osugi*) are concerned with pressure effects on chemical equilibria (e.g. for conformers, *cis–trans* double bond isomers, ionization reactions, etc.), and with kinetic isotope effects, especially the pressure dependence of the tunnel effect in hydrogen transfer reactions. Here the experimental results are compared with model calculations where these are available. In Chapter 5 (20 pp.) *T. Asano* discusses the effects of pressure on the hindered rotation in amides and on the *cis–trans* isomerization of compounds containing N=N, C=N and C=C bonds. The use of dynamic NMR spectroscopy at high pressures as a method for such studies is described. In Chapter 6 (61 pp.), which is devoted to pericyclic reactions, *G. Jenner* includes a detailed discussion of Diels-Alder reactions, whose pressure dependence has been studied very thoroughly. Also discussed here are other cycloaddition reactions ([2+2]-, [6+4]-, [8+2]- and 1,3-dipolar cycloadditions), en-reactions, and sigmatropic and electrocyclic rearrangements. Emphasis is placed here on the types of information which activation volumes and reaction volumes contain in relation to reaction mechanisms.

Chapters 7 (34 pp., *K. R. Brower*), 8 (16 pp., *E. Whalley* and *W. J. LeNoble*) and 9 (29 pp., *V. M. Zhulin*) deal with pressure effects on anionic, carbocationic and free radical reactions, respectively. Topics discussed in these chapters include acid-base equilibria, hydride transfer, nucleophilic substitutions, additions and eliminations, the problem of the classical versus the non-classical norbornyl cation, polymerization reactions, and the decomposition of azo and per-ester compounds. Here again mechanistic problems are in the foreground. In the following two chapters the main emphasis is on preparative organic chemistry. Chapter 10 (20 pp., *A. Rahm*) describes, amongst other reactions, the additions of organosilicon and organotin compounds to C=C and C=O bonds at high pressures, which are of particular interest for synthetic purposes. Under the title "Synthesis" in Chapter 11 (53 pp.), *J. Jurczak* provides an impressive review of reactions of importance in preparative chemistry which only proceed with good or very good yields at high pressures. This chapter is rounded off with examples of natural products syntheses in which the key steps require high pressures.

Chapter 12 (23 pp., *R. Schmidt* and *H.-D. Brauer*) and 13 (46 pp., *K. Heremans*) describe respectively the pressure dependence of photophysical and photochemical processes (such as intersystem crossing and the deactivation of excited states), and aspects of bioorganic chemistry, e.g. the effects of pressure on the structures of proteins and on enzyme activity. In the final contribution (Chapter 14, 12 pp.) *W. J. LeNoble* discusses the sorts of conclusions regarding mechanisms that can be drawn from pressure effects, taking a number of carbene and fragmentation reactions as examples.

Since this monograph has been written by a large number of authors representing very different chemical specialisms, which range from physical chemistry to preparative organic chemistry, it should appeal to readers with widely varying interests, and is a mine of information on published work which is scattered throughout the organic and physical chemistry journals, and is therefore difficult to keep track of. The literature citations extend up to 1986 inclusive. The coordination achieved by the editor is commendable. This has undoubtedly succeeded in avoiding over-frequent repetition of the same phenomena in different chapters. However, there are a few instances where it is pleasing to find the same experiment discussed from different points of view. There remains now the question as to what readership this book in the series "Studies in Organic Chemistry" is aimed at. Foremost undoubtedly is the research chemist who already has a basic knowledge of high pressure chemistry, and may need to carry out his or her own high pressure experiments.

It is difficult to understand why the price is so high. The authors' typescripts have been directly reproduced, and with modern text processing methods there can be no objection to this. However, one would expect the considerable reduction in production costs achieved by this means to keep down the purchase price. The fact that the price is much too high, unjustifiably so in my opinion, is unfortunately likely to prevent this monograph, which is full of useful information for non-specialists also, from reaching a wider readership.

Frank-Gerrit Klärner [NB 982 IE]
Fakultät für Chemie
der Universität Bochum (FRG)

Georg de Hevesy. 1885–1966. Festschrift. Edited by *G. Marx*. Akadémiai Kiadó, Budapest 1988. 165 pp., hard cover, DM 34.00. – ISBN 963-05-5230-2

This book contains the typewritten texts of the papers presented at a meeting held at the Eötvös University in Budapest on 26 September 1985 to commemorate the hundredth anniversary of the birth of *Georg von Hevesy*. First *György Marx* gives, by way of an introduction, an outline of *Hevesy*'s life and work. After studying in Budapest and at German universities he undertook a period of research with *Rutherford* in Manchester from 1911 to 1914. This familiarized him with radioactivity, and was also the start of a lifelong friendship with *Niels Bohr*. His teaching and research activities at Budapest University were interrupted by World War 1, and shortly after the end of the war they came to a stop due to the revolution. *Hevesy* emigrated to Denmark for the first time. From there he went in 1926 to Freiburg as Professor of Physical Chemistry. In 1934 he moved for the second time to Denmark. In 1943 he fled to Stockholm, and in 1945 became a Swedish citizen. His life ended in 1966 in Freiburg—perhaps finally reconciled? His relationship with Hungary is discussed at the end of this little book by *Gábor Palló*.

Hevesy's scientific work was extremely varied, as becomes clear from *Marx*'s article, and the quantity of it was also quite large, as is evident from the bibliography compiled by *Hilde Levi*, which lists 397 publications. In 1913, together with *Friedrich Paneth*, he invented radioactive labeling, and soon began to apply it to problems for which this was the only available method, such as self-diffusion in metals. The discovery of element 72, hafnium, using X-ray fluorescence spectroscopy, belongs to his first Copenhagen period. His time in Freiburg was dominated by geochemical topics such

as the dating of geological specimens using the radioactive decay of lead isotopes. Back once more in Copenhagen, he invented neutron activation analysis with *Hilde Levi*, then became increasingly involved in the applications of artificial radioactive isotopes in biology and medicine, initially using ^{32}P; from this work nuclear medicine developed. For his research on isotopes as tracers for investigating chemical reactions he received the Nobel Prize for Chemistry in 1943.

The lectures were linked under the general heading "Interdisciplinary Applications of Nuclear Methods". Only the first of these relates directly to *Hevesy;* in this *Gustaf Arrhenius* and *Hilde Levi* give a review of his geochemical and cosmochemical period from 1922 to 1935 (26 pp.). *Rudolf Mößbauer* describes the beginnings of the precision gamma-ray spectroscopy technique which is named after him (13 pp.), and following this *Vitalii Goldanskii* then discusses the method in greater detail, using examples of applications, mainly in the field of biomacromolecules (35 pp.). Next comes a contribution by *Ferenc Mezei* on the neutron spin-echo technique, again applied mainly to biomolecules; here an important field of research which originated at the place of the meeting was described (11 pp.). The book ends with a detailed review by *Kai Sieghahn* of the development and still continuing refinement of the ESCA (electron spectroscopy for chemical analysis) method (37 pp.).

This little book will be mainly useful to readers who are engaged in work in the fields dealt with in the individual papers. It should also be in every department library, as a way of keeping alive the memory of *Georg von Hevesy*, a gentleman scientist who had the resources to enable him to work for a considerable time without a salary, and thus to remain literally his own boss. There is something in the view which is occasionally put forward that the decline of science in this country began with the disappearance of the wealthy "Privatdozenten", for these people were truly independent.

Günter Herrmann [NB 990 IE]
Institut für Kernchemie
der Universität Mainz (FRG)

Carbocycle Construction in Terpene Synthesis. By *Tse-Lok Ho*. VCH Verlagsgesellschaft, Weinheim/VCH Publishers, New York 1988. xiv, 768 pp., hard cover, DM 260.00. – ISBN 3-527-26582-1/0-89573-279-3

This book by *Ho* on ring-forming reactions in terpene synthesis is a long one. It has 760 pages, 1600 references and about 7000 structural formulas which are correctly drawn in nearly every case. What does the book offer the reader that is new? *Ho* places the ring-forming reaction as the central step in every synthesis, with the synthesis proceeding around it, before it and following it. This viewpoint strikes the reviewer as misleading, or at least biased. It can sometimes be appropriate, as in some of the more spectacular cationic cyclizations, e.g. in the synthesis of alnusenone (page 290), but it is an overstatement in many cases, especially for syntheses of which ring formation is a comparatively insignificant part, e.g. the formation of the second cyclopentane ring in the synthesis of pentalenolactone (page 92). This overemphasis on ring formation is reminiscent of total syntheses of natural products in which, say, 15 laborious stages are needed to prepare the precursor for the ingenious one-stage ring-closing reaction.

The book treats the subject defined above in 11 chapters: Robinson annelations, aldol condensations, Michael aldol condensations, Claisen and Dieckmann reactions, intramolecular alkylations, cationic cyclizations, Diels-Alder reactions, other thermal processes (i.e. [3 + 2]-, [4 + 3]-additions, etc., Wittig and Claisen rearrangements, electrocyclizations, etc.), free radical cyclizations, small ring syntheses (Simmons-Smith reaction, carbene chemistry, photochemical formation of cyclobutane, etc.), ring enlarging and ring contraction reactions, and a chapter on "transitory" ring formation reactions, i.e. those that subsequently serve other purposes, e.g. cyclopropane → gem-dimethyl.

The book also takes into account the most recent published work. Even the main text contains quite a number of 1987 references, while the 50 or so references contained in the appendix are mainly to papers published in 1988.

Unfortunately the information content of the reaction schemes is very scanty. Only for the centrally placed ring-forming reaction are some details of the reactants rather casually included, and even here without giving yields. More information here would have been very useful for quick reference, and rapid access to information is without doubt one of the main purposes of such a book.

The content of the book overlaps to a large extent with the chapters on mono-, sesqui- and triterpenes in the series "The Total Synthesis of Natural Products" by *ApSimon*. While it is true that *Ho* is seven to eight years more up-to-date, *ApSimon* is better in information content and clarity.

Finally, a few errors will be mentioned, more in order to show that the reviewer has read the book carefully than by way of serious criticism. On page 481 a CH_3 group is missing from the route to nootkatone, on page 335 *E*/*Z*-ocimenone was converted using isoprene, not ocimene, and the relevant reference is *Adams* (1975), not *Ayar* (1973, 1975). On page 215 the CH_3 and $ClCH_2$ groups are shown in the wrong positions in the ishwarone synthesis. But, as has already been said, these are unimportant details in a work such as this.

To summarize, the book constitutes a new attempt at presenting the formidable variety of terpene syntheses according to a different method of classification based on their ring-forming reactions. Since every such new approach offers the possibility that in thumbing through the book one can learn something new, or see something which is already familiar from a different viewpoint, it is a useful book for the synthetic chemist and, although rather expensive, is worth buying.

Georg Fráter [NB 966 IE]
Givaudan Forschungsgesellschaft AG
Dübendorf (Switzerland)

Analytical Artifacts: GC, MS, HPLC, TLC and PC. (Journal of Chromatography Library, Vol. 44). Edited by *B. S. Middleditch*. Elsevier, Amsterdam 1989. 1033 pp., hard cover, HFl 495.00. – ISBN 0-444-87158-6

Every honest analyst has at some time detected in his samples substances whose presence has at first seemed astonishing. In many cases it turns out, after further careful investigation, that these have found their way into the analytical samples in mysterious ways, through the operation of "Murphy's Law", during some purification or sample preparation step, or even during sampling. In publications mention of such occurrences is either shyly omitted, since no one willingly admits to having been stupid, or hidden away in incidental minor comments. After all, why not let others make the same mistakes?

It is surprising, therefore, that despite this there are so many wrong chromatographic interpretations to be found in

the literature; in this work they are systematically collected together in more than 1000 pages. In each case the pitfalls are described and listed under either the name of the wrongly identified substance or that which was responsible for introducing them. For example, under the keyword "Tenax", which is a polymer often used for concentrating trace organic impurities present in the atmosphere, are listed more than 40 compounds and compound classes that have allegedly been found in environmental samples, but which originated from the polymer itself. Perhaps it is already sufficiently well known that samples purified by gas chromatography or in reverse phase columns can be contaminated with siloxanes, but the fact that difficulties can arise with chromatographic tests for drugs, as used in the USA, if one has been eating poppy-seed bread rolls, not only illustrates the sensitivity of the chromatographic test method, but also emphasizes the need for care in interpreting analytical results.

Under the keyword "filter paper" are listed over 60 compounds, from simple hydrocarbons to steroids, which have been introduced during filtration. The book is enriched by many practical hints, ranging from sample injection procedures to the problems encountered in the determination of nitrosamines, and precautions against both false positive and false negative results in this case. There are also historical anecdotes concerning false analyses (e.g. the poisoning of *Napoleon* by arsenic, or the theory that the Philadelphia legionnaires were poisoned by tetracarbonylnickel, which arose because the samples were contaminated by nickel from a spatula), which enliven the book.

In addition to keywords of a general type, all the compounds identified as artefacts are listed alphabetically. In addition to the molecular formula, molecular mass, trivial and systematic names, and CAS and Merck index numbers, the compilation also includes mass spectra in many cases. Also provided are detailed descriptions (with literature references) of how and where the substance appeared as an artefact, and precautions that were taken to avoid errors. In addition to the usual index of compounds, the mass spectrometric data (base peak and 2nd and 3rd peaks) are also indexed in such a way that the corresponding substance can be quickly found.

Despite the relatively high price of HFl 495.00, this book should be regarded as essential reading for everyone seriously engaged in chromatographic trace analysis. The price is small when compared with the trouble, annoyance and expense caused by incorrect analyses.

Heinz Engelhardt [NB 983 IE]
Institut für Physikalische Chemie
der Universität Saarbrücken (FRG)

Name Reactions and Reagents in Organic Synthesis. By *B. P. Mundy* and *M. G. Ellerd*. Wiley, Chichester 1988. ix, 546 pp., hard cover, £ 27.05. – ISBN 0-471-83626-5

This is neither an ordinary book nor a systematic encyclopedia; rather it is a well-ordered card index that has been put between covers. The following layout is repeated 120–130 times on the left-hand pages: a first section consisting of the named reaction with an equation, a mechanism, and comments on its applicability; a second section containing reagents with their formulas, areas of application and methods of preparation, followed by about five literature references. On the right-hand page in each case are about five examples (in large print) of reactions taken from the papers cited.

The following are two examples: 1) Vilsmeier reactions for the regioselective formylation of an open-chain triene and for preparing selenoaldehydes are described. No yield is given for the first reaction (are the other isomers also formed?); the second reaction means nothing to me in the absence of any discussion of selenoaldehydes. The three other Vilsmeier reactions cited are of "normal" types, and can also be found in standard textbooks. 2) The most common application of *Mitsonubu*'s reagent is for OH-substitution in alcohols with a change of configuration. Here one also finds the esterification of carbon dioxide using pentanol. This is certainly surprising, but what purpose does this serve in organic synthesis? (see the book's title). The examples throughout are either very familiar or very exotic. There are so few surprises in the information given (see, for example, under the keywords formic acid and potassium hydride) that one shrugs one's shoulders and dismisses it as inconsequential. There is, moreover, no index of reaction types, and consequently it is not possible to search for particular ones.

The never-failing references to pages in *March*'s "Advanced Organic Chemistry" and *Fieser*'s "Reagents for Organic Synthesis" are evidence of painstaking student work. Basically the book is nothing more than this. None of the material has been treated in a novel way or freshly evaluated; instead it has merely been collected together and, on the whole, faithfully reproduced (an exception is the incorrectly shown bonding in the chair form of cyclohexane, e.g. on page 477). To misquote *Arno Schmidt*, the book remains a Zettel-Alptraum (card-index nightmare). Throughout the whole of the five hundred-odd large-format pages the same question keeps coming to mind: what is it meant to be?

Jürgen-Hinrich Fuhrhop [NB 986 IE]
Institut für Organische Chemie
der Freien Universität Berlin

Mechanistic Principles of Enzyme Activity. Edited by *J. F. Liebman* and *A. Greenberg*. VCH Verlagsgesellschaft, Weinheim/VCH Publishers, New York 1988. 404 pp., hard cover, DM 204.00. – ISBN 3-527-26907-X/0-89573-706-X

The field of enzyme chemistry has undergone a significant mutation over the last ten years thanks to advances in cognate biological technologies and in instrumentation. As a result, the focus of attention has broadened from the substrate and mechanisms of chemical catalysis to include detailed consideration of the properties of the protein relevant to catalysis. To reflect such a change in emphasis in the title of a multi-author book is extremely difficult and the familiar ring of many of the chapter titles also disguises the high scientific and intellectual content of many of the chapters.

We are dealing here with a book that not only presents the information currently available on several important topics but also shows how ideas have developed, identifies problems in current understanding, and indicates potential lines for future research. Further, where appropriate, there is a concise exposition of the theory relevant to the understanding of the problem, for example in the discussion of electron transfer in cytochromes (*Dixon*). Several other chapters deal with specific classes of enzymes including peptidases (zinc proteases, *Christianson* and *Lipscomb*; serine proteases, *Schowen*) and oxidases (hemoproteins, *Bruice*; flavin mixed function oxidases, *Bruice*; glutathione dependent aldehyde oxidation, *Creighton* and *Pourtomabbed*). Two others of general significance discuss stereoelectronic analysis (*Benner*)

and a modern view of intramolecularity, proximity, and strain (*Czarnik*). A further chapter, unusual for this type of work, covers the topic of porphyrin metallation reactions (*Lavallee*).

As always in books of this length (ca. 400 pp.) many areas of equal interest and importance are not covered. However I found several of the chapters so exciting and stimulating to read that I would consider this book an obligatory purchase for libraries and very meritorious of inclusion in the private collections of researchers active in any field of mechanistic enzyme chemistry.

Colin J. Suckling [NB 995 IE]
Department of Pure and Applied Chemistry
University of Strathclyde
Glasgow (Scotland)

Sterol Biosynthesis Inhibitors. Pharmaceutical and Agrochemical Aspects. (Ellis Horwood Series in Biomedicine). Edited by *D. Berg* and *M. Plempel*. VCH Verlagsgesellschaft, Weinheim/VCH Publishers, New York 1988. 583 pp., hard cover, DM 220.00. – ISBN 3-527-26744-1/0-89573-671-3; ISSN 0930-3367

Inhibitors of sterol biosynthesis are nowadays indispensable for the treatment of fungal infections in human and veterinary medicine and for plant protection. Whereas 25 years ago they were still completely unknown, even in research laboratories, they now account for a considerable part of the sales of pharmaceutical and agrochemical manufacturers. An enormous amount of research on such products is carried out worldwide. The number of patents and publications has grown exponentially, and various classes of compounds with broad or selective activity have been discovered, some of which are yet to be introduced onto the market. There is a strong probability that the economic importance of sterol biosynthesis inhibitors will increase further and that they will find new applications. It is not surprising, therefore, that in addition to the monograph reviewed here two other books summarizing the current state of knowledge on these substances have been published during the last two years, viz: R. A. Fromtling (ed.): *Recent Trends in the Discovery, Development and Evaluation of Antifungal Agents*. J. R. Prous Science Publishers, Barcelona 1987, and V. St. Georgiev (ed.): *Antifungal Drugs (Ann. New York Acad. Sci. 544* (1988)). The latter two volumes concentrate on antifungal agents for human applications (all the important new antifungals are sterol biosynthesis inhibitors).

However, all three monographs contain contributions from the same authors on special aspects of particular agents, and these are even similar in content. How do the books differ, and what makes the present book especially valuable? It attempts for the first time to bring together the pharmaceutical and agrochemical aspects of sterol biosynthesis inhibitors, and also sets out to open a window on a possible new area of application. As is indicated below, the editors *D. Berg* and *M. Plempel* have essentially succeeded in these aims.

In Part 1 of the book the basic chemical and biochemical characteristics of the different classes of antifungal agents (e.g. azoles, morpholines, allylamines) are reviewed, covering work published up to 1987. This is followed by a chapter on the toxicology of azoles; it would have been better to include this in Part 3 with the article on the pharmacokinetics of this class of compounds, but it is nevertheless very useful. Toxicological aspects of azoles as a group, as they relate to the extent of investigations and the problems inherent in handling these compounds, are not usually discussed either at conferences or in scientific journals. The article here presents data from the Bayer toxicological laboratory on liver toxicity, embryo toxicity, and effects of steroidal hormones through inhibition of the cytochrome P-450 system. Other firms should follow this example!

Part 2 is devoted to the applications of sterol biosynthesis inhibitors in plant protection. The non-specialist reading this will be surprised at the similarity of the chemical structures, especially those of the new triazole fungicides, to those of the azole type human antifungal agents. Here one has a situation which is probably unique: substances of the same structural class which differ by only slight modifications are used in completely different market applications. Whether or not this situation can also lead to problems (e.g. through development of resistant strains) remains to be seen. By providing a wider circle of readers with a survey of the human and agricultural aspects of sterol biosynthesis inhibitors, this book may lead to a heightened awareness of such problems.

Part 3 deals with the chemotherapy of fungal infections in humans and animals, and indications for possible new treatments. Especially useful contributions are the article by *W. Ritter* on the pharmacokinetics of azoles, and the review of aromatase inhibitors by *D. F. Covey*. The latter article draws attention to a possible new application of azoles as an inhibitor of this cytochrome P-450 dependent enzyme, namely the inhibition of oestrogen-dependent tumors. The selective control of other processes that involve the synthesis of steroidal hormones and are regulated by highly specific cytochrome P-450 enzymes, by using specially tailored azoles, is still a utopian idea, but could soon become a reality.

This book is suitable both for newcomers to this rapidly developing field of research and application, and as a work of reference for the specialist. The way in which the book brings together information on these topics will contribute to useful discussion, and hence to the future development of the field.

Anton Stütz [NB 970 IE]
Sandoz Forschungsinstitut
Vienna (Austria)

Art in Organic Synthesis. 2nd Edition. By *N. Anand, J. S. Bindra* and *S. Ranganathan*. Wiley, Chichester 1988, xix, 427 pp., hard cover, £ 34.50. – ISBN 0-471-88738-2

"There is excitement, adventure, and challenge, and there can be great art, in organic synthesis." To illustrate this quotation from *Woodward*, by describing a selection of outstanding syntheses, was the declared objective of the authors in the first edition of "Art in Organic Synthesis", published in 1970. The rapid developments that have occurred since then in new synthetic targets, methods and reagents have necessitated a rewriting of this "state of the art" account.

The second edition which the same team of authors has now produced with a different publisher again presents, under about 100 subject headings, a colorful kaleidoscope of the power of organic synthetic methods. In the form of annotated flow charts, it summarizes important syntheses drawn from the whole spectrum of applications, providing a balanced mixture which contains about two-thirds on natural products and one-third on man-made compounds. An indication of the degree of topicality is given by the fact that the majority of the chapters of the first edition have been replaced by new ones; only a third or so are "classical"

teaching examples which have been retained almost unchanged. The examples range from simple structures such as adamantane, through many different steroids, alkaloids and antibiotics, spectacular polycyclic compounds such as [1.1.1]propellane, tetra-*tert*-butyltetrahedrane and dodecahedrane, through to gene synthesis. Although it is possible to quarrel with the authors' subjective selections in some cases, the wealth of topics included leaves only a very few others that one would have liked to see added. Each chapter begins with a brief introduction in which, after the occasional historical reference, the nub of the synthetic problem is described. This is followed by a concise diagrammatic representation of the synthetic route, amplified by footnotes and literature references. The main emphasis is on the strategic concept, and the list of reagents used is only occasionally supplemented by details of the reaction conditions. The book ends with detailed indexes of the structures synthesized, authors, reagents and reaction types (the latter are sometimes rather uncritically taken to excess, e.g. there are 50 references to the use of the commonplace reagent chromium trioxide, a number exceeded only by lithium aluminum hydride with 66 references).

The motives underlying such a compilation of "highlights" from organic synthesis are to be applauded. The authors have succeeded in compiling a selection of elegant applications of contemporary methods to both classical and currently topical problems, in such a way as to convey an appreciation of the changes that are developing in the type and complexity of the problems to be solved. However, although the examples chosen are very appropriate to the book's title, this makes it all the more regrettable that the presentation does not always meet a level of aesthetic excellence. The direct reproduction of the typescript which has been used to reduce the cost, evidently without editing by the publishers, has led to a large number of grammatical and typographical errors which detract from the enjoyment of reading the book (even the page headings, which are typeset, have not escaped this). One wishes that the authors and publishers had made better use of the 18 years that have passed since the first edition, so as to improve the content with more careful attention to details. Similarly the figures, and especially the structural formulas, are not free from defects (distorted geometries, missing or superfluous bonds, incomplete or incorrect representation of stereochemical relationships occurring at bond crossings or wedged projecting bonds). Occasionally one wishes that the perspectives used in the original papers had been followed more closely.

For some of the more important natural products and homologous series of polycyclic compounds, several known alternative synthetic routes are presented alongside each other, in the way adopted, for example, in the journal *Synform*. However, one cannot make a fair comparison of the different strategies and methods used in the various routes, as no yields are given. To suit this condensed method of presentation, an indication of the type of transformation (e.g. "Sharpless epoxidation") would in some cases be more informative, and more desirable from a didactic standpoint, than a mere listing of chemicals. The literature references extend in general up to 1985, and occasionally there are citations of 1986 papers; the older chapters have in general not been updated, and here the literature coverage only extends to 1969. Quite often one finds an early short communication cited rather than the more detailed article published later; often too there are no references to relevant or more recent review articles. Inadequate treatment of the literature also shows itself in inconsistencies in the form used for citations of the various journals (e.g. there are at least four versions of *Angew. Chem. Int. Ed. Engl.*).

One of the aims of the book is to serve as a textbook for advanced undergraduate and graduate students. However, in order to receive a recommendation without reservation it would need to be still further revised, e.g. in such a way as to take account of the merits of a rival "artist" from the same publishing house.[*] The question of what purpose the book can most appropriately serve is perhaps best answered by comparing it to a nice box of chocolates: an appropriate present for a friend, or for treating oneself to an occasional munch. However, this analogy is not fully satisfying, because even though the price is affordable one can get real truffles for less.

Wolf-Dieter Fessner [NB 971 IE]
Institut für Organische Chemie und Biochemie
der Universität Freiburg (FRG)

[*] M. E. Alonso: *The Art of Problem Solving in Organic Chemistry*, Wiley, New York 1987.

Registered names, trademarks, etc. used in this journal, even when not marked as such, are not to be considered unprotected by law.

© VCH Verlagsgesellschaft mbH, D-6940 Weinheim, 1989. – Printed in the Federal Republic of Germany by Konrad Triltsch Druck- und Verlagsanstalt Würzburg.

All rights reserved (including those of translation into foreign languages). No part of this issue may be reproduced in any form — by photoprint, microfilm, or any other means — nor transmitted or translated into a machine language without written permission from the publishers. Only single copies of contributions, or parts thereof, may be made for personal use. This journal was carefully produced in all its parts. Nevertheless, authors, editors and publisher do not warrant the information contained therein to be free of errors. Readers are advised to keep in mind that statements, data, illustrations, procedural details or other items may inadvertently be inaccurate.

Valid for users in the USA: The appearance of the code at the bottom of the first page of an article (serial) indicates the copyright owner's consent that copies of the article may be made for personal or internal use, or for the personal or internal use of specific clients. This consent is given on the condition, however, that the copier pay stated per-copy fee through the Copyright Clearance Center, Inc. (CCC), for copying beyond that permitted by Sections 107 or 108 of the U.S. Copyright Law. This consent does not extend to other kinds of copying, such as copying, for general distribution, for advertising or promotional purposes, for creating new collective works, or for resale. For copying from back volumes of this journal see 'Permissions to Photo-Copy: Publisher's Fee List' of the CCC.

Editorial office: Postfach 10 11 61, D-6490 Weinheim, Federal Republic of Germany, Telephone (06201) 60 22 55, Telex 465 516 vchwh d, Telefax (06201) 602 328.

Editor: *Peter Gölitz*

Associate editors: *D. I. Loewus, A. Stimson.* **Editorial assistant:** *E. Schweikart*

Publishers: VCH Verlagsgesellschaft mbH. (Managing Director: *Hans Dirk Köhler*), Pappelallee 3, D-6940 Weinheim, Federal Republic of Germany.

Advertising office (Advertising Manager *R. J. Roth*): Postfach 10 11 61, D-6940 Weinheim, Federal Republic of Germany, Telephone (0 62 01) 60 61 30, Telex 4 67 155, Telefax (0 62 01) 606 184.

ADVANCED MATERIALS

How to Tailor Molecular Electronics or Why is Nature Taking the 'Soft' Approach?**

Editorial Essay

By Dietrich Haarer*

Dedicated to Professor Wolfgang Hilger on the occasion of his 60th birthday

1. Introduction

The more we are able to understand the efficiency of biological systems, the more our mind is tempted to design *Molecular Devices* whose efficiency is comparable to the efficiency which nature has achieved during its evolutionary path. Here are three examples:

a) The **capacity of the human brain** is of the order of 10^{15} bits. To mimic this memory-capacity with magnetic disks (typically 60 MByte; 50 Watt power consumption) one would need about two million disks, consuming about 0.1 Gigawatts of electric power. Our human brain does this job for as little as a couple of Watts. Granted, a magnetic store of the above size would be more reliable than our brain; however, its energy consumption differs from the biological systems by some 7 orders of magnitude.

b) Highest performance can be achieved with **semiconductor devices,** but assuming a price of \$10 for a 1 MBit chip, we would have to pay about 10 billion dollars to assemble a semiconductor memory of the capacity of the human brain.

c) The **sensitivity of the human eye** is comparable to that of a photomultiplier tube. On our retina we have in the order of 10^8 photon receptors of roughly the sensitivity of a photomultiplier tube. If we assume that a photomultiplier costs around \$100 (including power supply), we would have to pay about 10 billion dollars in order to build, by conventional means, an optical device with the same performance as the human eye.

The above examples may be fortuitous, and it is certainly accidental that our 'multiplier eye' turns out to cost as much as our 'megabit brain'. The examples show, however, that nature must have some design secrets which we cannot yet handle.

Even more astounding than its price/performance is the accuracy with which nature is able to process molecular information. Consider that the rate of mutation per base pair per replication of DNA is of the order of 10^{-10} (drosophila; see[1]). Even the accuracy of the translation of the genetic information into amino acids with 10^{-5} to 10^{-4} errors per amino acid position is very impressive.[2] These numbers beat, by any means, what can be technically achieved by present magnetic, optical or chemical schemes.

With nature being able to perform the above 'miracles' and with the limits of the silicon based technologies becoming more and more visible, it was an obvious step to consider a synthesis of electronic schemes and molecular schemes, long before the word *'molecular electronics'* was coined. Starting with the possibility of creating quite accurate molecular assemblies it was shown in the early 70's[3] that by using monolayer techniques, molecules could be assembled at well defined distances and that energy transfer and tunneling processes could be investigated experimentally[3] as well as theoretically.[4]

The capability of achieving 'design' on a molecular level led to concepts like the *molecular rectifier*[5] and *molecular shift registers*,[6] where molecular and semiconductor terminologies were fused to give a new dimension, namely *'Molecular Electronics'*.

Speakers at two recent meetings, a workshop in Bangor (UK)[7] and a meeting in Strasbourg (France)[8] presented two aspects of molecular design. In Bangor, aspects of 'Molecular Metals' (*F. Garnier*), 'Monolayers and Thin-Films' (*D. Bloor*) and 'Spectroscopy on a Molecular Scale' (*D. Haarer*) were the center of attention, whereas in Strasbourg it was the chemistry of synthesizing molecules which are selective as to the size, shape and ionic state of other molecules (*Lehn*,[9] *Stoddart*[10]) as well as biological aspects which deal with very large molecules like bacteriorhodopsin (*G. H. Khorana*) and molecular schemes which fall into the category of 'Topobiology' (*G.Edelman*) which provided the central theme. All of these are topics which reflect the wide range of interests in the field of molecular design.

[*] Prof. D. Haarer
Physikalisches Institut und BIMF der Universität Bayreuth
Postfach 101251
D-8580 Bayreuth (FRG)

[**] This work was supported by the Deutsche Forschungsgemeinschaft, by the Stiftung Volkswagenwerk and by the Fonds der Chemischen Industrie. Moreover, I would like to thank my colleagues *Büttner* and *Blumen* for valuable comments and my students at the University of Bayreuth for their contributions to this work.

ADVANCED MATERIALS

The question which I would like to discuss briefly in this article is the following: Why does nature use such large units like phycobilisomes, bacteriorhodopsin and the photoreactive center of *Rps viridis*[11,12] to perform electronic functions? (In the above mentioned examples, 'electronic functions' are functions which are triggered by photon absorption). Figure 1 shows the reaction center.[11] It is about 130 Å in length and has an elliptical cross section of 70 and 30 Å

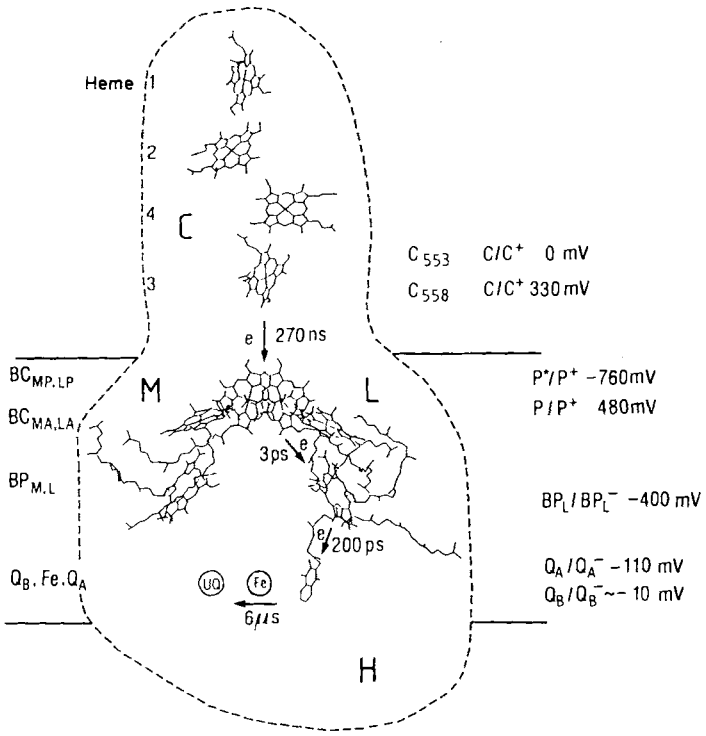


Fig. 1. Scheme of the structure of the reaction center of *Rps. viridis* showing the cofactor system, the outline of the protein subunits (C, M, L, H), the electron transfer half-times, and the redox potentials of defined intermediates [11].

respectively.[12] The total molecular weight is about 125 000, about 250 times larger than the dye molecule phthalocyanine, and about 1000 times as large as a small organic donor molecule like naphthalene.

Was nature wasteful with its valuable resources or does the large volume of 'biological machines' point towards a principle of *low densities of excited states* or *low charge carrier densities*, one of which may be the conditio sine qua non for the system to function? In typical configurations, as proposed for straightforward molecular electronics, one needs a high density of charge carriers where each charge carrier represents a bit of information and is, in general, confined to the space occupied by a small molecule. In other configurations one uses light to generate excited molecules at adjacent molecular sites (for instance donor-acceptor sites) in order to implement a clock which is able to shift molecular information along a molecular array. In other words, the charge density and the density of excited states tend to be of the order of one per small molecule. These situations are not easy to handle, as one knows from past experience with molecular crystals. Some of the following examples document what can happen if charges and excited states are brought into close proximity.

2. High Density of Excited States—Exciton Annihilation

Biological systems can be 'bleached' with low light levels and this seems to contradict the above statements about high densities. This contradiction, however, is not real, because nature has used certain construction principles:

- The dye-like molecules, absorbing in the visible spectral range, are present at a dilute concentration and surrounded by non-absorbing (and space filling) proteins.
- The systems are very complex, having subsystems with sub-picosecond electron transfer, nanosecond lifetimes, and microsecond to millisecond metastable states, which store chemical or electrical energy before allowing the systems to return to their ground state after the light has been switched off.

If one were to pack small molecules, similar to those which are often suggested for molecular electronics in close proximity to one another, and if one neglects long living interme-



Dietrich Haarer is Professor of Physics at the University of Bayreuth, FRG. A physicist by training, he received his Ph.D. in 1969 from the University of Stuttgart. With short interruptions he then worked until 1980 at the IBM research laboratory in San Jose, California, which he left as manager of the Organic Solids Department, to take up his current position. His research activities include laser spectroscopy and laser chemistry. He is an Editorial Advisor of Advanced Materials.

diates (which are undesirable in fast electronic systems because they would slow down molecular switches), one arrives at matrices resembling molecular crystals. Here we know that excited singlet states are delocalized (excitons, polarons) and annihilate i.e. transfer their valuable photon energy into heat if brought closer together than a typical distance of about 1000 Å.[13]

Having the above example in mind, nature has done two things to avoid annihilation: a) dye-like molecules with overlapping π-orbitals appear in dimers rather than in single crystal-like configurations and b) the dye molecules are surrounded by a large bulk of protein (solvent cage) which is transparent in the wavelength range of visible photons.

3. High Concentrations of Charge Carriers

3.1. The Electron-Hole Recombination Problem

Having made the point, that excited states do – in crystal-like media – not like to be packed closely, we have to discuss the same issue for charge carriers.

Light-induced charge carriers are always produced as electron-hole pairs, maintaining the total charge neutrality. Electron-hole pairs, however, have the tendency to annihilate unless they are created in a high electric field which is able to separate them. *Onsager* has calculated the probability of the geminate recombination of charge carriers performing a diffusionlike motion. Typical 'Onsager Radii', which define the distance at which the charge carriers thermalize, are of the order of 20 Å.[14, 15] Following the model of *Onsager*, the quantum yields for electron-hole separation approach unity as the field strength increases beyond 10^6 V/cm. For external fields this field strength is close to the dielectric breakdown. Molecular fields in biological systems may even be higher than the above quoted numbers for external technical fields.

3.2. The Space Charge Problem

One of the most severe problems if one wants to confine charge carriers to molecular-size boxes is the far reaching Coulomb force, which falls off slowly with $1/R$, where R is the distance between the charges. One problem, when dealing with molecular devices, will therefore be the difficulty of controlling charges using 'external fields', which are larger than the 'internal molecular fields' with which the charge carriers mutually interact. The simplest way of calculating the upper limit of how many charge carriers can be put into a molecular box, without exceeding the space charge conditions[16, 17] is the following: one calculates the capacitance C_m of a molecular capacitor of the size of a 'molecular device'. The condition to be fulfilled is that the molecular charge q_m must be smaller than $C_m \times U$, where U is the applied voltage. For simplicity I assume a plane parallel capacitor geometry with two disks of diameter R_D separated by a distance d (see also Fig. 2). This capacitor is filled with a dielectric medium of dielectric constant ε ranging between 10

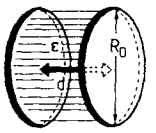


Fig. 2. Dimensions of a molecular capacitor – see text.

and 100. Now, the simple question to be answered will be the following: How many electrons can be packed into this device without running into space charge problems at a field of 10^6 V/cm (close to breakdown)? Doing this elementary calculation, one notes that the distance d does not enter into the figures, and one gets the result that it is only possible to pack 5×10^{-2} electrons into the box if ε is 10 and the diameter R_D is 10 Å.[18]

In spite of the crudeness of this estimate, I realize that it is quite difficult to control charges with external fields under conditions where the external field dominates (known from photoconduction experiments[15, 16, 19]). Since we cannot easily design a molecular deviced operating with 1/20 of an electronic charge, our recipe for avoiding space charge problems would be to take a capacitor diameter of 100 Å rather than 10 Å – and that's just what nature has done with biological devices, casting our mind back to the photoreactive center shown in Figure 1. A second comment should be made concerning the thickness d of the device. Since the thickness does not enter into the calculation (in our crude planar geometry model), it is always advantageous to deal with thin samples because here one can optimize the number of charges which can be controlled via external fields.

4. Conclusions

Admittedly, the above model assumptions are very crude, yet, they are based upon experiments with molecular crystals and polymer films and point to the fact that organic materials do not like high densities of excitated states. For instance, the molecular crystals, which were used for exciton annihilation experiments showed brown spots of carbonization after a few laser shots.[13] Organic materials also cannot accommodate many charges while still alowing us to control the charges individually. Certainly, one can make 'organic metals' like TTF-TCNQ and pack one electron and one hole into a charge transfer pair, but one is then dealing with metals, where the individual character of the charge carriers is lost in the Fermi-sea.

Taking into account all of the above 'hard restrictions' which must be satisfied in order to perform electronic processes on a molecular scale, we may not be so surprised that nature has chosen the 'soft' way in reaching its goals. It uses

ADVANCED MATERIALS

not so much the Coulombic approach with adjacent electrons and holes and not so much the excitonic approach with large single crystal-like structures and strongly coupling singlet excited states. More often, nature uses environments in which charges are screened, like *ionic* environments, *hydrogen bonded* environments and environments in which Van der Waals interactions dominate, and it also separates the active sites using bulky proteins. Fortunately, the fluid phase is an ideal medium for these interactions: geometries can be optimized, and defects which would be detrimental to a solid state device can heal in microseconds or milliseconds.

Not everybody will agree with this article, since it draws far reaching conclusions on the basis of simple model estimates. I hope, however, that the article is useful in the following sense: If some of the estimates turn out to be too skeptical, the article will stimulate experiments to prove that less severe conditions have to be fulfilled. Should the limitations be as severe as pointed out, we will have to proceed along the 'soft' path of molecular electronics. I believe that this can be done.

I will end the article with one example in a field of molecular electronics in which I have some knowledge and through this I would like to document that the soft approach can be realized. The example is photochemical hole burning.[20, 21] In these experiments, optical saturation is achieved by using a three level scheme (idealized here; in a true model more levels are involved). After exciting dye-like molecules to their first singlet state (two level picture), the photochemical change occurs mostly in states which are subsequently populated and have longer lifetimes (for instance triplet states). From these states the system then relaxes into a photochemical state (being labelled as the third state), whose lifetime can be infinitely long (at least at sufficiently low temperatures). In this scheme the photon information is *accumulated photochemically* in a third state, whose lifetime can be varied over wide ranges (microseconds to years). This kind of photochemistry even occurs at the lowest light levels. The system accumulates the photon information and, if enough photons have been accumulated a bit of digital information can be stored. This can occur at integrated energies of as little as one picojoule and it only works in systems in which the molecules which store molecular information are very dilute (10^{-3}–10^{-5} M)[21] So, from my present viewpoint, the future of molecular electronics is a bright one if we follow realistic design principles.

[1] J. W. Drake, *Nature 221* (1969) 1132.
[2] M. Yarus, *Prog. Nucleic Acid Res. 23* (1980) 195.
[3] H. Kuhn, D. Möbius, *Angew. Chem. Int. Ed. Engl. 10* (1971) 620; *Angew. Chem. 83* (1971) 672.
[4] J. J. Hopfield, *Proc. Nat. Acad. Sci. USA 71*, 3640 (1974).
[5] A. Aviram, M. A. Ratner, *Chem. Phys. Lett. 29* (1974) 277.
[6] J. J. Hopfield, J. N. Onuchic, D. N. Beratan, *Science 241* (1988) 817.
[7] 'Molecular Electronics', Future Developments and European Collaboration in Molecular Electronics, Bangor, April 5.–6., 1989.
[8] 'The Storage and Transfer of Molecular Information', Espaces Europeens des Sciences, Strasbourg, July 2.–7., 1989. For a report of the conference see *Jean-Paul Behr's* article in this issue.
[9] J. M. Lehn, *Angew. Chem. Int. Ed. Engl. 27* (1988) 89; *Angew. Chem. 100* (1988) 91.
[10] F. H. Kohnke, A. M. Z. Slawin, J. F. Stoddart, D. J. Williams, *Angew. Chem. Int. Ed. Engl. 26* (1987) 892; *Angew. Chem. 99* (1987) 941.
[11] R. Huber, *Angew. Chem. Int. Ed. Engl. 28* (1989) 848; *Angew. Chem. 101* (1989) 849.
[12] J. Deisenhofer, H. Michel, *Angew. Chem. Int. Ed. Engl. 28* (1989) 829; *Angew. Chem. 101* (1989) 872.
[13] D. Haarer, G. Castro, *J. Luminescence 12/13* (1976) 233.
[14] L. Onsager, *Phys. Rev. 54* (1938) 544.
[15] R. R. Chance, C. L. Braun, *J. Chem. Phys. 64* (1976) 3573.
[16] H. Kaul, D. Haarer, *Ber. Bunsenges. Phys. Chem. 91* (1987) 845.
[17] Space Charge Effects, Chapter 10 in F. Gutmann, L. E. Lyons (Eds.): *Organic Semiconductors*, Robert E. Krieger Publ. Co., Malabar, Florida 1981.
[18] The dielectric constant ε can be much larger for collective states like ferroelectric states but in these the 'molecular' nature of the approach is lost. See M. E. Lines, A. M. G. Lass: *Principles and Applications of Ferroelectrics and Related Materials* Chapter 8, Clarendon Press, Oxford 1977.
[19] E. Müller-Horsche, D. Haarer, H. Scher, *Phys. Rev. B35*, (1987) 1273.
[20] J. Friedrich, D. Haarer, *Angew. Chem. Int. Ed. Engl. 23* (1984) 113; *Angew. Chem. 96* (1984) 96. a) D. Haarer: Photochemical Hole Burning in Electronic Transitions in W. E. Moerner (Ed.): *Persistent Spectral Hole Burning, Science and Applications*, Topics in Current Physics Springer, Heidelberg 1988.
[21] D. Haarer, *Proc. Int. Symp. Optical Memories 1987*, Jpn. J. *Appl. Physics 26* (1987) Suppl. 26-4, 227.

The following review articles will be published early in 1990:

K. Bange, T. Gambke: Electrochromic Materials for Optical Switching Devices

P. Grant: High Temperature Superconductivity: Four Years since Bednorz and Müller

D. Reinhoudt: Molecular Systems for the Transduction of Host-Guest Complexation Reactions into Electronic Signals

H. Jäger: Superconductivity—Then and Now

B. Blümich et al.: Solid State NMR in Polymer Science

P. Comita: Surface Modification with Lasers

A. R. West: Characterization of Electroceramics by Impedance Spectroscopy

B. Lengeler: Applications of X-ray Absorption, Reflection, Fluorescence and Diffraction with Synchrotron Radiation in Materials Analysis

ADVANCED MATERIALS

Polymer Optical Fibers and Nonlinear Optical Device Principles**

Optoelectronics
Active LB Layers
Model Calculations
Fluorinated Polymers
Network Systems

By W. Groh, D. Lupo and H. Sixl*

Dedicated to Professor Wolfgang Hilger on the occasion of his 60th birthday

Basic principles of the present optoelectronic research activities at Hoechst AG are presented in this contribution. Within the diversified broad band spectrum of optoelectronic materials and applications our interest is focused on new types of polymer optical fibers and nonlinear optical device principles using organic Langmuir–Blodgett films and electrically poled polymers. The basic principles and the limits of the present research and development activities which have a high market potential are outlined.

1. Introduction

Polymeric materials have developed extraordinarily quickly in the last fifty years and now rank among the most important materials used in society and in industrial applications. New polymers with unusual optical and electrical properties are predicted to have a high market potential in the future. The combination of electrical and optical properties is especially attractive in modern electronics which develops more and more in the direction of optoelectronics with long term ambitions concerning all-optical devices. Optoelectronics plays a central role in computing and the handling of large amounts of data. Consequently material research using functionalized polymers with specially designed tailor-made properties becomes very important.

In the last few years, interest in polymer optical fibers (POF) has increased because of their low cost, easy handling and good flexibility even at large diameters.[1–5] These fibers are used for short-haul data transmission applications in computer links or in automobiles. However, the presently available fibers suffer from two major disadvantages, namely the relatively high loss of about 200 dB/km and the low maximum operating temperature of 80 to 90 °C, which is not sufficient for automotive applications. In distributed networks, even for short distance transmission, improvements in the optical loss are essential as will be shown in this contribution.

Nonlinear optical (NLO) effects have long ceased to be only a research curiosity or even research tool, and are being widely investigated and used in integrated optics and optoelectronic applications. For example, the electro-optic effect is used to build commercially available ultrafast electro-optic modulators, based on lithium niobate, which can modulate a continuous wave (CW) laser at multi-GHz frequencies. There are indications that for certain applications, organic materials will show significantly better performance than inorganic ones. The reasons for interest in organic materials and some of the problems to be solved before they can be used commercially are discussed in Section 3.

2. Polymer Optical Fibers

2.1. Model Calculations

The two important intrinsic loss factors in commercial polymethylmethacrylate (PMMA) optical fibers are C–H overtone absorption and Rayleigh scattering, which is mainly due to microscopic density fluctuations. Both factors lead to a theoretical lower loss limit of about 100 dB/km at 650 nm[1] with 90 dB/km due to overtone absorption as seen from Figure 1. Reduction of the loss is achieved by substituting the hydrogen atoms with heavier elements like deuterium which have lower energy absorption bands.

Deuteration, however, is a very expensive process and therefore other substituents have to be considered. Fluorination, for example, seems to be a good choice, but there is no information available in the literature about the positions and intensities of higher C–F vibrational overtones.

Light transmission measurements on perfluorinated compounds for a sample thickness of 10 cm show no C–F absorption in the visible spectral region as shown in Figure 2. Although this gives an upper limit for the C–F loss contribution the measurement is not sensitive enough to predict what loss a fiber consisting of this material would have, because

[*] Prof. H. Sixl, Dr. W. Groh, Dr. D. Lupo
Angewandte Physik, Hoechst AG
P.O. Box 800320, D-6230 Frankfurt am Main 80 (FRG)

[**] This work was supported by the Federal Ministry of Research and Technology (BMFT). The research projects are done in cooperation with other industrial and academic partners. We would like to thank our colleagues active in the project teams for many stimulating discussions and efficient cooperation.

ADVANCED MATERIALS

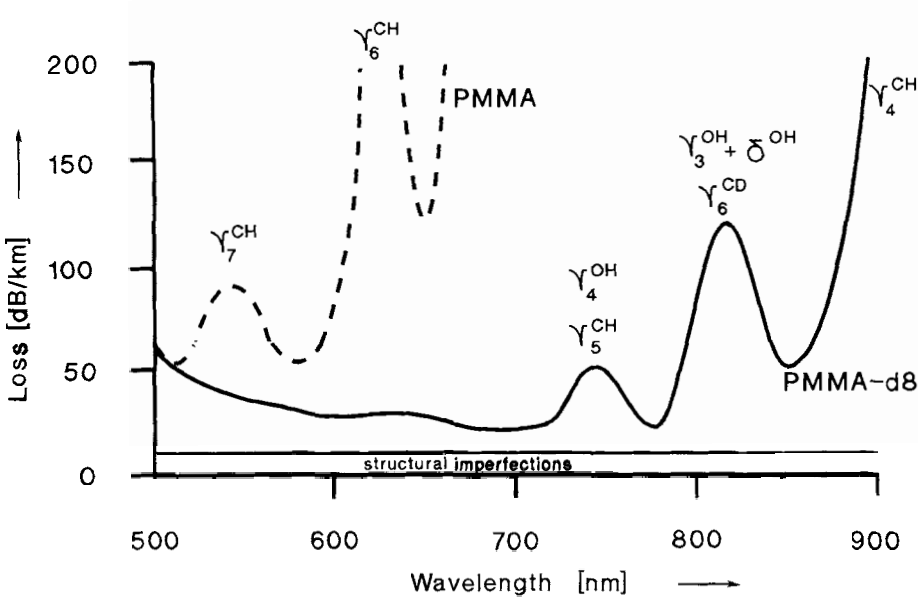


Fig. 1. Spectral loss of polymethylmethacrylate (PMMA) and d_8-PMMA polymer optical fibers.

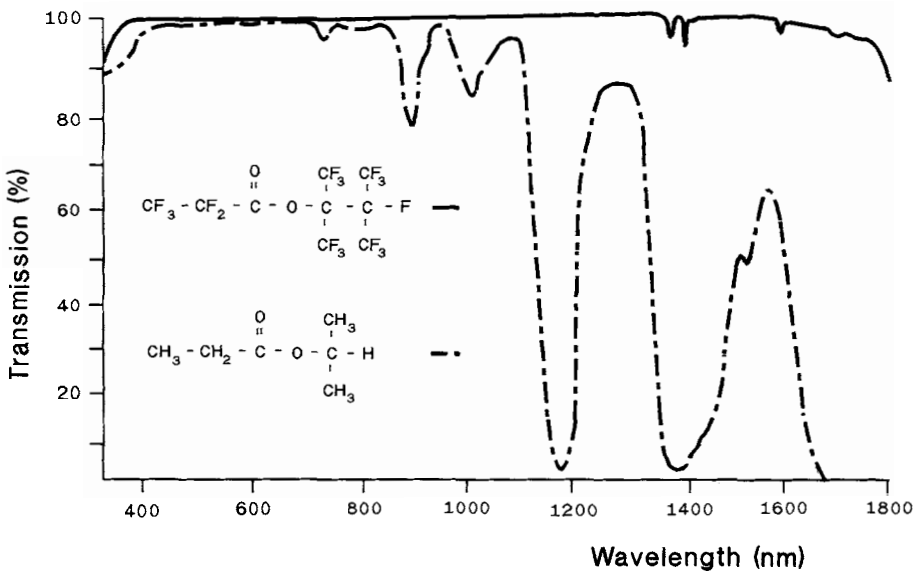


Fig. 2. Transmission spectra of a partially fluorinated and a perfluorinated compound (sample length: 10 cm).

the length of the fiber is 10^4 to 10^5 times larger. Therefore theoretical calculations on the expected overtone band positions and intensities have been made.[4-6]

Overtone bands appear because molecular vibrations are not perfectly harmonic. This is expressed in a nonsymmetric potential curve and a non-zero anharmonicity constant x. From the Morse potential approximation (Fig. 3) we obtain the energy levels and the corresponding transitions. We can calculate the spectral position of any overtone band if we know the position of the fundamental vibration and the anharmonicity constant. From infrared spectroscopic data on hydrogenated, deuterated or halogenated compounds one can find ν_1 and also ν_2 for all interesting vibrations, from which the x-values can be calculated. If, for example, ν_1 and ν_2 were known for a certain molecular vibration, the positions of all higher overtones can be calculated.

Energy levels (Morse potential)

$$G(v) = \nu_0(v + \tfrac{1}{2}) - \nu_0 x(v + \tfrac{1}{2})^2$$

Transitions

$$\nu_v = G(v) - G(0) \rightarrow \boxed{\nu_v = \frac{\nu_1 v - \nu_1 x v(v+1)}{1 - 2x} \qquad v = 2,3,4,\ldots}$$

or if e.g. ν_1 and ν_2 are known $\Rightarrow x$

For experimentally accessible overtones, for example from C–H or C–D vibrations, one can evaluate the band strength from the spectrum if the number of contributing bonds,

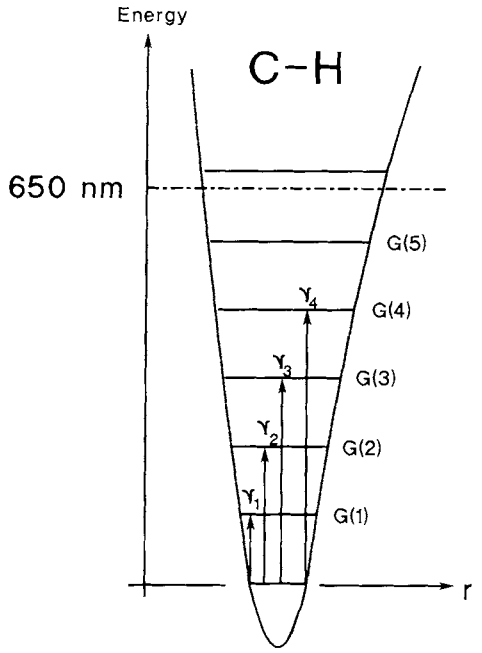


Fig. 3. Calculation of molecular vibrations with the Morse potential approximation.

molecular weight, density and sample thickness are known. Theoretical calculation of the interesting vibrations is also possible (with some approximations) due to the work of *Timm* and *Mecke*.[6, 7] We come out with a very simple equation for the band strength of an overtone normalized to the band strength of its fundamental. Any overtone band strength can be calculated if we know the anharmonicity constant x and the fundamental band strength $E(\nu_1)$, both of which can be extracted from an infrared spectrum of an appropriate compound.

This is illustrated in Figure 4, which shows selected parts of the infrared spectrum of a fluorinated model compound. Shown are the fundamental and overtone vibrational bands of the carbonyl group. From such spectra the exact band positions and intensities can be easily extracted. If, for example, the spectral positions of ν_1 and ν_2 are known, the anharmonicity constant and the positions of all other overtones can be calculated as shown above. We also obtain the band strength of the fundamental and can thus calculate all band strengths of the higher overtones which are not experimentally accessible.

The most important molecular vibrations in polymers are listed in Table 1. In a fluorine-containing methacrylate com-

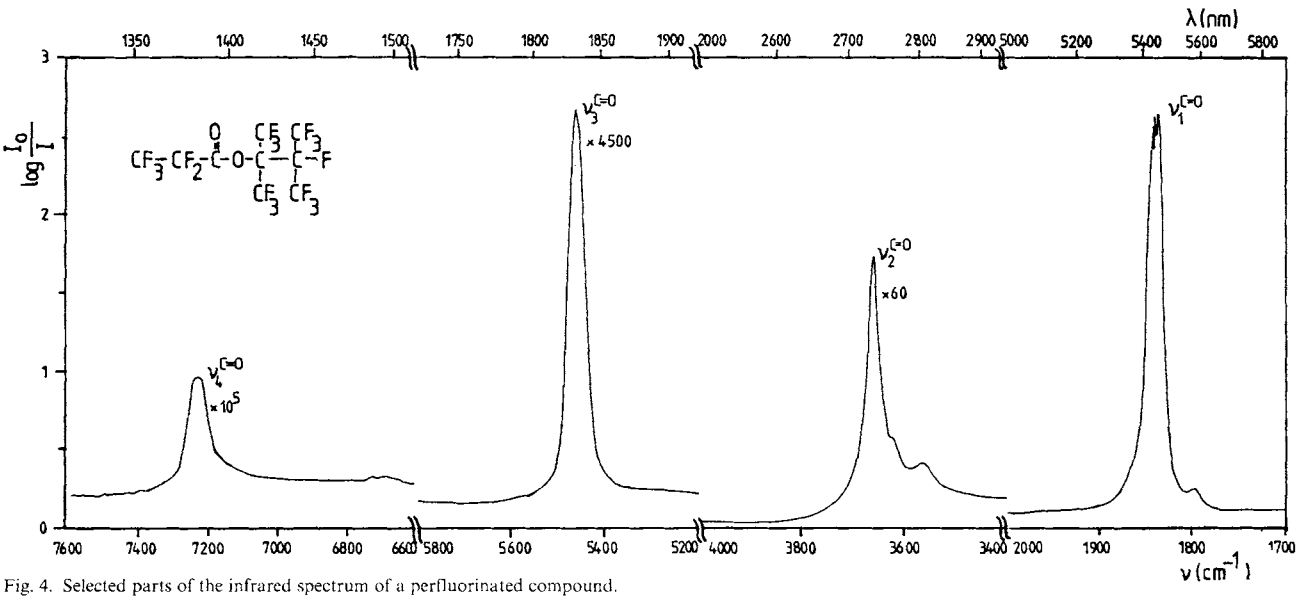


Fig. 4. Selected parts of the infrared spectrum of a perfluorinated compound.



Hans Sixl studied physics at the University of Stuttgart, FRG, gaining a Ph.D. in 1971 and habilitating in 1976. After this he spent some time at the Max Planck Institute for Solid State Research in Stuttgart and also in Grenoble working with Professor Dransfeld before returning to Stuttgart University to become Professor of Physics in 1981. Since 1986 he has been the Departmental Head of Applied Physics at Hoechst in Frankfurt, FRG.

ADVANCED MATERIALS

pound we have to consider the absorption due to the C–H bonds, the carbonyl group and the C–F bonds. Values for the spectral position of the fundamental, the band strengths and the anharmonicity constants are also given in Table 1. The C–H absorption is most pronounced because of its large anharmonicity constant.

Table 1. Important molecular vibrations in organic polymers.

bond	ν_1 [cm^{-1}]	$E(\nu_1)$ [cm mol^{-1}]	x	overtone quantum number in VIS
C–H	2950	6×10^5	1.9×10^{-2}	~ 5
C–D	2230	2.4×10^5	1.46×10^{-2}	~ 8
C=O	1846	9.6×10^6	6.5×10^{-3}	~ 9
C–F	1250	2.4×10^7	4×10^{-3}	~13
C–Cl	770	4.8×10^6	5.9×10^{-3}	~23

C–C and C–O vibrations cannot be treated using this simple model, because the dipole curves are much more complex and the approximation of a smooth dipole curve no longer holds. The spectral positions of the fundamental vibrations are known from the literature but there is little or no information about the corresponding overtone wavelengths and intensities. The intensity of the absorption of the C–C group, for example, depends strongly on the symmetry of the C–C bonds. There is experimental evidence that the fourth overtones of the C–C and C–O groups, expected in the 1200–1500 nm range, are already undetectable.[8, 9]

The results of the calculations are summarized in Figure 5. The symbols represent the calculated spectral overtone positions and the corresponding calculated band strengths. For the experimentally accessible low order C–H, C–D and C=O overtones we found very good agreement for the band positions. Experimental and theoretical band strengths coincide within a factor of 3 which is very good for such a simple model and sufficient for these considerations. The results for the experimentally inaccessibly high C–F and C=O, and also for C–Cl overtones are given. In the most important spectral region between 600 and 900 nm they are orders of magnitude lower in intensity than the C–H overtones and therefore should contribute negligibly to the losses in the fiber. The reasons are, firstly, the low anharmonicity constant of the C–F, C–Cl and C=O vibrations compared to C–H and, secondly, the low energy fundamentals which are in the far infrared. To get absorption in the visible spectral region, relatively high quantum states have to be excited which are therefore low in band strength. These are the two important factors dominating the absorption in the visible region.

The theoretical lower loss limit for fully halogenated polymers in the 600–900 nm region is therefore limited by Rayleigh scattering which is about 10 dB/km at 650 nm. From the theoretical point of view losses of a few dB/km should be attainable with optimized perfluorinated polymers.

Other expected advantages of fluorination are

- less scattering
- improved transparency at longer wavelengths where fast high power LEDs are available
- lower water uptake
- usually higher glass transition temperature.

The lower scattering losses of fluorinated polymers can be easily understood by considering the parameters responsible for scattering (Table 2). In the case of density fluctuations the loss is proportional to the eighth power of the refractive

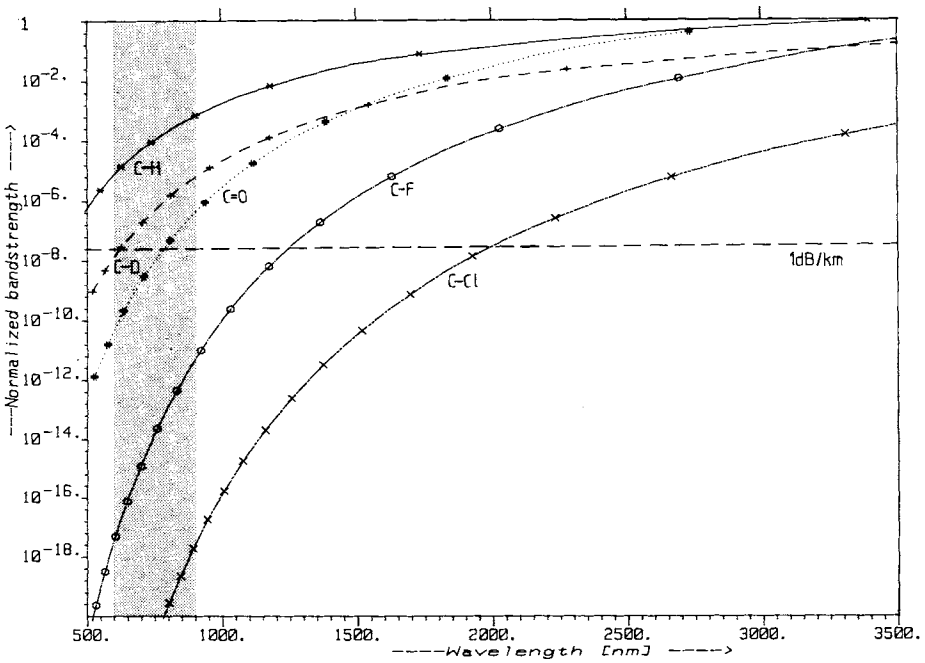


Fig. 5. Calculated spectral overtone positions and normalized integral band strengths for different C–X vibrations. The marked zone denotes the important spectral region for polymer optical fibers.

Density fluctuations

$$D_D \sim \frac{1}{\lambda^4} n^8 \beta_T$$

Anisotropy fluctuations

$$D_A \sim \frac{1}{\lambda^4} n^4 N p \delta_0^2$$

Concentration fluctuations

where λ: wavelength. n: refractive index. β_T: isothermal compressibility. N: monomer concentration in the polymer. p: number of parallel monomers per structural unit. δ_0: monomer anisotropy.

index. It is known that fluorination reduces the refractive index and thus leads to less scattering. The same is true for anisotropy fluctuations which are pronounced in polymers with aromatic groups. In special cases like copolymers or polymer blends, additional inhomogeneities on the molecular scale have to be considered. They are very difficult to predict theoretically because of unknown interaction parameters and exact microscopic structures.

Unfortunately a complete fluorination seems to be impossible from a chemical point of view. Our investigations showed that completely halogenated monomers do not polymerize well. Two or three C–H or C–D groups have to remain in the molecule and therefore a realistic lower loss limit for existing fluoropolymers is in the 40–70 dB/km range.

2.2. Local Area Networks

In POF-Network-Systems the fiber loss is an important factor but the total flux budget also depends on the system configuration and the properties of the active and passive components.

In Figure 6a and b two basic network topographies, the tapped bus and the star bus are compared. Calculating the total path attenuation we consider the fiber attenuation, average connector losses of 1 dB, typical POF-coupler losses and also different LED-output powers for different data rates.

To simplify the calculations a circular arrangement of nodes has been assumed. In the tapped bus network the coupler losses are divided into the insertion loss, the tap loss and the coupling loss. Typical values for commercial taps are given in Table 2. The worst case of path loss can be calculated using the equation under Table 2, where α_c is the connector loss, α_f the fiber loss, and N the number of nodes.

In a passive star bus network the nodes are connected by polymer optical fibers via a star coupler (Fig. 6b). In this system we have a splitting loss due to the equal intensity

Table 2. Optical properties of the tapped bus network topography.

	Loss values of the tap	
loss	definition	value [dB]
Tap	$-10 \log (P_3/P_1)$	9
Insertion	$-10 \log (P_2/P_1)$	1
Coupling	$-10 \log (P_2/P_4)$	4

$\alpha_{TB} = \alpha_{coup} + 2 N \alpha_c + (N-2) \alpha_{in} + \alpha_{tap} + \alpha_f 2 \pi R$

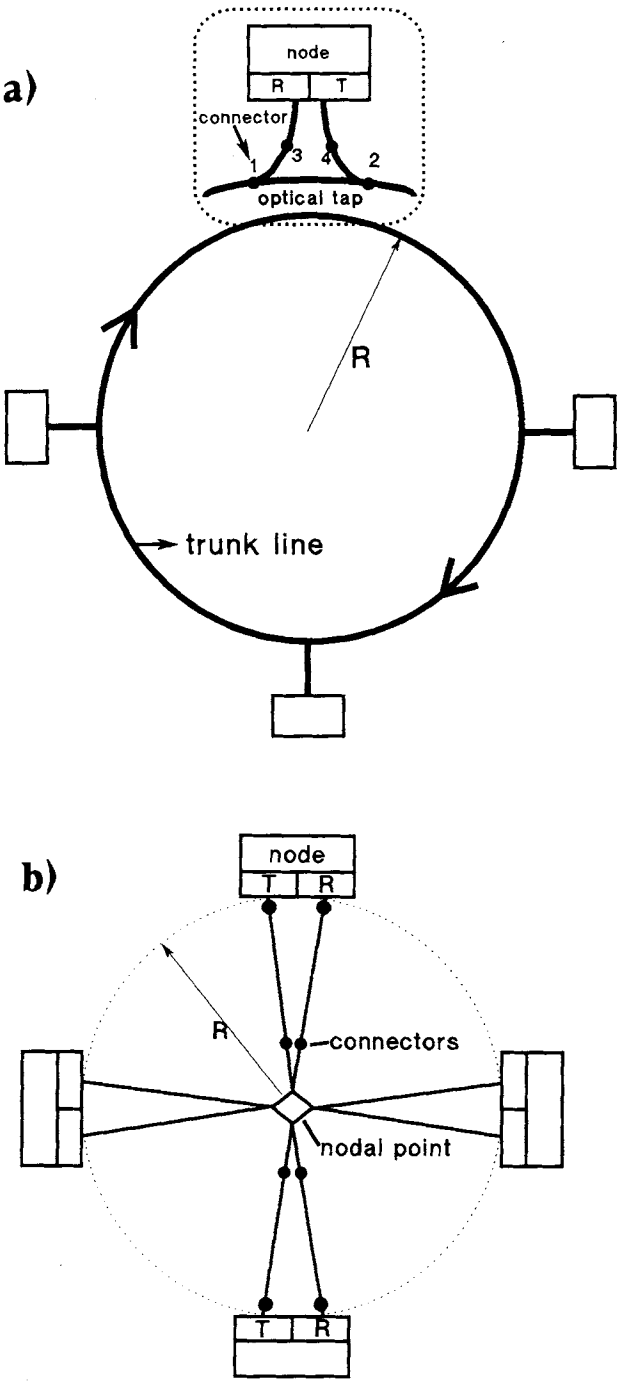


Fig. 6. Basic network topographies. a) Tapped bus network. b) Star bus network.

splitting to all nodes and an excess loss in the mixing region. The worst case of path attenuation can be calculated using the equation under Table 3. The system has four connectors, the excess loss depending on the number of nodes, the splitting loss which is 10 log N, and 2 R is the distance between an LED and a receiver. In a tapped bus the flux budget decreases linearly with the number of nodes, while for the star bus it decreases in proportion to the logarithm of the number of nodes.

ADVANCED MATERIALS

Table 3. Optical properties of the star bus network topography.

Loss values of the star		
nodes N	excess loss α_e [dB]	splitting loss α_{split} [dB]
2	1.5	3
4	2.5	6
6	3	7.8
8	3	9
10	3.5*	10

* extrapolated value

$\alpha_{SB} = 4\alpha_c + \alpha_e(N) + 10 \log N + \alpha_f \times 2R$

while for the star bus it decreases in proportion to the logarithm of the number of nodes.

Figure 7a shows the system budget for the tapped and star bus topography as a function of the number of nodes. The full lines correspond to a network radius of 2 meters, the dashed lines to 10 meters and the dashed-dotted lines to 50 meters radius. The horizontal lines at 16 dB and 28 dB indicate the flux ratio available for the network systems with 1.5 Mbaud and 40 Kbaud, respectively. The calculations were done for a PMMA fiber with 210 dB/km loss. Taking into account a system margin of 3 dB, only 3–5 subscribers can be connected via a star coupler in very local area networks like, for example, automobiles or robots. For short-haul, low data transmission, multinoded star-bus networks can be realized. Tapped bus systems only allow for low data transmission rates in networks of about 2 m size.

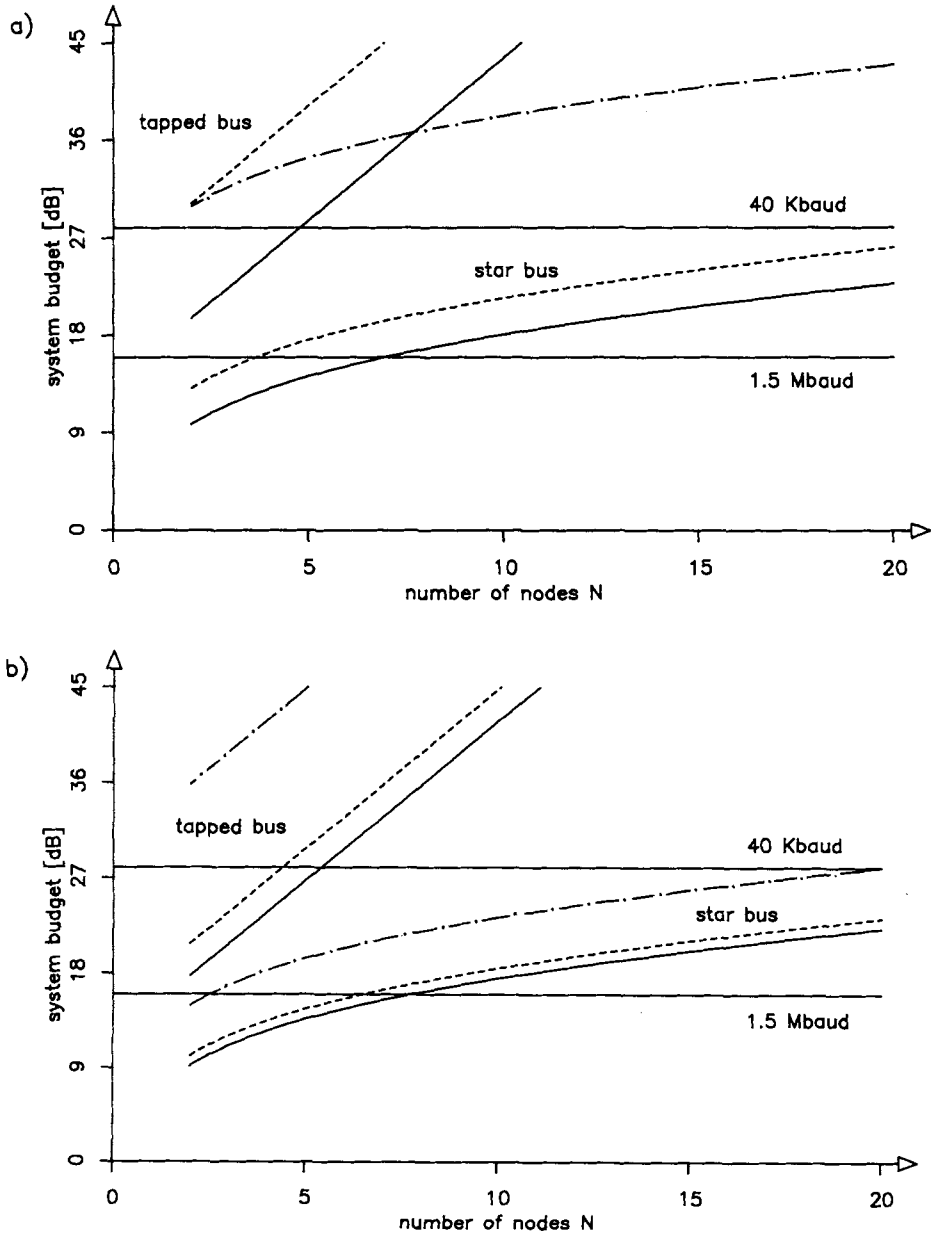


Fig. 7. System budget for tapped and star bus networks. a) Fiber loss: 210 dB/km. b) Fiber loss: 60 dB/km. The different network radii R = 2, 10, 50 meters are represented by full, dashed and dashed-dotted curves, respectively. The horizontal lines mark the assumed flux ratios of 28 and 16 dB for the indicated data transmission rates.

In very local area networks the system loss is mainly determined by the coupler losses and only to a much smaller degree by the fiber attenuation. For a radius of 2 meters, for example, the fiber loss contributes only 1 or 2 dB.

This can also be seen in Figure 7b, for which a fiber loss of only 60 dB/km was assumed. From the loss consideration explained above, 60 dB/km seems to be a realistic value for the loss of an optimized fluorinated polymer in the visible spectral region.

For very short distances the star bus system budgets do not differ significantly, due to the minor influence of the fiber attenuation compared to the coupler losses. For longer distances like 50 or 100 meters the improved fiber loss allows for multinoded star bus networks with a 40 Kbaud data rate, which is not possible with today's PMMA fibers. Even with a low loss fiber, high data rate applications can only be covered if not more than about 5 subscribers are connected. For tapped bus systems only very local area networks (2–10 m) with low data rates and not more than 5 subscribers are possible.

In conclusion a star bus system has the advantage of lower path attenuation, so a larger number of subscribers can be connected; it requires less receiver dynamic range, but the system has a larger overall fiber length. More complex systems can be made with a low loss fiber but the data rates have to be low and the system is still of limited size.

With the performances of the present active and passive components no complex high speed networks, working above 1 Mbaud, can be realized. To achieve a higher flux ratio improvements have to be made not only on passive components like fibers and couplers but also on transmitters and receivers.

3. Organic Materials for Nonlinear Optics

3.1. Basic Principles

The term "nonlinear optics" refers to effects which depend on quadratic or higher powers of the electric field strength. The interaction of an electric field $\vec{E}$ with a material can be described using a power series of the net polarization $\vec{P}$ of the material (Eq. 1).

$$\vec{P} = \vec{P}_0 + \chi^{(1)} \cdot \vec{E} + \chi^{(2)} : \vec{E}\vec{E} + \chi^{(3)} : \vec{E}\vec{E}\vec{E} + \ldots \quad (1)$$

$\chi^{(n)}$ is the nth order susceptibility which is a $(n+1)$th rank tensor. $\chi^{(1)}$ is responsible for the well known "linear" phenomenon of refraction. $\chi^{(2)}$, upon which we shall concentrate here, leads to quadratic effects such as optical second harmonic generation (SHG), parametric frequency mixing and the linear electro-optic effect. $\chi^{(3)}$ leads to such effects as intensity-dependent refractive indices and coherent anti-Stokes Raman spectroscopy (CARS).[10] Since the higher order susceptibilities are normally much smaller than $\chi^{(1)}$ nonlinear effects become noticeable only at high electric field strength, i.e. with lasers or with relatively high voltages over small distances.

In the mid-1970s it was discovered that certain types of organic molecules have much higher second-order nonlinearities and shorter switching times than the known inorganic materials such as potassium dihydrogen phosphate or lithium niobate.[11] The common characteristic of most such

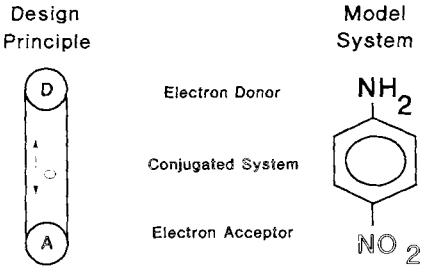


Fig. 8. Molecular design principle for high β species and the model system *p*-nitroaniline.

molecules is the presence of a conjugated π-electron system, providing easily polarized electrons, and donor and acceptor groups which provide the necessary asymmetry for second order effects. The design principles and a model system are shown in Figure 8. In organic systems one can thus speak of a *molecular* basis for the nonlinearity resulting from a polarization $\vec{p}$ of the charges in an individual molecule (Eq. 2).

$$\vec{p} = \vec{\mu}_0 + \alpha \cdot \vec{E} + \beta : \vec{E}\vec{E} + \gamma : \vec{E}\vec{E}\vec{E} + \ldots \quad (2)$$

where β and γ are the 2nd and 3rd order hyperpolarizabilities and μ_0 is the molecular dipole moment, although the absolute determination of these quantities presents considerable problems.[12]

A large value of β is not a sufficient condition for a high second order macroscopic susceptibility $\chi^{(2)}$, which is only non-zero for non-centrosymmetric systems. Furthermore the individual molecules should be aligned so that the individual nonlinearities add to each other as much as possible. β is related to $\chi^{(2)}$ through the relation (Eq. 3).

$$\chi^{(2)} = N\,\mathrm{F}\,\mathrm{D}\,\beta \quad (3)$$

where N is the density of nonlinear species, F stands for local-field correction factors and D stands for the effect of molecular orientation in converting from molecular coordinates and nonlinearity to macroscopic effects. Within the (sometimes questionable[13]) assumption that the molecular nonlinearity is dominated by the component β_{zzz} along the chromophore axis, a perfectly parallel orientation along the z-axis would for example lead to a maximum value of $\chi^{(2)}_{zzz}$. Of course such perfect orientations are practically nonexistent and can only be approximated.

Three main techniques are available to achieve a non-centrosymmetric orientation of the chromophores. One possi-

ADVANCED MATERIALS

bility is design of the molecule so that it crystallizes noncentrosymmetrically. High $\chi^{(2)}$ values and good quality single crystals have been achieved for several compounds,[14-16] and one can even buy organic frequency doubling crystals on the open market. However, the extension of organic crystal techniques to planar waveguided integrated optics devices is not straightforward and the crystal growth method does not seem to work for all chromophores.

Another technique is to put the chromophores into a polymer matrix, either physically (guest-host solutions) or chemically (side-chain polymers). The polymer is then heated to near the glass transition temperature and the (highly polar) chromophores are aligned by applying a high electric field ($\geq 10^5$ V/cm) across the polymer using either electrodes[17] or a corona discharge.[18] The polymer is subsequently cooled under continued application of the electric field to freeze in the orientation. This technique has the advantages of the flexibility of polymer processing techniques, chemical modification of polymer properties and the ability to make thin film waveguides of good optical quality. Limitations are the fairly low, Boltzmann-limited degree of order one can obtain in the poling field before dielectric breakdown and the tendency of the chromophores to relax after the electric field is removed, limiting the second order susceptibility one can attain in polymers for a given chromophore.

Susceptibilities well above that of the market leader for electro-optics, $LiNbO_3$, have been achieved with polymers which have been deposited in films, structured into waveguides and used to modulate light using the linear electro-optic (Pockels) effect. An example of such a device is shown schematically in Figure 9.[17,18] The active polymer with refractive index n_K, between cladding layers with n_M, forms a planar waveguide in which the optical electric field $\vec{E}(\omega)$ is confined through total internal reflection. An AC voltage is then applied perpendicular to the substrate and induces, through the Pockels effect, a modulation of the refractive index n in the active polymer (Eq. 4).

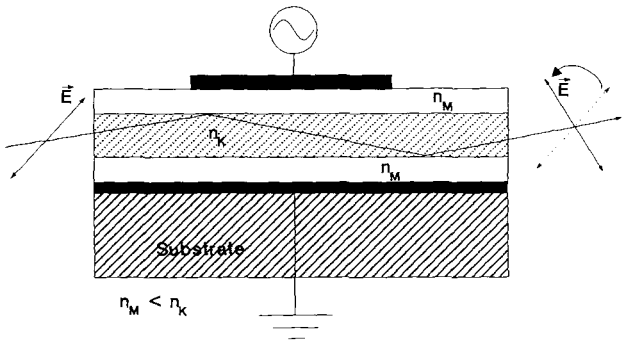


Fig. 9. Slab waveguide electro-optic modulator based on poled polymers.

The relationship between the Pockels coefficient Γ and $\chi^{(2)}$ is shown in Equation 5. The εs are the dielectric constants at the optical frequency ω and the much lower modulation frequency Ω. For light polarized diagonally to the substrate, i.e. coupled into TM (electric field perpendicular to the substrate) and TE (electric field parallel to the substrate) modes, the phase of the TM component relative to the TE mode is

$$(n^2)^{-1} = (n_0^2)^{-1} + \Gamma \vec{E} \tag{4}$$

$$\Gamma = \frac{2\chi^{(2)}}{\varepsilon(\omega)\,\varepsilon(\Omega)} \tag{5}$$

modulated. The resulting phase shift causes a rotation of the plane of polarized light; this polarization modulation can be converted to amplitude modulation by the addition of an analyzer after the device.

In order to take advantage of the fast switching times of organics and to design extremely high-speed modulators one must go to more sophisticated architectures which take the finite spatial extent of very short electrical impulses into account (so-called "traveling wave" electrode geometries). The NLO program at the Hoechst Celanese Corporation is

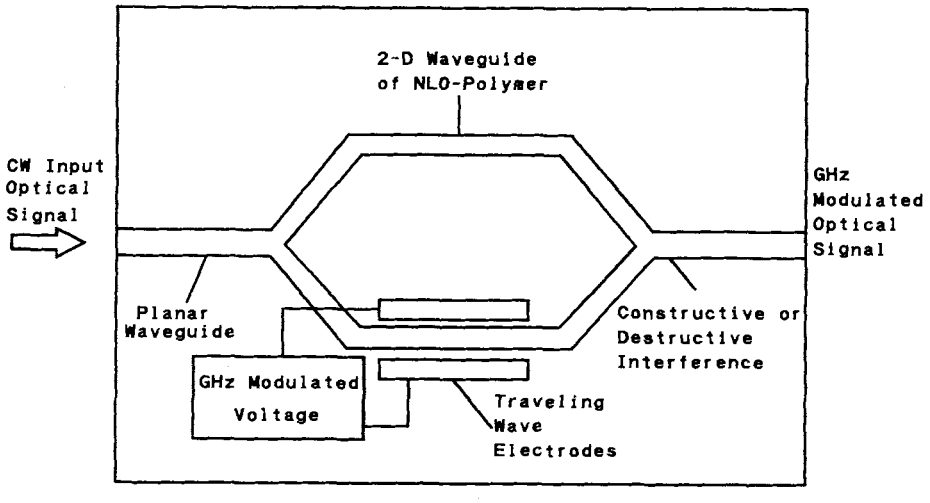


Fig. 10. Schematic representation of a polymeric Mach-Zehnder high frequency electro-optic modulator.

currently developing a multi-GHz traveling wave electro-optic modulator on the basis of a Mach-Zehnder interferometer[19] as shown in Figure 10. The microwave frequency electrical signal runs along a traveling wave electrode across one branch of the interferometer. Depending on the momentary voltage, one brings the two branches into or out of phase with each other, leading to constructive or destructive interference and thus direct intensity modulation of the light. Such devices are currently available based on $LiNbO_3$, but the ultimate attainable bandwidth is substantially less than that for organic materials.

3.2. NLO Active LB-Layers

Our investigations of nonlinear optical effects are focused on Langmuir–Blodgett (LB) films, which, due to their very high and often nearly ideal degree of order, yield the highest $\chi^{(2)}$ values measured to date,[20–22] but which are still at the stage of fundamental investigation. LB films with second order nonlinear optical properties are prepared using amphiphilic dyes, as shown in Figure 11, which contain a hydrophobic "tail", typically an alkyl chain, and a polar hydrophilic "head group", in NLO applications typically a donor-acceptor chromophore. A dilute solution of such species in a volatile solvent such as chloroform or methylene chloride is then spread onto a clean water surface in a film balance or "trough" (Fig. 12, top). After evaporation of the solvent (middle) the monolayer is compressed, leading to a highly oriented monolayer in which the head groups are next to the water surface and the tails are pointed away from it (bottom). This highly oriented monolayer can be transferred to a clean substrate a monolayer at a time, maintaining a high degree of order, by dipping the substrate through the interface into and out of the trough.

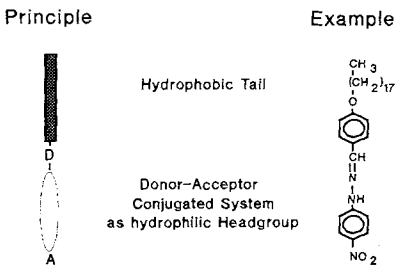


Fig. 11. Design of amphiphilic dyes for LB films with high second order optical nonlinearities.

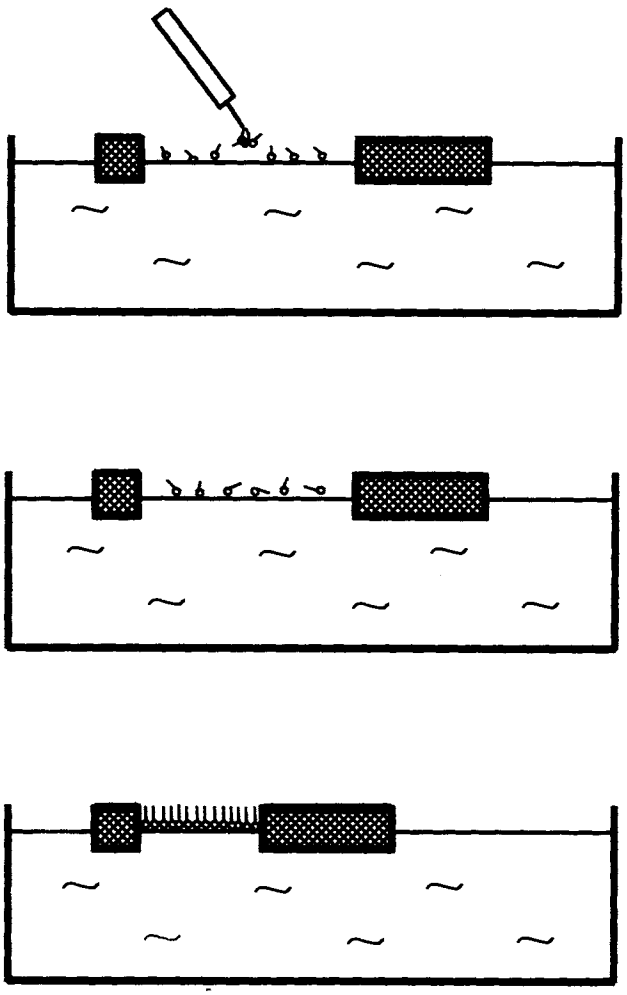


Fig. 12. Creation of oriented monolayers at the air-water interface.

By alternating an NLO active substance with a buffer layer (as shown in Fig. 13) or by alternating layers of molecules whose nonlinearities are in opposite directions with respect to the tails, using specially designed double well troughs, one can built up non-centrosymmetric multilayers with a high degree of order and thus very high susceptibilities. The exact control of film thickness (within the length of one molecule) and the possibility of film architecture on a molecular scale are two of the qualities which make Langmuir–Blodgett films promising for long-range applications in nonlinear integrated optics.

For fundamental studies of structure-property relationships and orientational phenomena, monolayers are practical model systems for study. The high susceptibilities of LB films lead to high signal to noise ratios even for a single

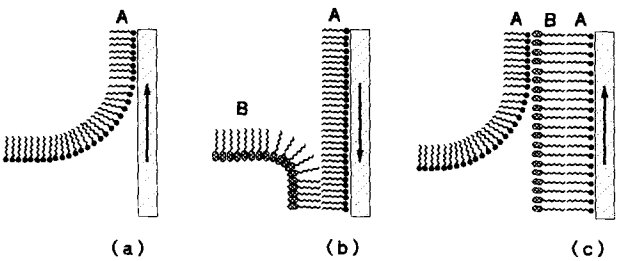


Fig. 13. Deposition of non-centrosymmetric Langmuir–Blodgett multilayers.

ADVANCED MATERIALS

monolayer. The experimental setup for studies of second harmonic generation in LB films is shown in Figure 14. The polarized beam from a pulsed Nd:YAG laser with a wavelength of 1064 nm is passed through the film deposited on a glass substrate, mounted on a rotation stage. Through the second order susceptibility of the film $\chi^{(2)}(-2\omega;\omega,\omega)$ a part of the laser light with circular frequency $\omega = 2\pi c/\lambda_0$ is converted to a harmonic wave at twice the frequency, i.e. with wavelength of 532 nm. The harmonic intensity, normalized by the intensity from a reference sample, is measured for different fundamental and harmonic polarizations as a function of incidence angle θ.

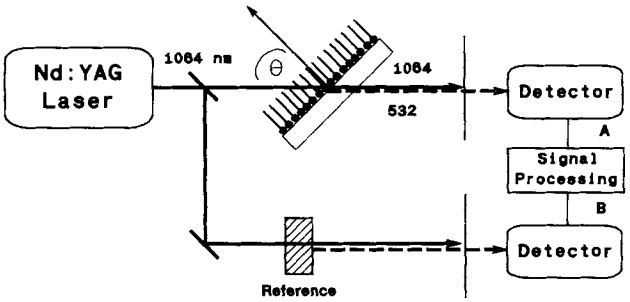


Fig. 14. Experimental apparatus for studying SHG in LB films.

A typical curve for a monolayer of a highly nonlinear hemicyanine dye deposited on both sides of a glass substrate is shown in Figure 15. One sees a superposition of two angular dependences of the second harmonic intensity. The fast fringing pattern is indicative of samples in which the film is deposited on both sides of the substrate and is due to the dispersion in glass between ω and 2ω, which causes interference between the harmonic waves generated at the front and back surfaces of the substrate. A clean fringing pattern with near zero minima is a good indication of film homogeneity. The shape and height of the slowly varying envelope function depends on the orientation (position of intensity maxima) and the nonlinearity (the height of the curve) of the chromophores in the monolayers. The curve in Figure 15 is consistent with the common assumption that the chromophores are tilted from the substrate normal with a narrow distribution in the tilt angle φ and a statistical distribution in the azimuthal angle. Table 4 shows the nonlinearities and average tilt angles for several amphiphilic dyes which we have investigated.[20] $\chi^{(2)}$ is here a purely scalar quantity with all projection factors removed; the specific tensor components relevant to a particular experiment must be obtained through multiplication by the appropriate projection

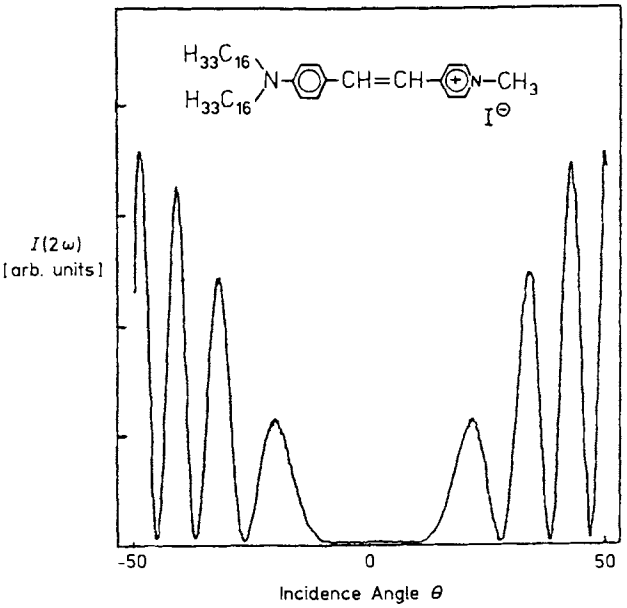
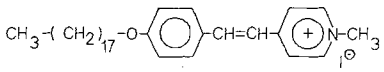
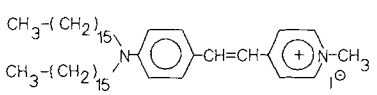
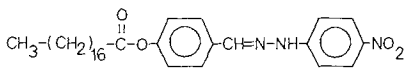
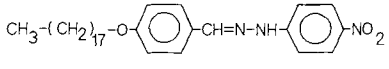
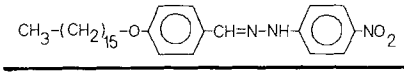


Fig. 15. Dependence of the second harmonic intensity on incidence angle for p-polarized fundamental and harmonic in a hemicyanine monolayer.

Table 4. Nonlinearities and average tilt angles for several amphiphilic dyes.

Structure	$X^{(2)}/10^{-6}$ esu	Ave. Tilt Angle/ °
	0.51	50
	6.25	50
	0.56	65
	1.80	60
	1.70	55

factors. For example, for a TM fundamental and a TM harmonic one would want $\chi^{(2)}_{zzz}$, which is in the simplest approximation given by $\chi^{(2)}_{zzz} \cong \chi^{(2)} \cos^3 \langle \varphi \rangle$.

Second harmonic generation can also be used as a probe of induced changes in orientation in LB films. Figure 16 shows two experimental SHG curves from measurements on the phenylhydrozone ester **1**, pure and diluted with acrylic acid *n*-octadecylamide.[23]

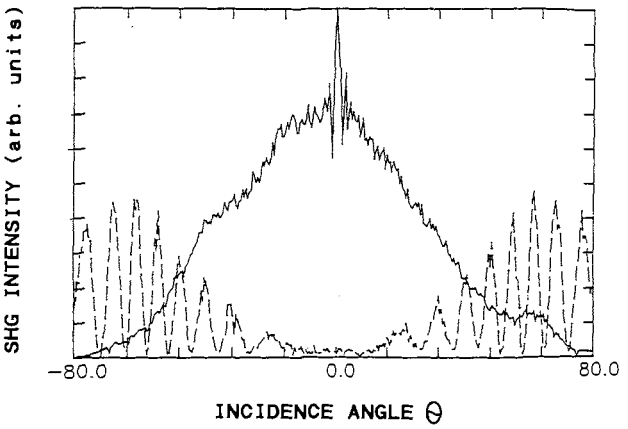
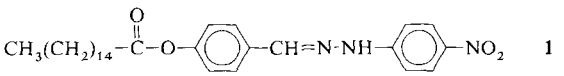


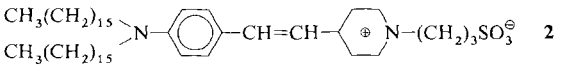
Fig. 16. SHG curves for monolayers of a phenylhydrazone ester, pure (solid line) and diluted with 40% acrylic acid *n*-octadecylamide (dashed line).

The curve for the pure dye is dramatically different from "normal" curves; the lack of fringes indicates poor sample homogeneity and the maximum intensity at normal incidence indicates that the chromophores are lying more or less flat. By diluting the dye with another amphiphilic species one can change the orientation drastically, improving the homogeneity and forcing the chromophores to "stand up".

In order to optimize deposited Langmuir-Blodgett films for nonlinear optics a better understanding of the nonlinear



1



2

optical properties of the monolayer films at the air-water interface is important. Second harmonic generation on reflection from the water surface can be used to monitor in situ the dependence of molecular orientation and nonlinearity on density, surface pressure, and relaxation and aggregation phenomena.[24] The experimental setup is shown schematically in Figure 17. The dependence of the reflected second harmonic intensity on the polarization of the fundamental and the harmonic is monitored as the film is compressed, expanded or held at constant pressure for a period of time. The second harmonic intensity for incidence angle θ is given by Equation 6.

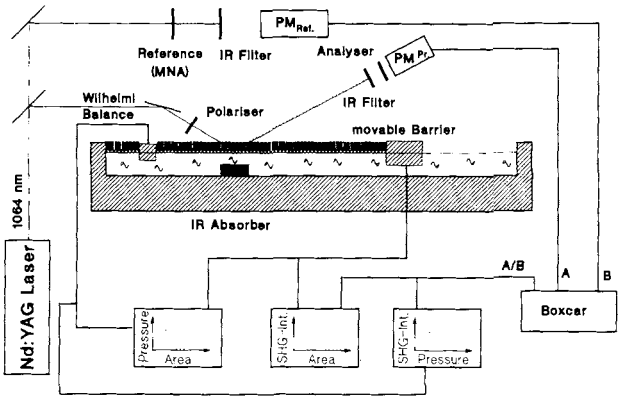


Fig. 17. Experimental apparatus for studies of SHG at the air-water interface.

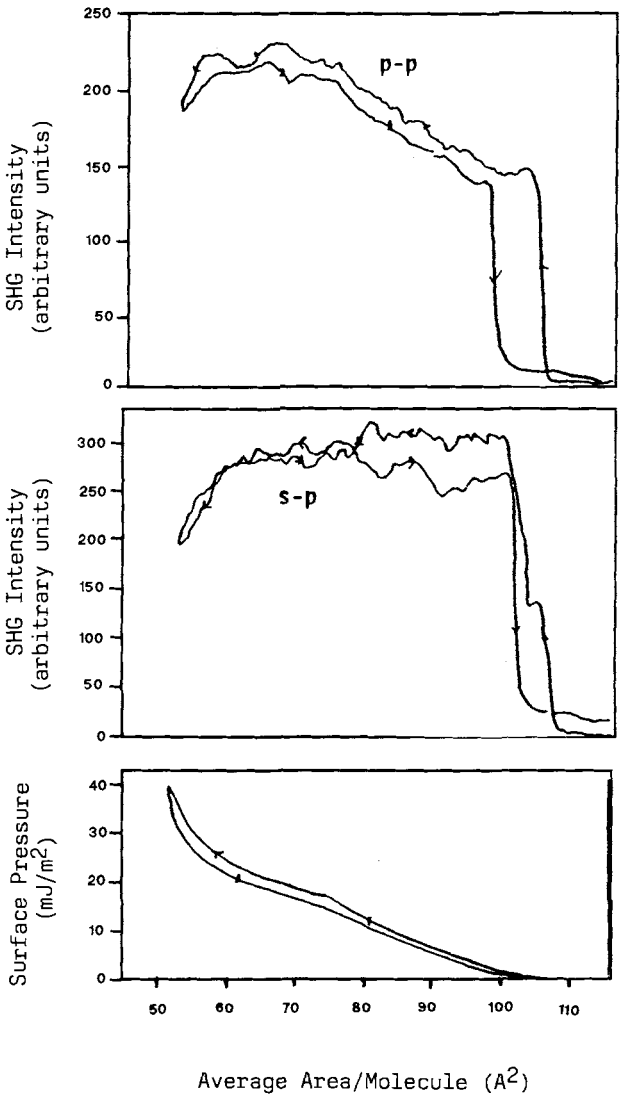


Fig. 18. Dependence of the second harmonic intensity from hemicyanine betaine **2** on water on surface area and the surface pressure-area isotherm. p–p: both fundamental and harmonic are p-polarized; s–p: fundamental is s-, harmonic p-polarized.

ADVANCED MATERIALS

$$I(2\omega) = \frac{32\, n^3\, \omega^3 \sec^2 \theta}{c^3} |\hat{e}(2\omega) \cdot \chi^{(2)} : \hat{e}(\omega)\hat{e}(\omega)|^2 I(\omega)^2 \quad (6)$$

where $I(\omega)$ is the intensity of the fundamental, the $\hat{e}$ are the polarization unit vectors for the fundamental and harmonic electric fields, c the speed of light and n the refractive index of the water substrate. The part between the modulus signs accounts for projection factors between fundamental, harmonic and the individual tensor components of $\chi^{(1)}$. Figure 18 shows the second harmonic intensity from the hemicyanine betaine **2** as a function of area per molecule. It is particularly interesting to note that the intensity does not increase significantly over the range of an almost twofold increase in density; in the absence of local field effects or orientational changes one would expect a fourfold increase in intensity over this range of surface areas.

4. Conclusion

A high susceptibility alone is of course not sufficient for applications of Langmuir–Blodgett films in nonlinear optics. Also necessary are high chemical and thermal stability, thick (a few hundred layers) films for planar waveguides with low loss coefficients and methods for forming structures in films without damaging their nonlinear optical properties. Progress has been made in each of these areas individually at Hoechst[25] and elsewhere.[26, 27] Combining all of these properties with high $\chi^{(2)}$ values is now the challenge.

Received August 7, 1989

[1] T. Kaino, M. Fujiki, K. Jinguji, *Rev. Electr. Commun. Lab. 32* (1984) 478.
[2] T. Kaino, *J. Polym. Sci. A 25* (1987) 37.
[3] R. M. Glen, *Chemitronics 1* (1986) 98.
[4] P. Herbrechtsmeier, W. Groh, *Laser und Optoelektronik 20 (5)* (1988) 60.
[5] W. Groh, J. Theis, P. Herbrechtsmeier, J. Coutandin, U. von Alpen, *Elektronikpraxis 10* (1988) 2.
[6] W. Groh, *Makromol. Chem. 189* (1988) 2861.
[7] B. Timm, R. Mecke, *Z. Phys. 98* (1936) 363.
[8] H. Günzler, H. Böck: *IR-Spektroskopie*, Verlag Chemie, Weinheim 1983.
[9] O. H. Wheeler, *Chem. Rev. 59* (1959) 629.
[10] Y. R. Shen: *The Principles of Nonlinear Optics*, Wiley, New York 1984.
[11] D. Williams (Ed.): *Nonlinear Optical Properties of Organic and Polymeric Materials*, Am. Chem. Soc., Washington 1983.
[12] G. Meredith, in J. Messier, F. Kajzar, P. Prasad, D. Ulrich: *Nonlinear Optical Effects in Organic Polymers*, Kluwer, Dordrecht 1989, p. 105, 385.
[13] T. L. Mazely, W. M. Hetherington III, *J. Chem. Phys. 86* (1987) 3640.
[14] P. A. Norman, D. Bloor, J. S. Obhi, S. A. Karavlov, M. B. Hursthouse, P. V. Kolinsky, R. J. Jones, S. R. Hall, *J. Opt. Soc. Amer. B, 4* (1987) 1013.
[15] C. Bosshard, K. Sutter, P. Günter, G. Chapuis, R. J. Twieg, D. Dobrowolski, in R. A. Hann, D. Bloor (Eds.): *Organic Materials for Nonlinear Optics*, R. Soc. Chem., London 1989.
[16] J. Zyss, D. S. Chemla, J. F. Nicoud, *J. Chem. Phys. 74* (1981) 4800.
[17] T. M. Leslie, C. C. Teng, unpublished.
[18] J. E. Sohn, K. D. Singer, M. G. Kuzyk, W. T. Holland, H. E. Katz, C. W. Dirk, M. C. Schilling, R. B. Comozoli, in reference [12]. J. Comizzoli, *J. Electrochem. Soc. 134* (1987) 424.
[19] A. Buckley, J. Stamatoff, in reference [12].
[20] D. Lupo, W. Praß, U. Scheunemann, A. Laschewsky, H. Ringsdorf, I. Ledoux, *J. Opt. Soc. America B 5* (1988) 300.
[21] I. R. Girling, P. V. Kolinsky, J. D. Evans, G. H. Cross, I. R. Peterson, *Thin Solid Films 132* (1985) 101.
[22] G. Marowsky, L. F. Chi, D. Möbius, R. Steinhoff, Y. R. Shen, D. Dorsch, B. Rieger, *Chem. Phys. Lett. 147* (1988) 420.
[23] J. Bauer, P. Jeckeln, D. Lupo, W. Praß, U. Scheunemann, R. Keosian, G. Khanarian, in reference [15].
[24] Y. R. Shen, *Annu. Rev. Mater. Sci. 16* (1986) 68.
[25] D. Lupo, W. Praß, U. Scheunemann, *Thin Solid Films*, in press.
[26] R. H. Tredgold, M. C. J. Young, P. Hodge, E. Khoshdel, *Thin Solid Films 151* (1987) 441.
[27] W. L. Barnes, J. R. Sambles, *Surf. Sci. 177* (1986) 399.

Superconductivity at the Temperature of Dry Ice?

J. T. Chen et al. from Wayne State University and the Ford Motor Company recently repeatedly observed zero resistance at temperatures above 200 K in several multi-phase Y-Ba-Cu-O samples. They presented their results at the Third Annual Conference on Superconductivity and Applications held in Buffalo in late September. In the past, *Chen* and others have claimed to have seen evidence of superconductivity above 200 K, but up to now these phenomena turned out to be instable and generally vanished after a few thermal cycles. The key to the stabilization of the effect, *Chen* says, is a low-temperature oxygenation process carried out at temperatures between 50 and 150 °C in an O_2 atmosphere at 0.1 and 13 MPa for four to seven days. Samples were kept in an oxygen atmosphere during all measurements.

Chen et al. prepared samples of various compositions by conventional solid state reaction techniques, but only observed stable zero-resistance phenomena in samples having the nominal composition $Y_3Ba_6Cu_{11}O_y$. X-ray spectra of these samples showed $YBa_2Cu_3O_{7-x}$, Y_2BaCuO_5, and CuO as the predominant phases, but a small number of unidentified peaks were also seen. $YBa_2Cu_3O_{7-x}$ peaks showed preferential orientation with the *c*-axis perpendicular to the surface.

Chen's team determined resistance and current-voltage characteristics by cooling with liquid nitrogen or a mixture of dry ice and acetone. Zero resistance was found in several samples near 250 K. The zero-resistance phenomenon was observed over eleven days and for as many as 29 thermal cycles. Current-voltage characteristics show ohmic behavior at room temperature and an onset of nonlinearity in the range of 260 to 290 K. Magnetization measurements with a SQUID magnetometer did not reveal a complete Meissner effect, but *Chen* et al. observed small diamagnetic deviations and some hysteresis.

Although the findings of the team were well documented and measurements appear to have been done very carefully, there are still some questions that have to be resolved before one can be sure that the observed phenomenon is indeed superconductivity. The fact that zero-resistance was only seen in mixed-phase samples together with the extreme weak diamagnetic signal, could indicate some sort of grain boundary superconductivity, a suggestion *Chen* made in a paper scheduled for the November issue of *Modern Physics Letters B*. The oxygen environment of the samples, even during low temperature measurements, was clearly shown to be crucial, since the zero-resistance state vanished upon evacuating the oxygen atmosphere. It will be interesting to see whether these experiments can be reproduced by *Chen* and, even more importantly, by others.

Herbert Jaeger, Max Planck Institute for Metals Research, Heisenbergstr. 5, D-7000 Stuttgart 80 (FRG)

ADVANCED MATERIALS

High-Performance Silicon Nitride Materials

Pressureless Sintering
Hot Isostatic Pressing
Sintering Aids
Powder Processing
Reinforced Ceramics
Silicon Slips

By Cornelia Boberski,* Rainer Hamminger, Marcell Peuckert, Fritz Aldinger, Reinhard Dillinger, Jürgen Heinrich and Jürgen Huber

Dedicated to Professor Wolfgang Hilger on the occasion of his 60th birthday

The past decade has seen greatly increased interest in ceramic materials with special combinations of properties. Their hardness, high resistance to abrasive and erosive wear, and their good corrosion resistance when used under extreme mechanical and thermal conditions have made ceramics increasingly attractive for applications in mechanical and apparatus engineering. Silicon nitride (Si_3N_4) in particular, is suitable for the development of a high-performance, high-temperature material for vehicle engine construction. Although the properties of Si_3N_4 materials have been consistently improved in the last few years, they are still not adequate to allow these materials to be used in series production parts, for example as valves in automotive engines. One of the main reasons for this is the wide scatter and low reproducibility of the property parameters, which means that component reliability does not yet meet market requirements. Hence, one aim of Si_3N_4 materials development is to reduce the structural flaws resulting from physical and chemical inhomogeneity. This objective can only be achieved through a fundamental understanding of all the processing steps, from powder production to the final processing of the components.

1. Introduction

Silicon nitride materials can be distinguished from one another by their composition and manufacturing technologies. Hot pressed (HPSN), pressureless sintered (SSN), reaction-bonded and post-sintered (SRBSN), hot isostatically pressed (HIPSN) and hot isostatically pressed post-densified reaction-bonded silicon nitride (HIPRBSN) all contain very small quantities of a second phase, which must be added as a sintering aid because of the high proportion of covalent bonding in Si_3N_4. In contrast, pure reaction-bonded silicon nitride (RBSN) is single-phased but still contains a residual porosity. This material is used successfully where chemical stability, rather than high strength, is of prime importance. If small amounts of sintering aids were added, the porous RBSN material then offers the possibility of post-densification and an increase in strength by means of hot isostatic pressing. On the other hand, dense silicon nitride materials are used wherever high strength is required, especially at high service temperatures.

However, the manufacture and utilization of ceramic materials can lead to difficulties. The thermal expansion, which is very low in comparison with that of metals, and the brittleness, i.e. the fact that it is impossible to reduce stresses by plastic deformation, require the especially careful design and handling of the manufactured parts. In brittle fracture, failure originates at defects that can arise during manufacture, processing, and also during application. The strength of the components is determined by the sizes and positions of the defects and by the fracture toughness and load. Consequently, strength is a probabilistic quantity that depends on the stressed volume. Failure always originates at a critical flaw in the specimen or component. These flaws in ceramics can be considered to be cracks, microcracks, pores, inclusions, grain boundaries or grain boundary phases and also structural inhomogeneities.

In developing high-performance Si_3N_4 materials it is necessary to avoid structural flaws $\geq 30\ \mu m$.[1] To achieve this goal, high-quality raw materials must be used and advanced processing applied where the optimization of each individual processing step is crucial. It must be assumed that the overall distribution of flaws in ceramic parts is the sum of different flaw distributions, each of which in turn represents a distribution with a specific physical content. Thus, the distribution of inherent flaws with small dimensions can adjoin or overlap processing, handling or randomly induced flaws, yielding the total observed technical distribution of structural flaws, and therefore the resulting technical range of strengths.[1] Consequently, to determine the probability of

[*] Dr. C. Boberski, Dr. R. Hamminger,
Dr. P. Peuckert, Dr. F. Aldinger
Hoechst Aktiengesellschaft
P.O. Box 800320, D-6230 Frankfurt am Main 80 (FRG)
Dr. R. Dillinger, Dr. J. Heinrich, Dr. J. Huber
Hoechst CeramTec AG
P.O. Box 1360, D-8672 Selb (FRG)

failure of an engineering part, it does not suffice to test specimens of only one geometry and size (which is usually very small). Hence, efforts are now being made to test larger specimens and to replace the customary four-point bending test by the more suitable tensile test, because the stress distribution in the specimen is more uniform, and at the same time substantially larger volumes are involved.[2] To clearly show the possibilities for a further quality increase the following discussion will examine the especially promising Si_3N_4 materials SSN, RBSN and HIPRBSN more closely.

2. Pressureless-Sintered Silicon Nitride (SSN)

Because of the high proportion of covalent bonding in silicon nitride, and the associated low self-diffusion coefficient, and owing to its dissociation to silicon and nitrogen at relatively low temperatures, Si_3N_4 cannot be densified in the conventional way without the addition of sintering aids. Through the addition of certain sintering aids (see Section 2.3) a liquid-phase sintering process can be initiated, producing dense ceramic bodies.[3] Densification is strongly affected by the purity and fineness of the initial powders, processing methods, type and amount of sintering aids and sintering parameters.

The glass phase in the ceramic resulting from the liquid phase sintering process is responsible for the strength reduction at high temperatures (> 1000 °C), and therefore, the proportion of additives should be kept as small as possible.[4] In order to minimize the quantity of the liquid phase, high pressures and temperatures must be used during the sintering process. In gas-pressure sintering, the process is carried out under, for example, 100 bar of nitrogen, which counteracts any tendency of Si_3N_4 to decompose. Furthermore, sintering processes under applied pressure mechanically effect the densification of the residual porosity[5] and under optimal conditions lead to a compaction of the grains and hence high mechanical strength. However, the appearance of pronounced internal stresses due to this process must be regarded as critical.[6] The pressureless sintering process, on the other hand, has the major advantage that even large-volume and highly complex components can be produced in virtually their final form, meaning that no expensive finishing is required.

2.1. Powder Synthesis

The quality of the Si_3N_4 powder has a decisive influence on the properties and quality of the ceramic materials. The development of optimal powders requires the most comprehensive knowledge possible of the powder properties. Powders are characterized chiefly by their morphology, chemical composition and phase content. Table 1 shows the degree to which the properties of the powders affect their processing.[7] Sinterable Si_3N_4 powders of the type required for the production of high-performance ceramics must meet the following main requirements:

Table 1. Features of powder characterization.

Category	Characteristic	Dependent properties
Morphology	Grain size	Powder density
	Grain form	Free-flowing properties
	Agglomeration	Specific surface
	Grain size distribution	Homogeneity
Chemical composition	Main constituents	Surface properties
	Impurities	Dispersibility
Phase content	Degree of crystallization	Densification behavior
	α/β phase ratio	

- mean particle size in the submicron range (0.1 μm < d < 1 μm)
- narrow grain size distribution (but not equal-sized particles)
- equiaxial particle shape
- $\alpha/(\alpha + \beta)$-Si_3N_4 ratio > 95 vol.-%
- low oxygen content (< 1.5 wt.-%)
- low carbon content (< 0.2 wt.-%)
- low metallic impurities content (< 0.1 wt.-%)

There are four ways of obtaining Si_3N_4 powders: direct nitridation of silicon (A), carbothermal nitridation (B), thermal decomposition of silicon diimide (C) and gas-phase reaction (D). While the production routes A to C are already being exploited industrially, the gas-phase reaction has so far been carried out only on a laboratory scale. Very pure powders can be produced especially by the diimide process. Examples of typical grain size distributions of powders produced via routes A, C and D are shown in Figure 1.

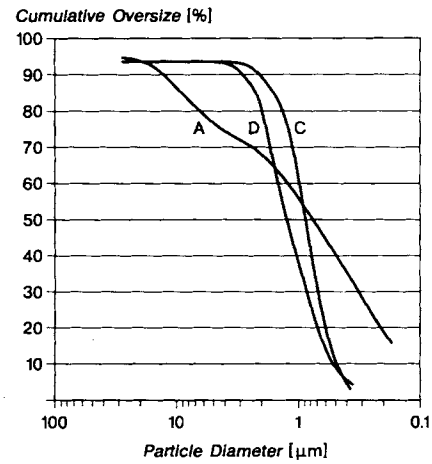


Fig. 1. Grain size distribution of silicon nitride powders produced by different methods: A: direct nitridation; C: diimide process; D: gas phase reaction.

The range between 0.1 and 1 μm for the average particle size is chosen in order to ensure a maximum green density[3] and low electrostatic forces.[7] The strength of the electrostatic attaction is determined by the synthesis process and the

post-treatment of the powders. However, the type of powder determines not only its agglomeration behavior but also its "deagglomeration" behavior in solution (dispersing behavior) which is important for molding by slip casting. Powder synthesized via route A can be very readily dispersed while it is considerably more difficult to disperse powders resulting from route C.

Figure 2 shows the mechanical strengths of sinter compacts composed of powders produced by different routes.

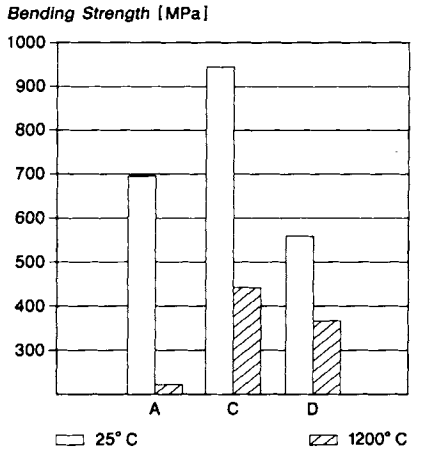


Fig. 2. Bending strength of ceramics composed of Si_3N_4-powders produced by different routes. A: direct nitridation; C: diimide process; D: gas phase reaction. α-Si_3N_4 powders were mixed with the sintering additives Y_2O_3, and Al_2O_3 in the ratio of Y_2O_3: Al_2O_3 of 2:1, and cold isostatically pressed and sintered in nitrogen at atmospheric pressure at 1800 °C. Strength was determined by the four-point bending test at 25 °C and 1200 °C.

Parts formed by cold isostatic pressing gave high strength at room temperature when powder C (diimide process) was used, which is characterized by high purity and very regular, equiaxial particles. In regard to the molding of parts from the powders, the powder type, the preparation methods and the molding processes must be very carefully adapted to one another.[8]

2.2. Powder Processing

During powder processing, the incorporation and homogeneous distribution of sintering aids, and the adjustment of a suitable grain size distribution of the mixed powders has to be achieved.

This is accomplished especially successfully by attritors or annular-gap ball mills. After the mixing and milling process, the preparation of agglomerates with a homogeneous particle distribution and appropriate shape follows. The drying and agglomeration of the mixture takes place in the spray dryer. After molding, either by cold isostatic pressing, slip casting or injection molding, any organic binder that may have been added must be removed. Finally, the high-temperature sintering process yields the densified ceramic component, which normally must be subjected to finishing work because of shrinkage imperfections and adhering firing skins. As an example of this production procedure, Figure 3 presents a typical processing sequence for the production of SSN components.

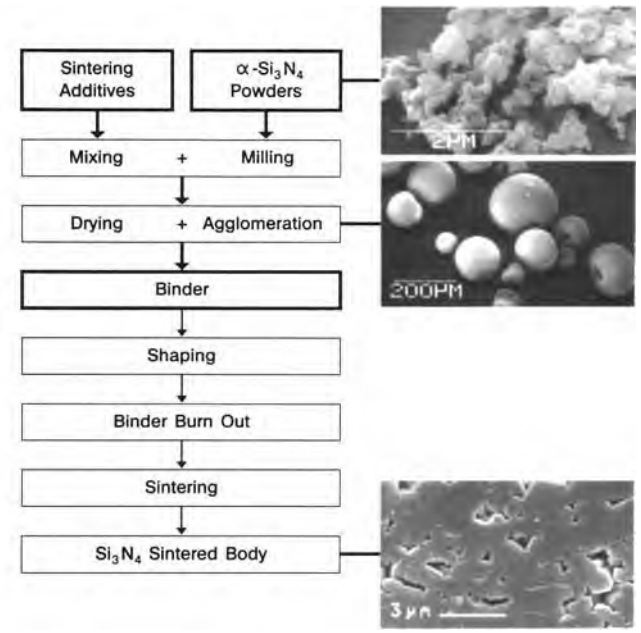


Fig. 3. Powder preparation and production of silicon nitride ceramics. (The introduction of raw materials is indicated by bold lines).

The experience of the last few years has shown that one of the major causes of failure of a ceramic component is the presence of foreign inclusions with diameters ≥ 30 µm. An analysis of these inclusions shows that even grains of dust can lead to the failure of ceramic components. Consequently, considerable efforts have been made to prepare the powder under cleanroom conditions in order to prevent contamination of the ceramic powder mixture with oversized dust particles. These facts are illustrated in Figure 4 with a typical structural flaw that is attributable to environmental contamination.

It must be pointed out in this connection that the results discussed in the following sections were obtained largely on materials that were produced under cleanroom (Class 3) conditions.

2.3. Reinforcement Concepts

The brittleness of ceramics is primarily caused by crack propagation. The objective of reinforcement concepts is, therefore, to increase the resistance of the microstructure to crack propagation.

ADVANCED MATERIALS

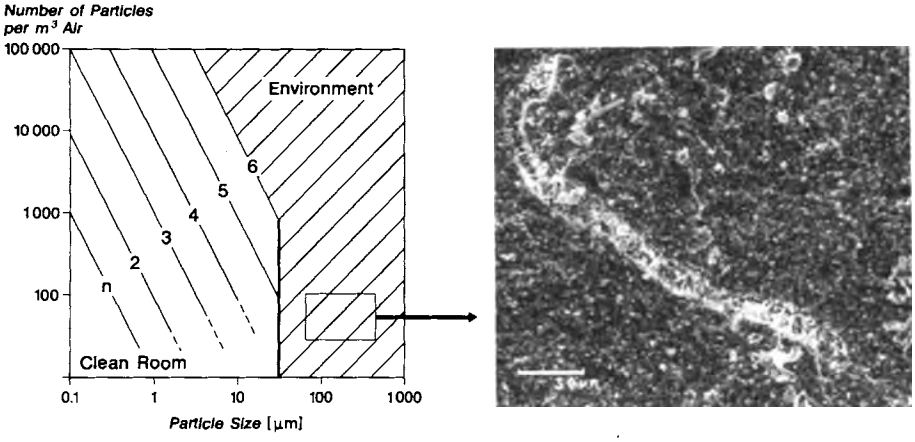


Fig. 4. Number and size of dust particles in different clean room classes. On the right, a fracture surface with a failure-initiating fault in a Si_3N_4 ceramic flaw can be seen. The flaw was caused by a dust particle of the kind found under normal environmental conditions.

The microstructure is determined essentially by the sintering aids which form a liquid phase during sintering. There are two possible types of sintering aids. First, oxides such as MgO, Y_2O_3 and Al_2O_3, which form amorphous or partially crystalline grain boundary phases because of their insolubility in Si_3N_4, and second, those which at suitable anion/cation ratios in Si_3N_4 lead to solid solutions (e.g. Be, Al).[9] In any case, the softening point, the viscosity and the amount of liquid phase are critical for densification and microstructural development. High viscosities always mean high aspect ratios of the precipitating β-Si_3N_4 grains.[4] This in turn acts to oppose good densification, meaning that these two mechanisms are frequently concurrent with each other. From the morphological point of view, good mechanical properties are best achieved by developing materials with high aspect ratios, with small mean grain sizes, low porosity and a minimal proportion of grain boundary phases. Below 1000 °C crack propagation under stress is influenced by different structural characteristics than at higher temperatures. Whereas at high temperatures strength is determined by the properties of grain boundary phases, at room temperature it is mainly the grain shape and size of Si_3N_4 that are decisive.[10]

In addition to specific structural development, two mechanisms essentially contribute to a reduction in crack propagation behavior at room temperature: first, crack deflection by mixed-in whiskers or fibers, or growth of in-situ whiskers or uniformly distributed micropores, and second, energy absorbtion by stress-induced phase conversion.[11] Most importantly, at high temperatures, the grain boundary slippage must be reduced by changing the chemical composition of the glassy phase and by the development of crystalline grain boundary phases.

Our own studies will therefore be presented below as typical examples of the reinforcement of SSN materials.

2.3.1. *In situ reinforcement by glass-forming additives*

Y_2O_3 and MgO have been the most often used sintering aids in the past. More recent work[12–14] has shown that the high-temperature properties in particular can be substantially improved by the use of oxides of the rare earth elements (RE*s*) as sintering aids. Therefore, Si_3N_4-powders have been mixed with various rare earth oxides and Al_2O_3 in a molar ratio of 2:1 (RE_2O_3: Al_2O_3 = 2:1).[15] The amounts used were chosen in such a way that in each trial the oxygen content contributed by the sintering additive was the same. In this way the influence of the rare earth oxides alone could be investigated. These powder mixtures were cold isostatically pressed and sintered under atmospheric pressure at 1800 °C.

In Figure 5 it can be seen that at room temperature as well as at high temperature the bending strength increases as the ionic radius of the rare earth oxides decreases.[16] Here the viscosity of the glass phases and the structural morphologies influenced by the rare earth oxides tend to counteract one another.[15] As a rule, densification can be improved by in-

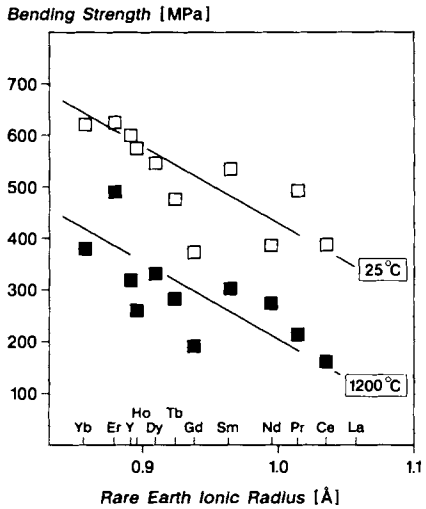


Fig. 5. In-situ reinforcement by the glass-forming intergranular phase. The Si_3N_4-powders were mixed with RE-oxides and Al_2O_3 as sintering aids (RE_2O_3:Al_2O_3 = 2:1). For specimen preparation compare the caption of Figure 2.

creasing the amount of additives with a lower melting point and lower viscosity[17] although exaggerated whisker growth can oppose densification. On the other hand, pronounced growth of elongated grains (Fig. 6) is very desirable in view of its reinforcement effect.

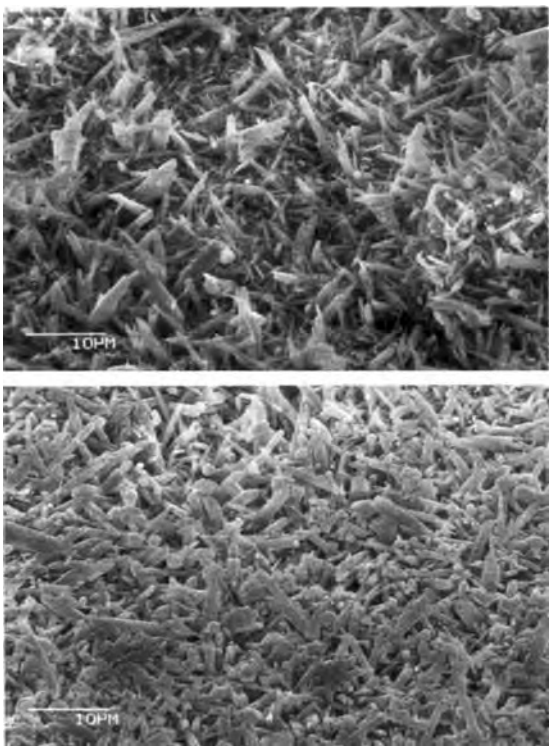


Fig. 6. Influence of the rare earths gadolinium (top) and dysprosium (bottom) on the growth of β-Si_3N_4 grains.

The higher the softening point of the glasses in the intergranular region, the more the grain boundary slippage will be prevented and the high-temperature strength improved. The exact composition of the glasses is not generally known. Probably, some nitrogen is dissolved in the glass phase. Studies of the Gd-Si-Al-O-N[18] and Nb-Si-Al-O-N[19] systems have shown that increasing substitution of nitrogen for oxygen in the glass network causes an increase in the glass transition temperature and a decrease of the thermal expansion coefficient. Possibly, the substitution of nitrogen is promoted by the incorporation of rare earth elements in the glass. Detailed studies with the help of advanced micro-analytical and surface analytical techniques,[20] are essential in verifying this interpretation.

2.3.2. *Crystallization of the amorphous grain boundary phases*

One further way of increasing the high-temperature strength is to crystallize the amorphous intergranular phase by tempering under nitrogen. Numerous investigations have been carried out on the Si_3N_4-SiO_2-Y_2O_3 system in order to study the crystallization of the glassy phase and its characterization,[21, 22] but rare earth oxides have also been investigated.[13, 14, 23] In further studies, the initial composition was again chosen in such a way that the ratio RE_2O_3:Al_2O_3 was exactly 2:1, i.e so that $RE_4Al_2O_9$ could crystallize. In practice, it was found that instead of $RE_4Al_2O_9$, mainly apatites $RE_5(SiO_4)_3N$, garnets $RE_3Al_5O_{12}$ and various silicate phases such as RE_2SiO_5 and $RE_2Si_2O_7$ crystallized at 1350 °C. When apatite was formed from any of the rare earth oxides the high-temperature strength was improved, while the crystallization of garnet and the silicate phases brought about only a slight improvement in strength.[16]

2.3.3. *Addition of dispersed crystalline phases*

The use of ZrO_2 as a sintering aid is known to improve the bending strength of Si_3N_4.[24] Apart from a minute glass phase fraction, ZrO_2 is present in the sintered structure as a crystalline intergranular phase. The strengthening mechanism of this Si_3N_4-ZrO_2 composite is based on a phase transformation mechanism, i.e. on the stress-induced change in the ZrO_2 from the tetragonal to the monoclinic modification, whereby the fracture energy can be absorbed.[25]

Since these mechanisms are effective only at temperatures below 1000 °C, trials were conducted with fully stabilized, cubic ZrO_2 and HfO_2. In these trials Al_2O_3 and Y_2O_3 were mixed with different proportions of HfO_2 and sintered at 1800 °C at atmospheric pressure. The proportion of Y_2O_3 was chosen to be so large that the cubic modification of HfO_2 is fully stabilized and, consequently, does not undergo a phase conversion on cooling.

Phase development during sintering is shown in Figure 7. The difference from a pure liquid-phase sintering process becomes very clear. The velocity of shrinkage is characterized by two maxima at about 1200 °C and 1400 °C (Fig. 7a). This shrinkage is accompanied by reaction of the sintering aids, formation of the glassy phase, and the phase transformation of Si_3N_4. The main shrinkage is associated with glass phase formation and α-β conversion of Si_3N_4.

Pure liquid-phase sintering is illustrated using the example of Y_2O_3/Al_2O_3 as the sintering aid (Fig. 7b). As soon as the additives react with one another, intergranular phases are formed which finally, at higher temperatures, are present only as a pure glassy phase. The α-β conversion of Si_3N_4 is associated with the formation of this glassy phase. After sintering, the original α-Si_3N_4-material has become β-Si_3N_4 with an oxinitride glass.

In contrast, the sintering aid HfO_2 remains crystalline but undergoes a phase conversion from the monoclinic to the cubic modification (Fig. 7c). It appears remarkable that this phase conversion is already concluded before the α-β phase conversion of Si_3N_4 takes place but seems to exert no influence on it. Thus, in addition to the β-Si_3N_4 grains and the glass phase with the constituents yttrium, aluminum, oxygen, silicon and nitrogen, the structure of the sinter compact

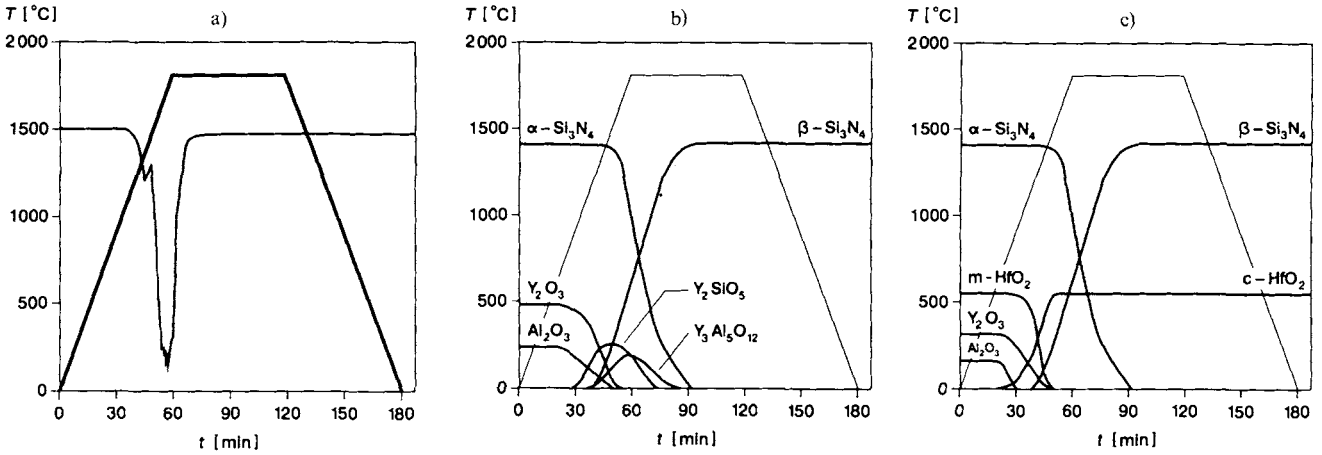


Fig. 7. Sintering behavior of Si_3N_4 with various sintering additives. The velocity of shrinkage is showin in (a) along with the sintering program (bold line): in 1 hour to 1800 °C, maintain for 1 hour; cool for 1 hour. Phase development with the glass-forming additives Y_2O_3 and Al_2O_3 (b) and additionally dispersed crystalline HfO_2 (c). The quantity and the quality of the crystalline phases were estimated by X-ray studies and are given schematically in the diagram.

consists additionally of cubic HfO_2. Corresponding micrographs of the structure are presented in Figure 8.

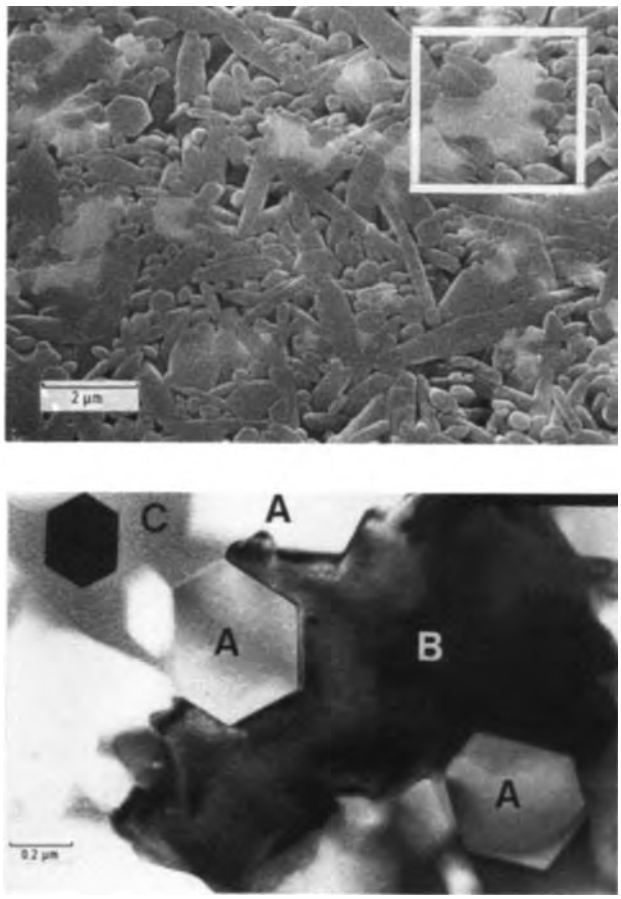


Fig. 8. Microstructure of ceramics that are reinforced with crystalline HfO_2; top, scanning electron micrograph, bottom, transmission electron micrograph (A: β-Si_3N_4; B: HfO_2; C: glass).

3. Reaction-Bonded and Hot Isostatically Pressed Reaction-Bonded Silicon Nitride

In contrast to the liquid-phase sintering process, in which the use of silicon nitride powders leads to a dense ceramic, in RBSN the ceramic is sintered making use of a gas-solid reaction between silicon and nitrogen. Ceramics which are produced in this way can be further densified by subsequent hot isostatic pressing.

3.1. Reaction-Bonded Silicon Nitride (RBSN)

Reaction-bonded silicon nitride is produced by the nitridation of moldings formed from silicon powder as shown in Equation 1.

$$3\,Si + 2\,N_2 \rightarrow Si_3N_4 \qquad (1)$$

The reaction in accordance with this equation can yield both the α- and the β-modifications. The accompanying volumetric expansion of approximately 22% leads in this reaction to a decrease in the overall porosity without any appreciable alteration in the outer dimensions of the specimen. The molding methods used include various pressing processes, slip casting, film casting and plastic processes such as extrusion and injection molding. After the molding aids are burned out, frequent presintering under an inert gas atmosphere follows. Following this step, the parts are strong enough to be worked (as graphite is worked) and in this way given their final shape. The moldings are then usually heat treated under nitrogen at atmospheric pressure and at temperatures between 1000 and 1450 °C. The attractiveness of this method lies in the minimal dimensional change which occurs during nitridation (< 0.1%), which means that no, or only minor machining of the final product is required. However, the components have a residual porosity of about 12%

to 30%, which has a strong influence on the mechanical properties.

The reaction between silicon and nitrogen is an exothermic process. The heat thus released can, because of an improperly programed temperature control, lead to excessive reaction rates and consequent local overheating. The result may be a melting of the silicon, which can bring the reaction to a standstill. No general rules governing the programing of temperature over time can be given for nitridation. However, the program depends on the furnace size, the amount of material being fired, the wall thickness of the parts, and the initial silicon grain size. The time required for complete nitridation can range from a few hours to several weeks, depending on the wall thickness. The maximum wall thickness that can be completely converted to silicon nitride is only approximately 30 mm, regardless of the length of the reaction time. For larger wall thicknesses the diffusion of nitrogen through silicon nitride becomes the rate-determining step, which causes the reaction rate to drop sharply.

In addition to the temperature control program, other nitridation conditions such as gas composition, gas pressure, temperature, time, and heating rate influence the course of the reaction and hence the structure and properties of this material.[4, 26] Whereas the molding process influences the packing density of the particles, the mean grain size and grain size distribution of the silicon powder, and the type and distribution of contaminants also affect the course of the reaction, and the structure and properties of RBSN.[27]

3.2. Hot Isostatically Pressed Reaction-Bonded Silicon Nitride (HIPRBSN)

Because of the relatively large shrinkage occurring during the densification of powder compacts, difficulties may appear during this process (contraction cracks, deformation), especially during the production of parts with complex shapes. For this reason RBSN with suitable sintering aids is also used as the starting material for hot isostatic pressing. In comparison with silicon nitride powder compacts the linear shrinkage here amounts only about 5–10%. The densification mechanisms are similar to those operating during the sintering of silicon nitride powder compacts. Pressure is applied to densify the material during the sintering process in order to accelerate the mechanisms responsible, such as particle rearrangement, diffusion, and plastic deformation. Pressure allows the amount of sintering aids to be reduced and improves especially the high-temperature strength. A reduction in the amount of sintering aids can also be achieved by crystallization of the amorphous grain boundary phase. Figure 9 shows a high-resolution micrograph of HIPRBSN, taken with a transmission electron microscope (TEM), showing a fully crystallized grain boundary phase: Y_2O_3 and Al_2O_3 were used as sintering aids.

The densification of RBSN by hot isostatic pressing permits the production of parts with narrow tolerances without,

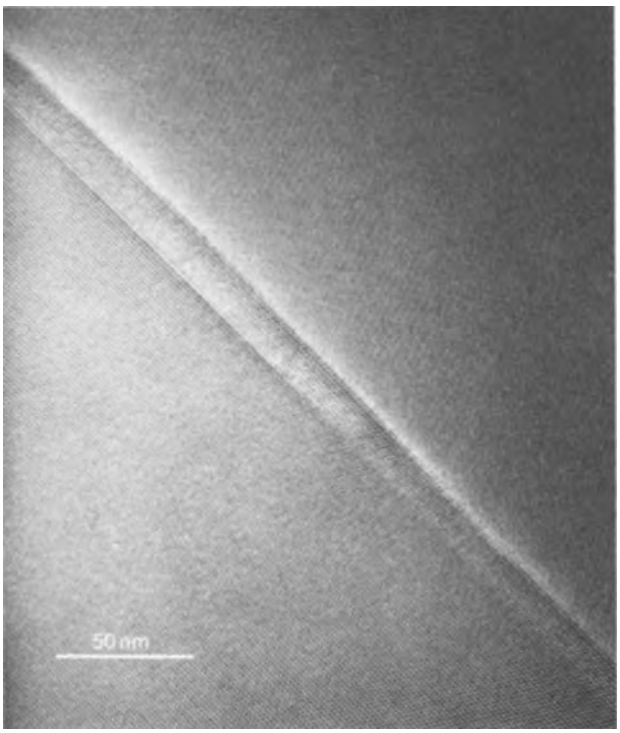


Fig. 9. TEM image of HIPRBSN with crystallized intergranular phase.

or with only minor machining being required. Furthermore, in comparison with conventional hot pressing, the uniform transmission of pressure results in isotropic material properties. Through the application of pressures up to more than 3000 bar, influence can be exerted on the densification behavior and grain growth and hence the optimization of material properties.[27] Below, the production of parts made of HIPRBSN is described in detail, with the slip casting of silicon powder in an aqueous system being used as the molding method, on which detailed reports have already been published.[28] In the first stage of slip development the silicon-water and silicon-sintering aid-water phase systems were investigated.

3.2.1. Hydrolysis in the silicon-water system

The addition of silicon powder to water should lead to intensive hydrolysis due to the normal electrode potential of the reaction shown in Equation 2.

$$Si + 2\,H_2O \rightarrow SiO_2 + 2\,H_2 \qquad (2)$$

The potential is strongly negative ($E = -0.875$ V), but silica is formed on the powder particle surface which produces a passivation layer which is insoluble in acids, thus preventing corrosion in acid media. Alkaline solution, however, can destroy the passivation layer according to Equation 3.

$$SiO_2 + 2\,OH^{\ominus} \rightarrow SiO_3^{2\ominus} + H_2O \qquad (3)$$

To characterize silicon hydrolysis, the amount of hydrogen formed was measured as a function of time at different pH values (Fig. 10).

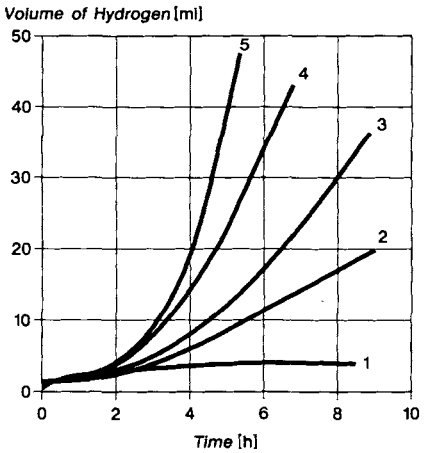


Fig. 10. Generation of hydrogen by the hydrolysis of silicon powder (50 wt.-%) in aqueous suspension plotted vs. time at different pH values: (1) pH = 2.4; (2) pH = 6.2; (3) pH = 10.0; (4) pH = 11.0; (5) pH = 12.0.

The higher the pH of the dispersion, the greater is the volume of hydrogen formed per unit time. Under strong alkaline conditions and at higher temperatures, the silicon is quantitatively decomposed, a reaction that is also used analytically for the determination of free silicon in SiSiC. In practice, it has been found that pH values above 9 are needed for the production of silicon slips.

3.2.2. *Viscosity of silicon slips*

Whereas at higher pH values hydrolysis of silicon powder can be observed, the usability of silicon slips under acid conditions is limited by a strong pH dependence of the slip viscosity. Towards the lower pH values the viscosity of the silicon powder dispersions increases sharply (Fig. 11).

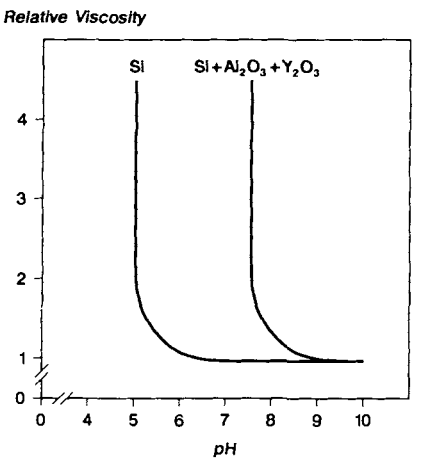


Fig. 11. Relative viscosity of an aqueous suspension with and without sintering aids as a function of pH (66.7 wt.-% solids; viscosity using Lehmann viscometer at pH 7).

Accordingly, below a certain pH-value the viscosity is too high to measure and therefore such dispersions are totally unsuitable for casting. The pH value at which the viscosity sharply rises depends on the powder concentration. At 75% powder content in the suspension it lies at pH 6, at 66% powder content at pH 4.5, while at 50% no such rise in viscosity can be observed down to a pH value of 2. To explain this phenomenon, reactions on the surface of the powder particles in the aqueous medium must be more closely examined (see 3.2.3.).

In summary, the pH range for preparing highly concentrated, chemically stable silicon slips of sufficiently low viscosity is limited to between 5 and 9.

3.2.3. *Surface reactions*

An analysis of silicon powders shows a silica content of about 1.5–2.0%. The silica forms a thin layer on the silicon particles and therefore the chemical behavior of the surface of silicon powder in water should be comparable with that of silica.

This behavior can be described as follows. Exposure to water leads to surface hydroxylation, enabling acid or base reactions to take place as shown in Equations 4 and 5.

$$\text{Si-OH} + \text{H}_3\text{O}^{\oplus} \rightarrow \text{Si-OH}_2^{\oplus} + \text{H}_2\text{O} \quad (4)$$

$$\text{Si-OH} + \text{OH}^{\ominus} \rightarrow \text{Si-O}^{\ominus} + \text{H}_2\text{O} \quad (5)$$

Silica is an acidic oxide, the reaction according to equation (5) can be expected to be dominant over a substantial range of pH values. That is the reason for the observation of a marked decrease of the pH when silicon powder is added to a basic solution. The reaction of the hydroxide ions with the silanol groups of the silicon surface reduces the $OH^{\ominus}$ concentration. The extent of this pH decrease depends on the specific surface of the dispersed particles and the degree of surface hydroxylation.

The following experimental finding can also be explained with equation (5). Over a wide range of pH values the zeta potential and hence the surface charge of the silicon particles is negative. For all powders examined, the particles were charged negatively at a pH greater than 2; this value represents the so-called "isoelectric point". At pH values higher than 2 the negative surface charge increases steadily, reaching its maximum at ca. -60 mV at a pH of around 7 (Fig. 12), and then remains constant up to higher pH values.

The zeta potential has an important influence on the state of particulate dispersion in suspensions.[30] Increasing surface potential generates an electrostatic barrier which prevents both contact between the individual particles and the formation of larger agglomerates of particles. The higher surface charge and the resulting electrostatic repulsion between the dispersed particles improves the properties of the dispersion, the viscosity is lowered and sedimentation decreases.

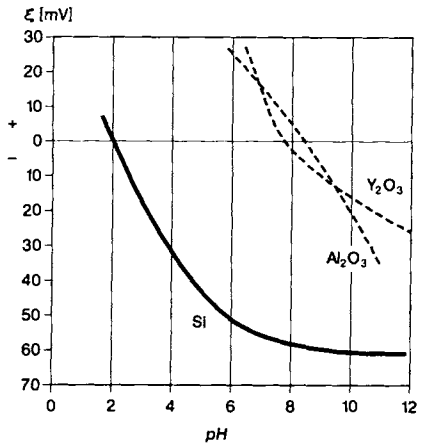


Fig. 12. Zeta potential (ζ) of silica, alumina and yttria powder particles in aqueous suspension as a function of pH.

3.2.4. *Addition of sintering aids*

The addition of the sintering aids Y_2O_3 and Al_2O_3 to an aqueous silicon suspension substantially influences the properties of the slip. Considering the importance of the surface charge to the sedimentation behavior, the viscosity, and the state of powder dispersion, the zeta potential of these powders was measured as a function of the pH value of the suspension (Fig. 12). For yttria the isoelectric point lies at a pH of ca. 8, the surface being charged positively at lower and negatively at higher pH values. Qualitatively the same result is observed for alumina powder dispersions with an isoelectric point at a pH of 8.5. Since the analogous point for silicon powder dispersions lies at a pH of 2, opposite signs of the surface charge of the components are observed in the pH range between 2 and 8.5 in aqueous suspensions of a mixture of these powders. This should lead to a higher viscosity of the slips because of the forces of electrostatic attraction. This assumption has been confirmed by experiment. For example, it is not possible to obtain a dispersion that contains all three powder types in an adequate concentration through mixing of the powders in distilled water (pH = 6.5). Because the silicon powder lowers the hydroxide ion concentration in alkaline dispersions, the initial pH must be chosen about three units higher than the desired final pH. The dependence of the relative viscosity of the sintering aid slip on pH has already been shown in Figure 11. The limit for the preparation of low-viscosity slips lies at pH 7.5.

3.2.5. *Material properties*

On the basis of the studies presented above, castable, low-viscosity and chemically stable slips can be prepared and cast. Depending on the silicon powder used, the densities of the slip cast and completely nitrided components lie between 2.40 and 2.65 g/cm^3. Subsequent densification is carried out in a high-pressure autoclave using nitrogen as the pressure transmission medium. For gas pressures at around 200 MPa the densification temperature lies at about 1800 °C. Holding times at the final temperature and the maximum pressure depend on the properties of the starting material. The linear shrinkage of the densified components is between 7 and 10%, depending on the initial density, much smaller than for other comparable sintering processes.

Figure 13 shows the distribution of four-point bending strengths in specimens cut from HIPRBSN sheets that had been produced by slip casting. The high Weibull modulus of $m = 23.42$ indicates that a structure with a very homogeneous distribution of flaws that could initiate failure can be achieved by the slip casting technique. Its strength exhibits a value of $\sigma_0 = 651$ MPa. It is possible to raise the strength of these materials through improvements in powder preparation that are especially designed for the purpose. A strength of 750 MPa with a Weibull modulus of 12 for isostatically pressed specimens could be achieved.

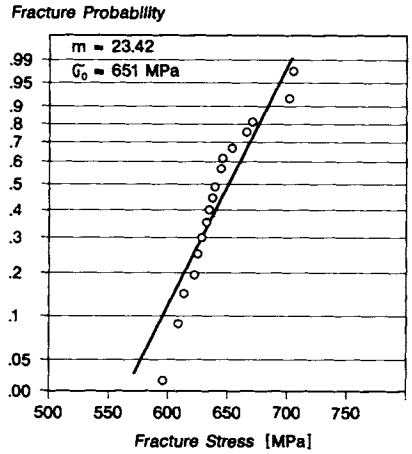


Fig. 13. Strength distribution of HIPRBSN slip cast moldings.

4. Conclusions

The results discussed in this report have revealed concepts that enable a fundamental improvement in the material properties of silicon nitride, such as the crystallization of the glass phase or the reduction in flaw frequency by using slip casting as the molding method. Additionally, these results demonstrate the different possibilities provided by the various processing methods for controlling material properties, component dimensions, shape, and production costs, etc. Although the process techniques for SSN and RBSN are fundamentally different, basic knowledge about the influence of the type and amount of sintering aids or the crystallization of the glassy phase can be applied to both types of material. Examples have been given here in order to show how basic knowledge can be expanded from findings in one subarea. These findings also clearly show that the powder preparation, the molding process or the sintering method

cannot be considered in isolation. In contrast, the individual steps of overall production must be adapted to one another. Thus the powder properties determine the suitability of the powder for a specific molding technique. That means that the developer of high-performance ceramics must be given the opportunity, as early as possible, to scale up his work in order to be able to incorporate the processing steps into the materials development with the help of parallel (and particularly nondestructive) testing methods.

Received: August 25, 1989

[1] R. Danzer, *Proc. 12. Int. Plansee-Seminar 2* (1989) 183–198.
[2] G. Grathwohl, *Int. J. High Techn. Ceram.* (1988) 123–142.
[3] M. Mitomo, N. Yang, Y. Kishi, Y. Bando, *J. Mater. Sci. 23* (1988) 3413–3419.
[4] G. Ziegler, J. Heinrich, G. Wötting, *J. Mater. Sci. 22* (1987) 3041–3086.
[5] J. Heinrich, E. Backer, M. Böhmer, *J. Am. Ceram. Soc. 71* (1988) C28–C31.
[6] G. R. Terwilliger, F. F. Lange, *J. Am. Ceram. Soc. 57* (1974) 25–31.
[7] G. Schwier, G. Nietfeld, *Werkst. Konstruktion 2* (1988), 149–154.
[8] F. Aldinger, H.-J. Kalz, *Angew. Chem. Int. Ed. Engl. 26* (1987) 371; *Angew. Chem. 99* (1987) 381–391.
[9] K. H. Jack in F. L. Riley (Ed.): *Nitrogen Ceramics*, Noordhoff-Leyden, Leyden 1977, 109–128.
[10] G. Wötting, B. Kanka, G. Ziegler in S. Hampshire (Ed.): *Non-Oxide Tech. Eng. Ceram.*, Elsevier, London 1985, 83–96.
[11] N. Claussen, J. Jahn, *J. Am. Ceram. Soc. 61* (1978) 94–95.
[12] Y. R. Xu, S. R. Fu, D. S. Yan, *Physica 150* (1988) 276–282.
[13] K. Ueno, *Yogyo-Kyokai-Shi 94* (1986) 702–705.
[14] B. Saruhan, M. J. Pomeroy, S. Hampshire in S. Hampshire (Ed.): *Non-Oxide Tech. Eng. Ceram.*, Elsevier, London 1985, 69–82.
[15] M. Peuckert, C. Boberski, P. Selgert, *Proc. 3rd. Int. Symp. Ceram. Mater. Compon. for Engines*, Elsevier, Amsterdam 1989, in press.
[16] C. Boberski, M. Peuckert, P. Selgert, *Proc. 1st Eur. Cer. Soc. Conf.*, Elsevier, Amsterdam 1989, in press.
[17] G. Wötting, G. Ziegler, *Ceram. Int. 10* (1984) 18–29.
[18] J. Rocherulle, P. Verdier, Y. Laurent, *Mater. Sci. Eng. 2* (1989) 265–268.
[19] J. Lang, P. Verdier, R. Pastuszak, R. Marchand, *Ann. Chim. (Paris) 5* (1970) 663.
[20] R. Hamminger, *Surf. Interface Anal. 12* (1988) 519–526.
[21] W. E. Lee, C. H. Drummond, G. E. Hilmas, J. D. Kiser, W. A. Sanders, *Ceram. Eng. Sci. Proc. 9* (1988) 1355–1366.
[22] L. J. Gauckler, H. Hohnke, T. Y. Tien, *J. Am. Ceram. Soc. 63* (1980) 35–37.
[23] W. A. Sanders, D. M. Mieskowski, *Am. Ceram. Soc. Bull. 64* (1985) 304–309.
[24] F. F. Lange, *J. Am. Ceram. Soc. 63* (1980) 38–40.
[25] K. Terao, Y. Miyamoto, M. Koizumi, *J. Am. Ceram. Soc. 71* (1988) C167–C169.
[26] J. A. Mangels, *Am. Ceram. Soc. Bull. 60* (1981) 613–617.
[27] J. Heinrich, D. Munz, G. Ziegler, *Powder Metall. Int. 3* (1982) 153–159.
[28] R. Dillinger, J. Heinrich, J. Huber, *Mater. Sci. and Eng. A 109* (1988) 373–378.
[29] I. Meisel: *Diploma Thesis*, Universität Bayreuth, 1987.
[30] M. D. Sacks, G. W. Scheiffele, *Ceram. Eng. Sci. Proc. 7–8* (1985) 1109–1123.

Communications

Manuscripts intended for publication as communications should be sent to ADVANCED MATERIALS PO Box 101161, D-6940 Weinheim, FRG. Authors are requested to consult the "Instructions to Authors" which are reproduced in the January issue of the journal or are available from the editorial office on request.

Spatially Selective Conducting Patterns in Transparent Films Derived from Ladder Type Polymers**

By *Igal Belaish, Dan Davidov*, Heny Selig, Malcolm R. McLean*, and *Larry Dalton*

Conducting patterns can be created in the insulating pristine ladder type polymer films BBL and BBB (see Fig. 1) by spatially selective heating using laser annealing. The conducting regions consist of cross-linked, stable, ladder polymers. Subsequent fluorination leads to conducting patterns embedded in a completely *transparent* film. These features may lead to a variety of possible applications.

In the last decades there has been significant progress in the synthesis, processing, and characterization of rigid rod polymers.[1] A few examples of such polymers are shown in Figure 1. These polymers have exceptional properties such as high tensile strength and modulus.[2, 3] They are stable at

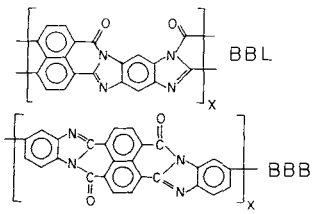


Fig. 1. Examples of ladder type polymers.

elevated temperatures (which may exceed 600 °C) and may be processed into fibers or highly packed films with excellent planar arrangements.[2] The conductivity of these rigid rod polymers can be controlled by thermal pyrolysis.[4]

Particularly, BBB polymer undergoes a phase transformation at a temperature T_p of 680 °C to a new ladder type polymer with high intrinsic conductivity.[4] Exposure of

[*] Prof. D. Davidov, I. Belaish and Prof. H. Selig
Racah Institute of Physics
Hebrew University
Jerusalem (Israel)
Prof. L. R. Dalton and Dr. M. R. McLean
Department of Chemistry
University of Southern California
Los Angeles, CA (USA)

[**] This research was supported by the US-Israel Binational Science Foundation. We thank Dr. *I. Palchan* for initial collaboration.

pristine BBB (and BBL) to fluorine leads to a colorless, transparent material, while the heat treated polymers ($T_p > 700\,°C$) are hardly affected by fluorination.

The synthesis and processing of BBB and BBL has been described previously.[1] In this work we have used free standing films as well as films on glass substrates, both having thicknesses of about 20 μm. These films exhibit excellent planar arrangement of the polymer chains as shown by the large anisotropic resistivity $\varrho_\perp/\varrho_{||} \cong 1000$. Here $\varrho_\perp$ and $\varrho_{||}$ are the resistivities perpendicular and parallel to the film, respectively. Films of BBB are shiny brown and exhibit a room temperature in-plane conductivity σ_{RT} of 10^{-9} S/cm and an optical energy gap of approximately 1.8 eV.[5, 6]

Heat treatment of ladder type polymers changes the conductivity dramatically. Figure 2a shows the in-plane room temperature conductivity, σ_{RT}, for BBB subsequent to heat treatment at a temperature T_p ($200° \leq T_p \leq 1000\,°C$) for several minutes in a vacuum oven. As clearly seen, the room temperature conductivity changes by 10 orders of magnitude and reaches a value of 30 S/cm for $T_p = 950\,°C$. Even higher in-plane conductivities were achieved for polymers with better in-plane ordering. This change in conductivity is associated with a $\sim 30\%$ weight loss[7] and color changes. The highly conducting films are silvery-gray and stable in air.

A most dramatic change in conductivity (Fig. 2a) occurs for a pyrolysis temperature near $T_p \cong 680\,°C$. Indeed, a plot

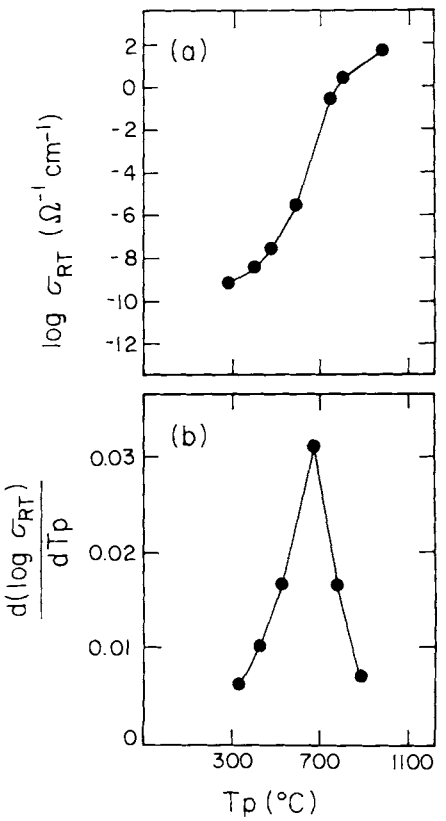


Fig. 2. a) The room temperature conductivity (but after annealing at T_p) vs. pyrolysis temperature T_p. b) A plot of $d(\log \sigma_{RT})/dT_p$. Note maximum at $T_p = 680\,°C$.

of $d(\log \sigma_{RT})/dT_p$ vs. T_p (Fig. 2b) shows the clear maximum at $T_p = 680\,°C$. We take this maximum as evidence for a transformation to a cross-linked network. Other evidence for such a phase transformation is provided by ESR studies[4] which indicate a clear maximum in the spin-density for $T_p \cong 680\,°C$. Photoluminescence measurements also suggest that the high temperature conducting, condensed aromatic structure is a different ladder polymer with a smaller band gap (1.4 eV).[8]

Pristine BBB and BBL were exposed to about 400 torr F_2 at room temperature. After exposure for several hours the brown shiny polymers became transparent and colorless. Optical absorption studies indicate that the energy gap is larger than 3.2 eV in the fluorinated material.[8] Infrared spectra of the product show strong absorptions in the C–F stretching region as well as absorptions in the 2900–3000 cm^{-1} range indicating the presence of C–H bonds. Weight uptake measurements (Table 1) using a Sartorius

Table 1. Weight uptake of pristine BBB and BBL.

material	initial weight (mg)	weight increase (mg)	F/BBL (BBB)
BBL	6.40	6.0	16.4 ± 0.5
	6.92	6.1	15.5 ± 0.5
	3.80	3.4	15.7 ± 0.5
BBB	12.26	13.5	23.6 ± 0.5
	12.40	12.7	22.0 ± 0.5
	7.49	7.0	20.1 ± 0.5

Magnetic Suspension Balance indicate that BBL and BBB take up about 16 and 22 fluorine atoms per monomer unit, respectively. This is exactly the number of aromatic carbon atoms per monomer unit (see Fig. 1) for BBL and BBB, respectively, suggesting formation of C–F bonds and partial or full conversion of the conjugated system to a saturated one. Exposure to air leads to a yellow transparent film after several days. The fluorinated materials are soluble in water, giving a yellow solution. Heat treated polymers ($T_p < 600\,°C$) also become transparent upon fluorination. However, *conducting polymers, heat treated at $T_p > 700\,°C$ are almost unaffected by exposure to fluorine* and retain their high conductivity and absorbance after exposure for several days. Exposure to higher fluorine pressure for longer periods converts the silvery-brown conducting polymers into a more bluish, rather than a transparent material. This shows that polymers heated above 700 °C exhibit different structures. In a few cases we found that fluorination of films which had been heat treated at around $T_p = 680\,°C$, may lead to transparent films with enhanced conductivities relative to pristine BBL and BBB.

The properties described above can be used to form spatially selective conductive patterns in a completely transparent film. This is achieved by shining laser light ($Ar^{\oplus}$, 2 watt/cm^2) through a metal mask or a slit onto the BBB insulating

ADVANCED MATERIALS

film on a glass substrate for several seconds. Figure 3a shows a series of embedded "conducting lines" of approximately 0.5 mm thickness in insulating BBB films treated in this way. The conductivity of these lines is approximately 50 S/cm. The conductivity of the shiny-brown polymer background remains unaffected by the laser heating. Using this masking technique, we can produce conducting lines approximately 10 μm in width (width is determined by the slit, laser focusing and exposure time). The pattern shown in Fig. 3a is stable in air and upon subsequent heating to 200 °C. We assume that laser annealing affects the polymer mainly through heating, so the "conducting lines" are composed of cross-linked polymers with the properties described above. Upon exposure to fluorine, the "conducting lines" remain unaffected, but the remaining pristine BBB becomes completely transparent and colorless. Figure 3b pictures this new structure consisting of "conducting lines" in a transparent material. This structure is stable in a humidity-free environment.

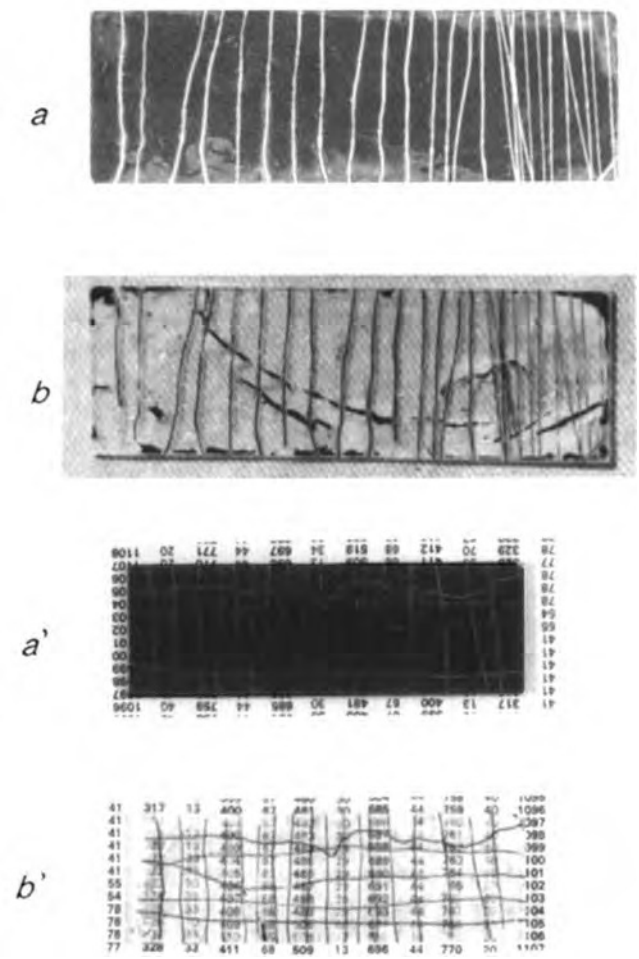


Fig. 3. a) "Conducting Lines" produced by the laser annealing technique in BBB polymer. The conducting lines are shiny-silver and reflect light and thus appear more bright in photo. a') Fine conducting lines produced by laser annealing of BBB. b) After fluorination: The "conducting lines" in a transparent film. b') Same as a', but after fluorination. (Numbers in background shown to emphasize degree of transparency).

We have now preliminary evidence that the heating and fluorination process affects other rigid-rod polymers as well. The transparent films so produced are optically anisotropic and less affected by humidity. The fluorination of polyacetylene was published recently[9] but in this case the fluorinated material is white rather than transparent.

The possibility to produce highly aligned transparent films with anisotropic optical properties and particularly the generation of spatially selective conductive patterns in insulating aligned transparent polymers opens new routes for applications in fields such as lithography, microelectronics, optics and molecular electronics. For instance, "writing" using selective laser heating and eliminating the rest of the film by fluorination and washing (using water or other solvents) might be important in both lithography and microelectronics. The fabrication of very fine grids composed of fine alternate stripes of conducting and transparent polymers with anisotropic optical properties is another interesting possibility. Optical disks should be considered as well. Generally speaking, the possibility to fabricate miniature conducting microstructures with novel electronic properties is now more realistic.

Received: August 2, 1989

[1] F. E. Arnold, R. L. Van-Deusen, *J. Appl. Polym. Sci. 15* (1971) 2035; R. L. Van Deusen, *J. Polym. Sci. B 4* (1966) 211; R. L. Van Deusen, O. K. Goins, A. J. Sicree, *J. Polym. Sci. A1* (1968) 1777; F. E. Arnold, R. L. Van Deusen, *Macromolecules 2* (1969) 497.
[2] S. R. Allen, R. J. Farris, E. L. Thomas, *J. Mater. Sci. 20* (1985) 4583.
[3] J. F. Wolfe, *Polym. Mater. Sci. Eng. (Proc. ACS Div.) 57* (1985) 99.
[4] I. Belaish, C. Rettori, D. Davidov, M. R. McLean, L. R. Dalton, *Proc. MRS Mtg. on Rigid-Rod Polymers, Boston, November 1989.*
[5] F. Coter, I. Belaish, D. Davidov, L. Dalton, E. Ehrenfreund, M. R. McLean, H. S. Nalwa, *Synth. Met. 29* (1989) E471.
[6] Oh Kil Kim, *Mol. Crys. Liq. Cryst. 105* (1984) 161.
[7] Oh Kil Kim, *J. Polym. Sci. Polym. Lett. 23* (1985) 137.
[8] F. Coter, et al., unpublished results.
[9] H. Selig, S. Luski, *J. Fluor. Chem. 39* (1988) 421.

Highly Conjugated, Substituted Polyacetylenes via the Ring-Opening Metathesis Polymerization of Substituted Cyclooctatetraenes**

By *Christopher B. Gorman, Eric J. Ginsburg, Seth R. Marder,* and *Robert H. Grubbs**

Soluble, highly conjugated polymers such as substituted polythiophenes, poly(*p*-phenylene vinylenes),[1] and most

[*] Prof. R. H. Grubbs, C. B. Gorman, E. J. Ginsburg.
Arnold and Mabel Beckman Laboratory of Chemical Synthesis
Division of Chemistry and Chemical Engineering
California Institute of Technology, Pasadena, CA 91125 (USA)
Dr. S. R. Marder
Jet Propulsion Laboratory
4800 Oak Grove Drive, Pasadena, CA 91109 (USA)

[**] The authors acknowledge financial support from the Office of Naval Research and Dr. Michael J. Sailor for helpful, serious discussions. SRM thanks the National Research Council and the National Aeronautics and Space Administration for a National Research Council Resident Research Associateship at the Jet Propulsion Laboratory.

recently polyalkylanilines,[2] have had a large impact on the study of conductive polymers. Soluble polymers can be more fully characterized and more easily processed. Despite intensive study and synthetic effort, there are few tractable or soluble conjugated derivatives of polyacetylene.[3, 4] Substitution of polyacetylene via the polymerization of substituted acetylenes results in materials with low effective conjugation lengths, as evidenced by their high-energy visible absorption spectra and comparatively low iodine-doped conductivities.[5] This low conjugation length is presumably due to twisting around the single bonds in polyacetylene resulting from steric repulsions of the side groups[6, 7] (Fig. 1).

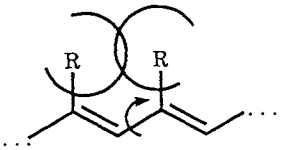


Fig. 1. Chain twisting in substituted polyacetylene.

Recently, *Klavetter* and *Grubbs* reported the synthesis of polyacetylene by the ring-opening metathesis polymerization[8] (ROMP) of cyclooctatetraene (COT).[9, 10] Here we report the ROMP of substituted cyclooctatetraenes: a route to a variety of highly conjugated, partially alkyl-substituted polyacetylenes. These polymers have a substituent on the average every eight carbons, rendering some of them partially soluble. Polymerization can be accomplished in a few minutes in a nitrogen drybox, resulting in free-standing films which are generally gold, shiny, and flexible.[11]

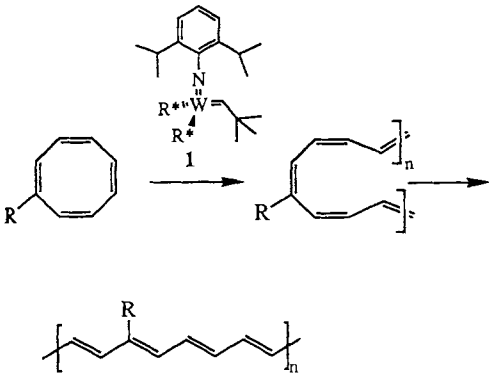


Fig. 2. Polymerization of Cycloocatatetraene Derivatives. R* = $(CF_3)_2(CH_3)CO$; R = Me, *n*Bu, octyl, octadecyl, Ph, *t*Bu, neopentyl.

These films can be iodine doped to a conductive state (Table 1). Moreover, in contrast to poly-cyclooctatetraene (polyacetylene) which shows large optical scattering losses due to its crystallinity, the alkylCOT polymers are amorphous and show low scattering losses.[12, 13]

Table 1. Conductivity and spectroscopic data.

polymer	σ(S/cm)	y [a]	abs. max. initially [b]	abs. max. T ≈ 6–12 hrs. [b]
Poly-MethylCOT	15–44	–	522 [c]	–
Poly-*n*-ButylCOT	0.25–0.7	0.10–0.13	462	614
Poly-OctylCOT	15–50	0.11–0.19	480	632
Poly-OctadecylCOT	0.60–3.65	0.14–0.16	538	630
Poly-PhenylCOT	0.3–0.6	0.19–0.28	522	620
Poly-*t*-ButylCOT	$<10^{-8}$	≈0.03	302	432
Poly-NeopentylCOT	0.2–1.5	0.11–0.18	412, 628	634
Poly-NeopentylCOT after recasting solution:	15–21	0.13–0.17	–	–

[a] Based on the molecular formula $(C[H/R]I_y)_x$. [b] Spectra taken in tetrahydrofuran. Wavelength in nm. [c] Very small amount of material that leached out of the film.

Whereas poly-methylCOT, like polyacetylene, is somewhat brittle and completely insoluble, films of poly-RCOT with straight chain alkyl substituents of at least four carbons are flexible and partially soluble in solvents such as tetrahydrofuran (THF) and dichloromethane. When a film of poly-*n*-butyl-, poly-octyl- or poly-octadecylCOT was stirred with THF, a red/brown solution resulted that contained 1–2 mg/mL of polymer, and which turned blue upon standing overnight. Solutions stored under argon at −50 °C in the dark did not turn blue. We propose that the color change is due to an increased electron delocalization arising from the *cis* double bonds in the nascent polymer isomerizing to give a material with predominantly *trans* double bonds, although aggregation phenomena cannot be ruled out at this time.[14] Similar changes have been observed in the optical spectra of films of polyacetylene,[15] and the related poly-trimethylsilylCOT.[16] Also, red-shifts in the absorption spectra of short polyenes upon *cis-trans* isomerization have been observed by *Schrock* and coworkers.[17] If not diluted at least tenfold before isomerization, 1–2 mg/mL solutions of the *cis* polymer gelled or precipitated. The predominantly *cis* isomer of these polymers is soluble whereas the *trans* isomer is much less so. This observation is consistent with previous observations on oligomeric polyenes.

Nascent poly-neopentylCOT was completely soluble, but also precipitated upon isomerization to the *trans* form if not diluted. Blue suspensions that resulted from the isomerization of concentrated solutions, however, were recast into gold films that displayed iodine-doped conductivities two orders of magnitude higher than the original material. The aromatic side-chain derivative poly-phenylCOT was about as soluble as poly-*n*-butylCOT in the *cis* form, but was almost completely insoluble in the *trans* form. Poly-*t*-butylCOT was freely soluble but was yellow-orange in color, indicating a low effective conjugation length. Thus, modifications to the polymer backbone which increase its solubility seem to reduce its conjugation length.

Gel permeation chromatography on solutions of the "*cis*" polymers indicated that the solutions contained high molec-

ADVANCED MATERIALS

ular weight materials (Table 2) although molecular weight distributions were very broad in several cases. The retention times of the polymers generally increased after isomerization, suggesting an increase in hydrodynamic radius.

Table 2. Molecular weights.

polymer	M_n	M_w
Poly-*n*-ButylCOT	33200	153400
Poly-OctylCOT	35900	369000
Poly-*t*-ButylCOT	58300	71900
Poly-NeopentylCOT	23400	27100
Poly-PhenylCOT	30600	121100

The polymers were examined by ^{1}H NMR and Raman spectroscopy. The NMR spectra of all the polymers showed broad multiplets between 6 and 7 ppm and broad signals in the regions expected for the side groups, indicative of a polymeric, olefinic chain. Raman spectroscopy provided further evidence of a conjugated chain. Two peaks, assigned as the A_g C-C stretch (ν_1) and A_g C=C stretch (ν_2) in *trans*-polyacetylene were observed in all the spectra (Table 3), except for that of poly-phenylCOT, which displayed a complicated

Table 3. Raman stretching vibrations of polyacetylene derivatives (cm^{-1}).

polymer	ν_1	ν_2
Polyacetylene[18]	1090–1120	1470
Poly-MethylCOT	1126–1132	1516
Poly-*n*-ButylCOT	1132	1514
Poly-OctylCOT	1114–1128	1485
Poly-*t*-ButylCOT	1147	1539–1547
Poly-NeopentylCOT	1131	1509

spectrum dominated by phenyl stretches. No peaks were seen that corresponded to the *cis* form of polyacetylene, probably since no precautions were taken to prevent isomerisation caused by the 488 nm laser light. In unsubstituted polyacetylene the infrared C-H stretching vibrations at 740 cm^{-1} and 1015 cm^{-1} are diagnostic for *cis* and *trans* material, respectively. The infrared spectra of the substituted polyacetylenes are not as useful, since the vibrations of the side chains obscured those of the main chain.

Several attempts have been made to correlate the effective conjugation length of a polyene with its absorbance maximum. Based on the extrapolation of polyene absorption data obtained from a variety of workers[19, 20] to the band gap of polyacetylene,[21] the *trans* form of these polymers have an effective conjugation length of at least 25 double bonds. Lower energy absorption maxima are seen in the solid state. A thin film of poly-octylCOT has a broad absorption centered around 650 nm which is comparable to that observed for a thin film of native polyacetylene.[21]

In summary, ROMP of alkyl-substituted cyclooctatetraenes produces polyacetylene derivatives in which the substituents are placed at a sufficient distance apart to allow conjugation along the backbone of the polymer and still provide for solubility in the *cis* configuration. Work is underway using the RCOT/ROMP methodology to develop other polyacetylene derivatives which are more soluble, more conductive, and air-stable.

Experimental

Polymerization was effected by adding 50–150 equivalents of the liquid monomer to 1–2 mg of the tungsten alkylidene catalyst [22] dissolved in a minimum (200 μL) of pentane and 1–2 μL of THF. After the yellow solution began to turn orange/brown, it was transferred by pipette onto a glass plate and allowed to harden into a film over the course of an hour or so. Films were peeled from the plate and used for conductivity measurements. Doping was accomplished by exposing the films to iodine vapor for 3 to 6 hours in a previously evacuated chamber followed by pumping (<0.01 torr) for approximately one hour to remove excess iodine. Films exposed to iodine immediately became blue-black in color and remained flexible. Conductivities were measured using a four-point probe in a nitrogen drybox or a four-wire probe attached to a Schlenk line. [23] Similar conductivities were seen using both methods.

Received: July 7, 1989
Revised version: September 8, 1989

[1] See, for example: a) K. Y. Jen, R. L. Oboodi, R. L. Elsenbaumer, *Polym. Mater. Sci. Eng. 53* (1985) 79. b) S. Hotta, S. D. D. V. Rughooputh, A. J. Heeger, F. Wudl, *Macromolecules 20* (1987) 212. c) S. D. D. V. Rughooputh, M. Nowak, S. Hotta, A. J. Heeger, F. Wudl, *Synth., Met. 21* (1987) 41. d) S. H. Askari, S. D. Rughooputh, F. Wudl, A. J. Heeger, *Polym. Prepr. 30* (1989) 157.

[2] (a) D. Macinnes, Jr., B. L. Funt, *Synth. Met. 25* (1988) 235. (b) M. Leclerc, J. Guay, L. H. Dao, *Macromolecules 22* (1989) 649.

[3] (a) T. A. Skotheim (Ed): *Handbook of Conducting Polymers. Vol. 1 and 2.* Marcel Dekker, New York 1989. (b) J. C. W. Chien: *Polyacetylene: Chemistry, Physics, and Material Science,* Academic, Orlando, 1984.

[4] A number of polyacetylene graft copolymers have been made. See: (a) S. P. Armes, B. Vincent, J. W. White, *J. Chem. Soc. Chem. Commun. 1986* 1525. (b) R. Dorsinville, R. Tubino, S. Krimchansky, R. R. Alfano, J. L. Birman, A. Bolognesi, S. Destri, M. Catellani, W. Porzio, *Phys. Rev. B32* (1985) 3377. (c) R. Tubino, R. Dorsinville, W. Lam, R. R. Alfano, J. L. Birman, A. Bolognesi, S. Destri, M. Catellani, W. Porzio, *Phys. Rev. B30* (1984) 6601. (d) G. L. Baker, F. S. Bates, *Macromolecules 17* (1984) 2619. (e) J. A. Stowell, A. J. Amass, M. S. Beevers, T. R. Farren, *Makromol. Chem. 188* (1987) 1635.

[5] (a) J. M. Zeigler, *U.S. Patent Appl.* US 760433 AO, 21 November, 1986; *Chem. Abstr. 20* (1986) 157042. (b) J. M. Zeigler, *Polym. Prepr. 25* (1984) 223. (c) Y. Okano, T. Masuda, T. Higashimura, *J. Polym. Sci. Polym. Chem. Ed. 22* (1984) 1603. (d) T. Masuda, T. Higashimura, *Adv. in Polymer Science 81* (1987) 121.

[6] M. Leclerc, R. E. Prudhomme, *J. Polym. Sci. Polym. Phys. Ed. 23* (1985) 2021.

[7] *Chien* has prepared copolymers of acetylene and methyl-acetylene, J. C. W. Chien, G. E. Wnek, F. E. Karasz, J. A. Hirsch, *Macromolecules 14* (1981) 479. However, extension of this method to other copolymerizations requires mixing a gas (acetylene) and a liquid (R-acetylene), and this two phase system is not expected to be well-behaved.

[8] (a) R. H. Grubbs in G. Wilkinson, F. G. A. Stone, E. W. Abel (Eds.): *Comprehensive Organometallic Chemistry,* Pergamon, Oxford 1982; Chapter 54. (b) J. K. Ivin: *Olefin Metathesis,* Academic, London 1983. (c) B. M. Novak, R. H. Grubbs in J. I. Kroschwitz (Ed): *Encyclopedia of Polymer Science and Engineering,* John Wiley & Sons, New York 1990. In press.

[9] Other methods reported for the polymerization of COT utilized Lewis-acidic metathesis catalysts, resulting in a polymer containing many sp^3 defects: (a) M. A. Tlenkopachev, Y. V. Korshak, A. V. Orlov, V. V. Korshak, *Dokl. Akad. Nauk SSSR (Engl. Transl.) 291* (1986) 1036; *Dokl. Akad. Nauk SSSR 29* (1986) 409. (b) Y. V. Korshak, V. Korshak, G. Kansichka, H. Höcker, *Makromol. Chem. Rapid Commun. 6* (1985) 685.

[10] F. L. Klavetter, R. H. Grubbs, *J. Am. Chem. Soc. 110* (1988) 7807.

[11] The polymer films could be folded almost in half without breaking.
[12] J. W. Perry, S. R. Marder, C. B. Gorman, E. J. Ginsburg, R. H. Grubbs, unpublished results.
[13] Only amorphous halos are observed in the wide angle X-ray profile of these polymers.
[14] D. N. Batchelder, *Contemp. Phys. 29* (1988) 3.
[15] Reference [3b], p. 225.
[16] E. J. Ginsburg, C. B. Gorman, S. R. Marder, R. H. Grubbs, *J. Am. Chem. Soc. 111* (1989) 7621.
[17] R. R. Schrock, S. A. Krouse, K. Knoll, J. Feldman, J. S. Murdzek, D. C. Yang, *J. Mol. Catal. 46* (1988) 243.
[18] S. Lichtmann, *PhD. Thesis*, Cornell University 1980.
[19] (a) Bohlmann, *Chem. Ber. 85* (1952) 387. (b) Bohlmann, *Chem. Ber. 86* (1953) 63. (c) Bohlmann, Kieslich, *Chem. Ber. 87* (1954) 1363. (d) P. Nayler, M. C. Whiting, *J. Chem. Soc. Chem. Commun. 1955*, 3037. (e) F. Sondheimer, D. Ben-Efriam, R. Wolovsky, *J. Am. Chem. Soc. 83* (1961) 1675. (g) Karrer, Eugster, *Helv. Chim. Acta 34* (1951) 1805. (h) A. Winston, P. Wichacheewa, *Macromolecules 6* (1973) 200.
[20] Similar values have been obtained by *R. Chance*, Exxon Corp., unpublished data.
[21] A. O. Patil, A. J. Heeger, F. Wudl, *Chem. Rev. 88* (1988) 183.
[22] R. R. Schrock, R. T. DePue, J. Feldman, C. J. Schaverien, J. C. Dewan, A. H. Liu, *J. Am. Chem. Soc. 110* (1988) 1423.
[23] S. M. Sze: *Physics of Semiconductor Devices*, Wiley, New York 1981, p. 30.

Research News

Monolayers and Langmuir–Blodgett Multilayers of Discotic Liquid Crystals?

By André Laschewsky*

1. Discotic Liquid Crystals

Discotic liquid crystals[1] were discovered in 1977. They are formed by disk-shaped molecules, i.e. typically by large planar aromatic, or by rather inflexible macrocyclic moieties, surrounded by a number of flexible so-called "wing groups". A selection of discotic liquid crystals (LCs) is shown in Figure 1.

Discotic LCs exhibit columnar mesophases which distinguish them from the well-known calamitic (rod-shaped) LCs. These columnar phases are characterized by stacks of the disk-shaped cores, packed in various ways.[1]

2. Monolayers and Langmuir–Blodgett Multilayers

Ordered monomolecular layers are formed by the self-organization of water-insoluble amphiphilic molecules at the gas-water interface.[3] The standard amphiphiles used for monolayers have a polar head group and one or two hydrophobic chains, e.g. fatty acids or phosphatidylcholines respectively. Under appropriate conditions, the monolayers of many amphiphiles can be transferred successively onto solid substrates, by dipping the substrate vertically or horizontally

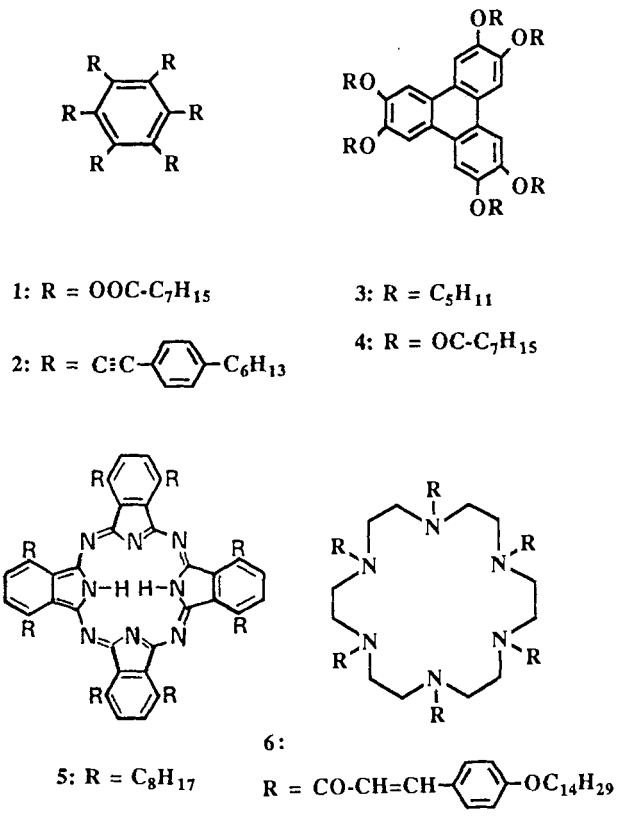


Fig. 1. A selection of discotic liquid crystals [2, 9, 10].

[*] Dr. A. Laschewsky
Institut für Organische Chemie, University of Mainz,
P.O. Box 3980, D-6500 Mainz (FRG)

ADVANCED MATERIALS

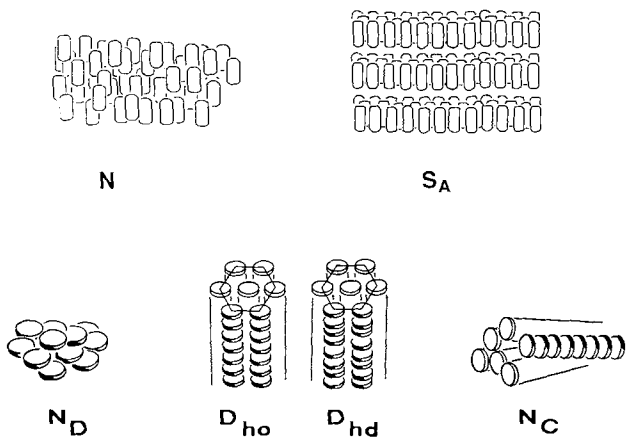


Fig. 2. Scheme of some mesophases: calamitic (rod-shaped) LCs: N = nematic, S_A = smectic A; discotic (disk-shaped) LCs: N_D = nematic discotic, N_C = nematic columnar, D_{ho} = discotic hexagonal ordered, D_{hd} = discotic hexagonal disordered.

through the monolayer.[3, 4] If the ordered monolayer structure is retained during the transfer process, these so-called Langmuir–Blodgett (LB) multilayers are characterized by molecularly defined thickness, defined anisotropic arrangement of the amphiphiles within the layers, and defined surface structure (Fig. 3). Therefore these ultrathin organic

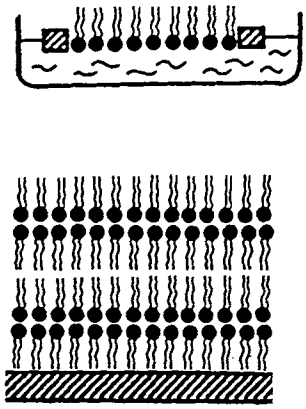


Fig. 3. Scheme of monolayers and Langmuir–Blodgett multilayers.

films are valuable systems for scientific studies, and many potential technical applications have been proposed.[4, 5]

The formation of monolayers is not restricted to standard amphiphiles. In principle any combination of the number of head groups and of hydrophobic chains is possible. Thus with hydrocarbon wing groups and polar cores, many discotic LCs meet the criteria of amphiphiles, even if they appear to be rather exotic. In fact, in the search for functionalized monolayers and multilayers, many rigid disk-shaped molecules have been investigated since the 1930s, in particular porphyrins and phthalocyanines.[3–5]

3. Theoretical Considerations on the Molecular Packing of Discotic LCs in Monolayers and Multilayers

The major interest in monolayers and LB-multilayers of discotic LCs derives from their "exotic" molecular shape. It is speculated as to whether this shape can modify the self-organization at the air–water interface to produce thin films of new structure. Perhaps, with a combination of liquid crystalline behavior and amphiphilic self-organization this can be achieved, as proposed in the concept of "amphotropic systems".[6] These ideas are illustrated in Figures 4 and 5.

When spread on the water surface, discotic LCs can orient in two extreme arrangements called "side on" and "edges on". With the wing groups acting as hydrophobic chains, four types of arrangements of the discotic LCs must be considered which are referred to as types A, B, C and D.

Through the deposition of the monolayers, four types of LB-multilayers of different structure can be produced, corresponding to the monolayer arrangements A–D.

Type A arrangement preserves the conformation of the discotic LCs in the bulk columnar phase, reduced to two-dimensions. Deposition of such monolayers, with the discotic cores of subsequent layers in register, would lead to columnar LC phases with molecularly defined heights of the columns[7] (Figs. 4a, 5a).

Type B arrangement (Figs. 4b, 5b) corresponds to classical amphiphilic behavior, as the disk-shaped core represents the polar part of the molecule. In this case, the conformation deviates considerably from the one in the bulk LC phase. The amphiphilic character is dominant. Deposition of type B monolayers produces the sandwich bilayer structure of classical LB multilayers, i.e. a structure similar to the smectic mesophases of rod-shaped LCs. Hence in bulk, unknown smectic phases of discotic LCs may be obtained via self-organization due to their amphiphilic character.

The "edge on" arrangements C and D imply that intermolecular interactions between the disk-shaped cores take place. In the special case of type C, strong interactions are required as some hydrophobic wing groups have unfavorably close contact with the water (Figs. 4c, 5c). That is, the discotic LC character of the molecules dominates the amphiphilic character. Such strong interactions may cause the

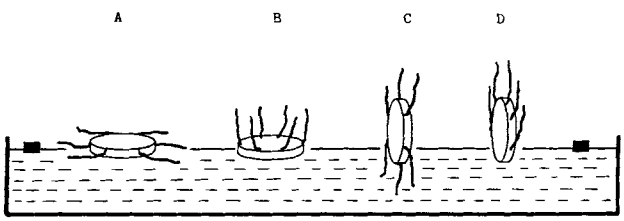


Fig. 4. Possible arrangements of discotic LCs at the gas–water interface: A = side on, chains random, B = side on, chains oriented, C = edge on, chains random, D = edge on, chains oriented.

discotic cores to form stacks, as seen for columnar mesophases (Fig. 2). If such "floating columns" are aligned in the monolayer, two-dimensional nematic columnar mesophases could be formed. If, however, such columns are deposited in register to LB-multilayers, thin columnar phases are produced where the columnar long axis is parallel to the surface of the support (Fig. 5c).

Type D arrangement (Figs. 4d, 5d) represents the compromise between self-organization due both to the amphiphilic and the discotic character. At the same time the interaction of the hydrophobic wing groups with water is small, whereas the interaction between the disk-shaped cores is fairly strong. As discussed for type C, type D arrangement would enable the formation of "floating columns" of the disks, with the possibility of two-dimensional nematic mesophases. Deposition of type D monolayers would create a novel hybrid structure of simultaneous columnar and smectic character (Fig. 5d).

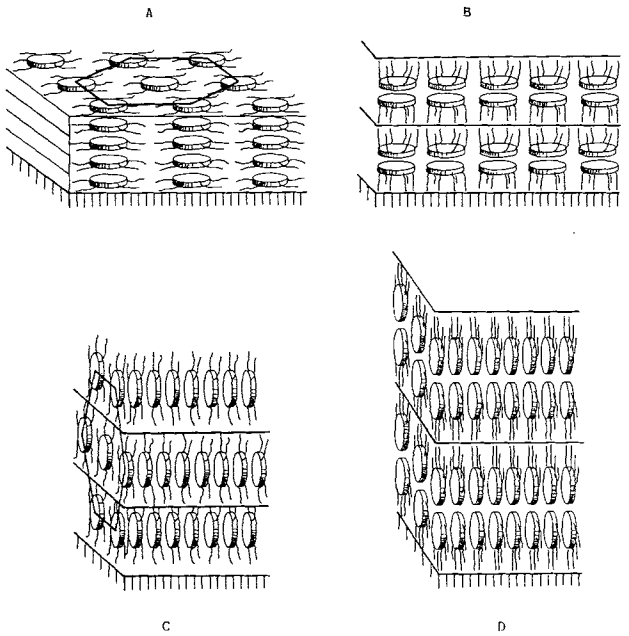


Fig. 5. Hypothetical structures of Langmuir-Blodgett multilayers obtained from discotic liquid crystals: A = side on, chains random, B = side on, chains oriented, C = edge on, chains random, D = edge on, chains oriented.

The monolayer and multilayer structures presented in Figs. 4 and 5 are only hypothetical, representing the "ideal cases". Intermediate or less ordered arrangements are possible, and three-dimensional aggregation may successfully compete with monolayer formation. Nevertheless, the possibility of designing such ordered structures of molecular dimensions is intriguing.

In addition to the unique structural combinations of liquid crystalline and amphiphilic structures, multilayers of many discotic LCs will be useful from the classical point of view as well. They could provide the particular properties expected from large non-liquid crystalline disk-shaped amphiphiles, e.g. improved thermal stability and conductivity or photoconductivity.[4, 5] In fact, the presence of the wing groups around the disk core in the discotic LCs will be an advantage in improving the solubility in the spreading solvents and probably decreasing the tendency to form microcrystallites at the gas–water interface.

4. Spreading Experiments with Discotic LCs

Up to now there have been only a few reports on spreading experiments with discotic LCs.[7–10, 17] Unfortunately, much of the experimental data available is ambiguous and therefore the conclusions drawn may be disputable. In general, surface pressure vs. area diagrams alone are not sufficient to determine the monolayer structure. Additional analysis, e.g. by ellipsometry, fluorescence microscopy, polarized UV/Vis/IR-spectroscopy, X-ray scattering or electron diffraction is required. Comparisons with the more plentiful investigations on non-liquid crystalline amphiphiles with disk-shaped moieties, e.g. porphyrins[11] and phthalocyanines, may prove to be helpful, but many of those results are also controversial.

Despite all shortcomings in monolayer experiments and their discussion, the present data suggest that extended hydrocarbon wing groups and strongly polar groups favor the "side on" arrangement of the disks, i.e. classical amphiphilic behavior, as observed for compound **6**.[10, 17] In contrast, weakly polar groups and rather short wing groups apparently favor "edge on" arrangements.[8] However, if the wing groups get too short, and the interaction of the disks too strong, three-dimensional crystallization may occur, as found for compound **2**.[12] In fact, the preferred arrangement of a discotic LC seems to depend on a subtle balance in the molecular architecture. The spreading behavior of the triphenylenes **2** and **3** may serve as such an example.[8] Thus, appropriate molecular design may allow us to control the type of self-organization in the monolayers.

5. LB-Multilayers of Discotic LCs

Reports on LB-multilayers of discotic LCs[8–9, 12] are even rarer than monolayer studies. As many of the monolayers are very stiff, deposition by the LB-technique can be difficult to achieve.[9] Successful transfer has been reported for triphenylenes **3** and **4**.[8] The presence of Bragg diffraction peaks in the X-ray data of the deposited LB-films (rarely observed in multilayers of disk-shaped amphiphiles) demonstrates an ordered layered structure, exemplifying the usefulness of discotic LCs for LB-multilayers. Their detailed structure is not yet clear, although the X-ray data of these triphenylene multilayers points to different types of arrangement of the discs such as type B for **4** and C for **3**.[8]

Interestingly, optical in-plane anisotropy has been observed in LB-multilayers of some phthalocyanines,[13, 14] supporting a two-dimensional nematoid arrangement of columnar stacks (implying types C or D). However, such in-plane anisotropies have recently been reported for the monolayers and multilayers of many amphiphiles,[5] and thus seem not to be unique for disk-shaped amphiphiles. The explanation of the in-plane anisotropy is still controversial.

6. Polymeric Discotic LCs

Because of the scarcity of data on low molecular weight discotic LCs, it is difficult to predict how polymeric discotic LCs will behave. The spreading behavior of classical polymeric amphiphiles is more complicated than that of their corresponding monomers,[3, 6] and this will also be true for the spreading behavior of monomeric and polymeric discotic LCs. If monolayer formation is still possible, a stabilization of the "edge on" arrangement of the disks may be expected. In particular, stack formation could be enhanced using a central polymer backbone.[15] However, with little data available,[12] it seems premature to discuss in depth the spreading of polymeric discotic LCs.

An alternative way to tailor "edge on" arranged monolayers may be the formation of charge-transfer complexes. The enhanced formation of molecular stacks and columnar mesophases by charge-transfer complexation has recently been shown in bulk discotic LCs,[16] and perhaps this method can be transferred to monolayers of discotic LCs.

7. Summary

The field of monolayer and multilayer films of discotic LCs is at its very beginning. The scope and limitations of this preparation method have not yet been explored, and little is known about the structures obtainable. However, the potential access to extraordinary, ordered thin films is fascinating, and will stimulate research in the future.

[1] a) S. Chandrasekhar, B. K. Sadashiva, K. A. Suresh, *Pramana 9* (1977) 471. b) J. Billard in W. Helfrich, G. Heppke (Eds.): *Liquid Crystals of One- and Two-Dimensional Order*, Springer, Berlin 1980. c) C. Destrade, P. Foucher, H. Gasparoux, N. Huu Tinh, A. M. Levelut, J. Malthete, *Mol. Cryst. Liq. Cryst. 106* (1984) 121.

[2] a) S. Chandrasekhar, B. K. Sadashiva, K. A. Suresh, N. V. Madhusudana, S. Kumar, R. Shashidar, G. Venkatesh, *J. Physique Coll. 40* (1979) C3-120. b) B. Kohne, K. Praefcke, *Chimia 41* (1987) 196. c) J. Billard, J. C. Dubois, N. Huu Tinh, A. Zann, *Nouv. J. Chim. 2* (1978) 535. d) C. Destrade, N. Huuh Tinh, H. Gasparoux, J. Malthete, A. M. Levelut, *Mol. Cryst. Liq. Cryst. 71* (1981) 111.

[3] a) G. L. Gaines: *Insoluble Monolayers at Liquid-Gas Interfaces*, Wiley Interscience, New York 1966. b) G. L. Gaines: *MTP International Review of Science, Inorganic Chemistry 7*, Butterworth, London 1973, p. 1.

[4] a) G. G. Roberts, *Adv. Phys. 34* (1985) 475. b) T. M. Ginnai, *Ind. Eng. Chem. Prod. Res. Div. 24* (1985) 188. c) M. Sugi, *J. Mol. Electr. 1* (1985) 3. d) *Thin Solid Films* Vols. 68, 99, 132-134, 152 and 159-160.

[5] Proceedings of the 4th International Conference on LB-Films, 25.-29.4.1989 Tsukuba Japan, *Thin Solid Films*, in press.

[6] H. Ringsdorf, B. Schlarb, J. Venzmer, *Angew. Chem. Int. Ed. Engl. 27* (1988) 113; *Angew. Chem. 100* (1988) 117.

[7] a) F. Rondelez, D. Koppel, B. Sadashiva, *J. Physique 43* (1982) 1371. b) K. A. Suresh, A. Blumstein, F. Rondelez, *J. Physique 46* (1985) 453. c) F. Rondelez, J. F. Baret, A. G. Bois, *J. Physique 48* (1987) 1225.

[8] O. Albrecht, W. Cumming, W. Kreuder, A. Laschewsky, H. Ringsdorf, *Colloid Polym. Sci. 264* (1986) 659.

[9] a) N. B. McKeown, M. J. Cook, A. J. Thompson, K. J. Harrison, M. F. Daniel, R. M. Richardson, S. J. Roser, *Thin Solid Films 159* (1988) 469. b) M. J. Cook, N. B. McKeown, A. J. Thompson, K. J. Harrison, R. M. Richardson, A. N. Davies, S. J. Roser, *Chem. Materials 1* (1989) 287.

[10] a) C. Mertesdorf, H. Ringsdorf, *Liq. Cryst. 5* (1989), in press. b) D. Ducharme, R. Leblanc, P. Meller, C. Mertesdorf, H. Ringsdorf, C. Salesse, unpublished.

[11] A. Miller, W. Knoll, H. Möhwald, A. Ruaudel-Teixier, *Thin Solid Films 133* (1985) 83.

[12] L. Häußling, O. Karthaus, H. Ringsdorf, P. Tschirner, C. Urban, unpublished results.

[13] M. Fujiki, H. Tabei, T. Kurihara, *Langmuir 4* (1988) 1123.

[14] K. Ogawa, S. Kinoshita, H. Yonehara, H. Nakahara, K. Fukuda, *J. Chem. Soc. Chem. Commun. 1989*, 477.

[15] E. Orthmann, G. Wegner, *Angew. Chem. Int. Ed. Engl. 25* (1986) 1105; *Angew. Chem. 98* (1986) 1114.

[16] H. Ringsdorf, R. Wüstefeld, E. Zerta, M. Ebert, J. H. Wendorff, *Angew. Chem. Int. Ed. Engl. 28* (1989) 914; *Angew. Chem. 101* (1989) 934.

[17] J. Malthête, D. Poupinet, R. Vilanove, J. M. Lehn, *J. Chem. Soc. Chem. Commun. 1989*, 1016.

ADVANCED MATERIALS

"is a heady mixture of essays, review and research communications, news and conference data and it works admirably"

"is perhaps the journal one would most like to have delivered to a busy desk"

"the articles can be read in a few minutes, yet they communicate at the highest level and reflect the perception of their often-distinguished authors"

Nature 341 (1989) 369

Surface Analysis I

Imaging Surfaces, Electric Charges and Magnetic Domains with the Atomic Force Microscope

By Jürgen P. Rabe*

The atomic force microscope (AFM) provides a means to record images of surfaces on the atomic length scale.[1, 2] It is closely related to both the scanning tunneling microscope (STM) and the stylus profilometer, combining atomic resolution with the ability to image insulating materials. In the AFM an ultrafine tip is mounted on a small lever and brought into close proximity of the sample (Fig. 1). For high resolution imaging, the force between tip and sample is measured sensitively by the deflection of the lever, using either electron tunneling or some optical detection scheme. As the tip is scanned across the sample, a contour map of constant force can be recorded. For true non-contact imaging at lower lateral resolution, a shift in the resonance frequency of the lever is detected, giving contours of constant force gradient. The key feature of the AFM is its ability to measure extremely small forces. In order to achieve this, the lever has to be as soft as possible. At the same time, it should have a high resonance frequency in order to minimize its sensitivity to vibrational noise from the environment. The solution to this is miniaturization. Indeed, with microfabricated levers and an optical detection system, a force sensitivity of the order of 10^{-9} N in water and 10^{-7} N in air has been achieved.[3] The number of forces contributing to the net force are manyfold, ranging from hard core repulsion at very small distances through van der Waals attraction and capillary forces to long range electrostatic and magnetic forces. In practice there exists a balance of several contributions.

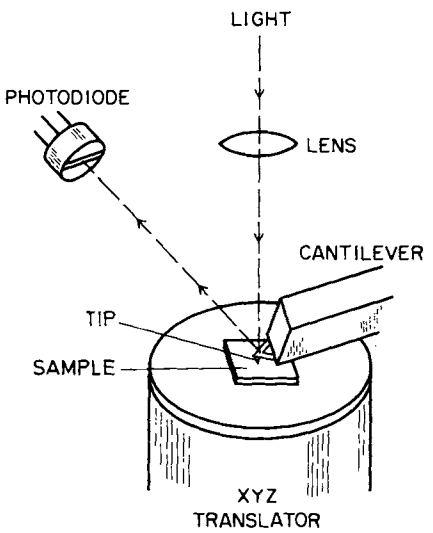


Fig. 1. The atomic force microscope (AFM) detects the vertical motion of the tip which is proportional to the force that the tip applies to the surface of the sample. The XYZ translator moves the sample in all three directions in space. In the particular detection scheme shown here the deflection of the laser beam, which is reflected from a cantilever, is measured sensitively by a two segment photodiode. The measurements can also be performed in fluid ambients like water [3].

Atomically resolved surface images have been obtained on both conducting and non-conducting materials like graphite,[2] boron nitride[4] or mica.[5] Also, the local step structure on some ionic crystal surfaces has been studied. For example, the (111) and (100) surfaces of chemically polished AgBr single crystals show some interesting differences.[6] While on the (111) surface, individual steps coinciding with both low index directions $\langle 0\bar{1}1 \rangle$ and $\langle 1\bar{2}1 \rangle$ were found, the (100) surface is dominated by crossing steps. These results may help to understand the different preferential J-aggregation of dyes occuring on these surfaces, a process which is of importance in photographic emulsion technology.

The ability of the AFM to image non-conductors enables it to be applied to organic materials, provided that the forces involved are small enough not to disrupt the sample. That this is indeed possible has been demonstrated for the surface of an amino acid crystal, DL-leucine,[7] and for a layer of polyalanine on glass.[5] Imaging an individual organic molecule, however, is even more demanding, since a single molecule can diffuse across the surface, particularly under the influence of the AFM tip. The adsorption energies must be particularly small if one wants to avoid a large distortion of the adsorbate on the surface. This, in turn, means that the forces applied by the AFM tip should be equally small. In this respect it is important to realize that surfaces in air are typically covered with an adsorbate layer of water and unknown contaminants causing a capillary force for small tip-

[*] Dr. J. P. Rabe
Max-Planck-Institut für Polymerforschung
Postfach 3148, D-6500 Mainz (FRG)

to-sample gaps which can exceed the externally applied forces. An elegant way to eliminate this force, besides operating in ultra high vacuum, appears to be operation under water or other fluid ambients.[3] Figure 2 shows ten AFM images of the clotting of the human blood protein, fibrinogen, adsorbed on mica before (A) and after introduction of the clotting enzyme thrombin into the aqueous ambient (B through J).[5] The role of the thrombin is to unmask some polymerization sites on the fibrinogen. The resulting fibrin monomers polymerize to form larger aggregates. Attempts to obtain high resolution images of single fibrinogen molecules suffered from a commonly encountered problem in both STM and AFM, namely that the adsorbates did not adhere well enough to the mica. However, as the fibrin monomers polymerized into the larger aggregates, they were more reproducibly imaged (Fig. 2B). The aggregates could still move, growing larger and connecting to each other (Figs. 2C through F) until a single chain spanned the whole field of view (Fig. 2G). Next, a second chain grew adjacent to the first (Fig. 2H), then a third (Fig. 2I) and finally nearly the whole field of view was covered with a fibrin net (Fig. 2J). While the resolution in these images is considerably lower than in the examples mentioned above, the results demonstrate the potential of the AFM to study processes occurring at the interphase between a solid and a liquid at molecular resolution and in real time. Also, higher resolution images may be achievable with microfabricated tips which are currently under development. A more fundamental limitation, namely the motion of the adsorbate on the surface may be circumvented by imaging in more viscous fluids or by lowering the temperature.

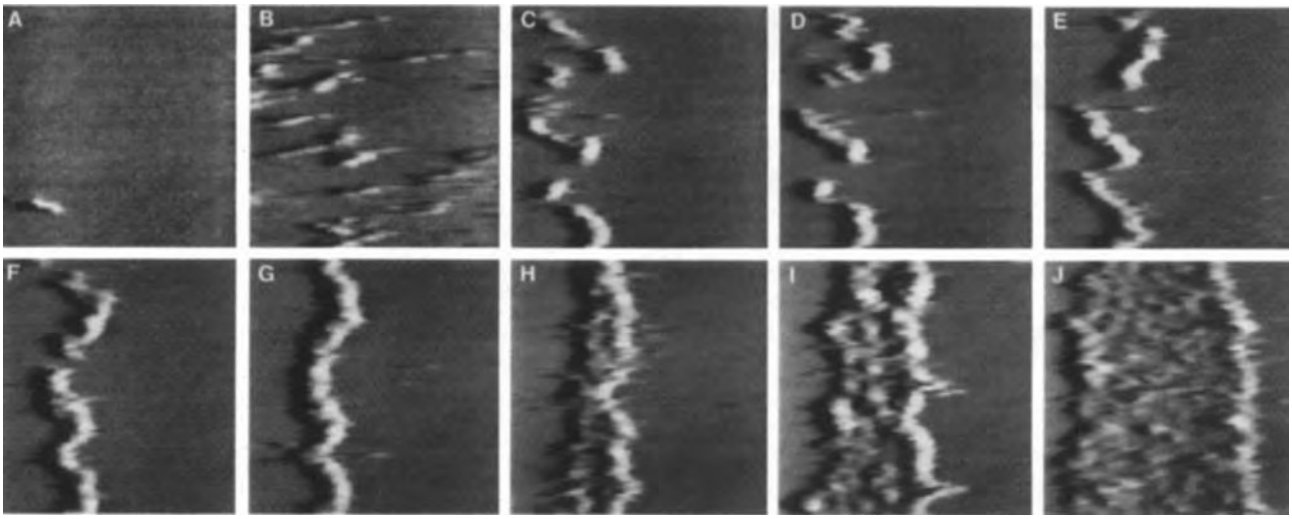


Fig. 2. Ten AFM images taken from a video tape that show clotting of the blood protein fibrinogen in real time. The images were selected from before introduction of the clotting enzyme thrombin (A), and at various times after its introduction between 9 min (B) through 33 min (J). Each image area is 450 nm × 450 nm [5].

The ability of the AFM to measure minute forces cannot only be used to image surface structure but also to elucidate other surface properties, for example, friction on an atomic scale.[8] Also intriguing is the imaging of electromagnetic forces at surfaces. Compared to the van der Waals force, electromagnetic forces are long range, i.e. they are dominating for large tip-to-sample separations. This makes imaging



Jürgen Rabe studied physics at RWTH Aachen, gaining his Diploma in 1981, and at the Technical University in Munich where he completed his doctoral work in 1984. He then spent two years as a Postdoctoral Fellow at the IBM Almaden Research Center in San Jose, California before taking up his present position on the Research Staff of the Max Planck Institute for Polymer Research in Mainz, FRG. His research interests include the chemical physics of ultrathin organic films, STM and related microscopies, and vibrational spectroscopy. From now on he will be writing regularly for Advanced Materials on aspects of surface analysis.

possible in a true non-contact mode. Recently it has been demonstrated that the AFM can be used to deposit and image localized charge on an insulator with a lateral resolution surpassing that of other currently available techniques.[9] A lever is oscillated near its resonance frequency at a tip-to-sample distance of the order of 100 nm. As the tip is scanned across the sample, variations in the tip-to-surface force gradient will alter the effective spring constant of the lever. The resulting change of its resonance frequency is detected as a change in the amplitude of the tip oscillation. If local charge is present on the surface, the tip will feel an additional force due to the coulomb attraction of the charge to its image charge in the tip. The measured force gradient contour will have a peak at the location of the charge. Moreover, by applying a voltage to an electrode behind the sample it is possible to determine the sign of the charge present. The amount of charge can be estimated by measuring the force as a function of distance. Initial experiments[9] have demonstrated the ability of the AFM to deposit and detect low charge levels on insulator surfaces with a lateral resolution of the order of 1 μm. The sensitivity was estimated to be about 100 electrons. The charge had been deposited by applying a voltage pulse to the tip. Interestingly, while charge on polymethylmethacrylate (PMMA) and sapphire samples was observed to decay over approximately 1 h in air, charge on mica and quartz appeared to dissipate so rapidly that it was impossible to obtain an image of a locally charged region.[9] An improved technique, employing a modulation of the bias of the back electrode on the sample[10] resulted in a further increase in resolution to 0.2 μm with an estimated sensitivity of 6 ± 3 electrons. With this, bipolar charging after contact charging has been observed in an area of about 10 μm diameter.[10] This is a surprising result, which could not be observed in previous tribocharging experiments with the lower lateral resolution. It may, however, help us to understand the spot-to-spot variations found in these earlier experiments. The above mentioned high resolution data may be complicated by the fact that they were obtained in air, with water possibly contributing to charge mobility at the surface. However, they demonstrate the ability of AFM to address very old but still unresolved problems on the underlying mechanisms in contact- or tribo-charging.

Magnetic forces can also be measured with a very similar setup, provided a magnetic tip of, for example, iron or nickel is used. Figure 3a shows an image of magnetic domains in a 2.5 μm thick NiFe film and Figure 3b shows the corresponding Kerr image, giving essentially the same structure.[11] Clearly, entire domains and domain walls are imaged with the AFM with submicron resolution. The inset in Figure 3 shows the direction of magnetization in each domain inferred from the images. The tip was scanned at a constant height of 150 nm above the surface, and it was concluded that the field of the tip did not move the walls significantly in this comparatively thick film. The image contrast at the wall is attributed to the sense of the rotation of the magnetization across the wall. However, a detailed interpretation of the complicated magnetic structure of domain walls in soft magnetic materials is still difficult. For a thinner film (30 nm), domain walls appeared to be narrower and more susceptible to stray magnetic fields. Therefore, the tip

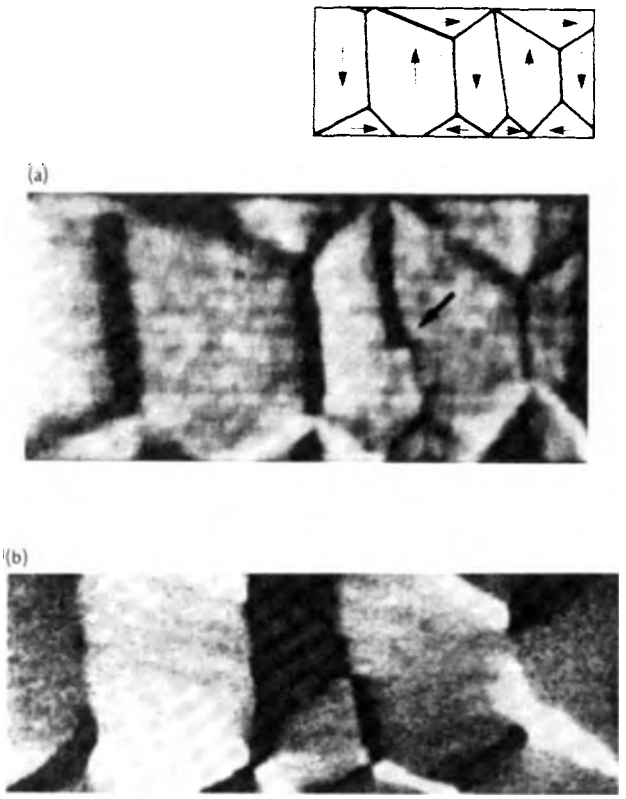


Fig. 3. (a) Magnetic force microscopy image and (b) Kerr image of domains in permalloy film. The imaged region is 50 μm × 30 μm; magnifications differ in horizontal and vertical directions. Arrow marks the location of a Bloch line [11].

could induce wall motion when brought sufficiently close to the surface.[11] While this may be disadvantageous in some cases, it is anticipated, that it will provide a means for studying magnetic properties such as wall motion coercivity on a microscopic scale. As far as resolution is concerned, a magnetic image of the domain pattern on a TbFeCo thin film on silicon has been obtained with a resolution of approximately 25 nm.[12] Clearly, a better understanding of the magnetic domain structure is of great fundamental and also technological interest as performance in magnetic recording devices depends on the detailed micromagnetic structure of the recording medium.

The results given above demonstrate the wide variety of forces which can be measured by the AFM on small lateral length scales. For high resolution surface imaging the advantage of AFM over STM is the ability of the former to image insulators. While this appears particularly promising for or-

ADVANCED MATERIALS

ganic systems, a further reduction of the forces applied during scanning is desirable.

[1] G. Binnig, C. F. Quate, C. Gerber, *Phys. Rev. Lett. 56* (1986) 930.
[2] G. Binnig, C. Gerber, E. Stoll, T. R. Albrecht, C. F. Quate, *Europhys. Lett. 3* (1987) 1281.
[3] A. L. Weisenhorn, P. K. Hansma, T. R. Albrecht, C. F. Quate, *Appl. Phys. Lett. 54* (1989) 2651.
[4] T. R. Albrecht, C. F. Quate, *J. Appl. Phys. 62* (1987) 2599.
[5] B. Drake, C. B. Prater, A. L. Weisenhorn, S. A. C. Gould, T. R. Albrecht, C. F. Quate, D. S. Cannell, H. G. Hansma, P. K. Hansma, *Science 243* (1989) 1586.
[6] H. Heinzelmann, E. Meyer, H. J. Güntherodt, *Surf. Sci. 221* (1989) 1.
[7] S. Gould, O. Marti, B. Drake, L. Hellemans, C. E. Bracker, P. K. Hansma, N. L. Keder, M. M. Eddy, G. D. Stucky, *Nature 332* (1988) 332.
[8] C. M. Mate, G. M. McClelland, R. Erlandson, S. Chiang, *Phys. Rev. Lett. 59* (1987) 1942.
[9] J. E. Stern, B. D. Terris, H. J. Mamin, D. Rugar, *Appl. Phys. Lett. 53* (1988) 2717.
[10] B. D. Terris, J. E. Stern, D. Rugar, H. J. Mamin, unpublished results.
[11] H. J. Mamin, D. Rugar, J. E. Stern, R. E. Fontana, Jr., P. Kasiraj, *Appl. Phys. Lett. 55* (1989) 318.
[12] H. K. Wickramasinghe, *J. Vac. Sci. Technol. A* (Proceedings of STM 89, January 15, 1990, in press).

Low Temperature Deposition of a CaF_2 Insulator Layer on GaAs*

Over recent years there has been widespread interest in the development of alternative insulators for silicon and GaAs, especially where these might be obtained in epitaxial layer form to permit the production of multilayer semiconductor-insulator structures.[1-3] Several workers have reported the growth of epitaxial CaF_2 on silicon[4-6] and GaAs.[7-9] The major problems in obtaining good quality films lie in the lattice mismatch between the layer and substrate (0.6% for Si; 3% for GaAs) and the thermal conductivity mismatch (α $CaF_2 = 1.9 \times 10^{-5}\ K^{-1}$; α Si $= 4 \times 10^{-6}\ K^{-1}$; α GaAs $= 6.9 \times 10^{-6}\ K^{-1}$). For GaAs applications the former has been overcome, partially at least, by the use of solid solutions of CaF_2–SrF_2, the composition $Ca_{0.44}Sr_{0.56}F_2$ being perfectly lattice-matched to GaAs at 25 °C.[10] The thermal expansion coefficient differences between GaAs, CaF_2, and SrF_2 produce strain at the film/substrate interface during cooling from the growth temperature. In the case of high elastic modulus material such as CaF_2 and CaF_2-rich alloys this leads to cracking, whilst the more plastic SrF_2 and SrF_2-rich alloys deform by dislocation generation, so that the layer becomes a poor substrate for subsequent semiconductor overgrowth. The best solution to this problem lies in a reduction of a growth temperature to minimize cooling strains. This demands a growth system which permits transport and low temperature decomposition of a suitable precursor, which must nevertheless remain sufficiently stable to withstand premature thermal decomposition.

Benac et al.[11] have recently reported polycrystalline growth by pyrolytic decomposition of bis(pentamethylcyclopentadienyl)calcium $(C_5Me_5)_2Ca$ in either SiF_4 or NF_3 at 150 °C. This low decomposition temperature may, however, lead to handling problems. At the observed growth rates of 10–100 μm/hr the product is polycrystalline CaF_2 with a grain size of 20–50 μm but X-ray photoelectron (XPS) studies show relatively high impurity levels (approximately 18% carbon and 7% oxygen) in these films.

Recent work at RSRE Malvern and Queen Mary College London has led to the development of a new approach to the deposition of CaF_2 on GaAs at low temperatures, which combines the advantages of the organometallic approach with those of photochemically-induced precursor decomposition. This permits the use of thermally stable precursors, thus reducing the risk of premature reaction outside the required deposition zone, and of gas phase reactions which generally result in poor epitaxy. Careful design of the photochemical reactor and the use of suitable projection masking in the incident photon beam can then be used to promote selected-area deposition.

The process is based on the photochemical decomposition of bis(1,1,1,5,5,5-hexafluoro-2,4-pentanedionato)calcium(II), $Ca(hfac)_2$, (Fig. 1) using xenon lamp radiation in the 180–300 nm waveband. The precursor compound was developed and synthesized at Queen Mary College, London.[12]

The material is obtained in the form of a pale yellow powder which sublimes at approximately 100 °C. It is impor-

[*] Dr. A. W. Vere, Dr. K. J. Mackey, Dr. D. C. Rodway, Dr. P. C. Smith
Electronic Materials Division
Royal Signals & Radar Establishment (RSRE)
St. Andrews Road, GT. Malvern
Worcestershire WR14 3PS (UK)
Dr. D. M. Frigo, Prof. D. C. Bradley
Department of Chemistry, Queen Mary College
University of London, Mile End Rd.
London E14NS (UK)

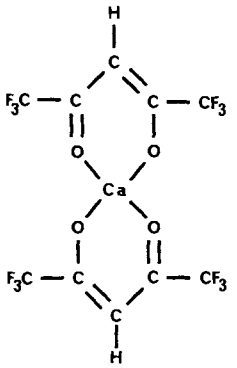


Fig. 1. Bis(1,1,1,5,5,5-hexafluoro-2,4-pentadionato)calcium(II) precursor for low temperature deposition of CaF_2.

tant to obtain the material in its anhydrous state as the hydrated or even partially hydrated compound does not appear to yield CaF_2 under the experimental conditions described here.[13] The material is thermally stable to approximately 300 °C, above which it can be pyrolytically decomposed to give CaF_2. In the photo-assisted decomposition process the precursor is transported from a bubbler held at 100 °C into a MOVPE reactor containing one or more substrates of GaAs heated to 100 °C (Fig. 2). The reactor pressure is approximately 10^{-1} Torr.

Radiation from a 450 watt xenon lamp is broad-band filtered (180–300 nm) and illuminates the substrate at normal incidence through an aperture in the furnace wall.

A deposited CaF_2 layer approximately 4000 Å thick is obtained at a deposition rate of around 30 Å min^{-1}. XPS analysis of the layer shows Ca and F peaks together with *small* carbon and oxygen (< 10%) peaks. X-Ray diffraction data indicate a polycrystalline CaF_2 layer with a high degree of preferred orientation. At this stage no attempt has been made to clean up the reactor or substrate prior to deposition and the polycrystallinity and impurity results are not unexpected. Work is now in progress to improve the layer structure. Further details of the photochemical process are awaiting publication.[14]

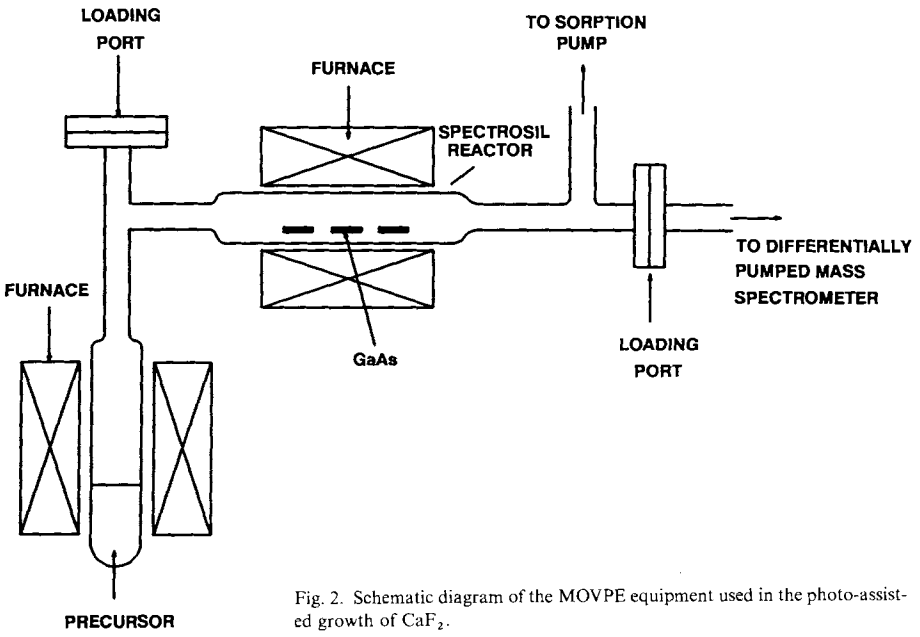


Fig. 2. Schematic diagram of the MOVPE equipment used in the photo-assisted growth of CaF_2.

[1] R. F. C. Farrow, P. W. Sullivan, G. M. Williams, G. R. Jones, D. C. Cameron, *J. Vac. Sci. Technol. 19 B3* (1981) 415–420.
[2] J. M. Philips, J. M. Gibson, *Mat. Res. Soc. Symp. Proc. 25* (1984) 381–391.
[3] A. Munoz-Yague, C. Fontaine, *Surf. Sci. 168* (1986) 626–634.
[4] H. Ishiwara, T. Asano, *Mat. Res. Soc. Symp. Proc. 25* (1984) 393–401.
[5] L. J. Schowalter, R. W. Fathauer, R. P. Goehner, L. G. Turner, R. W. de Blois, S. Hashimoto, J.-L. Peng, W. M. Gibson, J. R. Krusius, *J. Appl. Phys. 58* (1985) 302–308.
[6] J. M. Phillips, W. M. Augustyniak, *Mat. Res. Symp. Proc. 67* (1986) 115–118.
[7] P. W. Sullivan, J. E. Bower, G. M. Metze, *J. Vac. Sci. Technol. B3 (2)* (1985) 500–507.
[8] P. W. Sullivan, *Appl. Phys. Lett. 44* (1984) 190–192.
[9] S. Siskos, C. Fontaine, A. Munoz-Yague, *Appl. Phys. Lett. 44* (1984) 1146–1148.
[10] H. Heral, L. Bernard, A. Rocher, C. Fontaine, A. Munoz-Yague, *J. Appl. Phys. 61* (1987) 2410–2412.
[11] M. J. Benac, A. H. Cowley, R. A. Jones and A. F. Tasch, Jr., *Chem. Mater. 1* (1989) 289–290.
[12] M. Faktor, D. M. Frigo, D. C. Bradley, K. J. Mackey, A. W. Vere, *Patent Application*, PCT/GB89/00338, London.
[13] M. Hassan, D. C. Bradley, K. J. Mackey, unpublished results.
[14] K. J. Mackey, D. C. Rodway, P. C. Smith, A. W. Vere, *Appl. Surf. Sci.*, in press.

Conference Reports

Ceramics in Maastricht

By Richard J. Brook *

The combination of a new society and a new conference center brings a special atmosphere to any meeting. This proved true on the grand scale for the first meeting of the European Ceramic Society which was held in Maastricht, Netherlands, over the week 18.–23. June 1989.

The Society itself was founded in 1987 following negotiations between a number of the national ceramic societies in Europe. The coming into existence of the Society was in part prompted by discussions which took place between the American Ceramic Society and representatives of the several European societies at which the need for a coordinating group in Europe was clearly recognized. European colleagues will remember with gratitude the high professional standards which the American Ceramic Society followed in promoting these discussions and in sharing in the ensuing debates; the example of close professional collaboration at the international level afforded by these contacts is a notable and happy one.

The European Ceramic Society currently counts eleven countries among its membership: Belgium, France, Germany, Italy, the Netherlands, Norway, Portugal, Spain, Sweden, the United Kingdom and Yugoslavia. A major role for the new Society will be the organization of the set of conferences which are to continue the tradition established by the Science of Ceramics series. The first such meeting took the form of this conference organized by colleagues from the Netherlands Ceramic Society and the Netherlands Ceramic Federation at Maastricht.

The Maastricht Exhibition and Congress Center is a recently built facility opened in the Netherlands to cater for the holding of exhibitions, conferences, and business functions. The center consists of a group of auditoria, conference rooms, and exhibition halls coordinated into a building which also provides a range of shops, restaurants, cafeterias, hotels, and banks. The general impression is not unlike that given by the best quality of international airport except in that the participants have for the most part a less harassed appearance. The combination of a modern conference center and a neighboring town possessing a highly individual and charming character of the more established kind (open air cafés, tree-lined streets, a friendly and animated population – mostly on bicycles, buildings of high distinction) served to provide an atmosphere eminently suitable for concentrated scientific and technological discussion.

[*] Prof. R. J. Brook
Max Planck Institute for Metals Research, Powder Metallurgy Laboratory
Heisenbergstrasse 5, D-7000 Stuttgart 80 (FRG)

The meeting itself covered all aspects of the subject of ceramics. Focus was provided by a series of keynote lectures devoted to principal subject areas. These included treatments of basic science (*F. Thévenot*), of engineering ceramics (*F. Thümmler*), of traditional ceramics (*J. E. Enrique*), of electronic ceramics (*L. Cross*), of bioceramics (*G. Heimke*), of standardization (*G. C. Padgett*), and of high temperature superconductors (*S. Horiuchi*). A further plenary session was devoted to a lecture on the subject of microstructures (*R. J. Brook*) given to commemorate the striking contribution made to ceramics science and engineering by Prof. *A. L. Stuijts*. Professor *Stuijts* is everywhere acknowledged as having been a key figure in the development of magneto- and electroceramic materials; his special ability to operate at the interface between industrial applications and academic science served to make him a universally respected colleague, and it is fitting that his name should be associated with a plenary lecture that will form a regular feature at the conferences of the new Society.

The meeting spanned a full week and comprised a mix of technical presentations, of posters, of industrial visits and of exhibits of products from all sectors of the ceramics industry. Despite the length of the meeting, there were occasions when levels of concentration of an almost superhuman character were required on the part of participants (the digestion of 180 posters in parallel with a number of set sessions during a single day). Provision of the industrial visits as a caesura on the Wednesday afternoon gave just the degree of variety required to sustain energies.

In technical matters the meeting covered all aspects of ceramics but, as is common on such occasions, a degree of dominance on the part of the non-traditional ceramics sector could be recognized (the actual distribution of contributions was 180 from basic science, 115 from engineering ceramics, 64 from electrical ceramics, 42 from traditional ceramics, 18 from biological aspects, 27 from superconductors, and 3 from standardization). The integration of such themes within a common discipline will remain an important task for the new Society.

Dutch colleagues are to be congratulated for the imagination and effort which they devoted to the meeting. The assembly of 450 papers, of 80 exhibitors and of 1000 participants into a single professional community within Europe is no easy task; the fact that the meeting gave such a clear impression of a coherent group of participants is in no small part due to the vigor and enthusiasm with which the organizers set about their task. The role of the new Society as it seeks

to define its purpose will in the early stages be largely determined by such milestone events as this conference. The atmosphere of this first meeting was highly encouraging in this regard.

Responsibility for the Society now passes to the German Ceramic Society whose president, Prof. *Hans Hausner*, has succeeded Prof. *Rudi Metselaar* as president of the European Ceramic Society. On the basis of this first meeting one can look forward with confidence to the successor which will be held in Germany in two years time. Those who participated in Maastricht can have been left with little doubt that conferences of the European Ceramic Society will become a regular and respected element in the European materials scene.

Large Area Chromogenics in Gothenburg

By Tord Eriksson *

An international workshop on Large Area Chromogenics took place at Chalmers University of Technology in Gothenburg, Sweden, during a very full day, June 5th. It was organized by CoAT AB, The Center for Materials Science, and Chalmers Industri Teknik under the sponsorship of the Swedish Board for Technical Development. Eight invited researchers lectured on the state of the art of chromogenic materials. 50 invited representatives from industry listened and contributed to the ensuing discussions from, in particular, the applications point of view.

The workshop was opened by Professor *Olaf Meyer*, Head of the Eureka secretariat in Brussels, who gave a very much appreciated lecture entitled "Risk financing of hightech start-ups, especially in international cooperation".

The conference aimed at giving some answers to the following questions. What are the prospects and challenges for chromogenic materials? Where is the frontier in research? What are the applications, and when and how can they be commercially realized?

What is a chromogenic material? The question is certainly relevant since the concept was only recently introduced. The word comes from the greek χρωμα = color and γενεσιζ = creation. Chromogenic materials change their color – or more general optical properties such as transmission, reflection and absorption – due to an external influence such as applied voltage, incident light, temperature etc. These materials are classified as electrochromic, photochromic, thermochromic and some liquid crystal based materials.

Chromogenic materials could in the future be used to regulate the flow of light and/or solar energy through a window so that a suitable illumination and climatic comfort could be achieved. Other applications for these materials involve large area displays, rear view mirrors for cars, sun roofs etc.

[*] Dr. T. Eriksson
CoAT AB, Datavägen 21 B
S-43632 Askim (Sweden)

Professor *Granqvist* gave in his lecture a general insight into the prospects and challenges. A lot of applications sectors can be identified: architectural (energy efficiency, lighting), automotive (energy efficiency, anti-dazzling), aerospace (temperature control), information (displays of various kinds), military (camouflage/chamelionism). Technical problems still have to be solved before any commercialization is feasible. Large modulation of the optical properties is desired in many applications. The durability is sometimes an important requirement (in windows). The material has to be integrated in devices. A challenge of a more non-technical kind is that this technology is very interdisciplinary in nature. This means that, for instance, physicists and electrochemists have to cooperate to achieve an understanding of the coloration mechanism of electrochromic materials.

A lot of basic research has to be done in order to understand the mechanisms behind electrochromism. Dr. *Carl Lampert*, Lawrence Berkeley Laboratory, emphasized some research issues. The materials have to be characterized: optical properties, electrical properties, structure and chemistry, determination of coloration mechanism and overall stability. In addition a number of hitherto neglected materials should be studied. As to the complete devices the following aspects have to be considered: compatible ion storage electrodes, ion conductors for small positive ions such as $Li^{\oplus}$, $H^{\oplus}$, $K^{\oplus}$, polymeric electrolytes for lamination (an all solid state device is desirable), development of fabrication techniques, determination of device operating characteristics and stability testing of prototype devices.

Dr. *N. Lynam*, Donelly Corp., lectured on applications for electrochromic materials. Donelly is producing an electrochromic rear view mirror for cars. The design of such a device differs from that intended for a window in that it is not transparent but reflecting. The materials choice is also simpler since not all layers in the device have to be transparent.

ADVANCED MATERIALS

Dr. *Montgomery*, General Motors Res. Labs, reviewed the various existing liquid crystal systems and concentrated on those appearing to be most suited for large area switching devices. The polymer-dispersed and encapsulated liquid crystal films are either opaque (scattering) or transmitting, depending on the mismatch or match of the refractive indices of the liquid crystal particles and the host polymer. The operating temperatures are limited to the range $-20\,^{\circ}C$ to $+100\,^{\circ}C$. The response time makes them useful for most outdoor applications such as: solar control, automotive privacy, signs and eventually automotive displays. The on-state transmittance ($\sim 65\%$) restricts their use in areas where higher transmittances are required: windshields in cars and windows in buildings. For the future it seems important to reduce haze, increase durability, reduce operating voltage and improve solar attenuation characteristics so that this technology can find applications beyond its present technical limits.

Photochromism can be defined as a light-induced reversible photochemical process which results in a color change. The photochromic systems can be classified as either inorganic, organic, or those applying photophysical processes. Dr. *N. Chu*, American Optical Corp., suggested the following candidate materials: photochromic glasses, photochromic plastics activated by silver halides, and photochromic plastics activated by spirooxazines. The spirooxazines change from colorless to blue. They could find applications both in automotive windshields and sunroofs as well as for retrofit polyester films in glazings and window shades. However, the R&D program for the spirooxazines seems still to be in its infancy. The temperature sensitivity may be a problem, particularly in automotive applications. Also the light fatigue resistance limits the product lifetime and needs to be improved for window applications.

Dr. *T. Hjertberg* reported on research on conducting polymers. He identified the problems involved as: low stability, difficulties in processing due to bad mechanical properties and lower conductivity than desired. Dr. *O. Wennerström* reported on photochromic effects in organic materials.

A program that has caught a lot of interest is that reported by Professor *T. Lagervall*. His ferroelectric liquid crystal devices have an extremely short switching-time in addition to high contrast angles. This technology has already been commercialized by Canon for high definition information screens.

Professor *C.-G. Granqvist* reported on research carried out on a new electrochromic device based on Li_xWO_3 and VO_5. A new polymeric electrolyte with adhesive properties is applied as a lamination material in a five layer structure. He also reported on some very interesting results on thermochromic coatings made of VO_2. However, durability still has to be verified before marketing. The electrochromic device has reached the point of process development which has been triggered by the advent of the new solid polymeric electrolytes.

The workshop on Large Area Chromogenics was a very exciting and important meeting. Most intriguing is the fact that this area involves a large amount of high level basic research and will have a huge potential impact on daily life when this technology enters the market. It seems to be a supreme example of the synergetic effects achieved by combining academic research with industrial product development.

Storage and Transfer of Molecular Information in Strasbourg

By Jean-Paul Behr*

The European Parliament in Strasbourg housed the first congress "Espaces Européens des Sciences" from July 2–6, 1989. This symposium was organized by Fondation Alsace under the scientific direction of *J. M. Lehn* and *P. Chambon* and made possible the meeting of some thirty world renowned biologists, chemists and physicists to think over a common theme: "Storage and Transfer of Molecular Information". Although the time schedule was planned to imbricate disciplines and research fields, all lectures were centered on recognition processes at the molecular level, involving either the complex functions that workers in contemporary biology are trying to understand, or the highly elaborate molecules or molecular assemblies that chemists are able to make and handle, or approaches to the study of molecular signals and addressing that physicists are developing.

G. H. Khorana (MIT) opened the symposium by showing how light is transduced into chemical signals through rhodopsin molecules in highly organized systems as different as the eye's visual receptor cell and a photosensitive bacteria. The cascade of events in the former system was followed further down to the level of the nerve by *L. Stryer* (Stanford)

[*] Dr. J.-P. Behr
Institut Le Bel
Strasbourg (France)

whereas *M. Chabre* (Grenoble) proceeded to unravel the short term memory and signal amplification brought about by transducin; Other guanosine triphosphate (GTP)-binding proteins acting as intracellular messengers were reviewed by *Y. Kaziro* (Tokyo).

Soon it became clear that the crucial regions where things happen for biologists, chemists and physicists are liquid cristalline or solid-liquid interfaces. Electronic connection of the interior of redox enzymes to an electrode was cleverly done through a molecular charge relay by *A. Heller* (Austin) and his presentation was followed by other solid state aspects of information transfer (*H. C. Wolf*, Stuttgart; *H. McConnell*, Stanford). Oriented molecular films were reviewed by the pioneer of monolayer assemblies (*H. Kuhn*, Tschingel); chemical variations on bilayer membranes were introduced by *T. Kunitake* (Kyushu), and *H. Ringsdorf* (Mainz) reported in a humorous manner how these membranes could be made to perform complex molecular recognition functions. Supramolecular chemistry was brilliantly reviewed and illustrated with intertwined molecules by *F. Stoddart* (Sheffield).

Then a major question was raised. Are molecular computers feasible? This challenging call for new molecules was answered in the affirmative on a theoretical background (*J. Hopfield*, Caltech) but many technical difficulties appear at the interface between the molecular and macroscopic worlds (*D. Haarer*, Bayreuth—see the Editorial Essay in this issue) although the scanning tunneling microscope should allow us to address single molecules (*B. Michel*, IBM Rüschlikon). On the biomimetic side, *A. Eschenmoser* (ETH Zürich) and *C. Hélène* (Paris) have worked on chemical modifications of nucleic acids, whereas present and putative possibilities for tailored catalytic antibodies were presented by *R. A. Lerner* (La Jolla).

Immune response and morphogenesis are overwhelmingly complex physiological processes, yet after the lectures of *G. Edelman* (New-York) on topobiology, *R. Axel* (Columbia) on membrane receptors, and the more structural approach of *J. Strominger* (Harvard), even the journalists in the audience knew about cell to cell communication.

Where is the genetic information of living organisms stored, and how is it processed? Before the most eminent molecular geneticists took over, *M. Eigen* (Göttingen)



showed how the genetic code and self replicating molecules could originate, and *M. Lahav* (Rehovot) presented elegant interfacial crystallization experiments able to amplify chirality in a non-chiral environment. Then, *R. E. Dickerson* (UCLA), *S. C. Harrison* (Harvard), *A. Rich* (MIT) and *M. Ptashne* (Harvard) presented the various structural aspects of the regulation of gene expression at the transcriptional level, and *T. Steitz* (Yale) gave structural details of a tRNA synthetase. tRNA complexes are involved in translation of the genetic code.

The symposium ended with *S. Numa* (Kyoto) and *J. P. Changeux* (Paris) lecturing on a topic close to the first one: signal transfer in living systems, in this case, neurotransmitter receptors. On July 6, at 8 p.m., after some 35 hours of presentations and interdisciplinary discussions, the lecture theater was still full, a sign of the success of this meeting. This prompted *M. Neitzert*, President of Fondation Alsace (with the financial support of GMA, Matra, Rhône-Poulenc and Squibb) to plan the second meeting of this series for next year.

International Conference on Synthetic Metals (ICSM '90), 3–7 September 1990 in Tübingen, FRG

The conference will provide an interdisciplinary forum for the discussion of recent experimental and theoretical results in physics, chemistry, and the application of all synthetic metals (low-dimensional conductors). Sessions on the following topics are anticipated: Theory of organic conducting crystals, Synthesis and structure of new organic conducting crystals, Organic superconductors, Theory of organic conducting polymers, Synthesis and structure of organic conducting polymers, Properties of organic conducting polymers, Nonlinear optical properties, Pyropolymers and graphitic materials, Transition metal chalcogenides and oxides, Bronzes and other inorganic crystals, Other organic and inorganic conducting crystals, Ferromagnetic polymers and charge transfer salts, New low-dimensional materials, Application of synthetic metals.

Further information can be obtained from the German Chemical Society (GDCh) at the following address: GDCh, Dr. J. Wendenburg, Abt. Tagungen ICSM' 90, Varrentrappstr. 40, D-6000 Frankfurt 90, FRG, Telefax: 069/7917-475.

ADVANCED MATERIALS

Materials Science and Technology in Karlsruhe

By Bernd Eigenmann *

The scientific theme of the annual meeting of the German Society for Metals (Deutsche Gesellschaft für Metallkunde, DGM) held from May 16. to 18., 1989 in Karlsruhe (FRG) was "modern developments in materials science and materials technology". This title not only sketches out the course the DGM is intending to take in future, but also symbolizes the opening of the Society towards modern applications of metallic as well as non-metallic materials in materials science and technology. Since, in many cases, only compound materials of metallic and non-metallic components can meet the increasing specific requirements of modern structures, it appears necessary to include them into the field of activities. The subjects of many workshops of the DGM have already anticipated this trend. During this year's annual meeting, it was finally intended to symbolize the above described new developments in materials science and technology by changing the Society's name to German Society for Materials (Deutsche Gesellschaft für Materialkunde, DGM). This decision was supported by an overwhelming majority of the Society's members, and it terminated a process which lasted for more than a year in which the members of the Society tried to make up their minds about the consequences of the new requirements and tried to reconcile themselves with it.

At the opening ceremony, the president of the DGM, Prof. *G. Petzow* honored several members of the Society for their excellent research work. Prof. *Hans Warlimont* (Vacuumschmelze GmbH, Hanau) was awarded the Heyn Medal, the highest honor of the DGM, in recognition of his extraordinary contributions to the investigation of the basic principles of metallurgy and in the application of these principles to the development of metallic materials.

Dr. *Martin Bauser* (Wieland Werke AG, Ulm) and Prof. *Günther Sauer* (Hofmann KG, Wiesbaden) both received honorary memberships of the DGM for distinguished service to the Society, in particular for encouraging strong ties between industrial practice and scientific development.

The Tammann Medal was awarded to Prof. *Hans Paul Hougardy* (Max Planck Institute for Iron Research, Düsseldorf) recognizing his contribution to the quantitative understanding of structural transformations and their influence on stress in steel, and the Masing Memorial Prize went to Dr. *Werner Mader* (Max Planck Institute for Metals Research, Stuttgart) for his successful studies of the atomic structure of surfaces at oxide/metal boundaries.

[*] Dipl.-Ing. B. Eigenmann
Institut für Werkstoffkunde I, Universität Karlsruhe
P.O. Box 6980, D-7500 Karlsruhe (FRG)

In his annual report, the managing director of the DGM, Dr. *V. Schumacher*, pointed out that the spreading of the activities of the DGM to non-metallic materials would, however, not lead to an attempt to penetrate step by step into the field of research of other well-established scientific societies in Germany. The aim of the DGM was, according to Dr. *Schumacher*, rather to deepen interdisciplinary contacts and to promote common activities such as meetings, workshops, and conferences, and, of course, to establish and intensify personal contacts between DGM-members and other scientific organizations.

The annual meeting was terminated by a social evening, on the occasion of which not only a "Brigandebuffet" – whose roots in the history of Karlsruhe were explained by Prof. *E. Macherauch* – was offered, but also dancing, and finally Prof. F. *Thümmler* presented a humorous address to the ladies – especially the wives of scientists.

The annual meeting of the members was embedded in an impressive framework of scientific contributions. The conference was opened by a lecture traditionally dealing with a subject which is not related to materials science. Prof. *Wenzel* from the University of Karlsruhe, faculty of architecture, talked about the importance of new technologies for the renovation of old buildings. He explained different methods of reinforcing walls and entire buildings, using steel strings and cement and demonstrated how wooden structures can be reinforced either by wood or by steel. Special emphasis was laid on the refined techniques developed in Greece for the purpose of conserving ancient monuments.

During the conference, 10 plenary papers were presented dealing with the various aspects of modern developments in materials science and technology.

Prof. *Exner*, Max Planck Institute in Stuttgart, presented the advances in quantitative structure analysis. In his lecture, he discussed the stereometry, fractal geometry and mathematical morphology and pointed out the difficulties in describing complex dendritic structures of castings and pores in sintered materials.

Prof. *Cherdron*, Hoechst AG, Frankfurt, explained the chemical and structural differences between metals and organic polymers. The morphology and molecular structure of polymers was described and correlated with their properties. The theoretical aspects were well illustrated by a number of specific examples such as polymer liquid crystals, composites, and polymer alloys.

Generally, the properties of graphite are known. Up to now, however, they have only been exploited to a relatively

small extent. Prof. *Hüttinger*, University of Karlsruhe, showed that the high stiffness and toughness of this material up to high temperatures, due to the covalent bonding character in the graphite planes, offer potential applications, especially in the field of carbon fibers. On the other hand, it was shown that an economic production and use of these fibers as well as the minimization of their brittleness and their sensitivity to shear load parallel to the graphite planes still represents a challenge for both scientists and engineers.

Dr. *Meyer*, Thyssen Stahl AG, Duisburg, presented new developments in micro-alloyed steels. He showed that properties like the γ–α-transformation, texture formation, precipitation hardening, and yield strength can be varied over a wide range by small amounts of alloying elements, especially titanium. Good formability can be achieved as well as a high strength dual phase structure.

A survey of the most important methods of surface analysis was given by Dr. *Kirchheim*, Max Planck Institute, Stuttgart. He discussed the state of the art of AES, ESCA/XSP, SIMS, LEED, RHEED and the applications of these techniques to the study of catalyst surfaces, surface passivation, high temperature corrosion, and tribology. Moreover, he explained how inner surfaces can be analyzed, and how the effects of sintering additives in ceramics or the binding mechanisms of metal-polymer composites can be investigated.

Prof. *Holleck*, University of Karlsruhe, showed in an interesting way the relationship between the design and behavior of coatings. He explained the recent developments and trends in obtaining coatings by physical vapor deposition with improved properties, particularly emphasizing coatings with mixed phases, multilayer coatings and gradient coatings.

Prof. Dr. *Hougardy* gave an excellent survey of today's possibilities in calculating residual stresses and distortions resulting from the quenching and hardening processes of steels.

A review of the activities in developing superalloys was given by Dr. *Walser* from Sulzer AG, Winterthur. These efforts are mainly correlated with advances in aircraft and space technology where a permanent improvement of the performance of turbines and combustion chambers is needed. New materials can only be developed on the basis of an increasing knowledge of the influences of metal physics on the materials behavior. Besides the basic science, however, permanent improvements in production and application techniques of the materials are necessary.

Dr. *Riedel*, Fraunhofer Institute, Freiburg, reported on the modeling of deformation processes during the manufacturing and servicing of engine components. In this case, the term modeling has two meanings. On the one hand, the behavior of the component during manufacturing and service is described by means of numerical models, e.g. finite element calculations, and on the other hand, the derivation of macroscopic materials properties from microscopic models is attempted. For the time being, models for high temperature creep, which exceed the simple Newton creep model, are of particular interest. A model for ternary creep processes was presented, and examples for applications were given.

Finally, Prof. Dr. *Zum Gahr*, University of Karlsruhe, presented new results on the influence of the material used on friction and wear behavior, covering the field of metals, ceramics, and polymers. The wear mechanisms were illustrated, and the materials were classified with respect to their physical and chemical properties. Consequences on the wear behavior in the various tribological systems were explained, and optimized materials combinations were derived from this knowledge.

In addition to the plenary papers, 51 other papers and 145 posters were presented in 3 parallel sessions, covering the fields of plasticity, powder metallurgy, phase transformations, textures, recrystallization, fatigue, temperature resistance, surface layers, thermodynamics and constitution, engineering ceramics, computer aided modeling, fracture, high temperature fatigue, intermetallic phases, residual stresses, wear, interfaces, melting and crystallization, amorphous metals, superconductors, magnetism, composite materials, joining and cutting, and materials for nuclear technology.

The scientific program was enriched by a number of interesting visits to places of cultural and technological importance in and around Karlsruhe and, finally, by a well organized hiking tour through the Pfälzer Wald on Saturday. The wonderful sunny day made it possible to visit four castles in the surroundings of Nothweiler dating from the 12th to the 16th centuries.

Summarizing, one can say that the annual meeting of the DGM gave a well balanced survey of the state of the art in materials science and technology and also valuable insights into future developments.

1990 E-MRS Strasbourg Conferences: (Symposia)

Spring Meeting (May 29.–June 7. 1990)

A High-T_c Superconductor Materials
B Metal Matrix Composites
C Magnetic Thin Films, Multilayers
D Surface Modification and Coatings
E Surface Processing and Laser Assisted Chemistry

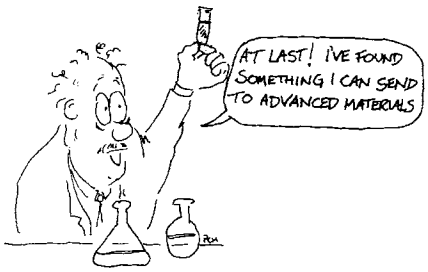
Fall Meeting (Nov. 27.–30. 1990)

A Semiconductors in Optoelectronics
B Nonlinear Optical Materials
C Wide Band-Gap Semiconductors
D Characterization of Compound Semiconductors

Details from Prof. *P. Siffert*, B.P. 20, F-67037 Strasbourg Cedex (France), Tel. 8828 6543, Fax 8828 0990

Materials Forum

Companies and individuals wishing their news and views on advanced materials issues and products to be considered for coverage in this section should send press releases, correspondence and other details, in English, to: Materials Forum, ADVANCED MATERIALS, P.O. Box 101161, D-6940 Weinheim, Federal Republic of Germany.



Conducting PPS-Compounds

The lowest electrical resistance of partially crystalline "conducting" thermoplastics previously achieved has been in the range 10^2 to 10^3 Ohm cm. Newly developed poly(phenylene sulphide) based compounds from Bayer, marketed under the trade name Tedur, combine a further reduced resistivity (to 1 Ohm cm) with high performance up to approx 200 °C and are stable at voltages of 220 V.

Additives such as metal fibers, carbon black and graphite improve the electrical properties of the polymeric materials. They are stable against oxidation and chemical decomposition and can possess a wide range of mechanical properties.

Several of the Tedur materials have been developed for antistatic applications, for example, housings in photocopiers, encapsulants for microchips or in the handling of flammable solvents. Others, of the conducting type will be applied in heating systems including preheaters for air/fuel mixtures.

Euromat '89

The Federation of European Materials Societies (FEMS) holds its first European materials conference from 22.–24. November 1989 in Aachen, FRG. The organization of the event is in the hands of the German Materials Society (DGM) and it is intended that the conference should bring together materials scientists from all over Europe and elsewhere to participate in plenary and short lectures, poster exhibitions and workshops. Six topics have been selected to from the basis of major symposia. They are: powder metallurgy, high temperature materials, materials in electronics, interface science, microscopy, and biomaterials.

The program and further information are available from DGM e.V., Adenauerallee 21, D-6370 Oberursel, FRG. Tel. (0 61 71) 40 81. Fax (0 61 71) 5 25 54.

Liquid Crystalline Polymers

Extruded bands of Polystal (a liquid crystalline polymer produced by Bayer) have a lower density than glass fiber reinforced expoxide materials and exhibit high strength and a better modulus of elasticity. Due to these properties the new reinforced materials have revolutionized the production of, amongst other things, cross country skis.

The leading world producers of cross country skis, Fischer (Ried, Austria) incorporated Polystal into 40 000 pairs of skis for the 1988/89 season and have been delighted by the results. In cross country skiing it is particularly important to have good shock absorbtion and insulation against vibration as well as light weight and high strength.

Liquid crystalline polymers can be looked upon as self-reinforcing polymers. The macromolecules which make up these materials are aligned parallel to one another in the melt but on extrusion the materials also take on a macroscopic parallel ordering. These fiber-like materials exhibit good performance at temperatures from 120 °C to those more likely to be found in a snow covered landscape.

Further information is available from Bayer AG, D-5090 Leverkusen, FRG, Tel. (0214) 30-31162.

New Man

Norwegian Talc have recently strengthened their materials business management by employing *Jens Adolf Döhle*, a chemist with experience in laser technology. *Döhle* took over responsibility for customer service and applications information on advanced materials in January. The Norwegian Talc program for which he is responsible includes high-purity chemicals, thin film materials especially for high-T_c superconductor work as well as materials for sputtering and CVD. This is a fast growing market area for the company which until now has concentrated mainly on Germany, Austria, and a number of Eastern-Block countries.

Crystalline Isotactic Polypropylene

The arrangement of the polymer chains in crystalline synthetic polymers is generally anisotropic. In other words, the macromolecules which make up the polymers are aligned parallel to one another. This chain-axis parallelism has become almost an unchallenged principle of polymer crystallization as it seems consistent with the packing requirements of the rods, although the polymers studied so far are almost exclusively of the fibrous type. However, in a recent article in *'Nature'*, *Sergio Brückner* and *Stefano Valdo Meille* of the University of Udine, and the Polytechnic of Milan, Italy, respectively, have reported a study of polymers which do not readily form fibrous specimens. They have found that the structure of isotactic γ-polypropylene comprises layers which are two chains wide, similar to the α-

phase, but with the chain axes aligned in the adjacent bilayers at an angle of 80° to one another (see figure) resulting in

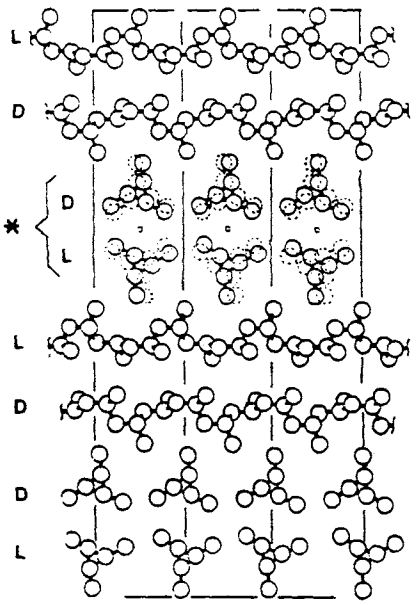


Fig. 1. Packing of γ-iPP. For the sake of clarity, coaxial anticlined helices are shown (dashed) only for some chains. The basic features of mutual chain arrangement and methyl-group interdigitation are shown. The labels D and L refer to the chirality of the helices belonging to the corresponding layer, and an asterisk identifies a bilayer of parallel chains.

favorable registration between helices. More about the unusual structure of γ-isotactic polypropylene where the non-parallel chains appear in a fully ordered array can be found in S. Brückner, S. V. Meille, *Nature 340* (1989) 455.

New Laser Glass

A new phosphate glass (APG-1) has been developed by Schott for use in high performance and high energy laser work. The glass is doped with neodymium and emits infrared light at a wavelength of 1053 nm. The new glass exhibits a high thermal shock stability and low thermal expansion ($\alpha = 7.6 \times 10^{-6}$/K) in the temperature range from 20 to 40 °C and is homogeneous.

Further details are available from Scott Glaswerke, Göttelmannstraße 17, P.O. Box 2480, D-6500 Mainz 1, FRG. Tel. (06131) 837328.

Quadrupole Mass Spectrometer

The QX 2000 Quadrupole Mass Spectrometer analyzes the composition of your process and residual gases – quickly and precisely. A single fingertip control lets you know immediately what gases are present in your vacuum chamber.

For ease of operation, the QX 2000 is menu driven via an integrated touch sensitive screen and uses a powerful computer (IBM AT compatible) with 640 kb RAM. Any important data can also be stored on a 3 1/2″ diskette drive floppy disk for recall and use at a later time.

The QX 2000 ensures early detection of problems which could otherwise jeopardize the operational integrity or safety of a process, such as: air leaks, changes in the water content of the process atmosphere, contamination due to oil or solvents, outgassing of materials under vacuum.



Typical applications include the areas of: IC and semiconductor fabrication, thin-film deposition techniques, laser industries, space simulation, materials research.

The QX 2000 offers more than conventional quadrupole mass spectrometers: simplicity of operation via the touch screen, high-resolution color monitor (640 × 350 Pixel, EGA standard), trend analysis for 12 user-selected masses, over a defined period of time. The display may be linear or logarithmic, covering up to 7 decades.

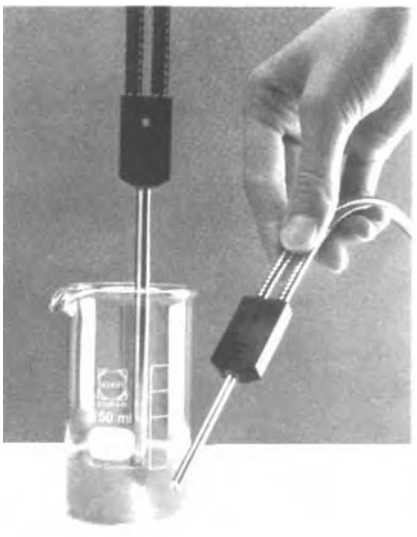
For further information please contact: Mr. M. Wasiletschko LEYBOLD, Bonner Strasse 498, D-5000 Köln 51, FRG, Phone: (0221) 347-1168 or in Great Britain: Mr. J. Holford, Phone: (01) 947 9744.

Materials Science in Bayreuth

The University of Bayreuth (FRG) in a northern area of Bavaria known as Oberfranken, has filled the first of three chairs in materials science which are to be the basis of the new Institute for Materials Science. Professor *Günther Ziegler*, previously at the German Research and Testing Establishment for Air and Space Travel (DLR) in Cologne takes up the challenge on November 1, 1989 and will be particularly responsible for the areas of ceramic composites. The other two planned chairs will be in polymer composites and metal surfaces and interfaces. The work in the institute will be applications oriented and will be based on the existing strengths of the university, solid state physics and polymer chemistry. Close cooperation with materials scientists at the University of Erlangen-Nürnberg some 85 km to the south is planned.

Fiber Optic Level Measurement

Schott have developed a level or depth measurement device for liquids based on fiber optic technology (see picture). The gauge is able to function in harsh conditions, for example, aggressive media, or in the region of explosions (highly shock



resistant), and can function at temperatures up to 200 °C. The recording and transfer of the measurement data is only affected by electromagnetic fields.

Further information is available from Schott Glaswerke, Göttelmannstraße 17, P.O. Box 2480, D-6500 Mainz 1, FRG, Tel. (06131) 837328.

Laser Power Monitor

OPhir Optics Jerusalem Ltd., have developed a new model, the PD-2A, to add to their range of power monitors. The newest addition to the range is based on a silicon photodiode where the spectral sensitivity with a resolution of 1 nm is recorded in the memory of the compact device. The desired wavelength is selected using a 4 way switch which also sets the corresponding calibration parameters from memory.

This calibration allows an accuracy of ±5% over the whole spectrum (350–1100 nm) to be achieved. For higher powers, to avoid saturation of the detector, a detachable filter is supplied extending the range of the device to 2 W.

Further details are available from agents Optiglas GmbH, Boschstr. 12, D-8039 Puchheim, FRG, Tel. (089) 80 10 35.

Magnetic-Bearing Turbomolecular Pump

LEYBOLD will introduce in Europe an improved magnetic bearing turbomolecular pump concept designed to substantially improve pump life and virtually eliminate pump maintenance.

The bearing system consists of a combination of passive permanent magnetic bearings and only one active controlled bearing. The lubricant-free pump (the Turbovac 340 M, see figure) can be



mounted in any position desired. Its built-in power generator assures active bearing control even during electrical fluctuations or in case of complete power failure.

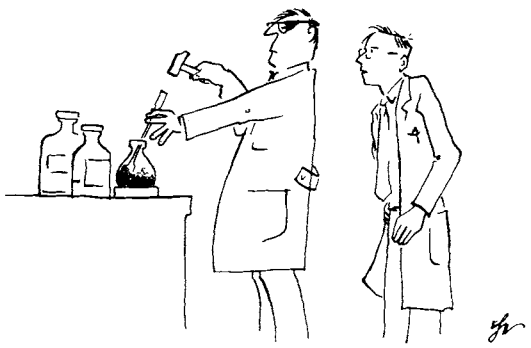
Highly resistant to shock and other currently known working conditions, this hydrocarbon-free pump will feature a maintenance-free, low vibration, and low noise level operation. Other features include: stable rotational speeds at high pressures, short start up and deceleration times and bearing purge gas protection. The solid state power control has built-in process control system for RS 232/24 V interfaces, drive control for backing pumps and pump set components and is sized for 1/2 19-inch rack mounting.

For further information, please contact Otmar Reuter, phone: West Germany (0221) 347-1556 or in Great Britain, John Holford, phone: 01-947 9744.

Materials Research in Germany – Annual Report

The annual report for 1988 on projects run under the aegis of the German BMFT, the government body concerned with research and technology, has recently appeared. The report, a healthy 1600+ pages, covers the progress made in projects concerning ceramics, powder metallurgy, polymers, composites, and tribology, projects which are running both in universities and in industry. The report has been produced by the BMFT in cooperation with the PLR, the Projektleitung Material- und Rohstofforschung and is available from the PLR, KFA Jülich, P.O. Box 1913, D-5170 Jülich, FRG. Tel. (02461) 61-0.

Call for Short Communications · Call for Short Communications · Call for Short Communications



... doesn't melt, won't dissolve, just can't be broken down – let's send it to ADVANCED MATERIALS!

ADVANCED MATERIALS

Book Reviews

Superconductors, Metals, Polymers, Electronics...

Introduction to the Modern Theory of Metals. By *Alan Cottrell*. The Institute of Metals, London 1988. 260 pp., hard cover, \$ 73.50, ISBN 0-904357-97-X

My first book review, written in Chicago in 1955, was on *Cottrell*'s "Theoretical Structural Metallurgy". At that time I was impressed by the non-physical argumentation which *Cottrell* used in that small book for the explanation of metallurgical phenomena, and it is a method I have often made use of during my career in physical metallurgy. Now, 35 years and many book reviews later, I have the opportunity to review the latest offering from *Cottrell*, another review of the basics of the metal state which attempts to incorporate the modern theories of today's metallurgists.

The book is intended to bring the post-war work of *Hume-Rothery* and *Raynor* up to date, work which *Cottrell* experienced at first hand during a stint as Professor in Birmingham from 1949 to 1955. Since that time he has worked at Harwell and at Cambridge, been a government science advisor, and Master of a college and Vice-Chancellor at the University of Cambridge. Here, during his retirement, he writes refreshingly on the electron theory of metals and alloys as if the intervening years had had no effect whatsoever. Truly a fascinating personality and performance!

The 10 chapters and 13 appendices (which make up more than one third of the book and contain the necessary mathematics) discuss the following points:

1. What is the definition of a metal? (Includes a discussion of the insulator-metal transition and electron delocalization).
2. Why are electrons 'free' (based on shielding and pseudopotentials)?
3. What is the effect of electron correlation?
4. What are the effects of band structure?
5. The cohesion in simple metals and the energies of lattice defects.
6. The d-shell transition metals and their magnetism.
7. The problems with Cu, Ag, and Au with respect to the Hume-Rothery rules for alloys.
8. The surface of metals.
9. Superconductors, including the high-T_c variety.

The physics of every example is explained well, the mathematical proofs being restricted to a minimum or confined to discussion in an appendix. The presentation makes the work highly readable, complete but concise. The metallurgist with some background in physics, or the physical chemist will gain much from reading the book. It is a masterpiece which provides an important education in the basic science that is applicable to many areas of materials science.

Peter Haasen
Institut für Metallphysik
Universität Göttingen
Hospitalstrasse 3/5, D-3400 Göttingen (FRG)

Studies of High Temperature Superconductors. Volume 1. Edited by *Anant Narlikar*. Nova Science Publishers, New York, 1989. xiv, 381 pp., bound, \$ 85.—ISBN 0-941743-44-3

The discovery of superconductivity in a La-Ba-Cu-O compound by *Bednorz* and *Müller* triggered a world wide race in the search for new superconducting materials with still higher transition temperatures. At the same time an enormous wave of publications was set in motion that continues today without any sign of diminishing. In order to ensure rapid publication, new journals mushroomed overnight everywhere, and it was extremely difficult to keep track of important developments.

Presently, three years after the beginning of high-T_c fever, the first books summarizing the current state of the art in the field are being published. The book in hand is the first volume of a series entitled *Studies of High Temperature Superconductors—Advances in Research and Applications*, edited by *Anant Narlikar* from the National Physical Laboratory in New Dehli, India. The underlying motivation for this series is the need for a convenient access to important advances in the field not only for scientists and engineers, but also for graduate students of physics, chemistry, materials science and related fields. Hence most of the chapters in each of the volumes have the character of a review article focusing on theoretical and experimental aspects of research in the field.

Volume one of this series contains 15 chapters, seven of which discuss theoretical approaches to high-T_c superconductivity. The remaining chapters summarize the processing of bulk and thin film materials, microstructural effects, elastic properties, and X-ray photon spectroscopy (XPS). *C. N. R. Rao* from the Indian Institute of Science gives an overview of the oxygen hole mechanism of superconductivity, including a review of available Auger and XPS data. *S. S. Jha* from the Tata Institute of Fundamental Research in Bombay reviews the generalized BCS pairing at the weak as well as the strong coupling limit, including a modified theory for layered crystals. A discussion of possible pairing mechanisms in high-T_c superconductors concludes this article.

J. P. Carbotte from McMaster University in Hamilton, Canada, and his colleague *F. Marsiglio* from the University of California at San Diego, USA, summarize boson exchange mechanisms and combined phonon-exciton mechanisms. A strong coupling approach to high-T_c superconductivity is considered by *J. Rammer* from the University of Bayreuth, FRG. Experimental studies allowing the assessment of the role of phonons in high-T_c superconductivity are included as well as a discussion of non-phonon and combined non-phonon and phonon mechanisms. *K. Machida* from Kyoto University considers electronically driven instabilities in a number of materials such as heavy Fermion superconductors, Cu-free cubic oxides, and the superconducting cuprates. *G. J. Hyland* from the University of Warwick, UK, looks at ground states of the parent compounds which are Mott-insulators and discusses the role of non-stoichiometry and altered valences in high-T_c superconductivity. Superconducting properties resulting from a short coherence length are discussed by *Y. Iye* from the University of Tokyo, Japan. He discusses fluctuations of diamagnetism and conductivity within the Ginzburg-Landau framework. Flux creep phenomena are discussed in the second part of the article.

Chemical aspects of the preparation of high-T_c superconductors are reviewed by *R. M. Iyer* and *J. V. Yakhmi* from Bhabba Atomic Research Center in Bombay, India. They discuss solid state and solution methods for the preparation of bulk superconductors. The oxygen stoichiometry of $YBa_2Cu_3O_{7-x}$ and processing for high critical current densities are reviewed as well as problems in synthesizing Bi and Tl superconductors. The following chapter by *A. V. Narlikar* et al. from National Physical Laboratory in New Delhi, India, is a comprehensive overview of substitution studies. Numerous tables and graphs summarize data and results of substitutions of the relevant lattice sites in $La_{2-x}Ba_xCuO_4$ and $YBa_2Cu_3O_{7-x}$ superconductors. A short section on substitutions in the Bi and Tl superconductors and an extensive bibliography with 144 entries concludes this review.

Sound velocity and measurements of the elastic constants are reviewed by *R. Srinivasan* from the Indian Institute of Technology. After a discussion of sound velocity data, he considers the possibility of structural change near 230 K; a number of measurements seem to point in that direction, e.g. sound velocity measurements, mechanical loss factors, specific heat, etc. Valence and conduction band XPS studies of high-T_c superconductors are summarized by *B. P. Padalia* and *P. K. Mehta* from the Indian Institute of Technology. The role of twins in $YBa_2Cu_3O_{7-x}$ is discussed at length by *C. J. Jou* and *J. Washburn* from the Lawrence Berkeley Laboratory, USA. Their proposed qualitative model for the formation of twins in $YBa_2Cu_3O_{7-x}$ is consistent with numerous experimental observations such as imperfect Meissner effect, remanent magnetization, etc.

Two chapters discuss thin film superconductors. *K. Wasa* and his colleagues from Matsushita Electric Industrial Co. Ltd. in Moriguchi, Japan, review basic thin film processing. After a short introduction listing the various deposition methods, the remainder of the article discusses deposition of a variety of high-T_c superconductors using RF-sputtering. *O. Meyer* from the Kernforschungszentrum in Karlsruhe, FRG, reviews the modification of thin films by ion beam irradiation and its effect on transport properties and electronic structure. The article closes with the discussion of application of ion beam modification techniques. Finally, the design, preparation, and characteristics of a superconducting three terminal device are discussed by *T. Kobay* and *U. Kabasawa* from Osaka University. Their "superconducting current switching transistor" shows a modest current modulation gain of 5 to 7. The authors close with a tentative interpretation of the current modulation mechanism on the basis of non-equilibrium superconductivity.

The volume certainly offers a wide range of topics and caters to a broad cross-section of scientists and engineers, just as the editor promised in the preface. Although the volume is somewhat heavily biased towards the theory side this will not be the case in future volumes as a glance into the list of planned articles reveals. The subject index in the back of the volume is a welcome supplement which enables the reader to cross-reference specific topics with other articles in the volume. On the negative side, some of the figures are of poor quality due either to the design of the responsible author or to the reproduction. It would improve this series if the editor would insist on higher quality supplied figures; a similar comment applies to the type styles, some of which are not suitable for camera-ready publications. Overall this first volume of the series is a good beginning and one can look forward to the forthcoming volumes.

Herbert Jaeger
Max-Planck-Institut für Metallforschung
Heisenbergstrasse 5, 7000 Stuttgart 80 (FRG)

Chambers Science and Technology Dictionary. Edited by P. Walker, W & R Chambers/CUP, Cambridge 1989. xvi 1008 pp., hard cover, £ 30 – ISBN 1-85296-150-3

Professor *Peter Walker*, a former Professor of natural history at the University of Edinburgh, Scotland, and a distinguished collection of collaborators from fields as disparate as acoustics and zoology have combined to produce a reference work of the highest quality which covers many areas of materials science as well as, amongst 100 other areas, biology, geology, and printing.

With the rate of development of science and technology ever increasing, it is not only the educated layman who becomes baffled, but one professional may have trouble understanding terms used by another in a neighboring field.

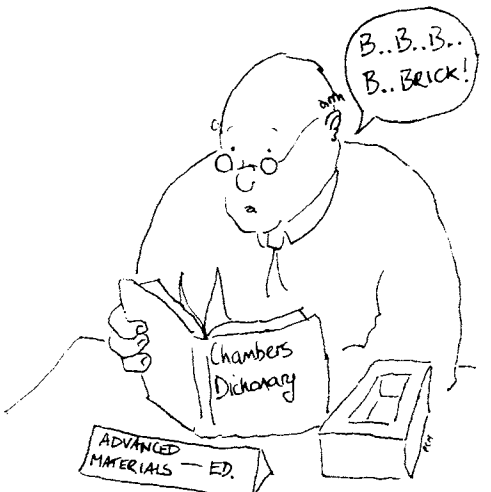
define your terms,
you will permit me again to say
or we shall never understand one another
— Voltaire

This book, to quote from the Preface, "will help a physician to understand a term in molecular biology, the layman to comprehend a medical term and both to talk to their builder in an informed manner."

Extending this philosophy to physicists, chemists, metallurgists, ceramists and engineers, which the dictionary does, is certainly a worthwhile task and one that is supported wholeheartedly in the Editorial Office of ADVANCED MATERIALS.

Chambers' technical dictionaries have a history of almost 50 years. The Technical Dictionary (1940), was supplemented substantially in 1958 and further revisions were made in 1971 and 1974. It seems a particular truism that changes in science and technology in the intervening years appear to have been as great as in the whole of earlier history.

The book, it is claimed, is not intended to replace the expert's own specialist dictionaries but should supplement them, giving the user a source of information which is multidisciplinary in character. To quote from the Preface once again "understanding specialist terms is the first step in applying intelligent controls" and the quality and composition of this work will take the reader a long way towards that goal.



"UNDERSTANDING SPECIALIST TERMS IS THE FIRST STEP IN APPLYING INTELLIGENT CONTROLS"

The main body of the dictionary, some 983 pages, starts with *a* and ends with *zymo-*, and the words in between are, unsurprisingly, arranged in alphabetical order. Joking apart, the coverage of the dictionary is satisfactory, the descriptions concise but clear, in many cases making interesting reading.

The book also contains a Greek alphabet (always useful) and appendices which contain information ranging from ISO paper sizes, through chemical formulae and nomenclature, information on the chemical elements and the classification of the animal and plant kingdoms, to a table mapping geological time and another describing and listing SI units and conversion factors.

All in all, the dictionary is well thought out, produced in high quality and is a valuable reference work which can be recommended without reservation to laymen and specialists alike.

Students of all ages, in all fields of materials technology will find it a valuable companion.

Knowledge is of two kinds. We know a subject ourselves or we know where we can find information upon it
—Samuel Johnson

Chambers are to be congratulated.

Peter Gregory
Advanced Materials
P.O. Box 101161, D-6940 Weinheim (FRG)

Electronics Reliability and Measurement Technology—Non-Destructive Evaluation. Edited by *Joseph S. Heyman*, Noyes Publications, 1988, xii, 188 pp., bound, $ 39.–. ISBN 0-8155-1171-X

The title of the book is misleading. The reader expecting to find a description of the main nondestructive methods for reliability evaluations of electronics will be disappointed. The book consists of a collection of papers presented at a workshop held in June 1986 at NASA Langley Research Center and sponsored by NASA, the U.S. Air Force, the National Security Industrial Association, and the Aerospace Industry Association.

The first paper "Measurement Science and Manufacturing Science Research" gives an overview of the activities at some U.S. universities, sponsored by the Semiconductor Research Corporation.

The paper "Nondestructive SEM for Surface and Subsurface Wafer Imaging" describes the use of a scanning electron microscope as a tool for both failure analysis as well as device characterization. The main emphasis is on capacitive coupling voltage contrast and on nondestructive subsurface imaging of semiconductors.

The paper "Surface Inspection – Research and Development" gives a brief overview of the industrial approach to semiconductor and magnetic disc surface inspection methods and the paper "Sensors Developed for In-Process Thermal Sensing and Imaging" describes a silicon thermophile array for fabrication process control.

The paper "Wafer Level Reliability for High-Performance VLSI Design" deals with the problem that the lifetimes of devices using new technologies are far shorter than older ones and are coming close to system lifetime. In order to monitor reliability on the wafer level, the paper proposes to introduce test structures on the wafer which allow the evaluation of certain failure modes, such as electromigration of mobile ions within a short time.

Some further papers deal with

- microfocus X-ray imaging for solder quality and structure inspection

- measurement of opaque-film thickness by thermal waves
- intelligent laser soldering inspection and process control
- rupture testing of electrodeposited copper interconnections (is this a non-destructive evaluation?)
- heterodyne holographic interferometry and
- "whole wafer" scanning electron microscopy.

The last four papers apparently only consist of copies of view graphs used for presentation at the workshop. The main part of the book describes activities at some companies and universities in 1986 in the area of measurement technology and process control in semiconductor manufacturing. This may be of some interest to a few specialists in the field, but of more interest is a summary of findings and recommendations in the first part of the book. On six pages, the deficiencies of the U.S. semiconductor industry with regard to quality and reliability are listed. These few pages should be read thoroughly by all executives in the U.S. semiconductor industry, but they are of equal interest to quality managers in companies using microelectronics, and for semiconductor competitors in Japan and Europe.

Hans Reiner
Standard Elektro Lorenz
Stuttgart, FRG

Analysis of Polymers. An Introduction By *T. R. Crompton*, Pergamon Press, Oxford 1989, viii, 362 pp., bound, DM 165.– ISBN 0-08-033942-5.

The number of commercially available polymers has been increasing over the last decade and is still increasing rapidly, due not only to the synthesis of new polymers, including new statistical copolymers or block copolymers, but also to the increasing use of polymer blends or of polymers containing various kinds of additives. Scientists in industry and in universities as well as potential users of such polymers frequently have the need to know what kind of polymers they are confronted with and which kind of additives they may contain. This is a formidable task. Fortunately the number of possible analytical techniques has also increased and some of them are highly sophisticated. It is therefore often not easy to decide which of the techniques is the most promising and what kind of information they are able to provide.

This is where the book "Analysis of Polymers" comes in very handy. It has been designed both as an introduction and as a practical guide for students and analytical chemists in universities or industrial laboratories. To serve this purpose it contains detailed descriptions on the various approaches which can be persued in order to analyze the chemical structure of homo- and copolymers and also the composition of multicomponent systems.

The organization of the book is primarily not so much technique-oriented but rather problem-oriented, as illustrated by the following titles of selected chapters: determination of elements, determination of functional groups, fingerprinting of polymers, polymer microstructure, fractionation and molecular weight, additives in polymers and adventitious volatiles in polymers.

Experimental techniques in turn are introduced within these chapters and their applications are demonstrated for a variety of examples in each of the chapters. Among the many techniques for which the basic theory is treated and applications demonstrated are gas chromatography, IR- and UV-spectroscopy, NMR- and ESR-spectroscopy, polarography, X-ray fluorescence spectroscopy, Neutron activation analysis, electron probe microanalysis, thermogravimetric and differential scanning calorimetry, titration methods, to mention just some.

The book is very well written and the examples have been selected well. It contains, in addition to the features mentioned so far, a large number of illustrations, extensive tables concerned with the properties of selected polymers as well as more than 1000 references. The book gives an impressive up-to-date exposition of the state of the art of polymer analysis and it seems certain that it will serve as a highly useful reference work.

J. H. Wendorff
Deutsches Kunststoffinstitut
Schlossgartenstrasse 6R, D-6100 Darmstadt (FRG)

Books received:

An Introduction to Rheology. By H. A. Barnes et al. Elsevier, Amsterdam 1989. X, 200 pp., soft cover, US $ 60.50. – ISBN 0-444-87469-0. **The Materials Revolution.** Edited by T. Forester. Basil Blackwell, Oxford 1988. XIII, 397 pp., paperback, £ 14.95. – ISBN 0-631-16701-3. **Practical Raman Spectroscopy.** Edited by D. J. Gardiner and P. R. Graves. Springer-Verlag, Heidelberg 1989. VIII, 157 pp., soft cover, DM 86. – ISBN 3-540-50254-8. **Chemistry and Physics of Carbon,** Vol. 22. Edited by P. A. Thrower. Marcel Dekker, New York 1989. XII, 264 pp., bound, US $ 162. – ISBN 0-8247-8113-9. **The MOCVD Challenge,** Vol. 1. By M. Razeghi. Adam Hilger, Bristol 1989. XII, 328 pp., bound, £ 55. – ISBN 0-85274-161-8. **The New Physics.** Edited by P. Davies. Cambridge University Press, Cambridge 1989. IX, 516 pp., bound, £ 30. – ISBN 0-521-30420-2. **Life of a Scientist.** By R. S. Mulliken. Springer-Verlag, Heidelberg 1989. XV, 256 pp., bound, DM 98. – ISBN 3-540-50375-7. **Polymer Processing.** By D. H. Morton-Jones. Chapman and Hall, London 1989. XI, 260 pp., soft cover, £ 16. – ISBN 0-412-26700-4. **Polymer Characterization.** By D. Campbell and J. R. White. Chapman and Hall, London 1989. VIII, 362 pp., soft cover, £ 19.95. – ISBN 0-412-27170-2. **NMR-Basic Principles and Progress,** Vol. 21. Edited by P. Diehl et al., Springer-Verlag, Heidelberg 1989. XII, 176 pp., bound, DM 128. – ISBN 3-540-50151-7.

Conference Calendar

The black hand symbol ☛ denotes new entries into the calendar. Send information concerning conferences to the editorial office.

December 1989

4–5 **Advanced Materials by Sol-Gel Techniques, Eurogel '89**
Eur. Conf.
Colmar (France)
Contact: Fraunhofer-Inst. f. Silicatforsch., "Eurogel '89", Neunerplatz 2, D-8700 Würzburg, FRG

11–13 **CBE/MOMBE and Related Growth Techniques**
2nd Int. Conf.
Houston, TX (USA)
Contact: H.-D. Shih, Univ. of Houston, Sci. and Res. One, 4800 Calhoun Rd., Houston, TX 77004, USA, Tel. 713-749-3701, Fax 713-747-7724

11–16 **Physics of Semiconductor Devices**
5th Int. Workshop
New Delhi (India)
Contact: Dr. S. K. Sharma, IWPSD-89, Nat. Physical Lab., Dr. K. S. Krishnan Rd., New Delhi-110012, India, Tel. 586087

12–15 **Pacific Polymer**
Hawaii (USA)
Contact: J. C. Vogl, Pacific Polym. Federation, Polytechnic Univ., 333 Jay St., Brooklyn, NY 11201, USA

20–22 **Thin Films and Multilayers**
Mtg.
Warwick (UK)
Contact: Inst. of Physics, Magnetism Group, 47, Belgrave Sq., London SW1X 8QX, UK

31–2 **Corrosion-Erosion-Wear of Materials at Elevated Temperatures**
4th Int. Conf.
Berkeley, CA (USA)
Contact: A. V. Levy, Lawrence Berkeley Lab., MS 62-203, Univ. of Calif., Berkeley, CA 94720, USA, Tel. 415-486-5822



January 1990

10–14 **Superconductivity**
Int. Conf.
Bangalore (India)
Contact: Prof. S. V. Subramanyam, ICSC, Dept. of Physics, Indian Inst. of Sci., Bangalore 560012, India, Tel. 91-812-344411, Fax 91-812-341683

14–19 **Electro-Optics**
Conf.
Los Angeles, CA (USA)
Contact: SPIE, POB 10, Bellingham, Wa 98227-0010, USA, Tel. 206-676-3290, Fax 206-647-14445

15–18 ☛ **Advances in Composite Materials**
Int. Conf.
Bombay (India)
Contact: Prof. P. Ramakrishnan, Indian Inst. of Techn., Dept. of Metallurg. Eng., Poway, Bombay 400076, India

21–24 ☛ **Gallium Arsenide**
Symp.
Atlanta, GA (USA)
Contact: K. J. Sieger, Naval Res. Lab., Code 6852, Washington, DC 20375, USA

22–26 **Recrystallization in Metallic Materials**
Int. Conf.
Wollongong (Australia)
Contact: T. Chandra, Dept. of Metallurgy and Materials Eng., Univ. of Wollongong, Wollongong NSW 2500, Australia, Tel. 042-270008, Fax 042-270477

February 1990

4–7 **Ceramic Powder Processing**
3rd Int. Conf.
San Diego, CA (USA)
Contact: G. L. Messing, Pennsylvania State Univ., University Park, PA 16802, USA, Tel. 814-865-2262, Fax 814-865-2917

4–8 **18th Australian Polymer Symposium**
Bendigo, Vic. (Australia)
Contact: Dr. J. D. Wells, Bendigo College of Adv. Education, Bendigo, Victoria 2550, Australia

19–21 ☛ **Advanced Ceramics**
Conf.
Rosemont (Italy)
Contact: Soc. of Manufacturing Eng., One SMF Dr., POB 930, Dearborn, MI 48121, USA

19–22 **Advanced Metals & Ceramics**
1990 TMS Annu. Mtg.
Int. Conf.
Anaheim, CA (USA)
Contact: M. Karl, TMS, Meetings Dept., 420 Commonwealth Drive, Warrendale, PA 15086, USA, Tel. 412-776-9050, Fax 412-776-3770

21 **Block-Copolymers**
Mtg.
London (UK)
Contact: Dr. K. Petrak, Ciba-Geigy ADDR Unit, Wimblehurst Road, Horsham, West Sussex RM124AB, UK

21–23 **Armed Forces Communications and Electronics**
Long Beach, CA (USA)
Contact: Armed Forces Communications and Electronics Assoc., Headquarters, 4400 Fair Lakes Court, Fairfax, VA 22033, USA

21–23 **Composites '90**
2nd Int. Congr.
Wiesbaden (Fed. Rep. Germany) Contact: D. Schnabel, Demat Exposition Managing, POB 110611, D-6000 Frankfurt 11, FRG, Tel. 069-234331, Fax 069-253071

25–27 **Interphase Reactions and Interactions**
Freiburg (Fed. Rep. Germany.)
Contact: Prof. Dr. H.-J. Cantow, Hermann-Staudinger-Haus, Stefan-Meier-Str. 31, D-7800 Freiburg, FRG

25–2 **Advanced Devices and Systems**
Symp.
Santa Clara, CA (USA)
Contact: SPIE, P.O. Box 10, Bellingham, WA 98227-0010, USA

March 1990

4–9 **Microlithography**
Symp.
San Jose, CA (USA)
Contact: Soc. of Photo-Optical Instrumentation Eng., Koblenzer Str. 34, D-5300 Bonn 2, FRG

12–16 **American Physical Society Meeting**
Anaheim, CA (USA)
Contact: W. W. Havens, J., Aps, 335 E., 45th St., New York, NY 10017, USA

12–16 **Optical Science and Engineering**
3rd Int. Congr.
The Hague (Netherlands)
Contact: Europtica Services I.C., 16, av. Bugeaud, F-75116 Paris, France

14–16 **Photovoltaic Solar Energy**
5th Int. Symp.
Staffelstein (Fed. Rep. Germany)
Contact: OTTI, D.-Martin-Luther-Str. 10, D-8400 Regensburg, FRG, Tel. 0941-58273/74/75, Fax 0941-54854

14–16 **Non-Metals in Metals**
Münster (Fed. Rep. Germany)
Contact: VDEh, Chemikerausschuß, POB 8209, D-4000 Düsseldorf 1, Tel. 0211-6707-441, Fax 0211-6707-310

17–21 **Advances in Semiconductors and Superconductors**
Symp.
San Diego, CA (USA)
Contact: Soc. of Photo-Optical Instrumentation Eng., Koblenzer Str. 34, D-5300 Bonn 2, FRG

19–20 **Materials Characterization**
Symp.
Philadelphia, PA (USA)
Contact: A. T. Riga, Lubrizol Corp., 29400 Lakeland Blvd., Wickliffe, OH 44092, USA

19–22 **Polymeric Materials**
2nd Arab. Int. Conf.
Alexandria (Egypt)
Contact: Prof. S. Morsi, ACM, Inst. Grad. Studies and Res., 163 Horreya Ave., POB 832, Shatby, Alexandria, Egypt

20–22 **Materials Testing**
10th show
Birmingham (UK)
Contact: J. Aspden, Mack Brooks Exhibitions, Forum Place, Hatfield, Herts AL10 ORN, UK

21–28 **Hannover Exhibition**
Hannover (Fed. Rep. Germany)
Contact: Dtsch. Messe AG, Messegelände, D-3000 Hannover 82, FRG

25–7 **Large-Scale Molecular Systems: Quantum and Stochastic Aspects**
Acquafredda di Maratea (Italy)
Contact: Dr. W. Gans, Inst. f. Physikal. Chemie d. FU, Takustr. 3, D-1000 Berlin 33.
Fax 49-308326561

26–28 **Microscopy of Oxidation**
Int. Conf.
Cambridge (UK)
Contact: J. Upton, Inst. of Metals, Conf. Dept., Carlton Hse. Terrace, London SW1Y 5DB, UK

26–30 **Solid State Physics**
Regensburg (Fed. Rep. Germany)
Contact: Prof. Dr. H. Hoffmann, Inst. f. Angew. Physik d. Univ., Universitätsstr. 31, D-8400 Regensburg, FRG

27–29 **Fiber Reinforced Composites**
4th Int. Conf.
Liverpool (UK)
Contact: Inst. of Mechanical Eng., Conf. Dept., 1, Birdcage Walk, London SW1H 9JJ, UK

April 1990

1–6 **Thin Films**
8th Int. Conf.
San Diego, CA (USA)
Contact: W. D. Sproul, Bas. Ind. Res. Lab., Northwestern Univ., 1801 Maple Ave., Evanston, IL 60201-3135, USA, Tel. 312-491-4108, Fax 312-491-4486

1–7 **Epitaxial Crystal Growth**
1st Int. Conf.
Budapest (Hungary)
Contact: E. Lendvay, Hung. Acad. of Sci., Res. Inst. for Techn. Physics, 1, Ujpest, POB 76, H-1325 Budapest, Hungary

2–5 **Advanced Materials – the Challenge for the Next Decade**
35th Int. Symp.
Anaheim, CA (USA)
Contact: SAMPE Headquarters, POB 2459, Covina, CA 91722, USA

2–6 **Applications of High-T_c Superconductors**
Greenbelt, MD (USA)
Contact: Dr. L. H. Bennett, Nat. Inst. of Standards and Technology, B 152, Materials Bldg., Gaithersburg, MD 20899, USA

3–6 **Engineering Ceramics**
5th Conf.
Petten (Netherlands)
Contact: Eur. Physical Soc., P.O. Box 69, CH-1211 Petit-Lancy 2, Switzerland

4–6 **Power Semiconductor Devices and ICs**
2nd Int. Symp.
Tokyo (Japan)
Contact: H. Ohasi, Toshiba Corp., R + D Center, Komukai Toshiba-cho 1, Kawasaki 210, Japan

4–6 **Composites**
25th Eur. Congr.
Paris (France)
Contact: Centre de Promotion des Composites, 65, rue de Prony, F-75854 Paris Cedex 17, France

8–13 **American Crystallographic Association Meeting**
New Orleans, LA (USA)
Contact: ACA, P.O. Box 96, Ellicott Station, Buffalo, NY 14025-0096, USA, Tel. 716-856-9600

9–10 **Ceramics in Energy Applications**
Mtg. Sheffield (UK)
Contact: Inst. of Energy, Conf. Dept., 18 Devonshire St., London W1N 2AU, UK

10–12 **New Materials and Their Applications**
2nd Conf.
Coventry (U.K.)
Contact: Inst. of Physics, Meetings Office, 47, Belgrave Square, London SWIX 8QX, UK

16–20 **EICS II**
2nd Eur. Inorg. Chem. Sem.
Wiesbaden (Fed. Rep. Germany)
Contact: Prof. Dr. P. Gütlich, Inst. f. Anorg. u. Analyt. Chemie der Univ., Staudinger-Weg 9, D-6500 Mainz, FRG, Tel. 06131-392373

16–20 **MRS Spring Meeting**
San Francisco, CA (USA)
Contact: M. Geil, Materials Res. Soc., 9800 McKnight Rd., Suite 327, Pittsburgh, PA 15237, USA, Tel. 412-367-3003, Fax 412-367-4373

17–20 **Polymer Processing Society**
6th Annu. Mtg.
Nice (France)
Contact: Ecole des Mines de Paris, CEMEF, Secr. PPS6, Sophia-Antipolis, F-06460 Valbonne, France

17–20 **Intermag '90**
Int. Conf.
Brighton (UK)
Contact: Intermag '90, c/o ITEL, Brighton Polytechnic, Brighton BN2 4GJ, UK

19–20 **Thermal Methods in the Study of High T_c Superconductors**
Manchester (UK)
Contact: Dr. F. R. Sale, Manchester Materials Sci. Center, Univ. of Manchester, UMIST, Grosvenor St., Manchester M1 7HS, UK

22–26 **American Ceramic Society**
92nd Annu. Mtg.
Dallas, TX (USA)
Contact: Am. Ceram. Soc. Inc., 757 Brooksedge Plaza Drive, Westerville, OH 43081, USA

23–26 **Low-Temperature Electronics**
Int. Conf.
Berkeley, CA (USA)
Contact: M. Vukovojac, Butterworth Scientific Ltd., POB 63, Westbury Hse., Bury St., Guildford, Surrey GU 2 5BH, UK, Tel. 0483-300966, Fax 0483-301563

24–26 **Fiber-Optics and Opto-Electronics**
8th Int. Conf.
London (UK)
Contact: Sira Ltd., Conf. Office, South Hill, Chislehurst, Kent BR7 5EH, UK

23–27 **MASHTEC '90**
Materials Science for High Technologies
Int. Symp.
Dresden (German Dem. Rep.)
Contact: Prof. W. Pompe, Zentralinst. f. Festkörperphysik u. Werkstofforsch. der AdW der DDR, Helmholtzstr. 20, DDR-8027 Dresden, GDR

23–27 **Corrosion '90**
Mtg.
Las Vegas, NV (USA)
Contact: Nat. Assoc. of Corrosion Eng., P.O. Box 218340, Houston, TX 77218, USA

24–27 **Cryogenic Engineering**
13th Int. Conf.
Beijing (PR of China)
Contact: C. S. Hong, Cryogenic Lab., AS, P.O. Box 2711, Beijing 100080, China, Tel. 256-4051, Fax 256-4049

25–27 **Cadcomp '90**
2nd Int. Conf.
Brussels (Belgium)
Contact: M. Bourlan, VUB-TW (KB), Pleinlaan 2, B-1050 Brussels, Belgium, Tel. 32(0)2.6412922

25–27 **Composite Building Blocks**
ITG-Fachtagung
Schwäbisch Gmünd (Fed. Rep. Germany)
Contact: Dr. B. Schwaderer, ANT Nachrichtentechnik GmbH, Grundlagenentw., POB

1120, D-7150 Backnang, Tel. 07191-132557, Fax. 07191-133212

29–4 **Transport Properties of Superconductors**
Int. Conf.
Rio de Janeiro (Brazil)
Contact: R. Nicolsky, Inst. de Física, Univ. Fed. do Rio de Janeiro, C.P. 68528, 21945 Rio de Janeiro, Brazil, Tel. 55-21-270-1191/270-1736, Fax 55-21-280-7693

30–4 **Thin Film Superconductors**
Conf.
Denver, CO (USA)
Contact: D. Christodaro, Solar Energy Res. Inst., Conf. Coordination Sect., 1617 Cole Blvd., Golden, CO, USA, Tel. 303-231-1158

May 1990

1–3 **Tribology of Composite Materials**
Conf.
Oak Ridge, TN (USA)
Contact: Am. Soc. for Metals, Metals Park, USA, OH 44073

2–4 **Biosensors '90**
1st World Congr.
Hong Kong
Contact: Prof. Dr. R. D. Schmid, GBF mbH, Ber. Enzymtechn. u. Naturstoffchemie, Mascheroder Weg 1, D-3300 Braunschweig, FRG

2–4 **Reinforced Plastics**
23rd Int. Conf.
Mainz (Fed. Rep. Germany)
Contact: AVK, Am Hauptbahnhof 12, D-6000 Frankfurt 1, Tel. 069-2710533, Fax 069-232799

6–8 **High-T_c Superconductors**
Symp.
Montreal (Canada)
Contact: S. Raider, IBM, T. J. Watson Res. Center, POB 218, Yorktown Heights, NY 10598, USA, Tel. 914-945-2203

6–9 **Characterization of Porous Solids**
2nd Int. Symp.
Alicante (Spain)
Contact: Prof. F. Rodriguez-Reinoso, Dept. de Quimica Inorgánica e Ingenieria Quimica, Facultad de Ciencias, Universidad de Alicante, Apartado 99, Alicante, Spain

6–11 **Metallized Plastics**
Symp.
Montreal (Canada)
Contact: K. L. Mittal, IBM US Techn. Education, 500 Columbus Ave., Thornwood, NY 10594, USA, Tel. 914-742-5747

7–9 **Polymers and Light**
Lecture Meeting
Bad Nauheim (Fed. Rep. Germany)
Contact: Ges. Dtsch. Chemiker, Abt. Tagungen, Varrentrappstr. 40–42, D-6000 Frankfurt, FRG

7–10 **Plastics Engineering**
48th Annu. Conf.
Dallas, TX (USA7
Contact: Soc. of Plastics Engineers, 14 Fairfield Dr., Brookfield Center, CT 06805, USA

9–11 **High-T_c Superconductors**
Garmisch-Partenkirchen (Fed. Rep. Germany) Contact: Dtsch. Gesellsch. f. Metallkd., Adenauerallee 21, D-6370 Oberursel, FRG, Tel. 06171-4081, Fax 06171-52552

14–15 **Spectroscopy**
11th World Conf.
Vienna (Austria)
Contact: Dr. V. M. Bhatnagar, Alena Enterprises of Can., POB 1779, Cornwall, Ontario K6H 5V7, Canada

17–18 **Nonmetallic Materials and Composites at Low Temperatures**
Heidelberg (Fed. Rep. Germany)
Contact: Dr. G. Hartwig, Kernforschungszentrum Karlsruhe, Inst. f. Material- u. Festkörperforschung IV, POB 3640 D-7500 Karslsruhe, FRG

21–24 **Advanced Aerospace Materials**
Conf.
Long Beach, CA (USA)
Contact: ASM Inst. Techn. Dept. Marketing Metals Park, OH 44073, USA

21–25 **Quantum Electronics**
17th Int. Conf.
Anaheim, CA (USA)
Contact: Optical Soc. of America Inc., 1816 Jefferson Pl., NW, Washington, DC 20036, USA

21–26 **Vacuum**
2nd Eur. Conf. + 11th Nat. Congr.
Trieste (Italy)
Contact: Dr. R. Molena, Consiglio Nazionale delle Ricerche, Istituto Tecnologia Materialii Metallici non Tradizionali, Via Bassini 15, I-20133 Milano, Italy

22–24 **Holography Applications**
Int. Conf.
Beijing (PR of China)
Contact: Prof. H. Da-hsiung, Beijing Inst. of Posts and Telecommunications, Beijing 100088, PR of China

22–26 **Optoelectronics**
Int. Symp.
Killarney (Ireland)
Contact: D. O'Connell, Trinity College, Dept. of Pure and Applied Physics, Dublin 2, Ireland

23–25 **Advances in Video Technology**
4th Symp.
Contact: ASTM, 1916 Race St., Philadelphia, PA 19103, USA

29–31 **Plastics-Metals-Ceramics**
11th Int. Conf.
Basel (Switzerland)
Contact: Dr. H. Hornfield, Consultex SA, CH-1261 Bogis-Bossey, Switzerland

June 1990

10–15 **Polycondensation and Related Reactions**
2nd Conf.
Gargano (Italy)
Contact: Prof. Er. E. Pilati, Dipart. di Chimica Appl. e Scienza dei Mat., Universita di Bologna, Viale Risorgimento 2, I-40136 Bologna, Italy

11–13 **Electroluminescence**
5th Workshop
Helsinki (Finland)
Contact: Prof. M. Leskelä, Dept. of Chem. Engineering, Helsinki Univ. of Technology, SF-02150 Espoo, Finland, Tel. 358-0-4512567, Fax 358-0-462373

11–14 **Precision Electromagnetic Measurements**
Conf.
Ottawa (Canada)
Contact: H. Lacoste, Nat. Res. Council of Can., Conf., Services, Ottawa, Ontario K1A ORA, Canada

11–15 **Metallurgical Coatings**
Int. Conf.
Beijing (PR of China)
Contact: Prof. Shi Changxu, No. 43 Baojia St., Xicheng District, Beijing, PR of China

13–15 **Atomic Layer Epitaxy**
1st Int. Symp.
Helsinki (Finland)
Contact: Prof. L. Niinistoe, Helsinki Univ. of Techn., Dept. of Chem. Eng., Kemistinitie 1, SF-02150 Espoo, Finland

18–21 **Metal-Organic Vapor Phase Epitaxy**
5th Int. Conf.
Aachen (Fed. Rep. Germany)
Contact: H. Henke, RWTH Aachen, Inst. f. Halbleitertechnik, Templergraben 55, D-5100 Aachen, FRG

18–22 **C-MRS International '90**
Beijing (PR of China)
Contact: Hengde Li, Dept. of Materials Sci. and Eng., Tsinghua Univ., Beijing 100084, China, Tel. 655646, Fax 861-256-2768

21–22 **Adhesion in Composites**
Symp.
Konstanz (Fed. Rep. Germany)
Contact: Dtsch. Gesellsch. f. Metallkd., Adenauerallee 21, D-6370 Oberursel, FRG

24–30 **Cimtec**
7th World Ceramics Congr.
Montecatini Terme (Italy)
Contact: World Ceramics Congress, POB 174, I-48018 Faenza, Italy, Tel. 546-664143, Fax 546-664138

25–27 **Surface Engineering**
Int. Conf.
Toronto (Canada)
Contact: Prof. S. A. Meguid, Univ. of Toronto, Dept. of Mechanical Eng., Toronto, Ontario M5S 1A4, Canada

July 1990

2–6 **Powder Metallurgy**
Int. Conf.
London (UK)
Contact: Inst. of Metals, Conf. Dept., Carlton Hse. Terrace, London SW1Y 5DB, UK

3–6 **Technology of Polymer Compounds and Energetic Materials**
21st Int. Annu. Conf.
Karlsruhe (Fed. Rep. Germany)
Contact: M. Wolff, Fraunhofer-Inst. f. Chem. Technologie, POB 1240, D-7507 Pfinztal 1, FRG

7–11 **Liquid Matter**
1st Conf.
Lyon (France)
Contact: S. Bratos, Univ. Pierre et Marie Curie, LPTL, Tour 16,5 et., 4 pl. Jussieu, F-75252 Paris Cedex 05, France

7–13 **Macromolecules**
33nd Int. Symp.
Montreal (Canada)
Contact: McGill Univ. Dept. of Chem. Eng., 3480 University St., Montreal, Quebec H3A 2A7, UK

Registered names, trademarks, etc. used in this journal, even when not marked as such, are not to be considered unprotected by law.

© VCH Verlagsgesellschaft mbH, D-6940 Weinheim, 1989. – Printed in the Federal Republic of Germany by Konrad Triltsch Druck- und Verlagsanstalt Würzburg.

All rights reserved (including those of translation into foreign languages). No part of this issue may be reproduced in any form — by photoprint, microfilm, or any other means — nor transmitted or translated into a machine language without written permission from the publishers. Only single copies of contributions, or parts thereof, may be made for personal use. This journal was carefully produced in all its parts. Nevertheless, authors, editors and publisher do not warrant the information contained therein to be free of errors. Readers are advised to keep in mind that statements, data, illustrations, procedural details or other items may inadvertently be inaccurate.

Valid for users in the USA: The appearance of the code at the bottom of the first page of an article (serial) indicates the copyright owner's consent that copies of the article may be made for personal or internal use, or for the personal or internal use of specific clients. This consent is given on the condition, however, that the copier pay stated per-copy fee through the Copyright Clearance Center, Inc. (CCC), for copying beyond that permitted by Sections 107 or 108 of the U.S. Copyright Law. This consent does not extend to other kinds of copying, such as copying, for general distribution, for advertising or promotional purposes, for creating new collective works, or for resale. For copying from back volumes of this journal see 'Permissions to Photo-Copy: Publisher's Fee List' of the CCC.

Editorial office: Postfach 10 11 61, D-6490 Weinheim, Federal Republic of Germany, Telephone (06201) 60 22 55, Telex 465 516 vchwh d, Telefax (06201) 602 328.

Editor: *Peter Gölitz*

Associate Editor: *Peter Gregory.* **Editorial Assistant:** *Susanne Stoll*

Publishers: VCH Verlagsgesellschaft mbH. (Managing Director: *Hans Dirk Köhler*), Pappelallee 3, D-6940 Weinheim, Federal Republic of Germany.

Advertising office (Advertising Manager *R. J. Roth*): Postfach 10 11 61, D-6940 Weinheim, Federal Republic of Germany, Telephone (0 62 01) 60 61 30, Telex 467 155 vchwh d, Telefax (0 62 01) 606 184.

ANGEWANDTE CHEMIE
International Edition in English
Volume 28 · Number 12
December 1989
Pages 1601–1766

Image Enhancement—Chemical, Digital, Visual

By Joachim Lohmann*

Digital image processing has become well known through the high quality of some spectacular satellite images. It has developed into a discipline in its own right within information science and now finds application, not only in space travel, but also in such diverse fields as, for example, robotics, medical imaging, and television technology. Image processing also occurs, however, in photographic films and biological visual systems. In these systems, too, recorded images are manipulated for better recognition. This poses the question as to whether similar principles of image processing are operative in these different image handling systems.

1. Introduction

The term "digital image processing" refers to the computer-aided modification of images and encompasses image enhancement (modification for better visual recognizability), image restoration (elimination of a systematic distortion), and image analysis (extraction of information) (Fig. 1). Several monographs on digital image processing are available.[1–5]

Generally the photographic film is known only as a means for image recording. But during chemical development the primary image—the latent image—is not only made visible but is improved in many respects. This forms the basis of modern color-negative films, which combine excellent reproduction of detail with high color saturation. The model for both digital image processing and, in many respects, for the photographic film is the visual system. It performs all the steps from image recording and image enhancement to image interpretation.

In this review the three systems—the chemical film, digital image processing, and the visual system—are compared solely from the standpoint of image enhancement. Naturally,

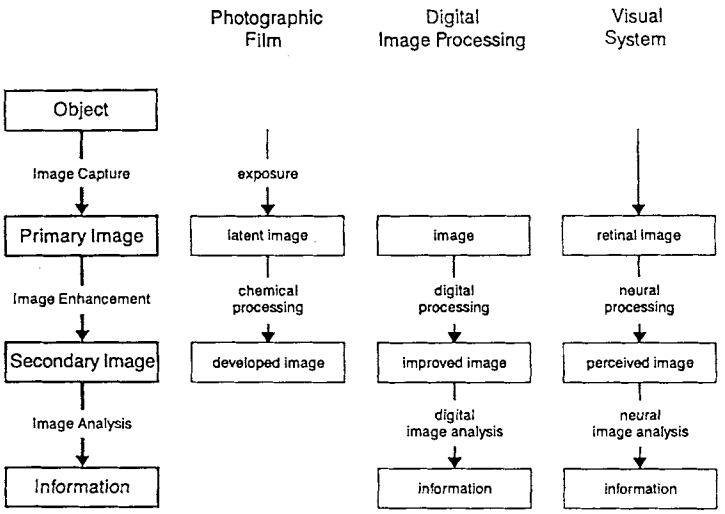


Fig. 1. Steps of image manipulation in the photographic film, in digital image processing and in the visual system.

very different physical and chemical mechanisms are operative in these systems, i.e. the image information is encoded in different languages; consequently, the comparison relates to the structure of these languages, to the algorithms of image processing. The discussion is restricted to the improvement

[*] Dr. J. Lohmann
Agfa-Gevaert AG
5090 Leverkusen 1 (FRG)

 © VCH Verlagsgesellschaft mbH, D-6940 Weinheim, 1989 0570-0833/89/1212-1601 $ 02.50/0

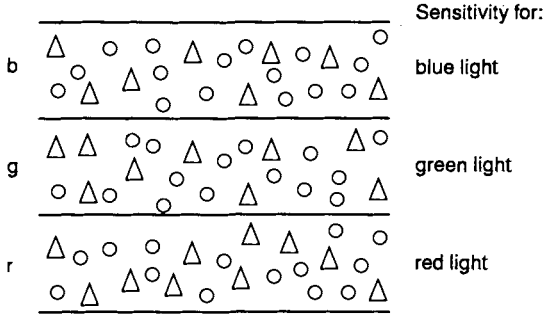
of three basic image properties, namely noise (Section 3), sharpness (Section 4) and color reproduction (Section 5).

2. Architecture of the Systems

In the following the essential elements of the three systems are briefly described.

2.1. Color Negative Film

Figure 2 shows the common three-layer structure of a color negative film. Each layer contains silver halide crystals which are sensitive to blue light or which are sensitized by appropriate dyes to green or red light. In addition, the layers contain dye-precursors, the couplers. Upon exposure to light, clusters of silver atoms Ag_n—the latent-image specks—are formed (Fig. 3). During the subsequent photographic development these silver clusters catalyze a redox reaction between the silver halide and the developer. The oxidized developer in turn reacts with the coupler to the image dye.



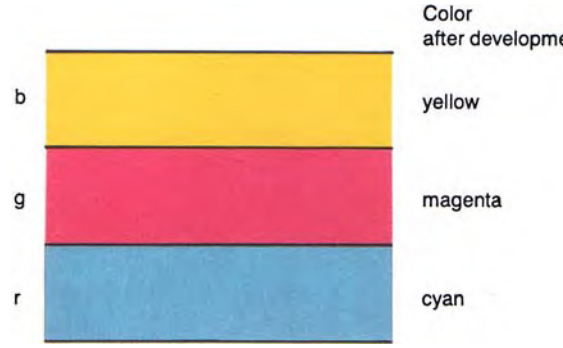


Fig. 2. General structure of a color negative film (△ silver halide crystals, ○ couplers); b blue-sensitive layer, g green-sensitive layer, and r red-sensitive layer; top: before development, bottom: after development.

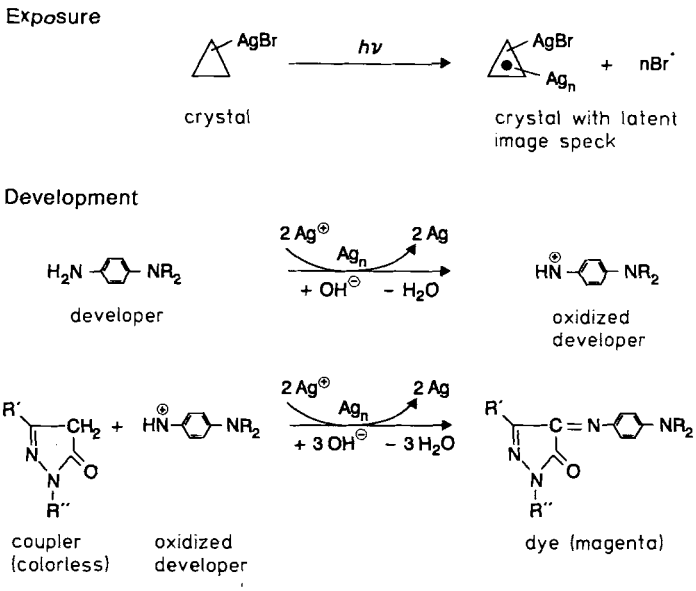


Fig. 3. Reactions during exposure and development of a color negative film (example: green-sensitive layer).

In modern color negative films there are some special couplers besides the standard couplers which fulfill image processing functions: colored couplers and development-inhibitor-releasing (DIR) couplers (Fig. 4).

The colored couplers are compounds which change their color on reaction with the oxidized developer[6]. In contrast, in the reaction of a DIR coupler with the oxidized developer, an inhibitor is released which can freely diffuse in the film in all directions[7]. Once adsorbed, the inhibitor contaminates the latent-image specks (Ag_n) and partially developed silver particles, thus decreasing their catalytic efficiency and retarding the development process.

The different reactions during chemical development of a color negative film are summarized in Figure 5.



Joachim Lohmann was born in 1939 in Hamburg. After a formal education (1959 to 1966) in Hamburg and Berlin he obtained his doctorate from the University of Hamburg in 1969 (supervisor H.-F. Grützmacher). He then spent a year carrying out postdoctoral research with Professor George Porter in London. Since 1971 he has been actively engaged in research at Agfa-Gevaert: at first, in Mortelsen (Belgium), where he was involved in research on silver-free photographic systems; since 1974 he has been working on photographic films and systems in Leverkusen, where he was appointed research director in 1981.

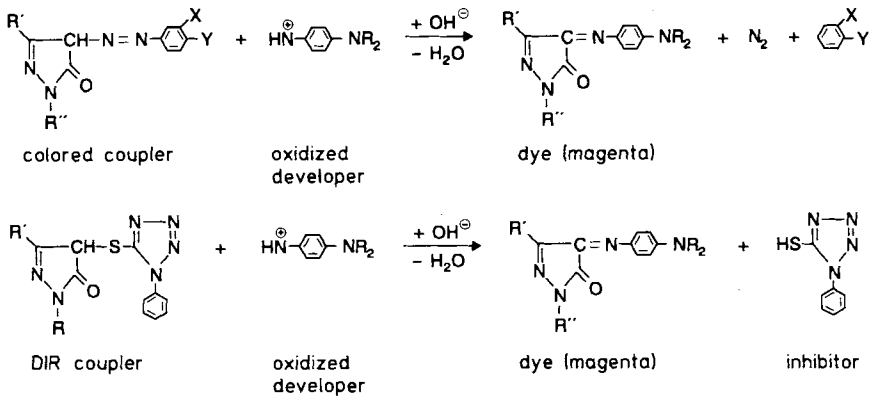


Fig. 4. Reactions of the oxidized developer with colored couplers and with DIR couplers in a color negative film.

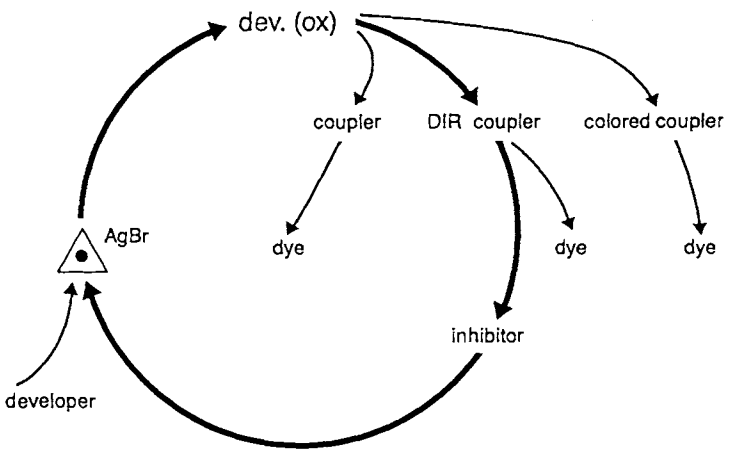


Fig. 5. Chemical processing of a color negative film.

2.2. Digital Image Processing

An analog image must first be digitized to render it accessible to digital processing (Fig. 6). A scanner reads the image by dividing the image area into discrete picture elements (pixels), and each element with the spatial coordinates x, y is assigned a quantized density value $f(x, y)$ (a pixel in a color image is assigned three quantized color densities). The smaller the pixels and the finer the density steps, the more precisely an image can be digitally described. The image function $f(x, y)$ corresponds to an array of numbers; processing results in a modified image function $g(x, y)$, the recording of which (e.g. by a laser on photographic paper) yields the improved image[8].

There are two modes in which the processing can be carried out (Fig. 7). In the spatial mode the numbers of the image function $f(x, y)$ are changed directly, either individually according to a given scheme (look-up tables) or as a function of the neighboring numbers. For processing in the frequency domain, the spatial function $f(x, y)$ is first transformed into a two-dimensional frequency function $F(u, v)$ using a Fourier transform, where u and v are the spatial frequency coordinates. The low frequencies contain information on luminance and coarse image structure, whereas the high frequencies contain information on reflectivity, edges, and granularity. Certain image properties can be enhanced or suppressed by amplification or reduction of the respective frequency range. A systematic distortion of the image produced by a moving camera or by an unfocussed objective lens (perturbation function **H**) can be eliminated by applying **H***, the inverse of the perturbation function.[3b] Thus, the frequency mode offers specific routes for image improvement, and in addition some mathematical operations are very much simplified. After processing the im-

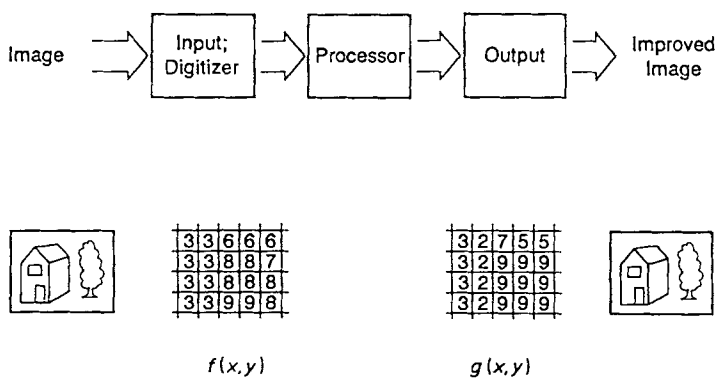


Fig. 6. Digital image processing.

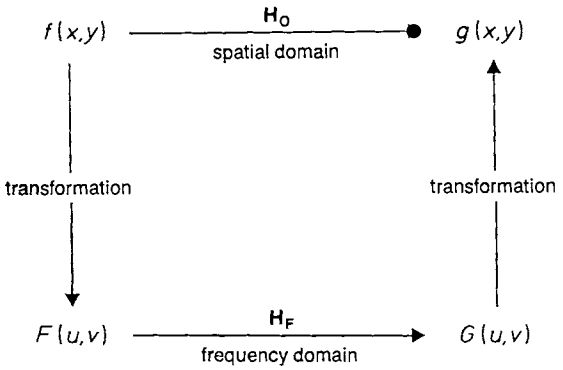


Fig. 7. Processing modes in digital image processing; x, y spatial coordinates; u, v spatial frequency coordinates; $f(x, y)$, $g(x, y)$ primary and improved image function in the spatial domain; $F(u, v)$, $G(u, v)$ primary and improved image function in the frequency domain; $\mathbf{H}_0$, $\mathbf{H}_F$ operators in the spatial and frequency domain.

proved frequency function $G(u, v)$ is transformed back into the modified spatial function $g(x, y)$.

Processing in the frequency domain is of great importance in digital image processing; frequency-dependent algorithms also seem to be operative in the visual system (see Section 4.3), but not in the photographic film. Processing in the frequency domain will therefore be dealt with only very briefly here.

2.3. Visual System

The human visual system consists of the eye (with its light-sensitive retina) and certain parts of the brain (Fig. 8). In the

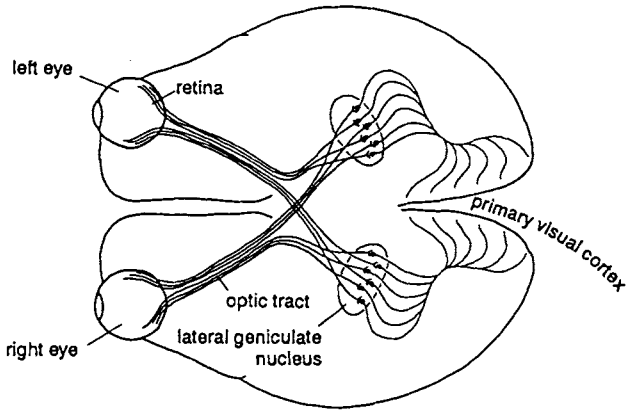


Fig. 8. Human visual system: view of the brain from below [9].

photoreceptor cells of the retina (Fig. 9) the incident light pulses are converted into electrical signals.[11, 12] The photoreceptor cells contain about 120 million rods which register only luminance, and about 6 million color-sensitive cones (three kinds of cone cells with different spectral sensitivities; absorption maxima at 440, 545 and 580 nm[6]). The signals flow via several intermediate cells which are connected crosswise to the ca. one million ganglion cells, and from there to the brain[13]. The complex network of cells in the retina indicates that image processing functions are carried out not only in the brain but also in the retina.

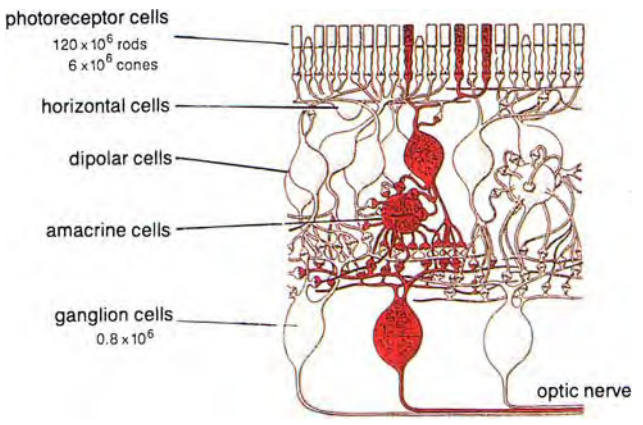


Fig. 9. Structure of the retina (taken from [10]).

3. Noise (Granularity)

Noise is the random variation of a signal and becomes more pronounced with increasing amplification.

3.1. Film

In photographic images the phenomenon of noise is known as granularity—the fluctuation of the optical density in a uniformly exposed image area on a microscopic scale. The relation between amplification and noise becomes evident by the fact that high-speed films are generally grainier and that push-processing (extension of development time to achieve higher speed) also increases granularity. The source for the granularity of a film lies in the random position and the response of the individual silver halide crystals. During development, the granularity of the silver image is translated into a granularity of the color image. This transformation, however, also provides the chance of improving the granularity.

In the presence of DIR couplers inhibitors are released during the development process which diffuse into the surrounding region and prevent the development of adjacent crystals; this leads to smaller dye clouds and results in less granularity (Fig. 10). Decisive in this method is that the sensitivity is not affected, for this is determined by the crystal size during exposure, which remains constant.

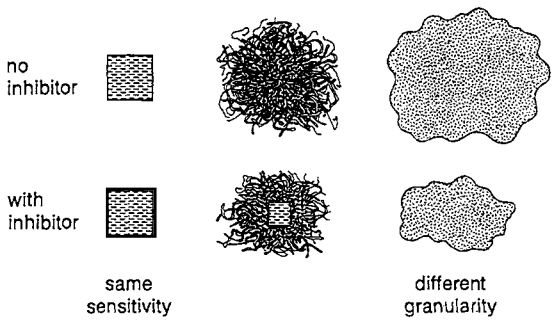


Fig. 10. Reduction of granularity in a color negative film by inhibitors which are released from DIR couplers.

This reduction of the granularity by DIR couplers is connected with the chemistry of chromogenic development. To exploit this effect for black-and-white films, the color "black" must be produced as a mixture of dyes. This is the concept of chromogenic black-and-white films.[14]

Furthermore, an incomplete transformation of the silver image into the dye image is achieved if the oxidized developer (see Fig. 5) is partially consumed by competitive non-chromogenic reactions. Potential competing reactions are the alkaline hydrolysis of the oxidized developer[15] (the more pronounced, the slower the coupling reaction), reactions with incorporated reducing compounds (e.g. dioctylhydroquinone), or reactions with incorporated couplers which produce colorless products.[16]

In all these cases the yield of dye based on the amount of silver halide is diminished. The reduced yield of dye must be

compensated for by an increase in silver halide coverage. An improvement of granularity thus has its price.

A completely different approach for decreasing the granularity is to design dyes with a certain diffusibility under the alkaline conditions of development.[17] Such a controlled diffusion smoothes out local differences in density and leads to a local density average. Figure 11 demonstrates by way of

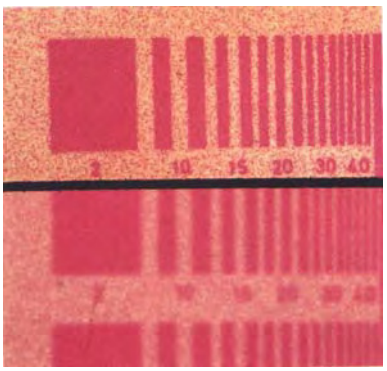


Fig. 11. Reduction of granularity in a color negative film by controlled diffusion of the image dyes.

example how the granularity is improved by this method, but at the same time it reveals the disadvantage of the method, namely the loss of definition with too much diffusion.

Similar to local averaging in one image, is averaging over several identical but independently taken images, which is achieved by exposure through a set of identical negatives. Owing to its random nature the granularity is reduced, but the image information is retained.

3.2. Digital Processing

In a digitized image, noise is the random fluctuation of the image function in a uniform field expressed as deviations of individual pixel values in an otherwise homogeneous field. Noise can be eliminated in a straightforward manner by substituting each number by the rounded-off local average (neighborhood averaging; spatial domain low pass filter). In the example shown in Figure 12, the local average is calculated as the algebraic mean of a particular number and its eight nearest neighbors.

Local digital averaging corresponds to averaging by diffusion in a film. In both cases the sharpness is affected. Therefore, rather complicated operators are applied in which adjacent pixels have lower weighting or in which the weighting of neighboring pixels is variable depending on the local gradient.[5] If the noise is characterized by a particularly high or

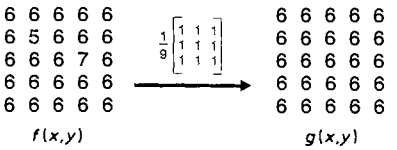


Fig. 12. Digital reduction of noise by local averaging.

low deviation of the signal from the local surround the noisy pixels can be improved selectively by defining thresholds. Only those pixel values are replaced by the local average value (i.e. the difference to the local surround is set equal to zero) whose differences from the local surround are higher or lower than preset thresholds (Fig. 13).[18] In this way, the

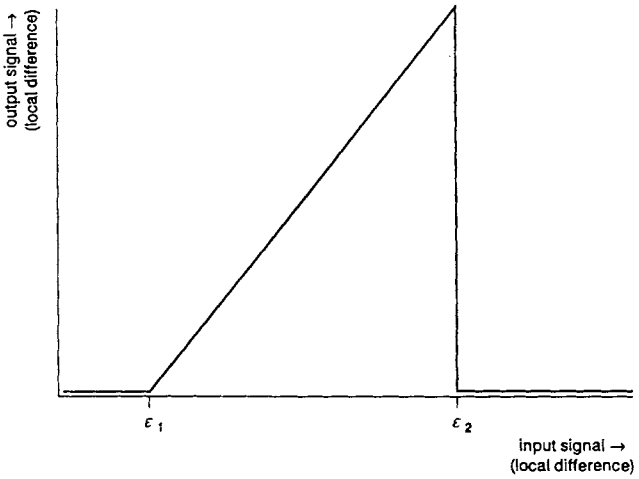


Fig. 13. Digital reduction of noise; restriction of local averaging to signals with low ($< \varepsilon_1$) or high ($> \varepsilon_2$) local differences from the surround.

white points in the lunar image of Figure 14 have been removed. In some cases it is advantageous to use the median of the surround pixels in place of the algebraic mean.[2]

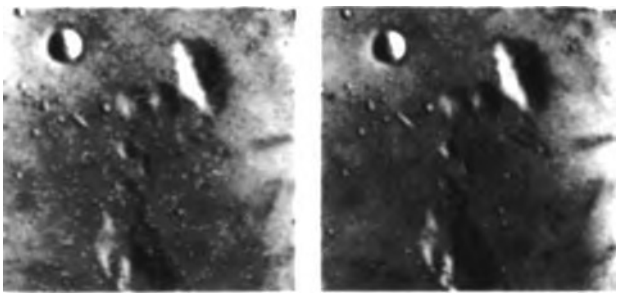


Fig. 14. Digital noise reduction by local averaging [2b].

Averaging over several independent images of the same object decreases granularity in digital images in the same way as in film images.

Another method having no parallel in film chemistry is carried out in the frequency domain. Noise is typically encoded in the high spatial frequencies. Filtering out the high frequencies preferentially suppresses noise (Fig. 15). However, this method also impairs the definition, but it is possible to minimize this by the use of special filters.[3c]

3.3. Visual System

We rarely experience noise in vision—only at near-darkness may we get an impression of flickering.[11, 19] Obviously, the visual system copes very effectively with noise.

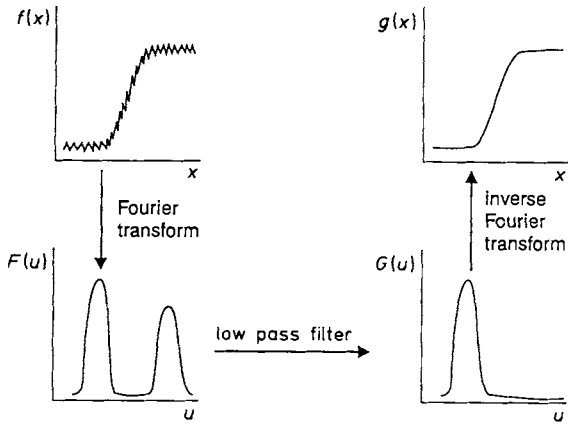


Fig. 15. Example of digital reduction of noise by application of a low-pass filter in the frequency domain (for explanation of symbols see Fig. 7).

Visual noise could have two sources: fluctuation of the input signal, which will be more pronounced at low light intensities (photon noise), or spatial-temporal deviations in the recording and transmission of the primary signals (system noise). The visual system masters intensity differences of $1:10^{10}$; the brain receives maximum differences of $1:10^{2}$.[20] This shows that the visual system can carefully control amplification, thus minimizing the noise problem.

Suppression of noise occurs in the visual system according to the same mechanism as applied in chemical and digital processing: by averaging both in spatial and in temporal mode.

- Spatial averaging: there are many more receptor cells than ganglion cells in the retina; each ganglion cell averages over approximately 100 receptor cells.
- Temporal averaging: the time resolution of the visual system is rather low; this forms the basis for cinematography. The eye cannot resolve individual images at frequencies of 20 images s^{-1} or higher[11, 21] but integrates the optical signals over a certain time span. The extent to which this improves granularity is immediately clear upon viewing an individual (still) image of a motion picture film. The temporal averaging is now no longer operative, and the coarse grain of the individual image becomes apparent.

An additional improvement of the signal-to-noise ratio is achieved in the visual system by transmitting only those signals to the brain which cross a certain (possibly adjustable) threshold.[22]

4. Sharpness

The sharpness of an image determines the quality of the reproduction of an edge (Fig. 16). The steeper the profile of a reproduced edge, the better the sharpness of the system. Improving sharpness means making an edge profile steeper or even overshooting the edges. Such an edge-effect improves the impression of sharpness.

4.1. Film

The sharpness of a color negative film can be chemically enhanced by two methods.

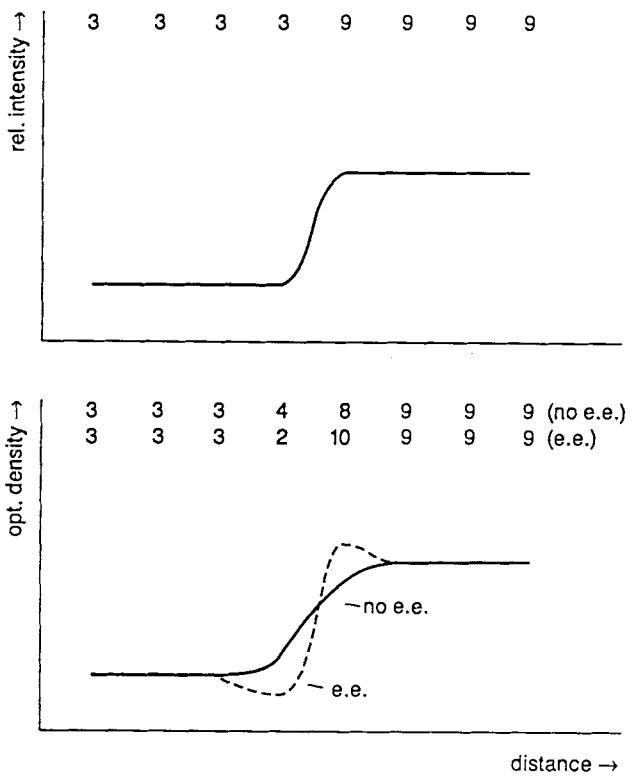


Fig. 16. Edge reproduction (in analog and digital notation). Top: original signal. Bottom: recorded signal with (e.e.) or without (no e.e.) edge effect.

The more important technique is that of "lateral inhibition" with inhibitors released from DIR couplers. Figure 17

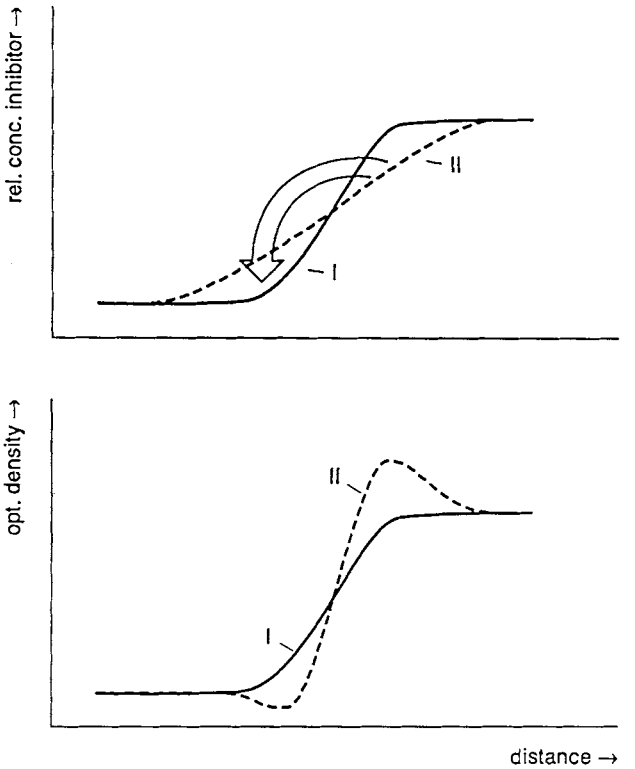


Fig. 17. Chemical generation of an edge effect in a film by lateral inhibition during the development process (schematic). Top: concentration of inhibitor without diffusion (—) and with diffusion (– – –). Bottom: corresponding optical densities.

shows the situation at an edge during development in the presence of a DIR couplers: image dye and inhibitor are formed on the high density side of the edge (see Section 2.1). Because of the concentration gradient the inhibitor diffuses in the direction indicated. That is, in the immediate vicinity of the edge the inhibitor concentration on the high density side decreases, while that on the low density side increases. The degree of development is affected accordingly. In this way an edge effect is generated. Chemical edge effects have been described quantitatively.[23]

The other method for improving sharpness is "unsharp masking", well known to darkroom specialists.[6] In this method a positive, unsharp image is printed in combination with the negative, sharp original image. Edge effects are thereby produced in the print. This principle can also be adapted for use in a film (Fig. 18). In this case a negative,

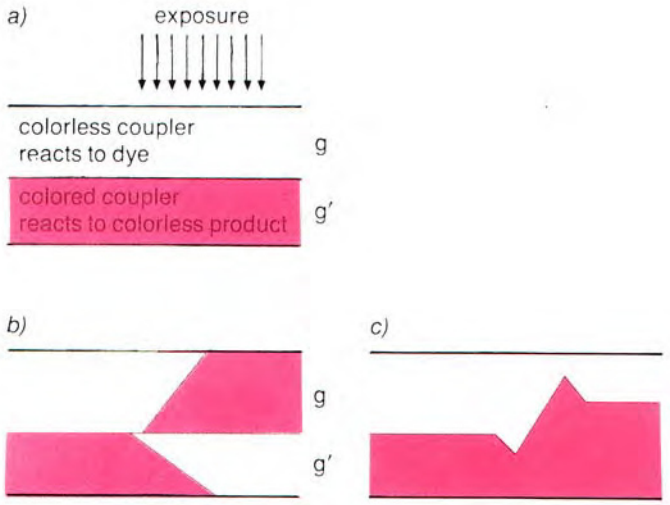


Fig. 18. Chemical generation of an edge effect by unsharp masking in the green-sensitive double layer of a color negative film (g, g': green-sensitive partial layers, K: coupler); a) before development, b) after development, c) summation of densities in the partial layers g and g'.

sharp partial image is generated in an upper layer and a positive unsharp, partial image in a lower layer. The total image from both partial images shows a clear edge effect.[24]

4.2. Digital Processing

There exist corresponding digital methods to both techniques for chemical enhancement of sharpness.

In digital "lateral inhibition" (center surround filter; high pass convolution mask[2]) each pixel value is modified, relative to its local surround. Figure 19 gives a simple example with the operator [− 1 3 − 1] to be applied to each number. The operator gives the instruction to take the threefold value of a particular number and to substract the values of both

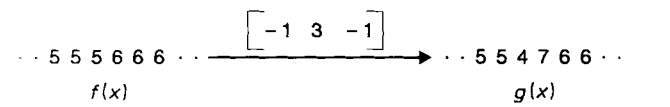


Fig. 19. Digital generation of an edge effect by lateral inhibition.

adjacent numbers. This operation transforms the left string $f(x)$ into the right string $g(x)$ exhibiting an edge effect. Thus, in digital lateral inhibition, each pixel is influenced in an inhibitory mode by its neighborhood—in analogy to chemical lateral inhibition.

Local differences are more or less emphasized depending on the form of the operator. For example, the operator [− 1 2 − 1] records differences only; this corresponds to a (negative) second derivative of the image function and leads to a contour image.

The calculation of local differences forms the basis of a whole class of methods for the enhancement of sharpness: gradient-technique,[3d] statistical differencing,[2c, 5] and use of second order derivative.[5] The combination of an original image function with its second order derivative results in an edge effect, as shown in the top portion of Figure 20.

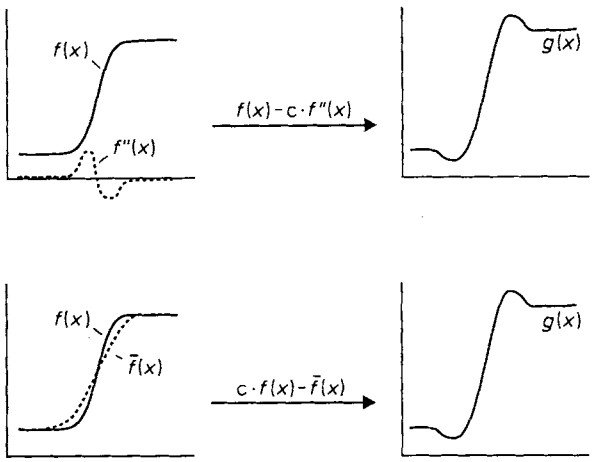


Fig. 20. Digital generation of an edge effect by combination of the original image function $f(x)$ — top: with its second order derivative $f''(x)$, bottom: with a function $\bar{f}(x)$ of reduced sharpness (unsharp masking).

Local lateral inhibition (or local differencing) amplifies signal differences and is therefore the counterpart of local averaging. Not only are edges enhanced, but also random signal differences, i.e. the noise. To overcome this dilemma, very sophisticated methods are applied or thresholds are introduced (see also Section 3.2). For example, the operator can be so modified that only local differences within preset threshold values ε_1 and ε_2 are amplified (Fig. 13), whereas local differences outside these thresholds are interpreted as noise and are suppressed.[5, 18]

In digital "unsharp masking" the original image function $f(x)$ is combined—in complete analogy to the corresponding chemical method—with a function of reduced sharpness $\bar{f}(x)$. Figure 20 (bottom) demonstrates that the resulting function exhibits an edge effect.[2, 4]

The digital methods for enhancing sharpness by processing in the frequency domain have no parallel in film chemistry. The information on edges is preferentially encoded in the high spatial frequencies; by amplification of this frequency range (high frequency emphasize filter) the edges can be emphasized.[2, 3, 5]

4.3. Visual System

An edge effect enhances recognition of details in the visual system, too. Figure 21 shows stepwise bands of different gray levels. This image gives the impression that the density in each band is increasing or decreasing near the edges. In fact, the density of the bands are completely uniform; the perceived edge effect is purely a visual phenomenon (Mach's bands[25]).

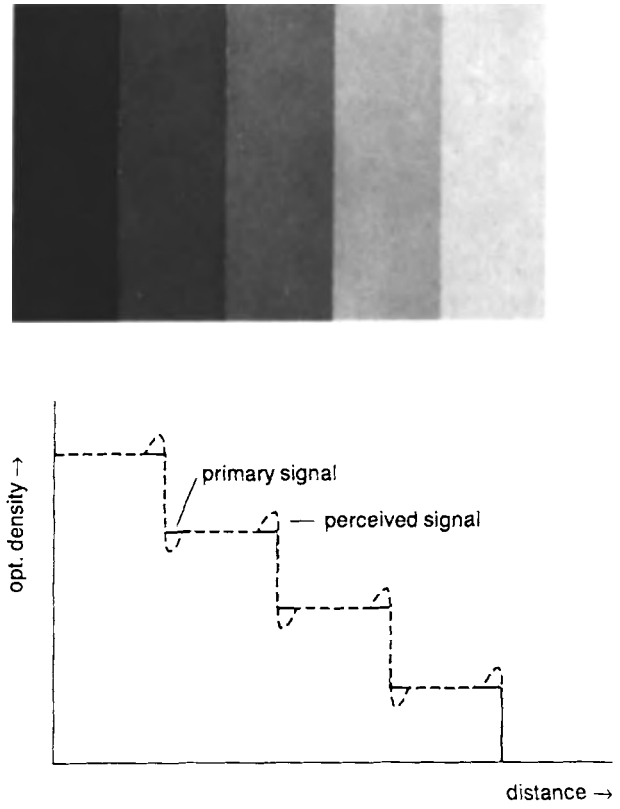


Fig. 21. Edge effect as visual phenomenon (Mach's bands).

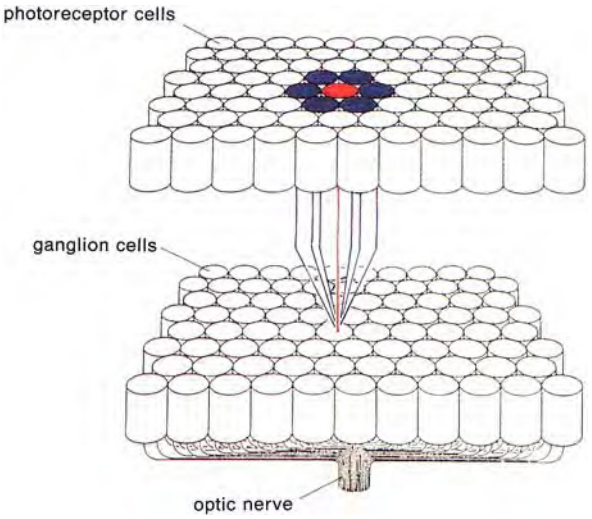


Fig. 22. Generation of edge effects in the visual system by lateral inhibition in the retina (from [26]).

The cause for the edge effects in the visual system is again lateral inhibition (Fig. 22). The receptor cells send activating signals (red) to the nearest ganglion cell but send inhibiting signals (blue) to more distant ganglion cells. Thus, each ganglion cell is subjected to a sum of activating and inhibiting signals. In complete analogy to chemical or digital lateral inhibition such a mechanism generates an edge effect.

The effect of lateral inhibition is also evident in the Hermann-effect: on viewing the black squares in Figure 23 ghost-spots are perceived at the intersections of the white bars between the black squares. At the intersections the lateral inhibition is relatively strong. Here, four inhibiting signals

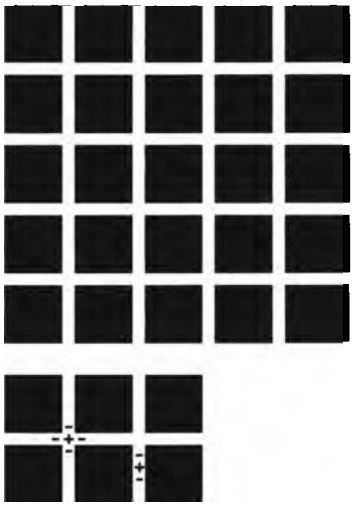


Fig. 23. Hermann effect; top: visual phenomenon; bottom: explanation.

from the surrounding region act on one activating signal, whereas in other white areas only two inhibiting signals act on one activating signal. The stronger lateral inhibition at the intersections gives the impression of lower brightness.[27]

Furthermore, the perception of sharpness in the visual system is spatial-frequency dependent: The visual resolution of a line pattern is better at medium spatial frequencies than at low or high spatial frequencies.[11, 25, 28]

5. Color Reproduction

Original colors are incorrectly recorded by any imaging system, e.g., by a film, because the dyes used have non-ideal absorptions (Fig. 24). When exposed, the color sensors of a film partially register wrong signals because of their non-ideal spectral response; for example, blue light is not only recorded in the blue-sensitive layer b, but to a certain extent also in the green-sensitive layer g. During printing the color information is falsified again, this time by the side-absorptions of the image dyes (the blue light of the printer is modulated not only by the yellow dye in b, but also to a minor extent by the magenta dye in g).

The situation can be described by a matrix of three equations (Fig. 25).[29] The equations contain six interference or

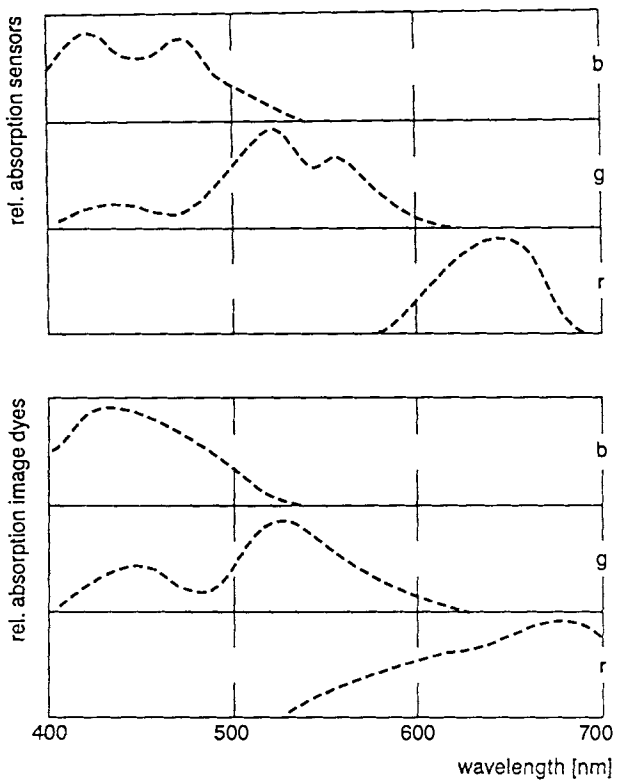


Fig. 24. Incorrect encoding of color signals in a color negative film by non-ideal absorption of the dyes used. Top: exposure. Bottom: read-out (printing).

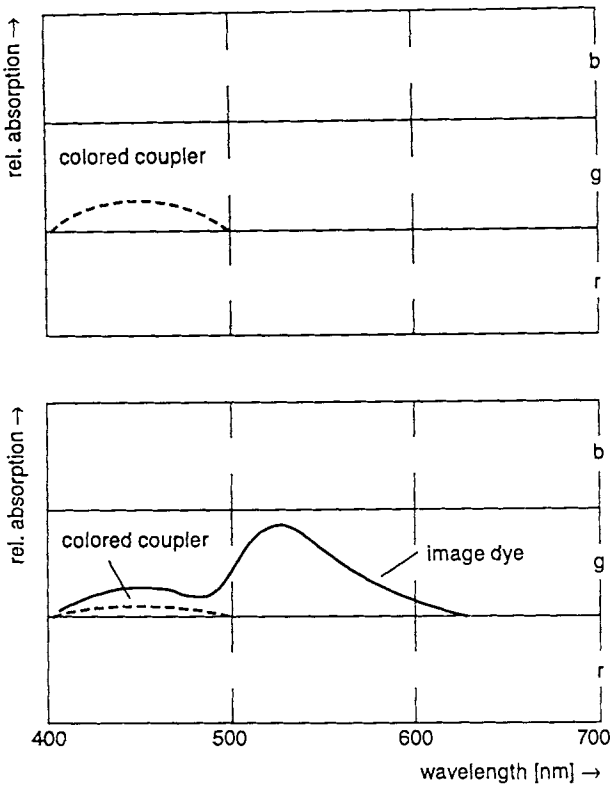


Fig. 26. Improvement of color reproduction in a color negative film by use of colored couplers; top: absorption of green-sensitive layer g before development; bottom: absorption of g after exposure and development.

correction terms which have different weighting. The mutual interference of the color signals affects color saturation and tone.

$$B' = +k_1B - k_2G - k_3R$$

$$G' = -k_4B + k_5G - k_6R$$

$$R' = -k_7B - k_8G + k_9R$$

Fig. 25. Calculation of the original color signals B', G' and R' from the degraded signals B, G and R; k_i are constants for a specific recording system.

5.1. Film

In the case of a film the color signals B,G, and R correspond to the optical densities (determined by the concentration of the respective dyes) as measured behind blue, green, and red filters.

The chemist has two methods available for improving (correcting) the color reproduction by interaction of the color signals with each other according to the matrix in Figure 25.[6, 29]

The first method involves the use of colored couplers (Fig. 26). For example, to correct for the yellow side-absorption of the magenta dye a yellow coupler is additionally incorporated into the green-sensitive layer; this coupler reacts with loss of its color. At a certain ratio of standard coupler and colored coupler the decrease in yellow density achieved by the reaction of the colored coupler compensates for the increase of the yellow density caused by the side-absorption of the magenta dye. The film exhibits a uniform yellow density before and after development which is filtered off in the printing process. Theoretically, all six interference terms can be corrected for by appropriate colored couplers. In practice only yellow colored couplers are used for the green-sensitive layer and red colored couplers for the red-sensitive layer. These colored couplers give color negative films an orange tint.

The other method "vertical inhibition", is based once again on the use of DIR couplers and the action of the inhibitors released during development. If, for example, a color negative film is exposed to a lot of green light and little blue light and red light, more magenta and less yellow dye and red dye are produced (Fig. 27). In the presence of a DIR coupler more inhibitor is released in layer g than in layers b and r. A vertical concentration gradient is built up, resulting in a diffusion of inhibitor from layer g into both adjacent layers, thus inhibiting development there. The situation can be arranged in such a way, that the development of the yellow dye in layer b is inhibited to such an extent that the undesired yellow side-absorption of the magenta dyeing is just compensated for. The diffusion of inhibitor out of the layer g simultaneously enhances the development in this layer. Both effects—the inhibition in the adjacent layers and the activation in the dominant layer—contribute to increased color saturation. The inhibitor of one layer acts on the other two layers (as shown in Fig. 27); incorporation of DIR couplers into all three layers generates a total of six inter-image effects, which correspond to the six correction terms in the matrix of Figure 25.

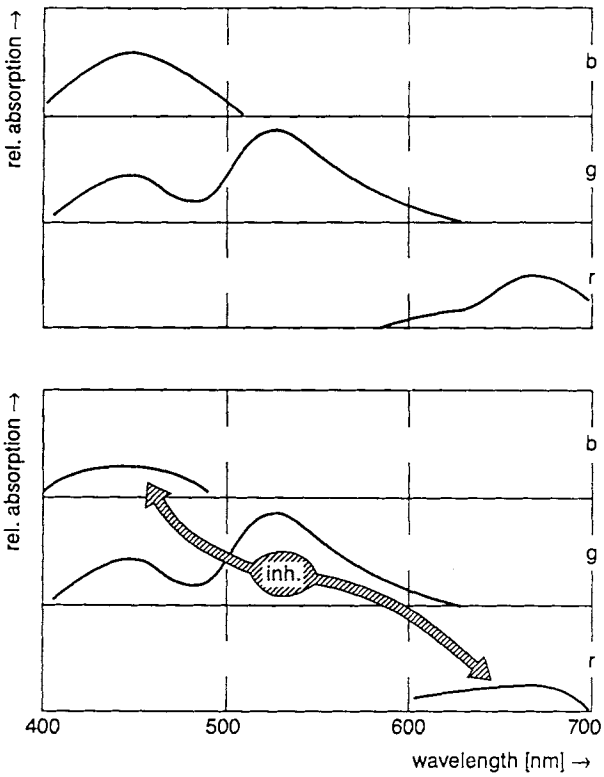


Fig. 27. Improvement of color reproduction in a color negative film by vertical inhibition. Top: absorption in the three partial layers of a developed film without vertical inhibition. Bottom: absorption in a film with vertical inhibition.

5.2. Digital Processing

In digital image processing the mutual interference of the color signals R, G and B can be eliminated by applying the matrix of Figure 25.[21a] The six correction terms are specific for a particular image system (for example for a particular type of film) which affords the input data for the digital image processing. After digital matrixing, the color failures of the original image are corrected with regard to tone and saturation.

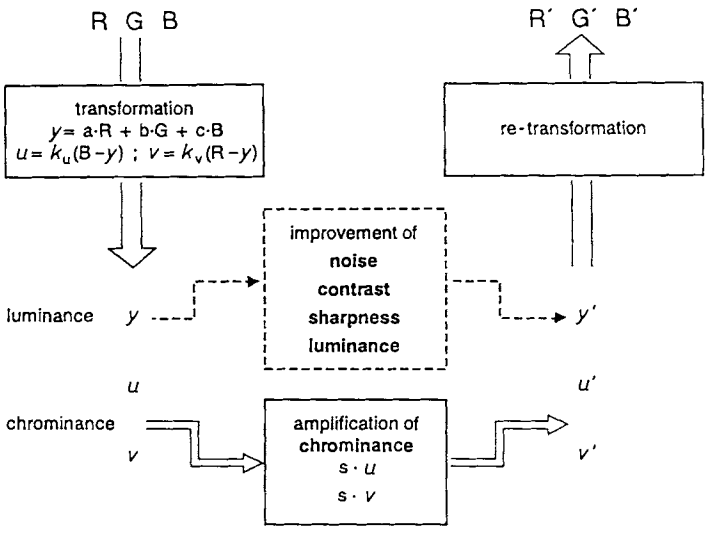


Fig. 28. Improvement of color saturation by digital amplification of chrominance and of image quality by modification of the luminance.

Another way to digitally influence color reproduction is by first transforming the input signals R, G and B into a luminance signal y and two chrominance signals u and v. The tranformations are given in Figure 28.[21c] The color saturation is increased if both chrominance signals are equally amplified. The luminance signal is used to improve noise, contrast, sharpness and brightness. The modified signals y', u' and v' are then converted into improved signals R′, G′ and B′. The increase in color saturation achieved by this method is shown in Figure 29.



Fig. 29. Top: conventional print of a slide. Bottom: print of same slide but with digital processing (digital image processing by CRT printer Agfa-Gevaert AG).

5.3. Visual System

Color results from a non-uniform excitation of the three kinds of color-sensitive receptor cells.

The visual system has the ability to perceive the colors of an object as constant regardless of the color of the illuminating light. This has been demonstrated by *Land*[30] in a decisive experiment shown in Figure 30: a color board is illuminated by three light sources (blue, green, red) and the reflectance striking the eye is measured. In the first case a certain reflectance R_1, G_1, B_1 strikes the eye from the blue field. In the second case the light sources are adjusted in such a way that exactly the same reflectance R_1, G_1, B_1 now comes from the formerly yellow-green field. We should expect that this field now appears blue. But this is not so; this field is seen as yellow-green in both cases, and similarly the other fields are perceived as unchanged with regard to their color. Obviously, the eye relates the color signals from any field to its surroundings. A triplet of relative signals determines the color perceived.

In the context of this comparison of processing algorithms it is also interesting that in the visual system the signals R, G

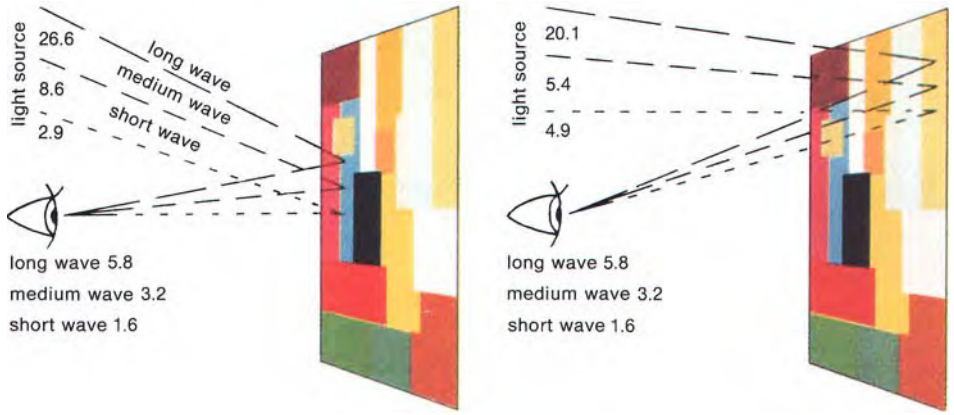


Fig. 30. Experiment for the demonstration of the eye's constancy of color perception. The values quoted are emission densities [$mWsr^{-1}m^{-2}$] (from [30]).

and B from the cone-shaped cells are combined locally in the retina in excitatory (+) and inhibitory (−) mode; the composite signals consist of two chrominance signals (R − G; B − R − G) and one luminance signal (R + G + B + rod signal). This model of opponent colors explains many phenomena of color perception[31, 32]; the model is similar to the mechanism of lateral inhibition (in the eye); whereby in both cases an activating center is surrounded by an inhibiting area.

6. Conclusion and Outlook

Table 1 summarizes and compares the methods for image enhancement discussed thus far. Although some methods are specific for certain systems, the analogies are evident.

Table 1. Comparison of image enhancing methods.

Image Property	FILM Chemical Processing	COMPUTER Digital Processing	VISUAL SYSTEM Neural Processing
Noise (Granularity)	• Averaging • Incomplete transform. Ag → Dye	• Averaging • Thresholding • Frequency filter	• Averaging • Thresholding
Sharpness	• Lateral inhibition • Unsharp masking	• Lateral inhibition • Unsharp masking • Frequency filter	• Lateral inhibition • Frequency filter
Color	• Matrixing – Colored couplers – Vertical inhibition	• Matrixing • Transformation RGB → Lum./Chrom. (Amplification Chrom.)	• Color Constancy • Transformation RGB → Lum./Chrom.

Noise is reduced by local or temporal averaging in all three image processing systems. Thresholds minimize the adverse effects of averaging on sharpness; they are applied in both digital and visual image processing.

Sharpness is improved in all three systems by edge effects caused by lateral inhibition. The method "unsharp masking" is used in chemical as well as in digital image processing. Frequency filters are common in digital processing and also in the visual system.

The correction of color reproduction in color negative films by matrixing (colored couplers or vertical inhibition) corresponds to matrixing in digital processing. In both cases, the R, G, and B color signals are corrected by mutual interaction. The transformation of the R, G and B signals into luminance and chrominance signals is used in both digital and visual processing.

Some striking analogies occur in the methods of image enhancement in these vastly different systems—the chemical film, the electronic computer, the biological visual system. The methods are written in codes specific to these systems; these are chemical reactions and diffusion in the film, electronic data processing in the computer, and neural mechanisms in the visual system.

The analogies described for image processing are relevant for the future of the photographic technology in two ways. Firstly, studying the similarities of digital and biological mechanisms for image enhancement may stimulate further improvement of the photographic film. Secondly, a competing technology becomes evident: A photographic image can be improved by chemical means incorporated into the film as well as by digital image processing in the finishing stage. Future films and their processing may perhaps be simplified because the computer takes over some processing functions. Whether chemical, parallel processing is superior to digital processing or whether the combination of both technologies will give the best results is still an open question.

I am very grateful to my colleague Dipl.-Ing. Eduard Wagensonner for his patience in explaining digital image processing to me.

Received: February 28, 1989 [A 741-IE]
German version: *Angew. Chem. 101* (1989) 1633

[1] P. Haberäcker: *Digitale Bildverarbeitung*, Hanser, München 1987.
[2] a) W. K. Pratt: *Digital Image Processing*, Wiley, New York 1978; b)[2a], p. 320; c)[2a], p. 323.
[3] a) R. C. Gonzalez, P. Wintz: *Digital Image Processing*, Addison-Wesley, London 1977; b)[3a], p. 199ff; c)[3a], p. 139; d)[3a], p. 153.
[4] E. L. Hall: *Computer Image Processing and Recognition*, Academic Press, New York 1979.
[5] D. C. C. Wang, A. H. Vagnucci, C. C. Li, *Computer Vision, Graphics and Image Processing 24* (1983) 363.

[6] R. W. G. Hunt: *The Reproduction of Colour*, Fountain Press, Tolworth 1987.
[7] G. Haist: *Modern Photographic Processing, Vol. 2*, Wiley, New York 1979, p. 501.
[8] T. M. Cannon, B. R. Hunt, *Sci. Am. 245* (1981) No. 4, p. 136.
[9] D. H. Hubel, T. N. Wiesel, *Sci. Am. 241* (1979) No. 3, p. 130; *Spektrum Wiss. 1979*, No. 11, p. 106.
[10] T. Poggio, C. Koch, *Sci. Am. 256* (1987) No. 5, p. 42; *Spektrum Wiss. 1987*, No. 7, p. 78.
[11] T. N. Cornsweet: *Visual Perception*, Academic Press, New York 1970.
[12] J. L. Schnepf, D. A. Baylor, *Sci. Am. 256* (1987) No. 4, p. 32.
[13] R. H. Masland, *Sci. Am. 255* (1986) No. 6, p. 90.
[14] R. Scheerer, E. Ranz, J. Lohmann, EP 0045427 (1981), Agfa-Gevaert.
[15] a) T. H. James (Ed.): *The Theory of the Photographic Process*, Macmillan, New York 1977; b) [15a], p. 343.
[16] W. Püschel, DBP 1099350 (1959), Agfa-Gevaert.
[17] a) [15a], p. 621; b) R. E. Booms, US-Pat. 4420556 (1981), Eastman Kodak.
[18] R. W. G. Hunt, *Phys. Technol. 16* (1985) 12.
[19] A. Rose: *Vision*, Plenum Press, New York 1973, p. 45.
[20] F. S. Werblin, *Sci. Am. 228* (1973) No. 1, p. 71.
[21] a) H. Lang: *Farbmetrik und Farbensehen*, R. Oldenbourg, München 1978; b) [21a] p. 284; c) [21a] p. 329.
[22] H. B. Barlow, T. P. Kaushal, M. Hawken, A. J. Parker, *J. Opt. Soc. Am. A 4* (1987) 2366.
[23] J. R. Jarvis, *J. Phot. Sci. 33* (1985) 212.
[24] M. Fujiwara, EP 0174873 (1984), Konishiroku.
[25] F. Ratliff, *Sci. Am. 226* (1972) No. 6, p. 90.
[26] T. Poggio, *Sci. Am. 250* (1984) No. 4, p. 68; *Spektrum Wiss. 1984*, No. 6, p. 114.
[27] J. P. Frisby: *Sehen*, Heinz Moos Verlagsges., Gütersloh, p. 156.
[28] F. W. Campbell, L. Maffei, *Sci. Am. 231* (1974) No. 5, p. 106.
[29] P. Kowaliski: *Applied Photographic Theory*, Wiley, London 1972, p. 258.
[30] E. H. Land, *Sci. Am. 237* (1977) No. 12, p. 108.
[31] M. S. Livingstone, D. H. Hubel, *J. Neurosci. 4* (1984) 309.
[32] D. H. Hubel: *Auge und Gehirn*, Spektrum der Wissenschaft Verlagsges., Heidelberg 1989.

Synthesis, Structure and Reactivity of Sulfur-Rich Cyclopentadienyl-Transition Metal Complexes: Sulfur Chemistry from an Organometallic Point of View

By Joachim Wachter*

Metal-sulfur centers play an important role in the activity of metalloproteins in enzymatic catalysis and the activity of metal sulfides as heterogeneous catalysts. The systematic search for M–S model compounds led to the discovery of an interesting and novel structural chemistry, which stems from the numerous coordination possibilities of sulfur ligands. The intention of this review article is to present and outline new approaches to sulfur chemistry from the organometallic point of view. Reactive cyclopentadienyl-transition metal fragments incorporate elemental sulfur to give polynuclear sulfur-rich complexes, which can contain either mono-, di- or polysulfido ligands or several such ligands in combined form. The versatile structural chemistry of the complexes formed and their reactivity towards organic, inorganic and organometallic compounds are discussed, and examples of some simple and rational procedures for their synthesis starting from cyclopentadienylcarbonyl- and cyclopentadienylhydrido-complexes are outlined. Their reactivity is manifested in numerous metal- and ligand-centered reactions. Finally the, albeit far less extensive, complex chemistry of the other chalcogens (O, Se, Te) is also considered for comparison, thus providing a more detailed survey of particular aspects of this area of chemistry.

1. Introduction

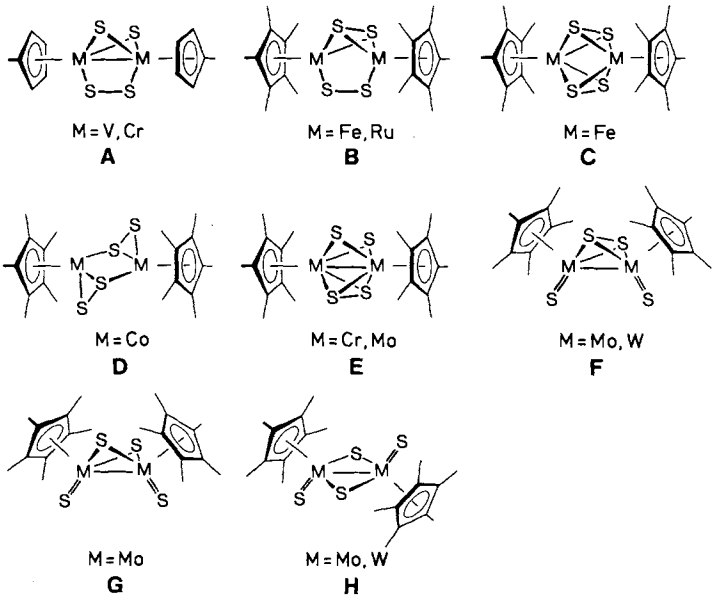
The chemistry of soluble transition metal sulfides is virtually inexhaustible. Whether one is considering the stabilization of unusual bonding systems or molecular model compounds, the immense range of possibilities available to sulfur in metal complex ligands is impressive.

Metal–sulfur complexes are, for example, of special interest with regard to the modes of action and the structures of many enzymes. The as yet unsolved problem of the structure of the active center of nitrogenase—the enzyme system that converts atmospheric nitrogen into ammonia—is often cited as example to demonstrate just how difficult it is to obtain structural information of biological centers indirectly using even the best possible model complexes.[1]

Metal sulfides also play a role in the desulfurization of fossil fuels by hydrogenation (e.g. hydrodesulfurization, HDS).[2] Utilization of the worlds sulfur-containing resources in an economic and environmentally unobjectionable way demands that basic research be carried out on soluble model systems—the HDS process actually occurs on a heterogeneous metall sulfide surface.

It is obvious from the examples already quoted that simple model systems in the form of soluble transition metal sulfides are required in order to extend our existing knowledge of sulfur coordination chemistry. The effort being made in this direction is reflected in the number of reviews of complexes with mono-,[3] di-[4] and polysulfido ligands.[5] Parallel to these investigations a new research area has been opened up with the chemistry of polynuclear sulfur-rich transition metal complexes. The addition of elemental sulfur to reactive cyclopentadienylmetal fragments and subsequent fragmentation of the generally unisolable primary products leads predominantly to binuclear complexes. The advantages offered by this chemistry are the generally uncomplicated synthetic strategies, the good solubility of the products, and the readiness of the products to undergo further reactions. The use of cyclopentadienyl carbonyl complexes often enables the spectroscopic observation and isolation of intermediates that can provide valuable information about the degradation of the S_8 ring.

As already demonstrated in an earlier review of the structures of binuclear sulfur-rich cyclopentadienyl complexes,[6] the sulfur: metal ratio varies from 1:2 to 10:2. The structure



Scheme 1. Examples of possible structure types (A–H) for $[Cp_2^{(*)}M_2S_4]$ complexes.

[*] Dr. J. Wachter,
Institut für Anorganische Chemie der Universität
Universitätsstrasse 31,
D-8400 Regensburg (FRG)

of the relatively simple molecules $[Cp_2^{(*)}M_2S_4]$[*] has alone been formulated in eight different ways to date (Scheme 1). This immediately calls for a clarification and comparison of the background information concerning the formation, structure and reactivity of all these complexes in relation to the nature of the central metal and to the influence of the substituents in the $Cp^{(*)}$ ligand.

The number of analogous Se- and Te-complexes is still relatively small, but nevertheless the existing results allow a comparison to be made between the differing reactivities of the chalcogens and a given CpM fragment. Oxygen is an exception since there already exists an extensive V-complex and Re-complex chemistry.[7] Even so, a discussion of the structural peculiarities of its complexes in comparison to the complexes of its higher homologues would appear stimulating.

2. Syntheses and Structures

2.1. Cyclopentadienyl Sulfides and Selenides of the Electron-Deficient Transition Metals

Rings with an even number of members in which two $Cp_2^{(*)}M$ fragments are present but do not directly interact with each other, are characteristic of the complexes **1** of the group 4 metals. There are many diverse methods available for the synthesis of such complexes. Ti-complexes **1**, for example, are accessible by desulfurization of $Cp_2^{(*)}TiS_5$ with PR_3 (the number n of bridging chalcogen atoms in the product depends on the nucleophilicity of the phosphane[8]) or by the reaction of Cp'_2TiCl_2 with Li_2Se_2 (n = 2).[9] Reaction of carbonyl derivatives such as $Cp_2^{(*)}Ti(CO)_2$ with H_2S[10] or H_2Se[11] yields the kinetically labile complexes **1** (n = 1). These form symmetrical clusters at higher temperatures, e.g. $[Cp_4Ti_4Se_4]$. A less pungent and less toxic way to complexes of type **1** is via the reaction of Cp'_2Zr, prepared in situ, with elemental S or Se.[12] Two different sorts of chalcogen bridges can be found in $[Cp_4Hf_2(\mu\text{-}O)(\mu\text{-}Se_4)]$,[13] the only known binuclear hafnium compound. It is formed from Cp_2HfSe_5 by exposure to air.

1, M = Ti, Zr
E = S, n = 1–3; E = Se, n = 1,2

The sulfur-rich vanadium complexes $[Cp_2^{(*)}V_2E_n]$ **2–4** (E = S, Se; n = 3–5) are structurally completely different from the binuclear complexes **1**. The diamagnetic compounds **2** can be prepared either by thermolysis of Cp'_2VE_5[14,15] or by dehalogenation of Cp_2VCl_2 with $Se(SiMe_3)_2$[16]. Since these reactions occur with the elimination of a $Cp^{(*)}$ ligand from each metal atom, the products strive to overcome their electron deficiency by utilizing three different chalcogen bridges as well as a metal–metal interaction (d_{V-V} 2.66–2.77 Å). An interesting and recurring phenomenon in complexes of the general composition $[Cp_2^{(*)}M_2S_n]$ ($n \geq 4$) is the stabilization of unusual electron configurations at the metal by M–E d_π–p_π interactions.[*] Such stabilizations may be the driving force for the unusual sulfur abstraction from **2a** ($Cp^{(*)} = Cp'$) by PBu_3 with formation of the 26e complexes **3**[18] and **4**.[17] Due to the very short V–S distances ($\bar{d}_{V-S}$ 2.23 Å) for *all* sulfur atoms, an alternative view of the general system of **3** and **4** with 34 valence electrons was suggested.[18]

E = S (a), Se (b)

2a,b

3 **4**

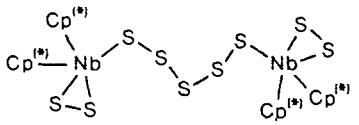
[*] If not otherwise indicated the following abbreviations for the cyclopentadienyl ligands apply: Cp = C_5H_5, Cp' = MeC_5H_4, Cp* = C_5Me_5, $Cp^{(*)}$ = any other substituted cyclopentadienyl ring. These ligands are η^5-coordinated in all cases.

[*] With a neutral charge distribution the contribution of the chalcogen ligands to the electron count of **2** is 2(μ-E) + 2(μ,η^1-E_2) + 6 (μ,η^2-E_2) electrons, which together with the 2 × 10 electrons from the two $Cp^{(*)}V$ units adds up to 30 e [3, 4]. The alternative view with μ-$E^{2\ominus}$, μ,η^1-$E_2^{2\ominus}$, and μ,η^2-E_2^{2-} ligands (4 + 4 + 8) and two $V^{4\oplus}$ centers leads to a similar result.



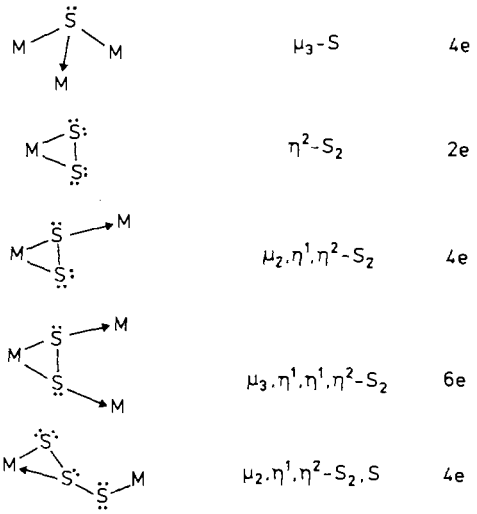
Joachim Wachter was born in 1945 in Böhmen and spent his early years in Riedenburg (Bavaria). He studied chemistry up to Diploma level at the University of Munich and received his doctorate from the University of Regensburg under Prof. Dr. H. Brunner. 1978/79 he carried out postdoctoral research with Prof. J. G. Riess in Nizza. Since 1977 he has been "Akademischer Oberrat" at the University of Regensburg. His research interests lie in the field of organometallic–chalcogen complexes and metal–metal multiple bonds.

The examples of sulfur-rich CpNb dimers known to date apparently show more similarities to Ti-complexes than to V-complexes. Thus, in principle, $[Cp_4Nb_2S_2]$[19] belongs to the same structure type as **1**, despite its weak Nb–Nb interaction (d_{Nb-Nb} 3.23 Å). A mixture of most likely very similar polysulfido complexes is formed upon reaction of $(t\mathrm{BuC_5H_4})_2NbH_3$ with S_8. The structure of **5**, in which the



5

two $(t\mathrm{BuC_5H_4})_2Nb(\eta^2\text{-}S_2)$ units are connected by an S_5-chain, was determined by an X-ray crystallographic analysis.[20] The above-mentioned mixture of polysulfido complexes can, depending on the large number of S–S bonds, be converted in toluene at 100 °C into three trinuclear clusters of slightly less sulfur content, of which **6** and **7** have been fully characterized (Fig. 1). The niobium-sulfur skeleton of **6** shows not less than five different ligand types (Scheme 2).[20] The core of the molecule (Fig. 1a) is a much flattened Nb_3S tetrahedron, whose base is spanned by a triply bridging S_2 group. Two Nb–Nb bonds are each bridged by an η^1, η^2-S_2 ligand. In contrast, Nb1–Nb2 is bridged by an η^1, η^2-S_3 ligand. The coordination sphere of Nb3 is completed by a terminal η^2-S_2 ligand.



Scheme 2. Overview of representative sulfur ligand types found in **6**, their bonding, and the number of electrons which they—assumed as neutral—contribute to the bonding.

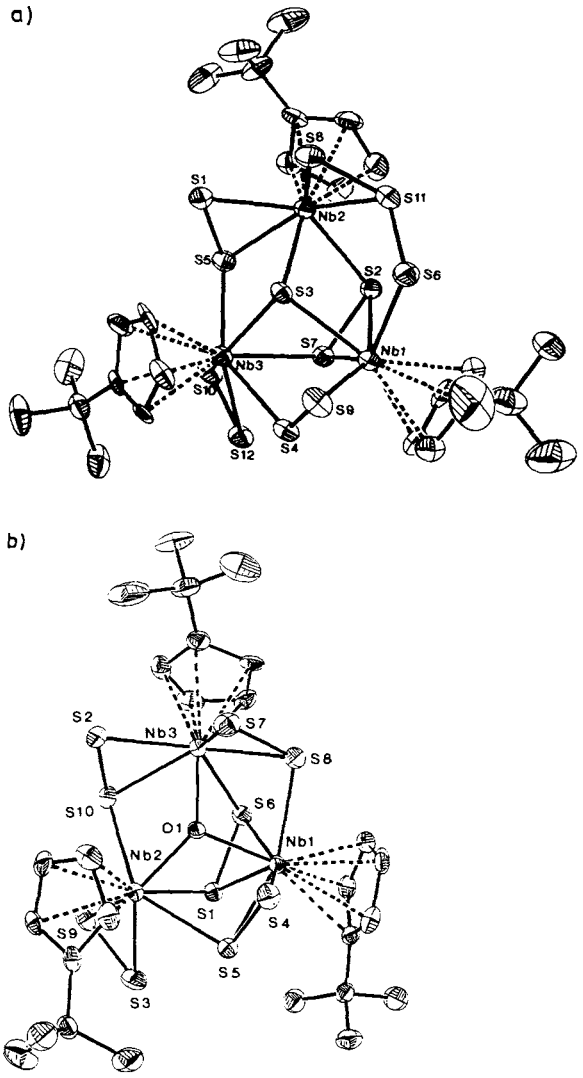


Fig. 1. a) Structure of $[(t\mathrm{BuC_5H_4})_3Nb_3S_{12}]$ **6** in the crystal. The S_2 ligand S4-S9 is bound η^2 to Nb1. b) Structure of $[(t\mathrm{BuC_5H_4})_3Nb_3S_{10}O]$ **7** in the crystal.

The structure of **7** (Fig. 1b), which can also be prepared directly from **6** by heating for a longer time in toluene solution, is closely related to that of **6**. At the apex of the central tetrahedron there is an oxygen atom, however, and instead of the S_3 ligand there is now only an η^1,η^2-S_2 ligand. This has no electronic consequences, but as a first principle of order a uniform orientation of the points of the edge-bridging S_2 ligands towards the top of the tetrahedron can be seen. This means that the compounds **6** and **7** differ in a remarkable way from the sulfur-bridged, but still halogen-containing clusters formed on reaction of $CpMHal_4$ (M = Nb, Ta) with $S(SiMe_3)_2$.[16]

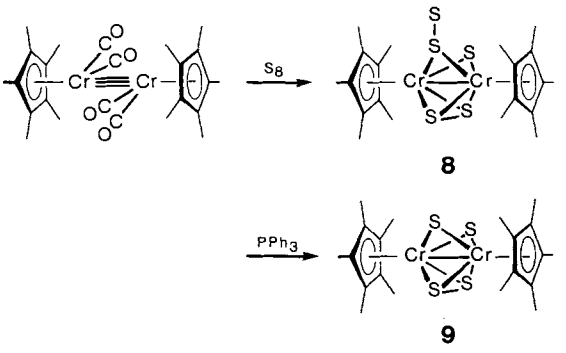
The sulfurization of Cp-carbonyl-Nb derivatives has until now only been investigated sporadically, although this entry to sulfur-rich cyclopentadienyl complexes has proven very successful for the later transition metal elements. Thus, reaction of $[CpNb(CO)_3(thf)]$ with S_8 leads to the CO-free complex of the composition $[Cp_2Nb_2S_5]$. Its structure, however, is still unclear.[21] It therefore remains to be seen whether the complexes $[\{CpNb(CO)_2\}_2(\mu\text{-}S)_n]$ (n = 2,3) are formed as intermediates en route to complexes with less CO- but a higher sulfur-content upon reaction of H_2S or MeSH and $[CpNb(CO)_3(thf)]$.[21]

2.2. Binuclear Cyclopentadienyl Chalcogenides of the Chromium Triad

2.2.1. Complexes of the Type $[Cp_2^{(*)}Cr_2S_n]$ (n = 4,5)

Due to the reactivity of their M–M triple bonds the complexes $[Cp'^{(*)}M(CO)_2]_2$ are generally the most suitable start-

ing materials for the synthesis of sulfur-rich binuclear complexes of the Cr triad. Thus for example, reaction of $[Cp^*Cr(CO)_2]_2$ and S_8 affords the complex **8**,[22] which in turn reacts with PPh_3 with elimination of sulfur to give **9**.[23] The complexes **8** and **9** are isoelectronic (each possessing 32



8

9

valence electrons) and therefore have similar structural frameworks resembling those of triple-decker compounds[22, 24] in which all bridging ligands lie in a plane perpendicular to the Cr–Cr vector and parallel to the Cp* rings. It is worth pointing out that **8** contains an η^1-S,S bridge, in which only one S atom is coordinated to both Cr atoms (Fig. 2). The bent character of this moiety (S5 is orien-

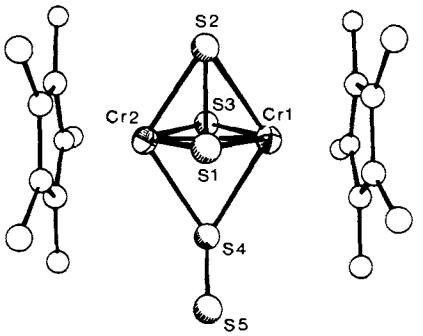
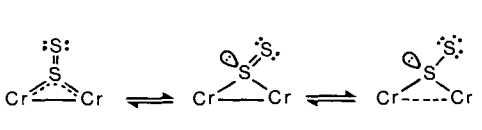


Fig. 2. Structure of **8** in the crystal.

tated towards the η^2-S_2 ligand) suggests a 2e donor (Scheme 3, **J** and **K**) and therefore not the valence tautomer **I**, in which the η^1-S_2 ligand would effectively be a 4e donor. In contrast its SO homologue $[\{Cp(CO)_2Mn\}_2(\mu\text{-SO})]$ has the structure corresponding to **I**.[25] A participation of the reso-

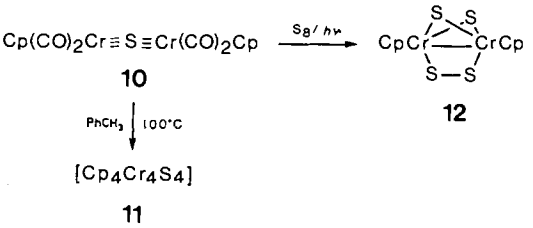


I **J** **K**

Scheme 3. Possible valence tautomerism of the μ,η^1-S,S ligand of **8**.

nance structure **K** explains the relatively long S–S bond (2.101 Å) and the higher nucleophilicity of the terminal sulfur atom.[23, 24] The formation of the η^1-S_2 ligand is surprising, since it does not differ electronically from a μ-S ligand.

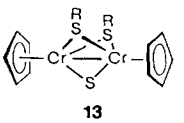
The reaction of $[CpCr(CO)_3]_2$ with S_8 is of a completely different character, since a relatively labile Cr–Cr single bond makes the insertion of sulfur possible. Other than in the case of dimers of the iron triad (see, for example, **36** and **41** in Section 2.4) with a Cr dimer maximally S_2 units are inserted into the M–M bond and only two CO ligands are substituted.[26] The main product **10** contains an almost linear CrSCr multiply bonded system.[27] Thermally, this readily undergoes cleavage of CO to give the 60e pseudocubane **11**. Photochemically, however, it can be transformed in the presence of sulfur into **12**.[28] From a structural point of view



10 **11** **12**

complex **12** has the same ligand set as the vanadium complex **3**. Formally, **12** (structure type **A** in Scheme 1) is related to **9** (structure type **E**) through a 90° rotation of the S_2 bridge (in contrast to the analogously built Mo sulfides (see Section 2.2.2) **9** and **12** are configurationally stable). Although the two complexes differ in their total electron count by four electrons, their magnetic behavior is very similar.

Also conceivable would be the existence of $[Cp_2Cr_2(\mu_1,\eta^2\text{-}S_2)(\mu\text{-S})]$, an even more sulfur-deficient compound than **9**. The isoelectronic dimethylthiolato complex **13** is al-



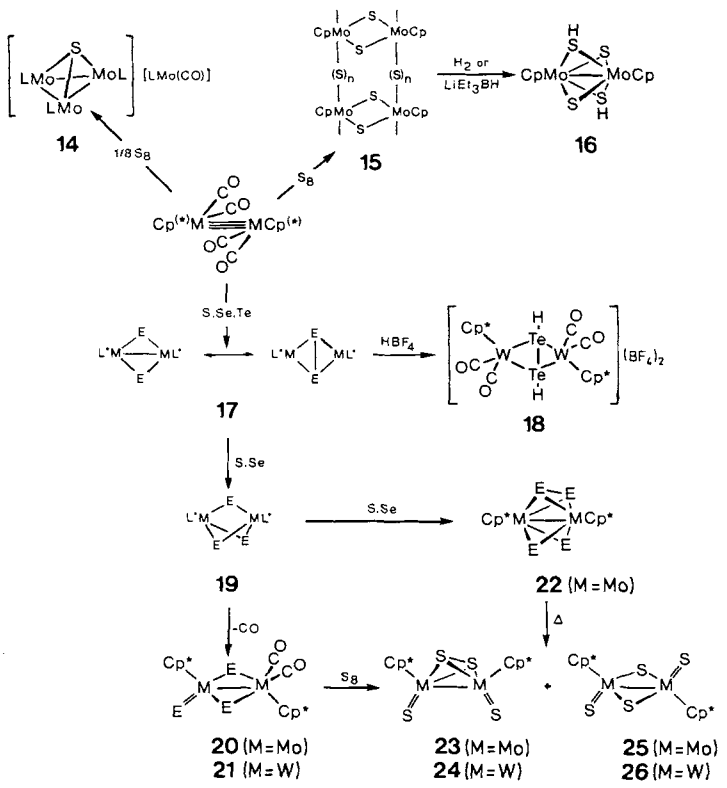
13

ready known. It shows antiferromagnetic behavior and serves as starting material for the synthesis of numerous S-bridged cluster compounds.[29]

2.2.2. *Cyclopentadienyl Sulfides and Selenides of Mo and W*

Since the M–M triple bond in $[Cp^{(*)}M(CO)_2]_2$ when M = Mo and W is generally more reactive than that when M = Cr,[30] the 'harvest' of sulfur-containing compounds is naturally richer. In contrast to the Cr system, even Se- und Te-containing compounds are occasionally isolated. As far as results up to now indicate, there are parallels between the reactivity of S and Se, while Te is distinctly less reactive. Particularly striking is the control of the course of reaction by the nature of the cyclopentadienyl ligand (Scheme 4), whereby steric effects may largely be decisive.

$[CpMo(CO)_2]_2$ reacts with substoichiometric amounts of sulfur to give **14**, whose cation contains an Mo_3S tetrahedron.[31] In contrast, with sulfur in excess the insoluble compound **15** is formed.[31–33] The formulation of **15** as a polymer would appear justified insofar as it can be converted under mild conditions with H_2[34] or $LiEt_3BH$ into the soluble hydrogensulfido-complex **16**.[35]



Scheme 4. Overview of the reactions of the chalcogens S,Se and Te with $[Cp^{(*)}M(CO_2)]_2$ (M = Mo, W; L = $Cp(CO)_2$, L* = $Cp^*(CO)_2$). **19**–**22**: **a**, E = S; **b**, E = Se. X-ray structurally characterized complexes shown in bold print.

As demonstrated by the occurrence of the kinetically labile di- and tri-chalcogen products **17** and **19** in the reaction of $[Cp^*M(CO)_2]_2$ (M = Mo, W) with condensed sulfur or selenium vapor at low temperatures, there must be a stepwise addition of chalcogen fragments to the M≡M bonds.[36] In contrast, in order to introduce the much less reactive Te the reaction must be carried out at the temperature of boiling THF. The intermediate **17**, for which there are two conceivable isomeric forms, can in the case of the W–Te compound be captured as a stable complex salt **18** by double protonation. This contains the unusual Te_2H_2 ligand.[36]

The formation of the complexes **20** and **21** from **19** can be interpreted in terms of an intramolecular rearrangement of the E-ligand framework with partial CO elimination and formation of an M–M bond. **21a** is the first structurally characterized complex whose sulfur bridges are not symmetrical owing to the unusual polarization of the molecule.[37] Whereas the CO ligands of the Mo-intermediates **19** (M = Mo) and **20** are relatively easily substituted by sulfur or selenium (45 °C, toluene), the W-complex **21a** reacts only with S_8 under substantially more drastic conditions (115 °C) to give well defined complexes.[37, 38] **23**–**26** are the thermally most stable complexes of the whole synthetic sequence. In agreement with this, **22a** isomerizes in solution to give **23** and **25**.[37] Whereas the transformation **22a** → **23** can be described as an opening of both monosulfur bridges, the reaction **22a** → **25** requires the additional cleavage of the η^2-bridge.[39] Interestingly, the entire process is photochemically reversible, since irradiation of any one isomer gives the two other isomers.[40]

Although even more $[Cp_2^{(*)}Mo_2S_4]$ isomers are conceivable (cf. Scheme 1 and Ref. [41]), the reaction products derived from the reaction of $[CpMo(CO)_3H]$ with methylthiirane[42] or $[Cp^*Mo(CO)_3H]$ with S_8[33] belong, just like $[Cp'_2Mo_2S_4]$[33] to structural type **H** (Scheme 1), which is also realized in **25**.

A comparison of the structures of **22a**[37] and **25**[33] reveals a 'clamping' effect of the bridging ligands in **22a**: the formal Mo–Mo bond orders (2 for **22a**, 32 valence electrons (VE) and 3 for **25**, 30 VE) contradict the observed Mo–Mo distances of 2.599 and 2.905 Å, respectively. On the other hand, the Mo–S bridging bonds of **25** are on average ca. 0.06 Å shorter than in **22a**, which could point to a delocalization of the electrons of the bridging sulfur atoms in **25**. Such a delocalization is further supported by the distinctly lower nucleophilicity found for **25**[23] compared to that for **22a**.[23]

An interesting by-product of the reaction of $[Cp^*Mo(CO)_3H]$ with S_8 is **27**, which contains three different types of S_2 ligands (Fig. 3),[33] including the seemingly rare nonplanar η^1–S_2 bridge[4] (Mo-S1-S1'-Mo').

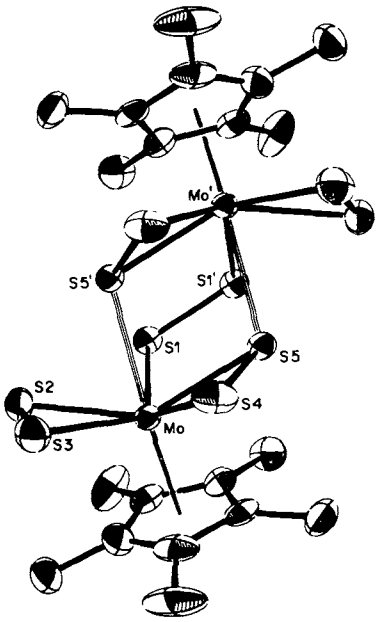
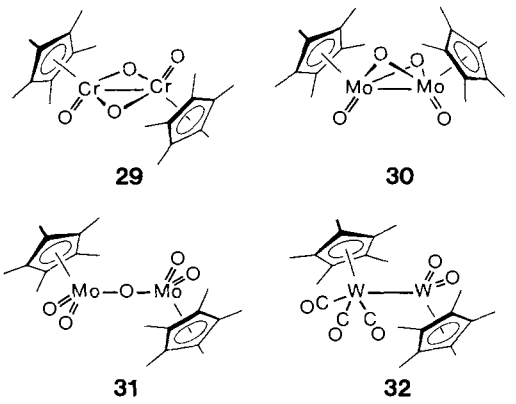


Fig. 3. Structure of $[Cp_2^*Mo_2S_{10}]$ **27** in the crystal [33].

2.2.3. *Cyclopentadienyl Oxo Complexes*

Even from the relatively few examples presented here (see Scheme 5) it can be seen that—with the exception of $[Cp_4Cr_4O_4]$[43] prepared by *E. O. Fischer* et al.—Cp-complexes of the Cr triad containing exclusively O-ligands have the same composition $[Cp_2^{(*)}M_2E_n]$ (n = 4,5) as their S-homologues. However, they differ considerably in many structural respects. One reason for this could be that the formal oxidation state of the metal center in the complexes with oxo ligands (Cr^V in **29**[45], Mo^{VI} in **31**,[45–47]) is frequently higher than in the complexes of the usual chalcogens. The only compound which can be directly derived from an already known sulfur complex, namely **25**, is $[Cp_2Mo_2(\mu\text{-}O)_2O_2]$ **28** with the structural type **H** (Scheme 1).[44]



Scheme 5. Examples for the structures of dinuclear Cp(*) oxo complexes of the chromium triad.

The absence of complexes with $O_2^{2\ominus}$ ligands is remarkable. Thus, e.g., the transfer of the peroxo ligand of $(t\text{BuNC})_2\text{Ni}(O_2)$ is only possible with the rupture of the O–O bond by the Mo≡Mo triple bond of $[Cp^*Mo(CO)_2]_2$.[48] The resulting complex **30** shows a folded Mo_2O_2 core like that of type **G** (Scheme 1). No structural equivalent in the $[Cp_2^{(*)}Mo_2S_4]$ system exists for the Cp^*MoO_2 moieties present in **31** and the nearly linear $O^{2\ominus}$ ligand that is linking them.[47]

There have been contradictory reports on the reaction of $[Cp^*W(CO)_2]_2$ with O_2: At first two products of the composition $[Cp_2^*W_2(CO)_2O_2]$ and $[Cp_2^*W_2O_4]$ were reported,[49] but then, in another experiment, the substitution of only one CO group could be established.[50] The X-ray structural analysis of **32** shows that, owing to the mixed oxidation states of its W atoms, this complex has a structure to some extent related to that of $[Cp_2^*W_2(CO)_2S_3]$ **21a**.[37]

Complexes which contain both oxo and thio ligands are accessible by reaction of the $[Cp_2^*Mo_2S_4]$ isomers **22a, 23** and **25** with atmospheric oxygen.[33, 51, 52] The progress of the reaction can be monitored quite well by ^{95}Mo-NMR spectroscopy, since the molybdenum centers suffer a shielding effect of $\Delta\delta = 400-600$ by introduction of oxygen.[53] The final products **33** are, according to X-ray structural

$$[Cp_2^*Mo_2S_4] \xrightarrow{O_2} [Cp_2^*Mo_2S_{4-n}O_n] + [Cp_2^*Mo_2S_4]\cdot SO_3$$

22a **33**, n = 1, 2 **34**

analyses, clearly of the structural types **G** and **H** (Scheme 1). The oxo ligands are always terminal, i.e. there are always two $S^{2\ominus}$ bridges present. Prerequisite for such a reaction with oxygen at the metal center (examples for an oxidation of the sulfur ligands have been well documented[54]) is obviously the presence of terminal sulfido or selenido ligands. Consistent with the course of the reaction of **22a** with O_2 is that the dioxo complex *syn*-$[Cp_2^*Mo_2(\mu\text{-Se})_2O_2]$ can be structurally characterized (type **G**), whereas this has not been possible for complexes with terminal Mo=Se moieties.[36, 38]

The sulfur released in the reaction of **22a, 23** and **25** with O_2 can be isolated in the form of an SO_3-adduct to the starting compound. It is assumed, however, that in such a reaction the complex with the most nucleophilic sulfur bridges, **22a**, is employed. Consistent with the comparatively large S–S distance (2.168(2) Å), **34** also chemically resembles

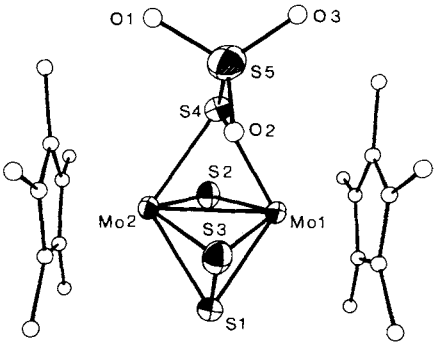


Fig. 4. Structure of **34** in the crystal.

an SO_3-adduct of the $S^{2\ominus}$ bridge rather than a complex with an η^1-thiosulfato bridge.[52a, 55] Further information about the mechanism of the reaction can be found in Section 3.4.

2.3. Cyclopentadienyl Chalcogenides of Mn and Re

Generally applicable methods for the preparation of chalcogen-rich complexes of Mn and Re have not yet been developed. Thus, the reaction of S, Se and Te with $[Cp(CO)_2ML]$ (M = Mn, Re; L = thf, Et_2O) leads only to mono- and dichalcogen-bridged products of the $CpM(CO)_2$ fragment.[56] With regard to the subject of this review these complexes are somewhat of a 'dead end', since they do not react any further with chalcogens. The only structurally characterized complex with a higher sulfur content is $[\{CpRe(CO)\}_2S_5]$, **35**. This contains a puckered seven-membered ring (Fig. 5), in which an S_2 bridge and an S_3 bridge connect two CpRe(CO) moieties.[57] Thus, each Re center has only 16 valence electrons.

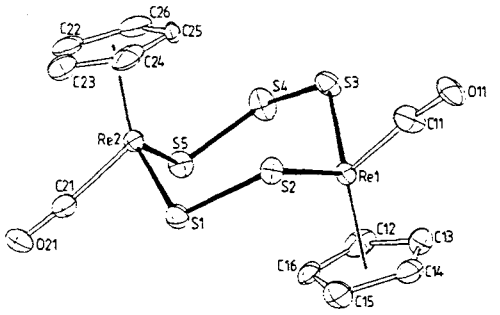


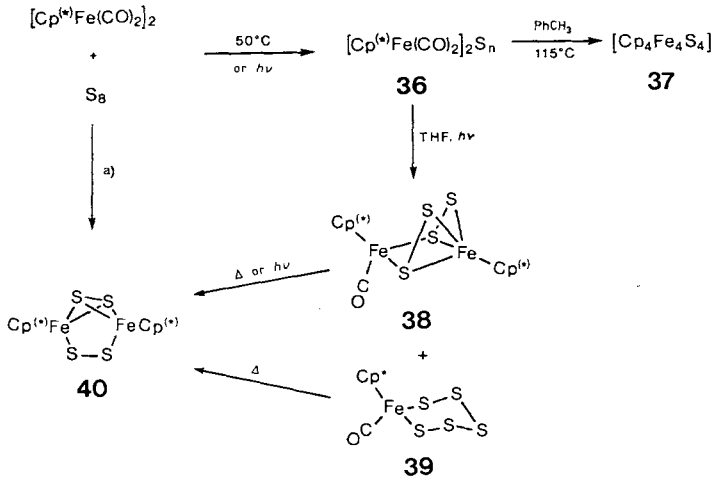
Fig. 5. Structure of **35** in the crystal [57].

Two CO-free dinuclear complexes of the composition $[Cp_2^*Mn_2S_4]$ have been prepared from the reactions of Cp_2^*Mn and $Cp_2^*Mn_2(\mu\text{-CO})_3$ (*Mn≡Mn*), respectively, with S_8. The elucidation of the structures of these extremely air-sensitive compounds still proves to be quite a challenge.[6] $[Cp_2^*Re_2S_4]$ is reported to be obtained upon reaction of Cp^*ReOCl_2 with $(Me_3Si)_2S$, but this too requires better

structural characterization.[7c] The oxygen homologue $[Cp^*_2Re_2O_4]$ (structural type **H**, Scheme 1) is a typical example of how the chemistry exhibited by O- and S-complexes differs. It can be obtained by careful deoxygenation of Cp^*ReO_3 and represents a preparatively important and very reactive intermediate.[7c, 58]

2.4. Cyclopentadienyl Sulfides of Fe and Ru

Sulfur-rich cyclopentadienyliron complexes have so far only been prepared from $[Cp^{(*)}Fe(CO)_2]_2$ and elemental sulfur. Scheme 6 covers the differing types of influence exhibited by the substituents on the $Cp^{(*)}$ ring in the thermal reac-



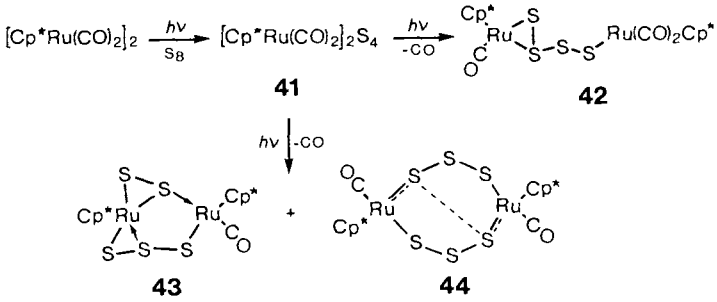
Scheme 6. Overview of the reactions in the system $[Cp^{(*)}Fe(CO)_2]_2$/sulfur. a) Toluene, 115 °C, only starting from $[Cp^*Fe(CO)_2]_2$.

tion: when $Cp^{(*)}=Cp$ the 60 e heterocubane **37**[32, 59] is obtained, whereas when $Cp^{(*)}=Cp^*$ one obtains the complex **40**(Cp*)[60]. **40**(Cp) can, in contrast, only be prepared photochemically.[61] Both complexes **40** exhibit an interesting structural feature in that two η^1-S_2 and η^2-S_2 bridges are found perpendicular to each another.[60, 61] These diamagnetic molecules (34 valence electrons from $2Cp^{(*)} + \eta^1$-S_2 and η^2-S_2 bridges $+2Fe = 10 + 2 + 6 + 16$) have relatively large Fe–Fe distances (ca. 3.50 Å) and shortened Fe–S distances. The latter fact in particular proves that there is increased π-donation from the η^1-S_2 ligand coplanar to the Fe–Fe vector. The mixing of the sulfur p_x-orbitals perpendicular to the Fe_2S_2 plane with a set of metal d-orbitals of suitable symmetry may explain this effect.[62]

The products **36** derived from insertion of sulfur into the Fe–Fe bond are of intermediate character, of which the derivatives with $Cp^{(*)}=Cp$ can even be isolated. **36**(Cp, n = 3) can be converted into **37** in boiling toluene,[63] **36**(Cp, n = 5) reacts photochemically in THF solution to give **38**(Cp), which in solution exists in three isomeric forms, of which that given in Scheme 6 has been characterized by an X-ray structure analysis.[61a]

Recently, the permethylated intermediates **38**(Cp*) and **39** formed during the photolytic preparation of **40**(Cp*) could also be isolated.[64] In contrast to **40, 39** is paramagnetic (ESR signal at $g = 2.056(3)$).

Since $[Cp^*Ru(CO)_2]_2$ dissociates easily under photochemical conditions to give reactive 17 e fragments,[65] it seems likely that the mechanism for the uptake of S_8 is radical in nature.[66] The primarily formed compound is the tetrasulfido-bridged complex **41** (Scheme 7). This is either stabilized



Scheme 7. Overview of the reactions in the system $[Cp^*Ru(CO)_2]_2$/sulfur.

intramolecularly in the form of **42** with elimination of CO or reacts further to give the sulfur-rich compounds **43** and **44**.[67] In the course of the latter process an S_4 bridge is broken down and the sulfur fragments that are released are apparently so reactive that they recombine to form a second bridging ligand. In this sense the formation of **43** and **44** is favored by the addition of S_8. Under thermal conditions (toluene 115 °C) only **41** and **43** are formed. The structure of **43** can be described as a Ru_2S_3-ring with two sulfur atoms bridging two adjacent Ru–S bonds (Fig. 6), i.e. the sulfur

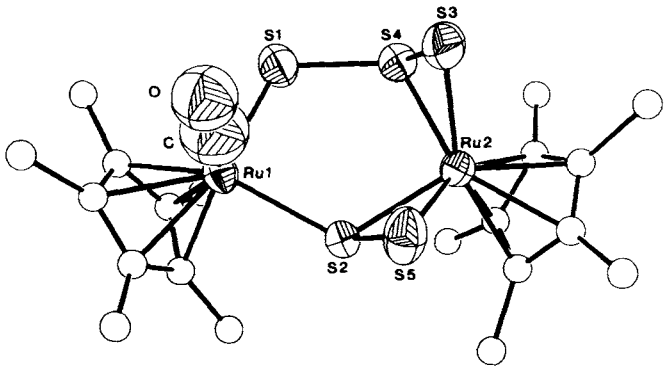


Fig. 6. Structure of **43** in the crystal.

bridges are effectively pure σ-donors. The assumption of a folded eight-membered ring in **44**, in which two S_3-ligands bridge the Cp*(CO)Ru centers, is based on an analogy to the structurally characterized $[\{Cp'RuPPh_3\}_2S_6]$, which can be prepared from $[Cp'_2Ru_2(PPh_3)_4S_2]^{2\oplus}$ and $S_6^{2\ominus}$.[68] Compared to **43**, there are rather different bonding modes, e.g. a bicyclic Ru_2S_6 core as a consequence of relatively important transannular S–S interactions (d_{S-S} 2.77 Å). Concomittantly, the different Ru–S distances ($\Delta d = 0.11$ Å) prove that there is an additional π-donor stabilization of the Ru centers by one S-atom in each case.

With **36**(Cp, n = 4) and **5** as examples it could be shown that complexes with polysulfido ligands tend to undergo

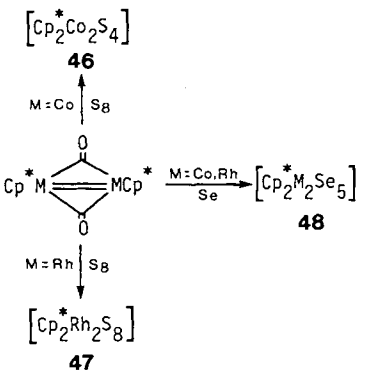
thermal decomposition with the formation of clusters. In contrast to this the metal-sulfur rings in **43** and **44** are so stable that up to now no way has been found to convert them, e.g., into the Ru-analogue of **40**. In this connection it is hard to explain why just a slight modification of the substituents of the Cp ring has such a large effect on the reaction: $[(EtC_5Me_4)_2Ru_2(CO)_4]$ reacts with S_8 in boiling toluene to give $[(EtC_5Me_4)_2Ru_2S_4]$ **45** (structure type **B**) and other still not fully characterized CO-free products.[69]

It is known from the higher sulfur homologues, that Se can be inserted into the Fe–Fe bond of $[CpFe(CO)_2]_2$. The number of bridging members in the products $[\{CpFe(CO)_2\}_2(\mu\text{-}Se)_n]$ appears, however, to be limited to n = 1 and 2, respectively.[70] An excess of Se leads to the 60e heterocubane $[Cp_4Fe_4Se_4]$.[71]

2.5. Cyclopentadienyl Chalcogenides of Co and Rh

The substrates from the Co triad that were chosen for reactions with chalcogens were the M=M double bonded dimers $[Cp^*M(CO)]_2$ (M = Co, Rh). These react with sulfur and selenium but not Te under mild conditions, finally giving CO-free products which have different structures (**46**–**48**), depending on the chalcogen and the metal. **46** has the structure type **D** (Scheme 1), in which the two η^1,η^2-S_2 bridges each act as 4e donors. (Fig. 7a).[60] In contrast, the molecular structure of **47** contains two RhS_4 chelates, which are coupled with formation of a slightly puckered Rh_2S_3 five-membered ring (Fig. 7b).[72] This asymmetric method of coordination allows the donation of four electrons per ligand and is thus quite interesting, since up to now all bridging S_4 ligands have been found to act as 6e donors coordinated via their terminal atoms.[5] In contrast, two non-bridging S_4 chelating ligands are present in **51** (see Scheme 8), which is the precursor of **47**. The elimination of sulfur from **47** to give a complex analogous to **46** with a $Rh_2S_4^{2\oplus}$ core has not yet been successfully carried out—although a core of this type is found in $[(triphos)_2Rh_2S_4](BPh_4)_2$ **54**.[73]

The 36e complexes **48** (M = Rh, Co) may be regarded as triple-decker complexes of a special kind.[74] The middle deck is a planar pseudo-five-membered ring which is σ-bound through three coordination sites and consists of a $Se^{2\ominus}$ ligand and a $Se_4^{2\ominus}$ ligand (Fig. 7c). The relatively short intramolecular Se···Se distances of about 3.10 Å could be responsible for the stabilization of this bonding system. Weaker intermolecular Van-der-Waals interactions ($d_{Se\cdots Se}$ 3.50 Å) seem to be responsible for the anisotropic orienta-



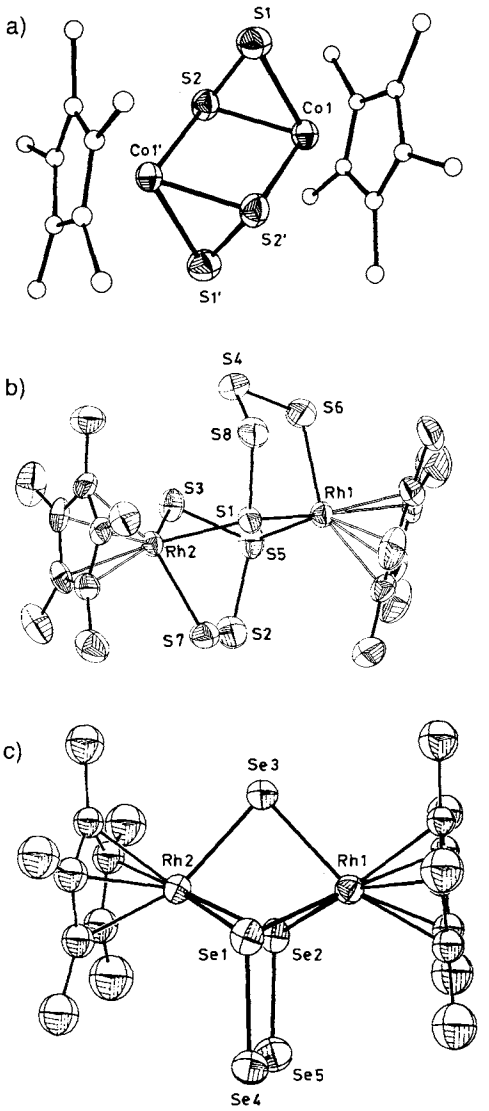


Fig. 7. Structures of a) **46**, b) **47** and c) **48** (M = Rh) in the crystal.

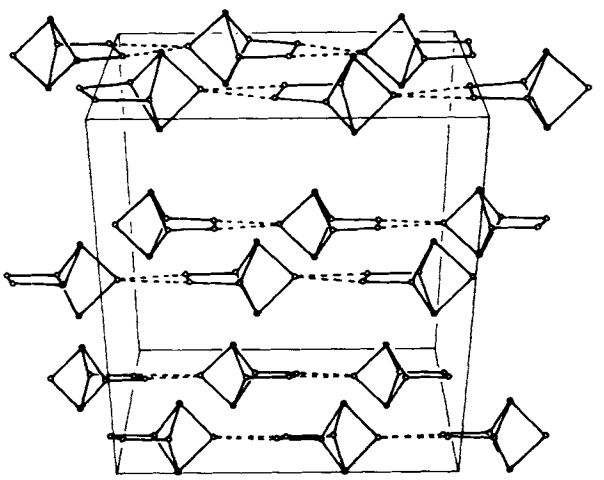
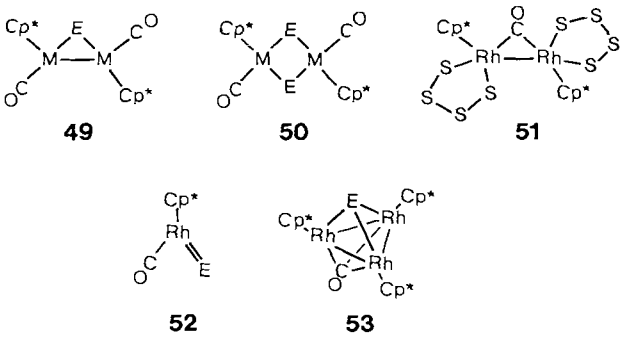


Fig. 8. Unit cell of **48** (M = Rh) (○ = Se atoms, ● = Rh atoms; the Cp* ligands have been omitted for clarity).

tion of the molecules in the crystal lattice. This is unusual for cyclopentadienyl complexes. All Se atoms lie in one plane, which, due to the parallel Cp* rings, gives it a compact layer structure (Fig. 8).

Investigations of the mechanism whereby the complexes **46**–**48** are formed must concentrate above all on evidence for and characterization of the mono- and dichalcogenide adducts at the M=M bond, **49** and **50** (Scheme 8), since the



49 **50** **51**

52 **53**

Scheme 8. Intermediates of the reactions of $[Cp^*M(CO)]_2$ (M = Co, Rh) with the chalcogens E (S, Se, Te).

incorporation and fragmentation of the chalcogen units occurs so quickly that they can hardly be followed, even by low-temperature IR spectroscopy.[74b] The stability of these complexes can certainly be traced to the influence of the central metal (some of the cobalt complexes are so labile that they can only be characterized by IR spectroscopy), but the reactivity of the chalcogen employed is also an important factor. The order of reactivity is $S_8 \approx Se_8 > Se_x > Te$. Due to oxidative addition of sulfur or selenium respectively (tellurium is not sufficiently reactive) at the metal centers of **49** and **50**, ME_4 chelating rings are ultimately formed. Only in the case of the Co/S system (**46**) does the degradation of the S_8 ring ultimately give an MS_2 unit. A further intermediate **51**[74b] with a symmetrically bridging CO ligand has been isolated in the Rh/S system. Solutions of **51** eliminate CO at room temperature with the formation of **47**.

Although it has not yet been directly proved, mononuclear complexes with metal-sulfur double bonds play a key role in the formation of sulfur-bridged binuclear complexes—this is at least true in the case of the $Cp^{(*)}(CO)_2M/S_8$ (M = Mn, Re) systems.[56] The complexes **52**, with noble gas configurations, also come into this category—indirect evidence for their existence has been obtained by studying the manner in which the complex **49** (M = Rh; E = S, Se) disproportionates to give the structurally characterized 48e clusters **53**.[64]

3. Reactions

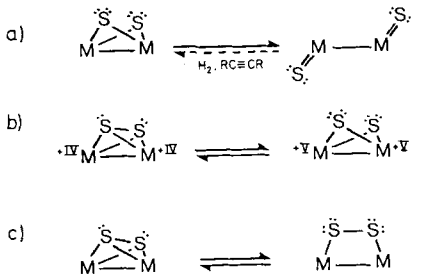
3.1. Tranformations of Mono- and Disulfido Ligands

Due to their clear structures the complexes of the type $[Cp_2^{(*)}M_2S_4]$ are especially suitable for the study of ligand transformations. A special case, limited as yet to Mo and W complexes, is the opening of a pair of monosulfido bridges to two terminal M = S units (Scheme 9). The reverse reaction is not only photochemically possible, it is also induced by H_2 or unsaturated organic molecules, giving complexes such as **16**[33].

During the course of the isomerization **22a** → **25**[37] (Scheme 4) a reductive opening of the η^2-S_2 bridge with consequent flattening of the folded Mo_2S_2 four-membered ring was also observed. According to recent experimental findings this reaction could even proceed via a dissociative mechanism.[52b] The bridge opening occurs formally with a change in the metal oxidation state [b) in Scheme 9] represented by Equation (a):

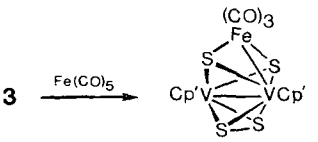
$$2Mo^{IV} + S_2^{2\ominus} \rightarrow 2Mo(V) + 2S^{2\ominus} \qquad (a)$$

The reverse reaction, whose inorganic equivalent is the redox-condensation reaction of oxothiomolybdates and -tungstates $[MO_nS_{4-n}]^{2\ominus}$ (M = Mo, W; n = 0–2),[75] can be carried out photochemically.

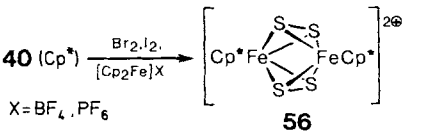


Scheme 9. Transformations of sulfur ligands in $[Cp_2^{(*)}M_2S_4]$ complexes. a) and b) M = Mo, W. c) M = V, Fe.

An elegant possibility of removing any electron deficiency arising at the metal centers, is the rearrangement of a μ,η^1-S_2 ligand to a μ,η^2-S_2 ligand [(c) in Scheme 9 from right to left]. This 90° rotation, which theoretically ought to be symmetry forbidden,[39] effectively gives the complex four more valence electrons. This explains, for example, why the 26e complex $[Cp'_2V_2S_4]$ **3** undergoes such a transformation to give the 48e trinuclear cluster **55** upon addition of an $Fe(CO)_3$ fragment at the monosulfido bridges.[76] In contrast to such chemically induced isomerizations[77] the electron-transfer induced η^1-$S_2 \rightarrow \eta^2$-S_2 isomerization of $[Cp^*_2Fe_2S_4]$



55



56

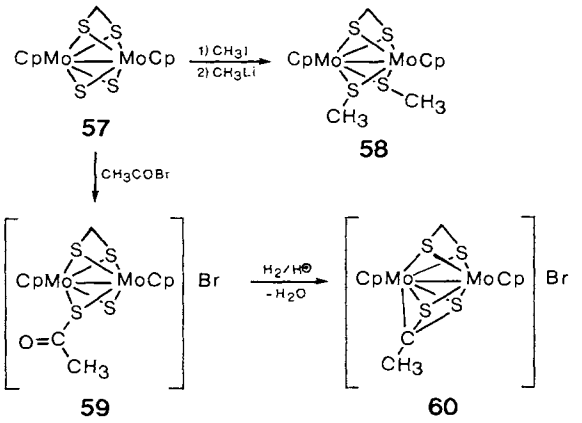
40(Cp*, structure type **B**) on oxidation is reversible—oxidation can be achieved with Br_2, I_2, $[Cp_2Fe]PF_6$ or even electrochemically, giving the dication **56** with an inert gas configuration. As in **40**(Cp*), the Fe–Fe distance in **56**, although

shortened by ca. 0.7 Å by the clamping effect of the two η^2-S_2 bridges, is non-bonding in nature.[78] Careful electrochemical investigations revealed the existence of an intermediate monocation, which quickly disproportionates to give **40**(Cp*) and **56**. Also remarkable is the stabilization of the S_2-bridges by the $Cp^{(*)}$-ligands, which, in principle, counteracts their possible elimination.[62]

3.2. Formation of S–C Bonds

3.2.1. The Alkylation of Sulfur Bridges

All sulfur ligands of the $Cp_2^{(*)}M_2S_4$ complexes presented in this paper have lone electron pairs and thus possess nucleophilic properties. Reaction with CH_3I leads predominantly to alkylation of the monosulfido bridges, whose nucleophilicity is only exceeded by the μ,η^1-S,S ligand in $[Cp^*_2Cr_2S_5]$ **8**.[23] Sulfur ligands whose lone pairs are withdrawn in order to stabilize the unsaturated metal centers via π-donation (e.g. in **2, 3, 40, 45**), are, in contrast, inert to alkylation by CH_3I. The monocationic complexes formed by such alkylation reactions are then susceptible to attack by nucleophiles, e.g. CH_3Li.[79] By such a reaction sequence, for example, the *cis*-dithiolato complex **58** is accessible from **57** (Scheme 10).[80]

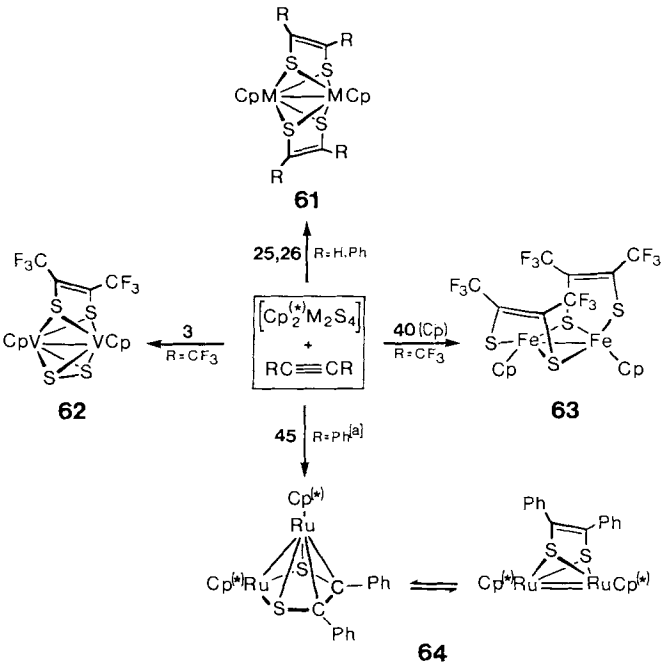


Scheme 10. Alkylation and acylation reactions at sulfur bridges using **57** as example.

In the complex **57**, which is accessible by reaction of the bis(hydrogensulfido) complex **16** with $CH_2Br_2/NaOCH_3$, two sulfur bridges are connected by a methylene bridge.[80] Owing to the two remaining cisoid $S^{2\ominus}$ bridges, **57** is without doubt a good model system for the molybdenum sulfide surfaces of commercial hydrotreating catalysts. Examples of alkylation reactions of **57** include, inter alia, the reductive cleavage of the C–Hal bonds of haloesters, acyl halides and vinyl bromides.[81] Of the complexes formed in this way the acetyl complex **59** is especially interesting, since it is able to activate H_2 with HHal elimination and then eliminate water in a complicated reaction sequence after addition of further acid. The complex salt **60** finally formed by this reaction contains a μ,η^2,η^3-dithioacetato ligand. Completely analogous to this C=O bond cleavage is the evolution of NH_3 from CH_3CN, whereby **60** is again formed.[82] Such reactions with expansion of the metal coordination sphere are very rare for the $[Cp_2^{(*)}M_2S_4]$-system. However, they show that, under certain circumstances, the central metal can act as a Lewis base.

3.2.2. Alkenedithiolato Complexes

It is impossible to arrange the reactions of complexes of the type $[Cp^*_2M_2S_4]$ with alkynes in a systematic scheme. This is again a consequence of the various reactivities of the sulfur ligands (Scheme 11).



Scheme 11. Overview of the formation of complexes with alkenedithiolato bridges from $[Cp_2^{(*)}M_2S_4]$ complexes ($Cp^{(*)}$ in **64** = η^5-C_5Me_4Et). [a] Reaction only in the presence of PBu_3.

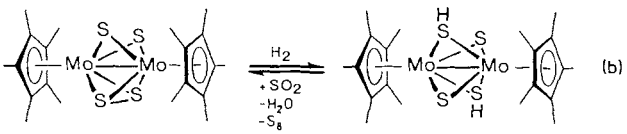
Only the Mo and W complexes **25** and **26**[33,83] react with unactivated alkynes. The bis(alkenedithiolato) complexes **61** thereby obtained can be reversibly hydrogenated under mild conditions to give bis(alkanedithiolato) complexes. The organic component of the dithiolato ligands is able to undergo exchange reactions with unsaturated hydrocarbons[41,83].

Complexes with π-donor sulfur ligands react only with electrophilic alkynes. Thus, $[Cp'_2V_2S_5]$, **2a**(Cp') reacts with hexafluorobutyne to give the mononuclear bischelate complex $[Cp'V\{SC(CF_3)=C(CF_3)S\}_2]$,[15] whereas $[Cp'_2V_2S_4]$ **3**, with 90° rotation of the η^1-S_2 ligand, affords **62** with a symmetrical alkenedithiolato bridge.[18] $[Cp_2Fe_2S_4]$ **40**(Cp) reacts with $CF_3C{\equiv}CCF_3$ with cleavage of both S_2 bridges to give the bisadduct **63**, in which the two μ,η^1,η^2-alkenedithiolato ligands are 4e donors. Of the two possible isomers only *cis*-**63** has been structurally characterized.[61b] The Ru-complex **45**, which is isostructural with **40**, (Section 2.4) reacts with PhC≡CPh only in the presence of the sulfur abstracting reagent PBu_3 to give the pentagonal-pyramidal *nido*-cluster **64**. ^{1}H-NMR spectroscopic findings in solution indicate that the equilibrium between the unusual μ,η^2,η^4-coordination and a symmetrically bridging η^2-coordination shown in Scheme 11 can be assumed for the cluster **64**.[69]

3.3. Formation of S–H Bonds

As long ago as 1949 it was shown that chemisorption of H_2 on MoS_2 occurs with the formation of SH ligands.[84] One such activation of H_2 on heterogeneous metal sulfide surfaces has been discussed as a possible step in the mechanism of the HDS catalysis.[85] In this context the complex $[Cp_2^{(*)}Mo_2S_2(SH)_2]$ (**16**; for synthesis see Scheme 4) is of special importance owing to the concomitant presence of sulfido- and mercapto-bridging ligands. For example **16** catalyzes the H/D exchange in a H_2D_2 mixture,[34] it hydrogenates N=N and C=N bonds under mild conditions[86] and adds thiols with elimination of H_2 to give thiolato complexes, and it reacts with C_2H_4 and C_2H_2, forming alkane- and alkenedithiolato complexes (e.g. **61**).[34]

An interesting reaction is the reduction of SO_2 with **65** to give H_2O and S_8 [Eq. (b)] which may proceed with formation of labile S–S bonds (see Section 3.4). The complex **22a** thus



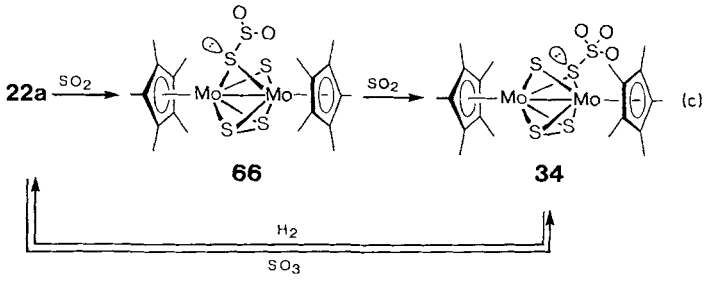
(b)

22a **65**

formed reacts with H_2 with cleavage of the disulfido bridge to give **65** again. The overall process can thus be formulated as a metal-catalyzed SO_2 reduction.[87] Attempts to hydrogenate the S_2 ligands in other $[Cp_2^{(*)}M_2S_4]$ complexes reveal that Mo is by a long way the most favorable center for such reactions. Thus, reactions of the Cr-complex **9**, which is isolobal with **22a**, and its more sulfur-rich precursor **8** with H_2 only proceed under high pressure and then with the formation of $[Cp_4^*Cr_4S_4]$. (Although the mechanism of this reaction is still not clear, it could be confirmed that the presence of H_2 is essential.)[23] In contrast, $[Cp_2^*Fe_2S_4]$ **40**(Cp*) is inert to H_2 up to 250 bar.[60]

3.4. Formation of S–S Bonds

As already indicated in Section 2.2.3 one of the products (**34**) formed upon reaction of **22a** with atmospheric oxygen contains a coordinated SO_3 ligand on the monosulfido bridge. The same product could be synthesized in much better yield by the direct reaction of SO_3·pyridine with **22a** [Eq. (c)].[88] This reaction can also be used to synthesize new



(c)

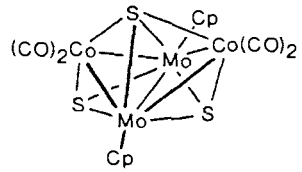
unusual ligands such as μ,η^1-S_3O_3 in **8**·SO_3[24] and μ,η^1-$SeSO_3$ in **49**·SO_3 (M=Rh, E=Se).[89]

34 can also be prepared in a two-step reaction from **22a** and SO_2 [Eq. (c)]. Remarkably the initially formed SO_2-adduct **66** is oxidized to **34** by SO_2 and not by O_2—this has been proved using ^{18}O-labeling experiments.[90]. During the oxidation elemental sulfur is formed. Results so far would suggest that the oxidation proceeds with inversion at the S-atom, thus indicating the existence of further as yet unidentified intermediates. For the air "oxidation" of **22a** and similar complexes (above all **8**) the presence of sulfur, which is easily activated, is essential.[24] The oxidation of SO_2 to SO_3 by excess SO_2 can be assumed not only to occur on the complex but also in solution by a disproportionation reaction. In solution the SO_3 being a very strong electrophile is an excellent coordination reagent not only for sulfur but also for other chalcogen ligands as well.[24, 88]

Since **34** can be reduced to **22a** with H_2 [Eq. (c)] and since an excess of H_2 causes the formation of **65**, it has been suggested that the processes in Equations (b) and (c) can be summarized in a cycle,[87, 90] that is as an organometallic variant of the Claus process (oxidation of H_2S to S with atmospheric oxygen).

3.5. Synthesis of Tri- and Tetranuclear Clusters

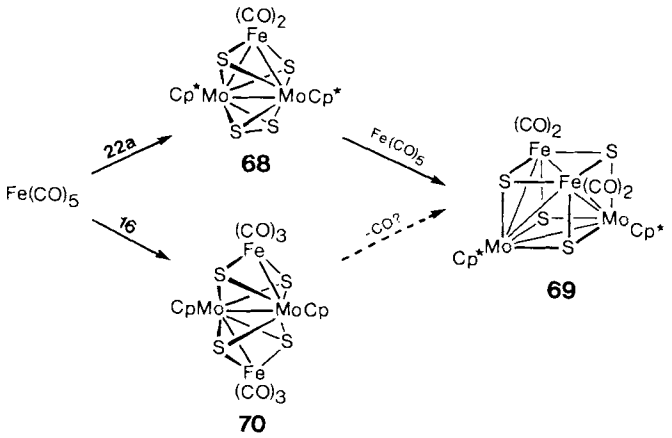
A further outstanding property of a large number of the $[Cp_2^{(*)}M_2S_4]$ complexes is their ability to coordinate reactive or unsaturated metal fragments using the lone pairs of the sulfur ligands. Thus, the sulfur ligands enlarge their connectivity from μ_2 to μ_3 and exceptionally to μ_4. Whereas simple



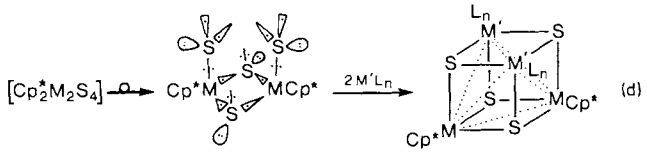
67

adducts can only as a rule be characterized with difficulty, the 48e trinuclear clusters such as for example **55** (Section 3.1) or **68** are stable enough to be isolated and structurally characterized.[76, 91] Particularly characteristic of these 48e clusters is a trigonal-bipyramidal $M_2M'(\mu_3\text{-}S)_2$ framework, the M–M edge of which is spanned by a μ,η^2-S_2 ligand. This arrangement is of special interest as a building block for the construction of multimetallic chains. It is also capable of oxidatively adding a further metal fragment, striving for a cubane type structure with a $M_2M'_2S_4$ core.[91, 92]

A simple and efficient concept for the synthesis of homo- and heterometallic clusters containing an $M_2M'_2S_4$ core is that developed on the basis of $[Cp_2^*Cr_2S_5]$ **8** (which loses its labile S atom on reaction) and $[Cp_2^*Mo_2S_4]$ presented in Equation (d). Starting from any structural framework (**E**, **G** or **H**) the Cr and Mo dimers can, after transformation of all mono- and disulfido-ligands into four-electron donors,[93] function as potential 38e substrate ($2Cp^*M + 4\mu_3\text{-}S =$



$2 \times 11 + 4 \times 4$). These give 60e and 62e clusters with formation of M–S and M–M bonds on addition of two 11e or 12e $M'L_n$ fragments respectively.



Typical examples of directed syntheses of homo- and bimetallic clusters are listed in Table 1. $Cp^{(*)}M$ (M = Cr, Mo),[94] Fe(NO)[95] and Co(CO)[96] can serve as 11e fragments, i.e. also complex-fragments with easily substituted ligands, so that ligand substitutions in the clusters are possible without destroying the cluster skeleton. Thus, e.g., the CO ligands in $[Cp_2^*Cr_2Co_2(CO)_2S_4]$ can be successively substituted by $P(OMe)_3$ without fragmentation of the cluster framework.[97]

All the 60e $M_2M'_2S_4$ clusters possess a distorted cubic ('pseudocubane') structure with incorporated M_4 and S_4 tetrahedra—they have six M–M bonds for electronic reasons.[29, 97, 98] The attainment of the same cubic structure is also the motive behind the formation of the 56e, 58e, and 60e clusters, even if the presence of the vanadium atoms provokes magnetic anomalies. All Vanadium clusters are accessible from the 36e building block **3** (Table 1).

Addition of the 12e fragments $Mo(CO)_3$, $Fe(CO)_2$ or Cu-Cl to **22a** leads ultimately to stable 62e heterocubanes (Table 1) containing only five M–M bonds.[91, 100] Clusters with both oxo- *and* thio-ligands can be prepared in the same way. Thus, for example, the cluster $[Cp_2^*Mo_2Cr_2(CO)_6O_2S_2]$ can be isolated from the reaction of $[Cp_2^*Mo_2O_2S_2]$ with $[Cr(CO)_3(MeCN)_3]$.[52a]

The results obtained from the analogous reactions with **16** are less consistent. The reaction with $Ni(CO)_4$ is the only reaction which gives a product, namely $[Cp_2Mo_2Ni_2(CO)_2S_4]$, with the expected 62e pseudocubane type structure.[101] In contrast, $Co_2(CO)_8$ reacts with **16** not only with elimination of CO but also of H_2S, thus yielding **67**. Two edge-sharing Mo_2CoS tetrahedra spanned by a μ_4-S ligand are characteristic of this cluster.[101] The reaction of **16** with $Fe(CO)_5$[102] or $Fe_2(CO)_9$[101] also yields a completely different sort of product, the 66e cluster **70**. This has only 3 M–M bonds, all metal atoms lying in one plane. Whether **70** can be converted into a cluster of the type **69**, has evidently not been investigated.

It is not the SH ligands that are responsible for the differing behavior of **16**, but rather the $Cp^{(*)}$ ligands: the permethylated derivative **65** reacts with $Co_2(CO)_8$ to give $[Cp_2^*Mo_2Co_2(CO)_2S_4]$, which has a 'normal' 60e M_4S_4 core.[103]

4. Conclusion and Perspectives

This review should hopefully have illustrated the appeal of the extremely variable structural chemistry of sulfur ligands from the organometallic point of view with particular reference to the dimeric cyclopentadienyl-transition metal complexes. The reactivity potential of these complexes has also been outlined. The unpredictable coexistence of mono-, di- and polysulfur ligands as well as the abilities to undergo ligand transformations and to be effective π-donor ligands, guarantee future developments in the structural chemistry and reactivity of these complexes. Although it is relatively difficult to present rigid principles, it was possible to show by

Table 1. Overview of the syntheses of homo- and heteronuclear clusters with the $M_2M'_2$ core from $[Cp_2^{(*)}M_2S_n]$ complexes (n = 4,5).

Substrate	Reactant	Conditions	Cluster	n [a]	Ref.
$[Cp'_2V_2S_4]$ **3**	$[Cp'_2V_2S_4]$	PBu_3; 20 °C	$[Cp'_4V_4S_4]$	56	[99]
	$Hg[Fe(CO)_3(NO)]_2$	toluene; 115 °C	$[Cp'_2V_2Fe_2(NO)_2S_4]$	58	[76b]
	$[Co(CO)_3(NO)]$	CH_2Cl_2; 20 °C	$[Cp'_2V_2Co_2(NO)_2S_4]$	60	[76b]
$[Cp_2^*Cr_2S_5]$ **8**	$[Cp_2Cr_2(CO)_4]$	THF; *hv*	$[Cp_2^*Cp_2Cr_4S_4]$	60	[94]
	$[Cp_2^*Cr_2S_5]$	H_2; 150 bar, 80 °C	$[Cp_2^*Cr_4S_4]$	60	[23]
	$[Fe(CO)_3(NO)][(Ph_3P)_2N]$	THF; *hv*	$[Cp_2^*Cr_2Fe_2(NO)_2S_4]$	60	[95]
	$Co_2(CO)_8$	toluene; 20 °C	$[Cp_2^*Cr_2Co_2(CO)_2S_4]$	60	[96]
$[Cp_2^*Mo_2S_4]$ **22a**	$[Cp_2Cr_2(CO)_4]$	THF; *hv*	$[Cp_2^*Mo_2Cp_2Cr_2S_4]$	60	[94]
	$[Cp_2Mo_2(CO)_4]$	toluene; 115 °C	$[Cp_2^*Cp_2Mo_4S_4]$	60	[94]
	$[Fe(CO)_3(NO)][(Ph_3P)_2N]$	THF; *hv*	$[Cp_2^*Mo_2Fe_2(NO)_2S_4]$	60	[95]
	$Co_2(CO)_8$	toluene; 20 °C	$[Cp_2^*Mo_2Co_2(CO)_2S_4]$	60	[96]
	$Mo(CO)_6$	toluene; 115 °C	$[Cp_2^*Mo_4(CO)_6S_4]$	62	[91]
	$Fe(CO)_5$	THF; 25 °C	$[Cp_2^*Mo_2Fe_2(CO)_4S_4]$ **69**	62	[91]
	CuCl	CH_2Cl_2; 20 °C	$[Cp_2^*Mo_2Cu_2(Cl)_2S_4]$	62	[100]
$[Cp_2Mo_2S_2(SH)_2]$ **16**	$Ni(CO)_4$	THF; 25 °C	$[Cp_2Mo_2Ni_2(CO)_2S_4]$	62	[101]

[a] Number of valence electrons in the cluster.

means of thermal, photochemical or electrochemical investigations that some relationships exist within groups of certain complex types. Above all, it would appear that electrochemistry will play an important role in the future, for such investigations should not only make up for the general lack of redox-active inorganic metal–sulfur complexes[104] but also open up the possibility of investigating new reaction types.[78, 80, 83]

The search for mixed chalcogen–pnicogen ligands could be a particularly fruitful field in which to extend our present knowledge of complexes of Cp with O, Se and Te ligands. This is immediately apparent on comparing the structural relationships between, e.g., **48** and $[Cp_2^*Cr_2P_5]$[105] or $[Cp_2Mo_2As_5]$[106] despite their differing bonding systems. In this connection, the first success in this search may have been the formal substitution of one and of three P atoms of the *cyclo*-P_5 ligand of $[Cp_2^*Mo_2P_5]$ by sulfur atoms.[107]

Because of the nucleophilicity of their monosulfido ligands the sulfur-rich complexes of the vanadium and chromium triads exhibit model character for the study of heterogeneous metal sulfide surfaces in commercially important hydrodesulfurization catalyses.[108] However, with regard to the excellent HDS properties of RuS_2 and Rh_2S_3[109] the suitability of sulfur-rich Ru- and Rh-complexes described in this contribution would be well worth investigation.

Since the active centers of commercial HDS catalysts also consist of MoM'S phases (M' = Fe, Co, Ni)[110] the preparation of heteronuclear clusters with an M_4S_4 core [Eq. (d)] using the synthetic concepts developed for the complexes $[Cp_2^{(*)}M_2S_4]$ could be of some importance. Actually, novel sulfur-resistant CO hydrogenation and HDS catalysts can be prepared[111] from **67** and **70** by coating them on oxidic supports which are then calcinated in an H_2 atmosphere. It should also be pointed out that striving for a high Fe:M ratio (particularly when M = Mo) or replacing the Cp ligands by, e.g., dithiocarbamato ligands could lead to the creation of clusters of physiological importance.[112]

I should once again thank my own co-workers cited in the reference section for their engaged contribution. Since conventional spectroscopic data on the compounds mentioned do not lead to a definite structural conclusion because of the very simple ligand situation, X-ray structural analysis has been of considerable importance. I would therefore particularly like to thank Prof. Dr. M. L. Ziegler (Universität Heidelberg) and his co-workers for their continued support since the very early stages of this work, and Dr. U. Klement (Universität Regensburg). I am particularly indebted to Prof. Dr. H. Brunner for generous material support and for the goodwill this work required and to Frau Karin Kilgert for the preparation of the manuscript.

Received: April 13, 1989 [A 743 IE]
German version: *Angew. Chem. 101* (1989) 1645

[1] An insight into the nature of the structural problems of the Fe-Mo cofactor of nitrogenase can be found, e.g., in the following works: S. D. Conradson, B. K. Burgess, W. E. Newton, L. E. Mortenson, K. O. Hodgson, *J. Am. Chem. Soc. 109* (1987) 7507; B. Hedman, P. Franck, S. F. Gheller, L. Roe, W. E. Newton, K. O. Hodgson, *ibid. 110* (1988) 3798. The synthetic efforts to solve this problem are summarized in R. H. Holm, E. D. Simhon in T. G. Spiro (Ed.): *Molybdenum Enzymes*, Wiley, New York 1985, p. 1 ff.

[2] F. E. Massoth, *Adv. Catal. 27* (1978) 265; W. Eltzner, M. Breysse, M. Lacroix, C. Lequlerq, M. Vrinat, A. Müller, E. Diemann, *Polyhedron 7* (1988) 2405.
[3] H. Vahrenkamp, *Angew. Chem. 87* (1975) 363; *Angew. Chem. Int. Ed. Engl. 14* (1975) 322.
[4] A. Müller, W. Jaegermann, J. H. Enemark, *Coord. Chem. Rev. 46* (1982) 245.
[5] a) M. Draganjac, T. B. Rauchfuss, *Angew. Chem. 97* (1985) 745; *Angew. Chem. Int. Ed. Engl. 24* (1985) 742; b) A. Müller, E. Diemann, *Adv. Inorg. Chem. 31* (1987) 89.
[6] J. Wachter, *J. Coord. Chem. 15* (1987) 219.
[7] a) F. Bottomley, J. Darkwa, L. Sutin, P. S. White, *Organometallics 5* (1986) 2165; F. Bottomley, L. Sutin, *Adv. Organomet. Chem. 28* (1988) 339; b) W. A. Herrmann, E. Herdtweck, M. Flöel, J. Kulpe, U. Küsthardt, J. Okuda, *Polyhedron 6* (1987) 1165; c) W. A. Herrmann, *Angew. Chem. 100* (1988) 1269; *Angew. Chem. Int. Ed. Engl. 27* (1988) 1297.
[8] D. M. Giolando, T. B. Rauchfuss, A. L. Rheingold, S. R. Wilson, *Organometallics 6* (1987) 667.
[9] D. M. Giolando, M. Papavassiliou, J. Pickardt, T. B. Rauchfuss, R. Steudel, *Inorg. Chem. 27* (1988) 2596.
[10] A. Shaver, J. M. McCall, *Organometallics 3* (1984) 1823; F. Bottomley, G. O. Egharevba, P. S. White, *J. Am. Chem. Soc. 107* (1985) 4353; F. Bottomley, D. F. Drummond, G. O. Egharevba, P. S. White, *Organometallics 5* (1986) 1620.
[11] F. Bottomley, T.-T. Chin, G. O. Egharevba, L. M. Kane, D. A. Pataki, P. S. White, *Organometallics 7* (1988) 1214.
[12] G. Erker, T. Mühlenbernd, R. Benn, A. Rufińska, G. Tainturier, B. Gautheron, *Organometallics 5* (1986) 1023; G. Erker, T. Mühlenbernd, R. Nolte, J. L. Petersen, G. Tainturier, B. Gautheron, *J. Organomet. Chem. 314* (1986) C21.
[13] N. Albrecht, E. Weiss, *J. Organomet. Chem. 355* (1988) 89.
[14] K. G. Muller, J. L. Petersen, L. F. Dahl, *J. Organomet. Chem. 111* (1976) 91.
[15] C. M. Bolinger, T. B. Rauchfuss, A. L. Rheingold, *Organometallics 1* (1982) 1551; A. L. Rheingold, C. M. Bolinger, T. B. Rauchfuss, *Acta Crystallogr. Sect. C 42* (1986) 1878.
[16] D. Fenske, J. Ohmer, J. Hachgenei, K. Merzweiler, *Angew. Chem. 100* (1988) 1300; *Angew. Chem. Int. Ed. Engl. 27* (1988) 1277.
[17] M. Herberhold, M. Kuhnlein, *New. J. Chem. 12* (1988) 357.
[18] C. M. Bolinger, T. B. Rauchfuss, A. L. Rheingold, *J. Am. Chem. Soc. 105* (1983) 6321.
[19] Y. V. Skripkin, I. L. Eremenko, A. A. Pasynskii, Y. T. Struchkov, V. E. Shklover, *J. Organomet. Chem. 267* (1984) 285.
[20] H. Brunner, U. Klement, J. Wachter, M. Tsunoda, J.-C. Leblanc, C. Moise, *Inorg. Chem.* in press; H. Brunner, W. Meier, J. Wachter, B. Nuber, M. L. Ziegler, *J. Organomet. Chem.* in press.
[21] W. A. Herrmann, H. Biersack, M. L. Ziegler, B. Balbach, *J. Organomet. Chem. 206* (1981) C33.
[22] H. Brunner, J. Wachter, E. Guggolz, M. L. Ziegler, *J. Am. Chem. Soc. 104* (1982) 1765.
[23] H. Brunner, H. Kauermann, W. Meier, J. Wachter, *J. Organomet. Chem. 263* (1984) 183.
[24] H. Brunner, J. Pfauntsch, J. Wachter, B. Nuber, M. L. Ziegler, *J. Organomet. Chem. 359* (1989) 179.
[25] I.-P. Lorenz, J. Messelhäuser, W. Hiller, K. Haag, *Angew. Chem. 97* (1985) 234; *Angew. Chem. Int. Ed. Engl. 24* (1985) 228.
[26] L. Y. Goh, T. W. Hambley, G. B. Robertson, *Organometallics 6* (1987) 1051.
[27] Complexes with the M-E-M skeleton (E = S, Se) are comprehensively referenced in W. A. Herrmann, *Angew. Chem. 98* (1986) 57; *Angew. Chem. Int. Ed. Engl. 25* (1986) 56.
[28] L. Y. Goh, T. C. W. Mak, *J. Chem. Soc. Chem. Commun. 1986*, 1474.
[29] A. A. Pasynskii, I. L. Eremenko, *Sov. Sci. Rev. Sect. B 10* (1987) 443.
[30] R. B. King, M. Z. Iqbal, A. D. King, Jr., *J. Organomet. Chem. 171* (1979) 53.
[31] M. D. Curtis, W. M. Butler, *J. Chem. Soc. Chem. Commun. 1980*, 998.
[32] R. A. Schunn, C. J. Fritchie, Jr., C. T. Prewitt, *Inorg. Chem. 5* (1966) 892.
[33] M. Rakowski DuBois, D. L. DuBois, M. C. Van Derveer, R. C. Haltiwanger, *Inorg. Chem. 20* (1981) 3064.
[34] M. Rakowski DuBois, M. C. Van Derveer, D. L. DuBois, R. C. Haltiwanger, W. K. Miller, *J. Am. Chem. Soc. 102* (1980) 7456.
[35] M. D. Curtis, P. D. Williams, *Inorg. Chem. 22* (1983) 2661.
[36] K. Endrich, E. Guggolz, O. Serhadli, M. L. Ziegler, R. R. Korswagen, *J. Organomet. Chem. 349* (1988) 323.
[37] H. Brunner, W. Meier, J. Wachter, E. Guggolz, T. Zahn, M. L. Ziegler, *Organometallics 1* (1982) 1107.
[38] H. Brunner, J. Wachter, H. Wintergerst, *J. Organomet. Chem. 235* (1982) 77.
[39] W. Tremel, R. Hoffmann, E. D. Jemmis, *Inorg. Chem. 28* (1989) 1213.
[40] A. E. Bruce, D. R. Tyler, *Inorg. Chem. 23* (1984) 3433.
[41] D. L. DuBois, W. K. Miller, M. Rakowski DuBois, *J. Am. Chem. Soc. 103* (1981) 3429; J. M. Newsam, T. R. Halbert, *Inorg. Chem. 24* (1985) 491.
[42] W. Beck, W. Danzer, G. Thiel, *Angew. Chem. 85* (1973) 625; *Angew. Chem. Int. Ed. Engl. 12* (1973) 582; W. Danzer, W. P. Fehlhammer, A. T.

Liu, G. Thiel, W. Beck, *Chem. Ber. 115* (1982) 1682; M. Rakowski DuBois, R. C. Haltiwanger, D. J. Miller, G. Glatzmeier, *J. Am. Chem. Soc. 101* (1979) 5245.
[43] E. O. Fischer, K. Ulm, H. P. Fritz, *Chem. Ber. 93* (1960) 2167; F. Bottomley, D. E. Paez, P. S. White, *J. Am. Chem. Soc. 104* (1982) 5651.
[44] M. Cousins, M. L. H. Green, *J. Chem. Soc. 1964*, 1567; C. Couldwell, K. Prout, *Acta Crystallogr. Sect. B 34* (1978) 933.
[45] M. Herberhold, W. Kremnitz, U. Thewalt, A. Razawi, H. Schöllhorn, *Angew. Chem. 97* (1985) 603; *Angew. Chem. Int. Ed. Engl. 24* (1985) 601.
[46] K. Isobe, S. Kimura, Y. Nakamura, *J. Organomet. Chem. 331* (1987) 221.
[47] J. W. Faller, Y. Ma, *J. Organomet. Chem. 340* (1988) 59; P. Gomez-Sal, E. de Jesus, A. Vazquez de Miguel, S. Martinez-Carrera, S. Garcia-Blanco, *ibid. 353* (1988) 191.
[48] H. Arzoumanian, A. Baldy, M. Pierrot, J.-F. Petrignani, *J. Organomet. Chem. 294* (1985) 327.
[49] W. A. Herrmann, *J. Organomet. Chem. 300* (1986) 111.
[50] H. G. Alt, H. I. Hayen, R. D. Rogers, *J. Chem. Soc. Chem. Commun. 1987*, 1795.
[51] P. M. Treichel, G. R. Wilkes, *Inorg. Chem. 5* (1966) 1182; D. L. Stevenson, L. F. Dahl, *J. Am. Chem. Soc. 89* (1967) 3721.
[52] a) H. Brunner, H. Kauermann, J. Pfauntsch, J. Wachter, J. H. Enemark, C. G. Young, *J. Organomet. Chem. 331* (1987) 45; b) L. D. Tanner, R. C. Haltiwanger, M. Rakowski DuBois, *Inorg. Chem. 27* (1988) 1741.
[53] C. G. Young, M. Minelli, J. H. Enemark, G. Miessler, N. Janietz, H. Kauermann, J. Wachter, *Polyhedron 5* (1986) 407; C. J. Casewitt, M. Rakowski DuBois, R. A. Grieves, J. Mason, *Inorg. Chem. 26* (1987) 1889.
[54] M. Herberhold, B. Schmidkonz, *J. Organomet. Chem. 308* (1986) 35.
[55] H. Brunner, U. Klement, J. Pfauntsch, J. Wachter, *Angew. Chem. 99* (1987) 268; *Angew. Chem. Int. Ed. Engl. 26* (1987) 230.
[56] M. Herberhold, B. Schmidkonz, *J. Organomet. Chem. 358* (1988) 301.
[57] M. Herberhold, D. Reiner, K. Ackermann, U. Thewalt, T. Debaerdemaeker, *Z. Naturforsch. B35* (1980) 1281.
[58] W. A. Herrmann, M. Flöel, J. Kulpe, J. K. Felixberger, E. Herdtweck, *J. Organomet. Chem. 355* (1988) 297.
[59] C. H. Wei, G. R. Wilkes, P. M. Treichel, L. F. Dahl, *Inorg. Chem. 5* (1966) 900.
[60] H. Brunner, N. Janietz, W. Meier, G. Sergeson, J. Wachter, T. Zahn, M. L. Ziegler, *Angew. Chem. 97* (1985) 1056; *Angew. Chem. Int. Ed. Engl. 24* (1985) 1060.
[61] a) H. Chanaud, A. M. Ducourant, G. Giannotti, *J. Organomet. Chem. 190* (1980) 201; b) R. Weberg, R. C. Haltiwanger, M. Rakowski DuBois, *Organometallics 4* (1985) 1315.
[62] P. J. Vergamini, R. Ryan, G. Kubas, *J. Am. Chem. Soc. 98* (1976) 1980; P. J. Vergamini, G. J. Kubas, *Prog. Inorg. Chem. 21* (1976) 261.
[63] M. A. El-Hinnawi, A. A. Aruffo, B. D. Santarsiero, R. McAlister, V. Schomaker, *Inorg. Chem. 22* (1983) 1585.
[64] N. Janietz, *Dissertation*, Universität Regensburg 1989.
[65] H. B. Abrahamson, M. C. Palazzotto, C. L. Reichel, M. S. Wrighton, *J. Am. Chem. Soc. 101* (1979) 4123.
[66] Concepts of the radical degradation of the S_8 molecule that are relevant to the reaction with $[Cp^*Ru(CO)_2]_2$ can be found, e.g., in C. Floriani, M. Fiallo, A. Chiesi-Villa, C. Guastini, *J. Chem. Soc. Dalton Trans. 1987*, 1367.
[67] H. Brunner, N. Janietz, J. Wachter, B. Nuber, M. L. Ziegler, *J. Organomet. Chem. 356* (1988) 85.
[68] J. Amarasekera, T. B. Rauchfuss, A. L. Rheingold, *Inorg. Chem. 26* (1987) 2017.
[69] T. B. Rauchfuss, D. P. S. Rodgers, S. R. Wilson, *J. Am. Chem. Soc. 108* (1986) 3114; J. Amarasekera, T. B. Rauchfuss, S. R. Wilson, *J. Chem. Soc. Chem. Commun. 1989*, 14.
[70] W. A. Herrmann, J. Rohrmann, E. Herdtweck, C. Hecht, M. L. Ziegler, O. Serhadli, *J. Organomet. Chem. 314* (1986) 295.
[71] R. M. Roder, *Ph. D. Thesis*, University of Wisconsin-Madison 1973; H. Ogino, H. Tobita, K. Yanagisawa, M. Shimoi, C. Kabuto, *J. Am. Chem. Soc. 109* (1987) 5847.
[72] H. Brunner, N. Janietz, W. Meier, B. Nuber, J. Wachter, M. L. Ziegler, *Angew. Chem. 100* (1988) 717; *Angew. Chem. Int. Ed. Engl. 27* (1988) 708.
[73] C. Bianchini, A. Meli, *Inorg. Chem. 26* (1987) 1346.
[74] a) H. Brunner, W. Meier, B. Nuber, J. Wachter, M. L. Ziegler, *Angew. Chem. 98* (1986) 907; *Angew. Chem. Int. Ed. Engl. 25* (1986) 908; b) H. Brunner, N. Janietz, W. Meier, J. Wachter, E. Herdtweck, W. A. Herrmann, O. Serhadli, M. L. Ziegler, *J. Organomet. Chem. 347* (1988) 237; H. Brunner, N. Janietz, J. Wachter, B. Nuber, M. L. Ziegler, *ibid. 367* (1989) 197.
[75] W. Rittner, A. Müller, A. Neumann, W. Bäther, R. C. Sharma, *Angew. Chem. 91* (1979) 565; *Angew. Chem. Int. Ed. Engl. 18* (1979) 530; S. Sarkar, M. A. Ansari, *J. Chem. Soc. Chem. Commun. 1986*, 342; M. A. Ansari, J. Chandrasekeran, S. Sarkar, *Polyhedron 7* (1987) 471.
[76] a) C. M. Bolinger, T. B. Rauchfuss, S. R. Wilson, *J. Am. Chem. Soc. 104* (1982) 7313; b) T. B. Rauchfuss, T. D. Weatherill, S. R. Wilson, J. P. Zebrowski, *ibid. 105* (1983) 6508.
[77] C. M. Bolinger, T. B. Rauchfuss, S. R. Wilson, *J. Am. Chem. Soc. 106* (1984) 7800.
[78] H. Brunner, A. Merz, J. Pfauntsch, O. Serhadli, J. Wachter, M. L. Ziegler, *Inorg. Chem. 27* (1988) 2055; H. Ogino, H. Tobita, S. Inomata, M. Shimoi, *J. Chem. Soc. Chem. Commun. 1988*, 586.
[79] H. Brunner, W. Meier, P. Weber, M. L. Ziegler, J. H. Enemark, C. G. Young, *J. Organomet. Chem. 309* (1986) 313.
[80] a) M. McKenna, L. L. Wright, D. J. Miller, L. Tanner, R. C. Haltiwanger, M. Rakowski DuBois, *J. Am. Chem. Soc. 105* (1983) 5329; b) C. J. Casewitt, R. C. Haltiwanger, J. Noordik, M. Rakowski DuBois, *Organometallics 4* (1985) 119.
[81] J. C. V. Laurie, L. Duncan, R. C. Haltiwanger, R. T. Weberg, M. Rakowski DuBois, *J. Am. Chem. Soc. 108* (1986) 6234; R. T. Weberg, R. C. Haltiwanger, J. C. V. Laurie, M. Rakowski DuBois, *ibid. 108* (1986) 6242; D. E. Coons, R. C. Haltiwanger, M. Rakowski DuBois, *Organometallics 6* (1987) 2417.
[82] D. E. Coons, J. C. V. Laurie, R. C. Haltiwanger, M. Rakowski DuBois, *J. Am. Chem. Soc. 109* (1987) 283.
[83] O. A. Rajan, M. McKenna, J. Noordik, R. C. Haltiwanger, M. Rakowski DuBois, *Organometallics 3* (1984) 831; L. D. Tanner, R. C. Haltiwanger, J. Noordik, M. Rakowski DuBois, *Inorg. Chem. 27* (1988) 1736.
[84] E. H. M. Badger, R. H. Friggith, W. S. B. Newling, *Proc. R. Soc. London Ser. A 197* (1949) 184.
[85] F. E. Massoth, C. L. Kibby, *J. Catal. 47* (1977) 300; F. E. Massoth, ibid. 47 (1977) 316; H. C. Kwart, G. C. A. Schuit, B. C. Gates, *ibid. 61* (1980) 128.
[86] C. J. Casewitt, D. E. Coons, L. L. Wright, W. K. Miller, M. Rakowski DuBois, *Organometallics 5* (1986) 951.
[87] G. J. Kubas, R. R. Ryan, *J. Am. Chem. Soc. 107* (1985) 6138.
[88] J. Pfauntsch, *Dissertation*, Universität Regensburg 1988.
[89] H. Brunner, N. Janietz, J. Wachter, H.-P. Neumann, B. Nuber, M. L. Ziegler, unpublished.
[90] G. J. Kubas, R. R. Ryan, K. A. Kubat-Martin, E. Larson, *J. Am. Chem. Soc. 111* (1989) 7823.
[91] H. Brunner, N. Janietz, J. Wachter, T. Zahn, M. L. Ziegler, *Angew. Chem. 97* (1985) 122; *Angew. Chem. Int. Ed. Engl. 24* (1985) 133.
[92] C. M. Bolinger, T. D. Weatherill, T. B. Rauchfuss, A. L. Rheingold, C. S. Day, S. R. Wilson, *Inorg. Chem. 25* (1986) 634.
[93] B. K. Teo, G. Longoni, F. R. K. Chung, *Inorg. Chem. 23* (1984) 1257.
[94] H. Brunner, H. Kauermann, J. Wachter, *J. Organomet. Chem. 265* (1984) 189.
[95] H. Brunner, H. Kauermann, J. Wachter, *Angew. Chem. 95* (1983) 567; *Angew. Chem. Int. Ed. Engl. 22* (1983) 549.
[96] H. Brunner, J. Wachter, *J. Organomet. Chem. 240* (1982) C41.
[97] H. Brunner, W. Meier, J. Wachter, H. Pfisterer, M. L. Ziegler, *Z. Naturforsch. B40* (1985) 923.
[98] J. A. Bandy, C. E. Davies, C. Green, M. L. H. Green, K. Prout, D. P. S. Rodgers, *J. Chem. Soc. Chem. Commun. 1983*, 1395.
[99] J. Darkwa, J. R. Lockemeyer, P. D. W. Boyd, T. B. Rauchfuss, A. L. Rheingold, *J. Am. Chem. Soc. 110* (1988) 141.
[100] H. Brunner, R. Grassl, J. Wachter, B. Nuber, M. L. Ziegler, unpublished.
[101] M. D. Curtis, P. D. Williams, W. M. Butler, *Inorg. Chem. 27* (1988) 2853.
[102] B. A. Cowans, R. C. Haltiwanger, M. Rakowski DuBois, *Organometallics 6* (1987) 995.
[103] N. Janietz, J. Wachter, unpublished results.
[104] See for example G. J. Kubas, P. J. Vergamini, *Inorg. Chem. 20* (1981) 2667; F. Cecconi, C. A. Ghilardi, S. Midollini, A. Orlandini, P. Zanello, *J. Chem. Soc. Dalton Trans. 1987*, 831.
[105] O. J. Scherer, J. Schwalb, G. Wolmershäuser, W. Kaim, R. Gross, *Angew. Chem. 98* (1986) 349; *Angew. Chem. Int. Ed. Engl. 25* (1986) 363.
[106] A. L. Rheingold, M. J. Foley, P. J. Sullivan, *J. Am. Chem. Soc. 104* (1982) 4727.
[107] H. Brunner, U. Klement, W. Meier, J. Wachter, O. Serhadli, M. L. Ziegler, *J. Organomet. Chem. 335* (1987) 339.
[108] For a summary of the catalytic uses of transition-metal complexes with sulfido ligands, see: M. Rakowski DuBois, *Chem. Rev. 89* (1989) 1.
[109] T. A. Pecoraro, R. R. Chianelli, *J. Catal. 67* (1981) 430.
[110] N.-Y. Topsøe, H. Topsøe, *J. Catal. 84* (1983) 386.
[111] M. D. Curtis, J. E. Penner-Hahn, J. Schwank, O. Baralt, D. J. McCabe, L. Thompson, G. Waldo, *Polyhedron 7* (1988) 2411.
[112] T. R. Halbert, S. A. Cohen, E. I. Stiefel, *Organometallics 4* (1985) 1689.

Fundamentals of Silicon Chemistry: Molecular States of Silicon-Containing Compounds**

By Hans Bock*

Dedicated to Professor Wolfgang Hilger on the occasion of his 60th birthday

Silicon and its compounds have made possible the design of new materials, which, from computers to space travel, have helped to shape the technology of our 20th century. Conversely, the demands of new technology have stimulated the fast development of silicon chemistry as part of the "renaissance" of inorganic chemistry. This article uses selected examples of predominantly organosilicon compounds to discuss in simplified terms the measurement and assignment of suitable spectroscopic "molecular fingerprints" as well as the resulting benefit for the preparative chemist. The comparison of "equivalent" states of "chemically related" molecules is emphasized, based on perturbation arguments and supporting quantum-chemical models. Special attention is given to the relation between structure and energy, which allows us to understand and to predict the connectivity between and the spatial arrangement of silicon "building blocks", the energy-dependent electron distribution over the effective nuclear potentials of a molecular framework, and, especially, the partly considerable effects of "silicon substituents" on molecular properties. Future-directed extensions and applications include polysilane band structures, Rydberg states of chromophores containing silicon centers, redox reactions and ion-pair formation of silicon-substituted π systems, and molecular dynamic phenomena in solution or on thermal fragmentation in the gas phase. The main objective is a set of clear and practical rules for interpreting measurements and planning experiments.

Measure everything and make the unmeasurable measurable.
Galileo Galilei

One must have hypotheses and theories in order to organize one's knowledge; otherwise everything merely remains rubble.
Georg Christoph Lichtenberg

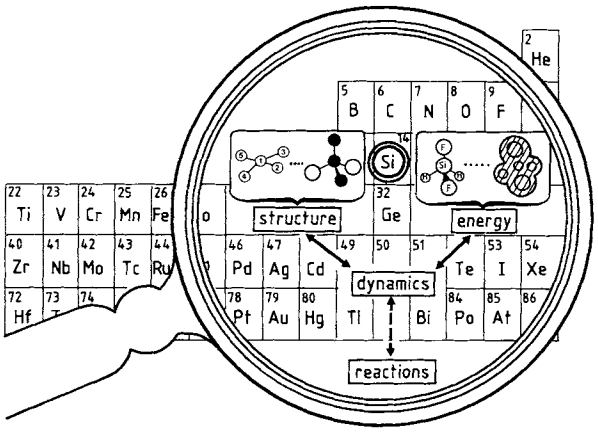
A sensible question can only be formulated with the help of a sensible theory.
Max Planck

1. What Can the Preparative Silicon Chemist Learn by Looking at Molecular Fingerprints?

In a time when at least one chemical publication appears in every one of the 525600 minutes of a 365-day year, the planning and evaluation of experiments as outlined by our scientific forefathers is a necessity.[8] In addition, the real building blocks of a chemist are no longer the over 10^7 molecules now known, but increasingly their numerous molecular and molecular-ion states[1-7] accessible via various routes of energy transfer (cf. Fig. 1a). These states are revealed by spectroscopic band or signal patterns, through which the respective compounds may be identified and characterized.[1, 3, 7] In addition to this analytical "ear-marking", such measurements afford as a rule valuable, but often unused information about the compound investigated, including the energies and the symmetries of its various states, as well as the energy-dependent electron distribution over its effective nuclear potentials. Let us, therefore, tentatively take a "molecular-state magnifying glass" (Scheme 1) and examine the relation between structure and energy for selected compounds of silicon, a nonmetal element. Let us also include equivalent states of chemically related molecules,[2] especially those containing the surrounding elements in the periodic table, in order to recognize additional useful relationships by correlating data from suitable measurements and/or quantum-chemical models. These correlations allow, for instance, the rationalization of the manifold of compounds and their diverse properties by a "red-line" subdivision into "parent systems" and their "substituent perturbations".[2, 4, 7] Thus, better use can be made of the extensive literature on valence-isoelectronic or structurally analogous compounds and of precalculable molecular properties[2, 5, 7] obtained by using quantum-chemical computer programs widely available for daily use. In addition, such a "static background" of structure–energy relationships will throw light on "dynamic phenomena", without which the largely

[*] Prof. Dr. H. Bock
Institut für Anorganische Chemie der Universität
Niederurseler Hang, D-6000 Frankfurt am Main 50 (FRG)

[**] 20th essay on molecular properties and models; shortened version of an introductory lecture at the US/Japan conference on "Advances in Silicon-Based Polymer Science", Makaha, Hawaii, 21 Nov. 1987. 19th Essay: [1]. See also earlier essays [2–6] as well as review [7].



Scheme 1. "Molecular-state magnifying glass" for the silicon chemist.

unknown microscopic pathways of chemical reactions, particularly those of medium-sized molecules,[6] cannot be described.

In general, molecules may be viewed[2] as self-dedicated computers, which, in "printing out" measurement data, provide complete (i.e., self-consistent and completely correlated) solutions of the Schrödinger equation. The question resulting from the rapid development of numerical quantum mechanics,[7a] as well as of vector computers, whether to measure or to calculate, is best answered with reference to how successful and stimulating the combination of the two proves to be. Among the numerous techniques of measurement now available, photoelectron (PE)[9] spectroscopy and electron spin resonance (ESR/ENDOR)[10] spectroscopy have proven themselves especially informative for preparatively oriented molecular-state investigations (Fig. 1a). "Vertically" recorded ionization energy patterns (i.e., those recorded with a time resolution on the order of 10^{-15} seconds) can be approximately correlated via Koopmans' theorem, $IE_n^v = -\varepsilon_j^{SCF}$, with the SCF eigenvalues[2] calculated for the neutral molecule M. PE spectrometers can thus be looked at as "eigenvalue meters". ESR/ENDOR signal patterns, on the other hand, are recorded "adiabatically" with a considerably smaller time resolution of about 10^{-7} seconds (i.e., long after the onset of molecular dynamics at about 10^{-13} seconds). These instruments can therefore be considered as "π-eigenfunction-squared meters", since the detected π-spin population ϱ_μ^π of radical and radical-ion centers can be correlated with the squared orbital coefficients, $\psi_\pi^2 \Rightarrow \sum_\mu c_{\pi\mu}^2$.[2] Obviously, the two methods complement each other owing to their different time resolutions and—coupled with quantum-chemical calculations—allow, for example, the determination of structural changes during one-electron oxidations, $M \rightarrow M^{\cdot\oplus} + e^{\ominus}$.

Starting from quantum-chemical precalculations and with extensive preparative efforts, the Frankfurt group[1-6] has carried out numerous investigations of compounds, especially those of the nonmetals B, C, N, P, S, and Si, by using the methods of measurement outlined in Figure 1a. For the element silicon, these investigations are summarized in the chronological pictogram of Scheme 2.

This article (cf. footnote to title) is based on the following results: the data obtained from measurements of the perturbation $\Delta\pi$ of π systems;[4] the PES ionization energies of various silicon compounds,[1] which allow the prediction of their oxidizability with $AlCl_3/H_2CCl_2$ to radical cations;[3] the thermal generation of unsaturated and reactive silicon compounds;[1] the development of ^{29}Si ENDOR spectroscopy[4] and its application to prove the existence of ion pairs in solution; experiments and hypersurface calculations[5] for the intramolecular elimination of H_2 from 1-silacyclohexa-2,5-diene. By way of introduction, both a PE-spectroscopically optimized gas-phase pyrolysis and an ESR-spectroscopically analyzed redox reaction in solution will illustrate the experimental procedure, the evaluation of molecular-state information, and the advantages of an approach combining preparation and measurement with supporting quantum-chemical calculations.

Generation of Phenyl Silaisocyanide in the Gas Phase: Starting from the literature report[11] that $H-N\equiv Si$ is produced on photolysis of H_3SiN_3 in a 4 K argon matrix, the



Hans Bock obtained his Ph.D. in 1958 from the Ludwigs Maximilians University in Munich, submitting a thesis on reactions of the rocket-fuel hydrazine, and his habilitation in 1964 based on investigations concerning relations between color and constitution of azo compounds. In the following three years as a visiting lecturer at the Federal Institute of Technology in Zurich, the three-volume book "The HMO Model and its Application" was compiled under the guidance of his mentor and friend Edgar Heilbronner and later translated into English, Japanese, and Chinese. In 1968 he received the Chemistry Award of the Academy of Science in Göttingen and the offer of an inorganic professorship at the Johann Wolfgang Goethe University of Frankfurt. Preparative nonmetal chemistry, in combination with physical measurements and quantum-chemical calculations has remained the trademark of his research group: Short-lived molecules, some of them found in interstellar space, are generated under nearly unimolecular conditions and identified by their PE-spectroscopic ionization fingerprints; radical ions and their ion pairs in aprotic solution are characterized by their ESR/ENDOR signal patterns and their respective molecular states; the accompanying structural changes are discussed based on calculated energy hypersurfaces. Professor Bock, a dedicated university teacher, has won numerous honors, among them the Frederic Stanley Kipping Award of the American Chemical Society and the Wilhelm Klemm Award of the German Chemical Society. Since 1977 he has been an External Scientific Member of the Max Planck Society, since 1981 an Adjunct Professor of The University of Michigan, Ann Arbor, and since 1984 a member of the Academy of Sciences and Literature at Mainz.

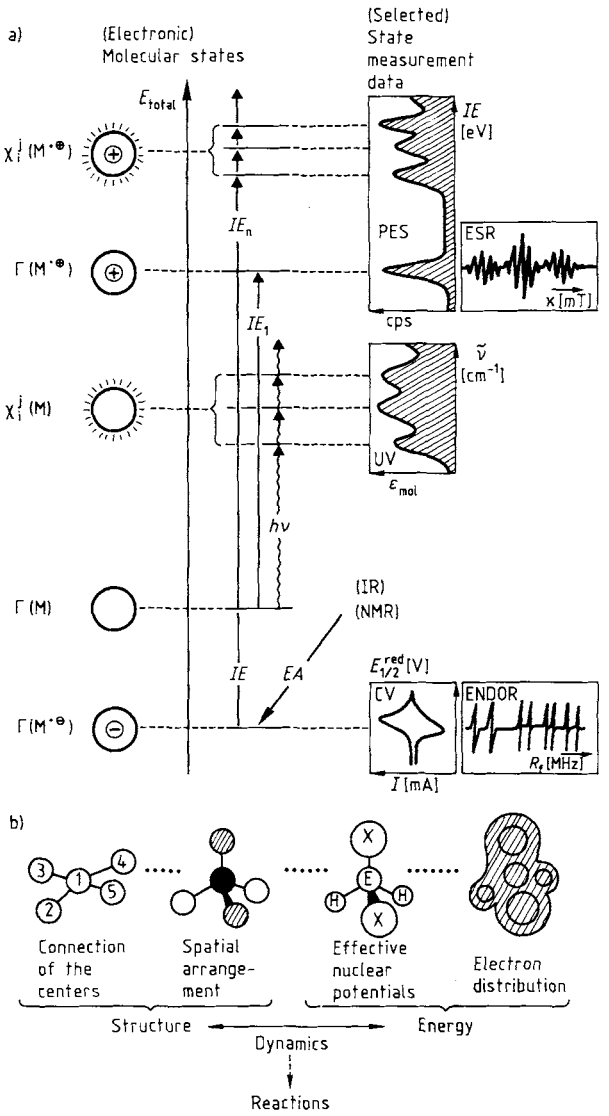
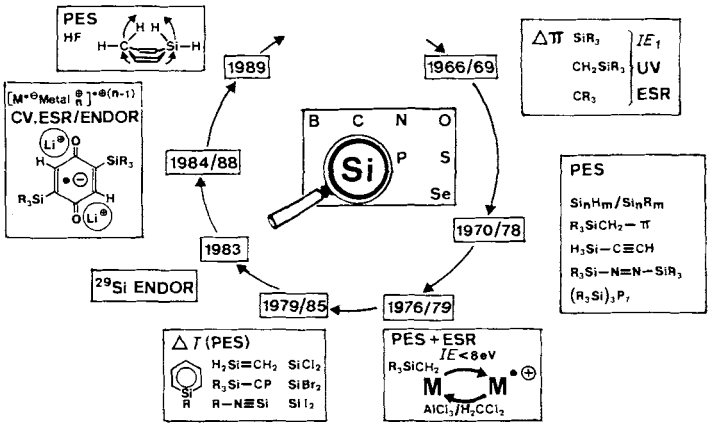


Fig. 1. Molecular states: (a) Schematic energy scale of electronic ground (Γ) and excited (χ_i^j) states of a neutral molecule M and its radical cation $M^{+\oplus}$ generated by ionization or oxidation or its radical anion $M^{-\ominus}$ resulting on electron attachment. As representative methods of measurement for many of the subsequently discussed silicon compounds, UV, PE, ESR, and ENDOR spectroscopy, as well as cyclovoltammetry (CV) have been selected. (b) Simplified scheme for the comparison of molecular states of chemically related compounds, emphasizing either the connection between centers, their spatial arrangement, their effective nuclear potentials, or the resulting electron distribution. Structural changes due to changes in energy involve molecular dynamics, which is of central importance for the still largely unknown reaction pathways of medium-sized molecules.

total energy, the structure, and the ionization pattern of the more stable phenyl derivative have been calculated (Scheme 3). Laboratory-scale azide exchange yields the starting material, triazido(phenyl)silane. Its controlled explosion in a flash pyrolysis apparatus under approximately unimolecular conditions ($p \approx 10^{-3}$ Pa, $c \approx 10^{-3}$ mM) can be carried out without danger.[12] Real-time PE-spectroscopic analysis of the band intensities revealed that the optimum reaction conditions required a temperature of 1100 K (i.e., red heat) for the complete elimination of four molecules of N_2 (Scheme 3: blackened ionization bands).

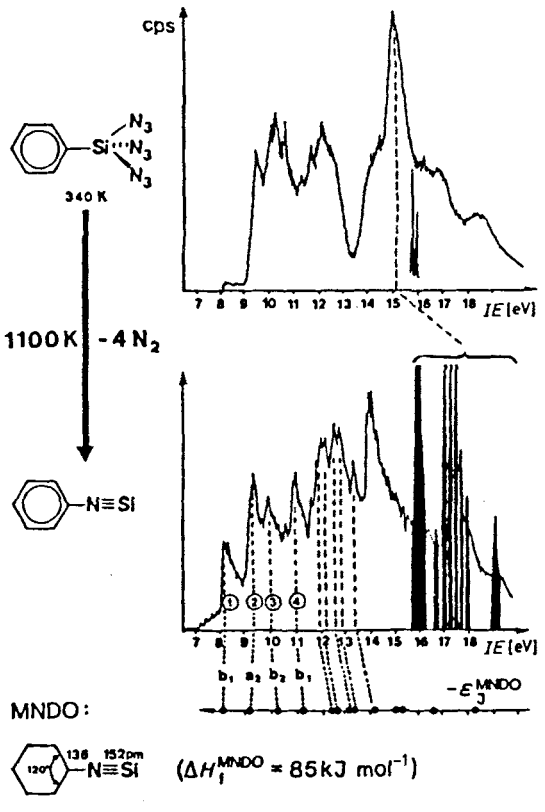
The identification of the first organosilicon compound with a triple bond to silicon and a silicon coordination number of 1 was accomplished by Koopmans' correlation of the



Scheme 2. The investigations on silicon compounds carried out by the Frankfurt group.

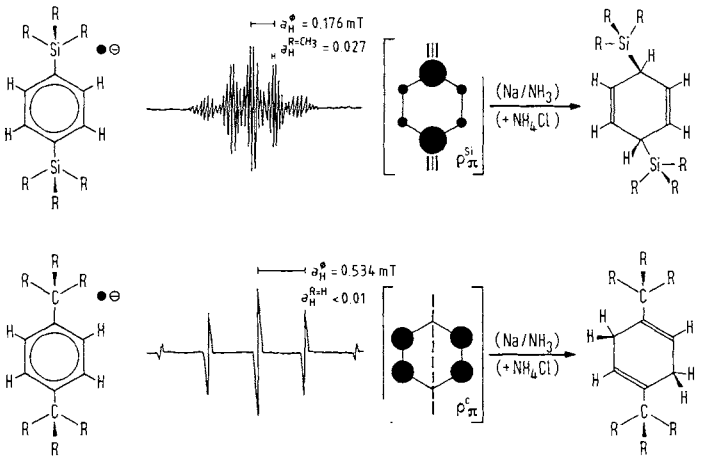
total of nine resolved low-energy ionization bands (Scheme 3) with calculated MNDO eigenvalues. The formation of the valence isomer H_5C_6-Si≡N, which is predicted to be 400 kJ mol^{-1} less stable, can be excluded, for example, by comparison of the radical-cation state sequence with that of the valence-isoelectronic carbon species $C_6H_5-N\equiv C$. Meanwhile, the PE-spectroscopic results have been confirmed by matrix isolation of H_5C_6-N≡Si.[7c, 11]

Birch Reduction of 1,4-Bis(trimethylsilyl)benzene: The ESR spectrum of the radical anion produced by treatment of a dimethoxyethane solution of this compound with potassium in a glass apparatus sealed under vacuum ($p \approx 10^{-1}$



Scheme 3. Generation of phenyl silaisocyanide by controlled explosion of triazido(phenyl)silane and its PE-spectroscopic identification. Triazido(phenyl)silane is prepared from trichloro(phenyl)silane by azide exchange with trimethylsilyl azide in the presence of $AlCl_3$ [12].

Pa)[13a] exhibits a quintet due to four equivalent phenyl protons. The signals, spaced 0.176 mT apart, are further split by the 18 equivalent methyl protons (R = CH_3; intensity ratio of outer line to inner line, 1:48 620). By contrast, the *p*-xylene radical anion, with a more strongly split quintet (R = H, a_H = 0.534 mT), shows no additional coupling with the six methyl protons; therefore, its substitution centers must be located in a nodal plane, in which the spin density ϱ_π is roughly zero and, concomitantly, the charge density negligible. In contrast, for the R_3Si-substituted radical anion, the spin density is small at the ring centers 2, 3, 5, and 6, as indicated by the smaller ring-proton couplings a_H, but large at the ring centers 1 and 4, as revealed by the resolved methyl proton splittings (Scheme 4, diagrams ϱ_π^{Si} and ϱ_π^{c}).



Scheme 4. Spin distribution in the valence-isoelectronic radical anions of 1,4-bis(trimethylsilyl)- and 1,4-dimethyl-substituted benzenes and the protonation products of their Birch reduction. R = H, CH_3; ∅ represents the phenyl protons.

The interpretation of the differing ESR signal patterns leads to the expectation that Birch reductions using Na/NH_3 followed by protonation of the respective dianions with NH_4Cl should take place at different centers (i.e., those with the highest charge density). This is indeed observed[13b] (Scheme 4; R = CH_3): reduction of 1,4-bis(trimethylsilyl)-benzene and 1,4-di-*tert*-butylbenzene exclusively yields the corresponding cyclohexa-2,5-diene and cyclohexa-1,4-diene, respectively.

These examples, chosen from the extensive literature, give the following answer to the question posed in the title of this section: "more than he might have expected". The conditions for the preparation of $H_5C_6-N\equiv Si$ by gas-phase pyrolysis of triazido(phenyl)silane could not have been optimized without PE real-time analysis, and the reactive intermediate could not have been identified in the gas flow without comparing experimental and calculated ionization patterns.[12] The Birch reductions of R_3Si- and R_3C-substituted *p*-benzene derivatives in solution would presumably not have been studied and compared without the ESR-spectroscopic evidence of differing spin and charge distribution in their radical anions.[13] Both examples, therefore, encourage use of the molecular-state magnifying glass (Scheme 1) to look at other silicon compounds as well.[1, 13]

2. Molecular-State Comparison of Silicon-Containing Compounds

2.1. Experimental and Quantum-Chemical Starting Points

The properties of a molecule depend on its energy and vary particularly on uptake or removal of electrons.[2] A particular state of a molecule or a molecular ion is characterized by the energy difference to the preceding or the following state and by its electron distribution, that is, by its structure and dynamics (Fig. 1). Information about energy differences between molecular states of, for example, silicon compounds,[1-7] as well as about their structures and their properties, is accessible by numerous physical measurements[1, 3, 7, 9, 10] or by precise quantum-chemical calculations.[5, 7a]

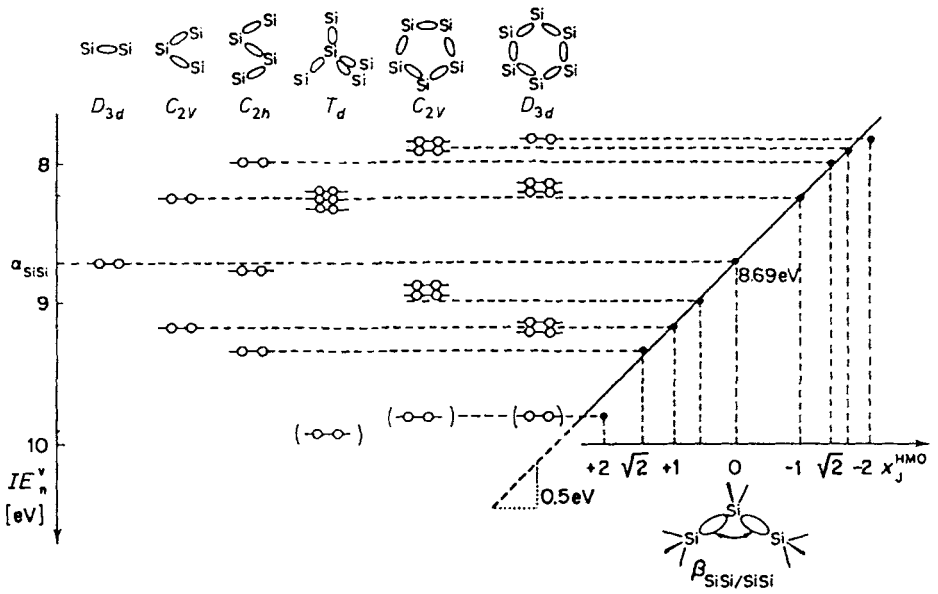
The multitude of states of a single molecule, especially on inclusion of its dynamics, and the numerous properties of each of these states are overwhelming and therefore inevitably outside the focus of interest of a synthetically oriented chemist, even if he analyzes and characterizes his compounds by physical measurements. What demands does he place on a suitable and useful molecular-state model? Above all, it should be as close to experiment, as flexible, and as general as possible, and it should allow him to use his extensive and detailed knowledge to define "chemically related" molecules and to compare their properties. These demands are largely fulfilled by a simplified molecular-state description (Fig. 1 b), which, depending on the specific requirements, emphasizes topological aspects, symmetry considerations, effective nuclear potentials, or electron distributions.[2] Quantum-chemical calculations,[5, 7a] performed with readily available computer programs or with the help of knowledgeable colleagues, are a valuable addition and allow these qualitative models to be extended further, especially with respect to structure–total energy relationships and pertinent total charge distributions. The following examples, taken predominantly from our investigations[1-6] (Scheme 2) and complemented by those from a recent comprehensive monograph on organosilicon compounds and their properties,[7] will illustrate procedures, advantages, and also some necessary caution.

2.2. The Connection of Silicon Building Blocks

Structural formulas of chemical compounds contain connecting lines, which correspond to the "handshaking" lemma of topology.[14] These lines should not be misinterpreted as representing two electrons each, since the historically developed shorthand notation for chemical formulas does not permit an exact description of the electron distribution, especially for multiple bonds or for higher coordination numbers. With this restriction, the application of topological connectivity concepts to the description of molecular states (Fig. 1 b) will be illustrated first for the PE-spectroscopic ionization patterns of polysilanes[1, 15] (Section 2.2.1) and then for the quantum-chemically predicted[16, 17] (1985/1987) and subsequently experimentally verified existence of three-dimensional polysilane polyhedra (Section 2.2.2).[18, 19]

2.2.1. SiSi Ionization Patterns of Polysilanes

The photoelectron spectra[1, 15] of permethylated polysilanes exhibit characteristic band patterns in the low-energy region up to 10 eV, which have been assigned to radical-cation states with predominantly SiSi framework contribution.[1, 15] This suggests a correlation between the vertical ionization energy IE_n^v [eV] and the topological eigenvalue coefficients,[20] x_j^{HMO}, for the differing number of dissimilarly connected σ_{SiSi} building blocks (Scheme 5).



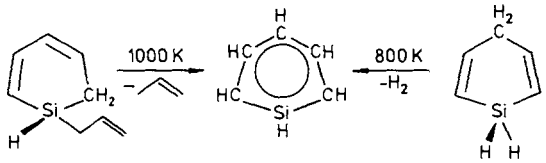
Scheme 5. SiSi ionization patterns of permethylated polysilanes and their correlation with topological eigenvalues.

The linear combination of bond orbitals (LCBO) model[15] clearly provides a fully occupied energy-level scheme, whose eigenvalues, $\varepsilon_j^{HMO} = \alpha_{SiSi} + x_j^{HMO}\beta_{SiSi/SiSi}$, on correlation with the vertical ionization energies IE_n^v [eV], yield a satisfactory linear regression. Its center is the Coulomb term $\alpha_{SiSi} = 8.69$ eV, and its gradient defines the interaction parameter $\beta_{SiSi/SiSi} \approx 0.5$ eV. For further elucidation, it should be noted that $\alpha_{SiSi} = 8.69$ eV is the first ionization energy of hexamethyldisilane and that the value $2\beta_{SiSi/SiSi} \approx 1.0$ eV corresponds to the difference between the two lowest ionization energies of octamethyltrisilane, $IE_{1,2}^v = 0.95$ eV. The applicability of a topological LCBO-MO model[1, 15] is further supported by the fact that the "alternating"[2, 20]—all the chains as well as the six-membered ring in Scheme 5—polysilanes show approximately equally spaced splitting patterns around α_{SiSi}[1] and that the highest SiSi ionization energies of the two rings, $IE_5^v = 9.80$ eV and $IE_6^v = 9.78$ eV,[1] agree, as expected from their identical eigenvalues, $\varepsilon_j^{HMO} = \alpha + 2\beta$. In addition, some of their lower-energy ionizations are predicted and found to be pairwise degenerate.[2, 20]

Altogether, the 21 IE_n^v values measured for polysilanes can be incorporated into the simple "isoconjugate" (i.e., consisting of equal subunits; cf. Fig. 3a) radical-cation-state model, which yields the experimental parameters α_{SiSi} and $\beta_{SiSi/SiSi}$. Comparison of the latter with the analogous π interaction in the $M^{\cdot\oplus}$ states of linear polyenes, $\beta_{C=C/C=C} \approx 1.2$ eV,[21] demonstrates that, despite the different values of the parameters, the positive charge in permethylated polysilane radical cations is largely delocalized over the SiSi skeleton[15] and thus explains the astoundingly small ionization energies measured.[1]

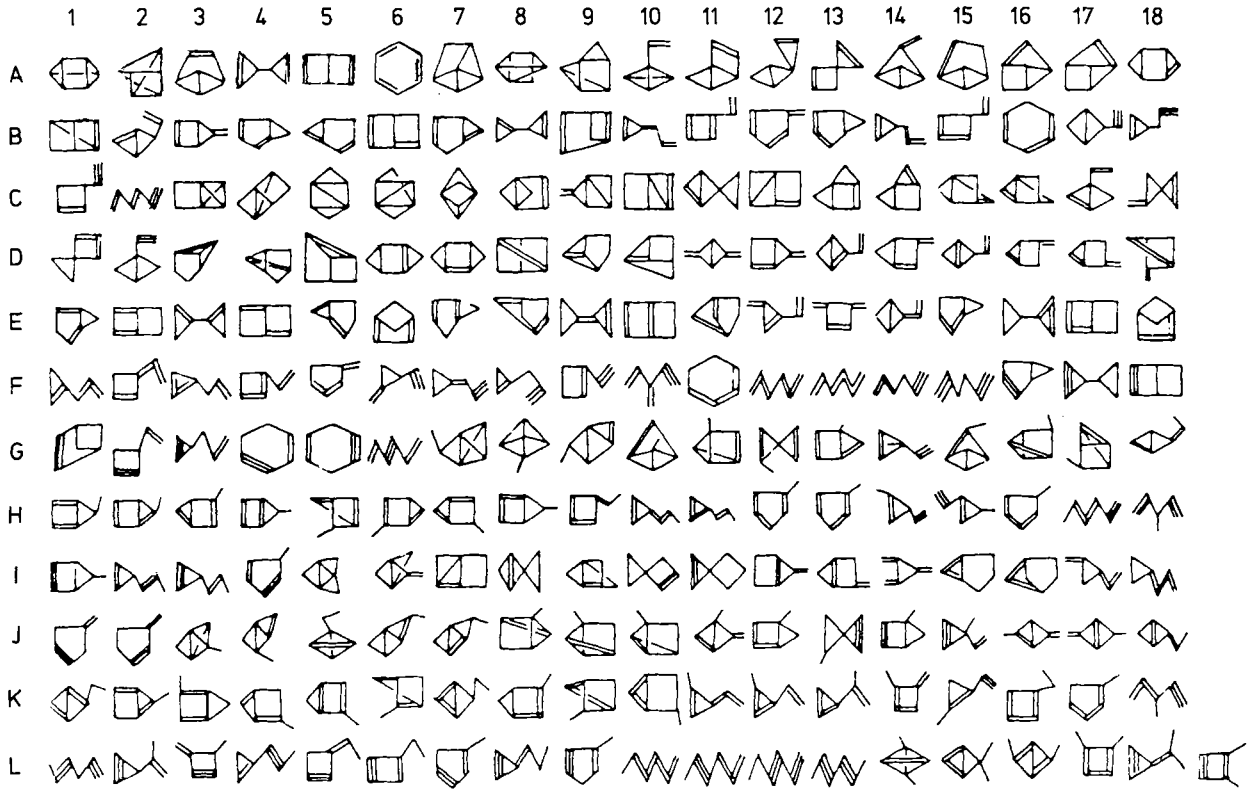
2.2.2. Structure and Total Energies of Polysilanes

Use of PE-spectroscopic ionization patterns (cf. Scheme 3) has also allowed the gas-phase thermolyses of 1-silacyclohexa-2,4-diene or 1-silacyclohexa-2,5-diene derivatives to silatoluene[22a] ($H \rightarrow CH_3$) or to silabenzene[22b] to be optimized for the first time (Scheme 6).[22]



Scheme 6. Preparation of silabenzene by gas-phase thermolysis of silacyclohexa-2,4-diene and silacyclohexa-2,5-diene.

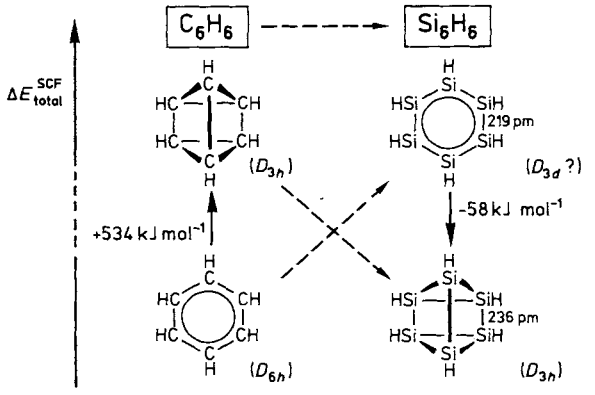
Assuming that sooner or later suitable starting materials for Si_6H_6 or its kinetically stabilized derivatives Si_6R_6 would be synthesized, spectacular structural proposals for these compounds have been put forward, based on quantum-chemical calculations,[16] partly including correlation energy (cf. Scheme 8). It should first be pointed out that molecules with n = 12 atoms possess $3n-6 = 30$ degrees of freedom. Therefore, the search for the respective total-energy minima has to be carried out in a 30-dimensional hyperspace. For the valence-isoelectronic system C_6H_6, when the coordination numbers were limited to ≤ 4 for carbon and 1 for hydrogen, an isomer computational program[23] "spat out" 217 topological possibilities (Scheme 7).



Scheme 7. Topological diagrams of the 217 C_6H_6 isomers with carbon coordination numbers ≤ 4.

In addition to the distillable D_{6h} hydrocarbon benzene (Scheme 7: A6), many of these molecular frameworks are known: the short-lived valence isomers prismane (A1), benzvalene (A3), and Dewar benzene (A5), as well as the more stable open-chain isomers such as 3-methylpenta-1,5-diyne (H18) and hexa-2,4-diyne (L13). On going from the "carbon world" to the neighboring "silicon world" with its reduced effective nuclear potential (see Section 2.4) and its larger covalent radius ($r_C = 77$ pm, $r_{Si} = 117$ pm)[24], calculations have predicted dramatic differences[16] (Scheme 8): In the case of Si_6H_6, the most stable valence isomer supposedly will not possess the famous Kekulé hexagon structure, but instead that of prismane, a highly explosive hydrocarbon.

Hexasilaprismane is calculated to be 58 kJ mol^{-1} more stable than hexasilabenzene,[16] whose SiSi bond lengths of 219 pm are predicted to be closer to that of disilene $H_2Si{=}SiH_2$ (215 pm) than of disilane (236 pm), and which might exhibit a fluctuating D_{3d} boat conformation.[7a] The considerable SCF total-energy difference of 534 kJ mol^{-1} calculated between the C_6H_6 valence isomers[16,17] prismane and benzene cannot be exclusively explained either by a more pronounced "magic" 6π-electron delocalization in benzene or by the reduced ring strain in hexasilaprismane; the preferred coordination number 4 of the Si centers[7a,16] may be the most important contributing factor (Fig. 2). This effect is also reflected in the ionization differences ΔIE_n^v between the $^2T_2$ and $^2A_1$ radical-cation states of CH_4 (Scheme 16: 8.7 eV) and SiH_4 (Scheme 16: 5.6 eV).



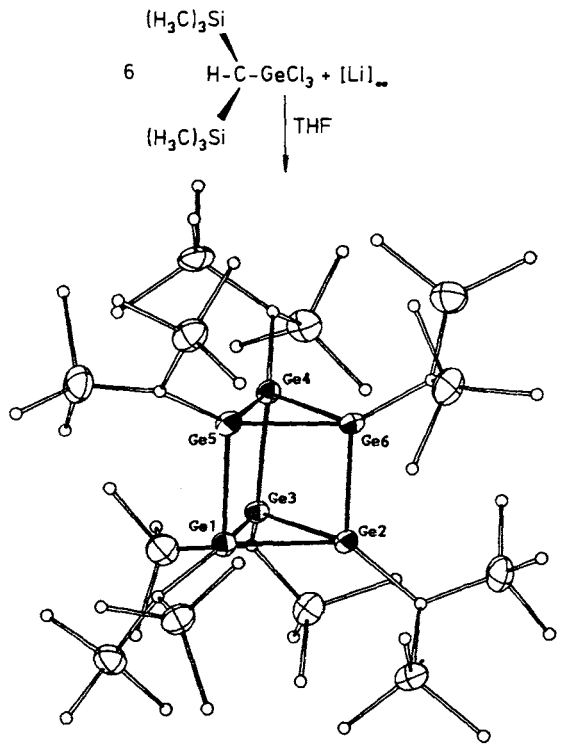
Scheme 8. Total energies of the six-membered ring and prismane isomers of the ensembles C_6H_6 and Si_6H_6.

The quantum-chemical calculations, extended in the meantime to include derivatives of the higher element homologues Ge, Sn, and Pb,[17] have been recently[18] and surprisingly confirmed experimentally. Selection of the substituents -$CH(Si(CH_3)_3)_2$, which are sterically suitable and kinetically shielding, led to the isolation and structural characterization of a hexagermaprismane (Scheme 9).

Within this context it should be pointed out that the strain energy in silicon polyhedra (e.g., $(SiH)_6$[17]) can be satisfactorily estimated quantum-chemically from the total-energy differences of "isodesmic" (constant composition) or—more precisely—"homodesmic" (unaltered subunits) reactions giving strain-free products.

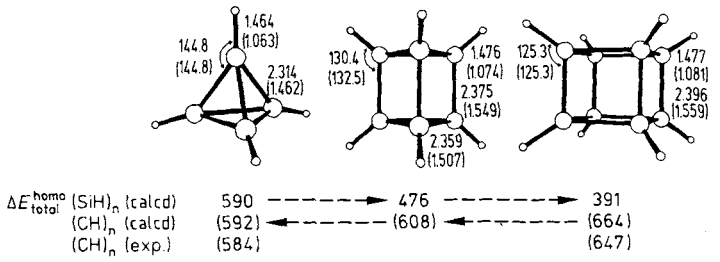
$$\text{isodesmic} \atop \text{homodesmic} \; (SiH)_6 \begin{cases} +12\,SiH_4 \rightarrow 9\,H_3SiSiH_3 \\ +9\,H_3SiSiH_3 \rightarrow 6\,(H_3Si)_3SiH \end{cases}$$

Calculations with 6-31 G* basis sets[17] predict for the $(SiH)_{4,6,8}$ polyhedra—and in parentheses for the valence-



Scheme 9. Preparation of the first hexagermaprismane and its kinetic stabilization by steric shielding.

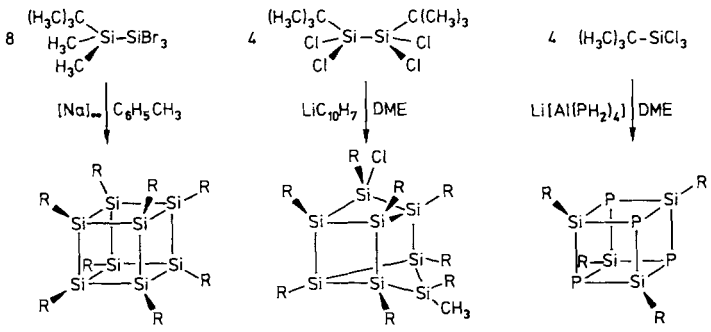
isoelectronic $(CH)_{4,6,8}$ polyhedra—the structures and strain energies ΔE_{total}^{homo} [kJ mol^{-1}] shown in Scheme 10.



Scheme 10. Ab initio SCF-calculated structures and strain energies of the valence-isoelectronic polyhedra $(SiH)_n$ and $(CH)_n$ with $n = 4$, 6, and 8. Values for $(CH)_n$ in parentheses. Bond angles in °, bond lengths in Å.

Comparison of these values with the experimental values[25] available for tetrahedrane and cubane support the reliability of the calculations. As the number of four-membered rings increases, the strain energy of Si_n polyhedra decreases, the value for octasilacubane being only 391 kJ mol^{-1}. This quantum-chemical prediction, suggesting to the preparative silicon chemist that octasilacubane and its derivatives should be preferred synthetic goals, has been repeatedly confirmed experimentally[19] (Scheme 11).

The quantum-chemically predicted[16, 17] (Schemes 8 and 10) and in the meantime—as the tip of an iceberg—synthesized[18, 19] (Schemes 9 and 11) novel polyhedra made up of group 14 elements should exhibit numerous interesting properties: thus, their calculated low first ionization energies suggest their oxidizability to the corresponding radical cations (cf. Section 2.5.4) and the PE spectra of polysilanes[1, 15] (Scheme 5) indicate an extensive delocalization of the positive charge. Additional predicted valence isomers[16] lead to the expectation of surprising dynamic phenomena,[26] and excitation into Rydberg states (cf. Section 3.2) should result in an interesting photochemistry[27] for suitable derivatives.



Scheme 11. Si_n ($n = 8$, 9) and Si_4P_4 polyhedral derivatives prepared in 1988/1989.

In terms of the stated goal of a simplified molecular-state description (Fig. 1), the SiSi ionization patterns (Scheme 5) illustrate different topological features of "isoconjugate" systems for the radical-cation states of polysilanes, just as the structure–energy relationships (Schemes 8 and 10) do for the ground states of polysilane polyhedra; that is, they reveal the dominant influence of connectivity between similar silicon building blocks. Both also demonstrate—in the rationalization of numerous measurement data and in suggestions for the synthesis of energetically favorable structures—the usefulness of such considerations for the silicon chemist.

2.3. The Silicon World: Coordination Numbers between 1 and 10

The "renaissance" of inorganic chemistry has also been inspired by the rapid development of the silicon sector. In the last ten years, countless "unsaturated" molecules with silicon centers of coordination numbers 1, 2, or 3 have been generated both in the gas phase[1, 28] and in matrices.[7c] Their isolation at room temperature could be achieved in most cases after introducing bulky substituents, that is, synthesis of kinetically stabilized derivatives[7c] (Fig. 2). Further progress has resulted from investigations of metal-rich silicide and Zintl phases,[29] which contain $Si_n^{m\ominus}$ polyanion-cluster lattice units such as $Si_4^{10\ominus}$ stars or $Si_4^{4\ominus}$ tetrahedra (Fig. 2). Unlike its neighboring element carbon, which prefers to form compounds with coordination numbers of 4 or less, the homologous silicon can rather easily accommodate five or six substituents.[7c] In the more recently reported bis(pentahapto) sandwich complexes[30] with cyclopentadienyl or dicarborane ligands,[30] the coordination sphere is enlarged to 10 (Fig. 2).

Future investigations will prove whether the existing "coordination number gap" between 6 and 10 can be filled and whether there is even a possibility of preparing novel silicon

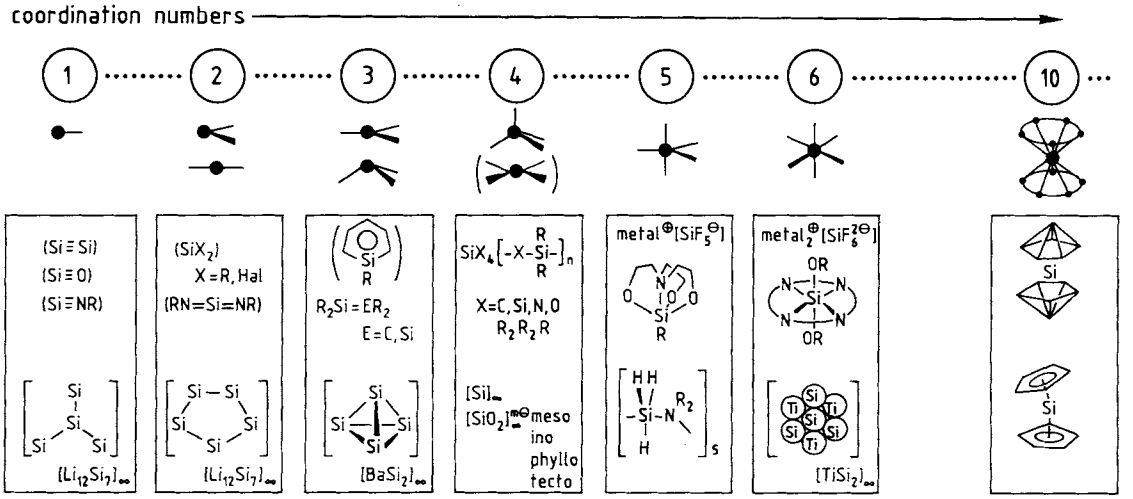


Fig. 2. Representative examples of a classification of silicon-containing molecules based on coordination numbers: silicon centers with coordination number 1 to 6 and 10 in covalent molecules and molecular ions and in solids (cf. text).

compounds with coordination numbers larger than 10—because it is perhaps difficult to imagine, reference is made to the uranium coordination number of 16 in $U(C_8H_8)_2$.[24] In the following discussion, which explicitly refers to recent literature surveys[7] concerning the current status of silicon chemistry and, in particular, the excellent summary of the quantum-chemical aspects contained therein,[7a] simplified molecular-state descriptions will be given for selected examples of compounds with coordination numbers 2, 5, and 10.

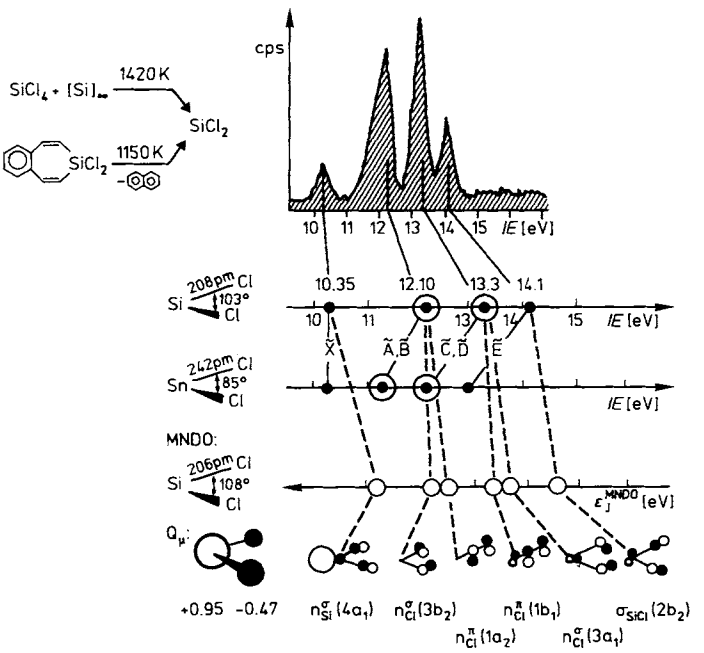
Dichlorosilanediyl (Dichlorosilylene), $SiCl_2$: This triatomic singlet molecule[7a] with a twofold-coordinated silicon center can be prepared via numerous routes.[4] It contains 18 valence electrons and, like the valence-isoelectronic compounds $SnCl_2$ and SO_2, is therefore bent according to the Walsh rules.[31] Its gas-phase structure (Scheme 12) has been determined by electron diffraction[32a] and its PE spectrum shows, as expected, six ionization bands in the He(I) region.[4, 32b]

The assignment of its radical-cation states can be accomplished by comparison with those of the valence-isoelectronic $SnCl_2$ or—via Koopmans' theorem—by use of MNDO-SCF calculations[32b] (Scheme 12), which, on complete geometry optimization, satisfactorily reproduce the structure and reveal that the $SiCl_2^{\bullet\oplus}$ radical ground state $\tilde{X}(^2A_1)$ originates from loss of one of the "nonbonding" electrons of the silicon electron pair in the molecular plane. The rather polar charge distribution Q_μ, calculated for the neutral molecule (Scheme 12), reflects the considerable differences in the effective Si and Cl nuclear potentials.

Silicon Pentahydride Anion, $SiH_5^\ominus$: This pentacoordinate silicon species was recently prepared in 32% yield by gas-phase reaction (a).[33a] According to extensive calculations,[7a, 33b] it possesses a D_{3h} trigonal-bipyramidal struc-

$$(H_5C_2)_3SiH_2^\ominus + SiH_4 \rightarrow SiH_5^\ominus + (H_5C_2)_3SiH \qquad (a)$$

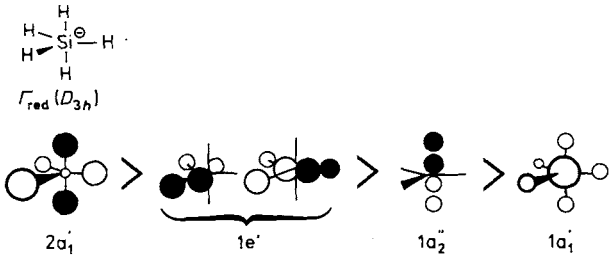
ture, in which the axial SiH distances are 10 pm longer than the equatorial distances. Only 9 kJ mol^{-1} higher on the energy hypersurface is a second minimum corresponding to a C_{4v} tetragonal pyramid. This result suggests fluxional behavior for $SiH_5^\ominus$ in the gas phase—as temperature-dependent NMR measurements have revealed for countless other pentacoordinate silicon compounds in solution.[7c]



Scheme 12. Gas-phase generation of $SiCl_2$ as well as PE-spectroscopic identification, molecular-state comparison with $SnCl_2$, and correlation with MNDO calculations.

Although noble-gas compounds such as XeF_2 have qualified the octet rule as a "closed shell-closed mind" intellectual exercise and multicenter bonding is not only generally accepted in electron-deficient compounds such as $H_2B(H)_2BH_2$,[34] a fictitious[35] "d-orbital participation" is

still erroneously invoked to explain certain properties of silicon compounds. Under the proviso that orbitals generally cannot be observables in experiments and that, at best, only the square of the wavefunction can be correlated with the electron density, the five occupied molecular orbitals of $SiH_5^{\ominus}$—without any 3d orbital contribution—are presented in Scheme 13.[7a]



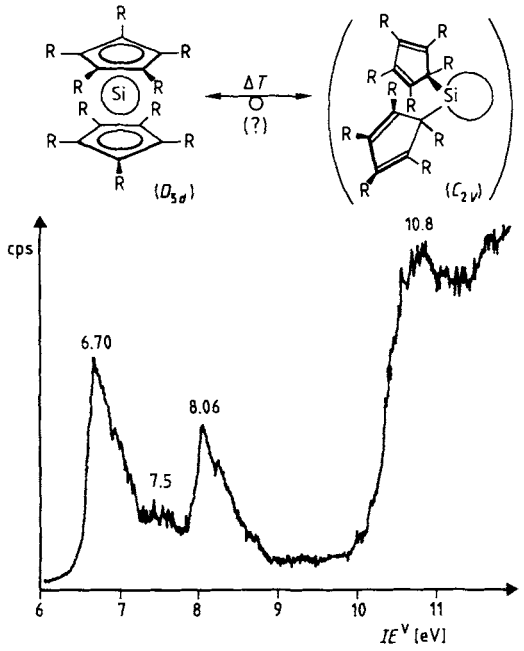
Scheme 13. Qualitative molecular orbitals of $SiH_5^{\ominus}$ obtained with a 3s,p basis set without 3d functions.

Independent of the preceding arguments, higher p, d, and f "polarization functions" are often included in high-quality basis sets for quantum-chemical calculations at all centers of the respective molecules to increase the occupied "electron density volume" covered. The "Shakespearean" question, "to d or not to d?", however, can be answered by the preparative chemist with a straightforward "not to".

Decamethylsilicocene, $(\eta^5\text{-}C_5R_5)_2Si$, $R = CH_3$: Syntheses of valence-isoelectronic sandwich complexes of Pb, Sn, Ge, $Bi^{\oplus}$, and $As^{\oplus}$ have been reported since 1956. In the absence of steric constraints, their five-membered ring planes are tilted from the coplanar D_{5d} or D_{5h} ideal structure by angles of between 30° and 50°.[36] The bis(pentamethylcyclopentadienyl) silicon derivative, also containing a tenfold-coordinated silicon center[30] (Fig. 2), shows two different conformers in the unit cell with interplane angles of 0° (D_{5d}) and 25° (C_{2v}).[30a] Extensive calculations[7a, 36] indicate a rather flat potential trough, inside which the R_5C_5 rings, exhibiting very long CSi distances (232–254 pm), can move relative to the silicon center, crossing only low energy barriers. This "fluctional behavior" renders the interpretation of the PE spectrum[37] (Scheme 14) more difficult.

Thus, the electron-rich silanediyl-like Si center leads to a low first ionization potential of only 6.7 eV.[37] The total electron population at the Si center, calculated to comprise 13.5 of the 14 electrons, is in agreement with this finding and also explains the long SiC distances, which are indicative of only weak π interactions with the five-membered ring. Moreover, despite the use of a basis set[36] with d polarization functions, they were found to play no significant role in the π bonding[36] in the silicon sandwich (cf. Scheme 13).

In summary, the multifaceted silicon world between coordination numbers 1 and 10 (Fig. 2) can be rationalized by known bonding principles—as long as each topological connecting line is not misleadingly associated with two electrons: (singlet) silanediyls, SiX_2, with twofold-coordinated Si, contain a "silicon electron pair", in analogy to $SnCl_2$; the bonding in $SiH_5^{\ominus}$, like that in PF_5 and SF_6, is best described without fictitious d functions, and silicocene, $(\eta^5\text{-}C_5R_5)_2Si$, like numerous valence-isoelectronic sandwich π complexes,



Scheme 14. Low-energy region of the PE spectrum of decamethylsilicocene.

can be formulated with centers of coordination number 10. As helpful as numerically exact SCF calculations are for molecules with only a few centers, the recommendation to the preparative silicon chemist for his usually multiatomic compounds with numerous degrees of freedom is to look instead for chemically related substances and to compare their equivalent molecular states.[2] Above all, such a procedure is usually of advantage for complex dynamic phenomena, for example in "pseudorotating" molecules with central Si atoms displaying fivefold or higher coordination.[7e]

2.4. Silicon Centers and Their Small Effective Nuclear Charge

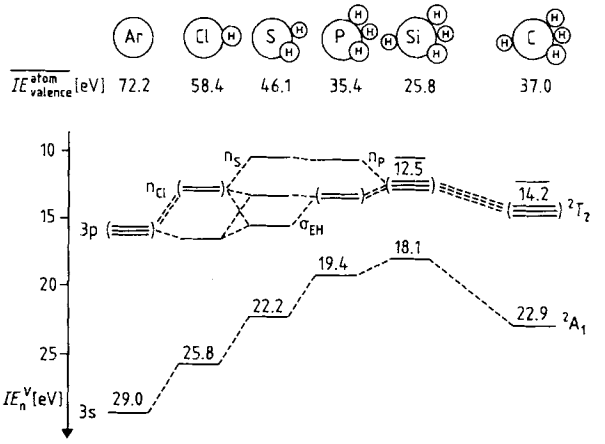
Let us return to the "normal" silicon coordination number of 4. The simplified molecular-state description (Fig. 1 b) ought to be expanded to include the effective nuclear charge Z_{eff}. Among the numerous literature suggestions, the concept of *Slater*,[38] in which the shielding contributions A_i of the nuclear charge Z are defined according to the quantum numbers n of the different electrons, has the following advantages: atoms or ionic radii can be rationalized in a lucid manner—for example, their contraction in the third period from Na (186 pm) through Si (117 pm) to Cl (99 pm) is a result of incomplete shielding ($A_i = 0.85$) of the respective increase ($\Delta Z = 1$) in nuclear charge (Table 1). Since the

Table 1. The dependence of effective nuclear charge, determined by the Slater method, on quantum numbers. A_i = shielding constant.

$Z_{eff} = Z - \sum_i A_i$

Electron orbitals	A_i for electrons in orbitals $n' > n$	$n' = n$	$n' = n-1$	$n' < n-1$
1s	0	0.30		
ns, np	0	0.35	0.85	1.00
nd, nf	0	0.35	1.00	1.00

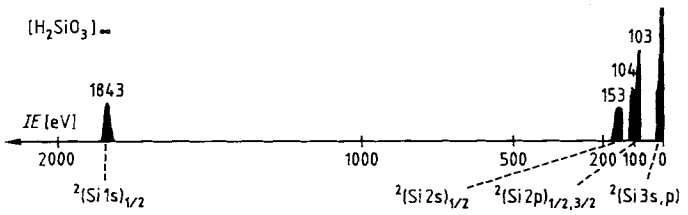
parameters A_i can be approximated from ionization energies,[38] they are "close to experiment" and contain electron correlation contributions. Furthermore, with small and justifiable additional assumptions, the Slater concept can also be used for molecules, even though their constituent atoms have lost their original identity. This approach, based on the numerous known vertical ionization energies into the different radical-cation states,[1,39,40] will be elaborated upon in the following selected examples: the X-PE spectrum of the inosilicate $[H_2SiO_3]_\infty$[39] (Scheme 15), the valence ionizations of the "united-atom" series from Ar to SiH_4[2] (Scheme 16), and a comparison of the radical-cation states of the valence-isoelectronic molecules H_3SiSiH_3 and H_3CCH_3[1] (Scheme 17). The "silicon-donor effect" derived from these examples and the resulting charge distribution will be qualitatively discussed by reference to the partly different structures of H_3C and H_3Si derivatives of the elements O, S, P, and N (Scheme 19).



Scheme 16. United-atom correlation of the valence ionization energies of Ar to SiH_4 and of CH_4.

2.4.1. PE-Spectroscopic Vertical Ionization Energies

X-PE Spectrum of $[H_2SiO_3]_\infty$: X-ray photoelectron spectroscopy (X-PES) conveys an impressive picture of "how electron shells are arranged about a certain effective nuclear potential" or—more precisely—what energies are required to generate a specific radical-cation state, a so-called electron-hole state. The X-PE spectrum of the polymeric inosilicate $[H_2SiO_3]_\infty$[39] (Scheme 15) reveals, for example, "how



Scheme 15. X-PE spectrum (ESCA ionization energies) of Si in the inosilicate $[H_2SiO_3]_\infty$.

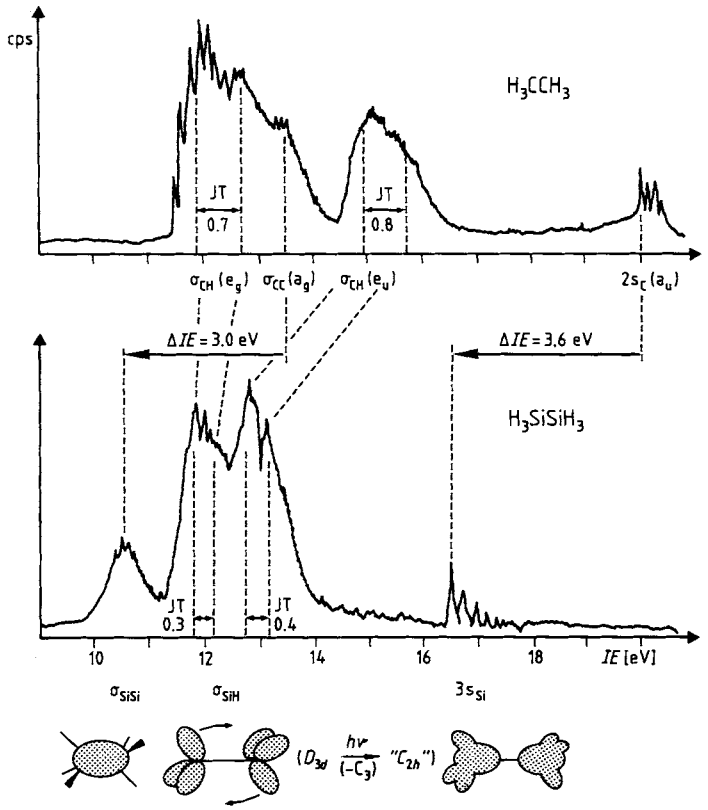
deep the 1s electrons are buried in the negative charge cloud" and shows that, owing to spin–orbit coupling, the Si(2p) doublet states, $^2(Si\,2p)_{1/2}$ and $^2(Si\,2p)_{3/2}$, are split, as expected, in the intensity ratio 2:4. It also shows that the Si(3s,p) valence-electron energy region, in which "all the chemistry takes place", is relatively narrow.

Valence Ionization Energies from Ar to SiH_4: If the end of the X-PES scale close to zero energy (Scheme 15) is expanded and, simultaneously, "nuclear protons" are pulled, one after another, from the noble gas argon as hydrogen atoms, then the united-atom molecular series HCl, H_2S, PH_3, SiH_4 results (Scheme 16). For characterization of the central nonmetal elements within the Slater concept, the mean atomic ionization energies $\overline{IE}^{atom}_{valence} = \sum IE_n/n$ for the respective n valence electrons may be considered.

The PE-spectroscopic comparison[2]—complemented by including CH_4[40]—shows both the region of the "3p valence band" and of the energetically higher 3s electron-hole states for Ar and the valence-isoelectronic species EH_n. In particular, the 3s ionization energies demonstrate the dominant influence of the effective nuclear charge. The "3s electron clouds", which are closer to the nucleus and approximately spherical, are increasingly more easily ionized[2] on decrease of the nuclear charges in steps of $\Delta Z = 1$ (compare also the mean atomic ionization energies $\overline{IE}^{atom}_{valence}$; Scheme 16), the difference between Ar and SiH_4 amounting to nearly 11 eV ($\triangleq$ 1060 kJ mol^{-1}). As expected, the ionizations of the 3p electrons, which are located farther from the nucleus, are more strongly influenced by the additional potentials of the hydrogens pulled from the united-atom argon and are therefore split into molecule-specific radical-cation states with dominant electron-pair (n_E) and bonding (σ_{EH}) contributions (Scheme 16). Nevertheless, the comparison of SiH_4 (principal quantum number $n_{Si} = 3$) and CH_4 ($n_C = 2$) demonstrates that, especially owing to the higher effective nuclear charge of carbon (Scheme 16: $\Delta\overline{IE}^{atom}_{valence} = 11.2$ eV), the two valence ionization energies increase by $\Delta IE(^2A_1) = 4.8$ eV and $\Delta IE(^2T_2) = 1.7$ eV.

Radical-Cation-State Comparison of H_3SiSiH_3 and H_3CCH_3: The considerable difference between the effective nuclear charges of Si and C centers and the differing influence of this Si electron-donor effect on the individual molecular states are particularly evident in the valence-electron ionization patterns of the "smallest polymers" disilane[1] and ethane,[40] generated with He(I) photons (Scheme 17). The repeatedly investigated sequence of $H_3CCH_3^{\bullet\oplus}$ is assigned in the usual D_{3d} symmetry-group notation as $\tilde{X}(^2E_g) < \tilde{A}(^2A_g) < \tilde{B}(^2E_u) < \tilde{C}(^2A_u)$.[38] The twofold-degenerate $\sigma_{CH}(^2E)$ states show relatively large Jahn–Teller splittings of 0.7 and 0.8 eV, presumably due to the symmetry reduction $D_{3d} \rightarrow C_{2h}$, that is, removal of the threefold axis (C_3).

A comparison with the valence-isoelectronic disilane reveals surprisingly large differences: for example, the energy of the $H_3SiSiH_3^{\bullet\oplus}$ state with the largest $3s_{Si}$ component is lowered by $\Delta IE^v = 3.6$ eV (cf. Scheme 17). Also, the center of gravity of the four σ_{SiH} states (cf. Scheme 17: $\sigma_{CH}(e_g) + (e_u)$) decreases from 13.9 eV in $H_3CCH_3^{\bullet\oplus}$ to 12.5 eV in $H_3SiSiH_3^{\bullet\oplus}$ and, as a result of the longer bond ($d_{CC} = 153$ pm, $d_{SiSi} = 235$ pm), both the $\sigma_{SiH}(e_g/e_u)$ band splitting and the Jahn–Teller distortions are simultaneously diminished. The small effective nuclear charge of the silicon



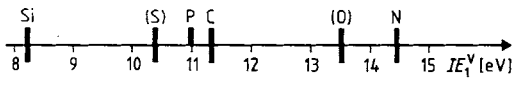
Scheme 17. Comparison of the radical-cation states of ethane and disilane.

centers even causes a change in the $M^{\bullet\oplus}$-state sequence: relative to the ionization $\sigma_{CC}(a_g)$, the σ_{SiSi} ionization band moves out of the SiH region and is (shifted by $\Delta IE^v = 3.0$ eV) the $H_3SiSiH_3^{\bullet\oplus}$ ground state. In general, the low σ_{SiSi} ionization energies resulting from the smaller effective nuclear charge of Si centers give rise to significant differences in the properties of silanes and alkanes: examples include the applicability of the $\sigma_{SiSi/SiSi}$ interaction model (Scheme 5), the band structure of polysilanes (Scheme 32), and the oxidizability of polysilanes like $(Si(CH_3)_2)_6$ to their radical cations in solution (Scheme 27).

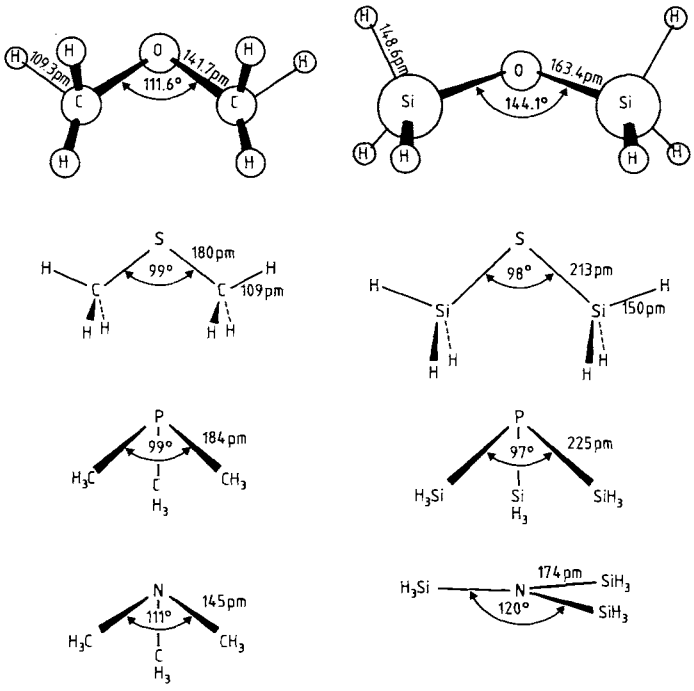
2.4.2. *Structures of H_3C and H_3Si Derivatives of the Elements O, S, P, and N*

The Slater concept of effective nuclear charges allows a comparative discussion of numerous molecular properties. The differing distribution of the same number of valence electrons over different skeletal potentials (Fig. 1 b) is exemplified by the gas-phase structures of the compounds $E(SiH_3)_n$ and $E(CH_3)_n$. The starting point of this discussion is supplied by the vertical ionization energies of nonmetal atoms (Scheme 18).

The single ionizations of O and S $(ns^2np^4) \rightarrow (ns^2np^3)^{\bullet\oplus}$ are placed in parentheses because they lead to energetically favorable cations with spherical symmetrical charge distributions and, therefore, the lower ionization energies deviate from a simplified Z_{eff} correlation. Nevertheless, a crude classification Si < C ~ P, S ≪ O, N is possible and suggests that especially the large difference in effective nuclear charge between Si and O and between Si and N will lead to considerably polar Si → O and Si → N bonds, that is, to high electron densities at the oxygen center of $H_3SiOSiH_3$ and at the N center of $N(SiH_3)_3$. From this point of view, the structures of the H_3C and H_3Si derivatives of the elements O, S, P, and N[41] (Scheme 19) can be comparatively discussed as follows: The differing gas-phase conformations of "doubly eclipsed" dimethyl ether and of "singly eclipsed" disiloxane and the widening of their internal angle (∢ COC = 111.6° to ∢ SiOSi = 144.1°) may be attributed to the considerable difference $Z_{eff}(Si) \ll Z_{eff}(O)$ and the high electron density consequently generated at the central oxygen. This, in turn, should lead to stronger "Coulombic repulsion" between the OSi bonds and, simultaneously, to improved hyperconjugative charge delocalization of the high n_O charge density into the four neighboring HSi bonds.[41a] Although such a line of reasoning touches on the limits of a simplified molecular-state description, it is supported by the comparable gas-phase structures of dimethylsulfide and disilathiane[41b] (Scheme 19). For these molecules, far smaller charge density differences on the two sulfur centers are expected ($Z_{eff}(Si) < Z_{eff}(C) \sim Z_{eff}(S)$). Also, the similar structures of $P(CH_3)_3$ and $P(SiH_3)_3$ and the dramatic differences between $N(CH_3)_3$ and $N(SiH_3)_3$ can be interpreted in an analogous manner: only the considerable difference $Z_{eff}(Si) \ll Z_{eff}(N)$ leads to such a large N electron density that a diminished repulsion between the NSi bonds and an improved π delocalization favors the observed planar NSi_3 molecular skeleton.[41]



Scheme 18. Vertical ionization energies of some nonmetal atoms (see text).



Scheme 19. Gas-phase structures of the methyl and silyl derivatives of O, S, P, and N.

As is often the case, the story is actually more complex.[42] Thus, disiloxane, despite its "vibrational distortion angle" of 144° determined by gas-phase electron diffraction (Scheme 19), exhibits IR excitations governed by D_{3d} selection rules;[42] that is, the molecule must possess a "quasi-linear" skeleton. The barrier to angle widening (∢ SiOSi from 144° to 180°) amounts to only 1.3 kJ mol^{-1}.[42] Therefore, qualitative structure–energy or structure–charge density discussions—like the preceding discussion based on Slater effective nuclear charges—although allowing chemically related compounds to be compared, can be put forward only with the proviso that the differing dynamic behavior of the individual molecules be neglected.

2.5. Silicon Substituent Effects on π Systems

Every chemist will presumably try—as indicated by the introductory quotations[8]—to disentangle the multitude of his compounds and to sort their molecular-state data (Fig. 1a) in the optimum way possible. There are countless different possibilities for selecting chemically related compounds within his area of research (Fig. 3). He may choose, for instance, topological features like coordination numbers (Fig. 2) or—especially for isoconjugate systems—the connection of the individual building blocks and their spatial arrangement (Section 2.2). For heteroconjugate systems, the different framework potentials (Section 2.4) and the respective number of valence electrons can be useful as the main criteria (Fig. 3).

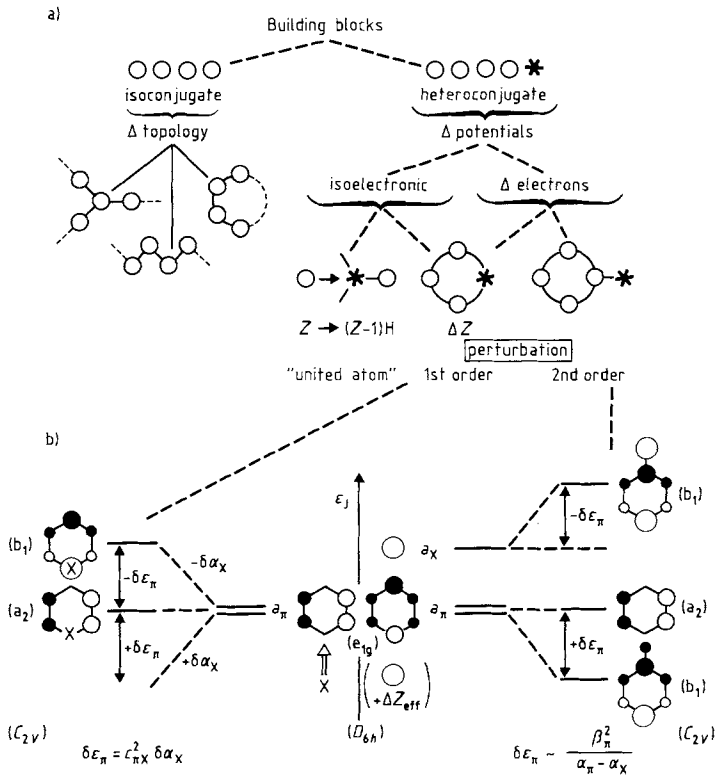


Fig. 3. Criteria for defining chemically related compounds. a) Subdivision into topologically determined isoconjugate and potential-determined heteroconjugate systems, which are appropriately further classified into valence isoelectronic systems and those with differing numbers of electrons as well as according to first-order perturbation by substitution within the molecular skeleton or according to second-order perturbation by additional substituents. b) First- and second-order perturbations are exemplified for benzene [20]: the lowering of the symmetry from D_{6h} to C_{2v} by monosubstitution lifts, among other things, the degeneracy of the $\pi(e_{1g})$ molecular orbitals. For first-order perturbation due to substitution (outside of a π nodal plane), electron donors lower the eigenvalue by $-\delta\varepsilon_\pi$ and electron acceptors raise it by $+\delta\varepsilon_\pi$. For second-order perturbation, the molecular orbitals of the same symmetry are "mixed" and will be lowered by $+\delta\varepsilon_\pi$ owing to additional bonding (O–O) interaction and raised by $-\delta\varepsilon_\pi$ owing to a corresponding antibonding (O–●) interaction. First-order perturbations like $\delta\alpha_x$ are proportional to the square of the coefficient ($c^2_{\pi\mu}$) of the perturbed center μ, while second-order perturbations increase with the square of the interaction parameter (β^2_π) as well as with the decreasing energy difference Δα between the starting levels.

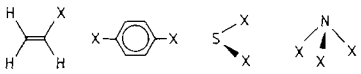
Every chemist will presumably try—as indicated by the introductory quotations[8]—to disentangle the multitude of his compounds and to sort their molecular-state data (Fig. 1a) in the optimum way possible. There are countless different possibilities for selecting chemically related compounds within his area of research (Fig. 3). He may choose, for instance, topological features like coordination numbers (Fig. 2) or—especially for isoconjugate systems—the connection of the individual building blocks and their spatial arrangement (Section 2.2). For heteroconjugate systems, the different framework potentials (Section 2.4) and the respective number of valence electrons can be useful as the main criteria (Fig. 3).

The widespread and useful subdivision of large molecules into parent systems and substituents and their comparison based on first- and second-order perturbation arguments[20] has proved to be tremendously valuable for organosilicon compounds as well. Therefore, the following examples are selected for additional illustration: the extreme σ-donor effects of β-trimethylsilyl groups[1,3] (Section 2.5.1), the "internal" and "external" first-order perturbations of the benzene π system[1,2,43] (Section 2.5.2), the second-order perturbation of the acetylene π system by H_3Si substituents[1,44] (Section 2.5.3), and the electron delocalization in organosilicon radical cations[3] (Section 2.5.4).

2.5.1. *Extreme Donor Effects of β-Trimethylsilyl Groups*

The donor effect of $(H_3C)_3SiCH_2$ substituents, discovered 20 years ago,[45] which, in particular, stabilizes the positive charge in radical cations (Section 2.5.3), is revealed by the low first ionization energies of π systems like ethene and benzene or of molecules with nonbonding electron pairs such as sulfides and amines[1,40,46] (Table 2).

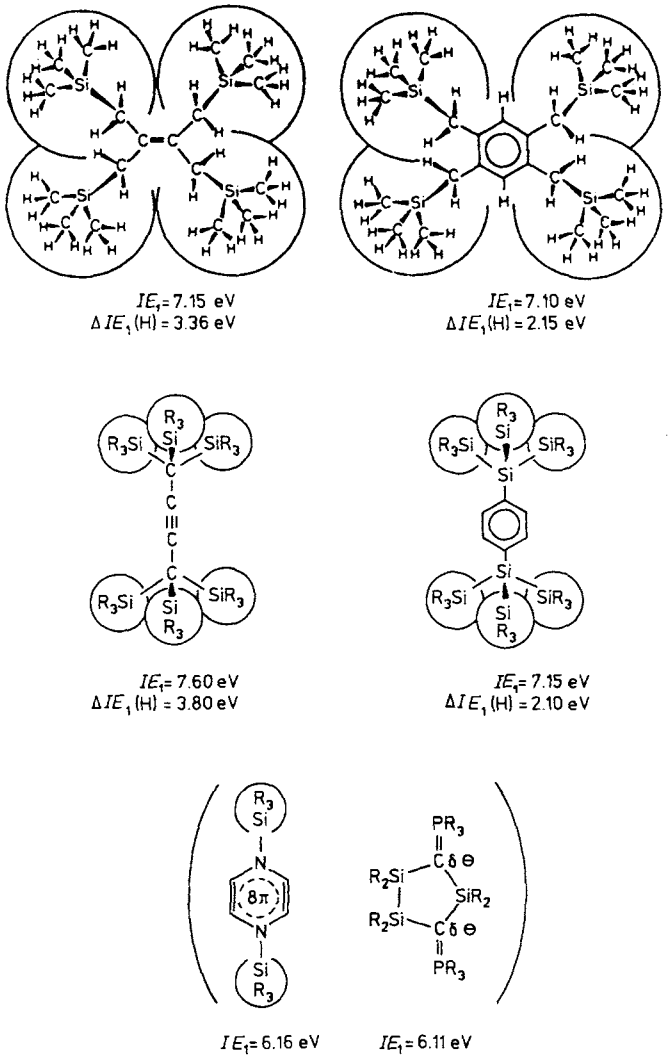
Table 2. Donor effect ΔIE^v_1(H) [eV] of substituents $CH_2Si(CH_3)_3$ on the π systems ethene and benzene as well as on the S and N systems containing lone pairs (see text). R = CH_3.



	X = H	SiH_3	R	SiR_3	CH_2SiR_3	ΔIE^v_1(H)
a	10.51	10.37	10.03	9.86	⇒9.10	1.41
b	9.25	(9.11)	8.44	8.7	⇒7.86	1.39
c	10.45	9.7	8.67	8.74	⇒8.04	2.41
d	10.85	9.7	8.44	8.60	⇒7.66	3.19

As demonstrated by the substituent effects $SiH_3 < CH_3 \sim Si(CH_3)_3 < CH_2Si(CH_3)_3$,[1,40] the vertical ionization energies are always lowered most by trimethylsilylmethyl groups.[1] The energy differences ΔIE^v_1(H) relative to the unsubstituted parent system depend, among other things, on the substituted center μ (ethene $c^2_{\pi,\mu} = 0.5 >$ benzene $c^2_{\pi,1/4} = 0.33$ and $Z_{eff}(N) > Z_{eff}(S)$) as well as on its steric shielding.

This is particularly obvious for the tetrasubstituted ethene and benzene derivatives (Scheme 20), whose bulky $(H_3C)_3Si$ groups are arranged alternately above and below the molecular plane: thus, in each case, the radical cations are almost tetrahedrally surrounded; their generation requires comparable ionization energies ($\sum_\mu c^2_{\pi\mu} = 1$[1]). Multiply R_3Si-substituted methyl and silyl groups also lead—al-



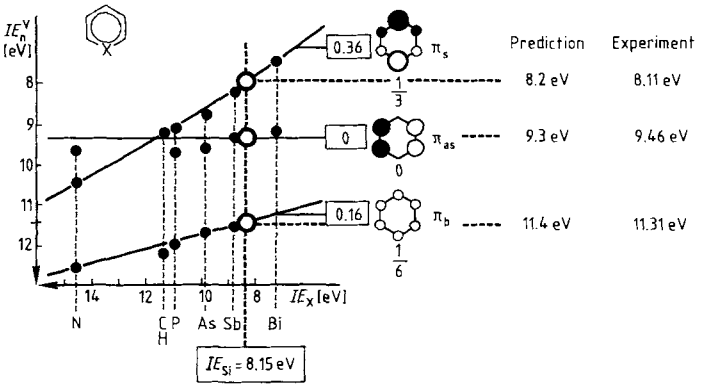
Scheme 20. Representative poly(trimethylsilyl)-substituted organosilicon compounds with unusually low vertical first ionization energies. R = CH_3.

though not additively[1, 43b]—to large ΔIE_1^v(H) values (Scheme 20). In contrast, the lowest first ionization energies of silicon compounds observed so far—only roughly 1 eV higher than that of the sodium atom—are not due to β-R_3Si substituents, but rather to molecule-specific factors, such as the eight π electrons in the 1,4-diazine system,[1] which formally contains eight π electrons, or to the interaction between the carbanionic centers in the five-membered ring bis-ylide[1] (Scheme 20, in parentheses). This assignment simultaneously sheds light on the origin of the "β-trimethylsilyl donor effect": the positive charge in the radical cation generated (Section 2.5.4) can be delocalized into the $(H_3C)_3Si$ groups predominantly by so-called π/σ_{CSi} or n_E/σ_{CSi} hyperconjugation and thus be stabilized (cf. Section 2.5.2).

2.5.2. Silicon First-Order Perturbation of the Benzene π System

Looking at organosilicon compounds with a "molecular-state-sensitive" eye (Scheme 1 and Fig. 1b) reveals numerous examples whose properties can be rationalized by first- and second-order perturbation arguments[2, 20] and thus be applied to chemically related molecules in equivalent states. The classical example is the 6π-electron system of benzene (Fig. 3b), for which substitution and the accompanying symmetry lowering lifts the degeneracy of the $\pi(e_{1g})$ states and, which, owing to its π-nodal planes (i.e., those of zero electron density), possesses unperturbed "standard states" for certain substitution patterns. In the following, "internal" first-order perturbations are illustrated by the prediction of the π-ionization energies of silabenzene[2] and "external" ones by the parameterization of the σ-donor effects of β-trimethylsilyl groups.[1, 43]

Prediction of the π-Ionization Energies of Silabenzene: A correlation (Scheme 21) between the PE-spectroscopically

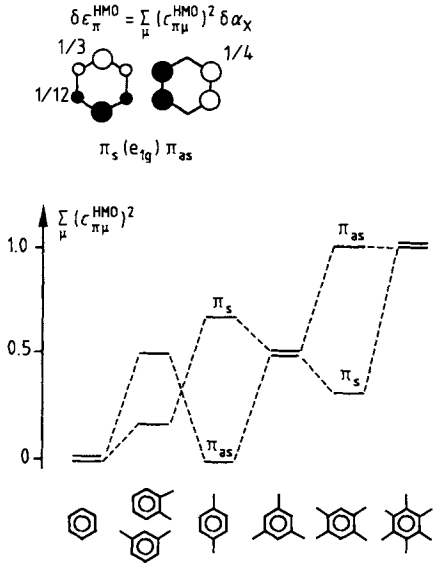


Scheme 21. Correlation of the π-ionization energies of heterobenzenes C_5H_5X and the correct prediction for silabenzene [2]. For the experiments see [22].

determined vertical π-ionization energies of benzene and its monohetero derivatives $(HC)_5ER$ and the ionization energies ($^4S_{3/2} \rightarrow {}^3P_0$) of the perturbing atoms E has been reported.[47] The gradients of the resulting regression lines reflect the squared coefficients, $c_{\pi\mu}^2$, of the perturbed center μ (cf. Fig. 3b).

The silicon-atom ionization energy of 8.15 eV was inserted into the regression (Scheme 21) in 1977[2] and yielded correct approximate predictions of the π-ionization energies of silabenzene. These were experimentally measured only two years later, after a shortpath pyrolysis apparatus[48] had been developed to generate silabenzene, a molecule only stable under "unimolecular" conditions[49] (Scheme 6). Especially its band at 8.11 eV helped considerably in optimizing the reaction conditions by PE-spectroscopic real-time gas analysis.[48]

Parameterization of the Donor Effect of β-Trimethylsilyl Groups: According to the simple benzene π-perturbation model (Fig. 3b), the sums of squared HMO coefficients, $\sum_{\mu}(c_{\pi,\mu}^{HMO})^2$, obtained from the given values for π_s (1/3 and 1/12) and π_{as} (1/4), yield characteristic perturbation eigenvalue patterns for the different derivatives (Scheme 22). Their correlation with the PES ionization energies requires an additional inductive correction, $\Delta\sigma_{CH_2SiR_3}$, since the ionization energies IE_2^v for the monosubstituted and 1,4-disubstituted derivatives (9.00 and 8.75 eV, respectively) differ from the expected constant value of $IE_2^v(\pi_{as}) = 9.24$ eV. Both parameters, $\delta\alpha_{CH_2SiR_3}$ and $\Delta\sigma_{CH_2SiR_3}$ can be determined by a linear regression calculation[1] (Scheme 22, Table 3).



Scheme 22. First-order π perturbations for $(H_3C)_3SiH_2C$-substituted benzene (cf. text). The substituents are only shown schematically by lines.

The linear relation (Table 3), which allows the prediction of π-ionization energies of $(H_3C)_3SiCH_2$-substituted benzenes to an accuracy of ±0.2 eV,[1, 43a] also demonstrates that, in addition to the "π/σ_{SiC} hyperconjugation", an inductive

Table 3. Values for Scheme 22. Benzene substituents: R = $CH_2Si(CH_3)_3$.

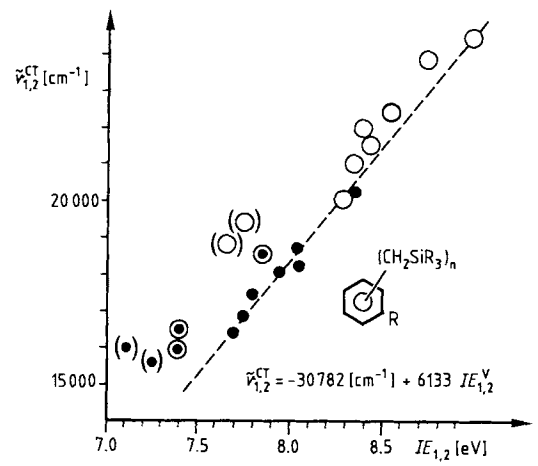
		Substitution pattern		
	C_6H_6	1	1,2	1,3
IE_1^v [eV]	9.24	8.35	8.05	8.05
IE_2^v [eV]	9.24	9.00	8.55	8.40
		Substitution pattern		
	1,4	1,3,5	1,2,4,5	complete
IE_1^v [eV]	7.75	7.85	7.10	7.40
IE_2^v [eV]	8.75	7.85	7.75	7.40

$IE_n^v = 9.24 - [\sum_\mu (c_{x\mu}^{HMO})^2 \delta\alpha_R + \sum_n \Delta\sigma_R] \Rightarrow \delta\alpha_R = 1.33$ eV; $\Delta\sigma_R = 0.24$ eV

component (Section 2.4: $Z_{eff}(Si) < Z_{eff}(C)$) also formally contributes to the extreme donor effect of β-trimethylsilyl groups (Section 2.5.1). Comparison with the analogously obtained parameters of the methyl groups, $\delta\alpha_{CH_3} = 0.86$ eV and $\sigma_{CH_3} = 0.09$ eV,[1, 43a] illustrates the considerable perturbation of the benzene π system caused by the $(H_3C)_3SiH_2C$ substituents, which, for instance, lower the first ionization energy of the 1,2,4,5-substituted derivative (7.1 eV, Table 3) below that of tetracyclic pyrene (7.4 eV) or of *p*-phenylenediamine (7.3 eV).

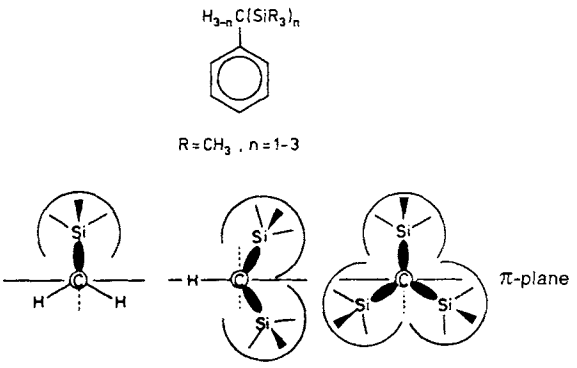
The steric overcrowding of poly(trimethylsilyl)-substituted benzenes can be demonstrated, for example, by correlation of the gas-phase ionization energies with the charge-transfer excitation energy of their tetracyanoethylene (TCNE) complexes in solution[43a] (Scheme 23).

The values in parentheses for the highly substituted derivatives deviate from the otherwise satisfactory linear relation because of the sterically enforced larger distances between the $(H_3C)_3SiH_2C$-surrounded donors and the acceptor molecule TCNE. The linear correlation (Scheme 23) allows, in addition, the determination of the first and second π-ionization energies of analogous benzene derivatives from the CT excitation energies of the respective donor–acceptor complexes formed in solution. These UV spectroscopic measurements are easy to perform, serving as a "test-tube photoelectron spectrometer".



Scheme 23. "Test-tube PE spectrometer": Correlation of the charge-transfer excitation energies of TCNE complexes with π ionization energies of $(H_3C)_3SiH_2C$-substituted benzenes (see text). ● = $IE_1^v/\tilde{\nu}_1^{CT}$; ○ = $IE_2^v/\tilde{\nu}_2^{CT}$.

The donor effects of poly(trimethylsilyl)methyl substituents $(R_3Si)_nH_{3-n}C$ (R = CH_3) can also be parameterized as first-order perturbations.[1, 43b] Starting with the simplifying assumption of constant squared coefficients for the six-membered ring, the differing numbers of β-$(H_3C)_3Si$ groups are accounted for by angle-dependent contributions ($<\cos^2\omega>$) of the d_{CSi} and d_{CH} π-bonding components (Scheme 24, Table 4).



Scheme 24. Hyperconjugation model of the first-order π perturbations caused by $CH_{3-n}(SiR_3)_n$ groups on benzene (cf. text).

For the substituents $(R_3Si)_2HC$ and $(R_3Si)_3C$ in the preferred conformations (Scheme 24; $2<\cos^2 30°> = 1.5$ and $1<\cos^2 0°> + 2<\cos^2 60°> = 1.5$, respectively), identical first ionization energies are predicted and the experimental results agree satisfactorily: as expected, the two different substituents give rise to identical perturbations (Table 4: $IE_1^v = 8.10$ eV).

Table 4. Substituents and values for $H_5C_6-CX^1X^2X^3$ (Scheme 24; R = CH_3).

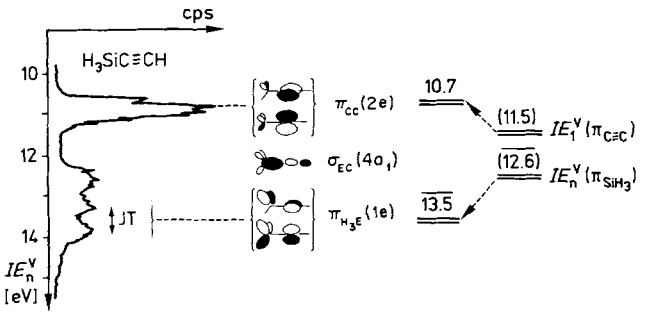
X^1	X^2	X^3	IE_1^v	IE_2^v
H	H	H	8.84	9.15
SiR_3	H	H	8.35	9.00
SiR_3	SiR_3	H	8.10	8.80
SiR_3	SiR_3	SiR_3	8.10	(< 8.9)

$IE_1 = 9.25 - \sum_{CX} d_{CX}^M \langle\cos^2\theta\rangle \Rightarrow d_{CSi} = 0.7$ eV, $d_{CH} = 0.3$ eV

2.5.3. Second-Order Silicon Perturbation of the Acetylene π System

In second-order perturbations (Fig. 3b), orbitals of the same symmetry are assumed to interact and, within the MO model, split into an antibonding and a bonding linear combination; their mixing increases with the square of the interaction parameter, β_π^2, and with decreasing energy difference $\Delta\alpha$. For radical-cation states of a molecule, in which the corresponding stabilization and destabilization become particularly apparent, this implies a different delocalization of the positive charge remaining after ionization.

The simplest example of such a second-order perturbation for organosilicon compounds and also for π_{CC}/σ_{SiH_3} hyperconjugation[1, 44] is represented by silylacetylene, which yields explosive mixtures with air. The molecule $H_3Si-C\equiv CH$ can be formally subdivided into a cylindrical electron cloud around the CC bond and the C_{3v}-symmetric "three-blade H_3Si propeller" (Scheme 25). The interaction



Scheme 25. Silylacetylene: the clearest example of hyperconjugative second-order perturbations (cf. text).

between the two ^2E radical-cation states of identical symmetry can be determined by calibration with the ionization energies IE_1^v of $HC\equiv CH$ and the mean value $IE_n^v(SiH_3)$ of H_3SiSiH_3 (Scheme 17).[1, 44]

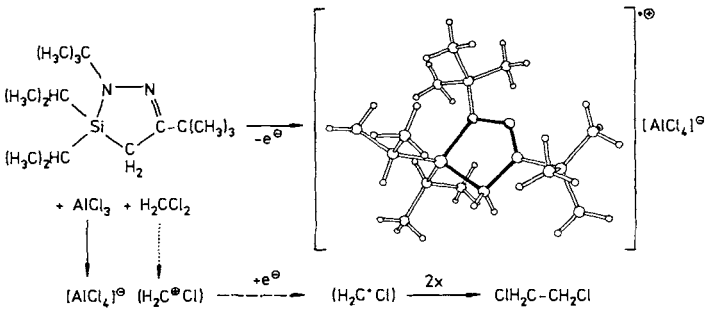
Inserting the respective ionization energies into the second-order interaction determinant (b) gives $\beta_{CC/SiH_3} = -1.2$ eV. Comparison with the analogous methylacetylene

$$\beta_\pi = \sqrt{(\alpha_{CC} - \varepsilon)(\alpha_{SiH_3} - \varepsilon)} = \sqrt{(IE_1^v(HC\equiv CH) - IE_1^v)(IE_n^v(SiH_3) - IE_1^v)} \quad (b)$$

interaction parameter $\beta_{CC/CH_3} = -2.1$ eV (cf. Scheme 17: $\alpha_{CH_3} = -14.2$ eV) shows that the π_{CC}/σ_{CH_3} hyperconjugation is even more effective—as expected from the shortening of the H_3C–C distance. By using the experimental parameters α_{CC}, α_{SiH_3}, and β_{CC/SiH_3}, the three π(e) ionization energies of doubly substituted disilylacetylene, $H_3SiC\equiv CSiH_3$, can also be correctly predicted.[44] Altogether, such hyperconjugative interaction models prove to be useful in the assignment and interpretation of numerous PES ionization patterns of silicon compounds: for example, the likewise C_{3v}-symmetric silicon halides H_3SiHal.[1]

2.5.4. One-Electron Oxidation of Organosilicon Compounds

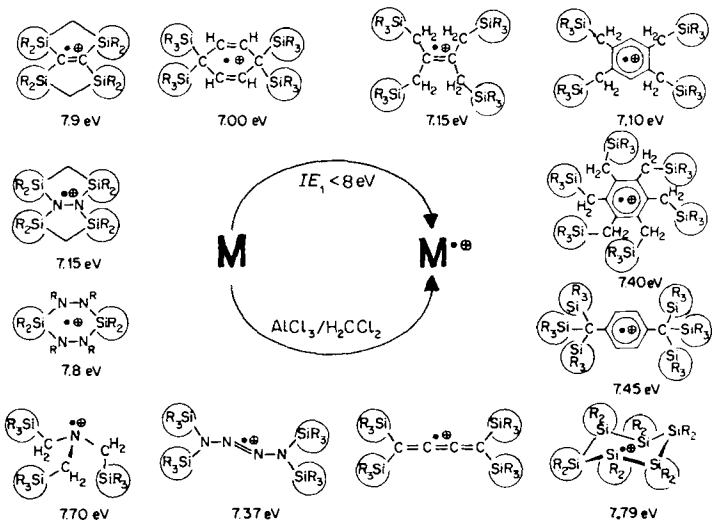
The small effective nuclear charge of silicon (Section 2.4) and, above all, the hyperconjugative charge delocalization by β-trimethylsilyl groups (Sections 2.5.1 and 2.5.2) lower the PE-spectroscopically determined first ionization energies of organosilicon compounds considerably relative to those of their carbon analogues[1] (cf. Table 2 and Schemes 20, 22, and 23). Thus, the experimentally proven stabilization of the positive charge in organosilicon radical cations generated by vertical photoionization within approximately 10^{-15} seconds, as well as the frequently observed parallel between ionization potentials in the gas phase and oxidation potentials in solvents of low polarity[1, 3, 50] leads to the expectation that a chemical and far slower ($< 10^{-10}$ s) adiabatic oxidation[1, 3] should also be possible and should allow the isolation of salts $[M^{\bullet\oplus}X^\ominus]$ with silicon-containing molecular cations $M^{\bullet\oplus}$. This is indeed the case (Scheme 26).[51]



Scheme 26. The assumed mechanism of selective one-electron oxidation by $AlCl_3/H_2CCCl_2$ (see text).

Discovered in 1976,[52] the selective one-electron oxidation of organosilicon compounds by $AlCl_3$ in water-free CH_2Cl_2 is most likely due to the chlorocarbenium ion, $H_2CCl^\oplus$, produced by $Cl^\ominus$ abstraction from the solvent H_2CCl_2, as substantiated by formation of the structurally characterized $AlCl_4^\ominus$ anion (Scheme 26). This carbenium ion, which presumably possesses an oxidation potential of +1.6 V as cyclovoltammetrically determined for the $AlCl_3/H_2CCl_2$ system,[50] could react to give the $H_2ClC^\bullet$ radical dimer, 1,2-dichloroethane,[51] which can be detected by gas chromatography (Scheme 26). The correlation of the (often irreversible) oxidation potentials of organosilicon molecules with their first ionization energies, $E^{ox}[V] = -4.58 + 0.78\ IE_1$ [eV],[50] allows an enormously useful prediction: all molecules[53] that exhibit a first ionization energy below 8 eV—as determined by either PE spectroscopy or UV spectroscopy of a suitable donor–acceptor complex (Scheme 23)—ought to be oxidized selectively to their radi-

cal cations by the oxygen-free $AlCl_3/H_2CCl_2$ system[1, 3, 53] (Scheme 27).

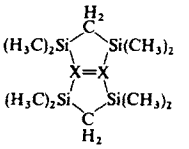


Scheme 27. Representative examples for organosilicon compounds with $IE_1 < 8$ eV and their $AlCl_3/CH_2Cl_2$ oxidation to radical cations. R = CH_3. Known IE_1^v values given.

ESR/ENDOR spectroscopy,[10] best suited to identify and characterize paramagnetic species in solution, yields a wealth of information about the ground states (Fig. 1a) of organosilicon radical cations generated so elegantly in $AlCl_3/CH_2Cl_2$ solution (Scheme 27): the recorded signal patterns allow the spin distributions to be "read off", thereby establishing the structural changes due to "adiabatic" relaxation. Temperature-dependent measurements allow, moreover, the observation of molecular dynamics on the ESR/ENDOR time scale of approximately 10^{-7} seconds, which is longer by orders of magnitude than the 10^{-15} seconds needed for vertical photoionization or the 10^{-13} seconds before the onset of molecular vibrations. From the extensive ESR/ENDOR data[3] for the numerous one-electron oxidation products of organosilicon compounds, the following have been selected as representative.

Spin Distribution: Radical cations of benzene derivatives that are considerably perturbed by 1,4-disubstitution (Scheme 22, $\sum_{\mu} c_{\pi\mu}^2 = 2/3$) show the coupling constants a_H^{ring} given in Scheme 28 for the four equivalent benzene protons.

The substituents $CH_{3-n}(SiR_3)_n$ clearly give rise to a more effective π-spin delocalization than "prototype" donors such as OR or NR_2. This result is—despite dissimilarity of spin and charge—in agreement with the PE-spectroscopically observed hyperconjugative stabilization of the positive charge (Schemes 20, 22, and 24) in the vertically generated radical cations. From the coupling constants $a_{^{29}Si}$ and $a_H^{Si(CH_3)_2}$ of the $M^{\bullet\oplus}$ and $M^{\bullet\ominus}$ radical ions of tetrasilabicyclo[3.3.0]octane, which are presumed to each exhibit a planar framework (Scheme 29),[3, 52, 54] one can "read off", in addition, how

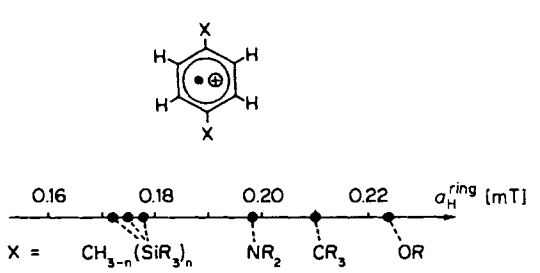


X=X	$C^{\bullet\oplus}=C$	$C^{\bullet\ominus}=C$	$N^{\bullet\oplus}=N$	
$a_{^{29}Si}$	2.271	0.685	0.500	[mT]
a_H	0.062	0.048	0.030	[mT]

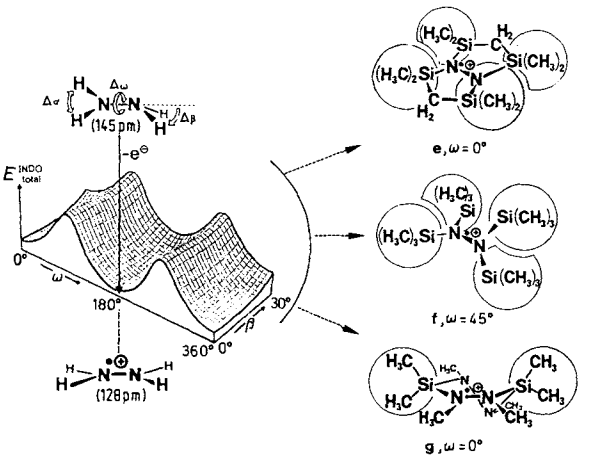
Scheme 29. Spin distribution in tetrasilabicyclo[3.3.0] radical cations (cf. text).

large the π-spin density in the $(H_3C)_2Si$ substituents of the $CC^{\bullet\oplus}$ radical cations actually is. In the two valence-isoelectronic $CC^{\bullet\ominus}$ and $NN^{\bullet\oplus}$ species, however, the unpaired electron is preferentially spread over the region of the central bond.

Structural Changes due to One-Electron Oxidation of Silylated Hydrazines: The changes in energy and electron distribution on vertical transition from the ground state of the neutral molecule to its radical-cation state ($\Gamma(M) \rightarrow \Gamma(M^{\bullet\oplus})$) (Fig. 1a) inevitably give rise, after the onset of molecular dynamics in the femtosecond region,[55] to "adiabatic changes in the "vertically frozen" molecular coordinates. When chemical oxidation in solution, $M + Ox^{\oplus} \rightarrow M^{\bullet\oplus} + Red$, is carried out instead of gas-phase photoionization, the structure of the oxidation product $M^{\bullet\oplus}$ can be determined from the ESR signal patterns[3, 53] and reproduced by quantum-chemical open-shell energy-hypersurface calculations.[1, 3, 5, 7a] For hydrazine and its $(H_3C)_nSi$ derivatives the following results are obtained (Scheme 30): The



Scheme 28. Spin distribution in substituted benzene radical cations (cf. text). R = CH_3.



Scheme 30. Energy hypersurface for the hydrazine radical cation and ESR-determined structures of organosilylhydrazine radical cations in solution (cf. text).

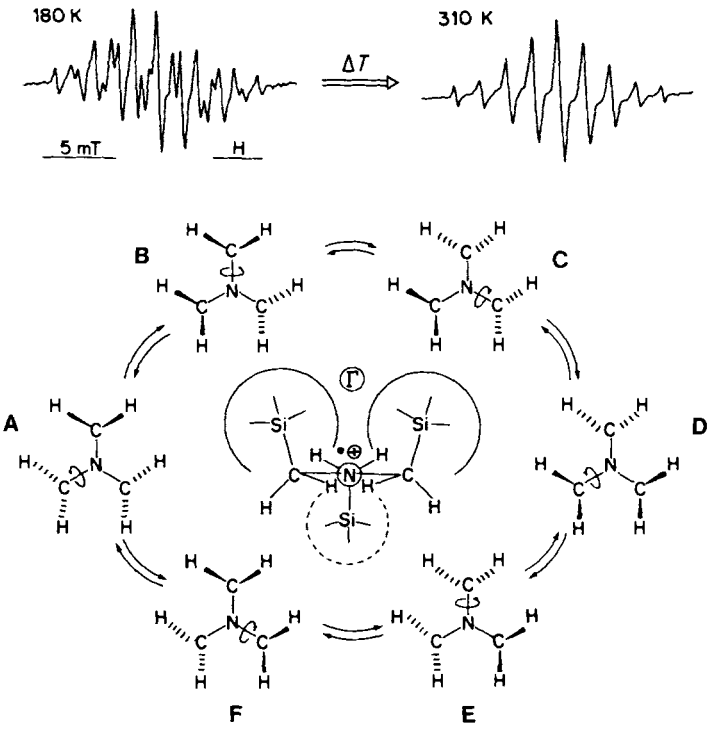
starting point is provided by INDO open-shell hypersurfaces for the six-atom parent radical cation $N_2H_4^{\bullet\oplus}$, the $3n - 6 = 12$ degrees of freedom of which are approximately covered by the three angular coordinates α(HNH), $\beta(NNH_2)$, and $\omega(H_2N-NH_2)$. According to the located energy minimum, the neutral C_2 molecule flattens on removal of an electron to a D_{2h} radical cation. For the three-electron two-center π bond formed, a shortening of the NN bond length from approximately 145 pm by $\Delta d_{NN} \approx$ 17 pm(!) to 128 pm has been calculated[56a] and, in the meantime, structurally confirmed.[56b]

From the simultaneously calculated angle-dependent ESR coupling constants,[56c] as well as by comparison with PES ionization energies, the following structural changes of the $(H_3C)_nSi$-substituted hydrazine derivatives result on one-electron oxidation[3] (Scheme 30): The bicyclic hydrazine is already almost planar in its neutral ground state—as confirmed by the enormous n_N/n_N splitting of $\Delta IE^v_{1,2} \approx$ 1.8 eV.[56c] In contrast, the dihedral angle of the open-chain derivative $M^{\bullet\oplus}$, which, according to the small difference in the ionization energies of only 0.2 eV, must possess two molecular halves almost perpendicular to each other, is diminished to the sterically enforced minimum value of $\omega \approx 45°$ in its radical cation, as proven by the a_N and a_H coupling constants.[56c] For the oxidized six-membered tetraazadisila ring **g**, the ESR signal pattern indicates a half-chair conformation with only one of $SiN^{\bullet\oplus}NSi$ molecular halves flattened. The intramolecular 'flipping" process is presumably slower than the ESR time scale of 10^{-7} seconds.[3] Altogether, the structural changes in the three chemically related silylhydrazine radical cations—despite compound-specific peculiarities—all occur in the same direction and, therefore, demonstrate the benefits of model energy-hypersurface calculations.[5, 7a]

Tris(trimethylsilyl)methylamine Radical Cation and Its "Cog Wheel" Dynamics: Many organosilicon radical cations with several β-trimethylsilyl groups (cf. Scheme 27) are sterically overcrowded and therefore rigid with respect to substituent rotations.[3] In contrast, the planar radical cation $[(H_3C)_3SiH_2C]_3N^{\bullet\oplus}$, which exhibits larger angles ($\sphericalangle$ CNC = 120°) between the individual ligands, shows a characteristic ESR line broadening on raising the temperature,[57] by which the 25 signals (1N + 3 × 2H) observed at 180 K are reduced to 9 (1N + 6H) at 310 K (Scheme 31).

This phenomenon is due to the rotation of each $(H_3C)_3SiH_2C$ substituent to the other side of the NC_3 molecular plane on the ESR time scale of 10^{-6} to 10^{-8} seconds. Because each side of the NC_3 plane offers room for only two of the bulky $(H_3C)_3Si$ groups, a "cog-wheel"-like coupled dynamic process (Scheme 31: **A** to **F**) results and the CH_2 protons become equivalent on the ESR time scale.[3, 57]

In summary, it has been established that all organosilicon compounds with first vertical ionization energies below 8 eV (Scheme 27) can be oxidized by $AlCl_3/H_2CCl_2$ (Scheme 26)[1, 13] to the corresponding radical cations.[1, 3] Their ESR/ENDOR signal patterns[3] show the influence of Si substitution on spin distributions (Schemes 28 and 29), characteristic changes in structure (Scheme 30), and molecular dynamics (Scheme 31) on the ESR time scale. The example of temperature-dependent ESR signal patterns reveals another molecular-state variable (Fig. 1), the storage of



Scheme 31. Temperature-dependent ESR spectra and the "cog wheel" molecular dynamics of the radical cation $N(CH_2SiR_3)_3^{\bullet\oplus}$, R = CH_3. In **A**–**F**, the R_3Si groups are omitted.

internal energy in the 3n − 6 degrees of freedom of n-atom three-dimensional molecules.

3. Silicon Chemistry: Molecular States as Retrospect or as Prospect?

Faced with the "torrent" of silicon compounds[7] and the "sea" of their molecular states,[7] this article can illustrate at best only some aspects of selected examples. Nevertheless, it should always be kept in mind that each chemical species, formally describable by connecting its centers exhibiting specific potentials, through electrons, will—depending on its energy—possess different structures and exhibit different dynamics and hence differing properties. Such a general statement, however, is of little help to the preparative chemist, who would like to classify the multiplicity of compounds by chemical intuition. The procedure[2] suggested here, to compare equivalent states of chemically related molecules based on their measurement data, that is, to stay as close to experiment as possible and to support experiment by quantum-chemical models and calculations, is—although useful and well tested[1–7]—not the only one possible; force-field approximations and statistical methods offer alternative approaches. This also applies to the especially emphasized techniques of PES[1, 9] and ESR/ENDOR[3, 10] spectroscopy, even though they advantageously cover different time domains, the molecular ions investigated by them show particularly strong perturbations, and the energy differences or measured spin populations can be correlated—for example, via Koopman's theorem or the McConnell relation—with results from approximate calculations, even for

larger molecules. With these and further reservations, one last question referring to the introductory quotations will be asked: To what extent can our knowledge be organized (Section 3.1) and sensible questions be formulated (Section 3.2)?

3.1. Retrospect: Structure, Energy, Charge Distribution

To begin with, attention is drawn once more to the fact that the preparative silicon chemist daily looks at molecular fingerprints, that is, molecular-state patterns, in order to characterize his compounds by spectroscopic analysis. For highly reactive species, such as phenyl silaisocyanide (Scheme 3), dichlorosilanediyl (Scheme 12), silabenzene (Schemes 6 and 21), and 1,4-bis(trimethylsilyl)benzene radical anion (Scheme 4), none of which can be "put in a bottle", spectroscopic methods are frequently the only possibility for obtaining proof that these molecules exist.[1, 3, 7e]

Additional information hidden in the spectroscopic molecular-state patterns of silicon compounds can often be profitably evaluated—despite the complexity of these patterns—if equivalent states of chemically related compounds are compared. Frequently, striking aspects (Fig. 1) can be emphasized in the interpretation—such as the connection of molecular building blocks (Fig. 3, Schemes 5, 8, 10, 22, and 25, as well as Tables 2 and 3), the small effective nuclear charge of Si (Section 2.4 and Schemes 5, 21, and 27), the concomitantly changed charge distribution (Section 2.5 and Schemes 4, 5, 16, 17 and 19), and structure–energy relationships (Section 2.2.2 and Schemes 3, 19, and 30). All these aspects overlap—as is demonstrated, for example, in the discussion of the extreme donor effect of β-$(H_3C)_3Si$ groups[58] (Section 2.5.1, Schemes 22–24 and 27, as well as Tables 3 and 4)—and have to be complemented by considering the specific dynamics of the respective molecular states (Scheme 31). Quantum-chemical models (Schemes 5, 13, 16, and 17), on which first- and second-order perturbations can be based (Sections 2.5.2 and 2.5.3 and Schemes 4, 12, 17, 28, and 29) and numerically exact calculations of molecular properties (Schemes 3, 8, 10, 12, and 30) may serve as starting points and are a most valuable help in the evaluation of experiments.[1–7] Quantum-chemical predictions quoted in the text and confirmed experimentally include the existence of $H_5C_6-N\equiv Si$ (Scheme 3), as well as of Ge_6-prismane and Si_8-cubane (Section 2.2.2). Hypersurface calculations have also been used to make predictions concerning the structural changes and the ESR signal patterns of organosilylhydrazine radical cations (Scheme 30). Molecular-state correlations[1–7] proved to be reliable in all examples selected in this article; for example, the Birch protonation of benzene radical anions (Scheme 4), the estimation of the silabenzene π-ionization pattern (Scheme 21), the linear regression $IE^{v}_{1,2}/\tilde{\nu}^{CT}_{1,2}$ (Scheme 23), and the one-electron oxidizability of molecules with first ionization energies below 8 eV by the $AlCl_3/CH_2Cl_2$ redox system (Scheme 27).

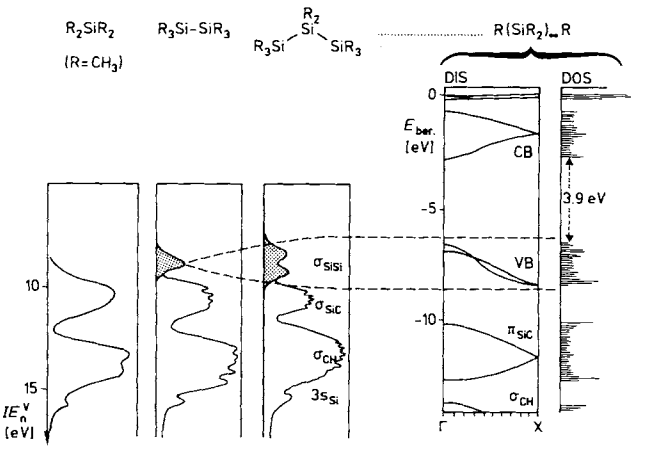
Altogether, these and further details of the molecular states of silicon-containing compounds[1–7] contribute to our essential knowledge of silicon chemistry. In particular, the molecular-state comparisons, for example with valence-isoelectronic carbon compounds,[1–7, 58] can be complemented by a variety of data obtained from other measurements and can be expanded to include numerous other compounds. This also helps in the determination of the differing substituent effects on individual molecular states (Fig. 1), which are useful for both the planning and the evaluation of experiments.[1–7, 58] The answer to the question concerning the benefits of molecular-state considerations for the preparative silicon chemist (Section 1) is, therefore, unequivocally a positive one. This statement can be further supported and extended by looking with the molecular-state magnifying glass (Scheme 1) at current and partially unsolved problems in silicon chemistry.

3.2. Prospect: Band Structures, Rydberg States, Contact Ion Pairs, Microscopic Reaction Pathways

The further development of silicon chemistry, which is in full swing, includes projects in which molecular-state measurements and their interpretation play an important role. Several of these projects will be outlined below.

Band Structures of Polysilanes: An understanding of band structures is of importance for developing novel photoconducting materials[7d, 59] with low ionization thresholds and narrow valence bands. As has already been discussed starting from a comparison of the radical-cation states of SiH_4/CH_4 (Scheme 16) and, especially, of H_3SiSiH_3/H_3CCH_3 (Scheme 17), the low effective nuclear charge of the silicon centers leads to low σ_{SiSi} ionization energies. This is particularly noteworthy in the case of permethylated polysilanes (Section 2.2.1), whose low-energy PE-spectroscopic band patterns were first interpreted 18 years ago[15] on the basis of a SiSi bond model (Scheme 5: $\alpha_{SiSi} \approx 8.7$ eV, $\beta_{SiSi/SiSi} \approx 0.5$ eV). Recently, the band structure[60] of the polymers $R(SiR_2)_\infty R$ of infinite chain length was calculated quantum-chemically (Scheme 32).[61]

The ab initio calculations using Bloch functions[60] were calibrated[61] with the PE ionization energies of silanes.[1, 15] The wave vector $\boldsymbol{k}$ runs from $\Gamma(\boldsymbol{k} = 0)$ to $X(\boldsymbol{k} = \pi/a)$, where a is the lattice constant. The state "dispersion" (Scheme 32:

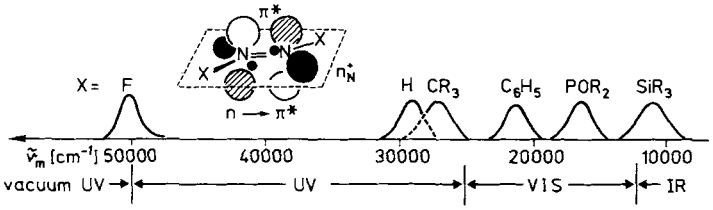


Scheme 32. Ionization patterns of permethylated silanes (cf. Scheme 5) and calculated band-structure dispersion (DIS) and state density (DOS) for polydimethylsilane $R(SiR_2)_\infty R$ [61].

DIS) shows a "$3p_{Si}$" valence band (VB) about 2 eV wide and an ionization threshold of 5.9 eV (cf. polyacetylene $H(HC=CH)_{\infty}H$:[59] threshold 2.2 eV, width 5–6 eV). Calculations revealed an unfilled $4s_{Si}$ conduction band (CB) some 3.9 eV above this valence band and, among others, π_{SiC}, σ_{CH}, and $3s_{Si}$ bands below it.[59, 61] The analogously scale-adjusted state-density diagram[61] (Scheme 32: DOS) agrees satisfactorily with the X-PES-determined values (cf. Schemes 15 and 16), which, conversely, confirm the calculated low ionization threshold and the narrow valence band width.[59] It should also be emphasized that the $M^{\bullet\oplus}$-state discussion of methylsilanes $R(SiR_2)_{1-5}R$[15] still serves today, 18 years later, as an interpretation tool and that the PES measurements[1, 15] are therefore of renewed use.

Rydberg States of the Blue Silicon Azo Compound $R_3Si-N=N-SiR_3$: One of the visible wonders of organosilicon chemistry is the unexpected blue color of bis(trimethylsilyl)diimine (-diazene).[62] Its $n_N^+ \rightarrow \pi^*$ excitation energy (cf. Scheme 33) is lowered relative to that of difluorodiimine by almost 40 000 $cm^{-1} \triangleq 5$ eV and even relative to that of the colorless valence-isoelectronic di-*tert*-butyl derivative by 14 500 $cm^{-1} \triangleq 1.8$ eV.[62]

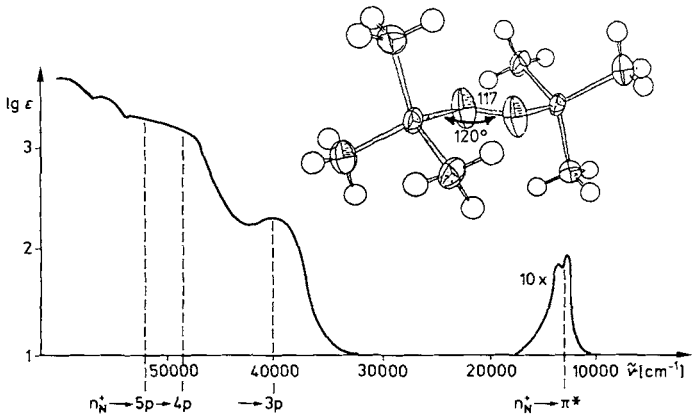
The crystal structure of $R_3Si-N=N-SiR_3$[1, 2, 62] (Scheme 34) offers some clues to the origin of this enormous bathochromic shift of the $n_N^+ \rightarrow \pi^*$ transition[62] in the blue four-center chromophore $Si-N=N-Si$, which exceeds the one caused by two phenyl substituents in the 14-center π system of orange azobenzene (Scheme 33). It shows normal



Scheme 33. The $n \rightarrow \pi^*$ excitation energies of representative azo compounds.

angles ($\sphericalangle$ SiNN = 120°) but a dramatically shortened N=N bond distance of only 117 pm, that is, halfway between that in carbon azo compounds ($d_{N\equiv N} \approx 125$ pm) and that in elemental nitrogen ($d_{N\equiv N} = 111$ pm). This is one more example (cf. Scheme 19) of a structural distortion due to the differing effective nuclear charges of Si and N (Section 2.4.2) and reconfirms the high electron density ($IE_1 = 7.1$ eV[1, 62]) around the Si-substituted N centers.

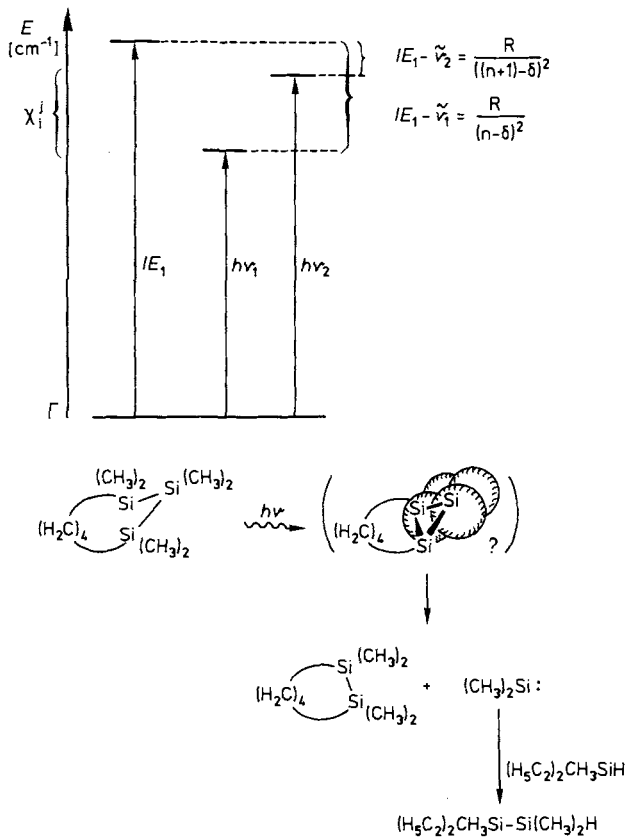
The assignment of the partially overlapping absorption bands in the UV and vacuum UV region of $R_3Si-N=N-SiR_3$ (Scheme 34) is of fundamental importance. According to an MO/CI estimate[1, 62] of the expected $n_N^- \rightarrow \pi^*$ and $\pi \rightarrow \pi^*$ transitions for carbon azo compounds $R'-N=N-R'$,[63] the latter presumably requires an excitation energy of more than 70 000 cm^{-1}. Therefore, by starting from the lowest first ionization energy, $IE_1^v = 7.1$ eV, of the trimethylsilyl derivative $R_3Si-N=N-SiR_3$[1, 62] and taking reported[63] term values $R/(n-\delta)^2$ (Scheme 34), excitation energies into N-centered Rydberg states could be estimated (R = Rydberg constant). The excellent agreement



Scheme 34. Structure of $R_3Si-N=N-SiR_3$ and Rydberg assignment of its UV bands. R = CH_3.

between the experimentally recorded (Schemes 34 and 35: $\tilde{\nu}_2 = 40\,000\ cm^{-1}$, $\tilde{\nu}_3 = 49\,000\ cm^{-1}$, $\tilde{\nu}_4 = 52\,000\ cm^{-1}$) and the expected Rydberg ($n_N^+ \rightarrow np$) excitation energies of 40 000 cm^{-1}, 48 500 cm^{-1}, and 51 900 cm^{-1}, respectively, supports such an assignment (Scheme 34: $n_N^+ \rightarrow$ 3p, 4p, 5p; series limit $IE_1 = 7.1$ eV = 57 300 cm^{-1}[1, 62]).

For other organosilicon derivatives, analogous estimates predict silicon-centered Rydberg states. For example, subtraction of the first UV excitation energy of 1,2,3-trisilacycloheptane ($\tilde{\nu}_m = 46\,000\ cm^{-1}$) from the first ionization energy of octamethyltrisilane ($IE_1^v = 8.19$ eV $\triangleq$ 66 000



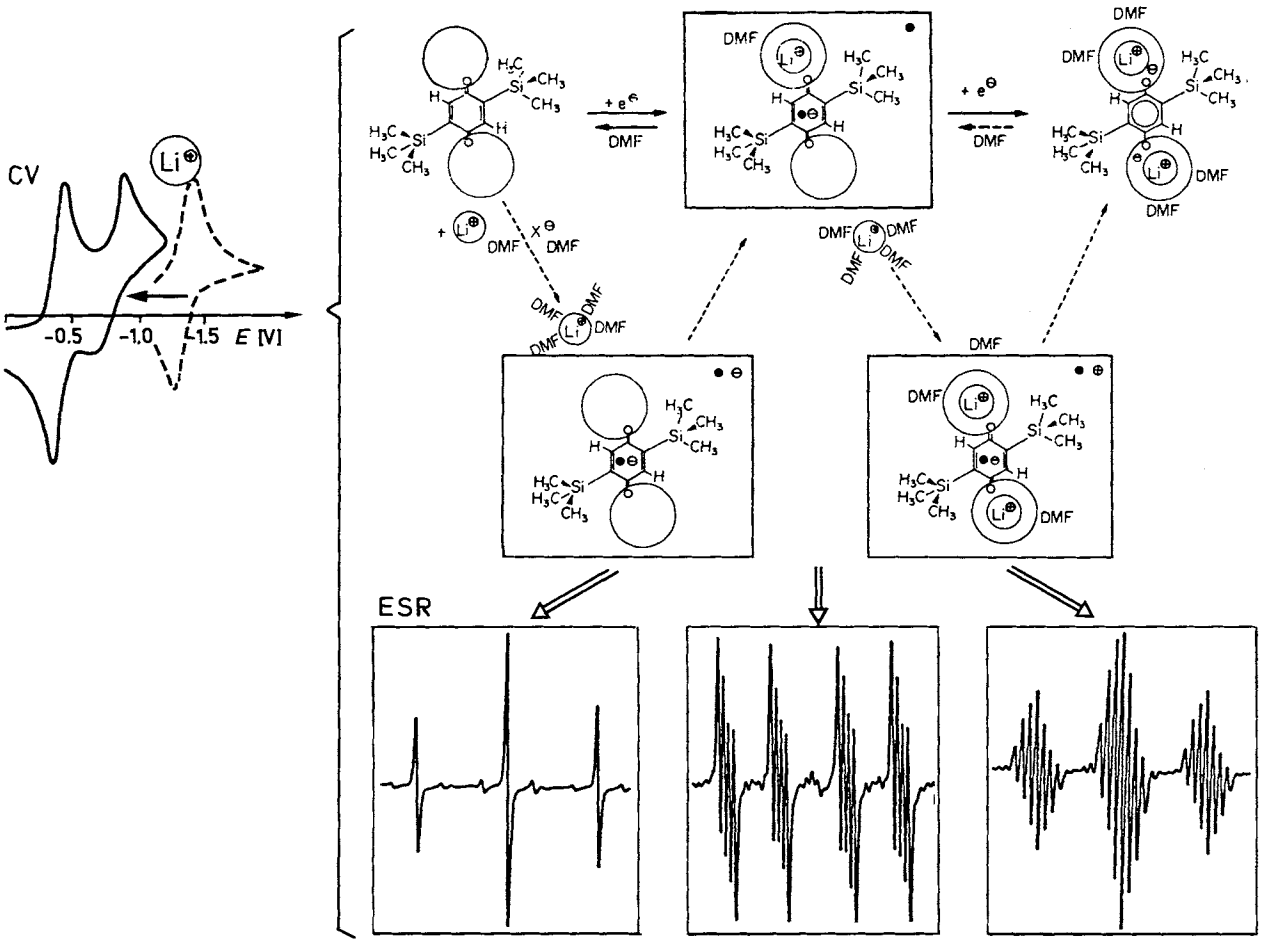
Scheme 35. Photochemical $(CH_3)_2Si$ elimination from trisilacycloheptane and suggestion of a "Rydberg excitation" transition state. R = Rydberg constant = 109 700 cm^{-1}; n = principal quantum number; δ = quantum defect. Term values $R/(n-\delta)^2$: d $\approx$ 12 000 cm^{-1}, p = 18 000 cm^{-1}, s $\approx$ 28 000 cm^{-1}.

cm^{-1} [1,15]; Scheme 5); gives a Rydberg term $R/(n-\delta)^2 \approx 20000\ cm^{-1}$. This term could correspond to a $\sigma_{SiSiSi} \rightarrow 4p_{Si}$ excitation and, in agreement with the measured UV intensity ($\varepsilon = 8000\ L\ mol^{-1}\ cm^{-1}$ [64]), would be allowed under local C_{2v} symmetry. Due to the enormous spatial extension of Rydberg states, which usually enclose large parts of a particular molecule,[63] such an assignment would explain the photochemical formation of a three-membered ring transition state and its relaxation by loss of dimethylsilanediyl, which can be captured by another disilane derivative[64] (Scheme 35).

Therefore, the loss of R_2Si from trisilanes upon irradiation with light of wavenumber $\tilde{\nu} = 39400\ cm^{-1}$, which is a key reaction for the preparation of the "dimer" $R_2Si{=}SiR_2$ (Fig. 2),[7b-d] presumably proceeds via a $4p_{Si}$ Rydberg excitation. The energetically relatively low-lying Rydberg states of organosilicon compounds could also be involved in many other photochemical reactions[7b] and, for example, contribute to the understanding of the still unsettled spin distribution in cyclosilane radical anions.[7d]

Contact Ion Pairs of Silylated p-Benzoquinones as Redox Intermediates: The microscopic pathway of the chemical reactions of medium-sized molecules, with their multifarious $3n-6$ degrees of freedom, is considered to be an almost unsolvable problem.[66] The preparative chemist can contribute partial information by specific synthesis, spectroscopic proof, and/or isolation of reactive intermediates.[69] In aprotic and largely nonpolar solvents, this often can be accomplished by additional "Coulombic interactions" between differently charged ions. Thus, by adding suitable salts $[Me^{\oplus}X^{\ominus}]$ to solutions of radical anions $M^{\bullet\ominus}$ (cf. Scheme 2), the formation of contact-ion-pair radicals $[M^{\bullet\ominus}Me^{\oplus}]^{\bullet}$ and triple-ion radical cations $[Me^{\oplus}M^{\bullet\ominus}Me^{\oplus}]^{\bullet\oplus}$ can be detected by ESR/ENDOR spectroscopy.[67] In some cases, these radical-anion salts can also be crystallized at low temperature and structurally characterized.[68]

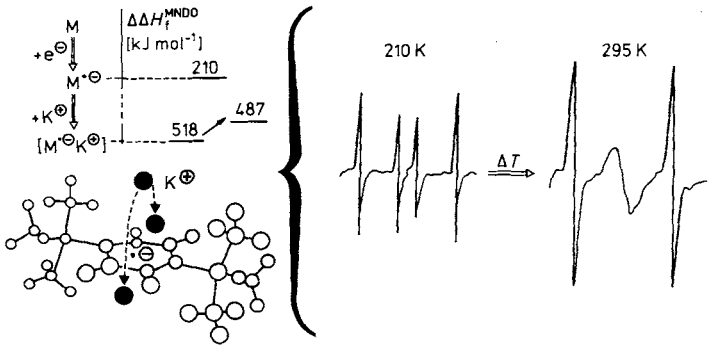
An especially illustrative example of an organosilicon compound is 2,5-bis(trimethylsilyl)-*p*-benzoquinone.[4,6,66] Its second, reversible half-wave potential (Scheme 36: CV- - -), on addition of the DMF-soluble $Li^{\oplus}[B(C_6H_5)_4)]^{\ominus}$ is lowered by 0.6 V and simultaneously becomes irreversible (Scheme 36: CV—). The presumed reduction pathway in the presence of excess lithium cation, which, owing to its small ionic radius ($r_{Li^{\oplus}} = 60$ pm), possesses a high effective ionic charge $1/r_{Li^{\oplus}}$, is supported by independent ESR/ENDOR measurements in THF.[4] A 1:2:1 triplet is observed for the solvated radical anion $M^{\bullet\ominus}$, owing to the two equivalent quinone hydrogens. The initially formed contact-ion-pair radical $[M^{\bullet\ominus}Li^{\oplus}]^{\bullet}$ shows a lowering of symmetry from C_{2v} to C_s owing to the "docking" of the $Li^{\oplus}$ ion and thus displays a doublet of doublets, the signals of which are each split into quartets by the ^7Li nuclear spin ($I = 3/2$). In the finally



Scheme 36. Electron transfer (CV) and ion-pair formation (ESR) on reduction of 2,5-bis(trimethylsilyl)-*p*-benzoquinone in aprotic solution, partly with added $Li^{\oplus}[B(C_6H_5)_4]^{\ominus}$ (cf. text).

resulting triplet radical cation $[Li^{\oplus}M^{\bullet\ominus}Li^{\oplus}]^{\bullet\oplus}$, the quinone hydrogens are again equivalent and the two docked $Li^{\oplus}$ ions cause an additional septet splitting. In this solvated contact triple ion, the final product, that is, the dilithium salt of 2,5-bis(trimethylsilyl)hydroquinone, is already preformed and, therefore, the second electron transfer takes place irreversibly at a dramatically lower reduction potential (Scheme 36; CV- - -).

The investigations concerning other contact ion pairs of 2,5-bis(trimethylsilyl)-*p*-benzosemiquinone with larger and, therefore, more loosely coordinated countercations,[4] such as $K^{\oplus}$ ($r_{K^{\oplus}} = 138$ pm), have been accompanied by approximate energy-hypersurface calculations[4] (cf. Scheme 37). They predict the geometry-optimized radical anion $M^{\bullet\ominus}$ to be more favorable relative to the neutral molecule M by $\Delta\Delta H_f^{MNDO} \approx 210$ kJ mol^{-1}, and the additional Coulomb stabilization in the contact ion pair, despite neglected solvation, should amount to 210 kJ mol^{-1}. Surprisingly, the energy-hypersurface calculations suggest that the $K^{\oplus}$ countercation should "fluctuate": to reach the saddlepoint 380 pm above the geometry-optimized quinone six-membered ring, an activation barrier of only approximately 30 kJ mol^{-1} would have to be surmounted[4] (Scheme 37).



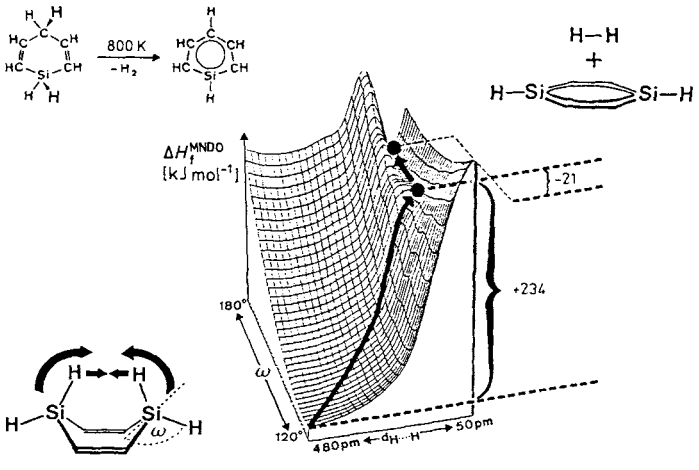
Scheme 37. Dynamics of the contact-ion-pair radical $[K^{\oplus}O_2C_6H_2(SiR_3)_2^{\bullet\ominus}]^{\bullet}$: Energy hypersurface calculations ($\Delta\Delta H_f^{MNDO}$) and temperature-dependent ESR spectra (cf. text).

The predicted dynamics of the $K^{\oplus}$ contact ion pair can be confirmed by ESR spectroscopy (Scheme 37): At 210 K, the expected doublet of doublets is measured for the nonequivalent quinone hydrogens, whereas at 295 K a ^{1}H triplet indicates that, owing to $K^{\oplus}$ fluctuation, the quinone protons become equivalent on the ESR time scale of 10^{-7} seconds.

Altogether the CV and ESR/ENDOR data,[4] in combination with the quantum-chemical hypersurface calculations, thus provide, as exemplified by 2,5-bis(trimethylsilyl)-*p*-benzoquinone, some insight into the pathway of a consecutive two-electron reduction, although solvent effects are still neglected. The partially dynamic contact ion pairs discovered in the investigation could be of interest both bioinorganically because of their carrier properties and industrially as molecular switches.

Does Thermal H_2 Elimination from Silacyclohexadiene to Give Silabenzene Proceed Intramolecularly? Dynamic phenomena have already been covered in some detail as important molecular-state properties (Fig. 1) by selecting as examples the radical cation $(R_3SiCH_2)_3N^{\bullet\oplus}$ (Scheme 31) and the contact-ion-pair radical $[(R_3Si)_2C_6H_2O_2^{\bullet\ominus}K^{\oplus}]^{\bullet}$ (Scheme 37). Along the microscopic pathways of chemical reactions, they often play a decisive role[55] and thus their importance should not be underestimated. As concerns medium-sized molecules, however, their $3n-6$ degrees of freedom are rather restrictive and mostly lead to a nearly hopeless situation of multidimensional complexity.[5, 6, 66] Even the five-atom molecule methanimine, $H_2C=NH$, which is generated upon pyrolysis of methyl azide as a "chemically activated" species[12, 69] (i.e., with considerable energy stored in its $3\times5-6=9$ degrees of freedom) and, in the subsequent reaction channel, loses H_2 to give HCN, would have to be calculated quantum-chemically in a nine-dimensional hyperspace! For specific molecular conformations, some of the numerous degrees of freedom can often be more or less neglected by introducing additional assumptions.[5] Such an approach, although it crudely simplifies the rather complex reality, will be illustrated for the pyrolysis of 1-silacyclohexa-2,5-diene to silabenzene and H_2[22e] (Scheme 6) in a yellow-glowing flow tube at 800 K and under 10^{-4} Pa pressure—that is, under nearly unimolecular conditions.

In order to carry out an approximate energy-hypersurface calculation, the 36 degrees of freedom of the 14-atom molecule silacyclohexadiene must be drastically reduced.[5] One possibility is to introduce a mirror plane into the sila derivative by incorporating an additional silicon atom at the 4 position and to select as the dominant vibrational modes of its boat conformation the intramolecular bending characterized by both the angle ω between the CSiC triangle and the $(C=C)_2$ plane and the $d_{H\cdots H}$ distance representing additional "joints" at the two Si centers[70] (Scheme 38). Their variation ($\Delta\omega = 120° \rightarrow 180°$ and $\Delta d_{H\cdots H} = 480 \rightarrow 50$ pm) in about 10^3 separate and, in each case, geometry-optimized MNDO calculations,[71] produces a folded total-energy hypersurface, on which the "product valley" for 1,4-disilabenzene + H_2 is reached by crossing the saddlepoint indicated in Scheme 38.



Scheme 38. Model energy hypersurface for the intramolecular H_2 elimination from disilacyclohexadiene to give disilabenzene (cf. text).

Additional calculations of selected points for the actually investigated 1-silacyclohexa-2,5-diene,[70] which exhibits only C_s symmetry, yield as values closer to experiment an acti-

vation enthalpy of 175 kJ mol^{-1}, a saddlepoint structure with $\omega = 140°$ and $d_{H\cdots H} = 120$ pm and, for the considerably deeper product valley of the ensemble "C_5SiH_8" with the energetically more favorable products silabenzene and hydrogen, an enthalpy difference of -120 kJ mol^{-1}. Both the correspondence between the calculated activation barrier[70] and the PE-spectroscopically determined pyrolysis temperatures,[22c] as well as a comparison with the respective data for cyclohexa-1,4-diene and 1,4-dihydropyridine,[70] support the basic assumption for the hypersurface calculations that the thermal H_2 elimination from silacyclohexadiene to give silabenzene should proceed intramolecularly.[72]

The examples discussed above represent rather different topics, including polysilane band structure, possible Rydberg states in photochemical reactions of organosilicon compounds, evidence for and dynamics of Si-containing contact ion pairs, and an approximately calculated energy hypersurface of the supposedly intramolecular H_2 elimination from silacyclohexadiene. All of them illustrate that molecular-state considerations (Figs. 1 and 3) are also useful in the diverse world of silicon compounds (Fig. 2). At the same time, they demonstrate the increasing impact of both the constantly improved and the newly developed techniques of physical measurement and, above all, the effect of the avalanche of applications made possible by ever faster and numerically more precise quantum-chemical calculations, even for larger molecules. Both hardware and software are widely distributed nowadays and thus readily accessible. Of increasing importance, therefore, is an "intellectual tunneling" between the only seemingly different viewpoints of preparative and theoretical chemistry, which both meet in the reality of molecular states. It is to be hoped that the examples discussed here, selected[1-6] from the wide area of silicon chemistry,[7] may also contribute to bridging the fictitious gap between experiment and theory. It would be most rewarding could they convince the preparative silicon chemist of how profitable it is to take a look for himself at his fast developing and interesting area of research through the molecular-state magnifying glass (Scheme 1).

Thanks are due, above all, to my "theoretical" teachers and friends Edgar Heilbronner and Michael J. S. Dewar, who convinced a preparative inorganic chemist some 20 years ago of the usefulness of simple molecular orbital models and semiempirical calculations. The cited results of our research group have been obtained by committed and competent co-workers—those cited in the references are Bahman Solouki, Hartmut Alt†, Georg Brähler, Ralph Dammel, Walter Enßlin, Peter Hänel, Hans-Friedrich Herrmann, Bernhard Hierholzer, Wolfgang Kaim, Mitsuo Kira, Ulrike Lechner-Knoblauch, Jochen Meuret, Philip Mollère, Klaus Oswald, Pavel Rosmus, Hans Seidl, Andrej Semkow, and Klaus Wittel. Cooperation and discussions have stimulated close links to numerous colleagues, including T. J. Barton (Ames, Iowa), G. Becker (Stuttgart), D. Fenske (Karlsruhe), G. Fritz (Karlsruhe), R. Janoschek (Graz), H. Kurrek (Berlin), G. Maier (Gießen), J. Michl (Austin, Texas), H. Nöth (Munich), H. Sakurai (Sendai), P. von R. Schleyer (Erlangen), H. G. von Schnering (Stuttgart), M. Veith (Saarbrücken), R. West (Madison, Wisconsin), and, last but not least, N. Wiberg (Munich). For the most generous funding of our research, we would like to thank the Deutsche Forschungsgemeinschaft, the Fonds der Chemischen Industrie, the State of Hessen, the Max Buchner, Adolf Messer, and Hermann Schlosser foundations, Hoechst AG, Degussa AG, and Dow Corning Corporation.

Received: June 6, 1989 [A 740 IE]
German version: *Angew. Chem. 101* (1989) 1659

[1] H. Bock, B. Solouki, "Photoelectron Spectra of Silicon Compounds" in S. Patai, Z. Rappoport (Eds.): *The Chemistry of Organic Silicon Compounds*, Wiley, Chichester 1989, pp. 555–653 (252 references cited therein).

[2] H. Bock, "Molekülzustände und Molekülorbitale", *Angew. Chem. 89* (1977) 631–655; *Angew. Chem. Int. Ed. Engl. 16* (1977) 613–637, and references cited therein.

[3] H. Bock, W. Kaim, "Organosilicon Radical Cations", *Acc. Chem. Res. 15* (1982) 9.

[4] H. Bock, B. Solouki, P. Rosmus, R. Dammel, P. Hänel, B. Hierholzer, U. Lechner-Knoblauch, H. P. Wolf, "Recent Investigations on Short-lived Organosilicon Molecules and Molecular Ions" in H. Sakurai (Ed): *Organosilicon and Bioorganosilicon Chemistry*, Ellis Horwood, Chichester 1985, pp. 45–73, and references cited therein.

[5] H. Bock, R. Dammel, B. Roth, "Molecular State Fingerprints and Semiempirical Hypersurface Calculations: Useful Correlations to Track Short-Lived Molecules" in A. H. Cowley, (Ed.): *Rings, Clusters and Polymers of the Main Group Elements, ACS Symp. Ser. 232* (1983) 139–165, and references cited therein.

[6] H. Bock, "Reaction of Carbon and Organosilicon Compounds as Viewed by a Preparative Chemist", *Rev. L'Actualité, Chim. 1986/3*, 33; cf. also *Abh. Math.-Naturwiss. Kl. Akad. Wiss. Lit. Mainz*, 1986/2, 1–35; cf. also *Polyhedron 7* (1988) 2429.

[7] A comprehensive review of silicon chemistry can be found in a recently published book: S. Patai, Z. Rappoport (Eds.): *The Chemistry of Organic Silicon Compounds*, Wiley, Chichester 1989. In addition to [1] the following contributions are emphasized within this context: a) Y. Apeloig, "Theoretical Aspects of Organosilicon Compounds", pp. 57–226 (377 references therein); b) A. G. Brook, "The Photochemistry of Organosilicon Compounds", pp. 965–1006 (161 references therein); c) G. Raabe, J. Michl, "Multiple Bonds to Silicon", pp. 1015–1142 (406 references therein); d) R. West, "Polysilanes", pp. 1208–1240 (132 references therein); e) R. J. P. Corriu, J. C. Young, "Hypervalent Silicon Compounds", pp. 1241–1288 (182 references therein).

[8] Source: H.-J. Quadbeck-Seeger: *Zwischen den Zeichen*, VCH, Weinheim 1988.

[9] Cf., for example, C. R. Brundle, A. D. Baker (Eds.): *Electron Spectroscopy: Theory, Techniques and Applications, Vol. 1–5*, Academic Press, London 1977–1984, and references cited therein.

[10] Cf., for example, H. Kurreck, B. Kirste, W. Lubitz: *Electron Nuclear Double Resonance Spectroscopy of Radicals in Solution*, VCH, Weinheim 1988, and references cited therein.

[11] J. F. Ogilvie, S. Cradock, *J. Chem. Soc. Chem. Commun. 1966*, 364; cf. additional calculations: J. N. Murrell, H. W. Kroto, M. F. Guest, *ibid. 1977*, 619; R. Preuss, R. J. Buenker, S. D. Peyerimhoff, *J. Mol. Struct. 49* (1978) 171.

[12] a) H. Bock, R. Dammel, *Angew. Chem. 97* (1985) 128; *Angew. Chem. Int. Ed. Engl. 24* (1985) 111; b) *ibid. 99* (1987) 518 and *26* (1987) 504, and references cited therein.

[13] a) F. Gerson, J. Heinzer, H. Bock, H. Alt, H. Seidl, *Helv. Chim. Acta 51* (1968) 707, and references cited therein; b) H. Alt, E. R. Franke, H. Bock, *Angew. Chem. 81* (1969) 538; *Angew. Chem. 8* (1969) 525, and references cited therein.

[14] Cf. for example, T. Balaban (Ed.): *Chemical Applications of Graph Theory*, Academic Press, London 1976; R. J. Wilson: *Introduction to Graph Theory*, Oliver & Boyd, Edinburgh 1972.

[15] H. Bock, W. Enßlin, *Angew. Chem. 83* (1971) 435; *Angew. Chem. Int. Ed. Engl. 10* (1971) 404; H. Bock, W. Enßlin, F. Feher, R. Freund, *J. Am. Chem. Soc. 98* (1976) 668; not cited in [7d].

[16] A. Sax, R. Janoschek, *Angew. Chem. 98* (1986) 634; *Angew. Chem. Int. Ed. Engl. 25* (1986) 651 and references cited therein; cf. *Phosphorus Sulfur 28* (1986) 151; S. Nagase, T. Kudo, M. Aoki, *J. Chem. Soc. Chem. Commun. 1985*, 1121 and references cited therein; cf. summary in [7a]; cf. R. Janoschek, *Chem. Unserer Zeit 21* (1988) 128.

[17] S. Nagase, *Angew. Chem. 101* (1989) 340; *Angew. Chem. Int. Ed. Engl. 28* (1989) 340 and references cited therein; particularly S. Nagase, M. Nakano, T. Kudo, *J. Chem. Soc. Chem. Commun. 1987*, 60; cf. also A. F. Sax, J. Kalcher, *ibid. 1987*, 809.

[18] A. Sekiguchi, C. Kabuto, H. Sakurai, *Angew. Chem. 101* (1989) 97; *Angew. Chem. Int. Ed. Engl. 28* (1989) 55.

[19] a) H. Matsumoto, K. Higuchi, Y. Hoshino, H. Koike, Y. Naoi, Y. Nagai, *J. Chem. Soc. Chem. Commun. 1988*, 1083; b) Y. Kabe, M. Kuroda, Y. Honda, O. Yamashita, T. Kawase, S. Masamune, *Angew. Chem. 100* (1988) 1793; *Angew. Chem. Int. Ed. Engl. 27* (1988) 1725; c) M. Baudler, G. Scholz, K.-F. Tebbe, M. Fehér, *ibid. 101* (1989) 352 and *28* (1989) 339 in analogy to the known heterocubane $(H_5C_6SnP)_4$: H. Schumann, H. Benda, *ibid. 80* (1968) 846 and *7* (1968) 813.

[20] Cf. E. Heilbronner, H. Bock: *Das HMO-Modell und seine Anwendung, Bd. 1*, 2nd ed., Verlag Chemie, Weinheim 1978.

[21] Cf. H. Bock, B. G. Ramsey, *Angew. Chem. 85* (1973) 773; *Angew. Chem. Int. Ed. Engl. 12* (1973) 734, and references cited therein.

[22] a) H. Bock, R. A. Bowling, B. Solouki, T.-J. Barton, G.-T. Burns, *J. Am. Chem. Soc. 102* (1980) 429; b) B. Solouki, P. Rosmus, H. Bock, G. Maier, *Angew. Chem. 92* (1980) 56; *Angew. Chem. Int. Ed. Engl. 19* (1980) 51; c) H. Bock, P. Rosmus, B. Solouki, G. Maier, *J. Organomet. Chem. 271* (1984) 145. Further investigations of silabenzene derivatives, cf. [7c].

[23] *Chem. Unserer Zeit 11* (1977), title picture of No. 4; cf. A. H. Schmidt, *ibid. 11* (1977) 118.

[24] Cf. A. F. Wells: *Structural Inorganic Chemistry*, 5th ed., Clarendon Press, Oxford 1987.

[25] K. B. Wiberg, *Angew. Chem. 98* (1986) 312; *Angew. Chem. Int. Ed. Engl. 25* (1986) 312, and references cited therein.

[26] In [16], other high-energy valence isomers of Si_6H_6 and other hexasila-Dewar-benzenes or hexasilabenzvalenes were observed. In this connection it should be pointed out that benzvalene, C_6H_6, is assumed as the intermediate in the ^{13}C equlibration of [1,2-$^{13}C_2$]benzene; L. T. Scott, N. H. Roelofs, T.-H. Tsang, *J. Am. Chem. Soc. 109* (1987) 5456.

[27] Thus, photolysis of hexakis(trifluoromethyl)benzene in perfluoro-*n*-pentane at 300 K provides an 82% yield of the kinetically stable benzvalene, Dewar benzene, and prismane valence isomers; D. M. Lemal, L. H. Dunlop, Jr., *J. Am. Chem. Soc. 94* (1972) 6562.

[28] Cf. also H. Bock, B. Solouki, S. Aygen, M. Bankmann, O. Breuer, R. Dammel, J. Dörr, M. Haun, T. Hirabayashi, D. Jaculi, J. Mintzer, S. Mohmand, H. Müller, P. Rosmus, B. Roth, J. Wittmann, H.-P. Wolf, *J. Mol. Struct. 173* (1988) 31, and references cited therein.

[29] Cf., for example, H. G. von Schnering, *Angew. Chem. 93* (1981) 44; *Angew. Chem. Int. Ed. Engl. 20* (1981) 33, and references cited therein; cf. also [24].

[30] a) $Si(\eta^5\text{-}C_5(CH_3)_5)_2$: P. Jutzi, D. Kaune, C. Krüger, *Angew. Chem. 98* (1986) 163; *Angew. Chem. Int. Ed. Engl. 25* (1986) 164; b) $Si(B_9C_2H_{11})_2$: W. S. Rees, Jr., D. M. Schubert, C. B. Knobler, M. F. Hawthorne, *J. Am. Chem. Soc. 108* (1986) 5369; c) $Si(B_4H_4(CSiR_3)_2)_2$, R = CH_3: N. S. Hosmane, P. de Meester, U. Siriwardane, M. S. Islam, S. S. C. Chu, *J. Chem. Soc. Chem. Commun. 1986*, 1421.

[31] A. D. Walsh, *J. Chem. Soc. 1953*, 2301; cf. R. J. Buenker, S. D. Peyerimhoff, *Chem. Rev. 74* (1974) 127; B. M. Gimarc, *J. Am. Chem. Soc. 100* (1978) 2346, and references cited therein.

[32] a) I. Hargittai, G. Schultz, J. Tremmel, N. D. Kagramanov, A. K. Maltsev, O. M. Nefedov, *J. Am. Chem. Soc. 105* (1983) 2895; b) H. Bock, B. Solouki, G. Maier, *Angew. Chem. 97* (1985) 205; *Angew. Chem. Int. Ed. Engl. 24* (1985) 205; cf. [1].

[33] a) D. J. Hajdasz, R. R. Squires, *J. Am. Chem. Soc. 108* (1986) 3139, and references cited therein; b) A. E. Reed, P. von R. Schleyer, *Chem. Phys. Lett. 133* (1987) 553, and references cited therein; cf. [13a].

[34] Cf. for example, J. I. Musher, *Angew. Chem. 81* (1969) 68; *Angew. Chem. Int. Ed. Engl. 8* (1969) 54 and references in [7a].

[35] Cf. [7a] and [1] as well as the references cited therein, for example, A. M. Semkow, P. Rosmus, H. Bock, P. Botschwina, *Chem. Phys. 35* (1978) 283.

[36] T. J. Lee, J. E. Rice, *J. Am. Chem. Soc. 111* (1989) 2011, and references cited therein; cf. also [7a].

[37] R. Gleiter, P. Jutzi, unpublished; cf. [1].

[38] J. C. Slater, *Phys. Rev. 36* (1930) 57. For a good didactic introduction, cf. K. F. Purcell, J. C. Kotz: *Inorganic Chemistry*, W. B. Saunders, Philadelphia 1977, p. 44f. Reparametrization starting from the experimental first ionization energy $IE_1(Si) = 8.1$ eV with $\Delta E = E(M^{\bullet\oplus}) - E(M)$ gives the higher shielding ($n' = n - 1$) of 0.91 instead of 0.85.

[39] Cf. K. Siegbahn, C. Nordling, A. Fahlman, R. Nordberg, K. Hamrin, J. Hedman, G. Johansson, T. Bergmark, S.-E. Karlsson, I. Lindgren, B. Lindberg: *ESCA—Atomic Molecular and Solid State Structure Studied by Means of Electron Spectroscopy*, Almquist & Wiksells, Uppsala 1967, and references cited therein.

[40] Cf. also K. Kimura, S. Katsumata, Y. Achiba, T. Yamazaki, S. Iwata: *Handbook of the He(1) Photoelectron Spectra of Fundamental Organic Molecules*, Halstead Press, New York 1981.

[41] Cf. [24] and E. A. V. Ebsworth, *Acc. Chem. Res. 20* (1987) 295, and references cited therein. Further details a) $H_3E\text{–}O\text{–}EH_3$: Structures: K. Kimura, M. Kubo, *Nature (London) 183* (1959) 533; A. Almeningen, O. Bastiansen, V. Ewing, K. Hedberg, M. Traetteberg, *Acta Chem. Scand. 17* (1963) 2455; CNDO calculations: H. Bock, P. Mollére, G. Becker, G. Fritz, *J. Organomet. Chem. 61* (1973) 113; b) $H_3E\text{–}S\text{–}EH_3$: Structures: I. Hargittai: *The Structure of Volatile Sulfur Compounds*, Reidel, Dordrecht 1985, and references cited therein; calculations: P. Mollére, H. Bock, G. Becker, G. Fritz, *J. Organomet. Chem. 61* (1973) 127; cf. also W. Wojnowski, B. Becker, K. Peters, E.-M. Peters, H. G. von Schnering, *Z. Anorg. Allg. Chem. 563* (1988) 48, 53, and references cited therein.

[42] Cf. J. Durig, M. J. Flanagan, V. F. Kalasinsky, *J. Chem. Phys. 66*(1977) 2775 and references cited therein; E. A. V. Ebsworth, *Acc. Chem. Res. 20* (1987) 295, and references cited therein; literature on quasi-linear behavior of nonmetal compounds is reviewed, for example, by D. Christen, H.-G. Mack, C. J. Marsden, H. Oberhammer, G. Schatte, K. Seppelt, H. Willner, *J. Am. Chem. Soc. 109* (1987) 4012. Cf. also unpublished calculations by R. Janoschek, University of Graz, personal communication.

[43] a) H. Bock, W. Kaim, *Chem. Ber. 111* (1978) 3552; b) H. Bock, W. Kaim, H. E. Rohwer, *ibid. 111* (1978) 3573.

[44] W. Enßlin, H. Bock, G. Becker, *J. Am. Chem. Soc. 96* (1974) 2757, and references cited therein.

[45] Cf. the summary: H. Bock, "Die Störung von π-Systmen als Molekülsonde für Substituenten-Effekte", *Jahrb. Akad. Wiss. Göttingen 1969*, 13–25 and [1, 4] and references cited therein.

[46] J. Meuret, *Diplomarbeit*, Universität Frankfurt 1989.

[47] C. Batich, E. Heilbronner, V. Hornung, A. J. Ashe, D. T. Clark, U. T. Cobley, D. Kilcast, I. Scanlan, *J. Am. Chem. Soc. 95* (1973) 928.

[48] H. Bock, B. Solouki, *Angew. Chem. 93* (1981) 425; *Angew. Chem. Int. Ed. Engl. 20* (1981) 427.

[49] Cf., for example, G. Märkl, W. Schlosser, *Angew. Chem. 100* (1988) 1009; *Angew. Chem. Int. Ed. Engl. 27* (1988) 963.

[50] H. Bock, U. Lechner-Knoblauch, *J. Organomet. Chem. 294* (1985) 295, and references cited therein.

[51] O. Graalmann, M. Hesse, U. Klingebiel, W. Clegg, M. Haase, G. M. Sheldrick, *Angew. Chem. 95* (1983) 630; *Angew. Chem. Int. Ed. Engl. 22* (1983) 621; *Angew. Chem. Suppl. 1983*, 874.

[52] H. Bock, G. Brähler, G. Fritz, E. Matern, *Angew. Chem. 88* (1976) 765; *Angew. Chem. Int. Ed. Engl. 15* (1976) 699; H. Bock, W. Kaim, J. W. Connolly, *ibid. 88* (1976) 766 and *15* (1976) 700; cf. [3].

[53] The prediction of selective $AlCl_3/CH_2Cl_2$ one-electron oxidizability based on first ionization energies $IE_1' < 8$ eV is also valid for other classes of compounds. For examples of ESR/ENDOR-detected radical cations or their rearrangement products, see: BN heterocycles: H. Nöth, W. Winterstein, W. Kaim, H. Bock, *Chem. Ber. 112* (1979) 2494; tetra-*tert*-butyltetrahedrane: H. Bock, R. Roth, G. Maier, *ibid. 117* (1984) 172; tetrakis(dimethylamino)-*p*-benzoquinone: H. Bock, P. Hänel, W. Kaim, U. Lechner-Knoblauch, *Tetrahedron Lett. 26* (1985) 5155; 1,2-dithiolane: H. Bock, B. L. Chenards, P. Rittmeyer, U. Stein, *Z. Naturforsch. B 43* (1988) 177, and references cited therein.

[54] ^{29}Si ENDOR measurements (Scheme 2) cf. H. Bock, B. Hierholzer, H. Kurreck, W. Lubitz, *Angew. Chem. 96* (1983) 817; *Angew. Chem. Int. Ed. Engl. 22* (1983) 787; *Angew. Chem. Suppl. 1983*, 1088–1105; cf. [10].

[55] A. H. Zewail, R. B. Bernstein, "Femtochemistry", *Chem. Eng. News 66* (1988) No. 45, pp. 24–43, and references cited therein.

[56] a) H. Bock, W. Kaim, A. M. Semkow, H. Nöth, *Angew. Chem. 90* (1978) 308; *Angew. Chem. Int. Ed. Engl. 17* (1978) 286; b) The independent structure determination of a sterically protected tetraalkylhydrazine (S. F. Nelson, W. C. Hollinsed, C. R. Kessel, J. C. Calabrese, *J. Am. Chem. Soc. 100* (1978) 7876) gives $d_{NN} = 126.9$ pm; c) H. Bock, W. Kaim, H. Nöth, A. Semkow, *J. Am. Chem. Soc. 102* (1980) 4421.

[57] H. Bock, W. Kaim, M. Kira, H. Osawa, H. Sakurai, *J. Organomet. Chem. 164* (1979) 295.

[58] For different substituent effects in different types of molecular states of $(H_3C)_3C$-, $(H_3C)_3Si$- and $(H_3C)_3SiH_2C$-substituted π-systems, cf. the data and references in [4], for example, H. Bock, H. Seidl, *J. Am. Chem. Soc. 90* (1968) 5694; *J. Chem. Soc. B 1968*, 1158; H. Bock, H. Alt, *J. Am. Chem. Soc. 91* (1969) 355; *J. Organomet. Chem. 13* (1968) 103; H. Bock, H. Alt, H. Seidl, *J. Am. Chem. Soc. 91* (1969) 355 and references cited therein.

[59] Cf. Lecture Abstracts "Advances in Silicon-Based Polymer Science", Makaha, Hawaii 1987, *ACS Symp. Ser. 224* (1989); G. Loubriel, J. M. Zeigler, *Phys. Rev. B33* (1986) 4203; L. A. Harrah, J. M. Zeigler, *Macromolecules 20* (1987) 601; cf. [7d] and references cited therein.

[60] Cf. the introduction to band-structure calculations with Bloch functions $\psi_k = \sum_n e^{ikna}\chi_n$ by R. Hoffmann, *Angew. Chem. 99* (1987) 871; *Angew. Chem. Int. Ed. Engl. 26* (1987) 846, and references cited therein.

[61] K. Takeda, H. Teramae, N. Matsumoto, *J. Am. Chem. Soc. 108* (1986) 8186; H. Teramae, K. Takeda, *ibid. 111* (1989) 1281, and references cited therein.

[62] H. Bock, K. Wittel, M. Veith, N. Wiberg, *J. Am. Chem. Soc. 98* (1976) 109, and references cited therein. For the violet color of diphosphaazo derivatives, cf. H. Bock, *Angew. Chem. 77* (1965) *Angew. Chem. Int. Ed. Engl. 4* (1965) 457. For bathochromic shifts in organometalloid chromophore excitations, cf. R. S. Grev, H. F. Schaefer III, *J. Am. Chem. Soc. 111* (1989) 6137.

[63] M. B. Robin: *Higher Excited States of Polyatomic Molecules*, Academic Press, New York; *Vol. I* 1974, *Vol. II* 1975, *Vol. III* 1985. Cf. especially *Vol. 1*, p. 309f, *Vol. II*, p. 68f. and 327 as well as *Vol. III*, p. 247f.

[64] H. Sakurai, Y. Kobayashi, Y. Nakadeira, *J. Am. Chem. Soc. 93* (1971) 5273.

[65] a) R. Janoschek, personal communication; b) cf. for example, R. S. Grev, H. F. Schaefer III, *J. Am. Chem. Soc. 109* (1987) 6576, and references cited therein.

[66] H. Bock, "What do we Actually Know about Reaction Pathways?", *Polyhedron 7* (1988) 2429, and references cited therein; cf. [6] and particularly [55].

[67] Our investigations; e.g., a) H. Bock, B. Hierholzer, F. Vögtle, G. Hollmann, *Angew. Chem. 96* (1984) 74; *Angew. Chem. Int. Ed. Engl. 23* (1984) 57; b) H. Bock, D. Jaculi, *ibid. 96* (1984) 298 and *23* (1984) 305; c) H. Bock, B. Hierholzer, P. Schmalz, *ibid. 99* (1987) 811, and *26* (1987) 791; d) H. Bock, B. Hierholzer, D. Jaculi, *Z. Naturforsch. B43* (1988) 1247; cf. also [4, 10] and references cited therein.

[68] H. Bock, H.-F. Herrmann, D. Fenske, H. Goesmann, *Angew. Chem. 100* (1988) 1125; *Angew. Chem. Int. Ed. Engl. 27* (1988) 1067.

[69] Cf. also H. Bock, R. Dammel, *J. Am. Chem. Soc. 110* (1988) 5261, and references cited therein; cf. also [12b].

[70] B. Solouki, H. Bock, unpublished results. For the thermal H_2 elimination from cyclohexa-1,4-diene and derivatives as well as additional hypersurface calculations for 1-sila-cyclohexa-2,5-diene; cf. K. Oswald, *Diplomarbeit*, Universität Frankfurt 1989.

[71] The MNDO procedure (M. J. S. Dewar, W. Thiel, *J. Am. Chem. Soc. 99* (1977) 4899), which best stands the test on application to all silicon compounds in the Frankfurt group, employs a Davidson/Fletcher/Powell subroutine for geometry optimization.

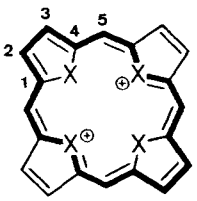
[72] G. Bruno: "Se non è vero, è ben trovato" from "Gil eroici furori", Paris 1585.

Communications may be submitted in English *or* in German. Further details regarding the submission of communications can be found in the "Notice to Authors" reproduced in the January issue of the journal. Copies thereof may be obtained from the editorial office upon request.

The Thiophene Analogue of Porphyrin: Tetrathiaporphyrin Dication

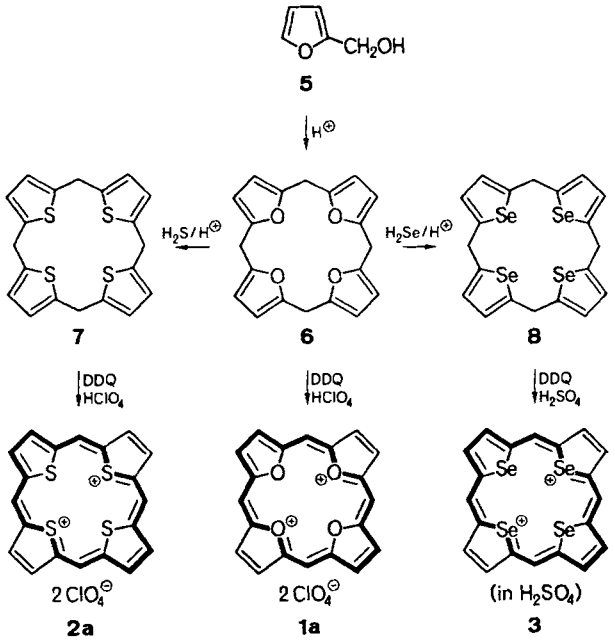
By *Emanuel Vogel,* Peter Röhrig, Martin Sicken, Bernd Knipp, Adalbert Herrmann, Michael Pohl, Hans Schmickler,* and *Johann Lex*

In spite of the long history of porphyrin chemistry,[1] tetraoxaporphyrin **1**, unlike porphyrin a dicationic species, was discovered only last year.[2] The synthesis of **1** (as perchlorate **1a**)—in the variant to be presented here—is surprising in its simplicity, for the compound can readily be prepared starting from furfuryl alcohol in merely a two-step sequence modeled after the biogenesis of porphyrin. **1** qualifies spectroscopically and in structural respects as an aromatic porphyrin, while its chemical behavior, as to be expected for a molecule with a carbenium ion/oxonium ion structure, is characterized by high reactivity towards nucleophiles.



1 X = O
2 X = S
3 X = Se
4 X = NCH_3

The current trend to broaden the basis of porphyrin chemistry by the development of novel porphyrinoid systems[3] and, not least, the discovery of **1**[2] has stimulated renewed interest in the tetrathiaporphyrin dication **2**,[4] which has hitherto escaped all efforts at its synthesis.[5] It seems certain that **2**, in contrast to **1**, does not have a planar ring skeleton, since the relatively large van-der-Waals radius of sulfur causes a marked steric hindrance in the S_4 core. According to force field calculations (MM2), **2** assumes a conformation in which all sulfur atoms protrude slightly out of the C_{20}-ring on the same side (C_{4v} symmetry).[6] Such a deviation from planarity should hardly affect the aromatic nature of **2** if one bears in mind the deformations porphyrins and bridged [4n+2]annulenes[8] are capable of tolerating without suffering serious loss of aromaticity. This conclusion derives added support from the presence of a pronounced diamagnetic ring current in the dicationic *N,N',N'',N'''*-tetramethyl-octakis(carbomethoxymethyl)porphyrin (derivative of **4**) described by *Franck* et al.,[9] in which the repulsion of the *N*-methyl groups leads to a strong puckering (or other deformation) of the molecule. Consequently, there is a good chance that the tetraselenaporphyrin dication **3**—despite an increase in the radius of the hetero atom by about 0.15 Å compared to sulfur—will likewise turn out to be an aromatic porphyrin.



We have now found that the crown ether tetraoxaporphyrinogen **6**[2b] not only enables the synthesis of the tetraoxaporphyrin dication **1** but also opens up an entry to the tetrathia- and tetraselenaporphyrin dications **2** and **3**, respectively. Interestingly, what was previously overlooked, tetraoxaporphyrinogen **6** is formed in small amounts in the much-investigated acid-catalyzed condensation of furfuryl alcohol **5**.[10] To prepare **6**, the most expedient way of carrying out the reaction involves treating a solution of **5** in dichloromethane with a solution of zinc chloride in 5% hydrochloric acid and vigorously stirring the mixture for 6 h. After conventional work-up of the reaction mixture, **6** is isolated by chromatography with toluene on silica gel; colorless needles from ethanol (m.p. 158–159 °C, yield 1%). Since **5** is a technical chemical and **6** is relatively easily separable, synthesizing the tetrafuranoid macrocycle on a preparative scale presents no difficulties, despite the preferred formation of linear condensation products. The conversion of **6** into the tetraoxaporphyrin dication **1** can be substantially improved compared to the original procedure,[2] namely by oxidizing **6** with 2,3-dichloro-5,6-dicyano-1,4-benzoquinone (DDQ) in benzene solution (room temperature, 10 min), filtering off the resulting amorphous product, and treating this with conc. nitric acid. There results a red solution, from which, after addition of 70% perchloric acid and brief standing, pure **1a** separates in the form of violet needlelike crystals (yield 86%).

Tetrathiaporphyrinogen **7** can be regarded as the key compound for the synthesis of the tetrathiaporphyrin dication **2**.

[*] Prof. Dr. E. Vogel, P. Röhrig, M. Sicken, B. Knipp, A. Herrmann, M. Pohl, Dr. H. Schmickler, Dr. J. Lex
Institut für Organische Chemie der Universität
Greinstrasse 4, D-5000 Köln 41 (FRG)

In view of the failure of all previous efforts to construct thiaporphyrinogens by coupling suitable 2,2'-dithienylmethane derivatives,[5] it was hardly surprising that the inevitably attempted extension of the acid-catalyzed cyclic condensation of **5** to α-hydroxymethylthiophene likewise met without success. A way out of this dilemma was offered by a well-known proven reaction in furan chemistry: the transformation of furans into thiophenes with hydrogen sulfide in acidic medium.[11] It was found that **6** does indeed exchange the oxygen atoms remarkably smoothly with formation of **7** when H_2S and HCl are passed simultaneously into a solution of **6** in ethanol for 2 h at 0 °C and then 3 h at room temperature and the reaction mixture finally allowed to stand for 24 h; after filtration in toluene over silica gel and crystallization from the same solvent, **7** is obtained in the form of colorless cubic-shaped crystals (decomp. at 235 °C, yield 66%). Like **6**, **7** is stable towards atmospheric oxygen.

Tetrathiaporphyrinogen **7**, which shows spectra (see Table 2) analogous to those of **6** is found by an X-ray structure analysis[12] to be a centrosymmetric molecule in the crystal (Fig. 1). The four CH_2 groups lie in a plane, from

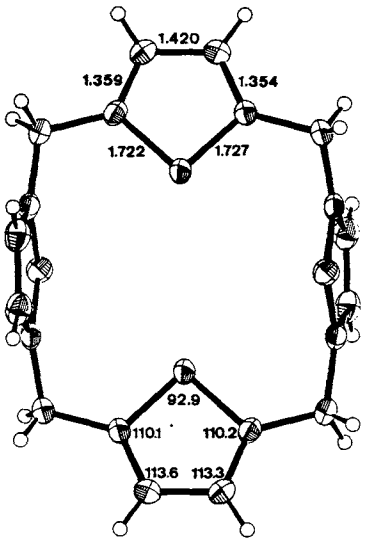


Fig. 1. Structure of **7** in the crystal. Selected bond lengths [Å] and angles [°]; standard deviations ca. 0.002 Å and 0.1°. The vibration ellipsoids are drawn at the 40% probability level.

which the thiophene rings are tilted in the way dictated by the symmetry center by 19.6 and 78.6°, respectively. In this conformation the shortest distance between sulfur atoms—given for neighboring thiophene rings—is 3.45 Å, which approximately corresponds to the spatial requirement of sulfur (twice the van-der-Waals radius: 3.70 Å).

The oxidation of **7** to the dication **2** (as perchlorate **2a**) is achieved by successive reaction of the thia crown ether with DDQ and perchloric acid,[13] whereby the following procedure is recommended: **7**, suspended in glacial acetic acid/nitromethane (5:1), is treated with DDQ in glacial acetic acid and the reaction mixture heated to 45 °C for 3 h. Upon evaporation of the homogeneous mixture to dryness there remains an amorphous residue; addition of 70% perchloric acid and subsequent stirring for 14 hours affords a deep-green solution with deposition of a black solid. When this solution is stored under a saturated water-vapor atmosphere for ca. 5 d, small violet (rodlike) crystals separate out, which according to the ^{1}H-NMR spectrum consist of pure **2a** (decomp. at 240 °C with deflagration, yield 25%). An analytically pure sample was obtained by dissolving the salt in 70% perchloric acid and repeating the crystallization procedure.

The tetrathia compound **2a** is taken up by common organic solvents, if at all, only with decomposition. With water, rapid nucleophilic attack resulting in a complex mixture of products takes place. Strong mineral acids, preferably sulfuric acid and perchloric acid (nitric acid leads to oxidative degradation) as well as liquid sulfur dioxide have proven to be the solvents of choice. Unlike **1a**, **2a** cannot be stored for extended periods of time; after several weeks, decomposition on the surface is noticed.

The ^{1}H-NMR spectrum of **2a** (Table 1), for which no temperature dependence could thus far be detected (room

Table 1. ^{1}H- NMR (300 MHz) and ^{13}C-NMR data (75.5 MHz) of **1a** and **2a** (68% $DClO_4$, CH_2Cl_2 int.) and of **3** (98% D_2SO_4, CH_2Cl_2 int.). Chemical shifts δ_H and δ_C and coupling constants J [Hz].

	2-H $^3J(H,H)$	5-H	C-1	C-2 $^1J(C,H)$	C-5
1a	11.17 *J(2,3) = 4.71* [a]	12.13	157.03 –	139.61 *188* [a]	104.87 *168* [a]
2a	10.52 *J(2,3) = 5.23* [b]	12.46	163.90 –	142.20 *180* [b]	136.47 *171* [b]
3	9.90 – [c]	11.81	– [c] –	142.89 *177*	147.05 *167*

[a] The coupling constants were taken from the spectrum of **1a** in 68% DNO_3 (better solubility); [b] taken from the spectrum of **2a** in 98% D_2SO_4; [c] so far not determinable.

temperature down to −75 °C), corresponds to that of **1a**, for it shows only two signals (δ = 12.46 and 10.52) in the resonance region to be expected for a dicationic, aromatic **2**. Also with regard to the ^{13}C-NMR spectrum there is a close analogy to **1a**. Very distinct differences are observed, however, in the UV/VIS spectra of **2a** and **1a**. Whereas the spectrum of **1a** exhibits a sharp Soret band with high extinction and a series of Q bands, that of **2a**, while being of the same type, shows all bands to be strongly broadened and shifted to longer wavelengths (Fig. 2). Noteworthily, the spectrum of **2a** is strikingly similar to that of the derivative of **4** (as bromide) mentioned at the outset.[9a] This observation can

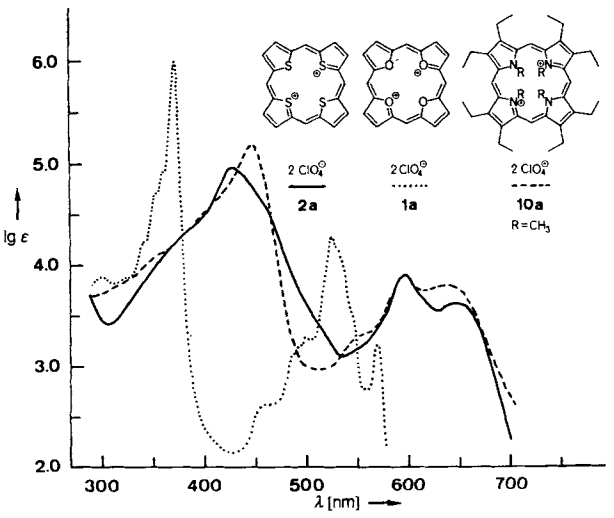


Fig. 2. UV/VIS spectra (96% H_2SO_4) of **1a**, **2a** and **10a**.

be regarded as the first experimental evidence that **2** deviates from planarity.

Concerning the IR spectrum of **2a** it should be noted that a certain relationship with that of **1a** exists regarding the band pattern; common to the spectra of both compounds is a relative paucity of bands.

The presumed non-planarity of **2** is confirmed by the X-ray structure analysis of the perchlorate **2a**[14] (Fig. 3). In **2**,

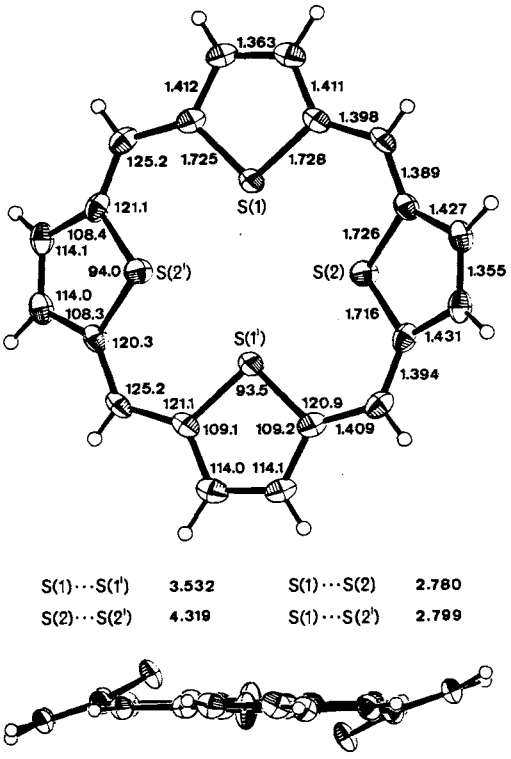


Fig. 3. Structure of **2a** in the crystal. Above: top view. Below: side view. Selected bond lengths and other distances [Å] together with bond angles [°]; standard deviations ca. 0.003 Å and 0.2°, respectively. The vibration ellipsoids are drawn at the 40% probability level.

which like **7** is centrosymmetric, the *meso*-methine carbon atoms lie in a plane, with respect to which the hetero five-membered rings are inclined by 3.7° and 22.8°, respectively. This deviation of the molecule from planarity is—in agreement with the conclusions drawn from the NMR findings—obviously too small to result in a significant loss of aromaticity, since the CC bonds in the hetero five-membered rings very markedly show the bond-length relation C_α-$C_\beta > C_\beta$-C_β[1b,c] typical for porphyrins (opposite to that in the parent heterocycles pyrrole, furan and thiophene). Consistent with the symmetry of the molecule the sulfur atoms also lie in a plane. The distance between neighboring sulfur atoms (2.78 and 2.80 Å, resp.) thereby falls about 1 Å short of double the van-der-Waals radius, so that it can be assumed that there are attractive interactions between these atoms.[15] Since the NMR spectra indicate only one sort of protons for the hetero five-membered rings, **2a** in solution—provided the nonplanar conformation in the solid state also applies in this case—must be a dynamic molecule in which the five-membered rings very rapidly exchange positions. The two perchlorate ions are, similarly to the situation in **1a**, arranged at normal distances above and below the dication.

The porphyrinogen **8** required for the synthesis of the tetraselenaporphyrin dication **3** was obtained from **6** and H_2Se under reaction conditions which essentially corresponded to those in the conversion of **6** into **7**;[16] microcrystalline powder from carbon disulfide (decomp. at 250 °C, yield 45%). **8** is air-stable and has spectra analogous to those of **6** and **7** (see Table 2). Reaction of **8** with DDQ in glacial

Table 2. Selected physical data of **7**, **2a**, **8** and **10a**.

7: ^{1}H-NMR (300 MHz, $CDCl_3$): δ = 6.61 (s, 2-H), 4.14 (s, 5-H); ^{13}C-NMR (75.5 MHz, $CDCl_3$): δ = 145.51, 123.56, 31.77; MS (70 eV): *m/z* 384 ($M^\oplus$, 100%); IR (KBr): $\tilde{\nu}$ = 3064, 2923, 2899, 2826, 1421, 1298, 1255, 803, 790, 746, 494, 476 cm^{-1}; UV/VIS (cyclohexane): λ_{max} = 241 nm (ε = 26 500), 247 (24 900) sh, 254 (18 300) sh

2a: ^{1}H- and ^{13}C-NMR data see table 1 (the investigation of the temperature dependence was carried out from room temperature down to −40 °C in 70% D_2SO_4 and at −75 °C in SO_2); IR (Nujol): $\tilde{\nu}$ = 3084, 3050, 3029, 1407, 1380, 1276, 1182, 1082 ($ClO_4^\ominus$), 1062, 1049 ($ClO_4^\ominus$), 964, 900, 835, 808, 658, 623 ($ClO_4^\ominus$), 546 cm^{-1}; UV/VIS (96% H_2SO_4): λ_{max} = 381 nm (ε = 21 700) sh, 426 (94 500), 456 (42 700) sh, 514 (2400) sh, 547 (1500) sh, 595 (8250), 646 (4300)

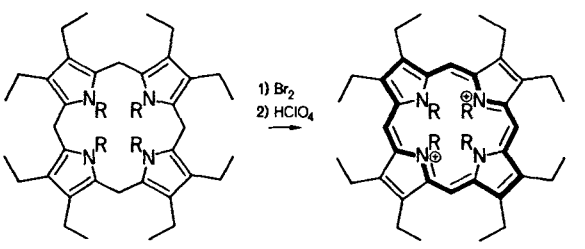
8: ^{1}H-NMR (300 MHz, $CDCl_3$): δ = 6.74 (s, 2-H), 4.17 (s, 5-H); ^{13}C-NMR (75.5 MHz, $CDCl_3$): δ = 155.19, 125.12, 37.04; MS (75 eV): *m/z* 576 [$M^\oplus$ (for ^{80}Se), 41%]; IR (KBr): $\tilde{\nu}$ = 3045, 3010, 2888, 1492, 1291, 1127, 1029, 817, 798, 729, 432 cm^{-1}; UV/VIS (dioxane): λ_{max} = 251 nm (ε = 25 000), 257 (22 700) sh

10a: ^{1}H-NMR (300 MHz, $CDCl_3$): δ = 9.94 (s, 5-H), 3.56 (m, 2a-H), 1.50 (t, 2b-H), −4.59 (s, N-CH_3); ^{13}C-NMR (75.5 MHz, $CDCl_3$): δ = 156.97, 141.51, 102.73, 34.54, 20.50, 16.56; MS (FAB): *m/z* 592 [(*M*- 2ClO_4)$^\oplus$, 100%]; UV/VIS (96% H_2SO_4): λ_{max} = 445 nm (ε = 157 000), 554 (2150) sh, 594 (8000), 637 (6550)

acetic acid and subsequent treatment of the residue remaining after removal of solvent with 98% sulfuric acid leads indeed to formation of the dication **3**—apparently still aromatic according to its NMR data (see Table 1)—but attempts to crystallize this as sulfate or other salt from the medium sulfuric acid have, as yet, met with no success. The use of perchloric acid is not helpful here, since **3** rapidly decomposes in its presence.

The previously noted close similarity of the UV/VIS spectra of **2a** and the octakis(carbomethoxymethyl) derivative of **4** invited attempts to determine the molecular geometry of an *N,N',N'',N'''*-tetramethylporphyrin dication by X-ray structure analysis. Compound **4**, regarded as especially desirable for the analysis (in combination with a suitable counterion), was ruled out because it was thus far not possible to gain access to the peripherally unsubstituted *N,N',N'',N'''*-tetramethylporphyrinogen. As alternative, therefore, the *N,N',N'',N'''*-tetramethyl-octaethylporphyrinogen **9** described by *Franck* and *Gosmann*[17] was subjected to oxidation employing the well proven reagent bromine in chloroform.[9] As confirmed by the NMR spectra and the elemental analysis of the product, this led to smooth formation of the expected *N,N',N'',N'''*-tetramethyl-octaethylporphyrin dication **10** as bromide.

Unfortunately, this could only be isolated in microcrystalline form, and thus, in view of the fact that the perchlo-



rates of **1** and **2** crystallize exceedingly well, it was converted into the perchlorate **10a** by addition of perchloric acid to a solution of the bromide in methanol/water (1:1); blue platelets from dichloromethane/hexane (1:4) (decomp. above 230 °C, yield 77% based on **9**).

In the ^{1}H-NMR spectrum (Table 2) of **10a** the resonance of 5-H (δ = 9.94) appears at noticeably higher field than in the spectra of **1a** and **2a** (Table 1); however, the strong shielding of the N-CH_3 protons (δ = −4.59) leaves no doubt that there is a pronounced diamagnetic ring current in the dication.[18]

The structure analysis of **10a**,[19] which presented no problems, revealed the dication **10** as a highly symmetric species characterized by a fourfold alternating axis (Fig. 4).

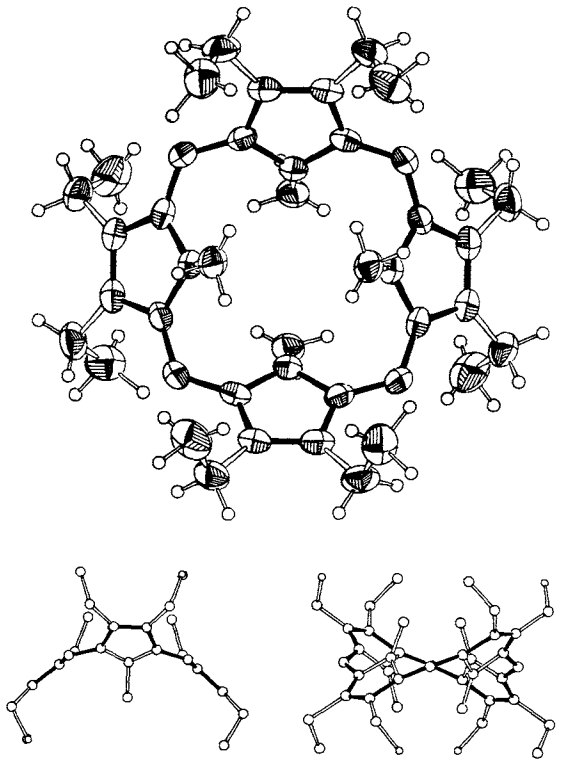


Fig. 4. Structure of **10a** in the crystal. The molecule has approximate D_{2d} symmetry (exactly S_4), as shown by the three chosen projections. Above: top view, looking in the direction of the crystallographic S_4 axis, vibration ellipsoids with 40% probability, selected bond lengths C_α–C_m: 1.411, C_α–C_β: 1.449, C_α–N: 1.391 (mean values), C_β–$C_{\beta'}$: 1.365 Å. Below: side views (without H atoms) from two directions differing by 45°: left, parallel to one of the two equivalent mirror planes; right, along one of the two equivalent C_2 axes.

As predicted, the conformation of **10** is largely determined by the steric hindrance of the *N*-methyl groups. The heterocyclic five-membered rings are each tilted by 39° with respect to the plane through the *meso*-methine carbon atoms, and torsion angles (C_β–C_α–C_m–$C_{\alpha'}$) of 29° occur at each of the eight C_α–C_m bonds of the ring skeleton. Moreover, the *N*-methyl groups are not coplanar with their respective five-membered rings but are bent at a significant angle (32°); this bending must be accompanied by a partial rehybridization of the nitrogen atoms from sp^2 to sp^3 (sum of the bond angles at nitrogen: 349.1°). Although the geometry of the ring skeleton in **10** should considerably impair p-orbital overlap, the pattern of the bond lengths in the dication, especially the CC bond-length relations in the heterocyclic five-membered rings (C_α-C_β > C_β-C_β), corresponds to the situation in porphyrins.[1b,c] Some interesting features of the arrangement of the perchlorate ions can only be alluded to at this juncture.[19]

The structurally closely related dicationic porphyrins **1**, **2** and **10** form a series in which the conformation of the ring skeleton varies from slightly puckered to strongly puckered. According to NMR and structural chemical criteria there is no significant decrease in aromaticity on going from **1** to **10**, impressively illustrating the ability of porphyrins of the present type to maintain an effective cyclic π-electron delocalization, even under unfavorable steric conditions.

Received: July 17, 1989 [Z 3446 IE]
German version: *Angew. Chem. 101* (1989) 1683

[1] a) H. Fischer, H. Orth: *Die Chemie des Pyrrols, Bd. II*, Akademische Verlagsgesellschaft, Leipzig 1937; b) K. M. Smith (Ed.): *Porphyrins and Metalloporphyrins*, Elsevier, Amsterdam 1975; c) D. Dolphin (Ed.): *The Porphyrins, Vol. I–VII*, Academic Press, New York 1978/1979.

[2] a) E. Vogel, W. Haas, B. Knipp, J. Lex, H. Schmickler, *Angew. Chem. 100* (1988) 445; *Angew. Chem. Int. Ed. Engl. 27* (1988) 406; b) W. Haas, B. Knipp, M. Sicken, J. Lex, E. Vogel, *ibid. 100* (1988) 448 and *27* (1988) 409.

[3] a) Sapphyrins: M. J. Broadhurst, R. Grigg, A. W. Johnson, *J. Chem. Soc. Perkin Trans. 1 1972*, 2111; V. J. Bauer, D. L. J. Clive, D. Dolphin, J. B. Paine III, F. L. Harris, M. M. King, J. Loder, S.-W. Chien Wang, R. B. Woodward, *J. Am. Chem. Soc. 105* (1983) 6429; b) Texaphyrins: J. L. Sessler, M. R. Johnson, V. Lynch, *J. Org. Chem. 52* (1987) 4394; c) Platyrins: E. LeGoff, O. G. Weaver, *ibid. 52* (1987) 710; d) [26]Porphyrin: M. Gosmann, B. Franck, *Angew. Chem. 98* (1986) 1107; *Angew. Chem. Int. Ed. Engl. 25* (1986) 1100; [34]Porphyrin: G. Knübel, B. Franck, *ibid. 100* (1988) 1203 and *27* (1988) 1170; e) Pentaphyrin: H. Rexhausen, A. Gossauer, *J. Chem. Soc. Chem. Commun. 1983*, 275; f) Homoporphyrins: H. J. Callot, E. Schaeffer, *J. Org. Chem. 42* (1977) 1567; g) Porphycenes: E. Vogel, M. Köcher, H. Schmickler, J. Lex, *Angew. Chem. 98* (1986) 262; *Angew. Chem. Int. Ed. Engl. 25* (1986) 257; E. Vogel, M. Balci, K. Pramod, P. Koch, J. Lex, O. Ermer, *ibid. 99* (1987) 909 and *26* (1987) 928.

[4] Various reports have appeared on mono- and dithiaporphyrins as well as on diselenaporphyrins: a) A. W. Johnson in K. M. Smith (Ed.): *Porphyrins and Metalloporphyrins*, Elsevier, Amsterdam 1975, p. 729; b) A. Ulman, J. Manassen, *J. Am. Chem. Soc. 97* (1975) 6540; c) R. L. Hill, M. Gouterman, A. Ulman, *Inorg. Chem. 21* (1982) 1450; d) P. Stein, A. Ulman, T. G. Spiro, *J. Phys. Chem. 88* (1984) 369; e) L. Latos-Grażyński, J. Lisowski, M. M. Olmstead, A. L. Balch, *Inorg. Chem. 28* (1989) 1183; see also a review of the literature in [2a].

[5] M. Ahmed, O. Meth-Cohn, *Chem. Commun. 1968*, 82; *Tetrahedron Lett. 1969*, 1493; *J. Chem. Soc. C 1971*, 2104.

[6] We thank Prof. *R. Gleiter*, Universität Heidelberg, for the calculations.

[7] a) Porphyrins: T. P. Wijesekera, J. B. Paine III, D. Dolphin, F. W. B. Einstein, T. Jones, *J. Am. Chem. Soc. 105* (1983) 6747; b) *N*-protonated porphyrins: N. Hirayama, A. Takenaka, Y. Sasada, E.-I. Watanabe, H. Ogoshi, Z.-I. Yoshida, *J. Chem. Soc. Chem. Commun. 1974*, 330; A. Stone, E. B. Fleischer, *J. Am. Chem. Soc. 90* (1968) 2735; *N*-substituted porphyrins: D. K. Lavallee: *The Chemistry and Biochemistry of N-Substituted Porphyrins*, VCH Publishers, New York, Weinheim 1987.

[8] E. Vogel in H. Nozaki (Ed.): *Current Trends in Organic Synthesis*, Pergamon Press, Oxford 1983, p. 379.

[9] a) R. Steinkamp, *Dissertation*, Universität Münster 1978; b) B. Franck, W. Bock, G. Bringmann, G. Fels, F. Grubenbecher, M. Marsmann, R. Pietschmann, K. Schäpers, U. Spiegel, R. Steinkamp, G. Ufer, C. Wegner, *Int. J. Biochem. 12* (1980) 671; c) B. Franck, *Angew. Chem. 94* (1982) 327; *Angew. Chem. Int. Ed. Engl. 21* (1982) 343.

[10] Earlier analytic investigations on furfuryl alcohol polycondensates containing a relatively high proportion of low-molecular weight products gave no indications of the formation of **6** or higher cyclooligomers: J. B. Barr, S. B. Wallon, *J. Appl. Polym. Sci. 15* (1971) 1079; E. M. Wewerka, E. D. Loughran, K. L. Walters, *ibid. 15* (1971) 1437.

[11] J. K. Jurjew, *Ber. Dtsch. Chem. Ges. 69* (1936) 440; Y. Miyahara, T. Inazu, T. Yoshino, *Chem. Lett. 1980*, 397; V. G. Kharchenko, T. I. Gubina, I. A. Markushina, *Zh. Org. Khim. 18* (1982) 394; *J. Org. Chem. USSR 18* (1982) 343.

[12] $C_{20}H_{16}S_4$, decomp. at 235 °C, crystals from toluene; monoclinic, space group $P2_1/c$, $Z = 2$; a = 9.743(2), b = 10.019(2), c = 9.336(2) Å, β = 109.80(2)°; ϱ_{calcd} = 1.490 g cm^{-3}; intensity measurements on a four-circle diffractometer, room temperature, λ_{Mo} = 0.71069 Å, Θ_{Mo} (max) = 27°; refinement (C,S anisotropic, H isotropic) taking into account 1879 reflections with $F_o > 4\sigma(F_o)$: R = 0.029, R_w = 0.038 [20].

[13] Tetrathiaporphyrinogen **7** shows a remarkably varying behavior towards oxidizing reagents: aside from being converted into the dication **2** (with

DDQ) it can also be converted into the corresponding tetraketone (ceric ammonium nitrate), into the monosulfone (peracids) as well as into a still unidentified red ionic species (electrochemically). By way of contrast, tetraoxaporphyrinogen **6** has thus far always afforded the dication **1** with all reagents which effect oxidation with retention of the ring skeleton. The electrochemical oxidation of **6** also gave **1** (private communication from Prof. *E. Steckhan*, Universität Bonn (FRG)).

[14] $C_{20}H_{12}Cl_2O_8S_4$, decomp. at 240 °C, crystals from $HClO_4$; triclinic, space group $P\bar{1}$, $Z = 1$; $a = 5.850(1)$, $b = 8.994(1)$, $c = 10.547(2)$ Å, $\alpha = 78.90(2)$, $\beta = 81.03(2)$, $\gamma = 82.19(2)°$; $\varrho_{calcd} = 1.800$ g cm^{-3}; measuring conditions as for **7**; refinement (C,Cl, O,S anisotropic, H isotropic) taking into account 1791 reflections with $F_o > 4\sigma(F_o)$; $R = 0.045$, $R_w = 0.053$ [20].

[15] In the case of **2a** there are no indications of bonding between sulfur atoms that lie opposite to each other in the porphyrin core—as has been assumed and is theoretically substantiated in the case of tetraphenyl-21,23-dithiaporphyrin on the basis of the extremely short S···S distances of 3.05 Å [4c, d].

[16] Concerning the acid-catalyzed conversion of furans into selenophenes see C. W. Bird, G. W. H. Cheeseman, A.-B. Hörnfeldt in A. R. Katritzky, C. W. Rees (Eds.): *Comprehensive Heterocyclic Chemistry, Vol. 4*, Pergamon Press, Oxford 1984, p. 968.

[17] M. Gosmann, *Dissertation*, Universität Münster 1986.

[18] *With regard to the δ values for 5-H and N-CH$_3$, the* ^{1}*H-NMR spectrum* of **10a** is, as expected, in good agreement with that of the octakis(carbomethoxymethyl) derivative of **4** (as bromide) [9a, c].

[19] $C_{40}H_{56}Cl_2N_4O_8$, decomp. at about 230 °C, crystals from dichloromethane/hexane (1:4); tetragonal, space group $P4/n$, $Z = 2$; $a = 14.866(3)$, $c = 9.441(2)$ Å; $\varrho_{calcd} = 1.260$ g cm^{-3}; measuring conditions as for **7**; refinement (C,Cl,N,O anisotropic, H isotropic), 1011 reflections with $F_o > 4\sigma(F_o)$; $R = 0.062$, $R = 0.065$. One of the two independent perchlorate ions is distorted [20].

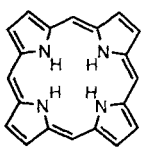
[20] Further details of the crystal structure investigations are available on request from the Fachinformationszentrum Karlsruhe, Gesellschaft für wissenschaftlich-technische Information mbH, D-7514 Eggenstein-Leopoldshafen 2 (FRG), on quoting the depository number CSD-54209, the names of the authors, and the journal citation.

A Pyrrolophanediene-Porphycene Redox System

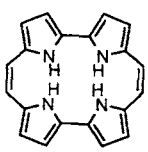
By *Emanuel Vogel,* Ilona Grigat, Matthias Köcher,* and *Johann Lex*

Isophlorin **1**, a still elusive dihydroporphyrin first referred to by *Woodward* some 30 years ago in connection with the synthesis of chlorophyll,[1] is a molecule equally interesting from the standpoint of porphyrin and annulene chemistry. It seems justified to regard **1** as a "cyclobutadiene homologue" since it constitutes an essentially planar [20]annulene associated with a degenerate, presumably very fast π-bond shift. As a consequence of its π-electron structure, **1** is expected to exhibit a pronounced tendency to undergo a two-electron oxidation with formation of resonance-stabilized diprotonated porphyrin, and hence to be a dihydroporphyrin of only fleeting existence.

The anticipated ready oxidizability of **1** would explain why *N,N'*-dihydroporphycene **2**, the analogue of **1** in the

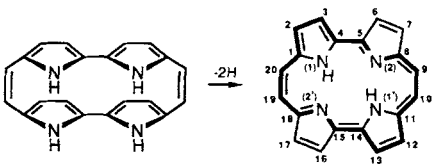


1



2

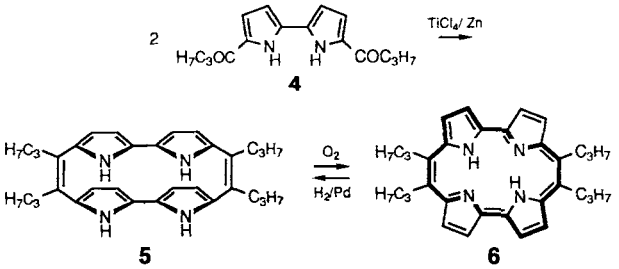
porphycene series and the obvious intermediate in the synthesis of porphycene[2], has hitherto defied all attempts at its detection. Other than in the case of **1**, there is considerable steric hindrance of the NH-hydrogen atoms in **2**. For this reason **2** is in all probability not planar but has the pyrrolophanediene structure **2a**.[3,4] We have now found that *N,N'*-dihydroporphycenes are in certain cases isolable, are in fact pyrrolophanedienes, and, what was unforeseen, form redox systems with the corresponding porphycenes.



2a **3**

Examination of the stereochemistry of porphycene **3** reveals that peripheral alkyl groups, particularly in the 9, 10, 19, 20 as well as in the 3, 6, 13, 16 positions are capable of modulating the geometry of the tetrapyrrolic macrocycle relatively strongly through non-bonding interactions. A representative example of this is the 9,10,19,20-tetrapropylporphycene **6**, which is obtainable analogously to the synthesis of **3** by reductive coupling of the bipyrrole derivative **4** with titanium tetrachloride and zinc.[5] According to an X-ray structure analysis, **6**, like **3**, has a planar ring skeleton, but due to the repulsion of the propyl groups there is a convergence of the oppositely disposed nitrogen atoms, so that the N_4 core with the distances N(1)···N(2′) = 2.528(4) Å[6] and N(1)···N(2) = 2.898(4) Å now becomes decidedly rectangular in shape. This structural change not only influences the strength of the N-H···N hydrogen bonds and the tendency to undergo metal complex formation but, as revealed by the most recent studies, also leads to unexpected chemical reactions.

One such reaction is found in the catalytic hydrogenation of **6** with palladium/carbon in ethyl acetate. While the parent porphycene **3** under these hydrogenation conditions regioselectively affords the red-violet 2,3-dihydroporphycene, which can be regarded as a chlorin analogue,[7] **6** surprisingly gives a colorless dihydro compound (rectangular crystals from dichloromethane/hexane, decomp. at 180 °C, yield 25%, losses by re-oxidation to **6**). The finding that saturation of only one formal double bond dramatically reduces the conjugation immediately made one suspect that the product is the pyrrolophanediene *N,N'*-dihydro-9,10,19,20-tetrapropylporphycene **5**. The spectra (Table 1) and the X-ray structure analysis of the compound confirmed this.



4 **5** **6**

The ^{1}H-NMR spectrum of **5** shows only one ABX system for the pyrrole protons at δ = 6.94 (NH), 6.09 (2,7,12,17-H) and 6.02 (3,6,13,16-H) with coupling constants ($^4J_{2,NH}$ = 2.70 Hz, $^4J_{3,NH}$ = 2.47 Hz and $^3J_{2,3}$ = 3.48 Hz) typical for

[*] Prof. Dr. E. Vogel, I. Grigat, Dr. M. Köcher, Dr. J. Lex
Institut für Organische Chemie der Universität
Greinstrasse 4, D-5000 Köln 41 (FRG)

pyrrole rings, and a quartet (α-CH_2), a multiplet (β-CH_2) and a triplet (CH_3) for the propyl protons at $\delta = 2.44$, 1.51 and 0.95, respectively.[8] The loss of porphycene aromaticity is impressively reflected in these NMR data, as marked high-field shifts are observed, both for the vinylic pyrrole protons ($\Delta\delta = 3.3$) and (in the corresponding gradation) for the α-, β- and CH_3-propyl protons ($\Delta\delta = 1.9$, 0.9 and 0.5). The approximate invariance ($\Delta\delta = 0.1$) of the NH resonance signal appears understandable when one considers that opposing effects occur in **5**, namely a high-field shift due to disappearance of the strong N-H···N hydrogen bonds[9] and a downfield shift as a result of the collapse of the diamagnetic ring current in the macrocycle. Complementary to the simple ^{1}H-NMR spectrum, indicating a high molecular symmetry, eight signals are found in the ^{13}C-NMR spectrum of **5**.

Table 1. Selected physical data of **5** and **7**.

5: ^{1}H-NMR (300 MHz, $CDCl_3$): $\delta = 6.94$ (br.s, 4H; NH), 6.09 (m, 4H; 2,7,12,17-H), 6.02 (m, 4H; 3,6,13,16-H), 2.44 (q, 8H; α-CH_2), 1.51 (m, 8H; β-CH_2), 0.95 (t, 12H; CH_3); ^{13}C-NMR (75.5 MHz, $CDCl_3$): $\delta = 133.29$, 128.42, 125.61 (quaternary C atoms), 108.81 (C-2,7,12,17), 106.29 (C-3,6,13,16), 34.86 (α-CH_2), 22.44 (β-CH_2), 14.25 (CH_3); MS (EI, 70 eV): m/z 480 ($M^{\oplus}$, 100%), 451 (14%), 437 (22%), 240 ($M^{2\oplus}$, 5%); IR (KBr): $\tilde{\nu}$ [cm^{-1}] = 3434, 3100, 2958, 2933, 2871, 1679, 1553, 1463, 1409, 1363, 1259, 1093, 1043, 772, 707, 586, 539; UV/VIS (cyclohexane): λ [nm] = 220 (ε = 23 700) sh, 278 (35 200), 320 (12 100) sh

7: ^{1}H-NMR (300 MHz, $CDCl_3$): $\delta = 10.20$ (br.s, 1H; NH2), 8.80 (d, 1H; 13-H), 8.74 (dd, 1H; 16-H), 8.70 (dd, 1H; 17-H), 8.62 (d, 1H; 6-H), 8.50 (d, 1H; 12-H), 8.43 (d, 1H; 7-H), 6.77 (br.s, 1H; NH2'), 4.64 (m, 2H; 3-H), 4.33 (m, 2H; 2-H), 4.00 (q, 2H; α-CH_2), 3.96 (q, 2H; α-CH_2), 3.89 (q, 2H; α-CH_2), 3.36 (q, 2H; α-CH_2), 2.25 (m, 2H; β-CH_2), 2.22 (m, 2H; β-CH_2), 2.10 (m, 2H; β-CH_2), 1.95 (m, 2H; β-CH_2), 1.35 (t, 3H; CH_3), 1.34 (t, 3H; CH_3), 1.30 (t, 3H; CH_3), 1.28 (t, 3H; CH_3); ^{13}C-NMR (75.5 MHz, $CDCl_3$): $\delta = 166.67$, 157.77,147.17, 143.55, 135.28, 134.32, 133.40, 130.55, 129.70, 127.10, 123.83, 120.31 (quaternary C atoms), 126.09 (C-17), 126.04 (C-6), 122.81 (C-7), 121.39 (C-12), 120.41 (C-13), 119.11 (C-16), 38.16, 37.83, 37.68 (α-CH_2), 35.98 (C-2), 31.50 (C-3), 29.27, 28.85, 28.67, 25.34 (β-CH_2), 15.28, 15.19, 15.17, 15.11 (CH_3); MS (EI, 70 eV): m/z 480 ($M^{\oplus}$, 100%), 451 (28%), 437 (30%), 240 ($M^{2\oplus}$, 19%); IR (CsI): $\tilde{\nu}$ [cm^{-1}] = 3103, 2950, 2859, 1603, 1420, 1381, 1330, 1204, 1167, 1067, 1061, 760; UV/VIS (dichloromethane) [a]: λ [nm] = 353 (ε = 60 000) sh, 372 (82 000), 394 (54 000), 415 (79 000), 554 (13 500) sh, 597 (31 000), 630 (26 100)

[a] UV/VIS spectrum corrected calculationally for the presence of 2% of **6**.

In the UV/VIS spectrum of **5** no absorption appears above 400 nm. The IR spectrum is informative insofar as it contains a sharp band for the NH stretching vibration and thus corroborates the disappearance of the strong hydrogen bonds (no NH band could be reliably located in the spectrum of **3**).[10]

According to an X-ray structure analysis,[11] the dihydro compound **5**, in the crystalline state, clearly has the phanediene structure deduced from the spectra (Fig. 1). The geometry of the compound derives from the hypothetical planar structure primarily in such a way that, within each bipyrrole moiety, the pyrrole rings have rotated out of the plane in opposite sense. The dihedral angle between the pyrrole rings, arising from twisting and slight bending of the rings with respect to the central α–α'-bond due to strain, is 64.3°. The pyrrole rings as such show no deviation from planarity. Oppositely disposed pyrrole rings are to a crude approximation arranged antiparallel, as would be expected, since there are attractive dipole-dipole interactions with this orientation of the rings.[12] It is a manifestation of the distortion of the pyrrolophanediene skeleton that the ethene units, at which torsions of 7° occur, are not oriented parallel to each other but are at an angle of 47.8°.

Following the successful isolation and characterization of **5** (in the hydrogenation of **6**) it also proved possible to isolate the compound under rigorous exclusion of oxygen in the reductive coupling of **4** (always accompanied by small amounts of **6**) and thus to confirm the assumed intermediary formation of *N,N'*-dihydroporphycenes in the synthesis of porphycenes. The easy aromatization of **5** to **6** by atmospheric oxygen and other oxidizing agents in combination with the above mentioned hydrogenation makes **5**/**6** an extraordinary redox system.

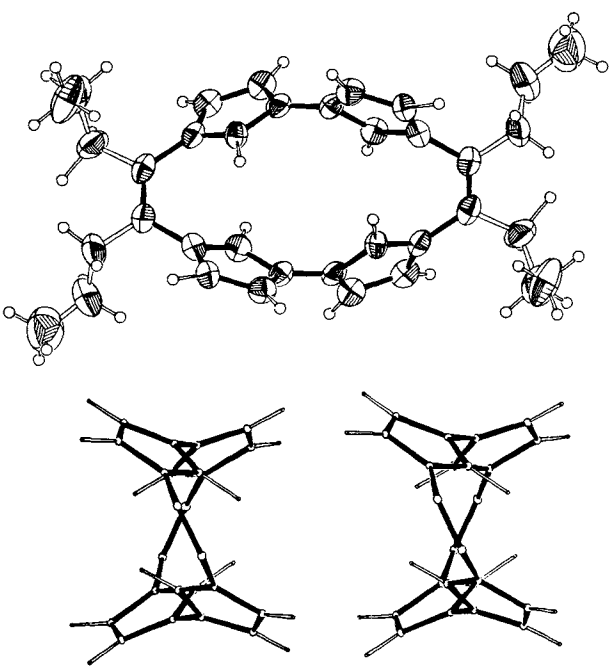
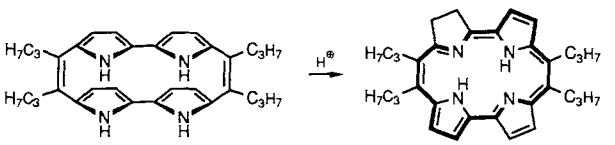


Fig. 1. Molecular structure of **5** in the crystal at −20 °C. Decisive for carrying out the analysis at the quoted temperature was that the D_2 symmetry of the molecule established at room temperature includes a dynamic disorder of the propyl groups (high temperature factors for the terminal carbon atoms). At −20 °C the propyl groups, which at the outset were crystallographically equivalent, adopt two different conformations, so that a lowering of the symmetry from D_2 to C_2 results for the overall molecule. The phane skeleton as such, on the other hand, retains D_2 symmetry at −20 °C. Top: view of the molecule in the direction of the C_2 axis, vibration ellipsoids (40% probability). Bottom: stereoview of the skeleton (without propyl groups), perpendicular to the C_2 axis along the bipyrrole units.



5 **7**

Concerning the course of the hydrogenation of **6** it is conceivable that, in parallel with the situation in the case of **3**, the 2,3-dihydro compound **7** is formed, and **5** therefore results from subsequent tautomerism of **7**. This alternative to direct *N,N'*-hydrogenation could, however, be ruled out, since, conversely, **5** tautomerizes to the 2,3-dihydro compound **7** upon treatment with a catalytic amount of conc. sulfuric acid in dichloromethane (yield 52%).[13] That **7** is stable under the conditions of the catalytic hydrogenation was confirmed by control experiments. The structure of **7** follows from the similarity of its spectra with those of 2,3-dihydroporphycene, and in particular from an X-ray structure analysis.[14]

The diminished oxidizability of *N,N'*-dihydro-9,10,19,20-tetrapropylporphycene **5** compared to that of the still unknown *N,N'*-dihydroporphycene parent compound **2**, which enabled its isolation, is apparently due to the fact that the rotation of the pyrrole rings into the planar or into a near-

planar conformation required for oxidation is hindered by non-bonding interactions between the propyl groups and the hydrogen atoms in the 2,7,12,17-positions. The favored hydrogenation of **6** with formation of **5** instead of the expected **7** is probably due to hitherto unexplained kinetic factors, since it is almost certain from the acid-catalyzed tautomerization of **5** to **7** that **7** is the thermodynamically more stable tautomer.

Received: July 17, 1989 [Z 3447 IE]
German version: *Angew. Chem. 101* (1989) 1687

CAS Registry numbers: **4**, 124044-97-9; **5**, 124044-96-8; **6**, 107985-44-4; **7**, 124044-98-0.

[1] R. B. Woodward, *Angew. Chem. 72* (1960) 651; R. B. Woodward, *Ind. Chim. Belge 27* (1962) 1293.

[2] E. Vogel, M. Köcher, H. Schmickler, J. Lex, *Angew. Chem. 98* (1986) 262; *Angew. Chem. Int. Ed. Engl. 25* (1986) 257; E. Vogel, M. Balci, K. Pramod, P. Koch, J. Lex, O. Ermer, *ibid. 99* (1987) 909 and *26* (1987) 928.

[3] Pyrrolophanes with oppositely disposed pyrrole rings are thus far known only in the form of [2.2](2,5)pyrrolophane and some of its derivatives; see the review by W. W. Paudler, M. D. Bezoari in P. M. Keehn, S. M. Rosenfeld: *Cyclophanes, Vol. II*, Academic Press, New York 1983, p. 359; W. Flitsch, H.-G. Kneip, *Liebigs Ann. Chem. 1985*, 1895.

[4] The furan analogue of **2** is present in the crystal as a planar molecule; E. Vogel, M. Sicken, P. Röhrig, H. Schmickler, J. Lex, O. Ermer, *Angew. Chem. 100* (1988) 450; *Angew. Chem. Int. Ed. Engl. 27* (1988) 411.

[5] E. Vogel, M. Köcher, J. Lex, O. Ermer, *Isr. J. Chem. 29* (1989) 257 (David-Ginsburg-Memorial Issue).

[6] Comparably short hydrogen bonds between N atoms have, to our knowledge, thus far only been observed in "proton sponges" in protonated form, see H. A. Staab, T. Saupe, *Angew. Chem. 100* (1988) 895; *Angew. Chem. Int. Ed. Engl. 27* (1988) 865; T. Saupe, C. Krieger, H. A. Staab, *ibid. 98* (1986) 460 and *25* (1986) 451; R. W. Alder, A. Casson, R. B. Sessions, *J. Am. Chem. Soc. 101* (1979) 3652.

[7] E. Vogel, M. Köcher, M. Balci, I. Teichler, J. Lex, H. Schmickler, O. Ermer, *Angew. Chem. 99* (1987) 912; *Angew. Chem. Int. Ed. Engl. 26* (1987) 931.

[8] In the ^{1}H-NMR spectrum, recorded between +70 °C and −80 °C, changes are observed below −30 °C which can be ascribed to an incipient hindrance to rotation of the alkyl groups.

[9] Information on the deshielding of protons which participate in strong hydrogen bonds is given in a review by J. Emsley, *Chem. Soc. Rev. 9* (1980) 91.

[10] Concerning the influence of strong hydrogen bonds on the band position and band shape of the element-hydrogen vibrations involved, see: C. Sandorfy, *Top. Curr. Chem. 120* (1984) 41; A. Novak, *Struct. Bonding (Berlin) 18* (1974) 177; see also reference [9].

[11] **5**: $C_{32}H_{40}N_4$, decomp. at 180 °C, rectangular crystals from dichloromethane/hexane; measurement at room temperature: tetragonal, space group $P4/ncc$, $Z = 4$, $a = 16.458(4)$, $c = 10.699(3)$ Å; $\varrho_{calcd} = 1.103\ g\,cm^{-3}$; intensity measurements on a four-circle diffractometer [$\lambda_{Mo} = 0.71069$ Å, $\Theta_{Mo}(max) = 27°$]; refinement (C, N anisotropic, H isotropic) taking into account 565 reflections with $F_o > 4\sigma(F_o)$; $R = 0.095$, $R_w = 0.097$; the hydrogen atoms of the propyl groups were not taken into account in the refinement because of disorder. Measurement at −20 °C: orthorhombic, space group $Pccn$, $Z = 4$; $a = 16.099(2)$, $b = 16.716(2)$, $c = 10.619(1)$ Å; $\varrho_{calcd} = 1.117\ g\,cm^{-3}$; intensity measurements on a four-circle diffractometer [$\lambda_{Mo} = 0.71069$ Å, $\Theta_{Mo}(max) = 27°$]; refinement (C, N anisotropic, H isotropic) taking into account 998 reflections with $F_o > 4\sigma(F_o)$; $R = 0.059$, $R_w = 0.060$ [15].

[12] A. Gossauer: *Die Chemie der Pyrrole*, Springer, Berlin 1974, p. 71.

[13] The rearrangement of **5** into **7** under the given reaction conditions is practically irreversible. Owing to ready oxidation to the porphycene **6**, **7** usually contains 1–2% of the oxidation product even on careful work-up.

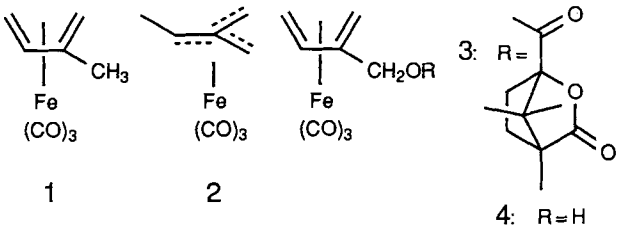
[14] **7**: $C_{32}H_{40}N_4$, m.p. 250–252 °C, rhombic crystals from dichloromethane/hexane; monoclinic, space group $P2_1/c$, $Z = 4$; $a = 17.507(3)$, $b = 9.938(2)$, $c = 15.742(3)$ Å, $\beta = 93.59(2)°$; $\varrho_{calcd} = 1.168\ g\,cm^{-3}$; intensity measurements on a four-circle diffractometer [room temperature, $\lambda_{Mo} = 0.71069$ Å, $\Theta_{Mo}(max) = 27°$]; refinement (C, N anisotropic, H isotropic) taking into account 1893 reflections with $F_o > 4\sigma(F_o)$; $R = 0.060$, $R_w = 0.062$. In analogy to the situation in the case of the porphycene 3/2,3-dihydroporphycene pair [7], the transition from **6** to **7** has no noticeable effect on the overall conformation of the ring skeleton (as before, planar). An accurate analysis of the bond lengths suggests that **7** is partially disordered in the crystal [15].

[15] Further details of the crystal structure investigations on **5** and **7** are available on request from the Fachinformationszentrum Karlsruhe, Gesellschaft für wissenschaftlich-technische Information mbH, D-7514 Eggenstein-Leopoldshafen 2 (FRG), on quoting the depository number CSD-54208, the names of the authors, and the journal citation.

Optically Active Isoprene(tricarbonyl)iron(0) and Methyltrimethylenemethane(tricarbonyl)iron(0)**

By *Dag Kappes, Hans Gerlach,* Peter Zbinden, Max Dobler, Wilfried A. König, Ralph Krebber,* and *Gerhard Wenz*

About thirty acyclic chiral 1,3-diene(tricarbonyl)iron(0) complexes have so far been prepared in optically active form.[1] Only in the case of two compounds[2,3], however, has the absolute configuration of the tricarbonyliron(0) complex been determined by X-ray structure analysis of a derivative. We report here on the first synthesis of (+)-tricarbonyl(η^4-2-methyl-1,3-butadiene)iron(0) (+)-**1** and (−)-tricarbonyl(η^4-2-methylene-1,3-butanediyl)iron(0) (−)-**2** from the ester (+)-**3**.



1 2

The ester (+)-**3** was prepared by reaction of (±)-tricarbonyl(η^4-2-methylene-3-buten-1-ol)iron(0) (±)-**4**[4] with (−)-(1*S*,4*R*)-camphanoyl chloride[5] in pyridine and isolated as pure diastereomer (m.p. 127.7–129.3 °C) by twofold recrystallization from cyclohexane. An X-ray structure analysis of (+)-**3** showed[6] that it is the (1*S*,4*R*)-camphanoate of (+)-(2*S*,3*R*)-**4** (Fig. 1), i.e. the chirality sense in the tricarbonyliron moiety of the complex can be derived from the observed structure.

Reduction of (+)-**3** with BF_3 and Et_3SiH in dichloromethane at −78 °C leads to formation of (−)-**2** and (+)-**1** in the ratio 91:9. During this ionic hydrogenation[7] the carbocation generated from (+)-**3** with BF_3 is trapped mainly by hydride transfer to C4. The ^{1}H-NMR spectrum of (−)-**2** is identical to that reported by *Ehrlich* and *Emerson*[8] for (±)-**2**. The main product (−)-**2** isomerizes quantitatively to (+)-**1** within 5 min in 85% H_2SO_4 (cf. Ref. [8]) at 25 °C, probably by a protonation-deprotonation reaction.

König et al.[9] recently introduced new alkylated cyclodextrins as stationary phases in capillary chromatography, and they have been found to be excellently suitable for the analytical separation of enantiomers. Signals separated to the base line can be obtained for the enantiomers of **1** and **2** on a 50 m × 0.25 mm glass capillary column coated with octakis-

[*] Prof. Dr. H. Gerlach, Dipl.-Chem. D. Kappes
Laboratorium für Organische Chemie der Universität
Postfach 10 12 51, D-8580 Bayreuth (FRG)
Dipl.-Chem. P. Zbinden, Prof. Dr. M. Dobler
Laboratorium für Organische Chemie
der Eidgenössischen Technischen Hochschule
Universitätstrasse 16, CH-8092 Zürich (Switzerland)
Prof. Dr. W. A. König, Dipl.-Chem. R. Krebber
Institut für Organische Chemie der Universität
Martin-Luther-King-Platz 6, D-2000 Hamburg 13 (FRG)
Dr. G. Wenz
Max-Planck-Institut für Polymerforschung
Jakob-Welder-Weg 11, D-6500 Mainz (FRG)

[**] This work was supported by the Fonds der Chemischen Industrie, by the Schweizerische Nationalfonds zur Förderung der Wissenschaftlichen Forschung and by the Bundesminister für Forschung und Technologie (Project No. 0319134A, "Polysaccharidforschung").

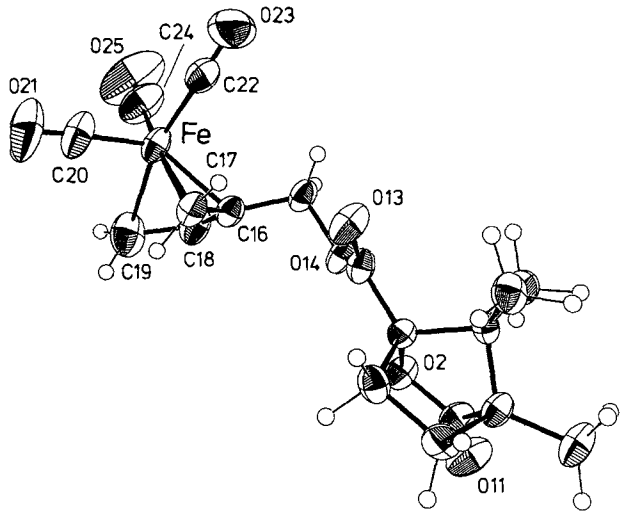


Fig. 1. Structure of **3** in the crystal (ORTEP, vibration ellipsoids with 50% probability); selected bond lengths [Å] and angles [°]: Fe-C16 2.040(4), Fe-C17 2.100(4), Fe-C18 2.058(5), Fe-C19 2.114(6), Fe-C20 1.778(4), Fe-C22 1.775(5), Fe-C24 1.811(5), C20-O21 1.137(5), C22-O23 1.144(7), C24-O25 1.126(6); Fe-C20-O21 177.8(7), Fe-C22-O23 179.1(6), Fe-C24-O25 177.7(6).

(2,3,6-tri-*O*-pentyl)-γ-cyclodextrin (Fig. 2).[10] The smooth separation of these unpolar enantiomers is indicative of an interaction with the inside of the cavity of the perpentylated γ-cyclodextrin (inclusion).

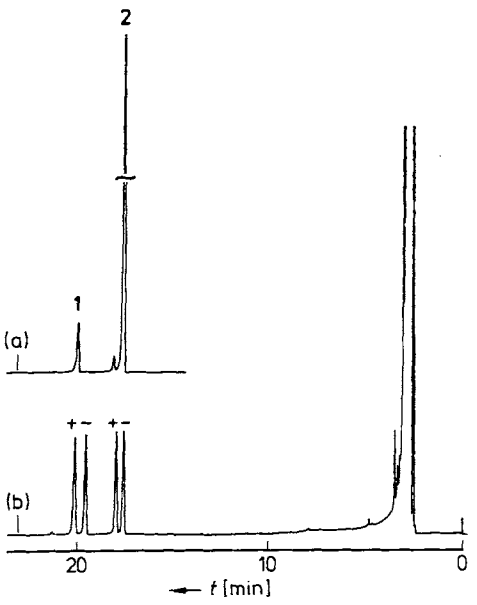


Fig. 2. a) Determination of the enantiomeric excess of the samples of (+)-**1** and (−)-**2**. b) For comparison chromatograms of (±)-**1** and (±)-**2** (50 m glass capillary column coated with perpentyl-γ-cyclodextrin, at 80 °C with hydrogen (1 bar) as carrier gas).

Using this method of separation the enantiomeric excess in the case of (−)-**2**, $[\alpha]_D = -68$, was found to be 96% *ee* and in the case of (+)-**1**, $[\alpha]_D = +63$, to be 88% *ee*. The ionic hydrogenation at −78 °C and the subsequent isomerization in H_2SO_4 apparently proceed almost without racemization. If both reactions are carried out at 25 °C, (−)-**2** is formed with 58% *ee* and—by subsequent isomerization—(+)-**1** with 54% *ee*, i.e. the carbocation intermediate of the ionic hydrogenation partially racemizes, presumably by rotation about the C2–C3 bond, before it is reduced by Et_3SiH. The maximum specific rotation of the pure enantiomers (+)-**1** and (−)-**2** can be calculated from the measured rotation values and the gas-chromatographically determined enantiomeric ratios to be $[\alpha]_D = +72$ ($CHCl_3$) and -71 ($CHCl_3$), respectively.

If it is assumed that the orientation of the organic ligands does not change during the ionic hydrogenation and acid-catalyzed isomerization, the (3*R*)-chirality sense for (−)-**2** and (2*S*,3*R*)-chirality sense for (+)-**1** can be derived from the known absolute configuration of the ester (+)-**3**, as given in the formula scheme.

It was of special interest to record the CD spectra of the complexes **1** and **2**.[11] The isoprene complex (+)-**1** shows two Cotton effects of opposite sign at 365 and 309 nm, while the complex (−)-**2** likewise shows two Cotton effects of opposite sign at 320 and 245 nm; these effects are presumably (cf. Ref. [3]) due to dissymmetrically perturbed iron d→d transitions. Both complexes show a strong negative Cotton effect at ca. 205 nm which can be ascribed to d → π* transitions.

Experimental

2: BF_3 gas was passed for ca. 5 min through a solution of (+)-**3** (1.007 g, 2.49 mmol) and Et_3SiH (730 mg, 6.3 mmol) in CH_2Cl_2 (30 mL) under N_2. After 2 hours' stirring at −78 °C the solution was treated with 20 mL of 2 N KOH and the resulting mixture, after warming, was extracted twice with 20 mL of CH_2Cl_2. The organic phases were washed with H_2O, filtered through a 5 cm-thick layer of silica gel, and evaporated down: 475 mg (91%) of (−)-**2** and (+)-**1** in the ratio 91:9 (GC). Chromatographic separation on silica gel with pentane afforded pure (−)-**2**, b.p. = 60 °C/10 torr; $[\alpha]_D = -68°$ ($c = 1.0$, $CHCl_3$).—UV (CH_3CN): $\varepsilon(\lambda[nm]) = 13000$ (240, shoulder).—CD (CH_3CN): $\Delta\varepsilon_{max}$ (λ[nm]) = −0.88 (320), +2.2 (245), −7 (206). −^{1}H-NMR (300 MHz, $CDCl_3$): $\delta = 1.33$ (d, $J = 6.8$ Hz, 3H), 1.61 (d, $J = 4.4$ Hz, 1H), 1.74 (s, 1H), 2.14 (d, $J = 2.3$ Hz, 1H), 2.53 (d, $J = 4.4$ Hz, 1H), 3.06 (qd, $J = 6.8$, 2.3 Hz, 1H).—^{13}C-NMR (75.5 MHz, $CDCl_3$): $\delta = 15.0$(q), 50.2(t), 52.3(t), 73.2(d), 103.9(s), 211.0(s), 211.5(s), 212.0(s).

1: The yellow solution of (−)-**2** (175 mg, 0.83 mmol) in 85% H_2SO_4 (2 mL), after 5 min at 25 °C, was diluted with 20 mL of H_2O and extracted twice with 30 mL of pentane. Residue from the organic phases: 95 mg (55%) (+)-**1** (after GC pure), b.p. = 60 °C/10 torr; $[\alpha]_D = +63°$ ($c = 0.9$, $CHCl_3$).—UV (CH_3CN): ε_{max} (λ[nm]) = 2100 (285).—CD (CH_3CN): $\Delta\varepsilon_{max}$ (λ[nm]) = −0.37 (365), +1.95(309), −8.0(202).—^{1}H-NMR and ^{13}C-NMR spectra ($CDCl_3$) identical to those given for (±)-**1** [12].

Received: July 26, 1989 [Z 3468 IE]
German version: *Angew. Chem. 101* (1989) 1744

CAS Registry numbers:
(+)-**1**, 123877-51-0; (−)-**2**, 123808-82-2; (+)-**3**, 123751-47-3; **4**, 82764-13-4; Et_3SiH, 617-86-7; (−)-(1*S*, 4*R*)-camphanoyl chloride 39637-74-6.

[1] R. Grée, *Synthesis 1989*, 341, and references cited therein.
[2] A. Monpert, *Dissertation*, Université de Rennes 1983, see Ref. [1].
[3] N. W. Alcock, D. H. G. Crout, C. M. Henderson, S. E. Thomas, *J. Chem. Soc. Chem. Commun. 1988*, 746.
[4] M. Franck-Neumann, D. Martina, M. Heitz, *J. Organomet. Chem. 301* (1986) 61.
[5] H. Gerlach, *Helv. Chim. Acta 68* (1985) 1815; *ibid. 51* (1968) 1587.
[6] (+)-**3**: yellow platelets from diethyl ether, single crystal (0.5 × 0.4 × 0.2 mm^3), monoclinic, space group $P2_1$, $a = 6.262(2)$, $b = 6.804(2)$, $c = 21.828(6)$ Å, $\beta = 90.79(2)°$, $V = 925.6(8)$ Å^3, $\varrho_{calc} = 1.450$ g cm^{-3}, Enraf-Nonius CAD-4 diffractometer, $Mo_{K\alpha}$ radiation, graphite monochromator, (2θ-ω) scan with $2\theta \leq 60°$, 2825 independent reflections, 2475 with $I > 3\sigma(I)$. Solution of structure: direct methods (Program SHELX 86, G. Sheldrick, Göttingen 1986), refinement by full matrix least squares method for 314 parameters (Program SHELX 76, G. Sheldrick, Göttingen 1976), all non-H atoms refined anisotropically and all H atoms isotropically with fixed C–H = 1.09 Å, $R = 0.040$ ($R_w = 0.037$, $w = \sigma^2(F_0)^{-1}$), maximal residual electron density = 0.36 eÅ^{-3}, minimal residual electron density −0.79 eÅ^{-3}. Further details of the crystal structure investigation are

available on request from the Director of the Cambridge Crystallographic Data Centre, University Chemical Laboratory, Lensfield Road, GB-Cambridge CB2 1EW, on quoting the full journal citation.
[7] M. Brossi, C. Ganter, *Helv. Chim. Acta 71* (1988) 848; M. G. Adlington, M. Orfanopoulos, J. L. Fry, *Tetrahedron Lett. 1976*, 2955; D. N. Kursanov, Z. N. Parnes, N. M. Loim, *Synthesis 1974*, 633.
[8] K. Ehrlich, G. F. Emerson, *J. Am. Chem. Soc. 94* (1972) 2464.
[9] W. A. König, *Nachr. Chem. Techn. Lab. 37* (1989) 471, and references cited therein.
[10] The preparation was accomplished analogously to that of perpentylated α-cyclodextrin [9].
[11] Recorded with a spectropolarimeter JASCO J600. We thank Prof. Dr. *G. Snatzke* (Bochum) for the measurements.
[12] C. M. Adams, G. Cerioni, A. Hafner, H. Kalchhauser, W. von Philipsborn, A. Schwenk, *Helv. Chim. Acta 71* (1988) 1116.

Copper(I)-Assisted Formation of an "Organic" Sandwich Structure: Structural Prerequisites for Luminescence of the Dinuclear Complexes [(μ-Bipyrimidine){Cu(PR$_3$)$_2$}$_2$]X$_2$**

By *Conny Vogler, Hans-Dieter Hausen, Wolfgang Kaim,* Stephan Kohlmann, Horst E. A. Kramer,* and *Jochen Rieker*

Weak inter- or intramolecular interactions, especially when combined and integrated into appropriate molecular "architecture", can lead to the formation of supramolecular structures with specific functionality.[1] Here we report a system that, owing to such interactions in the solid, shows strong luminescence from a metal-to-ligand charge-transfer (MLCT) excited state.

[(μ-bpym){Cu(PR$_3$)$_2$}$_2$](BF$_4$)$_2$ **1**

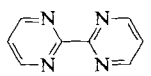
R = C_6H_5 (**a**), C_6D_5 (**b**), *o*-$C_6H_4CH_3$ (**c**), *m*-$C_6H_4CH_3$ (**d**), *p*-$C_6H_4CH_3$ (**e**), C_6F_5 (**f**), *p*-C_6H_4Cl (**g**), *p*-$C_6H_4N(CH_3)_2$ (**h**)

[(μ-bpym){Cu(PRR'$_2$)$_2$}$_2$](BF$_4$)$_2$ **2**

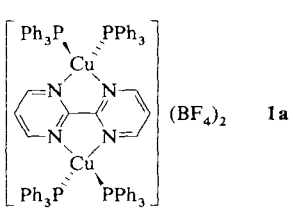
R = H, R' = C_6H_5; R = CH_3, R' = C_6H_5; R = *p*-$C_6H_4CH_3$, R' = CH_3

[(μ-bpym){Cu(Ph$_2$P(CH$_2$)$_n$PPh$_2$)}$_2$](BF$_4$)$_2$ **3**, n = 1–5

bpym =



Compounds **1**–**3**, which belong to the class of homodinuclear complexes containing the bridging ligand 2,2'-bipyrimidine (bpym),[2] can be synthesized by conventional procedures.[3] Compound **1a** exhibits a long-wavelength MLCT absorption band—$d^{10}(Cu) \rightarrow \pi_1^*$(bpym)—at λ_{max} = 438 nm (sh, lg ε ≈ 3.5) (see Fig. 1); π_1^*(bpym), the LUMO of **1a**, can also be populated electrochemically (E_{red} = −0.66 V vs. SCE in dichloromethane) and the resulting radical anion can be identified by absorption[4a] and ESR spectroscopy.[4b]



(BF$_4$)$_2$ **1a**

In the solid state, **1a**·CH_3OH·H_2O displays a surprisingly strong luminescence (Fig. 1), which is not as intense either in

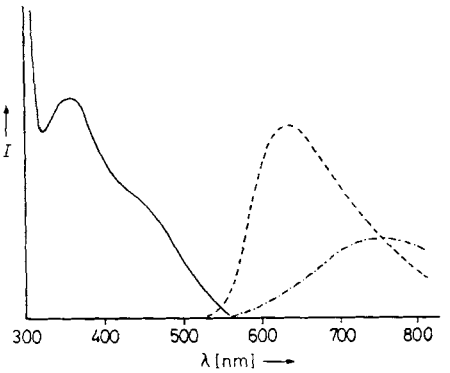


Fig. 1. **1a**: Absorption spectrum in $CHCl_3$ (—; λ_{max} = 357, 438 nm (sh)) as well as emission spectra in the solid state (– – –: λ_{max} = 630 nm) and ca. 10^{-4} M in $CHCl_3$ solution (–·–·–; λ_{max} = 758 nm), excitation with λ = 436 nm. Intensities not shown to scale.

solution (Fig. 1) or after anion exchange ($BF_4^{\ominus} \rightarrow PF_6^{\ominus}$, $ClO_4^{\ominus}$) or when most other monodentate phosphane ligands PR_3 (**1c, e–h, 2**) are used. Only complexes **1b**[5] and **1d**, in addition to the arsenic analogue of **1a**, show similar luminescence; of the complexes **3**, containing bidentate chelate ligands, only the complex with the 1,5-bis(diphenylphosphino)pentane ligand (n = 5) luminesces in the solid state.

Although luminescence has been observed for mononuclear complexes $[LCu(PPh_3)_2]^{\oplus}$ with L = 2,2-bipyridine or 1,10-phenanthroline derivatives, as well as similar ligands,[3] dinuclear bpym complexes with metal centers having d^6 configurations do not emit at all (Re^{I}[2b]) or only very weakly (Ru^{II},[2c] Mo^{0}[2a]).

The crystal structure analysis of **1a** (Fig. 2)[6] reveals the special prerequisites for solid-state luminescence. It is obvious that the intramolecular (562.2 pm)[7] and intermolecular (≥ 953.3 pm) metal–metal distances are appreciably greater than those in luminescing copper(I) halide clusters.[8] The space above and below the bpym bridging ligand of **1a** is just sufficient, however, to allow one (donor) phenyl ring of a triphenylphosphane ligand to interact in a π fashion with each side of the π-acceptor heterocycle. This results in a considerable distortion of the ligands from tetrahedral geometry around copper. The dihedral angles between the bpym plane and the Cu–P bonds are 98.0° for the two triphenylphosphane ligands involved in π coordination and 139.4° for the others. The angles between the best planes of the "organic" sandwich structure phenyl/bpym/phenyl are approximately 14°; the shortest atom–atom distance between the sandwich rings is only 315.0 pm for C1-C56. This value is significantly smaller than the sum of the van der Waals radii.

Phosphorus ligands with other aryl substituents are apparently no longer able to adopt the arrangement shown in Figure 2, which is required for π coordination of the bpym ligand, because of transannular repulsion between the

[*] Prof. Dr. W. Kaim, Dipl.-Chem. C. Vogler, Dr. H.-D. Hausen, Dr. S. Kohlmann
Institut für Anorganische Chemie der Universität
Pfaffenwaldring 55, D-7000 Stuttgart 80 (FRG)
Prof. Dr. H. E. A. Kramer, Dr. J. Rieker
Institut für Physikalische Chemie der Universität Stuttgart

[**] This work was supported by the Deutsche Forschungsgemeinschaft and the Volkswagen-Stiftung.

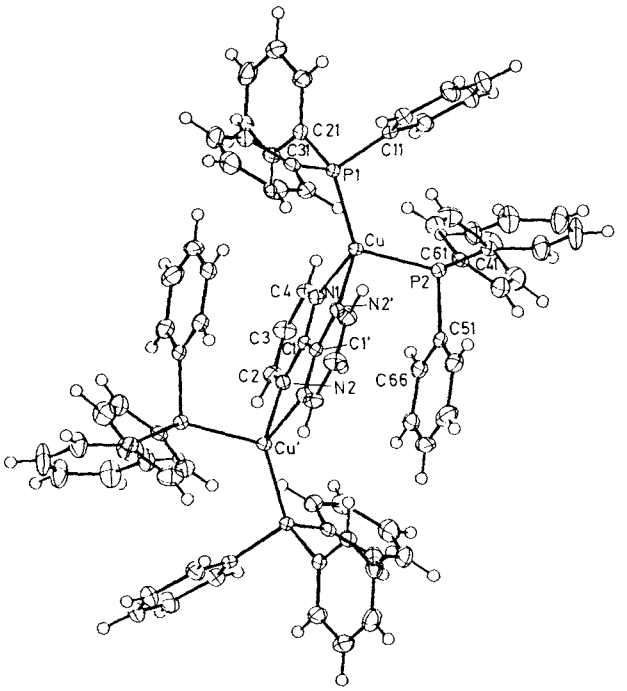


Fig. 2. Molecular structure of the dication of **1a**. Important distances [pm] and angles [°]: Cu-Cu' 562.2(1), Cu-N1 208.7(2), Cu-N2' 211.9(2), Cu-P1 223.1(1), Cu-P2 229.5(1), N1-C1 134.0(3), C1-N2 134.2(3), C1-C1' 146.1(4), N2-C2 133.5(4), C2-C3 137.1(4), C3-C4 137.9(4), C4-N1 133.1(4), P-C 181.7(4)–183.1(3); N1-Cu-N2' 79.1(1) P1-Cu-P2 122.7(<1), N1-Cu-P1 125.5(1), N1-Cu-P2 99.8(1), N2'-Cu-P1 119.9(1), N2'-Cu-P2 99.7(1), Cu-P1-C11 109.7(1), Cu-P1-C21 118.8(1) Cu-P1-C31 115.2(1), Cu-P2-C41 117.0(1), Cu-P2-C51 104.7(1), Cu-P2-C61 118.1(1), C-P-C 102.5(1)–108.1(1).

phenyl rings (*para* substituents, **1e, f, g, h**) or owing to considerable change in the cone angle[9] (*ortho* substituents, **1c, 2**). Accordingly, no luminescence is observed for those systems. On the other hand, substituents in *meta* position, as in **1d**, or the use of a bis(diphenylphosphino)alkane chelate ligand having a sufficiently large "bite" angle (**3**, n = 5, P-Cu-P ≈ 120°) do not prevent a "π-sandwich" interaction; these complexes also luminesce, especially in the solid state.

In contrast to the situation in other Cu^I complex salts with $BF_4^\ominus$ as counterion,[10] this anion is not disordered in crystals of **1a**·CH_3OH·H_2O; rather long distances (300–305 pm) to the O atoms of the solvent molecules indicate only weak hydrogen bonds F···H-O. On replacement of $BF_4^\ominus$ by the still less basic anions $PF_6^\ominus$ or $ClO_4^\ominus$, system **1a** shows no or orders of magnitude smaller (< 1%) luminescence in the solid state.

Apparently, the flexibility possible in solution is sufficient to reduce appreciably the luminescence of **1a** (see Fig. 1). NMR and emission measurements at very low temperatures in solution should help to clarify this finding. The intense solid-state luminescence of **1a** could thus be due to the noncovalent interactions which, in combination, result in an effective decrease in molecular degrees of freedom. Thus, in contrast to the usually negative results obtained with dinuclear complexes,[2] the rate of internal conversion is dramatically decreased, radiationless deactivation is suppressed, and the intensity of luminescence therefore markedly increased.[11]

System **1a** is thus a further example[12] of the superb suitability of structurally flexible Cu^I as a "template" center for interactions between coordinated ligands.

Experimental Procedure

Dinuclear Cu^I complexes with bpym: 2,2'-Bipyrimidine (158 mg, 1 mmol) was suspended in 50 mL of methanol together with copper powder (95 mg, 1.5 mmol), $Cu(BF_4)_2$ (237 mg, 1 mmol), and PR_3 or $AsPh_3$ (4 mmol) or Ph_2P-$(CH_2)_n$-PPh_2 (2 mmol) and the mixture was refluxed for approximately 1 h. After filtration of the hot reaction mixture, the product was allowed to crystallize at −15 °C and then recrystallized from methanol. Yield 60–85%; correct elemental analyses. The hexafluorophosphates and perchlorates were prepared with $[Cu(CH_3CN)_4](PF_6)$ and $Cu(ClO_4)_2$, respectively, instead of $Cu(BF_4)_2$.

Received: May 18, 1989 [Z 3345 IE]
German version: *Angew. Chem. 101* (1989) 1734

[1] J.-M. Lehn, *Angew. Chem. 100* (1988) 92; *Angew. Chem. Int. Ed. Engl. 27* (1988) 89.
[2] a) Mo^0 complexes: W. Kaim, S. Kohlmann, *Inorg. Chem. 26* (1987) 68; W. Kaim, S. Kohlmann, A. J. Lees, D. J. Stufkens, M. M. Zulu, unpublished; b) Re^I complexes: A. Vogler, J. Kisslinger, *Inorg. Chim. Acta 115* (1986) 193; c) Ru^{II} complexes: M. Hunziker, A. Ludi, *J. Am. Chem. Soc. 99* (1977) 7370.
[3] a) A. K. Ichinaga, J. R. Kirchhoff, D. R. McMillin, C. O. Dietrich-Buchecker, P. A. Marnot, J.-P. Sauvage, *Inorg. Chem. 26* (1987) 4290; b) W. Kaim, S. Kohlmann, *ibid. 26* (1987) 1469.
[4] a) P. S. Braterman, J.-I. Song, W. Kaim, C. Vogler, unpublished; b) $\mathbf{1a}^{\bullet\ominus}$: ESR coupling constants a [mT] at 300 K in CH_2Cl_2: $a(^{63}Cu/^{65}Cu)$ = 0.655, $a(^{31}P)$ = 0.655, $a(^{14}N)$ = 0.218, $a(H_{5,5'})$ = 0.437; g = 2.0017.
[5] W. Kaim, P. Hänel, H. Bock, *Z. Naturforsch. B37* (1982) 1382.
[6] Single crystals were obtained by slow cooling (65 °C → 50 °C) of a saturated solution in methanol (1% H_2O). Crystal data for **1a**·CH_3OH·H_2O: triclinic, space group $P\bar{1}$, Z = 1, a = 1192.4(2), b = 1253.7(3), c = 1457.3(3) pm, α = 65.57(2), β = 71.76(2), γ = 74.88(2)°, V = 1861.8(6) × 10^6 pm^3, μ = 7.5 cm^{-1}, ϱ_{calcd} = 1.39 g cm^{-3}. 6536 reflections were collected using a Syntex $P2_1$ diffractometer with $Mo_{K\alpha}$ radiation and a graphite monochromator for 2° < 2Θ < 50°: no absorption correction. Structure solution by Patterson synthesis; hydrogen atoms refined with isotropic thermal parameters, all other atoms with anisotropic thermal parameters (full matrix); R = 0.039 for 5395 observed reflections with $I > 2\sigma(I)$. R_w = 0.035. Further details of the crystal structure investigation may be obtained from the Fachinformationszentrum Karlsruhe, Gesellschaft für wissenschaftlich-technische Information mbH, D-7514 Eggenstein-Leopoldshafen 2 (FRG), on quoting the depository number CSD-53880, the names of the authors, and the journal citation.
[7] d(CuCu) ≈ 554 pm in Cu^{II} dimers of bpym: M. Julve, G. DeMunno, G. Bruno, M. Verdaguer, *Inorg. Chem. 27* (1988) 3160.
[8] J. Strähle, W. Hiller, D. Oelkrug, E. Eitel, *Z. Naturforsch. B35* (1980) 1247; cf. also A. Vogler, H. Kunkely, *J. Am. Chem. Soc. 108* (1986) 7211.
[9] C. A. Tolman, *Chem. Rev. 77* (1977) 313.
[10] D. Fenske, S. Kohlmann, J. Jordanov, W. Kaim, unpublished.
[11] T. Förster: *Fluoreszenz organischer Verbindungen*, Vandenhoeck & Ruprecht, Göttingen 1951, p. 110ff.
[12] a) J.-M. Lehn, A. Rigault, *Angew. Chem. 100* (1988) 1121; *Angew. Chem. Int. Ed. Engl. 27* (1988) 1095; b) C. O. Dietrich-Buchecker, J.-P. Sauvage, *ibid. 101* (1989) 192 and *28* (1989) 189.

Ta_2Se: A Tantalum-Rich Selenide with a New Layer Structure

By *Bernd Harbrecht**

Preparative investigations on tantalum-rich systems containing, as additional components, a metal M of the iron group and sulfur or selenium have led to $M_2Ta_9S_6$ and $M_2Ta_{11}Se_8$, novel intermetallic compounds with remarkable structural[1] and electronic[2] properties. Chalcogenides with extended three-dimensional bonding networks[3] have been found to consist of strikingly open clusterlike structures, penetrated by channels surrounded by chalcogen atoms. The binary tantalum sulfides Ta_2S and Ta_6S, the latter of which forms monoclinic crystals,[4] have completely different struc-

[*] Dr. B. Harbrecht
Fachbereich Chemie der Universität
Otto-Hahn-Strasse 6, D-4600 Dortmund 50 (FRG)

tures. Their metal frameworks consist of distorted, centered Ta_{13} icosahedra, which extend along a "fivefold axis of symmetry" to form chains, $^{1}_{\infty}[TaTa_{10/2}]$. New representatives of this class are the substitutional phases $M_xTa_{6-x}S$ (M = V, Cr; $x \leq 2.5$),[5] the triclinic modification of Ta_6S,[6] and $Ta_3S_{1.8}$.[7]

Similarly reduced tantalum selenides were previously unknown: TaSe, $Ta_{1.64}Se_2$, and Ta_2Se_3 are the most selenium-poor phases so far reported.[8] By reduction of $TaSe_2$ with tantalum in the melt, we were able to prepare Ta_2Se for the first time. Its simple structure reflects the unprecedented bonding in such metal-rich compounds.[3]

To synthesize Ta_2Se, a pellet (approximately 1 g) of Ta and $TaSe_2$, the latter formed from the elements (Ta:Se 2:1) in an evacuated and sealed quartz tube at 1170 K, was fused for a short period on both sides in an arc (35 V, approximately 60 A) on a water-cooled copper block under argon (0.11 Pa). Under these conditions, material loss caused by vaporization of selenium is less than 0.8%. The product, which has a metallic luster, decomposes slowly on exposure to air. In agreement with the single-crystal X-ray structure analysis,[9] examination of Guinier photographs of Ta- and Se-rich specimens reveals no evidence of a significant phase width.

Crystalline Ta_2Se represents a new structural type (Table 1), which is symmetry-related to the cubic, body-centered

Table 1. Structural parameters of Ta_2Se [9]: space group $P4/nmm$-D^7_{4h} (No. 129), $Z = 2$; $a = 337.5(1)$, $c = 983.2(1)$ pm; all atoms occupy the positions 2c (4mm symmetry): 1/4 1/4 z (center of inversion at the origin); B_{eq} in 10^4 pm^2, U_{ii} in pm^2, $U_{ij} = 0$.

Atom	z[a]	B_{aq}	U_{11}	U_{33}
Ta1	0.0776(2) [1/12]	0.36(2)	46(5)	44(8)
Ta2	0.7553(3) [3/4]	0.54(2)	63(6)	79(9)
Se1 [Ta3]	0.3665(6) [5/12]	0.70(6)	80(10)	110(20)

[a] For comparison, the positional parameters of bcc-Ta, transformed according to $P4/nmm$, are given in brackets [10].

modification of tantalum (bcc-Ta).[10] Viewed in terms of bcc-Ta, the structure of Ta_2Se can formally be regarded as an "ordered substitution phase" or as an "insertion phase". After every four Ta layers—the sequence corresponds to that along a in bcc-Ta—two Se layers are inserted (Fig. 1). The slightly oxidized metallic regions are formed by the Ta1 atoms, which, in each case, are surrounded by 13 Ta atoms (4×283.3, 4×289.7, 1×316.9, 4×337.5 pm) and one Se atom (284.1 pm). The peripheral layers adjacent to the Se atoms are formed from Ta2. They have four Se atoms (267.0 pm) and nine Ta atoms (4×289.7, 316.9, $4 \times$ 337.5 pm) as nearest neighbors. The Se atoms, which complete the coordination number to 14, lie in adjacent Se-Ta-Ta-Ta-Ta-Se networks. The Ta–Se separations (382.2 pm) are too large for Ta–Se bonds, which would lead to interpenetration of the layers. The structurally different functions of the Ta atoms are also revealed in the average distances Ta1-Ta (304.5 pm) and Ta2-Ta (313.6 pm); these differences are not as striking, however, as those in Ta_2S (289 and 314 pm).[4]

The greater distortions of the body-centered packing compared with those in the bcc-Ta fragments are revealed in specific displacements of the Se layers (cf. Table 1). The acentric coordination geometry about Se clearly indicates the disruption of the structure between the Se layers; there are strong bonds, such as that for atom Se3 in $Fe_2Ta_{11}Se_8$ ($< d$(Ta-Se)$> = 270.1$ pm[11]), to only five Ta atoms ($4 \times$ 267.0, 284.1 pm) of a tantalum fragment. The shortest distance between Se atoms of neighboring layers is 354.7 pm.

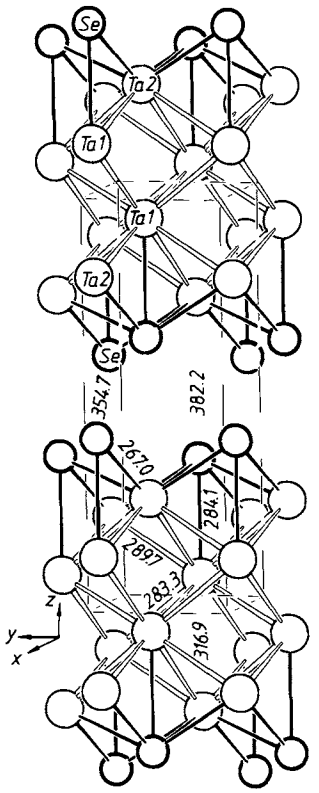


Fig. 1. SCHAKAL plot of the structure of Ta_2Se; atoms less than 315 pm apart are joined by lines.

Apparently, van der Waals interactions are responsible for holding together the Se–4Ta–Se networks.

According to these findings, Ta_2Se cannot be assigned structurally to the homomorphic ternary nitrides of the CrNbN type.[11] Their metal partial structure is isotypic to γ-CuTi,[12] likewise a bcc-related AB structure of the same symmetry. The N atoms occupy gaps within the distorted octahedra, which, in CrNbN, are formed by five Nb atoms and one Cr atom. In terms of the symmetry relationship to the bcc arrangement, the ideal $c:a$ ratio is 2 for γ-CuTi (γ-CuTi, 1.905; CaGaN, 2.117[13]), but 3 for Ta_2Se (actual value: 2.957).

Ta_2Se may be assigned to the class of quasi-two-dimensional materials and is the most metal-rich representative so far known. Its electronic properties should be of great interest (e.g., see Ref. [14]).

Received: May 23, 1989 [Z 3355 IE]
German version: *Angew. Chem. 101* (1989) 1696

[1] B. Harbrecht, H. F. Franzen, *J. Less-Common Met. 115* (1986) p. 177; B. Harbrecht, *ibid. 124* (1986) 125; *ibid. 141* (1988) 59.
[2] M. J. Calhorda, R. Hoffmann, *Inorg. Chem. 27* (1988) 4679.
[3] H. F. Franzen, *Prog. Solid State Chem. 12* (1978) 1; A. Simon, *Angew. Chem. 93* (1981) 23; *Angew. Chem. Int. Ed. Engl. 20* (1981) 1; B. Harbrecht, *Habilitationsschrift*, Universität Dortmund 1989.
[4] H. F. Franzen, J. G. Smeggil, *Acta Crystallogr. Sect. B 25* (1969) 1736; *ibid. B 26* (1970) 125.
[5] B. Harbrecht, H. F. Franzen, *Z. Anorg. Allg. Chem. 551* (1987) 74; B. Harbrecht, *Vortragstag. Fachgruppe Festkörperchemie (Ges. Dtsch. Chem.) 6th*, Erlangen 28–30 September 1988.
[6] B. Harbrecht, *J. Less-Common Met. 138* (1988) 225.
[7] H. Wada, M. Onoda, *Mater. Res. Bull. 24* (1989) 191.
[8] E. Revolinsky, B. E. Brown, D. J. Beerntsen, C. H. Armitage, *J. Less-Common Met. 8* (1965) 63; E. Bjerkelund, A. Kjekshus, *Acta Chem. Scand. 21* (1967) 513; R. Huisman, F. Kadijk, F. Jellinek, *J. Less-Common Met. 12* (1967) 423; *ibid. 21* (1970) 187.

[9] Crystal structure analysis: four-circle diffractometer CAD 4 B (Enraf-Nonius), $Ag_{K\alpha}$, graphite monochromator; Structure Determination Package (*B. A. Frenz*); graphics, SCHAKAL (*E. Keller*); crystal dimensions, $0.20 \times 0.10 \times 0.02$ mm^3, ω-2θ scans, $2\theta_{max} = 44°$, 652 reflections ($\pm h,k,l$), empirical absorption correction, $R_{int}(F_0) = 0.034$, 97 unique reflections with $I_0 \geq 1\,\sigma\,(I_0)$, 11 variables ($k_{ext} = 2.20 \times 10^{-7}$); $R(F_0)/R_w$ ($w = 1$) = 0.038/0.042; max. residual charge density normalized to ϱ_{max} (Se) = 0.027. Further details of the crystal structure investigation may be obtained from the Fachinformationszentrum Karlsruhe, Gesellschaft für wissenschaftlich-technische Information mbH, D-7514 Eggenstein-Leopoldshafen 2 (FRG), on quoting the depository number CSD-54191, the names of the authors, and the journal citation.

[10] bcc-Ta, after threefold minimal symmetry reduction ($I\ 4/m\ \bar{3}\ 2/m - t(3) \rightarrow I\ 4/m\ 2/m\ 2/m - k(2) \dashrightarrow -e(3)\,[c' = 3c] \rightarrow P\ 4/n\ 2_1/m\ 2/m$) can be placed in the space group of Ta_2Se. The cubic symmetry is then restored when the z parameter of the three otherwise unique Ta positions (position $2c$: 1/4 1/4 z) is 1/12, 5/12, 9/12 and $c = 3a$.

[11] D. H. Jack, K. H. Jack, *J. Iron Steel Inst. London 210* (1972) 790.

[12] N. Karlsson; *J. Inst. Met. 79* (1951) 391.

[13] P. Verdier, P. L'Haridon, M. Maunaye, R. Marchand, *Acta Crystallogr. Sect. B30* (1974) 226.

[14] G. Hutiray, J. Sólyom (Eds.): *Charge Density Waves in Solids, Lect. Notes Phys. 217* (1985).

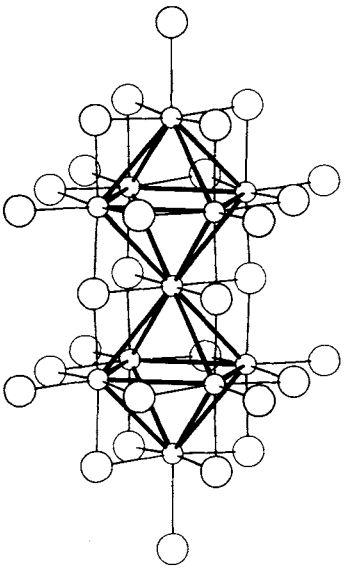


Fig. 1. $Nb_{11}O^i_{20}O^a_8F^a_2$ clusters in the compound $K_4Al_2Nb_{11}O_{20}F$. The O^i atoms lie above the edges, the O^a atoms above the vertices of the highlighted Nb_6 octahedron; the F^a atoms are located at the top and bottom of the cluster.

$K_4Al_2Nb_{11}O_{20}F$—The Missing Link in Cluster Condensation

By *Arndt Simon,* Jürgen Köhler, Robert Tischtau,* and *Gordon Miller*

Dedicated to Professor Reginald Gruehn on the occasion of his 60th birthday

Condensed metal clusters, that is, clusters linked by metal–metal bonds, are present in numerous compounds.[1] Particularly common are octahedral M_6 units joined to form one-, two-, and three-dimensional networks. These units are surrounded by nonmetal atoms above free edges or faces in such a way that M_6X_{12} and M_6X_8 clusters result.[2] The first steps of condensation have already been accomplished, namely, the synthesis and characterization of "oligomeric" clusters, though only those in which the octahedra are condensed through faces[3–5] or edges.[6–10] For nearly five years, we have attempted to realize the last remaining variant, condensation through the octahedral vertices. This "missing link"[11] has now been found in the compound $K_4Al_2Nb_{11}O_{20}F$.[12]

Figure 1 shows the discrete $Nb_{11}O^i_{20}O^a_8F^a_2$ clusters (for terminology see Ref. [2]) present in the structure of $K_4Al_2Nb_{11}O_{20}F$. These clusters contain two $Nb_6O^i_{12}$ units connected through the vertices of the Nb_6 octahedra.[13] All free octahedral vertices are coordinated by further O or F atoms (O^a, F^a). In the crystal, these clusters are linked to form $[Nb_{11}O^i_{12}O^{i-a}_{8/2}]O^{a-i}_{8/2}F^{a-a}_{2/2}$. The $Al^{3\oplus}$ ions occupy tetrahedral voids in the anion packing, and the $K^{\oplus}$ ions are surrounded cuboctahedrally by ten $O^{2\ominus}$ ions, one $F^{\ominus}$ ion, and one $K^{\oplus}$ ion (d_{K-K} = 330.5 pm). The $F^{\ominus}$ ion cannot be located unambiguously by X-ray analysis. The marked change in the c axis on introduction of $F^{\ominus}$ (cf. Ref. [12]), as well as summation of bond strengths, indicates that the $F^{\ominus}$ ion lies at the terminal, bridging X^{a-a} positions (Fig. 1). The electron count reveals that 24 electrons occupy M–M bonding states in the cluster. This experimental finding is in good agreement with extended Hückel MO calculations.[14]

Figure 2 shows the orbital correlations for the M–M bonding orbitals in the Nb_6O_{12} and $Nb_{11}O_{20}$ clusters. The condensation of two Nb_6O_{12} clusters raises the energy of an

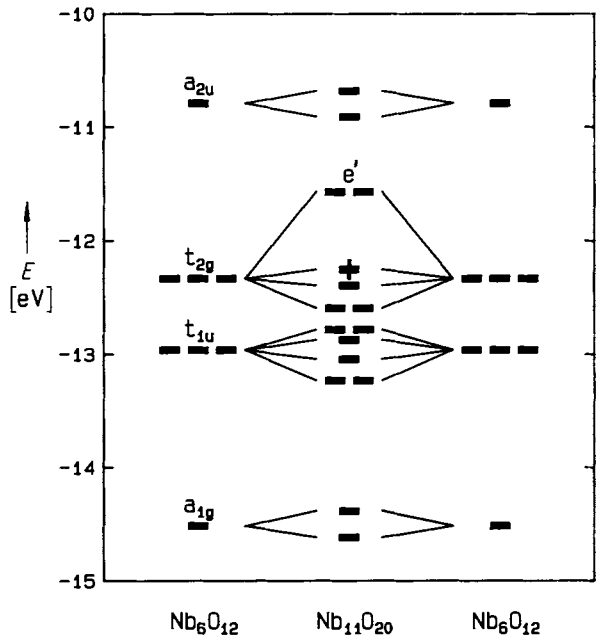


Fig. 2. Correlation of the MO diagram for the $Nb_{11}O_{20}$ cluster with the energy states of the isolated Nb_6O_{12} cluster.

e' orbital, arising from the bonding t_{2g} state of the octahedron, by nearly 0.9 eV. This is due, on the one hand, to an enhancement of the Nb–O^*_π interaction for the O atoms between the two octahedra and, on the other, to a weakening of the Nb–Nb bonding character of this orbital owing to the symmetry-determined node at the central Nb atom. Therefore, twelve low-lying M–M bonding orbitals are obtained; these can accept 24 electrons for maximum electronic stabilization.

In contrast to the large number of structures in which clusters of the M_6X_8 type, condensed through octahedral vertices, are present,[1,9] only a few examples involving the corresponding condensation of clusters of the M_6X_{12} type are known. Nonetheless, for the oxides, these examples rep-

[*] Prof. Dr. A. Simon, Dr. J. Köhler, R. Tischtau, Dr. G. Miller
Max-Planck-Institut für Festkörperforschung
Heisenbergstrasse 1, D-7000 Stuttgart 80 (FRG)

resent a nearly continuous series from discrete M_6X_{12} clusters toward increasing dimensionality of the cluster networks (Fig. 3).

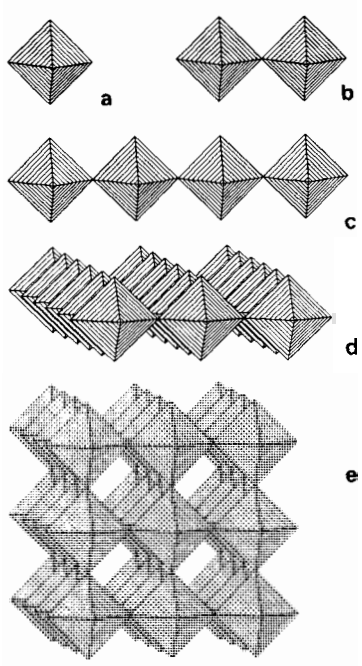


Fig. 3. Scheme for the condensation of M_6X_{12} clusters in various compounds. a) In all pictures the octahedron corresponds to the M_6 core in the M_6O_{12} cluster; b) octahedral pair in the $Nb_{11}O_{20}$ cluster; c) part of the octahedron chain in the structure of TiO (low-temperature modification); d) section of the octahedron layer in $Ba_2Nb_5O_9$; e) part of the NbO structure with octahedra linked through all vertices.

Many structures with discrete Nb_6O_{12} clusters are now known.[9, 15–21] The $Nb_{11}O_{20}$ cluster described here represents the first step in a condensation process leading, via the hypothetical oligomers of general composition $M_{5n+1}O_{8n+4}$ (n = number of octahedra), to the M_5O_8 chain, which is the only building unit in the structure of TiO (low-temperature modification).[1, 22] In the recently reported compounds $Sr_2Nb_5O_9$ and $Ba_2Nb_5O_9$, Nb_6O_{12} clusters are condensed through four octahedral vertices to form layers.[23, 24] The linking of all octahedral vertices according to $Nb_{6/2}O_{12/4}$ leads ultimately to the structure of NbO.[2] The existence of a "phasoid" in the Ba/Nb/O system with disordered fragments of the NbO structure in a perovskite matrix[24, 25] points to the possible existence of many other intermediates.

Received: July 17, 1989 [Z 3445 IE]
German version: *Angew. Chem. 101* (1989) 1695

[1] A. Simon, *Angew. Chem. 93* (1981) 23; *Angew. Chem. Int. Ed. Engl. 20* (1981) 1.
[2] H. Schäfer, H. G. Schnering, *Angew. Chem. 76* (1964) 833.
[3] M. Potel, R. Chevrel, M. Sergent, M. Decroux, Ø. Fischer, *C.R. Acad. Sci. Ser. C 288* (1979) 429.
[4] R. Chevrel, P. Gougeon, M. Potel, M. Sergent, *J. Solid State Chem. 57* (1985) 25.
[5] R. Chevrel, M. Sergent in J. Rouxel (Ed.): *Crystal Chemistry and Properties of Materials with Quasi One-Dimensional Structures*, Reidel, Dordrecht, The Netherlands 1986, p. 315.
[6] H. Mattausch, A. Simon, E.-M. Peters, *Inorg. Chem. 25* (1986) 3428.
[7] A. Simon, W. Mertin, H. Mattausch, R. Gruehn, *Angew. Chem. 98* (1986) 831; *Angew. Chem. Int. Ed. Engl. 25* (1986) 845.
[8] S. J. Hibble, A. K. Cheetham, A. R. L. Bogle, H. R. Wakerley, D. E. Cox, *J. Am. Chem. Soc. 110* (1988) 3295.
[9] A. Simon, *Angew. Chem. 100* (1988) 163; *Angew. Chem. Int. Ed. Engl. 27* (1988) 159.
[10] R. Dronskowski, A. Simon, *Angew. Chem. 101* (1989) 775; *Angew. Chem. Int. Ed. Engl. 28* (1989) 758.
[11] Like, for example, the coelacanth (*Crossopterygia*, especially *Latimeria*):



[12] Dried KF (Merck, p.a.), Al_2O_3, NbO, and NbO_2 (Ventron) in a ratio of 3:1:2:8 were pressed into a pellet and then annealed for 23 d at 880 °C in an Nb capsule, sealed under Ar and protected from oxidation by a quartz ampoule. The product consisted of small, black octahedra (EDAX: Al, Nb, K) and colorless crystals (Al, K) along with microcrystalline components. The product contained 1.00 (3)% F, corresponding to the formula $K_4Al_2Nb_{11}O_{20.0}F_{0.8}$ and showed only small amounts of other phases in the Guinier diagram (a = 878.6(1), c = 1263.7(1) pm). The compound exhibits temperature-independent paramagnetism between 50 and 350 K ($\chi_m \approx 1.26 \times 10^{-8}$ m^3 mol^{-1}) and is semiconducting. Under fluoride-free conditions ($KNbO_3$ (Puratronic), Al_2O_3, NbO and Nb (Alfa) in a ratio of 4:1:6:1; tablet, corundum crucible in quartz ampoule under Ar, 1 d at 1100 °C), heterogeneous product was obtained, which, according to Guinier photographs, contains much $K_4Al_2Nb_{11}O_{21}$ (a = 879.9(1), c = 1252.7(1) pm).
[13] Space group $I4/mmm$ (No. 139), Z = 2, a = 878, c = 1258 pm (CAD4 diffractometer); $Mo_{K\alpha}$; 229 reflections, 202 with $F_o \geq 3\sigma(F_o)$, $R_{(iso)}$ = 8.27, R_w(iso) = 6.09, ϱ_{calcd} = 5.35 g cm^{-3}. Further details of the crystal structure investigation may be obtained from the Fachinformationszentrum Karlsruhe, Gesellschaft für wissenschaftliche-technische Information mbH, D-7514 Eggenstein-Leopoldshafen 2 (FRG), on quoting the depository number CSD-53992, the names of the authors, and the journal citation.
[14] Details on the parameter set employed and the calculations are given in [15].
[15] J. Köhler, G. Miller, A. Simon, *Z. Anorg. Allg. Chem. 568* (1989) 8.
[16] D. M. Evans, L. Katz, *J. Solid State Chem. 6* (1973) 459.
[17] B. O. Marinder, *Chim. Scripta 11* (1977) 97.
[18] R. Burnus, J. Köhler, A. Simon, *Z. Naturforsch. B42* (1987) 536.
[19] J. Köhler, A. Simon, *Z. Anorg. Allg. Chem. 553* (1987) 106.
[20] J. Köhler, A. Simon, S. J. Hibble, A. K. Cheetham, *J. Less Common Met. 142* (1988) 123.
[21] J. Köhler and A. Simon, *Z. Anorg. Allg. Chem. 572* (1989) 7.
[22] D. Watanabe, J. R. Castles, A. Jostsons, A. S. Malin, *Acta Crystallogr. 23* (1967) 307.
[23] G. Svensson, *Mater. Res. Bull. 23* (1988) 437.
[24] G. Svensson, *Dissertation*, Stockholm 1989.
[25] G. Svensson, *Solid State Ionics*, in press.

An Electron-Rich [4]Radialene**

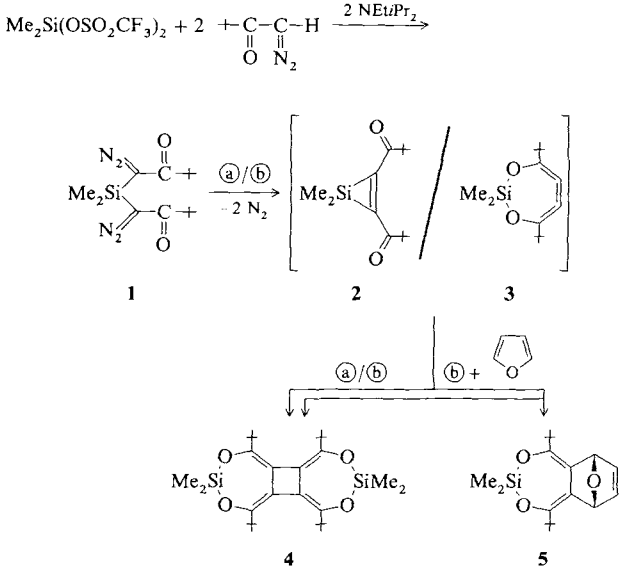
By *Antonio Fronda* and *Gerhard Maas**

[4]Radialenes (tetraalkylidenecyclobutanes), the unusual topologies of which raise questions concerning structural and spectroscopic properties as well as bonding, are relatively uninvestigated species. Besides the parent compound[1] and a series of alkyl-[2, 3] and aryl-substituted[2, 4] [4]radialenes, only scattered examples containing other substituents are known.[5] If the alkyl-substituted systems are ignored, only a few examples of electron-rich derivatives have been reported.[5d, e] Here we describe the synthesis and structure of a new electron-rich [4]radialene

[*] Prof. Dr. G. Maas, Dipl.-Chem. A. Fronda
Fachbereich Chemie der Universität
Erwin-Schrödinger-Strasse, D-6750 Kaiserslautern (FRG)

[**] This work was supported by the Deutsche Forschungsgemeinschaft and the Fonds der Chemischen Industrie.

The starting material **1**, the first bis(1-diazo-2-oxoalkyl)silane, is accessible from dimethylsilyl bis(trifluoromethanesulfonate) and 1-diazo-3,3-dimethyl-2-butanone[6] (Scheme 1). The bis-diazo compound **1**, which is relatively unstable as a pure substance, affords the [4]radialene **4** in 38% yield upon decomposition catalyzed by copper(I) trifluoromethanesulfonate in cyclohexane.[7] When palladium(II) acetate in ether is used, the reaction is appreciably slower (yield 40%).



Scheme 1. ⓐ $Cu(O_3SCF_3) \cdot 0.5\,C_6H_6$ (3 mol%)/cyclohexane/2 h. ⓑ $Pd(OAc)_2$ (6 mol%)/ether/24 h.

Possible intermediates in the formation of **4** are the diacylsilirene **2** (formally the product of an intramolecular carbene dimerization) and 1,3-dioxa-2-sila-4,5,6-cycloheptatriene (**3**). Acylsilirenes have not yet been reported. Although the direct transformation **2** → **4**, consisting of dimerization followed by a fourfold 1,3-Si (C → O) shift, cannot be excluded,[8] the pathway involving ring expansion **2** → **3** seems more plausible. The latter rearrangement can be regarded as an intramolecular variant of the insertion of carbonyl groups into the Si–C bond of silirenes.[9] Finally, the direct formation of **3** from **1**, without the intermediacy of **2**, should also be considered.[10] The ability of the strained cyclocumulene **3** to undergo thermal or metal-catalyzed[2, 3] dimerization to **4** is self-evident.

When the palladium(II) acetate–catalyzed decomposition of **1** is carried out in the presence of furan (10 molar equivalents), the tricyclic compound **5** (18%) is obtained in addition to **4** (6%). Again, it cannot be concluded with certainty whether **5** is the product of a [2+4] cycloaddition to **2** (followed by Si (C → O) shift) or, instead, to **3**.[11]

With one exception,[12] [4]radialenes substituted on the four-membered ring are known to be folded.[5f, 13] The crystal structure analysis of **4**[14] reconfirms this observation (Fig. 1). The folding angle of 35.0° (tilting of the plane C2′-C3-C3′ with respect to the plane C2′-C2-C3) lies within the range of the highest values known so far (37.4° in a tetrakis(α-methoxycarbonylbenzylidene)cyclobutane isomer,[5f] 34.7° in octaphenyl[4]radialene[13]). This strong deformation is obviously the result of minimization of steric interactions between the spatially neighboring *t*Bu groups. The same cause presumably explains the twisting (albeit small, see caption to Fig. 1) around the exocyclic C=C bonds as

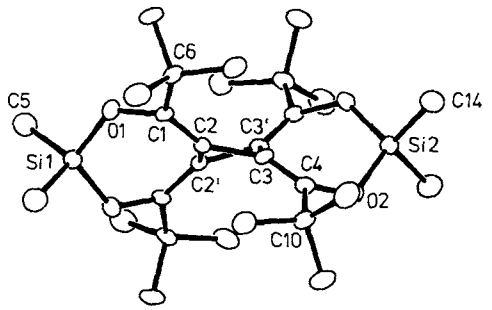
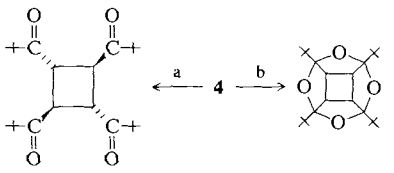


Fig. 1. Molecular structure of **4** (ORTEP). The molecule has crystallographic C_2 symmetry; the two Si atoms lie on the C_2 axis. Bond lengths [Å]: C2-C2′ 1.508(4), C2-C3 1.494(3), C2-C1 1.326(3), C3-C4 1.324(3), C1-O1 1.395(2), C4-O2 1.389(2), Si1-O1 1.638(2), Si2-O2 1.635(2); Bond angles [°]: C2′-C2-C3 87.3(1), C1-C2-C3 140.4(2), C1-C2-C2′ 126.8(2), C2-C3-C3′ 87.2(1), C2-C3-C4 140.6(2), C3′-C3-C4 127.0(2), C2-C1-C6 131.6(2), C3-C4-C10 130.9(2); Torsion angles [°]: C6-C1-C2-C3 − 6.9, O1-C1-C2-C2′ 18.6, C2-C3-C4-C10 − 5.1, C3′-C3-C4-O2 18.9, C2′-C2-C3-C3′ 24.5, C2-C3-C3′-C2′ − 24.7.

well as the pyramidalization of the cyclobutane carbon atoms (sum of angles at C2, 354.5°; at C3, 354.8°; deviation from the plane defined by the three bonding partners at C2, 0.180 Å; at C3, 0.175 Å). On the other hand, the *t*Bu-substituted C atoms nearly retain their planar coordination (sum of angles at C1, 359.4°; at C4, 359.3°).

Alkaline hydrolysis of **4** smoothly leads to tetra(1-oxoneopentyl)cyclobutane (**6**)[7] (Scheme 2); under the reaction conditions, the thermodynamically favored all-*trans* product is presumably favored. On the other hand, treatment of **4** with aqueous acid results in formation of the unusual pentacyclic polyketal **7**,[7] which displays an all-*cis* arrangement of



Scheme 2. a: MeOH, aq. NaOH (2.5 N) 1 h, 20 °C; 65% b: CH_2Cl_2/MeOH/HCl(6 N)(5/2/1), 4 h, reflux, 40%.

the substituents on the four-membered ring. The constitution of **7** is confirmed by the crystal structure analysis,[14] (Fig. 2) according to which **7** may be regarded as a tetra(oxa-

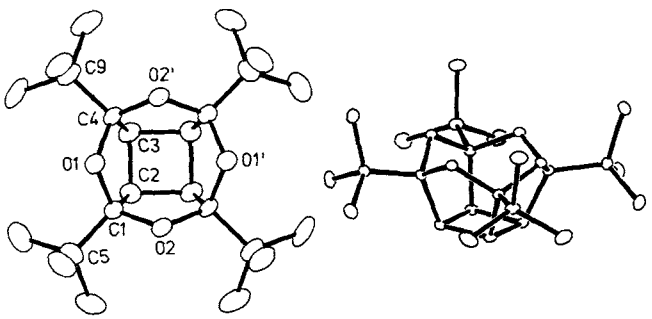


Fig. 2. Molecular structure of **7** (ORTEP). The molecule has crystallographic C_2 symmetry. Left: Viewed along the C_2 axis. Right: Viewed from the side. The average values for *d*(C–O) (1.472 Å), ∢ (C–O–C) (112.0°) and ∢ (O–C–O) (110.0°) in the crown-shaped tetraoxocane ring are significantly larger than those in isolated 1,3,5,7-tetraoxocane [17]. Further bond angles: C3-C4-C9 118.9(2), C2-C1-C5 118.9(2)°.

homo)cubane or as an oxygen analogue of [4]peristylane.[15] Furthermore, this result corroborates the constitutional assignment, based solely on the ^{1}H NMR and IR spectra, of a product obtained after ozonolysis of the *syn* dimer of tetramethylcyclobutadiene.[16]

Experimental Procedure

Dimethylsilyl bis(trifluoromethanesulfonate) (2.28 g, 6.4 mmol) was added dropwise at 0 °C to a solution of 1-diazo-3,3-dimethyl-2-butanone (1.61 g, 12.8 mmol) and ethyldiisopropylamine (2.23 mL, 12.8 mmol) in 40 mL of ether. After stirring for 5 h at room temperature, the reaction mixture was filtered and the solvent was replaced by 25 mL of cyclohexane. The resulting orange solution of **1** (IR(neat): $\tilde{\nu}$ (CN_2) = 2069 cm^{-1}) was then treated with copper(I) trifluoromethanesulfonate–benzene complex (90 mg, 0.3 mmol). After stirring for 12 h, the mixture was filtered, the solvent was removed at 20 °C/0.01 Torr, and the product was recrystallized from 4 mL of ether/methanol (1:1): 0.61 g (38%) of colorless **4** [7], m.p. 135 °C, was obtained.

Received: July 17, 1989 [Z 3450 IE]
German version: *Angew. Chem. 101* (1989) 1750

CAS Registry numbers:
1, 123624-32-8; **4**, 123624-33-9; **5**, 123624-34-0; **6**, 123624-35-1; **7**, 123624-36-2; $Me_2Si(OSO_2CF_3)_2$, 27607-78-9; $CuO_3SCF_3 \cdot 0.5\,C_6H_6$, 42152-46-5; $Pd(OAc)_2$, 3375-31-3; 1-diazo-3,3-dimethyl-2-butanone, 6832-15-1; furan, 110-00-9.

[1] a) G. W. Griffin, L. I. Peterson, *J. Am. Chem. Soc. 84* (1962) 3398; *ibid. 85* (1963) 2268; b) T. Bally, U. Buser, E. Haselbach, *Helv. Chim. Acta 61* (1978) 38; c) L. Trabert, H. Hopf, *Liebigs Ann. Chem. 1980*, 1786.
[2] M. Iyoda, S. Tanaka, H. Otani, M. Nose, M. Oda, *J. Am. Chem. Soc. 110* (1988) 8494, and references cited therein.
[3] G. Wilke, *Angew. Chem. 100* (1988) 189; *Angew. Chem. Int. Ed. Engl. 27* (1988) 185.
[4] K. Tanaka, F. Toda, *Tetrahedron Lett. 21* (1980) 2713.
[5] a) S. K. Koster, R. West, *J. Org. Chem. 40* (1975), 2300; b) H. Meier, T. Echter, O. Zimmer, *Angew. Chem. 93* (1981) 901; *Angew. Chem. Int. Ed. Engl. 20* (1981) *901*; c) B. Hagenbruch, K. Hesse, S. Hünig, G. Klug, *Liebigs Ann. Chem. 1981*, 256; d) M. Horner, S. Hünig, H.-U. Reißig, *ibid. 1983*, 658; e) T. Sugimoto, H. Awaji, Y. Misaki, Z.-i. Yoshida, Y. Kai, H. Nakagawa, N. Kasai, *J. Am. Chem. Soc. 107* (1985) 5792; f) F. W. Nader, C.-D. Wacker, H. Irngartinger, U. Huber-Patz, R. Jahn, H. Rodewald, *Angew. Chem. 97* (1985) 877; *Angew. Chem. Int. Ed. Engl. 24* (1985) 852.
[6] Analogous synthesis of (1-diazo-2-oxoalkyl)silanes: G. Maas, R. Brückmann, *J. Org. Chem. 50* (1985) 2801.
[7] **4**: IR (KBr): $\tilde{\nu}$ = 1603 cm^{-1} (C=C). 90-MHz ^{1}H NMR ($CDCl_3$): δ = 0.20 (s, 12H, $SiMe_2$), 1.10 (s, 36H, *t*Bu). 50.28-MHz ^{13}C NMR ($CDCl_3$): δ = −1.47 (s, $SiMe_2$), 28.6 (q, CMe_3), 37.0 (s, CMe_3), 122.0 (s, O–C=*C*), 145.8 (s, O–*C*=C). **5**: yellow, m.p. 51 °C; IR (KBr): $\tilde{\nu}$ = 1605 cm^{-1} (C=C). 90-MHz ^{1}H NMR ($CDCl_3$): δ = 0.17 (s, 3H, SiMe), 0.27 (s, 3H, SiMe), 1.23 (s, 18H, *t*Bu), 5.60 (s, 2H, =CH), 6.43 (s, 2H, O–CH). 100.6-MHz ^{13}C NMR ($CDCl_3$): δ = −2.9 (q, SiMe), −2.3 (q, SiMe), 30.2 (q, CMe_3), 38.5 (s, CMe_3), 80.1 (d, O–CH), 114.7 (s, O–C=*C*), 135.1 (d, =CH), 153.0 (s, O–*C*=C). **6**: m.p. 186 °C; IR (KBr): $\tilde{\nu}$ = 1690 cm^{-1} (C=O). 90-MHz ^{1}H NMR ($CDCl_3$): δ = 1.07 (s, *t*Bu), 4.03 (s, CH) 50.28-MHz ^{13}C NMR ($CDCl_3$): δ = 26.3 (q, CMe_3), 41.8 (s, CMe_3), 44.1 (d, CH), 212.9 (s, C=O). MS (70 eV): *m/z* calculated for $C_{24}H_{40}O_4$ 392.293, found 392.291.
7: m.p. 205 °C. 90-MHz ^{1}H NMR ($CDCl_3$): δ = 0.83 (s, *t*Bu), 3.08 (s, CH). 50.28-MHz ^{13}C NMR (CD_2Cl_2): δ = 26.9 (q, CMe_3), 38.7 (s, CMe_3), 44.8 (d, CH), 124.6 (s, O–C–O).
[8] Some silirenes undergo Pd^{II}-catalyzed dimerization to 1,4-disilacyclohexadienes: a) M. Ishikawa, T. Fuchikami, M. Kumada, *J. Chem. Soc. Chem. Commun. 1977*, 352; b) H. Sakurai, Y. Kamiyama, Y. Nakadaira, *J. Am. Chem. Soc. 99* (1977) 3879.
[9] D. Seyferth, S. C. Vick, M. L. Shannon, *Organometallics 3* (1984) 1897.
[10] One possibility is the intramolecular dimerization of a bis(β-siloxyalkyli-denecarbene(oid)). For thermal formation of β-siloxyalkylidenecarbenes, see R. Brückmann, G. Maas, *Chem. Ber. 120* (1987) 635.
[11] The all-carbon analogue of **3**, 1,2,3-cycloheptatriene, has also been trapped by [2+4] cycloadditions: H.-G. Zoch, G. Szeimies, R. Römer, R. Schmitt, *Angew. Chem. 93* (1981) 894; *Angew. Chem. Int. Ed. Engl. 20* (1981) 877.
[12] A. E. Learned, A. M. Arif, P. J. Stang, *J. Org. Chem. 53* (1988) 3122.
[13] M. Iyoda, H. Otani, M. Oda, *J. Am. Chem. Soc. 108* (1986) 5371, and references therein.
[14] X-ray structure analysis (Enraf-Nonius CAD 4 diffractometer, monochromatic $Mo_{K\alpha}$ radiation, full-matrix refinement (H atoms isotropic)): **4** ($C_{28}H_{48}O_4Si_2$, *M* = 504.9): monoclinic, space group *C*2/*c*, *a* = 11.482(4), *b* = 16.123(6), *c* = 17.912(8) Å, β = 101.07(3)°; $\varrho_{calcd.}$ = 1.025 g cm^{-3}, *Z* = 4; 2874 unique reflections with $2.0 \le \Theta \le 25.0°$, 2314 reflections with $I > 2\sigma(I)$; 259 variables, R = 0.0525, $R_w = (\sum\Delta^2F/\sum F_0^2)^{1/2}$ = 0.0520; maximal shift/error ratio 0.53. **7** ($C_{24}H_{40}O_4$, *M* = 392.6): monoclinic, space group *C*2/*c*; *a* = 19.607(12), *b* = 6.176(2), *c* = 19.681(6) Å, β = 105.78(3)°; $\varrho_{calcd.}$ = 1.14 g cm^{-3}, *Z* = 4; 1595 unique reflections with $2.0 \le \Theta \le 23.0°$, 1296 reflections with $I > 2.2\sigma(I)$; 207 variables, R = 0.066, R_w = 0.065; maximal shift/error ratio 1.29. Further details of the crystal structure investigation may be obtained from the Fachinformationszentrum Karlsruhe, Gesellschaft für wissenschaftlich-technische Information mbH, D-7514 Eggenstein-Leopoldshafen 2 (FRG), on quoting the depository number CSD-54042, the names of the authors, and the journal citation.
[15] L. A. Paquette, J. W. Fischer, A. R. Browne, C. W. Doecke, *J. Am. Chem. Soc. 107* (1985) 686; crystal structure analysis: P. Engel, J. W. Fischer, L. A. Paquette, *Z. Kristallogr. 166* (1984) 225.
[16] R. Criegee, G. Schröder, G. Maier, H.-G. Fischer, *Chem. Ber. 93* (1960) 1553; see also R. Criegee, W. Eberius, H.-A. Brune, *ibid. 101* (1968) 94.
[17] Y. Chatani, T. Yamauchi, Y. Miyake, *Bull. Chem. Soc. Jpn. 47* (1974) 583.

Pd Clusters Containing As and PPh_3 Ligands: The Structures of $[Pd_9As_6(PPh_3)_8]$, $[Pd_2(As_2)(PPh_3)_4]$, and $[Pd_{20}As_{12}(PPh_3)_{12}]$**

By *Dieter Fenske,* Holm Fleischer*, and *Claudia Persau*

Dedicated to Professor Gerhard Fritz on the occasion of his 70th birthday

The reactions of $PhAs(SiMe_3)_2$ with $[MCl_2(PPh_3)_2]$ (M = Co, Ni) lead, even at room temperature, to cleavage of the As–C bond and formation of Me_3SiCl. The resulting cluster compounds **1**–**3** contain Co_4 tetrahedra (**1**) or cubic body-centered Ni_9 clusters (**2**,**3**).[1] We have now attempted to synthesize analogous Pd complexes.

$[Co_4(\mu_3\text{-}As)_3(\mu_3,\eta^3\text{-}As_3)(PPh_3)_4]$ **1**
$[Ni_9(\mu_4\text{-}As)_6(PPh_3)_5Cl_3]$ **2**
$[Ni_9(\mu_4\text{-}As)_6(PPh_3)_6Cl_2]$ **3**

We allowed the trinuclear cluster **4** to react with $As(SiMe_3)_3$ in THF[2] and observed, after a short period, the formation of a deep brown solution, from which, upon addition of a layer of heptane, black crystals of **5** formed. As a second reaction product, PPh_3S was identified.

$$\underset{\mathbf{4}}{[Pd_3(\mu_3\text{-}S)_2Cl_2(PPh_3)_4]} + As(SiMe_3)_3 \xrightarrow{THF} \underset{\mathbf{5}}{[Pd_9As_6(PPh_3)_8]} + PPh_3S$$

The IR spectrum of the diamagnetic cluster **5** corresponds, except for small shifts of some bands, to the spectra of other PPh_3-substituted clusters and therefore provides little information. The X-ray structure analysis of **5**[3] revealed a body-centered Pd_8 cube with a threefold axis of symmetry (Fig. 1).

The Pd atoms at the corners of the cube are coordinated by three μ_4-As atoms and the phosphorus atom of a PPh_3 ligand in a distorted tetrahedral fashion. The distances between corner Pd atoms are about 41 pm longer than the distances between the central Pd atom and corner Pd atoms. Thus, the bonding resembles that in the nickel cluster **2**,[1b] although the corresponding distances in **2** are about 30 pm shorter.

The distances between the μ_4-As atoms and the corner Pd atoms of the cube (247.5–248.7 pm) are only 22 pm shorter than those between them and the interstitial Pd atom. This

[*] Prof. Dr. D. Fenske, Dipl.-Chem. H. Fleischer, Dipl.-Chem. C. Persau
Institut für Anorganische Chemie der Universität
Engesserstrasse, Gebäude Nr. 30.45, D-7500 Karlsruhe (FRG)

[**] This work was supported by the Deutsche Forschungsgemeinschaft, the Fonds der Chemischen Industrie, and Degussa Ag.

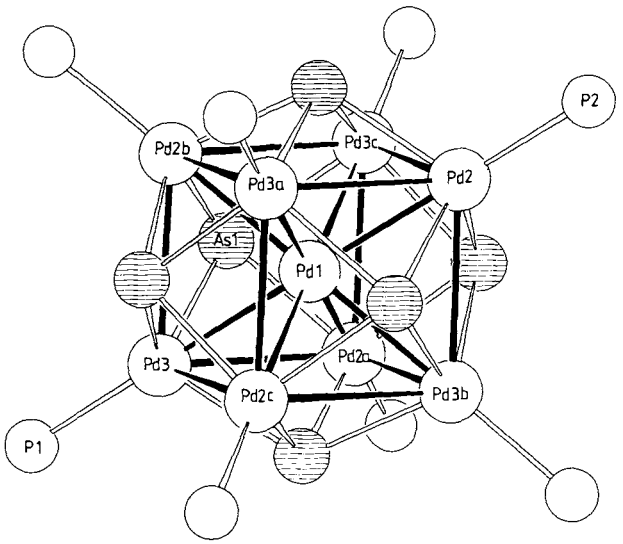


Fig. 1. Molecular structure of **5** (phenyl groups omitted). Important distances [pm] (±0.2 pm) and angles [°] (±0.05°): Pd1-Pd2 268.0, Pd1-Pd3 270.5, Pd2-Pd3a 310.9, Pd1-As1 270.4, Pd3-As1 248.7, Pd-P 230.5; Pd3a-Pd2-Pd3b 90.0, As1-Pd1-Pd2 125.26, As1-Pd1-Pd3 54.74 Pd2-Pd1-Pd3 180.0, Pd1-Pd2-P2 180.0.

central Pd atom has a coordination number of 14, since it is equally distant from the Pd and As atoms.

Cluster **5** contains 124 valence electrons (VE) and thus two electrons more than predicted by the 18-electron rule for body-centered cubes. The electron counting rules proposed by *Mingos* et al.[4] (VE = $12n_s + \Delta_i$) give 114 or 120 valence electrons for this type of cluster ($n_s = 8$; $\Delta_i = 18$ or 24, respectively); this result represents a substantial deviation from the actual number of valence electrons.

The following clusters can also be regarded as portions of cubic body-centered metal structures: $[Au_9(PPh_3)_8]^{\oplus}$,[5] $[Rh_{14}(CO)_{25}]^{4\ominus}$, and $[Rh_{14}(CO)_{26}]^{2\ominus}$.[6]

If, instead of **4**, the complex $[PdCl_2(PPh_3)_2]$ is allowed to react with $As(SiMe_3)_3$ in THF, dark yellow crystals of **6** can be isolated from the reaction solution after about two weeks.

$$[PdCl_2(PPh_3)_2] + As(SiMe_3)_3 \xrightarrow{THF} \underset{\mathbf{6}}{[Pd_2(As_2)(PPh_3)_4]} + \underset{\mathbf{7}}{[Pd_{20}As_{12}(PPh_3)_{12}]} + \mathbf{5}$$

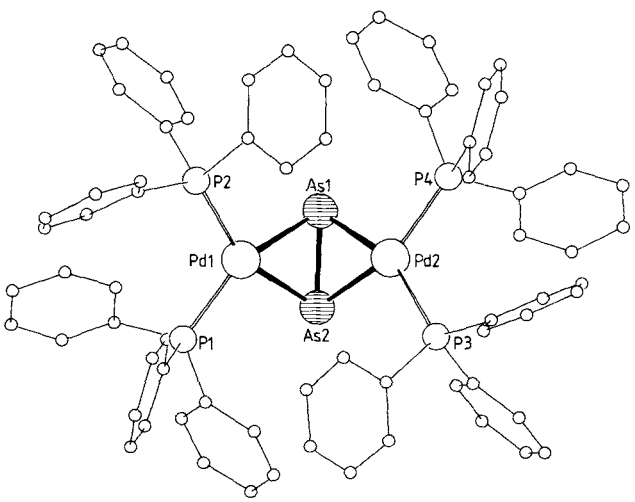


Fig. 2. Molecular structure of **6**. Important bond lengths [pm] (±0.1 pm) and angles [°] (±0.1°): Pd1-As1 252.2, Pd1-As2 245.5, Pd2-As1 245.8, Pd2-As2 251.5, As1-As2 227.4, Pd-P 232.8; As1-Pd1-As2 54.3, As1-Pd2-As2 54.4, Pd1-As1-Pd2 88.1, Pd1-As2-Pd2 88.3, P1-Pd1-P2 111.1, P3-Pd2-P4 110.9.

A crystal structure analysis[3] revealed that, in **6**, two $Pd(PPh_3)_2$ units are joined through a μ_2,η^2-As_2 bridge to form a "butterfly" structure. The As–As distance is similar to that in complexes such as $[Co_2As_2(CO)_6]$, $[Co_2(As_2)_2(CO)_5(PPh_3)]$, $[Cp_2M_2(CO)_4As_2]$ (M = Mo, W), and $[Cp^*_2Mn_2(CO)_4As_2]$.[7] Application of the usual counting rules gives 32 valence electrons for **6**. In agreement, a nonbonding Pd–Pd distance of 346 pm is found.

The formation of **6** is not surprising, since the reaction of $[(R_2PCH_2CH_2PR_2)NiCl_2]$ with $P(SiMe_3)_3$ also leads to a binuclear complex containing a bridging E_2 ligand.[8]

After separation of **6**, the filtrate was evaporated, the residue dissolved in toluene, and a layer of heptane added. A mixture of **5** and black crystals of a diamagnetic Pd_{20} cluster, **7**, crystallize within several days. The crystal structure analysis[3] shows that **7** consists of a Pd_8 cube (Pd11-Pd16, Pd18, Pd20), in which each edge is bridged by a μ_2-($PdPPh_3$) group (Fig. 3, top). Each of these bridges lies, within a deviation of 28–43 pm, within the best plane containing four Pd atoms

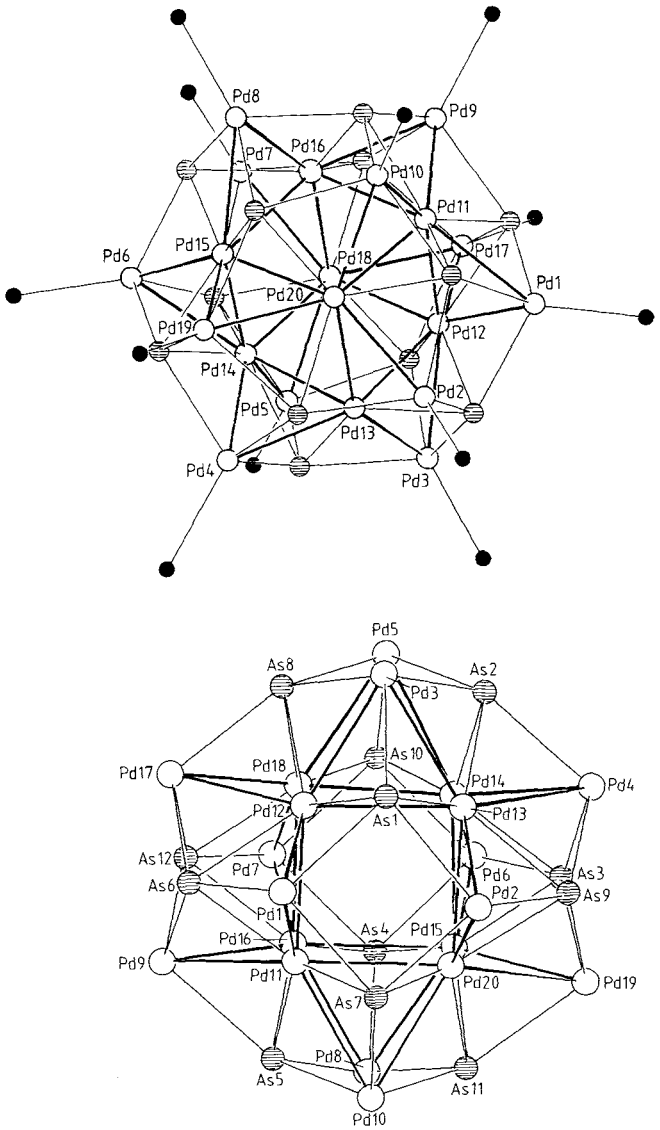


Fig. 3. Two views of the molecular structure of 7. Above: Phenyl groups omitted. Below: P atoms also omitted. ● = P atoms of the PPh_3 ligands, ◍ = As atoms. Important bond lengths [pm] (±0.2 pm) and angles (±0.2°): Pd-Pd (in the Pd_8 cube) 278.5–291.7, Pd-(μ_2-Pd) 274.1–279.8, Pd-P 229.6–230.7, As-Pd (in the Pd_8 cube) 240.0–247.2, As-(μ_2-Pd) 250.5–258.9; Pd-Pd-Pd (in the Pd_8 cube) 87.0–92.5, Pd-(μ_2-Pd)-Pd 60.3–61.3.

defining a side of the cube. Alternatively, the cluster framework of **7** can be described as a polyhedron formed by joining six Pd_6 rings and bridging the faces with μ_5-As atoms (Fig. 3, bottom).

The As–Pd distances are significantly shorter for the atoms of the Pd_8 cube than for the outer Pd atoms. These peripheral Pd atoms are each coordinated in a distorted tetrahedral fashion by three As ligands and one PPh_3 ligand.

The electron balance for clusters with $n > 13$ is often difficult to explain by using the usual models. If the As ligands are treated as three-electron donors and the PPh_3 ligands as two-electron donors, then **7** contains 260 valence electrons, that is, 28 electrons fewer than required by the 18-electron rule and 12 electrons more than expected according to the 16-electron rule. According to the concept proposed by *Mingos* ($n_s = 12$, $\Delta_i = 120$),[4] 264 valence electrons are obtained, that is, only four electrons more than the number calculated for **7**. Similarly large Pd clusters containing CO and PR_3 ligands have been synthesized and structurally characterized by *Mednikov* et al.: for example, $[Pd_{10}(CO)_{12}(PBu_3)_6]$, $[Pd_{23}(CO)_{22}(PEt_3)_{10}]$, and $[Pd_{38}(CO)_{28}(PEt_3)_{12}]$.[9]

Experimental Procedure

5: **4** (670 mg, 0.44 mmol) was suspended in 50 mL of THF and then treated with $As(SiMe_3)_3$ (0.26 mL, 0.88 mmol). Compound **4** dissolved rapidly with formation of a dark brown solution, which afforded 110 mg of a yellow microcrystalline precipitate of unknown composition after 7 d. Cluster **5** was obtained as black crystals by addition of a layer of heptane to the filtrate (yield 30% based on Pd).

6 and **7**: $[PdCl_2(PPh_3)_2]$ (2.12 g, 2.97 mmol) was suspended in 100 mL of THF and then treated with $As(SiMe_3)_3$ (2.97 g, 0.87 mL). Upon dissolution of the $[PdCl_2(PPh_3)_2]$ over 30–40 min, the solution turned dark brown. After about 1 h, the Pd complex had dissolved completely. The solution afforded small dark yellow crystals of **6** in small yield (15% based on Pd) when allowed to stand for 14 d. The solvent was removed from the still dark colored filtrate and the residue was washed with 50 mL of pentane and dissolved in 100 mL of toluene. After 2–3 weeks, a few large and uniform dark crystals of **7** had formed (yield 30%) together with crystals of **5** (yield 10%).

Received: July 31, 1989 [Z 3479 IE]
German version: *Angew. Chem. 101* (1989) 1740

[1] a) D. Fenske, J. Hachgenei, *Angew. Chem. 98* (1986) 165; *Angew. Chem. Int. Ed. Engl. 25* (1986) 175; b) D. Fenske, K. Merzweiler, J. Ohmer, *ibid. 100* (1988) 1572 and *27* (1988) 1512.

[2] D. Fenske, H. Fleischer, H. Krautscheid, J. Magull, unpublished.

[3] *X-ray structure analyses:* Stoe Stadi IV, $Mo_{K\alpha}$, empirical absorption correction. Data collection and refinement: ω scan, As, P, Pd anisotropic. **5**·3THF; crystals from THF; lattice constants (200 K): $a=b=c=$ 1961.5(9) pm, $\alpha=\beta=\gamma=90.0(0)°$, $V = 7546.8 \times 10^6$ pm^3; space group Pn_3, $Z = 2$, $\mu(Mo_{K\alpha}) = 24.7$ cm^{-1}. Profile analysis, $2\theta_{max} = 50°$, 5994 reflections, 1956 unique reflections, 1272 with $I > 2\sigma(I)$, 144 parameters (C anisotropic, H calculated), $R_1 = 0.077$, $R_2 = 0.046$. **6**: crystals from THF; lattice constants (293 K): $a = 1468.9(7)$, $b = 2319.3(12)$, $c = 1945.2(10)$ pm, $\beta = 109.07(3)°$, $V = 6305.9 \times 10^6$ pm^3; space group $P2_1/n$, $Z = 4$, μ ($Mo_{K\alpha}$) = 16.5 cm^{-1}. $2\theta_{max} = 54°$, 14311 reflections, 10876 with $I > 2\sigma(I)$, 961 parameters (C anisotropic, H isotropic), $R_1 = 0.036$, $R_2 = 0.036$. 7·2 toluene; crystals from toluene; lattice constants: (293 K): $a = 1972.2(5)$, $b = 2042.9(9)$, $c = 3410.8(19)$ pm, $\alpha = 74.85(3)$, $\beta = 84.11(4)$, $\gamma = 79.94(4)°$, $V = 13037.11 \times 10^6$ pm^3; space group $P\bar{1}$, $Z = 2$, μ ($Mo_{K\alpha}$) = 28.1 cm^{-1}. $2\theta_{max} = 44°$, 31852 reflections, 21894 with $I > 2\sigma(I)$, 820 parameters (Ph calculated as rigid groups), $R_1 = 0.082$, $R_2 = 0.0776$. Further details of the crystal structure investigation may be obtained from the Fachinformationszentrum Karlsruhe, Gesellschaft für wissenschaftlich-technische Information mbH, D-7514 Eggenstein-Leopoldshafen 2 (FRG), on quoting the depository number CSD-54074, the names of the authors, and the journal citation.

[4] D. M. P. Mingos, *J. Chem. Soc. Chem. Commun. 1985*, 1352; *Chem. Soc. Rev. 15* (1986) 31; D. M. P. Mingos, R. L. Johnston, *Struct. Bonding (Berlin) 68* (1987) 29.

[5] J. A. van der Velden, J. J. Bour, W. P. Bosman, J. H. Noordikand, P. T. Beurskens, *Recl. Trav. Chim. Pays-Bas 103* (1984) 13; J. G. M. van der Linden, M. L. H. Paulissen, J. E. J. Schmitz, *J. Am. Chem. Soc. 105* (1983) 1903.

[6] G. Ciani, A. Sironi, S. Martinengo, *J. Organomet. Chem. 192* (1980) C42; S. Martinengo, G. Ciani, A. Sironi, *J. Chem. Soc. Chem. Commun. 1980*, 1140; P. Chini, *J. Organomet. Chem. 200* (1980) 37.

[7] M. Müller, H. Vahrenkamp, *J. Organomet. Chem. 252* (1983) 95; A. S. Foust, M. S. Foster, L. F. Dahl, *J. Am. Chem. Soc. 91* (1969) 5633; P. J. Sullivan, A. L. Rheingold, *Organometallics 1* (1982) 1547; G. Huttner, B. Sigwarth, O. Scheidsteger, L. Zsolnai, O. Orama, *ibid. 4* (1985) 326; W. A. Herrmann, B. Koumbouris, T. Zahn, M. L. Ziegler, *Angew. Chem. 96* (1984) 802; *Angew. Chem. Int. Ed. Engl. 23* (1984) 812; W. A. Herrmann, B. Koumbouris, A. Schäfer, T. Zahn, M. L. Ziegler, *Chem. Ber. 118* (1985) 2472.

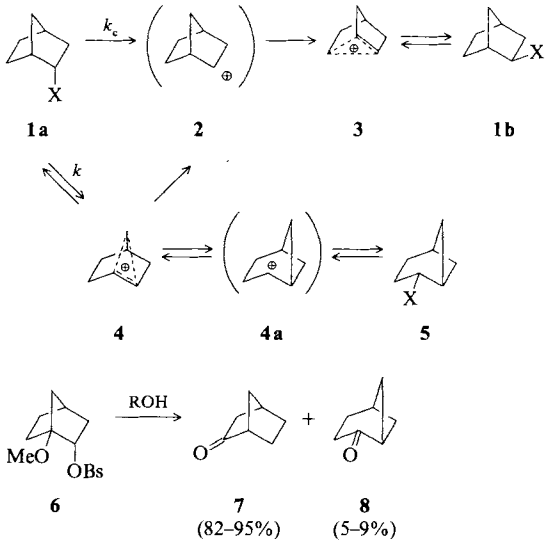
[8] H. Schäfer, D. Binder, D. Fenske, *Angew. Chem. 97* (1985) 523; *Angew. Chem. Int. Ed. Engl. 24* (1985) 522.

[9] E. G. Mednikov, N. K. Eremenko, V. A. Mikhailov, S. P. Gubin, Y. L. Slovokhotov, Y. T. Struckhov, *J. Chem. Soc. Chem. Commun. 1981*, 989; E. G. Mednikov, N. K. Eremenko, Y. L. Slovokhotov, Y. T. Struckhov, *J. Organomet. Chem. 301* (1986) C35; *J. Chem. Soc. Chem. Commun. 1987*, 218.

Si-Promoted Norbornyl–Norpinyl Rearrangements

By *Wolfgang Kirmse** and *Frank Söllenböhmer*

The ionization of *exo*-2-norbornyl derivatives (**1b**) occurs with participation of the C-1–C-6 bond (**1b** → **3**).[1] For *endo*-2-norbornyl derivatives (**1a**), a corresponding participation of the C-1–C-7 bond (**1a** → **4**) should likewise be possible. However, the ring strain thereby increases,[2] so that the k_c process **1** → **2** → **3** is often favored over the formation of the bridged ion **4** (Scheme 1). The large number of norpinyl–norbornyl rearrangements (**5** → **1**)[3] contrasts sharply, therefore, with the few examples of norbornyl–norpinyl rearrangements (**1** → **5**). Those few cases involve (1) the good leaving group nitrogen ($X = N_2^{\oplus}$) and (2) charge-destabilizing groups at C-3,[4] and/or charge-stabilizing groups at C-1.[5] Sulfonates, even in combination with (2), proved relatively ineffective as leaving groups; the best result so far is the formation of 5–9% of 2-norpinanone **8** from **6**.[6] We



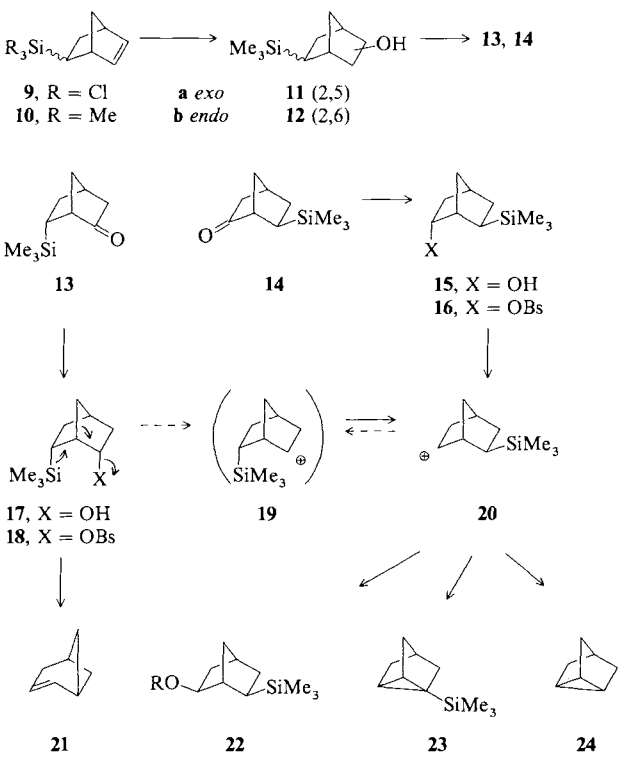
Scheme 1.

have now found predominant norbornyl–norpinyl rearrangement for *endo*-2-norbornyl brosylates bearing an *endo*-6-$SiMe_3$ group.

[*] Prof. Dr. W. Kirmse, Dr. F. Söllenböhmer
Fakultät für Chemie der Universität
Postfach 102148, D-4630 Bochum 1 (FRG)

To synthesize the starting material, we separated the adducts **9a,b**, obtained by Diels–Alder addition of trichlorovinylsilane to cyclopentadiene, by Spaltrohr® distillation.[7] Methylation with methylmagnesium bromide,[8] hydroboration, separation of the regioisomers **11**/**12** by column chromatography, and oxidation with chromium trioxide/pyridine afforded the ketones **13**[9] and **14**.

Reduction of the ketones with $LiAlH_4$ gave predominantly (**13**, 95:5; **14**, 96:4) the *endo* alcohols **17** and **15**, respectively, which were purified by column chromatography and transformed into their brosylates **18** and **16**, respectively, by reaction with brosyl chloride/pyridine (Scheme 2).



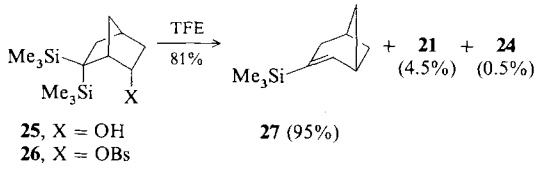
Scheme 2.

On solvolysis of **18** in trifluoroethanol (TFE), we obtained mainly (86%) norpinene **21**.[10] The byproducts **22**–**24** were produced in a ratio similar to that found in solvolyses of **6** (Table 1). They are formed from the ions **19** and **20** (Wagner–Meerwein rearrangement) by substitution, deprotonation, and desilylation. We did not find a substitution product with *endo*-$SiMe_3$; apparently, the *exo* position of the trimethylsilyl group is strongly preferred for steric reasons.[11] The formation of norpinene from **18** can occur in a concerted fashion (see arrows in Scheme 2) or via intermediates of type **4**. In a concerted mechanism, **18** is expected to exhibit a faster rate of reaction than *endo*-2-norbornyl brosylate. In fact, however, **18** reacts 30 times slower (TFE, 25 °C).[12] Since the special effect of the *endo*-6-$SiMe_3$ groups is exerted in the product-determining step rather than in the rate-determining step, a cationic intermediate is probable.

Table 1. Solvolysis products of brosylates **16** and **18** (TFE, 2,6-dimethylpyridine, 75 °C, 16 h).

	Yield [%]	Product distribution [%] 21	22	23	24
16	70	–	13	37	50
18	83	86	1.5	6	6.5

Brosylation of 6,6-bis(trimethylsilyl)bicyclo[2.2.1]heptan-*endo*-2-ol (**25**), a compound described elsewhere,[13] to give **26** could only be accomplished in moderate yield (39%). Solvolysis of **26** in TFE gave 3-trimethylsilylnorpinene (**27**) as the main product (Scheme 3, Table 2). The byproducts **21** and **24** could have been formed by acidolysis of **27**. The norbornyl–norpinyl rearrangement is nearly complete for **26**. The behavior of brosylate **26** does not lie midway between that of **16** and **18**; instead, the effect of the *endo*-6-$SiMe_3$ group in **18** is further enhanced by the additional *exo*-6-$SiMe_3$ group. The branched reaction pathway discussed above (Scheme 1) explains this finding: although the *exo*-6-$SiMe_3$ group cannot promote formation of **4** or **4a** (cf. **16**), it does increase the stability (β-Si effect)[14] and promote the desilylation of this cationic intermediate.



Scheme 3.

Table 2. Melting points and ^1H NMR data (400 MHz, $CDCl_3$) for **12**–**15**, **17** and **27**.

12a: m.p. 66 °C. $\delta = -0.05$ (s; Me_3Si), 0.23 (ddd, $J = 9.4$, 7.5, 1.5 Hz; 6-H), 1.05 (ddq, $J = 10.0$, 2.3, 1.5 Hz; *syn*-7-H), 1.18 (dddd, $J = 12.2$, 9.0, 2.3, 1.0 Hz; *endo*-5-H), 1.27 (m; *exo*-5- and *exo*-3-H), 1.48 (dquint, J = 10.0, 1.7 Hz; *anti*-7-H), 1.52 (s, br; OH), 1.65 (ddd, $J = 13.4$, 6.7, 2.2 Hz; *endo*-3-H), 2.03 (s, br; 1-H), 2.27 (tm, $J = 4$ Hz; 4-H), 3.71 (dm; $J = 6.7$ Hz, 2-H)

12b: m.p. 68.5 °C. $\delta = -0.02$ (s; Me_3Si), 0.89 (ddd, $J = 13.5$, 6.0, 4.2 Hz; 6-H), 0.91 (ddd, $J = 14.5$, 6.0, 1.8 Hz; *endo*-5-H), 1.12 (ddq, $J = 9.5$, 2.5, 1.3 Hz; *anti*-7-H), 1.25 (dm, $J = 13$ Hz; *exo*-3-H), 1.35 (s, br; OH), 1.57 (ddd, $J = 13.0$, 6.7, 2.5 Hz; *endo*-3-H), 1.61 (dddd, $J = 14.5$, 13.5, 4.5, 3.0 Hz; *exo*-5-H), 1.67 (dq, $J = 9.5$, 1.5 Hz; *syn*-7-H), 2.22 (dt, $J = 4.2$, 1.5 Hz; 1-H), 2.28 (tm, $J = 4.5$ Hz; 4-H), 3.90 (d,br, $J = 6.7$ Hz; 2-H)

13: $\delta = -0.05$ (s; Me_3Si), 1.20 (ddd; $J = 12.0$, 6.5, 4.0 Hz; 6-H), 1.28 (ddd, $J = 12.0$, 6.5, 1.5 Hz; *endo*-5-H), 1.51 (ddt, $J = 10.0$, 4.5, 1.5 Hz; *anti*-7-H), 1.65 (dd, $J = 17.8$, 4.5 Hz; *endo*-3-H), 1.70 (dq, $J = 10.0$, 1.5 Hz; *syn*-7-H), 1.95 (tdd, $J = 12.0$, 4.5, 2.8 Hz; *exo*-5-H), 1.98 (ddd, $J = 17.8$, 4.5, 2.8 Hz; *exo*-3-H), 2.55 (dm, $J = 4.0$ Hz; 1-H), 2.63 (tm, $J = 4.5$ Hz; 4-H)

14: $\delta = -0.02$ (s; Me_3Si), 0.82 (ddm, $J = 9.5$, 7.8 Hz; 6-H), 1.45 (ddt, $J = 10.0$, 4.0, 1.5 Hz; *anti*-7-H), 1.58 (m, 3H), 1.87 (dd, $J = 17.8$, 4.0 Hz; *endo*-3-H), 2.00 (dd, $J = 17.8$, 4.5 Hz; *exo*-3-H), 2.43 (s,br; 1-H), 2.60 (m; 4-H)

15: $\delta = -0.05$ (s; Me_3Si), 0.78 (ddd, $J = 13.0$, 4.0, 3.0 Hz; *endo*-3-H), 1.19 (ddt, $J = 10.0$, 3.0, 1.9 Hz; *anti*-7-H), 1.23 (dquint, $J = 10.0$, 1.5 Hz; *syn*-7-H), 1.28 (ddd, $J = 9.3$, 7.5, 1.5 Hz; 6-H), 1.40 (s,br, OH), 1.41 (ddm, $J = 12.5$, 7.5 Hz; *endo*-5-H), 1.90 (ddm, $J = 12.5$, 9.3 Hz; *exo*-5-H), 1.90 (ddm, $J = 13.0$, 10.0 Hz; *exo*-3-H), 2.07 (dt, $J = 4.0$, 1.5 Hz; 1-H), 2.15 (m; 4-H), 4.16 (dt, $J = 10.0$, 4.0 Hz; 2-H)

17: m.p. 37 °C. $\delta = 0.04$ (s; Me_3Si), 0.75 (dt, $J = 12.5$, 3.8 Hz; *endo*-3-H), 0.97 (dddd, $J = 12.7$, 6.7, 3.5, 1.2 Hz; *endo*-5-H), 1.23 (ddd, $J = 11.5$, 6.7, 1.7 Hz; 6-H), 1.25 (ddt, $J = 9.7$, 3.5, 1.7 Hz; 7-H), 1.32 (s,br; OH), 1.43 (dq, $J = 9.7$, 1.5 Hz; 7-H), 1.79 (dddd, $J = 12.7$, 11.5, 4.7, 3.0 Hz; *exo*-5-H), 1.94 (dddd, $J = 12.5$, 10.5, 5.0, 3.0 Hz; *exo*-3-H), 2.20 (ddm, $J = 5.0$, 4.7 Hz; 4-H), 2.32 (m; 1-H), 4.20 (dtm, $J = 10.5$, 3.8; 2-H)

27: $\delta = 0.05$ (s; Me_3Si), 1.32 (AA′ part of AA′XX′, $J = 8.1$, 7.8, 0.2 Hz; *endo*-6, 7-H), 2.11 (XX′ part of AA′XX′ split into a triplet, $J = 8.1$, 5.5, 0.7 Hz; *exo*-7-H), 2.41 (dd, $J = 2.9$, 2.0 Hz; 4-H), 2.47 (dq, $J = 6.2$, 5.5 Hz; 1-H), 2.64 (qt, $J = 5.5$, 2.9 Hz; 5-H), 6.61 (dtt, $J = 6.2$, 2.0, 0.7 Hz; 2-H)

With increasing number of silicon-controlled rearrangements[15] the examples of unusual reactions also increase. Recently, 1,3-aryl shifts were reported.[16] Our results show that the β-Si effect makes it possible for frameworks to rearrange in the direction of increasing strain.

Received: August 10, 1989 [Z 3491 IE]
German version: *Angew. Chem. 101* (1989) 1728

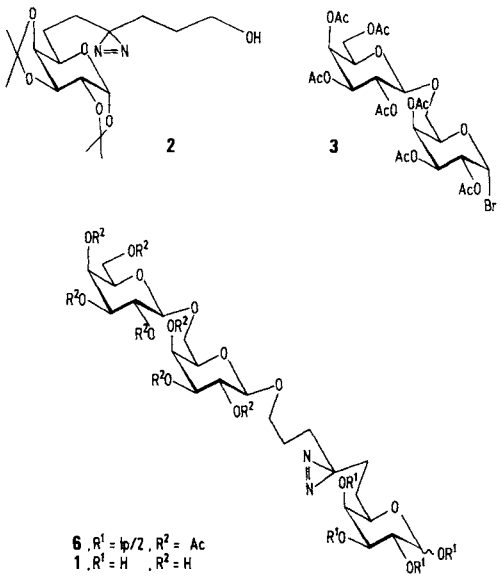
[1] Reviews: G. D. Sargent in G. A. Olah, P. von R. Schleyer (Eds.): *Carbonium Ions, Vol. III*, Wiley, New York 1972, p. 1099; H. C. Brown: *The Nonclassical Ion Problem* (with comments by *P. von R. Schleyer*), Plenum, New York 1977; W. Kirmse, *Top. Curr. Chem. 80* (1979) 125; V. A. Barkhash, *ibid. 116* (1984) 1; P. Vogel: *Carbocation Chemistry*, Elsevier, Amsterdam 1985; D. Lenoir, Y. Apeloig, D. Arad, P. von R. Schleyer, *J. Org. Chem. 53* (1988) 661.
[2] According to force-field calculations, the strain energy of bicyclo[3.1.1]heptane (norpinane, **5**, X = H) is 143.8 kJ mol^{-1}, that of bicyclo-[2.2.1]heptane (norbornane, **1**, X = H) 63.2 kJ mol^{-1}: W. F. Maier, P. von R. Schleyer, *J. Am. Chem. Soc. 103* (1981) 1891.
[3] Review: W. Kirmse, *Acc. Chem. Res. 19* (1986) 36.
[4] P. Yates, R. J. Crawford, *J. Am. Chem. Soc. 88* (1966) 1561; R. A. Blattel, P. Yates, *Tetrahedron Lett. 1972*, 1069, 1071; C. J. Collins, I. T. Glover, M. D. Eckart, V. F. Raen, B. M. Benjamin, B. S. Bemjaminov, *J. Am. Chem. Soc. 94* (1972) 899; R. Siegfried, *Chem. Ber. 107* (1974) 1472.
[5] W. Kirmse, G. Arend, R. Siegfried, *Angew. Chem. 82* (1970) 174; *Angew. Chem. Int. Ed. Engl. 9* (1970) 165; W. Kirmse, G. Arend, *Chem. Ber. 105* (1972) 2738, 2746; W. Kirmse, R. Siegfried, *ibid. 105* (1972) 2754; W. Kirmse, K. Loosen, *ibid. 114* (1981) 400; W. Kirmse, N. Knöpfel, K. Loosen, R. Siegfried, H. J. Wroblowsky, *ibid. 114* (1981) 1187; K. Banert, W. Kirmse, H. J. Wroblowsky, *ibid. 116* (1983) 3591.
[6] Y. Lin, A. Nickon, *J. Am. Chem. Soc. 92* (1970) 3496.
[7] GC separation and spectra: R. F. Cunico, *J. Org. Chem. 36* (1971) 929.
[8] H. G. Kuivila, C. R. Warner, *J. Org. Chem. 29* (1964) 2845.
[9] H. G. Kuivila, G. L. Grady, *J. Organomet. Chem. 21* (1970) 303.
[10] K. Grychtol, H. Musso, J. M. F. Oth, *Chem. Ber. 105* (1972) 1789; C. Herzog, R. Lang, D. Brückner, P. Kemmer, M. Christl, *ibid. 119* (1986) 3027.
[11] We obtained similar results with 6-methyl-2-norbornyl cations: W. Kirmse, M. Hartmann, R. Siegfried, H.-J. Wroblowsky, B. Zang, V. Zellmer, *Chem. Ber. 114* (1981) 1793.
[12] T. W. Bentley, unpublished.
[13] W. Kirmse, F. Söllenböhmer, *J. Chem. Soc. Chem. Commun. 1989*, 774.
[14] J. B. Lambert, G. Wang, R. B. Finzel, D. H. Teramura, *J. Am. Chem. Soc. 109* (1987) 7838, and references cited therein.
[15] I. Fleming, S. K. Patel, C. J. Urch, *J. Chem. Soc. Perkin Trans. 1 1989*, 115, and references cited therein.
[16] C. Eaborn, P. D. Lickiss, S. T. Najim, W. A. Stanczyk, *J. Chem. Soc. Chem. Commun. 1987*, 1461; C. Eaborn, K. L. Jones, P. D. Lickiss, *ibid. 1989*, 595.

A "Spacer"-Modified Trisaccharide as Photolabile Ligand for Affinity Labeling of Antigalactan IgA X24**

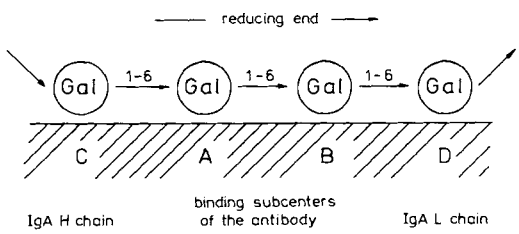
By *Cornelis P. J. Glaudemans, Jochen Lehmann,** and *Markus Scheuring*

Many carbohydrate-binding proteins—for example, endoglycanases, lectins, transport proteins for oligosaccharides, and antibodies directed against polysaccharides and glycoconjugates—recognize and bind not only individual monosaccharides but also whole oligosaccharide sequences. Intensively investigated examples of such carbohydrate-binding proteins are the amylases from various sources. In 1970, *J. F. Robyt* and *D. French*[1] used kinetic studies to formulate a so-called subsite model—binding to five centers—for the binding region of α-amylase from porcine pancreas, an enzyme that binds maltose as the minimal structural unit of starch and specifically hydrolyzes the maltosyl bond.

The design of the first "spacer"-modified disaccharide, a maltotriose analogue, was based on this concept. This analogue, containing two D-glucose moieties linked through a six-membered acyclic segment, was synthesized and found to be a competitive inhibitor of the enzyme.[2] Spacer-modified oligosaccharides were designed for use as reactive probes of receptor proteins. The spacer, a flexible unit, replaces one or more rigid, bulky monosaccharide moieties. It can bear a reactive or activable group for chemical modification of the binding region. The affinity of the whole molecule should not be affected appreciably by this group. Affinity labeling is suitable for probing the binding region of enzymes whose structure, as in the case of the antibody used here, is known.



The applicability of this principle is confirmed here by the ability of the spacer-modified trisaccharide 8-azi-6,7,8,9,10-pentadeoxy-11-*O*-[β-D-galactopyranosyl-(1→6)-β-D-galactopyranosyl-]-D-*galacto*-undecaose (**1**) to bind to the monoclonal antigalactan IgA X24.[3,4] This immunoglobulin displays optimum affinity for a tetrameric segment of (1→6)-β-D-galactopyranan (Table 1), in which the four binding centers A, B, C, and D (see Scheme 1) exhibit decreasing



Schema 1. Schematic drawing of the mode of binding of a β-(1→6)-D-galactopyranan segment to the variable region of an appropriate antibody [4, 7].

[*] Prof. Dr. J. Lehmann, Dipl.-Chem. M. Scheuring
Institut für Organische Chemie und Biochemie der Universität
Albertstrasse 21, D-7800 Freiburg (FRG)
Prof. C. P. J. Glaudemans
National Institutes of Health
Bethesda, MD 20892 (USA)

[**] This work was supported by the Deutsche Forschungsgemeinschaft and the Fonds der Chemischen Industrie.

binding affinity in that order for the monosaccharide moieties.[4] Photoaffinity labeling of IgA X24 was carried out previously with two β-D-galactosides of moderate affinity.[5, 6] In both cases, relatively unspecific labeling was observed; namely, both the L chain and the H chain were chemically modified. This result indicates either that binding occurred at various subcenters—that is, various ligand–receptor complexes were formed—or that the aglyconically bound, reactive groups were too flexible.

Compound **1** is designed so that, of the four subcenters,[4, 7] three, namely, A, C, and D, are occupied by galactosyl moieties and the fourth, B, is bridged by the spacer. The high affinity of compound **1** (1.1×10^5 M^{-1}), exceeding by far that of the structurally comparable disaccharide Gal_2[4] (Table 1), indicates an optimal, stable occupation of the four-

Table 1. Binding constants of some ligands to antigalactan IgA X24 [4, 6].

Compound	K_a [M^{-1}]
MeGal [a]	0.50×10^3
$MeGal_2$ [a]	2.10×10^4
$MeGal_3$ [a]	3.20×10^5
$MeGal_4$ [a]	5.70×10^5
Gal_4 [b]	2.70×10^5
1	1.10×10^5

[a] Methyl-β-D-glycopyranoside and methyl-β-D-(1→6)-linked β-D-galactooligosaccharide.
[b] The (1→6)-β-linked, reducing tetrasaccharide [16].

center binding region. Compound **1** can be prepared via a modified Koenigs–Knorr synthesis[8] by reaction of the undecaose derivative **2**, synthesized originally as a D-galactopyranose analogue,[9] with per-*O*-acetyl-*O*-β-D-galactopyranosyl-(1→6)-α-D-galactopyranosyl bromide (**3**)[10] followed by deprotection. Compound **3** was prepared according to a modified procedure[15] in improved yield (98% compared with 60%[10]). Treatment of **1** with β-galactosidase results in release of both galactose and the undecaose[9] of the reducing end. Both products were identified by thin layer chromatography with authentic samples.

Experimental Procedure

The affinity constants of **1** and IgA X24 were determined fluorometrically [5] (Table 1).

2,3,4,6-Tetra-*O*-acetyl-*O*-β-D-galactopyranosyl-(1→6)-1,2:3,4-di-*O*-isopropylidene-α-D-galactopyranose (**4**): 1,2:3,4-Di-*O*-isopropylidene-α-D-galactopyranose (7 g, 27 mmol) [11] was dissolved in 15 mL of chloroform. Ag_2O (6.88 g, 29 mmol), anhydrous $CaSO_4$ (12.5 g), and 3-Å molecular sieves (3 g) were then added. The reaction vessel was placed for 1 h in an ultrasonicating bath. After addition of iodine (1.77 g, 14 mmol) to the stirred mixture, 2,3,4,6-tetra-*O*-acetyl-α-D-galactosyl bromide (12.2 g, 29 mmol) [12] in 10 mL of chloroform was added dropwise over one hour. The reaction mixture was stirred for an additional 22 h and insoluble matter was then removed by filtration. The filtrate was washed first with dilute, aqueous sodium thiosulfate, then with water, and subsequently dried (Na_2SO_4) and evaporated. Compound **4** was obtained as a colorless oil (11.3 g, 71%) and was pure by thin layer chromatography; $R_f = 0.27$, ethyl acetate/cyclohexane, 1:1. Compound **4** was used without further purification.

Per-*O*-acetyl-*O*-β-D-galactopyranosyl-(1→6)-α-D-galactopyranosyl bromide (**3**) [13]: **4** (10 g, 17 mmol) was dissolved in 50 mL of glacial acetic acid and water was added until a clouded solution was obtained. The reaction mixture was refluxed for 5 × 30 min, 5 mL of water being added after each interval of 30 min. The solution was concentrated under vacuum to half the original volume, the acetic acid was removed by repeated codistillation with water under vacuum, and the mixture was then evaporated to dryness. The residue was acetylated, as usual, in 40 mL of pyridine/acetic anhydride (2:1), followed by workup [14]. Purification was carried out by column chromatography on silica gel with ethyl acetate/cyclohexane, 1:1; $R_f = 0.16$. After evaporation of the corresponding fractions, **5** [13] was obtained as a colorless, solid foam (10.7 g, 94%; $[\alpha]_D^{20}$ −5° (chloroform)). Bromination of **5** was carried out by modification of a known procedure [10] at lower temperature (−5 °C) in the presence of acetic anhydride: **5** (0.2 g, 0.294 mmol) was dissolved in 15 mL of a 2:1 mixture of acetic anhydride and 30% HBr in acetic acid at 0 °C and the resulting mixture was cooled to −5 °C. After 48 h, the starting material had undergone complete reaction [10]. The workup was performed as usual and the crude product **3** was purified by column chromatography on silica gel (ethyl acetate/cyclohexane, 1:1; $R_f = 0.23$).

6,7,8,9,10-Pentadeoxy-11-*O*-per-*O*-acetyl-β-D-galactopyranosyl-(1→6)-β-D-galactopyranosyl-[-1,2:3,4-di-*O*-isopropylidene-8-azi-]-D-*galacto*-undeca-1,5-pyranose (**6**) [13]: **2** (0.3 g, 0.84 mmol) was coupled with **3** (680 mg, 9.2 mmol) in the presence of 7 g of silver silicate–alumina catalyst according to a Koenigs–Knorr synthesis modified by *H. Paulsen* et al. [8]. Compound **6** was obtained as a colorless foam (272 mg, 34%); $R_f = 0.32$, ethyl acetate/cyclohexane, 1:1.

1: **6** (270 mg, 0.27 mmol) was dissolved in 20 mL of chloroform and 2 mL of 99% trifluoroacetic acid and the reaction mixture was allowed to stand for 48 h. After concentration of the reaction solution under vacuum accompanied by repeated codistillation with methanol, the residue was dissolved in 20 mL of methanol and treated with 1 M sodium methoxide until the solution was alkaline. After complete conversion ($R_f = 0.22$, ethyl acetate/MeOH/H_2O, 4:2:1), the methanolic solution was evaporated and **1** was purified by HPLC (reversed phase); yield 100 mg (60%), $[\alpha]_D^{23}$ +65° (water).

Received: August 7, 1989 [Z 3484 IE]
German version: *Angew. Chem. 101* (1989) 1730

[1] J. F. Robyt, D. French, *J. Biol. Chem. 245* (1970) 3917–3927.
[2] S. Jegge, J. Lehmann, *Carbohydr. Res. 133* (1984) 247–254.
[3] C. P. J. Glaudemans, M. E. Jolly, M. Potter, *Carbohydr. Res. 30* (1973) 409–413.
[4] C. P. J. Glaudemans, *Mol. Immunol. 24* (1987) 371–379, and references cited therein.
[5] G. L. Jung, K. R. Holm, C. P. J. Glaudemans, J. Lehmann, H. Lay, *Carbohydr. Res. 174* (1988) 87–98.
[6] C. S. Kuhn, C. P. J. Glaudemans, J. Lehmann, *Liebigs Ann. Chem. 1989*, 357–360.
[7] C. P. J. Glaudemans, P. Kovac, *Am. Chem. Soc. Symp. Ser. 374* (1988) 78–108.
[8] H. Paulsen, O. Lockhoff, *Chem. Ber. 114* (1981) 3102–3114.
[9] J. Lehmann, M. Scheuring, *Liebigs Ann. Chem.*, in press.
[10] E. M. Nashed, C. P. J. Glaudemans, *Carbohydr. Res. 158* (1986) 125–136.
[11] O. T. Schmidt, *Meth. Carbohydr. Chem. 2* (1963) 324–325.
[12] R. U. Lemieux, *Meth. Carbohydr. Chem. 2* (1963) 221–222.
[13] **3**: ^{1}H NMR (200 MHz, $CDCl_3$, 25 °C, TMS as standard): $\delta = 6.71$ (d, $J_{1,2} = 4.05$ Hz, 1H; H1), 5.49 (dd, $J_{3,4} = 3.15$, $J_{4,5} = 1.5$ Hz, 1H; H4), 5.38 (dd, $J_{2,3} = 7.5$, $J_{3,4} = 3.15$ Hz, 1H; H3), 5.37 (dd, $J_{3',4'} = 3.15$, $J_{4',5'} = 1.2$ Hz, 1H; H4'), 5.17 (dd, $J_{1',2'} = 7.8$, $J_{2',3'} = 7.65$ Hz, 1H; H2'), 5.03 (dd, $J_{1,2} = 4.05$, $J_{2,3} = 7.5$ Hz, 1H; H2), 4.99 (dd, $J_{2',3'} = 7.65$, $J_{3',4'} = 3.15$ Hz, 1H; H3'), 4.52 (d, $J_{7,8} = 7.8$ Hz, 1H; H1), 4.46 (t, $J_{4,5} = 1.5$, $J_{5,6} = 6.0$ Hz, 1H; H5), 4.2 (dd, $J_{6'b,5'} = 6.0$, $J_{6'a,6'b} = 11.25$ Hz, 1H, H6'b), 4.1 (dd, $J_{6'a,5'} = 6.0$, $J_{6'a,6'b} = 11.25$ Hz, 1H; H6'a), 3.91 (dt, $J_{4',5'} = 1.2$, $J_{5',6'} = 6.0$ Hz, 1H; H5'), 3.83 (dd, $J_{6b,5} = 6.0$, $J_{6a,6b} = 11.25$ Hz, 1H; H6b), 3.74 (dd, $J_{6a,5} = 6.0$, $J_{6a,6b} = 11.25$ Hz, 1H; H6a), 2.20–1.97 (m, 21H; OAc). **5**: ^{1}H NMR: $\delta = 6.37$ (d, $J_{1,2} = 1.5$ Hz, 1H; H1), 5.68 (d, $J_{1,2} = 8.25$ Hz, 1H; H1β), 4.51 (d, $J_{1',2'} = 7.65$ Hz, 1H; H1'), 4.47 (d, $J_{1',2'} = 7.65$ Hz, 1H; H1β) $[\alpha]_D^{20} = 5°$ ($CHCl_3$). **6**: ^{1}H NMR: $\delta = 5.49$ (d, $J_{1,2} = 4.8$ Hz, 1H; H1), 5.42–5.38 (m, 2H; H4',H2'), 5.18 (dd, $J_{2',3'} = 7.5$, $J_{3',4'} = 3.15$ Hz, 1H; H3'), 5.14 (dd, $J_{3'',4''} = 3.15$, $J_{4'',5''} = 1.2$ Hz, 1H; H4''), 5.02 (dd, $J_{1'',2''} = 7.8$, $J_{2'',3''} = 7.65$ Hz, 1H; H2''), 4.96 (dd, $J_{2'',3''} = 7.65$, $J_{3'',4''} = 3.15$ Hz, 1H; H3''), 4.58 (dd, $J_{2,3} = 2.7$, $J_{3,4} = 7.97$ Hz, 1H; H3), 4.52 (d, $J_{1'',2''} = 7.8$ Hz, 1H; H1''), 4.41 (d, $J_{1',2'} = 7.65$ Hz, 1H; H1'), 4.29 (dd, $J_{1,2} = 4.8$, $J_{2,3} = 2.7$ Hz, 1H; H2), 4.17 (dd, $J_{6''b,5''} = 6.0$, $J_{6''b,6''a} = 11.25$ Hz, 1H; H6''b), 4.13 (dd, $J_{6''a,5} = 6.0$, $J_{6''a,6''b} = 11.25$ Hz, 1H; H6''a), 4.05 (dd, $J_{3,4} = 7.97$, $J_{4,5} = 1.8$ Hz, 1H; H4), 3.91 (t, $J_{4'',5''} = 1.2$, $J_{5'',6} = 6.0$ Hz, 1H; H5''), 3.87 (dd, $J_{6'b,5} = 6.0$, $J_{6'b,6'a} = 11.25$ Hz, 1H, H6'b), 3.77 (dd, $J_{6'a,5} = 6.0$, $J_{6'a,6'b} = 11.25$ Hz, 1H; H6'a), 3.63–3.56 (m, 1H; H5), 3.5–4.91 (m, 1H; H5'), 2.2–1.96 (m, 21H; OAc), 1.75–1.23 (m, 21H; CH_2, CH_3); $C_{43}H_{62}O_{23}N_2$ (974.2): calcd C 53.01, H 6.34, N 2.87; found C 53.24, H 6.33, N 2.91.
[14] M. L. Wolfrom, A. Thompson, *Meth. Carbohydr. Chem. 2* (1963) 211–215.
[15] D. Shapiro, A. J. Acher, *Chem. Phys. Lipids 22* (1978) 197–206.
[16] M. E. Jolly, S. Rudikoff, M. Potter, C. P. J. Glaudemans, *Biochemistry 12* (1973) 3039–3044.

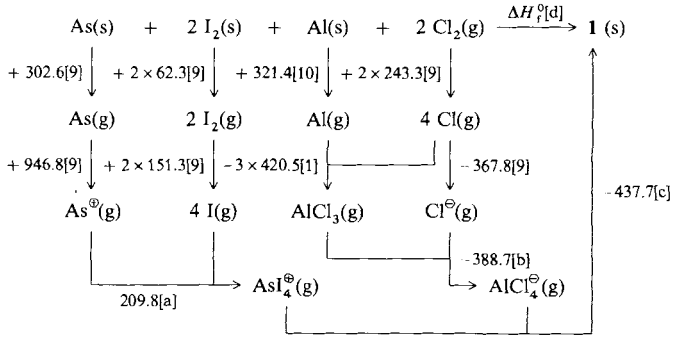
$AsI_4^{\oplus}AlCl_4^{\ominus}$, a Salt of the Last Missing Tetrahaloarsonium Ion**

By *Inis Tornieporth-Oetting* and *Thomas Klapötke**

In their highest oxidation states, the nonmetals of the fourth row of the periodic table, As, Se, and Br, form rather unstable compounds.[1] Whereas PCl_5 and $SbCl_5$ are stable under normal conditions,[2] metastable $AsCl_5$ exists only at low temperature.[3] However, stable salts containing the binary cation $AsCl_4^{\oplus}$ have been described.[4-6] $AsBr_5$ and AsI_5 are unknown, though the synthesis of the $AsBr_4^{\oplus}$ ion in $AsBr_4^{\oplus}AsF_6^{\ominus}$ was recently accomplished.[6] $AsBr_4^{\oplus}AsF_6^{\ominus}$ is unstable, however, and decomposes irreversibly above $-78\,^{\circ}C$ to AsF_3 and Br_2. We have now attempted to prepare the last missing member in the series of tetrahaloarsenic(v) cations, $AsI_4^{\oplus}$.

From thermodynamic data we estimated that the formation of $AsI_4^{\oplus}AsF_6^{\ominus}$ from AsF_3 and I_2 is not possible ($\Delta H >$ 230 kJ mol^{-1}).[7] Furthermore, since decomposition to AsF_3 and I_2 is strongly favored, oxidation of AsI_3/I_2 with AsF_5 also seems unsuitable. On the other hand, a simple estimate (not a calculation!) based on a Born–Haber cycle (Scheme 1) showed that the reaction should be thermodynamically possible according to Equation (a) ($\Delta H = -7$ kJ mol^{-1}).

$$AsI_3(s) + ICl(s) + AlCl_3(s) \rightarrow \underset{\mathbf{1}}{AsI_4^{\oplus}AlCl_4^{\ominus}}(s) \qquad (a)$$



Scheme 1. Thermodynamic cycle for estimating the enthalpy of formation ΔH_f^0 of $AsI_4^{\oplus}AlCl_4^{\ominus}$ (1). All energies in kJ mol^{-1}. [a] $As^{\oplus}$–I bond energies, assumed to be 1.05 × As–I bond energies in AsI_3 [1] in analogy to $2\,AsF_3 + 2\,Cl_2 \rightarrow AsCl_4^{\oplus}AsF_6^{\ominus}$, $\Delta H = -104.5$ kJ mol^{-1}, i.e., $As^{\oplus}$–Cl bond energy = 324.0 kJ mol^{-1} and therefore 5% larger than As–Cl bond energies in $AsCl_3$. [b] $Cl^{\ominus}$ ion affinity [11]. [c] Lattice energy calculated from the molecular volume V_M [Å^3] by use of the following linear relation: 2325 $V_M^{-0.33}$ + 110 [12, 13]; $V_M(AsI_4^{\oplus})$ was set equal to $V_M(GeI_4)$ = 223 Å^3 [10], $V_M(AlCl_4^{\ominus})$ = 144 Å^3 [11]. [d] $\Delta H_f^0(AsI_4^{\oplus}AlCl_4^{\ominus}(s)) = -807.6$ kJ mol^{-1}. For reaction (a), the following values are thereby obtained: $\Delta H = -7.1$ kJ mol^{-1} ($\Delta H_f^0(AsI_3(s)) = -58.1$ [10], $\Delta H_f^0(ICl(s)) = -35.5$ [2], $\Delta H_f^0(AlCl_3(s)) = -706.8$ kJ mol^{-1} [10]).

Since decomposition of **1** to AsI_3, $AsCl_3$, $AlCl_3$, and I_2 is appreciably favored [Eq. (b), $\Delta H = -119$ kJ mol^{-1}],[8] reaction (a) was performed at lower temperature ($-95\,^{\circ}C$)

$$3\,\mathbf{1}\,(s) \rightarrow 2\,AsI_3(s) + AsCl_3(l) + 3\,I_2(s) + 3\,AlCl_3(s) \qquad (b)$$

and the reaction products were kept frozen in liquid nitrogen. Their characterization was accomplished by low-temperature Raman spectroscopy ($-110\,^{\circ}C$).[14]

After assignment of the respective frequencies to the $AlCl_4^{\ominus}$ ion and to two byproducts ($ICl_2^{\ominus}$,[15] $I_2Cl^{\oplus}$[16]), the four strong bands remaining can be assigned to the complex cation $AsI_4^{\oplus}$, which has T_d symmetry (Fig. 1). The Raman

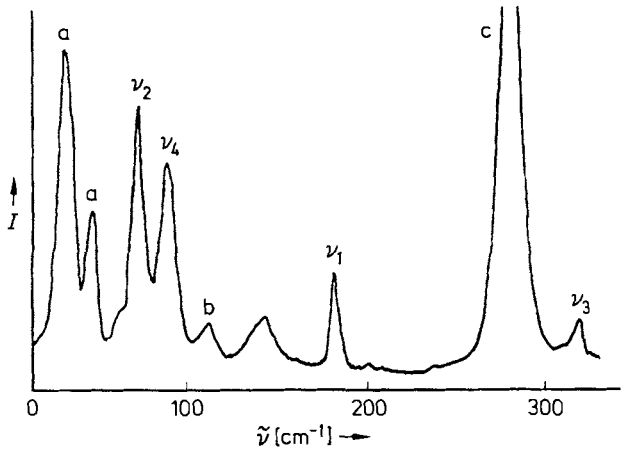


Fig. 1. Raman spectrum of **1** [14]. ν_1–ν_4: $AsI_4^{\oplus}$. Lattice vibrations: b, $AlCl_4^{\ominus}$; c, $ICl_2^{\ominus}$.

data for $AsI_4^{\oplus}$ are compared with those of the isoelectronic GeI_4 and the lighter homologues $AsBr_4^{\oplus}$ and $AsCl_4^{\oplus}$ in Table 1. As expected, the frequencies of $AsI_4^{\oplus}$ are all higher than those of GeI_4; the assignments are unambiguous owing to the relative intensities of the bands. Furthermore, the estimated values[17] for the ν_1 and ν_3 vibrational bands agree with the experimental values (Table 1). The spectrum displays neither AlI_3 bands nor the ν_1 band of I_2 (207 cm^{-1}[17]).

Table 1. Wavenumbers [cm^{-1}] and relative intensities (in parentheses) of the Raman-active fundamental vibrations ν_i of the tetrahedral $AsHal_4^{\oplus}$ ions (Hal = Cl, Br, I) and of GeI_4.

	$AsI_4^{\oplus}(AlCl_4^{\ominus})$ observed	$AsI_4^{\oplus}(AlCl_4^{\ominus})$ expected	GeI_4 [18]	$AsBr_4^{\oplus}$-($AsF_6^{\ominus}$) [6]	$AsCl_4^{\oplus}$-($AsF_6^{\ominus}$) [4]
ν_1	183 (40)	177	159 (80)	244 (100)	422 (100)
ν_2	72 (100)		60 (100)	88 (94)	156 (70)
ν_3	319 (20)	310	264 (20)	349 (28)	500 (50)
ν_4	87 (80)		80 (100)	115 (74)	187 (60)

[a] Calculated using $\tilde{\nu}(MI)/\tilde{\nu}(MCl) = 0.62$ for ν_3 and 0.42 for ν_1 [17].

At $-78\,^{\circ}C$, **1** decomposes spontaneously [Eq. (b), **danger of explosion**[19]] and both iodine and AsI_3 could be identified unequivocally by Raman spectroscopy; weak bands of $AlCl_3$ are observed in the IR spectrum of the decomposition product. In further experiments ($AsI_3/I_2/AlI_3$; AsI_3/IF/SbF_5; $AsI_3/0.5I_2/BF_3/0.5F_2$), we attempted to stabilize the $AsI_4^{\oplus}$ ion with other anions. $AlCl_4^{\ominus}$ proved to be the best suited counterion. The synthesis and characterization of the $AsI_4^{\oplus}$ ion in **1** confirms the existence of the last missing tetrahaloarsonium ion.

Experimental Procedure

1: ICl (0.1824 g, 1.123 mmol; Aldrich) was condensed into a thin-walled 5-mm-thick tube, distributed on the glass walls in the lower part of the tube (ca. 4 cm), and frozen in liquid nitrogen. After addition of a powdered mixture of AsI_3 (0.512 g, 1.124 mmol; Alfa) and $AlCl_3$ (0.300 g, 2.25 mmol; Aldrich) (two equivalents of $AlCl_3$ to prepare either the $AlCl_4^{\ominus}$ or the $Al_2Cl_7^{\ominus}$ salt), 0.5 mL of HCl(g) was condensed into the tube. The reaction mixture was warmed to

[*] Dr. T. Klapötke, Dipl.-Chem. I. Tornieporth-Oetting
Institut für Anorganische und Analytische Chemie der Technischen Universität
Strasse des 17. Juni 135, D-1000 Berlin 12

[**] This work was supported by the Deutscheforschungsgemeinschaft and the Fonds der Chemischen Industrie.

$-95\,^{\circ}C$, shaken for 30 min, and then allowed to warm slowly over 5-s periods at intervals of 5 min to $-78\,^{\circ}C$. The HCl was then removed under vacuum at $-95\,^{\circ}C$ and the remaining reaction mixture was kept frozen in liquid nitrogen until spectroscopic measurement.

Received: July 25, 1989 [Z 3464 IE]
German version: *Angew. Chem. 101* (1989) 1742

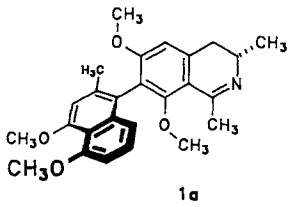
[1] J. E. Huheey: *Anorganische Chemie*, de Gruyter, Berlin 1988.
[2] J. C. Bailar, H. J. Emeléus, R. Nyholm, A. F. Trotman-Dickenson (Eds.): *Comprehensive Inorganic Chemistry*, 1st ed., Pergamon, Oxford 1973.
[3] K. Seppelt, *Angew. Chem. 88* (1976) 410; *Angew. Chem. Int. Ed. Engl. 15* (1976) 377.
[4] J. Weidlein, K. Dehnicke, *Z. Anorg. Allg. Chem. 337* (1965) 113.
[5] A. Müller, A. Fadini, *Z. Anorg. Allg. Chem. 349* (1968) 377.
[6] T. Klapötke, J. Passmore, E. G. Awere, *J. Chem. Soc. Chem. Commun. 1988*, 1426.
[7] $\Delta H_f^0(AsF_3(l)) = -956.4$ kJ mol^{-1} [9].
[8] $\Delta H_f^0(AsI_3(s)) = -58.1$ [10], $\Delta H_f^0(AsCl_3(l)) = -305$ [2], $\Delta H_f^0(AlCl_3(s)) = -706.8$ kJ mol^{-1} [10].
[9] D. A. Johnson: *Some Thermodynamic Aspects of Inorganic Chemistry*, 2nd ed., Cambridge University Press, Cambridge 1982, Appendix.
[10] N. N. Greenwood, A. Earnshaw: *Chemistry of the Elements*, Pergamon, Oxford 1984; *Chemie der Elemente*, VCH Verlagsgesellschaft, Weinheim 1988.
[11] P. Gowik, T. Klapötke, *J. Fluorine Chem.*, im Druck.
[12] T. E. Mallouk, G. L. Rosenthal, G. Müller, R. Brusasco, N. Bartlett, *Inorg. Chem. 23* (1984) 3167.
[13] T. J. Richardson, F. L. Tarzella, N. Bartlett, *J. Am. Chem. Soc. 108* (1986) 4937.
[14] Excitation wavelength, 647.09 nm; laser energy, 100 mW; T, $-110\,^{\circ}C$, $\tilde{\nu}$ [cm^{-1}] = 30(s), 45(m), 72 (s, ν_2 ($AsI_4^{\oplus}$)), 89 (s, ν_4($AsI_4^{\oplus}$)), 111 (m, ν_2 ($AlCl_4^{\ominus}$)), 144(m), 183 (m, ν_1 ($AsI_4^{\oplus}$)), 281 (s, ν_1 ($ICl_2^{\ominus}$)[15]), 319 (m, ν_3 ($AsI_4^{\oplus}$)), 350 (s,sh, ν_1 ($AlCl_4^{\ominus}$)), 355 (s, ν_1 ($I_2Cl^{\oplus}$)[16]).
[15] W. Gabes, H. Gerding, *J. Mol. Struct. 14* (1972) 267.
[16] W. Wilson, F. Aubke, *Inorg. Chem. 13* (1974) 326.
[17] K. Nakamoto: *Infrared and Raman Spectra of Inorganic and Coordination Compounds*, 4th ed. Wiley, New York 1986.
[18] H. Stammreich, R. Forneris, Y. Tavares, *J. Chem. Phys. 25* (1956) 1278.
[19] **Warning:** In another experiment, we photolyzed a mixture of AsI_3, ICl, and $AlCl_3$ in the absence of solvent at low temperature (150-W high-pressure Hg lamp, cooled with N_2 (l), $\lambda = 254$ nm); the sample exploded upon warming, resulting in injury to a co-worker.

Atropdiastereoselective Ring Opening of Bridged, "Axial-Prostereogenic" Biaryls: Directed Synthesis of (+)-Ancistrocladisine**

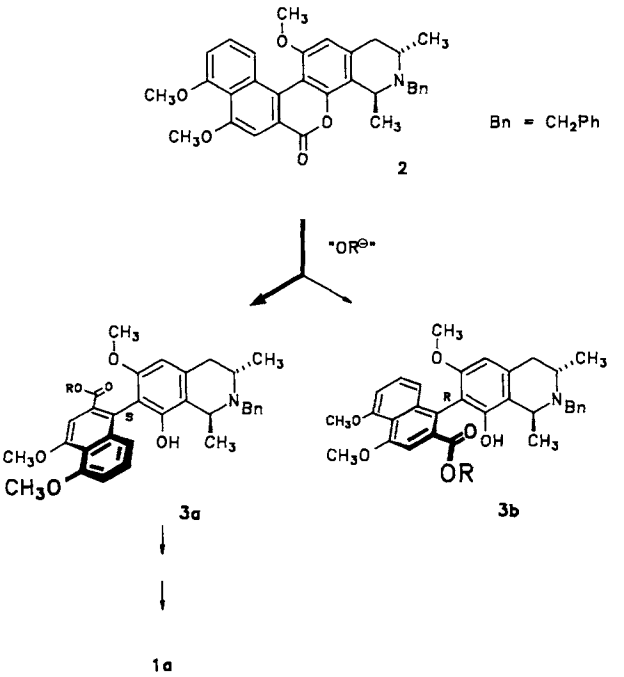
By *Gerhard Bringmann** and *Helmut Reuscher*

The biaryl axis[1] is a central structural feature of a broad spectrum of natural products derived via different biosynthetic pathways and exhibiting a broad range of biological activities. We have recently introduced a novel concept for the directed synthesis of highly hindered biaryls; according to this approach, the two arenes are brought into favorable proximity by an ether- or esterlike auxiliary bridge and then coupled *intra*molecularly.[2] This method made possible the first synthetic entry to the structurally interesting class of naphthylisoquinoline alkaloids,[3, 4] for example, ancistrocladisine (**1a**).[4, 5]

Of particular stereochemical interest is the optically active synthetic intermediate **2**. Although this lactone already contains the biaryl axis, the latter is still largely planar owing to the CO bridge, so that the barrier to atropisomerization is dramatically lowered relative to that for the nonbridged biaryls **1** and **3**. In consequence, lactone **2** does *not yet* consist of atropisomers; instead, it is still "*axial-prostereogenic*".[4, 5] Reaction with external oxygen nucleophiles—for example, methanolic sodium hydroxide solution—results in opening of the lactone ring and formation of the atropisomeric esters **3a** and **3b** (Scheme 1). The desired atropdiastereomer **3a** can be transformed into ancistrocladisine (**1a**), and also isomer **3b** can be recycled, for example, by recyclization to the axial-prostereogenic lactone **2**.[4, 5]



1a



Scheme 1. Atropdiastereoselective ring opening of the axial-prostereogenic lactone **2** (for details see Table 1).

Still more interesting would be the stereoselective control of this ring-opening step, which has proceeded so far without significant asymmetric induction. Here we report on the *kinetically controlled atropdiastereoselective ring opening of the axial-prostereogenic lactone* **2** with oxygen nucleophiles for the directed synthesis of ancistrocladisine (**1a**).

The results of the ring-opening experiments are summarized in Table 1. In determining the atropisomeric ratios, not only the esters themselves but also, in particular, their reduction products, alcohols **3a',b'** (CH_2OH instead of CO_2R), were used, because, on the one hand, this approach simplifies the analysis and, on the other, these alcohols afford a preparatively more relevant picture of the efficiency of the procedure, since they are configurationally stable. Particularly noteworthy are the atropisomeric excesses achieved—under kinetic control—with even such small oxygen nucleophiles as methanol and, especially, isopropyl alcohol.

[*] Prof. Dr. G. Bringmann, Dipl.-Chem. H. Reuscher
Institut für Organische Chemie der Universität
Am Hubland, D-8700 Würzburg (FRG)

[**] Acetogenic Isoquinoline Alkaloids, Part 15. This work was supported by the Deutsche Forschungsgemeinschaft and the Fonds der Chemischen Industrie. We thank *L. Kinzinger* for technical assistance. Part 14: [5].

Table 1. Atropisomeric ratios obtained in the reaction **2** → **3a** + **3b**.

"RO$^{\ominus}$"/solvent [a]	Reaction time	Ratio [c] **3a**:**3b**
$CH_3ONa/MeOH$	15 s	15.3:1
$CH_3ONa/MeOH$	5 min	1.3:1
$CH_3OH/NaHCO_3$ [b]	60 min	3.3:1
i-C_3H_7OK/i-C_3H_7OH	10 s	20.9:1
	22 h	1:1.1
Li-(+)-mentholate/THF	10 min	23.2:1
Li-(−)-mentholate/THF	10 min	1:1.8

[a] The reactions were carried out with 0.06 mmol of lactone **2** and 2.5 equivalents of the oxygen nucleophile in 10 mL of solvent at room temperature. The reaction mixture was subsequently acidified with concentrated hydrochloric acid and evaporated under vacuum. Analysis was performed after conversion of esters **3a, b** to alcohols **3a',b'** by treatment with $LiAlH_4$ in tetrahydrofuran. [b] Ten equivalents of sodium hydrogen carbonate were used. [c] The atropisomeric ratio was determined by analytical HPLC (Lichrosorb Si60 (Knauer AG), $CH_2Cl_2/MeOH/NEt_3$ = 99.6/0.2/0.2; the more rapidly eluting alcohol has the configuration of ancistrocladisine (**1a**).

Relatively small in comparison to the internal asymmetric induction is the effect exerted by the absolute configuration of the *O*-nucleophile mentholate. Even in the best case, the atropisomeric excesses obtained are hardly higher than those obtained with, for example, isopropoxide. Thus, taking into consideration the availability and separability of the oxygen nucleophile as well as the stability of the respective esters **3a,b** to isomerization, the reaction with isopropoxide is overall preferred for stereoselective ring opening on a preparative scale (e.g., on a gram scale): isolated overall yield 83%; **3a**, R = i-C_3H_7, amorphous, $[\alpha]_D^{25} = -4.0$ ($c = 0.47$, $CHCl_3$); **3b**, R = i-C_3H_7: m.p. 145–147 °C, $[\alpha]_D^{25} = -84.7$ ($c = 0.38$, $CHCl_3$).

The ring-opening reaction described here—the key step in the atropisomer-selective synthesis of ancistrocladisine (**1a**)—allows the first directed transformation of an easily accessible prostereogenic biaryl axis into a stereogenic axis of defined configuration by stereoselective attack on a prostereogenic *center* linked to the axis, the lactone carbonyl group.[6] To the best of our knowledge, this principle makes possible the *first stereoselective synthesis of a biaryl natural product in which the biaryl axis is flanked on one of the rings by two identical ortho substituents* (two OCH_3 groups).[7]

Received: August 24, 1989 [Z 3518 IE]
German version: *Angew. Chem. 101* (1989) 1725

CAS Registry numbers:
1a, 41787-65-9; **2**, 123858-65-1; **3a** (R = Me) 123858-6-2; **3a** (R = *i*Pr), 123858-67-3; **3a** (R = (+)-menthyl), 123858-68-4; **3a**, (R = (−)-menthyl), 123931-22-6; **3b**, (R = Me), 123931-23-7; **3b**, (R = *i*Pr), 123931-24-8; **3b**, (R = (−)-menthyl), 123931-25-9; **3b**, (R = (+)-menthyl, 123931-26-0.

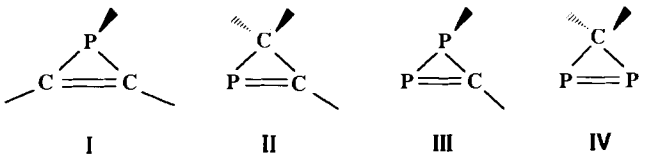
[1] Review on recently introduced methods of aryl coupling: H. J. Altenbach, *Nachr. Chem. Tech. Lab. 36* (1988) 1324.
[2] a) G. Bringmann, J. R. Jansen, *Tetrahedron Lett. 25* (1984) 2537; b) G. Bringmann, J. R. Jansen, *Heterocycles 28* (1989) 137; c) G. Bringmann, J. R. Jansen, H.-P. Rink, *Angew. Chem. 98* (1986) 917; *Angew. Chem. Int. Ed. Engl. 25* (1986) 913.
[3] a) T. R. Govindachari, P. C. Parthasarathy, *Heterocycles 7* (1977) 661; b) G. Bringmann in A. Brossi (Ed.): *The Alkaloids, Vol. 29*, Academic Press, New York 1986, p. 141.
[4] G. Bringmann, J. R. Jansen, A. Hille, H. Reuscher, Symposia, "6ème Colloque International, consacré aux Plantes Médicinales et Substances d'Origine Naturelle", Angers (France) 1988, p. 181.
[5] G. Bringmann, H. Reuscher, *Tetrahedron Lett. 30* (1989) 5249.
[6] The mechanism of this stereoselective twisting of previously planar biaryl units is under investigation. A proposal for the mechanism of such reactions is discussed in [4].
[7] Compare, for example, the nonstereoselective synthesis of a (presumably nonseparable) mixture of all four possible stereoisomeric ancistrocladisines: M. Rizzacasa, M. V. Sargent, *J. Chem. Soc. Chem. Commun. 1989*, 301.

Synthesis and Structure of a 1*H*-Diphosphirene**

By *Edgar Niecke,* Rainer Streubel, Martin Nieger,* and *Dietmar Stalke*

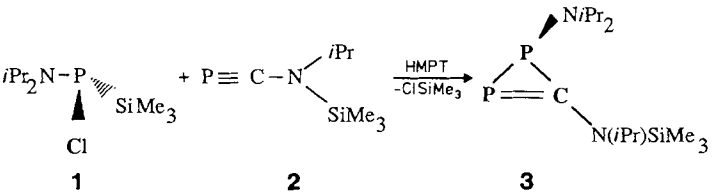
Dedicated to Professor Gerhard Fritz on the occasion of his 70th birthday

Phosphirenes, both in the 1*H*-form **I** as well as in the thermodynamically less favorable 2*H*-form **II**, have become well known in recent years through the works of *Mathey* et al.[1] and *Regitz* et al.[2] Replacement of a methylene group in **I** and **II** by a two-coordinate phosphorus atom leads to the previously unknown diphosphirenes **III** and **IV**, respectively (Scheme 1). As investigations on α-functional aminophosphanes have shown, halo(silyl)phosphanes such as **1** and compounds with polar double bonds react with formation of three-membered ring systems.[3] By extension of this synthetic principle to the P–C triple-bond system we have now gained access to **3**, the first 1*H*-diphosphirene **III**.[4]



Scheme 1. Phosphirenes and diphosphirenes; the lines symbolize bonds to arbitrary substituents.

The heterocycle **3**, accessible under mild conditions upon reaction of the functionalized aminophosphane **1**[5] with the phosphaalkyne **2**[6], is obtained as an extremely air-sensitive, deep-red liquid. By low-temperature crystallization from pentane, **3** can be obtained as a crystalline solid (m.p. −12 to −10 °C).

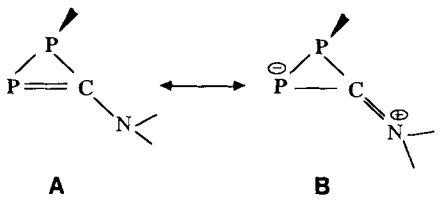


The composition and constitution of the compound are confirmed by elemental analysis, ^{31}P-, ^{1}H-, ^{13}C-NMR[8] and mass spectra[7] and by X-ray structure analysis. The occurrence of two pairs of signals in the ^{31}P-NMR spectrum is consistent with the presence of a diastereomeric pair (ratio 3:1). The position of the aminophosphane-phosphorus signal ($\delta = -118.7$ (−116.3)) corresponds to that of comparably substituted 1*H*-phosphirenes.[9] Unusual, on the other hand, is the high-field position of the σ^2-phosphorus signal

[*] Prof. Dr. E. Niecke, Dipl.-Chem. R. Streubel, Dr. M. Nieger
Anorganisch-chemisches Institut der Universität
Gerhard-Domagk-Strasse 1, D-5300 Bonn 1 (FRG)
Dr. D. Stalke
Institut für Anorganische Chemie der Universität
Tammannstr. 4, D-3400 Göttingen (FRG)

[**] Presented at the 11th International Conference on Phosphorus Chemistry. Tallinn, USSR, July 1989.—This work was supported by the Minister für Wissenschaft und Forschung des Landes Nordrhein-Westfalen and by the Fonds der Chemischen Industrie.

(14.9(4.6)) compared to the positions of the signals of other three-membered ring systems containing a phosphaalkene moiety.[2, 10] This would indicate substantial participation of resonance structure **B** as well as that of resonance structure **A** in the ground state of **3**. In any case, a comparison with the shielding of the ^{31}P nucleus in 2-amino-1,3-diphosphapropenes[11] suggests such an interpretation. Furthermore, the hindered rotation about the exocyclic C–N bond attributed to a participation of resonance structure **B** would also explain the occurrence of the diastereomeric pair recognizable in the NMR spectra.



A **B**

The presence of a four-electron 3-center (4e, 3c) PCN-p_π bond system is strongly supported by the result of the X-ray structure analysis (Fig. 1). The almost planar arrangement

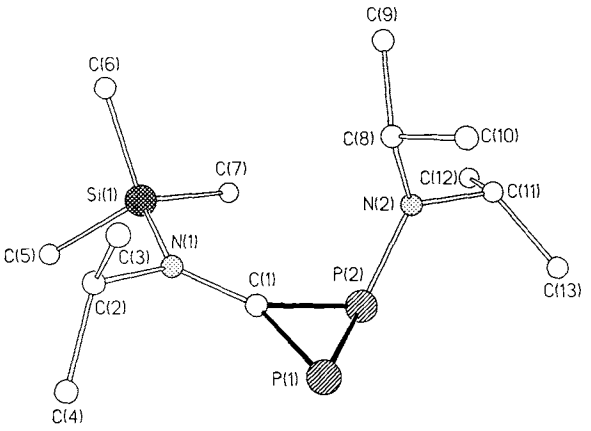
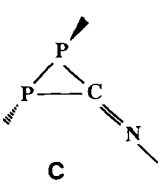


Fig. 1. Crystal structure of **3** with selected bond lengths [pm] and angles [°]: P(1)-C(1) 170.2(4), P(2)-C(1) 178.7(4), P(1)-P(2) 221.8(1), P(2)-N(2) 170.2(3), N(1)-C(1) 135.0(4); P(2)-P(1)-C(1) 52.3(1), P(1)-P(2)-C(1) 48.9(1), P(1)-P(2)-N(2) 111.5(1) [13].

of the P(1)–C(1)–N(1)–Si(1) atoms (dihedral angle: 178.6°) enables an effective π-donation of the amino nitrogen atom, which is manifested in the observed shortening of the C(1)–N(1) bond (135.0(4) pm) and stretching of the P(1)–C(1) bond (170.2(4) pm). Such a bonding situation is also found in the 2-amino-1,3-diphosphapropene $PhP=C(PPhSiMe_3)$-$N(o\text{-}ClC_6H_4)SiMe_3$, in which the P–C bond length (170.2 pm)[11] compares with that in **3**.

The weakening (stretching) of the P–C double bond brought about by the exocyclic π-donor is compensated by a comparable strengthening (shortening) of the P(2)–C(1) bond (178.7(4) pm). This correlation of the two P–C bond lengths and the shortening of the exocyclic C–N bond point to the structural transformation of the amino-1*H*-phosphirene into the thermodynamically more stable diphosphirane imine **C**.[12]



C

Experimental

3: 1.2 g (6.94 mmol) of **2** was cooled to 0 °C and slowly treated with stirring with 1.37 g (5.71 mmol) of **1**. The mixture was then treated with three drops of hexamethylphosphoric triamide and the cooling jacket removed. Stirring of the mixture was continued for ca. 1.5 h at room temperature and then all volatile components were removed in a high vacuum. The red, oily residue was taken up in a small amount of *n*-pentane and, after storage for 1 d at − 80 °C, orange crystals of **3** were obtained; these were isolated at low temperature (1.18 g, 67.9%). The melting point was found to be −12 to −10 °C.

Received: July 3, 1989 [Z 3421 IE]
German version: *Angew. Chem. 101* (1989) 1708

CAS Registry numbers:
1, 123542-38-1; **2**, 118375-89-6; **3**, 123542-39-2.

[1] A. Marinetti, F. Mathey, J. Fischer, A. Mitschler; *J. Chem. Soc. Chem. Commun. 1984*, 45.
[2] O. Wagner, G. Maas, M. Regitz, *Angew. Chem. 99* (1987) 1328; *Angew. Chem. Int. Ed. Engl. 26* (1987) 1257.
[3] R. Streubel, *Diplomarbeit*, Universität Bonn 1987,—presented at the *11th Int. Conf. Phosphorus Chem.* (Tallinn, UdSSR, July 1989).
[4] Recently the synthesis of a λ^5-diphosphirene has been described: E. Niecke, D. Barion, *Tetrahedron Lett. 30* (1989) 459.
[5] E. Niecke, M. Nieger, H. Westermann, unpublished.
[6] R. Appel, M. Poppe, *Angew. Chem. 101* (1989) 70; *Angew. Chem. Int. Ed. Engl. 28* (1989) 53.
[7] MS (30 °C/50 eV): *m/z* 304 ($M^{\oplus}$, 6%), 261(94), 231(16), 204(39), 162 ($iPr_2NP_2^{\oplus}$, 100).
[8] Numbering of the atoms as in Figure 1. 32 MHz, $^{31}P\{^1H\}$-NMR(C_6D_6): main isomer: δ = 14.9 (P(1)), − 118.7 (P(2)); $^1J(P,P)$ = 104.8 Hz; minor isomer: δ = 4.6 (P(1)), − 116.3 (P(2)); $^1J(P,P)$ = 108,8 Hz.—400 MHz ^1H-NMR(C_6D_6): main isomer: δ = 0.26 (s, 9H, $Si(CH_3)_3$), 1.07 (d, $^3J(H,H)$ = 7.2 Hz, 6H, $CH(CH_3)_2$), 1.08 (d, $^3J(H,H)$ = 7.2 Hz, 6H, $CH(CH_3)_2$), 1.33 (d, $^3J(H,H)$ = 7.2 Hz, 3H, N(1)CHCH_3), 1.51 (d, $^3J(H,H)$ = 7.2 Hz, 3H, N(1)CHCH_3), 3.15 (sept., $^3J(H,H)$ = 7.2 Hz, 2H, N(2)CH), 3.81 (sept., $^3J(H,H)$ = 7.2 Hz, 1H, N(1)CH); minor isomer: δ = 0.32 (s, 9H, $Si(CH_3)_3$), 0.93 (d, $^3J(H,H)$ = 7.2 Hz, 3H, N(1)CHCH_3), 1.19 (d, $^3J(H,H)$ = 7.2 Hz, 3H, N(1)CHCH_3), 1.23 (d, $^3J(H,H)$ = 7.2 Hz, 6H, $CH(CH_3)_2$), 1.25 (d, $^3J(H,H)$ = 7.2 Hz, 6H, $CH(CH_3)_2$), 3.17 (sept., $^3J(H,H)$ = 7.2 Hz, 2H, N(2)CH), 3.89 (sept., $^3J(H,H)$ = 7.2 Hz, 1H, N(1)CH).—100 MHz $^{13}C\{^1H\}$-NMR(C_6D_6): main isomer: δ = 0.8 (d, $^4J(P,C)$ = 4.9 Hz, $Si(CH_3)_3$), 18.7 (d, $^4J(P,C)$ = 6.1 Hz, N(1)CHCH_3) 19.6 (d, $^3J(P,C)$ = 3.8 Hz, N(1)CHCH_3), 23.7 (d, $^3J(P,C)$ = 4.1 Hz, $CH(CH_3)_2$), 24.0 (d, $^3J(P,C)$ = 13.3 Hz, $CH(CH_3)_2$), 43.8 (d, $^2J(P,C)$ = 6.2 Hz, N(2)CH), 53.4 (s, N(1)CH), 196.8 (dd, $^1J(P,C)$ = 83.4, 79.6 Hz, C(1)); minor isomer: δ = 0.2 (d, $^4J(P,C)$ = 4.8 Hz, $Si(CH_3)_3$), 23.2 (s, N(1)CHCH_3), 23.7 (d, $^4J(P,C)$ = 3.8 Hz, $CH(CH_3)_2$), 24.1(d,$^3J(P,C)$ = 12.6 Hz, $CH(CH_3)_2$), 24.6 (d, $^4J(P,C)$ = 7.6 Hz, N(1)CHCH_3),43.4(d, $^2J(P,C)$ = 6.6 Hz, N(2)CH), 55.5 (s, N(1)CH), 202.6 (dd, $^1J(P,C)$ = 87.7, 80.7 Hz, C(1)).
[9] O. Wagner, M. Ehle, M. Regitz, *Angew. Chem. 101* (1989) 227; *Angew. Chem. Int. Ed. Engl. 28* (1989) 225.
[10] A. Schäfer, M. Weidenbruch, W. Saak, S. Pohl, *Angew. Chem. 99* (1987) 806; *Angew. Chem. Int. Ed. Engl. 26* (1987) 776.
[11] R. Appel, B. Laubach, *Tetrahedron Lett. 21* (1980) 2497; R. Appel, F. Knoll, I. Ruppert, *Angew. Chem. 93* (1981) 771; *Angew. Chem. Int. Ed. Engl. 20* (1981) 731.
[12] M. Baudler, J. Simon, *Chem. Ber. 120* (1987) 421.
[13] X-ray structure analysis of **3** ($C_{13}H_{30}N_2P_2Si$, M_r = 304.4): space group $P2_12_12_1$ (No. 19), a = 946.3(1), b = 1324.3(2), c = 1493.8(2) pm, V = 1.872 nm^3, Z = 4, ϱ_{calc} = 1.08 g cm^{-3}, μ ($Mo_{K\alpha}$) = 0.28 mm^{-1}, T = 188 K; 3283 symmetry independent reflections ($2\theta_{max}$ = 50°), 2897 reflections with $F > 4\sigma(F)$ used for solution of structure (direct methods) and refinement (163 parameters); non-hydrogen atoms anisotropic, H atoms refined with a riding model; R = 0.061 (R_w = 0.059, $w^{-1} = \sigma^2(F) + 0.0010\,F^2$). Further details of the crystal structure investigation are available on request from the Fachinformationszentrum Karlsruhe, Gesellschaft für wissenschaftlich-technische Information mbH, D-7514 Eggenstein-Leopoldshafen 2 (FRG), on quoting the depository number CSD-53969, the names of the authors, and the journal citation.

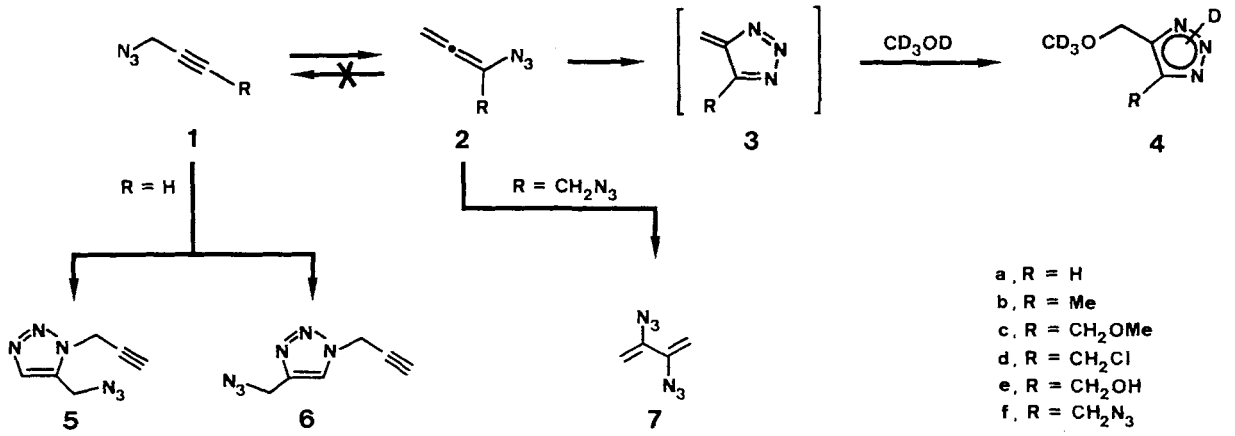
First Isolation of Allenyl Azides**

By *Klaus Banert** and *Manfred Hagedorn*

Whereas numerous synthetic methods are known for vinyl azides,[1] all attempts so far to isolate allenyl azides have failed.[2-4] Recently, we showed that propargyl azides of type **1** isomerize to the allenyl azides **2** by migration of the azide group.[5] These species proved to be short-lived intermediates that cyclized rapidly to the triazafulvenes **3**, which could be trapped by nucleophiles such as methanol[6] to afford 1,2,3-triazoles of type **4**. The transformation of propargyl azides into allenyl azides does not only occur by shift of the azido group, but also through base catalysis (prototropic rearrangement).[7] Preparatively interesting yields of 1,2,3-triazoles, which are also formed in the subsequent reactions of azidobutatriene,[8] are thereby obtained.

Here we report on the first spectroscopic characterization and the first isolation of allenyl azides, thereby showing that these species are not merely reactive intermediates. Dilute solutions of the propargyl azides[9] **1a–e**[9a, 10, 7, 8, 12, 5] in $CDCl_3$ or [D_4]methanol at 40 °C give polymeric triazoles or monomeric **4**, respectively. ^1H and ^{13}C NMR spectroscopic monitoring of the reactions reveals signals of allenyl azides **2a** (≤3%), **2b** (≤1%), **2c** (≤3%), **2d** (≤7%), and **2e** (≤8%) (Table 1). In each case, the ratio **1/2** remains almost constant during the reaction; therefore, **2** is a short-lived (quasi-stationary) intermediate. The donor substituent R = Me obviously accelerates the ring closure to **3b**, thereby allowing only a small concentration of **2b** to build up. By contrast, the concentration of **2b**, which bears the weak acceptor substituent R = CH_2Cl, reaches a higher value. In concentrated solution, **1a** displays a particular tendency toward 1,3-dipolar cycloaddition;[13] dimers **5** and **6** are thereby formed in a ratio of approximately 1:3.[14] Starting from **1f**,[15] it is possible to detect allene **2f** (≤0.8%), which does not cyclize to **3f**, but rather rearranges rapidly to **7**. Thus, the intermediacy of **2f** in the known[15, 16] reaction **1f** → **7** is demonstrated for the first time.

The azides **2a–e** could be separated from the isomeric propargyl compounds by preparative gas chromatography (25–50 °C). All allenyl azides were characterized spectroscopically (Table 1). Particularly informative are the long-range couplings in the ^1H NMR spectra (^4J = 6.4 Hz; ^5J = 1.8–3.3 Hz), the signals of the central allene carbon atoms in the ^{13}C NMR spectra ($\delta \approx 200$), and the intense azide band in the IR spectra ($\tilde{\nu} \approx 2100\ cm^{-1}$). IR absorptions for the allene moiety, which are often weak, could not be found for **2a–d**.[17] The pure allenes **2c** and **2d**, colorless liquids, are stable for a short period at room temperature. On the other hand, **2a** had to be isolated in a GC trap cooled to −80 °C and then diluted with solvent as rapidly as possible. Thus, whereas pure **2a** proved to be very unstable, solutions of this substance can be used at room temperature for NMR spectroscopy.



In [D_4]methanol, **2a–d** afford the triazoles **4** quantitatively in a first-order reaction; the backward reaction to **1** was not observed. A plot of the rate constants versus the Taft σ^*

Table 1. Selected physical data for **2a–f**, **5**, and **6** [a].

2a: IR (CCl_4): $\tilde{\nu}$ = 2170, 2110, 1330, 1255, 900. ^1H NMR (CD_3OD): δ = 5.46 (d, J = 6.4, 2H), 6.01 (br. t, $J \approx 6$, 1H). ^{13}C NMR (CD_3OD): δ = 88.0 (td, J = 170, 6.5; C-3), 100.5 (dt, J = 194, 9; C-1), 204.8 (s; C-2). GC-MS: m/z 81 ($M^{\oplus}$, 94%), 53 ([M-N_2]$^{\oplus}$, 44), 52 (100). UV (ether): λ_{max} = 240 nm ($\varepsilon \approx 6700$)

2b: IR ($CDCl_3$): $\tilde{\nu}$ = 2110, 1435, 1420, 1280, 1250, 1130. ^1H NMR (CD_3OD): δ = 1.78 (t, J = 3.3, 3H), 5.34 (q, J = 3.3, 2H). ^{13}C NMR ($CDCl_3$): δ = 17.2 (q; C-4), 86.2 (t; C-1), 108.8 (s; C-3), 201.3 (s; C-2). GC-MS: m/z 95 ($M^{\oplus}$, 45%), 66 (100), 52 (51)

2c: colorless liquid. IR ($CDCl_3$): $\tilde{\nu}$ = 2120. ^1H NMR ($CDCl_3$): δ = 3.37 (s, 3H), 3.95 (t, J = 2.0, 2H), 5.47 (t, J = 2.0, 2H). ^{13}C NMR (CD_3OD): δ = 57.3 (q; OCH_3), 71.7 (t; C-4), 87.4 (t; C-1), 110.4 (s; C-3), 202.6 (s; C-2)

2d: colorless liquid. IR (CCl_4): $\tilde{\nu}$ = 2120, 1270, 1245, 890. ^1H NMR ($CDCl_3$): δ = 4.02 (t, J = 1.8, 2H), 5.55 (t, J = 1.8, 2H). ^{13}C NMR ($CDCl_3$, −30 °C): δ = 43.3 (t; C-4), 89.2 (t; C-1), 109.9 (s; C-3), 200.4 (s; C-2). UV (cyclohexane): λ_{max} = 242 nm (ε = 5300)

2e: ^1H NMR (CD_3OD): δ = 4.01 (t, J = 2.3, 2H), 5.49 (t, J = 2.3, 2H). ^{13}C NMR (CD_3OD): δ = 61.8 (t, J = 147; C-1), 87.9 (t; J = 170, C-4), 114.0 (s; C-2), 201.8 (s; C-3)

2f: ^1H NMR ($CDCl_3$): δ = 3.72 (br. t, $J \approx 2$, 2H), 5.57 (t, J = 2.1, 2H). ^{13}C NMR ($CDCl_3$): δ = 50.6 (t; C-4), 88.4 (t; C-1), 108.5 (s; C-3), 200.3 (s; C-2)

5: ^1H NMR (CD_3OD): δ = 3.06 (t, J = 2.5, 1H), 4.72 (s, 2H), 5.33 (d, J = 2.5, 2H), 7.77 (s, 1H). ^{13}C NMR (CD_3OD): δ = 39.08 (t, J = 148), 43.30 (t, J = 146), 76.50 (dt, J = 52, 9), 76.54 (dt, J = 254, 4), 133.93(s), 134.83 (d, J = 196)

6: colorless liquid. IR (CCl_4): $\tilde{\nu}$ = 3300, 2100. ^1H NMR (CD_3OD): δ = 3.09 (t, J = 2.5, 1H), 4.47 (s, 2H), 5.31 (d, J = 2.5, 2H), 8.14 (s, 1H). ^{13}C NMR (CD_3OD): δ = 40.63 (t, J = 148), 45.94 (t, $J \approx 145$), 76.75 (dt, J = 51, 10), 76.78 (dt, J = 254, 4), 124.59 (d, J = 196), 144.02(s)

[a] ^1H NMR at 80 and 400 MHz, ^{13}C NMR at 100.6 MHz, J in Hz; $\tilde{\nu}$ in cm^{-1}; GC-MS at 70 eV.

[*] Dr. K. Banert, M. Hagedorn
Fachbereich 8, Organische Chemie II der Universität—Gesamthochschule Adolf-Reichwein-Strasse, D-5900 Siegen (FRG)

[**] Reactions of Unsaturated Azides, Part 9. This work was supported by the Deutsche Forschungsgemeinschaft. We thank *E. Reißaus* and *K. Vrobel* for careful assistance. Part 8: [8].

values[18] (Fig. 1) shows that acceptor substituents retard the ring closure to **3** and therefore the formation of **4**. In the absence of nucleophiles—for example, in chloroform solution—the allenyl azides polymerize. In the presence of tributyl(hexadecyl)phosphonium azide[19] in chloroform, **2d** is transformed into **2f**, which rapidly rearranges to **7** (maximum proportion of **2f**, 30%).

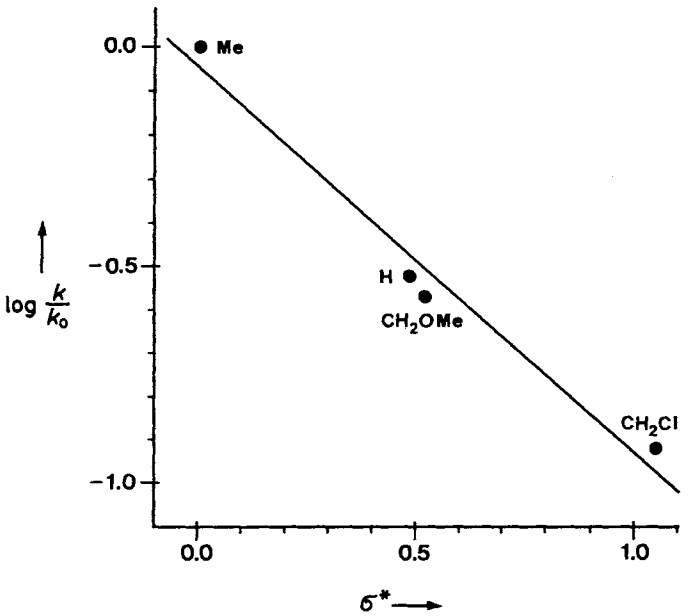


Fig. 1. Plot of $\log(k/k_0)$ versus Taft σ^* values for the reaction **2** → **4** in CD_3OD at 29 °C; $k(\mathbf{2a}) = 2.81 \times 10^{-5}\ s^{-1}$, $k_0 = k(\mathbf{2b}) = 9.34 \times 10^{-5}\ s^{-1}$, $k(\mathbf{2c}) = 2.53 \times 10^{-5}\ s^{-1}$, and $k(\mathbf{2d}) = 1.13 \times 10^{-5}\ s^{-1}$ give $\varrho^* = -0.87$.

Our results confirm that allenyl azides are better stabilized by acceptor substituents than by sterically demanding[2b] alkyl substituents which act as donors. The title compounds are of interest as potential precursors of the still unknown methylene azirines.[2b, c]

Received: August 16, 1989 [Z 3503 IE]
German version: *Angew. Chem. 101* (1989) 1710

CAS Registry numbers:
1a, 14989-89-0; **1b**, 105643-77-4; **1c**, 118724-01-9; **1d**, 119720-88-6; **1e**, 118723-98-1; **1f**, 91686-83-8; **2a**, 88596-79-6; **2b**, 123625-03-6; **2c**, 123625-04-7; **2d**, 123625-05-8; **2e**, 123625-06-9; **2f**, 91686-85-0; **3b**, 123625-13-8; **4a**, 123625-09-2; **4b**, 123625-10-5; **4c**, 123625-11-6; **4d**, 123625-12-7; **5**, 123625-07-0; **6**, 123625-08-1; **7**, 91686-86-1; $TsOCH_2C \equiv CCH_3$, 56563-37-2.

[1] G. Smolinsky, C. A. Pryde in S. Patai (Ed.): *The Chemistry of the Azido Group*, Wiley-Interscience, London 1971, pp. 555–585; G. L'abbé, A. Hassner, *Angew. Chem. 83* (1971) 103–109; *Angew. Chem. Int. Ed. Engl. 10* (1971) 98–104; A. Hassner in E. F. V. Scriven (Ed.): *Azides and Nitrenes*, Academic Press, Orlando (USA) 1984, pp. 35–94; E. F. V. Scriven, K. Turnbull, *Chem. Rev. 88* (1988) 297–368.

[2] a) V. J. Shiner, Jr., J. S. Humphrey, Jr., *J. Am. Chem. Soc. 89* (1967) 622–630; b) G. L'abbé, M. Mahy, M. Bollyn, G. Germain, G. Scheefer, *Bull. Soc. Chim. Belg. 92* (1983) 881–891; G. L'abbé, *ibid. 93* (1984) 579–592; c) A. Hassner, J. Keogh, *J. Org. Chem. 51* (1986) 2767–2770.

[3] The ^1H NMR signals mentioned in [2a] are not due, as suggested by the authors, to 1-azido-3-methyl-1,2-butadiene, but to 4-(1-azido-1-methylethyl)-1*H*-1,2,3-triazole; cf. [5].

[4] If the azide group and the allenyl system are separated by *one* carbon atom, an isolable compound is obtained: K. Banert, *Angew. Chem. 97* (1985) 231–232; *Angew. Chem. Int. Ed. Engl. 24* (1985) 216–217.

[5] K. Banert, *Chem. Ber. 122* (1989) 911–918.

[6] Investigations of the reaction of triazafulvenes with nucleophiles (e.g., methanol): E. M. Burgess, J. P. Sanchez, *J. Org. Chem. 38* (1973) 176–178; *ibid. 39* (1974) 940–948.

[7] K. Banert, *Chem. Ber. 122* (1989), 1963–1967.

[8] K. Banert, *Chem. Ber. 122* (1989) 1175–1178.

[9] Caution should be exercised during isolation of propargyl azides: a) M. G. Baldwin, K. E. Johnson, J. A. Lovinger, C. O. Parker, *J. Polym. Sci. Part B 5* (1967) 803–806; b) J. Almlöf, G. O. Braathen, P. Klaeboe, C. J. Nielsen, H. Priebe, S. H. Schei, *J. Mol. Struct. 160* (1987) 1–26.

[10] Azide **1b** can be prepared from the tosylate [11] of 2-butyn-1-ol and sodium azide in aqueous methanol in 78% yield: see also C. J. Nielsen, H. Priebe, R. Salzer, *J. Mol. Struct. 162* (1987) 41–56.

[11] A. Marszak-Fleury, *Bull. Soc. Chim. Fr. 1958*, 490–493.

[12] Pure **1d** (yield 77%) may be prepared by treatment of **1e** with thionyl chloride in pyridine and ether.

[13] In $[D_4]$methanol, slow H/D exchange of the alkyne proton further complicates the reaction **1a** → **2a** → → **4a**.

[14] For formation of a tricyclic dimer from **1a**, see, H. Priebe, *Acta Chem. Scand. Ser. B38* (1984) 623–626.

[15] H. Priebe, *Angew. Chem. 96* (1984) 728–729; *Angew. Chem. Int. Ed. Engl. 23* (1984) 736–737.

[16] K. Banert, *Chem. Ber. 120* (1987) 1891–1896; *Tetrahedron Lett. 26* (1985) 5261–5264.

[17] All attempts to record Raman spectra have failed so far—presumably owing to the low photostability of the title compounds.

[18] R. W. Taft, Jr., *J. Am. Chem. Soc. 75* (1953) 4231–4238.

[19] D. Landini, A. Maia, F. Montanari, *J. Am. Chem. Soc. 100* (1978) 2796–2801; *Nouv. J. Chim. 3* (1979) 575–577; D. Landini, A. Maia, F. Montanari, F. Rolla, *J. Org. Chem. 48* (1983) 3774–3777; K. Banert, W. Kirmse, *J. Am. Chem. Soc. 104* (1982) 3766–3767; K. Banert, *Chem. Ber. 118* (1985) 1564–1574.

Indications of Cesium in a Higher Oxidation State**

By *Klaus Moock* and *Konrad Seppelt**

The idea that alkali metals could exist in a higher oxidation state than +1 is older than the first demonstration of noble gas compounds with oxidation states up to +8. Earlier reports on the preparation of KF_2, RbF_3 and CsF_3,[1, 2] however, proved to be completely false; the authors had presumably mistaken KHF_2 $RbClF_4$, and $CsClF_4$ for these compounds.[3, 4] *R. Hoppe* et al. estimated the enthalpy of formation of CsF_3 to be about $-85\ kJ\ mol^{-1}$.[5, 6] Because of the high lattice energy of CsF, the decomposition into CsF and F_2 should be extremely exothermic ($-445\ kJ\ mol^{-1}$). Although the lattice energy should remain nearly constant on fluorination of $Cs^{\oplus}SbF_6^{\ominus}$ to $CsF_2^{\oplus}SbF_6^{\ominus}$, all such attempts failed completely.[7] Cocondensation of KF, RbF, and CsF and fluorine in argon matrices affords compounds whose IR spectra can be interpreted in terms of the presence of $F_3^{\ominus}$,[8] in complete analogy to the well known trihalides. Thus, attempts to synthesize higher valence alkali-metal compounds with fluorine have so far failed.

During cyclovoltammetric investigations on $OTeF_5$-compounds[9] we observed an electrochemical activity in the system $Cs^{\oplus}OTeF_5^{\ominus}/CH_3CN$ in the extremely oxidative region at ca. +3 V (versus SCE). By painstakingly accurate tests we were able to show that this oxidation, which is still irreversible at −35 °C, is dependent upon the cesium concentration but cannot be attributed to the solvent, the electrolyte or the anion $OTeF_5^{\ominus}$. Thus, $K^{\oplus}OTeF_5^{\ominus}$, $Rb^{\oplus}OTeF_5^{\ominus}$, $HOTeF_5$ and $(n\text{Bu})_4N^{\oplus}OTeF_5^{\ominus}$ are inert in the oxidative region. The findings are always reproducible, providing a vacuum-tight electrochemical cell[10] and extremely pure acetonitrile or propionitrile are used.[11] To support the assumption that

[*] Prof. Dr. K. Seppelt, Dr. K. Moock
Institut für Anorganische und Analytische Chemie der Freien Universität
Fabeckstraße 34–36, D-1000 Berlin 33

[**] This work was supported by the Fonds der Chemischen Industrie. We thank Dr. *U. Zenneck*, Universität Heidelberg, for recording the ESR spectra.

$Cs^{\oplus}$ is oxidized, we have also used cesium as $Cs^{\oplus}PF_6^{\ominus}$ and in the complexed forms as $[Cs^{\oplus}([18]crown-6)]PF_6^{\ominus}$ **1** and $[Cs^{\oplus}(crypt.2.2.2)]PF_6^{\ominus}$ **2**. The crown ethers/cryptands employed are obtainable in high purity, and they are "too small" for $Cs^{\oplus}$, so that a more stable complex is present after the oxidation through ion contraction. In fact, the oxidation takes place at a somewhat lower potential (+2.7 V in the case of the cryptate versus $\geq +3.0$ V in the case of $Cs^{\oplus}PF_6^{\ominus}$) (Table 1). The decrease of ca. 0.3 V through the cryptands

Table 1. Electrochemical data of $Cs^{\oplus}PF_6^{\ominus}$, $[Cs^{\oplus}([18]crown-6)]\ PF_6^{\ominus}$ **1**, and $[Cs^{\oplus}(crypt.2.2.2)]\ PF_6^{\ominus}$ **2**.

	Cyclovoltammogram (c.v.)			Alternating current polarogram (a.c.) [a]		
	E_{pa} [V] [b]	E_p	T [°C]	$E_{1/2}$	$E_{p/2}$ [mV] [c]	T [°C]
$Cs^{\oplus}PF_6^{\ominus}$ [d]	$\geq +3.0$	irrev.	−35	irrev.	–	+20
1 [d]	+3.0	irrev.	−35	irrev.	–	+20
2 [d]	+2.7	irrev.	−35	+2.6	360	+20

[a] $w = 1.3$ KHz, $\Delta E = 10$ mV. [b] All potentials are measured against $FeCp_2/FeCp_2^{\oplus}$ as internal standard referred to SCE. [c] Half-widths of the curves. [d] 0.1 mol L^{-1} in acetonitrile; supporting electrolyte $Et_4N^{\oplus}PF_6^{\ominus}$, three-electrode system (platinum).

corresponds to a change of energy of 29 kJ mol^{-1} and thus has the order of magnitude of a typical chelate effect. Once again it could be shown that the complex ligands, free or together with $K^{\oplus}$ or $Rb^{\oplus}$, are not oxidized. In the most favorable case of $[Cs^{\oplus}(crypt.2.2.2)]PF_6^{\ominus}$ **2** an oxidation could even be detected by alternating current polarography (Fig. 1).

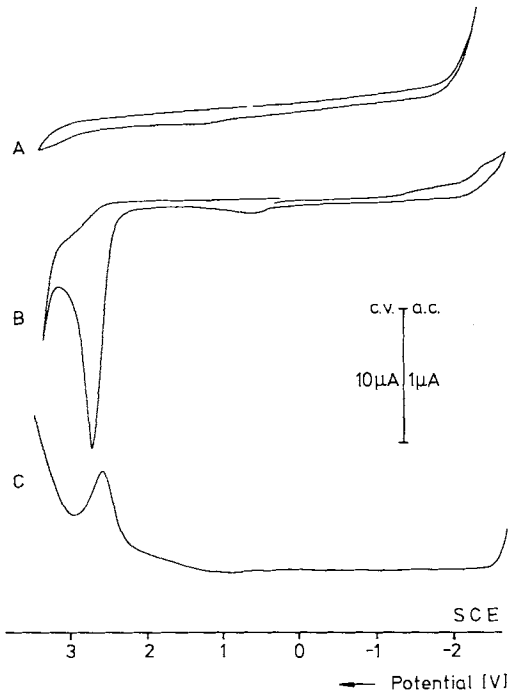


Fig. 1. Cyclovoltammogram (cv) of Kryptofix-2.2.2® (A) and $[Cs^{\oplus}(crypt.2.2.2)]PF_6^{\ominus}$ **2** (B), and alternating current polarogram (ac) of **2** (C).

H. Ahrens had already stated as long ago as 1956 that oxidations by chemical methods are possible if the relevant difference in ionization energy of the gas particle does not exceed 2400 kJ mol^{-1}.[12] In the case of $Cs^{\oplus}/Cs^{2\oplus}$ this is 2046 kJ mol^{-1}. From thermodynamic considerations and by analogy, however, it follows that not $Cs^{2\oplus}$ but at best $Cs^{3\oplus}$ should be stable. The gas reaction $2Cs^{2\oplus} \rightleftharpoons Cs^{3\oplus} + Cs^{\oplus}$ (856 kJ mol^{-1}) is exothermic and should not reverse, even upon solvation, because of the same total charge. Hence, we expect immediate further oxidation of $Cs^{2\oplus}$ to $Cs^{3\oplus}$. It would then also be understandable why ESR measurements were unsuccessful in simultaneous electrochemical oxidations. ($Cs^{2\oplus}$ with a nuclear spin 7/2 (100%) would be an excellent ESR probe—providing a minimum concentration of ca. 10^{-9} mol L^{-1} is achieved.) The isoelectronic system Xe/XeF_2, which is also irreversible, has a redox potential of 2.2 V in acid solution.[13] In this respect the higher values found for $Cs^{\oplus}/Cs^{2\oplus(3\oplus)}$ are fully consistent with expectation.[14]

A major argument against the conclusions drawn from the above findings is that an oxidation of the solvent, of the electrolyte, or of the cryptand takes place only with $Cs^{\oplus}$ catalysis. We do not refute that such oxidations proceed as secondary processes, but we cannot imagine a $Cs^{\oplus}$ catalysis without prior oxidation, because complex formation with the positive center (here $Cs^{\oplus}$) usually stabilizes the complex ligands against oxidation.

Although the isolation of a $Cs^{3\oplus}$ species has still to be reported, from the present results it would seem more feasible than was hitherto imagined. The use of cesium salts as oxidation transfer reagents in electrochemical processes is also conceivable.

Experimental

Electrochemical measurements: PAR 173 potentiostat, PAR 5208 lock-in-amplifier and PAR 175 programer, closed electrochemical cell [10]. Purification of acetonitrile as described in Ref. [11]; preparation of $OTeF_5$ salts according to Ref. [15].

$[Cs^{\oplus}(crypt\ 2.2.2)]PF_6^{\ominus}$: 0.57 g (2.05 mmol) of $CsPF_6$ and 0.77 g (2.05 mmol) of dried Kryptofix-2-2-2® (4,7,13,16,21,24-hexaoxa-1,10-diazabicyclo[8.8.8]hexacosane) were each transferred in a glove box into separate limbs of a two-limbed flask fitted with magnetic stirrers. 5 mL of acetonitrile were distilled under vacuum into each limb. The two solutions were then united in the first limb of the flask and stirred for 30 min at room temperature. After decantation of the clear solution into the second limb of the flask the solvent was removed in a vacuum. There remained a white crystalline solid in almost quantitative yield. Correct elemantal analysis. IR (Nujol): $\tilde{\nu}$ [cm^{-1}] = 1296, 1259, 1234, 1170, 1102, 1074, 1065, 1051, 1018, 945, 926, 910, 873, 840 ($\nu_3PF_6^{\ominus}$), 774, 746, 557 ($\nu_4PF_6^{\ominus}$), 521, 507. Raman (solid): $\tilde{\nu}$ [cm^{-1}] = 2971, 2956, 2919, 2902, 2874, 2841, 2830, 2807, 1121, 1075, 837, 819, 745 ($\nu_1\ PF_6^{\ominus}$), 564 ($\nu_2PF_6^{\ominus}$), 534, 520, 468 ($\nu_5PF_6^{\ominus}$), 390, 333, 259, 169.

Received: April 20, 1989 [Z 3302 IE]
German version: *Angew. Chem. 101* (1989) 1713

[1] H. Bode, *Naturwissenschaften 37* (1950) 477.
[2] H. Bode, E. Klesper, *Z. Anorg. Allg. Chem. 267* (1952) 97.
[3] L. B. Asprey, J. L. Margrave, M. E. Silverthorn, *J. Am. Chem. Soc. 83* (1961) 2955.
[4] H. Bode, E. Klesper, *Z. Anorg. Allg. Chem. 313* (1961/62) 161.
[5] R. Hoppe, *Fortschr. Chem. Forsch. 5* (1965) 213.
[6] R. Hoppe, H. Mattauch, M. Rödder, W. Dähme in H. H. Hyman (Ed.): *Noble Gas Compounds*, University of Chicago of Chicago Press 1963, S. 98.
[7] K. Seppelt, 1978, unpublished. The negative result of this experiment merely shows that the higher valent cesium is no longer stable at the high temperatures used. Under normal conditions the equilibrium $Cs^{\oplus}SbF_6^{\ominus} + F_2 \rightleftharpoons CsF_2^{\oplus}SbF_6^{\ominus}$ should lie on the right-hand side if the average Cs–F bond energy is greater than 76 kJ mol^{-1} (cf. average bond energy in XeF_2 136, in KrF_2 51 kJ mol^{-1}).
[8] B. S. Ault, L. Andrews, *J. Am. Chem. Soc. 98* (1976) 1591; *Inorg. Chem. 16* (1977) 2024. The reaction enthalpy $F_2 + F^{\ominus} \rightleftharpoons F_3^{\ominus}$ has been calculated to be −46.6 kJ mol^{-1}: R. A. Cahill, C. F. Dykstra, J. C. Martin, *J. Am. Chem. Soc. 107* (1985) 6359.

[9] K. Moock, K. Seppelt, *Z. Anorg. Allg. Chem. 561* (1988) 132.
[10] G. M. Anderson, J. Iqbal, D. W. A. Sharp, J. M. Winfield, J. H. Cameron, A. G. McLeod, *J. Fluorine Chem. 24* (1984) 303; G. A. Heath, K. H. Moock, D. W. A. Sharp, L. J. Yellowless, unpublished.
[11] J. M. Winfield, *J. Fluorine Chem. 25* (1984) 91.
[12] H. Ahrens, *J. Inorg. Nucl. Chem. 2* (1956) 290; *Geochim. Cosmochim. Acta 2* (1952) 155; *ibid. 3* (1953) 1.
[13] B. Jaselskis, *Science (Washington DC) 146* (1964) 263.
[14] An accurate estimation of the redox potential $Cs^{\oplus}/Cs^{3\oplus}$ was not possible. True, the ionization potentials and the solvation energy of $Cs^{\oplus}$ are known, but $Cs^{3\oplus}$ is presumably not spherical-shaped but disk-shaped with a radius ratio of 1:2. The solvation energy of a charged particle depends approximately on r^{-1}. All desired redox potentials can be predicted when $60 \leq r_1$, $r_2 \leq 120$ pm.
[15] S. H. Strauss, K. D. Abney, O. P. Anderson, *Inorg. Chem. 25* (1986) 2806; F. Sladky, H. Kropshofer, O. Leitzke, P. Peiger, *J. Inorg. Nucl. Chem. Herbert H. Hyman Mem. Vol. 1976*, 69.

Iron-Mediated Diastereoselective Spiroannelation to the Spiro[1,2,3,4-tetrahydroquinoline-4,1′-cyclohexane] System and a Novel Rearrangement to 2,3-Dihydroindole Derivatives**

By *Hans-Joachim Knölker,** *Roland Boese*, and *Konrad Hartmann*

The use of iron-diene complexes in the synthesis of heterocycles recently opened up a versatile entry to carbazole derivatives.[1] We have now extended this concept to the synthesis of other nitrogen-heterocycles. Cyclization, instead of being carried out oxidatively, as hitherto, was now achieved via nucleophilic substitution. This permitted closure of the C–C bond and the C–N bond in a one-pot reaction and thus the stereoselective synthesis of spirocycles.

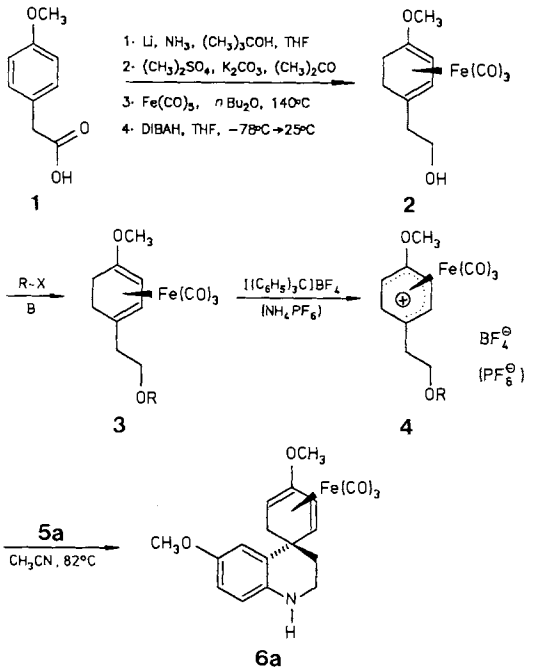
The discorhabdins[2] and prianosins[3] recently isolated from marine sources are distinguished by their high cytotoxic and antimicrobial activity. The discorhabdin D described only recently[4] also exhibits a strong antitumor activity in vivo. A common feature of these compounds is a spiro[1,2,3,4-tetrahydroquinoline-4,1′-cyclohexane] substructure. We report here on an iron-mediated diastereoselective entry to this ring system.

The addition of nucleophiles to tricarbonyl(η^5-1-alkyl-4-methoxycyclohexadienylium)iron cations enables the stereocontrolled synthesis of quaternary centers.[5] We have recently been able to show that iron-complexed cyclohexadienylium cations are very effective as mild electrophiles for the reaction with highly substituted electron-rich and thus oxidation-sensitive arylamines.[11] With the iron-complex salts **4** we have now succeeded for the first time in using this electrophilic substitution of aromatic systems for the diastereoselective generation of quaternary carbon atoms. Combination of this reaction with the subsequent in situ nucleophilic substitution of the leaving group in the side chain of **4** affords a new method for spiroannelation.

[*] Dr. H.-J. Knölker, Dipl.-Chem. K. Hartmann
Institut für Organische Chemie der Universität
Schneiderberg 1 B, D-3000 Hannover 1 (FRG)
Dr. R. Boese
Institut für Anorganische Chemie der Universität-Gesamthochschule
Universitätsstrasse 5–7, D-4300 Essen 1 (FRG)

[**] Transition-metal Diene Complexes in Organic Synthesis, Part 3. This work was supported by the Volkswagen foundation and the Deutsche Forschungsgemeinschaft. We thank Dr. *V. Wray*, Gesellschaft für Biotechnologische Forschung, Braunschweig-Stöckheim für the ^{13}C and 2D-NMR spectra and Dr. *K.-H. Geiss*, BASF AG, Ludwigshafen, for a supply of pentacarbonyliron.—Part 2: [1b].

The iron-complex **2** is readily accessible in four steps from *p*-methoxyphenylacetic acid **1**.[6] Compound **2** is converted by *O*-functionalization (**3**) and hydride abstraction into the complex salts **4**. The spiroannelation with *p*-anisidine **5** leads diastereoselectively to the spiro[1,2,3,4-tetrahydroquinoline-4,1′-cyclohexane] derivative **6a** (Schema 1). Cyclization to



Scheme 1. DIBAH = diisobutylaluminum hydride, B = base.

6a still takes place even with the methoxy derivative **4a**. A systematic optimization of the spiroannelation could be achieved by varying the leaving group in the side-chain (Table 1). In some cases (**4a, c, d**), owing to the stability of the salt, the hexafluorophosphate had to be used. The route via the *p*-nitrobenzoate derivatives **3f** and **4f** proved to be the best over all three steps (**2** → **3** → **4** → **6a**).

Table 1. Variation of the leaving group R in the complex salt **4**, and results of the spirocyclization to **6a**.

R	**3**, Yield [%]	**4**, Yield [%]	**6a**, Yield [%]
CH_3	**3a**, 96 [6]	**4a**, 69 (PF_6^-) [6]	20
CH_3SO_2	**3b**, 94	**4b**, 77	53
4-$CH_3(C_6H_4)SO_2$	**3c**, 87	**4c**, 27 (PF_6^-)	54
CH_3CO	**3d**, 98 [6]	**4d**, 74 (PF_6^-) [6]	68
CF_3CO	**3e**, 80	**4e**, 80	53
4-$NO_2(C_6H_4)CO$	**3f**, 98	**4f**, 92	80

The structure of **6a** follows from spectroscopic data (^1H-, ^{13}C- and COSY-NMR spectra) and an X-ray structure analysis (Fig. 1).[7] The latter revealed that the aryl ring is *anti* to the $Fe(CO)_3$ group referred to the cyclohexadiene ring plane. This can be explained by the stereodirecting effect of the $Fe(CO)_3$ group (*anti* selectivity). With the amines **5b**–**5e** the same diastereoselectivity is observed in the spiroannelation as with **5a** (Scheme 2, Table 2). The stereochemistry was established by comparison of the ^1H- and ^{13}C-NMR spectra of **6b**–**6e** with those of **6a**. In addition, the synthesis of **6d** clearly demonstrates that the reaction with 3,4-disubstituted anilines is regiospecific.

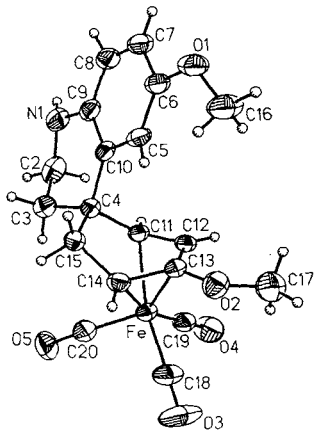
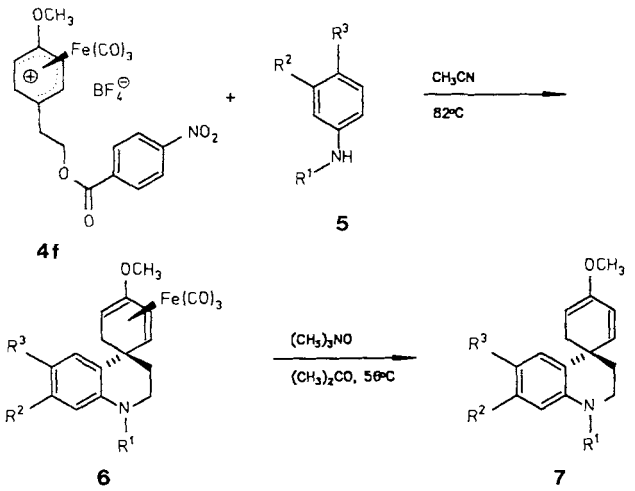


Fig. 1. Structure of **6a** in the crystal [7]. Selected bond lengths [Å]: Fe-C11 2.096(3), Fe-C12 2.054(4), Fe-C13 2.099(3), Fe-C14 2.116(4), C4-C11 1.529(5), C11-C12 1.432(6), C12-C13 1.412(6), C13-C14 1.437(6), C14-C15 1.516(6), C4-C15 1.561(6).



Scheme 2.

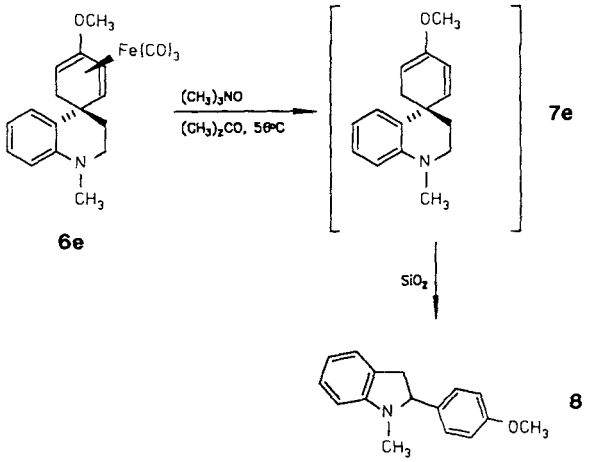
The complexes **6a–6d** can be demetalated with trimethylamine *N*-oxide[8] to give **7** (Scheme 2, Table 2). The yields of this reaction are strongly dependent on the reaction conditions (solvent, temperature, reaction time). Nevertheless, an optimization of the yields for each individual case was not carried out, since the metal complex **6** and its free ligand **7** each have the same R_f value. Thus all demetalations were performed under a standard set of conditions (10 equiv. Me_3NO, Me_2CO, 56 °C, 2–5 h).

Table 2. Yields of the spirocycles **6** and their demetalation to **7/8**.

5	R^1	R^2	R^3	**6**, Yield [%]	**7/8**, Yield [%]
5a	H	H	OCH_3	**6a**, 80	**7a**, 66
5b	H	H	H	**6b**, 55	**7b**, 47
5c	H	H	CH_3	**6c**, 58	**7c**, 48
5d	H	CH_3	CH_3	**6d**, 53	**7d**, 58
5e	CH_3	H	H	**6e**, 48	**8**, 68

Acid hydrolysis of the 2-methoxydiene moiety in **7a** to the corresponding enone affords a promising substrate for stereoselective Michael additions. Recomplexation of the free ligand **7a** (nonacarbonyldiiron, THF, 67 °C) leads exclusively to the *anti*-configurated complex **6a** again.

During the demetalation of **6a** a novel rearrangement occurs with ring contraction and aromatization to the dihydroindole derivative **8** (Scheme 3, Table 2). This reaction



Scheme 3.

proceeds via the free ligand **7e** which is oxidized to **8** during chromatography on silica gel. The structure of **8** was derived from spectroscopic data (^{1}H-, ^{13}C-, COLOC- and inverse ^{1}H-^{13}C-correlated NMR spectra). The driving force behind this rearrangement is undoubtedly aromatization of the cyclohexadiene ring. The influence of the substitution pattern of the arylamine component and the mechanism of this rearrangement are currently under investigation.

Received: June 30, 1989 [Z 3418 IE]
German version: *Angew. Chem. 101* (1989) 1745

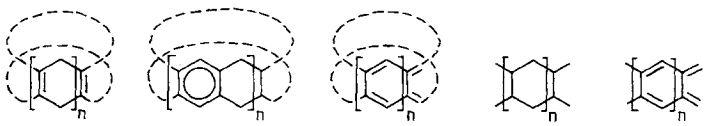
CAS Registry numbers:
2, 75969-38-9; **3a**, 75969-40-3; **3b**, 123774-94-7; **3c**, 123774-95-8; **3d**, 75969-39-0; **3e**, 123774-96-9; **3f**, 123774-97-0; **4a**, 75978-76-6; **4b**, 123751-42-8; **4c**, 123751-44-0; **4d**, 75969-42-5; **4e**, 123751-46-2; **4f**, 123774-99-2; **5a**, 104-94-9; **5b**, 62-53-3; **5c**, 106-49-0; **5d**, 95-64-7; **5e**, 100-61-8; **6a**, 123775-00-8; **6b**, 123775-01-9; **6c**, 123775-02-0; **6d**, 123775-03-1; **6e**, 123775-04-2; **7a**, 123751-36-0; **7b**, 123751-37-1; **7c**, 123751-38-2; **7d**, 123751-39-3; **8**, 123751-40-6.

[1] a) H.-J. Knölker, M. Bauermeister, D. Bläser, R. Boese, J.-B. Pannek, *Angew. Chem. 101* (1989) 225; *Angew. Chem. Int. Ed. Engl. 28* (1989) 223; b) H.-J. Knölker, M. Bauermeister, *J. Chem. Soc. Chem. Commun. 1989*, 1468.
[2] N. B. Perry, J. W. Blunt, M. H. G. Munro, *Tetrahedron 44* (1988) 1727.
[3] J.-F. Cheng, Y. Ohizumi, M. R. Wälchli, H. Nakamura, Y. Hirata, T. Sasaki, J. Kobayashi, *J. Org. Chem. 53* (1988) 4621.
[4] N. B. Perry, J. W. Blunt, M. H. G. Munro, T. Higa, R. Sakai, *J. Org. Chem. 53* (1988) 4127.
[5] A. J. Pearson, *Acc. Chem. Res. 13* (1980) 463; A. J. Pearson, in G. Wilkinson, F. G. A. Stone, E. W. Abel (Eds): *Comprehensive Organometallic Chemistry, Vol. 8*, Pergamon, Oxford 1982, Chap. 58, p. 939.
[6] A. J. Pearson, M. Chandler, *J. Chem. Soc. Perkin Trans. 1* 1980, 2238.
[7] **6a**: orthorhombic, $Pna2_1$, $a = 14.416(1)$, $b = 12.530(1)$, $c = 9.852(1)$ Å, $\alpha = \beta = \gamma = 90°$, $V = 1779.5(2)$ Å^3, $Z = 4$, $\varrho_{calcd} = 1.466$ g cm^{-3}, $\mu = 8.7$ cm^{-1}; $Mo_{K\alpha}$ radiation (graphite monochromator); $3° \leq 2\Theta \leq 50°$; 3156 unique reflections, 2999 with $F_o \geq 4\sigma(F)$, $R = 0.043$, $R_w = 0.056$. Further details of the crystal structure investigation are available on request from the Fachinformationszentrum Karlsruhe, Gesellschaft für wissenschaftlich-technische Information mbH, D-7514 Eggenstein-Leopoldshafen 2 (FRG), on quoting the depository number CSD-54049, the names of the authors, and the journal citation.
[8] Y. Shvo, E. Hazum, *J. Chem. Soc. Chem. Commun. 1974*, 336.

Double-Stranded Molecules: A [6]Beltene Derivative and the Corresponding Open-Chain Polymer**

By *Adelheid Godt, Volker Enkelmann,* and *Arnulf-Dieter Schlüter**

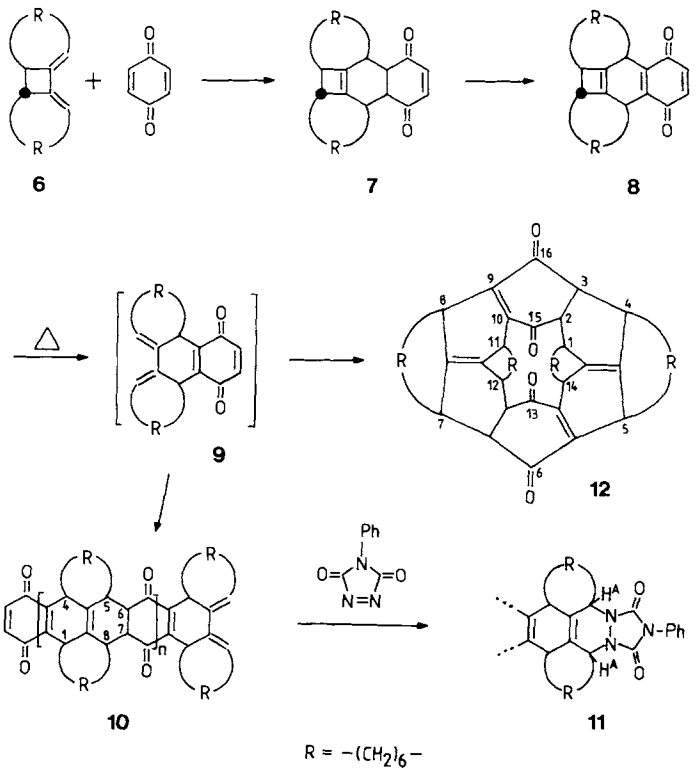
[n]Beltenes **1**, [n]collarenes **2** and [n]cyclacenes **3** have a double-stranded structure of linearly annelated, partly or completely unsaturated six-membered rings.[1] Owing to their cyclic, belt-like structure they are of interest, inter alia, for the study of orbital interactions and host/guest phenomena.[1, 2] A few representatives of this class of compounds recently became accessible, in particular, through the work of *Stoddart* et al.[3] Their open-chain, high molecular weight analogues, for example the ribbon-shaped polymers poly(butane-1,4:3,2-tetrayl) **4** and polyacene **5**, on the other hand, are still unknown, although they should attract great interest, especially from the materials science point of view.[4, 5] We report here on an efficient synthesis of the masked AB-type monomer **8**, which, depending upon the reaction conditions, can be used for the synthesis of the [6]beltene derivative **12** as well as for the synthesis of the corresponding ribbon-shaped polymer **10**. Both compounds are readily soluble, and the structure of **12** has been confirmed by a single-crystal structure analysis.



1 **2** **3** **4** **5**

We recently found that the repetitive Diels-Alder cyclization of bifunctional dienes and bifunctional dienophiles (AA and BB monomers, respectively) is a good method for the synthesis of structurally well-defined ribbon-shaped polymers.[6, 7] In order to gain access to polymers via a route free of stoichiometric problems we searched for an AB-type monomer. Our interest focussed on the compound **8**, which is readily accessible and should be reactive in the sense of the Diels-Alder cyclization.[8] Moreover, it contains flexible alkyl rings which are expected to lead to a significant increase in the solubility of the polymer.[9]

For the synthesis of **8**, the allene dimer **6**,[10] which is readily accessible on a 20 g-scale, was allowed to react with benzoquinone to give the cycloadduct **7** (Scheme 1). This was then oxidized to **8**.[11] When a highly concentrated solution of **8** is heated to 110 °C, an orbital symmetry allowed ring-opening of the cyclobutene ring[12] leads to formation of the required AB-type "monomer" **9**, which then polymerizes.[13] After work-up, an isolable low-molecular weight component and a polymer were obtained (ratio 1:3[14]; total mass balance 90%), the latter of which was assigned the structure **10**.[15] By fractional precipitation monomodally[16] distributed fractions could be obtained with osmometrically (toluene, room temperature) determined molecular weights $\bar{M}_n$ of 8500 (±300) to 116000 (±10000) g mol^{-1} (degree of polymerization $\bar{P}_n$ = 24–330).



6 **7** **8** **9** **10** **11** **12**

$R = -(CH_2)_6-$

Scheme 1.

The addition of the ring-opened monomer (and analogous terminal groups) to the quinoid terminal of the polymer in a growth step should lead to formation of *exo/endo* isomers, each of which can exhibit a different relative arrangement of the alkyl rings. It is therefore not surprising that the polymer **10** consists of a complex mixture of isomers. Its ^{13}C-NMR spectrum (Table 1) shows numerous closely grouped signals which still cannot be assigned individually. These groups lie in the expected shift regions.[17] Particularly informative are the ^{1}H-NMR spectra of low-molecular weight **10** ($n \approx 5$), which is easily accessible by fusion polymerization of **8**.[18] Not only are the typical signals for the polymer clearly recognizable but also the groups of signals for the two termini at $\delta = 5.9$ (diene H atoms) and $\delta = 6.7$ (quinone H atoms),

Table 1. ^{1}H- ($CDCl_3$, 300 MHz) and ^{13}C-NMR data ($CDCl_3$, 75 MHz) of **10** and **12**.

10: ^{1}H-NMR (all signals broad and unstructured): δ = 1.6 (24H), 2.6 (2H), 3.1 (2H), 3.7 (2H); ^{13}C-NMR (assignment via DEPT-sequence): δ = 26.3, 28.8 (CH_2), 32.9 (C-1(4)), 38.1 (CH_2), 43.5 (C-5(8)), 52.7 and 54.3 (C-6(7)), 131.8, 132.9 and 137.3 (C-4a(8a)), 147.1, 148.3, 149.5, 150.7, 151.0 and 151.7 (C-2(3)), 197.6 and 199.7 (C=O).

12: ^{1}H-NMR: δ = 1.15–2.15 (m, 24H), 2.64 (m, 4H; 1-,4-,7-,12-H), 2.86 (m, 4H; 5-,8-,11-,14-H), 3.05 (dd, J = 2.3, 4.2 Hz, 4H; 2-,3-,6a-,12a-H); ^{13}C-NMR: δ = 23.7–38.2 (6t), 37.4 (d; C-5,-8,-11,-14), 45.5 (d; C-1,-4,-7,-12), 53.2 (d; C-2,-3,-6a,-12a), 138.5 (s; C-4a,-7a,-11a,-14a), 154.8 (s; C-5a,-9,-10,-13a), 197.8 (s; C-6,-13,-15,-16).

[*] Dr. A.-D. Schlüter, Dipl.-Chem. A. Godt, Dr. V. Enkelmann
Max-Planck-Institut für Polymerforschung
Postfach 3184, D-6500 Mainz (FRG)

[**] This work was supported by the Bundesministerium für Forschung und Technologie (Project: "Planar Systems"). We thank Prof. Dr. *G. Wegner* for his interest in this work and for his continued support, *R. Dorn* for GPC and osmometric measurements, and *A. Wagner* for carrying out some of the experiments. *A.G.* thanks the Fonds der Chemischen Industrie for a Kekulé fellowship.

which, upon further heating of the material in solution disappear with a concomitant increase of the intensity of the polymer signals and of the molecular weight (GPC). Moreover, the dienoid terminal groups can be detected chemically by addition of *N*-phenyltriazoledione with formation of **11**.[19]

The low-molecular weight component, which was formed as by-product in the polymerization, was identified as the [6]beltene derivative **12**, the cyclic dimer of "**9**" (Table 1). This compound precipitated in stereochemically pure form (^{1}H- and ^{13}C-NMR spectra); the arrangement of the alkyl rings was established by a single-crystal structure analysis.[20] Figure 1 (ORTEP) shows a slightly flattened,[1a] double-stranded cyclic species, which according to the space-filling model (not shown) has only a small "unusable" cavity in the center. The smallest intramolecular distances between atoms that are not bound to each other are observed between the dihydroquinone rings (C3-C6a 3.70, C2-C12a, 3.47, C4-C5a 3.66, C1-C13a 3.60 Å); they lie in the range of the van-der-Waals distances.

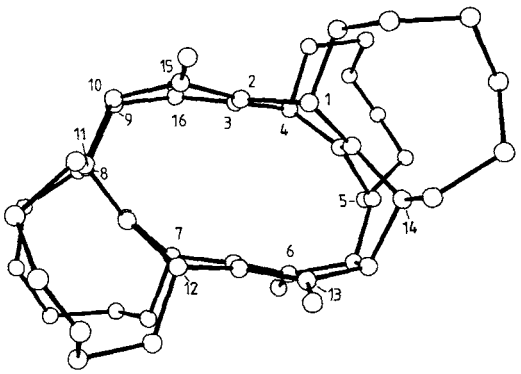
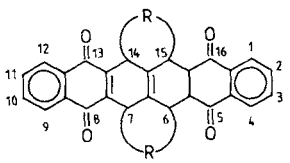


Fig. 1. Structure of **12** in the crystal.

By working in dilute solution it was possible to shift the polymer **10**:dimer **12** ratio from 3:1 to about 1:4 and thus to make the cyclic dimer conveniently accessible in g-amounts—for example, for investigations concerning the aromatizability (yield: 70%).[21]

The spatial shape of polymer **10** is determined by the double stranded structure with its many, presumably irregular kinks, such that a sort of "two-dimensional coil" could result. For investigation of the structure we synthesized the open-chain 2:1-adduct **13** as model compound.[11] This



13

compound (Fig. 2, ORTEP[20]) shows, apart from the benzene rings, a section of the chain of the polymer **10**. The intramolecular distances between the two limbs of the U-shaped adduct **13** lie in the range of the van-der-Waals distances (about 3.5 Å). Extrapolated to the case of polymer **10** this means that the double-stranded main chain is folded back on itself tightly at the corresponding kinks.

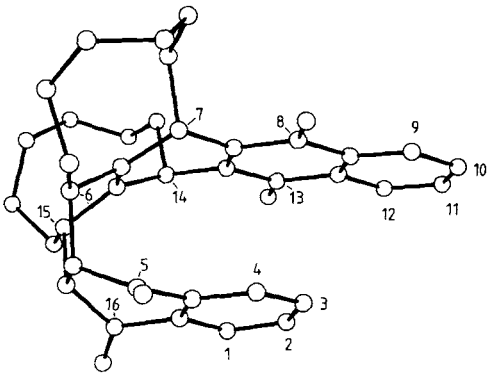


Fig. 2. Structure of **13** in the crystal. Selected distances [Å]: C13a-C16a 3.496(5), C7a-C4a 3.590(5), C7-C5 3.729(5), C14-C16 3.539(5).

Experimental

10: A solution of 3.6 g (10.3 mmol) of **8** in 3 mL of toluene was heated for 41 h at 110 °C, the mixture being diluted after 4 h with 5 mL of toluene. The resulting precipitate (**12**) was removed by filtration on a frit and the polymer recovered from the filtrate by addition of MeOH; yield of **10**: 2.5 g (69%).

12: A solution of **8** (1.62 g, 4.61 mmol) in toluene (300 mL) was heated under reflux for 3 h. After evaporating down the solution, yellowish crystals separated out; yield 1.13 g (70%). M.p. > 260 °C; EI-MS: *m/z* 700 ($M^{\oplus}$, 100%), 350 ($M/2^{\oplus}$, 22%).

Received: August 4, 1989 [Z 3482 IE]
German version: *Angew. Chem. 101* (1989) 1704

[1] a) R. W. Alder, R. B. Sessions, *J. Chem. Soc. Perkin Trans. 2 1985*, 1849; b) F. Vögtle, *Top. Curr. Chem. 115* (1983) 157.

[2] See, e.g. a) B. Kovac, M. Mohraz, E. Heilbronner, V. Boekelheide, H. Hopf, *J. Am. Chem. Soc. 102* (1980) 4314; b) H. C. Kang, A. W. Hanson, B. Eaton, V. Boekelheide, *ibid. 107* (1985) 1979; c) D. J. Cram, K. D. Stewart, I. Goldberg, V. N. Trueblood, *ibid. 107* (1985) 2574; d) A. B. McEwen, P. von R. Schleyer, *J. Org. Chem. 51* (1986) 4357; e) R. O. Angus, Jr., R. P. Johnson, *ibid. 53* (1988) 314.

[3] F. H. Kohnke, A. M. Z. Slawin, J. F. Stoddart, D. J. Williams, *Angew. Chem. 99* (1987) 941; *Angew. Chem. Int. Ed. Engl. 26* (1987) 892; P. R. Ashton, N. S. Isaacs, F. H. Kohnke, A. M. Z. Slawin, C. M. Spencer, J. F. Stoddart, J. J. Williams, *ibid. 100* (1988) 981; the synthesis of a [6]beltene derivative was alluded to in Ref. [2e].

[4] Review of ribbon-shaped polymers: C. G. Overberger, J. A. Moore, *Adv. Polym. Sci. 7* (1970) 113.

[5] Attempts at the synthesis of derivatives of **4** and **5** and descriptions of the expected properties of **5** and similar compounds: K. Messmer, P. Mehnert, *Colloid Polym. Sci. 252* (1974) 97; V. N. Salaurov, Y. G. Kryazhev, T. I. Yushmanova, T. I. Vakul'skaya, M. G. Voronkov, *Makromol. Chem. 175* (1974) 757; C. Clar: *Polycyclic Hydrocarbons, Vol. 1*, Academic Press, New York 1964; S. Kivelson, O. L. Chapman, *Phys. Rev. B28* (1983) 7236; Z. Iqbal, D. M. Ivory, J. Marti, J. L. Bredas, R. H. Baughman, *Mol. Cryst. Liq. Cryst. 118* (1985) 103; M. Ozaki, Y. Ikeda, I. Nagoya, *Synth. Met. 18* (1987) 485.

[6] K. Blatter, A.-D. Schlüter, G. Wegner, *J. Org. Chem. 54* (1989) 2396; K. Blatter, A.-D. Schlüter, *Chem. Ber. 122* (1989) 1351; *Macromolecules 22* (1989) 3506.

[7] T. Vogel, K. Blatter, A.-D. Schlüter, *Makromol. Chem. Rapid Commun. 10* (1989) 427; see also M. Wagner, W. Wohlfarth, K. Müllen, *Chimia 42* (1988) 377.

[8] See, e.g., A. T. Blomquist, J. A. Verdol, *J. Am. Chem. Soc. 78* (1956) 109; L. Skattebøl, S. Solomon, *ibid. 87* (1965) 4506; P. Heimbach, R. Schimpf, *Angew. Chem. 81* (1969) 186; *Angew. Chem. Int. Ed. Engl. 8* (1969) 206; H. Jendralla, K. Laumen, *Chem. Ber. 116* (1983) 2136.

[9] See, e.g., K. Opitz, A.-D. Schlüter, *Angew. Chem. 101* (1989) 513; *Angew. Chem. Int. Ed. Engl. 28* (1989) 456.

[10] S.-H. Dai, W. R. Dolbier, Jr., *J. Am. Chem. Soc. 94* (1972) 3946.

[11] A. Godt, A.-D. Schlüter, unpublished.

[12] See, e.g., R. Criegee, H. G. Reinhardt, *Chem. Ber. 101* (1968) 102.

[13] A similar reaction has been reported but no experimental procedure has been published as yet: W. J. Bailey in D. H. Solomon (Ed.): *Step Growth Polymerization*, Dekker, New York 1972, p. 322.

[14] Owing to a superposition of signals in the ^{1}H-NMR spectrum of the crude mixture of **10** and **12**, only a rough estimation of the ratio can be given.

[15] Polymer **10** forms transparent, free-standing films which are relatively fragile. Viscosity measurements (toluene, room temperature) on a sample with $\bar{M}_n = 20000$ (vapor pressure osmosis) gave a Staudinger index of $\eta = 0.11$ dL g^{-1} (measurement range: 1.4–0.5 gd L^{-1}). Thermogravimetric measurements (heating rate 5 K min^{-1}; under N_2) show that the degradation proceeds in two steps. Between 280 and 410 °C ca. 25% and from 410–700 °C the remaining 75% of the sample underwent degradation.

[16] Gel-permeation chromatography (GPC) in 1,2-dichlorobenzene at room temperature.

[17] H.-O. Kalinowski, S. Berger, S. Braun: *^{13}C-NMR-Spektroskopie*, Thieme, Stuttgart 1984.

[18] When the polymerization is carried out in the melt, the reaction mixture is so viscous, even at very low degrees of polymerization, that growth is brought to a standstill.

[19] The hydrogen atoms of **11** marked with an A appear as unstructured relatively broad signals at $\delta = 4.8$ or $\delta = 4.6$, presumably depending on their stereochemical arrangement.

[20] X-ray structure data of **12** and **13**: Enraf-Nonius CAD-4 diffractometer, room temperature, $Cu_{K\alpha}$ radiation, $\lambda = 1.5405$ Å, graphite monochromator. The structures were solved by direct methods (MULTAN). Empirical absorption correction, anisotropic temperature factors for O and C, refinement of the H atoms in the "riding mode" with fixed isotropic temperature factors. **12**: monoclinic, space group $P2_1/c$, $a = 13.0811(13)$, $b = 13.8608(34)$, $c = 11.1107(12)$ Å, $\beta = 114.602(8)$, $V = 1831.6$ Å^3, $Z = 2$, $\varrho_{calc} = 1.16$ g cm^{-3}, $\mu(Cu_{K\alpha}) = 5.2$ cm^{-1}. 2088 reflections, 873 observed [$I \geq 2\sigma(I)$]. $R = 0.049$, $R_w = 0.053$. **13**: monoclinic, space group $P2_1/c$, $a = 11.1588(6)$, $b = 16.4549(8)$, $c = 17.170(3)$ Å, $\beta = 114.353(10)$, $V = 2872$ Å^3, $Z = 4$, $\varrho_{calc} = 1.29$ g cm^{-3}, $\mu(Cu_{K\alpha}) = 6.12$ cm^{-1}. 4612 reflections, 3230 observed [$I \geq 2\sigma(I)$], $R = 0.053$, $R_w = 0.051$. Further details of crystal structure investigations are available on request from the Fachinformationszentrum Karlsruhe, Gesellschaft für wissenschaftlich-technische Information mbH, D-7514 Eggenstein-Leopoldshafen 2 (FRG), on quoting the depository number CSD-54210, the names of the authors, and the journal citation.

[21] In no case was the formation of [n]beltene derivatives with n ≠ 6 observed. GPC diagrams of representative mixtures show, apart from the polymer signal, only one further signal with longer retention time, which is unequivocally assigned to compound **12** by co-injection.

TlSPh and TlS*t*Bu, Thallium(I) Thiolates with Novel Cagelike Structural Units: $[Tl_5(SPh)_6]^{\ominus}[Tl_7(SPh)_6]^{\oplus}$ and $[Tl_8(StBu)_8]$**

By *Bernt Krebs** and *Andreas Brömmelhaus*

Dedicated to Professor Reginald Gruehn on the occasion of his 60th birthday

Very little has thus far been reported about molecular compounds of low-valent main group elements such as In^I, Tl^I, Sn^{II} and Pb^{II} with sulfur as ligand donor atom. This is especially true in the case of the thiolate complexes or mixed-ligand sulfide-thiolates of these elements, which, as oligomers and polymers, could have interesting structures and properties; further, they are of current interest as models for biologically important metal-coordination centers, e.g. in metallothioneins, and for studying the influence of the s^2 configuration of the metals and relativistic effects on reactivity, structure, bonding and possible metal–metal interactions. Although thallium(I) thiolates were first synthesized as long as 40 years ago,[1] their structural characterization has thus far not been possible. Novel electrochemical methods for their synthesis have been described recently.[2, 3] We have now been able to synthesize thallium(I) thiolates in crystalline form by direct reaction of Tl^I-salts with alkali-metal thiolates. As first compounds of this type, it was possible to characterize thallium(I) thiophenolate TlSPh **1** and thallium(I) *tert*-butyl sulfide TlS*t*Bu **2** by their vibrational spectra and by complete structural analyses. The yellow to orange-yellow compounds are sparingly soluble in all the usual solvents, are stable for a few days, but are sensitive to light.[4]

In the case of **1** the X-ray structure analysis[5] showed a remarkable polymeric structure. The highly symmetric crystal structure is made up of two novel cage-like structural units. They have the compositions $[Tl_5(SPh)_6]^{\ominus}$ **1a** and $[Tl_7(SPh)_6]^{\oplus}$ **1b** and are present in equal amounts in the structure; each unit **1a** is coupled with three units of **1b** and vice versa. **1a** has C_3 symmetry and can be described as a distorted octahedral array of sulfur atoms in which five of the eight faces of the octahedron are bridged by trigonal-pyramidally coordinated thallium atoms (Fig. 1, top). In a similar way **1b** (Fig. 1, bottom), which also has C_3 symmetry, consists of an almost regular octahedron of sulfur atoms in which now seven of the eight faces are bridged by trigonal-pyramidally coordinated thallium atoms. Three of these seven thallium atoms of **1b** (Tl6, 6a and 6b) are each addi-

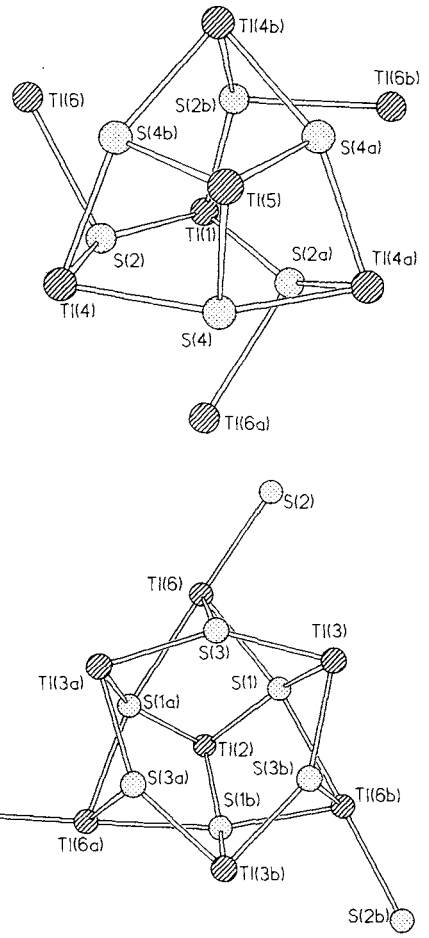


Fig. 1. Above: Structure of the Tl_5S_6 framework in the complex $[TlSPh]_n \equiv [\{Tl_5(SPh)_6\}\{Tl_7(SPh)_6\}]_n$ **1**. The phenyl groups of the SPh ligands have been omitted; Tl(6), Tl(6a), and Tl(6b) are part of neighboring $[Tl_7(SPh)_6]$ groups. Important bond lengths [Å] and angles [°]: Tl(1)-S(2) 2.936(11), Tl(4)-S(2) 2.876(12), Tl(4)-S(4) 2.989(12), Tl(4)-S(4b) 2.910(12), Tl(5)-S(4) 2.932(12); S(2)-Tl(1)-S(2a) 83.6(3), S(2)-Tl(4)-S(4) 91.8(3), S(2)-Tl(4)-S(4b) 79.9(3), S(4)-Tl(4)-S(4b) 77.0(4), S(4)-Tl(5)-S(4b) 77.6(3).—Below: Structure of the Tl_7S_6 framework in **1**. The phenyl groups of the SPh ligands are not shown. S(2), S(2a) and S(2b) are part of neighboring $[Tl_5(SPh)_6]$ groups. Important bond lengths [Å] and angles [°]: Tl(2)-S(1) 2.937(11), Tl(3)-S(1) 2.954(11), Tl(3)-S(3) 2.899(12), Tl(3)-S(3b) 2.891(12), Tl(6)-S(1) 3.163(11), Tl(6)-S(1a) 3.410(12), Tl(6)-S(2) 3.210(11), Tl(6)-S(3) 3.085(13); S(1)-Tl(2)-S(1a) 83.1(3), S(1)-Tl(3)-S(3) 76.3(3), S(1)-Tl(3)-S(3b) 81.7(3), S(3)-Tl(3)-S(3b) 91.0(4), S(1)-Tl(6)-S(1a) 72.5(3), S(1)-Tl(6)-S(2) 106.5(3), S(1)-Tl(6)-S(3) 70.8(3), S(2)-Tl(6)-S(1a) 175.9(3), S(2)-Tl(6)-S(3) 104.2(3), S(3)-Tl(6)-S(1a) 71.9(3).

[*] Prof. Dr. B. Krebs, Dipl.-Chem. A. Brömmelhaus
Anorganisch-chemisches Institut der Universität
Wilhelm-Klemm-Strasse 8, D-4400 Münster (FRG)

[**] This work was supported by the Deutsche Forschungsgemeinschaft and the Fonds der Chemischen Industrie.

tionally bound to a sulfur atom of three neighboring units of **1a** (S2, 2a and 2b), so that the Tl6 atoms are the only ones with a distorted pseudo-trigonal-bipyramidal coordination in the structure. The majority of sulfur atoms are surrounded by three thallium atoms and one phenyl C atom (S2,3,4), whereas S1 is bound square-pyramidally to four thallium atoms and one phenyl C atom.

TlS*t*Bu **2** consists of isolated octanuclear $[Tl_8(StBu)_8]$ molecules with the novel structure shown in Figure 2. The

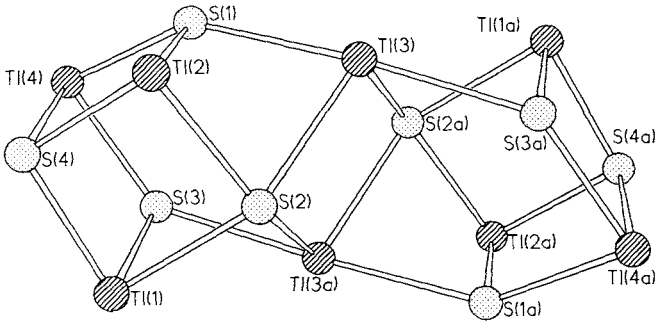


Fig. 2. Structure of the Tl_8S_8 framework in $[Tl_8(StBu)_8]$ **2**. The *tert*-butyl groups of the S*t*Bu ligands are not shown. Important bond lengths [Å] and angles [°]: Tl(1)-S(2) 3.004(5), Tl(1)-S(3) 2.818(7), Tl(1)-S(4) 2.832(8), Tl(2)-S(1) 2.846(7), Tl(2)-S(2) 2.980(8), Tl(2)-S(4) 2.849(7), Tl(3)-S(1) 3.264(6), Tl(3)-S(2) 3.093(6), Tl(3)-S(2a) 2.939(7), Tl(3)-S(3a) 3.193(6), Tl(4)-S(1) 2.830(6), Tl(4)-S(3) 2.863(7), Tl(4)-S(4) 3.030(7); S(2)-Tl(1)-S(3) 75.1(2), S(2)-Tl(1)-S(4) 88.3(2), S(3)-Tl(1)-S(4) 78.3(2), S(1)-Tl(2)-S(2) 83.2(2), S(1)-Tl(2)-S(4) 86.4(2), S(2)-Tl(2)-S(4) 88.4(2), S(1)-Tl(3)-S(2) 74.9(2), S(1)-Tl(3)-S(2a) 95.2(2), S(1)-Tl(3)-S(3a) 165.8(2), S(2)-Tl(3)-S(2a) 91.6(2), S(2)-Tl(3)-S(3a) 104.7(2), S(2a)-Tl(3)-S(3a) 70.6(2), S(1)-Tl(4)-S(3) 80.7(2), S(1)-Tl(4)-S(4) 83.3(2), S(3)-Tl(4)-S(4) 74.4(2).

centrosymmetric molecule consists of two cubane-like $[Tl_3(StBu)_4]$ subunits whose corners are alternately occupied by Tl and S, and in each of which one Tl corner is missing. Both halves of the molecule are coupled via two additional thallium atoms Tl3 and Tl3a with pseudo-trigonal-pyramidal coordination, resulting in formation of a central planar Tl_2S_2 four-membered ring. The thallium atoms of the cubane-like subunits are surrounded trigonal-pyramidally by three sulfur atoms, the sulfur atoms by three thallium atoms and one butyl-C-atom (S1, S3, S4) or tetragonal-pyramidally by four thallium atoms and one butyl-C-atom (S2).

Common features of the structures of **1** and **2** are, as expected, significantly longer Tl–S distances in the TlS_4 polyhedra (2.939–3.410 Å, mean value 3.170 Å) than in the trigonal-pyramidal TlS_3 polyhedra (2.818–3.030 Å, mean value 2.917 Å) and remarkably small S–Tl–S angles of 74.4–88.4° in the TlS_3 groups; the latter indicate repulsive Tl–Tl interactions within the cages and a large steric demand by the lone electron pairs on the Tl atoms. As indicated by the shortest intramolecular Tl–Tl distances of 4.235(3) Å (Tl4 $\cdots$ Tl5) in **1a**, 4.293(2) Å (Tl2 $\cdots$ Tl6) in **1b**, and 3.720(1) Å (Tl2 $\cdots$ Tl3) as well as 4.101(1) Å (Tl1 $\cdots$ Tl3a) in **2**, there are no structural arguments for bonding Tl–Tl interactions. However, there appear to be indications of specific intermolecular (weakly bonding) Tl–Tl interactions in TlS*t*Bu. Here, the stereochemically active lone electron pairs of Tl2 and Tl4 (Fig. 2) are closely neighboring in the channels of the crystal structure, whereby each $Tl_8(StBu)_8$ molecule is in close contact with four others via Tl2 $\cdots$ Tl2′ and Tl4 $\cdots$ Tl4′ distances of 3.864(3) and 3.749(2) Å, respectively.

The $[Tl_5(SPh)_6]^{\ominus}$, $[(Tl_7(SPh)_6]^{\oplus}$ and $[Tl_8(StBu)_8]$ cages have no counterparts in the chemistry of polynuclear metal-ligand systems. In the series of chemically related Tl^I–chalcogen complexes only di- and tetranuclear species have thus far been reported. Thus, thallium(I) methoxide TlOMe has a cubane-like $[Tl_4O_4]$ framework;[6] thallium(I) dithiocarbamates TlS_2CNR_2 contain dinuclear bipyramidal $[TlS_4Tl]$ cages with square-pyramidal coordination of the thallium, which are associated via weak Tl–S bonds in a variety of ways, depending upon the residue R, to give polymeric structures;[7] similarly, dinuclear TlO_2S_2Tl cages are present in the structures of thallium(I) D,L-cysteinate [Tl(D,L-CysH)][8] and thallium(I) tri-*tert*-butoxysilanethiolate [TlSSi(O*t*Bu)$_3$].[9]

Remarkable structural parallels exist between the hepta- and pentanuclear thallium(I) thiolate cages and some cage anions of the homoleptic thiolates of Cu^I and Ag^I, e.g. $[M_4(SR)_6]^{2\ominus}$, $[M_5(SR)_6]^{\ominus}$ and $[M_5(SR)_7]^{2\ominus}$,[10] in which, however, the metal atoms are surrounded linearly by two, or in a trigonal-planar coordination by three sulfur ligands, in contrast to the trigonal-pyramidal or pseudo-trigonal-bipyramidal coordination of the thallium.

Received: August 11, 1989 [Z 3493 IE]
German version: *Angew. Chem. 101* (1989) 1726

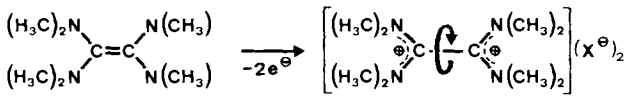
[1] H. Gilman, R. K. Abbott, *J. Am. Chem. Soc. 71* (1949) 659.
[2] R. Kumar, H. E. Mabrouk, D. G. Tuck, *J. Chem. Soc. Dalton Trans. 1988*, 1045.
[3] J. H. Green, R. Kumar, N. Seudeal, D. G. Tuck, *Inorg. Chem. 28* (1989) 123.
[4] *Procedures:* All preparative work was carried out in sealed apparatus under N_2 or Ar.—TlSPh **1**: A solution of NaSPh (665 mg, 5 mmol) in MeCN (50 mL) was added dropwise with stirring to a suspension of Tl_2CO_3 (1.17 g, 2.5 mmol) in MeCN (30 mL). After several days' stirring at 20 °C and removal of a yellow residue by filtration, TlSPh was isolated from the filtrate at 5 °C in the form of orange-yellow rectangular crystals. Yield 32%; correct elemental analysis. Raman spectrum: $\tilde{\nu}$[cm^{-1}] = 421(s), 320(m), 152(sh), 105(vs); IR spectrum: $\tilde{\nu}$[cm^{-1}] = 419(s), 410(m), 403(sh), 398(sh), 315(s), 291(m), 160(vs), 125(sh), 102(w).—TlS*t*Bu **2**: A suspension of 468 mg (1 mmol) of Tl_2CO_3 in 30 mL of MeOH was treated with a solution of 4 mmol of NaS*t*Bu (prepared from 2.6 mL of *t*BuSH and 96 mg of Na) in 30 mL of MeOH. Work-up as for TlSPh. TlS*t*Bu was obtained at −20 °C in the form of yellow needle-like crystals. Yield 40%; correct elemental analysis. Raman spectrum: $\tilde{\nu}$[cm^{-1}] = 410(w), 391(w), 323(m), 169(sh), 120(s); IR spectrum: $\tilde{\nu}$[cm^{-1}] = 362(m), 340(m), 324(w), 288(s), 260(w), 241(m), 180(vs), 132(vs), 120(vs), 104(w).
[5] *Crystal data:* Syntex $P2_1$ four-circle diffractometer, $Mo_{K\alpha}$ radiation, graphite monochromator, scintillation counter, $2\Theta-\Theta$ scan, T = 143 K, empirical absorption corrections. TlSPh **1**: cubic, space group $P2_13$, a = 19.943(3) Å, V = 7931.8 Å^3, Z = 48, ϱ_{calc} = 3.15 g cm^{-3}, $\mu(Mo_{K\alpha})$ = 248 cm^{-1}, crystal dimensions 0.23 × 0.27 × 0.12 mm^3, $2\Theta_{max}$ = 48°, 2298 independent reflections, $R(R_w)$ = 0.060 (0.055) for 1659 reflections with $F_0 \geq 3.92\,\sigma(F_0)$.—TlS*t*Bu **2**: triclinic, space group $P\bar{1}$, a = 11.490(3), b = 11.490(3), c = 12.698(4) Å, α = 108.31(3), β = 91.23(2), γ = 116.99(3)°, V = 1391.3 Å^3, Z = 8, ϱ_{calc} = 2.80 gcm^{-3}, $\mu(Mo_{K\alpha})$ = 235.4 cm^{-1}, crystal dimensions 0.13 × 0.21 × 0.10 mm^3, $2\Theta_{max}$ = 48°, 4403 independent reflections, $R(R_w)$ = 0.060 (0.056) for 3496 reflections with $F_0 \geq 3.92\,\sigma(F_0)$. EXTL and SHELXTL programs, structure solution by direct methods, least squares fit (anisotropic, C in TlSPh isotropic, H atoms isotropic at idealized positions with $U(H) = 1.2\,U_{eq}(C)$. Further details of the crystal structure investigations are available on request from the Fachinformationszentrum Karlsruhe, Gesellschaft für wissenschaftlich-technische Information mbH, D-7514 Eggenstein-Leopoldshafen 2 (FRG), on quoting the depository number CSD-54032, the names of the authors, and the journal citation.
[6] L. F. Dahl, G. L. Davis, D. L. Wampler, R. West, *J. Inorg. Nucl. Chem. 24* (1962) 357.
[7] a) L. Nilson, R. Hesse, *Acta Chem. Scand 23* (1969) 1951; b) P. Jennische, A. Olin, R. Hesse, *ibid. 26* (1972) 2799; c) P. Jennische, R. Hesse, *ibid. 27* (1973) 3531; d) H. Anacker-Eickhoff, P. Jennische, R. Hesse, *ibid. A 29* (1975) 51; e) H. Pritzkow, P. Jennische, *ibid. A 29* (1975) 60; f) E. Elfwing, H. Anacker-Eickhoff, P. Jennische, R. Hesse, *ibid. A 30* (1976) 335.
[8] H. C. Freeman, C. J. Moore, *Acta Crystallogr. B 33* (1977) 2690.
[9] W. Wojnowski, K. Peters, E.-M. Peters, H. G. von Schnering, *Z. Anorg. Allg. Chem. 531* (1985) 147.
[10] See e.g. a) G. Henkel, B. Krebs, P. Betz, H. Fietz, K. H. Saatkamp, *Angew. Chem. 100* (1988) 1373; *Angew. Chem. Int. Ed. Engl. 27* (1988) 1326; b) B. Krebs, G. Henkel, *Adv. Inorg. Chem.*, in press; c) G. A. Bowmaker, G. R. Clark, J. K. Seadow, I. G. Dance, *Polyhedron 3* (1984) 535; d) I. G. Dance, *ibid. 5* (1986) 1037.

Tetrakis(dimethylamino)ethylene Dication: Two CC Singly Bonded and Almost Perpendicularly Twisted $((H_3C)_2N)_2C^{\oplus}$ Carbenium Ions

By *Hans Bock,* Klaus Ruppert, Kurt Merzweiler, Dieter Fenske,** and *Helmut Goesmann*

Dedicated to Professor Edgar Heilbronner

The most simple hydrocarbon with a single π-bond, $H_2C=CH_2$, changes its structure on uptake of the $\pi \rightarrow \pi^*$ excitation energy by twisting of the two molecular halves.[1] Twofold adiabatic ionization requiring considerably higher energy, should produce a dication with a CC single bond between perpendicular $H_2C^{\oplus}$ subunits.[2] To substantiate this prediction, we allowed the fourfold $(H_3C)_2N$-donor-substituted and, therefore, more easily oxidized[3] tetrakis-(dimethylamino)ethylene to react with Cl_2 and Br_2[3,4] and determined the single crystal structures[5] of the resulting dichloride and dibromide salts (Fig. 1), which are stabilized by improved charge delocalization.[6]



Accordingly, the twofold oxidation of the electron-rich tetrakis(dimethylamino)ethylene **1** proceeds via tremendous structural changes (cf. Table 1 and Fig. 1). The two $((H_3C)_2N)_2C^{\oplus}$ molecular halves rotate relative to each other by up to 76° and the CC double bond lengthens to a CC single bond. Simultaneously, the CN single bonds are shortened by 16 pm (!) and the now planar $(H_3C)_2N^{\delta\oplus}$ groups are twisted to different extents out of the two CCN_2 planes. The energetically enforced two electron removal leads—according to geometry-optimized MNDO calculations, the results of which are supported by satisfactory agreement with the measured data—to the changes in charge distribution presented in Scheme 1.

Table 1. Calculated and experimentally determined characteristic structure parameters of tetrakis(dimethylamino)ethylene and its dication.

	M MNDO [2]	$M^{2\oplus}$ MNDO [2]	$[M^{2\oplus}](X^{\ominus})_2$ $X^{\ominus}=Cl^{\ominus}$ [5]	$Br^{\ominus}$ [5]
$\omega(N_2C\text{-}CN_2)$ [°]	14	62	76	67
d(CC) [pm]	136	155	152	151
d(CN) [pm]	147	136	131 [b]	131 [b]
α(CNC) [°]	105 [a]	120 [a]	120	120
ω(C-NC_2) [°]	0 [a]	29	18 [b]	23 [b]

[a] Not optimized. [b] Average value.

[*] Prof. Dr. H. Bock, Dipl.-Chem. K. Ruppert, Dr. K. Merzweiler
Institute of Inorganic Chemistry, University Frankfurt
Niederurseler Hang, D-6000 Frankfurt am Main 50 (FRG)
Prof. Dr. D. Fenske, Dr. H. Goesmann
Institute of Inorganic Chemistry, University Karlsruhe
Engesserstrasse, D-7500 Karlsruhe (FRG)

[**] Structures of Perturbed π Systems, Part 2, and Electron Transfer and Ion Pairing, Part 13. This work was supported by the Deutsche Forschungsgemeinschaft, the Fonds der Chemischen Industrie, and the Land Hessen.—Part 1: H. Bock, H.-F. Herrmann, D. Fenske, H. Goesmann, *Angew. Chem. 100* (1988) 1125; *Angew. Chem. Int. Ed. Engl. 27* (1988) 1067; part 12: H. Bock, H.-F. Herrmann, *J. Am. Chem. Soc. 111* (1989) 7622.

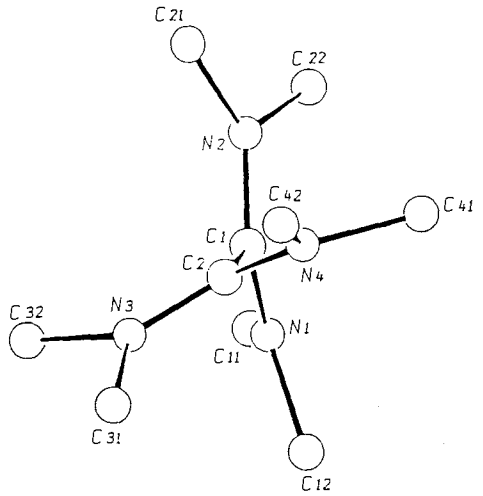
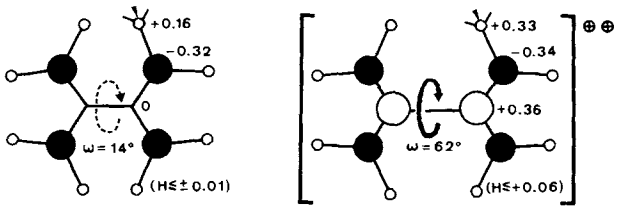


Fig. 1. Structure of the tetrakis(dimethylamino)ethylene dication in its dichloride and dibromide salts [5]. Most important distances [pm] and angles [°] for the dibromide (±1.5 pm, ±1°) and (in brackets) for the dichloride (±0.3 pm, ±0.2°), which contains a twofold crystallographic axis: C1-C2 151.2 (152.4), C1-N1 133.1 (132.0), C1-N2 131.9 (131.5), C2-N3 131.2 (131.5), C2-N4 129.7 (132.0); N1-C1-N2 125 (128.5), N3-C2-N4 127.2 (128.5), C11-N1-C12 113.8 (113.4), C21-N2-C22 115.7 (113.1), C31-N3-C32 115.1 (113.1), C41-N4-N42 112.3 (113.4); N1C1-C2N3 67.2 (75.8), C2C1-N1C11 23.0 (17.1), C2C1-N2C21 18.3 (18.5), C1C2-N3C31 24.4 (18.5), C1C2-N4C41 26.3 (17.1).

Owing to their higher effective nuclear charge, the pyramidally coordinated amino nitrogen centers in the neutral molecule are 'negativated' by the neighboring methyl groups, whereas the electron density at the trigonal planar coordinated carbon π centers remains balanced. In the dication on the other hand, 2/3 of the added positive charges are located at the threefold-coordinated carbon centers of the twisted CC single bond and 4/3 in the eight peripheral methyl groups. Thus, despite an almost constant negative charge on the amino nitrogens each $(H_3C)_2N$ substituent, as predicted by the MNDO valence electron densities (Scheme 1), carries a partial positive charge of about 1/3, i.e. the total charge distribution in the dication is also dominated by the high effective nuclear charge of the nitrogen centers. The Coulomb repulsion between the positive charges, delocalized in each of the $(R_2N)_2C^{\oplus}$ molecular halves, gives rise to both their twisting relative to each other as well as the charging of their "alkyl envelopes".



Scheme 1. MNDO charge distributions for tetrakis(dimethylamino)ethene and its dication.

The structures of the dications (Fig. 1, Table 1) are in accord with numerous other measured data.[3a] The ^{1}H-NMR spectrum,[3a] in contrast to that of the neutral molecule, shows two signals for the methyl group,[7] a result which confirms the fixation, also in solution, of the R_2N substituents due to drastically shortened R_2N–C bonds caused

 © VCH Verlagsgesellschaft mbH, D-6940 Weinheim, 1989 0570-0833/89/1212-1684 $ 02.50/0

by the π charge delocalization. The vibrational spectrum[3a] exhibits two slightly split $\tilde{\nu}_{CN^{\oplus}}$ bands at 1667 and 1672 cm^{-1}, which corroborate a distorted $(N_2C–CN_2)^{2\oplus}$ skeleton lacking an inversion center. A comparison of the UV excitation energies at 36630 and 48800 cm^{-1} with that of the tetramethylformamidinium ion $((H_3C)_2N)_2CH^{\oplus}$ at 44640 cm^{-1} reveals the continued existence of π interaction between both molecular halves, and supports, also in solution, a twist angle of $0° < \omega(N_2C–CN_2) < 90°$, which reflects the counteracting effects of π conjugation and sterically inflicted rotational distortion.

An extensive literature search concerning analogous structural changes in other ethylene dications provided a hint of twisting ($\omega(S_2^{\oplus}C–C^{\oplus}S_2) \approx 60°$)[8a] in the tetrathiafulvalene dication, and for a dihedral angle $\omega(C_2^{\oplus}C–C^{\oplus}C_2) = 41°$ in that of tetra(*p*-methoxyphenyl)ethylene, which is bent at the C=C bond.[8b] In addition, it is pointed out that the two-electron oxidation of 1,2,4,5-tetrakis(dimethylamino)benzene generates a twisted π-conformation of the six-membered ring containing two $[Me_2NC–CNMe_2]^{\oplus}$ subunits, each of which show CC bond distances of 153 pm and dihedral angles of $\omega(NC–CN)^{\oplus} = 49°$.[8c]

Summarizing, the—according to molecular state arguments[9]—inevitable structural changes accompanying differences in energy, and especially differences in the number of valence electrons of a given molecule, thus predominantly lead, in the simplest alkene, $H_2C=CH_2$, and its derivatives, $X_2C=CX_2$, to an elongated CC bond, shortened CX bonds and a twisting of the two molecular halves relative to each other.

Received: May 19, 1989 [Z 3348]
German version: *Angew. Chem. 102* (1989) 1715

[1] A summary of spectroscopic data and of quantum chemical results concerning the $\pi \rightarrow \pi^*$ excitation of ethylene ($\nu > 40000\ cm^{-1} = 5$ eV) into the singlet state $\tilde{A}(^1B_{1u})$ and its presumed D_{2d} structure exhibiting a dihedral angle $\omega = 90°$ between both molecular halves is given by M. B. Robin in: *Higher Excited States of Polyatomic Molecules, Vol. 2, 3,* Academic Press, New York 1975, 1985, pp: 2–22, 213–227, respectively; cf. also the references cited therein.

[2] K. Ruppert, *Diplomarbeit,* Universität Frankfurt 1989. Approximate geometry-optimized MNDO calculations predict for $[H_2C–CH_2]^{2\oplus}$ a total energy difference of $\Delta E \approx 27$ eV, a dihedral angle $\omega = 90°$ and a bond distance $d_{CC} = 146$ ppm. Ab initio SCF calculations (cf. e.g. K. Lammertsma, M. Barzaghi, G. A. Olah, J. A. Pople, A. J. Kos, P. von R. Schleyer, *J. Am. Chem. Soc. 105* (1983) 5252 or G. Frenking, W. Koch, H. Schwarz, *J. Comput. Chem. 7* (1986) 406) confirm the semiempirical result. The unknown structure of the 38-atom neutral molecule of the composition $((H_3C)_2N)_2C=C(N(CH_3)_2)_2$ is MNDO-optimized based on the assumption of pyramidal $(H_3C)_2N$ groups, and the resulting satisfactory correlation with measurement data can be illustrated by the calculated first vertical ionization energy of 7.0 eV (exp. 5.95 eV [3b]). For the dication, planar N_2C subunits with freely rotating R_2N groups are restrictively assumed and reasonable agreement with the slightly differing crystal structure data of the dibromide (2 H_2O, orthorhombic) [5] and the dichloride (2 H_2O, monoclinic C) [5] is achieved (cf. Table 1).

[3] Cf. a) redox investigations and preparation of salts: N. Wiberg, J. W. Buchler, *Chem. Ber. 96* (1963) 3223; summary: N. Wiberg, *Angew. Chem. 80* (1968) 809; *Angew. Chem. Int. Ed. Engl. 7* (1968) 766. b) PE spectrum: B. Cetinkaya, G. H. King, S. S. Krishnamurthy, M. F. Lappert, J. B. Pedley, *J. Chem. Soc. Chem. Commun. 1971,* 1370. c) Half-wave oxidation potential in aprotic ($c_{H^{\oplus}} < 1$ ppm) dimethylformamide solution (H. Bock, D. Jaculi, *Angew. Chem. 96* (1984) 298; *Angew. Chem. Int. Ed. Engl. 23* (1984) 305): the cyclovoltammogram exhibits an unstructured (two-electron) wave between $E_{pc} = -0.63$ V and $E_{pa} = -0.52$ V.

[4] Cf. [2]. Dichloride salt: 3 g (15 mmol) tetrakis(dimethylamino)ethylene were 'titrated' at −10 °C under Ar with an oxygen-free $Cl_2/HCCl_3$ solution until the orange color vanished. After solvent evaporation at room temperature in vacuo, the residue was dissolved in a minimum of CH_3OH and the salt precipitated by pouring the solution dropwise into 200 ml of cold diethyl ether; yield 4.0 g (97%), decomp. 243–247 °C, ^1H NMR (CD_3OD/TMS): $\delta = 3.41$ (s, 12H), 3.77 (s, 12H); IR cf. [3a]. The growth of a single crystal was achieved within six weeks in a two-limbed trap by slow difusion of *n*-hexane into the CH_3OH solution. Dibromide salt: After oxidation with 0.4 mL of Br_2 in 30 mL of carefully degassed $HCCl_3$ at 0 °C, 2.3 g (95%) of a hygroscopic powder precipitate from the orange-colored solution at room temperature. Decomposition at 280 °C; ^1H NMR identical to that of the dichloride; elemental analysis: C 33.06 (33.33), H 6.87 (6.67), N 15.29 (15.56). Growth of single crystal within about 24 h from 5 mL of a C_2H_5OH solution of 1 g of salt by superposing a layer of 3 mL of *n*-hexane (non-compliance of the concentrations quoted yields only powders).

[5] Crystal structure analysis: $[C_{10}H_{24}N_4]^{\oplus\oplus}Cl_2^{\ominus} \cdot 2\,H_2O$, space group *C*2/*c*, $Z = 4$, lattice constants (211 K): $a = 1524.3(8)$, $b = 763.7(4)$, $c = 1758.7(9)$ pm, $\beta = 125.25°(3)$, $V = 1672 \times 10^6$ pm^3, $\mu(Mo_{K\alpha}) = 3.38\ cm^{-1}$. Siemens AED-2 diffractometer, $3° < 2\Theta < 52°$, 1853 reflections, of which 1350 are independent with $I > 3\sigma(I)$. Direct methods, Cl, N, C and O positions anisotropically, detected H positions isotropically refined; $R = 0.039$, $R_w = 0.039$. The dication contains a twofold axis, crystallographically enforced. Angle sums around C1, C2, N1, N2, N3, N4 each 360°. Contact distances Cl–N 359–416 pm, O–N > 400 pm, Cl–O 323 pm. Additional structure parameters: $H_3C–N$ 147.5–148.3 pm. $[C_{10}H_{24}N_4]^{\oplus\oplus}Br_2^{\ominus} \cdot 2\,H_2O$: space group P_{cab}, $Z = 8$, lattice constants (218 K): $a = 928.3(9)$, $b = 2583.8(30)$, $c = 1474.0(15)$ pm, $V = 3535 \times 10^6$ pm^3. $\mu(Mo_{K\alpha}) = 44.81\ cm^{-1}$. Siemens AED-2 diffractometer, $3° < 2\Theta < 48°$, 6829 reflexes, of which 1718 are independent with $I > 2\sigma(I)$. Direct methods, Br, N, C and O positions anisotropically, detected H positions isotropically refined; $R = 0.085$, $R_w = 0.084$. Angle sums around C1, C2, N1, N2, N3, N4 each 360°. Most important contact distances Br–N 362–386 pm, O–N > 400 pm, Br–O 328–334 pm. Additional structural parameters: $H_3C–N$ 145.7–148.2 pm.—Details for both crystal structure determinations are available on request from the Fachinformationszentrum Karlsruhe, Gesellschaft für wissenschaftlich-technische Information mbH, D-7514 Eggenstein-Leopoldshafen 2 (FRG), on quoting the depository number CSD-54165, the names of the authors, and the literature citation.

[6] After submission of our manuscript, we were informed that the crystal structure of 1-$(PF_6^{\ominus})_2$ has been determined. In close agreement with our results for the dichloride and dibromide salts [4], a CC bond distance of 151 pm and a dihedral angle of 72° were found. C. Krieger, K. Elbl-Weiser, H. A. Staab, unpublished. We thank Professor *H. A. Staab,* Max-Planck Institut, Heidelberg, for communicating these unpublished data (cf. also [8c]).

[7] The signal pattern in the ESR spectrum of the radical cation $[((H_3C)_2N)_2C–C(N(CH_3)_2)]^{\cdot\oplus}$, generated by one-electron oxidation, also exhibits different ^1H couplings of 0.328 mT and 0.284 mT (K. Kuwata, D. H. Geske, *J. Am. Chem. Soc. 86* (1964) 2101; J. M. Fritsch, H. Weingarten, J. D. Wilson, *ibid. 92* (1970) 4038).

[8] a) The structure investigation announced for the tetrathiafulvalene dication (B. A. Scott, S. J. La Placa, J. B. Torrance, B. Silverman, B. Welber, *J. Am. Chem. Soc. 99* (1977) 6631) could not be traced. b) The tetra(*p*-methoxyphenyl)ethylene dication (cf. G. A. Olah, P. von R. Schleyer in *Carbonium Ions, Vol. 5,* Wiley Interscience, New York 1976, p. 2445, and references cited therein), however, possesses a shorter CC distance of 143 pm and angle sums around the ethylene carbon atoms of only 350°. c) K. Elbl, C. Krieger, H. A. Staab, *Angew. Chem. 98* (1986) 1024; *Angew. Chem. Int. Ed. Engl. 25* (1986) 1023.

[9] Cf. H. Bock, *Angew. Chem. 89* (1977) 631; *Angew. Chem. Int. Ed. Engl. 16* (1977) 613, and references cited therein.

Tetraphenylethylenedisodium: The Band Structure of the CC Singly Bonded, Twisted $(C_6H_5)_2C^{\ominus}$ Carbanions**

By *Hans Bock,* Klaus Ruppert,* and *Dieter Fenske**

Dedicated to Professor Jack D. Dunitz

Increased mastering of intricate reaction conditions permits "the preparative exploration of ever more shallow potential troughs"[2]—for instance, in the synthesis of air-,

[*] Prof. Dr. H. Bock, Dipl.-Chem. K. Ruppert
Institut für Anorganische Chemie der Universität
Niederurseler Hang, D-6000 Frankfurt am Main 50 (FRG)
Prof. Dr. D. Fenske
Institut für Anorganische Chemie der Universität
Engesserstrasse, D-7500 Karlsruhe (FRG)

[**] Structures of Perturbed π Systems, Part 3, and Electron Transfer and Ion Pairing, Part 14. The work was supported by the Deutsche Forschungsgemeinschaft, the Fonds der Chemischen Industrie, and the Land Hessen. Parts 2 and 13, respectively: [1a].

temperature-, and light-sensitive organic alkali-metal compounds. Their often complex crystal structures,[1b, 3] even after prolonged study, generate a rather "fairy-tale-like" impression, that is, one defying the usual bond rationalization based on formal charges. In our investigations[1a, 4] of dication and dianion salts of the simplest alkene, $H_2C=CH_2$, tetraphenylethylene was allowed to react in diethyl ether under argon (aprotic conditions, $c_H^{\oplus} < 1$ ppm) at room temperature with a sodium mirror obtained by vacuum distillation. After 24 hours of UV-controlled reaction in the dark-red diethyl ether solution, green crystals[5] can be isolated; they exhibit a metallic luster and possess a band structure[6] (Fig. 1).

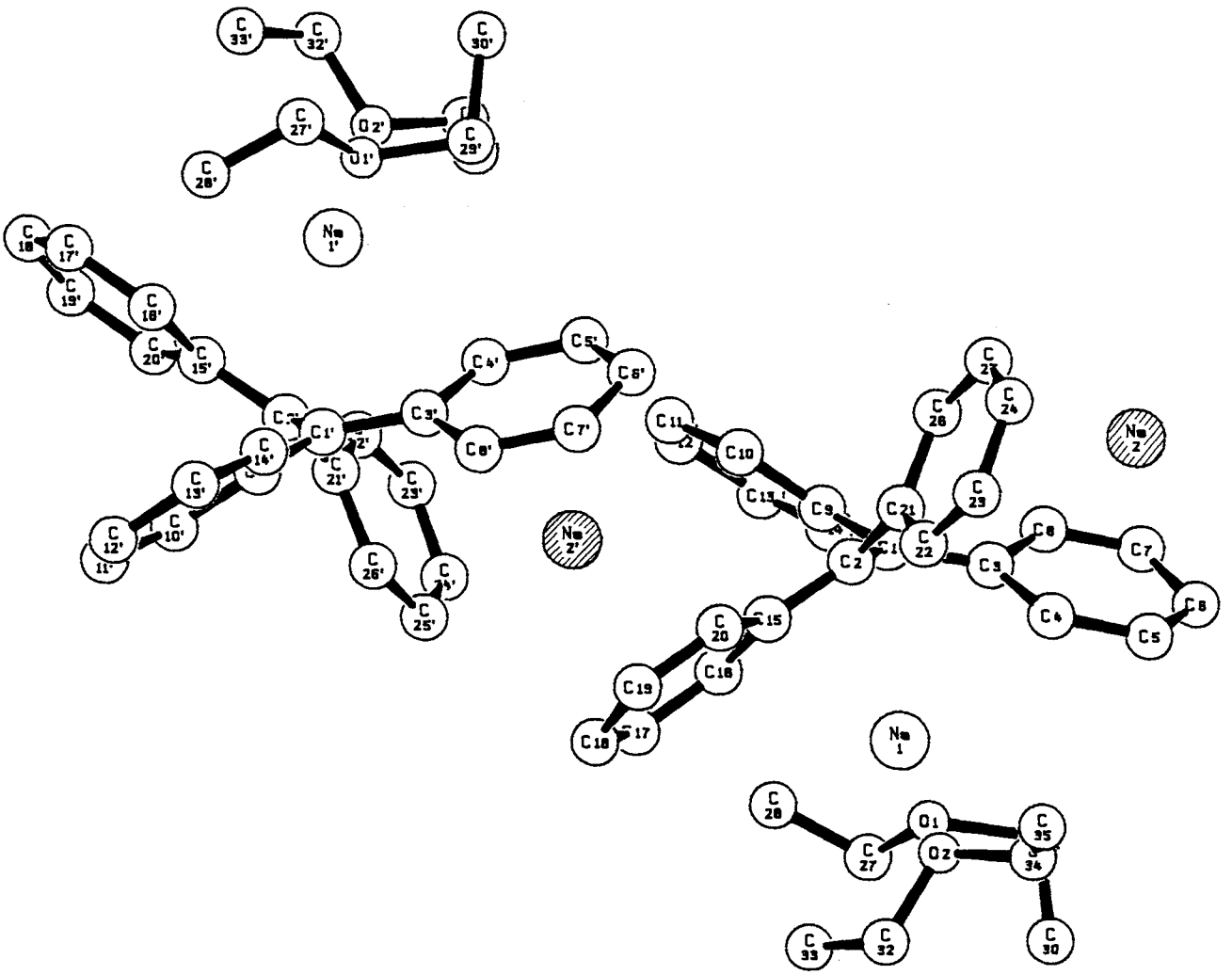


Fig. 1. Segment of the unit cell showing two ion pairs of tetraphenylethylenedisodium bis(diethyl ether), with the hatched sodium centers generating the band structure (cf. Figs. 2 and 3).

Advantageously, a discussion of the delicately balanced electron distribution along a tetraphenylethylenedisodium band starts with the organic chain links (Fig. 2). Upon two-electron reduction, the structure of tetraphenylethylene[7] is changed as follows: The two $(H_5C_6)_2C$ molecular halves twist through 56° relative to each other and the CC double bond is elongated by 13 pm (!) to a CC single bond. In contrast, the C–C_6H_5 distances are shortened by 3 to 6 pm and the twisting of the phenyl rings out of the C1–C3–C9 and C2–C15–C21 planes decreases to values between 10° and 40°. The simultaneous opening of the ethylene angles (e.g., C15–C2–C21 from 114° to 122°) provides further evidence that steric overcrowding is reduced in the dianion and, therefore, most of the structural changes are caused by electronic effects.[8] Partly geometry-optimized MNDO calculations[4] suggest that about 1/3 of the negative charge is localized at the carbon centers C1 and C2, whereas about 1/3 is delocalized in each of the four phenyl rings and causes substantial distortions of the still planar C_6 skeletons, especially in the predominantly Na-coordinating six-membered rings I and III. Thus, the *ipso* angle at C3 of the visibly stretched ring I is reduced to 113°[9] and, in the likewise elongated ring III, the CC bond distances differ by 6 pm (Fig. 2).

The sodium center, solvated by two diethyl ether ligands (Fig. 1: Na1), altogether is eightfold coordinated (Fig. 3, top). Its "zigzag" coordination sphere extends from the π bond C4–C3 in phenyl ring I via the negatively charged, trigonal-planar carbon centers C1 and C2 to the π bond C15–C16 of the phenyl substituent III. Comparable substructures containing metal (metal-ion) contacts to several different ligand parts are observed in numerous alkali-metal organometallic compounds.[3] Surprising, however, is the sandwichlike complexation of Na2, which is supposedly the first unsolvated sodium detected;[3] it connects two $[\{(H_5C_6)_2C\text{-}C(C_6H_5)_2\}^{2\ominus}Na^{\oplus}(OR_2)_2]^{\ominus}$ units and thus provides the link for the band structure (Fig. 1: Na2, hatched). This sodium center (Fig. 3) binds "hexahapto" to phenyl

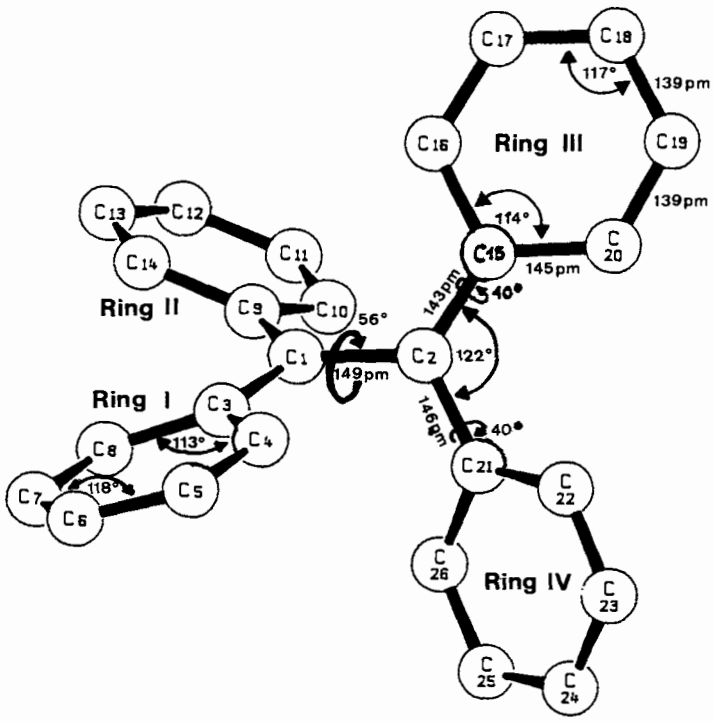
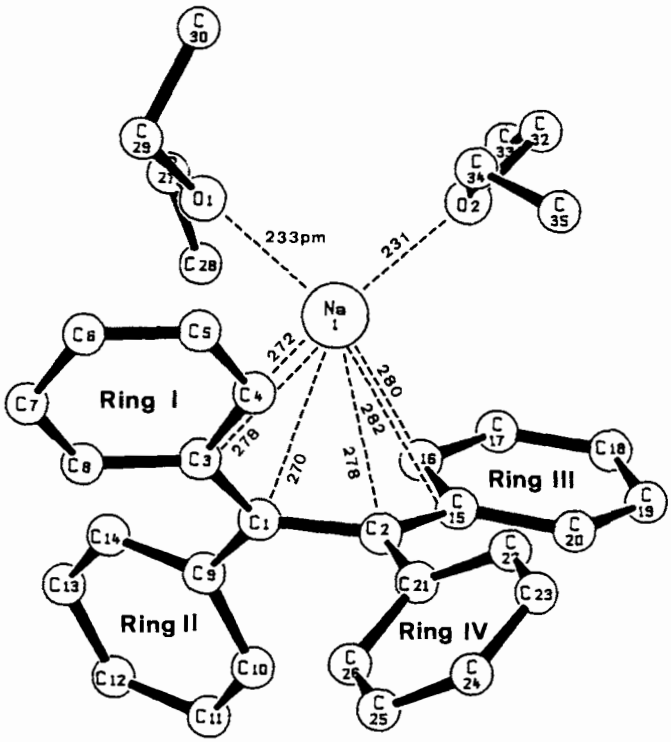


Fig. 2. Carbon skeleton of the tetraphenylethylene dianion.

ring III, which on its "backside" at the centers C15 and C16 already coordinates Na1, and "allyl-like" (C3′, C4′, and C5′) to phenyl ring I of the next tetraphenylethylene unit, which, conversely, on its backside at centers C3′ and C4′, complexes the respective Na1′. Additional contacts are formed to C26 of ring IV and, more distant, to C6′, C7′, and C8′ of ring III. Thus, altogether and depending on the "bond distance" limitation imposed, an Na2 coordination number between 10 and 14 results. In addition, it should be pointed out that the two phenyl rings I and III, each of which extend coordinative links on both sides to sodium centers, exhibit the smallest twist angles relative to the planes of the molecular halves (cf. Fig. 2: C2–C1–C3–C4 14° and C1–C2–C15–C16 10°) and also the longest CC bond distances between the respective Na-coordinated ring centers (Figs. 2 and 3).

For the rather unusual sandwichlike coordination of Na2, the following parallels have emerged from an extensive literature search: Lithium 7b*H*-indeno[1,2,3-*jk*]fluorenide contains a "dodecahapto" embedded Li center between each of its two coplanar, coaxial, and 386-pm-spaced phenyl ring pairs.[10a] In lithium 1,1,3,3-bis(2,2′-biphenylene)propenide diethyl ether, the Li-di(η^6-phenyl) sandwich between two different molecular units opens on one side by 56° owing to the additional R_2O solvation.[10b] In contrast, the Na center in $(H_5C_6)_3CNa \cdot TMEDA$, which also exhibits a band structure,[10c] prefers a rather short bond of only 264 pm to the carbanion center rather than a "polyhapto" coordination to the phenyl rings.

In tetraphenylethylenedisodium, which crystallizes from the diethyl ether solution after reduction with a sodium mirror, the two negative formal charges are largely delocalized,



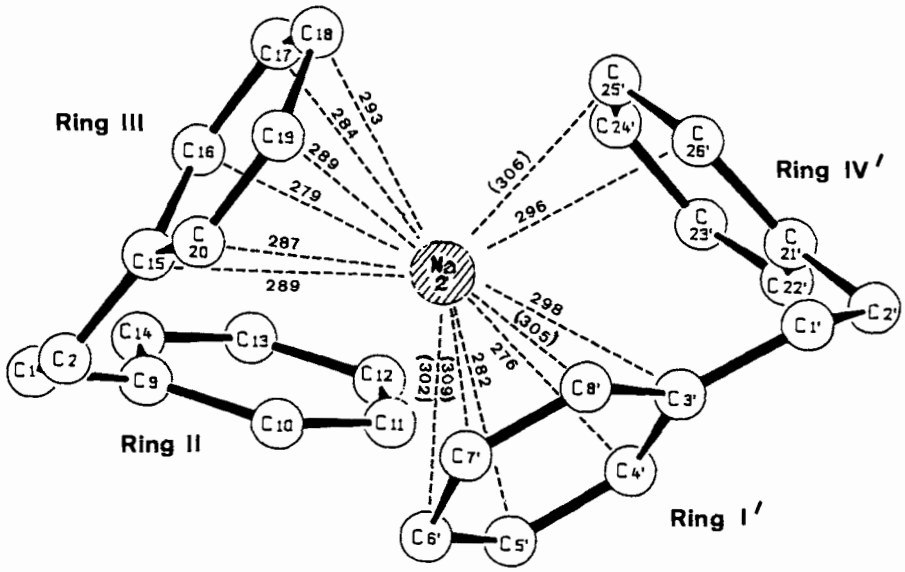


Fig. 3. Coordination spheres around the two different Na centers in tetraphenylethylenedisodium.

predominantly in the CC singly bonded and twisted diphenylcarbanion molecular halves and partly—owing to the sandwich complexation of Na2—also in the "one-dimensional" bands, which are separated from each other by the alternatingly "left-right" arranged countercations $^{\oplus}Na(OR_2)_2$. The unexpected formation of this solid-state structure may be tentatively rationalized by the following literature observations: tetraphenylethylene radical anion $M^{\bullet\ominus}$, generated by single electron transfer, is of comparable structure to the sterically overcrowded neutral molecule M[11a] and, therefore, in ether solution only forms "solvent separated", radical-ion pairs $(M^{\bullet\ominus}_{solv} \cdots Na^{\oplus}_{solv})$[11a] and thus preferentially disproportionates via $2\,M^{\bullet\ominus} \rightarrow M + M^{2\ominus}$ to its dianion.[11b] Owing to considerable structural changes, this can be stabilized as a contact ion pair $[M^{2\ominus}Na^{\oplus}_n]^{(2-n)\ominus}$ ($n \leq 2$), and presumably crystallizes under the reaction conditions chosen—like the dimer [fluorenone$^{\bullet\ominus}$Na$^{\oplus}$-(DME)$_2$]$_2$[11b]—in the band structure reported.

Received: May 19, 1989 [Z 3349 IE]
German version: *Angew. Chem. 101* (1989) 1717

[1] a) H. Bock, K. Ruppert, K. Merzweiler, D. Fenske, H. Goesmann, *Angew. Chem. 101* (1989) 1715, *Angew. Chem. Int. Ed. Engl. 28* (1989) 1684; b) cf. also H. Bock, H.-F. Herrmann, D. Fenske, H. Goesmann, *ibid. 100* (1988) 1125 and *27* (1988) 1067, and references cited therein.

[2] Remark by *J. D. Dunitz*, ETH Zürich, on the occasion of a lecture at the Universität Frankfurt on January 9, 1989.

[3] Cf. reviews on the structures of organolithium compounds (W. N. Setzer, P. von R. Schleyer, *Adv. Organomet. Chem. 24* (1985) 353) as well as on organometallic derivatives of higher alkali metals (C. Schade, P. von R. Schleyer, *ibid. 27* (1987) 169), and references cited therein.

[4] K. Ruppert, *Diplomarbeit*, Universität Frankfurt 1989. Approximative geometry-optimized MNDO calculations neglecting the countercations predict for the fictive ethylene dianion the following (gas-phase) data. $\Delta E_{total} \approx 10$ eV, $\omega = 90°$, $d_{CC} \approx 140$ pm (for $Li_2C_2H_4$ cf. A. J. Kos, E. D. Jemmis, P. von R. Schleyer, R. Gleiter, U. Fischbach, J. A. Pople, *J. Am. Chem. Soc. 103* (1981) 4996). For the tetraphenylethylene dianion, the calculations started from the crystal structure data (exception: hexagonal C_6 rings) and on partial MNDO optimization (keeping $d_{CC} = 150$ pm and $\omega = 56°$ constant) the bond distances $d_{C\ phenyl} \approx 145$ pm and twist angles ω(phenyl) $\approx 35°$ result. The MNDO charge distribution is: C1 = C2 = −0.29, $C^{ortho}_{phenyl} = -0.13$, $C^{para}_{phenyl} = -0.21$. Calculations with cation simulating "sparkles" do not converge, cf. [8].

[5] Cf. [2]. Vacuum distillation of 70 mg (3 mmol) of Na in a Schlenk trap under Ar yields a sodium mirror, which reacts with 505 mg (1.5 mmol) tetraphenylethylene in 30 mL of water-free diethyl ether under Ar at room temperature within 24 h to a dark-red solution. ESR and UV/VIS spectra ($\nu_m \approx 21000$ cm^{-1}) do not provide evidence for the radical anion as an intermediate, which in its blue dimethoxyethane solution shows a characteristic absorption ($\tilde{\nu}_m = 15400$ cm^{-1}). The green, shiny metallic crystals precipitated are extremely air-sensitive and, therefore, have to be handled in a stream of N_2.

[6] Crystal structure analysis of $C_{26}H_{20}Na_2 \cdot 2\,O(C_2H_5)_2$: space group $P2_1/n$, $Z = 4$, lattice constants (210 K): $a = 997.8(5)$, $b = 1545.4(9)$, $c = 2025.1(10)$ pm, $\beta = 100.59°(4)$, $V = 3069.5 \times 10^6$ pm^3 · $\mu(Mo_{K\alpha}) = 0.63$ cm^{-1}, Siemens AED-2 diffractometer, $3° < 2\Theta < 52°$, 6199 reflections, of which 2932 are independent with $I > 2\sigma(I)$. Direct methods, Na, O, and C positions anisotropic, detected H positions isotropically refined; $R = 0.099$, $R_w = 0.102$. The unsatisfactory high R value is due to decomposition of the crystal in the X-ray beam; for the decomposition correction, an approximate linear relation has been assumed. Deviations in structural parameters (Figs. 1–3): ±1.5 pm and ±0.8°; angle sums of all six-membered rings 720 ± 0.5°. Further details of the crystal structure determination are available on request from the Fachinformationszentrum Karlsruhe, Gesellschaft für wissenschaftlich-technische Information mbH, D-7514 Eggenstein-Leopoldshafen 2 (FRG), on quoting the depository number CSD-51466, the names of the authors and the literature citation.

[7] A. Hoekstra, A. Vos, *Acta Crystallogr. B31* (1975) 1722. Selected structural parameters: C1-C2 136 pm, C3-C1-C2-C15 8.4°, C15-C2-C21 114.4°, C-C_6H_5 150 pm, C1-C2-C_6H_5 43–57°, angle sum of all six-membered rings 720°. Cf. also the structure of the dianion of bifluorene, prepared by deprotonation (M. Walczack, G. D. Stucky, *J. Organomet. Chem. 97* (1975) 313), which possesses a CC bond distance elongated from 139 pm to 149 pm and a dihedral angle $\omega(C_2C\text{–}CC_2) = 48°$. In the largely interaction-free dianion of tetracyanoethylene (D. A. Dixon, J. S. Miller, *J. Am. Chem. Soc. 109* (1987) 3656) a central CC bond distance of 149 pm and a dihedral angle of 87° are observed. After submission of this publication, the crystal structure of tetrakis(trimethylsilyl)ethylenedilithium was published (A. Sekiguchi, T. Nakanishi, C. Kabuto, H. Sakurai, *J. Am. Chem. Soc. 111* (1989) 3748); the dihedral angle ($\omega = 34°$) is only slightly increased relative to that ($\omega = 34°$) of the sterically overcrowded parent molecule.

[8] Cf. M. A. Fox, D. Shultz, *J. Org. Chem. 53* (1988) 4386, and references cited therein. The MO calculations, according to which a planar dianion should be about 40 kJ mol^{-1} more stable than the one exhibiting orthogonal $(H_5C_6)_2C$ molecular halves, neglect the effect of the countercations (cf. also [2]); cf. also *J. Am. Chem. Soc. 111* (1989) 6311.

[9] For the substituent-dependence of *ipso* angles in benzene derivatives, cf. T. Maezke, D. Seebach, *Helv. Chim. Acta 72* (1989) 624, and references cited therein; an angle of 109° is reported for tBu$_3$C$_6$H$_2$Li · TMPN (TMPN = *N,N,N',N'*-tetramethylpropane-1,2-diamine). Cf. also U. Schümann, E. Weiss, *Angew. Chem. 100* (1988) 573, *Angew. Chem. Int. Ed. Engl. 27* (1988) 583), who determined an *ipso* angle of 111° in $[Li(C_6H_5)_4 \cdot (Na \cdot TMEDA)_3]$.

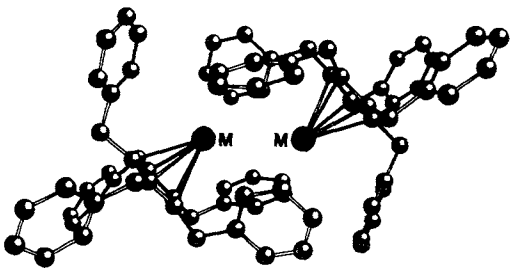
[10] a) B. Bladauski, H. Dietrich, H. J. Hecht, D. Rewicki, *Angew. Chem. 89* (1977) 490; *Angew. Chem. Int. Ed. Engl. 16* (1977) 474; b) D. Bladauski, D. Rewicki, *Chem. Ber. 110* (1977) 3920; c) H. Köster, E. Weiss, *J. Organomet. Chem. 168* (1979) 273; cf. also [3].

[11] Cf. [8] and references cited therein, especially a) R. C. Roberts, M. Szwarc, *J. Am. Chem. Soc. 87* (1965) 5542; b) J. F. Garst, *ibid. 93* (1972) 6312 and references cited therein.

Tl^I–Tl^I Interactions in the Molecular State—an MO Analysis**

By *Christoph Janiak* and *Roald Hoffmann**

Are direct bonds possible between Tl^I or In^I atoms? The question is raised by the pentabenzylcyclopentadienylthallium dimer, $[(PhCH_2)_5C_5Tl]_2$ (**1a**)[1] and its isostructural indium analogue (**1b**),[2] both synthesized by *Schumann* and coworkers.[3]



1a, M = Tl
1b, M = In

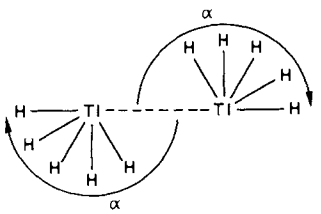
Both centrosymmetric dimers feature a relatively covalent metal–cyclopentadienyl interaction, a metal–metal contact of 363 pm and a Cp'(centroid)–M–M angle of 131.8° (**1a**) or 136.5° (**1b**).[1, 2] Unambiguous Tl^I–Tl^I or In^I–In^I bonds are not yet known in molecular complexes, as they are, for example, for the related Ge^{II} or Sn^{II} in $[\{(Me_3Si)_2CH\}_2M]_2$.[4] To us a Tl···Tl contact only about 20 pm longer than in Tl metal,[5] occurring in the absence of bridging, is definitely suggestive of direct metal–metal bonding. A few bridged complexes with similar length Tl···Tl contacts are also

[*] Prof. R. Hoffmann, Dr. C. Janiak
Department of Chemistry and Materials Science Center
Cornell University, Ithaca, NY 14853 (USA)

[**] This work was supported by the Deutscher Akademischer Austauschdienst (DAAD) through the award of a NATO postdoctoral fellowship for *C. J.* and by the National Science Foundation through grant CHE-8406119.

known.[6] However, the apparent consensus and a brief theoretical study[7] interpret these as resulting from the bridging coordination. A short Tl–Tl bond (284 pm), albeit between Tl^{II} centers, has recently been found in $Tl_{0.8}Sn_{0.6}Mo_7O_{11}$.[8]

An analysis of a model C_5H_5Tl dimer led us to focus on the significant role of the L–Tl–Tl angle (L = ligand). The gist of what we observe is retained as we simplify the C_5H_5 ligand to OCH_3,[6e] Te,[6f] and H. So in the sequel we focus on the simplest model, namely, HTlTlH (**2**), shown in



2

Scheme 1. Definition of the angle α in HTlTlH (**2**).

Scheme 1 with the important H–Tl–Tl angle α. Figure 1 shows a plot of the calculated overlap population as a function of α.[9]

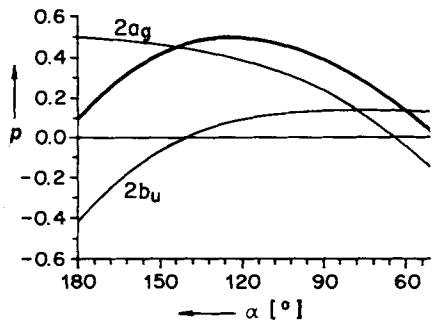


Fig. 1. Dependence of overlap population p on H–Tl–Tl angle α with Tl–Tl = 370 pm and Tl–H = 190 pm. Bold curve: total overlap populations. α = 180° corresponds to linear H_2Tl_2.

The surprising result is that the overlap population between the Tl atoms in **2** shows a dramatic increase, upon bending, to a substantial maximum at a H–Tl–Tl angle of around 120°, followed by an eventual decline towards the bridging geometry. For the more realistic Cp ligand, the Tl–Tl overlap populations at α = 180°, 131.6°, 120°, and 90° are 0.177, 0.347, 0.367, and 0.296, respectively (Tl–Tl = 370, Tl–Cp(centroid) = 249 pm).

Both the magnitude and the range of variation are extraordinary. The question raised in the beginning is answered with a definite yes: There is a Tl^I–Tl^I bond in these compounds, at least for a bent geometry.

How can there be a bond between two filled s^2 subshells, which is the way one might think of Tl^I or In^I? The answer is "it is a consequence of efficient mixing of formally vacant np orbitals, that is, hybridization". In the case at hand, a calculation on 120°-bent HTlTlH, using only a Tl 6s basis (i.e., no 6p orbitals) yields a Tl–Tl overlap population of − 0.026 (compare the + 0.490 from Fig. 1 for the case where both s and p orbitals on Tl are included). Changing an initial repulsion of closed subshells into an attraction, by inclusion of unfilled orbitals, is a general phenomenon. It can also be seen in d^{10}-d^{10} systems, such as Cu^I-Cu^I,[13] Pt^0-Pt^0,[14] and Au^I-Au^I,[15] whose bonding interactions are based on a d–s–p mixing. Relativistic effects may be important in the bonding of some of these systems as well as in the thallium dimer.[16]

For LTlTlL the relevant mixing is sp. In a sense this is no surprise—Tl is a main-group element. Perhaps it is worthwhile to draw an analogy with the "isoelectronic" $HCCH^{2\oplus}$. One would not doubt for a moment the necessity of sp hybridization or the presence of a C–C bond in this acetylene dication. But that just raises the further question: Why is LTlTlL bent? The acetylene analogy is not immediately helpful in this matter. There is also the remarkable sensitivity of the Tl–Tl bonding to the H–Tl–Tl angle displayed in Figure 1. We approach these questions by a decomposition of the total overlap population versus angle function (see Fig. 1) into its major components from the HOMO ($2b_u$) and the orbital below the HOMO ($2a_g$). From the slope of the curves, it is obvious that from 180° to 120° the $2b_u$ orbital dominates the changes in the overlap population, while from 120° to 60° the $2a_g$ orbital is the governing factor.

The origins of the bending can be traced with the help of a Walsh diagram for the relevant orbitals in **2** (Fig. 2). From

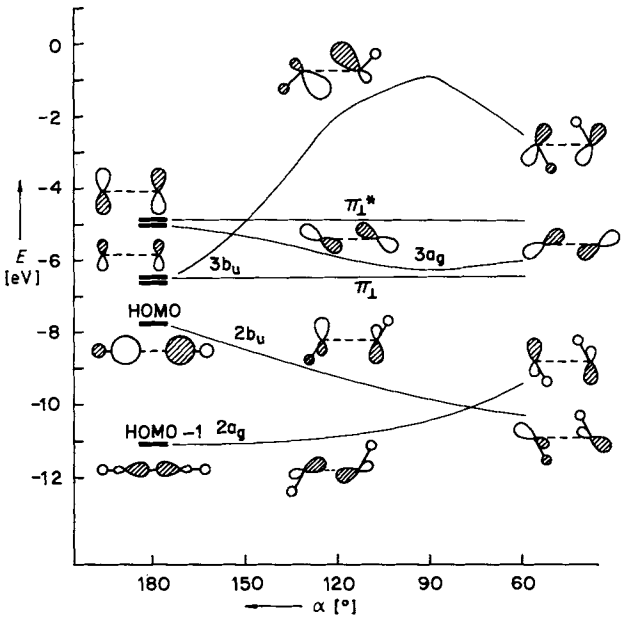
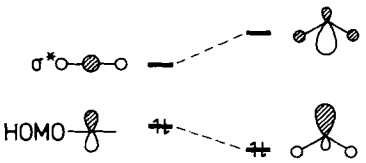


Fig. 2. Partial Walsh diagram for the bending in **2** with Tl–Tl = 370 pm and Tl–H = 190 pm. Symmetry labels are for point group C_{2h}; orbital drawings are schematic $\pi_\perp$, $\pi_\perp^*$: π sets perpendicular to the plane of the molecule.

the orbital sketches, it may be seen that the stabilization and change in character of $2b_u$ results from strong mixing with the empty $3b_u$ orbital—pushing both levels apart. The lowest energy for **2** is calculated around 105°.

What happens in the *trans* bending of HTlTlH is closely related to the critical orbital interactions in the pyramidalization of AH_3 systems (e.g., NH_3, $CH_3^\ominus$, PR_3) and the bending of AH_2 molecules (e.g., H_2O, H_2S).[17] The orbitals guiding these deformations are sketched for AH_2 in Scheme 2.

The controlling orbital (HOMO for both AH_3 and AH_2) is a lone pair centered on the A atom. This level decreases in



Scheme 2. The orbitals involved in bending of AH_2 molecules. Left: linear AH_2. Right: bent AH_2.

energy with bending, mixing in more s character and a hydrogen contribution from an empty A–H σ* orbital above, to give a stabilized filled orbital with A–H nonbonding character and an empty level which is destabilized and strongly A–H antibonding. The lone pair occupies a pure p orbital in the planar AH_3 or linear AH_2 geometry. The closer the higher σ* combination to the p orbital, the stronger is the tendency to bend. Essentially the same thing happens in HTlTlH. The only difference is that in the Tl case the upper orbital ($3b_u$) is of Tl p character, whereas in AH_3 and AH_2 it is the lower orbital. This can be traced to the long Tl–Tl separation. As soon as bending and therefore mixing begins, this distinction becomes unimportant. The $2b_u$ and $3b_u$ orbitals in **2** are close to each other in energy, which they are not in the isoelectronic $HCCH^{2\oplus}$.

While the $2b_u$ mixes very strongly with the $3b_u$ combination in the 180° to 120° range, thereby transforming its character from strongly antibonding to slightly bonding, the main Tl–Tl bonding orbital, $2a_g$, shows only very small interactions with orbitals of the same symmetry in this region. The $2a_g$ orbital thus retains its strongly bonding character (see Fig. 1). From 120° on, the mixing of $2a_g$ with other levels, however, gets much stronger as appropriate symmetry combinations come closer in energy. Hence, the $2a_g$ Tl–Tl overlap population drops rapidly to nonbonding as one approaches the bridging geometry. With the ligands in the bridging positions, both $2a_g$ and $2b_u$ can be considered as lone-pair combinations, with only a small overlap population between the thalliums. Another way of thinking about this mixing, governed by orbital level energies, is that it provides the opportunity for a stereochemically active lone pair.

To summarize: HTlTlH and CpTlTlCp want to bend at Tl as a result of a near resonance in the energy of the $2b_u$ (σ*) and $3b_u$ (π) orbitals. The factors favoring pyramidalization are similar to those for EL_2,EL_3 (and L_2EEL_2), except that the driving force is stronger in HTlTlH. There definitely is Tl^I–Tl^I bonding in these structures. The bonding in the formally s^2–s^2 closed subshell interaction is due to the mixing of formally empty p levels into the filled s combinations. We are now analyzing the full range of Tl^I–Tl^I interactions in molecular and extended structures.

Received: July 4, 1989 [Z 3424 IE]
German version: *Angew. Chem. 101* (1989) 1706

CAS Registry number:
TlH, 13763-69-4.

[1] H. Schumann, C. Janiak, J. Pickardt, U. Börner, *Angew. Chem. 99* (1987) 788; *Angew. Chem. Int. Ed. Engl. 26* (1987) 789.
[2] H. Schumann, C. Janiak, F. Görlitz, J. Loebel, A. Dietrich, *J. Organomet. Chem. 363* (1989) 243.
[3] For another modification of **1a** see H. Schumann, C. Janiak, M. A. Khan, J. J. Zuckerman, *J. Organomet. Chem. 354* (1988) 7.
[4] P. B. Hitchcock, M. F. Lappert, S. J. Miles, A. J. Thorne, *J. Chem. Soc. Chem. Commun 1984*, 480, and references therein.
[5] R. W. G. Wyckoff: *Crystal Structures, Vol. 1*, 2nd ed., Interscience Publishers, New York 1963. Shortest Tl–Tl distance in hexagonal closed packed lattice, 343.8 pm; in body-centered cubic lattice, 336.2 pm.
[6] See, for example, a) J. M. Cassidy, K. H. Whitmire, *Inorg. Chem. 28* (1989) 1432, and references herein; b) S. Harvey, M. F. Lappert, C. L. Raston, B. W. Skelton, G. Srivastava, A. H. White, *J. Chem. Soc. Chem. Commun 1988* 1216; c) M. Veith, F. Goffing, V. Huch, *Chem. Ber. 121* (1988) 943; d) J. Beck, J. Strähle, *Z. Naturforsch. B41* (1986) 1381; e) R. C. Burns, J. D. Corbett, *J. Am. Chem. Soc. 103* (1981) 2627; f) L. F. Dahl, G. L. Davis, D. L. Wampler, R. West, *J. Inorg. Nucl. Chem. 24* (1962) 357.
[7] K. H. Whitmire, R. R. Ryan, H. J. Wasserman, T. A. Albright, S.-K. Kang, *J. Am. Chem. Soc. 108* (1986) 6831.
[8] R. Dronskowski, A. Simon, *Angew. Chem. 101* (1989) 775; *Angew. Chem. Int. Ed. Engl. 28* (1989) 758.
[9] The computations were performed within the extended Hückel formalism [10] with weighted H_{ij}'s [10c]. The following atomic parameters were used in our calculations (H_{ij}, ζ) [11]: Tl 6s: − 11.6 eV, 2.3; 6p: − 5.8 eV, 1.6 [12]; H 1s: − 13.6 eV, 1.3 [10a]; C 2s: − 21.4 eV, 1.625; 2p: − 11.4 eV, 1.625 [10a].
[10] a) R. Hoffmann, *J. Chem. Phys. 39* (1963) 1397; b) R. Hoffmann, W. N. Lipscomb, *ibid. 36* (1962) 2179; *ibid. 37* (1962) 2872; c) J. H. Ammeter, H. B. Bürgi, J. C. Thibeault, R. Hoffmann, *J. Am. Chem. Soc. 100* (1978) 3686.
[11] Dr. *Gordon Miller*, Stuttgart, pointed out another Tl parameter set to us (cf. [9]) based on work by *Timothy Hughbanks* (College Station, TX, private communication) (6s: − 12.8 eV, 2.52; 6p: − 5.1 eV, 1.77). The use of this parameter set retains the dependence of overlap population on α but cuts the absolute value at the 120° maximum approximately in half.
[12] T. A. Albright (Houston), private communication 1988.
[13] a) P. K. Mehrotra, R. Hoffmann, *Inorg. Chem. 17* (1978) 2187; b) K. M. Merz, R. Hoffmann, *ibid. 27* (1988) 2120.
[14] A. Dedieu, R. Hoffmann, *J. Am. Chem. Soc. 100* (1978) 2074.
[15] Y. Jiang, S. Alvarez, R. Hoffmann, *Inorg. Chem. 24* (1985) 749.
[16] See a) W. C. Ermler, R. B. Ross, P. A. Christiansen, *Adv. Quantum Chem. 19* (1988) 139; b) P. Pyykkö, *Chem. Rev. 88* (1988) 563; c) F. Scherbaum, A. Grohmann, G. Müller, H. Schmidbaur, *Angew. Chem. 101* (1989) 464; *Angew. Chem. Int. Ed. Engl. 28* (1989) 463, and references therein.
[17] a) T. A. Albright, J. K. Burdett, M.-H. Whangbo: *Orbital Interactions in Chemistry*, Wiley-Interscience, New York 1985; b) B. M. Gimarc: *Molecular Structure and Bonding*, Academic Press, New York 1979.

Inter- and Intramolecular Photochemical C–H Activation in Matrices and in Solution with (η^6-Arene)(carbonyl)osmium Complexes**

By *Andrew McCamley, Robin N. Perutz,* Stefan Stahl,* and *Helmut Werner**

Dedicated to Professor Walter Strohmeier on the occasion of his 70th birthday

Matrix isolation has proved to be an effective means both for observing C–H activation of methane and for characterizing the coordinatively unsaturated complexes implicated in this process.[1, 2] However, the identification of the (methyl)hydride complexes resulting from insertion into methane [Eq. (a)] has rested so far on the observation of CO and

$$\left.\begin{matrix}[L_nMH_2] \xrightarrow[-H_2]{h\nu} \\ [L_nM(CO)] \xrightarrow[-CO]{h\nu}\end{matrix}\right\rangle \rightarrow [L_nM] \xrightarrow{CH_4} [L_nM(CH_3)H] \qquad \text{(a)}$$

MH stretching vibrations in the IR spectrum (e.g., in the formation of $[(\eta^5\text{-}C_5H_5)Ir(CO)(CH_3)H]$ from $[(\eta^5\text{-}C_5H_5)Ir(CO)_2]$).[1] Suitable precursors for such photochemi-

[*] Dr. R. N. Perutz, A. McCamley
Department of Chemistry, University of York
York Y01 5DD (UK)
Prof. Dr. H. Werner, Dipl.-Chem. S. Stahl
Institut für Anorganische Chemie der Universität Würzburg
Am Hubland, D-8700 Würzburg (FRG)

[**] This work was supported by SERC, the Deutsche Forschungsgemeinschaft, the Royal Society, the Fonds der Chemischen Industrie, NATO, British Gas, and Degussa AG.

cal reactions include metal carbonyl, dihydride, and ethene complexes. In the latter case, elimination of ethene may compete with insertion into the C–H bonds of ethene, as has been demonstrated in the matrix photolysis of $[(\eta^5\text{-}C_5H_5)Ir(C_2H_4)_2]$.[3a] Recent experiments have shown a close link between the matrix and the solution reactivity.[1b, 3, 4]

We have now found that (1) the (η^6-arene)osmium complexes **1**–**4** undergo *inter-* or *intra*molecular C–H activation reactions on photolysis in low-temperature matrices and (2) some of these reactions may also be carried out in solution. As far as we are aware, **1** is the first (η^6-arene)dicarbonylosmium complex.[5] It was synthesized from **3**[6] by an unusual route via $[(Mes)Os(CO)H_3]^{\oplus}$ and $[(Mes)Os(CO)_2H]^{\oplus}$.[7] Complex **2** is obtained in good yield from $[(Mes)Os(CO)(CH_3)I]$[6] by reaction with Na/Hg in THF/EtOH; **4a** is obtained from $[(Mes)Os(CO)(CH_3)_2]$ by a route analogous to that already described for **4b**.[5b, 7]

$[(Mes)Os(CO)_2]$ **1** $[(Mes)Os(CO)(CH_3)H]$ **2** $[(Mes)Os(CO)H_2]$ **3**

$[(Mes)Os(CO)(C_2H_4)]$ **4a** $[(\eta^6\text{-}C_6H_6)Os(CO)(C_2H_4)]$ **4b**

Mes = η^6-1,3,5-$Me_3C_6H_3$

Complexes **1**–**4** may be sublimed into a matrix at 35–60 °C without decomposition. Complex **1** is photostable in argon matrices,[8] but proves reactive when isolated in solid methane. On photolysis ($\lambda > 290$ nm), the ν(CO) bands of **1** (1981, 1909 cm^{-1}) decrease and the band of free CO (2136 cm^{-1}) appears. A pair of new IR bands is detected close to 2085 cm^{-1} (w, br) together with a group of bands close to 1955 cm^{-1} and ca. nine further bands between 1200 and 450 cm^{-1}. All of the IR bands of **2** (sublimed into a methane matrix) are observed within 4 cm^{-1} of the corresponding modes of the photoproduct of **1**. The high-frequency modes of the photoproduct are assigned to ν(OsH) (ca. 2085 cm^{-1}) and ν(CO) (ca. 1955 cm^{-1}); they are split into several components because of multiple conformations and sites in the matrix. The exact *splitting pattern* is different in the photochemically generated product from that of **2** isolated directly. Nevertheless, this comparison provides secure evidence that irradiation of **1** results in CO loss and formation of **2** in solid methane.

Complex **3** shows ν(OsH) and ν(CO) modes at ca. 2081 and 1970 cm^{-1} when isolated in a methane matrix. On photolysis ($\lambda > 220$ nm), very little CO is released, but formation of **2** can be recognized both from its ν(CO) band and its low frequency modes. The yield of **2** is higher than on photolysis of **1**, but the ν(OsH) mode of **2** is obscured by the corresponding band of the precursor, **3**. The ν(CO) mode and the low-frequency modes are now observed within 1 cm^{-1} of those of **2** (Fig. 1), indicating that the expelled H_2 from **3** causes less perturbation than the expelled CO from **1**.

Further evidence for the reductive elimination of H_2 from **3** is obtained by photolysis in nitrogen matrices, which yields complex **6** (Scheme 1), isoelectronic with **1**. The NN and CO stretching modes of **6** are observed at 2108 and 1917 cm^{-1}. In $^{14}N_2/^{15}N_2$ (55:45) matrices, two NN stretching modes are observed for the $^{14}N_2$ and $^{15}N_2$ complexes (2108 and 2042 cm^{-1}, respectively).

The coordinatively unsaturated monocarbonyl **5** (Scheme 1) may be generated either by photolysis of **2** or **3** in argon matrices ($\lambda > 220$ nm). The formation of **5** from **3** may be partially reversed by long-wavelength irradiation ($\lambda > 365$ nm). As expected, its ν(CO) mode (1885 cm^{-1} when formed from **2**, 1889 cm^{-1} from **3**) lies at lower frequency than that of **6** (1917 cm^{-1}), which has an additional Os–N_2 bond. Photolysis of **2** in argon matrices also causes release of free methane, which can be identified by its characteristic bands at 2910 and 1305 cm^{-1}. However, photolysis of either **2** or **3** in argon matrices is complicated by the formation of other carbonyl products with higher frequency ν(CO) bands. A similar phenomenon has been observed for $[(\eta^5\text{-}C_5H_5)Ir(CO)H_2]$.[1c] The observations on **1**–**3**, **5**, and **6** (Scheme 1) show that the reaction proceeds via dissociation of CO or H_2 from **1** or **3** and oxidative addition of methane to the coordinatively unsaturated fragment **5**.

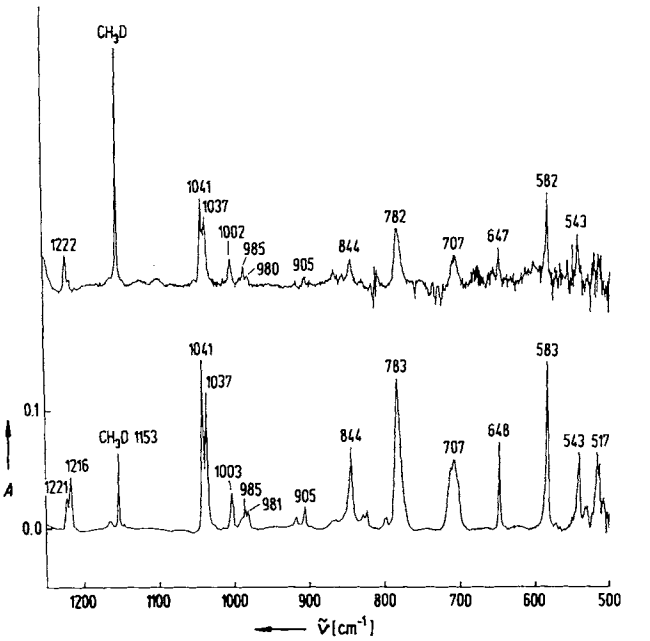
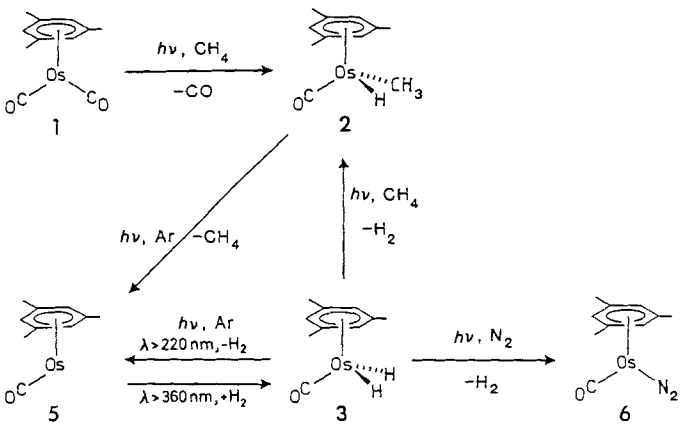


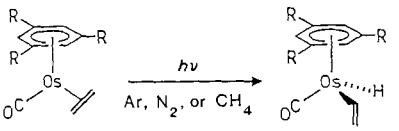
Fig. 1. Above: IR spectrum in the region $\tilde{\nu} < 1250$ cm^{-1} obtained following photolysis (620 min, $\lambda > 220$ nm) of **3** isolated in a methane matrix after computer subtraction of the residual bands of **3**. Below: **2**, deposited directly into a methane matrix. The band at 1153 cm^{-1} is due to CH_3D in natural abundance. The agreement between the two spectra demonstrates conclusively that **2** is formed by photolysis of **3**. A = absorbance.



Scheme 1. Photolysis of **1**–**3**.

Irradiation of **4a** in CH_4, N_2, and Ar matrices leads, not to **2**, **5**, or **6**, but to *intra*molecular C–H activation and formation of the hydrido(vinyl)osmium complex **7a** [Eq. (b)]. Complex **7a** has a ν(CO) mode shifted to high frequency

relative to **4a**, a ν(OsH) mode (ca. 2060 cm^{-1}), and three bands in the 1200–1600 cm^{-1} region characteristic of a vinyl group.[8] These bands occur within 9 cm^{-1} of those of $[(\eta^5\text{-}C_5H_5)Ir(C_2H_4)(C_2H_3)H]$ formed by the matrix photolysis of $[(\eta^5\text{-}C_5H_5)Ir(C_2H_4)_2]$.[3a] On photolysis of [(Mes)Os(CO)-(C_2D_4)], [D_4]**4a**, in argon matrices ($220 < \lambda < 360$ nm), no OsH vibration is detected at 2060 cm^{-1} and considerable shifts are observed in the bands below 1600 cm^{-1}. The absence of free C_2D_4 (722 cm^{-1}) demonstrates that ethene is not released in the reaction of [D_4]**4a**. Confirmation that insertion into the ethene C–H bonds has taken place, rather than into those of the mesitylene methyl groups, is obtained by repeating the experiments with **4b** and its C_2D_4-substituted analogue.



(b)

4a R=Me **7a** R=Me
4b R=H **7b** R=H

Irradiation of **4a** in solution ($\lambda > 290$ nm, [D_8]toluene, − 85 °C) also results in isomerization to **7a**.[9] As expected from recent investigations of related rhenium, iridium, and iron (vinyl)hydride complexes,[3a, 10–12] **7a** is stable in solution at room temperature. It isomerizes back to **4a** at 80 °C. The photolysis of **4a** in [D_8]toluene at − 80 °C under C_2D_4 (3 bar), or of [D_4] **4a** under C_2H_4 (3 bar), generates the corresponding isotopomer of **7a**. Since no C_2H_4/C_2D_4 exchange occurs, we conclude that the insertion into the ethene C–H bonds is either strictly intramolecular or occurs within the solvent cage. Preliminary results indicate that *inter*molecular C–H activation resulting in formation of [(Mes)Os(CO)(C_6H_4Me)H] occurs on photolysis of **1** or **3** in toluene *solution*.

Received: August 10, 1989 [Z 3490 IE]
German version: *Angew. Chem. 101* (1989) 1721

CAS Registry numbers:
1, 123725-74-6; **2**, 123725-75-7; **3**, 123725-76-8; **4a**, 123725-77-9; [D_4]**4a**, 123725-83-7; **4b**, 109013-47-0; **5**, 123725-78-0; **6**, 123725-79-1; **7a**, 123725-80-4; [D_4]**7a**, 123725-84-8; **7b**, 123725-81-5; (Mes)Os(CO)(CH_3)I, 123725-82-6; CH_4, 74-82-8; (C_6H_6)Os(CO)(C_2D_4), 123725-85-9.

[1] a) A. J. Rest, I. Whitwell, W. A. G. Graham, J. K. Hoyano, A. D. McMaster, *J. Chem. Soc. Dalton Trans. 1987*, 1181; b) P. E. Bloyce, A. J. Rest, I. Whitwell, W. A. G. Graham, R. Holmes-Smith, *J. Chem. Soc. Chem. Commun. 1988*, 846; c) P. E. Bloyce, A. J. Rest, I. Whitwell, *J. Chem. Soc. Dalton Trans. 1989*, in press.

[2] a) D. M. Haddleton, *J. Organomet. Chem. 311* (1986) C21; b) D. M. Haddleton, A. McCamley, R. N. Perutz, *J. Am. Chem. Soc. 110* (1988) 1810.

[3] a) D. M. Haddleton, R. N. Perutz, *J. Chem. Soc. Chem. Commun. 1986*, 1734; b) S. T. Belt, S. B. Duckett, D. M. Haddleton, R. N. Perutz, *Organometallics 8* (1989) 748.

[4] S. T. Belt, F.-W. Grevels, W. Klotzbücher, A. McCamley, R. N. Perutz, *J. Am. Chem. Soc.*, in press.

[5] The following complexes of the type [(Arene)M($CO)_2$] are known: a) [(C_6Me_6)Fe($CO)_2$]: S. R. Weber, H. H. Brintzinger, *J. Organomet. Chem. 127* (1977) 45; b) [(C_6Me_6)Ru($CO)_2$]: K. Roder, H. Werner, *Chem. Ber. 122* (1989) 833.

[6] a) S. Stahl, *Diplomarbeit*, Universität Würzburg 1987; b) H. Werner, S. Stahl, manuscript in preparation.

[7] **1**: Yellow solid. MS (70 eV): *m/z* 368 (57%; $M^{\oplus}$). IR (hexane): ν(CO) 1978, 1907 cm^{-1}. ^1H NMR (90 MHz, C_6D_6): $\delta = 4.82$ (s; $C_6H_3Me_3$), 1.90 (s; $C_6H_3Me_3$). **2**: Pale yellow solid. MS (70 eV): *m/z* 356 (5%; $M^{\oplus}$). IR (hexane): ν(OsH) 2060, ν(CO) 1951 cm^{-1}. ^1H NMR (90 MHz, C_6D_6): $\delta = 4.50$ (s; $C_6H_3Me_3$), 1.91 (s; $C_6H_3Me_3$), 0.90 (s; $OsCH_3$), − 10.19 (s, OsH). **3**: Colorless solid. MS (70 eV): *m/z* 342 (28%; $M^{\oplus}$). IR (C_6H_6): ν(OsH) 2060, ν(CO) 1935 cm^{-1}. ^1H NMR (90 MHz, C_6D_6): $\delta = 4.83$ (s; $C_6H_3Me_3$), 2.11 (s; $C_6H_3Me_3$), − 11.03 (s; OsH_2). **4a**: pale yellow solid. MS (70 eV): *m/z* 368 (62%; $M^{\oplus}$). IR (hexane): ν(CO) 1922 cm^{-1}. ^1H NMR (90 MHz, C_6D_6): $\delta = 4.59$ (s; $C_6H_3Me_3$), 1.94 (s; $C_6H_3Me_3$), 2.22 (m; 2H; C_2H_4), 1.53 (m; 2H; C_2H_4). Satisfactory C,H, and Os analyses were obtained for **1**–**4**.

[8] IR-bands in Ar matrices [cm^{-1}]: **1**: ν(CO) 1989, 1986, 1919, 1917. **4a**: ν(CO) 1941, 1937, 1934. **4b**: ν(CO) 1943, 1940. **7a**: ν(OsH) 2061, 2057; ν(CO) 1979, 1974; ν(C=C) 1565; $\delta(=CH_2)$ 1374, 1372; $\delta(=CH)$ 1257. [D_4]**7a**: ν(CO) 1979, 1974; ν(C=C) 1512; ν(OsD) 1493; $\delta(=CD_2)$ 1044, 1043; $\delta(=CD)$ 990. **7b**: ν(OsH) 2072, 2060; ν(CO) 1990, 1987; ν(C=C) 1567; $\delta(=CH_2)$ 1376; $\delta(=CH)$ 1256. [D_4]**7b**: ν(CO) 1987; ν(C=C) 1507; ν(OsD) 1481,1474; $\delta(=CD_2)$ 1044; $\delta(=CD)$ 989. (The ν(C=C) and ν(OsD) vibrations are probably strongly mixed in the deuterated complexes).

[9] IR (hexane): ν(CO): 1960 cm^{-1}. ^1H NMR (90 MHz, [D_8]toluene): $\delta =$ 7.90 (ddd, $J = 17.8$, 10.7, 1.2 Hz; $CHCH_2$), 6.79 (dd, $J = 10.7$, 3.7 Hz; $CHCH_2$), 5.89 (dd, $J = 17.8$, 3.7 Hz; $CHCH_2$), 4.53 (s; $C_6H_3Me_3$), 1.92 (s; $C_6H_3Me_3$), − 10.42 (s; OsH).

[10] P. O. Stoutland, R. G. Bergman, *J. Am. Chem. Soc. 107* (1985) 4581; *ibid. 110* (1988) 5732.

[11] T. T. Wenzel, R. G. Bergman, *J. Am. Chem. Soc. 108* (1986) 4856.

[12] M. V. Baker, L. D. Field, *J. Am. Chem. Soc. 108* (1986) 7433, 7436.

Encapsulation of Polypyrrole Chains in Zeolite Channels**

By *Thomas Bein** and *Patricia Enzel*

Fundamental studies of the electronic structure and conduction mechanism of conducting polymers[1–3] would benefit substantially if the low-dimensional structures were available as decoupled, structurally well-defined entities. The design of molecularly isolated conducting or semiconducting[4–6] structures (with modified electronic properties) could potentially reduce the size of electronic circuitry to molecular dimensions.[7, 8]

We report the first successful synthesis of polypyrrole (Ppy) as potential "molecular wires" within the crystalline channel systems of zeolite Y and mordenite (M) molecular sieves (Fig. 1).[9] Zeolite Y is composed of sodalite cages

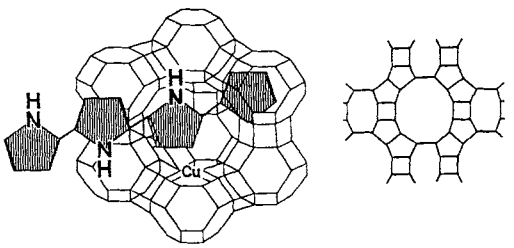


Fig. 1. Structures of zeolite Y with polypyrrole chain (left) and mordenite (right) viewed along the (001) axis.

(0.3-nm windows), interconnected by double six-rings of Si/Al, and of "supercages" with 0.8-nm windows, which together form a three-dimensional open framework with typical unit-cell composition $Na_{56}Al_{56}Si_{136}O_{384}$. Mordenite (M) features pseudo-one-dimensional twelve-ring channels, with

[*] Prof. Dr. T. Bein, P. Enzel
Department of Chemistry, University of New Mexico
Albuquerque, NM 87131 (USA)

[**] Instrumentation used in this work was acquired with funding from the National Science Foundation. We thank *F. Beuneu* and *L. Zuppiroli* (Ecole Polytechnique, Paris) for ESR studies, and *B. Crawford* (University of New Mexico) for Raman measurements.

basic unit-cell composition $Na_8Al_8Si_{40}O_{96}$. The polypyrrole/zeolite hybrid materials differ fundamentally from previous systems in larger scale host structures,[10, 11] because the zeolite hosts can isolate *single* molecular chains in their molecule-size channel systems.[12]

When pyrrole (py) is allowed to diffuse into large-pore zeolites containing Fe^{III} or Cu^{II} ions,[13] the color of the resulting adducts—for example, $Cu_{15}Na_{26}Y(py)_{50}$ (**1**) or $Cu_{2.5}Na_3M(py)_{0.75}$ (**2**)—changes slowly from yellowish or greenish to different shades of turquoise green and black [Eq. (1)]; Na or Fe^{II} forms do not react. The polymerization reaction is one to two orders of magnitude slower in the zeolite hosts than in homogeneous solution, indicating diffusional limitations for the pyrrole in the channel system.

$$NaY + Cu(NO_3)_2/aq \xrightarrow{620\ K/10^{-5}\ torr} Cu^{II}NaY \xrightarrow[295\ K]{py\ vapor/} Ppy/Cu^{I}NaY \quad (1)$$

Intrazeolite polypyrrole shows IR bands quite similar to the typical set of bands characteristic for bulk polypyrrole;[14] however, certain shifts, which vary with host and preparation conditions, are observed. For instance, characteristic modes of **1** occur at 1573 (1540), 1460 (1450–1470), and 1312 (1280–1300) cm^{-1}, with the positions for bulk polypyrrole in parentheses (D in Fig. 2).[15] Although

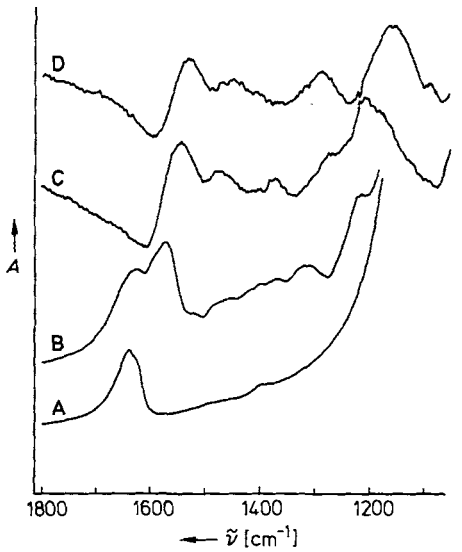


Fig. 2. FT-IR spectra (KBr pellets) of zeolite NaY (**A**), $Cu_{15}Na_{26}Y(py)_{50}$ **1** (**B**), polypyrrole extracted from **1** (**C**), and bulk polypyrrole (**D**). A = absorption.

proton generation is expected during polymerization, no clear hydroxyl features are resolved in the FT-IR spectra, probably due to strong electronic absorption features.[16] The resonance Raman spectrum of **1**[17] shows weak but resolved bands at 1598 and 1418 cm^{-1}, similar to those of Ppy film[18].

No deposition of polymer on the external surface of the zeolite crystals could be detected in electron micrographs. Since the polymerization depends upon a redox reaction with the *intrazeolite* Cu^{II} or Fe^{III} ions, most of the polymer must form inside the zeolite crystals. Consistent with the molecular-sieve properties of zeolites, treatment of the zeolite $Cu_8Na_{80}A$ (pore size 4.1 Å, smaller than pyrrole) with pyrrole did not produce detectable polymer (cf. **A** in Fig. 3).

The uptake of monomer into the zeolites is about two orders of magnitude higher than that expected from monolayer coverage of the surface of the zeolite crystals.[19] Based upon the optimal oxidant:pyrrole ratio of 2.4[14c] and the zeolite oxidant content, it follows that ca. six pyrrole molecules can be polymerized per unit cell in zeolite Y and ca. one in M. This corresponds to 13% of the pyrrole loading in Y and ca. 100% in M, fairly consistent with the amount of *polymer* recovered after dissolution of **1** in HF (4 pyrrole units per unit cell).[20] The excess monomer in the zeolites was below detection limits of the FT-IR measurements.

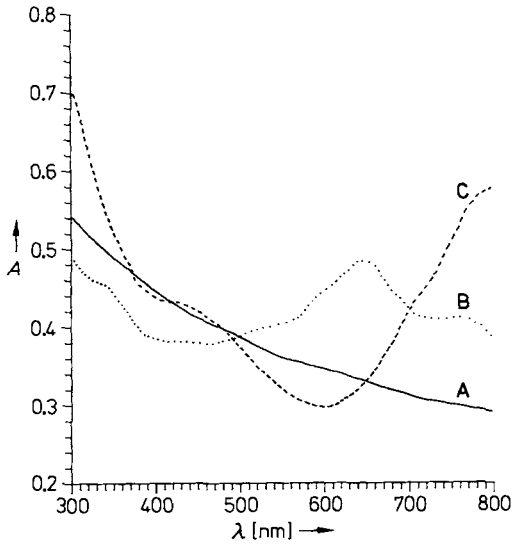


Fig. 3. UV/VIS spectra (glycerol dispersions) of $Cu_8Na_{80}A(py)_{0.3}$ (**3**) (**A**), $Cu_{2.5}Na_3M(py)_{0.75}$ (**2**) (**B**), and $Cu_{15}Na_{26}Y(py)_{50}$ (**1**) (**C**). A = absorption.

The UV/VIS spectrum of **1** shows features between 400 and 500 nm (ca. 2.7 eV) and below 650 nm (ca. 1.9 eV; **C** Fig. 3). Mordenite-based $Cu_{2.5}Na_3M(py)_{0.75}$ (**2**) also shows features at 650 and 330 nm (1.9 and 3.8 eV, **B** Fig. 3). Absorption maxima of electrochemically formed, highly doped polypyrrole at about 2.3 and 0.7 eV have been assigned to bipolaron states; the higher energy band shifted to lower values al lower oxidation levels.[21] The UV/VIS spectra probably reflect a higher oxidation level of polypyrrole in faujasite than in mordenite. ESR spectra of these samples confirm the low spin count expected for bipolaron formation,[22] and large line widths[23] (ca. 10 G) indicate strong dipolar interactions with the host. Preliminary conductivity measurements[24] of polypyrrole/zeolite samples show dramatic differences compared to bulk properties. Pressed zeolite samples deliberately coated with a thin film of polymer still show conductivities of about 10^{-6} S cm^{-1} versus 1–10 S cm^{-1} for bulk Ppy). In contrast, zeolites with *encapsulated* polymer chains do not show measurable conductivity (detection limit 10^{-9} S cm^{-1}). The agglomerated product resulting from dissolution of **1** in HF has spectroscopic properties very similar to bulk Ppy (cf. C in Fig. 2) and conductivity on the order of 0.0001 S cm^{-1}. These observations indicate that the *intrazeolite* heteroaromatic polymer chains are decoupled from each other and/or from the crystal surface, and that they probably have dramatically different transport properties. At this point is is not known if some chains in zeolite Y intersect in the spacious supercages (diameter 1.3 nm), while the one-dimensional channels of mordenite

force alignment along the (001) axis. NMR studies aimed at polymer chain-length determination are presently being carried out.

Continuing research on intrazeolite polypyrrole and other conducting polymers addresses issues such as the effect of different host pore sizes and topologies on the polymer chain length and transport properties of the resulting low-dimensional systems.

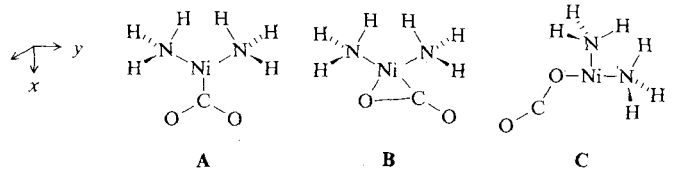
Received: July 14, 1989 [Z 3443 IE]
German version: *Angew. Chem. 101* (1989) 1737

[1] M. Aldissi (Ed.): *Proc. Int. Conf Sci. Technol. Synth. Met.* (ICSM 1988); *Synth. Met. 28* (1989) No. 1–3; *ibid. 29* (1989) No. 1.
[2] T. A. Skotheim (Ed.): *Handbook of Conducting Polymers, Vol. 1*, Marcel Dekker, New York 1986.
[3] L. Alcacer (Ed.): *Conducting Polymers. Special Applications*, Reidel, Dordrecht 1987.
[4] J. B. Parise, J. E. MacDougall, N. Herron, R. D. Farlee, A. W. Sleight, Y. Wang, T. Bein, K. Moller, L. M. Moroney, *Inorg. Chem. 27* (1988) 221.
[5] N. Herron, Y. Wang, M.M. Eddy, G. D. Stucky, D. E. Cox, K. Moller, T. Bein, *J. Am. Chem. Soc. 111* (1989) 530.
[6] K. Moller, M. M. Eddy, G. D. Stucky, N. Herron, T. Bein, *J. Am. Chem. Soc. 111* (1989) 2564.
[7] J. J. Hopfield, J. N. Onuchic, B. N. Beratan, *Science (Washington DC) 241* (1988) 817.
[8] F. L. Carter (Ed.): *Molecular Electronic Devices I, II*, Marcel Dekker, New York 1982 and 1987.
[9] D. W. Breck: *Zeolite Molecular Sieves*, R. E. Krieger Publishing Co., Malabar, FL, 1984.
[10] a) Polypyrrole monolayer-type films have been intercalated between the layers of FeOCl and V_2O_5. b) M. G. Kanatzidis, L. M. Tonge, T. J. Marks, H. O. Marcy, C. R. Kannewurf, *J. Am. Chem. Soc. 109* (1987) 3797; c) M. G. Kanatzidis, C.-G. Wu, H. O. Marcy, C. R. Kannewurf, *J. Am. Chem. Soc. 111* (1989) 4139.
[11] Polypyrrole fibrils with diameters between ca. 0.03 and 1 μm at 10-μm length have been synthesized in Nuclepore membranes: a) R. M. Penner, C. R. Martin, *J. Electrochem. Soc. 133* (1986) 2206; b) Z. Cai, C. R. Martin, *J. Am. Chem. Soc. 111* (1989) 4138.
[12] In situ polymerization of pyrrole in the 0.68-nm diameter channels of $[(Me_3Sn)_3Fe^{III}(CN)_6]_n$ has recently been reported: P. Brandt, R. D. Fischer, E. S. Martinez, R. Diaz Calleja, *Angew. Chem. 101* (1989) 1275; *Angew. Chem. Int. Ed. Engl. 28* (1989) 1265.
[13] Cu^{II} forms of zeolite Y (LZ-Y52; Alfa), mordenite (M; LZ-M5; Union Carbide), and zeolite A (Alfa 5A) were obtained by ion exchange with 0.1 M $Cu(NO_3)_2$ solution and dehydration at 620 K 10^{-5} torr, resulting in $Cu_{15}Na_{26}Y$, $Cu_{2.5}Na_3M$, and $Cu_8Na_{80}A$ (15, 2.5, and 8 Cu per unit cell, respectively). The dry zeolites were equilibrated with pyrrole vapor (1 torr) for 1 h at 295 K and then placed under vacuum for 1 h. Loadings were determined gravimetrically. Polymerization of pyrrole was also observed in Fe^{III} zeolite forms and when the monomer was introduced from solvents such as water, toluene, or hexane.
[14] a) Prepared by chemical oxidation of pyrrole with $FeCl_3$ in water; b) R. E. Myers, *J. Electron. Mater. 15* (1986) 61; c) S. P. Armes, *Synth. Met. 20* (1987) 365; d) S. Rapi, V. Bocchi, G. P. Gardini, *ibid. 24* (1988) 217.
[15] a) K. G. Neoh, T. C. Tan, E. T. Kang, *Polymer 29* (1988) 553; b) M. Zagorska, A. Pron, S. Lefrant, Z. Kucharski, J. Suwalski, P. Bernier, *Synth. Met. 18* (1987) 43.
[16] Similar observations were noted in the polypyrrole/FeOCl system: M. G. Kanatzidis, personal communication; see also [10].
[17] Obtained by excitation with an Ar ion laser at 457.9 nm, 5 mW.
[18] C. H. Olk, C. P. Beetz, Jr.; J. Heremans, *J. Mater. Res. 3* (1988) 984.
[19] The estimated surface capacity for 1-μm crystals is 0.2 (Y) and 0.05 (M) pyrrole per unit cell based on a 0.6-nm diameter for pyrrole.
[20] Pyrolysis mass spectra (up to 560 K) of all samples showed only desorption of some excess monomer but no indication of short-chain oligomeric products.
[21] J. H. Kaufman, N. Colaneri, J. C. Scott, K. K. Kanazawa, G. B. Street, *Mol. Cryst. Liq. Cryst. 118* (1985) 171.
[22] On average, ca. 0.001 Curie-type spins per adsorbed monomer were observed.
[23] J. C. Scott, P. Pfluger, M. T. Krounbi, G. B. Street, *Phys. Rev. B28* (1983) 2140.
[24] a) Carried out at 295 K with pressed wafers of the bulk polymers and of zeolite powders by use of the four-point technique; b) F. M. Smits, *Bell Syst. Tech. J. 37* (1958) 711.

Monohapto versus Dihapto CO_2 Coordination in Bis(amine)Ni^0 Complexes: A CAS-SCF Study

By *Alain Dedieu** and *Florent Ingold*

$[NiL_2(CO_2)]$ complexes (L = phosphane, amine) are known to play a key role in many processes of organometallic chemistry.[1] For instance, they may be critical intermediates in various coupling reactions of CO_2 with alkenes, alkynes, aldehydes, imines, or even oxygen at Ni^0 centers.[1e–g, 2] They also display an interesting fluxional behavior: ^{31}P NMR spectra of a bisphosphane CO_2 complex of nickel, both in solution[3] and in liquid CO_2,[4] show a single resonance. This has been attributed to an η^1 coordination of CO_2 at the carbon atom (**A**) or to a fast dynamic process averaging the two η^2 coordination modes (e.g., **B**) either through the η^1-C coordination mode or through a fast rotation around the Ni–(η^2-CO_2) bond.[5] We report here the result of ab initio CAS-SCF calculations (CAS = complete active space), which indicate that another structure, characterized by an η^1 coordination mode at the oxygen atom (**C**) and by a strong diradical character, is close in energy to the η^2-CO_2 structure **B**, thereby providing a new perspective on the reactivity pattern of this class of complexes.



A **B** **C**

Preliminary SCF calculations were first carried out with the ASTERIX system of programs,[6] using a split valence-type basis set[7] and geometries assumed from related X-ray crystal structures or previous calculations on similar systems.[13] CAS-SCF calculations[18, 19] were then performed using the same geometries and basis set. Such multiconfiguration SCF-type calculations are necessary to include nondynamical correlation effects and to give a balanced description of the bond-forming and bond-breaking processes.[21] In particular, they provide an appropriate way (1) to take into account the manifold of low-lying electronic configurations, which is usually characteristic of nickel systems with a low coordination number,[22] and (2) to treat the diradical and closed-shell species with a similar degree of accuracy. They are also a convenient starting point for the study of dynamical correlation effects (currently under way). Including these effects (and also adding polarization functions) will probably improve the overall accuracy of the calculation but should not alter the main conclusions obtained at the present level of theory.[21]

The first salient result of the CAS-SCF calculations is the fact that the η^1-O structure **C** is found to be only 1.3 kcal mol^{-1} higher in energy than the η^2-CO_2 ground-state structure **B**.[23] A complete optimization of the two geometries might, of course, change this value somewhat, but not to a great extent. Both structures are therefore close to each other in energy, a result that was not expected on the basis of the preliminary SCF calculations.[24] The η^1-C structure **A** is computed to be much higher in energy (by

[*] Dr. A. Dedieu, F. Ingold
Laboratoire de Chimie Quantique, UPR 139 du CNRS
Université Louis Pasteur
4, rue Blaise Pascal, F-67000 Strasbourg (France)

46.8 kcal mol^{-1} at the CAS-SCF level[23]). In addition, a natural orbital analysis of the corresponding CAS-SCF wave functions points to a strong diradical character for the η^1-O structure **C**. The orbital occupations of the the bonding orbital between $d_{x^2-y^2}$ and $\pi^*_{CO_2}$ (the HOMO in the SCF ground-state wave function) and its antibonding counterpart (the LUMO) are 1.288 and 0.714, respectively.[25] Since these two orbitals are equally spread over the metal and the CO_2 ligand, the η^1-O structure **C** is probably best regarded as a 1,3 diradical centered on the nickel and carbon atoms. Most probably **C** has a singlet ground state, since the triplet state was computed to lie 4.1 kcal mol^{-1} above the singlet state.

These results suggest that the coupling reaction of CO_2 and C_2H_4, which has been observed experimentally at a Ni^0 center,[2b] might well involve a coordinated CO_2 attacked by the incoming olefin rather than an electrophilic attack on a coordinated C_2H_4 by the carbon dioxide. In both cases the attacked ligand has to slip in one way or another from an η^2 to an η^1 coordination mode.[26] But the η^1 geometry for the corresponding ethylene complex $[Ni(NH_3)_2(C_2H_4)]$ is found to be 29.0 kcal mol^{-1} above the η^2-C_2H_4 ground-state structure; hence, deformation of the η^2 geometry to the η^1 geometry is much less easy than deformation of the η^2-CO_2 structure **B** to the η^1-CO_2 structure **C**. This is reflected in the results obtained from CAS-SCF calculations performed for two geometries corresponding either to a 3-Å approach of C_2H_4 to the nickel atom of $[Ni(NH_3)_2(\eta^1\text{-}CO_2)]$ or to a 3-Å approach of CO_2 to the nickel atom of $[Ni(NH_3)_2(\eta^1\text{-}C_2H_4)]$.[27] The energy needed to reach the first geometry from the separated reactants, $[Ni(NH_3)_2(\eta^2\text{-}CO_2)]$ and C_2H_4, amounts to 14.9 kcal mol^{-1}, whereas the energy needed to reach the second geometry from the separated reactants, $[Ni(NH_3)_2(\eta^2\text{-}C_2H_4)]$ and CO_2, amounts to 36.1 kcal mol^{-1}. All these features are therefore consistent with C_2H_4 attack as the favored pathway. Work is now in progress to investigate in more detail these two reaction pathways and the influence of the ligand coordination pattern.

Received: July 10, 1989 [Z 3427 IE]
German version: *Angew. Chem. 101* (1989) 1711

[1] Reviews; a) D. J. Darensbourg, R. A. Kudaroski, *Adv. Organomet. Chem. 22* (1983) 129; b) D. A. Palmer, R. Van Eldik, *Chem. Rev. 83* (1983) 51; c) R. Ziessel, *Nouv. J. Chim. 7* (1983) 613; d) D. J. Darensbourg, C. Ovalles, *CHEMTECH 1985* 636; e) D. Walther, *Coord. Chem. Rev. 79* (1987) 135; f) A. Behr, *Angew. Chem. 100* (1988) 681; *Angew. Chem. Int. Ed. Engl. 27* (1988) 661; g) P. Braunstein, D. Matt, D. Nobel, *Chem. Rev. 88* (1988) 747.

[2] a) H. Hoberg, Y. Peres, C. Krüger, Y.-H. Tsay, *Angew. Chem. 99* (1987) 799; *Angew. Chem. Int. Ed. Engl. 26* (1987) 771; b) H. Hoberg, Y. Peres, A. Milchereit, S. Gross, *J. Organomet. Chem. 345* (1988) C17.

[3] M. Aresta, E. Quaranta, I. Tommasi, *J. Chem. Soc. Chem. Commun 1988*, 450.

[4] M. G. Mason, J. A. Ibers, *J. Am. Chem. Soc. 104* (1982) 5153.

[5] M. Aresta, E. Quaranta, I. Tommasi, R. Gobetto, NATO-ASI Summer School on Enzymatic and Model Carboxylation and Reduction Reactions (Ginosa, Italy, 1989).

[6] M. Bénard, A. Dedieu, J. Demuynck, M.-M. Rohmer, A. Strich, A. Veillard, R. Wiest, *Asterix, a system of programs for the IBM 3090*, unpublished.

[7] Basis sets: (14,9,6) contracted to <6,4,3> for the nickel atom [8, 9]; (9,5) contracted to <3,2> for the first-row atoms [11]; and (4) contracted to <2> for the hydrogen atoms [12].

[8] I. Hyla-Kryspin, J. Demuynck, A. Strich, M. Bénard, *J. Chem. Phys. 75* (1981) 3954.

[9] The original (13,7,5) basis set [8] is modified by the addition of an s primitive of exponent 0.37458 to suppress the gap between the functions needed to describe the widely separated 3s and 4s shells and two p functions of exponents 0.30117 and 0.09739 to describe the 4p shell, and by replacing in the d shell the last function by two functions of exponents 0.40354 and 0.13013. These exponents were chosen according to the even-tempered criterion [10].

[10] R. Raffenetti, R. D. Bardo, K. Ruedenberg in D. W. Smith, W. B. McRae (Eds.): *Energy Structure and Reactivity*, Wiley, New York 1973, p. 164.

[11] S. Huzinaga: *Approximate Atomic Functions, Technical Report*, University of Alberta, Edmonton 1971.

[12] S. Huzinaga, *J. Chem. Phys. 42* (1965) 1293.

[13] Structural parameters: a) Dihapto complex **B**: The geometry of the CO_2 moiety was taken from the experimentally determined structure of $[Ni\{P(cyclo\text{-}C_6H_{11})_3\}_2(\eta^2\text{-}CO_2)]$ [14]; the Ni–N bond was set at 2.15 Å as in the previous SCF study of *Sakaki* et al. [15] and the N–Ni–N angle at 90° [16]. b) η^1-O structure **C**: The geometry of the $Ni(NH_3)_2$ unit was retained as in **B**, and the geometry of the Ni–CO_2 unit set as follows: Ni-O = 1.868 Å, C-O = 1.297 and 1.230 Å for the bound and nonbound C–O bonds, respectively; O–C–O angle = 130.3°. These values are taken from the X-ray crystal structure of the metallalactone complex $[Ni(dbu)_2(C_3O_2H_4)]$ (dbu = 1,8-diazabicyclo[5.4.0]undec-7-ene) [2a] and from an SCF optimization of the O–C–O angle. c) η^1-C structure **A**: The geometry of the $Ni(NH_3)_2$ unit was again retained as in **B**, and the geometry of the Ni–CO_2 unit was set according to the previous SCF calculation of *Sakaki* et al. [15]. For the NH_3 ligand the experimental geometry [17] was chosen.

[14] M. Aresta, C. F. Nobile, V. G. Albano, E. Forni, M. Manassero, *J. Chem. Soc. Chem. Commun 1975*, 636.

[15] S. Sakaki, K. Kitaura, K. Morokuma, *Inorg. Chem. 21* (1982) 760.

[16] CAS-SCF calculations carried out for an N–Ni–N angle of 120° in **B** showed that the energy was lowered by only 0.4 kcal mol^{-1}.

[17] *Tables of Interatomic Distances (Spec. Publ. Chem. Soc. 18* (1965)).

[18] a) B. O. Roos, P. R. Taylor, P. E. M. Siegbahn, *Chem. Phys. 48* (1980) 157; b) P. E. M. Siegbahn, J. Almlöf, A. Heiberg, B. O. Roos, *J. Chem. Phys. 74* (1981) 2384; c) B. O. Roos, *Int. J. Quantum Chem. Symp. 14* (1980) 175.

[19] The active space of the CAS-SCF calculations was made of six active orbitals populated by eight electrons for the $[Ni(NH_3)_2(CO_2)]$ system. These active orbitals (d_{z^2}, $d_{x^2-y^2}$, 4s, π_{CO_2}, n π_{CO_2}, and $\pi^*_{CO_2}$) account for the main bonding interactions as well as for the sd hybridization features. For the $[Ni(NH_3)_2(CO_2)] + C_2H_4$ system, the $\pi_{C_2H_4}$ and $\pi^*_{C_2H_4}$ orbitals were added, giving rise to a set of eight active orbitals populated by ten electrons. The frozen core approximation [20] was used throughout the calculations in order to avoid error effects due to basis-set superposition.

[20] L. Pettersson, U. Wahlgren, *Chem. Phys. 69* (1982) 185.

[21] See, for instance, a) J. E. Bäckvall, E. E. Björkman, L. Pettersson, P. Siegbahn, A. Strich, *J. Am. Chem. Soc. 107* (1985) 7408; b) M. R. A. Blomberg, P. E. M. Siegbahn, J. E. Bäckvall, *ibid. 109* (1987) 4450.

[22] See, for instance, a) M. R. A. Blomberg, U. B. Brandemark, P. E. M. Siegbahn, K. B. Mathisen, G. Karlström, *J. Phys. Chem. 89* (1985) 2171; b) P. O. Widmark, B. O. Roos, P. E. M. Siegbahn, *ibid. 89* (1985) 2180.

[23] The total CAS-SCF energies are: **B**, −1803.7096; **C**, −1803.7075; **A**, −1803.6351 Hartree (1 Hartree = 627.7 kcal mol^{-1}).

[24] The total SCF energies are: **B**, −1803.6196; **C**, −1803.5774; **A**, −1803.5190 Hartree.

[25] This corresponds to an important weight (35%) (in the CI expansion) of the configuration obtained through a double excitation from the HOMO to the LUMO with respect to the ground-state SCF configuration (whose weight in the CI expansion amounts to only 63%).

[26] The geometry of the metallactone ring corresponds either to an η^1-CO_2 or to an η^1-C_2H_4 unit. Moreover, the slippage of the ethylene ligand from the dihapto coordination mode to the monohapto coordination mode polarizes the C_2H_4 π orbital on the uncoordinated carbon atom, making it more prone to an electrophilic attack by CO_2.

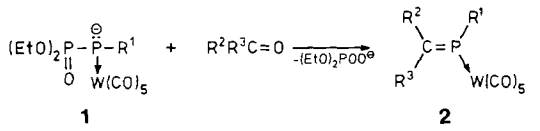
[27] This corresponds to a C–C distance of about 2.5 Å. SCF calculations, which were also carried out for an approach of 2.5 Å (corresponding to a C–C distance of about 2 Å), yielded total energies which were already lower than the energies of the separated reactants.

Phosphaalkenes from Monochlorophosphanes and Alkylidenetriphenylphosphoranes

By *Gottfried Märkl** and *Walter Bauer*

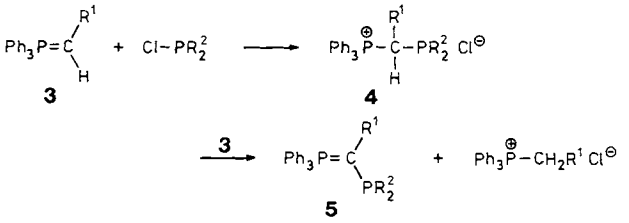
The recently published synthesis by *F. Mathey* et al.[1] of complex-stabilized phosphaalkenes **2** by carbonyl olefination with the phosphorylphosphide complexes **1** leads us to describe a new general synthesis of phosphaalkenes **10** involving the reaction of alkylidenetriphenylphosphoranes **3** with chloro-(2,4,6-tri-*tert*-butylphenyl)phosphane **6**.

[*] Prof. Dr. G. Märkl, Dipl.-Chem. W. Bauer
Institut für Organische Chemie der Universität
Universitätsstrasse 31, D-8400 Regensburg (FRG)



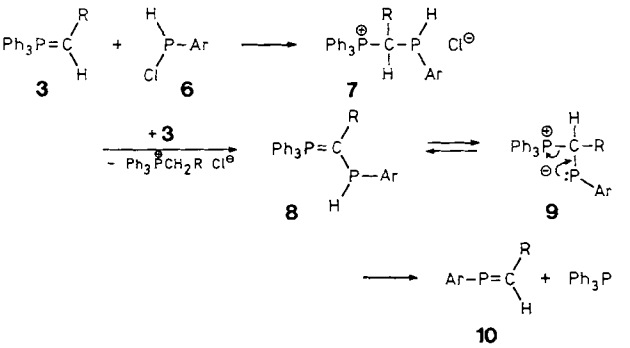
1 2

K. Issleib et al.[2] published several reports regarding the reaction of **3** with chlorophosphanes, a reaction that leads, depending upon the reaction conditions, either to the phosphonium salts **4** or—by transylidation with **3**[3]—to the phosphino-substituted alkylidenetriphenylphosphoranes **5**.



3 4 5

Treatment of chlorophosphane **6**[4] with two equivalents of a non-resonance stabilized monosubstituted methylenetriphenylphosphorane **3** (salt-containing ylide solution in THF, addition of **6** to **3**, benzene or THF as solvent, room temperature) initially causes rapid separation of one equivalent of phosphonium salt **7**. After 5 h it is possible to isolate phosphaalkenes **10** from the solution by column chromatography over heat-treated silica gel 60 with either petroleum ether (40–60 °C)/benzene (2:1) or petroleum ether alone. Benzene is suitable for subsequent elution of triphenylphosphane.

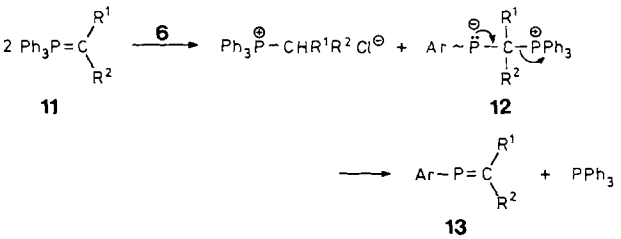


3 6 7 8 9 10

Ar = 2,4,6-tri-*tert*-butylphenyl; **a**: R = H, **b**: R = Me, **c**: R = Et, **d**: R = *n*-Pr, **e**: R = Ph

Phosphaalkenes **10** are formed by way of the phosphonium salts **7**, which undergo transylidation and are deprotonated with a second mole of ylide **3** to the phosphino-substituted alkylidenephosphoranes **8**. These are probably present in equilibrium with the betaines **9**, which ultimately fragment to **10** by elimination of triphenylphosphane (Table 1). A direct deprotonation of **7** to **9** cannot be ruled out (see below), but according to *K. Issleib* et al.[2] the relative pK_a values of **7** and protonated **3** make primary formation of the ylides **8** more probable.

Treatment of monochlorophosphane **6** with disubstituted methylenetriphenylphosphoranes **11** leads directly to the disubstituted phosphaalkenes **13** (Table 2). This means that intermediate phosphonium salts corresponding to **7**, which are incapable of forming ylides, must be deprotonated di-



11 12 13

Ar = 2,4,6-tri-*tert*-butylphenyl; **a**: $R^1 = R^2$ = Me, **b**: $R^1 = R^2$ = Et, **c**: $R^1, R^2 = (CH_2)_5$, **d**: R^1 = Me, R^2 = Ph

Table 1. Physical data for 1-(2,4,6-tri-*tert*-butylphenyl)-2-R-1-phosphaalkenes **10**.

10a, R = H [5]: Yield 45%, m.p. = 87–89 °C (from CH_3CN) (m.p. = 80 °C [5b]); ^{1}H NMR (250 MHz, $CDCl_3$, TMS): δ = 6.79 (dd, ^2J(P,H) = 28.2, ^2J(H,H) = 4.56 Hz, 1H; =CH), 7.13 (dd, ^2J(P,H) = 32.3 Hz, 1H; =CH); 1.51 (s, 18H; *o*-*t*Bu), 1.33 (s, 9H; *p*-*t*Bu), 7.39 (d, ^4J(P,H) = 1.17 Hz, 2H; aryl-H); ^{31}P{^{1}H}-NMR ($CDCl_3$, H_3PO_4): δ = + 290.0; MS (70 eV): *m*/*z* 290 ($M^{\oplus}$, 22%), 275 ($M^{\oplus}$-CH_3, 52) [6]

10b, R = Me: Yield 55%, oily *E*/*Z* isomeric mixture (50/50), b.p. = 200 °C/0.05 torr (Kugelrohr), *E* isomer: m.p. 53–55 °C (from CH_3CN), colorless crystals; ^{1}H NMR; δ = 7.42 (dquart, ^2J(P,H) = 26.0, ^3J(H,H) = 8.42 Hz, 1H; *E*, =CH), 2.14 (dd, ^3J(P,H) = 25.1, ^3J(P,H) = 25.1, ^3J(H,H) = 8.42 Hz, 3H; *E*, CH_3), 7.25 (dquart, ^2J(P,H) = 39.96, ^3J(H,H) = 7.84 Hz, 1H; *Z*, =CH), 1.27 (dd, ^3J(P,H) = 17.7, ^3J(H,H) = 7.84 Hz, 3H; *Z*, CH_3), 1.33 (s, 9H; *p*-*t*Bu); 1.49 (s, 18H; *o*-*t*Bu), 7.39 (d, ^4J(P,H) = 1.13 Hz, 2H, aryl-H; ^{31}P{^{1}H}-NMR: δ = + 251.9 (*E*); + 251.6 (*Z*); MS: *m*/*z* 304 ($M^{\oplus}$, 4%), 289 ($M^{\oplus}$-CH_3, 22), 276 ($M^{\oplus}$-C_2H_4, 6), 275 ($M^{\oplus}$-C_2H_5, 16) [6]

10c, R = Et: yield 44%; oily *E*/*Z* isomeric mixture (70/30), b.p. = 150 °C/0.05 torr (Kugelrohr), partially crystallizes upon cooling; ^{1}H NMR: δ = 7.47 (dt, ^2J(P,H) = 25.6, ^3J(H,H) = 8.48 Hz, 1H; *E*, =CH), 1.12 (*t*, ^3J(H,H) = 7.33 Hz, 3H; *E*, CH_2CH_3), 2.51 (ddt, ^3J(H,H) = 8.48, ^3J(P,H) = 19.2 Hz, 2H; *E*, CH_2CH_3), 1.33 (s, 9H; *E*, *p*-*t*Bu), 7.08 (dt, ^2J(P,H) = 32.1, ^3J(H,H) = 7.66 Hz, 1H; *Z*, =CH), 0.78 (t, ^3J(H,H) = 7.42 Hz, 3H; *Z*, CH_2CH_3), 1.25–1.75 (m, 2H; *Z*, CH_2CH_3), 1.34 (s, 9H, *Z*, *p*-*t*Bu), 1.50 (s, 18H; *o*-*t*Bu), 7.37 (d, ^4J(P,H) = 1.10 Hz, 2H, (*Z*)-aryl-H, 7.38 (d, ^4J(P,H) = 1.14 Hz, 2H, (*E*)-aryl-H; ^{31}P{^{1}H}-NMR: δ = + 247.4 (*E*), + 243.1 (*Z*); MS: *m*/*z* 318 ($M^{\oplus}$, 7%), 303 ($M^{\oplus}$-CH_3, 45), 276 ($M^{\oplus}$-C_3H_6, 16), 275 ($M^{\oplus}$-C_3H_7, 30) [6]

10d, R = *n*-Pr: yield 21%; oily *E*/*Z* isomeric mixture (80/20), b.p. ≃ 200 °C/0.05 torr; ^{1}H NMR: δ = 7.17 (dt, ^2J(P,H) = 39.9, ^3J(H,H) = 7.59 Hz, 1H; *Z*, =C*H*), 7.45 (dt, ^2J(P,H) = 21.1, ^3J(H,H) = 8.77 Hz, 1H; *E*, =C*H*), 0.70 (t, ^3J(H,H) = 7.26 Hz, 3H; *Z*, $CH_2CH_2CH_3$), 0.95 (t, ^3J(H,H) = 7.35 Hz, 3H; *E*, $CH_2CH_2CH_3$), 1.30–1.60 (m, 2H; $CH_2CH_2CH_3$), 2.40–2.58 (m, 2H; -$CH_2CH_2CH_3$), 7.38 (d, ^4J(P,H) = 1.09 Hz, 2H, aryl-H, 1.50 (s, 18H, *o*-*t*Bu), 1.33 (s, 9H, *p*-*t*Bu); ^{31}P{^{1}H}-NMR: δ = + 244.6 (*Z*), + 250.0 (*E*); MS: *m*/*z* 332 ($M^{\oplus}$, 3%), 317 ($M^{\oplus}$-CH_3, 14), 276 ($M^{\oplus}$-C_4H_8, 15), 275 ($M^{\oplus}$-C_4H_9, 38) [6]

10e, R = C_6H_5 [7]: yield 28%; oily *E*/*Z* isomeric mixture (75/25); recrystallization from CH_3CN/toluene (2/1) provides the pure *E* isomer, m.p. 135–137 °C; ^{1}H NMR: δ = 7.80 (d, ^2J(P,H) = 38.0 Hz, 1H; *Z*, =CH), 8.12 (d, ^2J(P,H) = 25.6 Hz, 1H; *E*, =CH), 1.36 (s, 9H; *p*-*t*Bu), 1.52 (s, 18H; *o*-*t*Bu), 7.44 (d, *J*(P,H) = 1.24 Hz, 2H; Aryl-H), 7.22–7.57 (m, 5H; phenyl-H); ^{31}P{^{1}H}-NMR: δ = + 260.4 (*E*), + 241.7 (*Z*); MS: *m*/*z* 366 ($M^{\oplus}$, 17%), 351 ($M^{\oplus}$-CH_3, 4), 310 ($M^{\oplus}$-C_4H_8, 5), 275 ($M^{\oplus}$-C_7H_7, 100) [6]

Table 2. Physical data for 1-(2,4,6-tri-*tert*-butylphenyl)-2-R^1-2-R^2-1-phosphaalkenes **13**.

13a, $R^1 = R^2$ = Me; yield 35%; m.p. = 85–86 °C (from CH_3CN); ^{1}H NMR: δ = 1.22 (dd, ^3J(P,H) = 13.6, ^4J(H,H) = 0.87 Hz, 3H; *Z*-CH_3), 2.11 (dd, ^3J(P,H) = 24.4 Hz, 3H; *E*-CH_3), 1.33 (s, 9H; *p*-*t*Bu), 1.47 (s, 18H; *o*-*t*Bu), 7.39 (d, *J*(P,H) = 1.14 Hz, 2H; Aryl-H); ^{31}P{^{1}H}-NMR: δ = +223.0; MS: *m*/*z* 318 ($M^{\oplus}$, 42%), 308 ($M^{\oplus}$-CH_3, 48), 276 ($M^{\oplus}$-C_6H_6, 63), 275 ($M^{\oplus}$-C_3H_7, 100) [6]

13b, $R^1 = R^2$ = Et; yield 42%, b.p. = 150 °C/0.05 torr (Kugelrohr), colorless oil; ^{1}H NMR: δ = 0.57 (t, ^3J(H,H) = 7.23 Hz, 3H; CH_2CH_3), 0.98 (t, ^3J(H,H) = 7.29 Hz, 3H; CH_2CH_3), 2.32 (dq, ^3J(P,H) = 21 Hz, 1H; CH_2CH_3), 1.25–1.75 (m, 1H; CH_2CH_3), 1.47 (s, 18H; *o*-*t*Bu), 1.33 (s, 9H; *p*-*t*Bu) 7.38 (d, ^4J(P,H) = 1.11 Hz, 2H, aryl-H); ^{31}P{^{1}H}-NMR: δ = +225.7; MS: *m*/*z* 346 ($M^{\oplus}$, 6%), 331 ($M^{\oplus}$-CH_3, 7), 317 ($M^{\oplus}$-C_2H_5, 95), 289 ($M^{\oplus}$-C_4H_9, 13), 276 ($M^{\oplus}$-C_5H_{10}, 26), 275 ($M^{\oplus}$-C_5H_{11}, 70) [6]

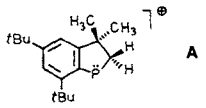
rectly to **12** in order to permit fragmentation to phosphaalkenes **13** and triphenylphosphane.

Reactions of **6** with **11c** and **11d** proceed less satisfactorily, probably for steric reasons. Thus, in addition to formation of phosphalkenes **13c, d,** which cannot be isolated in pure form, ylide dehydrochlorination of **6** is also observed, leading to the diphosphene Ar–P=P–Ar isolated as orange-red crystals, m.p. = 170–180 °C, in yields up to 31 %.

Received: June 5, 1989 [Z 3377 IE]
German version: *Angew. Chem. 101* (1989) 1698

CAS Registry numbers:
3a, 3487-44-3; **3b**, 1754-88-7; **3c**, 16666-78-7; **3d**, 3728-50-5; **3e**, 16721-45-2; **6**, 86120-24-3; **10a**, 84114-18-1; (*E*)-**10b**, 123542-40-5; (*Z*)-**10b**, 123542-41-6; (*E*)-**10c**, 123542-42-7; (*Z*)-**10c**, 123542-43-8; (*E*)-**10d**, 123542-44-9; (*Z*)-**10d**, 123542-81-1; (*E*)-**10e**, 99364-92-8; (*Z*)-**10e**, 99364-93-9; **11a**, 16666-80-1; **11b**, 21481-99-2; **13a**, 123542-45-0; **13b**, 123542-46-1.

[1] A. Marinetti, F. Mathey, *Angew. Chem. 100* (1988) 1435; *Angew. Chem. Int. Ed. Engl. 27* (1988) 1382.
[2] K. Issleib, R. Lindner, *Justus Liebigs Ann. Chem. 699* (1966) 40; *ibid. 707* (1967) 112, 120; K. Issleib, M. Lischewski, *J. Prakt. Chem. 311* (1969) 857.
[3] H. J. Bestmann, *Chem. Ber. 95* (1962) 58; see also: H. J. Bestmann, R. Zimmermann: *The Chemistry of Organophosphorus Compounds II, Fortschr. Chem. Forsch. 20* (1971) 6.
[4] Preparation from 2,4,6-tri-*tert*-butylphosphane by chlorination with CCl_4 in the presence of azobisisobutyronitrile according to *J. Escudie* (personal communication); see also: *G. Märkl, S. Reithinger, Tetrahedron Lett. 29* (1988) 463.
[5] a) K. Issleib, H. Schmidt, C. Wirkner, *Z. Anorg. Allg. Chem. 488* (1982) 75 (proof based solely on the ^{31}P-NMR spectrum, $\delta = 289.9$); b) R. Appel, C. Casser, M. Immenkeppel, *Angew. Chem. 96* (1984) 905; *Angew. Chem. Int. Ed. Engl. 23* (1984) 895; c) R. Appel, C. Casser, F. Knoch, *J. Organomet. Chem. 293* (1985) 213; d) G. Etemad-Moghadam, J. Bellan, C. Techon, M. Koenig, *Tetrahedron 43* (1987) 1793.
[6] The signal at *m/z* 275 in the spectra for all the phosphaalkenes **10, 13** corresponds to the phosphaindane fragment **A**.



A

[7] Data obtained for **10e** correspond to those reported in the literature: K. Issleib, H. Schmidt, E. Leißring, *Z. Chem. 26* (1986) 407; separation of the *E/Z* isomers and X-ray crystallographic structure determination: R. Appel, J. Menzel, F. Knoch, *Z. Anorg. Allg. Chem. 534* (1986) 100.

Anion Coordination and Cl–H···Cl Bridges in the Low-melting Poly(Hydrogen Chloride) $Me_3N \cdot 5\,HCl$**

By *Dietrich Mootz** and *Jörg Hocken*

Adduct formation with hydrogen halides in large molar excess (beyond the composition of hydrogen dihalides) and the underlying structural principles have been studied in a systematic way only in the case of hydrogen *fluoride*.[1] We now wish to report the first characterization also of certain poly(hydrogen *chlorides*),[2] including a highly HCl-enriched phase of the system trimethylamine–HCl with the composition $Me_3N \cdot 5\,HCl$, melting congruently at -54 °C[3].

A crystal structure analysis of this phase[4] revealed an ionic compound with the formula $(Me_3NH)^{\oplus}[Cl(HCl)_4]^{\ominus}$, an interesting combination of anion coordination, hydrogen bonding, and ion-pair formation. The cation formed by protonation of the base Me_3N is accompanied by a complex anion (Fig. 1) in which a central $Cl^{\ominus}$ ion is coordinated by

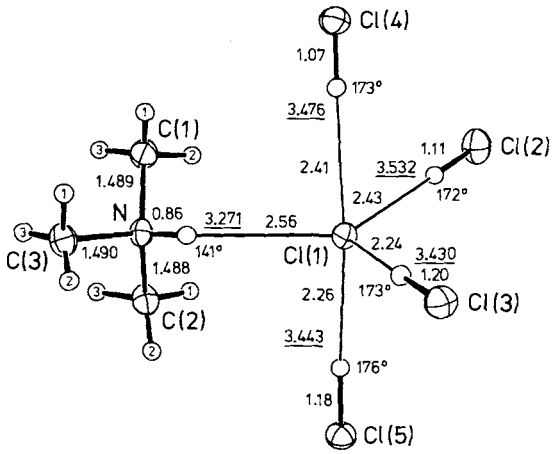


Fig. 1. The ion pair $(Me_3NH)^{\oplus}[Cl(HCl)_4]^{\ominus}$ as a structural element in the crystal structure of the phase $Me_3N-5\,HCl$, together with selected distances [Å] and angles [°]. Underlined values correspond to the overall distances Cl···Cl and N···Cl in the hydrogen bridges. Standard deviations are 0.001 Å for Cl···Cl, 0.002 Å for N···Cl, 0.004 Å for N–C, and 0.03–0.05 Å and 2–4° for distances and angles involving H atoms.

the remaining four HCl molecules of the formula unit via four hydrogen bonds of the relatively uncommon type Cl–H···Cl. In addition, the cation and complex anion are linked with each other by an N–H···Cl bridge. The overall coordination of the $Cl^{\ominus}$ ion thus constitutes a distorted trigonal bipyramid.

The significant deviation from linearity of the N–H···Cl bridge (with an angle at the H atom of only 141°) is explained by the fact that this bridge is but *one* component of a branched interaction N–H(···Cl)$_2$. The other component—leading to atom Cl(5) of an adjacent ion pair—is noticeably weaker, as indicated by the much larger N···Cl and H···Cl distances of 3.547 and 2.96 Å, respectively, and an even smaller angle at the H atom of 128°. The shortest Cl···Cl distance (apart from those involving hydrogen bonds) is one between $Cl^{\ominus}$ ions in adjacent ion pairs, determined to be 3.723 Å.

In contrast to the present case, complex anions in poly(hydrogen *fluorides*)[1] have never been found to possess more than four hydrogen bonds to a central halide ion. Provided the HF content is sufficiently high, these are characterized instead by extended or branched chains.

Received: July 24, 1989 [Z 3457 IE]
German version: *Angew. Chem. 101* (1989) 1713

CAS Registry number:
$Me_3N \cdot 5HCl$, 123624-31-7.

[*] Prof. Dr. D. Mootz, Dr. J. Hocken
Institut für Anorganische Chemie und Strukturchemie der Universität
Universitätsstrasse 1, D-4000 Düsseldorf (FRG)

[**] This work was supported by the Deutsche Forschungsgemeinschaft and the Fonds der Chemischen Industrie.

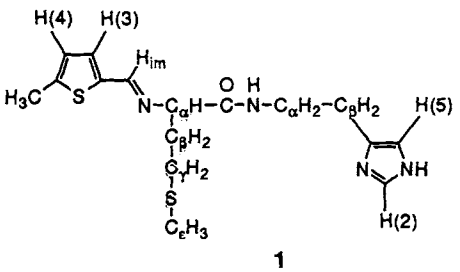
[1] a) D. Boenigk, D. Mootz, *J. Am. Chem. Soc. 110* (1988) 2135 and references cited therein; b) D. Mootz, D. Boenigk, *Z. Anorg. Allg. Chem. 544* (1987) 159 and references cited therein.

[2] J. Hocken, *Dissertation*, Universität Düsseldorf 1988.
[3] K. Angermund, *Diplomarbeit*, Universität Düsseldorf 1983.
[4] Crystal growth and structure determination: miniature zone melting with focussed heat radiation (D. Brodalla, D. Mootz, R. Boese, W. Osswald, *J. Appl. Crystallogr. 18* (1985) 316) in sealed quartz capillaries; Syntex-P2$_1$ diffractometer with low-temperature attachment; $Mo_{K\alpha}$ radiation, graphite monochromator, ω-scan; H atoms by difference electron density analysis; refinement by the method of least squares. Space group *Cc*, $Z = 4$; $a = 7.424(3)$, $b = 13.438(4)$, $c = 12.578(4)$ Å, $\beta = 107.61(3)°$ at -145 °C; 1470 observed independent reflections, $R = 0.023$. Further details of the crystal structure investigation are available on request from the Fachinformationszentrum Karlsruhe, Gesellschaft für wissenschaftlich-technische Information mbH, D-7514 Eggenstein-Leopoldshafen 2 (FRG) by quoting the depository number CSD-54041, the names of the authors, and the journal citation.

A Chiral Ag^I-Coordination Polymer with a Polydentate Chiral Ligand; Crystal Structure of the 1:1 Complex of CF_3SO_3Ag and *N*-[*N*-(5-Methylthenylidene)-L-methionyl]histamine**

By *Johan F. Modder, Gerard van Koten,* Kees Vrieze,* and *Anthony L. Spek*

Since chiral complexes play an essential role in many fields of chemistry,[1,2] the design and synthesis of chiral polydentate ligands, which on coordination to a metal center can selectively afford a complex in a single stereoisomeric form, is an important challenge. In research related to the modeling of the chromophore in copper proteins,[3] we recently embarked on a study of the coordination behavior of the chiral polydentate ligand *N*-[*N*-(5-methylthenylidene)-L-methionyl]histamine **1** towards the metal ions Ag^I and Cu^I. In **1** three different ligating groups are connected to the same stereogenic carbon center: a thioether group and an imidazole ring (both monodentate ligands) with S- and N-donor atoms, respectively, and a conjugated thiophenemethanimine unit as potential bidentate N,S-donor. CPK molecular model studies indicate that this ligand, when folded, might provide a cavity in which an N,N',S,S' donor array, related to the one present in Blue copper proteins,[4] is available for coordination to a single metal atom.



1

Reaction of **1** with AgO_3SCF_3 in a 1:1 molar ratio affords a product whose ^{1}H-NMR spectrum[5] is considerably different from that of the free ligand. Notable differences are the downfield shifts of the proton signals of the imine function ($\Delta\delta = 0.22$), of the methionine methyl group (0.18) and of the imidazole ring (H2 0.28, H5 0.21); furthermore, the histamine $C_\alpha H_2$-$C_\beta H_2$ signal pattern changes from an apparent A_2X_2 spin system for the free ligand to an apparent ABX_2 spin system for the complex.[6] These data indicate that there is coordination of the imine nitrogen, the methionine sulfur and at least one imidazole nitrogen atom together with spatial fixation of the histamine aliphatic chain.

An X-ray structure analysis[7] reveals that there are no discrete mononuclear units in the crystalline product, but, instead, a fascinating chiral polymer (Fig. 1) in which each ligand molecule is bound to three silver ions; this finding suggests that a folded geometry with coordination of one ligand to a single metal ion is energetically less favorable.[8] The unique rotation of this coordination polymer, which leads to a single stereoisomer with a Δ-helix,[9] seems to result from just a single stereogenic center—the C_α of L-methionine.

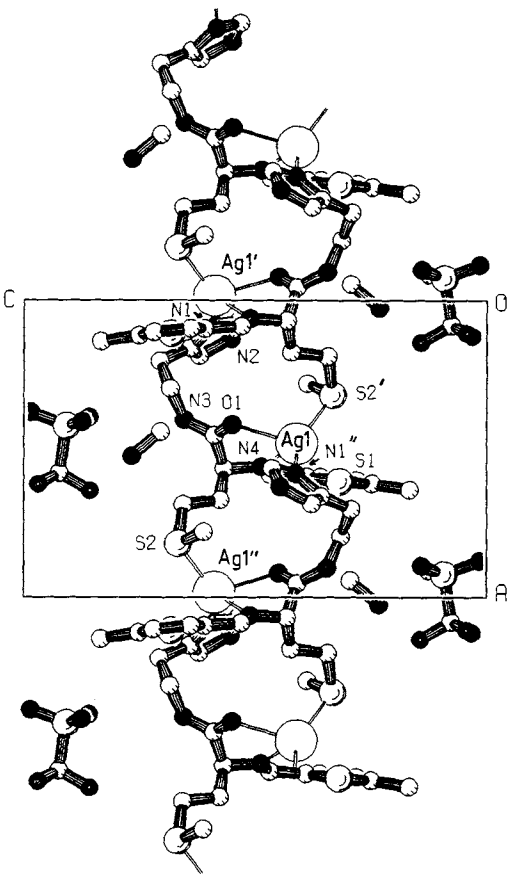


Fig. 1. Projection down the *b*-axis of part of the absolute structure of the polymeric 1:1-complex of AgO_3SCF_3 and *N*-[*N*-(5-methylthenylidene)-L-methionyl]histamine **1**. Symmetry operations by the screw axis are denoted by '(= $-1/2 + x$, $1/2 - y$, $1 - z$) and ''(= $1/2 + x$, $1/2 - y$, $1 - z$) respectively.

The compound also contains methanol, which acts as an acceptor for the amide hydrogen of the ligand and as a donor to an oxygen of an O_3SCF_3 anion. The nitrogen-bound imid-

[*] Prof. Dr. G van Koten,[+] J. F. Modder, Prof. Dr. K. Vrieze
Anorganisch Chemisch Laboratorium, Universiteit van Amsterdam
Nieuwe Achtergracht 166, NL-1018 WV Amsterdam (The Netherlands)
Dr. A. L. Spek
Vakgroep Algemene Chemie, Afdeling Kristal- en Structuurchemie, Universiteit van Utrecht
Padualaan 8, NL-3584 CH Utrecht (The Netherlands)
[+] Present adress:
Organisch Chemisch Laboratorium, Universiteit van Utrecht
Padualaan 8, NL-3584 CH Utrecht (The Netherlands)

[**] This work was supported by The Netherlands Foundation for Chemical Research (SON) and the Netherlands Organization for Scientific Research (NWO). Thanks are due to Dr. *C. J. Elsevier* for his interest and suggestions, to *A. J. M. Duisenberg* for the X-ray data collection and to Dr. *D. M. Grove* for his careful reading of the manuscript.

azole-H is hydrogen bonded directly to another oxygen of $O_3SCF_3^{\ominus}$. The O_3SCF_3 anion does not, as intended, coordinate to silver.

Each Ag^I center (Fig. 2) lies almost exactly in the plane of the methionine S2′, imine N4 and imidazole N1″ atoms to which it is tightly bound. The amide O1 atom lies above this plane, but not directly over the Ag ion, owing to rigidity of the ligand. The relatively long distance of O1 from the metal atom (2.568(4) Å) implies a weak bond. The thiophene S1 atom is located on the other side of the plane; however, the Ag–S1 distance of 3.081(2) Å is too long to be considered a bond.[10] This long range interaction between the thiophene sulfur atom and the silver cation was expected on the basis of the X-ray structure data of some Ag^I complexes with ligands which only contain thiophenemethane-imine moieties.[3]

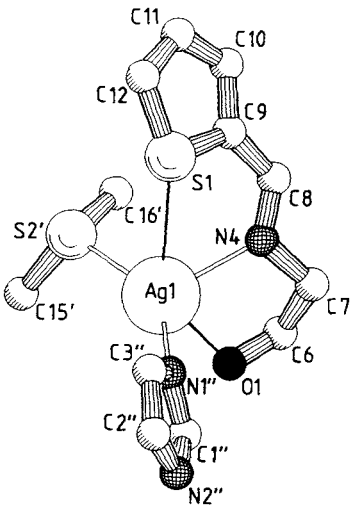


Fig. 2. Coordination geometry of the Ag-ion in the complex of AgO_3SCF_3 and **1**. Selected bond distances [Å] and angles [°]: Ag1-S2′, 2.509(2); Ag1-N1″ 2.219(4); Ag1-N4, 2.378(5); Ag1-O1, 2.568(4), Ag1-S1, 3.081(2); S2′-Ag1-N1″ 137.3(1), S2′-Ag1-N4, 106.7(1); N1″-Ag1-N4, 115.3(2); O1-Ag1-S2′, 110.6(1); O1-Ag1-N1″ 91.6(2); O1-Ag1-N4, 69.8(2).

The Ag^I-ion is best described as a trigonal-planar *N,N′,S*-coordinated, sp^2 hybridized ion, which binds the amide O1 atom and, to a lesser extent, the thiophene S1 atom via a dipole–cation interaction. Each Ag^I center in the sp^2 plane, when viewed along the axis perpendicular to it from S1 to O1, is *R* configurated.

The ^{1}H-NMR data of the complex are consistent with a structure of the complex in solution in which the Ag^I center is similarly coordinated as in the solid state; the degree of association is still unknown.

Some of the features of the metal coordination geometry found in this new complex may be relevant to a better understanding of the aspects that govern the structure and the physical and chemical properties of the Cu-N_2S_2 chromophore in Blue or Type I copper proteins.[4] Noteworthy in this respect are the M(I)–thioether-*S* bond, the M(I)–imidazole-*N* bond,[11,12] and perhaps also the long range M(I)–amide-*O* interaction.[12b]

From our results it is clear that **1** is not coordinated in a folded form to only one Ag^I center. On the contrary, the ligand is tailor-made to complex three silver ions, and, as a result of this coordination, a unique chiral polymer is formed. The occurrence of such a highly enantioselective polymerization, seemingly induced by a single stereogenic carbon center, is to our knowledge unprecedented. We are currently investigating the relevance of the ^{109}Ag-NMR shift found for this 1:1 complex of AgO_3SCF_3 and **1** (δ = 581).[13] Further studies include the synthesis and characterization of the corresponding Cu^I complex as well as modification of the ligand system (in order to create a pure N_2S_2 coordinated metal center) by replacing the thiophene by a sulfur donor with better coordinating properties.

Experimental

1: To protect the amino group, L-methionine (H-Met-OH) was converted quantitatively (295 K, commercial 2-*tert*-butyloxycarbonyloxyimino-2-phenylacetonitrile) into BOC-Met-OH. The latter was converted into its succinimide ester (273 K dicyclohexylcarbodiimide), thus activating the acid function, after which the histamine (Histam) unit was introduced via an amide bond. Subsequent removal of the amine protecting group with trifluoroacetic acid (TFA) yielded the salt H-Met-Histam · 2TFA. The free amine of this salt (generated *in situ*) was condensed with 5-methyl-2-thiophenecarbaldehyde in ethyl acetate at reflux over more than 3 equivalents of Na_2CO_3. Overall yield: 40%. Satisfactory elemental analyses were obtained[14].

[Ag **1**]$\infty(O_3SCF_3)\infty$: In a typical experiment, solutions of **1** (0.89 g, 2.5 mmol) in MeOH (25 ml) and of $Ag(I)O_3SCF_3$ (0.65 g, 2.5 mmol) in MeOH (25 ml) were mixed at room temperature, under exclusion of direct light. After stirring for 0.5 h, the solvent was evaporated and subsequently the solid, white residue was dried in vacuo. Satisfactory elemental analyses were obtained. Crystallization was achieved from a solvent mixture of MeOH, Et_2O and hexane cooled to 4 °C[7]; yield 0.92 g (60%).

Received: July 26, 1989 [Z 3467 IE]
German version: *Angew. Chem. 101* (1989) 1723

[1] J.-M. Lehn, *Angew. Chem. 100* (1989) 91; *Angew. Chem. Int. Ed. Engl. 27* (1988) 89, and references cited therein.

[2] J.-M. Lehn, A. Rigault, *Angew. Chem. 100* (1988) 1121; *Angew. Chem. Int. Ed. Engl. 27* (1988) 1095.

[3] a) G. C. van Stein, G. van Koten, K. Vrieze, A. L. Spek, E. A. Klop, C. Brevard, *Inorg. Chem. 24* (1985) 1367; b) G. C. van Stein, G. van Koten, F. Blank, L. C. Taylor, K. Vrieze, A. L. Spek, A. J. M. Duisenberg, A. M. M. Schreurs, B. Kojić-Prodić, C. Brevard, *Inorg. Chim. Acta 98* (1985) 107.

[4] a) J. A. Fee, Struct. Bonding (Berlin) 23 (1075) 1; b) A. E. G. Cass, H. A. O. Hill, *Ciba Found. Symp. 79* (1980) 71.

[5] ^{1}H-NMR data (CD_3OD, 250 MHz, TMS ext., room temperature) of a 1:1 mixture of AgO_3SCF_3 and **1**: δ = 2.20 (m, Met: H_2C_β), 2.24 (s, Met: H_3C_ε), 2.50 (s, (5 Me)Th: H_3C), 2.57 (m, Met: H_2C_γ), 2.91 (t, Histam: H_2C_β), 3.53 (m, Histam: H_bC_α), 3.67 (m, Histam: H_aC_α), 4.18 (t, Met: HC_α), 6.89 (d, (5 Me)Th: H(4)), 7.09 (s, Histam: H(5)), 7.44 (d, (5 Me)Th: H(3)), 7.87 (s, Histam: H(2)), 8.51 (s, (5 Me)Th: H_{im}). COSY and NOESY experiments were carried out to aid assignment.

[6] Theoretically this spin system is ABXY in the free as well as the complexed ligand, due to the presence of the chiral C_α of methionine. However at the magnetic field used (5.87 T) the diastereotopicity of the CH_2 protons is not necessarily evident. The AB character of the histamine $C_\alpha H_2$ pattern was identified by irradiating the XY virtual triplet of the $C_\beta H_2$ at δ = 2.91.

[7] Crystal data of the 1:1 complex of AgO_3SCF_3 and **1**: $[C_{16}H_{22}N_4S_2Ag]^{\oplus}$ $[O_3SCF_3]^{\ominus} \cdot CH_4O$, orthorhombic, space group $P2_12_12_1$, with a = 11.339(1), b = 13.122(1) and c = 17.451(1) Å, V = 2596.5(3) Å^3, Z = 4, ϱ_{calc} = 1.636 g cm^{-3}, $F(000)$ = 1296, $\mu(Mo_{K\alpha})$ = 10.5 cm^{-1}; 3369 reflections with $1.2° < \Theta < 27.5°$ were collected for a block-shaped, ivory-colored crystal [0.42 × 0.42 × 0.48 mm] at 100 K on an Enraf-Nonius CAD4 F diffractometer with Zr filtered $Mo_{K\alpha}$-radiation (λ = 0.71073 Å). The structure was solved by standard Patterson and Fourier methods (SHELXS-86) and refined by full matrix least-squares (SHELX-76) to a final R value of 0.037 [R_w = 0.043, $w^{-1} = \sigma^2(F)$, S = 1.78, 371 parameters] for 2827 observed reflections with $I > 2.5\sigma(I)$. Hydrogen atoms were located from a difference map and their positions refined (except for those of the methyl groups that were introduced at calculated positions and refined with fixed geometry) with four common isotropic thermal parameters. A final difference map did not show any features outside the range −0.68 to 0.75 e Å^{-3}. Both enantiomorphic structures were refined; the one with the lowest R value corresponds to the absolute *S* configuration of the ligand used (Figure 1). Further details of the crystal structure investigation may be obtained from the Director of the Cambridge Crystallographic Data Centre, Lensfield Road, Cambridge CB2 1EW (England), on quoting the full literature citation.

[8] *Bosnich* et al. suggest also that their coordination complexes of Cu^I and Cu^{II} with a quadridentate ligand, containing all the binding sites of blue

copper proteins, may have polymeric structures as a result of ligand flexibility: J. Whelan, B. Bosnich, *Inorg. Chem. 25* (1986) 3671.
[9] The helix can be visualized by following the chain Ag–imidazole $-C_\beta-C_\alpha-CO-N-C_\alpha-C=N-Ag$–imidazole- etc (Fig. 1).
[10] 3.08 Å > 1.59 Å (covalent radius Ag) + 1.02 Å (covalent radius S) + 0.40 Å (usual tolerance); radii: Manual Cambridge Crystallographic Data Base.
[11] a) J. M. Guss, H. C. Freeman, *J. Mol. Biol. 169* (1983) 521; b) J. M. Guss, P. R. Harrowell, M. Murata, V. A. Norris, H. C. Freeman, *ibid. 192* (1986) 361.
[12] a) E. T. Adman, L. H. Jensen, *Isr. J. Chem. 21* (1981) 8; b) G. E. Norris, B. F. Anderson, E. N. Baker, *J. Am. Chem. Soc. 108* (1986) 2784.
[13] ^{109}Ag-NMR spectrum (4.66 MHz, 10 mm tube, 0.67 g of the complex in 1.9 ml of CD_3OD, room temperature) was measured directly, the shift being relative to external $AgNO_3$ (5.9 M in D_2O). Acquisition time 1.64 s, delay time 200 s, number of scans: 1149.
[14] Details of the synthesis and X-ray structure analysis of **1**: J. F. Modder, G. van Koten, A. L. Spek, *J. Org. Chem.*, in press.

Generation, Stereochemistry, and Molecular Dynamics of a 1,3-Bis(phosphonio)propenide Cation**

By Hubert Schmidbaur, Christos Paschalidis, Oliver Steigelmann,* and *Gerhard Müller*

Allyl ions are the most simple resonance-stabilized π-systems in organic chemistry. Knowledge of their structure and molecular dynamics is of prime importance for an understanding of, e.g., allyl coordination to metals[1] and reaction pathways involving synthons with allyl-functionality.[2] Structural studies on classical metal propenide systems give ambiguous results regarding the stereochemistry of the free anions, since direct or indirect metal contacts cannot be excluded, either in the crystal or in the solution state[3]. The situation is not unlike the problem associated with the stereochemistry of "free" simple carbanions (or carbenium ions), where aggregation via the counterions $Li^\oplus$, $Na^\oplus$, $K^\oplus$, $MgX^\oplus$ etc. (or $X^\ominus$ in the case of carbenium ions) is a common feature.[4]

In previous studies we have been able to demonstrate that the configuration of carbanions can be determined by structural studies on phosphorus ylides, where the carbanionic charge is compensated intramolecularly by the phosphonium centers. Cyclopropanides and cyclobutanides[5] were shown to have distinctly pyramidal carbanionic centers, and even the simple methanides and 2-propanides are clearly species with nonplanar ylidic functions.[6] Moreover, it could be proven that bis(phosphonio)methanediides ("carbodiphosphoranes") are highly bent.[7] Following the preparation of a neutral phosphoniopropenide[8] we have now synthesized and structurally characterized the corresponding bis(phosphonio)propenide cation.

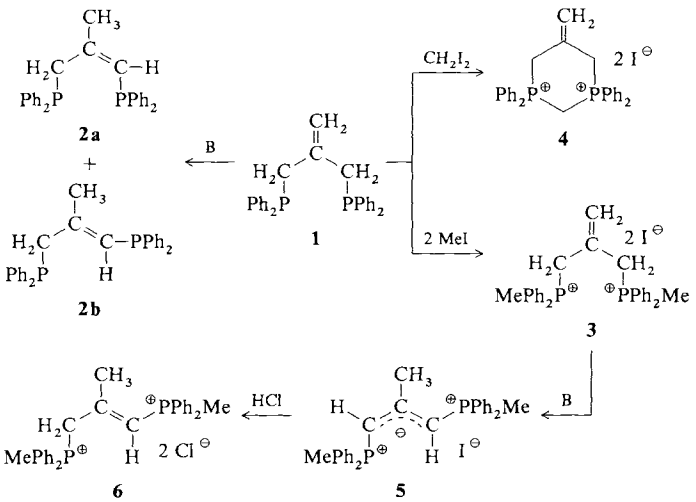
1,1,-Bis(diphenylphosphinomethyl)ethene, **1**,[9] was found to undergo facile base-catalyzed rearrangement, affording the two stereoisomers of 2-methyl-1,3-bis(diphenylphosphino)propene (**2a, b**; Scheme 1). This isomerization is not unexpected and has been observed previously in related systems.[10] In contrast, **1** reacts with excess iodomethane or diiodomethane to give **3**, containing a symmetrical open-chain dication, or **4**, containing a cyclic 1,3-diphosphonia dication, respectively.

[*] Prof. Dr. H. Schmidbaur, Dipl.-Chem. C. Paschalidis, Dipl.-Chem. O. Steigelmann [+], Dr. habil. G. Müller [+]
Anorganisch-chemisches Institut der Technischen Universität München
Lichtenbergstraße 4, D-8046 Garching (FRG)
[+] Röntgenstrukturanalyse

[**] This work was generously supported by the Deutsche Forschungsgemeinschaft (Leibniz-Programm), by the Fonds der Chemischen Industrie, and by Hoechst AG, Knapsack (FRG)

Careful deprotonation of the dication in **3** using triethylethylidenephosphorane[11] as a transylidating agent[12] leads to the 2-methyl-1,3-bis[(methyl)diphenylphosphonio]-propenide monocation, which crystallizes as the iodide salt **5** in almost quantitative yield (87%). The only other product is tetraethylphosphonium iodide. Organolithium reagents, sodamide, or other strong bases can also be used for the conversion of **3** into **5**.

According to analytical, spectroscopic, and X-ray diffraction data, **5** is present as only one isomer with a stereochemistry as indicated in Scheme 1. Surprisingly, the reprotonation of **5** with ethereal HCl is equally stereoselective and yields only one dication isomer in the form of the salt **6** (the assignment in Scheme 1 is tentative). It should be noted that the dications of **3** and **6** are regioisomers when referring to (de)protonation.



Scheme 1. Reactions starting from the diphosphino compound **1**. B = base.

The NMR spectra of the salt **5** indicate the presence of two slightly nonequivalent diphenylmethylphosphonio groups in the anion at ambient temperature in $C_6D_5NO_2$ or CD_3CN as solvent. Similarly, the allyl carbon atoms C1 and C3 and their hydrogen atoms are only marginally nonequivalent, as expected for a configuration where the onium centers reside in *syn/anti* (*E/Z*) positions relative to the allylic system. ^{31}P- and ^{13}C-NMR chemical shifts are in the range typical for ylidic bonding, where onium character can be assigned to the phosphorus atoms (δ(P) = 7.9, 7.2), while carbanionic character appears to predominate at the neighboring carbon centers, whose resonances (δ(C1/C3) = 56.7/58.5) are clearly upfield from the olefinic region. By contrast, the resonance of the central carbon atom (C2) has its position in the aromatic region (δ(C2) = 167.6), in agreement also with the simple MO diagram for allylic anions[13] and with previous NMR data.[3]

The magnetic nonequivalence of P1/P2, C1/C3, and H1/H3 affords proof of rigidity of the anion configuration in solution at room temperature on the NMR time scale. The spectra are, however, temperature-dependent, and on heating a reversible collapse of pertinent signals can be detected. From the coalescence temperatures, a free activation energy for the rotational barrier of the allylic anion can be calculated. The result ($\Delta G^\ddagger = 20.5 \pm 1.0$ kcal/mol)[14] is in good agreement with data obtained previously for alkali-metal propenide solutions.[3] It should be noted that for small

cations like $Li^{\oplus}$ even greater geometrical changes are to be expected for the anions, which would lead to a complete change also of the molecular dynamics.[14b]

Figure 1 shows the result of a single crystal structure analysis of compound **5**.[15] As expected the allylic moiety is

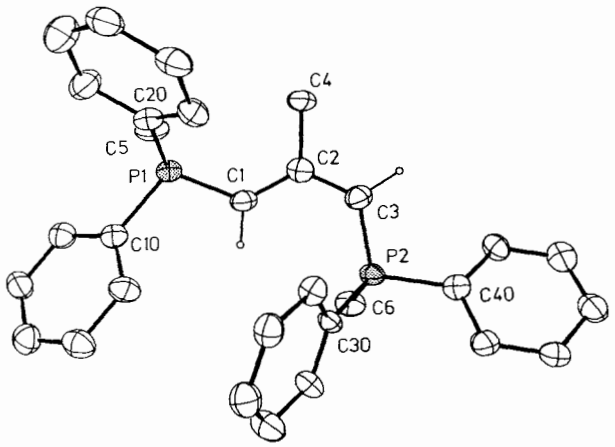


Fig. 1. Structure of the cation of **5** in the crystal (ORTEP, probability ellipsoids 50%; only the hydrogen atoms at C1/C3 are shown.) Selected bond distances [Å] and angles [°]: C1-C2 1.393(5), C2-C3 1.389(5), C2-C4 1.511(5); P1-C1 1.725(4), P2-C3 1.725(3); P1-C5 1.800(4), P2-C6 1.805(4); P1-C10 1.800(3) P1-C20 1.814(3), P2-C30 1.799(3), P2-C40 1.802(3). C1-C2-C3 124.8(3), C1-C2-C4 120.4(3), C3-C2-C4 114.8(3); P1-C1-C2 128.4(3), P2-C3-C2 125.9(3). Maximum deviation from the best plane through P1,P2,C1,C2,C3,C4 is 0.09 Å for C1. Iodide contacts are >3.8 Å.

planar, with the phosphorus substituents in *E*/*Z*-positions. The central carbon atom C2 is in a trigonal planar configuration with the methyl carbon at a normal aliphatic distance (C2–C4 = 1.511(5) Å) and two equidistant olefinic carbon atoms at C1–C2 = 1.393(5) and C2–C3 = 1.389(5) Å. Ylidic bonding is obvious from the distances P1–C1 = 1.725(4) and P2–C3 = 1.725(3) Å, when compard with the lengths of the other phosphorus-carbon bonds serving as "internal reference", and the lengths of the corresponding bonds of the precursor **1**.[9]

The iodide counteranion has no discrete cation contact in the crystal. In the absence of any prominent crystal packing effects, the propenide structure determined here can thus be taken as the unperturbed configuration of an (onium-stabilized) allylic anion. A comparison of the results with the numerous theoretical calculations on allyl systems that are now available will be dealt with in a future full paper.[16]

Experimental

The ^{1}H-, ^{13}C- and ^{31}P-NMR spectra were recorded at 270.05, 67.80 and 161.83 MHz. **2a, b**: A solution of 2.0 g (4.7 mmol) of **1** in 50 mL of tetrahydrofuran was treated with 10 g (0.91 mmol) of *t*BuOK and heated under reflux for 12 h. After removal of all volatile components by evaporation there remained a mixture of the two isomers as a colorless, viscous oil (1.9 g, 94%).—^{31}P{^{1}H}-NMR ($CDCl_3$): **2a**: $\delta = -13.5$, -30.7 (AB, $^4J(PP) = 5.7$ Hz); **2b**): $\delta = -17.1$, -27.2 (AB, $^4J(PP) = 2.8$ Hz).—^{13}C{^{1}H}-NMR ($CDCl_3$): **2a**: $\delta = 26.6$ (dd, $J(PC) = 10.27, 6.36$ Hz, CH_3), 36.0 (dd, $J(PC) = 24.94, 16.14$ Hz, CH_2), 151.7 (dd, $J(PC) = 25.9, 7.8$ Hz, =CP), 138.4 (A part of a AXX′ system, $N = 17.6$ Hz, $=CC_2$); **2b**: $\delta = 20.9$ (dd, $J(PC) = 24.9, 8.3$ Hz, CH_3), 42.2 (dd, $J(PC) = 16.1, 6.3$ Hz, CH_2), 150.1 (dd, $J(PC) = 26.4, 6.85$ Hz, =CP), 138.2 (A part of a AXX′ system, $N = 15.16$ Hz, CC_2). **3**: see Ref. [9]

4: A mixture of 2.0 g (4.7 mmol) of **1** and 0.38 mL (1.26 g, 4.7 mmol) of CH_2I_2 in 50 mL of CH_2Cl_2 was heated under reflux for 2 d. The precipitate was filtered off, washed, and dried in a vacuum (1.8 g, 56%), m.p. 215 °C (dec.). ^{31}P{^{1}H}-NMR ([D_6] DMSO): $\delta = 13.2$(s).—^{13}C{^{1}H}-NMR ([D_6] DMSO): $\delta = 13.27$ (t, $J(PC) = 40.0$ Hz, PCP), 26.89 (AA′ part of a AA′ XX′ system, $N = 50.36$ Hz, CCH_2P), 126.27 (t, $J(PC) = 10.3$ Hz, $=CH_2$), 127.98 (t, $J(PC) = 26.7$ Hz, $=CC_2$), one set of phenyl-C resonance signals.—^{1}H-NMR ([D_6] DMSO): $\delta = 4.8$ (A_2A_2' part of $A_2A_2'XX'$ system, $J(PH) = 14.65$ Hz, 4H, CCH_2P), 5.9 (t, $J(PH) = 15.26$ Hz, 2H, PCH_2P), 6.0 (br. s, 2H, $=CH_2$), 7.6–8.0 (m, 20H, Ph).

5: A suspension of 1.0 g (1.41 mmol) of the salt **3** in 100 mL of tetrahydrofuran was cooled to −40 °C and treated with a solution of 0.20 g (1.41 mmol) of $Et_3P=CHMe$ in 10 mL of the same solvent. The reaction mixture was allowed to warm to room temperature and stirred for 1 h. The precipitate was filtered off and recrystallized from toluene/acetonitrile (0.4 g Et_4PI). The filtrate was concentrated and the oily residue crystallized from benzene/hexane (**5**, 0.70 g, 87%, m.p. 174 °C).—^{31}P{^{1}H}-NMR (CD_3CN, 25 °C): $\delta = 7.89$, 7.18(s); ^{31}P{^{1}H}-NMR ($C_6D_5NO_2$, 25 °C): $\delta = 6.07$, 5.50; coalescence temperature (at 161.83 MHz): 369 K (96 °C).—^{13}C{^{1}H}-NMR (CD_3CN, −35 °C): $\delta = 10.93$ (d, $J(PC) = 63.1$ Hz, P*Me*), 13.13 (d, $J(PC) = 62.6$ Hz, P*Me*), 25.8 (dd, $J(PC) = 18.6, 8.3$ Hz, *Me*C), 56.7 (dd, $J(PC) = 118.6, 8.6$ Hz, PCH), 58.5 (dd, $J(PC) = 106.4, 17.8$ Hz, PCH), 167.6 (dd, $J(PC) = 6.86, 5.33$ Hz, *C*Me), two sets of phenyl-C resonance signals.—^{1}H-NMR ($C_6D_5NO_2$, 150 °C): $\delta = 1.98$ (s, MeC), 2.33 (d, $J(PH) = 12.9$ Hz, PMe), 3.51 (br. s, PCH), equivalent phenyl-H resonance signals.

Received: June 22, 1989 [Z 3410 IE]
German version: *Angew. Chem. 101* (1989) 1739

CAS Registry numbers:
1, 120658-80-2; **2a**, 123775-75-7; **2b**, 123775-76-8; **3**, 120883-37-6; **4**, 123775-77-9; **5**, 123775-78-0; **6**, 123775-79-1; CH_2I_2, 75-11-6; $Et_3P=CHMe$, 17847-85-7.

[1] C. Elschenbroich, A. Salzer: *Organometallics*, VCH Verlagsgesellschaft, Weinheim 1989, p. 280ff. Phosphoniopropenide Complexes: H. Schmidbaur, *Angew. Chem. 95* (1983) 980; *Angew. Chem. Int. Ed. Engl. 22* (1983) 907.

[2] J. March: *Advanced Organic Chemistry*, Wiley, New York 1985; R. H. DeWolfe, W. G. Young in S. Patai (Ed.): *The Chemistry of Alkenes*, Wiley-Interscience, New York 1964, p. 681ff.

[3] G. Fraenkel, W. R. Winchester, *J. Am. Chem. Soc. 111* (1989) 3794 (the most recent pertinent publication with leading references); M. Schlosser, M. Stähle, *Angew. Chem. 92* (1980) 497; *Angew. Chem. Int. Ed. Engl. 19* (1980) 487; S. Bywater, D. J. Worsfold, *J. Organometal. Chem. 159* (1978) 229; W. N. Setzer, P. von R. Schleyer, Adv. *Organomet. Chem. 24* (1985) 353.

[4] H. Schmidbaur, U. Deschler, B. Zimmer-Gasser, D. Neugebauer, U. Schubert, *Chem. Ber. 113* (1980) 902; H. Schmidbaur, U. Deschler, B. Zimmer-Gasser, B. Milewski-Mahrla, *ibid. 14* (1981) 608; H. Schmidbaur, U. Deschler, B. Milewski-Mahrla, *ibid. 115* (1982) 3290.

[5] H. Schmidbaur, A. Schier, B. Milewski-Mahrla, U. Schubert, *Chem. Ber. 115* (1982) 722; H. Schmidbaur, A. Schier, D. Neugebauer, *ibid. 116* (1983) 2173.

[6] H. Schmidbaur, A. Schier, C. M. F. Frazao, G. Müller, *J. Am. Chem. Soc. 108* (1986) 976; H. Schmidbaur, C. Krüger, J. Jeong, A. Schier, D. L. Wilkinson, G. Müller, *N. J. Chem.* 13 (1989) 341 and references cited therein.

[7] U. Schubert, C. Kappenstein, B. Milewski-Mahrla, H. Schmidbaur, *Chem. Ber. 114* (1981) 3070.

[8] H. Schmidbaur, W. Malisch, D. W. H. Rankin, *Chem. Ber. 104* (1971) 145.

[9] H. Schmidbaur, C. Paschalidis, O. Steigelmann, G. Müller, *Chem. Ber. 122* (1989) 1851.

[10] L. Horner, I. Ertel, H.-D. Ruprecht, O. Belowski, *Chem. Ber. 103* (1970) 1582.

[11] H. Schmidbaur, W. Tronich, *Chem. Ber. 101* (1968) 604.

[12] H. J. Bestmann, *Chem. Ber. 95* (1962) 58.

[13] F. A. Cotton: *Chemical Applications of Group Theory*, Wiley-Interscience, New York 1963, p. 156ff.

[14] a) G. Binsch, H. Kessler, *Angew. Chem. 92* (1980) 445; *Angew. Chem. Int. Ed. Engl. 19* (1980) 411; b) G. Boche, *Top. Curr. Chem. 146* (1988) 7.

[15] Crystal structure data of compound **5** ($C_{30}H_{31}IP_2$, $M_r = 580.43$): monoclinic, space group $P2_1/n$, $a = 10.018(1)$, $b = 15.522(2)$, $c = 17.937(2)$ Å, $\beta = 101.22(1)°$, $V = 2735.9$ Å^3, $Z = 4$, $\varrho_{calc.} = 1.409$ g cm^{-3}, $\mu(MoK_\alpha) = 12.9$ cm^{-1}, T = −50 °C. 4757 independent reflexions ($R_{int} = 0.028$), with 4110 'observed' at $F_o \geq 4.0\sigma(F_o)$, $[(\sin\Theta/\lambda)_{max} = 0.595$, *hkl*: +11, +18, ±21, $Mo_{K\alpha}$ radiation, $\lambda = 0.71069$ Å, graphite monochromator, Syntex $P2_1$ diffractometer]. Structure solution by Patterson methods (SHELXS-86), R (R_w) = 0.032 (0.036), $w = 1/\sigma^2(F_o)$; (anisotropic, H constant, SHELX-76). $\Delta\varrho_{fin}$(max/min) = 0.55/−0.41 e/Å^3. Further data are available from the Fachinformationszentrum Karlsruhe, Gesellschaft für wissenschaftlich-technische Information mbH, D-7514 Eggenstein-Leopoldshafen 2, on quoting the depository number CSD-54221, the names of the authors, and the journal citation.

[16] L. Radom in E. Buncel, T. Durst (Eds.): *Comprehensive Carbanion Chemistry* Part C, Elsevier, Amsterdam 1987, Chap. 1.

LiCaN and Li_4SrN_2, Derivatives of the Fluorite and Lithium Nitride Structures**

By *Gerhard Cordier, Axel Gudat, Rüdiger Kniep,* and *Albrecht Rabenau**

Dedicated to Robert Juza on the occasion of his 85th birthday

Ternary nitrides[1] preferentially crystallize in the fluorite structure when the ionic radius ratio[2] $r(Li^{\oplus})/r(M^{n\oplus}) \geq 1$. The cations occupy the tetrahedral holes of the approximately cubic close-packed matrix of nitride ions either statistically ($LiMgN$[3]) or fully ordered ($LiZnN$,[3] Li_3AlN_2,[4] Li_3GaN_2,[4] Li_5GeN_3,[5] Li_5TiN_3,[5] Li_7VN_4,[6] and Li_7MnN_4[7]). The recently determined crystal structures of Li_3FeN_2, $Li_{15}Cr_2N_9$, and $Li_6(M)N_4$ (M = Cr, Mo, W)[8] are also consistent with this generalization. Within the alkaline earth series of compounds, the only member other than LiMgN ($r(Li^{\oplus})/r(Mg^{2\oplus}) = 1.0$) whose crystal structure has been reported is LiSrN.[9] LiSrN ($r(Li^{\oplus})/r(Sr^{2\oplus}) < 1$) crystallizes in the YCoC structure,[10] which is energetically more favorable than a hypothetical fluorite structure.[11] The homologous compound LiCaN[12] offers the possibility to investigate a crystal-chemical link between the LiMgN and LiSrN structures. Moreover, a Li-rich phase of the ternary Li-Sr-N system (Li_4SrN_2) has been prepared and its crystal structure determined. The structure bears a close relationship to the Li_3N structure.[13] Intermediate phases[14,15] were observed from the systems Li-Be-N and Li-Ba-N, but no suitable single crystals have so far been obtained.

LiCaN was prepared from the elements. In order to obtain single crystals suitable for structural analysis a tantalum crucible was charged with a mixture of lithium and calcium (molar ratio 6:1) and fused under argon at 250 °C. The temperature was subsequently increased, under 1 atm nitrogen, to 850 °C. LiCaN is obtained (along with Li_3N) as orange-colored single crystals with a plate-like habit. Single phase, polycrystalline samples of Li_4SrN_2 (dark metallic luster) were prepared by reaction of lithium nitride with strontium (molar ratio Li:Sr = 4:1) under nitrogen (1 atm). The melt was cooled from 700 °C to room temperature over a 12 hour period.

The crystal structure of LiCaN[16] (Fig. 1) is directly related to the fluorite structure. The calcium atoms occupy half the tetrahedral holes whereas the lithium atoms are displaced from the tetrahedral center positions of the approximately cubic close-packed nitrogen matrix, being only 0.135 Å from a tetrahedral face but 3.570(8) Å from the fourth nitrogen atom. Lithium atoms are thus coordinated to three nitrogen atoms (Li–N: 2.071(4)–2.108(8) Å), a situation similar to that found in the crystal structure of Li_3N[13] where Li atoms are coordinated in a planar arrangement within the Li_2N layers (Li–N: 2.130(1) Å). As a result of the special distribution of the cations (Fig. 1) infinite $^1_\infty[LiN_{3/3}]$ bands occur, which run in the [010] direction. These are one dimensional sections from the Li_2N layers in Li_3N[13] which, through nitrogen atoms shared with CaN_4 tetrahedra (Ca–N: 2.436(4)–2.472(2) Å; N–Ca–N: 98.6(1)–120.1(1)°), become interconnected into a three-dimensional structural

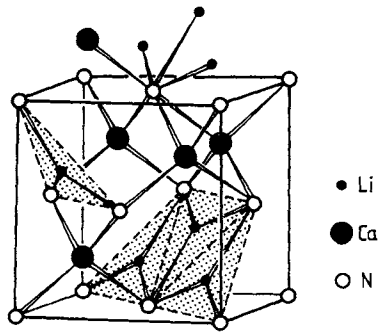


Fig. 1. Section from the crystal structure of LiCaN. Schematic representation: cubic face centered arrangement of nitrogen atoms; calcium in tetrahedral coordination; lithium displaced from the center of the tetrahedral hole to the tetrahedral face (LiN bands parallel to $[010]_{ortho}$); pentagonal bipyramidal coordination of the nitrogen atoms.

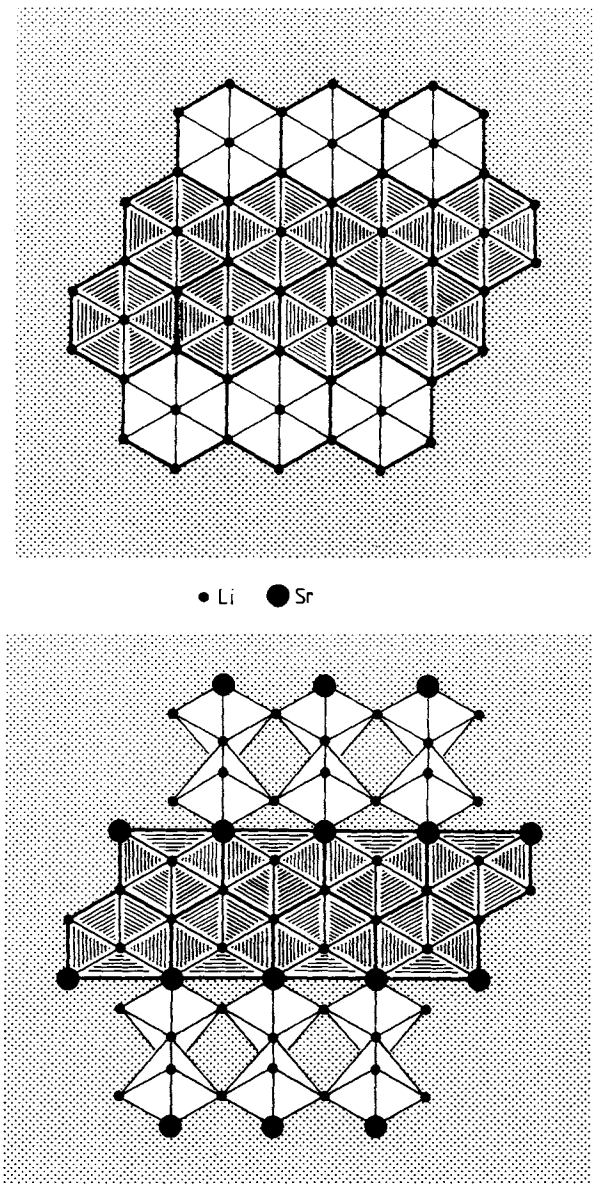


Fig. 2. Schematic representation of the coordination polyhedra (hexagonal and pentagonal bipyramids) around the nitrogen atoms in the structure of Li_3N (top, [001] projection) [13] and Li_4SrN_2 (bottom, [100] projection). In the second case, groups of layers are present in which the axes of pentagonal bipyramids lie either in the plane of the diagram (open polyhedra) or perpendicular to it (shaded polyhedra).

[*] Prof. Dr. A. Rabenau, Dr. G. Cordier [+], Dipl.-Chem. A. Gudat, Prof. Dr. R. Kniep [+]
Max-Planck-Institut für Festkörperforschung
Heisenbergstrasse 1, D-7000 Stuttgart 80 (FRG)

[+] Permanent Address:
Eduard-Zintl-Institut der Technischen Hochschule
Hochschulstrasse 10, D-6100 Darmstadt (FRG)

[**] This work was supported by the Fonds der Chemischen Industrie and the Freunde der TH Darmstadt.

arrangement. The nitrogen atoms are coordinated in the form of a distorted pentagonal bipyramid, axially by two calcium atoms and equatorially by two calcium and three lithium atoms. The Ca_{ax}–N–Ca_{ax} angle is nearly linear at 177.5(3)°; the Ca_{ax}–N–$(Ca, Li)_{eq}$ angles lie between 81.5(2)° and 96.9(2)°. In the equatorial plane the angle subtended at nitrogen between two calcium atoms is 94.7(1)°; that between two lithium atoms is 62.0(2)°.

In the crystal structure of Li_4SrN_2[16] (bottom of Fig. 2) the N atoms are also coordinated within distorted pentagonal bipyramids, in this case involving $2 \times Li_{ax}$ and $2 \times Sr_{eq} + 3 \times Li_{eq}$. The angular relationships are comparable to those in the calcium compound (vide supra): Li_{ax}–N–Li_{ax} 174.4(3)°; Li_{ax}–N–$(Sr,Li)_{eq}$ 87.2(2)°–92.0(2)°; Sr_{eq}–N–Sr_{eq} 92.4(2)°; Li_{eq}–N–Li_{eq} 62.8(2)°. As implied in Figure 2 (bottom), the Li_4SrN_2 structure can be derived directly from the structure of Li_3N (Fig. 2, top)[13]. The three-dimensional framework of hexagonal bipyramids interconnected through equatorial edges and axial vertices in Li_3N ($NLi_{2/2}Li_{6/3}$) is cut into layers which in Li_4SrN_2 ($NLi_{2/2}Li_{3/3}Sr_{2/4}$) are in turn made up of pentagonal bipyramids. The layers run along [001]; each is turned 90° relative to the next, and they are connected to one another through shared strontium atoms. Strontium is therefore coordinated to four nitrogen atoms in a distorted tetrahedral geometry (Sr–N: 2.648(3) Å; N–Sr–N: 92.4(2)°–118.6(3)°). The Li–N bond lengths within the layers (Li_{ax}–N: 1.913(2) Å, Li_{eq}–N: 2.112(2)–2.149(2) Å) are just as graded as those in the structure of Li_3N[13] (Li_{ax}–N: 1.938 Å, Li_{eq}–N: 2.130(1). Impedance measurements show Li_4SrN_2 to be an ion conductor (activation energy 0.9(5) eV) but with a considerably lower ionic conductivity than Li_3N[17]. At 430 °C the ionic conductivity of Li_4SrN_2 is still an order of magnitude lower than that of pure Li_3N measured at room temperature.

Received: May 26, 1989 [Z 3359 IE]
German version: *Angew. Chem. 101* (1989) 1689

[1] R. Juza, K. Langer, K. von Benda, *Angew. Chem. 80* (1968) 373; *Angew. Chem. Int. Ed. Engl. 7* (1968) 360.
[2] R. D. Shannon, *Acta Crystallogr. A 32* (1976) 751.
[3] R. Juza, F. Hund, *Z. Anorg. Allg. Chem. 257* (1948) 1.
[4] R. Juza, F. Hund, *Z. Anorg. Allg. Chem. 257* (1948) 13.
[5] R. Juza, H. H. Weber, E. Meyer-Simon, *Z. Anorg. Allg. Chem. 273* (1953) 48.
[6] R. Juza, W. Gieren, J. Haug, *Z. Anorg. Allg. Chem. 300* (1959) 61.
[7] R. Juza, E. Anschütz, H. Puff, *Angew. Chem. 71* (1959) 161.
[8] A. Gudat, R. Kniep, A. Rabenau, *German Chem. Soc., 5th Annu. Conf. Solid State Chem.*, Erlangen, September 28–30, 1988,
[9] G. Cordier, A. Gudat, R. Kniep, A. Rabenau, *Angew. Chem. 101* (1989) 204; *Angew. Chem. Int. Ed. Engl. 28* (1989) 201.
[10] M. H. Gerss, W. Jeitschko, *Z. Naturforsch. B41* (1986) 946.
[11] R. Nesper, *Z. Kristallogr.* manuscript in preparation. The observed distance d(Sr–N) ≃ 2.6 Å leads to a decidedly larger volume for the fluorite structure type than for the YCoC structure type. For d(Sr–N) > 2.44 Å, the fluorite structure type will be energetically less favorable than the latter.
[12] J. Aubry, M. Fromont, R. Streiff, *C.R. Hebd. Séances Acad. Sci. Ser. C 262* (1966) 1785.
[13] A. Rabenau, H. Schulz, *J. Less Common Met. 50* (1976) 155.
[14] J.-F. Brice, J.-P. Motte, R. Streiff, *C.R. Hebd. Séances Acad. Sci. Ser. C 269* (1969) 910.
[15] J.-F. Brice, J. Aubry, *C.R. Hebd. Séances Acad. Sci. Ser. C 271* (1970) 825.
[16] Crystallographic data: LiCaN: orthorhombic, *Pnma*, $a = 8.471(3)$, $b = 3.676(2)$, $c = 5.537(3)$ Å, $Z = 4$; 670 measured, 268 independent reflections; $R = 0.034$. Li_4SrN_2: tetragonal, $I4_1/amd$, $a = 3.822(2)$, $c = 27.042(9)$ Å, $Z = 4$; 1192 measured, 188 independent reflections; $R = 0.045$. Phillips PW-1100 single crystal diffractometer, $Mo_{K\alpha}$, 300 K. Further details of the crystal structure investigation are available on request from the Fachinformationszentrum Karlsruhe, Gesellschaft für wissenschaftlich-technische Information mbH, D-7514 Eggenstein-Leopoldshafen 2 (FRG) by quoting the depository number CSD 54206, the names of the authors, and the journal citation.
[17] A. Rabenau, *Solid State Ionics 6* (1982) 277.

Chirality and Isomerism in Binuclear Iron Complexes with Sulfur Ligands: $[Fe(CO)(\mu\text{-}"S_4")]_2$, a Model Complex for Oxidoreductases**

By *Dieter Sellmann,* Robert Weiss,* and *Falk Knoch*

Numerous oxidoreductases, including nitrogenases and hydrogenases, have an active center consisting of iron atoms in a coordination sphere of sulfur atoms. However, much uncertainty remains about the precise structures of such multinuclear centers and the molecular processes associated with the corresponding catalytic reactions.[1a] Previously described model compounds of these centers are all only of the structural type; i.e., they do incorporate iron atoms and sulfido or thiolato ligands,[1b] are usually highly symmetric, but fail to react with such relevant substrates as CO, N_2, or H_2. What has generally not been considered with respect to model complexes is the fact that the metal centers in oxidoreductases are always chirotopic as a consequence of bonding to the protein shell.[2] This generalization applies even when the catalyzed reaction involves only achiral substrates or, as in the case of the iron centers in ferredoxins, when the iron centers are constituents of highly symmetrical subunits such as $[Fe_4S_4(SR)_4]$ clusters.[1a] Metallic centers in oxidoreductases must also provide free or potentially free coordination sites for the attachment of substrates.

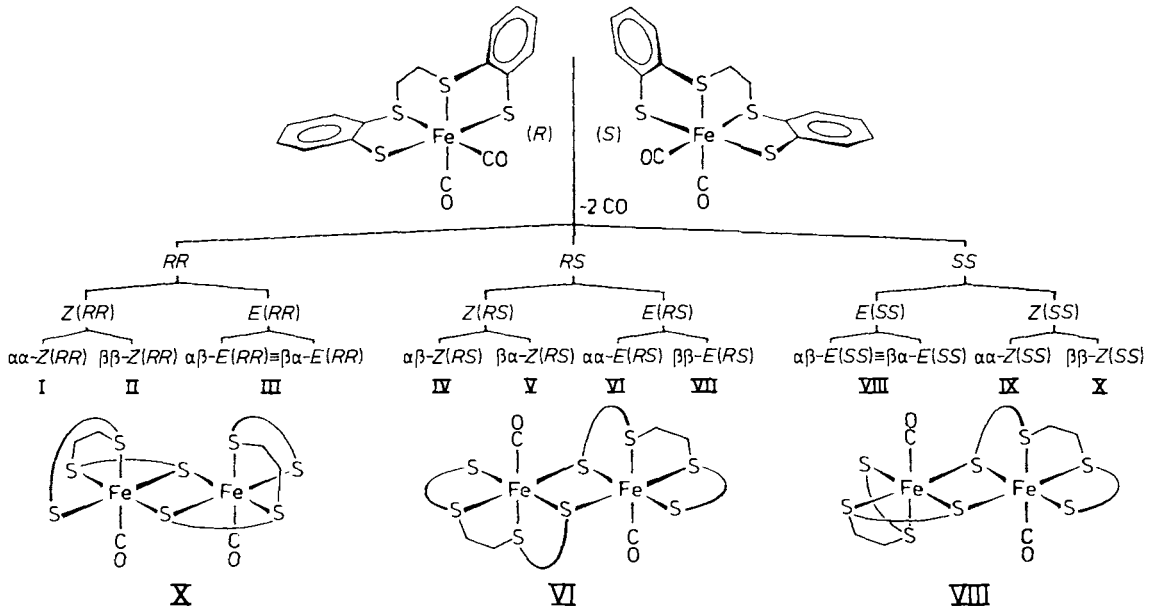
In our search for model complexes of the active centers in nitrogenases and hydrogenases we have attempted to elaborate the iron complex **1** in such a way as to create multicentered chiral units with free or potentially free coordination sites at the Fe centers. Since **1** itself is chiral, it was of particular interest to ascertain what diastereomers would form in the course of a dimerization. We now report the isolation and structural characterization of the binuclear complex **2**,[3] which represents a new type of chiral complex. **2** contains two homochiral fragments with low-valent Fe centers that bind σ-π ligands, and it is formed upon dimerization of racemic precursor complexes according to equation (a).[4]

$$\underset{\mathbf{1}}{2\,[Fe(CO)_2("S_4")]} \xrightarrow[-2CO]{DMF/90\,^\circ C} \underset{\mathbf{2}}{[Fe(CO)(\mu\text{-}"S_4")]_2} \qquad (a)$$

Theoretically, the dimerization of $[Fe(CO)("S_4")]$ fragments might lead to ten diastereomers (Scheme 1, **I**–**X**). This assertion is based on the assumption of configurational stability at the Fe centers, however, since otherwise the number of diastereomers would be even larger (e.g., isomers with planar orientation of the sulfur ligands). Molecular models reveal that the conformation of the C_2H_4 bridge in **1** is fixed due to the rigid $C_6H_4S_2$ units (i.e., "inversion" of the bridge would lead to serious distortion of the angles at the Fe atom). Thus, dimerization can only lead to *RR*, *RS* and *SS* isomers.[5] In contrast to previously known binuclear complexes with chiral fragments,[6] each of these combinations in **2** is in principle the source of four isomers. Members of two of the resulting "pairs" are in fact identical, so the overall result

[*] Prof. Dr. D. Sellmann, Dipl.-Chem. R. Weiss, Dr. F. Knoch
Institut für Anorganische Chemie der Universität Erlangen-Nürnberg
Egerlandstrasse 1, D-8520 Erlangen (FRG)

[**] $("S_4")^{2\ominus}$ = 2,2'-(ethylenedithio)dibenzenethiolate. Transition Metal Complexes with Sulfur Ligands, Part 51. This work was supported by the Deutsche Forschungsgemeinschaft and the Fonds der Chemischen Industrie. Part 50: D. Sellmann, O. Käppler, F. Knoch, M. Moll, *Z. Naturforsch.*, in press.



Scheme 1. Theoretically possible isomers of **2**, with schematic representations of the ββ-*Z*(*SS*), αα-*E*(*RS*), and βα-*E*(*SS*) isomers, ∩ = C_6H_4.

is ten structures that differ in the following ways:

a) The two CO ligands may point either in the same (*Z* isomers) or the opposite (*E* isomers) direction.

b) The bridging of the Fe centers takes place via two kinds of thiolato-S atoms which differ in only one respect: The *ortho* thioether-S atom at the respective benzene ring stands either *trans* to the remaining CO ligand (α-bridging) or *trans* to the second thiolato bridge (β-bridging).

Furthermore, in the case of the *RR* and *SS* isomers the *Z* form is only possible with αα- or ββ-, the *E* form only with βα- or αβ-linkage. The opposite is true for the *RS* isomers: the *Z* form is only possible with αβ- or βα-, and the *E* form only with αα- or ββ-bridging. The inversion-symmetric αα-*E*(*RS*) and ββ-*E*(*RS*) isomers **VI** and **VII** are *meso* forms of **2**.

Steric hindrance to dimerization is most likely to be associated with the various *Z* isomers. It was thus surprising to discover that the product **2** isolated upon reaction according to equation (a) could be shown by X-ray structural analysis[3] to consist of the enantiomeric pair αα-*Z*(*RR*)/αα-*Z*(*SS*). Figure 1 illustrates the structure of the αα-*Z*(*SS*) isomer of **2**.

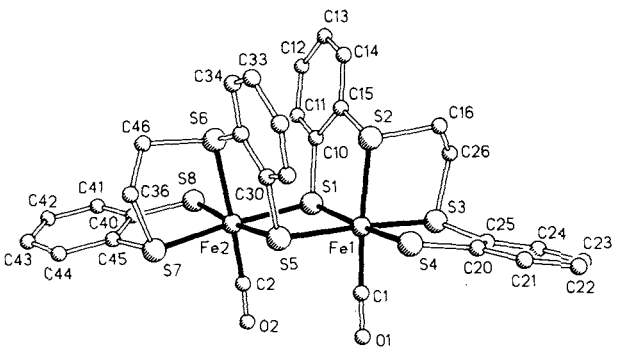


Fig. 1. Structure of αα-*Z*(*SS*)-**2** in the crystal (without H atoms). Important distances [*pm*] and angles [°]: Fe1-Fe2 342.0(1), Fe1-S1 230.2(3), Fe1-S2 230.5(3), Fe1-S3 225.8(3), Fe1-S4 229.8(3), Fe1-S5 232.7(3), Fe1-C1 174.4(11), Fe2-S1 233.0(3), Fe2-S5 229.4(3), Fe2-S6 231.3(3), Fe2-S7 225.1(3), Fe2-S8 230.5(3), Fe2-C2 174.5(10); Fe2-S1-Fe1 95.1(1), Fe2-S5-Fe1 95.4(1), S5-Fe1-S1 84.3(1), S5-Fe2-S1 84.4(1), C1-Fe1-S2 174.4(4), C2-Fe2-S6 177.1(4).

The diamagnetic complex **2** contains two homochiral [Fe(CO)("S_4")] fragments connected by thiolato ligands, and the resulting complex is also chiral. **2** possesses nearly C_2 symmetry, and the Fe^{II} centers, which have 18 e-configurations, are each coordinated pseudo-octahedrally to one CO ligand and five S atoms. Both the 18 e rule and the large Fe1-Fe2 separation argue against direct metal-metal interaction. The [Fe1-Fe2-S1-S5] four-membered ring is slightly folded, with a dihedral angle of 171°. The Fe–S distances are 225.1(3)–233.0(3) pm, and thus within the range regarded as typical for such complexes.

The differing steric requirements within the Fe coordination spheres in **2** is rather striking. One "half" of each molecule appears heavily overloaded due to the steric demands of the "S_4" ligands, while the other "half" is occupied only by the two CO ligands. In this respect, therefore, the structure of **2** is reminiscent of metalloproteins in which the folding of a peptide chain produces a distinctive spatial environment for the free coordination site. The two coordination sites on **2** that would result from release of CO should make it possible for bicentric and enantiofacial reactions to take place. That free coordination sites actually do result upon cleavage of CO from **2** is demonstrated by preliminary experiments leading to the isolation of $[Fe_2(CO)(NO)(\mu\text{-}"S_4")_2]PF_6$.

According to X-ray structural analysis, the homochiral [Fe(CO)("S_4")] fragments in **2** display exclusively α-bridging. This suggests that the regioselectivity observed during dimerization is due not to steric, but rather to electronic factors associated with the differing characteristics of the thiolate S atoms in the [Fe(CO)("S_4")] fragments. Attempts are currently being made to separate the racemic mixture.

Experimental Procedure

1270 mg (3.0 mmol) of **1** [7] *was dissolved in 50 mL of* dimethylformamide (DMF). The raspberry-colored solution was then filtered and warmed to 90 °C, causing it to turn reddish brown, and dark brown crystals of **2** began to separate. These were isolated after 48 h. Yield 70% (not optimized); IR (KBr): $\tilde{\nu}$ = 1965 cm^{-1} (CO); ^1H NMR ([D_7]DMF): $\delta \approx 6.8-8.4$ (m, 16H), 0.8–2.5 (m, 8H); correct elemental analysis.

Received: August 9, 1989 [Z 3488 IE]
German version: *Angew. Chem. 101* (1989) 1719

[1] Compare a) T. G. Spiro (Ed.): *Metal Ions in Biology, Vol. 4* (Iron Sulfur Proteins) and *Vol. 7* (Molybdenum Enzymes), Wiley, New York 1982 and 1987; b) M. J. Nelson, P. A. Lindahl, W. H. Orme-Johnson in G. L. Eichhorn, L. G. Marzilli (Ed.): *Adv. Inorg. Biochemistry, Vol. 4*, Elsevier, Amsterdam 1982, p. 1.

[2] Regarding terminology cf. K. Mislow, J. Siegel, *J. Am. Chem. Soc. 106* (1984) 3319.

[3] X-ray structure analysis of **2**: $P2_1/c$, $a = 1272.8(5)$, $b = 1534.1(23)$, $c = 1633.6(16)$ pm, $\beta = 104.76(8)°$; $V = 3085(2) \times 10^6$ pm^3; $Z = 4$. $T = 200$ K, $Mo_{K\alpha}$ irradiation; ω-scan; $3.0 < \omega < 15°$ min^{-1}, $4° < 2\Theta < 52°$. 5328 independent reflections, for 3287 of which $F > 6\sigma(F)$. SHELXTL-PLUS, direct methods, $R = 0.078$, $R_w = 0.065$. Further details of the crystal structure investigation are available on request from the Fachinformationszentrum Karlsruhe, Gesellschaft für wissenschaftlich-technische Information mbH, D-7514 Eggenstein-Leopoldshafen 2 (FRG), on quoting the depository number CSD-54803, the names of the authors, and the journal citation. A comparison between experimental and simulated powder diagrams (LAZY-Pulverix) for αα-*Z*(*RR*)/αα-*Z*(*SS*)-**2** shows that the isolated product, consisting of blocks and intertwined prisms, must contain an additional isomer of **2**.

[4] Regarding the dimerization of homochiral fragments or racemic heterochiral fragments cf. F. A. L. Anet, S. S. Miura, J. Siegel, K. Mislow, *J. Am. Chem. Soc. 105* (1983) 1419.

[5] *R,S* assignment according to R. S. Cahn, C. K. Ingold, V. Prelog, *Angew. Chem. 78* (1966) 413; *Angew. Chem. Int. Ed. Engl. 5* (1966) 385; based on IUPAC nomenclature the *R* and *S* isomers would be referred to as Δ and Λ isomers, respectively; cf. Deutsches Zentralausschuß für Chemie (Ed.): *Internationale Regeln für die chemische Nomenklatur und Terminologie, Band 1, Gruppe 1*, Verlag Chemie, Weinheim 1976, p. 100. As indicated in this source, the IUPAC nomenclature for describing octahedral complexes with multidentate ligands remains unsatisfactory.

[6] Compare a) C. H. Winter, A. M. Arif, J. A. Gladysz, *Organometallics 8* (1989) 219; b) G. Wilkinson, R. D. Gillard, J. A. McCleverty (Ed.): *Comprehensive Coordination Chemistry*, Pergamon, Oxford 1987; c) J. M. B. Harrowfield, S. B. Wild in [6b], *Vol. 1*, p. 179; D. A. House in [6b], *Vol. 2*, p. 23; G. B. Kaufmann, *Coord. Chem. Rev. 12* (1974) 105.

[7] D. Sellmann, H. E. Jonk, H. R. Pfeil, G. Huttner, J. von Seyerl, *J. Organomet. Chem. 191* (1980) 171.

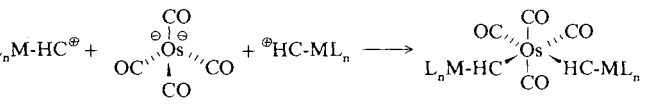
Directed Synthesis of Trinuclear Hydrocarbon-Bridged Complexes such as $[(OC)_5ReCH_2CH_2Os(CO)_4CH_2CH_2Re(CO)_5]$ **

By *Wolfgang Beck,* Burkhard Niemer,* and *Barbara Wagner*

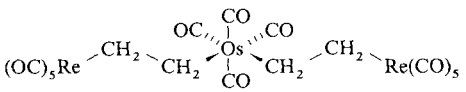
Dedicated to Professor Alfred Schmidpeter on the occasion of his 60th birthday

The nucleophilic addition of carbonylmetalates to coordinated, unsaturated hydrocarbons in cationic complexes is a method that lends itself to the directed synthesis of a variety of hydrocarbon-bridged complexes.[1] Previously we have utilized only monoanions for this purpose, for example $[Re(CO)_5]^{\ominus}$, leading to heterobimetallic complexes. We are now able to report that the dianion $[Os(CO)_4]^{2\ominus}$ [2, 3] permits the efficient synthesis of trinuclear hydrocarbon-bridged complexes (Scheme 1).

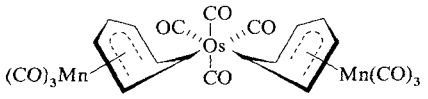
The complexes **1**–**4** were obtained in good yield by treatment of $[Os(CO)_4]^{2\ominus}$ with the cations **5**–**8** (in THF). The Re_2 compound **9** was identified as a byproduct of **1**. As in the case of the dialkyl(tetracarbonyl)osmium compounds *cis*-$[R_2Os(CO)_4]$,[3] the hydrocarbon bridges in **1**–**4** are *cis* to each other.



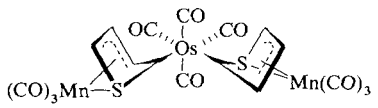
Scheme 1. HC = unsaturated hydrocarbon.



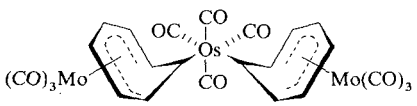
1



2



3



4

$[(OC)_5Re(\eta^2\text{-}C_2H_4)]^{\oplus}$ **5** [4] $[(OC)_3Mn(\eta^6\text{-}C_6H_6)]^{\oplus}$ **6** [5]

$[(OC)_3Mn(\eta^5\text{-thiophene})]^{\oplus}$ **7** [6] $[(OC)_3Mo(\eta^7\text{-}C_7H_7)]^{\oplus}$ **8** [7]

$[(OC)_5ReCH_2CH_2Re(CO)_5]$ **9** [4]

Compounds **1**–**4** were characterized on the basis of spectroscopic data (Table 1); in addition, **2**–**4** were the subject of X-ray structural analysis.[9] The mass spectrum of **1** reveals signals not only for the molecular ion but also for the cleavage products $[(OC)_4OsC_2H_4Re(CO)_5]^{\oplus}$ and $[(OC)_5Re(C_2H_4)]^{\oplus}$ and fragments corresponding to succes-

Table 1. IR[a] together with ^{1}H- and ^{13}C-NMR spectroscopic data for **1**–**4**.

1 (in pentane): $\tilde{\nu}$ = 2119w, 2110w, 2033s, 2009vs, 1983m
2 (in C_6H_6): $\tilde{\nu}$ = 2113w, 2067vw, 2040s,sh, 2030s, 2013vs, 2006vs, 1930vs,br
3 (in pentane): $\tilde{\nu}$ = 2138w, 2070m, 2053vs, 2044m, 2022m,sh, 2015vs, 2005vw, 1940s, 1926s
4 (in CH_2Cl_2): $\tilde{\nu}$ = 2121w, 2040s, 2015m, 1978vs,br, 1907s,br, 1872s,br

1 (CD_2Cl_2, 270 MHz): AA'BB' spectrum, δ = 2.08 – 1.91, 14 lines
2 [D$_8$]toluene, 90 MHz, −72 °C): δ = 5.20 (t, 4-H), 3.76 (dd, 3,5-H), 2.95 (t,1-H), 2.47 (dd,2,6-H); (+26 °C): δ = 3.73 (br); (+52 °C): δ = 3.80(s)
3 (C_6D_6): δ = 5.08 (br,1 H), 5.05 (br, 1 H), 4.71 (br, 2 H), 3.86 (br, 1 H), 3.79 (br, 1 H), 2.92 (br, 1 H), 2.86 (br,1 H)
4 (CD_2Cl_2): δ = 6.23 (dd,4,5-H), 4.50 (m, 3,6-H), 4.26 (t, 2,7-H), 3.68 (t,1-H)
1(CD_2Cl_2, 67.8 MHz): δ = 187.26 ($ReCO_{eq}$), 181.90 ($ReCO_{ax}$), 172.44 (OsCO), 12.04, 4.45
3 (C_6D_6): δ = 174.65 ($OsCO_{ax}$), 168.54 ($OsCO_{eq}$), 88.93, 88.75, 69.27, 69.19, 68.95, 68.75, 49.07, 48.63, MnCO signal not detectable
4 (CD_2Cl_2): δ = 176.71 ($OsCO_{ax}$), 169.57 ($OsCO_{aq}$), 100.87 (C-4,5), 97.94 (C-3,6), 82.77 (C-2,7), 18.09 (C-1), MoCO signal not detectable

[a] ν(CO) bands in cm^{-1}.

[*] Prof. Dr. W. Beck, Dipl.-Chem. B. Niemer, Dipl.-Chem. B. Wagner [†]
Institut für Anorganische Chemie der Universität
Meiserstrasse 1, D-8000 München 2 (FRG)

[†] X-ray structural analysis

[**] Hydrocarbon-Bridged Complexes, Part 14. This work was supported by the Deutsche Forschungsgemeinschaft and the Fonds der Chemischen Industrie. We wish to thank Professor Dr. *F. R. Kreissl*, Technische Universität München, for mass spectra, and Professor Dr. *G. Huttner*, Universität Heidelberg, and Dr. *K. Karaghiosoff*, Universität München, for helpful discussions. Part 13: J. Breimair, M. Steimann, B. Wagner, W. Beck, *Chem. Ber.*, in press.

sive loss of CO. The ^{1}H-NMR spectrum of **1** shows the typical pattern for an AA'BB' system at $\delta = 2.00$. **1** is isolobal[8] with *n*-heptane, and can be regarded as a 1,7-dirhena-4-osma-*n*-heptane.

The $OsMn_2$ complex **2** displays the same dynamic behavior in solution as the bimetallic complex $[(OC)_3Mn(\mu\text{-}\eta^5\text{:}\eta^1\text{-}C_6H_6)Re(CO)_5]$.[10] Thus, the ^{1}H-NMR spectrum of **2** at 25 °C in [D$_8$]toluene shows only a broad signal at $\delta = 3.73$. Below -45 °C fluctuation is suppressed, so signals for the frozen cyclohexadienyl bridges appear. A benzene-bridged structure $[\{(OC)_3Mn^{\ominus}(\mu\text{-}\eta^4\text{:}\eta^2\text{-}C_6H_6)\}_2Os^{2\oplus}(CO)_4]$ with 18 valence electrons on each of the metal atoms seems plausible as a transition state for the fluctuation. Both the ^{1}H- and ^{13}C-NMR spectra of **3** contain double sets of signals, suggesting the formation of isomers. The molecular structure of crystalline **3** (Fig. 1) reveals *exo* placement of the

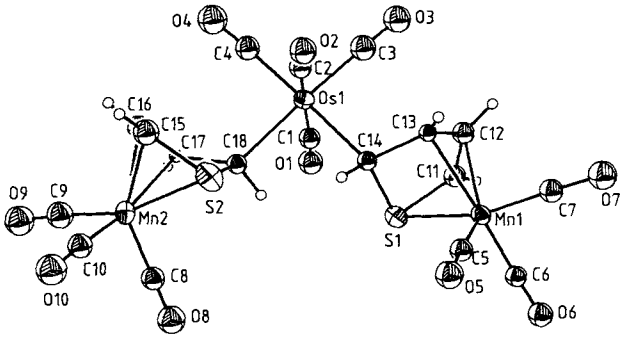


Fig. 1. Molecular structure of crystalline **3**; ellipsoids at the 20% probability level. Space group $P\bar{1}$, $a = 789.2(4)$, $b = 1158.1(7)$, $c = 1461(1)$ pm; $\alpha = 78.93(6)$, $\beta = 75.82(5)$, $\gamma = 87.81(4)°$; $V = 1.270(1)$ nm^3; $Z = 2$. λ ($Mo_{K\alpha}$) = 71.069 pm; crystal size = $0.2 \times 0.2 \times 0.4$ mm^3, $\mu(Mo_{K\alpha}) = 6.14$ mm^{-1} (corrected for absorption). ω-Scan, $\Delta\omega = 2.0°$, $8 \le \dot{\omega} \le 30$ min^{-1}, $4 \le 2\Theta \le 50°$; 4123 reflections collected, 3928 independent, 2450 observed [$I > 2\sigma(I)$]. Number of refined parameters, 159; heavy atoms Os, Mn, and S anisotropy. $R = 0.081$, $R_w = 0.079$, $w = [\sigma^2(F_o) + gF_o^2]^{-1}$, $g = 0.0006$. Maximum residual electron density 2.66, minimum residual electron density -1.55×10^{-6} e pm^{-3}. H-atoms placed in calculated positions.—Selected bond lengths [pm] and angles [°]: Os-C14 223(3), Os-C18 218(3), S1-C14 183(3), S1-C11 176(3), S2-C18 181(2), S2-C15 165(4), Mn1-S1 231(1), Mn2-S2 229(1); Os-C14-S1 119(1), Os-C14-C13 115(2), Os-C18-S2 120(1), Os-C18-C17 117(2), C18-Os-C14 87(1), C4-Os-C3 90(2).—Further details of the crystal structure investigation are available on request from the Fachinformationszentrum Karlsruhe, Gesellschaft für wissenschaftlich-technische Information mbH, D-7514 Eggenstein-Leopoldshafen 2 (FRG) by quoting the depository number CSD-54043, the names of the authors, and the journal citation.

$Os(CO)_4$ group on the two five-membered rings; the sulfur atoms are "*trans*" to each other. The two stereogenic carbon atoms bound to osmium have the same configuration. Bond lengths and angles in the $[Mn(CO)_3(thiophene)]$ unit are comparable to those in the adduct of cyanide with $[(CO)_3Mn(\eta^5\text{-thiophene})]^{\oplus}$, in which the C_4H_4S ring acts as an allylsulfide donor.[6] The Os–C σ-bonds of **3** have lengths (223(3) and 218(3) pm) similar to those in, for example, $[(OC)_4Os(CH_2C_6F_5)_2]$ (216(2) and 220(2) pm).[11] Addition of organic nucleophiles to metal-coordinated thiophene has been studied as a model reaction for the catalytic hydrodesulfurization of petroleum.[12]

Based on our experiences, $[Re(CO)_5]^{\ominus}$, $[Ru(CO)_2Cp]^{\ominus}$, and $[Os(CO)_4]^{2\ominus}$ are especially well-suited to the directed synthesis of hydrocarbon-bridged compounds. They are sufficiently nucleophilic for the purpose, and they also form stable metal-carbon σ-bonds. It is tempting to consider the preparation of higher polynuclear complexes through the use of highly reduced metal carbonyls[13] such as $[Re(CO)_4]^{3\ominus}$. Such polynuclear heterometallic complexes are of interest as potential precursors to heterogeneous catalysts.[14]

Experimental Procedure

All experiments were conducted under argon with carefully dried solvents.

4: To a beige suspension of 90 mg (0.26 mmol) of $Na_2Os(CO)_4$ in 5 mL of THF (−70 °C) were added 185 mg (0.52 mmol) of $[(C_7H_7)Mo(CO)_3][BF_4]$. The solvent was removed in vacuo at −25 °C from the red suspension after 1 h. The residue was then washed once with 10 mL of pentane, and **4** was extracted with 10 mL of CH_2Cl_2. Removal of solvent and drying (4 h) in high vacuum provided **4** as a red powder that gave dark red needles upon recrystallization from toluene (0 °C). Yield 190 mg (87%), decomposition above 110 °C.

The complexes **1** (colorless needles, yield 65%), **2**, and **3** (orange-yellow crystals, yield 40%) were prepared similarly, with slight modifications in the workup.

Received: July 3, 1989
Supplemented: August 28, 1989 [Z 3420]
German version: *Angew. Chem. 100* (1989) 1699

[1] W. Beck, *Polyhedron 7* (1988) 2255; W. Beck, B. Niemer, J. Breimair, J. Heidrich, *J. Organomet. Chem. 372* (1989) 79.
[2] R. D. George, S. A. R. Knox, F. G. A. Stone, *J. Chem. Soc. Dalton Trans. 1973*, 972; J. P. Collman, D. W. Murphy, E. B. Fleischer, D. Swift, *Inorg. Chem. 13* (1974) 1.
[3] F. L'Eplattenier, C. Pélichet, *Helv. Chim. Acta 53* (1970) 1091; W. J. Carter, J. W. Kelland, S. J. Okrasinski, K. E. Warner, J. R. Norton, *Inorg. Chem. 21* (1982) 3955.
[4] K. Raab, U. Nagel, W. Beck, *Z. Naturforsch. B 38* (1983) 1466; W. Beck, K. Raab, *Inorg. Synth.*, in press.
[5] G. Winkhaus, L. Pratt, G. Wilkinson, *J. Chem. Soc. 1961*, 3807.
[6] D. A. Lesch, J. W. Richardson, Jr., R. A. Jacobson, R. J. Angelici, *J. Am. Chem. Soc. 106* (1984) 2901.
[7] J. D. Munro, P. L. Pauson, *J. Chem. Soc. 1961*, 3475; R. B. King, M. B. Bisnette, *Inorg. Chem. 3* (1964) 785; A. Salzer, H. Werner, *Z. Anorg. Allg. Chem. 418* (1975) 88.
[8] R. Hoffmann, *Angew. Chem. 94* (1982) 725; *Angew. Chem. Int. Ed. Engl. 21* (1982) 711.
[9] The structural analyses of **2** and **4** will be described separately; M. Steimann, B. Wagner, B. Niemer, W. Beck, unpublished results.
[10] B. Niemer, M. Steimann, W. Beck, *Chem. Ber. 121* (1988) 1767.
[11] G. G. Aleksandrov, G. P. Zol'nikova, I. I. Kritskaya, Yu. T. Struchkov, *Sov. J. Coord. Chem. 6* (1980) 305.
[12] R. J. Angelici, *Acc. Chem. Res. 21* (1988) 387; G. N. Glavee, L. M. Daniels, R. J. Angelici, *Organometallics 8* (1989) 1856.
[13] G. F. P. Warnock, L. C. Moodie, J. E. Ellis, *J. Am. Chem. Soc. 111* (1989) 2131, and references cited therein.
[14] J. H. Sinfelt: *Bimetallic Catalysts: Discoveries, Concepts and Applications*, Wiley, New York 1983; P. Braunstein, R. Devenish, P. Gallezot, B. T. Heaton, C. J. Humphreys, J. Kervennal, S. Mulley, M. Ries. *Angew. Chem. 100* (1988) 972; *Angew. Chem. Int. Ed. Engl. 27* (1988) 927.

Stereoselective Synthesis of γ-Aminocarboxylates **

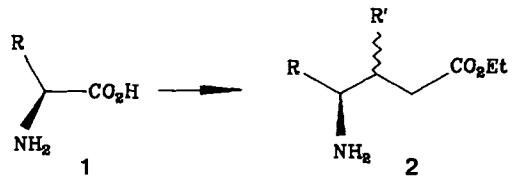
By *Manfred T. Reetz*,* and *Dirk Röhrig*

Owing to their well documented and potential biological and pharmacological activity the stereoselective synthesis of non-proteinogenic amino acids has assumed great importance.[1] We report here on a method whereby α-amino acids **1** can be converted into γ-amino acid esters of type **2** containing a new stereocenter. Accordingly, the stereoselective formation of the two possible diastereomers **2** can be controlled,

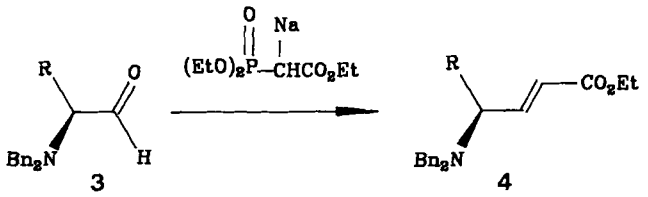
[*] Prof. Dr. M. T. Reetz, Dipl.-Chem. D. Röhrig
Fachbereich Chemie der Universität
Hans-Meerwein-Strasse, D-3550 Marburg (FRG)

[**] This work was supported by the Deutsche Forschungsgemeinschaft (SFB 260) and the Fonds der Chemischen Industrie.

and no racemization occurs at the original stereocenter of the amino acid **1**.

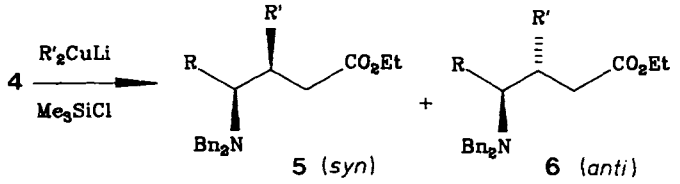


Our interest was focussed on the concept that optically active α,β-unsaturated carboxylates **4** could undergo stereoselective Michael additions with suitable organocopper reagents, providing they are accessible in a prochirally pure form. This prerequisite could be fulfilled, since Wittig-Horner olefination of the *N*,*N*-dibenzyl-protected aldehydes **3**,[2] which are readily accessible from the amino acids **1**, led exclusively to the *E*-configurated products in good yields.



a: R = CH_3 (yield 73%), **b**: R = $PhCH_2$ (79%), **c**: Me_2CHCH_2 (82%)

Although the decisive cuprate addition with the Gilman reagents R'_2CuLi proved unsuccessful, the desired 1,4-addition could nevertheless be accomplished in good yields[4] and high diastereoselectivity with formation of the *syn*-configurated adducts **5** when the reaction was carried out in the

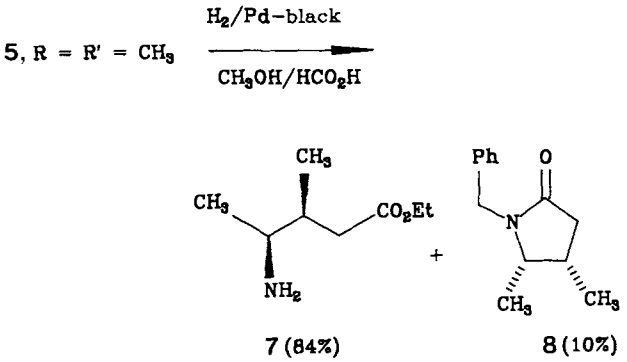


presence of trimethylchlorosilane[3] (Table 1). Not only the copper reagents but also the tin compound $(n\text{-}C_4H_9)_3SnLi$ could be added smoothly. Decisive for the high stereoselectivity are the nature and number of the protecting groups on the nitrogen: the mono-protected *tert*-butoxycarbonyl (Boc) analogue of **4b** reacts with cuprates with formation of 3:1 to 4:1 diastereomeric mixtures.[5]

In order to assign the relative configuration and check the enantiomeric purity, the protective groups of the pure diastereomers **5** were first removed with H_2/Pd black.[2] Thus, in the case of the adduct **5**, R = R′ = CH, the free amine could be isolated together with the mono-debenzylated and cyclized product **8**. NOE difference spectra provided proof of a *cis* arrangement of the substituents in the lactam **8** and thus conclusive evidence for a *syn*-configuration of the adducts **5**. The free amine was converted into the corresponding amide by reaction with (+)-3,3,3-trifluoro-2-methoxy-2-phenylpropionyl chloride according to the method of *Mosher* et al.[6] The ^1H-, ^{13}C- and ^{19}F-NMR spectra showed only a single set of signals—a clear indication that the synthesis and reactions of the α,β-unsaturated esters **4** are free of racemization.[7]

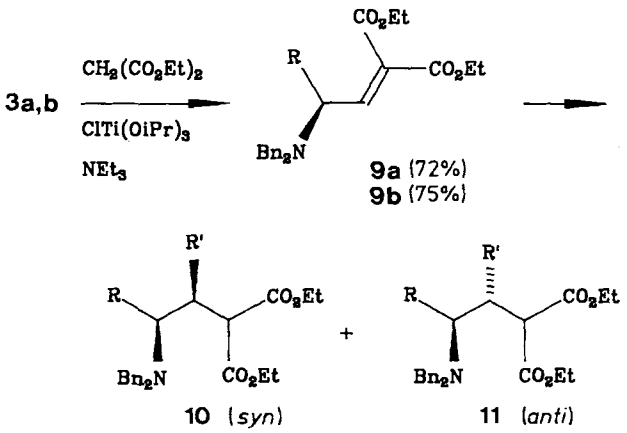
Table 1. Diastereoselective Michael additions to α,β-unsaturated carboxylates **4**.

Ester	Reagent	T/t [°C]/[h]	Yield of **5** [%]	*syn*/*anti* ratio **5**:**6**
4a	$(CH_3)_2CuLi/Me_3SiCl$	−78/20	80	94:6
4a	$(n\text{-}C_4H_9)_2CuLi/Me_3SiCl$	−78/12	82	>95:<5
4a	$(C_6H_5)_2CuLi/Me_3SiCl$	−78/16	80	95:5
4b	$(CH_3)_2CuLi/Me_3SiCl$	−65/24	84	92:8
4b	$(n\text{-}C_4H_9)_2CuLi/Me_3SiCl$	−78/16	80	>95:<5
4b	$(CH_2{=}CH)_2CuLi/Me_3SiCl$	−78/18	46	94:6
4b	$(C_6H_5)_2CuLi/Me_3SiCl$	−78/16	78	95:5
4c	$(n\text{-}C_4H_9)_3SnLi$	−78/1	74	92:8
4c	$(CH_3)_2CuLi/Me_3SiCl$	−78/24	87	93:7
4c	$(n\text{-}C_4H_9)_2CuLi/Me_3SiCl$	−78/12	81	>95:<5
4c	$(CH_2{=}CH)_2CuLi/Me_3SiCl$	−78/24	41	94:6
4c	$(C_6H_5)_2CuLi/Me_3SiCl$	−78/16	80	>95:<5
4c	$(CH_3)_2CuLi/BF_3 \cdot OEt_2$	−78/12	71	>95:<5
4c	$(n\text{-}C_4H_9)_2CuLi/BF_3 \cdot OEt_2$	−78/12	70	93:7



In order to reverse the direction of the diastereoselectivity,[8] the diesters **9a**, **b** were prepared from the aldehydes **3a**, **b** by means of a titanium-mediated Knoevenagel condensation[9] and then allowed to react with organometallic reagents.

The reactions with R_2CuLi led indeed to unusually selective formation of the *anti*-adducts **11**[11] (Table 2). Since the diesters **9** are clearly better Michael acceptors than the monoesters **4**, the use of trimethylchlorosilane as additive was

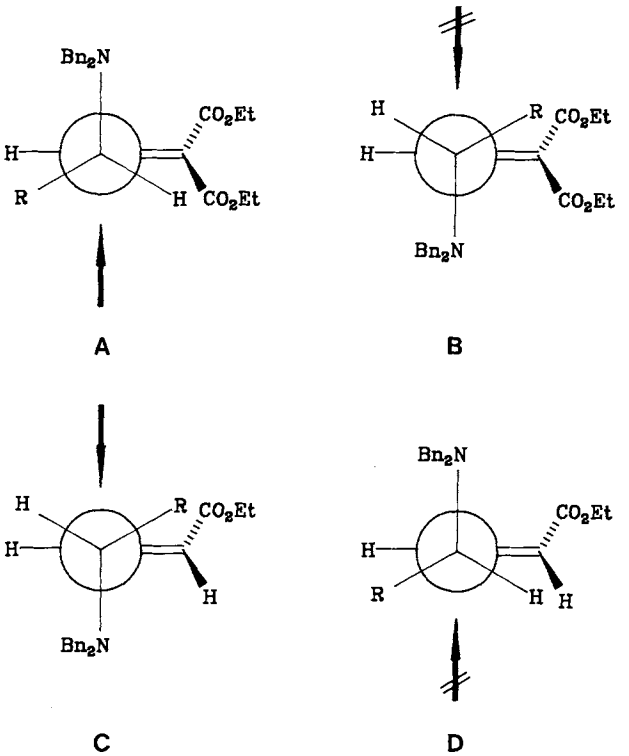


unnecessary. Even Grignard reagents underwent 1,4-addition, albeit with somewhat less diastereoselectivity (Table 2).

Table 2. Diastereoselective Michael additions to the diesters **9**.

Ester	Reagent	T/t [°C]/[h]	Yield of **11** [%]	*syn*/*anti* ratio **10**:**11**
9a	$(n\text{-}C_4H_9)_3SnLi$	−78/15	71	5:95
9a	$(CH_3)_2CuLi$	−78/24	68	21:79
9b	$(CH_3)_2CuLi$	−78/24	77	<5:>95
9b	$(n\text{-}C_4H_9)_2CuLi$	−78/12	81	<5:>95
9b	$(C_6H_5)_2CuLi$	−78/12	82	<5:>95
9b	CH_3MgBr	0/6	76	10:90
9b	C_2H_5MgBr	−35/12	71	6:94
9b	$(n\text{-}C_4H_9)_3SnLi$	−78/1	79	<5:>95

What is the origin of the diastereoselectivity in the above reactions? In the case of the diesters **9** a 1,3-allyl strain[12] possibly plays the decisive role. Accordingly, the conformation **A** would be preferred over **B**, since steric interaction between the residue R and the *cis*-oriented ester group would lead to an energetically unfavorable 1,3-allyl strain. The stereoselective formation of the *anti*-adducts is thus consistent with an *anti*-periplanar attack,[13] as indicated in conformation **A**. In the case of the monoester **4** the 1,3-allyl strain is of less importance (less interaction between R and H in conformation **C**), whereas the 1,2-allyl strain[14] in conformation **D** (interaction between R and H) gains importance



and even dominates. According to these concepts the *Z*-configurated analogues of the esters **4** should lead to the *anti*-adducts. The fact that only 40:60 diastereomeric mixtures were observed points to a possible *Z*/*E* isomerization during the cuprate addition.

No matter what the theoretical basis may be,[15] enantiomerically pure Michael acceptors of the type **4** and **9** with *N*,*N*-dibenzylamino moieties at the chirality center open up novel methods for the stereoselective synthesis of amino compounds with additional functional groups. Preliminary experiments show that the corresponding α,β-unsaturated ketones and sulfones are likewise readily accessible. Thus, the use of the "chiral pool" of the α-amino acids is extended.

Received: July 12, 1989 [Z 3432 IE]
German version: *Angew. Chem. 101* (1989) 1732

CAS Registry numbers:
3a, 111060-63-0; **3b**, 111060-64-1; **3c**, 111060-65-2; **4a**, 123725-86-0; **4b**, 123725-87-1; **4c**, 123725-88-2; **5** (R = R′ = CH_3), 123725-89-3; **5** (R = CH_3, R′ = n-C_4H_9), 123725-90-6; **5** (R = CH_3, R′ = C_6H_5), 123725-91-7; **5** (R = $PhCH_2$, R′ = CH_3), 123725-92-8; **5** (R = $PhCH_2$, R′ = n-C_4H_9), 123725-93-9; **5** (R = $PhCH_2$, R′ = CH_2=CH), 123725-94-0; **5** (R = $PhCH_2$, R′ = C_6H_5), 123725-95-1; **5** (R = Me_2CHCH_2, R′ = CH_3), 123725-96-2; **5** (R = Me_2CHCH_2, R′ = n-C_4H_9), 123725-97-3; **5** (R = Me_2CHCH_2, R′ = CH_2=CH), 123725-98-4; **5** (R = Me_2CHCH_2, R′ = Ph), 123725-99-5; **7**, 123726-00-1; **8**, 123807-64-7; **9a**, 123726-01-2; **9b**, 123726-02-3; **10** (R = R′ = CH_3) 123726-09-0; **11** (R = CH_3, R′ = n-C_4H_9), 123726-03-4; **11** (R = R′ = CH_3), 123726-04-5; **11** (R = $PhCH_2$, R′ = CH_3), 123726-05-6; **11** (R = $PhCH_2$, R′ = n-C_4H_9), 123726-06-7; **11** (R = $PhCH_2$, R′ = Ph), 123726-07-8; **11** (R = $PhCH_2$, R′ = C_2H_5), 123726-08-9; $(CH_3)_2CuLi$, 15681-48-8; $(n\text{-}C_4H_9)_2CuLi$, 24406-16-4; $(C_6H_5)_2CuLi$, 23402-69-9; $(CH_2{=}CH)_2CuLi$, 22903-99-7; $(n\text{-}C_4H_9)_3SnLi$, 4226-01-1; CH_3MgBr, 75-16-1; C_2H_5MgBr, 925-90-6; $(EtO)_2P(O)CH(Na)CO_2Et$, 123726-10-3; $CH_2(CO_2Et)_2$, 105-53-3.

[1] See, e.g., U. Schöllkopf, B. Hupfeld, S. Küper, E. Egert, M. Dyrbusch, *Angew. Chem. 100* (1988) 438; *Angew. Chem. Int. Ed. Engl. 27* (1988) 433; H. Kunz, W. Pfrengle, *Tetrahedron 44* (1988) 5487; T. Bretschneider, W. Miltz, P. Münster, W. Steglich, *ibid. 44* (1988) 5403; W. Oppolzer, R. Moretti, *ibid. 44* (1988) 5525; D. A. Evans, T. C. Britton, R. L. Dorow, J. F. Dellaria, *ibid. 44* (1988) 5525; F. Fitzi, D. Seebach, *ibid. 44* (1988) 5277; P. J. Sinclair, D. Zhai, J. Reibenspies, R. M. Williams, *J. Am. Chem. Soc. 108* (1986) 1103; S. Ikegami, H. Uchiyama, T. Hayama, T. Katsuki, M. Yamaguchi, *Tetrahedron 44* (1988) 5333.

[2] M. T. Reetz, M. W. Drewes, A. Schmitz, *Angew. Chem. 99* (1987) 1186; *Angew. Chem. Int. Ed. Engl. 26* (1987) 1141.

[3] Me_3SiCl-accelerated cuprate addition: E. J. Corey, N. W. Boaz, *Tetrahedron Lett. 26* (1985) 6015; A. Alexakis, J. Berlan, Y. Besace, *ibid. 27* (1986) 1047; Y. Horiguchi, S. Matsuzawa, E. Nakamura, I. Kuwajima, *ibid. 27* (1986) 4029; BF_3-accelerated additions: Y. Yamamoto, *Angew. Chem. 98* (1986) 945; *Angew. Chem. Int. Ed. Engl. 25* (1986) 947.

[4] A solution of 5 mmol of the organocuprate in 20 mL of THF was treated at the given temperatures with 1.1 mmol of chlorotrimethylsilane, and then immediately thereafter with 1 mmol of the relevant α,β-unsaturated ester in 2 mL of THF. The mixture was stirred for the given length of time and finally poured very carefully into concentrated ammonium chloride solution. After 15 minutes' vigorous stirring the mixture was extracted with ether and the organic phase separated off and dried over $MgSO_4$. After removal of the solvent, oily products were obtained. These were purified by flash chromatography on silica gel (ethyl acetate/petroleum ether). Preliminary experiments with only 2.2 mmol of the cuprate gave the same results. For removal of the protecting group from **5a**, about 200 mg was treated with 50 mg of Pd-black in 10 mL of anhydrous methanol and with 2 mL of formic acid and hydrogenated under 1 atm of hydrogen. The course of the reaction was monitored by thin-layer chromatography. On completion of reaction the solution was decanted from the catalyst and filtered. The residue was washed with methanol and the combined filtrates evaporated down. The mixture of **7** and **8** was separated by column chromatography on silica gel. Preliminary experiments with the Pearlman catalyst $Pd(OH)_2$ (Cf. K. Yoshida, S. Nakajima, T. Wakamatsu, Y. Ban, M. Shibasaki, *Heterocycles 7* (1988) 1167) on the adducts **5**, **6** and **10**, **11** point to a uniform reaction.

[5] Since racemic phenylalanine was used as starting compound, it is not clear whether the Wittig olefination of the corresponding Boc-protected aldehyde proceeds without racemization. Boc-protected α-aminoaldehydes are clearly configurationally more stable than the *N*,*N*-dibenzyl analogues first prepared by us [2].

[6] J. A. Dale, D. L. Dull, H. S. Mosher, *J. Org. Chem. 34* (1969) 2543.

[7] Control experiments with racemic starting compounds afforded (racemic) adducts whose NMR spectra showed a double set of signals after the Mosher acylation [6].

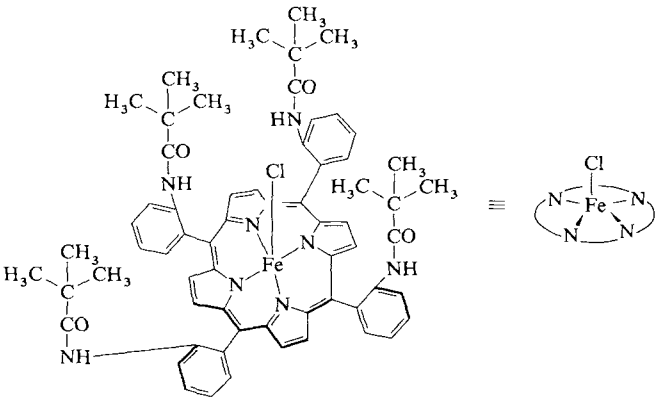
[8] In the case of cuprate additions in the series of alkoxy analogues [OCH_2Ph instead of $N(CH_2Ph)_2$ in the compounds **4** and **9**], the transition from the mono- to the diesters effects a reversal of the diastereoselectivity; however the direction of the stereoselectivity is in each case opposite to that in our experiments: Y. Yamamoto, S. Nishii, T. Ikuba, *J. Chem. Soc. Chem. Commun. 1987*, 464; see also [15].

[9] M. T. Reetz, R. Peter, M. von Itzstein, *Chem. Ber. 120* (1987) 121.
[10] The Knoevenagel condensation affords the isopropyl diester [9], which was transesterified with EtOH/NaOEt.
[11] The assignment was accomplished by saponifying decarboxylation, which led to the products **6**, and by an X-ray structure analysis (Dr. K. *Harms*) of the primary product **11**, R = $PhCH_2$, R' = CH_3. The latter was debenzylated with H_2/Pd-black [2] (85% yield) and the corresponding primary amine was converted with the „Mosher chloride" [6] into the amide. The usual analysis gave an *ee* value of >98%.
[12] F. Johnson, *Chem. Rev. 68* (1968) 375; R. W. Hoffmann, *Synthesis*, in press.
[13] K. N. Houk, M. N. Paddon-Row, N. G. Rondan, Y.-D. Wu, F. K. Brown, D. C. Spellmeyer, J. T. Metz, Y. Li, R. J. Loncharich, *Science (Washington DC) 231* (1986) 1108.
[14] 1,2-Allyl strain as controlling element in the stereoselective epoxidation of allyl alcohols: A. Narula, *Tetrahedron Lett. 23* (1982) 5579.
[15] Steric and electronic factors and, on some occasions, chelate effects have been discussed in the case of nucleophilic additions to activated olefins having *alkoxy* residues at the allylic stereocenter; see, for example, M. Larchevegue, G. Tamagnan, Y. Petit, *J. Chem. Soc. Chem. Commun. 1989*, 31; W. R. Roush, B. M. Lesur, *Tetrahedron Lett. 24* (1983) 2231; J. Mulzer, M. Kappert, *Angew. Chem. 95* (1983) 60; *Angew. Chem. Int. Ed. Engl. 22* (1983) 63; M. Isobe, Y. Ichicawa, Y. Funabashi, S. Mio, T. Goto, *Tetrahedron 42* (1986) 2863; M. Hirama, T. Iwakuma, S. Ito, *J. Chem. Soc. Chem. Commun. 1987*, 1523.

Oxoiron Porphyrin Species with High-Valent Iron: Formation by Solvent-Dependent Protonation of a Peroxoiron(III) Porphyrinate Derivative **

By *Dominique Mandon, Raymond Weiss,* Michaela Franke, Eckard Bill,* and *Alfred X. Trautwein**

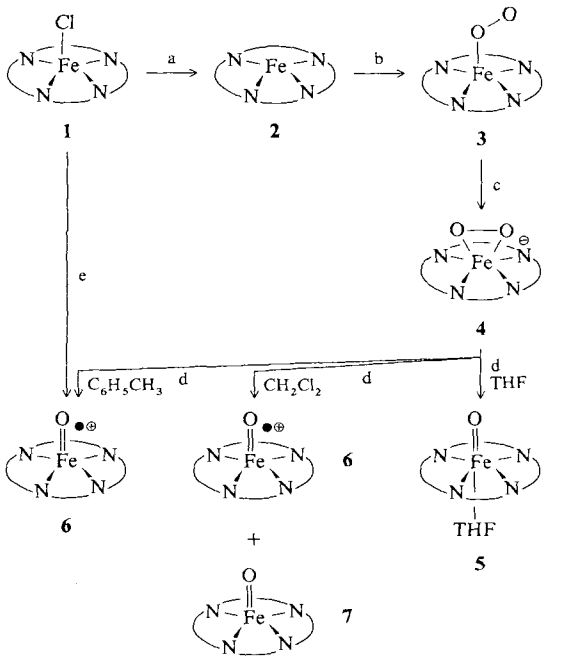
The mechanism by which molecular oxygen is converted into an active oxygen ("oxenoid") intermediate by cytochrome P450 monooxygenases is still poorly understood in chemical terms.[1] A generally accepted working hypothesis, however, is that: a peroxoiron(III) species is formed by reduction of the dioxygen adduct of cytochrome P450 which yields, by protonation and heterolytic O–O bond cleavage, a π radical-cationic oxoiron(IV) porphyrinate species, similar to the well characterized compound I of Horse Radish Peroxidase (HRP I). This oxoiron(IV) porphyrinate π radical cation is presently the most attractive candidate for the active oxygen intermediate.[2–4] However, neither the formation of the peroxoiron(III) intermediate of cytochrome P450 nor its conversion into the oxoiron(IV) radical cation have thus far been observed. Consequently, the chemical properties of the known synthetic peroxoiron porphyrinate species, are of particular interest.[5–8] We have recently shown that the reaction of carbon dioxide with the peroxoiron(III) picket-fence porphyrinate **1** (Scheme 1) affords an oxoiron(IV) porphyrinate (cf. **5** in Scheme 2), presumably by homolytic O–O bond cleavage of an iron(III) peroxycarbonate intermediate.[9–11] *Khenkin* and *Shteinmann*[12] have suggested that the reaction of an acylating reagent with a peroxoiron(III) porphyrinate in toluene/acetonitrile leads to an acylperoxoiron(III) porphyrinate that decomposes by heterolytic O–O bond cleavage into an oxoiron(IV) porphyrinate π radical cation. We have now studied the protonation of the peroxoiron(III) porphyrinate **1** with tetrafluoroboric acid–diethyl ether adduct and report here the characterization of the species obtained by this highly solvent-dependent reaction.



1

Scheme 1. Structural formula and schematic drawing of the starting material **1**.

Reduction of the chloroiron(III) 5,10,15,20-tetrakis(*o*-pivalamidophenyl)porphyrinate **1** (Scheme 1) with zinc amalgam in dry degassed solvents at normal temperature leads to the iron(II) porphyrinate derivative **2**, which is four-coordinated (toluene, CH_2Cl_2) or six-coordinated (THF (Scheme 2). Treatment of **2** with O_2 at 220 K affords the five-coordinated dioxygen adduct **3** in toluene and CH_2Cl_2 and the corresponding six-coordinate species in THF and DMF.[13] The UV/VIS spectrum of **3** in toluene at 220 K presents



Scheme 2. a) Zinc amalgam, room temperature; b) oxygenation, 220 K; c) hydride reduction, 230 K; d) $HBF_4 \cdot Et_2O$, 190 K; e) *m*-chloroperoxybenzoic acid, toluene, 190 K. The steps a and b were carried out in toluene, in CH_2Cl_2, or in THF.

[*] Prof. Dr. R. Weiss, Dr. D. Mandon
Laboratoire de Cristallochimie et de Chimie Structurale
(U.R.A. CNRS 424)
Institut Le Bel, Université Louis Pasteur
4, rue Blaise Pascal, 67070 Strasbourg Cedex (France).
[*] Prof. Dr. A. X. Trautwein, Dr. E. Bill, Dipl. Phys. M. Franke
Institut für Physik, Medizinische Universität,
Ratzeburger Allee 160, D-2400 Lübeck (FRG)

[**] This work was supported by the Centre National de la Recherche Scientifique and the Deutsche Forschungsgemeinschaft. *R. W.* is recipient of the Alexander von Humboldt award and thanks the Alexander von Humboldt Foundation for financial support.

bands at λ_{max} = 422 and 536 nm. Generation of the peroxo-iron(III) anion **4** was carried out at 220–230 K, as previously described,[10] by reaction of **3** with sodiumdihydrido bis(2-methoxyethoxy)aluminate in the molar ratio 1:1. The reaction time is longer in toluene than in more polar solvents such as THF and DMF. However, on the basis of UV/VIS spectroscopic data, which are solvent-independent in the case of **4**, total conversion of **3** into **4** occurs at 220–230 K within one hour in toluene (λ_{max} = 438, 563, 604 nm).

Reaction of **4** in THF at 220 K with a THF solution of $HBF_4 \cdot Et_2O$ yields a bright red species **5**. The UV/VIS spectrum of **5** shows bands at 419 and 550 nm. Its ^{1}H-NMR spectrum (Bruker SY 200, [D_8] THF, 220 K, TMS) displays signals close to +7.2 (pyrrole H) and +12.9 (*o*-phenyl H) ppm. The zero-field Mössbauer spectrum obtained at 4.2 K with a sample of **5** enriched in ^{57}Fe consists of a quadrupole doublet with $\delta = 0.11 \pm 0.02$ mm s^{-1} (relative to α-Fe) and $\Delta E_q = 2.20 \pm 0.03$ mm s^{-1}. These spectral data indicate that **5** is identical with the oxoiron(IV) derivative which was obtained previously by reaction of **4** with carbon dioxide in THF at 220 K.[10] Compound **5** does not react with cyclohexene, and upon warming in THF solution to ambient temperature gives the ferric starting material **1** nearly quantitatively.

In contrast, reaction of **4** in toluene at 190 K with a suspension of $HBF_4 \cdot Et_2O$ in a small amount of CH_2Cl_2 affords a greenish transient species **6**. The identification of **6** as a π radical cationic oxoiron(IV) porphyrinate derivative[14] is based on the following observations: The UV/VIS spectrum of **6** (Fig. 1) recorded after decantation of the heterogeneous

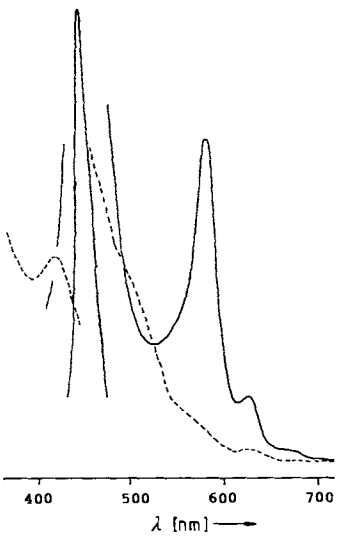


Fig. 1. Change in the UV/VIS. spectrum of **4** (—) upon addition of $HBF_4 \cdot Et_2O/CH_2Cl_2$ at 190 K in toluene (– – –) after 15 min. decantation).

medium, exhibits a weak and broad absorption in the Soret band region[15] (416 nm) and weak bands at 508 (shoulder) and 630 nm. The radical cation **6** is highly unstable; warming to 230 K causes bleaching of the sample. The Mössbauer spectrum of ^{57}Fe-enriched **6** obtained at 4.2 K, shows that approximately 75% of the sample[16] consisted of a species having an isomeric shift compatible with an iron(IV) species ($\delta = 0.09 \pm 0.02$ mm s^{-1}) but a much smaller quadrupole splitting ($\Delta E_q = 1.44 \pm 0.03$ mm s^{-1}) than the red oxo-iron(IV) porphyrinate derivative of type **5** which is obtained at 230 K in toluene upon reaction of **4** with carbon dioxide.

The zero-field Mössbauer spectrum of this species of type **5** obtained at 4.2 K consists of a quadrupole doublet characterized by an isomeric shift δ of 0.10 mm s^{-1} and a quadrupole splitting ΔE_q of 1.94 mm s^{-1}. A similar increase in the value of the quadrupole splitting has been observed at 4.2 K between the green π radical-cationic oxoiron(IV) tetramesitylporphyrinate (analogue of **6**) ($\delta = 0.06$, $\Delta E_q = 1.62$ mm s^{-1})[17, 18] and the corresponding neutral red oxoiron(IV) species (analogue of **5**) ($\delta = 0.04$, $\Delta E_q = 2.30$ mm s^{-1}).[19] Moreover, the external-field Mössbauer studies reveal that in **6** the π radical cation is only weakly coupled to the iron(IV) ($S = 1$) center. The Mössbauer spectra (Fig. 2) are superpo-

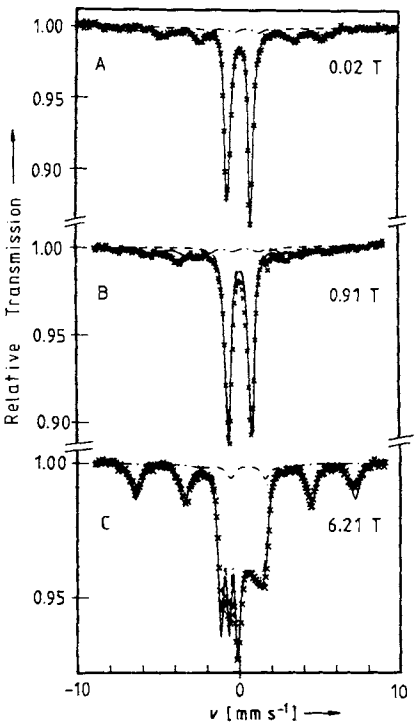


Fig. 2. Experimental Mössbauer spectra of **6** and a high-spin iron(III) species (75% and 25% of total absorption area) [16], recorded at 4.2 K with field applied perpendicular to the γ-beam; 0.02 T (A), 0.91 T (B), 6.21 T (C). The calculated powder spectra (broken lines: iron(III) species; unbroken lines: total spectrum of **6** and iron(III) species) represent spin-Hamiltonian simulations using the parameters listed in Table 1.

sitions of subspectra from **6** and a high-spin iron(III) contamination.[16] The calculated subspectra are spin-Hamiltonian simulations using the parameters listed in Table 1. The weak spin coupling of iron(IV) ($S = 1$) and the radical cationic porphyrinate moiety ($S' = 1/2$) is discerned in the weak-field spectra (Fig. 2A, 2B) from the slight magnetic splitting and the resultant asymmetry of the prominent line doublet. In particular, the magnetic-field dependence of this asymmetry cannot be simulated without spin coupling. Thus, **6** presents spectroscopic and magnetic properties which are very similar to those known for the well characterized HRP I.[21] We should mention, that strong spin coupling, as observed in oxoiron(IV) tetramesitylporphyrinate[18] yields completely different Mössbauer spectra in weak and in strong magnetic fields.

In order to further characterize this greenish species **6** we have studied its ^{1}H-NMR spectrum (Bruker SY200, [D_8]-toluene, 203 K). In contrast to the ^{1}H-NMR spectra of the π radical cationic oxoiron(IV) complexes of tetramesityl-

Table 1. Spin Hamiltonian [a] and Mössbauer parameters [b] of **6** and a high-spin iron(III) species used for the simulation [c] of powder spectra in the slow relaxation range (cf. Fig. 2).

Species	D [cm^{-1}]	E/D	ΔEq [$mm\,s^{-1}$]	η	$A_x = A_y = A_z$ [T]	δ [$mm\,s^{-1}$]	Γ [$mm\,s^{-1}$]	J [cm^{-1}]	S	S'
6	20	0	+1.44	0	−20	0.09	0.3	1	1	1/2
Iron(III) [d]	4.5	0	+0.30	0	−21	0.46	0.6	–	5/2	–

[a] The electronic Hamiltonian is given by $H_e = D[S_z^2 - 1/3\,S(S+1) + E/D\,(S_x^2 - S_y^2)] + S \cdot J \cdot S' + g\beta B \cdot (S+S')$. The electronic g-factor and the exchange coupling tensor are taken to be isotropic. D and E are zero-field splitting parameters, and B is the applied field. [b] The components of the hyperfine-coupling tensor A are part of the usual nuclear Hamiltonian used for simulating Mössbauer spectra. Quadrupole splitting ΔE_q, asymmetry parameter η, isomer shift δ and line width Γ correspond to 4.2 K; δ is given relative to α-Fe at room temperature. [c] For details see References [18, 20, 22]. [d] For the simulations of the iron(III) subspectra in Figure 2 we adopted axial symmetry, i.e. $E/D = 0$, $\eta = 0$ without further refinement.

porphyrin[17, 18, 21] and tetrakis(2,6-dichlorophenyl)porphyrin[22] the upfield shift of the β pyrrole protons and the downfield shift of the *m*-phenyl protons are less marked in the spectrum of **6**.[23] Indeed, this spectrum is characterized by two broad signals at $\delta = -6.5$ and $+13.0$ which we assign to the β-pyrrole and the *o*-phenyl proton resonances, respectively. Sharper signals at $\delta = +8.7$ and $+9.2$ are probably due to the *m*-, *m'*- and *p*-protons of the phenyl groups. Upon warming the sample, the signals of the π radical cation **6** already disappear at 230 K with formation of a weak residual spectrum typical for a high-spin iron(III) species.

Another route for the generation of **6** is the reaction in toluene at 190 K of the high-spin chloroiron(III) derivative **1** with two equivalents of *m*-chloroperoxybenzoic acid (*m*-CPBA). Both the stability, and spectroscopic features (UV/VIS, ^1H NMR, Mössbauer) are not significantly different from those displayed by **6**. Furthermore, in presence of catalytic amounts of **1**, cyclohexene is completely epoxidized in toluene at 220–230 K by *m*-CPBA.[24] Gas phase chromatography indicates that cyclohexene oxide is exclusively obtained without formation of hydroxylated or carbonylated derivatives.

In conclusion, the protonation at low-temperature of the peroxoiron(III) porphyrinate derivative **4** with $HBF_4 \cdot Et_2O$ yields in THF the red oxoiron(IV) porphyrinate species **5** and in toluene the greenish π radical cationic oxoiron(IV) porphyrinate **6**. This protonation reaction is highly solvent-dependent, only a mixture of **6** and **7** could be obtained in CH_2Cl_2. In DMF no oxoiron species with high-valent iron could be identified, only a mixture of iron(II) and iron(III) prophyrinates could be detected.[25]

Received: June 2, 1989;
revised: September 21, 1989 [Z 3371 IE]
German version: *Angew. Chem. 101* (1989) 1747

[1] T. L. Poulos in G. L. Eichhorn, L. G. Marzilli (Eds.): *Heme Proteins, Vol. 7*, Elsevier, Amsterdam 1988, p. 29.
[2] S. G. Sligar, B. S. Chastry, I. C. Gunsalus in V. Ulrich (Ed.): *Microsomes and Drug Oxidation*, Pergamon, London 1977, p. 202.
[3] R. V. Blake, M. J. Coon, *J. Biol. Chem 255* (1980) 4100–4111.
[4] J. T. Groves, Y. Watanabe, *J. Am. Chem. Soc. 110* (1988) 8443–8452.
[5] E. McCandlish, A. R. Miksztal, M. Nappa, A. Q. Sprenger, J. S. Valentine, J. D. Stong, T. G. Spiro, *J. Am. Chem. Soc. 102* (1980) 4268–4271.
[6] C. H. Welborn, D. Dolphin, B. R. James, *J. Am. Chem. Soc. 103* (1981) 2869–2871.
[7] P. Friant, J. Goulon, J. Fischer, L. Ricard, M. Schappacher, R. Weiss, M. Momenteau, *Nouv. J. Chim 9* (1985) 33–40.
[8] J. N. Burstyn, J. A. Roe, A. R. Miksztal, B. A. Shaevitz, G. Lang, J. S. Valentine, *J. Am. Chem. Soc. 110* (1988) 1382–1388.
[9] EXAFS studies of the peroxoiron(III) tetraphenylporphyrinate complex indicate that the O_2^{2-} group is side-on bonded to the metal in these derivatives (see Reference [7]).
[10] M. Schappacher, R. Weiss, R. Montiel-Montoya, A. X. Trautwein, A. Tabard, *J. Am. Chem. Soc. 107* (1985) 3736–3738.
[11] M. Schappacher, G. Chottard, R. Weiss, *J. Chem. Soc. Chem. Commun.* 1986, 93–94.
[12] A. M. Khenkin, A. Shteinman, *J. Chem. Soc. Chem. Commun.* 1984, 1219–1220.
[13] J. P. Collman, R. G. Gagne, C. A. Reed, T. H. Halbert, G. Lang, W. T. Robinson *J. Am. Chem. Soc. 96* (1975) 1427–1439.
[14] So far, it is not clear whether the oxo group present in **6** is located within the pickets or on the non-protected side of the porphyrin ring. We favor the former structure because **6**, although quite unstable, is still more stable than the radical cationic oxoiron(IV) species that one can generate at very low-temperature with non-protected porphyrins. Furthermore, the oxo group of **5** is located inside the molecular cavity of the picket-fence porphyrin (see Reference [10]).
[15] D. Dolphin, A. Forman, D. C. Borg, J. Fajer, R. H. Felton, *Proc. Natl. Acad. Sci. USA 68* (1971) 614–618.
[16] Approximately 25% of the sample correspond to a high-spin iron(III) species. The presence of iron(III) material could either be due to a non-quantitative reaction and/or to a partial decomposition of the sample during the transfer into the Mössbauer cell.
[17] J. T. Groves, R. C. Haushalter, M. Nakamura, T. E. Nemo, B. J. Evans, *J. Am. Chem. Soc. 103* (1981) 2884–2886.
[18] B. Boso, G. Lang, T. J. McMurry, J. T. Groves, *J. Chem. Phys. 79* (1983) 1122–1126.
[19] J. T. Groves, J. A. Gilbert, *Inorg. Chem. 25* (1986) 123–125.
[20] C. E. Schultz, R. Rutter, J. T. Sage, P. G. Debrunner, L. P. Hager, *Biochemistry 23* (1984) 4743–4754.
[21] A. L. Balch, L. Latos-Grazynski, M. W. Renner, *J. Am. Chem. Soc. 107* (1985) 2983–2985.
[22] A. Gold, K. Jayaray, P. Doppelt, R. Weiss, E. Bill, X.-Q. Ding, E. L. Bominaar, A. X. Trautwein, H. Winkler, *New. J. Chem. 13* (1989) 169–172.
[23] The upfield shift of the pyrrole protons and the downfield shift of the *m*-phenyl protons are also very small in the π radical cationic oxoiron(IV) tetrakis(2,4,6-methoxyphenyl)porphyrinate; A. Gold, private communication.
[24] No reaction of **6** with one equivalent of cyclohexene was detected in the UV/VIS cell, neither at 220 K nor at higher temperatures. However, if a large excess of cyclohexene is added to **6** at 220 K, when warming up the solution, instead of total bleaching, 20 to 30% of the starting material **1** is recovered at room temperature.
[25] D. Mandon, R. Weiss, unpublished.

Bicycloprop-2-enyl (C_6H_6)**

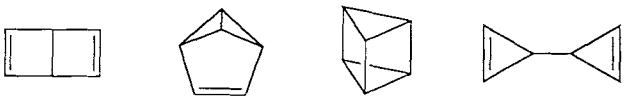
By *Wilbur E. Billups** and *Michael M. Haley*

The valence bond isomers of benzene have been the object of intensive theoretical and synthetic studies. Dewar benzene (**1**) was synthesized in 1963 by *van Tamelen* and *Pappas*.[1]

[*] Prof. Dr. W. E. Billups and Michael M. Haley
Department of Chemistry, Rice University
P.O. Box 1892, Houston, Texas 77251 (USA)

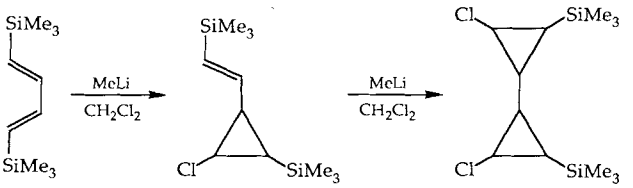
[**] We gratefully acknowledge The Robert A. Welch Foundation for support of this work. Acknowledgment is made to the donors of the Petroleum Research Fund, administered by the American Chemical Society, for partial support of this work. *MMH* gratefully acknowledges the support of the Dow Chemical Company in the form of a fellowship.

Benzvalene (**2**) was isolated in low yield from sensitized photolysis of benzene by *Wilzbach* et al. in 1967[2] and synthesized by *Katz* et al. in 1971.[3] Prismane (**3**) was prepared from **2** by *Katz* and *Acton* in 1973.[4] Although derivatives of bicycloprop-2-enyl **4** have been prepared,[5] the unsubstituted species, which has been calculated to be the $(CH)_6$ species of highest energy,[6] has eluded synthesis. We now wish to report the synthesis and characterization of this the remaining $(CH)_6$ isomer.



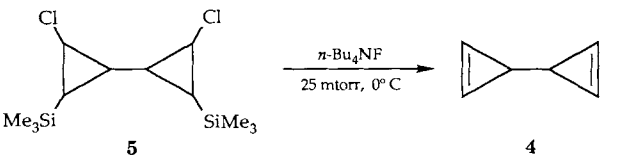
1 **2** **3** **4**

The starting material **5** was prepared from 1,4-bis(trimethylsilyl)buta-1,3-diene (**6**)[7] and chlorocarbene[8]. Treatment of **6** with an eightfold excess of chlorocarbene afforded the vinylcyclopropane **7** in 68% yield as a 60:40 mixture of *trans* and *cis* isomers.[9] Exposure of **7** to the same conditions resulted in the isolation of the bicyclopropyl **5** in 45% yield.[10]



6 **7** **5**

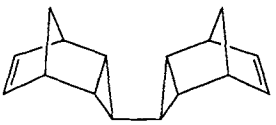
The slow introduction of **5** into a vacuum gas-solid reaction (VGSR) apparatus packed with tetra-*n*-butylammonium fluoride on glass helices[11] yielded bicycloprop-2-enyl **4** as the major product. The identity of **4** is based on its ^{1}H-NMR spectrum—a doublet at $\delta = 7.15$ (4H, $J = 1.3$ Hz) and a triplet at 1.45 (2H, $J = 1.3$ Hz). The NMR signals of **4** were persistent as a solution in CD_2Cl_2 was warmed from $-90\,^\circ C$ to $-10\,^\circ C$. Above $-10\,^\circ C$, however, these signals began to diminish. At room temperature **4** polymerizes into a solid yellow mass, in contrast to other bicycloprop-2-enyls which aromatize. Although the thermal rearrangement of bicycloprop-2-enyls to benzene derivatives is among the most exothermic unimolecular processes known ($\Delta H^\circ_{rxn} =$ 120 kcal/mol),[5] the polymerization of **4** is thought to proceed via an ene reaction characteristic of other simple cyclopropenes.[12]



5 **4**

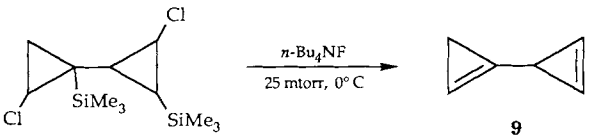
When the walls of the liquid nitrogen trap used to collect **4** were coated with cyclopentadiene, the Diels-Alder adduct **8** could be isolated in 72% yield.[13]

Treatment of a solution of **4** in $CDCl_3$ with $AgBF_4$ at 0 °C resulted in nearly quantitative conversion into **1** along with a small amount of polymer.[14] The identity of **1** was confirmed by comparison with the ^{1}H-NMR spectrum of an authentic sample and by its isomerization to benzene.[2]



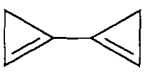
8

The fluoride-induced elimination of β-halosilanes in the gas phase has also been utilized in the synthesis of the isomeric bicyclopropenyl **9**.[15, 16]



9

Studies on the synthesis of the potentially useful synthon bicycloprop-1-enyl **10** will be reported shortly.



10

Received: August 16, 1989 [Z 3504 IE]
German version: *Angew. Chem. 101* (1989) 1735

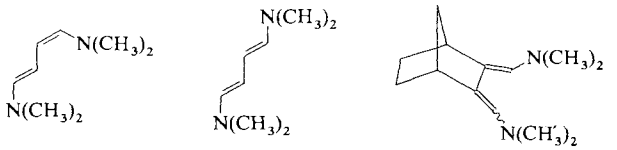
CAS Registry numbers:
1, 5649-95-6; **4**, 62595-44-2; **5**, 123725-71-3; **6**, 13625-90-6; **7**, 123725-72-4; **8**, 123725-73-5; **9**, 77160-46-4; 1-(2-chloro-1-trimethylsilyl-1-cyclopropanyl)-2-chloro-3-trimethylsilylcyclopropane, 123725-70-2; cyclopentadiene 542-92-7.

[1] a) E. E. van Tamelen, S. P. Pappas, *J. Am. Chem. Soc. 85* (1963) 3297; b) E. E. van Tamelen, S. P. Pappas, K. L. Kirk, *ibid. 93* (1971) 6092.
[2] a) K. E. Wilzbach, J. S. Ritscher, L. Kaplan, *J. Am. Chem. Soc. 89* (1967) 1031; b) L. Kaplan, K. E. Wilzbach, *ibid. 90* (1968) 3291; c) H. R. Ward, J. S. Wishnok, *ibid. 90* (1968) 1085.
[3] T. J. Katz, E. J. Wang, N. Acton, *J. Am. Chem. Soc. 93* (1971) 3782.
[4] T. J. Katz, N. Acton, *J. Am. Chem. Soc. 95* (1973) 2738.
[5] J. H. Davis, K. J. Shea, R. G. Bergman, *J. Am. Chem. Soc. 99* (1977) 1499, and references cited therein.
[6] A. Greenburg, J. F. Liebman, *J. Am. Chem. Soc. 103* (1981) 44.
[7] H. Bock, H. Seidl, *J. Am. Chem. Soc. 90* (1968) 5694.
[8] G. L. Closs, L. E. Closs, *J. Am. Chem. Soc. 82* (1960) 5723.
[9] **7**: b.p. 48–60 °C (0.1 torr); ^{1}H NMR (300 MHz, $CDCl_3$) *trans*-**7**: $\delta = 5.88$ (1H, d, $J = 18.1$ Hz), 5.83 (1H, dd, $J = 18.1$, 6.9 Hz), 3.16 (1H, dd, $J = 6.4$, 5.8 Hz), 1.62 (1H, AB, $J = 8.0$, 6.9 Hz), 0.30 (1H, dd, $J = 8.0$, 5.8 Hz), 0.07 (9H, s), 0.01 (9H, s); *cis*-**7**: $\delta = 5.73$ (1H, d, $J = 18.4$ Hz), 5.55 (1H, dd, $J = 18.4$, 7.9 Hz), 3.28 (1H, dd, $J = 8.4$, 2.9 Hz), 1.78 (1H, td, $J = 7.9$, 2.9 Hz), 0.31 (1H, dd, $J = 8.4$, 7.9 Hz), 0.14 (9H, s), 0.04 (9H, s); mass spectrum calculated for $C_{11}H_{23}ClSi_2$ 246.1027, found 246.1031.
[10] **5**: b.p. 70–120 °C (bath temperature) 0.03 torr; ^{1}H NMR: $\delta = 3.29$–3.01 (2H, m), 1.44–0.87 (2H, m), 0.54 to −0.21 (2H, m), 0.12 to −0.06 (18H, 8s); mass spectrum calculated for $C_{12}H_{24}Cl_2Si_2$ 294.0794, found 294.0791.
[11] W. E. Billups, L.-J. Lin, *Tetrahedron 42* (1986) 1575.
[12] a) B. Halton, M. G. Banwell in Z. Rappaport (Ed.): *The Chemistry of the Cyclopropyl Group*, Wiley, New York 1987, p. 1223; b) M. S. Baird, *Top. Curr. Chem. 144*, (1988) 137.
[13] **8**: m.p. 104–105 °C; ^{1}H NMR: $\delta = 5.67$ (4H, t, $J = 2.0$ Hz), 2.76 (4H, bs), 1.67 (2H, dt, $J = 6.6$, 1.5 Hz), 1.65 (2H, d, $J = 6.6$ Hz). 1.17 (4H, d, $J = 1.5$ Hz), 0.41 (2H, t, $J = 1.5$ Hz); mass spectrum calculated for $C_{16}H_{18}$ 210.1408, found 210.1407.
[14] I. J. Landheer, W. H. de Wolf, F. Bickelhaupt, *Tetrahedron Lett. 1975*, 349, and references cited therein.
[15] **9**: ^{1}H NMR: $\delta = 7.35$ (d, 2H, $J = 1.3$ Hz), 6.43 (t, 1H, $J = 1.8$ Hz), 2.57 (t, 1H, $J = 1.3$ Hz), 0.79 (d, 2H, $J = 1.8$ Hz); isolated in 57% yield as the Diels-Alder adduct of cyclopentadiene.
[16] For derivatives of **9** see: A. Padwa, M. J. Pulwer, R. J. Rosenthal, *J. Org. Chem. 49* (1984) 856.

[4+2]-Cycloadditions with 1,4-Bis(*N*,*N*-dimethylamino)-1,3-dienes: Stereochemical Studies and Observation of Radical Ions**

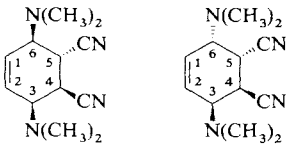
By *Reiner Sustmann,** *Karin Lücking, Gebhard Kopp,* and *Michael Rese*

For a long time, and particularly following the presentation of the Woodward-Hoffmann rules, it was assumed that there is one universally valid mechanism for [4+2]-cycloadditions. Recent investigations, however, indicate that the mechanism is dependent on the pattern of substitution of the diene and the dienophile.[1] Thus, some cycloadditions proceed via diradicals,[1,2] while others are reported to proceed via polar intermediates.[3] Even an electron transfer with formation of radical ions has been proposed as primary step.[4] The observation of charge-transfer (CT) complexes and the analysis of their significance in Diels-Alder reactions have stimulated further discussion on the degree of charge transfer during these cycloadditions.[5-8] Herein we report on cycloadditions of the stereoisomeric dienes **1** and **2** and of the bicyclic diene **3** with dienophiles of different acceptor strength. A combination of stereochemical studies with electrochemical measurements and ESR investigations should provide information on the significance of electron transfer in the reactions.



1 **2** **3**

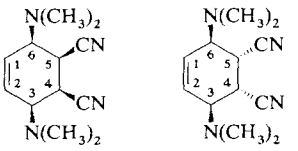
A solution of equimolar amounts ($c = 0.2$ M) of **1** and fumaric dinitrile in [D_6]benzene is dark violet (λ_{max} = 470 nm); this is attributed to a charge transfer (CT) complex. The solution of **2** with fumaric dinitrile absorbs at λ_{max} = 500 nm. In both cases a crude yield of 96% of the same cycloadduct **4** was determined ^{1}H-NMR spectroscopically after two weeks at 35 °C, i.e. the product obtained corresponded to what had been isolated earlier in 55% yield[9] upon reaction of **2** with fumaric dinitrile.



4 **5**

For **1**, this result can be explained in terms of a thermal isomerization of **1** to **2** prior to the cycloaddition and a rapid reaction of **2**, whereas for **2**, product formation can be rationalized in terms of concerted cycloaddition. This explanation is consistent with the observation that *Z*-1-substituted dienes react considerably slower than the *E* isomer.[10] It has been shown independently that **1** isomerizes quantitatively to **2** within 5 d at 35 °C. If the cycloaddition of **1** and fumaric dinitrile is carried out at 50 °C using the 16-fold higher concentration described in the literature,[9] the isomerization is suppressed and up to 96% of **5** is formed.[11] In each case it was demonstrated by mixing that 1.5% of the other isomer could have been detected by ^{1}H-NMR spectroscopy. The stereoselectivity of the reactions is accordingly ≥98.5%.

Maleic dinitrile reacts with **2** in benzene ($c = 0.2$ M for both components, $T = 35$ °C) within 23 d to give a mixture of **6a** and **6b** (96%, ratio 86:14, determined by ^{1}H-NMR spectroscopy). A CT complex is formed initially and absorbs at λ_{max} = 486 nm. The products could not be separated without decomposition and were characterized spectroscopically.[12] In the reaction of maleic dinitrile with **1** the same product was formed as in the reaction with **2**. Isomerization of **1** could not be suppressed upon reaction with the less reactive maleic dinitrile.



6a/6b

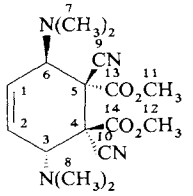
The reactions of the respective 1,2-dicyano-substituted dimethyl esters of fumaric acid and maleic acid with **1** and **2** were carried out (0.2 M solution of the components in methylene chloride) at −50 °C, since a higher temperature led to unidentifiable products. The reaction was complete within 5 min—the minimum time required for the recording of a ^{1}H-NMR spectrum after mixing the compounds—and a single adduct was always isolated (97%) with all four combinations of the reaction partners. At −95 °C formation of a bluish-green CT complex (λ_{max} = 540 nm) is briefly observed. The cycloadduct decomposes in solution at T ≥ −40 °C, but it can be isolated as a colorless microcrystalline solid by removal of the solvent at −50 °C. This cycloadduct is also unstable at higher temperatures, but it could be characterized spectroscopically.[13] In the mass spectrum the $M^{\oplus}$ peak appears at *m/z* 334 with a relative intensity of 1%. According to the spectroscopic data the cycloadduct must have either C_2 or C_s symmetry. In principle, six stereoisomers are possible, of which, however, two are already ruled out because of lack of symmetry. Of the remaining four, structure **7** is preferred since all the larger substituents can be arranged equatorially or pseudo-equatorially. In a concerted reaction, **7** would be formed upon reaction of the *E,Z*-diene **1** with the *E*-dienophile dimethyl 1,2-dicyanofumarate. The chemical shifts are consistent with those expected for such a substituted cyclohexene derivative.[14]

The *E,E*-diene **2** and the *E*-dienophile are configurationally stable for at least 3 h at −50 °C in methylene chloride even if the diene has been added to the dienophile or vice versa, as has been demonstrated ^{1}H-NMR spectroscopically. The *E,Z*-diene **1** and the *Z*-dienophile, however, isomerize when they are mixed at −50 °C in methylene chloride to give **2** and the *E*-dienophile, respectively. The rate of isomerization is a function of the concentration of the reaction partners. With 0.4 equivalents of the *Z*-dienophile the isomerization of **1** was complete after 5 min at −50 °C, whereas the dienophile was isomerized to only 60% under these conditions. Concomitant with the isomerization, the cycloadduct **7** was formed in amounts corresponding to that of the substoichiometric component. In the case of a concerted cy-

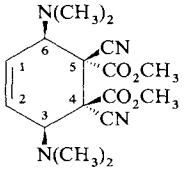
[*] Prof. Dr. R. Sustmann, Dr. K. Lücking, Dr. G. Kopp, Dipl.-Chem. M. Rese
Institut für Organische Chemie der Universität
Postfach 103764, D-4300 Essen 1 (FRG)

[**] This work was supported by the Deutsche Forschungsgemeinschaft.

cloaddition after isomerization, the adduct **8** would have been expected instead of **7**. Because of the lower symmetry, the ^{1}H-NMR spectrum of **8** must, however, show more lines than that of **7**.



7

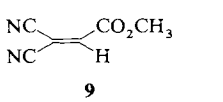


8

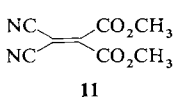
After mixing the *E,E*-diene **2** with the *E*-dienophile at $-95\,^\circ$C in CD_2Cl_2 a complex ^{1}H-NMR spectrum was obtained which showed hardly any signals left over from the starting materials and only very small signals for the product **7**. It was possibly the spectrum of conformers of a zwitterionic intermediate. On slow heating of this solution to $-50\,^\circ$C the signals of **7** became larger, while the other signals disappeared. **7** is thus clearly formed in a multistep reaction. After mixing the solutions of the components in CH_2Cl_2 at $-75\,^\circ$C, radical ions of both the diene as well as of the dienophile were observed ESR spectroscopically, as could be confirmed by the independent generation of $\mathbf{2}^{\bullet\oplus}$ (oxidation with $AgBF_4$) and of the dienophile (reduction in THF with Na/K alloy). Hyperfine coupling constants for the radical anion of dimethyl 1,2-dicyanofumarate were determined to be $a_H = 0.086$ mT (6H; OCH_3) and $a_N = 0.145$ mT (2N, CN). The large number of lines in the spectrum of $\mathbf{2}^{\bullet\oplus}$ precluded an accurate analysis.

The reaction of **3**—which had already been reacted with other dienophiles in earlier experiments[15]—with equimolar amounts of **9** at room temperature in the absence of solvent is strongly exothermic and yields only unidentifiable products. When the reaction was carried out in THF ($c = 0.17$ M, both components) a red solid could be isolated, which according to the ^{1}H- and ^{13}C-NMR spectra had the structure of the [4+2]-cycloadduct **10**.[16] The mass spectrum (chemical ionization CI) shows the expected $(M+H)^\oplus$ peak at 343 (54%). Attempts to purify this thermolabile adduct, which according to the ^{1}H-NMR spectrum is formed in 93% yield, met without success. Its coloration must be attributed to the presence of small amounts of an impurity. ESR spectroscopic examination of the solid revealed slight paramagnetism.

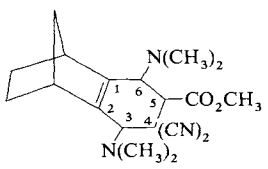
Equimolar amounts of **3** and **11** were allowed to react in THF at room temperature and in toluene at $-80\,^\circ$C. The ^{1}H- and ^{13}C-NMR spectra of the product, which was formed in 80% yield (^{1}H-NMR analysis with a standard), confirmed that a [4+2]-cycloaddition to give **12** had taken place.[16] The structure **12** is also supported by the CI-mass spectrum [m/z 401 ($M^\oplus+H$, 16%), 207 ($\mathbf{2}^\oplus+H$, 100%)]. Although **3** was allowed to react as a mixture of the *E,E*- and *E,Z*-isomers, only one diastereomer could be detected. Reaction of the isomeric mixture **3** with less reactive dienophiles leads to product mixtures.[17] The uniform product observed here points to a non-stereospecific, presumably multistep, reaction leading to the thermodynamically most stable product.



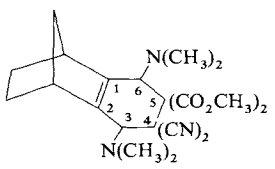
9



11



10



12

Radical ions are detectable in the ESR spectroscopic analysis of the reaction mixtures of **3** with **9** and **11**. Thus, the radical anion of **9** could be observed in THF between $-20\,^\circ$C and $+20\,^\circ$C. At $-20\,^\circ$C three sorts of radical ions are recognizable, of which two are assigned to conformers of $\mathbf{9}^{\bullet\ominus}$, because of their very similar splitting pattern. The third radical is $TCNE^{\bullet\ominus}$ (TCNE tetracyanoethylene). At $+20\,^\circ$C only one isomer of $\mathbf{9}^{\bullet\ominus}$ and $TCNE^{\bullet\ominus}$ are still recognizable [$\mathbf{9}^{\bullet\ominus}$: $a_H = 0.085$(3H), 0.343 mT(1H), $a_N = 0.135$(1N), 0.159 mT(1N)]. The presence of $TCNE^{\bullet\ominus}$ is surprising, but must result from a metathetical reaction of **9** with $\mathbf{9}^{\bullet\ominus}$. $TCNE^{\bullet\ominus}$ is the only radical ion that is detectable on mixing the solutions of **3** and **11**. The metathesis can only be of secondary importance, however, since the yields of cycloadducts are high.

The results show that the dienes **1**–**3** form radical ions with very reactive dienophiles. On the basis of polarographically determined redox potentials[18] the results can be interpreted quantitatively. Figure 1 shows the redox potentials

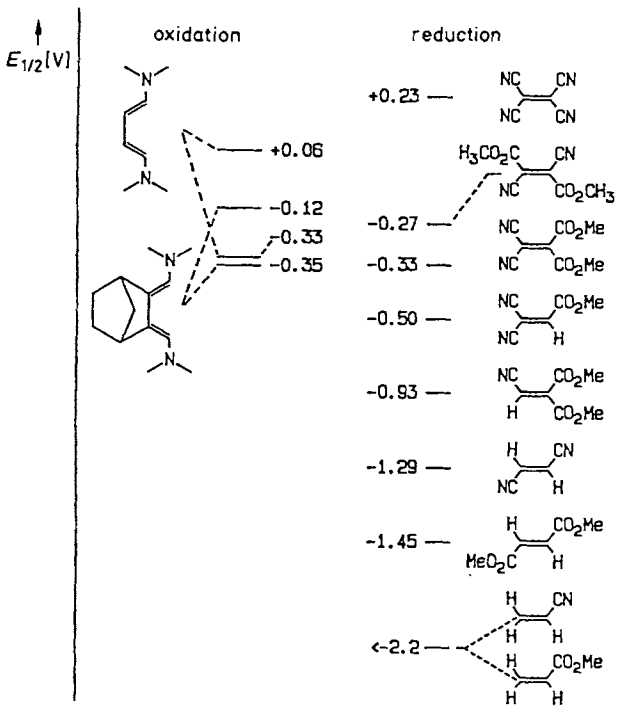


Fig. 1. Redox potentials $E_{1/2}$ vs. SCE for some dienes and dienophiles.

of the dienes and dienophiles, whereby two potentials are quoted for each of the dienes, one corresponding to the oxidation to the radical cation, and the other to the further oxidation to the dication. Owing to the measuring arrangement, reduction potentials ≤ -2.2 V could not be determined. *Hall* et al.[19] have investigated the reduction of the reactive dienophiles cyclovoltammetrically. With exception of TCNE and of the dimethyl esters of the 1,2-dicyanofumaric and 1,2-dicyanomaleic acids, the reductions were

irreversible. The sequences of the potentials determined polarographically by us and cyclovoltammetrically by *Hall* et al. are, with one exception, identical: we found a more negative reduction potential for dimethyl 2-cyanoethene-1,1-dicarboxylate than for methyl 3,3-dicyanoacrylate. Since the CN group is more strongly electron withdrawing than the CO_2Me group, the sequence found by us is in better agreement with that expected qualitatively.

From the experimental results, it emerges that electron transfer is observable when the reduction potential of the dienophiles is ≥ -0.50 V. Since no olefins with reduction potentials between -0.93 and -0.50 V are present, an exact limiting value cannot be quoted for the difference in redox potentials at which electron transfer is still visible. With the help of the Rehn-Weller equation,[20] not only can the free enthalpy of the reaction for the electron transfer be calculated but, assuming that the electron transfer has no additional activation barrier, also a maximum rate constant for this step.[21] According to Table 1, electron transfer is found

Table 1. ΔG and k_{max} for electron transfer from **3** to some dienophiles.

Dienophile	E_{red} [V] vs. SCE	ΔG_{SET} [a] [kcal mol^{-1}]	k_{max} [b] [M^{-1} s^{-1}]
$(NC)_2C=C(CN)_2$	+0.23	−13.37	1.0×10^{9}
$MeO_2C(NC)C=C(CN)CO_2Me$	−0.27	−1.84	1.0×10^{9}
$(NC)_2C=C(CO_2Me)_2$	−0.33	−0.46	1.0×10^{9}
$(NC)_2C=CHCO_2Me$	−0.50	+3.46	2.3×10^{8}
$NCHC=C(CO_2Me)_2$	−0.93	+13.37	2.1×10^{1}
NCHC=CHCN	−1.29	+21.68	2.0×10^{-5}
$MeO_2CHC=CHCO_2Me$	−1.45	+25.37	4.3×10^{-8}
$H_2C=CHCN$	<-2.2	$>+42.66$	$<1.3\times10^{-20}$
$H_2C=CHCO_2Me$	<-2.2	$>+42.66$	$<1.3\times10^{-20}$

[a] $\Delta G_{SET} = 23.06\,(E_{ox}\text{-}E_{Red}\text{-}C)$. [b] $1/k_{max} = 1/k_{diff} + 10^{-11}\exp(\Delta G_{SET}/RT)$.

when ΔG is negative or weakly positive. In these cases, the electron transfer should, according to the above premise, be diffusion controlled ($k_{max} \geq 10^9$ M^{-1} s^{-1}). The more positive ΔG is, the less likely is there an electron transfer. The cycloadditions of acrylonitrile and methyl acrylate with **3**[15] confirm that electron transfer-activation cannot participate in these reactions, since the rate constant for the electron transfer is prohibitively small.

The dramatic acceleration of reaction on occurrence of electron transfer could mean that it participates in product formation. However, it could also be that the diene/dienophile pairs are especially capable of forming zwitterions, either directly, starting from the neutral reaction partners, or from the radical ions. The stereochemical results, together with the results of the electron transfer studies lead to the following conclusions: If the electron transfer can be detected ESR spectroscopically, the product is formed in several steps. On the other hand, if no electron transfer can be observed spectroscopically, the cycloaddition is stereospecific. Since the large majority of diene/dienophile pairs, in [4+2]-cycloadditions have less pronounced donor/acceptor properties than the examples studied here, it may be assumed that electron transfer to form free radical ions is not the general mechanism for [4+2]-cycloadditions. Thus, the study of mechanistically limiting cases leads to an understanding of the behavior in "normal" cases.

Received: July 17, 1989;
revised: September 13, 1989 [Z 3451 IE]
German version: *Angew. Chem. 101* (1989) 1701

CAS Registry numbers:
1, 74894-01-2; **2**, 123931-19-1; **2**$^{\oplus\bullet}$, 123931-21-5; (*E,E*)-**3**, 45765-39-2; (*E, Z*)-**3**, 95765-38-1; **4**, 123858-31-1; **5**, 123858-32-2; **6a**, 123931-20-4; **6b**, 123858-36-6; **7**, 123881-39-0; **8**, 123858-33-3; **9**, 82849-50-1; **9**$^{\ominus\bullet}$, 123858-35-5; **10**, 123881-40-3; **11**, 82849-49-8; **12**, 123858-34-4; $TCNE^{\bullet-}$, 34512-48-6; (*E*)-$(NCCH\!\!\rightarrow_2$, 764-42-1; (*Z*)-$(NCCH\!\!\rightarrow_2$, 928-53-0; (*E*)-$[MeO_2C(CN)C\!\!\rightarrow_2$, 35234-87-8; (*Z*)-$[MeO_2C(CN)C\!\!\rightarrow_2$, 101342-44-3; $[(NC)_2C\!\!\rightarrow_2$, 670-54-2; $(MeO_2C)_2C=CHCN'$, 6293-70-3; (*E*)-$(MeO_2CH\!\!\rightarrow_2$, 624-49-7; $CH_2=CHCN$, 107-13-1; $CH_2=CHCO_2Me$, 96-33-3.

[1] J. Sauer, R. Sustmann, *Angew. Chem. 92* (1980) 773; *Angew. Chem. Int. Ed. Engl. 19* (1980) 779.
[2] W. von E. Doering, W. R. Roth, R. Breuckmann, L. Figge, H.-W. Lennartz, W.-D. Fessner, H. Prinzbach, *Chem. Ber. 121* (1988) 1.
[3] R. Gompper, *Angew. Chem. 81* (1969) 348; *Angew. Chem. Int. Ed. Engl. 8* (1969) 312.
[4] J. K. Kochi, *Angew. Chem. 100* (1988) 1331; *Angew. Chem. Int. Ed. Engl. 27* (1988) 1227.
[5] S. Fukuzumi, J. K. Kochi, *Tetrahedron 38* (1982) 1035.
[6] S. Fukuzumi, J. K. Kochi, *Bull. Chem. Soc. Jpn. 56* (1983) 969.
[7] R. Sustmann, M. Dern, R. Kasten, W. Sicking, *Chem. Ber. 120* (1987) 1315.
[8] V. D. Kiselev, J. G. Miller, *J. Am. Chem. Soc. 97* (1975) 4036.
[9] M. F. Fegley, N. M. Bortnick, C. H. McKeever, *J. Am. Chem. Soc. 79* (1957) 4736.
[10] C. Rücker, D. Lang, J. Sauer, H. Friege, R. Sustmann, *Chem. Ber. 113* (1980) 1663.
[11] **4**: ^{1}H NMR (200 MHz $CDCl_3$): δ = 5.87 (m, 2H; H-1, H-2), 3.40 (dd, 1H, ^3J = 9.6, ^5J = 1.7 Hz; H-3), 3.21 (dd, 1H, ^3J = 11.2, 9.6 Hz; H-4), 3.04 (dd, 1H, ^3J = 11.2, 4.4 Hz; H-5), 3.33 (m, 1H; H-6), 2.45, 2.35 (each s, 12H). ^{13}C-NMR (50.3 MHz, $CDCl_3$): δ = 127.41, 128.70 (each d; C-1,C-2), 57.51, 62.53 (each d; C-3,C-6), 28.18, 35.27 (each d, C-4,C-5), 40.80, 44.15 (each q; $N(CH_3)_2$), 117.75, 119.12 (each s, CN).—**5**: Only one of two stereoisomers is formed. ^{1}H NMR (200 MHz, $CDCl_3$): δ = 5.81 (s, 2H; H-1,H-2), 3.56 (m, 2H; H-3,H-6), 2.97 (m, 2H; H-4,H-5), 2.33 (s, 12H; $N(CH_3)_2$). ^{13}C-NMR (50.3 MHz, $CDCl_3$): δ = 128.32 (d; C-1, C-2), 62.21 (d; C-3,C-6), 53.53 (d; C-4,C-5), 40.53 (q; $N(CH_3)_2$), 118.34 (s; CN).
[12] **6**: ^{1}H NMR (200 MHz, C_6D_6); main component: δ = 5.36 (m, 2H; H-1,H-2), 2.47 (m, 2H; H-3,H-6), 2.27 (m, 2H; H-4, H-5), 2.27 (s, 12H; $N(CH_3)_2$); minor component: δ = 5.31 (m, 2H; H-1′, H-2′), 2.94 (m, 2H; H-3′, H-6′), 2.68 (m, 2H; H-4′, H-5′), 2.27 (s, 12H; $N(CH_3)_2$). ^{13}C NMR (50.3 MHz, $CDCl_3$), only the spectrum of the main component is visible: δ = 127.50 (d; C-1,C-2), 58.60 (d; C-3,C-6), 31.04 (d; C-4,C-5), 42.69 (q; $N(CH_3)_2$), 117.78 (s; CN).
[13] **7**: ^{1}H NMR (200 MHz, $CDCl_3$, −50 °C): δ = 2.49 (s; 12H), 3.95 (s; 6H), 4.47 (s; 2H), 6.05 (s; 2H). ^{13}C-NMR (50.3 MHz, $CDCl_3$, −50 °C): δ = 43.41 (q; C-7,C-8), 54.60 (q; C-11, C-12), 54.88 (s; C-4,C-5), 63.06 (d; C-3,C-6), 114.36 (s; C-9,C-10), 124.92 (d; C-1,C-2), 163.58 (s; C-13,C-14).
[14] H. O. Kalinowski, S. Berger, S. Braun: *^{13}C-NMR-Spektroskopie*, Thieme, Stuttgart 1984, pp. 237–238, pp. 122–124.
[15] M. Dern, H.-G. Korth, G, Kopp, R. Sustmann, *Angew. Chem. 97* (1985) 324; *Angew. Chem. Int. Ed. Engl. 24* (1985) 337.
[16] **10**: ^{1}H NMR (200 MHz, C_6D_6): δ = 0.80–1.20 (m, 6H), 2.15 (s, 6H; $N(CH_3)_2$), 2.22 (s, 6H; $(N(CH_3)_2)$, 2.26 (s, 1H), 2.77 (s, 1H), 3.21 (d, 1H, ^3J = 7 Hz), 3.23 (s, 1H), 3.41 (s, 3H; OCH_3), 3.70 (d, 1H, ^3J = 7 Hz). ^{13}C NMR (50.3 MHz, C_6D_6): δ = 138.8, 145.2(C-1,C-2), 61.0, 65.2(C-3,C-6), 40.5, 41.0, 24.8, 45.4 (norbornane skeleton), 44.4, 45.1($N(CH_3)_2$), 52.6(OCH_3), 28.3(C-4), 41.4(C-5), 113.8, 114.4(CN), 171.4(CO).—**12**: ^{1}H NMR (200 MHz, C_6D_6): δ = 0.82–1.48 (m, 6H), 2.41 (s, 6H; $N(CH_3)_2$), 2.61 (s, 6H; $N(CH)_3)_2$), 2.49 (s, 1H), 2.57 (s, 1H), 3.20 (s, 3H; OCH_3), 3.36 (s, 3H; OCH_3), 3.48 (d, ^5J = 1.5 Hz, 1H), 4.00 (d, ^5J = 1.5 Hz, 1H). ^{13}C NMR (50.3 MHz, C_6D_6): δ = 140.99, 141.89 (C-1,C-2), 62.41, 66.99 (C-3,C-6), 43.31, 46.05, 24.74, 25.43, 44.95 (norbornane skeleton), 44.91, 44.68 ($N(CH_3)_2$), 115.11, 116.41(CN), 52.61, 52.70(OCH_3), 165.97, 166.75 (CO_2Me at C-5).
[17] M. Dern, unpublished results.
[18] Measurements in 0.001 M solution in CH_3CN (tetraethylammonium perchlorate 0.1 M) with a Bruker E-310 polarograph.
[19] T. Gotoh, A. B. Padias, H. K. Hall, Jr., *J. Am. Chem. Soc. 108* (1986) 4920; J. E. Mulvaney, R. J. Cramer, H. K. Hall, Jr., *J. Polym. Sci. Polym. Chem. Ed. 21* (1983) 309.
[20] D. Rehm, A. Weller, *Ber. Bunsenges. Phys. Chem. 73* (1969) 839. The quantity *C*, which is generally considered as being small [21], is neglected in the calculation of ΔG.
[21] J. W. Verhoeven, W. van Gerresheim, F. M. Martens, S. M. van der Kerk, *Tetrahedron 42* (1986) 975.

Book Reviews are written by invitation from the editor. Suggestions for books to be reviewed and for book reviewers are welcome. Publishers should send brochures or (better) books to the following address: Redaktion Angewandte Chemie, Postfach 101161, D-6940 Weinheim, Federal Republic of Germany. The editor reserves the right of selecting which books will be reviewed. Uninvited books not chosen for review will not be returned.

Dictionary of Organophosphorus Compounds. Edited by *R. S. Edmundson*. Chapman & Hall, London 1988. 1347 pp., hardcover, £ 305.00.—ISBN 0-412-25790-4

Although organophosphorus compounds are covered in several series, the publication of a "Dictionary of Organophosphorus Chemistry" is unparalleled. In view of the great importance of phosphorus and its compounds, such a publication is therefore potentially of great interest. How does the sole author deal with this vast topic? Are his efforts successful?

The first question posed by the potential user of such a handbook concerns the definition of an organophosphorus compound as used by the author to define the scope of the text. According to the dust jacket, over 20000 organophosphorus compounds are discussed (in almost 900 pages). What does the author consider to be an organophosphorus compound? A glance through the text reveals that the definition goes beyond systems containing P–C bonds; for example, there are numerous entries treating phosphorus compounds containing C–N–P, C–O–P, or C–S–P groupings, to name just a few. C is part of an organic moiety. This realization is most welcome from the viewpoint of the user. However, the user will find no metal complexes of organophosphorus(III) compounds, even those containing organic moieties directly bonded to phosphorus. Thus, it is not fully clear what the author considers to be an organophosphorus compound.

An especially important question in using this handbook is the ease of finding a particular compound. Compounds can be located in a number of ways: for example, by name, empirical formula, CAS Registry Number, or type of compound ("Type of Compound Index"). Although the nomenclature of organophosphorus compounds is more straightforward than that of other groups of compounds, it may be difficult to find some compounds through their names. In such cases, the empirical formula is always sufficient. The huge amount of information collected by the author is therefore readily accessible to the user.

A typical entry in the "Dictionary of Organophosphorus Compounds" usually refers to a parent compound (for example, a phosphonic acid) followed by data on its derivatives (for example, its salts, esters, and amides). The information usually includes the structural formula, the molecular mass, and selected physical constants. NMR and other spectroscopic data are not directly included, though numerous references to the literature are given. Useful are short general comments on the typical chemical behavior and toxicity of the compounds, always supported by leading references.

The book begins with a lengthy discussion of the nomenclature of organophosphorus compounds and includes, under the title "Sources of Further Information", a comprehensive list of textbooks and handbooks, as well as of review articles, covering all aspects of the chemistry of organophosphorus compounds (six pages). This list is well suited in providing access to the original literature, especially when a general orientation about a certain aspect of organophosphorus chemistry is desired.

A further question concerns the depth in which the original literature is treated. Chronologically, the literature is covered through 1986, though it is less clear how far back the primary literature is taken into consideration. To a large extent, the references appear to date from the last twenty-five years, a period during which the most important progress has been made, both qualitatively and quantitatively, in organophosphorus chemistry. It is noted that a small part of the entries (< 10%) were already included in the 5th edition of the "Dictionary of Organic Compounds" (1982) and that the style of the current "Dictionary of Organophosphorus Compounds" is strongly reminiscent of that work.

Immediately noticeable in glancing through the numerous references to the literature is that the bulk of them are references to journals. However, it is not clear according to what criteria—particularly, how thoroughly—these references were evaluated. A large amount of information on organophosphorus compounds is available in the patent literature. Although this handbook contains references to that source, how exhaustively it was evaluated is not clear.

A random check revealed that the references are by no means complete and that not all organophosphorus compounds reported during the last decades have been included. Thus, if a compound of interest is not found, a further literature search, for example through *Chemical Abstracts*, is warranted. The author does not appear to have addressed the question of how exhaustively the original literature has been examined. Checking concrete examples reveals a certain arbitrariness in the choice of literature references for particular compounds. The original literature is covered in more of a representative than an exhaustive fashion. For example, a typical preparation rather than the first synthesis is often cited.

I did not like the use of only one author's name followed, if necessary, by *et al.* in the literature citations. Although the highly desirable preparation of an author index would demand considerable work, it would increase the usefulness of this handbook. In the case of patents, not only the name of the inventor or discoverer but also that of the company should be given. The literature is not always correctly cited; in some cases, the information taken from the publications is inaccurate. Such shortcomings are not unexpected for a work of this scale and can be corrected in preparing the next edition. The dust jacket states that "Supplements" are planned.

It would be easy to criticize particular details in a work of this magnitude. Although I wish to avoid nitpicking, I cannot resist making one critical comment. Under No. P-00002 (p. 645), Parathion (= diethyl p-nitrophenyl thiophosphate) is discussed in some detail. However, the synthesis cited is that by American authors in 1948, whereas *Gerhard Schrader* (then at I.G. Farbenindustrie, Eberfeld), who first synthesized the compound in December 1944 and called it E 605, is not mentioned at all.

 © VCH Verlagsgesellschaft mbH, D-6940 Weinheim, 1989 0570-0833/89/1212-1716 $ 02.50/0

These reservations and criticisms should in no way detract from the value of this work. Organophosphorus chemists should be thankful to Dr. *Edmundson* for his overall successful undertaking, which will make their own work easier. Although the price of £ 305 will almost certainly prevent wide dissemination of this book, it should be purchased by every chemistry library.

Reinhard Schmutzler [NB 1016 IE]
Institut für Anorganische und Analytische Chemie
der Technischen Universität Braunschweig (FRG)

The Technical Writer's Handbook. By *Matt Young*. University Science Books, Mill Valley, CA, 1989. xi, 232 pp., hardcover, $ 22.50.—ISBN 0-935702-60-1

Some style handbooks and usage dictionaries defeat their very purpose. They confront the well-intentioned writer with a jungle of dos, don'ts, and maybes and they beget rules having more to do with logic than with language. Like the much maligned schoolmarm who drilled students in a latinized English, they often discourage good writing by taking the fun out of writing. *The Technical Writer's Handbook* sidesteps these pitfalls. In the preface, *Matt Young* writes, "I ask for precision in writing, but I try to be flexible and have a healthy regard for usage." His highly readable book bears him out.

Despite its title, this book is primarily a usage dictionary, or, as Part II is titled, *An ABC of Technical Writing*. In Part I, only fourteen pages long, *Young* discusses three rules. To scientists who enjoy talking about their work but who, when forced to write, chew on their pencils or grow bleary-eyed staring at a computer display screen, he advises, "Write the way you talk; then polish." To scientists who find their sentences cluttered with commas, hyphens, and conjunctions, he suggests, "Write one thought per sentence." Following his own advice, he adds a corollary to the second rule: "Be explicit." To all scientists wanting to reach a wide audience, he recommends, "Write for the uninformed reader." These commonsense rules do not guarantee good scientific and technical writing, but they point the way. "Writing with Style and Clarity"—the subtitle of this book—requires pleasure in writing, a good feel for language, and, not least, the desire to be understood.

Part II, best read once through, contains an alphabetically organized discussion of word usage, grammar, and style. *False elegance*, for example, treats word choice and, in particular, elegant variation, the unjustified fear of repeating a word within a sentence or paragraph. "Comma-kazes"—those disposed to putting commas in the wrong places—will find help under *comma*. Other entries discuss such topics as parallel sentence structures (*principle of parallelism, list*), dangling participles and other wrongly placed modifiers (*dangling modifier, misplaced modifier*), problems with number (*singular or plural*), and the correct choice of verb tense (*tense*). The entries are short and to the point. *Young*'s conversational tone and effective use of humor spice the text. A *black hole*, for example, is defined as a noun that has collapsed under the weight of too many modifiers.

An ABC of Technical Writing is more than a mere usage dictionary, however. *Getting started, organization, manuscript preparation*, and *style manual*, not to mention *procrastination*, are just a few of the entries addressing the scientific paper itself. Under *private communication*, *Young* expresses the opinion that scientists with too many such connections should include complete mailing addresses as well. *Duplicate publications* condemns this practice and suggests, overoptimistically, that authors explicitly state that two papers are essentially the same. "Avoid implicit attacks on the writers rather than the manuscript" is one piece of advice in *refereeing*. The entry *Shakespeare* argues against using his work as a model for technical writing: "The language changes every day, and I look to modern writers for instruction on modern writing."

The Technical Writer's Handbook, like most language handbooks, contains much opinion and some questionable advice. For instance, *Young*'s efforts at spelling reform (he considers "analogue" obsolete) may or may not yield fruit. If *Noah Webster* had had his way, we would have "chimists" instead of chemists. Biologists might disagree with *Young*'s admonition against writing "wild-type bacterium" (see *type, -type*), which he thinks could refer to either a "modified wild bacterium" or a wild strain. "Wild type" is a well-defined term meaning the typical (nonmutant) form of an organism encountered in nature. Here *Young*'s training in physics makes him less of a pragmatist and more of a purist (see *permissivist, prescriptivist*). Moreover, his background also causes him to overlook some examples of relevance to, say, chemists. Under *vague words, vogue words*, for instance, he might have included the adjectives novel, elegant, and exquisite; so many compounds are novel, so many syntheses elegant, and so many processes exquisite these days that such words have become almost meaningless.

Unfortunately, the bibliography is inadequate. Comprehensive usage dictionaries, such as *Henry Fowler*'s *A Dictionary of Modern English Usage*, *Wilson Follet*'s *Modern American Usage*, or *A Dictionary of Contemporary American Usage* by *Bergen* and *Cornelia Evans*, are not mentioned. These sources contain more detailed discussions of many of the entries. The book contains few typographical errors, though *Young* should follow his own advice on spelling names correctly (see *names*) and change the name of the corecipient of the 1987 Nobel Prize in physics from Muller to Müller (or, arguably, Mueller) on page 151.

Correct use of language is just one element of style. It is common knowledge that the writing of some of the best stylists violates much conventional word usage, many of the rules of grammar, and all prescribed literary forms. The scientific writer would do well, however, to recall a word of advice from *The Elements of Style* by *William Strunk, Jr.*, and *E. B. White*: "No idiom is taboo, no accent forbidden; there is simply a better chance of doing well if the writer holds a steady course, enters the stream of English quietly, and does not thrash about." Like that classic, *The Technical Writer's Handbook* will help make writing that next paper or report a little easier and certainly more enjoyable. Indeed, pleasure in writing may be the most important element in writing with style and clarity. And remember: "If you have nothing more to say, just stop" (see *conclusions*).

David I. Loewus [NB 1030 IE]
Angewandte Chemie, Weinheim (FRG)

Immobilization of Cells. (Series: Biotechnology Monographs, Vol. 5). By *C. R. Phillips* and *Y. C. Poon*. Springer, Berlin 1988, viii, 167 pp., hardcover, DM 168.00.—ISBN 3-540-18637-9

The "Biotechnology Monographs", dealing in turn with various specific areas of biotechnology, have, within a very short period of time, developed into a series that is greatly valued by others besides biotechnologists.

Whereas most of the previous volumes have been concerned with special biotechnological processes such as the hydrolysis of cellulose, the anaerobic treatment of waste water, and the production of single cell protein, this latest volume is the second one (following that on coenzyme regeneration) to deal with a topic which is not specific to a particular process, namely the immobilization of cells for biological heterogeneous catalysis. In connection with this it is especially relevant to note that immobilized whole cells are now used in many biotechnological processes, and are in some cases an alternative to free cells. The reasons for this are not only the better control and higher cell densities that can be achieved, but also the lower costs, especially for large-scale processes.

The volume is divided into five chapters. Following an introductory chapter the basic techniques of immobilization are described. A broad distinction is made between mechanical containment of cells by pelletizing, encapsulation, or entrapment in polymers on the one hand, and covalent or ionic bonding to inert supports on the other.

By means of suitably chosen examples the third chapter deals with special, though frequently encountered, problems with immobilized cells, such as the inhibition of essential enzymes, or problems of solubility or mass transfer within the biocatalyst. Ways of overcoming these difficulties are suggested.

Chapter 4 focuses on the properties of immobilized biocatalysts, first considering each component of the system (the immobilized cells themselves, their active enzyme system, and the immobilization matrix), then looking at their interactions.

In the final chapter special emphasis is put on the engineering parameters. Variables already familiar from heterogeneous catalysis, such as the catalytic efficiency, the Sherwood number and the Thiele modulus are introduced, and their mathematical and technical relationships are described.

The book aims to provide an overview of the wide-ranging topic of cell immobilization. It gives an excellent account of the principles of the various immobilization methods, which is clear and detailed, citing numerous examples from the literature. It forms a very good introduction to the technology of cell immobilization, and is therefore also suitable as a textbook for advanced students of biology, chemistry, process engineering and biotechnology, although its use for this purpose will be limited to some extent by the relatively high price.

There is, regrettably, no adequately critical discussion of the different immobilization techniques. Also the scale of the processes described and the potential for scale-up are nowhere discussed in detail, and thus no clear distinction is made between laboratory processes and those that can be used on an industrial scale. One area with many applications in research and industry, the immobilization of mammalian cells, e.g. by means of the micro-carrier technique and related methods, is not mentioned at all. Despite these shortcomings, the book offers, both to beginners and to those experienced in the field, a good overview of cell immobilization, with a coverage which one could previously only obtain through a combination of several reviews and specialist articles.

Holger Ziehr [NB 987 IE]
Gesellschaft für Biotechnologische Forschung mbH
Braunschweig (FRG)

Registered names, trademarks, etc. used in this journal, even when not marked as such, are not to be considered unprotected by law.

© VCH Verlagsgesellschaft mbH, D-6940 Weinheim, 1989. – Printed in the Federal Republic of Germany by Konrad Triltsch Druck- und Verlagsanstalt Würzburg.

All rights reserved (including those of translation into foreign languages). No part of this issue may be reproduced in any form — by photoprint, microfilm, or any other means — nor transmitted or translated into a machine language without written permission from the publishers. Only single copies of contributions, or parts thereof, may be made for personal use. This journal was carefully produced in all its parts. Nevertheless, authors, editors and publisher do not warrant the information contained therein to be free of errors. Readers are advised to keep in mind that statements, data, illustrations, procedural details or other items may inadvertently be inaccurate.

Valid for users in the USA: The appearance of the code at the bottom of the first page of an article (serial) indicates the copyright owner's consent that copies of the article may be made for personal or internal use, or for the personal or internal use of specific clients. This consent is given on the condition, however, that the copier pay stated per-copy fee through the Copyright Clearance Center, Inc. (CCC), for copying beyond that permitted by Sections 107 or 108 of the U.S. Copyright Law. This consent does not extend to other kinds of copying, such as copying, for general distribution, for advertising or promotional purposes, for creating new collective works, or for resale. For copying from back volumes of this journal see 'Permissions to Photo-Copy: Publisher's Fee List' of the CCC.

Editorial office: Postfach 10 11 61, D-6490 Weinheim, Federal Republic of Germany, Telephone (06201) 60 22 55, Telex 465 516 vchwh d, Telefax (06201) 602 328.

Editor: *Peter Gölitz*

Associate editors: *D. I. Loewus, A. Stimson.* **Editorial assistant:** *E. Schweikart*

Publishers: VCH Verlagsgesellschaft mbH. (Managing Director: *Hans Dirk Köhler*), Pappelallee 3, D-6940 Weinheim, Federal Republic of Germany.

Advertising office (Advertising Manager *R. J. Roth*): Postfach 10 11 61, D-6940 Weinheim, Federal Republic of Germany, Telephone (0 62 01) 60 61 30, Telex 4 67 155, Telefax (0 62 01) 606 184.

ADVANCED MATERIALS

The Nature of Materials Science Publishing

Editorial Essay

By Peter Gregory *

The materials scientist, whether he thinks of himself as such, or whether he regards himself more as a metallurgist, chemist, physicist, ceramist or engineer must publish the results of his labors to complete the scientific process and to ensure career advancement or continued financial support. This is no different to scientists working in more clearly defined areas but a difference does arise when he consideres to which journal he should submit his manuscript.

As with other scientists, the worker in materials science would obviously wish that his "hot new results" are communicated to as large an audience of interested colleagues as possible. In the more classically defined areas of chemistry, biology, physics etc. there are a number of well established, high quality publications which cater for a specialist audience, as well as one or two highly popular journals which mix quality reports of new research results with articles of a more general nature. These more general articles are intended to bring new developments to the attention of the non-specialist but otherwise scientifically educated reader. These journals are namely *Nature* and *Science*.

This approach produces an excellent forum for the exchange of ideas and opinion across a wide range of disciplines. However, these highly respected journals, while catering well for the molecular biologists, earth scientists and astro- and particle physicists for example, cannot possibly blanket every area of science to an equal degree and therefore have weaknesses in their coverage of certain areas.

The nature of today's materials science is such that the interaction of experts from different fields is not only important but quite often essential and it is therefore unfortunate that those areas which are covered to a lesser extent by the leading journals of general science are just those with the greatest relevance to materials.

In the materials sector there are a large number of specialist journals serving restricted areas of the whole, and a few which purport, through their names, to be of a more general nature, but on closer inspection are found to lack true interdisciplinarity and to publish to a large extent only full papers.

Materials science, with its many facets and contributing technologies is ideally suited to the general forum approach to publishing where research results are combined with opinion, comment and information. The complexity of materials science, and the accompanying plethora of journals each dealing with their own specialist areas have made it increasingly difficult, alone on time grounds, to keep up with the literature in one field while maintaining an all important



overview of other areas. To provide that opportunity is exactly the intended function of *Advanced Materials*, the advent of which has been warmly welcomed, one reviewer[1] being moved to say:

"It is the (materials) journal one would most like to have delivered to a busy desk"

This is an opinion we are sure will be shared by an increasing number of ceramists, chemists, physicists, metallurgists and engineers as we move into what will undoubtedly be a fascinating and exciting future for materials science.

For our part, at *Advanced Materials*, we would like to thank both the readers and editorial team of *Angewandte Chemie* for their interest and support over the last eighteen months during which time the two journals were also published in a joint form. The complete separation of the two journals, which occurs in January, will give us the space and freedom to expand our coverage of all aspects of high-tech materials science while not giving *Angewandte Chemie* too strong a materials bias. We believe that we can provide the materials scientist with a readable, general forum for results and opinion which will help integrate all of our efforts and change the nature of materials science publishing.

[*] Dr. P. Gregory
Advanced Materials
P.O. Box 101161, D-6940 Weinheim (FRG)

[1] A. Windle, *Nature 341* (1989) 369.

ADVANCED MATERIALS

Structural Characterization of Non-Oxide Chalcogenide Glasses using Solid State NMR **

Magic Angle Spinning
Internal Interactions
Selective Averaging
B/Si/P Based Glasses
Infrared Optics
Semiconductor Technology

By Hellmut Eckert *

Dedicated to Prof. W. Müller-Warmuth on the occasion of his 60th birthday

In spite of the long-standing importance of non-oxide chalcogenide glasses in infrared optics and semiconductor technology, concepts describing the structural principles governing glass formation in these systems are just emerging. Most recently, modern quantitative solid state NMR techniques have offered new unique insights into the structural organization of these systems. In this review, we discuss the basic principles of various experimental approaches and their application to boron- silicon,- and phosphorus chalcogenide glasses.

1. Introduction

Non-oxide chalcogenide glasses, which are based on the sulfides, selenides, and tellurides of the main group III–V elements, have recently gained much interest as materials for infrared-transparent optical fibers,[1] reversible conductivity switching devices,[2] semiconductors,[3] photoconductors, photoresists,[4] and solid electrolytes for battery applications.[5] Generally, glasses are often preferred over crystalline compounds because of their favorable mechanical and interfacing characteristics, and because their materials properties can be tailored for specific applications by continuously varying their composition or processing conditions. In the area of non-oxide chalcogenide glasses, however, substantial challenges have remained due to the air- and moisture sensitivity and the low glass transition temperatures of many systems.

Figure 1 shows the most common constituent elements of such glasses. During the last two decades, much work has been devoted to the phase diagrams, regions of glass-formation, and the thermodynamic and physicochemical properties of these systems.[6] It has been much more recently that, driven by the search for structural guidelines to optimize materials properties, the microstructure of these glasses has moved into the focus of attention. At the same time (and for similar reasons) chalcogenide glasses have become an increasingly attractive subject for theoreticians and solid-state physicists.[7–10]

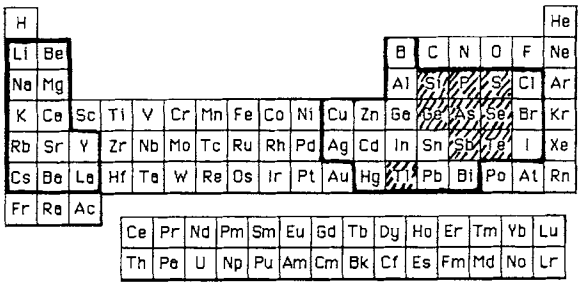


Fig. 1. Elements that participate in the formation of covalent non-oxidic glasses. Dashed lines indicates those elements that occur most commonly in such glasses.

According to most recent spectroscopic studies, the structure of chalcogenide glasses is characterized by several unique features not commonly found in other types of glasses. These features include: a) valence alternation pairs, b) new types of micro-environments not known in analogous crystalline compounds, and c) clusters or polymeric entities with a high degree of intermediate-range order. Figure 2 shows a few recent examples from the literature.

While these novel findings represent substantial progress, they mark only the beginning of a qualitative and quantitative understanding of chalcogenide glasses. The identification and quantification of specific structural features has often remained controversial, since most of the spectroscopic techniques used are not inherently quantitative and tend to emphasize ordered environments. Moreover, the proposals made for individual systems are conceptually somewhat divergent, which reflects a current inability to explain the

[*] Prof. H. Eckert
Department of Chemistry, University of California, Santa Barbara, Goleta, CA 93106 (USA)

[**] The author is very grateful to his scientific mentor, Prof. *W. Müller-Warmuth*, who, a decade ago, introduced him to solid state NMR theory and techniques. Thanks are due to my coworkers at UC Santa Barbara, *M. Drake, D. Lathrop, T. Luong, K. Moran, M. Tullius*, and *Zh. Zhang*, and my collaborators *Dr. J. H. Kennedy* and Dr. *M. Ribes* for their many contributions and stimulating discussions. Acknowledgment is made to the Donors of the Petroleum Research Fund administered by the American Chemical Society for partial support of this research. Financial support by the UCSB Academic Senate is also gratefully acknowledged.

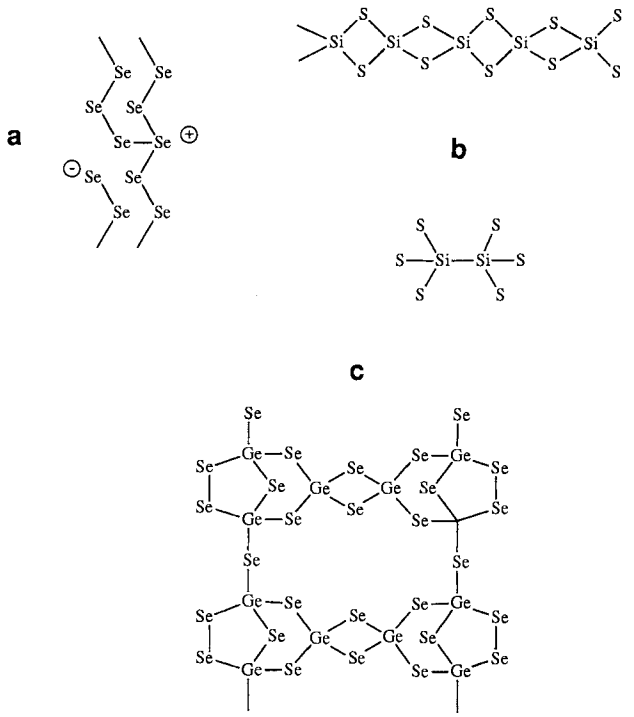


Fig. 2. Unique structural features postulated to occur in non-oxide chalcogenide glasses. a) valence alternation pairs in amorphous selenium [7]. b) edge-shared polymers and ethane-like units in Si–S glasses [8]. c) intermediate-range ordered cluster units in glassy $GeSe_2$ [9].

principles of non-oxide glass formation in more quantitative terms. There is a definite need for new experimental probes that can test the existing structural hypotheses in a more stringent manner than presently possible. Solid state NMR is an element-selective, inherently quantitative method ideally suited for this objective.[11] Since NMR is also spatially very selective, the spectroscopic information remains largely unaffected by the lack of periodicity in non-crystalline systems.

During 25 years of intense research, solid state NMR has proven very useful in developing structural concepts for oxide-based (silicate, borate, and phosphate) glasses.[12] In contrast, the unique power of this technique to provide structural information in chalcogenide systems is just emerging.

2. Information Content of Solid State NMR Spectra in Glasses

2.1. Fundamental Principles of the Technique

All nuclei containing an odd number of either protons or neutrons or both, possess angular momentum ("spin") and consequently, a magnetic moment. In the presence of an applied magnetic field B_0 (typical strength 1–14 T), these nuclei occupy quantized energy levels which are energetically non-degenerate and thus not equally populated. These population differences result in a macroscopic nuclear magnetization along the direction of B_0.

NMR spectroscopy measures the precise energy differences between such nuclear levels; this is done by stimulating transitions between them through the application of electromagnetic waves in the radio frequency region (1–600 MHz). At resonance, the condition

$$\omega = \gamma B_{\mathrm{loc}} \tag{1}$$

holds, where ω is the frequency of the electromagnetic radiation at which absorption occurs, γ is a nuclear constant, and B_{loc} is the strength of the magnetic field present at the nuclear sites. Usually, a short (1–10 μs length), intense (100–1000 W power) radiofrequency pulse is applied by the spectrometer that tips the magnetization into the plane perpendicular to the magnetic field direction ("90° pulse"). The precession of the magnetization in this plane then induces an ac voltage in a coil, which is amplified, detected, and stored in a computer. Fourier analysis of the acquired "free induction decay signal" then yields ω, the nuclear magnetic resonance frequency.

Signal averaging by repetitive pulsing is usually necessary. For truly quantitative information it is mandatory to allow for sufficient time between pulses to restore the magnetization along B_0 to its equilibrium value. The waiting time required depends on the relaxation time T_1 of the nuclei, which can range from a few ms to several hours in glasses.

2.2. Internal Interactions

The usefulness of NMR in addressing structural questions in matter stems from the fact that the magnitude of B_{loc} (and



Hellmut Eckert received his PhD in Physical Chemistry at the Westfälische Wilhelms Universität Münster, FRG, in 1982. After two postdoctoral years at Rutgers University, New Brunswick, New Jersey, he held a position as a staff Scientist at the Southern California Regional NMR Facility at the California Institute of Technology, from 1984–1987. Since July 1987, he has been an Assistant Professor of Chemistry at the University of California, Santa Barbara. Prof. Eckert's research is concerned with the synthesis of novel types of non-oxidic glasses and with the development of modern solid state NMR strategies for the structural analysis of disordered materials.

ADVANCED MATERIALS

hence the nuclear resonance frequency) is usually slightly different from B_0, due to various types of internal interactions: The *magnetic dipole-dipole interaction* describes the effect nearby magnetic moments from other atoms have on the local field of the nuclei under observation. The *chemical shift interaction* describes how the local field is modified by the electron clouds surrounding the nuclei, and finally, the *nuclear electric quadrupole coupling* describes the interaction of the asymmetric charge distribution in spin $> \frac{1}{2}$ nuclei with electrostatic field gradients generated by the chemical bonding environment. Each of these interactions is characterized by a few spectroscopic parameters, listed in Table 1.

Table 1. Interactions in solid state NMR, spectroscopic parameters and their selective measurement.

Interaction	Spectroscopic parameters	Selective measurement	Ref.
dipole-dipole	$M_{2hom.}$ (like nuclei)	$90°$–t_1–$180°$ echo decay	14
	$M_{2het.}$ (unlike nuclei)	$90_x°$–t_1–$90_y°$ echo decay	15
chemical shift	isotropic part, δ_{iso}	MAS-centerline position	13
	anisotropic part	MAS sideband intensities	17
quadrupole	coupling constant (e^2qQ/h)	MAS lineshape analysis, 2-D nutation NMR	16 16
	asym. parameter η	variable angle spinning	18

Mathematically, a tensorial description is used to appropriately reflect the fact that all of these interactions are anisotropic.[11] Consequently, the energy level perturbations (and hence the resonance conditions) depend on the orientation of the crystal (or molecule) with respect to the external magnetic field. Therefore, the spectrum observed in a powder or glass (the "NMR powder pattern") forms the envelope of all resonance conditions arising from all possible orientations.

If one of the three interactions discussed above is much larger than the other ones, the corresponding spectroscopic parameters are usually easily determined from such a powder pattern. However, frequently the various terms are of comparable magnitude, making the spectra difficult to analyze. The situation is complicated further in glasses, where the spectroscopic parameters would be more accurately represented in the form of distribution functions rather than unique values.

The NMR problem thus falls into two sub-tasks: a) accurate parametrization of the experimental spectra and b) correlating the spectroscopic parameters thus obtained with the desired structural information.

2.3. Selective Averaging Experiments

The first task is often approached by modifying the relative magnitudes of different interactions in a predictable fashion. Traditionally, this has been done by exploiting field dependence, isotopic dilution, or different isotopes of the same element. Alternatively, elegant selective averaging techniques that suppress certain interactions while leaving others unaffected are being increasingly utilized. Table 1 contains some of the approaches which are most generally applicable.[13–18] In the following, we will discuss briefly two of these techniques, which are of particular interest for the material covered in this review.

The first, most popular, selective averaging experiment uses mechanical sample rotation about an axis inclined by an angle β with respect to the external magnetic field direction.[13] This manipulation modulates the anisotropic part of the interaction by the term $(3\cos^2\beta - 1)$. At an angle of 54.7° the orientational dependence of the spectra is removed and a sharp, "liquid-like" resonance is observed at the isotropic chemical shift position. Solid state NMR spectra acquired with this technique are referred to as "MAS" (magic angle spinning) spectra. The isotropic chemical shift δ_{iso}, which is usually quoted in ppm with respect to a chosen reference standard (tetramethyl silane for ^{29}Si, 85% phosphoric acid for ^{31}P NMR), is the single most significant NMR observable for compound identification.

The second experiment involves the selective measurement of magnetic dipole-dipole couplings.[14, 15] The magnitude of the dipolar coupling is most commonly expressed in terms of the second moment M_2, the average squared local field present at the nuclei due to these interactions. This particular description in terms of a statistical quantity has the advantage that the details of the spin system (numbers and relative geometries of the interacting nuclei involved) need not be known for the analysis, and that homonuclear interactions (between like spins) and heteronuclear interactions (between unlike spins) can be separated.[19] The homonuclear part of M_2 can be measured selectively by spin-echo spectroscopy. Figure 3 illustrates the concept. In general, the free induction decay following a 90° radio frequency pulse on resonance can be refocused by a subsequent 180° pulse, resulting in a

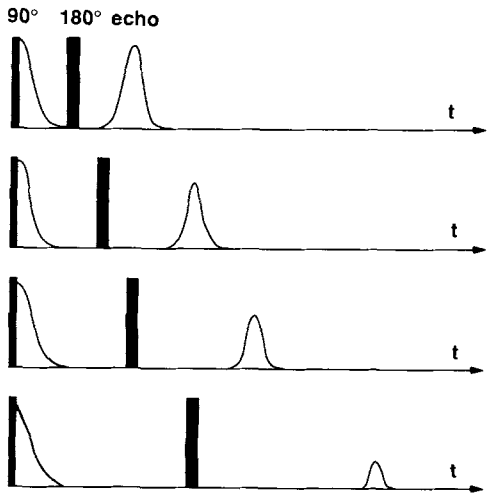


Fig. 3. NMR spin echo decay method for measuring homonuclear dipole-dipole couplings.

"spin echo" at a time $2t_1$ after the initial 90° pulse, where t_1 is the time delay between both pulses. Dipolar interactions among like nuclei, however, interfere with the refocusing process. Consequently the echo is diminished, depending on the length of the evolution time $2t_1$, i.e. the period over which the dipole coupling is operative.[14, 15] Very often, the echo height $I(2t_1)$ shows a Gaussian decay, whose steepness depends on the strength of the homonuclear interaction characterized by the second moment M_{2h}:

$$I(2t_1)/I(0) = \exp[-(2t_1)^2 M_{2h}/2] \quad (2)$$

Since most of the other solid state interactions are refocused by the above sequence, the measurement of the echo height under systematic incrementation of the evolution time $2t_1$ often affords a selective measurement of M_{2h} from the semi-logarithmic plot defined by Equation 2.

2.4. Correlation of NMR Parameters with Structural Information

Once the correct spectroscopic parameters have been extracted, the information needs to be related to concrete structural information. Important information is often already obtained from a detailed inspection of the compositional dependence of the spectra. Furthermore, the use of crystallographically well defined reference compounds is indispensible. These methodologically simple approaches are often combined with spectroscopic simulations based on computer-modeled trial structures. Of the various interactions summarized above, only the dipolar coupling is calculable from first principles. In contrast, the interpretation of chemical shifts and quadrupolar coupling constants requires the use of semi-empirical correlations. Furthermore, the specific information that can be obtained depends highly on the certain "personality" of the nucleus under study. Table 2 gives a summary of the basic properties of nuclei typically part of chalcogenide glasses. We will limit our discussion to ^{11}B, ^{29}Si, and ^{31}P, the prototype constituents of the glasses reviewed here.

^{11}B. ^{11}B NMR data in glasses show discrete sites B_3 and B_4, with triangular and tetrahedral coordination symmetries, respectively. These sites are separated by ca. 20 ppm in high-field ^{11}B MAS-NMR spectra,[20] and quantitative integration of the spectra yields N_4, the fraction of four-coordinate boron atoms:

$$N_4 = [B_4]/([B_4] + [B_3]) \quad (3)$$

A spectral separation can also be accomplished from traditional low-field NMR spectra on the basis of nuclear electric quadrupolar interactions.[12]

^{29}Si. ^{29}Si NMR data in glasses are usually interpreted in terms of various types of SiO_4 coordination polyhedra differing in the number of bridging Si–O–Si units. This is expressed by the $Q^{(n)}$ nomenclature, where n specifies the number of such bridges per silicon present. A large number of studies have been devoted to obtaining detailed quantitative information about the $Q^{(n)}$ speciation from MAS NMR data in crystalline silicates and silicate glasses.[21] Specifically, the NMR results on alkali-metal silicate glasses are in good agreement with the traditional network modification model, in which one mole of alkali-metal oxide generates two non-bridging oxygen atoms (see Figure 4).

Table 2. Nuclear properties of magnetic isotopes present in chalcogenide glasses.

nucleus	spin	natl. abund. [%]	resonance frequency at 7.05 T	comments on suitability for structural analysis in chalcogenide glasses
^{7}Li	3/2	92.58	116.59	sensitive, but limited range of δ
^{6}Li	1	7.42	44.15	limited range of δ, superior in resolution to ^{7}Li
^{11}B	3/2	80.42	96.25	sensitive, limited range of δ, MAS complicated by quadrupole effects
^{23}Na	3/2	100	79.35	sensitive, limited range of δ, MAS complicated by quadrupole effects
^{27}Al	5/2	100	78.17	sensitive, MAS complicated by quadrupole effects
^{29}Si	1/2	4.70	59.70	very long relaxation times (~ 1 h) wide range of δ small chemical shift anisotropies.
^{31}P	1/2	100	121.44	very sensitive, wide range of δ, large chemical shift anisotropies moderately long relaxation times
^{33}S	3/2	0.76	23.01	difficult to detect
^{73}Ge	9/2	7.76	10.47	large quadrupole moment,
^{75}As	3/2	100	51.38	poor resolution.
^{77}Se	1/2	7.58	57.20	difficult to detect, wide δ-range,
^{125}Te	1/2	7.00	94.79	extremely large chemical shift anisotropy, long relaxation times
^{205}Tl	1/2	70.50	173.12	very sensitive, wide δ range, extremely broad lines, difficult to detect with high-field instruments

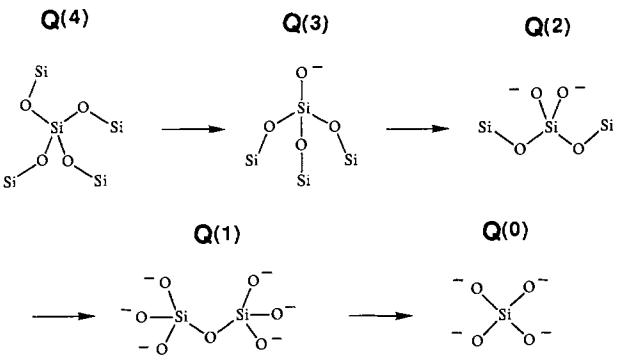


Fig. 4. Structural modification of silica glass by alkali-metal oxide modifiers, giving rise to the various $Q^{(n)}$ species. The arrow indicates increasing concentration of the modifier oxide.

ADVANCED MATERIALS

^{31}P. ^{31}P MAS-NMR has been used in a similar fashion to provide $Q^{(n)}$ speciation in a variety of phosphates and phosphate glasses.[22] In addition valuable information is available from the measurement of the internuclear ^{31}P–^{31}P interactions. Under rigid lattice conditions, M_{2h} (^{31}P) can be calculated from van Vleck theory:[19]

$$M_{2d} = 4/15\ (\mu_0/4\pi)^2\ I\ (I+1)\ \gamma^4\ \hbar^2\ N^{-1} \sum_{i \neq j} r_{ij}^{-6} \qquad (4)$$

where γ_I, I, N, and r_{ij} represent the ^{31}P gyromagnetic ratio, the spin quantum number (½), the number of nuclei involved, and the distances between them respectively. Equation 4 permits a direct calculation of an M_2 value from an assumed structure. The selective measurement of internuclear ^{31}P–^{31}P interactions affords a powerful tool for testing atomic distribution models in chalcogenide glasses.

3. Chalcogenide Glasses

3.1. Boron Based Glasses

Solid state NMR has been instrumental in the investigation of compound and glass formation in the systems B–S, B–Se, and B–S–Se.[23, 24] Specifically, NMR confirms that the structure of glassy B_2S_3 is based on the triangular $BS_{3/2}$ unit. In contrast, no such unit can be identified in corresponding B–Se glasses.[24] The composition "B_2Se_3" disproportionates into BSe_2 and an amorphous yellowish selenide B_xSe, which, according to the strong internuclear dipole couplings detected by NMR, must contain boron–boron bonds. This reflects the increasingly efficient competition of homoatomic (B–B and Se–Se) versus heteroatomic (B–Se) bond formation as the size of the chalcogen atom is increased.

Glassy B_2S_3 has a more uniform structure than glassy B_2O_3.[24] Nevertheless, the structural modification of B_2S_3 by Li_2S[25, 26] and Tl_2S[27] is an excellent analogy to the well-studied behavior of borate glasses.[12] Glasses in the systems $(Li_2S)_x(B_2S_3)_{1-x}$ and $(Tl_2S)_x(B_2S_3)_{1-x}$ are formed for $0 \leq x \leq 0.75$, with phase separation occurring at low x-values. In both cases, small amounts of Li_2S and Tl_2S cause a network transformation resulting in the production of four-coordinate boron atoms. Above a ratio $Li_2S(Tl_2S)/B_2S_3$ of 0.5, the number of four-coordinate boron atoms decreases again, because units containing non-bridging sulfur atoms are formed in this regime. This compositional dependence of N_4 is in good agreement with the respective oxygen-based systems.[12, 28]

3.2. Silicon Based Glasses

Besides offering promise for applications in infrared optics and semiconductor technology, silicon chalcogenide glasses are of fundamental interest in glass science. Vibrational spectroscopic data suggest that the structure of these glasses contains linear chain polymers composed of edge-sharing $SiSe_{4/2}$ units.[29] This finding is a striking exception from the general rule that glasses organize exclusively by corner-sharing of coordination polyhedra.

Figure 5 shows typical ^{29}Si MAS-NMR spectra in the system silicon–selenium.[30] Note that multiple sites are present, even in the stoichiometric glass of composition $SiSe_2$. The spectra show three distinct resonances which are assigned to Si atoms involved in zero, one and two edge-sharing tetrahedra, labeled $E^{(0)}$, $E^{(1)}$, and $E^{(2)}$ in Figure 5.[31] Increasing the selenium content in the glasses favors corner sharing. The evaluation of these units is made difficult by the extremely long T_1 values in these glasses.[30, 31] Absolute signal intensity calibrations with standards containing known amounts of silicon show that with 90° pulses and recycle delays of 2 h, 85–95% of the total Si atoms are detected in these systems.[30] This control experiment ensures that the speciation inferred from NMR is truly representative of the entire glass.

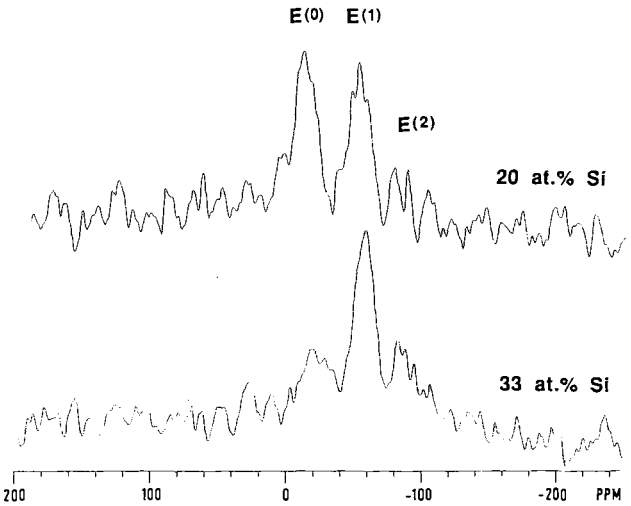


Fig. 5. ^{29}Si MAS-NMR spectra of glasses in the system Si–Se. The resonances are assigned to (from left to right in order of increasing field): corner-sharing $SiSe_{4/2}$ tetrahedra ($E^{(0)}$), $SiSe_{4/2}$ groups involved in one edge-sharing tetrahedron ($E^{(1)}$), and $SiSe_{4/2}$ groups involved in two edge-sharing tetrahedra ($E^{(2)}$), respectively. Note the compositional dependence. The poor signal-to-noise ratio arises from the extremely long spin-lattice relaxation times in these samples, requiring recycle delays of 2 h.

Lithium silicon sulfide glasses show promise for solid electrolyte applications.[32] The region of glass-formation of the system $(Li_2S)_x$-$(SiS_2)_{1-x}$ ranges from $x = 0$ to $x = 0.6$ (glasses formed in the compositional region $0 < x < 0.4$ may be phase separated). Given the unusual structural properties of the parent SiS_2 and $SiSe_2$ glasses, new types of microstructures might be expected in the glasses modified analogously by alkali metal sulfides. A detailed ^{29}Si MAS NMR study of the system Li_2S-SiS_2 was undertaken to test whether the $Q^{(n)}$

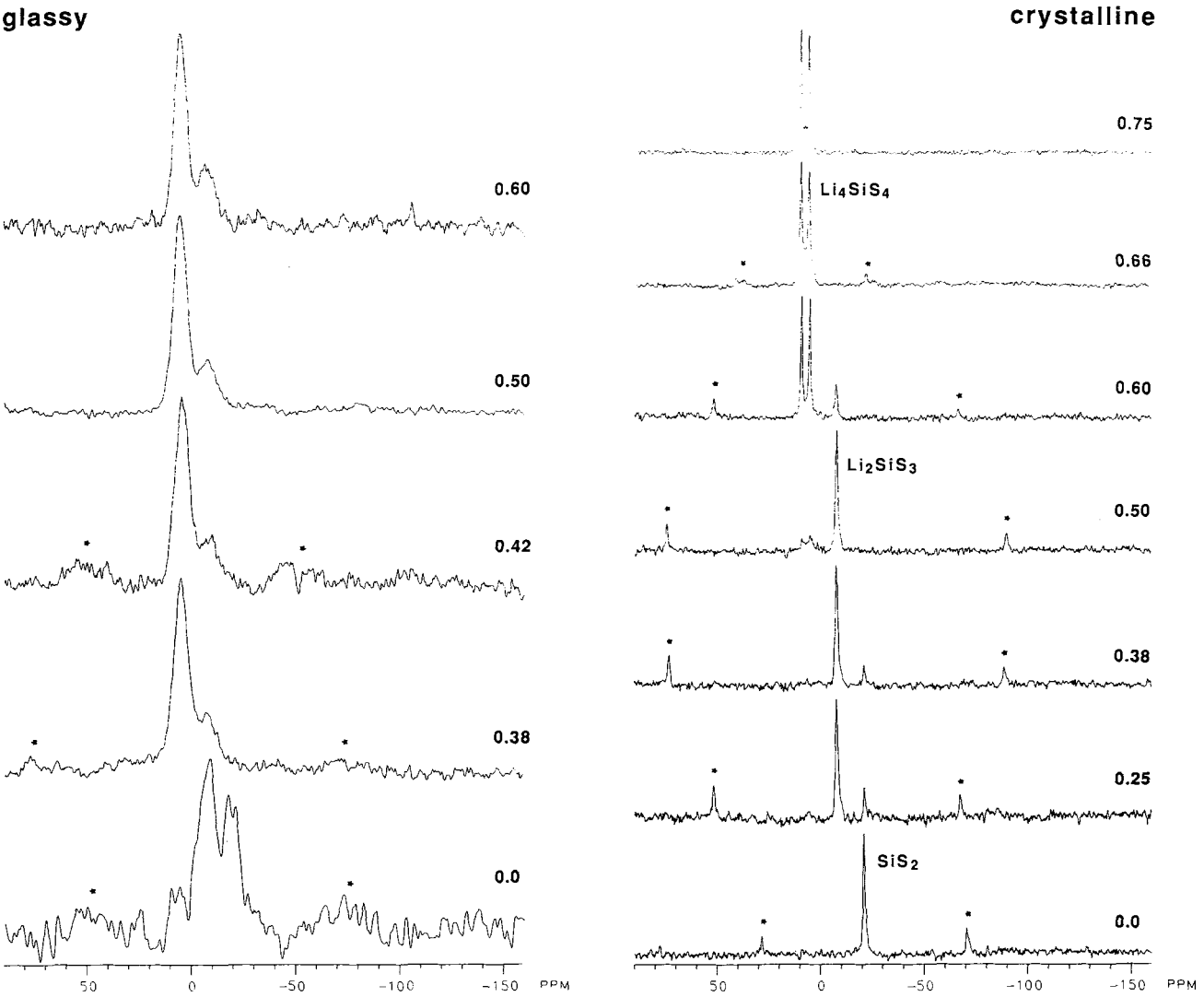


Fig. 6. 59.9 MHz ^{29}Si MAS-NMR spectra of glassy and crystalline samples in the system $(Li_2S)_x(SiS_2)_{1-x}$. For $x \geq 0.4$, the spectra show no obvious chemical shift evolution in the glasses, in contrast to the situation in the crystalline phases.

concept valid in the oxidic glasses (Figure 4) is also applicable to sulfide-based glasses.[33] The results are shown in Figure 6. Virtually no compositional evolution can be detected in the ternary glasses, whereas the corresponding crystallized specimens reveal marked changes. These findings were initially interpreted in terms of a constant number of non-bridging sulfur atoms regardless of Li_2S content. The two resonances were assigned to $Q^{(0)}$ species (major resonance around 4–8 ppm) and $Q^{(2)}$ species (minor peak around -6 to -10 ppm), based on previous assumptions in the literature[34] that the structures of Li_4SiS_4 and Li_2SiS_3 contain corner shared $Q^{(0)}$ and $Q^{(2)}$ environments (no single crystal X-ray work has been carried out). The original interpretation dismisses the traditional model of continous network modification and invokes a number of non-bridging sulfur atoms that is much larger than expected from the Li_2S content.

Subsequent work on a larger number of better characterized crystalline alkali thiosilicates[35] suggests that the chemical shift discrimination seen in the spectra of Figure 6a is most likely not due to the various $Q^{(n)}$ species but due to the number of edge sharing tetrahedra, $E^{(n)}$, in which the Si atom under consideration is involved.[36] According to this reinterpretation, the majority peak around 4–8 ppm arises from Si atoms involved exclusively in corner sharing with other tetrahedra ($E^{(0)}$), while the minority peak around -6 to -10 ppm is assigned to units engaging in edge-sharing with one other SiS_4 tetrahedron ($E^{(1)}$). Based on these assignments, the spectra reveal that Li_2S decreases the amount of edge-sharing dramatically, such that no $E^{(2)}$ units remain at 38 mole-% Li_2S or above. The work on the crystalline model compounds suggests further, that the chemical shift differences between Si atoms containing different numbers of non-bridging S atoms (i.e. the sulfide-analogs of the various $Q^{(n)}$

ADVANCED MATERIALS

species of Figure 4) are much smaller in sulfides than in oxides. Given the inherently broad MAS-NMR lines in the glasses, it is not possible to resolve individual peaks for these species. Therefore, there is no proof from NMR that the $Q^{(n)}$ concept is actually valid in sulfide glasses. If, however, the assumption is made as a working hypothesis, one arrives at the peak assignments summarized in Figure 7 in the form of

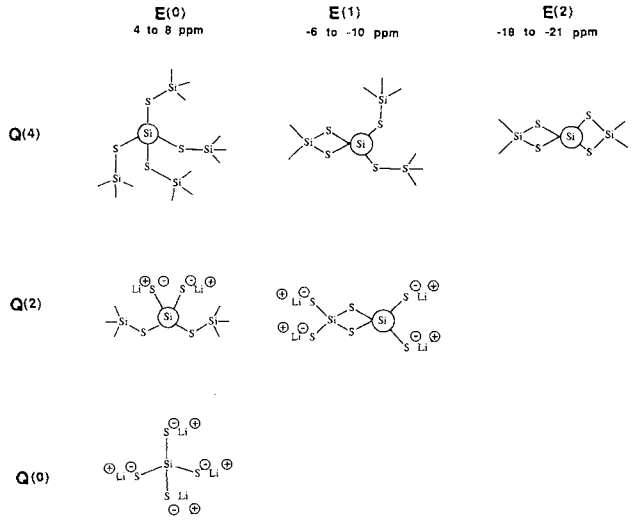


Fig. 7. Suggested peak assignments in the system Li_2S–SiS_2.

a matrix. Each microstructure can be represented by a $Q^{(n)}$ *and* an $E^{(n)}$ symbol. The NMR spectra then show that, at low Li_2S contents, the production of non-bridging sulfur atoms preferably occurs at the $E^{(1)}$ and $E^{(2)}$ sites. The constant ratio of $E^{(0)}$ to $E^{(1)}$ units at higher Li_2S contents suggests that some balance has been attained between the destruction of edge- and corner-sharing Si–S–Si units.

3.3. Phosphorus Based Glasses

Both the binary systems P–S and P–Se are well known to form stable glasses, with P concentrations ranging from 0–25 at.-% P in the former, and 0–52 as well as 62–80 at.-%.P in the latter system.[37–41] Phosphorus–Selenium glasses are of particular interest because of their infrared-transparency, their comparatively high stability in a moist atmosphere, and their resistance towards recrystallization. The microscopic structure of these glasses has been the subject of an interesting controversy. On the one hand, *Borisova* et al.[37] as well as *Blachnik* and coworkers[38] propose what basically amounts to a chemically ordered continuous random network model: at P contents below 40 at.-% the glasses contain $Se=PSe_{3/2}$, $PSe_{3/2}$ and Se–Se units only, whereas no P–P bonds exist. Above 40 at.-% P, these authors suggest an abrupt increase in the fraction of P–P bonds, hence rationalizing the steep increase of glass transition temperatures which is experimentally observed in this compositional region.

In sharp contrast, combined EXAFS and neutron diffraction studies point toward an entirely different glass structure based on P_4Se_n clusters ($5 \geq n \geq 3$, depending on the P/Se ratio) which are embedded in an Se-rich matrix.[42] Such an arrangement constitutes substantial intermediate range order, as has been recently suggested for other glass systems.

The two conflicting models differ largely with respect to the distribution of the P atoms in space. Figure 8 shows three

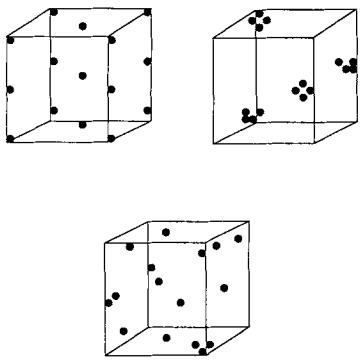


Fig. 8. Simple atomic distribution models for P atoms in P–Se glasses, corresponding to uniform, clustered, and random arrangements.

simplistic atomic distribution models for P–Se glasses, corresponding to a) a uniform, b) a clustered and c) a random distribution of P atoms. These arrangements are clearly distinguishable by the magnitude and the compositional dependence of the dipole-dipole couplings between the ^{31}P nuclear spins. Thus, using the spin-echo sequence discussed in Section 2, the second moments characterizing these internuclear

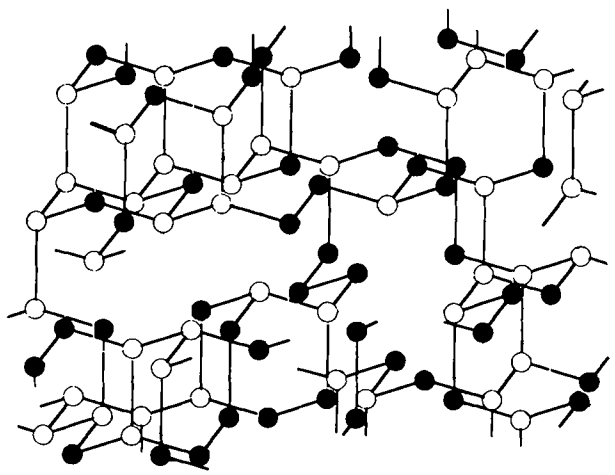


Fig. 9. Graphical illustration of the randomly occupied zinc blende structure used as a model for a P–Se glass containing 50 at.-% P. Open circles denote P atoms, filled circles Se atoms. The dotted lines represent non-bonding electron pairs pointing towards a vacancy in the structure.

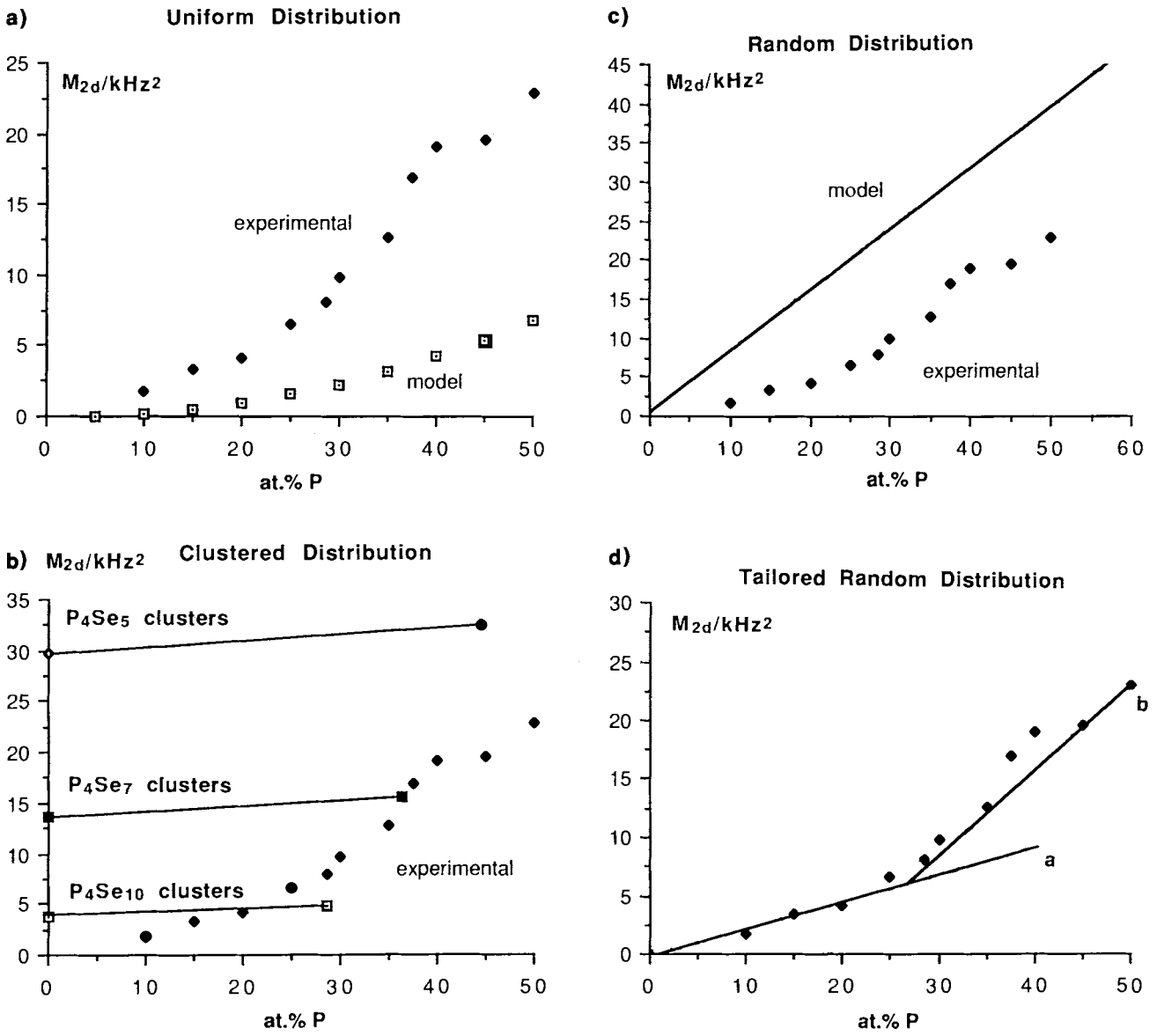


Fig. 10. Comparison of the compositional dependence of the ^{31}P dipolar second moment characterizing the strength of homonuclear ^{31}P–^{31}P dipolar interactions with calculations based on assumed atomic distribution models in P–Se glasses. See text for further discussion. The tailored random distribution assumes that no P–P bonds are present below 25 at.-% P (line a) and a probability of (X-25%) at all compositions with higher P contents X at.-% (line b).

interactions can be measured and compared with calculated values (using Equation 4) based on various assumed distribution models.

In order to simulate a random distribution, the P and Se atoms are positioned irregularly, according to their atomic percentages, over the sites of a cubic zinc blende structure. The chosen lattice constant (5.289 Å) constrains the nearest neighbor distance to 2.29 Å, corresponding to the average of typical P–P, P–Se, and Se–Se bond lengths. Furthermore, the random model incorporates the valency constraints of P and Se by distributing nonbonding electron pairs over additional lattice positions. Figure 9 shows an example of a random distribution generated in this way. This model reproduces the experimental densities of the glasses quite well (within 5–10%).

The comparison between calculated and experimental M_2 values is shown in Figure 10. Clearly, the experimental data are incompatible with either uniform, clustered or random distribution models. If however, the random model is adapted in terms of a reduced probability of P–P bonds, an excellent fit to the experimental data can be obtained. The comparison of Figure 10c with 10d indicates that, at any composition within the glass forming region, there is a distinct preference for P–Se over P–P bonds. Overall, the NMR results can be understood in terms of a random distribution of P and Se atoms over a glass structure, modeled as a defect

ADVANCED MATERIALS

zinc blende lattice, excluding P–P bonds below 25 at.-% P and admitting them in less than statistical proportions above 25 at.-%.[43,44]

While such dipolar measurements provide important insights concerning the statistics of P–P versus P–Se bonding in these glasses, they are unable to identify the distinct nearest neighbor environments present. Such information can be provided by MAS-NMR in conjunction with data obtained on crystalline reference compounds.[44–46] Figure 11 shows typical results in the P–Se system.[45] At P contents below 30 at.-%, two well-resolved peaks are observed which

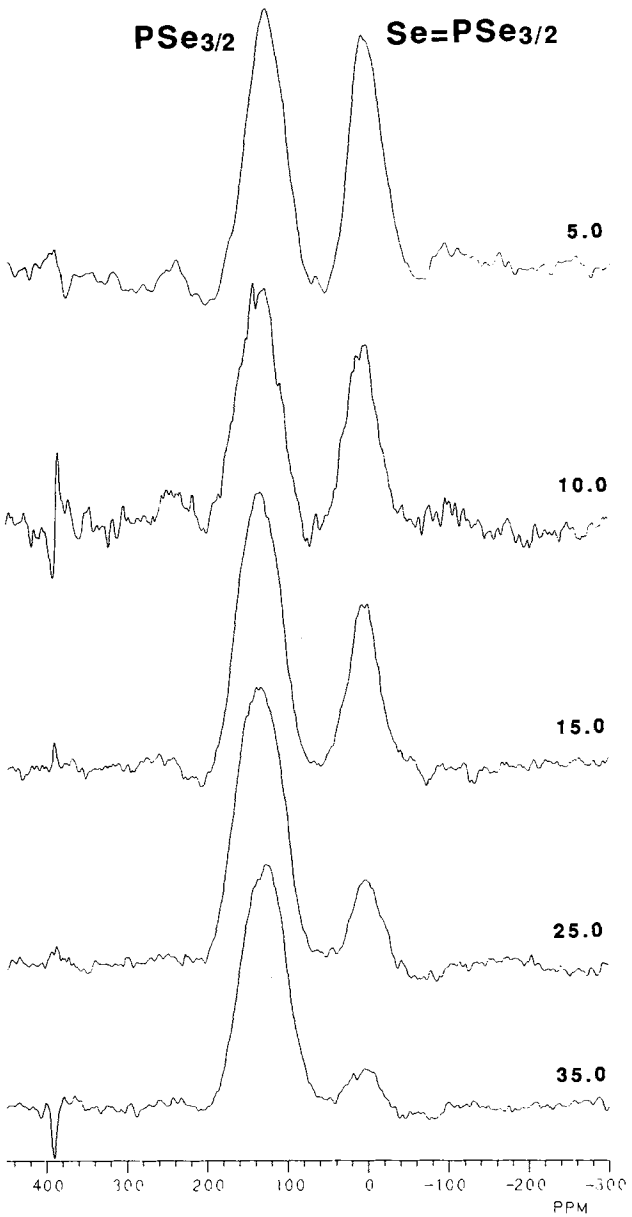


Fig. 11. 121.5 MHz ^{31}P MAS-NMR spectra of P–Se glasses. Numerals indicate at.-% phosphorus. The two resonances are assigned to three-coordinated ($PSe_{3/2}$ and $Se_{2/2}P–PSe_{2/2}$, downfield resonance, left) and four coordinated $Se=PSe_{3/2}$ species (upfield resonance, right), respectively.

are assigned to three-coordinated $PSe_{3/2}$ and tetrahedral $Se=PSe_{3/2}$ groups, respectively.

Quantitative integration of these spectra yields a phenomenological equilibrium constant K of 0.85 (at.-fraction)$^{-1}$ associated with the melt reaction $PSe_{3/2} + [Se_n]_{1/n} \rightarrow Se=PSe_{3/2}$. Figure 12 shows the experimental data for the fraction N_4 of

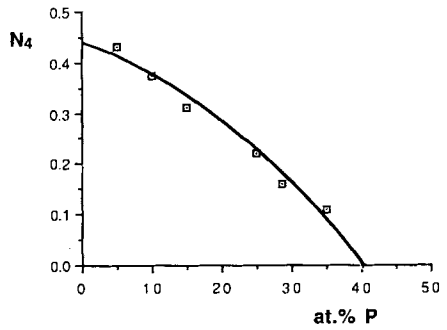


Fig. 12. Dependence of the fraction of four-coordinated $Se=PSe_{3/2}$ units, N_4, (open squares) on the atomic fraction of P atoms in P–Se glasses. The solid curve is calculated based on an equilibrium constant K = 0.85 (at.-fraction)$^{-1}$ of the reaction $PSe_{3/2} + Se \rightarrow Se=PSe_{3/2}$.

the four-coordinate P atoms as a function of composition and the corresponding theoretical fit. The near-unity value of K reflects the efficient competition of the three entities that take part in the above reaction, hence providing a thermodynamic rationale for the excessive tendency of glass-formation in this system.

It is interesting to compare these results with corresponding data obtained on the system P–S.[47] According to ^{31}P MAS and spin echo NMR data, the $S=PS_{3/2}$ grouping is the dominant structural unit within the entire glass forming region. This leads to crystallization of P_4S_9 and P_4S_{10} above 25 at.-% P. In fact, MAS-NMR studies of P–S glasses detect molecular P_4S_9 and P_4S_{10} entities well below the compositional glass-forming border. Likewise, NMR detects P_4Se_3 molecules in P–Se glasses with P contents well below the stoichiometry of this compound.[45] The presence of such molecular entities near and somewhat below the glass-forming border appears to be a general feature of glass formation in phosphorus chalcogenide systems.

4. Summary and Outlook

The experimental results covered in this review show that the degree to which the structural principles operative in non-oxide chalcogenide glasses differ from the bonding concepts used in the stoichiometrically analogous oxidic glasses depend greatly on the system under study. Specifically, in boron chalcogenide-based systems, there seems to be very close similarity between oxides and sulfides. In contrast, the edge-shared micro-environments identified in SiS_2, Si–Se,

and Li_2S–SiS_2 glasses are fundamentally new structures not known to exist in ordinary silica-based glasses. The latter statement also holds true for phosphorus chalcogenide glasses. Specifically in the P–Se glasses, there is a multitude of micro-environments, containing three- and four coordinate P atoms as well as various P–P bonded structures and, near the glassforming border, molecular cluster units.

The attractiveness of NMR spectroscopy for these systems lies in the opportunity of providing actual percentages with which these structural features occur, provided the experiments are done under quantitative conditions. Due to their element-selectivity, NMR methods have a decisive advantage over other competing structural probes for the compositionally more complex systems usually encountered in "real-life" practical applications. This advantage has already been exploited in our NMR studies of the co-former effect in Li_2S–B_2S_3–P_2S_5 and Li_2S–SiS_2–P_2S_5 glasses.[25,48] The studies reported here have laid the groundwork for such further investigations and the author hopes that this review will help to popularize the use of quantitative solid state NMR techniques in the structural elucidation of chalcogenide glasses.

Received: July 17, 1989

[1] P. C. Taylor, *Mater. Res. Soc. Bull. 1987*, p. 36. A. M. Andriesh, *J. Non-Cryst. Solids 77/78* (1985) 1219. A. R. Hilton, C. E. Jones, M. J. Brau, *Infrared Phys. 4* (1964) 213.
[2] S. R. Ovshinsky, *Phys. Rev. Lett. 21* (1968) 1450.
[3] M. Kastner, *J. Non-Cryst. Solids 35–36* (1980) 807. D. Adler, *J. Non-Cryst. Solids 73*, (1985) 205, and references therein.
[4] R. G. Brandes, F. P. Laming, A. D. Pearson, *Appl. Opt. 9* (1970) 1712.
[5] S. Sahami, S. W. Shea, J. H. Kennedy, *J. Electrochem. Soc. 132* (1985) 985. J. H. Kennedy, S. Sahami, S. W. Shea, Z. Zhang, *Solid State Ionics 18/19* (1986) 368.
[6] For early seminal work on glass formation in chalcogenide systems, see A. R. Hilton, C. E. Jones, M. Brau, *Phys. Chem. Glasses 7* (1966) 105. B. T. Kolomiets, *Phys. Status Solidi 7* (1964) 359, 713. See also: Z. U. Borisova: *Glassy Semiconductors*, Plenum Press, New York 1981, and references therein.
[7] S. A. Dembovskii, E. A. Chechetkina, *J. Non-Cryst. Solids 85* (1986) 364. J. Bicerano, S. R. Ovshinsky, *J. Non-Cryst. Solids 74* (1985) 75.
[8] M. Tenhover, M. A. Hazle, R. K. Grasselli, *Phys. Rev. B29* (1984) 6732. R. W. Johnson, D. L. Price, S. Susman, M. Arai, T. I. Morrison, G. K. Shenoy, *J. Non-Cryst. Solids 83* (1986) 251.
[9] P. Boolchand, *Hyperfine Interact. 27* (1986) 3. J. C. Phillips, *J. Non-Cryst. Solids 43* (1981) 37. J. C. Phillips, *ibid 34* (1979) 153.
[10] Comprehensive discussions of the structural problem in glasses can be found in R. Zallen: *The Physics of Amorphous Solids*, Wiley, New York 1983; R. A. Weeks, *J. Non-Cryst. Solids 73* (1985) 103. For recent molecular dynamics simulations, see C. A. Angell, *J. Non-Cryst. Solids 73* (1985) 1. P. Vashishta, R. K. Kalia, I. Ebbsjö, *J. Non-Cryst. Solids 106* (1988) 301. G. A. Antonio, R. K. Kalia, P. Vashishta, *J. Non-Cryst. Solids 106* (1988) 305.
[11] For an excellent review of solid state NMR, see T. M. Duncan, C. R. Dybowski, *Surf. Sci. Rep. 1* (1981) 157. See also M. Mehring: *Principles of High Resolution NMR in Solids*, Springer, Heidelberg 1983.
[12] Comprehensive reviews of NMR applications to glasses can be found in W. Müller-Warmuth, H. Eckert, *Phys. Rep. 88* (1982) 91. P. J. Bray, *J. Non-Cryst. Solids 73* (1985) 19. G. L. Turner, R. J. Kirkpatrick, S. H. Risbud, E. Oldfield, *Am. Ceram. Soc. Bull. 66* (1987) 656.
[13] E. R. Andrew, A. Bradbury, R. G. Eades, *Nature 183* (1959) 1802. I. J. Lowe, *Phys. Rev. Lett. 2* (1959) 285.
[14] M. Engelsberg, R. E. Norberg, *Phys. Rev. B5* (1972) 3395.
[15] N. Boden, M. Gibb, Y. K. Levine, M. Mortimer, *J. Magn. Reson. 16* (1974) 471.
[16] A. P. M. Kentgens, J. J. M. Lemmens, F. M. M. Geurts, W. S. Veeman, *J. Magn. Reson. 71* (1987) 62. A. Samoson, E. Kundla, E. Lippmaa, *J. Magn. Reson. 49* (1982) 350.
[17] M. M. Maricq, J. S. Waugh, *J. Chem. Phys. 70* (1979) 3300. J. Herzfeld, A. E. Berger, *J. Chem. Phys. 73* (1980) 6021.
[18] S. Ganapathy, S. Schramm, E. Oldfield, *J. Chem. Phys. 77* (1982) 4360.
[19] J. H. Van Vleck, *Phys. Rev. 74* (1948) 1168.
[20] G. L. Turner, K. A. Smith, R. J. Kirkpatrick, E. Oldfield, *J. Magn. Reson. 67* (1986) 544.
[21] E. Lippmaa, M. Mägi, A. Samoson, G. Engelhardt, A. R. Grimmer, *J. Am. Chem. Soc. 102* (1980) 4889. K. A. Smith, R. J. Kirkpatrick, E. Oldfield, D. M. Henderson, *Am. Mineral. 68* (1983) 1206. A. R. Grimmer, M. Mägi, M. Hähnert, H. Stade, A. Samoson, W. Wieker, E. Lippmaa, *Phys. Chem. Glasses 25* (1984) 105. R. Dupree, D. Holland, P. W. McMillan, R. F. Pettifer, *J. Non-Cryst. Solids 68* (1984) 399. J. B. Murdoch, J. F. Stebbins, I. S. E. Carmichael, *Am. Mineral. 70* (1985) 332. R. J. Kirkpatrick, K. A. Smith, R. A. Kinsey, E. Oldfield, *Am. Mineral. 70* (1985) 106. E. Schneider, J. F. Stebbins, A. Pines, *J. Non-Cryst. Solids 89* (1987) 371.
[22] G. L. Turner, K. A. Smith, R. J. Kirkpatrick, E. Oldfield, *J. Magn. Reson. 70* (1986) 408. M. Villa, K. R. Carduner, G. Chiodelli, *J. Non-Cryst. Solids 94* (1987) 101.
[23] M. Rubinstein, *Phys. Rev. B14* (1976) 2778.
[24] H. U. Hürter, B. Krebs, H. Eckert, W. Müller-Warmuth, *Inorg. Chem. 24* (1985) 1288.
[25] Z. Zhang, J. H. Kennedy, J. Thompson, S. Anderson, D. A. Lathrop, H. Eckert, *Appl. Phys. A* (1989) *49* (1989) 41.
[26] D. E. Hintenlang, P. J. Bray, *J. Non-Cryst. Solids 69* (1985) 243.
[27] H. Eckert, W. Müller-Warmuth, W. Hamann, B. Krebs, *J. Non-Cryst. Solids 65* (1984) 53.
[28] J. F. Baugher, P. J. Bray, *Phys. Chem. Glasses 10* (1969) 77.
[29] M. Tenhover, R. S. Henderson, D. Lukco, M. A. Hazle, R. K. Grasselli, *Solid State Commun. 51* (1984) 455. M. Tenhover, M. A. Hazle, R. K. Grasselli, *Phys. Rev. Lett. 51* (1983) 404.
[30] K. Moran, R. Shibao, H. Eckert, unpublished.
[31] M. Tenhover, R. D. Boyer, R. S. Henderson, T. E. Hammond, G. A. Shreve, *Solid State Commun. 65* (1988) 1517.
[32] J. H. Kennedy, Z. Zhang, *J. Electrochem. Soc. 135* (1988) 859.
[33] H. Eckert, Z. Zhang, J. H. Kennedy, *J. Non-Cryst. Solids*, 107 (1989) 271.
[34] A. Haas, *Angew. Chem. Int. Ed. Engl. 4* (1965) 1014; *Angew. Chem. 77* (1965) 1066. A. Weiss, G. Rocktaeschel, *Z. Anorg. Allg. Chem. 307* (1960) 1.
[35] J. Olivier-Fourcade, J. C. Jumas, M. Ribes, E. Phillipot, M. Maurin, *J. Solid State Chem. 23* (1978) 155. B. Krebs, *Angew. Chem. Int. Ed. Engl. 22* (1983) 113; *Angew. Chem. 95* (1983) 113.
[36] H. Eckert, J. H. Kennedy, A. Pradel, M. Ribes, unpublished.
[37] Z. U. Borisova, B. E. Kasatkin, E. I. Kim, *Izv. Akad. Nauk SSSR Neorg. Mater. 9* (1973) 822.
[38] R. Blachnik, A. Hoppe, *J. Non-Cryst. Solids 34* (1979) 191.
[39] F. Heyder, D. Linke, *Z. Chem. 13* (1973) 480.
[40] Y. Monteil, H. Vincent, *J. Inorg. Nucl. Chem. 37* (1975) 2053.
[41] Y. Monteil, H. Vincent, *Z. Anorg. Allg. Chem. 416* (1975) 181.
[42] D. L. Price, M. Misawa, S. Susman, T. I. Morrison, G. K. Shenoy, M. Grimsditch, *J. Non-Cryst. Solids 66* (1984) 443. M. Arai, R. W. Johnson, D. L. Price, S. Susman, M. Gay, J. E. Enderby, *J. Non-Cryst. Solids 83* (1986) 80.
[43] D. Lathrop, H. Eckert, *J. Am. Chem. Soc. 111* (1989) 3536.
[44] D. Lathrop, H. Eckert, *J. Non-Cryst. Solids 106* (1988) 417.
[45] D. Lathrop, H. Eckert, *J. Phys. Chem.* in press.
[46] H. Eckert, C. S. Liang, G. D. Stucky, *J. Phys. Chem. 93* (1989) 452.
[47] M. Tullius, D. Lathrop, H. Eckert, *J. Phys. Chem.* in press.
[48] H. Eckert, Z. Zhang, J. H. Kennedy, *Mater. Res. Soc. Symp. Proc. 135* (1989) 259.

ADVANCED MATERIALS

Polysilanes—A New Look at Some Old Materials

Radiation Sensitivity
Ceramic Precursors
Photoinitiators
Microlithography
Nonlinear Optics

By Robert D. Miller *

In spite of the fact that the first polysilane derivatives were probably prepared in the mid 1920's, there was little scientific interest until recently. The synthesis of the first soluble homo and copolymers about 10 years ago has stimulated an explosive development of this class of materials. This brief review traces the historical development of the polysilanes and focuses on recent studies of polymer structure, electronic properties, photochemical reactions and mechanisms and finally on new applications.

1. Introduction

Substituted silane polymers, i.e. materials which contain only silicon atoms in the polymer backbone, represent a new class of radiation sensitive materials with very unusual electronic properties.[1, 2] The unique combination of physical, mechanical and electronic properties has recently stimulated a flurry of theoretical and experimental studies and has resulted in the discovery of potential applications. In this regard, the polysilanes have been investigated as (i) new thermal precursors to β-silicon carbide,[3, 4] (ii) a new class of photo and charge conducting materials,[5, 6] (iii) radiation sensitive materials for microlithography,[7–9] (iv) broad spectrum photoinitiators for free radical vinyl polymerizations[10] and recently (v) as materials with interesting nonlinear optical properties.[11, 12]

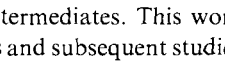
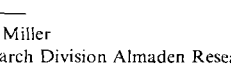
Historically these materials are quite old and the first aryl substituted materials were probably prepared in the 1920's by *Kipping*.[13] However, these early materials attracted little scientific attention, since they were highly crystalline, insoluble and intractable. In 1949, *Burkhard*[14] reported the preparation of the first alkyl derivative poly(dimethylsilane), (PDMS) by a similar synthetic route, i.e., the condensation of dichlorodimethylsilane with sodium metal. This material, like the earlier derivatives, also proved to be insoluble and intractable. The poor polymer properties of the early materials led workers to believe that these characteristics were generic to the class and as a result they attracted little interest until the middle 1970's when *Yajima* and coworkers[3] showed that PDMS could be converted to β-silicon carbide in a series of thermal steps which involved soluble and processable intermediates. This work rekindled the interest in polysilanes and subsequent studies produced the first soluble high molecular weight homo[15, 16] and copolymers.[17, 18] The preparation of the first soluble materials about 10 years ago initiated the modern era in the study of polysilane chemistry which continues today.

It is interesting that in spite of considerable efforts, the original Wurtz-type coupling shown below in Equation 1, with some experimental modifications, is still the most viable general procedure for the preparation of high molecular weight, linear polysilane derivatives. Usually the metal of choice for the condensation is sodium. Lithium tends to produce cyclic oligomers while potassium, particularly in polar solvents at elevated temperatures, often results in substantial degradation of the linear polymers to produce oligomers. In spite of the drawbacks of the Wurtz-type coupling procedure, i.e. low yields of high polymer and limited functional group tolerance, a large number of soluble, high molecular weight polysilanes have been prepared[1, 2] and a representative sample is shown in Table 1.

$$RR'SiCl_2 + 2\,Na \rightarrow \text{-}(RR'Si)_n\text{-} + 2\,NaCl \qquad (1)$$

When purified, most polysilanes are both thermally and oxidatively stable. Those with aromatic substituents attached to the backbone can often be melted and recast without significant decomposition. In general, the thermal stability of these materials is high and samples heated in nitrogen show little weight loss below 250 °C. The mechanical proper-

Table 1. Representative substituted silane polymers prepared by Wurtz-type coupling.

Entry	Polymer Structure	Yield (%)	$\bar{M}_w \times 10^{-3}$	R [a]
1.	$(n\text{-PrSiMe})_n$	32	64.4, 13.3	0.4
2.	$(n\text{-HexSiMe})_n$	11	524, 20.5	2.4
3.	$(n\text{-DodecylSiMe})_n$	8	1345, 9.4	2.7
4.	$(n\text{-Bu}_2\text{Si})_n$	34	110, 5.9	1.5
5.	$(n\text{-Hex}_2\text{Si})_n$	6	1982, 1.2	3.1
6.	$(n\text{-Tetradecyl}_2\text{Si})_n$	60	3071, 27.8	1.9
7.	$(\text{PhSiMe})_n$	55	193.5, 5.6	0.7
8.	$(p\text{-}t\text{-ButylPhMe})_n$	14	153	–
9.	$(p\text{-MeOPhSiMe})_n$	12	13	–
10.	$(p\text{-Me}_2\text{NPhSiMe})_n$	13	3.3	–
11.	$(\text{PhSiMe}_2\text{SiMe})_n$	9	13.2	–
12.	$(\beta\text{-NaphthylSiMe})_n$	20	30	
13.		6.2	231.6, 2.1	0.8
14.		8.5	1248, 2.6	0.8

[a] Ratio of high/low molecular weight fractions

[*] Dr. R. D. Miller
IBM Research Division Almaden Research Center
650 Harry Road, San Jose, California 95120-6099 (USA)

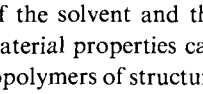
ties depend on the nature of the substituents and the polymer microstructure, and measured glass transition temperatures range from −75 °C to above 120 °C. In general, polymers with aromatic substituents tend to be more crystalline and higher melting.

Depending on the type of substituents and the reaction conditions employed, the Wurtz-type coupling procedure results in polymeric materials with a broad range of molecular weights varying from a few thousand to several million. The polymer molecular weights and dispersities can be controlled to some extent by judicious choice of the solvent and the polymerization conditions.[2, 7] The material properties can also be altered by the preparation of copolymers of structure $+R^1R^2Si)_n(SiR^3R^4+_m$, permitting further fine tuning of the mechanical and electronic characteristics. For this reason, a large number of structural and compositional copolymer variants have been described.[1, 2]

2. Spectral and Electronic Properties

It was the curious electronic properties of catenated silane oligomers which first attracted the attention of both theorists and experimentalists.[19] The spectral properties were consistent with significant delocalization of the sigma electrons in the sigma backbone. All soluble, high molecular weight polysilane derivatives absorb strongly in the UV and the absorption characteristics of a number of typical polysilane derivatives are shown in Table 2. Solution UV spectroscopic studies suggest that alkyl substituted polysilanes absorb in the region 300–325 nm, and the position of the absorption maximum depends on the steric bulk of the substituents.[20] Aryl substituents directly bonded to the backbone cause a red shift of 20–30 nm due to the electronic interaction of the substituent π orbitals with those of the silicon backbone. The absorption characteristics of linear substituted silane polymers also depend on the extent of catenation.[20] In this regard, both the position of the long wavelength absorption maxima and the molar absorptivities per silicon-silicon bond increase rapidly at first with increasing molecular weight, but approach limiting values beyond a degree of polymerization (chain length) of 40–50 as shown in Figure 1. The gross spectral characteristics of linear silicon catenates have been adequately rationalized computationally by simple linear

Table II. UV spectral characteristics of some polysilane derivatives. Data is listed for the longest wavelength transition only.

Entry	Polymer Structure	λ_{max} (nm)	ε/SiSi
1.	$(n\text{-PrSiMe})_n$	306	5600
2.	$(n\text{-DodecylSiMe})_n$	309	5000
3.	$(c\text{-HexylSiMe})_n$	320	7390
4.	$[(n\text{-Hexyl})_2Si]_n$	317	9700
5.	$[(n\text{-Tetradecyl})_2Si]_n$	322	8400
6.	$(PhSiMe)_n$	341	9300
7.	$(p\text{-MeOPhSiMe})_n$	346	8180
8.	$(\beta\text{-NaphthylSiMe})_n$	350	2800
9.	(*p*-BiphenylSiMe)	352	4000
10.		395	26600

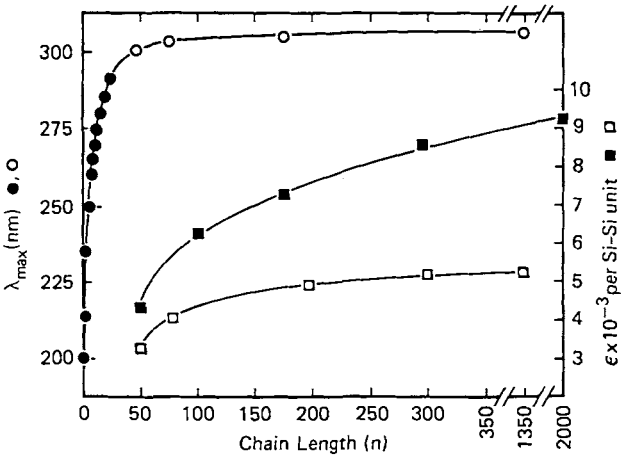


Fig. 1. Absorption wavelength maxima (λ_{max}, ●○) and extinction coefficients (ε_{sisi} ■□) as a function of oligomer/polymer chain length of n-units $+SiRR'+_n$. (●) $Me(Me_2Si)_nMe$, (○) [(*n*-dodecyl)(Me)Si]$_n$, (■) $(PhSiMe)_n$, (□) [(*n*-dodecyl)(Me)Si]$_n$.



Robert D. Miller received his Ph.D. in organic chemistry from Cornell University in 1968 working with Professor A. T. Blomquist. After post-doctoral work at Union Carbide Research Institute on low temperature spectral characterization of reactive intermediates generated by flash vacuum pyrolytic techniques, he joined IBM Research in Yorktown Heights, New York as a member of a multidisciplinary "basic studies" group. In 1971, he moved to the San Jose Research Laboratory. His current research interests include: basic photochemical processes, radiation sensitive polymers, synthetic methods involving multifunctional synthons, spectroscopy and chemistry of reactive intermediates, the synthesis and characterization of highly strained and/or theoretically interesting molecules, and novel rearrangements promoted by structural strain. He is a member of the American Chemical Society and is presently on the editorial board for Chemical Reviews.

ADVANCED MATERIALS

combination of atomic orbitals (LCAO) or Sandorfy-type theoretical treatments.[19] However, the absorption spectra of the polysilanes also depend strongly on the backbone conformation,[21, 22] a fact which was not predicted from the simple molecular orbital treatments. More sophisticated semiempirical and ab initio studies are required to adequately describe the electronic ground state and the nature of the electronic transitions.[2] INDO/S calculations rationalize the conformational dependence of the absorption spectra in terms of long range 1,4-orbital interactions and predict furthermore that *trans* sequences should absorb at longer wavelengths than *gauche*. Moreover, these studies also suggest that the electronic excitation energy tends to localize in the *trans* segments even when they are quite short.[23, 24] A solution model for the dialkyl polysilanes, which has emerged from wavelength dependent fluorescence polarization studies, is one of a polymer chain composed of discrete chromophoric segments (presumably *trans* or nearly *trans* units of varying lengths). The individual spectral characteristics depend on the segment length and are partially electronically decoupled by conformational twists or kinks. These segments apparently communicate by rapid energy transfer.[24, 25] Such a model is also supported by the INDO/S calculations. Consistently, the experimental absorption and emission characteristics of polysilanes in solution may be adequately modeled[26] using rotational isomeric state theory (RIMS) assuming both a statistical distribution of chromophoric segments of varying lengths, and conformational defects which mediate the electronic interaction between the chromophores. As expected from such a model, the polysilanes are predicted to be thermochromic as is often the case, although the detailed conformational interpretation of the solution thermochromism[26, 27] is complicated by possible aggregation effects.

The fluorescence emission from most polysilane derivatives in solution is short-lived (75–200 ps)[24, 29] and the band width is much narrower than the corresponding absorption bands.[24, 26, 28] The short radiative lifetimes, narrow spectral band width, and lack of fine structure of the fluorescence is suggestive of a highly delocalized excited state. Comparison of the absorption and emission spectra of poly(di-*n*-hexylsilane) in solution suggests that emission is occurring from segments containing 20–36 silicon atoms, assuming that the oscillator strength is independent of the chromophore length.[24, 29] In contrast to the intense, narrow fluorescence reported for poly(di-*n*-alkylsilanes), a weak, broad, long-lived emission is often observed at longer wavelengths in rigid media. This has tenatively been attributed to phosphorescence.[25, 26, 28, 41] On the basis of band structure and width, *Zeigler* et al.[26, 41] have suggested that the triplet excitation is more localized and hence, may be responsible for the polymer photolability. While the apparent localized nature of the triplet excitation is more consistent with the observed photolability (vide infra), this connection has been unambiguously established only for poly(methyl-*n*-propylsilane).[28]

Many polysilane derivatives are strongly thermochromic in the solid state. This effect was first reported for poly(di-*n*-hexylsilane) (PDHS) (see Fig. 2)[22] and this material has been the object of many structural studies.[21, 30] In this case,

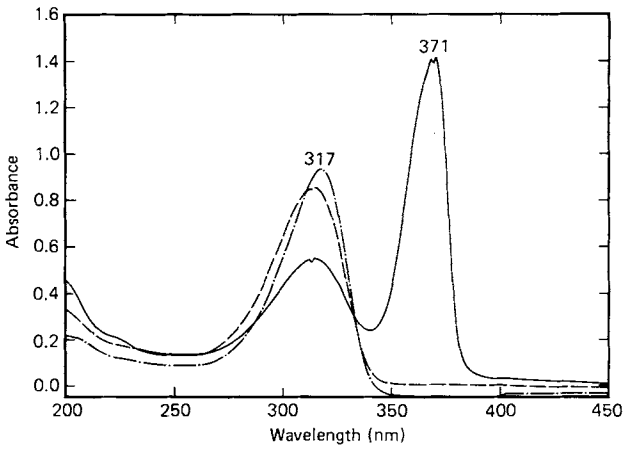


Fig. 2. UV absorption spectra of poly(di-*n*-hexylsilane): (●—●) solution in hexane; (—) thin film run immediately after baking at 100 °C, (—) thin film after standing at 20 °C for 3 h.

crystallization of the *n*-alkyl side chains enforces an all-*trans* planar backbone conformation which is responsible for the ~ 60 nm spectral red-shift. Above the transition temperature, which for PDHS is around 42 °C, the backbone conformationally disorders. It appears that for polysilane derivatives with sterically demanding substituents some type of intermolecular interaction in the solid state is necessary to enforce a stable planar all-*trans* conformation. This characteristic leads to a series of very subtle substituent effects which can dramatically effect the spectral properties. For example, poly(di-*n*-pentylsilane) (PDPS), in which side chain crystallization does not occur to a significant extent, adopts a 7/3 helical backbone conformation in the solid state at room temperature.[21] In this case, a deviation in the polymer backbone of only ~ 30° from *trans* planar results in a spectral blue-shift of almost 60 nm.

Recent studies suggest, however, that side chain crystallization does not always assure the formation of a stable, planar all-*trans* conformation for polysilanes with sterically demanding alkyl substituents. For example, poly(di-*n*-tetradecylsilane) (PDTDS) adopts a non-planar TGTG′ backbone conformation in spite of spectral evidence of side chain crystallization.[31] Apparently, the backbone retains sufficient flexibility for derivatives with long chain *n*-alkyl substituents, even in the presence of strong intermolecular interactions to allow alternative non-planar conformations. It is also interesting that PDTDS is still thermochromic, suggesting that the observation of a spectral red-shift need not necessarily be uniquely associated with the formation of planar all-*trans* backbone segments. We have also observed that the

introduction of sterically unsymmetrical substituents such as aryl groups, which can minimize intrachain steric interactions by rotation around the silicon-carbon substituent bond, can also produce dramatic spectral effects. For example, the poly(bis-alkylphenylsilanes) are among the most red-shifted of all polysilanes ($\lambda_{max} \sim 400$ nm) and the spectral data supports the presence of long *trans* sequences which persist even in solution.[32]

3. Radiation Sensitivity

Polysilane derivatives are sensitive to light and ionizing radiation both in solution and in the solid state. Irradiation causes a rapid bleaching of the long wavelength absorption, and the formation of lower molecular weight fragments.[20] This spectral bleaching, which is key to a number of applications (vide infra) is unusual and occurs because the absorption characteristics are a function of the polymer's molecular weight. The measured quantum yields for polymer scission in solution are high (0.25–1.0) although competitive crosslinking is often observed particularly when pendant unsaturated substituents are directly attached to the polymer backbone.[8, 20] The efficiency of both processes decreases markedly (50–100 fold) in the solid state. However, in every case that we have examined, photoscissioning predominates and this behavior can be considered to be characteristic of the linear polysilanes.

Exhaustive irradiation of soluble polysilanes at 254 nm in solution in the presence of trapping reagents such as trialkylsilanes or alcohols suggests that both silylenes and silyl radicals are intermediates (Equations 2a and 2b). Thermodynamic considerations and experimental studies[34] suggest that the silylene-forming reaction and the pathway to the silyl radicals are uncoupled and competing processes. In many respects, the photochemical decomposition of substituted silane high polymers resembles that previously reported for shorter chain oligosilanes.[33]

$$-\mathrm{SiRR'SiRR'SiRR'}- \xrightarrow{h\nu} \begin{cases} \ddot{\mathrm{S}}\mathrm{iRR'} + -\mathrm{SiRR'SiRR'}- & (2a) \\ -\mathrm{RR'Si}\cdot + \cdot\mathrm{SiRR'SiRR'}- & (2b) \end{cases}$$

However, recent mechanistic studies in solution suggest that the polymer photochemistry is more complex than first imagined. There is an unusual wavelength dependency and the quantum yield for the extrusion of silylenes decreases markedly with increasing irradiation wavelength, becoming very small above 300 nm.[34] On the other hand, the photodegradation proceeds at all wavelengths absorbed by the polymer as evidenced by the continuous spectral bleaching and decrease in molecular weight. Studies on isotopically labeled polymers show that silyl radicals produced by polymer chain scission disproportionate in addition to recombining. In addition, a new photochemical chain-cleavage reaction, i.e., 1,1-reductive elimination (see Equations 3a and 3b)[35] has been identified. The wavelength dependent photochemistry has been rationalized in terms of the proposed solution model for the polysilanes consisting of a statistical collection of chain segments of varying lengths with differing absorption characteristics which are only weakly electronically coupled due to conformational defects.[23, 24, 25, 26, 28]

$$-\mathrm{SiRR'SiRR'SiRR'}- \xrightarrow{h\nu} \begin{cases} -\mathrm{SiR_2R'} + \ddot{\mathrm{S}}\mathrm{iR'SiRR'}- & (3a) \\ -\mathrm{SiRR'_2} + \ddot{\mathrm{S}}\mathrm{iRSiRR'}- & (3b) \end{cases}$$

In summary, mechanistic studies in solution suggest that there are at least three photochemical pathways leading to polysilane molecular weight reduction: (i) substituted silylene extrusion and chain abridgement; (ii) silicon-silicon bond homolysis to produce chain-cleaved silyl radicals and (iii) 1,1-reductive elimination to produce chain silylenes. Current evidence indicates that these pathways are uncoupled and competing.

4. Potential Applications

4.1. Preceramic Precursors

The excellent thermal and mechanical properties, unusual electronic characteristics and photolability of the polysilanes have led to a number of potential applications, as enumerated in the introduction. The earliest uses for these materials were as preceramic precursors to β-silicon carbide. In the middle 1970's, *Yajima* and coworkers[3, 36] discovered that poly(dimethylsilane) (PDMS) could be converted, in the series of steps shown in Equation 4, to silicon carbide fibers of exceptional strength. Fibers of this type are now marketed under the trade-name of Nicalon. The intermediate carbosilanes are crucial intermediates, as they are soluble and can be either cast or spun. The initial thermolysis step can be bypassed by using soluble silane homo and copolymers and materials of this type can be employed either as impregnating reinforcing materials for porous ceramics such as silicon nitride or directly for the formation of β-silicon carbide.[4] Dimensional stability of fibers can be introduced either by surface oxidation, as in the *Yajima* process, or by the photocrosslinking of unsaturated polysilanes, prior to firing to 1200 °C.

$$(\mathrm{Me_2Si})_n \xrightarrow[\mathrm{Ar}]{450\,^\circ\mathrm{C}} \left(\mathrm{Si}(\mathrm{H})(\mathrm{Me})-\mathrm{CH_2}-\mathrm{Si}(\mathrm{H})(\mathrm{Me})-\mathrm{CH_2}\right)_n \xrightarrow[(2)\ \Delta,\ 1300\,^\circ\mathrm{C},\ \mathrm{N_2}]{(1)\ \Delta,\ 350\,^\circ\mathrm{C},\ \mathrm{Air}} \beta\text{-SiC} \qquad (4)$$

4.2. Photoinitiators for Vinyl Polymerizations

Recently *West* and *Wolff* have utilized the broad spectrum photolability of polysilane derivatives for the photoinitiation of a variety of vinyl polymerization reactions.[10] The polydispersities obtained for poly(ethyl acrylate) and poly-

ADVANCED MATERIALS

(styrene) produced in this manner were very similar to those observed in standard free radical initiated polymerizations suggesting that silyl radicals generated by chain scission may be responsible for initiation. Although the initiation efficiency is relatively low, this is partially compensated by the broad, active spectral range of the initiators and their very high extinction coefficients. In addition, vinyl polymerizations initiated by polysilane derivatives are curiously insensitive to the presence of oxygen. This sensitivity can be further decreased by the addition of certain antioxidants such as *tert*-amines and phosphines. The authors speculate that the in-situ generation of certain oxygen scavengers such as silenes, which are expected products from radical disproportionation, may be responsible for the reduced oxygen sensitivity.

4.3. Photo and Charge Conduction

The reduced spectral band gap of most polysilane derivatives relative to that of polymers with saturated carbon skeletons (~ 4 eV versus 8 eV) suggests that these material may comprise a new class of charge conducting and/or photoconducting media. In this regard, conducting films of a number of polysilane derivatives have been prepared either by doping with arsenic pentafluoride[18] or by casting from sulfuric acid solutions.[37] Similarly, the photo and charge conducting characteristics of a number of polysilane derivatives have been studied in some detail.[5,6] Drift mobilities of $\sim 10^{-4}$ cm^2/Vs have been measured both for the direct photogeneration of carriers[5] and for hole injection[6] from a variety of light absorbing substrates. For the polysilanes, charge conduction is by holes only. The measured charge drift mobilities are among the highest reported for amorphous polymers and are approximately four orders of magnitude greater than those described for poly(*N*-vinylcarbazole). Similarly, the measured activation energies (0.25–0.28 eV) which are associated with hole hopping, are also very low for an amorphous organic polymer. In photoconductivity studies on poly(methylphenylsilane), *Kepler* et al.[5] have estimated that the hole generation quantum efficiency approaches 1% at high electric fields and that the carrier lifetimes are in excess of several milliseconds.

The high discharge efficiencies, coupled with the large drift mobilities and nondispersive transport characteristics of the polysilanes are promising for potential Xerographic applications.

4.4. Microlithographs

The polysilanes have a number of unique material characteristics for certain lithographic applications, particularly those utilizing multilayer techniques. They are (i) thermally and oxidatively stable yet photochemically labile; (ii) strongly absorbing over a broad spectral range, yet bleachable; (iii) good film formers which are incompatible with most common organic carbon polymers; (iv) high in silicon content and hence, very resistant to etching under oxygen plasma conditions and (v) sensitive not only to light but also to various types of ionizing radiation (γ-ray, X-ray, e-beam, etc.). This combination of characteristics is ideally suited for a variety of multilayer lithographic processes. Accordingly they have been used as soluble, oxygen reactive ion etch (O_2-RIE) resistant barrier layers in trilevel schemes,[7] as new resists for ionizing radiation imaging,[21,38] as combined imaging and etch barrier layers in bilayer processes utilizing both wet[7–9,21,39] and dry development techniques[8,9,38–43] and as short wavelength contrast enhancing materials.[8,9,42,44] Space limitations prevent the detailed discussion of each application and the interested reader is referred to the reference list. The important concepts of bilayer imaging and contrast enhancement are discussed in more detail below.

Multilayer resist imaging schemes for the production of high resolution images offer certain advantages, particularly where troublesome chip topography causes difficulties for single layer schemes. In a bilayer process (see Fig. 3) the substrate with its topographic features is initially coated with a thick (1–5 μm) layer of a planarizing polymer which is usually not photosensitive. A thin imaging layer (0.15–0.5 μm) is then coated on top of the planarizing layer. Upon exposure, the top layer can be imaged and developed with high resolution because the imaging layer is very thin, flat and of uniform thickness. In principle, the initial develop-

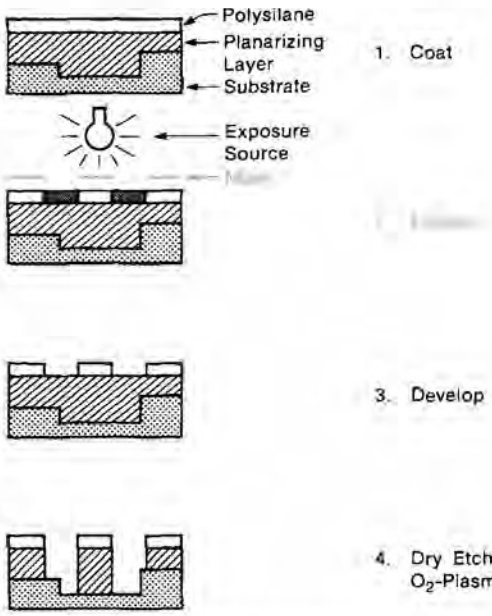


Fig. 3. Bilayer lithographic scheme utilizing a polysilane as the combination imaging and O_2-RIE resistant barrier layer. For ablative self-development in an all-dry process, the image is produced and developed directly during the exposure step.

ment could be either by a classical wet process or by dry, photoablative development. Transfer of these high resolution images through the planarizing polymer layer is usually accomplished by O_2-RIE plasma techniques, since highly anisotropic etching conditions can be employed to assure that the transfer of the initial photoimages maintains near-vertical side wall profiles. The successful utilization of such a scheme requires a photosensitive imaging layer which is also significantly more resistant to etching in the oxygen plasma than the planarizing polymer. The polysilanes are ideally suited for such procedures, since they are strongly absorbing in thin films and permit efficient light absorption, photosensitive over a broad spectral range, and resistant to O_2-RIE conditions due to the formation of a thin skin (50–100 Å) of etch-resistant SiO_x on the polymer surface. Accordingly, they have been utilized in a bilayer configuration for the production and transfer of high resolution images generated by exposure in either the near UV (350–400 nm)[8] or in the mid UV (300–340 nm) spectral regions.[7–9, 39] The use of shorter wavelength exposure sources (e.g., KrF excimer laser, 248 nm) in a 10X projection printing tool leads to significantly improved resolution and allows the delineation of sub 0.5 μm features in a bilayer configuration (see Fig. 4).[45]

The bilayer processes described above used classical wet development steps for the production of images in the irradiated polysilane layer. However, high resolution images can also be produced directly in a thin polysilane layer by photoablative imaging. In this process, the polysilane is exposed to a high intensity radiation source (e.g., an excimer laser) during which the polymer spontaneously degrades and volatilizes. Since the image thus produced is subsequently transferred by gas phase O_2-RIE techniques, the procedure constitutes an all-dry, solventless lithographic process requiring no wet development step. The production and transfer of submicron images in such an all-dry process utilizing certain polysilane derivatives for imaging and an UV excimer laser exposure source have been successfully demonstrated.[8, 9]

The generation of images by projection printing in cases where the photomask features are of comparable size to the exposure wavelength is complicated by diffraction distortion of the mask features at the photoresist surface. Contrast enhanced lithography[46] is a technique which employs a thin layer of an appropriate contrast enhancing layer coated on top of a conventional photoresist to improve the diffraction distorted mask image incident on the photoresist. Although a discussion of the concepts involved in the contrast enhancement of images is beyond the scope of this article, the reader is referred to the background information contained in the literature.[46] However, consideration of the process suggests that a workable contrast enhancing material should possess a number of characteristics: (i) it should be thermally and oxidatively stable; (ii) the material should be very strongly absorbing at the exposure wavelength and bleach rapidly upon irradiation and (iii) it should be incompatible with the underlying photoresist so that the material

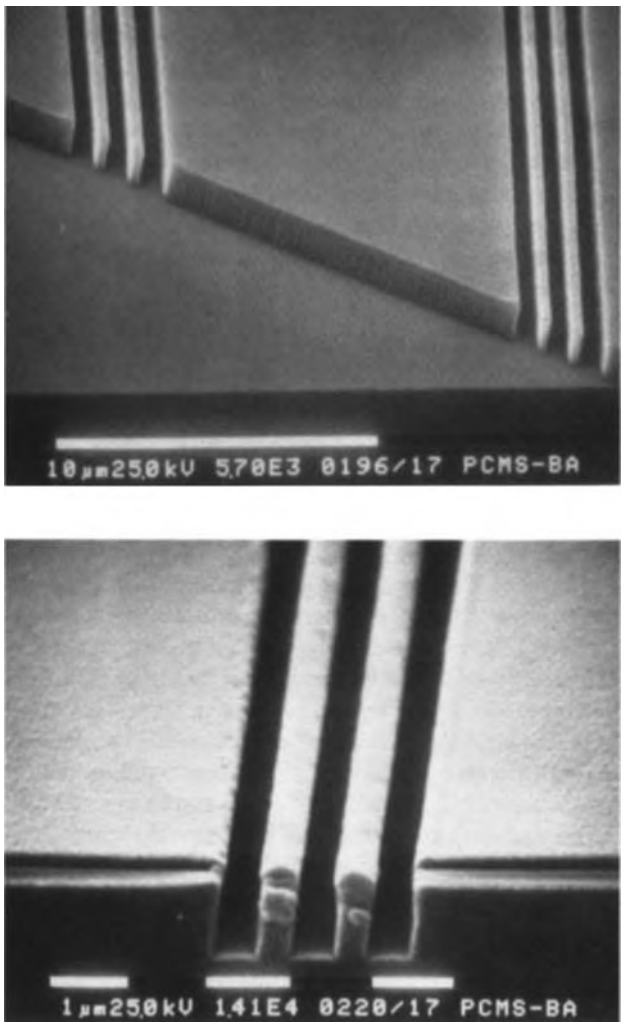


Fig. 4. Images produced in a polysilane bilayer configuration using a deep UV, KrF excimer laser exposure source (248 nm). Bilayer: 170 nm poly(cyclohexylmethylsilane) over 1.0 μm of hard baked AZ-type photoresist; 248 nm. 150 mJ/cm^2, developed 80/20 butyl acetate-isopropanol, O_2-RIE image transfer; (Top) 0.45 and 0.5 μm features, (Bottom) 0.4 μm features.

boundaries are clearly delineated. Initially it was also felt that the contrast enhancing layer should be removable prior to the development of the exposed photoresist, but recent studies indicate that this characteristic is not essential.

Certain of the polysilane derivatives not only satisfy the above criteria but also absorb and bleach at shorter wavelengths than commercial materials thus providing the possibility of realizing the enhanced resolution intrinsic to short wavelength exposure sources.[8, 9, 42, 44] A system composed of a conventional diazoquinone-novolac type photoresist overcoated with a thin layer of poly(cyclohexylmethylsilane) has been studied in detail and significant improvements in the image quality relative to the same photoresist without the contrast enhancing layer have been demonstrated.[8, 9, 44] Similar image enhancement for mid UV exposure using other polysilane derivatives[42] has been reported recently.

ADVANCED MATERIALS

4.5. Nonlinear Optical Properties

Finally, there is currently increased interest in the nonlinear optical properties of the materials due to their potential utility in optoelectronic or opto-optic devices for telecommunications and optical computing. In this regard, organic materials are of considerable interest because of their intrinsically large nonlinear susceptibilities, rapid response times and high threshold radiation damage values.[47] Furthermore, the utilization of third order effects eliminates the stringent requirements for an acentric molecular environment thus expanding the range of useful materials to polymeric systems.

Studies of the third order susceptibilities ($\chi^{(3)}$) of polymers to date have focused on highly polarizable materials containing conjugated π electron systems such as the polyacetylenes and diacetylenes, rigid rod aromatic polymers, ladder polymers, etc. While these materials have high intrinsic susceptibilities, many have other drawbacks such as limited processability, thermal and/or oxidative liability, nonideal spectral matching, etc.

The polysilanes represent a new class of potentially interesting nonlinear optical (NLO) materials. They are: (i) thermally and oxidatively stable, (ii) the σ-conjugated backbone is highly delocalized and absorbs very strongly in the UV region, (iii) electronic substituent effects can be transmitted over large distances and (iv) the polarizability is large, anisotropic and dependent on backbone conformation. In fact, many of the electronic properties of the polysilanes more closely resemble conjugated π systems than saturated σ bonded carbon-based polymers. In addition, the polysilanes are imagable to high resolution using standard lithographic techniques, an attribute potentially useful for guided wave applications.

Initial NLO measurements on polysilane derivatives have revealed some interesting properties. Relatively large $\chi^{(3)}$ values ranging from 10^{-11} to 10^{-12} esu[11,12,48,49] have been measured and the variation in these numbers with the film thickness suggests possible polymer orientational effects.[12] The resonant $\chi^{(3)}$ value measured for thin films of poly(di-*n*-hexylsilane) ($\sim 10^{-11}$ esu) is the largest reported for a polymeric system which is transparent in the visible and is comparable to values reported for rigid aromatic polymers such as poly(*p*-phenylenevinylene) and poly(*p*-phenylenebenzobisthiazole). Thermal effects on the third harmonic generation efficiency have been correlated with the known thermochromic characteristics of the polymers[12] and the picosecond time response[48] of the nonlinearity reported for poly(methylphenylsilane) is consistent with an electronic mechanism. In addition, biphotonic nonablative, nonlinear photochemical processes have been observed upon exposure to high intensity visible laser light. This photochemistry is anisotropic, and refractive index changes of greater than 2.5×10^{-2} (at 632.8 nm) have been induced due to selective polymer chain degradation in a direction parallel to the electric field of the laser light.[50] Birefringence changes of this magnitude are adequate for the fabrication of channel waveguides and birefringent grating structures.

Although the study of the NLO properties of polysilane derivatives is in its infancy, the unusual spectral properties, the substantial nonlinearities, the capacity for polymer orientation and the anisotropic photolability suggest that these materials are worthy of future investigation.

In summary, the polysilanes represent a new class of radiation sensitive polymers whose unusual electronic structure and properties, and thermochromic behavior are attracting considerable attention. Although most of the work to date has been science-oriented, the modern era of investigation is less than 10 years old. In spite of this, a number of potential applications for these interesting materials have been discovered and described.

Received: July 3, 1989

[1] R. J. West, *Organomet. Chem. 300* (1986) 327.
[2] R. D. Miller, J. Michl, *Chem. Rev. 89* (1989) 1359.
[3] S. Yajima, J. Hayashi, M. Omori, *Chem. Lett. 1975*, 931.
[4] R. West in L. L. Hensch, D. R. Ulrich (Eds.): *Ultrastructure Processing of Ceramics, Glasses and Composites*, John Wiley, New York 1984, Chapt. 19.
[5] R. G. Kepler, J. M. Zeigler, L. A. Harrah, S. R. Kurtz, *Phys. Rev. B35* (1987) 2818.
[6] M. Stolka, H.-J. Yuh, K. McGrane, D. M. Pai, *J. Polym. Sci. Polym. Chem. Ed. 25* (1987) 823.
[7] R. D. Miller, D. Hofer, D. R. McKean, C. G. Willson, R. West, P. T. Trefonas III in L. F. Thompson, C. G. Willson, J. M. J. Fréchet (Eds.): *Materials for Microlithography*, ACS Symposium Series No. 266, Am. Chem. Soc. Washington D.C. 1984, Chapt. 14.
[8] R. D. Miller, D. Hofer, J. F. Rabolt, R. Sooriyakumaran, C. G. Willson, G. N. Fickes, J. E. Guillet in M. J. Bowden, S. R. Turner (Eds.): *Polymers for High Technology: Electronics and Photonics*, ACS Symposium Series No. 346, Am. Chem. Soc. Washington D.C. 1987, Chapt. 15.
[9] R. D. Miller, D. Hofer, G. N. Fickes, C. G. Willson, E. E. Marinero, P. T. Trefonas III, R. West, *Polym. Eng. Sci. 26* (1986) 1129.
[10] A. Wolff, R. West, *Appl. Organomet. Chem. 1* (1987) 7.
[11] F. Kajzar, J. Messier, C. Rosilio, *J. Appl. Phys. 60* (1986) 3040.
[12] J. C. Baumert, G. C. Bjorklund, D. H. Jundt, M. C. Jurich, H. Looser, R. D. Miller, J. F. Rabolt, R. Sooriyakumaran, J. D. Swalen, R. Twieg, *J. Appl. Phys. Lett. 53* (1989) 1147.
[13] F. S. Kipping, *J. Chem. Soc. 125* (1924) 2291.
[14] C. Burkhard, *J. Am. Chem. Soc. 71* (1949) 963.
[15] R. E. Trujillo, *J. Organomet. Chem. 198* (1980) C27.
[16] P. T. Trefonas III, P. I. Djurovich, X.-H. Zhang, R. West, R. D. Miller, D. Hofer, *J. Polym. Sci. Polym. Lett. Ed. 21* (1983) 819.
[17] J. P. Wesson, T. C. Williams, *J. Polym. Sci. Polym. Chem. Ed. 18* (1980) 959.
[18] R. West, L. D. David, P. I. Djurovich, K. L. Stearley, K. S. V. Srinivasan, H. Yu, *J. Am. Chem. Soc. 103* (1981) 7352.
[19] C. G. Pitt, in A. L. Rheingold (Ed.): *Homoatomic Rings, Chains and Macromolecules of Main Group Elements*, Elsevier Scientific Publishing Co., New York 1977, Chapt. 8 and references cited therein.
[20] P. Trefonas, R. West, R. D. Miller, D. Hofer, *J. Polym. Sci. Polym. Lett. Ed. 21* (1983) 823 and references cited therein.
[21] R. D. Miller, J. F. Rabolt, R. Sooriyakumaran, W. Fleming, G. N. Fickes, B. L. Farmer, H. Kuzmany in M. Zeldin, K. J. Wynne, H. R. Allcock (Eds.): *Inorganic and Organometallic Polymers*, ACS Symposium Series No. 360, Am. Chem. Soc., Washington D.C. 1988, Chapt. 4 and references cited therein.
[22] R. D. Miller, D. Hofer, J. Rabolt, G. N. Fickes, *J. Am. Chem. Soc. 107* (1985) 2172.
[23] K. A. Klingensmith, J. W. Downing, R. D. Miller, J. Michl, *J. Am. Chem. Soc. 108* (1986) 7438.
[24] J. Michl, J. W. Downing, T. Karatsu, K. A. Klingensmith, G. M. Wallraff, R. D. Miller in M. Zeldin, K. J. Wynne, H. A. Allcock (Eds.): *Inorganic*

and Organometallic Polymers, ACS Symposium Series No. 360, Am. Chem. Soc., Washington D.C. 1988, Chapt. 5.
[25] G. E. Johnson, K. M. McGrane in C. E. Hoyle, J. M. Torkelson (Eds.): *Photophysics of Polymers,* ACS Symposium Series No. 258, Am. Chem. Soc., Washington D.C. 1987, 499.
[26] L. A. Harrah, J. M. Zeigler, *ibid.,* 482.
[27] P. T. Trefonas III, J. R. Jr. Damewood, R. West, R. D. Miller, *Organometallics 4* (1985) 1318.
[28] J. Michl, J. W. Downing, T. Karatsu, A. J. McKinley, G. Poggi, G. M. Wallraff, R. Sooriyakumaran, R. D. Miller, *Pure Appl. Chem. 60* (1988) 959.
[29] Y. R. Kim, M. Lee, J. R. G. Thorne, R. M. Hochstrasser, J. M. Zeigler, *Chem. Phys. Lett. 145* (1988) 75.
[30] A. J. Lovinger, F. C. Schilling, F. A. Bovey, J. M. Zeigler, *Macromolecules 19* (1985) 2657.
[31] B. L. Farmer, R. D. Miller, J. F. Rabolt, W. W. Fleming, G. N. Fickes, *Bull. Am. Phys. Soc. 33 (3)* (1988) 657.
[32] R. D. Miller, R. J. Sooriyakumaran, *Polym. Sci. Polym. Lett. Ed. 25* (1987) 32.
[33] M. Ishikawa, M. Kumada, *Adv. Organomet. Chem. 19* (1986) 51.
[34] T. Karatsu, R. D. Miller, R. Sooriyakumaran, J. Michl, *J. Am. Chem. Soc. 111* (1989) 1140.
[35] A. J. McKinley, T. Karatsu, G. M. Wallraff, R. D. Miller, R. Sooriyakumaran, J. Michl, *Organometallics 7* (1988) 2567.
[36] Y. Hasegawa, M. Iimura, S. Yajima, *J. Mater. Sci. 15* (1980) 720.
[37] H. Naarman, N. Theophilou, L. Geral, J. Sledz, F. Schien, *German Patent* DE 3634281 (1981).
[38] G. N. Taylor, M. Y. Hellman, T. Wolf, J. M. Zeigler, *Proc. SPIE 920* (1988) 274.
[39] D. C. Hofer, R. D. Miller, C. G. Willson, *Proc. SPIE 469,* (1984) 16.
[40] E. E. Marinero, R. D. Miller, *Appl. Phys. Lett. 50* (1987) 1041.
[41] J. M. Zeigler, L. A. Harrah, A. W. Johnson, *Proc. SPIE 539* (1985) 160.
[42] C. Rosilio, A. Rosilio, B. Serre, *Microelectronic Eng. 8* (1988) 55.
[43] S. G. Hansen, T. E. Robitalli, *J. Appl. Phys. 62* (1987) 1394.
[44] D. C. Hofer, R. D. Miller, C. G. Willson, A. R. Neureuther, *Proc. SPIE 469* (1984) 108.
[45] R. D. Miller, C. G. Willson, G. H. Wallraff, N. Clecak, R. Sooriyakumaran, J. Michl, T. Karatsu, A. J. McKinley, K. A. Klingensmith, F. Downing, *Proc. SPE Conf. Photopolymers: Principles, Processes and Materials,* Ellenville, New York 1988, 111.
[46] B. F. Griffing, P. R. West, *Polym. Eng. Sci. 23* (1983) 947.
[47] D. J. Williams (Ed.): *Nonlinear Optical Properties of Organic and Polymeric Materials,* ACS Symposium Series No. 233, Am. Chem. Soc., Washington D.C. 1983.
[48] D. J. McGraw, A. E. Siegman, G. M. Wallraff, R. D. Miller, *Appl. Phys. Lett. 54* (1989) 1713.
[49] L. Yang, Q. Z. Wang, P. P. Ho, R. Dorsenville, R. R. Alfano, W. K. Zou, N. L. Yang, *Appl. Phys. Lett. 53* (1988) 1245.
[50] F. M. Schellenberg, R. L. Byer, R. D. Miller, R. Sooriyakumaran, Abstracts *Int. Conf. Quantum Electronics,* Springer Tokyo 1988, p. 192.

1990 E-MRS Strasbourg Conferences: (Symposia)

Spring Meeting (May 29.–June 1. 1990)

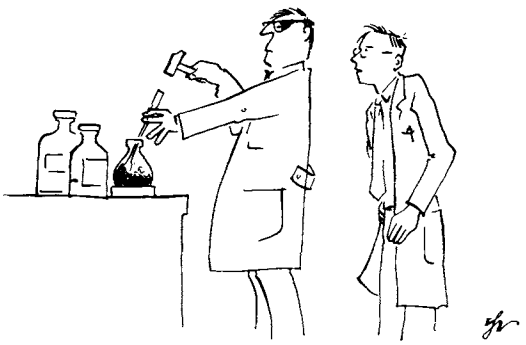
A High-T_c Superconductor Materials
B Metal Matrix Composites
C Magnetic Thin Films, Multilayers
D Surface Modification and Coatings
E Surface Processing and Laser Assisted Chemistry

Fall Meeting (Nov. 27.–30. 1990)

A Semiconductors in Optoelectronics
B Nonlinear Optical Materials
C Wide Band-Gap Semiconductors
D Characterization of Compound Semiconductors

Details from Prof. *P. Siffert,* B.P. 20, F-67037 Strasbourg Cedex (France), Tel. 8828 6543, Fax 8828 0990

Call for Short Communications · Call for Short Communications · Call for Short Communications



... doesn't melt, won't dissolve, just can't be broken down – let's send it to ADVANCED MATERIALS!

Communications

^{15}N CPMAS NMR Study of the Structure of Polyaniline**

By *Bernd Wehrle, Hans-Heinrich Limbach,* John Mortensen,* and *Jürgen Heinze**

Dedicated to Professor Christoph Rüchardt on the occasion of his 60th birthday

In the last few years the structure and properties of polyaniline (PANI) have attracted much interest.[1-12] Among the different techniques used in these studies, high resolution solid state ^{13}C NMR spectroscopy under the conditions of ^{1}H cross-polarization (CP), magic angle spinning (MAS), and proton decoupling[13-16] has been employed in order to elucidate the structure and the reactivity of this compound.[17-22] Using this method on chemically synthesized PANI, evidence for the emeraldine structure **I** (Fig. 1), which

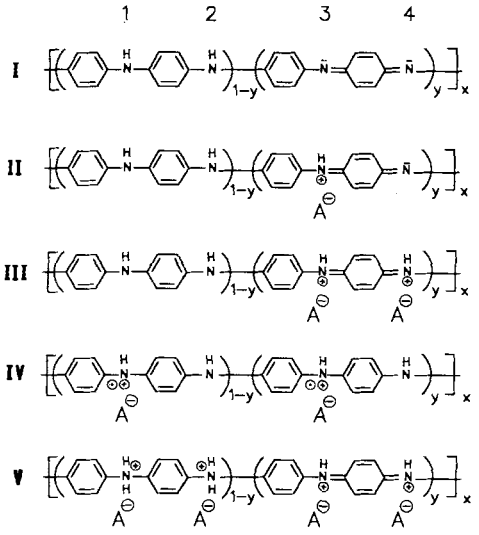


Fig. 1. Possible structures of polyaniline (PANI). Leucoemeraldine: **I**, y = 0; emeraldine: **I**, y = 0.5; pernigraniline: **I**, y = 1.

consists of alternating phenylenediamine and chinonimine units with y = 0.5 has been obtained. It is not known, however, whether PANI prepared by electropolymerization in media of different acidities[1, 7, 8, 20] is characterized by the same structure or whether structures with different y values as well as structures **II** to **V** (Fig. 1) also have to be considered.

Since solid, nitrogen containing heterocycles can conveniently be studied by ^{15}N CPMAS NMR spectroscopy of ^{15}N enriched materials[23-32] it is surprising that only one preliminary ^{15}N CPMAS paper on chemically synthesized PANI has been published.[32] Therefore, we report here the results of ^{15}N CPMAS NMR experiments[33] on various PANI-samples synthesized by electropolymerization[35] in $HClO_4$/water mixtures and subsequent discharge in acetonitrile.

Figure 2 shows ^{15}N CPMAS NMR spectra of three samples. The spectrum of sample 1 (Figure 2a) contains a sharp

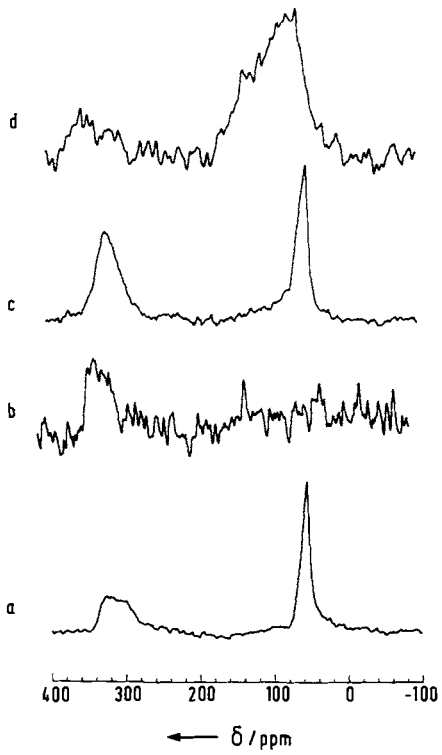


Fig. 2. ^{15}N CPMAS NMR spectra of electrochemically synthesized polyanilines (PANI): a) discharged sample 1; b) dephasing experiment performed on sample 1 with a delay of 100 μs; c) sample 2, as sample 1 but after thorough washing; d) sample 3, prepared in highly acidic conditions.

high field signal at ~ 60 ppm and a broad band at ~ 320 ppm. Figure 2b shows the result of a dipolar dephasing experiment[37] on the same sample in which only the magnetization of non-protonated nitrogen atoms survives. When sample 1 is carefully washed[35] we observe in

[*] Prof. H. H. Limbach, Dr. B. Wehrle,[+] Prof. J. Heinze, Dr. J. Mortensen,[‡] Institut für Physikalische Chemie der Universität Freiburg, Albertstr. 21, D-7800 Freiburg (FRG)

[+] Present address: Bayer AG, D-5090 Leverkusen (FRG)

[‡] Present address: Department of Chemistry, University of Roskilde (Denmark)

[**] This work was supported by the Stiftung Volkswagenwerk, Hannover, the Deutsche Forschungsgemeinschaft, Bonn-Bad Godesberg, and the Fonds der Chemischen Industrie, Frankfurt.

the ^{15}N spectra of the resulting sample 2 slight changes of the signal at low field as shown in Figure 2c.

The ^{15}N spectra of samples 1 and 2 are very similar to the spectrum shown in the literature[32] which was interpreted in terms of the emaraldine structure **I** with $y \approx 0.5$. The dipolar dephasing experiment in Figure 2b supports the assignment of the high field line to the protonated nitrogen atoms 1 and 2 in **I**. Their chemical shift is consistent with what is known about the chemical shifts of model compounds such as diphenylamine (65 ppm)[38] or the NH-nitrogen atoms of azophenine (Figure 3).[31] Note that unsubstituted aniline

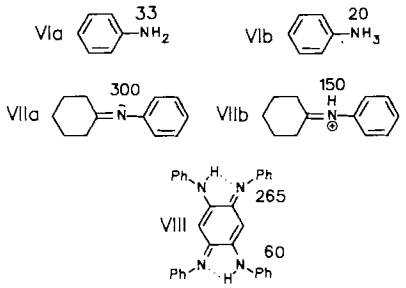


Fig. 3. ^{15}N chemical shifts of model compounds for PANI. **VI**: aniline, [38] **VII**: N-phenylcyclohexanonimine, [39] **VIII**: azophenine [31].

and anilinium appear at higher field, i.e. at 33 ppm and 20 ppm.[38] The dephasing experiment strongly indicates that the low field line has to be assigned to the non-protonated nitrogen 3 and 4 in **I** although they absorb at slightly lower field than the corresponding atoms in azophenine ($\sim$ 265 ppm).[31] Thus, our results support similar structures of PANI when synthesized chemically and electrochemically.

Dramatic changes of the spectra are, however, found when PANI is prepared electrochemically under strongly acid conditions (sample 3).[35] For such material, salt structures **III** and **IV** (Fig. 1) have been proposed.[20, 32] As shown in Figure 2d we observe for sample 3 two very broad lines at $\sim$ 100 and $\sim$ 350 ppm which represents a shift to lower field. The observation that the relative intensity of the high field line has increased, indicates a higher mole fraction of protonated ^{15}N atoms in sample 3.

These results are consistent with the presence of a superposition of all structures **I**, **II** and **III** in sample 3. Also, structure **V** cannot be completely excluded. We tentatively assign the low-field line in Figure 2d to the non-protonated nitrogen atoms 4 in **II**. By comparison with the protonation shift of compound **VII** in Figure 3 which is of the order of +150 ppm[39] we also tentatively assign the low field part of the high field line to atoms 3 and 4 in **III** as well as to atom 3 in **II**. The high field part stems then probably from the atoms 1 and 2 in **II** and **III**.

There are different phenomena which might contribute to the broadness of the high field line in Figure 2d. Firstly, one has to consider the effect of proton disorder arising from a superposition of **I, II,** and **III**. One also has to take a distribution of intermolecular interactions of the PANI subunits with the anions $A^{\ominus}$ into account. A look at structure **III** shows that the positive charge can only be localized as indicated if the $A^{\ominus}$ ions interact with particular nitrogen atoms. At longer distances between the nitrogen atoms and counter ions the differences of electronic charges and, subsequently, of nitrogen chemical shifts between the two subunits in **III** will disappear. Thus, a broad nitrogen-anion distribution function will lead to a broad distribution of chemical shifts in the region between 150 and 50 ppm, as observed in Figure 2d. Note that we can also not exclude the presence of semiquinone structures **IV**. Evidence for the existence of **IV** has been obtained by EPR[40] and magnetic susceptibility measurements.[41] Unfortunately, it is difficult to know where the ^{15}N signals of **IV** appear because they might be subject to paramagnetic or Knight shifts as well as to line broadening.

Finally, the linewidths in Figure 2d could also be influenced by electron and nuclear motions as well as spin dynamics. A fast migration of anions should lead to a breakdown of the nitrogen-anion distribution function, i.e. to line broadening and line narrowing of the lines in Figure 2d. Since the *p*-tolylsulfonate anions are bulky it is, however, not very probable that this phenomenon occurs within the NMR timescale. However, the situation could be different if smaller anions were employed.

We have shown that ^{15}N CPMAS NMR spectroscopy is a promising technique, useful for studying the structure of nitrogen containing heterocyclic polymers. Besides PANI we have also studied other materials such as polypyrrole (PPy) and related compounds. In contrast to PANI, we find for PPy only one inhomogeneously broadened ^{15}N signal at 120 ppm which is not significantly altered when the substance is oxidized. This means that even in neutral PPy, only protonated nitrogen atoms can be detected, as expected for a structure $(P^{y\oplus}X_y^{\ominus})_n$, $y \geq 0$. Further ^{15}N CPMAS results obtained for a completely different class of nitrogen containing polymers have been reported.[42]

Received: September 27, 1989

[1] J. C. Chiang, A. G. MacDiarmid, *Synth. Met. 13* (1986) 193.
[2] W. W. Focke, G. E. Wnek, Y. Wei, *J. Phys. Chem. 91* (1987) 5813.
[3] A. G. MacDiarmid, J. C. Chiang, W. S. Huang, B. D. Humphrey, N. L. D. Somasiri, W. Wu, S. I. Yaniger, *Mol. Cryst. Liq. Cryst. 121* (1985) 173.
[4] D. S. Boudreaux, R. R. Chance, J. F. Wolf, L. W. Shacklette, J. L. Bredas, B. Themans, J. M. André, R. Silbey, *J. Chem. Phys. 85* (1986) 4584.
[5] M. Nechtschein, C. Santier, J. P. Travers, J. Chroboczek, A. Alix, M. Ripert, *Synth. Met. 18* (1987) 311.
[6] J. P. Travers, M. Nechtschein, *Synth. Met. 21* (1987) 135.
[7] T. Hagiwara, T. Demura, K. Iwata, *Synth. Met. 18* (1987) 317.
[8] E. M. Genies, M. Lapkowski, C. Santier, E. Vieil, *Synth. Met. 18* (1987) 631.
[9] W. R. Salaneck, I. Lundstrom, T. Hjertberg, C. B. Duke, E. M. Conwell,

ADVANCED MATERIALS

A. Paton, A. G. MacDiarmid, N. L. D. Somasiri, W. S. Huang, A. F. Richter, *Synth. Met. 18* (1987) 291.
[10] R. Kessel, G. Hansen, G. J. W. Schultze, *Ber. Bunsenges. Phys. Chem. 92* (1988) 710.
[11] F. Wudl, R. O. Angus, Jr., F. L. Lu, P. M. Allemand, D. F. Vachon, M. Novak, Z. X. Liu, A. J. Heeger, *J. Am. Chem. Soc. 109* (1987) 3677.
[12] L. W. Shacklette, J. F. Wolf, S. Gould, R. H. Baughman, *J. Chem. Phys. 88* (1988) 3955.
[13] J. Schaeffer, E. O. Stejskal, *J. Am. Chem. Soc. 98* (1986) 1031.
[14] J. R. Lyerla, C. S. Yannoni, C. A. Fyfe, *Acc. Chem. Res. 15* (1982) 208.
[15] C. A. Fyfe: *Solid State NMR for Chemists*, C.F.C. Press, Guelph, Ontario, 1983.
[16] R. A. Komoroski: *High Resolution NMR Spectroscopy of Synthetic Polymers in Bulk*, VCH-Verlag, Weinheim 1986.
[17] F. Devreux, G. Bidan, A. A. Syed, C. Tsintavis, *J. Phys. 46* (1985) 1595.
[18] T. Hjertberg, W. R. Salaneck, I. Lundstrom, N. L. D. Somasiri, A. G. MacDiarmid, *J. Polym. Sci. Polym. Lett. 23* (1985) 503; *J. Phys. 46* (1985) 1595.
[19] S. Stafström, B. Sjörgen, O. Wennerström, T. Hjertberg, *Synth. Met. 16* (1986) 31.
[20] S. Kaplan, E. M. Conwell, A. F. Richter, A. G. MacDiarmid, *J. Am. Chem. Soc. 110* (1988) 7647.
[21] S. Kaplan, E. M. Conwell, A. F. Richter, A. G. MacDiarmid, *Synth. Met. 29* (1989) E235.
[22] Y. Wei, W. W. Focke, G. E. Wnek, A. Ray, A. G. MacDiarmid, *J. Phys. Chem. 93* (1989) 495.
[23] H. H. Limbach, J. Hennig, R. D. Kendrick, C. S. Yannoni, *J. Am. Chem. Soc. 106* (1984) 4059.
[24] H. H. Limbach, B. Wehrle, M. Schlabach, R. D. Kendrick, C. S. Yannoni, *J. Magn. Reson. 77* (1988) 84.
[25] H. H. Limbach, B. Wehrle, H. Zimmermann, R. D. Kendrick, C. S. Yannoni, *Angew. Chem. Int. Ed. Engl. 26* (1987) 247; *Angew. Chem. 99* (1987) 241.
[26] R. D. Kendrick, S. Friedrich, B. Wehrle, H. H. Limbach, C. S. Yannoni, *J. Magn. Reson. 65* (1985) 159.
[27] B. Wehrle, H. H. Limbach, *Chem. Phys. 136* (1989) 223.
[28] H. H. Limbach, B. Wehrle, H. Zimmermann, R. D. Kendrick, C. S. Yannoni, *J. Am. Chem. Soc. 109* (1987) 929.
[29] B. Wehrle, H. H. Limbach, M. Köcher, O. Ermer, E. Vogel, *Angew. Chem. Int. Ed. Engl. 26* (1987) 934; *Angew. Chem. 99* (1987) 914.
[30] B. Wehrle, H. Zimmermann, H. H. Limbach, *Ber. Bunsenges. Phys. Chem 91* (1987) 941; B. Wehrle, H. H. Limbach, H. Zimmermann, *J. Am. Chem. Soc. 110* (1988) 7014.
[31] H. Rumpel, H. H. Limbach, *J. Am. Chem. Soc. 111* (1989) 5429.
[32] A. F. Richter, A. Ray, K. V. Ramanathan, S. K. Mannohar, G. T. Furst, S. J. Opella, A. G. MacDiarmid, *Synth. Met. 29* (1989) E243–E249.
[33] The NMR experiments were performed on a Bruker CXP 100 spectrometer working at 90.02 MHz for protons, using a 5 mm Doty MAS probe [34]. The rotation frequencies of the 5 mm o.d. rotors were between 2.5 and 3.5 kHz; thus, rotational sideband free spectra could be obtained. All spectra were referenced to external $^{15}NH_4Cl$.
[34] F. D. Doty, P. D. Ellis, *Rev. Sci. Instrum. 52* (1981) 1868.
[35] The PANI-samples were prepared with equipment described previously [36] as follows. Aniline-^{15}N was electropolymerized galvanostatically at a current density of 1 mA/cm^2 at a concentration of 0.1 mol l^{-1} using $HClO_4$/water mixtures as solvent. Samples 1 and 2 were prepared at a $HClO_4$ concentration of 1 mol l^{-1}, sample 3 at a concentration of 3 mol l^{-1}. The precipitates on the electrodes were washed with acetonitrile and dried in vacuo. Then the samples were discharged at a potential of -0.4 V vs. Ag/AgCl in acetonitrile containing 0.5 mol l^{-1} $LiClO_4$ as supporting electrolyte. Sample 2 was thoroughly washed with water and then with acetonitrile in contrast to sample 1 which was washed only superficially. Finally, all samples were dried in vacuo.
[36] J. Heinze, R. Bilger, K. Meerholz, *Ber. Bunsenges. Phys. Chem. 92* (1988) 1266.
[37] J. S. Opella, M. H. Frey, *J. Am. Chem. Soc. 101* (1979) 5854.
[38] G. J. Martin, M. L. Martin in P. Diehl, E. Fluck, R. Kosfeld, *^{15}N NMR Spectroscopy, NMR Basic Principles and Progress*, Vol. 18, Springer, Berlin 1981.
[39] I. I. Schuster, J. D. Roberts, *J. Org. Chem. 44* (1979) 3864.
[40] A. G. MacDiarmid, J. C. Chiang, A. F. Richter, A. J. Epstein, *Synth. Met. 18* (1987) 285.
[41] J. M. Ginder, A. F. Richter, A. G. MacDiarmid, A. J. Epstein, *Solid State Commun. 63* (1987) 97.
[42] B. Wehrle, H. H. Limbach, T. Zipplies, M. Hanack, *Adv. Mater. 1989*, No. 12; *Angew. Chem. Int. Ed. Engl. Adv. Mater. 28* (1989) No. 12; *Angew. Chem. Adv. Mater. 101* (1989) No. 12.

^{15}N CPMAS NMR Study of the Structure and Reactions of Phthalocyaninatopolysiloxane and its Precursors in the Solid State**

By *Bernd Wehrle, Hans-Heinrich Limbach*, Tilman Zipplies*, and *Michael Hanack**

Dedicated to Professor Christoph Rüchardt on the occasion of his 60th birthday

The class of phthalocyaninatopolymetalloxanes $(PcMO)_n$ (Pc ≡ phthalocyanine, M ≡ Si, Ge, Fig. 1) has attracted considerable interest because of the high conductivity of these molecules after doping with iodine or other electron acceptors.[1–5] Since it has not yet been possible to perform crystal structure analyses on these compounds, information about the molecular structure of these materials has mainly been obtained[1–5] by solid state ^{13}C CPMAS NMR spectroscopy under the conditions of cross polarization (CP) and magic angle spinning (MAS).[6–9] Unfortunately, the ^{13}C CPMAS spectra of $(PcMO)_n$ contain a manifold of various aromatic carbon atoms sites which differ only slightly in their chemical shifts and which are difficult to assign.

In the past it has been shown that the structure and reactions of solid, nitrogen containing heterocycles can conveniently be studied using ^{15}N CPMAS NMR spectroscopy which requires, however, ^{15}N enriched samples.[10] We show here that this technique is also useful for studying the structure and the solid state reactivity of phthalocycaninatopolymetalloxanes.

The ^{15}N labeled compounds studied were prepared according to standard methods from 95% ^{15}N enriched phthalodinitrile via diimidoisoindoline.[11] This was reacted with $SiCl_4$ in quinoline to form dichlorophthalocyaninatosilicon $PcSiCl_2$ which was hydrolyzed in a mixture of pyridine and NaOH to form dihydroxyphthalocyaninatosilicon ^{15}N labeled $PcSo(OH)_2$, (**I**) whose structure is shown in Figure 1. **I** was then polymerized in a thermal balance under nitrogen at 450 °C to form ^{15}N labeled μ-oxo-phthalocyaninatosilicon $[PcSiO]_n$ (**II**); **II** was subsequently doped with iodine according to a literature method.[2] Thus, the ^{15}N labeled product $[(PcSiO)I_{1.1}]_n$ (**III**) was obtained. ^{15}N NMR experiments were carried out on all compounds **I**–**III** using instrumentation previously described.[11] For the low temperature experiments a self-built heat exchanger[12] was employed.

The room temperature ^{15}N CPMAS NMR spectra of the various phases of phthalocyaninatopolysiloxanes are shown

[*] Prof. H. H. Limbach, Dr. B. Wehrle,[+]
Institut für Physikalische Chemie der Universität Freiburg,
Albertstr. 21, D-7800 Freiburg (FRG)
Prof. M. Hanack, Dr. T. Zipplies,[‡]
Institut für Organische Chemie der Universität Tübingen,
Auf der Morgenstelle 18, D-7400 Tübingen (FRG)
[+] Present address: Bayer AG, Zentrale Forschung,
D-5090 Leverkusen (FRG)
[‡] Present address: Hoechst AG, Werk Gendorf, D-8261 Burgkirchen (FRG)
[**] This work was supported by the Stiftung Volkswagenwerk, Hannover, and the Fonds der Chemischen Industrie, Frankfurt

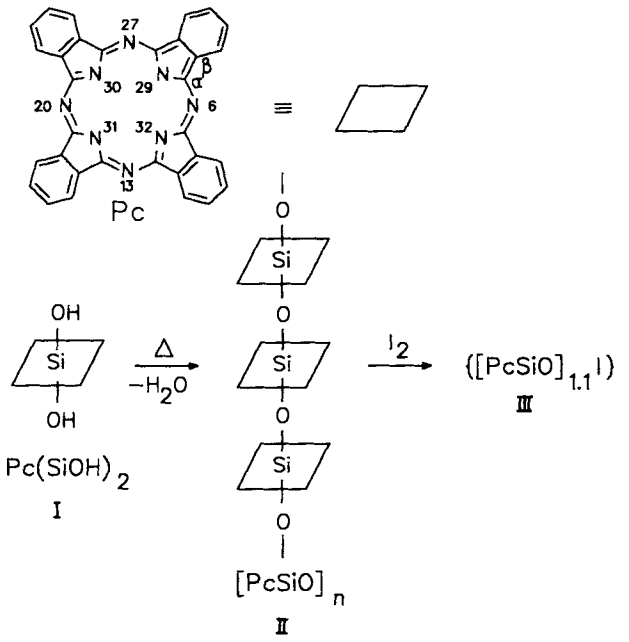


Fig. 1. Solid state polymerization of $PcSi(OH)_2$ to $(PcSiO)_n$ and subsequent oxidation to $[(PcSiO)I_{1.1}]_n$ with iodine; Pc ≡ phthalocyanine.

in Figure 2. For the monomeric precursor $PcSi(OH)_2$ three resonances are observed at 211, 199 and 170 ppm respectively. The assignment of the individual resonances are based on former ^{15}N CPMAS NMR studies of free base phthalocyanine.[11,12] The two low field lines stem from the outer nitrogen atoms N-6, N-13, N-20, and N-27. The inner core nitrogens give rise to the resonance at ~ 170 ppm. The inequivalence of the outer nitrogen atoms has been observed previously in the case of free base phthalocyanine.[11] The differences in the chemical shifts may either result (i) from a small deviation of the Pc macrocycle from a D_{4h} symmetry or (ii) from O–H···N hydrogen bonds between adjacent molecules as a consequence of intermolecular stacking.[13] In contrast to the monomeric form, the spectrum of the dehydrated polymeric form reveals only two resonances as shown in Figure 2b. The low field line which stems from the outer nitrogen atoms appears exactly in the middle of the monomer at 200 ppm, indicating a D_{4h} symmetry of the Pc macrocycle on the ^{15}N NMR timescale. This symmetry could be real or arise from rapid 90° jumps of the Pc macrocycle in **II**. The high field line has been shifted slightly upfield to 167 ppm as a result of small change of the electronic environment. The different signal intensities arise from different cross polarization dynamics and indicate the loss of the nearby OH protons in the polymer which facilitate cross polarization to the inner nitrogen atoms in $PcSi(OH)_2$, (**I**). Attempts to detect spin diffusion[14,15] between the outer and inner nitrogens in $[PcSiO]_n$, (**II**) were unsuccessful.

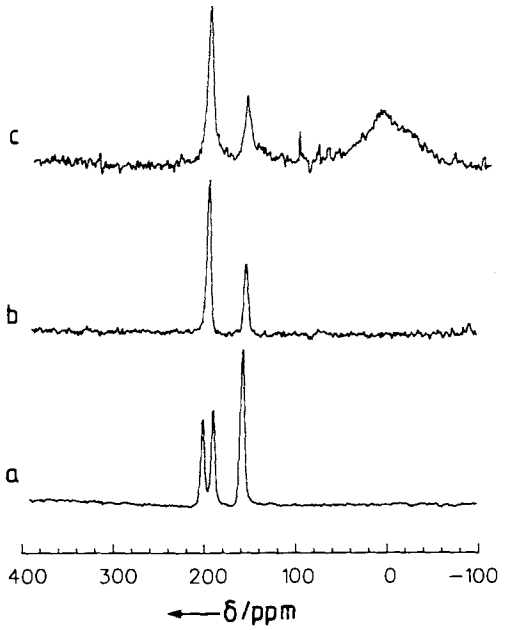


Fig. 2. ^{15}N CPMAS NMR spectra of 95% ^{15}N enriched phthalocyaninatosiloxanes at 9.12 MHz. (a) monomeric $PcSi(OH)_2$; (b) polymeric $(PcSiO)_n$; (c) partly oxidized polymeric $[(PcSiO)I_{1.1}]_n$. Experimental conditions: room temperature spectra, 5 mm o.d. rotors, spinning speed between 2.5 and 3.5 kHz, external reference $^{15}NH_4Cl$, 3 μs 90° pulses, 2.773 s repetition time, 7 kHz spectral width, 73 ms acquisition time; (a) 15 ms cross polarization time, 1480 scans; (b) and (c) 25 ms cross polarization time, 1390 scans.

In doping $[PcSiO]_n$ with iodine the spectra change dramatically as shown in Figure 2c. In addition to the familiar lines, a broad high field shifted resonance is observed. Careful line shape analysis shows that the signal consists of two lines, the stronger component appearing at 25 and the smaller component at 8 ppm; thus, in the doped compound the nitrogen signals are shifted between −160 and −180 ppm to high field. Note that not all material could be oxidized by doping with iodine; the observation of the presence of both shifted and unshifted signals in Figure 2c indicates the presence of coexisting clusters of conducting and isolating regions.

In order to obtain more information about **III** we have performed variable temperature measurements on this compound. The results are shown in Figure 3. Although the center of the broad high-field line seems to shift slightly to lower field as the temperature is raised, there is almost no temperature dependence on the line positions within the margin of error. This result is expected for Knight shifts resulting from interactions with conducting electrons; paramagnetic shifts arising from interactions with localized electrons should experience a much stronger temperature dependence.[16] Knight shifts are independent of the gyromagnetic ratio of the nucleus studied but proportional to the electron spin density at the latter;[16] the sign of spin densities is known to vary between adjacent atoms in π-electron systems. Thus, we can directly compare our results with the ^{13}C-Knight shifts reported previously for **III**.[6] These are + 280 ppm for the α-^{13}C atoms and −78 ppm for the β-^{13}C atoms. Thus, all carbon and nitrogen atoms adjacent to the α-^{13}C atom experience a positive Knight shift as expected. Whereas the small shift of the β-^{13}C atom signal is plausible, the much larger

ADVANCED MATERIALS

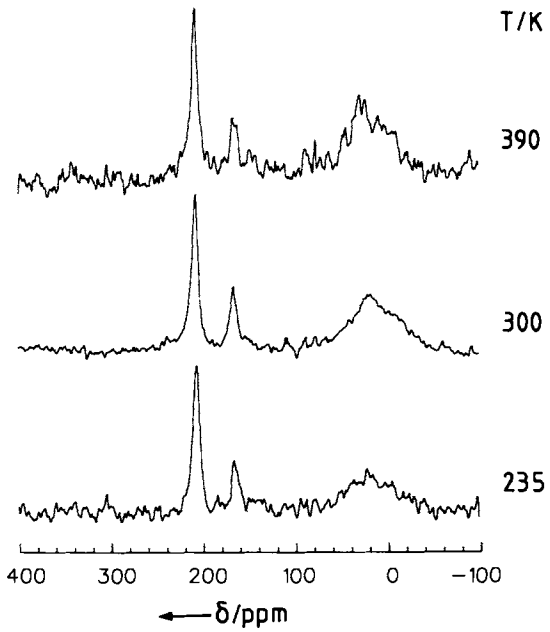


Fig. 3. ^{15}N CPMAS NMR spectra of partly oxidized $[(PcSiO)I_{1.1}]_n$ as a function of temperature. The spectra indicate slightly temperature dependent Knight-shifts of the oxidized material. Experimental conditions: 10 ms cross polarization time, 10 kHz spectral width, 52 ms acquisition time, otherwise same as Figure 2; (a) 2902 scans, (b) 15000 scans, (c) 7082 scans.

shift of the α-^{13}C spins as compared to the ^{15}N shifts needs further study.

In summary, it has been shown that structural changes of the solid state polymerization and the subsequent oxidation of ^{15}N labeled phthalocyaninatometalloxanes can be monitored by ^{15}N CPMAS NMR spectroscopy. In the oxidized state these materials are highly conductive, a fact confirmed by the observation of a ^{15}N Knight shift similar to the one observed by ^{13}C CPMAS spectroscopy. Conductive and non-conductive regions coexist and their relation can be estimated. Thus, ^{15}N CPMAS NMR spectroscopy provides interesting information on the structure and the reactions of this class of compounds.

Received: September 27, 1989

[1] W. Kroenke, C. E. Sutton, R. D. Joyner, M. E. Kenney, *Inorg. Chem. 2* (1963) 1064.
[2] B. N. Diel, T. Inabe, J. W. Lyding, K. F. Schoch jr., C. R. Kannewurf, T. J. Marks, *J. Am. Chem. Soc. 105* (1983) 1551; C. W. Dirk, T. Inabe, K. F. Schoch jr., T. J. Marks, *J. Am. Chem. Soc. 105* (1983) 1539; T. J. Marks, *Science 227* (1985) 881.
[3] J. Metz, G. Pawlowski, M. Hanack, *Z. Naturforsch. 38b* (1983) 378.
[4] M. Hanack, T. Zipplies, *J. Am. Chem. Soc. 107* (1985) 6127.
[5] M. Hanack, S. Deger, A. Lange, T. Zipplies, *Synth. Met. 15* (1986) 207.
[6] P. J. Toscano, T. J. Marks, *J. Am. Chem. Soc. 108* (1986) 437.
[7] J. Schaeffer, E. O. Stejskal, *J. Am. Chem. Soc. 98* (1976) 1031.
[8] J. R. Lyerla, C. S. Yannoni, C. A. Fyfe, *Acc. Chem. Res. 15* (1982) 208.
[9] C. A. Fyfe: *Solid State NMR for Chemists*, C.F.C. Press, Guelph, Ontario 1983.
[10] B. Wehrle, H. H. Limbach, J. Mortensen, J. Heinze, *Adv. Mater. 1989*, No. 12; *Angew. Chem. Int. Ed. Engl. Adv. Mater. No. 12; Angew. Chem. Adv. Mat. No. 12* and references cited therein.
[11] B. Wehrle, H. H. Limbach, *Chem. Phys. 1989*, in press.
[12] R. D. Kendrick, S. Friedrich, B. Wehrle, H. H. Limbach, C. S. Yannoni, *J. Magn. Reson. 65* (1985) 159.
[13] T. Krämer, Dissertation, Universität Tübingen, 1985.
[14] H. H. Limbach, B. Wehrle, H. Zimmermann, R. D. Kendrick, C. S. Yannoni, *J. Am. Chem. Soc. 109* (1987) 929.
[15] H. H. Limbach, B. Wehrle, M. Schlabach, R. D. Kendrick, C. S. Yannoni, *J. Magn. Reson. 77* (1988) 84.
[16] a) A. Abragam: *The Principles of Nuclear Magnetism*, Clarendon Press, Oxford University Press 1983. b) C. P. Slichter, *Principles of Magnetic Resonance*, 2nd ed.; Springer Verlag, Berlin 1978.

A New Route to Highly Conducting Polyenes

By *Henning Hopf**, *Olaf Kretschmer*, and *Herbert Naarmann**

Dedicated to Professor Wolfgang Lüttke on the occasion of his 70th birthday

Since doped polyacetylene was shown to possess metallic conductivity in 1977 this class of organic polymers has been studied intensively.[1] The polyacetylenes used for these experiments may be prepared by various routes,[2] the polymerization of acetylene with Ziegler catalysts according to Shirakawa being a widely employed method.[3] Under certain conditions this approach provides mechanically stable polymer films which are of particular importance for the preparation of conducting material.

Regardless of the catalyst system used, it is an inherent disadvantage of this type of polymerization that ultimately a washing process will be required to remove the catalyst or its residues from the desired polymer preparation. In this communication we describe a method which avoids this pitfall and provides polyene films which form a solid layer on glass surfaces, ceramic plates, tubes etc.

Allene (propadiene) is condensed under high-vacuum into a 2l-round bottomed flask, and after several freeze-and-pump cycles to remove residual oxygen and volatile impurities the reaction vessel is sealed (internal pressure at room temperature ca. 1000 mb). After 20 h at 460 °C (high-temperature drying oven) the inner surface of the flask is covered completely by a deep-black, shiny-film which can be removed in patches and whose electric conductivity is 10^{-8} S/cm. When this film is doped by treating it for 30 min with a saturated solution of iodine in carbon tetrachloride[4] its appearance changes to a shiny gold. After solvent removal the conductivity has increased by a factor of 10^9.

Since allene is known to isomerize to propyne at elevated temperatures[5] we also investigated the polymerization of this hydrocarbon and several other alkynes under the above conditions. The results of these experiments are summarized in Table 1.

[*] Prof. H. Hopf, Cand.Chem. O. Kretschmer
Institut für Organische Chemie, Universität Braunschweig
Hagenring 30, D-3300 Braunschweig (FRG)
Dr. H. Naarmann
BASF Aktiengesellschaft, D-6700 Ludwigshafen (FRG)

Table 1. High-temperature polymerization of alkynes and diynes.

monomer	electric conductivity of polymer film [a] [S/cm]	
	undoped	doped with I_2
propyne	10^{-8}	10^{-1}
1-hexyne	10^{-9}	10^{-2}
butadiyne	10^{-8}	10
1,5-hexadiyne	10^{-6}	60

[a] Determined with the four-probe technique [4]

The reaction time of the polymerization experiments may be reduced considerably (8 h) by carrying out the above thermal processes in the presence of small amounts of various Lewis acids such as $FeCl_3$ or $MoCl_5$.

The undoped polymer films are insoluble in common solvents, possess up to 10% sp^3-hybridized carbon atoms as determined by ^{13}C NMR spectroscopy, and are more stable to air than a Shirakawa-polymer film. The oxygen-uptake of the latter amounts to 6% after 1 hour (in air, room temperature, humidity 50%) and reaches 14% after 24 hours under the same conditions. A polyene film prepared from propyne by our approach only absorbed 1.5 and 2.7% of oxygen after 1 and 24 hours respectively.

The simplicity of this new approach to conducting organic polymers makes it amenable to other highly unsaturated systems (other allenes, cumulenes, alkylacetylenes) and the results of presently performed experiments along these lines will be published in due course.

Received: August 30, 1989

[1] For recent summaries of the vast literature see a) C. Kröhnke, G. Wegner, *Houben-Weyl-Müller E20/2* (1986) 1312, Thieme Verlag, Stuttgart, 1986; b) H. J. Mair, S. Roth (Eds.): *Elektrisch leitende Kunststoffe*, C. Hanser Verlag, Munich 1986; c) M. G. Chauser, Yu. M. Rodionov, V. M. Misin, M. I. Cherkasin, *Russ. Chem. Rev. 45* (1976) 348.
[2] H. Naarmann, *Angew. Makromol. Chem. 109/110* (1982) 295.
[3] H. Shirakawa, S. Ikeda, *Polymer J. 2* (1971) 2, 231.
[4] H. Naarmann, N. Theophilou, *Synth. Met. 22* (1987) 7.
[5] H. Hopf, H. Priebe, R. Walsh, *J. Am. Chem. Soc. 102* (1980) 1210.

Research News/Inorganic Materials I

Glass-Ceramics in the Scheme of Inorganic Materials

By Graham Partridge*

1. Introduction

Glass and ceramic materials have been known for several thousands of years, the technology of preparation and diversity of composition and properties increasing, perhaps relatively slowly at first, but latterly much faster leading to the advanced materials which are becoming established in todays technology and which are expected to form the backbone of developments into the 21st century.

Originally it was considered that the various materials should be classed as insulating, and were distinct in composition and properties. However, these distinctions have become very blurred at the edges, for example, conducting ceramics such as silicon carbide and the superconducting materials such as yttrium–barium–copper oxide have appeared together with semiconducting glasses of the chalcogenide type. Indeed the blurring has gone even further with the advent of such materials as amorphous metals or metallic glasses. How should these be classified—as special glasses or special metals?

[*] G. Partridge
GEC ALTHSTOM Engineering Research Centre
P.O. Box 30, Lichfield Road, Stafford ST17 4LN (UK)

A further type of material which bridges the original gap between glasses and ceramics are glass-ceramics. These are much more recent in concept and possess many of the useful properties of the earlier materials. Essentially, they help to extend the overall range of materials and provide the technologist and materials designer with more opportunities to meet the increasing technological demands of today.

The present article, intended to form part of a series describing and discussing recent developments in these materials is aimed at introducing the materials and outlining their properties and general position in the overall scheme of inorganic materials. By way of introduction it is useful to consider what is meant by the various terms used for these materials.

2. Description of the Materials

2.1. Ceramics

The definition of ceramics provided by *Kingery*; "the art and science of making and using solid articles which have as their essential component, and are composed in large part of

inorganic, non-metallic materials"[1], covers not only porcelains and refractories, which are normally considered to be ceramics, but also glasses and glass-ceramics. More specifically, however, ceramics are polycrystalline materials, generally with some interstitial glassy phase present, the material being a product of high temperature solid and/or liquid phase reactions occurring between the initial inorganic crystal forms resulting in regrowth and restructuring of the crystal phases present.

Many of the earlier ceramics, such as porcelains and refractories, were essentially silicate-based materials, but many other types now exist which have been developed as the technological demands increase. These include pure oxide ceramics, for example alumina (Al_2O_3) and zirconia (ZrO_2) ceramics, nitrides such as silicon nitride (Si_3N_4) and boron nitride (BN), and carbides such as silicon carbide (SiC). All these are polycrystalline materials and can truly be considered as ceramics which are made by the sintering of powder precursors.

2.2. Glasses

There have been a number of attempts to provide a satisfactory definition of glass which would enable this type of material to be differentiated from the "all embracing" ceramic definition given above. These attempts have tried to take into account the fact that glasses are essentially supercooled, high viscosity liquids, possess an amorphous structure and can be obtained from a wide range of both inorganic and organic compositions.[2] Perhaps the most satisfactory definition is "glass is a non-crystalline solid"[3], since this includes all solid materials which are non-crystalline regardless of their composition and mode of formation. This latter definition comes closest to overcoming the great difficulty of attempting a broad classification of such widely diverse substances.

The majority of glasses which are known and made on a commercial scale consist of glass-forming systems based on silica (SiO_2) and boric oxide (B_2O_3). However, many other glass forming systems are known within the overall range of technical glasses based on oxides such as phosphorus pentoxide (P_2O_5) and alumina (Al_2O_3) and non-oxide glasses such as the chalcogenides (glasses based on sulphur, selenium or tellurium)[3b] and indeed elemental glasses, for example amorphous alloys. With these, as with all glass-forming systems, the range of compositions which will form glasses is influenced to some degree by the rates of cooling which may be employed from temperatures above the liquidus: fast rates extend the composition range. Limits are imposed, however, by what is achievable in practice, being influenced by the size of the article and constraints such as thermal stress build-up and resistance to thermal shock.

2.3. Glass-Ceramics

Glass-ceramics are essentially polycrystalline solids prepared by the controlled crystallization of what is now a wide range of glass compositions.[4, 5] These technologically important materials may perhaps be described as "wonder materials", and the first wonder may be that they exist at all. Glass is essentially a meta-stable material, with a disordered liquid-like structure, and would prefer to exist in a more ordered, crystallized condition. Nevertheless, for many glass compositions, particularly those which are produced commercially in large quantities, the emphasis over the years has been to prevent devitrification occurring. If the glass can be cooled successfully through the temperatures at which crystallization occurs, the high viscosity of the material prevents the structural reorganization which would develop crystals, and the product possesses an amorphous structure.

Devitrification, as it is normally understood in the glass industry, is an uncontrolled process which has a harmful effect since it can lead to sudden and unpredictable changes in viscosity which interfere with the working of glass making machinery. Additionally, localized high stresses can be generated arising from differential contraction between glass and crystal phases formed, resulting in a mechanically weak product.

It has been appreciated, for some time, however, that if crystallization could be controlled then useful materials



Graham Partridge graduated from the University of Sheffield in 1953 with a Batchelor of Science Degree in Chemistry and Physics. After National Service in the Royal Corps of Signals as a Radio Mechanic Instructor, during which he rose to the dizzy heights of Corporal, he joined the then English Electric Company in 1956 to work on glass and glass-ceramic materials. After the Company was merged with the General Electric Company in the late 1960s he was appointed head of the laboratory, now known as the Glass/Ceramics Group in 1972. Currently the Group forms part of the Engineering Research Centre (Stafford) of the joint UK/French Company GEC ALSTHOM. Graham has been responsible for the development of special glasses, glass-ceramics, ceramics and ceramic matrix composites, together with fabrication and processing technology to provide materials for use in many aspects of engineering and electronics. He has authored and co-authored more than 25 publications and is named as co-inventor on more than 25 patents on which a number of international patents have been based. From now on he will write regularly for Advanced Materials.

might be produced. Indeed, *Reaumur*,[6] in 1739 tried to produce a polycrystalline material by heating articles of a soda-lime-silica composition immersed in a mixture of sand and gypsum. However, crystallization occurred from the surface, resulting in weak and brittle articles. Although surface crystallization in certain glass compositions can now be controlled to provide high mechanical strength materials,[7] in the context of the discussion on bulk derived glass-ceramics this is an undesirable form of crystallization.

In the 1950's, research at Corning Glass Works in the USA led to the realization (it is claimed by serendipity) that, under suitable conditions and (at that time) in a restricted range of compositions, it was possible to produce a usable polycrystalline material by the controlled devitrification of a glass provided that sufficient nuclei were developed within the bulk of the glass on which crystals could subsequently grow.

The glass-ceramic process may thus be essentially divided into two parts. In the first, nuclei are developed in the glass body either by phase separation of the glass or by precipitation of a primary crystal phase during the first stages of a heat-treatment process as depicted in Figure 1. In order to

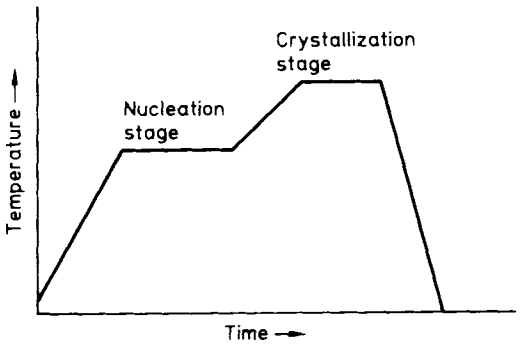


Fig. 1. Typical heat-treatment schedule for the production of glass-ceramics showing nucleation and crystallization holding stages.

develop the required quantity of nuclei it is usual to incorporate in the glass composition a nucleating agent. There have been many and varied such agents over the years of glass-ceramic development but the ones that are generally preferred in current developments are the oxides P_2O_5, TiO_2, and ZrO_2. Further heat-treatment to higher temperatures causes crystals to grow on the nuclei to form a closely interlocking crystal structure, with crystal sizes generally in the region of 1 μm, with a small proportion of interstitial residual glassy phase. In many cases, the crystallization processes can be very complex and the simple heat-treatment schedule depicted has to be modified to incorporate further holding stages in order to produce the desired materials and properties.

Alternatively, the glass may be reduced to powder and then processed in a similar manner to that discussed above for sintered ceramics. In this case the glass powder particles react together and because of the highly damaged state of the particles, surface crystallization may become dominant over bulk crystallization. Two possibilities exist in the use and development of sintered glass-ceramic materials. In the first, the compacted material is sintered to a vitreous body and is then subsequently heat-treated as in the case of the bulk materials above. Alternatively, nucleation and bulk crystallization occur during the same firing cycle as that used for the sintering step and this is to be preferred from an economic point of view.

The majority of glass-ceramic compositions are silicate based, although a number are known based on aluminate compositions. The many and varied compositions which can now be prepared as glass-ceramics the materials possess very different properties from those of the glasses from which they are derived. Mechanical properties are often improved and the linear thermal expansion characteristics of a glass-ceramic can be considerably different to those of its parent glass. Good electrical, particularly dielectric, properties are also produced as a result of the conversion of glass to glass-ceramic.

3. Properties

The general properties of the three types of inorganic materials discussed above are reviewed in this section. Detailed properties of materials relating to specific applications will be reviewed in future articles. Table 1 provides limited data for a number of inorganic materials.

3.1. Mechanical Properties

Although glass in its pristine state, for example newly drawn fiber, can possess very high mechanical strength with moduli of rupture above 7000 MPa, in practice, owing to surface damage, this is not realized and the practical moduli of rupture of glasses are in the range 50–120 MPa. Glass-ceramics are somewhat stronger and moduli of rupture up to 750 MPa have been realized. However, by far the strongest ceramic materials are derived from the sintered type of material with high strengths being obtained in oxide, carbide and nitride materials and particularly in materials such as yttria stabilized zirconia.

3.2. Electrical Properties

Owing to the presence of closed pores in sintered ceramics, their dielectric breakdown strengths are usually no higher than 20–25 $kV mm^{-1}$ whereas both glasses and glass-ceramics which do not contain closed pores can show dielectric breakdown strengths of 40–50 $kV mm^{-1}$. The dielectric properties of sintered ceramics and glass-ceramics cover sim-

Table 1. Properties of typical inorganic materials.

Property		Ceramics					Glasses			Glass-ceramics [8]			
		Al_2O_3	SiC	Si_3N_4	ZrO_2/Y_2O_3	SiO_2	Na_2O-CaO-SiO_2	B_2O_3-SiO_2	Li_2O-Al_2O_3-SiO_2	Li_2O-Al_2O_3-SiO_2	Li_2O-ZnO-SiO_2	MgO-Al_2O_3-SiO_2	ZnO-Al_2O_3-SiO_2
									low α	med α			
Modulus of rupture at RT	MPa	250–350	400–600	250–700	650–2000	50	120	90	100	255	200	350	95
Elastic modulus at RT	GPa	250	360	160–300	300	70	60	70	90	80	97		
Density	$kg \cdot m^{-3}$	360–390		240–310		220	220	255	255	244	260	265	370
Dielectric breakdown strength	$kVmm^{-1}$	20–25					25–30	44		45	50		
Volume resistivity	ohm cm	$>10^{16}$					10^{10}	10^{12}					
Dielectric constant	1 MHz	8.6–10					5	7			5.4		
	10 GHz	8.8–9.2		9		3.4			5.9	5.6		5.7	6.8
Loss angle, $\tan\delta \times 10^4$	1 MHz	5–8					38	40		22			
	10 GHz	1–10				4			1300	106		3	5
Linear thermal expansion coefficient, α, 20–500 °C $\times 10^7\,°C^{-1}$		78				5	92	32	~0	52	145	53	30
Thermal conductivity	$Wm^{-1}K^{-1}$	26	300	34	2	3			1	2	3	3	3

ilar ranges, the properties being strongly dependent on the crystal phases (and interstitial glass phase) present in the material. In general, glasses show higher dielectric losses than crystalline materials at high frequencies although fused silica (SiO_2) is very good in this respect.

3.3. Thermal Properties

The linear thermal expansion characteristics of sintered ceramics and glasses cover similar ranges although it is difficult to obtain a satisfactory sintered material which possesses a very low expansion comparable to that of fused silica. At the high expansion end, linear thermal expansion coefficients greater than about $140 \times 10^7\,°C^{-1}$ can be obtained for sintered ceramics but the materials possessing such expansions are generally poor in terms of strength and resistance to attack by atmospheric moisture. Glass-ceramic materials, however, enable the overall expansion range to be extended and usable materials with linear thermal expansion coefficients ranging from negative to as high as $180 \times 10^{-7}\,°C^{-1}$ can readily be obtained. The thermal conductivities of glasses and glass-ceramics are low, comparable with those of zirconia ceramics. High thermal conductivities can only be obtained in selected sintered ceramics, for example, Al_2O_3, BeO, SiC.

In addition, in terms of increasing resistance to high temperatures, the order is glass, glass-ceramics, ceramics. Many glasses cannot withstand temperatures in excess of 500–600 °C for long periods although fused silica may be used to temperatures in the region of 1000 °C before devitrification becomes a problem. Glass-ceramics can operate for extended periods at temperatures of 700 °C to over 1200 °C. Sintered ceramics, however, can provide operational capability to temperatures of 2000 °C although protection by means of a neutral or reducing atmosphere may be necessary to achieve this.

4. Selection

The selection of an inorganic material depends, perhaps obviously it could be argued, on the properties specified for a particular application. Often the properties are interactive so that whilst it is relatively easy to optimize one or two properties required, the problem becomes increasingly more severe when three or more properties must be optimized. However, properties are not always the overriding criteria and attention frequently has to be paid to fabrication routes. A fabrication route necessary for the highest strength material may not be practical in a specific application and compromises have to be made. Thus selection of a material for a given application may be guided, perhaps on economic terms, and the materials expert then has to obtain the best properties possible with the designated material. Examples of selection will be given in future articles and reasons discussed.

[1] W. D. Kingery, H. K. Bowen, D. R. Uhlmann, *Introduction to Ceramics*, Wiley, New York 1976.
[2] L. D. Pye, H. J. Stevens, W. C. LaCourse (Eds.): *Introduction to Glass Science*, Plenum Press, 1972.
[3] D. R. Secrist, J. D. McKenzie, *Modern Aspects of the Vitreous State*, Butterworths, 1960.
[4] P. W. McMillan, *Glass-ceramics*, Academic Press, 1979.
[5] Z. Strnad, *Glass-ceramic Materials, Glass Science and Technology 8*, Elsevier, Amsterdam 1986.
[6] M. de Réaumur, *Art de Faire une Nouvelle Espece de Porcelaine*, Memoirs de l'Academic Royale, 1740, p. 370–388.
[7] G. Partridge, *Glass Technol. 28* (1987) 9–18.
[8] M. H. Lewis (Ed.): *Glasses and Glass-ceramics*, Chapman and Hall, 1989, Chapter 7.

Conference Reports

Powder Metallurgy (PM'89) in San Diego

By Rainhard Laag*

1. Introduction

At the PM'89 conference, held 10–14 June 1989 in San Diego, USA, the present state of metal powder injection molding (MIM) in the USA was presented in five sessions, each with 15 presentations where the leading researchers, producers and consumers of MIM parts demonstrated impressive progress in development and application. Currently, the most extended activities in institutional research and development are being made at Rensselaer Polytechnic Institute (RPI), Troy, NY. A considerable number of companies are also developing improved processing, but it is mostly of a proprietary nature.

Before discussing the individual presentations given at San Diego, the general state of the art will be briefly described. The development of new, high performance metal alloys requires rapid solidification process to control the microscale homogeneity of the chemical constituents. Investigations of powder production are, therefore, closely connected with the development of advanced forming and consolidation processes. Two examples of recent developments are Metal Powder Injection Molding (MIM) and sinter-hot isostatic pressing (Sinter-HIP). Both, as concepts, are attempts to conserve the physical properties of powders on a macroscopic scale. Between concept and finished part, however, the processing steps change the initial conditions of homogeneity and freedom from exogenous materials—both solids and gases.

Sinter-HIPing of powder compacts is a pressure assisted consolidation technique and is applicable to a wide size range of parts made from powders. It is beneficial to form a stable green body either by cold isostatic or by uniaxial pressing. Advanced metals like superalloy and intermetallic phase powders do not compact well. Therefore, the powder must be filled in glass or metal containers for consolidation. This encapsulating process increases the production costs (an additional step) especially since the containers are not reusable after HIPing. The advantage of Sinter-HIP consolidation is that relatively coarse powders can be used without any contamination being caused by binders or additives. This simplifies the conservation of the physical properties of the powders and helps to achieve an optimum in mechanical properties.

MIM is a hydrostatic-pressure forming and consolidation process used to produce small and complex shaped parts inexpensively in large quantities. A mixture of approximately 60 vol.-% fine metal powder and 40 vol.-% binder and lubricant can be formed much like a conventional plastic. The use of waxes like polyethylene or other thermoplastics provides the rheological basis allowing the mixture to flow into undercuts and corners in a way that the uniaxial pressing of lubricated metal powders cannot achieve. Dependent on the shape complexity, this process needs very fine powders to achieve homogeneous form filling. The forming process is a combination of thermoplastic pressure casting and conventional powder metallurgical technologies. Like all known processes, MIM has some advantages and disadvantages. The limitations are mainly in the compatibility of the powder/binder interface, the complete binder removal and the pressureless sinterability of the metal powders to near full density.

In order to combine the advantages of MIM with its achievable shape complexity with, for example, the high performance of superalloy and intermetallic phase materials, it is necessary to enhance the ability of MIM either to process coarser powder particles or to develop powder production techniques that allow the inexpensive preparation of fine prealloyed powders on an industrial scale. Because of MIM's potential to produce large quantities of parts, the use of fine powders produced by conventional techniques is currently much more expensive than the use of coarse powders. The savings are twofold, in powder costs and in economies of scale which often result in an exponential increase in cost effectiveness with the quantity of produced parts.

The main disadvantage of MIM is that the savings in processing are connected with an increase in impurity of the part because group III–IV metallic elements and refractory metals are highly reactive towards anionic elements like oxygen or nitrogen. A reduction of the powder particle size far below 100 μm increases the specific surface area of the powder so that the content of impurities can reach 1–2 wt.-%. At the higher temperatures necessary for consolidation, these impurities diffuse to grain boundaries and promote brittleness by forming strong oriented covalent bonds. The me-

[*] R. Laag
Max-Planck-Institut für Metallforschung
Institut für Werkstoffwissenschaft, Pulvermetallurgisches Laboratorium
Heisenbergstraße 5, D-7000 Stuttgart 80 (FRG)

chanical properties are very dependent on the amount of impurities. Another advantage of using coarse and spherical powder particles is their lower mechanical friction and their higher packing densities. This allows a higher powder loading in the binder. An additional increase in density can be achieved if special particle size distributions like bimodal or trimodal distributions are used. The higher the density of the green shape compared to the theoretical density, the smaller is the resulting shrinkage during sintering.

Today, the use of coarser particles is, however, limited. This has three main reasons:

- Super solidus sintering does not work as well with coarse particles because the surface area decreases with an increase in particle size.
- The internal friction of coarser particles is lower. After debinding, the parts are very sensitive to fragmentation before presintering. Typically the debinding process ends at much lower temperatures than necessary for presintering. This difference is especially noticeable for high temperature alloys.
- Solid state sintering of single phase high temperature alloys like intermetallic aluminides does not work because of the low diffusion rates in ordered lattice structures.

The overall advantage to the processing of fine powders is the superior form filling during molding which allows more complex shapes to be molded and gives a homogeneous distribution of binder and powder in the green body. Spherically shaped particles simplify the critical debinding process, enhance sinterability, and cause uniform dimensional shrinkage which reduces effort in tool design, quality control and finishing of the parts. The application of prealloyed powders achieves the additional advantage of a more homogeneous microstructure after sintering compared to the component or multicomponent powder mixtures.



Injection molding consists of four basic steps: powder-binder-formulation, injection molding, debinding and sintering. Although each step appears independent they are in some ways all related. Currently the interchange between the processing steps is not understood adequately. The procedure of producing parts is based on empirical results which are connected with long and expensive trial and error investigations. Up to now it is clear that the most sensitive factors are the powder properties, the constituents of the binder, the powder binder interfaces and the process variables of debinding and sintering. All these problems were addressed by the presentations in San Diego.

2. Powders

In the section on powders the need for the production of ultrafine powders below 20 μm in diameter was outlined. Three different atomization processes and one high energy milling process were shown. The microatomization of GTE Products Corporation, presented by *M. Pliwal* and *R. J. Holland*, produces spherical powders of tungsten, copper, aluminum and stainless steel by remelting sintered powder mixtures and forming prealloyed powders in a plasma jet. This relatively expensive procedure allows the production of prealloyed powders made from alloys with very high melting points. Another method, ultrasonic gas atomization, provides particles below 45 μm. The volume fraction of powders below 20 μm was small in comparison to the yield of other methods presented. The reason may be the low gas-mass stream that divides the melt stream into the required fine droplets. *K. P. Kao* (Defense Metallurgical Research Laboratory) presented fluid energy milling which he has used to process iron sponges to fine particles of spherical shape. These have a shorter debinding time and a better sinterability in comparison to iron carbonyl powder. With the exception of the ultrasonic gas atomization, all processes described in this session had the same disadvantage in being an additional production step in working with MIM and being expensive when larger quantities are produced.

3. Process Variables

The presentation by *D. Lee, K. F. Hens* and *L. A. Najmi* (RPI) was focused on the understanding of the conditions under which the injection molded parts could be produced. They have developed software packages which allow the examination of the form filling conditions with respect to the powder/binder mixture. The basic concept of the calculations is known from plastic injection molding. Additional difficulties arise due to the variation in molding temperature. If the binder shows a rapid change in viscosity, and segregation occurs inside the die, then density variations occur in the molded parts. The optimization of process parameters by extensive computer calculations demonstrates the need for

careful process control. The second presentation of this session (*D. A. Issitt*, European Advanced Materials Institute) illustrated the influence of powder characteristics, binder selection, rheology of the mixture, green strength, debinding, shrinkage and tolerance on the properties of the finished part. Here, the audience was told that only the carefully adjusted optimization of each individual process parameter will result in a product with the properties required for advanced technological applications. In the last presentation *T. Tonomura* (Multimaterial Japan Limited) illustrated factors that affect size tolerance and physical and mechanical properties. The high performance of injection molding was demonstrated even for cases where elemental powders were used.

4. Binders

This session dealt with the key problem of successful injection molding, the evaluation of binder systems and their compatibility to the surface chemistry of the powders. The presentation "Optimization of the Powder–Binder Mixture for Powder Injection Molding" given by *R. M. German* (RPI) was the highlight of the injection molding sessions. Based on his long term practical experience, he gave the audience an assessment of the powders and binders currently used in injection molding. A body of mathematics was described which is used to predict and optimize the design of injection molding powder/binder mixtures. Several factors were included in calculating the inherent packing density of a powder. It was shown how the packing characteristics are dependent on particle size, distribution and shape, agglomeration, surface active agents, internal powder porosity, mixture homogeneity, interparticle friction and the size of the mold. Modeling of the viscosity of the powder binder mixture, using several equations developed for concentrated suspension behavior was demonstrated. The method resulted in a predicted optimal mixture for injection molding for a given set of powder and binder attributes.

After the discussion of particle characteristics, the second presentation "Requirements of Binder for Powder Injection Molding" by *C. I. Chung* (RPI) tried to illuminate some of the secrets in binder development. As expected the specific requirements of a binder depend on the complexity, size and metallurgy of the desired part. The performance of the binder can be enhanced by mixing or blending the binder with other materials. The molecular length of all components of the binder must be smaller than the interstitial free path length between powders in order to obtain a microscopically uniform mixture.

5. Research

The purpose of this session included the evaluation of new materials applicable for injection molding in the future. Highly sensitive materials like titanium powder were shown to be moldable if the binder does not violate the surface chemistry of the powder. In the presentation given by *K. Ameyama* (Ritsumeikan University) on injection molding of fine titanium powder it was reported that binder consisting mainly of polybutylmethacrylate can be completely removed after molding and the titanium sintered to a density of about 94% theoretical density. Impact properties were measured and fracture was characterized in order to evaluate the processing (molding, sintering). Correlations between processing parameters and mechanical properties were established.

"Supersolidus Sintering of Coarse Powders and Its Application to Injection Molding", given by *P. F. Murley* (RPI) was an attempt to evaluate the applicability of injection molding for coarse powders. Here, obtaining a homogeneous distribution of binder, and debinding were the most critical steps of the process. Experiments with higher volume fractions of metal in the mixture showed that the disadvantages caused by a homogeneous binder distribution—pore formation during molding and incomplete debinding even after long cycle times—counteract the advantages expected from higher metal fractions. Microstructure development during super solidus sintering of bronze and nickel alloy powder was found to be highly sensitive to local temperature variations.

6. Applications

Three presentations covered the evaluation of profitable applications of MIM. Nickel–Steel parts for the automotive industry, office equipment, oil drilling and camera components were shown. Other profitable examples made from stainless steel are parts for computer equipment, dental instrumentation, orthodontic devices, chemical components, marine equipment, aerospace equipment and a Fender bass guitar. Parts made from some exotic materials like Kovar, Tungsten, Invar and Molybdenum were supplied to the electronics industry in the form of hermetically sealed packages—headers, eyelets, flanges, heatsinks and bases.

The problem of building inexpensive prototyes of mold forms for experiment and process optimization was sketched. A minimum production quantity of about 20,000 pieces per year was thought necessary to amortize tooling costs.

The PM'89 conference in San Diego covered the present state of the research, development and production of MIM. Much effort was made to develop processing and new applications for parts which should be very competitive with other powder metallurgical routes and castings. Standard processing known from plastic injection molding has been successfully transferred to the production of small parts made from carbonyl iron and nickel powders. The transition to more complex materials and the systematic evaluation of new compatible binder systems needs a lot more scientific work

ADVANCED MATERIALS

towards understanding the principles and dependency of the process. An ideal process would use inexpensively produced, gas atomized, fine and small sized powders of about 10 μm diameter with a compatible multicomponent binder system which provides a mild decomposition at relatively low debinding temperatures. Debinding, presintering and consolidation of injection molded parts in a Sinter-HIP furnace offers the possibility of a one step heat treatment which avoids handling of the debinded parts. Full density can be achieved by pressure assisted final stage HIP. In the USA, a multimillion dollar project, part of the Advanced Powder Processing program at Rensselaer Polytechnic Institute, is the beginning of a move from empirically based process development to a systematic development of the theoretical background.

The basic elegance and simplicity of the injection molding process must not lead to the assumption that fully dense parts of predictable final dimensions are produceable as easily as in plastic injection molding. Up to now the main problems arise after the actual molding, during debinding and sintering. Only complete control over all process parameters will result in high quality reproducable parts.

Macromolecular Physics in Lodz

By Hugh J. Byrne *

To the French Cistercians who founded the Abbey in Sulejow Lodz, Poland, the terms charge transport and activation energy had little meaning, and seldom were they to be seen meandering through the grounds digesting the importance of bipolarons and multiphoton resonances. However, for one week in September, the serenity of this decaying 12th century house of learning was disturbed as it played host to the 21st Euro-Physics Conference on Macromolecular Physics, held from 4–8 September.

The conference was focused on the topic of "Electrically and Optically Active Polymers", a field which has attracted the expertise of a diverse range of scientists including polymer and solid-state physicists as well as physical and synthetic chemists. Interest in these materials was generated by the discovery that it was possible to make thin films of polyacetylene, and was increased by the subsequent discovery that the conductivity of this material could be increased to metallic values by chemical doping. Since then, a great deal of activity has produced a large range of processible organic polymers whose properties have been studied. Of similar interest to the electrical properties of these materials are the optical and, in particular, the nonlinear optical properties. The highly delocalized π-electron backbone of these polymers should give rise to large nonlinear susceptibilities which may render these materials a possible alternative to inorganic materials in the developing fields of all-optical switching and signal processing. This conference was designed to review the progress and problems of understanding the nature and origins of these materials properties.

The key-note address was delivered by the conference chairman, *Prof. M. Kryszevski*, from the Polymer Institute of the Technical University of Lodz, who outlined the objectives of the conference. Particular importance was attributed to the necessity for a greater understanding of the dependence of the electrical and optical properties of these materials on their structure and morphology. In a field where the range of materials available is ever increasing and where the polymer morphology may vary from that of single crystal to that of solution, an understanding of this structure-properties relationship is as important as understanding the microscopic molecular properties. Indeed, the problems facing "homo polymerius" were effectively portrayed by *V. Enkelmann* from Mainz, FRG. In his presentation he described the number of possible inter and intra chain effects contributing to a bulk measurement of any polymer parameter. He stressed the need to control the macroscopic conductivity by means of molecular parameters. The approach taken was to move towards single crystal materials in which interchain hopping is controlled by the size of the molecular structure. In polythiophene and polyparaphenylene, substitution was employed to systematically control the interchain distance by steric effects. The temperature dependence of the conductivity was found to increase as the size of the substituent increased, indicating an increasing activation energy although the conductivity itself decreased. The transition from the dominance of interchain effects to that of intrachain effects was thus shown, and an empirical relationship between the activation energy and the interchain parameter was presented. A similarly strong correlation between the

[*] Prof. H. J. Byrne
Department of Pure and Applied Physics
Trinity College
Dublin 2 (Ireland)

structural and electronic properties of these systems was evident in the presentation of *P. Bernier* from Montpelier, France. NMR and ESR studies of the doping process of polyacetylene appear to confirm the stage-like nature of this process indicative of a step-wise restructuring of the material with increasing dopant concentration. They also reported that a new, dilute phase was identified. This correlation was highlighted by the work of *M. Stolka* et al. from Xerox in New York in which the charge transport in Si and Ge backbone polymers was studied over a wide range of temperatures, encompassing the glass transition temperature. At the glass transition temperature the activation energy of transport abruptly decreases to very low values, raising the comment from *H. Bässler* from Marburg, FRG, that transport in these materials is controlled by disorder.

The importance and nature of interchain transport mechanisms were outlined by *A. A. Zakhidov* of Tashkent, USSR and the stabilization of solitons, polarons, and bipolarons by interchain coupling effects between neighboring polyacetylene chains was proposed. This stabilization leads to the possibility of interchain optical transitions, influencing the nature of the photoinduced absorption spectrum.

In terms of electrical conductivity, the most promising material at the present time is the so-called Naarmann polyacetylene. The question as to why this particular form of polyacetylene (and indeed, only some samples within a batch) shows such high conductivities ($\sim 10^5\ S\,cm^{-1}$) was addressed by Dr. *T. Schimmel* of Bayreuth, FRG. The anisotropy of the conductivity was found to be ~ 50 but temperature independent, indicating a common limiting mechanism in both directions. This dependence was reported to fit best to the model of *Sheng* describing large, highly conducting regions separated by small gaps, with the rate of gap hopping being proportional to temperature. These barriers contribute to only 30–40% of any sample resistance and do not vary much between high and low conductivity samples. Transport is therefore deemed to be limited by the resistance of the high conductivity regions. As yet, however, the recipe for these highly conducting regions appears to be empirical.

The importance of new materials exhibiting new properties and of new processing techniques was also stressed in the key note address. The influence of the structural properties of poly(vinylidene fluoride) which has a strong piezoelectric activity, on the macroscopic polarization was discussed by *D. Geiss* from Taltow, GDR. It was demonstrated that even poorly crystalline polymers such as dye-doped poly(methylmethacrylate) can exhibit a significant piezoelectric activity upon poling. Polymer blends of poly(3-alkylthiophenes) were shown to exhibit improved mechanical properties by Dr. *V. Laakso* of Porvoo, Finland, whereas the soluble forms of polyacetylene described by *J. P. Pfleger* from Prague, Czechoslovakia, provided good optical quality materials for nonlinear optical measurements. In samples of poly(bisalkylthio-acetylene) a dramatic increase of conductivity was observed by *H. K. Roth* from Leipzig, GDR, upon laser treatment. This increase is associated with a color change from red to blue-black and a loss of solubility, and the process appears to be similar to polymer doping. The advantages of this technique over doping is the high spatial resolution available by using small laser focal diameters.

Investigation of the nonlinear optical properties of organic conjugated polymers is a field of research equally as active as that of their electrical properties, and already device applications have become realistic. Exploiting the large second order polarizability of poled organic polymers, guided wave structures may be made which act as phase and intensity modulators. A 2X2 electro-optic switch has been realized, as reported by *G. Mohlmann* from Akzo in the Netherlands. Waveguide losses are as low as, or lower than, $1\ dB\,cm^{-1}$, and further development should produce devices competitive with rival lithium niobate structures.

The second order nonlinearities utilized in these devices are not, however, intrinsic to the polymer backbone and exploitation of such an intrinsic nonlinearity for device applications appears to be further from realization. Highly conjugated polymers have been predicted to possess a large ultrafast nonlinearity which should be real in nature. Investigations of the nature of this nonlinearity using the technique of third harmonic generation were carried out by *F. Kajzar* of Saclay, France and also by *D. Neher* from Mainz. In the latter case, the materials studied were substituted polyphenyl acetylenes and poly(3-decylthiophenes) whereas in the former, they were poly(thienylthiophene) and poly(dithienyl benzene). In all cases a strong resonant enhancement of the process was observed. The influence of such multiphoton resonances on the degenerate four wave mixing signals at 1.064 μm in a range of polymers was discussed by *H. J. Byrne*, from Dublin, Ireland. In the case of poly(3-butyl thiophene) a strong three photon enhancement was observed, whereas in the much studied polyacetylenes poly 3 and 4 (BCMU) a two photon enhancement was observed. In poly(anthracene phenylenine) however, the nonlinearity is purely third order although a large imaginary contribution is measured. It appears therefore that in all cases, the nonlinearity is dominated by imaginary contributions, and it was suggested by *Byrne* that this represents an inherent limit to the material polarizability since all resonances in these materials are localized by virtue of the strong excitation-lattice coupling. The ultrafast nature of the nonlinearities in polyacetylene/poly methylmethacrylate copolymers was demonstrated by *Pfleger*, who also showed the detrimental effect of doping on the polymer nonlinearity. This observation highlights the divergence of the disciplines of electrically active and (nonlinear) optically active polymers.

As the intensity of research increases in this area, the number of realistic applications increases. As previously mentioned, electrooptic switching devices based on poled polymers are already approaching the standards set by their rival lithium niobate based devices. The strong mechanical properties of *Laakso*'s poly(3-alkyl thiophene) blends make them good materials for antistatic packaging. An impressive piece

ADVANCED MATERIALS

of precision work with a wide range of applications was presented by *J. Kikas* from Estonia. Spectral hole burning of dyes in polymer matrices produces holes with a spectral width as low as 10^{-2}–10^{-3} cm^{-1}. With this resolution, up to 10^3 holes may be burned per inhomogeneous band. The listed applications of such hole burning techniques included frequency selective optical memory, space and time domain holography, and the materials may be used as narrow band optical filters. Application of an external electric field gives rise to stark shifting of the holes, an effect which may be exploited as an optical modulator.

Within one week it is only possible to cover a small portion of the current developments in this expanding field. Presented above is merely a cross-section of the week, but a number of issues were, however, highlighted. Firstly, whereas the nature of the optical and nonlinear optical properties of conjugated polymers are still considered to be primarily determined by interchain effects, the material structure and morphology appears to be critical for the electrical properties. This structure-properties relationship was discussed at length, resulting in the recognition of the need for well defined structures, and systematic studies. In such a way, understanding and enhancement of electrical properties may be achieved through manipulation of material structure. On the other hand, in the case of the nonlinear optical properties of conjugated polymers, the suggestion of an intrinsic molecular limit to the magnitude of the response infers the need for further systematic studies on well defined molecular structures. The division between the two fields of research is highlighted by the fact that good electrical properties require material doping, a process which as a devastating effect on the nonlinear optical properties.

Despite the continuing complexity of both areas, progress towards an understanding of the dominant physical processes involved is being made. The resulting feeling of optimism was reflected in the atmosphere of a conference designed as an exchange between Eastern and Western Europe, held in a country in transition from one political idealogy to the other. Amidst this political, economic, and scientific complexity, the conference was a success.

Surface Modification Technology in Neuchâtel

By Peter K. Bachmann*

The "Third International Conference on Surface Modification Technologies" (SMT III) was held from 28 August–1 September in Neuchâtel, Switzerland. After Phoenix, Arizona and Chicago, Illinois, SMT III was the first of this series of conferences to take place outside the United States of America.

Neuchâtel, beautifully located at the foot of Mount Chaumont and at the shore of Lake Neuchâtel was chosen because it is also the home of the University of Neuchâtel and of CSEM, the Centre Suisse d'Electronique et de Microtechnique S.A., a private, non-profit R&D organization active in the fields of microelectronics, optoelectronics, sensors, micromechanics and material science. CSEM and TSM jointly organized and sponsored SMT III along with many other Swiss scientific societies, Swiss government agencies and the University of Neuchâtel, which provided the rooms and the infrastructure for the conference.

The objective of the "Surface Modification Technologies" conference series is to bring together physicists, chemists, metallurgists, manufacturing engineers, and other materials scientists from around the world to interact and utilize each other's capabilities in the cross pollination of ideas, and, indeed, 82 contributions from 20 different countries including Europe, Asia, Australia and North America are listed in the technical program. Quite interestingly for a conference held in Europe, the USA with 22 papers outnumbered Switzerland with 13 and West Germany with 10 contributions. Japan, on the other hand, had only two entries.

The sessions offered to an audience of approximately 160 participants included ● Diamond and Related Coatings, ● Characterization of Coatings, ● Physical Vapor Deposition, ● Chemical Vapor Deposition, ● Laser Alloying, ● Alternate Coating techniques, ● Laser Surface Treatment, ● Coatings for Space Applications, ● Ion Implantation, ● Electroplating, ● High Temperature Coatings, and were accompanied by an additional half-day poster session.

1. Wear and Corrosion Resistance

Similar to other coating oriented conferences, SMT III illustrated that many practical applications of modified surfaces are related to improved wear resistance or increased

[*] Dr. P. K. Bachmann
Philips Research Laboratories
P. O. Box 1980, D-5100 Aachen (FRG)

lifetime of bearings and cutting tools. Contributions to this field were scattered throughout the processing technology oriented sessions and made up approximately 30% of the conference papers. Examples of this topic include a presentation by *O. Knotek* (RWTH Aachen, FRG) on reactively sputtered ceramic coatings. The properties of Si_3N_4 ceramics were improved by adding a thin layer of Si–Al–O–N using reactive magnetron sputtering techniques. *W. Ensinger* (University of Heidelberg, FRG) presented a paper on the low temperature generation of ceramic coatings, for instance nitrides or carbides of boron, titanium, chromium aluminum or silicon using ion beam assisted deposition. Deposition temperatures well below 200 °C were made possible using this technique. *D. G. Bhat* (GTE Valenite, Troy, MI, USA), one of the conference co-organizers describing in his contribution how to improve the chemical wear resistance of Si_3N_4 cutting tools for the machining of steel by applying a computer-modeled titanium nitride layer that adheres excellently to the surface of the tool material.

An alternative to applying vapor deposited coatings to improve the performance of cutting tools was presented by *T. L. VanderWert*. (Innovex, Hopkins, MN, USA). By applying a pulsed magnetic field to relieve internal stresses the lifetime of any cutting tool material was shown to increase by 40% to 180%.

Another alternative to the deposition of carbide and nitride coatings that has gained attention in the Japanese industries was pointed out by *T. Arai* (Toyota, Aichi, Japan). In this approach, carbon or nitrogen containing materials are immersed into molten salt baths containing carbide or nitride forming elements. The coating is formed by chemical reaction on the substrate surface. The performance of this material is comparable to CVD or PVD coatings but the preparation process was found to be more efficient.

2. Superconductors

This topic was covered in three papers. The results of R.F. magnetron sputtering experiments (by *P. K. Srivastava*, CSEM, Neuchâtel), chemical vapor deposition (by *G. Wahl*, Asea Brown Boveri, Heidelberg) and spray pyrolysis of aqueous Y-Ba-Cu nitrates (by *S. P. S. Arya*, CSEM, Neuchâtel) were outlined. All of the methods are capable of producing the standard 1-2-3 material with transition temperatures around 90 K. The width of the transition region of films made by spray pyrolysis on alumina decreases upon applying a Y_2BaCuO_5 interfacial layer prior to the formation of the 1-2-3 coating.



3. Miscellaneous Coatings and Processes

The preparation of unusual material combinations was tackled by *J. W. Dini* (Lawrence Livermore Laboratory, Livermore, CA, USA) by utilizing combinations of processes. Thick (1 mm) copper coatings on glass which can subsequently be precision machined for optical purposes were obtained by first applying a PVD coating followed by the electroplating of the newly generated surface.

Part of a review by *P. K. Bachmann* (Philips Research Laboratories, Aachen) was devoted to a sucessfully industrialized CVD application, the preparation of high quality optical fibers for telecommunications applications by means of thermal and plasma induced chemical vapor deposition methods. Up to now the stringent requirements of ultraclean processing and the close matching of a desired refractive index profile are only met by CVD techniques. With respect to efficiency, dopability and refractive index profiling, plasma induced CVD has advantages over thermally initiated deposition processes. A number of papers in various sessions were related to the characterization of surfaces modified by laser treatment, plasma treatment, and ion bombardment. Special attention was on the characterization, modification, optimization and modeling of substrate-deposit interfaces to improve the adhesion of deposits.

4. Diamond and Related Coatings

After more than 6 years of continuous research and development efforts in Japan and about 4 years after major US groups entered (or re-entered) the field, CVD grown diamond coatings are now considered a reality in Western Europe. This is illustrated by the first major diamond-related conference session held as part of SMT III as well as by the announcement of the first European conference solely devoted to diamond and related coatings, the "Diamond Films '90" planned for September 1990 in Montreux, Switzerland (for further information, please contact the author). Eight papers and one poster were associated with this emerging technology.

In his invited presentation on diamond as a heat sink material *M. Seal* (D. Drukker, Amsterdam, Holland) provided the link between the well established applications of

natural or high pressure synthesized diamond and the utilization of vapor deposited diamond thin and thick films. Diamond is known to be the material with the highest heat conductivity of any solid at room temperature and is applied as a heat sink for high power electronics. When designed and prepared properly, diamond films deposited from hydrocarbon/hydrogen mixtures at low pressure and substrate temperatures of approximately 1000 °C can be used for this purpose thus circumventing the size limitations of natural or high pressure synthesized diamond stones.

As a pleasant surprise to the organizers, *Boris V. Spitzyn* of the USSR Academy of Science in Moscow, USSR, was able to attend the conference. *Spitzyn* has been actively involved in diamond CVD since the early 1950's and was the first to ever apply for a patent on the vapor growth of diamond (on diamond substrates) in 1956. This patent, coauthored by *B. V. Derjaguin*, was finally granted in 1980. He outlined the history of diamond CVD which he rightfully terms diamond "crystallization" from the vapor phase and gave some insight into the basic mechanisms of diamond formation. The main trick is to etch the growing deposit with atomic hydrogen. Due to the higher etch rate, the thermodynamically more stable graphite is removed and pure diamond remains to form a film.

Various preparation methods, including thermal and plasma enhanced CVD techniques can be applied to form polycrystalline coatings on metals, semiconductors and insulators, e.g. Mo, Si and silica glass, as pointed out by *P. K. Bachmann* in the second part of his review on selected CVD applications. He also described applications other than heat sinks, such as cutting tool coatings, loudspeaker membranes, optical coatings and, using semiconducting doped diamond, high power/high speed electronics. Some of these applications are already commercially available, e.g. loudspeakers and certain tools, while additional efforts are still necessary to get the others to the market place. The main problems are currently adhesion for tool applications, scattering of the polycrystalline material for optical applications, and heteroepitaxy of single crystals for larger size electronics applications.

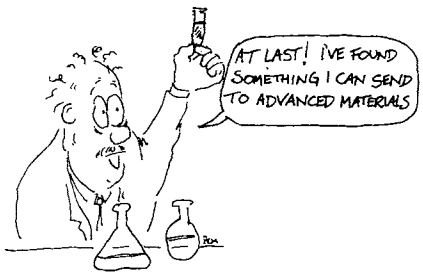
Homoepitaxial growth of diamond on various types of natural diamond is possible, however. In a contribution of *A. Badzian* (Materials Research Laboratory, Pennsylvania State University, PA, USA) the successful preparation of 160 μm thick vapor grown single crystal diamond layers was reported. The differences between the Raman spectra of the substrate and the deposit are neglegible, indicating the high quality of the deposited material. These findings were supported by the X-ray and infrared data of the epitaxial layer. This paper also covered some materials aspects of the C–N and the B–C–N system. The plasma CVD preparation of ternary phases that easily scratch diamond was claimed. Hardening of diamond by the implantation of nitrogen ions was also the topic of *S. Prawer* (Royal Inst. of Technology, Melbourne, Australia). The ion bombardment that improved the wear properties of diamond single crystals had to be applied at elevated temperatures. Another paper on post-growth treatment of diamond, given by *N. Chapliev* (Academy of Science, Moscow, USSR) described the effects of CO_2 laser pulses on CVD diamond surfaces. Pattern etching, the formation of well defined holes and surface smoothing were achieved using different atmospheres during the treatment. Two papers of the session were solely devoted to preparation techniques. *C. Benndorf* (University of Hamburg, FRG) presented a simple set up for microwave plasma CVD of diamond. His modification of this widely used method was to use a cylindrical, tunable resonator along with parts from a commercial microwave oven. Diamond deposition using a DC plasma torch was described by *P. K. Bachmann*. DC thermal plasmas are capable of diamond deposition rates of up to 500 μm/hour on small substrate areas. As pointed out in this presentation, a major drawback is the radially inhomogeneous composition of the coating. Only the central portion of the coating consists of high quality material. Other parts of the deposit are contaminated with graphitic phases. The method is suitable, however, for the preparation of bulk material on small areas. Diamonds also won the prize for "best poster" of the poster session. A presentation by *R. Haubner* (University of Vienna, Austria) outlined the influence of nitrogen added to the CVD gas phase. For nitrogen concentrations of more than 5% (in the gas phase) the crystallinity of the coatings deteriorates. At about 2%, large textured growth regions are observed. They exploited the "heated" filament thermal CVD method to grow diamond. All major preparation techniques currently applied worldwide for diamond CVD were, therefore, represented at SMT III.

SMT III was the first of its kind held outside the USA. The organizers will certainly benefit from this experience and further improve some organizational weak spots. The final program with a valid schedule of the papers should be available at least two weeks prior to the conference to allow attendees to plan their stay. The adjustment of the schedules of parallel sessions is a problem for any major conference and will certainly be improved at the next SMT. Despite these minor problems the conference was highly successful in providing a forum to freely exchange surface related ideas and collect results in various scientific fields. The proceedings of SMT III containing the peer reviewed full length papers will appear in book form (2 vols.) in November 1989 (available from TMS, 420 Commonwealth Drive, Warrendale, PA). The organization for SMT IV is already under way. The conference will be held 2–7 September, 1990 in Paris, France and the abstract deadline is December 1, 1989.

Erratum: In Figure 6 of the article Liquid Crystalline Elastomers by R. Zentel, *Adv. Mater. 1989*, 321; *Angew. Chem. Int. Ed. Engl. Adv. Mater. 28* (1989) 1407; *Angew. Chem. Adv. Mater. 101* (1989) 1437, the frequencies quoted in the legend should read "between 10^{-4} and 10^{2} Hz".

Materials Forum

Companies and individuals wishing their news and views on advanced materials issues and products to be considered for coverage in this section should send press releases, correspondence and other details, in English, to: Materials Forum, ADVANCED MATERIALS, P.O. Box 101161, D-6940 Weinheim, Federal Republic of Germany.



Seasons Greetings

The *Advanced Materials* production team would like to wish all our readers worldwide, a most merry Christmas and an enjoyable and happy New Year. Many of you will not know that *Advanced Materials* has, for the last year, also been published as part of the leading chemistry journal *Angewandte Chemie*. This will stop at the end of 1989, after which *Advanced Materials* will begin a totally independent existence, and its future, we are sure, will give us all cause to celebrate a successful New Year.

Japanese Materials

The Japanese Ministry for International Trade and Industry have just published the results of a survey on the commercialization of new materials. Of the 453 companies surveyed, 302 had been developing, producing or selling new materials with a total of 1822 new materials being recorded. These figures represent a three-fold increase in both companies and products over the period 1985–1988. The chemical industry had shown the best performance in penetrating the new materials market followed by the ceramics, non-ferrous metals, steel and textile industries.

The report, and further information can be obtained from Pera-Otis, Melton Mowbray, Leicestershire LE13 OPB, UK.

Low Pressure Plasma

The integration of the plasma treatment of materials or devices into the regular production line has, in the past, been hindered by the slowness of the treatment, which requires high vacuum and long plasma generation times. Using a combination of high performance pumps, and using microwaves to generate the plasma instead of the traditional megahertz frequency generators, the company Technics Plasma has developed a plasma treatment system which has an turnover time one-third that of previous ones. The system has already been successfully incorporated into the production of plastic housings for ignition coils by the company Beru, Ruprecht (Ludwigsburg, FRG). The housings have to be coated with epoxy resin but before this is done the surfaces are conditioned with plasma, ensuring strong bonding with the resin.

Further information on this first, fully automatic plasma treatment system is available from Technics Plasma GmbH, Dieselstrasse 22, D-8011 Kirchheim bei München, FRG. Tel. (089) 903 8021. Fax. (089) 903 9553.

Optical Storage Media

Six years since its introduction, the Audio Compact Disc (CD) has firmly established itself in entertainment electronics. Some 450 million of these silver discs were sold worldwide in 1988. Bayer AG played a decisive role in the development of suitable products for this application. Almost half the CDs sold around the world today are made from Makrolon CD 2000, a polycarbonate plastic from Bayer. Now that internationally valid standards for so-called "write once media" (WORM—write once read many) have been adopted, not only the WORM and CD ROM disc but also the CD video single have put life into the market for optical storage media for picture and data processing. Makrolon CD 2000 is also used successfully for these discs.

While the use of optical storage media was up to now limited to replacing old distribution techniques, such as records and print, the WORM disc is a new product which complements the newer techniques, such as micro-filming. With this system, the user is himself able to write data onto an optical storage disc and then read them out again as often as desired and without wear.

The Philips and Du Pont Optical (PDO) company has been selling WORM discs with a diameter of



The new WORM (write once read many) discs from Philips and Du Pont Optical (PDO) are made from Makrolon CD 2000, a polycarbonate from Bayer AG. They can be written on on both sides and are protected by a cassette. The formatted 5.25" disc offers the user 600 megabytes of free storage capacity. This corresponds to about 150,000 DIN sides of A4, written in binary code.

130 mm based on Makrolon CD 2000 since the end of 1988. Intensive efforts to improve the product quality, especially in the production area, enabled PDO to meet even the highest requirements for WORM discs, a raw bit error rate of 10^{-6}, with Makrolon. WORM discs can be written on on both sides and are protected by a cassette. The formatted disc offers the user approximately 600 megabytes of free storage capacity. This corresponds to approximately 150,000 sides of A4, written in binary code.

A new medium in entertainment electronics is the CD video single with a diameter of 120 mm, which boasts not only a digital audio section, but also a video part about 5 minutes long. Philips and Sony first introduced this disc on the US market at the start of 1988, launching it in Europe at the end of 1988.

The MO (magneto-optic) storage technique (erasable system) being tested at the moment makes particularly great demands on the birefringence which can only be met with difficulty by the polycarbonate grades available today. Bayer is developing new substrate materials based on thermoplastics and thermosetting plastics for this application. The products are undergoing market trials.

Further details are available from Abteilung Öffentlichkeitsarbeit, Bayer AG, D-5090 Leverkusen, Bayerwerk, FRG Tel. (0214) 30-81725

Materials Database

The first electronic materials database to be made available freely to the plastics industry was created by ICI. K'89 in Düsseldorf, 2–9 November, provided the launchpad for an updated version of the company's Engineering Plastics On Screen materials database EPOS 90.

The new version will not only be faster and more user friendly, but will also contain a more comprehensive coverage of available ICI polymers. As before, price data will be included, and EPOS 90 will be complemented by the latest version of the EPOS F fluoropolymer database.

The new system has been devised with a general, unified approach in mind which will be more compact, outline the technical advantages of using ICI materials, and will contain more detailed information for the design engineer.

Disks will be available in 5.25″ and 3.5″ formats and are designed to run on IBM PC's and compatible hardware.

Further information is available from Madeline Whitfield, ICI Advanced Materials, P.O. Box 6, Shire Park, Bessemer Road, Welwyn Garden City, Hertfordshire AL 7 1HD, UK. Tel. (0707) 323400. Fax. (0707) 335556.

Wiring Board Inspection System

Nippon Steel, and Eastern Co., Ltd., a leading manufacturer of printed wiring boards, have started production and sales of a jointly-developed automatic printed wiring board inspection system, the PT Series.

Printed wiring boards are having to accommodate an increasingly high density of components, and board manufacturers have been responding to these needs by providing multilayer boards and finer circuit lines.

With visual checks becoming unfeasible, there is a strong demand for systems which are capable of checking boards automatically. The PT Series was developed as the answer to these needs. Its principal features are:

1. A high-detection accuracy of 80 microns (the minimum width for inspection) and a maximum resolution of 5 microns.
2. A high-speed check can be performed at a rate of 3 m^2/min.
3. Two methods, feature extraction and comparison, can be used in parallel, so it can cover a wide range of applications, including checks of external and internal layers and phototools.
4. Full use of computers allows checking conditions to be set and imaging system settings to be determined automatically.

Nippon Steel accumulated its image processing and pattern recognition technology as a result of the surface inspection of steel sheets. Information processing technologies using computers have also been developed. In addition, the defect detection algorithm was applied to the system, which is based on the cross operator method developed by Professor *Gotaro Odawara* of the University of Tokyo's engineering faculty. The final link in the system was the advanced manufacturing capabilities and experience of Eastern.

Further information is available from Nippon Steel Corporation, Königsallee 30, D-4000 Düsseldorf, FRG. Tel. (0211) 320791. Fax (0211) 329368.

Intermetallic Alloys

Intermetallic alloys based on titanium, nickel and niobium aluminides are potentially interesting and important materials for future aircraft and aerospace applications. They can be used as monolithic or matrix materials for fiber reinforced compound materials.

For material development work in this field, Marko Materials, North Billerica, Massachusetts, USA, have developed a laboratory melt spinning unit for the production of rapidly solidified filaments, fibers and powder.

The Marko melt spinner permits the production of alloys of high purity, for example Fe-Nd-B magnet materials and high melting refractory alloys with melting temperatures up to 3000 °C (Tungsten, Columbium, Molybdenum). Another promising application is to produce high temperature superconductors based on Y-Ba-Cu.

The fully assembled, turnkey systems, many of which are already operating in research institutes in the USA and Japan, are now marketed in Europe by Industriekontor Rolf Hardt, Benrather Schlossufer 51, D-4000 Düsseldorf 13, FRG. Tel. (0211) 712828. Fax (0211) 71 31 86.

Book and Video Reviews

Nonlinear Optics, Lasers, Surface Analysis, NMR, etc. ...

Organic Materials for Non-linear Optics. Edited by *R. A. Hann* and *D. Bloor*, Royal Society of Chemistry, London 1989. xiv, 423 pp., bound, £ 45.00. – ISBN 0-85186-806-1

This book consists of the proceedings of the conference "Organic Materials for Non-linear Optics 1988" held at Oxford University in June 1988, and contains the manuscripts to the plenary lectures, short talks and posters presented at this meeting. The breadth of material covered here corresponds to the generality of the title and includes contributions over almost all current general themes in organic nonlinear optics research.

The first section of this volume deals primarily with theoretical calculations of molecular nonlinearities. The plenary contributions from *Hurst, Munn, Morley* and *Pugh* point out the significant progress made in calculating second order nonlinearities. Other contributions, e.g. from *Garito* et al., indicate that progress has been made in understanding the microscopic basis of third order effects, but that our understanding is still full of gaps and uncertainties, as is our understanding of the correlation between molecular structure and crystal packing, as pointed out in the section on crystals by *Gavezzotti*.

The short section on materials characterization contains a discussion by *Meredith* of the pros and cons of various methods of characterization of NLO materials, as well as an interesting discussion of an application of parametric effects in fast infrared detection by *Hierle* et al.

The next section of the book contains numerous contributions on small organic molecules, as crystals, in solution, or in films, where "small" is taken to include oligomers as well. Here, there is a balance of detailed characterizations of previously reported compounds (*Bailey* et al. and *Bosshard* et al.) and reports of novel structures for both second and third order effects (e.g. *Blanchard-Desce* et al., *Davis* et al., but not limited to these). This aspect is continued in the subsequent short section on organometallics, which have up to now received probably too little attention.

The section on polymeric materials covers several aspects and types of effects in nonlinear optical polymers, from an overview of materials and possible devices (e.g. *Ulrich* and *Möhlmann*) to ultrafast third-order processes (*Prasad*), with contributions as well on synthesis, liquid crystalline polymers and gels. The next section on materials deals with Langmuir-Blodgett films and monolayers at the air-water interface. Among the plenary lectures, *Peterson* summarizes the use of LB films as media for characterization and the requirements for an eventual use of such films in all-optical or electro-optic devices. *Shen*'s contribution summarizes the utility of nonlinear optical methods to study interfacial phenomena in situ. Further short contributions deal with such subjects as polymer amphiphilics, orientation and deposition methods.

An eventual application of organic materials in nonlinear optics depends to a large extent on the ability to construct working devices out of them and integrate them into other systems. The contribution from *Stegeman* reviews proof-of-principle all optical $\chi^{(3)}$ based devices, e.g. interferometers and directional couplers, but offers as well the sobering observation that we are several orders of magnitude away from substances which would lead to practical devices. The contribution from *Lytel* et al. shows on the other hand that we are much closer to commercial integrated optic devices on the basis of $\chi^{(2)}$ polymeric substances, demonstrating that high speed electro-optic modulation in waveguides has already been achieved.

There is quite a bit of information on numerous subjects in this volume. With the plenary lectures, one often has the feeling that one has seen a good deal of it before, but such talks are usually intended to be overviews. The newer information is concentrated in the short poster contributions, which were however too numerous to mention individually here, and it is in these contributions that one is more likely to find results that have not yet been published elsewhere. A critical discussion of both the merits and disadvantages of organic materials in view of advances in inorganic materials would have been welcome, but this was perhaps more the responsibility of the participants than of the editors.

"Organic Materials for Non-linear Optics" summarizes the state of the art in organics for NLO, with a European emphasis, and contains contributions from many of the leading researchers in many aspects of the field. Thus the book can be useful to the researcher trying to attain or maintain an overview of the wide field of organic materials for nonlinear optics. For more detailed information one can always refer to further work from the numerous authors represented in the book.

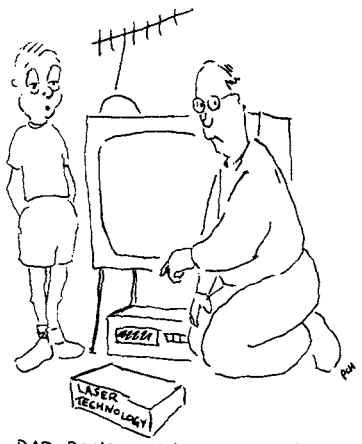
D. Lupo
Hoechst AG, Angewandte Physik
Postfach 800320, D-6230 Frankfurt 80 (FRG)

Lasertechnik. Grundlagen, Eigenschaften, Anwendung. VDI-Verlag, Düsseldorf 1989. DM 68. – ISBN 3-18-400879-0 (German language video cassette, 17 min.)

'Laser Technology' a la video show—Much too often we come home with a briefcase loaded with 'things to do' for the

weekend or for the evening and, in many cases, we return to work with the briefcase untouched because we were too tired in the evening and we needed some relaxation over the weekend. The video-quick-education may change this situation for the better or worse (who knows?).

After coming home from a long day, I had in my briefcase—among other things—the above video educational quicky (17 minutes) on 'Laser Technology'. The activation barrier of watching a video tape is low—in the case of this video tape, the message is presented at a level which is easy to understand and the pictures are fascinating. When my 16 year old son joined me at the TV and saw the pictures of a laser beam cutting through metal and welding steel he made the following remark: "Dad, I didn't know that your work was so interesting."



Now back to the content of the video cassette which was put together by the VDI (Verein Deutscher Ingenieure; German professional society of engineers) and which was sponsored by the BMFT (Germany Ministry of Research and Technology). The tape starts with a description of the main mechanisms of the laser, introducing words like 'stimulated emission' and 'inversion' without going into the intricacies of explaining why inversion can, in most cases, only be achieved by quite complex atomic schemes. Also the words 'coherence' and 'monochromaticity' are described on a rather qualitative level.

The video tape shows in greater detail and with very good graphical documentation technical applications like cutting, welding and surface hardening. For that purpose the main laser-tools are introduced briefly: The CO_2 laser, the solid state laser and the excimer laser. The subsequent applications are commented on from an engineering viewpoint and are very helpful for those who wonder why lasers are, in many cases, superior to conventional techniques for welding and hardening: it is the ease of handling the light beam via lightpipes and the ease of focusing power on a narrow spot or dissipating power in a thin layer. All the above features reduce the thermal stress which conventional methods often cause. So—all in all—the video cassette is, in my opinion, a success and its application will expand in the near future.

The only critical remark concerns the title. The title should be: 'Laser Technology in Materials Processing'. What has been left out are large areas of laser technology and laser applications. *Semiconductor lasers* which are in every laser printer which we use on a daily basis and lasers in data processing and communication technologies (glass fiber techniques) are completely omitted. This may reflect on some less developed areas of the German engineering menu or it may just be that the authors of the cassette forgot to implement the above area of 'information technology'. These are, however,—without doubt—part of the engineering sciences.

Since medical applications are also missing in the tape we come to the conclusion that it may be rather difficult to treat the full subject of 'laser technology' in one tape.

The only part of the tape which goes beyond materials technology is the part on holography; but that would have to be expanded because there are also optical memories and holographical optical schemes for storing and processing information, let alone the question of whether the complex subject of 'pattern recognition' by holographical schemes could be part of an educational tape.

In summary I think that the video tape is a success and – if it were not for the misleading title—I would rate it as excellent because I think that it will stimulate others to describe science and technology in a way which we can handle in the time between coming home and dinner. It may make our lives easier or the opposite—to answer this question I would have to consult my wife.

Dietrich Haarer
Lehrstuhl für Experimentalphysik IV, der Universität
Postfach 101251, D-8580 Bayreuth (FRG)

Inverse Gas Chromatography. Characterization of Polymers and Other Materials. Edited by *D. R. Lloyd, T. C. Ward,* and *H. P. Schreiber,* ACS Symposium Series 391, American Chemical Society, Washington, DC 1989. xi, 318 pp., bound, US $ 83.95. – ISBN 0-8412-1610-X

The book originates from a Symposium on Polymer Characterization held in Toronto, Canada in June 1988. As mentioned in the Preface, it contains 19 of 20 papers presented there, and three additional chapters were incorporated to broaden the scope of the book.

Inverse Gas Chromatography (IGC), first mentioned in 1966 as an analytical technique for studying bulk samples, has developed since then to become a viable and powerful method for the investigation of surface and bulk properties, especially of polymer materials. The name for this chromatographic technique was coined because the material under investigation is not introduced as a (temporary) component of the mobile phase, but it constitutes—at least in part—the

stationary phase. The aim of the experimenter is not the separation of a mixture of injected compounds but to inspect the retention behaviour of molecules introduced as probes in order to obtain information on the interactions between a probe molecule and the substrate under investigation.

The book reviewed here is the first to focus exclusively on IGC and therefore merits attention if for no other reason. Moreover, the editors have been successful in collecting contributions which cover a variety of applications which make obvious the wide spectrum of applications of the method.

The first, introductory chapter, written by two of the editors (*D. R. Lloyd, H. P. Schreiber*), gives a short overview of IGC and, in particular, of the contents of the volume. The remaining 21 chapters are divided into six sections. Chapters 2–4 are concerned with methodology and instrumentation. The next three sections focus on sorption and diffusion in polymers (4 chapters), polymer blend characterization (4 chapters), and surface and interface characterization (6 chapters). Analytical applications and special applications (2 chapters each) are covered by the last two sections.

The methodology and instrumentation section starts with a chapter by *A. E. Bolvari, T. C. Ward, P. A. Koning*, and *D. P. Sheehy* describing experimental techniques for IGC. Column techniques and their advantages and disadvantages are discussed: capillary columns (the substrate is coated on to the inner wall of the capillary), packed columns (packed with a solid support on to which the polymer has been coated) and fiber columns (the column is packed with the polymer fibers). In addition, some instrumental aspects are briefly considered, including the necessity for automation in IGC. Automation is also the subject of chapter 3 (by *J. E. Guillet, M. Romansky, G. J. Price*, and *R. van der Mark*). The authors give a review on fundamental aspects of measurements by IGC, such as the determination of transition temperatures, crystallinity, solubility, interaction parameters, surface areas, and adsorption isotherms. In chapter 4 (by *P. Hattam, Q. Du*, and *P. Munk*) results from a computer simulation study of the elution behavior of probes are compared with experiment. This study aims at improving the "quality" of the conclusions that can be drawn from IGC data.

In the next section, sorption and diffusion processes in polymers are covered. Chapter 5 by *G. J. Price* is concerned with an important application of IGC: the determination of solubility parameters δ. The author shows very interesting results; unfortunately, not a single equation is given which correlates variables measured by IGC to thermodynamic functions. Thus, it remains unclear from this chapter how the δ values have been calculated. The next chapter (by *B. Shiyao, S. Sourirajan, F. D. F. Talbot*, and *T. Matsuura*) is concerned with adsorption measurements on cellulosic materials and on polyethersulfone. Different gases and vapors of organic compounds were used as the probe molecules. Of particular interest are the results obtained with binary mixtures of gases and vapors. Thermodynamics of water sorption by two copolymers composed of vinylidene chloride and vinyl chloride or acrylonitrile are the subject of chapter 7 (by *P. G. Demertzis* and *M. G. Kontominas*). In addition to thermodynamic parameters of sorption (free energy, entropy, enthalpy, and activity coefficient), diffusion coefficients and activation energies for the diffusion of water vapor in the two copolymers were calculated from the chromatographic data. Solute diffusion in polymers is also the subject of the last chapter in this section. *D. Arnould* and *R. L. Lawrence* report on measurements carried out with different probes and polymethyl methacrylate as the substrate; the capillary column technique was used. The results are discussed with respect to the mechanism of diffusion and to the validity of different models of the diffusion process.

The next section starts with a chapter by *G. DiPaola-Baranyi* on studies of the thermodynamics of polymer blends by IGC. Three binary blends were studied at different compositions; thus interaction parameters were obtained as a function of the composition of the blends. It will be interesting to see the remarkable results confirmed by other techniques. That care has to be taken with experimental and data acquisition techniques in IGC when studying polymer blends is a conclusion drawn in chapter 10 by *M. J. El-Hibri, W. Cheng, P. Hattam*, and *P. Munk* from their theoretical and practical work. Phase diagrams for two polystyrene blends as based on IGC data are shown by *S. Klotz, H. Gräter*, and *H.-J. Cantow* in chapter 11. These authors report that a correct interpretation of the thermodynamics of mixtures of molten polymers can be obtained via IGC. *A. C. Su* and *J. R. Fried* (chapter 12) compared—on the basis of IGC data—the miscibility of the components of two binary blends and found the results to be in agreement with conclusions from studies on thermal and mechanical behavior.

The next four chapters deal with the surface and interface characterization of carbon fibers. *A. J. Vukov* and *D. G. Gray* (chapter 13) studied the dependence of surface characteristics on pretreatment at different temperatures, while *S. P. Wesson* and *R. E. Allred* (chapter 15) report on the surface energetics of plasma-treated fiber. In the contributions of *J. Schultz* and *L. Lavielle* (chapter 14) and *A. E. Bolvari* and *T. C. Ward* (chapter 16) adhesion between carbon fibers and different matrices is correlated with acid-base interactions. Altogether, these four chapters give an extensive overview on surface and adhesion properties of carbon fibers. Acid-base interactions are also shown to play an important role in adsorption of polymers on glass surfaces, as demonstrated by *E. Osmont* and *H. P. Schreiber* in chapter 17 for glass materials with differently treated surfaces. In the last chapter of this section, *E. Papirer, A. Vidal*, and *H. Balard* report on the use of IGC for the determination of surface energy characteristics of silica materials of different polarity, as obtained by heat treatment or by grafting reactions.

The next section (Analytical Applications) contains two chapters dealing with the characterization of polymers which can be used as stationary phases in gas chromatography. *R. J. Laub* and *O. S. Tyagi* made use of the correlation between retention and saturation vapor pressure of different solutes for characterizing the stationary phase. In chap-

ter 20, *J. H. Raymer, S. D. Cooper,* and *E. D. Pellizzari* compare the retention properties of four polyimide-based materials and a well-established polyphenylene oxide stationary phase by means of a deuterated tracer pulse technique.

The last two chapters are combined in a "Special Applications" section. *P. H. Neill* and *R. E. Winans* (chapter 21) report on the use of IGC to determine the alterations that coals and oxidized coals undergo when heated to 450 °C. Interpretation of the observed effects is made on the basis of results obtained by pyrolysis, plastometry, and microdilatometry. The final chapter of the volume (by *S. G. Gilbert*) deals with the determination of water sorption isotherms of starch materials.

A general drawback of multi-authored books also applies to this volume: although the contributions are well written, some information can be found in almost every chapter whereas other useful information may have been omitted. Unfortunately, the work which has been done by the editorial staff cannot be recognized by the reader of the book since he does not know anything about the original versions of the contributions. Nevertheless, contributions to a book should be "harmonized" to a certain extent. Thus, symbols should be used consistently throughout the volume. In this book, however, almost every author uses his own special symbols (e.g., five different symbols are used for the hold-up or dead time). Another example: Figure 3 of chapter 14 appears again in a much better version two chapters later; the latter version alone would have been sufficient. Finally, the last chapter is only of minor quality compared to the other chapters; in fact, it looks like a manuscript for an oral presentation, the figures are not explained in the text, and "the product tcKt" turns out to be a product of the factors "tc" and "Kt"!

Only a few errors have been observed (e.g., sub- and superscripts are missing with the symbols and units of Table 1 in chapter 13, and the heading of the last column of Table I in chapter 14 should read "γ_s^P" instead of "γ_s^D"). The subject index is of sufficient length (but, as an example, the entry "absorption" is missing). The reference lists of the individual chapters cover the literature until the beginning of 1988, thus providing the reader with information also on recent work.

In all, the book contains a wealth of highly interesting information, and it will be of value for specialists in the field as well as for the interested newcomer.

Franz Peter Schmitz
Lehrstuhl für Makromolekulare Chemie der RWTH
Worringerweg 1, D-5100 Aachen (FRG)

Transmission Electron Microscopy. By *L. Reimer.* Springer Series in Optical Sciences, Springer-Verlag, Second Edition, 1989, xiii, 547 pp., paperback, DM 128.—ISBN 3-540-50499-0

In 1906 *J. J. Thomson* was awarded the Nobel Prize for demonstrating that the electron was a particle. Thirty-one years later his son, *G. P. Thomson,* was awarded the Nobel Prize for demonstrating that the electron was a wave. In 1986 *Ernst Ruska* was awarded the Nobel Prize (long overdue) for utilizing both the particle and wave properties of electrons in designing the first electron microscope in 1931.

Electron microscopes are amongst the most widely used and the most important scientific instruments. They are essential equipment for biologists, chemists, geologists, materials scientists, physicists and others. There are many books on the subject, but this book by *Reimer* is, quite simply, the best. This second edition is a revision of his earlier book on Transmission Electron Microscopy (TEM), first published in 1984. In the last five years the field of TEM has expanded enormously and this revision very thoroughly updates and extends growth areas such as electron holography, lattice imaging with atomic resolution, electron energy-loss spectroscopy, etc.

The scope of the book covers both TEM and analytical electron microscopy. Even subjects like reflection electron microscopy from surfaces are discussed. Contents include the types of electron microscopes available, particle optics and electron lenses, wave optics, imaging, scanning transmission electron microscopy (STEM), electron-specimen interactions, contrast theory, high resolution electron microscopy (HREM) and analytical electron microscopy.



The main thrust of the book is to explain as clearly as possible the basic physical principles underlying transmission electron microscopy in all its various forms. In this Professor *Reimer* succeeds admirably. Although the book adopts a theoretical approach it is also full of useful practical advice. For example on p. 458 we are advised that 'Vacuum leaks can never be cured by heavy greasing but only by carefully polishing the sealing surfaces. Viton rings should be used in preference to rubber. All surfaces should be washed with methyl alcohol, which evaporates completely in air. Finger-marks should be avoided by wearing gloves'. This quotation also illustrates the easy-to-read crisp sentences that the author adopts.

The value of this book lies in its breadth, depth and accuracy. I have indicated its breadth above, but the book also digs deep into the fundamentals of the subject: for example there is a particularly clear exposition of the dynamical theory of electron diffraction, and of applications ranging from the critical voltage effect to the imaging of surface steps.

Concerning accuracy, there are many books on TEM which contain fundamental errors in understanding. This book, on the other hand, is reliable and accurate and reflects the scholarship one expects from Professor *Reimer*.

The book is for research students, post-doctoral scientists, lecturers and professors. It is good for teaching purposes and for reference. If you are an electron microscopist this book is the best: you should have it on your book shelves: I cannot recommend it too strongly.

C. J. Humphreys
Department of Materials Science and Engineering
The University of Liverpool
P.O. Box 147, Liverpool L69 3BX (UK)

Methods of Surface Analysis. Edited by *J. M. Walls*. Cambridge University Press, Cambridge 1989. x, 342 pages, bound, $ 80.– ISBN 0-521-30564-0

At present, surface analysis and related methods represent one of the fastest progressing technological fields. Therefore there is an increasing demand for appropriate books, introducing the newcomer to the principles of these methods and their range of applications.

The above mentioned book is a compendium of articles from experts who cover one method or one field of interest each. The book contains 9 chapters dealing with the 6 most common methods of surface analysis (AES, XPS, SSIMS, DSIMS, ISS, RBS) and 3 more general topics which aim at supplying the reader with the essential basic knowledge. This selection out of the large number of different surface analysis techniques is wise and concentrates on those methods with a broad range of applications. Three more methods are briefly dealt with: Sputtered Neutral Mass Spectrometry (SNMS), Laser Microprobe Analysis (LIMA) and Atom Probe Microanalysis.

The book is composed well, contains instructive drawings and images, but mainly deals with VG products, almost neglecting all other products, instrument manufactures and construction principles. There is, for example, in the chapter "State-of-the-art XPS" only a short remark about small spot ESCA and no reference to the SSL instrument and the new Uppsala machine, the XPS "jumbo" ESCA-300. Also the world's finest scanning SIMS instrument, built by Levi-Setti in Chicago, is not mentioned at all. The spatial resolution in Scanning Auger Microanalysis is about 350 Å with commercially available instruments (e.g. PHI-660) and not 2000 Å as stated in Chapter 1.

The more practically oriented analyst, who has to struggle with the tricky every-day samples, would like to find some more examples of typical applications in the many fields in which surface analytical instruments are used today. In addition, the sections on data processing and curve fitting are very brief and confined to a list of possible computer routines. More information would have been helpful.

If there are many authors, who contribute to a book, it is obviously always difficult to make it up in such a way, that everything fits together, that each writer uses the same formulas and expressions and that unnecessary repetition is avoided. The reviewer is of the opinion that these problems have been solved satisfactory.

Generally only few literature references are given, in some cases even too few, and they are often not mentioned in the text.

The book can be recommended without reservations for all VG instrument users and those being non-specialists, who are looking for an introduction into those surface analytical methods which are frequently used today, and who want to get information quickly on the appropriate technique to choose for a special applicational purpose.

Harald Hantsche
Bundesanstalt für Materialforschung u. -prüfung
Unter den Eichen 44–46, 1000 Berlin 45 (West)

Nuclear Magnetic Resonance, Vol. 18, Edited by *G. A. Webb*. Royal Society of Chemistry, Cambridge 1989. LVI, 511 pp., bound, $ 232.-, ISBN 0-85186-412-0.

The number of applications of nuclear magnetic resonance (NMR) spectroscopy is growing rapidly and NMR is increasingly used also in non-traditional areas of application like the investigation of solid and macromolecular materials. To a considerable degree its increasing popularity is a result of the continuing development of innovative methods and measurement procedures for instance in solid state and two-dimensional NMR. A comprehensive literature review about current NMR activities can be of value not only for the specialist but also for those interested in the applicational potential of the method.

The book reviews the NMR literature published between June 1987 (1986 in some cases) and May 1988. The 13 chapters cover different subjects, which are reviewed by specialists. The individual chapters are preceeded by a compilation of citations of 588 books and reviews. For this list, a subdivision into type of publication (books, regular review series, reviews in periodicals, etc.) has been chosen and not a classification according to subjects. Considering that there are references to reviews in each chapter on individual subjects the list seems redundant.

Chapter 1 (*C. J. Jameson*) covers the theory and physics of chemical shielding tensor values. Known as chemical shift in isotropic liquids, these values are essential for quantitative structural and dynamic solid state NMR. Chapter 2 (*M. J. Foster*) deals with the applications of nuclear shielding. Apart from ^{1}H and ^{13}C, chemical shift studies of nuclei such as ^{6}Li, ^{9}Be, $^{14,15}N$, ^{17}O, ^{19}F, etc. are reported. Spin-spin couplings are treated in Chapters 3 (theory: *J. Ostershede*) and 4 (applications: *J. C. Lindon* and *J. M. Williams*). Like the chemical shift values, the coupling constants give important information on molecular conformation. Different liquid state NMR techniques for their measurement as well as coupling between particular nuclei other than ^{1}H and ^{13}C

are reviewed. Chapter 5 (*H. Weingärtner*) is on nuclear spin relaxation in liquids and gases. Relaxation time studies which give information about molecular dynamics and molecular distance determination in biological macromolecules are included. Chapter 6 (*R. Dupree*) reviews solid state NMR. The chapter is subdivided into new techniques, theory, experimental, and several sections on different substances and areas of application like silicates, zeolites, ceramics, phase transitions, glasses, organic and inorganic solids, wood and coal. A number of tables efficiently guide the reader through the literature. Chapter 7 (*L. Y. Lian*) is entitled "Multiple Pulse NMR", a terminus technicus from solid state NMR, but deals with multi-dimensional NMR in liquids including the development of special excitation pulses. Chapter 8 (*D. B. Davies* and *H. G. Parkes*) surveys natural macromolecules, excluding biological studies, with many tables in the text. Chapter 9 (*F. Hatley*) reviews synthetic macromolecules, again largely in appealing tabular form. References to reviews are followed by sections on solution NMR studies of polymer structure by 1D and 2D NMR, polymer-polymer interaction in solution and gels, and on bulk polymers. The last section is subdivided into wideline ^{1}H NMR, high resolution NMR, NMR of deuterons and other nuclei, and applications to cellulose polymers. Relaxation and lineshape studies for the investigation of polymer dynamics are included as well as new magic angle spinning and cross-polarization techniques for the investigation of molecular order and polymer morphology. Chapter 10 (*C. Jones*) is dedicated to conformational analysis in liquid state NMR based on the measurement of indirect couplings, distance determination by cross-relaxation, and computer refinement. Chapter 11 (*P. G. Morris*) is concerned with NMR of living systems with subsections on NMR imaging and high resolution NMR. Chapter 12 (*K. G. Orrell*) treats NMR of paramagnetic species and Chapter 13 (*A. Khan*) NMR of liquid crystals and micellar solutions. The latter starts with a helpful introduction to the subject, which is missing in many of the other chapters. The smaller part of the material (4 pages) covers thermotropic liquid crystals, where solid state deuteron NMR is increasingly used for investigations of molecular order and mobility. The larger part (17 pages) deals with micellar solutions and lyotropic liquid crystals. Phase diagrams and phase structures in complex amphiphilic systems are investigated as well as multicomponent self-diffusion coefficients. Solid state NMR is applied more and more for studies of lipids and protein-lipid interactions.

The readability of the chapters is adequate and the chapters cover the subjects in sufficient depth to gain an understanding of the current state of research. The use of tables in some chapters (1, 6, 8, 9, 12) provides quick and easy access to the information and should be encouraged in future volumes. A list of symbols and an author index are helpful features. For materials science oriented NMR research, chapters 1, 6, 9 and 13 are most relevant. The book is in competition with review papers and computer literature searches on dedicated subjects. Considering also the price, the book is unlikely to be found in every science library.

Bernhard Blümich
Max-Planck-Institut für Polymerforschung
Postfach 3148, D-6500 Mainz (FRG)

Conference Calendar

The black hand symbol ☞ denotes new entries into the calendar. Send information concerning conferences to the editorial office

January 1990

10–14 **Superconductivity**
Int. Conf.
Bangalore (India)
Contact: Prof. S. V. Subramanyam, ICSC, Dept. of Physics, Indian Inst. of Sci., Bangalore 560012, India, Tel. 91-812-344411, Fax 91-812-341683

14–19 **Electro-Optics**
Conf.
Los Angeles, CA (USA)
Contact: SPIE, POB 10, Bellingham, Wa 98227-0010, USA, Tel. 206-676-3290, Fax 206-647-14445

15–18 **Advances in Composite Materials**
Int. Conf.
Bombay (India)
Contact: Prof. P. Ramakrishnan, Indian Inst. of Techn., Dept. of Metallurg. Eng., Poway, Bombay 400076, India

21–24 **Gallium Arsenide**
Symp.
Atlanta, GA (USA)
Contact: K. J. Sieger, Naval Res. Lab., Code 6852, Washington, DC 20375, USA

22–26 **Recrystallization in Metallic Materials**
Int. Conf.
Wollongong (Australia)
Contact: T. Chandra, Dept. of Metallurgy and Materials Eng., Univ. of Wollongong, Wollongong NSW 2500, Australia, Tel. 042-270008, Fax 042-270477

February 1990

4–7 **Ceramic Powder Processing**
3rd Int. Conf.
San Diego, CA (USA)
Contact: G. L. Messing, Pennsylvania State Univ., University Park, PA 16802, USA, Tel. 814-865-2262, Fax 814-865-2917

4–8 **18th Australian Polymer Symposium**
Bendigo, Vic. (Australia)
Contact: Dr. J. D. Wells, Bendigo College of Adv. Education, Bendigo, Victoria 2550, Australia

5–6 **High Temperature Corrosion**
Frankfurt (Fed. Rep. Germany)
Contact: Dr. M. Schütze, DECHEMA, Theodor-Heuss Allee 25, D-6000 Frankfurt 97, FRG

19–21 **Advanced Ceramics**
Conf.
Rosemont (Italy)
Contact: Soc. of Manufacturing Eng., One SMF Dr., POB 930, Dearborn, MI 48121, USA

19–22 **Advanced Metals & Ceramics**
1990 TMS Annu. Mtg.
Int. Conf.
Anaheim, CA (USA)
Contact: M. Karl, TMS, Meetings Dept., 420 Commonwealth Drive, Warrendale, PA 15086, USA, Tel. 412-776-9050, Fax 412-776-3770

21 **Block-Copolymers**
Mtg.
London (UK)
Contact: Dr. K. Petrak, Ciba-Geigy ADDR Unit, Wimblehurst Road, Horsham, West Sussex RM124AB, UK

21–23 **Armed Forces Communications and Electronics**
Long Beach, CA (USA)
Contact: Armed Forces Communications and Electronics Assoc., Headquarters, 4400 Fair Lakes Court, Fairfax, VA 22033, USA

21–23 **Composites '90**
2nd Int. Congr.
Wiesbaden (Fed. Rep. Germany) Contact: D. Schnabel, Demat Exposition Managing, POB 110611, D-6000 Frankfurt 11, FRG, Tel. 069-234331, Fax 069-253071

25–2 **Advanced Devices and Systems**
Symp.
Santa Clara, CA (USA)
Contact: SPIE, P.O. Box 10, Bellingham, WA 98227-0010, USA

March 1990

1–3 **Interphase Reactions and Interactions**
Freiburg (Fed. Rep. Germany.)
Contact: Prof. Dr. H.-J. Cantow, Hermann-Staudinger-Haus, Stefan-Meier-Str. 31, D-7800 Freiburg, FRG

4–9 **Microlithography**
Symp.
San Jose, CA (USA)
Contact: Soc. of Photo-Optical Instrumentation Eng., Koblenzer Str. 34, D-5300 Bonn 2, FRG

12–16 **American Physical Society Meeting**
Anaheim, CA (USA)
Contact: W. W. Havens, J., Aps, 335 E., 45th St., New York, NY 10017, USA

12–16 **Optical Science and Engineering**
3rd Int. Congr.
The Hague (Netherlands)
Contact: Europtica Services I.C., 16, av. Bugeaud, F-75116 Paris, France

14–16 **Photovoltaic Solar Energy**
5th Int. Symp.
Staffelstein (Fed. Rep. Germany)
Contact: OTTI, D.-Martin-Luther-Str. 10, D-8400 Regensburg, FRG, Tel. 0941-58273/74/75, Fax 0941-54854

14–16 **Non-Metals in Metals**
Münster (Fed. Rep. Germany)
Contact: VDEh, Chemikerausschuß, POB 8209, D-4000 Düsseldorf 1, Tel. 0211-6707-441, Fax 0211-6707-310

17–21 **Advances in Semiconductors and Superconductors**
Symp.
San Diego, CA (USA)
Contact: Soc. of Photo-Optical Instrumentation Eng., Koblenzer Str. 34, D-5300 Bonn 2, FRG

Registered names, trademarks, etc. used in this journal, even when not marked as such, are not to be considered unprotected by law.

© VCH Verlagsgesellschaft mbH, D-6940 Weinheim, 1989. – Printed in the Federal Republic of Germany by Konrad Triltsch Druck- und Verlagsanstalt Würzburg.

All rights reserved (including those of translation into foreign languages). No part of this issue may be reproduced in any form — by photoprint, microfilm, or any other means — nor transmitted or translated into a machine language without written permission from the publishers. Only single copies of contributions, or parts thereof, may be made for personal use. This journal was carefully produced in all its parts. Nevertheless, authors, editors and publisher do not warrant the information contained therein to be free of errors. Readers are advised to keep in mind that statements, data, illustrations, procedural details or other items may inadvertently be inaccurate.

Valid for users in the USA: The appearance of the code at the bottom of the first page of an article (serial) indicates the copyright owner's consent that copies of the article may be made for personal or internal use, or for the personal or internal use of specific clients. This consent is given on the condition, however, that the copier pay stated per-copy fee through the Copyright Clearance Center, Inc. (CCC), for copying beyond that permitted by Sections 107 or 108 of the U.S. Copyright Law. This consent does not extend to other kinds of copying, such as copying, for general distribution, for advertising or promotional purposes, for creating new collective works, or for resale. For copying from back volumes of this journal see 'Permissions to Photo-Copy: Publisher's Fee List' of the CCC.

Editorial office: Postfach 10 11 61, D-6490 Weinheim, Federal Republic of Germany, Telephone (06201) 60 22 55, Telex 465 516 vchwh d, Telefax (06201) 602 328.

Editor: *Peter Gölitz*

Associate Editor: *Peter Gregory*

Publishers: VCH Verlagsgesellschaft mbH. (Managing Director: *Hans Dirk Köhler*), Pappelallee 3, D-6940 Weinheim, Federal Republic of Germany.

Advertising office (Advertising Manager *R. J. Roth*): Postfach 10 11 61, D-6940 Weinheim, Federal Republic of Germany, Telephone (0 62 01) 60 61 30, Telex 467 155 vchwh d, Telefax (0 62 01) 606 184.

AUTHOR INDEX [*Angew. Chem. Int. Ed. Engl. 28* (1989)]

The (first) page numbers in square brackets refer to the German edition [*Angew. Chem. 101* (1989)] of Angewandte Chemie. In the case of book reviews the names of the authors and of the reviewers are given; the corresponding GE reference can be found in the Author Index of the German Edition. AM: Reference to *Advanced Materials 1989*. Page numbers in round brackets indicate errata.

Ache, H. J. 1 [1]
Ackermann, T. 981 [1005]
Adachi, T. 1040 [1053]
Adams, F. 101, 1060, 1063 [–, 1043, 1046]
Ahlers, A. 1216 [1304]
Ahlers, F.-P. 187 [190]
Ahlrichs, R. 1379 [1401]
Albert, K. 327, 1029 [336, 1033]
Albright, T. A. 750 [789]
Aldinger, F. 1560 [1592; AM 378]
Alexander, J. 1531 [1530]
Allcock, H. R. 528 [544; AM 132]
Allenmark, S. G. 1281
Allwohn, J. 781, 784 [759, 761]
Amann, A. 268 [277]
Anand, N. 1539
Anders, E. 1371 [1420]
Antonietti, M. 673 [689; AM 175]
Aoshima, T. 1040 [1053]
Aoyama, Y. 921 [922]
Appel, R. 53 [70]
Armstrong, A. R. 810 [830; AM 196]
Arya, P. 1016 [1069]
Asano, Y. 450 [511]
Ashton, P. R. 1258, 1261, 1396 [1266, 1269, 1404]
Asmus, K.-D. 1275 [1247]
Aso, Y. 1222 [1254]
Astruc, D. 460 [459]
Auberson, Y. 1498 [1554]
Augart, N. 342 [354]
Aumann, D. C. 453 [495]
Aviram, A. 520 [536; AM 124]
Aye, K.-T. 767 [765]

Baceiredo, A. 621, 1250 [617, 1253]
Bachmann, P. K. 1755 [1795; AM 455]
Bahr, U. 760 [805]
Bai, Y. 754 [788]
Bain, C. D. 506 [522; AM 110]
Ballauff, M. 253, 382, 383, 1130 [261, 396, 397, 1156; AM –, 92, 93, 302]
Banert, K. 1675 [1710]
Bankmann, M. 911 [950]
Bantel, H. 1059 [1084]
Bär, M. 1379 [1401]
Barbe, B. 614 [645]
Barr, D. 1044, 1241 [1048, 1279]
Bart, H. 634
Bartlett, R. A. 316 [325]
Basset, J.-M. 347 [360]
Batail, P. 588, 1249 [607, 1251]
Bats, J. W. 480, 1528 [471, 1539]
Baudler, M. 339 (502), 1231 [352 (–), 1245]
Bauer, F. 1056 [1092]
Bauer, W. 1695 [1698]
Bauermeister, M. 223 [225]
Baumgartner, C. 1053 [1059]
Bayer, E. 327, 1029 [336, 1033]
Beale, J. M. 146 [147]
Beattie, I. R. 313 [322]
Beaucourt, J.-P. 755 [794]
Bechgaard, K. 588 [607]
Beck, F. 821 [841; AM 207]
Beck, W. 1529, 1705 [1532, 1699]
Becker, B. 458 [501]
Becker, S. 1237 [1287]
Behl, H. 1219 [1303]
Behr, J.-P. 1585 [1617; AM 403]
Behrens, D. 385, 819 [399, 839; AM 95, 205]
Behrens, U. 476 [481]
Bein, T. 1692 [1737]
Belaish, I. 1569 [1601; AM 387]
Bell, P. 473, 1239 [503, 1298]
Belyik, V. J. 1441 [1471; AM 355]
Bender, R. 923 [931]
Benn, R. 610 [647]
Bennett, M. A. 1296 [1349]
Berg, D. 1539
Berlitz, T. F. 611 [623]
Berndt, A. 186, 781, 784 [188, 759, 761]
Berrisford, D. J. 1044 [1048]
Bertman, S. B. 330 [342]
Bertrand, G. 621, 1250 [617, 1253]
Bestmann, H. J. 1219 [1303]
Betz, P. 630, 1011 [644, 1066]
Beutler, U. 333 [344]
Bever, M. B. 820 [840; AM 206]
Bharathi, P. 465 [506]
Biagini, P. 1009 [1079]
Biali, S. E. 199 [202]
Bicknell-Tassius, R. N. 1441 [1471; AM 355]
Bierbach, U. 776 [796]
Bill, E. 1709 [1747]
Billeb, G. 1028 [1074]
Billups, W. E. 1711 [1735]
Bindra, J. S. 1539
Binger, P. 610 [647]
Black, Sir J. W. 886 [910]
Bläser, D. 206, 223 [209, 225]
Blau, W. 1440 [1470; AM 354]
Bloor, D. 1760 [1800; AM 460]
Blümich, B. 1429, 1764 [1459, 1804; AM 343, 464]
Boberski, C. 1560 [1592; AM 378]
Boche, G. 72, 73, 277, 337, 468, 932, 1392 [57, 58, 286, 349, 470, –, 1424]
Bock, H. 88, 911, 1373, 1627, 1684, 1685 [77, 950, 1378, 1659, 1715, 1717]
Bodwell, G. 455 [509]
Boese, R. 206, 223, 342, 1379, 1500, 1678 [209, 225, 354, 1401, 1563, 1745]
Bögge, H. 1518 [1527]
Boguth, G. 1008 [1058]
Boland, W. 178, 1379 [180, 1401]
Bold, G. 497 [491]
Bonamico, M. 1049 [1067]
Bonrath, W. 772 [790]
Boons, G. J. P. H. 1504 [1538]
Born, D. 1050 [1085]
Born, L. 483 [462]
Borrmann, H. 180 [182]
Bos, M. 746 [800]
Bosold, F. 337 [349]
Boubekeur, K. 588 [607]
Bournonville, J. P. 347 [360]
Bovenschulte, E. 202 [204]
Boyer, J. 1016 [1069]
Bradley, D. C. 1581 [1613; AM 399]
Brandmeier, V. 486 [466]
Brandsma, L. 631, 1224 [–, 1261]
Brandt, P. 1263, 1265 [1274, 1275]
Braschwitz, W.-D. 1348 [1383]
Brauer, H. 1028 [1074]
Braun, K. 1056 [1092]
Braun, Manfred 895, 896 [953, 948]
Braun, Max 601 [636]
Braun, S. 1025 (1282) [1061 (–)]
Braunstein, P. 100, 923, 1361 [931, 1414]
Bremer, M. 486, 1042, 1219, 1224, 1226 [466, 1063, 1303, 1261, 1264]
Brett, W. A. 206 [209]
Brieden, W. 477 [477]
Brimah, A. K. 1263 [1274]
Bringmann, G. 1672 [1725]
Brömmelhaus, A. 1682 [1726]
Brook, R. J. 1137, 1583 [1163, 1615; AM 309, 401]
Brown, H. C. 354
Brückner, H. 327 [336]
Brunner, H. 1521 [1558]
Brzezinski, V. 323 [332]
Bube, R. H. 671 [687; AM 173]
Buchholz, S. 72, 73 [57, 58]
Buddrus, J. 738 [797]
Bujacz, G. 97 [87]
Bullock, E. 1088 [1114; AM 260]
Bunsell, A. R. 1443 [1473; AM 357]
Burgess, J. 103
Bürgi, H. B. 1534
Buser, U. 902 [938]
Bussmann-Holder, A. 379 [393; AM 89]
Büttner, H. 379, 671 [393, 687; AM 89, 173]
Byrne, H. J. 1753 [1793; AM 453]

Cahn, R. W. 123, 246, 524, 820, 1128 [123, 254, 540, 840, 1154; AM 19, 56, 128, 206, 300]
Calabrese, J. C. 90, 92, 205 [79, 81, 207]
Calderazzo, F. 471 [469]
Campbell, A. K. 933
Canceill, J. 1246, 1249 [1249, 1251]
Candy, J. P. 347 [360]
Caneschi, A. 1365 [1408]
Cannon, R. D. 930 [923]
Caporusso, A. M. 1009 [1079]
Carré, F. 489, 1016 [474, 1069]
Casas, J. M. 748 [782]
Castan, F. 1250 [1253]
Cayton, R. H. 1523 [1547]
Cederbaum, L. S. 88, 761, 1281 [77, 770, –]
Cerveau, G. 489 [474]
Cesario, M. 1246 [1249]
Chacon, S. T. 1523 [1547]
Chadwick, A. V. 75 [69]
Chan, C. 1502 [1559]
Chardon-Noblat, S. 593 [631]
Charles, R. 192 [195]
Chelikowsky, J. R. 1441 [1471; AM 355]
Chen, C.-S. 695 [711]
Chen, H. 316 [325]
Chiesi-Villa, A. 64, 66, 1376 [91, 93, 1430]
Chisholm, M. H. 432, 1368, 1523 [446, 1399, 1547]
Chou, T.-W. 1442 [1472; AM 356]

Chuit, C. 489 [474]
Chung, J. Y. L. 1502 [1559]
Chung, T. 98 [83]
Clark, D. L. 432 [446]
Clark, R. J. H. 963 [987; AM 241]
Clayson, D. B. 931
Clegg, W. 1241 [1279]
Clooth, G. 453 [495]
Clough, S. 1124 [1150; AM 296]
Cohen, M. L. 1441 [1471; AM 355]
Collet, A. 1246, 1249 [1249, 1251]
Collette, J. W. 638 [654; AM 140]
Collins, T. J. 912, 1509 [924, 1552]
Coors, C. 626 [624]
Corazza, F. 64, 66 [91, 93]
Cordier, G. 201, 1702 [204, 1689]
Corriu, R. J. P. 489, 1016 [474, 1069]
Cosmo, R. 604 [638]
Cossu, S. 766 [767]
Cotton, F. A. 1073
Cottrell, A. 1592 [1624; AM 410]
Cowley, A. H. 1018, 1208 [1089, 1235]
Cramer, F. 1403
Cramer, R. E. 98 [83]
Cremer, D. 898 [920]
Crompton, T. R. 1595 [1627; AM 413]
Czekay, G. 1277 [1306]
Czjzek, M. 770 [786]

Dalton, L. 1569 [1601; AM 387]
Damerius, R. 769 [783]
Daub, J. 1494 [1541]
Davidov, D. 1569 [1601; AM 387]
Davies, S. J. 624 [613]
de Jeu, V. A. 383 [397; AM 93]
De Lucchi, O. 766 [767]
de Meijere, A. 595, 1037 [626, 1071]
Deacon, G. B. 1370 [1374]
Dedieu, A. 923, 1694 [931, 1711]
Deisenhofer, J. 829 [872]
Deiseroth, H.-J. 1251 [1286]
Della Vedova, B. S. P. C. 763 [780]
Delogu, G. 766 [767]
Denisenko, S. N. 1381 [1397]
Depezay, J.-C. 614 [645]
Desbois, M.-H. 460 [459]
Dettlaff-Weglikowska, U. 623 [615]
Dhal, P. K. 196, 383 [198, 397; AM –, 93]
Diaz Calleja, R. 1265 [1275]
Dickert, F. L. 813 [833; AM 199]
Dietrich, A. 1370 [1374]
Dietrich-Buchecker, C. O. 189 [192]
Dillinger, R. 1560 [1592; AM 378]
Dixon, D. A. 90, 92 [79, 81]
Dobler, M. 1657 [1744]
Dominguez, L. 1122 [1148; AM 294]
Dötz, K. H. 1384 [1425]
Dougherty, D. A. 961 [985; AM 239]
Douglas, T. 1367 [1394]
Drabowicz, J. 97 [87]
Dresselhaus, G. 526 [542; AM 130]
Dresselhaus, M. S. 526 [542; AM 130]
Drewello, T. 1275 [1247]
Drieß, M. 217, 1038 [219, 1087]
Dronskowski, R. 758 [775]
Duff, D. G. 590 [610]
Düll, B. 1343 [1375]
Dumas, J. 614 [645]
Dunne, B. J. 737 [798]
Dürr, H. 413 [427]
Durst, H. 323 [332]
Dusausoy, Y. 923 [931]
Duthaler, R. O. 494, 495, 497 [488, 490, 491]
Dyer, A. 964 [988; AM 242]
Dykstra, C. E. 1404

Ebert, M. 914 [934]
Ebmeyer, F. 79 [95]
Eckert, H. 1723 [1763; AM 423]
Economy, J. 229 [237; AM 39]
Edelmann, F. T. 445 [496]
Edmundson, R. S. 1716
Edwards, P. P. 590, 810 [610, 830; AM –, 196]
Effenberg, G. 524 [540; AM 128]
Effenberger, F. 1053 [1059]
Egert, E. 67 [65]
Egli, M. 1147 [1173]
Ehle, M. 225 [227]
Ehrenfreund, M. 1531 [1530]
Eichhorn, B. W. 1032 [1081]
Eidenschink, R. 1424 [1454; AM 338]
Eigenmann, B. 1587 [1619; AM 405]
Eilenberg, W. 927 [955]
Eisenbach, C. D. 504 [520; AM 108]
El Mansour, A. 347 [360]
Elion, G. B. 870 [893]
Eller, K. 607, 1277 [634, 1306]
Eller, S. 1263 [1274]
Ellerd, M. G. 1538
Ellis, D. E. 1357 [1410]
Ellis, P. D. 1523 [1547]
Emberger, R. 1022 [1039]
Emmelius, M. 1445 [1475]
Engel, J. 102
Engelhardt, H. 353, 1537
Engels, J. W. 716 [733]
Englert, U. 471 [469]
Enkelmann, V. 458, 1680 [501, 1704]
Entian, K.-D. 616 [618]
Enzel, P. 1692 [1737]
Eriksson, T. 1584 [1616; AM 402]
Erk, P. 1245 [1297]
Erker, G. 179, 397, 628, 630 [181, 411, 642, 644]
Erman, B. 673 [689; AM 175]
Ermer, O. 105, 473, 1239 [–, 503, 1298]
Ernst, L. 455, 1279, 1507 [509, 1290, 1549]
Espinet, P. 1065 [1076]
Ettel, F. 1496 [1525]
Etxebarría, J. 1065 [1076]
Evans, J. 590 [610]

Fabbri, D. 766 [767]
Fabian, J. 677 [693]
Fachinetti, G. 1009 [1079]
Falbe, J. 634
Falk-Heppner, M. 1253 [1281]
Famulok, M. 337, 468 [349, 470]
Fanta, A. D. 1038 [1087]
Fanwick, P. E. 1377 [1431]
Fares, V. 1049 [1067]
Fawzi, R. 448 [460]
Fehér, M. 339 (502), 1231 [352 (–), 1245]
Feigel, M. 486 [466]
Felixberger, J. K. 334 [346]
Fennen, J. 1371 [1420]
Fenske, D. 1390, 1665, 1684, 1685 [1412, 1740, 1715, 1717]
Ferch, H. 385 [399; AM 95]
Ferguson, G. 767 [765]
Ferraro, F. 1365 [1408]
Ferretti, O. A. 347 [360]
Feser, R. 935
Fessner, W.-D. 1539
Fiedler, J. 1531 [1530]
Finckh, P. 619 [629]
Finklea, H. O. 386 [400; AM 96]
Fisch, K. 1521 [1558]
Fischer, C. 1494 [1541]
Fischer, E. 925 [925]
Fischer, H. 354, 491 [–, 486]
Fischer, R. D. 1263, 1265 [1274, 1275]
Fitjer, L. 94 [55]
Fitzgerald, J. A. 649 [665; AM 151]
Fitzky, H.-G. 483 [462]
Flamini, A. 1049 [1067]
Fleischer, H. 315, 1665 [324, 1740]
Fleischer, U. 1042 [1063]
Flintjer, B. 95 (228) [89 (–)]
Floriani, C. 64, 66, 1376 [91, 93, 1430]
Floss, H. G. 146 [147]
Folting, K. 1368, 1523 [1399, 1547]
Forniés, J. 748 [782]
Förster, H. 741 [753]
Forsyth, C. M. 1370 [1374]
Fourmigué, M. 588 [607]
Frahm, J. 791
Franck, B. 1243, 1519 [1292, 1550]
Franke, M. 1709 [1747]
Frankhauser, P. 217 [219]
Fráter, G. 1537
Frelek, J. 1515 [1543]
Frigo, D. M. 1581 [1613; AM 399]
Frischat, G. H. 820 [840; AM 206]
Fritz, G. 315 [324]
Fritz, H. 300, 305, 310, 1345, 1348 [309, 314, 319, 1381, 1383]
Fritz, H. P. 786
Frohn, H. J. 1506 [1534]
Fronda, A. 1663 [1750]
Fuchs, J. 1526 [1528]
Fueß, H. 770 [786]
Fuhrhop, J.-H. 1538
Fukunishi, K. 71 [64]
Fülling, G. 1519 [1550]
Funaioli, T. 1009 [1079]

Gabelica, Z. 81 [60]
Gäbler, A. 178 [180]
Gais, H.-J. 349 (1282), 1025 (1282) [362 (1434), 1061 (–)]
Galm, W. 345 [357]
Gans, W. 268, 633 [277, –]
Garnier, F. 513 [529; AM 117]
Gatteschi, D. 1365 [1408]
Gauntlett, J. T. 590 [610]
Gaus, H. 1019 [1037]
Gauss, J. 898 [920]
Gcib, S. J. 1388 [1422]
Gerlach, H. 1657 [1744]
Gernoth, H. 1441 [1471; AM 355]
Gerson, F. 902 [938]
Gescheidt, G. 902 [938]
Giannis, A. 218 [220]
Giese, B. 325, 969 [334, 993]
Gigou, A. 755 [794]
Gijbels, R. 101
Gil-Av, E. 192, 1281 [195, –]
Gillard, R. 786
Gillette, G. R. 54 [90]
Ginovker, A. S. 1441 [1471; AM 355]
Ginsburg, E. J. 1571 [1603; AM 389]
Glaudemans, C. P. J. 1669 [1730]
Gleiter, R. 925, 1379, 1525 [925, 1401, 1561]
Glitsch, H. G. 1359 [1417]
Göbel, E. O. 672 [688; AM 174]
Godt, A. 1680 [1704]
Goesmann, H. 1684 [1715]

Gogu, E. 953 [977; AM 231]
Goldberg, H. A. 526 [542; AM 130]
Gölitz, P. 107 [107; AM 3]
Gompper, R. 1060, 1063 [1043, 1046]
Goodnow, T. T. 1396 [1404]
Görgen, G. 178 [180]
Görling, A. 1357 [1410]
Gorman, C. B. 1571 [1603; AM 389]
Goto, K. S. 821 [841; AM 207]
Gouzerh, P. 1363 [1377]
Grainger, D. W. 1137 [1163; AM 309]
Graml, H. J. 1442 [1472; AM 356]
Gray, G. W. 1120 [1146; AM 292]
Gréc, R. 755 [794]
Greenberg, A. 1401, 1538
Gregory, K. 1224 [1261]
Gregory, P. 1139, 1593, 1721 [1165, 1625, 1761; AM 311, 411, 421]
Greidanus, F. J. A. M. 235, 958 [243, 982; AM 45, 236]
Grellmann, K.-H. 338 [350]
Grennberg, A. 1538
Gribov, L. A. 1281
Griesinger, C. 1071
Grigat, I. 1655 [1687]
Grimm, F.-T. 198 [201]
Grimm, H. 953 [977; AM 231]
Grimme, W. 1353 [1390]
Gritsenko, V. A. 1441 [1471; AM 355]
Groh, W. 1548 [1580; AM 366]
Grohmann, A. 463 [464]
Gross, H.-J. 1245 [1297]
Grotjahn, D. 1384 [1425]
Grove, D. M. 341 [351]
Grubbs, R. H. 1571 [1603; AM 389]
Grunze, M. 963 [987; AM 241]
Grützmacher, H. 740 [768]
Guastini, C. 64, 66, 1376 [91, 93, 1430]
Gudat, A. 201, 1702 [204, 1689]
Guenter, P. 1440 [1470; AM 354]
Guhl, D. 1035 [1091]
Guilhem, J. 1246 [1249]
Günther, H. 1025 (1282) [1061 (–)]
Guth, J.-L. 81 [60]
Gütlich, P. 334 [346]

Haaland, A. 992 [1017]
Haarer, D. 504, 1544, 1760 [520, 1576, 1800; AM 108, 362, 460]
Haase, D. 344 [355]
Haasen, P. 1592 [1624; AM 410]
Haenel, M. W. 455 [509]
Hafner, A. 499 [493]
Hagedorn, M. 1675 [1710]
Hake, D. 1364 [1416]
Haley, M. M. 1711 [1735]
Hamilton, T. P. 485 [500]
Hämmerle, M. 908 [940]
Hamminger, R. 1560 [1592; AM 378]
Hammond, C. E. 1368 [1399]
Hampden-Smith, M. J. 432, 1523 [446, 1547]
Hampp, N. 245 [253; AM 55]
Hanack, M. 1057, 1743 [1083, 1783; AM –, 443]
Handreck, D.-R. 1351 [1386]
Hann, R. A. 1760 [1800; AM 460]
Hansert, B. 1059 [1084]
Hantsche, H. 1764 [1804; AM 464]
Harbrecht, B. 1660 [1696]
Harel, M. 466 [515]
Hargittai, I. 1534
Hargittai, M. 1534
Harkema, S. 746 [800]
Harlow, R. L. 92 [81]
Harms, K. 72, 73, 1384, 1392 [57, 58, 1425, 1424]
Harrison, M. R. 810 [830; AM 196]
Härter, P. 1008 [1058]
Hartmann, K. 1678 [1745]
Hartmann, K.-P. 1267 [1288]
Hartung, J. 325 [334]
Hartweg, M. 56 [98]
Hartweg, U. 56 [98]
Hartwig, U. 221 [224]
Hassel, T. 483 [462]
Haug, H. 672 [688; AM 174]
Haupt, E. 603 [640]
Hausen, H.-D. 1659 [1734]
Haushalter, R. C. 743, 1032 [802, 1081]
Hausmann, I. 319 [328]
Hazen, R. M. 1139 [1165; AM 311]
He, J. 325 [334]
Hedtmann, U. 1515 [1543]
Heimke, G. 111, 518, 956, 1431 [111, 534, 980, 1461; AM 7, 122, 234, 345]
Heinrich, J. 1560 [1592; AM 378]
Heinze, J. 604, 1741 [638, 1781; AM –, 441]
Heitele, H. 619 [629]
Heitz, W. 633
Helbing, J. 1235 [1259]
Hellmann, G. 1025 (1282) [1061 (–)]
Hemmerle, H. 349 (1282) [362 (1434)]
Hendrickson, D. N. 1388 [1422]
Henisch, H. K. 381 [395; AM 91]
Henkel, G. 61, 202, 1506 [54, 204, 1534]
Henzler, M. 523 [539; AM 127]
Herberich, G. E. 319, 737 [328, 798]
Herborn, C. 1399 [1392]
Herbst, R. 67 [65]
Herbst, W. 1073
Herdtweck, E. 334, 1008, 1511 [346, 1058, 1536]
Herold, P. 495 [490]
Herrmann, A. 1651 [1683]
Herrmann, G. 1536
Herrmann, W. A. 334, 786, 1511 [346, –, 1536]
Heßner, B. 737 [798]
Hester, R. E. 963 [987; AM 241]
Heuer, L. 1507 [1549]
Heuschmann, M. 1267 [1288]
Hevesi, L. 227
Heyman, J. S. 1594 [1626; AM 412]
Heywang, G. 483 [462]
Hidai, M. 1040 [1053]
Higuchi, T. 1040 [1053]
Hill, A. F. 210 [213]
Hill, J. S. 1120 [1146; AM 292]
Hillen, W. 104
Hillenkamp, F. 760 [805]
Hiller, W. 448 [460]
Hillermeier, K. 1442 [1472; AM 356]
Hinrichs, H. 1499 [1546]
Hipskind, P. A. 1502 [1559]
Hitchings, G. H., Jr. 879 [903]
Ho, T.-L. 1537
Hoberg, H. 1035 [1091]
Hobert, K. 1515 [1543]
Hobza, P. 502
Hochstrasser, R. 181 [183]
Hock, R. 179 [181]
Hocken, J. 1697 [1713]
Höcker, H. 384 [398; AM 94]
Hocker, J. 483 [462]
Hodge, P. 383 [397; AM 93]
Hodgson, S. M. 1241 [1279]
Hoffman, D. M. 432 [446]
Hoffmann, H. 529 [545; AM 133]
Hoffmann, R. 1070, 1688 [–, 1706]
Hoffmann, U. 630 [644]
Hofmann, P. 354, 786, 908 [–, –, 940]
Höfner, A. 186 [188]
Holla, E. W. 220 [222]
Hollnagel, A. 1390 [1412]
Hölscher, A. 1443 [1473; AM 357]
Holz, B. 1269 [1301]
Hondros, E. D. 1088 [1114; AM 260]
Höner, P. 1353 [1390]
Hönle, W. 56, 623 [98, 615]
Hopf, H. 455, 904, 1279, 1745 [509, 942, 1290, 1785; AM –, –, –, 445]
Hopp, R. 1022 [1039]
Hoppe, D. 67, 69 [65, 67]
Hoppe, I. 67 [65]
Horchler, K. 918, 1500 [945, 1563]
Horn, E.-M. 342 [354]
Hoser, A. 1526 [1528]
Howard, J. A. K. 210, 624 [213, 613]
Hu, D. 900 [929]
Huang, S.-P. 1513 [1556]
Huber, J. 1560 [1592; AM 378]
Huber, R. 848 [849]
Huber, W. 1531 [1530]
Huch, V. 603, 1237 [640, 1287]
Hucker, J. 904 [942]
Huffman, J. C. 1032, 1368, 1523 [1081, 1399, 1547]
Huggins, B. A. 1523 [1547]
Huignard, J.-P. 1440 [1470; AM 354]
Humphreys, C. J. 1077, 1763 [1103, 1803; AM 249, 463]
Hunger, K. 1073
Hünig, S. 104, 1245 [–, 1297]
Hunkler, D. 298, 1351 [307, 1386]
Hunold, R. 781, 784 [759, 761]
Huser, M. 1386 [1427]
Hüter, O. 325 [334]
Huttner, G. 446, 1496 [482, 1525]

Iatridou, H. 447 [485]
Igau, A. 621 [617]
Ilg, M. 1029 [1033]
Immergut, E. W. 382 [396; AM 92]
Imperatori, P. 1049 [1067]
Ingendoh, A. 760 [805]
Ingold, F. 1694 [1711]
Ingold, K. U. 183 [186]
Isaacs, N. S. 1258, 1261 [1266, 1269]
Ishii, D. 353
Ivanov, I. B. 527 [543; AM 131]

Jachow, H. 1231 [1245]
Jacobsen-Bauer, A. 603 [640]
Jacobson, R. 597 (1074) [605 (–)]
Jacoby, D. 1376 [1430]
Jaeger, H. 124, 125, 1592 [124, 125, 1624; AM 20, 21, 410]
Jäger, V. 469 [512]
Jakobi, R. 334 [346]
Jakobs, S. 1506 [1534]
Janiak, C. 1688 [1706]
Jauch, J. 1022 [1039]
Jayasooriya, U. A. 930 [923]
Jeannin, Y. 1363 [1377]
Jefferson, D. A. 590, 810 [610, 830; AM –, 196]
Johann, R. 920 [952]
Johnson, B. F. G. 590 [610]
Johnston, M. D. 1071
Jones, P. G. 1279, 1521 [1290, 1558]
Jones, P. J. 313 [322]

Jones, R. A. 1018, 1208 [1089, 1235]
Jones, R. V. H. 1044 [1048]
Jost, N. 815 [835; AM 201]
Josten, M. 616 [618]
Joyce, B. A. 1098 [1124; AM 270]
Jung, D. 750 [789]
Jung, G. 616 [618]
Jutzi, P. 600, 762, 1518 [628, 769, 1527]

Kabuto, C. 55, 757 [97, 778]
Kaesz, H. D. 354
Kagoshima, S. 526 [542; AM 130]
Kahl, G. 104
Kahlich, S. 953 [977; AM 231]
Kaifer, A. E. 1396 [1404]
Kaim, W. 1073, 1659 [–, 1734]
Kaletta, C. 616 [618]
Kalinowski, H.-O. 1232 [1293]
Kalló, D. 381 [395; AM 91]
Kambe, N. 452 [476]
Kaminaka, M. 1040 [1053]
Kaminsky, W. 1216 [1304]
Kämmerling, H. T. 1353 [1390]
Kanatzidis, M. G. 1513 [1556]
Känel, H. von 822 [842; AM 208]
Kanellakopulos, B. 1055 [1055]
Kang, S.-J. L. 522 [538; AM 126]
Kappes, D. 1657 [1744]
Karas, M. 760 [805]
Karpfen, A. 502
Karraß, S. 607 [634]
Kaschube, W. 772 [790]
Käss, V. 448 [460]
Kato, Y. 450 [511]
Kaulen, J. 462 [507]
Kaupp, G. 1381 [1397]
Kautz, C. 604 [638]
Kawanaka, H. 1268 [1258]
Kaysser, W. A. 817, 820 [837, 840; AM 203, 206]
Kearley, G. J. 930 [923]
Keim, W. 1011 [1066]
Keller, H. J. 953 [977; AM 231]
Keller, M. 1253 [1281]
Kellner, R. 616 [618]
Kelly, P. F. 1047 [1052]
Kiedrowski, G. von 1235 [1259]
Kiprof, P. 334 [346]
Kirkland, A. I. 590, 810 [610, 830; AM –, 196]
Kirmse, W. 1667 [1728]
Kirste, B. 792
Kiss, K. 964 [988; AM 242]
Kiss, L. 935
Kissler, B. 1525 [1561]
Kiyoshige, K. 320 [329]
Klaff, N. 319 [328]
Klahn, S. 235 [243; AM 45]
Klapötke, T. 1671 [1742]
Klärner, F. G. 1535
Kleemann, A. 102
Klein, E. 751 [792]
Klein, K.-D. 83 [63]
Klein, L. C. 1137 [1163; AM 309]
Kleinschmit, P. 1416 [1446; AM 330]
Klintz, R. 1515 [1543]
Klockenkämper, R. 964 [988; AM 242]
Klöne, A. 1515 [1543]
Klusener, P. A. A. 1224 [1261]
Kneeland, J. B. 791
Kniep, R. 201, 951, 1702 [204, 975, 1689; AM –, 229, –]
Knipp, B. 1651 [1683]
Knoch, F. 1271, 1703 [1244, 1719]
Knöchel, T. 1494 [1541]
Knölker, H.-J. 223, 1678 [225, 1745]
Knorr, M. 1361 [1414]
Knotter, D. M. 341 [351]
Ko, F. 1442 [1472; AM 356]
Kobayashi, Y. 1052 [1090]
Koch, A. 325 [334]
Koch, W. 1042 [1063]
Köcher, J. 1028 [1074]
Köcher, M. 1655 [1687]
Kodas, T. T. 794 [814; AM 180]
Köhler, F. H. 786
Köhler, J. 1662 [1695]
Kohlmann, S. 1659 [1734]
Kohnke, F. H. 1103, 1258, 1261 [1129, 1266, 1269; AM 275, –, –]
Kohnz, H. 1343 [1375]
Kojo, S. 71 [64]
Kondo, K. 450, 452 [511, 476]
König, W. A. 178, 1657 [180, 1744]
Kono, Y. 1222 [1254]
Kopf, J. 777 [764]
Kopp, G. 1713 [1701]
Köppel, H. 761 [770]
Köpsel, M. 1022 [1039]
Korth, H.-G. 183 [186]
Koscielniak, T. 614 [645]
Köster, R. 918 [945]
Kovačević, M. 1147 [1173]
Kramer, B. 215 [217]
Kramer, H. E. A. 1659 [1734]
Krause, A. 1379 [1401]
Krebber, R. 1657 [1744]
Krebs, A. 603 [640]
Krebs, B. 61, 187, 1682 [54, 190, 1726]
Kreissl, F. R. 354
Kreiter, C. G. 1013 [1035]
Kremer, M. 1373 [1378]
Kretschmer, O. 1745 [1785; AM 445]
Kreuder, W. 323 [332]
Kriechbaum, G. W. 1416 [1446; AM 330]
Krief, A. 227
Krieger, C. 84, 86, 491 [72, 73, 486]
Krimmel, E. F. 938 [962; AM 216]
Kroos, R. 600 [628]
Krug, H. 323 [332]
Krüger, C. 628, 630, 772, 786, 1011 [642, 644, 790, –, 1066]
Krüger, T. 61 [54]
Kubiak, C. P. 1377 [1431]
Kuck, D. 595 [626]
Kühlwein, J. 1053 [1059]
Kuhn, H. J. 738 [797]
Kuhn, N. 342 [354]
Kujath, E. 1060 [1043]
Kunkely, H. 1494 [1541]
Kunz, H. 1067, 1068 [1041, 1042]
Kuperman, A. 359 [373; AM 69]
Kurreck, H. 792
Kutzelnigg, W. 1042 [1063]

Laag, R. 1750 [1790; AM 450]
Lacey, D. 1120 [1146; AM 292]
Lacher, R. C. 633
Lacombe, L. 1246 [1249]
Laggner, P. 959 [983; AM 237]
Lahav, M. 466 [515]
Lai, F. W. 743 [802]
Lajzerowicz, J. 1249 [1251]
Lallement, R. 357 [371; AM 67]
Lambert, J. 738 [797]
Lammertsma, K. 1321 [1313]
Lamming, G. R. 1241 [1279]
Lamparter, P. 951 [975; AM 229]
Lancaster Jr., J. R. 632
Langhals, H. 478 [497]
Langohr, U. 1245 [1297]
Lanneau, G. 1016 [1069]
Lapasset, J. 1016 [1069]
Laschewsky, A. 1574 [1606; AM 392]
Laszlo, P. 636 [652]
Le Merrer, Y. 614 [645]
Lebrilla, C. B. 1275 [1247]
Lee, P. R. 1033 [1073]
Lehmann, J. 1669 [1730]
Lehnert, A. 780 [773]
Lehnig, M. 792
Leis, C. 203 [206]
Leiserowitz, L. 466 [515]
Leitenberger, V. 929 [946]
Lellouche, J.-P. 755 [794]
Lenfers, J. B. 777 [764]
LeNoble, W. J. 1535
Lentz, D. 321 [330]
Lesueur, W. 66 [93]
Leutenegger, U. 60 [61]
Lewerenz, H.-J. 386 [400; AM 96]
Lex, J. 902, 1651, 1655 [938, 1683, 1687]
Liang, W. Y. 810 [830; AM 196]
Licini, G. 766 [767]
Lieberknecht, A. 333, 929 [344, 946]
Liebman, J. F. 1401, 1538
Lieser, B. 1231 [1245]
Limbach, H.-H. 76, 1741, 1743 [84, 1781, 1783; AM –, 441, 443]
Lindner, Ekkehard 448 [460]
Lindner, Ernst 102
Lindner, H. J. 1025 (1282) [1061 (–)]
Lindoy, L. F. 1534
Link, R. 194 [197]
Linti, G. 478 [497]
Lintz, H.-G. 708 [725]
Lloyd, D. R. 1761 [1801; AM 461]
Loebel, J. 1033 [1073]
Loewus, D. I. 1717
Lohmann, J. 1601 [1633]
Lohse, K. 1528 [1539]
Lopez, F. 1025 (1282) [1061 (–)]
Lorberth, J. 611, 735 [623, 793]
Lorenz, I.-P. 1342 [1389]
Lork, K. D. 327 [336]
Lößel, G. 62 [75]
Lösking, O. 1255 [1283]
Lottenbach, W. 495 [490]
Lotz, R. 344 [355]
Lough, A. J. 767 [765]
Lowe, K. C. 670 [686; AM 172]
Lozach, B. 1246 [1249]
Lubitz, W. 792
Lücke, M. 493 [480]
Lücking, K. 1713 [1701]
Lührs, E. 187 [190]
Lukas, H. L. 524 [540; AM 128]
Lupo, D. 1548, 1760 [1580, 1800; AM 366, 460]
Lusztyk, J. 183 [186]
Lüttke, W. 1073
Lutz, G. 298 [307]
Lutz, H. D. 477 [477]
Lutz, S. 178 [180]
Łyżwa, P. 97 [87]

Maas, G. 1663 [1750]
Mackay, K. D. 810 [830; AM 196]
Mackey, K. J. 1581 [1613; AM 399]
Madappat, K. V 1256 [1284]
Maddox, P. J. 808 [828; AM 194]
Madin, A. 60 [61]

Maercker, A. 83, 477 [63, 477]
Mahjoub, A. R. 1526 [1528]
Mahler, H. 896 [948]
Maier, G. 1050, 1232 [1085, 1293]
Maier, W. F. 135 [135]
Maligres, P. 1272 [1255]
Malm, J.-O. 778 [772]
Mandon, D. 1709 [1747]
Mannschreck, A. 199 [202]
Marcos, M. 1065 [1076]
Marder, S. R. 1571 [1603; AM 389]
Margaretha, P. 1499 [1546]
Margaritondo, G. 791
Marinero, E. 1134 [1160; AM 306]
Mark, J. E. 673 [689; AM 175]
Märkl, G. 1695 [1698]
Marsch, M. 72, 1392 [57, 1424]
Martin, G. E. 1071
Martin, J. D. 1368 [1399]
Martin Jr., F. J. 932
Marx, G. 1536
Mason, S. A. 1239 [1298]
Massa, W. 72, 73, 186, 611, 735, 781, 784 [57, 58, 188, 623, 793, 759, 761]
Matern, E. 315 [324]
Mathias, J. P. 1103, 1258 [1129, 1266; AM 275, –]
Mathis, P. 593 [631]
Mathy, A. 1122 [1148; AM 294]
Matusch, R. 626 [624]
Maxka, J. 54 [90]
Mayer, B. 895 [953]
Mayer, J. M. 790
McArdle, C. B. 1140 [1166; AM 312]
McBride, J. M. 330, 377 [342, 391; AM –, 87]
McCall, D. W. 640 [656; AM 142]
McCamley, A. 1690 [1721]
McCleverty, J. A. 786
McLean, M. R. 1569 [1601; AM 387]
Mechmann, S. 1359 [1417]
Meerholz, K. 604 [638]
Mega, I. 1040 [1053]
Meier, H. 227
Meisel, M. 1373 [1378]
Meixner, H. 1245 [1297]
Melandri, M. C. 1365 [1408]
Melder, J.-P. 300, 305, 310 [309, 314, 319]
Mendenhall, D. 933
Menger, F. M. 1218 [1277]
Mensching, L. 597 (1074) [605 (–)]
Merz, A. 807 [827; AM 193]
Merzweiler, K. 1684 [1715]
Metselaar, R. 1406 [1436; AM 320]
Metz, P. 202 [204]
Meurs, J. H. H. 927 [955]
Meyer, R. 929 [946]
Meyer, W. H. 1122 [1148; AM 294]
Micas-Languin, D. 614 [645]
Michael, H. 321 [330]
Michaeli, W. 644 [660; AM 146]
Michel, H. 829 [872]
Michel-Beyerle, M. E. 619 [629]
Middleditch, B. S. 1537
Miguel, D. 1014 [1078]
Miguel, J. A. 1014 [1078]
Mikołajczyk, M. 97 [87]
Miller, G. 1662 [1695]
Miller, G. J. 1070
Miller, J. S. 90, 92, 638, 961 [79, 81, 654, 985; AM –, –, 140, 239]
Miller, L. L. 597 (1074) [605 (–)]
Miller, R. D. 1733 [1773; AM 433]
Minachev, Kh. M. 381 [395; AM 91]
Mißlitz, U. 472 [484]
Mittendorf, J. 613 [633]
Miyamoto, H. 1222 [1254]
Miyashi, T. 1052 [1090]
Mizobe, Y. 1040 [1053]
Mizuno, T. 452 [476]
Modder, J. F. 1698 [1723]
Mohr, E. 105
Möhrke, A. 762, 1518 [769, 1527]
Möhwald, H. 527 [543; AM 131]
Moll, M. 1271 [1244]
Möller, U. 1359 [1417]
Möller-Lindenhof, N. 1216 [1304]
Montforts, F.-P. 480 [471]
Moock, K. 1676 [1713]
Mootz, D. 1697 [1713]
Mortensen, J. 1741 [1781; AM 441]
Morun, B. 778 [772]
Motomura, T. 921 [922]
Müllen, K. 458, 604, 904, 1343, 1531 [501, 638, 942, 1375, 1530]
Müller, A. 600, 1518 [628, 1527]
Müller, G. 203, 463, 1700 [206, 464, 1739]
Müller, H.-K. 483 [462]
Müller, P. 610 [647]
Müller, U. 185, 1011 [187, 1066]
Müller, Winfried 1029 [1033]
Müller, Wolfgang 183 [186]
Müller-Buschbaum, Hk. 1472 [1503]
Mulvey, R. E. 1241 [1279]
Mulzer, J. 354
Mundy, B. P. 1538
Murakami, S. 452 [476]
Murata, I. 1268 [1258]
Musgrove, R. J. 624 [613]
Musso, H. 1379 [1401]
Mutter, M. 535 [551]
Myers, D. 936
Mynott, R. 610 [647]

Naarmann, H. 1745 [1785; AM 445]
Nagasawa, H. 526 [542; AM 130]
Nagase, S. 329 [340]
Nakamura, A. 98 [83]
Nakazawa, A. 450 [511]
Narlikar, A. 1592 [1624; AM 410]
Neef, G. 773 [776]
Neher, A. 1342 [1389]
Neibecker, D. 500 [479]
Nelson, R. D. 385 [399; AM 95]
Nesper, R. 58 [99]
Neubold, P. 763 [780]
Neugebauer, F. A. 491 [486]
Neumann, C. 178 [180]
Neumann, W. P. 1028 [1074]
Newsom, I. 84 [72]
Nicolaou, K. C. 587, 1272 [621, 1255]
Niecke, E. 215, 751, 1673 [217, 792, 1708]
Nieger, M. 215, 751, 1673 [217, 792, 1708]
Niemer, B. 1705 [1699]
Niessen, W. von 88, 597 (1074) [77, 605 (–)]
Nobel, D. 208 [211]
Nolte, R. 628 [642]
Noltemeyer, M. 338, 609, 754, 1383 [350, 609, 788, 1419]
Nöth, H. 478 [497]
Nowotny, H.-P. 736 [785]
Nuber, B. 763, 1055 [780, 1055]
Nugent, W. A. 790
Nunn, C. M. 1018 [1089]

Oertle, K. 495 [490]
Oeynhausen, M. von 1221 [1295]
Offerhaus, R. 1056 [1092]
Ogawa, A. 452 [476]
Ogoshi, H. 921 [922]
Ogura, F. 1222 [1254]
Ohlhorst, B. 595 [626]
Opitz, K. 456 [513]
Oppolzer, W. 38 [39]
Ortholand, J.-Y. 1394 [1402]
Orville-Thomas, W. J. 1281
Osborn, J. A. 1386 [1427]
Ossig, J. 194 [197]
Otsubo, T. 1222 [1254]
Otten, T. 1348 [1383]
Ottow, E. 773 [776]
Overhand, M. 1504 [1538]
Ozin, G. A. 359 [373; AM 69]

Paetzold, P. 88, 1401 [77, –]
Palazon, J. M. 587 [621]
Pampaloni, G. 471 [469]
Pannek, J.-B. 223 [225]
Parkin, I. P. 1047 [1052]
Partridge, G. 1132, 1746 [1158, 1786; AM 304, 446]
Pascard, C. 1246 [1249]
Pasch, E. 1381 [1397]
Paschalidis, C. 1700 [1739]
Patai, S. 933, 1070
Patyk, A. 898 [920]
Pawlowski, G. 1445 [1475]
Pelter, A. 354
Penk, M. 600 [628]
Pérez, J. 1065 [1076]
Perrot, M. 1016 [1069]
Persau, C. 1665 [1740]
Perutz, R. N. 1690 [1721]
Peter, M. G. 555, 741, 933 [572, 753, –]
Petzow, G. 524 [540; AM 128]
Peuckert, M. 1560 [1592; AM 378]
Pfaltz, A. 60 [61]
Pfleiderer, B. 327 [336]
Pfrengle, W. 1067 [1041]
Phillips, B. R. 649 [665; AM 151]
Phillips, C. R. 1717
Piantini, U. 499 [493]
Pickardt, J. 1269 [1301]
Pickering, I. J. 808 [828; AM 194]
Pilz, M. 781, 784 [759, 761]
Pinkos, R. 303, 305, 310 [312, 314, 319]
Pittel, B. 483 [462]
Platz, G. 384, 936 [398, –; AM 94, –]
Plempel, M. 1539
Ploog, K. 819 [839; AM 205]
Plößl, K. 446 [482]
Pohl, M. 1651 [1683]
Pohl, S. 95 (228), 198, 344, 776 [89 (–), 201, 355, 796]
Poli, N. 1049 [1067]
Politzer, P. 932
Pongs, O. 1515 [1543]
Poon, Y. C. 1717
Poppe, M. 53 [70]
Pörschke, K. R. 772 [790]
Potrawa, T. 478 [497]
Powell, A. K. 318, 1059 [327, 1084]
Powell, D. 1038 [1087]
Powell, P. 934
Power, P. P. 316 [325]
Prelog, V. 1147 [1173]
Priebsch, W. 1221 [1295]
Prigogine, I. 1403
Prinzbach, H. 298, 300, 303, 305, 310, 1253, 1345, 1348, 1351 [307, 309, 312, 314, 319, 1281, 1381, 1383, 1386]
Priou, C. 1016 [1069]

Pritzkow, H. 217, 221, 345, 740, 900 [219, 224, 357, 768, 929]
Proust, A. 1363 [1377]
Puddephatt, R. J. 767 [765]
Pulay, P. 1042 [1063]
Pusch, H. 1359 [1417]
Pustet, N. 199 [202]

Quabeck, U. 94 [55]
Quack, M. 571, 932 [588, –]

Rabalais, J. W. 385 [399; AM 95]
Rabe, J. P. 117, 1127, 1578 [117, 1153, 1610; AM 13, 299, 396]
Rabenau, A. 201, 1702 [204, 1689]
Rademacher, P. 206 [209]
Räder, H.-J. 904, 1531 [942, 1530]
Rall, K. 221 [224]
Ramphal, J. Y. 587 [621]
Rang, H. 1232 [1293]
Ranganathan, S. 1539
Rapp, K. M. 1494 [1541]
Rappoport, Z. 199, 933, 1070 [202, –, –]
Raptis, K. 1055 [1055]
Rauwald, H. W. 1528 [1539]
Réau, R. 500 [479]
Recknagel, A. 445 [496]
Reddington, M. V. 1396 [1404]
Redlich, H. 777 [764]
Reetz, M. T. 1706 [1732]
Regitz, M. 225, 1013 [227, 1035]
Rehder, D. 1221 [1295]
Reichardt, C. 103, 104
Reimer, L. 1763 [1803; AM 463]
Reiner, H. 1594 [1626; AM 412]
Reinhoudt, D. N. 746 [800]
Reinking, M. K. 1377 [1431]
Reiser, O. 1037 [1071]
Reißig, H.-U. 632
Reitmeier, S. 807 [827; AM 193]
Remón, A. 1065 [1076]
Renault, A. 1249 [1251]
Repinsky, S. M. 1441 [1471; AM 355]
Rese, M. 1713 [1701]
Reuscher, H. 1672 [1725]
Reuter, H. 1437 [1467; AM 351]
Rey, P. 1365 [1408]
Réyé, C. 489 [474]
Rheingold, A. L. 1388 [1422]
Riede, J. 1008 [1058]
Riediker, M. 494, 495, 497, 499 [488, 490, 491, 493]
Rieker, J. 1659 [1734]
Riera, V. 1014 [1078]
Riesen, A. 902 [938]
Rihs, G. 298, 303, 499 [307, 312, 493]
Ringsdorf, H. 323, 914 [332, 934]
Robert, F. 1363 [1377]
Rodway, D. C. 1581 [1613; AM 399]
Roesky, H. W. 445, 493, 609, 754, 1383 [496, 480, 609, 788, 1419]
Röhrig, D. 1706 [1732]
Röhrig, P. 1651 [1683]
Rohrmann, J. 1511 [1536]
Romanowski, F. 480 [471]
Rösch, N. 1357 [1410]
Rosmus, P. 88 [77]
Rosoff, M. 1137 [1163; AM 309]
Roth, H. D. 1193 [1220]
Roth, S. 483 [462]
Roth, W. R. 1056 [1092]
Rücker, C. 1348 [1383]
Ruedenberg, K. 597 (1074) [605 (–)]
Rumpel, H. 76 [84]
Ruppert, K. 1684, 1685 [1715, 1717]
Ryu, I. 452 [476]

Saak, W. 95 (228), 198, 344, 776 [89 (–), 201, 355, 796]
Saalfrank, R. W. 631
Sachse, H. 105
Sahl, H.-G. 616 [618]
Sakurai, H. 55, 757, 1028 [97, 778, 1074]
Salbeck, J. 1494, 1521 [1541, 1558]
Salkind, M. 655 [671; AM 157]
Sambongi, T. 526 [542; AM 130]
Sanchez Martinez, E. 1265 [1275]
Sander, W. 898 [920]
Sandhoff, K. 218 [220]
Saniere, M. 614 [645]
Sasaki, N. 1040 [1053]
Sauer, J. 1404
Sauthoff, G. 243 [251; AM 53]
Sauvage, J.-P. 189, 593 [192, 631]
Sawada, M. 1222 [1254]
Sawluk, A. 906 [927]
Schaefer III, H. F. 485 [500]
Schäfer, J. 473 [503]
Schanzenbach, D. 1068 [1042]
Schäufele, H. 900 [929]
Scheer, P. 1019 [1037]
Scheller, M. 761 [770]
Schenk, R. 904 [942]
Scherbaum, F. 463 [464]
Scherer, O. J. 212, 1355 [214, 1395]
Scheuring, M. 1669 [1730]
Schindler, M. 1042 [1063]
Schlabach, M. 76 [84]
Schleyer, P. von R. 781, 1042, 1224, 1226, 1321 [759, 1063, 1261, 1264, 1313]
Schlosser, D. 918 [945]
Schlüter, A.-D. 456, 1680 [513, 1704]
Schmähl, D. 931
Schmalzing, D. 736, 1022 [785, 1039]
Schmalzried, H. 1436 [1466; AM 350]
Schmickler, H. 1651 [1683]
Schmid, G. 778, 780 [772, 773]
Schmidbaur, H. 463, 786, 1357, 1700 [464, –, 1410, 1739]
Schmidt, C. 1529 [1532]
Schmidt, H.-W. 940, 1140 [964, 1166; AM 218, 312]
Schmidt, M. P. 241 [249; AM 51]
Schmidt, T. 477 [477]
Schmidt, U. 333, 929 [344, 946]
Schmitz, F. P. 1761 [1801; AM 461]
Schmutzler, R. 1716, 1507 [–, 1549]
Schneider, H.-J. 753 [757]
Schneider, J. 1013 [1035]
Schneider, S. 213 [215]
Schnering, H. G. von 56, 623, 1019 [98, 615, 1037]
Schöllkopf, U. 613 [633]
Scholz, G. 339 (502) [352 (–)]
Scholz, M. 1383 [1419]
Schomburg, D. 1507 [1549]
Schönherr, E. 381 [395; AM 91]
Schötz, K. 1042 [1063]
Schreiber, H. P. 1761 [1801; AM 461]
Schrobilgen, G. J. 636 [652]
Schrock, R. R. 354
Schröder, D. 1277, 1519 [1306, 1550]
Schubert, U. 354, 934
Schuegraf, K. K. 822 [842; AM 208]
Schulte, K. 1443 [1473; AM 357]
Schultz, P. G. 1283 [1336]
Schulz, G. E. 1023 [1056]
Schulz, H. 356
Schulze, C. 607 [634]
Schumacher, K.-H. 1243 [1292]
Schumann, H. 1033, 1370 [1073, 1374]
Schümann, U. 476 [481]
Schurig, V. 194, 736, 1019, 1022 [197, 785, 1037, 1039]
Schuster, A. 595 [626]
Schütz, J. U. von 1245 [1297]
Schwager, H. 206 [209]
Schwarz, H. 607, 1275, 1277, 1321 [634, 1247, 1306, 1313]
Schwarz, P. 1263 [1274]
Schwarz, W. H. E. 597 (1074), 1071 [605 (–), –]
Schweiger, E. J. 1272 [1255]
Schweitzer, D. 526, 953 [542, 977; AM 130, 231]
Schwemlein, H. P. 1296 [1349]
Schwerdtfeger, P. 1228 [1271]
Scott, A. J. 1241 [1279]
Sebata, M. 98 [83]
Sebba, F. 384 [398; AM 94]
Seebach, D. 472 [484]
Seidel, G. 918 [945]
Sekiguchi, A. 55, 757 [97, 778]
Sekiguchi, Y. 98 [83]
Selig, H. 1569 [1601; AM 387]
Sellmann, D. 1271, 1703 [1244, 1719]
Seppelt, K. 769, 1526, 1676 [783, 1528, 1713]
Serrano, J. L. 1065 [1076]
Sessoli, R. 1365 [1408]
Setton, R. 1434 [1464; AM 348]
Sharma, G. V. M. 465 [506]
Shaw, D. 791
Sheldrick, G. M. 338 [350]
Sherrington, D. C. 383 [397; AM 93]
Shin, S.-H. 735 [793]
Sibilia, J. P. 385 [399; AM 95]
Sibley, J. S. 356
Sicken, M. 1651 [1683]
Sicking, W. 1023 [1056]
Siebert, W. 217 [219]
Sigwart, C. 1525 [1561]
Sih, C. J. 695 [711]
Silberzahn, W. 1022 [1039]
Simmrock, H.-U. 1122 [1148; AM 294]
Simon, A. 180, 758, 1662 [182, 775, 1695]
Simon, J. 528 [544; AM 132]
Sinitasa, S. P. 1441 [1471; AM 355]
Sinning, H. 185 [187]
Sinnwell, V. 595 [626]
Sitzmann, H. 212 [214]
Sixl, H. 1548 [1580; AM 366]
Skokotas, G. 1272 [1255]
Slawin, A. M. Z. 1044, 1047, 1394, 1396 [1048, 1052, 1402, 1404]
Smith, D. J. 590 [610]
Smith, K. 354
Smith, P. C. 1581 [1613; AM 399]
Snaith, R. 1044, 1241 [1048, 1279]
Soglowek, W. 1271 [1244]
Soláns, X. 1014 [1078]
Solari, E. 64 [91]
Söllenböhmer, F. 1667 [1728]
Solouki, B. 88, 1373 [77, 1378]
Sonoda, N. 452 [476]
Sopher, D. W. 927 [955]
Spain, I. L. 526 [542; AM 130]
Spaleck, W. 1511 [1536]
Spanevello, R. A. 587 [621]
Spaniol, T. P. 210 [213]
Spek, A. L. 208, 341, 1698 [211, 351, 1723]
Spencer, N. 1394, 1396 [1402, 1404]

Staab, H. A. 84, 86 [72, 73]
Stadler, M. 781, 784 [759, 761]
Stagno d'Alcontres, G. 1261 [1269]
Stahl, S. 1690 [1721]
Staley, D. L. 1388 [1422]
Stalke, D. 445, 1673 [496, 1708]
Stammler, H.-G. 447 [485]
Stanger, A. 206 [209]
Steckhan, E. 1399 [1392]
Steeb, S. 951 [975; AM 229]
Steffan, B. 453 [495]
Steglich, W. 453 [495]
Steigelmann, O. 1700 [1739]
Steimann, M. 1529 [1532]
Stein, A. 359 [373; AM 69]
Steudel, R. 1269 [1301]
Stirling, C. 1070
Stoddart, J. F. 1044, 1103, 1258, 1261, 1394, 1396, 1534 [1048, 1129, 1266, 1269, 1402, 1404, –; AM –, 275, –, –, –, –, –]
Stone, F. G. A. 210, 624 [213, 613]
Strähle, J. 471, 790 [469, –]
Strangmann-Dickmann, M. 1515 [1543]
Stratmann, M. 385, 819 [399, 839; AM 95, 205]
Streubel, R. 1673 [1708]
Strunck, A. 1251 [1286]
Stuhrmann, H. 791
Sturm, F. von 526 [542; AM 130]
Stütz, A. 1539
Stüwer, D. 101
Suckling, C. J. 1538
Sugihara, K. 526 [542; AM 130]
Sugihara, Y. 1268 [1258]
Sundermeyer, J. 609 [609]
Sundermeyer, W. 221 [224]
Sustmann, R. 1023, 1713 [1056, 1701]
Suzuki, T. 1134 [1160; AM 306]
Szameitat, J. 210 [213]
Szeimies, G. 473 [503]
Szyperski, T. 1228 [1271]

Tadros, T. F. 529 [545; AM 133]
Takagi, T. 819 [839; AM 205]
Talham, D. 1249 [1251]
Tamaru, Y. 351 [358]
Tanaka, T. 1222 [1254]
Tanigawa, H. 351 [358]
Tanner, D. 649 [665; AM 151]
Tarantelli, F. 761 [770]
Tasi, M. 318, 1059 [327, 1084]
Tatsumi, K. 98 [83]
Tauer, E. 338 [350]
Tebbe, K.-F. 339 (502), 1231 [352 (–), 1245]
Thayer, J. S. 100
Theis, I. 753 [757]
Theopold, K. H. 1367 [1394]
Thomas, J. M. 75, 808, 964, 1079 [69, 828, 988, 1105; AM –, 194, 242, 251]
Thompson, J. S. 205 [207]
Thrasher, J. S. 769, 1256 [783, 1284]
Tietze, L. F. 1371 [1420]
Tiripicchio, A. 1361 [1414]
Tiripicchio Camellini, M. 1361 [1414]
Tischtau, R. 1662 [1695]
Toda, F. 320 [329]
Togni, A. 499 [493]
Tölg, G. 1072
Tomás, M. 748 [782]
Tornieporth-Oetting, I. 1671 [1742]
Torssell, K. B. G. 227
Toshima, K. 1272 [1255]
Toupet, L. 755 [794]
Trautwein, A. X. 1709 [1747]
Trinquier, G. 621 [617]
Trofimenko, S. 205 [207]
Trost, B. M. 213, 1173, 1502 [215, 1199, 1559]
Trupp, B. 1345 [1381]
Tsay, Y.-H. 628 [642]
Tsukamoto, I. 71 [64]

Ueda, T. 1040 [1053]
Uffelman, E. S. 1509 [1552]
Uhlmann, E. 716 [733]
Uhlmann, P. 472 [484]
Unger, K. K. 327 [336]
Urland, W. 1364 [1416]
Usón, R. 748 [782]

Vaahs, T. 315 [324]
Vahrenkamp, H. 180, 318, 1059 [182, 327, 1084]
Valentine, J. S. 632
Valtazanos, P. 597 (1074) [605 (–)]
van Boom, J. H. 1504 [1538]
van der Marel, G. A. 1504 [1538]
Van Grieken, R. 101
van Koten, G. 208, 341, 1698 [211, 351, 1723]
van Maanen, H. L. 341 [351]
van Mil, J. 466 [515]
van Veggel, F. C. J. M. 746 [800]
Vandecasteele, C. 1072
Vasilyeva, L. L. 1441 [1471; AM 355]
Vayenas, C. G. 708 [725]
Veith, M. 603, 1237 [640, 1287]
Verboom, W. 746 [800]
Vere, A. W. 1581 [1613; AM 399]
Vertogen, G. 383 [397; AM 93]
Vicent, C. 1396 [1404]
Viebahn, S. 1028 [1074]
Vierling, P. 670 [686; AM 172]
Vogel, E. 902, 1651, 1655 [938, 1683, 1687]
Vogel, P. 1498 [1554]
Vogl, O. 382 [396; AM 92]
Vogler, C. 1659 [1734]
Vogt, T. 770 [786]
Vögtle, F. 79 [95]
Voigt-Martin, I. G. 323 [332]
Volf, M. B. 820 [840; AM 206]
Vollhardt, K. P. C. 206 [209]
Vollmann, H. W. 1445 [1475]
Vondung, J. 1355 [1395]
Vorbrüggen, H. 102
Voß, J. 906, 1070 [927, –]
Vrieze, K. 1698 [1723]
Vuilleumier, S. 535 [551]

Wachter, J. 1613 [1645]
Wadepohl, H. 345 [357]
Wagner, B. 1529, 1705 [1532, 1699]
Wagner, O. 225, 1013 [227, 1035]
Wagner, P. 1359 [1417]
Wakefield, B. J. 632
Waldmüller, D. 895 [953]
Waldraff, R. 1353 [1390]
Walker, P. 1593 [1625; AM 411]
Walls, J. M. 1764 [1804; AM 464]
Walz, L. 623, 1019 [615, 1037]
Wamhoff, H. 227
Ward, T. C. 1761 [1801; AM 461]
Warlimont, H. 947 [971; AM 225]
Wasserman, E. 466 [515]
Watabe, K. 192 [195]
Webb, G. A. 1764 [1804; AM 464]
Webb, R. J. 1388 [1422]
Weber, M. 1037 [1071]
Wegner, G. 667, 1122 [683, 1148; AM 169, 294]
Wehner, V. 469 [512]
Wehrle, B. 1741, 1743 [1781, 1783; AM 441, 443]
Wehrli, F. W. 791
Weidenbruch, M. 95 (228), 198 [89 (–), 201]
Weikert, H.-G. 761 [770]
Weinges, K. 447 [485]
Weiß, R. 1703 [1719]
Weiss, E. 476 [481]
Weiss, J. 447, 763 [485, 780]
Weiss, K. 62, 354 [75, –]
Weiss, R. 1709 [1747]
Weitkamp, J. 381 [395; AM 91]
Welzel, P. 1359, 1515 [1417, 1543]
Wendeborn, S. 1272 [1255]
Wendorff, J. H. 914, 1595 [934, 1627; AM –, 413]
Wenz, G. 178, 1657 [180, 1744]
Werkhoff, P. 1022 [1039]
Werner, H. 1690 [1721]
Werner, H.-P. 1245 [1297]
Werner, U. 1359 [1417]
West, R. 54, 1038 [90, 1087]
Westmoreland, D. L. 1018 [1089]
Wettling, T. 1013 [1035]
Whangbo, M.-H. 750 [789]
White, R. P. 930 [923]
Whitesides, G. M. 506 [522; AM 110]
Wiechert, R. 773 [776]
Wieczorek, M. 97 [87]
Wieghardt, K. 763, 1153 [780, 1179]
Wienold, R. 1529 [1532]
Wilhelm, B. 1057 [1083]
Wilke, G. 772 [790]
Wilkinson, D. L. 203 [206]
Wilkinson, G. 786, 1073
Williams, D. F. 662 [678; AM 164]
Williams, D. J. 1044, 1047, 1394, 1396 [1048, 1052, 1402, 1404]
Williams, J. O. 1110 [1136; AM 282]
Williams, R. E. 1401
Willner, H. 1255 [1283]
Winter, A. 1511 [1536]
Wirz, J. 181, 1353 [183, 1390]
Witulski, B. 1279 [1290]
Wlotzka, B. 1235 [1259]
Wocadlo, S. 735 [793]
Wolf, H. C. 1245 [1297]
Wolff, C. 67 [65]
Wolmershäuser, G. 212, 920, 1355 [214, 952, 1395]
Wood, M. G., Jr. 1218 [1277]
Woollins, J. D. 1047 [1052]
Workman, J. M. 912 [924]
Wrackmeyer, B. 918, 1500 [945, 1563]
Wright, D. S. 1241 [1279]
Wulff, G. 21, 196, 383 [22, 198, 397; AM –, –, 93]
Wüstefeld, R. 914 [934]
Wynne, K. J. 528 [544; AM 132]
Wypych, J. 384 [398; AM 94]

Yagi, M. 320 [329]
Yamamoto, T. 351 [358]
Yamashita, Y. 1052 [1090]
Yatabe, T. 757 [778]
Yee, K. A. 750 [789]

Yoshida, T. 1040 [1053]
Yoshida, Z. 351 [358]
Youinou, M.-T. 1386 [1427]
Young, M. 1717
Young, N. A. 313 [322]

Zahradnik, R. 502, 677 [–, 693]
Zare, R. N. 932
Zarges, W. 1392 [1424]
Zbinden, P. 1657 [1744]
Zehnder, M. 902 [938]
Zektzer, A. S. 1071
Zeldin, M. 528 [544; AM 132]
Zeltner, D. 813 [833; AM 199]
Zenneck, U. 900 [929]
Zentel, R. 1407 (1757) [1437 (1797); AM 321 (455)]
Zerta, E. 914 [934]
Zhou, W. 75, 810 [69, 830; AM –, 196]
Ziegler, B. 186 [188]
Ziegler, M. L. 1055 [1055]
Ziehr, H. 1717
Zietlow, A. 1399 [1392]
Zipplies, T. 1743 [1783; AM 443]
Zirnstein, M. A. 84, 86 [72, 73]
Zschage, O. 69 [67]
Zsolnai, L. 446, 1496 [482, 1525]
Zuccarello, G. 1272 [1255]
Zwettler, R. 630 [644]
Zybill, C. 203 [206]
Zylka, C. 1359 [1417]

SUBJECT INDEX

(a second page number to an entry indicates an erratum to the corresponding article)

(R) = Review Article (C) = Short Communication (B) = Book Review (L) = Correspondence (AM) = Advanced Materials

Ab initio calculations, Ab initio calculation of the structures and properties of molecules (B) 1404
- Aurophilicity as concerted effect: relativistic MO calculations on carbon-centered gold clusters (C) 1357
- Diisocyanogen or isocyanogen? (C) 761
- Electron densities, deformation densities, and chemical bonding (C) 597, 1074
- Monohapto versus dihapto CO_2 coordination in bis(amine)Ni^0 complexes: a CAS-SCF study (C) 1694
- Much less strained cubane analogues with Si, Ge, Sn, and Pb skeletons (C) 329
- On the stability of trioxo(η^5-cyclopentadienyl) compounds of manganese, technetium, and rhenium: an ab initio SCF study (C) 1228
- Organic dications: gas phase experiments and theory in concert (R) 1321
- Sodium pentaphosphacyclopentadienide (NaP_5) and the pentaphosphacyclopentadienide ion ($P_5^{\ominus}$): theoretical predictions of molecular structures, infrared and Raman spectra (C) 485
- The 7-norbornadienyl cation: an NMR/IGLO validation of its ab initio structure (C) 1042
- Tl^I-Tl^I interactions in the molecular state—an MO analysis (C) 1688
- Very short C—C single bonds and their origin. The central bond length in bitetrahedryl (C) 1226

Acepentalenes, Towards tribenzoacepentalene: tribenzotriquinacene, dihydrotribenzoacepentalenediide, and the tribenzoacepentalene radical anion (C) 595

Acetylacetonates, N-analogues of metal acetylacetonates: bis(1,2,6,7-tetracyano-3,5-diimino-3,5-dihydro-pyrrolizinido)metal(II), (metal = Fe, Ni, Cu, Zn); crystal structure of the copper derivative (C) 1049

Acetylene, Preparative acetylenic chemistry (B) 631

Additions, Addition of carboxamides to alkynyl trifluoromethyl sulfones (C) 1057

Advanced materials, editorial, Paving the way... (AM) 107

Affinity labeling, A "spacer"-modified trisaccharide as photolabile ligand for affinity labeling of antigalactan IgA X24 (C) 1669

Alkali-metal compounds, *N*-Cesiocarbazole · pmdta and *N*-potassiocarbazole · pmdta (PMDTA = *N,N,N',N'',N''*-pentamethyldiethylenetriamine). Cation size and multihapto bonding (C) 1224
- A new coordinating chiral lithium amide (C) 1044
- Are lithiosulfones configurationally stable? (C) 1025, 1282
- Asymmetric homoaldol reaction by enantioselective lithiation of a prochiral 2-butenyl carbamate (C) 69
- $[Et_4N]_6[Na_{14}Mo_{24}P_{17}O_{97}(OH)_{31}] \cdot xH_2O$: a hollow cluster filled with 12 $Na^{\oplus}$ ions and a H_3PO_4 molecule (C) 743
- $[H_2C(CH_2)_5NLi]_6$, the first cyclized lithium amide ladder: synthesis and structure of hexamethyleneimidolithium (C) 1241
- Hg_8 ("Mercubane") clusters in $Rb_{15}Hg_{16}$ (C) 1251
- Indications of cesium in a higher oxidation state (C) 1676
- K_4P_3, a compound containing the radical anion $P_3^{4\ominus}$ (C) 56
- LiSrN—a three dimensional structural arrangement of corner and edge sharing orthorhombic bipyramids, $NLi_{2/2}Sr_{4/4}$ (C) 201
- Model of a solvent-shared ion pair with N—H · · · C hydrogen bonds between amine and carbanion—crystal structure of [fluorenyllithium · 2 ethylenediamine]$_\infty$ (C) 72
- $Na_xMg_{5-x}Ga_9$, a new intermetallic phase as a link between Zintl phases and metals (C) 58
- Non-chelate-controlled addition of 1-bromo-1-lithio-1-alkenes to *O*-protected lactaldehydes (C) 896
- Organolithium methods (B) 632
- Pentabenzylcyclopentadienylpotassium · 3THF, an organopotassium compound with "piano stool" geometry (C) 735
- Stable open-chain 1,3-dilithium compounds by reaction of methylenecyclopropanes with lithium powder: 2,4-dilithio-1-butenes (C) 83
- Synthesis and structure of a phenylsodium solvate, bis[μ-phenyl(pentamethylenetriamine)-sodium] (C) 476
- The dienolate of (*R*)-2-*tert*-butyl-6-methyl-1,3-dioxin-4(2*H*)-one—a chiral acetoacetic ester d^4-reagent (C) 472
- The first PE-spectroscopic investigations of lithium, sodium, and potassium *tert*-butoxide (C) 895
- The structure of lithium compounds of sulfones, sulfoximides, sulfoxides, thioethers and 1,3-dithianes, nitriles, nitro compounds and hydrazones (R) 277
- The structures of 1,n-bis(9-lithio-9-fluorenyl)ethane · 8THF and -hexane · 8THF as models for solvent-separated ion pairs (C) 458
- X-ray structure analysis of α-lithiophenylacetonitrile · lithium diisopropylamide · 2 tetramethylethylenediamine —a "quasi-dianion complex" (C) 1392

Alkaline earth metal compounds, LiCaN and Li_4SrN_2, derivatives of the fluorite and lithium nitride structures (C) 1702

Alkaloids, Carbohydrates as chiral templates: stereoselective tandem Mannich-Michael reactions for the synthesis of piperidine alkaloids (C) 1067

Alkenes, Addition of free Me_2Ge: to alkenes and alkynes on glass surfaces in the presence of water (C) 1028
- $[\{Ph_3PCH_2C(CF_3)_2O\}NiH(PCy_3)]$: support for a nickel hydride mechanism in ethene oligomerization (C) 1011

Alkynes, A new class of DNA-cleaving molecules: pH-dependent DNA cleavage by propargylic and allenic sulfones (C) 1272
- Addition of carboxamides to alkynyl trifluoromethyl sulfones (C) 1057
- Addition of free Me_2Ge: to alkenes and alkynes on glass surfaces in the presence of water (C) 1028
- Hydrooligomerization of alkynes, a new catalytic reaction promoted by $[Co(py)_6]^{\oplus}$ in the presence of H_2 (C) 1009
- New intermediates in the cyclocotrimerization of thioxophosphorus(v) cations with alkynes (C) 448
- Triorganolead cations stabilized by side-on coordination to the C≡C bond in alkynylborates (C) 1500

Allenes, Versatile modes of allene bonding in the structures of $[W_2(OtBu)_6(C_3H_4)]$, $[W_2(OtBu)_6(C_3H_4)(CO)_2]$, and $[W_2(OtBu)_6(C_3H_4)_2]$ (C) 1523

Allenyl azides, First isolation of allenyl azides (C) 1675

Allonojirimycin, Total synthesis of allonojirimycin (5-amino-5-deoxy-D-allopyranose) (C) 1498

Alloys, Aluminum-rich metallic glasses (AM) 123
- Conference report (AM) 815
- Phase equilibria under stress (AM) 1128
- Production and application of rapidly quenched materials (AM) 947
- Ternary alloys—a comprehensive compendium of evaluated constitutional data and phase diagrams: volumes 1 and 2, ternary silver alloys (B) 524

Allyl anions, Generation, stereochemistry, and molecular dynamics of a 1,3-bis(phosphonio)propenide cation (C) 1700

Aloin, Establishment of configurations for the two diastereomeric C-glucosylanthrones aloin A und aloin B (C) 1528

Aluminum oxide, Structure of anodic coatings on aluminum (AM) 951

Amides, The first macrocyclic square-planar cobalt(III) complex relieves ring strain by forming a nonplanar amide (C) 1509

Amines, Anion coordination and Cl—H · · · Cl bridges in the low-melting poly(hydrogen chloride) $Me_3N \cdot 5HCl$ (C) 1697
- Formation of *N*-(deoxyguanosin-8-yl)-aniline in the in vitro reaction of *N*-acetoxyaniline with deoxyguanosine and DNA (C) 468
- Synthesis of *O*-acetyl-*N*-(4-biphenylyl)-hydroxylamine ("*N*-acetoxy-4-aminobiphenyl"), an ultimate metabolite of carcinogenic 4-aminobiphenyl, and its reaction with deoxyguanosine (C) 337
- The structure of hexaaminobenzene (C) 90

Amino acids, carbohydrates as chiral templates: stereoselective synthesis of β-amino acids (C) 1068
- Discovery of a D-stereospecific aminopeptidase and its use as a catalyst in organic synthesis (C) 450
- Stereoselective synthesis of γ-aminocarboxylates (C) 1706

Amorphous metals, Production and application of rapidly quenched materials (AM) 947

Analytical chemistry, Activation analysis with charged particles (B) 1072

Analytical methods, A guide to materials characterization and chemical analysis (B) 385
- Analysis of polymers. An introduction (B) 1595
- Analytical artifacts: GC, MS, HPLC, TLC and PC (B) 1537
- Imaging surfaces, electric charges and

magnetic domains with the atomic force microscope (AM) 1578
- Methods of surface analysis (B) 1764
- Problem-solving with microbeam analysis (B) 964
- Stereochemical applications of gas-phase electron diffraction. Parts A and B (B) 1534
- Using crystal birefringence to study molecular recognition (C) 330
Ancistrocladisine, Atropdiastereoselective ring opening of bridged, "axial-prostereogenic" biaryls: directed synthesis of (+)-ancistrocladisine (C) 1672
Annulenes, Di(1-pyridinio)- and di(1-bipyridindiio)dihydrodibenzotetraaza[14]annulenes (C) 1060
- Di(4-pyridinio)-, di(2-benzothiazolio)-, di(2[1,3-dithiolylio])- and diformyltetraaza[14]annulenes and tetraaza[14]annulenylene-homologous tetrathiafulvalenes (C) 1063
- From the bicyclo[3.3.0]octane framework to multiply bridged [12]annulenes and semibullvalenes (C) 1343
- Stack-type redox systems: synthesis via repeated carbanion alkylation and electron transfer studies (C) 1531
- The radical cation of *N,N'*-tetramethylene-*syn*-1,6:8,13-diimino[14]annulene. An experimental study of the N-N three-electron σ bond (C) 902
Anthrones, Establishment of configurations for the two diastereomeric *C*-glucosylanthrones aloin A und aloin B (C) 1528
Antibiotics, Biosynthetic studies on antibiotics (R) 146
- Intramolecular Diels–Alder reaction of vinylsulfonic acid esters (C) 202
- Pep5: structure elucidation of a large lantibiotic (C) 616
- Total synthesis of the antitumor antibiotic WF-3161 (C) 333
- Unsaturated 1,4-*cis*- and 1,4-*trans*-diaminotetradeoxycycloheptites—enantiomerically pure, polyfunctionalized tropa derivatives by enzymatic hydrolysis (C) 1253
Antibodies, Catalytic antibodies (R) 1283
Antigalactan, A "spacer"-modified trisaccharide as photolabile ligand for affinity labeling of antigalactan IgA X24 (C) 1669
Antimony compounds, $[Mes_2SbCu(PMe_3)_2]_2$: the first Cu^I antimonide (C) 1018
- Structural diversity in iodoantimonates; the anions $Sb_3I_{11}^{2\ominus}$, $Sb_5I_{18}^{3\ominus}$ and $Sb_6I_{22}^{4\ominus}$ (C) 344
Arene complexes, $(C_4Me_4NBH_3)_2Fe$—a metal complex isosteric with decamethylferrocene with characteristic metallocene disorder (C) 342
- Inter- and intramolecular photochemical C-H activation in matrices and in solution with (η^6-arene)(carbonyl)osmium complexes (C) 1690
- Synthesis and structure of a binuclear *syn*-coordinated μ-cycloheptatrienylhydrido complex with hindered C_7H_7 rotation (C) 345
Arenes, Activated aminocarbene complexes of the Fischer type: synthesis, structure, and annelation reactions (C) 1384
- Oxidative fluorination of arenes (C) 927
- Radical tri- and pentaanions of benzenedi- and benzenetriglyoxylate thioesters (C) 906
- The structure of hexaaminobenzene (C) 90
- The structure of the tetracation of hexaazaoctadecahydrocoronene, a simple substituted benzene (C) 92
Aromaticity, 3,3':4,4'-Bis(thieno[2,3-*b*]thiophene): a novel fused heteroarene (C) 1222
- Di(1-pyridinio)- and di(1-bipyridindiio)dihydrodibenzotetraaza[14]annulenes (C) 1060
- Di(4-pyridinio)-, di(2-benzothiazolio)-, di(2[1,3-dithiolylio])- and diformyltetraaza[14]annulenes and tetraaza[14]annulenylene-homologous tetrathiafulvalenes (C) 1063
- 1-Phenalenol: isolation and disproportionation (C) 1268
- $S_4(CN)_8$, a blue-black high-molecular sulfur-cyanogen compound with 6π- and 8π-electron structural elements (C) 609
- Towards tribenzoacepentalene: tribenzotriquinacene, dihydrotribenzoacepentalenediide, and the tribenzoacepentalene radical anion (C) 595
Arsenic compounds, $AsI_4^{\oplus}AlCl_4^{\ominus}$, a salt of the last missing tetrahaloarsonium ion (C) 1671
- Hexaarsabenzene as complex ligand (C) 212
- Insertion of $Cr(CO)_3$ into $As_7^{3\ominus}$ to form $[As_7Cr(CO)_3]^{3\ominus}$: an inorganic nortricyclane-to-norbornadiene conversion (C) 1032
- Octabromocyclohexaarsenate, $[As_6Br_8]^{2\ominus}$ (C) 185
- Pd clusters containing As and PPh_3 ligands: the structures of $[Pd_9As_6(PPh_3)_8]$, $[Pd_2(As_2)(PPh_3)_4]$, and $[Pd_{20}As_{12}(PPh_3)_{12}]$ (C) 1665
Aryl complexes, 2,4,6-Triisopropylphenylcopper, a new tetranuclear organocopper aggregate with unsymmetrically bridging σ-π bonded aryl ligands (C) 208
Arynes, Metal complexes of small cycloalkynes and arynes (A) 1296
Asymmetric syntheses, 3-Arylsulfonyloxazolidines as chiral templates: asymmetric synthesis of 2-substituted 2-hydroxycyclohexanecarbaldehydes from 2-hydroxymethylenecyclohexanone (C) 67
- Asymmetric homoaldol reaction by enantioselective lithiation of a prochiral 2-butenyl carbamate (C) 69
- Asymmetric oligomerization of propene and 1-butene with a zirconocene/alumoxane catalyst (C) 1216
- Chiral building blocks for the synthesis of triquinane sesquiterpenes: derivatives of 2-methylbicyclo[3.3.0]octan-3-ol from catalpol (C) 447
- Copper(I)-promoted Michael-addition reaction of organozincs of esters, nitriles, and α-amino acids (C) 351
- Flexible syntheses of optically active isocarbacyclins (C) 1282, 349
- Stereocontrolled total synthesis of (5*S*,6*R*)-, (5*S*,6*S*)-, (5*R*,6*R*)-, and (5*R*,6*S*)-, (7*E*,9*E*,11*Z*,14*Z*)-5,6-dihydroxy-7,9,11,14-icosatetraenoic acid (5,6-DiHETE) methyl esters (C) 587
- The enantiomers of the azole fungicide HWG-1608—asymmetric synthesis of a 2-hydroxyethyl azole fungicide (C) 462
Atomic force microscope, Imaging surfaces, electric charges and magnetic domains with the atomic force microscope (AM) 1578
Aurivillius phases, Aurivillius phases: a possible new class of metal oxide superconductors (C) 750
Aurophilicity, Aurophilicity as concerted effect: relativistic MO calculations on carbon-centered gold clusters (C) 1357
- Synthesis, structure, and bonding of the cation $[\{(C_6H_5)_3PAu\}_5C]^{\oplus}$ (C) 463
Azides, First isolation of allenyl azides (C) 1675
Bay boletus, Complexation of cesium 137 by the cap pigments of the bay boletus (*Xerocomus badius*) (C) 453
Beltenes, Double-stranded molecules: a [6]beltene derivative and the corresponding open-chain polymer (C) 1680
Benzene isomers, Bicycloprop-2-enyl (C_6H_6) (C) 1711
Benzodiquinoline, Benzo[1,2-*h*:4,3-*h'*]diquinoline ("1,14-diaza[5]helicene"): synthesis, structure, and properties (C) 86
Benzopyrenes, Selective 1:3 coupling of norbornene and iodobenzene: a facile synthesis of benzo[*e*]pyrenes with annelated cycloaliphatic moieties (C) 1037
Benzvalene, Photocycloadditions of benzvalene (C) 601
Benzylglyceraldehyde, 2-*O*-benzylglyceraldehyde: a synthetic building block available in both enantiomeric forms and configurationally stable owing to rapid oligomerization (C) 469
Best synthetic methods, Borane reagents (B) 354
- Organolithium methods (B) 632
Biaryls, Atropdiastereoselective ring opening of bridged, "axial-prostereogenic" biaryls: directed synthesis of (+)-ancistrocladisine (C) 1672
Bicyclobutanes, Shortened C-C bonds in coupled bicyclo[1.1.0]butanes (C) 473
Bicyclopropenyl, Bicycloprop-2-enyl (C_6H_6) (C) 1711
Binaphthalenes, Ethylenebis(sulfonyl)-bridged 1,1'-binaphthalene, an atropisomeric dienophile for highly diastereoselective Diels–Alder reactions (C) 766
Biochemistry, A new class of DNA-cleaving molecules: pH-dependent DNA cleavage by propargylic and allenic sulfones (C) 1272
- A structural basis of light energy and electron transfer in biology (Nobel lecture) (R) 848
- Catalytic antibodies (A) 1283
- Chaos und Ordnung: Die komplexe Struktur des Lebendigen (B) 1403
- Chemical modifications of biopolymers by quinones and quinone methides (R) 555
- The photosynthetic reaction center from the purple bacterium *Rhodopseudomonas viridis* (Nobel lecture) (R) 829
Bioinorganic chemistry, The bioinorganic chemistry of nickel (B) 632
Biomaterials, Advanced ceramics for biomedical applications (AM) 111
- Bone replacements: implant materials and the modes of implant fixation (AM) 1431
- Conference report (AM) 245
- Materials for biomedical applications—bone and joint replacements (AM) 518
- Materials for biomedical applications—high long-term success rates might pose new problems (AM) 956
Biomimetic syntheses, Biomimetic synthesis of an inverted porphyrinoid with peripheral N atoms (C) 1243
Biopolymers, Calorimetric studies of biopolymers and aggregates of phospholipids (R) 981
Biosynthesis, Biosynthetic studies on antibiotics (R) 146
Biotechnology, Immobilization of cells (B) 1717
Birefringence, Using crystal birefringence to study molecular recognition (C) 330
Bismuth compounds, A new oxygen sensor based on the thermoelectric power of solid solutions of Nb_2O_5 and Bi_2O_3 (C) 75

- $[\{Cp(CO)_2Mn\}_2(\mu\text{-}H)]^{\ominus}$: a new, versatile reagent (C) 446

Blood substitutes, blood substitutes, preparation, physiology and medical applications (B) 670

Boron compounds, A tetraborylphosphonium ion with a spiroheterocyclic structure (C) 217
- Advances in boron and the boranes (B) 1401
- Borane reagents (B) 354
- $LiBH_4(NaBH_4)/Me_3SiCl$, an unusually strong and versatile reducing agent (C) 218
- Methylboron oxide, $H_3C-B\equiv O$ (C) 88
- $[M(NMesBMes_2)_2]$(M = Cr, Ni): stable, distorted, two-coordinate d^4 and d^8 complexes (C) 316
- $NaBH_4$ reduction of ketones in the solid state (C) 320
- Phosphonioboratoacetylenes: C_2 stabilized by donor and acceptor molecules (C) 1219
- Stable methyleneboranes of high Lewis acidity (C) 781
- Tetraalkylidene-1,4-diboracyclohexanes from 3,4-dilithio-2,5-dimethyl-2,4-hexadiene; the first "hetero[6]radialene" with chair conformation (C) 477
- The solid-state structure of $Me_2B-O-BMe_2$ (C) 180
- The structure of a *C*-borylborirene with strong C-B hyperconjugation (C) 186
- Thermal cleavage and isomerization of 1,3-diboretanes to stable methyleneboranes (C) 784
- Triorganolead cations stabilized by side-on coordination to the $C\equiv C$ bond in alkynylborates (C) 1500

Bridging ligands, A phosphane—dithioformate adduct as a five-electron bridging ligand $[Mn_2(CO)_6\{S_2C(H)P(cyclo\text{-}C_6H_{11})_3\}_2]$ (C) 1014
- Complexes with an η^2-μ_2-SiO bridge. Structure of the bimetallic complex $[Fe(CO)_3\{\mu\text{-}Si(OMe)_2\text{-}OMe\}(\mu\text{-}dppm)PdCl]$(*Fe-Pd*) (C) 1361
- Directed synthesis of trinuclear hydrocarbon-bridged complexes such as $[(OC)_5ReCH_2CH_2Os(CO)_4CH_2CH_2\text{-}Re(CO)_5]$ (C) 1705
- $[Ir_2(\mu\text{-}CH_2)(CO)_4(Me_2PCH_2PMe_2)_2][CF_3SO_3]_2$, an unprecedented electrophilic methylene complex; $H^{\ominus}$ addition to prepare a bridging methyl complex (C) 1377
- Synthesis, structure and magnetic properties of a dinuclear manganese(II) complex with one μ-aqua and two μ-carboxylato bridges (C) 1365
- The first heterodinuclear complexes with bis(cyclopentadienyl)methane bridges (C) 1008

Bromoselenates, Bromoselenates(II,IV), a novel type of mixed valence compounds (C) 187

Butterfly clusters, A systhematic entry to butterfly-type $[M_4(CO)_{12}(\mu_4\text{-}XY)]$ clusters (C) 1059

Cage compounds, Cryptophane radical cations as components of three-dimensional charge-transfer salts (C) 1249
- Selective molecular recognition of trihydroxybenzenes (C) 79
- Structure and properties of the cryptophane-E/$CHCl_3$ complex, a stable van der Waals molecule (C) 1246
- The pagodane route to dodecahedranes: chemistry and structure of bissecododecahedranes (C) 298
- The pagodane route to dodecahedranes: polyfunctionalized homologous dodecahedranes and dodecahedrenes (C) 310
- The pagodane route to dodecahedranes: polyfunctionalized pentagonal dodecahedranes and dodecahedrenes (C) 305
- The pagodane route to dodecahedranes: 4,9,14,19-tetrasubstituted [1.1.1.1]pagodanes by intramolecular functionalization (C) 303
- The pagodane route to dodecahedranes: total synthesis and chemistry of 4,9,14,-19-tetrasubstituted [1.1.1.1]pagodanes (C) 300
- TlSPh and TlS*t*Bu, Thallium(I) thiolates with novel cagelike structural units: $[Tl_5(SPh)_6]^{\ominus}/[Tl_7(SPh)_6]^{\oplus}$ and $[Tl_8(StBu)_8]$ (C) 1682
- Trinacrene—a product of structure-directed synthesis (C) 1261

Calixarenes, Aggregation of metal ions with functionalized calixarenes: synthesis and structure of an octanuclear copper(I) chloride complex (C) 1376

Calorimetry, Calorimetric studies of biopolymers and aggregates of phospholipids (R) 981

Carbanions, Are lithiosulfones configurationally stable? (C) 1025, 1282
- Bis-stilbene systems: reduction to the tetraanions (C) 904
- Highly reduced porphyrins (C) 604
- Hydrogen bonds between an $NH_4^{\oplus}$ ion and a carbanion—crystal structure of ammonium 1,2,4-tricyanocyclopentadienide (C) 73
- Model of a solvent-shared ion pair with $N-H\cdots C$ hydrogen bonds between amine and carbanion—crystal structure of [fluorenyllithium · 2 ethylenediamine]$_\alpha$ (C) 72
- Stable open-chain 1,3-dilithium compounds by reaction of methylenecyclopropanes with lithium powder: 2,4-dilithio-1-butenes (C) 83
- Synthesis and structure of a phenylsodium solvate, bis[μ-phenyl(pentamethylenetriamine)-sodium] (C) 476
- Tetraphenylethylenedisodium: the band structure of the CC singly bonded, twisted $(C_6H_5)_2C^{\ominus}$ carbanions (C) 1685
- The structures of 1,n-bis(9-lithio-9-fluorenyl)ethane · 8THF and -hexane · 8THF as models for solvent-separated ion pairs (C) 458
- X-ray structure analysis of α-lithiophenylacetonitrile · lithium diisopropylamide · 2 tetramethylethylenediamine—a "quasi-dianion complex" (C) 1392

Carbazoles, *N*-Cesiocarbazole · pmdta and *N*-potassiocarbazole · pmdta (PMDTA = *N*,*N*,*N*′,*N*″,*N*″-pentamethyldiethylenetriamine). Cation size and multihapto bonding (C) 1224

Carbazomycin A, Highly selective oxidations of $Fe(CO)_3$-cyclohexadiene complexes: synthesis of 4b,8a-dihydrocarbazol-3-ones and the first total synthesis of carbazomycin A (C) 223

Carbene complexes, Activated aminocarbene complexes of the Fischer type: synthesis, structure, and annelation reactions (C) 1384
- Heterogeneous, metathesis-active Schrock-type carbene complexes by reaction of carbyne tungsten(VI) complexes with silica gel (C) 62
- Metallocene carbene complexes and related compounds of titanium, zirconium, and hafnium (R) 397
- The mechanism of the Dötz reaction: chromacyclobutenes by alkyne-carbene coupling? (C) 908
- Vinylcarbene complexes of titanocene (C) 610

Carbenes, [Bis(diisopropylamino)phosphino]trimetylsilylcarbene: a stable nucleophilic carbene (C) 621

Carbenium ions, Tetrakis(dimethylamino)ethylene dication: two CC singly bonded and almost perpendicularly twisted $((CH_3)_2N)_2C^{\oplus}$ carbenium ions (C) 1684
- Unusual geometry of a sterically congested analogue of $(CH)_5^{\oplus}$ (C) 1232

Carbocycles, all-*cis*-1,4,7,10-cyclododecatetraene—X-ray structure analysis and photoelectron spectrum (C) 1379
- Bicycloprop-2-enyl (C_6H_6) (C) 1711
- 4,6-Dimethylenetricyclo[3.3.0.0^{3,7}]octane-2-one and 2,4,6-trimethylenetricyclo[3.3.0.0^{3,7}]octane (C) 1525
- Structure, deformation electron densities, photoelectron spectra, and reactivity of 3,4-dihydro-1*H*-cyclobuta[*a*]cyclopropa[*d*]benzene (C) 206

Carbohydrates, A "spacer"-modified trisaccharide as photolabile ligand for affinity labeling of antigalactan IgA X24 (C) 1669
- Application of the dimethyl(phenyl)silyl group as a masked form of the hydroxy group in the synthesis of an L-*glycero*-α-D-*manno*-heptopyranoside-containing trisaccharide from the dephosphorylated inner core region of *neisseria meningitidis* (C) 1504
- Carbohydrates as chiral templates: stereoselective synthesis of β-amino acids (C) 1068
- Carbohydrates as chiral templates: stereoselective tandem Mannich-Michael reactions for the synthesis of piperidine alkaloids (C) 1067
- Chiral cyclobutanones by [2 + 2]-cycloaddition of dichloroketene to carbohydrate enol ethers (C) 777
- Enantioselective aldol reaction of *tert*-butyl acetate using titanium-carbohydrate complexes (C) 495
- Enantioselective allylation of carbonyl compounds with titanium-carbohhydrate complexes (C) 494
- Enantioselective synthesis of D-*threo*-β-hydroxy-α-amino acids with titanium-carbohydrate complexes (C) 497
- Structure of chloro(cyclopentadienyl)-bis(1,2:5,6-di-*O*-isopropylidene-α-D-glucofuranos-3-*O*-yl) titanate, a novel titanium-carbohydrate complex (C) 499
- Unsaturated 1,4-*cis*- and 1,4-*trans*-diaminotetradeoxycycloheptites—enantiomerically pure, polyfunctionalized tropa derivatives by enzymatic hydrolysis (C) 1253

Carbon-carbon bond lengths, Shortened C-C bonds in coupled bicyclo[1.1.0]butanes (C) 473
- Very short C—C single bonds and their origin. The central bond length in bitetrahedryl (C) 1226

Carbon-carbon linkage, Activated aminocarbene complexes of the Fischer type: synthesis, structure, and annelation reactions (C) 1384
- [Bis(diisopropylamino)phosphino]trimetylsilylcarbene: a stable nucleophilic carbene (C) 621
- Carbocycle construction in terpene synthesis (B) 1537
- Cyclizations via palladium-catalyzed allylic alkylations (R) 1173
- Enantioselective aldol reaction of *tert*-butyl acetate using titanium-carbohydrate complexes (C) 495
- Enantioselective allylation of carbonyl compounds with titanium-carbohhydrate complexes (C) 494
- Enantioselective synthesis of D-*threo*-β-

hydroxy-α-amino acids with titanium-carbohydrate complexes (C) 497
- Formation of a phosphaferracyclopentadiene ring by coupling of a phosphaalkyne with two fluoromethylidyne ligands (C) 321
- Hydrooligomerization of alkynes, a new catalytic reaction promoted by $[Co(py)_6]^{\oplus}$ in the presence of H_2 (C) 1009
- Intramolecular, stoichiometric (Li, Mg, Zn) and catalytic (Ni, Pd, Pt) metalloene reactions in organic synthesis (R) 38
- 2-Isocyanato-2-alkenoates—synthesis and reactions (C) 1053
- Monohapto versus dihapto CO_2 coordination in bis(amine)Ni^0 complexes: a CAS-SCF study (C) 1694
- Nickel(0)-catalyzed preparation of isomeric carboxamides—ligand-controlled β-H or β′-H elimination (C) 1035
- Non-chelate-controlled addition of 1-bromo-1-lithio-1-alkenes to *O*-protected lactaldehydes (C) 896
- On the formation of "free radicals" from alkylcobalt complexes (C) 325
- $[\{Ph_3PCH_2C(CF_3)_2O\}NiH(PCy_3)]$: support for a nickel hydride mechanism in ethene oligomerization (C) 1011
- Selective 1:3 coupling of norbornene and iodobenzene: a facile synthesis of benzo[*e*]pyrenes with annelated cycloaliphatic moieties (C) 1037
- The effect of acetylene substituents on a Pd^{II}-catalyzed cycloisomerization. Total synthesis of (−)-sterepolide and assignment of absolute stereochemistry (C) 1502
- The mechanism of the Dötz reaction: chromacyclobutenes by alkyne-carbene coupling? (C) 908
- Vinylcarbene complexes of titanocene (C) 610

Carbonylation, Chlorocarbon activation: catalytic carbonylation of dichloromethane and chlorobenzene (C) 1386

Carbyne complexes, Carbyne complexes (B) 354
- Alkyl and alkylidyne complexes of rhenium (C) 334
- Reactions of mono- and dinuclear metal-alkylidyne complexes with phosphaalkynes: C≡P and C≡Mo metathesis (C) 210

Carcinogenicity, Chemicals carcinogens. Activation mechanisms, structural and electronic factors, and reactivity (B) 932
- Combination effects in chemical carcinogenesis (B) 931
- Formation of *N*-(deoxyguanosin-8-yl)aniline in the in vitro reaction of *N*-acetoxyaniline with deoxyguanosine and DNA (C) 468
- Synthesis of *O*-acetyl-*N*-(4-biphenylyl)-hydroxylamine ("*N*-acetoxy-4-aminobiphenyl"), an ultimate metabolite of carcinogenic 4-aminobiphenyl, and its reaction with deoxyguanosine (C) 337

Catalysis, A *trans*-dimethyl derivative of octahedral Ti^{IV}: alkylation and arylation of Ti^{IV}-Schiff base complexes (C) 64
- A highly selective montmorillonite catalyst for hydrogenation of alkynes, alkenynes, and alkadienes (C) 465
- A joint structural characterization of colloidal platinum by EXAFS and high-resolution electron microscopy (C) 590
- A sensitive spectroscopic probe for monitoring changes in the coordination sphere of titanium: eight-membered dioxatitanacycles and their organometallic derivatives (C) 66
- Addition of free Me_2Ge: to alkenes and alkynes on glass surfaces in the presence of water (C) 1028
- Advanced catalysts: interfaces in the physical and biological sciences (AM) 1079
- Amide bond scission via bifunctional activation with bimetallic porphyrin systems with two different metal centers (C) 921
- Asymmetric oligomerization of propene and 1-butene with a zirconocene/alumoxane catalyst (C) 1216
- Catalysis on zeolites (B) 381
- Catalytic antibodies (A) 1283
- Chlorocarbon activation: catalytic carbonylation of dichloromethane and chlorobenzene (C) 1386
- Coupling of epoxides to Pt^{II}-complexes with carbon dioxide and the structure of a cyclic metallacarbonate (C) 767
- Cyclizations via palladium-catalyzed allylic alkylations (R) 1173
- Dimeric $[Cp_2Zr(CH_2O)]$, a novel (η^2-formaldehyde)metal complex from carbon monoxide (C) 630
- Double stereodifferentiation in the formation of isotactic polypropylene at chiral $(C_5H_4CHMePh)_2ZrCl_2$/methylalumoxane catalysts (C) 628
- Enantioselective reduction of α,β-unsaturated carboxylates with $NaBH_4$ and catalytic amounts of chiral cobalt semicorrin complexes (C) 60
- Heterogeneous, Metathesis-active Schrock-type carbene complexes by reaction of carbyne tungsten(VI) complexes with silica gel (C) 62
- Hydrooligomerization of alkynes, a new catalytic reaction promoted by $[Co(py)_6]^{\oplus}$ in the presence of H_2 (C) 1009
- Immobilization of cells (B) 1717
- Intramolecular, stoichiometric (Li, Mg, Zn) and catalytic (Ni, Pd, Pt) metalloene reactions in organic synthesis (R) 38
- Location of *para*-xylene in Yb-faujasite (zeolite Y) by neutron diffraction (C) 770
- Nickel(0)-catalyzed preparation of isomeric carboxamides—ligand-controlled β-H or β′-H elimination (C) 1035
- Phosphanorbornadienes as ligands in the transition metal-catalyzed synthesis of fine chemicals (C) 500
- $[\{Ph_3PCH_2C(CF_3)_2O\}NiH(PCy_3)]$: support for a nickel hydride mechanism in ethene oligomerization (C) 1011
- Probing changes in the structure and performance of a lithium nickel oxide catalyst by in situ X-ray diffraction during the high-temperature oxidative coupling of methane (AM) 808
- Pyrones as substrates for palladium-catalyzed [4+3] cycloadditions (C) 213
- Reaction mechanisms in heterogeneous catalysis; C-H activation as a case study (R) 135
- Revision and modification of the traditional mechanism of C-H/C-C activation by "naked" transition-metal ions (C) 607
- Selective 1:3 coupling of norbornene and iodobenzene: a facile synthesis of benzo[*e*]pyrenes with annelated cycloaliphatic moieties (C) 1037
- Selective hydrogenation of esters to alcohols with a catalyst prepared from Rh_2O_3, $Sn(n\text{-}C_4H_9)_4$, and SiO_2: evidence for site isolation (C) 347
- Selenium-catalyzed synthesis of *S*-alkyl thiocarbamates from amines, carbon monoxide, sulfur, and alkyl halides (C) 452
- Solid ion conductors in heterogeneous catalysis (R) 708
- The first example of an *ethylene*-selective soluble Ziegler catalyst of the zirconocene class (C) 1511

Catechol, *catena*-Poly[bis-μ-(*o*-oxyphenyleneoxy)silicon]: crystal structure of the orthosilicate of catechol (C) 623

Catenanes, A [2]catenane made to order (C) 1396

C_2 stabilization, Phosphonioboratoacetylenes: C_2 stabilized by donor and acceptor molecules (C) 1219

C-Cl activation, Chlorocarbon activation: catalytic carbonylation of dichloromethane and chlorobenzene (C) 1386

C-H activation, Reaction mechanisms in heterogeneous catalysis; C-H activation as a case study (R) 135
- Inter- and intramolecular photochemical C-H activation in matrices and in solution with (η^6-arene)(carbonyl)osmium complexes (C) 1690
- Multiple "remote functionalization" of different sites in flexible molecules by "anchored" bare Fe^I ions (C) 1277
- Revision and modification of the traditional mechanism of C-H/C-C activation by "naked" transition-metal ions (C) 607

Ceramics, Advanced ceramics for biomedical applications (AM) 111
- Conference report (AM) 1132, 1437, 1583, 522
- Generation of complex metal oxides by aerosol processes: superconducting ceramic particles and films (AM) 794
- Glass-ceramics in the scheme of inorganic materials (AM) 1746
- High-performance silicon nitride materials (AM) 1560
- Substituted silane polymers—a new look at some old materials (AM) 1733

Cesium compounds, Complexation of cesium 137 by the cap pigments of the bay boletus (*Xerocomus badius*) (C) 453
- Indications of cesium in a higher oxidation state (C) 1676

Chalcogen compounds, Reaction of decamethylsilicocene with sulfur, selenium, and tellurium: from a p_π-p_π system to new heterocycles (C) 1518

Chaos, Chaos und Ordnung: Die komplexe Struktur des Lebendigen (B) 1403

Chelate ligands, A chiral Ag^I-coordination polymer with a polydentate chiral ligand; crystal structure of the 1:1 complex of CF_3SO_3Ag and *N*-[*N*-(5-Methylthenylidene)-L-methionyl]histamine (C) 1698
- A novel trimeric chiral copper(I) thiophenolate with intramolecular coordination (C) 341
- Bis[cyclooctane-1,5-diyl)di(pyrazol-1-yl)borato]cobalt: a polypyrazolylborate complex with two agostic hydrogen bonds (C) 205
- Indigo-metal complexes: synthesis and structure of Pd^{II} and Pt^{II} compounds containing the anions of indigo and octahydroindigo as mono- and bis-chelate ligands (C) 1529

Chemical abstracts, From CA to CAS online (B) 356

Chemical bonding, Covalent versus dative bonds to main group metals, a useful distinction (R) 992
- Electron densities, deformation densities, and chemical bonding (C) 597, 1074
- Solids and surfaces: a chemist's view of bonding in extended structures (B) 1070
- The novel complex $[LRu^{IV}(\mu\text{-}O)_3Ru^{IV}L][PF_6]_2 \cdot H_2O$—a molecular section of the structures of $BaRu^{IV}O_3$(high-pressure phase) and $Ba_{5/6}Sr_{1/6}Ru^{IV}O_3$ (C) 763

Chemical transport, $HoAl_3Cl_{12}$ in crystalline form (C) 1364
Chemiluminescence, Chemiluminescence (B) 933
Chemistry and language, The technical writer's handbook (B) 1717
Chemotherapy, Selective inhibitors of dihydrofolate reductase (Nobel lecture) (R) 879
- The purine path to chemotherapy (Nobel lecture) (R) 870
Chirality, A chiral Ag^I-coordination polymer with a polydentate chiral ligand; crystal structure of the 1:1 complex of CF_3SO_3Ag and *N*-[*N*-(5-Methylthenylidene)-L-methionyl]histamine (C) 1698
- A new coordinating chiral lithium amide (C) 1044
- Are lithiosulfones configurationally stable? (C) 1025, 1282
- Can polystyrene be optically active? (C) 196
- Chirality and isomerism in binuclear iron complexes with sulfur ligands: $[Fe(CO)(\mu\text{-}"S_4")]_2$, a model complex for oxidoreductases (C) 1703
- (4*RS*,5*R*)- and (4*RS*,5*S*)-4-Methoxy-5-methyloxazolidin-2-one derivatives of threonine—interesting chiral amidoalkylating reagents (C) 1399
- One-dimensional metal chains in a chiral environment—the crystal structure of helical bis(dicarbonylrhodium(I))-3,3'-hexafluoroglutarylbis-(1*R*)-camphorate (C) 1019
- Optically active isoprene(tricarbonyl)iron(0) and methyltrimethylenemethane(tricarbonyl)iron(0) (C) 1657
- Residual enantiomerism and chromatographic resolution of a 1,1,2-triarylalkene (C) 199
- Structure and dynamics of chiral molecules (R) 571
- Thermal and electrocatalytic epimerization at iron as the chiral center (C) 1521
- Thiosulfinic acids: a new class of chiral organosulfur compounds (C) 97
Chlorins, A simple synthesis of dioxoisobacteriochlorins from hematoporphyrin (C) 480
Chromatography, Analytical artifacts: GC, MS, HPLC, TLC and PC (B) 1537
- Chromatographic enantioseparation—methods and applications (B) 1281
- Chromatographic separation of the excess enantiomer under achiral conditions (C) 626
- Correlation of the dynamic behavior of *n*-alkyl ligands of the stationary phase with the retention times of paracelsin peptides in reserved phase HPLC (C) 327
- Introduction to microscale high-performance liquid chromatography (B) 353
- Residual enantiomerism and chromatographic resolution of a 1,1,2-triarylalkene (C) 199
- Visualization of chromatographic separations by NMR imaging (C) 1029
Chromium compounds, Direct observation of ground state splitting in the chromium(III) acetate trimer by inelastic neutron scattering (C) 930
- Insertion of $Cr(CO)_3$ into $As_7^{3\ominus}$ to form $[As_7Cr(CO)_3]^{3\ominus}$: an inorganic nortricyclane-to-norbornadiene conversion (C) 1032
Chromogenics, Conference report (AM) 1584
Clusters, Aurophilicity as concerted effect: relativistic MO calculations on carbon-centered gold clusters (C) 1357
- A novel type of anionic cluster containing a Pt_4Ag_2 core (C) 748
- A systhematic entry to butterfly-type $[M_4(CO)_{12}(\mu_4\text{-}XY)]$ clusters (C) 1059
- Agostic-type gold ligand and incipient μ_3-PPh_2 coordination in the $Au_2Pt_2P_6$ "hammock" skeleton of the cluster $[Au_2Pt_2(\mu\text{-}PPh_2)_2(PPh_3)_4][PF_6]_2$ (C) 923
- Alkoxide clusters of molybdenum and tungsten as templates for organometallic chemistry: comparison with carbonyl clusters of the later transition elements (R) 432
- Comments on the molecular structure and bonding in $[W_4Cl(O)(O\mathit{i}Pr)_9]$ and $[W_4(O)(O\mathit{i}Pr)_{10}]$. Analogies with tetranuclear carbonyl clusters (C) 1368
- Direct observation of ground state splitting in the chromium(III) acetate trimer by inelastic neutron scattering (C) 930
- $[Et_4N]_6[Na_{14}Mo_{24}P_{17}O_{97}(OH)_{31}] \cdot xH_2O$: a hollow cluster filled with 12 $Na^{\oplus}$ ions and a H_3PO_4 molecule (C) 743
- Formation of a phosphaferracyclopentadiene ring by coupling of a phosphaalkyne with two fluoromethylidyne ligands (C) 321
- Hg_8 ("Mercubane") clusters in $Rb_{15}Hg_{16}$ (C) 1251
- $K_4Al_2Nb_{11}O_{20}F$—the missing link in cluster condensation (C) 1662
- Nickel complexes containing sterically demanding thiolate ligands: $[Ni_8S(SC_4H_9)_9]^{\ominus}$, a mixed-valence nickel sulfide thiolate cluster, and $[Ni_4(SC_3H_7)_8]$, a homoleptic nickel thiolate (C) 61
- Novel nickel clusters with Se and Cp' as ligands: $[Ni_4Se_2(CO)BrCp'_3]$, $[Ni_6Se_4Cp'_5]$, $[Ni_{15}Se_{10}(CO)_3Cp'_8]$, and $[Ni_{15}Se_{10}(CO)Cl_2Cp'_8]$ (C) 1390
- $PbMo_5O_8$ and $Tl_{0.8}Sn_{0.6}Mo_7O_{11}$, novel clusters of molybdenum and thallium (C) 758
- Pd clusters containing As and PPh_3 ligands: the structures of $[Pd_9As_6(PPh_3)_8]$, $[Pd_2(As_2)(PPh_3)_4]$, and $[Pd_{20}As_{12}(PPh_3)_{12}]$ (C) 1665
- $Pt_{309}Phen_{36}O_{30\pm10}$, a four-shell platinum cluster (C) 778
- Stabilization of niobium(0) and tantalum(0) in mixed metal clusters containing silver atoms (C) 471
Coatings, Conference report (AM) 1755
Cobalt compounds, Amides nonplanar solely by C-N bond rotation (C) 912
- Bis[cyclooctane-1,5-diyl)di(pyrazol-1-yl)borato]cobalt: a polypyrazolylborate complex with two agostic hydrogen bonds (C) 205
- On the formation of "free radicals" from alkylcobalt complexes (C) 325
- The first macrocyclic square-planar cobalt(III) complex relieves ring strain by forming a nonplanar amide (C) 1509
Cocomplexation, The organization of two "soft" ($Cu^{2\oplus}$, $Ni^{2\oplus}$) metal centers in heterotrinuclear complexes of a macrocyclic ligand by cocomplexation with $Ba^{2\oplus}$ (C) 746
Colloids, A joint structural characterization of colloidal platinum by EXAFS and high-resolution electron microscopy (C) 590
- Foams and biliquid foams—aphrons (B) 384
- The complexation of gold colloids (C) 780
Complexes, Chain complexes with eleven metal atoms (C) 624
- Intermolecular complexes (B) 502
Complexes with chalcogen ligands, Novel nickel clusters with Se and Cp' as ligands: $[Ni_4Se_2(CO)BrCp'_3]$, $[Ni_6Se_4Cp'_5]$, $[Ni_{15}Se_{10}(CO)_3Cp'_8]$, and $[Ni_{15}Se_{10}(CO)Cl_2Cp'_8]$ (C) 1390
Complexes with hydrido ligands, $[\{Cp(CO)_2Mn\}_2(\mu\text{-}H)]^{\ominus}$: a new, versatile reagent (C) 446
- $[\{Ph_3PCH_2C(CF_3)_2O\}NiH(PCy_3)]$: support for a nickel hydride mechanism in ethene oligomerization (C) 1011
- Synthesis and structure of a binuclear *syn*-coordinated μ-cycloheptatrienyl hydrido complex with hindered C_7H_7 rotation (C) 345
Complexes with nitrogen ligands, *N*-Arylation and *N,N*-dibenzylation of coordinated N_2 with organic halides; differences in the reactivity of *trans*-$[Mo(N_2)_2(Me_8[16]aneS_4)]$ and its phosphane analogues (C) 1040
- A novel approach to ferroelectric liquid crystals: the first organotransition metal compound displaying this behavior (C) 1065
- Aminebis(ethene)nickel(0) complexes; structure of 1-azabicyclo[2.2.2]octanebis(ethene)nickel(0) (C) 772
- Copper(I)-assisted formation of an "organic" sandwich structure: structural prerequisites for luminescence in the dinuclear complexes $[(\mu\text{-bipyrimidine})\{Cu(PR_3)_2\}_2]X_2$ (C) 1659
- $[M(NMesBMes_2)_2](M=Cr, Ni)$: stable, distorted, two-coordinate d^4 and d^8 complexes (C) 316
- Nitrogenase model compounds: $[\mu\text{-}N_2H_2\{Fe("N_HS_4")\}_2]$, the prototype for the coordination of diazene to iron sulfur centers and its stabilization through strong N—H···S hydrogen bonds (C) 1271
- Platinum complexes of the anions $Se_2N_2^{2\ominus}$ and $Se_2N_2H^{\ominus}$; X-ray structure analysis of $[Pt(Se_2N_2H)(PMe_2Ph)_2]Cl$ (C) 1047
- Synthesis and analysis of polymetallaphosphazenes (C) 493
- Trigonal-bipyramidal lanthanoid complexes with interstitial oxygen atoms (C) 1033
- Two novel polyoxomolybdates containing the $(MoNO)^{3\oplus}$ unit: $[Mo_5Na(NO)O_{13}(OCH_3)_4]^{2\ominus}$ and $[Mo_6(NO)O_{18}]^{3\ominus}$ (C) 1363
Complexes with oxygen ligands, Indium 2,4,6-tris(trifluoromethyl)phenoxide—a dimer with the coordination number two at the indium atoms (C) 1383
- On the stability of trioxo(η^5-cyclopentadienyl) compounds of manganese, technetium, and rhenium: an ab initio SCF study (C) 1228
- Oxoiron porphyrin species with high-valent iron: formation by solvent-dependent protonation of a peroxoiron(III) porphyrinate derivative (C) 1709
- $[VO(O_2C\mathit{t}Bu)_3]$ and $[V_6O_6(\mu\text{-}O)_4(\mu\text{-}O_2CPh)_9]$: structural characterization of a mononuclear V^V and a (2+4)-nuclear $V^{IV}V^V_5$ carboxylato complex. Models for vanadate-dependent peroxidases (C) 1221
Complexes with phosphorus ligands, A phosphane—dithioformate adduct as a five-electron bridging ligand $[Mn_2(CO)_6\{S_2C(H)P(\mathit{cyclo}\text{-}C_6H_{11})_3\}_2]$ (C) 1014
- Aggregation of metal ions with functionalized calixarenes: synthesis and structure of an octanuclear copper(I) chloride complex (C) 1376
- Agostic-type gold ligand and incipient μ_3-PPh_2 coordination in the $Au_2Pt_2P_6$ "hammock" skeleton of the cluster $[Au_2Pt_2(\mu\text{-}PPh_2)_2(PPh_3)_4][PF_6]_2$ (C) 923

- New intermediates in the cyclocotrimerization of thioxophosphorus(v) cations with alkynes (C) 448
- Reductive dimerization of a phosphaalkyne with complexation to samarium (C) 445
- Tetraphosphacyclobutadiene as complex ligand (C) 1355

Complexes with sulfur ligands, A novel trimeric chiral copper(I) thiophenolate with intramolecular coordination (C) 341
- A phosphane—dithioformate adduct as a five-electron bridging ligand $[Mn_2(CO)_6\{S_2C(H)P(cyclo\text{-}C_6H_{11})_3\}_2]$ (C) 1014
- Chirality and isomerism in binuclear iron complexes with sulfur ligands: $[Fe(CO)(\mu\text{-}"S_4")]_2$, a model complex for oxidoreductases (C) 1703
- 17- to 19-Electron pentamethylcyclopentadienyl iron dithiocarbamate complexes. Formation of a Cp^*Fe^{IV} complex (C) 460
- $FeI_3SC(NMe_2)_2$, a neutral thiourea complex of iron(III) iodide (C) 776
- Nickel complexes containing sterically demanding thiolate ligands: $[Ni_8S(SC_4H_9)_9]^{\ominus}$, a mixed-valence nickel sulfide thiolate cluster, and $[Ni_4(SC_3H_7)_8]$, a homoleptic nickel thiolate (C) 61
- Self-reduction of $[Ph_4P][Nb(SCH_2CH_2CH_2S)_3]$ with formation of a Nb_2^{IV} complex (C) 98
- Synthesis and structure of $[(C_5H_5)_2TiS_4AsCH_3]$—a new reagent for the synthesis of sulfur-rich heterocycles (C) 1269
- Synthesis, structure and reactivity of sulfur-rich cyclopentadienyl-transition metal complexes: sulfur chemistry from an organometallic point of view (R) 1613

Composite materials, Conference report (AM) 817
- Fiber reinforcement for composite materials (B) 1443
- Textile structural composites (B) 1442

Composites, Aerospace materials research opportunities (AM) 655

Computer, Computational chemistry. An emphasis on practical calculations (B) 1071
- Image enhancement—chemical, digital, visual (R) 1601
- Materials for optical data storage (R) 1445
- Math/Chem/Comp 1987 (B) 633

Conducting patterns, Spatially selective conducting patterns in transparent films derived from ladder type polymers (AM) 1569

Configuration, Establishment of configurations for the two diastereomeric *C*-glucosylanthrones aloin A und aloin B (C) 1528

Conformation, 2'-Aminomethylbiphenyl-2-carboxylic acid as component of a cyclopeptide; crystal structure and conformation in solution (C) 486
- The first macrocyclic square-planar cobalt(III) complex relieves ring strain by forming a nonplanar amide (C) 1509
- Zur Konformation des Cyclohexans. (Ostwalds Klassiker der exakten Wissenschaft, Band 274) (B) 105

Conjugation, Bis-stilbene systems: reduction to the tetraanions (C) 904
- The search for highly colored organic compounds (R) 677

Coordination, A new coordinating chiral lithium amide (C) 1044
- A novel trimeric chiral copper(I) thiophenolate with intramolecular coordination (C) 341
- A sensitive spectroscopic probe for monitoring changes in the coordination sphere of titanium: eight-membered dioxatitanacycles and their organometallic derivatives (C) 66
- Amides nonplanar solely by C-N bond rotation (C) 912
- Anion coordination and $Cl-H\cdots Cl$ bridges in the low-melting poly(hydrogen chloride) $Me_3N \cdot 5HCl$ (C) 1697
- *catena*-Poly[bis-μ-(*o*-oxyphenyleneoxy)silicon]: crystal structure of the orthosilicate of catechol (C) 623
- *N*-Cesiocarbazole · pmdta and *N*-potassiocarbazole · pmdta (PMDTA = *N,N,N',N'',N''*-pentamethyldiethylenetriamine). Cation size and multihapto bonding (C) 1224
- Complexation of a novel organoytterbium(II) ligand with dimethylplatinum(II): crystal structure of the resulting heterobimetallic complex (C) 1370
- Indium 2,4,6-tris(trifluoromethyl)phenoxide—a dimer with the coordination number two at the indium atoms (C) 1383
- Metal complexes of small cycloalkynes and arynes (A) 1296
- $[M(NMesBMes_2)_2]$(M = Cr, Ni): stable, distorted, two-coordinate d^4 and d^8 complexes (C) 316
- Monohapto versus dihapto CO_2 coordination in bis(amine)Ni^0 complexes: a CAS-SCF study (C) 1694
- Pentacoordinated elements of the 4th main group with four organic residues (C) 918
- Triorganolead cations stabilized by side-on coordination to the C≡C bond in alkynylborates (C) 1500
- Versatile modes of allene bonding in the structures of $[W_2(OtBu)_6(C_3H_4)]$, $[W_2(OtBu)_6(C_3H_4)(CO)_2]$, and $[W_2(OtBu)_6(C_3H_4)_2]$ (C) 1523

Coordination chemistry, Comprehensive coordination chemistry. The synthesis, reactions, properties and applications of coordination compounds (B) 786

Copper compounds, A novel trimeric chiral copper(I) thiophenolate with intramolecular coordination (C) 341
- Aggregation of metal ions with functionalized calixarenes: synthesis and structure of an octanuclear copper(I) chloride complex (C) 1376
- Binary alloys of 2,5-disubstituted DCNQI radical anion salts of copper and their electrical conductivity (C) 1245
- Copper(I)-assisted formation of an "organic" sandwich structure: structural prerequisites for luminescence in the dinuclear complexes $[(\mu\text{-bipyrimidine})\{Cu(PR_3)_2\}_2]X_2$ (C) 1659
- $[Mes_2SbCu(PMe_3)_2]_2$: the first Cu^I antimonide (C) 1018
- N-analogues of metal acetylacetonates: bis(1,2,6,7-tetracyano-3,5-diimino-3,5-dihydro-pyrrolizinido)metal(II), (metal = Fe, Ni, Cu, Zn); crystal structure of the cooper derivative (C) 1049
- 2,4,6-Triisopropylphenylcopper, a new tetranuclear organocopper aggregate with unsymmetrically bridging σ-π bonded aryl ligands (C) 208

Correspondence, 636

Corrosion, DECHEMA corrosion handbook, Vol. 2 (B) 385

Crystal growth, Crystals in Gels and Liesegang rings (B) 381

Crystal structure analysis, A structural basis of light energy and electron transfer in biology (Nobel lecture) (R) 848
- Benzo[1,2-*h*:4,3-*h'*]diquinoline ("1,14-diaza[5]helicene"): synthesis, structure, and properties (C) 86
- *catena*-Poly[bis-μ-(*o*-oxyphenyleneoxy)silicon]: crystal structure of the orthosilicate of catechol (C) 623
- Formation and reactivity of silicon-sulfur and silicon-selenium double bonds. The first X-ray structure of a silanethione (C) 1016
- Hydrogen bonds between an $NH_4^{\oplus}$ ion and a carbanion—crystal structure of ammonium 1,2,4-tricyanocyclopentadienide (C) 73
- LiSrN—a three dimensional structural arrangement of corner and edge sharing orthorhombic bipyramids, $NLi_{2/2}Sr_{4/4}$ (C) 201
- Model of a solvent-shared ion pair with $N-H\cdots C$ hydrogen bonds between amine and carbanion—crystal structure of [fluorenyllithium · 2 ethylenediamine]$_\infty$ (C) 72
- Pentabenzylcyclopentadienylpotassium · 3THF, an organopotassium compound with "piano stool" geometry (C) 735
- Pentamethylcyclopentadienylmercury chloride: an organomercury compound with novel battlement-like structure (C) 611
- Probing changes in the structure and performance of a lithium nickel oxide catalyst by in situ X-ray diffraction during the high-temperature oxidative coupling of methane (AM) 808
- Structure of chloro(cyclopentadienyl)-bis(1,2:5,6-di-*O*-isopropylidene-α-D-glucofuranos-3-*O*-yl) titanate, a novel titanium-carbohydrate complex (C) 499
- Structures of quino[7,8-*h*]quinoline and quino[8,7-*h*]quinoline (C) 84
- Synthesis and structure of a phenylsodium solvate, bis[μ-phenyl(pentamethylenetriamine)sodium] (C) 476
- The photosynthetic reaction center from the purple bacterium *Rhodopseudomonas viridis* (Nobel lecture) (R) 829
- The solid-state structure of $Me_2B-O-BMe_2$ (C) 180
- The structure of hexaaminobenzene (C) 90
- The structure of lithium compounds of sulfones, sulfoximides, sulfoxides, thioethers and 1,3-dithianes, nitriles, nitro compounds and hydrazones (R) 277
- The structure of the tetracation of hexaazaoctadecahydrocoronene, a simple substituted benzene (C) 92
- The structures of 1,n-bis(9-lithio-9-fluorenyl)ethane · 8THF and -hexane · 8THF as models for solvent-separated ion pairs (C) 458

Cubanes, $(t\text{BuSiP})_4$—the first silaphosphacubane (C) 339, 502
- Much less strained cubane analogues with Si, Ge, Sn, and Pb skeletons (C) 329
- Tetra-*tert*-butyltetraphosphacubane: the first thermal cyclooligomerization of a phosphaalkyne (C) 1013

Cyclacenes, Stereoregular oligomerization by repetitive Diels–Alder reactions (C) 1258

Cyclizations, Cyclizations via palladium-catalyzed allylic alkylations (R) 1173
- New intermediates in the cyclocotrimerization of thioxophosphorus(v) cations with alkynes (C) 448
- Stereo- and regiospecific 6-*endo-trig*-cyclization of aryl radicals, an entry to novel progesterone-antagonists of the androstane series (C) 773
- Tetra-*tert*-butyltetraphosphacubane:

the first thermal cyclooligomerization of a phosphaalkyne (C) 1013
Cycloadditions, [4+2]-cycloadditions with 1,4-bis(*N*,*N*-dimethylamino)-1,3-dienes: stereochemical studies and observation of radical ions (C) 1713
- Chiral cyclobutanones by [2+2]-cycloaddition of dichloroketene to carbohydrate enol ethers (C) 777
- Disilene *versus* silanediyl ("silylene") additions to CN and NCO bonds (C) 95, 228
- Does cyanoacetylene dimerize thermally to 1,3-cyclobutadiene-1,2-dicarbonitrile? (C) 1279
- Photocycloadditions of benzvalene (C) 601
- Pyrones as substrates for palladium-catalyzed [4+3] cycloadditions (C) 213
- Regiochemistry of the intramolecular [2+2]-photocycloaddition of cyclohexenone to vinyl ethers (C) 925
- Surprising reactions of decamethylsilicocene with π-systems of the type X=C=Y (C) 762
Cycloalkynes, Metal complexes of small cycloalkynes and arynes (A) 1296
Cyclobutadienes, Does cyanoacetylene dimerize thermally to 1,3-cyclobutadiene-1,2-dicarbonitrile? (C) 1279
Cyclobutanones, Chiral cyclobutanones by [2+2]-cycloaddition of dichloroketene to carbohydrate enol ethers (C) 777
Cyclododecatetraene, all-*cis*-1,4,7,10-cyclododecatetraene—X-ray structure analysis and photoelectron spectrum (C) 1379
Cycloheptenes, From 2,5-dihydropyrazines to 2*H*-1,4-diazepines and from benzodihydroarenes to benzocycloheptene derivatives, structural variants of the antidepressant protriptyline (C) 613
Cyclohexane, Zur Konformation des Cyclohexans. (Ostwalds Klassiker der exakten Wissenschaft, Band 274) (B) 105
Cyclooctatetraenes, Highly conjugated, substituted polyacetylenes via the ring-opening metathesis polymerization of substituted cyclooctatetraenes (AM) 1571
Cyclopentandiyls, Energy wells of diradicals; 4-methylene-1,3-cyclopentanediyl (C) 1056
Cyclophanes, A pyrrolophanediene-porphycene redox system (C) 1655
- Does cyanoacetylene dimerize thermally to 1,3-cyclobutadiene-1,2-dicarbonitrile? (C) 1279
- 1,2,9,10,17,18-Hexasila[2.2.2](1,3,5)cyclophane, a cage-like phane containing three Si-Si units (C) 757
- *syn*- and *anti*-[2.2]orthometacyclophane (C) 455
Cyclovoltammetry, Indications of cesium in a higher oxidation state (C) 1676

Data storage, Magneto-optical recording and data storage materials (AM) 235
- Materials for optical data storage (R) 1445
DECHEMA, DECHEMA corrosion handbook, Vol. 2 (B) 385
Detergents, Surfactant science and technology (B) 936
Diastereoselectivity, Atropdiastereoselective ring opening of bridged, "axial-prostereogenic" biaryls: directed synthesis of (+)-ancistrocladisine (C) 1672
- Carbohydrates as chiral templates: stereoselective synthesis of β-amino acids (C) 1068
- Carbohydrates as chiral templates: stereoselective tandem Mannich-Michael reactions for the synthesis of piperidine alkaloids (C) 1067
- Ethylenebis(sulfonyl)-bridged 1,1'-binaphthalene, an atropisomeric dienophile for highly diastereoselective Diels–Alder reactions (C) 766
- Intramolecular Diels–Alder reaction of vinylsulfonic acid esters (C) 202
- Iron-mediated diastereoselective spiroannelation to the spiro[1,2,3,4-tetrahydroquinoline-4,1'-cyclohexane] system and a novel rearrangement to 2,3-dihydroindole derivatives (C) 1678
- Stereoselective synthesis of γ-aminocarboxylates (C) 1706
Diazepines, From 2,5-dihydropyrazines to 2*H*-1,4-diazepines and from benzodihydroarenes to benzocycloheptene derivatives, structural variants of the antidepressant protriptyline (C) 613
Diaziridines, The first tricyclic diaziridines—a simple synthetic route (C) 1381
Diboretanes, Thermal cleavage and isomerization of 1,3-diboretanes to stable methyleneboranes (C) 784
Dictionaries, Chambers science and technology dictionary (B) 1593
- Dictionary of organophosphorus compounds (B) 1716
Diels–Alder reactions, Diels–Alder adducts on the *b* side of naphthalene: rapid cycloreversion of *o*-quinodimethanes (C) 1353
- Double-stranded molecules: a [6]beltene derivative and the corresponding open-chain polymer (C) 1680
- Ethylenebis(sulfonyl)-bridged 1,1'-binaphthalene, an atropisomeric dienophile for highly diastereoselective Diels–Alder reactions (C) 766
- Intramolecular Diels–Alder reaction of vinylsulfonic acid esters (C) 202
- Isolation of a zwitterion in a Diels–Alder reaction with inverse electron demand (C) 1267
- Mechanism of the hetero-Diels–Alder reaction of oxadienes and alkenes: calculation of the acrolein/ethene system (C) 1371
- Stereoregular oligomerization by repetitive Diels–Alder reactions (C) 1258
- Structure-directed synthesis of new organic materials (AM) 1103
- Trinacrene—a product of structure-directed synthesis (C) 1261
Diisocyanogen, Diisocyanogen or isocyanogen? (C) 761
Diisotyrosine, Synthesis of (*S*,*S*)-diisotyrosine and its incorporation in an ansa tripeptide (C) 929
Diphosphenes, Synthesis, structure, and reactivity of diphosphenes having a *cis*-configuration (C) 215
Discotic polymers, Induction of liquid crystalline phases: formation of discotic systems by doping amorphous polymers with electron acceptors (C) 914
- Microstructure of a discotic polymer as revealed by electron diffraction and high-resolution imaging (C) 323
Dispersions, Sol-gel technology for thin films, fibers, preforms, electronics and specialty shapes (B) 1137
- Solid/liquid dispersions (B) 529
DNA cleavage, A new class of DNA-cleaving molecules: pH-dependent DNA cleavage by propargylic and allenic sulfones (C) 1272
Dodecahedranes, The pagodane route to dodecahedranes: 4,9,14,19-tetrasubstituted [1.1.1.1]pagodanes by intramolecular functionalization (C) 303
- The pagodane route to dodecahedranes: chemistry and structure of bissecododecahedranes (C) 298
- The pagodane route to dodecahedranes: polyfunctionalized homologous dodecahedranes and dodecahedrenes (C) 310
- The pagodane route to dodecahedranes: polyfunctionalized pentagonal dodecahedranes and dodecahedrenes (C) 305
- The pagodane route to dodecahedranes: total synthesis and chemistry of 4,9,14,19-tetrasubstituted [1.1.1.1]pagodanes (C) 300
Donor-acceptor systems, A polymolecular donor-acceptor stack made of paraquat and a 1,5-dihydroxynaphthalene-derived crown ether (C) 1394
- Covalent versus dative bonds to main group metals, a useful distinction (R) 992
- Phosphonioboratoacetylenes: C_2 stabilized by donor and acceptor molecules (C) 1219
Dyes, Dichroic dyes and liquid crystalline side chain polymers (AM) 940
- Industrielle Organische Pigmente. Herstellung, Eigenschaften, Anwendung (B) 1073
- The search for highly colored organic compounds (R) 677
Dynamics, Correlation of the dynamic behavior of *n*-alkyl ligands of the stationary phase with the retention times of paracelsin peptides in reserved phase HPLC (C) 327
- Structure and dynamics of chiral molecules (R) 571

Ecology, Chemicals carcinogens. Activation mechanisms, structural and electronic factors, and reactivity (B) 932
- Combination effects in chemical carcinogenesis (B) 931
- Complexation of cesium 137 by the cap pigments of the bay boletus (*Xerocomus badius*) (C) 453
- Metal-induced reduction of sulfur dioxide to sulfur monoxide and sulfur (C) 1342
- Polymer benzo[15]crown-5 complexes as sensor materials for solvent vapors—aromatic halogenated hydrocarbons and polar solvents (AM) 813
Editorial essay, Advanced materials R&D—planning for the future (AM) 229
- European materials societies (AM) 357
- How to tailor molecular electronics or why is nature taking the 'soft' approach? (AM) 1544
- Materials research—current issues and future directions (AM) 638
- Materials science and engineering in Britain (AM) 1077
- Paving the way... (AM) 107
- Polymers as advanced materials (AM) 504
- The European ceramic society (ECerS) (AM) 1406
- The European materials research society (E-MRS) (AM) 938
- The nature of materials sciencepublishing (AM) 1721
Elastomers, Liquid crystalline elastomers (AM) 1407, 1757
Electrochemistry, Kinetics of electrochemical metal dissolution (B) 935
- Semiconductor electrodes (B) 386
Electrocyclizations, Perspectives in photochromism: a novel system based on the 1,5-electrocyclization of heteroanalogous pentadienyl anions (R) 413
Electron density, Electron densities, deformation densities, and chemical bonding (C) 597, 1074
- Structure, deformation electron densi-

ties, photoelectron spectra, and reactivity of 3,4-dihydro-1*H*-cyclobuta[*a*]cyclopropa[*d*]benzene (C) 206
Electron diffraction, Stereochemical applications of gas-phase electron diffraction. Part A and B (B) 1534
Electron microscopy, A joint structural characterization of colloidal platinum by EXAFS and high-resolution electron microscopy (C) 590
– High resolution electron microscopy of the high-T_c superconductor $Bi_{2+x}Sr_2Ca_{1-x}Cu_2O_{8+\delta}$ (AM) 810
– Microstructure of a discotic polymer as revealed by electron diffraction and high-resolution imaging (C) 323
– $Pt_{309}Phen^*_{36}O_{30\pm10}$, a four-shell platinum cluster (C) 778
– The complexation of gold colloids (C) 780
– Transmission electron microscopy (B) 1763
Electron transfer, Light-sensitive molecular building blocks with electron transfer activity: synthesis and properties of a photochemically switchable, dicyanovinyl-substituted furan (C) 1494
– Stack-type redox systems: synthesis via repeated carbanion alkylation and electron transfer studies (C) 1531
– Synthesis of a rigid electron-donor/acceptor compound—evidence for intramolecular charge separation (C) 619
Electronic industry, Electronics reliability and measurement technology—non-destructive evaluation (B) 1594
Electronic structure, Direct observation of ground state splitting in the chromium(III) acetate trimer by inelastic neutron scattering (C) 930
– The novel complex $[LRu^{IV}(\mu\text{-}O)_3Ru^{IV}L][PF_6]_2 \cdot H_2O$—a molecular section of the structures of $BaRu^{IV}O_3$(high-pressure phase) and $Ba_{5/6}Sr_{1/6}Ru^{IV}O_3$ (C) 763
Emulsions, Dispersing powders in liquids (B) 385
– Foams and biliquid foams—aphrons (B) 384
Enantiomer separation, Chromatographic enantioseparation—methods and applications (B) 1281
– Chromatographic separation of the excess enantiomer under achiral conditions (C) 626
– Evidence for a temperature dependent reversal of the enantioselectivity in complexation gas chromatography on chiral phases (C) 194
– Gas chromatographic determination of the enantiomeric composition of epoxy alcohols (C) 178
– Gas-chromatographic enantiomer separation of unfunctionalized cycloalkanes on permethylated β-cyclodextrin (C) 736
– Temperature dependent inversion of elution sequence in the resolution of α-amino acid enantiomers on chiral diamide selectors (C) 192
Enantioselectivity, Enantioselective aldol reaction of *tert*-butyl acetate using titanium-carbohydrate complexes (C) 495
– Enantioselective allylation of carbonyl compounds with titanium-carbohydrate complexes (C) 494
– Enantioselective reduction of α,β-unsaturated carboxylates with $NaBH_4$ and catalytic amounts of chiral cobalt semicorrin complexes (C) 60
– Enantioselective synthesis of D-*threo*-β-hydroxy-α-amino acids with titanium-carbohydrate complexes (C) 497
– General aspects and optimization of enantioselective biocatalysis in organic solvents: the use of lipases (R) 695
– Lipophilic tartaric acid esters as enantioselective ionophores (R) 1147
– Total enantiospecific synthesis of (9*S*)- and (9*R*)-9-hydroxyeicosatetraenoic acid (9-HETE) methyl ester (C) 614
Encyclopediae, PARAT. Index of acronyms and abbreviations in electrical and electronic engineering (B) 1442
ENDOR spectroscopy, Electron nuclear double resonance spectroscopy of radicals in solution (B) 792
Ene reactions, Intramolecular, stoichiometric (Li, Mg, Zn) and catalytic (Ni, Pd, Pt) metallo-ene reactions in organic synthesis (R) 38
Energy transport, Efficient photoinduced intramolecular energy transfer in an oblique bis-porphyrin system (C) 593
Enzyme catalysis, Advanced catalysts: interfaces in the physical and biological sciences (AM) 1079
– Discovery of a D-stereospecific aminopeptidase and its use as a catalyst in organic synthesis (C) 450
– Enzymatic synthesis of selectively protected glycals (C) 220
– General aspects and optimization of enantioselective biocatalysis in organic solvents: the use of lipases (R) 695
Enzyme inhibitors, Chain-substituted lipids as substrates for phospholipase A_2 (C) 1218
– Selective inhibitors of dihydrofolate reductase (Nobel lecture) (R) 879
– Sterol biosynthesis inhibitors. Pharmaceutical and agrochemical aspects (B) 1539
– The enantiomers of the azole fungicide HWG-1608—asymmetric synthesis of a 2-hydroxyethyl azole fungicide (C) 462
– The purine path to chemotherapy (Nobel lecture) (R) 870
– Total synthesis of allonojirimycin (5-amino-5-deoxy-D-allopyranose) (C) 1498
Enzyme models, Nitrogenase model compounds: $[\mu\text{-}N_2H_2\{Fe(\text{“}N_HS_4\text{”})\}_2]$, the prototype for the coordination of diazene to iron sulfur centers and its stabilization through strong N–H ··· S hydrogen bonds (C) 1271
– $[VO(O_2CtBu)_3]$ and $[V_6O_6(\mu\text{-}O)_4(\mu\text{-}O_2CPh)_9]$: structural characterization of a mononuclear V^V and a (2+4)-nuclear $V^{IV}V^V_5$ carboxylato complex. Models for vanadate-dependent peroxidases (C) 1221
Enzymes, Mechanistic principles of enzyme activity (B) 1538
– The active site of glutathione reductase: *an example of near transition-state* structures (C) 1023
Epoxides, Coupling of epoxides to Pt^{II}-complexes with carbon dioxide and the structure of a cyclic metallacarbonate (C) 767
Epoxy alcohols, Gas chromatographic determination of the enantiomeric composition of epoxy alcohols (C) 178
Errata, 228, 502, 1074, 1282
ESR spectroscopy, Radical tri- and pentaanions of benzenedi- and benzenetriglyoxylate thioesters (C) 906
– The radical cation of *N,N'*-tetramethylene-*syn*-1,6:8,13-diimino[14]annulene. An experimental study of the N-N three-electron σ bond (C) 902
– Well-resolved ESR spectra of arenecarboxyl radicals in solution (C) 183
Ethylene dianions, Tetraphenylethylenedisodium: the band structure of the CC singly bonded, twisted $(C_6H_5)_2C^{\ominus}$ carbanions (C) 1685
Ethylene dications, Tetrakis(dimethylamino)ethylene dication: two CC singly bonded and almost perpendicularly twisted $((CH_3)_2N)_2C^{\oplus}$ carbenium ions (C) 1684
Ethynol, photochemical generation in an argon matrix, IR spectrum, and photoisomerization to ketene (C) 181
Evolution, Retention of configuration in the non-Darwinian evolution of cytochrome c (C) 71

Felkin-Anh selectivity, Non-chelate-controlled addition of 1-bromo-1-lithio-1-alkenes to *O*-protected lactaldehydes (C) 896
Ferroelectricity, A novel approach to ferroelectric liquid crystals: the first organotransition metal compound displaying this behavior (C) 1065
– Ferroelectricity and superconductivity (AM) 379
Fibers, Graphite fibers and filaments (B) 526
Filbertone, Isolation, synthesis, and absolute configuration of filbertone—the principal flavor component of the hazelnut (C) 1022
Flavor compounds, Isolation, synthesis, and absolute configuration of filbertone—the principal flavor component of the hazelnut (C) 1022
Fluorescence, Synthesis of a rigid electron-donor/acceptor compound—evidence for intramolecular charge separation (C) 619
– The influence of packing effects on the solid-state fluorescence of diketopyrrolopyrroles (C) 478
Fluorinations, Oxidative fluorination of arenes (C) 927
Fluorine compounds, Sulfur-cyanide pentafluoride SF_5NC (C) 1255
– Sulfur-pentafluoride isocyanide, SF_5NC (C) 1256
– The structure of $BrF_6^{\ominus}$ and related compounds (C) 1526
Fractals, Theoretical chemistry en route to a theory of chemistry (R) 268
Fulvalenes, *p*-Quinodimethane analogues of tetrathiafulvalene (C) 1052
– Di(4-pyridinio)-, di(2-benzothiazolio)-, di(2[1,3-dithiolylio])- and diformyltetraaza[14]annulenes and tetraaza[14]annulenylene-homologous tetrathiafulvalenes (C) 1063
Fungicides, The enantiomers of the azole fungicide HWG-1608—asymmetric synthesis of a 2-hydroxyethyl azole fungicide (C) 462
Furans, Light-sensitive molecular building blocks with electron transfer activity: synthesis and properties of a photochemically switchable, dicyanovinyl-substituted furan (C) 1494

Gallium arsenide, Single-source III/V precursors: a new approach to gallium arsenide and related semiconductors (R) 1208
Gallium compounds, $Na_xMg_{5-x}Ga_9$, a new intermetallic phase as a link between Zintl phases and metals (C) 58
Gas chromatography, Evidence for a temperature dependent reversal of the enantioselectivity in complexation gas chromatography on chiral phases (C) 194
– Gas chromatographic determination of the enantiomeric composition of epoxy alcohols (C) 178

- Gas-chromatographic enantiomer separation of unfunctionalized cycloalkanes on permethylated β-cyclodextrin (C) 736
- Inverse gas chromatography. Characterization of polymers and other materials (B) 1761
- Temperature dependent inversion of elution sequence in the resolution of α-amino acid enantiomers on chiral diamide selectors (C) 192

Gels, Crystals in Gels and Liesegang rings (B) 381

Generation of current, Chemical aspects of fusion technology (R) 1

Genes, Architecture of eukaryotic genes (B) 104
- Gene synthesis (R) 716

Germanium compounds, A base-stabilized Ge–S double bond (C) 1237
- A polyhedral oligogermane: 4,8-dibromoocta-*tert*-butyltetracyclo-[3.3.0.0^{2,7}.0^{3,6}]octagermane (C) 198
- A silicogermanate with a Si:Ge ratio ≥ 2—an MFI zeolite of novel composition (C) 81
- Addition of free Me_2Ge: to alkenes and alkynes on glass surfaces in the presence of water (C) 1028
- $[(Me_3Si)_2CHGe]_6$, the first hexagermaprismane (C) 55
- Synthesis and structure of digerma- and distannacyclobutenes (C) 603

Glass, Addition of free Me_2Ge: to alkenes and alkynes on glass surfaces in the presence of water (C) 1028

Glasses, Aluminum-rich metallic glasses (AM) 123
- Conference report (AM) 1132
- Glass-Ceramics in the scheme of inorganic materials (AM) 1746
- Structural characterization of non-oxide chalcogenide glasses by modern solid state NMR techniques (AM) 1723

Glycals, Enzymatic synthesis of selectively protected glycals (C) 220

Gold, The complexation of gold colloids (C) 780

Gold compounds, Agostic-type gold ligand and incipient μ_3-PPh_2 coordination in the $Au_2Pt_2P_6$ "hammock" skeleton of the cluster $[Au_2Pt_2(\mu\text{-}PPh_2)_2(PPh_3)_4][PF_6]_2$ (C) 923
- Aurophilicity as concerted effect: relativistic mo calculations on carbon-centered gold clusters (C) 1357
- Synthesis, structure, and bonding of the cation $[\{(C_6H_5)_3PAu\}_5C]^{\oplus}$ (C) 463

Graphite, Graphite fibers and filaments (B) 526

Halogen compounds, Alkylidene sulfur difluorides: $F_5S(F_3C)C{=}SF_2$ and $(F_3C)_2C{=}SF_2$. Synthesis, structure, and structure predictions (C) 769
- $AsI_4^{\oplus}AlCl_4^{\ominus}$, a salt of the last missing tetrahaloarsonium ion (C) 1671
- Bromoselenates (II,IV), a novel type of mixed valence compounds (C) 187
- $FeI_3SC(NMe_2)_2$, a neutral thiourea complex of iron(III) iodide (C) 776
- Structural diversity in iodoantimonates; the anions $Sb_3I_{11}^{2\ominus}$, $Sb_5I_{18}^{3\ominus}$ and $Sb_6I_{22}^{4\ominus}$ (C) 344

Helix, One-dimensional metal chains in a chiral environment—the crystal structure of helical bis(dicarbonylrhodium(I))- 3,3′-hexafluoroglutarylbis-(1*R*)-camphorate (C) 1019

HETE, A new synthesis of key intermediates for the preparation of 5,6-DiHETE and lipoxin A_4 (C) 755
- Stereocontrolled total synthesis of (5*S*,6*R*)- (5*S*,6*S*)- (5*R*,6*R*)-, and (5*R*,6*S*)- (7*E*,9*E*,11*Z*,14*Z*)-5,6-dihydroxy-7,9,11,14-icosatetraenoic acid (5,6-DiHETE) methyl esters (C) 587
- Total enantiospecific synthesis of (9*S*)- and (9*R*)-9-hydroxyeicosatetraenoic acid (9-HETE) methyl ester (C) 614

Heteroallyl anions, Synthesis, structure, and reactivity of a 1,3-diphospha-2-silaallyl anion (C) 751

Heteroarenes, 3,3′:4,4′-Bis(thieno[2,3-*b*]-thiophene): a novel fused heteroarene (C) 1222
- Azonia derivates of arenes: synthesis and properties of 10c-azoniafluoranthene (C) 588
- Benzo[1,2-*h*:4,3-*h*′]diquinoline ("1,14-diaza[5]helicene"): synthesis, structure, and properties (C) 86
- Di(1-pyridinio)- and di(1-bipyridindiio)dihydrodibenzotetraaza[14]annulenes (C) 1060
- Di(4-pyridinio)-, di(2-benzothiazolio)-, di(2[1,3-dithiolylio])- and diformyltetraaza[14]annulenes and tetraaza[14]annulenylene-homologous tetrathiafulvalenes (C) 1063
- Light-sensitive molecular building blocks with electron transfer activity: synthesis and properties of a photochemically switchable, dicyanovinyl-substituted furan (C) 1494
- New intermediates in the cyclocotrimerization of thioxophosphorus(v) cations with alkynes (C) 448
- Poly-[*N*,*N*-(1,4-divinylbenzene-β,β′-diyl)-4,4′-bipyridinium dibromide], a novel conducting viologen polymer (AM) 807
- Structures of quino[7,8-*h*]quinoline and quino[8,7-*h*]quinoline (C) 84
- Synthesis and crystal structure of a phospholyl anion (C) 1367

Heterocycles, A base-stabilized Ge–S double bond (C) 1237
- 3-Arylsulfonyloxazolidines as chiral templates: asymmetric synthesis of 2-substituted 2-hydroxycyclohexanecarbaldehydes from 2-hydroxymethylenecyclohexanone (C) 67
- 2-Chloro-2*H*-phosphirene/1-chloro-1*H*-phosphirene isomerization by [1,3]-chlorine shift (C) 225
- Azaoctabisvalenes (C) 1345
- Dimethyldioxasilirane (C) 898
- Formation of 2,4,4-trimethylthiete by photodecarbonylation of 3,3,5-trimethyl-2(3*H*)-thiophenone (C) 1499
- From 2,5-dihydropyrazines to 2*H*-1,4-diazepines and from benzodihydroarenes to benzocycloheptene derivatives, structural variants of the antidepressant protriptyline (C) 613
- Iron-mediated diastereoselective spiroannelation to the spiro[1,2,3,4-tetrahydroquinoline-4,1′-cyclohexane] system and a novel rearrangement to 2,3-dihydroindole derivatives (C) 1678
- Pentacoordinated elements of the 4th main group with four organic residues (C) 918
- Perspectives in photochromism: a novel system based on the 1,5-electrocyclization of heteroanalogous pentadienyl anions (R) 413
- Phosphanorbornadienes as ligands in the transition metal-catalyzed synthesis of fine chemicals (C) 500
- Reaction of decamethylsilicocene with sulfur, selenium, and tellurium: from a p_π-p_π system to new heterocycles (C) 1518
- $S_4(CN)_8$, a blue-black high-molecular sulfur-cyanogen compound with 6π- and 8π-electron structural elements (C) 609
- Surprising reactions of decamethylsilicocene with π-systems of the type $X{=}C{=}Y$ (C) 762
- Synthesis and structure of $[(C_5H_5)_2TiS_4AsCH_3]$—a new reagent for the synthesis of sulfur-rich heterocycles (C) 1269
- Synthesis and structure of digerma- and distannacyclobutenes (C) 603
- Synthesis and structure of $[\{(\eta^5\text{-}C_5Me_5)Ti(NH)\}_3N]$, a titanium imide nitride (C) 754
- Synthesis, characterization, and complexation of an unusual P_2Si_2 bicyclobutane with butterfly-structure: 2,2,4,4-tetramesityl-1,3-diphospha-2,4-disilabicyclo[1.1.0]butane (C) 1038
- Synthesis of the novel ring systems 1,2,3,4-oxazadisiletidine and 1,3,4,2,5-dioxazadisilolidine (C) 54
- Tellurobenzaldehyde by Staudinger-chalcogenation of the ylide benzylidenetriphenylphosphorane (C) 179
- Tetraalkylidene-1,4-diboracyclohexanes from 3,4-dilithio-2,5-dimethyl-2,4-hexadiene; the first "hetero[6]radialene" with chair conformation (C) 477
- 1,3,5-Trithia-2,4,6-triazapentalenyl—a stable sulfur-nitrogen radical (C) 920

Heterometallic compounds, A novel type of anionic cluster containing a Pt_4Ag_2 core (C) 748
- The first heterodinuclear complexes with bis(cyclopentadienyl)methane bridges (C) 1008

Heteropolyanions, $[Et_4N]_6$-$[Na_{14}Mo_{24}P_{17}O_{97}(OH)_{31}]\cdot x\,H_2O$: a hollow cluster filled with 12 $Na^{\oplus}$ ions and a H_3PO_4 molecule (C) 743
- $PbMo_5O_8$ and $Tl_{0.8}Sn_{0.6}Mo_7O_{11}$, novel clusters of molybdenum and thallium (C) 758

Hexaaminobenzene, The structure of hexaaminobenzene (C) 90

Hexaazaoctadecahydrocoronene, The structure of the tetracation of hexaazaoctadecahydrocoronene, a simple substituted benzene (C) 92

High pressure chemistry, Organic high pressure chemistry (B) 1535

Histamines, A chiral Ag^{I}-coordination polymer with a polydentate chiral ligand; crystal structure of the 1:1 complex of CF_3SO_3Ag and *N*-[*N*-(5-Methylthenylidene)-L-methionyl]histamine (C) 1698

History of chemistry, Georg de Hevesy. 1885–1966. Festschrift (B) 1536
- One pioneer or several pioneers? The discovery of noble-gas compounds (L) 636
- Superconductors: the breakthrough (B) 1139
- The beginnings of organic photochemistry (A) 1193
- The Kevlar story—an advanced materials case study (AM) 649
- Zur Konformation des Cyclohexans. (Ostwalds Klassiker der exakten Wissenschaft, Band 274) (B) 105

Homobenzenes, Bridged *cis*-Tris-σ-homobenzenes: Heterodiademanes (C) 1351
- Stabilized *cis*-Tris-σ-homobenzenes: syntheses, [σ2+σ2+σ2] cycloreversions (C) 1348

Hormone antagonists, Drugs from emasculated hormones: the principle of syntopic antagonism (Nobel lecture) (R) 886

Host-guest chemistry, A polymolecular donor-acceptor stack made of paraquat and a 1,5-dihydroxynaphthalene-derived crown ether (C) 1394

- Additivities of electrostatic and hydrophobic interactions in host-guest complexes (C) 753
- Efficient Ion exchangers and receptors for organic and organometallic cations (C) 1263
- Encapsulation of polypyrrole chains in zeolite channels (C) 1692
- Spontaneous oxidation and in-situ polymerization of pyrrole in channels of the three-dimensional coordination polymer $[(Me_3Sn)_3Fe^{III}(CN)_6]_\infty$ (C) 1265

Houben-Weyl, Houben-Weyl. Methoden der Organischen Chemie. Band E20, Teil 1-3: Makromolekulare Stoffe (B) 634

Hydrogen bonds, A structure for the H-bonded complex of nylon-66 with perfluoroglutaric acid (C) 466
- Anion coordination and Cl−H···Cl bridges in the low-melting poly(hydrogen chloride) $Me_3N \cdot 5HCl$ (C) 1697
- Bis[cyclooctane-1,5-diyl)di(pyrazol-1-yl)borato]cobalt: a polypyrazolylborate complex with two agostic hydrogen bonds (C) 205
- hydrogen bonds between an $NH_4^\oplus$ ion and a carbanion—crystal structure of ammonium 1,2,4-tricyanocyclopentadienide (C) 73
- Model of a solvent-shared ion pair with N−H···C hydrogen bonds between amine and carbanion—crystal structure of [fluorenyllithium · 2 ethylenediamine]$_\infty$ (C) 72
- Nitrogenase model compounds: $[\mu\text{-}N_2H_2\{Fe(\text{“}N_HS_4\text{”})\}_2]$, the prototype for the coordination of diazene to iron sulfur centers and its stabilization through strong N−H···S hydrogen bonds (C) 1271

Hydrogenation, A highly selective montmorillonite catalyst for hydrogenation of alkynes, alkenynes, and alkadienes (C) 465
- Selective hydrogenation of esters to alcohols with a catalyst prepared from Rh_2O_3, $Sn(n\text{-}C_4H_9)_4$, and SiO_2: evidence for site isolation (C) 347

Hydrooligomerization, hydrooligomerization of alkynes, a new catalytic reaction promoted by $[Co(py)_6]^\oplus$ in the presence of H_2 (C) 1009

Hydroxyecdysone, Side-chain homologues of 20-hydroxyecdysone: synthesis, configurational assignment, and biochemical characterization (C) 1515

Hyperconjugation, The structure of a *C*-borylborirene with strong C-B hyperconjugation (C) 186

Image processing, Image enhancement—chemical, digital, visual (R) 1601

Implant devices, Advanced ceramics for biomedical applications (AM) 111
- Bone replacements: implant materials and the modes of implant fixation (AM) 1431
- Challenges in materials for health care applications (AM) 662

Indigo, Indigo-metal complexes: synthesis and structure of Pd^{II} and Pt^{II} compounds containing the anions of indigo and octahydroindigo as mono- and bischelate ligands (C) 1529

Indium compounds, Indium 2,4,6-tris(trifluoromethyl)phenoxide—a dimer with the coordination number two at the indium atoms (C) 1383

Industrial chemistry, Industrielle Organische Pigmente. Herstellung, Eigenschaften, Anwendung (B) 1073
- Materials for optical data storage (R) 1445
- Polymer optical fibers and nonlinear optical device principles (AM) 1548

Inorganic chemistry, Advanced inorganic chemistry (B) 1073

Intercalation, Conference report (AM) 1434
- Location of *para*-xylene in Yb-faujasite (zeolite Y) by neutron diffraction (C) 770

Interhalogene compounds, The structure of $BrF_6^\ominus$ and related compounds (C) 1526

Intermetallics, Conference report (AM) 243

Ion conductors, Solid ion conductors in heterogeneous catalysis (R) 708

Ion exchangers, Efficient ion exchangers and receptors for organic and organometallic cations (C) 1263

Ionophores, Lipophilic tartaric acid esters as enantioselective ionophores (R) 1147

Ions, Ions in solution: basic principles of chemical interactions (B) 103
- The structure of the tetracation of hexaazaoctadecahydrocoronene, a simple substituted benzene (C) 92

Iridium compounds, $[Ir_2(\mu\text{-}CH_2)(CO)_4(Me_2PCH_2PMe_2)_2][CF_3SO_3]_2$, an unprecedented electrophilic methylene complex; $H^\ominus$ addition to prepare a bridging methyl complex (C) 1377

Iron compounds, 17- to 19-electron pentamethylcyclopentadienyl iron dithiocarbamate complexes. Formation of a Cp^*Fe^{IV} complex (C) 460
- Chirality and isomerism in binuclear iron complexes with sulfur ligands: $[Fe(CO)(\mu\text{-}\text{“}S_4\text{”})]_2$, a model complex for oxidoreductases (C) 1703
- $(C_4Me_4NBH_3)_2Fe$—a metal complex isosteric with decamethylferrocene with characteristic metallocene disorder (C) 342
- Complexes with an $\eta^2\text{-}\mu_2$-SiO bridge. Structure of the bimetallic complex $[Fe(CO)_3\{\mu\text{-}Si(OMe)_2\text{-}OMe\}(\mu\text{-}dppm)PdCl]$(*Fe-Pd*) (C) 1361
- $FeI_3SC(NMe_2)_2$, a neutral thiourea complex of iron(III) iodide (C) 776
- Formation of a phosphaferracyclopentadiene ring by coupling of a phosphaalkyne with two fluoromethylidyne ligands (C) 321
- Highly selective oxidations of $Fe(CO)_3$-cyclohexadiene complexes: synthesis of 4b,8a-dihydrocarbazol-3-ones and the first total synthesis of carbazomycin A (C) 223
- Identification of $[(OC)_4Fe{=}Si(CH_3)_2 \cdot \{(H_3C)_2N\}_3PO]$ as intermediate in the formation of polysilanes from $(H_3C)_2SiCl_2$ and $[Na_2Fe(CO)_4]$ (C) 203
- Multiple “remote functionalization” of different sites in flexible molecules by “anchored” bare Fe^I ions (C) 1277
- Nitrogenase model compounds: $[\mu\text{-}N_2H_2\{Fe(\text{“}N_HS_4\text{”})\}_2]$, the prototype for the coordination of diazene to iron sulfur centers and its stabilization through strong N−H···S hydrogen bonds (C) 1271
- Optically active isoprene(tricarbonyl)-iron(0) and methyltrimethylenemethane(tricarbonyl)iron(0) (C) 1657
- Oxoiron porphyrin species with high-valent iron: formation by solvent-dependent protonation of a peroxoiron(III) porphyrinate derivative (C) 1709
- Pronounced anion dependence of valence detrapping temperature in mixed-valence 1′,1‴-disubstituted biferrocenium salts (C) 1388
- Thermal and electrocatalytic epimerization at iron as the chiral center (C) 1521
- Two ferrole isomers in equilibrium: experimental confirmation of an old hypothesis (C) 318

Isocarbacyclins, Flexible syntheses of optically active isocarbacyclins (C) 1282, 349

Isocyanatoalkenoates, 2-Isocyanato-2-alkenoates—synthesis and reactions (C) 1053

Isocyanogen, Diisocyanogen or isocyanogen? (C) 761

Isomerization, The effect of acetylene substituents on a Pd^{II}-catalyzed cycloisomerization. Total synthesis of (−)-sterepolide and assignment of absolute stereochemistry (C) 1502
- Thermal and electrocatalytic epimerization at iron as the chiral center (C) 1521
- Two ferrole isomers in equilibrium: experimental confirmation of an old hypothesis (C) 318

Kinetics, Additivities of electrostatic and hydrophobic interactions in host-guest complexes (C) 753
- Kinetics of electrochemical metal dissolution (B) 935

Knot compounds, A synthetic molecular trefoil knot (C) 189

Lanthanoid compounds, Complexation of a novel organoytterbium(II) ligand with dimethylplatinum(II) : crystal structure of the resulting heterobimetallic complex (C) 1370
- $HoAl_3Cl_{12}$ in crystalline form (C) 1364
- Magneto-optical recording and data storage materials (AM) 235
- Reductive dimerization of a phosphaalkyne with complexation to samarium (C) 445
- Trigonal-bipyramidal lanthanoid complexes with interstitial oxygen atoms (C) 1033

Lasers, Lasertechnik (B) 1760

Lead compounds, $[\{Cp'(CO)_2Mn\}_2PbS\textit{t}Bu]^\ominus$; completion of an isoelectronic series of binuclear complexes containing trigonal-planar coordinated main group elements (C) 1496
- Triorganolead cations stabilized by side-on coordination to the C≡C bond in alkynylborates (C) 1500

Ligand transfers, Triple-decker complexes as intermediates in ring-ligand transfers (C) 737

Lipoxin A_4, A new synthesis of key intermediates for the preparation of 5,6-DiHETE and lipoxin A_4 (C) 755

Liquid crystals, A novel approach to ferroelectric liquid crystals: the first organotransition metal compound displaying this behavior (C) 1065
- Conference report (AM) 959, 961
- Dichroic dyes and liquid crystalline side chain polymers (AM) 940
- Induction of liquid crystalline phases: formation of discotic systems by doping amorphous polymers with electron acceptors (C) 914
- Liquid crystalline elastomers (AM) 1407
- Liquid crystals—new compounds, new applications (AM) 1424, 1757
- Materials processing—a key factor (AM) 644
- Monolayers and Langmuir-Blodgett multilayers of discotic liquid crystals? (AM) 1574
- Side chain liquid crystal polymers (B) 1140
- Siloxane copolymers with laterally and terminally attached mesogenic side chains (AM) 1120

- Thermotropic liquid crystals, fundamentals (B) 383
Liquid films, Thin liquid films (B) 527
Luminescence, Copper(I)-assisted formation of an "organic" sandwich structure: structural prerequisites for luminescence in the dinuclear complexes [(μ-bipyrimidine){Cu(PR$_3$)$_2$}$_2$]X$_2$ (C) 1659

Macrocycles, A [2]catenane made to order (C) 1396
- A polymolecular donor-acceptor stack made of paraquat and a 1,5-dihydroxynaphthalene-derived crown ether (C) 1394
- Polymer benzo[15]crown-5 complexes as sensor materials for solvent vapors—aromatic halogenated hydrocarbons and polar solvents (AM) 813
- Stereoregular oligomerization by repetitive Diels–Alder reactions (C) 1258
- The chemistry of macrocyclic ligand complexes (B) 1534
- The first macrocyclic square-planar cobalt(III) complex relieves ring strain by forming a nonplanar amide (C) 1509
- The organization of two "soft" ($Cu^{2\oplus}$, $Ni^{2\oplus}$) metal centers in heterotrinuclear complexes of a macrocyclic ligand by cocomplexation with $Ba^{2\oplus}$ (C) 746

Macromolecular chemistry, Houben-Weyl. Methoden der Organischen Chemie. Band E20, Teil 1-3: Makromolekulare Stoffe (B) 634
Macromolecular physics, Conference report (AM) 1753
Magnesium compounds, $Na_xMg_{5-x}Ga_9$, a new intermetallic phase as a link between zintl phases and metals (C) 58
Magnetic materials, Conference report (AM) 1134, 958, 961
Magneto-optics, Conference report (AM) 1134
- Magneto-optical recording and data storage materials (AM) 235

Manganese compounds, A phosphane–dithioformate adduct as a five-electron bridging ligand [Mn$_2$(CO)$_6${S$_2$C(H)P(*cyclo*-C$_6$H$_{11}$)$_3$}$_2$] (C) 1014
- [{Cp(CO)$_2$Mn}$_2$(μ-H)]$^{\ominus}$: a new, versatile reagent (C) 446
- [{Cp′(CO)$_2$Mn}$_2$PbS*t*Bu]$^{\ominus}$; completion of an isoelectronic series of binuclear complexes containing trigonal-planar coordinated main group elements (C) 1496
- Synthesis, structure and magnetic properties of a dinuclear manganese(II) complex with one μ-aqua and two μ-carboxylato bridges (C) 1365
- The active sites in manganese-containing metalloproteins and inorganic model complexes (A) 1153
- The first heterodinuclear complexes with bis(cyclopentadienyl)methane bridges (C) 1008

Mass spectrometry, Dithia dications from cyclic and acyclic precursors by gas-phase oxidation ("charge stripping") of 3e/2c-radical cations (C) 1275
- Inorganic mass spectrometry (B) 101
- Laser desorption/ionization mass spectrometry of proteins of mass 100000 to 250000 Dalton (C) 760
- Multiple "remote functionalization" of different sites in flexible molecules by "anchored" bare Fe^{I} ions (C) 1277
- Organic dications: gas phase experiments and theory in concert (A) 1321

Materials science, Advanced materials R&D—planning for the future (AM) 229
- Conference report (AM) 1587, 246
- European materials societies (AM) 357
- Improving effectiveness in materials research (AM) 667
- Materials for optical data storage (R) 1445
- Materials for the next millenium (AM) 1088
- Materials research—current issues and future directions (AM) 638
- Materials science and engineering in Britain (AM) 1077
- The European ceramic society (ECerS) (AM) 1406
- The European materials research society (E-MRS) (AM) 938
- The nature of materials science publishing (AM) 1721

Matrix isolation, Ethynol: photochemical generation in an argon matrix, IR spectrum, and photoisomerization to ketene (C) 181
- Dimethyldioxasilirane (C) 898

Mercury compounds, Hg_8 ("Mercubane") clusters in $Rb_{15}Hg_{16}$ (C) 1251
- Pentamethylcyclopentadienylmercury chloride: an organomercury compound with novel battlement-like structure (C) 611

Metal chains, Chain complexes with eleven metal atoms (C) 624
- One-dimensional metal chains in a chiral environment—the crystal structure of helical bis(dicarbonylrhodium(I))-3,3′-hexafluoroglutarylbis-(1*R*)-camphorate (C) 1019

Metallacycles, Dimeric [Cp$_2$Zr(CH$_2$O)], a novel (η^2-formaldehyde)metal complex from carbon monoxide (C) 630
- Single-source III/V precursors: a new approach to gallium arsenide and related semiconductors (R) 1208

Metalloproteins, The active sites in manganese-containing metalloproteins and inorganic model complexes (R) 1153
Metal-metal bonds, Tl^{I}-Tl^{I} interactions in the molecular state—an MO analysis (C) 1688
Metal-metal multiple bonds, Alkoxide clusters of molybdenum and tungsten as templates for organometallic chemistry: comparison with carbonyl clusters of the later transition elements (R) 432
- [{Cp(CO)$_2$Mn}$_2$(μ-H)]$^{\ominus}$: a new, versatile reagent (C) 446

Metal oxides, The crystal chemistry of high-temperature oxide superconductors and materials with related structures (R) 1472
Metals, Introduction to the modern theory of metals (B) 1592
Metathesis, Heterogeneous, metathesis-active Schrock-type carbene complexes by reaction of carbyne tungsten(VI) complexes with silica gel (C) 62
- Reactions of mono- and dinuclear metal-alkylidyne complexes with phosphaalkynes: C≡P and C≡Mo metathesis (C) 210

Michael additions, Copper(I)-promoted Michael-addition reaction of organozincs of esters, nitriles, and α-amino acids (C) 351
Mixed-valence compounds, bromoselenates(II,IV), a novel type of mixed valence compounds (C) 187
- Nickel complexes containing sterically demanding thiolate ligands: [Ni$_8$S(SC$_4$H$_9$)$_9$]$^{\ominus}$, a mixed-valence nickel sulfide thiolate cluster, and [Ni$_4$(SC$_3$H$_7$)$_8$], a homoleptic nickel thiolate (C) 61
- Pronounced anion dependence of valence detrapping temperature in mixed-valence 1′,1‴-disubstituted biferrocenium salts (C) 1388

Molecular beam epitaxy, Metal organic chemical vapor deposition (MOCVD) perspectives and prospects (AM) 1110
- Tailoring semiconductor crystals to atomic dimensions (AM) 1098

Molecular design, Structure-directed synthesis of new organic materials (AM) 1103
Molecular electronics, Conference report (AM) 520
- How to tailor molecular electronics or why is nature taking the 'soft' approach? (AM) 1544

Molecular recognition, Conference report (AM) 1585
- Selective molecular recognition of trihydroxybenzenes (C) 79
- Using crystal birefringence to study molecular recognition (C) 330

Molybdenum compounds, Alkoxide clusters of molybdenum and tungsten as templates for organometallic chemistry: comparison with carbonyl clusters of the later transition elements (R) 432
- *N*-Arylation and *N,N*-dibenzylation of coordinated N$_2$ with organic halides; differences in the reactivity of *trans*-[Mo(N$_2$)$_2$(Me$_8$[16]aneS$_4$)] and its phosphane analogues (C) 1040
- Hexaarsabenzene as complex ligand (C) 212
- Two novel polyoxomolybdates containing the $(MoNO)^{3\oplus}$ unit: [Mo$_5$Na(NO)-O$_{13}$(OCH$_3$)$_4$]$^{2\ominus}$ and [Mo$_6$(NO)O$_{18}$]$^{3\ominus}$ (C) 1363

Montmorillonites, A highly selective montmorillonite catalyst for hydrogenation of alkynes, alkenynes, and alkadienes (C) 465
Multiple bonds, A base-stabilized Ge–S double bond (C) 1237
- Alkylidene sulfur difluorides: F$_5$S(F$_3$C)C=SF$_2$ and (F$_3$C)$_2$C=SF$_2$. Synthesis, structure, and structure predictions (C) 769
- Bis(trifluoromethyl)sulfene (CF$_3$)$_2$C=SO$_2$, isolated as adduct (C) 221
- *t*Bu$_2$P-P=PBr*t*Bu$_2$ · LiBr and formation of *t*Bu$_2$P-P (C) 315
- [{Cp′(CO)$_2$Mn}$_2$PbS*t*Bu]$^{\ominus}$; completion of an isoelectronic series of binuclear complexes containing trigonal-planar coordinated main group elements (C) 1496
- Formation and reactivity of silicon-sulfur and silicon-selenium double bonds. The first X-ray structure of a silanethione (C) 1016
- Metal-ligand multiple bonds (B) 790
- Methylboron oxide, H$_3$C–B≡O (C) 88
- Stable methyleneboranes of high Lewis acidity (C) 781
- Synthesis, structure, and reactivity of diphosphenes having a *cis*-configuration (C) 215
- The structure of a *C*-borylborirene with strong C-B hyperconjugation (C) 186
- Thermal cleavage and isomerization of 1,3-diboretanes to stable methyleneboranes (C) 784
- Versatile modes of allene bonding in the structures of [W$_2$(O*t*Bu)$_6$(C$_3$H$_4$)], [W$_2$(O*t*Bu)$_6$(C$_3$H$_4$)(CO)$_2$], and [W$_2$(O*t*Bu)$_6$(C$_3$H$_4$)$_2$] (C) 1523

Name reactions, name reactions and reagents in organic synthesis (B) 1538
Natural products, A new synthesis of key intermediates for the preparation of 5,6-DiHETE and lipoxin A$_4$ (C) 755

- Biosynthetic studies on antibiotics (R) 146
- Chemical modifications of biopolymers by quinones and quinone methides (R) 555
- Chiral building blocks for the synthesis of triquinane sesquiterpenes: derivatives of 2-methylbicyclo[3.3.0]octan-3-ol from catalpol (C) 447
- Enzymatic synthesis of selectively protected glycals (C) 220
- Establishment of configurations for the two diastereomeric *C*-glucosylanthrones aloin A und aloin B (C) 1528
- Flexible syntheses of optically active isocarbacyclins (C) 1282, 349
- Highly selective oxidations of $Fe(CO)_3$-cyclohexadiene complexes: synthesis of 4b,8a-dihydrocarbazol-3-ones and the first total synthesis of carbazomycin A (C) 223
- Intramolecular, stoichiometric (Li, Mg, Zn) and catalytic (Ni, Pd, Pt) metalloene reactions in organic synthesis (R) 38
- Isolation, synthesis, and absolute configuration of filbertone—the principal flavor component of the hazelnut (C) 1022
- On the structure of eumelanins: identification of constitutional patterns by solid-state NMR spectroscopy (C) 741
- Stereo- and regiospecific 6-*endo*-*trig*-cyclization of aryl radicals, an entry to novel progesterone-antagonists of the androstane series (C) 773
- Stereocontrolled total synthesis of (5*S*,6*R*)-, (5*S*,6*S*)-, (5*R*,6*R*)-, and (5*R*,6*S*)-, (7*E*,9*E*,11*Z*,14*Z*)-5,6-dihydroxy-7,9,11,14-icosatetraenoic acid (5,6-DiHETE) methyl esters (C) 587
- The effect of acetylene substituents on a Pd^{II}-catalyzed cycloisomerization. Total synthesis of (−)-sterepolide and assignment of absolute stereochemistry (C) 1502
- Total enantiospecific synthesis of (9*S*)- and (9*R*)-9-hydroxyeicosatetraenoic acid (9-HETE) methyl ester (C) 614
- Total synthesis of the antitumor antibiotic WF-3161 (C) 333

Neisseria meningitidis, Application of the dimethyl(phenyl)silyl group as a masked form of the hydroxy group in the synthesis of an L-*glycero*-α-D-*manno*-heptopyranoside-containing trisaccharide from the dephosphorylated inner core region of *neisseria meningitidis* (C) 1504

Neutron diffraction, Double-bond geometry of norbornene: neutron diffraction measurement of a derivative at 15 K (C) 1239

Nickel compounds, Aminebis(ethene)-nickel(0) complexes; structure of 1-azabicyclo[2.2.2]octanebis(ethene)nickel(0) (C) 772
- Monohapto versus dihapto CO_2 coordination in bis(amine)Ni^0 complexes: a CAS-SCF study (C) 1694
- Nickel(0)-catalyzed preparation of isomeric carboxamides—ligand-controlled β-H or β′-H elimination (C) 1035
- Nickel complexes containing sterically demanding thiolate ligands: $[Ni_8S(SC_4H_9)_9]^{\ominus}$, a mixed-valence nickel sulfide thiolate cluster, and $[Ni_4(SC_3H_7)_8]$, a homoleptic nickel thiolate (C) 61
- Novel nickel clusters with Se and Cp′ as ligands: $[Ni_4Se_2(CO)BrCp'_3]$, $[Ni_6Se_4Cp'_5]$, $[Ni_{15}Se_{10}(CO)_3Cp'_8]$, and $[Ni_{15}Se_{10}(CO)Cl_2Cp'_8]$ (C) 1390
- $[\{Ph_3PCH_2C(CF_3)_2O\}NiH(PCy_3)]$: support for a nickel hydride mechanism in ethene oligomerization (C) 1011
- The bioinorganic chemistry of nickel (B) 632

Niobium compounds, A new oxygen sensor based on the thermoelectric power of solid solutions of Nb_2O_5 and Bi_2O_3 (C) 75
- $K_4Al_2Nb_{11}O_{20}F$—the missing link in cluster condensation (C) 1662
- Self-reduction of $[Ph_4P][Nb(SCH_2CH_2CH_2S)_3]$ with formation of a Nb_2^{IV} complex (C) 98
- Stabilization of niobium(0) and tantalum(0) in mixed metal clusters containing silver atoms (C) 471

Nirile imines, A distillable *C*- and *N*-silylated nirile imine (C) 1250

Nitrides, LiCaN and Li_4SrN_2, derivatives of the fluorite and lithium nitride structures (C) 1702
- Synthesis and structure of $[\{(\eta^5\text{-}C_5Me_5)Ti(NH)\}_3N]$, a titanium imide nitride (C) 754

Nitrogen compounds, A distillable *C*- and *N*-silylated nirile imine (C) 1250
- *N*-Arylation and *N*,*N*-dibenzylation of coordinated N_2 with organic halides; differences in the reactivity of *trans*-$[Mo(N_2)_2(Me_8[16]aneS_4)]$ and its phosphane analogues (C) 1040
- Azonia derivates of arenes: synthesis and properties of 10c-azoniafluoranthene (C) 588
- 2,3-Dihydro-1*H*-1,2,4-triazol-1-yls, a novel group of stable radicals (C) 491
- N-analogues of metal acetylacetonates: bis(1,2,6,7-tetracyano-3,5-diimino-3,5-dihydro-pyrrolizinido)metal(II), (metal = Fe, Ni, Cu, Zn); crystal structure of the copper derivative (C) 1049
- Nitrile oxides, nitrones and nitronates in organic synthesis. Novel strategies in synthesis (B) 227
- The first tricyclic diaziridines—a simple synthetic route (C) 1381
- 1,3,5-Trithia-2,4,6-triazapentalenyl—a stable sulfur-nitrogen radical (C) 920

NMR imaging, Biomedical magnetic resonance imaging. Principles, methodology and applications (B) 791

NMR spectroscopy, A sensitive spectroscopic probe for monitoring changes in the coordination sphere of titanium: eight-membered dioxatitanacycles and their organometallic derivatives (C) 66
- A synthetic molecular trefoil knot (C) 189
- Are lithiosulfones configurationally stable? (C) 1025, 1282
- Biomedical magnetic resonance imaging. Principles, methodology and applications (B) 791
- Biosynthetic studies on antibiotics (R) 146
- Complete identification of C-C connectivities by two-dimensional INADEQUATE NMR spectroscopy with composite pulses (C) 738
- High resolution solid state NMR of quadrupolar nuclei (AM) 1429
- Investigation of the tautomerism of ^{15}N-labeled hydroporphyrins by dynamic NMR spectroscopy (C) 76
- ^{15}N CPMAS NMR study of the structure and reactions of phthalocyaninato-polysiloxane and its precursors in the solid state (AM) 1743
- ^{15}N CPMAS NMR study of the structure of polyaniline (AM) 1741
- Nuclear magnetic resonance (B) 1764
- On the structure of eumelanins: identification of constitutional patterns by solid-state NMR spectroscopy (C) 741
- Pentacoordinated elements of the 4th main group with four organic residues (C) 918
- Synthesis of the novel ring systems 1,2,3,4-oxazadisiletidine and 1,3,4,2,5-dioxazadisilolidine (C) 54
- Structural characterization of non-oxide chalcogenide glasses by modern solid state NMR techniques (AM) 1723
- The 7-norbornadienyl cation: an NMR/IGLO validation of its ab initio structure (C) 1042
- Two-dimensional NMR methods for establishing molecular connectivity. A chemist's guide to experiment selection, performance and interpretation (B) 1071
- Visualization of chromatographic separations by NMR imaging (C) 1029

Nobel lecture, A structural basis of light energy and electron transfer in biology (Nobel lecture) (R) 848
- Drugs from emasculated hormones: the principle of syntopic antagonism (Nobel lecture) (R) 886
- Selective inhibitors of dihydrofolate reductase (Nobel lecture) (R) 879
- The photosynthetic reaction center from the purple bacterium *Rhodopseudomonas viridis* (Nobel lecture) (R) 829
- The purine path to chemotherapy (Nobel lecture) (R) 870

Noble-gas compounds, One pioneer or several pioneers? The discovery of noble-gas compounds (L) 636
- The acetonitrile(pentafluorophenyl)xenon(II) cation, $[MeCN-Xe-C_6F_5]^{\oplus}$: the first structural characterization of a xenon-carbon bond (C) 1506

Nonlinear optics, Polymer optical fibers and nonlinear optical device principles (AM) 1548

Nonplanar amides, Amides nonplanar solely by C-N bond rotation (C) 912

Norbornadienyl cation, The 7-norbornadienyl cation: an NMR/IGLO validation of its ab initio structure (C) 1042

Norbornanes, Si-promoted norbornyl-norpinyl rearrangements (C) 1667

Norbornenes, Double-bond geometry of norbornene: neutron diffraction measurement of a derivative at 15 K (C) 1239

Norpinanes, Si-promoted norbornyl-norpinyl rearrangements (C) 1667

Nuclear chemistry, Chemical aspects of fusion technology (R) 1
- Georg de Hevesy. 1885–1966. Festschrift (B) 1536

Nucleic acids, Sequence dependence of template-directed syntheses of hexadeoxynucleotide derivatives with 3′–5′ pyrophosphate linkage (C) 1235

Oligomerizations, Asymmetric oligomerization of propene and 1-butene with a zirconocene/alumoxane catalyst (C) 1216
- Hydrooligomerization of alkynes, a new catalytic reaction promoted by $[Co(py)_6]^{\oplus}$ in the presence of H_2 (C) 1009
- $[\{Ph_3PCH_2C(CF_3)_2O\}NiH(PCy_3)]$: support for a nickel hydride mechanism in ethene oligomerization (C) 1011
- Stereoregular oligomerization by repetitive Diels–Alder reactions (C) 1258

Optics, Conference report (AM) 1584
- Electronic structure and optical properties of semiconductors (B) 1441
- Organic materials for non-linear optics (B) 1760
- Photorefractive materials and their applications I: fundamental phenomena (B) 1440

- Polymer optical fibers and nonlinear optical device principles (AM) 1548
- Polymers with a high refractive index and low optical dispersion (AM) 1122
- Structural characterization of non-oxide chalcogenide glasses by modern solid state NMR techniques (AM) 1723
- Substituted silane polymers—a new look at some old materials (AM) 1733

Organic chemistry, Organic high pressure chemistry (B) 1535

Organic conductors, A new route to highly conducting polyenes (AM) 1745
- Binary alloys of 2,5-disubstituted DCNQI radical anion salts of copper and their electrical conductivity (C) 1245
- Functionalized conducting polymers—towards intelligent materials (AM) 513
- One-dimensional conductors (Springer series in solid state science 72) (B) 526
- Poly-[*N*,*N*-(1,4-divinylbenzene-β,β'-diyl)-4,4'-bipyridinium dibromide], a novel conducting viologen polymer (AM) 807
- Radical anion salts of naphthalenetetracarboxylic acid derivatives—a novel class of electrically conducting compounds (C) 483
- Spatially selective conducting patterns in transparent films derived from ladder type polymers (AM) 1569
- Superconductivity at 7.5 K and ambient pressure in polycrystalline pressed samples of β_p-(BEDT-TTF)$_2$I$_3$ (AM) 953

Organic synthesis, A synthetic molecular trefoil knot (C) 189
- Art in organic synthesis (B) 1539
- Nitrile oxides, nitrones and nitronates in organic synthesis. Novel strategies in synthesis (B) 227
- Organoselenium chemistry I. Functional group transformations (B) 227
- The dienolate of (*R*)-2-*tert*-butyl-6-methyl-1,3-dioxin-4(2*H*)-one—a chiral acetoacetic ester d^4-reagent (C) 472

Organometallic chemistry, An overview (B) 100
- Principles of organometallic chemistry (B) 934

Osmium compounds, Directed synthesis of trinuclear hydrocarbon-bridged complexes such as [(OC)$_5$ReCH$_2$CH$_2$-Os(CO)$_4$CH$_2$CH$_2$Re(CO)$_5$] (C) 1705
- Inter- and intramolecular photochemical C-H activation in matrices and in solution with (η^6-arene)(carbonyl)osmium complexes (C) 1690

Oxalic acid orthoamides, Photochemical formation of a stable oxalic acid orthoamide with a propellane structure (C) 338

Oxazolidines, 3-Arylsulfonyloxazolidines as chiral templates: asymmetric synthesis of 2-substituted 2-hydroxycyclohexanecarbaldehydes from 2-hydroxymethylenecyclohexanone (C) 67

Oxazolidinones, (4*RS*,5*R*)- and (4*RS*,5*S*)-4-Methoxy-5-methyloxazolidin-2-one derivatives of threonine—interesting chiral amidoalkylating reagents (C) 1399

Oxidations, Highly selective oxidations of Fe(CO)$_3$-cyclohexadiene complexes: synthesis of 4b,8a-dihydrocarbazol-3-ones and the first total synthesis of carbazomycin A (C) 223
- Spontaneous oxidation and in-situ polymerization of pyrrole in channels of the three-dimensional coordination polymer [(Me$_3$Sn)$_3$Fe^{III}(CN)$_6$]$_\infty$ (C) 1265

Oxygen compounds, Trigonal-bipyramidal lanthanoid complexes with interstitial oxygen atoms (C) 1033

Oxygen sensors, A new oxygen sensor based on the thermoelectric power of solid solutions of Nb_2O_5 and Bi_2O_3 (C) 75

Pagodane route, The pagodane route to dodecahedranes: chemistry and structure of bissecododecahedranes (C) 298
- The pagodane route to dodecahedranes: polyfunctionalized homologous dodecahedranes and dodecahedrenes (C) 310
- The pagodane route to dodecahedranes: polyfunctionalized pentagonal dodecahedranes and dodecahedrenes (C) 305
- The pagodane route to dodecahedranes: 4,9,14,19-tetrasubstituted [1.1.1.1]pagodanes by intramolecular functionalization (C) 303
- The pagodane route to dodecahedranes: total synthesis and chemistry of 4,9,14,19-tetrasubstituted [1.1.1.1]pagodanes (C) 300

Palladium compounds, A novel approach to ferroelectric liquid crystals: the first organotransition metal compound displaying this behavior (C) 1065
- Complexes with an η^2-μ_2-SiO bridge. Structure of the bimetallic complex [Fe(CO)$_3${μ-Si(OMe)$_2$-OMe}(μ-dppm)PdCl] (*Fe-Pd*) (C) 1361
- Indigo-metal complexes: synthesis and structure of Pd^{II} and Pt^{II} compounds containing the anions of indigo and octahydroindigo as mono- and bis-chelate ligands (C) 1529
- Pd clusters containing As and PPh$_3$ ligands: the structures of [Pd$_9$As$_6$(PPh$_3$)$_8$], [Pd$_2$(As$_2$)(PPh$_3$)$_4$], and [Pd$_{20}$As$_{12}$(PPh$_3$)$_{12}$] (C) 1665

Parat, PARAT. Index of acronyms and abbreviations in electrical and electronic engineering (B) 1442

Peptides, 2'-Aminomethylbiphenyl-2-carboxylic acid as component of a cyclopeptide; crystal structure and conformation in solution (C) 486
- Correlation of the dynamic behavior of *n*-alkyl ligands of the stationary phase with the retention times of paracelsin peptides in reserved phase HPLC (C) 327
- Pep5: structure elucidation of a large lantibiotic (C) 616
- Synthesis of (*S*,*S*)-diisotyrosine and its incorporation in an ansa tripeptide (C) 929

Pharmaceuticals, Arzneimittel—Fortschritte 1972 bis 1985 (B) 102
- Controlled release of drugs: polymers and aggregate systems (B) 1137
- Drugs from emasculated hormones: the principle of syntopic antagonism (Nobel lecture) (R) 886
- Selective inhibitors of dihydrofolate reductase (Nobel lecture) (R) 879
- Synthesis and pharmacological properties of a novel cardioactive steroid (C) 1359
- The purine path to chemotherapy (Nobel lecture) (R) 870

Phenalenol, 1-Phenalenol: isolation and disproportionation (C) 1268

Phosphaalkenes, A new route to phosphaalkenes (C) 740
- Phosphaalkenes from monochlorophosphanes and alkylidenetriphenyl Phosphoranes (C) 1695

Phosphaalkynes, A stable amino-substituted phosphaalkyne (C) 53
- Formation of a phosphaferracyclopentadiene ring by coupling of a phosphaalkyne with two fluoromethylidyne ligands (C) 321
- Reactions of mono- and dinuclear metal-alkylidyne complexes with phosphaalkynes: C≡P and C≡Mo metathesis (C) 210
- Reductive dimerization of a phosphaalkyne with complexation to samarium (C) 445
- Tetra-*tert*-butyltetraphosphacubane: the first thermal cyclooligomerization of a phosphaalkyne (C) 1013

Phosphazenes, Synthesis and analysis of polymetallaphosphazenes (C) 493

Phospholipids, Calorimetric studies of biopolymers and aggregates of phospholipids (R) 981
- Chain-substituted lipids as substrates for phospholipase A$_2$ (C) 1218

Phosphorus compounds, A tetraborylphosphonium ion with a spiroheterocyclic structure (C) 217
- [Bis(diisopropylamino)phosphino]trimetylsilylcarbene: a stable nucleophilic carbene (C) 621
- tBu$_2$P-P=PBrtBu$_2$ · LiBr and formation of tBu$_2$P-P (C) 315
- (tBuSiP)$_4$—the first silaphosphacubane (C) 339, 502
- 2-Chloro-2*H*-phosphirene/1-chloro-1*H*-phosphirene isomerization by [1,3]-chlorine shift (C) 225
- Dictionary of organophosphorus compounds (B) 1716
- Generation and ionization pattern of the iso(valence)electronic compounds ClP(=O)$_2$ and ClP(=S)$_2$ (C) 1373
- Generation, stereochemistry, and molecular dynamics of a 1,3-bis(phosphonio)propenide cation (C) 1700
- K$_4$P$_3$, a compound containing the radical anion $P_3^{4\ominus}$ (C) 56
- [P$_4$Aryl$_6$][Me$_3$SnF$_2$]$_2$ (Aryl = 2,6-(MeO)$_2$C$_6$H$_3$): an unusual ion pair consisting of a planar 2,4-diphospha-1,3-diphosphoniacyclobutane dication and the difluorotrimethylstannate anion (C) 1507
- Phosphaalkenes from monochlorophosphanes and alkylidenetriphenyl Phosphoranes (C) 1695
- Phosphanorbornadienes as ligands in the transition metal-catalyzed synthesis of fine chemicals (C) 500
- Phosphonioboratoacetylenes: C$_2$ stabilized by donor and acceptor molecules (C) 1219
- Polycyclic polyphosphorus hydrocarbons (C) 900
- Synthesis and crystal structure of a phospholyl anion (C) 1367
- Synthesis and structure of a 1*H*-Diphosphirene (C) 1673
- Synthesis, characterization, and complexation of an unusual P$_2$Si$_2$ bicyclobutane with butterfly-structure: 2,2,4,4-tetramesityl-1,3-diphospha-2,4-disilabicyclo[1.1.0]butane (C) 1038
- Synthesis, structure, and reactivity of a 1,3-diphospha-2-silaallyl anion (C) 751
- Synthesis, structure, and reactivity of diphosphenes having a *cis*-configuration (C) 215
- Water elimination from phosphorus-oxygen compounds: the formation of 2-phosphapropene by thermolysis of dimethylphosphane oxide (C) 911

Phosphorus homocycles, P$_6$(C$_5$Me$_5$)$_2$, a tricyclic polyphosphane (C) 600
- P$_{14}$*i*Pr$_4$—the first hexacyclic organophosphane (C) 1231
- Sodium pentaphosphacyclopentadienide (NaP$_5$) and the pentaphosphacyclopentadienide ion ($P_5^\ominus$): theoretical predictions of molecular structures, infrared and Raman spectra (C) 485
- Tetra-*tert*-butyltetraphosphacubane:

the first thermal cyclooligomerization of a phosphaalkyne (C) 1013
- Tetraphosphacyclobutadiene as complex ligand (C) 1355
Photochemistry, Efficient photoinduced intramolecular energy transfer in an oblique bis-porphyrin system (C) 593
- Ethynol: photochemical generation in an argon matrix, IR spectrum, and photoisomerization to ketene (C) 181
- Formation of 2,4,4-trimethylthiete by photodecarbonylation of 3,3,5-trimethyl-2(3*H*)-thiophenone (C) 1499
- Inter- and intramolecular photochemical C-H activation in matrices and in solution with (η^6-arene)(carbonyl)osmium complexes (C) 1690
- Light-sensitive molecular building blocks with electron transfer activity: synthesis and properties of a photochemically switchable, dicyanovinyl-substituted furan (C) 1494
- Photocycloadditions of benzvalene (C) 601
- Photochemical formation of a stable oxalic acid orthoamide with a propellane structure (C) 338
- Regiochemistry of the intramolecular [2+2]-photocycloaddition of cyclohexenone to vinyl ethers (C) 925
- The beginnings of organic photochemistry (R) 1193
Photochromism, Perspectives in photochromism: a novel system based on the 1,5-electrocyclization of heteroanalogous pentadienyl anions (R) 413
Photoelectron spectroscopy, all-*cis*-1,4,7,10-cyclododecatetraene—X-ray structure analysis and photoelectron spectrum (C) 1379
- Diisocyanogen or isocyanogen? (C) 761
- Fundamentals of silicon chemistry: molecular states of silicon-containing compounds (R) 1627
- Generation and ionization pattern of the iso(valence)electronic compounds $ClP(=O)_2$ and $ClP(=S)_2$ (C) 1373
- Methylboron oxide, $H_3C-B\equiv O$ (C) 88
- Structure, deformation electron densities, photoelectron spectra, and reactivity of 3,4-dihydro-1*H*-cyclobuta[*a*]cyclopropa[*d*]benzene (C) 206
- The first PE-spectroscopic investigations of lithium, sodium, and potassium *tert*-butoxide (C) 895
Photography, Image enhancement—chemical, digital, visual (R) 1601
Photosensitizers, Water-soluble porphyrin diglycosides with photosensitizing properties (C) 1519
Photosynthesis, A structural basis of light energy and electron transfer in biology (Nobel lecture) (R) 848
- Synthesis, structure and magnetic properties of a dinuclear manganese(II) complex with one μ-aqua and two μ-carboxylato bridges (C) 1365
- The photosynthetic reaction center from the purple bacterium *Rhodopseudomonas viridis* (Nobel lecture) (R) 829
Phthalocyaninatopolysiloxane, ^{15}NCPMAS NMR study of the structure and reactions of phthalocyaninatopolysiloxane and its precursors in the solid state (AM) 1743
Physical chemistry, Angular momentum: understanding spatial aspects in chemistry and physics (B) 932
Pigments, Industrielle Organische Pigmente. Herstellung, Eigenschaften, Anwendung (B) 1073
Platinum, A joint structural characterization of colloidal platinum by EXAFS and high-resolution electron microscopy (C) 590
Platinum compounds, A novel type of anionic cluster containing a Pt_4Ag_2 core (C) 748
- Agostic-type gold ligand and incipient μ_3-PPh_2 coordination in the $Au_2Pt_2P_6$ "hammock" skeleton of the cluster $[Au_2Pt_2(\mu\text{-}PPh_2)_2(PPh_3)_4][PF_6]_2$ (C) 923
- Complexation of a novel organoytterbium(II) ligand with dimethylplatinum(II): crystal structure of the resulting heterobimetallic complex (C) 1370
- Coupling of epoxides to Pt^{II}-complexes with carbon dioxide and the structure of a cyclic metallacarbonate (C) 767
- Indigo-metal complexes: synthesis and structure of Pd^{II} and Pt^{II} compounds containing the anions of indigo and octahydroindigo as mono- and bis-chelate ligands (C) 1529
- Platinum complexes of the anions $Se_2N_2^{2\ominus}$ and $Se_2N_2H^{\ominus}$; X-ray structure analysis of $[Pt(Se_2N_2H)(PMe_2Ph)_2]Cl$ (C) 1047
- $Pt_{309}Phen^{*}_{36}O_{30\pm10}$, a four-shell platinum cluster (C) 778
Polyacetylenes, Highly conjugated, substituted polyacetylenes via the ring-opening metathesis polymerization of substituted cyclooctatetraenes (AM) 1571
Polyaniline, ^{15}N CPMAS NMR study of the structure of polyaniline (AM) 1741
Polycycles, A polyhedral oligogermane: 4,8-dibromo-octa-*tert*-butyltetracyclo[3.3.0.0^{2,7}.0^{3,6}]octagermane (C) 198
- Diels-Alder adducts on the *b* side of naphthalene: rapid cycloreversion of *o*-quinodimethanes (C) 1353
- 4,6-Dimethylenetricyclo[3.3.0.0^{3,7}]octane-2-one and 2,4,6-trimethylenetricyclo[3.3.0.0^{3,7}]octane (C) 1525
- From tetraspiranes to bispropellanes (C) 94
- From the bicyclo[3.3.0]octane framework to multiply bridged [12]annulenes and semibullvalenes (C) 1343
- $[(Me_3Si)_2CHGe]_6$, the first hexagermaprismane (C) 55
- Polycyclic polyphosphorus hydrocarbons (C) 900
- Synthesis of a rigid electron-donor/acceptor compound—evidence for intramolecular charge separation (C) 619
- Tri-*tert*-butyl(trimethylsilyl)tricyclo-[1.1.0.0^{2,4}]butane—a second tetrahedrane derivative (C) 1050
Polymerization, Encapsulation of polypyrrole chains in zeolite channels (C) 1692
- Highly conjugated, substituted polyacetylenes via the ring-opening metathesis polymerization of substituted cyclooctatetraenes (AM) 1571
Polymers, A new route to highly conducting polyenes (AM) 1745
- A polymeric technetium compound of the composition $[Tc_2O_3(C_5Me_5)]_n$ (C) 1055
- A structure for the H-bonded complex of nylon-66 with perfluoroglutaric acid (C) 466
- Analysis of polymers. An introduction (B) 1595
- Can polystyrene be optically active? (C) 196
- Challenges in materials for health care applications (AM) 662
- Dichroic Dyes and liquid crystalline side chain polymers (AM) 940
- Double stereodifferentiation in the formation of isotactic polypropylene at chiral $(C_5H_4CHMePh)_2ZrCl_2$/methylalumoxane catalysts (C) 628
- Double-stranded molecules: a [6]beltene derivative and the corresponding open-chain polymer (C) 1680
- Functionalized conducting polymers—towards intelligent materials (AM) 513
- Induction of liquid crystalline phases: formation of discotic systems by doping amorphous polymers with electron acceptors (C) 914
- Inorganic and organometallic polymers (ACS symposium series 360) (B) 528
- Inverse gas chromatography. Characterization of polymers and other materials (B) 1761
- Liquid crystalline elastomers (AM) 1407
- Materials processing—a key factor (AM) 644
- Microstructure of a discotic polymer as revealed by electron diffraction and high-resolution imaging (C) 323
- ^{15}N CPMAS NMR study of the structure of polyaniline (AM) 1741
- Networks composed of rigid rod polymers (AM) 1130
- 2-Pentyltricyclo[1.1.1.0^{1,3}]pentane and its homopolymer, a soluble poly([1.1.1]-propellane) (C) 456
- Poly-[*N,N*-(1,4-divinylbenzene-β,β'-diyl)-4,4'-bipyridinium dibromide], a novel conducting viologen polymer (AM) 807
- Polymer modified textile materials (B) 384
- Polymer optical fibers and nonlinear optical device principles (AM) 1548
Polymer science, in the next decade, an international symposium honoring Hermann F. Mark on his 90th birthday (B) 382
- Polymers as advanced materials (AM) 504
- Polymers with a high refractive index and low optical dispersion (AM) 1122
- Rubberlike elasticity—a molecular primer (B) 673
- Side chain liquid crystal polymers (B) 1140
- Siloxane copolymers with laterally and terminally attached mesogenic side chains (AM) 1120
- Spatially selective conducting patterns in transparent films derived from ladder type polymers (AM) 1569
- Stiff-chain polymers—structure, phase behavior, and properties (R) 253
- Substituted silane polymers—a new look at some old materials (AM) 1733
- Synthesis and separations using functional polymers (B) 383
- Synthesis and analysis of polymetallaphosphazenes (C) 493
- The Kevlar story—an advanced materials case study (AM) 649
Polypyrroles, Encapsulation of polypyrrole chains in zeolite channels (C) 1692
- Spontaneous oxidation and in-situ polymerization of pyrrole in channels of the three-dimensional coordination polymer $[(Me_3Sn)_3Fe^{III}(CN)_6]_\infty$ (C) 1265
Porphycenes, A pyrrolophanediene-porphycene redox system (C) 1655
Porphyrins, A simple synthesis of dioxoisobacteriochlorins from hematoporphyrin (C) 480
- Amide bond scission via bifunctional activation with bimetallic porphyrin systems with two different metal centers (C) 921
- Biomimetic synthesis of an inverted porphyrinoid with peripheral N atoms (C) 1243

- Di(1-pyridinio)- and di(1-bipyridindiio)dihydrodibenzotetraaza[14]annulenes (C) 1060
- Di(4-pyridinio)-, di(2-benzothiazolio)-, di(2[1,3-dithiolylio])- and diformyltetraaza[14]annulenes and tetraaza[14]annulenylene-homologous tetrathiafulvalenes (C) 1063
- Efficient photoinduced intramolecular energy transfer in an oblique bis-porphyrin system (C) 593
- Highly reduced porphyrins (C) 604
- Investigation of the tautomerism of ^{15}N-labeled hydroporphyrins by dynamic NMR spectroscopy (C) 76
- Oxoiron porphyrin species with high-valent iron: formation by solvent-dependent protonation of a peroxoiron(III) porphyrinate derivative (C) 1709
- The thiophene analogue of porphyrin: tetrathiaporphyrin dication (C) 1651
- Water-soluble porphyrin diglycosides with photosensitizing properties (C) 1519

Powder metallurgy, Conference report (AM) 1750

Prismanes, $[(Me_3Si)_2CHGe]_6$, the first hexagermaprismane (C) 55

Processing, Aerospace materials research opportunities (AM) 655
- Conference report (AM) 1750
- High-performance silicon nitride materials (AM) 1560
- Materials processing—a key factor (AM) 644
- The Kevlar story—an advanced materials case study (AM) 649

Propellanes, From tetraspiranes to bispropellanes (C) 94
- 2-Pentyltricyclo[1.1.1.$0^{1,3}$]pentane and its homopolymer, a soluble poly([1.1.1]-propellane) (C) 456
- Photochemical formation of a stable oxalic acid orthoamide with a propellane structure (C) 338

Proteins, A chemical approach to protein design—template-assembled synthetic proteins (TASP) (R) 535
- Laser desorption/ionization mass spectrometry of proteins of mass 100000 to 250000 Dalton (C) 760
- Retention of configuration in the non-Darwinian evolution of cytochrome c (C) 71
- The active sites in manganese-containing metalloproteins and inorganic model complexes (A) 1153

Proton sponges, Benzo[1,2-*h*:4,3-*h'*]diquinoline ("1,14-diaza[5]helicene"): synthesis, structure, and properties (C) 86
- Structures of quino[7,8-*h*]quinoline and quino[8,7-*h*]quinoline (C) 84

Publications, The technical writer's handbook (B) 1717

Publishing, The nature of materials science publishing (AM) 1721

Purple bacterium, The photosynthetic reaction center from the purple bacterium *Rhodopseudomonas viridis* (Nobel lecture) (R) 829

Pyrenes, Selective 1:3 coupling of norbornene and iodobenzene: a facile synthesis of benzo[*e*]pyrenes with annelated cycloaliphatic moieties (C) 1037

Pyrones, pyrones as substrates for palladium-catalyzed [4+3] cycloadditions (C) 213

Pyrrolopyrroles, The influence of packing effects on the solid-state fluorescence of diketopyrrolopyrroles (C) 478

Quinodiimines, Binary alloys of 2,5-disubstituted DCNQI radical anion salts of copper and their electrical conductivity (C) 1245

Quinodimethanes, Diels–Alder adducts on the *b* side of naphthalene: rapid cycloreversion of *o*-quinodimethanes (C) 1353
- *p*-Quinodimethane analogues of tetrathiafulvalene (C) 1052

Quinones, Chemical modifications of biopolymers by quinones and quinone methides (R) 555
- On the structure of eumelanins: identification of constitutional patterns by solid-state NMR spectroscopy (C) 741
- The chemistry of the quinonoid compounds. Vol. 2. parts 1 and 2 (B) 933

Quinoquinoline, Structures of quino[7,8-*h*]quinoline and quino[8,7-*h*]quinoline (C) 84

Radialenes, An electron-rich [4]radialene (C) 1663

Radical ions, Azonia derivates of arenes: synthesis and properties of 10c-azoniafluoranthene (C) 588
- Binary alloys of 2,5-disubstituted DCNQI radical anion salts of copper and their electrical conductivity (C) 1245
- Cryptophane radical cations as components of three-dimensional charge-transfer salts (C) 1249
- [4+2]-cycloadditions with 1,4-bis(*N,N*-dimethylamino)-1,3-dienes: stereochemical studies and observation of radical ions (C) 1713
- Dithia dications from cyclic and acyclic precursors by gas-phase oxidation ("charge stripping") of 3e/2c-radical cations (C) 1275
- 17- to 19-Electron pentamethylcyclopentadienyl iron dithiocarbamate complexes. Formation of a Cp^*Fe^{IV} complex (C) 460
- K_4P_3, a compound containing the radical anion $P_3^{4\ominus}$ (C) 56
- Organic dications: gas phase experiments and theory in concert (A) 1321
- Radical anion salts of naphthalenetetracarboxylic acid derivatives—a novel class of electrically conducting compounds (C) 483
- Radical tri- and pentaanions of benzenedi- and benzenetriglyoxylate thioesters (C) 906
- The radical cation of *N,N'*-tetramethylene-*syn*-1,6:8,13-diimino[14]annulene. An experimental study of the N-N three-electron σ bond (C) 902
- Towards tribenzoacepentalene: tribenzotriquinacene, dihydrotribenzoacepentalenediide, and the tribenzoacepentalene radical anion (C) 595

Radicals, 2,3-Dihydro-1*H*-1,2,4-triazol-1-yls, a novel group of stable radicals (C) 491
- Electron nuclear double resonance spectroscopy of radicals in solution (B) 792
- Energy wells of diradicals; 4-methylene-1,3-cyclopentanediyl (C) 1056
- On the formation of "free radicals" from alkylcobalt complexes (C) 325
- Stereo- and regiospecific 6-*endo*-*trig*-cyclization of aryl radicals, an entry to novel progesterone-antagonists of the androstane series (C) 773
- The stereoselectivity of intermolecular free radical reactions (R) 969
- 1,3,5-Trithia-2,4,6-triazapentalenyl—a stable sulfur-nitrogen radical (C) 920
- Well-resolved ESR spectra of arenecarboxyl radicals in solution (C) 183

Radioactivity, Complexation of cesium 137 by the cap pigments of the bay boletus (*Xerocomus badius*) (C) 453

Radiochemistry, Chemical aspects of fusion technology (R) 1
- Georg de Hevesy. 1885–1966. Festschrift (B) 1536

Reaction mechanisms, A compound containing hexacoordinated silicon—a model for nucleophilic attack on anionic, pentacoordinated silicon species? (C) 489
- [4+2]-cycloadditions with 1,4-bis(*N,N*-dimethylamino)-1,3-dienes: stereochemical studies and observation of radical ions (C) 1713
- Does cyanoacetylene dimerize thermally to 1,3-cyclobutadiene-1,2-dicarbonitrile? (C) 1279
- Energy wells of diradicals; 4-methylene-1,3-cyclopentanediyl (C) 1056
- Isolation of a zwitterion in a Diels–Alder reaction with inverse electron demand (C) 1267
- Mechanism of the hetero-Diels–Alder reaction of oxadienes and alkenes: calculation of the acrolein/ethene system (C) 1371
- Probing changes in the structure and performance of a lithium nickel oxide catalyst by in situ X-ray diffraction during the high-temperature oxidative coupling of methane (AM) 808
- Reaction mechanisms in heterogeneous catalysis; C-H activation as a case study (R) 135
- Regiochemistry of the intramolecular [2+2]-photocycloaddition of cyclohexenone to vinyl ethers (C) 925
- Revision and modification of the traditional mechanism of C-H/C-C activation by "naked" transition-metal ions (C) 607
- The stereoselectivity of intermolecular free radical reactions (R) 969
- The mechanism of the Dötz reaction: chromacyclobutenes by alkyne-carbene coupling? (C) 908
- Water elimination from phosphorusoxygen compounds: the formation of 2-phosphapropene by thermolysis of dimethylphosphane oxide (C) 911

Reagents, A new coordinating chiral lithium amide (C) 1044
- A new synthesis of key intermediates for the preparation of 5,6-DiHETE and lipoxin A_4 (C) 755
- 2-*O*-benzylglyceraldehyde: a synthetic building block available in both enantiomeric forms and configurationally stable owing to rapid oligomerization (C) 469
- Chiral building blocks for the synthesis of triquinane sesquiterpenes: derivatives of 2-methylbicyclo[3.3.0]octan-3-ol from catalpol (C) 447
- $[H_2C(CH_2)_5NLi]_6$, the first cyclized lithium amide ladder: synthesis and structure of hexamethyleneimidolithium (C) 1241
- (4*RS*,5*R*)- and (4*RS*,5*S*)-4-Methoxy-5-methyloxazolidin-2-one derivatives of threonine—interesting chiral amidoalkylating reagents (C) 1399
- Name reactions and reagents in organic synthesis (B) 1538
- Synthesis and structure of $[(C_5H_5)_2TiS_4AsCH_3]$—a new reagent for the synthesis of sulfur-rich heterocycles (C) 1269
- The dienolate of (*R*)-2-*tert*-butyl-6-methyl-1,3-dioxin-4(2*H*)-one—a chiral acetoacetic ester d^4-reagent (C) 472

Rearrangements, From 2,5-dihydropyrazines to 2*H*-1,4-diazepines and from benzodihydroarenes to benzocyclohep-

tene derivatives, structural variants of the antidepressant protriptyline (C) 613
- From tetraspiranes to bispropellanes (C) 94
- Insertion of $Cr(CO)_3$ into $As_7^{3\ominus}$ to form $[As_7Cr(CO)_3]^{3\ominus}$: an inorganic nortricyclane-to-norbornadiene conversion (C) 1032
- Iron-mediated diastereoselectivespiroannelation to the spiro[1,2,3,4tetrahydroquinoline-4,1'-cyclohexane] system and a novel rearrangement to 2,3-dihydroindole derivatives (C) 1678
- Si-promoted norbornyl-norpinyl rearrangements (C) 1667

Redox systems, A pyrrolophanediene-porphycene redox system (C) 1655
- Stack-type redox systems: synthesis via repeated carbanion alkylation and electron transfer studies (C) 1531

Reductions, Enantioselective reduction of α,β-unsaturated carboxylates with $NaBH_4$ and catalytic amounts of chiral cobalt semicorrin complexes (C) 60
- Highly reduced porphyrins (C) 604
- $LiBH_4(NaBH_4)/Me_3SiCl$, an unusually strong and versatile reducing agent (C) 218
- Metal-induced reduction of sulfur dioxide to sulfur monoxide and sulfur (C) 1342
- $NaBH_4$ reduction of ketones in the solid state (C) 320
- Self-reduction of $[Ph_4P][Nb(SCH_2CH_2CH_2S)_3]$ with formation of a Nb_2^{IV} complex (C) 98

Rhenium compounds, Alkyl and alkylidyne complexes of rhenium (C) 334
- Directed synthesis of trinuclear hydrocarbon-bridged complexes such as $[(OC)_5ReCH_2CH_2Os(CO)_4CH_2CH_2Re(CO)_5]$ (C) 1705

Rhodium compounds, Amide bond scission via bifunctional activation with bimetallic porphyrin systems with two different metal centers (C) 921
- One-dimensional metal chains in a chiral environment—the crystal structure of helical bis(dicarbonylrhodium(I))-3,3'-hexafluoroglutarylbis-(1*R*)-camphorate (C) 1019
- Selective hydrogenation of esters to alcohols with a catalyst prepared from Rh_2O_3, $Sn(n\text{-}C_4H_9)_4$, and SiO_2: evidence for site isolation (C) 347

Rotation, Angular momentum: understanding spatial aspects in chemistry and physics (B) 932

Ruthenium compounds, The novel complex $[LRu^{IV}(\mu\text{-}O)_3Ru^{IV}L][PF_6]_2 \cdot H_2O$—a molecular section of the structures of $BaRu^{IV}O_3$(high-pressure phase) and $Ba_{5/6}Sr_{1/6}Ru^{IV}O_3$ (C) 763

Sandwich complexes, $(C_4Me_4NBH_3)_2Fe$—a metal complex isosteric with decamethylferrocene with characteristic metallocene disorder (C) 342
- Hexaarsabenzene as complex ligand (C) 212
- Pronounced anion dependence of valence detrapping temperature in mixed-valence 1',1'''-disubstituted biferrocenium salts (C) 1388
- Reaction of decamethylsilicocene with sulfur, selenium, and tellurium: from a p_π-p_π system to new heterocycles (C) 1518
- Tetraphosphacyclobutadiene as complex ligand (C) 1355
- The 30-electron rule for triple-decker complexes—vanadium, niobium and tantalum complexes as illustrative examples (C) 319
- Triple-decker complexes as intermediates in ring-ligand transfers (C) 737

Scanning Tunneling Microscopy, Imaging organic molecules with the scanning tunneling microscope (AM) 1127
- Surface chemistry with the scanning tunneling microscope (AM) 117

Selenium compounds, bromoselenates(II,IV), a novel type of mixed valence compounds (C) 187
- Counterion dependent structural diversity in silver polyselenides; structures of the new complex anions $[Ag(Se_4)]_4^{4\ominus}$, $[Ag(Se_5)]_n^{n\ominus}$ and $[Ag_4(Se_4)_3]^{2\ominus}$ (C) 1513
- Organoselenium chemistry I. Functional group transformations (B) 227
- Platinum complexes of the anions $Se_2N_2^{2\ominus}$ and $Se_2N_2H^{\ominus}$; X-ray structure analysis of $[Pt(Se_2N_2H)(PMe_2Ph)_2]Cl$ (C) 1047
- Selenium-catalyzed synthesis of *S*-alkyl thiocarbamates from amines, carbon monoxide, sulfur, and alkyl halides (C) 452
- Ta_2Se: a tantalum-rich selenide with a new layer structure (C) 1660
- The thiophene analogue of porphyrin: tetrathiaporphyrin dication (C) 1651

Semibullvalenes, From the bicyclo[3.3.0]-octane framework to multiply bridged [12]annulenes and semibullvalenes (C) 1343

Semiconductors, Electronic structure and optical properties of semiconductors (B) 1441
- Low temperature deposition of a CaF_2 insulator layer on GaAs (AM) 1581
- Materials issues in electronic systems (AM) 640
- Metal organic chemical vapor deposition (MOCVD) perspectives and prospects (AM) 1110
- Optical nonlinearities and instabilities in semiconductors (B) 672
- Semiconductor electrodes (B) 386
- Silicon-nitride in electronics (B) 1441
- Single-source III/V precursors: a new approach to gallium arsenide and related semiconductors (A) 1208
- Structural characterization of non-oxide chalcogenide glasses by modern solid state NMR techniques (AM) 1723
- Tailoring semiconductor crystals to atomic dimensions (AM) 1098

Semi-empirical calculations, Generation and ionization pattern of the iso(valence)electronic compounds $ClP(=O)_2$ and $ClP(=S)_2$ (C) 1373
- Mechanism of the hetero-Diels–Alder reaction of oxadienes and alkenes: calculation of the acrolein/ethene system (C) 1371
- Tetrakis(dimethylamino)ethylene dication: two CC singly bonded and almost perpendicularly twisted $((CH_3)_2N)_2C^{\oplus}$ carbenium ions (C) 1684
- Tetraphenylethylenedisodium: the band structure of the CC singly bonded, twisted $(C_6H_5)_2C^{\ominus}$ carbanions (C) 1685

Sensors, A new oxygen sensor based on the thermoelectric power of solid solutions of Nb_2O_5 and Bi_2O_3 (C) 75
- Advanced zeolite materials science (AM) 359
- Functionalized conducting polymers—towards intelligent materials (AM) 513
- Polymer benzo[15]crown-5 complexes as sensor materials for solvent vapors—aromatic halogenated hydrocarbons and polar solvents (AM) 813
- Structure-directed synthesis of new organic materials (AM) 1103

Separations, Synthesis and separations using functional polymers (B) 383

Sesquiterpenes, Chiral building blocks for the synthesis of triquinane sesquiterpenes: derivatives of 2-methylbicyclo[3.3.0]octan-3-ol from catalpol (C) 447

Silanediyls, Disilene *versus* silanediyl ("silylene") additions to CN and NCO bonds (C) 95, 228

Silicon compounds, A compound containing hexacoordinated silicon—a model for nucleophilic attack on anionic, pentacoordinated silicon species? (C) 489
- A silicogermanate with a Si:Ge ratio ≥ 2—an MFI zeolite of novel composition (C) 81
- An electron-rich [4]radialene (C) 1663
- $(t\text{BuSiP})_4$—the first silaphosphacubane (C) 339, 502
- *catena*-Poly[bis-μ-(*o*-oxyphenyleneoxy)-silicon]: crystal structure of the orthosilicate of catechol (C) 623
- Dimethyldioxasilirane (C) 898
- Disilene *versus* silanediyl ("silylene") additions to CN and NCO bonds (C) 95, 228
- Formation and reactivity of silicon-sulfur and silicon-selenium double bonds. The first X-ray structure of a silanethione (C) 1016
- Fundamentals of silicon chemistry: molecular states of silicon-containing compounds (R) 1627
- 1,2,9,10,17,18-Hexasila[2.2.2](1,3,5)cyclophane, a cage-like phane containing three Si-Si units (C) 757
- High-performance silicon nitride materials (AM) 1560
- Identification of $[(OC)_4Fe{=}Si(CH_3)_2 \cdot \{(H_3C)_2N\}_3PO]$ as intermediate in the formation of polysilanes from $(H_3C)_2SiCl_2$ and $[Na_2Fe(CO)_4]$ (C) 203
- ^{15}N CPMAS NMR study of the structure and reactions of phthalocyaninato-polysiloxane and its precursors in the solid state (AM) 1743
- Siloxane copolymers with laterally and terminally attached mesogenic side chains (AM) 1120
- Substituted silane polymers—a new look at some old materials (AM) 1733
- Surprising reactions of decamethylsilicocene with π-systems of the type $X{=}C{=}Y$ (C) 762
- Synthesis, characterization, and complexation of an unusual P_2Si_2 bicyclobutane with butterfly-structure: 2,2,4,4-tetramesityl-1,3-diphospha-2,4-disilabicyclo[1.1.0]butane (C) 1038
- Synthesis of the novel ring systems 1,2,3,4-oxazadisiletidine and 1,3,4,2,5-dioxazadisilolidine (C) 54

Silver compounds, A chiral Ag^I-coordination polymer with a polydentate chiral ligand; crystal structure of the 1:1 complex of CF_3SO_3Ag and *N*-[*N*-(5-Methylthenylidene)-L-methionyl]histamine (C) 1698
- A novel type of anionic cluster containing a Pt_4Ag_2 core (C) 748
- Amide bond scission via bifunctional activation with bimetallic porphyrin systems with two different metal centers (C) 921
- Counterion dependent structural diversity in silver polyselenides; structures of the new complex anions $[Ag(Se_4)]_4^{4\ominus}$, $[Ag(Se_5)]_n^{n\ominus}$ and $[Ag_4(Se_4)_3]^{2\ominus}$ (C) 1513
- Stabilization of niobium(0) and tantalum(0) in mixed metal clusters containing silver atoms (C) 471

Sol-gel processing, Conference report (AM) 1437

Solid solutions, A new oxygen sensor based on the thermoelectric power of solid solutions of Nb_2O_5 and Bi_2O_3 (C) 75
– Symmetry reduction in solid solutions: a new method for materials design (AM) 377
Solid state chemistry, Conference report (AM) 1436
– Electrons in solids: an introductory survey (B) 671
– High resolution solid state NMR of quadrupolar nuclei (AM) 1429
– $K_4Al_2Nb_{11}O_{20}F$—the missing link in cluster condensation (C) 1662
– LiCaN and Li_4SrN_2, derivatives of the fluorite and lithium nitride structures (C) 1702
– $NaBH_4$ reduction of ketones in the solid state (C) 320
– Solids and surfaces: a chemist's view of bonding in extended structures (B) 1070
– Ta_2Se: a tantalum-rich selenide with a new layer structure (C) 1660
– The crystal chemistry of high-temperature oxide superconductors and materials with related structures (R) 1472
– The influence of packing effects on the solid-state fluorescence of diketopyrrolopyrroles (C) 478
Solid state physics, Gauge theory—a new outlook on solid state dynamics (AM) 1124
Solutions, ions in solution: basic principles of chemical interactions (B) 103
Solvent effects, Solvents and solvent effects in organic chemistry (B) 104
Spectroscopy, spectroscopy of surfaces (B) 963
– Theory and methods of calculation of molecular spectra (B) 1281
Spiro compounds, A tetraborylphosphonium ion with a spiroheterocyclic structure (C) 217
– From tetraspiranes to bispropellanes (C) 94
– Iron-mediated diastereoselective spiroannelation to the spiro[1,2,3,4tetrahydroquinoline-4,1′-cyclohexane] system and a novel rearrangement to 2,3-dihydroindole derivatives (C) 1678
Stereochemistry, Retention of configuration in the non-Darwinian evolution of cytochrome c (C) 71
– Stereochemical applications of gas-phase electron diffraction. Part A and B (B) 1534
Stereoselectivity, The stereoselectivity of intermolecular free radical reactions (R) 969
Sterepolide, The effect of acetylene substituents on a Pd^{II}-catalyzed cycloisomerization. Total synthesis of (−)-sterepolide and assignment of absolute stereochemistry (C) 1502
Steroids, Side-chain homologues of 20-hydroxyecdysone: synthesis, configurational assignment, and biochemical characterization (C) 1515
– Stereo- and regiospecific 6-*endo*-*trig*-cyclization of aryl radicals, an entry to novel progesterone-antagonists of the androstane series (C) 773
– Synthesis and pharmacological properties of a novel cardioactive steroid (C) 1359
Sterols, Sterol biosynthesis inhibitors. Pharmaceutical and agrochemical aspects (B) 1539
Stiff-chain polymers, 2-Pentyltricyclo-[1.1.1.$0^{1,3}$]pentane and its homopolymer, a soluble poly([1.1.1]propellane) (C) 456
– Stiff-chain polymers—structure, phase behavior, and properties (R) 253
Stilbenes, Bis-stilbene systems: reduction to the tetraanions (C) 904
Strained rings, Azaoctabisvalenes (C) 1345
– Bridged *cis*-Tris-σ-homobenzenes: Heterodiademanes (C) 1351
– 4,6-Dimethylenetricyclo[3.3.0.$0^{3,7}$]octane-2-one and 2,4,6-trimethylenetricyclo[3.3.0.$0^{3,7}$]octane (C) 1525
– Shortened C-C bonds in coupled bicyclo[1.1.0]butanes (C) 473
– Stabilized *cis*-Tris-σ-homobenzenes: syntheses, [$\sigma2+\sigma2+\sigma2$] cycloreversions (C) 1348
– Structure, deformation electron densities, photoelectron spectra, and reactivity of 3,4-dihydro-1*H*-cyclobuta[*a*]cyclopropa[*d*]benzene (C) 206
– Synthesis and structure of a 1*H*-Diphosphirene (C) 1673
– Synthesis, characterization, and complexation of an unusual P_2Si_2 bicyclobutane with butterfly-structure: 2,2,4,4-tetramesityl-1,3-diphospha-2,4-disilabicyclo[1.1.0]butane (C) 1038
– Tri-*tert*-butyl(trimethylsilyl)tricyclo-[1.1.0.$0^{2,4}$]butane—a second tetrahedrane derivative (C) 1050
– Unusual geometry of a sterically congested analogue of $(CH)_5^{\oplus}$ (C) 1232
– Very short C—C single bonds and their origin. The central bond length in bitetrahedryl (C) 1226
Strontium compounds, LiSrN—a three dimensional structural arrangement of corner and edge sharing orthorhombic bipyramids, $NLi_{2/2}Sr_{4/4}$ (C) 201
Structure elucidation, Anion coordination and Cl−H···Cl bridges in the low-melting poly(hydrogen chloride) $Me_3N \cdot 5HCl$ (C) 1697
– *N*-Cesiocarbazole · pmdta and *N*-potassiocarbazole · pmdta (PMDTA = *N*,*N*,*N*′,*N*″,*N*″-pentamethyldiethylenetriamine). Cation size and multihapto bonding (C) 1224
– Complete identification of C-C connectivities by two-dimensional INADEQUATE NMR spectroscopy with composite pulses (C) 738
– all-*cis*-1,4,7,10-cyclododecatetraene—X-ray structure analysis and photoelectron spectrum (C) 1379
– Do any AB_n molecules have anomalous shapes? ν_3 of TiF_4 and TiF_3 and their relevance to the shape of TiF_2 (C) 313
– Double-bond geometry of norbornene: neutron diffraction measurement of a derivative at 15 K (C) 1239
– $K_4Al_2Nb_{11}O_{20}F$—the missing link in cluster condensation (C) 1662
– LiCaN and Li_4SrN_2, derivatives of the fluorite and lithium nitride structures (C) 1702
– Organic dications: gas phase experiments and theory in concert (A) 1321
– $[P_4Aryl_6][Me_3SnF_2]_2$ (Aryl = 2,6-$(MeO)_2C_6H_3$): an unusual ion pair consisting of a planar 2,4-diphospha-1,3-diphosphoniacyclobutane dication and the difluorotrimethylstannate anion (C) 1507
– Structure of anodic coatings on aluminum (AM) 951
– Ta_2Se: a tantalum-rich selenide with a new layer structure (C) 1660
– The acetonitrile(pentafluorophenyl)xenon(II) cation, $[MeCN-Xe-C_6F_5]^{\oplus}$: the first structural characterization of a xenon-carbon bond (C) 1506
– Two-dimensional NMR methods for establishing molecular connectivity. A chemist's guide to experiment selection, performance and interpretation (B) 1071
– X-ray structure analysis of α-lithiophenylacetonitrile · lithium diisopropylamide · 2 tetramethylethylenediamine—a "quasi-dianion complex" (C) 1392
Studies in organic chemistry, Preparative acetylenic chemistry (B) 631
Studies in physical and theoretical chemistry, kinetics of electrochemical metal dissolution (B) 935
– Computational chemistry. An emphasis on practical calculations (B) 1071
– Intermolecular complexes (B) 502
Sulfenes, Bis(trifluoromethyl)sulfene $(CF_3)_2C=SO_2$, isolated as adduct (C) 221
Sulfur compounds, Alkylidene sulfur difluorides: $F_5S(F_3C)C=SF_2$ and $(F_3C)_2C=SF_2$. Synthesis, structure, and structure predictions (C) 769
– 3,3′:4,4′-Bis(thieno[2,3-*b*]thiophene): a novel fused heteroarene (C) 1222
– Bis(trifluoromethyl)sulfene $(CF_3)_2C=SO_2$, isolated as adduct (C) 221
– Dithia dications from cyclic and acyclic precursors by gas-phase oxidation ("charge stripping") of 3e/2c-radical cations (C) 1275
– Formation and reactivity of silicon-sulfur and silicon-selenium double bonds. The first X-ray structure of a silanethione (C) 1016
– Formation of 2,4,4-trimethylthiete by photodecarbonylation of 3,3,5-trimethyl-2(3*H*)-thiophenone (C) 1499
– Metal-induced reduction of sulfur dioxide to sulfur monoxide and sulfur (C) 1342
– Modeling organic surfaces with self-assembled monolayers (AM) 506
– $S_4(CN)_8$, a blue-black high-molecular sulfur-cyanogen compound with 6π- and 8π-electron structural elements (C) 609
– Sulfur-cyanide pentafluoride SF_5NC (C) 1255
– Sulfur-pentafluoride isocyanide, SF_5NC (C) 1256
– Synthesis, structure and reactivity of sulfur-rich cyclopentadienyl-transition metal complexes: sulfur chemistry from an organometallic point of view (R) 1613
– The chemistry of sulphones and sulphoxides (B) 1070
– The thiophene analogue of porphyrin: tetrathiaporphyrin dication (C) 1651
– Thiosulfinic acids: a new class of chiral organosulfur compounds (C) 97
– TlSPh and TlS*t*Bu, Thallium(I) thiolates with novel cagelike structural units: $[Tl_5(SPh)_6]^{\ominus}/[Tl_7(SPh)_6]^{\oplus}$ and $[Tl_8(StBu)_8]$ (C) 1682
– 1,3,5-Trithia-2,4,6-triazapentalenyl—a stable sulfur-nitrogen radical (C) 920
Superconductors, aurivillius phases: a possible new class of metal oxide superconductors (C) 750
– Ferroelectricity and superconductivity (AM) 379
– Conference report (AM) 124
– Generation of complex metal oxides by aerosol processes: superconducting ceramic particles and films (AM) 794
– High resolution electron microscopy of the high-T_c superconductor $Bi_{2+x}Sr_2Ca_{1-x}Cu_2O_{8+\delta}$ (AM) 810
– Materials issues in electronic systems (AM) 640
– Studies of high temperature superconductors (B) 1592
– Superconductivity at 7.5 K and ambient pressure in polycrystalline pressed samples of β_p-$(BEDT\text{-}TTF)_2I_3$ (AM) 953

- Superconductors: the breakthrough (B) 1139
- The crystal chemistry of high-temperature oxide superconductors and materials with related structures (R) 1472

Surfaces, Addition of free Me_2Ge: to alkenes and alkynes on glass surfaces in the presence of water (C) 1028
- Conference report (AM) 1755, 523
- Imaging organic molecules with the scanning tunneling microscope (AM) 1127
- Imaging surfaces, electric charges and magnetic domains with the atomic force microscope (AM) 1578
- Metal organic chemical vapor deposition (MOCVD) perspectives and prospects (AM) 1110
- Methods of surface analysis (B) 1764
- Modeling organic surfaces with self-assembled monolayers (AM) 506
- Solids and surfaces: a chemist's view of bonding in extended structures (B) 1070
- Spectroscopy of surfaces (B) 963
- Structure of anodic coatings on aluminum (AM) 951
- Surface chemistry with the scanning tunneling microscope (AM) 117
- Tailoring semiconductor crystals to atomic dimensions (AM) 1098

Symmetry reduction, symmetry reduction in solid solutions: a new method for materials design (AM) 377

Synchrotron radiation, Introduction to synchrotron radiation (B) 791

Synthetic methods, Application of the dimethyl(phenyl)silyl group as a masked form of the hydroxy group in the synthesis of an L-*glycero*-α-D-*manno*-heptopyranoside-containing trisaccharide from the dephosphorylated inner core region of *neisseria meningitidis* (C) 1504
- Cyclizations via palladium-catalyzed allylic alkylations (R) 1173
- Gene synthesis (R) 716
- General aspects and optimization of enantioselective biocatalysis in organic solvents: the use of lipases (R) 695
- Intramolecular, stoichiometric (Li, Mg, Zn) and catalytic (Ni, Pd, Pt) metalloene reactions in organic synthesis (R) 38
- Side-chain homologues of 20-hydroxyecdysone: synthesis, configurational assignment, and biochemical characterization (C) 1515
- The stereoselectivity of intermolecular free radical reactions (R) 969

Tantalum compounds, Stabilization of niobium(0) and tantalum(0) in mixed metal clusters containing silver atoms (C) 471
- Ta_2Se: a tantalum-rich selenide with a new layer structure (C) 1660

Tartaric acid esters, Lipophilic tartaric acid esters as enantioselective ionophores (R) 1147

Tautomerization, Ethynol: photochemical generation in an argon matrix, IR spectrum, and photoisomerization to ketene (C) 181
- Investigation of the tautomerism of ^{15}N-labeled hydroporphyrins by dynamic NMR spectroscopy (C) 76

Technetium compounds, A polymeric technetium compound of the composition $[Tc_2O_3(C_5Me_5)]_n$ (C) 1055

Tellurobenzaldehyde, tellurobenzaldehyde by Staudinger-chalcogenation of the ylide benzylidenetriphenylphosphorane (C) 179

Template syntheses, A chemical approach to protein design—template-assembled synthetic proteins (TASP) (R) 535
- A synthetic molecular trefoil knot (C) 189
- 3-Arylsulfonyloxazolidines as chiral templates: asymmetric synthesis of 2-substituted 2-hydroxycyclohexanecarbaldehydes from 2-hydroxymethylenecyclohexanone (C) 67
- Carbohydrates as chiral templates: stereoselective synthesis of β-amino acids (C) 1068
- Carbohydrates as chiral templates: stereoselective tandem Mannich-Michael reactions for the synthesis of piperidine alkaloids (C) 1067
- Sequence dependence of template-directed syntheses of hexadeoxynucleotide derivatives with 3′—5′ pyrophosphate linkage (C) 1235

Terpenes, Carbocycle construction in terpene synthesis (B) 1537

Tetrahedranes, Tri-*tert*-butyl(trimethylsilyl)tricyclo[1.1.0.$0^{2,4}$]butane—a second tetrahedrane derivative (C) 1050

Textiles, Polymer modified textile materials (B) 384

Thallium compounds, Tl^I-Tl^I interactions in the molecular state—an MO analysis (C) 1688
- TlSPh and TlS*t*Bu, Thallium(I) thiolates with novel cagelike structural units: $[Tl_5(SPh)_6]^{\ominus}[Tl_7(SPh)_6]^{\oplus}$ and $[Tl_8(StBu)_8]$ (C) 1682

The chemistry of functional groups, The chemistry of sulphones and sulphoxides (B) 1070

Theoretical chemistry, theoretical chemistry en route to a theory of chemistry (R) 268
- Covalent versus dative bonds to main group metals, a useful distinction (R) 992
- Fundamentals of silicon chemistry: molecular states of silicon-containing compounds (R) 1627
- Introduction to the modern theory of metals (B) 1592
- Structure and dynamics of chiral molecules (R) 571
- The active site of glutathione reductase: an example of near transition-state structures (C) 1023
- Theory and methods of calculation of molecular spectra (B) 1281

Thermolysis, Water elimination from phosphorus-oxygen compounds: the formation of 2-phosphapropene by thermolysis of dimethylphosphane oxide (C) 911

Thin films, A novel monolithic thin-film electroluminescent device with extrinsic memory (AM) 241
- Generation of complex metal oxides by aerosol processes: superconducting ceramic particles and films (AM) 794
- Low temperature deposition of a CaF_2 insulator layer on GaAs (AM) 1581
- Monolayers and Langmuir-Blodgett multilayers of discotic liquid crystals? (AM) 1574

Thiocarbamates, Selenium-catalyzed synthesis of *S*-alkyl thiocarbamates from amines, carbon monoxide, sulfur, and alkyl halides (C) 452

Thioesters, Radical tri- and pentaanions of benzenedi- and benzenetriglyoxylate thioesters (C) 906

Thiosulfinic acids, a new class of chiral organosulfur compounds (C) 97

Tin compounds, $[P_4Aryl_6][Me_3SnF_2]_2$ (Aryl = 2,6-$(MeO)_2C_6H_3$): an unusual ion pair consisting of a planar 2,4-diphospha-1,3-diphosphoniacyclobutane dication and the difluorotrimethylstannate anion (C) 1507
- Synthesis and structure of digerma- and distannacyclobutenes (C) 603

Titanium compounds, A *trans*-dimethyl derivative of octahedral Ti^{IV}: alkylation and arylation of Ti^{IV}-Schiff base complexes (C) 64
- A sensitive spectroscopic probe for monitoring changes in the coordination sphere of titanium: eight-membered dioxatitanacycles and their organometallic derivatives (C) 66
- Do any AB_n molecules have anomalous shapes? ν_3 of TiF_4 and TiF_3 and their relevance to the shape of TiF_2 (C) 313
- Enantioselective aldol reaction of *tert*-butyl acetate using titanium-carbohydrate complexes (C) 495
- Enantioselective allylation of carbonyl compounds with titanium-carbohydrate complexes (C) 494
- Enantioselective synthesis of D-*threo*-β-hydroxy-α-amino acids with titanium-carbohydrate complexes (C) 497
- Metallocene carbene complexes and related compounds of titanium, zirconium, and hafnium (R) 397
- Structure of chloro(cyclopentadienyl)-bis(1,2:5,6-di-*O*-isopropylidene-α-D-glucofuranos-3-*O*-yl) titanate, a novel titanium-carbohydrate complex (C) 499
- Synthesis and structure of $[(C_5H_5)_2TiS_4AsCH_3]$—a new reagent for the synthesis of sulfur-rich heterocycles (C) 1269
- Synthesis and structure of $[\{(\eta^5\text{-}C_5Me_5)Ti(NH)\}_3N]$, a titanium imide nitride (C) 754
- Vinylcarbene complexes of titanocene (C) 610

Trace analysis, Activation analysis with charged particles (B) 1072

Transition state, Mechanism of the hetero-Diels–Alder reaction of oxadienes and alkenes: calculation of the acrolein/ethene system (C) 1371
- The active site of glutathione reductase: an example of near transition-state structures (C) 1023

Triazoles, 2,3-Dihydro-1*H*-1,2,4-triazol-1-yls, a novel group of stable radicals (C) 491
- First isolation of allenyl azides (C) 1675

Trinacrene, trinacrene—a product of structure-directed synthesis (C) 1261

Tropa derivatives, Unsaturated 1,4-*cis*- and 1,4-*trans*-diaminotetradeoxycycloheptites—enantiomerically pure, polyfunctionalized tropa derivatives by enzymatic hydrolysis (C) 1253

Tungsten compounds, Alkoxide clusters of molybdenum and tungsten as templates for organometallic chemistry: comparison with carbonyl clusters of the later transition elements (R) 432
- Comments on the molecular structure and bonding in $[W_4Cl(O)(OiPr)_9]$ and $[W_4(O)(OiPr)_{10}]$. Analogies with tetranuclear carbonyl clusters (C) 1368
- Versatile modes of allene bonding in the structures of $[W_2(OtBu)_6(C_3H_4)]$, $[W_2(OtBu)_6(C_3H_4)(CO)_2]$, and $[W_2(OtBu)_6(C_3H_4)_2]$ (C) 1523

Valenes, Azaoctabisvalenes (C) 1345

Vanadium compounds, $[VO(O_2CtBu)_3]$ and $[V_6O_6(\mu\text{-}O)_4(\mu\text{-}O_2CPh)_9]$: structural characterization of a mononuclear V^V and a (2+4)-nuclear $V^{IV}V^V_5$ carboxylato complex. Models for vanadate-dependent peroxidases (C) 1221

Van der Waals molecules, Structure and properties of the cryptophane-E/$CHCl_3$ complex, a stable van der Waals molecule (C) 1246

Vapor Deposition, Conference report (AM) 1755
Vinylsulfonic acid esters, Intramolecular Diels–Alder reaction of vinylsulfonic acid esters (C) 202
Viologens, Poly-[*N*,*N*-(1,4-divinylbenzene-β,β'-diyl)-4,4'-bipyridinium dibromide], a novel conducting viologen polymer (AM) 807

Wade's rules, The 30-electron rule for triple-decker complexes—vanadium, niobium and tantalum complexes as illustrative examples (C) 319

Xenon compounds, The acetonitrile-(pentafluorophenyl)xenon(II) cation, $[MeCN-Xe-C_6F_5]^{\oplus}$: the first structural characterization of a xenon-carbon bond (C) 1506

Ylides, Tellurobenzaldehyde by Staudinger-chalcogenation of the ylide benzylidenetriphenylphosphorane (C) 179

Zeolites, A silicogermanate with a Si:Ge ratio ≥ 2—an MFI zeolite of novel composition (C) 81
- Advanced zeolite materials science (AM) 359
- Catalysis on zeolites (B) 381
- Encapsulation of polypyrrole chains in zeolite channels (C) 1692
- Location of *para*-xylene in Yb-faujasite (zeolite Y) by neutron diffraction (C) 770
- Zeolite molecular sieves (B) 964

Ziegler catalysts, The first example of an *ethylene*-selective soluble Ziegler catalyst of the zirconocene class (C) 1511
Zinc compounds, Copper(I)-promoted Michael-addition reaction of organozincs of esters, nitriles, and α-amino acids (C) 351
Zintl phases, $Na_xMg_{5-x}Ga_9$, a new intermetallic phase as a link between zintl phases and metals (C) 58
Zirconium compounds, Asymmetric oligomerization of propene and 1-butene with a zirconocene/alumoxane catalyst (C) 1216
- Dimeric $[Cp_2Zr(CH_2O)]$, a novel (η^2-formaldehyde)metal complex from carbon monoxide (C) 630
- Double stereodifferentiation in the formation of isotactic polypropylene at chiral $(C_5H_4CHMePh)_2ZrCl_2$/methylalumoxane catalysts (C) 628
- Metallocene carbene complexes and related compounds of titanium, zirconium, and hafnium (R) 397
- The first example of an *ethylene*-selective soluble Ziegler catalyst of the zirconocene class (C) 1511